

Hereditary pancreatitis

Richard M Charnley

Richard M Charnley, Consultant Surgeon, Freeman Hospital, Newcastle upon Tyne, NE7 7DN, UK

Correspondence to: Richard M Charnley, DM FRCS, Consultant Surgeon, Freeman Hospital, Newcastle upon Tyne, NE7 7DN, UK. richard.charnley@nuth.northy.nhs.uk

Received: 2002-11-30 **Accepted:** 2002-12-08

Abstract

Hereditary pancreatitis is an autosomal dominant condition, which results in recurrent attacks of acute pancreatitis, progressing to chronic pancreatitis often at a young age. The majority of patients with hereditary pancreatitis express one of two mutations (R122H or N29I) in the cationic trypsinogen gene (PRSS1 gene). It has been hypothesised that one of these mutations, the R122H mutation causes pancreatitis by altering a trypsin recognition site so preventing deactivation of trypsin within the pancreas and prolonging its action, resulting in autodigestion. Families with these two mutations have been identified in many countries and there are also other rarer mutations, which have also been linked to hereditary pancreatitis.

Patients with hereditary pancreatitis present in the same way as those with sporadic pancreatitis but at an earlier age. It is common for patients to remain undiagnosed for many years, particularly if they present with non-specific symptoms. Hereditary pancreatitis should always be considered in patients who present with recurrent pancreatitis with a family history of pancreatic disease. If patients with the 2 common mutations are compared, those with the R122H mutation are more likely to present at a younger age and are more likely to require surgical intervention than those with N29I. Hereditary pancreatitis carries a 40 % lifetime risk of pancreatic cancer with those patients aged between 50 to 70 being most at risk in whom screening tests may become important.

Charnley RM. Hereditary pancreatitis. *World J Gastroenterol* 2003; 9(1): 1-4
<http://www.wjgnet.com/1007-9327/9/1.htm>

INTRODUCTION

Hereditary pancreatitis (HP) is an autosomal dominant condition characterised by recurrent attacks of acute pancreatitis and progressing to the development of chronic pancreatitis over a variable period of time. Symptoms usually begin in childhood or adolescence and with time, exocrine and/or endocrine insufficiency may develop. The clinical spectrum of hereditary pancreatitis was first reported in 1952^[1]. Mutations causing HP have been identified in the PRSS1 gene which encodes cationic trypsinogen^[2-4]. This article discusses the genetics of HP, its pathophysiology and clinical spectrum.

THE GENETICS OF HEREDITARY PANCREATITIS

HP is an autosomal dominant condition with 80 % penetrance. The specific mutations responsible for HP were identified in 1996 when it was confirmed that the hereditary pancreatitis

gene could be mapped to chromosome 7q35^[5,6]. Whitcomb *et al* demonstrated that a mutation in these patients existed in the third exon of the cationic trypsinogen gene (PRSS1)^[7]. This mutation, a guanine (G) to adenine (A) transition, alters arganine (CGC) to histidine (CAC) at codon 117 (using the chymotrypsin numbering system) and was originally known as R117H. This first mutation is easily identified because it creates a novel recognition site for the restriction endonuclease *Afl*III. More recently, it has been shown that a neutral polymorphism within this enzyme recognition site may produce a false negative result^[8]. A second mutation in the cationic trypsinogen gene was subsequently discovered, which was found to be a single A to thiamine (T) transversion mutation in exon 2 resulting in an asparagine (ACC) to isoleucine (ATC) substitution at amino acid 21^[9]. These two mutations (R117H and N21I) have now been identified in families with hereditary pancreatitis from many countries including France^[4], Germany^[9], United Kingdom^[10], Japan^[11] and the USA^[3,7]. A further mutation, which appears to be much less common, is the A16V mutation, which was originally identified in three patients with idiopathic pancreatitis and in one patient with HP^[12]. There is also evidence that mutations in genes other than the cationic trypsinogen gene might be associated with HP^[13]. Since the discovery of the cationic trypsinogen gene mutations, a new nomenclature system for human gene mutations has been devised and accepted. This has changed the names of the common mutations from R117H to R122H and N21I to N29I^[14].

PATHOPHYSIOLOGY

The mechanism by which mutations of the cationic trypsinogen gene cause hereditary pancreatitis is important for several reasons. Firstly, the cellular mechanisms of acute pancreatitis and progression to chronic pancreatitis are poorly understood. Secondly it is not known why the pancreas of one individual is susceptible to alcohol whilst the pancreas of another is not. Thirdly, focusing on the link between genetics and pancreatitis might provide a clue to the etiology of pancreatic cancer which can occur as a complication in sporadic and hereditary pancreatitis.

Trypsinogen is secreted by the pancreatic acinar cell^[15]. It is activated to trypsin within the duodenum by enterokinase, which cleaves an 8-aminoacid N-terminal peptide. Trypsin then activates a cascade of digestive enzyme precursors. A number of mechanisms exist to prevent inappropriate activation of trypsin within the pancreas before its secretion into the duodenum. It is hypothesised that the R122H mutation alters a trypsin recognition site, which would prevent deactivation of trypsin within the pancreas, thus prolonging its action^[2]. The mechanism whereby the N29I mutation causes pancreatitis is unclear. It has been speculated, however, that the N29I mutation would enhance autoactivation of trypsinogen, altering the binding of pancreatic secretory trypsin inhibitor (PSTI)^[3] or impairing trypsin inactivation by altering the accessibility of the initial hydrolysis site to trypsin. Predicted molecular conformational changes in the structure of trypsin support this^[16]. The pathogenic mechanism whereby the A16V mutation causes pancreatitis is speculative but it is thought to alter the cleavage site of the signal peptide^[12]. Because the two common mutations, R122H and N29I produce such a similar

clinical picture, it has been speculated that these mutations, rather than being the cause of hereditary pancreatitis, simply represent markers for a number of linked pancreatic defects. There appears no doubt, however, that inappropriate prevention of the deactivation of trypsin within the pancreas is responsible for HP in the majority of cases.

The penetrance of cationic trypsinogen gene mutations remains at approximately 80 % in the majority of studies. To investigate factors contributing to this, a study of monozygotic twins with HP was carried out^[17]. Of 11 sets of twins, seven were suitable for this study. Whereas four of these seven sets were concordant for pancreatitis, three of the seven sets of twins (43 %) were discordant for phenotypic expression of pancreatitis. The overall penetrance in the seven pairs of twins was 78 %. The conclusion from this study was that genetic and/or environmental factors contribute to the expression and age of onset of HP. As yet the mechanism of non-penetrance remains unclear.

CLINICAL PRESENTATION IN HEREDITARY PANCREATITIS

The initial presentation of a patient with HP is usually indistinguishable from a case of sporadic pancreatitis. The clinical presentation is variable but typical patients present with recurrent attacks of acute pancreatitis in childhood, progressing to chronic pancreatitis with time^[1,18]. The presentation during an acute attack is identical to an attack of gallstone-induced, alcoholic or idiopathic, acute pancreatitis. The presentation of chronic pancreatitis in these patients is likewise indistinguishable from alcoholic, idiopathic or other forms of chronic pancreatitis^[18-20]. Pediatric patients with HP have a similar presentation to idiopathic juvenile chronic pancreatitis^[21]. It is however very common for these patients to remain undiagnosed for many years having often suffered from chronic symptoms since childhood. We have found that recognition of the disease within a family often results in several relatives being newly diagnosed with pancreatitis whereas previously they had been labelled as "peptic ulcer" or "chronic abdominal pain". In Newcastle upon Tyne, UK, the pancreatic clinic now has individuals belonging to thirteen families with hereditary pancreatitis. Data on nine of these families has been previously published^[10]. The R122H (R117H) mutation was identified in three families and the N29I (N21I) mutation was demonstrated in a further five families. In a remaining family, no mutations were demonstrated in any of the five exons of the PRSS1 gene. The families and patients belonging to the R122H group were compared with those belonging to the N29I group. Comparison of clinical details including complications of pancreatitis was carried out. The mean age at onset of symptoms of pancreatitis was lower in the R122H group at 8.4 vs 6.5 years, ($P=0.007$) and more patients with the R122H mutation had developed symptoms by the age of 20 years (89 vs 64 %). More patients with the R122H mutation required surgical intervention (8 of 12 vs 4 of 17, $P=0.029$) and this occurred at an earlier age. There was also a tendency for more patients with the R122H mutation to develop exocrine failure but the incidence and age of onset of endocrine failure (as measured by the development of insulin dependent diabetes mellitus) was similar in both groups. Patients in both groups identified alcohol as a provoking factor for the symptoms. These observations were also noted in the original description of the N21I mutation in 1997^[3] and have also been noted by the European Registry of Hereditary Pancreatitis and Pancreatic Cancer (EUROPAC)^[22]. It is also clear that as well as hereditary pancreatitis being identical to other forms of pancreatitis in terms of the mode of clinical presentation, radiological and histopathological features are also identical^[23]. Apart from earlier onset and delay in diagnosis, hereditary pancreatitis has been found to have a

natural history similar to that of chronic alcoholic pancreatitis in terms of a similar prevalence of pancreatic calcification, a similar amount of pancreatic insufficiency both endocrine and exocrine but a higher prevalence of pseudocysts^[24].

CATIONIC TRYPSINOGEN GENE MUTATIONS IN NON-HEREDITARY PANCREATITIS

Taking a family history is very important in all patients with pancreatitis because the majority of patients with cationic trypsinogen gene mutations have a clear cut family history of pancreatitis. It is, however, common for patients to be referred to a pancreatic specialist with so-called idiopathic pancreatitis without a reliable family history having been obtained^[25]. It has also been considered whether idiopathic chronic pancreatitis might be due to PRSS1 gene mutations. An investigation of patients with chronic alcoholic pancreatitis showed no evidence of the R122H or N29I mutation in 21 patients^[26] but a much larger and important study investigated 221 patients with idiopathic chronic pancreatitis and no family history. The entire PRSS1 gene was sequenced in these patients. Only three patients had mutations, one with R122H and two patients with A16V^[27]. A genetic background has also been investigated in patients with idiopathic juvenile chronic pancreatitis, a disease which closely mimics the clinical pattern of hereditary pancreatitis^[28]. The R122H mutation was detected in one patient with idiopathic juvenile chronic pancreatitis and the A16V mutation was also found in one patient. It is clear from these studies that new mutations do occur and that screening of individuals with idiopathic pancreatitis for cationic trypsinogen gene mutations is worthwhile. It is, therefore, our policy in patients with idiopathic pancreatitis, after exclusion of other causes, to perform genetic counselling and genetic testing. We have found that patients are keen to know their genetic status in relation to this disease.

RISK OF CANCER IN HEREDITARY PANCREATITIS

Sporadic chronic pancreatitis carries a significantly increased risk of pancreatic cancer. This has been clearly demonstrated by a multi-centre historical cohort study of over 2000 patients^[29]. The standardized incidence ratio, i.e. the ratio of observed to expected pancreatic cancers was 16.5. This study may have been subject to detection bias in that increased surveillance of chronic pancreatitis patients may have increased the number of cancers diagnosed compared with the general population. A study of Swedish patients, however, confirmed an increased risk of pancreatic cancer in sporadic chronic pancreatitis but with a standardised incidence ratio of 3.8^[30]. Patients with HP have not been included in either of these studies but have since been examined for the risk of developing pancreatic cancer by the International Hereditary Pancreatitis Study Group. A cohort of 246 patients with hereditary pancreatitis was identified from ten countries with a mean follow-up period of over 14 years^[31]. Eight patients with pancreatic adenocarcinoma were identified yielding a standardized incidence ratio of 53.3. The estimated cumulative risk of pancreatic cancer developing in these patients was nearly 40 % and was greater for patients with a paternal inheritance pattern. These figures have been confirmed by the Midwest Multicentre Pancreatic Study Group^[32]. The conclusions from these cancer studies are that, firstly chronic pancreatitis is a risk factor for pancreatic cancer and secondly hereditary pancreatitis puts patients at an even higher risk of developing cancer than the sporadic disease. Although it is not absolutely clear whether the risk of cancer is due to prolonged inflammatory change or whether it is related to the presence of a cationic trypsinogen mutation per se, the evidence available at present indicates that those patients with HP who

develop cancer, are those with a prolonged history of chronic pancreatitis^[32]. The number of cancers, which have developed in HP patients have so far not allowed an investigation into which mutation (s) might predispose to cancer more than another. This data, however, will be available with time. A study of pancreatic tissue from 34 patients with sporadic ductal adenocarcinoma has shown no specific relationship between the R122H mutation and pancreatic cancer^[33]. Further such studies are expected as tissue from patients with hereditary pancreatitis becomes available for analysis.

MANAGEMENT DILEMMAS IN HEREDITARY PANCREATITIS

When faced with a patient or a family with a possible diagnosis of HP, three questions are commonly asked. Firstly, what can be done about the patient with pancreatitis? Secondly, are other relatives likely to be affected? Thirdly, what can be done to reduce the risk of cancer?

Management of the pancreatitis

There are no specific medical therapies recommended in patients with HP. The management of acute attacks of pancreatitis are the same as for the sporadic disease that is, rehydration, analgesia and careful monitoring. Severe necrotising pancreatitis is rare in HP but pseudocysts seem to be relatively common. It has been suggested that antioxidant therapy may be helpful to prevent acute attacks but there is no evidence to support this and it is not recommended. Chronic pancreatitis should be treated as for any other patients. Enzyme supplements are likely to be required and analgesics as necessary. If diabetes mellitus occurs it is likely to require insulin therapy. Surgical treatment is for complications such as pseudocyst, biliary obstruction or duodenal obstruction. In older patients requiring surgery, a total pancreatectomy should be considered in order to abolish the cancer risk (see below).

Genetic counselling of relatives

Relatives should be told that although the majority of HP cases are revealed by the age of 18, the disease may not manifest itself until the age of 30 or older. In these unaffected individuals, genetic testing confers no advantage and should be discouraged. Since unaffected (non-carrier) individuals and unaffected carriers do not have pancreatitis, they carry no increased risk of developing cancer.

Screening of hereditary pancreatitis patients for cancer

Since patients with this disease exhibit a 53-fold increased risk of pancreatic cancer with a cumulative risk of 40 % by the age of 70, an attempt at screening would appear to be essential. Unfortunately, no adequate screening test exists. The measurement of tumor markers, endoscopic techniques and radiological imaging lack the sensitivity and specificity for early diagnosis. Tumors are particularly difficult to detect on a background of chronic pancreatitis. It is thought therefore that molecular based strategies are likely to offer the best opportunities for the screening of these high risk patients for pancreatic ductal adenocarcinoma^[34]. It has been suggested that the banking of blood and pancreatic juice samples should be mandatory in any screening protocol and that imaging of the pancreas should be carried out by endoscopic ultrasound^[35]. One such protocol for the secondary screening of patients with HP has been established by EUROPAC (European Registry of Hereditary Pancreatitis and Pancreatic Cancer). As part of a research program only, affected individuals over the age of 30 are offered imaging by CT and endoscopic ultrasound (EUS), followed after genetic counselling, by genetic analysis of pancreatic juice obtained at ERCP for K-ras mutations. Patients negative for K-ras continue with repeat screening at

3 yearly intervals by CT, EUS and K-ras analysis of pancreatic juice. Patients who are K-ras positive undergo further genetic analysis in the form of p53, p16 and aberrant methylation. If positive, these patients may be at risk of pancreatic ductal carcinoma and an attempt should be made to obtain cells for cytology by ERCP brushing of the pancreatic duct. The ultimate preventative measure in these patients would be a total pancreatectomy but this is a relatively high morbidity operation with the certainty of becoming diabetic. Certainly any patient with HP aged 30 or over, who requires surgery for relief of symptoms should undergo a total pancreatectomy in order to abolish the cancer risk rather than a lesser procedure. This is not, however, appropriate in patients who are well unless there is clear evidence that they possess cellular atypia or a focal abnormality suspicious of cancer.

CONCLUSIONS

Hereditary pancreatitis is a fascinating condition which has provided new insights into the pathophysiology of pancreatitis. There are however many unanswered questions particularly in relation to the ways in which these mutations relate to pancreatitis and cancer. Management of these patients should be carried out by a team of experienced pancreatic specialists who are also able to provide genetic counselling. Registration of patients with one of the large Hereditary Pancreatitis Registries is essential if management strategies are to be improved and genetic research to be continued.

REFERENCES

- 1 **Comfort MW**, Steinberg AG. Pedigree of a family with hereditary chronic relapsing pancreatitis. *Gastroenterology* 1952; **21**: 54-63
- 2 **Whitcomb DC**. Hereditary pancreatitis: new insights into acute and chronic pancreatitis. *Gut* 1999; **45**: 317-322
- 3 **Gorry MC**, Ghabbaizadeh D, Furey W, Gates LK Jr, Preston RA, Aston CE, Zhang Y, Ulrich C, Ehrlich GD, Whitcomb DC. Mutations in the cationic trypsinogen gene are associated with recurrent acute and chronic pancreatitis. *Gastroenterology* 1997; **113**: 1063-1068
- 4 **Ferec C**, Raguene O, Salomon R, Roche C, Bernard JP, Guillot M, Quere I, Faure C, Mercier B, Audrezet MP, Guillausseau PJ, Dupont C, Munnich A, Bignon JD, Le Bodic L. Mutations in the cationic trypsinogen gene and evidence for heterogeneity in hereditary pancreatitis. *J Med Genet* 1999; **36**: 228-232
- 5 **Whitcomb DC**, Preston RA, Aston CE, Sossenheimer MJ, Barua PS, Zhang Y, Wong-Chong A, White GJ, Wood PG, Gates LK Jr, Ulrich C, Martin SP, Post JC, Ehrlich GD. A gene for hereditary pancreatitis maps to chromosome 7q35. *Gastroenterology* 1996; **110**: 1975-1980
- 6 **Pandya A**, Blanton SH, Landa B, Javaheri R, Melvin E, Nance WE, Markello T. Linkage studies in a large kindred with hereditary pancreatitis confirms mapping of the gene to a 16-cM region on 7Q. *Genomics* 1996; **38**: 227-230
- 7 **Whitcomb DC**, Gorry MC, Preston RA, Furey W, Sossenheimer MJ, Ulrich CD, Martin SP, Gates LK Jr, Amann ST, Toskes PP, Liddle R, McGrath K, Uomo G, Post JC, Ehrlich GD. Hereditary pancreatitis is caused by a mutation in the cationic trypsinogen gene. *Nat Genet* 1996; **14**: 141-145
- 8 **Howes N**, Greenhalf W, Rutherford S, O'Donnell M, Mountford R, Ellis I, Whitcomb D, Imrie C, Drumm B, Neoptolemos JP. A New polymorphism for the R122H mutation in hereditary pancreatitis. *Gut* 2001; **48**: 247-250
- 9 **Teich N**, Mossner J, Keim V. Mutations of the cationic trypsinogen in hereditary pancreatitis. *Hum Mutat* 1998; **12**: 39-43
- 10 **Creighton JE**, Lyall R, Wilson DI, Curtis A, Charnley RM. Mutations of the cationic trypsinogen gene in patients with hereditary pancreatitis. *Br J Surgery* 2000; **87**: 170-175
- 11 **Nishimori I**, Kamakura M, Fujikawa-Adachi K, Morita M, Onishi S, Yokoyama K, Makino I, Ishida H, Yamamoto M, Watanabe S, Ogawa M. Mutations in exons 2 and 3 of the cationic trypsinogen gene in Japanese families with hereditary pancreatitis. *Gut*

- 1999; **44**: 259-263
- 12 **Witt H**, Luck W, Becker M. A signal peptide cleavage site mutation in the cationic trypsinogen gene is strongly associated with chronic pancreatitis. *Gastroenterology* 1999; **117**: 7-10
- 13 **Bartness MA**, Duerr RH, Ford MA, Zhang L, Aston CE, Barmada M. Potential linkage of a pancreatitis associated gene to chromosome 12. *Pancreas* 1998; **17**: 426
- 14 **Antonarakis SE**. Recommendations for a nomenclature system for human gene mutations. Nomenclature Working Group. *Hum Mutat* 1998; **11**: 1-3
- 15 **Scheele G**, Kern H. The exocrine pancreas. In: Desnuelle P, Sjöström H, Norén O, eds. *Molecular and Cellular Basis of Digestion*. Amsterdam: Elsevier 1986: 173-194
- 16 **Whitcomb DC**. Hereditary pancreatitis: new insights into acute and chronic pancreatitis. *Gut* 1999; **45**: 317-322
- 17 **Amann ST**, Gates LK, Aston CE, Pandya A, Whitcomb DC. Expression and penetrance of the hereditary pancreatitis phenotype in monozygotic twins. *Gut* 2001; **48**: 542-547
- 18 **Perrault J**. Hereditary pancreatitis. *Gastroenterol Clin North Am* 1994; **23**: 743-752
- 19 **Konzen KM**, Perrault J, Moir C, Zinsmeister AR. Long-term follow-up of young patients with chronic hereditary or idiopathic pancreatitis. *Mayo Clinic Proc* 1993; **68**: 1993
- 20 **Kattwinkel J**, Lapey A, Di Sant' Agnese PA, Edwards WA. Hereditary pancreatitis: three new kindreds and a critical review of the literature. *Paediatrics* 1973; **51**: 55-69
- 21 **DuBay D**, Sandler A, Kimura K, Bishop W, Eimen M, Soper R. The modified Puestow procedure for complicated hereditary pancreatitis in children. *Journal of Paediatric Surgery* 2000; **35**: 343-348
- 22 **Howes N**, Rutherford S, McRonald F, Ellis I, Whitcomb D, Mountford R, Neoptolemos JP. For the UK and Ireland Consortium of EUROPAC. Trypsinogen mutations in families with Hereditary Pancreatitis in the UK and Ireland. *Int J Pancreatol* 1999; **25**: 237
- 23 **Sossenheimer MJ**, Aston CE, Preston RA, Gates LK Jr, Ulrich CD, Martin SP, Zhang Y, Gorry MC, Ehrlich GD, Whitcomb DC. Clinical characteristics of hereditary pancreatitis in a large family, based on high-risk haplotype. The Midwest Multi-Centre Pancreatic Study Group (MMPCG). *Am J Gastroenterol* 1997; **92**: 1113-1116
- 24 **Paolini O**, Hastier P, Buckley M, Maes B, Demarquay JF, Staccini P, Bellon S, Caroli-Bosc FX, Dumas R, Delmont J. The natural history of hereditary chronic pancreatitis: a study of 12 cases compared to chronic alcoholic pancreatitis. *Pancreas* 1998; **17**: 226-271
- 25 **Creighton J**, Lyall R, Wilson DI, Curtis A, Charnley R. Mutations of the cationic trypsinogen gene in patients with chronic pancreatitis. *Lancet* 1999; **354**: 42-43
- 26 **Teich N**, Mossner J, Keim V. Screening for mutations of the cationic trypsinogen gene: are they of relevance in chronic alcoholic pancreatitis? *Gut* 1999; **44**: 413-416
- 27 **Chen JM**, Piepoli Bis A, Le Bodic L, Ruzsniowski P, Robaszekiewicz M, Deprez PH, Ragueneo O, Quere I, Andriulli A, Ferec C. Mutational screening of the cationic trypsinogen gene in a large cohort of subjects with idiopathic chronic pancreatitis. *Clinical Genetics* 2001; **59**: 189-193
- 28 **Truninger K**, Kock J, Wirth HP, Muellhaupt B, Arnold C, von Weizsacker F, Seifert B, Ammann RW, Blum HE. Trypsinogen gene mutations in patients with chronic or recurrent acute pancreatitis. *Pancreas* 2001; **22**: 18-23
- 29 **Lowenfels AB**, Maisonneuve P, Cavallini G, Ammann RW, Lankisch PG, Andersen JR, Dimagno EP, Andren-Sandberg A, Domellof L. Pancreatitis and the risk of pancreatic cancer. International Pancreatitis Study Group. *N Engl J Med* 1993; **328**: 1433-1437
- 30 **Ekbom A**, McLaughlin JK, Karlsson BM, Nyren O, Gridley G, Adami HO, Fraumeni JF Jr. Pancreatitis and pancreatic cancer: a population-based study. *J Natl Cancer Ins* 1994; **86**: 625-627
- 31 **Lowenfels AB**, Maisonneuve P, DiMagno EP, Elitsur Y, Gates LK Jr, Perrault J, Whitcomb DC. Hereditary pancreatitis and the risk of pancreatic cancer. International Hereditary Pancreatitis Study Group. *J Natl Cancer Ins* 1997; **89**: 442-446
- 32 **Whitcomb DC**, Applebaum S, Martin SP. Hereditary pancreatitis and pancreatic carcinoma. *Ann NY Acad Sci* 1999; **880**: 201-209
- 33 **Hengstler JG**, Bauer A, Wolf HK, Bulitta CJ, Tanner B, Oesch F, Gebhard S, Boettger T. Mutation analysis of the cationic trypsinogen gene in patients with pancreatic cancer. *Anticancer Research* 2000; **20**: 2967-2974
- 34 **Howes N**, Greenhalf W, Neoptolemos J. Screening for early pancreatic ductal adenocarcinoma in hereditary pancreatitis. *Medical Clinics North Am* 2000; **84**: 719-738
- 35 **Martin SP**, Ulrich CD 2nd. Pancreatic cancer surveillance in a high-risk cohort. Is it worth the cost? *Medical Clinics North Am* 2000; **84**: 739-747

Edited by Ma JY

Design of a ribozyme targeting human telomerase reverse transcriptase and cloning of it's gene

Zhi-Ming Hao, Jin-Yan Luo, Jin Cheng, Quan-Yin Wang, Guang-Xiao Yang

Zhi-Ming Hao, Department of Gastroenterology, 1st Hospital, Xi'an Jiaotong University, Xi'an 710061, Shaanxi Province, China

Jin-Yan Luo, Jin Cheng, Department of Gastroenterology, 2nd Hospital, Xi'an Jiaotong University, Xi'an 710061, Shaanxi Province, China

Supported by the National Natural Science Foundation, No. 39800061. (Reversal of malignant proliferation of a telomerase-specific ribozyme on colonic carcinoma cells)

Correspondence to: Dr. Zhi-Ming Hao, Department of Gastroenterology, 1st Hospital, Xi'an Jiaotong University, 1 Jiankanglu, Xi'an 710061, Shaanxi Province, China. haozhm@public.xa.sn.cn

Telephone: +86-029-5265523

Received: 2002-04-13 **Accepted:** 2002-04-27

Abstract

AIM: To design a hammerhead ribozyme targeting human telomerase reverse transcriptase (hTERT) and clone it's gene for future use in the study of tumor gene therapy.

METHODS: Using the software RNAstructure, the secondary structure of hTERT mRNA was predicted and the cleavage site of ribozyme was selected. A hammerhead ribozyme targeting this site was designed and bimolecular fold between the ribozyme and hTERT was predicted. The DNA encoding the ribozyme was synthesized and cloned into pGEMEX-1 and the sequence of the ribozyme gene was confirmed by DNA sequencing.

RESULTS: Triplet GUC at 1742 of hTERT mRNA was chosen as the cleavage site of the ribozyme. The designed ribozyme was comprised of 22nt catalytic core and 17nt flanking sequence. Computer-aided prediction suggested that the ribozyme and hTERT mRNA could cofold into a proper conformation. Endonuclease restriction and DNA sequencing confirmed the correct insertion of the ribozyme gene into the vector pGEMEX-1.

CONCLUSION: This fundamental work of successful designing and cloning of an anti-hTERT hammerhead ribozyme has paved the way for further study of inhibiting tumor cell growth by cleaving hTERT mRNA with ribozyme.

Hao ZM, Luo JY, Cheng J, Wang QY, Yang GX. Design of a ribozyme targeting human telomerase reverse transcriptase and cloning of it's gene. *World J Gastroenterol* 2003; 9(1): 104-107

<http://www.wjgnet.com/1007-9327/9/104.htm>

INTRODUCTION

Telomeres form the ends of eukaryotic chromosomes consisting of an array of tandem repeats of the hexanucleotide 5'-TTAGGG-3'. Their functions are protecting the ends of chromosomes against exonucleases and ligase, preventing the activation of DNA-damage checkpoints, and countering the loss of terminal DNA segments that occur during linear DNA replication^[1,2]. Telomerase, a ribonucleoprotein enzyme, add

the hexanucleotides to the ends of replicating chromosomes^[3]. It is believed that telomerase plays a crucial role in cellular senescence and immortalization^[3-5]. Telomerase is strongly repressed in most human somatic cells, and telomeres shorten progressively with each cell division^[6]. Most cancer cells express telomerase activity^[3,6-9]. The restoration of telomerase activity is considered to immortalize cells and to be an important step in carcinogenesis. Inhibition of telomerase can lead to telomere shorting and tumor cell death. Thus, specific inhibition of human telomerase is suggested to be an efficient means of tumor therapy. Nowadays, a limited number of means can be used experimentally to inhibit the activity of human telomerase including chemical agents^[10], antisense oligonucleotide^[11,12], peptide nucleic acid^[13], and ribozyme^[14-16]. Telomerase is composed of at least three subunits^[17]. The RNA subunit and the catalytic subunit are the essential components for telomerase activity^[18]. The RNA subunit of telomerase serves as the template for addition of short sequence repeats to the chromosome 3' ends^[19]. And the catalytic subunit, telomerase reverse transcriptase (TERT), is the most important component in telomerase complex which is responsible of catalytic activity of telomerase. The expression of TERT correlates with the presence of telomerase activity^[20]. These studies suggest that hTERT is a good target for cancer gene therapy.

Ribozymes are *sis-* or *trans-*acting, sequence-specific catalytic RNA molecules. Based on the studies about natural ribozymes, we can design site-specific *trans-*acting ribozymes to suppress the expression of genes by recognize and splice the mRNA. Hammerhead ribozyme and hairpin ribozyme are intensively studied because of their simple structures and dual activity of splicing as well as blocking^[21]. Ribozymes may surpass the efficiency of the antisense oligonucleotide and are considered a promising means of gene therapy^[22,23]. In this study, we designed a hammerhead ribozyme targeting hTERT and cloned the gene encoding the ribozyme for future study of this ribozyme in the treatment of malignancies.

MATERIALS AND METHODS

Materials

Plasmid vector pGEMEX-1, X-gal and IPTG were Promega products. T4 DNA ligase, Klenow fragment and restriction endonucleases used in this study were purchased from Sino-America Biotechnology Co.

Design of the hammerhead ribozyme

Using the software RNAstructure 3.6 (mFOLD for windows version), the full-length telomerase mRNA (GenBank NM003219) was analyzed and the second structure of telomerase mRNA was predicted. Since *trans-*acting hammerhead ribozymes preferentially recognize and cleave the GUC sequence, all the fragments containing GUC were candidate target sequences for ribozyme binding and cleavage. Considering the predicted local conformation near the GUC triplets and the nucleotide sequences flanking the GUCs, triplet GUC located at 1742 of the hTERT mRNA was chosen as the target site of ribozyme. According to the rules of hammerhead ribozyme design suggested by Haseloff *et al*^[24], the ribozyme

was primarily designed. Then, bimolecular fold between the ribozyme and substrate RNA was predicted and modification of the ribozyme sequence was made according to the prediction to improve the binding between the ribozyme and the substrate. The hammerhead ribozyme designed was comprised of 39 nucleotides, including 22nt catalytic core and 17nt (5' 7nt and 3' 10nt) flanking antisense sequence. The sequence is 5' - TCTCCGTCTGATGAGTCCGTGAGGACGAAACATAAAAAGA - 3' (The underlined are nucleotides complementary to the substrate).

Synthesis of the ribozyme gene

DNA synthesis was carried out by Shanghai Sangon Biotechnology Co. LTD. with 3 900 DNA autosynthesis instrument. The primers used for the ribozyme were as follows: 5' - CCCAAGCTTCTCCGTCTGATGAGTC - CGTGAGGACGAAAC - 3' (strand A) and 5' - GGAATTCATCGATAGATCTTTTATGTTTCGTCTCA - 3' (strand B). Twelve nucleotides from the 3' ends of the two strands were complementary to each other. A HindIII restriction site was introduced into the 5' end of strand A. And restriction sites of BglII, ClaI and EcoRI were introduced into the 5' end of strand B. Equal molecule of the two strands were mixed and annealed to form a hemiduplex. The hemiduplex was extended with Klenow fragment to form full duplexes. The reaction mixture contained 50 mM Tris-HCl (pH 7.2), 10 mM MgSO₄, 0.1 mM DTT, 0.4 mM dNTP mixture, 4 µg each of the two single strand oligonucleotides, 20 U Klenow fragment in a final volume of 50 µl. The reaction was carried out at 37 °C for an hour. The reaction mixture was extracted with phenol-chloroform and precipitated with sodium acetate ethanol (The methods referred to Sambrook *et al.*^[25]).

Cloning of ribozyme gene

The double strand DNA was digested with HindIII and EcoRI. The product was electrophoresed in 2 % agarose for purification followed by electroelution in a dialysis bag for DNA recovery. The recovered fragment was inserted into the HindIII/EcoRI site of plasmid vector pGEMEX-1 with T4 DNA ligase. *E. coli* JM109 was transformed with the recombinant plasmid and cultured on a solid medium containing ampicillin, X-gal and IPTG. Six white colonies were picked and plasmid was extracted by alkaline lysis. The plasmid was digested by HindIII, NotI, EcoRI, BglII, respectively. Endonuclease digests of plasmid DNA were analyzed on 1 % agarose. DNA sequencing was carried out to further confirm the inserted sequence of ribozyme gene (The methods referred to Sambrook *et al.*^[25]).

RESULTS

Selection of cleavage site and design of the ribozyme

Aided by computer prediction of RNA secondary structure, we selected the triplex GUC situated at 1 742 of the hTERT mRNA as the cleavage site (Figure 1). The ribozyme could co-fold with the substrate RNA to form a desired conformation in computer-aided prediction (Figure 2).

Analysis of the transformants

Six white colonies were picked. All the plasmids were cleaved into two fragments (1.0kb+3.0kb) by BglII. The plasmid from colony number 6 was digested with HindIII, NotI and EcoRI respectively. The plasmid DNA was linearized by HindIII or EcoRI but not by NotI. This result suggested plasmid from colony number 6 was a correct recombinant (Figure 3,4).

DNA sequencing

The DNA sequencing of the plasmid DNA from colony number

6 confirmed that the ribozyme gene was correctly inserted into the vector pGEMEX-1. This recombinant was named pGEMEX-1-RZ. The diagram of DNA sequencing is shown in Figure 5.

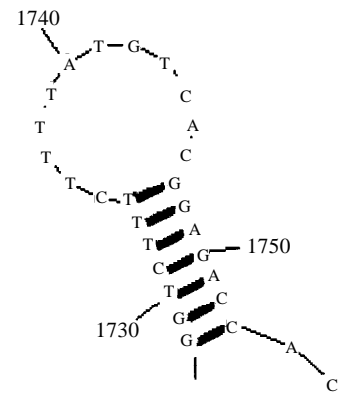


Figure 1 Predicted second structure of the substrate RNA surrounding the selected cleavage site

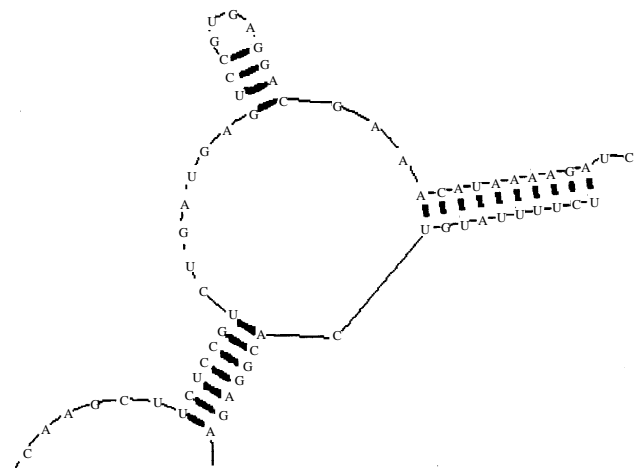


Figure 2 Predicted bimolecular co-fold between the hammerhead ribozyme and the substrate RNA

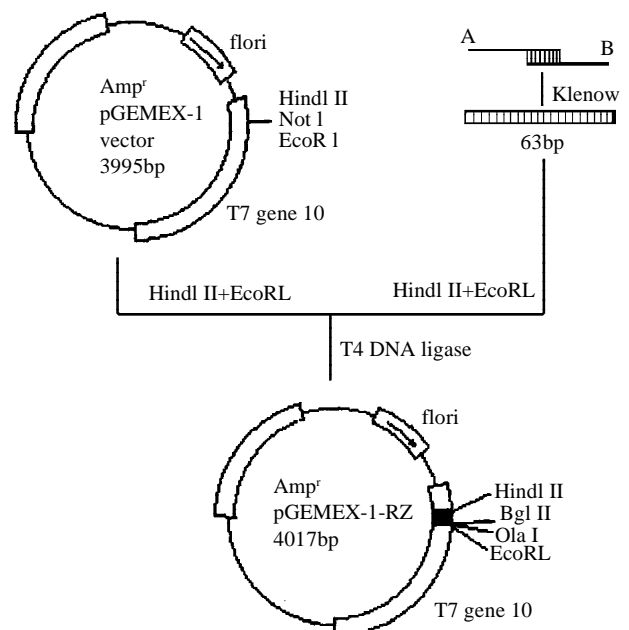


Figure 3 Diagram of the cloning of the hammerhead ribozyme

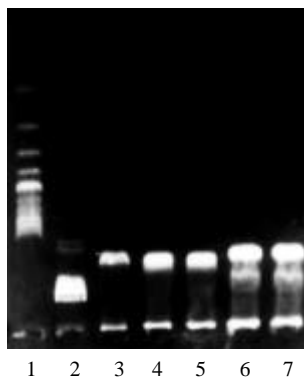


Figure 4 Gel analysis of the plasmid containing the ribozyme gene. Lane 1: 200 bp DNA ladder; lane 2: λ DNA/*Hind*III marker; lane 3: pGEMEX-1-RZ/*Bgl*II; lane 4: pGEMEX-1-RZ/*Hind*III; lane 5: pGEMEX-1-RZ/*Eco*RI; lane 6: pGEMEX-1-RZ/*Not*I; lane 7: pGEMEX-1-RZ

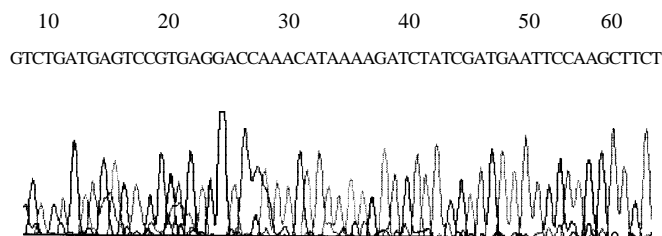


Figure 5 DNA sequencing of ribozyme gene

DISCUSSION

A hammerhead ribozyme is composed of a 22nt or 23nt catalytic core and the flanking complementary sequences. The catalytic core determines the cleavage activity of the ribozyme. And the nucleotide sequence of the catalytic core is conserved. Whereas the flanking sequences determine the recognition specificity of the ribozyme^[24]. The catalytic mechanisms of hammerhead ribozyme and related factors have been intensively studied^[26]. Hammerhead ribozyme can cleave the triplet sequence NUH (N is anyone of A, U, C or G, and H could be C, U or A), but the triplet GUC is most efficiently cleaved^[27]. The length of complementary sequence also influences the catalytic activity. Short complementary sequence will decrease the recognition specificity of the ribozyme and the annealing between ribozyme and substrate. In contrary, long complementary sequence will influence the dissociation of ribozyme from the substrate and hence the turnover of the ribozyme. Commonly, the proper length of each of the flanking sequence is 6-8nt^[28,29] although some studies suggested that longer antisense flanking arms have higher intracellular cleavage efficacy^[30,31]. This opinion is also supported by the estimation that stretches of 11-15 nucleotides define unique sequences for cellular RNA^[32]. It was reported that asymmetric ribozymes (longer helixIII, shorter helixI) have higher cleavage activity than symmetric ribozyme^[33]. In this study, we designed a asymmetric hammerhead ribozyme which had 7nt helixI and 10nt helixIII.

The premise of ribozyme cleavage is the base pairing between flanking sequence of the ribozyme and the substrate mRNA^[34]. This step is akin to the antisense oligodeoxyribonucleotides used for the same purpose. And the base pairing is determined by the secondary structure of the target site, Triplet NUH situated in a loop, protruding or linker of the substrate is advantageous to the annealing between

ribozyme and substrate and then the cleavage of the substrate RNA by the ribozyme^[35]. The selection of the cleavage sites is most important in the design of ribozymes. Nowadays, two approaches are available in the selection of the cleavage sites of ribozymes. One approach is to use *in vitro* accessibility assays. The other is to use theoretical prediction, that is, computer-aided prediction. A number studies aimed to compare the two approaches in their consistency have suggested that theoretical prediction is positively correlate with the intracellular accessibility of the target sites in mRNA^[35-37]. So we performed computer-aided analysis of the secondary structure of the substrate RNA. mFOLD is a commonly used software for RNA secondary structure^[38], so we used mFOLD to predict the secondary structure of hTERT mRNA previous to designing the ribozyme. We choose 1742 GUC as the cleavage site of ribozyme in total 57 triplet GUC in hTERT mRNA. The reasons included: (1) 1 744 triplet RNA is located in coding region of an essential motif of telomerase activity-T motif, and T motif is unique to telomerase in all kinds of reverse transcriptase^[39]. (2) 1 742 triplet GUC is situated in a rather large loop of the predicted secondary structure of telomerase RNA where comparatively more unpaired bases are present near the cleavage triplet. It was reported this kind of structure was correlated with the hybridization accessibility for hammerhead ribozymes^[35]. (3) The sequence surrounding 1742 triplet GUC is rich of adenosine and uridine. It is reported that for efficient catalytic turnover, the free energy of the ribozyme-substrate duplex should be less than -16 kal/mol, that is, higher ratio of A+U will be advantageous to the annealing between ribozyme and substrate^[28]. Next, we performed a computer-aided bimolecular fold prediction between the ribozyme and the substrate and modified the complementary sequences until the ribozyme and the substrate can co-fold into a correct conformation in computer-aided prediction.

Commonly, cloning of short double-strand DNA is carried out by synthesizing the full-length sense strand and antisense strand, annealing and then inserting into a cloning vector. In this study, both the sense strand and antisense strand synthesized were partial of the ribozyme gene which were 12 nucleotides complementary to each other on the 3' ends. After annealing to form a hemiduplex, the hemiduplex was extended with Klenow fragment to obtain full-length double-strand DNA. The reliability of this method is proven by the present study. The advantages of this method including comparative simplicity, higher precision and lower cost to synthesize shorter single-strand DNA.

Since the hammerhead ribozyme gene is only about 50 bps in length, primary analysis of the recombinant relies on PAGE conventionally. Because PAGE is comparatively complex, in this study, we introduced *Bgl*II and *Cl*A restriction sites to the 3' end of the ribozyme gene for the convenience of restriction analysis. As shown in figure, correct recombinants can be linearized by *Cl*A as well as cleaved into two fragments (1.0kb+3.0kb) by *Bgl*II. Also, because *Not*I restriction site in pGEMEX-1 had been removed, correct recombinant could not be cleaved by *Not*I. Then agarose electrophoresis can be used to analyze the recombinants. One of the six recombinants selected by this strategy was sequenced, and the sequence of the inserted ribozyme gene was confirmed. The result suggests that this strategy is applicable. The recombinant plasmid pGEMEX-1-RZ also would be used as an *in vitro* transcription vector to test the *in vitro* cleavage activity of the ribozyme. The recovered 2.0 kb fragment after *Bgl*II restriction would be used as the transcription template. The transcribed product would have two additional nucleotides on the 3' end of the ribozyme, but these two additional nucleotides have no influence on the secondary structure of the ribozyme predicted by computer.

Design and cloning of a ribozymes are the essential work of

studies about ribozymes. In this study, we designed and cloned the anti-hTERT ribozyme successfully. Next, we will test the *in vitro* cleavage activity of the ribozyme and will investigate the growth inhibition effect of this ribozyme on colonic tumor cell lines.

REFERENCES

- 1 **Greider CW.** Chromosome first aid. *Cell* 1991; **6**: 645-647
- 2 **Levy MZ, Allsopp RC, Futcher AB, Greider CW, Harley CB.** Telomere end-replication problem and cell aging. *J Mol Biol* 1992; **225**: 951-960
- 3 **de Lange T.** Activation of telomerase in a human tumor. *Proc Natl Acad Sci USA* 1994; **91**: 2882-2885
- 4 **Rhyu MS.** Telomeres, telomerase, and immortality. *J Natl Cancer Inst* 1995; **87**: 884-893
- 5 **Shen ZY, Xu LY, Li EM, Cai WJ, Chen MH, Shen J, Zeng Y.** Telomere and telomerase in the initial stage of immortalization of esophageal epithelial cell. *World J Gastroenterol* 2002; **8**: 357-362
- 6 **Bodnar AG, Ouellette M, Frolkis M, Holt SE, Chiu CP, Morin GB, Harley CB, Shay JW, Lichtsteiner S, Wright WE.** Extension of life-span by introduction of telomerase into normal human cells. *Science* 1998; **279**: 349-352
- 7 **Harley CB.** Telomerase loss: Mitotic clock or genetic time bomb? *Mutat Res* 1991; **256**: 271-282
- 8 **Dhaene K, van Marck E, Parwaresch R.** Telomeres, telomerase, and cancer: an up-date. *Virchows Arch* 2000; **437**: 1-16
- 9 **Zhan WH, Ma JP, Peng JS, Gao JS, Cai SR, Wang JP, Zheng ZQ, Wang L.** Telomerase activity in gastric cancer and its clinical implications. *World J Gastroenterol* 1999; **5**: 316-319
- 10 **Yakoob J, Hu GL, Fan XG, Zhang Z.** Telomere, telomerase and digestive cancer. *World J Gastroenterol* 1999; **5**: 334-337
- 11 **Xu D, Gruber A, Peterson C, Pisa P.** Suppression of telomerase activity in HL60 cells after treatment with differentiating agents. *Leukemia* 1996; **10**: 1354-1357
- 12 **Herbert BS, Pitts AE, Backer SI, Hamilton SE, Wright WE, Shay JW, Corey DR.** Inhibition of human telomerase in immortal human cells lead to progressive telomere shortening and cell death. *Proc Natl Acad Sci USA* 1999; **96**: 14276-14281
- 13 **Zhang FX, Zhang XY, Fan DM, Deng ZY, Yan Y, Wu HP, Fan JJ.** Antisense telomerase RNA induced human gastric cancer cell apoptosis. *World J Gastroenterol* 2000; **6**: 430-432
- 14 **Shammas MA, Simmons CG, Corey DR, Shmookler-Reis RJ.** Telomerase inhibition by peptide nucleic acids reverse "immortality" of transformed human cells. *Oncogene* 1999; **8**: 6191-6200
- 15 **Yokoyama Y, Takahashi Y, Shinohara A, Lian Zenglin, Wan Xiaoyun, Niwa K, Tamaya T.** Attenuation of telomerase activity by a hammerhead ribozyme targeting the template region of telomerase RNA in endometrial carcinoma cells. *Cancer Res* 1998; **58**: 5406-5410
- 16 **Ludwig A, Saretzki G, Holm PS, Tiemann F, Lorenz M, Emrich T, Harley CB, von Zglinick T.** Ribozyme cleavage of telomerase mRNA sensitizes breast epithelial cells to inhibitors of topoisomerase. *Cancer Res* 2001; **61**: 3053-3061
- 17 **Yokoyama Y, Takahashi Y, Shinohara A, Wan X, Takahashi S, Niwa K, Tamaya T.** The 5' -end of hTERT mRNA is a good target for hammerhead ribozyme to suppress telomerase activity. *Biochem Biophys Res Commun* 2001; **273**: 316-321
- 18 **Ramakrishnan S, Sharma HW, Farris AD, Kaufman KM, Harley JB, Collins K, Prujin GJ, van Venrooij WJ, Martin ML, Narayanan R.** Characterization of human telomerase complex. *Proc Natl Acad Sci USA* 1997; **94**: 10075-10079
- 19 **Masutomi K, Kaneko S, Hayashi N, Yamashita T, Shiota Y, Kobayashi K, Murakami S.** Telomerase activity reconstituted *in vitro* with purified human telomerase reverse transcriptase and human telomerase RNA component. *J Bio Chem* 2000; **275**: 22568-22573
- 20 **Feng J, Funk WD, Wang SS, Weinrich SL, Ailion AA, Chiu CP, Adams RR, Chang E, Allsopp RC, Yu J, Le S, West MD, Harley CB, Andrews WH, Greider CW, Villeponteau.** The RNA component of human telomerase. *Science* 1995; **269**: 1236-1241
- 21 **Martin-Rivera L, Herrera E, Albar JP, Blasco MA.** Expression of mouse telomerase catalytic subunit in embryos and adult tissues. *Proc Natl Acad Sci USA* 1998; **95**: 10471-10476
- 22 **Cristoffersen RE, Marr JJ.** Ribozymes as human therapeutic agents. *J Med Chem* 1995; **38**: 2023-2037
- 23 **Jen KY, Gewirtz AM.** Suppression of gene expression by targeted disruption of messenger RNA: Available options and current strategies. *Stem Cell* 2000; **18**: 307-319
- 24 **Haseloff J, Gerlach WL.** Simple RNA enzymes with new and highly specific endoribonuclease activity. *Nature* 1988; **334**: 585-591
- 25 **Sambrook J, Fritsch EF, Maniatis T, eds.** Molecular cloning A laboratory manual, 2nd ed. Cold spring harbor laboratory press, 1989
- 26 **Vaish NK, Kore AR, Eckstein F.** Recent development in the hammerhead ribozyme field. *Nucleic Acid Res* 1998; **26**: 5237-5242
- 27 **Kore AR, Vaish NK, Kutzke U, Eckstein F.** Sequence specificity of the hammerhead ribozyme revisited; the NHH rule. *Nucleic Acids Res* 1998; **26**: 4116-4120
- 28 **Herschlag D.** Implications of ribozyme kinetics for targeting the cleavage of specific RNA molecules *in vivo*: More isn't always better. *Proc Natl Acad Sci USA* 1991; **88**: 6921-6925
- 29 **Hertel KJ, Herschlag D, Uhlenbeck OC.** A kinetic and thermodynamic framework for the hammerhead ribozyme reaction. *Biochemistry* 1994; **33**: 3374-3385
- 30 **Hormes R, Homann M, Oelze I, Marschall P, Tabler M, Eckstein F, Sczakiel G.** The subcellular localization and length of hammerhead ribozyme determine efficacy in human cells. *Nucleic Acids Res* 1997; **25**: 769-775
- 31 **Sloud M.** Effects of variations in length of hammerhead ribozyme antisense arms upon the cleavage of longer RNA substrates. *Nucleic Acids Res* 1997; **25**: 333-338
- 32 **Helene C, Toulme JJ.** Specific regulation of gene expression by antisense, sense and antigene nucleic acids. *Biochim Biophys Acta* 1990; **1049**: 99-125
- 33 **Tabler M, Homann M, Tzortzakaki S, Sczakiel G.** A three nucleotide helix I is sufficient for full activity of a hammerhead ribozyme: Advantages of an asymmetric design. *Nucleic Acid Res* 1994; **22**: 395
- 34 **Campbell TB, McDonald CK, Hagen M.** The effect of structure in a long target RNA on ribozyme cleavage efficiency. *Nucleic Acids Res* 1997; **25**: 4985-4993
- 35 **Amarguoui M, Brede G, Babaie E, Grotli M, Sproat B, Prydz H.** Secondary structure prediction and *in vitro* accessibility of mRNA as tools in the selection of target sites for ribozyme. *Nucleic Acids Res* 2000; **28**: 413-4124
- 36 **Patzel V, Steidl U, Kronenwett R.** A theoretical approach to select effective antisense oligodeoxyribonucleotides at high statistical probability. *Nucleic Acid Research* 1999; **27**: 4328-4334
- 37 **Scherr M, Ross JJ, Sczakiel G, Patzel V.** RNA accessibility prediction: a theoretical approach is consistent with experimental studies in cell extracts. *Nucleic Acids Res* 2000; **28**: 2455-2461
- 38 **Mathews DH, Sabina J, Zuker M, Turner DH.** Expanded sequence dependence of thermodynamic parameters improves prediction of RNA secondary structure. *J Mol Biol* 1999; **288**: 911-940
- 39 **Nakamura TM, Morin GB, Chapman KB, Weinrich SL, Andrews WH, Lingner J, Harley CB, Cech TR.** Telomerase catalytic subunit homologs from fission yeast and human. *Science* 1997; **277**: 955-959

HBV DNA vaccine with adjuvant cytokines induced specific immune responses against HBV infection

De-Wei Du, Zhan-Sheng Jia, Guang-Yu Li, Yong-Ying Zhou

De-Wei Du, Zhan-Sheng Jia, Guang-Yu Li, Yong-Ying Zhou,
Department of Infectious Diseases, Tangdu Hospital, Fourth Military Medical University, Xi'an 710038, Shaanxi Province, China
Supported by the National Natural Science Foundation of China, No. 39770665

Correspondence to: Dr. De-Wei Du, Department of Infectious Diseases, Tangdu Hospital, the Fourth Military Medical University, Xi'an 710038, Shaanxi Province, China. ddw0715@yahoo.com.cn

Received: 2002-05-02 **Accepted:** 2002-07-30

Abstract

AIM: To seek for an effective method to improve the immune responses induced by DNA vaccine expressing HBV surface antigen (pCR3.1-S) in Balb/c mice (H-2^d).

METHODS: The pCR3.1-S plasmid and the eukaryotic expression vectors expressing murine IL-2 (pDOR-IL-2) or IL-12 (pWRG3169) were injected into mice subcutaneously. The immune responses to pCR3.1-S and the adjuvant effect of the cytokines plasmid were studied. Meanwhile the effect of pCR3.1-S on anti-translated subcutaneous tumor of P815 mastocytoma cells stably expressing HBsAg (P815-HBV-S) was also studied. Anti-HBs in serum was detected by enzyme-linked immunosorbent assay (ELISA) and HBsAg specific cytotoxic T lymphocytes (CTLs) activity was measured by ⁵¹Cr release assay. After three weeks of DNA immunization, the cells of P815-HBV-S were inoculated into mice subcutaneously and the tumor growth was measured every five days. The survival rate and living periods of mice were also calculated.

RESULTS: After 8 wk DNA immunization, the A 450 nm values of sera in mice immunized with pCR3.1, pCR3.1-S and pCR3.1-S codelivered with IL-2 or IL-12 plasmids were 0.03±0.01, 1.24±0.10, 1.98±0.17 and 1.67±0.12 respectively. Data in mice codelivered pCR3.1-S with IL-2 or IL-12 plasmids were significantly higher than that of mice injected pCR3.1 or pCR3.1-S only. The HBsAg specific CTL activities in mice coinjected with pCR3.1-S and IL-2 or IL-12 eukaryotic expression vectors were (61.9±7.1) % and (73.3±8.8) % , which were significantly higher than that of mice injected with pCR3.1 (10.1±2.1) % or pCR3.1-S (50.5±6.4) %. The HBsAg specific CTL activities in mice injected with pCR3.1, pCR3.1-S, pCR3.1-S combined with IL-2 or IL-12 eukaryotic expression vectors decreased significantly to (3.2±0.8) %, (10.6±1.4) %, (13.6±1.3) % and (16.9±2.3) % respectively after the spleen cells were treated by anti-CD8⁺ monoclonal antibody, but presented no significant change to anti-CD4⁺ monoclonal antibody or unrelated to monoclonal antibody. The HBV-S DNA vaccine (pCR3.1-S) could evidently inhibit the tumor growth, prolong the survival period of mice and improve the survival rate of mice and these effects could be improved by IL-12 gene codelivered.

CONCLUSION: HBV DNA vaccine has a strong antigenicity in humoral and cellular immunities, which can be promoted by plasmid expressing IL-2 or IL-12. CD8⁺ cells executed

the CTL activities. DNA vaccine may be useful for both prophylaxis and treatment of HBV infection.

Du DW, Jia ZS, Li GY, Zhou YY. HBV DNA vaccine with adjuvant cytokines induced specific immune responses against HBV infection. *World J Gastroenterol* 2003; 9(1): 108-111

<http://www.wjgnet.com/1007-9327/9/108.htm>

INTRODUCTION

Many animal models of infectious diseases have been reported^[1-3] which shows DNA vaccine induced broad range of protective immunities, including antibodies, CD8⁺CTL, CD4⁺Th cells against challenge with the pathogens, such as plasmodium^[4], influenza virus^[5] simplex virus^[6] and HIV-1^[7]. Application of this genetic vaccination approach has been extended to the treatment of cancers^[8,9] as well as allergic diseases^[10,11] and autoimmune disease^[12]. Because DNA vaccines can induce weak and short-lived immune responses in large out-bred animal^[13], seeking for an effective way to promote the immune responses of DNA immunization is an urgent case. Relying on the knowledge above, we constructed a recombination vector expressing HBV S protein, pCR3.1-S, to study the possibility of DNA vaccine in controlling and preventing the HBV infection. In addition, the eukaryotic expression vectors expressing murine IL-2 or IL-12 were coimmunized to mice with pCR3.1-S and their effects as adjuvants for immune responses were also studied. Meanwhile, we established the HBV-infectious animal model through the inoculating of the P815-HBV-S and observed the treatment and preventive effect of pCR3.1-S to HBV infection *in vivo*.

MATERIALS AND METHODS

Plasmids, cell lines and mice

Plasmid expressing hepatitis B virus surface antigen (pCR3.1-S)^[14] was constructed by Prof. Yao ZHQ (in this Department). Plasmids expressing murine IL-2 (pDOR-IL-2) and IL-12 (pRW1369)^[15] were generous gift from Dr. Feng ZHH (in this Department). P815 mastocytoma cells were generous gift from Dr. Zhao (Department of Pathology, the Fourth Military Medical University). Female Balb/c (H-2^d) mice were obtained from the Center for Experimental Animals of the Fourth Military Medical University and used at the age of 5-8 weeks.

Transfection and expression of pCR3.1-S in P815

P815 cells were maintained in RPMI 1640 (Sigma) with 10 mL·L⁻¹ fetal bovine serum in a six-well tissue culture plate at 37 °C in 5 % CO₂ humidified atmosphere and then transfected with the pCR3.1-S or the pCR3.1 alone by using lipofectamine (GIBCO). For each transfection 20 μg of plasmid and 15 μL of lipofectamine in 0.2 mL of serum free medium were mixed in tube for 30 minutes. After 0.8 mL of serum-free medium were added to the tube, the DNA-lipofectamine complexes were overlaid onto the cells. After incubated 12 hours, the cells were washed two times with the complete culture medium and

the medium was replaced with 2 mL of the complete culture medium. After another 24-48-hour incubation, the cells were transferred from the culture medium, which was then replaced by medium contained $300 \text{ mg} \cdot \text{L}^{-1}$ G_{418} (Promega). Two weeks later, the G_{418} -resistant clones were selected and the expression of HBsAg was detected by using of indirect immunofluorescence (IIF). The HBsAg expressed cells were designated as P815-HBV-S and used as the target cells for CTL assay.

DNA immunization in mice

Four groups of mice were used, each consisting of 5 mice which were immunized with one of the following regiments in 100 μL of sterile saline: (1) 100 μg of pCR3.1-S; (2) mixture of 100 μg of pCR3.1-S and 100 μg of pDOR-IL-2 (IL-2); (3) mixture of 100 μg of pCR3.1-S and 100 μg of pRW1369 (IL-12); (4) 100 μg of pCR3.1 vector. The mice in the last group served as negative control. All injections were done intramuscularly into the left thigh quadriceps muscle of mice at 0, 2, 4, 6 and 8 weeks.

HBsAg-specific antibody assay

Sera samples were collected by tail bleeding at different times, beginning at 1 wk after immunization, and the presence of HBsAg-specific antibody was analyzed by ELISA. The ELISA kits for the HBsAg-specific antibody detection were purchased from Huamei Co. and performed according to the manufacturer's instructions.

CTL assay

Spleen cells of mice were segregated 8 weeks after immunization and the CTL activities were measured by ^{51}Cr releases assay. $\text{Na}^{51}\text{CrO}_4$ was purchased from Dubang Co. Target cells (1×10^6) were labeled with 3.7MBq radiolabeled sodium chromate. The assays were performed in triplicate with 1×10^5 targets/well at various effector cell/target cell (E:T) ratios of 100:1. Results were expressed according to the formula: % specific lysis = (experimental release - spontaneous release) / (maximum release - spontaneous release). Experimental release represents the mean count per-minute released by target cells in the presence of effector cells. Maximum release represents the radioactivity released after lysis of target cells with $50 \text{ g} \cdot \text{L}^{-1}$ Triton X-100. Spontaneous release represents the radioactivity present in medium derived from target cells alone.

Blocking of CTL response by monoclonal antibodies

At the effector cell/target cell ratio of 100:1, CTL assays were performed in the presence of $10 \text{ mg} \cdot \text{L}^{-1}$ of anti- CD4^+ or anti- CD8^+ monoclonal antibody added to the spleen cells in 96-well plates. As a control an unrelated antibody was added to the spleen cells. The monoclonal antibodies to mouse CD4^+ or CD8^+ cell were purchased from Sigma Chemical Co.

DNA vaccine against subcutaneous translated tumor

Four groups of mice were used, each consisting of 5 mice immunized with one of the following regiments in 100 μL of sterile saline: (1) 100 μg of pCR3.1-S; (2) mixture of 100 μg of pCR3.1-S and 100 μg of pRW1369 (IL-12). (3) 100 μg of pCR3.1; one group of mice without immunization. Three weeks after DNA immunization, cells of P815-HBV-S were inoculated into mice by subcutaneous injection in abdomen. The growing tumors were measured every five days with a calipers using average diameter. The survival period of mice was observed and the survival rate of mice was calculated.

Statistical analysis

Data were reported as $\bar{x} \pm s$ and were analyzed by professional statistical computer software SPSS. Significance was set at $P < 0.05$.

RESULTS

Codelivery of cytokines gene augmented the titer of antibody induced by pCR3.1-S

The pCR3.1-S showed a strong antigenicity in humoral immunity and the anti-HBsAg could be detected in sera of mice after pCR3.1-S vaccination. The serum titres of anti-HBsAg in mice increased with the times of immunization in a period of time. The titres of anti-HBsAg in sera of mice were significantly promoted by genes expressed murine IL-2 or IL-12, especially by IL-2 gene (Figure 1).

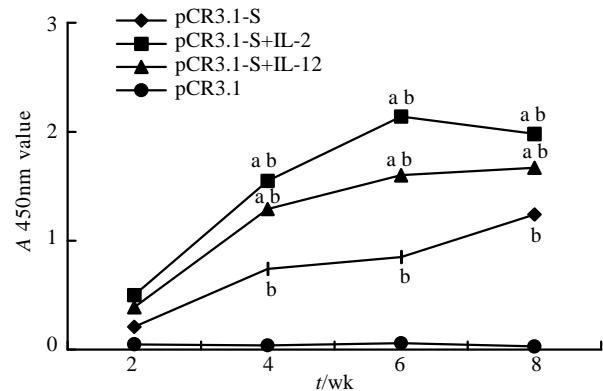


Figure 1 Serum anti-HBsAg level of Balb/c mice. $^bP < 0.01$ vs pCR3.1; $^aP < 0.05$ vs pCR3.1-S

Cytokines gene effected on the CTL activity induced by pCR3.1-S

The HBsAg specific CTL activities were developed in the mice after pCR3.1-S immunization. The CTL activities were augmented by coimmunized with IL-2 or IL-12 gene. The mice immunized with pCR3.1 alone did not elicited detectable HBsAg specific CTL activities. IL-12 was more effective than IL-2 in promoting the HBsAg specific CTL activities. The CTL activity was blocked by anti- CD8^+ monoclonal antibody but not by anti- CD4^+ monoclonal antibody or unrelated antibody (Table 1). Taken together, these results indicated that the CTL activity induced by pCR3.1-S *in vivo* was executed by cells expressing $\text{CD8}^+/\text{CD4}^-$ surface phenotype and the CTL activity could be enhanced or suppressed depending on the cytokines gene expressed.

Table 1 The effect of cytokines gene on CTL activity induced by pCR3.1-S ($n=5$; $\bar{x} \pm s$ %)

Group	Untreated	mAb		
		Unrelated	Anti- CD4^+	Anti- CD8^{+b}
pCR3.1	10.1 \pm 2.1	10.7 \pm 1.9	9.7 \pm 1.2	3.2 \pm 0.8
pCR3.1-S	50.5 \pm 6.4	49.7 \pm 6.1	48.3 \pm 5.9	10.6 \pm 1.4
pCR3.1-S+IL-2	61.9 \pm 7.1	62.0 \pm 6.8	56.2 \pm 7.5	13.5 \pm 1.9
pCR3.1-S+IL-12	73.3 \pm 8.8	69.9 \pm 7.6	75.6 \pm 9.1	16.9 \pm 2.3

$^bP < 0.01$ vs unrelated mAb or CD4^+ mAb

DNA vaccine inhibits the formation of subcutaneous translating tumor derived from P815-HBV-S

After inoculated with P815-HBV-S, all five mice with or without pCR3.1 (100%) formed the tumor. The rate of tumor formation was 20% (1/5) in mice immunized with pCR3.1-S and there was no tumor formed in mice coimmunized with pCR3.1-S and IL-12. The survival rate of mice immunized with pCR3.1-S alone or coimmunized with IL-12 increased significantly (Figure 2) and the tumor growth was evidently slower than that of mice immunized with or without pCR3.1 (Figure 3).

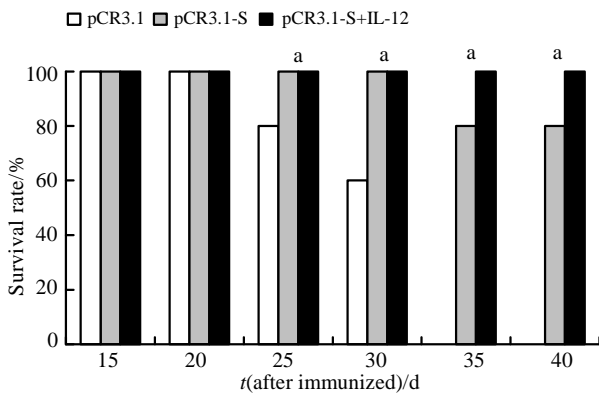


Figure 2 Survival rate in different group. ^a*P*<0.05 vs pCR3.1

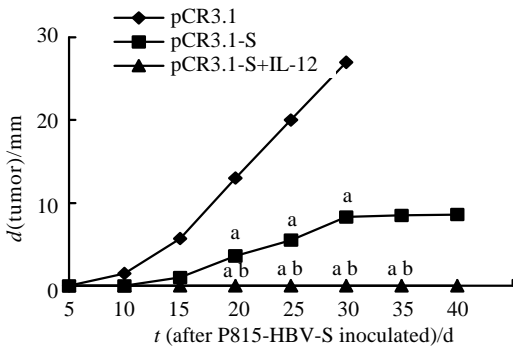


Figure 3 Growth curve of subcutaneous translating tumor in different group of mice. ^b*P*<0.01 vs pCR3.1; ^a*P*<0.05 vs pCR3.1-S

DISCUSSION

HBV infection is very common in China^[16-23]. It is estimated that approximately 130 million people in the world is infected by hepatitis B virus (HBV). These people are at risk of developing chronic hepatitis leading to liver cirrhosis and hepatocellular carcinoma. Up to now, vaccination is a main way in prevention^[24-31].

It has been suggested that the MHC class II and I restricted T cell responses to the virus are relatively weak during chronic HBV infection^[28] and there are no specific therapies to cope with it. DNA vaccine contains the gene for an antigenic portion of a pathogen, such as the core or the envelope protein, usually under the transcriptional control of a viral promoter^[29,30]. In DNA-based vaccination, immunogenic proteins are expressed in transfected cells of the vaccine recipients in their native conformation with correct post-translational modifications from antigen-encoding expression plasmid DNA *in vivo*. This ensures the integrity of antibody-defined epitopes and supports the generation of protective antibody. DNA vaccination is furthermore an exceptionally potent strategy to stimulate CD8+ cytotoxic T lymphocyte (CTL) responses because antigenic peptides are efficiently generated by endogenous processing of intracellular protein antigen^[31].

The results of our experiment indicate that the plasmids expressing either IL-2 or IL-12 can enhance the specific humoral and cellular immune responses against HBV infection elicited by pCR3.1-S in mice. The former mainly enhances the level of the HBsAg specific antibody and the latter mainly enhances the HBsAg specific CTL activity.

IL-2 can enhance the immune responses through promoting proliferation and differentiation of B cells and the antibody development. The proliferation and activation of many kinds of T-cells and the production of various cytokins can also be promoted and stimulated by IL-2. The effect of IL-2 enhancing the level of antibody may be related to its ability to induce the

increase of the Th1 cells but not Th2 cells. This can increase IgG2a type of antibody and lead to the increase of the total level of the antibody subsequently^[32-34]. IL-12 is so far the most potent cytokine with the widest scope of modulation of immune responses. The immune responses can be modulated by IL-12 promoting the production of Th1 type T cells and secretion of other cytokines, stimulating the polarization and proliferation of T cells and through promoting the maturity of CTL cells and LAK cells. All of these can enhance the ability of the host to kill and eliminate pathogens. The adjuvantivities of cytokines were also observed by others^[25,32-36].

The situations *in vivo* are different from that *in vitro* after all. In order to search the preventive and therapeutical effects of HBV DNA vaccine to the HBV infection *in vivo*, we serve the mouse injected with P815-HBV-S cells subcutaneously for an animal model of HBV infection. The preventive and therapeutical effects of pCR3.1-S on HBV infectious animal model were investigated by observing the inhibiting effects of pCR3.1-S on the neoplasia of P815-HBV-S cells inoculated by subcutaneous injection. The result indicates that the pCR3.1-S can reduce the formative rate of the subcutaneous translating tumor significantly, inhibit the growth of tumor, prolong the living periods and promote the survival rate of mice injected with the P815-HBV-S cells. Maybe all of these relate to the specific killing effect of CTLs to P815-HBV-S cells induced by DNA vaccine. Furthermore, these effects of pCR3.1-S can be enhanced obviously by IL-12 gene as shown in the experiment. The therapeutic potential of DNA-based immunization for the chronic HBV carrier states has also been demonstrated in a transgenic mouse model^[37]. This mode of immunization has been shown to successfully eliminate HBsAg in circulation.

These features of DNA-based immunization make it an attractive strategy for prophylactic and therapeutic vaccination against extra- and intracellular pathogens. Recently, DNA vaccines induced the specific humoral^[38] and cellular^[39-41] immune responses were observed in human experiments. The results of these experiments suggest that DNA vaccine might be a potential therapy for chronic HBV infection.

REFERENCES

- Loirat D, Lemonnier FA, Michel ML. Multiepitopic HLA-A*0201-restricted immune response against hepatitis B surface antigen after DNA-based immunization. *J Immunol* 2000; **165**: 4748-4755
- Dunham SP, Flynn JN, Rigby MA, Macdonald J, Bruce J, Cannon C, Golder MC, Hanlon L, Harbour DA, Mackay NA, Spibey N, Jarrett O, Neil JC. Protection against feline immunodeficiency virus using replication defective proviral DNA vaccines with feline interleukin-12 and -18. *Vaccine* 2002; **20**: 1483-1496
- Huang ZH, Zhuang H, Lu S, Guo RH, Xu GM, Cai J, Zhu WF. Humoral and cellular immunogenicity of DNA vaccine based on hepatitis B core gene in rhesus monkeys. *World J Gastroenterol* 2001; **7**: 102-106
- Le TP, Coonan KM, Hedstrom RC, Charoenvit Y, Sedegah M, Epstein JE, Kumar S, Wang R, Doolan DL, Maguire JD, Parker SE, Hobart P, Norman J, Hoffman SL. Safety, tolerability and humoral immune responses after intramuscular administration of a malaria DNA vaccine to healthy adult volunteers. *Vaccine* 2000; **18**: 1893-1901
- Cox RJ, Mykkeltvedt E, Robertson J, Haaheim LR. Non-lethal viral challenge of influenza haemagglutinin and nucleoprotein DNA vaccinated mice results in reduced viral replication. *Scand J Immunol* 2002; **55**: 14-23
- Strasser JE, Arnold RL, Pachuk C, Higgins TJ, Bernstein DI. Herpes simplex virus DNA vaccine efficacy: effect of glycoprotein D plasmid constructs. *J Infect Dis* 2000; **182**: 1304-1310
- Fuller DH, Rajakumar PA, Wilson LA, Trichel AM, Fuller JT, Shipley T, Wu MS, Weis K, Rinaldo CR, Haynes JR, Murphey-Corb M. Induction of mucosal protection against primary, heterologous simian immunodeficiency virus by a DNA vaccine. *J Virol*

- 2002; **76**: 3309-3017
- 8 **Gavarasana S**, Kalasapudi R S, Rao T D, Thirumala S. Prevention of carcinoma of cervix with human papillomavirus vaccine. *Indian J Cancer* 2000; **37**: 57-66
 - 9 **Thirdborough SM**, Radcliffe JN, Friedmann PS, Stevenson FK. Vaccination with DNA encoding a single-chain tcr fusion protein induces anticonotypic immunity and protects against t-cell lymphoma. *Cancer Res* 2002; **62**: 1757-1760
 - 10 **Horner AA**, Van Uden JH, Zubeldia JM, Broide D, Raz E. DNA-based immunotherapeutics for the treatment of allergic disease. *Immunol Rev* 2001; **179**: 102-118
 - 11 **Lee YL**, Ye YL, Yu CI, Wu YL, Lai YL, Ku PH, Hong RL, Chiang BL. Construction of single-chain interleukin-12 DNA plasmid to treat airway hyperresponsiveness in an animal model of asthma. *Hum Gene Ther* 2001; **12**: 2065-2079
 - 12 **Garren H**, Ruiz PJ, Watkins TA, Fontoura P, Nguyen LT, Estline ER, Hirschberg DL, Steinman L. Combination of gene delivery and DNA vaccination to protect from and reverse Th1 autoimmune disease via deviation to the Th2 pathway. *Immunity* 2001; **15**: 15-22
 - 13 **Chaplin PJ**, De Rose R, Boyle JS, McWaters P, Kelly J, Tennent JM, Lew AM, Scheerlinck JP. Targeting improves the efficacy of a DNA vaccine against *Corynebacterium pseudotuberculosis* in sheep. *Infect Immun* 1999; **67**: 6434-6438
 - 14 **Li WB**, Yao ZQ, Zhou YY, Feng ZH. Studies on immunization with HBV gene vaccine plus HBsAg protein in mice. *Shijie Huaren Xiaohua Zazhi* 1999; **7**: 188-190
 - 15 **Rakhmievich AL**, Turner J, Ford MJ, McCabe D, Sun WH, Sondel PM, Grota K, Yang NS. Gene gun-mediated skin transfection with interleukin 12 gene results in regression of established primary and metastatic murine tumors. *Proc Natl Acad Sci USA* 1996; **93**: 6291-6296
 - 16 **Guan XJ**, Wu YZ, Jia ZC, Shi TD, Tang Y. Construction and characterization of an experimental ISCOMS-based hepatitis B polypeptide vaccine. *World J Gastroenterol* 2002; **8**: 294-297
 - 17 **Chen XS**, Wang GJ, Cai X, Yu HY, Hu YP. Inhibition of hepatitis B virus by oxymatrine *in vivo*. *World J Gastroenterol* 2001; **7**: 49-52
 - 18 **Huang ZH**, Zhuang H, Lu S, Guo RH, Xu GM, Cai J, Zhu WF. Humoral and cellular immunogenicity of DNA vaccine based on hepatitis B core gene in rhesus monkeys. *World J Gastroenterol* 2001; **7**: 102-106
 - 19 **Fang JN**, Jin CJ, Cui LH, Quan ZY, Choi BY, Ki MR, Park HB. A comparative study on serologic profiles of virus hepatitis B. *World J Gastroenterol* 2001; **7**: 107-110
 - 20 **Guo SP**, Wang WL, Zhai YQ, Zhao YL. Expression of nuclear factor- κ B in hepatocellular carcinoma and its relation with the X protein of hepatitis B virus. *World J Gastroenterol* 2001; **7**: 340-344
 - 21 **You J**, Zhuang L, Tang BZ, Yang H, Yang WB, Li W, Zhang HL, Zhang YM, Zhang L, Yan SM. Interferon alpha with Thymopeptide in the treatment of chronic hepatitis B. *Shijie Huaren Xiaohua Zazhi* 2001; **9**: 388-391
 - 22 **He XS**, Huang JF, Chen GH, Fu Q, Zhu XF, Lu MQ, Wang GD, Guan XD. Orthotopic liver transplantation for fulminant hepatitis B. *World J Gastroenterol* 2000; **6**: 398-399
 - 23 **Zhao LS**, Qin S, Zhou TY, Tang H, Liu L, Lei BJ. DNA-based vaccination induces humoral and cellular immune responses against hepatitis B virus surface antigen in mice without activation of C-myc. *World J Gastroenterol* 2000; **6**: 239-243
 - 24 **Du DW**, Zhou YX, Feng ZH, Li GY, Yao ZQ. Study on immunization of anti-subcutaneous transplanting tumor induced by gene vaccine. *Shijie Huaren Xiaohua Zazhi* 1999; **7**: 955-957
 - 25 **Du DW**, Zhou YX, Feng ZH, Yao ZQ, Li GY. Immune responses to interleukin 12 and hepatitis B gene vaccine in H²-d mice. *Shijie Huaren Xiaohua Zazhi* 2000; **8**: 128-130
 - 26 **Liu HB**, Meng ZD, Ma JC, Han CQ, Zhang YL, Xing ZC, Zhang YW, Liu YZ, Cao HL. A 12-year cohort study on the efficacy of plasma-derived hepatitis B vaccine in rural newborns. *World J Gastroenterol* 2000; **6**: 381-383
 - 27 **Li H**, Wang L, Wang SS, Gong J, Zeng XJ, Li RC, Nong Y, Huang YK, Chen XR, Huang ZN. Research on optimal immunization strategies for hepatitis B in different endemic areas in China. *World J Gastroenterol* 2000; **6**: 392-394
 - 28 **Geissler M**, Tokushige K, Wakita T, Zurawski VR Jr, Wands JR. Differential cellular and humoral immunization using chimeric constructs. *Vaccine* 1998; **16**: 857-867
 - 29 **Reyes-Sandoval A**, Ertl H C. DNA vaccines. *Curr Mol Med* 2001; **1**: 217-243
 - 30 **Kwissa M**, Unsinger J, Schirmbeck R, Hauser H, Reimann J. Poly-valent DNA vaccines with bidirectional promoters. *J Mol Med* 2000; **78**: 495-506
 - 31 **Schirmbeck R**, Reimann J. Revealing the potential of DNA-based vaccination: lessons learned from the hepatitis B virus surface antigen. *Biol Chem* 2001; **382**: 543-452
 - 32 **Du DW**, Liu QQ, Chen HM, Li JG, Lian JQ, Feng ZH, Zhou YX, Yao ZQ. Immune adjuvant effect of eukaryotic expression vector with Interleukin-2 on hepatitis B gene vaccine. *Shanghai Mianyixue Zazhi* 2001; **21**: 77-79
 - 33 **Geissler M**, Bruss V, Michalak S, Hockenjos B, Ortman D, Offensperger WB, Wands JR, Blum HE. Intracellular retention of hepatitis B virus surface proteins reduces interleukin-2 augmentation after genetic immunizations. *J Virol* 1999; **73**: 4284-4292
 - 34 **Li WB**, Yao ZQ, Zhou YX, Feng ZH. Effect of interleukin-2 on the potency of genetic vaccines of hepatitis B virus. *Di-si Junyi Daxue Xuebao* 1999; **20**: 747-749
 - 35 **Scheerlinck JP**, Casey G, McWaters P, Kelly J, Woollard D, Lightowlers MW, Tennent JM, Chaplin PJ. The immune response to a DNA vaccine can be modulated by co-delivery of cytokines gene using a DNA prime-protein boost strategy. *Vaccine* 2001; **19**: 4053-4060
 - 36 **Noormohammadi AH**, Hochrein H, Curtis JM, Baldwin TM, Handman E. Paradoxical effects of IL-12 in leishmaniasis in the presence and absence of vaccinating antigen. *Vaccine* 2001; **19**: 4043-4052
 - 37 **Oka Y**, Akbar SM, Horiike N, Joko K, Onji M. Mechanism and therapeutic potential of DNA-based immunization against the envelope proteins of hepatitis B virus in normal and transgenic mice. *Immunology* 2001; **103**: 90-97
 - 38 **Tacket CO**, Roy MJ, Wiedera G, Swain WF, Broome S, Edelman R. Phase 1 safety and immune response studies of a DNA vaccine encoding hepatitis B surface antigen delivered by a gene delivery device. *Vaccine* 1999; **17**: 2826-2829
 - 39 **Roy MJ**, Wu MS, Barr LJ, Fuller JT, Tussey LG, Speller S, Culp J, Burkholder JK, Swain WF, Dixon RM, Wiedera G, Vessey R, King A, Ogg G, Gallimore A, Haynes JR, Heydenburg Fuller D. Induction of antigen-specific CD8⁺ T cells, T helper cells, and protective levels of antibody in humans by particle-mediated administration of a hepatitis B virus DNA vaccine. *Vaccine* 2001; **19**: 764-778
 - 40 **Weber R**, Bossart W, Cone R, Luethy R, Moelling K. Phase I clinical trial with HIV-1 gp160 plasmid vaccine in HIV-1-infected asymptomatic subjects. *Eur J Clin Microbiol Infect Dis* 2001; **20**: 800-803
 - 41 **Swain WE**, Heydenburg Fuller D, Wu MS, Barr LJ, Fuller JT, Culp J, Burkholder J, Dixon RM, Wiedera G, Vessey R, Roy MJ. Tolerability and immune responses in humans to a PowderJect DNA vaccine for hepatitis B. *Dev Biol (Basel)* 2000; **104**: 115-119

Expression of hepatitis B virus X protein in transgenic mice

Jun Xiong, Yu-Cheng Yao, Xiao-Yuan Zi, Jian-Xiu Li, Xin-Min Wang, Xu-Ting Ye, Shu-Min Zhao, Yong-Bi Yan, Hong-Yu Yu, Yi-Ping Hu

Jun Xiong, Yu-Cheng Yao, Xiao-Yuan Zi, Jian-Xiu Li, Xin-Min Wang, Xu-Ting Ye, Shu-Min Zhao, Yong-Bi Yan, Yi-Ping Hu, Department of Cell Biology, Second Military Medical University, Shanghai 200433, China

Hong-Yu Yu, Department of Pathology, Changzheng Hospital, Second Military Medical University, Shanghai 200433, China

Supported by Projects of the Science Development Foundation of Shanghai (No.994919033) and Tackling Key Problems in Science and Technology from the State Science and Technology Ministry (No.TJ99-LA01)

Correspondence to: Yi-Ping Hu, Department of Cell Biology, Department of Basic Medicine, Second Military Medical University, Shanghai, 200433, China. yphu@smmu.edu.cn

Telephone: +86-21-25070291 **Fax:** +86-21-25070291

Received: 2002-01-14 **Accepted:** 2002-07-26

Abstract

AIM: To establish a mice model harboring hepatitis B virus *x* gene (adr subtype) for studying the function of hepatitis B virus X protein, a transactivator of viral and cellular promoter/enhancer elements.

METHODS: Expression vector pcDNA3-*HBx*, containing CMV promoter and hepatitis B virus *x* gene open reading fragment, was constructed by recombination DNA technique. Hela cells were cultured in DMEM and transfected with pcDNA3-*HBx* or control pcDNA3 plasmids using FuGENE6 Transfection Reagent. Expression of pcDNA3-*HBx* vectors in the transfected Hela cells was confirmed by Western blotting. After restriction endonuclease digestion, the coding elements were microinjected into male pronuclei of mice zygotes. The pups were evaluated by multiplex polymerase chain reaction (PCR) at genomic DNA level. The *x* gene transgenic mice founders were confirmed at protein level by Western blotting, immunohistochemistry and immunogold transmission electron microscopy.

RESULTS: Expression vector pcDNA3-*HBx* was constructed by recombination DNA technique and identified right by restriction endonuclease digestion and DNA direct sequencing. With Western blotting, hepatitis X protein was detected in Hela cells transfected with pcDNA3-*HBx* plasmids, suggesting pcDNA3-*HBx* plasmids could express in eukaryotic cells. Following microinjection of coding sequence of pcDNA3-*HBx*, the embryos were transferred to oviducts of pseudopregnant females. Four pups were born and survived. Two of them were verified to have the *HBx* gene integrated in their genomic DNA by multiplex PCR assay, and named C57-TgN(*HBx*)SMMU1 and C57-TgN(*HBx*)SMMU3 respectively. They expressed 17KD X protein in liver tissue by Western blotting assay. With the immunohistochemistry, X protein was detected mainly in hepatocytes cytoplasm of transgenic mice, which was furthermore confirmed by immunogold transmission electron microscopy.

CONCLUSION: We have constructed the expression vector pcDNA3-*HBx* that can be used to study the function of *HBx* gene in eukaryotic cells *in vitro*. We also established *HBx*

gene (adr subtype) transgenic mice named C57-TgN (*HBx*)SMMU harboring *HBx* gene in their genome and express X protein in hepatocytes, which might be a valuable animal system for studying the roles of *HBx* gene in hepatitis B virus life cycle and development of hepatocellular carcinoma *in vivo*.

Xiong J, Yao YC, Zi XY, Li JX, Wang XM, Ye XT, Zhao SM, Yan YB, Yu HY, Hu YP. Expression of hepatitis B virus X protein in transgenic mice. *World J Gastroenterol* 2003; 9(1): 112-116
<http://www.wjgnet.com/1007-9327/9/112.htm>

INTRODUCTION

Human hepatitis B virus (HBV) is the prototype for a family of viruses, referred to as *Hepadnaviridae*^[1,2]. It has at least 4 subtypes, ayw, adr, ayr, and adw, among which adr is the most prevailing subtype in China. The complete genomic DNA of subtype adr has been cloned and demonstrated only 3.2kbp in length, and which is different from the other 3 subtypes in DNA and protein sequence^[3]. HBV genome has 4 open reading frames (ORFs), including envelope genes coding region (*pre-s1*, *pre-s2* and *s* gene coding region), precore (*pc*) gene and core (*c*) gene coding region, polymerase (*p*) gene coding region, *x* gene coding region^[4-6].

Chronic HBV infection is associated with a high incidence of liver disease, including hepatocellular carcinoma (HCC)^[7-9]. Based on epidemiologic studies involving chronic HBV infection, it is estimated that the relative risk of developing HCC for HBV carriers may be 100- to 200-fold higher than that for non-carriers. It is proposed that the role of HBV played in HCC predisposition is modifying host gene regulation. Integration of viral DNA into the host genome can mediate host gene deregulation by a variety of mechanisms^[10-15]. X protein may alter host gene expression leading to the development of HCC^[16]. It has been demonstrated that X protein is a transactivator of a variety of viral and cellular promoter/enhancer elements and can mediate the activation of signal transduction pathways. Besides, it may affect DNA repair, cell cycle control, and apoptosis^[17-22]. It is now clear that X-defective virus is unable to initiate infection *in vivo*. However, the physiological role of X protein during the course of an infection remains a major issue unresolved in hepadnavirus biology^[23-27].

To explore the function of *HBx* gene *in vivo*, we generated transgenic mice harboring *HBx* gene from subtype adr by microinjection method, in which *HBx* gene could be expressed. This model might be valuable for the study of *HBx* biology and its associated biomedical issues *in vivo*.

MATERIALS AND METHODS

Reagents, antibodies, cells and animals

Restriction Endonucleases and T₄ DNA ligase were obtained from Promega Co. (USA). The mouse monoclonal antibody against X protein was purchased from DAKO (USA). Sheep anti mouse IgG-HRP was obtained from CALBIOCHEM (Germany). Gel extraction kit was purchased from QIAGEN. Hela cells were preserved in our laboratory. C57BL/6 mice were maintained in our Transgenic Animal Laboratory (SPF level).

Plasmid constructions

Plasmids pBR322-HBV (containing two tandem copies of the HBV genome of adr subtype) and pcDNA3 (containing CMV promoter) were preserved in our laboratory. Expression plasmid pcDNA3.1 (containing CMV promoter) was generously provided by Dr. Yu Hong-Yu. An 0.894-Kilobase pair DNA fragment containing *HBx* gene was isolated by gel extraction from plasmid pBR322-HBV after *Hind*III and *Bgl*II restriction digest. The fragment was then subcloned into plasmid pcDNA3.1 that has been digested by *Hind*III and *Bam*HI to yield intermediate plasmid pcDNA3.1-*HBx*, which was employed as a template for polymerase chain reaction (PCR) amplification of the *HBx* coding fragments. The primers (A: 5' -ACACA AGCTT CATAT GGCTG CTCGG G-3', B: 5' -CATGA ATTCT AGATG ATTAG GCAGA GGTG-3') were synthesized by Sangon Co. (Shanghai). Thirty five cycles of amplification were done in a total volume of 50 μ l with an annealing temperature of 58 $^{\circ}$ C. PCR product and pcDNA3 were isolated after *Hind*III and *Xba*I digestion. After ligation, the plasmid of pcDNA3-*HBx* was confirmed by restriction endonucleases digestion and direct DNA sequencing.

Cell culture and DNA transfection

Hela cells were cultured in DMEM (Gibco) supplemented with 10 % FCS (Gibco) to confluence. Cells at 50 % confluency were transfected with pcDNA3-*HBx* or control pcDNA3 plasmids using FuGENE6 Transfection Reagent (Roche) with a total of 1 μ g of DNA per 3.5-cm plate of cells. Selection in medium containing geneticin (G418; Gibco) at a concentration of 500 μ g/ml was started 48 hours later. After 2 weeks selection, positive clones that were named Hela-*HBx* were isolated and further expanded.

Assay pcDNA3-*HBx* expression in hela cells

Hela-*HBx* cells cultured in 10-cm dishes were rinsed with phosphate-buffered saline (pH7.4) three times and collected in a microcentrifuge tube by trypsinization. Cells were lysed with lysis buffer^[18]. Supernatants were then diluted 5 times with phosphate-buffered saline (pH7.4) to assay the expression of the transfected pcDNA3-*HBx* vectors in Hela cells by Western blotting.

Microinjection and production of *HBx* transgenic mice

The pcDNA3-*HBx* plasmid was digested by *Sal*I and purified by gel extraction (Qiagen gel extraction kit). Purified coding fragment containing CMV promoter and *HBx* ORF were dissolved in TE buffer (10 mM Tris-HCl, 0.2 mM EDTA, pH7.5) at a final concentration of 2 μ g/L (-4 000 copies/ μ l) and microinjected into zygotes. Microinjection and embryo manipulation were performed according to standard protocols.

Analysis of *HBx* gene integration

Genomic DNA was extracted from tail tissue of pups mice or normal mouse and dissolved in TE buffer. It was used for PCR assays to identify founders of transgenic mice with *HBx* gene. In order to set an internal control of the efficiency of PCR amplification, we developed a multiplex PCR, using two sets of primers to amplify the *HBx* gene and the autosomal *IL3* gene in the same reaction tube^[28,29]. PCR reaction was performed using 1 μ l of dissolved DNA, 0.2 μ l *HBx* gene specific primers (C: 5' -GGACG TCCTT TGTCT ACGTC CCGTC-3', D: 5' -CCTAA TCTCC TCCCC CAACT CCTCC-3', synthesized by Sangon Co. /Shanghai), and 0.1 μ l *IL3* gene specific primers (E: 5' -GGGAC TCCAA GCTTC AATCA-3', F: 5' -TGGAG GAGGA AGAAA AGCAA-3', synthesized by Sangon Co. /Shanghai) in a total volume of 50 μ l according to the cycling program: 94 $^{\circ}$ C, 40 s; 61 $^{\circ}$ C, 40 s; 72 $^{\circ}$ C, 60 s; 35 cycles.

Analysis of *HBx* gene expression in transgenic mice

Western blotting Liver samples were obtained from the transgenic mice with *HBx* gene and normal C57BL/6 mice. Specimens (approximately 100 mg) were homogenized in a screw-capped 1.5 ml microcentrifuge tube and lysed in lysis buffer (0.5 % Nonidet P-40, 10 mM Tris (pH7.4), 150 mM NaCl, 1 mM EDTA and 1 mM phenylmethanesulfonyl fluorid). 100 mg lysate was separated via 15 % SDS-polyacrylamide gel electrophoresis with Tris-Glycine buffer (pH8.3). One electrophoresis gel was stained with commassie brilliant blue R-250, and another was blotted to nitrocellulose filter. After blocked with 50 g/L defatted milk, the filter was incubated with X protein mouse monoclonal antibody for 40 min at 37 $^{\circ}$ C, then washed with TBS (three times, 15 min each time) and incubated with HRP-conjugated sheep anti-mouse IgG for 30 min at 37 $^{\circ}$ C. Finally, the filter was incubated with peroxidase substrate solution Diaminobenzidine (DAB) for 5 min to visualize the positive bands.

Immunohistochemistry analysis Hepatic tissue samples were fixed in 10 % neutral buffered formalin, paraffin-embedded and sectioned. Briefly paraffin-embedded sections were blocked with 3 % hydrogen peroxide (H₂O₂) for 10 min at 37 $^{\circ}$ C and washed with PBS. Subsequently, the sections were incubated in the X protein mouse monoclonal antibody (diluted 1:100) for 2hr at 37 $^{\circ}$ C. After washing with PBS, the sections were incubated in horseradish peroxidase-labeled sheep anti mouse IgG (diluted 1:50) for 40 min at 37 $^{\circ}$ C. Washed with PBS three times, the sections were subjected to color reaction with 0.02 % 3, 3-diaminobenzidine tetrahydrochloride containing 0.005 % H₂O₂ in PBS and counterstained with hematoxylin lightly.

Immunogold transmission electron microscopy The immunohistochemical X protein-positive mouse liver tissue was selected to be cut into small pieces (0.1 cm in diameter) and fixed first in 2 % paraformaldehyde and 0.5 % glutaraldehyde mixture buffer for 2hr at 4 $^{\circ}$ C, washed three times with PBS, acted upon by 0.25 % Triton X-100 for 10 min. After being blocked with blocking buffer, the pieces were incubated with X protein mouse monoclonal antibody over night at 4 $^{\circ}$ C, washed with TBS and incubated with avidin-gold (15 nm) for 2hr at room temperature; then postfixed in 1 % osmium tetroxide for 1hr at room temperature, dehydrated in gradient ethanol and embedded in epoxy resin. The sections were cut on an LKB Ultralome III, mounted on copper grids, stained with uranyl acetate and lead citrate, and examined by transmission electron microscopy.

RESULTS

pcDNA3-*HBx* vector construction and expression in Hela cells

A 0.465kb *HBx* gene was amplified from HBV genomic DNA and subcloned into the expression vector pcDNA3, with which the pcDNA3-*HBx* was constructed. The sequence of *HBx* gene in the plasmid was coincident with that reported before^[3], as identified by restriction endonucleases digestion and confirmed by DNA direct sequencing. After purification by gel extraction, pcDNA3-*HBx* plasmids were transfected into Hela cells. Positive clones, Hela-*HBx* cells were isolated by G418 selection. With Western blotting, hepatitis X protein was detected in Hela cells, suggesting pcDNA3-*HBx* plasmids expressed in eukaryotic cells (Figure 1).

Production of transgenic mice

The pcDNA3-*HBx* plasmid was digested by *Sal*I and target fragments containing CMV promoter and *HBx* ORF were purified by gel extraction. Target fragments then were microinjected into male pronuclei of zygotes from C57BL/6

mice. 45 zygotes were microoperated. 41 microinjected eggs were implanted into oviducts of 3 pseudopregnant recipient mice, and 4 pups were born and survived. The born rate was 11 %. By multiplex PCR screening, two of the pups were identified to harbour *HBx* gene in their genomic DNA, named C57-TgN *HMU1* and C57-TgN(*HBx*)SMMU3 (Figure 2).



Figure 1 Detected hepatitis X protein expression in transfected HeLa cells. *M*_{17 000} X protein was detected in HeLa-*HBx* cells. Lane1: control cells; Lane 2: HeLa-*HBx* cells.

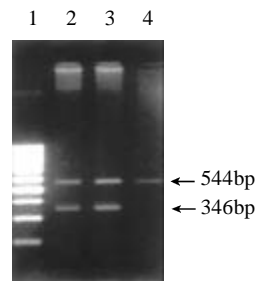


Figure 2 Analysis of *HBx* gene integration in transgenic mice by PCR. 544 bp *IL3* gene fragment and 346 bp fragment were amplified with positive and negative primers. Lane 1: 100 bp ladder Marker; Lane 2: C57-TgN (*HBx*) SMMU1 transgenic mice; Lane3: C57-TgN(*HBx*)SMMU3 transgenic mice; Lane 4: normal C57BL/6 mice.

Expression of *HBx* gene in transgenic mouse

To detect the expression of hepatitis X protein in transgenic mice, liver samples were obtained from C57-TgN(*HBx*) SMMU1 mice and normal C57BL/6 mice. Specimens were homogenized and lysed in lysis buffer. 100 mg lysate was used to assay HBX protein. A component of relative molecular mass 17 000 befitting the X protein was specifically detected with anti X protein monoantibody by Western blotting (Figure 3A), suggesting the transgenic mice with *HBx* gene could express X protein in the liver tissue. The distribution of X protein in hepatocytes was determined by immunohistochemistry and immunogold electron microscopy, which revealed that X protein was mainly distributed in hepatocytic cytoplasm, little on plasm membrane and in nucleus (Figure 3B-3D).

DISCUSSION

Transgenic mice are the valuable animal models to study the functions of genes^[30]. Although transgenic mice containing different HBV genes, including the entire viral genome, have been established and analysed before, there is little evidence to suggest that the virus plays a direct role in inducing hepatocellular carcinoma^[31-41]. Hepatitis X protein is essential for HBV genes expression and replication^[42,43]. *In vitro*, X protein exhibits a plethora of activities. From cell culture studies, it is believed that X protein can activate the transcription of host genes, including the major histocompatibility complex and *c-myc*, as well as viral genes. Aside from the transactivation of many promoters, the other activities linked to X protein include

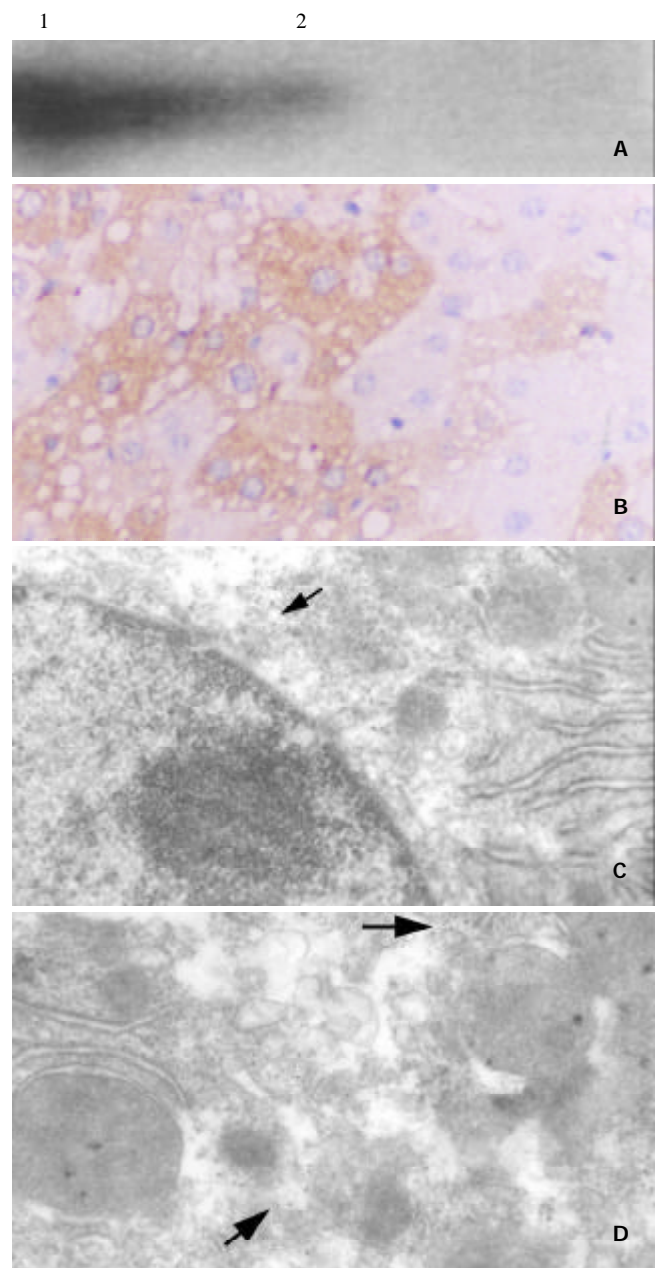


Figure 3 Expression of *HBx* gene in transgenic mice. (A) Western blot analysis of *HBx* gene expression in liver tissue from transgenic mouse. *M*_{17 000} X protein was detected with X protein mouse monoclonal antibody; Lane 1: C57-TgN(*HBx*) SMMU1 transgenic mice; Lane 2: normal C57BL/6 mice; (B): *HBx* gene expression mainly in hepatocytes cytoplasm of C57-TgN(*HBx*)SMMU1 transgenic mice demonstrated by immunohistochemistry (×132). (C, D) *HBx* gene Expression in hepatocyte cytoplasm of C57-TgN (*HBx*) SMMU1 transgenic mice detected by immunogold electron microscopy (arrows) 3C: ×20 000; 3D: ×40 000.

stimulation of signal transduction and binding, to various degrees, to well-known protein targets such as p53, proteasome subunit, and UV-damaged DNA binding protein^[44-58].

However, the role of *HBx* gene in the course of HBV infection and in inducing HCC is unknown. In the present study, we constructed an *HBx* gene (adr subtype) expression vector pcDNA3-*HBx* containing CMV promoter and *HBx* gene ORF. By Western blotting, we found that it could express X protein in eukaryotic cells. pcDNA3-*HBx* may be a useful vector to study the role of X protein and explore the mechanism of transactivation *in vitro*. We also generated two founders of transgenic mice with *HBx* gene (adr subtype) by microinjections,

named C57-TgN(*HBx*)SMMU1 and C57-TgN(*HBx*)SMMU3, which harboured *HBx* gene in their genomic DNA. The birth rate of the pups was lower than that of other transgenic mice, including entire hepatitis viral genome transgenic mice. This indicated that X protein was probably involved in some phases of development. The hepatitis X protein was expressed in the liver tissue of transgenic mice and distributed mainly in hepatocytes cytoplasm by Western blotting, immunohistochemistry and immunogold electron microscopy, which suggested that the transgenic mice could be an important tool in studying the function of *HBx* gene *in vivo*. Besides, we also developed a multiplex PCR to rapidly and accurately screen the transgenic mice with *HBx* gene. This method, using an optimized ratio of primer pairs, allows for the detection of *HBx* gene in transgenic mice, which can not only amplify target genes, but also show its amplification efficiency.

In conclusion, we have established *HBx* (adr subtype) transgenic mice as a model system for defining the function of *HBx* gene (adr subtype) and the role of X protein in the virus life cycle and HCC. And the multiplex PCR is a rapidly and accurately method to detect the transgenic mice with *HBx* gene.

REFERENCES

- Tiollais P**, Pourcel C, Dejean A. The hepatitis B virus. *Nature* 1985; **317**: 489-495
- Ganem D**, Varmus HE. The molecular biology of the hepatitis B viruses. *Annu Rev Biochem* 1987; **56**: 651-693
- Gan RB**, Chu MJ, Shen LP, Qian SW, Li ZP. The complete nucleotide sequence of the cloned DNA of hepatitis B virus subtype adr in pADR-1. *Sci Sin B* 1987; **30**: 507-521
- Seeger C**, Mason WS. Hepatitis B virus biology. *Micro Mol Bio Rev* 2000; **64**: 51-68
- Stuyver LJ**, Locarnini SA, Lok A, Richman DD, Carman WF, Dienstag JL, Schinazi RF. Nomenclature for antiviral-resistance human hepatitis B virus mutations in the polymerase region. *Hepatology* 2001; **33**: 751-757
- Wu X**, Zhu L, Li ZP, Koshy R, Wang Y. Functional organization of enhancer (EN) of hepatitis B virus. *Virology* 1992; **191**: 490-494
- Chisari FV**, Ferran C. Hepatitis B virus immunopathogenesis. *Annu Rev Immunol* 1995; **13**: 29-60
- Chisari FV**. Viruses, immunity, and cancer: lessons from hepatitis B. *Am J Pathol* 2000; **156**: 1117-1132
- Montalto G**, Cervello M, Giannitrapani L, Dantona F, Terranova A, Castagnetta LA. Epidemiology, risk factors, and natural history of hepatocellular carcinoma. *Ann N Y Acad Sci* 2002; **963**: 13-20
- Arbuthnot P**, Kew M. Hepatitis B virus and hepatocellular carcinoma. *Int J Exp Pathol* 2001; **82**: 77-100
- Honda M**, Kaneko S, Kawai H, Shirota Y, Kobayashi K. Differential gene expression between chronic hepatitis B and C hepatic lesion. *Gastroenterology* 2001; **120**: 955-966
- Liu H**, Wang Y, Zhou Q, Gui SY, Li X. The point mutation of p53 gene exon7 in hepatocellular carcinoma from Anhui Province, a non HCC prevalent area in China. *World J Gastroenterol* 2002; **8**: 480-482
- Li Y**, Tang ZY, Ye SL, Liu YK, Chen J, Xue Q, Chen J, Gao DM, Bao WH. Establishment of cell clones with different metastatic potential from the metastatic hepatocellular carcinoma cell line MHCC97. *World J Gastroenterol* 2001; **7**: 630-636
- Cao XY**, Liu J, Lian ZR, Clayton M, Hu JL, Zhu MH, Fan DM, Feitelson M. Differentially expressed genes in hepatocellular carcinoma induced by woodchuck hepatitis B virus in mice. *World J Gastroenterol* 2001; **7**: 575-578
- Lee JH**, Ku JL, Park YJ, Lee KU, Kim WH, Park JG. Establishment and characterization of four human hepatocellular carcinoma cell lines containing hepatitis B virus DNA. *World J Gastroenterol* 1999; **5**: 289-295
- Madden CR**, Finegold MJ, Slagle BL. Hepatitis B virus X protein acts as a tumor promoter in development of diethylnitrosamine-induced preneoplastic lesions. *J Virol* 2001; **75**: 3851-3858
- Koike K**, Moriya K, Yotsuyanagi H, Iino S, Kurokawa K. Induction of cell cycle progression by hepatitis B virus HBx gene expression in quiescent mouse fibroblasts. *J Clin Invest* 1994; **94**: 44-49
- Shih WL**, Kuo ML, Chuang SE, Cheng AL, Doong SL. Hepatitis B virus X protein inhibits transforming growth factor- α -induced apoptosis through the activation of phosphatidylinositol 3-kinase pathway. *J Bio Chem* 2000; **275**: 25858-25864
- Benn J**, Schneider RJ. Hepatitis B virus HBx protein deregulates cell cycle checkpoint controls. *Proc Natl Acad Sci* 1995; **92**: 11215-11219
- Ogden SK**, Lee KC, Barton MC. Hepatitis B viral transactivator HBx alleviates p53-mediated repression of α -fetoprotein gene expression. *J Bio Chem* 2000; **275**: 27806-27814
- Su F**, Theodosios CN, Schneider RJ. Role of NK-kappaB and myc proteins in apoptosis induced by hepatitis B virus HBx protein. *J Virol* 2001; **75**: 215-225
- Diao J**, Garces R, Richardson CD. X protein of hepatitis B virus modulates cytokine and growth factor related signal transduction pathways during the course of viral infections and hepatocarcinogenesis. *Cytokine Growth Factor Rev* 2001; **12**: 189-205
- Kaneko S**, Miller RH. X-region-specific transcript in mammalian hepatitis B virus-infected liver. *J virol* 1988; **62**: 3979-3984
- Terradillos O**, Pollicino T, Lecoeur H, Tripodi M, Gougeon ML, Tiollais P, Buendia MA. p53-independent apoptotic effects of the hepatitis B virus HBx protein *in vivo* and *in vitro*. *Oncogene* 1998; **17**: 2115-2123
- Su F**, Schneider RJ. Hepatitis B virus HBx protein sensitizes cells to apoptotic killing by tumor necrosis factor alpha. *Proc Natl Acad Sci U S A* 1997; **94**: 8744-8749
- Murakami S**. Hepatitis B virus X protein: a multifunctional viral regulator. *J Gastroenterol* 2001; **36**: 651-660
- Feitelson MA**, Duan LX. Hepatitis B virus x antigen in the pathogenesis of chronic infections and the development of hepatocellular carcinoma. *Am J Pathol* 1997; **150**: 1141-1157
- Miyatake S**, Yokota T, Lee F, Arai K. Structure of the chromosomal gene for murine interleukin 3. *Proc Natl Acad Sci USA* 1985; **82**: 316-320
- Lambert JF**, Benoit BO, Colvin GA, Carlson J, Delville Y, Quesenberry PJ. Quick sex determination of mouse fetuses. *J Neurosci Method* 2000; **95**: 127-132
- Rall GF**, Lawrence DM, Patterson CE. The application of transgenic and knockout mouse technology for the study of viral pathogenesis. *Virology* 2000; **271**: 220-226
- Koike K**. Hepatocarcinogenesis in hepatitis viral infection: lessons from transgenic mouse studies. *J Gastroenterol* 2002; **37** (suppl13): 55-64
- Chen XS**, Wang GJ, Cai X, Yu HY, Hu YP. Inhibition of hepatitis B virus by oxymatrine *in vivo*. *World J Gastroenterol* 2001; **7**: 49-52
- Aragona E**, Burk RD, Ott M, Shafritz DA, Gupta S. Cell type-specific mechanisms regulate hepatitis B virus transgene expression in liver and other organs. *J Pathol* 1996; **180**: 441-449
- Xu Z**, Yen TS, Wu L, Madden CR, Tan W, Slagle BL, Ou JH. Enhancement of hepatitis B virus replication by its X protein in transgenic mice. *J Virol* 2002; **76**: 2579-2584
- Guidotti LG**, Matzke B, Schaller H, Chisari FV. High-level hepatitis B virus replication in transgenic mice. *J Virol* 1995; **69**: 6158-6169
- Zhu HZ**, Cheng GX, Chen JQ, Kuang SY, Cheng Y, Zhang XL, Li HD, Xu SF, Shi JQ, Qian GS, Gu JR. Preliminary study on the production of transgenic mice harboring hepatitis B virus X gene. *World J Gastroenterol* 1998; **4**: 536-539
- Chemin I**, Ohgaki H, Chisari FV, Wild CP. Altered expression of hepatic carcinogen metabolizing enzymes with liver injury in HBV transgenic mouse lineages expressing various amounts of hepatitis B surface antigen. *Liver* 1999; **19**: 81-87
- Schweizer J**, Valenza-Schaerly P, Goret F, Pourcel C. Control of expression and methylation of a hepatitis B virus transgene by strain-specific modifiers. *DNA Cell Biol* 1998; **17**: 427-435
- Kim CM**, Koike K, Saito I, Miyamura T, Jay G. HBx gene of hepatitis B virus induces liver cancer in transgenic mice. *Nature* 1991; **351**: 317-320
- Hu YP**, Hu WJ, Zheng WC, Li JX, Dai DS, Wang XM, Zhang SZ, Yu HY, Sun W, Hao GR. Establishment of transgenic mouse harboring hepatitis B virus (adr subtype) genomes. *World J Gastroenterol* 2001; **7**: 111-114
- Hu YP**, Yao YC, Li JX, Wang XM, Li H, Wang ZH, Lei ZH. The

- cloning of 3' -truncated preS/S gene from HBV genomic DNA and its expression in transgenic mice. *World J Gastroenterol* 2000; **6**: 734-737
- 42 **Ganem D**. The X files-one step closer to closure. *Science* 2001; **294**: 2299-2300
- 43 **Bouchard MJ**, Wang LH, Schneider RJ. Calcium signaling by HBx protein in hepatitis B virus DNA replication. *Science* 2001; **294**: 2376-2378
- 44 **Yun C**, Um HR, Jin YH, Wang JH, Lee MO, Park S, Lee JH, Cho H. NF-kappaB activation by hepatitis B virus X (HBx) protein shifts the cellular fate toward survival. *Cancer Lett* 2002; **184**: 97-104
- 45 **Bergametti F**, Sitterlin D, Transy C. Turnover of hepatitis B virus X protein is regulated by damaged DNA-binding complex. *J Virol* 2002; **76**: 6495-6501
- 46 **Li J**, Xu Z, Zheng Y, Johnson DL, Ou JH. Regulation of hepatocyte nuclear factor 1 activity by wild-type and mutant hepatitis B virus X proteins. *J Virol* 2002; **76**: 5875-5881
- 47 **Han HJ**, Jung EY, Lee WJ, Jang KL. Cooperative repression of cyclin-dependent kinase inhibitor p21 gene expression by hepatitis B virus X protein and hepatitis C virus core protein. *FEBS Lett*, 2002; **518**: 169-172
- 48 **Wang XZ**, Jiang XR, Chen XC, Chen ZX, Li D, Lin JY, Tao QM. Seek protein which can interact with hepatitis B virus X protein from human liver cDNA library by yeast two-hybrid system. *World J Gastroenterol* 2002; **8**: 95-98
- 49 **Guo SP**, Wang WL, Zhai YQ, Zhao YL. Expression of nuclear factor-kappa B in hepatocellular carcinoma and its relation with the X protein of hepatitis B virus. *World J Gastroenterol* 2001; **7**:340-344
- 50 **Lee S**, Tarn C, Wang WH, Chen S, Hullinger RL, Andrisani OM. Hepatitis B virus X protein differentially regulates cell cycle progression in X-transforming versus nontransforming hepatocyte (AML12) cell lines. *J Biol Chem* 2002; **277**: 8730-8740
- 51 **Qiao L**, Leach K, McKinstry R, Gilfor D, Yacoub A, Park JS, Grant S, Hylemon PB, Fisher PB, Dent P. Hepatitis B virus X protein increases expression of p21(Cip-1/WAF1/MDA6) and p27(Kip-1) in primary mouse hepatocytes, leading to reduced cell cycle progression. *Hepatology* 2001; **34**: 906-917
- 52 **Waris G**, Huh KW, Siddiqui A. Mitochondrially associated hepatitis B virus X protein constitutively activates transcription factors STAT-3 and NF-kappa B via oxidative stress. *Mol Cell Biol* 2001; **21**: 7721-7730
- 53 **Nag A**, Datta A, Yoo K, Bhattacharyya D, Chakraborty A, Wang X, Slagle BL, Costa RH, Raychaudhuri P. DDB2 induces nuclear accumulation of the hepatitis B virus X protein independently of binding to DDB1. *J Virol* 2001; **75**: 10383-10392
- 54 **Lin-Marq N**, Bontron S, Leupin O, Strubin M. Hepatitis B virus X protein interferes with cell viability through interaction with the p127-kDa UV-damaged DNA-binding protein. *Virology* 2001; **287**: 266-274
- 55 **Tarn C**, Lee S, Hu Y, Ashendel C, Andrisani OM. Hepatitis B virus X protein differentially activates RAS-RAF-MAPK and JNK pathways in X-transforming versus non-transforming AML12 hepatocytes. *J Biol Chem* 2001; **276**: 34671-34680
- 56 **Jaitovich-Groisman I**, Benlimame N, Slagle BL, Perez MH, Alpert L, Song DJ, Fotouhi-Ardakani N, Galipeau J, Alaoui-Jamali MA. Transcriptional regulation of the TFIIF transcription repair components XPB and XPD by the hepatitis B virus x protein in liver cells and transgenic liver tissue. *J Biol Chem* 2001; **276**: 14124-14132
- 57 **Pan J**, Duan LX, Sun BS, Feitelson MA. Hepatitis B virus X protein protects against anti-Fas-mediated apoptosis in human liver cells by inducing NF-kappa B. *J Gen Virol* 2001; **82**: 171-182
- 58 **Sitterlin D**, Bergametti F, Transy C. UVDDDB p127-binding modulates activities and intracellular distribution of hepatitis B virus X protein. *Oncogene* 2000; **19**: 4417-4426

Edited by Zhu L

Changes in serum and histology of patients with chronic hepatitis B after interferon alpha-2b treatment

Hong-Lei Han, Zhen-Wei Lang

Hong-Lei Han, Zhen-Wei Lang, Department of Pathology, Beijing Youan Hospital, Beijing 100054, Beijing City, China

Correspondence to: Professor Zhen-Wei Lang, Department of Pathology, Beijing Youan Hospital, Beijing 100054, Beijing City, China
Telephone: +86-10-63292211-2402

Received: 2001-07-19 **Accepted:** 2001-09-21

Abstract

AIM: Chronic hepatitis B is a serious health problem. Interferon has long been used to treat Chronic hepatitis B. To evaluate the effects of interferon on chronic hepatitis B better, we designed the study to investigate the changes in sera and liver histology of patients with chronic hepatitis B after interferon alpha-2b treatment.

METHODS: Twenty-four patients with chronic hepatitis B were enrolled in this study. They all received interferon alpha-2b treatment as following: 3 million units, i.m., t.i.w., for 18 weeks. Sera of all patients were obtained respectively for evaluation of ALT, HBsAg, HBeAg, HBV DNA and TIMP-1 before and after interferon treatment, also a liver biopsy pre- and post-treatment was performed for comparison of HAI, HBsAg, HBeAg, TIMP-1 and activated HSC in the liver tissue.

RESULTS: Patients who had normalization of serum ALT and seroconversion of HBeAg and/or HBV DNA (blot hybridization) after treatment were defined as responders. The response rate in this study group was 37.5 % (7/24). Compared to pretreatment, the serum HBV DNA and TIMP-1 decreased significantly ($P < 0.05$), so did the HAI, HBsAg, HBeAg, TIMP-1 and activated HSC ($P < 0.05$).

CONCLUSION: The significant decrease in HBV DNA in sera, the seroconversion of HBeAg, and the decrease of viral expression in liver indicated that interferon alpha-2b treatment can inhibit viral replication. The normalization of ALT in sera and the improvement of HAI in liver showed that interferon alpha-2b can improve the liver histology of patients with chronic hepatitis B. At the same time, interferon alpha-2b treatment can reduce the TIMP-1 in serum and liver and decrease the number of activated HSC, which may alleviate or inhibit hepatic fibrosis. Although the response rate was unsatisfactory, interferon play a beneficial role on patients with chronic hepatitis B in other respects. We still need further studies to improve the therapy effects.

Han HL, Lang ZW. Changes in serum and histology of patients with chronic hepatitis B after interferon alpha-2b treatment. *World J Gastroenterol* 2003; 9(1): 117-121

<http://www.wjgnet.com/1007-9327/9/117.htm>

INTRODUCTION

Chronic hepatitis B is a serious problem threatening public health, especially in our country. Interferon has been used to treat it for a long time. It has been proved that after interferon

treatment, the response rate in patients with chronic hepatitis B is about 30-50 %, with normalization of ALT, seroconversion of HBeAg and HBV DNA and improvement of liver HAI^[1-11]. However, the effects on hepatic fibrosis and viral antigen in liver tissue have been seldom reported. In this study, we evaluated mainly the effects of interferon treatment on some indexes of sera and liver histology.

MATERIALS AND METHODS

Materials

Patients Twenty-four patients were enrolled in this study. Of these, 21 were male, 3 were female. The mean age was 38.4. All patients had moderately elevated serum ALT. All patients were negative for hepatitis C and D. None had alcoholic liver disease, autoimmune or drug-induced liver disease, no patients had received antiviral or immunomodulatory therapy. Informed consent was obtained from each patient before the study. All patients were treated with recombinant IFN- α -2b 3MU thrice a week for 18 weeks (The IFN- α -2b was a product of Anke Company of biological technic of Anhui Province). Liver biopsy was performed in each patient before and after IFN treatment and serum specimens were obtained at the same time.
Response to IFN-a-2b treatment Patients who had normalization of serum ALT and seroconversion of HBeAg and/or HBV DNA (blot hybridization) after treatment were defined as responders, while those with negative result were taken as non-responders.

Methods

Assay for serum HBV, HCV, CMV and EBV markers All markers were measured by using the enzyme linked immunosorbent assay (ELISA). Antibodies to HBsAg, anti-HBs, HBeAg, anti-HBe, anti-HBc-IgM, anti-HBc-IgG, anti-HCV-IgG and anti-HCV-IgM were products of American Abbott Company. Anti-CMV-IgG and anti-EBV-IgG were purchased from Italian Deyi Company. The reagents for HBV DNA blot hybridization were products of Yuanli Reagent Company of Shanghai Medical University.

Quantitative PCR of serum HBV DNA Blood samples were obtained under fasting conditions before and after the IFN treatment. All sera were stored at -40 °C until assay. Quantitative polymerized chain reaction (PCR) of HBV DNA was performed as the method introduced by American Biotronics Company^[12]. The logarithms of the HBV DNA levels were statistically analyzed.

Assay for serum TIMP-1 Serum TIMP-1 was evaluated by using sandwich method of ELISA. Multiclonal antibody to TIMP-1 was bought from Beijing Zhongshan Biological Company, while monoclonal antibody to TIMP-1 was from Fujian Maxim Biological Company. Other reagents for ELISA were purchased from Beijing Zhongshan Biological Company.

Histological analysis Liver specimens were graded by 2 pathologists blinded to the response to treatment, using the histological activity index (HAI) described by Knodell^[13].

Assay for viral antigen in liver Expression of HBsAg, HBeAg and HBeAg in liver were evaluated using immunohistochemical S-P method. S-P kit was produced by Fujian Maxim Biological

Company. The procedures were performed according to the kit instruction. Expression of viral antigen in the liver was evaluated by semi-quantitative scoring system referring to the method introduced by Lindh^[14]. Based on the ratio of positive cells, the score was 0-3 respectively, corresponding to the positivity in 0 %, 1-20 %, 20-50 %, and more than 50 % of hepatocytes examined.

Liver fibrosis (1) Using α -smooth muscle actin (α -SMA) as a marker of activated hepatic stellate cell (HSC), the changes of activated HSC in the liver were analysed. (2) The expression of TIMP-1 in the liver was also investigated by using immunohistochemical method. The reagents for both HSC and TIMP-1 were bought from Fujian Maxim Biological Company. Scoring systems were the same as that for viral antigens.

Statistical analysis

All statistics were performed by using statistical procedure of social science (SPSS), including chi-square test and Wilcoxon's rank sum test. The probability values less than 5 % were considered significant.

RESULTS

Responders and non-responders

After interferon treatment, 7/24 (37.5 %) of patients were responders who had normalization of ALT and seroconversion of HBeAg and/or HBV DNA. The other 15 (62.5%) patients were non-responders.

Changes in serum level of HBV DNA

The average logarithm of serum HBV DNA before interferon treatment was 8.20 ± 0.60 m, which changed to 7.21 ± 1.14 after treatment (Table 1 and Figure 1). Compared to pretreatment, the serum level of HBV DNA decreased significantly ($P < 0.05$). Moreover, the decrease of serum HBV DNA level of responders was significant ($P < 0.05$).

Table 1 Changes of serum HBV DNA of patients with chronic hepatitis B (Logarithm of the value expressed by copy/ml) ($\bar{x} \pm s$)

	responders (n=9)	non-responders (n=15)	all patients (n=24)
pretreatment	8.52 ± 0.39	8.00 ± 0.64	8.20 ± 0.60
post-treatment	7.24 ± 0.83	7.16 ± 0.14	7.21 ± 1.14
P value	$P = 0.028$	$P = 0.051$	$P = 0.002$

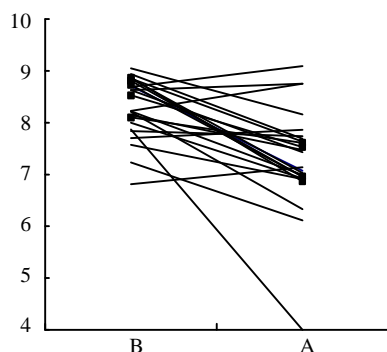


Figure 1 Changes of the logarithm value of serum HBV DNA of patients with chronic hepatitis B (B: before IFN treatment; A: after IFN treatment)

Changes in serum TIMP-1

Because of limited samples, only the serum TIMP-1 of 13

patients (4 responders and 9 non-responders) were evaluated. After the IFN treatment was completed, the optical density (OD) values of serum TIMP-1 of 10/13 (76.9 %) of patients decreased. Compared to pretreatment, the decrease was significant (pretreatment 0.481 ± 0.199 , post-treatment 0.367 ± 0.210 , $P < 0.05$) (Figure 2), regardless of the responders or non-responders.

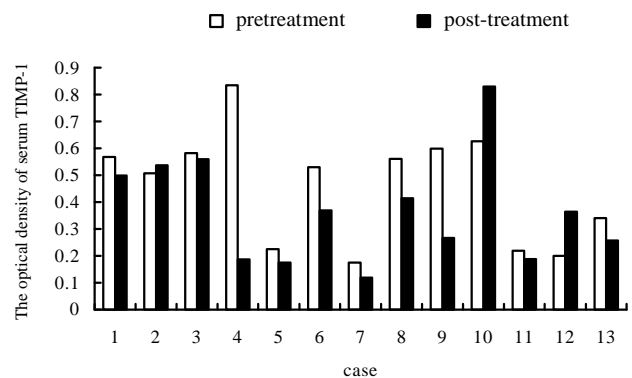


Figure 2 Changes of OD value of serum TIMP-1 of patients with chronic hepatitis B

Changes in HAI

Before IFN treatment, there was no significant difference of the HAI between the responders and non-responders ($P > 0.05$). After treatment, the HAI of patients decreased markedly ($P < 0.05$), especially the necrosis and intralobular inflammation ($P < 0.05$), but not the portal inflammation and fibrosis ($P > 0.05$). The changes of HAI of responders was significant ($P < 0.05$), while that of non-responders was insignificant ($P > 0.05$). (Table 2).

Table 2 Changes of HAI of patients with chronic hepatitis B ($\bar{x} \pm s$)

	responders (n=9)		nonresponders (n=15)		all patients (n=24)	
	pre-treatment	post-treatment	pre-treatment	post-treatment	pre-treatment	post-treatment
necrosis	2.57 ± 1.51	2.14 ± 1.21	2.82 ± 0.98	1.91 ± 1.04	2.72 ± 1.18^a	2.06 ± 1.11
lob. inf.	3.29 ± 0.49^a	1.57 ± 0.98	2.67 ± 0.82	2.36 ± 0.92	2.72 ± 0.89^a	1.78 ± 1.00
portal inf.	3.00 ± 1.00	2.29 ± 1.25	2.32 ± 0.96	2.09 ± 0.94	2.58 ± 1.00	2.39 ± 0.98
necrosis	1.71 ± 1.25	1.57 ± 1.13	1.91 ± 1.14	1.36 ± 1.12	1.82 ± 1.15	1.44 ± 1.10
HAI	10.57 ± 3.6^a	7.57 ± 4.12	9.41 ± 3.04	7.45 ± 3.11	9.86 ± 3.22^a	7.78 ± 3.30

^a $P < 0.05$

Viral antigens in liver

In the liver, HBsAg was expressed in the following pattern: membranous, submembranous, cytoplasmic or inclusion body. In this study, before IFN treatment, HBsAg was mainly located in the cytoplasm of hepatocytes, and was positive in 22/24 (91.7 %). The positivity of HBsAg in the liver of responders was not considerably different from that of non-responders ($P > 0.05$). After IFN treatment, 17 patients were found to have HBsAg expression in the liver, which was not significantly different from that of pretreatment (pretreatment 1.50 ± 1.79 , post-treatment 1.11 ± 0.83 , $P > 0.05$), regardless of responders or non-responders (Responders: pretreatment 1.33 ± 0.52 , post-treatment 1.17 ± 0.75 , $P > 0.05$; Non-responders: pretreatment 1.50 ± 0.80 , post-treatment 1.08 ± 0.90 , $P > 0.05$). The location of HBsAg switched from a diffuse cytoplasmic pattern to a membranous and/or sub membranous pattern.

HBcAg can be mainly detected in hepatocyte nucleus and cytoplasm (Figure 3). HBcAg expression was positive in 20/

24 (83.3 %). There was no significant difference between HBcAg expression in the liver of the responders and non-responders ($P>0.05$). However 12/20 (60 %) of patients were found to have a decrease in HBcAg expression in liver after IFN treatment, and the location of HBcAg changed to nucleic pattern mostly. Statistics showed that HBcAg expression in the liver declined significantly, Compared to pretreatment (pretreatment 1.28 ± 0.75 , post-treatment 0.61 ± 0.85 , $P<0.05$). The decrease in the responders was marked, but not that in the non-responders (Responders: pretreatment 1.67 ± 0.52 , post-treatment 0.17 ± 0.47 , $P<0.05$; Non-responders: pretreatment 1.08 ± 0.79 , post-treatment 0.83 ± 0.94 , $P>0.05$).

Positive HBeAg expression in liver was mainly located in cytoplasm and nucleus of hepatocytes (Figure 4). HBeAg was detected in the liver of 12/24 (50 %) of patients before IFN treatment and 4/24 (16.7 %) after treatment. Statistics proved that HBeAg expression decreased remarkably (pre-treatment 0.78 ± 0.94 , post-treatment 0.22 ± 0.43 , $P<0.05$). But the decrease in the responders was not significantly different from that in the non-responders ($P>0.05$).

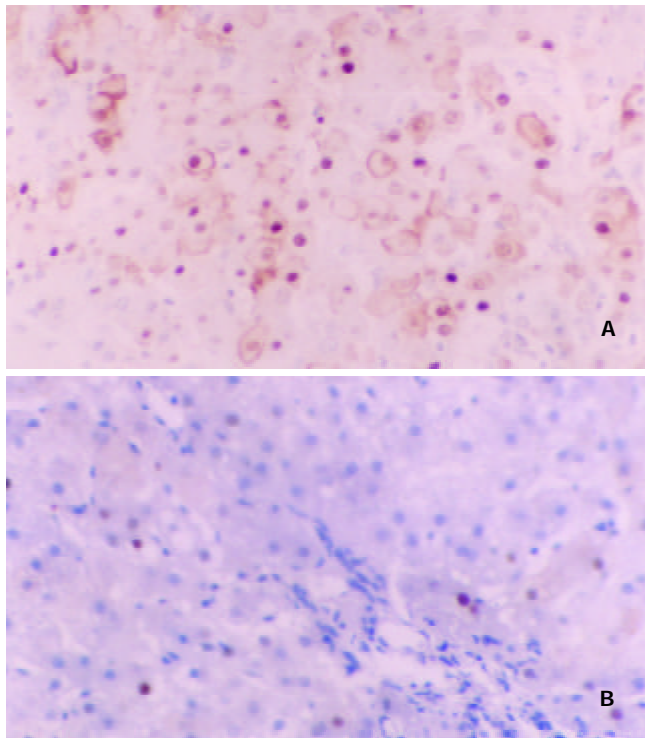


Figure 3 Changes of HBcAg expression in liver of patients with chronic hepatitis B. A: before IFN treatment; B: after IFN treatment

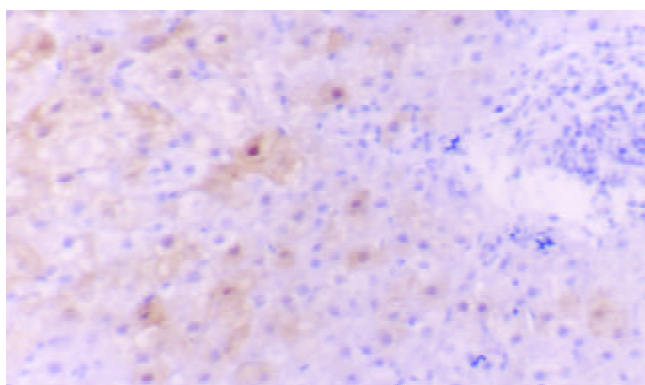


Figure 4 HBeAg expression in liver of patients with chronic hepatitis B before IFN treatment

Liver fibrosis

HSC in liver Normally, there are only several activated HSCs which contain α -SMA. But in the liver of patients with chronic hepatitis B, there were large number of α -SMA-positive HSC, diffusely located in the sinusoids (Figure 5). This showed that the number of α -SMA-positive HSC in the liver decreased significantly after treatment (pre-treatment 1.39 ± 0.35 , post-treatment 0.61 ± 0.70 , $P<0.05$). The marked change of HSC was related to the change of HAI ($P<0.05$), but not to the fibrosis score in accordance with HAI.

TIMP-1 in liver TIMP-1 in the liver was located in cytoplasm of hepatocyte (Figure 6). Before IFN- α treatment, 21/24 (87.5 %) of patients were detected positive TIMP-1 in their livers. In addition, there was no significant difference in TIMP-1 expression between responders and non-responders ($P>0.05$). After treatment, the TIMP-1 in liver of 18/21 (85.6 %) patients decreased. Compared to pretreatment, TIMP-1 in liver decreased significantly (pre-treatment 1.765 ± 1.033 , post-treatment 0.588 ± 0.441 , $P<0.01$), regardless of the responders or non-responders.

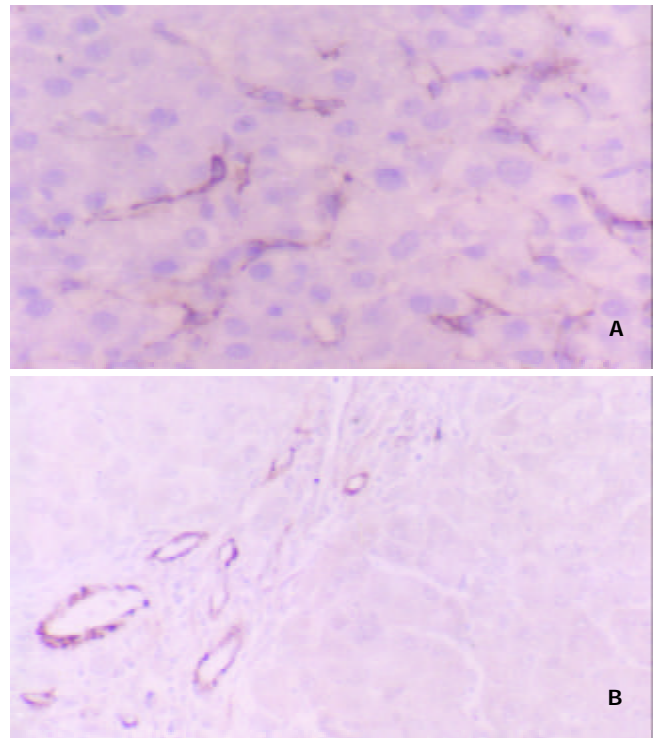


Figure 5 Changes of α -SMA-positive HSC in liver of patients with chronic hepatitis B. A: before IFN treatment; B: after IFN treatment

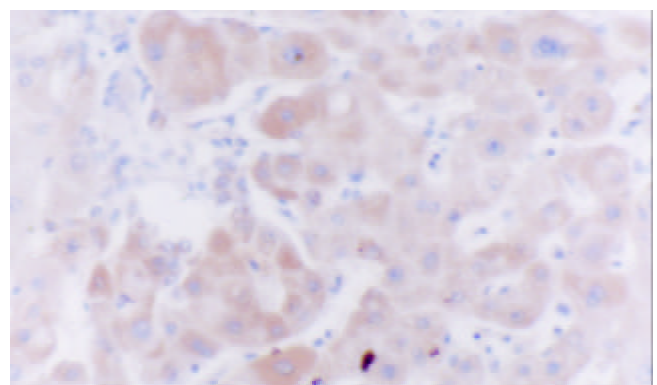


Figure 6 TIMP-1 in liver of patients with chronic hepatitis B before IFN treatment

DISCUSSION

Interferon- α treatment is effective in decreasing serum alanine transferase (ALT), converting serum HBeAg and HBVDNA to negative, and improving necroinflammation in the liver of patients with chronic hepatitis B. In this study, we evaluated the effect of interferon- α on both liver histology and serum parameters.

Viral markers in sera

Among the patients, 9/24 (37.5 %) showed response reaction after interferon treatment, which agreed with other studies^[14]. The serum ALT of responders became normal, and the serum HBeAg and/or HBVDNA became negative after treatment. Compared to pre-treatment, the serum HBVDNA of the patients decreased significantly ($P < 0.05$), especially that of the responders ($P < 0.05$). The results suggested that interferon- α could inhibit the viral replication.

Viral antigen in liver

It was reported that interferon- α can inhibit all hepatitis B virus antigens expression in primary hepatocyte culture^[15]. Moreover, interferon can change the location of HBsAg in hepatocyte from cytoplasm to the cell membrane or submembrane region^[15], which may enhance immune recognition and clearance of infected hepatocytes. Our study evaluated the effect of interferon- α on viral antigen in liver of chronic hepatitis B. In this group, the decline of HBsAg expression in liver was not significant, but the HBsAg expression switched from cytoplasmic to membranous/submembranous, which supported some previous studies^[5,6]. However, the HBcAg and HBeAg in the liver decreased significantly after interferon treatment, especially in the responders, but not in the non-responders. This might be related to the fact that HBcAg and HBeAg of hepatocytes were target antigens of immune reaction mediated by HBV. IFN could enhance the recognition of immune system on the infected hepatocytes.

HAI

Shiratori *et al* proved that interferon therapy can improve liver histology of hepatitis C by alleviating hepatic inflammation and fibrosis^[16]. Our study showed that after interferon treatment, HAI of liver of all the patients decreased significantly ($P < 0.05$), mainly in the aspects of necrosis and intralobular inflammation. The change in responders was significant, but not that in the non-responders. This indicated interferon treatment can improve the hepatic lesions of patients with chronic hepatitis B.

Liver fibrosis

Many patients with chronic hepatitis B progress slowly to liver fibrosis even cirrhosis. During this course, HSC plays a key role in the process of fibrosis. Proliferation and transformation of HSC is basic characteristic of liver fibrosis. On the one hand, liver injury and cytokines released stimulate HSC to proliferate, differentiate and acquire myofibroblast phenotype, with increase of collagen synthesis, expression of α -SMA, secretion and desposition of extracellular matrix (ECM)^[17,18]. On the other hand, HSC can secrete matrix metalloproteinase (MMP) which can degrade ECM. It is worth noting that HSC also secretes tissue inhibitor of metalloproteinase (TIMP)-the inhibitor of MMP. TIMP can noncovalently bind with MMP to inhibit the degradation of ECM, and promote liver fibrosis. Researches showed that in liver of patients with liver disease related to hepatitis B, the expression of TIMPs and MMP altered to make the liver tend to develop fibrosis^[19-22]. Certain medicine can improve liver cirrhosis^[23]. Several reports suggested that interferon treatment can alleviate hepatic fibrosis caused by viral hepatitis^[24-30]. The mechanism is not clear. Some evidence

supported that interferon reduced HSCs^[31], probably by inducing the apoptosis of HSCs^[32]. Others believed that interferon changed the amount of enzymes, such as MMP and TIMPs^[33,34].

HSC in liver

In our study, the number of HSC containing α -SMA decreased significantly after interferon treatment ($P < 0.05$). The α -SMA expression by HSC decreased in 50 % of patients. This suggested that interferon treatment might inhibit the proliferation or transformation of HSC with the same conclusion by Guido's^[31]. The significant association of α -SMA to liver HAI ($P < 0.05$) suggested that the effect of interferon on HSC maybe related to its anti-inflammatory function. But there was no significant relation between reduction of HSC and change of fibrosis according to Knodell's HAI, which might be due to the small size of our patients.

TIMP-1 in serum and liver

Mitsuda *et al* found that IFN- α could not only reduce the TIMP-1 in serum to enhance fibrinolysis, but also inhibit the fibrogenesis of patients with chronic hepatitis C^[33]. Whether IFN- α has similar effect on the patients with chronic hepatitis B remains to be seen.

In this study, TIMP-1 in both serum and liver of patients with chronic hepatitis B decreased markedly after IFN- α treatment. This phenomenon suggests that IFN- α can inhibit production or TIMP-1 expression to improve fibrinolysis and inhibit fibrosis.

In conclusion, our study suggests that IFN- α treatment can inhibit viral replication, alleviate liver injury, inhibit activation of HSC, decrease TIMP-1 in liver and serum and inhibit liver fibrosis. The detailed mechanism and the optimal dose and course of IFN- α still deserve more studies. Although the interval of two biopsy was not very long, evidence suggested that interferon has long-term beneficial effect in patients with chronic hepatitis B^[35]. The result was not very satisfactory. Maybe we should combine interferon and other medicines to treat chronic hepatitis B, as some study did^[36].

REFERENCES

- 1 **Pessoa MG**, Wright TL. Update on clinical trials in the treatment of hepatitis B. *J Gastroenterol Hepatol* 1999; **14** (Suppl): S6-S11
- 2 **Lau GKK**, Carman WF, Locarnini SA, Okuda K, Lu ZM, Williams R, Lam SK. Treatment of chronic hepatitis B virus infection: An Asia-Pacific perspective. *J Gastroenterol Hepatol* 1999; **14**: 3-12
- 3 **Yao GB**. Treatment of chronic hepatitis B in China. *J Gastroenterol Hepatol* 2000; **15**(Suppl): E61-E66
- 4 **Ishikawa T**, Kakumu S. Update of liver disease related to chronic hepatitis B virus infection. *Intern Med* 2001; **40**: 178-179
- 5 **Liaw YF**. Management of patients with chronic hepatitis B. *J Gastroenterol hepatol* 2002; **17**: 406-408
- 6 **Wang XZ**, Chen YX, Ma LS, Ma JY, Pan BR. Antiviral therapy of chronic hepatitis B in China. *Shijie Huaren Xiaohua Zazhi* 2002; **10**: 745-748
- 7 **Hoofnagle JH**, Peters M, Mullen KD, Jones DB, Rustgi V, Bisceglie AD, Hallahan C, Park Y, Meschivetz C, Jones EA. Randomized, controlled trial of recombinant human α -interferon in patients with chronic hepatitis B. *Gastroenterol* 1988; **95**: 1318-1325
- 8 **Oliveri F**, Santantonio T, Bellati G, Colombatto P, Mels GC, Carriero L, Dastoli G, Pastore G, Ideo G, Bonino F, Brunetto MR. Long term response to therapy of chronic anti-HBe-Positive Hepatitis B is poor independent of type and schedule of interferon. *Am J Gastroenterol* 1999; **94**: 1366-1372
- 9 **Brunetto MR**, Oliveri F, Coco B, Leandro G, Colombatto P, Gorin JM, Bonino F. Outcome of anti-HBe positive chronic hepatitis B in alpha-interferon treated and untreated patients: a long term cohort study. *J Hepatol* 2002; **36**: 263-270
- 10 **You J**, Zhuang L, Tang BZ, Yang WB, Ding SY, Li W, Wu RX,

- Zhang HL, Zhang YM, Yan SM, Zhang L. A randomized controlled clinical trial on the treatment of Thymosin a1 versus interferon- α in patients with hepatitis B. *World J Gastroenterol* 2001; **7**: 411-414
- 11 **Zhuang L**, You J, Tang BZ, Ding SY, Yan KH, Peng D, Zhang YM, Zhang L. Preliminary results of Thymosins-a1 versus interferon- α -treatment in patients with HBeAg negative and serum HBV DNA positive chronic hepatitis B. *World J Gastroenterol* 2001; **7**: 407-410
- 12 **Kaneko S**, Feinstone SM, Miller RH. Rapid and sensitive method for the detection of serum hepatitis B virus DNA using the Polymerase Chain Reaction Technique. *J Clin Microbiol* 1989; **27**: 1930-1933
- 13 **Knodell RG**, Ishak KG, Black WC, Chen TS, Craig R, Kaplowitz N, Kiernan TW, Wollman J. Formulation and application of a numerical scoring system for assessing histological activity in asymptomatic chronic active hepatitis. *Hepatology* 1981; **1**: 431-435
- 14 **Lindh M**, Savage K, Rees J, Garwood L, Horal P, Norrans G, Dhillon AP. HBeAg immunostaining of liver tissue in various stages of chronic hepatitis B. *Liver* 1999; **19**: 294-298
- 15 **Lau JYN**, Bain VG, Naoumov NV, Smith HM, Alexander GJM, Williams R. Effect of interferon- γ on hepatitis B viral antigen expression in primary hepatocyte culture. *Hepatology* 1991; **14**: 975-979
- 16 **Shiratori Y**, Imazeki F, Moriyama M, Yano M, Arakawa Y, Yokosuka O, Kuroki T, Nishiguchi S, Sata M, Yamada G, Fujiyama S, Yoshida H, Omata M. Histological improvement of fibrosis in patients with hepatitis C who have sustained response to interferon therapy. *Ann Intern Med* 2000; **132**: 517-524
- 17 **Qin JP**, Jiang MD. Phenotype and regulation of hepatic stellate cell and liver fibrosis. *Shijie Huaren Xiaohua Zazhi* 2001; **9**: 801-804
- 18 **Huang GC**, Zhang JS. Signal transduction in the cells activated by hepatic stellate cells. *Shijie Huaren Xiaohua Zazhi* 2001; **9**: 1056-1060
- 19 **Xie YM**, Nie QH, Zhou YX, Cheng YQ, Kang WZ. Detection of TIMP-1 and TIMP-2 RNA expressions in cirrhotic liver tissue using digoxigenin labeled probe by in situ hybridization. *Shijie Huaren Xiaohua Zazhi* 2001; **9**: 251-254
- 20 **Nie QH**, Cheng YQ, Xie YM, Zhou YX, Bai XG, Cao YZ. Methodologic research on TIMP-1, TIMP-2 detection as a new diagnostic index for hepatic fibrosis and its significance. *World J Gastroenterol* 2002; **8**: 282-287
- 21 **Liu HL**, Li XH, Wang DY, Yang SP. Matrix metalloproteinase-2 and tissue inhibitor of metalloproteinase -1 expression in fibrotic rat liver. *World J Gastroenterol* 2000; **6**: 881-884
- 22 **Wu CH**. Fibrodynamics-elucidation of the mechanisms and sites of liver fibrogenesis. *World J Gastroenterol* 1999; **5**: 388-390
- 23 **Wang LT**, Zhang B, Jie J. Effect of anti-fibrosis compound on collagen expression of hepatic cells in experimental liver fibrosis of rats. *World J Gastroenterol* 2000; **6**: 877-880
- 24 **Li XQ**, Zeng MX, Ling QH. Effects of interferon- γ on DNA synthesis and collagen production of cultured rat hepatocytes. *Shijie Huaren Xiaohua Zazhi* 1998; **6**: 488-490
- 25 **Cheng ML**, Wu YY, Huang KF, Luo TY, Ding YS, Lu YY, Liu RC, Wu J. Clinical study on the treatment of liver fibrosis due to hepatitis B by IFN- α 1 and traditional medicine preparation. *World J Gastroenterol* 1999; **5**: 267-269
- 26 **Cheng ML**, Lu YY, Wu J, Luo TY, Huang KF, Ding YS, Liu RC, Li J, Li Z. Three-year follow-up study on hepatic fibrosis due to chronic hepatitis B is treated by interferon- α -1b and traditional medicine preparation. *World J Gastroenterol* 2000; **6**(suppl 3): 81
- 27 **Zavaglia C**, Airoidi A, Pinzello G. Antiviral therapy of HBV- and HCV-induced liver cirrhosis. *J Clin Gastroenterol* 2000; **30**: 234-241
- 28 **Du XF**, Weng HL, Cai WM. Histological changed in 20 hepatic fibrosis with chronic hepatitis B after human interferon- α treatment. *Chin J Hepatol* 2001; **9**: 273-275
- 29 **Weng HL**, Cai WM, Liu RH. Animal experiment and clinical study of effect of gamma2interferon on hepatic fibrosis. *World J Gastroenterol* 2001; **7**: 42-48
- 30 **Deuffic-Burban S**, Poynard T, Valleron AJ. Quantification of fibrosis progression in patients with chronic hepatitis C using a Markov model. *J Viral Hepatitis* 2002; **9**: 114-122
- 31 **Guido M**, Rugge M, Chemello L, Leandro G, Fattovich G, Giustina G, Cassaro M, Alberti A. Liver stellate cells in chronic viral hepatitis: the effect of interferon therapy. *J Hepatol* 1996; **24**: 301-307
- 32 **Xu WH**, Lü XX, Zhu JR. Apoptosis of hepatic stellate cell of rats with liver fibrosis. *Shijie Huaren Xiaohua Zazhi* 2002; **10**: 972-974
- 33 **Mitsuda A**, Suou T, Ikuta Y, Kawasaki H. Changes in serum tissue inhibitor of matrix metalloproteinase-1 after interferon alpha treatment in chronic hepatitis C. *J Hepatol* 2000; **32**: 666-672
- 34 **Wang Y**, Gao Y, Yu JL, Huang YQ, Jiang XQ. Effect of interferon-alpha on interstitial collagenase gene expression in rat liver fibrosis. *Shijie Huaren Xiaohua Zazhi* 2001; **9**: 20-23
- 35 **Lin SM**, Sheen IS, Chien RN, Chu CM, Liaw YF. Long term beneficial effect of interferon therapy in patients with chronic hepatitis B virus infection. *Hepatology* 1999; **29**: 971-975
- 36 **You J**, Zhuang L, Tang BZ, Yang H, Yang WB, Li W, Zhang HL, Zhang YM, Zhang L, Yan SM. Interferon alpha with thymopeptide in the treatment of chronic hepatitis B. *Shijie Huaren Xiaohua Zazhi* 2001; **9**: 388-391

Edited by Wu XN

Expression of Lewis^b blood group antigen in *Helicobacter pylori* does not interfere with bacterial adhesion property

Peng-Yuan Zheng, Jiesong Hua, Han-Chung Ng, Khay-Guan Yeoh, Ho Bow

Peng-Yuan Zheng, Jiesong Hua, Han-Chung Ng, Ho Bow, Department of Microbiology, Faculty of Medicine, National University of Singapore, 5 Science Drive 2, Singapore 117597, Republic of Singapore

Khay-Guan Yeoh, Department of Medicine, Faculty of Medicine, National University of Singapore, 5 Science Drive 2, Singapore 117597, Republic of Singapore

Supported by a grant from the National University of Singapore, No. 6431

Correspondence to: Peng-Yuan Zheng, MD, PhD, Division of Gastroenterology/Nutrition, The Hospital for Sick Children, University of Toronto, 555 University Ave. Toronto, ON, Canada M5G 1X8. pengyuan.zheng@sickkids.ca

Telephone: +1-416-8137072 **Fax:** +1-416-8136531

Received: 2002-08-03 **Accepted:** 2002-08-19

Abstract

AIM: The finding that some *Helicobacter pylori* strains express Lewis b (Le^b) blood group antigen casts a doubt on the role of Le^b of human gastric epithelium being a receptor for *H. pylori*. The aim of this study was to determine if expression of Le^b in *H. pylori* interferes with bacterial adhesion property.

METHODS: Bacterial adhesion to immobilized Le^b on microtitre plate was performed in 63 *H. pylori* strains obtained from Singapore using *in vitro* adherence assay. Expression of Lewis blood group antigens was determined by ELISA assay.

RESULTS: Among 63 *H. pylori* strains, 28 expressed Le^b antigen. *In vitro* adhesion assay showed that 78.6 % (22/28) of Le^b-positive and 74.3 % (26/35) of Le^b-negative *H. pylori* isolates were positive for adhesion to immobilized Le^b coated on microtitre plate ($P=0.772$). In addition, blocking of *H. pylori* Le^b by prior incubation with anti-Le^b monoclonal antibody did not alter the binding of the bacteria to solid-phase coated Le^b.

CONCLUSION: The present study suggests that expression of Le^b in *H. pylori* does not interfere with the bacterial adhesion property. This result supports the notion that Le^b present on human gastric epithelial cells is capable of being a receptor for *H. pylori*.

Zheng PY, Hua J, Ng HC, Yeoh KG, Bow H. Expression of Lewis^b blood group antigen in *Helicobacter pylori* does not interfere with bacterial adhesion property. *World J Gastroenterol* 2003; 9(1):122-124

<http://www.wjgnet.com/1007-9327/9/122.htm>

INTRODUCTION

Helicobacter pylori is the major etiologic agent of chronic active gastritis, and is generally accepted as a causative factor in the pathogenesis of gastritis, peptic ulcer (PU) disease and gastric adenocarcinoma^[1-3]. It is estimated that over 50 % of the world's population are infected with *H. pylori*.

The bacterium shows a strict tropism for gastric epithelium and is usually isolated from gastric epithelium and duodenal mucosa with gastric metaplasia. The presence of specific receptors for *H. pylori* on the gastric mucosa may explain its gastric tropism. The Lewis^b (Le^b) blood group antigen has been reported to be a receptor of *H. pylori*, and the blood-group antigen-binding adhesin, BabA, has been shown to mediate binding of *H. pylori* to human Le^b on gastric epithelium^[4]. Following the finding that Le^b was expressed in some strains of *H. pylori*^[5], the role of host Le^b as a receptor for *H. pylori* has been questioned considering the *H. pylori* lipopolysaccharide (LPS) Le^b may interfere with the interaction between the bacteria BabA and Le^b on gastric epithelium^[5, 6]. This may be more important for the Asian strains where there is a higher frequency of *H. pylori* strains expressing type 1 blood-group antigens (Le^a, Le^b) (43.5 % for Le^b)^[7, 8] comparing with Western strains (<10 % for Le^b). The high frequency of Le^b expression in *H. pylori* strains in our population offers a unique opportunity to investigate the potential influence of Le^b in *H. pylori* on the bacterial adhesion property.

MATERIALS AND METHODS

Patients and H. pylori isolates

H. pylori strains were isolated from the gastric biopsies of 108 patients undergoing upper gastrointestinal endoscopy for dyspepsia at the National University Hospital, Singapore. Informed consent was obtained from all the patients for gastroscopy and biopsies. A subset of 63 *H. pylori* strains from these 108 strains which were performed in our previous study^[8] was randomly chosen for the *in vitro* adherence assay. Of these, 36 were isolated from male patients and 27 were from female patients. The average age of the patients was 43 years (16-78 years). Based on endoscopic and histologic examination, the patients were classified into the following groups: peptic ulcer ($n=33$), and chronic gastritis ($n=30$). The bacteria were isolated and identified as described previously^[8]. Each strain was cultured on chocolate agar for 3-4 days at 37 °C in a humid incubator (Forma Scientific, Mountain View, USA) supplemented with 5 % CO₂.

In vitro adherence assay

The adherence assay was performed according to Gerhard *et al*^[9] with minor modifications. Briefly, for each of the 63 *H. pylori* strains, the 4-day-old culture was harvested and washed twice in 0.05 M carbonate buffer (pH 9.6) before resuspending in 1 ml of the same buffer. A 10 µl of 10 mg·ml⁻¹ of digoxigenin (Roche Diagnostics, Mannheim, Germany) solution was added to the bacterial suspension and incubated for 60 min at RT. Polysorb 96-well- microtiter plates (Nunc, Rochester, USA) were coated with 50 ng per well of Le^a, Le^b, Le^x and Le^y, (IsoSep, Tullinge, Sweden) in 50 µl of 0.05 M carbonate buffer (pH 9.6) while 50 µl of the same buffer was added as negative control. Following overnight incubation at RT, the solution was decanted without washing, and 100 µl of blocking buffer (0.5 % non-fat milk/0.2 % Tween-20) was added. After the plate was further incubated at RT for 1 hour, the solution was decanted without washing, and then 50 µl of digoxigenin

labeled bacteria diluted to an OD of 0.5 at 600 nm were added to each well of the plates and incubated for another 1 hour at RT with gentle agitation. After washing with PBS, 50 μ l of 150 mU·ml⁻¹ of anti-digoxigenin-HRP antibody (Roche Diagnostics, Mannheim, Germany) was added and incubated for 1 hour at RT. The plates were washed 3 times with PBS before adding 50 μ l of o-phenylenediamine dihydrochloride (Sigma, Louis, USA) (0.4 mg·ml⁻¹ in citric acid buffer with 0.025 % H₂O₂). The reaction was stopped with the addition of 2.5 M sulfuric acid. The OD value was read at 490 nm in an ELISA reader (Bio-Tek, Houston, USA). The strains were considered positive for adhesion to the antigen if the ratio of OD_{Ag}/OD_{control} was >2.0^[9]. The assay was carried out in duplicate for all the strains tested.

Lewis antigen expression

The expression of Lewis blood group antigens (Le^a, Le^b, Le^x and Le^y) was determined by enzyme-linked immunosorbent assay (ELISA) as described previously^[8, 10]. The following murine monoclonal antibodies (mAb) were used: mAb 54-1F6A, specific for Lewis^x (Le^x); mAb 1E52, specific for Le^y; mAb 7Le, specific for Le^a and mAb 225Le, specific for Le^b. Bacterial whole cells from 3-day cultures (7.5×10⁶ ml⁻¹) were suspended in 1 ml phosphate buffered saline (PBS) at pH 7.4. One hundred ml of suspension was added to each well of 96-well microtitre plate (Nunc, Rochester, USA) and incubated overnight at room temperature (RT). Plates were then washed three times with PBS containing 0.05 % Tween-20 (PBST). Subsequently, an aliquot of 100 ml of mAbs (100 ng·ml⁻¹) was added and incubated overnight at RT. After washing three times with PBST, a 100 ml solution of 1:1 000 horseradish peroxidase-labelled goat anti-mouse immunoglobulin (DAKO, Glostrup, Denmark) diluted in PBST with 0.5 % goat serum was added. Color development occurred with the addition of H₂O₂ and o-phenylenediamine dihydrochloride (Sigma, St. Louis, USA) in phosphate citrate buffer (pH 5.4) in the dark for 30 min at RT. A 50 ml of 2.5 M H₂SO₄ solution was added to each well to stop the reaction. The optical density (OD) was read at 490 nm. OD of 0.2 was chosen as the cut-off value because the sum of non-specific background binding value for mAbs never exceeded an OD of 0.1. Synthetic protein-linked Lewis antigens, i.e., Le^a, Le^b, Le^x and Le^y (IsoSep, Tullinge, Sweden) were used as positive controls for the mAbs.

Adherence blocking assay by anti-Le^b mAb

To test if blocking LPS Le^b would alter the binding of the bacteria to Le^b on ELISA plate, two chemically characterized strains with Le^b (H428 and H507)^[7] were subjected to adherence blocking assay by incubation with mAb 225Le, specific for Le^b^[8, 11]. The bacteria were incubated with 225Le mAb (1.0, 10.0, and 100.0 μ g·ml⁻¹) for 1 hour at RT, and then washed twice with PBST (PBS + 0.05 % Tween-20). The adherence assay was performed as described earlier.

Statistical analysis

Frequencies were compared using 2-tailed Fisher's exact test (SPSS 9.0, Chicago, USA). The ratios of OD values were expressed as means \pm standard deviations, and the distributions of the ratios were compared by using Student's *t* test for comparison of means of independent samples. A *P* value <0.05 was considered statistically significant.

RESULTS

In vitro adherence assay

Of the 63 *H. pylori* strains tested, 48 (76.2 %) were positive for adhesion to immobilized Le^b antigen on microtitre plate. The positive *H. pylori* strains showed ratios of OD_{Ag}/OD_{control}

between 2.0-4.1 while the negative strains exhibited values between 0.89-1.67. None of the *H. pylori* strains bound to Le^a, Le^x or Le^y.

Effect of Le^b expression in *H. pylori* on bacterial adhesion property

In the test for expression of Lewis antigen in *H. pylori*, 28 out of the 63 *H. pylori* strains expressed Le^b while 35 did not express Le^b based on ELISA. Among these 28 Le^b-positive strains, 22 (78.6 %) were positive for adhesion to immobilized Le^b antigen coated on plate as compared to 26 (74.3 %) of 35 Le^b-negative strains (*P*=0.772). Furthermore, the ratio of OD_{Ag}/OD_{control} was not significant difference between LPS Le^b-positive strains and Le^b-negative strains (2.3±0.7 vs 2.3±0.7, *P*=0.988).

Adherence blocking assay by anti-Le^b mAb

Two chemically characterized Le^b positive *H. pylori* strains H428 and H507^[7] were subjected to adherence blocking assay by prior incubation with the bacteria with specific mAb 225Le (100.0 μ g·ml⁻¹). The ratio of OD_{Ag}/OD_{control} for strain H428 was changed from 2.7 to 2.6 after incubation with mAb 225Le. The value of adhesion assay for strain H507 was showed minimal change from 1.1 to 1.0. No difference of the ratio of OD_{Ag}/OD_{control} was observed when the bacteria were incubated with different concentrations (1.0, 10.0, and 100.0 μ g·ml⁻¹) of mAb 225Le, which suggested that Le^b expression in *H. pylori* did not interfere with the bacterial adhesion to Le^b.

Effect of mixed Lewis expression on bacterial adhesion property

Of the 63 *H. pylori* strains tested, 55 expressed 2 or more Lewis antigens (Le^a, Le^b, Le^x or Le^y), and the remaining 8 strains expressed 1 Lewis antigen. Among the 55 strains with expression of 2 or more Lewis antigens, 42 (76.4 %) were positive for adhesion to immobilized Le^b compared with 6 (75 %) of 8 strains with 1 Lewis antigen expression (*P*=1.000). Furthermore, the ratio of OD_{Ag}/OD_{control} was not significant difference between the strains with expression of 2 or more Lewis antigen and strains with 1 Lewis antigen (2.3±0.7 vs 2.2±0.8, *P*=0.836).

DISCUSSION

Attachment of *H. pylori* to gastric epithelium is important for its colonization and survival. This adhesion property protects the bacteria from the displacement from the stomach by gastric emptying and peristalsis^[12]. A recent study has demonstrated that the *H. pylori* blood-group antigen-binding adhesin, BabA, facilitates bacterial colonization and augments a nonspecific immune response^[13]. The fucosylated blood group antigens of Le^b and H type 1 have been proposed as receptors of *H. pylori*^[4]. In addition, a study using transgenic mice expressing the human Le^b epitope in gastric epithelial cells indicated that Le^b antigen functioned as a receptor for *H. pylori* adhesin and mediated its attachment to gastric pit and surface mucous cells. However, following the observation^[5] that some *H. pylori* strains also express Le^b, the question on the possible role of host Le^b as a receptor for *H. pylori* has been raised by Wirth *et al*^[5] as well as Clyne and Drumm^[6]. Furthermore, if host Le^b is the principle receptor for *H. pylori*, one might then expect a decreased prevalence of *H. pylori* in the secretor subjects because Le^b present in saliva or gastric mucus in secretor individuals would competitively inhibit the binding of *H. pylori*. However, numerous studies have shown that there is no association between prevalence of *H. pylori* and host secretor status^[14], which indicates that competitive inhibition by Le^b in gastric mucus in secretor individuals may not be able to effectively prevent the colonization of *H. pylori*.

In this study, it was shown that there was no significant difference between Le^b-positive and Le^b-negative *H. pylori* strains with respect to their ability to adhere to immobilized Le^b, mimicking the epithelial cell Le^b antigen. This suggests that expression of Le^b in *H. pylori* strains in our study population does not interfere with the bacterial adhesion to immobilized Le^b *in vitro*. Furthermore, the blocking experiment using anti-Le^b mAb on two Le^b expressing strains (H428 and H507) showed that the expression of Le^b in *H. pylori* had no effect on the adhesion property of *H. pylori*. Additionally, our study population are mainly of Chinese origin which are predominantly Le (b+) phenotype^[8], and *H. pylori* strains isolated from Asian population have a tendency to express type 1 Lewis antigen (Le^a and Le^b)^[7,8]. However, a high prevalence of *H. pylori* infection has been found in this population. These data further support our observation that expression of Le^b in *H. pylori* does not affect the bacterial adhesion.

Our previous study found that increased expression of Lewis antigens in *H. pylori* was associated with peptic ulceration in our population^[8]. We, therefore, attempted to determine whether strains with Lewis antigen expression have advantage for binding to immobilized Le^b, but only observed that the increased expression of a combination of Le antigens in *H. pylori* had no influence on bacterial adhesion.

The chemical structures of Le^a, Le^b, Le^x, Le^y, i antigen, H type 1 and blood group A antigens expressed by *H. pylori* have been elucidated^[7,15,16]. These antigens are also expressed on gastric mucosa^[14]. The possible interaction between Lewis antigens expressed by *H. pylori* and gastric epithelium is intriguing. Le^x-Le^x homotypic interaction has been found to be important in eukaryotic cell interaction, and Le^x structure has recently been proven to be involved in the formation of adhesion pedestal between *H. pylori* and gastric epithelium^[14]. More recently, Le^x structure in *H. pylori* has been demonstrated to promote the bacterial adhesion to gastric epithelium^[17]. However, Le^b-Le^b homotypic interaction has not been proven, and our *in vitro* study does not support such an interaction of *H. pylori* LPS Le^b with epithelial Le^b. The next question is how a *H. pylori* population can manage to exist as single bacterium *in vivo* but not autoaggregative, when bacterium expresses both BabA adhesin and Le^b? *H. pylori* lectins such as BabA may evolve an ability to distinguish between host and bacterial ligands based on differences in their core structure, and thus avoid bacterial autoaggregation^[18,19].

In conclusion, expression of Le^b blood group antigen in *H. pylori* strains in our Asian population does not interfere with the bacterial adhesion to immobilized Le^b on microtitre plate. This result supports the notion that host Le^b present on the gastric epithelium is capable of being a receptor for *H. pylori*.

ACKNOWLEDGEMENTS

The authors are grateful to Dr. Ben J. Appelmelk (Amsterdam Free University, The Netherlands) for generously providing all the monoclonal antibodies. We thank Dr. Mario A. Monteiro (Institute for Biological Sciences, National Research Council, Ottawa, Canada) for analyzing the chemical structures of the *H. pylori* strains. This work was partly present in the European *Helicobacter pylori* 2000 conference in Rome, Italy.

REFERENCES

- Hunt RH, Sumanac K, Huang JQ. Should we kill or should we save *Helicobacter pylori*? *Aliment Pharmacol Ther* 2001; **15** (Suppl 1): 51-59
- Cai L, Yu SZ, Zhang ZF. *Helicobacter pylori* infection and risk of gastric cancer in Changle County, Fujian Province, China. *World J Gastroenterol* 2000; **6**: 374-376
- Uemura N, Okamoto S, Yamamoto S, Matsumura N, Yamaguchi S, Yamakido M, Taniyama K, Sasaki N, Schlemper RJ. *Helicobacter pylori* infection and the development of gastric cancer. *N Engl J Med* 2001; **345**: 784-789
- Iiver D, Arnqvist A, Ogren J, Frick IM, Kersulyte D, Incecik ET, Berg DE, Covacci A, Engstrand L, Boren T. *Helicobacter pylori* adhesin binding fucosylated histo-blood group antigens revealed by retagging. *Science* 1998; **279**: 373-377
- Wirth HP, Yang M, Karita M, Blaser MJ. Expression of the human cell surface glycoconjugates Lewis x and Lewis y by *Helicobacter pylori* isolates is related to *cagA* status. *Infect Immun* 1996; **64**: 4598-4605
- Clyne M, Drumm B. Absence of effect of Lewis A and Lewis B expression on adherence of *Helicobacter pylori* to human gastric cells. *Gastroenterology* 1997; **113**: 72-80
- Monteiro MA, Zheng PY, Ho B, Yokota BSI, Amano KI, Pan ZJ, Berg DE, Chan KH, MacLean LL, Perry MB. Expression of histo-blood group antigens by lipopolysaccharides of *Helicobacter pylori* strains from Asian hosts: the propensity to express type 1 blood-group antigens. *Glycobiology* 2000; **10**: 701-713
- Zheng PY, Hua J, Yoeh KG, Ho B. Association of peptic ulcer with increased expression of Lewis antigens but not *cagA*, *iceA* and *vacA* in *Helicobacter pylori* isolates in an Asian population. *Gut* 2000; **47**: 18-22
- Gerhard M, Lehn N, Neumayer N, Boren T, Rad R, Schepp W, Miehlke S, Classen M, Prinz C. Clinical relevance of the *Helicobacter pylori* gene for blood-group antigen-binding adhesin. *Proc Natl Acad Sci USA* 1999; **96**: 12778-12783
- Zheng PY, Hua J, Ng HC, Ho B. Unchanged characteristics of *Helicobacter pylori* during its morphological conversion. *Microbios* 1999; **98**: 51-64
- Appelmelk BJ, Monteiro MA, Martin SL, Moran AP, Vandenbroucke-Grauls CM. Why *Helicobacter pylori* has Lewis antigens. *Trends Microbiol* 2000; **8**: 565-570
- Falk PG, Syder AJ, Guruge JL, Kirschner D, Blaser MJ, Gordon JI. Theoretical and experimental approaches for studying factors defining the *Helicobacter pylori*-host relationship. *Trends Microbiol* 2000; **8**: 321-329
- Rad R, Gerhard M, Lang R, Schoniger M, Rosch T, Schepp W, Becker I, Wagner H, Prinz C. The *Helicobacter pylori* blood group antigen-binding adhesin facilitates bacterial colonization and augments a nonspecific immune response. *J Immunol* 2002; **168**: 3033-3041
- Taylor DE, Rasko DA, Sherburne R, Ho C, Jewell LD. Lack of correlation between Lewis antigen expression by *Helicobacter pylori* and gastric epithelial cells in infected patients. *Gastroenterology* 1998; **15**: 1113-1122
- Monteiro MA, Chan KH, Rasko DA, Taylor DE, Zheng PY, Appelmelk BJ, Wirth HP, Yang M, Blaser MJ, Hynes SO, Moran AP, Perry MB. Simultaneous expression of type 1 and type 2 Lewis blood group antigens by *Helicobacter pylori* lipopolysaccharides. Molecular mimicry between *H. pylori* lipopolysaccharides and human gastric epithelial cell surface glycoforms. *J Biol Chem* 1998; **273**: 11533-11543
- Monteiro MA, Appelmelk BJ, Rasko DA, Moran AP, Hynes SO, MacLean LL, Chan KH, Michael FS, Logan SM, O'Rourke J, Lee A, Taylor DE, Perry MB. Lipopolysaccharide structures of *Helicobacter pylori* genomic strains 26695 and J99, mouse model *H. pylori* Sydney strain, *H. pylori* P466 carrying sialyl lewis X, and *H. pylori* UA915 expressing lewis B classification of *H. pylori* lipopolysaccharides into glycoform families. *Eur J Biochem* 2000; **267**: 305-320
- Edwards NJ, Monteiro MA, Faller G, Walsh EJ, Moran AP, Roberts IS, High NJ. Lewis X structures in the O antigen side-chain promote adhesion of *Helicobacter pylori* to the gastric epithelium. *Mol Microbiol* 2000; **35**: 1530-1539
- Karlsson KA. The human gastric colonizer *Helicobacter pylori*: a challenge for host-parasite glycobiology. *Glycobiology* 2000; **10**: 761-771
- Falk P. Why does *Helicobacter pylori* actually have Lewis antigens? *Trends Microbiol* 2001; **9**: 61-62

N-acetylcysteine attenuates alcohol-induced oxidative stress in the rat

Resat Ozaras, Veysel Tahan, Seval Aydin, Hafize Uzun, Safiye Kaya, Hakan Senturk

Resat Ozaras, Department of Infectious Diseases and Clinical Microbiology, University of Istanbul, Istanbul, Turkey

Veysel Tahan, Hakan Senturk, Department of Internal Medicine, University of Istanbul, Istanbul, Turkey

Seval Aydin, Hafize Uzun, Safiye Kaya, Department of Biochemistry, University of Istanbul, Istanbul, Turkey

This study was presented in Digestive Disease Week, 20-23rd May, 2001, Atlanta, Georgia as an oral presentation

Supported by the research Fund of the University of Istanbul. No: T-589/240698

Correspondence to: Resat Ozaras, M.D., Altimermer Cad. 27/4, Kucukhamam TR-34303 Fatih, Istanbul, Turkey. rozaras@yahoo.com

Telephone: +90-212-5882840 **Fax:** +90-212-5882840

Received: 2002-07-26 **Accepted:** 2002-11-22

Abstract

AIM: There is increasing evidence that alcohol-induced liver damage may be associated with increased oxidative stress. We aimed to investigate free-radical scavenger effect of n-acetylcysteine in rats intragastrically fed with ethanol.

METHODS: Twenty-four rats divided into three groups were fed with ethanol (6 g/kg/day, Group 1), ethanol and n-acetylcysteine (1 g/kg, Group 2), or isocaloric dextrose (control group, Group 3) for 4 weeks. Then animals were sacrificed under ether anesthesia, intracardiac blood and liver tissues were obtained. Measurements were performed both in serum and in homogenized liver tissues. Malondialdehyde (MDA) level was measured by TBARS method. Glutathione peroxidase (GSH-Px) and superoxide dismutase (SOD) levels were studied by commercial kits. Kruskal-Wallis test was used for statistical analysis.

RESULTS: ALT and AST in Group 1 (154 U/L and 302 U/L, respectively) were higher than those in Group 2 (94 U/L and 155 U/L) and Group 3 (99 U/L and 168 U/L) ($P=0.001$ for both). Serum and tissue levels of MDA in Group 1 (1.84 nmol/mL and 96 nmol/100 mg-protein) were higher than Group 2 (0.91 nmol/mL and 64 nmol/100 mg-protein) and Group 3 (0.94 nmol/mL and 49 nmol/100 mg-protein) ($P<0.001$ for both). On the other hand, serum GSH-Px level in Group 1 (8.21 U/g-Hb) was lower than Group 2 (16 U/g-Hb) and Group 3 (16 U/g-Hb) ($P<0.001$). Serum and liver tissue levels of SOD in Group 1 (11 U/mL and 26 U/100 mg-protein) were lower than Group 2 (18 U/mL and 60 U/100 mg-protein) and Group 3 (20 U/mL and 60 U/100 mg-protein) ($P<0.001$ for both).

CONCLUSION: This study demonstrated that ethanol-induced liver damage is associated with oxidative stress, and co-administration of n-acetylcysteine attenuates this damage effectively in rat model.

Ozaras R, Tahan V, Aydin S, Uzun H, Kaya S, Senturk H. N-acetylcysteine attenuates alcohol-induced oxidative stress in the rat. *World J Gastroenterol* 2003; 9(1): 125-128
<http://www.wjgnet.com/1007-9327/9/125.htm>

INTRODUCTION

Reactive oxygen intermediates contributes to the pathogenesis of various hepatic disorders such as paracetamol intoxication, hemochromatosis, toxic hepatitis, and alcoholic liver injury^[1-4]. Increased oxygen radical production leads to lipid peroxidation by induced cytochrome P4502E1^[5,6]. Enhanced generation of acetaldehyde was shown to cause lipid peroxidation in isolated perfused livers^[7]. Oxidative damage correlates with the amount of ethanol consumed^[8].

Antioxidants such as vitamin E have been suggested as therapeutic options in acute and chronic liver diseases^[9,10]. N-acetylcysteine (NAC) exerts a strong antioxidant activity, and is the treatment of choice in acetaminophen intoxication. NAC provides protection from toxic liver damage by elevating intracellular glutathione concentrations^[11,11]. It has also been used in the treatment of CCl₄ poisoning^[12].

In this study, we tested whether NAC attenuates alcohol-induced free radical damage in the liver in a rat model.

MATERIALS AND METHODS

Male Wistar-Albino rats weighing 220-250 g obtained from University of Istanbul Animal Research Laboratory were kept in the same unit and fed chow (Eris Chow Industry, Istanbul, Turkey) *ad libitum*. All rats had free access to tap water. All animals received humane care in compliance with the National Institutes of Health criteria for care of laboratory animals.

Twenty-four rats divided into three groups and were given ethanol (Group 1) or both ethanol and NAC (Group 2) or isocaloric dextrose (Group 3). NAC and alcohol were administered respectively 4 hours apart. Ethanol and NAC were given intragastrically at doses of 6 g/kg/day and 1 mg/kg/day respectively.

All rats were sacrificed at 1 month under ether anesthesia. After exploration of the thorax, intracardiac blood and liver samples were quickly obtained. Serum alcohol levels were measured on the day the rats were sacrificed.

Glutathione peroxidase levels in erythrocytes, serum alcohol level and biochemistry were studied immediately. For the remaining studies, serum and liver tissue samples were stored at -70 °C.

Tissue Homogenization: Liver samples were weighed and homogenized in 0.15 M NaCl for lipid peroxidation parameters and for the other studies, and homogenates of 20 % were obtained. Tissue homogenates were sonicated two times at 30 sec. intervals. Homogenization and sonication were performed at 4 °C. After sonication, homogenates for lipid peroxidation and biochemical studies were centrifuged at 3 000 rpm for 10 minutes and at 15 000 rpm for 15 minutes respectively. Aliquots of the supernatants were used for both studies^[13]. The assayed parameters were expressed per mg protein and protein content of the aliquots was determined by the method of Lowry *et al*^[14].

Lipid peroxidation

Lipid peroxidation was measured by thiobarbituric acid method, a modified form of the procedure described by Beuge and Aust^[15]. This method measures several aldehydes derived

from lipid hydroperoxides and also known as TBARS (thiobarbituric acid reactive substances) method.

Superoxide dismutase (SOD) level

Serum and homogenized liver tissue SOD levels were measured by using commercial kits. (Randox-Ransod, Cat No:SD 125).

Glutathione level

Glutathione concentration was determined according to the method of Beutler *et al*^[16], using metaphosphoric acid for protein precipitation and 5' 5-dithiobis-2-nitrobenzoic acid for colour development. Erythrocyte and tissue glutathione concentrations were expressed as mg/grHb, mg/gr wet weight respectively.

Glutathione peroxidase level

Serum and homogenized liver tissue glutathione peroxidase levels were also measured by using commercial kits. (Randox-Ransel, Cat No: RS 505).

Biochemical studies were performed by using autoanalyser (Hitachi 717). Hemoglobin level was measured manually by cyanmethemoglobin method.

Alcohol level

Serum alcohol level was measured by fluorescent polarizing immunoassay using commercial kits (Abbot TDx, Cat No: 378190100).

Statistical analysis

All results are expressed as mean \pm standard deviation. Comparisons between the groups were performed by Kruskal-Wallis variance analysis and a *P* value <0.05 was accepted as statistically significant.

RESULTS

Blood alcohol levels of Group 1 and 2 were comparable (207 ± 33 mg/dL vs 182 ± 27 mg/dL).

AST level in Group 1 (302.00 ± 70.68 U/L), was higher than those in Group 2 (155.25 ± 24.07 U/L), and in Group 3 (168.25 ± 32.08 U/L) (*P*=0.001). ALT level also in Group 1 (154.13 ± 33.59 U/L), was higher than those in Group 2 (94.25 ± 16.02 U/L), and in Group 3 (99.00 ± 19.86 U/L) (*P*=0.001) (Figure 1).

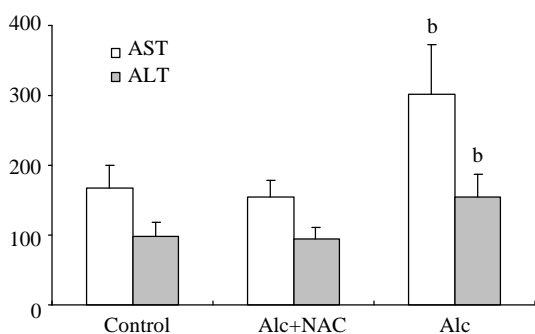


Figure 1 Serum AST and ALT levels (U/L). Alc: alcohol, NAC: N-acetylcysteine, ^b*P*=0.001 vs control and Alc+NAC group.

Although serum GGT level in Group 1 (8.50 ± 3.16 U/L) tend to be higher than those in Group 2 (8.25 ± 3.92 U/L) and Group 3 (6.88 ± 3.76 U/L), the difference was not significant. However tissue GGT level in Group 1 (18.75 ± 5.90 U/g-protein) was significantly higher than those in Group 2 (7.23 ± 6.09 U/g-protein) and Group 3 (6.25 ± 3.33 U/g-protein) (*P* <0.001) (Figure 2).

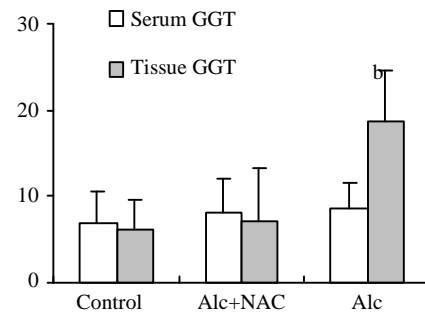


Figure 2 Serum (U/L) and tissue (U/g-protein) GGT levels. Alc: alcohol, NAC: N-acetylcysteine, ^b*P* <0.001 vs control and Alc+NAC group.

Although serum ALP level in Group 1 (131.38 ± 33.84 U/L) tend to be higher than those in Group 2 (109.50 ± 49.75 U/L) and Group 3 (93.13 ± 32.42 U/L), the difference was not significant either. But tissue ALP level in Group 1 (26.88 ± 3.31 U/g-protein) was significantly higher than those in Group 2 (12.63 ± 2.67 U/g-protein) and Group 3 (11.25 ± 2.49 U/g-protein) (*P* <0.001) (Figure 3).

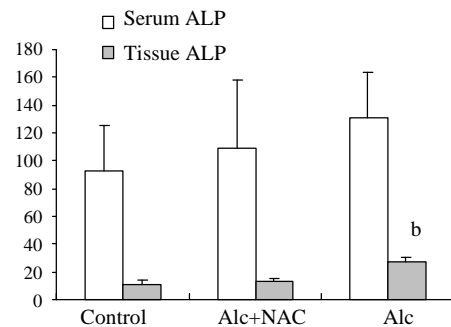


Figure 3 Serum (U/L) and Tissue (U/g-protein) ALP levels. Alc: alcohol, NAC: N-acetylcysteine, ^b*P* <0.001 vs control and Alc+NAC group.

Erythrocyte glutathione level was lower in Group 1 (356.2 ± 18.3 mg/g-Hb) when compared to Group 2 (387.8 ± 13.1 mg/g-Hb) and Group 3 (398.0 ± 18.0 mg/g-Hb) (*P* <0.01) (Figure 4).

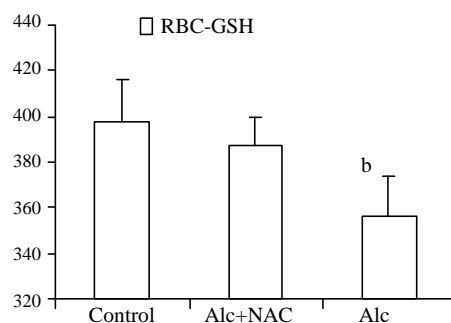


Figure 4 Erythrocyte glutathione levels (U/g-Hb). Alc: alcohol, NAC: N-acetylcysteine, ^b*P* <0.01 vs control and Alc+NAC group.

Blood glutathione peroxidase level was lower in Group 1 (8.21 ± 1.15 U/g-Hb) when compared to Group 2 (16.04 ± 2.38 U/g-Hb) and Group 3 (16.84 ± 2.68 U/g-Hb) (*P* <0.001) (Figure 5). Also serum SOD level was lower in Group 1 (11.08 ± 1.13 U/mL) when compared to Group 2 (17.92 ± 0.81 U/mL) and Group 3 (19.68 ± 1.76 U/mL) (*P* <0.001). The same was true for the tissue SOD levels: it was lower in Group 1 (26.04 ± 8.49 U/100 mg-protein) when compared to Group 2 (59.96 ± 10.23 U/100 mg-protein) and Group 3 (60.34 ± 8.24 U/100 mg-protein.) (*P* <0.001) (Figure 6).

Serum MDA level was significantly higher in Group 1 (1.84 ± 0.14 nmol/mL) than those in Group 2 (0.91 ± 0.14 nmol/mL) and Group 3 (0.94 ± 0.11 nmol/mL) ($P < 0.001$) (Figure 7). For the tissue levels, it was higher also in Group 1 (96.00 ± 18.20 nmol/100 mg-protein) than those in Group 2 (64.00 ± 11.63 nmol/100 mg-protein) and Group 3 (49.63 ± 12.11 nmol/100 mg-protein) ($P < 0.001$) (Figure 8).

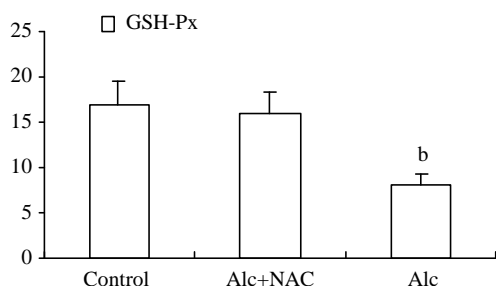


Figure 5 Blood glutathione peroxidase levels (U/g-Hb). Alc: alcohol, NAC: N-acetylcysteine, ^a $P < 0.001$ vs control and Alc+NAC group.

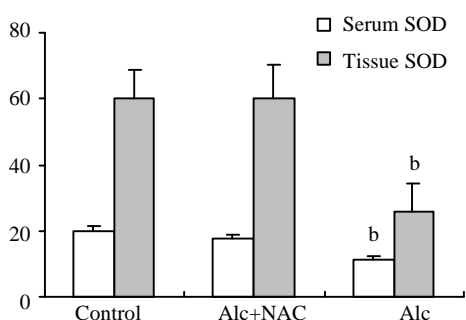


Figure 6 Serum (U/mL) and tissue (U/100 mg-protein) superoxide dismutase (SOD) levels. Alc: alcohol, NAC: N-acetylcysteine, ^b $P < 0.001$ vs control and Alc+NAC group.

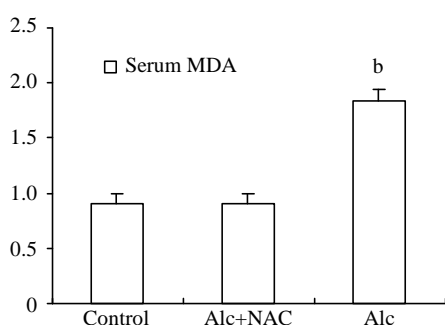


Figure 7 Serum MDA level (nmol/mL). Alc: alcohol, NAC: N-acetylcysteine, ^b $P < 0.001$ vs control and Alc+NAC group.

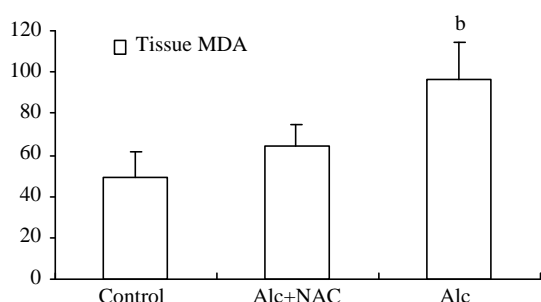


Figure 8 Tissue MDA level (nmol/100 mg-protein). Alc: alcohol, NAC: N-acetylcysteine, ^b $P < 0.001$ vs control and Alc+NAC group.

DISCUSSION

Ethanol is capable of generating oxygen radicals, inhibiting glutathione synthesis, producing glutathione loss from the tissue, increasing malonyldialdehyde levels and impairing antioxidant defense systems in humans and experimental animals. Lipid peroxidation results from the increased oxygen radical production by the induced 2E1^[6]. Enhanced generation of acetaldehyde was also shown to be capable of causing lipid peroxidation in isolated perfused livers^[7]. Lipid peroxidation is not only a reflection of tissue damage, it may also play a pathogenic role, for instance by promoting collagen production^[17]. The removal of the toxic metabolites is believed to be the vital initial step in providing cell survival during ethanol intoxication^[18].

Genc *et al*^[19], used melatonin in preventing lipid peroxidation due to acute alcohol intoxication. They found that melatonin administration prior to alcohol did not alter MDA and GSH levels of the tissue but an antioxidant enzyme (CuZn-SOD) was higher in animals receiving alcohol+melatonin. However since absorption and kinetics of this hormone are not widely known, and its antioxidant effect depend on both the tissue studied and the dose applied, the results of a melatonin study may not reflect the effects of other antioxidants.

Nanji *et al*^[20], used thromboxane inhibitors in alcoholic liver disease in rats. They found that treatment with thromboxane inhibitors prevented necrosis and inflammation, and suggested a role for the use of thromboxane inhibitors in the treatment of alcoholic liver disease. Flora *et al*^[21] tested NAC and a chelator agent meso 2,3-dimercaptosuccinic acid combination in the treatment of arsenic-induced oxidative stress, and found that these agents had a capability of reversing the toxic effects.

Bruck *et al*^[11], have used NAC in the treatment of thioacetamide-induced fulminant hepatic failure in the rat model. They found no protective effect of NAC. In this model, total hepatic glutathione content is not affected. Instead, other free radical scavengers, dimethylsulfoxide and dimethylthiourea having additional modes of action such as inhibition of nitric oxide formation prevented liver injury.

The results of our study show that co-administration of NAC diminishes oxidative stress, by increasing antioxidant enzymes. This restoration of oxidant/antioxidant balance is reflected by lower levels of transaminases, ALP, and GGT. Although the decrease in serum level of the latter two enzymes was not significant, tissue levels were lower. NAC has been used in acetaminophen intoxication. It reduces the incidence of organ failure and enhances survival^[22]. It acts by reducing tissue hypoxia, mediated by the activity of the nitric oxide/soluble guanylate cyclase system^[11]. Cysteine derived from NAC also serves as a precursor of glutathione which forms conjugates with carbon tetrachloride metabolites^[23] and increases intracellular glutathione concentrations^[11]. In a recent study, NAC - in a lower dose than used in the current study- has been shown to prevent the fatty acid changes produced by ethanol and also reduce inflammatory response by reducing the level of prostaglandin^[24].

Antioxidant protective mechanisms are both enzymatic and nonenzymatic. Impairments in these defense systems have been shown in alcoholics: alterations in ascorbic acid levels, glutathione, selenium, and vitamin E have been observed^[25,26]. Reduced hepatic alpha-tocopherol content after long-term ethanol feeding in rats under adequate intake of vitamin E^[27] and also in alcoholics^[28] has been reported. Alpha-tocopherol level was found to be reduced in the blood of the alcoholics^[29]. In addition to acetaldehyde and free radical generation by the ethanol-induced microsomes, these deficient defense systems were suggested to contribute to liver damage via lipid peroxidation^[17]. Lipid peroxidation is a reflection of tissue

damage and plays a pathogenic role by promoting collagen production^[30].

A growing body of experimental and clinical experience shows the importance of free radicals in ethanol-induced liver damage. Free radical scavenging property may be beneficial as ascertained by previous studies of NAC in both acetaminophen and carbon tetrachloride intoxication. In this rat model, we have used NAC to attenuate ethanol-induced free radical damage. In both serum and tissue levels, we observed a favorable result. The results of this study suggest a role for NAC in the management of ethanol-induced liver damage as a safe, cheap, and effective option.

REFERENCES

- 1 **Bruck R**, Aeed H, Shirin H, Matas Z, Zaidel L, Avni Y, Halpern Z. The hydroxyl radical scavengers dimethylsulfoxide and dimethylthiourea protect rat against thioacetamide-induced fulminant hepatic failure. *J Hepatol* 1999; **31**: 27-38
- 2 **Bacon BR**, Tavill AS, Brittenham GM, Park CH, Recknagel RO. Hepatic lipid peroxidation *in vivo* in rats with chronic iron overload. *J Clin Invest* 1983; **71**: 429-439
- 3 **Kyle ME**, Miccadei S, Nakae D, Farber JL. Superoxide dismutase and catalase protect cultured hepatocytes from the cytotoxicity of acetaminophen. *Biochem Biophys Res Commun* 1987; **149**: 889-896
- 4 **Shaw S**, Jayatilleke E, Ross WA, Gordon E, Lieber CS. Ethanol-induced lipid peroxidation: potentiation by long-term alcohol feeding and attenuation by methionine. *J Lab Clin Med* 1981; **98**: 417-424
- 5 **Dai Y**, Rashba-Step J, Cederbaum AI. Stable expression of human cytochrome P4502E1 in HepG2 cells: characterization of catalytic activities and production of reactive oxygen intermediates. *Biochemistry* 1993; **32**: 6928-6937
- 6 **Castillo T**, Koop DR, Kamimura S, Triadafilopoulos G, Tsukamoto H. Role of cytochrome P-450 2E1 in ethanol-, carbon tetrachloride- and iron-dependent microsomal lipid peroxidation. *Hepatology* 1992; **16**: 992-996
- 7 **Muller A**, Sies H. Role of alcohol dehydrogenase activity and the acetaldehyde in ethanol-induced ethane and pentane production by isolated perfused rat liver. *Biochem J* 1982; **206**: 153-156
- 8 **Clot P**, Tabone M, Arico S, Albano E. Monitoring oxidative damage in patients with liver cirrhosis and different daily alcohol intake. *Gut* 1994; **35**: 1637-1643
- 9 **Liu SL**, Esposti SD, Yao T, Diehl AM, Zern MA. Vitamin E therapy of acute CCl₄-induced hepatic injury in mice is associated with inhibition of nuclear factor kappa B binding. *Hepatology* 1995; **22**: 1474-1481
- 10 **Brown KE**, Poulos JE, Li L, Soweid AM, Ramm GA, O' Neill R, Britton RS, Bacon BR. Effect of vitamin E supplementation on hepatic fibrogenesis in chronic dietary iron overload. *Am J Physiol* 1997; **272**: G116-G123
- 11 **Lauterburg BH**, Corcoran GB, Mitchell JR. Mechanism of action of N-acetylcysteine in the protection against the hepatotoxicity of acetaminophen in rats *in vivo*. *J Clin Invest* 1983; **71**: 980-991
- 12 **Howard RJ**, Blake DR, Pall H, Williams A, Green ID. Allopurinol/N-acetylcysteine for carbon monoxide poisoning. *Lancet* 1987; **2**: 628-629
- 13 **Brown KE**, Kinter MT, Oberley TD, Freeman ML, Frierson HF, Ridnour LA, Tao Y, Oberley LW, Spitz DR. Enhanced gamma-glutamyl transpeptidase expression and selective loss of CuZn superoxide dismutase in hepatic overload. *Free Radic Biol Med* 1998; **24**: 545-555
- 14 **Lowry OH**, Rosebrough NJ, Farr AL, Landall RJ. Protein measurement with Folin phenol reagent. *J Biol Chem* 1951; **193**: 265-275
- 15 **Buege JA**, Aust SD. Microsomal lipid peroxidation. *Methods Enzymol* 1978; **52**: 302-310
- 16 **Beutler E**, Duran O, Kelly MB. Improved method for the determination of blood glutathione. *J Lab Clin Med* 1963; **61**: 882-888
- 17 **Lieber CS**. Alcohol and the liver: 1994 update. *Gastroenterology* 1994; **106**: 1085-1105
- 18 **Nordmann R**, Ribiere C, Rouach, H. Implication of free radical mechanisms in ethanol-induced cellular injury. *Free Radic Biol Med* 1992; **12**: 219-240
- 19 **Genc S**, Gurdol F, Oner-Iyidogan Y, Onaran I. The effect of melatonin administration on ethanol-induced lipid peroxidation in rats. *Pharmacol Res* 1998; **37**: 37-40
- 20 **Nanji AA**, Khwaja S, Rahemtulla A, Miao L, Zhao S, Tahan SR. Thromboxane inhibitors attenuate pathological changes in alcoholic liver disease in the rat. *Gastroenterology* 1997; **112**: 200-207
- 21 **Flora SJS**. Arsenic-induced oxidative stress and its reversibility following combined administration of n-acetylcysteine and meso 2,3-dimercaptosuccinic acid in rats. *Clin Exp Pharmacol Physiol* 1999; **26**: 865-869
- 22 **Prescott LF**, Illingworth RN, Critchley JA, Stewart MJ, Adam RD, Proudfoot AT. Intravenous N-acetylcysteine: the treatment of choice for paracetamol poisoning. *Br Med J* 1979; **2**: 1097-1100
- 23 **Mathiseon PW**, Williams G, MacSweeney JE. Survival after massive ingestional carbon tetrachloride treated by intravenous infusion of acetylcysteine. *Hum Toxicol* 1985; **4**: 627-631
- 24 **Raja, krishnan V**, Menon VP. Potential role of antioxidants during ethanol-induced changes in the fatty acid composition and arachidonic acid metabolites in male Wistar rats. *Cell Biol Toxicol* 2001; **17**: 11-22
- 25 **Tanner AR**, Bantock I, Hinks L, Lloyd B, Turner NR, Wright R. Depressed selenium and vitamin E levels in alcoholic population. Possible relationship to hepatic injury through increased lipid peroxidation. *Dig Dis Sci* 1986; **31**: 1307-1312
- 26 **Bonjour JP**. Vitamins and alcoholism. I. Ascorbic acid. *Int J Vit Nutr Res* 1979; **49**: 434-441
- 27 **Bjorneboe GE**, Bjorneboe A, Hagen BF, Morland J, Drevon CA. Reduced hepatic a-tocopherol content after long-term administration of ethanol to rats. *Biochem Biophys Acta* 1987; **918**: 236-241
- 28 **Leo MA**, Rosman A, Lieber CS. Differential depletion of carotenoids and tocopherol in liver diseases. *Hepatology* 1993; **17**: 977-986
- 29 **Bjorneboe GE**, Johnsen J, Bjorneboe A, Marklund SL, Skylv N, Hoiseth A, Bache-Wiig JE, Morland J, Drevon CA. Some aspects of antioxidant status in blood from alcoholics. *Alcohol Clin Exp Res* 1988; **12**: 806-810
- 30 **Geesin JC**, Hendricks LJ, Falkenstein PA, Gordon JS, Berg RA. Regulation of collagen synthesis by ascorbic acid: characterization of the role of ascorbate-stimulated lipid peroxidation. *Arch Biochem Biophys* 1991; **290**: 127-132

Edited by Xu JY and Xu XQ

Mechanisms for regulation of gastrin and somatostatin release from isolated rat stomach during gastric distention

Yong-Yu Li

Yong-Yu Li, Department of Pathophysiology, Medical College of Tongji University, Shanghai 200331, China

Correspondence to: Yong-Yu Li, M.D., Professor of Pathophysiology, Department of Pathophysiology, Medical College of Tongji University, Shanghai 200331, China. liyyu@163.net

Telephone: +86-21-51030563

Received: 2002-09-13 **Accepted:** 2002-10-21

Abstract

AIM: To investigate the intragastric mechanisms for regulation of gastric neuroendocrine functions during gastric distention in isolated vascularly perfused rat stomach.

METHODS: Isolated vascularly perfused rat stomach was prepared, then the gastric lumen was distended with either 5, 10 or 15 ml pH7 isotonic saline during a period of 20 min. During the distention, the axonal blocker tetrodotoxin (TTX), the cholinergic antagonist atropine, or the putative somatostatin-antagonist cyclo [7-aminoheptanoyl-Phe-D-Trp-Lys-Thr(Bzl)] were applied by vascular perfusion. The releases of gastrin and somatostatin were then examined by radioimmunoassay.

RESULTS: The graded gastric distention caused a significant volume-dependent decrease in gastrin secretion [-183±75 (5 ml), -385±86 (10 ml) and -440±85 (15 ml) pg/20 min] and a significant increase of somatostatin secretion [260±102 (5 ml), 608±148 (10 ml) and 943±316 (15 ml) pg/20 min]. In response to 10 ml distention, the infusion of either axonal blocker TTX (10^{-6} M) or cholinergic blocker atropine (10^{-7} M) had a similar affect. They both attenuated the decrease of gastrin release by approximately 50 %, and attenuated the increase of somatostatin release by approximately 40 %. The infusion of somatostatin-antagonist cyclo [7-aminoheptanoyl-Phe-D-Trp-Lys-Thr (Bzl)] (10^{-6} M) attenuated the decrease of gastrin release by about 60 %. Furthermore, combined infusion of the somatostatin-antagonist and atropine completely abolished distention-induced inhibition of gastrin release.

CONCLUSION: The present data suggest that distention of isolated rat stomach stimulates somatostatin release via cholinergic and non-cholinergic TTX-insensitive pathways. Both somatostatin and intrinsic cholinergic pathways are responsible for distention-induced inhibition of gastrin release.

Li YY. Mechanisms for regulation of gastrin and somatostatin release from isolated rat stomach during gastric distention. *World J Gastroenterol* 2003; 9(1): 129-133
<http://www.wjgnet.com/1007-9327/9/129.htm>

INTRODUCTION

Early in 1948, Grossman first proposed that intragastric neurones could regulate gastric neuroendocrine response to gastric distention independent of the extrinsic nervous system^[1], and later Schubert and Makhlof reported that

distention of the distal part of the isolated rat stomach activates the intrinsic VIP neurones and the intrinsic cholinergic mechanism, thereby regulating gastrin and somatostatin release^[2]. However, the intrinsic pathways, independent of extrinsic nerves, which are activated by gastric distention and which modify gastrin release, have remained largely obscure until now.

After finding that distention of isolated rat stomach results in an inhibition of gastrin release and that distention of the extrinsically innervated stomach stimulates gastrin release *in vivo*^[3], we performed this study to examine the intragastric mechanisms involved in regulation of gastrin and somatostatin response to gastric distention. For the study, gastric distention was performed *in vitro* in isolated vascularly perfused rat stomach, an extrinsically denervated preparation that retains the integrity of intramural neurones as well as intragastric paracrine pathways^[4-7]. In this model the effect of graded gastric distention on the release of gastrin and somatostatin was determined. The importance of the intrinsic nervous system and, in particular, its cholinergic part was investigated by performing distention in presence of the axonal blocker tetrodotoxin (TTX) and the cholinergic antagonist atropine. The putative somatostatin-antagonist cyclo [7-aminoheptanoyl-Phe-D-Trp-Lys-Thr(Bzl)] was employed in order to evaluate the role of endogenous somatostatin on regulation of gastrin release during gastric distention.

MATERIALS AND METHODS

Materials

Male Wistar rats ($n=101$), body weight 250-300 g (Charles River Wiga GmbH, Sulzfelden, Germany); dextran T-70 (Pharmacia, Uppsala, Sweden); bovine serum albumine (Serva, Heidelberg, Germany); cyclo [7-aminoheptanoyl-Phe-D-Trp-Lys-Thr(Bzl)] (Bachem, Hannover, Germany); commercial gastrin-kit (Becton and Dickinson, Heidelberg, Germany); tetrodotoxin (TTX), atropine, somatostatin-14 and porcine gastrin-releasing peptide (GRP) (Sigma Chemie, Munich, Germany).

Experimental design

We first prepared the rat stomach. The stomach was isolated from rats fasted overnight using a procedure described by McIntosh *et al*^[8,9]. The isolated stomach was perfused through the celiac artery in a single pass perfusion system at a rate of 1.5 ml/min with a modified Krebs-Ringer buffer solution. The perfusion medium contained 4 % dextranT-70, 0.2 % bovine serum albumin and 5.5 mM glucose and was gassed with 95 % O₂ and 5 % CO₂. The gastric venous effluent was collected via a catheter in the portal vein at two-minute intervals and frozen immediately for subsequent radioimmunoassay. A further catheter was placed in the stomach via the esophagus with the tip at the cardia. A distal catheter was placed in the stomach at the ligated pylorus to drain gastric contents.

After insertion of the gastric catheters, the lumen of the stomach was gently rinsed with isotonic pH7 saline until clear. Thereafter gastric lumen was continuously perfused with saline (1.5 ml/min) during an equilibration period of 25 min and a basal period of 10 min and the perfusate was allowed to flow off via a distal catheter. Subsequently, graded gastric distention

was initiated by instillation of 5, 10 or 15 ml saline through the esophageal catheter at a rate of 2 ml per 10 sec while the distal catheter was blocked. After a distention period of 20 min the distal catheter was reopened and the gastric lumen was again perfused for a period of 20 min with saline. After instillation of the saline load, a fluid filled pressure transducer was connected to the esophageal catheter for recording of the intragastric pressure. During distention, intragastric pressure increased to 5.0 ± 0.4 cm water at 5 ml saline load, to 10.4 ± 0.9 cm water at 10 ml saline load and to 15.0 ± 1.1 cm water at 15 ml saline load. The increase in intragastric pressure induced by the tested distention volumes caused no visible mucosal damage and no impairment of vascular perfusion.

For neural blockade, either the neurotoxin TTX (10^{-6} M) or the cholinergic blocker atropine (10^{-7} M) was added to the vascular perfusate. In further experiments the putative somatostatin-antagonist cyclo [7-aminoheptanoyl-Phe-D-Trp-Lys-Thr(Bzl)] (10^{-6} M) was added to the perfusate alone or in combination with atropine (10^{-7} M). Since the somatostatin-antagonist did not completely abolish distention-induced inhibition of gastrin release, its effectiveness was tested against the inhibitory action of somatostatin-14 (10^{-8} M) on gastrin release prestimulated by mammalia bombisin peptide GRP (10^{-8} M), which is well known in stimulating gastrin secretion^[10-12]. In each stomach only one experiment was performed.

Radioimmunoassay

Gastrin levels in the venous effluent were measured by radioimmunoassay as described elsewhere^[13] employing a commercial gastrin-kit. Somatostatin was determined as described in detail previously^[14], by employing antibody 80C which was generously provided by Dr. R.H. Unger (Dallas, TX, USA).

Data analysis

All data are expressed as mean \pm SE. Integrated peptide secretion was calculated as the sum of the differences between the value of each time point during gastric distention and the mean value of the preceding baseline period. For statistical evaluation of the point-to-point variations, the Friedman two-way analysis of variance was used, followed by the Wilcoxon matched-pairs signed rank test if the former allowed rejection of the null hypothesis. The difference in the values between the treatment groups was statistically evaluated by analysis of variance for multiple determinations. Differences resulting in *P*-values of 0.05 or less were considered significant.

RESULTS

Effect of graded gastric distention on release of gastrin and somatostatin

Graded distention of isolated rat stomach elicited a significant and volume dependent decrease in gastrin release from a mean baseline of 63 ± 4 to a minimum of 50 ± 3 pg/min ($P < 0.05$; $n = 8$), during distention with 5 ml, from 69 ± 6 to 41 ± 3 pg/min ($P < 0.01$; $n = 15$), with 10 ml and from 60 ± 7 to 25 ± 5 pg/min, and with 15 ml saline ($P < 0.01$; $n = 8$) (Figure 1). Gastrin secretion decreased throughout the distention period and returned promptly to baseline values after removal of the intragastric saline load. Integrated gastrin release decreased during distention by -183 ± 75 pg/20 min ($P < 0.05$) at 5 ml, by -385 ± 86 pg/20 min ($P < 0.01$) at 10 ml, and by -440 ± 85 pg/20 min ($P < 0.01$) at 15 ml saline distention (Figure 2).

Somatostatin levels rose volume-dependently during gastric distention from a mean baseline of 41 ± 5 to a maximum level of 61 ± 6 pg/min ($P < 0.05$) at 5 ml, from 40 ± 5 to 92 ± 12 pg/min ($P < 0.01$) at 10 ml and from 39 ± 6 to 116 ± 22 pg/min ($P < 0.01$) at 15 ml saline load (Figure 1). After distention,

somatostatin secretion decreased to its baseline level. The integrated incremental somatostatin release was 260 ± 102 pg/20 min ($P < 0.05$) during distention with 5 ml, 608 ± 148 pg/20 min ($P < 0.01$) during distention with 10 ml and 943 ± 316 pg/20 min ($P < 0.05$) during distention with 15 ml saline (Figure 2).

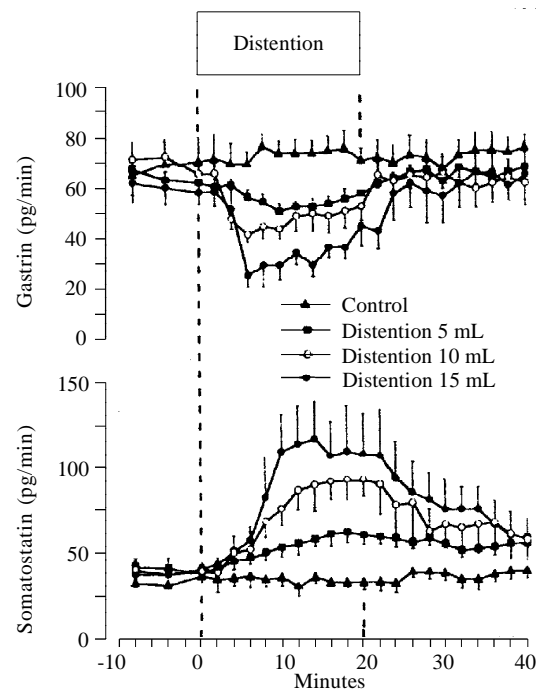


Figure 1 Release of gastrin and somatostatin from perfused rat stomachs in control ($n = 8$) and during gastric distention with 5 ml ($n = 8$), 10 ml ($n = 15$) and 15 ml ($n = 8$) saline (mean \pm SE)

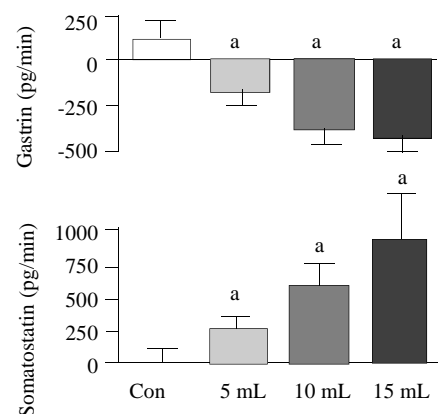


Figure 2 Integrated release of gastrin, somatostatin from perfused rat stomachs in control ($n = 8$) and during gastric distention with 5 ml ($n = 8$), 10 ml ($n = 15$) and 15 ml ($n = 8$) saline. (mean \pm SE) ^a $P < 0.05$ vs 10 ml distention in control

Effect of TTX and atropine on release of gastrin and somatostatin during gastric distention

The axonal blocker TTX (10^{-6} M) and the cholinergic antagonist atropine (10^{-7} M) elicited similar effects on distention-induced inhibition of gastrin. The decrease of gastrin release in response to distention with 10 ml saline was attenuated by approximately 50% [from -385 ± 86 pg/20 min to -189 ± 89 pg/20 min ($P < 0.05$ vs control)] during infusion of TTX ($n = 10$), and to -224 ± 95 pg/20 min ($P < 0.05$ vs control) during infusion of atropine ($n = 10$) (Figure 3). The effects of TTX and atropine on distention-stimulated somatostatin release were also nearly identical, and the incremental somatostatin response to a 10 ml intragastric saline load was reduced about

40% [from 608 ± 148 pg/20 min to 370 ± 100 pg/20 min ($P < 0.05$ vs control) in presence of TTX, and to 404 ± 77 pg/20 min ($P < 0.05$ vs control) during infusion of atropine] (Figure 3).

Effect of the somatostatin-antagonist on release of gastrin during gastric distention

In presence of the somatostatin-antagonist (10^{-6} M), the decrease in gastrin release induced by gastric distention with 10 ml saline was significantly attenuated (-167 ± 73 pg/20 min with somatostatin-antagonist vs -385 ± 86 pg/20 min without somatostatin-antagonist; $P < 0.05$, $n = 15$). Combined administration of the somatostatin-antagonist and atropine ($n = 15$) nearly completely abolished distention-induced inhibition of gastrin release (Figure 3).

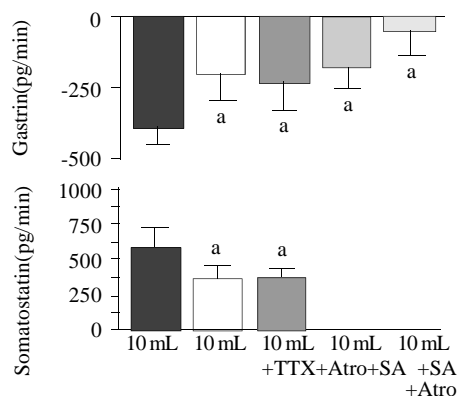


Figure 3 Integrated release of gastrin and somatostatin from perfused rat stomachs during gastric distention with 10 ml in control ($n = 15$) and in presence of tetrodotoxin (TTX, 10^{-6} M; $n = 10$), atropine (Atro, 10^{-7} M; $n = 10$), somatostatin-antagonist (SA, 10^{-6} M; $n = 15$) and a combination of somatostatin-antagonist and atropine ($n = 15$), (mean \pm SE). ^a $P < 0.05$ vs 10 ml distention in control.

Effect of the somatostatin-antagonist on the inhibitory action of exogenous somatostatin-14 on GRP-prestimulated gastrin release

Infusion of GRP (10^{-8} M) produced a significant increase in gastrin release, from a baseline value of 58 ± 6 to a maximum of 136 ± 11 pg/min. GRP-prestimulated gastrin release was reduced significantly from 136 ± 11 pg/min to 84 ± 4 pg/min by exogenous somatostatin-14 (10^{-8} M; $n = 11$) ($P < 0.05$). When somatostatin-14 was removed from the perfusate, gastrin release promptly returned to prestimulated levels. At a dose of 10^{-6} M the somatostatin-antagonist did not change the baseline gastrin release, but completely blocked the inhibitory action of exogenous somatostatin-14 on GRP-prestimulated gastrin release ($n = 9$). (Figure 4).

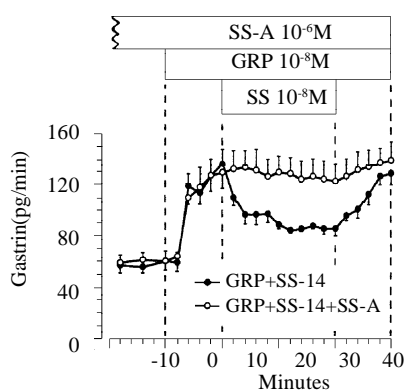


Figure 4 Effect of somatostatin-14 (10^{-6} M) on gastrin release from perfused rat stomachs prestimulated by GRP (10^{-8} M) in control ($n = 11$) and during perfusion with somatostatin-antagonist (10^{-6} M; $n = 9$). (mean \pm SE.)

DISCUSSION

It is well established that gastric distention *in vivo* activates vagal mechanoreceptors within the gastric wall. The afferent vagal nerve fibers activate brainstem neurones which regulate vagal efferent fibers and thereby exocrine and endocrine functions of the stomach^[15-19]. Apart from this extrinsic nervous system, the stomach itself contains regulatory systems within the gastric wall such as intrinsic neurons and intrinsic paracrine pathways^[20-22]. The importance of these intragastric mechanisms on regulation of gastrin in response to gastric distention is largely unknown. Isolated perfused stomach allows examination of the remaining intragastric regulatory mechanisms since this model is separated from the extrinsic innervation and the systemic humoral signals, whereas the integrity of intrinsic neurocrine and paracrine pathways is maintained.

As previously reported, distention of the isolated stomach causes a decrease of gastrin release in proportion to the applied intragastric volume and intragastric pressure^[3]. To examine the functional role of the intragastric nervous system we employed the neurotoxin tetrodotoxin (TTX) which blocks all neural elements that are activated by an influx of Na^+ . This comprises all the adrenergic and cholinergic neurons and, presumably, the majority of peptidergic neurons as well. The effect was observed while using a very low concentration of TTX (10^{-6} - 10^{-8} M) which had no noticeable effect on other membrane parameters^[23]. The present data suggest that the inhibition of gastrin release during gastric distention is mediated in part by neural, particularly cholinergic, mechanisms.

However, the classical cholinergic neurotransmitter acetylcholine and its stable analogue carbachol stimulate gastrin release *in vivo* in the isolated stomach preparation and in cultured antral G-cells^[24-27]. Therefore the inhibitory effect of the cholinergic system on gastrin release in our experiment seems to be indirect, perhaps via peptidergic neurotransmitters. Furthermore, the present data suggest that gastric distention activates endogenous somatostatin through cholinergic and non-cholinergic TTX insensitive pathways, and endogenously released somatostatin can cause distention-induced inhibition of gastrin release. Several studies have shown a reciprocal relationship between stimulation of somatostatin and inhibition of gastrin, suggesting a functional linkage between somatostatin and gastrin release^[28-32]. Accordingly, the importance of endogenous somatostatin for regulation of gastrin release is supported by studies with antisomatostatin serum, demonstrating an augmented gastrin release after neutralization of endogenously released somatostatin in isolated rat stomach^[33]. These findings imply that endogenous somatostatin exerts its inhibitory effect on gastrin release via intragastric mechanisms. The secretion and expression of gastrin are under the paracrine control of somatostatin, produced by D cells situated in close contact with gastrin-producing G cells, and gastric D-cells extend the long cytoplasmatic processes that terminate close to gastrin-secreting G-cells in antral mucosa of both humans and rats^[34,35]. This morphological evidence for a paracrine mode of action is consistent with the functional study results.

The putative somatostatin-antagonist cyclo [7-aminoheptanoyl-Phe-D-Trp-Lys-Thr (Bzl)] has been described as an antagonist of somatostatin in some peripheral tissues such as endocrine rat pancreas, the papillary muscle of the guinea pig heart and the ferret trachea, as well as in neural tissues such as avian choroid, rat cortex, rat hippocampus and rat pituitary^[36]. In the present study the somatostatin antagonist completely blocked the inhibitory effect of a high infusion rate of somatostatin-14 on gastrin release. During infusion of somatostatin-14 (10^{-8} M), somatostatin measured in the portal venous effluent of the isolated rat stomach rose to levels

between 1 000 and 1 600 pg/min, whereas somatostatin secretion during gastric distention was only between 60 and 120 pg/min. Since the inhibitory effect of exogenous somatostatin was sufficiently antagonized by the dose of the somatostatin-antagonist employed, it seems most likely that a sufficient amount of antagonist was administered to block all the effects of endogenously released somatostatin during gastric distention. Therefore the residual inhibition of gastrin during gastric distention in presence of the somatostatin-antagonist seems to be independent of endogenous somatostatin and may be mediated by inhibitory cholinergic pathways.

Schubert and Makhlof have previously shown that low distention of the antral part of the isolated rat stomach stimulated somatostatin and inhibited gastrin release probably via VIP-dependent mechanisms, whereas high distention caused an increase in gastrin and a decrease in somatostatin secretion via cholinergic pathways^[2]. Distention of the whole stomach seems to activate other regulatory mechanisms than selective distention of the distal part of the stomach, since Debas *et al.* have shown that distention of the oxyntic gland area of the stomach can modulate antral gastrin release^[37]. Furthermore the mechanoreceptors in the antrum have been reported to respond mainly to gastric contractions, while those located in the corpus and fundus respond primarily to distention^[38].

In conclusion, the present data suggest that distention of the isolated rat stomach inhibits gastrin release via intrinsic neurocrine and paracrine pathways. Both somatostatin and intrinsic cholinergic pathways are responsible for distention-induced inhibition of gastrin release. Somatostatin release is activated by gastric distention through cholinergic and non-cholinergic TTX-insensitive pathways.

ACKNOWLEDGEMENT

The author sincerely thanks Dr. N. Weigert and Professor V. Schusdzarra in the Department of Internal Medicine II, Technical University of Munich, Germany, for their expert guidance in this experimental research.

REFERENCES

- Grossman MI**, Robertson CR, Ivy AC. The proof of a hormonal mechanism for gastric secretion: the humoral transmission of the distention stimulus. *Am J Physiology* 1948; **153**: 1-9
- Schubert ML**, Makhlof GM. Gastrin secretion induced by distention is mediated by gastric cholinergic and vasoactive intestinal peptide neurons in rats. *Gastroenterology* 1993; **104**: 834-839
- Weigert N**, Li YY, Schick RR, Coy DH, Classen M, Schusdzarra V. Role of vagal fibers and bombesin/gastrin-releasing peptide-neurons in distention-induced gastrin release in rats. *Regul pept* 1997; **69**: 33-40
- Lippl F**, Schusdzarra V, Huepfgens K, Allescher HD. Inhibitory effect of nociceptin on somatostatin secretion of the isolated perfused rat stomach. *Regul Pept* 2002; **107**: 37-42
- Weigert N**, Schepp W, Haller A, Schusdzarra V. Regulation of gastrin, somatostatin and bombesin release from the isolated rat stomach by exogenous and endogenous gamma-aminobutyric acid. *Digestion* 1998; **59**: 16-25
- Weigert N**, Schaffler A, Reichenberger J, Madaus S, Classen M, Schusdzarra V. Effect of endogenous opioids on vagally induced release of gastrin, somatostatin and bombesin-like immunoreactivity from the perfused rat stomach. *Regul Pept* 1995; **55**: 207-215
- Saffouri B**, DuVal JW, Makhlof GM. Stimulation of gastrin secretion in vitro by intraluminal chemicals: regulation by intramural cholinergic and noncholinergic neurons. *Gastroenterology* 1984; **87**: 557-561
- McIntosh CH**, Pederson RA, Koop H, Brown JC. Gastric inhibitory polypeptide stimulated secretion of somatostatin-like immunoreactivity from the stomach: inhibition by acetylcholine or vagal stimulation. *Can J Physiol Pharmacol* 1981; **59**: 468-472
- Li YY**. Effect of neuromedin C on gastrin secretion from isolated and perfused rat stomach. *Shengli Xuebao* 1996; **48**: 77-82
- Tokita K**, Hocart SJ, Coy DH, Jensen RT. Molecular basis of the selectivity of gastrin-releasing peptide receptor for gastrin-releasing peptide. *Mol Pharmacol* 2002; **61**: 1435-1443
- Schubert ML**, Jong MJ, Makhlof GM. Bombesin/GRP-stimulated somatostatin secretion is mediated by gastrin in the antrum and intrinsic neurons in the fundus. *Am J Physiol* 1991; **261**: G885-889
- Schepp W**, Prinz C, Hakanson R, Schusdzarra V, Classen M. Bombesin-like peptides stimulate gastrin release from isolated rat G-cells. *Regul Pept* 1990; **28**: 241-253
- Barber WD**, Burks TF. Brain stem response to phasic gastric distension. *Am J Physiol* 1983; **245**: G242-248
- Blackshaw LA**, Grundy D, Scratcherd T. Involvement of gastrointestinal mechano- and intestinal chemoreceptors in vagal reflexes: an electrophysiological study. *J Auton Nerv Syst* 1987; **18**: 225-234
- Ladabaum U**, Minoshima S, Hasler WL, Cross D, Chey WD, Owyang C. Gastric distention correlates with activation of multiple cortical and subcortical regions. *Gastroenterology* 2001; **120**: 369-376
- Tuo BG**, Yan YH, Ge ZL, Ou GW, Zhao K. Ascorbic acid secretion in the human stomach and the effect of gastrin. *World J Gastroenterol* 2000; **6**: 704-708
- Voutilainen M**, Juhola M, Pitkanen R, Farkkila M, Sipponen P. Immunohistochemical study of neuroendocrine cells at the gastric cardia mucosa. *J Clin Pathol* 2002; **55**: 767-769
- Mailliard ME**, Wolfe MM. Effect of antibodies to the neuropeptide GRP on distention-induced gastric acidsecretion in the rat. *Regul Pept* 1989; **26**: 287-296
- Kovacs TO**, Walsh JH, Maxwell V, Wong HC, Azuma T, Katt E. Gastrin is a major mediator of the gastric phase of acid secretion in dogs: proof by monoclonal antibody neutralization. *Gastroenterology* 1989; **97**: 1406-1413
- Lindstrom LM**, Ekblad E. Origins and projections of nerve fibres in rat pyloric sphincter. *Auton Neurosci* 2002; **97**: 73-82
- Kawashima K**, Ishihara S, Karim Rumi MA, Moriyama N, Kazumori H, Suetsugu H, Sato H, Fukuda R, Adachi K, Shibata M, Onodera S, Chiba T, Kinoshita Y. Localization of calcitonin gene-related peptide receptors in rat gastric mucosa. *Peptides* 2002; **23**: 955-966
- Blackshaw LA**, Grundy D, Scratcherd T. Vagal afferent discharge from gastric mechanoreceptors during contraction and relaxation of the ferret corpus. *J Auton Nerv Syst* 1987; **18**: 19-24
- Ulbricht W**. Kinetics of drug action and equilibrium results at the node of Ranvier. *Physiol Rev* 1981; **61**: 785-828
- Weigert N**, Schaffer K, Wegner U, Schusdzarra V, Classen M, Schepp W. Functional characterization of a muscarinic receptor stimulating gastrin release from rabbit antral G-cells in primary culture. *Eur J Pharmacol* 1994; **264**: 337-344
- Leib MS**, Wingfield WE, Twedt DC, Williams AR, Bottoms GD. Gastric distention and gastrin in the dog. *Am J Vet Res* 1985; **46**: 2011-2015
- Konturek SJ**. Cholinergic control of gastric acid secretion in man. *Scand J Gastroenterol Suppl* 1982; **72**: 1-5
- Schiller LR**, Walsh JH, Feldman M. Distention-induced gastrin release: effects of luminal acidification and intravenous atropine. *Gastroenterology* 1980; **78**: 912-917
- Chiba T**, Taminato T, Kadowaki S, Abe H, Chihara K, Seino Y, Matsukura S, Fujita T. Effects of glucagon, secretin and vasoactive intestinal polypeptide on gastric somatostatin and gastrin release from isolated perfused rat stomach. *Gastroenterology* 1980; **79**: 67-71
- Buscail L**, Vernejoul F, Faure P, Torrisani J, Susini C. Regulation of cell proliferation by somatostatin *Ann Endocrinol* 2002; **63**: 2S13-18
- Soehartono RH**, Kitamura N, Yamagishi N, Taguchi K, Yamada J, Yamada H. An immunohistochemical study of endocrine cells in the abomasum of vagotomized calf. *J Vet Med Sci* 2002; **64**: 11-15

- 31 **Zavros Y**, Rieder G, Ferguson A, Samuelson LC, Merchant JL. Hypergastrinemia in response to gastric inflammation suppresses somatostatin. *Am J Physiol Gastrointest Liver Physiol* 2002; **282**: G175-183
- 32 **Li YY**, Gao JT. Somatostatin: the important factor for regulating digestive functions. *Shengli Kexue Jinzhan* 1995; **26**: 65-68
- 33 **Short GM**, Doyle JW, Wolfe MM. Effect of antibodies to somatostatin on acid secretion and gastrin release by the isolated perfused rat stomach. *Gastroenterology* 1985; **88**: 984-988
- 34 **Larsson LI**, Goltermann N, DeMagistris L, Rehfeld JF, Schwartz TW. Somatostatin cell processes as pathways for paracrine secretion. *Science* 1979; **205**: 1393-1395
- 35 **Larsson LI**. Developmental biology of gastrin and somatostatin cells in the antropyloric mucosa of the stomach. *Microsc Res Tech* 2000; **48**: 272-281
- 36 **Shibata S**, Koga Y, Hamada T, Watanabe S. Facilitation of 2-deoxyglucose uptake in rat cortex and hippocampus slices by somatostatin is independent of cholinergic activity. *Eur J Pharmacol* 1993; **231**: 381-388
- 37 **Debas HT**, Walsh JH, Grossman MI. Evidence for oxyntopyloric reflex for release of antral gastrin. *Gastroenterology* 1975; **68**: 687-690
- 38 **Andrews PL**, Grundy D, Scratcherd T. Vagal afferent discharge from mechanoreceptors in different regions of the ferret stomach. *J Physiol* 1980; **298**: 513-524

Edited by Zhang JZ

Effects of tetrandrine on calcium and potassium currents in isolated rat hepatocytes

Hong-Yi Zhou, Fang Wang, Lan Cheng, Li-Ying Fu, Ji Zhou, Wei-Xing Yao

Hong-Yi Zhou, Fang Wang, Lan Cheng, Li-Ying Fu, Ji Zhou, Wei-Xing Yao, Department of Pharmacology, Tongji medical college of Huazhong university of science and technology, Wuhan 430030, Hubei Province, China

Correspondence to: Hong-Yi Zhou, Department of Pharmacology, Tongji medical college of Huazhong university of science and technology, 13 hangkong Road, Wuhan 430030, China. zhouhy518@yahoo.com.cn
Telephone: 027-83644206

Received: 2002-06-27 **Accepted:** 2002-07-25

Abstract

AIM: To study the effects of tetrandrine (Tet) on calcium release-activated calcium current (I_{CRAC}), delayed rectifier potassium current (I_K), and inward rectifier potassium currents (I_{K1}) in isolated rat hepatocytes.

METHODS: Hepatocytes of rat were isolated by using perfusion method. Whole cell patch-clamp techniques were used in our experiment.

RESULTS: The peak amplitude of I_{CRAC} was -508 ± 115 pA ($n=15$), its reversal potential of I_{CRAC} was about 0 mV. At the potential of -100 mV, Tet inhibited the peak amplitude of I_{CRAC} from -521 ± 95 pA to -338 ± 85 pA ($P < 0.01$ vs control, $n=5$), with the inhibitory rate of 35 % at 10 μ mol/L and from -504 ± 87 pA to -247 ± 82 pA ($P < 0.01$ vs control, $n=5$), with the inhibitory rate of 49 % at 100 μ mol/L, without affecting its reversal potential. The amplitude of I_{CRAC} was dependent on extracellular Ca^{2+} concentration. The peak amplitude of I_{CRAC} was -205 ± 105 pA ($n=3$) in tyrode's solution with Ca^{2+} 1.8 mmol/L ($P < 0.01$ vs the peak amplitude of I_{CRAC} in external solution with Ca^{2+} 10 mmol/L). Tet at the concentration of 10 and 100 μ mol/L did not markedly change the peak amplitude of delayed rectifier potassium current and inward rectifier potassium current ($P > 0.05$ vs control).

CONCLUSION: Tet protects hepatocytes by inhibiting I_{CRAC} , which is not related to I_K and I_{K1} .

Zhou HY, Wang F, Cheng L, Fu LY, Zhou J, Yao WX. Effects of tetrandrine on calcium and potassium currents in isolated rat hepatocytes. *World J Gastroenterol* 2003; 9(1): 134-136
<http://www.wjgnet.com/1007-9327/9/134.htm>

INTRODUCTION

Tetrandrine (Tet) is a bisbenzylisoquinoline alkaloid from a Chinese medicinal herb (*Stephania tetrandra* S. Moore). In the past decade, lots of studies demonstrated that Tet possessed multiple bioactivities, such as potential immunomodulating, anticarcinoma^[1] and protective effect on CCl₄-injured hepatocytes^[2]. It has also been used in the treatment of ischemic heart diseases^[3] and hypertension^[3,4]. Recently, the antifibrotic effects of Tet have been received considerable attention^[1,5-10]. The former researches of Tet on the liver have probed into cellular and molecular levels^[9,10]. In the present paper, we used

whole-cell patch-clamp technique to observe the effects of Tet on I_{CRAC} , I_K , I_{K1} in normal isolated rat hepatocytes, in order to have a better understanding its hepatoprotective and antifibrotic effects.

MATERIALS AND METHODS

Solutions and drugs

Tet was from Jinhua Pharmaceutical Co. The stock solution (10 mmol/L) was dissolved in distilled water after acidification with 0.1 mol/L HCl and neutralized with 0.1 mol/L NaOH. Ca^{2+} -free Hank's solution was prepared without Ca^{2+} and Mg^{2+} . KB solution contained (mmol/L): glutamic acid 70, taurine 15, KCl 130, KH_2PO_4 10, HEPES 10, glucose 11, egtazic acid 0.5, pH was adjusted to 7.4 with KOH. The external solution used to record I_{crac} contained (mmol/L): NaCl 140, KCl 2.8, $CaCl_2$ 10, $MgCl_2$ 0.5, glucose 11, HEPES 10, pH was adjusted to 7.4 with NaOH. The internal solution used to record I_{CRAC} contained (mmol/L): potassium-glutamate 145, NaCl 8, $MgCl_2$ 1, Mg-ATP 0.5, egtazic acid 10, HEPES 10, pH was adjusted to 7.2 with KOH. The external solution used to record I_K contained (mmol/L): NaCl 144, KCl 4, $CaCl_2$ 1.8, $MgCl_2$ 0.53, NaH_2PO_4 0.33, glucose 5.5, HEPES 5, pH was adjusted to 7.4 with NaOH. The internal solution used to record I_K contained (mmol/L): KCl 130, K_2ATP 5, creatine phosphate 5, HEPES 5, pH was adjusted to 7.2 with KOH. The same external and internal solutions used to record I_{K1} contained (mmol/L): KCl 7, $MgCl_2$ 2, egtazic acid 1, potassium-glutamate 130, HEPES 10, pH was adjusted to 7.4 with KOH.

Isolation of single hepatocytes

Hepatocytes were isolated with the modified method reported by Seglen^[11]. Briefly, adult wistar rats of either sex (175 ± 25 g) were anesthetized by intraperitoneal injection of pentobarbital sodium (50 mg/kg). The portal vein was cannulated and perfused with oxygenated Ca^{2+} -free Hank's solution 30 ml/min at 37 °C for 4-5 min followed by perfusion with Ca^{2+} -free Hank's solution containing collagenase (Type 1, Sigma) (0.3g/L) for 10 min. The liver was chopped in 10 ml Ca^{2+} -free Hank's solution. The cell suspension was filtered through 200 mesh gauze and then centrifuged three times (50 g, 2 min) to separate liver cells. Cells were plated onto the coverslips and incubated in KB medium for 2 hour and preserved in DMEM at 4 °C.

Electrophysiologic recording

Whole-cell recordings were performed using a PC-II patch clamp amplifier (Huazhong university of science and technology). The recording chamber (1.5 ml) was perfused with the corresponding external solution. The pipettes were pulled in two stages from hard glass capillaries using a vertical microelectrode puller (Narishige, Japan). Electrode has a resistance of 2-5M Ω for whole-cell recording when filled with electrode internal solution. All experiments were conducted at 22 ± 2 °C.

Statistic analysis

The data were expressed as $\bar{x} \pm s$. Statistical significances were analyzed by a unpaired *t*-test. A value of $P < 0.05$ was considered significant.

RESULTS

Effect of Tet on calcium release-activated calcium current (I_{CRAC})

I_{CRAC} was elicited for 200 ms from the holding potential of 0 mV to various potentials ranging from -10 mV to +80 mV with the step of 20 mV every 5 s^[12]. The peak amplitude of I_{CRAC} was -508 ± 115 pA ($n=15$) and the reversal potential of I_{CRAC} was about 0 mV, the current was steady and without run-down in 5 mins. Tet inhibited the peak amplitude of I_{CRAC} from -521 ± 95 pA to -338 ± 85 pA ($P < 0.01$ vs control, $n=5$), with the inhibitory rate of 35 % at 10 $\mu\text{mol/L}$ and from -504 ± 87 pA to -247 ± 82 pA ($P < 0.01$ vs control, $n=5$), with the inhibitory rate of 49 % at 100 $\mu\text{mol/L}$. Tet did not affect the shape of its current voltage curve (Figure 1, 2).

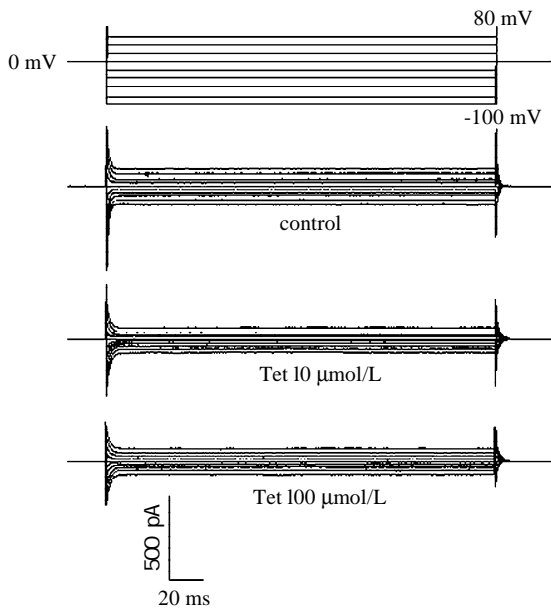


Figure 1 Effect of Tet on I_{CRAC} in isolated rat hepatocytes. I_{CRAC} traces before and after Tet 10 $\mu\text{mol/L}$ and 100 $\mu\text{mol/L}$. I_{CRAC} was elicited for 200 ms from the holding potential of 0 mV to various potentials ranging from -100 mV to +80 mV with step of 20 mV.

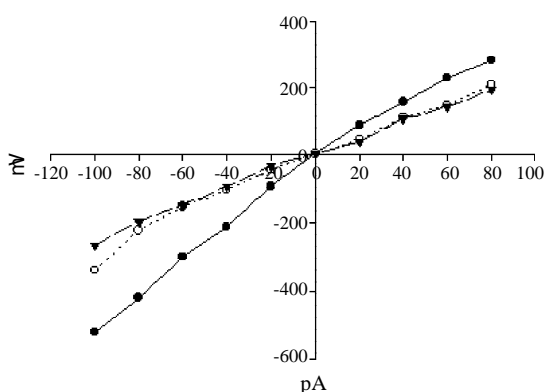


Figure 2 Effect of Tet on I-V relationship of I_{CRAC} in isolated rat hepatocytes. Especially at the potential of -100 mV, Tet inhibited the peak amplitude of I_{CRAC} with the inhibitory rate of 35 % at 10 $\mu\text{mol/L}$ and with the inhibitory rate of 49 % at 100 $\mu\text{mol/L}$. ● control; ○ 10 $\mu\text{mol/L}$; □ 100 $\mu\text{mol/L}$.

The amplitude of I_{CRAC} was dependent on extracellular Ca^{2+} concentration. The peak amplitude of I_{CRAC} was -205 ± 105 pA ($n=3$) in tyrode's solution with Ca^{2+} 1.8 mmol/L ($P < 0.01$ vs the peak amplitude of I_{CRAC} in external solution with Ca^{2+} 10 mmol/L). Tet at 10 $\mu\text{mol/L}$ decreased I_{CRAC} from -205 ± 105 pA to -148 ± 96 pA ($n=3$).

Effect of Tet on delayed rectifier potassium current (I_K)

I_K was elicited by 900 ms depolarization steps from +30 mV to +140 mV with step of 10 mV at holding potential of -50 mV^[13]. Tet at 10 and 100 $\mu\text{mol/L}$ did not change the peak amplitude of I_K [from 2014 ± 686 pA to 2030 ± 692 pA and 2047 ± 710 pA respectively, $n=5$, cells from 3 rats, $P > 0.05$]. Tet did not affect the shape of its current voltage curve.

Effect of Tet on inward rectifier potassium current (I_{K1})

I_{K1} was elicited by a number of step pulses (40 ms) from the holding potential (E_h) of 0 mV to test potentials from -200 mV to +175 mV with the step of 10 mV^[14]. Tet at 10 and 100 $\mu\text{mol/L}$ did not change the peak amplitude of I_{K1} [from 2254 ± 718 pA to 2239 ± 700 pA and 2224 ± 658 pA respectively, $n=5$, cells from 3 rats, $P > 0.05$]. Tet did not affect the shape of its current voltage curve.

DISCUSSION

Hepatic fibrosis is a common consequence of chronic liver injury from many causes^[15-19], and the sustained hepatic injury is a primary factor for hepatic fibrogenesis^[20-28]. Preventing hepatocyte from injury is a matter of primary importance in blocking the fibrogenic pathway. Tet has been considered as an effective antifibrotic and hepatoprotective agent^[1,2,5-10], but its protection against toxic cell death has never been well illustrated.

The Ca^{2+} influx is mainly mediated by voltage-operated Ca^{2+} channels and receptor-activated Ca^{2+} channels. Voltage-operated Ca^{2+} channels are not present in hepatocytes^[29]. Calcium influx in isolated hepatocytes mainly depend on receptor-mediated Ca^{2+} entry which has been identified by indirect methods^[30]. Previous studies have shown that one type of receptor-activated Ca^{2+} channels, most likely a store-operated Ca^{2+} channel, in freshly isolated rat hepatocytes is inhibited by high concentrations of L-type voltage-operated Ca^{2+} channels antagonists^[30,31]. Besides, the mRNA encoding isoforms of L-type voltage-operated Ca^{2+} channels has been detected in rat hepatocytes, these observation suggested that receptor-activated Ca^{2+} channels in rat hepatocytes exhibit some characteristics of voltage-operated Ca^{2+} channels^[32]. Cui *et al* reported that I_{CRAC} (an important sub-type of store-operated Ca^{2+} channels) existed in isolated rat hepatocytes and 50 $\mu\text{mol/L}$ of verapamil, diltiazem and nifedipine could decrease the amplitude of I_{CRAC} effectively^[12]. The results in our experiment showed that Tet at the concentration of 10 and 100 $\mu\text{mol/L}$ could decrease the peak amplitude of I_{CRAC} . The concentration that Tet made a half-maximal inhibition of I_{CRAC} was approximately 100 $\mu\text{mol/L}$, which was substantially higher than that needed for the half-maximal inhibition of L-type voltage-operated Ca^{2+} channels by Tet. It suggested that Tet could protect hepatocytes by inhibiting I_{CRAC} and decreasing intracellular Ca^{2+} concentration, in which a higher concentration of Tet was needed.

Nietsch's study demonstrated that the activation of potassium and chloride channels by TNF- α induced apoptosis and death of the HTC rat hepatoma cells, which could be significantly delayed by K^+ channel blockers (Ba^{2+} and quinine)^[33]. Our result showed that Tet had no effect on I_K and I_{K1} , which suggested that the hepatoprotection of Tet might not relate to potassium channels. However, whether calcium activated potassium channels exist in rat hepatocytes or not remains controversial^[34,35]. The effect of Tet on potassium channels requires further investigation.

In conclusion, Tet protects hepatocytes by inhibiting I_{CRAC} , which is not related to I_K and I_{K1} .

REFERENCES

- 1 Li DG, Wang ZR, Lu HM. Pharmacology of tetrandrine and its therapeutic use in digestive diseases. *World J Gastroenterol* 2001; 7: 627-629

- 2 **Chen XH**, Hu YM, Liao YQ. Protective effects of tetrandrine on CCl₄-injured hepatocytes. *Acta Pharmacol Sin* 1996; **17**: 348-350
- 3 **Wong TM**, Wu S, Yu XC, Li HY. Cardiovascular actions of Radix Stephaniae Tetrandrae: a comparison with its main component, tetrandrine. *Acta Pharmacol Sin* 2000; **21**: 1083-1088
- 4 **Cheng D**, Chen W, Mo X. Acute effect of tetrandrine pulmonary targeting microspheres on hypoxic pulmonary hypertension in rats. *Chin Med J (Engl)* 2002; **115**: 81-83
- 5 **Lee SH**, Nan JX, Sohn DH. Tetrandrine prevents tissue inhibitor of metalloproteinase-1 messenger RNA expression in rat liver fibrosis. *Pharmacol Toxicol* 2001; **89**: 214-216
- 6 **Liu D**, Li G, Liu D, Cao Y. Effects of tetrandrine on the synthesis of collagen and scar-derived fibroblast DNA. *Zhonghua Shaoshang Zazhi* 2001; **17**: 222-224
- 7 **Park PH**, Nan JX, Park EJ, Kang HC, Kim JY, Ko G, Sohn DH. Effect of tetrandrine on experimental hepatic fibrosis induced by bile duct ligation and scission in rats. *Pharmacol Toxicol* 2000; **87**: 261-268
- 8 **Ma JY**, Barger MW, Hubbs AF, Castranova V, Weber SL, Ma JK. Use of tetrandrine to differentiate between mechanisms involved in silica-versus bleomycin-induced fibrosis. *J Toxicol Environ Health A* 1999; **57**: 247-266
- 9 **Li DG**, Lu HM, Chen YW. Progression on antifibrotic effects of tetrandrine. *Shijie Huaren Xiaohua Zazhi* 1999; **7**: 171-172
- 10 **Li DG**, Lu HM, Chen YW. Progress in studies of tetrandrine against hepatofibrosis. *World J Gastroenterol* 1998; **4**: 377-379
- 11 **Seglen PO**. Preparation of isolated rat liver cells. *Methods Cell Biol* 1976; **13**: 29-83
- 12 **Cui GY**, Li JM, Cui H, Hao LY, Liu DJ, Zhang KY. Effects of calcium channel blockers on calcium release-activated calcium currents in rat hepatocytes. *Acta Pharmacol Sin* 1999; **20**: 415-418
- 13 **Li JM**, Cui GY, Liu DJ, Cui H, Chang TH, Wang YP, Zhang KY. Effects of N-methyl berbamine on delayed outward potassium current in isolated rat hepatocytes. *Acta Pharmacol Sin* 1998; **19**: 24-26
- 14 **Henderson RM**, Graf J, Boyer JL. Inward-rectifying potassium channels in rat hepatocytes. *Am J Physiol* 1989; **256**: G1028-1035
- 15 **Wu CH**. Fibrodynamics-elucidation of the mechanisms and sites of liver fibrogenesis. *World J Gastroenterol* 1999; **5**: 388-390
- 16 **Albanis E**, Friedman SL. Hepatic fibrosis. Pathogenesis and principles of therapy. *Clin Liver Dis* 2001; **5**: 315-334
- 17 **Friedman SL**. Molecular regulation of hepatic fibrosis, an integrated cellular response to tissue injury. *J Biol Chem* 2000; **275**: 2247-2250
- 18 **Brenner DA**, Waterboer T, Choi SK, Lindquist JN, Stefanovic B, Burchardt E, Yamauchi M, Gillan A, Rippe RA. New aspects of hepatic fibrosis. *J Hepatol* 2000; **32**(Suppl 1): 32-38
- 19 **Maddrey WC**. Alcohol-induced liver disease. *Clin Liver Dis* 2000; **4**: 115-131
- 20 **Liu Y**, Shimizu I, Omoya T, Ito S, Gu XS, Zuo J. Protection effect of estradiol on hepatocytic oxidative damage. *World J Gastroenterol* 2002; **8**: 363-366
- 21 **Wei HS**, Li DG, Lu HM, Zhan YT, Wang ZR, Huang X, Zhang J, Cheng JL, Xu QF. Effects of AT1 receptor antagonist, losartan, on rat hepatic fibrosis induced by CCl₄. *World J Gastroenterol* 2000; **6**: 540-545
- 22 **Hu YY**, Liu CH, Wang RP, Liu C, Liu P, Zhu DY. Protective actions of salvianolic acid A on hepatocyte injured by peroxidation *in vitro*. *World J Gastroenterol* 2000; **6**: 402-404
- 23 **Chen PS**, Zhai WR, Zhou XM, Zhang JS, Zhang YE, Ling YQ, Gu YH. Effects of hypoxia, hyperxia on the regulation of expression and activity of matrix metalloproteinase-2 in hepatic stellate cells. *World J Gastroenterol* 2001; **7**: 647-651
- 24 **Hamasaki K**, Nakashima M, Naito S, Akiyama Y, Ohtsuru A, Hamanaka Y, Hsu CT, Ito M, Sekine I. The sympathetic nervous system promotes carbon tetrachloride-induced liver cirrhosis in rats by suppressing apoptosis and enhancing the growth kinetics of regenerating hepatocytes. *J Gastroenterol* 2001; **36**: 111-120
- 25 **Hu Y**, Wang R, Zhang X, Liu C, Liu C, Liu P, Zhu D. Effects of carbon tetrachloride-injured hepatocytes on hepatic stellate cell activation and salvianolic acid A preventive action *in vitro*. *Zhonghua Ganzangbing Zazhi* 2000; **8**: 299-301
- 26 **Kim KY**, Choi I, Kim SS. Progression of hepatic stellate cell activation is associated with the level of oxidative stress rather than cytokines during CCl₄-induced fibrogenesis. *Mol Cells* 2000; **10**: 289-300
- 27 **Shi J**, Aisaki K, Ikawa Y, Wake K. Evidence of hepatocyte apoptosis in rat liver after the administration of carbon tetrachloride. *Am J Pathol* 1998; **153**: 515-525
- 28 **Greenwel P**, Dominguez-Rosales JA, Mavi G, Rivas-Estilla AM, Rojkind M. Hydrogen peroxide: a link between acetaldehyde-elicited alpha1 (I) collagen gene up-regulation and oxidative stress in mouse hepatic stellate cells. *Hepatology* 2000; **31**: 109-116
- 29 **Sawanobori T**, Takanashi H, Hiraoka M, Iida Y, Kamisaka K, Maezawa H. Electrophysiological properties of isolated rat liver cells. *J Cell Physiol* 1989; **139**: 580-585
- 30 **Strigrow F**, Bohnsack R. Verapamil and diltiazem inhibit receptor-operated calcium channels and intracellular calcium oscillations in rat hepatocytes. *FEBS Lett* 1993; **318**: 341-344
- 31 **Hughes BP**, Milton SE, Barritt GJ, Auld AM. Studies with verapamil and nifedipine provide evidence for the presence in the liver cell plasma membrane of two types of Ca²⁺ inflow transporter which are dissimilar to potential-operated Ca²⁺ channels. *Biochem Pharmacology* 1986; **35**: 3045-3052
- 32 **Breterton HM**, Harland ML, Frosco M, Petronijevic T, Barritt GJ. Novel variants of voltage-operated calcium channel alpha 1-subunit transcripts in a rat liver-derived cell line: deletion in the IVS4 voltage sensing region. *Cell Calcium* 1997; **22**: 39-52
- 33 **Nietsch HH**, Roe MW, Fiekers JF, Moore AL, Lidofsky SD. Activation of potassium and chloride channels by tumor necrosis Factor α role in liver cell death. *J Biol Chem* 2000; **275**: 20556-20561
- 34 **Takanashi H**, Sawanobori T, Kamisaka K, Maezawa H, Hiraoka M. Ca²⁺-activated K⁺ channel is present in guinea-pig but lacking in rat hepatocytes. *Jpn J Physiol* 1992; **42**: 415-430
- 35 **Duszynski J**, Elensky M, Cheung JY, Tillotson DL, Lanoue KF. Hormone-regulated Ca²⁺ channel in rat hepatocytes revealed by whole cell patch clamp. *Cell Calcium* 1995; **18**: 19-29

Edited by Zhu L

Influence of intrauterine injection of rat fetal hepatocytes on rejection of rat liver transplantation

Yan-Ling Yang, Ke-Feng Dou, Kai-Zong Li

Yan-Ling Yang, Ke-Feng Dou, Kai-Zong Li, Department of Hepatobiliary Surgery, Xijing Hospital, Fourth Military Medical University, Xi'an 710032, Shaanxi Province, China
Supported by the National Nature Science Foundation of China, No. 30070741

Correspondence to: Kai-Zong Li, Department of Hepatobiliary Surgery, Xijing Hospital, Fourth Military Medical University, 710032 Xi'an, Shaanxi Province, China. gdwk@fmmu.edu.cn
Telephone: +86-29-3375259 **Fax:** +86-29-3375561
Received: 2002-08-01 **Accepted:** 2002-08-27

Abstract

AIM: To investigate the influence of immune tolerance induced by intrauterine exposure to fetal hepatocytes on liver transplantation in the adult rat.

METHODS: LOU/CN rat fetal hepatocytes were injected into the fetuses of pregnant CHN rats (14-16 days of gestation). At 7-9 weeks of age, the surviving male rats received orthotopic liver transplantation (OLT) from male LOU/CN donors and the survival period was observed and monitored by mixed lymphocyte reaction assay and cytotoxicity test.

RESULTS: (1) A total of 31 pregnant CHN rats with 172 fetuses received fetal hepatocytes from LOU/CN rats via intrauterine injection. Among them, thirteen pregnant rats showed normal parturition, with 74 neonatal rats growing up normally. (2) The mean survival period after OLT in rats with fetal exposure to fetal hepatocytes was 32.1 ± 3.7 days, which was significantly different from the control (11.8 ± 2.3 days, $P < 0.01$) in rats without fetal induction of immune tolerance. (3) Mixed lymphocyte proliferation assays yielded remarkable discrepancies between the groups of rats with- or without fetal exposure to fetal hepatocytes, with values of 8411 ± 1361 and 22473 ± 1856 (CPM \pm SD, $P < 0.01$) respectively. (4) Cytotoxicity assays showed values of $21.2 \pm 6.5\%$ and $64.5 \pm 7.2\%$ ($P < 0.01$) in adult rats with or without fetal induction of immune tolerance.

CONCLUSION: Intrauterine injection of fetal hepatocytes into rat fetuses can prolong the survival period of liver transplant adult male rats recipients, inducing immune tolerance in OLT.

Yang YL, Dou KF, Li KZ. Influence of intrauterine injection of rat fetal hepatocytes on rejection of rat liver transplantation. *World J Gastroenterol* 2003; 9(1): 137-140
<http://www.wjgnet.com/1007-9327/9/137.htm>

INTRODUCTION

In both experimental study and clinical practice, rejection responses induced by organ transplants necessitate the use of potent immunosuppressive drugs^[1-7]. It should be noted, however, that excessive dosage of immunosuppressive agents may result in severe side effects such as hypertension and

hepatic and/or renal toxicity. Moreover, prolonged usage of immunosuppressants often leads to severe infection and increased susceptibility to malignancy, thus critically affecting the health of recipients. Particularly in juvenile patients, immunosuppressive drugs can lead to stunted growth. It is therefore imperative to assess, as an alternative to immunosuppressants, the protective effect of induced immune tolerance on organ transplantation. The ideal strategy is to induce a low responsiveness or irresponsiveness in the recipients toward donors' grafts, while preserving normal immunological functions for the recognition of tumor antigens and prevention of infection. Thus immunosuppressive agents can be avoided or be used at dramatically reduced dosage. The key steps toward successful transplantation therefore include either attenuated immune reactions or induced immune tolerance to grafts^[8-15].

In utero, the stem cell transplantation represents a new therapeutic approach of experimental nature toward the treatment of hematopoietic diseases, immunodeficiency diseases, metabolic disorders and genetic diseases^[16-19]. Some reports support the possibility of using this method to induce immunologic tolerance in both human subjects and animals receiving organ transplantation^[20-22]. But the effect of *in utero* fetal exposure to fetal hepatocytes on liver transplantation in adulthood is unclear. In the present study, we injected fetal hepatocytes intraperitoneally into rat fetuses and then performed orthotopic liver transplantation (OLT) in surviving adult male rats. Some parameters were tested in order to confirm the anti-rejection effect of *in utero* injection of fetal hepatocytes.

MATERIALS AND METHODS

Animals

Male and female LOU/CN and CHN rats weighing 200-250 g were obtained from the Laboratory Animal Center of The Fourth Military Medical University, and fed with standard rat chow.

Timed pregnancy of CHN rats

Male CHN rats, or male LOU/CN rats, were housed individually in standard cages with a metal divider with 0.25-inch holes. One female CHN or LOU/CN rat was placed in the corresponding empty side. The cage divider was then removed 48 hrs later. Pairs of CHN or LOU/CN rats were allowed to mate overnight separately. The pairs were then separated with the females placed singly in cages. The presence of vaginal plug marked day 0 of gestation. Normal gestation is about 21 days.

Preparation of LOU/CN fetal rat hepatocytes

Pregnant LOU/CN females were killed by cervical dislocation at 15 to 16 days of gestation. All subsequent handling was done under sterile conditions. The uterine horns were removed and dissected in phosphate-buffered saline (PBS). Fetuses were separated from decidua and extraembryonic membranes and transferred to 35 mm petri dishes filled with PBS. Fetal livers were removed, with 5 to 10 livers placed in 1 to 2 ml RPMI 1640 medium (GIBCO BRL, Grand Island, CA) with 15% fetal calf serum (FCS, GIBCO BRL, Grand Island, CA). Cell suspensions were prepared by repeated pipetting of the livers

through a 23-gauge needle attached to a 1ml pipette. The mononuclear cells were separated by centrifugation at 500 g for 20 minutes and filtered through a Nitex filter with a 41 μm pore size (Huamei chemical company, Henan province, China). Cell viability counting (usually greater than 90 %) was done using trypan blue exclusion test, and the final cell suspension was prepared in PBS/15 % FCS at a concentration of $5 \times 10^7/\text{ml}$. The cell suspension was used for intrauterine injection within 4 hours of preparation.

In utero intraperitoneal injection into CHN rat fetuses with LOU/CN fetal rat hepatocytes

Micropipettes were prepared from capillaries using a Brown and Flaming micropipette puller. The end of the needle was cut under a microscope with ophthalmological forceps, and the tip was sharpened on a micro-grinding wheel. Pregnant (11 to 13 days of gestation) CHN rats were anesthetized i.p. with sodium pentobarbital, and the uterine horns were exteriorized with ophthalmological forceps. Fetal hepatocytes from LOU/CN rats were injected into CHN fetuses through a hand-drawn glass micropipette with a beveled edge. The placenta was penetrated at an oblique angle. The number of cells injected per fetus was 10^6 (about 5×10^{10} cells/kg of recipient weight), except in experiments in which the effects of different cell concentrations and volumes of cell suspension used were examined. Muscle layers were closed with 4-0 silk suture, and 1-0 silk thread was used for skin suture.

Orthotopic liver transplantation (OLT)

Orthotopic whole-liver transplantation was performed^[23-26] using the simplified cuff technique for portal and intrahepatic vena cava anastomosis, whereas the hepatic artery was not reconstructed. The twenty male CHN rats, aged 7 to 9 weeks that survived intraperitoneal injection with fetal liver cells from LOU/CN rats, were taken as graft recipients, with normal male LOU/CN rats as liver donors. Both donors and recipients were anesthetized with methoxyflurane. After explantation, livers were stored at 0-4 °C for 1 hr in UW solution. Grafts were connected to suprahepatic vena cava with a running 7-0 prolene suture. We insert cuffs into the corresponding vessels, and anastomose the bile duct and hepatic artery over an intraluminal polyethylene splint. Transplantation required less than 40 min, while the portal vein was clamped for 12-15 min during this period. After transplantation, the recipients had free access to standard laboratory chow and tap water. Animals that died within 3 days were considered technical failures and were excluded from data collection. The rate of success of liver transplantation was more than 90 % in this study. Five rats were sacrificed at 5 days after OLT. Immediately before sacrifice, the livers were removed for histological investigation. Liver samples from 10 normal male CHN rats were taken as controls.

Mixed lymphocyte reaction assay

Mixed spleen cells were used for setting up lymphocyte cultures. Briefly, the spleens were aseptically removed from experimental CHN rats that survived *in utero* intraperitoneal injection of fetal LOU/CN rat liver cell, and from control CHN rats. Then they were separately disrupted mechanically using a pair of sterile forceps. LOU/CN spleen cells were treated with 25 $\mu\text{g}/\text{ml}$ mitocin-C (Kyowa Hakko Kogyo, Tokyo, Japan) at 37 °C for 45 min. Then the two groups of cells were washed by PBS, followed by lysis of erythrocytes in Tris-NH₄Cl solution (pH 7.2). After further washes, the cells were finally resuspended in RPMI 1640 with 10 % FCS. The numbers of two groups of spleen cells were adjusted, and 5×10^5 spleen cells from each of the two sources were mixed together (final

volume 0.2 ml) and added to triplicate wells of 96-well round-bottomed microtiter plates. Cells were cultured for 120 hr, and 1 μCi [3H]-thymidine was added into wells 18hr before cell harvesting. Radioactive thymidine incorporation rate was measured by a liquid scintillation counter (1205 Betaplate), with data expressed as $\text{CPM} \pm \text{SD}$ ^[27,28].

Complement-dependent cytotoxicity test

Recipient CHN rats were tested one week after OLT for complement-dependent cytotoxicity test against lymphocytes suspensions from LOU/CN donor rats. Sera from recipients were prepared and added into the wells of 96-well round-bottomed microtiter plates (1 μl per well). Then 1 μl lymphocytes (about 2 000 cells per 1 μl volume) were added into the same wells. They were gently mixed and incubated for 30 min at 22 °C \pm 2 °C, then 5 μl rabbit complement (Huamei chemical company, Henan province, China) was added, and the mixture incubated for 60 min at 22 °C \pm 2 °C. Afterwards, the mixtures were stained with eosin (50 g/L) for 5 min. The cells were fixed in 36 % formalin for 2 hr and observed with an inverted phase-contrast microscope (Olympus, Tokyo, Japan). Cytotoxicity was determined by eosin exclusion and percentage enumeration of cells killed by sera from OLT^[29,30].

Histology

Livers from CHN rats that underwent OLT were fixed in 10 % neutral formalin for five days and then embedded in paraffin. Five micron sections were cut and stained with hematoxylin and eosin for histological examination. Sections from normal rat livers served as controls.

Diagnostic criterion of graft rejection

Several diagnostic criteria were used to determine the existence of rejection response following hepatic transplantation. The first is survival of recipients over 7 days post-transplantation. The second entails the occurrence of acute hepatic dysfunction as typified by inappetence, weight loss, auricle or nail jaundice, depressed mood, with incidental diarrhea or ascites in some cases. The third criterion involves typical histological changes, such as enlarged liver bulk, yellowish white appearance of the liver, and the presence of liver conglutination to muscles or abdominal walls, and viscera. Also frequently encountered are apparent degeneration or necrosis of hepatic cells, and infiltration of numerous lymphocytes, especially at liver sinusoidal area. The fourth denotes the presence in good condition of the recipients plus good appetite, accompanied with normal weight 3 days after successful transplantation. The recipients that died from post-surgical complications such as necrosis of bile duct, intra-abdominal hemorrhage and infection were excluded from data collection.

Statistics

All the data were analyzed by Student's *t* test and expressed as mean \pm S. The statistical difference $P < 0.05$ was considered significant and $P < 0.01$ as very significant.

RESULTS

Influence of intraperitoneal injection into fetus in utero on survival of neonatal CHN rats

Thirty-one pregnant CHN recipients who later delivered 172 fetal CHN rats were injected into their fetuses with isolated fetal hepatocytes from LOU/CN rats. Among them, eleven pregnant females died from various surgical complications, and seven females aborted or consumed their litters. There were 17 pregnant rats with normal parturition, and 74 neonatal rats grew up normally.

Suppression of rejection response to rat liver transplantation after intrauterine injection

The mean survival period of rats with fetal intraperitoneal injection of fetal hepatocytes prior to OLT was 32.1 ± 3.7 day, in comparison to control values of 11.8 ± 2.3 day ($P < 0.01$) obtained from rats without this procedure.

Inhibitory effect of intraperitoneal injection in utero on mixed lymphocytes reaction assay

Mixed lymphocytes reaction assay showed significant differences in [³H]-thymidine incorporation rates in groups of CHN rats that were either fetally exposed (8411 ± 1361 , CPM \pm SD) or not (22473 ± 1856 , CPM \pm SD) to intraperitoneal injection of fetal hepatocytes in utero ($P < 0.01$).

Suppressive effect of fetal intraperitoneal injection in utero on cytotoxicity test after rat liver transplantation in adulthood

Cytotoxicity test revealed percentage values of dead cells to be 21.2 ± 6.5 % vs 64.5 ± 7.2 % ($P < 0.01$) respectively from the two groups of CHN rats with or without fetal intraperitoneal injection in utero prior to OLT in the adult rats, the difference being statistically significant.

DISCUSSION

With rapid advances in antenatal diagnostic technology, many prenatal diseases (congenital metabolic liver disorders, congenital heart disease and hemophilia, e.g.) can be diagnosed. Therefore organ transplantation becomes a very useful choice for treating these diseases in afflicted children. However, routine regime of immunosuppression in use today suffered from many serious side effects, including stunted growth seen in children using most immunosuppressive drugs^[31-34]. If we can induce low responsiveness or even irresponsiveness in the recipients to the donors' grafts, immunosuppressive drugs can then be used at much reduced dosage. Until now, low responsiveness or irresponsiveness to the graft has not been achieved in clinical practice. Therefore, induction of immunologic tolerance becomes imperative in clinical transplantation^[35-42].

Clonal deletion theory maintains that burst of cell proliferation during embryonic period is very frequent, with resultant formation of multiple specific clones of lymphocytes capable of responding to respective antigens^[43,44]. During embryonic period, the lymphocyte clones encounter internal antigens or artificially introduced antigens, with consequent damage to, or suppression of these clones, the so-called abstinence clones. In postnatal life, the abstinence clone remains inactive to an internal antigen or an artificially introduced foreign antigen that has been present in utero, a status of immunologic tolerance in the adult to an antigen following prior exposure during the embryonic period. On the contrary, if a lymphocyte clone meets an antigen that has never been introduced during the embryonic period, the specific immunological response would ensue. According to the theory, intrauterine injection is considered a useful tool for the induction of immunologic tolerance, especially for clinical transplantation. Some advantages of intrauterine injection for evoking immunologic tolerance should be noted. Firstly, because the host at fetal stage can't recognize a foreign substance and thus display immunologic tolerance to a xenogen (the earlier the fetal stage of the host, the stronger the tolerance effect to the antigen), no immunologic reaction is seen between the host and ecdemic grafts. Therefore intrauterine injection spares tissue-matching work needed in routine transplantation and makes easier graft transplantation. Meanwhile, immunologic tolerance induced by intrauterine injection makes unnecessary pretreatment with immunosuppressive drugs, thus

avoiding possible side effects of immunosuppressive agents on the body. Secondly, fewer fetal liver cells are needed for transplanting into the recipients during embryonic period because of their small body size and weight. The latter assures little influence and gentle torture for the recipients. Thirdly, in addition to exempt from infection due to microorganism, the maternal body offers adequate nutrition and energy to the fetuses, thus the uterus can be seen as an ideal 'isolation room'^[45-51].

We also compared the effect of using rat spleen or bone marrow cells, with that of fetal liver cells, for intraperitoneal injection in utero into fetuses in pregnant rats. It was observed that the survival birth rate using fetal liver cells was much greater than that with spleen or bone marrow cells. Several factors may help to explain the discrepancy. The most important one may be that the response against the host is induced by active lymphocytes located in the spleen or bone marrow cells. In contrast, the main components of fetal liver cells are hematopoietic stem cells possessing two effects, with the first reducing graft versus host reaction, and the other for the maintenance of chimerism because hematopoietic stem cells are characterized by self-renewal and multipotential for differentiation^[52,53].

As evidenced by both *in vivo* and *in vitro* data in the present study, the method of fetal hepatocytes in utero injection can prolong the survival period of rat liver transplants. Although complete immune tolerance can not be induced, partial immune tolerance observed in our study is sufficient for liver transplantation. Further work will be needed to reveal if chimerism is induced by transplantation itself, as well as its possible influence on the immune system in the grafted recipients.

REFERENCES

- 1 **Karim M**, Steger U, Bushell AR, Wood KJ. The role of the graft in establishing tolerance. *Front Biosci* 2002; **7**: 129-154
- 2 **Riordan SM**, Williams R. Transplantation of primary and reversibly immortalized human liver cells and other gene therapies in acute liver failure and decompensated chronic liver disease. *World J Gastroenterol* 2000; **6**: 636-642
- 3 **Tang ZY**. Hepatocellular carcinoma-cause, treatment and metastasis. *World J Gastroenterol* 2001; **7**: 445-454
- 4 **Zhu XF**, Chen GH, He XS, Lu MQ, Wang GD, Cai CJ, Yang Y, Huang JF. Liver transplantation and artificial liver support in fulminant hepatic failure. *World J Gastroenterol* 2001; **7**: 566-568
- 5 **Platell CF**, Coster J, McCauley RD, Hall JC. The management of patients with the short bowel syndrome. *World J Gastroenterol* 2002; **8**: 13-20
- 6 **Ouyang EC**, Wu CH, Walton C, Promrat K, Wu GY. Transplantation of human hepatocytes into tolerized genetically immunocompetent rats. *World J Gastroenterol* 2001; **7**: 324-330
- 7 **Waldmann H**, Cobbold S. Approaching tolerance in transplantation. *Int Arch Allergy Immunol* 2001; **126**: 11-22
- 8 **Yu X**, Carpenter P, Anasetti C. Advances in transplantation tolerance. *Lancet* 2001; **357**: 1959-1963
- 9 **Qian YB**, Cheng GH, Huang JF. Multivariate regression analysis on early mortality after orthotopic liver transplantation. *World J Gastroenterol* 2002; **8**: 128-130
- 10 **Shi LB**, Peng SY, Meng XK, Peng CH, Liu YB, Chen XP, Ji ZL, Yang DT, Chen HR. Diagnosis and treatment of congenital choledochal cyst: 20 years' experience in China. *World J Gastroenterol* 2001; **7**: 732-734
- 11 **Bramhall S**, Minford E, Gunson B, Buckels JA. Liver transplantation in the UK. *World J Gastroenterol* 2001; **7**: 602-611
- 12 **Womer KL**, Lee RS, Madsen JC, Sayegh MH. Tolerance and chronic rejection. *Philos Trans R Soc Lond B Biol Sci* 2001; **356**: 727-738
- 13 **Zavazava N**, Kabelitz D. Alloreactivity and apoptosis in graft rejection and transplantation tolerance. *J Leukoc Biol* 2000; **68**: 167-174
- 14 **Hong JC**, Kahan BD. Immunosuppressive agents in organ transplantation: past, present, and future. *Semin Nephrol* 2000; **20**: 108-125
- 15 **Bartlett A**, McCall J, Munn S. Co-stimulatory blockade and tolerance induction in transplantation. *BioDrugs* 2001; **15**: 491-500

- 16 **Jones DR**. In utero stem cell transplantation: two steps forward but one step back? *Expert Opin Biol Ther* 2001; **1**: 205-212
- 17 **Hayashi S**, Flake AW. In utero hematopoietic stem cell therapy. *Yonsei Med J* 2001; **42**: 615-629
- 18 **Flake AW**. In utero transplantation of haemopoietic stem cells. *Best Pract Res Clin Haematol* 2001; **14**: 671-683
- 19 **Cowan MJ**, Chou SH, Tarantal AF. Tolerance induction post in utero stem cell transplantation. *Ernst Schering Res Found Workshop* 2001; **33**: 145-171
- 20 **Kim HB**, Shaaban AF, Milner R, Fichter C, Flake AW. In utero bone marrow transplantation induces donor-specific tolerance by a combination of clonal deletion and clonal anergy. *J Pediatr Surg* 1999; **34**: 726-729
- 21 **Rubin JP**, Cober SR, Butler PE, Randolph MA, Gazelle GS, Ierino FL, Sachs DH, Lee WP. Injection of allogeneic bone marrow cells into the portal vein of swine in utero. *J Surg Res* 2001; **95**: 188-194
- 22 **Takahashi T**, Kakita A, Sakamoto I, Takahashi Y, Hayashi K, Tadokoro F, Yamashina S. Immunohistochemical and electron microscopic study of extrinsic hepatic reinnervation following orthotopic liver transplantation in rats. *Liver* 2001; **21**: 300-308
- 23 **Boros P**, Tarcsafalvi A, Wang L, Megyesi J, Liu J, Miller CM. Intrahepatic expression and release of vascular endothelial growth factor following orthotopic liver transplantation in the rat. *Transplantation* 2001; **72**: 805-811
- 24 **Okano S**, Eto M, Tomita Y, Yoshizumi T, Yamada H, Minagawa R, Nomoto K, Sugimachi K, Nomoto K. Cyclophosphamide-induced tolerance in rat orthotopic liver transplantation. *Transplantation* 2001; **71**: 447-456
- 25 **He XS**, Huang JF, Chen GH, Zheng KL, Ye XM. A successful case of combined liver and kidney transplantation for autosomal dominant polycystic liver and kidney disease. *World J Gastroenterol* 1999; **5**: 79-80
- 26 **Zhang SG**, Wu MC, Tan JW, Chen H, Yang JM, Qian QJ. Expression of perforin and granzyme B mRNA in judgement of immunosuppressive effect in rat liver transplantation. *World J Gastroenterol* 1999; **5**: 217-220
- 27 **Genden EM**, Mackinnon SE, Yu S, Hunter DA, Flye MW. Pretreatment with portal venous ultraviolet B-irradiated donor alloantigen promotes donor-specific tolerance to rat nerve allografts. *Laryngoscope* 2001; **111**: 439-447
- 28 **Horimoto H**, Nakai Y, Nakahara K, Nomura Y, Mieno S, Sasaki S. HMG-CoA reductase inhibitor cerivastatin prolonged rat cardiac allograft survival by blocking intercellular signals. *J Heart Lung Transplant* 2002; **21**: 440-445
- 29 **Hehmke B**, Schroder D, Kloting I, Kohnert KD. Complement-dependent antibody-mediated cytotoxicity (CAMC) to pancreatic islet cells in the spontaneously diabetic BB/OK rat: interference from cell-bound and soluble inhibitors. *J Clin Lab Immunol* 1991; **35**: 71-81
- 30 **Tange S**, Scherer MN, Graeb C, Weiss T, Justl M, Frank E, Andrassy J, Jauch KW, Geissler EK. The antineoplastic drug Paclitaxel has immunosuppressive properties that can effectively promote allograft survival in a rat heart transplant model. *Transplantation* 2002; **73**: 216-223
- 31 **Reyes J**, Mazariegos GV, Bond GM, Green M, Dvorchik I, Kosmach-Park B, Abu-Elmagd K. Pediatric intestinal transplantation: Historical notes, principles and controversies. *Pediatr Transplant* 2002; **6**: 193-207
- 32 **Bassas AF**, Chehab MS, Al-Shahed MS, Djurberg HG, Al-Shurafa HA, Jawdat MT, Al-Hussaini HF, Zuleika MA, Al-Hebby HA, Wali SH. Pediatric living-related liver transplantation in Saudi Arabia. *Saudi Med J* 2002; **23**: 640-644
- 33 **Robinson LG**, Hilinski J, Graham F, Hymes L, Beck-Sague CM, Hsia J, Nesheim SR. Predictors of cytomegalovirus disease among pediatric transplant recipients within one year of renal transplantation. *Pediatr Transplant* 2002; **6**: 111-118
- 34 **Samsonov D**, Briscoe DM. Long-term care of pediatric renal transplant patients: from bench to bedside. *Curr Opin Pediatr* 2002; **14**: 205-210
- 35 **Rela M**, Dhawan A. Liver transplantation in children. *Indian J Pediatr* 2002; **69**: 175-183
- 36 **Fine RN**. Growth following solid-organ transplantation. *Pediatr Transplant* 2002; **6**: 47-52
- 37 **Bucuvalas JC**, Ryckman FC. Long-term outcome after liver transplantation in children. *Pediatr Transplant* 2002; **6**: 30-36
- 38 **Shneider BL**. Pediatric liver transplantation in metabolic disease: clinical decision making. *Pediatr Transplant* 2002; **6**: 25-29
- 39 **He XS**, Huang JF, Chen GH, Fu Q, Zhu XF, Lu MQ, Wang GD, Guan XD. Orthotopic liver transplantation for fulminant hepatitis B. *World J Gastroenterol* 2000; **6**: 398-399
- 40 **Guan WX**, Li KZ, Dou KF. Hepatocellular carcinoma and liver transplantation. *Shijie Huaren Xiaohua Zazhi* 2001; **9**: 1292-1295
- 41 **Song WL**, Wang WZ, Wu GS, Dong GL, Ling R, Ji G, Zhao JX. Evaluation of perioperative serum cytokine level in acute rejection in human living-related small bowel transplantation. *Shijie Huaren Xiaohua Zazhi* 2001; **9**: 401-404
- 42 **He XS**, Huang JF, Chen GH, Zheng KL, Ye XM. A successful case of combined liver and kidney transplantation for autosomal dominant polycystic liver and kidney disease. *World J Gastroenterol* 1999; **5**: 79-80
- 43 **Prevot A**, Martini S, Guignard JP. Exposure in utero to immunosuppressives. *Rev Med Suisse Romande* 2001; **121**: 283-291
- 44 **Tanaka SA**, Hiramatsu T, Oshitomi T, Imai Y, Koyanagi H. Induction of donor-specific tolerance to cardiac xenografts in utero. *J Heart Lung Transplant* 1998; **17**: 888-891
- 45 **Mackenzie TC**, Shaaban AF, Radu A, Flake AW. Engraftment of bone marrow and fetal liver cells after in utero transplantation in MDX mice. *J Pediatr Surg* 2002; **37**: 1058-1064
- 46 **Taylor PA**, McElmurry RT, Lees CJ, Harrison DE, Blazar BR. Allogenic fetal liver cells have a distinct competitive engraftment advantage over adult bone marrow cells when infused into fetal as compared with adult severe combined immunodeficient recipients. *Blood* 2002; **99**: 1870-1872
- 47 **Barker JE**, Deveau S, Lessard M, Hamblen N, Vogler C, Levy B. In utero fetal liver cell transplantation without toxic irradiation alleviates lysosomal storage in mice with mucopolysaccharidosis type VII. *Blood Cells Mol Dis* 2001; **27**: 861-873
- 48 **Casal ML**, Wolfe JH. In utero transplantation of fetal liver cells in the mucopolysaccharidosis type VII mouse results in low-level chimerism, but overexpression of beta-glucuronidase can delay onset of clinical signs. *Blood* 2001; **97**: 1625-1634
- 49 **Surbek DV**, Holzgreve W, Nicolaidis KH. Haematopoietic stem cell transplantation and gene therapy in the fetus: ready for clinical use? *Hum Reprod Update* 2001; **7**: 85-91
- 50 **Surbek DV**, Gratwohl A, Holzgreve W. In utero hematopoietic stem cell transfer: current status and future strategies. *Eur J Obstet Gynecol Reprod Biol* 1999; **85**: 109-115
- 51 **Flake AW**, Zanjani ED. In utero transplantation for thalassemia. *Ann N Y Acad Sci* 1998; **850**: 300-311
- 52 **Pschera H**. Stem cell therapy in utero. *J Perinat Med* 2000; **28**: 346-354
- 53 **Stanworth SJ**, Newland AC. Stem cells: progress in research and edging towards the clinical setting. *Clin Med* 2001; **1**: 378-382

Functional changes of dendritic cells derived from allogeneic partial liver graft undergoing acute rejection in rats

Ming-Qing Xu, Zhen-Xiang Yao

Ming-Qing Xu, Zhen-Xiang Yao, Department of General Surgery, The First affiliated Hospital, Chongqing University of Medical Science, Chongqing 400016, China

Supported by the Medical Scientific Foundation of Chongqing City, No. 01-2-029

Correspondence to: Dr. Ming-Qing Xu, Liver Transplantation Center, West China Hospital, Sichuan University, Chengdu 610041, Sichuan Province, China. xumingqing@hotmail.com

Telephone: +86-28-85400588

Received: 2002-07-04 **Accepted:** 2002-09-12

Abstract

AIM: To investigate functional change of dendritic cells (DCs) derived from allogeneic partial liver graft undergoing acute rejection in rats.

METHODS: Allogeneic (SD rat to LEW rat) whole and 50 % partial liver transplantation were performed. DCs from liver grafts 0 hr and 4 days after transplantation were isolated and propagated in the presence of GM-CSF *in vitro*. Morphological characteristics of DCs propagated for 4 days and 10 days were observed by electron microscopy. Phenotypical features of DCs propagated for 10 days were analyzed by flow cytometry. Expression of IL-12 protein and IL-12 receptor mRNA in DCs propagated for 10 days was also measured by Western blotting and semiquantitative RT-PCR, respectively. Histological grading of rejection were determined.

RESULTS: Allogeneic whole liver grafts showed no features of rejection at day 4 after transplantation. In contrast, allogeneic partial liver grafts demonstrated moderate to severe rejection at day 4 after transplantation. DCs derived from allogeneic partial liver graft 4 days after transplantation exhibited typical morphological characteristics of DC after 4 days' culture in the presence of GM-CSF. DCs from allogeneic whole liver graft 0 hr and 4 days after transplantation did not exhibit typical morphological characteristics of DC until after 10 days' culture in the presence of GM-CSF. After 10 days' propagation *in vitro*, DCs derived from allogeneic whole liver graft exhibited features of immature DC, with absence of CD40, CD80 and CD86 surface expression, and low levels of IL-12 proteins (IL-12 p35 and IL-12 p40) and IL-12 receptor (IL-12R β_1 and IL-12R β_2) mRNA, whereas DCs from allogeneic partial liver graft 4 days after transplantation displayed features of mature DC, with high levels of CD40, CD80 and CD86 surface expression, and as a consequence, higher expression of IL-12 proteins (IL-12 p35 and IL-12 p40) and IL-12 receptors (IL-12R β_1 and IL-12R β_2) mRNA than those of DCs both from partial liver graft 0 hr and whole liver graft 4 days after transplantation ($P < 0.001$) was observed.

CONCLUSION: DCs derived from allogeneic partial liver graft undergoing acute rejection display features of mature DC.

Xu MQ, Yao ZX. Functional changes of dendritic cells derived from allogeneic partial liver graft undergoing acute rejection in rats. *World J Gastroenterol* 2003; 9(1): 141-147
<http://www.wjgnet.com/1007-9327/9/141.htm>

INTRODUCTION

The shortage of donor organs remains a major obstacle to the widespread application of liver transplantation in patients with end-stage liver disease. Although split grafting was used to increase the number of donor livers, the accelerated rejection induced by liver regeneration^[1,2] can interfere with the outcome of these liver grafts. Therefore, it is important to investigate the mechanism responsible for the accelerated rejection of split liver grafting.

After organ transplantation, interstitial donor dendritic cells (DCs) migrate to recipient lymphoid tissue. In the case of experimental skin, heart, or kidney allografts, these cells have been implicated as the principal instigators of rejection. Despite similar patterns of donor DCs migration, liver grafts are accepted without immunosuppressive therapy between MHC-mismatched mouse, and certain rat strains, and induce donor-specific tolerance. These phenomena and the persistence of donor hematopoietic cells, including DCs, in successful, long-term graft recipients, have raised important questions about the possible role of donor DCs in liver transplant tolerance. The capacity of DCs to initiate immune responses is determined by their surface expression of MHC gene products and costimulatory molecules (CD40, CD80 and CD86), and the secretion of the immune regulator, interleukin (IL)-12^[3-12]. Immature DCs resident in nonlymphoid tissues such as normal liver are deficient at antigen capture and progressing^[3,13], whereas mature DCs, resident in secondary lymphoid tissues, are potent antigen-presenting cells, which can induce naive T-cell activation and proliferation^[3-7]. Immature DCs that express surface MHC class II, but that are deficient in surface costimulatory molecules, can induce T-cell hyporesponsiveness^[13-15] and inhibit immune reactivity^[16,17]. It has been observed that liver-derived^[13,18] or bone marrow-derived immature DCs^[17], propagated *in vitro* and lacking surface costimulatory molecules, can prolong heart or pancreatic islet allograft survival. Whereas, marked augmentation of DCs numbers and maturation of DCs in liver allografts by donor treatment with the hematopoietic growth factor fms-like tyrosine kinase 3 (Flt3) ligand (FL) results in acute liver graft rejection^[19,20].

Recent findings have revealed increased immune responses to regenerating allogeneic partial liver graft in rats^[1,2], but little is known about the mechanism responsible for the accelerated rejection. The purpose of this study was to investigate the property of DCs isolated from allogeneic partial liver graft in comparison with DCs isolated from allogeneic whole liver graft, in an attempt to elucidate the possible mechanism responsible for the accelerated rejection of allogeneic partial liver graft. Given mature DC can induce naive T-cell activation and proliferation^[3-7], and consequently induce acute rejection^[19,20], we suspected that maturation of DCs derived from liver graft would be a key inducer of the accelerated rejection of allogeneic partial liver graft. In the present study, we first demonstrated that DCs derived from partial liver graft undergoing acute rejection displayed features of mature DC, including positive expression of costimulatory molecules, higher level expression of IL-12 protein and IL-12 receptor mRNA in these mature DCs.

MATERIALS AND METHODS

Animals

One hundred male LEW rats and one hundred male SD rats weighing 220-300 g were used in all the experiments. Allogeneic whole and 50 % partial liver transplantation were performed using a combination of SD rats to LEW rats. The animals were purchased from Chinese Academy of Science and Sichuan University. They were maintained with a 12-hr light/dark cycle in a conventional animal facility with water and commercial chow provided ad libitum, with no fasting before the transplantation.

Liver transplantation

All operation were performed under ether anesthesia in clean but not sterile conditions. All surgical procedures were performed from 8 a.m. to 5 p.m. Donors and recipients of similar weight (± 10 g) were chosen. Liver reduction was achieved by removing the left lateral lobe and the two caudate lobes, which resulted in a 50 % reduction of the liver mass. Whole liver transplantation (WLT) and partial liver transplantation (PLT) were performed with the two-cuff method described by Kammada and Calne^[21], Knoop *et al*^[22] and Uchiyama *et al*^[23]. Briefly, the whole and partial liver were perfused with 20 ml of chilled lactated Ringer's solution containing 200 U of heparin through the aorta. The liver was removed and immersed in chilled University of Wisconsin solution. Immediately after cuffs were placed on the portal vein and the infrahepatic vena cava, the liver graft was perfused with 8 ml of chilled University of Wisconsin solution through the portal vein and 2 ml of the same solution through the hepatic artery, and then the hepatic artery was ligated. Cold preservation time was approximately 1 hr in all experiments. After a total hepatectomy was performed in the recipient, the suprahepatic vena cava was anastomosed in a continuous fashion with 8-0 sutures. The portal vein and infrahepatic vena cava were then connected by a 6-FG and 8-FG polyethylene tube cuff, respectively. The bile duct was internally stented with a 22-gauge i.v. catheter. The portal vein was clamped for <18 min in all animals. In each group, the survival rate after grafting was >89 % at 24 hr after surgery. Deaths that occurred within this period were defined as resulting from technical failure. Penicillin was given perioperatively.

Histology

Part of liver graft tissues 4 days after transplantation were sectioned and preserved in 10 % Formalin, embedded in paraffin, cut with microtome, and stained with hematoxylin and eosin.

Propagation and purification of liver graft-derived DC populations

DCs from liver graft 0 hr and 4 days after transplantation were propagated in GM-CSF from nonparenchymal cells (NPC) isolated from collagenase-digested liver graft tissue, as described by Lu^[18]. Nonadherent cells, released spontaneously from proliferating cell clusters, were collected after 4 days' and 10 days' culture, and purified by centrifugation 500 \times g, 10 min at room temperature on a 16 % w/v metrizamide gradient (DC purity 80-85 %).

Morphological and Phenotypical features of DCs

Morphological characteristics of DCs derived from liver graft were observed by electron microscopy. Expression of cell surface molecules was quantitated by flow cytometry as described by Mehling *et al*^[4]. Aliquots of 2×10^5 DCs propagated for 10 days *in vitro* were incubated with the following primary mouse anti-rat mAbs against OX62, CD40, CD80, CD86

(Serotec, USA), or rat IgG as an isotype control for 60 min on ice (1 μ g/ml diluted in PBS/1.0 % FCS). The cells were washed with PBS/1.0 % FCS and labeled with FITC-conjugated goat anti-mouse IgG, diluted 1/50 in PBS/1.0 % FCS for 30 min on ice. At the end of this incubation cells were washed, PBS were added, and the cells were subsequently analyzed in an FACS-4200 flow cytometer (Becton-Dikison, USA).

Semiquantitative RT-PCR for expression of IL-12R mRNA in DCs

Analysis of expression of IL-12R β_1 and IL-12R β_2 mRNA was determined by reverse transcription-PCR (RT-PCR) amplification in contrast with house-keeping gene GAPDH. Total RNA from 1×10^7 DCs propagated for 10 days *in vitro* was isolated using TripureTM reagent (Promega, USA). First-strand cDNA was transcribed from 1 μ g RNA using AMV and an Oligo (dT)₁₅ primer. PCR was performed in a 25 μ l reaction system containing 10 μ l cDNA, 2 μ l 10 mM dNTP, 2.5 μ l 10 \times buffer, 2.5 μ l 25 mmol \cdot L⁻¹ MgCl₂, 2 μ l specific primer, 5 μ l water and 1 μ l Taq. IL-12R β_1 and IL-12R β_2 were amplified using specific primer for IL-12R β_1 ^[24] and IL-12R β_2 ^[25]. Specific primers for GAPDH^[26] were also used for control. Thermal cycling of IL-12R β_1 and IL-12R β_2 and GAPDH primers were performed as follows^[25]: denaturation at 94 $^{\circ}$ C for 1 min, annealing at 55 $^{\circ}$ C for 1 min, and extension at 72 $^{\circ}$ C for 1 min, all cycling were performed for 35 cycles. The predicted PCR product size were 331 bp for IL-12R β_1 , 1 200 bp for IL-12R β_2 and 576 bp for GAPDH. PCR products of each sample were subjected to electrophoresis in a 15g \cdot L⁻¹ agarose gel containing 0.5 mg \cdot L⁻¹ ethidium bromide. Densitometrical analysis using NIH image software was performed for semiquantification of PCR products, and the expression level of each sample were expressed by IL-12R mRNA/GAPDH mRNA (%).

Western blotting for IL-12 protein expression in DCs

DCs cultured for 10 days *in vitro* were starved in serum-free medium for 4hr at 37 $^{\circ}$ C. These cells were washed twice in cold PBS, resuspended in 100 μ l lysis buffer (1 % Nonidet P-40, 20mM Tris-HCl, pH8.0, 137mM NaCl, 10 % glycerol, 2mM EDTA, 10 μ g/ml leupeptin, 10 μ g/ml aprotinin, 1mM PMSF, and 1 mM sodium orthovanadate), and total cell lysates were obtained. The homogenates were centrifuged at 10 000 \times g for 10 min at 4 $^{\circ}$ C. Cell lysates (20 μ g) were electrophoresed on SDS-PAGE gels, and transferred to PVDC membranes for Western blot analysis. Briefly, PVDC membranes were incubated in a blocking buffer for 1 hr at room temperature, then incubated for 2 hr with Abs raised against IL-12 p35 (M-19, goat anti-rat, Santa Cruz, CA), IL-12p40 (H-306, rabbit anti-rat, Santa Cruz, CA). The membranes were washed and incubated for 1 hr with HRP-labeled horse anti-goat or HRP-labeled goat anti-rabbit IgG. Immunoreactive bands were visualized by ECL detection reagent.

Statistics

Statistic analysis of data was performed using the Student's *t*-test; $P < 0.05$ was considered statistically significant.

RESULTS

Histological rejection

Histology features of allografted livers were compared between the whole and partial groups on Day 4 after transplantation, allogeneic whole liver grafts demonstrated no rejection. In contrast, partial liver grafts demonstrated moderate to severe rejection, including inflammatory cellular infiltration in the portal tract, and endothelialitis and bile duct damage.

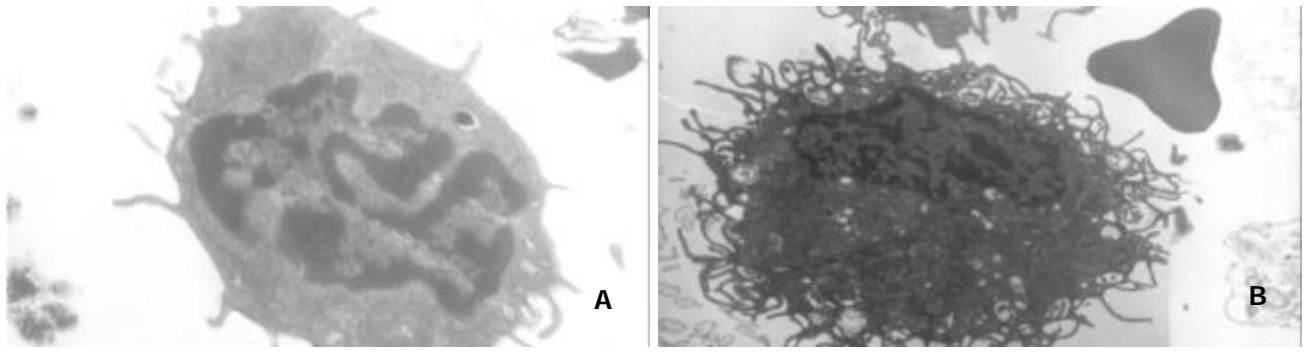


Figure 1 Morphological characteristics of liver graft-derived DCs propagated for 4 days in the presence of GM-CSF. **A:** DC from whole liver graft 4 days after transplantation ($\times 1\ 200$ b). **B:** DC from partial liver graft 4 days after transplantation ($\times 600$ b).

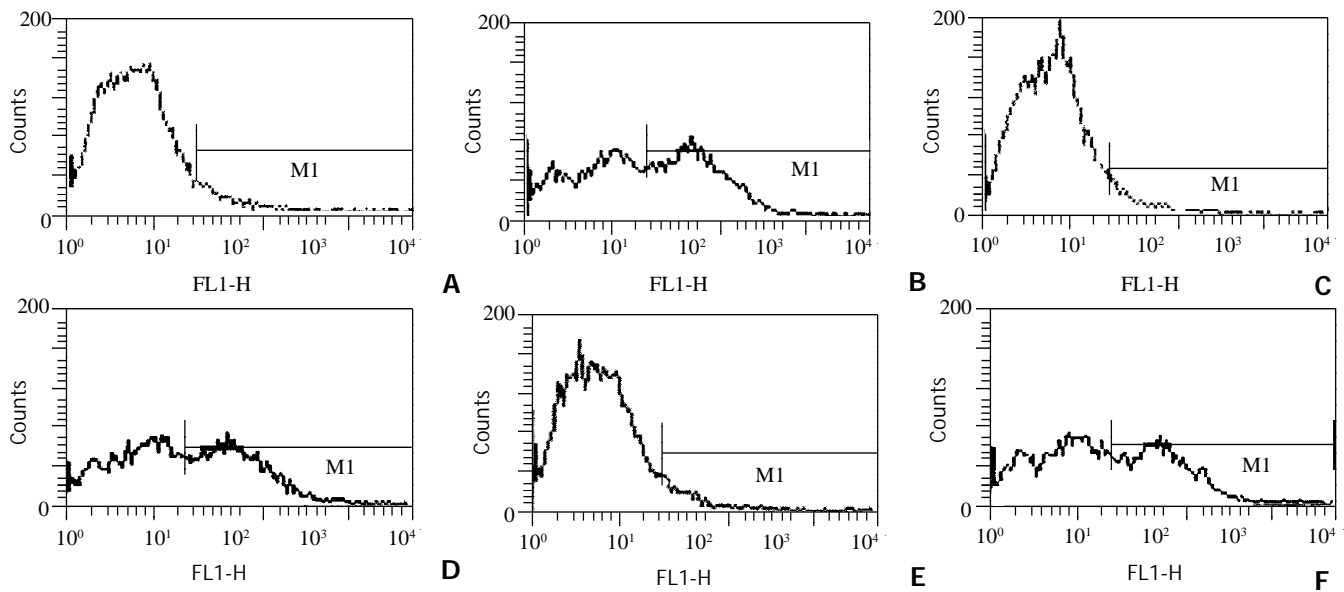


Figure 2 Expression of costimulatory molecules in DCs from liver grafts 4 days after transplantation by FCM. **A:** Expression of CD40 in whole liver graft-derived DCs; **B:** Expression of CD40 in partial liver graft-derived DCs; **C:** Expression of CD80 in whole liver graft-derived DCs; **D:** Expression of CD80 in partial liver graft-derived DCs; **E:** Expression of CD86 in whole liver graft-derived DCs; **F:** Expression of CD86 in partial liver graft-derived DCs.

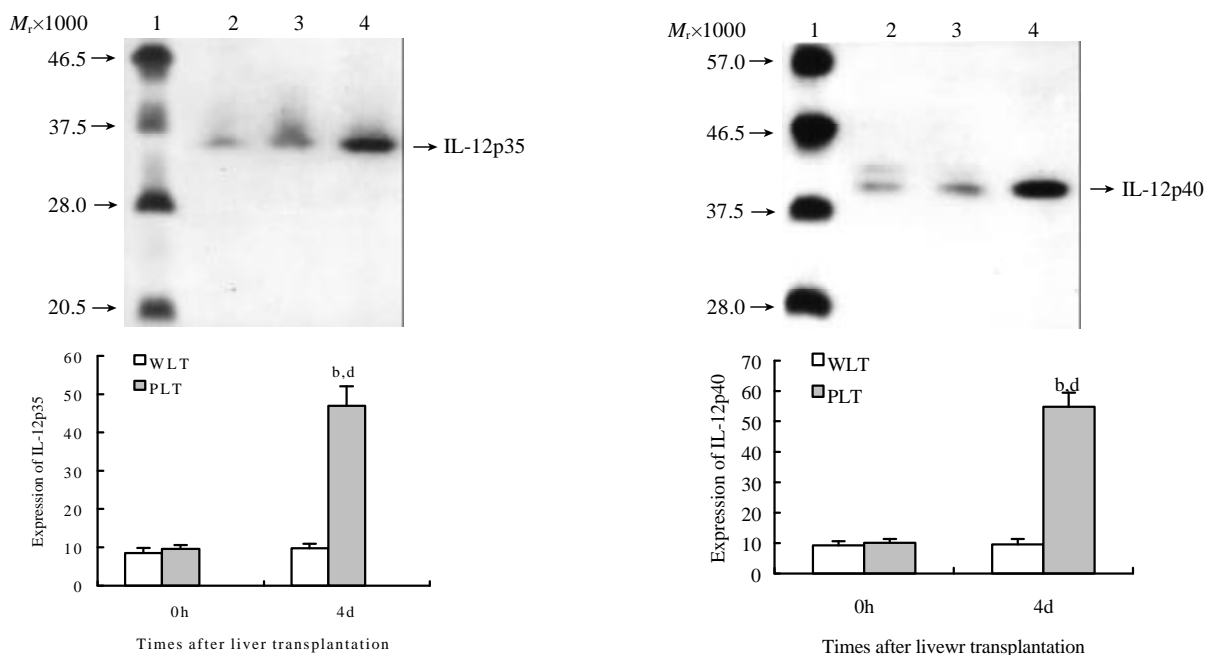


Figure 3 Detection of IL-12 proteins in liver graft-derived DCs by Western blotting. Lanes 1: protein marker. Lanes 2-4: extracts derived from DCs from liver graft 0 h after transplantation, whole liver graft (WLT) and partial liver graft (PLT) 4 days after transplantation, respectively. Compared with 4 d WLT group, ^b $P < 0.001$; Compared with 0 h PLT group, ^d $P < 0.001$.

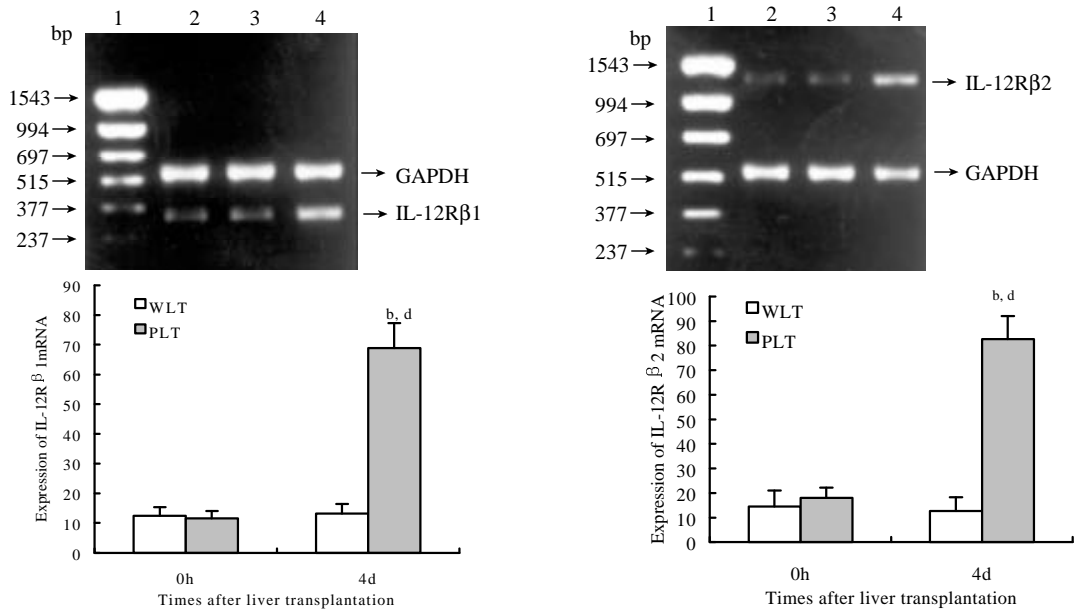


Figure 4 Detection of IL-12 R mRNA in liver graft-derived DCs by RT-PCR. Lanes 1: marker; Lanes 2- 4: extracts derived from DCs from liver graft 0 h after transplantation, whole liver graft (WLT) and partial liver graft (PLT) 4 days after transplantation, respectively. Compared with 4 d WLT group, ^b $P < 0.001$; Compared with 0 h PLT group, ^d $P < 0.001$.

Phenotypic characteristics of liver graft-derived DCs propagated *in vitro*

After 4 days' culture in the presence of GM-CSF, liver graft-derived DCs were observed with electron microscopy, DCs from whole liver grafts 0 hr and 4 days after transplantation exhibited round shape, smaller body, bigger nucleus, and a few shorter dendrites, whereas DCs derived from partial liver graft 4 days after transplantation displayed typical morphological features of DC including anomalous shape, bigger body, and numerous longer dendrites (as shown in Figure 1). Flow cytometry showed 80-85 % of DCs both from whole and partial liver grafts strongly expressed rat DC-specific OX62 antigen molecule (as shown in Table 1), which was suggested high purity DCs were obtained. After 10 day' culture in the presence of GM-CSF, although DCs both from whole and partial liver grafts exhibited typical morphological features of DC by electron microscopy, flow cytometric analysis showed (as shown in Figure 2 and Table 1) whole liver graft-derived DCs displayed low amounts of costimulatory molecules (CD40, CD80 and CD86), whereas DCs from partial liver graft 4 days after transplantation expressed moderate to high levels of these markers. These results suggested allogeneic partial liver transplant could promote maturation of DCs derived from partial liver graft.

Table 1 Comparison of expression of DC surface markers from whole liver graft and partial liver graft ($\bar{x} \pm s$, $n=13$)

Groups	OX62	CD40	CD80	CD86
Whole liver graft-DC	85.63±3.81	7.24±1.87	6.58±2.39	7.01±2.54
Partial liver graft-DC	88.42±5.75	50.18±3.26 ^b	45.31±3.67 ^b	43.29±2.03 ^b

^b $P < 0.001$ vs whole liver graft-DC

IL-12 protein expression in liver graft-derived DCs

To investigate the functional change of DCs derived from liver grafts, we evaluated IL-12 protein expression in these DCs. As shown in Figure 3, DCs derived from both whole and liver grafts 0 hr after transplantation expressed detectable but low levels of IL-12 p35 and IL-12 p40, and expression levels of

IL-12 p35 and IL-12 p40 in DCs from whole liver graft 4 days after transplantation were similar to those of DCs from whole liver graft 0 hr after transplantation ($P > 0.05$). However, expression of IL-12 p35 and IL-12 p40 in DCs from partial liver graft 4 days after transplantation was markedly increased, and their expression levels were significantly higher than those of DCs both from partial liver graft 0 hr and whole liver graft 4 days after transplantation ($P < 0.001$).

IL-12R mRNA expression in liver graft-derived DCs

As shown in Figure 4, semiquantitative RT-PCR analysis revealed detectable but low levels of IL-12R β_1 and IL-12R β_2 mRNA expression in DCs both from whole and partial liver grafts 0 hr after transplantation, expression levels of IL-12R β_1 and IL-12R β_2 mRNA in DCs from whole liver graft 4 days after transplantation were not markedly changed compared with those of DCs from whole liver graft 0 hr after transplantation ($P > 0.05$). Whereas DCs from partial liver graft 4 days after transplantation expressed higher levels of IL-12R β_1 mRNA and IL-12R β_2 mRNA, and their expression levels were markedly higher than those of DCs both derived from partial liver graft 0 hr and whole liver graft 4 days after transplantation ($P < 0.001$).

DISCUSSION

DCs play critical roles in the initiation and modulation of immune responses^[27-34]. After vascularized organ transplantation, donor passenger leukocytes (mainly interstitial DCs) are mobilized out of the graft via peripheral blood to the recipient lymphoid and nonlymphoid tissues^[35-39]. Maturation of donor DC from thyroid, pancreatic islet, skin, or kidney allografts in recipient lymphoid organs lead to the activation of naive, alloreactive Th0 lymphocytes, and thus provides the primary stimulus for acute allograft rejection. However, in mouse and certain rat strain combinations, fully MHC-mismatched liver allografts accepted without any of immune suppression, and fail to elicit an effective rejection response^[38,39]. Moreover, in humans, the liver is considered the least immunogenic of transplanted whole organs. In a tolerant rat strain combination, depletion of interstitial leukocytes from liver by pretransplant donor radiation prevents the tolerogenic effect, and results in acute rejection^[40]. On the other hand, it has been reported that

immature, costimulatory molecule-deficient DCs (such as normal liver or bone marrow-derived DCs) propagated *in vitro* can promote graft survival in allogeneic recipients^[14,41,42], and posttransplant administration of donor leukocytes induces long-term acceptance of liver transplants^[43].

Therefore, passenger leukocytes (most likely DCs) may have a dualistic role with potential to elicit T cell activation and graft rejection, or induce T cell tolerance and graft acceptance. The sustained release from the transplanted liver of immature DCs, may contribute to allogeneic liver graft tolerance induction. These liver-derived DCs migrate *in vivo* to T cells areas of secondary lymphoid tissue, where they persisted for weeks in allogeneic recipients^[18, 44]. It is accepted that alloantigen-specific Th1 cells initiate allograft rejection, and that Th2 cells exert an inhibitory influence on the development of Th1 clones. It has been proposed that preferential induction of alloantigen-specific Th2 lymphocytes could suppress the development of Ag-specific Th1 cells, and as a consequence, inhibit allograft rejection. Liver-derived DCs might induce the proliferation of Th2 clones with capacity to inhibit Th1 responses^[18]. Liver-derived DCs display an immature phenotype with absence of costimulatory molecules (CD40, CD80 and CD86) surface expression, low levels of MHC class I and II, and as a consequence, low stimulatory capacity for naive allogeneic T cells. Unlike mature DC, these liver-derived DCs do not induce detectable levels of intracytoplasmic IFN- γ in allogeneic CD4⁺ cells in 72-h MLR, and elicited very low levels of CTLs *in vitro*^[3,13,18]. In contrast, acute liver graft rejection would be induced by maturation of liver grafts derived-DCs^[20]. These findings point to a pivotal role for donor immature or mature DCs in determining the outcome of liver transplantation. Mature DCs express high levels of costimulatory molecules such as CD40, CD80 and CD86. Activation of T cells by mature DCs has been shown to require direct contact between T cells and DCs through CD40-CD40L interaction^[45], upon ligation of CD40L on T cells with CD40 on DCs, DCs are triggered to produce even high quantities of IL-12, thus consigning T cells to Th1 responses^[46].

IL-12 is an important immune regulator produced primarily by DCs and macrophages that drives the preferential induction of Th1 immune responses. IL-12 appears to be a central mediator of acute graft-vs-host disease in mice^[47], whereas neutralization of bioactive IL-12 enhances allogeneic myoblast survival^[48]. Moreover, exogenous IL-12 mediates liver allograft rejection^[49], and IL-12 antagonism could promote liver graft tolerance^[19]. IL-12 binds to a unique, high affinity receptor on activated Th cells and NK cells, enhances the expression of antiapoptotic factors (bcl₂ and bcl_{xl}), and facilitates activated T cell and NK-lymphokine activated killer cell expansion. IL-12 indirectly promotes Th1 and inhibits Th2 development by inducing the secretion of IFN- γ by Th1 and NK cells^[19, 50-54]. Recent investigation showed IL-12 also induce autologous IL-12 production of DC by interaction with IL-12 receptor^[25]. Previous studies have shown that IL-12R is detected in T cells and NK cells, and IL-12R plays a crucial role for IL-12 mediated activation of these cell types^[25, 55-60]. IL-12R β_1 is the subunit primarily responsible for binding IL-12, and IL-12R β_2 plays an essential role in mediating the biological functions of IL-12. IL-12-induced phosphorylation of STAT4 and IFN- γ production are absent in Con A and anti-CD3-activated splenocytes from IL-12R β_2 ^{-/-} mice^[56]. Recent investigations suggested that DCs exhibited expression of IL-12R β_1 and IL-12R β_2 ^[25,61-66], and mature DCs express high level of IL-12R β_1 and IL-12R β_2 ^[25,64].

Although Omura T *et al*^[1] and Shiraishi M *et al*^[2] reported that allogeneic partial liver grafts exhibited increased immune response compared with allogeneic whole liver grafts as early as 3 days after transplantation, little is known about the exact

mechanism responsible for the accelerated rejection. In the present study, accelerated rejection was demonstrated in allogeneic partial liver graft 4 days after transplantation. Our results first demonstrated that DCs derived from allogeneic whole liver graft without acute rejection 4 days after transplantation exhibited an immature phenotype with absence of CD40, CD80 and CD86 surface expression, and low expression of IL-12 proteins (IL-12 p35 and IL-12 p40) and IL-12 receptor (IL-12R β_1 and IL-12R β_2) mRNA. In contrast with immature DCs derived from whole liver graft, DCs derived from partial liver graft undergoing acute rejection 4 days after transplantation displayed a mature phenotype with high level of CD40, CD80 and CD86 surface expression, and as a consequence, high level expression of IL-12 proteins (IL-12 p35 and IL-12 p40) and IL-12 receptors (IL-12R β_1 and IL-12R β_2) mRNA. Given immature DCs can induce T-cell hyporesponsiveness^[13-15] and immune reactivity inhibition^[16,17], whereas mature DCs can stimulate Th1 response and the development of alloantigen-specific CTLs^[3-7,27-34], together with IL-12 is an important inducer of liver graft rejection, we suggest that maturation of liver graft-derived DCs may be an important mechanism of the accelerated rejection of allogeneic partial liver graft, and inhibition of maturation of liver graft-derived DCs may suppress rejection of allogeneic partial liver graft.

REFERENCES

- 1 **Omura T**, Nakagawa T, Randall HB, Lin Z, Huey M, Ascher NL, Emond JC. Increased immune responses to regenerating partial liver grafts in the rat. *J Surg Res* 1997; **70**: 34-40
- 2 **Shiraishi M**, Csete ME, Yasunaga C, Drazan KE, Jurim O, Cramer DV, Busuttill RW, Shaked A. Regeneration-induced accelerated rejection in reduced-size liver grafts. *Transplantation* 1994; **57**: 336-340
- 3 **Morelli AE**, O'Connell PJ, Khanna A, Logar AJ, Lu LN, Thomson AW. Preferential induction of Th1 responses by functionally mature hepatic (CD8 α and CD8 α^+) dendritic cells. *Transplantation* 2000; **69**: 2647-2657
- 4 **Mehling A**, Grabbe S, Voskort M, Schwarz T, Luger TA, Beissert S. Mycopheolate mofetil impairs the maturation and function of murine dendritic cells. *J Immunol* 2000; **165**: 2374-2381
- 5 **Stuart LM**, Lucas M, Simpson C, Lamb J, Savill J, Lacy HA. Inhibitory effects of apoptotic cell ingestion upon endotoxin-driven myeloid dendritic cell maturation. *J Immunol* 2002; **168**: 1627-1635
- 6 **Ismaili J**, Rennesson J, Aksoy E, Vekemans J, Vincart B, Amraoui Z, Van Laethem F, Goldman M, Dubois PM. Monophosphoryl lipid A activates both human dendritic cells and T cells. *J Immunol* 2002; **168**: 926-932
- 7 **Sato K**, Nagayama H, Enomoto M, Tadokoro K, Juji T, Takahashi TA. Autocrine activation-induced cell death of T cells by human peripheral blood monocyte-derived CD4⁺ dendritic cells. *Cellular Immunology* 2000; **199**: 115-125
- 8 **Zheng H**, Dai J, Stoilova D, Li Z. Cell surface targeting of heat shock protein gp96 induces dendritic cell maturation and antitumor immunity. *J Immunol* 2001; **167**: 6731-6735
- 9 **Morel Y**, Truneh A, Sweet RW, Olive D, Costello RT. The TNF superfamily members LIGHT and CD154 (CD40 ligand) costimulate induction of dendritic cell maturation and elicit specific CTL activity. *J Immunol* 2001; **167**: 2479-2486
- 10 **Kobayashi M**, Azuma E, Ido M, Hirayama M, Jiang Q, Iwamoto S, Kumamoto T, Yamamoto H, Sakurai M, Komada Y. A pivotal role of Rho GTPase in the regulation of morphology and function of dendritic cells. *J Immunol* 2001; **167**: 3585-3591
- 11 **Hertz CJ**, Kiertscher SM, Godowski PJ, Bouis DA, Norgard MV, Roth MD, Modlin RL. Microbial lipopeptides stimulate dendritic cell maturation via Toll-like receptor 2. *J Immunol* 2001; **166**: 2444-2450
- 12 **Thoma-Uszynski S**, Kiertscher SM, Ochoa MT, Bouis DA, Norgard MV, Miyake K, Godowski PJ, Roth MD, Modlin RL. Activation of toll-like receptor 2 on human dendritic cells triggers induction of IL-12, but not IL-10. *J Immunol* 2000; **165**: 3804-3810

- 13 **Khanna A**, Morelli AE, Zhong CP, Takayama T, Lu LN, Thomson AW. Effects of liver-derived dendritic cell progenitors on Th1- and Th2-like cytokine responses *in vitro* and *in vivo*. *J Immunol* 2000; **164**: 1346-1354
- 14 **Hirano A**, Luke PP, Specht SM, Fraser MO, Takayama T, Lu L, Hoffman R, Thomson AW, Jordan ML. Graft hyporeactivity induced by immature donor-derived dendritic cells. *Transpl Immunol* 2000; **8**: 161-168
- 15 **Lee WC**, Zhong C, Qian S, Wan Y, Gauldie J, Mi Z, Robbins PD, Thomson AW, Lu L. Phenotype, function, and *in vivo* migration and survival of allogeneic dendritic cell progenitors genetically engineered to express TGF-beta. *Transplantation* 1998; **66**: 1810-1817
- 16 **Hayamizu K**, Huie P, Sibley RK, Strober S. Monocyte-derived dendritic cell precursors facilitate tolerance to heart allografts after total lymphoid irradiation. *Transplantation* 1998; **66**: 1285-1291
- 17 **Khanna A**, Steptoe RJ, Antonysamy MA, Li W, Thomson AW. Donor bone marrow potentiates the effect of tacrolimus on nonvascularized heart allograft survival: association with microchimerism and growth of donor dendritic cell progenitors from recipient bone marrow. *Transplantation* 1998; **65**: 479-485
- 18 **Lu L**, Woo J, Rao AS, Li Y, Watkins SC, Qian S, Starzl TE, Demetris AJ, Thomson AW. Propagation of dendritic cell progenitors from normal mouse liver using granulocyte/macrophage colony-stimulating factor and their maturational development in the presence of type-1 collagen. *J Exp Med* 1994; **179**: 1823-1834
- 19 **Li W**, Lu L, Wang Z, Wang L, Fung JJ, Thomson AW, Qian S. IL-12 antagonism enhances apoptotic death of T cells within hepatic allografts from Flt3 ligand-treated donors and promotes graft acceptance. *J Immunol* 2001; **166**: 5619-5628
- 20 **Steptoe RJ**, Fu F, Li W, Drakes ML, Lu L, Demetris AJ, Qian S, McKenna HJ, Thomson AW. Augmentation of dendritic cells in murine organ donors by Flt3 ligand alters the balance between transplant tolerance and immunity. *J Immunol* 1997; **159**: 5483-5491
- 21 **Kamada N**, Calne RY. A surgical experience with five hundred thirty liver transplantation in the rat. *Surgery* 1983; **93**: 64-69
- 22 **Knoop M**, Bachmann S, Keck H, Steffen R, Neuhaus P. Experience with cuff rearterialization in 600 orthotopic liver grafts in the rat. *Am J Surg* 1994; **167**: 360-363
- 23 **Uchiyama H**, Yanaga K, Nishizaki T, Soejima Y, Yoshizumi T, Sugimachi K. Effects of deletion variant of hepatocyte growth factor on reduced-size liver transplantation in rats. *Transplantation* 1999; **68**: 39-44
- 24 **Collison K**, Saleh S, Parhar R, Meyer B, Kwaasi A, Al-Hussein K, Al-Sedairy S, Al-Mohanna F. Evidence for IL-12-activated Ca²⁺ and tyrosine signaling pathways in human neutrophils. *J Immunol* 1998; **161**: 3737-3745
- 25 **Nagayama H**, Sato K, Kawasaki H, Enomoto M, Morimoto C, Tadokoro K, Juji T, Asano S, Takahashi TA. IL-12 responsiveness and expression of IL-12 receptor in human peripheral blood monocyte-derived dendritic cells. *J Immunol* 2000; **165**: 59-66
- 26 **Vos TA**, Hooiveld GJ, Koning H, Childs S, Meijer DK, Moshage H, Jansen PL, Muller M. Up-regulation of the multidrug resistance genes, Mrp1 and Mdr1b, and down-regulation of the organic anion transporter, Mrp2, and the bile salt transporter, Spgp, in endotoxemic rat liver. *Hepatology* 1998; **28**: 1637-1644
- 27 **Zhang JK**, Chen HB, Sun JL, Zhou YQ. Effect of dendritic cells on LPAK cells induced at different times in killing hepatoma cells. *Shijie Huaren Xiaohua Zazhi* 1999; **7**: 673-675
- 28 **Li MS**, Yuan AL, Zhang WD, Chen XQ, Tian XH, Piao YJ. Immune response induced by dendritic cells induce apoptosis and inhibit proliferation of tumor cells. *Shijie Huaren Xiaohua Zazhi* 2000; **8**: 56-58
- 29 **Luo ZB**, Luo YH, Lu R, Jin HY, Zhang PB, Xu CP. Immunohistochemical study on dendritic cells in gastric mucosa of patients with gastric cancer and precancerous lesions. *Shijie Huaren Xiaohua Zazhi* 2000; **8**: 400-402
- 30 **Li MS**, Yuan AL, Zhang WD, Liu SD, Lu AM, Zhou DY. Dendritic cells *in vitro* induce efficient and special anti-tumor immune response. *Shijie Huaren Xiaohua Zazhi* 1999; **7**: 161-163
- 31 **Wang FS**, Xing LH, Liu MX, Zhu CL, Liu HG, Wang HF, Lei ZY. Dysfunction of peripheral blood dendritic cells from patients with chronic hepatitis B virus infection. *World J Gastroenterol* 2001; **7**: 537-541
- 32 **Zhang JK**, Li J, Chen HB, Sun JL, Qu YJ, Lu JJ. Antitumor activities of human dendritic cells derived from peripheral and cord blood. *World J Gastroenterol* 2002; **8**: 87-90
- 33 **Tang ZH**, Qiu WH, Wu GS, Yang XP, Zou SQ, Qiu FZ. The immunotherapeutic effect of dendritic cells vaccine modified with interleukin-18 gene and tumor cell lysate on mice with pancreatic carcinoma. *World J Gastroenterol* 2002; **8**: 908-912
- 34 **Zhang J**, Zhang JK, Zhuo SH, Chen HB. Effect of a cancer vaccine prepared by fusions of hepatocarcinoma cells with dendritic cells. *World J Gastroenterol* 2001; **7**: 690-694
- 35 **Maestroni GJ**. Dendritic cell migration controlled by alpha 1b-adrenergic receptors. *J Immunol* 2000; **165**: 6743-6747
- 36 **Qian S**, Demetris AJ, Murase N, Rao AS, Fung JJ, Starzl TE. Murine liver allograft transplantation: tolerance and donor cell chimerism. *Hepatology* 1994; **19**: 916-924
- 37 **Thomson AW**, Lu L, Murase N, Demetris AJ, Rao AS, Starzl TE. Microchimerism, dendritic cell progenitors and transplantation tolerance. *Stem Cells* 1995; **13**: 622-639
- 38 **Jonsson JR**, Hogan PG, Thomas R, Steadman C, Clouston AD, Balderson GA, Lynch SV, Strong RW, Powell EE. Peripheral blood chimerism following human liver transplantation. *Hepatology* 1997; **25**: 1233-1236
- 39 **Spriewald BM**, Wassmuth R, Carl HD, Kockerling F, Reichstetter S, Kleeburger A, Klein M, Hohenberger MW, Kalden JR. Microchimerism after liver transplantation: prevalence and methodological aspects of detection. *Transplantation* 1998; **66**: 77-83
- 40 **Sun J**, McCaughan GW, Gallagher ND, Sheil AG, Bishop GA. Deletion of spontaneous rat liver allograft acceptance by donor irradiation. *Transplantation* 1995; **60**: 233-236
- 41 **Rastellini C**, Lu L, Ricordi C, Starzl TE, Rao AS, Thomson AW. Granulocyte/macrophage colony-stimulating factor-stimulated hepatic dendritic cell progenitors prolong pancreatic islet allograft survival. *Transplantation* 1995; **60**: 1366-1370
- 42 **Gao JX**, Madrenas J, Zeng W, Cameron MJ, Zhang Z, Wang JJ, Zhong R, Grant D. CD40-deficient dendritic cells producing interleukin-10, but not interleukin-12, induce T-cell hyporesponsiveness *in vitro* and prevent acute allograft rejection. *Immunology* 1999; **98**: 159-170
- 43 **Yan Y**, Shastry S, Richards C, Wang C, Bowen DG, Sharland AF, Painter DM, McCaughan GW, Bishop GA. Posttransplant administration of donor leukocytes induces long-term acceptance of kidney or liver transplants by an activation-associated immune mechanism. *J Immunol* 2001; **166**: 5258-5264
- 44 **Thomson AW**, Lu L, Subbotin VM, Li Y, Qian S, Rao AS, Fung JJ, Starzl TE. In vitro propagation and homing of liver-derived dendritic cell progenitors to lymphoid tissues of allogeneic recipients. Implications for the establishment and maintenance of donor cell chimerism following liver transplantation. *Transplantation* 1995; **59**: 544-551
- 45 **Kitamura H**, Iwakabe K, Yahata T, Nishimura SI, Ohta A, Ohmi Y, Sato M, Takeda K, Okumura K, Van Kaer L, Kawano T, Taniguchi M, Nishimura T. The natural killer T (NKT) cell ligand α -galactosylceramide demonstrates its immunopotentiating effect by inducing interleukin (IL)-12 production by dendritic cells and IL-12 receptor expression on NKT cells. *J Exp Med* 1999; **189**: 1121-1127
- 46 **Cella M**, Scheidegger D, Palmer-Lehmann K, Lane P, Lanzavecchia A, Alber G. Ligation of CD40 on dendritic cells triggers production of high levels of interleukin-12 and enhances T cell stimulatory capacity: T-T help via APC activation. *J Exp Med* 1996; **184**: 747-752
- 47 **Williamson E**, Garside P, Bradley JA, Mowat AM. IL-12 is a central mediator of acute graft-versus-host disease in mice. *J Immunol* 1996; **157**: 689-699
- 48 **Kato K**, Shimozato O, Hoshi K, Wakimoto H, Hamada H, Yagita H, Okumura K. Local production of the p40 subunit of interleukin 12 suppresses T-helper 1-mediated immune responses and prevents allogeneic myoblast rejection. *Proc Natl Acad Sci USA* 1996; **93**: 9085-9089
- 49 **Thai NL**, Li Y, Fu F, Qian S, Demetris AJ, Duquesnoy RJ, Fung JJ. Interleukin-2 and interleukin-12 mediate distinct effector mechanisms of liver allograft rejection. *Liver Transpl Surg* 1997; **3**: 118-129
- 50 **Heuffer C**, Koch F, Stanzl U, Topar G, Wysocka M, Trinchieri G, Enk A, Steinman RM, Romani N, Schuler G. Interleukin-12 is

- produced by dendritic cells and mediates T helper 1 development as well as interferon-gamma production by T helper 1 cells. *Eur J Immunol* 1996; **26**: 659-668
- 51 **Shibuya K**, Robinson D, Zonin F, Hartley SB, Macatonia SE, Somoza C, Hunter CA, Murphy KM, O'Garra A. IL-1 alpha and TNF- α are required for IL-12-induced development of Th1 cells producing high levels of IFN- γ in BALB/c but not C57BL/6 mice. *J Immunol* 1998; **160**: 1708-1716
- 52 **Sin JI**, Kim JJ, Arnold RL, Shroff KE, McCallus D, Pachuk C, McElhiney SP, Wolf MW, Pompa-de Bruin SJ, Higgins TJ, Ciccarelli RB, Weiner DB. IL-12 gene as a DNA vaccine adjuvant in a herpes mouse model: IL-12 enhances Th1-type CD4⁺ T cell-mediated protective immunity against herpes simplex virus-2 challenge. *J Immunol* 1999; **162**: 2912-2921
- 53 **Bhardwaj N**, Seder RA, Reddy A, Feldman MV. IL-12 in conjunction with dendritic cells enhances antiviral CD8⁺ CTL responses *in vitro*. *J Clin Invest* 1996; **98**: 715-722
- 54 **Schmidt CS**, Mescher MF. Adjuvant effect of IL-12: conversion of peptide antigen administration from tolerizing to immunizing for CD8⁺ T cells *in vivo*. *J Immunol* 1999; **163**: 2561-2567
- 55 **Kim J**, Uyemura K, Van Dyke MK, Legaspi AJ, Rea TH, Shuai K, Modlin RL. A role for IL-12 receptor expression and signal transduction in host defense in leprosy. *J Immunol* 2001; **167**: 779-786
- 56 **Wu CY**, Wang X, Gadina M, O' Shea JJ, Presky DH, Magram J. IL-12 receptor β 2 (IL-12R β 2)-deficient mice are defective in IL-12-mediated signaling despite the presence of high affinity IL-12 binding sites. *J Immunol* 2000; **165**: 6221-6228
- 57 **Wang KS**, Frank DA, Ritz J. Interleukin-2 enhances the response of natural killer cells to interleukin-12 through up-regulation of the interleukin-12 receptor and STAT4. *Blood* 2000; **95**: 3183-3190
- 58 **Chang JT**, Shevach EM, Segal BM. Regulation of interleukin (IL)-12 receptor β 2 subunit expression by endogenous IL-12: a critical step in the differentiation of pathogenic autoreactive T cells. *J Exp Med* 1999; **189**: 969-978
- 59 **Kawashima T**, Kawasaki H, Kitamura T, Nojima Y, Morimoto C. Interleukin-12 induces tyrosine phosphorylation of an 85-kDa protein associated with the interleukin-12 receptor β 1 subunit. *Cell Immunol* 1998; **186**: 39-44
- 60 **Lawless VA**, Zhang S, Ozes ON, Bruns HA, Oldham I, Hoey T, Grusby MJ, Kaplan MH. Stat4 regulates multiple components of IFN- γ -inducing signaling pathways. *J Immunol* 2000; **165**: 6803-6808
- 61 **Ohteki T**, Fukao T, Suzue K, Maki C, Ito M, Nakamura M, Koyasu S. Interleukin 12-dependent interferon γ production by CD8 α ⁺ lymphoid dendritic cells. *J Exp Med* 1999; **189**: 1981-1986
- 62 **Fukao T**, Matsuda S, Koyasu S. Synergistic effects of IL-4 and IL-18 on IL-12-dependent IFN-gamma production by dendritic cells. *J Immunol* 2000; **164**: 64-71
- 63 **Fukao T**, Frucht DM, Yap G, Gadina M, O' Shea JJ, Koyasu S. Inducible expression of Stat4 in dendritic cells and macrophages and its critical role in innate and adaptive immune responses. *J Immunol* 2001; **166**: 4446-4455
- 64 **Fukao T**, Koyasu S. Expression of functional IL-2 receptors on mature splenic dendritic cells. *Eur J Immunol* 2000; **30**: 1453-1457
- 65 **Grohmann U**, Belladonna ML, Bianchi R, Orabona C, Ayroldi E, Fioretti MC, Puccetti P. IL-12 acts directly on DC to promote nuclear localization of NF- κ B and primes DC for IL-12 production. *Immunity* 1998; **9**: 315-323
- 66 **Grohmann U**, Bianchi R, Belladonna ML, Vacca C, Silla S, Ayroldi E, Fioretti MC, Puccetti P. IL-12 acts selectively on CD8 α dendritic cells to enhance presentation of a tumor peptide *in vivo*. *J Immunol* 1999; **163**: 3100-3105

Edited by Zhang JZ

Cloning and analyzing the up-regulated expression of transthyretin-related gene (LR_1) in rat liver regeneration following short interval successive partial hepatectomy

Cun-Shuan Xu, Yu-Chang Li, Jun-Tang Lin, Hui-Yong Zhang, Yun-Han Zhang

Cun-Shuan Xu, Yu-Chang Li, Jun-Tang Lin, Hui-Yong Zhang,
College of Life Science, Henan Normal University, Xinxiang 453002,
Henan Province, China

Yun-Han Zhang, Henan Key Laboratory for Tumor Pathology,
Zhengzhou, 450052, Henan Province, China

Supported by grants from National Natural Science Foundation of
China, No. 39970362; Tackle Key of Scientific and Technical Problem
of Henan Province, No. 0122031900

Correspondence to: Prof. Dr. Cun-Shuan Xu, College of Life
Science, Henan Normal University, Xinxiang, 453002, Henan
Province, China. xucs@x263.net

Telephone: +86-373-3326341/3326609 **Fax:** +86-373-3326524

Received: 2002-03-12 **Accepted:** 2002-04-20

Abstract

AIM: Cloning and analyzing the up-regulated expression of transthyretin-related gene following short interval successive partial hepatectomy (SISPH) to elucidate the mechanism of differentiation, division, dedifferentiation and redifferentiation in rat liver regeneration (LR).

METHODS: Lobus external sinister and lobus centralis sinister, lobus centralis, lobus dexter, lobus candatus were removed one by one from rat liver at four different time points 4, 36, 36 and 36 hr (total time: 4 hr, 40 hr, 76 hr, 112 hr) respectively. Suppression subtractive hybridization (SSH) was carried out by using normal rat liver tissue as driver and the tissue following short interval successive partial hepatectomy (SISPH) as tester to construct a highly efficient forward-subtractive cDNA library. After screening, an interested EST fragment was selected by SSH and primers were designed according to the sequence of the EST to clone the full-length cDNA fragment using RACE (rapid amplification of cDNA end). Homologous detection was performed between the full-length cDNA and Genbank.

RESULTS: Forward suppression subtractive hybridization (FSSH) library between 0 h and 112 h following SISPH was constructed and an up-regulated full-length cDNA (named LR_1), which was related with the transthyretin gene, was cloned by rapid amplification of cDNA end. It was suggested that the gene is involved in the cellular dedifferentiation in LR following SISPH.

CONCLUSION: Some genes were up-regulated in 112 h following SISPH in rat. LR_1 is one of these up-regulated expression genes which may play an important role in rat LR.

Xu CS, Li YC, Lin JT, Zhang HY, Zhang YH. Cloning and analyzing the up-regulated expression of transthyretin-related gene (LR_1) in rat liver regeneration following short interval successive partial hepatectomy. *World J Gastroenterol* 2003; 9 (1): 148-151

<http://www.wjgnet.com/1007-9327/9/148.htm>

INTRODUCTION

In mammals, liver is the only organ that possesses the strong capability of regeneration^[1-7]. Since Higgins and Anderson^[8] established the model of partial hepatectomy (PH), it has been widely used to study the reconstruction and regeneration of tissue and organs, cellular multiplication, dedifferentiation, stress response and the regulation of physiology and biochemistry^[8-16]. But due to the complexity of liver regeneration, the molecular mechanism of LR remains to be elucidated. In order to better understand the mechanism of PH, researchers have established a series of successive partial hepatectomy (SPH) models. These included the long interval successive partial hepatectomy (LISPH) that involved an interval of more than three weeks and short interval successive partial hepatectomy (SISPH) which had an interval of 4 and/or 36 hr^[17]. Because the hepatocytic initiation, dedifferentiation, division and redifferentiation mainly occurred within 144 hr following PH^[18-22]. It is doubtless that the study on the change of liver tissue, cellular morphology, structure, physiology and biochemistry in every crucial point following SISPH can offer more data about LR. In this paper, we used the normal liver tissue as control and the liver tissue in 112 hr SISPH as experimental materials, and adopted the whole-mount research strategy of genome and resorted to SSH technique to construct a differential expressed forward-subtracted cDNA library. From the library, we picked some significant expressed sequence tags (ESTs) clones. Then the primers were designed according to these ESTs. By RACE PCR, some full-length cDNAs were obtained. After sequencing these full-length cDNAs, it showed that one of them belonged to the gene of related transthyretin, termed LR_1 gene, which was up-regulated expression in LR.

MATERIALS AND METHODS

Making SISPH model and preparation of samples

Adult Spargue-Dawley rats (weighing 200-250 g) were provided by the experimental animal house of Henan Normal University and 0-4-36-36-36 hr SISPH model was made according to the method of Xu *et al*^[17]. Lobus external sinister and lobus centralis sinister, lobus centralis, lobus dexter, lobus candatus were removed one by one at four different time points 4, 36, 36 and 36 hr (total time: 4 hr, 40 hr, 76 hr, 112 hr) respectively. The control and the four resected liver hepatic lobus were washed with precooled phosphate-buffered saline (PBS) thoroughly before these samples were frozen in liquid nitrogen and transferred to the -80 °C freezer for storage.

Preparation of control mRNA and the 112 hr SISPH mRNA

Isolation of total RNA and mRNA was carried out according to the protocol of RNAease kit and oligotex mRNA spin column purification kit (Qiagen). The quantity and integrity of mRNA were detected by ultraviolet spectrometer and by electrophoresing on a denaturing formaldehyde agarose

stained by EtBr. Chemicals and reagents used were at least of analytical grade.

Generating of a subtracted cDNA library

SSH was performed between the aforementioned tester and driver liver tissue mRNA preparations using a PCR select™ cDNA subtraction kit and 50×PCR enzyme kit (Clontech, Heidelberg, Germany) following the instructions of the manufacturer. Briefly, 2 µg aliquots each of poly (A⁺) mRNA from the tester and the pooled driver were subjected to cDNA synthesis. Thereafter, the tester and driver cDNAs were digested with Rsa I. The tester cDNA was subdivided into two portions, and each was ligated with a different cDNA adaptor. In the first hybridization reaction, an excess of driver was added to each sample of tester. The samples were heat denatured and allowed to anneal. Due to the second-order kinetics of hybridization, the concentration of high- and low-abundance sequence is equalized among the single-stranded tester molecules. At the same time, single-stranded tester molecules are significantly enriched for differentially expressed sequences. During the second hybridization, the two primary hybridization samples were mixed together without denaturation, only the remaining equalized and subtracted single-stranded tester cDNAs can reassociate to form double-stranded tester molecules with different ends. After filling in the ends with DNA polymerase, the entire population of molecules was subjected to nested PCR with two adaptor-specific primer pairs. The tester control was amplified with primer1 and nested primer 1 and 2 provided in the kit. The subtraction efficiency was evaluated by house-keeping gene *g3pdh*.

Cloning the subtracted library into a TA vector

Products from the secondary PCR reactions were ligated into a pGEM-T vector (Promega) and the resultant ligation products were then transformed into JM109 *E. coli* competent cells. The bacterial were subsequently grown in 800 µl of liquid Luria-Bertani medium and allowed to incubate for 45 min at 37 °C with shaking at 150 rpm. Thereafter, the cells were plated onto agar plates containing ampicillin (50 µg/ml), 5-bromo-4-chloro-3-indolyl-β-D-galactoside (x-gal; 20 µg/cm²) and isopropyl-β-D-thiogalactoside (IPTG; 12.1 µg/cm²) and incubated overnight at 37 °C. Individual recombinant white clones were picked and grown in single line pattern onto Luria-Bertani agar solid medium containing ampicillin and allowed to incubate at 37 °C for 6-7 hr before single clone was picked from single-line pattern agar medium and allowed to grow in Luria-Bertani liquid medium containing ampicillin overnight at 37 °C with shaking of 150 rpm.

Identifying the subtracted clones

Plasmids were isolated from bacterial clones harboring differentially expressed cDNA sequences as described by Sambrook *et al.* Plasmids containing cDNA inserts were amplified by PCR with nested primer 1 and primer 2 and the amplified product of every plasmid was detected by agarose gel electrophoresis. After that, the inserts that appeared as distinct bands were sequenced by T7/SP6 chain termination reaction in TaKaRa (DaLian, China). Nucleic acid homology searches were subsequently performed at the National Center of Biotechnology Information (National Institutes of Health, Bethesda, Md., NCBI).

RACE

An interested EST fragment was chosen from the established cDNA library for primer design according to the instructions of the 5' /3' RACE kit (Roche) manufacturer. RACE, a procedure to amplify nucleic acid sequences from a mRNA template between a defined internal site and unknown

sequences at 5' -and 3' -end of mRNA, was then performed by using 5' /3' RACE kit and following the supplier's protocol. The primer used for 3' RACE was SP5: 5' -AGCTGGGAG CCGTTTGC-3' and the primer used for 5' RACE was SP1: 5' -TGCTGTAGGAGTACGGGCT-C3' , SP2: 5' -A C C A G A G T C A T T G G C T G T -3' , SP3: 5' -GCCCGTGCAGCTCT-3' respectively. Proofreading *pfu* DNA polymerase was purchased from MBI and the 3' RACE PCR parameters were: predenaturation at 94 °C for 2 min before amplification was done for 40 cycles at 94 °C for 45 sec, annealing at 65 °C for 1 min and extension at 72 °C for 1 min and 30 sec followed by an additional extension period at 72 °C for 5 min. The 5' RACE used touchdown PCR and amplification was carried out with the following conditions: 94 °C for 2 min, 25 cycles including a denaturation step at 94 °C for 15 sec, an annealing step from 68 °C to 55 °C for 30 sec, and extension at 72 °C for 1 min and 30 sec; 15 cycles as above except that the annealing step at 55 °C; a final extension step at 72 °C for 7 min ended the PCR reaction. The products were subjected to electrophoresis in a 1 % agarose gel, purified according to qiaquick PCR purification kit protocol and added dATP-tailing to blunt-ended fragments at 70 °C for 30 min in the presence of Taq DNA polymerase before ligated into the pGEM-T vector. Transformation, screening, and sequencing were then performed as described above.

Splicing the full-length nucleotide sequence

Alignment of the sequences was spliced, in light of contig of 5' /3' sequencing result, to get a full-length nucleotide sequence. Homology search was performed using the BLAST program at NCBI.

RESULTS

Construction of the subtracted cDNA library and screening of the differential fragments

By means of suppression subtractive hybridization (SSH) technique, we prepared driver cDNAs and tester cDNAs of liver tissue from control and liver tissue 112 hr following SISPH. After two rounds hybridization and two PCR reactions, we obtained the forward-subtractive cDNA library (Figure 1). The subtracted cDNA was evaluated by the house-keeping gene *g3pdh* (Figure 2). Our results showed that the constructed forward-subtracted cDNA library was highly efficient after cDNA library was subcloned into pGEM-T vector and transformed into JM109, we obtained 120 white clones and 40 clones randomly selected were then subjected to sequencing (Figure 3). The sequencing results were sent to NCBI for BLAST searches.

Determination of the full-length nucleotide sequence of LR₁ cDNA by RACE

The original cDNA isolated from the cDNA subtraction screening was about 311bp long. This cDNA fragment was used to design primers according to 5' /3' RACE kit. After amplification, ligation, screening and sequencing, we obtained the sequence of the 3' end and 5' end (Figure 4). Alignment of contig sequences enabled us to delineate the entire cDNA sequence (Figure 5). We found a single long ORF starting with a methionine codon ATG at nucleotide 47 and ending with a TAA stop codon at 625 and a putative polyadenylation signal AATAAA upstream from the poly (A⁺). Homology search using *LR₁* cDNA sequence revealed that it is 88.8 % homologous to rat transthyretin gene and 88.4 % homologous to albumin gene. Protein homology (Swissport database) search of the peptide encoded by the *LR₁* ORF revealed that it is 91% homologous to rat transthyretin, submitting this full-length cDNA to NCBI and obtain GenBank Accession No. AF479660.

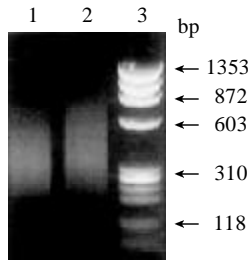


Figure 1 Gel electrophoresis of SSH results. 1. Control; 2. Forward subtractive; 3. Marker.

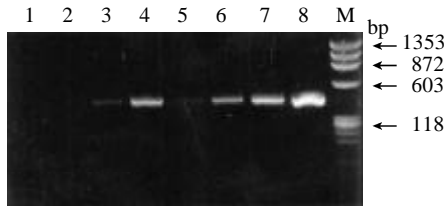


Figure 2 Efficiency of subtracted library. 1-4. Subtracted products with *g3pdh* primer; 5-8. Control products with *g3pdh* primer; M. Marker.

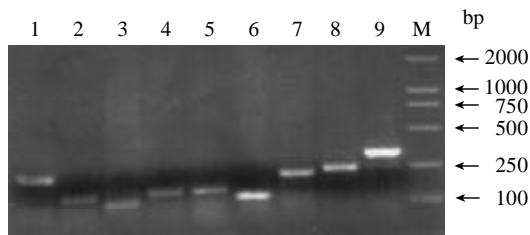


Figure 3 Gel electrophoresis of clones inserted fragments. 1-9. Different EST fragments; M. Marker.

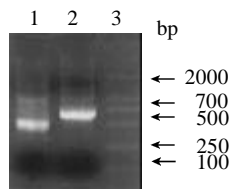


Figure 4 RACE PCR results. 1. 3' RACE result; 2. 5' RACE result; 3. Marker.

```

1   ggccattacg gccggggatc gtagagatcc gctggtcct gacaggatgg cttcccttcg
61  cctgttctc ctctgcctcg ctggactgat atttgcgtct gaagctggcc ctgggggtgc
121 tggagaatcc aagtgtcctc tgatgtcaaa agtctctggat gctgtccgag gcagccctgc
181 tgtcgatgtg gccctgaaag tgttcaaaaa gactgcagac ggaagctggg agccgtttgc
241 ctctgggaag accgccgagt ctggagagct gcacgggctc accacagatg agaagttcac
301 ggaaggggtg tacagggtag aactggacac caaatgtac tggaaaggctc ttggcatttc
361 cccattccat gaatacgcag aggtggtttt cacagccaat gactctgtgc atcgccaata
421 caccatcgca gccctgcctca gccctgtact ctacagcacc actgctgtcg tcagtaacctc
481 ccagaactga gggaccaccg ccaggaggac caggatcttg ccaaaagcagt agcttcccat
541 ttgtactgaa acagtgttct tgctctataa accgtgttag caactcggga agatgccgtg
601 aaacgttctt attaaaccac ctttatttca tccaaaaaaa aaaaaaaaaa aaaaaaaaaa
661 a
    
```

Figure 5 Full-length cDNA of *LR_γ*

DISCUSSION

SSH technique was developed based primarily on a recently described technique called cDNA suppression PCR which combines normalization and subtraction in a single procedure

to generate subtracted cDNA library^[23-25]. Compared to the methods of mRNA differential display^[26], representational difference analysis of DNA^[27], it has two distinct advantages: (1) it has a high subtraction efficiency; (2) it harbors an equalized representation of differentially expressed sequences which can separate effectively both high and low copy expressed genes mainly because of normalization. The normalization step equalizes the abundance of cDNAs within the target population and the subtraction step excludes the common sequences between the target and the driver populations^[23,28,29]. The experimental results showed the SSH technique can enrich for rare sequences over 1 000-5 000 fold in one round of subtractive hybridization^[23,24,30]. By resorting to SSH and high-density array scanning technique, using non-metastatic counterpart Bsp73-1AS as driver, metastatic adenocarcinoma cell line Bsp73-ASML as tester, Von Stein^[31] found up to 252 over-expressed clones among 625 clones with no homologous sequences in GenBank. By using an EST fragment derived from the forward-subtracted cDNA library as probe, we have cloned a novel gene from the liver tissue 112 hr cDNA library following SISPH. These results suggest that SSH technique is applicable to many molecular genetic and positional cloning studies for the identification of disease, developmental, tissue-specific or other differentially expressed genes.

With the aim to shed light on the molecular mechanism of PH, Xu *et al*^[17] established the SISPH model which selected the intervals at the crucial periods, e.g. the peak of cell activation (4 hr after PH), the peak of cell division (36 hr after PH) and the peak of re-differentiation (48 hr after PH). We have examined some biological activated factors, heat shock proteins (HSPs), proteases, proteins related to cell proliferation and dephosphoralization^[13,14,17,18,32]. These data have provided useful information to reveal the molecular mechanism of LR. The results suggested that SISPH model may offer more abundant data than that of PH. In present study, We took 0 h and 112 hr as driver and tester respectively in 0-4-36-36-36hr SISPH model when resorting to SSH strategy, then we constructed a forward-subtractive cDNA library in short time by using RACE, subsequently we cloned a full-length cDNA and blast search showed that the cDNA is 88.8 % and 88.4 % homologous to the transthyretin and albumin in rat respectively. This suggested that the gene may exert partial function identical to transthyretin. It is well known that thyroxine and its metabolic products integrated thyroxine-binding prealbumin and albumin is derived from liver to operate. In the physiological conditions, 99.9 % 3,3' 5,5' -tetraiodothyronine (T₄) and 99.7 % 3,3' 5-triiodothyronine (T₃) are complexed with proteins which contain over 60 % transthyretin and 15-30 % thyroxine-binding prealbumin and 10 % albumin. Our present study showed that the injured liver released abundant analogs of transthyretin. As we know, the changes of transthyretin concentration is regarded as one of the important reasons that metabolic or biochemical abnormality in thyroid gland responsible for hepatopathy^[33,34]. The up-regulations of transthyretin in liver tissue is speculated to have following functions: (1) breaking the balance of HSS (hepatocyte stimulate substrate) and inhibitor and thus enhancing the dedifferentiation. We have cloned two up-regulated genes, one of which is 78.6 % homologous to rat transferring gene and the other is 72 % homologous to mouse embryonic stem cell gene from 112 hr cDNA library following SISPH (remains to be published), It is also known that over-expression of transferring gene and embryonic stem cell gene have close relations with the cellular dedifferentiation; (2) influencing the induction of enzyme and consumption of oxygen. Compensatory respiration was promoted in mitochondrion responsible for partial hypoxia following PH, but the energy produced from tricarboxylic acid cycle couldn't meet the

structural recovery of damaged liver due to successive partial hepatectomy and thus triggered the related genes to express in hypoxia metabolism. The over-expressed gene of alcohol dehydrogenase have cloned from 112 hr cDNA library following SISPH (remains to be published) seems to explain this hypothesis which is consistent with the result of Cheng Lingzhong.

In conclusion, complicated physiological and biochemical reaction changed in the liver tissue following SISPH, we postulated that this kind of up-regulated gene *LR₁* expression involve in liver regeneration may (1) relate with compensated increase of stress molecules following SISPH; (2) lead to the initiation of other metabolism; (3) maintain the homeostasis in the body. As to, whether severe dedifferentiation happened following SISPH and what are the key dedifferential factors and how they influence the dedifferentiation, remain to be further investigated.

REFERENCES

- 1 **Michael M**, Awad, Philip A. Gruppuso. Cell cycle control during liver development in the rat: Evidence indicating a role for cyclin d1 posttranscriptional regulation. *Cell Growth Differ* 2000; **11**: 325-334
- 2 **Jiang YP**, Ballou LM, Lin RZ. Apamycin-insensitive regulation of 4E-BP1 in regenerating rat Liver. *J Biol Chem* 2001; **276**: 10943-10951
- 3 **Zakko WF**, Berg CL, Gollan JL, Green RM. Hepatocellular expression of glucose-6-phosphatase is unaltered during hepatic regeneration. *Am J Physiol Gastrointest Liver Physiol* 1998; **275**: 717-722
- 4 **Iimuro YJ**, Nishiura T, Hellerbrand C, Behrns KE, Schoonhoven R, Grisham JW, Brenner DA. NFκB prevents apoptosis and liver dysfunction during liver regeneration. *J Clin. Invest* 1998; **101**: 802-811
- 5 **Laconi E**, Oren R, Mukhopadhyay DK, Hurston E, Laconi S, Pani P, Dabeva MD, Shafritz DA. Long-Term. Near-total liver replacement by transplantation of isolated hepatocytes in rats treated with retrorsine. *Am J Pathol* 1998; **153**: 319-329
- 6 **Ying C**, Rory O, Conolly B, Russell S, Thomas, Yihua X, Melvin E, Andersen, Laura S, Chubb, Henry C, Pitot, Raymond S, Yang H. A clonal growth model: time-course simulations of liver foci growth following penta-or hexachlorobenzene treatment in a medium-term bioassay. *Cancer Res* 2001; **61**: 1879-1889
- 7 **Kooby DA**, Zakian KL, Challa SN, Matei C, Petrowsky H, Yoo HH, Koutcher JA, Fong Y. Use of phosphorous-31 nuclear magnetic resonance spectroscopy to determine safe timing of chemotherapy after hepatic resection. *Cancer Res* 2000; **60**: 3800-3806
- 8 **Michalopoulos GK**, DeFrance MC. Liver regeneration. *Science* 1997; **275**: 60-66
- 9 **Sigal SH**, Rajvanshi P, Gorla GR, Sokhi RP. Partial hepatectomy-induced polyploidy attenuates hepatocyte replication and activates cell aging events. *Am J Physiol Gastrointest Liver Physiol* 1999; **276**: 1260-1272
- 10 **Ikeda Y**, Matsumata T, Utsunomiya T, Yamagata M, Takenaka K, Sugimachi K. Effects of doxorubicin on cancer cells after two-thirds hepatectomy in rats. *J Surg Onco* 1995; **58**: 101-103
- 11 **Shih HH**, Xiu M, Berasi SP, Sampson EM, Leiter A, Yee AS. HMG box transcriptional repressor hbp1 maintains a proliferation barrier in differentiated liver tissue. *Mol Cell Biol* 2001; **21**: 5723-5732
- 12 **Xu CS**, Xia M, Lu AL, Li XY, Li YH, Zhao XY, Hu YH. Changes in the content and activity of HSC70/HSP68, proteinase and phosphatases during liver regeneration. *Sheng Li Xue Bao* 1999; **51**: 546-556
- 13 **Hayami S**, Yaita M, Ogiri Y, Sun F, Nakata R, Kojo S. Change in caspase-3-like protease in the liver and plasma during rat liver regeneration following partial hepatectomy. *Biochem Pharmacol* 2000; **60**: 1883-1886
- 14 **Rissler P**, Torndal UB, LC Eriksson. Induced drug resistance inhibits selection of initiated cells and cancer development. *Carcinogenesis* 1997; **18**: 649-655
- 15 **Aaron W**, Bell, Jie-Gen Jiang, Qiuyan Chen, Youhua Liu, Reza Zarnegar. The upstream regulatory regions of the hepatocyte growth factor gene promoter are essential for its expression in transgenic mice. *J Biol Chem* 1998; **273**: 6900-6908
- 16 **Lu AL**, Xu CS. Effect of heat shock before and after rat partial hepatectomy on HSC/HSP68, acid and alkaline phosphatases. *World J Gastroenterol* 2000; **6**: 730-733
- 17 **Xu CS**, Li YH, Duan RF, Lu AL, Xia M, Ji AL. Effects of the short interval successive partial hepatectomy on rat survival and liver tissue structure. *Dongwu Xuebao* 2001; **47**: 659-665
- 18 **Ankoma-Sey V**. Hepatic regeneration-revisiting the myth of Prometheus. *News in physiological Sciences* 1999; **14**: 149-155
- 19 **Diehl AM**. Liver regeneration. *Front Biosci* 2002; **7**: e301-314
- 20 **Russell WE**, Dempsey PJ, Sitaric S, Peck AJ, Coffey RJ. Transforming growth factor-alpha concentrations increase in regenerating rat liver: evidence for a delayed accumulation of mature TGF alpha. *Endocrinology* 1993; **133**: 1731-1738
- 21 **Schirmacher P**, Geerts A, Pietrangelo A, Dienes HP, Rogler CE. Hepatocyte growth factor/hepatopoietin A is expressed in fat-storing cells from rat liver but not myofibroblast-like cells derived from fat-storing cells. *Hepatology* 1992; **15**: 5-11
- 22 **Yamada Y**, Kirillova I, Peschon JJ, Fausto N. Initiation of liver growth by tumor necrosis factor deficient liver regeneration in mice lacking type I tumor necrosis factor receptor. *Proc Acad Sci USA* 1997; **94**: 1441-1446
- 23 **Diatchenko L**, Lukyanov S, Lau YF, Siebert PD. Suppression subtractive hybridization: a versatile method for identifying differentially expressed genes. *Methods Enzymol* 1999; **303**: 349-380
- 24 **Nishizuka S**, Tsujimoto H, Stanbridge EJ. Detection of differentially expressed genes in hela x fibroblast hybrids using subtractive suppression hybridization. *Cancer Res* 2001; **61**: 4536-4540
- 25 **Shridhar V**, Sen A, Chien J, Staub J, Avula R, Kovats S, Lee J, Lillie J, Smith DI. Identification of under expressed genes in early- and late-stage primary ovarian tumors by suppression subtraction hybridization. *Cancer Res* 2002; **62**: 262-270
- 26 **Liang P**, Pardee AB. Differential display of eukaryotic messenger RNA by means of the polymerase chain reaction. *Science* 1992; **257**: 967-971
- 27 **Duguin JL**, Dinauer MC. Library subtraction of in vitro cDNA libraries to identify differentially expressed genes in scrapie infection. *Nucleic Acids Res* 1990; **18**: 2789-2792
- 28 **Hara E**, Kato T, Nakada S, Sekiya L, Oda K. Subtractive cDNA cloning using oligo (dT)30-latex and PCR: isolation of cDNA clones specific to undifferentiated human embryonal carcinoma cells. *Nucleic Acids Res* 1991; **19**: 7097-7104
- 29 **Hubank M**, Schatz DG. Identifying differences in mRNA expression by representational analysis of cDNA. *Nucleic Acids Res* 1994; **22**: 5640-5648
- 30 **Fabrikant JL**. The kinetics of the cellular proliferation in the regeneration liver. *Cell Biol* 1968; **36**: 551-565
- 31 **Von Stein OD**, Thies WG, Hofmann MA. High through put screening for rarely transcribed differentially expressed genes. *Nucleic Acids Research* 1997; **25**: 2598-2602
- 32 **Joan M**, Boylan, Padmanabhan Anand, Philip A, Gruppuso. Ribosomal protein S6 phosphorylation and function during Late Gestation liver development in the rat. *J Biol Chem* 2001; **276**: 44457-44463
- 33 **Schreiber G**. The evolutionary and integrative roles of transthyretin in thyroid hormone homeostasis. *J Endocrinol* 2002; **175**: 61-73
- 34 **Toshi D**, Shen CN, Slack JM. Differentiated properties of hepatocytes induced from pancreatic cells. *Hepatology* 2002; **36**: 534-543

Effects of pentoxifylline on the hepatic content of TGF- β 1 and collagen in *Schistosomiasis japonica* mice with liver fibrosis

Li-Juan Xiong, Jian-Fang Zhu, Duan-De Luo, Lin-Lan Zen, Shu-Qing Cai

Li-Juan Xiong, Duan-De Luo, Lin-Lan Zen, Shu-Qing Cai, Department of Infectious Diseases, Union Hospital, Tongji Medical College, Huazhong University of Science and Technology, Wuhan 430022, Hubei Province, China

Jian-Fang Zhu, Department of Central Laboratory, Union Hospital, Tongji Medical College, Huazhong University of Science and Technology, Wuhan 430022, Hubei Province, China

Supported by the Science Research Foundation of Schistosomiasis of Hubei Province, No.2000

Correspondence to: Dr. Li-Juan Xiong, Department of Infectious Disease, Union Hospital, Tongji Medical College, Huazhong University of Science and Technology, Wuhan 430022, Hubei Province, China. kljxiong@public.wh.hb.cn

Telephone: +86-27-85726109

Received: 2002-08-15 **Accepted:** 2002-09-12

Abstract

AIM: To study the effects of pentoxifylline (PTX) on the content of hepatic TGF- β 1, type I and type III collagen in schistosomiasis japonica mice with liver fibrosis and its mechanism of anti-fibrosis.

METHODS: Forty mice with schistosomiasis were divided into four groups: one group as control without any treatment, other three were treated with Praziquantel 500 mg/(kg·d) for 2 d, high dose PTX 360 mg/(kg·d) for 8 wk, and low dose PTX 180 mg/(kg·d) for 8 wk respectively. Immunohistochemical technique and multimedia color pathographic analysis system were applied to observe the content change of hepatic TGF- β 1, type I and type III collagen in schistosomiasis japonica mice with liver fibrosis before and after PTX treatment.

RESULTS: Effects of PTX on the content change of hepatic TGF- β 1, type I and type III collagen in schistosomiasis japonica mice with liver fibrosis were related to the dosage of PTX, high dose PTX treated group could significantly reduce the content of TGF- β 1 (0.709 ± 0.111), type I (0.644 ± 0.108) and type III (0.654 ± 0.152) collagen compared with those of control group (0.883 ± 0.140 , 0.771 ± 0.156 , 0.822 ± 0.129) with statistical significance ($P<0.05$). Low dose PTX could also reduce the hepatic content of TGF- β 1 (0.752 ± 0.152), type I (0.733 ± 0.117) and type III (0.788 ± 0.147) collagen, but without statistical significance ($P>0.05$). Both high dose and low dose PTX groups have significant differences on the content of TGF- β 1, type I and type III collagen ($P<0.05$, $P<0.05$, $P<0.01$, respectively).

CONCLUSION: High dose of PTX treatment could reduce the content of hepatic TGF- β 1, type I and type III collagen significantly in schistosomiasis japonica mice with liver fibrosis, and thus plays its role of antifibrosis.

Xiong LJ, Zhu JF, Luo DD, Zen LL, Cai SQ. Effects of pentoxifylline on the hepatic content of TGF- β 1 and collagen in *Schistosomiasis japonica* mice with liver fibrosis. *World J Gastroenterol* 2003; 9(1): 152-154

<http://www.wjgnet.com/1007-9327/9/152.htm>

INTRODUCTION

Liver fibrosis is the main reason for portal hypertension and hemorrhagic of upper digestive tract in schistosomiasis and there fore the main reason for the mortality of schistosomiasis. The basic pathological changes of liver fibrosis are the disturbance and degradation of extracellular matrix (ECM), which causes accumulation of ECM in the liver^[1,2]. Within the major components of ECM, type I and type III collagen constitute more than 95 % of the total content of increased collagen in liver fibrosis^[3-5]. It is well known that fibrosis is reversible whereas cirrhosis is irreversible, so it is important to prevent fibrosis progressing to cirrhosis^[6,7]. However, there is no ideal antifibrosis drug to date. Recent researches found that PTX has antifibrosis function^[8,9], while its effects on hepatic fibrosis of schistosomiasis japonica are still unknown. Since the main pathological characteristic of schistosomiasis japonica is the deposition of type I and III collagen and TGF β 1 has very important influence on the fibrosis development, it is considered the key cytokine to accelerate cirrhotic procession^[10-15], we studied the effects of PTX on the expression of collagen I and III and TGF β 1 in mice with schistosomiasis japonica and intended to evaluate the roles of PTX in hepatic fibrosis.

MATERIALS AND METHODS

Materials

Forty female Kunming mice, weighted 16-20 g and aged 4-6 w, provided by Experimental Animal Center of Tongji Medical College, were infected with 25 cercaria of schistosomiasis japonica (provided by Wuhan Institute of Schistosomiasis Prophylactic and Therapy) and fed for 2 weeks and then divided randomly and equally into 4 groups: one group as control without any treatment, other three were treated with Praziquantel 500 mg/(kg·d) for 2 d, high dose PTX (provided as SHUANLIN tablet by Shijiazhuang Pharmaceutics CO.) 360 mg/(kg·d) for 8 wk, and low dose PTX 180 mg/(kg·d) for 8 wk respectively. The mice were then deceased and hepatic tissue sections were prepared for examination. Immunohistochemical technique and multimedia color pathographic analysis system were applied to observe the content of hepatic TGF- β 1, type I and type III collagen before and after treatment.

Assay of TGF β 1, collagen I and collagen III

Rabbit anti-mouse TGF β 1 was purchased from Santa Cruz. Rabbit anti-mouse collagen I and III, and SABC kit were provided by Boster Biological Technology Co., Ltd. The immunohistochemical studies were performed by the avidin-biotin-peroxidase method, briefly described as following. The tissue sections were blocked in 3 % hydrogen peroxide, washed in buffer solution, and then incubated in mixed digestive solution for 5 min in room temperature. The sections were washed in PBS and then incubated in goat serum blocking solution for 10 min. The sections were then incubated with the primary antibodies at 37 °C for 30 min, washed and then incubated with biotin conjugated secondary antibodies at 37 °C for 20 min, washed with PBS, and then labeled with peroxidase-conjugated streptavidin for 20 min at 37 °C. The washed

sections were then incubated with Diaminobenzidine (DAB), counterstained and prepared for microscopic examination.

Results analysis

The sections were analyzed with MPZAS-500 multimedia color pathological graph analyzing system. The average integral light density (ILD) of positive staining in each section was obtained and presented as $\bar{x} \pm s$. Results were then analyzed with student *t* test.

RESULTS

Effects of PTX on TGF- β 1 expression

The contents of TGF β 1 in praziquantel group, high dose PTX group and low dose PTX group decrease by 44.62 %, 19.71 %, 14.84 % respectively compared with control group. The difference between praziquantel group and control group is very significant ($P < 0.01$). The effect of PTX on TGF β 1 content is dose related and there is significant difference on TGF β 1 contents between high and low dose groups. The TGF β 1 content in high dose PTX group is significantly ($P < 0.05$) different from that of control group while no significant difference between low dose PTX group and control group. Both high dose and low dose PTX groups have significant difference on TGF β 1 contents between praziquantel group and themselves. The results are shown in Table 1.

Table 1 Content of TGF- β 1, collagen I and III in liver of each treated group and control group ($\bar{x} \pm s$, ILD, $n = 10$)

Group	TGF- β 1	Collagen I	Collagen III
Control	0.883 \pm 0.140	0.771 \pm 0.156	0.822 \pm 0.129
Praziquantel	0.489 \pm 0.105 ^a	0.596 \pm 0.103 ^a	0.613 \pm 0.116 ^a
High dose PTX	0.709 \pm 0.111 ^{bd}	0.644 \pm 0.108 ^{bd}	0.654 \pm 0.152 ^{be}
Low dose PTX	0.752 \pm 0.152 ^{cd}	0.733 \pm 0.117 ^{cd}	0.788 \pm 0.147 ^{cdg}

^a $P < 0.01$, vs control group; ^b $P < 0.05$, vs control group; ^c $P > 0.05$, vs control group; ^d $P < 0.01$, vs praziquantel group; ^e $P > 0.05$, vs praziquantel group; ^f $P < 0.05$, vs high dose PTX group; ^g $P < 0.01$, vs high dose PTX group.

Effects of PTX on collagen I expression

The contents of collagen I in praziquantel group, high dose PTX group and low dose PTX group decrease by 22.70 %, 16.47 %, 4.93 % respectively compared with control group. The difference between praziquantel group and control group is very significant ($P < 0.01$). The effect of PTX on collagen I content is dose related and there is significant difference on collagen I contents between high and low dose groups. The collagen I content in high dose PTX group is significantly ($P < 0.05$) different from that of control group while no significant difference between low dose PTX group and control group. Both high and low dose PTX groups have significant difference on collagen I contents between praziquantel group and themselves. The results are shown in Table 1.

Effects of PTX on collagen III expression

The contents of collagen III in praziquantel group, high dose PTX group and low dose PTX group decrease by 25.43 %, 20.44 %, 4.14 % respectively compared with control group. The difference between praziquantel group and control group is very significant ($P < 0.01$). The effect of PTX on collagen III content is dose related and there is significant difference on collagen III contents between high and low dose groups ($P < 0.01$). The collagen III content in high dose PTX group is significantly ($P < 0.05$) different from that of control group while no

significant difference between low dose PTX group and control group ($P > 0.05$). Compared with praziquantel group, high dose PTX group has no difference on collagen III contents ($P > 0.05$), whereas low dose PTX group has significant difference ($P < 0.01$). The results are shown in Table 1.

DISCUSSION

PTX is a trimethylated xanthine derivative product. As an inhibitor of phosphodiesterase, it can induce the increase of intracellular cAMP, dilation of the blood vessels and smooth muscles, ameliorating the microcirculation. It has been used to improve the peripheral blood vessel disease for many years^[16,17]. Recently, PTX has been found to have antifibrosis effect. *In vitro* studies show that PTX can inhibit the proliferation of myofibroblast from hepatitis patients and depress the synthesis of collagen. Treatment with PTX in early stage can alleviate the hepatic lesion and inflammatory reaction^[18]. In animal hepatic fibrosis models, PTX also has anti-fibrosis effect. It has been reported that treated with PTX prior to the inducing of hepatic fibrosis with CCL₄-acetone can alleviate the proliferation of hepatic stellate cell (HSC), and previous treatment with PTX decelerate the differentiation of HSC in mouse with hepatic fibrosis induce by bile duct ligation^[19]. It was reported that previous treatment with PTX could improve the regeneration and function of liver after partial hepatectomy in mice with hepatic fibrosis and alleviate the hepatic fibrosis. But there is no report on the effects of PTX on schistosomal hepatic fibrosis^[20]. The fibrosis in schistosomal has its special characteristics against those caused by hepatic cell lesion or bile duct obstruction. Therefore, the effects of PTX in the schistosomal hepatic fibrosis should be explored.

Hepatic stellate cell (HSC) plays a pivotal role in the fiber synthesis and degradation. The activation of HSC is mediated by various cytokines and reactive oxygen species released from the damaged hepatocytes and activated Kupffer cells^[21-26]. HSC can release TGF β 1 by autocrine^[27,28] and TGF β 1 has been proved to be a strong mitogen to HSC. This autocrine effect is upgraded when HSC has been activated. TGF β 1 depresses the regeneration of hepatic cells, activates and promotes HSC to synthesize extracellular matrix such as collagen, fibronectin proteinopolysaccharide, promotes the synthesis of TIMP and inhibits the synthesis of MMPs^[29-37].

We established a mouse hepatic fibrosis model induced by cercaria of schistosomiasis japonica infection and studied the effect of PTX on the fibrosis development in the early stage. We found that PTX could inhibit the development of fibrosis in this model significantly. The quantitative immunohistochemical evaluation of TGF β 1, type I and III collagens shows that, high dose of PTX can reduce the content of TGF β 1, type I and III collagens in hepatic tissue of mice with schistosomal hepatic fibrosis. Its capability to reduce the hepatic content of type III collagen is similar to praziquantel ($P > 0.05$) and its effects on TGF β 1 and type I collagen are weaker than praziquantel. Compared with the control group, low dose of PTX can also reduce the contents of TGF β 1, type I and III collagens but the effects have no statistical significance.

The results indicate that PTX treatment in the early stage inhibits the development of schistosomal hepatic fibrosis by reducing the content of TGF β 1, type I and III collagens.

REFERENCES

- 1 **Qing JP**, Jiang MD. Phenotype and regulation of hepatic stellate cell and liver fibrosis. *Shijie Huaren Xiaohua Zazhi* 2001; **9**: 801-804
- 2 **Dai WJ**, Jiang HC. Advances in gene therapy of liver cirrhosis: a review. *World J Gastroenterol* 2001; **7**: 1-8

- 3 **Wang GQ**, Lu HQ, Wang H, Kong XT, Zhong RQ, Huang C, Gao F. Effects of Decorin on collagen of hepatic stellate cells. *Xin Xiaohuabingxue Zazhi* 2001; **9**: 1395-1398
- 4 **Wang JY**, Guo JS, Yang CQ. Expression of exogenous rat collagenase *in vitro* and in a rat model of liver fibrosis. *World J Gastroenterol* 2002; **8**: 901-907
- 5 **Zhang YT**, Chang XM, Li X, Li HL. Effects of spironolactone on expression of type I/III collagen proteins in rat hepatic fibrosis. *Xin Xiaohuabingxue Zazhi* 2001; **9**: 1120-1124
- 6 **Jiang SL**, Yao XX, Sun YF. Therapy of liver fibrosis. *Shijie Huaren Xiaohua Zazhi* 2000; **8**: 684-686
- 7 **Okazaki I**, Watanabe T, Hozawa S, Niioka M, Arai M, Maruyama K. Reversibility of hepatic fibrosis: from the first report of collagenase in the liver to the possibility of gene therapy for recovery. *Keio J Med* 2001; **50**: 58-65
- 8 **Reis LF**, Ventura TG, Souza SO, Arana-Pino A, Pelajo-Machado M, Pereira MJ, Lenzi HL, Conceicao MJ, Takiya CM. Quantitative and qualitative interferences of pentoxifylline on hepatic *Schistosoma mansoni* granulomas: effects on extracellular matrix and eosinophil population. *Mem Inst Oswaldo Cruz* 2001; **96**: 107-112
- 9 **Raetsch C**, Jia JD, Boigk G, Bauer M, Hahn EG, Riecken EO, Schuppan D. Pentoxifylline downregulates profibrogenic cytokines and procollagen I expression in rat secondary biliary fibrosis. *Gut* 2002; **50**: 241-247
- 10 **Jiang HQ**, Zhang XL. Mechanism of liver fibrosis. *Shijie Huaren Xiaohua Zazhi* 2000; **8**: 687-689
- 11 **Kanzler S**, Baumann M, Schirmacher P, Dries V, Bayer E, Gerken G, Dienes HP, Lohse AW. Prediction of progressive liver fibrosis in hepatic C infection by serum and tissue levels of transforming growth factor-beta. *J Viral Hepat* 2001; **8**: 430-437
- 12 **Chen WX**, Li YM, Yu CH, Cai WM, Zheng M, Chen F. Quantitative analysis of transforming growth factor beta1 mRNA in patients with alcoholic liver disease. *World J Gastroenterol* 2002; **8**: 379-381
- 13 **Kmiec Z**. Cooperation of liver cells in health and disease. *Adv Anat Embryol Cell Biol* 2001; **161**: 1-151
- 14 **Du WD**, Zhang YE, Zhai WR, Zhou XM. Dynamic changes of type I,III and IV collagen synthesis and distribution of collagen-producing cells in carbon tetrachloride-induced rat liver fibrosis. *World J Gastroenterol* 1999; **5**: 397-403
- 15 **Bissell DM**. Chronic liver injury, TGF-beta, and cancer. *Exp Mol Med* 2001; **33**: 179-190
- 16 **Schuppan D**, Koda M, Bauer M, Hahn EG. Fibrosis of liver, pancreas and intestine: common mechanisms and clear targets? *Acta Gastroenterol Belg* 2000; **63**: 366-370
- 17 **Windmeier C**, Gressner AM. Pharmacological aspects of pentoxifylline with emphasis on its inhibitory actions on hepatic fibrogenesis. *Gen Pharmacol* 1997; **29**: 181-196
- 18 **Preaux AM**, Mallat A, Rosenbaum J, Zafrani ES, Mavier P. Pentoxifylline inhibits growth and collagen synthesis of cultured human hepatic myofibroblast-like cells. *Hepatology* 1997; **26**: 315-322
- 19 **Desmouliere A**, Xu G, Costa AM, Yousef LM, Gabbiani G, Tuchweber B. Effects of pentoxifylline on early proliferation and phenotypic modulation of fibrogenic cells in two rat models of liver fibrosis and on cultured hepatic stellate cells. *J Hepatol* 1999; **30**: 621-631
- 20 **Moser M**, Zhang M, Gong Y, Johnson J, Kneteman N, Minuk GY. Effects of preoperative interventions on outcome following liver resection in a rat model of cirrhosis. *J Hepatol* 2000; **32**: 287-292
- 21 **Wu J**, Zern MA. Hepatic stellate cells: a target for the treatment of liver fibrosis. *J Gastroenterol* 2000; **35**: 665-672
- 22 **Reeves HL**, Friedman SL. Activation of hepatic stellate cells-a key issue in liver fibrosis. *Front Biosci* 2002; **7**: D808-826
- 23 **Tsukamoto H**. Cytokine regulation of hepatic stellate cells in liver fibrosis. *Alcohol Clin Exp Res* 1999; **23**: 911-916
- 24 **Bataller R**, Brenner DA. Hepatic stellate cells as a target for the treatment of liver fibrosis. *Semin Liver Dis* 2001; **21**: 437-451
- 25 **Beljaars L**, Meijer DK, Poelstra K. Targeting hepatic stellate cells for cell-specific treatment of liver fibrosis. *Front Biosci* 2002; **7**: e214-222
- 26 **Wu J**, Zern MA. Hepatic stellate cells: a target for the treatment of liver fibrosis. *J Gastroenterol* 2000; **35**: 665-672
- 27 **Liu T**, Hu JH, Cai Q, Ji YP. The signal transducing molecular in HSC. *Shijie Huaren Xiaohua Zazhi* 2001; **9**: 805-807
- 28 **Huang GC**, Zhang JS. Activated *in vivo* signal transduction of HSC. *Xin Xiaohuabingxue Zazhi* 2001; **9**: 1056-1060
- 29 **Dooley S**, Delvoux B, Streckert M, Bonzel L, Stopa M, Ten Dijke P, Gressner AM. Transforming growth factor beta signal transduction in hepatic stellate cells via Smad2/3 phosphorylation, a pathway that is abrogated during *in vitro* progression to myofibroblasts. TGFbeta signal transduction during transdifferentiation of hepatic stellate cells. *FEBS Lett* 2001; **502**: 1-3
- 30 **Garcia-Trevijano ER**, Iraburu MJ, Fontana L, Dominguez-Rosales JA, Auster A, Covarrubias-Pinedo A, Rojkind M. Transforming growth factor beta1 induces the expression of alpha1(I) procollagen mRNA by a hydrogen peroxide-C/EBPbeta-dependent mechanism in rat hepatic stellate cells. *Hepatology* 1999; **29**: 960-970
- 31 **Yata Y**, Gotwals P, Koteliensky V, Rockey DC. Dose-dependent inhibition of hepatic fibrosis in mice by a TGF-beta soluble receptor: implications for antifibrotic therapy. *Hepatology* 2002; **35**: 1022-1030
- 32 **Tahashi Y**, Matsuzaki K, Date M, Yoshida K, Furukawa F, Sugano Y, Matsushita M, Himeno Y, Inagaki Y, Inoue K. Differential regulation of TGF-beta signal in hepatic stellate cells between acute and chronic rat liver injury. *Hepatology* 2002; **35**: 49-61
- 33 **Okuno M**, Akita K, Moriwaki H, Kawada N, Ikeda K, Kaneda K, Suzuki Y, Kojima S. Prevention of rat hepatic fibrosis by the protease inhibitor, camostat mesilate, via reduced generation of active TGF-beta. *Gastroenterology* 2001; **120**: 1784-1800
- 34 **Breitkopf K**, Lahme B, Tag CG, Gressner AM. Expression and matrix deposition of latent transforming growth factor beta binding proteins in normal and fibrotic rat liver and transdifferentiating hepatic stellate cells in culture. *Hepatology* 2001; **33**: 387-396
- 35 **Suzuki C**, Kayano K, Uchida K, Sakaida I, Okita K. Characteristics of the cell proliferation profile of activated rat hepatic stellate cells *in vitro* in contrast to their fibrogenesis activity. *J Gastroenterol* 2001; **36**: 322-329
- 36 **Liu F**, Liu JX. The role of transforming growth factor beta1 in liver fibrosis. *Shijie Huaren Xiaohua Zazhi* 2000; **8**: 86-88
- 37 **Preaux AM**, Mallat A, Nhieu JT, D'ortho MP, Hembry RM, Mavier P. Matrix metalloproteinase-2 activation in human hepatic fibrosis regulation by cell-matrix interactions. *Hepatology* 1999; **30**: 944-950

Effects of Tetrandrine and QYT on ICAM-1 and SOD gene expression in pancreas and liver of rats with acute pancreatitis

Yong-Yu Li, Xue-Li Li, Cui-Xiang Yang, Hong Zhong, Hong Yao, Ling Zhu

Yong-Yu Li, Hong Zhong, Hong Yao, Ling Zhu, Department of Pathophysiology, Medical College of Tongji University, Shanghai 200331, China

Xue-Li Li, Cui-Xiang Yang, Department of Biochemistry, Medical College of Tongji University, Shanghai 200331, China

Supported by the National Natural Scientific Foundation of China, No. 30060031

Correspondence to: Yong-Yu Li, M.D., Professor of Pathophysiology, Department of Pathophysiology, Medical College of Tongji University, Shanghai 200331, China. liyyu@163.net

Telephone: +86-21-51030563

Received: 2002-09-13 **Accepted:** 2002-10-21

Abstract

AIM: Available experimental evidence from both clinical and animal models shows that both Chinese medicines tetrandrine (Tet) and Qing Yi Tong (QYT) have positive treatment effects on acute pancreatitis (AP). This investigation was conducted to explore the treatment mechanisms of Tet and QYT on AP at the molecular level and thereby explain their therapeutic effects. It included an investigation of the effects of these drugs on gene expression of both intercellular adhesion molecule 1 (ICAM-1) and superoxide dismutase (Mn-SOD and Cu, Zn-SOD) in a rat model with AP.

METHODS: AP in the test rats was induced by subjecting them to laparotomy followed by a retrograde injection of 4 % sodium taurocholate into the bilio-pancreatic duct. The test rats with AP were divided into three groups. One was treated with Tet, one with QYT, and one with normal saline solution. The sham-operated control group (SO) rats were only subjected to laparotomy. They were given no further treatment. For the Tet group, Tet was injected intraperitoneally, and for the QYT group, QYT was given with a nose-gastric catheter. These procedures were done at both 10 min and 5 h after AP induction. The levels of ICAM-1 mRNA expression and of SOD (Mn-SOD and Cu, Zn-SOD) mRNA expression in the pancreas and liver tissues were measured by RT-PCR at 1, 5, and 10 h after AP induction.

RESULTS: When compared with the SO group during the observation time, rats with AP showed a higher expression of ICAM and a lower expression of Mn-SOD in both pancreas and liver tissues, and a lower expression of Cu, Zn-SOD in the pancreas. Tet treatment attenuated changes in the expression of both ICAM-1, and SOD (Mn-SOD and Cu, Zn-SOD) to a significant degree. A similar effect on the expression of SOD (Mn-SOD and Cu, Zn-SOD) was also found in the QYT group, but no obvious suppressive effect on ICAM-1 expression was observed.

CONCLUSION: The results of this study suggest that one of the main mechanisms of Tet and QYT in treating AP is to enhance anti-oxidation of the body. The results also suggest that the anti-inflammatory effect of Tet is involved in the reduction of ICAM-1 expression. This explains why Tet and QYT are beneficial in treating AP.

Li YY, Li XL, Yang CX, Zhong H, Yao H, Zhu L. Effects of Tetrandrine and QYT on ICAM-1 and SOD gene expression in pancreas and liver of rats with acute pancreatitis. *World J Gastroenterol* 2003; 9(1): 155-159

<http://www.wjgnet.com/1007-9327/9/155.htm>

INTRODUCTION

Acute pancreatitis (AP) is a severe disease with both high morbidity and high mortality. Therefore, much research has been focused on the specific and effective therapies for AP^[1-6]. Tetrandrine (Tet) is a kind of dibenzyl quinoline alkaloid extracted from the root of *Stephania tetrandra* S., a Chinese herbal medicine. Qing Yi Tang (QYT) is a medicine composed of several Chinese herbs. Both Tet and QYT have shown positive treatment effects on AP clinical patients and on animal models. These include attenuation of clinical symptoms, improvement of morphology and biochemistry changes in the tissues and blood, prolongation of survival time, and decrease of mortality^[7-10]. In order to explore some of the molecular mechanisms combating AP, the effects of Tet and QYT on gene expression of both intercellular adhesion molecule 1 (ICAM-1) and superoxide dismutase (Mn-SOD and Cu,Zn-SOD) were investigated in a rat model with AP.

MATERIALS AND METHODS

Chemicals

Chemicals used in this experiment were purchased as follows: Sodium pentobarbital and sodium taurocholate (NaTc) from Shanghai Chemical Reagent Company; TRIzol reagent and SuperscriptTM II from GIBCO-BRL (Shanghai); Oligonucleotide primer pairs from Chinese Academy of Science, Institute of Cell and Biology (Shanghai); Taq DNA polymerase from Promega (Shanghai); Tet from the Department of Pharmacology of Second Military Medical University (Shanghai); QYT from Zunyi Medical College (Zunyi); other reagents from Sigma Chemical (Shanghai).

Animals and AP model

The subjects for the experiment were adult male and female Sprague-Dawley rats weighing 170-230 g ($n=36$; the Animal Center, Fudan University Medical College, Shanghai). After fasting with free access to water overnight, the rats were anesthetized by an intraperitoneal (ip) injection of 40 mg/kg sodium pentobarbital. AP was induced by a retrograde injection of 4 % NaTc into the bilio-pancreatic duct (BPD) according to the method of Aho *et al*^[11]. Briefly, a small median laparotomy was performed first, and then the pancreas was exteriorized and the BPD was temporarily closed at the liver hilum with a soft microvascular clamp to prevent reflux of the infused material into the liver. A retrograde injection of 4 % NaTc into the distal BPD was then given (100 ul/100body wt, pressure 50cmH₂O). The clamp was removed 5 min after the injection. In the sham-operated control group (SO) rats only underwent laparotomy. Finally, the abdomen was closed with a silk suture and the rats were placed back into their cages with free access to water and food.

Animal group

The test rats with AP were divided into three groups: Tet, QYT and normal saline (NS). The Tet group ($n=9$) received an injection (ip) of 4% Tet at a dosage of 80 mg/kg body wt. The QYT group ($n=9$) received an infusion of QYT (1 ml/100 g body wt), and the NS group ($n=9$) received an infusion of NS (1 ml/100 g body wt), by use of a nose-gastric catheter. Rats in the SO group received the same infusion as the NS group. All groups were treated two times (at 10 min and 5 h after the AP operation).

Preparation of RNA and RT-PCR assay

At selected times (1, 5, 10 h) after the AP induction or sham operation, the rats ($n=3$ at each time point) underwent relaparotomy under pentobarbital anesthesia, and samples of the pancreas and liver were rapidly collected. Total RNA was extracted from pancreatic and liver tissues using the TRIzol reagent. RNA quality was verified by ethidium bromide staining of ribosomal RNA bands on agarose gel. Total RNA was precipitated and re-suspended in diethylpyrocarbonate-treated sterile H_2O , quantified by spectrophotometry (A260/A280 ratio >1.80) and diluted to a concentration of 1.0 $\mu\text{g}/\mu\text{l}$. Then the extracted RNA was used for a semi-quantitative reverse transcription-polymerase chain reaction (RT-PCR). Total RNA (5 $\mu\text{g}/\text{sample}$) was reverse-transcribed using oligo (dT) as a primer. The oligonucleotide primer pairs were designed from published sequences for each gene studied. The sequences used as G3PDH, SOD and ICAM-1 specific primers are shown in Table 1.

Table 1 Sequence of primers and length of fragments

Gene	Primer (5' → 3')	Length
G3PDH	ACCACAGTCCATGCCATCAC	452 bp
	TCCACCACCTGTTGCTGTA	
Mn-SOD	ATTAACGCGCAGATCATGCAG	483 bp
	TTTCAGATAGTCAGGTCTGACGTT	
CuZn-SOD	TTCGAGCAGAAGGCAAGCGGTGAA	396 bp
	AATCCCAATCACACCACAAGCCAA	
ICAM-1	CCTTAGGAAGGTGTGATATCCGG	415 bp
	AGGTGGTCACCCATGCTGGTGCT	

Two-microliter aliquots of cDNA were used as a target for separate PCR reactions in the presence of 0.5 units of Taq DNA polymerase, 50 $\mu\text{mol}/\text{L}$ of a primer pair specific for G3PDH, SOD or ICAM-1, and amounts of the corresponding constructs. The total volume of the reaction fluid was 25 μl .

The amplification cycles were carried out in a DNA Thermalcycler (Perkin Elmer) under the following conditions: initial denaturation at 94 for 2 min, followed by amplification cycles of 1 min at 94 $^{\circ}\text{C}$, 1 min at 58 $^{\circ}\text{C}$ and 1 min at 72 $^{\circ}\text{C}$. This procedure was repeated for 30 cycles. PCR products were separated by polyacrylamide gel electrophoresis and then visualized by ethidium bromide staining. The intensities of gene-specific bands were photographed and quantified by measuring the optical density (OD) of the bands in a UVP (white/UV transilluminator, GDS 7500). In the same sample, mRNA levels were normalized to the density of an internal control housekeeping gene RT-PCR product, glyceraldehyde-3-phosphate dehydrogenase (G3PDH), which is commonly used as an internal standard control in mRNA expression studies. RT-PCR was performed independently at least twice starting from the same RNA.

Statistical analysis

Data were expressed as mean \pm SE. Statistical differences between values from two groups were determined by the unpaired Student's *t*-test and statistical significance was set at $P < 0.05$.

RESULTS

G3PDH level

The level of G3PDH was approximately the same for all pancreas and liver samples tested (Figure 1), which indirectly showed that the cDNA concentration did not differ in the samples from each group.

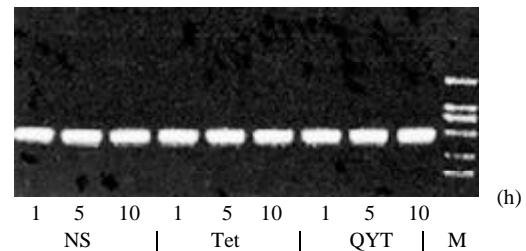


Figure 1 GAPDH mRNA expression in the liver in the parts of different group.

ICAM-1 mRNA expression in the pancreas and liver

Semi-quantitative evaluation of ICAM-1 level was obtained by measuring its gene expression by RT-PCR. As shown in Figure 2 and Figure 2B, the pancreas showed an increased ICAM-1 mRNA expression in the NS group at 5 h and 10 h after AP induction when compared to the SO group. Tet attenuated the increase at the same time-points. But QYT showed an increase effect for ICAM-1 mRNA expression at 10 h after AP. In the liver, compared with the SO group, the level of ICAM-1 mRNA expression in the NS group was elevated at 1 h and sustained up to 10 h, with a maximum increase (2-fold) at 5 h after AP induction. A similar change but at a lower level was observed in the Tet group. And in the QYT group a modest increase of ICAM mRNA expression occurred only at 5 h and 10 h after AP induction. (Figure 3 and Figure 3B).

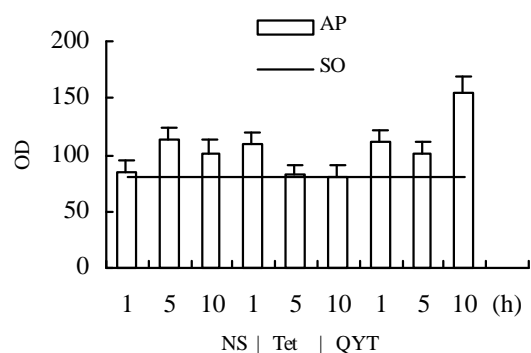


Figure 2A ICAM-1 mRNA expression in the pancreas in the different groups.

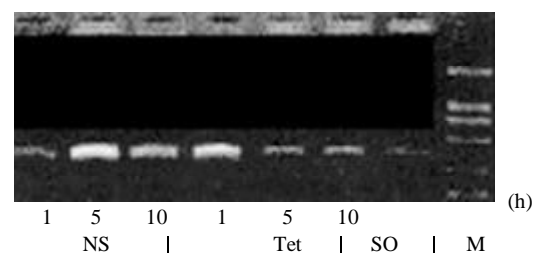


Figure 2B ICAM-1 mRNA expression in the pancreas in the different groups.

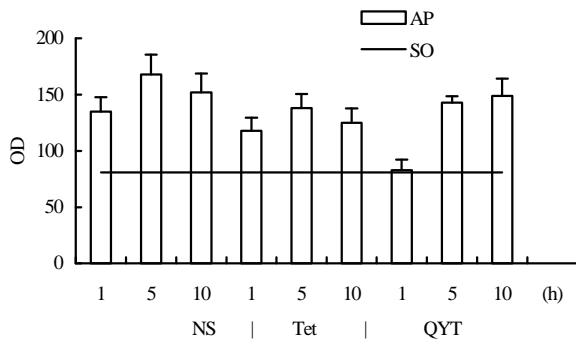


Figure 3A ICAM-1 mRNA expression in the liver in the different groups.

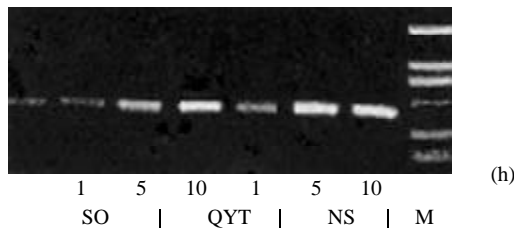


Figure 3B ICAM-1 mRNA expression in the liver in the parts of different groups.

Mn-SOD mRNA expression in the pancreas and liver

As shown in Figure 4 and Figure 4B, in the pancreas, compared to the SO group, Mn-SOD mRNA expression in the NS group was lower from 1 h to 5 h after AP induction. The Tet-treated group had a higher expression at the same time-points, and the QYT-treated group had a much higher expression at 10 h, nearly a 2-fold increase compared to that of the NS group. As shown in Figure 5 and Figure 5B, the NS group showed a similar decrease of Mn-SOD mRNA expression in the liver to that in the pancreas at 1 h and 5 h. When compared to the NS group, the Tet-treated group had a higher Mn-SOD mRNA expression from 1 h to 10 h, and the QYT group had a higher Mn-SOD mRNA expression from 5 h to 10 h, after AP induction.

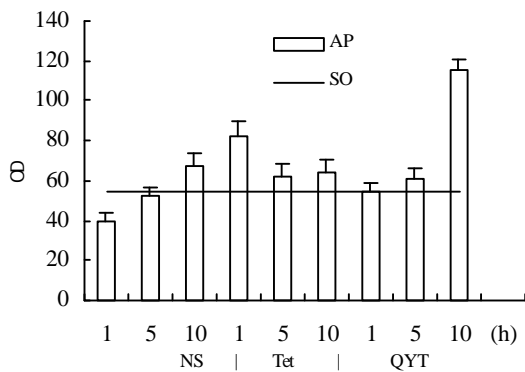


Figure 4A Mn-SOD mRNA expression in the pancreas in the different groups.

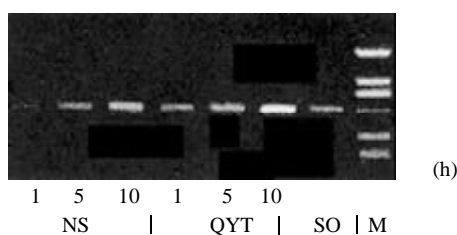


Figure 4B Mn-SOD mRNA expression in the pancreas in the parts of different groups.

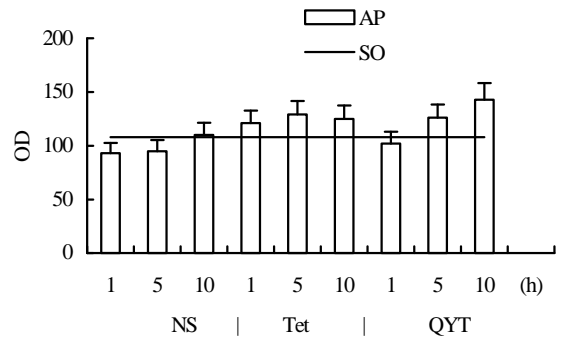


Figure 5A Mn-SOD mRNA expression in the liver in the different groups.

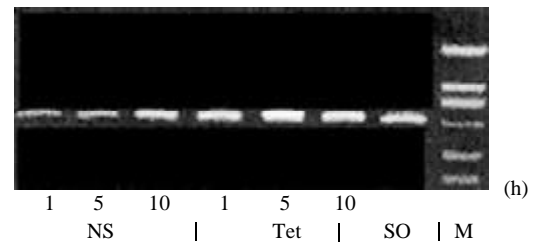


Figure 5B Mn-SOD mRNA expression in the liver in the parts of different groups.

Cu,Zn-SOD mRNA expression in the pancreas and the liver

As shown in Figure 6 and Figure 6B, in the pancreas, the NS group decreased significantly in Cu, Zn-SOD mRNA expression after AP induction to 1/3 of that in SO group. The Tet and QYT- treated groups had much higher levels of Cu, Zn-SOD mRNA expression at 1 h and 10 h respectively. These high levels were a 2-fold increase when compared with the SO group, and a 4-fold increase when compared with the NS group at the same time points. In the liver, no obvious changes of SOD expression were observed (Figure7).

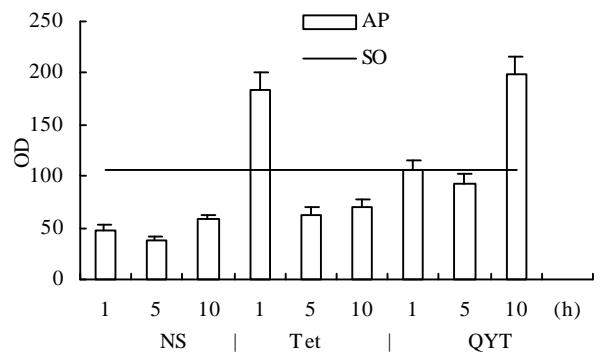


Figure 6A Cu, Zn-SOD mRNA expression in the pancreas in the different groups.

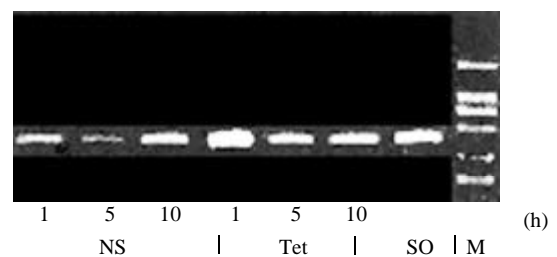


Figure 6B Cu, Zn-SOD mRNA expression in the pancreas in the parts of different groups.

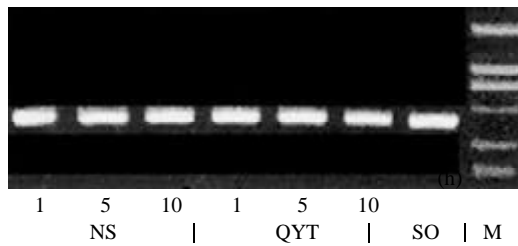


Figure 7 Cu, Zn-SOD mRNA expression in the liver in the parts of different groups.

DISCUSSION

Research on AP can be traced back at least one hundred years, yet the treatment of AP continues to be a difficult aspect of clinical practice, especially for severe acute pancreatitis (SAP). SAP is recognized to be a multiple-stage disease where the pathological events at the pancreatic acinar cell level are paralleled by an exaggerated local and systemic inflammatory response (SIRS), and even by multiple-organ damage (MODS) or failure (MOF), with a high mortality^[12-15]. Considerable progress in understanding of pathophysiologic events during the early stage of AP has been made over the years, but the underlying pathogenic processes responsible for the inflammatory cascade and MOF are still unknown to a large extent. Most recent studies have revealed that the excessive releases of oxygen-derived free radicals (OFRs), destructive inflammatory mediators and cytokines, such as TNF-alpha, IL-1beta, IL-6, IL-8, IL-10, PAF, ICAM-1, play key roles in the AP process^[16-19]. Recent evidence suggests that, besides their directly detrimental effects on AP, OFRs may activate certain gene transcription factors, notably the nuclear transcription factor-kappa B (NF-kB) and activator protein-1 (AP-1), which then mediate the induction of certain adhesion molecules (ICAM, VCAM, etc.) and other cytokines^[15,20-23]. These factors prompt neutrophil aggregation, adherence and activation, then tremendous amounts of inflammatory mediators and cytokines are released. The pancreas and remote organs are then severely injured and MOF occurs. Meanwhile, activation of leukocyte may release more OFRs, and the vicious circle continues^[24-27].

The manganese superoxide dismutase (Mn-SOD) and copper/zinc superoxide dismutase (Cu, Zn-SOD) existing in the mitochondria or cytoplasm of cells are the major OFR scavengers of the body. Previous experiments have demonstrated that the pathological changes in AP could be reduced by SOD^[28,29]. By immunohistochemistry, Su *et al* have proved the localization of SOD in acinar cells and have found Mn-SOD mRNA expression peaked at 2 hours after the addition of arginine to the cell culture medium^[30]. These data suggest that increased SOD expression reflects a defensive mechanism of acinar cells against oxidative stress. G. Teleck *et al* discovered that the increase of OFRs and ICAM expression could be measured within one hour and lasted for the 24 hour observation period^[31]. These findings, along with others from different laboratories, suggest that OFRs and ICAM induce morphologic change, aggregation, adherence, and activation of polymorphonuclears (PMNs), which then shift out of blood vessels and consequently cause microcirculation dysfunction^[32,33]. Our experimental results showed that during the process of AP, the expression of ICAM-1 in both the pancreas and the liver (especially in liver) was significantly increased, while the expressions of Mn-SOD and Cu-Zn-SOD were decreased in the pancreas by 1/3 as compared to the SO control group. This was similar to the finding of the experiment by L. Czako *et al*^[28]. These results provide further evidence that the increased ICAM-1 and decreased OFRs scavengers take part in the

pathophysiologic processes of AP.

Tet is a kind of dibenzyl quinoline alkaloid extracted from the root of *Stephania tetrandra* S., a Chinese herbal medicine with the effect of a non-selective calcium channel blocker (CCB). It has recently been found that Tet also has a widely anti-inflammatory effect by reducing the activity of PLA2 from inflammatory leukocytes, inhibiting the release of inflammatory mediators, eliminating OFRs and dilating blood vessels, and then improving microcirculation function of the body^[7,8,34,35]. QYT is a combined medication of Chinese herbs containing *Rheum officinale* Baillon, *ructus gardeniae*, etc., and also has the effects of anti-inflammation, cleaning OFRs, eliminating hazardous metabolite, dilating blood vessels and improving microcirculation^[9,10]. We found in this experiment that Tet reduced ICAM expression in the pancreatic and hepatic tissues during AP, while increasing the expression of Mn-SOD, and Cu, Zn-SOD. QYT had no significant effect on the expression of ICAM-1, but significantly enhanced the expression of Mn-SOD, and Cu, Zn-SOD. These findings suggest that Tet and QYT demonstrate the potentially useful effects of eliminating OFRs and reducing their damage, and also demonstrate the ability of Tet inhibiting ICAM production. The experiment provided a molecular level explanation of why clinical treatment of AP using Tet and QYT has been successful.

It is generally recognized that the induction of AP follows a uniform mechanism independent of different etiologic causes such as gallstones, alcohol, ischemia, hyperlipidemia, hypercalcemia, heredity and others. Firstly, each cause seems to affect primarily the acinar cell, resulting in intracellular activation of trypsinogen and other digestive enzymes and over-production of OFRs, which injure the acinar cells and pancreatic tissue. Then tremendous amounts of inflammatory mediators and cytokines, mentioned above, are released into the tissue and result in microcirculation disturbance. This not only worsens the local damage, but also influences the remote organs and causes systemic inflammatory response syndrome (SIRS). In the final stage of the pathophysiological process, multi-organ damage develops and multi-organ failure (MOF) may happen due to the combined effects of all the factors. Klar *et al* pointed out^[36] that since the initial enzyme activation and cytokine release were irreversible by the time of clinical presentation, specific therapy must be directed towards microperfusion failure as a secondary pathogenic stage. The beneficial therapeutic principles of this included the inhibition of leukocyte-endothelium interaction with ICAM-1 antibodies and the control of local vasoconstriction to stop the progression of the disease. Therefore, based on previously observed clinical effects and on the experimental results with Tet and QYT in this study, we conclude that Tet and QYT which inhibit ICAM-1 and enhance SOD expression are beneficial in treating AP.

REFERENCES

- 1 **Slavin J**, Ghaneh P, Sutton R, Hartley M, Rowlands P, Garvey C, Hughes M, Neoptolemos J. Mngement of necrotizing pancreatitis. *World J Gastroenterol* 2001; **7**: 476-481
- 2 **Masamune A**, Shimosegawa T, Satoh A, Fujita M, Sakai Y, Toyota T. Nitric oxide decreases endothelial activation by rat experimental severe pancreatitis-associated ascitic fluids. *Pancreas* 2000; **20**: 297-304
- 3 **Hughes CB**, el-Din AB, Kotb M, Gaber LW, Gaber AO. Calcium channel blockade inhibits release of TNF alpha and improves survival in a rat model of acute pancreatitis. *Pancreas* 1996; **13**: 22-28
- 4 **Eibl G**, Buhr HJ, Foitzik T. Therapy of microcirculatory disorders in severe acute pancreatitis: what mediators should we block? *Intensive Care Med* 2002; **28**: 139-146
- 5 **Rau B**, Bauer A, Wang A, Gansauge F, Weidenbach H, Nevalainen T, Poch B, Beger HG, Nussler AK. Modulation of

- endogenous nitric oxide synthase in experimental acute pancreatitis: role of anti-ICAM-1 and oxygen free radical scavengers. *Ann Surg* 2001; **233**: 195-203
- 6 **Deng Q**, Wu C, Li Z. The prevention of infection complicating acute necrotizing pancreatitis: an experimental study. *Zhonghua Waikexue* 2000; **38**: 625-629
 - 7 **Leng DY**, Yu J, Luo JR, Yu JB. Tet was used in the treatment of patients with severe acute pancreatitis. *Dangdai Yishi* 1997; **2**: 59-60
 - 8 **Zhang H**, Li YY. Therapeutic effect of Tetrandrine on experimental acute pancreatitis. *Zunyiyi Xueyuan Xuebao* 2000; **23**: 91-95
 - 9 **Li ZL**, Wu CT, Lu LR, Zhu XF, Xiong DX. Traditional Chinese medicine Qing Yi Tang alleviates oxygen free radical injury in acute necrotizing pancreatitis. *World J Gastroenterol* 1998; **4**: 357-359
 - 10 **Wu C**, Li Z, Xiong D. An experimental study on curative effect of Chinese medicine qing yi tang in acute necrotizing pancreatitis. *Zhongguo Zhongxiyi Jiehe Zazhi* 1998; **18**: 236-238
 - 11 **Aho HJ**, Koskensalo SM, Nevelainen TJ. Experimental pancreatitis in the rat. Sodium taurocholate-induced acute haemorrhagic pancreatitis. *Scand J Gastroenterol* 1980; **15**: 411-416
 - 12 **Zhang H**, Li YY. The study progresses on the mechanisms of pancreatitis. *Zhongguo Weizhongbing Jijiu Yixue* 2000; **12**: 116-119
 - 13 **Li YY**, Zhang H. The pathogenesis role of intracellular calcium overload in acute pancreatitis. *Zhongguo Zhongxiyi Jiehe Waikexue* 2001; **7**: 123-125
 - 14 **Li YY**, Gao ZF. The possible role of nuclear factor-kB in the pathogenesis of acute pancreatitis. *Shijie Huaren Xiaohua Zazhi* 2001; **9**: 420-421
 - 15 **Wu XZ**. Therapy of acute severe pancreatitis awaits further improvement. *World J Gastroenterol* 1998; **4**: 285-286
 - 16 **Telek G**, Regoly-Merei J, Kovacs GC, Simon L, Nagy Z, Hamar J, Jakab F. The first histological demonstration of pancreatic oxidative stress in human acute pancreatitis. *Hepatogastroenterology* 2001; **48**: 1252-1258
 - 17 **Bhatia M**, Neoptolemos JP, Slavin J. Inflammatory mediators as therapeutic targets in acute pancreatitis. *Curr Opin Investig Drugs* 2001; **2**: 496-501
 - 18 **Menger MD**, Plusczyk T, Vollmar B. Microcirculatory derangements in acute pancreatitis. *J Hepatobiliary Pancreat Surg* 2001; **8**: 187-194
 - 19 **Bhatia M**, Brady M, Shokuhi S, Christmas S, Neoptolemos JP, Slavin J. Inflammatory mediators in acute pancreatitis. *J Pathol* 2000; **190**: 117-125
 - 20 **Blanchard JA 2nd**, Barve S, Joshi-Barve S, Talwalker R, Gates LK Jr. Antioxidants inhibit cytokine production and suppress NF-kappaB activation in CAPAN-1 and CAPAN-2 cell lines. *Dig Dis Sci* 2001; **46**: 2768-2772
 - 21 **Vaquero E**, Gukovsky I, Zaninovic V, Gukovskaya AS, Pandol SJ. Localized pancreatic NF-kappaB activation and inflammatory response in taurocholate-induced pancreatitis. *Am J Physiol Gastrointest Liver Physiol* 2001; **280**: G1197-1208
 - 22 **Jaffray C**, Yang J, Carter G, Mendez C, Norman J. Pancreatic elastase activates pulmonary nuclear factor kappa B and inhibitory kappa B, mimicking pancreatitis-associated adult respiratory distress syndrome. *Surgery* 2000; **128**: 225-231
 - 23 **Han B**, Logsdon CD. Cholecystokinin induction of mob-1 chemokine expression in pancreatic acinar cells requires NF-kappaB activation. *Am J Physiol* 1999; **277**: C74-82
 - 24 **Chang CK**, Albarillo MV, Schumer W. Therapeutic effect of dimethyl sulfoxide on ICAM-1 gene expression and activation of NF-kB and Ap-1 in septic rats. *J Surg Res* 2001; **95**: 181-187
 - 25 **Yeh LH**, Kinsey AM, Chatterjee S, Alevriadou BR. Lactosylceramide mediates shear-induced endothelial superoxide production and intercellular adhesion molecule-1 expression. *J Vasc Res* 2001; **38**: 551-559
 - 26 **Zaninovic V**, Gukovskaya AS, Gukovsky I, Mouria M, Pandol SJ. Cerulein upregulates ICAM-1 in pancreatic acinar cells, which mediates neutrophil adhesion to these cells. *Am J Physiol Gastrointest Liver Physiol* 2000; **279**: G666-676
 - 27 **Jaffray C**, Yang J, Norman J. Elastase mimics pancreatitis-induced hepatic injury via inflammatory mediators. *J Surg Res* 2000; **90**: 95-101
 - 28 **Czako L**, Takacs T, Varga IS, Tiszlavicz L, Hai DQ, Hegyi P, Matkovics B, Lonovics J. Oxidative stress in distant organs and the effects of allopurinol during experimental acute pancreatitis. *Int J Pancreatol* 2000; **27**: 209-216
 - 29 **Rau B**, Poch B, Gansauge F, Bauer A, Nussler AK, Nevelainen T, Schoenberg MH, Beger HG. Pathophysiologic role of oxygen free radicals in acute pancreatitis: initiating event or mediator of tissue damage. *Ann Surg* 2000; **231**: 352-360
 - 30 **Su SB**, Motoo Y, Xie MJ, Mouri H, Asayama K, Sawabu N. Superoxide dismutase is induced during rat pancreatic acinar cell injury. *Pancreas* 2002; **24**: 146-152
 - 31 **Telek G**, Ducroc R, Scoazec JY, Pasquier C, Feldmann G, Roze C. Differential upregulation of cellular adhesion molecules at the sites of oxidative stress in experimental acute pancreatitis. *J Surg Res* 2001; **96**: 56-67
 - 32 **Zhou ZG**, Chen YD, Sun W, Chen Z. Pancreatic microcirculatory impairment in experimental acute pancreatitis in rats. *World J Gastroenterol* 2002; **8**: 933-936
 - 33 **Masamune A**, Shimosegawa T, Kimura K, Fujita M, Sato A, Koizumi M, Toyota T. Specific induction of adhesion molecules in human vascular endothelial cells by rat experimental pancreatitis-associated ascitic fluids. *Pancreas* 1999; **18**: 141-150
 - 34 **Jiang JM**, Dai DZ. The study progress for tetrandrine-a calcium channel blocker. *Zhongguo Yaolixue Tongbao* 1998; **14**: 297-300
 - 35 **Zhang H**, Li YY. Therapeutic effect of tetrandrine on pancreas and lung injury in rats with experimental acute pancreatitis. *Tongji Daxue Xuebao (Yixue Branch)* 2002; **23**: 363-367
 - 36 **Klar E**, Werner J. New pathophysiologic knowledge about acute pancreatitis. *Chirurg* 2000; **71**: 253-264

Alterations of p53 and PCNA in cancer and adjacent tissues from concurrent carcinomas of the esophagus and gastric cardia in the same patient in Linzhou, a high incidence area for esophageal cancer in northern China

Hong Chen, Li-Dong Wang, Mei Guo, She-Gan Gao, Hua-Qin Guo, Zong-Min Fan, Ji-Lin Li

Hong Chen, Li-Dong Wang, She-Gan Gao, Zong-Min Fan, Hua-Qin Guo, Laboratory for Cancer Research, College of Medicine, Zhengzhou University, Zhengzhou, Henan Province, 450052, China
Mei Guo, Anyang City Tumor Hospital, Anyang, Henan Province, 455000, China

Ji-Lin Li, Yaocun Esophageal Hospital of, Anyang, Henan Province, 456592, China

Supported by National Outstanding Young Scientist Award of China, No.30025016 and Foundation of Henan Education Committee

Correspondence to: Li-Dong Wang, Laboratory for Cancer Research, College of Medicine, Zhengzhou University, Zhengzhou 450052, Henan Province, China. ldwang@371.net

Telephone: +86-371-6970165 **Fax:** +86-371-6970165

Received: 2002-07-23 **Accepted:** 2002-08-07

Abstract

AIM: To characterize the alteration and significance of p53 and PCNA in cancer and adjacent tissues of concurrent cancers from the esophagus and gastric cardia in the same patient.

METHODS: P53 and PCNA protein accumulation in 25 patients with concurrent cancers from the esophagus and gastric cardia (CC, concurrent carcinomas of esophageal squamous cell carcinoma and gastric cardia adenocarcinoma) were detected by immunohistochemical method (ABC).

RESULTS: In CC patients, both esophageal squamous cell carcinoma (SCC) and gastric cardia adenocarcinoma (GCA) tissues showed different positive immunostaining extent of p53 and PCNA protein ($P > 0.05$). The positive immunostaining rates for p53 and PCNA were 60 % (15/25) and 92 % (23/25), respectively in SCC; and 40 % (10/25) and 88 % (22/25), respectively in GCA. "Diffuse" immunostaining pattern was frequently observed in both p53 and PCNA. High coincidence rates for p53 and PCNA positive staining were observed in SCC and GCA from the same patients, and accounted for 56 % and 96 %. In SCC patients, with the lesions progressed from normal esophageal epithelium (NOR) to basal cell hyperplasia (BCH) to dysplasia (DYS) to carcinoma *in situ* (CIS) to SCC, the positive rates for p53 were 27 %, 50 %, 50 %, 29 % and 72 %, and 55 %, 70 %, 75 %, 71 % and 93 % for PCNA, respectively. In GCA, with the lesions progressed from normal gastric cardia epithelium to DHS to CIS to GCA, the positive rates of p53 expression were 44 %, 27 %, 22 % and 36 % respectively, the difference was not significant; the positive rates of PCNA protein expression were 67 %, 64 %, 67 % and 86 %, respectively. The χ^2 test, Fisher's Exact Test, Mantel-Haenszel χ^2 Test and Kappa Test were used for the statistics.

CONCLUSION: The high coincident alterations for P53 and PCNA in SCC and GCA from the same patient indicate the possibility of similar molecular basis, which provides important molecular basis and etiological clue for similar geographic distribution and risk factors in SCC and GCA.

Chen H, Wang LD, Guo M, Gao SG, Guo HQ, Fan ZM, Li JL. Alterations of p53 and PCNA in cancer and adjacent tissues from concurrent carcinomas of the esophagus and gastric cardia in the same patient in Linzhou, a high incidence area for esophageal cancer in northern China. *World J Gastroenterol* 2003; 9(1): 16-21

<http://www.wjgnet.com/1007-9327/9/16.htm>

INTRODUCTION

Esophageal squamous cell carcinoma (SCC) and gastric cardia adenocarcinoma (GCA) are the two most frequent malignant diseases in the world^[1-3]. SCC is characterized by its remarkable geographic distribution; the ratio between the incident rates of high- and low-risk areas can be as high as 500:1. Consistent geographic distribution with SCC in the same high-incidence area (HIA) is the remarkable epidemiological characteristic of GCA^[3], and in America and Europe the incidence of GCA increased dramatically in recent decades^[4-8]. Linzhou and the nearby counties in Henan province, have the highest incidence and mortality for SCC and GCA in the world, SCC and GCA remain the leading cause of cancer-related death in these areas^[9].

It is noteworthy that the concurrent cancers from esophagus and gastric cardia in the same patient (CC) is not uncommon in this area, with an incidence of 0.4-2.5 %^[10-13]. This special pattern indicates that there may be same or similar risk factors and mechanism involved in the carcinogenesis. The molecular mechanism of SCC/GCA is still not clear, and the information from the concurrent cancers of SCC & GCA in the same patient in the HIA is very limited. It is apparent to further characterize the molecular changes of CC patients may provide not only more information on the molecular mechanism but also the etiological clues for SCC and GCA.

Recent studies indicate that esophageal and gastric cardia carcinogenesis is a multistep progressive process involving multiple genetic changes (accumulation or overlap). The accumulation of p53 protein and p53 gene mutation were observed in the very early stage of esophageal carcinogenesis, even in the microscopically normal esophageal epithelium, with positive immunostaining and mutation rates increasing with the progression of lesions^[14-24]. In addition, recent study showed that PCNA protein overexpression was also observed in the carcinogenesis of GCA^[25].

To elucidate the molecular mechanisms of SCC/GCA carcinogenesis and to expand the knowledge for early detection of SCC/GCA and screening high-risk population, the present study was undertaken to analyze the alternations of p53 and PCNA in cancer tissues and adjacent cancerous tissues with different degrees of precancerous lesions in CC patients.

MATERIALS AND METHODS

Tissue collection and processing

25 cases with concurrent cancers of SCC & GCA enrolled in this study were from Linzhou City Hospital, Yaocun

Esophageal Cancer Hospital and Anyang City Tumor Hospital, the high-incidence area for EC, including 16 males and 9 females, with a mean age of 59 (59±9.88) in male and 60.6 (60.6±11.44) in female. None of these patients received any treatment of chemotherapy or radiotherapy before operation. All the resected tissues and biopsied tissues were fixed with 85 % alcohol, embedded with paraffin and serially sectioned at 5 µm. The sections were mounted onto the histostick-coated slides. Four or five adjacent ribbons were collected for histopathological diagnosis (hematoxylin and eosin stain) and immunohistochemical staining.

Histopathology analysis

Histopathological diagnosis for esophageal and gastric cardia epithelia was based on the changes in cellular morphology and tissue architecture using previously established criteria^[26-32]. The normal esophageal epithelium (NOR) contained 1 to 3 basal-cell layers; the papillae were confined to the lower half of the epithelium. In basal cell hyperplasia (BCH), the number of proliferating basal cells was increased to more than 3-cell layers. Dysplasia (DYS) was characterized by the partial loss of cell polarity and nuclear atypia. SCC was characterized by confluent and invasive sheets of cohesive, polymorphous cells with hyperchromatic nuclei. The following histopathological classification was used for the gastric-cardia epithelia: dysplasia (DYS), neoplastic features including nuclear atypia and/or architectural abnormalities confined to the gastric epithelium, without invasion; GCA: invasion of neoplastic gastric cells through the basement membrane. The diagnosis of CC was based on the following criteria: (1) the tumors must be clearly separated on histological phenotype; (2) the tumors must be malignant; (3) Metastasis must be excluded.

Immunohistochemical staining (IHC)

Anti-p53 antibody is a monoclonal mouse anti-serum against p53 of human origin, and recognizes both wild and mutant type p53 (Ab-6, Oncogen Science, Manhasset, NY). Anti-PCNA antibody is a monoclonal mouse anti-serum against PCNA of human origin (Mab, DAKO, Carpinteria, CA). The avidin-biotin-peroxidase complex method was used for the immunostaining of p53, PCNA. In brief, after dewaxing, inactivating endogenous peroxidase activity and blocking cross-reactivity with normal serum (Vectastain Elite Kit; Vector, Burlingame, CA), the sections were incubated overnight at 4 °C with a diluted solution of the primary antibodies (1:500 for p53 and 1:200 for PCNA). Location of the primary antibodies was achieved by subsequent application of a biotinylated anti-primary antibody, an avidin-biotin complex conjugated to horseradish peroxidase, and diaminobenzidine (Vectastain Elite Kit, Vector, Burlingame, CA). The slides were counter-stained by hematoxylin. Negative controls were established by replacing the primary antibody with PBS and normal mouse serum. Known immunostaining-positive slides were used as positive controls.

Specific staining for each protein was categorized as either positive or negative based on the presence of brown coloration staining. More than 10 % positively stained cells were graded as positive^[33,34]. Clear staining for nuclei was the criterion for a positive reaction. Immunostaining patterns^[26] were graded into the “focus”, “scattered”, “diffuse”, according to cell distribution in one microscopic eyeshot (×40). All the immunostaining slides were observed by two pathologists independently. The slides with different diagnosis by two pathologists were reviewed again (less than 5 %) until the agreed diagnosis was made.

Statistics analysis

The χ^2 test, Fisher's Exact Test, Mantel-Haenszel χ^2 Test and

Kappa Test were used for the statistics ($P < 0.05$ was considered significant).

RESULTS

Histopathological results

Histopathologically, primary SCC and GCA in the same patient were verified in all 25 cases by two pathologists using an Olympus microscope independently. Of the 14 CC patients (both with cancer and adjacent tissues) examined, in esophagus 11 samples were diagnosed as normal, 10 as BCH, 8 as DYS, 7 as CIS and 14 as SCC; in gastric cardia 9 as normal, 11 as DYS, 9 as CIS and 14 as GCA.

Expression of p53 protein in CC patients (Table 1)

P53 positive immunostaining was observed in the epithelial and tumor cells of esophagus and gastric cardia. In CC patients, both SCC and GCA tissues showed a different extent positive immunostaining of p53 protein (Figure 1,2). In 25 CC patients, the immunostaining rate of p53 protein in SCC was 60 % (15/25) and in GCA was 40 % (10/25), and statistical analysis showed that the difference was not significant ($P > 0.05$). “Diffuse” was the most frequent immunostaining pattern observed in both SCC (60 %, 9/15) and GCA (70 %, 7/10). High coincidence alteration for positive staining of p53 was observed in SCC and GCA from the same patients, and accounted for 56 %.

Table 1 Expression of P53 protein in 25 CC patients

Number	Sex/age	P53 immunostaining			
		SCC		GCA	
		(+/-) ^a	Immunostaining pattern	(+/-) ^a	Immunostaining pattern
001	M/63	+ ^a	Diffuse	- ^a	-
002	M/60	-	-	+	Focus & Scattered
003	M/55	+	Diffuse	-	-
004	M/71	+	Diffuse & Scattered	+	Scattered
005	F/56	+	Scattered & Diffuse	-	-
006	M/59	-	-	-	-
007	F/67	-	-	-	-
008	M/62	+	Diffuse	+	Diffuse
009	F/61	+	Diffuse	-	-
010	F/64	+	Scattered	-	-
011	M/65	+	Diffuse	-	Diffuse
012	M/68	+	Diffuse	-	Diffuse
013	M/57	-	-	-	-
014	M/51	+	Diffuse	-	-
015	M/50	-	-	-	-
016	M/67	+	Scattered	-	Diffuse
017	M/70	+	Focus	-	-
018	M/67	+	Scattered	-	Scattered
019	F/74	-	-	+	Diffuse
020	M/49	-	-	+	Diffuse
021	M/36	-	-	-	-
022	M/70	+	Diffuse	-	-
023	F/74	-	-	-	-
024	F/56	-	-	-	-
025	F/38	+	Scattered	+	Diffuse & Scattered

^a+: positive immunostaining of P53, -: negative immunostaining of P53.

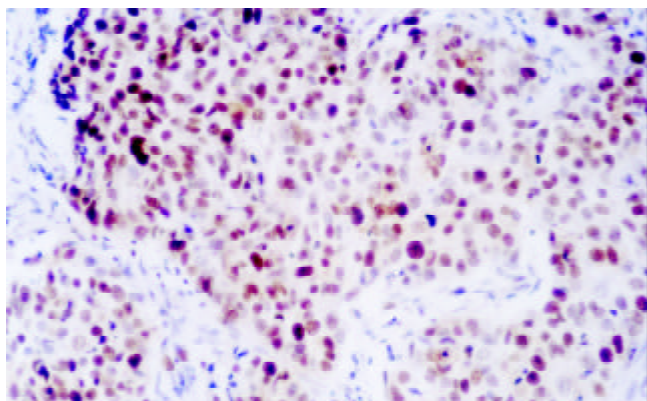


Figure 1 Expression of p53 in SCC ($\times 200$)

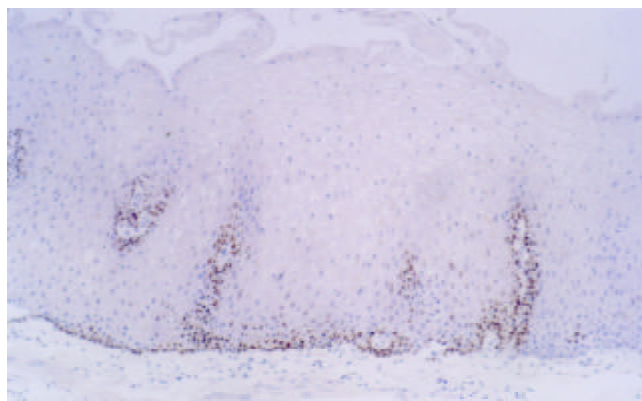


Figure 5 Expression of p53 in NOR (Esophagus) ($\times 200$)

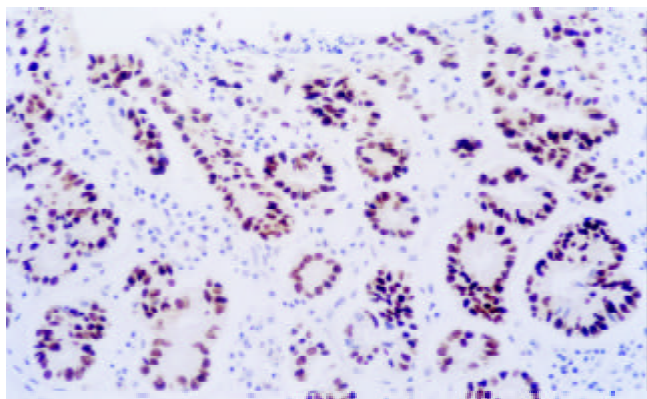


Figure 2 Expression of p53 in GCA ($\times 200$)

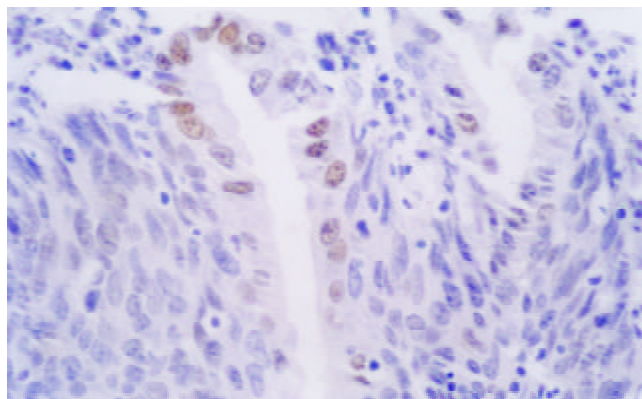


Figure 6 Expression of p53 in NOR (Gastric cardia) ($\times 400$)

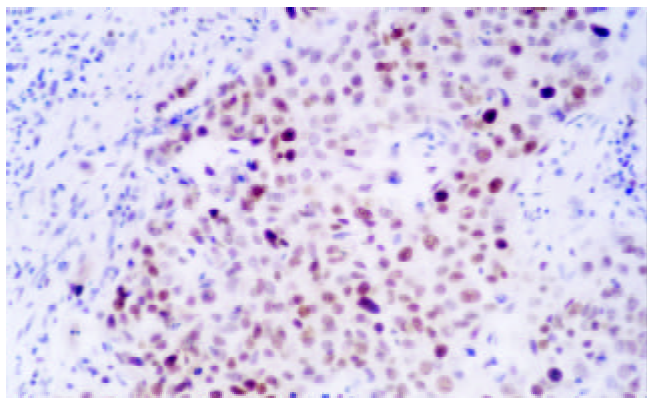


Figure 3 Expression of PCNA in SCC ($\times 200$)

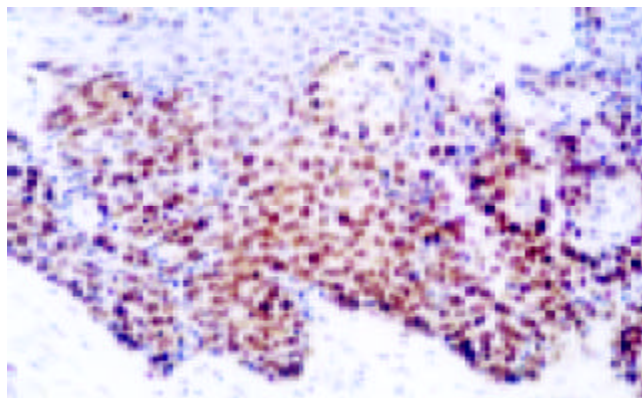


Figure 7 Expression of p53 in CIS (Esophagus) ($\times 200$)

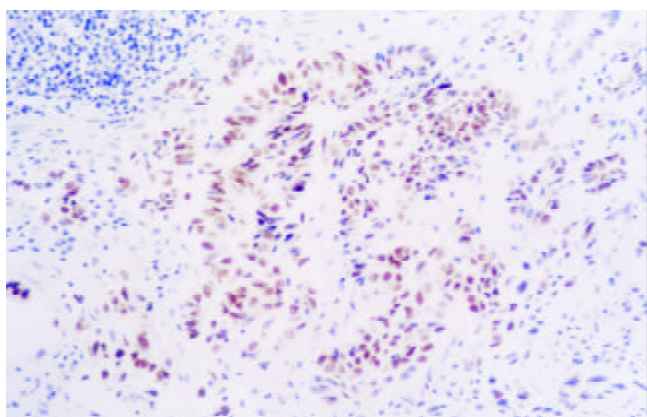


Figure 4 Expression of PCNA in GCA ($\times 200$)

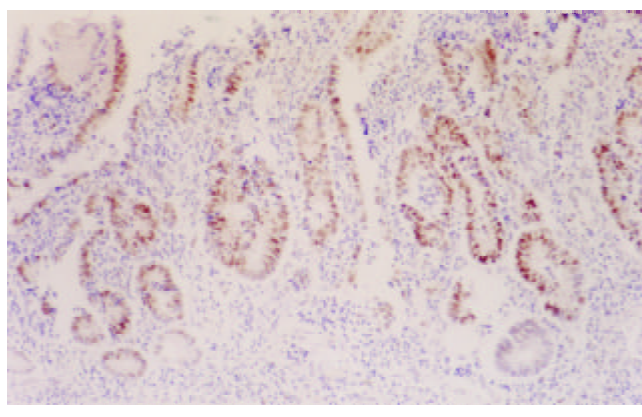


Figure 8 Expression of p53 in DYS (Gastric cardia) ($\times 100$)

Expression of PCNA protein in CC patients (Table 2)

In CC patients, both SCC and GCA tissues showed a different extent positive immunostaining of PCNA protein (Figure 3,4). And the positive immunostaining was observed in the cell nuclei of tumor and epithelial tissues. In 25 CC patients, the immunostaining rate of PCNA protein in SCC was 92 % (23/25) and in GCA was 86 % (19/22), and statistical analysis showed that the difference was not significant ($P>0.05$). "Diffuse" was the most frequent immunostaining pattern observed in both SCC 57 % (13/23) and GCA 86 % (19/22). High coincidence alteration for positive staining of PCNA was observed in SCC and GCA from the same patients, and accounted for 96 % (24/25).

Table 2 Expression of PCNA protein in 25 CC patients

Number	Sex/age	PCNA immunostaining			
		SCC		GCA	
		(+/-) ^a	Immunostaining pattern	(+/-) ^a	Immunostaining pattern
001	M/63	+ ^a	Diffuse	+ ^a	Diffuse
002	M/60	+	Scattered	+	Focus & Scattered
003	M/55	+	Diffuse	+	Diffuse
004	M/71	+	Scattered & Focus	+	Diffuse
005	F/56	+	Scattered & Diffuse	+	Diffuse
006	M/59	+	Scattered & Focus	+	Diffuse
007	F/67	+	Diffuse	+	Focus
008	M/62	+	Diffuse	+	Diffuse
009	F/61	+	Diffuse	+	Diffuse
010	F/64	+	Scattered	+	Diffuse
011	M/65	+	Focus	+	Diffuse
012	M/68	+	Diffuse	+	Diffuse
013	M/57	-	-	-	-
014	M/51	+	Diffuse	-	-
015	M/50	+	Scattered	+	Diffuse
016	M/67	+	Scattered	+	Diffuse
017	M/70	+	Focus	+	Scattered & Focus
018	M/67	+	Diffuse	+	Scattered
019	F/74	+	Diffuse	+	Diffuse
020	M/49	+	Scattered & Focus	+	Diffuse
021	M/36	+	Diffuse	+	Diffuse
022	M/70	-	-	-	-
023	F/74	+	Diffuse	+	Diffuse
024	F/56	+	Scattered & Focus	+	Diffuse
025	F/38	+	Scattered	+	Diffuse

^a+: positive immunostaining of PCNA, -: negative immunostaining of PCNA.

Expression of p53 and PCNA in adjacent cancerous tissues

In SCC patients, with the lesions progressed from normal esophageal epithelium to BCH to DYS to CIS to SCC, an increasing tendency of p53 protein accumulation and PCNA expression were observed, the positive rates for p53 were 27 %, 50 %, 50 %, 29 % and 72 %, and 55 %, 70 %, 75 %, 71 % and 93 % for PCNA, respectively. In GCA, with the lesions progressed from normal gastric cardia epithelium to DYS to

CIS to GCA, the positive rates of p53 expression were 44 %, 27 %, 22 % and 36 % respectively, the difference was not significant; the positive staining of PCNA protein expression were 67 %, 64 %, 67 % and 86 %, respectively, positive rates of PCNA expression in GCA was generally higher than those in precancerous lesions (Table 3) (Figure 5-8).

Table 3 Expression of P53 & PCNA in precancerous lesions of adjacent cancerous tissues

	Number of samples	P53		PCNA	
		+	%	-	%
Esophagus					
NOR	11	3	27	6	55
BCH	10	5	50	7	70
DYS	8	4	50	6	75
CIS	7	2	29	5	71
SCC	14	10	71	13	93
Gastric cardia					
NOR	9	4	44	6	67
DYS	11	3	27	7	64
CIS	9	2	22	6	67
CGA	14	5	36	12	86

DISCUSSION

In this study, indistinguishable overexpressions of p53 and PCNA protein and the same main immunostaining pattern (Diffuse) of immunoreaction were observed in primary SCC and GCA from the same patient. We also found that in CC patient p53 and PCNA had high coincident alteration in both SCC and GCA. These results indicated that SCC and GCA in the same patient might have the similar molecular basis and mechanism of carcinogenesis. These results might be a molecular explanation of the consistent geographic distribution of SCC and GCA. That further characterized the molecular alterations in different stages of SCC and GCA and their relations with morphological changes would provide more information to elucidate the carcinogenesis of SCC and GCA. In this study, high PCNA positive staining rates were observed in CC patient, both in esophageal and gastric cardia epithelia. It inferred that in this high-incidence area, the alimentary canal of patients exposed to similar risk factor might lead the esophageal and gastric cardia epithelial cells to become the hotspot of hyperproliferation, which might be a molecular evidence of hypothesis of field cancerization^[35,36]. The hypothesis of field cancerization is an explanation of multiple primary malignant neoplasms, which consider the tissues of similar architecture exposed to similar pathogen might occur independently as precancerous lesions in multiple sites of the organ.

It is very important for the diagnosis of CC and multiple primary SCC/GCA to exclude local metastasis. In this study, microscopic observation showed that mixed of SCC and GCA tissue was observed occasionally in some patients, and the tissues adjacent to SCC and GCA had different patterns of precancerous lesions, which were characterized by either isolated or in succession. These unique information provided important clues to study the molecular basis of SCC/GCA carcinogenesis and sensibility.

Through the contrast study of adjacent cancerous tissues of SCC and GCA, we found that different extent of overexpressions of p53 and PCNA were already observed in the apparently normal epithelia and very early precancerous

lesions of esophagus and gastric cardia. Especially, from normal epithelia (NOR) to different precancerous lesions to SCC, of both p53 and PCNA protein positive staining rate increased accordingly in the esophagus, and PCNA increased in gastric cardia, but did not show the tendency of increase. Other researchers' results showed that from NOR to precancerous lesions to SCC/GCA, positive staining of p53 and PCNA showed a continuous increasing tendency^[14,25,37-44]. So the explanation of our result might be that IHC qualitative analysis cannot reflect the number of immunostaining cells, and only show the alteration of immunostaining rates. The use of quantitative analysis may solve this problem. In this study we also found that in the stage of CIS, both esophagus and gastric cardia tissues showed a decrease of positive staining rate of p53. It might due to that precancerous lesions have an instable characteristic of bidirectional development, that is, in the multistage progression course of carcinogenesis precancerous lesions might progress to cancer, or reverse to low-grade lesion or even normal^[14]. These results inferred that the molecular changes of SCC and GCA not only were similar in the ultimate stages but also in the early stages, so the CC patient might have similar carcinogenetic course in primary SCC and GCA, but their precise mechanism and biological significance need further study.

REFERENCES

- 1 **Wang LD**, Zhou Q, Yang CS. Esophageal and gastric cardia epithelial cell proliferation in northern Chinese subjects living in a high-incidence area. *J Cell Biochem Suppl* 1997; **28/29**: 159-165
- 2 **Correa P**. Precursors of gastric and esophageal cancer. *Cancer* 1982; **50**: 2554-2565
- 3 **Lu JB**, Yang WX, Zu SK, Chang QL, Sun XB, Lu WQ, Quan PL, Qin YM. Cancer mortality and mortality trends in Henan, China, 1974-1985. *Cancer Detect Prev* 1988; **13**: 167-173
- 4 **Blot WJ**, Devesa SS, Kneller RW, Fraumeni JF. Rising incidence of adenocarcinoma of the esophagus and gastric cardia. *JAMA* 1991; **265**: 2960
- 5 **Blot WJ**, Devesa SS, Fraumeni JF. Continuing climb in rates of esophageal adenocarcinoma: An update. *JAMA* 1993; **270**: 1320
- 6 **Pera M**, Cameron AJ, Trastek VF, Carpenter HA, Zinsmeister AR. Increasing incidence of adenocarcinoma of the esophagus and esophagogastric junction. *Gastroenterology* 1993; **104**: 510-513
- 7 **Botterweck AA**, Schouten LJ, Volovics A, Dorant E, van den Brandt PA. Trends in incidence of adenocarcinoma of the oesophagus and gastric cardia in ten European countries. *Int J Epidemiol* 2000; **29**: 645-654
- 8 **Hainaut P**, Soussi T, Shomer B, Hollstein M, Greenblatt M, Hovig E, Harris CC, Montesano R. Database of p53 gene somatic mutation in human tumors and cell lines: updated compilation and future prospects. *Nucleic Acid Res* 1997; **25**: 151-157
- 9 **Gao SS**, Zhou Q, Li YX, Bai YM, Zheng ZY, Zou JX, Liu G, Fan ZM, Qi YJ, Zhao X, Wang LD. Comparative studies on epithelial lesions at gastric cardia and pyloric antrum in subjects from a high incidence area for esophageal cancer in Henan, China. *World J Gastroenterol* 1998; **4**: 332-333
- 10 **Zhou HP**, Cao XF. Six cases of esophageal carcinoma with concomitant tumors of the gastric cardia. *Zhonghua Waike Zazhi* 1987; **25**: 700
- 11 **Yao SC**. Nine cases report of primary esophageal and gastric cardia cancers. *Zhongliu* 1987; **7**: 121
- 12 **Zhou FY**, Ma JS, Han XC. Repetitive primary carcinomas concurrently occurring in the esophagus and gastric cardia. *Henan Zhongliuxue Zazhi* 1996; **9**: 357-358
- 13 **Wang L**, Zhang S. Twenty-eight cases report of the concurrent cancers of esophagus and gastric cardia. *Jining Yixueyuan Xuebao* 1996; **19**: 43-44
- 14 **Wang LD**, Chen H. Alterations of tumor suppressor gene p53-Rb system and human esophageal esophageal carcinogenesis. *Shijie Huaren Xiaohua Zazhi* 2002; **9**: 367-371
- 15 **Gao H**, Wang LD, Zhou Q, Hong JY, Huang TY, Yang CS. p53 tumor suppressor gene mutation in early esophageal precancerous lesions and carcinoma among high-risk populations in Henan, China. *Cancer Res* 1994; **54**: 4342-4346
- 16 **Hainaut P**, Hernandez T, Robinson A, Rodriguez-Tome P, Flores T, Hollstein M, Harris CC, Montesano R. IARC database of p53 gene mutation in human tumors and cell lines: updated compilation, revised formats and new visualization tools. *Nucleic Acids Res* 1998; **26**: 205-213
- 17 **Bennett WP**, Hollstein MC, He A, Zhu SM, Resau JH, Trump BF, Metcalf RA, Welsh JA, Midgley C, Lane DP. Archival analysis of p53 genetic and protein alterations in Chinese esophageal Cancer. *Oncogene* 1991; **6**: 1779-1784
- 18 **Shi ST**, Yang GY, Wang LD, Xue Z, Feng B, Ding W, Xing EP, Yang CS. Role of P53 gene mutations in human esophageal carcinogenesis: results from immunohistochemical and mutation analysis of carcinomas and nearby non-cancerous lesions. *Carcinogenesis* 1999; **20**: 591-597
- 19 **Harris CC**. Structure and function of the p53 tumor suppressor gene: clues for rational cancer therapeutic strategies. *J Natl Cancer Inst* 1996; **88**: 1442-1455
- 20 **Sidransky D**, Hollstein M. Clinical implications of the p53 gene. *Annu Rev Med* 1996; **47**: 285-301
- 21 **Li HC**, Lu SX. Mutation of p53 gene in human cancers of the esophagus and gastric cardia. *Zhonghua Zhongliu Zazhi* 1994; **16**: 172-176
- 22 **Yue WB**, Wang LD, Ding I. Detection of angiogenic growth factors in patients with precancerous and cancerous lesions of esophagus from high-risk area in Henan, China. *World J Gastroenterol* 1998; **4**(Suppl 2): 109
- 23 **He LJ**, Wu M. The distribution of esophageal and cardiac carcinoma and precancerous of 2238. *World J Gastroenterol* 1998; **4**(Suppl 2): 100
- 24 **Xu T**, Fang LP, Li J, Liu WQ, Zhou ZY, Qiu CP, Yu XH, Si TP, He LJ, Fang XL, Meng ZH, Li YH, Jiang LH, Luo DY. A pathologic analysis of 4451 cases with digestive tract cancer. *World J Gastroenterol* 1998; **4**(Suppl 2): 65-66
- 25 **Gerdes J**, Schwab U, Seeub H. Production of a mouse monoclonal antibody reactive with a human nuclear antigen associated with cell proliferation. *Int J Cancer* 1983; **31**: 13-20
- 26 **Wang LD**, Hong JY, Qiu SL, Gao HG, Yang CS. Accumulation of p53 protein in human esophageal precancerous lesions: a possible early biomarker for carcinogenesis. *Cancer Res* 1993; **53**: 1783-1787
- 27 **Hermanek P**, Hutter RVP, Sobin LH. International Union Against Cancer (UICC). TNM atlas, 4th edition. *Berlin: Springer* 1997
- 28 **Warren S**, Gates P. Multiple primary malignant tumors. A survey of literature and a statistical study. *Am J Cancer* 1932; **16**: 1358-1414
- 29 **Moertel CG**. Multiple primary malignant neoplasms. *Cancer* 1977; **40**: 1786
- 30 **Esophageal Cancer**. Du BL (editor). *Beijing: Chinese Science And Technology Publishing Company* 1994
- 31 **Wang LD**, Shi ST, Zhou Q, Goldstein S, Hong JY, Shao P, Qiu SL, Yang CS. Changes in P53 and cyclin D1 protein level and cell proliferation in different stages of Henan esophageal and gastric-cardia Carcinogenesis. *Int J Cancer* 1994; **59**: 514-519
- 32 **Shen MZ**, Wang G, Qiu SL. Stomach cancer, Chinese stomach tumor collaborative research group editor. *Shenyang: Liaoning People Publishing Company* 1981
- 33 **Biemer-Huttman AE**, Walsh MD, McGuckin MA, Ajioka Y, Watanabe H, Leggett BA, Jass JR. Immunohistochemical staining patterns of Mucin1, Mucin2, Mucin4 and Mucin5AC mucins in hyperplastic polyps, serrated adenomas, and traditional adenomas of the colorectum. *J Histochem Cytochem* 1999; **47**: 1039-1048
- 34 **Reis CA**, David L, Correa P, Carneiro F, de Bolos C, Garcia E, Mandel U, Clausen H, Sobrinho-Simoes M. Intestinal metaplasia of human stomach displays distinct patterns of mucin expression. *Cancer Res* 1999; **59**: 1003-1007
- 35 **Moertel CG**, Dockerty MB. Multiple primary malignant neoplasms: tumors of different tissues or organs. *Cancer* 1961; **14**: 231-237
- 36 **Slaughter TP**, Soutwick HW, Smejkel W. Field cancerization in

- oral stratified epithelium. *Cancer* 1953; **6**: 963-968
- 37 **Lu SX**. Alterations of oncogenes and tumor suppressor genes in esophageal cancer in China. *Mutation Res* 2000; **462**: 343-353
- 38 **Liu B**, Wang LD. Barrett's esophagus. *Huaren Xiaohua Zazhi* 1999; **3**: 3-7
- 39 **Mandard AM**, Hainaut P, Hollstein M. Genetic steps in the development of squamous cell carcinoma of the esophagus. *Mutation Res* 2000; **462**: 335-342
- 40 **Zou JX**, Wang LD, Shi Stephanie T, Yang GY, Xue ZH, Gao SS, Li YX, Yang Chung S. p53 gene mutations in multifocal esophageal precancerous and cancerous lesions in patients with esophageal cancer in high-risk northern China. *Shijie Huaren Xiaohua Zazhi* 1999; **7**: 280-284
- 41 **Wang YK**, Ji XL, Gu YG, Zhang SC, Xiao JH. P53 and PCNA expression in glandular dilatation of gastric mucosa. *China Natl J New Gastroenterol* 1996; **2**: 106-108
- 42 **Wang LD**, Zhou Q, Gao SS, Li YX, Yang WC. Measurements of cell proliferation in esophageal and gastric cardia epithelia of subjects in a high incidence area for esophageal cancer. *China Natl J New Gastroenterol* 1996; **2**: 82-85
- 43 **Wang LD**, Yang WC, Zhou Q, Xing Y, Jia YY, Zhao X. Changes of p53 and Waf1p21 and cell proliferation in esophageal carcinogenesis. *China Natl J New Gastroenterol* 1997; **3**: 87-89
- 44 **Wang LD**, Zhou Q, Wei JP, Yang WC, Zhao X, Wang LX, Zou JX, Gao SS, Li YX, Yang CS. Apoptosis and its relationship with cell proliferation, p53, Waf1p21, bcl-2 and *c-myc* in esophageal carcinogenesis studied with a high-risk population in northern China. *World J Gastroenterol* 1998; **4**: 287-293

Edited by Wu XN

Relationship between overexpression of NK-1R, NK-2R and intestinal mucosal damage in acute necrotizing pancreatitis

Xin Shi, Nai-Rong Gao, Qing-Ming Guo, Yong-Jiu Yang, Ming-Dong Huo, Hao-Lin Hu, Helmut Friess

Xin Shi, Nai-Rong Gao, Yong-Jiu Yang, Ming-Dong Huo, Hao-Lin Hu, Department of General Surgery, Zhong-Da Hospital, Southeast University, Nanjing 210009, Jiangsu Province, China
Qing-Ming Guo, Department of Pathology, Zhong-Da Hospital, Southeast University, Nanjing 210009, Jiangsu Province, China
Helmut Friess, Department of General Surgery, University of Heidelberg, Im Neuenheimer Feld 110, D-69120 Heidelberg, Germany
Supported by the scientific research funding for the returned overseas Chinese scholars, State Personnel Ministry, No. 7690004027
Correspondence to: Dr. Xin Shi, Department of General Surgery, Zhong-Da Hospital, Southeast University, Nanjing, 210009, Jiangsu Province, China. shixined@hotmail.com
Telephone: +86-25-3272196 **Fax:** +86-25-3272196
Received: 2002-07-01 **Accepted:** 2002-08-05

Abstract

AIM: To study the expression of neurokinin-1 receptor (NK-1R) and neurokinin-2 receptor (NK-2R) in distal ileum of acute necrotizing pancreatitis (ANP) and to evaluate the relationship between expression of these two receptors and intestinal mucosal damage.

METHODS: A total of 130 adult Sprague-Dawley rats were randomly divided into two groups: the rats in ANP group ($n=80$) were induced by the retrograde intraductal infusion of $30 \text{ g} \cdot \text{L}^{-1}$ sodium taurocholate. And the rats in normal control group ($n=50$) received laparotomy only. Sacrifices were made 6 h, 12 h, 24 h and 48 h later in ANP and normal control group after induction respectively. Intestinal mucosal permeability was studied by intrajejunal injection of 1.5 mCi radioactive isotope $^{99\text{m}}\text{Tc}$ -diethylene triamine pentacetic acid (DTPA) and the radioactivity of $^{99\text{m}}\text{Tc}$ -DTPA content in urine was measured 6 h, 12 h, 24 h and 48 h after induction. Then the pancreas and intestine were prepared for pathology. Reverse transcription polymerase chain reaction (RT-PCR) was used to determine the mRNA expression of NK-1R and NK-2R, and Western blot was used to investigate the protein level of NK-1R and NK-2R.

RESULTS: In ANP rats, serious histologic damages in intestinal mucosa were observed, and the radioactivity of $^{99\text{m}}\text{Tc}$ -DTPA in urine increased significantly in the ANP group. RT-PCR revealed that NK-1R and NK-2R mRNA level was overexpressed in the distal ileum of ANP as compared with the normal control group. Western blot discovered stronger NK-1R (14-fold increase) and NK-2R (9-fold increase) immunoreactivity in the intestinal mucosa of ANP rats. Moreover, the overexpression of NK-1R was associated with mucosal pathological score ($r=0.77$, $P<0.01$) and intestinal permeability ($r=0.68$, $P<0.01$) in ANP rats.

CONCLUSION: NK-1R and NK-2R contribute to disrupted neuropeptides loop balance, deteriorate intestinal damage, and are involved in pathophysiological changes in ANP.

Shi X, Gao NR, Guo QM, Yang YJ, Huo MD, Hu HL, Friess H. Relationship between overexpression of NK-1R, NK-2R and intestinal mucosal damage in acute necrotizing pancreatitis. *World J Gastroenterol* 2003; 9(1): 160-164
<http://www.wjgnet.com/1007-9327/9/160.htm>

INTRODUCTION

Acute necrotizing pancreatitis (ANP) has a complicated and ill-defined pathophysiology. It is associated with a high complication rate and unpredictable outcome, with a mortality rate of 10-45 %^[1]. The hypothesis that ANP promotes bacterial translocation, leading to infection in the inflamed pancreas and peripancreatic tissue, has been studied in rats fed with fluorescent beads, sensitive inert markers of translocation^[2]. The results suggested a translocated bacteria route for pancreatic infection. Normal intestinal mucosal barrier can keep the bacteria from translocation, however, this barrier is damaged in ANP^[3,4]. The mechanism, which leads to the dysfunction of mucosal barrier, remains unclear^[5-9].

Recent studies have revealed the important role of Substance P (SP) and its receptors in ANP^[10-13]. However, the expression of SP's two receptors- neurokinin-1 receptor (NK-1R) and neurokinin-2 receptor (NK-2R) in intestinal mucosa of ANP, remains unclear. And their roles in mucosal damage has not been revealed.

Therefore, in the present study the mRNA of NK-1R and NK-2R in intestinal mucosa of ANP was analyzed using reverse transcription polymerase chain reaction (RT-PCR), the protein level of these two receptors was analyzed by Western blot. And the relationship between mRNA level and intestinal mucosal damage/intestinal permeability was also investigated.

MATERIALS AND METHODS

Animals

Adult Sprague-Dawley rats weighing 250-300 g were obtained from the Laboratory Animal Center of Southeast University, and fed with standard rat chow. Animals were fasted overnight and anesthetized with $20 \text{ g} \cdot \text{L}^{-1}$ sodium pentobarbital (intraperitoneal injection). ANP models ($n=80$) were induced by the retrograde intraductal infusion of $30 \text{ g} \cdot \text{L}^{-1}$ sodium taurocholate ($0.1 \text{ ml} \cdot \text{min}^{-1} \cdot \text{kg}^{-1}$). And the rats in normal control group ($n=50$) received laparotomy, the duodenum was taken out of the abdominal cavity and the pancreas was turned over for three times.

Sacrifices were made 6 h, 12 h, 24 h and 48 h later in ANP and normal control group after induction respectively. The distal ileum, pancreas and blood in portal vein were obtained for further studies. Freshly removed tissue samples were immediately fixed in paraformaldehyde solution for 12-24 hours and paraffin-embedded for routine histopathologic analysis. Concomitantly, tissue samples destined for RNA and protein extraction were immediately snap-frozen in liquid nitrogen and maintained at $-80 \text{ }^\circ\text{C}$ until use. Blood was obtained for serum amylase determinations.

Pathological examination for intestinal mucosa and pancreas

Paraffin-embedded tissue sections (2-3 mm thick) were subjected to hematoxylin & eosin staining. Intestinal mucosal damage was evaluated blindly under microscope by two pathologists^[14, 15].

Determinants of intestinal mucosal permeability

Intestinal mucosal permeability was investigated by intrajejunal

injection of 1.5mCi radioactive isotope ^{99m}Tc (Chinese Institute of Nuclear Power)-diethylene triamine pentacetic acid (DTPA, Chinese Institute of Nuclear Power) and the radioactivity of ^{99m}Tc -DTPA content in urinary were measured 6 h, 12 h, 24 h and 48 h after induction. Urinary volume was measured and radioactive impulse was determined using radio-immunity γ counter. Intestinal mucosal permeability was calculated using the following formula: Intestinal mucosal permeability (%) = ^{99m}Tc -DTPA excretory rate (%) = [(urine-background) \times volume] / (standard-background) \times 100%^[16, 17].

RNA extraction and RT-PCR

Total RNA was extracted using the single-step guanidinium isothiocyanate method, as previously reported^[18, 19]. Following DNase treatment, total RNA was reversely transcribed into cDNA using random hexamers according to the manufacturer's instructions (Roche Diagnostics, Rotkreuz, Switzerland). The primers were designed using Primer Express software (Germany) and synthesized by Amplimmun (Amplimmun AG, Madulain, Switzerland). The sequence is shown in Table 1.

Table 1 The sequence of primers used for RT-PCR

Primers	Sequence	Primer size (bp)	PCR products size (bp)
NK-1R			
Forward primer	5'- CAT CAA CCC AGA TCT CTA CC -3'	20	380
Reverse primer	5'- GCT GGA GCT TTC TGT CAT GGA -3'	21	
NK-2R			
Forward primer	5'-CAT CAC TGT GGA CGA GGG GG-3'	20	491
Reverse primer	5'-TGT CTT CCT CAG TTG GTG TC-3'	20	
GAPDH			
Forward primer	5'-TGA AGG TCG GTG TCA ACG GATTTG GC-3'	26	999
Reverse primer	5'- CAT GTA GGC CAT GAG GTC CAC CAC-3'	24	

PCR amplification was carried out using either NK-1R or NK-2R or GAPDH in a final volume of 25 μl with a Perkin-Elmer GeneAmp System 9 700 and 0.625 U of Taq DNA polymerase (Roche Diagnostics GmbH, Mannheim, Germany). Cycling conditions were as follows: 35 cycles of denaturation at 94 $^{\circ}\text{C}$ for 1 min, annealing at 62 $^{\circ}\text{C}$ for 1 min and elongation at 72 $^{\circ}\text{C}$ for 2.5 min. The first PCR cycle was preceded by denaturation at 94 $^{\circ}\text{C}$ for 3 min, and last PCR cycle was followed by incubation at 72 $^{\circ}\text{C}$ for 10 min.

For each PCR reaction, an identical tube containing the same amount of reagent, and same amount of water was substituted for cDNA in these tubes. These tubes served as negative control of PCR.

RNA concentrations and PCR were titrated to establish standard curves to document linearity and to permit semiquantitative analysis of signal strength^[20-22]. Amplified PCR products were separated by electrophoresis through a 1 % agarose gel at 45 V for 120 min. The cDNA bands were visualized by ultraviolet illumination after the gels were stained with 0.5 $\text{g} \cdot \text{L}^{-1}$ ethidium bromide dissolved in Tris-borate-EDTA buffer (89 mM Tris, 89 mM boric acid, 2.5 mM EDTA, pH 8.2). The gels were photographed, and the films were scanned and analyzed with a computerized densitometer (Image-Pro Plus, Version 3.0.01).

Western blot

Western blot for NK-1R and NK-2R was performed as previously reported with certain modifications^[18, 19]. Briefly, 200 mg of tissue samples were powdered in liquid nitrogen and

then homogenized in lysis buffer (50 mM Tris-HCl, pH 7.5, 150 mM NaCl, 2 mM EDTA, 1 % SDS) supplemented with a protease inhibitor cocktail (Roche Diagnostics, Rotkreuz, Switzerland). The lysate was collected and centrifuged at 4 $^{\circ}\text{C}$ for 10 min with 14 000 rpm to remove the insoluble material. The protein concentration was measured by spectrophotometry using the BCA protein assay (Pierce, Rockford, IL, USA). For each sample, 40 mg of protein was separated on 12 % SDS-polyacrylamide gels and electroblotted onto nitrocellulose membranes.

The blots were incubated in blocking solution (50 $\text{g} \cdot \text{L}^{-1}$ non-fat milk in 20 mM Tris-HCl, 150 mM NaCl, 1 $\text{g} \cdot \text{L}^{-1}$ Tween-20 [TBS-T]), followed by incubation with 1:1 000 dilution of goat anti-rat NK-1R antibody (Santa Cruz Biotechnology, Santa Cruz, CA, USA) or 1:1 000 dilution of goat anti-rat NK-2R antibody (Santa Cruz Biotechnology, Santa Cruz, CA, USA) at 4 $^{\circ}\text{C}$ overnight. The membranes were then washed with TBS-T and incubated with donkey anti-goat IgG (1:3 000 dilution) for 60 min at room temperature. Antibody detection was performed with an enhanced chemiluminescence reaction (ECL Western blotting detection, Amersham Life Science, Amersham, UK).

Statistical analysis

Results were expressed as mean \pm SD. Statistical analysis was made using the Prism software (Prism, GraphPad Software Inc., San Diego, CA, USA). The comparative statistical evaluations among groups were done using the Mann-Whitney U test or Chi-square test. Spearman correlation analysis was used for correlation analysis of the parameters. Significance was defined as $P < 0.05$.

RESULTS

Serum amylase and pathological examination

Serum amylase increased significantly in ANP group as compared with normal controls ($P < 0.01$). The diagnoses of ANP were confirmed by gross appearance and microscopy. In ANP group, mucosal edema, epithelia degeneration, necrosis or even abscission were observed after 6 h. Hemangiectasia, hemorrhage and inflammatory cell infiltration were revealed in mucosa or submucosa (Table 2).

Table 2 The pathological score of intestinal mucosa

Groups	0 h	6 h	12 h	24 h	48 h
Control	0.92 \pm 0.47	0.90 \pm 0.35	0.93 \pm 0.38	0.93 \pm 0.29	1.07 \pm 0.36
ANP		2.11 \pm 0.47 ^a	2.65 \pm 0.49 ^b	3.91 \pm 0.82 ^b	4.89 \pm 1.21 ^b

^a $P < 0.05$ vs each time point of control group, respectively; ^b $P < 0.01$ vs each time point of control group, respectively

Intestinal mucosal permeability change in ANP rats

The intestinal mucosal permeability was determined using isotope. The results revealed that permeability increased significantly after 6 h (Table 3).

Table 3 Changes of intestinal mucosal permeability

Groups	0 h	6 h	12 h	24 h	48 h
Control	0.0411 \pm 0.0156	0.0455 \pm 0.0174	0.0532 \pm 0.0188	0.0693 \pm 0.0153	0.0698 \pm 0.0223
ANP		0.2367 \pm 0.1132 ^a	0.3457 \pm 0.0473 ^a	0.6651 \pm 0.1411 ^a	0.7021 \pm 0.1523 ^a

^a $P < 0.01$ vs each time point of control group, respectively

mRNA expression of NK-1R and NK-2R in distal ileum

The rats were sacrificed 6 h, 12 h, 24 h or 48 h after model inducing, distal ileum was obtained for determination of NK-1R and NK-2R mRNA. Figure 1 shows the amplification plot at the time point of 6 h. The gene above had been amplified effectively, and amplification of GAPDH was comparable in each sample, which suggested comparable mRNA in each sample (Figure 1B, 1D), whereas amplification of NK-1R in normal controls was so weak that some of the samples could only be observed in the gel. In contrast, the amplification of NK-1R in ANP group was relatively stronger (Figure 1A). The expression of NK-2R was similar to NK-1R (Figure 1C). After 12 h, 24 h or 48 h, the expression of above genes maintained the same pattern as before.

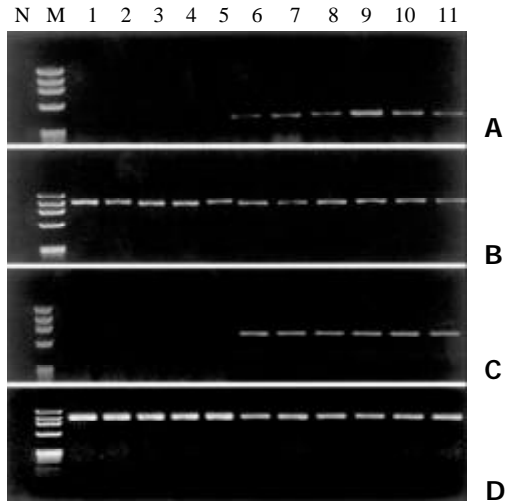


Figure 1 Amplification results of NK-1R, NK-2R and GAPDH from RT-PCR in control and ANP intestinal tissue. A: amplification results of NK-1R; C: amplification results of NK-2R; B, D: amplification results of GAPDH. N: PCR negative control; M: PCR Marker (upper to lower: 1 000, 800, 600, 400, 200 and 100bp); 1-5: group of normal control; 6-11: group of ANP

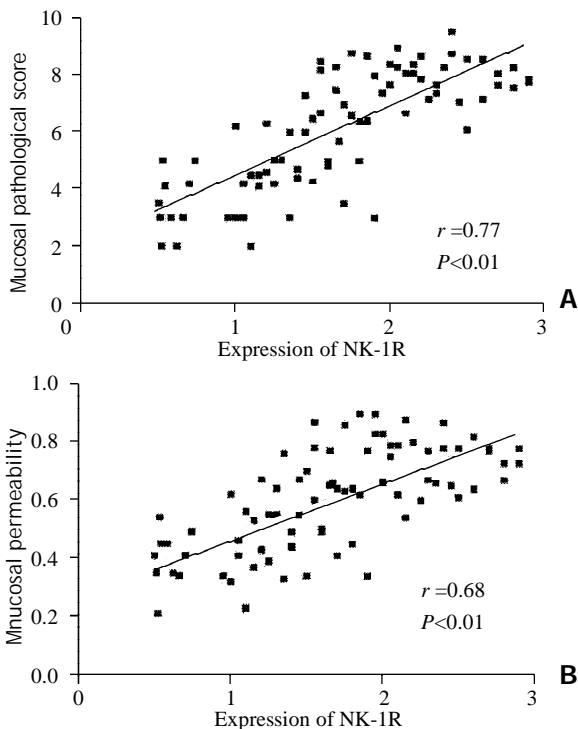


Figure 2 The expression level of NK-AR mRNA was correlated with intestinal mucosal pathological score (A) and mucosal permeability (B) in ANP rats

Correlation of expression of NK-1R and NK-2R with intestinal mucosal damage

We then evaluated whether there was a relationship between the expression levels of these two genes and intestinal mucosal pathological score and permeability. A significant relationship between NK-1R mRNA and mucosal pathological score ($r=0.77, P<0.01$) was found (Figure 2A). Furthermore, statistical analysis revealed a significant relationship between NK-1R mRNA and mucosal permeability ($r=0.68, P<0.01$, Figure 2B). Although NK-2R mRNA was overexpressed in ANP, there was no significant relationship between this gene expression and intestinal mucosal pathological score ($r=0.32, P=0.31$) and permeability ($r=0.28, P=0.21$).

NK-1R and NK-2R protein expression in distal ileum

We then performed the Western blot analysis in controls and ANP group. All the normal controls exhibited approximately 46 kDa band of NK-1R protein of weak intensity. In contrast, the ANP samples showed a more intense signal (Figure 3A). The densitometric analysis demonstrated a 14-fold increase of NK-1R protein level in ANP ileum compared with the normal ileum ($P<0.01$).

When Western blot analysis for NK-2R was performed, similar pattern was observed, protein signal was weak in normal control, but much stronger in ANP group (Figure 3B). Densitometry revealed a 9-fold increase of NK-2R in ANP ileum ($P<0.01$).

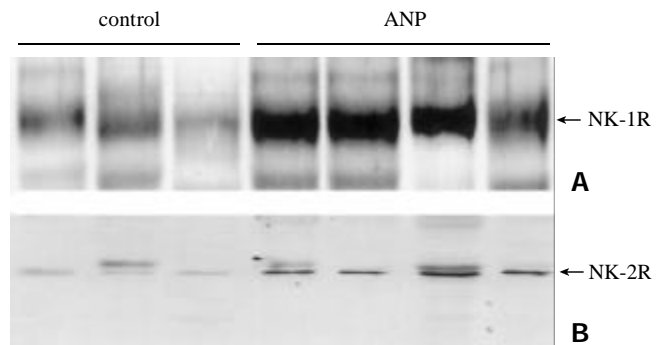


Figure 3 Western blot revealed the protein level of NK-1R (A) and NK-2R (B) in normal control and ANP intestinal tissue

DISCUSSION

Intestinal bacterial translocation is the main source leading to infection of pancreas, whereas this translocation is dependent, to some degree, on the function of intestinal mucosal barrier. Intestinal mucosal barrier is made up of mechanical, biological, immunologic and chemical barrier, while the mechanical barrier is the fundamental one, which can prevent large molecule and bacteria from passing through^[23,24]. More and more evidence showed that gut barrier dysfunction is related to multiorgan system failure in sepsis and immune dysregulation^[25-35]. Pancreatitis-induced hypovolaemia due to endothelial barrier leakage and gut arteriovenous shunting causes intestinal ischaemia and reperfusion injury with concomitant gut barrier dysfunction. Gut endothelial barrier dysfunction probably plays a central role. Potential molecular mechanisms could be associated with alterations in intracellular signal transduction, intercellular signal and expression of adhesion molecules on endothelial cells. Bacterial infections are often seen during the progression of ANP, concomitant with the potential development of multiple organ dysfunction^[36,37]. The mechanisms underlying gut barrier dysfunction in acute pancreatitis are thus complex and still not fully elucidated.

SP is synthesized by small-diameter C sensory 'pain' fibers, and release of this peptide into the dorsal horn of the spinal cord following intense peripheral stimulation was thought to promote central hyperexcitability (central sensitization)^[38,39]. In addition, it could result in plasma extravasation, neutrophil infiltration, and vasodilatation. In rats, both SP and NK-1R selective agonist stimulated pancreatic plasma extravasation, and this response was blocked by the NK-1R antagonist. Selective agonist of NK-2R showed no effect^[12]. Continuous infusion of SP stimulated plasma extravasation in rat pancreas via activation of NK-1R^[40-42].

In the present study, expression of NK-1R and NK-2R mRNA was investigated by RT-PCR and the protein levels of NK-1R and NK-2R were determined using Western blot analysis in normal control and ANP intestines. The results revealed that both NK-1R and NK-2R were overexpressed in ANP intestines, and the overexpression of NK-1R was correlated with mucosal damage in ANP rats. Increased level of SP^[43] in ANP, together with overexpression of its receptors-NK-1R and NK-2R, results in excessive biological effect, such as aggregation of neutrophilic granulocyte, cascade release of inflammatory transmitter, tissue fluid and plasma extravasation, thus resulting in deterioration of intestinal pathological changes and gut barrier dysfunction, and facilitating gut bacterial translocation.

Better understanding of the molecular biological changes in ANP will provide novel therapies to this disease. Once specific receptors were identified, selective antagonists which blocked these receptors would have therapeutic effects. Antagonists against NK-1R have showed some effects in acute pancreatitis on animal models^[12,42]. Knowledge about the regulating events will probably make future pharmacological therapy available for prevention and treatment of the severe complications of ANP, including gut barrier dysfunction.

REFERENCES

- Buchler MW**, Gloor B, Muller CA, Friess H, Seiler CA, Uhl W. Acute necrotizing pancreatitis: treatment strategy according to the status of infection. *Ann Surg* 2000; **232**: 619-626
- Medich DS**, Lee TK, Melhem MF, Rowe MI, Schraut WH, Lee KK. Pathogenesis of pancreatic sepsis. *Am J Surg* 1993; **165**: 46-50
- Juononen PO**, Alhava EM, Takala JA. Gut permeability in patients with acute pancreatitis. *Scand J Gastroenterol* 2000; **35**: 1314-1318
- Liu Q**, Djuricin G, Nathan C, Gattuso P, Weinstein RA, Prinz RA. The effect of interleukin-6 on bacterial translocation in acute canine pancreatitis. *Int J Pancreatol* 2000; **27**: 157-165
- Li JY**, Lu Y, Hu S, Sun D, Yao YM. Preventive effect of glutamine on intestinal barrier dysfunction induced by severe trauma. *World J Gastroenterol* 2002; **8**: 168-171
- Simsek I**, Mas MR, Yasar M, Ozyurt M, Saglamkaya U, Devenci S, Comert B, Basustaoglu A, Kocabalkan F, Refik M. Inhibition of inducible nitric oxide synthase reduces bacterial translocation in a rat model of acute pancreatitis. *Pancreas* 2001; **23**: 296-301
- Colak T**, Ipek T, Paksoy M, Polat E, Uygun N, Kayabasi B. The effects of cefepim, G-CSF, and sucralfate on bacterial translocation in experimentally induced acute pancreatitis. *Surg Today* 2001; **31**: 502-506
- Cicalese L**, Sahai A, Sileri P, Rastellini C, Subbotin V, Ford H, Lee K. Acute pancreatitis and bacterial translocation. *Dig Dis Sci* 2001; **46**: 1127-1132
- Buttenschoen K**, Berger D, Hiki N, Buttenschoen DC, Vasilescu C, Chikh-Torab F, Seidelmann M, Beger HG. Endotoxin and antiendotoxin antibodies in patients with acute pancreatitis. *Eur J Surg* 2000; **166**: 459-466
- Bhatia M**, Neoptolemos JP, Slavin J. Inflammatory mediators as therapeutic targets in acute pancreatitis. *Curr Opin Investig Drugs* 2001; **2**: 496-501
- Steer ML**. Relationship between pancreatitis and lung diseases. *Respir Physiol* 2001; **128**: 13-16
- Grady EF**, Yoshimi SK, Maa J, Valeroso D, Vartanian RK, Rahim S, Kim EH, Gerard C, Gerard N, Bunnett NW, Kirkwood KS. Substance P mediates inflammatory oedema in acute pancreatitis via activation of the neurokinin-1 receptor in rats and mice. *Br J Pharmacol* 2000; **130**: 505-512
- Bhatia M**, Brady M, Shokuhi S, Christmas S, Neoptolemos JP, Slavin J. Inflammatory mediators in acute pancreatitis. *J Pathol* 2000; **190**: 117-125
- Denham JW**, Hauer-Jensen M, Kron T, Langberg CW. Treatment-time-dependence models of early and delayed radiation injury in rat small intestine. *Int J Radiat Oncol Biol Phys* 2000; **48**: 871-887
- Park PO**, Haglund U, Bulkeley GB, Falt K. The sequence of development of intestinal tissue injury after strangulation ischemia and reperfusion. *Surgery* 1990; **107**: 574-580
- Weiss DJ**, Evanson OA, MacLeay J, Brown DR. Transient alteration in intestinal permeability to technetium Tc99m diethylenetriaminopentaacetate during the prodromal stages of alimentary laminitis in ponies. *Am J Vet Res* 1998; **59**: 1431-1434
- Li YS**, Li JS, Jiang JW, Liu FN, Li N, Qin WS, Zhu H. Glycyl-glutamine-enriched long-term total parenteral nutrition attenuates bacterial translocation following small bowel transplantation in the pig. *J Surg Res* 1999; **82**: 106-111
- Kleeff J**, Shi X, Bode HP, Hoover K, Shrikhande S, Bryant PJ, Korc M, Buchler MW, Friess H. Altered expression and localization of the tight junction protein ZO-1 in primary and metastatic pancreatic cancer. *Pancreas* 2001; **23**: 259-265
- Koliopoulos A**, Friess H, Kleeff J, Shi X, Liao Q, Pecker I, Vlodavsky I, Zimmermann A, Buchler MW. Heparanase expression in primary and metastatic pancreatic cancer. *Cancer Res* 2001; **61**: 4655-4659
- King KA**, Hu C, Rodriguez MM, Romaguera R, Jiang X, Piedimonte G. Exaggerated neurogenic inflammation and substance P receptor upregulation in RSV-infected weanling rats. *Am J Respir Cell Mol Biol* 2001; **24**: 101-107
- Piedimonte G**, Rodriguez MM, King KA, McLean S, Jiang X. Respiratory syncytial virus upregulates expression of the substance P receptor in rat lungs. *Am J Physiol* 1999; **277(4 Pt 1)**: L831-840
- Kaltreider HB**, Ichikawa S, Byrd PK, Ingram DA, Kishiyama JL, Sreedharan SP, Warnock ML, Beck JM, Goetzl EJ. Upregulation of neuropeptides and neuropeptide receptors in a murine model of immune inflammation in lung parenchyma. *Am J Respir Cell Mol Biol* 1997; **16**: 133-144
- Andersson R**, Wang XD. Gut barrier dysfunction in experimental acute pancreatitis. *Ann Acad Med Singapore* 1999; **28**: 141-146
- Wang XD**, Borjesson A, Sun ZW, Wallen R, Deng XM, Zhang HY, Hallberg E, Andersson R. The association of type II pneumocytes and endothelial permeability with the pulmonary macrophage system in experimental acute pancreatitis. *Eur J Clin Invest* 1998; **28**: 778-785
- Hirsh M**, Dyugovskaya L, Bashenko Y, Krausz MM. Reduced rate of bacterial translocation and improved variables of natural killer cell and T-cell activity in rats surviving controlled hemorrhagic shock and treated with hypertonic saline. *Crit Care Med* 2002; **30**: 861-867
- Shimizu T**, Tani T, Endo Y, Hanasawa K, Tsuchiya M, Kodama M. Elevation of plasma peptidoglycan and peripheral blood neutrophil activation during hemorrhagic shock: plasma peptidoglycan reflects bacterial translocation and may affect neutrophil activation. *Crit Care Med* 2002; **30**: 77-82
- Doty JM**, Oda J, Ivatury RR, Blocher CR, Christie GE, Yelon JA, Sugerma HJ. The effects of hemodynamic shock and increased intra-abdominal pressure on bacterial translocation. *J Trauma* 2002; **52**: 13-17
- Koyluoglu G**, Bakici MZ, Elagoz S, Arpacik M. The effects of pentoxifylline treatment on bacterial translocation after hemorrhagic shock in rats. *Clin Exp Med* 2001; **1**: 61-66
- Ling YL**, Meng AH, Zhao XY, Shan BE, Zhang JL, Zhang XP. Effect of cholecystokinin on cytokines during endotoxin shock in rats. *World J Gastroenterol* 2001; **7**: 667-671
- Cui DX**, Zeng GY, Wang F, Xu JR, Ren DQ, Guo YH, Tian FR, Yan XJ, Hou Y, Su CZ. Mechanism of exogenous nucleic acids and their precursors improving the repair of intestinal epithelium after gamma-irradiation in mice. *World J Gastroenterol* 2000; **6**: 709-717
- Wu XN**. Current concept of pathogenesis of severe acute

- pancreatitis. *World J Gastroenterol* 2000; **6**: 32-36
- 32 **Indaram AV**, Nandi S, Weissman S, Lam S, Bailey B, Blumstein M, Greenberg R, Bank S. Elevated basal intestinal mucosal cytokine levels in asymptomatic first-degree relatives of patients with Crohn's disease. *World J Gastroenterol* 2000; **6**: 49-52
- 33 **Zhu L**, Yang ZC, Li A, Cheng DC. Protective effect of early enteral feeding on postburn impairment of liver function and its mechanism in rats. *World J Gastroenterol* 2000; **6**: 79-83
- 34 **Meng AH**, Ling YL, Zhang XP, Zhao XY, Zhang JL. CCK-8 inhibits expression of TNF-alpha in the spleen of endotoxic shock rats and signal transduction mechanism of p38 MAPK. *World J Gastroenterol* 2002; **8**: 139-143
- 35 **Zhu L**, Yang ZC, Li A, Cheng DC. Reduced gastric acid production in burn shock period and its significance in the prevention and treatment of acute gastric mucosal lesions. *World J Gastroenterol* 2000; **6**: 84-88
- 36 **Schwarz M**, Thomsen J, Meyer H, Buchler MW, Beger HG. Frequency and time course of pancreatic and extrapancreatic bacterial infection in experimental acute pancreatitis in rats. *Surgery* 2000; **127**: 427-432
- 37 **Hongo H**, Takano H, Imai A, Yamaguchi T, Boku Y, Fujii T, Naito Y, Yoshida N, Yoshikawa T, Kondo M. Pancreatic phospholipase A2 induces bacterial translocation in rats. *Immunopharmacol Immunotoxicol* 1999; **21**: 717-726
- 38 **Duggan AW**, Hendry IA, Morton CR, Hutchison WD, Zhao ZQ. Cutaneous stimuli releasing immunoreactive substance P in the dorsal horn of the cat. *Brain Res* 1988; **451**: 261-273
- 39 **Cao YQ**, Mantyh PW, Carlson EJ, Gillespie AM, Epstein CJ, Basbaum AI. Primary afferent tachykinins are required to experience moderate to intense pain. *Nature* 1998; **392**: 390-394
- 40 **Maa J**, Grady EF, Kim EH, Yoshimi SK, Hutter MM, Bunnett NW, Kirkwood KS. NK-1 receptor desensitization and neutral endopeptidase terminate SP-induced pancreatic plasma extravasation. *Am J Physiol Gastrointest Liver Physiol* 2000; **279**: G726-732
- 41 **Maa J**, Grady EF, Yoshimi SK, Drasin TE, Kim EH, Hutter MM, Bunnett NW, Kirkwood KS. Substance P is a determinant of lethality in diet-induced hemorrhagic pancreatitis in mice. *Surgery* 2000; **128**: 232-239
- 42 **Kirkwood KS**, Kim EH, He XD, Calastro EQ, Domush C, Yoshimi SK, Grady EF, Maa J, Bunnett NW, Debas HT. Substance P inhibits pancreatic exocrine secretion via a neural mechanism. *Am J Physiol* 1999; **277**(2 Pt 1): G314-320
- 43 **Bhatia M**, Saluja AK, Hofbauer B, Frossard JL, Lee HS, Castagliuolo I, Wang CC, Gerard N, Pothoulakis C, Steer ML. Role of substance P and the neurokinin 1 receptor in acute pancreatitis and pancreatitis-associated lung injury. *Proc Natl Acad Sci U S A* 1998; **95**: 4760-4765

Edited by Ma JY

Effect of oxytocin on contraction of rabbit proximal colon *in vitro*

Dong-Ping Xie, Lian-Bi Chen, Chuan-Yong Liu, Jing-Zhang Liu, Ke-Jing Liu

Dong-Ping Xie, Lian-Bi Chen, Chuan-Yong Liu, Jing-Zhang Liu, Ke-Jing Liu, Department of Physiology, Medical School, Shandong University, Jinan 250012, Shandong Province, China

Supported by Scientific Initiating Grants of Shandong University and Shandong Science Foundation

Correspondence to: Lian-Bi Chen, Department of Physiology, School of Medicine, Shandong University, Jinan 250012, Shandong Province, China. clb@sdu.edu.cn

Telephone: +86-531-8382037 **Fax:** +86-531-8382156

Received: 2002-06-08 **Accepted:** 2002-07-03

Abstract

AIM: To investigate the effects of oxytocin (OT) on isolated rabbit proximal colon and its mechanism.

METHODS: Both longitudinal muscle (LM) and circular muscle (CM) were suspended in a tissue chamber containing 5 mL Krebs solution (37 °C), bubbled continuously with 950 mL·L⁻¹ O₂ and 50 mL·L⁻¹ CO₂. Isometric spontaneous contractile responses to oxytocin or other drugs were recorded in circular and longitudinal muscle strips.

RESULTS: OT (0.1 U·L⁻¹) failed to elicit significant effects on the contractile activity of proximal colonic smooth muscle strips ($P>0.05$). OT (1 to 10 U·L⁻¹) decreased the mean contractile amplitude and the contractile frequency of CM and LM. Hexamethonium (10 μmol·L⁻¹) partly blocked the inhibition of oxytocin (1 U·L⁻¹) on the contractile frequency of CM. N^ω-nitro-L-arginine-methylester (L-NAME, 1 μmol·L⁻¹), progesterone (32 μmol·L⁻¹) and estrogen (2.6 μmol·L⁻¹) had no effects on OT-induced responses.

CONCLUSION: OT inhibits the motility of proximal colon in rabbits. The action is partly relevant with N receptor, but irrelevant with that of NO, progesterone or estrogen.

Xie DP, Chen LB, Liu CY, Liu JZ, Liu KJ. Effect of oxytocin on contraction of rabbit proximal colon *in vitro*. *World J Gastroenterol* 2003; 9(1): 165-168

<http://www.wjnet.com/1007-9327/9/165.htm>

INTRODUCTION

Oxytocin (OT) is a very abundant neuropeptide. The structure of the OT gene was elucidated in 1984^[1], and the sequence of the OT receptor was reported in 1992^[2]. OT exerted a wide spectrum of central and peripheral effects^[3-5]. It was reported that hypothalamic paraventricular nucleus is a site of controlling gastric function^[6], oxytocin facilitated the manifestation of inhibitory effects of hypothalamus on the motor function of gastrointestinal tract^[7]. The experiments on rats had shown that gastric motility was inhibited by microinjection of oxytocin into the dorsal motor nucleus of the vagus (DMN), and that the inhibition of gastric motility after electrical stimulation of the hypothalamic paraventricular nucleus was blocked by microinjection of an oxytocin receptor antagonist directly into the DMN. These results suggested that oxytocin acted on the gastric motility via DMN^[8]. The reports on peripheral action of oxytocin to influence gastrointestinal

(GI) motility were controversial: OT decreases the contractions of the guinea pig stomach *in vitro*, and inhibits the tone and peristaltic contractions of stomach and small intestines in fasting dogs *in vivo*^[9]; but increases the gastric emptying of semisolid food in normal human and the contractions of gastric smooth muscle strips in rats^[10]. The effect of oxytocin on colonic motility is still unknown.

OTR is functionally coupled to GTP binding proteins, stimulates the activity of phospholipase C-β isoforms. Finally, a variety of cellular events are initiated. For example, the forming Ca²⁺-calmodulin complexes triggers the activation of neuronal and endothelial isoforms of nitric oxide (NO) synthase^[11]. Steroid hormones were reported to control oxytocin receptor (OTR) activity via both genomic and nongenomic pathways^[12]. Estrogen induces the OTR mRNA expression, and then increases the OTR density on the membrane of the uterus smooth muscle and central nervous system^[13,14]; on the other hand, progesterone inhibits the nuclear OTR mRNA expression, and decreases the sensitivity of the target cell on OT stimulation^[15,16]; progesterone was also reported to bind to OTR with high affinity and inhibit the receptor function^[17]. In this study, we investigated the effect of OT on proximal colonic motility of rabbits; We also investigated if the OT-induced responses were relevant with NO, steroid hormones or N receptor.

MATERIALS AND METHODS

Animal preparation

Rabbits of both sexes, weighing 1.5-2 kg, were fasted for 24-hour and sacrificed. The proximal colon (1 cm from the cecocolonic junction) was removed. The segment of the colon was opened along the mesentery. Muscle strips (8×2 mm) were cut, parallel to either the circular or the longitudinal fibers, and named circular muscle (CM) and longitudinal muscle (LM). The mucosa on each strip was carefully removed.

Experiments

The muscle strip was suspended in a tissue chamber containing 5 mL Krebs solution (37 °C) and bubbled continuously with 950 mL·L⁻¹ O₂ and 50 mL·L⁻¹ CO₂^[18]. One end of the strip was fixed to a hook on the bottom of the chamber. The other end was connected to an external isometric force transducer (JZ-BK, BK). Motility of colonic strips (under an initial tension of 1 g) in 2 tissue chambers were simultaneously recorded on ink-writing recorders (LMS-ZB, Cheng-Du). After 1 h equilibration, OT (0.1, 1, 10 U·L⁻¹) was added in the tissue chamber to observe their effects on proximal colon; N^ω-nitro-L-arginine-methylester (L-NAME, 1 μmol·L⁻¹), hexamethonium (10 μmol·L⁻¹), progesterone (32 μmol·L⁻¹) or estrogen (2.6 μmol·L⁻¹), given 3 min before the administration of OT (1 U·L⁻¹), was added separately to investigate whether the actions of OT were relevant with NO, N receptor or steroids. The resting tension, the contractile frequency, and the mean contractile amplitude of LM and CM were measured.

Drugs preparation

The following agents were used: oxytocin (Biochemical Pharmaceutical Company, Shanghai, China), N^ω-nitro-L-arginine-methylester (L-NAME) and hexamethonium (Sigma Chemical Company), progesterone and estrogen (The Ninth Pharmaceutical Factory in Shanghai).

Data analysis

The results were presented as $\bar{x} \pm s$, and statistically analyzed by paired *t* test, $P < 0.05$ was considered to be significant.

RESULTS

Effect of OT on the spontaneous contraction of colonic smooth muscle strips

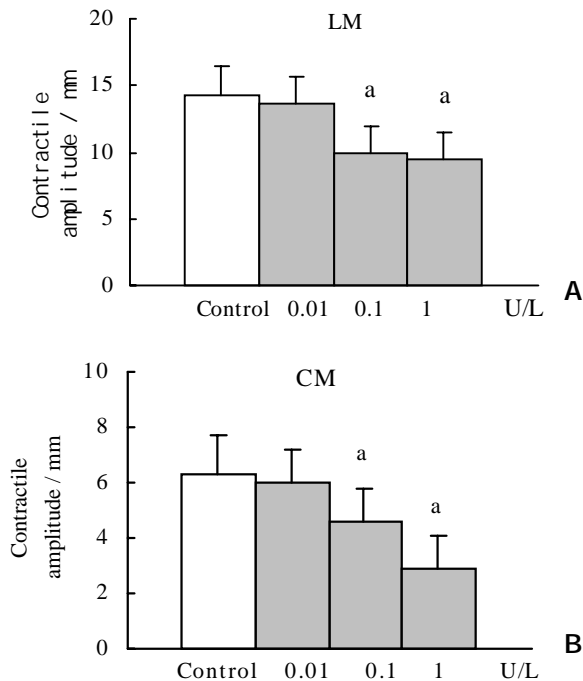


Figure 1 A: Effect of oxytocin on the mean contractile amplitude of longitudinal muscle (LM) of proximal colon in rabbits. B: Effect of oxytocin on the mean contractile amplitude of circular muscle (CM) of proximal colon in rabbits. ^a $P < 0.05$ vs control, $n = 10$.

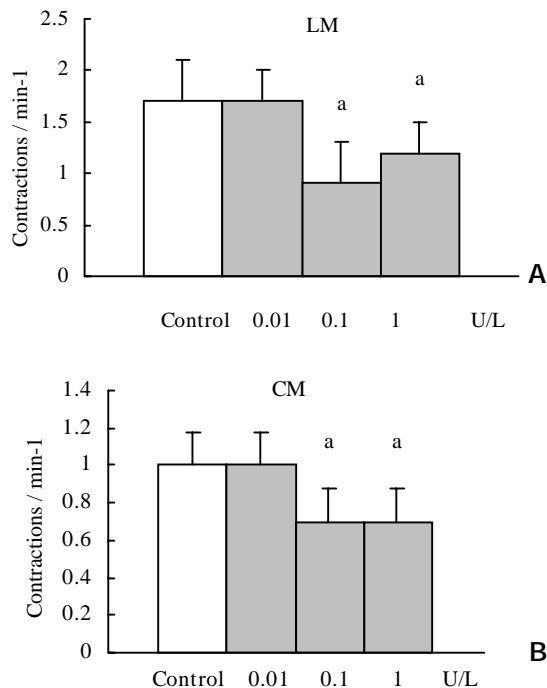


Figure 2 A: Effect of oxytocin on the contractile frequency of longitudinal muscle (LM) of proximal colon in rabbits. B: Effect of oxytocin on the contractile frequency of circular muscle (CM) of proximal colon in rabbits. ^a $P < 0.05$ vs control, $n = 10$.

OT ($0.1 \text{ U} \cdot \text{L}^{-1}$) failed to elicit significant effects on the contractile activity of proximal colonic smooth muscle strips ($P > 0.05$). OT (1 to $10 \text{ U} \cdot \text{L}^{-1}$) decreased the mean contractile amplitude and the contractile frequency of CM and LM (Figure 1, Figure 2). It had no significant effects on the resting tension of CM and LM.

Effect of hexamethonium on the OT-induced responses

Hexamethonium ($10 \mu\text{mol} \cdot \text{L}^{-1}$) had no significant effect on the contractile activity of each colonic smooth muscle strip. Hexamethonium given 3 minute before administration of OT ($1 \text{ U} \cdot \text{L}^{-1}$) decreased OT-induced inhibition on the contractile frequency of CM (Figure 3). It had no significant effects on the other action of OT.

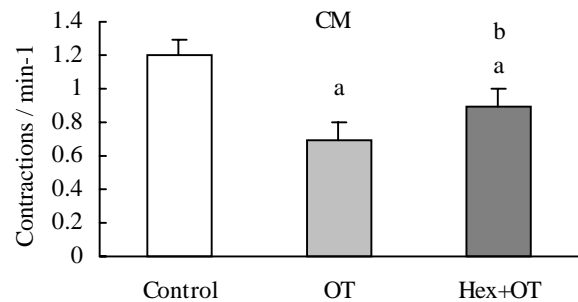


Figure 3 Effect of oxytocin on the contractile frequency of circular muscle (CM) of proximal colon after hexamethonium pretreatment in rabbits. OT, oxytocin; Hex, hexamethonium. ^a $P < 0.05$ vs control, ^b $P < 0.05$ vs oxytocin, $n = 6$.

Effect of L-NAME on the OT-induced responses

L-NAME ($1 \mu\text{mol} \cdot \text{L}^{-1}$) itself had no significant effects on proximal colon in rabbits. When given 3 min before the administration of OT ($1 \text{ U} \cdot \text{L}^{-1}$), it had no significant effects on OT-induced responses.

Effect of progesterone and estrogen on the OT-induced responses

Progesterone ($32 \mu\text{mol} \cdot \text{L}^{-1}$) and estrogen ($2.6 \mu\text{mol} \cdot \text{L}^{-1}$) had no significant effects on proximal colonic motility. When given 3 min before the administration of OT ($1 \text{ U} \cdot \text{L}^{-1}$), neither progesterone nor estrogen had significant effects on OT-induced responses.

DISCUSSION

The present study revealed that oxytocin $1 \text{ U} \cdot \text{L}^{-1}$ to $10 \text{ U} \cdot \text{L}^{-1}$ inhibited the spontaneous contractile motility of proximal colonic smooth muscle in rabbits. Petring *et al* reported that veinjection of oxytocin could increase the gastric emptying of semisolid food in normal human^[10]. Oxytocin 10 - $100 \text{ U} \cdot \text{L}^{-1}$ stimulated the spontaneous contractile motility of gastric body and gastric antrum in rats *in vitro*. But oxytocin ($10 \text{ pmol} \cdot \text{L}^{-1}$ - $10 \text{ nmol} \cdot \text{L}^{-1}$) suppressed the spontaneous contractions of circular smooth muscle from guinea-pig gastric antrum and gastric emptying in male rats^[19,20]. Therefore, it seems that there are species, region and OT concentration differences in OT-induced contractions in gastrointestinal tract.

Our results showed that hexamethonium partly blocked the decreasing action of oxytocin on the contractile frequency of colonic strips, but not that of the contractile amplitude of the strips. These results suggested that oxytocin partly inhibited the contractile frequency of colonic strips via ganglion N receptor.

NO is found to be an inhibitory neurotransmitter of enteric neurons. NOS neurons has been identified in the myenteric plexus^[21-23]. The action of OT has been reported to relevant

with NO^[24] We observed the effect of L-NAME (inhibitor of NOS activity) on the inhibitory action of oxytocin to decide whether oxytocin inhibits the colonic contraction via NO synthetic pathway. The results showed that L-NAME had no effect on the inhibitory action of oxytocin, which suggested that the inhibitory action of oxytocin on colonic motility was irrelevant with NO.

OT has been identified to exert the actions via OT receptors in many tissues, including the hypothalamus, uterus, kidney, pancreas, heart, vasculature, and thymus^[25-30]. Oxytocin receptor are suggested to be present on the members of guinea-pig antral smooth muscle cells^[19]. OT might act on the proximal colonic smooth muscle via selective oxytocin receptor, which still need to be further studied.

The function and physiological regulation of the OT system has been reported to be strongly steroid dependent^[31,32]. But our results showed that both progesterone and estrogen had no significant effects on OT-induced responses.

Effects on the gastrointestinal tract muscle during pregnancy are caused primarily by hormonal changes, such as progesterone, estrogen, and other hormones^[33]. Motility changes occur throughout the gastrointestinal tract during pregnancy, including colonic transit manifested primarily as abdominal bloating and constipation^[34]. Both progesterone and estrogen have been shown to inhibit colonic motility and transit in rats^[35]. But Hinds and associates^[36] reported that no significant differences in colon transit were found between phase of the menstrual cycle or between women and men. Our results also showed that neither progesterone nor estrogen affected the proximal colonic motility in rabbits. OT was another hormone relate to pregnancy, and its plasma concentration was higher in late pregnancy^[37,38]. Our results showed that OT inhibited the colonic motility. Results from these studies provided new insight into the mechanisms controlling colonic motility during pregnancy and may form the basis for drug treatments of colonic motility disorders.

In conclusion, oxytocin inhibit the contractile activity of proximal colonic smooth muscle of rabbits *in vitro*. The action is partly relevant with N receptor, but irrelevant with that of NO, progesterone or estrogen.

REFERENCES

- Ivell R, Richter D. Structure and comparison of the oxytocin and vasopressin genes from rat. *Proc Natl Acad Sci USA* 1984; **81**: 2006-2010
- Kimura T, Tanizawa O, Mori K, Brownstein MJ, Okayama H. Structure and expression of a human oxytocin receptor. *Nature* 1992; **356**: 526-529
- Arletti R, Bertolini A. Oxytocin acts as an antidepressant in two animal models of depression. *Life Sci* 1987; **41**: 1725-1730
- Arletti R, Benelli A, Bertolini A. Influence of oxytocin on feeding behavior in the rat. *Peptides* 1989; **10**: 89-93
- Ackerman AE, Lange GM, Clemens LG. Effects of paraventricular lesions on sex behavior and seminal emission in male rats. *Physiol Behav* 1997; **63**: 49-53
- Flanagan LM, Dohanics J, Verbalis JG, Stricker EM. Gastric motility and food intake in rats after lesions of hypothalamic paraventricular nucleus. *Am J Physiol* 1992; **263**: R39-44
- Dobrovol'skaia ZA, Kosenko AF. The role of oxytocin in realizing hypothalamic effects on the motor function of the digestive tract. *Fiziol Zh SSSR* 1989; **75**: 734-737
- Flanagan LM, Olson BR, Sved AF, Verbalis JG, Stricker EM. Gastric motility in conscious rats given oxytocin and an oxytocin antagonist centrally. *Brain Research* 1992; **578**: 256-260
- Milenov K, Barth T, Jost K, Kasakov L. Effect of deamino-dicarboxy-tocin and oxytocin on myoelectrical and mechanical activity of uterus, stomach and small intestine in dog. *Endocrinol Exp* 1979; **13**: 177-183
- Petring OU. The effect of oxytocin on basal and pethidine - induced delayed gastric emptying. *Br J Clin Pharmacol* 1989; **28**: 329-332
- Melis MR, Argiolas A. Reduction of drug-induced yawning and penile erection and of noncontact erections in male rats by the activation of GABAA receptors in the paraventricular nucleus: involvement of nitric oxide. *Eur J Neurosci* 2002; **15**: 852-860
- Zingg HH, Grazzini E, Breton C, Larcher A, Rozen F, Russo C, Guillon G, Mouillac B. Genomic and non - genomic mechanisms of oxytocin receptor regulation. *Adv Exp Med Biol* 1998; **449**: 287-295
- Engstrom T, Bratholm P, Christensen NJ, Vilhardt H. Up-regulation of oxytocin receptors in non-pregnant rat myometrium by isoproterenol: effects of steroids. *J Endocrinol* 1999; **161**: 403-411
- Terenzi MG, Jiang QB, Cree SJ, Wakerley JB, Ingram CD. Effect of gonadal steroids on the oxytocin-induced excitation of neurons in the bed nuclei of the stria terminalis at parturition in the rat. *Neuroscience* 1999; **91**: 1117-1127
- Behrendt-Adam CY, Adams MH, Simpson KS, McDowell KJ. Oxytocin - neurophysin I mRNA abundance in equine uterine endometrium. *Domes Anim Endocrinol* 1999; **16**: 183-192
- Murata T, Murata E, Liu CX, Narita K, Honda K, Higuchi T. Oxytocin receptor gene expression in rat uterus: regulation by ovarian steroids. *J Endocrinol* 2000; **166**: 45-52
- Grazzini E, Guillon G, Mouillac B, Zingg HH. Inhibition of oxytocin receptor function by direct binding of progesterone. *Nature* 1998; **392**: 509-512
- Xie DP, Li W, Qu SY, Zheng TZ, Yang YL, Ding YH, Wei YL, Chen LB. Effect of areca on contraction of colonic muscle strips in rats. *World J Gastroenterol* 2002; **8**: 350-352
- Duridanova DB, Nedelcheva MD, Gagov HS. Oxytocin induced changes in single cell K⁺ currents and smooth muscle contraction of guinea-pig gastric antrum. *Eur J Endocrinol* 1997; **136**: 531-538
- Liu CY, Chen LB, Liu PY, Xie DP, Wang PS. Effects of progesterone on gastric emptying and intestinal transit in male rats. *World J Gastroenterol* 2002; **8**: 338-341
- Peng X, Feng JB, Yan H, Zhao Y, Wang SL. Distribution of nitric oxide synthase in stomach myenteric plexus of rats. *World J Gastroenterol* 2001; **7**: 852-854
- Venkova K, Krier J. A nitric oxide and prostaglandin-dependent component of NANC off-contractions in cat colon. *Am J Physiol* 1994; **266**: G40-G47
- Powell AK, Bywater RA. Endogenous nitric oxide release modulates the direction and frequency of colonic migrating motor complexes in the isolated mouse colon. *Neurogastroenterol Motil* 2001; **13**: 221-228
- Haraldsen L, Soderstrom-Lauritzen V, Nilsson GE. Oxytocin stimulates cerebral blood flow in rainbow trout (*Oncorhynchus mykiss*) through a nitric oxide dependent mechanism. *Brain Res* 2002; **929**: 10-14
- Adan RA, Van Leeuwen FW, Sonnemans MA, Brouns M, Hoffman G, Verbalis JG, Burbach JP. Rat oxytocin receptor in brain, pituitary, mammary gland, and uterus: partial sequence and immunocytochemical localization. *Endocrinology* 1995; **136**: 4022-4028
- Jasper JR, Harrell CM, O'Brien JA, Pettibone DJ. Characterization of the human oxytocin receptor stably expressed in 293 human embryonic kidney cells. *Life Sci* 1995; **57**: 2253-2261
- Jeng YJ, Lolait SJ, Strakova Z, Chen C, Copland JA, Mellman D, Hellmich MR, Soloff MS. Molecular cloning and functional characterization of the oxytocin receptor from a rat pancreatic cell line (RINm5F). *Neuropeptides* 1996; **30**: 557-565
- Jankowski M, Hajjar F, Kawas SA, Mukaddam DS, Hoffman G, McCann SM, Gutkowska J. Rat heart: a site of oxytocin production and action. *Proc Natl Acad Sci USA* 1998; **95**: 14558-14563
- Jankowski M, Wang D, Hajjar F, Mukaddam DS, McCann SM, Gutkowska J. Oxytocin and its receptors are synthesized in the rat vasculature. *Proc Natl Acad Sci USA* 2000; **97**: 6207-6211
- Elands J, Resink A, De Kloet ER. Neurohypophysial hormone receptors in the rat thymus, spleen, and lymphocytes. *Endocrinology* 1990; **126**: 2703-2710
- Gimpl G, Fahrenholz F. The oxytocin receptor system: structure, function, and regulation. *Physiol Rev* 2001; **81**: 629-683

- 32 **Soloff MS**, Grzonka Z. Binding studies with rat myometrial and mammary gland membranes on effects of mannanase on relative affinities of receptors for oxytocin analogs. *Endocrinology* 1986; **119**: 1564-1569
- 33 **Everson GT**. Gastrointestinal motility in pregnancy. *Gastroenterol Clin North Am* 1992; **21**: 751-776
- 34 **Baron TH**, Ramirez B, Richter JE. Gastrointestinal motility disorder during pregnancy. *Ann Intern Med* 1993; **118**: 366-375
- 35 **Ryan JP**, Bhojwani A. Colonic transit in rats: effect of ovariectomy, sex steroid hormones, and pregnancy. *Am J Physiol* 1986; **251**:G46-50
- 36 **Hinds JP**, Stoney B, Wald A. Does gender or the menstrual cycle affect colonic transit? *Am J Gastroenterol* 1989; **84**: 123-126
- 37 **Mizutani S**, Hayakawa H, Akiyama H, Sakura H, Yoshino M, Oya M, Kawashima Y. Simultaneous determinations of plasma oxytocin and serum placental leucine aminopeptidase (P-LAP) during late pregnancy. *Clin Biochem* 1982; **15**: 141-145
- 38 **Kumaresan P**, Subramanian M, Anandarangam PB, Kumaresan M. Radioimmunoassay of plasma and pituitary oxytocin in pregnant rats during various stages of pregnancy and parturition. *J Endocrinol Invest* 1979; **2**: 65-70

Edited by Wu XN

A new cytokine: the possible effect pathway of methionine enkephalin

Xin-Hua Liu, Dong-Ai Huang, Fei-Yi Yang, Yan-Sheng Hao, Guo-Guang Du, Ping-Feng Li, Gang Li

Xin-Hua Liu, Fei-Yi Yang, Yan-Sheng Hao, Guo-Guang Du, Ping-Feng Li, Gang Li, Department of Biochemistry and Molecular Biology, Health Science Center, Peking University, Beijing 100083, China
Dong-Ai Huang, Department of Biochemistry, Hainan Medical College, Haikou 571101, Hainan Province China

Supported by National Science Foundation of China, No. 30060091

Correspondence to: Dr. Gang Li and Ping-Feng Li, Department of Biochemistry and Molecular Biology, Peking University Health Science Center, Beijing 100083, China. ligang55@263.net

Telephone: +86-10-62092454

Received: 2002-06-01 **Accepted:** 2002-07-06

Abstract

AIM: To investigate experimentally the effects of methionine enkephalin on signal transduction of mouse myeloma NS-1 cells.

METHODS: The antigen determinate of delta opioid receptor was designed in this lab and the polypeptide fragment of antigen determinate with 12 amino acids residues was synthesized. Monoclonal antibody against this peptide fragment was prepared. Proliferation of Mouse NS-1 cells treated with methionine enkephalin of 1×10^{-6} mol·L⁻¹ was observed. The activities of protein kinase A (PKA) and protein kinase C (PKC) were measured and thereby the mechanism of effect of methionine enkephalin was postulated.

RESULTS: The results demonstrated that methionine enkephalin could enhance the proliferation of NS-1 cells and the effect of methionine enkephalin could be particularly blocked by monoclonal antibody. The activity of PKA was increased in both cytosol and cell membrane. With reference to PKC, the intracellular activity of PKC in NS-1 cells was elevated at 1×10^{-7} mol·L⁻¹ and then declined gradually as the concentration of methionine enkephalin was raised. The effects of methionine enkephalin might be reversed by both naloxone and monoclonal antibody.

CONCLUSION: Coupled with the findings, it indicates that the signal transduction systems via PKA and PKC are involved in the effects of methionine enkephalin by binding with the traditional opioid receptors, and therefore resulting in different biological effects.

Liu XH, Huang DA, Yang FY, Hao YS, Du GG, Li PF, Li G. A new cytokine: the possible effect pathway of methionine enkephalin. *World J Gastroenterol* 2003; 9(1): 169-173
<http://www.wjgnet.com/1007-9327/9/169.htm>

INTRODUCTION

A number of studies have documented the involvement of endogenous opioid peptide on the cellular functions. It has been known that opioid receptors exist on the surface of cells pertinent to immune function, and that the activation or inhibition of these receptors may enhance or down regulate

some cell activities. Methionine enkephalin, the native opioid peptide, has been identified and defined as a cytokine because of its non-neurotransmitter function and sharing all of the major properties of cytokines^[1-4]. Although numerous studies have shown that opioid-induced alteration of cellular function can be mediated indirectly via the central nervous system (CNS) or through direct interaction with cells, the precise cellular mechanisms underlying the immunomodulatory effects of opioids are largely unknown.

It is especially true that the opioid receptors contain consensus sites for phosphorylation by numerous protein kinases. Protein kinase C (PKC) has been shown to catalyze the *in vitro* phosphorylation of delta-opioid receptors and to potentiate agonist-induced receptor desensitization^[5,6]. On the other hand, studies suggest that acute and chronic opioid can regulate the cAMP-dependent protein kinase (PKA) signaling pathway and the changes in this pathway may be involved in opioid tolerance^[7-9]. It has been documented that increased PKA activity can maintain cellular tolerance to opioid receptor agonist by chronic opioid treatment^[10].

Although there is mounting evidence supporting the concept that opioids are members of the cytokine-like family, the relative contribution of the opioids to immunoregulation remains unclear. Furthermore, little has been studied how methionine enkephalin acts as binding with the receptor of cell surface and trigger the intracellular biological events via some kinases. In this series of experiments, we analyzed the effect of methionine enkephalin, the endogenous opioid, on the activities of PKA and PKC at various dosages. The effects of monoclonal antibody and naloxone were also determined so that the mechanism of effect of methionine enkephalin on the signal transduction will be further clarified.

MATERIALS AND METHODS

Materials

Methionine enkephalin, naloxone, dithiothreitol (DTT), leupeptin, histone, phosphatidyl serine (PS), diacylglycerol (DG) and ATP were purchased from SIGMA; DMEM medium, bovine serum albumin (BSA) and 1-eth-3-3-dimethylaminopropyl carbodimide-HCl (EDC) were purchased from GIBCO; phenylmethyl sulfonyl fluoride (PMSF) and egtazic acid (EGTA) were from SERVAL.

Methods

Design of polypeptide fragment of delta opioid receptor

Delta opioid receptor is composed of 372 amino acids residues. Hydrophilic analysis and structure prediction were performed in our laboratory by typing the sequence of opioid receptor into a special computer program designed according to the principle of prediction of antigen determinants, and by which fragment of antigen determinant was selected^[11]. The amino acids residues sequence of antigen determinant was selected from the 3rd hydrophilic peak based on the feature of possibility of antigen determinant and listed as follows: NH₂-Gly-Ser-Leu-Arg-Arg-Pro-Arg-Gln-Ala-Thr-Thr-Arg-COOH.

Synthesis of polypeptide fragment and preparation of monoclonal antibody Polypeptide fragment with 12 amino

acids residues of delta opioid receptor was synthesized in North West University, USA. Monoclonal antibody against this polypeptide fragment was prepared according to the routine procedure. In short, BALB/C mice was immunized with synthesized polypeptide fragment conjugated with bovine serum albumin in complete Freund's adjuvant at 2- to 3-week intervals. The splenic cells separated from mice were fused with myeloma cells to form a stable antibody-producing hybridoma cell line. Positive clones were screened by the method of ELISA and inoculated into BALB/C mice. The antibody was harvested from ascitic fluid and purified with affinity chromatography. The titers of monoclonal antibodies were higher than 3 000. The specificity and effects of monoclonal antibody were verified in this experiment.

Effect of methionine enkephalin on proliferation of NS-1 cell lines NS-1, Mouse myeloma cell line, was cultured in DMEM medium containing 10 % fetal calf serum at 37 °C in a humidified atmosphere of 5 % CO₂. After the cell growth occupied full of the bottom of the flasks, the cells were washed once and resuspended in medium at a density of 5×10⁴ cells per ml. 1 ml of the cells per well was liquated in a 24 wells plate. When the cells were grown about 70 % full of wells, the supernatant was taken out. Then the cells were resuspended in 1 ml of medium without serum and cultured for one more day. After 1 d, supernatants in all wells were removed and the cells were resuspended in 1 ml of medium (with 10 % fetal calf serum). The cells were administrated with 1×10⁻⁶ mol·L⁻¹ of methionine enkephalin. Different concentrations of monoclonal antibody (0.1-10×10⁻⁹ mol·L⁻¹) were used to block the effect of methionine enkephalin. The culture was continued for 2 d and then pulsed with 18.5×10³ Bq of ³H-TdR in each well. 4 h later, the cells were harvested onto glass microfiber filter using a multiple sample harvester. The incorporation of ³H-TdR was measured by using LKB 1209 Rackbeta liquid scintillation counter.

Determination of protein kinase A activity NS-1 cells were adjusted to 5×10⁴ cells per ml with DEME medium (containing 10 % fetal calf serum) and aliquot into 24 well plate at 1 ml cell suspension per well. When the cells were grown about 70 % full of the wells, the supernatant was taken out. Then the cells were resuspended in 1 ml of medium without serum, cultured for one more day and added 1×10⁻⁶ mol·L⁻¹ of methionine enkephalin. For the blocking assay, the different concentration of monoclonal antibody (0.1-10×10⁻⁶ mol·L⁻¹) and naloxone (0.1-10×10⁻⁶ mol·L⁻¹) were added at the same time. After 24 h, the cells were collected, resuspended in 500 μl of buffer A (containing 200 mmol·L⁻¹ Tris-HCl pH 7.5, 0.25 mol·L⁻¹ sucrose, 2 mmol·L⁻¹ edetic acid, 2 mmol·L⁻¹ dithiothreitol, 10 mg·L⁻¹ leupeptin and 0.5 mmol·L⁻¹ PMSF) and destroyed by supersonic instrument for 2 min in ice bath. The supernatants were collected following a spin at 10 000 g for 45 min and defined as the cytosol fraction. The pellet was resuspended in 400 μl of buffer A containing 0.5 % Triton X-100, supersonically destroyed for 2 min and defined as the membrane fraction. The measurement of PKA activity was carried out as described with modifications^[12]. In short, 40 μl of extracted enzyme fractions were mixed with 160 μl of the solution at the final concentration of 20 mmol·L⁻¹ Tris-HCl pH 7.5, 5 mmol·L⁻¹ MgCl₂, 0.25 g·L⁻¹ BSA, 0.5 g·L⁻¹ histone, 2×10⁻⁷ mol·L⁻¹ ATP (γ-³²P ATP, 3.7×10⁴ Bq) and 8.0 μmol·L⁻¹ of cAMP at 37 °C for 10 min. After followed by incubation in ice bath for 5 min to terminate the reaction, 150 μl of the solution from each sample was collected onto Whatmen GF/C filter paper. After washing 2× with 10 % TCA-2 % phosphoric acid for 30 min at room temperature followed by 2× wash with 5 % TCA for 30 min, the activities of PKA were measured by using liquid scintillation counter and expressed as pmol value of ³²P in histone catalyzed by per mg protein per min.

Determination of protein kinase C activity The procedures of cell treatment and enzyme extraction were similar to that described in the determination of PKA instead of cells resuspended in 500 μl of buffer B (buffer A+10 mmol·L⁻¹ egtazic acid). The final volume was 200 μl with final concentration of 20 mmol·L⁻¹ Tris-HCl pH 7.5, 5 mmol·L⁻¹ MgCl₂, 0.25 g·L⁻¹ BSA, 0.5 g·L⁻¹ histone, 2×10⁻⁵ mol·L⁻¹ ATP (γ-³²P ATP, 3.7×10⁴ Bq), and 40 μl of extracted enzyme fraction. The measurement of activity of PKC was performed as described by Choi *et al.* with modification^[13]. Briefly, 5 mmol·L⁻¹ CaCl₂, 80 mg·L⁻¹ PS and 3 mg·L⁻¹ DG were added into reaction system. The collection and assay of samples and the addition of methionine enkephalin, also monoclonal antibody and naloxone, were according to the measurement of PKA. The activities of PKC were expressed with pmol value of ³²P in histone catalyzed by per mg protein per min (pmol·mg⁻¹·min⁻¹).

Statistical analysis

The data were expressed as $\bar{x} \pm s$ obtained from at least 3 independent experiments and analyzed by *t* test.

RESULTS

Effects of methionine enkephalin on the proliferation of NS-1 cells

Methionine enkephalin could stimulate the proliferation of NS-1 cells. When 1×10⁻⁶ mol·L⁻¹ of methionine enkephalin was added into the cultured cells, the cells could proliferate up to 109 %. Monoclonal antibody at a lower concentration of 0.1×10⁻⁹ mol·L⁻¹ could not block the effect of methionine enkephalin. Whereas 1 and 10×10⁻⁹ mol·L⁻¹ of monoclonal antibody could reverse the enhancing effect of methionine enkephalin on the cell proliferation that showed significantly the differences as compared with treatment group of methionine enkephalin alone (Figure 1).

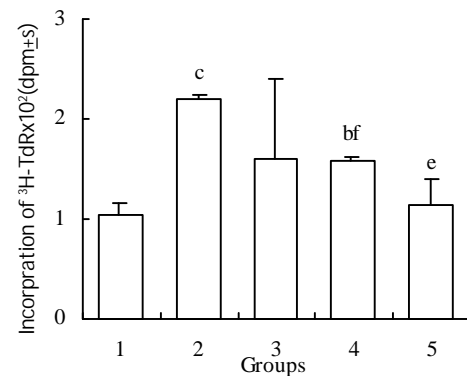


Figure 1 Blockage of monoclonal antibody to the effect of methionine enkephalin on the proliferation of NS-1 cells. Treatment groups; 1: control group; 2; 1×10⁻⁶ mol·L⁻¹ methionine enkephalin; 3; 1×10⁻⁶ mol·L⁻¹ methionine enkephalin plus 1×10⁻¹⁰ mol·L⁻¹ monoclonal antibody. 4; 1×10⁻⁶ mol·L⁻¹ methionine enkephalin plus 1×10⁻⁹ mol·L⁻¹ monoclonal antibody. 5; 1×10⁻⁶ mol·L⁻¹ methionine enkephalin plus 1×10⁻⁸ mol·L⁻¹ monoclonal antibody. *n*=3 from 3 independent experiments. ^b*P*<0.05 and ^c*P*<0.01 vs control group, ^e*P*<0.05 and ^f*P*<0.01 vs group 2

Effects of methionine enkephalin on the activity of PKA

Methionine enkephalin at various concentrations could enhance the level of activity of PKA in cytosol and cell membrane. The effects could be observed at the concentration of 0.1-10×10⁻⁶ mol·L⁻¹ in cytosol and 0.01-10×10⁻⁶ mol·L⁻¹ in cell membrane. The effects of methionine enkephalin on the activity of PKA were consistent in the cytosol and the cell membrane (Figure 2).

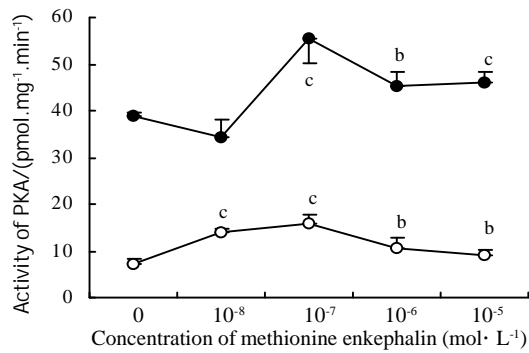


Figure 2 The influences of different concentrations of methionine enkephalin on the activity of PKA in cytosol (●) and cell membrane (○) of NS-1 cells. $n=3$ from 3 independent experiments. $^bP<0.05$ and $^cP<0.01$ vs control ($0 \text{ mol} \cdot \text{L}^{-1}$)

Antagonism of monoclonal antibody and naloxone on the activity of PKA

$1 \times 10^{-6} \text{ mol} \cdot \text{L}^{-1}$ of methionine enkephalin was used for the blocking assay of monoclonal antibody on the activity of PKA. The reversed effects could be observed at the concentration of 1×10^{-10} and $1 \times 10^{-9} \text{ mol} \cdot \text{L}^{-1}$ of antibody (Table 1). After administration of different concentrations of naloxone in the case of cytosol, the reversed effects were also obvious (Figure 3).

Table 1 Antagonism of different concentrations of monoclonal antibody (MAB) to methionine enkephalin (MENK) at $1 \times 10^{-6} \text{ mol} \cdot \text{L}^{-1}$ on the activity of PKA in cytosol and membrane of NS-1 cells. $n=3$ from 3 independent experiments. $^bP<0.05$ and $^cP<0.01$ vs control, $^eP<0.05$ and $^fP<0.01$ vs group 2

MENK+MAB	Activity of PKA in cytosol / $\text{pmol} \cdot \text{mg}^{-1} \cdot \text{min}^{-1}$	Activity of PKA in membrane / $\text{pmol} \cdot \text{mg}^{-1} \cdot \text{min}^{-1}$
Control	21.10 ± 1.09	6.81 ± 1.63
MENK	24.69 ± 0.49^c	10.42 ± 0.71^b
MENK+ $10^{-11} \text{ mol} \cdot \text{L}^{-1}$ MAB	29.98 ± 0.59^{cf}	13.73 ± 1.84^{ce}
MENK+ $10^{-10} \text{ mol} \cdot \text{L}^{-1}$ MAB	20.03 ± 1.47	7.59 ± 0.35^e
MENK+ $10^{-9} \text{ mol} \cdot \text{L}^{-1}$ MAB	12.99 ± 0.95^{cf}	7.11 ± 2.04^e

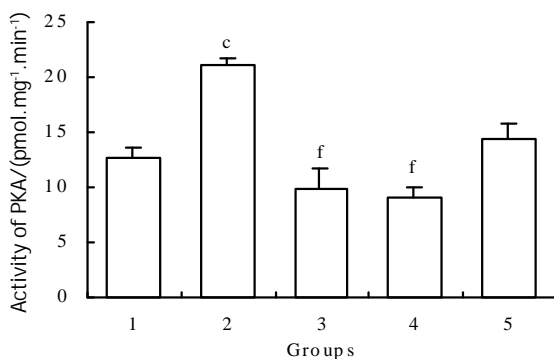


Figure 3 The effects of different concentration of naloxone on the activity of PKA in cytosol of NS-1 cells. Treatment groups: 1: control; 2: $1 \times 10^{-6} \text{ mol} \cdot \text{L}^{-1}$ methionine enkephalin; 3: $1 \times 10^{-6} \text{ mol} \cdot \text{L}^{-1}$ methionine enkephalin plus $1 \times 10^{-7} \text{ mol} \cdot \text{L}^{-1}$ naloxone; 4: $1 \times 10^{-6} \text{ mol} \cdot \text{L}^{-1}$ methionine enkephalin plus $1 \times 10^{-6} \text{ mol} \cdot \text{L}^{-1}$ naloxone; 5: $1 \times 10^{-6} \text{ mol} \cdot \text{L}^{-1}$ methionine enkephalin plus $1 \times 10^{-5} \text{ mol} \cdot \text{L}^{-1}$ naloxone. $n=3$ from 3 independent experiments. $^cP<0.01$ vs control, $^fP<0.01$ vs group 2

Effects of methionine enkephalin on the activity of PKC

In Figure 4, a narrow effective range of methionine enkephalin was displayed. At the concentration of $1 \times 10^{-7} \text{ mol} \cdot \text{L}^{-1}$,

methionine enkephalin could enhance the intracellular activity of PKC (Figure 4), but the higher concentration (10^{-6} - $10^{-5} \text{ mol} \cdot \text{L}^{-1}$) of methionine enkephalin showed a suppressive effect compared with control ($0 \text{ mol} \cdot \text{L}^{-1}$).

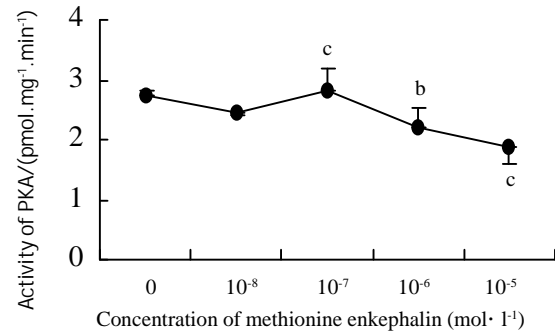


Figure 4 The influences of different concentrations of methionine enkephalin on the intracellular activity of PKC in NS-1 cells. $n=3$ from 3 independent experiments. $^bP<0.05$ and $^cP<0.01$ vs control ($0 \text{ mol} \cdot \text{L}^{-1}$).

Antagonism of monoclonal antibody and naloxone on the activity of PKC

Based on the data in Figure 4, $1 \times 10^{-6} \text{ mol} \cdot \text{L}^{-1}$ of methionine enkephalin was used to inhibit the PKC. Like observed in the case of PKA, the effect of methionine enkephalin could be blocked by different concentrations of monoclonal antibody (Table 2). Naloxone at concentrations of 1×10^{-6} and $1 \times 10^{-5} \text{ mol} \cdot \text{L}^{-1}$ could also reverse the suppressed effect of methionine enkephalin in the cytosol (Figure 5).

Table 2 Antagonism of different concentrations of monoclonal antibody (MAB) to methionine enkephalin (MENK) at $1 \times 10^{-6} \text{ mol} \cdot \text{L}^{-1}$ on the intracellular activity of PKC in NS-1 cells. $n=3$ from 3 independent experiments. $^bP<0.05$ vs control, $^eP<0.05$ and $^fP<0.05$ vs group 2

MENK+MAB	Activity of PKC ($\text{pmol} \cdot \text{mg}^{-1} \cdot \text{min}^{-1}$)
Control	3.06 ± 0.19
MENK	2.26 ± 0.03^b
MENK+ $10^{-11} \text{ mol} \cdot \text{L}^{-1}$ MAB	2.92 ± 0.02^e
MENK+ $10^{-10} \text{ mol} \cdot \text{L}^{-1}$ MAB	2.80 ± 0.4^e
MENK+ $10^{-9} \text{ mol} \cdot \text{L}^{-1}$ MAB	3.13 ± 0.45^{ff}

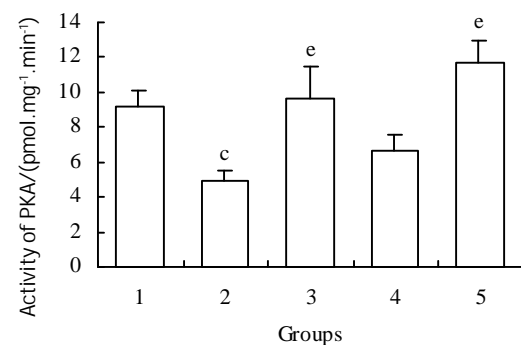


Figure 5 The effects of different concentration of naloxone on the intracellular activity of PKC in NS-1 cells. Treatment groups: 1: control; 2: $1 \times 10^{-6} \text{ mol} \cdot \text{L}^{-1}$ methionine enkephalin; 3: $1 \times 10^{-6} \text{ mol} \cdot \text{L}^{-1}$ methionine enkephalin plus $1 \times 10^{-7} \text{ mol} \cdot \text{L}^{-1}$ naloxone; 4: $1 \times 10^{-6} \text{ mol} \cdot \text{L}^{-1}$ methionine enkephalin plus $1 \times 10^{-6} \text{ mol} \cdot \text{L}^{-1}$ naloxone; 5: $1 \times 10^{-6} \text{ mol} \cdot \text{L}^{-1}$ methionine enkephalin plus $1 \times 10^{-5} \text{ mol} \cdot \text{L}^{-1}$ naloxone. $n=3$ from 3 independent experiments. $^cP<0.01$ vs control, $^eP<0.05$ vs group 2

DISCUSSION

The biological and clinical effects of opiate interaction with immune cells are well appreciated. In recent years, investigations from several laboratories have indicated that opioids can operate as cytokines, the principal communication signals of the immune system^[1,2]. Our previous studies have also proved the cellular modulation of methionine enkephalin^[3,4]. In this experiment, the results that methionine enkephalin could enhance the proliferation of NS-1 cells and perform the effect of growth factor-like, were consistent with the conclusion.

One possible component in the receptor signal cascade that can be responsible for these differences is the ligand-receptor interaction site. Receptor chimera studies followed by mutational analysis have revealed that functions of receptor domains were different for various opioid alkaloids and opioid peptides^[14-19]. Based on the principle of antigen determinant, we prepared the monoclonal antibody against delta opioid receptor. Our data showed that the effects of methionine enkephalin were reversible in the presence of different concentration of monoclonal antibody, which indicating the existence of a functional domain at the peptides segment.

Although some laboratories have provided evidences that supporting agonist-induced down-regulation of opioid receptors appear to require the phosphorylation of the receptor protein^[20-24], the identities of the specific protein kinases that perform this task remain uncertain. Moreover, it is unknown whether the change of protein kinase activation was dependent on the effect of methionine enkephalin. Our data showed that the activities of PKA were up-regulated in both cytosol and membrane of NS-1 cells in a variety of concentrations of methionine enkephalin. The elevation of PKA activity showed dose-independent and the most efficient concentration of methionine enkephalin was at 10^{-7} mol·L⁻¹. It had been shown that increased PKA activity related to the maintenance of cellular tolerance to opioid receptor agonists^[10, 25, 26].

However, in the case of PKC, the enzyme activity was elevated when methionine enkephalin at the concentration of 1×10^{-7} mol·L⁻¹ and declined gradually at 1×10^{-6} to 10^{-5} mol·L⁻¹. The coincident results have also been observed in other laboratory. It had been reported that a biphasic response of opioid on expression of some cytokines had been demonstrated that nanomolar concentration of opioid augmented the secretion of both IL-6 and TNF-alpha, whereas micromolar concentration inhibited their synthesis^[27]. It had also been reported that opioid-induced PKC translocation followed a time-dependent and biphasic pattern beginning 2 h after opioid addition, when a pronounced translocation of PKC to the plasma membrane occurred. When exposure to opioids was lengthened to >12 h, both cytosolic and particulate PKC levels dropped significantly below those of control-treated cells because of the decrease of membrane-bound PKC density^[15, 28].

From our data, the effect of methionine enkephalin could be reversed by a lower concentration of monoclonal antibody. Although little previous information was available to compare the usage of antibody, it was postulated that a complex ligand-receptor interaction was involved. The results that an antagonism of monoclonal antibody to the effect of methionine enkephalin on the activity of PKA or PKC indicated that the antigen determinant of the receptor fragment was also the functional domain of the receptor. The postulate was reinforced by studies involving μ/δ receptor chimeras that investigated the function of each domain^[14, 15]. Likewise, the same results could be observed in the assay of naloxone, the antagonist of opioid receptor. The effect of naloxone abolishing the effect of opioid on the activity of PKA had been reported^[29, 30]. Thus, a traditional opioid mechanism on signaling pathway of PKA and PKC was thereby involved.

REFERENCES

- 1 **Peterson PK**, Molitor TW, Chao CC. The opioid-cytokine connection. *J Neuroimmunology* 1998; **83**: 63-69
- 2 **Plotnikoff NP**, Faith RE, Murgo AJ, Herberman RB, Good RA. Methionine enkephalin: a new cytokine-human studies. *Clin Immunol Immunopathol* 1997; **82**: 93-101
- 3 **Li G**, Fraker PJ. Methionine enkephalin alteration of mitogenic and mixed lymphocyte culture responses in zinc-deficient mice. *Acta Pharmacol Sin* 1989; **10**: 216-221
- 4 **Li G**, Yu J. Inhibition of bone marrow immature B lymphocytes from zinc deficient mice by methionine enkephalin. *Acta Pharmacol Sin* 1991; **12**: 500-503
- 5 **Kramer HK**, Simon EJ. Role of protein kinase C(PKC) in agonist-induced mu-opioid receptor down-regulation:II. Activation and involvement of the alpha, epsilon, and zeta isoform of PKC. *J Neurochem* 1999; **72**: 594-604
- 6 **Narita M**, Mizoguchi H, Kampine JP, Tseng LF. Role of protein kinase C in desensitization of spinal delta-opioid-mediated antinociception in the mouse. *Br J Pharmacol* 1996; **118**: 1829-1835
- 7 **Shen J**, Benedict GA, Gallagher A, Stafford K, Yoburn BC. Role of camp-dependent protein kinase (PKA) in opioid agonist-induced mu-opioid receptor downregulation and tolerance in mice. *Synapse* 2000; **38**: 322-327
- 8 **Avidor-Reiss T**, Bayewitch M, Levy R, Matus-Leibovitch N, Nevo I, Vogel Z. Adenylylcyclase supersensitization in mu-opioid receptor-transfected Chinese hamster ovary cells following chronic opioid treatment. *J Biol Chem* 1995; **270**: 29732-29738
- 9 **Liu JG**, Anand KJ. Protein kinases modulate the cellular adaptations associated with opioid tolerance and dependence. *Brain Res Brain Res Rev* 2001; **38**: 1-19
- 10 **Wagner EJ**, Ronnekleiv OK, Kelly MJ. Protein kinase A maintains cellular tolerance to mu opioid receptor agonists in hypothalamic neurosecretory cells with chronic morphine treatment: convergence on a common pathway with estrogen in modulating mu opioid receptor/effector coupling. *J Pharmacol Exp Ther* 1998; **285**: 1266-1273
- 11 **Hopp TP**, Woods KR. Prediction of protein antigenic determinants from amino acid sequences. *Proc Natl Acad Sci USA* 1981; **78**: 3824-3828
- 12 **Li MS**, Li PF, He SP, Du GG, Li G. The promoting molecular mechanism of alpha-fetoprotein o the growth of human hepatoma Bel7402 cell line. *World J Gastroenterol* 2002; **8**: 469-475
- 13 **Choi SW**, Park HY, Rubeiz NG, Sachs D, Gilchrist BA. Protein kinase C-alpha levels are inversely associated with growth rate in cultured human dermal fibroblasts. *J Dermatological Sci* 1998; **18**:54-63
- 14 **Fukuda K**, Kato S, Mori K. Location of regions of the opioid receptor involved in selective agonist binding. *J Biol Chem* 1995; **270**: 6702-6709
- 15 **Pepin MC**, Yue SY, Roberts E, Wahlestedt C, Walker P. Novel "restoration of function" mutagenesis strategy to identify amino acids of the δ -opioid receptor involved in ligand binding. *J Biol Chem* 1997; **1272**: 9260-9267
- 16 **Meng F**, Ueda Y, Hoversten MT, Thompson RC, Taylor L, Watson SJ, Akil H. Mapping the receptor domains critical for the binding selectivity of delta-opioid receptor ligands. *Eur J Pharmacol* 1996; **311**: 285-292
- 17 **Metzger TG**, Paterlini MG, Ferguson DM, Portoghesi PS. Investigation of the selectivity of oxymorphone- and naltrexone-derived ligands via site-directed mutagenesis of opioid receptors: exploring the "address" recognition locus. *J Med Chem* 2001; **44**: 857-862
- 18 **Ide S**, Sakano K, Seki T, Awamura S, Minami M, Satoh M. Endomorphin-1 discriminates the mu-opioid receptor from the delta- and kappa-opioid receptors by recognizing the difference in multiple regions. *Jpn J Pharmacol* 2000; **83**: 306-311
- 19 **Bonner G**, Meng F, Akil H. Selectivity of mu-opioid receptor determined by interfacial residues near third extracellular loop. *Eur J Pharmacol* 2000; **403**: 37-44
- 20 **Krupnick JG**, Benovic JL. The role of receptor kinases and arrestins in G protein-coupled receptor regulation. *Ann Rev Pharmacol Toxicol* 1998; **38**: 289-319
- 21 **Whistler JL**, Tsao P, von Zastrow M. A phosphorylation-regulated brake mechanism controls the initial endocytosis of opioid

- receptors but is not required for post-endocytic sorting to lysosomes. *J Biol Chem* 2001; **276**: 34331-34338
- 22 **Chaturvedi K**, Bandari P, Chinen N, Howells RD. Proteasome involvement in agonist-induced down-regulation of mu and delta opioid receptors. *J Biol Chem* 2001; **276**: 12345-12355
- 23 **Law PY**, Kouhen OM, Solberg J, Wang W, Erickson LJ, Loh HH. Deltorphin II-induced rapid desensitization of delta-opioid receptor requires both phosphorylation and internalization of the receptor. *J Biol Chem* 2000; **275**: 32057-32065
- 24 **Kramer HK**, Andria ML, Esposito DH, Simon EJ. Tyrosine phosphorylation of the delta-opioid receptor. Evidence for its role in mitogen-activated protein kinase activation and receptor internalization. *Biochem Pharmacol* 2000; **60**: 781-792
- 25 **Yoshikawa M**, Nakayama H, Ueno S, Hirano M, Hatanaka H, Furuya H. Chronic fentanyl treatments induce the up-regulation of mu opioid receptor mRNA in rat pheochromocytoma cells. *Brain Res* 2000; **859**: 217-223
- 26 **Wang Z**, Sadee W. Tolerance to morphine at the mu-opioid receptor differentially induced by camp-dependent protein kinase activation and morphine. *Eur J Pharmacol* 2000; **389**: 165-171
- 27 **Roy S**, Cain KJ, Chapin RB, Charboneau RG, Barke RA. Morphine modulates NF kappa B activation in macrophages. *Biochem Biophys Res Commun* 1998; **245**: 392-396
- 28 **Kramer HK**, Simon EJ. Role of protein kinase C (PKC) in agonist-induced mu-opioid receptor down-regulation: I. PKC translocation to the membrane of SH-SY5Y neuroblastoma cells is induced by mu-opioid agonists. *J Neurochem* 1999; **72**: 585-593
- 29 **Chakrabarti S**, Law PY, Loh HH. Distinct differences between morphine-and [D-Ala2,N-MePhe4,Gly-ol5]-enkephalin-mu-opioid receptor complexes demonstrated by cyclic AMP-dependent protein kinase phosphorylation. *J Neurochem* 1998; **71**: 231-239
- 30 **Sharma P**, Kumar Bhardwaj S, Kaur Sandhu S, Kaur G. Opioid regulation of gonadotropin release: role of signal transduction cascade. *Brain Res Bull* 2000; **52**: 135-142

Edited by Wu XN

Is analysis of lower esophageal sphincter vector volumes of value in diagnosing gastroesophageal reflux disease?

Robert E. Marsh, Christopher L. Perdue, Ziad T. Awad, Patrice Watson, Mohamed Selima, Richard E. Davis, Charles J. Filipi

Robert E. Marsh, Christopher L. Perdue, Ziad T. Awad, Mohammed Selima, Richard E. Davis, Charles J. Filipi, Department of Surgery, Creighton University School of Medicine, Omaha Nebraska USA
Patrice Watson, Department of Preventive Medicine, Creighton University School of Medicine, Omaha Nebraska USA
Correspondence to: Dr. Charles J. Filipi, Department of Surgery, Creighton University School of Medicine, 601 N 30th Street, Suite 3740, Omaha, NE 68131. cjfilipi@creighton.edu
Telephone: +402-280-4213 **Fax:** +402-280-4278
Received: 2002-07-23 **Accepted:** 2002-07-27

Abstract

AIM: With successful surgical treatment of gastroesophageal reflux disease (GERD), there is interest in understanding the anti-reflux barrier and its mechanisms of failure. To date, the potential use of vector volumes to predict the DeMeester score has not been adequately explored.

METHODS: 627 patients in the referral database received esophageal manometry and ambulatory 24-hour pH monitoring. Study data included LES resting pressure (LESP), overall LES length (OL) and abdominal length (AL), total vector volume (TVV) and intrabdominal vector volume (IVV).

RESULTS: In cases where LESP, TVV or IVV were all below normal, there was an 81.4 % probability of a positive DeMeester score. In cases where all three were normal, there was an 86.9 % probability that the DeMeester score would be negative. Receiver-operating characteristics (ROC) for LESP, TVV and IVV were nearly identical and indicated no useful cut-off values. Logistic regression demonstrated that LESP and IVV had the strongest association with a positive DeMeester score; however, the regression formula was only 76.1 % accurate.

CONCLUSION: While the indices based on TVV, IVV and LESP are more sensitive and specific, respectively, than any single measurement, the measurement of vector volumes does not add significantly to the diagnosis of GERD.

Marsh RE, Perdue CL, Awad ZT, Watson P, Selima M, Davis RE, Filipi CJ. Is analysis of lower esophageal sphincter vector volumes of value in diagnosing gastroesophageal reflux disease? *World J Gastroenterol* 2003; 9(1): 174-178
<http://www.wjgnet.com/1007-9327/9/174.htm>

INTRODUCTION

With the recognition of gastroesophageal reflux disease (GERD) as a surgical pathology, there is deep interest in understanding the anatomical and physiological anti-reflux barrier and its mechanisms of failure^[1-8]. The anatomical components of the barrier include the crural fibers of the diaphragmatic esophageal hiatus, the smooth muscle sling fibers of the gastric cardia, and the semicircular and clasp fibers of the distal esophagus^[1-5]. Augmented by positive intrabdominal pressure over the most

distal portion of the lower esophagus and proximal cardia, the sphincter approximates the mucosal epithelium covering the internal surface area of the esophagogastric junction. This distinct high-pressure zone is a critical factor in the barrier against reflux of gastric contents^[5-8]. The anatomical function of the lower esophageal sphincter (LES) is complemented by neutralization of refluxate by alkaline oral secretions and rapid clearance of esophageal contents by intermittent and reflex peristalsis^[8].

Various means have been devised to measure the mechanical integrity of the LES^[8-11]. Traditional pull-through manometry has been succeeded in some laboratories by sophisticated equipment and software that allows measurement of the closure pressure generated by the three-dimensional sphincter mechanism. Directional pressures can be summated over the length of the sphincter to produce a vector volume that describes the overall physical resistance of the barrier to continuous reflux^[11,12]. Other measures of the sphincter competence include resting pressure of the LES at various points along its length, the vector volume of the intrabdominal portion of the LES as well as overall and intrabdominal lengths of the LES. While many observers have noted the relationship between abnormal manometry and GERD^[4-14], we have sought to quantify this relationship in a way that describes the comparative ability of such measurements to predict positive ambulatory pH monitoring as described by DeMeester and colleagues^[15]. It was our goal to compare traditional manometric measurements, vector volume analysis and results of 24-hour pH monitoring. We postulated that one or more of the manometric measurements would yield a statistically significant relationship to a positive DeMeester score. Because of the complexity of the procedure, expense, and general discomfort to the patient, it was hoped that detection of a defective LES would obviate the need for subsequent pH monitoring in certain cases.

MATERIALS AND METHODS

Materials

Manometric studies were performed using a 9-lumen catheter (ESM38R, Arndorfer, Greendale, Wisconsin) coupled to a hydraulic capillary infusion system (Arndorfer). The catheter consisted of a central lumen of 1.8 mm internal diameter surrounded by 8 lumens of 0.8 mm internal diameter. Four channels extended to the distal end of the catheter with ports at the same level and oriented radially at 90° intervals. The remaining 4 ports were spaced contiguously at 5 cm intervals proximal to, and offset by 45° from, the radial ports, providing 20 cm of working length. The central lumen was not used. The catheter was pulled at a 3 mm/second using a mechanical puller. The transducer information was translated into digital information using a polygraph (Medtronic Synectics, Shoreview, Minnesota). External transducers were also used to detect swallow and respiratory waves. The information was saved for real-time and retrospective review using Polygram software (Medtronic Synectics).

Methods

The original audit population consisted of 1 900 patients referred to the Esophageal Function Laboratory in the

Department of Surgery at Creighton University. This population received either esophageal manometry, 24-hour pH monitoring or both. Patients were referred to the laboratory for typical or atypical symptoms thought to represent GERD. Of the 1 900 patients in the referral database, only 627 received both esophageal manometry with measurement of LES vector volumes and ambulatory 24-hour pH monitoring. Vector volume data were available for the total length of the lower esophageal sphincter (total vector volume, TVV) and for the intrabdominal length (intrabdominal vector volume, IVV). The vector volume is a calculated value representing the directional pressures within the LES over a specific portion of the sphincter. Additional data included age, weight, resting pressure of the LES (LESP), overall LES length (OL) and abdominal LES length (AL).

In preparation for station pull-through (SPT), the catheter assembly was introduced through either nare and advanced into the stomach. SPT was performed using a mechanized puller (Medtronic Synectics) at 3 mm/sec to avoid swallowing with pauses every centimeter to allow pressure measurement. Using the gastric baseline pressure as the reference point, a port entered the LES when a sustained positive deflection away from the baseline was observed. A wet swallow of 5 mL tap water was performed at this level to observe relaxation of the LES. The SPT proceeded through the entirety of the LES resulting in five measurements from separate channels which were averaged to produce the final value. The patient was instructed to breathe regularly and not to swallow. Swallowing (except for the wet swallow) required another attempt.

The resting pressure of the LES (LESP) was defined as the mean pressure at the respiratory inversion point (RIP). The RIP was the place on the pressure waveform where the positive deflections in the abdomen caused by inspiration changed to negative deflections in the chest. OL was the distance between the distal and proximal borders of the LES; AL was the distance between the distal border of the LES and the RIP. Both measurements were obtained during SPT.

Measurements for vector volume calculations were obtained from transducers attached to the 4 radial ports located at the same level on the catheter. Each channel yielded a separate pressure and direction (pressure vector) over the length of the LES. The distal border of the LES was defined as the position at which two or more of the four channels deflected positively from the gastric baseline. The crural component, often represented as the distal hump in the bimodal waveform, was intentionally included in the TVV. The proximal border was defined as that position in which two or more of the four channels returned and stayed below the gastric baseline. Computer software summated the pressure vector measurements into a single vector volume (mm Hg^3). A three-dimensional image was also generated but not included in the database.

IVV was determined similarly. The proximal endpoint of the IVV was the RIP; the distal endpoint was the same as for TVV. As with TVV determination, when two or more of the four channels reached the RIP, all were considered to be at the RIP. Computer software similarly produced a value for the vector volume.

Upon completion of manometry, the pressure catheter was replaced with a pH probe catheter (Ingold Bipolar Glass pH Probe, Mui Scientific, Mississauga, Ontario). All patients had been off their medication (PPI's for 7 days, H2 blockers for 3 days) for the appropriate time. The catheter was passed through the nose and into the stomach to obtain a baseline reading from the ambulatory recording equipment to be carried by the patient (Digitrapper, Medtronic Synectics). The catheter was then withdrawn to a position 5 cm above the LES as determined by SPT. A baseline reading was again obtained. The catheter was secured to the nose and patients were given instructions to eat at

least three meals (limited to foods in which the pH was known), to stay upright at least 4 hours after eating, and to be recumbent for no more than 8 hours during sleep. Patients were instructed to note in a diary the time of each symptom occurrence, when and what they ate, and when they retired for bed.

At the completion of the 24-hour period, the catheter was removed and the information in the Digitrapper was downloaded and analyzed using pH-metry software (EsopHagram, Synectics). A DeMeester score was then tabulated by the computer and recorded for both acid and alkaline reflux. A score <14.8 was considered negative for GERD.

Except for the logistic regression, sensitivities and specificities for the receiver-operating characteristics (ROC) were calculated manually. The purpose of the ROC was to find an optimal cut-off point, if any, for measurements that would yield the greatest combination of sensitivity and specificity. The formulas for calculations involving LESP (for example) were:

$$\text{Sensitivity} = \frac{[\text{'n' patients with GERD and LESP} \leq \text{'x'}]}{[\text{'n' patients with GERD}]}$$

$$\text{Specificity} = \frac{[\text{'n' patient without GERD and LESP} > \text{'x'}]}{[\text{'n' patient without GERD}]}$$

In those calculations, 'x' refers to a progressively larger cut-off value for LESP (following the example above). Therefore, a particular sensitivity represented the probability that a patient with an $\text{LESP} \leq \text{'x'}$ would have GERD. Likewise, the specificity represents that probability that a patient with an $\text{LESP} > \text{'x'}$ would not have GERD. Cut-off values were chosen at increments that resulted in enough data points to provide adequate resolution to the curve but with enough cases within each range to reflect real trends. This was done for LESP, TVV, IVV, AL and OL.

All other calculations were performed by SAS statistical software (version 6.12). The logistic regression process was automated and resulted in a formula for predicting GERD-positive or GERD-negative. According to its program, the statistical software started with all predictors in a test formula, then through backward selection, removed predictors that failed to meet the appropriate confidence interval. The software rejected predictors when p-values were $>0.05\%$. There were no attempts at relating the manometry measurements directly to DeMeester score in a continuous fashion. Rescaling in order to account for outliers consisted of setting values above the 95th percentile for any measurement equal to the value of that measurement at the 95th percentile. Values for normal were derived from a prior study in this laboratory using 50 healthy (non-GERD) volunteers. No attempts were made to sort patients or data according to age, sex or weight.

RESULTS

Demographic data with respect to the diagnosis of GERD is presented in Table 1. There were no attempts at age or sex matching. Table 2 includes the means, standard deviations, p-values, sensitivities and specificities for the measured parameters. The sensitivity and specificity of LESP, TVV and IVV, respectively, were 67.3 % and 73.3 %; 72.5 % and 62.6 %; and 58.5 % and 77.3 % at the lower values for normal. The sensitivity and specificity for AL and OL reflect the fact that very few patients had abnormal values of either (4 and 2 patients, respectively); this was also reflected in the similarity relatively large standard deviations between the average AL and OL for GERD and non-GERD sufferers. Because AL and OL were so weakly sensitive for reflux disease, Any-low refers only to cases where LESP, TVV or IVV were below normal. The sensitivity of Any-low indicated an 81.4 % probability a patient with either abnormally low LESP, TVV or IVV will have GERD. Similarly, AL and OL were also excluded from calculations of the All-low values. There was an 86.9 %

probability that a patient with all three normal measurements will not have an abnormal esophageal acid exposure; this is the specificity for All-low.

Table 1 Demographic data for study cases

	Range	non-GERD mean ± SD	GERD mean ± SD
Age (years)	4 - 86	47.0±16.1 (n=308)	48.5±14.9 (n=319)
Weight (lbs)	87-397	173.6±42.2 (n=310)	190.2±38.0 (n=317)
Sex	F: 313M: 314	F: 101 M: 80	F: 108 M: 162

Table 2 Summary of manometric data

	Normal range	Range of measurements	non-GERD mean ± SD	GERD mean ± SD	P	Sens. %	Spec. %
LESP	6.1-25.6	0-59.3	10.9±8.4 (n=319)	5.7±4.8 (n=308)	<0.001	67.3	71.3
IVV	1855-10953	0-45830	4090±4709 (n=321)	1712±2080 (n=306)	<0.001	72.5	62.6
TVV	2060-14135	80-60740	5429±5564 (n=321)	2533±2626 (n=306)	<0.001	58.5	77.3
AL	1.0-5.0	0-9.8	2.6±1.0 (n=280)	2.2±1.0 (n=347)	0.013	4.5	98.4
OL	2.4-5.5	1.2-27.4	4.7±1.8 (n=287)	4.6±1.4 (n=340)	<0.047	2.6	99.0
Any low	-	-	-	-	-	81.4	51.0
All ow	-	-	-	-	-	49.3	86.9

LESP=Lower esophageal sphincter resting pressure (mm-Hg), IVV=Intraabdominal vector volume (mm-Hg³), TVV=total vector volume (mm-Hg³), AL=abdominal length of the LES (mm), OL=overall length of the LES (mm). "Any-low" refers to cases where LESP, IVV or TVV are lower than normal. "All-low" refers to cases where LESP, IVV and TVV are all lower than normal. SD=Standard deviation, Sens.=Sensitivity, Spec.=Specificity. 'P' is the probability value from the chi-squared test for GERD vs. non-GERD; P<0.05 is significant. Sensitivities and specificities are calculated using the lowest normal value.

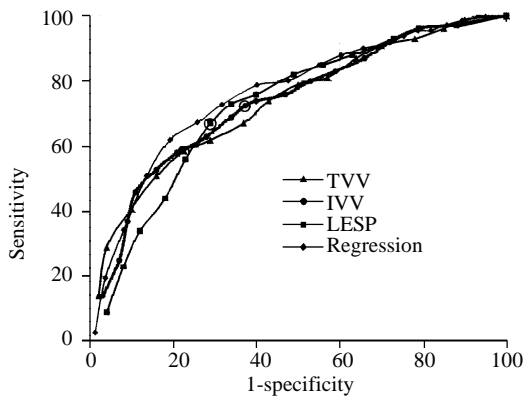


Figure 1 Receiver-operating characteristics for total vector volume (TVV), intrabdominal vector volume (IVV) and LES resting pressure (LESP). Included is a comparable ROC for the logistic regression. The points on the curves that correspond to the normal values in Table 1 are circled

Figure 1 shows the receiver-operating characteristics for LESP, TVV, and IVV. The curves for AL and OL fell below all of the other curves and (for clarity) have not been depicted. There are no obvious points at which both specificity and sensitivity are optimal for any of the measurements. Cut-off values equal to the lowest normal values are indicated by the circled data points. Also shown in Figure 1 is an ROC curve for the regression formula (below) indicating that it does not

have a better combination of sensitivity and specificity than the measurements themselves.

The logistic regression formula following backward selection was

$$Y = 1.24 + [LESP](-0.1056) + [IVV] (-0.00019)$$

where Y is equal to a nominal value for GERD (1=the presence and 2=absence of GERD). P-values for the factor estimates were all <0.0001. Various attempts were made at rescaling the data (as described in Materials and Methods) and ranking without effect. The "native" logistic regression (unscaled and unranked) was superior or equal in every case with 76.1 % concordance, 23.6 % discordance and 0.3 % tied. Table 3 contains data from the logistic regression process. TVV, OL and AL were excluded by the software from the regression formula because of P-values >0.05 %. When ranked values were used for logistic regression, similar estimates were obtained for the y-intercept, LESP and IVV factors and the P-values were all <0.0001. The formulas for the ranked and rescaled data were equally good or worse at predicting GERD and have been excluded from further discussion.

Table 3 Logistic regression with the results of backward selection

Variable	Estimate	P
Intercept	+1.241	<0.0001
LESP	-0.106	<0.0001
IVV	-0.00019	<0.0001
TVV	(rejected)	0.43
AL	(rejected)	0.089
OL	(rejected)	0.79
Concordant = 76.1%		
Discordant = 23.6%		
Tied = 0.3%		

DISCUSSION

Intraabdominal vector volume is more sensitive than TVV or LESP, but only marginally, and no more than 72.5 % (Table 2). Measurements of TVV and LESP are more specific for GERD; that is, findings of normal TVV and LESP are 77.3 % and 71.3 % likely in a non-GERD patient, respectively. While the mean values for LESP, TVV and IVV are all significantly lower in GERD patients (P<0.0001), the standard deviations are nearly equal to the means themselves in every measurement (Table 2). Intraabdominal length (AL) and overall length (OL) of the LES are clearly unimportant in the assessment of gastroesophageal reflux disease. Only 4 and 2 patients, respectively, had abnormally low values for AL or OL.

When measurements are viewed as ROC curves (Figure 1), there are no points where a measurement has both a high sensitivity and high specificity. That is to say that there appears to be no optimal cut-off value for predicting GERD. Ideally, an ROC curve is a parabolic figure with the apex in the upper right corner (using the axes as in Figure 1) which drops sharply from a point where sensitivity and specificity are both high to a point where sensitivity is very low and specificity is very high. In fact, there are no values for which there is a high sensitivity and even a moderately useful specificity. At cut-off values representing 85 % sensitivity for GERD (≤1 600 mm-Hg³ for TVV; ≤1 000 mm-Hg³ for IVV; and ≤3 mm-Hg for LESP), the specificities of the measurements fall between 35 % and 45 %. Finding significantly lower-than-average TVV, IVV and LESP in GERD patients (Table 2.) reiterates our understanding of the pathological consequences of a weakened LES. It also confirms our present understanding that there is a more complex relationship between the

anatomical correlates of the LES and function than can be expressed by a single measurement.

Use of the "Any-low," "All-low," and logistic regression models were attempts to use the measurements in a combined fashioned, similar to the calculation of the DeMeester ambulatory pH score. While Any-low had a relatively better sensitivity (81.4 %) and All-low had relatively better specificity (86.9 %) for the DeMeester score than the original measurements, the logistic regression-presumably the more rigorous mathematical model-was little better than the ROC curves for LESP, IVV or TVV. The computer generated a series of sensitivities and specificities for predictions made by the regression formula. This data is represented in Figure 1 as a means of comparison. Interestingly, total vector volume of the LES (TVV) was rejected by the computer due to a failure to meet the 95 % correlation confidence interval. The logistic regression formula was only 76.1 % accurate in predicting the real data. Attempts at ranking the data and rescaling in order to account for a number of outlying measurements made no improvement in the accuracy of the formula. The regression formula was clearly unable to improve on the predictive power of the raw measurements. As such, the formula has no practical use in the laboratory.

We have been motivated to find a way to identify surgical candidates without directly measuring distal esophageal reflux because of the inherent difficulty with ambulatory pH monitoring (patient discomfort, cost, compliance). Recently, Fass and colleagues have suggested that the test itself may have the effect of reducing reflux-provoking activities, thereby reducing the sensitivity of the test^[16]. In studies of different patient populations where vector volumes were found to have greater use^[11-14] we are unaware of the degree to which they were able to control patient compliance with ambulatory pH monitoring protocols (either maintaining a normal daily diet and activities or maintaining a controlled regimen). Certainly, patient compliance would be expected to be higher when he or she is made to understand the importance of maintaining normal habits. This is also an uncontrolled factor in the present study. In a sense, this might be a form of "compliance bias" reflected in the sensitivity of the test, where poor compliance (relatively less daily activity, smaller meals, more conservative food choices) results in more falsely negative screening tests. Quigley has also referred to the multiple difficulties with pH-metry as the gold standard for diagnosing GERD, namely the issue of patient compliance with testing conditions^[17]. It remains to be seen if patient compliance, or any other factors, have any real effect on 24-hour pH monitoring and the treatment indications for GERD.

To improve surgical results, it is helpful but not mandatory to find evidence that a defective lower esophageal sphincter is the cause for GERD. This is based on the reports by numerous authors who have sought to describe the sphincter and its mechanisms of failure^[1-10]. Studies have demonstrated the effectiveness of anti-reflux surgery to improve symptom scores, esophagitis and LES resting pressure^[2,7,11,13]. Authors have asserted that measurement of vector volumes would be superior to standard lower esophageal manometry for detecting a defective LES^[11-15]. Wetscher and colleagues made the observation that IVV was more sensitive than LESP (i.e. standard manometry) and TVV at detecting a defective lower esophageal sphincter^[12]. They concluded that measurement of vector volumes would be a valuable adjunct to current esophagogastric studies. Our study suggests that measurement of vector volumes is not greatly more valuable than traditional manometry.

There is an 81.4 % chance that a patient with either a low LESP, TVV or IVV (when all three are measured) will have a positive DeMeester score. Whether or not this would suffice

as an indication for surgery would require inclusion of surgical outcome data into the analysis. Alternatively, a priority ranking system used by Martinez-Serna and colleagues might serve as an effective adjunct to manometry data^[18]. Those authors found a positive association between high symptom priority ranking for heartburn and regurgitation and abnormal pH and manometry results. Analysis of traditional manometry, vector volumes, symptom scores and surgical outcomes will be necessary to confidently define indications for surgery without ambulatory pH monitoring.

Transient relaxation of the lower esophageal sphincter may be an important etiology for pathologic reflux^[8-19]. Dodds and colleagues found that 65 % of reflux episodes in GERD patients were due to transient relaxation of the LES^[8]. This finding is difficult to interpret when 82 % of normal reflux in non-GERD patients can also be attributed to transient LES relaxation^[20]. Sloan and colleagues found that abrupt increases in intrabdominal pressure resulted in a higher occurrence of reflux in GERD patients who also had hiatal hernia and low LES resting tone^[21]. Kahrilas *et al.* found the degree of separation of the LES from the crura is associated with the transient relaxations^[22]. This separation can be detected by manometry and is described as the double hump.

Based on our findings, we draw the following conclusions: (1) a patient with a low TVV, IVV or LESP (when all three are measured) is 81.4 % likely to have a positive DeMeester score; and (2) when LESP, TVV and IVV are normal, a patient is 86.9 % likely to have a negative DeMeester score. This is a marginal improvement over the sensitivities and specificities of the native measurements, but the probabilities are not large enough to justify omission of the ambulatory pH study despite its inherent challenge to patient compliance and reliability. It appears that vectors volumes, particularly intrabdominal vector volume, are just as sensitive and specific for GERD as LES resting pressure, and thus cannot be considered superior in the evaluation of GERD.

REFERENCES

- 1 **Liebermann-Meffert D**, Allgower M, Schmid P, Blum AL. Muscular equivalent of the lower esophageal sphincter. *Gastroenterology* 1979; **76**: 31-38
- 2 **Stein HJ**, Crookes PF, DeMeester TR. Three-dimensional manometric imaging of the lower esophageal sphincter. *Surg Annu* 1995; **27**: 199-214
- 3 **Bonavina L**, Evander A, DeMeester TR, Walther B, Cheng SC, Palazzo L, Concannon JL. Length of the distal esophageal sphincter and competency of the cardia. *Am J Surg* 1986; **151**: 25-34
- 4 **Stein HJ**, Liebermann-Meffert D, DeMeester TR, Siewert JR. Three-dimensional pressure image and muscular structure of the human lower esophageal sphincter. *Surgery* 1995; **117**: 692-698
- 5 **DeMeester TR**, Wernly JA, Bryant GH, Little AG, Skinner DB. Clinical and *in vitro* analysis of determinants of gastroesophageal competence. A study of the principles of antireflux surgery. *Am J Surg* 1979; **137**: 39-46
- 6 **Stein HJ**, Barlow AP, DeMeester TR, Hinder RA. Complications of gastroesophageal reflux disease. Role of the lower esophageal sphincter, esophageal acid and acid/alkaline exposure, and duodenogastric reflux. *Ann Surg* 1992; **216**: 35-43
- 7 **Costantini M**, Zaninotto G, Anselmino M, Boccu C, Nicoletti L, Ancona E. The role of a defective lower esophageal sphincter in the clinical outcome of treatment for gastroesophageal reflux disease. *Arch Surg* 1996; **131**: 655-659
- 8 **Dodds WJ**, Dent J, Hogan WJ, Helm JF, Hauser R, Patel GK, Egide MS. Mechanisms of gastroesophageal reflux in patients with reflux esophagitis. *N Engl J Med* 1982; **307**: 1547-1552
- 9 **Crookes PF**, Kaul BK, DeMeester TR, Stein HJ, Oka M. Manometry of individual segments of the distal esophageal sphincter. Its relation to functional incompetence. *Arch Surg* 1993; **128**: 411-415

- 10 **Byrne PJ**, Stuart RC, Lawlor P, Walsh TN, Hennessy TP. A new technique for measuring lower oesophageal sphincter competence in patients. *Ir J Med Sci* 1993; **162**: 351-354
- 11 **Bombeck CT**, Vaz O, DeSalvo J, Donahue PE, Nyhus LM. Computerized axial manometry of the esophagus. A new method for the assessment of antireflux operations. *Ann Surg* 1987; **206**: 465-472
- 12 **Wetscher GJ**, Hinder RA, Perdakis G, Wiescheimer T, Stalzer R. Three-dimensional imaging of the lower esophageal sphincter in healthy subjects and gastroesophageal reflux. *Dig Dis Sci* 1996; **41**: 2377-2382
- 13 **Stein HJ**, DeMeester TR, Naspetti R, Jamieson J, Perry RE. Three-dimensional imaging of the lower esophageal sphincter in gastroesophageal reflux disease. *Ann Surg* 1991; **214**: 374-383
- 14 **DeMeester TR**, Wang CI, Wernly JA, Pellegrini CA, Little AG, Klementsich P, Bermudez G, Johnson LF, Skinner DB. Technique, indications, and clinical use of 24 hour esophageal pH monitoring. *J Thorac Cardiovasc Surg* 1980; **79**: 656-670
- 15 **Stein HJ**, Korn O, Liebermann-Meffert D. Manometric vector volume analysis to assess lower esophageal sphincter function. *Ann Chir Gynaecol* 1995; **84**: 151-158
- 16 **Fass R**, Hell R, Sampliner RE, Pulliam G, Graver E, Hartz V, Johnson C, Jaffe P. Effect of ambulatory 24-hour esophageal pH monitoring on reflux- provoking activities. *Dig Dis Sci* 1999; **44**: 2263-2269
- 17 **Quigley EM**. 24 h pH monitoring for gastroesophageal reflux disease: already standard but not yet gold? *Am J Gastroenterol* 1992; **87**: 1071-1075
- 18 **Martinez-Serna T**, Tercero F, Jr., Filipi CJ, Dickason TJ, Watson P, Mittal SK, Tasset MR. Symptom priority ranking in the care of gastroesophageal reflux: a review of 1 850 cases. *Dig Dis* 1999; **17**: 219-224
- 19 **Holloway RH**, Kocyan P, Dent J. Provocation of transient lower esophageal sphincter relaxations by meals in patients with symptomatic gastroesophageal reflux. *Dig Dis Sci* 1991; **36**: 1034-1039
- 20 **Schoeman MN**, Tippett MD, Akkermans LM, Dent J, Holloway RH. Mechanisms of gastroesophageal reflux in ambulant healthy human subjects. *Gastroenterology* 1995; **108**: 83-91
- 21 **Sloan S**, Rademaker AW, Kahrilas PJ. Determinants of gastroesophageal junction incompetence: hiatal hernia, lower esophageal sphincter, or both? *Ann Intern Med* 1992; **117**: 977-982
- 22 **Kahrilas PJ**, Shi G, Manka M, Joehl RJ. Increased frequency of transient lower esophageal sphincter relaxation induced by gastric distention in reflux patients with hiatal hernia. *Gastroenterology* 2000; **118**: 688-695

Edited by Zhang JZ

Role of NF- κ B in multiple organ dysfunction during acute obstructive cholangitis

Bin Tu, Jian-Ping Gong, Hu-Yi Feng, Chuan-Xin Wu, Yu-Jun Shi, Xu-Hong Li, Yong Peng, Chang-An Liu, Sheng-Wei Li

Bin Tu, Jian-Ping Gong, Hu-Yi Feng, Chuan-Xin Wu, Yu-Jun Shi, Xu-Hong Li, Yong Peng, Chang-An Liu, Sheng-Wei Li, Department of General Surgery, the Second College of Clinical Medicine & the Second Affiliated Hospital of Chongqing University of Medical Science, 74 Linjiang Road, Chongqing 400010, China
Supported by the National Natural Science Foundation of China, No.39970719, 30170919

Correspondence to: Dr Jian-Ping Gong, Department of General Surgery, the Second College of Clinical Medicine & the Second Affiliated Hospital of Chongqing University of Medical Science, 74 Linjiang Road, Chongqing 400010, China. gongjianping11@hotmail.com
Telephone: +86-23-63766701 **Fax:** +86-23-63822815
Received: 2002-06-24 **Accepted:** 2002-07-22

Abstract

AIM: To elucidate the role of NF- κ B activation in the development of multiple organ dysfunction (MOD) during acute obstructive cholangitis (AOC) in rats.

METHODS: Forty-two Wistar rats were divided into three groups: the AOC group, the group of bile duct ligation (BDL group), and the sham operation group (SO group). All the animals in the three groups were killed in the 6th and 48th hour after operation. Morphological changes of vital organs were observed under light and electron microscopy. NF- κ B activation was determined with Electrophoretic Mobility Shift Assay (EMSA). Arterial blood gas analyses and the serum levels of lactate dehydrogenase (LDH), alanine aminotransferase (ALT), blood urea nitrogen (BUN) and creatinine were performed. The concentrations of TNF- α and IL-6 in plasma were also measured.

RESULTS: The significant changes of histology and ultrastructure of vital organs were observed in AOC group. By contrast, in BDL group, all the features of organs damage were greatly reduced. Expression of NF- κ B activation in various tissues increased in AOC group when compared to other two groups. At 6 h, the arterial pH in three groups was 7.52 ± 0.01 , 7.46 ± 0.02 , and 7.45 ± 0.02 , and the blood pCO₂ was 33.9 ± 0.95 mmHg, 38.1 ± 0.89 mmHg, 38.9 ± 0.94 mmHg, there was difference in three groups ($P<0.05$). At 48 h, the blood pH values in three groups was 7.33 ± 0.07 , 7.67 ± 0.04 , and 7.46 ± 0.03 , and blood HCO₃⁻ was 20.1 ± 1.29 mmol·L⁻¹, 26.7 ± 1.45 mmol·L⁻¹ and 27.4 ± 0.35 mmol·L⁻¹, there was also difference in three groups ($P<0.05$). In AOC group, Levels of LDH, ALT, BUN and creatinine were 16359.9 ± 2278.8 nkat·L⁻¹, 5796.2 ± 941.9 nkat·L⁻¹, 55.7 ± 15.3 mg/dl, and 0.72 ± 0.06 mg/dl, which were higher than in SO group (3739.1 ± 570.1 nkat·L⁻¹, 288.4 ± 71.7 nkat·L⁻¹, 12.5 ± 2.14 mg/dl, and 0.47 ± 0.03 mg/dl) ($P<0.05$). Levels of plasma TNF- α and IL-6 in AOC at 48 h were 429 ± 56.62 ng·L⁻¹ and 562 ± 57 ng·L⁻¹, which increased greatly when compared to BDL group (139 ± 16 ng·L⁻¹, 227 ± 43 ng·L⁻¹) and SO group (74 ± 10 ng·L⁻¹, 113 ± 19 ng·L⁻¹) ($P<0.05$).

CONCLUSION: The pathological damages and the NF- κ B activation of many vital organs existed during AOC. These

findings have an important implication for the role of NF- κ B activation in MOD during AOC.

Tu B, Gong JP, Feng HY, Wu CX, Shi YJ, Li XH, Peng Y, Liu CA, Li SW. Role of NF- κ B in multiple organ dysfunction during acute obstructive cholangitis. *World J Gastroenterol* 2003; 9 (1): 179-183

<http://www.wjgnet.com/1007-9327/9/179.htm>

INTRODUCTION

In humans with acute obstructive cholangitis (AOC) or other sepsis, the onset of multiple organ dysfunction (MOD), especially involving the liver, the heart, the lungs, and the kidneys, is a well known complication that is associated with a high mortality rate^[1-10]. MOD in either humans or animals appears to emerge as a consequence of progressive development of activation of mononuclear phagocytes system and an unregulated release into the blood of a variety of proinflammatory mediators (interleukins, cytokines, chemokines)^[11-14]. NF- κ B is highly activated at sites of inflammation in diverse diseases and can induce transcription of proinflammatory cytokines^[15-17]. For example, NF- κ B is overexpressed in neutrophil, peripheral blood mononuclear cells (PBMC), dendritic cells (DC), and Kupffer cell, and so on. Its activity may enhance recruitment of inflammatory cells and production of proinflammatory mediators like IL-1, IL-6, IL-8, and TNF- α ^[18-21]. These events may be associated with the development of MOD.

In our original study of patients with AOC, the changes of NF- κ B activation were documented^[1], but evidence of MOD and the effects of NF- κ B were not assessed. In the current studies, we observed the pathological changes of the damages of many vital organs and correlated the role of NF- κ B activation with MOD in animal model with AOC.

MATERIALS AND METHODS

Reagents

E. coli and type IV of collagenase were obtained from Sigma Chemical Company (St. Louis, Mo.). The kits of TNF- α and IL-6 were obtained from Beijing Bang Bing Co.. Other reagents were purchased from Ke Hua Co. or Zhong Sheng Co..

Animals and experimental groups

Forty-two male Wistar rats, weighing 250-300 g, were obtained from the Laboratory Animal Center of Chongqing University of Medical Science. The animals were fed with standard rat food and water *ad libitum* for 1 wk before use and kept in a climate-controlled environment with a 12 h light-dark cycle. The animals were handled in accordance with the guidelines set by the Experimental Animals Society of Chongqing University of Medical Science. These animals were randomized into three groups: the AOC group, the group of bile duct ligation (BDL), and sham operation (SO). All the animals in these groups were killed in the 6th and 48th hour after operation. Seven rats from each group at each time point were examined.

Preparation of animal models

All rats were starved overnight and underwent an upper midline laparotomy with an intraperitoneal injection of 30 mg·kg⁻¹ sodium pentobarbital for anesthesia. In AOC group, a median incision was made on the upper abdomen. The common bile duct was mobilized and doubly ligated. 0.2 ml of the *E. coli* suspension (5×10¹²cfu·L⁻¹) was injected into the ligated common bile duct. In BDL group, the common bile duct was doubly ligated but no *E. coli* suspension was injected. In SO group, neither *E. coli* suspension injection nor common bile duct ligation was done, but only routine operative procedure was performed.

Histology

Morphological changes of liver, heart, lungs, and kidneys were observed by light microscope and transmission electron microscope (TEM). These samples from different organs were fixed with 10 % buffered formalin or 2.5 % glutaraldehyde immediately. For optical microscopy, the tissue blocks were embedded in paraffin, and the sections were stained with hematoxylin and eosin (H&E). For TEM, the tissue blocks were embedded in Epon 618 resin and ultrathin sections were stained with uranyl acetate and lead citrate. A transmission electron microscope (JEM-2000) was used.

Electrophoretic mobility shift assay for NF-κB

Isolation of nuclear proteins Nuclear proteins were isolated as previously described^[1,22]. In brief, the liver, heart, lungs, and kidneys tissues were placed in 0.8 mL of ice-cold hypotonic buffer [10 mmol·L⁻¹ HEPES (pH7.9), 10 mL KCl, 0.1 mmol·L⁻¹ EDTA, 0.1 mmol·L⁻¹ ethylene glycol tetraacetic acid, 1 mmol·L⁻¹ DTT; Protease inhibitors (aprotinin, pepstatin, and leupeptin, 10 mg·L⁻¹ each)]. The homogenates were incubated on ice for 20 min, vortexed for 20 s after adding 50 μL of 10 per cent Nonidet P-40, and then centrifuged for 1 minute at 4 °C in an Eppendorf centrifuge. Supernatants were decanted, the nuclear pellets after a single wash with hypotonic buffer without Nonidet P-40 were suspended in an ice-cold hypertonic buffer [20 mmol·L⁻¹ HEPES (pH7.9), 0.4 mol·L⁻¹ NaCl, 1 mmol·L⁻¹ EDTA, 1 mmol·L⁻¹ DTT; Protease inhibitors], incubated on ice for 30 min at 4 °C, mixed frequently, and centrifuged for 15 min at 4 °C. The supernatants were collected as nuclear extracts and stored at -70 °C. Concentrations of total proteins in the samples were determined according to the method of Bradford.

Electrophoretic mobility shift assay (EMSA) NF-κB binding activity was performed in a 10-μL binding reaction mixture containing 1×binding buffer [50 mg·L⁻¹ of double-stranded poly (dI-dC), 10 mmol·L⁻¹ Tris-HCl (pH 7.5), 50 mmol·L⁻¹ NaCl, 0.5 mmol·L⁻¹ EDTA, 0.5 mmol·L⁻¹ DTT, 1 mmol·L⁻¹ MgCl₂, and 100 mL·L⁻¹ glycerol], 5 μg of nuclear protein, and 35 fmol of double-stranded NF-κB consensus oligonucleotide (5' -AGT TGA GGG GAC TTT CCC AGG-3') that was endly labeled with γ-³²P(111TBq mmol⁻¹ at 370GBq L⁻¹) using T4 polynucleotide kinase. The binding reaction mixture was incubated at room temperature for 20 min and analyzed by electrophoresis on 7 per cent nondenaturing polyacrylamide gels. After electrophoresis the gels were dried by Gel-Drier (Bio-Rad Laboratories, Hercules, CA) and exposed to Kodak X-ray films at -70 °C. The binding bands were quantified by scanning densitometer of a Bio-Image Analysis System.

Arterial blood gas analyses

In some animals, a carotid artery catheter was placed through an anterior cervical area, and arterial blood samples were collected to measure blood lactate, pH, pO₂, pCO₂, and HCO₃⁻ using a blood gas analyzer.

Measurement of biochemical parameters

Blood was obtained from the inferior vena cava at the time of

sacrifice, heart, liver, kidney injury were assessed by measuring the serum lactate dehydrogenase (LDH), alanine aminotransferase (ALT), blood urea nitrogen (BUN) and creatinine, respectively, which were performed with an Automatic Biochemical Analyser.

Assay of TNF-α and IL-6 in plasma

The concentrations of TNF-α and IL-6 in plasma were measured by a commercially available enzyme-linked immunosorbent assay (ELISA) according to the manufacture instructions which has a low detection limit of 50 ng·L⁻¹. Briefly, microtitre plates were coated with anti TNF-α or IL-6 mAb overnight at room temperature on a plate shaker and then, after they had been blocked, samples were added. The detecting antibody was biotinylated anti TNF-α or IL-6. The results were determined at 492 nm with DG 3022 Enzyme Linkage Essay Instrument.

Statistical analysis

The results are presented as means ±SEM. Data sets were analyzed with a one-way ANOVA. The differences were regarded significant when the *P* value was less than <0.05.

RESULTS

The changes of histology and ultrastructure of vital organs

In AOC group, in the liver, there was multifocal and patchy lytic necrosis. hepatocytes showed swelling and partly fatty degeneration, focal cytoplasmic degeneration and many myelin figures could be seen in the cytoplasm (Figure 1), Kupffer cells showed proliferation and many myelin figures in the cytoplasm (Figure 2). In the lungs, polymorphonuclear neutrophil (PMN) aggregated in alveolar capillary. In the heart, mitochondria were swollen or even vacuolated (Figure 3). In the kidneys, there was extensive fusion of foot processes of podocytes in glomeruli. The cells had lost their cell membranes and exhibited mitochondrial swelling together with intracellular edema in proximal convoluted tubules (Figure 4).

Changes of NF-κB activation

In AOC group, The NF-κB activity increased significantly in liver, nearly fivefold over other organs after 6 h. At 48 h, the NF-κB activity increased also significantly in lung and heart besides liver (Figure 5). In BDL group and SO group, the active form of NF-κB was minimal in hepatic tissue and other tissues.

Arterial blood gas analyses

In AOC group, arterial blood gases showed early respiratory alkalosis and late metabolic acidosis. At 6 h there was a mild respiratory alkalosis, with the arterial pH rising from 7.45±0.02 to 7.52±0.01, the blood pCO₂ fell from a value of 37.9±0.86 to 34.23±0.89. At 48 h, similar group showed evidence of metabolic acidosis, with the blood pH values falling from 7.46±0.003 to 7.33±0.007, and blood HCO₃⁻ (mmol·L⁻¹) falling from 27.4±0.35 to 20.1±1.29. In contrast, in BDL group, the blood pH and pCO₂ values were the same as those values obtained in SO group (Table 1).

Biochemical parameters

Biochemical parameters in three groups were showed in Table 2.

Cytokines contents in plasma

In AOC group, Levels of plasma TNF-α and IL-6 increased greatly in 6 h and 48 h. Levels of two cytokines were over 4-fold and 5-fold higher than that in other two groups. In BDL group, the levels of TNF-α and IL-6 in 48 h increased modestly when compared to that in SO group (*P*<0.05). Low levels of TNF-α and IL-6 was detectable in plasma in SO group (Table 3).

Table 1 Arterial blood gas analyses in three groups animals

Parameter	Early Phase (6 h)			Late Phase (48 h)		
	AOC	BDL	SO	AOC	BDL	SO
pH	7.52 \pm 0.01 ^a	7.46 \pm 0.02	7.45 \pm 0.02	7.33 \pm 0.07 ^a	7.67 \pm 0.04	7.46 \pm 0.03
pCO ₂ (mmHg)	33.9 \pm 0.95 ^a	38.1 \pm 0.89	38.9 \pm 0.94	40.4 \pm 4.23	37.8 \pm 3.51	37.5 \pm 0.72
HCO ₃ ⁻ (mmol/L)	26.6 \pm 0.63	28.3 \pm 0.86	27.8 \pm 1.04	20.1 \pm 1.57 ^a	26.7 \pm 1.45	27.82 \pm 1.25
pO ₂ (mmHg)	105.1 \pm 6.4	108.3 \pm 4.2	106.5 \pm 5.8	67.3 \pm 6.9 ^a	104.7 \pm 5.3	110.7 \pm 4.6

^a P <0.05, vs other groups.

Table 2 Biochemical parameters in three groups animals

Parameter	Early Phase (6 h)			Late Phase (48 h)		
	AOC	BDL	SO	AOC	BDL	SO
LDH (nkat·L ⁻¹)	13632.7 \pm 891.8 ^a	4107.4 \pm 951.9	3655.7 \pm 576.8	16359.9 \pm 2278.8 ^a	6793 \pm 885.1 ^c	3742.4 \pm 570.1
ALT (nkat·L ⁻¹)	2213.8 \pm 391.7 ^a	343.4 \pm 103.3	311.7 \pm 91.7	5796.2 \pm 941.9 ^a	955.2 \pm 175 ^c	288.4 \pm 75
BUN (mg/dl)	16.3 \pm 13.3	12.9 \pm 2.8	11.8 \pm 2.2	55.7 \pm 15.3 ^a	16.7 \pm 4.6	12.5 \pm 2.14
Cr (mg/dl)	0.48 \pm 0.03	0.42 \pm 0.02	0.41 \pm 0.03	0.72 \pm 0.06 ^a	0.51 \pm 0.03	0.47 \pm 0.03

^a P <0.05, vs other groups. ^c P <0.05, vs SO group.

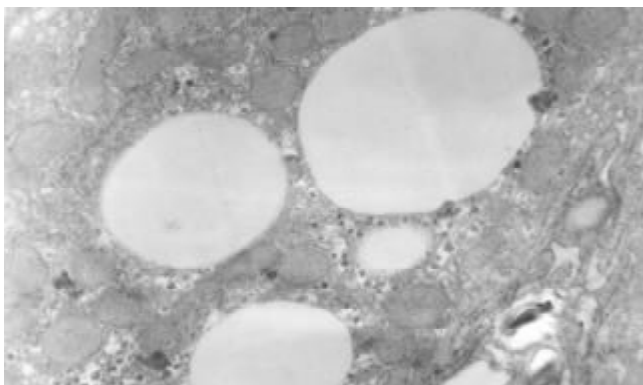


Figure 1 Fatty degeneration, focal cytoplasmic degeneration and myelin figures in the cytoplasm of hepatocyte in AOC group TEM \times 12 000.

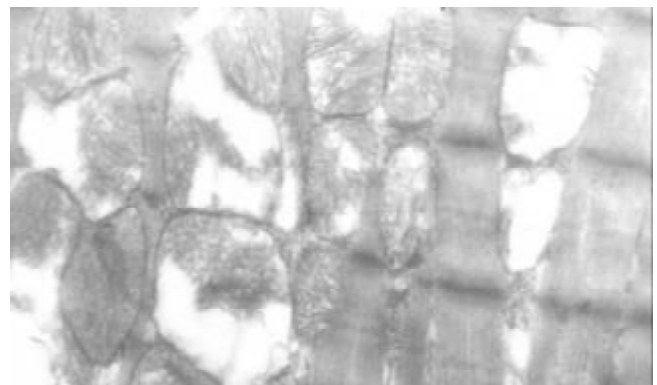


Figure 3 Myocyte mitochondria of heart were swollen or even vacuolated in AOC group TEM \times 20 000.

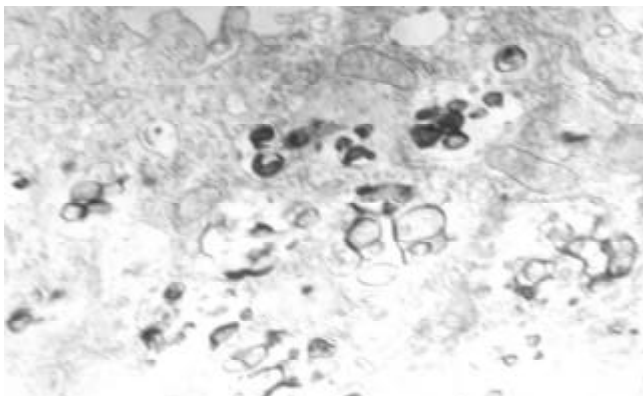


Figure 2 Kupffer cells showed proliferation and focal cytoplasmic degeneration and many myelin figures could be seen in the cytoplasm in AOC group TEM \times 15 000.

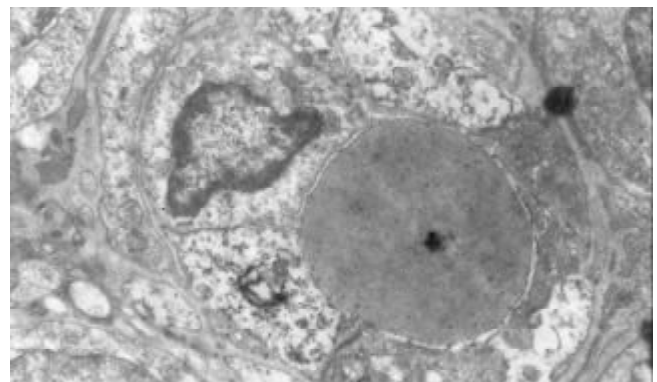


Figure 4 Proximal convoluted tubules was full of electron dense phagosomes, the cells had lost their cell membranes and exhibited mitochondrial swelling together with intracellular edema In AOC group TEM \times 3 000.

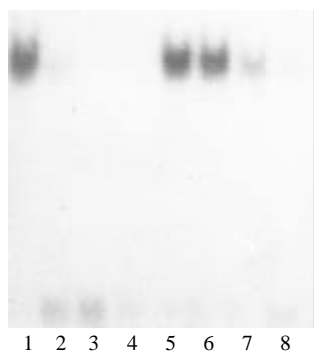


Figure 5 Activation of NF- κ B in AOC group. Lane 1, 2, 3, and 4 represents the Liver, the lungs, the heart, and the kidneys in 4 kw, respectively. Lane 5, 6, 7, and 8 represents the Liver, the lungs, the heart, and the kidneys in 8 kw, respectively.

Table 3 TNF- α and IL-6 levels in plasma ($n=7$)

Groups	TNF- α (ng·L ⁻¹)		IL-6(ng·L ⁻¹)	
	6 h	48 h	6 h	48 h
AOC	235±39.23 ^a	429±56.62 ^a	253±23.41 ^a	562±57.58 ^a
BDL	73±11.52	139±16.21 ^c	113±21.39	227±43.02 ^c
SO	72±12.45	74±10.53	109±18.37	113±19.81

^a $P<0.05$, vs other two groups. ^c $P<0.05$, vs SO group.

DISCUSSION

AOC in humans often leads to progressive MOD, which is still associated with a high mortality rate^[1-5]. Recent studies showed NF- κ B is rapidly in response to many pathologic signals that may be relevant during surgical trauma, including cytokines, adhesion molecules, endotoxin, hypoxia, and shear^[23-27]. Activation of NF- κ B results in the transcription of genes that can participate in the inflammatory reaction by inducing the production of cytokines, immunoreceptors, and cell adhesion molecules^[28-32]. These cytokines and proinflammatory mediators are therefore a potentially attractive target inducing MOD during sepsis and endotoxemia^[33-47]. Information on the role of NF- κ B in sepsis, AOC and MOD is limited but shows that NF- κ B is increased during inflammation and sepsis^[1,18].

The role of NF- κ B activation in sepsis and in complication such as MOD is a debatable issue. Pennington *et al*^[20] observed the degree of NF- κ B activation with severity of acute appendicitis and found that NF- κ B binding activity is elevated in these patients and correlates with symptoms longer than 24 hours. Arnalich *et al*^[18] determined NF- κ B activation in peripheral blood mononuclear cells of 34 patients with severe sepsis and serial concentrations of inflammatory cytokines and resulted the prognosis value of early measurement of NF- κ B activity in patients with severe sepsis. Gong and Paterson *et al*^[1,20] determined NF- κ B activation in mononuclear and neutrophils from critically ill patients and compared NF- κ B activation with circulating concentrations of IL-6, IL-8 and soluble intercellular adhesion molecule (sICAM)-1, and found NF- κ B activation in patients systemic inflammatory response syndrome, which increased markedly before death. However, Chen *et al*^[48] observed intrahepatic changes in TNF- α and NF- κ B activation in Sprague-Dawley rats with cecal ligation and puncture, and their results implied NF- κ B activation was not linked to the outcome in sepsis. In our original study of patients with AOC, the changes of NF- κ B activation were documented, but evidence of MOD and the effects of NF- κ B were not assessed. So it would be helpful to further analyze the expression with the inflamed tissues. There is, however, no published information about a key role of NF- κ B in

development of multiple organ dysfunction during biliary infection. In this study, we investigated the role NF- κ B in the development of MOD in rats with AOC.

The present study shows a correlation among the pathological damages of many vital organs, NF- κ B activation and release of proinflammatory cytokines. This is only one published investigation about the correlation of NF- κ B activation and MOD during AOC. The present study demonstrated that NF- κ B activation plays a key role during AOC. The finding that prompt surgical inflammatory condition of the inflammatory focus results in a rapid normalization of NF- κ B activation adds further validity to this assay.

Perhaps other important finding of this study was the marked difference in NF- κ B levels among various organs during AOC. During AOC, Expression of NF- κ B was observed first in liver at 6 h. At 48 h, NF- κ B also expressed in the lung, the heart, and the kidney besides the liver. The liver was the main organ which was injured by bacteria during AOC, liver and other organs influence each other in their function, the liver plays a key role in host defense. Matuschak *et al* reported that the liver failure affected on the incidence and resolution of the adult respiratory distress syndrome. Seki *et al*^[49] Hepatocytes produce acute phase protein and complement in bacterial infections. KCs are activated by various bacterial stimuli, including LPS and bacterial superantigens, and produce IL-12 and other monokines. So the liver plays a crucial role in the first line of defense against bacterial infections^[50-52]. However, if this defense system is inadequately activated, sepsis and shock associated with MOD takes place. It was found in our previous study that when liver was injured, especially KCs function failed, gram-negative bacteria normally restricted to the biliary tract invaded the bloodstream and were trapped in vital organs, and NF- κ B activation occurred, eventually MOD ensued. Further clinical trials are indicated to confirm that this "molecular biology" marker indeed will be a useful clinical tool in the management of the patients with AOC^[53-56].

In conclusion, we have shown the expression of NF- κ B and the pathological changes of the damages occurred in many vital organs, especially in liver during AOC. These findings have an important implication for the role of NF- κ B activation in MOD during AOC.

REFERENCES

- Gong JP, Liu CA, Wu CX, Li SW, Shi YJ, Li XH. Nuclear factor κ B activity in patients with acute severe cholangitis. *World J Gastroenterol* 2002; **8**: 346-349
- Huang ZQ. New development of biliary surgery in China. *World J Gastroenterol* 2000; **6**: 187-192
- Kimmings AN, Deventer SIH, Rauws EAJ, Huibregtse K, Gouma DJ. Systemic inflammatory response in acute cholangitis and after subsequent treatment. *Eur J Surg* 2000; **166**: 700-705
- Lillemoe KD. Surgical treatment of biliary tract infections. *Am Surg* 2000; **66**: 138-144
- Fry DE. Sepsis syndrome. *Am Surg* 2000; **66**: 126-132
- Parker SJ, Watkins PE. Experimental models of gram-negative sepsis. *Br J Surg* 2001; **88**: 22-30
- Tabrizi AR, Zehnbauser BA, Freeman BD, Buchman TG. Genetic markers in sepsis. *J Am Coll Surg* 2001; **192**: 106-117
- Jackson GDF, Dai Y, Sewell WA. Bile mediates intestinal pathology in endotoxemia in rats. *Infect Immun* 2000; **68**: 4714-4719
- Islam AFMW, Moss ND, Dai Y, Smith MSR, Collins AM, Jackson GDF. Lipopolysaccharide-induced biliary factors enhance invasion of *salmonella enteritidis* in a rat model. *Infect Immun* 2000; **68**: 1-5
- Erwin PJ, Lewis H, Dolan S, Tobias PS, Schumann RR, Lamping N, Wisdom GB, Rowlands BJ, Halliday MI. Lipopolysaccharide binding protein in acute pancreatitis. *Crit Care Med* 2000; **28**: 104-109
- Kordzaya DJ, Goderdzishvili VT. Bacterial translocation in obstructive jaundice in rats: role of mucosal lacteals. *Eur J Surg* 2000; **166**: 367-374

- 12 **Kimmings AN**, van Deventer SJH, Obertop H, Rauws EAJ, Huijbregtse K, Gouma DJ. Endotoxin, cytokines, and endotoxin binding proteins in obstructive jaundice and after preoperative biliary drainage. *Gut* 2000; **46**: 725-731
- 13 **Bone-Larson CL**, Simpson KJ, Colletti LM, Lukacs NW, Chen SC, Lira S, Kunkel SL, Hogaboam CM. The role of chemokines in the immunopathology of the liver. *Immunol Rev* 2000; **177**: 8-20
- 14 **Ito Y**, Machen NW, Urbaschek R, McCuskey RS. Biliary obstruction exacerbates the hepatic microvascular inflammatory response to endotoxin. *Shock* 2000; **14**: 599-604
- 15 **Zhao SY**, Qi Y, Liu XC, Jiang QB, Liu SY, Jiang Y, Jiang ZF. Activation of NF- κ B in bronchial epithelial cells from children with asthma. *Chin Med J* 2001; **114**: 909-911
- 16 **West MA**, Clair L, Kraatz J, Rodriguez JL. Endotoxin tolerance from lipopolysaccharide pretreatment induces nuclear factor- κ B alterations not present in C3H/HeJ mice. *J Trauma* 2000; **49**: 298-305
- 17 **Reddy SAG**, Huang JH, Liao WSL. Phosphatidylinositol 3-kinase as a mediator of TNF-induced NF- κ B activation. *J Immunol* 2000; **164**: 1355-1363
- 18 **Paterson RL**, Galley HF, Dhillon JK, Webster NR. Increased nuclear factor κ B activation in critically ill patients who die. *Crit Care Med* 2000; **28**: 1047-1051
- 19 **Arnalich F**, Garcia-Palomero E, Lopez J, Jimenez M, Madero R, Renart J, Vazquez JJ, Montiel C. Predictive value of nuclear factor κ B activity and plasma cytokine levels in patients with sepsis. *Infect Immun* 2000; **68**: 1942-1945
- 20 **Pennington C**, Dunn J, Li C, Ha T, Browder W. Nuclear factor κ B activation in acute appendicitis: a molecular marker for extent of disease? *Am Surgeon* 2000; **66**: 914-919
- 21 **Foulds S**, Galustian C, Mansfield AO, Schachter M. Transcription factor NF- κ B expression and postsurgical organ dysfunction. *Ann Surg* 2001; **233**: 70-78
- 22 **Reising H**, Jaeschke H, Bauer I, Patau C, Datene V, Pannen BHJ, Bauer M. Differential activation pattern of redox-sensitive transcription factors and stress-inducible dilator systems heme oxygenase-1 and inducible nitric oxide synthase in hemorrhagic and endotoxic shock. *Crit Care Med* 2001; **29**: 1962-1971
- 23 **Kono H**, Wheeler MD, Rusyn I, Lin M, Seabra V, Rivera CA, Bradford BU, Forman DT, Thurman RG. Gender differences in early alcohol-induced liver injury: role of CD14, NF- κ B, and TNF- α . *Am J Physiol Gastrointest Liver Physiol* 2000; **278**: G652-G661
- 24 **Ninomiya-Tsuji J**, Kishimoto K, Hiyama A, Inoue JI, Cao Z, Matsumoto K. The kinase TAK1 can activate the NIK-I κ B as well as the MAP kinase cascade in the IL-1 signalling pathway. *Nature* 1999; **398**: 252-256
- 25 **Hedin KE**, Kaczynski JA, Gibson MR, Urrutia R. Transcription factors in cell biology, surgery, and transplantation. *Surgery* 2000; **128**: 1-5
- 26 **Starkel P**, Horsmans Y, Sempoux C, Saeger CD, Wary J, Lause P, Maiter D, Lambotte L. After portal branch ligation in rat, nuclear factor κ B, interleukin-6, signal transducers and activators of transcription 3, *c-fos*, *c-myc*, and *c-jun* are similarly induced in the ligated and nonligated lobes. *Hepatology* 1999; **29**: 1463-1470
- 27 **Liu Y**, Wang Y, Yamakuchi M, Isowaki S, Nagata E, Kanmura Y, Kitajima I, Maruyama I. Upregulation of Toll-like receptor 2 gene expression in macrophage response to peptidoglycan and high concentration of lipopolysaccharide is involved in NF- κ B activation. *Infect Immun* 2001; **69**: 2788-2796
- 28 **Jiang QQ**, Akashi S, Miyake K, Petty HR. Cutting Edge: lipopolysaccharide induces physical proximity between CD14 and Toll-like receptor 4 (TLR4) prior to nuclear translocation of NF- κ B. *J Immunol* 2000; **165**: 3541-3544
- 29 **Adib-Conquy M**, Adrie C, Moine P, Asehounne K, Fitting C, Pinsky MR, Dhainaut JF, Cavaillon JM. NF- κ B expression in mononuclear cells of patients with sepsis resembles that observed in lipopolysaccharide tolerance. *Am J Respir Crit Care Med* 2000; **162**: 1877-1883
- 30 **Abraham E**, Arcaroli J, Shenkar R. Activation of extracellular signal-regulated kinases, NF- κ B, and cyclic adenosine 5' -monophosphate response element-binding protein in lung neutrophils occurs by differing mechanisms after hemorrhage or endotoxemia. *J Immunol* 2001; **166**: 522-530
- 31 **Belich MP**, Salmeron A, Johnston LH, Ley SC. TPL-2 kinase regulates the proteolysis of the NF- κ B-inhibitory protein NF- κ B1 p105. *Nature* 1999; **397**: 363-368
- 32 **Choi JH**, Ko HM, Kim JW, Lee HK, Han SS, Chun SB, Im SY. Platelet-activating factor-induced early activation of NF- κ B play a crucial role for organ clearance of *Candida albicans*. *J Immunol* 2001; **166**: 5139-5144
- 33 **Han DW**. The clinical sine of subsequent liver injury induced by gut derived endotoxemia. *Shijie Huaren Xiaohua Zazhi* 1999; **7**: 1055-1058
- 34 **Lin E**, Calvano SE, Lowry SF. Inflammatory cytokines and cell response in surgery. *Surgery* 2000; **127**: 117-126
- 35 **Li SW**, Gong JP, Wu CX, Shi YJ, Liu CA. Lipopolysaccharide induced synthesis of CD14 proteins and its gene expression in hepatocytes during endotoxemia. *World J Gastroenterol* 2002; **8**: 124-127
- 36 **Hardaway RM**. A review of septic shock. *Am Surg* 2000; **66**: 22-27
- 37 **Sindram D**, Porte RJ, Hoffman MR, Bentley RC, Clavien PA. Synergism between platelets and leukocytes in inducing endothelial cell apoptosis in the cold ischemic rat liver: a Kupffer cell mediated injury. *FASEB J* 2001; **15**: 1230-1232
- 38 **Wu RQ**, Xu YX, Song XH, Chen LJ, Meng XJ. Adhesion molecule and proinflammatory cytokine gene expression in hepatic sinusoidal endothelial cells following cecal ligation and puncture. *World J Gastroenterol* 2001; **7**: 128-130
- 39 **Baldwin AS**. The transcription factor NF- κ B and human disease. *J Clin Invest* 2001; **107**: 3-6
- 40 **Assy N**, Jacob G, Spira G, Edoute Y. Diagnostic approach to patients with cholestatic jaundice. *World J Gastroenterol* 1999; **5**: 252-262
- 41 **Blunck R**, Scheel O, Muller M, Brandenburg K, Seitzer U, Seydel U. New insights into endotoxin-induced activation of macrophages: involvement of a K⁺ channel in transmembrane signaling. *J Immunol* 2001; **166**: 1009-1015
- 42 **Tak PP**, Firestein GS. NF- κ B: a key role in inflammatory diseases. *J Clin Invest* 2001; **107**: 7-11
- 43 **Ling YL**, Meng AH, Zhao XY, Shan BE, Zhang JL, Zhang XP. Effect of cholecystokinin on cytokines during endotoxic shock in rats. *World J Gastroenterol* 2001; **7**: 667-671
- 44 **Gordon H**. Detection of alcoholic liver disease. *World J Gastroenterol* 2001; **7**: 297-302
- 45 **Bai XY**, Jia XH, Cheng LZ, Gu YD. Influence of IFN α -2b and BCG on the release of TNF and IL-1 by Kupffer cells in rats with hepatoma. *World J Gastroenterol* 2001; **7**: 419-421
- 46 **Wang LS**, Zhu HM, Zhou DY, Wang YL, Zhang WD. Influence of whole peptidoglycan of bifidobacterium on cytotoxic effectors produced by mouse peritoneal macrophages. *World J Gastroenterol* 2001; **7**: 440-443
- 47 **Zuo GQ**, Gong JP, Liu CH, Li SW, Wu XC, Yang K, Li Y. Expression of lipopolysaccharide binding protein and its receptor CD14 in experimental alcoholic liver disease. *World J Gastroenterol* 2001; **7**: 836-840
- 48 **Chen J**, Raj N, Kim P, Andrejko KM, Deutschman CS. Intrahepatic nuclear factor- κ B activity and α_1 -acid glycoprotein transcription do not predict outcome after cecal ligation and puncture in the rat. *Crit Care Med* 2001; **29**: 589-596
- 49 **Seki S**, Habu Y, Kawamura T, Takeda K, Dobashi H, Ohkawa T, Hiraide H. The liver as a crucial organ in the first line of host defense: the roles of Kupffer cells, natural killer (NK) cells and NK 1.1 Ag⁺ T cells in T helper 1 immune responses. *Immunol Rev* 2000; **174**: 35-46
- 50 **Wu RQ**, XU YX, Song XH, Chen LJ, Meng XJ. Relationship between cytokine mRNA expression and organ damage following cecal ligation and puncture. *World J Gastroenterol* 2002; **8**: 131-134
- 51 **Gong JP**, Wu CX, Liu CA, Li SW, Shi YJ, Li XH, Peng Y. Liver sinusoidal endothelial cell injury by neutrophils in rats with acute obstructive cholangitis. *World J Gastroenterol* 2002; **8**: 342-345
- 52 **Gong JP**, Dai LL, Liu CA, Wu CX, Shi YJ, Li SW, Li XH. Expression of CD14 protein and its gene in liver sinusoidal endothelial cells during endotoxemia. *World J Gastroenterol* 2002; **8**: 551-554
- 53 **Shang D**, Guan FL, Jin PY, Chen HL, Cui JH. Effect of combined therapy of Yinchenhao Chengqi decoction and endoscopic sphincterotomy for endotoxemia in acute cholangitis. *World J Gastroenterol* 1998; **4**: 443-445
- 54 **Tiscornia OM**, Hamamura S, de Lehmann ES, Otero G, Waisman H, Tiscornia WP, Bank S. Biliary acute pancreatitis: a review. *World J Gastroenterol* 2000; **6**: 157-168
- 55 **Gong JP**, Wu CX, Liu CA, Li SW, Shi YJ, Yang K, Li Y, Li XH. Intestinal damage mediated by Kupffer cells in rats with endotoxemia. *World J Gastroenterol* 2002; **8**: 923-927
- 56 **Zhang WZ**, Chen YS, Wang JW, Chen XR. Early diagnosis and treatment of severe acute cholangitis. *World J Gastroenterol* 2002; **8**: 150-152

Proliferative activity of bile from congenital choledochal cyst patients

Gao-Song Wu, Sheng-Quan Zou, Xian-Wen Luo, Jian-Hong Wu, Zheng-Ren Liu

Gao-Song Wu, Sheng-Quan Zou, Xian-Wen Luo, Jian-Hong Wu, Zheng-Ren Liu, Department of General Surgery, Tongji Hospital, Tongji Medical College, Huazhong University of Science and Technology, Wuhan, 430030, Hubei Province, China

Correspondence to: Dr. Gao-Song Wu, Department of General Surgery of Tongji Hospital, 1095 Jiefang Road, Wuhan, 430030, Hubei Province, China. wugaosong9172@sina.com

Telephone: +86-27-83662851 **Fax:** +86-27-83662851

Received: 2002-07-08 **Accepted:** 2002-07-31

Abstract

AIM: To explore the potential carcinogenicity of bile from congenital choledochal cyst (CCC) patients and the mechanism of the carcinogenesis in congenital choledochal cyst patients.

METHODS: 20 bile samples from congenital choledochal cyst patients and 10 normal control bile samples were used for this study. The proliferative effect of bile was measured by using Methabenzthiazuron (MTT) assay; Cell cycle and apoptosis were analyzed by using flow cytometry (FCM), and the PGE₂ levels in the supernatant of cultured cholangiocarcinoma cells were quantitated by enzyme-linked immunosorbent assay (ELISA).

RESULTS: CCC bile could significantly promote the proliferation of human cholangiocarcinoma QBC939 cells compared with normal bile ($P=0.001$) and negative control group ($P=0.002$), and the proliferative effect of CCC bile could be abolished by addition of cyclooxygenase-2 specific inhibitor celecoxib (20 μ M). The QBC939 cells proliferative index was increased significantly after treated with 1 % bile from CCC patient ($P=0.008$) for 24 h, the percentage of S phase (29.48 ± 3.27)% was increased remarkably ($P<0.001$) compared with normal bile (11.72 ± 2.70) %, and the percentage of G0/G1 phase (54.19 ± 9.46) % was decreased remarkably ($P=0.042$) compared with normal bile (69.16 ± 10.88) %, however, bile from CCC patient had no significant influence on apoptosis of QBC939 cells ($P=0.719$).

CONCLUSION: Bile from congenital choledochal cyst patients can promote the proliferation of human cholangiocarcinoma QBC939 cells via COX-2 and PGE₂ pathway.

Wu GS, Zou SQ, Luo XW, Wu JH, Liu ZR. Proliferative activity of bile from congenital choledochal cyst patients. *World J Gastroenterol* 2003; 9(1): 184-187
<http://www.wjgnet.com/1007-9327/9/184.htm>

INTRODUCTION

Congenital choledochal cyst (CCC) is a rare disease in Western countries^[1-3]. Most of the reported cases come from Asia, particularly from Japan^[4-7]. In recent years, cases of CCC are reported increasingly in China^[8-17]. The incidence of carcinoma arising in the wall of a congenital bile duct cyst is high and this lesion is considered as a precancerous state of the biliary

tract, but its underlying precise mechanisms remain unclear. For the purpose of resolving these mechanisms we used the whole bile of CCC patients to act directly on the QBC939 cells to determine the effects of CCC bile on the growth of cholangiocarcinoma cells.

MATERIALS AND METHODS

Materials

Bile samples collection and treatment: Experiments were classified into CCC bile group, normal control bile group and negative control group. 20 CCC bile samples were obtained from the common bile duct of patients (5 male, 15 female, age range 5-49 years, mean 26.8 years) with CCC underwent operation at the Department of Surgery, Tongji hospital, Wuhan, China. 10 normal control bile samples were obtained from the common bile duct of patients (5 male, 5 female, age range 23-51 years, mean 42.3 years) with a normal hepatobiliary tract underwent surgery at the Department of Surgery, Tongji hospital, Wuhan, China. All patients didn't take any nonsteroid anti-inflammatory drugs, antibiotics or anti-tumor drugs before operation. Bile samples were filtered (0.22 μ m, Millipore) by sterile technique immediately twice and stored at -80 °C. PBS (pH7.2) instead of bile sample was used as negative control. Human extra-hepatic cholangiocarcinoma cell line QBC939 was established and given to us through the courtesy of professor Xu-Guang Wang (Third Military Medical University, China)^[18], cells were maintained as mono-layers in Dulbecco's modified Eagle's medium (DMEM) supplemented with 10 % fetal bovine serum (FBS, Gibco, USA.), 100 units/ml penicillin and 100 mg/ml streptomycin in a humidified atmosphere of 95 % air and 5 % CO₂ at 37 °C. They were subcultivated every 3-5 days and given fresh medium every other day. 70-80 % subconfluent monolayers of human cholangiocarcinoma cells were employed in all experiments. PGE₂ ELISA detection kit was purchased from Jingmei Biotech Co., Wuhan, China. Celecoxib was synthesized and given as a gift by Dr Zhi-Nan Mei (Wuhan University, China)^[19]. Stock solution was prepared in dimethylsulfoxide (DMSO) and stored at -20 °C. In all experiments DMSO final concentration in the medium was ≤ 0.1 %.

Methods

Cytotoxicity pretesting Cytotoxicity pretesting was taken with each of the gradient diluted bile sample to determine the concentration of experimental bile samples. Our results showed that 1 % bile (10 μ L bile/mL medium) had no significant cytotoxic influence on QBC939 cells.

MTT assay The human cholangiocarcinoma cells QBC939 in proliferating status was determined by using MTT assay. Cholangiocarcinoma cells were seeded at a density of 1×10^4 cells per well in flat-bottomed 96-well microplates. 12 h after incubation, cells were treated with 1 % bile samples with or without 20 μ M celecoxib. After 24 h incubation, 20 μ L MTT (5 g/L) was added to each well, cultured for 4 h. After removed of supernatant, 150 μ L DMSO was added and shaken for 5 min until the crystal was dissolved. OD490nm value was

measured by using an enzyme-linked immunosorbent assay reader. The negative control well had no cells and was used as zero point of absorbance. Each assay was performed three times in triplicate.

ELISA The PGE₂ levels in the supernatant of cultured human cholangiocarcinoma cells QBC939 were quantitated by ELISA: Cells were seeded into 24-well microplates (4.0×10⁵/well) and allowed to adhere overnight. The cells were then incubated in the presence 1 % bile samples with or without 20 μM celecoxib for 24 h. The supernatants were aspirated and centrifuged to prepare for the detection of PGE₂. 0.5 mL supernatant was added into 0.1 mL 1N HCl and centrifuged for 10 min at room temperature; then 0.1 mL 1.2N NaOH was used to neutralize the acidified samples. Standard solution (200 μL per well) or activated samples were added into the microplates. Then the steps were proceeded as instructed. The value of OD of each well was determined at 450nm. The supernatants were harvested in triplicate and the experiment was performed three times.

Flow cytometric analysis Cholangiocarcinoma cells QBC939 were trypsinized and plated in 6-well culture dishes in the presence of 1 % CCC bile or 1 % normal bile. After 24 h, cells were harvested, centrifuged at low speed and fixed in 70 % ethanol. After overnight incubation at 4 °C, cells were stained with 50 μg/ml propidium iodide in the presence of Rnase A (10 μg/ml) and 0.1 % Triton X-100 and determined by using a flow cytometer.

Statistical analysis

Data were expressed as $\bar{x} \pm s$. Student's *t*-test was used for statistical analysis. *P*<0.05 indicates significant difference.

RESULTS

Assay of COX-2 activity

The COX-2 activity was determined by PGE₂ levels in the supernatant released by the cultured human cholangiocarcinoma cells QBC939. The concentrations of PGE₂ in culture medium of QBC939 cells treated with 1 % CCC bile, 1 % normal bile or 1 % PBS (pH7.2) with or without 20 μM celecoxib for 24 h were quantitated by ELISA (Table 1). CCC bile could induce the release of PGE₂ in QBC939 cells: the PGE₂ level was higher significantly (*P*<0.001) in CCC bile group (184.0±9.7 ng/well) compared with that in normal control bile group (131.0±7.3 ng/well) and negative control group (123.3±8.4). Celecoxib could suppress QBC939 cells PGE₂ production, the PGE₂ concentration was 80.3±7.1 ng/well, 74.1±9.7 ng/well and 72.4±10.8 ng/well in CCC bile group, normal control bile group and negative control bile group respectively, when pre-treated with 20 μM celecoxib, there was no statistical difference (*P*>0.05).

Table 1 PGE₂ level released by QBC939 in the existence of bile with or without celecoxib

Group	<i>n</i>	PGE ₂	<i>P</i>	+CE PGE ₂	<i>P</i>
A	20	184.0±9.7	^b <i>P</i> <0.001, ^d <i>P</i> <0.001	80.3±7.1	^b <i>P</i> =0.057, ^d <i>P</i> =0.055
B	10	131.0±7.3	^b <i>P</i> =0.087	74.1±9.7	^b <i>P</i> =0.771
C	5	123.3±8.4		72.4±10.8	

The concentrations of PGE₂ (ng/well) in culture medium of QBC939 cells treated with 1 % CCC bile (A), 1 % normal bile (B) or 1 % PBS (C) with or without 20 μM celecoxib (+CE) for 24 h were quantitated by ELISA. Data were expressed as $\bar{x} \pm s$, b vs C, d vs B.

Effects of bile on the growth of QBC939

QBC939 cells were incubated in 1 % bile samples with or without 20 μM celecoxib, and the cell density was measured by using MTT assay (Table 2). CCC bile could significantly promote the proliferation of human cholangiocarcinoma QBC939 cells compared with normal bile (*P*=0.001) and negative control group (*P*=0.002), and the proliferative effect of CCC bile could be abolished by addition of cyclooxygenase-2 specific inhibitor celecoxib.

Table 2 Effects of bile on the growth of QBC939 with or without celecoxib

Group	<i>n</i>	OD ₄₉₀	<i>P</i>	+CE OD ₄₉₀	<i>P</i>
A	20	0.59±0.17	^b <i>P</i> =0.002, ^d <i>P</i> =0.001	0.29±0.09	^b <i>P</i> =0.089, ^d <i>P</i> =0.190
B	10	0.47±0.14	^b <i>P</i> =0.398	0.26±0.07	^b <i>P</i> =0.052
C	5	0.43±0.10		0.24±0.09	

QBC939 cells were incubated in 1 % CCC bile (A), 1 % normal bile (B) or 1 % PBS (C) with or without 20 μM celecoxib (+CE), and the cells density (OD_{490nm}) was measured by using MTT assay. Data were expressed as $\bar{x} \pm s$, b vs C, d vs B.

Flow cytometric analysis of cell cycle and apoptosis

The QBC939 cells proliferative index (PI) increased significantly (*P*=0.008) after treated with 1 % CCC bile (41.53±5.68) compared with normal bile (25.46±4.41), PI=(S+G2/M) % × 100. The percentage of S phase cells was increased remarkably (*P*<0.001) in CCC bile group (29.48±3.27) % compared with that in normal bile group (11.72±2.70) %, and the percentage of G0/G1 phase cells was decreased remarkably (*P*=0.002) in CCC group (54.19±9.46) % compared with that in normal group (69.16±10.88) %, CCC bile had no significant influence on the apoptosis of QBC939 cells compared with normal bile (*P*=0.719). The percentage of apoptotic cells in CCC bile group and normal bile group were (2.38±0.41) % and (2.09±0.36) % respectively (Figure 1).

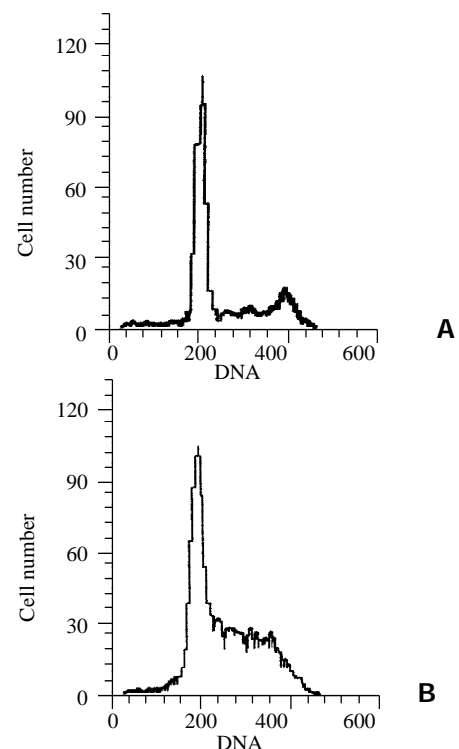


Figure 1 Representative data of cell cycle and apoptosis from QBC939 cells in the presence of 1 % CCC bile (B) or 1 % normal bile (A) for 24 h was analyzed by using flow cytometry.

DISCUSSION

As one of the high risk factors of cholangiocarcinoma, CCC is a common disease in eastern countries. Choledochal cysts are associated with a 10 % overall incidence of cholangiocarcinoma: there is a 1 % cumulative risk which plateaus after 15-20 years^[20]. In almost all cases congenital bile duct cysts are related to anomalous arrangements of the pancreaticobiliary duct system (APBDU) which seems to play a crucial role in the development of cystic bile ducts and biliary carcinogenesis. Bile stasis together with reflux of pancreatic juice causing longstanding inflammation and activation of bile acids might be the factors in carcinogenesis of the exposed bile duct epithelium in the cystic wall^[21]. Ohtsuka^[22] have reported that bile presented one possible explanation for the predisposition to carcinoma in choledochoceles as bile containing amylase may stagnate in the choledochoceles and then carcinoma may develop in the inner epithelium of the choledochoceles by the same mechanism as that leading to carcinogenesis in patients with APBDU.

Elevation of the secondary and free bile acid concentrations is considered as a risk factor for biliary carcinogenesis in CCC patients. Yuzuru *et al*^[23], have suggested that elevation of the lysolecithin (LL) in the bile is one of the factors for development of biliary tract carcinoma in patients with CCC: the LL in the phospholipid, which is produced from lecithin by activated phospholipase A₂ in refluxed pancreatic juice, was significantly elevated in the CCC group. Yoon *et al*^[24], have indicated that bile acids both induced EGFR phosphorylation and enhanced COX-2 protein expression. EGFR was activated by bile acids and functioned to induce COX-2 expression by a MAPK cascade. The induction of COX-2 might participate in the genesis and progression of cholangiocarcinomas.

In an effort to delineate the underlying mechanisms of the carcinogenesis in CCC patients, we used the whole bile from CCC patients for the first time to act directly on the human cholangiocarcinoma QBC939 cells *in vitro* to determine the effects of CCC bile on the growth of human cholangiocarcinoma cells. Our data showed that CCC bile could significantly promote the proliferation of human cholangiocarcinoma QBC939 cells compared with normal bile, and the proliferative effect of CCC bile could be abolished by addition of cyclooxygenase-2 specific inhibitor celecoxib. Our research indicated that CCC bile promoted the proliferation of human cholangiocarcinoma QBC939 cells via COX-2 and PGE₂ pathway.

Substantial evidences have shown that COX-2 is important in carcinogenesis^[25-33]. Celecoxib as a new COX-2 selective inhibitor has shown its safety and efficiency in human and animal. Several studies have demonstrated that celecoxib has significant efficacy in animal models: Celecoxib inhibited intestinal tumor multiplicity up to 71 % compared with controls in the Min mouse model, inhibited colorectal tumor burden in the rat azoxymethane (AOM) model^[34-36]. Recently celecoxib has been approved by FDA to reduce the number of adenomatous colorectal polyps in patients with familial adenomatous polyposis (FAP). Our data suggested that celecoxib as a chemopreventive and chemotherapeutic agent might be effective in cholangiocarcinomas and could be used as a chemopreventive strategy in the people of high-risk conditions for the development of cholangiocarcinoma such as CCC patients. Our research demonstrated that the QBC939 cells proliferative index increased significantly after treated with CCC bile for 24 h, the percentage of S phase was increased remarkably compared with normal bile, and the percentage of G0/G1 phase was decreased remarkably compared with normal bile, however, CCC bile had no significant influence on apoptosis of QBC939 cells. These data suggested that CCC bile could effect on the QBC939 cell proliferation cycle and

the proliferative activity of CCC bile was on cell cycle but not on apoptosis.

In conclusion, CCC bile can promote the proliferation of human cholangiocarcinoma QBC939 cells and these effects are via COX-2 and PGE₂ pathway.

REFERENCES

- 1 **Cucinotta E**, Palmeri R, Lazzara S, Salamone I, Melita G, Melita P. Diagnostic problems of choledochal cysts in the adult. *Chir Ital* 2002; **54**: 245-248
- 2 **Nassar AH**, Chakhtoura N, Martin D, Parra-Davila E, Sleeman D. Choledochal cysts diagnosed in pregnancy: a case report and review of treatment options. *J Matern Fetal Med* 2001; **10**: 363-365
- 3 **Wienke J**, Falen S, McCartney W. Hepatobiliary scan showing type II choledochal cyst. *Clin Nucl Med* 2001; **26**: 1010-1012
- 4 **Komuro H**, Makino SI, Yasuda Y, Ishibashi T, Tahara K, Nagai H. Pancreatic complications in choledochal cyst and their surgical outcomes. *World J Surg* 2001; **25**: 1519-1523
- 5 **Li L**, Yamataka A, Yian-Xia W, Da-Yong W, Segawa O, Lane GJ, Kun W, Jin-Zhe Z, Miyano T. Ectopic distal location of the papilla of Vater in congenital biliary dilatation: Implications for pathogenesis. *J Pediatr Surg* 2001; **36**: 1617-1622
- 6 **O'Neill JA**. Choledochal cyst. *Curr Probl Surg* 1992; **29**: 361-410
- 7 **Tsuchida Y**, Takahashi A, Suzuki N, Kuroiwa M, Murai H, Toki F, Kawarasaki H, Hashizume K, Honna T. Development of intrahepatic biliary stones after excision of choledochal cysts. *J Pediatr Surg* 2002; **37**: 165-167
- 8 **Shi LB**, Peng SY, Meng XK, Peng CH, Liu YB, Chen XP, Ji ZL, Yang DT, Chen HR. Diagnosis and treatment of congenital choledochal cyst: 20 years' experience in China. *World J Gastroenterol* 2001; **7**: 732-734
- 9 **Liu H**, Lu XH. The diagnosis of choledochal cyst (A report of 50 cases). *Xin Xiaohuabingxue Zazhi* 1996; **4**: 259
- 10 **Zhang Z**, Wei HL. Congenital choledochal dilatation in adult (A report of 3 cases). *Xin Xiaohuabingxue Zazhi* 1996; **4**(Suppl 5): 32
- 11 **Qiao Q**, Sun Z, Huang Y. Diagnosis and treatment of congenital choledochal cysts in adults. *Zhonghua Waike Zazhi* 1997; **35**: 610-612
- 12 **Wang L**, Wang SF, Li YG. Choledochal cyst (A report of 2 cases). *Xin Xiaohuabingxue Zazhi* 1996; **4**(Suppl 5): 210
- 13 **Tao K**, Li K, Dou K. Analysis and prevention of reoperation on congenital choledochal cyst. *Zhonghua Waike Zazhi* 1999; **37**: 344-346
- 14 **Dou K**, Guan W, Li K. Living related liver transplantation: a case report. *Zhonghua Waike Zazhi* 1998; **36**: 203-205
- 15 **Lin JTH**, Chen YH, Ni YH, Lai HS, Peng SS. Magnetic resonance cholangiopancreatography diagnosed pancreatitis associated choledochal cyst: report of one case. *Acta Paediatr Taiwan* 2001; **42**: 363-366
- 16 **Li M**, Jin Q, Feng J. Early postoperative complications of choledochal cyst excision and reconstruction of biliary tract. *Zhonghua Waike Zazhi* 2001; **39**: 686-689
- 17 **Zhao L**, Li Z, Ma H, Zhang X, Mou X, Zhang D, Lin W, Niu A. Congenital choledochal cyst with pancreatitis. *Chin Med J* 1999; **112**: 637-640
- 18 **Wang SG**, Han BL, Duan HC, Chen YS, Peng ZM. Establishment of the extrahepatic cholangiocarcinoma cell line. *Zhonghua Waike Zazhi* 1997; **14**: 67-68
- 19 **Mei ZY**, Shi Z, Wang XH, Luo XD. Synthesis of COX-2 Inhibitor Celecoxib. *Zhongguo Yiyao Gongye Zazhi* 2000; **31**: 433-434
- 20 **Chapman RW**. Risk factors for biliary tract carcinogenesis. *Ann Oncol* 1999; **10** (Suppl 4): 308-311
- 21 **Holzinger F**, Baer HU, Schilling M, Stauffer EJ, Buchler MW. Congenital bile duct cyst: a premalignant lesion of the biliary tract associated with adenocarcinoma—a case report. *Z Gastroenterol* 1996; **34**: 382-385
- 22 **Ohtsuka T**, Inoue K, Ohuchida J, Nabae T, Takahata S, Niiyama H, Yokohata K, Ogawa Y, Yamaguchi K, Chijiwa K, Tanaka M. Carcinoma arising in choledochoceles. *Endoscopy* 2001; **33**: 614-619
- 23 **Sugiyama Y**, Kobori H, Hakamada K, Seito D, Sasaki M. Altered bile composition in the gallbladder and common bile duct of patients with anomalous pancreaticobiliary ductal junction. *World J Surg* 2000; **24**: 17-21

- 24 **Yoon JH**, Higuchi H, Werneburg NW, Kaufmann SH, Gores GJ. Bile acids induce cyclooxygenase-2 expression via the epidermal growth factor receptor in a human cholangiocarcinoma cell line. *Gastroenterology* 2002; **122**: 985-993
- 25 **Gao HJ**, Yu LZ, Sun G, Miao K, Bai JF, Zhang XY, Lu XZ, Zhao ZQ. The expression of Cox-2 Proteins in gastric cancer tissue and accompanying tissue. *Shijie Huaren Xiaohua Zazhi* 2000; **8**:578-579
- 26 **Zhuang ZH**, Wang LD. Non-steroid anti-inflammatory drug and digestive tract tumors. *Shijie Huaren Xiaohua Zazhi* 2001; **9**: 1050-1053
- 27 **Tian G**, Yu JP, Luo HS, Yu BP, Yue H, Li JY, Mei Q. Effect of Nimesulide on proliferation and apoptosis of human hepatoma SMMC-7721 cells. *World J Gastroenterol* 2002; **8**: 483-487
- 28 **Sun B**, Wu YL, Zhang XJ, Wang SN, He HY, Qiao MM, Zhang YP, Zhong J. Effects of Sulindac on growth inhibition and apoptosis induction in human gastric cancer cells. *Shijie Huaren Xiaohua Zazhi* 2001; **9**: 997-1002
- 29 **Tian G**, Yu TP, Luo HS, Yu BP, Li JY. The expression and effect of cyclooxygenase-2 in acute hepatic injury. *Shijie Huaren Xiaohua Zazhi* 2002; **10**: 24-27
- 30 **Li JY**, Yu JP, Luo HS, Yu BP, Huang JA. Effects of nonsteroidal anti-inflammatory drugs on the proliferation and cyclooxygenase activity of gastric cancer cell line SGC7901. *Shijie Huaren Xiaohua Zazhi* 2002; **10**: 262-265
- 31 **Wu YL**, Sun B, Zhang XI, Wang SN, He HY, Qiao MM, Zhong J, Xu JY. Growth inhibition and apoptosis induction of sulindac on human gastric cancer cells. *World J Gastroenterol* 2001; **7**: 796-800
- 32 **Sirica AE**, Lai GH, Zhang Z. Biliary cancer growth factor pathways, cyclo-oxygenase-2 and potential therapeutic strategies. *J Gastroenterol Hepatol* 2001; **16**: 363-372
- 33 **Chariyalertsak S**, Sirikulchayanonta V, Mayer D, Kopp-Schneider A, Furstenberger G, Marks F, Muller-Decker K. Aberrant cyclooxygenase isozyme expression in human intrahepatic cholangiocarcinoma. *Gut* 2001; **48**: 80-86
- 34 **Hosomi Y**, Yokose T, Hirose Y, Nakajima R, Nagai K, Nishiwaki Y, Ochiai A. Increased cyclooxygenase 2 (COX-2) expression occurs frequently in precursor lesions of human adenocarcinoma of the lung. *Lung Cancer* 2000; **30**: 73-81
- 35 **Tsubouchi Y**, Mukai S, Kawahito Y, Yamada R, Kohno M, Inoue K, Sano H. Meloxicam inhibits the growth of non-small cell lung cancer. *Anticancer Res* 2000; **20**: 2867-2872
- 36 **Souza RF**, Shewmake K, Beer DG, Cryer B, Spechler SJ. Selective inhibition of cyclooxygenase-2 suppresses growth and induces apoptosis in human esophageal adenocarcinoma cells. *Cancer Res* 2000; **60**: 5767-5772

Edited by Xu JY

K-ras gene mutation in the diagnosis of ultrasound guided fine-needle biopsy of pancreatic masses

Min Zheng, Lian-Xin Liu, An-Long Zhu, Shu-Yi Qi, Hong-Chi Jiang, Zhu-Ying Xiao

Min Zheng, Zhu-Ying Xiao, Department of Ultrasound, the First Clinical College, Harbin Medical University, Harbin 150001, Heilongjiang Province, China

Lian-Xin Liu, An-Long Zhu, Hong-Chi Jiang, Department of Surgery, the First Clinical College, Harbin Medical University, Harbin 150001, Heilongjiang Province, China

Shu-Yi Qi, Department of VIP, the First Clinical College, Harbin Medical University, Harbin 150001, Heilongjiang Province, China
Support by Natural Scientific Foundation of Heilongjiang Province, No.97024

Correspondence to: Dr. An-Long Zhu, Department of Surgery, the First Clinical College, Harbin Medical University, No.23 Youzheng Street, Nangang District, Harbin 150001, Heilongjiang Province, China. anlonge@163.com

Telephone: +86-451-4213684 **Fax:** +86-451-3670428

Received: 2002-07-08 **Accepted:** 2002-08-02

Abstract

AIM: To investigate the utility of K-ras mutation analysis of ultrasound guided fine-needle aspirate biopsy of pancreatic masses.

METHODS: Sixty-six ultrasound guided fine-needle biopsies were evaluated by cytology, histology and k-ras mutation. The mutation at codon 12 of the k-ras oncogene was detected by artificial restriction fragment length polymorphisms using *Bst* NI approach.

RESULTS: The presence of malignant cells was reported in 40 of 54 pancreatic carcinomas and K-ras mutations were detected in 45 of the 54 FNABs of pancreatic carcinomas. The sensitivity of cytology and k-ras mutation were 74 % and 83 %, respectively. The speciality of cytology and k-ras mutation were both 100 %. The sensitivity and speciality of k-ras mutation combined with cytology were 83 % and 100 %, respectively.

CONCLUSION: High diagnostic accuracy with acceptable discomfort of FNAB make it useful in diagnosis of pancreatic carcinoma. Ultrasound guided fine-needle biopsy is a safe and feasible method for diagnosing pancreatic cancer. Pancreatic carcinoma has the highest K-ras mutation rate among all solid tumors. The mutation rate of k-ras is about 80-100 %. The usage of mutation of codon 12 of k-ras oncogene combined with cytology is a good alternative for evaluation of pancreatic masses.

Zheng M, Liu LX, Zhu AL, Qi SY, Jiang HC, Xiao ZY. K-ras gene mutation in the diagnosis of ultrasound guided fine-needle biopsy of pancreatic masses. *World J Gastroenterol* 2003; 9(1):188-191 <http://www.wjgnet.com/1007-9327/9/188.htm>

INTRODUCTION

Pancreatic adenocarcinoma is a very aggressive carcinoma and has the worst prognosis in common abdominal cancer^[1-3]. Despite the poor prognosis, patients with localized disease may be cured with surgery^[4-6]. However, it is difficult to diagnose

pancreatic cancer in the earlier stages. This dismal prognosis is a result not only of biological aggressiveness but also of diagnosis late in the chronological progression of the tumor. If pancreatic cancer can be resected when it is small, the prognosis is much better, with a 5-year survival of approximately 40 %^[7-9]. When pancreatic cancer is clinically suspected and a pancreatic mass identified by ultrasonography or computed tomography scan, a guided percutaneous fine-needle biopsy (FNAB) can be obtained; this may be the only sample available for diagnosis in most patients^[10-12].

Even though alternative techniques for sampling cellular or tissue material have been developed, FNAB is still widely used for morphological verification of intra-abdominal malignancies, especially in pancreatic cancer. Although it has been questioned because of the risk of peritoneal seeding and seeding of tumor cells along the needle tract. It is still widely used for the diagnosis of pancreatic cancer combined with modern molecular biological techniques^[13].

The high incidence of mutations at codon 12 of the K-ras gene (65-100 %) leads to consider them as a potential tumor marker at the tissue level^[14-19]. The development of PCR-based techniques for detection of K-ras mutations has allowed its use in the clinical setting. The high incidence of mutation suggests that it may be used as a tumor marker at the tissue level. The role of k-ras detection in the clinical evaluation of pancreatic mass has to be established in a large series of patients. Data suggest that a combination of cytological examination and K-ras mutation detection in cellular material may improve diagnostic accuracy^[20-26]. In this study we evaluated the diagnostic utility of cytological and histological examination and k-ras mutation detection, alone and in combination under the ultrasound guided FNAB from 66 patients with pancreatic masses.

MATERIALS AND METHODS

Patients and samples

Between January 1997 and May 2001, 66 consecutive patients (38 men and 28 women, mean age of 54±9 years) with pancreatic masses were included. In all cases FNAB of the masses were percutaneously obtained under ultrasonographic guidance. A portion (50 %) of each FNAB was immediately examined by pathologist. The other 50 % of the same specimen was frozen and stored in liquid nitrogen.

Final diagnosis of pancreatic carcinoma was established if malignant cells were identified in the FNAB or in surgically resected specimens or when death occurred within six months after diagnosis, with clinical evolution compatible with disseminated cancer disease. Other types of neoplasm were diagnosed on the basis of pathological findings. The diagnosis of chronic pancreatitis was based on standard clinical criteria. In chronic pancreatitis, a minimum of 6-month (range, 6-27 months) follow-up period with no evidence of cancer was available. Pancreatic tuberculosis was confirmed by positive Lowenstein culture.

Detection of K-ras codon 12 mutations

DNA was extracted following standard procedures. We utilized

*Bst*NI (Promega, USA) restriction fragment length polymorphism/polymerase chain reaction (RFLP/PCR) method that enriches for the amplification of mutant codon 12 K-ras alleles by cleaving amplified wild-type allele through intermediate digestion between first- and second-round PCR^[27]. To create the restriction site for the enzyme *Bst*NI [CCTGG], which is lost when a K-ras codon 12 mutation exists, the first-round amplification was performed using the mutant primers K-ras 5' and DD5P (Table 1) in a volume of 50 µL containing PCR buffer (50 mmol/L KCl, 20 mmol/L Tris HCl, pH 8.4), 1.5 mmol/L MgCl₂, 0.2 mmol/L each dNTP (Promega, USA), 1U of Taq polymerase (Life Technologies, USA), and 150 ng of PCR primers^[28]. The reactions were 10 cycles of 92 °C (15s), 44 °C (15s) and 72 °C (15s). An aliquot of 5 µL of the amplified product was enzymatically digested with *Bst*NI following the manufacturer's directions. One microliter of the digested product was reamplified using a heminested reaction with mutant amplimers K-ras 5' and K-ras 3'^[28]. The reaction conditions were 35 cycles of 92 °C (15s), 54 °C (15s) and 72 °C (15s). The latter primer artificially introduces an internal control to assure the completion of enzymatic digestion. After polyacrylamide gel electrophoresis (6 %) and ethidium bromide (0.5 g/L) staining, the 143-bp band depicted the mutant allele, and the 114-bp band the wild-type allele. RFLP/PCR method consistently detected a mutant allele in serial dilutions containing at least 1 mutant allele in 1 000 wild-type alleles. Positive bands were always clearly identifiable when DNA obtained from FNAB was examined. All samples were analyzed in duplicate. Results were available 48-72 h after the tissue sample was obtained.

Table 1 Primers for K-ras mutation detection

Round	Primer	Sequence
First	K-ras 5'	5'-ACTGAARARAACTTGTGGTAGTTGGACCT-3'
	DD5P	5'-TCATGAAAATGGTCAGAGAA-3'
Second	K-ras 5'	5'-ACTGAATATAACTTGTGGTAGTTGGAACCT-3'
	K-ras 3'	5'-TCAAAGAATGGTCCTGGACC-3'

RESULTS

Cytological examination

Final diagnoses were as follows: 54 pancreatic carcinomas, 3 other malignancies (1 lymphoma, and 2 cholangiocarcinomas), 6 benign diseases (5 chronic pancreatitis and 1 tuberculosis), and 3 endocrine tumors. The presence of malignant cells was reported in 40 of 54 pancreatic carcinomas with no false positives. However, in 14 of the 54 FNABs of pancreatic carcinomas, the cytological report was not conclusive: 12 because of insufficient material and 2 because of suspicion. The sensitivity of cytology was 74 % in the diagnosis of pancreatic cancer.

Molecular diagnosis

Molecular analysis was possible in 54 of 66 FNABs. K-ras mutations were detected in 45 of the 54 FNABs of pancreatic carcinomas, with no false positives. The combination of cytology and enriched RFLP/PCR analysis was always informative and showed a sensitivity of 83.3 %, with a specificity of 100 %. Only nine pancreatic carcinomas failed to be correctly classified after the combined cytological and molecular analysis.

In three cases, a K-ras positive analysis in combination with the presence of suspicious cells was considered confirmation of pancreatic cancer, and no further studies were performed. Two of these patients died 1 and 3 months later, respectively,

with a clinical course consistent with advanced pancreatic cancer. In the other, positive peritoneal disease was present at surgery. In one patient with insufficient material at cytology, molecular analysis was the endpoint of the diagnostic work-up, and laparotomy was not performed because of the poor clinical status of the patient. Finally, in the remaining one patient with insufficient material for cytological evaluation and K-ras positive analysis, surgical resection of a histologically confirmed pancreatic carcinoma was performed.

DISCUSSION

The influence of biopsy on the natural history of pancreatic carcinoma is still unclear, considering the increasing intention to treat and the development of new multimodality therapies^[29,30]. Our data indicate the FNAB of pancreatic malignancy can be easily performed without serious side effects and is still a safe and useful procedure for establishing the diagnosis of pancreatic carcinoma. High diagnostic accuracy with acceptable patient discomfort has also been reported when using an 18-gauge cutting needle with an automatic spring-loaded sample device. The large amount of tissue obtained could improve the microscopic evaluation, but it has not been verified that microhistology offers advantages over cytology in the diagnosis of pancreatic cancer. The complication rate, including needle tract seeding, in pancreatic carcinoma is lower than in other tumors^[31,32].

The main limitation of cytological analysis is the substantial proportion of cases in which a conclusive report is not possible, and where a second procedure to confirm diagnosis is required. FNAB can get a bigger tissues for microhistological examination. The molecular approach allows detection of K-ras mutants even when cells are present in a small proportion. Mutation detection would have complemented the cytological evaluation of FNAB when cellular material was insufficient, suspicious cells were present, or when healthy-appearing duct cells were reported^[33].

Pancreatic carcinoma is known to have the highest K-ras mutation rate among all tumors. The codon 12 of this gene is affected in 80-100 % of the cases^[34-36]. Only a minority of pancreatic cancers (9 cases) failed to be correctly classified by the combined histological and molecular approach in our studies. Although inaccurate sampling of the lesion may account for some of the false negatives observed, the molecular approach has some limitations^[26,37]. The discrepancies between the results of the various studies are based on the wide range of investigated cases, the selection of lesion types, and the sensitivity of the microdissection and PCR techniques employed. The clinical usefulness of ras mutations relies on the development of rapid, sensitive, and reproducible techniques for their detection. Moreover, a positive molecular diagnosis avoided iterative pancreatic fine-needle aspiration or further diagnostic procedures in these patients.

In Japanese studies, a comparison of the K-ras mutation pattern in ductal lesions with that of the adjacent carcinomas revealed nearly identical mutation patterns^[38,39], whereas in a study from North America a concordance rate of only 50 % was reported^[40]. The results of our analysis showed identical mutation patterns in the primary tumor confirming the results of the Japanese authors. There are large differences in the incidence of ras mutations between Japanese and Western populations, although the reason is still unclear and the number of subjects is limited. In Japan, the frequency of K-ras mutation ranged from 55-80 %^[41-44], whereas in West it was relatively low, ranging from 0-31 %^[45,46]. The current data suggest that most patients have ras gene mutations in the tumor itself, which is similar to previous Japanese reports.

In conclusion, the results of the present study indicate that

K-ras analysis is a highly specific and sensitive approach in pancreatic carcinoma patients and suggest that a k-ras assay may have a role in the diagnostic assessment of these patients. Further investigations are needed to confirm these results, to improve the technique's sensitivity, and to establish its usefulness in the early.

REFERENCES

- 1 **Yoshida T**, Matsumoto T, Sasaki A, Morii Y, Aramaki M, Kitano S. Prognostic factors after pancreatoduodenectomy with extended lymphadenectomy for distal bile duct cancer. *Arch Surg* 2002; **137**: 69-73
- 2 **Shankar A**, Russell RC. Recent advances in the surgical treatment of pancreatic cancer. *World J Gastroenterol* 2001; **7**: 622-626
- 3 **Zhao XY**, Yu SY, Da SP, Bai L, Guo XZ, Dai XJ, Wang YM. A clinical evaluation of serological diagnosis for pancreatic cancer. *World J Gastroenterol* 1998; **4**: 147-149
- 4 **Ahmad NA**, Lewis JD, Ginsberg GG, Haller DG, Morris JB, Williams NN, Rosato EF, Kochman ML. Long term survival after pancreatic resection for pancreatic adenocarcinoma. *Am J Gastroenterol* 2001; **96**: 2532-2534
- 5 **Guo XZ**, Friess H, Shao XD, Liu MP, Xia YT, Xu JH, Buchler MW. KAI1 gene is differently expressed in papillary and pancreatic cancer: influence on metastasis. *World J Gastroenterol* 2000; **6**: 866-871
- 6 **Ghaneh P**, Slavin J, Sutton R, Hartley M, Neoptolemos JP. Adjuvant therapy in pancreatic cancer. *World J Gastroenterol* 2001; **7**: 482-489
- 7 **Huang JJ**, Yeo CJ, Sohn TA, Lillemoe KD, Sauter PK, Coleman J, Hruban RH, Cameron JL. Quality of life and outcomes after pancreatoduodenectomy. *Ann Surg* 2000; **231**: 890-898
- 8 **Sakorafas GH**, Tsiotou AG. Multi-step pancreatic carcinogenesis and its clinical implications. *Eur J Surg Oncol* 1999; **25**: 562-565
- 9 **Liu B**, Staren E, Iwamura T, Appert H, Howard J. Taxotere resistance in SUIT Taxotere resistance in pancreatic carcinoma cell line SUIT and its sublines. *World J Gastroenterol* 2001; **7**: 855-859
- 10 **Cui JH**, Krueger U, Henne-Bruns D, Kremer B, Kalthoff H. Orthotopic transplantation model of human gastrointestinal cancer and detection of micrometastases. *World J Gastroenterol* 2001; **7**: 381-386
- 11 **Liu B**, Staren E, Iwamura T, Appert H, Howard J. Effects of Taxotere on invasive potential and multidrug resistance phenotype in pancreatic carcinoma cell line SUIT-2. *World J Gastroenterol* 2001; **7**: 143-148
- 12 **Xu HB**, Zhang YJ, Wei WJ, Li WM, Tu XQ. Pancreatic tumor: DSA diagnosis and treatment. *World J Gastroenterol* 1998; **4**: 80-81
- 13 **Linder S**, Blasjo M, Sundelin P, von Rosen A. Aspects of percutaneous fine-needle aspiration biopsy in the diagnosis of pancreatic carcinoma. *Am J Surg* 1997; **174**: 303-306
- 14 **Villanueva A**, Reyes G, Cuatrecasas M, Martinez A, Erill N, Lerma E, Farre A, Lluís F, Capella G. Diagnostic utility of K-ras mutations in fine-needle aspirates of pancreatic masses. *Gastroenterology* 1996; **110**: 1587-1594
- 15 **Yuan P**, Sun MH, Zhang JS, Zhu XZ, Shi DR. APC and K-ras gene mutation in aberrant crypt foci of human colon. *World J Gastroenterol* 2001; **7**: 352-356
- 16 **Wang Q**, Lin ZY, Feng XL. Alterations in metastatic properties of hepatocellular carcinoma cell following H-ras oncogene transfection. *World J Gastroenterol* 2001; **7**: 335-339
- 17 **Yin ZZ**, Jin HL, Yin XZ, Li TZ, Quan JS, Jin ZN. Effect of *Boschniakia rossica* on expression of GST-P, p53 and p21(ras) proteins in early stage of chemical hepatocarcinogenesis and its anti-inflammatory activities in rats. *World J Gastroenterol* 2000; **6**: 812-818
- 18 **Li J**, Feng CW, Zhao ZG, Zhou Q, Wang LD. A preliminary study on ras protein expression in human esophageal cancer and precancerous lesions. *World J Gastroenterol* 2000; **6**: 278-280
- 19 **Ward R**, Hawkins N, O'Grady R, Sheehan C, O'Connor T, Impey H, Roberts N, Fuery C, Todd A. Restriction endonuclease-mediated selective polymerase chain reaction: a novel assay for the detection of K-ras mutations in clinical samples. *Am J Pathol* 1998; **153**: 373-379
- 20 **Ikeda N**, Nakajima Y, Sho M, Adachi M, Huang CL, Iki K, Kanehiro H, Hisanaga M, Nakano H, Miyake M. The association of K-ras gene mutation and vascular endothelial growth factor gene expression in pancreatic carcinoma. *Cancer* 2001; **92**: 488-499
- 21 **Fukushima H**, Yamamoto H, Itoh F, Nakamura H, Min Y, Horiuchi S, Iku S, Sasaki S, Imai K. Association of matrilysin mRNA expression with K-ras mutations and progression in pancreatic ductal adenocarcinomas. *Carcinogenesis* 2001; **22**: 1049-1052
- 22 **Lohr M**, Muller P, Mora J, Brinkmann B, Ostwald C, Farre A, Lluís F, Adam U, Stubbe J, Plath F, Nizze H, Hopt UT, Barten M, Capella G, Liebe S. p53 and K-ras mutations in pancreatic juice samples from patients with chronic pancreatitis. *Gastrointest Endosc* 2001; **53**: 734-743
- 23 **Mora J**, Puig P, Boadas J, Urgell E, Montserrat E, Lerma E, Gonzalez-Sastre F, Lluís F, Farre A, Capella G. K-ras gene mutations in the diagnosis of fine-needle aspirates of pancreatic masses: prospective study using two techniques with different detection limits. *Clin Chem* 1998; **44**: 2243-2248
- 24 **Pabst B**, Arps S, Binmoeller K, Thul R, Walsemann G, Fenner C, Klapdor R. Analysis of K-ras mutations in pancreatic tissue after fine needle aspirates. *Anticancer Res* 1999; **19**: 2481-2484
- 25 **Li D**, Firozi PF, Zhang W, Shen J, DiGiovanni J, Lau S, Evans D, Friess H, Hassan M, Abbruzzese JL. DNA adducts, genetic polymorphisms, and K-ras mutation in human pancreatic cancer. *Mutat Res* 2002; **513**: 37-48
- 26 **Ha A**, Watanabe H, Yamaguchi Y, Ohtsubo K, Wang Y, Motoo Y, Okai T, Wakabayashi T, Sawabu N. Usefulness of supernatant of pancreatic juice for genetic analysis of K-ras in diagnosis of pancreatic carcinoma. *Pancreas* 2001; **23**: 356-363
- 27 **Kahn SM**, Jiang W, Culbertson TA, Weinstein IB, Williams GM, Tomita N, Ronai Z. Rapid and sensitive nonradioactive detection of mutant K-ras genes via "enriched" PCR amplification. *Oncogene* 1991; **6**: 1079-1083
- 28 **Jiang W**, Kahn SM, Guillem JG, Lu SH, Weinstein IB. Rapid detection of ras oncogenes in human tumors: applications to colon, esophageal, and gastric cancer. *Oncogene* 1989; **4**: 923-928
- 29 **Schramm H**, Urban H, Arnold F, Penzlin G, Bosseckert H. Intraoperative pancreas cytology. *Pancreas* 2002; **24**: 210-214
- 30 **Freeny PC**. Pancreatic carcinoma: imaging update 2001. *Dig Dis* 2001; **19**: 37-46
- 31 **Chang KJ**, Nguyen P, Erickson RA, Durbin TE, Katz KD. The clinical utility of endoscopic ultrasound-guided fine-needle aspiration in the diagnosis and staging of pancreatic carcinoma. *Gastrointest Endosc* 1997; **45**: 387-393
- 32 **Gloor B**, Todd KE, Reber HA. Diagnostic workup of patients with suspected pancreatic carcinoma: the University of California-Los Angeles approach. *Cancer* 1997; **79**: 1780-1786
- 33 **Puig P**, Urgell E, Capella G, Sancho FJ, Pujol J, Boadas J, Farre A, Lluís F, Gonzalez-Sastre F, Mora J. A highly sensitive method for K-ras mutation detection is useful in diagnosis of gastrointestinal cancer. *Int J Cancer* 2000; **85**: 73-77
- 34 **Suwa H**, Hosotani R, Kogire M, Doi R, Ohshio G, Fukumoto M, Imamura M. Detection of extrapancreatic nerve plexus invasion of pancreatic adenocarcinoma. Cytokeratin 19 staining and K-ras mutation. *Int J Pancreatol* 1999; **26**: 155-162
- 35 **Luttges J**, Kloppel G. Update on the pathology and genetics of exocrine pancreatic tumors with ductal phenotype: precursor lesions and new tumor entities. *Dig Dis* 2001; **19**: 15-23
- 36 **Matsubayashi H**, Watanabe H, Nishikura K, Ajioka Y, Kijima H, Saito T. Determination of pancreatic ductal carcinoma histogenesis by analysis of mucous quality and K-ras mutation. *Cancer* 1998; **82**: 651-660
- 37 **Esikinen MJ**, Haglund UH. Prognosis of human pancreatic adenocarcinoma: review of clinical and histopathological variables and possible uses of new molecular methods. *Eur J Surg* 1999; **165**: 292-306
- 38 **Tsuchida T**, Kijima H, Hori S, Oshika Y, Tokunaga T, Kawai K, Yamazaki H, Ueyama Y, Scanlon KJ, Tamaoki N, Nakamura M. Adenovirus-mediated anti-K-ras ribozyme induces apoptosis and growth suppression of human pancreatic carcinoma. *Cancer Gene Ther* 2000; **7**: 373-383
- 39 **Kimura W**, Zhao B, Futakawa N, Muto T, Makuuchi M. Significance of K-ras codon 12 point mutation in pancreatic juice in the diagnosis of carcinoma of the pancreas. *Hepatogastroenterology* 1999; **46**: 532-539

- 40 **Futakawa N**, Kimura W, Yamagata S, Zhao B, Ilsoo H, Inoue T, Sata N, Kawaguchi Y, Kubota Y, Muto T. Significance of K-ras mutation and CEA level in pancreatic juice in the diagnosis of pancreatic cancer. *J Hepatobiliary Pancreat Surg* 2000; **7**:63-71
- 41 **Theodor L**, Melzer E, Sologov M, Idelman G, Friedman E, Bar-Meir S. Detection of pancreatic carcinoma: diagnostic value of K-ras mutations in circulating DNA from serum. *Dig Dis Sci* 1999; **44**: 2014-2019
- 42 **Caldas C**. Biliopancreatic malignancy: screening the at risk patient with molecular markers. *Ann Onco* 1999; **10**: 153-156
- 43 **Matsubayashi H**, Watanabe H, Yamaguchi T, Ajioka Y, Nishikura K, Iwafuchi M, Yamano M, Kijima H, Saito T. Multiple K-ras mutations in hyperplasia and carcinoma in cases of human pancreatic carcinoma. *Jpn J Cancer Res* 1999; **90**: 841-848
- 44 **Nakaizumi A**, Uehara H, Takenaka A, Uedo N, Sakai N, Yano H, Ohigashi H, Ishikawa O, Ishiguro S, Sugano K, Tatsuta M. Diagnosis of pancreatic cancer by cytology and measurement of oncogene and tumor markers in pure pancreatic juice aspirated by endoscopy. *Hepatogastroenterology* 1999; **46**: 31-37
- 45 **Castells A**, Puig P, Mora J, Boadas J, Boix L, Urgell E, Sole M, Capella G, Lluís F, Fernandez-Cruz L, Navarro S, Farre A. K-ras mutations in DNA extracted from the plasma of patients with pancreatic carcinoma: diagnostic utility and prognostic significance. *J Clin Oncol* 1999; **17**: 578-584
- 46 **Tamagawa E**, Ueda M, Takahashi S, Sugano K, Uematsu S, Mukai M, Ogata Y, Kitajima M. Pancreatic lymph nodal and plexus micrometastases detected by enriched polymerase chain reaction and nonradioisotopic single-strand conformation polymorphism analysis: a new predictive factor for recurrent pancreatic carcinoma. *Clin Cancer Res* 1997; **3**: 2143-2149

Edited by Xu JY

A new three-layer-funnel-shaped esophagogastric anastomosis for surgical treatment of esophageal carcinoma

Han-Lei Dan, Yang Bai, Hui Meng, Cong-Lin Song, Jie Zhang, Yong Zhang, Lei-Chi Wan, Ya-Li Zhang, Zhen-Shu Zhang, Dian-Yuan Zhou

Han-Lei Dan, Yang Bai, Ya-Li Zhang, Zhen-Shu Zhang, Dian-Yuan Zhou, Research Institute of Digestive Disease, South Hospital, First Military Medical University, Guangzhou 510515, Guangdong Province, China

Hui Meng, Department of Cardio-Thoracic Surgery, South Hospital, First Military Medical University, Guangzhou 510515, Guangdong Province, China

Cong-Lin Song, Jie Zhang, Department of Surgery, No. 520 Hospital, Mianyang City 621000, Sichuan Province, China

Yong Zhang, Yanting Oncology Research Institute, Yanting County 621042, Sichuan Province, China

Lei-Chi Wan, Department of Cardio-Thoracic Surgery, Pearl River Hospital, Guangzhou 510282, Guangdong Province, China

Correspondence to: Dr. Han-Lei Dan, M.D., Doctor-in-chief of Surgery Department. Prf. Ya-Li Zhang, M.D., Ph. D., Research Institute of Digestive Disease, South Hospital (Nanfang Hospital), First Military Medical University, Guangzhou 510515, Guangdong Province, China. henrydan@sina.com

Telephone: +86-20-85141531 **Fax:** +86-20-85141531

Received: 2002-05-14 **Accepted:** 2002-06-16

Abstract

AIM: To reduce the incidence of postoperative anastomotic leak, stenosis, gastroesophageal reflux (GER) for patients with esophageal carcinoma, and to evaluate the conventional method of esophagectomy and esophagogastric anastomosis modified by a new three-layer-funnel-shaped (TLF) esophagogastric anastomotic suturing technique.

METHODS: From January 1997 to October 1999, patients with clinical stage I and II (IIa and IIb) esophageal carcinoma, which met the enrollment criteria, were surgically treated by the new method (Group A) and by conventional operation (Group B). All the patients were followed at least for 6 months. Postoperative outcomes and complications were recorded and compared with the conventional method in the same hospitals and with that reported previously by McLarty *et al* in 1997 (Group C).

RESULTS: 58 cases with stage I and II (IIa and IIb) esophageal carcinoma, including 38 males and 20 females aged from 34 to 78 (mean age: 57), were surgically treated by the TLF anastomosis and 64 by conventional method in our hospitals from January 1997 to October 1999. The quality of swallowing was improved significantly (*Wilcoxon W*=2 142, *P*=0.001) 2 to 3 months after the new operation in Group A. Only one patient had a blind anastomotic fistula diagnosed by barium swallow test 2 months but healed up 3 weeks later. Postoperative complications occurred in 25 (43 %) patients, anastomotic stenosis in 8 (14 %), and GER in 13 (22 %). The incidences of postoperative anastomotic leak, stenosis and GER were significantly decreased by the TLF anastomosis method compared with that of conventional methods ($\chi^2=6.566$, *P* =0.038; $\chi^2=10.214$, *P*= 0.006; $\chi^2=21.265$, *P*=0.000).

CONCLUSION: The new three-layer-funnel-shaped

esophagogastric anastomosis (TLFEGA) has more advantages to reduce postoperative complications of anastomotic leak, stricture and GER.

Dan HL, Bai Y, Meng H, Song CL, Zhang J, Zhang Y, Wan LC, Zhang YL, Zhang ZS, Zhou DY. A new three-layer-funnel-shaped esophagogastric anastomosis for surgical treatment of esophageal carcinoma. *World J Gastroenterol* 2003; 9(1): 22-25
<http://www.wjgnet.com/1007-9327/9/22.htm>

INTRODUCTION

Surgical therapy is considered the major method for treatment of operable esophageal cancer^[1-2]. Unfortunately, there are many operative complications after classical standard esophagectomy and esophageal reconstruction with stomach in patients with esophageal carcinoma. Anastomotic leak, with a rate of about 12-14 % as reported, is the most severe complication and the principal cause of death after operation^[3-7]. Anastomotic stenosis and gastroesophageal reflux (GER), with higher rates of about 36.4-40 % and 50-60 % respectively, result in dysphagia, heartburn, regurgitation and nausea^[3-7].

We modified the conventional method of esophagectomy and created a new three-layer-funnel-shaped (TLF) esophagogastric anastomotic suturing technique, which significantly reduced postoperative complications of anastomotic leak, stricture and GER.

MATERIALS AND METHODS

Patients and preoperative examination

From January 1997 to October 1999, the patients with clinical stage I and II (IIa and IIb) esophageal carcinoma, which met the enrollment criteria, were allocated into two groups and surgically treated by a new method (Group A) and the conventional operation (Group B) in our hospitals. All patients were diagnosed by esophagoscopy and biopsy. Barium swallow test confirmed that the cancer length was <5 cm, there was absence of sinus or fistula. No lung or liver metastases were detected by radiography and/or computed tomography (CT) scan of the chest and ultrasonography of the upper abdomen. Supraclavicular lymph nodes were not involved by physical examination in all patients. Karnofsky performance status was >70. All patients assessed by pulmonary functional test were fit for thoracotomy. Patients with stage III or IV esophageal carcinoma, inoperable conditions, receiving chemotherapy or radiotherapy before or after operation were precluded.

Methods of operation

Partial or sub-total resection of esophagus was routinely performed through left or right thoracic incision, some cases need cervical incision, with removal of paraesophageal, subcarinal, supradiaphragmatic, perihialal, as well as left gastric and coeliac lymph node group. Partial gastrectomy was performed with esophagogastric junction carcinoma. The stomach remained and was reconstructed as a tube-like pouch to replace the resected part of the esophagus. The anastomotic

techniques were improved as follows:

When the gastric tube was constructed, an adequate amount of greater omentum was reserved for protecting the right gastroepiploic vessels and the blood supply of the gastric tube. The gastric tube was kept long enough to avoid tension and pulled along the esophageal bed, anchored to the back of the chest wall beside the mediastinum (The cervical cancer need a cervical incision to perform the anastomotic suture in the neck). First, the esophageal muscular layer was cut 3.0-3.5 cm in length into the inclined cycle, and the esophageal mucosa was kept 1.0-1.5 cm longer. Between the short gastric vessel, the sero-muscular layer was incised 4.0-4.5 cm, and its posterior aspect was hand-sewn to the same aspect of esophageal muscular layer. Then, excised the inner circular muscle layer and mucosa of stomach for 2.5-3.0 cm long and anastomosed to the esophageal mucosa by interrupted suture. The anterior aspect of the esophageal muscular and the gastric sero-muscular layer was sewn finally with fundoplication by inversion suture. The fundoplication suture cycle is 1.0 -2.0 cm larger than the suture cycle of the esophageal muscular-to-sero-muscular layer of the stomach (Figure 1). The other procedures were performed as usual.

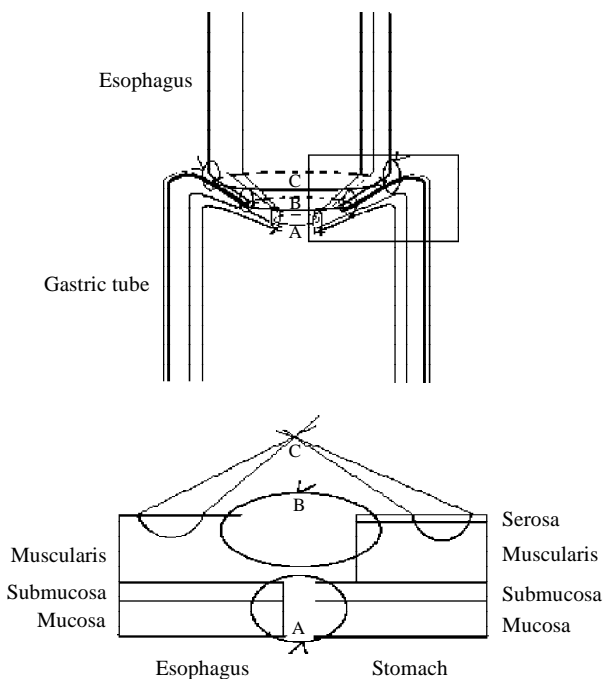


Figure 1 Technique of three-layer-funnel-shaped (TLF) esophagogastric anastomosis. A: mucosa-to-mucosa suture cycle; B: the esophagus muscular to gastric sero-muscular suture cycle; C: fundoplication suture cycle.

Postoperative management and follow-up

After the operation, all patients were treated routinely by thoracic drainage, nutrition support, and antibiotics. The swallowing ability and symptoms of anastomotic leak, stricture and GER were observed clinically as reported^[3-7]. All patients were evaluated clinically by their general condition, eating habits, swallowing ability and barium swallow test or esophagoscopy 2 to 3 months after the completion of all treatments and followed up at intervals of 2-3 months for at least 6 months.

Postoperative anastomotic leak was diagnosed clinically by leakage of gastrointestinal contents and radiographically extravasation of water-soluble contrast medium at the site of anastomosis. The anastomotic stricture was defined as any form of narrowing in the anastomosis region by contrast swallow study (≤ 2.0 cm in diameter in obverse and lateral posture)

and any symptom of dysphagia when swallowing solid food, semisolids or liquids, requiring endoscopic dilation. GER was present if the patient had intermittent or continuous heartburn, regurgitation and nausea, especially that required antacids for relief of heartburn, or barium regurgitation at horizontal posture or Trendelenburg’s position on radiographic examination.

Statistical analysis

All patients’ general characteristics, pathological pattern of carcinoma, clinical staging, swallowing ability, postoperative complications, and incidences of anastomotic leak, stricture, and GER were recorded and compared to that treated by conventional methods in the same hospitals and that reported previously by McLarty *et al*^[7]. Quantitative data were compared by using Independent-Samples *t* test and qualitative data by Chi-square, Fisher’s exact test, and Wilcoxon rank test. Statistical significance was assumed at $P \leq 0.05$.

RESULTS

58 patients (Group A), including 38 males and 20 females aged from 34 to 78 (mean age: 57), 54 cases with dysphagia, 4 without any symptom by routine examination, were successfully treated by the new method and 64 (Group B) by the conventional operation. There were no severe intraoperative complications, no operative mortality, no abscesses or uncontrolled infections occurred in all patients. Treated by the new method, the quality of swallowing of the patients improved significantly ($P=0.0001$) 2 to 3 months after the operation (Table 1). In Group A, only one patient had a minute blind anastomotic fistula into the immediate paraesophageal soft tissues without causing any symptoms which was diagnosed by barium swallowing test 2 months after the operation, but healed up automatically without any treatment 3 weeks afterwards. Postoperative complications occurred in 25 patients (43%), including incision and/or thoracic cavity bleeding in 2, wound infection in 1, pneumonia in 1, anastomotic stenosis in 8 (14%), and GER in 13 (22%). There were 7 of 8 cases with symptom of dysphagia but dilated successfully by endoscopy, 1 case with moderate stricture could only eat semisolid or liquid food 1 year after the operation.

Table 1 Evaluation of swallowing quality after operation (Group A, $n=58$)

	No symptom of dysphagia	With symptom of dysphagia		
		Solid Food	Semisolids	Liquids
Preoperation	4 (6.9%)	23 (39.7%)	26 (44.8%)	5 (8.6%)
Postoperation	50 (86.2%)	5 (8.6%)	2 (3.4%)	1 (1.7%)

Analysed by wilcoxon rank test (*Wilcoxon W*=2 142, $P=0.0001$), swallowing quality of patients after operation increased significantly compared with that before operation.

Except the difference of pathological type of carcinoma in the west from that in China, which was not the major factor that affected the operation modality and the early outcomes, the patients’ general characteristics, tumor site and clinical staging in Group A were analogous to those in Group B and that reported previously by Allison *et al* (Table 2). Although the total incidence of postoperative complications were not different due to different method of calculation, the incidences of anastomotic leak, stricture, and GER in our new method therapy group were significantly reduced compared with that of conventional therapy groups (Table 3).

Table 2 Characteristics and pathological condition of patients in different groups

	A New method (n=58)	B Conventional (n=64)	C Reported ^a (n=107)	Statistical analysis	
				χ^2/t	P Value
Sex (male /female)	46/12	43/21	81/26	2.563	0.279
Mean age (range) (years)	57 (34-78)	54(28-76)	62 (30-81)		
Tumor site					
Upper (include cervical)	4 (7%)	3 (4.6%)	2 (2%)	2.731	0.604
Middle	21 (36%)	24 (37.5%)	43 (40%)		
Lower(junctional part)	33 (57%)	37 (57.8%)	62 (58%)		
Pathological type ^b					
Squamous	32 (55%)	34(53%)	28 (26%)	14.399	0.001 ^b
Adenocarcinoma	22 (38%)	28(44%)	72 (67%)	1.155	0.561 ^c
Others	4 (7%)	2(3%)	7 (7%)		
Tumor Diameter (Mean±SD)(cm)	3.1±1.94	3.6 ± 1.58	ND	1.551(t)	0.084
Clinical Staging					
Stage I	18 (31%)	22 (35%)	34 (32%)	7.272	0.122
StageIIA	31 (53%)	29 (45%)	65 (61%)		
StageIIB	9 (16%)	13 (22%)	8 (8%)		

^aBy McLarty AJ, Deschamps C, Trastek VF, *et al.* Ann Thorac Surg, 1997;63:1568-1572. ^bThe pathological type of esophageal carcinoma was different as reported in the west from that in China ($P=0.001$), but it was not the major factor that affected the methods and early outcomes of operation. ^cCompared the pathologic type of cancer treated by the new(Group A) and the conventional (Group B) methods. ND: No data available.

Table 3 Postoperative Outcomes and Complications of Patients in the above Groups

	A New method (n=58)	B Conventional (n=64)	C Reported ^a (n=107)	Statistical analysis	
				χ^2/t	P Value
No complication	33(56.9%)	26(40.6%)	17 (16%)	29.716	0.000
Complications	25 (43%)	38(59.3%)	43 (40%)	2.258	0.353
Anastomotic leak	1 (2%)	4(6%)	13 (12%)	6.566	0.038
Anastomotic stricture					
Dysphagia to food	8 (13%)	24(37.5%)	40 (37%)	10.214	0.006
Postoperative dilation	8 (14%)	23(35.9%)	46(43%)	14.746	0.001
Gastroesophageal reflux					
Reflux Symptoms	13 (22%)	33(52%)	64 (60%)	21.265	0.000
Required antacids	11 (19%)	20(32%)	31 (29%)	2.026	0.363

^aBy McLarty AJ, *et al.* Ann Thorac Surg, 1997;63:1568-1572.

DISCUSSION

There are clear evidences that patients with earlier stage esophageal carcinoma have relatively good outcomes when treated with resection only, especially through thoracic incision which is easy to remove the regional lymph nodes and to carry out the whole operation^[1,2,8]. Multimodality treatment with neoadjuvant chemotherapy or chemoradiotherapy was recommended for esophageal carcinoma by some studies but the results are debatable recently by other studies due to poor outcomes at present^[9-12]. Yet there are still many postoperative complications such as leaks, stricture, and GER, which affect the esophageal function and quality of life, as well as long-term survival of the patients^[3-7].

Anastomotic leak is mainly caused by ischemia of the anastomosis and errors in surgical technique^[7]. Except few recurrence of carcinoma which occurs usually above 6 months after operation, small-bore anastomosis and fibrotic stenosis are the principal causes of anastomotic stricture that results in poor function of swallowing^[3,4,7]. Some studies show that there is a trend toward slightly higher leaking rate for one-layer

anastomosis and a higher stricture rate for two-layer anastomosis^[4,13,14]. As for GER, it is basically caused by loss or alteration of normal anatomical structure, location, and function of esophagus, cardia and stomach^[3,5,6].

The new three-layer-funnel-shaped esophagogastric anastomotic suturing technique, we report here, has more advantages than the classical ones. First, it not only maintains adequate arterial perfusion and venous drainage by reserving enough amount of greater omentum, protecting the right gastroepiploic vessels, and avoiding excessive tension of gastric tube and esophagus, but also maintains accurate mucosa-to-mucosa, muscular-to-muscular apposition and enhances the anastomosis by three-layer sutures, as well as omentum or pleura covering. This significantly avoids the occurrence of anastomotic leak according to our clinical data.

Second, it forms three inclined suture cycles in different diameters at different levels (Figure 1). The fundoplication suture cycle and the esophageal muscular-to-gastric sero-muscular suture cycle are ellipse like and big enough to form a large-bore anastomosis that reduces stricture formation. That

is why the incidence of anastomotic strictures being low and dilated easily and effectively in our study.

Third, with adequate mucosa-to-mucosa suture, the new method reconstructed a soft mucosa petal which forms the third suture cycle, smaller in diameter and easier to open or shrink automatically, and prevents GER effectively. Although postoperative GER still occurred in 22 % which need further study, it was significantly decreased compared to the conventional method^[15]. Twenty-four-hour esophageal pH monitor is a new method to diagnose GER and we plan to carry out a further randomized clinical trial to more scientifically evaluate the anti-GER effects of the mucosa petal created by the new anastomosis^[16].

Like all conventional anastomotic suture techniques, we also emphasize that it is important for the anastomotic healing to prevent infection, malnutrition, influence of chemotherapy and radiotherapy and other related factors in perioperative stage. To prevent the anastomotic tissue injury from strangulation, one should never suture too tightly, or place an excessive number of sutures. In addition, each suture 'bite' of esophageal muscular layer may be transversely sewn so as to overcome the problem because the longitudinally oriented esophageal muscle holds suture poorly.

Some studies recommend that the stapled esophagogastric anastomosis after resection for esophagogastric or cardia cancer is a simple and expeditious procedure, carrying an acceptable perioperative morbidity and cancer recurrence rate^[17-19]. But except the technical problems caused by the staples, the stricture rate of stapled anastomosis was higher^[17-21]. Beitler *et al* systemically reviewed the related randomized controlled trials and pointed out that both stapled and hand-sewn techniques are acceptable but both need further improvement^[22]. GER is recently demonstrated as a main risk factor for esophageal adenocarcinoma and is the main factor that decreases the quality of life of patients after operation^[7,23-30]. The new three-layer-funnel-shaped esophagogastric anastomotic suturing technique is a pilot study, its effect on anti-GER has not been very ideal, and we are making further efforts for improvement, especially that on the prevention of anastomotic leak, stricture and GER.

REFERENCES

- Simchuk EJ**, Alderson D. Oesophageal surgery. *World J Gastroenterol* 2001; **7**: 760-765
- Law S**, Fok M, Chow S, Chu KM, Wong J. Preoperative chemotherapy versus surgical therapy alone for squamous cell carcinoma of the esophagus: a prospective randomized trial. *J Thorac Cardiovasc Surg* 1997; **114**: 210-217
- Whooley BP**, Law S, Alexandrou A, Murthy SC, Wong J. Critical appraisal of the significance of intrathoracic anastomotic leakage after esophagectomy for cancer. *Am J Surg* 2001; **181**: 198-203
- Swisher SG**, Hunt KK, Holmes EC, Zinner MJ, McFadden DW. Changes in the surgical management of esophageal cancer from 1970 to 1993. *Am J Surg* 1995; **169**: 609-614
- Urschel JD**. Esophagogastric anastomotic leaks complicating esophagectomy: a review. *Am J Surg* 1995; **169**: 634-640
- Bruns CJ**, Gawenda M, Wolfgarten B, Walter M. Cervical anastomotic stenosis after gastric tube reconstruction in esophageal carcinoma. Evaluation of a patient sample 1989-1995. *Langenbecks Arch Chir* 1997; **382**: 145-148
- McLarty AJ**, Deschamps C, Trastek VF, Allen MS, Pairolero PC, Harmsen WS. Esophageal resection for cancer of the esophagus: long-term function and quality of life. *Ann Thorac Surg* 1997; **63**: 1568-1572
- Miller JD**, Jain MK, de Gara CJ, Morgan D, Urschel JD. Effect of surgical experience on results of esophagectomy for esophageal carcinoma. *J Surg Oncol* 1997; **65**: 20-21
- Walsh TN**, Noonan N, Hollywood D, Kelly A, Keeling N, Hennessy TP. A comparison of multimodal therapy and surgery for esophageal adenocarcinoma. *N Engl J Med* 1996; **335**: 462-467
- Bosset JF**, Gignoux M, Triboulet JP, Tiret E, Manton G, Elias D, Lozach P, Ollier JC, Pavy JJ, Mercier M, Sahmoud T. Chemoradiotherapy followed by surgery compared with surgery alone in squamous-cell cancer of the esophagus. *N Engl J Med* 1997; **337**: 161-167
- Stein HJ**, Sendler A, Fink U, Siewert JR. Multidisciplinary approach to esophageal and gastric cancer. *Surg Clin North Am* 2000; **80**: 659-682
- Urba SG**, Orringer MB, Turrisi A, Iannettoni M, Forastiere A, Strawderman M. Randomized trial of preoperative chemoradiation versus surgery alone in patients with locoregional esophageal carcinoma. *J Clin Oncol* 2001; **19**: 305-313
- Zieren HU**, Muller JM, Pichlmaier H. Prospective randomized study of one- or two-layer anastomosis following oesophageal resection and cervical oesophagogastric anastomosis. *Br J Surg* 1993; **80**: 608-611
- Wang SJ**, Wen DG, Zhang J, Man X, Liu H. Intensify standardized therapy for esophageal and stomach cancer in tumor hospitals. *World J Gastroenterol* 2001; **7**: 80-82
- Wang Q**, Liu J, Zhao X. Can esophagogastric anastomosis prevent gastroesophageal reflux. *Zhonghua Waike Zazhi* 1999; **37**: 71-73
- Sun M**, Wang WL, Wang W, Wen DL, Zhang H, Han YK. Gastroesophageal manometry and 24-hour dual pH monitoring in neonates with birth asphyxia. *World J Gastroenterol* 2001; **7**: 695-697
- Bisgaard T**, Wojdemann M, Larsen H, Heindorff H, Gustafsen J, Svendsen LB. Double-stapled esophagogastric anastomosis for resection of esophagogastric or cardia cancer: new application for an old technique. *J Laparoendosc Adv Surg Tech A* 1999; **9**: 335-339
- Singh D**, Maley RH, Santucci T, Macherey RS, Bartley S, Weyant RJ, Landreneau RJ. Experience and technique of stapled mechanical cervical esophagogastric anastomosis. *Ann Thorac Surg* 2001; **71**: 419-424
- Stone CD**, Heitmiller RF. As originally published in 1994: Simplified, standardized technique for cervical esophagogastric anastomosis. Updated in 2000. *Ann Thorac Surg* 2000; **70**: 999-1000
- Valverde A**, Hay JM, Fingerhut A, Elhadad A. Manual versus mechanical esophagogastric anastomosis after resection for carcinoma: a controlled trial. French Associations for Surgical Research. *Surgery* 1996; **120**: 476-483
- Berrisford RG**, Page RD, Donnelly RJ. Stapler design and strictures at the esophagogastric anastomosis. *J Thorac Cardiovasc Surg* 1996; **111**: 142-146
- Beitler AL**, Urschel JD. Comparison of stapled and hand-sewn esophagogastric anastomoses. *Am J Surg* 1998; **175**: 337-340
- Shaheen N**, Ransohoff DF. Gastroesophageal reflux, Barrett esophagus, and esophageal cancer: clinical applications. *JAMA* 2002; **287**: 1982-1986
- Lagergren J**, Bergstrom R, Lindgren A, Nyren O. Symptomatic gastroesophageal reflux as a risk factor for esophageal adenocarcinoma. *N Engl J Med* 1999; **340**: 825-831
- Johanson JF**. Critical review of the epidemiology of gastroesophageal reflux disease with specific comparisons to asthma and breast cancer. *Am J Gastroenterol* 2001; **96**: S19-21
- El-Serag HB**, Hepworth EJ, Lee P, Sonnenberg A. Gastroesophageal reflux disease is a risk factor for laryngeal and pharyngeal cancer. *Am J Gastroenterol* 2001; **96**: 2013-2018
- Ferguson MK**, Durkin A. Long-term survival after esophagectomy for Barrett's adenocarcinoma in endoscopically surveyed and nonsurveyed patients. *J Gastrointest Surg* 2002; **6**: 29-35
- Ye W**, Chow WH, Lagergren J, Yin L, Nyren O. Risk of adenocarcinomas of the esophagus and gastric cardia in patients with gastroesophageal reflux diseases and after antireflux surgery. *Gastroenterology* 2001; **121**: 1286-1293
- Incarbone R**, Bonavina L, Saino G, Bona D, Peracchia A. Outcome of esophageal adenocarcinoma detected during endoscopic biopsy surveillance for Barrett's esophagus. *Surg Endosc* 2002; **16**: 263-266
- Shaheen N**, Ransohoff DF. Gastroesophageal reflux, barrett esophagus, and esophageal cancer: scientific review. *JAMA* 2002; **287**: 1972-1981

Silencing-specific methylation and single nucleotide polymorphism of *hMLH1* promoter in gastric carcinomas

Da-Jun Deng, Jin Zhou, Bu-Dong Zhu, Jia-Fu Ji, Jeffrey C. Harper, Steven M. Powell

Da-Jun Deng, Jin Zhou, Bu-Dong Zhu, Jia-Fu Ji, Peking University Health Science Center and Beijing Institute for Cancer Research, Beijing, 100034, China

Jeffrey C. Harper, Steven M. Powell, University of Virginia Health Science Center, Charlottesville, VA 22908-0708, USA

Supported by grant (2000-A-29) from Peking University Center for Human Disease Genomics, grant (0106) from Peking University Cancer Research Center, grant (3171045) from National Natural Science Foundation of China, and by NIH Grant CA67900

Correspondence to: Professor Da-Jun Deng, Department of Cancer Etiology, Peking University School of Oncology and BICR, Da-Hong-Luo-Chang Street, Western District, Beijing, 100034, China. dengdajun@sina.com

Telephone: +86-10-66162978 **Fax:** +86-10-66175832

Received: 2002-09-13 **Accepted:** 2002-10-18

Abstract

AIM: To investigate CpG methylation and single nucleotide polymorphism (SNP) of a specific promoter region of *hMLH1* in primary gastric carcinoma.

METHODS: Primary gastric carcinomas ($n=80$), their corresponding normal mucosal samples, and gastric mucosal biopsies from normal/gastritis control patients ($n=54$) were used. Hypermethylation at -253 nt and -251 nt in relation with the translational start site and SNP of a silencing specific region (-339 nt-46 nt) in the *hMLH1* promoter were analyzed by *Bst* UI-combined bisulfite assay (COBRA), denaturing high performance liquid chromatogram (DHPLC), and sequencing.

RESULTS: (A) The specific methylation at -253 nt and -251 nt was observed in 2 of 60 primary gastric carcinomas, but neither in all of the corresponding mucosa nor in normal/gastritis samples, by *Bst* UI-COBRA and DHPLC. (B) The *hMLH1* promoter was methylated homogeneously in the xenograft of the primary gastric carcinoma with the methylated and unmethylated *hMLH1*. (C) The pattern of SNP at -93 nt of the *hMLH1* promoter in 54 Chinese patients with gastric carcinoma was the same as that in the control patients: 51 % was A/G heteroalleles, 34 % and 15 % were A/A and G/G homoalleles, respectively.

CONCLUSION: Biallelic inactivation of *hMLH1* by epigenetic silencing existed in human primary gastric carcinoma homogeneously. Hypermethylation of *hMLH1* may play a role in the early stage of development of a few gastric carcinomas. The SNP at -93 nt is not related to the susceptibility of gastric carcinomas.

Deng DJ, Zhou J, Zhu BD, Ji JF, Harper JC, Powell SM. Silencing-specific methylation and single nucleotide polymorphism of *hMLH1* promoter in gastric carcinomas. *World J Gastroenterol* 2003; 9(1): 26-29

<http://www.wjgnet.com/1007-9327/9/26.htm>

INTRODUCTION

Hypermethylation of CpG islands in upstream is an epigenetic

mechanism of lost of functions of tumor suppressor genes, DNA repair genes, *etc*^[1-3]. The methylated *hMLH1* was observed in most of primary gastric carcinomas with the microsatellite instability-H phenotype (MSI-H)^[4-12]. Silencing of *hMLH1* by CpG methylation may play an important role in the development of MSI-H tumors. However, the *hMLH1*-methylated proportions in MSI-L and MSI-stable sporadic gastric carcinoma varied greatly (0-75 %) in previous reports. Nakajima *et al.* reported that *hMLH1* methylation was detected in 8 of 100 primary gastric carcinoma cases, but not detected in their corresponding normal mucosa or in intestine metaplastic mucosa^[13]. Kang *et al.* reported a much higher rate of *hMLH1* methylation in gastric carcinoma (20.3 %), adenoma (9.8 %), and intestine metaplastic mucosa (6.3 %)^[14]. Different results might result from applications of both different markers used to classify MSI tumors, and different approaches or primers used to detect methylation of CpG island of *hMLH1*. It was reported recently that the methylation of CpGs in a small C-region (-270 nt ~ -199 nt) of the *hMLH1* promoter was invariably correlated with the absence of gene expression^[15-17]. Thus, it is of interest to further explore the silencing specific methylation of the *hMLH1* promoter in primary gastric carcinomas. In the present study, we analyzed the silencing specific *hMLH1* methylation at -253 nt and -251 nt in the C-region in primary gastric carcinoma and normal/gastritis control.

Deng *et al.* established a novel approach to detect CpG methylation by denaturing high performance liquid chromatography (DHPLC)^[18,19], which was further developed to quantify CpG methylation and SNP of CpG islands simultaneously^[20,21]. It was reported that there is a SNP at -93 nt of the *hMLH1* promoter^[22]. In order to evaluate the possible role of the SNP in the gastric carcinogenesis, the pattern of the SNP in patients with gastric carcinoma was also compared with that in control patients without malignant diseases using DHPLC.

MATERIALS AND METHODS

Gastric samples

60 primary gastric carcinomas and their corresponding normal gastric mucosa were collected: 34 from the Beijing Institute for Cancer Research (BICR) surgically (28 males and 6 females, 29-59 years old, average age: 47.7 years old), and 26 from the University of Virginia Health System (Uva) (18 males and 8 females, 41-84 years old, the average age: 63.8 years old). Three Uva xenografted human GC were obtained from nude mice as described^[23]. In addition, 56 biopsy samples of gastric epithelial tissues were collected from normal/gastritis patients at BICR (50 males and 4 female, 18-47 years old, the average age: 29.7 years old). All samples were used in the analysis of both methylation and SNP. Additional 18 corresponding normal gastric mucosal samples from BICR (Chinese patients, 13 males and 5 females, 26-78 years old, average age: 48.7 years old) with gastric carcinoma were used in SNP analysis in order to have the same number of cases as control. All clinical samples and histopathological information for each case were obtained according to approved institutional guidelines.

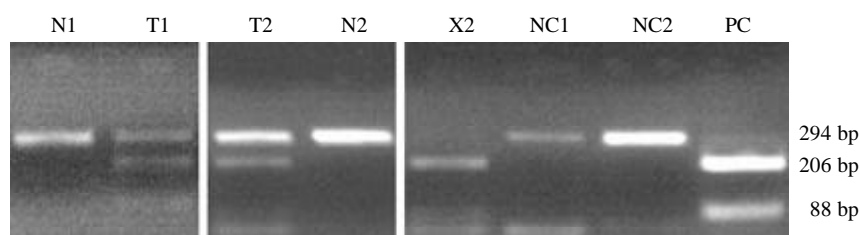


Figure 1 Detection of *hMLH1* methylation by *Bst*UI-COBRA assay. PCR products and methylated ssPCR products (294 bp) were digested into two small fragments (206 bp and 88 bp). Unmethylated ssPCR products were not digested by *Bst*UI. T1, T2: primary gastric carcinomas; N1, N2: corresponding normal gastric mucosal samples; X2: xenograft of primary gastric carcinomas (T2) with *hMLH1* methylation; NC1, NC2: negative control xenografts of primary gastric carcinomas without *hMLH1* methylation; PC: PCR products of the *hMLH1* templates not treated by bisulfite

DNA extraction and bisulfite modification

Genomic DNA of tissue samples was isolated with QIAGEN DNA Purification Kits. Two mg genomic DNA was treated with sodium bisulfite in order to convert the unmethylated C to U (T in PCR products) as described^[24].

Design of Primers and PCR Conditions

Primers were designed according to the specific region (-339 nt ~ -46 nt in relation to the translational start site) of CpG islands of the sense strand of *hMLH1* (GenBank accession number U83845, gi: 2511457) as described^[18, 20]. The strand-specific primers for the modified CpG islands included *hMLH1*-mF (5' -gtatgtttttttttattgttgata-3') and *hMLH1*-mR (5' -aatacctcaaccaatcacctcaata-3'). Primers for the templates without bisulfite-treatment included *hMLH1*-wF (5' -gcatctctgctcctattggctggata-3') and *hMLH1*-wR (5' -agtgccttcagccaatcacctcagt-3'). Hot-started touchdown PCR (-1.0 °C per cycle, total 35 cycles) was used to amplify *hMLH1* without bisulfite-treatment (72 °C → 58 °C), and the sense strand templates with bisulfite-treatment (ssPCR, 65 °C → 50 °C for *hMLH1*)^[18, 20].

Detection of CpG methylation by combined bisulfite restriction analysis (COBRA) and DHPLC

The specific region of the methylated CpG island contain a *Bst*UI restriction site (CGCG) that is converted to UGUG in the unmethylated CpG island after bisulfite modification. Hence the methylation of the bisulfite-modified *hMLH1* could be analyzed directly by *Bst*UI-COBRA. In the confirmation study, methylation status was detected further by DHPLC. Basic mechanism to detect methylation by DHPLC is that the retention time of the methylated PCR products is longer than that of the unmethylated ones, because of higher denaturing temperature of the methylated sequence resulted from higher G+C content after bisulfite modification^[20].

Analysis for SNP by DHPLC and sequencing

The SNP at -93 nt in the corresponding normal mucosal samples and the gastric biopsies from the control patients was detected by DHPLC and confirmed by sequencing as described^[20]. Because all control normal/gastritis samples were collected from Chinese patients, therefore only corresponding normal samples from Chinese cases with gastric carcinomas hospitalized in BICR were used in the SNP analysis.

RESULTS AND DISCUSSION

Silencing-specific methylation of *hMLH1* promoter

One *Bst*UI restriction site (CGCG) exists in the silencing-specific C-region of the CpG island that was invariably correlated with the absence of gene expression^[15]. This site remains only in the methylated templates but not in the

unmethylated ones after bisulfite modification. Therefore, *Bst*UI-COBRA was used to detect the methylation of the specific region^[18]. If the template is methylated, its ssPCR product (294 bp) is digested into a 206 bp and an 88 bp fragments. If not methylated, not digested. The specific CpG methylation of the *hMLH1* promoter was observed in only 3.3 % (2 of 60) of primary gastric carcinoma cases by this assay (Figure 1-T1, T2). T1 sample was distal adenocarcinoma (mod-poor differentiation) from BICR, and T2 was gastro-esoph junction adenocarcinoma (poor differentiation) from UVa. Such methylation was neither observed in all 60 corresponding normal gastric mucosa (Figure 1-N1, N2) nor in 54 normal/gastritis samples from the BICR control patients. The unmethylated *hMLH1* was detectable in all tested human samples (Figure 1-T1, T2, N1, N2). The same result was observed by DHPLC analysis (Figure 2-A, B).

The positive rate (3.3 %) of the specific CpG hypermethylation of *hMLH1* in the present study was lower than those reported by others. Nakajima *et al.* reported that *hMLH1* methylation was observed in 8 of 100 primary gastric carcinomas (8 %) by *Rsa*I-COBRA (restriction site GTAC)^[13]. Although the specific C-region was also included in the ssPCR products in Nakajima's work, the *Rsa*I restriction site GTAC is at -76 nt in the D-region where the correlation between CpG methylation and gene expression is not as well as the C-region^[15]. Kang *et al.* reported that *hMLH1* methylation was detected in 20.3 % of gastric carcinoma cases^[14]. The possible reason for the higher positive rate might result from detection of CpG methylation in A-region of the *hMLH1* promoter that are methylated partially even in cells expressing *hMLH1*^[15]. Another reason was that they used a very sensitive assay, methylation-specific PCR (MSP)^[24], which would result in a positive result even if 0.1 % of testing cells were methylated. Detection of methylation by *Bst*UI-COBRA used in the present study reflects the exact status of the *hMLH1* methylation in the testing samples. Therefore, the low methylation rate in the present study most likely represents the true state of these gastric cancers.

Only the methylated *hMLH1* was detectable in the xenograft of primary gastric carcinoma

It was reported that bialleles of *hMLH1* were inactivated by CpG methylation in cell lines^[25]. Unlike in cell lines, both the methylated and unmethylated *hMLH1* were observed in primary gastric carcinomas (Figure 1-T1, T2). In order to confirm that *hMLH1* is methylated homogeneously in malignant cells, we detected the status of *hMLH1* methylation in UVa xenografts originated from *hMLH1*-methylated and -unmethylated primary gastric carcinomas by *Bst*UI-COBRA. No *hMLH1* methylation was detected in two xenografts from two *hMLH1*-unmethylated primary gastric carcinoma (Figure 1-NC1, NC2). Only methylated *hMLH1* was observed in the X2 xenograft from primary gastric carcinoma T2, in which both the methylated and unmethylated *hMLH1* were observed

(Figure 1-X2, T2). This result was also confirmed by results of DHPLC (Figure 2-B). These results suggested that bialleles of *hMLH1* was methylated homogeneously in all of the malignant cells. The unmethylated *hMLH1* in T2 should come from normal cells such as fibrocytes, fibroblasts, and lymphocytes comprising the primary carcinoma. To best of our knowledge, this is the first report to describe the distribution of methylation status of CpG islands in primary carcinoma.

Thus, all of the malignant cells in the primary gastric cancer T2 appear originate from a single initiated cell with biallelic aberrant methylation of the *hMLH1* promoter. It is useful to study whether certain extent of methylation in the specific C-region of *hMLH1* CpG island is detectable in precancerous gastric lesions by sensitive assays such as MSP^[24] and Methylight^[26]. Taken together, the *hMLH1* methylation may play an important role in the initiation stage of a few gastric carcinomas. In addition to inactivation of *hMLH1* by germline defects^[27-32], silencing of *hMLH1* by CpG methylation is an alternative way to inactivate *hMLH1*.

Table 1 Pattern of the SNP at -93 nt of the *hMLH1* promoter in patients with and without gastric carcinoma

Patients	n	G/G	A/G	A/A
Without gastric carcinoma	56	9(16.1%)	29(51.8%)	18(32.1%)
With gastric carcinoma	54	8(14.9%)	27(50.0%)	19(35.2%)
Total	110	17(15.5%)	56(50.9%)	37(33.6%)

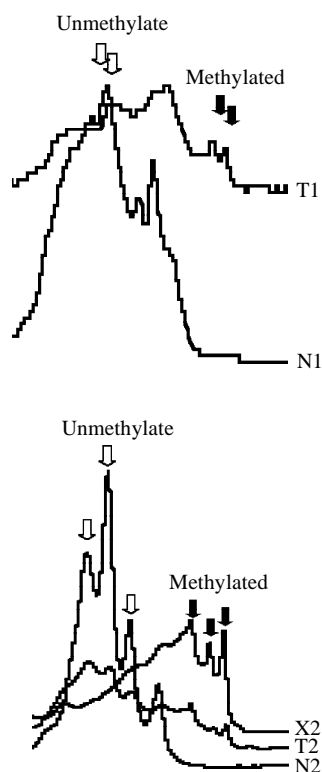


Figure 2 DHPLC Chromatograms of the specific methylation of the *hMLH1* promoter ssPCR products were analyzed at partial denaturing temperature 54 °C, point mutation mode. T1 and T2, primary gastric carcinomas; N1 and N2, the corresponding normal gastric mucosal samples; X2, the xenograft of T2 in nude mouse

SNP at -93 of the *hMLH1* promoter is not correlated with gastric carcinoma

There is a SNP at -93 of the *hMLH1* promoter^[22], which is located within the D-region tested in the present study. In order

to evaluate the correlation of the SNP with risk of gastric cancer, we compared the pattern of the SNP in 54 Chinese patients with gastric carcinoma with that in 56 Chinese control patients through DHPLC and sequencing. Similar percentages of homoalleles (G/G and A/A) and heteroalleles (A/G) were observed in samples from both groups (Table 1). The result suggested that this SNP was not correlated with the risk of gastric carcinoma. Similar result was observed in hereditary nonpolyposis colorectal cancer (HNPCC) and non-HNPCC populations^[22].

REFERENCES

- Bird A. DNA methylation de Novo. *Science* 1999; **286**: 2287-2288.
- Jones PA, Laird PW. Cancer epigenetics comes of age. *Nature Genet* 1999; **21**: 163-167
- Yakoob J, Fan XG, Hu GL, Zhang Z. DNA methylation and carcinogenesis in digestive neoplasms. *World J Gastroenterol* 1998; **4**: 174-177
- Leung SY, Yuen ST, Chung LP, Chu KM, Chan AS, Ho JC. *hMLH1* promoter methylation and lack of *hMLH1* expression in sporadic gastric carcinomas with high-frequency microsatellite instability. *Cancer Res* 1999; **59**: 159-164
- Fleisher AS, Esteller M, Wang S, Tamura G, Suzuki H, Yin J, Zou TT, Abraham JM, Kong D, Smolinski KN, Shi YQ, Rhyu MG, Powell SM, James SP, Wilson KT, Herman JG, Meltzer SJ. Hypermethylation of the *hMLH1* gene promoter in human gastric cancers with microsatellite instability. *Cancer Res* 1999; **59**: 1090-1095
- Kang GH, Shim YH, Ro JY. Correlation of methylation of the *hMLH1* promoter with lack of expression of *hMLH1* in sporadic gastric carcinomas with replication error. *Lab Invest* 1999; **79**: 903-909
- Bevilacqua RA, Simpson AJ. Methylation of the *hMLH1* promoter but no *hMLH1* mutations in sporadic gastric carcinomas with high-level microsatellite instability. *Int J Cancer* 2000; **87**: 200-203
- Pinto M, Oliveira C, Machado JC, Cirnes L, Tavares J, Carneiro F, Hamelin R, Hofstra R, Seruca R, Sobrinho-Simoes M. MSI-L gastric carcinomas share the *hMLH1* methylation status of MSI-H carcinomas but not their clinicopathological profile. *Lab Invest* 2000; **80**: 1915-1923
- Jung HY, Jung KC, Shim YH, Ro JY, Kang GH. Methylation of the *hMLH1* promoter in multiple gastric carcinomas with microsatellite instability. *Pathol Int* 2001; **51**:445-451
- Sakata K, Tamura G, Endoh Y, Ohmura K, Ogata S, Motoyama T. Hypermethylation of the *hMLH1* gene promoter in solitary and multiple gastric cancers with microsatellite instability. *Br J Cancer* 2002; **86**: 564-567
- Oue N, Sentani K, Yokozaki H, Kitadai Y, Ito R, Yasui W. Promoter methylation status of the DNA repair genes *hMLH1* and *MGMT* in gastric carcinoma and metaplastic mucosa. *Pathobiology* 2001; **69**: 143-149
- Baek MJ, Kang H, Kim SE, Park JH, Lee JS, Paik YK, Kim H. Expression of *hMLH1* is inactivated in the gastric adenomas with enhanced microsatellite instability. *Br J Cancer* 2001; **85**:1147-1152
- Nakajima T, Akiyama Y, Shiraishi J, Arai T, Yanagisawa Y, Ara M, Fukuda Y, Sawabe M, Saitoh K, Kamiyama R, Hirokawa K, Yuasa Y. Age-related hypermethylation of the *hMLH1* promoter in gastric cancers. *Int J Cancer* 2001; **94**: 208-211
- Kang GH, Shim YH, Jung HY, Kim WH, Ro JY, Rhyu MG. CpG island methylation in premalignant stages of gastric carcinoma. *Cancer Res* 2001; **61**:2847-2851
- Deng G, Chen A, Hong J, Chae HS, Kim YS. Methylation of CpG in a small region of the *hMLH1* promoter invariably correlates with the absence of gene expression. *Cancer Res* 1999; **59**: 2029-2033
- Deng G, Peng E, Gum J, Terdiman J, Sleisenger M, Kim YS. Methylation of *hMLH1* promoter correlates with the gene silencing with a region-specific manner in colorectal cancer. *Br J Cancer* 2002; **86**: 574-579
- Kang YH, Bae SI, Kim WH. Comprehensive analysis of promoter methylation and altered expression of *hMLH1* in gastric cancer cell lines with microsatellite instability. *J Cancer Res Clin Oncol* 2002; **128**: 119-124

- 18 **Deng DJ**, Deng GR, Zhou J, Xin HJ. Detection of CpG methylations in human mismatch repair gene *hMLH1* promoter by denaturing high-performance liquid chromatography (DHPLC). *Chin J Cancer Res* 2000; **12**: 171-191
- 19 **Deng D**, Deng G, Lu Y. Analysis of the methylation in CpG island by denaturing high-performance liquid chromatography. *Zhonghua Yixue Zazhi* 2001; **81**: 158-161
- 20 **Deng D**, Deng G, Smith MF, Zhou J, Xin H, Powell SM, Lu Y. Simultaneous detection of CpG methylation and single nucleotide polymorphism by denaturing high performance liquid chromatography. *Nucleic Acids Res* 2002; **30**: e13
- 21 **Deng D**, El-Rifai W, Jil J, Zhu B, Tramont P, Li J, Smith MF, Powell SM. Hypermethylation of Metallothionein-3 CpG island in gastric carcinoma. *Carcinogenesis* 2003; **24**: in press
- 22 **Ito E**, Yanagisawa Y, Iwahashi Y, Suzuki Y, Nagasaki H, Akiyama Y, Sugano S, Yuasa Y, Maruyama K. A core promoter and a frequent single-nucleotide polymorphism of the mismatch repair gene hMLH1. *Biochem Biophys Res Commun* 1999; **256**: 488-494
- 23 **El-Rifai W**, Frierson HF, Harper JC, Powell SM, Knuutila S. Expression profiling of gastric adenocarcinoma using cDNA array. *Int J Cancer* 2001; **92**: 832-838
- 24 **Herman JG**, Graff JR, Myöhänen S, Nelkin BD, Baylin SB. Methylation-specific PCR: A novel PCR assay for methylation status of CpG islands. *Proc Natl Acad Sci USA* 1996; **93**: 9821-9826
- 25 **Veigl ML**, Kasturi L, Olechnowicz J, Ma AH, Lutterbaugh JD, Periyasamy S, Li GM, Drummond J, Modrich PL, Sedwick WD, Markowitz SD. Biallelic inactivation of hMLH1 by epigenetic gene silencing, a novel mechanism causing human MSI cancers. *Proc Natl Acad Sci USA* 1998; **95**: 8698-8702
- 26 **Eads CA**, Danenberg KD, Kawakami K, Saltz LB, Blake C, Shibata D, Danenberg PV, Laird PW. MethyLight: a high-throughput assay to measure DNA methylation. *Nucleic Acids Res* 2000; **28**: e32
- 27 **Leach FS**, Nicolaides NC, Papadopoulos N, Liu B, Jen J, Parsons R, Peltomaki P, Sistonen P, Aaltonen LA, Nystrom-Lahti M. Mutations of a mutS homolog in hereditary nonpolyposis colorectal cancer. *Cell* 1993; **75**: 1215-1225
- 28 **Kinzler KW**, Vogelstein B. Lessons from hereditary colorectal cancer. *Cell* 1996; **87**: 159-170
- 29 **Eshleman JR**, Markowitz SD. Microsatellite instability in inherited and sporadic neoplasms. *Curr Opin Oncol* 1995; **7**: 83-89
- 30 **Marra G**, Boland CR. Hereditary nonpolyposis colorectal cancer: the syndrome, the genes, and historical perspectives. *J Natl Cancer Inst* 1995; **87**: 1114-1125
- 31 **Zhao B**, Wang ZJ, Xu YF, Wan YL, Li P, Huang YT. Report of 16 kindreds and one kindred with hMLH1 germline mutation. *World J Gastroenterol* 2002; **8**: 263-266
- 32 **Cai Q**, Sun MH, Lu HF, Zhang TM, Mo SJ, Xu Y, Cai SJ, Zhu XZ, Shi DR. Clinicopathological and molecular genetic analysis of 4 typical Chinese HNPCC families. *World J Gastroenterol* 2001; **7**: 805-810

Edited by Xu XQ

A novel gene, GCRG224, is differentially expressed in human gastric mucosa

Gang-Shi Wang, Meng-Wei Wang, Ben-Yan Wu, Wei-Di You, Xin-Yan Yang

Gang-Shi Wang, Meng-Wei Wang, Ben-Yan Wu, Wei-Di You, Xin-Yan Yang, Department of Gastroenterology, General Hospital of Chinese PLA, Beijing 100853, China

Supported by Key project grant in medical sciences from the tenth five-year plan of Chinese PLA; Contract Grant number: 01Z035

Correspondence to: Gang-Shi Wang, MD., Ph.D., Department of Gerontal Gastroenterology, General Hospital of Chinese PLA, Beijing 100853, China. wanggangshi@hotmail.com

Telephone: +86-10-66937393

Received: 2002-03-25 **Accepted:** 2002-04-20

Abstract

AIM: To clone genes that may predispose us to human gastric cancer and to analyze its expression in gastric tissues.

METHODS: Specimens of paired tumor, paratumor and normal gastric mucosa tissues collected from fifteen patients who suffered from stomach antrum adenocarcinoma were used for analysis. Seven out of the fifteen cases were first studied by fluorescent differential display reverse transcription polymerase chain reaction (DDTR-PCR) analysis. The differentially expressed bands of interest were cloned, analyzed by Northern blot, sequencing and RT-PCR. Through BLAST, the sequencing results were compared with GenBank database for homology analysis. *In situ* hybridization with DIG-labeled cRNA probes was used to analyze the expression of interesting cDNA bands in paraffin embedded paired normal gastric mucosa and cancer tissues isolated from 30 gastric adenocarcinoma patients.

RESULTS: DDRT-PCR showed that one of the interesting cDNA bands, which was named W2, expressed much higher in all seven tested tumor and paratumor samples than in their normal counterparts, it was sub-cloned into a pGEM-T Easy vector. Two subclones were subsequently obtained. One of the subclone, GCRG224, was studied further. The sequencing result showed that GCRG224 consisted of 1 159 base pairs and had one open reading frame (ORF). It located at human chromosome 11q14. No homologue was found in GenBank database with GCRG224-ORF. This nucleotide sequence data were submitted to GenBank with accession No. AF438406. RT-PCR showed that GCRG224 expressed higher in 11/15 gastric cancer tissues than in non-tumor tissues. However, the result of Northern blot analysis showed a higher GCRG224 expression in the non-tumor tissue than in the tumor one. Human multiple tissue Northern blot analysis revealed that GCRG224 also expressed in human normal colon tissue, and peripheral blood leukocyte. *In situ* hybridization analysis showed that only 5/30 adenocarcinoma, 3/18 dysplasia and 6/18 intestinal metaplasia showed higher GCRG224 expression level than the normal gastric glands. However, GCRG224 was over-expressed predominantly in 26/30 cases of normal mucosal epithelium.

CONCLUSION: A novel gene named GCRG224 was identified from human gastric mucosal tissue. It

overexpressed in almost all gastric mucosal epithelium but only a small portion of cancer and precancerous lesions. The role of GCRG224 expression in gastric epithelium needs further study.

Wang GS, Wang MW, Wu BY, You WD, Yang XY. A novel gene, GCRG224, is differentially expressed in human gastric mucosa. *World J Gastroenterol* 2003; 9(1): 30-34
<http://www.wjgnet.com/1007-9327/9/30.htm>

INTRODUCTION

Gastric cancer is one of the most commonly diagnosed malignancies and remains an important cause of mortality world wide^[1]. Considerable evidence supports the pivotal role of genetic factors in the pathogenesis of gastric cancer^[2-7]. However, the mechanism of the process of multistage carcinogenesis is still unknown for gastric cancer. Abundant clinical and histopathological data suggest that most, if not all, intestinal-type gastric cancer arise from precancerous lesions, which indicated intestinal-type gastric cancer to be an excellent model for studying the genetic alterations involved in the development of human neoplasms. It would be desirable, therefore, to screen directly from human intestinal-type gastric cancer and its precursor lesions the differentially expressed genes that are closely related to human gastric cancer.

In this study, differential display reverse transcription polymerase chain reaction (DDRT-PCR) analysis was used to identify and characterize differentially expressed genes in human gastric cancer tissues in comparison with their surrounding paratumor and nontumor counterparts. One novel cDNA with a complete cds was identified. We designated this gene as gastric cancer related gene 224 (GCRG224). Expression of GCRG224 in gastric tissues was analyzed using RT-PCR and *In situ* hybridization (ISH).

MATERIALS AND METHODS

Tissue acquisition

Fresh primary intestinal-type gastric adenocarcinoma, paratumor tissue which is 1.0 cm away from the tumor mass and their surrounding noncancerous stomach mucosal tissues obtained from 15 patients (11 male, 4 female, with average age 54±15 years) undergoing surgery were used for reverse transcription polymerase chain reaction (RT-PCR) analysis. 7 cases (4 male, 3 female, with average age 51±18 years) out of the 15 patients were used for differential display analyses. Paraffin embedded gastric adenocarcinoma and their corresponding normal gastric mucosal tissues obtained from 30 advanced gastric adenocarcinoma patients (21 male, 9 female, with average age 59±10 years) were used for ISH analysis. All tissues were histologically confirmed by pathologists.

RNA preparation and differential display

Total RNA was extracted from tissues using TRIzol reagent (Life Technologies, Inc., Rockville, Maryland). The fluorescent

DDRT-PCR procedure was performed essentially as described previously^[8]. The primers used in the assay included 4 T₁₂MN primers and 20 arbitrary oligonucleotide primers (ARP-1 to ARP-20) (Genomix Corporation, Foster City, CA).

Cloning and sequencing

The cDNA fragment of interest were subcloned into pGEM-T Easy vector (Promega Corporation, Madison, WI) and confirmed by EcoR I (Life Technologies, Bethesda, MD) digestion according to the manufacturer's instruction. Sequence analysis was performed with CEQ™ 2000 DNA sequencer (Beckman Coulter, Fullerton, CA). The sequenced cDNA were analyzed via the BLAST program for homology matches in the GenBank database^[9].

Northern blot analysis

Samples containing 20 µg of total nontumor and tumor RNAs were fractionated on an 1.2 % agarose gel containing 5.5 % formaldehyde and 1×MOPS and transferred to a nylon membrane. Fix the RNA to the membrane by baking at 80 °C for 2 hours. Human multiple tissue Northern (MTN) blot II membrane (Clontech Laboratories, Inc., Palo Alto, CA) was used for analysis. Anti-sense cRNA probe labeled with digoxigenin was generated from a digested cDNA insert using Dig Northern Starter Kit (Roche Diagnostic Corporation, Indianapolis, IN) by means of *in vitro* transcription. The membrane was prehybridized and then hybridized according to the manufacturer's protocol. The results were detected using chemiluminescent detection.

RT-PCR

First-strand cDNAs were synthesized by SuperscriptII Rnase H reverse transcriptase (Life Technologies, Bethesda, MD) using oligo d(T) primers according to the protocol. PCR primers were designed using Primer Premier software (Premier biosoft international, Palo Alto, CA). The PCR primers used were: forward primer: 5' AAGGGTCACCTCTGTTCAAAGTG3', reverse primer: 5' GCAGGGTTTATGGGCTCAATAG3', Product length: 929 bp. G3PDH was used as internal control. Reactions were carried out in 10 µl solutions containing 100 ng cDNA, 0.2 µM of each primer, 50 µM of each dNTP, and 0.5 U of AmpliTaq DNA polymerase (Life Technologies, Bethesda, MD). The amplification conditions were (25 cycles): 1 min at 94 °C, 40 sec at 56 °C, 1 min at 72 °C.

In situ hybridization

Specimens were fixed in 10 % neutral buffered formalin and embedded in paraffin wax. A series of 5 µm sections were cut for analysis. The antisense cRNA probe was prepared according to procedure described in Northern blot analysis section. ISH was performed as described previously^[10,11]. Negative control (no probe applied) was performed. Slides were examined using an Olympus microscope. Images were captured using a cooled CCD camera (JVC, Japan). Cytoplasmic staining was noted.

Any appreciable blue staining was considered positive, and graded as ± if very light blue were barely detectable, 1+ if light blue staining were seen diffusely throughout the cytoplasm, 2+ if easily seen fine staining were present throughout the cytoplasm, and 3+ when dark blue were observed. Generally, more than 100 cells (nontumor or tumor) were quantified in each measurement and at least one measurement was taken per slide. H&E slides were then reviewed to determine diagnosis and to map the location of the various histological patterns and correlate with the staining patterns observed in the ISH preparations.

Informed consents

The study protocol was approved by the Institutional Review Board of the hospital under the guidelines of the 1975 Declaration of Helsinki. Written informed consents were obtained from patients.

RESULTS

Isolation of differentially expressed cDNA by DDRT-PCR in gastric cancer

In order to run the assay efficiently, among 80 combinations of primer pairs (4 T₁₂MN primers vs 20 ARP primers), 4 pairs able to amplify more bands in one set of paired tissues were chosen and used to amplify cDNA from 7 sets of paired tissues. One primer pair (T₁₂GG vs ARP-3: 5' GACCATTGCA3') was found to amplify genes expressed differentially in 7 of 7 sets of the paired tissues. As shown in Figure 1, in comparison with results in the normal tissues, a cDNA fragment (arrowed) was found to be more abundant in the tumor and paratumor samples in all tested patients. The results of mRNA differential display were reproducible. This differentially expressed cDNA band was named as W2.

Sub-clone and sequence analysis

Two subclones, GCRG213 and GCRG224, were identified from the subcloning procedure. GCRG213 consisted of 1 194 base pairs, while GCRG224 consisted of 1 159 base pairs and had one open reading frame (ORF). The GCRG224-ORF consists of 35 amino acids with an estimated molecular weight of 3.8 kDa. BLAST analysis revealed that GCRG224 nucleotide sequence had 98 % homologue with Homo sapiens clone RP11-718B12, but the deduced amino acid sequence of GCRG224-ORF had no homology with any known peptide in the GenBank database. GCRG224 nucleotide sequence data was submitted to GenBank with accession No.AF438406. Further bioinformatic study in the GenBank database showed that GCRG224 is located at human chromosome 11q14.

RT-PCR and northern blot analysis

To confirm the expression pattern of GCRG224 in human gastric cancer, we performed RT-PCR analyses in 15 cases of paired gastric adenocarcinoma, paratumor and non-tumor

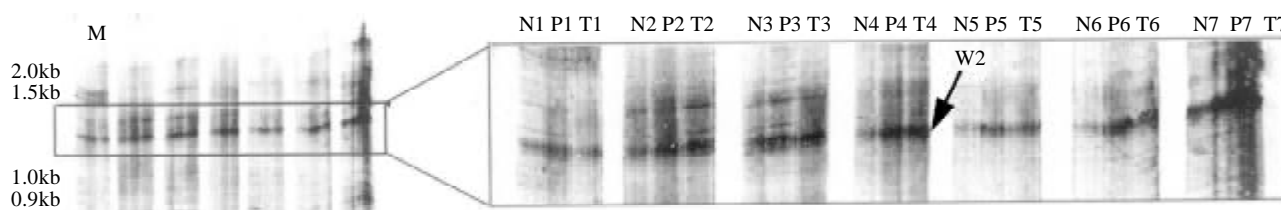


Figure 1 Differential analysis of expressed genes among human gastric cancer, paratumor and normal stomach mucosal tissues by means of fluorescent differential display. The differentially expressed cDNA fragment W2 (arrowed) showed higher expression in tumor and paratumor tissues than that in normal ones. N: normal; P: paratumor; T: tumor; 1-7: patient number.

tissues. GCRG224 expressed higher in 11/15 gastric cancer tissues than non-tumor tissues. However, the result of Northern blot analysis was contrary to that of DDRT-PCR, the non-tumor tissue showed higher GCRG224 expression level than the tumor did (Figure 2a). MTN results showed that GCRG224 also expressed in human normal colon tissues and peripheral blood leukocyte (Figure 2b).

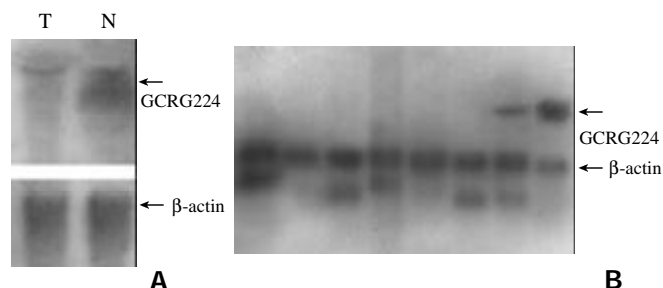


Figure 2 Northern blot analysis of GCRG224 expression in (a) human gastric cancer T/N pairs. T: tumor, N: non-tumor. (b) various adult human tissues. From left to right: spleen, thymus, prostate, testis, ovary, small intestine, colon, peripheral blood leukocyte.

In situ hybridization

GCRG224 expression was analyzed at mRNA level. The hybridization signal that appears as blue is restricted to the cytoplasmic portion. All normal gastric glands showed \pm -1+ staining. Only 5 out of 30 cases of adenocarcinoma had 2+ staining while the rest had \pm staining. Of the 18 cases of intestinal metaplasia (IM) and dysplasia found in the paratumor site, 6/18 IM and 3/18 dysplasia had 2+ staining, respectively. Interestingly, in 26/30 cases the gastric mucosal epithelial cells were stained 2+-3+ (Table 1, Figure 3).

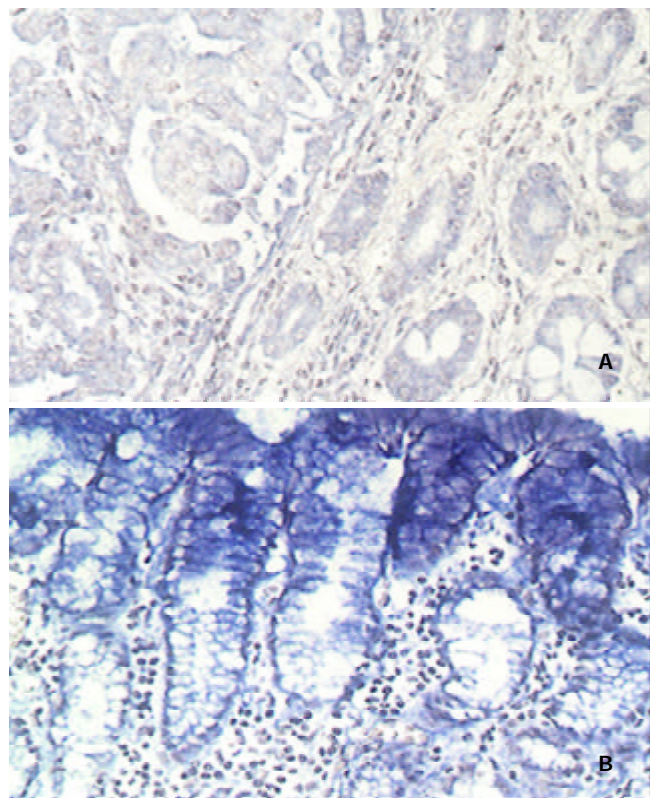


Figure 3 ISH analysis of GCRG224-ORF mRNA in formaldehyde-fixed, paraffin-embedded gastric tissues with a digoxigenin-labeled anti-sense probe, NBT/BCIP was used as

alkaline phosphatase substrates, the expression appeared as cytoplasmic staining (blue precipitates). (a): Mild expression in tumor (left) and intestinal metaplasia glands (right) (200 \times); (b): Strong expression in gastric mucosal epithelium cells, while the adjacent normal gastric glands showed little staining (200 \times).

Table 1 GCRG224 expression in different types of cells in gastric mucosa

	gastric mucosal epithelium	Gastric glands	IM	DYS	adenocarcinoma
\pm	0	19	8	13	25
1+	4	11	4	2	0
2+	15	0	6	3	4
3+	11	0	0	0	1
Total	30	30	18	18	30

DISCUSSION

Advances in molecular biology have revealed a consistent set of genetic alterations that may correspond to multi-step stomach cancer development. Aberrant expression and amplification of oncogenes such as c-met, c-myc, K-ras, c-erbB-2^[12-16], etc., inactivation of tumor suppressor genes such as p53, p16, Rb, DCC, APC, PTEN^[17-24], etc, DNA ploidy and microsatellite instability^[25-28], abnormal transcript of genes related to metastasis like nm23, CD44, E-cadherin^[29,30], etc., are reported common events in the steps of carcinogenesis. Newly found cancer related genes such as COX-2, survivin, metallothionein II and RUNX3, etc. were also expressed abnormally in gastric cancer^[31-38]. Recognition of genetic factors had also improved the the treatment of cancer^[39-41]. However, very little is currently known about genes that may predispose us to gastric cancer. The primary aim of this study was to identify genes that were closely related to human gastric cancer by means of DDRT-PCR.

DDRT-PCR has been widely applied to identify cancer-related genes^[42-47], some of these genes look like to be of clinical value. It might reflect the true patterns of genetic changes in human gastric cancer if we identify gastric cancer-related genes directly from human gastric tissues.

One of the defects when using tissues for DDRT-PCR analysis is that some cDNA fragments amplified in the tumor tissues may actually originate from normal cells present in the tumor tissues, which may affect the results of the analyses. In order to decrease the chance of error in this study, we used 7 sets of tumor, paratumor and non-tumor tissues for the assay, displayed the results simultaneously and chose interesting bands showing distinctive patterns in all sets of specimens. One cDNA fragment which is up-regulated in gastric cancer tissues was identified. However, two subclones were identified from the subsequent subcloning procedure. Sequencing results revealed that these two subclones contained nucleotides of nearly the same size but of totally different sequences. This should be the result of PCR amplification in which arbitrary primers were used.

Because the deduced amino acid sequence of GCRG224-ORF had no homology with any known peptide in the GenBank database, further study was focused on this gene. The result of RT-PCR analysis was consistent with that of DDRT-PCR, but Northern blot analysis revealed an opposite result. Furthermore, ISH analysis also failed to see a general higher expression of GCRG224 in tumor cells. On the other hand, ISH showed an extensively strong expression of GCRG224 in gastric mucosal epithelial cells in almost all tested cases. This indicated GCRG224 might come mainly from normal gastric epithelium

other than tumor cells. Although the tissues applied for DDRT-PCR, Northern blot and RT-PCR in this study were examined by pathologists before their usage, they were actually a mixture of different types of cells, the exact percentage of tumor and non-tumor cells in each tissue could not be identified, this resulted in the contradiction we faced. It would be better, therefore, to separate different types of cells using techniques such as microdissection in tissues like gastric mucosa prior to the analyses^[48-51].

Correlations between prognoses and the expression of genes such as p53, ras, myc, nm23, etc. were studied extensively in gastric cancer^[15-17,52-57]. However, the results turned out to be controversial. It is meaningful to find a biomarker that might predict the diagnosis or prognosis of gastric cancer. The consistent over-expression of GCRG224 in all tested tumor tissues in the DDRT-PCR and RT-PCR analyses prompted us to study further the expression pattern of GCRG224 in gastric mucosal tissues using ISH. However, GCRG224 did not show the expression pattern in gastric cancer and its precancerous lesions as RT-PCR revealed. Only around 20 percent tumor and precancerous lesions showed GCRG224 over-expression comparing with their normal gastric glands. Thus, GCRG224 may not serve as a potential marker for the diagnosis of gastric cancer.

A significant finding in this study is the extensive staining of GCRG224 in gastric epithelium. Up till now, the function of gastric mucosal cells is believed to be a barrier of the stomach as well as secretion of alkali and other ions such as Na⁺, K⁺ and Cl⁻. It will be of great interest to study the role of GCRG224 expression in gastric mucosal epithelium.

REFERENCES

- 1 **Stadlander CT**, Waterbor JW. Molecular epidemiology, pathogenesis and prevention of gastric cancer. *Carcinogenesis* 1999; **20**: 2195-2208
- 2 **Becker KF**, Keller G, Hoefler H. The use of molecular biology in diagnosis and prognosis of gastric cancer. *Surg Oncol* 2000; **9**: 5-11
- 3 **Boussioutas A**, Taupin D. Towards a molecular approach to gastric cancer management. *Intern Med J* 2001; **31**: 296-303
- 4 **Palli D**. Epidemiology of gastric cancer: an evaluation of available evidence. *J Gastroenterol* 2000; **35**(Suppl 12): 84-89
- 5 **Yasui W**, Oue N, Kuniyasu H, Ito R, Tahara E, Yokozaki H. Molecular diagnosis of gastric cancer: present and future. *Gastric Cancer* 2001; **4**: 113-121
- 6 **Maltoni M**, Volpi A, Nanni O, Bajorko P, Belletti E, Vecchi AM, Liverani M, Danesi S, Calistri D, Ricotti L, Amadori D. Gastric cancer: epidemiologic and biological aspects. *Forum (Genova)* 1998; **8**: 199-207
- 7 **Meltzer SJ**. Tumor genomics vs. tumor genetics: a paradigm shift? *Gastroenterology* 2001; **121**: 726-729
- 8 **Wang GS**, Wang MW, You WD, Wang HF, Feng MF. Fluorescent mRNA differential display technique. *Zhongguo Yingyong Shenglixue Zazhi* 2000; **16**: 373-376
- 9 **Altschul SF**, Madden TL, Schäffer AA, Zhang J, Zhang Z, Miller W, Lipman DJ. Gapped BLAST and PSI-BLAST: a new generation of protein database search programs. *Nucleic Acids Res* 1997; **25**: 3389-3402
- 10 **Komminoth P**, Merk FB, Leav I, Wolfe HJ, Roth J. Comparison of 35S- and digoxigenin-labeled RNA and oligonucleotide probes for *In situ* hybridization. Expression of mRNA of the seminal vesicle secretion protein II and androgen receptor genes in the rat prostate. *Histochemistry* 1992; **98**: 217-228
- 11 **Komminoth P**. Digoxigenin as an alternative probe labeling for *In situ* hybridization. *Diagn Mol Pathol* 1992; **1**: 142-150
- 12 **Kubicka S**, Claas C, Staab S, Kuhnelt F, Zender L, Trautwein C, Wagner S, Rudolph KL, Manns M. p53 mutation pattern and expression of c-erbB2 and c-met in gastric cancer: relation to histological subtypes, *Helicobacter pylori* infection, and prognosis. *Dig Dis Sci* 2002; **47**: 114-121
- 13 **Hiyama T**, Haruma K, Kitadai Y, Masuda H, Miyamoto M, Tanaka S, Yoshihara M, Shimamoto F, Chayama K. K-ras mutation in helicobacter pylori-associated chronic gastritis in patients with and without gastric cancer. *Int J Cancer* 2002; **97**: 562-566
- 14 **Yokozaki H**, Yasui W, Tahara E. Genetic and epigenetic changes in stomach cancer. *Int Rev Cytol* 2001; **204**: 49-95
- 15 **Nakajima M**, Sawada H, Yamada Y, Watanabe A, Tatsumi M, Yamashita J, Matsuda M, Sakaguchi T, Hirao T, Nakano H. The prognostic significance of amplification and overexpression of c-met and c-erbB-2 in human gastric carcinomas. *Cancer* 1999; **85**: 1894-1902
- 16 **Gurel S**, Dolar E, Yerci O, Samli B, Ozturk H, Nak SG, Gulden M, Memik F. The relationship between c-erbB-2 oncogene expression and clinicopathological factors in gastric cancer. *J Int Med Res* 1999; **27**: 74-78
- 17 **Gurel S**, Dolar E, Yerci O, Samli B, Ozturk H, Nak SG, Gulden M, Memik F. Expression of p53 protein and prognosis in gastric carcinoma. *J Int Med Res* 1999; **27**: 85-89
- 18 **Sato K**, Tamura G, Tsuchiya T, Endoh Y, Usuba O, Kimura W, Motoyama T. Frequent loss of expression without sequence mutations of the DCC gene in primary gastric cancer. *Br J Cancer* 2001; **85**: 199-203
- 19 **He XS**, Su Q, Chen ZC, He XT, Long ZF, Ling H, Zhang LR. Expression, deletion and mutation of p16 gene in human gastric cancer. *World J Gastroenterol* 2001; **7**: 515-521
- 20 **Liu DH**, Zhang XY, Fan DM, Huang YX, Zhang JS, Huang WQ, Zhang YQ, Huang QS, Ma WY, Chai YB, Jin M. Expression of vascular endothelial growth factor and its role in oncogenesis of human gastric carcinoma. *World J Gastroenterol* 2001; **7**: 500-505
- 21 **Liu XP**, Tsushimi K, Tsushimi M, Kawauchi S, Oga A, Furuya T, Sasaki K. Expression of p21(WAF1/CIP1) and p53 proteins in gastric carcinoma: its relationships with cell proliferation activity and prognosis. *Cancer Lett* 2001; **170**: 183-189
- 22 **Fei G**, Ebert MP, Mawrin C, Leodolter A, Schmidt N, Dietzmann K, Malfertheiner P. Reduced PTEN expression in gastric cancer and in the gastric mucosa of gastric cancer relatives. *Eur J Gastroenterol Hepatol* 2002; **14**: 297-303
- 23 **Kang YH**, Lee HS, Kim WH. Promoter methylation and silencing of PTEN in gastric carcinoma. *Lab Invest* 2002; **82**: 285-291
- 24 **Ebert MP**, Fei G, Kahmann S, Muller O, Yu J, Sung JJ, Malfertheiner P. Increased beta-catenin mRNA levels and mutational alterations of the APC and beta-catenin gene are present in intestinal-type gastric cancer. *Carcinogenesis* 2002; **23**: 87-91
- 25 **Laghi L**, Ranzani GN, Bianchi P, Mori A, Heinimann K, Orbetegli O, Spauo MR, Luinetti O, Francisconi S, Roncalli M, Solcia E, Malesci A. Frameshift mutations of human gastrin receptor gene (hGARE) in gastrointestinal cancers with microsatellite instability. *Lab Invest* 2002; **82**: 265-271
- 26 **Sakata K**, Tamura G, Endoh Y, Ohmura K, Ogata S, Motoyama T. Hypermethylation of the hMLH1 gene promoter in solitary and multiple gastric cancers with microsatellite instability. *Br J Cancer* 2002; **86**: 564-567
- 27 **Baba H**, Korenaga D, Kakeji Y, Haraguchi M, Okamura T, Maehara Y. DNA ploidy and its clinical implications in gastric cancer. *Surgery* 2002; **131** (Suppl): S63-70
- 28 **Russo A**, Bazan V, Migliavacca M, Tubiolo C, Macaluso M, Zanna I, Corsale S, Latteri F, Valerio MR, Pantuso G, Morello V, Dardanoni G, Latteri MA, Colucci G, Tomasino RM, Gebbia N. DNA aneuploidy and high proliferative activity but not K-ras-2 mutations as independent predictors of clinical outcome in operable gastric carcinoma; results of a 5-year gruppo oncologico dell'italia meridionale prospective study. *Cancer* 2001; **92**: 294-302
- 29 **Nesi G**, Palli D, Pernice LM, Saieva C, Paglierani M, Kroning KC, Catarzi S, Rubio CA, Amorosi A. Expression of nm23 gene in gastric cancer is associated with a poor 5-year survival. *Anticancer Res* 2001; **21**: 3643-3649
- 30 **Cai J**, Ikeguchi M, Tsujitani S, Maeta M, Liu J, Kaibara N. Significant correlation between micrometastasis in the lymph nodes and reduced expression of E-cadherin in early gastric cancer. *Gastric Cancer* 2001; **4**: 66-74
- 31 **van Rees BP**, Saukkonen K, Ristimaki A, Polkowski W, Tytgat GN, Drillenburger P, Offerhaus GJ. Cyclooxygenase-2 expression during carcinogenesis in the human stomach. *J Pathol* 2002; **196**: 171-179
- 32 **Kikuchi T**, Itoh F, Toyota M, Suzuki H, Yamamoto H, Fujita M, Hosokawa M, Imai K. Aberrant methylation and histone deacetylation of cyclooxygenase 2 in gastric cancer. *Int J Cancer* 2002; **97**: 272-277
- 33 **Krieg A**, Mahotka C, Krieg T, Grabsch H, Muller W, Takeno S,

- Suschek CV, Heydthausen M, Gabbert HE, Gerharz CD. Expression of different survivin variants in gastric carcinomas: first clues to a role of survivin-2B in tumour progression. *Br J Cancer* 2002; **86**: 737-743
- 34 **Ebert MP**, Gunther T, Hoffmann J, Yu J, Miehle S, Schulz HU, Roessner A, Korc M, Malfertheiner P. Expression of metallothionein II in intestinal metaplasia, dysplasia, and gastric cancer. *Cancer Res* 2000; **60**: 1995-2001
- 35 **Bai YQ**, Yamamoto H, Akiyama Y, Tanaka H, Takizawa T, Koike M, Kenji Yagi O, Saitoh K, Takeshita K, Iwai T, Yuasa Y. Ectopic expression of homeodomain protein CDX2 in intestinal metaplasia and carcinomas of the stomach. *Cancer Lett* 2002; **176**: 47-55
- 36 **Li QL**, Ito K, Sakakura C, Fukamachi H, Inoue K, Chi XZ, Lee KY, Nomura S, Lee CW, Han SB, Kim HM, Kim WJ, Yamamoto H, Yamashita N, Yano T, Ikeda T, Itohara S, Inazawa J, Abe T, Hagiwara A, Yamagishi H, Ooe A, Kaneda A, Sugimura T, Ushijima T, Bae SC, Ito Y. Causal relationship between the loss of RUNX3 expression and gastric cancer. *Cell* 2002; **109**: 113-124
- 37 **Saitoh T**, Mine T, Katoh M. Up-regulation of WNT8B mRNA in human gastric cancer. *Int J Oncol* 2002; **20**: 343-348
- 38 **Li Z**, Wang Y, Song J, Kataoka H, Yoshii S, Gao C, Wang Y, Zhou J, Ota S, Tanaka M, Sugimura H. Genomic structure of the human beta-PIX gene and its alteration in gastric cancer. *Cancer Lett* 2002; **177**: 203-208
- 39 **Shinohara H**, Morita S, Kawai M, Miyamoto A, Sonoda T, Pastan I, Tanigawa N. Expression of HER2 in human gastric cancer cells directly correlates with antitumor activity of a recombinant disulfide-stabilized anti-HER2 immunotoxin. *J Surg Res* 2002; **102**: 169-177
- 40 **Takehana T**, Kunitomo K, Kono K, Kitahara F, Iizuka H, Matsumoto Y, Fujino MA, Ooi A. Status of c-erbB-2 in gastric adenocarcinoma: a comparative study of immunohistochemistry, fluorescence in situ hybridization and enzyme-linked immunosorbent assay. *Int J Cancer* 2002; **98**: 833-837
- 41 **Kodera Y**, Nakanishi H, Ito S, Yamamura Y, Kanemitsu Y, Shimizu Y, Hirai T, Yasui K, Kato T, Tatematsu M. Quantitative detection of disseminated free cancer cells in peritoneal washes with real-time reverse transcriptase-polymerase chain reaction: a sensitive predictor of outcome for patients with gastric carcinoma. *Ann Surg* 2002; **235**: 499-506
- 42 **You H**, Xiao B, Cui DX, Shi YQ, Fan DM. Two novel gastric cancer-associated genes identified by differential display. *World J Gastroenterol* 1998; **4**: 334-336
- 43 **Tortola S**, Marcuello E, Risques RA, Gonzalez S, Aiza G, Capella G, Peinado MA. Overall deregulation in gene expression as a novel indicator of tumor aggressiveness in colorectal cancer. *Oncogene* 1999; **18**: 4383-4387
- 44 **Yoshikawa Y**, Mukai H, Hino F, Asada K, Kato I. Isolation of two novel genes, down-regulated in gastric cancer. *Jan J Cancer Res* 2000; **91**: 459-463
- 45 **Wang X**, Lan M, Shi YQ, Lu J, Zhong YX, Wu HP, Zai HH, Ding J, Wu KC, Pan BR, Jin JP, Fan DM. Differential display of vincristine-resistance-related genes in gastric cancer SGC7901 cell. *World J Gastroenterol* 2002; **8**: 54-59
- 46 **Shiozaki K**, Nakamori S, Tsujie M, Okami J, Yamamoto H, Nagano H, Dono K, Umeshita K, Sakon M, Furukawa H, Hiratsuka M, Kasugai T, Ishiguro S, Monden M. Human stomach-specific gene, CA11, is down-regulated in gastric cancer. *Int J Onco* 2001; **19**: 701-707
- 47 **Wang G**, Wang M, You W, Li H. Cloning and primary expression analyses of down-regulated cDNA fragment in human gastric cancer. *Zhonghua Yixue Yichuanxue Zazhi* 2001; **18**: 43-47
- 48 **Fend F**, Kremer M, Quintanilla-Martinez L. Laser capture microdissection: methodical aspects and applications with emphasis on immuno-laser capture microdissection. *Pathobiology* 2000; **68**: 209-214
- 49 **Maitra A**, Wistuba I I, Gazdar A F. Microdissection and the study of cancer pathways. *Curr Mol Med* 2001; **1**: 153-162
- 50 **Rekhter MD**, Chen J. Molecular analysis of complex tissues is facilitated by laser capture microdissection: critical role of upstream tissue processing. *Cell Biochem Biophys* 2001; **35**: 103-113
- 51 **Cor A**, Vogt N, Malfroy B. Microdissection techniques for cancer analysis. *Folia Biol (Praha)* 2002; **48**: 3-8
- 52 **Noda H**, Maehara Y, Irie K, Kakeji Y, Yonemura T, Sugimachi K. Increased proliferative activity caused by loss of p21WAF1/CIP1 expression and its clinical significance in patients with early-stage gastric carcinoma. *Cancer* 2002; **94**: 2107-2112
- 53 **Saadat I**, Saadat M. Glutathione S-transferase M1 and T1 null genotypes and the risk of gastric and colorectal cancers. *Cancer Lett* 2001; **169**: 21-26
- 54 **Kuniyasu H**, Oue N, Wakikawa A, Shigeishi H, Matsutani N, Kuraoka K, Ito R, Yokozaki H, Yasui W. Expression of receptors for advanced glycation end-products (RAGE) is closely associated with the invasive and metastatic activity of gastric cancer. *J Pathol* 2002; **196**: 163-170
- 55 **Mori M**, Mimori K, Yoshikawa Y, Shibuta K, Utsunomiya T, Sadanaga N, Tanaka F, Matsuyama A, Inoue H, Sugimachi K. Analysis of the gene-expression profile regarding the progression of human gastric carcinoma. *Surgery* 2002; **131**: S39-47
- 56 **Endo K**, Maejara U, Baba H, Tokunaga E, Koga T, Ikeda Y, Toh Y, Kohnoe S, Okamura T, Nakajima M, Sugimachi K. Heparanase gene expression and metastatic potential in human gastric cancer. *Anticancer Res* 2001; **21**: 3365-3369
- 57 **Wang CS**, Lin KH, Hsu YC. Alterations of thyroid hormone receptor alpha gene: frequency and association with Nm23 protein expression and metastasis in gastric cancer. *Cancer Lett* 2002; **175**: 121-127

PTEN encoding product: a marker for tumorigenesis and progression of gastric carcinoma

Lin Yang, Li-Ge Kuang, Hua-Chuan Zheng, Jin-Yi Li, Dong-Ying Wu, Su-Min Zhang, Yan Xin

Lin Yang, Li-Ge Kuang, Hua-Chuan Zheng, Jin-Yi Li, Dong-Ying Wu, Su-Min Zhang, Yan Xin, No.4 Lab, Cancer Institute, The First Affiliated Hospital, China Medical University, Shenyang 110001, China

Ying Chen, Shen Yang, Gynecology & Obstetrics Hospital, Shenyang 110014, China

Supported by the National Natural Science Foundation of China No.30070845, "Outstanding Research Training Program", Ministry of Education No. [1999] 2, and Science Foundation of Liaoning Education Bureau No. 20121031

Correspondence to: Prof. Xin Yan, No.4 Lab, Cancer Institute, The First Affiliated Hospital, China Medical University, Shenyang 110001, China. yxin@mail.cmu.edu.cn

Telephone: +86-24-23256666 Ext. 6351

Received: 2002-04-13 **Accepted:** 2002-06-01

Abstract

AIM: To detect the expression of PTEN encoding product in normal mucosa, intestinal metaplasia (IM), dysplasia and carcinoma of the stomach, and to investigate its clinical implication in tumorigenesis and progression of gastric carcinoma.

METHODS: Formalin-fixed paraffin embedded specimens from 184 cases of gastric carcinoma, their adjacent normal mucosa, IM and dysplasia were evaluated for PTEN protein expression by SABC immunohistochemistry. PTEN expression was compared with tumor stage, lymph node metastasis, Lauren's and WHO's histological classification of gastric carcinoma. Expression of VEGF was also detected in 60 cases of gastric carcinoma and its correlation with PTEN was concerned.

RESULTS: The positive rates of PTEN protein were 100 % (102/102), 98.5 % (65/66), 66.7 % (4/6) and 47.8 % (88/184) in normal mucosa, IM, dysplasia and carcinoma of the stomach, respectively. The positive rates in dysplasia and carcinoma were lower than in normal mucosa and IM ($P < 0.01$). Advanced gastric cancers expressed less frequent PTEN than early gastric cancer (42.9 % vs 67.6 %, $P < 0.01$). The positive rate of PTEN protein was lower in gastric cancer with than without lymph node metastasis (40.3 % vs 63.3 %, $P < 0.01$). PTEN was less expressed in diffuse-type than in intestinal-type gastric cancer (41.5 % vs 57.8 %, $P < 0.05$). Signet ring cell carcinoma showed the expression of PTEN at the lowest level (25.0 %, 7/28); less than well and moderately differentiated ones ($P < 0.01$). Expression of PTEN was not correlated with expression of VEGF ($P > 0.05$).

CONCLUSION: Loss or reduced expression of PTEN protein occurs commonly in tumorigenesis and progression of gastric carcinoma. It is suggested that PTEN can be an objective marker for pathologically biological behaviors of gastric carcinoma.

Yang L, Kuang LG, Zheng HC, Li JY, Wu DY, Zhang SM, Xin Y. PTEN encoding product: a marker for tumorigenesis and progression of gastric carcinoma. *World J Gastroenterol* 2003; 9(1): 35-39

<http://www.wjgnet.com/1007-9327/9/35.htm>

INTRODUCTION

PTEN/MMAC1/TEP1 gene (phosphatase and tensin homology deleted from chromosome ten/mutated in multiple advanced cancer 1/TGF- β -regulated and epithelial cell enriched phosphatase 1) was the firstly defined tumor suppressor which product acted as phosphatase and shared extensive homology with cytoskeletal protein, mapping to human chromosome 10q23.3. PTEN encoding product could not only dephosphorylate the phosphatidylinositol-3, 4, 5-triphosphate (PIP₃), but also be involved in cytoskeletal reconstruction and cellular mobility^[1-6]. Recently, many studies showed there were several putative mechanisms relating to tumor suppression as follows: inhibiting cell invasion and metastasis by dephosphorylating focal adhesion kinase (FAK); inhibiting cell apoptosis and increasing cell growth by dephosphorylating PIP₃; restraining cell differentiation by inhibiting mitogen-activated protein kinase (MAPK) signal pathway^[7-9]. Mutation or abnormal expression of PTEN protein occurred commonly in multiple tumors and significantly correlates with tumorigenesis and progression of different malignancies^[10-20]. It was reportedly suggested that deletion or mutation of PTEN could enhance the expression of vascular epithelial growth factor (VEGF) and stimulate the proliferation of microvessels in tumor tissues, which in turn closely correlated with tumor invasion and metastasis^[21-28].

Gastric carcinoma was one of the commonest malignancies in the world, and even the most frequent in China^[29]. Although the achievement of early diagnosis and treatment have somewhat improved the patients' outcome, gastric cancer still remains the major killer among Chinese because the mechanisms of its tumorigenesis and progression were unclear^[30]. In this study, we detected the expression of PTEN proteins in gastric cancer and its adjacent noncancerous mucosa, compared PTEN protein expression with its pathologically biological behaviors, and discussed the relationship between the expression of PTEN and VEGF in order to explore the role of PTEN gene product in tumorigenesis and progression of gastric cancer, and to provide scientific foundation for evaluating prognosis of gastric carcinoma.

MATERIALS AND METHODS

Pathology

One hundred and eighty-four cases of surgically removed specimens of gastric carcinoma were collected from Cancer Institute, China Medical University. This study included 102 cases of adjacent normal mucosa, 63 cases of adjacent IM and 6 cases of adjacent dysplasia. According to clinical staging, 37 cases were early, and 147 cases advanced. According to metastasis, 124 cases were accompanied with lymph node metastasis, 6 with liver metastasis (4 of them with lymph node metastasis) and 2 with ovary metastasis. All gastric specimens were classified according to the Lauren's and WHO's histological classification criteria.

Immunohistochemistry

All specimens were fixed in 4 % formaldehyde solution,

embedded in paraffin and incised into 5 μm sections. The rabbit anti-human polyclonal antibody against PTEN (ready to use) and mouse anti-human monoclonal antibody against VEGF (ready to use) were purchased from Maixim Biotech. SABC complex kit was from Boster Biotech. For negative control, sections were incubated with PBS (0.01 mol/L, pH7.4) instead of the primary antibodies.

Evaluation of PTEN and VEGF expression

Clearly brown staining was restricted to cytoplasm, which was considered as positive for PTEN or VEGF. Slides were scored semi-quantitatively based on staining intensity and distribution. Two pathologists assessed the positive rate according to the percent of positive cells in all counted cells from 5 randomly selected representative fields. The degree of staining was graded in the light of proportion of positive cells as follows: negative (-), positive rate <5 %; weakly positive (+); 5-25 %; moderately positive (++) : 25-50 %; strongly positive (+++~++++): >50 %.

Statistical analysis

Statistical evaluation was performed by chi-square test to differentiate the rates between two groups. *P*-value less than 0.05 was considered as statistically significant. SPSS 10.0 software was employed to analyze all data.

RESULTS

PTEN was expressed in normal mucosa, intestinal metaplasia, dysplasia and carcinoma of the stomach at the rate of 100 % (102/102), 98.5 % (65/66), 66.7 % (4/6), 47.8 % (88/184), respectively. Dysplasia and carcinoma expressed less frequent than normal mucosa or intestinal metaplasia ($P < 0.01$) (Table 1, Figure 1,2).

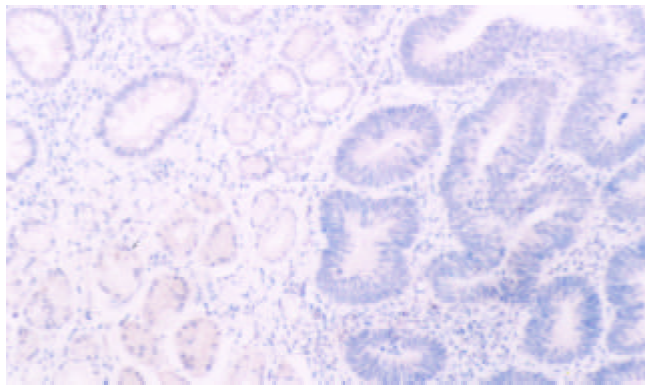


Figure 1 PTEN protein was restricted to cytoplasm. It was moderately expressed in normal mucosa (below), while decreased in IM (left top) and dysplasia (right), (20 \times)

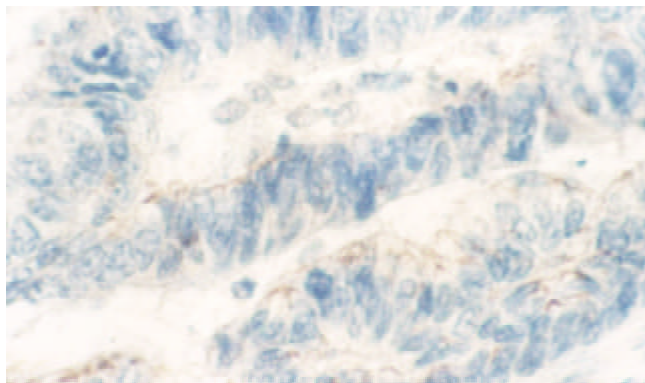


Figure 2 Well differentiated papillary-tube adenocarcinoma showed weakly positive expression of PTEN protein (40 \times)

Table 1 PTEN expression in normal mucosa, intestinal metaplasia, dysplasia and carcinoma of the stomach

	<i>n</i>	PTEN expression		%
		+~++++	-	
"Normal" mucosa	102	102	0	100.0
Intestinal metaplasia	66	65	1	98.5
Dysplasia	6	4	2	66.7 ^a
Carcinoma	184	88	96	47.8 ^b

^aCompared with "normal" mucosa or intestinal metaplasia, $P < 0.01$ (modified $\chi^2 = 18.729$, 7.115); ^bCompared with "normal" mucosa or intestinal metaplasia, $P < 0.01$ ($\chi^2 = 80.106$, 52.499)

Positive rate of PTEN in advanced gastric carcinoma (AGC) was 42.9 % (63/147), lower than in early one (EGC) (67.6 %, 25/37) ($P < 0.01$). In 124 cases with lymph node metastasis, 50 expressed PTEN protein (40.3 %), whose positive rate of PTEN was higher than those without lymph node metastasis (63.3 %, 38/60) ($P < 0.01$). 41.5 percent of 118 diffuse-type gastric cancers expressed PTEN, less than that of intestinal-type ones (51.8 %, 37/64). Signet ring cell carcinoma expressed PTEN protein at the lowest level (25.0 %, 7/28), more than well and moderately differentiated adenocarcinoma (61.8 %, 21/34) ($P < 0.01$).

None of the gastric normal mucosa showed expression of VEGF, while 75.0 percent of gastric carcinoma expressed it (45/60) ($P < 0.05$) (Figure 3,4). The PTEN-positive cases expressed VEGF at the rate of 78.1 % (25/32), whereas PTEN-negative ones did it at the rate of 71.4 % (20/28). Both rates were not significantly different by statistical analysis ($P > 0.05$).

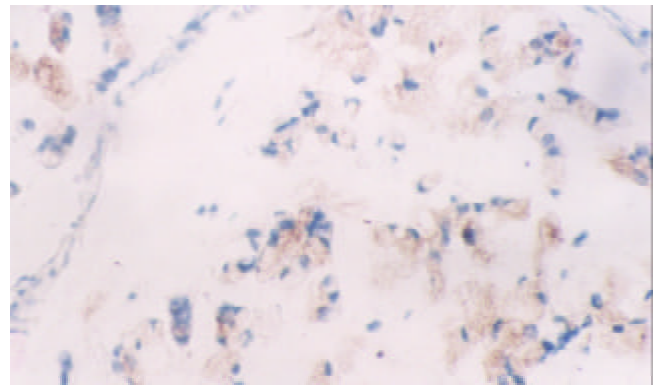


Figure 3 Mucinous adenocarcinoma of the stomach moderately expressed VEGF (20 \times)

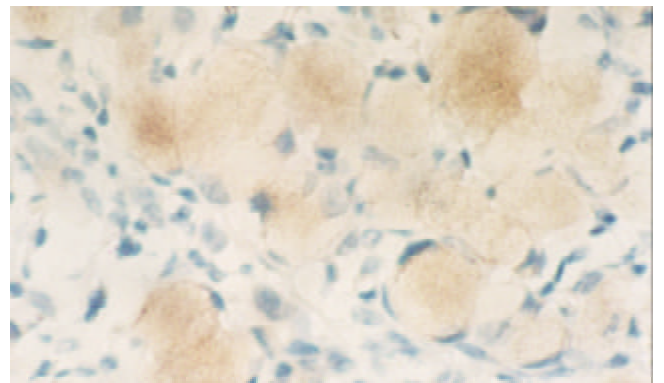


Figure 4 SRC showed strongly positive expression of VEGF protein (40 \times)

Table 2 Relationship between expression of PTEN and the biological behaviors of gastric carcinoma

	n	PTEN expression		%
		+~+++++	-	
Clinicopathological staging				
Early	37	25	12	67.6
Advanced	147	63	84	42.9 ^a
Lymph node metastasis				
+	124	50	74	40.3 ^b
-	60	38	22	63.3
Lauren's classification				
Intestinal type	64	37	27	57.8
Diffused type	118	49	96	41.5 ^c
Mixed type	2	2	0	100.0
WHO's histological classification				
Papillary adenocarcinoma	20	10	10	50.0
Well-differentiated adenocarcinoma	9	5	4	55.6
Moderated-differentiated adenocarcinoma	25	16	9	64.0
Poorly-differentiated adenocarcinoma	85	39	64	45.9
Undifferentiated adenocarcinoma	5	3	2	60.0
Signet ring-cell carcinoma(SRC)	28	7	21	25.0 ^d
Mucinous adenocarcinoma	10	6	4	60.0
Carcinoid	1	1	0	-
Squamous cell carcinoma	1	1	0	-

^aCompared with early gastric carcinoma, $P < 0.01$ ($\chi^2 = 26.504$);

^bCompared with non-lymph node metastasis, $P < 0.01$ ($\chi^2 = 8.580$);

^cCompared with intestinal-type gastric carcinoma, $P < 0.05$ ($\chi^2 = 4.416$);

^dCompared with well and moderately differentiated gastric carcinoma, $P < 0.01$ ($\chi^2 = 8.380$)

DISCUSSION

Deletion or down-regulation of tumor suppressing genes plays an important role in the multiple steps of tumorigenesis and progression of gastric carcinoma. Previous studies on the relationship between alteration of tumor suppressor genes and the development of gastric carcinoma focused on p53^[31, 32], p16^[33], p27^[34], p33 (ING1)^[35], RB^[36], DCC^[37] etc. However, few reports were involved in the newly discovered tumor suppressing gene- PTEN in tumorigenesis and progression of gastric carcinoma.

As a tumor-suppressing gene, PTEN makes great contribution to cellular differentiation, reproduction and apoptosis, as well as cellular adhesion and mobility. Some studies showed down-regulation of PTEN protein expression due to genetic changes like mutation, loss of heterozygosity, hypermethylation in gastric cancer, prostate cancer and breast cancer^[2, 14, 16, 19, 38]. Our results showed that decreased expression of PTEN during the courses of normal mucosa → intestinal metaplasia → dysplasia → carcinoma. Gastric dysplasia or carcinoma expressed less PTEN than normal mucosa or intestinal metaplasia ($P < 0.01$), revealing that genetic changes of PTEN gene may play an important role in malignant transition of epithelial cells of gastric mucosa.

Low expression of PTEN gene product was involved in clinicopathological stage and metastasis of stomach neoplasms. We found that 42.9 percent of AGC expressed PTEN, less than EGC ($P < 0.01$). Positive rate of PTEN was lower in gastric cancer with than without lymph node metastasis (40.3 % vs

63.3 %, $P < 0.01$). One of the six liver metastases showed negative expression of PTEN in primary or liver metastasis, while the other five cases with liver metastasis showed reduced expression of PTEN protein. These results were similar to other kinds of tumors^[39-46]. It is suggested that deletion or reduced expression of PTEN protein probably facilitate the metastatic ability of gastric cancer cells. Hwang *et al.* found that PTEN could enhance mobility and metastasis of tumor cells by regulating matrix metalloproteinases (MMPs) and VEGF^[47]. There was another report that PTEN dephosphorated FAK so as to be involved in cellular adhesion^[7]. Deletion or reduced expression of PTEN could result in decreasing cellular adhesion, increasing synthesis of MMPs and VEGF, which subsequently contributed to invasion and angiogenesis of cancer cells. These biological effects possibly underlay prelude of invasion and metastasis of tumor. Our results revealed that reduced expression of PTEN was implicated in progression of gastric cancer probably by decreasing cellular adhesion, increasing cellular mobility and angiogenesis and could act as an objective marker to reflect the biological behaviors of gastric cancer.

In addition, signet ring cell carcinoma showed the lowest expression of PTEN among histological classifications, less than well and moderately differentiated adenocarcinoma ($P < 0.01$), suggesting that decreased expression of PTEN was closely associated with carcinogenesis of signet ring cell carcinoma. Diffuse-type cancer showed less expression of PTEN at the rate of 41.5 % than intestinal-type one. ($P < 0.05$). In this sense, it supported that there were different tumorigenic pathways between diffuse and intestinal -type gastric carcinoma. Diffuse-type gastric cancer, main part of which was signet ring cell carcinoma, showed diffusely invasive growth pattern. It is possible that down-regulation of PTEN could affect the function of cellular skeleton, mobility and adhesion of cancer cells.

Some reports suggested that decreased expression of PTEN encoding product could down-regulate PI₃K/AKT pathway, leading to increasing synthesis of VEGF induced by hypoxia inducing factor-1 (HIF-1)^[48-50]. Our study showed that 75.0 percent of gastric carcinomas expressed VEGF (45/60), significantly more than normal mucosa (0/5) ($P < 0.05$), indicating that VEGF was up-regulated in gastric cancer. But PTEN was down-regulated in gastric cancer. Both PTEN and VEGF showed negative correlation, which was not statistically significant ($P > 0.05$). The relationship between expression of both PTEN and VEGF in tumorigenesis and progression of gastric cancer need proving by amplifying the sample.

In all, loss or reduced expression of PTEN protein occurred commonly in gastric carcinogenesis. Altered expression of PTEN contributed to progression of gastric cancer by increasing cell adhesion, angiogenesis, cell mobility and so on. It was suggested that PTEN could be a useful marker for pathologically biological behaviors of gastric carcinoma. However, the role of PTEN gene and its encoding protein in tumorigenesis and progression of gastric cancer need further investigation.

REFERENCES

- 1 **Steck PA**, Pershouse MA, Jasser SA, Yung WK, Lin H, Ligon AH, Langford LA, Baumgard ML, Hattier T, Davis T, Frye C, Hu R, Swedlund B, Teng DH, Tavtigian SV. Identification of a candidate tumour suppressor gene, MMAC1, at chromosome 10q23.3 that is mutated in multiple advanced cancers. *Nat Genet* 1997; **15**: 356-362
- 2 **Li J**, Yen C, Liaw D, Podsypanina K, Bose S, Wang SI, Puc J, Miliareis C, Rodgers L, McCombie R, Bigner SH, Giovannella BC, Ittmann M, Tycko B, Hibshoosh H, Wigler MH, Parsons R. PTEN, a putative protein tyrosine phosphatase gene mutated in human brain, breast, and prostate cancer. *Science* 1997; **275**:1943-1947
- 3 **Li DM**, Sun H. TEP1, encoded by a candidate tumor suppressor

- locus, is a novel protein tyrosine phosphatase regulated by transforming growth factor beta. *Cancer Res* 1997; **57**: 2124-2129
- 4 **Cantley LC**, Neel BG. New insights into tumor suppression: PTEN suppresses tumor formation by restraining the phosphoinositide 3-kinase/AKT pathway. *Proc Natl Acad Sci U S A* 1999; **96**: 4240-4245
 - 5 **Wu X**, Senechal K, Neshat MS, Whang YE, Sawyers CL. The PTEN/MMAC1 tumor suppressor phosphatase functions as a negative regulator of the phosphoinositide 3-kinase/Akt pathway. *Proc Natl Acad Sci U S A* 1998; **95**: 15587-15591
 - 6 **Sun H**, Lesche R, Li DM, Liliental J, Zhang H, Gao J, Gavrillova N, Mueller B, Liu X, Wu H. PTEN modulates cell cycle progression and cell survival by regulating phosphatidylinositol 3,4,5-trisphosphate and Akt/protein kinase B signaling pathway. *Proc Natl Acad Sci U S A* 1999; **96**: 6199-6204
 - 7 **Maehama T**, Taylor GS, Dixon JE. PTEN and myotubularin: novel phosphoinositide phosphatases. *Annu Rev Biochem* 2001; **70**: 247-279
 - 8 **Besson A**, Robbins SM, Yong VW. PTEN/MMAC1/TEP1 in signal transduction and tumorigenesis. *Eur J Biochem* 1999; **263**: 605-611
 - 9 **Waite KA**, Eng C. Protean PTEN: form and function. *Am J Hum Genet* 2002; **70**: 829-844
 - 10 **Tanno S**, Tanno S, Mitsuuchi Y, Altomare DA, Xiao GH, Testa JR. AKT activation up-regulates insulin-like growth factor I receptor expression and promotes invasiveness of human pancreatic cancer cells. *Cancer Res* 2001; **61**: 589-593
 - 11 **Rubin MA**, Gerstein A, Reid K, Bostwick DG, Cheng L, Parsons R, Papadopoulos N. 10q23.3 loss of heterozygosity is higher in lymph node-positive (pT2-3,N+) versus lymph node-negative (pT2-3,N0) prostate cancer. *Hum Pathol* 2000; **31**: 504-508
 - 12 **Depowski PL**, Rosenthal SI, Ross JS. Loss of expression of the PTEN gene protein product is associated with poor outcome in breast cancer. *Mod Pathol* 2001; **14**: 672-676
 - 13 **Meng Q**, Goldberg ID, Rosen EM, Fan S. Inhibitory effects of Indole-3-carbinol on invasion and migration in human breast cancer cells. *Breast Cancer Res Treat* 2000; **63**: 147-152
 - 14 **Garcia JM**, Silva JM, Dominguez G, Gonzalez R, Navarro A, Carretero L, Provencio M, Espana P, Bonilla F. Allelic loss of the PTEN region (10q23) in breast carcinomas of poor pathophenotype. *Breast Cancer Res Treat* 1999; **57**: 237-243
 - 15 **Dillon DA**, Howe CL, Bosari S, Costa J. The molecular biology of breast cancer: accelerating clinical applications. *Crit Rev Oncog* 1998; **9**: 125-140
 - 16 **Lin WM**, Forgacs E, Warshal DP, Yeh IT, Martin JS, Ashfaq R, Muller CY. Loss of heterozygosity and mutational analysis of the PTEN/MMAC1 gene in synchronous endometrial and ovarian carcinomas. *Clin Cancer Res* 1998; **4**: 2577-2583
 - 17 **Shao X**, Tandon R, Samara G, Kanki H, Yano H, Close LG, Parsons R, Sato T. Mutational analysis of the PTEN gene in head and neck squamous cell carcinoma. *Int J Cancer* 1998; **77**: 684-688
 - 18 **Hosoya Y**, Gemma A, Seike M, Kurimoto F, Uematsu K, Hibino S, Yoshimura A, Shibuya M, Kudoh S. Alteration of the PTEN/MMAC1 gene locus in primary lung cancer with distant metastasis. *Lung Cancer* 1999; **25**: 87-93
 - 19 **Celebi JT**, Shendrik I, Silvers DN, Peacocke M. Identification of PTEN mutations in metastatic melanoma specimens. *J Med Genet* 2000; **37**: 653-657
 - 20 **Tsao H**, Zhang X, Fowlkes K, Haluska FG. Relative reciprocity of NRAS and PTEN/MMAC1 alterations in cutaneous. *Cancer Res* 2000; **60**: 1800-1804
 - 21 **Huang J**, Kontos CD. PTEN modulates vascular endothelial growth factor-mediated signaling and angiogenic effects. *J Biol Chem* 2002; **277**: 10760-10766
 - 22 **Ferrara N**, Gerber HP. The role of vascular endothelial growth factors in angiogenesis. *Acta Haematol* 2001; **106**: 148-156
 - 23 **Harmey JH**, Bouchier-Hayes D. Vascular endothelial growth factor (VEGF), a survival factor for tumour cells: implications for anti-angiogenic therapy. *Bioessays* 2002; **24**: 280-283
 - 24 **Lin R**, LeCouter J, Kowalski J, Ferrara N. Characterization of endocrine gland-derived vascular endothelial growth factor signaling in adrenal cortex capillary endothelial cells. *J Biol Chem* 2002; **277**: 8724-8729
 - 25 **Dias S**, Choy M, Alitalo K, Rafii S. Vascular endothelial growth factor (VEGF)-C signaling through FLT-4 (VEGFR-3) mediates leukemic cell proliferation, survival, and resistance to chemotherapy. *Blood* 2002; **99**: 2179-2184
 - 26 **Inoki I**, Shiomi T, Hashimoto G, Enomoto H, Nakamura H, Makino K, Ikeda E, Takata S, Kobayashi K, Okada Y. Connective tissue growth factor binds vascular endothelial growth factor (VEGF) and inhibits VEGF-induced angiogenesis. *FASEB J* 2002; **16**: 219-221
 - 27 **Umeda N**, Ozaki H, Hayashi H, Kondo H, Uchida H, Oshima K. Non-paralleled increase of hepatocyte growth factor and vascular endothelial growth factor in the eyes with angiogenic and nonangiogenic fibroproliferation. *Ophthalmic Res* 2002; **34**: 43-47
 - 28 **Suzuma K**, Takahara N, Suzuma I, Isshiki K, Ueki K, Leitges M, Aiello LP, King GL. Characterization of protein kinase C beta isoform's action on retinoblastoma protein phosphorylation, vascular endothelial growth factor-induced endothelial cell proliferation, and retinal neovascularization. *Proc Natl Acad Sci U S A* 2002; **99**: 721-726
 - 29 **Parkin DM**. Global cancer statistics in the year 2000. *Lancet Oncol* 2001; **2**: 533-543
 - 30 **Chen XY**, van Der Hulst RW, Shi Y, Xiao SD, Tytgat GN, Ten Kate FJ. Comparison of precancerous conditions: atrophy and intestinal metaplasia in Helicobacter pylori gastritis among Chinese and Dutch patients. *J Clin Pathol* 2001; **54**: 367-370
 - 31 **Gunther T**, Schneider-Stock R, Hackel C, Kasper HU, Pross M, Hackelsberger A, Lippert H, Roessner A. Mdm2 gene amplification in gastric cancer correlation with expression of Mdm2 protein and p53 alterations. *Mod Pathol* 2000; **13**: 621-626
 - 32 **Liu XP**, Tsushimi K, Tsushimi M, Oga A, Kawachi S, Furuya T, Sasaki K. Expression of p53 protein as a prognostic indicator of reduced survival time in diffuse-type gastric carcinoma. *Pathol Int* 2001; **51**: 440-444
 - 33 **Jang TJ**, Kim DI, Shin YM, Chang HK, Yang CH. p16(INK4a) Promoter hypermethylation of non-tumorous tissue adjacent to gastric cancer is correlated with glandular atrophy and chronic inflammation. *Int J Cancer* 2001; **93**: 629-634
 - 34 **Migaldi M**, Zunarelli E, Sgambato A, Leocata P, Ventura L, De Gaetani C. P27Kip1 expression and survival in NO gastric carcinoma. *Pathol Res Pract* 2001; **197**: 231-236
 - 35 **Oki E**, Maehara Y, Tokunaga E, Kakeji Y, Sugimachi K. Reduced expression of p33 (ING1) and the relationship with p53 expression in human gastric cancer. *Cancer Lett* 1999; **147**: 157-162
 - 36 **Lee WA**, Woo DK, Kim YI, Kim WH. p53, p16 and RB expression in adenosquamous and squamous cell carcinomas of the stomach. *Pathol Res Pract* 1999; **195**: 747-752
 - 37 **Yoshida Y**, Itoh F, Endo T, Hinoda Y, Imai K. Decreased DCC mRNA expression in human gastric cancers is clinicopathologically significant. *Int J Cancer* 1998; **79**: 634-639
 - 38 **Kang YH**, Lee HS, Kim WH. Promoter methylation and silencing of PTEN in gastric carcinoma. *Lab Invest* 2002; **82**: 285-291
 - 39 **Lee JI**, Soria JC, Hassan KA, El-Naggar AK, Tang X, Liu DD, Hong WK, Mao L. Loss of PTEN expression as a prognostic marker for tongue cancer. *Arch Otolaryngol Head Neck Surg* 2001; **127**: 1441-1445
 - 40 **Verma RS**, Manikal M, Conte RA, Godec CJ. Chromosomal basis of adenocarcinoma of the prostate. *Cancer Inves* 1999; **17**: 441-447
 - 41 **McMenamin ME**, Soung P, Perera S, Kaplan I, Loda M, Sellers WR. Loss of PTEN expression in paraffin-embedded primary prostate cancer correlates with high Gleason score and advanced stage. *Cancer Res* 1999; **59**: 4291-4296
 - 42 **Rustia A**, Wierzbicki V, Marrocco L, Tossini A, Zamponi C, Lista F. Is exon 5 of the PTEN/MMAC1 gene a prognostic marker in anaplastic glioma? *Neurosurg Rev* 2001; **24**: 97-102
 - 43 **Nozaki M**, Tada M, Kobayashi H, Zhang CL, Sawamura Y, Abe H, Ishii N, Van Meir EG. Roles of the functional loss of p53 and other genes in astrocytoma tumorigenesis and progression. *Neuro-oncol* 1999; **1**: 124-137
 - 44 **Minaguchi T**, Yoshikawa H, Oda K, Ishino T, Yasugi T, Onda T,

- Nakagawa S, Matsumoto K, Kawana K, Taketani Y. PTEN mutation located only outside exons 5, 6, and 7 is an independent predictor of favorable survival in endometrial carcinomas. *Clin Cancer Res* 2001; **7**: 2636-2642
- 45 **Tada K**, Shiraishi S, Kamiryo T, Nakamura H, Hirano H, Kuratsu J, Kochi M, Saya H, Ushio Y. Analysis of loss of heterozygosity on chromosome 10 in patients with malignant astrocytic tumors: correlation with patient age and survival. *J Neurosurg* 2001; **95**: 651-659
- 46 **Mills GB**, Lu Y, Kohn EC. Linking molecular therapeutics to molecular diagnostics: inhibition of the FRAP/RAFT/TOR component of the PI3K pathway preferentially blocks PTEN mutant cells *in vitro* and *in vivo*. *Proc Natl Acad Sci USA* 2001; **98**: 10031-10033
- 47 **Hwang PH**, Yi HK, Kim DS, Nam SY, Kim JS, Lee DY. Suppression of tumorigenicity and metastasis in B16F10 cells by PTEN/MMAC1/TEP1 gene. *Cancer Lett* 2001; **172**: 83-91
- 48 **Laughner E**, Taghavi P, Chiles K, Mahon PC, Semenza GL. HER2 (neu) signaling increases the rate of hypoxia-inducible factor 1alpha (HIF-1alpha) synthesis: novel mechanism for HIF-1-mediated vascular endothelial growth factor expression. *Mol Cell Biol* 2001; **21**: 3995-4004
- 49 **Zhong H**, Chiles K, Feldser D, Laughner E, Hanrahan C, Georgescu MM, Simons JW, Semenza GL. Modulation of hypoxia-inducible factor 1alpha expression by the epidermal growth factor/phosphatidylinositol 3-kinase/PTEN/AKT/FRAP pathway in human prostate cancer cells: implications for tumor angiogenesis and therapeutics. *Cancer Res* 2000; **60**: 1541-1545
- 50 **Zundel W**, Schindler C, Haas-Kogan D, Koong A, Kaper F, Chen E, Gottschalk AR, Ryan HE, Johnson RS, Jefferson AB, Stokoe D, Giaccia AJ. Loss of PTEN facilitates HIF-1-mediated gene expression. *Genes Dev* 2000; **14**: 391-396

Edited by Ma JY

Relationship between lymph node sinuses with blood and lymphatic metastasis of gastric cancer

Tong Yin, Xiao-Long Ji, Min-Shi Shen

Tong Yin, Xiao-Long Ji, Min-Shi Shen, General Hospital of PLA, 28 Fu Xing Road, Beijing 100853, China

Correspondence to: Dr. Xiao-Long Ji, Department of Pathology of General Hospital of PLA, 28 Fu Xing Road, Beijing 100853, China. xljji@public.bta.net.cn

Telephone: +86-10-66936455 **Fax:** +86-10-68228362

Received: 2002-03-25 **Accepted:** 2002-04-23

Abstract

AIM: To elucidate the relationship between lymph node sinuses with blood and lymphatic metastasis of gastric cancer.

METHODS: Routine autopsy was carried out in the randomly selected 102 patients (among them 100 patients died of various diseases, and 2 patients died of non-diseased reasons), their superficial lymph nodes locating in bilateral necks (include supraclavicle), axilla, inguina, thorax, and abdomen were sampled. Haematoxylin-Eosin staining was performed on 10 % formalin-fixed and paraffin-embedded lymph node tissue sections (5um). The histological patterns of the lymph sinuses containing blood were observed under light microscope. The expression of CD31, a marker for endothelial cell, was detected both in blood and non-blood containing lymph node sinuses with the method of immunohistochemistry.

RESULTS: Among the 1322 lymph nodes sampled from the autopsies of 100 diseased cases, lymph node sinuses containing blood were found in 809 lymph nodes sampled from 91 cases, but couldn't be seen in the lymph nodes sampled from the non-diseased cases. According to histology, we divided the blood containing lymph node sinuses into five categories: vascular-opening sinus, blood-deficient sinus, erythrophago-sinus, blood-abundant sinus, vascular-formative sinus. Immunohistochemical findings showed that the expression of CD31 was strongly positive in vascular-formative sinuses and some vascular-opening sinuses while it was faint in blood-deficient sinuses, erythrophago-sinuses and some vascular-opening sinuses. It was almost negative in blood-abundant sinus and non-blood containing sinus.

CONCLUSION: In the state of disease, the phenomenon of blood present in the lymph sinus is not uncommon. Blood could possibly enter into the lymph sinuses through the lymphaticovenous communications between the veins and the sinuses in the node. Lymph circulation and the blood circulation could communicate with each other in the lymph node sinuses. The skipping and distal lymphatic metastasis of gastric cancer may have some connection with the blood containing lymph node sinuses.

Yin T, Ji XL, Shen MS. Relationship between lymph node sinuses with blood and lymphatic metastasis of gastric cancer. *World J Gastroenterol* 2003; 9(1): 40-43

<http://www.wjgnet.com/1007-9327/9/40.htm>

INTRODUCTION

It is well known that one of the most common behaviours of lymphatic metastasis of gastric cancer is their great tendency to produce skipping metastasis with the tumor emboli traversing the proximal lymph nodes encountered on their route or even bypassing them to form distant nodal metastasis (mainly at left supraclavicle). Skipping metastasis is a peculiar kind of lymphatic metastasis. Until now, there have been few reports of this condition and its pathogenesis has not yet been clarified. Blood present in lymph node sinuses is a phenomenon that haven't been deeply researched too. In the routine lymph node biopsy, erythrocytes in the lymph node sinuses could occasionally be seen. In the early literature, vascular transformation of lymph node sinus (VTS) and haemal lymph node sinus (HLs) have been reported. Their common feature is blood presenting in the lymph node sinus. Since lymph node sinus is also the place where the metastatic malignant tumor is located, we speculated there might be some inner relationships between the two phenomena. The purpose of this study is to find out the relationship between lymph node sinuses with blood and lymphatic metastasis of gastric cancer.

MATERIALS AND METHODS

When routine autopsy was carried out in the randomly selected 102 patients died of different reasons, their superficial lymph nodes locating in the bilateral necks (include supraclavicle), axilla, inguina, thorax, and abdomen were sampled. Haematoxylin-Eosin staining was performed on 10 % formalin-fixed and paraffin-embedded 5 um lymph node tissue sections. The histological patterns of the lymph node sinuses containing blood were observed under light microscope. The expression of CD31, a marker for endothelial cell, was detected both in blood and non-blood containing lymph node sinuses by immunohistochemistry.

RESULTS

Clinical findings

The randomly selected 102 cases included 62 males and 38 females whose ages ranged from 2 months to 90 years (mean 45.08 years, median 57 years). Among the 102 cases, 100 patients died of various diseases, and 2 died of non-diseased reasons. The total number of the sampled lymph nodes was 1 362 (1 322 from the 100 patients died of various diseases and 40 from the 2 patients died of non-diseased reasons).

Light microscopic findings

Among the 1 322 lymph nodes sampled from the 100 autopsy diseased cases, blood containing lymph node sinuses were found in 809 lymph nodes sampled from 91 cases, whereas such sinuses couldn't be seen in the lymph nodes sampled from the non-diseased cases. According to the histology, we divided the blood containing lymph node sinuses into five categories: vascular-opening sinus (in 338 lymph nodes from 68 cases), blood-deficient sinus (in 291 lymph nodes from 69 cases), erythrophago-sinus (in 344 lymph nodes from 69 cases), blood-

abundant sinus (in 80 lymph nodes from 34 cases), and vascular-formative sinus (in 364 lymph nodes from 82 cases). In the vascular-opening sinus, venules and/or capillaries in the cortex and medulla extended or opened directly in the lymph node sinuses. Through the opening, blood could enter into the sinus (Figure 1). Blood-deficient sinus was defined as a small quantity of erythrocytes present in the lymph node sinuses (Figure 2). When erythrocytes in the sinuses were phagocytosed, erythrophago-sinus appeared. When the sinuses filled with blood, we called it blood-abundant sinus (Figure 3). Vascular-formative sinus was defined as vascular formation in the sinuses. We could see short to long sinuous vascular slits or vascular channels with round or oval contours lined by flat or plump endothelium. The channels were either empty or filled with an amorphous lymph-like materials and some red cells, occasionally they were markedly engorged with blood (Figure 4).

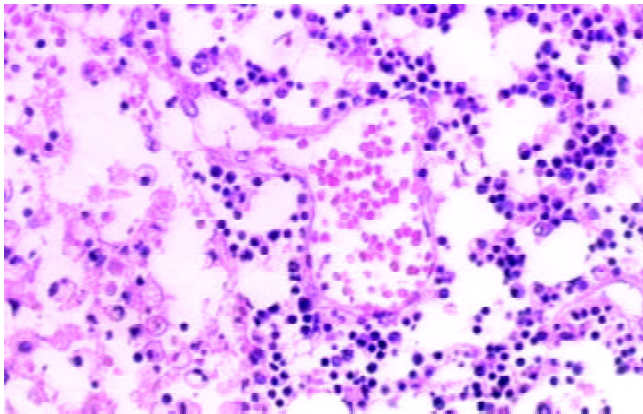


Figure 1 Vascular-opening lymph node sinus HE×200

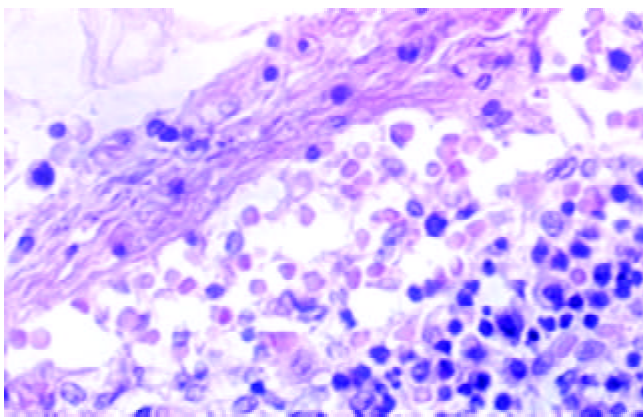


Figure 2 Blood-deficient lymph node sinus HE×400

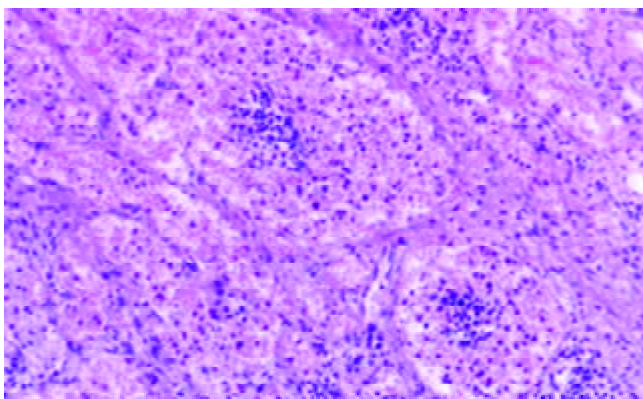


Figure 3 Blood-abundant lymph node sinus HE×100

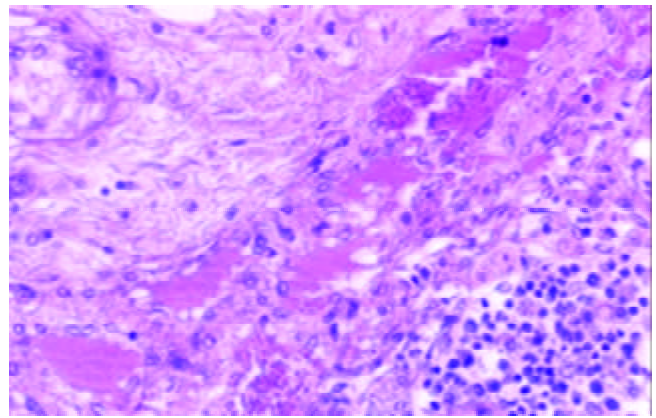


Figure 4 Vascular-formative lymph node sinus HE×200

Immunohistochemical findings

Immunohistochemical findings showed that the expression of CD31 was strongly positive in vascular-formative sinuses and some vascular-opening sinuses while it was faint in blood-deficient sinuses, erythrophago-sinuses and some vascular-opening sinuses. It was almost negative in blood-abundant sinuses and non-blood containing sinuses.

DISCUSSION

One of the most prominent features of the behaviour of carcinomas is their great tendency to produce secondary growths in regional lymph nodes. The early lymphatic metastasis of cancers almost invariably appear in the lymph nodes in the direction of normal lymph flow and the marginal sinus is the place where the metastatic growths are initially situated for the afferent lymphatics of lymph node enter the marginal sinus^[1-7]. As for the spread of the tumor to the lymph nodes in the direction contrary to the normal lymph flow or the lymph nodes far from the primary carcinomas, what is called skipping metastasis, it has always been convinced to be the consequence of the cancerous occlusion of the principal lymphatics; the lymph flow is diverted or sometimes reversed, into collateral channels passing to neighbouring unaffected nodes. Skipping metastasis is a peculiar kind of lymphatic metastasis. It was mostly recognised in the metastasis of gastric cancer to the supraclavicular lymph nodes which could be found as the earliest clinical symptom^[8-11]. There have been some reports of this condition, but most were concerning with how to detect the metastatic foci and the relationship with clinical nodal stage^[12,13]. Few mentioned the pathogenesis of skipping metastasis. The presence of previously unknown lymphatic tracts have been reported to explain the phenomenon^[14]. The skipping of intact lymph nodes can also be explained by anatomically demonstrable intra- and perinodal short circuit connections. Apart from this, preexisting lymph node changes (silicosis, fibrosis) also play an important part^[15].

Blood present in lymph node sinus is a phenomenon that haven't been deeply researched. How the blood entering the sinus remains to be elucidated^[16-29]. It's well recognized that there are two circulations in the lymph node, one is the lymphatic circulation, the other is the blood circulation. They could communicate via the high endothelial venules (HEV) in the paracortex, but it is not certain whether there is some other pathway for the communication in human lymph node. In 1961, Pressman and Simon^[24] devised experiments in dog to show that there were some other lymphatic-venous communications in lymph node. They inferred that the lymph node contained numerous lymphaticovenous communications between the lymph node sinuses and the veins. This claim has such far

reaching implications that the work should be repeated both in the dog and in other species. When it come to the human lymph node, the studies of blood containing lymph node sinus were concentrated on the vascular transformation of sinuses (VTS) and Hemolymph nodes (HLs). The term VTS was first coined by Haferkamp *et al*^[16] in 1971 for a distinctive benign vasoproliferative lesion of lymph node, which needed to be distinguished from Kaposi's sarcoma(KS); venous obstruction was thought to be the underlying mechanism, but it was still controversial^[30,31]. VTS is characterized by conversion of nodal sinuses into capillary-like channels, often accompanied by fibrosis^[21,32]. Hemolymph nodes (HLs) were another target for the study of the communication between lymph circulation and blood circulation in the lymph node sinuses. HLs are unique lymph nodes, because their lymphatic sinuses contain numerous erythrocytes. In 1969, Turner DR^[25] reported that blood entered the sinus through the communication between venule and sinuses, but it is still controversial^[26-29]. From the above-mentioned phenomenons and the researches, we hypothesized that the two circulations in the lymph node could communicate in the lymph node sinus.

In this study, blood in the lymph node sinuses could be found frequently in the lymph nodes sampled from the patients died of disease. The histologic patterns of the changes were not limited to HLs and VTS. According to the histologic patterns, the blood containing lymph node sinuses were divided into 5 categories. Vascular-opening sinus was characterized by venules or capillaries stretching into the sinus with blood in the vascular releasing into the lymph node sinuses (Figure 1). So that, it testified the existence of lymph-venule communication in human lymph node sinuses. Through the vascular-opening sinus, blood could enter the lymph node sinuses directly. This finding was in accordance with Pressman and Simon^[24]. Blood deficient sinus was possibly formed in the early period of the formation of sinuses containing blood, but the artifact factors should be excluded (Figure 2). The erythrophago-sinus was formed as a result of the phagocytosis of sinus-histocytes in the sinus. The red cells entered into the sinus were recognised as foreign bodies and engulfed by histocytes. When the pressure in venule increased for the stasis, plenty of red cells could rush into the sinus and the blood abundant sinus came into being due to the communication between lymph node sinus and venule (Figure 3). When the blood kept staying in the sinuses, an exceptional sinus containing blood -vascular formative sinus emerged. This kind of sinus was characterized by vascular formation in the lymph node sinus (Figure 4).

In order to clarify the features of endothelial cells of the lymph node sinus containing blood, monoclonal antibody CD31 was used to label the endothelial cells by immunohistochemistry^[33-36]. The expression of CD31 was different in the 5 blood contained sinuses. It was strongly positive in vascular-formative sinus and some vascular-opening sinus while it was weak in blood-deficient sinus, erythrophago-sinus and some vascular-opening sinus. It was almost negative in blood-abundant sinus and non-blood containing sinus. According to the expression of CD31 in different lymph node sinuses, we could speculated that the endothelial cells might experience the transformation from the lymph node sinus endothelial cells to the vascular endothelial cells. This course may have some connection with the blood in the sinuses^[37]. The Prompt recognition of the ultrastructure and the mechanism of the phenomenon was needed.

Since lymph node sinus is the place where the metastatic malignant tumor is located and we found in this study that in the state of disease, there was the communication between lymph and blood circulations in the sinus, we speculated there might be some inner relationships between lymphatic skipping metastasis of gastric cancer and blood containing lymph node sinuses.

Early clinical observations let to the impressions that

carcinomas frequently spread and grew in the lymphatic system, whereas tumors of mesenchymal origin spread more frequently by way of the blood stream^[38]. In fact, this division is arbitrary because these two routes are actually interlinked and inseparable. Cancer cells may invade the lymphatics directly or gain access to them via blood vessels. Tumor cells can readily pass from blood to lymphatic communication via the interstitial spaces of lymph nodes and other tissues exist. When tumor cells entered the local blood circulation and was brought to the distant area, through the communications between the lymph circulation and the blood circulation in lymph node sinuses, they could enter the lymph node and stay in the lymph node sinuses where the foci of skipping metastatic tumors are formed. When the lymph circulation was obstructed, through the communication, blood metastasis of tumor cell could also be accelerated.

Although, lymph node sinus containing blood was only found in the cases died of disease in our study, it was not certain if this kind of lymph node could also be found in non-diseased cases, because such cases were limited. An in-depth study in a larger cohort of gastric cancer patients is needed to confirm whether lymph node sinus containing blood is also very common in such alived human lymph nodes, and their physiological and pathological significance in the skipping metastasis.

REFERENCES

- 1 **del Regato JA**. Pathways of metastatic spread of malignant tumors. *Semin Oncol* 1977; **4**: 33-38
- 2 **Scanlon EF**. James Ewing lecture. The process of metastasis. *Cancer* 1985; **55**: 1163-1166
- 3 **Wittekind C**. Principles of lymphogenic and hematogenous metastasis and metastasis classification. *Zentralbl Chir* 1996; **121**: 435-441
- 4 **Hermanek P**. Lymph nodes and malignant tumors. *Zentralbl Chir* 2000; **125**: 790-795
- 5 **Passlick B**, Pantel K. Detection and relevance of immunohistochemically identifiable tumor cells in lymph nodes. *Recent Results Cancer Res* 2000; **157**: 29-37
- 6 **Kawaguchi T**. Pathological features of lymph node metastasis. 2) From morphological aspects. *Nippon Geka Gakkai Zasshi* 2001; **102**: 440-444
- 7 **Gendreau KM**, Whalen GF. What can we learn from the phenomenon of preferential lymph node metastasis in carcinoma? *J Surg Oncol* 1999; **70**: 199-204
- 8 **Maruyama K**, Gunven P, Okabayashi K, Sasako M, Kinoshita T. Lymph node metastases of gastric cancer. General pattern in 1931 patients. *Ann Surg* 1989; **210**: 596-602
- 9 **Siewert JR**, Sandler A. Potential and futility of sentinel node detection for gastric cancer. *Recent Results Cancer Res* 2000; **157**: 259-269
- 10 **Arai K**, Iwasaki Y, Takahashi T. Clinicopathological analysis of early gastric cancer with solitary lymph node metastasis. *Br J Surg* 2002; **89**: 1435-1437
- 11 **Kitagawa Y**, Ohgami M, Fujii H, Mukai M, Kubota T, Ando N, Watanabe M, Otani Y, Ozawa S, Hasegawa H, Furukawa T, Matsuda J, Kumai K, Ikeda T, Kubo A, Kitajima M. Laparoscopic detection of sentinel lymph nodes in gastrointestinal cancer: a novel and minimally invasive approach. *Ann Surg Oncol* 2001; **8**: 86S-89S
- 12 **Ichikura T**, Furuya Y, Tomimatsu S, Okusa Y, Ogawa T, Mukoda K, Mochizuki H, Tamakuma S. Relationship between nodal stage and the number of dissected perigastric nodes in gastric cancer. *Surg Today* 1998; **28**: 879-883
- 13 **Aikou T**, Higashi H, Natsugoe S, Hokita S, Baba M, Tako S. Can sentinel node navigation surgery reduce the extent of lymph node dissection in gastric cancer? *Ann Surg Oncol* 2001; **8**: 90S-93S
- 14 **Yamamoto Y**, Takahashi K, Yasuno M, Sakoma T, Mori T. Clinicopathological characteristics of skipping lymph node metastases in patients with colorectal cancer. *Jpn J Clin Oncol* 1998; **28**: 378-382
- 15 **Junker K**, Gumprich T, Muller KM. Discontinuous lymph node metastases ("skipping") in malignant lung tumors. *Chirurg* 1997;

- 68:** 596-599
- 16 **Haferkamp O**, Rosenau W, Lennert K. Vascular transformation of lymph node sinuses due to venous obstruction. *Arch Pathology* 1971; **92:** 81-83
 - 17 **Steinmann G**, Foldi E, Foldi M, Racz P, Lennert K. Morphologic findings in lymph nodes after occlusion of their efferent lymphatic vessels and veins. *Lab Invest* 1982; **47:** 43-50
 - 18 **Michael M**, Koza V. Vascular transformation of lymph node sinuses-a diagnostic pitfall. Histopathologic and immunohistochemical study. *Pathol Res Pract* 1989; **185:** 441-444
 - 19 **Scherrer C**, Maurer R. Vascular sinus transformation of the lymph nodes. Morphological and immunohistochemical analysis of 6 cases. *Ann Pathol* 1985; **5:**231-238
 - 20 **Lucke VM**, Davies JD, Wood CM, Whitbread TJ. Plexiform vascularization of lymph nodes: an unusual but distinctive lymphadenopathy in cats. *J Comp Pathol* 1987; **97:** 109-119
 - 21 **Chan JKC**, Warnke RA, Dorfman R. Vascular transformation of sinuses in lymph node. A study of its morphological spectrum and distinction from Kaposi's sarcoma. *Am J Surg Pathol* 1991; **15:** 732-743
 - 22 **Ostrowski ML**, Siddiqui T, Barnes RE, Howton MJ. Vascular transformation of lymph node sinuses, a process displaying a spectrum of histologic features. *Arch Pathol Lab Med* 1990; **114:** 656-660
 - 23 **Cook PD**, Czerniak B, Chan JKC, Mackay B, Ordonez NG, Ayala AG, Rosai J. Nodular spindle-cell vascular transformation of lymph nodes. A benign process occurring predominantly in retroperitoneal lymph nodes draining carcinomas that can simulate Kaposi's sarcoma or metastatic tumor. *Am J Surg Pathol* 1995; **19:** 1010-1020
 - 24 **Pressman JJ**, Simon MB. Communication between lymph and blood circulations in lymph node. *Surg Gynec Obstet* 1961; **113:** 537
 - 25 **Turner DR**. The vascular tree of the haemal node in the rat. *J Anat* 1969; **104:** 481
 - 26 **Cerutti P**, Marcaccini A, Guerrero F. A scanning and immunohistochemical study in bovine haemal node. *Anat Histol Embryol* 1998; **27:** 387-392
 - 27 **Hogg CM**, Reid O, Scothorne RJ. Studies on hemolymph nodes. III. Renal lymph as a major source of erythrocytes in the renal hemolymph node of rats. *J Anat* 1982; **135:** 291-299
 - 28 **Abu-Hijleh MF**, Scothorne RJ. Studies on haemolymph nodes. IV. Comparison of the route of entry of carbon particles into parathymic nodes after intravenous and intraperitoneal injection. *J Anat* 1996; **188:** 565-573
 - 29 **He YC**, Shen LS, Yang CL, Fang WN, Li Hong. The distribution of lymphatic channels and red cells in the lymph nodes of rat blood. *Jieyou Xuebao* 1991; **22:** 239-241
 - 30 **Samet A**, Gilbey P, Talmon Y, Cohen H. Vascular transformation of lymph node sinuses. *J Laryngol Otol* 2001; **115:** 760-762
 - 31 **Jindal B**, Vashishta RK, Bhasin DK. Vascular transformation of sinuses in lymph nodes associated with myelodysplastic syndrome-a case report. *Indian J Pathol Microbiol* 2001; **44:** 453-455
 - 32 **Ostrowski ML**, Siddiqui T, Barnes RE, Howton MJ. Vascular transformation of lymph node sinuses. A process displaying a spectrum of histologic features. *Arch Pathol Lab Med* 1990; **114:**656-660
 - 33 **Newman PJ**. The role of PECAM-1 in vascular cell biology. *Ann N Y Acad Sci* 1994; **714:** 165-174
 - 34 **DeLisser HM**, Christofidou-Solomidou M, Strieter RM, Burdick MD, Robinson CS, Wexler RS, Kerr JS, Garlanda C, Merwin JR, Madri JA, Albelda SM. Involvement of endothelial PECAM/CD31 in angiogenesis. *Am J Pathol* 1997; **151:** 671-677
 - 35 **Newman PJ**. The biology of PECAM-1 in vascular cell biology. *J Clin Invest* 1997; **99:** 3-8
 - 36 **Watt SM**, Gschmeissner SE, Bates PA. PECAM-1: its expression and function as a cell adhesion molecule on hemopoietic and endothelial cells. *Leuk Lymphoma* 1995; **17:** 229-244
 - 37 **Fujiwara K**, Masuda M, Osawa M, Kano Y, Katoh K. Is PECAM-1 a mechanoresponsive molecule? *Cell Struct Funct* 2001; **26:** 11-17
 - 38 **Weiss L**, Greep RO. Histology, Fourth Edition. USA: McGraw-Hill, Inc 1977: 523-543

Edited by Zhao M

Inhibition of conjugated linoleic acid on mouse forestomach neoplasia induced by benzo (a) pyrene and chemopreventive mechanisms

Bing-Qing Chen, Ying-Ben Xue, Jia-Ren Liu, Yan-Mei Yang, Yu-Mei Zheng, Xuan-Lin Wang, Rui-Hai Liu

Bing-Qing Chen, Ying-Ben Xue, Jia-Ren Liu, Yan-Mei Yang, Department of Nutrition and Food Hygiene, Public Health College, Harbin Medical University, Harbin 150001, Heilongjiang Province, China
Rui-Hai Liu, Food Science and Toxicology, Department of Food Science, 108 Stocking Hall, Cornell University, Ithaca, NY 14853-7201, USA
Supported by the National Natural Science Foundation of China, No. 30070658

Correspondence to: Prof. Bing-Qing Chen, Department of Nutrition and Food Hygiene, Public Health College, Harbin Medical University, 199 Dongdazhi Street, Nangang District, Harbin 150001, Heilongjiang Province, China. bingqingchen@sina.com

Telephone: +86-451-3608014 **Fax:** +86-451-3648617

Received: 2002-08-24 **Accepted:** 2002-10-12

Abstract

AIM: To explore the inhibition of conjugated linoleic acid isomers in different purity (75 % purity c9,t11-, 98 % purity c9,t11- and 98 % purity t10,c12-CLA) on the formation of forestomach neoplasm and chemopreventive mechanisms.

METHODS: Forestomach neoplasm model induced by B(a)P in KunMing mice was established. The numbers of tumor and diameter of each tumor in forestomach were counted; the mice plasma malondialdehyde (MDA) were measured by TBARS assay; TUNEL assay was used to analyze the apoptosis in forestomach neoplasia and the expression of MEK-1, ERK-1, MKP-1 protein in forestomach neoplasm were studied by Western Blotting assay.

RESULTS: The incidence of neoplasm in B(a)P group, 75 % purity c9, t11-CLA group, 98 % purity c9,t11-CLA group and 98 % purity t10, c12-CLA group was 100 %, 75.0 % ($P>0.05$), 69.2 % ($P<0.05$) and 53.8 % ($P<0.05$) respectively and the effect of two CLA isomers in 98 % purity on forestomach neoplasia was significant; CLA showed no influence on the average tumor numbers in tumor-bearing mouse, but significantly decreased the tumor size, the tumor average diameter of mice in 75 % purity c9,t11-CLA group, 98 % purity c9,t11-CLA group and 98 % purity t10, c12-CLA group was 0.157 ± 0.047 cm, 0.127 ± 0.038 cm and 0.128 ± 0.077 cm ($P<0.05$) and 0.216 ± 0.088 cm in B(a)P group; CLA could also significantly increase the apoptosis cell numbers by 144.00 ± 20.31 , 153.75 ± 23.25 , 157.25 ± 15.95 ($P<0.05$) in 75 % purity c9,t11-CLA group, 98 % purity c9, t11-CLA group and 98 % purity t10,c12-CLA group (30.88 ± 3.72 in BP group); but there were no significant differences between the effects of 75 % purity c9,t11-CLA and two isomers in 98 % purity on tumor size and apoptotic cell numbers; the plasma levels of MDA in were increased by 75 % purity c9,t11-CLA, 98 % purity c9,t11-CLA and 98 % purity t10,c12-CLA. The 75 % purity c9,t11-CLA showed stronger inhibition; CLA could also inhibit the expression of ERK-1 protein and promote the expression of MKP-1 protein, however no influence of CLA on MEK-1 protein was observed.

CONCLUSION: Two isomers in 98 % purity show stronger inhibition on carcinogenesis. However, the inhibitory

mechanisms of CLA on carcinogenesis is complicated, which may be due to the increased mice plasma MDA, the inducing apoptosis in tumor tissues. And the effect of CLA on the expression of ERK-1 and MKP-1 may be one of the mechanisms of the inhibition of CLA on the tumor.

Chen BQ, Xue YB, Liu JR, Yang YM, Zheng YM, Wang XL, Liu RH. Inhibition of conjugated linoleic acid on mouse forestomach neoplasia induced by benzo(a)pyrene and chemopreventive mechanisms. *World J Gastroenterol* 2003; 9(1): 44-49
<http://www.wjgnet.com/1007-9327/9/44.htm>

INTRODUCTION

Conjugated linoleic acid (CLA) refers to a group of dienoic derivatives of linoleic acid that can be found in natural foods, such as the milk fat and meat of ruminant animals^[1-4]. CLA can also be synthesized in the laboratory and is available commercially as a dietary supplement and has shown to be non-toxic^[5]. In several animal experiments, supplementation of feeding with CLA showed an anticarcinogenic effect against chemical-induced cancers of the skin, forestomach, colon and breast^[6-9]. Moreover, of the individual isomers of CLA, c9,t11 isomer has been implicated as most active biologically because it is the predominant isomer incorporated into the phospholipids of cell membrane, however recent evidence showed the t10, c12-CLA isomer might also exert biological activity^[10]. To date, the sample used for animal experiment or cell experiment is the isomer mixture of conjugated linoleic acid which mainly containing c9,t11-, t10,c12-, t9,t11-, t10,t12-CLA. Potent anticarcinogenic effects have been attributed to a synthetic mixture of CLA containing c9,t11- and t9,c11-CLA (43 %) and t10,c12-CLA (45.3 %)^[7,11-14]. For example, CLA used in Ha's report contained c9,t11-, t10,c12-, t9,t11-, t10,t12-CLA which accounted for about 90 % of the material^[7]; Hubbard applied a mixture of CLA isomers with 32.5 % c9,t11-CLA and 32.5 % t10,c12-CLA isomers making up 66 % to mammary tumor metastasis^[14], etc. In summary, there were few reports assessing the effects of CLA monomer on the carcinogenesis in animal model.

Now the effect of CLA on carcinogenesis had been confirmed and there were evidences to support CLA action on the every stage of cancer, including initiation^[15,16], post-initiation (promotion)^[17,18], progression^[19] and metastasis^[14,20-22]. However the mechanisms through which CLA inhibits tumorigenesis are moot. Ha *et al*^[7] suggested an antioxidant mechanism; Schonberg reported that the biochemical mechanisms by which CLA exerted its anticancer activity possibly including the formation of cytotoxic lipid peroxidation products, but this might not be sufficient to explain all the effects of these naturally occurring isomers of CLA^[23]; Ip's data showed an effect on growth and development of certain types of mammary cells^[24,25]; Reduced formation of carcinogen-DNA adducts had been implicated^[15,16]; Durgam's work showed CLA inhibit cancer by influences on the oestrogen response system^[26]; Others suggested inhibition mechanisms of CLA including its effects on eicosanoid metabolism^[27-31], apoptosis^[32,33], the gene

expression such as stearoyl-CoA desaturase^[34,35], PPARA^[36-38], cyclin A,B(1), D(1) cyclin-dependent kinases inhibitors and (CDKI)(P16 and P21)^[39] ect.

In our research group, we found that 75 % purity c9,t11-CLA inhibit cancer incidence by 40 %; at the same time that 98 % purity c9,t11 and t10,c12-CLA showed stronger inhibition on human gastric cancer (SGC-7901) and breast cancer cells(MCF-7)^[39-42]. Our study was designed to investigate the inhibition effects of synthetically-prepared individual isomer of CLA in different purity (75 % purity c9,t11-CLA, 98 % purity c9,t11-CLA and 98 % purity t10,c12-CLA) on the forestomach neoplasia induced by B(a)P and the mechanism whereby CLA acted as an anticarcinogen, especially in terms of lipid peroxidation, apoptosis and MAPKs pathway.

MATERIALS AND METHODS

Material

BP was purchased from Fluka Chemie AG of Switzerland. Salad oil was purchased from a local grocery. 75 % purity c9, t11-CLA, 98 % purity c9,t11-CLA and 98 % purity t10,c12-CLA were provided by Dr. Ruihai Liu at Cornell University.

Treatment of mice (43)

KunMing mice, 6 to 7 wk of age, were purchased from Cancer Research Institute of HarBin Medical University in China. Two weeks later the animals were randomized by body weight and divided into 7 groups (15 mice/group). They were then subjected to a forestomach tumorigenesis as follows: each animal except animals in salad control group was given 0.2 ml salad oil solution per 20 mg body weight (1 mg BP in 0.2 ml of salad oil solution) by gavage and animals in salad control group were given 0.2 ml salad oil only twice every week for over after 4 wk. And the following diets were given after 2 weeks of giving BP and continue for 7 wk (Table 1). Beginning with the first intubation and continuing thereafter, the body weight and food intake were recorded twice weekly. All surviving mice were sacrificed 26 wk after the first dose of BP.

Table 1 The diets given after 2 wk of giving BP

Group	diets
Salad oil Control(A)	Standard diet+salad oil: fat(salad oil) concentration was 20 %
BP Control(B)	Standard diet+salad oil: fat(salad oil) concentration was 20 %
BP+75 % c9,t11-CLA(C)	Standard diet+salad oil+75 %c9,t11-CLA: Fat (salad oil) concentration was 20 %, CLA 0.8 %
BP+98 % c9,t11-CLA(D)	Standard diet+salad oil+98 % c9,t11-CLA: Fat (salad oil) concentration was 20%, CLA 0.5 %
BP+98 %t10,c12-CLA(E)	Standard diet+salad oil+98 %t10,c12-CLA: Fat (salad oil) concentration was 20 %, CLA 0.5 %

Gross pathology and histopathology

At termination of the study, the forestomach was removed. Tumor numbers and size were recorded, and then fixed in 10 % formalin and paraffin-embedded; 4 μ m sections were cut and stained with hematoxylin and eosin (HE).

Lipid peroxidation analysis

The TBARS test was used to measure malonaldehyde (MDA). The mouse plasma MDA levels was determined by TBARS kits (Jiancheng Biotechnology Institute, NanJing, P.R. China).

Measurement of apoptosis cell numbers in forestomach neoplasia

In situ Cell Death Detection Kit, Fluorescein, were purchased from Boehringer Mannheim. Briefly, Fixed and permeabilized

apoptotic tissue sections, incubated the tissue section with the TUNEL reaction mixture containing TdT and fluorescein-dUTP, detected the incorporated fluorescein with an anti-fluorescein antibody POD conjugate and at last visualized the immunocomplex with a substrate reaction were in light microscope. The apoptosis cell number was counted in 10³ cells.

Protein extract and western blotting

Three mice forestomachs in each group were homogenated and lysed in RIPA buffer (150 mM NaCl, 0.1 % NP40, 0.5 % deoxycholic acid, 0.1 % SDS, 50 mM Tris, pH 7.4) with protease inhibitor, leupeptin and aprotinin. Equal amounts of protein (80 μ g/lane) were resolved by SDS-polyacrylamide gel electrophoresis, transferred onto nitrocellulose membranes, and immunoblotted with a mouse anti-MEK-1, rabbit anti-ERK-1 and rabbit anti-MKP-1 antibody, then incubated with horseradish peroxidase secondary antibodies. Immunoreactive bands were detected using DAB (diaminobenzidine tetrahydrochloride) substrate and analyzed with a ChemiImagerTM 4 000 Low Light Imaging System (Alpha Innotech Corporation, at the same time used GAPDH as house-keeping protein.

RESULTS

Establishment of mouse forestomach model

Figure 1(A) showed the normal forestomach with smooth surface and without tumor. However, the white-yellow cauliflower-like neoplasia in different size appeared in the forestomach of mice induced B(a)P(Figure 1B,C). The structure of mouse forestomach in Figure 2(A) was normal and squamous epithelial cells and glandular epithelium cells were in order; The pathological analysis of B(a)P-induced forestomach neoplasia showed atypical hyperplasia in Figure 2(B) with stratified squamous epithelium excessively cornified, with focal proliferative basal cells and hypertrophic echinocyte; The basal cells, proliferating actively and out of order, grew through basement membrane and developed carcinoma *in situ* (Figure 2C).

Effect of CLA on forestomach neoplasia

The effect of CLA on BP-induced neoplasia of the forestomach in female KunMing mice was shown in Table 2. The incidence of the tumor and average diameter of tumor in 98 % purity c9, t11-CLA group and 98 % purity t10,c12-CLA group were significantly lower than that in B(a)P group ($P<0.05$). 75 % Purity c9,t11-CLA only decreased the tumor incidence which was no significant ($P>0.05$), but its influence on the average diameter being significant ($P<0.05$). The average tumor number of each tumor-bearing mouse showed no statistical significance ($P>0.05$).

Table 2 Inhibition of BP-induced forestomach neoplasia in female KunMing mice by CLA

Group	No. of mice (No. of tumor-bearing mice) /treatment	Total number of tumors	Tumor incidence (%)	Tumors/ tumor-bearing mouse ^d	Diameter/ tumor (CM)
A	14(0)	0	0	0	0
B	12(12)	31	100	2.58 \pm 0.90	0.216 \pm 0.088
C	12(9)	23	75.0 ^a	2.56 \pm 0.73	0.157 \pm 0.047 ^e
D	13(9)	22	69.2 ^{bc}	2.44 \pm 0.53	0.127 \pm 0.038 ^e
E	13(7)	21	53.8 ^{bc}	3.00 \pm 0.58	0.128 \pm 0.077 ^e

^a $P>0.05$ compared to the group B; ^b $P<0.05$ compared to the group B; ^c $P>0.05$ compared to the group C; ^d $P>0.05$, ^e $P<0.05$ compared to the group B

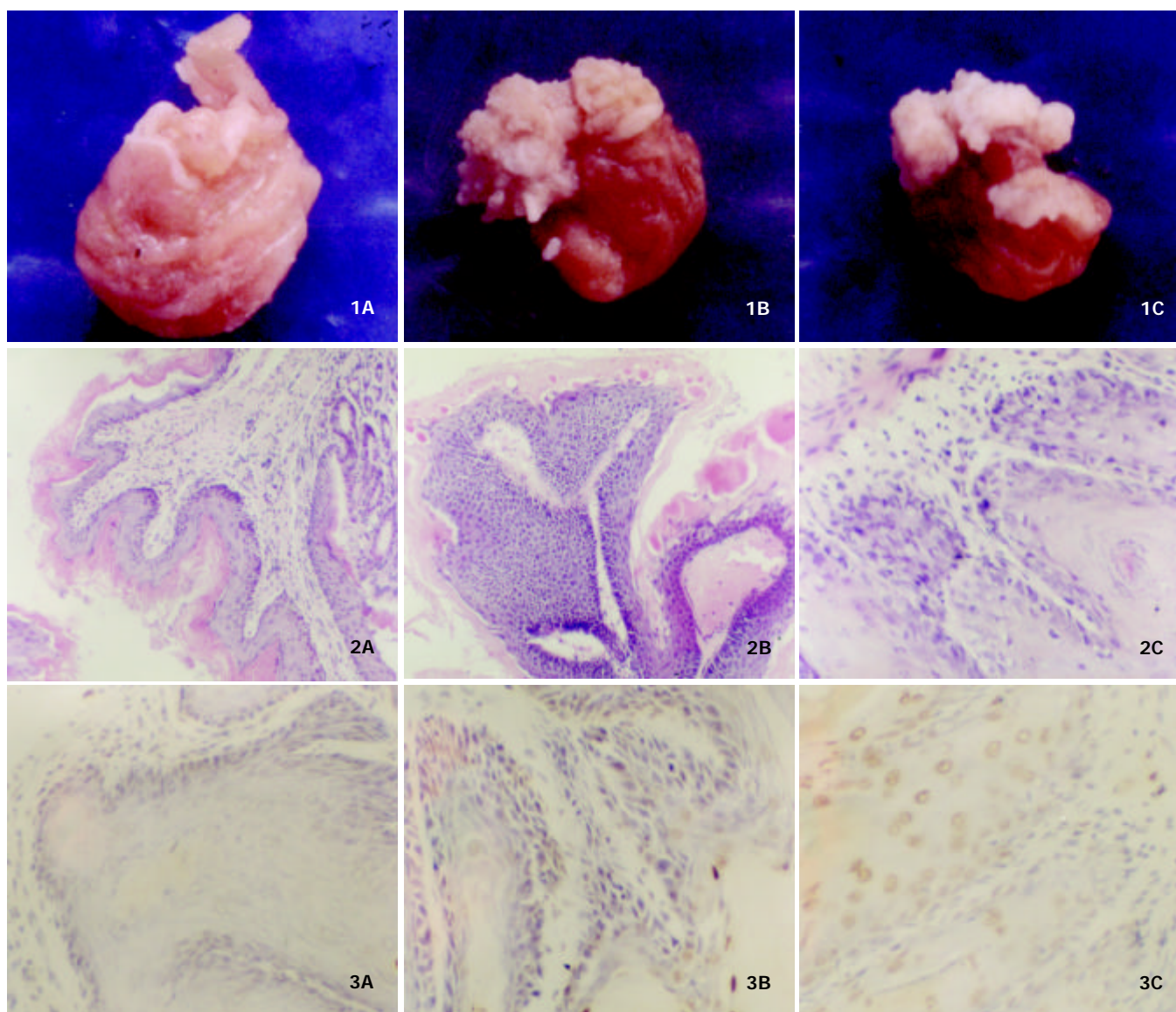


Figure 1 The establishment of mouse neoplasia model induced by B(a)P. (A): normal forestomach; (B, C): forestomach neoplasia.

Figure 2 The pathological analysis of mouse forestomach. (A): normal forestomach $\times 10$; (B): Atypical hyperplasia $\times 10$; (C): Carcinoma *in situ* $\times 4$.

Figure 3 Apoptosis induced by CLA in mice forestomach. (A or B): there were few apoptotic cells in group A and B; (C): the apoptosis induced by CLA. Arrow showed apoptotic cells $\times 40$.

Analysis on lipid peroxidation

The plasma levels of MDA measured by the TBARS assay increased in mice treated by 75 % purity c9,t11-CLA, 98 % purity c9,t11-CLA and 98 % purity t10,c12-CLA ($P < 0.05$). Moreover, 75 % purity c9,t11-CLA were more effective than purity 98 % c9,t11-CLA and 98 % purity t10,c12-CLA.

Table 3 The effects of CLA on mouse plasma lipid peroxidation

Group	MDA in plasma(nmol/L)
A	9.995 \pm 1.634
B	9.937 \pm 1.854
C	17.668 \pm 4.610 ^{ab}
D	14.005 \pm 4.116 ^a
E	13.303 \pm 3.593 ^a

^a $P < 0.05$ compared to the group A, B; ^b $P < 0.05$ compared to the group D, E.

The effect of CLA on apoptosis in forestomach neoplasia

Figure 3 showed the apoptosis in forestomach neoplasia. Table 4 showed that 75 % c9,t11-CLA, purity 98 % c9,t11-CLA and 98 % purity t10,c12-CLA can significantly induce apoptosis but with no statistical difference ($P < 0.05$).

Table 4 The effects of CLA on apoptosis in mice stomach(10^3 cells)

Group	Apoptotic cell numbers
A	42.63 \pm 6.02
B	30.88 \pm 3.72
C	144.00 \pm 20.31 ^a
D	153.75 \pm 23.25 ^a
E	157.25 \pm 15.95 ^a

^a $P < 0.01$ compared to the group A, B.

The effect of CLA on the MAPKs pathway

Figure 4, 5, 6 showed that 98 % purity t10,c12-CLA decreased

the expression of MEK-1 protein, but no influence was observed in mice treated by 75 % purity c9,t11-CLA and 98 % c9,t11-CLA. The expression of ERK-1 protein in 75 % purity c9,t11-CLA group, 98 % purity c9,t11-CLA group and 98 % purity t10,c12-CLA group was inhibited significantly, and 98 % purity c9,t11-CLA and 98 % purity t10,c12-CLA showed more effective than 75 % purity c9,t11-CLA. The expression of MKP-1 was increased in mice treated by 75 % purity c9,t11-CLA, 98 % purity c9,t11-CLA and 98 % purity t10,c12-CLA.

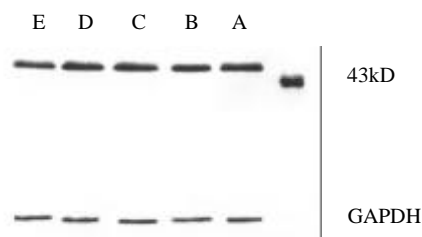


Figure 4 The effect of CLA on the expression of MEK-1 protein.



Figure 5 The effect of CLA on the expression of ERK-1 protein.

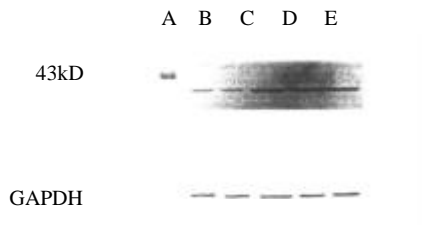


Figure 6 The effect of CLA on the expression of MKP-1 protein.

DISCUSSION

To date, all of the *in vivo* work with CLA has been done with a commercial free fatty acid preparation containing a mixture of c9,t11-, t10,c12-, c11, t13-isomers, although food CLA is predominately the c9,t11-isomer present in triacylglycerols (80-90 %). Ha *et al* reported that dietary mixture of c9,t11-CLA, t10,c12-CLA, t9,t11-CLA and t10,t12-CLA significantly decreased the incidence of mouse neoplasm induced B(a)P (up to 20 %) [7]. In DMBA-induced mammary adenocarcinoma model, the incidence in mice treated with dietary 0.05 %, 0.1 %, 0.25 %, 0.5 % CLA isomer mixture was 58 %, 42 %, 34 %, 36 %, respectively (that of the control was 56 %) [9]. In this study, we found that the incidence in mice fed with diet containing 75 % purity c9,t11-CLA (75 %), 98 % purity c9,t11-CLA (69.2 %), 98 % purity t10,c12-CLA (53.8 %) had been decreased, moreover, 98 % purity isomers showed significant influences in the inhibition of carcinogenesis; although 75 % purity c9,t11-CLA decreased tumor incidence with no statistical significance, it still significantly decreased the tumor size; all of which suggested that the effect of CLA on carcinogenesis was possibly related to the CLA purity. In addition, the different isomers of CLA in different purities decreased the average diameter of the tumors, but no influence was observed in

average tumor numbers of each tumor-bearing mouse, which might be one of characteristics of the inhibition of food components on carcinogenesis.

Lu reported that arachidonic acid and linoleic acid may promote HSC proliferation, but increased concentration can be cytotoxic to HSC [44]. As one of the positional and structural isomer of linoleic acid, more interests in conjugated linoleic acid promoting oxidation in cancer cells were paid upon. The study results in Stanton's group showed that CLA could make breast cancer cell more susceptible to lipid peroxidation, moreover, the extent of lipid peroxidation of CLA treated cells was related to CLA-induced cytotoxicity against cancer cell lines. At the same time, they found that milk fat triglyceride-bound CLA, consisting primarily of the c9,t11 isomer, was also cytotoxic towards MCF-7 cells [45-47]. In our study, 75 % purity c9,t11-CLA, 98 % purity c9,t11-CLA and 98 % purity t10,c12-CLA increased the levels of MDA in mouse plasma and 75 % purity c9,t11-CLA was most effective, but 75 % purity c9,t11-CLA did not show strongest inhibition of carcinogenesis, which suggested that the cytotoxic effect of lipid peroxidation to tumor cells might be one of mechanisms by which CLA exerted its biochemical activity. And Schönberg also reported that the formation of MDA induced by 40 $\mu\text{mol} \cdot \text{L}^{-1}$ CLA in lung adenocarcinoma cell lines was completely abolished by 30 μM vitamin E, but the growth rates were only partially restored, which indicated that cytotoxic lipid peroxidation products were only in part responsible for the growth inhibitory effects of CLA [24]. Furthermore, the lipid peroxidation product induced played important role in apoptosis [48]. We found that purity 75 % c9,t11-CLA, purity 98 % c9,t11-CLA and 98 % purity t10,c12-CLA induced significant apoptosis cells in forestomach neoplasia, but there were no differences between 75 % purity c9,t11-CLA group, 98 % purity c9,t11-CLA and 98 % purity t10,c12-CLA groups. The MAPK family consists of at least three different subgroups which include: ERKs, JNKs (SAPKs), and p38 MAPK kinase [49-53]. The Ras-Raf-MEK1/2-ERK1/2 pathway has been explained more clearly. Lavoie found that the transcription of cyclin D1 requires the long-term activation of ERK, which suggests that ERK can regulate cell cycle. In one report, there is a homeostasis between JNK/SAPKs and ERK systems: when ERK cascade is predominant in lymphocyte, cells will proliferate; by contraries, JNK/SAPK cascade will activate cell apoptosis [54]. It is found that the abnormalities of Ras/Raf/MAPK cascade reaction may contribute to malignant transformation of hepatocytes and activation of MAPK proteins may be an early event in hepatocellular carcinogenesis [55]. In summary, The activation of Ras-Raf-MEK-ERK can promote cell proliferation and inhibit cell apoptosis. In addition, The product of the immediate early gene MAP kinase phosphatase (MKP-1), is able to dephosphorylate phosphoserine/threonine as well as phosphotyrosine residues, and shows selectivity for ERKs 1 and 2 *in vitro*, with lower activity toward other MAP kinases such as JNK and P38 MAP kinase [56]. MKP-1 inactivates ERK following growth factor stimulation in intact cells and also suppresses signaling downstream of ERK at the level of gene transcription and proliferation [57], most likely through its inhibitory effects on MAP kinase. In our study, we found that CLA could inhibit the expression of ERK-1 protein, and at the same time inactivate the ERK-1 by increasing the expression of MKP-1, which might be one of mechanisms of CLA anticarcinogen.

In summary, it is confirmed that CLA shows inhibition on forestomach neoplasia induced by B(a)P, which is possibly related with CLA purity. Although the inhibition of different isomers (c9,t11- and t10,c12-CLA) on carcinogenesis is different, they show no significant difference. Moreover, the

inhibition mechanism of CLA is complicated and difficult to be explained by an mechanism.

ACKNOWLEDGEMENTS

We thank Dr. Rui-Hai Liu at Cornell University for helps and 75 % purity c9,t11-CLA, 98 % purity c9,t11-CLA, 98 % purity t10,c12-CLA.

REFERENCES

- 1 **Ha YL**, Grimm NK, Pariza MW. Anticarcinogens from fried ground beef: heated-altered derivatives of linoleic acid. *Carcinogenesis* 1987; **8**: 1881-1887
- 2 **Kritchevsky D**. Antimutagenic and some other effects of conjugated linoleic acid. *Br J Nutr* 2000; **83**: 459-465
- 3 **Pariza MW**, Park Y, Cook ME. Mechanisms of action of conjugated linoleic acid: evidence and speculation. *Proc Soc Exp Biol Med* 2000; **223**: 8-13
- 4 **Pariza MW**, Park Y, Cook ME. Conjugated linoleic acid and the control of cancer and obesity. *Toxicol Sci* 1999; **52**: 107-110
- 5 **Scimeca JA**. Toxicological evaluation of dietary conjugated linoleic acid in male Fischer 344 rats. *Food Chem Toxicol* 1998; **36**: 391-395
- 6 **Belury MA**, Nickel KP, Bird CE, Wu Y. Dietary conjugated linoleic acid modulation of phorbol ester skin tumor promotion. *Nutr Cancer* 1996; **26**: 149-157
- 7 **Ha YL**, Storkson J, Pariza MW. Inhibition of benzo(a)pyrene-induced mouse forestomach neoplasia by conjugated dienoic derivatives of linoleic acid. *Cancer Res* 1990; **50**: 1097-1101
- 8 **Xu M**, Dashwood RH. Chemoprevention studies of heterocyclic amine-induced colon carcinogenesis. *Cancer Lett* 1999; **143**: 179-183
- 9 **Ip C**, Singh M, Thompson HJ, Scimeca JA. Conjugated linoleic acid suppresses mammary carcinogenesis and proliferative activity of the mammary gland in the rat. *Cancer Res* 1994; **54**: 1212-1215
- 10 **Sebedio JL**, Gnaedig S, Chardigny JM. Recent advances in conjugated linoleic acid research. *Curr Opin Clin Nutr Metab Care* 1999; **2**: 499-506
- 11 **Ip C**, Chin SF, Scimeca JA, Pariza MW. Mammary cancer prevention by conjugated dienoic derivative of linoleic acid. *Cancer Res* 1991; **51**: 6118-6124
- 12 **Schut HA**, Cummings DA, Smale MH, Josyula S, Friesen MD. DNA adducts of heterocyclic amines: formation, removal and inhibition by dietary component. *Mutation Res* 1997; **376**: 185-194
- 13 **Pariza MW**, Hargraves WA. A beef derived mutagenesis modulator inhibits initiation of mouse epidermal tumors by 7, 12-dimethylbenz(a)anthracene. *Carcinogenesis* 1985; **6**: 591-593
- 14 **Hubbard NE**, Lim D, Summers L, Erickson KL. Reduction of murine mammary tumor metastasis by conjugated linoleic acid. *Cancer Lett* 2000; **150**: 93-100
- 15 **Josyula S**, Schut HA. Effect of dietary conjugated linoleic acid on DNA adduct formation of PhIP and IQ after bolus administration to female F344 rats. *Nutr Cancer* 1998; **32**: 139-145
- 16 **Josyula S**, He YH, Ruch RJ, Schut HA. Inhibition of DNA adduct formation of PhIP in female F344 rats by dietary conjugated linoleic acid. *Nutr Cancer* 1998; **32**: 132-138
- 17 **Ip C**, Jiang C, Thompson HJ, Scimeca JA. Retention of conjugated linoleic acid in the mammary gland is associated with tumor inhibition during the post-initiation phase of carcinogenesis. *Carcinogenesis* 1997; **18**: 755-759
- 18 **Kimoto N**, Hirose M, Futakuchi M, Iwata T, Kasai M, Shirai T. Site-dependent modulating effects of conjugated fatty acids from safflower oil in a rat two-stage carcinogenesis model in female Sprague-Dawley rats. *Cancer Lett* 2001; **168**: 15-21
- 19 **Ip C**, Scimeca JA, Thompson H. Effect of timing and duration of dietary conjugated linoleic acid on mammary cancer prevention. *Nutr Cancer* 1995; **24**: 241-247
- 20 **Xue YB**, Chen BQ, Zheng YM, Yuan LL, Liu RH. Effects of conjugated linoleic acid on the metastasis of mouse melanoma B16-MB. *Weisheng Yanjiu* 2001; **30**: 37-39
- 21 **Chen BQ**, Xue YB, Feng WJ, Zheng YM, Liu RH. The effects of conjugated linoleic acid on the adhesion and migration of B16-MB mouse melanoma cells. *J Health Toxicology* 2001; **1**: 20-23
- 22 **Cesano A**, Visonneau S, Scimeca JA, Kritchevsky D, Santoli D. Opposite effects of linoleic acid and conjugated linoleic acid on human prostatic cancer in SCID mice. *Anticancer Res* 1998; **18**: 1429-1434
- 23 **Visonneau S**, Cesano A, Tepper SA, Scimeca JA, Santoli D, Kritchevsky D. Conjugated linoleic acid suppresses the growth of human breast adenocarcinoma cells in SCID mice. *Anticancer Res* 1997; **17**: 969-973
- 24 **Schonberg S**, Krokan HE. The inhibitory effect of conjugated dienoic derivatives (CLA) of linoleic acid on the growth of human tumor cell lines is in part due to increased lipid peroxidation. *Anticancer Res* 1995; **15**: 1241-1246
- 25 **Ip C**, Banni S, Angioni E, Carta G, McGinley J, Thompson HJ, Barbano D, Bauman D. Conjugated linoleic acid-enriched butter fat alters mammary gland morphogenesis and reduces cancer risk in rats. *J Nutr* 1999; **129**: 2135-2142
- 26 **Durgam VR**, Fernandes G. The growth inhibitory effect of conjugated linoleic acid on MCF-7 cells is related to estrogen response system. *Cancer Lett* 1997; **116**: 121-130
- 27 **Cunningham DC**, Harrison LY, Shultz TD. Proliferative responses of normal human mammary and MCF-7 breast cancer cells to linoleic acid, conjugated linoleic acid and eicosanoid synthesis inhibitors in culture. *Anticancer Res* 1997; **17**: 197-203
- 28 **Liu KL**, Belury MA. Conjugated linoleic acid modulation of phorbol ester-induced events in murine keratinocytes. *Lipids* 1997; **32**: 725-730
- 29 **Igarashi M**, Miyazawa T. The growth inhibitory effect of conjugated linoleic acid on a human hepatoma cell line, HepG2, is induced by a change in fatty acid metabolism, but not the facilitation of lipid peroxidation in the cells. *Biochim Biophys Acta* 2001; **1530**: 162-171
- 30 **Thompson H**, Zhu Z, Banni S, Darcy K, Loftus T, Ip C. Morphological and biochemical status of the mammary gland as influenced by conjugated linoleic acid: implication for a reduction in mammary cancer risk. *Cancer Res* 1997; **57**: 5067-5072
- 31 **Miller A**, Stanton C, Devery R. Modulation of arachidonic acid distribution by conjugated linoleic acid isomers and linoleic acid in MCF-7 and SW480 cancer cells. *Lipids* 2001; **36**: 1161-1168
- 32 **Ip MM**, Masso-Welch PA, Shoemaker SF, Shea-Eaton WK, Ip C. Conjugated linoleic acid inhibits proliferation and induces apoptosis of normal rat mammary epithelial cells in primary culture. *Exp Cell Res* 1999; **250**: 22-34
- 33 **Ip C**, Ip MM, Loftus T, Shoemaker S, Shea-Eaton W. Induction of apoptosis by conjugated linoleic acid in cultured mammary tumor cells and premalignant lesions of the rat mammary gland. *Cancer Epidemiol Biomarkers Prev* 2000; **9**: 689-696
- 34 **Choi Y**, Park Y, Storkson JM, Pariza MW, Ntambi JM. Inhibition of stearoyl-CoA desaturase activity by the cis-9,trans-11 isomer and the trans-10,cis-12 isomer of conjugated linoleic acid in MDA-MB-231 and MCF-7 human breast cancer cells. *Biochem Biophys Res Commun* 2002; **294**: 785-790
- 35 **Choi Y**, Park Y, Pariza MW, Ntambi JM. Regulation of stearoyl-CoA desaturase activity by the trans-10,cis-12 isomer of conjugated linoleic acid in HepG2 cells. *Biochem Biophys Res Commun* 2001; **284**: 689-693
- 36 **Thuillier P**, Anchiraico GJ, Nickel KP, Maldve RE, Gimenez-Conti I, Muga SJ, Liu KL, Fischer SM, Belury MA. Activators of peroxisome proliferator-activated receptor-alpha partially inhibit mouse skin tumor promotion. *Mol Carcinog* 2000; **29**: 134-142
- 37 **Moya-Camarena SY**, Vanden Heuvel JP, Blanchard SG, Leesnitzer LA, Belury MA. Conjugated linoleic acid is a potent naturally occurring ligand and activator of PPARalpha. *J Lipid Res* 1999; **40**: 1426-1433
- 38 **Moya-Camarena SY**, Van den Heuvel JP, Belury MA. Conjugated linoleic acid activates peroxisome proliferator-activated receptor alpha and beta subtypes but does not induce hepatic peroxisome proliferation in Sprague-Dawley rats. *Biochim Biophys Acta* 1999; **1436**: 331-342
- 39 **Liu JR**, Li BX, Chen BQ, Han XH, Xue YB, Yang YM, Zheng YM, Liu RH. Effect of cis-9, trans-11-conjugated linoleic acid on cell cycle of gastric adenocarcinoma cell line (SGC-7901). *World J Gastroenterol* 2002; **8**: 224-229
- 40 **Liu JR**, Chen BQ, Deng H, Han XH, Liu RH. Cellular Apoptosis Induced by Conjugated Linoleic Acid in Human Gastric Cancer

- (SGC-7901) Cells. *Gongye Weisheng Yu Zhiyebing* 2001; **27**: 129-133
- 41 **Liu JR**, Chen BQ, Xue YB, Han XH, Yang YM, Liu RH. Conjugated linoleic acid inhibits the growth of mammary carcinoma cells. *Zhonghua Yufang Yixue* 2001; **35**: 244-247
- 42 **Zhu Y**, Qiou J, Chen BQ, Liu RH. The inhibitory effect of conjugated linoleic acid on mice forestomach neoplasia induced by benzo(a)pyrene. *Zhonghua Yufang Yixue* 2001; **35**: 19-22
- 43 **Wu K**, Shan YJ, Zhao Y, Yu JW, Liu BH. Inhibitory effects of RRR- α -tocopheryl succinate on benzo(a)pyrene (B(a)P)-induced forestomach carcinogenesis in female mice. *World J Gastroenterol* 2001; **7**: 60-65
- 44 **Lu LG**, Zeng MD, Li JQ, Hua J, Fan JG, Qiu DK. Study on the role of free fatty acids in proliferation of rat hepatic stellate cells (II). *World J Gastroenterol* 1998; **4**: 500-502
- 45 **Devery R**, Miller A, Stanton C. Conjugated linoleic acid and oxidative behaviour in cancer cells. *Biochem Soc Trans* 2001; **29**: 341-344
- 46 **O'Shea M**, Stanton C, Devery R. Antioxidant enzyme defence responses of human MCF-7 and SW480 cancer cells to conjugated linoleic acid. *Anticancer Res* 1999; **19**: 1953-1959
- 47 **O'Shea M**, Devery R, Lawless F, Murphy J, Stanton C. Milk fat conjugated linoleic acid (CLA) inhibits growth of human mammary MCF-7 cancer cells. *Anticancer Res* 2000; **20**: 3591-3601
- 48 **Hawkins RA**, Sangster K, Arends MJ. Apoptotic death of pancreatic cancer cells induced by polyunsaturated fatty acids varies with double bond number and involves an oxidative mechanism. *J Pathol* 1998; **185**: 61-70
- 49 **Cobb MH**. MAP kinase pathways. *Prog Biophys Mol Biol* 1999; **71**: 479-500
- 50 **Chang L**, Karin M. Mammalian MAP kinase signalling cascades. *Nature* 2001; **410**: 37-40
- 51 **Meng AH**, Ling YL, Zhang XP, Zhao XY, Zhang JL. CCK-8 inhibits expression of TNF- α in the spleen of endotoxic shock rats and signal transduction mechanism of p38 MAPK. *World J Gastroenterol* 2002; **8**: 139-143
- 52 **Fleischer F**, Dabew R, Goke B, Wagner AC. Stress kinase inhibition modulates acute experimental pancreatitis. *World J Gastroenterol* 2001; **7**: 259-265
- 53 **Wu K**, Liu BH, Zhao DY, Zhao Y. Effect of vitamin E succinate on expression of TGF- β 1, c-Jun and JNK1 in human gastric cancer SGC-7901 cells. *World J Gastroenterol* 2001; **7**: 83-87
- 54 **Jarvis WD**, Fornari FA, Auer KL, Freermerman AJ, Szabo E, Birrer MJ, Johnson CR, Barbour SE, Dent P, Grant S. Coordinate regulation of stress- and mitogen-activated protein kinases in the apoptotic actions of ceramide and sphingosine. *Mol Pharmacol* 1997; **52**: 935-947
- 55 **Feng DY**, Zheng H, Tan Y, Cheng RX. Effect of phosphorylation of MAPK and Stat3 and expression of c-fos and c-jun proteins on hepatocarcinogenesis and their clinical significance. *World J Gastroenterol* 2001; **7**: 33-36
- 56 **Dai T**, Rubie E, Franklin CC, Kraft A, Gillespie DA, Avruch J, Kyriakis JM, Woodgett JR. Stress-activated protein kinases bind directly to the delta domain of c-Jun in resting cells: implications for repression of c-Jun function. *Oncogene* 1995; **10**: 849-855
- 57 **Sun H**, Charles CH, Lau LF, Tonks NK. MKP-1 (3CH134), an immediate early gene product, is a dual specificity phosphatase that dephosphorylates MAP kinase *in vivo*. *Cell* 1993; **75**: 487-493

Edited by Wu XN

Helicobacter pylori infection and respiratory diseases: a review

Anastasios Roussos, Nikiforos Philippou, Konstantinos I Gourgoulianis

Anastasios Roussos, Nikiforos Philippou, 9th Department of Pulmonary Medicine, "SOTIRIA" Chest Diseases Hospital, Athens, Greece

Konstantinos I Gourgoulianis, Pulmonary Department, Medical University of Thessaly, Larisa, Greece

Correspondence to: Dr Anastasios Roussos, 20 Ierosolimon Street, PO: 11252, Athens, Greece. roumar26@yahoo.com

Telephone: +301-8646215 **Fax:** +301-8646215

Received: 2002-10-25 **Accepted:** 2002-11-07

Abstract

In the past few years, a variety of extradigestive disorders, including cardiovascular, skin, rheumatic and liver diseases, have been associated with *Helicobacter pylori* (*H. pylori*) infection. The activation of inflammatory mediators by *H. pylori* seems to be the pathogenetic mechanism underlying the observed associations. The present review summarizes the current literature, including our own studies, concerning the association between *H. pylori* infection and respiratory diseases.

A small number of epidemiological and serologic, case-control studies suggest that *H. pylori* infection may be associated with the development of chronic bronchitis. A frequent coexistence of pulmonary tuberculosis and *H. pylori* infection has also been found. Moreover, recent studies have shown an increased *H. pylori* seroprevalence in patients with bronchiectasis and in those with lung cancer. On the other hand, bronchial asthma seems not to be related with *H. pylori* infection.

All associations between *H. pylori* infection and respiratory diseases are primarily based on case-control studies, concerning relatively small numbers of patients. Moreover, there is a lack of studies focused on the pathogenetic link between respiratory diseases and *H. pylori* infection. Therefore, we believe that larger studies should be undertaken to confirm the observed results and to clarify the underlying pathogenetic mechanisms.

Roussos A, Philippou N, Gourgoulianis KI. *Helicobacter pylori* infection and respiratory diseases: a review. *World J Gastroenterol* 2003; 9(1): 5-8

<http://www.wjgnet.com/1007-9327/9/5.htm>

INTRODUCTION

Helicobacter pylori (*H. pylori*) is a slow-growing, microaerophilic, gram-negative bacterium, whose most striking biochemical characteristic is the abundant production of urease. This bacterium colonizes gastric mucosa and elicits both inflammatory and immune lifelong responses, with release of various bacterial and host-dependent cytotoxic substances^[1]. Pathological studies and extensive clinical trials, carried out in the past few years, have proved the causative role of *H. pylori* in the development of chronic gastritis^[2] and peptic ulcer disease^[3]. It seems that this bacterium is also causally related to low-grade B-cell lymphoma of gastric mucosa-associated-lymphoid-tissue (MALT-lymphoma)^[4]. Moreover, *H. pylori* infection has been established as a risk factor for the development of both diffuse and intestinal types of gastric cancer^[5].

Recent studies suggest an epidemiological association

between *H. pylori* infection and several extragastrointestinal pathologies, including cardiovascular, skin, rheumatic and liver diseases (Table 1)^[6,7]. Unfortunately, such epidemiological studies are influenced by a wide variety of confounding factors, i.e. socioeconomic status, time of acquisition of the infection, presence of different bacterial strains and previous antibiotic therapy. However, according to many authors, the observed associations might be true and explained by a role of *H. pylori* infection in the pathogenesis of certain extradigestive disorders. It is well known that *H. pylori* colonization of the gastric mucosa stimulates the release of various proinflammatory substances, such as cytokines, eicosanoids and proteins of the acute phase^[8]. Moreover, a cross mimicry between bacterial and host antigens exists in *H. pylori* infected patients^[9]. Therefore, a pathogenetic link between *H. pylori* infection and diseases characterized by activation of inflammatory mediators and/or induction of autoimmunity might exist.

Chronic inflammation and increased immune response have been observed in a variety of respiratory diseases, including chronic bronchitis^[10,11] and bronchiectasis^[12]. Moreover, both chronic obstructive pulmonary disease^[13,14] and pulmonary tuberculosis^[15] are more prevalent in peptic ulcer patients than in the general population. Based on these facts, many recent studies have focused on the potential association between *H. pylori* infection and various respiratory disorders. Table 2 summarizes those respiratory diseases whose relation with *H. pylori* infection has been studied in the literature.

The aim of the present report is to provide a critical review of the current literature, including our own studies, as regards the association between *H. pylori* infection and respiratory diseases.

Table 1^[6,7] Extradigestive diseases associated with *H. pylori* infection

Vascular diseases

Ischaemic heart disease
Primary Raynaud's phenomenon
Primary headache

Skin diseases

Idiopathic chronic urticaria
Rosacea
Alopecia areata

Autoimmune diseases

Sjogren's syndrome
Autoimmune thyroiditis
Autoimmune thrombocytopenia
Schoenlein-Henoch purpura

Other diseases

Liver cirrhosis
Growth retardation
Chronic idiopathic sideropenia
Sudden infant death
Diabetes mellitus

Table 2 Respiratory diseases studied for a relationship with *H. pylori* infection

Chronic bronchitis

Pulmonary tuberculosis
Bronchiectasis
Lung cancer
Bronchial asthma

HELICOBACTER PYLORI INFECTION AND CHRONIC BRONCHITIS

Chronic bronchitis is a pulmonary disease characterized by, primarily irreversible, airflow obstruction due to the chronic inflammation of the small airways. The presence of airflow obstruction that is not fully reversible is confirmed by spirometry (postbronchodilator FEV₁<80 % of the predicted value, in combination with an FEV₁/FVC<70 %). Although its true prevalence remains unknown, it is estimated that approximately 12.5 million persons in the United States suffer from chronic bronchitis^[16].

Chronic bronchitis had been associated with gastroduodenal ulcer many years before the identification of *H. pylori* infection as a cause of peptic ulcer disease. Three epidemiological studies, carried out between 1968 and 1986, showed that the prevalence of chronic bronchitis in peptic ulcer patients was increased two-to-three fold compared with that in ulcer-free controls^[13,14,17]. Moreover, a follow-up study demonstrated that chronic bronchitis was a major cause of death among patients with peptic ulcer disease^[18].

The reported association between these two diseases was originally attributed to the known role of cigarette smoking as an independent factor in both ulcerogenesis and development of chronic bronchitis. However, in 1998, Gaseli and colleagues carried out a prospective pilot study in a sample of 60 Italian patients with chronic bronchitis and found an increased seroprevalence of *H. pylori* infection compared to that detected in 69 healthy controls (81.6 % versus 57.9 % respectively, $P=0.008$). In this study, the odds ratio for chronic bronchitis in the presence of *H. pylori* infection, calculated after adjustment for age and social status, was 3.4^[19]. These results suggested, for the first time, that *H. pylori* infection per se might be related to an increased risk of developing chronic bronchitis. Two years later, a large epidemiological study in 3608 Danish adults showed that chronic bronchitis might be more prevalent in *H. pylori* IgG seropositive women than in uninfected ones (odds ratio 1.6, with a 95 % confidence interval of 1.1-2.5)^[20]. In order to further investigate the reported association between *H. pylori* infection and chronic bronchitis, we recently performed a case-control study in a cohort of 144 Greek patients with chronic bronchitis and 120 control subjects. Our results were in accordance with those of Gaselli and associates, as we also found that *H. pylori* seropositivity in patients was significantly higher than that in controls (83.3 % vs 60 %, $P=0.007$)^[21].

The mechanisms underlying the suggested association between *H. pylori* infection and chronic bronchitis remain unclear. This association might reflect either susceptibility induced by common factors or a kind of causal relationship between these two conditions. It is well known that age, sex and socioeconomic status are related with both *H. pylori* infection^[11] and risk of developing chronic bronchitis^[16]. However, in all mentioned studies above patients with chronic bronchitis were well matched with control subjects for these parameters. Tobacco use could be another confounding factor. Cigarette smoking is the major cause of chronic bronchitis^[16]. On the other hand, data on the relation between *H. pylori* infection and smoking habits are controversial. The prevalence of *H. pylori* infection in smokers has been variously reported as low^[22], normal^[23], and high^[24]. As the relation between smoking and *H. pylori* infection has not been clarified yet, the possible impact of cigarette smoking on both chronic bronchitis and *H. pylori* infection should be regarded as a potential limitation of the reviewed studies.

Unfortunately, there are no studies in the literature focused on the potential aetio-pathogenetic role of *H. pylori* infection in chronic bronchitis. Some authors hypothesized that the chronic

activation of inflammatory mediators induced by *H. pylori* infection might lead to the development of a non-specific inflammatory process, such as chronic bronchitis^[19,21]. It is well known that *H. pylori* and particularly those strains bearing the cytotoxin associated gene-A (cagA positive strains), stimulates the release of a variety of proinflammatory cytokines, including interleukin-1 (IL-1), IL-8 and tumour necrosis factor-alpha^[25,26]. The eradication of *H. pylori* leads to normalization of serum cytokines levels^[27]. Recent studies showed that the same cytokines might be released during the course and exacerbations of chronic bronchitis^[10,11,28]. The underlying mechanisms, which induce and control this inflammatory process in chronic bronchitis, are still unclear. Therefore, we could hypothesize that *H. pylori* infection might play a proinflammatory role and co-trigger chronic bronchitis with other more specific environmental, genetic and unknown yet factors.

In conclusion, the primary evidence for an association between *H. pylori* infection and chronic bronchitis rests on serologic, case-control studies. Studies estimating the relative risk of developing chronic bronchitis for *H. pylori* infected patients and the effect of *H. pylori* eradication on the natural history of chronic bronchitis should be undertaken. The pathogenetic mechanisms underlying this association need also further evaluation. Future studies concerning this aspect should be focused on the prevalence of cagA positive *Helicobacter* strains and their induced proinflammatory markers, in patients with chronic bronchitis.

HELICOBACTER PYLORI INFECTION AND PULMONARY TUBERCULOSIS

Tuberculosis (TB) is a chronic bacterial infection caused by *Mycobacterium tuberculosis* and characterized by the formation of granulomas in infected tissues and by cell-mediated hypersensitivity. The lungs are primarily infected. However, any other organ may be involved. Although there is a lack of epidemiological evidence concerning the worldwide prevalence of TB, it has been estimated that one third of the world population is infected with *Mycobacterium tuberculosis* and there are ten million new cases of active TB each year. The vast majority of them occur in the developing countries, where TB remains a common health problem^[29].

In 1992, Mitchell *et al* carried out a large cross-sectional study concerning the *H. pylori* epidemiology in a southern China population. They found that a history of pulmonary TB might be associated with an increased prevalence of *H. pylori* infection^[30]. More recently, Woeltje *et al* assessed the prevalence of tuberculin skin test (TST) positivity in a cohort of 346 newly hospitalized patients. A history of peptic ulcer disease was one of the identified risk factors for a positive TST test (odds ratio: 4.53, $P=0.017$)^[31]. In order to further investigate the possible association between pulmonary TB and *H. pylori* infection, Sanaka *et al* performed, in 1998, a serologic case-control study in a hospitalized population. No difference in *H. pylori* seroprevalence among 40 inpatients on antituberculosis chemotherapy for less than three months, 43 TB patients on chemotherapy for more than three months and 60 control subjects was detected (73.3 %, 65 % and 69.8 % respectively, $P>0.5$ in all comparisons)^[32]. However, in this study the eradication of *H. pylori* by antituberculosis drugs could not be excluded. Rifampicin and Streptomycin, two drugs commonly used in antituberculosis regimens, are effective against *H. pylori* and decrease in *H. pylori* seroprevalence during antituberculosis therapy has been reported^[33,34]. Therefore, we recently carried out a case-control study focused on the seroprevalence of *H. pylori* in TB patients, before the initiation of antituberculosis treatment. A total of 80 TB patients and 70 control subjects, well matched for age, sex and social

status, were recruited into this study. We found that the *H. pylori* seropositivity in the TB group was significantly higher than that of controls (87.5 % vs 61.4 %, $P=0.02$). The mean serum concentration of IgG antibodies against *H. pylori* was also significantly higher in TB patients than in control subjects (39.0 ± 25.2 U/ml vs 26.1 ± 21.2 U/ml, $P=0.001$)^[35].

Taken together, data in the literature on the relationship between *H. pylori* infection and pulmonary TB are still insufficient. The observed frequent coexistence of both infections must be confirmed in a larger number of patients. This coexistence might reflect susceptibility to both *H. pylori* and *Mycobacterium tuberculosis* induced by common host genetic factors. It has been suggested that HLA-DQ serotype may contribute to enhanced mycobacterial survival and replication^[36]. Recent studies showed that the same serotype is also associated with increased susceptibility to *H. pylori* infection^[37,38]. Poor socioeconomic and sanitary conditions during childhood could be another factor responsible for the association between the two infections, as it is well known that in developing countries acquisition of both *H. pylori* and *Mycobacterium tuberculosis* occurs early in life^[39,40]. Therefore, we believe that studies focused on the common, either genetic or environmental, predisposition to both bacteria are needed.

HELICOBACTER PYLORI INFECTION AND BRONCHIECTASIS

Bronchiectasis is an abnormal and permanent dilation of bronchi, due to inflammation and destruction of the structural components of the bronchial wall. Persistent or recurrent cough, purulent sputum production and/or hemoptysis are symptoms presented during the clinical course of this disorder. A wide variety of respiratory infections, toxic substances and rare congenital syndromes are associated with the development of bronchiectasis. However, a great percentage of cases are of unknown cause^[41].

In 1998, Tsang *et al* found that the *H. pylori* seroprevalence in 100 patients with bronchiectasis (76 %) was higher than that in the controls (54.3 %, $P=0.001$). Further analysis in studied patients revealed an association between *H. pylori* seropositivity and 24-hours sputum volume ($P=0.03$)^[42].

As far as we know, the study of Tsang *et al* is the only report in the literature concerning the association between *H. pylori* infection and bronchiectasis. The authors hypothesized that the spilling or inhalation of *H. pylori* into the respiratory tract might lead to a chronic bronchial inflammatory disorder such as bronchiectasis. However, although *H. pylori* has been identified in the tracheobronchial aspirates in mechanically ventilated patients^[43], neither identification in human bronchial tissue nor isolation from bronchoalveolar lavage (BAL) fluid have been achieved yet^[1]. On the other hand, recent studies have shown that inflammation in bronchiectasis is primarily cytokine-mediated^[12,44]. Therefore, the activation of systemic inflammatory mediators by chronic *H. pylori* infection could represent a possible pathogenetic link between these two diseases.

In conclusion, the possible association between *H. pylori* and bronchiectasis seems intriguing and might have a pathogenetic basis. However, studies in larger series are needed to confirm this association and to clarify the underlying mechanisms. As pulmonary TB is a common cause of bronchiectasis, we believe that the increased prevalence of *H. pylori* infection in TB patients should be taken into account in the design of these future studies.

HELICOBACTER PYLORI INFECTION AND OTHER RESPIRATORY DISEASES

Lung cancer A recent study showed a higher *H. pylori* seroprevalence (89.5 %) among 50 patients with lung cancer than that in control subjects (64 %, $P<0.05$). The CagA strain

seropositivity was about thrice as high as in controls. (63 % vs 21.5 % respectively, $P<0.05$). Lung cancer patients were characterized by a significant increase of gastrin concentration in both serum and bronchoalveolar lavage (BAL). An enhanced m-RNA expression for gastrin and its receptor, as well as for cyclooxygenase (COX)-2, in the tumor tissue was also detected. Therefore, the authors hypothesized that *H. pylori* might contribute to lung carcinogenesis, via enhancement of gastrin synthesis. Gastrin might induce increased mucosal cell proliferation of bronchial epithelium and lead to atrophy and induction of COX-2, as it happens in gastric cancer. Finally, the authors proposed that *H. pylori* should be eradicated in lung cancer patients, in order to reduce the *H. pylori* provoked hypergastrinemia and COX-2 expression^[45].

Chronic bronchitis, which is associated with both lung cancer and *H. pylori* infection, might be a confounding factor in this study. Moreover, although some authors have also showed an increased gastrin concentration in serum and BAL fluid in lung cancer patients^[46,47], others did not confirm this finding^[48]. Therefore, we believe that before adapting the *H. pylori* eradication in lung cancer patients, further studies are needed to examine whether the reported epidemiological association between these two diseases has a pathogenetic basis.

Bronchial asthma In 2000, Tsang *et al* estimated the prevalence of *H. pylori* infection in a cohort of 90 patients with bronchial asthma. *Helicobacter pylori* seroprevalence did not differ significantly between asthmatic and control subjects (47.3 % vs 38.1 %, $P>0.05$), while serum concentration of IgG antibodies against *H. pylori* did not correlate with spirometric values and duration of asthma. The authors concluded that bronchial asthma might not be associated with *H. pylori* infection^[49]. Moreover, as far as we know there is a lack of a theoretical hypothesis that might explain a possible association between these two diseases. Therefore, we believe that our knowledge on the association between *H. pylori* infection and respiratory diseases is unlikely to be advanced by more studies concerning the prevalence of *H. pylori* infection in patients with bronchial asthma.

CONCLUSIONS-FUTURE CHALLENGES

At present, the primary evidence for a link between *H. pylori* infection and respiratory diseases rests on case-control studies, concerning relatively small numbers of patients. Future studies should be large enough for moderate-sized effects to be assessed or registered reliably. The activation of inflammatory mediators by *H. pylori* infection might be the pathogenetic mechanism underlying the observed associations. Therefore, the role of genetic predisposition of the infected host, the presence of strain-specific virulence factors and the serum concentration of proinflammatory markers in *H. pylori* infected patients with respiratory diseases needs further evaluation. Finally, randomized control studies should be undertaken, in order to clarify the effect of the *H. pylori* eradication on the prevention, development and natural history of these disorders.

REFERENCES

- 1 **Peterson WL**, Graham DY. *Helicobacter pylori*. In: Feldman M, Scharschmidt BF, Sleisenger MH editors *Gastrointestinal and liver Disease. Pathophysiology, diagnosis, management*. 6th ed. Philadelphia: WB Saunders 1998; p: 604-619
- 2 **Cave DR**. Chronic gastritis and *Helicobacter pylori*. *Semin Gastrointestinal Dis* 2001; **12**: 196-202
- 3 **Cohen H**. Peptic ulcer and *Helicobacter pylori*. *Gastroenterol Clin North Am* 2000; **29**: 775-789
- 4 **Parsonnet J**, Hansen S, Rodriguez L, Gelb AB, Warnke RA, Jellum E, Orentreich N, Vogelman JH, Friedman GD. *Helicobacter pylori* and gastric lymphoma. *N Engl J Med* 1994; **330**: 1267-1271

- 5 **Xue FB**, Xu YY, Wan Y, Pan BR, Ren J, Fan DM. Association of *H. pylori* infection with gastric carcinoma. A Meta analysis. *World J Gastroenterol* 2001; **7**: 801-804
- 6 **Realdi G**, Dore MP, Fastame L. Extradigestive manifestations of *Helicobacter pylori* infection. Fact and fiction. *Dig Dis Sci* 1999; **44**:229-236
- 7 **Gasbarrini A**, Franceschi F, Armuzzi A, Ojetti V, Candelli M, Sanz Torre E, Lorenzo AD, Anti M, Pretolani S, Gasbarinni G. Extradigestive manifestations of *Helicobacter pylori* gastric infection. *Gut* 1999; **45**(Suppl 1): 9-12
- 8 **Crabtree JE**. Role of cytokines in pathogenesis of *Helicobacter pylori* induced mucosal damage. *Dig Dis Sci* 1998; **43**(Suppl 9): 46-55
- 9 **Negrini R**, Savio A, Poesi C, Appelmelk BJ, Buffoli F, Paterlini A, Cesari P, Graffeo M, Vaira D, Franzin G. Antigenic mimicry between *H. pylori* and gastric mucosa in the pathogenesis of body atrophic gastritis. *Gastroenterology* 1996; **111**: 655-665
- 10 **Huang SL**, Su CH, Chang SC. Tumor necrosis factor- α gene polymorphism in chronic bronchitis. *Am J Resp Crit Care Med* 1997; **156**: 1436-1439
- 11 **Nelson S**, Summer WR, Mason CM. The role of the inflammatory response in chronic bronchitis: therapeutic implications. *Semin Respir Infect* 2000; **15**: 24-31
- 12 **Silva JR**, Jones JA, Cole P, Poulter L. The immunological component of the cellular inflammatory infiltrate in bronchiectasis. *Thorax* 1989; **44**: 668-673
- 13 **Langman MJ**, Cooke AR. Gastric and duodenal ulcer and their associated diseases. *Lancet* 1976; **1**: 680-683
- 14 **Kellow JE**, Tao Z, Piper DW. Ventilatory function in chronic peptic ulcer. *Gastroenterology* 1986; **91**: 590-595
- 15 **Lundegardh G**, Helmick C, Zack M, Adami HO. Mortality among patients with partial gastrectomy for benign ulcer disease. *Dig Dis Sci*1994; **39**: 340-346
- 16 **Gomez FP**, Rodriguez-Roisin R. Global Initiative for Chronic Obstructive Lung Disease (GOLD) guidelines for chronic obstructive pulmonary disease. *Curr Opin Pulm Med* 2002; **8**: 81-86
- 17 **Arora OP**, Kapoor CP, Sobti P. Study of gastroduodenal abnormalities in chronic bronchitis and emphysema. *Am J Gastroenterol* 1968; **50**: 289-296
- 18 **Bonnevie O**. Causes of death in duodenal and gastric ulcer. *Gastroenterology* 1977; **73**: 1000-1004
- 19 **Gaselli M**, Zaffoni E, Ruina M, Sartori S, Trevisani L, Ciaccia A, Alvisi V, Fabbri L, Papi A. *Helicobacter pylori* and chronic bronchitis. *Scand J Gastroenterol* 1999; **34**: 828-830
- 20 **Rosenstock SJ**, Jorgensen T, Andersen LP, Bonnevie O. Association of *Helicobacter pylori* infection with lifestyle, chronic disease, body indices and age at menarche in Danish adults. *Scand J Public Health* 2000; **28**: 32-40
- 21 **Roussos A**, Tsimpoukas F, Anastasakou E, Alepopoulou D, Paizis I, Philippou N. *Helicobacter pylori* seroprevalence in patients with chronic bronchitis. *J Gastroenterol* 2002; **37**: 332-335
- 22 **Ogihara A**, Kikuchi S, Hasegawa A, Kurosawa M, Miki K, Kaneko E, Mizukoshi H. Relationship between *Helicobacter pylori* infection and smoking and drinking habits. *J Gastroenterol Hepatol* 2000; **15**: 271-276
- 23 **Brenner H**, Rothenbacher D, Bode G, Adler G. Relation of smoking and alcohol and coffee consumption to active *Helicobacter pylori* infection: cross sectional study. *BMJ* 1997; **315**: 1489-1492
- 24 **Parasher G**, Eastwood GL. Smoking and peptic ulcer in the *Helicobacter pylori* era. *Eur J Gastroenterol Hepatol* 2000; **12**: 843-853
- 25 **Perri F**, Clemente R, Festa V, De Ambrosio CC, Quitadamo M, Fusillo M, Grossi E, Andriulli A. Serum tumour necrosis factor- α is increased in patients with *Helicobacter pylori* infection and CagA antibodies. *Ital J Gastroenterol Hepatol* 1999; **31**: 290-294
- 26 **Russo F**, Jirillo E, Clemente C, Messa C, Chiloiro M, Riezzo G, Amati L, Caradonna L, Di Leo A. Circulating cytokines and gastrin levels in asymptomatic subjects infected by *Helicobacter pylori* (*H. pylori*). *Immunopharmacol Immunotoxicol* 2001; **23**: 13-24
- 27 **Kountouras J**, Boura P, Lygidakis NJ. Omeprazole and regulation of cytokine profile in *Helicobacter pylori*-infected patients with duodenal ulcer disease. *Hepatogastroenterology* 2000; **47**: 1301-1304
- 28 **Keatings VM**, Collins PD, Scott DM, Barnes PJ. Differences in interleukin-8 and tumor necrosis factor- α in induced sputum from patients with chronic obstructive pulmonary disease or asthma. *Am J Respir Crit Care Med* 1996; **153**: 530-534
- 29 **Daniel TM**. Tuberculosis In Harrison's Principles of internal medicine 14th edition. *New York: McGraw-Hill inc* 1998; **p**: 710-718
- 30 **Mitchell HM**, Li YY, Hu PJ, Liu Q, Chen M, Du GG, Wang ZL, Lee A, Hazell SL. Epidemiology of *Helicobacter pylori* in southern China: identification of early childhood as the critical period for acquisition. *J Infect Dis* 1992; **166**: 149-153
- 31 **Woetje KF**, Kilo CM, Johnson K, Primack J, Frases VJ. Tuberculin skin test of hospitalized patients. *Infect Control Hosp Epidemiol* 1997; **18**: 561-565
- 32 **Sanaka M**, Kuyama Y, Iwasaki M, Hanada Y, Tsuchiya A, Haida T, Hiramasa S, Yamaoka S, Yamanaka M. No difference in seroprevalences of *Helicobacter pylori* infection between patients with pulmonary tuberculosis and those without. *J Clin Gastroenterol* 1998; **27**: 331-334
- 33 **Sanaka M**, Kuyama Y, Yamanaka M, Iwasaki M. Decrease of serum concentrations of *Helicobacter pylori* IgG antibodies during antituberculosis therapy: the possible eradication by Rifampicin and Streptomycin. *Am J Gastroenterol* 1999; **94**: 1983-1984
- 34 **Heep M**, Beck D, Bayerdorffer E, Lehn N. Rifampin and rifabutin resistance mechanisms in *Helicobacter pylori*. *Antimicrob Agents Chemother* 1999; **43**: 1497-1499
- 35 **Filippou N**, Roussos A, Tsimboukas F, Tsimogianni A, Anastasakou E, Mavrea S. *Helicobacter pylori* seroprevalence in patients with pulmonary tuberculosis. *J Clin Gastroenterol* 2002; **34**: 189
- 36 **Goldfeld AE**, Delgado JC, Thim S, Bozon MV, Uglialoro AM, Turbay D, Cohen C, Yunis EJ. Association of an HLA-DQ allele with clinical tuberculosis. *JAMA* 1998; **29**: 226-228
- 37 **Azuma T**, Konishi J, Tanaka Y, Hirai M, Ito S, Kato T, Kohli Y. Contribution of HLA-DQA gene to host's response against *Helicobacter pylori*. *Lancet* 1994; **343**: 542-543
- 38 **Beales ILP**, Davey NJ, Pusey CD, Lechler RI, Calam J. Long-term sequelae of *Helicobacter pylori* gastritis. *Lancet* 1995; **346**: 381-382
- 39 **Graham DY**, Adam E, Reddy GT, Agarwal JP, Agarwal R, Evans DJ, Malaty HM, Evans DG. Seroepidemiology of *Helicobacter pylori* infection in India: Comparison of developing and developed countries. *Dig Dis Sci* 1991; **36**: 1084-1088
- 40 **Martin G**, Lazarus A. Epidemiology and diagnosis of tuberculosis. Recognition of at-risk patients is key to prompt detection. *Postgrad Med* 2000; **108**: 42-54
- 41 **Cole PJ**. Bronchiectasis In RL Brewis, B Corrin, DM Geddes, GJ Gibson, editors. *Respiratory Medicine. Philadelphia: WB Saunders* 1995: 1286-1317
- 42 **Tsang KW**, Lam SK, Lam WK, Karlberg J, Wong BC, Yew WW, Ip MS. High seroprevalence of *Helicobacter pylori* in active bronchiectasis. *Am J Resp Crit Care Med* 1998; **158**: 1047-1051
- 43 **Mitz HS**, Farber SS. Demonstration of *Helicobacter pylori* in tracheal secretions. *J Am Osteopath Assoc* 1993; **93**: 87-91
- 44 **Eller J**, Lapa JR, Poulter RW, Lode H, Cole PJ. Cells and cytokines in chronic bronchial infection. *Ann NY Acad Sci* 1994; **725**: 331-345
- 45 **Gocyk W**, Nikliski T, Olechnowicz H, Duda A, Bielanski W, Konturek P, Konturek S. *Helicobacter pylori*, gastrin and cyclooxygenase-2 in lung cancer. *Med Sci Monit* 2000; **6**: 1085-1092
- 46 **Zhou Q**, Yang Z, Yang J, Tian Z, Zhang H. The diagnostic significance of gastrin measurement of bronchoalveolar lavage fluid for lung cancer. *J Surg Oncol* 1992; **50**: 121-124
- 47 **Zhou Q**, Zhang H, Pang X, Yang J, Tain Z, Wu Z, Yang Z. Pre- and postoperative sequential study on the serum gastrin level in patients with lung cancer. *J Surg Oncol* 1993; **51**: 22-25
- 48 **Dowlati A**, Bury T, Corhay JL, Weber T, Lamproye A, Mendes P, Radermecker M. Gastrin levels in serum and bronchoalveolar lavage of patients with lung cancer: comparison with chronic obstructive pulmonary disease. *Thorax* 1996; **51**: 1270-1272
- 49 **Tsang KW**, Lam WK, Chan KN, Hu W, Wu A, Kwok E, Zheng L, Wong BC, Lam SK. *Helicobacter pylori* seroprevalence in asthma. *Respiratory medicine* 2000; **94**: 756-759

Association between pepsinogen C gene polymorphism and genetic predisposition to gastric cancer

Hui-Jie Liu, Xiao-Lin Guo, Ming Dong, Lan Wang, Yuan Yuan

Hui-Jie Liu, Xiao-Lin Guo, Ming Dong, Lan Wang, Yuan Yuan, Cancer Institute, First Affiliated Hospital, China Medical University, Shenyang, 110001, Liaoning Province, China

Supported by The National Basic Research Program (973) of China, No.G1998051203 and National Natural Science Foundation of China, No.30171054

Correspondence to: Dr. Yuan Yuan, Cancer Institute, First Affiliated Hospital, China Medical University, 155 Northern Nanjing Street, Heping District, Shenyang 110001, Liaoning Province, China. yyuan@mail.cmu.edu.cn

Telephone: +86-24-23256666-6153 **Fax:** +86-24-22703576

Received: 2002-06-28 **Accepted:** 2002-07-25

Abstract

AIM: To identify a molecular marker for gastric cancer, and to investigate the relationship between the polymorphism of pepsinogen C (PGC) gene and the genetic predisposition to gastric cancer.

METHODS: A total of 289 cases were involved in this study. 115 cases came from Shenyang area, a low risk area of gastric cancer, including 42 unrelated controls and 73 patients with gastric cancer. 174 cases came from Zhuanghe area, a high-risk area of gastric cancer, including 113 unrelated controls, and 61 cases from gastric cancer kindred families. The polymorphism of PGC gene was detected by polymerase chain reaction (PCR) and the relation between the genetic polymorphism of PGC and gastric cancer was examined.

RESULTS: Four alleles, 310bp (allele 1), 400bp (allele 2), 450bp (allele 3), and 480bp (allele 4) were detected by PCR. The frequency of allele 1 was higher in patients with gastric cancer than that in controls. Genotypes containing homogenous allele 1 were significantly more frequent in patients with gastric cancer than that in controls (0.33, 0.14, $\chi^2=3.86$, $P<0.05$). There was no significant difference between the control group of Zhuanghe and the group of gastric cancer kindred. But the frequency of allele 1 was higher in control group of Zhuanghe area than that in control group of Shenyang area and genotypes containing homogenous allele 1 were significantly more frequent in the control group of Zhuanghe area than those in control group of Shenyang area (0.33, 0.14, $\chi^2=4.32$, $P<0.05$). In the group of gastric cancer kindred the frequency of allele 1 was significantly higher than that in control group of Shenyang area (0.5164, 0.3571, $\chi^2=4.47$, $P<0.05$). Genotypes containing homogenous allele 1 were significantly more frequent in the group of gastric cancer kindred than those in control group of Shenyang area (0.36, 0.14, $\chi^2=4.91$, $P<0.05$).

CONCLUSION: These results suggest that there is some relation between pepsinogen C gene polymorphism and gastric cancer, and the person with homogenous allele 1 predisposes to gastric cancer than those with other genotypes. Pepsinogen C gene polymorphism may be used as a genetic marker for a genetic predisposition to gastric

cancer. The distribution of pepsinogen C gene polymorphism in Zhuanghe, a high-risk area of gastric cancer, is different from that in Shenyang, a low risk area of gastric cancer.

Liu HJ, Guo XL, Dong M, Wang L, Yuan Y. Association between pepsinogen C gene polymorphism and genetic predisposition to gastric cancer. *World J Gastroenterol* 2003; 9(1): 50-53 <http://www.wjgnet.com/1007-9327/9/50.htm>

INTRODUCTION

Gastric cancer is the second most common cancer in the world. Especially in China and other eastern Asian countries, the mortality of gastric cancer is still in the leading status of all cancers. The 5-year survival rate of gastric cancer is low, and identification and a better control of risk factors seem to be the most effective means of prevention. It was showed that many factors were ascribing to the cause of gastric cancer, including the living habit, nutrition^[1-3], microbe^[4-6], and genetic predisposition^[7-10]. Recently, following the primary completion of Human Genome Project, the association of genetic polymorphisms with diseases came to the study frontier^[11-14]. Genetic polymorphisms are defined as variations in DNA that are observed in 1 % or more of the population. The study of genetic polymorphisms promises to help define pathophysiologic mechanisms^[15,16], to identify individuals at risk for disease^[17-19] and to suggest novel targets for drug design and treatment^[20-24].

Pepsinogen C (PGC), also known as progastricsin, is the precursor of pepsin C or gastricsin. PGC can be detected throughout the stomach and proximal duodenum from the period of late infant stages to adult. Therefore it is also considered to be a mature marker of stomach cells^[25]. PGC consists of two electrophoretic isozymogens^[26]. No genetic variation was reported at the protein level. At the DNA level, however, an about 100bp insertion-deletion polymorphism was observed between exon 7 and exon 8 with several restriction enzymes. The polymorphism in PGC gene locus can be identified by both Southern blot and PCR methods.

In this study, we analyzed the PGC gene polymorphism of patients with gastric cancer and members with gastric cancer family history, and then examined the association between PGC gene polymorphism and gastric cancer.

MATERIALS AND METHODS

Patients

A total of 289 cases were involved in this study. 42 cases as health control came from the Blood Bank of the First Affiliated Hospital, China Medical University, whose health condition were checked up before blood was collected. 73 gastric cancer patients came from the Department of Oncology. 174 cases came from Zhuanghe, an area with high gastric cancer mortality, in the eastern Liaoning Province, China as described previously^[27], including 61 members from seven gastric cancer kindred families and 113 health controls whose family do not have gastric cancer history. In every gastric cancer kindred, at least two persons of the family are gastric cancer patients.

Analysis of PGC gene polymorphism

The genomic DNA from peripheral blood was amplified by PCR. The primers used were: upstream, 5'-AGCCCTAAGCCTGTTTTTGG-3'; and the downstream, 5'-GGCCAGATCTGCGTGTTTTA-3'^[28]. The reaction mixture including 32.15pmol of each primer was subjected to 5 minutes at 95 °C; 35 cycles of one minute at 94 °C, one minute at 57 °C, one minute at 72 °C; with a final extension at 72 °C for 5 minutes. The amplification reaction proceeded in a thermocycler (PE-9 600). 12 µl of reaction mixture (50 µl in total volume) underwent electrophoresis in 2 % agarose gel, and the gel was stained with ethidium bromide.

Statistical analysis

The association between the polymorphism of PGC gene and gastric cancer was tested using χ^2 test, with significance assigned to values below $P < 0.05$.

RESULTS

Detection of PGC gene polymorphism

After PCR, four alleles with different size were obtained: 310bp (allele 1), 400bp (allele 2), 450bp (allele 3), and 480bp (allele 4) (Figure 1). These results showed a little difference from the data showed by Southern blot, which demonstrated two different alleles (3.5kb and 3.6kb). According to the study of Ohtaki *et al.*, the 400bp, 450bp and 480bp of the PCR products correspond to the 3.6kb, and the 310bp correspond to 3.5bp of EcoRI fragments in Southern blot^[28].

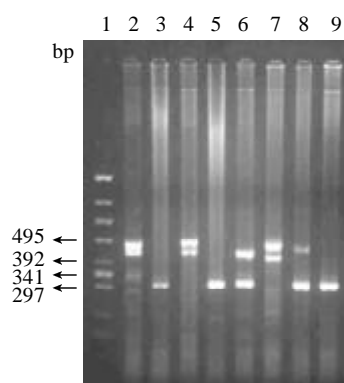


Figure 1 Analysis of PCR products. 1: The standard of molecule (174 HincII); 2-9: Genotype of samples--450bp/480bp; 310bp/310bp; 450bp/480bp; 310bp/310bp; 310bp/400bp; 400bp/480bp; 310bp/480bp; 310bp/310bp.

Distribution of PGC gene polymorphism

Ten different genotypes were obtained from the four alleles. Table 1 showed the distribution of these ten genotypes of PGC gene polymorphism in gastric cancer patients, members of gastric cancer kindred, health controls of Shenyang and Zhuanghe areas. Table 2 showed an estimated frequency of the four alleles in the four groups, and Table 3 showed the distribution of allele 1 homogenotype in above four groups. The frequency of allele 1 was higher in patients with gastric cancer than that in controls of Shenyang. Genotypes containing homogenous allele 1 were significantly more frequent in patients with gastric cancer than those in controls of Shenyang ($P < 0.05$). In the group of gastric cancer kindred the frequency of allele 1 was significantly higher than that in control group of Shenyang area ($P < 0.05$). Genotypes containing homogenous allele 1 were significantly more frequent in the group of gastric cancer kindred than those in control group of Shenyang area ($P < 0.05$). The frequency of allele 1 was higher in control group

of Zhuanghe area than that in control group of Shenyang area and genotypes containing homogenous allele 1 were significantly more frequent in the control group of Zhuanghe area than those in control group of Shenyang area ($P < 0.05$). There was no significant difference between the control group of Zhuanghe area and the group of gastric cancer kindred.

Table 1 The distribution of genotypes of PGC gene polymorphism in health control, gastric cancer patients, and gastric cancer kindred group

Genotypes	Controls (Shenyang)	Gastric cancer patients	Controls (Zhuanghe)	Gastric cancer kindred
1:1	6(0.14)	24(0.33)	37(0.33)	22(0.36)
1:2	10(0.24)	10(0.14)	9(0.08)	13(0.21)
1:3	7(0.17)	4(0.05)	14(0.12)	4(0.07)
1:4	1(0.02)	1(0.01)	9(0.08)	2(0.03)
2:2	4(0.10)	8(0.11)	10(0.09)	7(0.11)
2:3	5(0.12)	8(0.11)	9(0.08)	5(0.08)
2:4	1(0.02)	1(0.01)	13(0.12)	1(0.16)
3:3	2(0.05)	10(0.14)	2(0.02)	3(0.05)
3:4	3(0.07)	5(0.07)	8(0.07)	3(0.05)
4:4	3(0.07)	2(0.03)	2(0.02)	1(0.16)
Total	42	73	113	61

Table 2 The frequency of four alleles of PGC gene polymorphism in health control, gastric cancer patients, and gastric cancer kindred group

	n	Alleles of PGC gene polymorphism			
		1(310bp)	2(400bp)	3(450bp)	4(480bp)
Controls (Shenyang)	42	0.3571	0.2857	0.2262	0.1310
Gastric cancer patients	73	0.4315	0.2397	0.2534	0.0753
Controls (Zhuanghe)	113	0.4663	0.2389	0.1549	0.1504
Gastric cancer kindred	61	0.5164 ^a	0.2705	0.1475	0.0656

^a $P < 0.05$ vs compared with control group of Shenyang $\chi^2 = 4.47$.

Table 3 The distribution of allele 1 homogenotype in health control, gastric cancer patients, and gastric cancer kindred

	n	1:1	others
Controls (Shenyang)	42	6(0.14)	36
Gastric cancer patients	73	24(0.33) ^a	49
Controls (Zhuanghe)	113	37(0.33) ^c	76
Gastric cancer kindred	61	22(0.36) ^c	39

^a $P < 0.05$ vs compared with control group of Shenyang, $\chi^2 = 3.86$;

^c $P < 0.05$ vs compared with control group of Shenyang, $\chi^2 = 4.32$;

^c $P < 0.05$ vs compared with control group of Shenyang, $\chi^2 = 4.91$.

DISCUSSION

Family members of gastric cancer patients have been found to have a 1.5-fold to 3-fold increase in the risk of developing this cancer^[29]. This familial aggregation may be due to genetic or environmental factors shared by family members^[30-32]. To understand the genetic predisposition to gastric cancer, we selected pepsinogen C gene as a marker gene, and focused first on the distribution of the PGC gene polymorphism in gastric cancer patient group and health control. After PCR,

four alleles of pepsinogen C gene with different size were obtained. The frequency of allele 1 was higher in patients with gastric cancer than that in controls. Genotypes containing homogenous allele 1 were significantly more frequent in patients with gastric cancer than those in controls. This result showed that there is relation between the pepsinogen C gene polymorphism and gastric cancer, and the person with homogenous allele 1 seems to predispose to gastric cancer than those with other genotypes.

To further study the relation of the PGC gene polymorphism to gastric cancer and the genetic background of Zhuanghe, the high-risk area of gastric cancer, we selected three groups as our next research objects: gastric cancer kindred group in Zhuanghe, the control group of Zhuanghe and the control group of Shenyang. There was no significant difference in the distribution of PGC gene polymorphism between the health control group of Zhuanghe and gastric cancer kindred group, though the frequency of allele 1 in gastric cancer kindred group was a little higher than that in the control group of Zhuanghe. Our understanding for this phenomenon was that the persons who lived in Zhuanghe did not move frequently because of the historical reason, and this consanguinity between the two groups was the main factor responsible for the above result. But the frequency of allele 1 was higher in control group of Zhuanghe area than that in control group of Shenyang area, and genotypes containing homogenous allele 1 were significantly more frequent in the control group of Zhuanghe area than those in control group of Shenyang area. The frequency of allele 1 in the group of gastric cancer kindred was significantly higher than that in control group of Shenyang area. Genotype containing homogenous allele 1 was significantly more frequent in the group of gastric cancer kindred than that in the control group of Shenyang area. The result showed the distribution of PGC gene polymorphism in Shenyang area was different from that in Zhuanghe area.

The mortality of gastric cancer in Zhuanghe area is more than 50 per five hundred thousand. In the low risk area of that cancer, such as Shenyang, however, the mortality is less than 10 per five hundred thousand. From gastric cancer kindred group, the control groups of Zhuanghe and Shenyang, the risk ratio of gastric cancer becomes lower in turn. The data in this study showed that the frequency of allele 1 and Genotype containing homogenous allele 1 in the gastric cancer kindred group, the control groups of Zhuanghe and Shenyang in turn decreases, which is consistent with the risk ratio of gastric cancer in the above three groups. Therefore, we could conclude that the polymorphism of PGC gene may be related to the predisposition of gastric cancer, and the allele 1 associated with the risk of gastric cancer.

The mechanism of the association between PGC gene polymorphism and gastric cancer is not clear, in this study however, several hypotheses can be proposed. One is that the PGC gene itself is one of the genes responsible for gastric cancer. PGC, distributed throughout the stomach and proximal duodenum, is an important enzyme in stomach. It was reported that PGC not only was a digestive enzyme, but also might be a growth factor during the healing of gastric lesions^[33] and the change of serum PGC was associated with many gastric diseases^[34-37]. The polymorphism of PGC gene is in the intron between exon 7 and exon 8. Whether this polymorphism could affect the expression of PGC gene or regulate the PGC gene expression when the stomach was attacked by some pathogenetic factors was not known. In the following study, we will concentrate on the association of the PGC gene polymorphism and the PGC gene expression. It is interesting to note that in this study the frequency of allele 1 of PGC in the group of gastric cancer kindred was also higher than that in the group of gastric cancer group. As we know, the members

of the gastric cancer kindred all come from Zhuanghe, a place in which the incidence of gastric cancer is higher, and so is that of some other gastric diseases. In the study of Ohtaki's group, their data showed the polymorphism of PGC gene was associated with gastric body ulcer^[28]. Comparing with our data, we can conclude the polymorphism of PGC is related to gastric lesions.

Another possible explanation of the association between the PGC gene polymorphism and gastric cancer was that the PGC gene was not itself responsible for the predisposition but one of the responsible genes was closely linked to it. It is interesting to note that the PGC gene was localized to human chromosome 6p21.1-pter by analysis of mouse x human somatic cell hybrids. The recent linkage analysis demonstrated that the PGC gene is 22cM proximal to HLA cluster which has been investigated to determine the associated with gastric disease^[38-41], between D6S5 and D6S4, at a distance of 4.5 and 13.1cM. Further molecular biological studies using polymorphism markers for this chromosome region will clarify whether PGC polymorphism is linked to disequilibria of the causative genetic variations for gastric cancer. Lastly, the presence of reduced penetrance, other modifier genes, or an interaction with the environment may explain the association.

REFERENCES

- 1 **Botterweck AAM**, Van den Brandt PA, Goldbohm RA. Vitamins carotenoids, dietary fiber, and the risk of gastric carcinoma: results from a prospective study after 6.3 years of follow-up. *Cancer* 2000; **88**: 737-748
- 2 **Cai L**, Yu SZ, Zhang ZF. Cytochrome P450 2E1 genetic polymorphism and gastric cancer in Changde, Fujian Province. *World J Gastroenterol* 2001; **7**: 792-795
- 3 **Ye WM**, Yi YN, Luo RX, Zhou TS, Lin RT, Chen GD. Diet and gastric cancer: a case control study in Fujian Province, China. *World J Gastroenterol* 1998; **4**: 516-518
- 4 **Zhang ZF**, Kurtz RC, Klimstra DS, Yu GP, Sun M, Harlap S, Marshall JR. *Helicobacter pylori* infection on the risk of stomach cancer and chronic atrophic gastritis. *Cancer Detect Prev* 1999; **23**: 357-367
- 5 **Melato M**, Sidari L, Rizzardi C, Kovac D, Stimac D, Baxa P, Jonjic N. Gastric epithelium proliferation in early Hp+ and Hp- gastritis: a flow cytometry study. *Anticancer Res* 2001; **21**: 1347-1353
- 6 **Marinone C**, Martinetti A, Mestriner M, Seregini E, Geuna M, Ferrari L, Strola G, Bonardi L, Fea E, Bombardieri E. p53 evaluation in gastric mucosa of patients with chronic *Helicobacter pylori* infection. *Anticancer Res* 2001; **21**: 1115-1118
- 7 **Oue N**, Shigeishi, H, Kuniyasu H, Yokozaki H, Kuraoka K, Ito R, Yasui W. Promoter hypermethylation of MGMT is associated with protein loss in gastric carcinoma. *Int J Cancer* 2001; **93**: 805-809
- 8 **Deguchi R**, Takagi A, Kawata H, Inoko H, Miwa T. Association between CagA+ *Helicobacter pylori* infection and p53, bax and transforming growth factor-beta-RII gene mutations in gastric cancer patients. *Int J Cancer* 2001; **91**: 481-485
- 9 **Yao XX**, Yin L, Sun ZC. The expression of hTERT mRNA and cellular immunity in gastric cancer and precancerosis. *World J Gastroenterol* 2002; **8**: 586-590
- 10 **Zhou Y**, Gao SS, Li YX, Fan ZM, Zhao X, Qi YJ, Wei JP, Zou JX, Liu G, Jiao LH, Bai YM, Wang LD. Tumor suppressor gene p16 and Rb expression in gastric cardia precancerous lesions from subjects at a high incidence area in northern China. *World J Gastroenterol* 2002; **8**: 423-425
- 11 **El-Omar EM**, Carrington M, Chow WH, McColl KEL, Bream JH, Young HA, Herrera J, Lissowska J, Yuan C-C, Hothman N, Lanyon G, Martin M, Fraumeni Jr JF, Rabkin CS. Interleukin-1 polymorphism associated with increased risk of gastric cancer. *Nature* 2000; **404**: 398-402
- 12 **Yea S S**, Yang YI, Jang W H, Lee YI, Bae HS, Paik KH, Wei Q. Association between TNF- α promoter polymorphism and *Helicobacter pylori* cagA subtype infection. *J Clin Pathol* 2001; **54**: 703-706
- 13 **Shen H**, Xu Y, Zheng Y, Yu R, Qin Y, Wang X, Spitz MR, Wei Q. Polymorphisms of 5, 10-methylenetetrahydrofolate reductase and risk of gastric cancer in a Chinese population: a case-control

- study. *Int J Cancer* 2001; **95**: 332-336
- 14 **Liu MR**, Pan KF, Li ZF, Wang Y, Deng DJ, Zhang L, Lu YY. Rapid screening mitochondrial DNA mutation by using denaturing high-performance liquid chromatography. *World J Gastroenterol* 2002; **8**: 426-430
 - 15 **Pfutzer RH**, Barmada MM, Brunskill AP, Finch R, Hart PS, Neoptolemos J, Furey WF, Whitcomb DC. SPINK1/PSTI polymorphisms act as disease modifiers in familial and idiopathic chronic pancreatitis. *Gastroenterology* 2000; **119**: 615-623
 - 16 **Prkacin I**, Novak B, Sertic J, Mrzljak A. Angiotensin-converting enzyme gene polymorphism in patients with systemic lupus. *Acta Med Croatica* 2001; **55**: 73-76
 - 17 **Wu MS**, Huang SP, Chang YT, Lin MT, Shun CT, Chang MC, Wang HP, Chen CJ, Lin JT. Association of the -160 C a promoter polymorphism of E-cadherin gene with gastric carcinoma risk. *Cancer* 2002; **94**: 1443-1448
 - 18 **Takezaki T**, Gao CM, Wu JZ, Li ZY, Wang JD, Ding JH, Liu YT, Hu X, Xu TL, Tajima K, Sugimura H. hOGG1 Ser(326)Cys polymorphism and modification by environmental factors of stomach cancer risk in Chinese. *Int J Cancer* 2002; **99**: 624-627
 - 19 **Hiyama T**, Tanaka S, Kitadai Y, Ito M, Sumii M, Yoshihara M, Shimamoto F, Haruma K, Chayama K. p53 Codon 72 polymorphism in gastric cancer susceptibility in patients with *Helicobacter pylori*-associated chronic gastritis. *Int J Cancer* 2002; **100**: 304-308
 - 20 **Tsukino H**, Kuroda Y, Qiu D, Nakao H, Imai H, Katoh T. Effects of cytochrome P450 (CYP) 2A6 gene deletion and CYP2E1 genotypes on gastric adenocarcinoma. *Int J Cancer* 2002; **100**: 425-428
 - 21 **Zhang Z**, Zhang X, Hou G, Sha W, Reynolds GP. The increased activity of plasma manganese superoxide dismutase in tardive dyskinesia is unrelated to the Ala-9Val polymorphism. *J Psychiatr Res* 2002; **36**: 317-324
 - 22 **Wootton JC**, Feng X, Ferdig MT, Cooper RA, Mu J, Baruch DI, Magill AJ, Su XZ. Genetic diversity and chloroquine selective sweeps in *Plasmodium falciparum*. *Nature* 2002; **418**: 320-323
 - 23 **Clark AG**. Population genetics: malaria variorum. *Nature* 2002; **418**: 283-285
 - 24 **Feng Z**, Curtis J, Minchella DJ. The influence of drug treatment on the maintenance of schistosome genetic diversity. *J Math Biol* 2001; **43**: 52-68
 - 25 **Kageyama T**, Ichinose M, Tsukada-Kato S, Omata M, Narita Y, Moriyama A, Yonezawa S. Molecular cloning of neonate/infant-specific pepsinogens from rat stomach mucosa and their expression change during development. *Biochem Biophys Res Commun* 2000; **267**: 806-812
 - 26 **Kageyama T**. Pepsinogens, progastricsins, and prochymosins: structure, function, evolution, and development. *Cell Mol Life Sci* 2002; **59**: 288-306
 - 27 **Guo XL**, Wang LE, Wang L, Dong M, Yuan Y. The significant of measuring serum *Hp* CagA on the high risk population in the high-risk area of gastric cancer. *Shijie Huaren Xiaohua Zazhi* 2001; **9**: 595-596
 - 28 **Ohtaki Y**, Azuma T, Konishi J, Ito S, Kuriyama M. Association between genetic polymorphism of the pepsinogen C gene and gastric body ulcer: the genetic predisposition is not associated with *Helicobacter pylori* infection. *Gut* 1997; **41**: 469-474
 - 29 **Brenner H**, Arndt V, Sturmer T, Stegmaier C, Ziegler H, Dhom G. Individual and joint contribution of family history and *Helicobacter pylori* infection to the risk of gastric carcinoma. *Cancer* 2000; **88**: 274-279
 - 30 **Kim JC**, Kim HC, Roh SA, Koo KH, Lee DH, Yu CS, Lee JH, Kim TW, Lee HL, Beck NE, Bodmer WF. hMLH1 and hMSH2 mutations in families with familial clustering of gastric cancer and hereditary non-polyposis colorectal cancer. *Cancer Detect Prev* 2001; **25**: 503-510
 - 31 **Bakir T**, Can G, Erkul S, Siviloglu C. Stomach cancer history in the siblings of patients with gastric carcinoma. *Eur J Cancer Prev* 2000; **9**: 401-408
 - 32 **Dhillon PK**, Farrow DC, Vaughan TL, Chow WH, Risch HA, Gammon MD, Mayne ST, Stanford JL, Schoenberg JB, Ahsan H, Dubrow R, West AB, Rotterdam H, Blot WJ, Fraumeni JF Jr. Family history of cancer and risk of esophageal and gastric cancers in the United States. *Int J Cancer* 2001; **93**: 148-152
 - 33 **Kishi K**, Kinoshita Y, Matsushima Y, Okada A, Maekawa T, Kawanami C, Watanabe N, Chiba T. Pepsinogen C gene product is a possible growth factor during gastric mucosal healing. *Biochem Biophys Res Commun* 1997; **238**: 17-20
 - 34 **Fernandez R**, Vizoso F, Rodriguez JC, Merino AM, Gonzalez LO, Quintela I, Andicoechea A, Truan N, Diez MC. Expression and prognostic significance of pepsinogen C in gastric carcinoma. *Ann Surg Oncol* 2000; **7**: 508-514
 - 35 **Kikuchi S**, Kurosawa M, Sakiyama T, Tenjin H, Miki K, Wada O, Inaba Y. Long-term effect of *Helicobacter pylori* infection on serum pepsinogens. *Jpn J Cancer Res* 2000; **91**: 471-476
 - 36 **Fujisawa T**, Kumagai T, Goto A, Fujimori K, Akamatsu T, Kiyosawa K. Investigation about usefulness of serum antibody of *Helicobacter pylori* and serum pepsinogen I/II ratio as a marker of the judgment after eradication therapy. *Nippon Rinsho* 1999; **57**: 101-106
 - 37 **Araki H**, Miyazaki R, Matsuda T, Gejyo F, Koni I. Significance of serum pepsinogens and their relationship to *Helicobacter pylori* infection and histological gastritis in dialysis patients. *Nephrol Dial Transplant* 1999; **14**: 2669-2675
 - 38 **Magnusson PKE**, Enroth H, Eriksson I, Held M, Nyren O, Engstrand L, Hansson L-E, Gyllensten UB. Gastric cancer and human leukocyte antigen: distinct DQ and DR alleles are associated with development of gastric cancer and infection by *Helicobacter pylori*. *Cancer Res* 2001; **61**: 2684-2689
 - 39 **Archimandritis A**, Sougioultzis S, Foukas PG, Tzivras M, Davaris P, Moutsopoulos HM. Expression of HLA-DR, costimulatory molecules B7-1, B7-2, intercellular adhesion molecule-1 (ICAM-1) and Fas ligand (FasL) on gastric epithelial cells in *Helicobacter pylori* gastritis; influence of *H. pylori* eradication. *Clin Exp Immunol* 2000; **119**: 464-471
 - 40 **Sakai T**, Aoyama N, Satonaka K, Shigeta S, Yoshida H, Shinoda Y, Shirasaka, D, Miyamoto M, Nose Y, Kasuga M. HLA-DQB1 locus and the development of atrophic gastritis with *Helicobacter pylori* infection. *J Gastroenterol* 1999; **34**: 24-27
 - 41 **Yoshitake S**, Okada M, Kimura A, Sasazuki T. Contribution of major histocompatibility complex genes to susceptibility and resistance in *Helicobacter pylori* related diseases. *Eur J Gastroenterol Hepatol* 1999; **11**: 875-880

Helicobacter pylori infection generated gastric cancer through p53-Rb tumor-suppressor system mutation and telomerase reactivation

Jing Lan, Yong-Yan Xiong, Yi-Xian Lin, Bi-Cheng Wang, Ling-Ling Gong, Hui-Sen Xu, Guang-Song Guo

Jing Lan, Yong-Yan Xiong, Yi-Xian Lin, Bi-Cheng Wang, Ling-Ling Gong, Hui-Sen Xu, Guang-Song Guo, Department of Pathology, Zhongnan Hospital, Wuhan University, Wuhan city 430071, Hubei Province, China

Supported by the National Science Fund of Hubei Province, No. 98J087 and the Department of Health of Hubei Province, No. WJ01572

Correspondence to: Dr. Jing Lan, Department of Pathology, Zhongnan Hospital, Wuhan University, Wuhan 430071, Hubei Province, China. lanjing_2002@hotmail.com

Telephone: +86-27-87661547

Received: 2002-03-12 **Accepted:** 2002-04-20

Abstract

AIM: To investigate the relationship between *Helicobacter pylori* (*H.pylori*) infection and the expressions of the p53, Rb, c-myc, bcl-2 and hTERT mRNA in a series of diseases from chronic gastritis (CG), intestinal metaplasia type I or II (IMI-II), intestinal metaplasia type III (IMIII), mild or modest dysplasia (DysI-II), severe dysplasia (DysIII) to gastric cancer (GC) and to elucidate the mechanism of gastric carcinogenesis relating to *H.pylori* infection.

METHODS: 272 cases between 1998 and 2001 were available for the study including 42 cases of CG, 46 cases of IMI-II, 25 cases of IMIII, 48 cases of DysI-II, 27 cases of DysIII, 84 cases of GC. *H.pylori* infection and the expressions of p53, Rb, c-myc, bcl-2 were detected by means of streptavidin-peroxidase (SP) immunohistochemical method. hTERT mRNA was detected by *in situ* hybridization (ISH).

RESULTS: The expressions of p53, Rb, c-myc, hTERT mRNA and bcl-2 were higher in the GC than in CG, IM, Dys. The expression of c-myc was higher in IMIII with *H.pylori* infection (10/16) than that without infection (1/9) and the positive rate in DysI-II and DysIII with *H.pylori* infection was 18/30 and 13/17, respectively, higher than that without infection (4/18 and 3/10, respectively). In our experiment mutated p53 had no association with *H.pylori* infection, the expression of Rb was associated with *H.pylori* infection in GC, but the p53-Rb tumor-suppressor system abnormal in DysI-II cases, DysIII and GC cases with *H.pylori* infection was 21/30, 15/17 and 48/48 respectively, higher than non-infection groups (4/18, 3/10, 28/36). Furthermore the level of hTERT mRNA in GC with *H.pylori* infection (47/48) was higher than that without infection (30/36), however the relationship between bcl-2 and *H.pylori* was only in IMIII. C-myc had a close association with hTERT mRNA in DysIII and GC ($P=0.0253, 0.0305$ respectively).

CONCLUSION: In the gastric carcinogenesis, *H.pylori* might cause the severe imbalance of proliferation and apoptosis in the precancerous lesions (IMIII and GysIII) first, leading to p53-Rb tumor-suppressor system mutation and telomerase reactivation, and finally causes gastric cancer.

Lan J, Xiong YY, Lin YX, Wang BC, Gong LL, Xu HS, Guo GS. *Helicobacter pylori* infection generated gastric cancer through p53-Rb tumor-suppressor system mutation and telomerase reactivation. *World J Gastroenterol* 2003; 9(1): 54-58
<http://www.wjgnet.com/1007-9327/9/54.htm>

INTRODUCTION

Gastric cancer is one of the most fatal malignancies and in the world about 628 000 persons die of it every year. A close association between *Helicobacter pylori* (*H.pylori*) and gastric cancer has been found^[1-14], mainly on the basis of seroepidemiological data. Recently the animal models that developed gastric cancer owing to *H.pylori* infection provided powerful evidence^[15]. Although *H.pylori* has been classified as a type I carcinogen for gastric cancer by the International Agency for Research on Cancer (IARC)^[16], the exact nature and strength of the association with gastric cancer has remained indistinct.

A two-stage pattern has been introduced to explain the escape from senescence of the cultured human cells^[17,18]. The mortality stage 1 (M1) mechanism causes senescence, where normal human diploid cells become incapable of further division. However this cessation of cellular division can be overcome by the inactivation of human tumor suppressor genes p53 and Rb in fibroblasts^[18,19] that are mutated in a variety of human neoplasm. In non-neoplastic cells, wild type p53 modulates cell proliferation and differentiation by regulating the transcription of several gene products, inducing p21^{waf1} expression which acts as a regulator of the cell cycle at the G1 checkpoint^[20,21], and plays a crucial role in repairing damaged DNA through inducing GADD45 (growth arrest and DNA damage)^[22]. Moreover p53 induces the Bax gene, which is followed by apoptosis, in contrast to bcl-2^[23]. The cells which have overcome the M1 mechanism are able to divide until crisis occurs, which is caused by the mortality stage2 (M2) mechanism. It is difficult for human cells to escape from this crisis, but in rare instances some populations can achieve immortality by overcoming this M2 mechanism through the reactivation of the enzyme telomerase^[24-29]. Telomerase is a unique ribonucleoprotein enzyme that is responsible for adding the telomeric repeats onto the 3' end of chromosomes and composed of a catalytic protein subunit (hTERT, for human telomerase reverse transcription) and a template RNA (TR), and hTERT is the rate-limiting enzyme in the telomerase complex^[30-34].

From all the above it is apparent that the understanding of the association of *H.pylori* infection with some genes (for example p53, Rb) as well as telomerase can contribute to the elucidation of the mechanisms that regulate the development of gastric cancer. The aim of the present study, therefore, was to examine this association by detecting the expressions of *H.pylori*, hTERT, p53, Rb, c-myc and bcl-2 in a series of gastric diseases.

MATERIALS AND METHODS

Patients

Two hundred seventy-two patients (174 men, 98 women, ranging in age from 21 to 80 years, mean 54.22 years) underwent endoscopy (noncancerous patients) or curative gastrectomy (gastric cancer patients) in our hospital between 1998 to 2001, including 42 cases of CG, 46 cases of IMI-II, 25 cases of IMIII, 48 cases of DysI-II, 27 cases of DysIII, 84 cases of GC diagnosed according to the updated Sydney System^[35] and the Japanese Research Society for Gastric Cancer^[36]. No patients had received chemotherapy or radiation therapy before surgery.

All specimens were fixed in 10 % buffered neutral formalin and embedded in paraffin and serial sections (4 µm thick).

Histochemical staining

Hematoxylin-eosin (HE) staining was used for the histopathological diagnosis, evaluation and grading of gastritis, atrophy, intestinal metaplasia, dysplasia and cancer. High iron diamine (HID)-alcian blue (AB) (PH 2.5)-periodic acid schiff (PAS) method was used to distinguish sulphates, neutral and acid mucus, which were stained brown-black, red and blue respectively. Using both morphological and histochemical criteria, the cases of intestinal metaplasia were classified into three types^[37].

Immunohistochemistry

Was performed using the streptavidin-peroxidase (sp) method. The following primary antibodies and the kit were used: monoclonal antibodies against p53, Rb, c-myc, bcl-2 and the kit (Maixin-Bio, Fujian), polyclonal antibodies against *H.pylori* (antibody, diagnostica Inc. USA). Dewaxed sections were heated in a microwave oven (700W) for 12 min to retrieve the antigens and cooled to room temperature. Endogenous peroxidase was blocked by 3 % hydrogen peroxide (H₂O₂) for 15 min in methanol. After being washed with phosphate-buffered-saline (PBS, 0.01M), the sections were further blocked by 10 % rabbit serum for 15 min to reduce nonspecific antibody binding and then incubated with the primary antibodies of p53, Rb, c-myc, bcl-2 or *H.pylori* (1:60 dilution) at 4 °C overnight. After being washed with PBS for 2×5 min, the sections were incubated with the secondary anti-mouse immunoglobulin (Ig) conjugated with biotin at room temperature for 15 min, washed again with PBS, followed by incubation with streptavidin-peroxidase complex for 15 min. The reaction products of peroxidase were visualized by incubation with 0.05 M Tris-HCL buffer (PH7.6) containing 20 mg 3,3'-diaminobenzidine (Maixin-Bio, Fujian) and 100 µl 5 % hydrogen peroxide per 100 ml. Finally, the sections were counterstained for nuclei by hematoxylin solution. To examine the specificity of immunostaining, PBS was used to replace the primary antibodies as the control. The assessment of all the samples was conducted by an observer who did not know any details of this study by calculating the average ratio of positive cells (the nuclei or the plasma, staining brown-yellow) under ten 400× microscopes. If the ratio was more than 10 %, this

sample was considered positive. However the *H.pylori* immunostaining was assessed positive as long as the brown-black dotish, stake or bend material was stained on the surface of mucosa or in the gland's cave.

In situ hybridization

(ISH) was used to detect hTERT (human telomerase reverse transcriptase) mRNA. The probe (5' -CCCAG GCGCC GCACG AACGT GGCCA GCGGC-3') and the kit were bought from Boster Bio (Wuhan). Dewaxed sections were incubated with 3 % hydrogen peroxide for 30 min to reduce the non-specific binding and then with 1 µg/ml pepsin for 5-8 min to improve the penetration of the probe. The prehybridization was performed at 40 °C for 3 h to enhance hybridization efficiency, and the hybridization was conducted in a 42 °C water bath with each section covered with a coverslip, then the thorough washing procedure was followed: 2×SSC (sodium chloride and sodium citrate) at 37 °C for 15 min, 0.5 ×SSC for 15 min, 0.2×SSC for 15 min. Then the sections were visualized according to the kit manufacturer's instructions. We calculated the positive cells ratio to assess the positive sample by calculating the average ratio of positive cells (the plasma was stained brown-yellow) under ten 400× microscopes. If the ratio was more than 10 %, this sample was considered positive.

Statistics

The chi-square test and the Fisher's exact probability test were used to compute the frequencies by SPSS 10.0 for Windows. $P < 0.05$ was considered to be statistically significant.

RESULTS

With the development of the diseases from CG, IM, Dys to GC, the positive expressions of p53, Rb, c-myc, bcl-2 and hTERT mRNA were augmented significantly (Table 1). In particular, the frequencies of Rb, c-myc and hTERT mRNA in IMIII (8/25, 11/25, 4/25, respectively) were statistically higher than those in IMI-II (4/46, 8/46, 1/46, respectively) ($P < 0.05$). The expressions of all variables in GC were statistically higher than in DysIII and IMIII, higher in DysIII e than in IMIII ($P < 0.05$). In general the frequencies of them in *H.pylori* infection groups were higher than those in non-infection groups. The expression of c-myc was 10/10, 18/30,

Table 1 Expressions of c-myc, bcl-2, p53, Rb and hTERT mRNA in the different gastric diseases (%)

	GC	IMI-II	IMIII	DysI-II	DysIII	GC
c-myc	5(11.90)	8(17.39)	11(44.00)	22(45.83)	16(59.26)	74(88.09)
bcl-2	3(7.14)	17(36.96)	10(40.00)	24(50.00)	18(66.67)	55(65.48)
p53	0(0.00)	3(6.52)	5(20.00)	14(29.17)	10(37.04)	64(76.19)
Rb	3(7.14)	4(8.70)	8(32.00)	14(29.17)	12(44.44)	61(72.62)
HTERTmRNA	0(0.00)	1(2.17)	4(16.00)	10(16.67)	12(44.44)	78(92.86)

Table 2 The correlations between p53, Rb, c-myc, hTERT, bcl-2 and *H.pylori* in benign diseases and gastric cancer

<i>H.pylori</i>	CG		IMI-II		IMIII		DysI-II		DysIII		GC	
	+(31)	-(11)	+(32)	-(14)	+(16)	-(9)	+(30)	-(18)	+(17)	-(10)	+(48)	-(36)
c-myc	5	0	7	1	10 ^a	1	18 ^a	4	13 ^a	3	44	30
bcl-2	3	0	12	5	9 ^a	1	17	7	13	5	38	17
p53	0	0	2	1	3	2	12 ^a	2	6	4	39	25
Rb	3	0	4	0	6	2	11	3	9	3	40 ^a	21
P53-Rb	3	0	4	1	6	3	21 ^a	4	15 ^a	3	48 ^a	28
hTERT	0	0	1	0	4	0	8	2	9	3	47 ^a	30

^a $P < 0.05$ vs the non-infected group.

13/17 in IMIII, DysI-II and DysIII with *H.pylori* infection respectively, higher than non-infection group (1/9, 4/18, 3/10, respectively). In our experiment mutated p53 had no association with *H.pylori* infection, the expression of Rb was associated with *H.pylori* infection in GC, but the p53-Rb tumor-suppressor system abnormal in DysI-II cases, DysIII and GC cases with *H.pylori* infection was 21/30, 15/17 and 48/48, respectively, higher than that in non-infection groups (4/18, 3/10, 28/36, respectively). The association between bcl-2 and *H.pylori* only existed in IMIII (9/16, 1/9). The expression of hTERT mRNA in GC with *H.pylori* infection was 47/48, higher than non-infection group (30/36) (Table 2). We also found the association between c-myc and hTERT mRNA in GC and DysIII ($P<0.05$) (Table 3).

Table 3 Correlation between c-myc and hTERT in the gastric benign diseases and gastric cancer

c-myc	CG		IMI-II		IMIII		DysI-II		DysIII		GC	
	(+)	(-)	(+)	(-)	(+)	(-)	(+)	(-)	(+)	(-)	(+)	(-)
hTERT(+)	0	0	1	0	3	1	7	3	10 ^a	2	70 ^a	7
(-)	5	37	7	39	8	13	15	23	6	9	4	3

^a $P<0.05$ vs the negative group.

DISCUSSION

Gastric cancer occurs after a multi-step process of alterations in oncogenes, tumor-suppressor genes, cell-adhesion molecules, telomerase as well as genetic instability at several microsatellite loci. Studies have demonstrated that *H.pylori* infection is closely associated with these abnormal alterations. Konturek's study^[38] showed that *H.pylori* induced apoptosis in gastric mucosa through upregulation of Bax and bcl-2 expression. The bcl-2 gene family plays an important role in regulating apoptosis. In our studies, *H.pylori* enhanced the expression of c-myc and bcl-2 significantly in IMIII ($P<0.05$). The c-myc protein is a critical component for the control of normal cell growth, but the altered c-myc activity by translocation, amplification, overexpression, and mutation is widespread in tumor cells and important for multi-step carcinogenesis^[39,40]. C-myc is a strong inducer of proliferation and it is believed to be critical for the oncogenic properties. Some studies showed that the abnormal c-myc expression derived cells inappropriately through the cell cycle, leading to uncontrolled proliferation, a characteristic of neoplastic cells. From our study we found that *H.pylori* infection caused a higher proliferation and a lower apoptosis in IMIII than in CG and IMI-II and accelerated cell proliferation, leaving a good chance for all kinds of genes and proteins to mutate or overexpress, presumably heightening the genetic instability consistent with the development of carcinoma^[41,42].

Mutations in the tumor suppressor genes p53 and Rb are common events in human cancers that exert their control on the cell cycle at the G1-S phase transition through independent but interconnected pathways^[43-50]. Williams' studies showed that germ-line mutation in p53 and Rb might have cooperative tumorigenic effects in mice^[51]. It has been generally accepted that p53 and Rb tumor-suppressor system, including p53, Rb, p16, p15, p14 and p21waf1^[52-60], play an important role in carcinogenesis. Some studies observed this phenomenon that NO (nitric oxide) generated by *H.pylori* caused p53 mutation at the spot C:G to A:T and at the same time p53 was found mutated at the same spot in IM, Dys and GC, thus *H.pylori* probably caused p53 mutation. In our study, we found that the expressions of p53-Rb were continually enhanced from chronic gastritis (3/42) to gastric cancer (76/84) and in the DysIII and

GC which had a close association with *H.pylori* ($P<0.05$). Chen^[61] reported that the mRNA levels of p53-Rb in gastric cancer were significantly lower than those in their non-cancerous tissues using quantitative analysis method. Some studies favored the view that c-myc drove initial proliferation and subsequent differentiation, concomitant with the activation of the p53-Rb pathway is required for immortalization through overexpression of Myc^[62,63]. Although c-myc and p53-Rb had no direct association in our study, *H.pylori* infection might initially provoke the c-myc and bcl-2 more than in non-infection group in IMIII and then inactivate the p53-Rb tumor-suppress system in Dys and they collaborated in GC.

Telomerase activity has been found in 85-90 % of all human cancers but not in adjacent normal cells^[27]. It has thus been hypothesized that for a cancer cell to undergo sustained proliferation beyond the limits of cell senescence, it must reactivate telomerase or an alternative mechanism in order to maintain telomeres. This makes telomerase a target not only for the novel etiology agent but also a mark for cancer diagnosis. Many studies showed that telomerase activity was higher in cancers than in non-cancerous tissues and higher in IM than in CG^[64-69], which was similar to our results. The association between *H.pylori* infection and telomerase activity is still controversial. Suzuki' study^[67] indicated that hTERT mRNA which was expressed in precancerous lesions and gastric cancer could be induced at an early stage of gastric carcinogenesis, but it was not correlated with *H.pylori*. Kuniyasu^[70] found that *H.pylori* evidently caused the release of reactive oxygen species (ROMs) and reactive nitrogen species (NO) which might be strong triggers for "stem cell" hyperplastic in IM, followed by telomere reduction and increased telomerase activity as well as hTERT overexpression. We found in GC hTERT expression was significantly higher in infection group (47/48) than in non-infection group (30/36) but had no association in Dys or IM, maybe because there exist two different genetic pathways to two histological types: intestinal-type and diffuse-type gastric cancer. Some studies showed c-myc could stimulate expression of hTERT and thereby enhance telomerase activity which was an important step in carcinogenesis^[71-80]. In our study c-myc had an association with hTERT in Dys and GC, which suggests that *H.pylori* stimulates telomerase directly or indirectly by the overexpression of c-myc. We did not find the association between hTERT and p53-Rb or bcl-2.

There maybe exit this mechanism of gastric caicinogenesis relating to chronic *H.pylori* infection, which leads to imbalance of proliferation and apoptosis in the early stage, and furthermore p53-Rb tumor-suppressor system mutation, telomerase reactivation and finally gastric cancer generation. Hence this molecular pathology mechanism should be applied in routine diagnostic procedures, classification systems, disease monitoring, and even prognostic assessment.

ACKNOWLEDGMENTS

The authors thank the faculty of Department of Pathology and Wang Zhifeng of Stomatology of hospital for their excellent technical assistance throughout this investigation.

REFERENCES

- 1 **Sipponen P**, Kosunen TU, Valle J, Riihela M, Seppala K. *Helicobacter pylori* infection and chronic gastritis in gastric cancer. *J Clin Pathol* 1992; **45**: 319-323
- 2 **Blaser MJ**. Hypotheses on the pathogenesis and natural history of *Helicobacter pylori*-induced inflammation. *Gastroenterology* 1992; **102**: 720-727
- 3 **Forman D**, Newell DG, Fullerton F, Yarnell JW, Stacey AR, Wald

- N, Sitas F. Association between infection with *Helicobacter pylori* and risk of gastric cancer: Evidence from a prospective investigation. *BMJ* 1991; **302**: 1302-1305
- 4 **Parsonnet J**, Friedman GD, Vandersteen DP, Chang Y, Vogelstein JH, Orentreich N, Sibley RK. *Helicobacter pylori* infection and the risk of gastric carcinoma. *N Engl J Med* 1991; **325**: 1127-1131
 - 5 **Talley NJ**, Zinsmeister AR, Weaver A, DiMugno EP, Carpenter HA, Perez-perez GI, Blaser MJ. Gastric adenocarcinoma and *Helicobacter pylori* infection. *J Natl Cancer Inst* 1991; **83**: 1734-1739
 - 6 **The Eurogast Study Group**. An association between *Helicobacter pylori* infection and gastric cancer: An international study. *Lancet* 1993; **341**: 1359-1362
 - 7 **Hansson LE**, Engstrand L, Nyren O, Evans DJ Jr, Lindgren A, Bergstrom R, Andersson B, Athlin L, Bendtsen O, Tracz P. *Helicobacter pylori* infection: Independent risk indicator of gastric adenocarcinoma. *Gastroenterology* 1993; **105**: 1098-1103
 - 8 **Blaser MJ**. *Helicobacter pylori* and gastric diseases. *BMJ* 1998; **316**: 1507-1510
 - 9 **Wang TC**, Fox JG. *Helicobacter pylori* and gastric cancer: Koch's postulates fulfilled? *Gastroenterology* 1998; **115**: 780-783
 - 10 **Vandenplas Y**. *Helicobacter pylori* infection. *World J Gastroenterol* 2000; **6**: 20-31
 - 11 **Cai L**, Yu SZ, Zhang ZF. *Helicobacter pylori* infection and risk of gastric cancer in Changle County, Fujian Province, China. *World J Gastroenterol* 2000; **6**: 374-376
 - 12 **Zhuang XQ**, Lin SR. Research of *Helicobacter pylori* infection in precancerous gastric lesions. *World J Gastroenterol* 2000; **6**: 428-429
 - 13 **Xia HH**, Talley NJ. Apoptosis in gastric epithelium induced by *Helicobacter pylori* infection: implications in gastric carcinogenesis. *Am J Gastroenterol* 2001; **96**: 16-26
 - 14 **Meining A**, Bayerdorffer E, Stolte M. Extent, topography and symptoms of *Helicobacter pylori* gastritis. Phenotyping for accurate diagnosis and therapy? *Pathologie* 2001; **22**: 13-18
 - 15 **Fujioka T**, Honda S, Tokieda M. *Helicobacter pylori* infection and gastric carcinoma in animal models. *J Gastroenterol Hepatol* 2000; **15**(Suppl): D55-D59
 - 16 International Agency for research on Cancer. Schistosomes, Liver flukes and *Helicobacter pylori*. Evaluation of carcinogenic risks to humans. *IARC Monograph Evaluating Carcinogenic Risks to Humans* 1994: 61
 - 17 **Wright WE**, Pereira-Smith OM, Shay JW. Reversible cellular senescence: implications for immortalization of normal human diploid fibroblasts. *Mol Cell Biol* 1989; **9**: 3088-3092
 - 18 **Shay JW**, Pereira-Smith OM, Wright WE. A role for both RB and p53 in the regulation of human cellular senescence. *Exp Cell Res* 1991; **196**: 33-39
 - 19 **Shay JW**, Wright WE, Brasiskyte D, Van der Haegen BA. E6 of human papillomavirus type 16 can overcome the M1 stage of immortalization in human mammary epithelial cells but not in human fibroblasts. *Oncogene* 1993; **8**: 1407-1413
 - 20 **el-Deiry WS**, Harper JW, O'Connor PM, Velculescu VE, Canman CE, Jackman J, Pietenpol JA, Burrell M, Hill DE, Wang Y. WAF1/CIP1 is induced in p53-mediated G1 arrest and apoptosis. *Cancer Res* 1994; **54**: 1169-1174
 - 21 **Sheikh MS**, Rochefort H, Garcia M. Overexpression of p21WAF1/CIP1 induces growth arrest giant cell formation and apoptosis in human breast carcinoma cell lines. *Oncogene* 1995; **11**: 1899-1905
 - 22 **Zhan Q**, Bae I, Kastan MB, Fornace AJ Jr. The p53-dependent gamma-ray response of GADD45. *Cancer Res* 1994; **54**: 2755-2760
 - 23 **Zhan Q**, Fan S, Bae I, Guillouf C, Liebermann DA, O'Connor PM, Fornace AJ Jr. Induction of bax by genotoxic stress in human cells correlates with normal p53 status and apoptosis. *Oncogene* 1994; **9**: 3743-3751
 - 24 **Harley CB**. Telomere loss: mitotic clock or genetic time bomb? *Mutat Res* 1991; **256**: 271-282
 - 25 **Harley CB**, Vaziri H, Counter CM, Allsopp RC. The telomere hypothesis of cellular aging. *Exp Gerontol* 1992; **27**: 375-382
 - 26 **Shay JW**, Wright WE, Werbin H. Toward a molecular understanding of human breast cancer: a hypothesis. *Breast Cancer Res Treat* 1993; **25**: 83-94
 - 27 **Wright WE**, Shay JW. The two-stage mechanism controlling cellular senescence and immortalization. *Exp Gerontol* 1992; **27**: 383-389
 - 28 **Kim NW**, Piatyszek MA, Prowse KR, Harley CB, West MD, Ho PL, Coviello GM, Wright WE, Weinrich SL, Shay JW. Specific association of human telomerase activity with immortal cells and cancer. *Science* 1994; **266**: 2011-2015
 - 29 **Shay JW**, Wright WE. Haylick, his limit, and cellular ageing. *Nat Rev Mol Cell Biol* 2000; **1**: 72-76
 - 30 **Blackburn EH**. Structure and function of telomeres. *Nature* 1991; **350**: 569-573
 - 31 **Feng J**, Funk WD, Wang SS, Weinrich SL, Avilion AA, Chiu CP, Adams RR, Chang E, Allsopp RC, Yu J. The RNA component of human telomerase. *Science* 1995; **269**: 1236-1241
 - 32 **Kyo S**, Takakura M, Tanaka M, Kanaya T, Sagawa T, Kohama T, Ishikawa H, Nakano T, Shimoya K, Inoue M. Expression of telomerase activity in human chorion. *Biochem Biophys Res Commun* 1997; **241**: 498-503
 - 33 **Nakayama J**, Tahara H, Tahara E, Saito M, Ito K, Nakamura H, Nakanishi T, Tahara E, Ide T, Ishikawa F. Telomerase activation by hTERT in human normal fibroblasts and hepatocellular carcinomas. *Nat Genet* 1998; **18**: 65-68
 - 34 **Takakura M**, Kyo S, Kanaya T, Tanaka M, Inoue M. Expression of human telomerase subunits and correlation with telomerase activity in cervical cancer. *Cancer Res* 1998; **58**: 1558-1561
 - 35 **Dixon MF**, Genta RM, Yardley JH, Correa P. Classification and grading of gastritis. The updated Sydney System. International workshop on the histopathology of gastritis, Houston 1994. *Am J Surg Pathol* 1996; **20**: 1161-1181
 - 36 Japanese Research Society for Gastric Cancer: The General Rules for the Gastric Cancer Study, First English Edition. *Kanehara, Tokyo* 1995
 - 37 **Jass JR**. Role of intestinal metaplasia in the histogenesis of gastric carcinoma. *J Clin Pathol* 1980; **33**: 801-810
 - 38 **Konturek PC**, Pierzchalski P, Konturek SJ, Meixner H, Faller G, Kirchner T, Hahn EG. *Helicobacter pylori* induces apoptosis in gastric mucosa through an upregulation of Bax expression in humans. *Scand J Gastroenterol* 1999; **34**: 375-383
 - 39 **Felsher DW**, Bishop JM. Reversible tumorigenesis by MYC in hematopoietic lineages. *Mol Cell* 1999; **4**: 199-207
 - 40 **Pelengaris S**, Littlewood T, Khan M, Elia G, Evan G. Reversible activation of c-Myc in skin: induction of a complex neoplasia phenotype by a single oncogenic lesion. *Mol Cell* 1999; **3**: 565-577
 - 41 **Conchillo JM**, Houben G, de Bruine A, Stockbrugger R. Is type III intestinal metaplasia an obligatory precancerous lesion in intestinal-type gastric carcinoma? *Eur J Cancer Prev* 2001; **10**: 307-312
 - 42 **Rubio CA**, Jonasson JG, Filipe I, Cabanne AM, Hojman R, Kogan Z, Nesi G, Amorosi A, Zampi G, Klimstra D. Gastric carcinoma of intestinal type concur with distant changes in the gastric mucosa. A multicenter study in the Atlantic basin. *Anticancer Res* 2001; **21**: 813-818
 - 43 **Jacks T**, Fazeli A, Schmitt EM, Bronson RT, Goodell MA, Weinberg RA. Effects of an Rb mutation in the mouse. *Nature* 1992; **359**: 295-300
 - 44 **Donehower LA**, Harvey M, Slagle BL, McArthur MJ, Montgomery CA Jr, Butel JS, Bradley A. Mice deficient for p53 are developmentally normal but susceptible to spontaneous tumours. *Nature* 1992; **356**: 215-221
 - 45 **Williams BO**, Remington L, Albert DM, Mukai S, Bronson RT, Jacks T. Cooperative tumorigenic effects of germline mutations in Rb and p53. *Nat Genet* 1994; **7**: 480-484
 - 46 **Kamb A**, Gruis NA, Weaver-Feldhaus J, Liu Q, Harshman K, Tavitgian SV, Stockert E, Day RS 3rd, Johnson BE, Skolnick MH. A cell cycle regulator potentially involved in genesis of many tumor types. *Science* 1994; **264**: 436-440
 - 47 **Gotz C**, Montenarh M. p53: DNA damage, DNA repair, and apoptosis. *Rev Physiol Biochem Pharmacol* 1996; **127**: 65-95
 - 48 **Sherr CJ**. Cancer cell cycles. *Science* 1996; **274**: 1672-1677
 - 49 **Platz A**, Hansson J, Mansson-Brahme A, Lagerlof B, Linder S, Lundqvist E, Sevigny P, Inganas M, Ringborg U. Screening of germline mutations in the CDKN2A and CDKN2B genes in Swedish families with hereditary cutaneous melanoma. *J Natl Cancer Inst* 1997; **89**: 697-702
 - 50 **Walker DG**, Duan W, Popovic EA, Kaye AH, Tomlinson FH, Lavin M. Homozygous deletion of the multiple tumor suppressor gene 1 in the progression of human astrocytomas. *Cancer Res* 1995; **55**: 20-23
 - 51 **Williams BO**, Remington L, Albert DM, Mukai S, Bronson RT,

- Jacks T. Cooperative tumorigenic effects of germline mutations in Rb and p53. *Nat Genet* 1994; **7**: 480-484
- 52 **Sherr CJ**. Tumor surveillance via the ARF-p53 pathway. *Genes Dev* 1998; **12**: 2984-2991
- 53 **Cordon-Cardo C**, Zhang ZF, Dallbagni G, Drobnjak M, Charytonowicz E, Hu SX, Xu HJ, Renter VE, Benedict WF. Cooperative effects of p53 and pRB alterations in primary superficial bladder tumors. *Cancer Res* 1997; **57**: 1217-1221
- 54 **Cote RJ**, Dunn MD, Chatterjee SJ, Stein JP, Shi SR, Tran QC, Hu SX, Xu HJ, Groshen S, Taylor CR, Skinner DG, Benedict WF. Elevated and absent pRb expression is associated with bladder cancer progression and has cooperative effects with p53. *Cancer Res* 1998; **58**: 1090-1094
- 55 **Kastan MB**, Onyekwere O, Sidransky D, Vogelstein B, Craig RW. Participation of p53 protein in the cellular response to DNA damage. *Cancer Res* 1991; **51**: 6304-6311
- 56 **Murakami Y**, Hayashi K, Hirohashi S, Sekiya T. Aberrations of the tumor suppressor p53 and retinoblastoma genes in human hepatocellular carcinoma. *Cancer Res* 1991; **51**: 5520-5525
- 57 **Wang J**, Coltrera MD, Gown AM. Abnormalities of p53 and p110RB tumor suppressor gene expression in human soft tissue tumors: correlations with cell proliferation and tumor grade. *Mod Pathol* 1995; **8**: 837-842
- 58 **Gleich LL**, Li YQ, Biddinger PW, Gartside PS, Stambrook PJ, Pavelic ZP, Gluckman JL. The loss of heterozygosity in retinoblastoma and p53 suppressor genes as a prognostic indicator for head and neck cancer. *Laryngoscope* 1996; **106**: 1378-1381
- 59 **Dosaka-Akita H**, Hu SX, Fujino M, Harada M, Kinoshita I, Xu HJ, Kuzumaki N, Kawakami Y, Benedict WF. Altered retinoblastoma protein expression in nonsmall cell lung cancer: its synergistic effects with altered ras and p53 protein status on prognosis. *Cancer* 1997; **79**: 1329-1337
- 60 **Ferron PE**, Bagni I, Guidoboni M, Beccati MD, Nenci I. Combined and sequential expression of p53, Rb, Ras and Bcl-2 in bronchial preneoplastic lesions. *Tumori* 1997; **83**: 587-593
- 61 **Chen YJ**, Shih LS, Chen YM. Quantitative analysis of CDKN2, p53 and retinoblastoma mRNA in human gastric carcinoma. *Int J Oncol* 1998; **13**: 249-254
- 62 **Pelengaris S**, Rudolph B, Littlewood T. Action of Myc *in vivo* proliferation and apoptosis. *Curr Opin Genet Dev* 2000; **10**: 100-105
- 63 **Dazard JE**, Piette J, Basset-Seguain N, Blanchard JM, Gandarillas A. Switch from p53 to MDM2 as differentiating human keratinocytes lose their proliferative potential and increase in cellular size. *Oncogene* 2000; **19**: 3693-3705
- 64 **Okusa Y**, Ichikura T, Mochizuki H, Shinomiya N. Clinical significance of telomerase activity in biopsy specimens of gastric cancer. *J Clin Gastroenterol* 2000; **30**: 61-63
- 65 **Zhang F**, Zhang X, Fan D. Expression of telomere and telomerase in human primary gastric carcinoma. *Zhonghua Binglixue Zazhi* 1998; **27**: 429-432
- 66 **Kameshima H**, Yagihashi A, Yajima T, Kobayashi D, Denno R, Hirata K, Watanabe N. *Helicobacter pylori* infection: augmentation of telomerase activity in cancer and noncancerous tissues. *World J Surg* 2000; **24**: 1243-1249
- 67 **Suzuki K**, Kashimura H, Ohkawa J, Itabashi M, Watanabe T, Sawahata T, Nakahara A, Muto H, Tanaka N. Expression of human telomerase catalytic subunit gene in cancerous and precancerous gastric conditions. *J Gastroenterol Hepatol* 2000; **15**: 744-751
- 68 **Hur K**, Gazdar AF, Rathi A, Jang JJ, Choi JH, Kim DY. Overexpression of human telomerase RNA in *Helicobacter pylori*-infected human gastric mucosa. *Jpn J Cancer Res* 2000; **91**: 1148-1153
- 69 **Hahn WC**, Meyerson M. Telomerase activation, cellular immortalization and cancer. *Ann Med* 2001; **33**: 123-129
- 70 **Kuniyasu H**, Yasui W, Yokozaki H, Tahara E. *Helicobacter pylori* infection and carcinogenesis of the stomach. *Langenbechs Arch Surg* 2000; **385**: 69-74
- 71 **Latil A**, Vidaud D, Valeri A, Fournier G, Vidaud M, Lidereau R, Cussenot O, Biache I. Htert expression correlates with MYC overexpression in human prostate cancer. *Int J Cancer* 2000; **89**: 172-176
- 72 **Kyo S**, Takakura M, Taira T, Kanaya T, Itoh H, Yutsudo M, Ariga H, Inoue M. Sp1 cooperates with c-Myc to active transcription of the human telomerase reverse transcriptase gene (hTERT). *Nucleic Acids Res* 2000; **28**: 669-677
- 73 **Cerni C**. Telomeres, telomerase, and myc. An update. *Mutat Res* 2000; **462**: 31-47
- 74 **Kumamoto H**, Kinouchi Y, Ooya K. Telomerase activity and telomerase reverse transcriptase (TERT) expression in ameloblastomas. *J Oral Pathol Med* 2001; **30**: 231-236
- 75 **Xu D**, Popov N, Hou M, Wang Q, Bjorkholm M, Gruber A, Menkel AR, Henriksson M. Switch from Myc/Max to Mad1/Max binding and decrease in histone acetylation at the telomerase reverse transcriptase promoter during differentiation of HL60 cells. *Proc Natl Acad Sci USA* 2001; **98**: 3826-3831
- 76 **Kyo S**, Takakura M, Inoue M. Telomerase activity in cancer as a diagnostic and therapeutic target. *Histol Histopathol* 2000; **15**: 813-824
- 77 **Eberhardy SR**, D' Cunha CA, Farnham PJ. Direct examination of histone acetylation on Myc target genes using chromatin immunoprecipitation. *J Biol Chem* 2000; **275**: 33798-33805
- 78 **Kitagawa Y**, Kyo S, Takakura M, Kanaya T, Koshida K, Namiki M, Inoue M. Demethylating reagent 5-azacytidine inhibits telomerase activity in human prostate cancer cells through transcriptional repression of hTERT. *Clin Cancer Res* 2000; **6**: 2868-2875
- 79 **Nozawa K**, Maehara K, Isobe K. Mechanism for the reduction of telomerase expression during muscle cell differentiation. *J Biol Chem* 2001; **276**: 22016-22023
- 80 **Sagawa Y**, Nishi H, Isaka K, Fujito A, Takayama M. The correlation of TERT expression with c-myc expression in cervical cancer. *Cancer Lett* 2001; **168**: 45-50

Angiostatin up-regulation in gastric cancer cell SGC7901 inhibits tumorigenesis in nude mice

Jing Wu, Yong-Quan Shi, Kai-Chun Wu, De-Xin Zhang, Jing-Hua Yang, Dai-Ming Fan

Jing Wu, Yong-Quan Shi, Kai-Chun Wu, De-Xin Zhang, Jing-Hua Yang, Dai-Ming Fan, Institute of Gastrointestinal Diseases Research, Xijing Hospital, Fourth Military Medical University, Xi'an 710032, Shannxi Province, China

Supported by the National Natural Science Foundation of China No.39800156

Correspondence to: Dr. Jing Wu, Institute of Gastrointestinal Diseases Research, Xijing Hospital, Fourth Military Medical University, Xi'an 710032, Shannxi Province, China. wujingliu@sina.com.cn

Telephone: +86-29-3375229

Received: 2002-05-16 **Accepted:** 2002-06-09

Abstract

AIM: To explore the influence of angiostatin up-regulation on the biologic behavior of gastric cancer cells *in vitro* and *in vivo*, and the potential of angiostatin gene therapy in the treatment of human gastric cancer.

METHODS: Mouse angiostatin cDNA was subcloned into the eukaryotic expression vector pcDNA3.1(+) and identified by restriction endonucleases digestion and sequencing. The recombinant vector pcDNA3.1(+)-angio was transfected into human gastric cancer cells SGC7901 with liposome and paralleled with the vector control and the mock control. Angiostatin transcription and protein expression were examined by RT-PCR and Western blot in the stable cell lines selected by G418. Cell proliferation and growth *in vitro* of the three groups were observed respectively under microscope, cell number counting and FACS. The cells overexpressing angiostatin, vector transfected and untreated were respectively implanted subcutaneously into nude mice. After 30 days the size of tumors formed was measured, and microvessel density count (MVD) in the tumor tissues was assessed by immunohistochemistry with the primary anti-vWF antibody.

RESULTS: The recombinant vector pcDNA3.1(+)-angio was confirmed with the correct sequence of mouse angiostatin under the promoter CMV. After 30 d of transfection and selection with G418, macroscopic resistant cell clones were formed in the experimental group transfected with pcDNA 3.1(+)-angio and the vector control. But no untreated cells survived in the mock control. Angiostatin mRNA transcription and protein expression were detected in the experimental group. No significant differences were observed among the three groups in cell morphology, cell growth curves and cell cycle phase distributions *in vitro*. However, in nude mice model, markedly inhibited tumorigenesis and slowed tumor expansion were observed in the experimental group as compared with the controls, which was paralleled with decreased microvessel density in and around tumor tissues ($P < 0.05$).

CONCLUSION: Angiostatin does not directly inhibit human gastric cancer cell proliferation and growth *in vitro*, but exerts its anti-tumor functions through antiangiogenesis in a paracrine way *in vivo*.

Wu J, Shi YQ, Wu KC, Zhang DX, Yang JH, Fan DM. Angiostatin up-regulation in gastric cancer cell SGC7901 inhibits tumorigenesis in nude mice. *World J Gastroenterol* 2003; 9(1):59-64
<http://www.wjgnet.com/1007-9327/9/59.htm>

INTRODUCTION

Angiogenesis is indispensable for various physiological processes including reproduction, development, wound repair, and tissue regeneration. However, abnormal neovascularization is also involved in the development and progression of pathogenic processes in a variety of disorders, including diabetic retinopathy, psoriasis, chronic inflammation, lepra alphas, rheumatoid arthritis and cardiovascular diseases. Since Folkman put forward the hypothesis that malignant tumor is angiogenesis dependent, direct and indirect evidences have shown that tumor growth and metastasis are accompanied by the growth of new blood vessels, which proves the rationality and feasibility of anti-angiogenic therapy in treatment of cancer^[1,2]. Shifting the balance within the tumor microenvironment from overproduction of angiogenic stimulators toward an overproduction of angiogenic inhibitors represents one potential anti-angiogenic strategy^[3,4]. To date, a number of angiogenic inhibitors have been demonstrated to inhibit experimental tumor growth in animal models, and some of them have already entered clinical trials^[5].

Gastric cancer is a malignant neoplasm, for which the common treatment is suboptimal and the prognosis of patients remains dismal. It is suggested that tumor-mediated angiogenesis due to high levels of angiogenic stimulators and down-regulation of endogenous angiogenic inhibitors play a fundamental role in the pathogenesis of malignant gastric cancer^[6,7]. Molecular mechanisms of angiogenesis in gastric cancer have indicated an attractive therapeutic strategy by targeting those angiogenic regulators^[8].

Angiostatin, a potent specific inhibitor of proliferating endothelial cells, shows significant antiangiogenic and anticarcinogenic efficacies on various tumors *in vivo*. It specifically inhibits the proliferation, migration, and formation of capillary tubes *in vitro* or *in vivo*, and induces apoptosis in endothelial cells^[9-11]. Although no directed inhibition on tumor cell growth *in vitro* is observed, evidence shows that angiostatin inhibits the occurrence of the primary as well as metastatic tumor, and remains dormant. Systemic delivery of purified angiostatin protein, however, raises a number of difficult practical problems which make the large-scale implementation inefficient and/or inefficacious. And these problems also make it unavailable logically and pharmaceutically, including difficulties in producing large quantities of biologically active protein, the short half-life of such proteins *in vivo*, and the requirement for long-term intermittent or continuous treatment. The transfer of angiostatin gene, therefore, may represent a useful alternative delivery strategy. Transducing tissues at risk for tumor progression *in vivo* with genes encoding antiangiogenic proteins offers the potential of creating a local antiangiogenic microenvironment that can be stably maintained through continuous expression of the transduced transgene

from surrounding tumor cells.

We have constructed and administered eukaryotic vector encoding mouse angiostatin into human gastric cancer cells to further characterize the antitumor function of angiostatin and explore the potential activity in gene therapy for gastric cancer. Our data demonstrated statistically significant inhibition of tumor formation and growth in nude mice accompanied by decreased microvascular density and upregulation of angiostatin, meanwhile no cytostatic effect on gastric cancer cells was observed *in vitro*. These results suggested that the delivery of angiostatin gene may represent a potentially new treatment modality for malignant gastric cancer, accounting for antiangiogenic activity in a paracrine way on surrounding endothelial cells.

MATERIALS AND METHODS

Cell culture and reagents

The human gastric cancer cell line SGC7901 was obtained from the Japanese Cancer Research Resources Bank (Tokyo, Japan). Cells were cultured in RPMI1640 (Gibco) supplemented with 10 % fetal bovine serum (FBS) (Sijiqing, Hangzhou, China), penicillin (100 units/ml) and streptomycin (100 mg/ml) in a humidified atmosphere of 5 % CO₂ at 37 °C. Liposome (Tfx™ Reagent) was purchased from Promega Company; total RNA Isolation System (Sino-American Biotechnology Company) G418 from Gibco company; and bicinchoninic acid (BCA) protein assay kit was obtained from Pierce Chemicals (Rockford, Illinois).

Recombinant eukaryotic expression vector pcDNA3.1(+)-angio construction and transfection

Mouse angiostatin cDNA fragment encoding for the NH₂-terminal secretory signal sequence(SS) and kringle1-4(K1-4) regions of mouse plasminogen, fused with an antigenic epitope tag HA(HA tag) to the COOH terminus of kringle 4 was inserted into eukaryotic expression vector pcDNA3.1(+). The structure of the recombinant vector pcDNA3.1(+)-angio was confirmed by the restriction enzyme digest and DNA sequencing.

Gastric cancer cells SGC7901 in logarithmic growth phase were planted in 6-well plates at 5×10⁵ cells/well, and reached approximately 80 % confluent after overnight incubation on the day of the transfection. DNA/liposome (Tfx™ Reagent) complexes were prepared and transfected according to the protocol provided by the manufacturer. The experimental group was transfected with pcDNA3.1(+)-angio 2 μg/liposome 10 μL, the vector control with pcDNA3.1(+)-angio 2 μg/liposome 10 μL and the mock control with liposome 10 μL. After 48 h of transfection, the selective medium containing G418 (400 mg/L) was used to culture cells for 30 d. Then the isolated resistant cell clones were then selected and amplified.

RNA dot blot analysis of angiostatin transcription

Total RNA was extracted with total RNA isolation system, resuspended in DEPC-treated water, quantitated with OD260 and OD280, and dotted onto nitrocellulose filters. The linear mouse angiostatin cDNA fragment was released from the vector pcDNA3.1(+)-angio and labeled with [α -³²P] in nick translation reaction as the probe. The specific activity of the probe was examined by TCA method. Hybrid was performed sequentially: prehybridized at 42 °C for 3 h, the probe denatured in water-bath at 100 °C for 10 min and cooled on ice for 5 min, hybridized at 42 °C overnight, washed in 2×SSC and 0.2×SSC at RT, and then hybrid signals were detected by autoradiograph.

Western blot analysis of HA-tagged protein

The cells were cultured in conditioned media for 5 d. Cell

supernatants was mixed with Lysine-sepharose and incubated at 4 °C overnight. The resin was washed with 50 mM Tris-HCl (pH8.0), and protein was eluted and stored at -20 °C. Protein concentration was determined by bicinchoninic acid assay (BCA) with bovine serum albumin as standard. Equal aliquots (40 μg) of protein from cell supernatants were subjected to electrophoresis on a 10 % sodium dodecyl sulfate (SDS)-polyacrylamide gel, followed by transfer to PVDF membranes (mMillipore) using the transfer buffer for 2 hours and detection with the rabbit polyclonal anti-HA antibody (diluted 1:500; Santa Cruz Biotechnology, Santa Cruz, CA) overnight at 4 °C and a secondary peroxidase-conjugated goat anti-rabbit antibody (Santa Cruz Biotechnology, Santa Cruz, CA). Final detection was performed by the enhanced chemiluminescence (ECL) Western blotting analysis system.

Viable cell number counting and FACS analysis of cell cycle

Cell viability and cell growth *in vitro* were determined by cell number counting. Briefly, the three groups of cells were plated on 24-well plates at 1×10⁴ cells/well and cultured for 7 d. Everyday viable cell numbers of the three groups were counted under microscope.

Three groups of cells 3×10⁵ in the logarithmic growth phase were collected and fixed in 70 % ethanol overnight. After being dyed with PI at 4 °C avoid of light for 30 minutes, the cells through screening were checked in FACS to estimate the changes in cell cycle.

Animal studies

In vitro tumorigenesis assay. BalBc nude mice were randomly divided into three groups, 5 in each group and injected subcutaneously with gastric cancer cells SGC7901 at 1.2×10⁷ cells/mouse, the experimental group with pcDNA3.1(+)-angio/SGC7901, the vector control with pcDNA3.1(+)/SGC7901 and the mock control with SGC7901 untransfected. After 30 d, the mice were sacrificed to measure the size of tumor formed and calculate the percentage of inhibition on tumorigenesis *in vivo*.

Quantitative analyses for microvessel densities (MVD)

The tumor tissues were fixed and embedded in paraffin and MVD were detected by SABC method. Briefly, the sections were incubated with 0.3 % H₂O₂ and methanol for 30 min, blocked with normal goat serum at RT for 2 h, stained with a primary anti-mouse vWF monoclonal antibody at 4 °C overnight and then biotin-conjugated anti-mouse IgG antibody at RT for 1 h. After being incubated with ABC compounds for 40 min, DAB was used to develop color reaction. Under light microscope, MVD was counted in 4 fields (400×) selected randomly.

Statistical analysis

The results were verified by variance analysis and χ^2 analysis with SPLM statistical software offered by the Department of Statistics, the Fourth Military Medical University.

RESULTS

Identification of the recombinant eukaryotic expression vector encoding angiostatin cDNA

Angiostatin cDNA was cloned into an eukaryotic expression vector pcDNA3.1(+), under the cytomegalovirus promoter, encoding for the NH-terminal secretory signal sequence (SS), the preactivation peptide (PA), and kringle1-4(K1-4) regions of mouse plasminogen, and an antigenic epitope tag derived from the influenza HA fused to the COOH terminus of kringle4 (Figure 1). As shown in electrophoresis, the linear recombinant plasmid was about 7.0kb, and a fragment 1.4kb was released by restrictive digest with HindIII and XbaI, which confirmed

that the targeted gene was cloned into pcDNA3.1(+)-angio successfully (Figure 2). Gene sequencing showed that it had the same sequence as supposed.

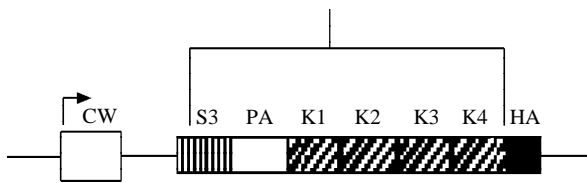


Figure 1 Schematic diagram of angiostatin cDNA fragment.

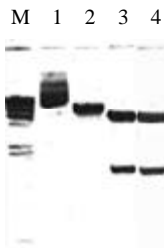


Figure 2 Identification of angiostatin cDNA insertion in pcDNA3.1(+)-angio. M: λ dsDNA/HindIII marker; 1: pcDNA3.1(+)-angio/HindIII; 2: pcDNA3.1(+)-angio; 3: pcDNA3.1(+)-angio/HindIII+XbaI; 4: pcDNA3.1(+)-angio/BamHI.

Vector-mediated expression and secretion of angiostatin in vitro

To determine the level of transgene-encoded angiostatin transcription and protein expression and secretion, gastric cancer cells SGC7901 transfected with the corresponding vectors were selected by G418 for 30 d and formed macroscopic cell clones in the experimental and vector control groups (Figure 3). The mock group of cells, however, were dead completely after 7 d of selection. Strong RNA hybrid signals of angiostatin mRNA were detected in the experimental group of cell clones genetically engineered but not in the controls (Figure 4). Western blot analysis of cell supernatants (Figure 5) revealed the detected protein of the size consistent with angiostatin in the experiment group, whereas no specific band was observed in the controls.

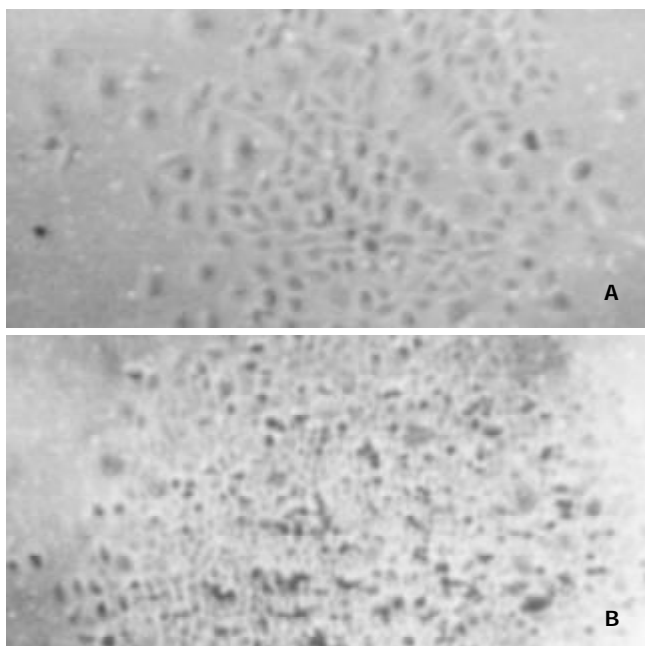


Figure 3 Cell clones transfected with pcDNA3.1(+)-angio and pcDNA3.1(+) respectively. A: Cell clone pcDNA3.1(+)-angio transfected; B: Cell clone pcDNA3.1(+) transfected.



Figure 4 Angiostatin mRNA expression by Dot Blot analysis. 1: SGC7901; 2: SGC7901(+); 3:SGC7901-pcDNA3.1(+)-angio.

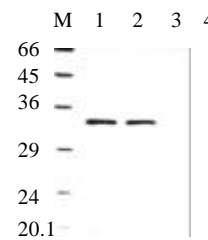


Figure 5 Angiostatin protein expression by Western Blot analysis. M: Marker; 1: SGC7901pcDNA3.1(+)-angio; 2: SGC7901pcDNA3.1(+)-angio; 3: SGC7901pcDNA3.1(+); 4: SGC7901.

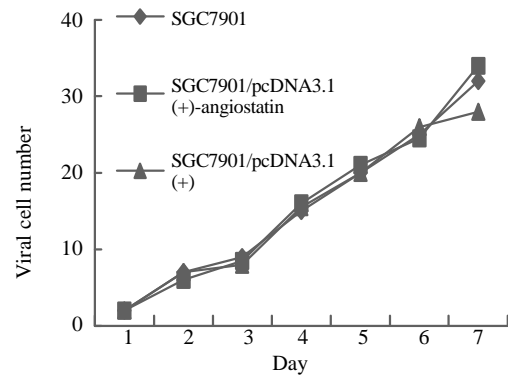


Figure 6 Cell growth curves.

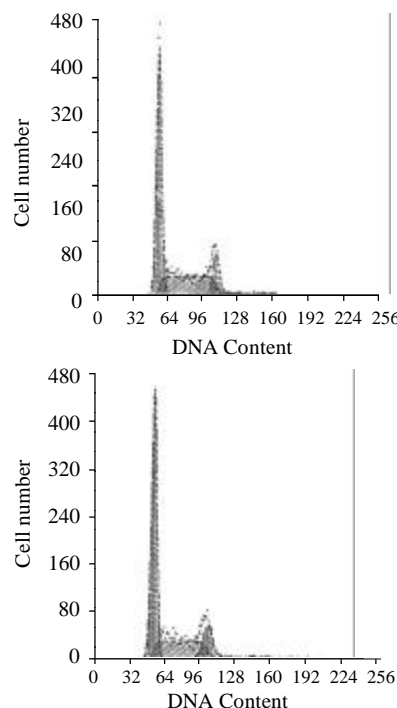


Figure 7 Cell cycle distributions by FACS analysis. A: SGC7901 transfected with pcDNA3.1(+)-angio; B: SGC7901.

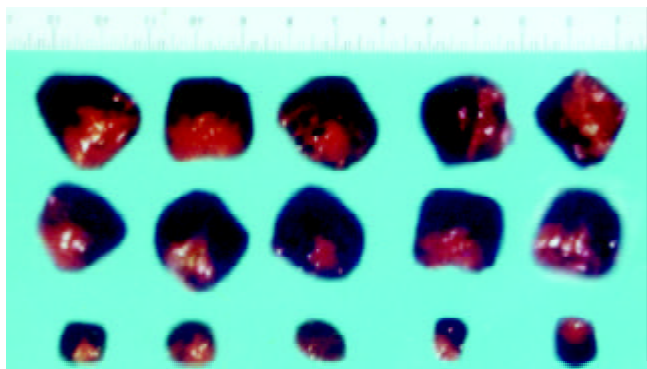


Figure 8 Tumors formed in nude mice by SGC7901/pcDNA-angio, SGC7901/pcDNA, and SGC7901 cells ($n=5$). A:SGC7901; B: SGC7901/pcDNA3.1(+); C: SGC7901/pcDNA3.1(+)-angio.

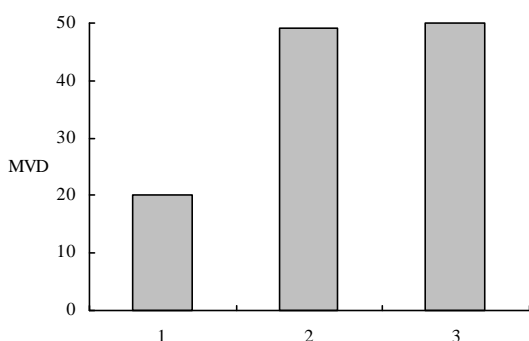


Figure 9 MVD in immunochemistry staining. 1: SGC7901/pcDNA-angio; 2: SGC7901/pcDNA; 3: SGC7901.

Biological activity of angiostatin proteins expression *in vitro*

To assay for biological activity of the encoded angiostatin *in vitro*, tumor cells transduced with and without the corresponding vectors were cultured for 7 d to make cell growth curve (Figure 6). Under microscope, no obvious difference was observed in the cell morphology among the three groups of cells. And cell growth curves indicated no change in cell growth speed and doubling time among the three groups. Comparing the cell cycle of the three groups, no significant differences were found in the distribution of G0/G1, S and G2/M (Figure 7). These results indicated that up-regulated angiostatin expression neither directly inhibits cell growth and proliferation nor affects cell cycle *in vitro*.

Biological activity of angiostatin proteins expression *in vivo*

The macroscopic tumors were observed on day 7 after injection and expanded fast in the vector and mock control groups of nude mice. However, no tumors were observable until day 10 after injection in the experimental group of nude mice, and tumors expanded slowly. After 30 d of injection, no mice died in the three groups and the tumors were resected and measured. Small, pale tumor nodules were observed in the angiostatin-transfected tumors, whereas large, red and hypervascularized tumors were present in the vector-transfected control and mock control tumor cells. The average size of tumors in the experimental group was $2.11 \times 0.53 \text{ cm}^3$, much less than the average size of the vector control $4.32 \times 1.00 \text{ cm}^3$ and the mock control (Figure 8). The inhibition by angiostatin overexpression reached 72 %.

The tumor tissues in the experimental group showed more typical symptoms of poor vascularization than the control groups. More markedly diminished microvascular densities were detected by immunohistochemical staining in the tumors in the experimental group than in the vector or mock control

groups respectively ($P < 0.01$) (Figure 9), which indicated that overexpression of angiostatin probably decreased tumorigenesis by inhibiting neovascularization in tumors *in vivo*. And angiostatin exerted its inhibitory actions in some paracrine ways on ECs surrounding tumor tissues and indirectly inhibited tumorigenesis.

DISCUSSION

Since Dr. Folkman raised the hypothesis of tumor angiogenic dependence, experimental evidences have validated that tumor growth requires the company of new blood vessel growth. At the prevascular stage, the tumor is unable to grow to a size beyond $2\text{-}3 \text{ mm}^3$ and remains in its dormant state. However, once the angiogenic phenotype of the tumor is switched on, tumor growth rate changes from linear to exponential^[12-14]. Metastases are also dependent on angiogenesis in at least two steps of the metastatic events^[15]. First, metastatic tumor cells must exit from a primary tumor which has been vascularized. Second, upon arrival at their target organ, metastatic tumor cells must undergo neovascularization in order to grow to a clinically detectable size. It is speculated that complete inhibition of tumor angiogenesis may result in a loss of survival factors essential for tumor cells from the endothelial cell as paracrine factors^[16]. The regulation of tumor angiogenesis is a complex process involving enzymatic and signal-transduction cascades that function in fibrinolysis, matrix remodeling, inflammation, hemodynamic control of oxygenation, and growth regulation^[17-19]. The local balance between positive and negative factors determines the net tendency toward angiogenesis or angiostasis^[20].

Angiogenesis is closely related to gastric cancer as a pertinent predictive factor in addition to having prognostic value^[21]. The average number of blood vessels is significantly higher in gastric cancer specimens than in normal gastric specimens, higher in advanced disease than in early-stage disease, higher in specimens with metastases or blood vessel invasion than in those without such metastasis or invasion^[22,23]. VEGF positive immunostaining is observed in the gastric tissues with different severities of lesions, the positive rates increased with the lesion progressing from CAG to IM to DYS^[24]. And its expression is associated with hematogenous invasion, metastasis, and clinical prognosis of gastric cancer^[25]. As a malignant disease with the highest mortality rates in China, gastric cancer is refractory to the routine chemotherapy and radiotherapy, which are mainly adopted as the adjunctive therapy during and/or post operation to prolong the survival rates^[26,27]. Moreover, chemotherapy has obvious toxicity and is subject to drug resistance in the treatment of gastric cancer^[28]. Until now the only method possible to cure gastric cancer is surgical resection, despite its importance for the late-stage cancer and various types of high-rate recurrences. Meanwhile the chromosomal instability in DNA of gastric cancer cells unfavorably obstructs the curative effects of the methods directly attacking tumor cells.

Thus antiangiogenic treatment may be necessary and potential for gastric cancer, which has been validated in many experiments. In *in vivo* experiments, antiangiogenic agents with cytotoxic anticancer drugs formed a highly effective modulator combination for the treatment against primary and metastatic carcinoma. The combination of anti-VEGF antibody with mitomycin C markedly enhanced anti-tumor and anti-metastasis effects in nude mice transplanted with human gastric cancer SGC-7901^[29]. The VEGF receptor KDR/Flk-1 antisense strategy significantly increases the number of gastric cancer cells undergoing apoptosis, and decreases tumor dissemination^[30]. Angiogenesis inhibitor endostatin inhibits both tumor growth and metastasis of human gastric cancer in nude mice^[31]. And

octreotide inhibits the migration and invasion of SGC-7901 gastric cancer cells *in vitro* and the metastasis of cancer *in vivo* through down-regulation of MMP-2 expression and tumor angiogenesis^[32]. And the clinical applications of antivasular, anti-angiogenic and angiostatic agents for the treatment of gastric carcinoma may be valuable for long-term administration to maintain tumor dormancy because drug resistance does not develop, and these agents have a sustained effect with less side effects than the traditional methods.

Angiostatin was firstly isolated as a circulating angiogenesis inhibitor, whose sequence has greater than 98 % identity with an internal fragment of plasminogen, containing the first four of five triple loop disulfide-linked kringle structures. Purified angiostatin specifically and reversibly inhibits proliferation of endothelial lineages in a dose-dependent manner, but not proliferation of normal and neoplastic nonendothelial cell lines^[9-11]. Systemic administration of human angiostatin potently inhibits the growth of transplanted human breast carcinoma by 95 %, colon carcinoma by 97 % and prostate carcinoma by almost 100 % in mice, without obvious weight loss or other toxicity observed^[33,34]. It causes human primary carcinomas to regress to a dormant state by a net balance of tumor cell proliferation and apoptosis. And in the presence of angiostatin, metastatic tumor cells form microscopic perivascular cuffs around the pre-existing microvessel, rarely expanding beyond 0.3 mm in diameter^[35-37]. Although angiostatin is a potent inhibitor of angiogenesis and tumor growth, the need of high dosages, repeated injections and long-term administration of this protein into the body have made it less attractive for clinical trials.

In order to develop alternative strategies for therapy, the potential of angiostatin in gene therapy has been investigated. In our study, human gastric cancer cells SGC7901 are transfected with mouse angiostatin cDNA and stable cell lines expressing the secreted form of angiostatin are established. Despite the high levels of its expression in cell clones, angiostatin has no direct influence on tumor-cell growth *in vitro*. Implantation of the stable cell clones in nude mice produces inhibition of primary tumor growth by an average of 72 %. Inhibition of tumor growth is correlated with reduced vascularization, suggesting that angiostatin exerts the antitumor effects through antiangiogenesis. These results are similar to the previously report that angiostatin cDNA transfection into the murine T241 fibrosarcoma cells inhibits primary tumor growth by an average of 77 % in C57Bl6/J mice^[38]. Thus angiostatin gene therapy is possibly available for gastric cancer, especially for its simple manipulation, highly specificity, wide-spectrum inhibitory effects on various tumors. It has been observed that retroviral transduction of angiostatin in rat glioma cells inhibits tumor growth by 70 % *in vivo*, however, a relatively ineffective process^[39]. Stable gene transfer of the angiostatin cDNA by retroviral vectors in Kaposi' s sarcoma KS-IMM cells resulted in delayed tumor growth in nude mice, which was associated with reduced vascularization^[40]. Direct injections of replication-deficient angiostatin-expressing adenoviral vector inhibit tumor growth, and represent a potentially new treatment modality for malignant ascites, which are efficient and capable of transducing dividing cells as well as non-dividing cells *in vivo*^[39,41]. The specific targeting of tumors to inhibit angiogenesis using an adenovirus expressing angiostatin, may deliver localized concentrations of protein having a greater impact on inhibition of tumor growth^[42]. AAV-mediated antiangiogenesis gene therapy offers efficient and sustained systemic delivery of the therapeutic product, which in turn effectively suppresses glioma growth in the brain^[43]. Considering the possibility of viral immunoreaction and toxicity, non-viral angiostatin-delivery system has also been explored. Intravenous injection of cationic liposome-

angiostatin cDNA complex produced a significant antimetastatic effect on murine B16 melanoma compared to either reporter gene-treated and untreated controls^[44]. These results support that angiostatin-gene therapy is a potential strategy in the clinical treatment of gastric cancer.

In order to modify the specificity, we are exploiting gastric cancer specific single-chained antibodies to guide the angiostatin-gene therapy. Another potential pathway is delivering angiostatin gene directly into gastric cancer tissues under the endoscope. Because neovascularization in tumors is a multi-step process, the key molecules involved in various steps are potentially combined to improve anti-cancer efficacy of angiogenic gene therapy, including inhibition of endothelial cell proliferation, migration, invasion and matrix degradation. More effective inhibition has been observed in the combined gene therapy of angiostatin and endostatin than the angiostatin-or endostatin-therapy respectively^[45]. Meanwhile, angiogenic genes are possibly combined with other curative molecules, such as immunoregulators, suppressors of oncogene, enzymatic precursor drugs. When angiostatin-mediated antiangiogenic therapy is used in combination with intratumor delivery of the IL-12 gene, this produces a synergistic therapeutic effect^[46]. It has been validated the potential of combining a destructive strategy directed against the tumor cells with an anti-angiogenic approach to fight cancer. The combination of radiotherapy and angiostatin intratumoral injection reveals a significant inhibition of tumor growth as compared with either treatment^[47]. These combined therapies will open new possibilities of being less toxic and more effective than the traditional therapies in the clinical treatment of gastric cancer.

In conclusion, it is the first time that approves the potential of angiostatin anti-cancer effect has been proved on gastric cancer and its functional mechanism of antiangiogenesis in tumor has been revealed. And these data offers a new way to comeover the disadvantages in traditional therapies in clinic.

REFERENCES

- 1 **Hayes AJ**, Li LY, Lippman ME. Science, medicine, and the future antivasular therapy: a new approach to cancer treatment. *BMJ* 1999; **318**: 353-356
- 2 **Rosen LS**. Angiogenesis inhibition in solid tumors. *Cancer J* 2001; **7** (Suppl 3): S120-128
- 3 **Sugimachi K**, Tanaka S, Terashi T, Taguchi K, Rikimaru T, Sugimachi K. The mechanisms of angiogenesis in hepatocellular carcinoma: angiogenic switch during tumor progression. *Surgery* 2002; **131** (Suppl 1): S135-141
- 4 **Cao Y**. Endogenous angiogenesis inhibitors and their therapeutic implications. *Int J Biochem Cell Biol* 2001; **33**: 357-369
- 5 **Hagedorn M**, Bikfalvi A. Target molecules for anti-angiogenic therapy: from basic research to clinical trials. *Crit Rev Oncol Hematol* 2000; **34**: 89-110
- 6 **Saito H**, Tsujitani S. Angiogenesis, angiogenic factor expression and prognosis of gastric carcinoma. *Anticancer Res* 2001; **21**: 4365- 4372
- 7 **Takeji Y**, Maehara Y, Sumiyoshi Y, Oda S, Emi Y. Angiogenesis as a target for gastric cancer. *Surgery* 2002; **131** (1 Suppl): S48-54
- 8 **Gibaldi M**. Regulating angiogenesis: a new therapeutic strategy. *J Clin Pharmacol* 1998; **38**: 898-903
- 9 **Gupta N**, Nodzenski E, Khodarev NN, Yu J, Khorasani L, Beckett MA, Kufe DW, Weichselbaum RR. Angiostatin effects on endothelial cells mediated by ceramide and RhoA. *EMBO Rep* 2001; **2**: 536-540
- 10 **Lucas R**, Holmgren L, Garcia I, Jimenez B, Mandriota SJ, Borlat F, Sim BK, Wu Z, Grau GE, Shing Y, Soff GA, Bouck N, Pepper MS. Multiple forms of angiostatin induce apoptosis in endothelial cells. *Blood* 1998; **92**: 4730-4741
- 11 **Hari D**, Beckett MA, Sukhatme VP, Dhanabal M, Nodzenski E, Lu H, Mauceri HJ, Kufe DW, Weichselbaum RR. Angiostatin induces mitotic cell death of proliferating endothelial cells. *Mol Cell Biol Res Commun* 2000; **3**: 277-282

- 12 **Papetti M**, Herman IM. Mechanisms of normal and tumor-derived angiogenesis. *Am J Physiol Cell Physiol* 2002; **282**: C947-970
- 13 **Ellis LM**, Liu W, Ahmad SA, Fan F, Jung YD, Shaheen RM, Reinmuth N. Overview of angiogenesis: Biologic implications for antiangiogenic therapy. *Semin Oncol* 2001; **28** (5 Suppl 16): 94-104
- 14 **Cavallaro U**, Christofori G. Molecular mechanisms of tumor angiogenesis and tumor progression. *J Neurooncol* 2000; **50**: 63-70
- 15 **Bashyam MD**. Understanding cancer metastasis: an urgent need for using differential gene expression analysis. *Cancer* 2002; **94**: 1821-1829
- 16 **Reinmuth N**, Stoeltzing O, Liu W, Ahmad SA, Jung YD, Fan F, Parikh A, Ellis LM. Endothelial survival factors as targets for anti-neoplastic therapy. *Cancer J* 2001; **7** (Suppl 3): S109-119
- 17 **VanMeter TE**, Roprai HK, Kibble MM, Fillmore HL, Broaddus WC, Pilkington GJ. The role of matrix metalloproteinase genes in glioma invasion: co-dependent and interactive proteolysis. *J Neurooncol* 2001; **53**: 213-235
- 18 **Izumi Y**, Xu L, di Tomaso E, Fukumura D, Jain RK. Tumour biology: herceptin acts as an anti-angiogenic cocktail. *Nature* 2002; **416**: 279-280
- 19 **Giatromanolaki A**, Harris AL. Tumour hypoxia, hypoxia signaling pathways and hypoxia inducible factor expression in human cancer. *Anticancer Res* 2001; **21**: 4317-4324
- 20 **Dixelius J**, Cross M, Matsumoto T, Sasaki T, Timpl R, Claesson-Welsh L. Endostatin regulates endothelial cell adhesion and cytoskeletal organization. *Cancer Res* 2002; **62**: 1944-1947
- 21 **Saito H**, Tsujitani S. Angiogenesis, angiogenic factor expression and prognosis of gastric carcinoma. *Anticancer Res* 2001; **21**: 4365-4372
- 22 **Chen CN**, Cheng YM, Lin MT, Hsieh FJ, Lee PH, Chang KJ. Association of color Doppler vascularity index and microvessel density with survival in patients with gastric cancer. *Ann Surg* 2002; **235**: 512-518
- 23 **Erenoglu C**, Akin ML, Uluutku H, Tezcan L, Yildirim S, Batkin A. Angiogenesis predicts poor prognosis in gastric carcinoma. *Dig Surg* 2000; **17**: 581-586
- 24 **Feng C**, Wang L, Jiao L, Liu B, Zheng S, Xie X. Expression of p53, inducible nitric oxide synthase and vascular endothelial growth factor in gastric precancerous and cancerous lesions: correlation with clinical features. *BMC Cancer* 2002; **2**: 8
- 25 **Tao HQ**, Lin YZ, Wang RN. Significance of vascular endothelial growth factor messenger RNA expression in gastric cancer. *World J Gastroenterol* 1998; **4**: 10-13
- 26 **Meyerhardt JA**, Fuchs CS. Chemotherapy options for gastric cancer. *Semin Radiat Oncol* 2002; **12**: 176-186
- 27 **Wilson KS**. Postoperative chemoradiotherapy helps in gastric adenocarcinoma. *BMJ* 2002; **324**: 977
- 28 **Wang X**, Lan M, Shi YQ, Lu J, Zhong YX, Wu HP, Zai HH, Ding J, Wu KC, Pan BR, Jin JP, Fan DM. Differential display of vincristine-resistance-related genes in gastric cancer SGC7901 cell. *World J Gastroenterol* 2002; **8**: 54-59
- 29 **Tao HQ**, Lin YZ, Wang RN. Significance of vascular endothelial growth factor messenger RNA expression in gastric cancer. *World J Gastroenterol* 1998; **4**: 10-13
- 30 **Kamiyama M**, Ichikawa Y, Ishikawa T, Chishima T, Hasegawa S, Hamaguchi Y, Nagashima Y, Miyagi Y, Mitsuhashi M, Hyndman D, Hoffman RM, Ohki S, Shimada H. VEGF receptor antisense therapy inhibits angiogenesis and peritoneal dissemination of human gastric cancer in nude mice. *Cancer Gene Ther* 2002; **9**: 197-201
- 31 **Zhang GF**, Wang YH, Zhang MA, Wang Q, Luo YB, Han CR, Lu YQ, Rao YY. Inhibition of growth and metastasis of human gastric cancer implanted in nude mice by the angiogenesis inhibitor endostatin. [Article in Chinese]. *Zhonghua Waike Zazhi* 2002; **40**: 59-61
- 32 **Wang CH**, Tang CW. Inhibition of human gastric cancer metastasis by ocreotide *in vitro* and *in vivo*. [Article in Chinese] *Zhonghua Yixue Zazhi* 2002; **82**: 19-22
- 33 **Sim BK**, O'Reilly MS, Liang H, Fortier AH, He W, Madsen JW, Lapcevic R, Nagy CA. A recombinant human angiostatin protein inhibits experimental primary and metastatic cancer. *Cancer Res* 1997; **57**: 1329-1334
- 34 **Kirsch M**, Strasser J, Allende R, Bello L, Zhang J, Black PM. Angiostatin suppresses malignant glioma growth *in vivo*. *Cancer Res* 1998; **58**: 4654-4659
- 35 **Apte RS**, Niederkorn JY, Mayhew E, Alizadeh H. Angiostatin produced by certain primary uveal melanoma cell lines impedes the development of liver metastases. *Arch Ophthalmol* 2001; **119**: 1805-1809
- 36 **Yanagi K**, Onda M, Uchida E. Effect of angiostatin on liver metastasis of pancreatic cancer in hamsters. *Jpn J Cancer Res* 2000; **91**: 723-730
- 37 **Drixler TA**, Rinkes IH, Ritchie ED, van Vroonhoven TJ, Gebbink MF, Voest EE. Continuous administration of angiostatin inhibits accelerated growth of colorectal liver metastases after partial hepatectomy. *Cancer Res* 2000; **60**: 1761-1765
- 38 **Cao Y**, O'Reilly MS, Marshall B, Flynn E, Ji RW, Folkman J. Expression of angiostatin cDNA in a murine fibrosarcoma suppresses primary tumor growth and produces long-term dormancy of metastases. *J Clin Invest* 1998; **101**: 1055-1063
- 39 **Indraco S**, Morini M, Gola E, Carrozzino F, Habeler W, Minghelli S, Santi L, Chieco-Bianchi L, Cao Y, Albini A, Noonan DM. Effects of angiostatin gene transfer on functional properties and *in vivo* growth of Kaposi's sarcoma cells. *Cancer Res* 2001; **61**: 5441-5446
- 40 **Gyorffy S**, Palmer K, Gaudie J. Adenoviral vector expressing murine angiostatin inhibits a model of breast cancer metastatic growth in the lungs of mice. *Am J Pathol* 2001; **159**: 1137-1147
- 41 **Tanaka T**, Cao Y, Folkman J, Fine HA. Viral vector-targeted antiangiogenic gene therapy utilizing an angiostatin complementary DNA. *Cancer Res* 1998; **58**: 3362-3369
- 42 **Hampf M**, Tanaka T, Albert PS, Lee J, Ferrari N, Fine HA. Therapeutic effects of viral vector-mediated antiangiogenic gene transfer in malignant ascites. *Hum Gene Ther* 2001; **12**: 1713-1729
- 43 **Ma HI**, Guo P, Li J, Lin SZ, Chiang YH, Xiao X, Cheng SY. Suppression of intracranial human glioma growth after intramuscular administration of an adeno-associated viral vector expressing angiostatin. *Cancer Res* 2002; **62**: 756-763
- 44 **Rodolfo M**, Cato EM, Soldati S, Ceruti R, Asioli M, Scanziani E, Vezzoni P, Parmiani G, Sacco MG. Growth of human melanoma xenografts is suppressed by systemic angiostatin gene therapy. *Cancer Gene Ther* 2001; **8**: 491-496
- 45 **Scappaticci FA**, Smith R, Pathak A, Schloss D, Lum B, Cao Y, Johnson F, Engleman EG, Nolan GP. Combination angiostatin and endostatin gene transfer induces synergistic antiangiogenic activity *in vitro* and antitumor efficacy in leukemia and solid tumors in mice. *Mol Ther* 2001; **3**: 186-196
- 46 **Wilczynska U**, Kucharska A, Szary J, Szala S. Combined delivery of an antiangiogenic protein (angiostatin) and an immunomodulatory gene (interleukin-12) in the treatment of murine cancer. *Acta Biochim Pol* 2001; **48**: 1077-1084
- 47 **Griscelli F**, Li H, Cheong C, Opolon P, Bennaceur-Griscelli A, Vassal G, Soria J, Soria C, Lu H, Perricaudet M, Yeh P. Combined effects of radiotherapy and angiostatin gene therapy in glioma tumor model. *Proc Natl Acad Sci USA* 2000; **97**: 6698-6703

Synergistic effect of cell differential agent-II and arsenic trioxide on induction of cell cycle arrest and apoptosis in hepatoma cells

Jian-Wei Liu, Yi Tang, Yan Shen, Xue-Yun Zhong

Jian-Wei Liu, Department of General Surgery, **Yi Tang, Yan Shen**, Cell Culture Laboratory, Guangzhou Red Cross Hospital, Jinan University, Guangzhou 510220, Guangdong Province, China
Xue-Yun Zhong, Department of Pathology, Jinan University Medical College, Guangzhou 510632, Guangdong Province, China
Supported by the Scientific Research Fund of Guangdong Province, No.1998110

Correspondence to: Dr. Jian-Wei Liu, Department of General Surgery, Guangzhou Red Cross Hospital, Jinan University, Guangzhou 510220 Guangdong Province, China. mabeliu@public.guangzhou.gd.cn
Telephone: +86-20-84412233 **Fax:** +86-20-84429803
Received: 2002-06-03 **Accepted:** 2002-07-03

Abstract

AIM: To illustrate the possible role of cell differential agent-II (CDA-II) in the apoptosis of hepatoma cells induced by arsenic trioxide (As_2O_3).

METHODS: Hepatoma cell lines BEL-7402 and HepG2 were treated with As_2O_3 together with CDA-II. Cell surviving fraction was determined by MTT assay; morphological changes were observed by immunofluorescence staining of Hoechst 33 258; and cell cycle and the apoptosis index were determined by flow cytometry (FCM).

RESULTS: Cytotoxicity of CDA-II was low. Nevertheless, CDA-II could strongly potentiate arsenic trioxide-induced apoptosis. At 1.0 g/L CDA-II, IC_{50} of As_2O_3 in hepatoma cell lines was reduced from 5.0 $\mu\text{mol/L}$ to 1.0 $\mu\text{mol/L}$ ($P < 0.01$). The potentiation of apoptosis was dependent on the dosage of CDA-II. FCM indicated that in hepatoma, cell growth was inhibited by CDA-II at lower concentrations (< 2.0 g/L) primarily by arresting at S and G_2 phase, and at higher concentrations (> 2.0 g/L) apoptotic cell and cell cycle arresting at G_1 phase increased proportionally. The combination of two drugs led to much higher apoptotic rates, as compared with the either drug used alone.

CONCLUSION: CDA-II can strongly potentiate As_2O_3 -induced apoptosis in hepatoma cells, and two drugs can produce a significant synergic effect.

Liu JW, Tang Y, Shen Y, Zhong XY. Synergistic effect of cell differential agent-II and arsenic trioxide on induction of cell cycle arrest and apoptosis in hepatoma cells. *World J Gastroenterol* 2003; 9(1): 65-68
<http://www.wjgnet.com/1007-9327/9/65.htm>

INTRODUCTION

It has been reported that arsenic trioxide (As_2O_3), a newly found apoptosis inducer, possesses a greater apoptotic effect on hepatoma cells as compared with some drugs used in chemotherapy^[1-5]. However, because of its toxicity and the drug resistance of cancer cells, it has not been widely used in the treatment of cancers^[6-10]. As a biological preparation purified from human urine, cell differential agent-II(CDA-II) can

effectively induce cell differentiation and reverse drug resistance of cancer cells against chemotherapeutic agents^[11,12]. Clinical application of CDA-II has demonstrated its low toxicity and satisfactory therapeutic effect^[13-15]. This report is intended to investigate the effect of CDA-II on As_2O_3 -induced apoptosis of hepatoma cells in an attempt to find a better combination therapy for hepatoma.

MATERIALS AND METHODS

Materials

Human hepatoma cell lines HepG2 and Bel-7402 were obtained from the cell laboratory in the Medical School of Zhongshan University; cell differential agent (CDA-II) was provided by Everlife Pharmaceutical Co. Ltd, Hefei; arsenic trioxide (As_2O_3 , $M_r=197.84$), MTT, Hoechst 33 258 and PI were purchased from Sigma Co., USA; PRMI 1 640 was purchased from GIBCO, USA; agar, RNase, proteinase were purchased from Huamei Company; DEME purchased from Evergreen Company, Hangzhou, dimethyl sulfoxide (DMSO) was imported and individually packed, and λ -DNA Marker VII was purchased from Roche Company, USA.

Experimental group

The preliminary experiment showed that 1.0-5.0 $\mu\text{mol/L}$ of As_2O_3 could induce apoptosis in hepatoma cells to various degrees, and 1.0-5.0 g/L of CDA-II could inhibit proliferation and induce differentiation of hepatoma cells. The experiment was divided into 4 groups: group A, control without any drug; group B, As_2O_3 was added only to final concentrations of 1.0, 2.0, 3.0, 4.0 and 5.0 $\mu\text{mol/L}$; group C, CDA-II was added to final concentrations of 1.0, 2.0, 3.0, 4.0 and 5.0 g/L; and group D, 1.0 g/L of CDA-II + various concentrations of As_2O_3 used in the group A.

Cell culture and survival rate tested with MTT

Cells were cultured in PRMI1640 with 10 % calf serum, 100 U/ml penicillin and 100 $\mu\text{g/ml}$ streptomycin in a humidified atmosphere of 5 % CO_2 at 37 °C. With a density between 2×10^6 and 6×10^6 , two cell lines grew in the same way as typical epithelial cells, and reproduced once every two days. During the experiment, the density of cells was adjusted to $1 \times 10^6/\text{mL}$ with culture medium PRMI1640, and transferred to 96-well plates, 100 μL cell suspension per well, to incubate for 24 hours. Drugs of different concentrations were added to the plate, 4 plate wells for each drug concentration according to the aforementioned group division: 100 μL drug and 100 μL culture medium were added to each well with a total volume of 200 μL for group B and C; 100 μL of two drugs each was added with a total volume of 200 μL for group D; and 200 μL culture medium was added to each well of control group. All the groups had concentrations of 4 compound wells. After incubation for 24 h, 48 h, 72 h and 96 h, 20 μL of 0.5 % MTT was added to each well and incubated for another 4 hours. The supernatant was discarded and 200 μL of DMSO was added. When the stain was dissolved, the optical density ABS value of each well was read on MinireaderIIat 570 nm. Cell survival

rate was calculated with the following equation: average A value of experimental group/average A value of control group \times 100 %. Each experiment was repeated at least three times.

The rate of apoptosis tested by fluorescence of live cells

After the aforementioned cells were cultured with drugs for 72 h, cells were harvested and fixed with 1:3 glacial acetic acid/methanol twice, first for 5 min and then 10 min and washed with phosphate buffer solution (PBS). Hoechst 33 258 was put into cell suspension to a final concentration of 1.0 mg/L and the cells were stained fluorescent for 15 minutes away from light. An Olympus BH-2 fluorescence microscope was used to observe the fluorescent associated with DNA of cells nuclei. Graphs were drawn based on different concentrations of drugs and apoptotic rate of cells.

Agarose gel electrophoresis of DNA

Cells treated with drugs for 96 h were collected. After lysis with Nicoletti lysis buffer, DNA was extracted with an equal volume of phenol, phenol/chloroform and chloroform once each, incubated with RNase and precipitated with ethanol and sodium acetate. DNA was sedimented by centrifugation, air dried and dissolved in Tris-EDTA buffer. Each DNA sample was analyzed by gel electrophoreses in 1.2 % agarose gel for 1.5 h and visualized under ultra-violet light.

Apoptosis index (PI) determined by flow cytometry (FCM)

The cells described above were harvested, and 1×10^6 cells were centrifuged to get rid of supernatant, fixed with ethanol, and incubated with 200 μ L RNase A at 37 $^{\circ}$ C for 1 h; 800 μ L PI staining solution was mixed into it and the subsequent mixture was stored in the refrigerator at 4 $^{\circ}$ C for 30 minutes. Flow cytometry was then used to analyze the cell cycle. The cells with content of DNA in sub G_1 were apoptotic cells.

Statistics

Software SPSS 10.1 was employed to process the data with test of index deviation, and to analyze the causes of the deviation in data concerning multiple factors of the experimental design.

RESULTS

Effects of CDA-II and As_2O_3 on the growth of hepatoma cells

Cytotoxicity of CDA-II was low. At 1.0 g/L, the respective survival rate of cell lines HepG2 and BEL-7402 were 92 % and 89 %. When the concentration was increased to 3.0 g/L, the survival rate dropped to 76 % and 65 % respectively. The combined usage of two drugs markedly increased the cytotoxicity of As_2O_3 on the two cell lines. The addition of 1.0 g/L CDA-II caused IC_{50} of As_2O_3 to fall from 5.0 μ mol/L to 1.0 μ mol/L ($P<0.01$, Table 1).

Table 1 Survival rate of hepatoma cell lines HepG2 treated with drugs ($\bar{x}\pm s$)%

Groups	$c_{B,B}/(\mu\text{mol}\cdot\text{L}^{-1})^a$ or $\rho_{B,C}/(\text{g}\cdot\text{L}^{-1})^b$				
	1.0	2.0	3.0	4.0	5.0 ^c
A (Comtrols)	100	100	100	100	100
B (As_2O_3, c_B) ^d	80.06 \pm 3.27	70.58 \pm 5.42	67.82 \pm 3.43	59.33 \pm 7.33	49.12 \pm 4.25
C (CDA-II, ρ_B) ^e	92.41 \pm 4.25	81.22 \pm 7.34	70.23 \pm 2.32	68.22 \pm 4.56	67.12 \pm 9.23
D (B+C _{1.0}) ^f	50.67 \pm 3.56	47.88 \pm 6.42	47.34 \pm 4.25	45.54 \pm 8.22	41.55 \pm 3.75

^a $c_{B,B}/(\mu\text{mol}\cdot\text{L}^{-1})$ is for group B(As_2O_3, c_B); $\rho_{B,C}/(\text{g}\cdot\text{L}^{-1})$ is for group C (CDA-II, ρ_B); ^bgroup D (B+C_{1.0}) refers to every each group B

($As_2O_3, c_{B,B}$) plus $\rho_{B,C}=1.0 \text{ g}\cdot\text{L}^{-1}$; ^cConcentration grads effect: $F=32.270$, sig.=0.000, $P<0.05$; ^dMain effect for group B (As_2O_3, c_B): $F=22.856$, sig.=0.000, $P<0.05$; ^eMain effect for group C (CDA-II, ρ_B): $F=0.831$, sig.=0.059, $P>0.05$; Interaction effect for group D (B+C_{1.0}): $F=27.178$, sig.=0.000, $P<0.05$

Effect of two drugs on apoptosis in hepatoma cells

Under fluorescent microscope, cell nuclei of the control group displayed fluorescence evenly. Treated by the two drugs in combination, a large proportion of cells underwent apoptosis. Uneven and more dense particulate fluorescence could be observed in cell nuclei (Figure 1). The rate of apoptosis of 500 cells was calculated. The result showed (Figure 2) that when As_2O_3 was employed at 1.0 μ mol/L, the number of apoptotic cells was only slightly above that of control, and the difference was not significant ($P=0.063$). However, the apoptotic rate rose greatly with the increase of drug concentrations above 1.0 μ mol/L, and the significance of differences became obvious as against the control ($P<0.01$). When CDA-II was used alone, the concentration must be above 3.0 g/L showed significant difference from the control ($P<0.015$). CDA-II greatly potentiated the apoptosis induced by As_2O_3 . The apoptotic rate of 1.0 μ mol/L of As_2O_3 together with 1.0 g/L of CDA-II approached that of 4.0 μ mol/L As_2O_3 .

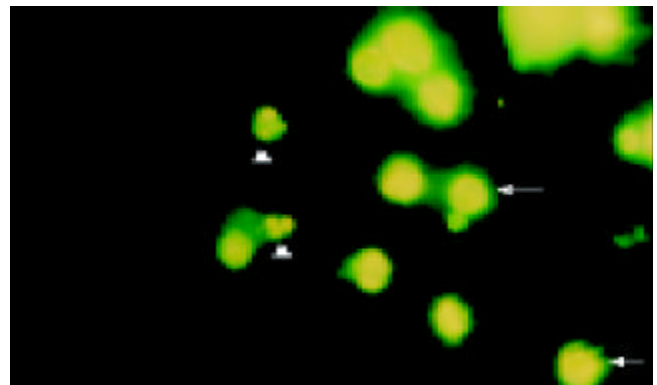


Figure 1 Immunofluorescence staining of Hoechst 33 258 72 h after 1.0 μ mol/L As_2O_3 +1.0 g/L CDA-II administered in HepG2 cells ($\times 400$). \rightarrow : dispersive fluorescences in normal cells nuclei; \triangle : compact particulate fluorescences in apoptosis cell nuclei

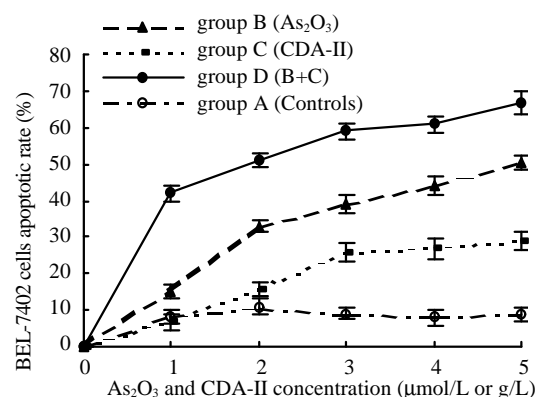


Figure 2 Comparison of different groups on numbers of BEL-7402 cell apoptosis. A. Main effect(As_2O_3): $F=0.387$, sig.=0.063, $P>0.05$; B. Main effect(CDA-II): $F=0.670$, sig.=0.785, $P>0.05$; C. Interaction (As_2O_3 + CDA-II): $F=22.450$, sig.=0.000, $P<0.05$

DNA of cells undergoing apoptosis showed a ladder pattern in agarose gel electrophoresis. In the present study, DNA ladders were characteristically identified in the cells treated with 5.0 μ mol/L As_2O_3 or 1.0 g/L CDA-II+1 μ M As_2O_3 for 72 h as shown in Figure 3.

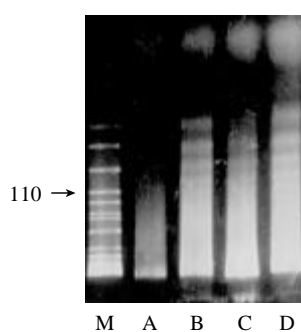


Figure 3 DNA agarose gel electrophore I of hepatoma cell lines treated by As_2O_3 or CDA-II+ As_2O_3 for 72 h. M: λ -DNA Marker VII; A (HepG2): controls; B (HepG2): $1.0 \mu\text{mol} \cdot \text{L}^{-1} \text{As}_2\text{O}_3 + 1.0 \text{g} \cdot \text{L}^{-1} \text{CDA-II}$; C (BEL-7402): $1.0 \mu\text{mol} \cdot \text{L}^{-1} \text{As}_2\text{O}_3 + 1.0 \text{g} \cdot \text{L}^{-1} \text{CDA-II}$; D (HepG2): $5.0 \mu\text{mol} \cdot \text{L}^{-1} \text{As}_2\text{O}_3$

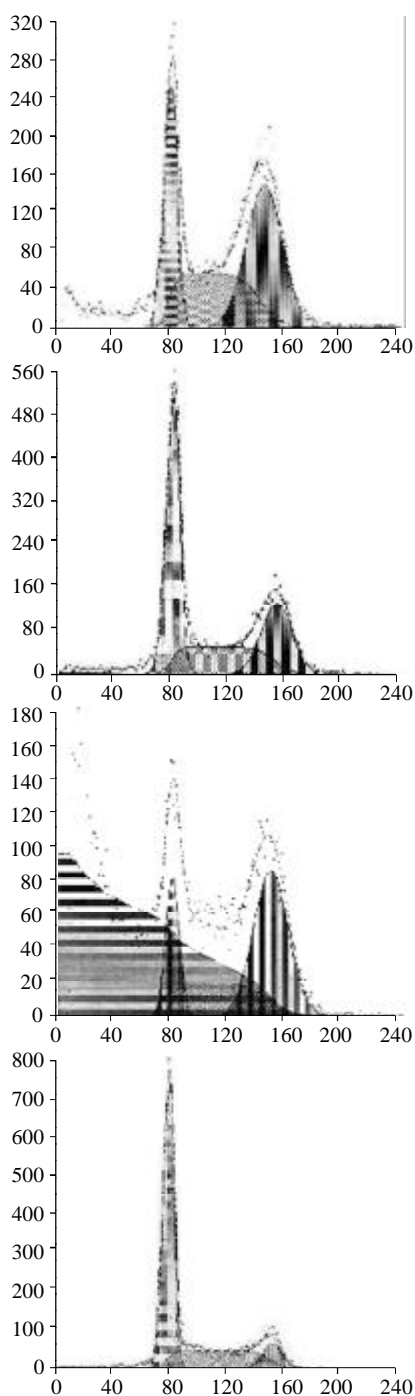


Figure 5 Flow cytometry 4 days after medicinal treatment. (A). $1.0 \mu\text{mol/L} \text{As}_2\text{O}_3$; (B). $1.0 \text{g/L} \text{CDA-II}$; (C). $1.0 \mu\text{mol/L} \text{As}_2\text{O}_3 + 1.0 \text{g/L} \text{CDA-II}$; (D). Control.

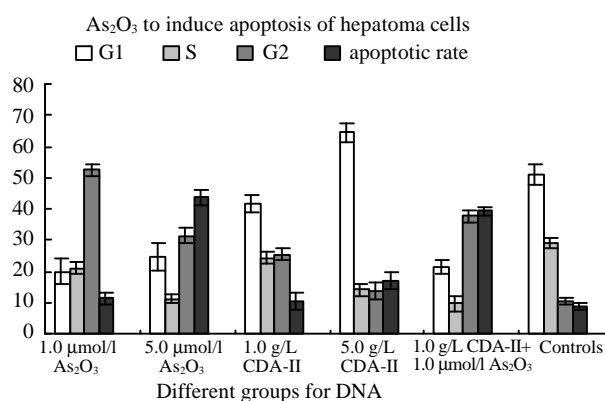


Figure 4 Comparison of DNA in various groups 4 days after medicinal treatment. $P < 0.05$ Compared with the controls

Flow cytometry study of cell apoptosis

Four days after treatment with As_2O_3 , sub- G_1 cells, namely apoptotic cells, became evident in HepG2 and BEL-7402, and the number of apoptotic cells was in direct proportion to drug concentration (Figure 4). As_2O_3 at $5.0 \mu\text{mol/L}$ induced 46.7 % of HepG2 and 53.1 % of BEL-7402, respectively to undergo apoptosis. When CDA-II was employed alone below 2.0g/L , the apoptotic rate of hepatoma cells was not significantly different from that of the control. At such low concentration ($< 2.0 \text{g/L}$), the cells arrested in G_2 exceeded those in the control, whereas at concentrations above 2.0g/L , both apoptotic cells and cells arrested in G_1 increased. The combination of $1.0 \text{g/L} \text{CDA-II}$ and $1.0 \mu\text{mol/L} \text{As}_2\text{O}_3$ in hepatoma cells resulted in reduced vitality of the two cell lines, and the apoptotic rate rose from 11.3 % in the presence of $1.0 \mu\text{mol/L} \text{As}_2\text{O}_3$ alone to 40.2 % (Figure 5). The potentiation of As_2O_3 -induced apoptosis by CDA-II was concentration-dependent. The percentage of sub- G_1 cells induced by $3.0 \text{g/L} \text{CDA-II}$ and $1.0 \mu\text{mol/L} \text{As}_2\text{O}_3$ reached 63 %, as against 57 % caused by $5.0 \mu\text{mol/L} \text{As}_2\text{O}_3$. All these findings indicated that CDA-II could synergistically potentiate As_2O_3 to induce apoptosis of hepatoma cells.

DISCUSSION

Toxicity of cell apoptotic agents and drug resistance of cancer cells are major factors contributing to the failure of chemotherapy. It has been reported by Cai *et al.*^[16], that one-third of 47 patients with normal liver function but suffering from recurrent acute promyelocytic leukemia who were treated with As_2O_3 , had their livers damaged. Obviously, the patients with damaged liver function must choose smaller dosage of As_2O_3 . In this regard it particularly fits the recommend combination therapy with CAD-II, because CAD-II is a very effective drug to protect liver from hepatotoxin-induced injuries^[17-20]. In vitro, hepatoma cell growth and proliferation were only inhibited by arsenic trioxide at lower concentrations ($0.25-2.0 \mu\text{mol/L}$), with no significant apoptosis, at higher concentration ($> 2.0 \mu\text{mol/L}$) can induce cell apoptosis^[21-26]. According to the sensitive standard of chemotherapeutic agents devised by Abe *et al.*^[27,28], hepatoma cells in this experiment are sensitive to the dosage of $5.0 \mu\text{mol/L} \text{As}_2\text{O}_3$. Based on the following formula^[29]: drug concentration (mg/L) = [(drug mg \times surface size)/body weight] \times (100/60), the sensitive dosage in clinical application is 20mg/m^2 . In the presence of 1g/L of CDA-II, IC_{50} of As_2O_3 can be reduced from $5.0 \mu\text{mol/L}$ to $1.0 \mu\text{mol/L}$. That means 4mg/m^2 is equally as effective in the combination protocol as 20mg/m^2 of single As_2O_3 . CAD-II is a biological preparation purified from human urine which is a selective inhibitor of abnormal cancer methylation enzymes^[16,30,31]. DNA hypermethylation attributable to abnormal methylation enzymes is related to the evolution of drug resistance of cancer cells^[32,33]. It is likely that the modulation of abnormal

methylation enzymes is responsible for the reverse of drug resistance and the potentiation of As₂O₃-induced apoptosis. Shen *et al.* reported that abnormal DNA methylation plays an important role in the process of hepatocellular carcinogenesis. DNA methylation level is closely correlated with the biological characteristic of liver cancer, the lower the level of DNA methylation, the stronger the infiltration and metastatic capacity^[34-36]. Animal experiments on have demonstrated that CAD-II could effectively prevent the growth and metastasis of xenografted hepatoma^[37].^{38]} Analysis of cell cycle revealed that CAD-II at low concentrations could arrest more hepatoma cells in G₂ and S, and at high concentrations could bring about more apoptosis and relatively more cells arrested in G₁. It is remarkable that CAD-II at a low dosage is not capable to induce apoptosis, nevertheless, it can strongly potentiate As₂O₃-induced apoptosis. With 1.0 g/L of CAD-II, the apoptosis-inducing capability of As₂O₃ can be reduced from 5.0 to 1.0 μmol/L. Therefore, only 4.0 mg/m² of As₂O₃ is needed in clinical treatment giving an equivalence of 20 mg/m² of As₂O₃. Thus, the combined therapy of As₂O₃ and CAD-II offers a great advantage to reduce toxic side effect and to improve the therapeutic efficacy for hepatoma.

REFERENCES

- 1 **Wang W**, Qin SK, Chen BA, Chen HY. Experimental study on antitumor effect of arsenic trioxide in combination with cisplatin or doxorubicin on hepatocellular carcinoma. *World J Gastroenterol* 2001; **7**: 702-705
- 2 **Pu YS**, Hour TC, Chen J, Huang CY, Guan JY, Lu SH. Arsenic trioxide as a novel anticancer agent against human transitional carcinoma-characterizing its apoptotic pathway. *Anticancer Drugs* 2002; **13**: 293-300
- 3 **Qian J**, Qin SK, He ZM, Wang L, Chen YX, Shao ZJ, Liu XF. Arsenic trioxide for the treatment of medium and advanced primary liver cancer. *Zhonghua Ganzhangbing Zazhi* 2002; **10**: 63
- 4 **Qian J**, Qin S, He Z. Arsenic trioxide in the treatment of advanced primary liver and gallbladder cancer. *Zhonghua Zhongliu Zazhi* 2001; **23**: 487-489
- 5 **Chen JQ**, Li SS, Peng MH, Lu YF, Qiu QM, Lu BY, Liao QH. Experimental study on arsenic trioxide and other 6 kinds of anti-tumor drugs' effects on human hepatic cancer cell lines BEL-7404, SMMC-7721. *Zhongguo Puwai Jichu Yu Linchuang Zazhi* 2001; **8**:367-369
- 6 **Vernhet L**, Allain N, Payen L, Anger JP, Guillouzo A, Fardel O. Resistance of human multidrug resistance-associated protein 1-overexpressing lung tumor cells to the anticancer drug arsenic trioxide. *Biochem Pharmacol* 2001; **61**: 1387-1391
- 7 **Gartenhaus RB**, Prachand SN, Paniaqua M, Li Y, Gordon LI. Arsenic trioxide cytotoxicity in steroid and chemotherapy-resistant myeloma cell lines: enhancement of apoptosis by manipulation of cellular redox state. *Clin Cancer Res* 2002; **8**: 566-572
- 8 **Hu X**, Ma L, Hu N. Ailing No. I in treating 62 cases of acute promyelocytic leukemia. *Zhongguo Zhongxixi Jiehe Zazhi* 1999; **19**: 473-476
- 9 **Kundu SN**, Mitra K, Bukhsh AR. Efficacy of a potentized homeopathic drug (Arsenicum-album-30) in reducing cytotoxic effects produced by arsenic trioxide in mice: III. Enzymatic changes and recovery of tissue damage in liver. *Complement Ther Med* 2000; **8**: 76-81
- 10 **Jing Y**, Wang L, Xia L, Chen GQ, Chen Z, Miller WH, Waxman S. Combined effect of all-trans retinoic acid and arsenic trioxide in acute promyelocytic leukemia cells *in vitro* and *in vivo*. *Blood* 2001; **97**: 264-269
- 11 **Xu JY**, Zhou Q, Lu P, Tang W, Tong LF. Induction of apoptosis and reversal of drug resistance in human tumor cell line KBV 200 by cell differentiation agent-II. *Zhonghua Neike Zazhi* 2000; **39**: 37-39
- 12 **Xu JY**, Zhou Q, Lu P, Tang W, Dong LF. Research on induction of apoptosis and reversal of multidrug resistance in human tumor cell line KBV200 by hyperthermia. *Zhonghua Liliao Zazhi* 2000; **23**: 33-36
- 13 **Chen ZS**, Ni M, Cheng HH, Ouyang XN, Lin J, Dai XH, Tu XH, Wu XG, Guo WH. Therapeutic efficacy of CDA-II on advanced cancer patients a comparison with cytotoxic chemotherapy. *Zhongguo Zhong Liu Linchuang Yu Kangfu* 1999; **6**: 84-87
- 14 **Gao YT**, Shi SQ, Gu FL, Wu MC. The effect of uroacitides on advanced liver cancer in 15 case. *Zhongguo Zhongliu* 2002; **11**: 110-112
- 15 **Feng FY**, Li Q, Wang ZJ. The effect of uroacitides on improving quality of life in advanced cancer patients. *Zhongguo Zhongliu* 2002; **11**: 108-110
- 16 **Cai X**, Shen YL, Zhu Q, Jia PM, Yu Y, Zhou L, Huang Y, Zhang JW, Xiong SM. Arsenic trioxide-induced apoptosis and differentiation are associated respectively with mitochondrial transmembrane potential collapse and retinoic acid signaling pathways in acute promyelocytic leukemia. *Leukemia* 2000; **14**: 262-270
- 17 **Lin WC**, Wu YW, Lai TY, Liao MC. Effect of CDA-II, urinary preparation, on lipofuscin lipid peroxidation and antioxidant systems in young and middle-aged rat brain. *Am J Chin Med* 2001; **29**: 91-99
- 18 **Lai TY**, Wu YW, Lin WC. Effect of a urinary preparation on liver injury by short-term carbon tetrachloride treatment in rats. *Am J Chin Med* 1999; **27**: 241-250
- 19 **Lai TY**, Wu YW, Lin JG, Lin WC. Effect of pretreatment of rats with an urinary preparation on liver injuries induced by carbon tetrachloride and alpha-naphthylisothiocyanate. *Am J Chinese Med*. 1998; **26**: 343-351
- 20 **Lai TY**, Wu YW, Lin WC. Ameliorative effect of an urinary preparation on acetaminophen and D-galactosamine induced hepatotoxicity in rats. *Am J Chinese Med* 1999; **27**: 73-81
- 21 **Li JT**, Ou QJ, Wei J. Studies on arsenic trioxide induces apoptosis in hepatoma cell lines Bel-7402. *Aizheng* 2000; **19**: 1087-1089
- 22 **Xu HY**, Yang YL, Gao YY, Wu QL, Gao GQ. Effect of arsenic trioxide on human hepatoma cell line BEL-7402 cultured *in vitro*. *World J Gastroenterol* 2000; **6**: 681-687
- 23 **Oketani M**, Kohara K, Tuvdendorj D, Ishitsuka K, Komorizono Y, Ishibashi K, Arima T. Inhibition by arsenic trioxide of human hepatoma cell growth. *Cancer Lett* 2002; **183**: 147-153
- 24 **Siu KP**, Chan JY, Fung KP. Effect of arsenic trioxide on human hepatocellular carcinoma HepG2 cells: inhibition of proliferation and induction of apoptosis. *Life Sci* 2002; **71**: 275-285
- 25 **Kito M**, Akao Y, Ohishi N, Yagi K, Nozawa Y. Arsenic trioxide-induced apoptosis and its enhancement by buthionine sulfoximine in hepatocellular carcinoma cell lines. *Biochem Biophys Res Commun* 2002; **291**: 861-867
- 26 **Chen H**, Qin SK, Pan QH, Chen HY, Ma J. Antitumor effect of arsenic trioxide on mice experimental liver cancer. *Zhonghua Ganzhangbing Zazhi* 2000; **8**: 27-29
- 27 **Abe R**, Ueo H, Akiyoshi T. Evaluation of MTT assay in agarose for chemosensitivity testing of human cancers: comparison with MTT assay. *Oncology* 1994; **51**: 416-425
- 28 **Van Thiel DH**, Brems J, Holt D, Hamdani R, Yong S. Chemosensitivity of primary hepatic neoplasms: a potential new approach to the treatment of hepatoma. *Hepatogastroenterology* 2002; **49**: 730-734
- 29 **Zhong XY**, Chen YX, Sun XD. Study of apoptotic threshold of cis-diamminedichloroplatinum and adriamycin on hepatocellular carcinoma. *Zhongguo Bingli Shengli Zazhi* 2000; **16**: 199-202
- 30 **Liao MC**. Differentiation therapy for cancer. *Zhongguo Zhongliu* 2002; **11**: 104-107
- 31 **Liao MC**, Liao CP. Methyltransferase inhibitors as excellent differentiation helper inducers for differentiation therapy of cancer. *Zhongguo Zhongliu* 2002; **11**: 166-168
- 32 **Plumb JA**, Strathdee G, Sludden J, Kaye SB, Brown R. Reversal of drug resistance in human tumor xenografts by 2'-deoxy-5-azacytidine-induced demethylation of the hMLH1 gene promoter. *Cancer Res* 2000; **60**: 6039-6044
- 33 **Wang C**, Mirkin BL, Dwivedi RS. DNA (cytosine) methyltransferase overexpression is associated with acquired drug resistance of murine neuroblastoma cells. *Int J Oncol* 2001; **18**: 323-329
- 34 **Shen L**, Fang J, Qiu D, Zhang T, Yang J, Chen S, Xiao S. Correlation between DNA methylation and pathological changes in human hepatocellular carcinoma. *Hepatogastroenterology* 1998; **45**:1753-1759
- 35 **Shen L**, Ahuja N, Shen Y, Habib NA, Toyota M, Rashid A, Issa JP. DNA methylation and environmental exposures in human hepatocellular carcinoma. *J Natl Cancer Inst* 2002; **94**: 755-761
- 36 **Shen L**, Qui D, Fang J. Correlation between hypomethylation of *c-myc* and *c-N-ras* oncogenes and pathological changes in human hepatocellular carcinoma. *Zhonghua Zhongliu Zazhi* 1997; **19**: 173-176
- 37 **Wu MF**, Han CH, Liu CC, Lai JM, Li ZJ, Xu KS. Establishment of animal models for the evaluation of differentiation inducing agents. *Zhongguo Zhongliu* 2002; **11**: 163-165
- 38 **Sun JJ**, Zhou XD, Liu YK, Wang ZY. Effect of CDA-II on prevention and therapy for metastasis and recurrence of liver cancer in nude mice. *Zhonghua Gangdan Waikie Zazhi* 1999; **5**: 14-16

Relationship between the imaging features and pathologic alteration in hepatoma of rats

Jia-He Yang, Tian-Geng You, Nan Li, Qi-Jun Qian, Ping Wang, Zhen-Lin Yan, Meng-Chao Wu

Jia-He Yang, Tian-Geng You, Nan Li, Qi-Jun Qian, Ping Wang, Zhen-Lin Yan, Meng-Chao Wu, Eastern Hepatobiliary Hospital, 225 Changhai Road, Shanghai 200433, China

Supported by two National Natural Science Foundation of China, No. 39870760 and No. 39970838

Correspondence to: Dr. Jie-He Yang, Department of Comprehensive Treatment III, Eastern Hepatobiliary Hospital, Second Military Medical University, Changhai Road 225, Shanghai 200433, China. tgyou59@hotmail.com

Telephone: +86-21-25070786 **Fax:** +86-21-65562400

Received: 2001-12-05 **Accepted:** 2002-02-23

Abstract

AIM: The imaging features of MRI and DSA, using the models of implanted and induced hepatoma, were investigated in rats.

METHODS: CBRH3 cancer cells were implanted for different liver site of rat liver and the diethylnitrosoamine was given orally to rats in order to induce liver cancer. Both experimental groups were detected by magnetic resonance imaging (MRI), digital subtraction angiography (DSA) and morphologic assay.

RESULTS: Hypointensity on T1WI and homogenous high signal intensity on T2WI in MRI, and ring-like abnormal stain on DSA were found in implanted cancer. Induced cancers appeared as homogeneous or heterogeneous hypointensity on T1WI (10 cases), and equal or slight high intensity on T2WI (8 cases), but some as hypointensity on T2WI (2 cases).

CONCLUSION: The imaging features of implanted cancers were similar to that of human liver metastases. Therefore, it could serve as an experimental model of human liver metastatic tumor. The imaging feature of induced cancers, whereas, were similar to that of human primary liver cancer. It could be used as an experimental model of human primary liver cancer.

Yang JH, You TG, Li N, Qian QJ, Wang P, Yan ZL, Wu MC. Relationship between the imaging features and pathologic alteration in hepatoma of rats. *World J Gastroenterol* 2003; 9(1): 69-72
<http://www.wjgnet.com/1007-9327/9/69.htm>

INTRODUCTION

It is important to investigate the relationship between the biologic properties of liver tumor and the findings with modern imaging techniques. MRI affords the possibility in coronal and sagittal views, which are very helpful in liver surgery because surgical techniques are described in these planes^[1-2]. In addition, targeted gene therapy, for instance, cytokines gene therapy, angiogenesis inhibitor and granulocyte-macrophage colony-stimulating factor (GM-CSF) gene-transduced tumor vaccine for patients, may be useful in developing anticancer drugs that prolong or stabilize the progression of tumors with minimal systemic toxicities. These drugs may also be used as novel imaging and radiomunotherapeutic agents in cancer therapy^[3-7].

However, little is known on experimental work of both scan imaging and liver cancer. The present study, using the model of

implanted and induced hepatoma of rats, was undertaken to investigate the relationship between the morphologic alterations and imaging characteristics of magnetic resonance imaging (MRI) and digital subtraction angiography (DSA), and more to improve level of diagnostic and treatment for liver cancer. Finally, interleukin 2 was therapeutic effect on liver tumors^[8], so the our further study of interleukin gene therapy for liver cancer was based on the present outcome of implanted and induced hepatoma.

MATERIALS AND METHODS

Imaging Instruments

MRI equipment was produced by Siemens AG (1.0 T). Its SE rank, 128*128 matrix, T1-weighted sequence (T1WI) were TR/TE 350-480/15 ms; T2-weighted sequence (T2WI) was TR/TE 2 200/90 ms. Slice thickness was 2 mm and scan space was 0.5 mm. Both of coronal and sagittal scanning was fulfilled. Hepatic artery was scanned by DSA (Toshiba DFP-0.3A) with perfusing iodized oil (Lipiodol). Instruments and drugs were sterilized routinely.

Animals and Hepatoma cell

Male Wister rats (200-250 g wt) were obtained from Animal Center of Chinese Academy of Sciences. Animals were maintained on a standard diet. Cellular strains of hepatoma CBRH3 were provided kindly by Prof. Xie Hong (Shanghai Institute of Biochemistry and Cell Biology, Chinese Academy of Science).

Implanted liver cancer model in rat

Hepatoma CBRH3 cells were injected into abdominal cavity of rat. Rats were sacrificed and tumors were removed from abdominal cavity 7-9 days late. The tumors were cut into pieces of 0.05-0.75 cm and then was inoculated into rat liver for one or more locations respectively. The tumor was grown up to diameter in 0.6-1 cm after 7-10 days of inoculation.

Induced liver cancer model in rat

Male Wister rats (age for 8 weeks) took orally 1:10 000 diethylnitrosamine for 80 days to induce liver cancer. The micro-nodules of hepatoma were developed 14 weeks late and 0.2-1 cm of tumor masses were observed 16-18 weeks late. There were poly-cysts in rat liver. This model was used to study for poly-nodules of hepatoma. The success rate of induced cancer was 100 %^[9,10].

Experimental procedure

Both of 10 implanted tumor rats (age of 9 days) and 10 induced tumor rats (age of 16-18 weeks) was divided to experimental group and control group, randomly. While rats were scanned by MRI, they were anesthetized by injecting ketamine into muscle. In addition, the hepatic artery and gastroduodenal artery were isolated carefully and micro-catheter was inserted into these artery for injection of iodine oil before DSA^[11].

RESULTS

A stable model of rat hepatoma was established by either implanted tumor with cancer piece or inducing tumor with diethylnitrosamine.

Imaging features of the implanted tumors in MRI and DSA and the pathology: The 10 implanted models showed 18 nodules of tumor in MRI and DSA. 11 nodules of them were round shape and 7 of them were ellipse. The margin of tumors was smooth. Implanted cancer showed homogeneous hypointensity on T1WI (Figure 1) and homogeneous hyperintensity on T2WI. The rat liver showed normal signal and normal organ shape.

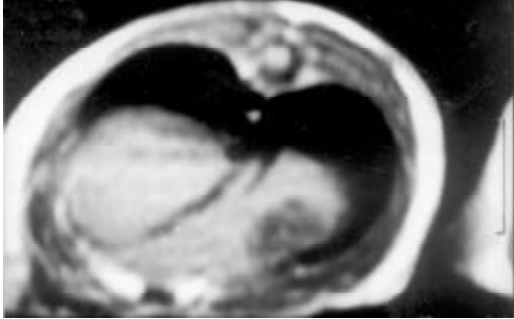


Figure 1 MR imaging showed low signal on T1WI in implanted hepatoma of rat

In DSA, the tumors showed no stain for blood vessels in the center of tumor (vacancy of vessel) and abnormal ring-like staining of vessel around tumor. The liver tissues were normal. Necrosis and colliquational cavity were shown on the core of tumors in all of 18 tumor mass and the yellow-gray tissue could be seen in cross section of tumors. The cancer cells were small or mediate in size with great nucleus. The parenchyma of liver was normal (Figure 2).

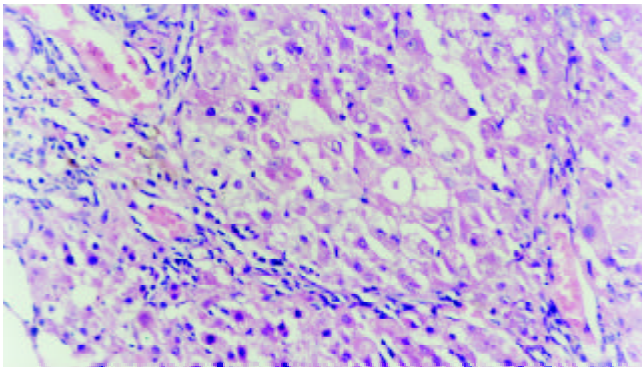


Figure 2 Distribution of microscopy ($\times 200$) in implanted liver cancer that abnormal type and arrangement of cancer cell. There were abundant vascular proliferation and lymphocyte infiltration growth around tumor

The scanning pictures of MRI and DSA and the pathological alteration in induced cancer: Liver cirrhosis with different degree and multiple nodules of cancer were observed in 10 tumor cases. Eight among 10 tumors showed homogeneous slight hypo-intensity on T1WI (Figure 3) and inhomogeneous slight hyper-intensity on T2WI with different shapes, but some of them were with normal signal or more contrast enhancement (Figure 4). Two among 10 tumor livers were shown inhomogeneous slight low signal on T1WI, but equal signal was found in interval. Hypointensity was observed on T2WI.

In DSA the distribution of internal hepato-vascularity was disorder and the angio-clumps were different in sizes in tumor (Figure 5). Pathology: Tumor liver showed poly-nodules, tumor diffusion and inequality of size. The tumor was light yellow. In microscopy examination, distribution of tumor and liver tissue was in interval. The cancer tissue showed plenty and dilation of vessel. The cell plasma of cancer was not abundant. The arrangement of tumor cell was nest and bunch. Liver tissue was

easy for proliferation of nodule with acid-like change and water-alteration. The dilation of lymphatic tube and the proliferation of bile duct were shown between hepato-lobule. Hepato-lobule was divided by proliferation of fibre. The artery and vein were not distinguished because of dilation of vessel (Figure 6).



Figure 3 Homogeneous slight hypointensity on T1WI was found in poly-nodules of tumor

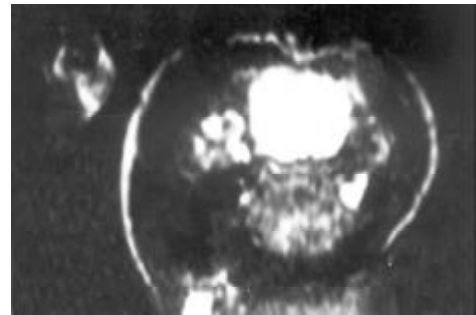


Figure 4 Inhomogeneous slight hyperintensity was indicated on T2WI in different shape, but some of them were showed normal signal or more contrast enhancement in interval



Figure 5 The disorder of distribution of internal hepato-vascularity was found and the angio-clump showed different size in tumor in DSA

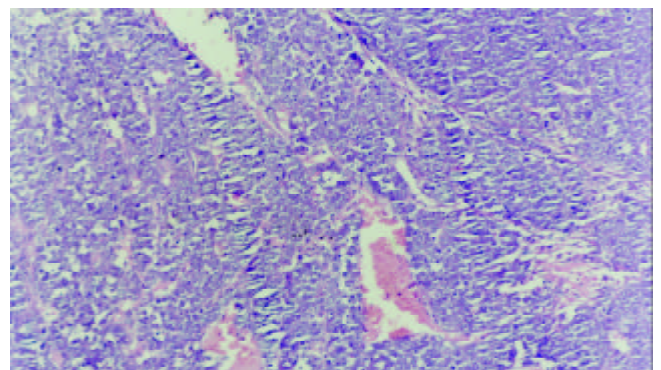


Figure 6 Distribution of microscopy ($\times 100$) in induced liver cancer that tumor and liver tissue was in interval. There was plenty and dilation of vessel

DISCUSSION

Characterization of image technique of rat

The available MR image photos were taken because technique is as follow. (1) Technique of eye surface loop: To avoid disturbing factors for image definition that focus on the location of rat liver, this technique was used. (2) Folium technique keeps away the cabin effect on conceal of small tumor nodules. (3) False shadow caused by move of body act and breath was prevented by suitable anesthesia for rats. On DSA image, deep anesthesia and careful anatomy of hepatic artery with catheter were necessary. But it is difficulty to puncture femoral artery. In order to find available condition of exposure time, we try to test more times^[12].

The relation of image and pathology in implanted cancer

The component of tumor is of long longitudinal relaxation time (T1) and long transverse relaxation time (T2) since the implanted cancer show low signal on T1WI and equal signal on T2WI in MRI. Equal signal intensity implies that there are no tissue component in the core of tumor apart from necrosis, liquefaction and cystic change. Therefore, the situation of blood supply was not described due to no-contrast enhancement of Gadolinium-DTPA^[13,14].

On DSA, the imaging of blood vessel around tumor was found such as folium annularity, whereas central liquefaction and necrosis were existed in tumor. Thus, cancer cell on the border of tumor grows actively because of blood supply in plenty and cancer cell in center of tumor does not grow because of insufficient blood supply. There is no liver cirrhosis because signal intensity of liver tissue in MRI and distribution of blood vessel in DSA are normal compared to normal liver parenchyma^[19].

Necrosis at core of tumor and the proliferated nodule of tumor cell were found around blood sinus and dilation of blood vessel after 9 days of implanted cancer^[16,17]. The change in MRI and DSA was accord to pathology.

The relation of image and pathology in induced cancer

Resent study has suggested that a random clonal origin of hepatocyte carcinoma from mature hepatocytes is seen in the diethylnitrosamine model of hepatocarcinogenesis^[18].

Induced cancer is of two different signal intensities including 1. slight low signal intensity on T1WI and slight high signal intensity on T2WI in 8 cases and 2. inhomogeneous low signal on T1WI and low signal on T2WI with regular appearance in 2 cases. We hypothesize that both signals is caused by the difference in hepatoma component and hepatoma cellular arrange. Amount of fibrocyte, apart from tumor cells, is found in these 2 cases which result in extended longitudinal relaxation time (T1) and contracted transverse relaxation time (T2) with low signal on T1WI and low signal on T2WI. Irregular liver shape and liver nodule proliferation in deferent degree with liver cyst could be manifested on MRI because of liver cirrhosis and degeneration resulting from taking carcinogen for long time. To differentiate with cirrhosis nodules and tumor nodules, some investigators reported that the early-enhancing single nodule with cirrhosis is high predictive to hepatocyte cancer in patient. This phenomenon is also seen in our data of photo and microscopy examination^[20,21]. On DAS, the tumor stain is displayed by reason of disorder of blood vessel and angio-clamp^[22].

Comparison imaging of implanted, induced and human hepatoma

Primary liver cancer Based on the liver cirrhosis, primary liver cancer display the slight low signal intensity on T1WI and equal or slight high signal intensity following extended echo time without raise of signal in MRI^[23]. In DSA, the plenty

amateur vessel is observed^[24].

Liver metastases MRI shows the low signal intensity on T1WI, high signal on T2WI and annular enhancement by Gadolinium. In DSA, annular staining is displayed without background of cirrhosis^[15].

Compared with manifestation of MRI and DSA, studies confirm that implanted hepatoma lead that the signal intensity is high following the extended echo time and annular staining around tumor is occurred without liver cirrhosis^[25].

In induced cancer, liver cirrhosis with slight high signal or low signal due to extended echo time without raise of signal is observed in MRI. The abundant malignant vessel stain is indicated that it is similar to human primary liver cancer^[26].

In conclusion, the imaging features of implanted cancers were similar to human liver metastases in manifestation of MRI and DSA. Therefor, it could serve as an experimental model of human liver metastatic tumor. The imaging feature of induced cancers, whereas, were similar to that of human primary liver cancer. It could be use as an experimental model of human primary liver cancer.

REFERENCES

- Foley LM**, Towner RA, Painter DM. *In vivo* image-guided H-magnetic resonance spectroscopy of the serial development of hepatocarcinogenesis in an experimental animal model. *Biochim Biophys Acta* 2001; **15**: 230-236
- Eliat PA**, Lechaux D, Gervais A, Rioux-Leclerc N, Franconi F, Lemaire L, Dazord L, Catros-Quemener V, de Certaines JD. Is magnetic resonance imaging texture analysis a useful tool for cell therapy *in vivo* monitoring? *Anticancer Res* 2001; **21**: 3857-3860
- Scappaticci FA**. Mechanisms and future directions for angiogenesis-based cancer therapies. *J Clin Oncol* 2002; **20**: 3906-3927
- Kawai K**, Tani K, Yamashita N, Tomikawa S, Eriguchi M, Fujime M, Okumura K, Kakizoe T, Clift S, Ando D, Mulligan R, Yamauchi A, Noguchi M, Asano S, Akaza H. Advanced renal cell carcinoma treated with granulocyte-macrophage colony-stimulating factor gene therapy: A clinical course of the first Japanese experience. *Int J Urol* 2002; **9**: 462-466
- Parkes AT**, Speirs V. British cancer research meeting, 30 june-3 july 2002, glasgow. *Breast Cancer Res* 2002; **4**: 202-204
- Zhang L**, Gu J, Lin T, Huang X, Roth JA, Fang B. Mechanisms involved in development of resistance to adenovirus-mediated proapoptotic gene therapy in DLD1 human colon cancer cell line. *Gene Ther* 2002; **9**: 1262-1270
- Gillies SD**, Lan Y, Brunkhorst B, Wong WK, Li Y, Lo KM. Bifunctional cytokine fusion proteins for gene therapy and antibody-targeted treatment of cancer. *Cancer Immunol Immunother* 2002; **51**: 449-460
- Zhao W**, Kobayashi M, Ding W, Yuan L, Seth P, Cornain S, Wang J, Okada F, Hosokawa M. Suppression of *in vivo* tumorigenicity of rat hepatoma cell line KDH-8 cells by soluble TGF-beta receptor type II. *Cancer Immunol Immunother* 2002; **51**: 381-388
- Balansky RM**, Ganchev G, Agostini F, De Flora S. Effects of N-acetylcysteine in an esophageal carcinogenesis model in rats treated with diethylnitrosamine and diethyldithiocarbamate. *Int J Cancer* 2002; **98**: 493-497
- Rao MS**, Kashireddy P. Effect of castration on dehydroepian drosterone-induced hepatocarcinogenesis in male rats. *Anticancer Res* 2002; **22**: 1409-1411
- Thorlacius H**, Larmark M, Randell M, Hultberg B, Jeppsson B. Isolated liver perfusion permits administration of high doses of chemotherapeutic agents. Comparison with hepatic artery infusion. *Eur Surg Res* 2001; **33**: 342-347
- Zhang H**, Liu Y, Cao W, Liu Y, Fan A. Establishment of modified model of Vx-2 carcinoma in rabbit liver and DSA imagining features of the tumor. *Zhonghua Ganzangbing Zazhi* 2002; **10**: 149
- Krupski G**, Ameis D, Cataldegirmen G, Herbst H, Henschel MG, Nicolas V, Rogiers X, Bucheler E. Native magnetic resonance tomography imaging of the Morris hepatoma (MH-7777A) in the rat. *Rofu Fortschr Geb Rontgenstr Neuen Bildgeb Verfahr* 2001; **173**: 639-642

- 14 **Lauenstein TC**, Goehde SC, Herborn CU, Treder W, Ruehm SG, Debatin JF, Barkhausen J. Three-dimensional volumetric interpolated breath-hold MR imaging for whole-body tumor staging in less than 15 minutes: a feasibility study. *Am J Roentgenol* 2002; **179**: 445-449
- 15 **Turler A**, Schaefer H, Schaefer N, Wagner M, Maintz D, Qiao JC, Hoelscher AH. Experimental low-level direct current therapy in liver metastases: influence of polarity and current dose. *Bioelectromagnetics* 2000; **21**: 395-401
- 16 **Kuppen PJ**, Gorter A, Hagensmaars M, Jonges LE, Giezeman-Smits KM, Nagelkerke JF, Fleuren G, van de Velde CJ. Role of NK cells in adoptive immunotherapy of metastatic colorectal cancer in a syngeneic rat model. *Immunol Rev* 2001; **184**:236-243
- 17 **Nakamoto T**, Inagawa H, Nishizawa T, Honda T, Kanou J, Nagasue N, Soma G. Antitumor effects of isolated hypoxic hepatic perfusion (IHHP) with high-dose TNF against colonic liver metastases in a rat model. *Anticancer Res* 2002; **22**: 2455-2459
- 18 **Bralet MP**, Pichard V, Ferry N. Demonstration of direct lineage between hepatocytes and hepatocellular carcinoma in diethylnitrosamine-treated rats. *Hepatology* 2002; **36**: 623-630
- 19 **Guo WJ**, Li J, Ling WL, Bai YR, Zhang WZ, Cheng YF, Gu WH, Zhuang JY. Influence of hepatic arterial blockage on blood perfusion and VEGF, MMP-1 expression of implanted liver cancer in rats. *World J Gastroenterol* 2002; **8**: 476-479
- 20 **Dean CE Jr**, Benjamin SA, Chubb LS, Tessari JD, Keefe TJ. Non-additive hepatic tumor promoting effects by a mixture of two structurally different polychlorinated biphenyls in female rat livers. *Toxicol Sci* 2002; **66**: 54-61
- 21 **Stoker J**, Romijn MG, de Man RA, Brouwer JT, Weverling GJ, van Muiswinkel JM, Zondervan PE, Lameris JS, Ijzermans JN. Prospective comparative study of spiral computer tomography and magnetic resonance imaging for detection of hepatocellular carcinoma. *Gut* 2002; **51**: 105-107
- 22 **Carroll NM**, Alexander HR Jr. Isolation perfusion of the liver. *Cancer J* 2002; **8**: 181-193
- 23 **Jeong YY**, Mitchell DG, Kamishima T. Small (<20 mm) enhancing hepatic nodules seen on arterial phase MR imaging of the cirrhotic liver: clinical implications. *AJR Am J Roentgenol* 2002; **178**:1327-1334
- 24 **Vogl TJ**, Balzer JO, Mack MG, Bett G, Oppelt A. Hybrid MR interventional imaging system: combined MR and angiography suites with single interactive table. Feasibility study in vascular liver tumor procedures. *Eur Radiol* 2002; **12**: 1394-1400
- 25 **Teng GJ**, He SC, Guo JH, Cai XL, Gao GR. Preoperative transcatheterhepatic arterial embolization for hepatic malignancy. *Investradiol*, 1993; **28**: 235-241
- 26 **An Y**, Bie P, Dong J. Hepatic artery and portal vein dual perfusion chemotherapy in combination with injection of lipiodol-ethanol in treatment of advanced primary hepatocellular carcinoma. *Zhonghua Waike Zazhi* 2001; **39**: 593-595

Edited by Pang LH

Synergetic anticancer effect of combined quercetin and recombinant adenoviral vector expressing human wild-type p53, GM-CSF and B7-1 genes on hepatocellular carcinoma cells *in vitro*

Ming Shi, Fu-Sheng Wang, Zu-Ze Wu

Ming Shi, Fu-Sheng Wang, Division of Biological Engineering, Institute of Infectious Disease, the 302 Hospital of PLA, Beijing 100039, China

Zu-Ze Wu, Institute of Radiation Medicine, Academy of Military Medical Sciences, Beijing 100850, China

Correspondence to: Dr. Fu-Sheng Wang, Division of Biological Engineering, Institute of Infectious Disease, the 302 Hospital of PLA, 26 Fengtai Lu, Beijing 100039, China. fswang@public.bat.net.cn

Telephone: +86-10-66933332 **Fax:** +86-10-63831870

Received: 2002-07-26 **Accepted:** 2002-08-16

Abstract

AIM: This study investigated the anti-cancer effect of combined quercetin and a recombinant adenovirus vector expressing the human p53, GM-CSF and B7-1 genes (designated BB-102) on human hepatocellular carcinoma (HCC) cell lines *in vitro*.

METHODS: The sensitivity of HCC cells to anticancer agents was evaluated by 3-(4,5-dimethylthiazol-2-yl)-2,5-diphenyl tetrazolium bromide (MTT) assay. The viability of cells infected with BB-102 was determined by trypan blue exclusion. The expression levels of human wild-type p53, GM-CSF and B7-1 genes were determined by Western blot, enzyme-linked immunosorbent assay (ELISA) and flow cytometric analysis, respectively. The apoptosis of BB-102-infected or quercetin-treated HCC cells was detected by terminal deoxynucleotidyl transferase (TdT) assay or DNA ladder electrophoresis.

RESULTS: Quercetin was found to suppress proliferation of human HCC cell lines BEL-7402, HuH-7 and HLE, with peak suppression at 50 $\mu\text{mol/L}$ quercetin. BB-102 infection was also found to significantly suppress proliferation of HCC cell lines. The apoptosis of BB-102-infected HCC cells was greater in HLE and HuH-7 cells than in BEL-7402 cells. Quercetin did not affect the expression of the three exogenous genes in BB-102-infected HCC cells ($P > 0.05$), but it was found to further decrease proliferation and promote apoptosis of BB-102-infected HCC cells.

CONCLUSION: BB-102 and quercetin synergetically suppress HCC cell proliferation and induce HCC cell apoptosis, suggesting a possible use as a combined anti-cancer agent.

Shi M, Wang FS, Wu ZZ. Synergetic anticancer effect of combined quercetin and recombinant adenoviral vector expressing human wild-type p53, GM-CSF and B7-1 genes on hepatocellular carcinoma cells *in vitro*. *World J Gastroenterol* 2003; 9(1): 73-78

<http://www.wjgnet.com/1007-9327/9/73.htm>

INTRODUCTION

Hepatocellular carcinoma (HCC) is one of the most malignant diseases known. Surgical resections are incapable of removing

all HCC cells and the disease is very resistant to anticancer agents, making chemotherapy an equally ineffective option^[1]. Therefore, anti-tumor gene therapy strategies seem a good future option for the treatment of HCC^[2]. Numerous studies have shown that tumor occurrence and progression are often related to mutations in tumor suppressor genes or loss of host anti-tumor immunity^[3-9]. Therefore, a promising approach is transfer of tumor suppressor genes to cause tumor cell growth arrest or apoptosis, combined with cytokine genes to induce an effective immune response directly against both the genetically modified and the parental tumor cells^[10].

In HCC, mutation or loss of tumor suppressor gene p53 is associated with malignancy and chemoresistance^[11-13], making the wild-type p53 (WT-p53) gene a good candidate for replacement by gene therapy. Granulocyte-macrophage colony stimulating factor (GM-CSF) has been proven to be a potent, long-lasting inducer of antitumor immunity that promotes maturation of dendritic cells and enhances the function of antigen-presenting cells and natural killer (NK) cells^[14-17]. In addition, the expression of members of the B7 gene family has been shown to be important in antitumor responses in both mice and humans^[18-20]. However, most tumor cells, including HCC cells, lack B7-1 molecules on their surface, and as a result they escape recognition by the immune system^[21]. Kim *et al.* found an increased antitumor effect with the combined expression of GM-CSF and B7-1 in athymic nude mice, suggesting that coexpression of GM-CSF and B7-1 may enhance antitumor activity^[22]. Recombinant adenovirus vector BB-102, which expresses p53, GM-CSF and B7-1 genes^[23], has been shown to inhibit the growth of various human carcinoma cells, such as hepatocellular carcinoma, lung cancer^[24], and laryngeal cancer^[25], and enhances carcinoma cell chemosensitivity to anti-cancer agents.

Quercetin (3,3',4',5,7-pentahydroxyflavone) is one of most widely distributed bioflavonoids in the plant kingdom and is a common component of most edible fruits and vegetable. Humans consume approximately 1 g of dietary flavonoid daily. This compound has been shown to inhibit the growth of various human cancer cell lines^[26-34], including leukemia, hepatocellular carcinoma, and estrogen-receptor positive breast carcinoma MCF-7, suggesting that quercetin may have anti-cancer and anti-metastasis potential^[35-39]. The growth inhibitory effect of quercetin on tumor cells is found to be consequence of its ability to interfere with the enzymatic processes involved in the regulation of cellular proliferation: DNA, RNA and protein biosynthesis^[40-43]. Quercetin also has shown to down-regulate or inhibit the phosphatidylinositol (PI) and phosphatidylinositol phosphate (PIP) kinase activities in human carcinoma cells, leading to a marked reduction of second messengers IP3 concentration and cell death^[44,45]. Therefore, quercetin may be useful in the treatment of carcinomas with increased or down-regulated signal transduction capacity^[45-47].

These results suggest that the combination of quercetin with BB-102 may synergetically suppress the growth of carcinoma cells. Accordingly, this study addressed the synergetic action of quercetin combined with BB-102 against HCC cells *in vitro*.

MATERIALS AND METHODS

Agents

Quercetin was purchased from Sigma (St Louis, MO). Western blot detection system ECL+plus Kit was purchased from Amersham Pharmacia Biotech (Arlinton Heights, IL). GM-CSF ELISA kit was bought from Genzyme (Cambridge, MA). The TdT FragEL™ DNA fragmentation detection kit was from Calbiochem (Cambridge, MA). Ad-GFP (Ad5 vector expressing green fluorescence protein) was kindly provided by the Gene Therapy Unit, Baxter Healthcare Corporation, USA. BB-102 was reconstructed by Dr ZH Qu. Quercetin was dissolved in medium containing 0.1 % dimethyl sulfoxide (DMSO), and the same concentration of DMSO was used in control experiments.

Quercetin inhibits the growth of HCC cells

The BEL-7402, HLE and HuH-7 cell lines were seeded in 96-well plates at a density of 5×10^3 cells/well. After 24 h, the cells were exposed to various concentrations of quercetin from 3.125 $\mu\text{mol/L}$ to 100 $\mu\text{mol/L}$. After 72 h, the number of viable cells was determined by MTT assay.

Growth suppression in BB-102-infected HCC cells

HCC cell lines were seeded in six-well plates at a density of 5×10^5 cells/well. Twelve hours later, the cells were infected with BB-102 and Ad-GFP at a MOI of 50 pfu/cell. Culture medium was used for mock infection. Triplicate wells of each treatment group were counted every 2 days for a total of four times after infection. The viability of the cells was determined by trypan blue exclusion.

Assay of apoptosis

Apoptosis induced by BB-102 was analyzed by terminal deoxynucleotidyl transferase (TdT) assay. Briefly, HCC cells were seeded in 12-well plates at a density of 5×10^5 cells/well. After 24 h, they were infected with BB-102 or Ad-GFP at a MOI of 50 pfu/cell. Culture medium was used for mock infection. Seventy-two hours later, cell monolayers were fixed with 4 % formaldehyde diluted in phosphate-buffered saline (PBS) for 15 min at room temperature. Apoptosis of the cells was detected using a TdT FragEL™ DNA fragmentation detection kit according to the protocol.

Cellular apoptosis induced by quercetin or quercetin combined with BB-102 was analyzed by agarose gel-electrophoresis as described based on the pattern of DNA cleavage. Briefly, cells (1×10^6) were lysed with 0.5 ml lysis buffer, followed by the addition of RNase A to a final concentration of 200 $\mu\text{g/ml}$, and incubated for 1 h at 37 °C. Cells were then treated with 300 $\mu\text{g/ml}$ of proteinase K for 1 h at 37 °C. After addition of 4 μl loading buffer, 20 μl samples in each lane were subjected to electrophoresis on a 1.5 % agarose at 50 V for 3 h. DNA was stained with ethidium bromide and laddering was visualized under UV light.

p53 gene expression by western blot

Three cell lines were seeded in 6-well plates at a density of 1×10^5 cells/well. Group II was treated with 100 $\mu\text{mol/L}$ quercetin, group III was infected with BB-102 at a MOI of 50 pfu/cell, group IV was infected with BB-102 and then treated with 100 $\mu\text{mol/L}$ quercetin, and group I was mock-infected with culture medium infected with empty adenovirus vector as control. After 48 h incubation, cells were washed with phosphate buffered saline, disrupted by addition of lysing buffer (100 mmol/L Tris·Cl pH 6.8, 200 mmol/L DTT, 4 % SDS, 0.2 % bromophenol blue, 20 % glycerol), and electrophoresed. Western blot detection system ECL+plus Kit was used to determine p53 expression according to the instruction manual.

ELISA of GM-CSF gene expression

Expression of human GM-CSF was detected by enzyme-linked immunosorbent assay. Briefly, the cells were seeded in 6-well plates at a density of 1×10^6 cells/well. After 24 h, the cells were infected with BB-102 at a MOI of 50 pfu/cell for 1 h, then BB-102 suspensions were replaced with either culture medium alone, or culture medium containing 100 $\mu\text{mol/L}$ quercetin. After 48 h, the suspension was collected. The GM-CSF present in each suspension was quantified using the ELISA kit according to the protocol.

FCM of B7-1 gene expression

HCC cells were seeded in 6-well plates at a density of 5×10^5 cells/well. After 24 h, the cells were either treated with 100 $\mu\text{mol/L}$ quercetin, infected with BB-102 at a MOI of 50 pfu/cell, or infected with BB-102 at a MOI of 50 pfu/cell then treated with 100 $\mu\text{mol/L}$ quercetin. Culture medium was used for mock infection. After 48 h incubation, the cells were collected. Cells were washed twice in PBS and resuspended in PBS containing 1 % bovine serum albumin (BSA) prior to incubation with anti-human B7-1 monoclonal antibody (MoAb) for 30 min at 4 °C in the dark, followed by two washes in PBS/BSA. The cells were stained with FITC-conjugated goat anti-mouse IgG for 30 min at 4 °C. Nonspecific binding was controlled by incubation with isotypic controls. Fluorescence was measured with FACSCalibur flow cytometer (Becton Dickinson).

Proliferation of cells treated with both quercetin and BB-102

HCC cells were seeded in 96-well plates at a density of 5×10^3 cells/well. After 24 h, cells were infected with Ad-GFP or BB-102 at a MOI of 50 pfu/cell. Culture medium was used for mock infection. After 48 h, cells were treated with various concentrations of quercetin from 3.125 to 50 $\mu\text{mol/L}$. Culture medium was used for mock treatment. After 72 h, the viable cell numbers were tested by MTT assay.

RESULTS

Antitumor effect of quercetin on HCC cells

Quercetin was shown to inhibit HCC proliferation and induce HCC apoptosis *in vitro* in a dose-dependent manner until it reached peak inhibition at 50 $\mu\text{mol} \cdot \text{L}^{-1}$ (Figure 1).

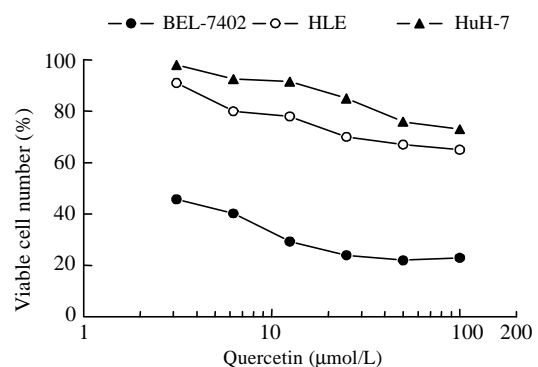


Figure 1 The suppressive effect of quercetin on the proliferation of BEL-7402, HLE and HuH-7 cell lines *in vitro*.

BB-102 inhibit the growth of HCC cells

Introduction of p53, GM-CSF and B7-1 through BB-102 infection led to significant suppression of growth proliferation in BEL-7402, HLE and HuH-7 cells compared with those infected with Ad-GFP or mock infected (Figure 2). Among them, there was a lower suppression in BEL-7402 cell line compared with HLE and HuH-7 cell lines ($P < 0.05$), which might be related

to the fact that BEL-7402 expresses an endogenous wild-type p53, while HLE and HuH-7 both express endogenous mutant p53, resulting in BEL-7402 being less sensitive to the effects of the exogenous p53 protein expressed by BB-102.

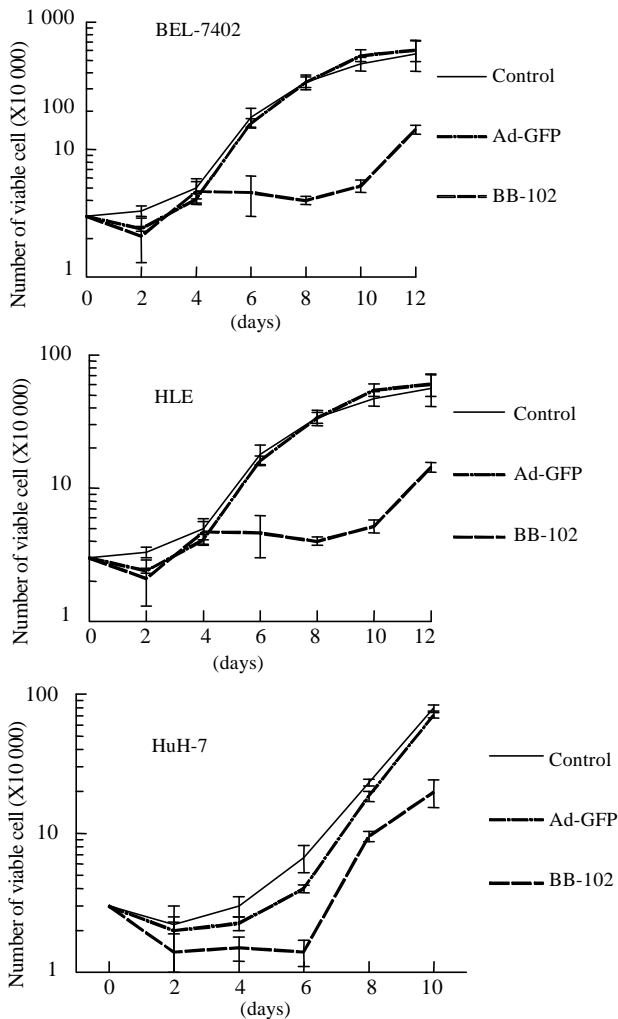


Figure 2 Proliferation inhibition of HCC cell lines transduced with BB-102.

BB-102 induces HCC cells apoptosis

As measured by TdT assay, apoptotic rates in BEL-7402, HLE and HuH-7 cells lines were 12.75 %, 57 % and 49.5 %, respectively. This suggests that HLE and HuH-7 cells were more sensitive to BB-102 than BEL-7402 cells.

Quercetin induces apoptosis of HCC cells

DNA laddering (Figure 3) suggests that quercetin induces HCC cell apoptosis, and that BB-102 further promoted the quercetin-treated cell apoptosis.

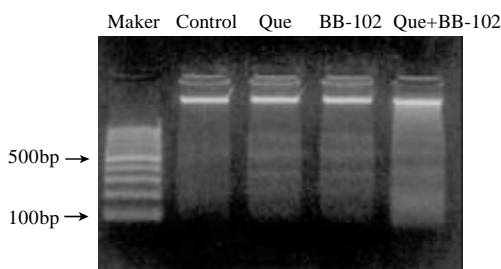


Figure 3 The promotion of Que on HCC cell apoptosis induced by BB-102.

Quercetin does not affect exogenous gene expression in BB-102-infected cells

Expression of exogenous P53 in BB-102-infected cells By using Western blot analysis, high levels of p53 protein were detected in BB-102-infected HCC cell lines. These levels were not affected by treatment with quercetin (Figure 4).

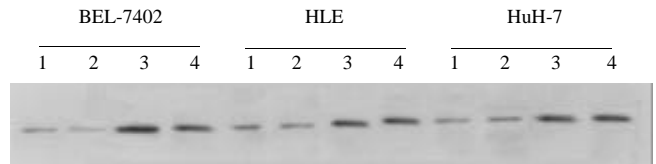


Figure 4 Effect of Que on the p53 expression in HCC cell lines transferred with BB-102. (lane1: control; lane2: with Que; lane3: with BB-102; lane4: with Que and BB-102).

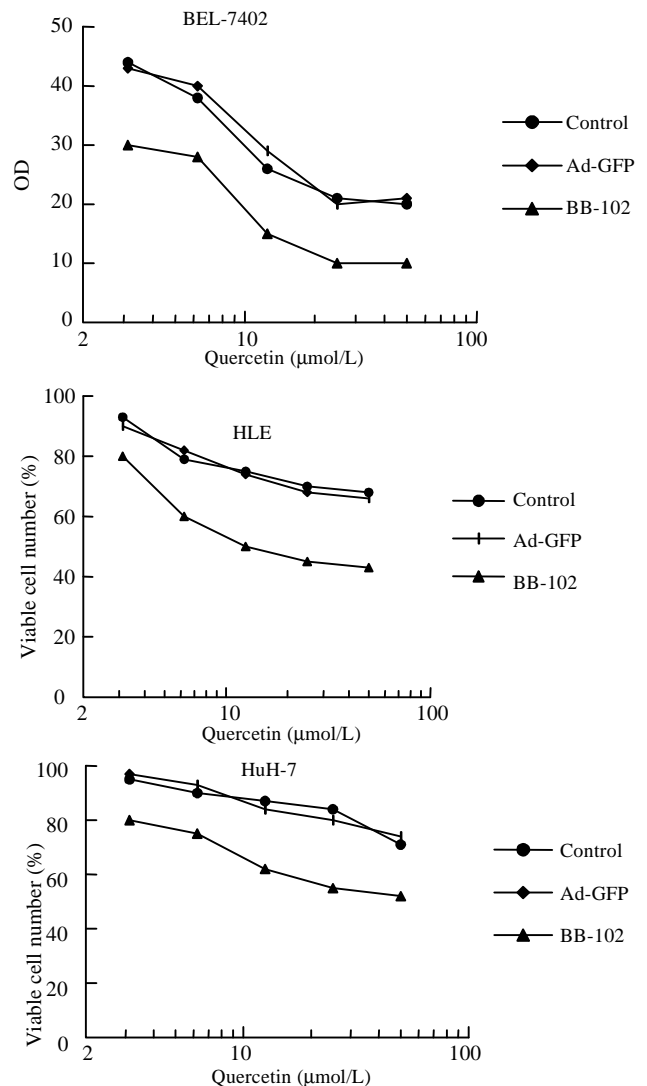


Figure 5 Synergistic effect of BB-102 on quercetin suppression of growth of HCC cell lines.

Expression of exogenous GM-CSF protein in BB-102-infected cells

ELISA assay showed that a high-level expression of GM-CSF was detected in the culture suspension of BB-102-infected cells 48 h after infection. There was no statistical difference in GM-CSF level between the cells treated with quercetin and untreated cells (Table 1).

Expression of exogenous B7-1 protein in BB-102-infected cells

B7-1 gene expression was observed flow cytometric analysis 48 h after BB-102 infection (Table 2). There was no

significant difference in B7-1 expression between cells treated with quercetin and untreated cells.

Table 1 Effect of Que on the GM-CSF expression in HCC cell lines transferred with BB-102 (pg·L⁻¹), ($\bar{x}\pm s$), (n=6)

Cell line	Infected with BB-102	Infected with BB-102+Que
BEL-7402	118.9±29.9	147.7±13.2
HLE	209.6±55.7	248.3±15.9
HuH-7	250.7±21.9	283.7±21.6

Table 2 Effect of Que on the B7-1 expression in HCC cell lines transferred with BB-102 (%) (n=4)

Cell line	Control	Que	BB-102	Que+BB-102
BEI-7402	10.0±2.5	11.2±1.7	80.0±10.3 ^b	85.0±12.0 ^b
HLE	15.3±2.1	14.0±2.0	31.0±7.8 ^a	35.2±5.6 ^b
HuH-7	20.0±2.6	22.0±3.0	59.8±8.5 ^b	64.0±8.8 ^b

^aP<0.01, ^bP<0.001, vs their controls

Quercetin enhances the inhibition of the proliferation in BB-102-infected HCC cell lines

The proliferation suppression pattern of HCC cells treated with quercetin was not significantly different between Ad-GFP-infected cells and Ad-mock infected cells. In contrast, BB-102-infected cells showed a significant increase of suppression when treated with quercetin. This implies that BB-102 transduction and quercetin treatment synergistically suppress HCC proliferation (Figure 5). The control data indicates that it was the exogenous gene expression that induced this effect, not the adenovirus.

DISCUSSION

Gene therapy, the introduction of functional genes into cells to treat or prevent a disease, is a promising approach for the treatment of human cancer. In an effort to explore potential gene therapy approaches to the treatment of stubborn HCC, we investigated the synergetic effects of dietary component (quercetin) plus gene transfer (BB-102 infection). BB-102 is a recombinant adenoviral vector expressing the genes for human wild-type p53, GM-CSF and B7-1^[23]. Our study showed that BB-102 infection arrested the growth of HCC cell lines BEL-7402, HLE, HuH-7, and induced their apoptosis by the expression of exogenous wild-type p53 (a transcriptional activator that induces cell cycle arrest and apoptosis^[48-50]). BB-102 also enhanced immunogenicity of HCC cells and improved host antitumor immune reaction.

We then examined the possible synergy between these exogenous genes and quercetin, which is thought to have a long-term preventive effect on chemical carcinogenesis, especially in people who eat a diet rich in fruits and vegetables^[30,31,36,51,52]. Previously, we had found that antineoplastic drug concentrations exerting cytotoxic activity were markedly lower when cells were pretreated with quercetin^[28,35]. In addition, quercetin has been shown to inhibit the growth of human breast cancer cell line MDA-MB468 in a dose-dependent fashion by specifically inhibiting the expression of mutant p53 in cellular transformation^[53]. Because HCC patients are generally resistant to chemotherapy (possibly due to the loss of a functional p53 gene^[54], which is known to occur in 50 % of cancers^[55-58]), we

questioned whether quercetin could reverse the multi-drug resistance of HCC cells, perhaps through down-regulation of mutated p53 or glycoprotein^[53,59,60]. In addition to its possible role in adjusting p53 levels, quercetin is also known to inhibit the synthesis of HSP70 (heat shock protein 70) and change its intracellular distribution. HSP70 is involved in apoptosis, and the link between the two suggests that quercetin may be involved in the induction of apoptosis^[35,61].

We found enhancement of apoptosis and inhibition of the proliferation of BB-102-infected HCC cell lines treated with quercetin, suggesting that there is a synergetic anticancer effect between quercetin and BB-102. There was no change in p53, GM-CSF and B7-1 gene expressions in BB-102-infected HCC cell lines following quercetin treatment, indicating that quercetin did not affect exogenous gene expression in BB-102-infected HCC cells. We believe it is possible that this synergetic effect might be due to BB-102 transduction promoting the chemosensitivity of HCC cells to quercetin, but this and other mechanisms will need further study.

BEL-7402 cells were more sensitive to quercetin than HLE and HuH-7 cells. At a concentration of 50 μmol/L quercetin (peak proliferation inhibition), proliferation inhibition was 78 %, 33 % and 24 % for BEL-7402, HLE and HuH-7, respectively. Our previous studies have shown that the doubling time of BEL-7402 is the shortest among these cells. This suggests that the cells that proliferate quickly are more sensitive to quercetin in this study. In addition, quercetin induced apoptosis in HCC cells at G1 and S in a dose- and time-dependent manner, and the effect was enhanced by BB-102 infection. This enhancement was less in BEL-7402, possibly due to its wild-type endogenous p53 status^[62]. Overall, HCC cells treated with both quercetin and BB-102 showed inhibition of proliferation and increased apoptosis, suggesting that quercetin may be useful as an adjuvant in chemotherapy treatment of HCC patients. The combination of quercetin and BB-102 transduction is a promising new strategy for the treatment of typically chemo-resistant hepatomas.

REFERENCES

- 1 Venook AP. Hepatocellular carcinoma. *Curr Treat Options Oncol* 2000; **1**: 407-415
- 2 Mohr L, Geissler M, Blum HE. Gene therapy for malignant liver disease. *Expert Opin Biol Ther* 2002; **2**: 163-175
- 3 Peller S. Clinical implications of p53: effect on prognosis, tumor progression and chemotherapy response. *Semin Cancer Biol* 1998; **8**: 379-387
- 4 Friess H, Kleeff J, Korc M, Buchler MW. Molecular aspects of pancreatic cancer and future perspectives. *Dig Surg* 1999; **16**: 281-290
- 5 Rocco JW, Sidransky D. p16(MTS-1/CDKN2/INK4a) in cancer progression. *Exp Cell Res* 2001; **264**: 42-55
- 6 Canote R, Du Y, Carling T, Tian F, Peng Z, Huang S. The tumor suppressor gene RIZ in cancer gene therapy (review). *Oncol Rep* 2002; **9**: 57-60
- 7 Farid NR. P53 mutations in thyroid carcinoma: tidings from an old foe. *J Endocrinol Invest* 2001; **24**: 536-545
- 8 Muschen M, Warskulat U, Beckmann MW. Defining CD95 as a tumor suppressor gene. *J Mol Med* 2000; **78**: 312-325
- 9 Behrens J. Cadherins and catenins: role in signal transduction and tumor progression. *Cancer Metastasis Rev* 1999; **18**: 15-30
- 10 Wu Q, Moyana T, Xiang J. Cancer gene therapy by adenovirus-mediated gene transfer. *Curr Gene Ther* 2001; **1**: 101-122
- 11 Xu GW, Sun ZT, Forrester K, Wang XW, Coursen J, Harris CC. Tissue-specific growth suppression and chemosensitivity promotion in human hepatocellular carcinoma cells by retroviral-mediated transfer of the wild-type p53 gene. *Hepatology* 1996; **24**: 1264-1268
- 12 Qin LX, Tang ZY. The prognostic molecular markers in hepatocellular carcinoma. *World J Gastroenterol* 2002; **8**: 385-392
- 13 Buendia MA. Genetics of hepatocellular carcinoma. *Semin Can-*

- cer Biol* 2000; **10**: 185-200
- 14 **Yu JS**, Burwick JA, Dranoff G, Breakefield XO. Gene therapy for metastatic brain tumors by vaccination with granulocyte-macrophage colony-stimulating factor-transduced tumor cells. *Hum Gene Ther* 1997; **8**: 1065-1072
 - 15 **Hogge GS**, Burkholder JK, Culp J, Albertini MR, Dubielzig RR, Keller ET, Yang NS, MacEwen EG. Development of human granulocyte-macrophage colony-stimulating factor-transfected tumor cell vaccines for the treatment of spontaneous canine cancer. *Hum Gene Ther* 1998; **9**: 1851-1861
 - 16 **Lu L**, Hsieh M, Oriss TB, Morel PA, Starzl TE, Rao AS, Thomson AW. Generation of DC from mouse spleen cell culture in response to GM-CSF: Immunophenotypic and functional analyses. *Immunology* 1995; **84**: 127-134
 - 17 **Ogawa T**, Kusumoto M, Mizumoto K, Sato N, Tanaka M. Adenoviral GM-CSF Gene Transduction into Breast Cancer Cells Induced Long-Lasting Antitumor Immunity in Mice. *Breast Cancer* 1999; **6**: 301-304
 - 18 **Felzmann T**, Ramsey WJ, Blaese RM. Anti-tumor immunity generated by tumor cells engineered to express B7-1 via retroviral or adenoviral gene transfer. *Cancer Lett* 1999; **135**: 1-10
 - 19 **Horig H**, Lee DS, Conkright W, Divito J, Hasson H, LaMare M, Rivera A, Park D, Tine J, Guito K, Tsang KW, Schlom J, Kaufman HL. Phase I clinical trial of a recombinant canarypoxvirus (ALVAC) vaccine expressing human carcinoembryonic antigen and the B7.1 co-stimulatory molecule. *Cancer Immunol Immunother* 2000; **49**: 504-514
 - 20 **Takahashi T**, Hirano N, Takahashi T, Chiba S, Yazaki Y, Hirai H. Immunogene therapy against mouse leukemia using B7 molecules. *Cancer Gene Ther* 2000; **7**: 144-150
 - 21 **Nakatsuka K**, Sugiyama H, Nakagawa Y, Takahashi H. Purification of antigenic peptide from murine hepatoma cells recognized by class- I major histocompatibility complex molecule-restricted cytotoxic T-lymphocyte induced with B7-1-gene-transfected hepatoma cells. *J Hepatol* 1999; **30**: 1119-1129
 - 22 **Kim KY**, Kang MA, Nam MJ. Enhancement of natural killer cell-mediated cytotoxicity by coexpression of GM-CSF/B70 in hepatoma. *Cancer Lett* 2001; **166**: 33-40
 - 23 **Qiu ZH**, Lao MF, Wu ZZ. Construction of recombinant adenovirus co-expressing human wild-type p53, GM-CSF and B7-1 genes. *Zhongguo Shengwuxuaxue Yu Fengzishengwu Xuebao* 2001; **17**: 33-38
 - 24 **Qiu ZH**, Lao MF, Wang YF, Wu ZZ. Adenovirus mediate multigenes expressing in lung cancer and inducing apoptosis. *Zhongguo Zhongliu Shengwuzhiliao Zazhi* 1999; **6**: 83-86
 - 25 **Qiu ZH**, Lao MF, Wu ZZ. Co-transfer of human wild-type p53 and granulocyte-macrophage colony-stimulating factor genes via recombinant adenovirus induces apoptosis and enhances immunogenicity in laryngeal cancer cells. *Cancer Lett* 2001; **167**: 25-32
 - 26 **Larocca LM**, Teofili L, Sica S, Piantelli M, Maggiano N, Leone G, Ranelletti FO. Quercetin inhibits the growth of leukemic progenitors and induces the expression of transforming growth factor-beta 1 in these cells. *Blood* 1995; **85**: 3654-3661
 - 27 **Scambia G**, Panici PB, Ranelletti FO, Ferrandina G, De Vincenzo R, Piantelli M, Masciullo V, Bonanno G, Isola G, Mancuso S. Quercetin enhances transforming growth factor beta 1 secretion by human ovarian cancer cells. *Int J Cancer* 1994; **57**: 211-215
 - 28 **Ranelletti FO**, Ricci R, Larocca LM, Maggiano N, Capelli A, Scambia G, Benedetti-Panici P, Mancuso S, Rumi C, Piantelli M. Growth-inhibitory effect quercetin and presence of type II estrogen-binding sites in human colon-cancer cell lines and primary colorectal tumors. *Int J Cancer* 1992; **50**: 486-492
 - 29 **Choi JA**, Kim JY, Lee JY, Kang CM, Kwon HJ, Yoo YD, Kim TW, Lee YS, Lee SJ. Induction of cell cycle arrest and apoptosis in human breast cancer cells by quercetin. *Int J Oncol* 2001; **19**: 837-844
 - 30 **Pawlikowska-Pawlega B**, Jakubowicz-Gil J, Rzymowska J, Gawron A. The effect of quercetin on apoptosis and necrosis induction in human colon adenocarcinoma cell line LS180. *Folia Histochem Cytobiol* 2001; **39**: 217-218
 - 31 **Kampa M**, Hatzoglou A, Notas G, Damianaki A, Bakogeorgou E, Gemetzi C, Kouroumalis E, Martin PM, Castanas E. Wine antioxidant polyphenols inhibit the proliferation of human prostate cancer cell lines. *Nutr Cancer* 2000; **37**: 223-233
 - 32 **Iwashita K**, Kobori M, Yamaki K, Tsushida T. Flavonoids inhibit cell growth and induce apoptosis in B16 melanoma 4A5 cells. *Biosci Biotechnol Biochem* 2000; **64**: 1813-1820
 - 33 **Uddin S**, Choudhry MA. Quercetin, a bioflavonoid, inhibits the DNA synthesis of human leukemia cells. *Biochem Mol Biol Int* 1995; **36**: 545-550
 - 34 **Caltagirone S**, Rossi C, Poggi A, Ranelletti FO, Natali PG, Brunetti M, Aiello FB, Piantelli M. Flavonoids apigenin and quercetin inhibit melanoma growth and metastatic potential. *Int J Cancer* 2000; **87**: 595-600
 - 35 **Sliutz G**, Karlseder J, Tempfer C, Orel L, Holzer G, Simon MM. Drug resistance against gemcitabine and topotecan mediated by constitutive hsp70 overexpression in vitro: implication of quercetin as sensitizer in chemotherapy. *Br J Cancer* 1996; **74**: 172-177
 - 36 **Yang CS**, Landau JM, Huang MT, Newmark HL. Inhibition of carcinogenesis by dietary polyphenolic compounds. *Annu Rev Nutr* 2001; **21**: 381-406
 - 37 **Wang HK**. The therapeutic potential of flavonoids. *Expert Opin Investig Drugs* 2000; **9**: 2103-2119
 - 38 **Asaam J**, Matsuzaki H, Kawasak S, Kuroda M, Takeda Y, Kishi K, Hiraki Y. Effects of quercetin on the cell growth and the intracellular accumulation and retention of adriamycin. *Anticancer Res* 2000; **20**: 2477-2483
 - 39 **Damianaki A**, Bakogeorgou E, Kampa M, Notas G, Hatzoglou A, Panagiotou S, Gemetzi C, Kouroumalis E, Martin PM, Castanas E. Potent inhibitory action of red wine polyphenols on human breast cancer cells. *J Cell Biochem* 2000; **78**: 429-441
 - 40 **Yamashita N**, Kawanishi S. Distinct mechanisms of DNA damage in apoptosis induced by quercetin and luteolin. *Free Radic Res* 2000; **33**: 623-633
 - 41 **Musonda CA**, Helsby N, Chipman JK. Effects of quercetin on drug metabolizing enzymes and oxidation of 2',7-dichlorofluorescein in HepG2 cells. *Hum Exp Toxicol* 1997; **16**: 700-708
 - 42 **Exon JH**, Magnuson BA, South EH, Hendrix K. Dietary quercetin, immune functions and colonic carcinogenesis in rats. *Immunopharmacol Immunotoxicol* 1998; **20**: 173-190
 - 43 **Drewa G**, Wozqak A, Palgan K, Schachtschabel DO, Grzanka A, Sujkowska R. Influence of quercetin on B16 melanotic melanoma growth in C57BL/6 mice and on activity of some acid hydrolases in melanoma tissue. *Neoplasma* 2001; **48**: 12-18
 - 44 **Weber G**, Shen F, Yang H, Prajda N, Li W. Regulation of signal transduction activity in normal and cancer cells. *Anticancer Res* 1999; **19**: 3703-3709
 - 45 **Weber G**, Shen F, Prajda N, Yeh YA, Yang H, Herenyiova M, Look KY. Increased signal transduction activity and down-regulation in human cancer cells. *Anticancer Res* 1996; **16**: 3271-3282
 - 46 **Richter M**, Ebermann R, Marian B. Quercetin-induced apoptosis in colorectal tumor cells: possible role of EGF receptor signaling. *Nutr Cancer* 1999; **34**: 88-99
 - 47 **Shen F**, Herenyiova M, Weber G. Synergistic down-regulation of signal transduction and cytotoxicity by tiazofurin and quercetin in human ovarian carcinoma cells. *Life Sci* 1999; **64**: 1869-1876
 - 48 **Levine AJ**. p53, the cellular gatekeeper for growth and division. *Cell* 1997; **88**: 323-331
 - 49 **Greenblatt MS**, Bennett WP, Hollstein M, Harris CC. Mutation in the P53 tumor suppressor gene: clues to cancer etiology and molecular pathogenesis. *Cancer Res* 1994; **54**: 4855-4878
 - 50 **Hui AM**, Makuuchi M, Li X. Cell cycle regulators and human hepatocarcinogenesis. *Hepatogastroenterology* 1998; **45**: 1635-1642
 - 51 **Yang CS**, Landau JM, Huang MT, Newmark HL. Inhibition of carcinogenesis by dietary polyphenolic compounds. *Annu Rev Nutr* 2001; **21**: 381-406
 - 52 **Hollman PC**, Katan MB. Health effects and bioavailability of dietary flavonols. *Free Radic Res* 1999; **31** (Suppl): S75-80
 - 53 **Avila MA**, Velasco JA, Cansado J, Notario V. Quercetin mediate the down-regulation of mutation p53 in the human breast cancer cell line MDA-MB468. *Cancer Research* 1994; **54**: 2424-2428
 - 54 **Thottassery**, Zambetti GP, Arimori K, Schuetz EG, Schuetz JD.

- p53-dependent regulation of *mdr1* gene expression causes selective resistance to chemotherapeutic agents. *Proc Natl Sci USA* 1997; **94**: 11037-11042
- 55 **Wang D**, Shi JQ. Overexpression and mutations of tumor suppressor gene p53 in hepatocellular carcinoma. *China Natl J New Gastroenterol* 1996; **2**: 161-164
- 56 **Wang XJ**, Yuan SL, Li CP, Iida N, Oda H, Aiso S, Ishikawa T. Infrequent p53 gene mutation and expression of the cardia adenocarcinomas from a high incidence area of Southwest China. *Shijie Huaren Xiaohua Zazhi* 2000; **6**: 750-753
- 57 **Li ZX**, Liu PY, Xu WX, Cong B, Ma ZX, Li Y. p53 gene mutations in primary gastric cancer. *China Natl J New Gastroenterol* 1996; **2**: 41-43
- 58 **Peng XM**, Peng WW, Yao JL. Codon 249 mutations of p53 gene in development of hepatocellular carcinoma. *World J Gastroenterol* 1998; **4**: 125-127
- 59 **Scambia G**, Ranelletti FO, Panici PB, De Vincenzo R, Bonanno G, Ferrandina G, Piantelli M, Bussa S, Rumi C, Cianfriglia M. Quercetin potentiates the effect of adriamycin in a multidrug-resistant MCF-7 human breast-cancer cell line: P-glycoprotein as a possible target. *Cancer Chemother Pharmacol* 1994; **34**: 459-464
- 60 **Beniston RG**, Morgan IM, O'Brien V, Campo MS. Quercetin, E7 and p53 in papillomavirus oncogenic cell transformation. *Carcinogenesis* 2001; **22**: 1069-1076
- 61 **Wei YQ**, Zhao X, Kariya Y, Fukata H, Teshigawara K, Uchida A. Induction of apoptosis by quercetin: Involvement of heat shock protein. *Cancer Research* 1994; **54**: 4952-4957
- 62 **Shi M**, Wang FS, Liu MX, Jin L, Shi H, Lei ZY. The examination of p53 gene status in BEL-7402, HLE and HuH-7 cells. *Shijie Huaren Xiaohua Zazhi* 2001; **9**: 1330-1332

Edited by Wu XN

Construction of IL-2 gene-modified human hepatocyte and its cultivation with microcarrier

Nan-Hong Tang, Yian-Ling Chen, Xiao-Qian Wang, Xiu-Jin Li, Feng-Zhi Yin, Xiao-Zhong Wang

Nan-Hong Tang, Xiao-Qian Wang, Yian-Ling Chen, Xiu-Jin Li, Feng-Zhi Yin, Hepato-Biliary Surgery Institute of Fujian Province, Union Hospital Affiliated to Fujian Medical University, Fuzhou 350001, Fujian Province, China

Xiao-Zhong Wang, Gastroenterology Department, Union Hospital Affiliated to Fujian Medical University, Fuzhou 350001, Fujian Province, China

Supported by Science and Technology Development Foundation of Fujian Province, No. 98-Z-214

Correspondence to: Nan-Hong Tang, Hepato-Biliary Surgery Institute of Fujian Province, Union Hospital, 29 Xinquan Road, Fuzhou 350001, Fujian Province, China. fztmh@sina.com

Telephone: +86-591-3671667

Received: 2002-08-24 **Accepted:** 2002-10-12

Abstract

AIM: To construct interleukin-2 gene-modified human hepatocyte line (L-02/IL-2) and investigate the changes of the function of liver cells and IL-2 secretion in culture with microcarrier, laying the foundation for further experimentation on hepatocyte transplantation.

METHODS: hIL-2 gene was transduced into L-02 hepatocytes by recombinant retroviral vector pLNCIL-2, and the changes of morphology and clonogenicity rate of the transduced cells were observed, the secretion levels of hIL-2 in cultural supernatant were detected by ELISA and NeoR gene was amplified by PCR. The growth of L-02/IL-2, the special biochemistry items and the levels of IL-2 were detected after cultivation with microcarrier.

RESULTS: The clonogenicity rate of the L-02/IL-2 cells was lower than that of L-02/Neo cells and L-02 cells. The levels of hIL-2 could reach 32 000 pg/10⁶ cells per day and kept secreting for more than ten weeks. NeoR gene segment was respectively obtained by PCR from both L-02/IL-2 and L-02/Neo cell's genomic DNA. At the 6th day in culture with microcarrier, the matrix-induced liver cell aggregates were formed, the number of alive L-02/IL-2 cell were 16.8±0.53 ×10⁶/flask and the levels of ALB and UREA were 52.54±1.28 mg/L and 5.29±0.17 mmol/L, respectively. These data had not significantly changed as compared with those of L-02 cells ($P>0.05$); However, the levels of IL-2 in IL-2/L-02 cells remarkably exceeded that in L-02 cells in the whole culture process ($P<0.001$).

CONCLUSION: The IL-2 gene-modified hepatocyte line has been successfully constructed. The L-02/IL-2 cellular aggregates cultured with microcarrier have a high capacity of IL-2 production as well as protein synthesis and amino acid metabolism.

Tang NH, Chen YL, Wang XQ, Li XJ, Yin FZ, Wang XZ. Construction of IL-2 gene-modified human hepatocyte and its cultivation with microcarrier. *World J Gastroenterol* 2003; 9(1): 79-83
<http://www.wjgnet.com/1007-9327/9/79.htm>

INTRODUCTION

Gene therapy has become an important therapeutic alternative in recent years, thanks to the growing improvement of gene-transduction techniques in eukaryotic cells. There are a large number of proteins expression in hepatocyte with high levels, and many genes that are involved in metabolism also express in hepatocytes, so hepatocyte is one of the crucial tools for gene therapy^[1], for example, the therapeutic implement for patient with hyperbilirubinemia by hepatocyte transplantation after gene modification *in vitro*, which was approved by FDA^[2].

As an important approach for inhibiting the growth of tumor, immune therapy of cytokines further broadens the prospect of clinical application of hepatocytes and gene therapy of cytokines. Recent studies have demonstrated the feasibility of cytokine gene transference to enhance the antitumor activities of host immune cell^[3]. With regards to therapy for hepatocarcinoma, there are many good results obtained from the study of hepatocarcinoma cells modified by cytokine genes^[4-11], especially using IL-2 gene modified hepatocarcinoma cells that conquered the substantial toxicity from administration of high doses of IL-2^[9,12]. However, few studies focus on the antitumor immune function of hepatocyte transduced with cytokine gene in hepatocyte transplantation. In this study, IL-2 gene was transduced into human hepatocyte line L-02 by recombinant retroviral vector. The experiments of its biologic activities and cultivation with microcarriers were performed, laying the foundation for further experimentation on hepatocyte transplantation.

MATERIALS AND METHODS

Material

Human hepatocyte line L-02, amphotropic packaging cell PA317 and mouse fibroblast cell line NIH3T3 were purchased from Shanghai Cell Biology Institute, Chinese Academy of Science and grown in DF medium (DMEM: Ham's F12=3:1) containing 100 mL·L⁻¹ fetal calf serum, penicillin 1×10⁵U·L⁻¹ and streptomycin 100 mg·L⁻¹. The cells were kept at 37 °C in a 50 mL/LCO₂ humidified atmosphere and subcultured from one to three when the cells proliferated into a full monolayer. Recombinant retroviral vector, LNCX and LNCIL-2, were kindly provided by Prof. Joo Hang Kim from Yonsei University in Korea. Plasmid extraction and purification kit, Wizard® Plus SV Minipreps DNA, and transfection kit TransFast™ were from Promega. hIL-2 ELISA kit was purchased from Jingmei Biological Engineering, Shenzhen. Microcarrier Cytodex3 was from Pharmacia. Poly-HEMA, DMEM and Ham's F12 medium were the products of Sigma. Calf serum were purchased from Four Season Green Biological Co., Hangzhou, China.

Methods

Construction of recombinant retrovirus producer cell line
Transformation of recombinant retroviral vector was performed as previously described^[13]. The extraction and purification of the product was operated according to the manufacturer's protocol. The purified products were quantitated by spectrophotometer (DU 640), digested with *Hind* III at 37 °C for 2 h and identified by electrophoresis through a 10 g/L

formaldehyde agarose gel. The amphotropic packaging cells PA317 were plated into 12-well plates and cultured till nearly 60-70 % confluence. Then LNCX or LNCIL-2 transduction to PA317 cell line was made with lipo-transfection technique. The PA317/Neo and PA317/IL-2 cell clones which produced pLNCX and pLNCIL-2 were respectively selected by G418 and subcultured for amplification in G418-free DF media for 24 h. Furthermore, the supernatant of above cells containing recombinant retrovirus were collected, and the retrovirus titer was detected by NIH3T3 cells according to that described^[14], quantitated highest titer was kept at -70 °C.

Transduction of IL-2 gene into the hepatocyte cell line The L-02 hepatocyte line were grown to a confluence of 60-70 % in 24-well plate. The supernatant were discarded and replaced with 1 mL recombinant retroviral supernatant supplemented with 8 µg of Polybrene. Two hours later, 2 mL fresh DF media containing 800 mg/L were added and cultured at 37 °C for 24 h. The whole process of the cell clone against G418 selection lasted 15 days followed by amplified cultivation.

Growth of transfected cells The growth of transfected cells were observed and photographed, total of 3×10^3 L-02, L-02/Neo and L-02/IL-2 cells were put into the media respectively with a final volume of 200 µL, and then plated on a 96-well plate and incubated at 37 °C in 5 mL/LCO₂ humidified atmosphere for 7 days. Each group had six wells. The assay of cell proliferation was performed by MTT every 24 h. Briefly, 20 µL of 5 g/L MTT were added into each well and cultured for another 4 h. The supernatant was discarded and replaced with 200 µL of dimethyl sulfoxide (DMSO). When the crystals were dissolved, the absorbance (A) value of the slides was read at 490 nm. In addition, 1×10^3 cells per well of the three kinds of cell were plated into 24-well plate in 1 mL media and cultured for 7 days, respectively. The colonogenicity rate (CR) of transferred cells were calculated by using the following equation: $CR = (\text{average clones per well} / 1000) \times 100 \%$.

NeoR gene analysis of the transfected cells by PCR The total genomic DNA were extracted from 1.0×10^6 of L-02, L-02/Neo and L-02/IL-2 cells in 200 mL TE buffer respectively, then quantitated by spectrophotometer and digested with *Bam*H1. The NeoR gene was amplified under following conditions: denaturation at 94 °C for 5 min followed by 94 °C 1 min, 62 °C 1 min and 72 °C 1 min 15 s for 30 cycles. The sequence of NeoR gene primers and length of PCR products were as follows: forward-5' -CAAGATGGATTGCACGCAGG-3' and reverse-5' -CCCGCTCAGAAGAAGACTCGTC-3', size, 790 bp. For analysis, 10 µL of reaction product were checked in 10 g/L agarose gel with ethidium bromide staining and followed by camera photographing.

Detection of the levels of hIL-2 secreted by the transduced cells The supernatant of 1.0×10^6 of L-02, L-02/Neo and L-02/IL-2 cells that cultured in flask for 24 h were obtained and stored at -70 °C after centrifugation. L-02/IL-2 cells were especially cultured for 10 wk and the supernatants were collected every week. The levels of hIL-2 were measured by ELISA according to the manufacturer's protocol.

Cultivation with microcarriers All glassware with which Cytodex3 came into contact, should be siliconized before use. The hydration of Cytodex3 was carried out as the protocol. Briefly, 200 mg Cytodex3 were dipped in Ca²⁺ and Mg²⁺-free PBS in a siliconized container overnight and sterilized by autoclaving, then replaced with fresh DF media; The flasks were covered with 0.1 mL/cm² 120 g/L Poly-HEMA dissolved in ethanol and then air-dried sterilizedly. The hydrated Cytodex3, 20 mg a flask, along with L-02 and L-02/IL-2 cells, 3.0×10^6 a flask in 2 mL media, were seeded into Poly-HEMA covered flasks, respectively. Each group had five bottles. They were all cultured in incubator at 37 °C for 4 h following shakes twice for 1 min every 4 h, the media were replaced every 24 h,

and the supernatants were kept at -70 °C after centrifugation at 1000r/min.

Morphologic observation and cell proliferation The culture process was observed and photographed. The cell samples at 6th day were fixed by 25 g/L glutaraldehyde and observed by HU-12A electronmicroscope. The proliferation was performed as follows: (1) 100 µL cell suspension were taken out from every flask at day 2, 4, 6, 8 and 10 in culture and added into a new flask without Poly-HEMA; (2) When all microcarriers went down, the supernatants were discarded, 100 µL 2.5 g/L trypsinase were added and cultured at 37 °C for 5 min; (3) After 100 µL DF media were added for termination of trypsinization, the flasks were put up slowly with all microcarriers anchored to the bottom of the flask, and the supernatant were rapidly dipped out for cell calculation with trypan blue dye exclusion method.

Measurement of biochemical items and IL-2 in the supernatant With γ calculator (SN-682), the concentration of human ALB was detected by RIA kit from North Biotechnique Institute, Beijing, others as UREA (BUN $\times 2.14$), AST and LDH were measured by biochemical autoanalyzer (CX Δ 7, Beckman).

RESULTS

Identification of amplified retroviral vector

The amplified products of LNCX and LNCIL-2 were digested with *Hind* III, and then checked with 20 g/L agarose gel electrophoresis (Figure 1). The length of LNCX (6 620 bp) and LNCIL-2 (7 293 bp) were identical with that predicted, showing the success of amplification, extraction and purification.

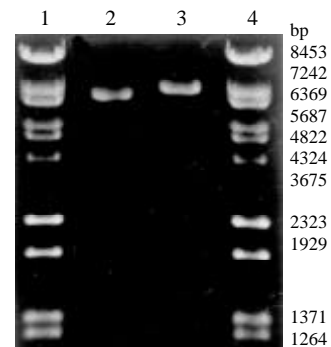


Figure 1 Restriction enzyme analysis of pLNCX and pLNCIL-2

Cultivation of virus producer cell and measurement of viral concentration

21 and 25 anti-G418 clones appeared after PA317 cells were transduced by LNCX and LNCIL-2 and cultured in media containing 800 mg/L of G418 for 2 weeks. 10 clones selected were performed amplified culture, respectively. The titer of retrovirus of all collected supernatants was between 5.4×10^7 cfu/L and 1.4×10^9 cfu/L.

Morphological changes

Under the light microscope, L-02 cells were seen flake-like growth (Figure 2A), L-02/Neo and L-02/IL-2 cells represented the trend of island-like growth with clear margin (Figure 2B). The growing speed of L-02/IL-2 cells was slightly slower than that of L-02 and L-02/Neo cells (Figure 3). Clonogenicity rate of the L-02/IL-2 cells were significantly lower than those of L-02/Neo and L-02 cells ($P < 0.01$) (Table 1).

PCR analysis of NeoR gene

NeoR gene segment (790 bp) was amplified by PCR from genomic DNA of L-02/Neo and L-02/IL-2 cells and tested with 20 g/L agarose gel electrophoresis, but none from L-02 cells

(Figure 4). These suggested that LNCX and LNCIL-2 were successfully integrated into the genome of L-02 cells.

IL-2 secretion from IL-2 transduced hepatocyte line

After IL-2 transduction and G418 selection using LNCX and LNCIL-2 retroviral vector, maximal amount of IL-2 production in L-02/IL-2 cells was 32 000 pg/10⁶ cells· 24 h, remarkably exceeding 56 pg/10⁶ cells· 24 h in L-02 cells and 48 pg/10⁶ cells· 24 h in L-02/Neo cells. Moreover, more than ten weeks later the levels of hIL-2 could rise to 27 500 pg/10⁶ cells· 24 h.

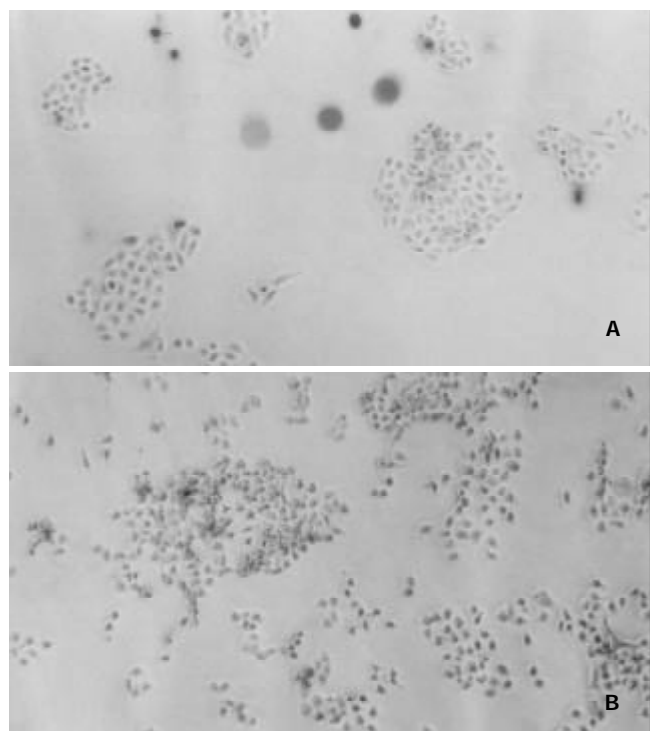


Figure 2 Morphological changes of cultured L-02/IL-2 and L-02 cells at 24 hours (×100). A: L-02/IL-2 cells; B: L-02 cells

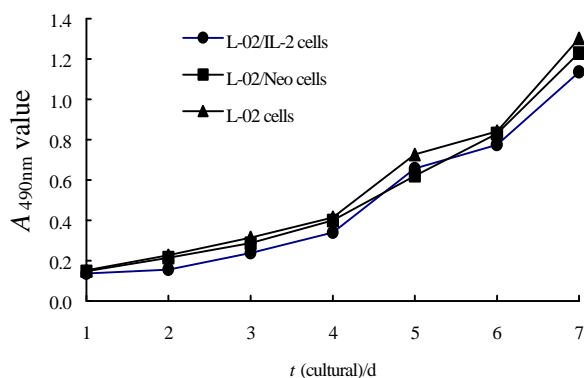


Figure 3 The growth curves of L-02/IL-2, L-02/Neo and L-02 cells

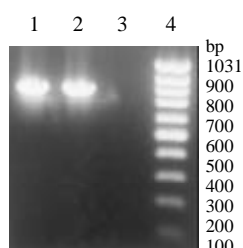


Figure 4 Integration of NeoR gene into L-02 cells' genomic DNA by PCR. 1: L-02/IL-2 cells; 2: L-02/Neo cells; 3: L-02 cells; 4: PCR DNA marker

Table 1 The clonogenicity rate of L-02/IL-2, L-02/Neo and L-02 cells

No. of repeated wells	L-02/IL-2	L-02/Neo	L-02
1	124	148	150
2	135	144	157
3	133	154	144
4	144	141	153
5	128	166	162
6	123	152	156
Mean value	131.2(13.1%) ^b	150.8(15.1%)	153.7(15.4%)

^bP<0.01, vs L-02/Neo and L-02 cells

Morphology and proliferation of cells in culture with microcarrier

After cultivation with microcarrier for 4 h, all the cells anchored to microcarriers. At the 4th day 70 % of microcarriers were filled with cells, at the 6th day all microcarriers' s surface were full of cells or cellular mass (Figure5), at the 8th day some dead cells could be seen shedded from microcarriers. Under the electronmicroscope, L-02 and L-02/IL-2 cells had normal super-microstructure, such as integral cell membrane, affluent mitochondria, glycogen and rough endoplasmic reticulum (Figure 6); 3) L-02 and L-02/IL-2 began an exponential growth after two days in culture. At the 6th day, the number of alive L-02 was 17.1±0.76×10⁶/flask and L-02/IL-2 was 16.8±0.53×10⁶/flask. At the day of 10, the number of alive cells were 6.1±0.34×10⁶/flask and 5.9±0.52×10⁶/flask, respectively.



Figure 5 Hepatocytes-anchored microcarriers linked in mass(×200)

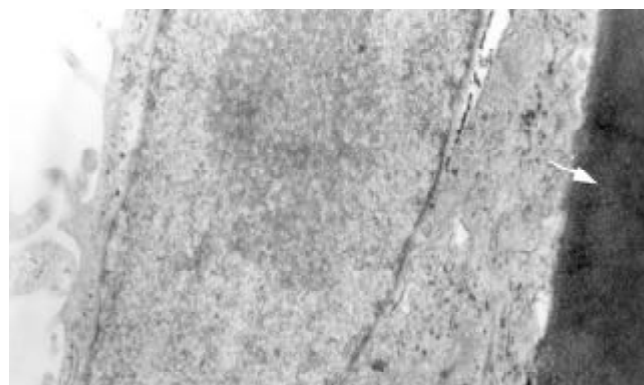


Figure 6 Hepatocyte with normal super-microstructures tightly anchors microcarrier (↑) (×15 000)

Values of biochemical items and IL-2 in the supernatant

The trend levels of ALB and UREA of L-02/IL-2 cells were consistent with the cell proliferation. The values reached the peak at the 6th day and decreased with growing cell death. The

Table 2 Values of biochemical items and IL-2 in supernatant of L-02/IL-2 cells cultured with microcarrier

	Cultivation of day					
	0	2	4	6	8	10
ALB(mg/L)						
L-02	0	8.58±0.30	25.01±0.50	53.81±1.64	39.13±1.22	12.16±0.68
L-02/IL-2	0	8.23±0.39	26.14±0.33	52.54±1.28	40.42±1.15	11.87±0.51
UREA(mmol/L)						
L-02	0.64±0.03	0.90±0.06	2.45±0.14	5.35±0.13	2.92±0.11	1.15±0.07
L-02/IL-2	0.60±0.05	0.85±0.03	2.57±0.23	5.29±0.17	2.93±0.14	1.08±0.09
AST(IU/L)						
L-02	1.0±0.58	3.3±0.75	14.0±0.58	17.6±0.98	46.6±1.62	70.3±1.80
L-02/IL-2	1.0±0.43	3.5±0.93	15.1±0.65	18.6±0.72	47.0±1.69	72.1±2.04
LDH(IU/L)						
L-02	15.9±0.69	25.3±0.95	63.0±1.41	87.4±2.07	522±11.7	687±13.4
L-02/IL-2	14.5±0.62	25.0±1.05	64.6±1.57	88.7±2.35	534±14.6	694±15.7
IL-2 (pg/L)						
L-02	0	<10	33.2±2.6	78.3±3.5	43.6±3.1	21.7±1.8
L-02/IL-2	0	6 456±373 ^b	23 765±688 ^b	52 180±1483 ^b	38 643±1104 ^b	4 360±587 ^b

^b $P < 0.001$, vs L-02 cells.

levels of AST and LDH elevated slowly before the 6th day and rapidly increased with the cell death after the peak of growth. These data had not significantly changed as compared with L-02 cells. However, the levels of IL-2 in IL-2/L-02 cells remarkably exceeded that in L-02 cells in the whole cultural process ($P < 0.001$) (Table 2).

DISCUSSION

IL-2, an important regulatory factor in immune network, can induce proliferation of T cell and enhance the immune response function of T cell, B cell, NK cell and monocytes. It plays an important role in antitumor and antiinfection immune function in the body^[15-17]. As one of the most therapeutically effective genes, IL-2 gene has been transduced into a varieties of cells in research^[8,12,18]. Recently, there were some reports about direct injection of viral vector that expressed IL-2 gene for therapy of hepatocarcinoma^[7]. Worldwide, 80 % of gene-therapy projects that were applied clinically with approval were using retroviral vector, for example, LNCX, LXCN, LXSNSX, etc.^[19,20]. LNCX, which contained the immediate early promoter of human cytomegalovirus (CMV), was not limited by cell type or animal species and it was more powerful than the other types of enhancer^[21]. In our study, LNCX, and its derivation LNCIL-2 were transduced into human hepatocyte line L-02. Clonogenicity rate of the L-02 /IL-2 cells were obviously lower than that of L-02/Neo cells and L-02 cells, due to the change of function of IL-2 as an inhibited signal in cell proliferation. The levels of IL-2 in supernatant of L-02/IL-2 cells were remarkably higher than that of L-02/Neo cells and L-02 cells, and the L-02/IL-2 cells could secrete IL-2 for more than ten weeks. These data showed that IL-2 gene was successfully integrated into the genome of L-02 cells.

Highly differentiated liver cell line were easy to proliferate in culture *in vitro*, and had many features of normal hepatocyte, so the construction of hepatocyte line is a very significant subject^[22]. Japanese scholars had constructed immortalized hepatocyte lines and used them for hepatocyte transplantation and bioartificial liver system with high efficacy^[23-26]. In this study, the hepatocyte line we used, L-02, was histologically originated from normal human liver tissue and immortalized. High levels of ALB and UREA reflected the cell's good

biological activity in protein synthesis and amino acid metabolism. When IL-2 gene was inserted, these characteristics were not notably changed.

As a alternative for amplifying the number of cells, the technique of cultivation with microcarrier is increasingly playing an important role in bio-engineering. For example, researchers can use it to produce monoclonal antibody^[27], hormone^[28], vaccine^[29], cytokine^[30] and even viral vector for gene therapy^[31], and moreover use it to culture hepatocyte for bioartificial liver system^[32,33] or hepatocyte transplantation^[34,35] for clinical use. Regardless of the type of liver cell, two requirements must be considered: First, the number of cell is adequate and easily available. Second, the cells should form congeries, because the work of hepatocytes depends on the contact between the cells or cell and the matrix. With charges-free, Cytodex3, formed by chemically coupling a thin layer of denatured collagen to the cross-linked dextran matrix, has a good adhesive character. So Cytodex3 became the core of hepatocyte aggregation and gradually formed the matrix-induced liver cell aggregates (MILCA)^[36].

The significances of construction of L-02/IL-2 cell are as follow. Theoretically, if hepatocytes modified by IL-2 gene can be transplanted into a patient with HCC who is subjected to operation, these cells might provide some functions of hepatocyte as well as antitumor immune function of IL-2 that can induce the regression of cancer cells and inhibit the metastasis, due to the activation of T-cell and other effector cells. Of course, the immune rejection of transplantation should be taken into account, two strategies are available. (1) The fetal hepatocytes, which are poor in immunogenicity and susceptible to retrovirus^[25,37], can be selected to be transfected by target-gene and cultured with microcarrier. (2) Microencapsular technique can be used to encapsule transgenetically immortalized hepatocytes, realizing the continuous expression of exogenous gene^[38,39], which can be testified by further animal experimentation.

REFERENCES

- 1 **Strauss M.** Liver-directed gene therapy: prospects and problems. *Gene Ther* 1994; **1**: 156-164
- 2 **Raper SE.** Hepatocyte transplantation and gene therapy. *Clin Transplant* 1995; **9**: 249-254

- 3 **Ojeifo JO**, Su N, Ryan US, Verma UN, Mazumder A, Zwiebel JA. Towards endothelial-cell-directed cancer immunotherapy: in vitro expression of human recombinant cytokine genes by human and mouse primary endothelial cells. *Cytokines Mol Ther* 1996; **2**: 89-101
- 4 **Tang ZY**. Hepatocellular carcinoma-cause, treatment and metastasis. *World J Gastroenterol* 2001; **7**: 445-454
- 5 **Tang YC**, Li Y, Qian GX. Reduction of tumorigenicity of SMMC-7721 hepatoma cells by vascular endothelial growth factor antisense gene therapy. *World J Gastroenterol* 2001; **7**: 22-27
- 6 **Wang Z**, Qiu SJ, Ye SL, Tang ZY, Xiao X. Combined IL-12 and GM-CSF gene therapy for murine hepatocellular carcinoma. *Cancer Gene Ther* 2001; **8**: 751-758
- 7 **Barajas M**, Mazzolini G, Genova G, Bilbao R, Narvaiza I, Schmitz V, Sangro B, Melero I, Qian C, Prieto J. Gene therapy of orthotopic hepatocellular carcinoma in rats using adenovirus coding for interleukin 12. *Hepatology* 2001; **33**: 52-61
- 8 **Hirschowitz EA**, Naama HA, Evoy D, Lieberman MD, Daly J, Crystal RG. Regional treatment of hepatic micrometastasis by adenovirus vector-mediated delivery of interleukin-2 and interleukin-12 cDNAs to the hepatic parenchyma. *Cancer Gene Ther* 1999; **6**: 491-498
- 9 **Kim JH**, Gong SJ, Yoo NC, Lee H, Shin DH, Uhm HD, Jeong SJ, Cho JY, Rha SY, Kim YS, Chung HC, Roh JK, Min JS, Kim BS. Effects of interleukin-2 transduction on the human hepatoma cell lines using retroviral vector. *Oncol Rep* 1999; **6**: 49-54
- 10 **Bui LA**, Butterfield LH, Kim JY, Ribas A, Seu P, Lau R, Glaspy JA, McBride WH, Economou JS. *In vivo* therapy of hepatocellular carcinoma with a tumor-specific adenoviral vector expressing interleukin-2. *Hum Gene Ther* 1997; **8**: 2173-2182
- 11 **Caruso M**, Pham-Nguyen K, Kwong YL, Xu B, Kosai KI, Finegold M, Woo SL, Chen SH. Adenovirus-mediated interleukin-12 gene therapy for metastatic colon carcinoma. *Proc Natl Acad Sci USA* 1996; **93**: 11302-11306
- 12 **Huang H**, Chen SH, Kosai K, Finegold MJ, Woo SL. Gene therapy for hepatocellular carcinoma: long-term remission of primary and metastatic tumors in mice by interleukin-2 gene therapy *in vivo*. *Gene Ther* 1996; **3**: 980-987
- 13 **Sambrook J**, Fritsch EF, Maniatis T. Molecular cloning: A laboratory manual, 2nd edition. *Cold spring harbor* 1996: 55
- 14 **Byun J**, Kim JM, Kim SH, Yim J, Robbins PD, Kim S. A simple and rapid method for the determination of recombinant retrovirus titer by G418 selection. *Gene Ther* 1996; **3**: 1018-1020
- 15 **Correale P**, Campoccia G, Tsang KY, Micheli L, Cusi MG, Sabatino M, Bruni G, Sestini S, Petrioli R, Pozzessere D, Marsili S, Fanetti G, Giorgi G, Francini G. Recruitment of dendritic cells and enhanced antigen-specific immune reactivity in cancer patients treated with hr-GM-CSF (Molgramostim) and hr-IL-2. results from a phase Ib clinical trial. *Eur J Cancer* 2001; **37**: 892-902
- 16 **Zheng N**, Ye SL, Sun RX, Zhao Y, Tang ZY. Effects of cryopreservation and phenylacetate on biological characters of adherent LAK cells from patients with hepatocellular carcinoma. *World J Gastroenterol* 2002; **8**: 233-236
- 17 **Chen B**, Timiryasova TM, Gridley DS, Andres ML, Dutta-Roy R, Fodor I. Evaluation of cytokine toxicity induced by vaccinia virus-mediated IL-2 and IL-12 antitumor immunotherapy. *Cytokine* 2001; **15**: 305-314
- 18 **Cao XT**, Zhang WP, Tao Q. Enhanced immune functions and antitumor activity of fibroblast-mediated interleukin-2 gene therapy. *Zhonghua Yixue Zazhi* 1995; **75**: 521-524
- 19 **Wang X**, Liu FK, Li X, Li JS, Xu GX. Inhibitory effect of endostatin expressed by human liver carcinoma SMMC7721 on endothelial cell proliferation in vitro. *World J Gastroenterol* 2002; **8**: 253-257
- 20 **Fakhrai H**, Shawler DL, Van Bevern C, Lin H, Dorigo O, Solomon MJ, Gjerset RA, Smith L, Bartholomew RM, Boggiano CA, Gold DP, Sobol RE. Construction and characterization of retroviral vectors for interleukin-2 gene therapy. *J Immunother* 1997; **20**: 437-448
- 21 **Boshart M**, Weber F, Jahn G, Dorsch-Hasler K, Fleckenstein B, Schaffner W. A very strong enhancer is located upstream of an immediate early gene of human cytomegalovirus. *Cell* 1985; **41**: 521-530
- 22 **Cascio SM**. Novel strategies for immortalization of human hepatocytes. *Artif Organs* 2001; **25**: 529-538
- 23 **Kobayashi N**, Noguchi H, Fujiwara T, Westerman KA, Leboulch P, Tanaka N. Establishment of a highly differentiated immortalized adult human hepatocyte cell line by retroviral gene transfer. *Transplant Proc* 2000; **32**: 2368-2369
- 24 **Kobayashi N**, Miyazaki M, Fukaya K, Inoue Y, Sakaguchi M, Noguchi H, Matsumura T, Watanabe T, Totsugawa T, Tanaka N, Namba M. Treatment of surgically induced acute liver failure with transplantation of highly differentiated immortalized human hepatocytes. *Cell Transplant* 2000; **9**: 733-735
- 25 **Kobayashi N**, Noguchi H, Watanabe T, Matsumura T, Totsugawa T, Fujiwara T, Tanaka N. Role of immortalized hepatocyte transplantation in acute liver failure. *Transplant Proc* 2001; **33**: 645-646
- 26 **Kobayashi N**, Noguchi H, Watanabe T, Matsumura T, Totsugawa T, Fujiwara T, Tanaka N. A tightly regulated immortalized human fetal hepatocyte cell line to develop a bioartificial liver. *Transplant Proc* 1999; **31**: 1948-1949
- 27 **Voigt A**, Zintl F. Hybridoma cell growth and anti-neuroblastoma monoclonal antibody production in spinner flasks using a protein-free medium with microcarriers. *J Biotechnol* 1999; **68**: 213-226
- 28 **Hamid M**, McCluskey JT, McClenaghan NH, Flatt PR. Culture and function of electrofusion-derived clonal insulin-secreting cells immobilized on solid and macroporous microcarrier beads. *Biosci Rep* 2000; **20**: 167-176
- 29 **Junker BH**, Wu F, Wang S, Waterbury J, Hunt G, Hennessey J, Aunins J, Lewis J, Silberklang M, Buckland BC. Evaluation of a microcarrier process for large-scale cultivation of attenuated hepatitis A. *Cytotechnology* 1992; **9**: 173-187
- 30 **Bing RJ**, Dudek R, Kahler J, Narayan KS, Ingram M. Cytokine production from freshly harvested human mononuclear cells attached to plastic beads. *Tissue Cell* 1992; **24**: 203-209
- 31 **Wu SC**, Huang GY, Liu JH. Production of retrovirus and adenovirus vectors for gene therapy: a comparative study using microcarrier and stationary cell culture. *Biotechnol Prog* 2002; **18**: 617-622
- 32 **Gao Y**, Xu XP, Hu HZ, Yang JZ. Cultivation of human liver cell lines with microcarriers acting as biological materials of bioartificial liver. *World J Gastroenterol* 1999; **5**: 221-224
- 33 **Suh KS**, Lilja H, Kamohara Y, Eguchi S, Arkadopoulos N, Neuman T, Demetriou AA, Rozga J. Bioartificial liver treatment in rats with fulminant hepatic failure: effect on DNA-binding activity of liver-enriched and growth-associated transcription factors. *J Surg Res* 1999; **85**: 243-250
- 34 **Demetriou AA**, Levenson SM, Novikoff PM, Novikoff AB, Chowdhury NR, Whiting J, Reisner A, Chowdhury JR. Survival, organization, and function of microcarrier-attached hepatocytes transplanted in rats. *Proc Natl Acad Sci USA* 1986; **83**: 7475-7479
- 35 **Nyberg SL**, Peshwa MV, Payne WD, Hu WS, Cerra FB. Evolution of the bioartificial liver: the need for randomized clinical trials. *Am J Surg* 1993; **166**: 512-521
- 36 **Kong LB**, Chen S, Demetriou AA, Rozga J. Matrix-induced liver cell aggregates (MILCA) for bioartificial liver use. *Int J Artif Organs* 1996; **19**: 72-78
- 37 **Koch KS**, Brownlee GG, Goss SJ, Martinez-Conde A, Leffert HL. Retroviral vector infection and transplantation in rats of primary fetal rat hepatocytes. *J Cell Sci* 1991; **99**: 121-130
- 38 **Aoki K**, Hakamada K, Umehara Y, Seino K, Itabashi Y, Sasaki M. Intra-peritoneal transplantation of microencapsulated xenogeneic hepatocytes in totally hepatectomized rats. *Transplant Proc* 2000; **32**: 1118-1120
- 39 **Umehara Y**, Hakamada K, Seino K, Aoki K, Toyoki Y, Sasaki M. Improved survival and ammonia metabolism by intra-peritoneal transplantation of microencapsulated hepatocytes in totally hepatectomized rats. *Surgery* 2001; **130**: 513-520

Effects of p16 gene on biological behaviour in hepatocellular carcinoma cells

Jian-Zhao Huang, Sui-Sheng Xia, Qi-Fa Ye, Han-Ying Jiang, Zhong-Hua Chen

Jian-Zhao Huang, Department of Hepatobiliary Surgery, DaPing Hospital, Third Military Medical University, Chongqing 400042, China
Sui-Sheng Xia, Qi-Fa Ye, Han-Ying Jiang, Zhong-Hua Chen, Institute of Organ Transplantation, Tong Ji Hospital, School of Medicine, Hua Zhong University of Science and Technology, Wuhan 430030, Hubei Province, China

Correspondence to: Dr. Jian-Zhao Huang, Department of Hepatobiliary Surgery, Daping Hospital, 10 Chang Jiang Road, Chongqing 400042, China. hjz999@mail.tmmu.com.cn

Telephone: +86-23-68757247

Received: 2002-06-11 **Accepted:** 2002-07-12

Abstract

AIM: To investigate the effects of p16 gene on biological behaviour in hepatocellular carcinoma cells.

METHODS: HCC cell lines SNU-449 and HepG2.2.15 were infected respectively by a replication defective, recombinant retrovirus capable of producing a high level of p16 protein expression (pCLXSN-p16). G418 resistant stable P16 protein expression cell lines were selected. And the biological behaviours of the p16 gene transfected HCC cells were observed.

RESULTS: Initial *in vitro* experiments in HCC cell line SNU-449 with loss of p16 protein expression demonstrated the pCLXSN-p16 treatment significantly inhibited cell growth. But there was no treatment effect when the pCLXSN-p16 was used in another HCC cell line HepG2.2.15 which has positive p16 protein expression. Subsequent study in a nude mouse model demonstrated that the p16 gene transfected SNU-449 had a lower succeeding rate in the first time establishment of tumors and grew more slowly in the nude mice when compared with non-transfected SNU-449. Moreover, the nude mice inoculated with transfected SNU-449 had a longer surviving time than those inoculated with non-transfected SNU-449.

CONCLUSION: Our results show that the p16INK4a gene transfer can inhibit the proliferation and reduce the invasion ability of hepatocellular carcinoma.

Huang JZ, Xia SS, Ye QF, Jiang HY, Chen ZH. Effects of p16 gene on biological behaviour in hepatocellular carcinoma cells. *World J Gastroenterol* 2003; 9(1): 84-88

<http://www.wjgnet.com/1007-9327/9/84.htm>

INTRODUCTION

Hepatocellular carcinoma (HCC) is a common malignant tumor with a increasing incidence^[1], and the treatment has been extremely difficult. HCCs are generally highly resistant to chemotherapeutic agents and radiotherapy. Despite a variety of treatment options including surgical resection, chemoembolization, percutaneous injection of ethanol or acetic acid, and liver transplantation, the prognosis of HCC patients is poor^[2]. Thus, new treatment strategies are necessary

to improve the survival rate. It is believed that molecular changes that occur during carcinogenesis, such as overexpression of the multidrug resistant gene and the loss of tumor suppressor genes may allow many kinds of tumor cell populations to become resistant to most therapeutic approaches. Gene therapy may offer certain advantages in the treatment of HCC.

P16 gene encoded for a protein that was initially identified as a specific inhibitor of the CDKs, CDK4 and CDK6. By binding to and inhibiting CDK4 and CDK6, p16 prevents both pRb phosphorylation and subsequent progression into the S phase of the cell cycle. P16 gene alterations were found in many kinds of cancers^[3-13]. Our previous study has showed that the frequency of P16 gene inactivation was high (36 %)^[14] in HCC. Other's Reports have also showed frequent P16 gene inactivations^[15-21]. Thus, P16 gene may be an ideal candidate for the treatment of HCC. In this study, we constructed the retrovirus p16 expression vector and then investigated whether it could control the proliferation of HCC cell lines.

MATERIALS AND METHODS

P16 cDNA subcloning and construction of pCLXSN-p16

The original P16 cDNA was amplified from the total RNA of normal human lymphocytes by reverse transcription PCR. The PCR product was subcloned into pCLXSN expression vector, a deficient retrovirus vector which derived from pLXSN (IMAGENEX). Then the recombinant p16 expression vector was cotransfected with the pCL-Ampho packaging construct into 293 cells by using a modification of the HEPES-buffered saline calcium phosphate method^[22]. Two days after infection the 293 cells were placed under G418 selection (800 µg/ml) and grew for 10 days. Then the G418 resistant 293 cells were amplified and the supernatant which contained the pCLXSN-p16 pseudo retrovirus were collected and filtered through a 0.45 µm pore size filter. The pseudo retroviruses were tited through infecting NIH 3T3 cells^[22]. We also packaged a reporter gene expression vector pCLMFG-LacZ as a control. The viral titer was 1.6×10⁵CFU/ml.

Cell lines

Human HCC cell lines SNU-449 (with loss of p16 expression) and HepG2.2.15 (with p16 expression) were kindly provided by Dr. Zhang Mingyi (Tumor Hospital of Sichuan Province, Chengdu, China,) and Dr. Gao Yong (the Union Hospital, Tong Ji Medical University, Wuhan, China) respectively. They were grown in RPMI 1640 containing 10 % fetal bovine serum.

Infection of retroviral vectors and selection of stable expression cell lines

SNU-449 and HepG2.2.15 cell lines were seeded and cultured in two 6 cm plates at a density of 2×10⁵ cells for 24hs respectively. Immediately before infection, the culture medium was replaced and 1 ml viral supernatant of pCLXSN-p16 or pCLMFG-LacZ (control) was added. Then the polybrene was added to the medium in 8 µg/ml. The infected cells were grown for 24hs and split into 10 cm plates at 1:10 dilution, then grown in the medium containing G418 in 800 µg/ml. The

medium was replaced every 3-4 days and the G418 resistant cells were selected and named SNU-449/pCLXSN-p16, HepG2.2.15/pCLXSN-p16, SNU-449/pCLMFG-LacZ and HepG2.2.15/pCLMFG-LacZ, respectively.

Immunohistochemical analysis and western blotting

SNU-449 cells were collected 24hs after infected by pCLXSN-p16. The stable G418 resistant SNU-449/pCLXSN-p16 cells were also collected. Both of them were examined for p16 expression immunohistochemically by the labeled streptavidin-biotin method. The SNU-449/pCLXSN cells were also screened for p16 expression by Western blotting. The cells for immunochemical analysis were grown on the glass slides.

Immunohistochemical detection procedure was carried out according to the manufacture's recommendations. Western blotting was performed as previously described^[23].

Growth curves

The effect of p16 expression on cell growth was examined in all six cell lines, including SNU-449, SNU-449/pCLXSN-p16, SNU-449/pCLMFG-LacZ, HepG2.2.15, HepG2.2.15/pCLXSN-p16, and HepG2.2.15/pCLMFG-LacZ. Triplicate samples of log phase cells were seeded at a density of 1×10^4 in 6 holes culture plates. Cells were harvested for counting by digestion with trypsin/EDTA for 3 min, followed by the addition of fresh media to inhibit further digestion. Cells were then pelleted by centrifugation at 1000rpm for 5 min, followed by resuspension in fresh media. Triplicate sets of cells were counted at 1, 3 and 5 days after seeded. The mean cell number for each harvesting was calculated, and cell growth curves were determined.

Cell cycle and apoptosis analysis

The effect of pCLXSN-p16 expression on cell cycle dynamics and cell apoptosis was examined in both the SNU-449/pCLXSN-p16 and HepG2.2.15/pCLXSN-p16 cell lines using FACS analysis. In the meanwhile, the cell cycle distribution and apoptosis analysis of SNU-449, SNU-449/pCLMFG-LacZ and HepG2.2.15 cells were also examined for controls. Briefly, 1×10^6 cells of each cell line were collected by centrifugation at 1000 rpm for 5 min, followed by two washes in ice-cold PBS. Cells were then fixed in 2.0 ml of 70 % ethanol and stored at 4 °C for a minimum of 1 h. Prior to FACS analysis, cells were washed twice with ice-cold PBS, and the cell pellet was resuspended in 10 µg/ml of propidium iodide (Sigma Chemical Co.). Add 100 µg/ml of RNase (Sigma Chemical Cop.) and incubated at 37 °C for 30 min. Then the FACS analysis was performed.

In vivo studies

Nude mice were used at the weight of 23-27 grams. Log phase SNU-449/pCLXSN-p16 and SNU-449 cells were harvested and centrifuged at 1000 rpm for 5 min, then resuspended in 0.9 % salt solution at 1×10^8 , respectively. Cells were immediately implanted subcutaneously into the right flank of nude mice (1×10^7 cells for each animal). Tumor formation and subsequent growth were monitored. The tumor volume at 23 days after implantation and the survival rate of the mice at 52 days after implantation were also observed. Statistical significance was assessed by Mann-Whitney statistical analysis (Statmost for windows).

RESULTS

Detection of p16 protein expression

SNU-449 cells exhibited a loss of p16 protein expression (Figure 1), and HepG2.2.15 cells showed positive p16 staining. About 20 % SNU-449 cells showed positive p16 staining 24 hours after infected by pCLXSN-p16 pseudo virus. All the

G418 resistant SNU-449/pCLXSN-p16 cells exhibited p16 protein expression (Figure 2). Western blot analysis also confirmed that SNU-449 cells showed loss of p16 protein expression and SNU-449/pCLXSN-p16 cells could express p16 protein (Figure 3).

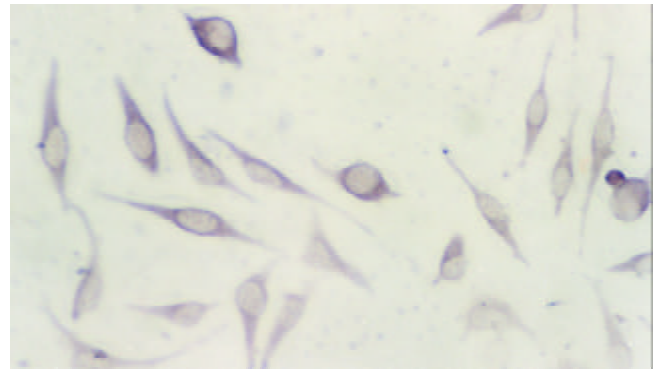


Figure 1 SNU-449 cells show negative p16 staining (original magnification $\times 400$).

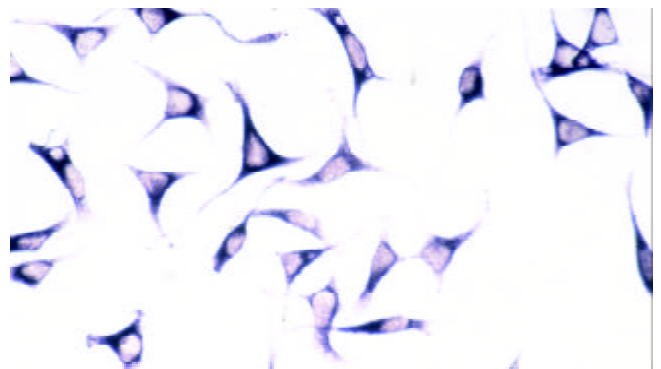


Figure 2 SNU-449/pCLXSN-p16 cells show positive p16 staining (original magnification $\times 200$).

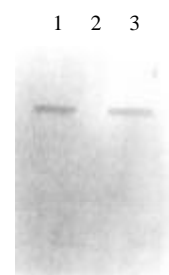


Figure 3 Western blot analysis. Lanes 1 and 3: SNU-449/pCLXSN-p16 cells; Lane 2: SNU-449 cells.

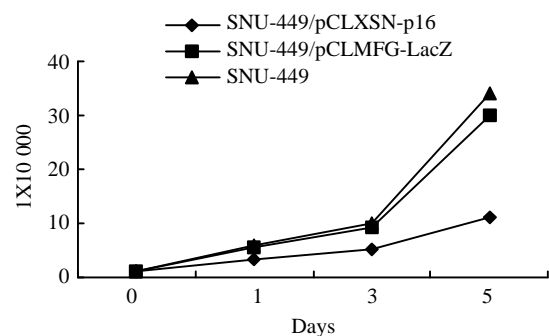


Figure 4 *In vitro* growth curves of SNU-449/pCLXSN-p16, SNU-449/pCLMFG-LacZ and SNU-449 cell lines.

Cell growth curves

As shown in Figure 4, *in vitro* growth rates of SNU-449/pCLXSN-p16 cell line, a selected stable p16 protein expression cell line, were significantly inhibited when compared with cell lines SNU-449 and SNU-449/pCLMFG-LacZ in which p16 protein expression was lost. Nearly equal growth rates were observed in both HepG 2.2.15 and HepG 2.2.15/pCLXSN-p16 cell lines.

Cell cycle distribution and cell apoptosis status

The underlying mechanism of *in vitro* growth inhibition seen in the pCLXSN-p16 treated cell line SNU-449/pCLXSN-p16 was investigated by cell cycle analysis using flow cytometry. As shown in table 1, SNU-449/pCLXSN-p16 cell line exhibited significant increase in the percentage of cells in G₀-G₁ phase (68%), consistent with a cell cycle arrest at the G₁ transition when compared with cell lines SNU-449 and SNU-449/pCLMFG-LacZ. However there was no obvious cell cycle difference between cell lines HepG2.2.15/pCLXSN-p16 and HepG2.2.15.

Table 1 Cell cycle analysis

Cell type	Cell cycle(%)		
	G ₀ -G ₁	G ₂ -M	S
SNU-449	37	36	27
SNU-449/pCLXSN-p16	68	21	11
SNU-449/pCLMFG-LacZ	39	38	23
HepG2.2.15	29	42	29
HepG2.2.15/pCLXSN-p16	32	43	25

Cell apoptosis analysis was performed in cell lines SNU-449, SNU-449/pCLXSN-p16, HepG2.2.15 and HepG2.2.15/pCLXSN-p16 and showed no difference between these cell lines.

Effects of pCLXSN-p16 treatment on HCC tumor growth in vivo

The therapeutic potential of pCLXSN-p16 to treat HCC tumors *in vivo* was studied in nude mice. Tumors were created by injecting 1×10⁷ SNU-449 or SNU-449/pCLXSN-p16 cells in 100 μl 0.9% salt solution into the right flank of nude mice as described above. The succeed rate of tumor establishment at the first time injection of tumor cells SNU-449/pCLXSN-p16 in nude mice was 70% (7/10). At the same time only 40% (4/10) nude mice succeeded to establish tumors at the first time injection of SNU-449 cells. Animals who were succeeded to establish tumors were observed over a period of 52 days from the day of injecting tumor cells. During the observing period animals injected with SNU-449/pCLXSN-p16 cell line survived significantly longer than those injected with SNU-449 (*P*<0.05). The mean survival time of animals injected with SNU-449/pCLXSN-p16 and SNU-449 were 42.1±9 days and 32.7±6.7 days, respectively (Table 2). The survival rate of nude mice injected with SNU-449/pCLXSN-p16 cell line was higher than that of those injected with SNU-449. Figure 5 was the survival curves of nude mice injected with cell lines SNU-449/pCLXSN-p16 and SNU-449, respectively.

Two groups of nude mice with each of 6 animals were established with tumors by injection of cell lines SNU-449/pCLXSN-p16 and SNU-449, respectively and were observed for a period of 23 days. All the animals survived during the observing period. At 23th day after injection of tumor cells they were all sacrificed for measurement of tumor volumes. The tumor volume in nude mice injected with SNU-449/

pCLXSN-p16 was 234±125 mm³, significantly smaller than that in those injected with SNU-449 cell line (726±513 mm³).

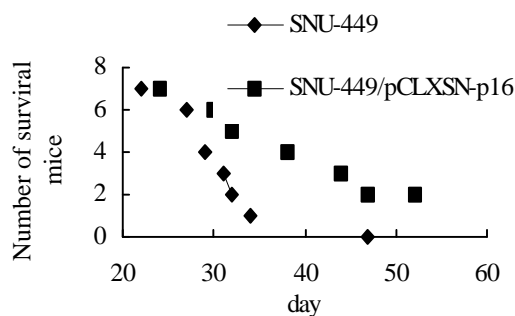


Figure 5 Survival curves of nude mice.

Table 2 The survival time and survival rate of nude mice

Group	animal number	survival time(d)	survival rate
Salt solution	5	52.0±0.0	100%
SNU-449	7	32.7±6.7	0%
SNU-449/pCLXSN-p16	7	42.1±9.0 ^a	28.6%

^a*P*<0.05 Compared with group SNU-449

DISCUSSION

The hypothesis that the inactivation or loss of certain genes, specially tumor suppressor genes, leads to both tumor growth and progression is now well established and provides a unique opportunity in cancer gene therapy. The decision to use p16 gene as a therapeutic agent against human hepatocellular carcinoma was based on our earlier work where we had found p16 gene was frequently inactivated in HCCs^[14]. In the fact, P16 gene was widely used in the study of tumor gene therapy and showed obvious tumor suppressing effects in many kinds of tumors^[23-31]. In the present study we cloned human p16 cDNA and constructed a replication-defective, recombinant retrovirus that express high levels of the tumor suppressor protein p16.

The pCLXSN vector was modified from pLXSN vector. It's more safe and can produce higher titers of retrovirus when cotransfected with the pCL-Ampho packaging construct into 293 cells than its' prototype pLXSN. It permits the expression of a number of cell cycle-regulatory proteins such as p16 that are otherwise difficult to study in retroviruses because of their potent cytostatic or cytotoxic effects^[22]. In this study we cotransfected a report gene LacZ expression vector pLMFG-LacZ and packaging constructs pCL-Ampho into 293 cells. The transfecting efficiency was determined and only 1% (data not shown), much lower than reported 30%^[15]. Considering the lower transfecting efficiency we selected a stable virus-producing cell lines after the p16 protein expression vector pCLXSN-p16 was cotransfected with pCL-Ampho into 293 cells. The titer of pCLXSN-p16 retrovirus produced by the stable virus-producing cell line was determined to be 1.6×10⁵CFU/ml. It is much lower than reported 5×10⁵-2×10⁶^[22]. Only 20% SNU-449 cells showed positive p16 protein expression 24hs after infected by the pCLXSN-p16 pseudo retroviruses. We then determined to select a SNU-449 cell line which stably expresses p16 protein after infected by the pCLXSN-p16 and use it to study the treatment effect of p16 gene transfer to the HCC cells.

Initial *in vitro* experiments demonstrated that the reintroduction of p16 gene significantly inhibited cell growth

by inducing G1-S cell cycle arrest in the SNU-449 HCC cell line in which p16 gene was originally inactivated. In contrast, no inhibition of cell growth was found when wild type p16 gene was transfected into another HCC cell line HepG2.2.15 in which p16 protein was normally expressed. This suggested that inactivation of p16 gene and its downstream gene may contributed to the carcinogenesis of HCC. Our results were similar to others' reports about treatment study of some tumors using p16 gene transfer^[32-35]. No changes of tumor cell apoptosis were found when wild type p16 gene was introduced to cell lines SNU-449 or HepG2.2.15. This suggested that introduction of p16 gene may not cause apoptosis of HCC cells.

Subsequent *in vivo* studies showed that the first time establishment of tumors in nude mice was more difficult using p16 gene treated SNU-449 cells (SNU-449/pCLXSN-p16) than using the cells without treatment. This suggested that reintroduction of p16 gene could reduce the invasion ability of HCC tumor cells. Further observation demonstrated that reintroduction of p16 gene into tumor cells significantly inhibited tumor growth rate in tumor-established animals and extended the survival time and survival rate of these animals during the observing period. The results of *in vitro* and *in vivo* study were consistent.

Our results support the use of retrovirus-mediated p16 gene treatment for HCC and provide an important foundation from which to build future preclinical studies and initiate future human clinical trials. If pCLXSN-p16 is proved to be effective in the clinical setting, it will offer a much useful addition to present therapeutic regimens. PCLXSN-p16 may potentially develop into an important adjuvant therapy, expedient in treating unresectable HCC or microscopic residual disease after surgical resection. However, the titer of pCLXSN-p16 pseudo retrovirus must be boosted in the future studies.

REFERENCES

- Ince N**, Wands JR. The increasing incidence of hepatocellular carcinoma. *N Engl J Med* 1999; **340**: 798-799
- Bruix J**. Treatment of hepatocellular carcinoma. *Hepatology* 1997; **25**: 259-262
- He XS**, Su Q, Chen ZC, He XT, Long ZF, Ling H, Zhang LR. Expression, deletion [was deletion] and mutation of p16 gene in human gastric cancer. *World J Gastroenterol* 2001; **7**: 515-521
- Yi J**, Wang ZW, Cang H, Chen YY, Zhao R, Yu BM, Tang XM. P16 gene methylation in colorectal cancers associated with Duke's staging. *World J Gastroenterol* 2001; **7**: 722-725
- Liu LH**, Xiao WH, Liu WW. Effect of 5-Aza-2'-deoxycytidine on the P16 tumor suppressor gene in hepatocellular carcinoma cell line HepG2. *World J Gastroenterol* 2001; **7**: 131-135
- Simon M**, Park TW, Koster G, Mahlberg R, Hackenbroch M, Bostrom J, Loning T, Schramm J. Alterations of INK4a(p16-p14ARF)/INK4b(p15) expression and telomerase activation in meningioma progression. *J Neurooncol* 2001; **55**: 149-158
- Hibi K**, Taguchi M, Nakayama H, Takase T, Kasai Y, Ito K, Akiyama S, Nakao A. Molecular detection of p16 promoter methylation in the serum of patients with esophageal squamous cell carcinoma. *Clin Cancer Res* 2001; **7**: 3135-3138
- Sanchez-Beato M**, Saez AI, Navas IC, Algara P, Sol-Mateo M, Villuendas R, Camacho F, Sanchez-Aguilera A, Sanchez E, Piris MA. Overall survival in aggressive B-cell lymphomas is dependent on the accumulation of alterations in p53, p16, and p27. *Am J Pathol* 2001; **159**: 205-213
- Bazan V**, Zanna I, Migliavacca M, Sanz-Casla MT, Maestro ML, Corsale S, Macaluso M, Dardanoni C, Restivo S, Quintela PL, Bernaldez R, Saleno S, Morello V, Tomasino RM, Cebbia N, Russo A. Prognostic significance of p16INK4a alterations and 9p21 loss of heterozygosity in locally advanced laryngeal squamous cell carcinoma. *J Cell Physiol* 2002; **192**: 286-293
- Sato N**, Ueki T, Fukushima N, Iacobuzio-Donahue CA, Yeo CJ, Cameron JL, Hruban RH, Goggins M. Aberrant methylation of CpG islands in intraductal papillary mucinous neoplasms of the pancreas. *Gastroenterology* 2002; **123**: 365-372
- Costentin L**, Pages P, Bouisson M, Berthelemy P, Buscail L, Escourrou J, Pradayrol L, Vaysse N. Frequent deletions of tumor suppressor genes in pure pancreatic juice from patients with tumoral or nontumoral pancreatic diseases. *Pancreatol* 2002; **2**: 17-25
- Child FJ**, Scarisbrick JJ, Calonje E, Orchard G, Russell-Jones R, Whittaker SJ. Inactivation of tumor suppressor genes p15(INK4b) and p16(INK4a) in primary cutaneous B cell lymphoma. *J Invest Dermatol* 2002; **118**: 941-948
- Hasegawa M**, Nelson HH, Peters E, Ringstrom E, Posner M, Kelsey KT. Patterns of gene promoter methylation in squamous cell cancer of the head and neck. *Oncogene* 2002; **21**: 4231-4236
- Huang J**, Shen W, Li B, Luo Y, Liao S, Zhang W, Cheng N. Molecular and immunohistochemical study of the inactivation of the p16 gene in primary hepatocellular carcinoma. *Chin Med J (Engl)* 2000; **113**: 889-893
- Herath NI**, Kew MC, Walsh MD, Young J, Powell LW, Leggett BA, MacDonald GA. Reciprocal relationship between methylation status and loss of heterozygosity at the p14(ARF) locus in Australian and South African hepatocellular carcinomas. *J Gastroenterol Hepatol*, 2002; **17**: 301-307
- Roncagli M**, Bianchi P, Bruni B, Laghi L, Destro A, Di Gioia S, Gennari L, Tommasini M, Malesci A, Coggi G. Methylation framework of cell cycle gene inhibitors in cirrhosis and associated hepatocellular carcinoma. *Hepatology* 2002; **36**: 427-432
- Azechi H**, Nishida N, Fukuda Y, Nishimura T, Minata M, Katsuma H, Kuno M, Ito T, Komeda T, Kita R, Takahashi R, Nakao K. Disruption of the p16/cyclin D1/retinoblastoma protein pathway in the majority of human hepatocellular carcinomas. *Oncology* 2001; **60**: 346-354
- Liew CT**, Li HM, Lo KW, Leow CK, Lau WY, Hin LY, Lim BK, Lai PB, Chan JY, Wang XQ, Wu S, Lee JC. Frequent allelic loss on chromosome 9 in hepatocellular carcinoma. *Int J Cancer* 1999; **81**: 319-324
- Liew CT**, Li HM, Lo KW, Leow CK, Chan JY, Hin LY, Lau WY, Lai PB, Lim BK, Huang J, Leung WT, Wu S, Lee JC. High frequency of p16INK4A gene alterations in hepatocellular carcinoma. *Oncogene* 1999; **18**: 789-795
- Wong IH**, Lo YM, Zhang J, Liew CT, Ng MH, Wong N, Lai PB, Lau WY, Hjeltn NM, Johnson PJ. Detection of aberrant p16 methylation in the plasma and serum of liver cancer patients. *Cancer Res* 1999; **59**: 71-73
- Saito Y**, Kanai Y, Sakamoto M, Saito H, Ishii H, Hirohashi S. Expression of mRNA for DNA methyltransferases and methyl-CpG-binding proteins and DNA methylation status on CpG islands and pericentromeric satellite regions during human hepatocarcinogenesis. *Hepatology* 2001; **33**: 561-568
- Naviaux RK**, Costanzi E, Hass M, Verma IM. The pCL vector system: rapid production of helper-free, high-titer, recombinant retroviruses. *J Virol* 1996; **70**: 5701-5705
- Urashima M**, Teoh G, Akiyama M, Yuza Y, Anderson KC, Maekawa K. Restoration of p16INK4A protein induces myogenic differentiation in RD rhabdomyosarcoma cells. *Br J Cancer* 1999; **79**: 1032-1036
- Kim SK**, Wang KC, Cho BK, Chung HT, Kim YY, Lim SY, Lee CT, Kim HJ. Interaction between p53 and p16 expressed by adenoviral vectors in human malignant glioma cell lines. *J Neurosurg* 2002; **97**: 143-150
- Rui HB**, Su JZ. Co-transfection of p16(INK4a) and p53 genes into the K562 cell line inhibits cell proliferation. *Haematologica* 2002; **87**: 136-142
- Calbo J**, Marotta M, Cascallo M, Roig JM, Celpi JL, Fueyo J, Mazo A. Adenovirus-mediated wt-p16 reintroduction induces cell cycle arrest or apoptosis in pancreatic cancer. *Cancer Gene Ther* 2001; **8**: 740-750
- Wang TJ**, Huang MS, Hong CY, Tse V, Silverberg GD, Hsiao M. Comparisons of tumor suppressor p53, p21, and p16 gene therapy effects on glioblastoma tumorigenicity *in situ*. *Biochem Biophys Res Commun* 2001; **287**: 173-180
- Ghaneh P**, Greenhalf W, Humphreys M, Wilson D, Zumstein L, Lemoine NR, Neoptolemos JP. Adenovirus-mediated transfer of p53 and p16(INK4a) results in pancreatic cancer regression *in vitro* and *in vivo*. *Gene Ther* 2001; **8**: 199-208

- 29 **Frizelle SP**, Rubins JB, Zhou JX, Curiel DT, Kratzke RA. Gene therapy of established mesothelioma xenografts with recombinant p16INK4a adenovirus. *Cancer Gene Ther* 2000; **7**: 1421-1425
- 30 **Campbell I**, Magiocco A, Moyana T, Zheng C, Xiang J. Adenovirus-mediated p16INK4 gene transfer significantly suppresses human breast cancer growth. *Cancer Gene Ther* 2000; **7**: 1270-1278
- 31 **Kawabe S**, Roth JA, Wilson DR, Meyn RE. Adenovirus-mediated p16INK4a gene expression radiosensitizes non-small cell lung cancer cells in a p53-dependent manner. *Oncogene* 2000; **19**: 5359-5366
- 32 **Lee SH**, Kim MS, Kwon HC, Park IC, Park MJ, Lee CT, Kim YW, Kim CM, Hong SI. Growth inhibitory effect on glioma cells of adenovirus-mediated p16/INK4a gene transfer *in vitro* and *in vivo*. *Int Mol Med* 2000; **6**: 559-563
- 33 **Todd MC**, Scalfani RA, Langan TA. Ovarian cancer cells that coexpress endogenous Rb and p16 are insensitive to overexpression of functional p16 protein. *Oncogene* 2000; **19**: 258-264
- 34 **Allay JA**, Steiner MS, Zhang Y, Reed CP, Cockroft J, Lu Y. Adenovirus p16 gene therapy for prostate cancer. *World J Urol* 2000; **18**: 111-120
- 35 **Kobayashi S**, Shirasawa H, Sashiyama H, Kawahira H, Kaneko K, Asano T, Ochiai T. P16INK4a expression adenovirus vector to suppress pancreas cancer cell proliferation. *Clin Cancer Res* 1999; **5**: 4182-4185

Edited by Ma JY

Mutation analysis of novel human liver-related putative tumor suppressor gene in hepatocellular carcinoma

Cheng Liao, Mu-Jun Zhao, Jing Zhao, Hai Song, Pascal Pineau, Agnès Marchio, Anne Dejean, Pierre Tiollais, Hong-Yang Wang, Tsai-Ping Li

Cheng Liao, Mu-Jun Zhao, Jing Zhao, Hai Song, Tsai-Ping Li, State Key Laboratory of Molecular Biology, Institute of Biochemistry and Cell Biology, Shanghai Institutes for Biological Sciences, Chinese Academy of Sciences, Shanghai, 200031, China

Pascal Pineau, Agnès Marchio, Anne Dejean, Pierre Tiollais, Unité de Recombinaison et Expression Génétique, INSERM U163, Institute Pasteur, Paris, France

Hong-Yang Wang, Shanghai Eastern Hepatobiliary Surgery Hospital, Shanghai, 200433, China

Supported by a grant from National High Technology "863" Program of China, No. 2001AA221021, a grant from Special Funds for Major State Basic Research "973" of China, No. 001CB510205, a grant from the National Natural Sciences Foundation of China, No. 30170524 and Chine-France PRA dans le domaine de la Biologie 2001, No. PRA B 01-05

Correspondence to: Professor Mu-Jun Zhao, State Key Laboratory of Molecular Biology, Institute of Biochemistry and Cell Biology, Shanghai Institutes for Biological Sciences, Chinese Academy of Sciences, 320 Yueyang Road, Shanghai, 200031, China. mjzhao@sunm.shnc.ac.cn
Telephone: +86-21-64315030 Ext.5295 **Fax:** +86-21-64338357

Received: 2002-07-26 **Accepted:** 2002-08-23

Abstract

AIM: To find the point mutations meaningful for inactivation of liver-related putative tumor suppressor gene (LPTS) gene, a human novel liver-related putative tumor suppressor gene and telomerase inhibitor in hepatocellular carcinoma.

METHODS: The entire coding sequence of LPTS gene was examined for mutations by single strand conformation polymorphism (SSCP) assay and PCR products direct sequencing in 56 liver cancer cell lines, 7 ovarian cancer and 7 head & neck tumor cell lines and 70 pairs of HCC tissues samples. The cDNA fragment coding for the most frequent mutant protein was subcloned into GST fusion expression vector. The product was expressed in *E.coli* and purified by glutathione-agarose column. Telomeric repeat amplification protocol (TRAP) assays were performed to study the effect of point mutation to telomerase inhibitory activity.

RESULTS: SSCP gels showed the abnormal shifting bands and DNA sequencing found that there were 5 different mutations and/or polymorphisms in 12 tumor cell lines located at exon2, exon5 and exon7. The main alterations were A(778)A/G and A(880)T in exon7. The change in site of 778 could not be found in HCC tissue samples, while the mutation in position 880 was seen in 7 (10 %) cases. The mutation in the site of 880 had no effect on telomerase inhibitory activity.

CONCLUSION: Alterations identified in this study are polymorphisms of LPTS gene. LPTS mutations occur in HCC but are infrequent and of little effect on the telomerase inhibitory function of the protein. Epigenetics, such as methylation, acetylation, may play the key role in inactivation of LPTS.

Liao C, Zhao MJ, Zhao J, Song H, Pineau P, Marchio A, Dejean A, Tiollais P, Wang HY, Li TP. Mutation analysis of novel human liver-related putative tumor suppressor gene in hepatocellular carcinoma. *World J Gastroenterol* 2003; 9(1): 89-93
<http://www.wjgnet.com/1007-9327/9/89.htm>

INTRODUCTION

Human hepatocellular carcinoma (HCC), the predominant histological subtype of primary liver cancer is one of the most common malignancies of the liver worldwide. The development of human cancer results from the clonal expansion of genetically modified cells that acquired selective growth advantage through accumulated alterations of proto-oncogenes and tumor suppressor genes^[1]. Chromosomal analysis using polymorphic DNA markers that distinguish different alleles has revealed loss of heterozygosity (LOH) of specific chromosomal regions in various types of cancers and mapping of regions with a high frequency of LOH has been critical for identifying negative regulators of tumor growth, which will be of great help in positional cloning of tumor suppressor genes^[2].

We have cloned a novel human liver-related putative tumor suppressor gene, LPTS by means of allelic-loss mapping and positional candidate cloning^[3]. LPTS gene mapped to chromosome 8p23, a locus with high-frequency LOH and a hot spot of tumor suppressor in HCC^[2, 4]. The expression of LPTS was ubiquitous in normal human tissues, whereas levels appeared to be significantly reduced, or sometimes undetectable in HCC cells and neoplastic tissues. The gene for LPTS is a growth-arrest gene that acts directly or indirectly to control the proliferation of cells, and might be a tumor suppressor gene^[3]. LPTS gene has 7 exons totally and encodes two transcripts, one is LPTS-S, lacking exon6 and encoding a 174-a.a. protein; the other is LPTS-L, encoding a 328-a.a. protein with entire 7 exons. The LPTS-L is highly homologous to PinX1 identified recently^[5]. LPTS-L and PinX1 have quite different 3' -untranslated region and encode a same protein, referred to LPTS-L/PinX1. LPTS-L/PinX1 has strong telomerase inhibitory activity both *in vivo* and *in vitro*.

In this study, we collected 56 HCC cell lines, 7 ovarian cancer cell lines and 7 head & neck tumor cell lines to perform single strand conformation polymorphism (SSCP) assay^[6,7] to screen the point mutations in LPTS gene. Then we detected those mutations identified from SSCP assay in 70 pairs of HCC tissues to confirm the existence of real mutations in HCC tissue samples. Finally, telomerase activity assay was done to study the effect of the point mutation on the function of protein *in vitro*.

MATERIALS AND METHODS

Tumor cells and HCC tissue samples

The cell lines, including 56 liver cancer cell lines, 7 ovarian cell lines and 7 head and neck tumor cell lines, were from mainland of P.R. China, Japan, France, Taiwan, Hongkong and America separately. The cell lines were cultured in Dulbecco's Modified Eagle Medium (DMEM, Life Technologies Inc., Grand Island, NY) or in RPMI medium 1 640 (Life Technologies Inc.),

supplemented with 10 % fetal calf serum (FCS, Life Technologies Inc.) with or without non-essential amino acid (Life Technologies Inc.) according to suppliers. All the samples of primary HCC (Ks), adjacent samples of nontumorous tissues (Ls), were obtained from Shanghai Eastern Hepatobiliary Surgery Hospital (Shanghai, P.R. China), with the agreement of each patient. The serial numbers were those recorded by the hospital. All tissues were placed in liquid nitrogen immediately after surgical resection.

Point mutation assay

According to the genome sequence of LPTS gene, we synthesized 11 pairs of primers covering 7 exons of the gene, with length of each PCR product around 170 to 250 bp (Table 1). Genomic DNA was separated as described^[8]. PCR was performed in a 25- μ L reaction mixture that contained 2 μ L Genomic DNA (around 50 ng) from each cell line as template, 2 μ L primers mix (20 μ M each), 0.4 μ L dNTP mix (12.5 mM each), 4.75 μ L H₂O, 0.25 μ L Taq DNA polymerase (Life Technologies Inc.), and 15.6 μ L premix (16 mM TrisHCl pH8.4, 80 mM KCl, 2.4mM MgCl₂ and 0.16 % Tween-20). PCR reaction conditions were described in Table 1. In Table 1, SD referred to the step-down PCR, the annealing temperature was declined 3 °C every 3 cycles for 94 °C 45 sec, annealing temperature 1 min and 72 °C 1 min from 68 °C until the indicated temperature and then for another 25 cycles of standard PCR reaction. The products of PCR were separated by electrophoresis on 2 % agarose gel to check the specificity of each PCR reaction. The PCR products were sequenced directly or performed SSCP assay as described below.

Table 1 Primer sequences for the coding region of the LPTS gene

Exon	Nucleotide sequences	PCR conditions	Product size (bp)
1	Forward: 5' -CGTGCTCGAGGAGCGAGTCG-3' Reverse: 5' -ACCCGGCATCTTACCAACG-3'	52 °C SD	241
2	Forward: 5' -TCCATTGCTGATGATAATGC-3' Reverse: 5' -CTTCCAGTCTCCTAAGAAGG-3'	50 °C SD	230
3	Forward: 5' -TGAGAGGAATGTTCTAACTC-3' Reverse: 5' -AGCCAAYYAYGCAAAGACAC-3'	50 °C SD	178
4	Forward: 5' -AACTACAGGCTTACCTCTCG-3' Reverse: 5' -AACATATTTGCATTGAGAAC-3'	55 °C SD	196
5	Forward: 5' -CAAGACTATCCACTGTTAGG-3' Reverse: 5' -GGACAAACACGTAGATTTCAATAAC-3'	52°C Standard	220
6	Forward: 5' -GCTGCATAGTTCATGTCTGC-3' Reverse: 5' -CACAGGTGAAAATCAGACAG-3'	50 °C SD	194
7.1	Forward: 5' -CTGCCITTTAACTCTTCTGC-3' Reverse: 5' -GGCTGGAGGTAACCTTCCAC-3'	50 °C SD	247
7.2	Forward: 5' -GGCCACAGGTAAAGATGTGG-3' Reverse: 5' -CAGGCGGCTGCACATGGTCC-3'	55 °C Standard	200
7.3	Forward: 5' -GCCTCTGCTCAGGATGCAGG-3' Reverse: 5' -GCCCCGGCTGGGAAGGATTC-3'	50 °C SD	191

SD: step-down PCR

For SSCP assay^[9,10], 3 μ L PCR product, added with 4 μ L denaturing buffer (95 % formamide, 10 mM NaOH, 0.25 % bromophenol blue and 0.25 % xylene cyanol), were kept at 95 °C for 5 min and then loaded 5 μ L denatured mixture sample

directly into each of sample wells of GeneGel Excel, 0.5 mm thin, pre-cast polyacrylamide ready-to-run gel for DNA electrophoresis (Amersham Pharmacia Biotech Inc.). Electrophoresis was done on GenePhor DNA separation system (Amersham Pharmacia Biotech Inc.) at 150 Voltage for 10 min and then 600 Voltage for 2 hours at 4 °C. At the end of running, silver stained the gel with DNA silver staining kit (Amersham Pharmacia Biotech Inc.) in accordance with the manufacturer's protocol.

Expression and purification of GST fusion protein

The coding sequence of protein fragment for expression was cloned in frame into the *E.coli* GST fusion expression vector pGEX-4T2 (Amersham Pharmacia Biotech Inc.), then transfected the construct into *E.coli* BL21(DE3). The protein was expressed with IPTG induction for 3 hours and purified by glutathione-agarose (Sigma) column.

TRAP telomerase activity assay

HCC cells SMMC-7721 were lysed in lysis buffer (10 mM TrisHCl pH7.5, 1 mM MgCl₂, 1 mM EGTA, 0.1 mM PMSF, 5 mM 2-mercaptoethanol, 0.5 % CHAPS, 10 % glycerol) on ice for 30 min and then centrifuged at high speed for 30 min, the suspension containing telomerase was used for TRAP assay. The GST-fused protein was incubated with cell extract for 10 min at 4 °C before subjecting to telomerase extension according reference^[11]. Telomerase products were separated on 10 % polyacrylamide gels, which were stained with silver nitrate.

RESULTS

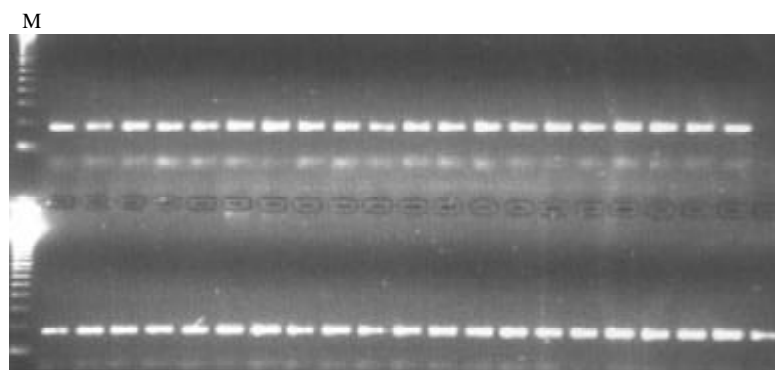
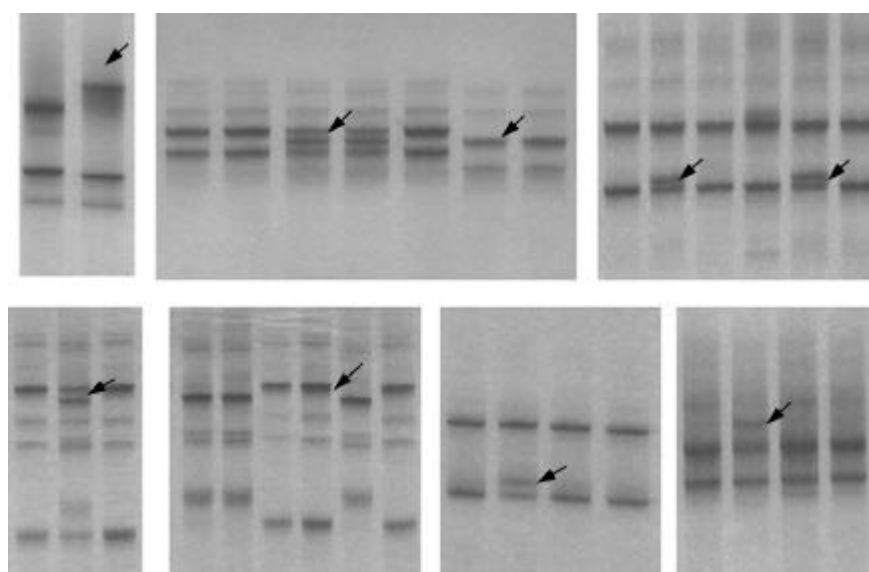
5 alterations were found in 12 tumor cell lines

We mainly screened the point mutations of LPTS gene in 56 liver cancer cell lines by means of SSCP. For chromosome 8p23 is a hot spot containing tumor suppressor in many types of tumors except for liver, including ovarian cancer and head and neck tumors, we checked LPTS gene in another 7 ovarian cancer cell lines and 7 head and neck tumor cell lines altogether. Among the cell lines analyzed, about half of those are homozygous in region between D8S550 and D8S518 on chromosome 8p23, covering the LPTS gene, by fine mapping of allele deletion (loss of heterozygosity) in Chromosome 8p.

After PCR amplification the fragment, PCR products were checked for specificity on 2 % agarose gel. Only the good specific amplification could be used in the latter assay (Figure 1). The specific PCR products were separated in PAGE gel and stained with silver nitrate. The abnormal band patterns, such as loss or gain of extra bands, different migration of bands, comparing to the negative and positive controls which had been sequenced in advance, suggested this sample might have point mutations (Figure 2). The products with abnormal migration pattern were sequenced and determined. The point mutations as shown in Table 2, were mainly located in exon 2, exon 5 and exon 7. In exon 2, there were two types of alterations, C (161) changed to T, predicted effect was the change from alanine to valine in cholangiocarcinoma cell CCLP1, and the other was C (183) to T, which was silent at the protein level and might therefore be considered as a polymorphism. In exon 5, only one point mutation of A (497) to G in HCC cell line PLCPRF5 was found, causing the encoded amino acid changing from tyrosine to cysteine. Two frequent mutations clustering at positions 778 and 880 were found in exon 7. The A778G changed the threonine residue to an alanine. All cell lines harboring this polymorphism were heterozygous at position 778 with the second allele retaining the wild type. The second mutation cluster A880T caused a change from serine to cysteine.

Table 2 The alterations of LPTS-S and LPTS-L in tumor cell lines

Cell line	Cell type	Mutation	Exon	Codon	Predicted effect
CCLP1	Cholangiocarcinoma	C161T	Exon 2	gct→gtt	Ala→Val
HepG2	HCC	A701A, G(LPTS-S)	Exon 7	Outside ORF	/
		A778A, G(LPTS-L)		aca→gca	Thr→Ala
HepT1	HCC	C183T	Exon 2	gcc→gct	Ala
MEK	HCC	A701A, G(LPTS-S)	Exon 7	Outside ORF	/
		A778A, G(LPTS-L)		aca→gca	Thr→Ala
SNU182	HCC	A701A, G(LPTS-S)	Exon 7	Outside ORF	/
		A778A, G(LPTS-L)		aca→gca	Thr→Ala
Li7A	HCC	A803T(LPTS-S)	Exon 7	Outside ORF	/
		A880T(LPTS-L)		agc→tgc	Ser→Cys
Li21	HCC	C183T	Exon 2	gcc→gct	Ala
		A803T(LPTS-S)	Exon 7	Outside ORF	/
		A880T(LPTS-L)		agc→tgc	Ser→Cys
MZCHA1	HCC	A803T(LPTS-S)	Exon 7	Outside ORF	/
		A880T(LPTS-L)		agc→tgc	Ser→Cys
PCI-SG231	HCC	G111C	Exon 1	Before ATG	/
		A803T(LPTS-S)	Exon 7	Outside ORF	/
		A880T(LPTS-L)		agc→tgc	Ser→Cys
PLCPRF5	HCC	A497G	Exon 5	tat→tgt	Tyr→Cys
IGR-OV1	Ovarian tumor	A701A, G(LPTS-S)	Exon 7	Outside ORF	/
		A778A, G(LPTS-L)		aca→gca	Thr→Ala
SW579	Head and neck tumor	C183C, T	Exon 2	gcc→gct	Ala

**Figure 1** Agarose gel analysis of PCR products for SSCP assay. Agarose gel separation was used to determine the specificity of PCR reaction. PCR products with only one specific band of right size in the gel can be used to SSCP assay. M: 100 bp ladder.**Figure 2** Some different electrophoresis patterns in SSCP assay of each exon. Arrows showed the differences, including extra bands, differential bands shifting, and so on.

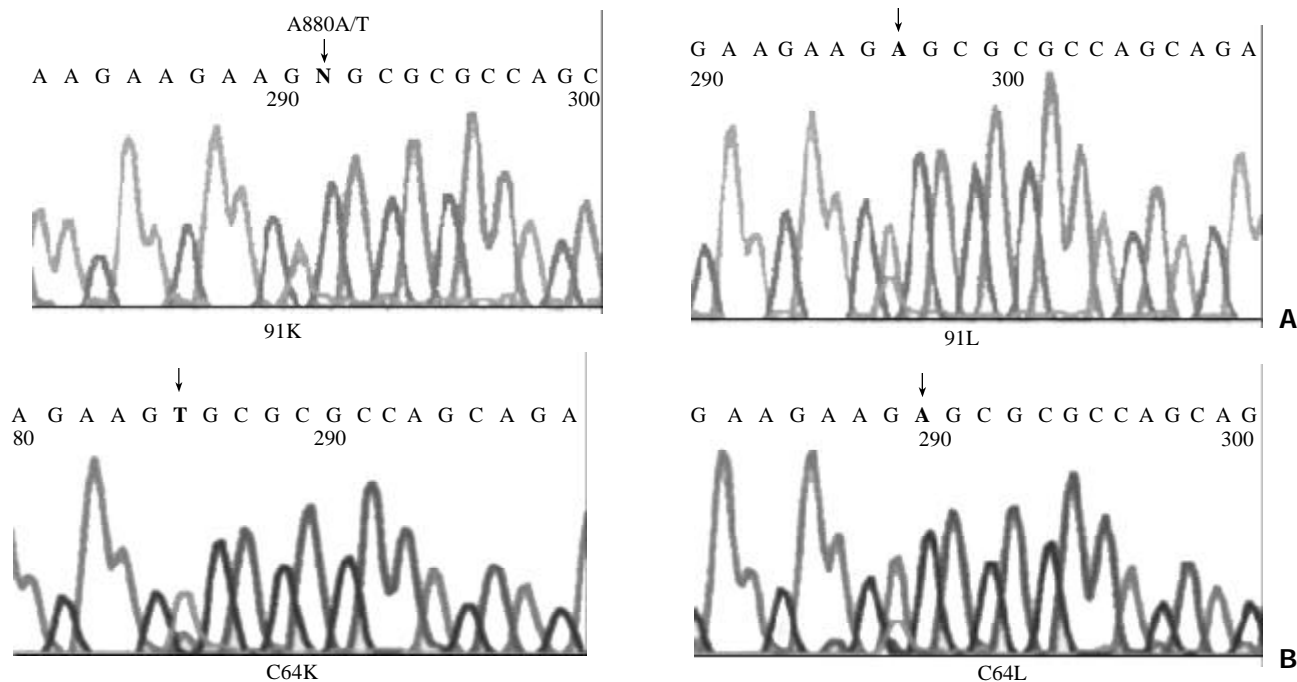


Figure 3 The sequences of mutation site of 880 in two pairs of HCC tissues. (A) HCC sample 91K, 91L; (B) HCC sample C64K, C64L. 'K' represents HCC tissue and 'L' represents adjacent nontumorous liver tissue. Arrow indicated the site of 880.

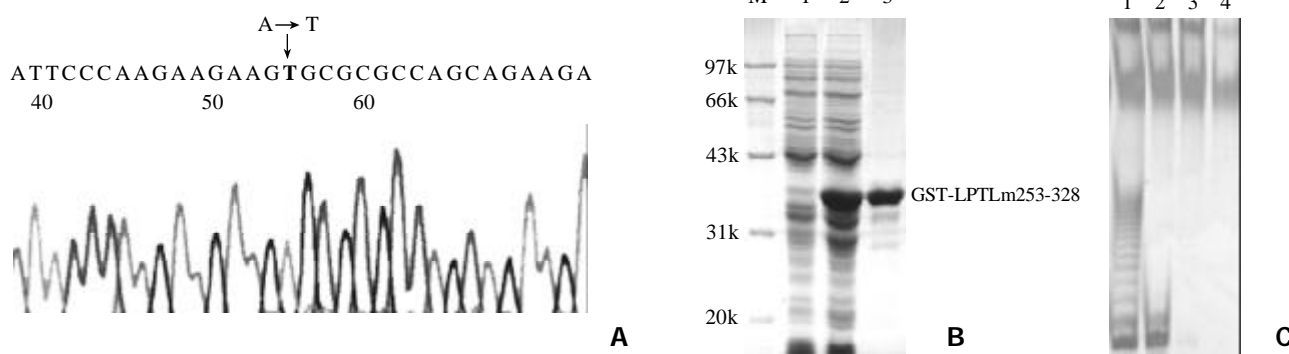


Figure 4 The point mutation in position 880 has no effect on the telomerase inhibitory activity of LPTS-L. A. The 'A' in position 880 of LPTS-L transcript was mutated to 'T'; B. The expression and purification of GST-LPTLm253-328, 1, without IPTG induction; 2, IPTG induction; 3, purified protein. C. The telomerase inhibiting activity assay *in vitro* of mutant protein LPTLm253-328 in SMMC-7721 cell extract. 1-4 were 0.1, 0.5, 1, 5 μ g protein added in cell extract for 10 min, respectively.

Position (880) A to T was identified in 7 patients (10 %)

From the assay in HCC and other tumor cell lines, we can see that the major point mutations are in exon 7. The point mutation in 778 and 880 nt caused threonine and serine which being the candidate sites for phosphorylation changed to alanine and cysteine. The mutation in 880 nt turned to the cysteine, which might form disulfide bond and affect the conformation of the protein. It would be very important to confirm the existence of these two mutations in HCC tissues. Next, we collected 70 pairs of HCC samples, amplified the exon 7 and sequenced directly. In all 70 pairs samples, we could not find the point mutation in position 778, whereas the mutation in site of 880 was detected in 7 HCC samples and the mutation frequency was 10 %. The mutation in the site of 880 was also A/T heterozygous, which was shown double pits in sequence reaction (Figure 3).

The significance of A(880) mutation

LPTS-L/PinX1 possessing strong telomerase inhibitory activity had been determined by *in vivo* and *in vitro* experiments. To

study the effect of telomerase inhibitory function of A(880) mutant, we designed PCR primer with point mutation at the site of 880, 5'-GAA TTC CCA AGA AGA AGT GCG CGC CA-3', the mutated site of 'T' was indicated in italic type. We subcloned the mutated cDNA fragment (from amino acid subunit 253 to 328) into GST fusion expression vector pGEX-4T2 and purified the GST-fused mutant protein. After TRAP telomerase activity assay, we found that the mutant protein still had strong telomerase inhibitory activity in HCC cell line SMMC-7721 cell extract (Figure 4). From these results, we concluded that the point mutation in position 880 of LPTS gene had no effect on telomerase inhibition.

DISCUSSION

Somatic inactivation of a tumor suppressor gene is usually achieved by intragenic mutation in one allele of the gene, with subsequent by loss of a chromosome region that spans the second allele, showed loss of heterozygosity (LOH). Among the various deleted chromosome regions identified by several laboratories, chromosome 8p has a particularly high frequency

of LOH^[2, 12-14] and a growing body of evidence suggests that chromosome 8p is active in many types of carcinogenesis and metastasis including liver, breast, colorectal, prostate, lung, head and neck, pancreatic and urinary bladder carcinomas^[14-18]. However, there have been no reports of the identification of a tumor suppressor gene on 8p.

LPTS gene is a possible candidate tumor suppressor localized in 8p23 region, which is a negative regulator in cell proliferation^[3]. According to Kundson's tumor suppressor "two-hit" model^[19], one tumor suppressor needs to be hit twice to be inactivated. To clarify the relationship between LPTS gene and HCC, we searched for point mutations in all seven exons of LPTS gene in HCC tissue samples and HCC cell lines. In 70 tumor cell lines and 70 pairs of HCC tissues analyzed, there were mainly two point mutations in exon 7, position 778 and 880. The mutation at the site of 778 was found only in several HCC cell lines, but not in clinical HCC tissues. The mutation at the site of 880 has the mutation frequency of 10 % in HCC tissues, but the mutation has no effect of the telomerase inhibitory activity of LPTS-L/PinX1 protein, suggesting that this position is a polymorphism site of LPTS gene.

During our preparation of this manuscript, another research group in Korea reported their research work of genetic analysis of LPTS gene in HCC sample from South Korea. They also found that LPTS gene indeed had very high LOH frequency (34.5 %) in HCC patients, but also no point mutations could be found in HCC patients from South Korea, same with our results in Chinese HCC patients^[20]. Taken the above data together, LPTS gene has high frequency of LOH in HCC, but has no point mutation in the last allele, suggesting that inactivation of LPTS gene may not be caused by point mutation. However, we cannot rule out completely the epigenetic inactivation, such as methylation, acetylation etc^[21-23]. Indeed, we found that there were two CpG islands, about 1.2 kb in length, in the upstream of LPTS gene transcription initiating site. Study of the methylation status in the regulation of LPTS gene is being performed now.

REFERENCES

- 1 **Weinberg RA.** Tumor suppressor genes. *Science* 1991; **254**: 1138-1146
- 2 **Nagai H,** Pineau P, Tiollais P, Buendia MA, Dejean A. Comprehensive allelotype of human hepatocellular carcinoma. *Oncogene* 1997; **14**: 2927-2933
- 3 **Liao C,** Zhao M, Song H, Uchida K, Yokoyama KK, Li T. Identification of the gene for a novel liver-related putative tumor suppressor at a high-frequency loss of heterozygosity region of chromosome 8p23 in human hepatocellular carcinoma. *Hepatology* 2000; **32**: 721-727
- 4 **Pineau P,** Nagai H, Prigent S, Wei Y, Gyapay G, Weissenbach J, Tiollais P, Buendia MA, Dejean A. Identification of three distinct regions of allelic deletions on the short arm of chromosome 8 in hepatocellular carcinoma. *Oncogene* 1999; **18**: 3127-3134
- 5 **Zhou XZ,** Lu KP. The Pin2/TRF1-interacting protein PinX1 is a potent telomerase inhibitor. *Cell* 2001; **107**: 347-359
- 6 **He XS,** Su Q, Chen ZC, He XT, Long ZF, Ling H, Zhang LR. Expression, deletion and mutation of p16 gene in human gastric cancer. *World J Gastroenterol* 2001; **7**: 515-521
- 7 **Peng XM,** Yao CL, Chen XJ, Peng WW, Gao ZL. Codon 249 mutations of p53 gene in non-neoplastic liver tissues. *World J Gastroenterol* 1999; **5**: 324-326
- 8 **Sambrook J,** Fritsch E F, Maniatis T ed, *Molecular cloning.* Cold spring harbor laboratory press, 1989: 463-467
- 9 **Bailey A.** Single-stranded conformational polymorphisms, PCR strategies. *Academic Press, Inc* 1995: 121-129
- 10 **Yap EPH,** McGee JO. Non-isotopic single-strand conformation polymorphism (SSCP) analysis of PCR products, PCR Technology: Current Innovations, Chapter 20. *CRC Press Inc* 1994: 165-177
- 11 **Kim NW,** Piatyszek MA, Prowse KR, Harley CB, West MD, Ho PL, Coviello GM, Wright WE, Weinrich SL, Shay JW. Specific association of human telomerase activity with immortal cells and cancer. *Science* 1994; **266**: 2011-2015
- 12 **Marchio A,** Meddeb M, Pineau P, Danglot G, Tiollais P, Bernheim A, Dejean A. Recurrent chromosomal abnormalities in hepatocellular carcinoma detected by comparative genomic hybridization. *Genes Chromosomes & Cancer* 1997; **18**: 59-65
- 13 **Fujimori M,** Tokino T, Hino O, Kitagawa T, Imamura T, Okamoto E, Mitsunobu M, Ishikawa T, Nakagama H, Harada H. Allelotype study of primary hepatocellular carcinoma. *Cancer Res* 1991; **51**: 89-93
- 14 **Emi M,** Fujiwara Y, Nakajima T, Tsuchiya E, Tsuda H, Hirohashi S, Maeda Y, Tsuruta K, Miyaki M, Nakamura Y. Frequent loss of heterozygosity for loci on chromosome 8p in hepatocellular carcinoma, colorectal cancer, and lung cancer. *Cancer Res* 1992; **52**: 5368-5372
- 15 **Bieche I,** Lidereau R. Genetic alterations in breast cancer. *Genes, Chromosomes Cancer* 1995; **14**: 227-251
- 16 **Macoka JA,** Trybus TM, Benson PD, Sakr WA, Grignon DJ, Wojno KD, Pietruk T, Powell JJ. Evidence for three tumor suppressor gene loci on chromosome 8p in human prostate cancer. *Cancer Res* 1995; **55**: 5390-5395
- 17 **Wistuba II,** Behrens C, Virmani AK, Milchgrub S, Syed S, Lam S, Mackay B, Minna JD, Gazdar AF. Allelic losses at chromosome 8p21-23 are early and frequent events in the pathogenesis of lung cancer. *Cancer Res* 1999; **59**: 1973-1979
- 18 **el-Naggar AK,** Hurr K, Batsakis JG, Luna MA, Goepfert H, Huff V. Sequential loss of heterozygosity at microsatellite motifs in preinvasive and invasive head and neck squamous carcinoma. *Cancer Res* 1995; **55**: 2656-2659
- 19 **Knudson AG.** Mutation and cancer: statistical study of retinoblastoma. *Proc Natl Acad Sci USA* 1971; **68**: 820-823
- 20 **Park WS,** Lee JH, Park JY, Jeong SW, Shin MS, Kim HS, Lee SK, Lee SN, Lee SH, Park CG, Yoo NJ, Lee JY. Genetic analysis of the liver putative tumor suppressor (LPTS) gene in hepatocellular carcinomas. *Cancer Letters* 2002; **178**: 199-207
- 21 **Esteller M,** Herman JG. Cancer as an epigenetic disease: DNA methylation and chromatin alterations in human tumours. *J Pathol* 2002; **196**: 1-7
- 22 **Jones PA,** Takai D. The role of DNA methylation in mammalian epigenetics. *Science* 2001; **293**: 1068-1070
- 23 **Ponder BA.** Cancer genetics. *Nature* 2001; **411**: 336-341

Gene expression profiles at different stages of human esophageal squamous cell carcinoma

Jin Zhou, Li-Qun Zhao, Mo-Miao Xiong, Xiu-Qin Wang, Guan-Rui Yang, Zong-Liang Qiu, Min Wu, Zhi-Hua Liu

Jin Zhou, Xiu-Qin Wang, Min Wu, Zhi-Hua Liu, National Laboratory of Molecular Oncology, Cancer Institute, Peking Union Medical College and Chinese Academy of Medical Sciences, Beijing 100021, China

Li-Qun Zhao, Guan-Rui Yang, Zong-Liang Qiu, Medical Science Institute of Henan Province, Zhengzhou 450052, China

Mo-Miao Xiong, Health Genetics Center, School of Public Health, The University of Texas Houston, Houston, Texas 77225, USA

Supported by China Key Program on Basic Research, No. G1998051021; the Chinese Hi-tech R&D program, No.2001AA231310 and National Natural Science Foundation of China, No.30170519

Correspondence to: Zhi-Hua Liu, Ph.D. Professor, National Laboratory of Molecular Oncology, Cancer Institute, Peking Union Medical College and Chinese Academy of Medical Sciences, Beijing 100021, China. liuzh@pubem.cicams.ac.cn

Telephone: +86-10-67723789 **Fax:** +86-10-67715058

Received: 2002-05-06 **Accepted:** 2002-07-26

Abstract

AIM: To characterize the gene expression profiles in different stages of carcinogenesis of esophageal epithelium.

METHODS: A microarray containing 588 cancer related genes was employed to study the gene expression profile at different stages of esophageal squamous cell carcinoma including basal cell hyperplasia, high-grade dysplasia, carcinoma *in situ*, early and late cancer. Principle component analysis was performed to search the genes which were important in carcinogenesis.

RESULTS: More than 100 genes were up or down regulated in esophageal epithelial cells during the stages of basal cell hyperplasia, high-grade dysplasia, carcinoma *in situ*, early and late cancer. Principle component analysis identified a set of genes which may play important roles in the tumor development. Comparison of expression profiles between these stages showed that some genes, such as P160ROCK, JNK2, were activated and may play an important role in early stages of carcinogenesis.

CONCLUSION: These findings provided an esophageal cancer-specific and stage-specific expression profiles, showing that complex alterations of gene expression underlie the development of malignant phenotype of esophageal cancer cells.

Zhou J, Zhao LQ, Xiong MM, Wang XQ, Yang GR, Qiu ZL, Wu M, Liu ZH. Gene expression profiles at different stages of human esophageal squamous cell carcinoma. *World J Gastroenterol* 2003; 9(1): 9-15

<http://www.wjgnet.com/1007-9327/9/9.htm>

INTRODUCTION

Cancer development is a complex multi-step process, involving various genetic and epigenetic changes. Progress of phenotypes from normal to advanced carcinoma is controlled by a transcriptional hierarchy that coordinates the action of hundreds

of genes. Conventional approaches investigating one or several candidate genes at a time can not show the whole story of carcinogenesis. The generation of vast amounts of DNA sequence information, coupled with advances in technologies developed for the experimental use of such information, allows the description of biological processes from a view of global genetic perspective. One such technology, DNA microarray, permits simultaneous monitoring of thousands of genes^[1,2]. Fuller *et al*^[3] and Sgroi *et al*^[4] have used this new technique in analyzing gene expression profiles in human glioblastoma, human breast cancer and matched normal tissues. However, little is known about the exact expression changes in each stage of tumorigenesis, which will help us identify the exact series of events that leads to the initiation and progression of cancer development.

In this study, esophageal cancer was chosen as a model to analyze the changes of expression profiles in different stages of carcinogenesis. By using microarray membranes, expression of 588 known cellular genes were profiled in normal esophageal tissues, basal cell hyperplasia, high-grade dysplasia, carcinoma *in situ*, early and advanced cancer. Our results revealed some genes differently expressed in a certain stage, and some kept up or down regulated in all stages toward cancer.

MATERIALS AND METHODS

Biopsy specimens and primary esophageal cancer tissues

Biopsy specimens were collected from the individuals who were more than 35 years old, underwent endoscopy examination in a screening for early cases of esophageal cancer in Henan province in North China, where has the highest incidence rate of this fatal cancer in the world. Agreements have been obtained from all individuals informed consents issued. In each case, 4 pieces of tissues with the size of 0.01 cm³ were separately removed from the mucosa, two of them were instantly frozen and kept in liquid nitrogen until use, and the other two underwent pathologic diagnosis according to the criteria of Riddell and associates. Specimens of normal esophagus, basal cell hyperplasia, high-grade dysplasia, carcinoma *in situ*, and early carcinoma were obtained in this study. Every tissue specimen was mostly composed of normal or abnormal epithelial cells.

Cancer and adjacent almost normal tissues with size of about 0.5 cm³ were collected from patients with primary esophageal cancer in Cancer Hospital of the Chinese Academy of Medical Sciences after informed consent was obtained. Fresh samples were dissected manually to remove mixed connective tissue and stored in liquid nitrogen. Pathological diagnosis showed that the cancers were from squamous cell at medium to high grade differentiation, the matched almost normal mucosa did not show any invasion of cancer cells.

Human cancer cDNA expression array

Human cancer cDNA expression array membrane was purchased from Clontech Laboratories Inc. (Palo Alto, CA), each membrane contains of 588 well characterized genes along with 9 housekeeping genes as internal control. During this study, membranes of the same lot were used to ensure the reproducibility.

RNA extraction

The biopsy specimens of the same histological diagnosis were pooled and the total RNA of different kinds of samples was extracted with Micro RNA isolation kit (Stratagene, La Jolla, CA). Before labeling, 5 µg total RNA of each type was treated with 2 µl DNase I (10 unit/ml, Boehringer Mannheim, Mannheim, Germany), 1 µl RNasin (40 units/µl, Promega) at 37 °C for 15 min to remove contaminated DNA.

Hybridization and exposure

Following the recommendation of the manufacturer, ³²P-labelled cDNA probes were generated by reverse transcription from 5 µg of RNA sample in the presence of [α -³²P]dATP (3 000 ci/mmol, Du Pont). Each cDNA probe was then hybridized to a membrane at 65 °C overnight. The membranes were washed twice in 2×SSC, 0.5 % SDS at 65 °C for 30 minutes, then twice in 0.2×SSC, 0.5 % SDS at 65 °C for 30 minutes, then exposed to X-ray film at -80 °C for 2-3 days.

Hybridization pattern analysis

Images of individual autoradiography for each stage of carcinogenesis were digitalized by Fluor-S™ MultiImager System (Bio-Rad Laboratories, Inc.) The hybridization pattern of arrays was analyzed and compared using AtlasImage™ 1.01 software (Clontech). To normalize the relative gene expression, beta-actin and alpha tubulin were used as internal references whose expression level was found stable in different developmental stages in our study. These genes were preferred also because they are conventionally used as internal references for measuring gene expression levels in Northern blot, RNase protection and semi-quantitative RT-PCR.

Confirmation by semi-quantitative RT-PCR analysis

To validate the expression pattern identified on the expression arrays, 5 genes were randomly picked and semi-quantitative RT-PCR was performed to confirm their differential expression with cDNA template from esophageal cancer and adjacent almost normal tissues. First strand cDNA was synthesized from 5 µg RNase-free DNase treated total RNA using the Superscript™ Preamplification system for First Strand cDNA Synthesis (Life Technologies, Inc) as described by the manufacturer. An aliquot of 1/20 of the reverse transcribed product was used as template in the following PCR amplification. Reactions undergone in 25 µl total volume containing 1×PCR buffer, 1.5 mmol/L MgCl₂, 200 µmol/L dNTPs, 1.5 u Taq Polymerase (Life Technologies, Inc) and 40 µmol/L gene specific primers under the conditions: 94 °C 5 min, followed by 25-28 cycles each of 94 °C 20 sec, 58 °C 30 sec, 72 °C 1 min. Amplification of beta actin with same aliquot of cDNA template was used as internal reference to determine the relative gene expression.

Gene specific primers: Rho8 5' -GGACACTTCGGGTTCTCCTTAC-3', 5' -TGTGGCTCTGTGATTTGTTTC-3'; IL-1 beta 5' -GCAGAAAGGGAACAGAAAGGTT-3', 5' -AAGGAGGCACACCAGTCCAAAT-3'; Interleukin 1 receptor antagonist 5' -ACTCTCCTCCTTCTCCTGTTCC-3', 5' -GCTTGTCTGCTTTCTGTTCTC-3'; Cytokeratin 4 5' -GGGAAACAAGCATCTCCAT-3', 5' -ATCTCAGGGTCAATCTCCAC-3'; Wnt-13 5' -GCCAAAGTTAGATGGGACAAAG-3', 5' -TTGAACAGGCAGCAAGTAAGC-3'.

Principle component analysis

A principle component analysis was used to explain the variance-covariance structure of the gene expressions in 6 stages of tumor development. The purpose of principle component analysis is data reduction, and interpretation through a few linear combinations of the original variables (gene expressions)^[5].

Principle component analysis starts with k variables which

represent the expression profiles of k genes. The t th element of the j variable corresponds to the expression level of the j th gene in the t stage of the tumor development. Principle component analysis intends to replace the k variables by p principle components where p is smaller than k , while minimizing loss of information. The principle component is a linear combination of the variables x_1, x_2, \dots, x_k and can be constructed by the eigenvector e_i ($i=1,2,\dots,k$) of the covariance matrix V of the variables x_1, x_2, \dots, x_k , where the eigenvector e_i of the matrix V is defined as any vector satisfying the equation $V e_i = \lambda_i e_i$, and λ_i is called the corresponding eigenvalue associated with the eigenvector e_i . The elements of the eigenvector measure the importance (loading score) of the genes to the principle component and the eigenvalue measures the variance of the corresponding principle component explaining variations of expressions of a linear combination of genes represented by the principle component. The first principle component with the largest eigenvalue has the largest variance, the second principle component with the second largest eigenvalue has the second largest variance and so on. It can be shown that λ_i is equal to the variance of the i th principle component.

Although k variables are required to reproduce the total system variability, often much of this variability can be accounted for by a small number of principle components with larger eigenvalues (variances) which explain large proportions of variations of gene expressions underlying some biological processes. Principle component analysis was used to identify a set of genes which may contribute to the tumor development.

RESULTS

Expression pattern of 588 known genes in progression of carcinoma

High quality total RNA was isolated from biopsy specimens. The RNA was reverse-transcribed into ³²P-labeled cDNA probe and hybridized to Atlas™ Human Cancer cDNA expression array to profile the expression of 588 known genes. The hybridization patterns were imaged by the Fluor-S™ MultiImage System and analyzed by AtlasImage™ 1.01 software. Genes with adjusted intensity difference >20 000 or ratio >2 between two stages were supposed to be regulated differentially. Figure 1 showed the cDNA array images along with color charts indicating up-regulated genes with red, down-regulated ones with blue, and non-changed with green.

There were more than 100 genes up or down regulated substantially in every abnormal stage when compared to human normal mucosa. In stage of basal cell hyperplasia II, there were 122 genes up regulated and 17 down regulated; in stage of high grade dysplasia, there were 134 genes up regulated and 33 down regulated; in stage of squamous cell carcinoma in situ, there were 114 genes up regulated and 10 down regulated; in stage of early cancer, there were 169 genes up regulated and 13 down regulated; In stage of late cancer, there were 77 genes up regulated and 60 down regulated. As shown in the color charts of Figure 1 the types as well as expression level of genes are different among each stage.

Validation of Array Data with RT-PCR

To further investigate the reliability of our array data, we randomly picked 5 differentially expressed genes and measured the expression of the genes in the paired cancer and adjacent almost normal tissues using RT-PCR. Figure 2 showed that the different expression pattern of each of the five genes as determined by RT-PCR were similar to those observed with cDNA array in more than half of 12 pairs of matched tissues (squamous esophageal cancer and matched adjacent almost normal tissue), confirming the reliability of our array data. Our observed correlation between the cDNA array and RT-PCR are consistent with that observed by others^[6,7].

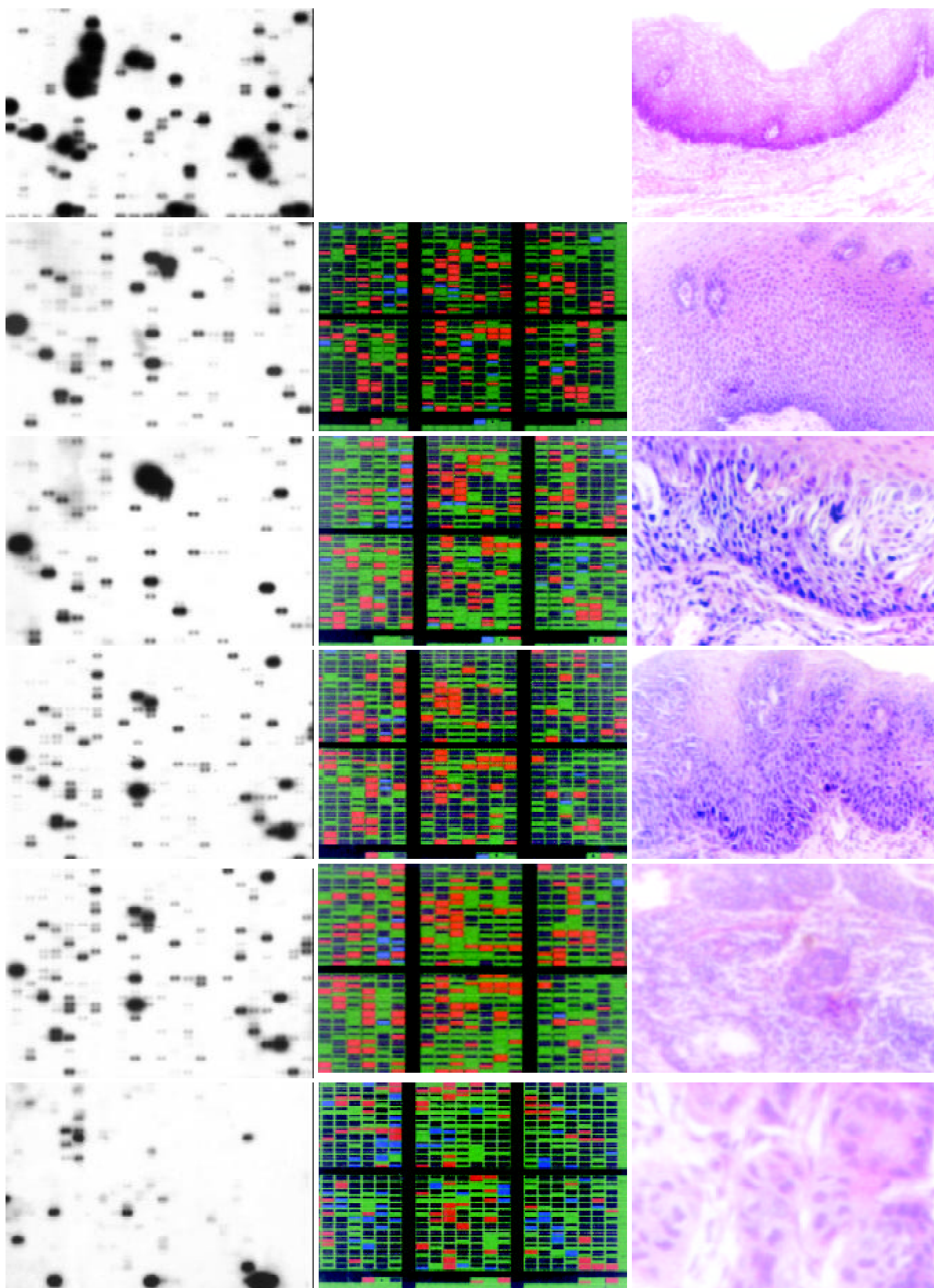


Figure 1 Expression patterns of genes in esophageal tissue of normal, basal cell hyperplasia, high-grade dysplasia, carcinoma in situ, early and advanced cancer. Total RNAs were isolated from these tissues, reverse-transcribed into ^{32}P -labeled cDNAs and hybridized to AtlasTM Human Cancer cDNA expression arrays. A complete list of names and location of the arrayed gene can be

found in the instruction manual and website from Clontech. Data was analyzed by AtlasImage™ 1.01 software. A,B,C,D,E,F showed hybridization result of normal cells, basal cell hyperplasia, high-grade dysplasia, carcinoma in situ, early and advanced cancer; G, H, I, J, K showed the color charts indicating up-regulated genes with red, down-regulated genes with blue, and non-changed genes with green in the later 5 stages when compared to normal tissue; L, M, N, O, P showed the pathological image of normal, basal cell hyperplasia, high-grade dysplasia, carcinoma in situ, early and advanced cancer respectively.

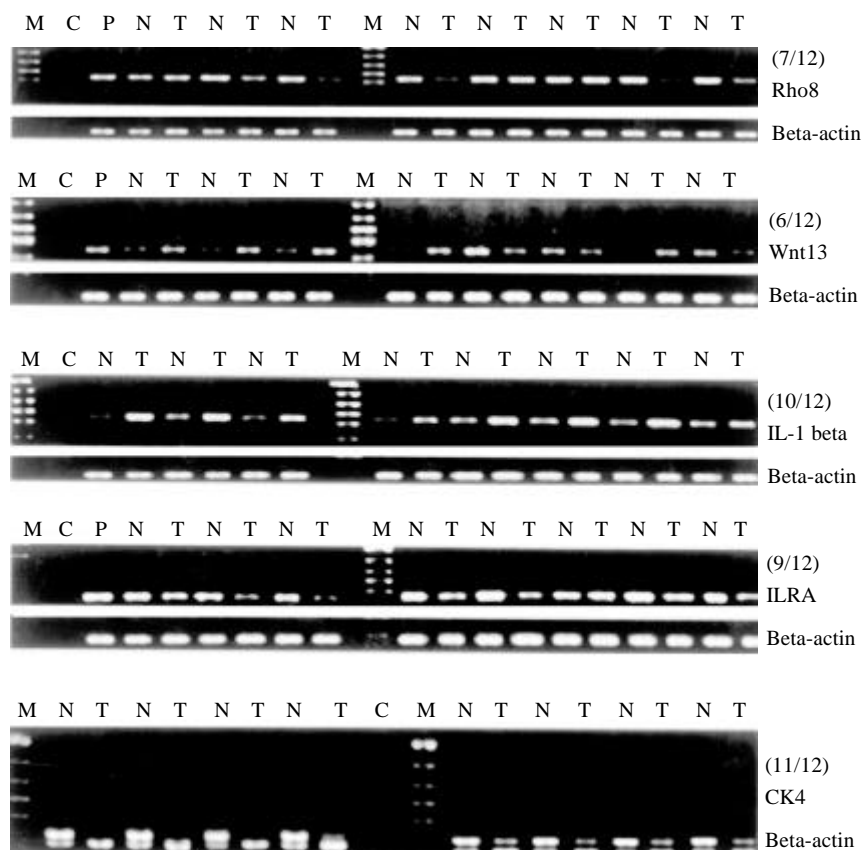


Figure 2 Validation of array data with RT-PCR: Rho8, Wnt 13, IL-1 beta, IL-1 receptor antagonist and cytokearin 4 were chosen to further investigate the reliability of the array data using RT-PCR. The figures showed part of the RT-PCR results of five genes in cancer (designated T) and matched almost normal tissues(designated N). P means positive control.

Principle component analysis Identified a set of genes which may play important roles in cancer development

Principle component analysis showed that there were 5 principle components in the 6 stages of cancer development. The three principle components with eigenvalues 233.52, 121.59 and 101.34 respectively, accounted 92 % of total variations of gene expressions in 6 stages. Table 1 showed a set of genes with largest loading score (negative or positive) in the first three principle components in the ascending order. The loading scores are highly correlated with the expression level of genes. In Table 1 we also listed the ratio of the gene expressions in the corresponding stages of the tumor development. From Table 1 we can see that the first principle component roughly describes the changes of the gene expression level in the first and last stage of tumor development. Nine genes in the upper of the table were up-regulated in the stages of basal cell hyperplasia and early cancer, meanwhile seven genes in the bottom of the table were down-regulated in these stages. Genes GAF, CAPR, CASP8, BMP5, MIF and MYC may play important roles in the esophagus tumorigenesis. GAF (Glial-activating factor) is a novel heparin-binding growth factor purified from the culture supernatant of a human glioma cell line with growth-stimulating effect on glial cells *in vitro*. GAF domains are ubiquitous motifs present in cyclic GMP (cGMP)-regulated cyclic nucleotide phosphodiesterases and form a new class of cyclic nucleotide receptors distinct from the regulatory domains of cyclic nucleotide-regulated protein

kinases and ion channels^[8], the role of GAF in tumor development has not been characterized yet; CAPR is cadherin-associated protein related, also named as alpha 2 catenin, the abnormal expression of adhesion molecules (E-cadherin, alpha-catenin) has been reported as markers of high malignant potential in esophageal cancer^[9], and it was suggested that alpha catenin has prognostic significance in colorectal and prostate cancer^[10]; The human CASP8 gene, whose product is also well known as caspase 8, encodes an interleukin-1beta converting enzyme (ICE)-related cysteine protease that is activated by the engagement of several different death receptors. Caspase 8 is a cysteine protease regulated in both a death-receptor-dependent and -independent manner during apoptosis, it is well characterized in apoptosis and tumor development^[11]; BMP5 (Bone morphogenetic protein-5) is a signaling molecule which have the ability to induce ectopic bone when placed under the skin of an animal^[12]; MIF (macrophage migration inhibitory factor) is involved in tumorigenesis via promotion of angiogenesis^[13], it is an ubiquitous cytokine whose expression has been investigated in tumors, showing a correlation between tumor aggressiveness and production of this protein by neoplastic cells. MIF is known to function as a cytokine, hormone, and glucocorticoid-induced immunoregulator, it is likely that MIF may function as a novel growth factor that stimulates incessant growth and invasion of melanoma concomitant with neovascularization; Myc is a well known oncogene which was involved in most of tumorigenesis, and

obviously it plays an important role in esophageal cancer development.

The second component involves three stages of the tumor development: basal cell hyperplasia, dysplasia and carcinoma in situ. Table 1 listed nine genes which were up-regulated and eight genes which were down-regulated in the stages of basal cell hyperplasia and dysplasia. The third principle component reflects the changes of the gene expression level in the transition from normal to basal cell hyperplasia and from basal cell hyperplasia to dysplasia. The table listed genes may play an important role in these transitions.

Table 1A Ratio of expression level for a set of genes with the largest loading scores in the first two principal components

Component 1			Component 2		
Gene	Ratio ELCA/LaCa	Ratio BCH/N	Gene	Ratio BCH/N	Ratio DYS/CAIN
GAF	131	16	PCTK1	122	8
CAPR	582	25	DAXX	5	95
CASP8	743	37	P70	7	62
MMp16	143	17	CCNH	174	87
DCC Precursor	316	12	CD153 antigen	70	31
Tenascin-R	742	21	TLAA	9	39
ZAP70	157	83	XPG	90	26
IL-13	110	22	Apoptosis Inhibitor Survivin	3	107
TRAIL receptor	66	82	Bcl-1 oncogene	122	19
	LaCa/ELCA	N/BCH		N/BCH	CAIN/DYS
BMP5	284	170	MERLIN	3	411
MIF	79	72	LERK-8	31	334
N-myc	14	110	DSG2; HDGC	355	395
RPSA	19	68	MMP11	2	271
RBL2	33	18	CDK2	13	51
RAD52	27	9	CLK1	60	798
RBQ1	15	55	MDMX	3	225

N: Normal; BCH: Basal cell hyperplasia; DYS: Dysplasia; CAIN: Carcinoma in situ; ELCA: Early cancer; LaCa: Late cancer.

Table 1B Ratio of expression level for a set of genes with the largest loading scores in the third principal components

Gene	Ratio N/BCH	Ratio DYS/BCH
Bcl-2L8	803	227
SRC1	333	141
Muscle cadherin precursor	299	111
Neurogenic locus notch protein	488	104
CASP3	232	92
BCL2A1;GRS protein	133	665
Type 1 cytoskeletal 10 protein	302	370
TRAF5	83	650
Transcription factor E2F5	615	30
MAP kinase p38	147	86
	BCH/N	BCH/DYS
KRT7	2	105
GRB-IR	5	96
GAS1	4	210
BMP8	21	21
DVL	12	187
CAM-PDE1B	18	18
Apoptosis regulator bcl-2	60	59

N: Normal; BCH: Basal cell hyperplasia; DYS: Dysplasia.

Table 2 Genes up or down regulated in all five stages of grade II basal cell hyperplasia, high-grade dysplasia, carcinoma in situ, early and advanced squamous cell carcinoma. Position indicates the gene position on the microarray membrane

Position	Gene Name
Up Regulated Genes	
A2k	G1/S-specific cyclin C
A4i	ERK5
A4j	ERK6
A5b	ERK activator kinase 1
A5l	transcription factor DP2
B3g	caspase-8 precursor
B3i	caspase-9 precursor
B3j	caspase-10 precursor (CASP10)
C1a	DNA-dependent protein kinase
C2c	DNA-repair protein XRCC1
C2j	RAD1
C4b	Wnt-5A
C4k	DVL1
C6m	CCK4
C7k	retinoic acid receptor epsilon
C7l	retinoic acid receptor gamma 1
C7m	retinoic acid receptor beta
D4b	integrin alpha 8
D4j	integrin beta 7 precursor
D4k	integrin beta 8 precursor
D5g	ezrin; cyto villin 2; villin 2
D5j	CD56 antigen
D7f	placenta growth factor 1
E1f	MMP9
E2a	MMP18
F3j	early growth response protein 1
F4l	IL-6
F5e	IL-13
F5k	interferon gamma precursor
F5l	leukocyte interferon-inducible peptide
Down regulated Genes	
C6c	insulin-like growth factor binding protein 2 (IGFBP2)
F4d	interleukin-1 receptor antagonist protein precursor (IL-1RA; IRAP)

Some genes are activated in particular stages

According to their specificity to stages, differentially expressed genes fall into two main categories. The first category contains genes that are up or down regulated in the same way in all 4 abnormal stages. 77 genes belong to this category, including G1/S-specific cyclin C, proliferating cyclic nuclear antigen (PCNA), E2F dimerization partner 2, Wnt5A, retinoic acid receptors (epsilon, gamma 1, beta), early growth response protein 1 (hEGR1), etc. Part of these genes are listed in Table 2. Most of which are genes related to cell proliferation or differentiation. These expression profiles are accordant with the generality of characteristic phenotype of all of the 4 abnormal stages, i.e. decrease in extent of differentiation and increase in rate of proliferation.

The second category contains genes that were up or down regulated in particular stages, some of them seemed to be activated in early stages of carcinogenesis, p160ROCK is one of such genes. Figure 3 showed the expression level of

p160ROCK in 5 stages. P160 ROCK peaked its expression level in the stage of high grade dysplasia, down-regulated rapidly after this stage, recovered its expression level in early and late cancer, which revealed that this gene was transcriptionally activated at pre-cancerous stage.

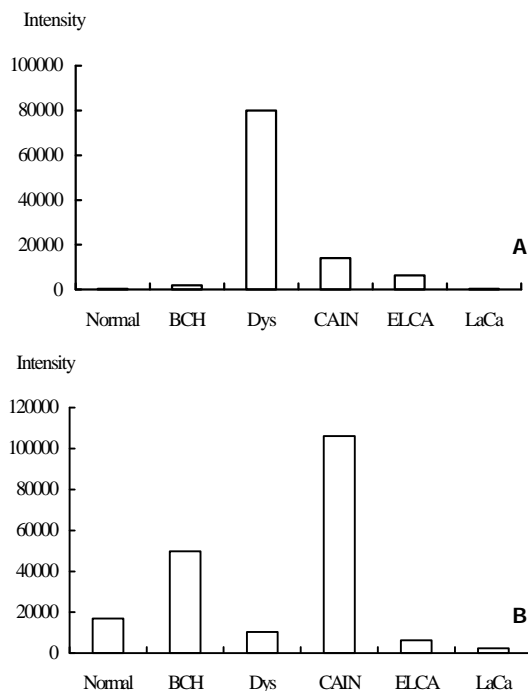


Figure 3 Expression level of p160ROCK (3A) and JNK2 (3B) in 6 different stages, p160ROCK peaked its expression at stage of high-grade dysplasia and JNK2 peaked its expression at stage of carcinoma in situ. The column chart indicated expression levels of p160ROCK and JNK2 in stages of normal mucosa (designated normal), basal cell hyperplasia II (designated BCH), high grade dysplasia (designated Dys), squamous cell carcinoma in situ (designated CAIN), early cancer (designated ELCA) and late cancer (designated LaCa).

p160ROCK belongs to a family of Rho-associated serine/threonine kinase isozymes and has been identified as a new class of Rho effectors. Its main function is participating the reorganization of the cytoskeletal, and plays an important role in signal transduction from Rho to cytoskeletal^[14] and also get involved in cell motility and morphological changes^[15]. In human hepatocellular carcinoma cells, dominant active p160ROCK transfectants showed increased motility, and dominant negative p160ROCK transfectants showed reduced motility under stimulation. Furthermore, implantation of dominant negative p160ROCK transfectants resulted in a reduced metastatic rate *in vivo* compared with the parent cells or a control transfectant^[16]. In this study, p160ROCK was found transcriptionally activated at the stage of high grade dysplasia, a pre-malignant stage, which imply that activation of the gene may be one of the early events during progress of esophageal carcinogenesis and may be one of the events responsible for morphological changes and increase in cell motility in early stages of carcinogenesis.

JNK2 is another representative gene which peaked its expression level in the stage of carcinoma in situ. Its expression levels in the 5 stages were shown in Figure 3. JNK2, c-Jun N-terminal kinase 2, also named as protein kinase mitogen-activated 9, is a proline-directed serine/threonine kinase activated by dual phosphorylation on threonine and tyrosine residues in response to a wide array of extracellular stimuli. Multiple research showed that JNK2 plays a critical role in coordinating the cellular response to stress and has been

implicated in regulating cell growth and transformation, antisense JNK2 induced growth inhibition which correlated with significant apoptosis^[17]. It was shown that JNK2 plays an important role in cell transformation and carcinogenesis. In this study, JNK2 was found activated at stage of carcinoma in situ, and down regulated in early and late cancer, which showed that this may also be an early events of carcinogenesis and one of the forces pushing the cell from pre-malignancy to malignancy.

DISCUSSION

Tumorigenesis is a complex and multistage process with many genes involved in. As a step toward understanding the complicated changes between normal and malignant cells, this report focused on gene expression profile variations among normal and abnormal esophageal epithelium tissues. Analyzing alterations of gene expression profiles in different stages of neoplasia is necessary for establishing the preventive, diagnostic, therapeutic, and prognostic potential of each related gene. To illustrate the mechanisms controlling malignant changes at molecular level may provide a further understanding of tumorigenesis, as well as new approaches in early detection and treatment of esophageal cancer. Furthermore, since it is impossible to get tissue samples of different stages from one patient, we got the biopsy specimens from different patients and pooled the samples with same pathologic diagnosis together to avoid the individual differences, and semi-quantitative RT-PCR was performed to confirm the reliability of the data. Moreover, we observed that many genes expressed abnormally in this complicated process and those changes mainly involved in cell proliferation, apoptosis, DNA repair, growth factors and cytokines. These genes and their expression alteration constitute a molecular atlas that is stage-specific and esophageal cancer-specific, and possibly being an important supplement to the traditional morphological diagnosis.

Principle component analysis identified a set of genes which plays important role in different stages of tumor development. Although many genes were related to tumorigenesis and development of esophageal cancer, further investigation is still needed to elucidate which gene (s) is the most critical one (s) to this complex process.

REFERENCES

- 1 **DeRisi J**, Penland L, Brown PO, Bittner ML, Meltzer PS, Ray M, Chen M, Su YA, Trent JM. Use of a cDNA microarray to analyze gene expression patterns in human cancer. *Nat Genet* 1996; **14**: 457-460
- 2 **Schena M**, Shalon D, Davis RW, Brown PO. Quantitative monitoring of gene expression patterns with a complementary DNA microarray. *Science* 1995; **270**: 467-470
- 3 **Fuller GN**, Rhee CH, Hess KR, Caskey LS, Wang R, Bruner JM, Yung WK, Zhang W. Reactivation of insulin-like growth factor binding protein 2 expression in glioblastoma multiforme: a revelation by parallel gene expression profiling. *Cancer Res* 1999; **59**: 4228-4232
- 4 **Sgroi DC**, Teng S, Robinson G, LeVangie R, Hudson JR, Elkahoulou AG. *In vivo* gene expression profile analysis of human breast cancer progression. *Cancer Res* 1999; **59**: 5656-5661
- 5 **Johanson RA**, Wichern DW. Applied multivariate statistical analysis, Prentice Hall, Inc., New York. 1982
- 6 **Lyer VR**, Eisen MB, Ross DT, Schuler G, Moore T, Lee JC, Trent JM, Staudt LM, Hudson J, Boguski MS, Lashkari D, Shalon D, Botstein D, Brown PO. The transcriptional program in the response of human fibroblasts to serum. *Science* 1999; **283**: 83-87
- 7 **Luo L**, Salunga RC, Guo H, Bittner A, Joy KC, Galindo JE, Xiao H, Rogers KE, Wan JS, Jackson MR, Erlander MG. Gene expression profiles of laser-captured adjacent neuronal subtypes. *Nat Med* 1999; **5**: 117-122
- 8 **Ho YS**, Burden LM, Hurley JH. Structure of the GAF domain, a

- ubiquitous signaling motif and a new class of cyclic GMP receptor. *EMBO J* 2000; **19**: 5288-5299
- 9 **Krishnadath KK**, Tilanus HW, van Blankenstein M, Hop WC, Kremers ED, Dinjens WN, Bosman FT. Reduced expression of the cadherin-catenin complex in oesophageal adenocarcinoma correlates with poor prognosis. *J Pathol* 1997; **182**: 331-338
- 10 **Aaltomaa S**, Lipponen P, Ala-Opas M, Eskelinen M, Kosma VM. Alpha-catenin expression has prognostic value in local and locally advanced prostate cancer. *Br J Cancer* 1999; **80**: 477-482
- 11 **Teitz T**, Wei T, Valentine MB, Vanin EF, Grenet J, Valentine VA, Behm FG, Look AT, Lahti JM, Kidd VJ. Caspase 8 is deleted or silenced preferentially in childhood neuroblastomas with amplification of MYCN. *Nat Med* 2000; **6**: 529-535
- 12 **DiLeone RJ**, Marcus GA, Johnson MD, Kingsley DM. Efficient studies of long-distance Bmp5 gene regulation using bacterial artificial chromosomes. *Proc Natl Acad Sci USA* 2000; **97**:1612-1617
- 13 **Shimizu T**, Abe R, Nakamura H, Ohkawara A, Suzuki M, Nishihira J. High expression of macrophage migration inhibitory factor in human melanoma cells and its role in tumor cell growth and angiogenesis. *Biochem Biophys Res Commun* 1999; **264**: 751-758
- 14 **Maekawa M**, Ishizaki T, Boku S, Watanabe N, Fujita A, Iwamatsu A, Obinata T, Ohashi K, Mizuno K, Narumiya S. Signaling from Rho to the actin cytoskeleton through protein kinases ROCK and LIM-kinase. *Science* 1999; **285**: 895-898
- 15 **Hirose M**, Ishizaki T, Watanabe N, Uehata M, Kranenburg O, Moolenaar WH, Matsumura F, Maekawa M, Bito H, Narumiya S. Molecular dissection of the Rho-associated protein kinase (p160ROCK)-regulated neurite remodeling in neuroblastoma N1E-115 cells. *J Cell Biol* 1998; **141**: 1625-1636
- 16 **Genda T**, Sakamoto M, Ichida T, Asakura H, Kojiro M, Narumiya S, Hirohashi S. Cell motility mediated by rho and Rho-associated protein kinase plays a critical role in intrahepatic metastasis of human hepatocellular carcinoma. *Hepatology* 1999; **30**: 1027-1036
- 17 **Potapova O**, Gorospe M, Dougherty RH, Dean NM, Gaarde WA, Holbrook NJ. Inhibition of c-Jun N-terminal kinase 2 expression suppresses growth and induces apoptosis of human tumor cells in a p53-dependent manner. *Mol Cell Biol* 2000; **20**: 1713-1722

Edited by Xu JY

Application of poly-lactide-co-glycolide-microspheres in the transarterial chemoembolization in an animal model of hepatocellular carcinoma

Jun Qian, Jochen Truebenbach, Florian Graepler, Philippe Pereira, Peter Huppert, Thomas Eul, Gundula Wiemann, Claus Claussen

Jun Qian, Jochen Truebenbach, Florian Graepler, Philippe Pereira, Peter Huppert, Thomas Eul, Gundula Wiemann, Claus Claussen, Department of Diagnostic Radiology, Eberhard-Karls-University Tubingen, Hoppe-Seyler-Strasse-3, Tubingen 72076, Germany

Supported by Bundesministerium fuer Bildung, Wissenschaft, Forschung und Technologie (Germany), No. 01KS9602

Correspondence to: Dr. Jun Qian, Department of Radiology, Xiehe Hospital, Tongji Medical College, Huazhong University of Science and Technology, Wuhan 430022, China. junqian_tjmc@yahoo.com.cn

Telephone: +86-27-85726432 **Fax:** +86-27-85727002

Received: 2002-01-28 **Accepted:** 2002-02-20

Abstract

AIM: To introduce an animal model of hepatocellular carcinoma (HCC) in ACI-rats, and to evaluate the therapeutic effects of Poly-lactide-co-glycolide(Plcg)-microspheres in the transarterial chemoembolization (TACE) in this model, as well the value of this model in the experiments of interventional therapy.

METHODS: Subcapsular implantation of a solid Morris Hepatoma 3 924A (1 mm³) in the livers was carried out in 11 male ACI-rats. The tumor volume (V1) was measured by magnetic resonance imaging (MRI) (13 days after implantation). After laparotomy and retrograde placement of catheter into the gastroduodenal artery (14 days after implantation), the following protocols of interventional treatment were performed: (A) mitomycin C+Poly-lactide-co-glycolide(Plcg)-microspheres ($n=4$); (B) 0.9 % NaCl (control group, $n=7$). 13 days after these therapies the change of the tumor volume (V2) was determined by MRI again.

RESULTS: The success rate of tumor implantation reached to 100 %. The mean tumor volume before TACE (V1) were 0.082 cm³ in group A and 0.096 cm³ in group B respectively. The mean tumor volume after TACE (V2) were 0.230 cm³ in group A and 1.347 cm³ in group B respectively. The mean V2/V1 were 2.860 in group A and 27.120 in group B respectively. Compared to the control group (group B), groups A showed a significant reduction of tumor growth ($P=0.004$) in the period of observation.

CONCLUSION: The growth of liver tumor could be obviously prevented by utilizing Plcg-mitomycin-microspheres in TACE in animal model. This rat model of HCC is suitable for the experimental studies of interventional therapy.

Qian J, Truebenbach J, Graepler F, Pereira P, Huppert P, Eul T, Wiemann G, Claussen C. Application of poly-lactide-co-glycolide-microspheres in the transarterial chemoembolization in an animal model of hepatocellular carcinoma. *World J Gastroenterol* 2003; 9(1): 94-98

<http://www.wjgnet.com/1007-9327/9/94.htm>

INTRODUCTION

Hepatocellular carcinoma (HCC) is one of the most common malignancies in the world, responsible for an estimated one million deaths annually^[1,2]. In China, HCC has been ranked second of cancer mortality since 1990s^[3]. It has a poor prognosis due to its rapid infiltrating growth and complicating liver cirrhosis^[4]. Surgical resection is still the only potentially curative treatment for HCC, particularly for small HCC^[3]. To date, the resection rate for HCC is unfortunately less than 30 %^[5, 6]. Transarterial chemoembolization (TACE) is currently the first choice of treatment for most unresectable HCC and improve the survival rate in selected patients^[7-13]. However, the technical variants of TACE have often been chosen on an empirical basis and it is not always safe and effective^[14-16]. Although TACE advantageously combines arterial embolization of the vascular supply of HCC with controlled intra-arterial infusion of chemotherapeutic drugs, its application is limited by the lack of appropriate and reliable embolization materials^[15,16]. Recently, poly-lactide-co-glycolide (Plcg)-microspheres has been proved to be a new promising embolic agent^[17,18]. In order to study the interventional therapeutic strategies for HCC, it is necessary to establish a suitable and reproducible animal model. The aim of the present study was to introduce an animal model of HCC with the technique of tumor implantation in ACI-rats, and to evaluate the therapeutic effect of different methods of TACE, including the efficiency of Plcg-microspheres in this animal model. MRI was performed for measuring the tumor volume before and after the TACE in this study.

MATERIALS AND METHODS

Tumor

Morris hepatoma 3 924A, a rapidly growing, poorly differentiated hepatocellular carcinoma, was induced by dietary administration of N-2-fluorenyldiacetamide in an ACI rat. The hepatoma specimens were obtained from the German Cancer Research Center in Heidelberg (DKFZ).

Animal

Inbred male ACI-rats weighing 200 to 220 g ($n=15$) were obtained from the company of Harlan Winkelmann in Germany. The animals were kept under conventional conditions with a temperature of 22 ± 2 °C, a relative humidity of 55 ± 10 %, a dark-light rhythm of 12 hr, and were fed standard laboratory chow and tap water ad libitum.

Anesthesia

All interventional and imaging procedures were carried out under intraperitoneally applied anesthesia with ketamine hydrochloride (Ketanest, Parke-Davis, Germany; 100 mg·kg⁻¹), Xylazinehydrochlorid (Rompun, Bayer, Germany; 15 mg·kg⁻¹) and atropine sulfate (Atropinsulfat Braun, Braun, Germany; 0.1 mg·kg⁻¹).

Tumor implantation (At day 1)

The technique for tumor implantation was basically similar to that described by Yang *et al*^[19,20] with minor modifications^[21].

The Morris Hepatoma 3 924A tumor tissue, recovered from the passaged animals 2 weeks after subcutaneous implantation (corresponding to 5×10^6 tumor cells), was cut into small cubes about 1 mm^3 .

The recipient ACI-rats were intraperitoneally anesthetized, and the upper abdomen was shaved. A small subcapsular incision on the left lateral lobe of the liver was made. The tumor fragment was gently placed into the pocket with a small cotton swab on the liver surface as hemostasis and the abdominal wall was then closed.

Catheterization and TACE (At day 14)

A PE-10 polyethylene catheter (inner diameter 0.28 mm, outer diameter 0.61 mm; Wenzel/Heidelberg, Germany) was used for experiments of TACE under a second laparotomy. By using a binocular operative microscope (M651, Leica/Wetzler, Germany), the catheter was retrograde inserted into the gastroduodenal artery (Figure 1). After slightly drawing the thin rope around the common hepatic artery, the following different agents were injected through the catheter: Group A ($n=4$): TACE with mitomycin C ($0.25 \text{ mg} \cdot \text{kg}^{-1}$) and Plcg-microspheres ($200 \text{ mg} \cdot \text{kg}^{-1}$, diameter: $40 \mu\text{m}$; Institute of Pharmacological Technology, Philipps University, Marburg/Germany).

Group B (control group, $n=7$): injection of 0.9 % NaCl alone.

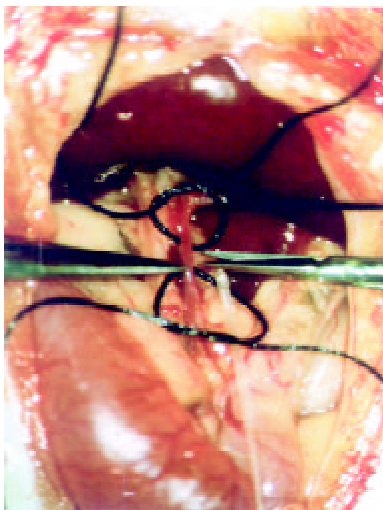


Figure 1 Catheterization of the gastroduodenal artery *in vivo*

MRI

MRI was performed in a 1.0 Tesla Magnetom superconducting system (Siemens, Erlangen, Germany) supplemented by a commercial coil (Small Field of View) before and after the catheterization (At day 13 and 27). T1-weighted (TR/TE, 400/14 ms) and T2-weighted (TR/TE, 3 000/96 ms) axial SE images with spatial presaturation for controlling the flow artifact were acquired. Slice thickness was 2.0 mm, Matrix was 192×256 . There was no gap between sections. The findings on T1- and T2-weighted SE images were examined in all 11 rats. Tumor volume was determined and evaluated according to the formula: Tumor volume (mm^3) = $\text{Length}(\text{mm}) \times \text{Width}^2(\text{mm})^2 / 2^{[22]}$.

RESULTS

In all the rats receiving tumor implantation with Morris Hepatoma 3 924A, the rate of tumor implantation reached 100 %. None of the animals died during implantation or in the postoperative period.

The sensitivity of MRI for detecting HCC reached 100 %. HCC showed a hypointense pattern on T1-weighted images and a hyperintense pattern on T2-weighted images in the left lateral lobe of the liver (Figure 2, Figure 3). Necrosis,

hemorrhage and metastase of the tumor were not observed. The liver tumor was well discernible from the surrounding liver tissue on each image.

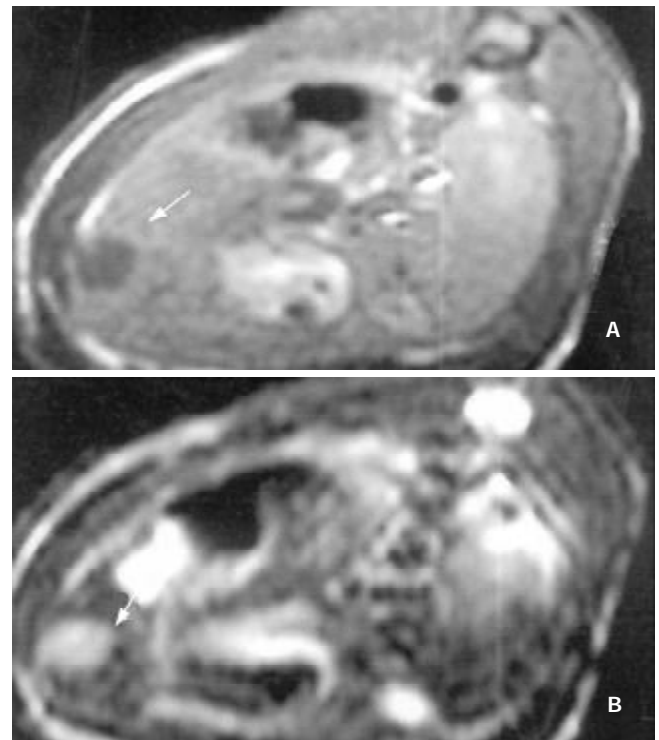


Figure 2 MR images of HCC before the application of Plcg-Mitomycin-microspheres: (a) T1-weighted image (400/14 ms) showed a hypointense pattern in the left lateral lobe of the liver, (b) T2-weighted image (3 000/96 ms) showed a hyperintense pattern in the liver. Necrosis, hemorrhage and metastase of the tumor were not observed.

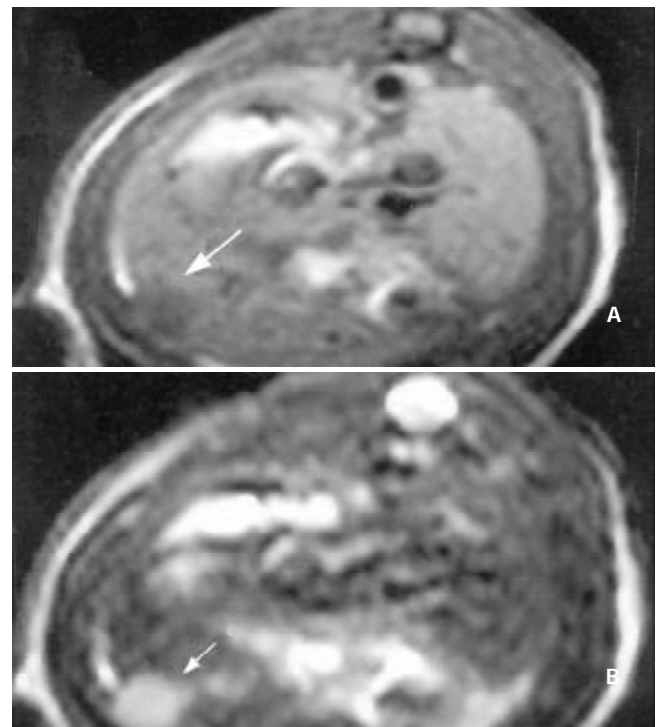


Figure 3 MR images of HCC after the application of Plcg-Mitomycin-microspheres: (a) MRI T1WI (400/14 ms); (b) MRI T2WI (3 000/96 ms). The tumor volume after the application of Plcg-Mitomycin-microspheres was not changed compared to that before the application.

The efficiencies of Plcg-Mitomycin-microspheres in the interventional therapy of HCC in ACI-rats were shown in Table 1.

Table 1 The efficiencies of Plcg-Mitomycin-microspheres in the interventional therapy of HCC in ACI-rats

	Group A (Plcg)	Group B (control group)
Mean volume (V1) before TACE (cm ³)	0.082	0.096
Mean volume (V2) after TACE (cm ³)	0.230	1.347
Mean V2/V1	2.86	27.12

Compared to the control group (group B), groups A showed a significant reduction of tumor growth ($P=0.004$) in the period of observation by *t*-test.

DISCUSSION

In order to investigate the efficiency of TACE for HCC, it is necessary to have a suitable and reproducible animal model. Various animal models of liver tumor have been established. The diethylnitrosamine model for hepatic tumor induction was simple, and provided a more representative range of tumors for experimental evaluation. However, the high mortality of the animals and various localization/number/size of the tumor in the liver were the major shortcomings. Therefore, the application of this model was extremely limited. The technique with a needle injection of tumor cells into hepatic parenchyma often caused tumor spill from the puncture channel and might result direct injection of the tumor cells into the circulation^[19]. Although a relative high tumor take rate could be obtained by using the Walker-256/VX2 model in rats or rabbits with the technique of tumor implantation, these animal models belonged to carcinosarcoma or adenocarcinoma and were usually utilized for the study of liver metastases^[23-27]. It is well known that the metastasis way and the therapeutic strategies as well the related effects of HCC and sarcoma are quite different from the aspect of histopathology, and a characteristic of HCC which distinguishes it from most metastases to the liver is that it is a highly vascular tumor^[28], so that these animal models are unsatisfactory and not suitable for studying the interventional therapy.

In our present study, an animal model of HCC with the technique of tumor implantation previously described by Yang *et al*^[19,20] was established. The rate of tumor implantation reached 100 %^[17]. Necrosis, hemorrhage and metastases of the tumor were not observed. Histopathologically, Morris hepatoma 3 924A was a poorly differentiated hepatocellular carcinoma, mimicking the Edmondson grade-III hepatoma in humans^[20] (Edmondson's classification is based on the degree of differentiation of HCC). The appropriate growth speed of the liver tumor made it easy for MRI examination^[29]. The blood supply of the tumor mainly came from hepatic arteries which was similar to that in human liver cancers^[19, 29]. As is known to all, HCC was usually hypervascular except for differentiated HCC and TACE was usually effective only for hypervascular HCC^[30-33]. Compared to other animal models, our rat model was more suitable for the study of interventional therapy of HCC, and the related conclusion of the study was more convincing.

MRI examination for measuring the tumor volume without utilizing contrast media was carried out in our experiments. There was no single parameter better than tumor growth rate that could give information on the effects of different therapeutic maneuvers on tumor growth^[22]. In another study of ours, we have demonstrated that MRI as an invasive imaging modality was superior to CT, DSA in the diagnosis of HCC in experiments^[29]. It was supported by histological examination that MRI was also superior to ultrasonography for judging the tumor dimensions^[29]. Another advantage of MRI was its

excellent soft-tissue contrast resolution^[34]. T1-weighted imaging was superior to T2-weighted imaging in depicting early HCC, but the latter could be useful in evaluating the progression of HCC in the histopathologically early stages^[35]. The signal intensity on T2-weighted images correlated with the histological grade and histopathological change of HCC^[35-37]. The detectability of MRI was 100 % in the present study. HCC showed a hypointense pattern on T1-weighted images and a hyperintense pattern on T2-weighted images in the left lateral lobe of the liver. Necrosis, hemorrhage and metastase of the tumor were not observed. The contrast between the tumor and surrounding normal liver parenchyma was clear to observe. Based on these results, we concluded that MRI was useful in the assessment of the therapeutic effects of TACE in HCC.

TACE is one choice of the palliative treatment for unresectable HCC, particularly for patients with multifocal HCC and with acceptable liver functions. TACE caused tumor necrosis by occlusion of the feeding artery of HCC, and its clinical efficiencies have been generally recognized^[38-41]. By using TACE with a combination of cytostatic drugs (mitomycin, doxorubicin, epirubicin, cisplatin, 5-Fu), a reduction of vital tumor tissue could be achieved^[42-44], although the prolongation of survival remained questionable^[45, 46]. As stated before, although TACE advantageously combined arterial embolization of the vascular supply of a neoplasm with controlled intra-arterial infusion of chemotherapeutic drugs, its application was limited by the lack of appropriate and reliable embolic agents. The major problem with embolic agents are twofold^[47]: first, they could often completely obstruct the hepatic artery, leading to difficulties in administration of subsequent courses of hepatic artery chemotherapy. With a relative short half-life of embolic agents, the effectiveness of TACE was not significantly improved; and second, it was easy to aggravate the liver cirrhosis and lead to hepatic failure after repeated TACE. The optimal treatment modality of TACE was unknown^[14, 48].

Recently, Plcg-microspheres have been proved to be a new promising embolic agent in TACE in experiments^[17,18]. Verrijck and co-workers^[49,50] reported that TACE with Plcg-microspheres and CDDP significantly improved the delivery of cytotoxic drugs to liver tumor and simultaneously reduced systemic toxicity in animals. Plcg-microspheres are biodegradable polymers with high molecular size and possess a good tissue compatibility. The degradation rate of polylactides is known to depend on the polymer microstructure that may be of the L, D or D, L type. The polyester lifetime could be controlled in a range of a few days or months^[49-51]. It has been suggested that this drug could slowly release into the tumor tissues principally by a diffusion mechanism. It has also been indicated that the microspheres size of 40 μ m allows a distal and homogeneous migration of the embolic agent within the targeted organ, without passing through the capillary filter^[18], it is this reason that Plcg-microspheres with the size of 40 μ m were chosen in our experiments. Verrijck *et al*^[49,50] also demonstrated, that the absence of a burst effect and an adequate CDDP release from Plcg-CDDP-microspheres then significantly prolonged the first-pass effect, with the result that low systemic platinum levels were maintained while a liver platinum concentration was achieved which was high enough for an antitumor effect. The results of our present studies indicated that Plcg-microspheres could effectively retard the growth of HCC. Compared to the control group (group B), groups A (Plcg) showed a significant reduction of tumor growth ($P=0.004$) in the period of observation by *t*-test. The therapeutic efficiencies of Plcg-mitomycin-microspheres was similar to Gelform+Mitomycin+Lipiodol in our another study (Mean V2/V1=2.86, $P=0.748$, unpublished results).

To conclude, the growth of liver tumor was markedly

prevented by the use of Plcg-mitomycin-microspheres in the TACE in an animal model. This effective and reliable embolic agent might be useful in clinic in future. However, the mechanism of effect of Plcg-microspheres is not clear so far. Data on a large number of animals and the test of application of various cytotoxic agents in the TACE, as well the repeated TACE will be required.

REFERENCES

- 1 **Cha C**, DeMatteo RP, Blumgart LH. Surgery and ablative therapy for hepatocellular carcinoma. *J Clin Gastroenterol* 2002; **35**: S130-137
- 2 **Teo EK**, Fock KM. Hepatocellular carcinoma: an Asian perspective. *Dig Dis* 2001; **19**: 263-268
- 3 **Tang ZY**. Hepatocellular carcinoma-cause, treatment and metastasis. *World J Gastroenterol* 2001; **7**: 445-454
- 4 **Yuen MF**, Cheng CC, Lauder IJ, Lam SK, Ooi CG, Lai CL. Early detection of hepatocellular carcinoma increases the chance of treatment: Hong Kong experience. *Hepatology* 2000; **31**: 330-335
- 5 **Sturm JW**, Keese MA, Bonninghoff RG, Wustner M, Post S. Locally ablative therapies of hepatocellular carcinoma. *Onkologie* 2001; **24** (Suppl 5): 35-45
- 6 **Chung JW**. Transcatheter arterial chemoembolization of hepatocellular carcinoma. *Hepatogastroenterology* 1998; **45** (Suppl 3): 1236-1241
- 7 **Acunas B**, Rozanes I. Hepatocellular carcinoma: treatment with transcatheter arterial chemoembolization. *Eur J Radiol* 1999; **32**: 86-89
- 8 **Rose DM**, Chapman WC, Brockenbrough AT, Wright JK, Rose AT, Meranze S, Mazer M, Blair T, Blanke CD, Debelak JP, Pinson CW. Transcatheter arterial chemoembolization as primary treatment for hepatocellular carcinoma. *Am J Surg* 1999; **177**: 405-410
- 9 **Liado L**, Virgill J, Figueras J, Valls C, Dominguez J, Rafecas A, Torras J, Fabregat J, Guardiola J, Jaurrieta E. A prognostic index of the survival of patients with unresectable hepatocellular carcinoma after transcatheter arterial chemoembolization. *Cancer* 2000; **88**: 50-57
- 10 **Zangos S**, Gille T, Eichler K, Engelmann K, Woitaschek D, Balzer JO, Mack MG, Thalhammer A, Vogl TJ. Transarterial chemoembolization in hepatocellular carcinomas: technique, indications, results. *Radiologe* 2001; **41**: 906-914
- 11 **Tang ZY**. Hepatocellular carcinoma. *J Gastroenterol Hepatol* 2000; **15** (Suppl): G1-7
- 12 **Livraghi T**. Treatment of hepatocellular carcinoma by interventional methods. *Eur Radiol* 2001; **11**: 2207-2219
- 13 **Loewe C**, Cejna M, Schoder M, Thurnher MM, Lammer J, Thurnher SA. Arterial embolization of unresectable hepatocellular carcinoma with use of cyanoacrylate and lipiodol. *J Vasc Interv Radiol* 2002; **13**: 61-69
- 14 **Camma C**, Schepis F, Orlando A, Albanese M, Shahied L, Trevisani F, Andreone P, Craxi A, Cottone M. Transarterial chemoembolization for unresectable hepatocellular carcinoma: meta-analysis of randomized controlled trials. *Radiology* 2002; **224**: 47-54
- 15 **Poon RT**, Ngan H, Lo CM, Liu CL, Fan ST, Wong J. Transarterial chemoembolization for inoperable hepatocellular carcinoma and postresection intrahepatic recurrence. *J Surg Oncol* 2000; **73**: 109-114
- 16 **Trinchet JC**, Ganne-Carrie N, Beaugrand M. Intra-arterial chemoembolization in patients with hepatocellular carcinoma. *Hepatogastroenterology* 1998; **45** (Suppl 3): 1242-1247
- 17 **Qian J**, Feng GS, Truebenbach J, Pereira PL, Huppert PE, Graepler F, Eul T, Claussen CD. Experimentelle Untersuchung zur Effektivität der Transarteriellen Chemoembolisation (TACE) im Tiermodell des hepatozellulären Karzinom. *Acta Universitatis Medicinæ Tongji* 2001; **21**: 115-118
- 18 **Bastian P**, Bartkowski R, Kohler H, Kissel T. Chemo-embolization of experimental liver metastases. Part I: distribution of biodegradable microspheres of different sizes in an animal model for the locoregional therapy. *Eur J Pharm Biopharm* 1998; **46**: 243-254
- 19 **Yang R**, Rescorla FJ, Reilly CR, Faught PR, Sanghvi NT, Lumeng L, Franklin TD, Grosfeld JL. A reproducible rat liver cancer model for experimental therapy: Introducing a technique of intrahepatic tumor implantation. *Journal of Surgical Research* 1992; **52**: 193-198
- 20 **Yang R**, Liu Q, Rescorla FJ, Grosfeld JL. Experimental liver cancer: Improved response after hepatic artery ligation and infusion of tumor necrosis factor-alpha and interferon-gamma. *Surgery* 1995; **118**: 768-774
- 21 **Trubenbach J**, Pereira PL, Graepler F, Huppert PE, Eul T, König CW, Duda SH, Claussen CD. Animal experiment studies on the effectiveness of permanent occlusion of the hepatic artery in transarterial chemoembolization. *Fortschr Röntgenstr* 2000; **172**: 274-277
- 22 **Carlsson G**, Gullberg B, Hafstrom L. Estimation of liver tumor volume using different formulas -an experimental study in rats. *J Cancer Res Clin Oncol* 1983; **105**: 20-23
- 23 **Yarmentis SD**, Kalogeropoulou CP, Hatjikondi O, Ravazoula P, Petsas T, Siambli D, Kalfarentzos F. An experimental approach of the Doppler perfusion index of the liver in detecting occult hepatic metastases: histological findings related to the hemodynamic measurements in wistar rats. *Eur Radiol* 2000; **10**: 417-424
- 24 **Ishida H**, Murata N, Yamada H, Nomura T, Shimomura K, Fujioka M, Idezuki Y. Effect of CO(2) pneumoperitoneum on growth of liver micrometastases in a rabbit model. *World J Surg* 2000; **24**: 1004-1008
- 25 **Kuszyk BS**, Boitnott JK, Choti MA, Bluemke DA, Sheth S, Magee CA, Horton KM, Eng J, Fishman EK. Local tumor recurrence following hepatic cryoablation: radiologic-histopathologic correlation in a rabbit model. *Radiology* 2000; **217**: 477-486
- 26 **Goldberg SN**, Walovitch RC, Straub JA, Shore MT, Gazelle GS. Radio-frequency-induced coagulation necrosis in rabbits: immediate detection at US with a synthetic microsphere contrast agent. *Radiology* 1999; **213**: 438-444
- 27 **Guo WJ**, Li J, Ling WL, Bai YR, Zhang WZ, Cheng YF, Gu WH, Zhuang JY. Influence of hepatic arterial blockage on blood perfusion and VEGF, MMP-1 expression of implanted liver cancer in rats. *World J Gastroenterol* 2002; **8**: 476-479
- 28 **Carr BI**. Hepatic artery chemoembolization for advanced stage HCC: experience of 650 patients. *Hepatogastroenterology* 2002; **49**: 79-86
- 29 **Trubenbach J**, Graepler F, Pereira PL, Ruck P, Lauer U, Gregor M, Claussen CD, Huppert PE. Growth characteristics and imaging properties of the Morris Hepatoma 3924A in ACI rats: A suitable model for transarterial chemoembolization. *Cardiovasc Intervent Radiol* 2000; **23**: 211-217
- 30 **Nakashima Y**, Nakashima O, Hsia CC, Kojiro M, Tabor E. Vascularization of small hepatocellular carcinomas: correlation with differentiation. *Liver* 1999; **19**: 12-18
- 31 **Tang ZY**. Treatment of hepatocellular carcinoma. *Digestion* 1998; **59**: 556-562
- 32 **Hayashi M**, Matsui O, Ueda K, Kawamori Y, Gabata T, Kadoya M. Progression to hypervascular hepatocellular carcinoma: correlation with intranodular blood supply evaluated with CT during intraarterial injection of contrast material. *Radiology* 2002; **225**: 143-149
- 33 **Kamura T**, Kimura M, Sakai K, Ichida T, Seki H, Yamamoto S, Ozaki T. Small hypervascular hepatocellular carcinoma versus hypervascular pseudolesions: differential diagnosis on MRI. *Abdom Imaging* 2002; **27**: 15-24
- 34 **Mueller-Lisse UG**, Heuck AF. Control and monitoring of focal radiotherapy with magnetic resonance tomography-An overview. *Radiologe* 1998; **38**: 200-209
- 35 **Honda H**, Kaneko K, Maeda T, Kuroiwa T, Fukuya T, Yoshimitsu K, Irie H, Aibe H, Takenaka K, Masuda K. Small hepatocellular carcinoma on magnetic resonance imaging: Relation of signal intensity to angiographic and clinicopathologic findings. *Invest Radiol* 1997; **32**: 161-168
- 36 **Inoue E**, Kuroda C, Fujita M, Narumi Y, Kadota T, Kuriyama K, Ishiguro S, Kasugai H, Sasaki Y, Imaoka S. MR features of various histological grades of small hepatocellular carcinoma. *J Comput Assist Tomogr* 1993; **17**: 75-79
- 37 **Yan FH**, Zhou KR, Cheng JM, Wang JH, Yan ZP, Da RR, Fan J, Ji Y. Role and limitation of FMPSG dynamic contrast scanning in the follow-up of patients with hepatocellular carcinoma treated by TACE. *World J Gastroenterol* 2002; **8**: 658-662
- 38 **Vogl TJ**, Schroeder H, Trapp M, Straub R, Schuster A, Schuster

- M, Mack M, Souchon F, Neuhaus P. Multi-sequential arterial chemoembolization of advanced hepatocellular carcinomas: Computerized tomography follow-up parameters for evaluating effectiveness of therapy. *Fortschr Rontgenstr* 2000; **172**: 43-50
- 39 **Li L**, Wu PH, Li JQ, Zhang WZ, Lin HG, Zhang YQ. Segmental transcatheter arterial embolization for primary hepatocellular carcinoma. *World J Gastroenterol* 1998; **4**: 511-512
- 40 **Chen MS**, Li JQ, Zhang YQ, Lu LX, Zhang WZ, Yuan YF, Guo YP, Lin XJ, Li GH. High-dose iodized oil transcatheter arterial chemoembolization for patients with large hepatocellular carcinoma. *World J Gastroenterol* 2002; **8**: 74-78
- 41 **Fan J**, Ten GJ, He SC, Guo JH, Yang DP, Weng GY. Arterial chemoembolization for hepatocellular carcinoma. *World J Gastroenterol* 1998; **4**: 33-37
- 42 **Kamada K**, Nakanishi T, Kitamoto M, Aikata H, Kawakami Y, Ito K, Asahara T, Kajiyama G. Long-term prognosis of patients undergoing transcatheter arterial chemoembolization for unresectable hepatocellular carcinoma: Comparison of cisplatin lipiodol suspension and doxorubicin hydrochloride emulsion. *J Vasc Interv Radiol* 2001; **12**: 847-854
- 43 **Gattoni F**, Dova S, Uslenghi CM. Three-year follow-up of 62 cirrhotic patients with hepatocellular carcinoma treated with chemoembolization. *Minerva Chir* 2000; **55**: 31-37
- 44 **Poyanli A**, Rozanes I, Acunas B, Sencer S. Palliative treatment of hepatocellular carcinoma by chemoembolization. *Acta Radiol* 2001; **42**: 602-607
- 45 **Roche A**. Therapy of HCC-TACE for liver tumor. *Hepatogastroenterology* 2001; **48**: 3-7
- 46 **Yip D**, Findlay M, Boyer M, Tattersall MH. Hepatocellular carcinoma in central Sydney: a 10 year review of patients seen in a medical oncology department. *World J Gastroenterol* 1999; **5**: 483-487
- 47 **Iwai K**, Maeda H, Konno T. Use of oily contrast medium for selective drug targeting to tumor: Enhanced therapeutic effect and x-ray image. *Cancer Research* 1984; **44**: 2115-2121
- 48 **Lorenz M**, Liermann D, Staib-Sebler E, Gog C, Encke A, Kollath J. Noradrenalin guided selective chemoembolization of hepatocellular carcinoma. *Zentralbl Chir* 1994; **119**: 777-786
- 49 **Verrijck R**, Smolders JJ, Bosnie N, Begg AC. Reduction of systemic exposure and toxicity of cisplatin by encapsulation in poly-lactide-co-glycolide. *Cancer Research* 1992; **52**: 6653-6656
- 50 **Verrijck R**, Smolders JJ, McVie JG, Begg AC. Polymer-coated albumin microspheres as carriers for intravascular tumor targeting of cisplatin. *Cancer Chemother Pharmacol* 1991; **29**: 117-121
- 51 **Hagiwara A**, Sakakura C, Tsujimoto H, Imanishi T, Ohgaki M, Yamasaki J, Sawai K, Takahashi T, Fujita T, Yamamoto A, Muranishi S, Ikada Y. Selective delivery of 5-fluorouracil (5-FU) to i.p. tissues using 5-FU microspheres in rats. *Anticancer Drug* 1997; **8**: 182-188

Edited by Pang LH

Nested case-control study on the risk factors of colorectal cancer

Kun Chen, Jian Cai, Xi-Yong Liu, Xi-Yuan Ma, Kai-Yan Yao, Shu Zheng

Kun Chen, Jian Cai, Department of Epidemiology, Zhejiang University School of Public Health, Hangzhou, 310006, Zhejiang Province, China

Xi-Yong Liu, Shu Zheng, Cancer Institute of Zhejiang University, Hangzhou, 310009, Zhejiang Province, China

Xin-Yuan Ma, Kai-Yan Yao, Institute of Cancer Research and Prevention, Jiashan County, 314000, Zhejiang Province, China

Supported by the National Natural Science Foundation of China, No. 30170828

Correspondence to: Kun Chen, Department of Epidemiology, Zhejiang University School of Public Health, 353 Yan-an Road, Hangzhou, 310006 Zhejiang Province, China. ck@zjuem.zju.edu.cn

Telephone: +86-571-87217190

Received: 2002-04-29 **Accepted:** 2002-06-08

Abstract

AIM: To investigate the risk factors of colon cancer and rectal cancer.

METHODS: A nested case-control study was conducted in a cohort of 64 693 subjects who participated in a colorectal cancer screening program from 1989 to 1998 in Jiashan county, Zhejiang, China. 196 cases of colorectal cancer were detected from 1990 to 1998 as the case group and 980 non-colorectal cancer subjects, matched with factors of age, gender, resident location, were randomly selected from the 64 693 cohort as controls. By using univariate analysis and multivariate conditional logistic regression analysis, the odds ratio (OR) and its 95 % confidence interval (95 %CI) were calculated between colorectal cancer and personal habits, dietary factors, as well as intestinal related symptoms.

RESULTS: The multivariate analysis results showed that after matched with age, sex and resident location, mucous blood stool history and mixed sources of drinking water were closely associated with colon cancer and rectal cancer, OR values for the mucous blood stool history were 3.508 (95 %CI: 1.370-8.985) and 2.139 (95 %CI: 1.040-4.402) respectively; for the mixed drinking water sources, 2.387 (95 %CI: 1.243-4.587) and 1.951 (95 %CI: 1.086-3.506) respectively. All reached the significant level with a *P*-value less than 0.05.

CONCLUSION: The study suggested that mucous blood stool history and mixed sources of drinking water were the risk factors of colon cancer and rectal cancer. There was no any significant association between dietary habits and the incidence of colorectal cancer.

Chen K, Cai J, Liu XY, Ma XY, Yao KY, Zheng S. Nested case-control study on the risk factors of colorectal cancer. *World J Gastroenterol* 2003; 9(1): 99-103

<http://www.wjgnet.com/1007-9327/9/99.htm>

INTRODUCTION

Colorectal cancer is one of the most common malignant tumors^[1-6]. During the past decades, the incidence of colorectal cancer was increased all around the world, more than 500 000 cases were diagnosed as colorectal cancer per year. In the east

of China, there has been a higher incidence of colorectal cancer. In Jiashan County, the mortality rate of colorectal cancer was the highest among China, which is about 20/100 000 per year^[7].

The causes of colorectal cancer are generally regarded as two aspects: heredity and environment^[8-10]. The former includes family history of cancer, intestinal polyp history, and so on. The later includes particularly dietary habit and physical activity.

Nested Case-Control Study (NCCS), an analytical epidemiological study method, was first presented by Mantel N, an American epidemiologist, in 1973^[11], and it was widely used after 1980's^[12-21]. All the subjects in such study are selected from a whole cohort, which is generally called cohort set. Compared with the cohort study, NCCS has the privilege of time-saving, money-saving, and trouble-saving; while compared to case-control study, since the exposure data are collected before the incident of disease, it is certain of the causes and time consequences relationship, and observational bias could be controlled efficiently. All of these characteristics of NCCS are suitable to the study of chronic disease, such as cancer.

There are many reports on the risk factors of colorectal cancer using classical case-control study method, however, few studies used nested case-control study method^[22-29]. The purpose of this study is to explore the risk factors of colorectal cancer, providing evidence for the prevention of colorectal cancer.

MATERIALS AND METHODS

Selection of cases and controls

A colorectal cancer screening program beginning on 1st May 1989 and ending on 30th April 1990 was conducted in ten countries which belonged to Jiashan county, Zhejiang province, China, including Weitan town, Yangmiao country, Xiadianmiao country, *et al*. From 75 842 eligible subjects aged 30 years and over, 64 693 subjects were enrolled as the base cohort set, the response rate was 85.3 %. Moreover, Jiashan county has founded cancer registration system and colorectal cancer report system, monitoring new cancer cases, including colorectal cancer. The cases in this study, who had participated in the 1989-1990 screening program, were the new colorectal cancer patients reported by Institute of Cancer Research and Prevention of Jiashan county. Up to 1998, the total number was 196 cases. Of which, 151 cases were pathological diagnosed, account for 77.1 %, 20 cases were diagnosed in the operation, 10.2 %, 23 cases were diagnosed by endoscopy, 11.7 %. Under the principle of same-country or town, same-sex, and no more than 3 years age disparity, 980 non-colorectal cancer subjects in the cohort set were selected as controls, resulting the final study subjects of 196 cases and 980 controls.

Contents of the study

The study contents composed of three parts as follow: (1). General characteristics: including age, sex, job types, educational levels, address *et al*; (2). Personal habits: including dietary habits, drinking water sources, alcohol consumption and cigarette smoking, *et al*; (3). Symptoms and disease history related with colorectal cancer: including changes of stool status, abdominal operation history, intestinal disease history, asthma history and allergy history, family cancer history, ancylostomiasis history, drug using history, psychic stimulation history, and so on.

Investigation methods and quality control

In the 1989-1990 screening investigation, a well-built *Investigation Manual* as the uniform criteria for inquiring the subjects and filling up the constructed questionnaire was used. All interviewers were trained focusing on the skills of inquiring. No subjects refused to be interviewed except that they were out of towns. For building the database, the questionnaires were coded and put into computer twice to control bias. The data used in this study were taken from this database.

Statistical analysis

Classical analysis methods of case-control study can be used to NCCS data, usually calculating OR value. In this study, Chi-square test was used in the univariate analysis of the data; conditional logistic regression was used in the multivariate analysis. The SPSS 10.0 for windows and the SAS system for windows, version 6.12, were used for completing all the statistical analyses.

RESULTS

General information

In this study, there were 196 cases (84 colon cancer, 112 rectal cancer) and 980 controls. The distribution of age between cases and controls for male and female was shown in Table 1.

Table 1 The distribution of subjects by age and sex

age	male		female	
	case	control	case	control
30-	3	15	7	35
35-	9	49	3	15
40-	14	69	3	19
45-	11	52	14	66
50-	21	110	14	78
55-	24	114	22	104
60-	11	57	13	63
65-	11	54	3	15
70-	2	10	5	26
75-	2	10	3	14
80-	0	0	1	5
Total	108	540	88	440

The average age of case group was 54.5 ± 10.6 years, while that of the control group was 54.3 ± 10.6 year, there was no statistically significant difference ($t=0.127$, $P=0.899$). For sex, there was also no difference statistically ($\chi^2=0.001$, $P=0.979$).

Univariate analysis

In order to control the possible confounding bias the age, sex and resident location were matched in the study design. Given that the risk factors of colon cancer might be different from that of rectal cancer, the analysis of the risk factors were separated into colon cancer and rectal cancer, instead of colorectal cancer. The OR and its 95 % confidence intervals (95 % CI), χ^2 and P values in the univariate analysis were showed respectively in Table 2 and Table 3 (the variables showed $P>0.20$ were excluded).

Table 2 Results of univariate analysis for colon cancer (cases $n=84$, controls $n=420$)

factors	OR	95 % CI	χ^2	P
pork eating($y=1, n=0$)	1.481	0.846 2.593	1.890	0.169
drining mixed water source* ($y=1, n=0$)	2.273	1.255 4.117	7.332	0.007
drining gutter water ($y=1, n=0$)	1.639	0.777 3.457	1.680	0.195
drining well water ($y=1, n=0$)	0.542	0.338 0.870	6.445	0.011
chronic diarrhea history($y=1, n=0$)	2.018	1.003 4.060	3.871	0.049
constipaton history($y=1, n=0$)	0.483	0.171 1.363	1.888	0.169
appendicitis history($y=1, n=0$)	1.697	0.966 2.981	3.386	0.066
appendix operating history($y=1, n=0$)	1.707	0.873 3.334	2.446	0.118
intestinal polyps history($y=1, n=0$)	6.503	2.009 21.049	9.762	0.002

*drinking mixed water source refers to the subjects drinking different type of water sources through his/her lifetime, mostly drinking river water and gutter water. So is Table 2,3 and 4

Table 3 Results of univariate analysis for rectal cancer (cases $n=112$, controls $n=560$)

factors	OR	95 % CI	χ^2	P
drining mixed water source ($y=1, n=0$)	2.021	1.170 3.491	6.363	0.011
mucious blood history ($y=1, n=0$)	2.138	1.122 4.072	5.335	0.021
defaecation drug using ($y=1, n=0$)	2.280	0.711 7.312	1.923	0.166
cholecyst excision history ($y=1, n=0$)	2.294	0.715 7.352	1.195	0.163

In Table 2, it was showed that four variables, well water drinking, mixed water source drinking, chronic diarrhea history and intestinal polyp history, were significantly associated with colon cancer ($P<0.05$). The factor of appendicitis history showed an OR value close to significant level ($P=0.066$). For rectal cancer in Table 3, there were two variables reached the significant level of $P=0.05$, which were mixed water source drinking (OR=2.02) and mucous blood stool history (OR=2.14).

Multivariate analysis

The variables showing associations with the risk of colon cancer and rectal cancer at $P<0.15$ level were further tested in forward stepwise conditional logistic regression models. The final model consisted of those variables showing a significant association with the risk of colorectal cancer at $P<0.05$ level. Results were showed in Table 4 and Table 5 for colon and rectal cancers, respectively.

Table 4 Results of multivariate analysis for colon cancer

factors	OR	95 % CI	P
drining mixed source water ($y=1, n=0$)	2.387	1.243 4.587	0.009
mucous blood history ($y=1, n=0$)	3.508	1.370 8.985	0.009

Table 4 and Table 5 illustrated that, at $P=0.05$ level, both for colon cancer and rectal cancer, the final logistic regression model comprised two factors: mixed water source drinking and mucous blood stool history.

Table 5 Results of multivariate analysis for rectal cancer

factors	OR	95%CI	P
drinking mixed water source ($y=1, n=0$)	1.951	1.086 3.506	0.025
mucous blood history ($y=1, n=0$)	2.139	1.040 4.402	0.039
factors	2.870	1.117 7.371	0.029

DISCUSSION

It is generally believed that colorectal cancer is the combined outcome of heredity and environment^[8-10,30]. Despite uncertainties regarding the underlying association between heredity and colorectal cancer, the genetic factors may affect the individual sensitivity to cancer^[3,30-37]; many documents had reported that the environmental factors might also influence colorectal cancer^[37-49]. On the secondary prevention for colorectal cancer, symptoms and/or disorders of pre-cancer, such as intestinal polyps, ulcerative colitis, should be considered^[50,51].

Univariate analysis results of this study showed that drinking well water is a protective factor for colon cancer, OR value was 0.542, ($P < 0.05$); drinking mixed water, mostly drinking river water and gutter water, was a risk factor both for colon cancer and rectal cancer, OR values were 2.387 (95 % CI: 1.247-4.587) and 1.951 (95 % CI: 1.086-3.506) in multivariate conditional logistic model, respectively. The association between drinking mixed water and colorectal cancer is consistent with former study. In this study, country subjects account for about 75 %, most of the mixed water drinking aggregated in country. In the local country, people usually were drinking river water and well water. It reflects that uncertainty of drinking water source, especially mixed drinking river water and guttering water would increase the incidence of colon cancer and rectal cancer. The findings in this study resembled other study reports^[47,52].

Chronic diarrhea, mucous blood stool and constipation history are the pre-clinical symptoms of colorectal cancer^[53-56]. This study has found the positive association between mucous blood stool history and colorectal cancer. In final colon cancer logistic model and rectal cancer logistic model, the OR values of mucous blood stool history were 3.508 (95 % CI: 1.370-8.985) and 2.139 (95 % CI: 1.04-4.402) respectively, both reached statistical significant level. Univariate analysis also showed that, for colon cancer, the OR value of chronic diarrhea history was 2.018 (95 % CI: 1.023-4.06), $P < 0.05$, but did not enter the final logistic regression model.

Intestinal polyp history commonly regarded as a high risk factor for colorectal cancer^[57-65]. Although the univariate analysis result showed a positive association between intestinal polyp history and colon cancer, OR=6.503 (95 % CI: 2.009-21.049), $P < 0.05$, after being matched with age, sex and location, the factor did not enter the final logistic regression model. However, the association between intestinal polyp history and rectal cancer could not reach the significant level even in the univariate analysis.

Although the association between dietary habits and colorectal cancer has been reported^[35,38,39,41,45,49, 66,67], this study was not able to confirm such a positive association. It was reported that increasing fat while reducing fibrous in diet would increase the incidence of colorectal cancer^[68-70]. In this study, after merging the two variables, pork eating and vegetable eating, into one variable by cross-difference method, we got a negative association. Red meat eating, such as fish cooked with soy sauce, was reported to be the risk factor of colorectal cancer^[71], but the result of this did not agree with that. Moreover, recent reports were not consistent with each other about the association between cigarette smoking and colorectal cancer, nor does the alcohol consumption^[71-76]. This study did not find any statistical association between cigarette smoking, nor was alcohol consumption and colorectal cancer.

Nested case control study, namely case control study within cohort, is based on a cohort set. After baseline investigation for the cohort set, including population structure, exposure factors and pertinent factors, the study subjects are divided into two groups: the disease individuals form the case group and the individuals of control group need to be randomly

selected from the non-disease subjects. This kind of study can be analyzed statistically as a case-control study. The risk factors found in nested one are certain in cause and time consequence. In addition, the number of case in this study was abundance after ten years of follow-up; the controls were randomly selected from the whole disease-free cohort set and can represent the normal public population well. All of these endue the results with persuasion.

It should be noted that, after ten years of follow-up, some exposure factors may have changed, factors such as dietary habits, drinking water sources, intestinal disease history may be different from the primate investigation. All the changes may discount the preciseness of the conclusion. That the association between dietary habits and colorectal cancer could not be put forward any positive evidence might be explained by such changes.

REFERENCES

- 1 **Zhang YL**, Zhang ZS, Wu BP, Zhou DY. Early diagnosis for colorectal cancer in China. *World J Gastroenterol* 2002; **8**: 21-25
- 2 **This Evensen E**, Hoff GS, Sauar J, Majak BM, Vatn MH. Flexible sigmoidoscopy or colonoscopy as a screening modality for colorectal adenomas in older age groups? Findings in a cohort of the normal population aged 63-72 years. *GUT* 1999; **45**: 834-839
- 3 **Colonna M**, Grosclaude P, Faivre J, Revzani A, Arveux P, Chaplain G, Tretarre B, Launoy G, Lesec'h JM, Raverdy N, Schaffer P, Buemi A, Menegoz F, Black RJ. Cancer registry data based estimation of regional cancer incidence: application to breast and colorectal cancer in French administrative regions. *J Epidemiol Community Health* 1999; **53**: 558-564
- 4 **Smalley W**, Ray WA, Daugherty J, Griffin MR. Use of nonsteroidal anti-inflammatory drugs and incidence of colorectal cancer: a population-based study. *Arch Int Med* 1999; **159**: 161-166
- 5 **Soliman AS**, Smith MA, Cooper SP, Ismail K, Khaled H, Ismail S, McPherson RS, Seifeldin IA, Bondy ML. Serum organochlorine pesticide levels in patients with colorectal cancer in Egypt. *Arch Environ Health* 1997; **52**: 409-415
- 6 **Kee F**, Wilson R, Currie S, Sloan J, Houston R, Rowlands B, Moorehead J. Socioeconomic circumstances and the risk of bowel cancer in Northern Ireland. *J Epidemiol Community Health* 1996; **50**: 640-644
- 7 **Liu XY**, Zheng S, Chen K, Ma XY, Zhou L, Yu H, Yao KY, Chen K, Cai SR, Zhang SZ. Randomized controlled trial of sequence mass screening program for colorectal cancer. *Zhonghua Liuxing Bingxue Zazhi* 2000; **21**: 430-433
- 8 **Haile RW**, Siegmund KD, Gauderman WJ, Thomas DC. Studydesign issues in the development of the University of Southern California Consortium's Colorectal Cancer Family Registry. *J Natl Cancer Inst Monogr* 1999; **26**: 89-93
- 9 **Campbell T**. Colorectal cancer. Part 1: Epidemiology, aetiology, screening and diagnosis. *Prof Nurse* 1999; **14**: 869-874
- 10 **Coughlin SS**, Miller DS. Public health perspectives on testing for colorectal cancer susceptibility genes. *Am J Prev Med* 1999; **16**: 99-104
- 11 **Mantel N**. Synthetic retrospective studies and related topics. *Biometrics* 1973; **29**: 479-490
- 12 **Hellard ME**, Sinclair MI, Fairley CK, Andrews RM, Bailey M, Black J, Dharmage SC, Kirk MD. An outbreak of cryptosporidiosis in an urban swimming pool: why are such outbreaks difficult to detect? *Aust N Z J Public Health* 2000; **24**: 272-275
- 13 **McDonald AD**, McDonald JC, Rando RJ, Hughes JM, Weill H. Cohort mortality study of North American industrial sand workers. I. Mortality from lung cancer, silicosis and other causes. *Ann Occup Hyg* 2001; **45**: 193-199
- 14 **Coker AL**, Gerasimova T, King MR, Jackson KL, Pirisi L. High-risk HPVs and risk of cervical neoplasia: a nested case-control study. *Exp Mol Pathol* 2001; **70**: 90-95
- 15 **Josefsson AM**, Magnusson PK, Ylitalo N, Sorensen P, Qvarforth Tubbin P, Andersen PK, Melbye M, Adami HO, Gyllenstein UB. Viral load of human papilloma virus 16 as a determinant for development of cervical carcinoma in situ: a nested case-control study. *Lancet* 2000; **355**: 2189-2193

- 16 **Akre O**, Lipworth L, Tretli S, Linde A, Engstrand L, Adami HO, Melbye M, Andersen A, Ekbom A. Epstein-Barr virus and cytomegalovirus in relation to testicular-cancer risk: a nested case-control study. *Int J Cancer* 1999; **82**: 1-5
- 17 **DeLamo J**, Petruckevitch A, Phillips AN, De Cock KM, Stephenson J, Desmond N, Hanscheid T, Low N, Newell A, Obasi A, Paine K, Pym A, Theodore C, Johnson AM. Risk factors for tuberculosis in patients with AIDS in London: a case-control study. *Int J Tuberc Lung Dis* 1999; **3**: 12-17
- 18 **Mathews WC**, Caperna J, Toerner JG, Barber RE, Morgenstern H. Neutropenia is a risk factor for gram-negative bacillus bacteremia in human immunodeficiency virus-infected patients: results of a nested case-control study. *Am J Epidemiol* 1998; **148**: 1175-1183
- 19 **Wideroff L**, Potischman N, Glass AG, Greer CE, Manos MM, Scott DR, Burk RD, Sherman ME, Wacholder S, Schiffrin M. A nested case-control study of dietary factors and the risk of incident cytological abnormalities of the cervix. *Nutr Cancer* 1998; **30**: 130-136
- 20 **Deacon JM**, Evans CD, Yule R, Desai M, Binns W, Taylor C, Peto J. Sexual behaviour and smoking as determinants of cervical HPV infection and of CIN3 among those infected: a case-control study nested within the Manchester cohort. *Br J Cancer* 2000; **83**: 1565-1572
- 21 **Ylitalo N**, Sorensen P, Josefsson AM, Magnusson PK, Andersen PK, Ponten J, Adami HO, Gyllensten UB, Melbye M. Consistent high viral load of human papillomavirus 16 and risk of cervical carcinoma *in situ*: a nested case-control study. *Lancet* 2000; **355**: 2194-2198
- 22 **Garcia Rodriguez LA**, Huerta Alvarez C. Reduced incidence of colorectal adenoma among long-term users of nonsteroidal anti-inflammatory drugs: a pooled analysis of published studies and a new population-based study. *Epidemiology* 2000; **11**: 376-381
- 23 **Knekt P**, Hakulinen T, Leino A, Heliovaara M, Reunanen A, Stevens R. Serum albumin and colorectal cancer risk. *Eur J Clin Nutr* 2000; **54**: 460-462
- 24 **Bertario L**, Russo A, Crosignani P, Sala P, Spinelli P, Pizzetti P, Andreola S, Berrino F. Reducing colorectal cancer mortality by repeated faecal occult blood test: a nested case-control study. *Eur J Cancer* 1999; **35**: 973-977
- 25 **Collet JP**, Sharpe C, Belzile E, Boivin JF, Hanley J, Abenheim L. Colorectal cancer prevention by non-steroidal anti-inflammatory drugs: effects of dosage and timing. *Br J Cancer* 1999; **81**: 62-68
- 26 **Kato I**, Dnistrian AM, Schwartz M, Toniolo P, Koenig K, Shore RE, Akhmedkhanov A, ZeleniuchJacquotte A, Riboli E. Serum folate, homocysteine and colorectal cancer risk in women: a nested case-control study. *Br J Cancer* 1999; **79**: 1917-1922
- 27 **Kato I**, Dnistrian AM, Schwartz M, Toniolo P, Koenig K, Shore RE, ZeleniuchJacquotte A, Akhmedkhanov A, Riboli E. Iron intake, body iron stores and colorectal cancer risk in women: a nested case-control study. *Int J Cancer* 1999; **80**: 693-698
- 28 **Karlen P**, Kornfeld D, Brostrom O, Lofberg R, Persson PG, Ekbom A. Is colonoscopic surveillance reducing colorectal cancer mortality in ulcerative colitis? A population based case control study. *Gut* 1998; **42**: 711-714
- 29 **Meijer GA**, Baak JP, Talbot IC, Atkin WS, Meuwissen SG. Predicting the risk of metachronous colorectal cancer in patients with rectosigmoid adenoma using quantitative pathological features. A case-control study. *J Pathol* 1998; **184**: 63-70
- 30 **Hemminki K**, Lonnstedt I, Vaittinen P, Lichtenstein P. Estimation of genetic and environmental components in colorectal and lung cancer and melanoma. *Genet Epidemiol* 2001; **20**: 107-116
- 31 **Chapman PD**, Burn J. Genetic predictive testing for bowel cancer predisposition: the impact on the individual. *Cytogenet Cell Genet* 1999; **86**: 118-124
- 32 **Thorson AG**, Knezetic JA, Lynch HT. A century of progress in hereditary nonpolyposis colorectal cancer (Lynch syndrome). *Dis Colon Rectum* 1999; **42**: 1-9
- 33 **Briskey EN**, Parnies RJ. Colorectal cancer: update on recent advances and their impact on screening protocols. *J Natl Med Assoc* 2000; **92**: 222-230
- 34 **Lichtenstein P**, Holm NV, Verkasalo PK, Iliadou A, Kaprio J, Koskenvuo M, Pukkala E, Skytthe A, Hemminki K. Environmental and heritable factors in the causation of cancer-analyses of cohorts of twins from Sweden, Denmark, and Finland. *N Engl J Med* 2000; **343**: 78-85
- 35 **Marchand LL**. Combined influence of genetic and dietary factors on colorectal cancer incidence in Japanese Americans. *J Natl Cancer Inst Monogr* 1999; **26**: 101-105
- 36 **Bonaiti Pellie C**. Genetic risk factors in colorectal cancer. *Eur J Cancer Prev* 1999; **8** (Suppl 1): S27-32
- 37 **Ponz de Leon M**, Pedroni M, Benatti P, Percesepe A, Rossi G, Genuardi M, Roncucci L. Epidemiologic and genetic factor in colorectal cancer: development of cancer in dizygotic twins in a family with Lynch syndrome. *Ital J Gastroenterol Hepatol* 1999; **31**: 218-222
- 38 **Prichard PJ**, Tjandra JJ. Colorectal cancer. *Med J Aust* 1998; **169**: 493-498
- 39 **Rafter J**, Glinghammar B. Interactions between the environment and genes in the colon. *Eur J Cancer Prev* 1998; **7** (Suppl 2): S69-74
- 40 **Gandhi SK**, Reynolds MW, Boyer JG, Goldstein JL. Recurrence and malignancy rates in a benign colorectal neoplasm patient cohort: results of a 5-year analysis in a managed care environment. *Am J Gastroenterol* 2001; **96**: 2761-2767
- 41 **Ritenbaugh C**. Diet and prevention of colorectal cancer. *Curr Oncol Rep* 2000; **2**: 225-233
- 42 **Hemminki K**, Lonnstedt I, Vaittinen P, Lichtenstein P. Estimation of genetic and environmental components in colorectal and lung cancer and melanoma. *Genet Epidemiol* 2001; **20**: 107-116
- 43 **Lichtenstein P**, Holm NV, Verkasalo PK, Iliadou A, Kaprio J, Koskenvuo M, Pukkala E, Skytthe A, Hemminki K. Environmental and heritable factors in the causation of cancer-analyses of cohorts of twins from Sweden, Denmark, and Finland. *N Engl J Med* 2000; **343**: 78-85
- 44 **Park JG**, Park YJ, Wijnen JT, Vasen HF. Gene-environment interaction in hereditary nonpolyposis colorectal cancer with implications for diagnosis and genetic testing. *Int J Cancer* 1999; **82**: 516-519
- 45 **Jansen MC**, Bueno de Mesquita HB, Buzina R, Fidanza F, Menotti A, Blackburn H, Nissinen AM, Kok FJ, Kromhout D. Dietary fiber and plant foods in relation to colorectal cancer mortality: the Seven Countries Study. *Int J Cancer* 1999; **81**: 174-179
- 46 **Gertig DM**, Hunter DJ. Genes and environment in the etiology of colorectal cancer. *Semin Cancer Biol* 1998; **8**: 285-298
- 47 **Gulis G**, Fitz O, Wittgruber J, Suchanova G. Colorectal cancer and environmental pollution. *Cent Eur J Public Health* 1998; **6**: 188-191
- 48 **Van Kranen HJ**, van Iersel PW, Rijnkels JM, Beems DB, Alink GM, van Kreijl CF. Effects of dietary fat and a vegetable-fruit mixture on the development of intestinal neoplasia in the ApcMin mouse. *Carcinogenesis* 1998; **19**: 1597-1601
- 49 **Kenji T**, Hedio O, Yasuharu O, Iwao Y, Tomohiro S, Katsuya Y, Kiichi M, Shigeru T, Hideki A. Dietary factors and prevention of colon cancer. *Nippon Geka Gakkai Zasshi* 1998; **99**: 368-372
- 50 **Charalambopoulos A**, Syrigos KN, Ho JL, Murday VA, Leicester RJ. Colonoscopy in symptomatic patients with positive family history of colorectal cancer. *Anticancer Res* 2000; **20**: 1991-1994
- 51 **Winawer SJ**. Natural history of colorectal cancer. *Am J Med* 1999; **106**: 3S-6S, 50S-51S
- 52 **Wang ZQ**, He J, Chen W, Chen Y, Zhou TS, Lin YC. Relationship between different sources of drinking water, water quality improvement and gastric cancer mortality in Changle County-A retrospective-cohort study in high incidence area. *World J Gastroenterol* 1998; **4**: 45-47
- 53 **Martinez Martinez L**, Lopez Santamaria M, Prieto Bozano G, Molina Arias M, Jimenez Alvarez C, Tovar Larrucea JA. Diagnosis and therapeutic options in chronic idiopathic intestinal pseudo-obstruction: review of 16 cases. *Cir Pediatr* 1999; **12**: 71-74
- 54 **Browning SM**. Constipation, diarrhea, and irritable bowel syndrome. *Prim Care* 1999; **26**: 113-139
- 55 **Ho KY**, Kang JY, Seow A. Prevalence of gastrointestinal symptoms in a multiracial Asian population, with particular reference to reflux-type symptoms. *Am J Gastroenterol* 1998; **93**: 1816-1822
- 56 **Iacono G**, Cavataio F, Montalto G, Florena A, Tumminello M, Soresi M, Notarbartolo A, Carroccio A. Intolerance of cow's milk and chronic constipation in children. *N Engl J Med* 1998; **339**: 1100-1104
- 57 **Lal G**, Ash C, Hay K, Redston M, Kwong E, Hancock B, Mak T, Kargman S, Evans JF, Gallinger S. Suppression of intestinal polyps in Msh2-deficient and non-Msh2-deficient multiple intesti-

- nal neoplasia mice by a specific cyclooxygenase-2 inhibitor and by a dual cyclooxygenase-1/2 inhibitor. *Cancer Res* 2001; **61**: 6131-6136
- 58 **Rex DK**. Surveillance colonoscopy following resection of colorectal polyps and cancer. *Can J Gastroenterol* 2001; **15**: 57-59
- 59 **Anderson J**. Clinical practice guidelines. Review of the recommendations for colorectal screening. *Geriatrics* 2000; **55**: 67-73, quiz 74
- 60 **Katsumata T**, Igarashi M, Kobayashi K, Sada M, Yokoyama K, Saigenji K. Usefulness of endoscopic polypectomy in early colorectal cancer. *Nippon Geka Gakkai Zasshi* 1999; **100**: 782-786
- 61 **Tobi M**. Polyps as biomarkers for colorectal neoplasia. *Front Biosci* 1999; **4**: 329-338
- 62 **Gruber M**, Lance P. Colorectal cancer detection and screening. *Lippincotts Prim Care Pract* 1998; **2**: 369-376, quiz 377-378
- 63 **Kennedy BP**, Soravia C, Moffat J, Xia L, Hiruki T, Collins S, Gallinger S, Bapat B. Overexpression of the nonpancreatic secretory group II PLA2 messenger RNA and protein in colorectal adenomas from familial adenomatous polyposis patients. *Cancer Res* 1998; **58**: 500-503
- 64 **Luo YQ**, Ma LS, Zhao YL, Wu KC, Pan BR, Zhang XY. Expression of proliferating cell nuclear antigen in polyps from large intestine. *World J Gastroenterol* 1999; **5**: 160-164
- 65 **Steindorf K**, Tobiasz Adamczyk B, Popiela T, Jedrychowski W, Penar A, Matyja A, Wahrendorf J. Combined risk assessment of physical activity and dietary habits on the development of colorectal cancer. A hospital-based case-control study in Poland. *Eur J Cancer Prev* 2000; **9**: 309-316
- 66 **Negri E**, Franceschi S, Parpinel M, La Vecchia C. Fiber intake and risk of colorectal cancer. *Cancer Epidemiol Biomarkers Prev* 1998; **7**: 667-671
- 67 **Jarvinen R**, Knekt P, Hakulinen T, Rissanen H, Heliovaara M. Dietary fat, cholesterol and colorectal cancer in a prospective study. *Br J Cancer* 2001; **85**: 357-361
- 68 **Franceschi S**, Favero A. The role of energy and fat in cancers of the breast and colon-rectum in a southern European population. *Ann Oncol* 1999; **10**(Suppl): 661-663
- 69 **Rieger MA**, Parlesak A, Pool Zobel BL, Rechkemmer G, Bode C. A diet high in fat and meat but low in dietary fibre increases the genotoxic potential of "faecal water". *Carcinogenesis* 1999; **20**: 2311-2316
- 70 **Giovannucci E**. An updated review of the epidemiological evidence that cigarette smoking increases risk of colorectal cancer. *Cancer Epidemiol Biomarkers Prev* 2001; **10**: 725-731
- 71 **Gertig DM**, Stampfer M, Haiman C, Hennekens CH, Kelsey K, Hunter DJ. Glutathione S-transferase GSTM1 and GSTT1 polymorphisms and colorectal cancer risk: a prospective study. *Cancer Epidemiol Biomarkers Prev* 1998; **7**: 1001-1005
- 72 **Terry P**, Ekblom A, Lichtenstein P, Feychting M, Wolk A. Long-term tobacco smoking and colorectal cancer in a prospective cohort study. *Int J Cancer* 2001; **91**: 585-587
- 73 **Chao A**, Thun MJ, Jacobs EJ, Henley SJ, Rodriguez C, Calle EE. Cigarette smoking and colorectal cancer mortality in the cancer prevention study II. *J Natl Cancer Inst* 2000; **92**: 1888-1896
- 74 **Yoshioka M**, Katoh T, Nakano M, Takasawa S, Nagata N, Itoh H. Glutathione S-transferase (GST) M1, T1, P1, N-acetyltransferase (NAT) 1 and 2 genetic polymorphisms and susceptibility to colorectal cancer. *J UOEH* 1999; **21**: 133-147
- 75 **Sinha R**, Chow WH, Kulldorff M, Denobile J, Butler J, Garcia Closas M, Weil R, Hoover RN, Rothman N. Well done, grilled red meat increases the risk of colorectal adenomas. *Cancer Res* 1999; **59**: 4320-4324
- 76 **Neugut AI**, Rosenberg DJ, Ahsan H, Jacobson JS, Wahid N, Hagan M, Rahman MI, Khan ZR, Chen L, Pablos Mendez A, Shea S. Association between coronary heart disease and cancers of the breast, prostate, and colon. *Cancer Epidemiol Biomarkers Prev* 1998; **7**: 869-873

Edited by Zhao M

Current treatment for liver metastases from colorectal cancer

Lian-Xin Liu, Wei-Hui Zhang, Hong-Chi Jiang

Lian-Xin Liu, Wei-Hui Zhang, Hong-Chi Jiang, Department of Surgery, the First Clinical College, Harbin Medical University, Harbin 150001, Heilongjiang Province, China

Supported by Youth Natural Science Foundation of Heilongjiang Province

Correspondence to: Dr Lian-Xin Liu, Department of Surgery, First Clinical College, Harbin Medical University, No. 23 Youzheng Street, Nangang District, Harbin 150001, Heilongjiang Province, China. liulianxin@sohu.com

Telephone: +86-451-3643849-5885 **Fax:** +86-451-3670428

Received: 2002-07-24 **Accepted:** 2002-08-07

Abstract

The liver is the commonest site of distant metastasis of colorectal cancer and nearly half of the patients with colorectal cancer ultimately develop liver involved during the course of their diseases. Surgery is the only therapy that offers the possibility of cure for patients with hepatic metastatic diseases. Five-year survival rates after resection of all detectable liver metastases can be up to 40 %. Unfortunately, only 25 % of patients with colorectal liver metastases are candidates for liver resection, while the others are not amenable to surgical resection. Regional therapies such as radiofrequency ablation and cryotherapy may be offered to patients with isolated unresectable metastases but no extrahepatic diseases. Hepatic artery catheter chemotherapy and chemoembolization and portal vein embolization are often used for the patients with extensive liver metastases but without extrahepatic diseases, which are not suitable for regional ablation. For the patients with metastatic colorectal cancer beyond the liver, systemic chemotherapy is a more appropriate choice. Immunotherapy is also a good option when other therapies are used in combination to enhance the efficacy. Selective internal radiation therapy is a new radiation method which can be used in patients given other routine therapies without effects.

Liu LX, Zhang WH, Jiang HC. Current treatment for liver metastases from colorectal cancer. *World J Gastroenterol* 2003; 9(2): 193-200

<http://www.wjgnet.com/1007-9327/9/193.htm>

INTRODUCTION

Colorectal cancer is one of the commonest solid tumors in human beings and is responsible for approximately 10 percent of the cancer death in Western world^[1-5]. The incidence of colorectal cancer is also increased recently in China^[6-8]. The liver is the commonest site of distant metastasis in this disease and nearly half of the patients with colorectal cancer ultimately develop liver involved during the course of their diseases. Treatment of primary colorectal cancer with surgical resection, combined with chemotherapy and radiotherapy in some cases, is effective in many patients. But, about 10-25 % patients had liver metastases at the time of primary diagnosis and another 20-25 % patients developed metachronous liver metastases^[9-12].

Death of colorectal cancer is often a result of liver metastases. Over half patients died from their metastatic liver diseases.

Surgical resection of distant metastases in colorectal cancer can produce long-term survival and cure in some selected patients. Surgery is the only therapy that offers any possibility of cure for the patients with hepatic metastatic diseases. The five-year survival rates after resection of all detectable liver metastases can reach up to 40 %. Unfortunately, only 25 % of the patients with colorectal liver metastases are candidates for liver resection, while the others are not amenable to surgical resection. Chemotherapy and some newer therapies are expected to raise the survival time for the unresectable colorectal liver metastases^[13-15].

This article reviews the natural history of colorectal cancer liver metastases, pretreatment assessment of patients, surgical resection of liver metastases, systemic and hepatic artery chemotherapy (hepatic artery infusion, HAC, HAI), hepatic artery chemoembolization, portal vein embolization, immunotherapy and selective intra-artery radiation therapy (SIRT), and other regional therapies, including cryotherapy, radiofrequency ablation (RFA).

NATURAL HISTORY

Understanding the natural history of colorectal cancer is useful to assess the value of various treatments. About 60 % patients who underwent curative surgery for colorectal cancer will develop local, regional, or distant recurrence. Nearly 85 % of tumors recurrence are detected within 2.5 years after resection of primary colorectal cancer, and the remaining 15 % are detected within the next 2.5 years. Median survival for these patients was found to be between 5 and 9 months^[16,17]. However, the majority of patients in former studies had advanced diseases diagnosed without modern imaging techniques. Several previous studies have retrospectively determined the survival of patients with potentially resectable colorectal cancer liver metastases that left untreated. It was found that a 0 % five-year survival for patients with untreated but potentially resectable liver metastases compared with a 28 % five-year survival for operated patients with resected liver metastases^[18]. Another study found that patients untreated but potentially resectable liver metastases had a mean survival of 21.3 months^[19]. Other study found patients with an untreated single liver metastasis had a median survival of 19 months, with no patients surviving 5 years, while patients with a resected single liver metastasis had a median survival of 36 months with 25 % of patients surviving five years^[20]. It is well known that resection of colorectal cancer liver metastases improves long-term survival.

PRETREATMENT ASSESSMENT

Synchronous liver metastases from colorectal cancer may be detected before operation or during operation. Suspicious liver lesions should be biopsied and send to freezing pathology during the operation. Metachronous liver metastases may be found after the operation of colorectal cancer by physical examination, blood test, and radiological imaging. Further evaluation of patients with colorectal cancer liver metastases depends on the available treatment procedures. If the patients are not suitable to operation, confirmation of the presence of metastatic lesions by ultrasound and CT scan is sufficient, no

matter of number and size of the lesions. If patients are candidates for surgical resection of liver metastases, a series of examinations should be done to determine the liver function and general condition to tolerate liver resection, to delineate exactly the anatomy of the lesions including the number, size and relationship with vessels and bile ducts, and to exclude the presence of extrahepatic disease.

Candidates for surgical resection of colorectal cancer liver metastases should be under a detailed history and physical examination, hematology test, liver function test, chest X-ray, and abdominal and pelvic CT scans. Patients should undergo colonoscopy to rule out the recurrence of the original primary colorectal cancer or development of a second primary colorectal cancer, if they had not already done within the past 6 months. A range of imaging techniques, including transabdominal ultrasound, CT scan, CT arteriography (CTAP), magnetic resonance imaging (MRI), and positron emission tomography (PET) can provide information of liver metastases and extrahepatic diseases^[21]. Transabdominal ultrasound examination of liver correctly identifies around 52-58 % of patients who had liver metastases. Ultrasound may be most appropriately used because it is cheapest and readily available. But transabdominal ultrasound plays no role in the preoperative evaluation of potential liver resection candidates^[22-24]. Abdominal CT scan is mostly used for the assessment of liver metastases, in which images are usually hypoattenuated relative to normal liver. The use of intravenous contrast increases the detectability of liver metastases because normal liver is perfused primarily by portal vein and liver metastases are perfused mostly by hepatic artery. Hypoattenuated liver metastases are more easily recognized following the intravenous contrast on CT scan during the portal venous phase. The sensitivity of helical CT of liver metastases was 80 %^[25,26]. We often used more sensitive CT arteriography (CTAP) which is an invasive method to investigate the metastatic liver lesions. We firstly placed a catheter into the superior mesenteric artery and then captured the liver CT images during the arterial and portal venous phase following contrast injection. The overall sensitivity for detection of liver metastases helical CTAP exceeded 90 %. But, perfusion abnormalities and pseudolesions were frequently observed with CTAP, thereby significantly reducing the specificity of this technique^[27-29]. Magnetic resonance imaging (MRI) is increasingly utilized for the diagnosis and characterization of liver lesions, particularly the liver-specific contrast agents and dynamic scanning have been incorporated. One liver-specific contrast agent, manganese-pyridoxal diphosphate (Mn-DPDP), is a paramagnetic agent taken up preferentially by hepatocytes and excreted in the bile. The popularity of MRI is also due to its non-invasiveness in some centers^[30,31]. PET is a newer technique which can scan the whole body. It is mainly used to rule out the potential extrahepatic diseases which could not be identified by other methods before operation^[32,33].

Laparoscopy is usually used for preoperative evaluation of metastatic liver diseases. Laparoscopy with laparoscopic ultrasound may be the most sensitive imaging technique for detection of liver metastases. Laparoscopy can prevent laparotomy in some unresectable cases with liver metastases which were judged resectable preoperatively by conventional imaging studies^[34]. But it is still an invasive procedure which need general anesthesia. Therefore, laparoscopy was not routinely used unless the resectability of the lesions was not determined by other methods.

SURGERY

Patients without extrahepatic diseases and with good liver function and general condition are candidates for surgical

resection, while all liver metastases can be resected with at least 1 cm tumor-free margin. Up to 75 % of the liver can be removed if the liver function is normal. Recognition of the segmental basis of liver anatomy led to the evolution of the segment-based resection. This has had a particular influence on surgery for colorectal metastases because it allows excision of bilateral or multiple liver lesions that might previously have been deemed unresectable. Staged resection is another means and may be useful for bulky bilateral lesions. In fact, one or more segmental resections can often spare more normal liver than a major resection or allow resection of metastases not encompassed by a traditional major resection^[35-39].

The surgical resection of liver metastases from colorectal cancer first involves an exploratory laparotomy through a right subcostal incision. The abdominal cavity is explored for signs of extrahepatic disease, and suspicious areas are biopsied. The liver is fully mobilized by dissection of its supporting ligaments and palpated to identify lesions. Intraoperative ultrasound is used at this point to identify nonpalpable lesions and delineate vascular anatomy. No matter traditional liver resection or segmental resection is performed, the goal of the operation is complete removal of all metastases with at least a 1cm tumor-free margin. Although there are various methods of dividing hepatic parenchyma, I prefer using ultrasonic surgical aspirator in normal liver and a combination of ultrasonic surgical aspirator and clamp fracture in cirrhotic liver. Small vessels are controlled with electrocautery or hemoclips, and large vessels are controlled with sutures. An argon beam coagulator can also be used to achieve hemostasis in resection margin^[40-42].

Vascular occlusion techniques, particularly the Pringle maneuver, have had a major impact in minimizing blood loss and reducing the morbidity associated with liver resection. Selective vascular occlusion has been popularly accepted in segment resection in patients with limited liver function. Total vascular exclusion has become widely accepted as a means of minimizing blood loss when we operated on difficult lesions. Although few surgeons use total vascular exclusion routinely, it is a technique that facilitates excision of lesions involving the vena cava or those lying near the junction of the hepatic veins and the vena cava. Some lesions which were previously been thought unresectable can now be resected with the reconstructed segments of hepatic inflow or outflow vascular structure. Replacement of hepatic vein and vena cava with autologous vein and prosthetic grafts respectively had been fasciated by the use of total vascular exclusion and a number of techniques of liver transplantation. The use of venovenous bypass in combination with *in situ* hypothermic perfusion and *ex situ* resection and autotransplantation, have both been important additions to the liver surgeons^[43,44].

The operative mortality for major liver resections has declined with improved operative techniques and postoperative care, but still significant. Operative mortality ranged from 0 % to 7 %. The causes of death include hemorrhage, sepsis, and liver failure. The Morbidity of liver resection was between 22-39 %, and the causes of morbidity included hemorrhage, biliary leak or fistula, liver failure, abscess around liver, wound infection, and pneumonia. Median survival ranged from 28 to 46 months. The five-year survival was between 24 % and 38 %^[45-48].

How many lesions are too many in colorectal cancer liver metastases underlying liver resections? Many surgeons consider four or more tumors in the liver to be a contraindication for surgical resection before. But more and more authors think that the number was not a limitation in liver resection of colorectal cancer liver metastases with the use of new techniques. The follow-up showed that there was no significant difference in the mortality, morbidity and five-year survival between patients whose lesions more than four and those less than four^[49].

RADIOFREQUENCY ABLATION (RFA)

The so-called RF thermal ablation works by converting RF waves into heat. A high-frequency alternating current (100 to 500 kHz), mostly 460kHz, passes from an insulated electrode tip into the surrounding tissues and causes ionic vibration as the ions attempt to follow the change in the direction of the rapidly alternating current. This ionic vibration causes frictional heating of the tissues surrounding the electrode, rather than the heat being generated from the probe itself. The goal of RFA is to achieve local temperatures to make tissue destruction occur^[50-55]. Tissue heating also drives extracellular and intracellular water out of the tissue and results in further destruction of the tissue due to coagulative necrosis. Besides these, different studies have shown that hyperthermia can cause accelerated emigration and migration of peripheral blood mononuclear cells, activation of effect cells, induction and secretion of cytokines, expression of heat shock proteins, and increased induction of apoptosis^[56-58].

Most of the early reports on the use of RFA for colorectal cancer liver metastases came from Rossi in Italy. In 1996, they reported their results with percutaneous RFA in 50 patients, of whom 11 patients had 13 metastases ranging from 1 to 9 cm in diameter. Monopolar and bipolar needles were utilized and multiple probe insertions and treatment sessions were performed. There were no associated complications or deaths. Of the 11 patients with metastases, two underwent subsequent surgical resection, one of them had complete tumor necrosis by histopathologic examination. At a median follow-up of 22.6 months, 10 (90 %) of 11 patients were alive, two (18 %) had a local recurrence and seven (64 %) had persistent or distant disease. Only one (9 %) patient, therefore, was alive without disease. These studies suggested that although RFA was effective in preventing local recurrence of metastases, it may not affect the progressive course of the cancer^[59].

Wood TF reported 231 tumors in 84 patients treated with 91 RFA procedures. The majority of the patients had metastatic lesions (213 lesions in 73 patients). RFA was given in 51 of the 91 treatments alone. The other 40 included RFA combined with surgical resection, cryoablation, and hepatic artery infusion of chemotherapy. Of the 91 RFA treatments, 39 were ablated at laparotomy, 27 by laparoscopy and 25 percutaneously. Tumors ranged in size from 0.3 to 9.0 cm. Three deaths occurred, one (1 %) of which was directly related to the RFA procedure. Ten patients underwent a second RFA procedure (sequential ablations). It is due to progressive (seven patients), and recurrent (three patients) lesions. A third RFA procedure for large was performed in one patient. At a median follow-up of 9 months (range 1-27 months), 15 (18 %) patients had developed a local recurrence. Of the remaining 69 patients, 34 were alive without disease, 14 were alive with disease, and 21 died. New hepatic tumors or extrahepatic diseases occurred in 35 patients. The average hospital stay was 3.6 days^[60].

Although RFA has a lot of advantages in the treatment of metastatic liver tumors, it still has a few disadvantages and complications. These complications included symptomatic pleural effusion, fever, pain, subcutaneous hematoma, subcapsular liver hematoma, and ventricular fibrillation. The severe complication is treatment-related death. Interms of the methods related to tumors, the outcome of RF thermal ablation involves the skill of a surgeon performing the procedure. Exact placement of the ablation needles requires considerable skill and some degree of guess work by the radiologist and surgeon, who may be the most experienced in interventional procedures. Recurrence at the treatment margin may result from an inability to adequately kill the tumor the hepatic parenchyma adjacent to the treated tumors. The abundant portal venous blood flow present in normal hepatic parenchyma acts as a heat pump, which makes the creation of thermal injury in normal liver

more difficult than that it is in liver tumors. RF also caused skin burn in percutaneous procedures, hemorrhage, diaphragmatic necrosis, hepatic abscess, hepatic artery injuries, bile duct injuries, renal failure, coagulopathy and liver failure, which were severe and eventually fatal^[61-64].

Although long-term observations are not available, RFA will definitely give the surgeon a helpful hand and bring the patients a better prognosis. But, RFA is unlikely to be curative for most patients, it can relieve the symptoms of patients and improve the quality of life of patients. RFA has been shown to be safer and better tolerated as compared with other ablative techniques, such as cryotherapy, laser ablation and microwave ablation. RFA has been associated with fewer local recurrence. RFA for unresectable liver tumors provides a relatively safe, highly effective method to control local disease in some liver metastatic patients who are not candidates for liver resection. RFA also showed some better respect in combination with surgical resection, hepatic artery chemotherapy. The most interesting feature of RFA is the minimal-invasiveness with zero mortality rate, significantly lower complications, reduced costs and hospital days compared with surgery and other therapies. Furthermore, in combination with other procedures, RFA will improve the survival of patients with colorectal cancer liver metastases^[65,66].

CRYOTHERAPY

Cryotherapy has been mostly used as a regional therapy all over the world for a long time^[67,68]. Hepatic cryotherapy involves the freezing and thawing of liver tumors by means of a cryoprobe inserted into the tumors. During freeze/thaw cycles, intracellular and extracellular ice formation occurs in an area termed "the iceball", leading to tumor destruction. Hepatic cryotherapy is generally reserved for patients with liver metastases from colorectal cancer in whom one or more lesions are not surgically resectable. Some centers offer liver cryotherapy as an alternative to surgical resection^[69-71]. Cryotherapy can treat multiple lesions and salvages more uninvolved liver parenchyma than surgical resection. Cryotherapy may also be used to treat tumors intimately associated with major vessels. But, major vessels may serve as "heat-sinks" and prevent adequate freezing of immediately adjacent tumors. Hepatic inflow occlusion may reduce the incidence of inadequate freezing of tumors adjacent to large blood vessels. Cryotherapy can also treat patients who are left with a positive surgical margin after hepatic resection which is called "edge cryotherapy". Cryotherapy can also be used in patients in whom underlying illness or hepatic insufficiency precludes surgical resection^[72-74].

Hepatic cryotherapy is performed by making an abdominal incision, followed by exploration of the abdomen to search for extrahepatic metastases. Intraoperative ultrasound is used to identify and assess intrahepatic lesions^[75,76]. For superficial lesions, a cryoprobe can be placed into the center of the lesion under direct vision. For deeper lesions, the probe can be inserted into the center of the tumor under ultrasound guidance. Sometimes two or three probes may be used for large lesions. Freezing is continued until the iceball is at least 1 cm beyond the tumor. Two or three cycles should be performed or combine freezing with occlusion of hepatic inflow to increase tumor destructive ice ball and negative edge of ice ball in some lesions. It can also be done percutaneously under the guide of ultrasound and CT scan^[77].

The complications of cryotherapy include subsequent hemorrhage of cracking frozen liver, bile collection, biliary fistula, right-sided pleural effusion, liver abscess, thrombocytopenia, myoglobinuria, arrhythmia, acute renal failure, and cryoshock due to multi-organ failure with DIC.

Overall morbidity rates range from 6 % to 29 %. Mortality rates range from 0 % to 8 %, with an overall mortality rate of 1.6 %. Median survival ranged from 8 to 43 months. New or improved liquid nitrogen delivery systems and together with intraoperative ultrasound have led to significant advances in cryotherapy over the past few years and its feasibility and safety are now well accepted. Although long-term survival following hepatic cryotherapy for liver metastases from colorectal cancer is unclear, hepatic cryotherapy is still an option for patients who are not candidates for surgical resection but enough to cryoablation of all lesions. Cryotherapy is also an important supplement of surgical resection and beneficial to the patients with liver metastasis from colorectal cancer when combined with surgery^[78,79].

HEPATIC ARTERY CHEMOTHERAPY

Following resection of liver metastases from colorectal cancer, recurrence will occur in 60-70 % of patients, most commonly in the liver, so effective postoperative adjuvant treatment is also required, during which chemotherapy is the main method. Chemotherapy is also required in unresectable liver metastases to sustain the survival rate^[80-83]. However, the optimum regimen and route of delivery should be clarified. As most drugs have a steep dose-dependent curve, it is a basic pharmacokinetic principle that if drug delivery is increased to tumors, the response rates can be elevated. An alternative approach to liver metastases is therefore, to deliver the drug intra-arterially^[84,85]. Hepatic artery catheter chemotherapy has been a therapeutic possibility for unresectable liver metastases for many years. The rationale for hepatic artery catheter chemotherapy is based on the fact that liver metastases over 1 cm derive most their blood supply from hepatic artery. The other rationale is the high first pass hepatic extraction of the drug used for this approach. Both factors cause high local drug concentrations with reduced systemic toxicity and allow relatively higher dosages as compared with intravenous treatment^[86,87].

Some studies compared intra-arterial chemotherapy with conventional systemic chemotherapy and showed consistently higher response rates in patients receiving intra-arterial chemotherapy^[88]. In the United Kingdom, patients were randomized to receive intra-arterial chemotherapy through a totally implantable infusion device; patients were given systemic chemotherapy in other group. Survival was significantly longer in the intra-arterial group (median survival 405 days compared with 226 days). The intra-arterial group also had a better quality of life than those received systemic chemotherapy^[89]. Other studies showed that the response rate was 43 % in the intra-arterial group compared with 9 % in the systemic chemotherapy group. Furthermore, the intra-arterial group showed a significant increase in the one-year survival (64 % vs 44 %) and two-year survival (23 % vs 13 %). Other studies also showed a higher response rates in intra-arterial chemotherapy than in systemic chemotherapy^[90].

In all studies, 5-FU and FUDR were chosen for the arterial route of administration. As 84-99 % of FUDR is extracted by the liver on first pass, it seemed logical to use FUDR to achieve the dual objective of high levels within the tumor and low plasma levels, thereby increasing the probability of the tumor's response while minimizing the systemic toxicity^[91]. But 55 % of patients using FUDR in the UK and French studies developed extra-hepatic progress, suggesting that these patients may have had occult extra-hepatic disease at the time of entry into the trial or during the intra-arterial chemotherapy. The lower plasma level of drugs has been misplaced, while 5-FU, which has a higher plasma level than FUDR, should be preferred. Although there are some complications in HAC, it is still a feasible method for liver metastases from colorectal cancer.

Most complications was related to the technique of surgery and care of patients^[92].

Comparison of intra-arterial with systemic chemotherapy is an important topic that has not been resolved adequately. Some groups were unable to detect any difference in recurrence of hepatic colorectal metastases after liver resection among groups treated with systemic, intra-arterial or intra-portal chemotherapy. There are a lot of new agents such as Xeloda, currently being assessed as adjuvant treatment for both primary colorectal cancer and following resection of metastatic liver lesions^[93-102].

HEPATIC ARTERY CHEMOEMBOLIZATION

Hepatic artery chemoembolization (HACE) was developed to treat unresectable non-disseminated liver tumors^[103,104]. Although HACE has not shown any benefit on survival, it increased the response rate compared with systemic administration of cytotoxic agents. HACE has been studied mostly in the treatment of hepatocellular carcinoma, which was also used in colorectal cancer liver metastases for some clinical trials^[105]. Preoperative HACE has been proposed as a possible means of decreasing perioperative tumor dissemination, but only in a small number of patients. Some centers reported that HACE in patients with borderline resectable tumors caused sufficient tumor shrinkage to allow resection. Routine HACE produced no survival benefit on patients with resectable tumors. It was only used in unresectable tumors as an adjacent treatment^[106,107].

PORTAL VEIN EMBOLIZATION

Preoperative portal vein embolization induced hypertrophy in the normal liver which will be remnant and decreased the likelihood of liver insufficiency occurring after extensive liver resection^[108,109]. It has not only mostly used in cholangiocarcinoma but sometimes used in liver metastases from colorectal cancer. Portal vein embolization may be performed either by percutaneous ultrasonographically guided puncture of a portal vein radical or by operative exposure of an ileocolic vein to access portal vein. It can not only be performed in the right portal vein to allow the left side hypertrophy in those who will receive right hepatectomy, but also in left portal vein to allow the right side hypertrophy in those who will receive extend left hepatectomy. Portal vein embolization was well tolerated and produced a less severe systemic reaction than intra-arterial chemoembolization^[110-113].

IMMUNOTHERAPY

Immunotherapy is mainly used in advanced diseases which have failed to respond to conventional therapy. Levamisole, a non-specific immune stimulant, was used in adjunctive treatment with 5-FU as an immune modulator^[114]. More exploration of different combinations may provide new adjuvant regimens. Some scientists have recently reported a phase I-II clinical trial of neoadjuvant immunotherapy with interleukin 2 before hepatectomy for liver metastases from colorectal cancer in 19 patients. Pretreatment with interleukin 2 prevented the postoperative immunodepression seen in the control patients^[115,116]. Clinical trials have also shown that the monoclonal antibody 17-1A was effective in increasing the survival following resection of Dukes C primary colorectal tumors. It can also be used as an adjuvant treatment before or after liver resection for liver metastases from colorectal cancer^[88,117-119].

RADIOTHERAPY

Traditional external beam irradiation has found little place in

the management of liver tumors because of the particularly radiosensitive nature of normal liver tissues, which limits the total dosage to 30-35 Gy^[120-122]. Selective internal radiation therapy (SIRT) is a new modality that may be valuable in colorectal cancer liver metastatic patients which was not suitable to resection, RFA and cryotherapy. SIRT is a technique that allows high average doses of radiation of 200-300Gy to liver tumors with minimal serious effects on the non-tumorous liver. The treatment entails delivery of usually a single dose of ⁹⁰Yttrium microspheres into the hepatic artery, which by virtue of the almost exclusive arterial supply to liver tumors compared with the predominant portal supply to normal liver, resulting in selective tumor uptake and irradiation. ⁹⁰Yttrium is a particularly suitable isotope for medical use in this situation. As a pure beta emitter, it is simpler to handle and use than gamma or mixed beta and gamma emitters such as ¹³¹Iodine^[123,124]. In addition, its half-life of 2.7 days and maximum penetration in soft tissues of 11 mm both are suitable for the purpose. The microspheres do not degrade and are of a size of 29-35 µm that means they are trapped in the arteriolar capillaries. To avoid the potential radiation pneumonitis and pancreatitis and ulceration of stomach and duodenum caused by inadvertent perfusion. The placement of a hepatic artery port is particularly important in terms of safety and efficacy. The high rate of response and encouraging survival from SIRT have been reported for hepatocellular and liver metastases from colorectal cancer^[125,126].

CONCLUSION

Patients with liver metastases from colorectal cancer that are potentially resectable should be evaluated by experienced surgeons and radiologists, because surgical resection remains best treatment for long-term survival, although a minority of patients are amenable to the resection. Patients who are not suitable to surgical resection and who have no extrahepatic disease can be considered for regional therapies such as RFA and cryotherapy. Patients with extensive liver metastases, Hepatic artery catheter chemotherapy and chemoembolization can be considered as an alternative to systemic chemotherapy. Portal vein embolization may be combined in the treatment of patients with huge metastases. SIRT should be used for patients without extrahepatic metastases who failed in the treatment with 5-FU and other cytotoxic agents prefer. Systemic chemotherapy should be administered in patients with extrahepatic diseases. Immunotherapy can only be used to amplify the efficacy of antitumor cytotoxic agents in combination.

REFERENCES

- 1 Renehan AG**, Egger M, Saunders MP, O' Dwyer ST. Impact on survival of intensive follow up after curative resection for colorectal cancer: systematic review and meta-analysis of randomised trials. *BMJ* 2002; **324**: 813
- 2 Gwyn K**, Sinicrope FA. Chemoprevention of colorectal cancer. *Am J Gastroenterol* 2002; **97**: 13-21
- 3 Iyer RB**, Silverman PM, DuBrow RA, Charnsangavej C. Imaging in the diagnosis, staging, and follow-up of colorectal cancer. *AJR Am J Roentgenol* 2002; **179**: 3-13
- 4 Johns LE**, Houlston RS. A systematic review and meta-analysis of familial colorectal cancer risk. *Am J Gastroenterol* 2001; **96**: 2992-3003
- 5 Landheer ML**, Therasse P, van de Velde CJ. The importance of quality assurance in surgical oncology in the treatment of colorectal cancer. *Surg Oncol Clin N Am* 2001; **10**: 885-914
- 6 Li XW**, Ding YQ, Cai JJ, Yang SQ, An LB, Qiao DF. Studies on mechanism of Sialy Lewis-X antigen in liver metastases of human colorectal carcinoma. *World J Gastroenterol* 2001; **7**: 425-430
- 7 Zhang YL**, Zhang ZS, Wu BP, Zhou DY. Early diagnosis for colorectal cancer in China. *World J Gastroenterol* 2002; **8**: 21-25
- 8 Liu QZ**, Tuo CW, Wang B, Wu BQ, Zhang YH. Liver metastasis models of human colorectal carcinoma established in nude mice by orthotopic transplantation and their biologic characteristic. *World J Gastroenterol* 1998; **4**: 409-411
- 9 Ruers T**, Bleichrodt RP. Treatment of liver metastases, an update on the possibilities and results. *Eur J Cancer* 2002; **38**: 1023-1033
- 10 Biasco G**, Gallerani E. Treatment of liver metastases from colorectal cancer: what is the best approach today? *Dig Liver Dis* 2001; **33**: 438-444
- 11 Yoon SS**, Tanabe KK. Multidisciplinary management of metastatic colorectal cancer. *Surg Oncol* 1998; **7**: 197-207
- 12 Cromheecke M**, de Jong KP, Hoekstra HJ. Current treatment for colorectal cancer metastatic to the liver. *Eur J Surg Oncol* 1999; **25**: 451-463
- 13 Geoghegan JG**, Scheele J. Treatment of colorectal liver metastases. *Br J Surg* 1999; **86**: 158-169
- 14 Chiappa A**, Zbar AP, Biella F, Staudacher C. Survival after repeat hepatic resection for recurrent colorectal metastases. *Hepatogastroenterology* 1999; **46**: 1065-1070
- 15 Fong Y**, Fortner J, Sun RL, Brennan MF, Blumgart LH. Clinical score for predicting recurrence after hepatic resection for metastatic colorectal cancer: analysis of 1001 consecutive cases. *Ann Surg* 1999; **230**: 309-318
- 16 Luna-Perez P**, Rodriguez-Coria DF, Arroyo B, Gonzalez-Macouzet J. The natural history of liver metastases from colorectal cancer. *Arch Med Res* 1998; **29**: 319-324
- 17 Heslin MJ**, Medina-Franco H, Parker M, Vickers SM, Aldrete J, Urist MM. Colorectal hepatic metastases: resection, local ablation, and hepatic artery infusion pump are associated with prolonged survival. *Arch Surg* 2001; **136**: 318-323
- 18 Wilson SM**, Adson MA. Surgical treatment of hepatic metastases from colorectal cancer. *Arch Surg* 1976; **111**: 330-334
- 19 Wagner JS**, Adson MA, Van Heerden JA, Adson MH, Ilstrup DM. The natural history of hepatic metastases from colorectal cancer. A comparison with resective treatment. *Ann Surg* 1984; **199**: 502-508
- 20 Wanebo HJ**, Semoglou C, Attiyeh F, Stearns MJ Jr. Surgical management of patients with primary operable colorectal cancer and synchronous liver metastases. *Am J Surg* 1978; **135**: 81-85
- 21 Glover C**, Douse P, Kane P, Karani J, Meire H, Mohammadtaghi S, Allen-Mersh TG. Accuracy of investigations for asymptomatic colorectal liver metastases. *Dis Colon Rectum* 2002; **45**: 476-484
- 22 Ryzewski B**, Dehdashti F, Gordon BA, Teefey SA, Strasberg SM, Siegel BA. Usefulness of intraoperative sonography for revealing hepatic metastases from colorectal cancer in patients selected for surgery after undergoing FDG PET. *AJR Am J Roentgenol* 2002; **178**: 353-358
- 23 Gruenberger T**, Zhao J, King J, Chung T, Clingan PR, Morris DL. Echogenicity of liver metastases from colorectal carcinoma is an independent prognostic factor in patients treated with regional chemotherapy. *Cancer* 2002; **94**: 1753-1759
- 24 Cervone A**, Sardi A, Conaway GL. Intraoperative ultrasound (IOUS) is essential in the management of metastatic colorectal liver lesions. *Am Surg* 2000; **66**: 611-615
- 25 Li L**, Wu PH, Mo YX, Lin HG, Zheng L, Li JQ, Lu LX, Ruan CM, Chen L. CT arterial portography and CT hepatic arteriography in detection of micro liver cancer. *World J Gastroenterol* 1999; **5**: 225-227
- 26 Schmidt J**, Strotzer M, Fraunhofer S, Boedeker H, Zirngibl H. Intraoperative ultrasonography versus helical computed tomography and computed tomography with arteriography in diagnosing colorectal liver metastases: lesion-by-lesion analysis. *World J Surg* 2000; **24**: 43-47
- 27 Okano K**, Yamamoto J, Okabayashi T, Sugawara Y, Shimada K, Kosuge T, Yamasaki S, Furukawa H, Muramatsu Y. CT imaging of intrabiliary growth of colorectal liver metastases: a comparison of pathological findings of resected specimens. *Br J Radiol* 2002; **75**: 497-501
- 28 Valls C**, Andia E, Sanchez A, Guma A, Figueras J, Torras J, Serrano T. Hepatic metastases from colorectal cancer: preoperative detection and assessment of resectability with helical CT. *Radiology* 2001; **218**: 55-60
- 29 Park JH**, Nazarian LN, Halpern EJ, Feld RI, Lev-Toaff AS, Parker L, Wechsler RJ. Comparison of unenhanced and contrast-en-

- hanced spiral CT for assessing interval change in patients with colorectal liver metastases. *Acad Radiol* 2001; **8**: 698-704
- 30 **Zheng WW**, Zhou KR, Chen ZW, Shen JZ, Chen CZ, Zhang SJ. Characterization of focal hepatic lesions with SPIO-enhanced MRI. *World J Gastroenterol* 2002; **8**: 82-86
- 31 **Ward J**, Naik KS, Guthrie JA, Wilson D, Robinson PJ. Hepatic lesion detection: comparison of MR imaging after the administration of superparamagnetic iron oxide with dual-phase CT by using alternative-free response receiver operating characteristic analysis. *Radiology* 1999; **210**: 459-466
- 32 **Zealley IA**, Skehan SJ, Rawlinson J, Coates G, Nahmias C, Somers S. Selection of patients for resection of hepatic metastases: improved detection of extrahepatic disease with FDG pet. *Radiographics* 2001; **21**: S55-69
- 33 **Boykin KN**, Zibari GB, Lilien DL, McMillan RW, Aultman DF, McDonald JC. The use of FDG-positron emission tomography for the evaluation of colorectal metastases of the liver. *Am Surg* 1999; **65**: 1183-1185
- 34 **Figueras J**, Valls C. The use of laparoscopic ultrasonography in the preoperative study of patients with colorectal liver metastases. *Ann Surg* 2000; **232**: 721-723
- 35 **Parks RW**, Garden OJ. Liver resection for cancer. *World J Gastroenterol* 2001; **7**: 766-771
- 36 **Petrowsky H**, Gonen M, Jarnagin W, Lorenz M, DeMatteo R, Heinrich S, Encke A, Blumgart L, Fong Y. Second liver resections are safe and effective treatment for recurrent hepatic metastases from colorectal cancer: a bi-institutional analysis. *Ann Surg* 2002; **235**: 863-871
- 37 **Malafosse R**, Penna C, Sa Cunha A, Nordlinger B. Surgical management of hepatic metastases from colorectal malignancies. *Ann Oncol* 2001; **12**: 887-894
- 38 **Rees M**, John TG. Current status of surgery in colorectal metastases to the liver. *Hepatogastroenterology* 2001; **48**: 341-344
- 39 **Taylor I**, Gillams AR. Colorectal liver metastases: alternatives to resection. *J R Soc Med* 2000; **93**: 576-579
- 40 **Rodgers MS**, McCall JL. Surgery for colorectal liver metastases with hepatic lymph node involvement: a systematic review. *Br J Surg* 2000; **87**: 1142-1155
- 41 **Fiorentini G**, Poddie DB, Giorgi UD, Guglielminetti D, Giovanis P, Leoni M, Latino W, Dazzi C, Cariello A, Turci D, Marangolo M. Global approach to hepatic metastases from colorectal cancer: indication and outcome of intra-arterial chemotherapy and other hepatic-directed treatments. *Med Oncol* 2000; **17**: 163-173
- 42 **Yamaguchi J**, Yamamoto M, Komuta K, Fujioka H, Furui JI, Kanematsu T. Hepatic resections for bilobar liver metastases from colorectal cancer. *J Hepatobiliary Pancreat Surg* 2000; **7**: 404-409
- 43 **Bozzetti F**, Bignami P, Baratti D. Surgical strategies in colorectal cancer metastatic to the liver. *Tumori* 2000; **86**: 1-7
- 44 **Bozzetti F**, Bignami P. Recommendation for surgical treatment of colorectal liver metastases. *Ann Oncol* 2000; **11**: 243-244
- 45 **Choti MA**, Sitzmann JV, Tiburi MF, Sumetchotimetha W, Rangsiri R, Schulick RD, Lillemoe KD, Yeo CJ, Cameron JL. Trends in long-term survival following liver resection for hepatic colorectal metastases. *Ann Surg* 2002; **235**: 759-766
- 46 **Bolton JS**, Fuhrman GM. Survival after resection of multiple bilobar hepatic metastases from colorectal carcinoma. *Ann Surg* 2000; **231**: 743-751
- 47 **Primrose JN**. Treatment of colorectal metastases: surgery, cryotherapy, or radiofrequency ablation. *Gut* 2002; **50**: 1-5
- 48 **Lorenz M**, Staib-Sebler E, Hochmuth K, Heinrich S, Gog C, Vetter G, Encke A, Muller HH. Surgical resection of liver metastases of colorectal carcinoma: short and long-term results. *Semin Oncol* 2000; **27**: 112-119
- 49 **Morris DL**. Surgery for liver metastases: How many? *ANZ J Surg* 2002; **72**: 2
- 50 **Liu LX**, Jiang HC, Piao DX. Radiofrequency ablation in liver cancer. *World J gastroenterol* 2002; **8**: 393-399
- 51 **Wood BJ**, Ramkaransingh JR, Fojo T, Walther MM, Libutti SK. Percutaneous tumor ablation with radiofrequency. *Cancer* 2002; **94**: 443-451
- 52 **Parikh AA**, Curley SA, Fornage BD, Ellis LM. Radiofrequency ablation of hepatic metastases. *Semin Oncol* 2002; **29**: 168-182
- 53 **Choi H**, Loyer EM, DuBrow RA, Kaur H, David CL, Huang S, Curley S, Charnsangavej C. Radio-frequency ablation of liver tumors: assessment of the therapeutic response and complications. *Radiographics* 2001; **21**: S41-54
- 54 **Goldberg SN**. Radiofrequency tumor ablation: Principles and techniques. *Eur J Ultrasound* 2001; **13**: 129-147
- 55 **Liu CL**, Fan ST. Nonresectional therapies for hepatocellular carcinoma. *Am J Surg* 1997; **173**: 358-365
- 56 **Buscarini L**, Buscarini E, Di Stasi M, Vallisa D, Quaretti P, Rocca A. Percutaneous radiofrequency ablation of small hepatocellular carcinoma: long-term results. *Eur Radiol* 2001; **11**: 914-921
- 57 **Hager ED**, Dziambor H, Hohmann D, Gallenbeck D, Stephan M, Popa C. Deep hyperthermia with radiofrequencies in patients with liver metastases from colorectal cancer. *Anticancer Res* 1999; **19**: 3403-3408
- 58 **Rossi S**, Di Stasi M, Buscarini E, Quaretti P, Garbagnati F, Squassante L, Paties CT, Silverman DE, Buscarini L. Percutaneous RF interstitial thermal ablation in the treatment of hepatic cancer. *AJR Am J Roentgenol* 1996; **167**: 759-768
- 59 **Wood TF**, Rose DM, Chung M, Allegra DP, Foshag LJ, Bilchik AJ. Radiofrequency ablation of 231 unresectable hepatic tumors: Indications, limitations, and complications. *Ann Surg Oncol* 2000; **7**: 593-600
- 60 **Solbiati L**, Ierace T, Tonolini M, Osti V, Cova L. Radiofrequency thermal ablation of hepatic metastases. *Eur J Ultrasound* 2001; **13**: 149-158
- 61 **Machi J**. Radiofrequency ablation for multiple hepatic metastases. *Ann Surg Oncol* 2001; **8**: 379-380
- 62 **Bilchik AJ**, Wood TF, Allegra DP. Radiofrequency ablation of unresectable hepatic malignancies: lessons learned. *Oncologist* 2001; **6**: 24-33
- 63 **Wong SL**, Edwards MJ, Chao C, Simpson D, McMasters KM. Radiofrequency ablation for unresectable hepatic tumors. *Am J Surg* 2001; **182**: 552-557
- 64 **Pearson AS**, Izzo F, Fleming RY, Ellis LM, Delrio P, Roh MS, Granchi J, Curley SA. Intraoperative radiofrequency ablation or cryoablation for hepatic malignancies. *Am J Surg* 1999; **178**: 592-599
- 65 **Curley SA**, Izzo F, Delrio P, Ellis LM, Granchi J, Vallone P, Fiore F, Pignata S, Daniele B, Cremona F. Radiofrequency ablation of unresectable primary and metastatic hepatic malignancies: results in 123 patients. *Ann Surg* 1999; **230**: 1-8
- 66 **Gillams AR**, Lees WR. Survival after percutaneous, image-guided, thermal ablation of hepatic metastases from colorectal cancer. *Dis Colon Rectum* 2000; **43**: 656-661
- 67 **Sotsky TK**, Ravikummar TS. Cryotherapy in the treatment of liver metastases from colorectal cancer. *Semin Oncol* 2002; **29**: 183-191
- 68 **Seifert JK**, Achenbach T, Heintz A, Bottger TC, Junginger T. Cryotherapy for liver metastases. *Int J Colorectal Dis* 2000; **15**: 161-166
- 69 **Neeleman N**, Wobbes T, Jager GJ, Ruers TJ. Cryosurgery as treatment modality for colorectal liver metastases. *Hepatogastroenterology* 2001; **48**: 325-359
- 70 **Ruers TJ**, Jager GJ, Wobbes T. Cryosurgery for colorectal liver metastases. *Semin Oncol* 2000; **27**: 120-125
- 71 **Sikma MA**, Coenen JL, Kloosterziel C, Hasselt BA, Ruers TJ. A breakthrough in cryosurgery. *Surg Endosc* 2002; **16**: 870
- 72 **Finlay IG**, Seifert JK, Stewart GJ, Morris DL. Resection with cryotherapy of colorectal hepatic metastases has the same survival as hepatic resection alone. *Eur J Surg Oncol* 2000; **26**: 199-202
- 73 **Rivoire M**, De Cian F, Meeus P, Gignoux B, Frering B, Kaemmerlen P. Cryosurgery as a means to improve surgical treatment of patients with multiple unresectable liver metastases. *Anticancer Res* 2000; **20**: 3785-3790
- 74 **Seifert JK**, Morris DL. Prognostic factors after cryotherapy for hepatic metastases from colorectal cancer. *Ann Surg* 1998; **228**: 201-208
- 75 **Seifert JK**, Morris DL. Indicators of recurrence following cryotherapy for hepatic metastases from colorectal cancer. *Br J Surg* 1999; **86**: 234-240
- 76 **Wallace JR**, Christians KK, Pitt HA, Quebbeman EJ. Cryotherapy extends the indications for treatment of colorectal liver metastases. *Surgery* 1999; **126**: 766-772
- 77 **Huang A**, McCall JM, Weston MD, Mathur P, Quinn H, Henderson DC, Allen-Mersh TG. Phase I study of percutaneous cryotherapy for colorectal liver metastasis. *Br J Surg* 2002; **89**: 303-310
- 78 **Gruenberger T**, Jourdan JL, Zhao J, King J, Morris DL. Reduction in recurrence risk for involved or inadequate margins with

- edge cryotherapy after liver resection for colorectal metastases. *Arch Surg* 2001; **136**: 1154-1157
- 79 **Ruers TJ**, Joosten J, Jager GJ, Wobbes T. Long-term results of treating hepatic colorectal metastases with cryosurgery. *Br J Surg* 2001; **88**: 844-849
- 80 **Ragnhammar P**, Hafstrom L, Nygren P, Glimelius B. SBU-group. Swedish Council of Technology Assessment in Health Care. A systematic overview of chemotherapy effects in colorectal cancer. *Acta Oncol* 2001; **40**: 282-308
- 81 **Kohne CH**, Cunningham D, Di CF, Glimelius B, Blijham G, Aranda E, Scheithauer W, Rougier P, Palmer M, Wils J, Baron B, Pignatti F, Schoffski P, Micheel S, Hecker H. Clinical determinants of survival in patients with 5-fluorouracil-based treatment for metastatic colorectal cancer: results of a multivariate analysis of 3825 patients. *Ann Oncol* 2002; **13**: 308-317
- 82 **Piedbois P**, Zelek L, Cherqui D. Chemotherapy of nonoperable colorectal liver metastases. *Hepatogastroenterology* 2001; **48**: 711-714
- 83 **Hasuike Y**, Takeda Y, Mishima H, Nishishou I, Tsujinaka T, Kikkawa N. Systemic chemotherapy for advanced colorectal cancer with liver metastasis. *Gan To Kagaku Ryoho* 2002; **29**: 866-872
- 84 **Ensminger WD**. Intrahepatic arterial infusion of chemotherapy: pharmacologic principles. *Semin Oncol* 2002; **29**: 119-125
- 85 **van Riel JM**, van Groenigen CJ, Giaccone G, Pinedo HM. Hepatic arterial chemotherapy for colorectal cancer metastatic to the liver. *Oncology* 2000; **59**: 89-97
- 86 **Aldrighetti L**, Arru M, Angeli E, Venturini M, Salvioni M, Ronzoni M, Caterini R, Ferla G. Percutaneous vs. surgical placement of hepatic artery indwelling catheters for regional chemotherapy. *Hepatogastroenterology* 2002; **49**: 513-517
- 87 **Howell JD**, Warren HW, Anderson JH, Kerr DJ, McArdle CS. Intra-arterial 5-fluorouracil and intravenous folinic acid in the treatment of liver metastases from colorectal cancer. *Eur J Surg* 1999; **165**: 652-658
- 88 **Lygidakis NJ**, Sgourakis G, Dedemadi G, Safioleus MC, Nestoridis J. Regional chemoimmunotherapy for nonresectable metastatic liver disease of colorectal origin. A prospective randomized study. *Hepatogastroenterology* 2001; **48**: 1085-1087
- 89 **Allen-Mersh TG**, Earlam S, Fordy C, Abrams K, Houghton J. Quality of life and survival with continuous hepatic-artery floxuridine infusion for colorectal liver metastases. *Lancet* 1994; **344**: 1255-1260
- 90 **Howell JD**, McArdle CS, Kerr DJ, Buckles J, Ledermann JA, Taylor I, Gallagher HJ, Budden J. A phase II study of regional 2-weekly 5-fluorouracil infusion with intravenous folinic acid in the treatment of colorectal liver metastases. *Br J Cancer* 1997; **76**: 1390-1393
- 91 **Pelosi E**, Bar F, Battista S, Bello M, Bucchi MC, Alabiso O, Molino G, Bisi G. Hepatic arterial infusion chemotherapy for unresectable confined liver metastases: prediction of systemic toxicity with the application of a scintigraphic and pharmacokinetic approach. *Cancer Chemother Pharmacol* 1999; **44**: 505-510
- 92 **Kemeny N**, Fata F. Hepatic-arterial chemotherapy. *Lancet Oncol* 2001; **2**: 418-428
- 93 **Weinreich DM**, Alexander HR. Transarterial perfusion of liver metastases. *Semin Oncol* 2002; **29**: 136-144
- 94 **Sasson AR**, Watson JC, Sigurdson ER. Hepatic artery infusional chemotherapy for colorectal liver metastases. *Cancer Treat Res* 2001; **109**: 279-298
- 95 **Mathur P**, Allen-Mersh TG. Hepatic arterial chemotherapy for colorectal liver metastases. *Hepatogastroenterology* 2001; **48**: 317-319
- 96 **Bloom AI**, Gordon RL, Ahl KH, Kerlan RK Jr, LaBerge JM, Wilson MW, Venook AP, Warren R. Transcatheter embolization for the treatment of misperfusion after hepatic artery chemoinfusion pump implantation. *Ann Surg Oncol* 1999; **6**: 350-358
- 97 **Kohnoe S**, Endo K, Yamamoto M, Ikeda Y, Toh Y, Baba H, Tajima T, Okamura T. Protracted hepatic arterial infusion with low-dose cisplatin plus 5-fluorouracil for unresectable liver metastases from colorectal cancer. *Surgery* 2002; **131**: S128-134
- 98 **Link KH**, Sunelaitis E, Kornmann M, Schatz M, Gansauge F, Leder G, Formentini A, Staib L, Pillasch J, Beger HG. Regional chemotherapy of nonresectable colorectal liver metastases with mitoxantrone, 5-fluorouracil, folinic acid, and mitomycin C may prolong survival. *Cancer* 2001; **92**: 2746-2753
- 99 **Muller H**, Nakchbandi W, Chatzissavvidis I, Valek V. Intra-arterial infusion of 5-fluorouracil plus granulocyte-macrophage colony-stimulating factor (GM-CSF) and chemoembolization with melphalan in the treatment of disseminated colorectal liver metastases. *Eur J Surg Oncol* 2001; **27**: 652-661
- 100 **Fiorentini G**, De Giorgi U, Giovanis P, Guadagni S, Cantore M, Marangolo M. International Society of Regional Cancer Treatment and Societa Italiana di Terapie Integrate Locoregionali in Oncologia. Intra-arterial hepatic chemotherapy (IAHC) for liver metastases from colorectal cancer: need of guidelines for catheter positioning, port management, and anti-coagulant therapy. *Ann Oncol* 2001; **12**: 1023
- 101 **Copur MS**, Capadano M, Lynch J, Goertzen T, McCowan T, Brand R, Tempero M. Alternating hepatic arterial infusion and systemic chemotherapy for liver metastases from colorectal cancer: a phase II trial using intermittent percutaneous hepatic arterial access. *J Clin Oncol* 2001; **19**: 2404-2412
- 102 **van Riel JM**, van Groenigen CJ, Albers SH, Cazemier M, Meijer S, Bleichrodt R, van den Berg FG, Pinedo HM, Giaccone G. Hepatic arterial 5-fluorouracil in patients with liver metastases of colorectal cancer: single-centre experience in 145 patients. *Ann Oncol* 2000; **11**: 1563-1570
- 103 **Chen MS**, Li JQ, Zhang YQ, Lu LX, Zhang WZ, Yuan YF, Guo YP, Lin XJ, Li GH. High-dose iodized oil transcatheter arterial chemoembolization for patients with large hepatocellular carcinoma. *World J Gastroenterol* 2002; **8**: 74-78
- 104 **Wu ZQ**, Fan J, Qiu SJ, Zhou J, Tang ZY. The value of postoperative hepatic regional chemotherapy in prevention of recurrence after radical resection of primary liver cancer. *World J Gastroenterol* 2000; **6**: 131-133
- 105 **Huang XQ**, Huang ZQ, Duan WD, Zhou NX, Feng YQ. Severe biliary complications after hepatic artery embolization. *World J Gastroenterol* 2002; **8**: 119-123
- 106 **Abramson RG**, Rosen MP, Perry LJ, Brophy DP, Raeburn SL, Stuart KE. Cost-effectiveness of hepatic arterial chemoembolization for colorectal liver metastases refractory to systemic chemotherapy. *Radiology* 2000; **216**: 485-491
- 107 **Popov I**, Lavrnjc S, Jelic S, Jezdic S, Jasovic A. Chemoembolization for liver metastases from colorectal carcinoma: risk or a benefit. *Neoplasma* 2002; **49**: 43-48
- 108 **Azoulay D**, Castaing D, Smail A, Adam R, Cailiez V, Laurent A, Lemoine A, Bismuth H. Resection of nonresectable liver metastases from colorectal cancer after percutaneous portal vein embolization. *Ann Surg* 2000; **231**: 480-486
- 109 **Azoulay D**, Castaing D, Krissat J, Smail A, Hargreaves GM, Lemoine A, Emile JF, Bismuth H. Percutaneous portal vein embolization increases the feasibility and safety of major liver resection for hepatocellular carcinoma in injured liver. *Ann Surg* 2000; **232**: 665-672
- 110 **Kemeny N**, Fata F. Arterial, portal, or systemic chemotherapy for patients with hepatic metastasis of colorectal carcinoma. *J Hepatobiliary Pancreat Surg* 1999; **6**: 39-49
- 111 **Kokudo N**, Tada K, Seki M, Ohta H, Azekura K, Ueno M, Ohta K, Yamaguchi T, Matsubara T, Takahashi T, Nakajima T, Muto T, Ikari T, Yanagisawa A, Kato Y. Proliferative activity of intrahepatic colorectal metastases after preoperative hemihepatic portal vein embolization. *Hepatology* 2001; **34**: 267-272
- 112 **Elias D**, Ouellet JF, De Baere T, Lasser P, Roche A. Preoperative selective portal vein embolization before hepatectomy for liver metastases: long-term results and impact on survival. *Surgery* 2002; **131**: 294-299
- 113 **Imamura H**, Kawasaki S, Miyagawa S, Ikegami T, Kitamura H, Shimada R. Aggressive surgical approach to recurrent tumors after hepatectomy for metastatic spread of colorectal cancer to the liver. *Surgery* 2000; **127**: 528-535
- 114 **Lode HN**, Xiang R, Becker JC, Gillies SD, Reifeld RA. Immunocytokines: a promising approach to cancer immunotherapy. *Pharmacol Ther* 1998; **80**: 277-292
- 115 **Okuno K**, Kaneda K, Yasutomi M. Regional IL-2-based immunochemotherapy of colorectal liver metastases. *Hepatogastroenterology* 1999; **46**: 1263-1267
- 116 **Okuno K**, Hirai N, Takemoto Y, Kawai I, Yasutomi M. Interleukin-2 as a modulator of 5-fluorouracil in hepatic arterial immunochemotherapy for liver metastases. *Hepatogastroenterology* 2000; **47**: 487-491

- 117 **Lou C**, Chen ZN, Bian HJ, Li J, Zhou SB. Pharmacokinetics of radioimmunotherapeutic agent of direct labeling mAb 188Re-HAb18. *World J Gastroenterol* 2002; **8**: 69-73
- 118 **Buchegger F**, Roth A, Allal A, Dupertuis YM, Slosman DO, Delaloye AB, Mach JP. Radioimmunotherapy of colorectal cancer liver metastases: combination with radiotherapy. *Ann N Y Acad Sci* 2000; **910**: 263-269
- 119 **Buchegger F**, Allal AS, Roth A, Papazyan JP, Dupertuis Y, Mirimanoff RO, Gillet M, Pelegrin A, Mach JP, Slosman DO. Combined radioimmunotherapy and radiotherapy of liver metastases from colorectal cancer: a feasibility study. *Anticancer Res* 2000; **20**: 1889-1196
- 120 **Malik U**, Mohiuddin M. External-beam radiotherapy in the management of liver metastases. *Semin Oncol* 2002; **29**: 196-201
- 121 **Liu L**, Jiang Z, Teng GJ, Song JZ, Zhang DS, Guo QM, Fang W, He SC, Guo JH. Clinical and experimental study on regional administration of phosphorus 32 glass microspheres in treating hepatic carcinoma. *World J Gastroenterol* 1999; **5**: 492-505
- 122 **Gong Y**, Liu KD, Zhou G, Xue Q, Chen SL, Tang ZY. Tumor radioimmunoinaging of chimeric antibody in nude mice with hepatoma xenograft. *World J Gastroenterol* 1998; **4**: 7-9
- 123 **Stubbs RS**, Cannan RJ, Mitchell AW. Selective internal radiation therapy (SIRT) with ⁹⁰Yttrium microspheres for extensive colorectal liver metastases. *Hepatogastroenterology* 2001; **48**: 333-337
- 124 **Stubbs RS**, Cannan RJ, Mitchell AW. Selective internal radiation therapy with ⁹⁰yttrium microspheres for extensive colorectal liver metastases. *J Gastrointest Surg* 2001; **5**: 294-302
- 125 **Dancey JE**, Shepherd FA, Paul K, Sniderman KW, Houle S, Gabrys J, Hendler AL, Goin JE. Treatment of nonresectable hepatocellular carcinoma with intrahepatic ⁹⁰Y-microspheres. *J Nucl Med* 2000; **41**: 1673-1681
- 126 **Campbell AM**, Bailey IH, Burton MA. Analysis of the distribution of intra-arterial microspheres in human liver following hepatic yttrium-90 microsphere therapy. *Phys Med Biol* 2000; **45**: 1023-1033

Edited by Ma JY

Hepatic stem cells: existence and origin

Ying Zhang, Xue-Fan Bai, Chang-Xing Huang

Ying Zhang, Xue-Fan Bai, Chang-Xing Huang, The center of diagnosis and treatment for infectious diseases of PLA, Tang Du Hospital, Fourth Military Medical University, Xi'an 710038, Shaanxi Province, China

Correspondence to: Prof. Xue-Fan Bai, The center of diagnosis and treatment for infectious diseases of PLA, Tang Du Hospital, Fourth Military Medical University, Xi'an 710038, Shaanxi Province, China. zfyfmmu@sohu.com

Telephone: +86-29-3377452 **Fax:** +86-29-3377452

Received: 2002-07-04 **Accepted:** 2002-08-02

Abstract

Stem cells are not only units of biological organization, responsible for the development and the regeneration of tissue and organ systems, but also are units in evolution by natural selection. It is accepted that there is stem cell potential in the liver. Like most organs in a healthy adult, the liver maintains a perfect balance between cell gain and loss. It has three levels of cells that can respond to loss of hepatocytes: (1) Mature hepatocytes, which proliferate after normal liver tissue renewal, less severe liver damage, etc; they are numerous, unipotent, "committed" and respond rapidly to liver injury. (2) Oval cells, which are activated to proliferate when the liver damage is extensive and chronic, or if proliferation of hepatocytes is inhibited; they lie within or immediately adjacent to the canal of Hering (CoH); they are less numerous, bipotent and respond by longer, but still limited proliferation. (3) Exogenous liver stem cells, which may derive from circulating hematopoietic stem cells (HSCs) or bone marrow stem cells; they respond to allyl alcohol injury or hepatocarcinogenesis; they are multipotent, rare, but have a very long proliferation potential. They make a more significant contribution to regeneration, and even completely restore normal function in a murine model of hereditary tyrosinaemia. How these three stem cell populations integrate to achieve a homeostatic balance remains enigmatic. This review focuses on the location, activation, markers of the three candidates of liver stem cell, and the most importantly, therapeutic potential of hepatic stem cells.

Zhang Y, Bai XF, Huang CX. Hepatic stem cells: existence and origin. *World J Gastroenterol* 2003; 9(2): 201-204
<http://www.wjgnet.com/1007-9327/9/201.htm>

INTRODUCTION

The considerable excitement surrounding the stem cell field is based on the unique biological properties of these cells and their capacity to self-renew and regenerate tissue and organ systems^[1-3]. Although the existence of a liver stem cell has been debated for many years, it is now generally accepted that the liver contains cells with stem-like properties and that these cells can be activated to proliferate and differentiate into mature hepatic epithelial cells under certain pathophysiologic circumstances^[4-8]. Cellular therapy with liver stem cells and their progeny is a promising new approach which will contribute to gene therapy of liver diseases^[9-11].

HEPATOCYTES AS HEPATIC STEM CELLS

It has been estimated that the liver is replaced by normal tissue renewal approximately once a year. The participation of putative liver stem cells has never been demonstrated in this process^[12,13]. Replacement of lost liver tissues is accomplished by proliferation of mature hepatocytes (and supporting sinusoidal cells)^[14]. In the classic partial hepatectomy (PH) experiments, the loss of two-thirds of the rat liver is replaced within 2 weeks by proliferation of hepatocytes^[15-17]. Although periportal hepatocytes appear to proliferate early after PH, all hepatocytes, including those immediately adjacent to the central vein, may undergo mitosis and proliferate promptly, continuously replenish the lost cells. Overturf *et al*^[18] performed serial transplantation of a limited number of unfractionated adult parenchymal hepatocytes in fumarylacetoacetate hydrolase (FAH) deficiency mice. The results document that such cells can divide at least 69 times without loss of functions. So it can be concluded that hepatocytes are highly proliferative and have growth potential similar to that of hematopoietic stem cells.

A cell population that has an extensive self-maintaining capacity is the definition of stem cells. In this context, the adult liver, having the extensive capacity of maintaining parenchymal cell number throughout the life span of the organism, can be considered as a single lineage stem cell system in which the hepatocyte is the stem cell. Potten and Loeffler^[19] proposed stem cells as actual stem cells, potential stem cells, and committed stem cells. So hepatocytes appear to be "committed stem cells" that are normally quiescent, but can be activated to produce progeny whose only differentiation option is hepatocytic.

HEPATIC STEM CELLS IN CANAL OF HERING

In the development of liver, the early fetal hepatocytes or hepatoblasts are progenitors for both adult hepatocytes and bile epithelial cells, which suggests that hepatoblasts are at least bipotential precursors^[20]. The question then arises whether either or both of the cell lineages derived from the hepatoblast retain the "bipotential capacity" of the precursor cells. There is at present no substantial evidence indicating that adult hepatocytes are more than a unipotential committed stem cell system, while adequate data have been accumulated to show that there really exist so-called "oval cells" in adult liver. Oval cells have lineage options similar to those displayed by hepatoblasts in early stages of liver development^[21]. As such, oval cells can be regarded as "bipotential precursors" for the two hepatic parenchymal cell lineages. They are able to differentiate into mature hepatocytes or cholangiocytes in response to various types of stress or injury.

Morphologically, oval cells are small in size (approximately 10 μm), with a large nucleus-to-cytoplasm ratio, with an oval-shaped nucleus (hence their name). Oval cells are heterogeneous, and may display features of both bile duct cells and hepatocytes. Oval cells are activated to proliferate after hepatocyte loss in the mature liver if liver damage is extensive and chronic, or if proliferation of hepatocytes is inhibited, such as by viral infection. Then their progeny extended across the liver lobule and differentiated into either hepatocytes or bile duct cells, ultimately rebuilt the liver^[22,23]. In rodents, the concept of the bipotential cell, the so-called oval cell, is now

widely accepted, the existence of a human equivalent remains controversial. In Heather's experiments^[24], immunolocalization of OV-6 and two biliary markers, cytokeratin 19(CK19) and human epithelial antigen 125(HEA-125) was compared in normal adult human livers and in primary biliary cirrhosis (PBC) and primary sclerosing cholangitis (PSC) liver sections. It is proposed that the small OV-6-positive oval cells are analogous to those seen in rat models and may represent human liver progenitor cells that may differentiate into OV-6-positive ductal cells or lobular hepatocytes. The most commonly recognized tissue reaction in support of oval cells in human is the appearance of "ductular reactions"^[25]. Ductular reaction is the proliferative response to many types of liver injury in human, characterized by an increase of bile duct-like structures. In a number of morphological studies, the presence of cells with a distinctive "small" or oval cell-like appearance have been reported in diseased human liver tissue^[26,27]. This includes severe hepatic necrosis, alcoholic cirrhosis, focal nodular hyperplasia, hepatoblastoma, and biliary diseases such as primary biliary cirrhosis or biliary atresia. These oval cell-like cells are proliferative and can differentiate into hepatocytes and cholangiocytes.

The anatomic location of oval cell has also been a subject of controversy. Results from a detailed time course study of activation of hepatic stem cells in the AAF/PH model, utilizing a combination of immunohistochemistry with OV-6 and desmin antibodies and autoradiography after [³H]thymidine administration shortly after the PH, indicate that the earliest population of proliferating OV-6 positive cells is located in the small bile ductules. In addition, these early population of OV-6 positive cells express albumin and α -fetoprotein(AFP)^[28]. Therefore, it seems likely that the major source of oval cells, at least in the AAF/PH model, is derived from the lining cells of the biliary ductules and that these cells constitute the dormant/facultative hepatic stem cell compartment. Theise *et al*'s experimental work^[29] suggests that oval cells lie within or immediately adjacent to the canal of Hering(CoH), which is the anatomic juncture of the hepatocyte canalicular system, and the terminal branches of the biliary tree.

Oval cells express similar markers to hepatocytes or bile duct cells, like AFP, certain keratin markers (e.g., cytokeratin 19 [CK19]), and γ -glutamyl transpeptidase. Monoclonal antibodies such as OV-6, OC2, and BD1 also aid in their characterization. High levels of certain mRNAs like AFP and stem cell factor (SCF) can also be expressed by oval cells. OV-6 identifies a cytokeratin of molecular weight 56 000, with epitopes shared on cytokeratins (CKs) 14 and 19. It is present in rat liver on bile ducts, oval cells, and nodular hepatocytes as well as transitional hepatocytes^[30]. In human liver, OV-6 identifies cells in the ductal plate, oval cells and bile ducts and ductules in fetal tissue, and oval cells found in focal nodular hyperplasia^[31,32]. AFP is an abundant serum glycoprotein in developing mammals. During embryonic development, AFP is first detected in the yolk sac and later in the fetal liver. The full-length AFP RNA and protein are highly expressed in the primitive hepatoblasts and postnatal hepatocytes^[33]. Full length AFP has been shown to be expressed in oval cells and small basophilic hepatocytes during the early stages of carcinogenesis^[34]. Hence, AFP expression can be used as an indicator for an early hepatic lineage, and has also served as an important marker for the activation of the hepatic stem cell compartment. SCF, also called c-kit ligand, encodes a transmembrane tyrosine kinase protein and belongs to the subfamily of platelet derived growth factor. The SCF/c-kit system is believed to play an important role in stem cell biology during hematopoiesis, gametogenesis, and melanogenesis^[35,36]. Studies have shown that both SCF and c-kit are expressed in the bile duct cells and the expression of both the genes is increased in

oval cells in the 2-acetylaminofluorene and partial hepatectomy model^[37].

HEPATIC STEM CELLS FROM BONE MARROW

In the experiment by Yavorkovsky *et al*^[38], periportal necrosis of allyl alcohol toxicity resulted in a "null cell" proliferation that was negative not only for hepatocyte markers, but also for cholangiocyte markers. This phenomenon suggests that oval cells are not the only source of hepatic stem cells. This hypothesis might be correct as suggested by the research in transdifferentiation of marrow stem cells^[39]. The ability of marrow stem cells to give rise to cells of different organs is being increasingly identified, for example, bone marrow turning into skeletal muscle^[40,41], renal^[42], or into brain^[43].

Correlation between bone marrow and liver has been discovered. (1) Hematopoiesis and hepatic development share common stages^[44]. During fetal development, hematopoietic stem cells move out of the yolk sac and into the developing liver. The liver remains hematopoietic during the entire fetal period and for approximately the first week after birth in the neonates. Simultaneously with the appearance of hematopoiesis, hematopoietic stem cells (HSCs) can be detected in the fetal liver. In the latter part of gestation and after birth, the hematopoietic function of the liver is considerably reduced, if not totally absent. Although the liver loses its hematopoietic functions, hematopoiesis often returns in adult life in disease states. (2) Some studies show that hepatic oval cells and hematopoietic stem cells share CD34, Thy-1, and c-kit mRNA and protein^[45-49]. Oval cells also express mRNA for the flt-3 receptor, previously reported to be restricted to hematopoietic stem cells^[50]. (3) In Theise ND *et al*'s research work^[51], a cohort of lethally irradiated female mice received whole bone marrow transplants from age-matched male donors. Fluorescence *in situ* hybridization (FISH) for the Y-chromosome was performed on liver tissues. Y-chromosome positive hepatocytes were identified in all animals sacrificed 2 months or longer post-transplantation. Simultaneous FISH for the Y-chromosome and albumin messenger RNA confirmed male-derived cells were mature hepatocytes. The experiments show that bone marrow cells transplanted from male donors to syngeneic recipients are able to localize in the two largest lobes of the liver, differentiating into mature hepatocytes carrying the Y-chromosome. In human experiment, biopsy and autopsy liver specimens from recipients of therapeutic bone marrow or liver transplants were analyzed for marrow-derived hepatocytes and cholangiocytes^[52,53]. In view of these bone marrow-liver inter-relationships, it is expected that a closer relationship might exist in the two lineages^[54]. Hepatocytes and cholangiocytes could derive from bone marrow stem cells. In both of human subjects and in the experimental animals, engraftment by bone marrow cells as hepatocytes could be seen in the absence of severe injury, suggesting that such movement might occur as a low level, baseline, physiologic phenomenon.

The mechanism of entry and differentiation of the transplanted bone marrow cells within the liver cell plates might also occur in different ways. First, circulating. Marrow-derived cells might enter the liver plates directly from the sinusoidal circulation. These cells are most often scattered throughout the parenchyma and intercalate randomly into pre-existent liver cords directly as hepatocytes. On the other hand, given previous demonstrations that oval cells derive from CoH, and that not only hepatocytes, but oval cells derive from marrow cells^[55-57], we can speculate that marrow cells might enter into liver through the circulation, then translocate across basement membranes into CoH and/or the terminal branches of the biliary tree, and differentiate into cytokeratin 19-positive small cholangiocyte-like cells. Proliferation and differentiation into

hepatocytes would follow in proportion to the type and extent of hepatocyte injury. Thus, hepatic regeneration through marrow cells may have multiple and perhaps overlapping pathways to accomplish cell replacement and organ repair.

MSCs are not only highly self-regenerative, but also can transdifferentiate into liver endogenous stem cells and liver parenchymal cells. So MSCs can repair damaged liver. Compared with liver transplantation and hepatocyte transplantation, there are much more marrow donors than liver and liver cells donors. If we utilize a patient's own MSCs as a new therapeutic option to treat liver diseases, immunological rejection will be avoided completely. Now MSCs has been used in animal experiments and clinical trails^[68,59]. Orlic *et al*^[60,61] sorted lineage-negative (Lin⁻) bone marrow cells from transgenic mice expressing enhanced green fluorescent protein by fluorescence-activated cell sorting on the basis of c-kit expression. Then they injected these Lin⁻c-kit^{pos} cells into the contracting wall bordering the infarct shortly after coronary ligation. The results show that newly formed myocardium occupied 68 % of the infarcted portion of the ventricle 9 days after transplanting the bone marrow cells. The developing tissues comprised proliferating myocytes and vascular structures. Their studies indicate that it is possible to rebuild heart-attack-damaged hearts with adult stem cells from bone marrow. Also, in order to determine whether bone marrow contains cells that can correct liver diseases, Lagasse *et al*^[62] used bone marrow transplantation in the fumarylacetoacetate hydrolase (FAH)-deficient mouse, an animal model of fatal hereditary tyrosinemia type I. The results show that bone marrow transplantation rescued the mouse and restored the biochemical functions of its liver.

PROSPECT

The liver is an organ known to have tremendous regenerative capacity. It is confirmed that liver stem cells exist in humans and that they can be of endogenous (hepatocytes or oval cells) or exogenous (most likely bone marrow) origin. The marked degree of hepatic engraftment from extrahepatic cells in cases of severe liver injury indicates that there may be therapeutic utility for bone marrow transplantation to correct defects in hepatocyte metabolic or synthetic function. The researches mentioned above represent significant advances in liver stem cell biology. However, questions regarding some respects of liver stem cells remain open and need to be resolved: how to activate liver stem cells^[63,64]? How to isolate and characterize a plenty of liver stem cells with high purification^[65,66]? How to set up a tracking system to make clear the ultimate fate of liver stem cells *in vivo*^[67,68]? How to develop a stable *ex vivo* culture system of liver stem cells and adjust their differentiation^[69,70]? Excellent *in vitro* and *in vivo* researches will pave the way for a much broader understanding of the biological properties and clinical use of liver stem cells.

REFERENCES

- 1 **Quesenberry PJ**, Colvin GA, Lambert JF, Frimberger AE, Dooner MS, Mcauliffe CI, Miller C, Becker P, Badiavas E, Falanga VJ, Effenbein G, Lum LG. The new stem cell biology. *Trans Am Clin Climatol Assoc* 2002; **113**: 182-206
- 2 **Aldhous P**. Can they rebuild us? *Nature* 2001; **410**: 622-625
- 3 **Wang ZH**, Chang XT, Fu XB. Proliferation and differentiation of the small intestinal stem cells and small intestinal development. *Shijie Huaren Xiaohua Zazhi* 2001; **9**: 1445-1448
- 4 **Crosby HA**, Strain AJ. Adult liver stem cells: bone marrow, blood, or liver derived? *Gut* 2001; **48**: 153-154
- 5 **Nagai H**, Terada K, Watanabe G, Ueno Y, Aiba N, Shibuya T, Kawagoe M, Kameda T, Sato M, Senoo H, Sugiyama T. Differentiation of liver epithelial (stem-like) cells into hepatocytes induced by coculture with hepatic stellate cells. *Biochem Biophys Res Commun* 2002; **293**: 1420-1425
- 6 **Jackson KA**, Majka SM, Wulf GG, Goodell MA. Stem cells: a minireview. *J Cell Biochem* 2002; (**Suppl 38**): 1-6
- 7 **Monga SP**, Tang Y, Candotti F, Rashid A, Wildner O, Mishra B, Iqbal S, Mishra L. Expansion of hepatic and hematopoietic stem cells utilizing mouse embryonic liver explants. *Cell Transplant* 2001; **10**: 81-89
- 8 **Suzuki A**, Zheng YW, Fukao K, Nakauchi H, Taniguchi H. Hepatic stem/progenitor cells with high proliferative potential in liver organ formation. *Transplant Proc* 2001; **33**: 585-586
- 9 **Chen XP**, Xue YL, Li XJ, Zhang ZY, Li YL, Huang ZQ. Experimental research on TECA-I bioartificial liver support system to treat canines with acute liver failure. *World J Gastroenterol* 2001; **7**: 706-709
- 10 **Xue YL**, Zhao SF, Zhang ZY, Wang YF, Li XJ, Huang XQ, Luo Y, Huang YC, Liu CG. Effects of a bioartificial liver support system on acetaminophen induced acute liver failure canines. *World J Gastroenterol* 1999; **5**: 308-311
- 11 **Riordan SM**, Williams R. Transplantation of primary and reversibly immortalized human liver cells and other gene therapies in acute liver failure and decompensated chronic liver disease. *World J Gastroenterol* 2000; **6**: 636-642
- 12 **Fausto N**. Liver regeneration: from laboratory to clinic. *Liver Transpl* 2001; **7**: 835-844
- 13 **Tateno C**, Takai-Kajihara K, Yamasaki C, Sato H, Yoshizato K. Heterogeneity of growth potential of adult rat hepatocytes *in vitro*. *Hepatology* 2000; **31**: 65-74
- 14 **Katayama S**, Tateno C, Asahara T, Yoshizato K. Size-Dependent *in vivo* Growth Potential of Adult Rat Hepatocytes. *Am J Pathol* 2001; **158**: 97-105
- 15 **Gordon GJ**, Coleman WB, Grisham JW. Temporal analysis of hepatocyte differentiation by small hepatocyte-like progenitor cells during liver regeneration in retrorsine-exposed rats. *Am J Pathol* 2000; **157**: 771-786
- 16 **Alison MR**, Poulsom R, Forbes SJ. Update on hepatic stem cells. *Liver* 2001; **21**: 367-373
- 17 **Kountouras J**, Boura P, Lygidakis NJ. Liver regeneration after hepatectomy. *Hepatogastroenterology* 2001; **48**: 556-562
- 18 **Overturf K**, al-Dhalimy M, Ou CN, Finegold M, Grompe M. Serial transplantation reveals the stem-cell-like regenerative potential of adult mouse hepatocytes. *Am J Pathol* 1997; **151**: 1273-1280
- 19 **Potten CS**, Loeffler M. Stem cells: attributes, cycles, spirals, pitfalls and uncertainties. *Development* 1990; **110**: 1001-1020
- 20 **Kruglov EA**, Jain D, Dranoff JA. Isolation of primary rat liver fibroblasts. *J Investig Med* 2002; **50**: 179-184
- 21 **Vessey CJ**, de la Hall PM. Hepatic stem cells: a review. *Pathology* 2001; **33**: 130-141
- 22 **Yang L**, Li S, Hatch H, Ahrens K, Cornelius JG, Petersen BE, Peck AB. *In vitro* trans-differentiation of adult hepatic stem cells into pancreatic endocrine hormone-producing cells. *Proc Natl Acad Sci U S A* 2002; **99**: 8078-8083
- 23 **Bustos M**, Sangro B, Alzuguren P, Gil AG, Ruiz J, Beraza N, Qian C, Garcia-Pardo A, Prieto J. Liver damage using suicide genes. A model for oval cell activation. *Am J Pathol* 2000; **157**: 549-559
- 24 **Crosby HA**, Hubscher S, Fabris L, Joplin R, Sell S, Kelly D, Strain AJ. Immunolocalization of putative human liver progenitor cells in livers from patients with end-stage primary biliary cirrhosis and sclerosing cholangitis using the monoclonal antibody OV-6. *Am J Pathol* 1998; **152**: 771-779
- 25 **Kiss A**, Schnur J, Szabo Z, Nagy P. Immunohistochemical analysis of atypical ductular reaction in the human liver, with special emphasis on the presence of growth factors and their receptors. *Liver* 2001; **21**: 237-246
- 26 **Roskams T**, De Vos R, Van Eyken P, Myazaki H, Van Damme B, Desmet V. Hepatic OV-6 expression in human liver disease and rat experiments: evidence for hepatic progenitor cells in man. *J Hepatol* 1998; **29**: 455-463
- 27 **Crosby HA**, Hubscher SG, Joplin RE, Kelly DA, Strain AJ. Immunolocalisation of OV-6, a putative progenitor cell marker in human fetal and diseased pediatric liver. *Hepatology* 1998; **28**: 980-985
- 28 **Evarts RP**, Hu Z, Fujio K, Marsden ER, Thorgeirsson SS. Activation of hepatic stem cell compartment in the rat: role of trans-

- forming growth factor alpha, hepatocyte growth factor, and acidic fibroblast growth factor in early proliferation. *Cell Growth Differ* 1993; **4**: 555-561
- 29 **Theise ND**, Saxena R, Portmann BC, Thung SN, Yee H, Chiriboga L, Kumar A, Crawford JM. The canals of Hering and hepatic stem cells in humans. *Hepatology* 1999; **30**: 1425-1433
- 30 **Lorenti AS**. Hepatic stem cells. *Medicina (B Aires)* 2001; **61**: 614-620
- 31 **Libbrecht L**, Desmet V, Van Damme B, Roskams T. Deep intralobular extension of human hepatic 'progenitor cells' correlates with parenchymal inflammation in chronic viral hepatitis: can 'progenitor cells' migrate? *J Pathol* 2000; **192**: 373-378
- 32 **Libbrecht L**, De Vos R, Cassiman D, Desmet V, Aerts R, Roskams T. Hepatic progenitor cells in hepatocellular adenomas. *Am J Surg Pathol* 2001; **25**: 1388-1396
- 33 **Poliard AM**, Bernuau D, Tournier I, Legres LG, Schoevaert D, Feldmann G, Sala-Trepat JM. Cellulur analysis by *in situ* hybridization and immunoperoxidase of alpha-fetoprotein and albumin gene expression in rat liver during the perinatal period. *J Cell Biol* 1986; **103**: 777-786
- 34 **Kubota H**, Storms RW, Reid LM. Variant forms of alpha-fetoprotein transcripts expressed in human hematopoietic progenitors: Implications for their developmental potential toward endoderm. *J Biol Chem* 2002; **277**: 27629-27635
- 35 **Hassan HT**, Zander A. Stem cell factor as a survival and growth factor in human normal and malignant hematopoiesis. *Acta Haemat* 1996; **95**: 257-262
- 36 **Sandlow JL**, Feng HL, Cohen MB, Sandra A. Expression of c-kit and its ligand stem cell factor in normal and subfertile human testicular tissue. *J Androl* 1996; **17**: 403-408
- 37 **Gordon GJ**, Coleman WB, Hixson DC, Grisham JW. Liver regeneration in rats with retrorsine-induced hepatocellular injury proceeds through a novel cellular response. *Am J Pathol* 2000; **156**: 607-619
- 38 **Yavorkovsky L**, Lai E, Ilic Z, Sell S. Participation of small intraportal stem cells in the restitutive response of the liver to periportal necrosis induced by allyl alcohol. *Hepatology* 1995; **21**: 1702-1712
- 39 **Vescovi A**, Gritti A, Cossu G, Galli R. Neural stem cells: plasticity and their transdifferentiation potential. *Cells Tissues Organs* 2002; **171**: 64-76
- 40 **McKay R**. Mammalian deconstruction for stem cell reconstruction. *Nat Med* 2000; **6**: 747-748
- 41 **Hirschi KK**, Goodell MA. Hematopoietic, vascular and cardiac fates of bone marrow-derived stem cells. *Gene Ther* 2002; **9**: 648-652
- 42 **Forbes SJ**, Poulosom R, Wright NA. Hepatic and renal differentiation from blood-borne stem cells. *Gene Ther* 2002; **9**: 625-630
- 43 **Kopen GC**, Prockop DJ, Phinney DG. Marrow stromal cells migrate throughout forebrain and cerebellum, and they differentiate into astrocytes after injection into neonatal mouse brains. *Proc Natl Acad Sci U S A* 1999; **96**: 10711-10716
- 44 **Pahal GS**, Jauniaux E, Kinnon C, Thrasher AJ, Rodeck CH. Normal development of human fetal hematopoiesis between eight and seventeen weeks' gestation. *Am J Obstet Gynecol* 2000; **183**: 1029-1034
- 45 **Baumann U**, Crosby HA, Ramani P, Kelly DA, Strain AJ. Expression of the stem cell factor receptor c-kit in normal and diseased paediatric liver. *Hepatology* 1999; **30**: 112-117
- 46 **Petersen BE**, Goff JP, Greenberger JS, Michalopoulos GK. Hepatic oval cells express the hematopoietic stem cell marker Thy-1 in the rat. *Hepatology* 1998; **27**: 433-445
- 47 **Lemma ER**, Shepard EG, Blakolmer K, Kirsch RE, Robson SC. Isolation from human fetal liver of cells co-expressing CD34 haematopoietic stem cell and CAM5.2 pancytokeratin markers. *J Hepatol* 1998; **29**: 450-454
- 48 **Krause DS**. Plasticity of marrow-derived stem cells. *Gene Ther* 2002; **9**: 754-758
- 49 **Crosby HA**, Kelly DA, Strain AJ. Human hepatic stem-like cells isolated using c-kit or CD34 can differentiate into biliary epithelium. *Gastroenterology* 2001; **120**: 534-544
- 50 **Omori M**, Omori N, Evarts RP, Teramoto T, Thorgeirsson SS. Coexpression of flt-3 ligand/flt-3 and SCF/c-kit signal transduction systems in bile duct ligated SI and W mice. *Am J Pathol* 1997; **150**: 1179-1187
- 51 **Theise ND**, Badve S, Saxena R, Henegariu O, Sell S, Crawford JM, Krause DS. Derivation of hepatocytes from bone marrow cells in mice after radiation-induced myeloablation. *Hepatology* 2000; **31**: 235-240
- 52 **Alison MR**, Poulosom R, Jeffery R, Dhillon AP, Quaglia A, Jacob J, Novelli M, Prentice G, Williamson J, Wright NA. Hepatocytes from non-hepatic adult stem cells. *Nature* 2000; **406**: 257
- 53 **Theise ND**, Nimmakayalu M, Gardner R, Illei PB, Morgan G, Teperman L, Henegariu O, Krause DS. Liver from bone marrow in humans. *Hepatology* 2000; **32**: 11-16
- 54 **Mitaka T**. Hepatic stem cells: from bone marrow cells to hepatocytes. *Biochem Biophys Res Commun* 2001; **281**: 1-5
- 55 **Petersen BE**, Bowen WC, Patrene KD, Mars WM, Sullivan AK, Murase N, Boggs SS, Greenberger JS, Goff JP. Bone marrow as a potential source of hepatic oval cells. *Science* 1999; **284**: 1168-1170
- 56 **Housset C**. Biliary epithelium, hepatocytes and oval cells. *Rev Prat* 2000; **50**: 2106-2111
- 57 **Liu ZC**, Chang TM. Increased viability of transplanted hepatocytes when hepatocytes are co-encapsulated with bone marrow stem cells using a novel method. *Artif Cells Blood Substit Immobil Biotechnol* 2002; **30**: 99-112
- 58 **Takahashi T**, Ku Y, Tominaga M, Iwasaki T, Fukumoto T, Takamatsu M, Tsuchida S, Sendou H, Suzuki Y, Kuroda Y. Phase I study of super high-dose chemotherapy for liver cancer with percutaneous isolated hepatic perfusion (PIHP) and peripheral blood stem cell transplantation (PBSCT). *Gan To Kagaku Ryoho* 2000; **27**: 1801-1804
- 59 **Libbrecht L**, Desmet V, Van Damme B, Roskams T. Deep intralobular extension of human hepatic 'progenitor cells' correlates with parenchymal inflammation in chronic viral hepatitis: can 'progenitor cells' migrate? *J Pathol* 2000; **192**: 373-378
- 60 **Orlic D**, Kajstura J, Chimenti S, Jakoniuk I, Anderson SM, Li B, Pickel J, McKay R, Nadal-Ginard B, Bodine DM, Leri A, Anversa P. Bone marrow cells regenerate infarcted myocardium. *Nature* 2001; **410**: 701-705
- 61 **Sussman M**. Cardiovascular biology. Hearts and bones. *Nature* 2001; **410**: 640-641
- 62 **Lagasse E**, Connors H, Al-Dhalimy M, Reitsma M, Dohse M, Osborne L, Wang X, Finegold M, Weissman IL, Grompe M. Purified hematopoietic stem cells can differentiate into hepatocytes *in vivo*. *Nat Med* 2000; **6**: 1229-1234
- 63 **Hamazaki T**, Iiboshi Y, Oka M, Papst PJ, Meacham AM, Zon LI, Terada N. Hepatic maturation in differentiating embryonic stem cells *in vitro*. *FEBS Lett* 2001; **497**: 15-19
- 64 **Suzuki A**, Taniguchi H, Zheng YW, Takada Y, Fukunaga K, Seino K, Yazawa K, Otsuka M, Fukao K, Nakauchi H. Clonal colony formation of hepatic stem/progenitor cells enhanced by embryonic fibroblast conditioning medium. *Transplant Proc* 2000; **32**: 2328-2330
- 65 **Avital I**, Inderbitzin D, Aoki T, Tyran DB, Cohen AH, Ferraresso C, Rozga J, Arnaout WS, Demetriou AA. Isolation, characterization, and transplantation of bone marrow-derived hepatocyte stem cells. *Biochem Biophys Res Commun* 2001; **288**: 156-164
- 66 **Suzuki A**, Zheng Y, Kondo R, Kusakabe M, Takada Y, Fukao K, Nakauchi H, Taniguchi H. Flow-cytometric separation and enrichment of hepatic progenitor cells in the developing mouse liver. *Hepatology* 2000; **32**: 1230-1239
- 67 **Dabeva MD**, Petkov PM, Sandhu J, Oren R, Laconi E, Hurston E, Shafritz DA. Proliferation and differentiation of fetal liver epithelial progenitor cells after transplantation into adult rat liver. *Am J Pathol* 2000; **156**: 2017-2031
- 68 **Wagers AJ**, Christensen JL, Weissman IL. Cell fate determination from stem cells. *Gene Ther* 2002; **9**: 606-612
- 69 **Hoekstra R**, Chamuleau RA. Recent developments on human cell lines for the bioartificial liver. *Int J Artif Organs* 2002; **25**: 182-191
- 70 **Suzuki A**, Zheng YW, Fukao K, Nakauchi H, Taniguchi H. Clonal expansion of hepatic stem/progenitor cells following flow cytometric cell sorting. *Cell Transplant* 2001; **10**: 393-396

Overexpression of ETS2 in human esophageal squamous cell carcinoma

Xin Li, Jia-Yun Lu, Li-Qun Zhao, Xiu-Qin Wang, Gui-Lin Liu, Zhong Liu, Chuan-Nong Zhou, Min Wu, Zhi-Hua Liu

Xin Li, Jia-Yun Lu, Xiu-Qin Wang, Chuan-Nong Zhou, Min Wu, Zhi-Hua Liu, National Laboratory of Molecular Oncology, Cancer Institute, Chinese Academy of Medical Sciences & Peking Union Medical College, Beijing 100021, China

Xin Li, Li-Qun Zhao, Medical Science Institute of Henan Province, Zhengzhou 450052, China

Gui-Lin Liu, Zhong Liu, Huixian Ren Min Hospital, Huixian 453600, China

Supported by China key program on basic research, No. G1998051021; The Chinese Hi-tech R&D program (2001AA231041); National Natural Science Foundation of China, No. 39993402

Correspondence to: Zhi-Hua Liu, Ph.D., Professor, National Laboratory of Molecular Oncology, Cancer Institute, Chinese Academy of Medical Sciences & Peking Union Medical College, Beijing 100021, China. liuzh@pubem.cicams.ac.cn

Telephone: +86-10-67723789 **Fax:** +86-10-67723789

Received: 2002-07-26 **Accepted:** 2002-09-04

Abstract

AIM: To study the expression pattern of ETS2 (erythroblastosis virus oncogene homolog 2) in human esophageal squamous cell carcinoma (ESCC).

METHODS: Reverse transcription polymerase chain reaction (RT-PCR) and Northern blot were performed to examine the expression level of ETS2 mRNA in 37 pairs of ESCC tissue samples. Western blot and immunohistochemistry were carried out to check the expression level of ETS2 protein in 30 pairs of ESCC tissue specimens.

RESULTS: RT-PCR and Northern blot analysis showed that ETS2 mRNA upregulated in 75.7 % (28/37) examined ESCC tissues relative to matched normal tissues. From those 37 cases, 14 cases were randomly selected to perform Western blot and the results revealed that ETS2 protein overexpressed in 71.4 % (10/14) checked ESCC tissues compared with the corresponding normal tissues. Moreover, the expression patterns of ETS2 protein in those 14 cases were identical to those of ETS2 mRNA displayed by RT-PCR or Northern Blot. Immunohistochemistry analysis showed that the expression level of ETS2 protein rose in 75 % (12/16) tumor epithelial cells contrasted to the normal cells. Altogether the expression level of ETS2 protein increased in 73.3 % (22/30) checked ESCC tissue samples contrary to their normal counterparts.

CONCLUSION: The results suggested that ETS2 overexpressed in paired human ESCC tissue samples at both mRNA and protein levels and may be associated with the tumorigenesis of esophagus.

Li X, Lu JY, Zhao LQ, Wang XQ, Liu GL, Liu Z, Zhou CN, Wu M, Liu ZH. Overexpression of ETS2 in human esophageal squamous cell carcinoma. *World J Gastroenterol* 2003; 9(2): 205-208
<http://www.wjgnet.com/1007-9327/9/205.htm>

INTRODUCTION

Erythroblastosis virus oncogene homolog 2 (ETS2) is a pro-

oncogene, which is located in human chromosomal region 21q22.3 and encodes a 56 kD protein that is phosphorylated by a Ca²⁺-dependent mitogenic signal process^[1,2]. ETS2 gene expresses in various tissues, including blood, breast and prostate. ETS2 may be involved in the regulation of cellular proliferation and differentiation and may play a critical role in T-cell activation and cytokines production^[3-6].

As a member of ETS oncogene family, ETS2 gene has the oncogenic potential. It is similarly transposed as a consequence of nonrandom chromosomal translocations; especially, the *t* (8;21)(q22;q22) translocation is the most frequently noted breakpoint involving chromosome 21 for acute myelogenous leukemia^[7]. An acute non-lymphoblastic leukemia with a complex *t* (6;18;21) chromosomal translocation, has so far been associated with higher expression level of ETS2^[8]. It had been reported that ETS2 gene was associated with the growth and invasion of breast carcinoma cells and was required to maintain the transformed state for human prostate cancer cells^[9,10].

Esophageal cancer ranks among the 10 most frequent cancers in the world, with a predominant distribution in developing countries. Our previous study showed that genetic susceptibility to esophageal cancer was one of the important causes for the high prevalence and familial aggregation of this disease in some areas of northern China^[11]. We observed the upregulation of ETS2 gene in human esophageal squamous cell carcinoma (ESCC) using cDNA microarray technique^[12]. To our best knowledge, this study first investigated the expression patterns of ETS2 gene and ETS2 protein in ESCC by reverse transcription polymerase chain reaction (RT-PCR), Northern blot, Western blot and immunohistochemistry. Both the expression levels of ETS2 gene and ETS2 protein increased in ESCC tissues contrary to their normal counterparts. The results were consistent with the microarray results. Therefore, it indicated that ETS2 gene might be related to the formation of human ESCC and its further study may provide the insight into the mechanisms of carcinogenesis of esophagus.

MATERIALS AND METHODS

Human tissues

Samples of ESCC and matched normal esophagus tissues were collected from 37 patients who had not receive chemotherapy or radiotherapy before surgery. The tissues were immediately stored in liquid nitrogen until analysis and each sample was confirmed by histological examination. Total RNA and total protein of the samples were extracted using Trizol solution (Life Technologies, Rochville, ML) per manufacturer's protocol. Total RNA was quantitated and assessed for purity by means of UV spectrophotometry and electrophoresis in denaturing formaldehyde gel. The standard curve of protein was prepared to determine the protein concentration of tissue samples with Bicinchoninic Acid Protein Assay Kit (SIGMA, St. Louis, MO). Sixteen pairs of ESCC paraffin slides were obtained from Department of Pathology, Cancer Hospital, Chinese Academy of Medical Sciences & Peking Union Medical College.

RT-PCR

Before reverse-transcription, 5 µg total RNA of each sample was treated with 20 units DNase I (Promega, Madison, WI), 40 units RNasin (Promega, Madison, WI) at 37 °C for 15 min to remove contaminated genomic DNA. Then first strand cDNA was synthesized with SuperScript Preamplification System For First Strand cDNA Synthesis kit (Life Technologies, Rochville, ML). Two microliters of reverse-transcription product were used as the template to amplify specific fragment of ETS2 gene. PCR conditions were as follows: initial denaturation at 94 °C for 3 min, followed by 28 cycles of 94 °C for 30 s, 58 °C for 30 s and 72 °C for 1 min. The expression of housekeeping gene, glyceraldehyde-3-phosphate dehydrogenase (GAPDH), was used to normalize the template input. The sequences of the PCR primer pairs of ETS2 and GAPDH were as follows: ETS2, 5' -GTGGACCTATTTCAGCTGTGG-3', 5' -TTCCCCGACGTCTTGTGGAT-3'; GAPDH, 5' -ACCACAGTCCATGCCATCAC-3', 5' -TCCACCACCCTGTTGCTGTA-3'.

Northern blot

Briefly, 30 µg total RNA of each sample was dissolved in loading buffer containing formamide and formaldehyde, heated at 70 °C for 10 min, electrophoresed on the 2 % formaldehyde agarose gel and transferred to a positively charged nylon membrane. The membrane was prehybridized in 5 ml hybridization solution (6×SSC, 2×Denhart's solution, 0.1 % SDS, 100 µg/ml denatured salmon sperm DNA) at 68 °C for 2 h. Then ³²P-labelled probe (bases 1202-1952) was added and hybridization was performed at 68 °C for 18 h. The membrane was washed twice at room temperature in 2×SSC, 0.1 % SDS for 20 min, once at 65 °C in 0.5×SSC, 0.1 % SDS for 20 min and exposed to X-ray films at -70 °C for 72 h.

Western blot

Anti-ETS2 antibody was purchased from Santa Cruz biotechnology, Inc (Santa Cruz, CA). Thirty-microgram total protein of each sample was mixed with 20 µl sample buffer (100 mM Tris·Cl, 200 mM DTT, 4 % SDS, 20 % glycerol and 0.2 % bromophenol blue) before separation by SDS-PAGE (10 %) electrophoresis system. Samples were then transferred to PVDF membrane and nonspecific binding was blocked with 5 % nonfat dry milk for 1 h at room temperature. Then the filter was incubated with anti-ETS2 antibody (1:500) for 2 h at room temperature. An enhanced chemiluminescence system (Santa Cruz, Santa Cruz, CA) was used for signal detection.

Immunohistochemistry

Four-micron paraffin-embedded slides were dewaxed in xylene, rehydrated in ethanol and treated with H₂O₂ to block the endogenous peroxidase activity. Antigen retrieval was achieved by microwaving in a citrate buffer (pH 6.0) for 15 min. The slides were incubated with anti-ETS2 antibody at a 1:50 dilution for 2 h at 37 °C. Biotinylated secondary antibody and peroxidase-conjugated streptavidin steps were performed using UltraSensitive™ S-P kit (Maxim Biotech, Fujian, China) according to the manufacturer's protocol. DAB was used as the chromogen and hematoxylin as the counterstain. Negative control was performed by substituting PBS for the primary antibody.

RESULTS

Overexpression of ETS2 in paired ESCC tissue samples at mRNA level

RT-PCR and Northern blot were performed to confirm the differential expression of ETS2 in ESCC at transcriptional level.

RT-PCR analysis showed that ETS2 gene overexpressed in 24 pairs of tumor versus normal tissues among a total of 31 tested cases (Figure 1). Northern blot analysis showed that the expression level of ETS2 gene increased in 4 of 6 cases of tumor tissues relative to the matched normal tissues (Figure 2).

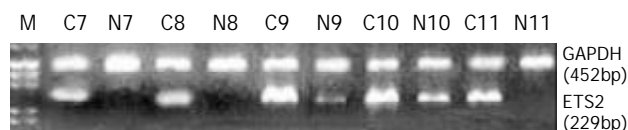


Figure 1 RT-PCR analysis of ETS2 expression in ESCC tissues (Lanes C) and matched normal esophagus tissues (Lanes N). Glyceraldehyde-3-phosphate dehydrogenase (GAPDH) was used as an internal control. PCR product sizes were 229bp for ETS2 and 452bp for GAPDH.

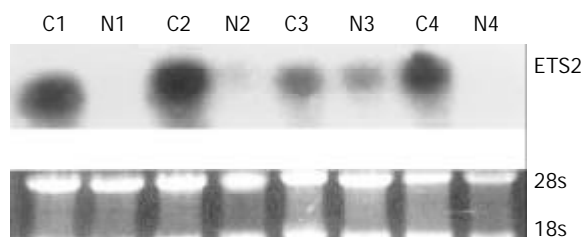


Figure 2 Northern blot results of ETS2 gene in ESCC tissues (designated as C) and matched normal esophagus tissues (designated as N). Thirty-microgram total RNA of each sample was resolved by formaldehyde gel electrophoresis, transferred to a nylon membrane, and hybridized with ³²P-labelled ETS2 probe.

Upregulation of ETS2 in paired ESCC tissue samples at protein level

Western blot and immunohistochemistry were conducted to verify the differential expression of ETS2 in ESCC at translational level. From the above mentioned 37 cases, 14 pairs of ESCC tissue samples were randomly selected to carry out Western blot and the results showed that ETS2 protein was upregulated in 71.4 % (10/14) examined ESCC tissues relative to the corresponding normal tissues (Figure 3). The expression patterns of ETS2 protein in those 14 cases were identical to those of ETS2 mRNA revealed by RT-PCR or Northern Blot.

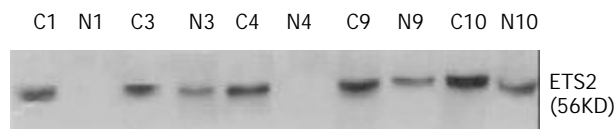


Figure 3 Elevation of ETS2 protein expression in paired ESCC tissue samples detected by Western blot. Total protein was extracted from the tissues and equal amounts of total protein of each sample (30 µg) were loaded. Blots were hybridized with anti-ETS2 antibody (1:500). An enhanced chemiluminescence system (ECL) was used for signal detection. The molecular weight of ETS2 protein is 56 kD.

Immunohistochemistry results displayed that 75 % (12/16) checked ESCC cases existed diffuse and strong staining in the nucleus of tumor cells, while sporadic and weak staining was observed in the nucleus of the matched normal esophageal epithelial cells (Figure 4).

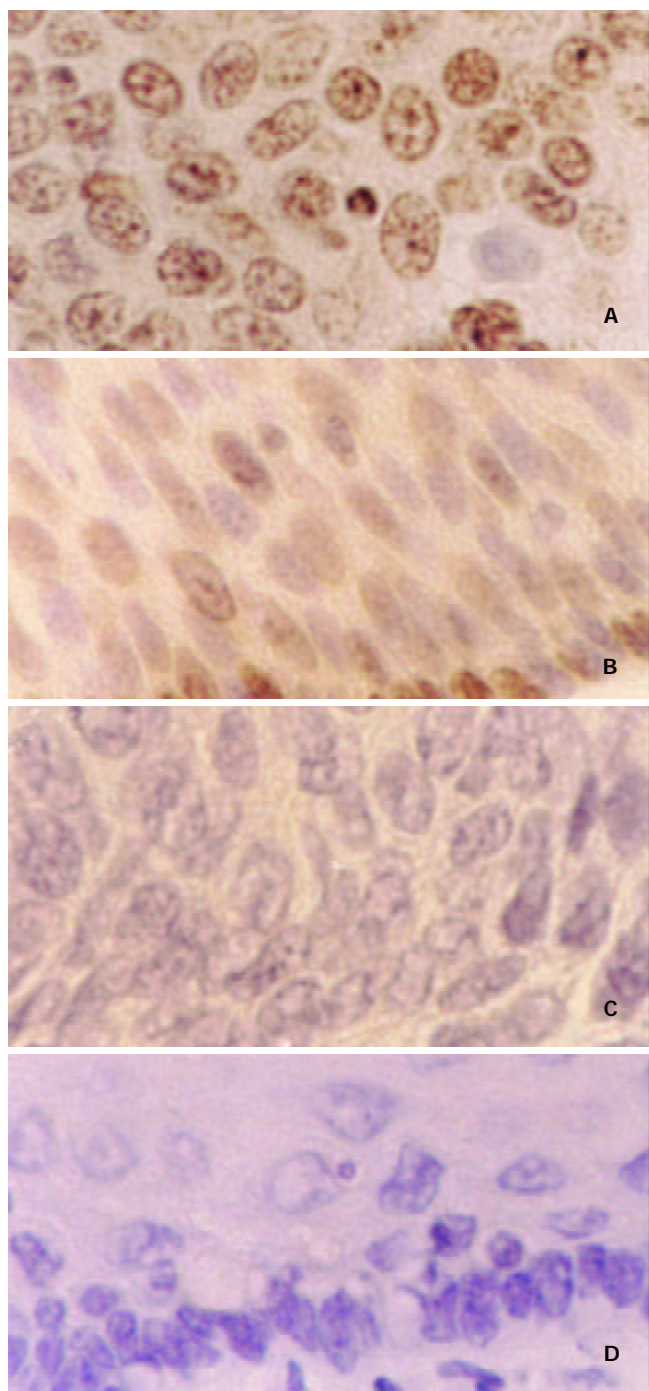


Figure 4 Immunohistochemistry analysis for ETS2 protein in paired ESCC tissue samples using anti-ETS2 antibody (1:50). Diffuse and strong staining was detected in the nucleus of the ESCC epithelial cells (A), while sporadic and weak staining was observed in the nucleus of matched normal esophageal epithelial cells (B). No positive staining was observed in negative controls (C, D). (original magnification $\times 400$).

DISCUSSION

The understanding of the molecular basis of tumor development has progressed dramatically in the last two decades. It is well known that tumor is essentially a genetic disease. So it is important to demonstrate what genes are and how they work in carcinogenesis. Identifying the genetic differences between normal and tumor cells or tissues will discover the genes that directly cause tumor or be associated with tumorigenesis and provide novel markers for early detection and appropriate therapy.

In our previous study, ETS2 gene showed upregulation in

human ESCC tissue^[12]. To verify this differential expression, we explored the expression pattern of ETS2 in paired ESCC tissue samples at both mRNA and protein levels. The results of RT-PCR and Northern blot revealed that ETS2 overexpressed in 75.7 % (28/37) examined tumor tissues relative to the corresponding normal tissues. From those 37 cases, 14 cases were randomly selected to perform Western blot and the results showed that the expression level of ETS2 protein elevated in 71.4 % (10/14) checked ESCC tissues compared with the corresponding normal tissues. Moreover, the expression patterns of ETS2 protein in those 14 cases were identical to those of ETS2 mRNA displayed by RT-PCR or Northern Blot. Immunohistochemistry analysis showed that the expression level of ETS2 protein raised in 75 % (12/16) examined tumor epithelial cells contrasted to the normal counterparts. Altogether ETS2 protein overexpressed in 73.3 % (22/30) tested ESCC tissues relative to the matched normal tissues. Therefore, the data suggested that ETS2 abnormally expressed not only in the transcriptional level but also in the translational level for human ESCC and the increasing transcription of ETS2 mRNA in ESCC may result in increasing translation of ETS2 protein.

As a transcription factor, ETS2 protein controls the transcription of some important genes participating in a number of biological processes including cell growth and apoptosis. Although many studies have been done, the accurate function of ETS2 in biological and pathophysiologic state is still unclear. Previous studies showed that the overexpression of ETS2 led to different results in different cells. Some promoted tumorigenesis^[13,14], while others were arresting^[15]. So it indicated that ETS2 could mediate multiple different signal pathways and might be involved in carcinogenesis with some unlike ways. In the present study, we found the overexpression of ETS2 in ESCC at both mRNA and protein levels. It suggested that ETS2 might be associated with the formation of ESCC. But how ETS2 acts during the neoplasia of esophagus and whether its function is tissue-specific or organ-specific are still unknown. Although a lot of work was focused on the chromosomal aberrations of human ESCC^[16-18] and even in several studies frequent loss of 21q was observed^[19,20], 21q had not yet been investigated in detail. Hence the variation of 21q22.3 in human ESCC, and which ETS2 gene is located in remain unclear. Further investigations will help us to make clear whether the overexpression of ETS2 is caused by the gain of 21q22.3 in human ESCC. As mentioned above, the higher expression level of ETS2 was found in an acute non-lymphoblastic leukemia with a complex *t*(6;18;21) chromosomal translocation^[8]. Another speculation is that the upregulation of ETS2 in human ESCC may be associated with the chromosomal translocation of 21q22.3. More studies about chromosomal aberrations will be helpful to demonstrate the precise function of ETS2 and its molecular mechanisms in tumorigenesis of esophagus.

REFERENCES

- 1 **Watson DK**, McWilliams-Smith MJ, Nunn MF, Duesberg PH, O'Brien SJ, Papas TS. The ets sequence from the transforming gene of avian erythroblastosis virus, E26, has unique domains on human chromosomes 11 and 21: both loci are transcriptionally active. *Proc Natl Acad Sci U S A* 1985; **82**: 7294-7298
- 2 **Fujiwara S**, Fisher RJ, Seth A, Bhat NK, Showalter SD, Zweig M, Papas TS. Characterization and localization of the products of the human homologs of the v-ets oncogene. *Oncogene* 1988; **2**: 99-103
- 3 **Villena JA**, Martin I, Vinas O, Cormand B, Iglesias R, Mampel T, Giral M, Villarroya F. ETS transcription factors regulate the expression of the gene for the human mitochondrial ATP synthase beta-subunit. *J Biol Chem* 1994; **269**: 32649-32654

- 4 **Bhat NK**, Thompson CB, Lindsten T, June CH, Fujiwara S, Koizumi S, Fisher RJ, Papas TS. Reciprocal expression of human ETS1 and ETS2 genes during T-cell activation: regulatory role for the protooncogene ETS1. *Proc Natl Acad Sci U S A* 1990; **87**: 3723-3727
- 5 **Ma X**, Neurath M, Gri G, Trinchieri G. Identification and characterization of a novel Ets-2-related nuclear complex implicated in the activation of the human interleukin-12 p40 gene promoter. *J Biol Chem* 1997; **272**: 10389-10395
- 6 **Blumenthal SG**, Aichele G, Wirth T, Czernilofsky AP, Nordheim A, Dittmer J. Regulation of the human interleukin-5 promoter by Ets transcription factors. Ets1 and Ets2, but not Elf-1, cooperate with GATA3 and HTLV-I Tax1. *J Biol Chem* 1999; **274**: 12910-12916
- 7 **Sacchi N**, Cheng SV, Tanzi RE, Gusella JF, Drabkin HA, Patterson D, Haines JH, Papas TS. The ETS genes on chromosome 21 are distal to the breakpoint of the acute myelogenous leukemia translocation (8;21). *Genomics* 1988; **3**: 110-116
- 8 **Santoro A**, Maggio A, Carbone P, Mirto S, Caronia F, Acuto S. Amplification of ETS2 oncogene in acute nonlymphoblastic leukemia with t(6;21;18). *Cancer Genet Cytogenet* 1992; **58**: 71-75
- 9 **Sapi E**, Flick MB, Rodov S, Kacinski BM. Ets-2 transdominant mutant abolishes anchorage-independent growth and macrophage colony-stimulating factor-stimulated invasion by BT20 breast carcinoma cells. *Cancer Res* 1998; **58**: 1027-1033
- 10 **Sementchenko VI**, Schweinfest CW, Papas TS, Watson DK. ETS2 function is required to maintain the transformed state of human prostate cancer cells. *Oncogene* 1998; **17**: 2883-2888
- 11 **Zhang W**, Bailey-Wilson JE, Li W, Wang X, Zhang C, Mao X, Liu Z, Zhou C, Wu M. Segregation analysis of esophageal cancer in a moderately high-incidence area of northern China. *Am J Hum Genet* 2000; **67**: 110-119
- 12 **Lu J**, Liu Z, Xiong M, Wang Q, Wang X, Yang G, Zhao L, Qiu Z, Zhou C, Wu M. Gene expression profile changes in initiation and progression of squamous cell carcinoma of esophagus. *Int J Cancer* 2001; **91**: 288-294
- 13 **Sumarsono SH**, Wilson TJ, Tymms MJ, Venter DJ, Corrick CM, Kola R, Lahoud MH, Papas TS, Seth A, Kola I. Down's syndrome-like skeletal abnormalities in Ets2 transgenic mice. *Nature* 1996; **379**: 534-537
- 14 **Neznanov N**, Man AK, Yamamoto H, Hauser CA, Cardiff RD, Oshima RG. A single targeted Ets2 allele restricts development of mammary tumors in transgenic mice. *Cancer Res* 1999; **59**: 4242-4246
- 15 **Foos G**, Hauser CA. Altered Ets transcription factor activity in prostate tumor cells inhibits anchorage-independent growth, survival, and invasiveness. *Oncogene* 2000; **19**: 5507-5516
- 16 **Pack SD**, Karkera JD, Zhuang Z, Pak ED, Balan KV, Hwu P, Park WS, Pham T, Ault DO, Glaser M, Liotta L, Detera-Wadleigh SD, Wadleigh RG. Molecular cytogenetic fingerprinting of esophageal squamous cell carcinoma by comparative genomic hybridization reveals a consistent pattern of chromosomal alterations. *Genes Chromosomes Cancer* 1999; **25**: 160-168
- 17 **Yen CC**, Chen YJ, Chen JT, Hsia JY, Chen PM, Liu JH, Fan FS, Chiou TJ, Wang WS, Lin CH. Comparative genomic hybridization of esophageal squamous cell carcinoma: correlations between chromosomal aberrations and disease progression/prognosis. *Cancer* 2001; **92**: 2769-2777
- 18 **Roth MJ**, Hu N, Emmert-Buck MR, Wang QH, Dawsey SM, Li G, Guo WJ, Zhang YZ, Taylor PR. Genetic progression and heterogeneity associated with the development of esophageal squamous cell carcinoma. *Cancer Res* 2001; **61**: 4098-4104
- 19 **Mayama T**, Nishihira T, Satomi S, Horii A. Frequent loss of heterozygosity on the long arm of chromosome 21 in human esophageal, squamous cell carcinoma. *Gan To Kagaku Ryoho* 1998; **25** (Suppl 3): 459-463
- 20 **Mayama T**, Fukushige S, Shineha R, Nishihira T, Satomi S, Horii A. Frequent loss of copy number on the long arm of chromosome 21 in human esophageal squamous cell carcinoma. *Int J Oncol* 2000; **17**: 245-252

Edited By Wu XN

An analysis of esophageal cancer incidence in Cixian county from 1974 to 1996

Yu-Tong He, Jun Hou, Cui-Yun Qiao, Zhi-Feng Chen, Guo-Hui Song, Shao-Sen Li, Fan-Shu Meng, Hong-Xin Jin, Chao Chen

Yu-Tong He, Jun Hou, Zhi-Feng Chen, Hebei Cancer Institute, Shijiazhuang 050011, Hebei Province China

Cui-Yun Qiao, Guo-Hui Song, Shao-Sen Li, Fan-Shu Meng, Hong-Xin Jin, Chao Chen, Cixian Cancer Institute, Cixian county 056500, Hebei Province China

Supported by The National Ninth-Five-Year Scientific Championship Project No.96-906-01-01

Correspondence to: Dr.Jun Hou, Hebei Cancer Institute, Jiankanglu 5, Shijiazhuang 050011, Hebei Province China. hytong69@yahoo.com

Telephone: +86-311-6033511 **Fax:** +86-311-6077634

Received: 2002-09-13 **Accepted:** 2002-10-21

Abstract

AIM: To describe the incidence of esophageal cancer (EC) in Cixian, a county of Hebei province during 1974-1996. We analyzed the sex and age characteristics as well as the geographic distribution of EC, in order to determine the impact so that methods of preventing and controlling EC in Cixian can be put in place.

METHODS: Since the early 1970s, the cancer registry system has been established, which collects the cancer incidence in Cixian county. The malignant tumors were coded according to International Classification of Disease IX (ICD-9). All the data were checked and analyzed using EPIINFO.

RESULTS: The trend of the incidence rate of EC from 1974 to 1996 had declined, (229.9/100 000 vs 178.5/100 000, Odds ratio=1.47, 95 % CI:1.32~1.63, $\chi^2=52.89$, trend $\chi^2=26.54$, $P<0.001$). The incidence rate of males declined significantly (281.81/100 000 vs 157.96/100 000, Odds ratio=1.61, 95 % CI: 1.41~1.84, $\chi^2=47.85$, Trend $\chi^2=44.86$, $P<0.001$), whereas, the females remained steady (157.96/100 000 vs 133.41/100 000, odds ratio=1.28, 95 % CI:1.17~1.49, $\chi^2=9.26$, trend $\chi^2=2.69$, $P>0.05$). Male average annual incidence rate was 142.80/100 000 and the female's was 95.18/100 000. The sex ratio (males to females) was 1.50:1. The incidence rate was increasing along with the age. As to the geographic distribution, the incidence rate in mountainous areas and hilly areas showed a significantly declining trend (mountainous areas, trend $\chi^2=149.93$, $P<0.001$; hilly areas, trend $\chi^2=42.70$, $P<0.001$). The incidence rate of EC in plain areas had increased (trend $\chi^2=22.39$, $P<0.001$).

CONCLUSION: The incidence rate of EC in Cixian county shows a trend and has declined after two decades, especially in mountainous area. But compared to other regions in the world, Cixian county still had a high incidence rate of EC.

He YT, Hou J, Qiao CY, Chen ZF, Song GH, Li SS, Meng FS, Jin HX, Chen C. An analysis of esophageal cancer incidence in Cixian county from 1974 to 1996. *World J Gastroenterol* 2003; 9(2): 209-213 <http://www.wjgnet.com/1007-9327/9/209.htm>

INTRODUCTION

Cixian county is one of the highest incidence rates of

esophageal cancer (EC) in China, as well as in the world^[1-7]. At the start of the 1970s, a field study of EC prevention and treatment was set up^[8]. At the same time the population-based cancer registry system, so called the three-level prevention web, was established. Each clinic doctor in every township was required to report each new case of cancer occurring in the township using a standard card, then the cards were sent to the clinic of the rural administration unit. The unit sorted the cards and sent them to the Cixian Cancer Registry. To this day the Cixian Cancer Registry continues to collect incidence data. This present report came from "A study of incidence, mortality and surveillant method of risk factors of common carcinoma" carried out in the Cixian county of Hebei province, which is adjacent to the Linxian county of Henan province. This study was one of The National Ninth-Five-Year Scientific Championship Project.

MATERIALS AND METHODS

Materials

Cixian is located at latitude 36° 30' North and longitude 114° 40' East. It is situated on the east side of the Taihang Mountain, along the Zhanghe River and it lies in the south of the Handan City. Across the Zhanghe River to the south is the Anyang City of Henan Province. Cixian county occupies an area about 951 square kilometers, composed of 35 districts, and its population is 574 828, consisting of 289 391 males and 285 437 females. There is a remarkable variation in the earth stratum of the county, with mountainous, hilly, and level land each constituting about one-third of its total area. The climate is influenced mainly by the warm mainland seasonal winds. The temperature range is between 18-25 °C and the rainfall range is between 600-700 millimeters. The major soil there is brown and light colored weed earth. Farm products include wheat, corn, millet, rice, red potato and beans. Iron and coal are the main minerals, and coal is the main local fuel of the county.

Cixian Cancer Registry is a population-based registry that was established in 1974. Its aim is to collect and analyze data on every new case of cancer occurring in Cixian county. Initially, it was mainly concerned with collecting data on the incidence and mortality rates of EC in Cixian. However, from 1988, it began to also collect information on the histopathology of the cancers reported.

Methods

The register was conducted by the three-level prevention web. Each clinic doctor in every township (prevention web I) was required to report each new case of cancer occurring in the township by a standard card, then the cards were sent to the clinic of the rural administration unit (prevention web II). They were sorted and sent to the Cixian Cancer Registry (prevention web III) once a month, these cards were checked, analyzed, coded and stored there. At the end of each year, a sample survey was conducted, to check the quality of the registration.

The carcinoma were coded according to International Classification of Disease IX (ICD-9)^[9]. All the data was checked and analyzed by EPIINFO software. Age-standardized

rates (ASR) were standardized to the world population using the direct method and the statistical analysis was carried out by using χ^2 and U-test, a probability value of less than 0.05 was considered statistically significant.

RESULTS

Incidence of esophageal cancer

Between the years 1974 and 1996 there were 14 207 cases of EC in the county. The annual average incidence rate was 119.43/100 000, the ASR was 167.22/100 000. In 1974, the incidence rate of EC was 165.81/100 000. It declined to 113.49/100 000 in 1996, representing a decline of 31.5 percent. From Table 1 and Figure 1, we can see that the incidence rate of EC in Cixian had a trend of gradual decline. The trend test revealed that $\chi^2=26.54$, $P<0.001$. The incidence rate among males declined significantly ($\chi^2=44.86$, $P<0.001$), whereas, the females remained steady ($\chi^2=2.69$, $P>0.05$). In total, the incidence rate between 1970s and 1990s showed significant differences (U test: $P<0.01$). While the difference between 1980s and 1990s was not significant.

The sex and age distribution

During the period there were 8 559 males and 5 648 females with EC. The incidence rate among males was 142.80/100 000, while females was 95.18/100 000. The sex ratio was 1.50:1. The sex ratios (males to females) in 1970s, 1980s and 1990s

respectively was 1.57:1, 1.56:1 and 1.35:1.

The minimum age group of incidence was 1-year group over 23 years. The incidence rate of EC increased with age after 30 years old. It reached the highest at 80 years old group. In 1970s, the minimum age group was 25 years old group. The incidence rate had significantly increased after 35 years of age, and reached the highest level at 70 years old, then declined in 75-year old group. In 1980s, the minimum incidence group was one-year group. The incidence rate increased with age after that 25-year old group. The male incidence rate reached the highest at 80-year-old group. In females at the 60-year-old group it declined a little and reached the highest at 80-year-old group. In 1990s the minimum incidence group was 10-year-old group. The incidence rate increased with age after 25-year-old group and reached the highest at 80-year-old group. The male incidence rate reached the highest at 80 years old group, while the female declined a little at 60-year-old group and reached the highest at 80-year-old group.

Geographic Distribution

In the mountainous area there were 2 106 EC cases from 1974 to 1996. The annual average incidence rate was 112.14/100 000. The incidence rate of EC in 1974 was 213.60/100 000, which declined to 82.55/100 000 in 1996. Decreased by 131.05/100 000, and the decline rate was 61.35 percent. From Table 2 and Figure 3 we could find that the incidence rate of EC in mountainous

Table 1 Cixian EC incidence rate state from 1974 to 1996

Year	Male				Female			
	Population	Case	Incidence rate	ASR	Population	Case	Incidence rate	ASR
74	221842	450	202.85	281.81	217799	279	128.10	157.96
75	224063	392	174.95	244.74	220937	279	126.28	162.8
76	226098	407	180.01	247.68	222526	236	106.06	131.44
77	227998	335	146.93	195.17	224094	193	86.12	103.31
78	227677	320	140.55	186.94	228524	191	83.58	104.51
79	231485	302	130.46	197.31	229242	190	82.88	108.11
80	235881	323	136.93	199.38	232902	221	94.89	124.86
81	242181	301	124.29	193.06	239136	191	79.87	101.76
82	242211	334	137.90	210.05	244007	194	79.51	106.98
83	251237	348	138.51	220.67	249751	229	91.69	122.07
84	253097	367	145.00	240.89	251332	192	76.39	103.22
85	256616	324	126.26	217.06	254526	214	84.08	113.06
86	260149	374	143.76	250.52	257671	205	79.56	100.92
87	265498	331	124.67	202.98	261498	231	88.34	114.62
88	262726	404	153.80	250.76	264539	287	108.49	153.86
89	272643	401	147.10	237.16	285840	258	90.26	131.13
90	289391	443	153.10	248.1	285437	322	112.81	151.55
91	294993	446	151.20	260.53	287546	305	106.07	139.36
92	299306	430	143.70	240.72	291905	302	103.46	139.6
93	299498	408	136.20	216.73	296060	283	95.59	126.12
94	303761	379	124.80	197.96	295104	260	88.10	114.01
95	302782	359	118.60	192.95	294867	289	98.01	125.92
96	302538	381	125.90	203.65	298596	297	99.47	133.41
Total of 70' s	1595044	2529	158.55	—	1576024	1589	100.82	—
Total of 80' s	2595749	3627	139.73	—	2593737	2323	89.56	—
Total of 90' s	1802878	2403	133.29	—	1764078	1736	98.41	—
Total	5993671	8559	142.80	—	5933839	5648	95.18	—

Table 2 The geographic distribution of esophageal cancer in Cixian from 1974 to 1996 (1/100 000)

Year	Mountainous area			Hilly area			Level land area		
	Population	Cases	Incidence rate	Population	Cases	Incidence rate	Population	Cases	Incidence rate
74	77240	165	213.60	145428	241	165.71	216973	323	148.81
75	77581	151	194.63	147830	232	156.93	219589	288	131.15
76	77981	132	169.27	148692	221	148.62	221951	290	130.65
77	78231	116	148.27	149995	192	128.00	223866	220	98.27
78	78257	85	108.60	151456	220	145.25	226488	226	99.78
79	78112	80	102.41	152682	173	113.11	229933	239	103.94
80	78331	92	117.45	155341	210	135.18	235111	242	102.93
81	78555	79	100.56	160010	157	98.12	242752	256	105.45
82	79271	92	116.05	162756	161	98.92	244191	275	112.62
83	80023	100	124.96	166662	186	111.60	254303	290	114.04
84	80294	95	118.32	168296	144	85.56	259276	320	123.42
85	80877	80	98.92	170916	173	101.22	262624	285	108.52
86	82214	101	122.85	172888	179	103.54	266119	296	111.23
87	82291	78	94.79	175132	173	98.78	269573	310	115.00
88	81953	114	139.10	177724	215	120.97	263222	340	129.17
89	82289	91	110.58	179502	206	114.76	275391	355	128.91
90	84228	62	73.61	190411	239	125.52	298185	449	150.58
91	85459	48	56.17	192370	262	136.20	302601	425	140.45
92	85498	59	69.01	194281	250	126.68	307073	405	131.90
93	86484	68	78.63	195963	225	114.88	308956	386	124.94
94	87881	68	77.38	198956	188	94.49	312984	374	119.50
95	87661	78	88.98	198715	195	98.13	311510	413	132.58
96	87221	72	82.55	198276	191	96.33	311009	409	131.51
Total of 70' s	545733	821	150.44	1051424	1489	141.62	1573911	1828	116.14
Total of 80' s	811995	892	109.85	1724297	1833	106.30	2635636	3176	120.50
Total of 90' s	520204	393	75.55	1178561	1311	111.24	1854133	2412	130.09
Total	1877932	2106	112.14	3954282	4633	117.16	6063680	7416	122.30

area had significantly decreased. The result of trend test was $\chi^2=149.93$, $P<0.001$. The incidence rates of EC in 1970s, 1980s, and 1990s were 150.44/100 000, 109.85/100 000 and 75.55/100 000, respectively. The U test result between 1970s and 1990s, between 1980s and 1990s was $P<0.01$. Both of them had significant difference.

In the hilly area there were 4 633 EC cases. The annual average rate was 117.16/100 000. From 1974 to 1996, the incidence rate changed from 165.71/100 000 to 96.33/100 000. Decreasing in number was 69.38/100 000. And declining rate was 41.86 percent. The result of trend test was $\chi^2=42.70$, $P<0.001$. From Table 2 and Figure 3, we could see that from 1970s to 1980s the incidence rate of EC declined significantly, from 141.62/100 000 to 106.30/100 000 (U test: $P<0.01$). While comparing the incidence rate of EC of 1980s with that of the 1990s', it increased from 106.30/100 000 to 111.24/100 000 (U test: $P<0.01$).

On level land there were 7 416 EC cases over 23 years. The annual average incidence rate was 122.30/100 000. According to Table 2 and Figure 3 we can see that during the past 23 years incidence rate of EC increased steadily. The result of trend test was $\chi^2=22.39$, $P<0.001$. Comparing 1970s' incidence rate with 1990s', it increased from 116.14/100 000 to 130.09/100 000. The increasing in number was 13.95/100 000 and the increasing rate was 12.01 percent (U test: $P<0.01$). Comparing the incidence rate of 1980s with the 1990s', which increased from 120.50/100 000 to 130.09/100 000. The increasing in number was 9.59/100 000 and the increasing rate

was 7.95 percent (U test: $P<0.01$). We could see that the incidence rate of EC in level land was increasing steadily.

There are 35 townships in Cixian County. In the 1970s, Linfeng township had the highest incidence rate of EC, which was 211.90/100 000. While Dudang township had the lowest, which was 66.57/100 000. The highest male incidence rate existed in Linfeng and the number was 298.02/100 000. While the highest female incidence rate existed in Guanglu township and the number was 164.49/100 000. The lowest incidence rate of EC of both male and female existed in Dudang, which was 79.71/100 000 and 51.51/100 000, respectively. The highest rate was 3.18 times as much as the lowest. Cixian County had two high risk areas, one was the mountainous area which was centered around Baitu district (132.23/100 000), the other was hilly area which was centered around Lintan district (128.64/100 000). Level land had the lowest incidence rate (116.01/100 000). After 1980s, the highest incidence rate existed in Guanglu township (232.04/100 000) and the lowest existed in Dudang (55.08/100 000). Linfeng had the highest male incidence rate of EC (285.37/100 000). While Cizhou town had the lowest (64.77/100 000). Guanglu had the highest female incidence rate of EC (214.28/100 000), while Dudang had the lowest (38.65/100 000). The highest EC incidence rate was 4.21 times as much as the lowest. There were 20 townships whose incidence rate were higher than the average of county wide, forming a high-risk hilly area, which was centered around Lintan district. After 1990s, Ducun township had the highest EC incidence rate of 275.80/100 000. While Dudang township

had the lowest whose number was 45.92/100 000. The highest male incidence rate existed in Ducun township which was 341.08/100 000. The highest female incidence rate existed in Guanglu which was 213.26/100 000. While the lowest male incidence rate lay in Wuhe township which number was 36.20/100 000. The lowest female incidence rate lay in Huangsha township which was 26.98/100 000. The highest EC incidence rate was 6.01 times as much as the lowest. There were 19 townships whose incidence rate were higher than the average of county wide, forming a high-risk level land area which was centered around Ducun township.

In the 1970s, the high incidence area existed in mountainous areas which are centered around Baitu district and in hilly area which was centered around Lintan district. After 1990s, the incidence rate of EC in Cixian declined significantly. But the hilly area still had high incidence rate, declining slowly. While the level land area had increasing trend, forming a high risk area which was centered around Ducun township.

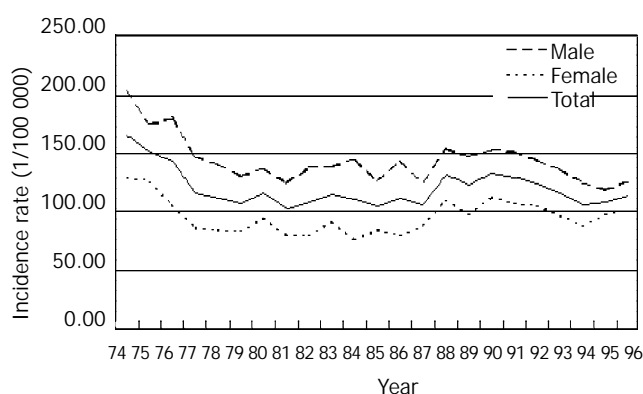


Figure 1 Cixian EC Incidence Rate State from 1974 to 1996.

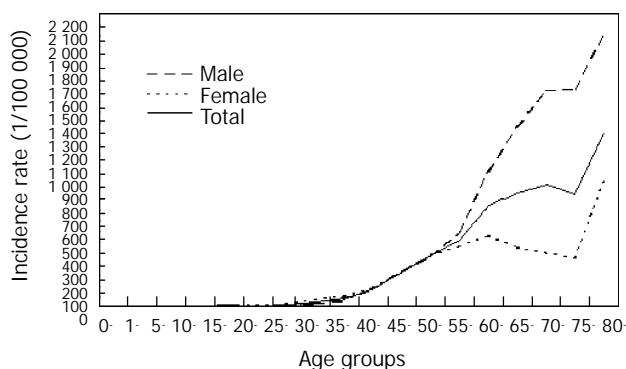


Figure 2 Cixian EC Incidence Rate of Groups from 1983 to 1997.

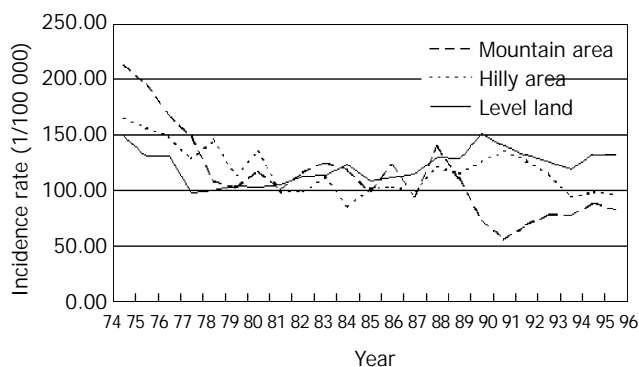


Figure 3 The Geography Distribution of Cixian EC Incidence from 1974 to 1996.

DISCUSSION

Cixian county is one of the highest EC incidence rate areas in China, as well as in the world. Since the early 1970s, cancer registry system has been established where began to collected the cancer incidence in Cixian county^[10-21]. Until now Cixian Cancer Registry have piled up the incidence data of more than twenty years. In this study we found the trend of the incidence rate of EC from 1974 to 1996 had declined after two decades. As for the possible causes of EC^[22-27], we advocate the inhabitant to take follow prevention: (1) To improve the quality of the drinking water condition; (2) To administer the farm products storage, not to eat the food with mold; (3) Eating more vegetables and fruits, changing the bad life style; (4) Conducting screening survey to find the carcinoma in situ or intramucosal carcinoma especially esophageal epithelium dysplasia (EED). EED is a precancerous lesion which can either develop further into a more severe stage or cancer, stay unchanged, or reverse back to normal again for a period of several years or even a decade^[28-34]. It is therefore very promising to detect patients with EED and treat the precancerous lesions before they transform into the irreversible malignant stage. There are several techniques and chemicals or nutrients that have been reported to be effective in blocking precancerous lesions from transforming into cancer^[35-38].

The incidence rate among males declined significantly however, females remained steady. As to the geographic distribution, the incidence rate in mountainous area and hilly area showed a declining trend. The incidence rate of EC in level land area had increased. The reasons why these happened needs to be further studied and analysed.

In conclusion, the trend of the EC incidence rate in Cixian county had declined after two decades, especially in mountainous areas. But compared to the other regions in the world Cixian county still had a high incidence rate of EC. By using a register the information can provide the scientific data for cancer prevention and control.

REFERENCES

- 1 **Puttawibul P**, Chanvitan A, Pornpatanarak C, Sangthong B. Esophageal carcinoma in Southern Thailand. *J Med Assoc Thai* 2001; **84**: 1-5
- 2 **Adanja B**, Gledovic Z, Pekmezovic T, Vlajinac H, Jarebinski M, Zivaljevic V, Pavlovic M. Mortality trends of malignant tumours of digestive organs in Belgrade, Yugoslavia, 1975-1997. *Dig Liver Dis* 2000; **32**: 386-391
- 3 **Vega KJ**, Jamal MM. Changing pattern of esophageal cancer incidence in New Mexico. *Am J Gastroenterol* 2000; **95**: 2352-2356
- 4 **Martin IG**. Gastro-oesophageal malignancy in New Zealand: 1995-97. *N Z Med J* 2002; **115**: 64-67
- 5 **Corley DA**, Buffler PA. Oesophageal and gastric cardia adenocarcinomas: analysis of regional variation using the Cancer Incidence in Five Continents database. *Int J Epidemiol* 2001; **30**: 1415-1425
- 6 **Aksel' EM**, Davydov MI, Ushakova TI. Statistics of lung, stomach and esophageal cancer: status of oncological care, morbidity and mortality. *Vestn Ross Akad Med Nauk* 2001; **9**: 61-65
- 7 **Kocher HM**, Linklater K, Patel S, Ellul JP. Epidemiological study of oesophageal and gastric cancer in south-east England. *Br J Surg* 2001; **88**: 1249-1257
- 8 **Hou J**, Lin PZ, Chen ZF, Ding ZW, Li SS, Men FS, Guo LP, He YT, Qiao CY, Guo CL, Duan JP, Wen DG. Field Population-based blocking treatment of esophageal epithelia dysplasia. *World J Gastroenterol* 2002; **8**: 418-422
- 9 **World health organization**. International classification of diseases of the international statistical classification of diseases, injuries, and causes of death. Volume 1. *Geneva* 1977: 115-163
- 10 **Zhang WH**, Bailey-Wilson JE, Li WD, Wang XQ, Zhang CL, Mao XZ, Liu ZH, Zhou CN, Wu M. Segregation analysis of esophageal cancer in a moderately high-incidence area of northern

- China. *Am J Hum Genet* 2000; **67**: 110-119
- 11 **Wang G**, Hao C, Lai S. Endoscopic study on cancer of gastric cardia in the high incidence areas of China. *Zhonghua Zhongliu Zazhi* 2002; **24**: 381-383
 - 12 **Wu MY**, Chen MH, Liang YR, Meng GZ, Yang HX, Zhuang CX. Experimental and clinicopathologic study on the relationship between transcription factor Egr-1 and esophageal carcinoma. *World J Gastroenterol* 2001; **7**: 490-495
 - 13 **Tan LJ**, Jiang W, Zhang N, Zhang XR, Qiu DH. Fas/FasL expression of esophageal squamous cell carcinoma, dysplasia tissues and normal mucosa. *Shijie Huaren Xiaohua Zazhi* 2001; **9**: 15-19
 - 14 **Wu QM**, Li SB, Wang Q, Wang DH, Li XB, Liu CZ. The expression of COX-2 in esophageal carcinoma and its relation to clinicopathologic characteristic. *Shijie Huaren Xiaohua Zazhi* 2001; **9**: 11-14
 - 15 **Liu HF**, Liu WW, Fang DC. Study of the relationship between apoptosis and proliferation in gastric carcinoma and its precancerous lesion. *Shijie Huaren Xiaohua Zazhi* 1999; **7**: 649-651
 - 16 **Liu J**, Su Q, Zhang W. Relationship between HPV-E6 P53 protein and esophageal squamous cell carcinoma. *Shijie Huaren Xiaohua Zazhi* 2000; **8**: 494-496
 - 17 **Lin J**, Deng CS, Sun J, Zhou Y, Xiong P, Wang YP. Study on the genetic susceptibility of HLA-DQB1 alleles in esophageal cancer of Hubei Chinese Hans. *Shijie Huaren Xiaohua Zazhi* 2000; **8**: 965-968
 - 18 **Ma QF**, Jiang H, Feng YQ, Wang XP, Zhou YA, Liu K, Jia ZL. Detection of human papillomavirus DNA in squamous cell carcinoma of the esophagus. *Shijie Huaren Xiaohua Zazhi* 2000; **8**: 1218-1224
 - 19 **Dong Z**, Tang P, Li L, Wang G. The strategy for esophageal cancer control in high-risk areas of China. *Jpn J Clin Oncol* 2002; **32** (Suppl): S10-12
 - 20 **Lu Z**, Chen K, Guo M. Detection of HPV in human esophageal cancer in high-incidence area and its correlation with p53 expression. *Zhonghua Zhongliu Zazhi* 2001; **23**: 220-223
 - 21 **Chen KN**, Xu GW. Diagnosis and treatment of esophageal cancer. *Shijie Huaren Xiaohua Zazhi* 2000; **8**: 196-202
 - 22 **Wang AH**, Sun CS, Li LS, Huang JY, Chen QS. Relationship of tobacco smoking CYP1A1 GSTM1 gene polymorphism and esophageal cancer in Xi'an. *World J Gastroenterol* 2002; **8**: 49-53
 - 23 **Su M**, Lu SM, Tian DP, Zhao H, Li XY, Li DR, Zheng ZC. Relationship between ABO blood groups and carcinoma of esophagus and cardia in Chaoshan inhabitants of China. *World J Gastroenterol* 2001; **7**: 657-661
 - 24 **Yu GQ**, Zhou Q, Ivan D, Gao SS, Zheng ZY, Zou JX, Li YX, Wang LD. Changes of p53 protein blood level in esophageal cancer patients and normal subjects from a high incidence area in Henan, China. *World J Gastroenterol* 1998; **4**: 365-366
 - 25 **Liu DW**, Wanf BY, Zhou Y, Cui WF, Liu B, Zhou Q, Ying JY, Zheng S, Gao SS, Jin XX, Min FZ, Min NH, Hao ZZ, Yang CS, Min BY, Jun QY. Endoscopic screening and determination of p53 and proliferating cell nuclear antigen in esophageal multistage carcinogenesis: a comparative study between high- and low-risk populations in Henan, northern China. *Dis Esophagus* 2002; **15**: 80-84
 - 26 **Bachmann MO**, Alderson D, Edwards D, Wotton S, Bedford C, Peters TJ, Harvey IM. Cohort study in South and West England of the influence of specialization on the management and outcome of patients with oesophageal and gastric cancers. *Br J Surg* 2002; **89**: 914-922
 - 27 **Li T**, Lu ZM, Chen KN, Guo M, Xing HP, Mei Q, Yang HH, Lechner JF, Ke Y. Human papillomavirus type 16 is an important infectious factor in the high incidence of esophageal cancer in Anyang area of China. *Carcinogenesis* 2001; **22**: 929-934
 - 28 **Zuo L**, Lin P, Qi F, Zhang L, Guo J, Liu J. Quantitative detection of multi-gene expressions and DNA content in the precancerous cells of esophageal carcinoma. *Zhonghua Zhongliu Zazhi* 2002; **24**: 30-33
 - 29 **Griffin SM**, Shaw IH, Dresner SM. Early complications after Ivor Lewis subtotal esophagectomy with two-field lymphadenectomy: risk factors and management. *J Am Coll Surg* 2002; **194**: 285-297
 - 30 **Zhang J**, Yan XJ, Yan QJ, Duan J, Hou Y, Su CZ. Cloning and expression of HPV16 L2 DNA from esophageal carcinoma in *E. coli*. *Shijie Huaren Xiaohua Zazhi* 2001; **9**: 273-278
 - 31 **Wei ZB**, Wang LB, Tian BS, Wang JL, Sun XF, Wei JP, Liu N, Wang JH. Lugol's staining with p53 oncoproteins in detecting early esophageal cancer. *Shijie Huaren Xiaohua Zazhi* 2001; **9**: 495-498
 - 32 **Gu HP**, Shang PZ, Su H, Li ZG. Association of CD15 antigen expression with cathepsin D in esophageal carcinoma tissues. *Shijie Huaren Xiaohua Zazhi* 2000; **8**: 259-261
 - 33 **Huang ZZ**, Wu XY, Liang YR, Li QS, Shen J. Immunohistochemical study of esophageal basaloid squamous cell carcinoma. *Shijie Huaren Xiaohua Zazhi* 2000; **8**: 1097-1100
 - 34 **Liu J**, Chen SL, Zhang W, Su Q. P21^{WAF1} gene expression with P53 mutation in esophageal carcinoma. *Shijie Huaren Xiaohua Zazhi* 2000; **8**: 1350-1353
 - 35 **Corley DA**, Levin TR, Habel LA, Weiss NS, Buffler PA. Surveillance and survival in Barrett's adenocarcinomas: a population-based study. *Gastroenterology* 2002; **122**: 633-640
 - 36 **Anderson MR**, Jankowski JA. The treatment, management and prevention of oesophageal cancer. *Expert Opin Biol Ther* 2001; **1**: 1017-1028
 - 37 **Wilson KS**, Wilson AG, Dewar GJ. Curative treatment for esophageal cancer: Vancouver Island Cancer Centre experience from 1993 to 1998. *Can J Gastroenterol* 2002; **16**: 361-368
 - 38 **Zhang LJ**, Chen KN, Xu GW, Xing HP, Shi XT. Congenital expression of mdr-1 gene in tissues of carcinoma and its relation with pathomorphology and prognosis. *World J Gastroenterol* 1999; **5**: 53-56

Risk factors for the gastric cardia cancer: a case-control study in Fujian Province

Lin Cai, Zong-Li Zheng, Zuo-Feng Zhang

Lin Cai, Zong-Li Zheng, Department of Epidemiology, Fujian Medical University, Fuzhou, 350004, China

Zuo-Feng Zhang, Department of Epidemiology, UCLA School of Public Health, Los Angeles California, USA

Supported by the Natural Science Foundation of Fujian Province, China, No. C001009 and the Foundation for the Author of National Excellent Doctoral Dissertation of P. R. China, No. 200157

Correspondence to: Lin Cai, Department of Epidemiology, Fujian Medical University, Fuzhou, 350004, Fujian Province, China. zjcailin@pub5.fz.fj.cn

Telephone: +86-591-3569264

Received: 2002-06-14 **Accepted:** 2002-07-15

Abstract

AIM: The incidence of gastric cardia cancer has greatly increased in the past 2-3 decades, however, the risk factors for the disease are still not clearly understood. The investigations among Chinese population on the risk factors of gastric cardia cancer were also scarcely reported. We therefore conducted a case-control study in Fujian province, China, to investigate the potential risk and protective factors of this disease.

METHODS: 191 cardia and 190 non-cardia gastric cancer cases, and a total of 222 control cases were included in this study. Standard questionnaires were used in collecting epidemiological factors and the data were then analyzed by the unconditional logistic regression model.

RESULTS: As the factors such as age, gender, smoking, alcohol consumption, and family history of gastric cancer were controlled, a multivariable analysis was conducted, which revealed that there was a significant correlation between the dietary habits such as irregular meal, over and fast eating, and the gastric cardia cancer with the odds ratios (ORs) of 4.2 (95 % confidence interval: 2.3-7.7), 4.7 (2.1-10.8), and 2.7 (1.3-5.3) respectively. Other correlations were also observed between the gastric cardia cancer and the consumption of salty fish or pickled vegetable, smoking, and the family cancer history with the ORs of 5.5 (1.4-19.5), 1.8 (1.0-3.0), 2.1 (1.3-3.5), and 3.8 (2.3-6.2) respectively. In contrast, the negative correlations were found existing between the intake of fresh vegetables and fruits, the use of refrigerator, and the gastric cardia cancer, with the ORs of 0.4 (0.2-0.9), 0.2 (0.1-0.5), and 0.2 (0.1-0.4), respectively. However, dietary habits were associated less with non-cardia gastric cancer compared with its cardia counterpart.

CONCLUSION: Dietary habits might be one of the risk factors for the cardia carcinogenesis among Chinese population.

Cai L, Zheng ZL, Zhang ZF. Risk factors for the gastric cardia cancer: a case-control study in Fujian Province. *World J Gastroenterol* 2003; 9(2): 214-218

<http://www.wjgnet.com/1007-9327/9/214.htm>

INTRODUCTION

While the total incidence and mortality of gastric cancer manifested a declining trend world wide, the incidence of gastric cardia cancer has increased considerably in the past few decades^[1-4]. The explanations for this phenomenon, however, have not been fully elucidated yet^[5-6]. Although certain dietary factors have been suggested to be associated with the gastric carcinogenesis, there are few investigations performing the etiological analysis further on the anatomical sub-site of the cancer^[7-11], whose divergent carcinogenesis patterns suggested that there might exist differences in etiological factors between the cardia and non-cardia gastric cancers. To verify this hypothesis, we have conducted a case-control study in Fujian Province, China.

MATERIALS AND METHODS

Subjects

191 cardia and 190 non-cardia primary gastric cancer cases, which were pathologically confirmed or diagnosed through surgical operation between April 2000 and June 2001 in six hospitals in Fuzhou, were employed as the observation group and the cancer controls respectively. The 222 cases of normal control, which came from the department of orthopedics in the same hospitals, were selected without cancers or gastric diseases and frequency-matched to the observation cases by age (± 3 year) and gender. All subjects in our study must have resided in Fujian Province for more than 20 years and can answer questions clearly.

Investigation

Face-to-face interviews were conducted in the hospitals by trained interviewers, in which a structured questionnaire containing socio-demographic characteristics, personal medical history, tobacco and alcohol consumption habits, family cancer history, dietary history and dietary habits was used. As for the dietary habits, the exposure time of 10 years before the interview was emphasized to ensure the assessment of potential risk factors with a reasonable latent period before the onset of cancer. Although the dietary habits could be changed presently by the course of the disease, they would never be influenced 10 years earlier. With the agreement to be interviewed, the observed case and his or her control counterparts were investigated by the same interviewer.

Statistical analysis

The data were statistically evaluated with Epi-info by the univariate and multivariate analysis. The relationship between the putative risk factors and the sub-sites of gastric cancer was assessed by odds ratios (ORs) and their 95 % confidence intervals (CIs) derived from unconditional logistic regression model. Multivariate logistic regression analysis was used to evaluate simultaneously the effects of multiple factors and other potential confounding factors.

RESULTS

A total of 603 subjects from 30 to 79 years old were included

in this study. In the observation group, there were 156 male and 35 female with the average age of 61.2 (± 9.7) and 57.3 (± 10.9) years old respectively. Table 1 shows the demographic characteristics of age and gender for the observed cases and controls. To minimize the possible confounding effects on the investigation results, the age and the gender were taken as the confounding factors to be controlled in all of our analyses.

The relationship between the dietary habits and gastric cancers are shown in Table 2 with the factors such as age, gender, smoking, alcohol consumption and family cancer history being controlled. Irregular meal, over and fast eating could increase the risk of cardia carcinogenesis. Intake of salty fish, pickled vegetables, lard oil and drinking of the well water were also the risk factors for the cardia cancer. In contrast, the intake of fresh vegetables and fruits and the use of refrigerator were belong to the protective factors against the cancer. Besides, it was found that low income, poor education and bearing a family cancer history in the first-degree relatives were associated with the cardia cancer risk. However, the dietary habits

were associated less with non-cardia cancer compared with its cardia counterpart. Alcohol consumption was not observed relating to the cardia cancer risk in the present study.

Table 3 shows the interrelation between cardia cancer and smoking. In smokers, the odds ratio for cardia cancer is 2.09 after adjusted by age, gender, alcohol drinking and family cancer history. For those who smoke more than 20 cigarettes a day, the risk for cardia cancer was 2-fold or more compared with non-smokers. We also noted a significant dose-risk relationship existed between the daily consumed cigarettes, smoking duration and the cardia cancer. However, it was not existed between smoking and the non-cardia gastric cancer.

Unconditional logistic analyses were made by a backward elimination approach to select a possible best subset of risk factors for cardia cancer. The results showed that the best subset of risk factors included family cancer history, irregular meal, fast eating, well-water drinking, smoking, and poor-educated. Fresh fruit intake and the use of refrigerator have protective effect against cardia cancer.

Table 1 Age and sex distribution of the observed cases and the controls

	Age (yrs)	Controls		Cardia cancer		Gastric cancer		Total		P value
		n	(%)	n	(%)	n	(%)	n	(%)	
Female	30 -	13	(22.8)	2	(5.7)	9	(15.8)	24	(16.1)	0.209
	45 -	15	(26.3)	15	(42.9)	13	(22.8)	43	(28.9)	
	55 -	13	(22.8)	9	(25.7)	19	(33.3)	41	(27.5)	
Male	65 -	16	(28.1)	9	(25.7)	16	(28.1)	41	(27.5)	
	30 -	29	(17.6)	10	(6.4)	17	(12.8)	56	(12.3)	
	45 -	37	(22.4)	27	(17.3)	31	(23.3)	95	(20.9)	
	55 -	44	(26.7)	49	(31.4)	42	(31.6)	135	(29.7)	
	65 -	55	(33.3)	70	(44.9)	43	(32.3)	168	(37.0)	0.025

Table 3 The interrelation between smoking and kinds of gastric cancers

Variables	Controls		Cardia cancer				Non-cardia gastric cancer			
	n	n	OR*	95%CI	P	n	OR*	95%CI	P	
Smoking										
No	120	74				99				
Yes	102	117	2.090	1.261-3.464	0.004	91	1.325	0.814-2.157	0.257	
Daily consumed cigarettes										
0	120	74				99				
< 19	37	28	1.443	0.753-2.766	0.270	27	1.092	0.579-2.062	0.785	
≥ 20	65	89	2.513	1.455-4.339	0.001	64	1.478	0.863-2.531	0.155	
P For trend			0.000				0.472			
Smoking duration (yrs)										
0	120	74				99				
< 30	53	37	1.408	0.755-2.625	0.282	36	1.073	0.596-1.933	0.814	
≥ 30	49	80	2.717	1.548-4.768	0.000	55	1.600	0.906-2.825	0.105	
P For trend			0.000				0.289			

*Adjusted by age, gender, drinking and family cancer history in the first-degree relatives

Table 4 Multivariate logistic regression analysis

Selected variable	β	$S\chi$	OR	95% CI	P
Family cancer history	1.455	0.289	4.286	2.431-7.554	0.000
Irregular meal	0.647	0.160	1.909	1.396-2.610	0.000
Fast eating	0.707	0.185	2.028	1.412-2.912	0.000
Fresh fruit intake	-0.439	0.195	0.645	0.439-0.945	0.025
Well-water drinking	0.555	0.262	1.741	1.042-2.910	0.034
Use of refrigerator	-0.313	0.158	0.731	0.536-0.997	0.048
Daily cig. consumption	0.298	0.158	1.347	0.989-1.835	0.059
Years of education	-0.759	0.269	0.468	0.276-0.794	0.005

Table 2 Potential risk or protective factors for cardia and non- cardia gastric cancers, odds ratios & 95 % confidence Interval (CI)

Variables	Controls		Cardia cancer			Non-cardia gastric cancer			
	<i>n</i>	<i>n</i>	<i>OR*</i>	<i>95%CI</i>	<i>P</i>	<i>n</i>	<i>OR*</i>	<i>95%CI</i>	<i>P</i>
Irregular meals									
No	165	101				98			
Sometimes	36	45	1.971	1.152-3.374	0.013	50	2.310	1.375-3.897	0.002
Frequently	21	45	4.184	2.260-7.747	0.000	42	3.662	1.997-6.717	0.000
<i>P</i> For trend			0.000				0.000		
Over eating for each meal									
No	105	103				156			
Sometimes	55	58	1.864	1.139-3.050	0.013	63	1.806	1.122-1.908	0.015
Frequently	11	28	4.720	2.067-10.781	0.000	24	3.499	1.569-7.801	0.002
<i>P</i> For trend			0.034				0.000		
Eating speed									
Slow	33	18				20			
Moderate	110	67	1.058	0.531-2.107	0.874	85	1.308	0.688-2.485	0.412
Fast	79	106	2.645	1.318-5.307	0.006	85	1.878	0.968-3.644	0.063
<i>P</i> For trend			0.000				0.043		
Years of education									
≤ 6	90	121				96			
> 6	132	70	0.317	0.204-0.492	0.000	94	0.643	0.426-0.972	0.036
Monthly Food Expense (RMB)									
<80	62	79				65			
80-	61	60	0.653	0.387-1.102	0.110	64	0.971	0.580-1.625	0.911
100-	59	34	0.397	0.223-0.710	0.002	46	0.697	0.405-1.199	0.192
200-	40	18	0.313	0.155-0.630	0.001	15	0.356	0.175-0.726	0.004
<i>P</i> For trend			0.000				0.044		
Salty fish intake									
< 1 times/M	170	139				134			
< 3 times/W	49	41	1.019	0.615-1.690	0.941	41	1.058	0.646-1.730	0.824
≥ 3 times/W	3	11	5.518	1.367-19.461	0.015	15	5.706	1.588-20.49	0.008
<i>P</i> For trend			0.111				0.020		
Fresh vegetables intake									
< 3 times/W	14	25				18			
≥ 3 times/W	208	166	0.439	0.212-0.909	0.027	172	0.644	0.303-1.367	0.252
Fresh fruit intake									
< 1 times/M	30	52				44			
< 3 times/W	127	116	0.565	0.328-0.973	0.040	115	0.586	0.339-1.015	0.057
≥ 3 times/W	65	23	0.225	0.112-0.452	0.000	31	0.289	0.149-0.561	0.000
<i>P</i> For trend			0.000				0.000		
Pickled vegetables intake									
< 1 times/M	88	61				69			
< 3 times/W	76	63	1.335	0.804-2.214	0.264	64	1.139	0.701-1.852	0.598
≥ 3 times/W	58	67	1.762	1.044-2.974	0.034	57	1.269	0.766-2.103	0.355
<i>P</i> For trend			0.038				0.367		
Cooking oil									
Other type	56	32				28			
Peanut oil	149	103	0.533	0.347-0.820	0.004	115	0.738	0.485-1.124	0.157
Lard oil	93	117	2.327	1.521-3.562	0.000	107	1.853	1.230-2.794	0.003
Drinking water									
Other type	27	30				32			
Well water	60	98	2.822	1.826-4.360	0.000	76	1.804	1.176-2.768	0.007
Tap water	135	63	0.301	0.195-0.464	0.000	82	0.461	0.306-0.694	0.000
Use of refrigerator									
No	83	108				86			
< 10 yrs	45	46	0.764	0.449-1.302	0.323	53	1.155	0.689-1.935	0.585
≥ 10 yrs	94	37	0.242	0.143-0.409	0.000	51	0.426	0.263-0.693	0.001
<i>P</i> For trend			0.000				0.007		
Family Cancer History									
No	190	122				131			
Yes	32	69	2.090	1.261-3.464	0.004	59	1.325	0.814-2.157	0.257

*Adjusted by age, gender, smoking, drinking, and family cancer history in the first-degree relatives

DISCUSSION

Epidemiological studies have indicated that while the overall incidence of gastric cancer has been decreasing, the morbidity of cardia gastric cancer has constantly gone up, which might reflect a different etiology for the cardia gastric cancer^[12-14]. However, little attention has been paid to the risk factors for this increasing trend of cardia gastric cancer. The correlation between the risk factors and the location of gastric cancer has also seldom been investigated^[15-17].

In our study the dietary habits were identified as the risk factors for cardia cancer. Irregular meal, over-eating, and the fast eating may cause injures to the digestive tract mucosa and promote the carcinogenesis. The protective effects of taking in fresh vegetables and fruits against gastric cancer may be mediated by anti-oxidants such as ascorbic acid. Therefore, intake of more fresh fruits and vegetables may significantly lower the risk of gastric cancer, which is consistent with the former epidemiological studies^[18-21]. The present study also showed that the more the pickled vegetables and salty fish were taken in, the more the risk for cardia cancer were increasing, which might be attributed to the potential carcinogens, such as nitroso compounds contained in these foods, and may also involved the increased cell replication and susceptibility to carcinogenesis from salt intake^[22-24]. Lard oil intake was also associated with the increased risk of gastric ca cancer, probably because of excessive exposures of people to the saturated fatty acids. We found that in comparison of the cardia with non-cardia cancer, the carcinogenic risk with specific food or food groups were similar; however, the dietary habits associated more closely with the cardia cancer than with the other stomach carcinomas.

Long-term use of refrigerators could decrease the risk of both cardia and non-cardia gastric cancer with the adjusted OR of 0.242 (95 % CI: 0.143-0.409) and 0.426 (95 % CI: 0.263-0.693) respectively. Refrigerator may keep foods and vegetables fresh for longer period of time, reduce the possibility of generating nitroso compounds, and maintain vitamins and other antioxidants at a higher level, which in turn protect the individuals from exposure to nitroso compounds and other carcinogens. Effective food preservation, which slows down the conversion of nitrates ions to highly carcinogenic nitrites, has been suggested to be at least partially responsible for the overall decreasing trend of gastric cancer incidence.

Well-water, especially shallow well-water may be more easily polluted than tap water. In this study, the fact that well-water drinking was related to an increased risk of cardia cancer suggested that potentially detrimental materials in polluted drinking water might be involved in the cardia carcinogenesis.

After adjusted by age, gender, drinking water and family cancer history in the first-degree relatives, cigarette smoking manifested as a risk factor for the cardia cancer in this study. There was a longer smoking exposure history in the cardia cancer cases than in both cancer-free controls and non-cardia gastric cancer patients. Significant positive dose-effect relationship was found both in the daily cigarette consumption ($P < 0.001$) and the smoking duration ($P < 0.001$). These findings suggested that the smoking exposure was a specific risk factor for the cardia cancer, and the results were influenced less by the recall bias, as it is implausible that patients with cardia cancer would recall smoking exposure more accurately than the non-cardia gastric cancer cases. It is also impossible for the cardia cancer patients to think the more about smoking as the possible cause of their illness than the non-cardia gastric cancer patients, even though cancer cases were aware of their disease status. Therefore, taking multiple controls of different types can be valuable for exploring alternate hypotheses and for taking into account possible potential bias such as recall bias^[25].

Low socio-economic status and poor education were also related to the gastric cancer risk^[26]. The cancer-free controls tended to be better educated than the cancer cases in this study. Family aggregation of the cardia gastric cancer has been confirmed in this study with adjusted OR of 2.09. The correlation between the cardia gastric cancer and family cancer history in the first-degree relatives suggested that inherited genetic susceptibility and shared environmental risk factors might contribute to the cardia carcinogenesis^[27, 28].

In conclusion, our study indicated that dietary habits and family cancer history are the risk factors both for cardia and non-cardia gastric cancer. However, dietary habits and smoking were associated more with the cardia cancer than the non-cardia carcinomas. The different epidemiological features between the cardia and the non-cardia gastric cancer suggested that these tumors might have different etiologic profiles. Therefore, further studies on environmental and host determinants of gastric cardia cancer are needed. Our study also suggested that interventions against cigarette smoking and bad dietary habits may be important for the prevention of gastric cancer. As part of the strategy for the cancer control, healthy lifestyle should be emphasized as every one's responsibility^[29, 30]. Daily intake of fresh vegetables and fruits should be encouraged^[31-33].

REFERENCES

- 1 **Devesa SS**, Fraumeni JF Jr. The rising incidence of gastric cardia cancer. *J Natl Cancer Inst* 1999; **91**: 747-749
- 2 **Walther C**, Zilling T, Perfekt R, Moller T. Increasing prevalence of adenocarcinoma of the oesophagus and gastro-oesophageal junction: a study of the Swedish population between 1970 and 1997. *Eur J Surg* 2001; **167**: 748-757
- 3 **Lagergren J**, Bergstrom R, Nyren O. Association between body mass and adenocarcinoma of the esophagus and gastric cardia. *Ann Intern Med* 1999; **130**: 883-890
- 4 **Botterweck AA**, Schouten LJ, Volovics A, Dorant E, van Den Brandt PA. Trends in incidence of adenocarcinoma of the oesophagus and gastric cardia in ten European countries. *Int J Epidemiol* 2000; **29**: 645-654
- 5 **Pera M**. Epidemiology of esophageal cancer, especially adenocarcinoma of the esophagus and esophagogastric junction. *Recent Results Cancer Res* 2000; **155**: 1-14
- 6 **Kocher HM**, Linklater K, Patel S, Ellul JP. Epidemiological study of oesophageal and gastric cancer in south-east England. *Br J Surg* 2001; **88**: 1249-1257
- 7 **Cai L**, Yu SZ. A molecular epidemiologic study on gastric cancer in Changle, Fujian Province. *Shijie Huaren Xiaohua Zazhi* 1999; **7**: 652-655
- 8 **Cai L**, Yu SZ, Ye WM, Yi YN. Fish sauce and gastric cancer: an ecological study in Fujian Province, China. *World J Gastroenterol* 2000; **6**: 671-675
- 9 **Cai L**, Yu SZ, Zhang ZF. *Helicobacter pylori* infection and risk of gastric cancer in Changle County, Fujian Province, China. *World J Gastroenterol* 2000; **6**: 374-376
- 10 **Cai L**, Yu SZ, Zhang ZF. Glutathione S-transferases M1, T1 genotypes and the risk of gastric cancer: A case-control study. *World J Gastroenterol* 2001; **7**: 506-509
- 11 **Cai L**, Yu SZ, Zhang ZF. Cytochrome P450 2E1 genetic polymorphism and gastric cancer in Changle, Fujian Province. *World J Gastroenterol* 2001; **7**: 792-795
- 12 **Ye WM**, Ekstrom AM, Hansson LE, Bergstrom R, Nyren O. Tobacco, alcohol and the risk of gastric cancer by sub-site and histologic type. *Int J Cancer* 1999; **83**: 223-229
- 13 **Ye W**, Chow WH, Lagergren J, Boffetta P, Boman G, Adami HO, Nyren O. Risk of adenocarcinomas of the oesophagus and gastric cardia in patients hospitalized for asthma. *British J Cancer* 2001; **85**: 1317-1321
- 14 **Shen H**, Xu Y, Zheng Y, Qian Y, Yu R, Qin Y, Wang X, Spitz MR, Wei Q. Polymorphisms of 5, 10-methylenetetrahydrofolate reductase and risk of gastric cancer in a Chinese population: a case-control study. *Int J Cancer* 2001; **95**: 332-336
- 15 **Terry P**, Lagergren J, Ye W, Wolk A, Nyren O. Inverse associa-

- tion between intake of cereal fiber and risk of gastric cardia cancer. *Gastroenterology* 2001; **120**: 387-391
- 16 **Ye W**, Chow WH, Lagergren J, Yin L, Nyren O. Risk of adenocarcinomas of the esophagus and gastric cardia in patients with gastroesophageal reflux diseases and after antireflux surgery. *Gastroenterology* 2001; **121**: 1286-1293
- 17 **Hansen S**, Melby KK, Aase S, Jellum E, Vollset SE. *Helicobacter pylori* infection and risk of cardia cancer and non-cardia gastric cancer. A nested case-control study. *Scand J Gastroenterol* 1999; **34**: 353-360
- 18 **Liu XM**, Wang QS, Ma J, Lin XP. A case-control study on the factors of stomach cancer in Tianjin city. *Zhonghua Liuxing Xingxue Zazhi* 2001; **22**: 362-363
- 19 **Li SP**, Ding JH, Gao CM, Zhou JN, Wu JZ, Su P, Zang Y, Liu YT, Zhou XF, Ding BG, Wang RH. A case-control study of esophageal and stomach cancers in high incidence area of upper-digestive tract cancer. *Zhongliu* 2001; **21**: 277-279
- 20 **Ward MH**, Lopez-Carrillo L. Dietary factors and the risk of gastric cancer in Mexico City. *Am J Epidemiol* 1999; **149**: 925-932
- 21 **Hill MHJ**. Nutritional and metabolic aspects of gastrointestinal cancer. *Current Opinion Clinical Nutrition Metabolic Care* 1998; **1**: 405-407
- 22 **Deng DJ**, E Z. Overview on recent studies of gastric carcinogenesis: human exposure of N-nitrosamides. *Shijie Huaren Xiaohua Zazhi* 2000; **8**: 250-252
- 23 **Ye WM**, Yi YN, Luo RX, Zhou TS, Lin RT, Chen GD. Diet and gastric cancer: a case-control study in Fujian Province, China. *World J Gastroenterol* 1998; **4**: 516-518
- 24 **Ji BT**, Chow WH, Yang G, Mclaughlin JK, Zheng W, Shu XO, Jin F, Gao RN, Gao YT, Fraumeni JF, JR. Dietary habits and stomach cancer in Shanghai, China. *Int. J Cancer* 1998; **76**: 659-664
- 25 **Gordis L**. Case-control and cross-sectional studies. In: *Epidemiology*. Second edition, New York: W.B.Saunders Company 2000: 140-157
- 26 **Brewster DH**, Fraser LA, McKinney PA, Black RJ. Socioeconomic status and risk of adenocarcinoma of the oesophagus and cancer of the gastric cardia in Scotland. *Br J Cancer* 2000; **83**: 387-390
- 27 **Slattery ML**, Edwards SL, Samowitz W, Potter J. Associations between family history of cancer and genes coding for metabolizing enzymes (United States). *Cancer Causes Control* 2000; **11**: 799-803
- 28 **Dhillon PK**, Farrow DC, Vaughan TL, Chow WH, Risch HA, Gammon MD, Mayne ST, Stanford JL, Schoenberg JB, Ahsan H, Dubrow R, West AB, Rotterdam H, Blot WJ, Fraumeni JF Jr. Family history of cancer and risk of esophageal and gastric cancers in the United States. *Int J Cancer* 2001; **93**: 148-152
- 29 **Stadtlander CTKH**, Waterhor JW. Molecular epidemiology, pathogenesis and prevention of gastric cancer. *Carcinogenesis* 1999; **20**: 2195-2207
- 30 **Lagergren J**, Bergstrom R, Lindgren A, Nyren O. The role of tobacco, snuff and alcohol use in the aetiology of cancer of the oesophagus and gastric cardia. *Int J Cancer* 2000; **85**: 340-346
- 31 **Mayne ST**, Risch HA, Dubrow R, Chow WH, Gammon MD, Vaughan TL, Farrow DC, Schoenberg JB, Stanford JL, Ahsan H, West AB, Rotterdam H, Blot WJ, Fraumeni JF Jr. Nutrient intake and risk of subtypes of esophageal and gastric cancer. *Cancer Epidemiol Biomarkers Prev* 2001; **10**: 1055-1062
- 32 **Terry P**, Lagergren J, Hansen H, Wolk A, Nyren O. Fruit and vegetable consumption in the prevention of oesophageal and cardia cancers. *European J Cancer Prev* 2001; **10**: 365-369
- 33 **Kurtz RC**, Zhang ZF. Gastric cardia cancer and dietary fiber. *Gastroenterology* 2001; **120**: 568-575

Edited By Zhu L

Preoperative TN staging of esophageal cancer: Comparison of miniprobe ultrasonography, spiral CT and MRI

Ling-Fei Wu, Bing-Zhou Wang, Jia-Lin Feng, Wei-Rong Cheng, Guo-Re Liu, Xiao-Hua Xu, Zhi-Chao Zheng

Ling-Fei Wu, Bing-Zhou Wang, Department of Gastroenterology, **Jia-Lin Feng**, Department of Information, **Guo-Rui Liu**, Department of Medical Imaging, **Wei-Rong Cheng**, **Xiao-Hua Xu**, Department of Surgery, **Zhi-Chao Zheng**, Department of Pathology, Second Affiliated Hospital, Shantou University Medical College, Shantou 515041, Guangdong Province China

Supported by Guangdong Medical Science Fund, No. A1999429

Correspondence to: Dr. Ling-Fei Wu, Department of Gastroenterology, Second Affiliated Hospital, Shantou University Medical College, Shantou 515041, Guangdong Province China. lingfeiwu@21cn.com

Telephone: +86-754-8355461 **Fax:** +86-754-8346543

Received: 2002-07-20 **Accepted:** 2002-08-29

Abstract

AIM: To evaluate the value of miniprobe sonography (MPS), spiral CT and MR imaging (MRI) in the tumor and regional lymph node staging of esophageal cancer.

METHODS: Eight-six patients (56 men and 30 women; age range of 39-73 years, mean 62 years) with esophageal carcinoma were staged preoperatively with imaging modalities. Of them, 81 (94 %) had squamous cell carcinoma, 4(5 %) adenocarcinoma, and 1(1 %) adenoacanthoma. Eleven patients (12 %) had malignancy of the upper one third, 41 (48 %) of the mid-esophagus and 34 (40 %) of the distal one third. Forty-one were examined by spiral CT in whom 13 were co-examined by MPS, and forty-five by MRI in whom 18 were also co-examined by MPS. These imaging results were compared with the findings of the histopathologic examination for resected specimens.

RESULTS: In staging the depth of tumor growth, MPS was significantly more accurate (84 %) than spiral CT and MRI (68 % and 60 %, respectively, $P < 0.05$). The specificity and sensitivity were 82 % and 85 % for MPS; 60 % and 69 % for spiral CT; and 40 % and 63 % for MRI, respectively. In staging regional lymph nodes, spiral CT was more accurate (78 %) than MPS and MRI (71 % and 64 %, respectively), but the difference was not statistically significant. The specificity and sensitivity were 79 % and 77 % for spiral CT; 75 % and 68 % for MPS; and 68 % and 62 % for MRI, respectively.

CONCLUSION: MPS is superior to spiral CT or MRI for T staging, especially in early esophageal cancer. However, the three modalities have the similar accuracy in N staging. Spiral CT or MRI is helpful for the detection of far-distance metastasis in esophageal cancer.

Wu LF, Wang BZ, Feng JL, Cheng WR, Liu GR, Xu XH, Zheng ZC. Preoperative TN staging of esophageal cancer: Comparison of miniprobe ultrasonography, spiral CT and MRI. *World J Gastroenterol* 2003; 9(2): 219-224

<http://www.wjgnet.com/1007-9327/9/219.htm>

INTRODUCTION

Patients with esophageal cancer have a poor prognosis because

on the onset of symptoms and the final diagnosis, most tumors have reached an advanced stage^[1-5]. Resection of esophageal cancers is the only curative method, but is limited to the early stages of the disease^[6-10]. Therefore, the early diagnosis and an accurate staging are very important for the surgery.

Esophageal tumor is a common disease in China^[11-17]. Shantou is a high-risk region. The incidence of the disease ranges from 60-150 per 100 000 population and the mortality is as high as 90-134 per 100 000 population^[18,19]. Currently, several cross sectional imaging techniques, such as endoscopic ultrasonography (EUS), computed tomography (CT) and magnetic resonance imaging (MRI) have been widely used to provide preoperative staging and follow-up information in these patients^[1, 20-26]. Unfortunately, all these techniques have their limitations.

Miniprobe endosonography (MPS) is a new intracavitary technique^[27], especially in China^[28,29]. In staging esophageal tumors, previously most studies used the 1987 TNM classification system^[30]. In this study, we adopted the new (1997) TNM classification standard^[31]. The purpose of our study is to compare the accuracy of the three different modalities in preoperative TN staging in patients with esophageal tumors and to analyze their advantages and limitations.

MATERIALS AND METHODS

Patients

From February 1997 to May 2001, 86 patients (56 men and 30 women; age range of 39-73 years, mean 62 years) with esophageal carcinoma were staged preoperatively with imaging modalities. All patients were operated on and staging was done either by histopathological assessment of the resected specimens, or by intraoperative findings, or both. The findings of histopathologic examination were as a gold standard and compared with the results of MPS, spiral CT, and MRI. Of the 86 patients, 81 (94 %) had squamous cell carcinoma, 4(5 %) adenocarcinoma, and 1(1 %) had adenoacanthoma. Eleven patients (12 %) had malignancy of the upper one third, forty-one (48 %) of the mid-esophagus and thirty-four (40 %) of the distal one third. Forty-one patients were examined by spiral CT in which 13 were co-examined by MPS, and 45 patients were examined by MRI in whom 18 were also co-examined by MPS. Of the 22 stenotic tumors in this group, 12 were examined by MPS and the others by spiral CT or MRI.

Imaging procedure

Miniprobe sonography system (Sp-501, Fujinon Co. Ltd, Japan) was used to obtain ultrasound images. A miniprobe (2.6 mm in diameter, 2.05 m in length, 12 MHz or 15 MHz in frequency) was passed through the biopsy channel of a video-endoscope (Olympus XQ-200) during routine endoscopy. Examinations were performed by one endoscopist using the following technique. Premedication with 5 mg midazolam was administered intravenously to 31 patients. First, a standard endoscopy was performed to determine the exact location and size of the tumor. Then the tip of the endoscope was placed 2 to 3 cm proximally to the tumor. The lumen was filled with 50-300 ml of deaerated water to achieve acoustic coupling

between transducer and wall. The normal esophageal wall is known to be visualized by MPS as a five-layer structure: (1) mucosa (hyperechoic), (2) muscularis mucosa (hypoechoic), (3) submucosa (hyperechoic), (4) muscularis propria (hypoechoic), and (5) adventitia (hyperechoic). TN staging of MPS was modified according to the 1997 standard of TNM classification^[31]. Depth of invasion of the primary tumor was assessed as follows: T1, tumor invading the lamina propria or submucosa; T2, tumor invading the muscularis propria and leading to complete or nearly complete loss of the layer structure, but with a smooth outer margin; T3, tumor invading the adventitia and surrounding fat tissues; and T4, tumor invading adjacent structures. The criteria for the assessment of lymph node metastasis were used according to our previous standard^[28]. In short, the hypoechoic pattern, clearly defined boundaries, especially the direct extension from the primary tumor were considered malignant nodes. In contrast, the hyperechoic pattern and fuzzy borders were considered benign nodes.

Spiral CT scans were obtained by means of a commercially available unit (Tomoscan AV EP-Plus, Phillip) with 10-mm thick contiguous sections from the pulmonary apices to the adrenal region. Enhanced CT scan was performed in a biphasic mode with a rapid intravenous injection of 50 ml iohalamate meglumine (Ultravist) in 38 patients. Three hundred ml of water was administered to the patients with distal neoplasms before the CT scanning in order to assess gastric extension. Spiral CT images were reviewed by an experienced radiologist, and TN stages were evaluated using the same criteria described below for MR examinations.

MR imaging was performed with a permanent magnet operating at 0.15T (ASP-015, Annke) with a 128×256 acquisition matrix. Multiple spin-echo pulse sequences were obtained in the transaxial plane at repetition times (TR) of 500, 1 800, or 2 500 msec and echo times (TE) of 35, 90 or 120 msec. In some patients, the sagittal and coronal images were obtained. T₁-weighted images were obtained at repetition times (TR) of 500msec and echo times (TE) of 30 msec, and T₂-weighted images were obtained at TR of 1 500-1 800 msec and TE of 90-120msec. Transaxial images with contiguous 8-10 mm sections were obtained from the pulmonary apices, including supra clavicular fossas to the upper abdomen, including the entire liver. Coronal and sagittal images with contiguous 8-10 mm sections were obtained in 37 patients, and 0.5 % Gd-DTPA was orally administered to distend the stomach before the MR examination. ECG-gated scans were not used in all patients. Five mm esophageal thickness was used as the upper limits of normal esophageal wall. Any increase beyond this was considered abnormal. Since CT or MRI cannot differentiate each layer of the esophageal wall, according to Botet *et al* standard^[32], thickening of the wall greater than 5 mm and less than 15 mm was diagnosed as modified T2, thickening of the wall greater than 15 mm with irregularity of the outer margin as T3, and tumor invasion of adjacent structures such as the trachea, aortic pericardium, or vertebral body as T4. Lymph nodes greater than 10 mm in shortaxis diameter were considered abnormal. In contrast, lymph nodes less than 10 mm in diameter were considered benign nodes.

Statistics

The accuracy, sensitivity and specificity of MPS, spiral CT and MRI were calculated using histopathologic staging as a gold standard. For T stage, the sensitivity is a measure of the ability of the three modalities to correctly stage T1/T2 and not overstage tumors as T3/T4, and conversely the specificity is a measure of the ability of the three modalities to correctly stage T3/T4 and not understage tumors as T1/T2^[30]. A Chi-squared test was performed to assess the differences in staging accuracy

by different methods. A *P* value of less than 0.05 was considered to be statistically significant.

RESULTS

Evaluation of tumor growth (T stage)

Tables 1 shows the accuracy of the three modalities for predicting the T category. Of the 86 patients, 4 patients had T1 tumor, 8 T2, 34 T3 and 40 T4 by final histopathologic examination.

Thirty-one patients were examined by MPS. It correctly diagnosed all 4 (100 %) T1 tumors, 5 of 7 (71 %) T2, 8 of 9 (89 %) T3, and 9 of 11 (82 %) T4. In stage T2, one was understaged and another was overstaged. In stage T3, only one tumor was misdiagnosed as T2. In stage T4, two tumors were understaged. The sensitivity and specificity were 82 % and 85 %, respectively. The overall accuracy of MPS was 84 %.

Spiral CT was performed in 41 patients. Among them, 2 had T1 tumor, 3 T2, 14 T3 and 22 T4 by final histopathologic examination. In 5 T1/T2 tumors, 2 were overstaged, and 3 were staged as modified T2 correctly (75 %). In stage T3, 2 tumors were understaged as T2 and 1 was overstaged, 11 of 14 were staged correctly (79 %). In stage T4, 8 were misdiagnosed, and only 14 of 22 were staged correctly (64 %). The sensitivity and specificity of T staging by spiral CT were 60 % and 69 %, respectively. The overall accuracy was 68 %.

MRI was performed in 45 patients. Among them, 5 had T2 tumor, 20 T3 and 20 T4 by final histopathologic examination. No T1 tumor was examined by MRI. In stage T2, one was understaged and 2 were overstaged, only 2 T2 were staged correctly (40 %). In stage T3, 2 tumors were understaged as T2 and 4 were overstaged, 14 of 20 were staged correctly (70 %). In stage T4, 9 were misdiagnosed, and only 11 of 20 were staged correctly (55 %). The sensitivity and specificity were 40 % and 63 %. The overall accuracy of MRI was 60 %.

Table 1 Accuracy of T classification in esophageal cancers: MPS, spiral CT, MRI compared with histopathologic staging

Histopathology	n	Accuracy (%)		
		MPS	Spiral CT	MRI
T1	4	4/4 (100)		
T2	8	5/7 (71)	3/5 (75)	2/5 (40)
T3	34	8/9 (89)	11/14 (79)	14/20 (70)
T4	40	9/11 (82)	14/22 (64)	11/20 (55)
Total	86	26/31 (84)	28/41 (68)	27/45 (60)

Evaluation of lymph node involvement (N stage)

Tables 2 shows the accuracy of the three modalities for predicting the overall N category differentiated as N0 or N1. Among the 86 patients, 47 had histopathologically proved lymph node involvement.

In 31 patients investigated by MPS, 19 had lymph node involvement and 12 had not by histopathologic examination. MPS correctly diagnosed 13 patients in 19 positive nodes. In 12 patients without lymph node involvement, MPS diagnosed 9 patients correctly. There were 3 false-positive and 6 false-negative. The sensitivity, specificity and accuracy were 68 %, 75 %, and 71 %, respectively.

Of 41 patients examined by spiral CT, 22 had lymph node involvement. Spiral CT showed 17 patients had regional lymph node metastasis in 22 positive patients. In 19 patients without lymph node involvement, spiral CT diagnosed 15 patients correctly. There were 4 false-positive and 5 false-negative.

The sensitivity, specificity and accuracy were 77 %, 79 %, and 78 %, respectively.

Among 45 patients examined by MRI, 26 had lymph node involvement. MRI showed 16 had regional lymph node metastasis in 26 positive patients. In 19 patients without lymph node involvement, MRI diagnosed 13 patients correctly. There were 6 false-positive and 10 false-negative. The sensitivity, specificity and accuracy were 62 %, 68 %, and 64 %, respectively.

Table 2 Accuracy of N classification in esophageal cancers: MPS, spiral CT, MRI compared to histopathologic staging

Histopathology	n	Accuracy (%)		
		MPS	Spiral CT	MRI
N0	39	9/12 (75)	15/19 (79)	13/19 (68)
N1	47	13/19 (68)	17/22 (77)	16/26 (62)
Total	86	22/31 (71)	32/41 (78)	29/45 (64)

DISCUSSION

It was reported that accuracy rates of EUS were approximately 52-92 % in the assessment of the infiltration depth of esophageal cancer^[33-39]. In our study, the overall accuracy of T staging was 84 %. We think that the high resolution of MPS contributes the good results, 12MHz translator made it possible to differentiate esophageal histological structures and delineate the entire margins of tumors, especially in the superficial esophageal cancer. The penetration depth of good resolution ultrasound was about 6-8 cm, which could clearly visualize the tumor and the adjacent organs^[40]. In some reports, T1 tumors were often overstaged as T2 because of the resultant obliteration of the submucosa and the muscularis propria^[33]. Although one study reported no benefit of miniprbes in esophageal cancers^[41], Menzel *et al* carefully compared the effects of higher frequency miniprbes with conventional probes and concluded that MPS had a higher accuracy for T staging and similar accuracy for N staging in esophageal tumors^[42]. Akahoshi *et al* also demonstrated the benefit of MPS in early gastric cancers^[43]. In this series, 4 T1 tumors (including one superficial mucosal carcinoma) were all correctly diagnosed because the tact border of muscularis propria was clearly visualized. In T2 tumor, the accuracy was 71 %. One T2 tumor was overstaged as T3 because the inflammation and fibrosis were mistakenly interpreted as tumor extension through the muscularis propria. Another T2 tumor was understaged because the microscopic invasion beyond the submucosa was not discerned. For T3 tumors, only one was understaged due to inexperience. The tumor was larger and the invasion outside the muscularis propria was interpreted as an irregular outer margin of the muscularis propria. In T4 stage, two tumors were understaged because the adjacent malignant stricture (tracheal or bronchial invasion) was not discerned in a limited field of view. We thought that endosonographic wall penetration was a critical factor. Richards *et al* also observed that ultrasound attenuation was a commonest reason which led to the error of diagnosis in the advanced tumor^[44], in particular in stenotic tumors^[45]. In addition, artifacts due to oblique scanning may also give rise to misrepresentation of the true depth of penetration, which was another deficient of MPS.

CT or MRI has been widely used in staging tumors of the upper intestinal tract. However, their diagnostic accuracy in evaluating esophageal carcinoma is controversial. Both of them have the same limitations, i.e. unable to discriminate the layer of the esophageal wall and to detect tumor spread through the muscular wall into adjacent tissues^[32]. Evaluation of direct invasion by CT or MRI is based on two criteria: mass effect

and loss of fat planes. When the trachea or bronchial wall is indented or displaced away by a tumor mass, the mass effect is present and invasion is presumed. The loss of fat plane between tumor and adjacent tissues is commonly used to predict aortic and pericardial invasion. According to the reports, the accuracy of CT or MRI in staging the local tumor infiltration ranged from 45 % to 73 %^[46-51]. Quint *et al* compared MRI with CT in the staging of esophageal tumors^[52]. In 12 patients evaluated, they found that both CT and MRI were 100 % accurate in prediction of tracheobronchial invasion with an accuracy rate of 75 % for aortic invasion and 88 % for pericardial invasion. In a late review, Kelly *et al* reported that the sensitivity of CT ranged from 40 % to 80 % and the specificity from 14 % to 97 %^[30]. In present study, the sensitivity of the three modalities ranged from 40 % to 82 % and the specificity from 63 % to 85 %. Three patients misdiagnosed by spiral CT and five patients by MRI were staged correctly by MPS, especially in T1-T2 tumors, which demonstrated the superiority of MPS. Spiral CT is an inspiring new technique. Our primary data showed that spiral CT was not optimistic, although spiral CT had a higher accuracy than MRI, no significant difference was found ($P>0.05$). MPS appeared more accurate (84 %) than spiral CT or MRI (68 % or 60 %, respectively, $P<0.05$). Although strictly blinded approach was not taken in this study, our results continue to support the hypothesis that endosonography is superior to CT or MRI in the T staging of esophageal cancer^[53-55].

MPS can only visualize lymph nodes close to the esophageal wall whereas CT and MRI can demonstrate both regional and distant lymph node metastases. For MPS, the differentiation of malignant lymph nodes from benign nodes could be made according to its size, distance from tumor and echo features. The round hypoechoic lymph nodes with a smoothly demarcated border and size greater than 5 mm had the greatest probability of malignancy^[56]. Murata *et al*^[57] used MPS to evaluate lymph nodes in different periesophageal areas and the accuracy being 88 %. Other reported that the accuracy of EUS ranged from 68 % to 92 %^[29,58-60]. In this study, the overall accuracy of MPS for diagnosing the N category was 71 %, with a sensitivity of 75 % and a specificity of 68 %. Our results were consistent with these reports.

We think that the lack of reliable criteria in N staging may be the main reason of low accuracy for MPS. The judging value of node size is still controversial. Some authors reported that nodes larger than 5 mm were not inflammatory in the resection specimens^[33, 61-64]. Tio *et al* thought that enlarged lymph nodes were not necessarily cancerous and small nodes might be involved by tumors^[33]. We also observed that lymph nodes larger than 5 mm were inflammatory by pathological examination^[28]. However, we believed that nodes greater than 10 mm, especially close to the primary tumor, rounder, darker, and more homogeneous had much more possibility of malignancy^[20]. In addition, the morphology of tumors would also be another important factor affecting these results.

Holscher *et al*^[65] thought that MPS was more accurate than CT or MRI in the diagnosis of lymph node metastases. Tio *et al*^[33], however, pointed out that CT was superior to EUS for evaluating celiac lymph nodes due to nontraversable stenoses. In this series, the accuracy of spiral CT (78 %) was higher than that of MPS or MRI (68 %, 64 %, respectively), but without significant difference ($P>0.05$). The cause was not clear. We think that methodologies of study designs are related to these results, because different assessment conditions, such as technical parameters, anatomical location of tumors and patient characteristics could lead to different results^[66]. For example, stenotic tumors were not included or accounted for different percentages in some studies^[65]. Hordijk *et al* assessed the influence of tumor stenosis on T staging accuracy of

miniprubes. A lower accuracy (46 %) was obtained with stenotic tumors than those with nontraversable tumors (82 %). They postulated that the main reason lay in the short focal distance between the ultrasonic transducer and tumor hampered clear visualization of the wall layers and tumor penetration depth^[45]. On the other hand, Kallimanis *et al*^[66] reported that the degree of esophageal stenosis was an important criteria for lymph node involvement. Brugge *et al* pointed out that T3 and T4 tumors were significantly thicker than T1 and T2 tumors^[67]. In our previous reports, about half of severe stenotic tumors were T3 and the other half T4^[18]. Tio *et al* indicated that the incidence of positive lymph nodes in the advanced tumors (T3/T4) was higher than the intramural tumors (T1/T2)^[33]. In this study, 23 (27 %) patients had stenotic tumors, in whom 10 patients had T3 and 13 had T4 and all had the lymph node involvement. No one had T2 or T1 stage. In other words, stenotic tumors had more possibilities of advanced stage and lymph node metastasis^[18, 68-72]. Our results strongly supported Brugge's view^[67]. However, in 12 stenotic tumors examined by MPS, only 5 (42 %) were correctly diagnosed. In another 10 stenotic tumors, 5 (5/6) were correctly diagnosed by Spiral CT and 3(3/4) by MRI. Spiral CT and MRI appeared more accurate than MPS in stenotic tumors^[30,71].

In clinical practice, two methods are commonly used to improve the accuracy of diagnosis. One is the use of contrast material, such as Ultravist on spiral CT or Gd-TDPA on MR imaging. Enhanced imaging can provide useful information of the blood supply of the lesions, which is helpful to distinguishing the malignant from the benign mass. The other one is the regulation of the section thickness. A section gap of 1-2 mm can help discover micro-lesions. However, Gd-DTPA has several disadvantages, such as non-specific distribution and slightly nephrotic toxicity^[73]. To develop new tissue-specific contrast material would further improve the accuracy of spiral CT and MRI in TNM staging of gastroesophageal carcinoma. In addition, it should be taken into consideration that in our study the MR equipment was of (first generation), which was also a reason for its low accuracy.

We think that the experience is an important factor to improve the accuracy of diagnosis^[28]. Some problems such as the lack of training facilities, EUS courses and EUS laboratories limit the wider use of MPS. No atlas of endosonography for different diseases has been published in the world so far. The interpretation of endosonographic images is dependent on the ultrasound knowledge or the results of animal experiments. The lack of experience in transabdominal ultrasonography hinders the reasonable interpretation for some complex image patterns. The ultrasound images are also unsteady. We observed that the esophageal wall can be visualized as a five-layer structure, but sometimes as a three-layer structure^[28]. Other authors also reported the similar results^[35,57]. The reason remains to be demonstrated. Many hospitals diagnosed the disease in cooperation between endoscopists and ultrasoundists. In addition, many surgeons have still doubted the role of endosonography. They would rather believe the results of spiral CT or MRI. In fact, CT or MRI plays an increasing role in ruling out the intra-abdominal metastasis so as to avoid unnecessary surgery^[74]. We also think it unnecessary to make MPS examination for those patients who have lost the operation chance. To our knowledge, surgeons in our hospital make the therapeutic plans for the patients with advanced tumors mainly relying on the results of spiral CT or MRI. As a matter of contrast, they select the surgical procedures for the patients with stage T1 and T2 much more depending on the results of MPS. As a matter of fact, MPS appears superior to CT or MRI mainly in staging early tumors and the latter have much higher accuracy in determining the presence or extent of more distant metastases. A combination of endoscopic ultrasound including

computer-assisted analysis and spiral CT or MRI are expected to provide a higher TNM accuracy^[75].

REFERENCES

- Krasna MJ**, Jiao X, Sonett JR, Gamliel Z, Eslami A, Raefaly Y, Mao Y. Thoracoscopic and laparoscopic lymph node staging in esophageal cancer: do clinicopathological factors affect the outcome? *Ann Thorac Surg* 2000; **73**: 1710-1713
- Wang N**, Liu ZH, Ding F, Wang XQ, Zhou CN, Wu M. Down-regulation of gut-enriched Kruppel-like factor expression in esophageal cancer. *World J Gastroenterol* 2002; **8**: 966-970
- Shen ZY**, Xu LY, Chen MH, Shen J, Cai WJ, Zeng Y. Progressive transformation of immortalized esophageal epithelial cells. *World J Gastroenterol* 2002; **8**: 976-981
- Wilson KS**, Wilson AG, Dewar GJ. Curative treatment for esophageal cancer: Vancouver Island Cancer Centre experience from 1993 to 1998. *Can J Gastroenterol* 2002; **16**: 361-368
- Nishimaki T**, Tanaka O, Ando N, Ide H, Watanabe H, Shinoda M, Takiyama W, Yamana H, Ishida K, Isono K, Endo M, Lkeuchi T, Mitomi T, Koizumi H, Imamura M, Iizuka T. Evaluation of the accuracy of preoperative staging in thoracic esophageal cancer. *Ann Thorac Surg* 1999; **68**: 2059-2064
- Ando N**, Niwa Y, Ohmiya N, Ito B, Sasaki Y, Goto H. Simultaneous multiple early cancers of esophagus and stomach treated by endoscopic mucosal resection. *Endoscopy* 2002; **34**: 667-669
- Drudi FM**, Trippa F, Cascone F, Righi A, Iascone C, Ricci P, David V, Passariello R. Esophagogram and CT vs endoscopic and surgical specimens in the diagnosis of esophageal carcinoma. *Radiol Med* 2002; **103**: 344-352
- Wu MY**, Liang YR, Wu XY, Zhuang CX. Relationship between Egr-1 gene expression and apoptosis in esophageal carcinoma and precancerous lesions. *World J Gastroenterol* 2002; **8**: 971-975
- Leung SF**, Griffith JF, Ahuja A, Chan AC. Influence of staging thoracic computed tomography on radiation therapy planning for esophageal carcinoma. *J Thorac Imaging* 2002; **17**: 145-150
- Christein JD**, Hollinger EF, Millikan KW. Prognostic factors associated with resectable carcinoma of the esophagus. *Am Surg* 2002; **68**: 258-262
- Shen ZY**, Shen J, Li QS, Chen CY, Chen JY, Zeng Y. Morphological and functional changes of mitochondria in apoptotic esophageal carcinoma cells induced by arsenic trioxide. *World J Gastroenterol* 2002; **8**: 31-35
- Gao F**, Yi J, Shi GY, Li H, Shi XG, Tang XM. The sensitivity of digestive tract tumor cells to As₂O₃ is associated with the inherent cellular level of reactive oxygen species. *World J Gastroenterol* 2002; **8**: 36-39
- Shen ZY**, Shen WY, Chen MH, Shen J, Cai WJ, Yi Z. Nitric oxide and calcium ions in apoptotic esophageal carcinoma cells induced by arsenite. *World J Gastroenterol* 2002; **8**: 40-43
- Gu ZP**, Wang YJ, Li JG, Zhou YA. VEGF₁₆₅ antisense RNA suppresses oncogenic properties of human esophageal squamous cell carcinoma. *World J Gastroenterol* 2002; **8**: 44-48
- Wang AH**, Sun CS, Li LS, Huang JY, Chen QS. Relationship of tobacco smoking, CYP1A1, GSTM1 gene polymorphism and esophageal cancer in Xi'an. *World J Gastroenterol* 2002; **8**: 49-53
- Zou JX**, Wang LD, Shi ST, Yang GY, Xue ZH, Gao SS, Li YX, Yang CS. p53 gene mutations in multifocal esophageal precancerous and cancerous lesions in patients with esophageal cancer in high risk northern China. *Shijie Huaren Xiaohua Zazhi* 1999; **7**: 280-284
- Deng LY**, Zhang YH, Xu P, Yang SM, Yuan XB. Expression of interleukin 1 β converting enzyme in 5-FU induced apoptosis in esophageal carcinoma cells. *World J Gastroenterol* 1999; **5**: 50-52
- Wu LF**, Yao JG, Wu ZD, Wu MY. The significance of endoscopic classification in esophageal cancer. *Najing Neijing* 1995; **12**: 146-148
- Chen HB**, Chen L, Zhang JK, Shen ZY, Su ZI, Cheng SB, Chew EC. Human papillomavirus 16E6 is associated with the nuclear matrix of esophageal carcinoma cells. *World Gastroenterol* 2001; **7**: 788-791
- Rice TW**. Clinical staging of esophageal carcinoma. CT, EUS, and PET. *Chest Surg Clin N Am* 2000; **10**: 471-485
- Nguyen NT**, Roberts PF, Follette DM, Lau D, Lee J, Urayama S, Wolfe BM, Goodnight JE. Evaluation of minimally invasive sur-

- gical staging for esophageal cancer. *Am J Surg* 2001; **182**: 702-706
- 22 **Giovannini M**, Monges G, Seitz JF, Moutardier V, Bernardini D, Thomas P, Houvenaeghel G, Delpero JR, Giudicelli R, Fuentes P. Distant lymph node metastases in esophageal cancer: impact of endoscopic ultrasound-guided biopsy. *Endoscopy* 1999; **31**: 536-540
 - 23 **Pfau PR**, Ginsberg GG, Lew RJ, Faigel DO, Smith DB, Kochman ML. Esophageal dilation for endosonographic evaluation of malignant esophageal strictures is safe and effective. *Am J Gastroenterol* 2000; **95**: 2813-2815
 - 24 **Slater MS**, Holland J, Faigel DO, Sheppard BC, Deveney CW. Does neoadjuvant chemoradiation downstage esophageal carcinoma? *Am J Surg* 2001; **181**: 440-444
 - 25 **Greenberg J**, Durkin M, Van Drunen M, Aranha GV. Computed tomography or endoscopic ultrasonography in preoperative staging of gastric and esophageal tumors. *Surgery* 1994; **116**: 696-702
 - 26 **Nishimaki T**, Tanaka O, Ando N, Ide H, Watanabe H, Shinoda M, Takiyama W, Yamana H, Ishida K, Isono K, Endo M, Ikeuchi T, Mitomi T, Koizumi H, Imamura M, Iizuka I. Evaluation of the accuracy of preoperative staging in thoracic esophageal cancer. *Ann Thorac Surg* 1999; **68**: 2059-2064
 - 27 **McLoughlin RF**, Cooperberg PL, Mathieson JR, Stordy SN, Halparin LS. High resolution endoluminal ultrasonography in the staging of esophageal carcinoma. *J Ultrasound Med* 1995; **14**: 725-730
 - 28 **Wu LF**, Wang BZ, Wang YZ, Xu XH, Zheng ZC. Evaluation of Miniprobe Endosonography in Preoperative TN staging of Esophageal Cancer: Comparison of water rinsing method with balloon method. *J CAUME* 1999; **5**: 10-13
 - 29 **Wang Y**, Sun Y, Li YY. Clinical application of transesophageal intraluminal ultrasonography to the esophageal carcinoma. *Zhonghua Waikexue* 1998; **36**: 620-623
 - 30 **Kelly S**, Harris KM, Berry E, Hutton J, Roderick P, Cullingworth J, Gathercole L, Smith MA. A systematic review of the staging performance of endoscopic ultrasound in gastro-oesophageal carcinoma. *Gut* 2001; **49**: 534-539
 - 31 **Sobin LH**, Wittekind C, eds. TNM classification of malignant tumours, 5th ed. *New York: Springer-Verlag* 1997
 - 32 **Botet JF**, Lightdale CJ, Zaubler AG, Gerdes H, Urmacher C, Brennan MF. Preoperative staging of esophageal cancer: comparison of endoscopic US and dynamic CT. *Radiology* 1991; **181**: 419-425
 - 33 **Tio TL**, Cohen P, Coene PP, Udding J, Den Hartog Jager FC, Tytgat GN. Endosonography and computed tomography of esophageal carcinoma. Preoperative classification compared to the new (1987) TNM system. *Gastroenterology* 1989; **96**: 1478-1486
 - 34 **Rice TW**, Zuccaro G Jr, Adelstein DJ, Rybicki LA, Blackstone EH, Goldblum JR. Esophageal carcinoma: depth of tumor invasion is predictive of regional lymph node status. *Ann Thorac Surg* 1998; **65**: 787-792
 - 35 **Hasegawa N**, Niwa Y, Arisawa T, Hase S, Goto H, Hayakawa T. Preoperative staging of superficial esophageal carcinoma: comparison of an ultrasound probe and standard endoscopic ultrasonography. *Gastrointest Endosc* 1996; **44**: 388-393
 - 36 **Vazquez-Sequeiros E**, Wiersema MJ. High-frequency US catheter-based staging of early esophageal tumors. *Gastrointest Endosc* 2002; **55**: 95-99
 - 37 **Vickers J**. Role of endoscopic ultrasound in the preoperative assessment of patients with oesophageal cancer. *Ann R Coll Surg Engl* 1998; **80**: 233-239
 - 38 **Peters JH**, Hoeft SF, Heimbucher J, Bremner RM, Demeester TR, Bremner CG, Clark GW, Kiyabu M, Parisky Y. Selection of patients for curative or palliative resection of esophageal cancer based on preoperative endoscopic ultrasonography. *Arch Surg* 1994; **129**: 534-539
 - 39 **Fockens P**, Van den Brande JH, Van Dullemen HM, Van Lanschot JJ, Tytgat GN. Endosonographic T-staging of esophageal carcinoma: a learning curve. *Gastrointest Endosc* 1996; **44**: 58-62
 - 40 **Nesje LB**, Svanes K, Viste A, Laerum OD, Odegaard S. Comparison of a linear miniature ultrasound probe and a radial-scanning echoendoscope in TN staging of esophageal cancer. *Scand J Gastroenterol* 2000; **35**: 997-1002
 - 41 **Vickers J**, Alderson D. Influence of luminal obstruction on esophageal cancer staging using endoscopic ultrasonography. *Br J Surg* 1998; **85**: 999-1001
 - 42 **Menzel J**, Hoepffner N, Nottberg H, Schulz C, Senninger N, Domschke W. Preoperative staging of esophageal carcinoma: miniprobe sonography versus conventional endoscopic ultrasound in a prospective histopathologically verified study. *Endoscopy* 1999; **31**: 291-297
 - 43 **Akahoshi K**, Chijiwa Y, Sasaki I, Hamada S, Iwakiri Y, Nawata H, Kabemura T. Pre-operative TN staging of gastric cancer using a 15 MHz ultrasound miniprobe. *Br J Radiol* 1997; **70**: 703-707
 - 44 **Richards DG**, Brown TH, Manson JM. Endoscopic ultrasound in the staging of tumours of the oesophagus and gastro-oesophageal junction. *Ann R Coll Surg Engl* 2000; **82**: 311-317
 - 45 **Hordijk ML**, Zander H, van Blankenstein M, Tilanus HW. Influence of tumour stenosis on the accuracy of endosonography in preoperative T staging of esophageal cancer. *Endoscopy* 1993; **25**: 171-175
 - 46 **Ampil FL**, Caldito G, Li BD, Pelsler R. Computed tomographic staging of esophageal cancer and prognosis. *Radiat Med* 2001; **19**: 127-129
 - 47 **Luketich JD**, Meehan M, Nguyen NT, Christie N, Weigel T, Yousem S, Keenan RJ, Schauer PR. Minimally invasive surgical staging for esophageal cancer. *Surg Endosc* 2000; **14**: 700-702
 - 48 **Rosch T**, Lorenz R, Zenker K, von Wichert A, Dancygier H, Hofier H, Siewert JR, Classen M. Local staging and assessment of resectability in carcinoma of esophagus, stomach and duodenum by endoscopic ultrasonography. *Gastrointest Endosc* 1992; **38**: 460-467
 - 49 **Irie H**, Honda H, Kaneko K, Kuroiwa T, Yoshimitsu K, Masuda K. Comparison of helical CT and MR imaging in detecting and staging small pancreatic adenocarcinoma. *Abdom Imaging* 1997; **22**: 429-433
 - 50 **Drudi FM**, Trippa F, Cascone F, Righi A, Iascone C, Ricci P, David V, Passariello R. Esophagogram and CT vs endoscopic and surgical specimens in the diagnosis of esophageal carcinoma. *Radiol Med* 2002; **103**: 344-352
 - 51 **Willis J**, Cooper GS, Isenberg G, Sivak MV Jr, Levitan N, Clayman J, Chak A. Correlation of EUS measurement with pathologic assessment of neoadjuvant therapy response in esophageal carcinoma. *Gastrointest Endosc* 2002; **55**: 655-661
 - 52 **Quint LE**, Glazer GM, Orringer MB. Esophageal imaging by MR and CT: study of normal anatomy and neoplasms. *Radiology* 1985; **156**: 727-731
 - 53 **Chandawarkar RY**, Kakegawa T, Fujita H, Yamana H, Hayabuchi N. Comparative analysis of imaging modalities in the preoperative assessment of nodal metastasis in esophageal cancer. *J Surg Oncol* 1996; **61**: 214-217
 - 54 **Massari M**, Cioffi U, De Simone M, Lattuada E, Montorsi M, Segalin A, Bonavina L. Endoscopic ultrasonography for preoperative staging of esophageal carcinoma. *Surg Laparosc Endosc* 1997; **7**: 162-165
 - 55 **Pang W**, Tao J, Chen W. Preoperative staging of esophageal carcinoma: comparison of endoesophageal ultrasonography, computerized tomography and conventional clinical staging. *Zhonghua Waikexue* 1998; **36**: 617-619
 - 56 **Yanai H**, Yoshida T, Harada T, Matsumoto Y, Nishiaki M, Shigemitsu T, Tada M, Okita K, Kawano T, Nagasaki S. Endoscopic ultrasonography of superficial esophageal cancers using a thin ultrasound probe system equipped with switchable radial and linear scanning modes. *Gastrointest Endosc* 1996; **44**: 578-582
 - 57 **Murata Y**, Suzuki S, Ohta M, Mitsunaga A, Hayashi K, Yoshida K, Ide H. Small ultrasonic probes for determination of the depth of superficial esophageal cancer. *Gastrointest Endosc* 1996; **44**: 23-28
 - 58 **Heidemann J**, Schilling MK, Schmassmann A, Maurer CA, Buchler MW. Accuracy of endoscopic ultrasonography in preoperative staging of esophageal carcinoma. *Dig Surg* 2000; **17**: 219-224
 - 59 **Wallace MB**, Hawes RH, Sahai AV, VanVelse A, Hoffman BJ. Dilation of malignant esophageal stenosis to allow EUS guided fine-needle aspiration: safety and effect on patient management. *Gastrointest Endosc* 2000; **51**: 309-313
 - 60 **Kim LS**, Koch J. Do we practice what we preach? Clinical decision making and utilization of endoscopic ultrasound for staging esophageal cancer. *Am J Gastroenterol* 1999; **94**: 1847-1852
 - 61 **Rosch T**, Dittler HJ, Strobel K, Meining A, Schusdziarra V, Lorenz R, Allescher HD, Kassem AM, Gerhardt P, Siewert JR, Hofier H, Classen M. Endoscopic Ultrasound criteria for vascular invasion in the staging of cancer of the head of the pancreas: a blind re-

- evaluation of videotapes. *Gastrointest Endosc* 2000; **52**: 469-477
- 62 **Faige DO**. EUS in patients with benign and malignant lymphadenopathy. *Gastrointest Endosc* 2001; **53**: 593-598
- 63 **Reed CE**, Mishra G, Sahai AV, Hoffman BJ, Hawes RH. Esophageal cancer staging: improved accuracy by endoscopic ultrasound of celiac lymph nodes. *Ann Thorac Surg* 1999; **67**: 319-321
- 64 **Zuccaro G Jr**, Rice TW, Goldblum J, Medendorp SV, Becker M, Pimentel R, Gitlin L, Adelstein DJ. Endoscopic ultrasound cannot determine suitability for esophagectomy after aggressive chemoradiotherapy for esophageal cancer. *Am J Gastroenterol* 1999; **94**: 906-912
- 65 **Holscher AH**, Dittler HJ, Siewert JR. Staging of squamous esophageal cancer: accuracy and value. *World J Surg* 1994; **18**: 312-320
- 66 **Kallimanis GE**, Gupta PK, Al-Kawas FH, Tio LT, Benjamin SB, Bertagnolli ME, Nguyen CC, Gomes MN, Fleischer DE. Endoscopic ultrasound for staging esophageal cancer, with or without dilation, is clinically important and safe. *Gastrointest Endosc* 1995; **41**: 540-546
- 67 **Brugge WR**, Lee MJ, Carey RW, Mathisen DJ. Endoscopic ultrasound staging criteria for esophageal cancer. *Gastrointest Endosc* 1997; **45**: 147-152
- 68 **Van Dam J**, Rice TW, Catalano MF, Kirby T, Sivak MV Jr. High-grade malignant stricture is predictive of esophageal tumor stage. Risks of endosonographic evaluation. *Cancer* 1993; **71**: 2910-2917
- 69 **Meining A**, Dittler HJ, Wolf A, Lorenz R, Schusdziarra V, Siewert JR, Classen M, Höfler H, Rösch T. You get what you expect? A critical appraisal of imaging methodology in endosonographic cancer staging. *Gut* 2002; **50**: 599-603
- 70 **Rice TW**, Zuccaro G Jr, Adelstein DJ, Rybicki LA, Blackstone EH, Goldblum JR. Esophageal carcinoma: depth of tumor invasion is predictive of regional lymph node status. *Ann Thorac Surg* 1998; **65**: 787-792
- 71 **Bhutani MS**, Barde CJ, Markert RJ, Gopalswamy N. Length of esophageal cancer and degree of luminal stenosis during upper endoscopy predict T stage by endoscopic ultrasound. *Endoscopy* 2002; **34**: 461-463
- 72 **Parmar KS**, Zwischenberger JB, Reeves AL, Waxman I. Clinical impact of endoscopic ultrasound-guided fine needle aspiration of celiac axis lymph nodes (M1a disease) in esophageal cancer. *Ann Thorac Surg* 2002; **73**: 916-920
- 73 **Zheng WW**, Zhou KR, Chen ZW, Shen JZ, Chen CZ, Zhang SJ. Characterization of focal hepatic lesions with SPIO-enhanced MRI. *World J Gastroenterol* 2002; **8**: 82-86
- 74 **Wang YH**, Zhang LZ, Wang GH. Clinical value of preoperative CT examination in esophageal cancer. *Huaren Xiaohua Zazhi* 1998; **6**(T7): 461
- 75 **Loren DE**, Seghal CM, Ginsberg GG, Kochman ML. Computer-assisted analysis of lymph nodes detected by EUS in patients with esophageal carcinoma. *Gastrointest Endosc* 2002; **56**: 742-746

Edited by Ma JY

Expression of e-cadherin and b-catenin in human esophageal squamous cell carcinoma: relationships with prognosis

Xi-Jiang Zhao, Hui Li, Hua Chen, Yan-Xue Liu, Li-Hua Zhang, Su-Xiang Liu, Qing-Lai Feng

Xi-Jiang Zhao, Qing-Lai Feng, Department of Thoracic Surgery, Cancer Hospital, Tianjin Medical University, Tianjin 300060, China
Hui Li, Department of Thoracic Surgery, Shandong Cancer Hospital & Institute, Jinan 250117, Shandong Province, China
Hua Chen, Yan-Xue Liu, Li-Hua Zhang, Su-Xiang Liu, Department of Pathology, Cancer Hospital & Institute, Tianjin Medical University, Tianjin 300060, China

Correspondence to: Dr Xi-Jiang Zhao, Department of Thoracic Surgery, Cancer Hospital of Tianjin Medical University, Tiyuanbei Street, Block Hexi, Tianjin 300060, China. zhaoxij@china.com
Telephone: +86-22-23359929 Ext 322

Received: 2002-04-29 **Accepted:** 2002-07-03

Abstract

AIM: To elucidate the expression of E-cadherin and β -catenin correlating with its clinical outcome in patients with esophageal squamous cell carcinoma (ESCC), by analyzing their interrelationship with clinicopathological variables and their effects on progress and prognosis.

METHODS: Expression of E-cadherin and β -catenin was determined by SP immunohistochemical technique in patients with ESCC consecutively, their correlation with clinical characteristics was evaluated and analyzed by multivariate analysis.

RESULTS: The rate of expression of E-cadherin decreased to 66.03 % (70/106) in ESCC and the protein level was negative correlated with histologic grade, tumor size, clinical staging, lymph node metastasis and venous invasion. Whereas the expression rate of β -catenin was reduced to 69.8 % (74/106) and the level of protein expression correlated only with histologic grade. There obviously existed inverse correlation between level of E-cadherin protein and survival, especially in stage I, IIa, IIb ($P=0.0033$). Patients with low-expressing tumors for β -catenin and non-expressing tumors for E-cadherin/ β -catenin had lower survival period than those with normal-expressing ones ($P=0.0501$ and $P=0.0080$, respectively). Patients with diminished expression of E-cadherin as grade II or III had shorter survival period than those with normally expressing and grade I, no significance existed between grade I and grade II or III with respect to different status of E-cadherin expression. Furthermore, Correlation analysis showed level of E-cadherin correlated with that of β -catenin ($P=0.005$). Cox proportional hazards model analysis suggested downregulation of E-cadherin was an important factor indicating poor prognosis.

CONCLUSION: As a probable independent prognostic factor, it correlates with overall and disease free survival period, expression of E-cadherin but not β -catenin may predict prognosis in patients with ESCC.

Zhao XJ, Li H, Chen H, Liu YX, Zhang LH, Liu SX, Feng QL. Expression of e-cadherin and β -catenin in human esophageal squamous cell carcinoma: relationships with prognosis. *World J Gastroenterol* 2003; 9(2): 225-232
<http://www.wjgnet.com/1007-9327/9/225.htm>

INTRODUCTION

Esophageal carcinoma is generally considered as one of the most extremely aggressive carcinomas with dismal prognosis identified thus far^[1-5]. In recent years, postoperative survival of the patients with esophageal carcinoma have been improved. However, 5-year survival rate of operative advanced esophageal carcinoma is still 20-25 %. Early diagnosis and treatment are still important^[2,3,6-9]. TNM system is always considered as a classic criterion to provide treatments and evaluate prognoses. Unfortunately tumor heterogeneity and individual differences influence its accurate estimation^[10]. Therefore, to establish a "molecular staging" system based on materials combining biomarkers and clinical parameters including histologic grade and tumor stage may be helpful to guide individualized treatment and evaluate prognosis. Then some potential molecules remain to be identified^[16,8,9,11-15].

Invasion and metastatic processes themselves consist of sequential multi-stage, multi-step involving host-tumor interactions^[16]. Some studies showed status of intercellular adherens junction plays a pivotal role in tumor growth, invasion, metastasis and prognosis and the suppression of cell-cell adhesiveness may trigger the release of cancer cells from the primary cancer nests and confer invasive properties on a tumor^[16-18]. Detecting expression of adhesion molecules may reflect biological behavior and characteristics of tumor and are conducive to predict and evaluate risk of relapse and metastasis of the patients with postoperative esophageal carcinoma, thus having realistic significance to guide individualized treatment.

The cadherins that exist in many kinds of cells, belong to a family of transmembrane glycoproteins responsible for homophilic interaction of calcium-dependent cell-cell adhesion. Among them, E-cadherin (120 kDa, chromosome 16q22.1) is a classical cadherin and forms the functional component of adherens junctions between epithelial cells, and β -catenin, a multifunctional cytoplasmic protein which links E-cadherin and α -catenin to cytoskeleton constituted E-cadherin-catenin complex, both have important roles in maintaining integrity of cellular structure^[16-20]. Reduction and loss of expression in cancer cells may destroy the junctional structure which can affect the intercellular adhesion, and facilitate tumor differentiation, infiltration and metastasis, Their expression are related to survival and prognosis in a portion of cancer. It had been formed that E-cadherin might be an independent predictor of occult lymph node or micrometastasis in nodes classified as N₀ by routine histopathological methods. However, only few studies were available in ESCC^[18,21,22].

β -catenin has recently been found as a member in Wnt signaling^[23-25]. In the absence of a mitotic signal outside the cell, β -catenin is sequestered in a complex with the APC (adenomatous polyposis coli) gene product, a serine threonine glycogen synthetase kinase (GSK-3 β) and an adapter protein axin (or a homologue conductin), enabling phosphorylation and degradation of free β -catenin by the ubiquitin-proteasome system^[23-25]. When a mitotic signal is delivered by the Wnt pathway, by association of the Wg/Wnt family of secreted glycoproteins and their membrane receptors frizzled, it leads

to activation of the dishevelled (Dsh) protein, which is recruited to the cell membrane. The activated Dsh downregulates the protein complex, so that it can no longer phosphorylate β -catenin. The release of β -catenin from the phosphorylation and degradation complex promotes β -catenin stabilization and signaling. This results in an increase of free cytosolic β -catenin which translocates to the nucleus and directly binds the transcription factors Lef and Tcf, leading to activation of gene expression^[26,27].

Here, we performed E-cadherin and β -catenin expression analysis in a 106 ESCC in order to elucidate whether the expression of E-cadherin and β -catenin correlate with clinicopathological variables and clinical outcome, by analyzing their interrelationships and effects on progression of cancer and their prognostic evaluations in ESCC. Furthermore, may provide some considerable suggestions for clinical treatments.

MATERIALS AND METHODS

Clinicopathologic data

The specimens of cancer tissues and non-cancerous adjacent tissues were taken from 106 consecutive patients with esophageal squamous cell carcinoma who had undergone esophagectomy from January 1990 to December 1995 at Cancer Hospital of Tianjin Medical University, Tianjin, China. None of them received irradiation or chemotherapy preoperatively. The patients included 76 men and 30 women with a mean age of 59 (range 37-76) years. Ten tumors were in the upper segment, 68 in the middle segment and 28 in the lower segment. With respect to their growth pattern, they were 20 medullary type, 42 fungating, 34 ulcerative, 9 scirrhous and 1 other type. Of seventy-three patients underwent left thoracic approach esophagectomy, 60 cases had esophagogastric anastomosis above the aortic arch, 10 below the aortic arches and 3 cervical esophagogastric reconstruction, 25 patients underwent right thoracic posteriolateral, abdominal and cervical approach esophagectomy and 8 with other approach. Tumors were staged again according to the TNM classification (UICC1997): 2 patients with stage I, 31 IIa, 10 IIb, 60 III and 3 IV. Postoperative radiotherapy was performed in 12 patients and chemotherapy in 15, Survival periods were calculated from the date of operation to death from recurrence of the disease, Follow-up period ranged from 2 to 117 months with an average of 32.4 months.

Immunohistochemical staining

For parallel analyses of staining characteristic of the tumor and normal mucosa, representative tissue section comparing the most part of the tumor and adjacent normal mucosa were selected after the H&E stained slides were reviewed. In brief, Four micrometers thick sections prepared from 100 ml·l⁻¹ neutral buffered formalin-fixed and paraffin-embedded tumor tissue on the slides were deparaffinized, dehydrated and blocked from removing endogenous peroxides activating with 3 ml·l⁻¹ H₂O₂ in methanol for 30 min. The sections were microwaved in 0.1 mol·l⁻¹ citrate buffer pH 6.0 at 750 W for 12 min. After incubation with 10 % normal goat serum to block non-specific binding and were then incubated with the primary antibodies such as mouse monoclonal anti-human E-cadherin (4A2C×7, Santa Cruz Biotechnology, USA, ready to use) and polyclonal rabbit anti- β -catenin (Sigma Chemical Company, USA, diluted 1:1 000 in PBS) overnight at 4 °C. After washing antibody with the SP kit (Zymed, USA) the peroxides reaction was performed using 3, 3'-diaminobenzidine tetrahydrochloride (DAB) (Zhongshan Biological Technology, Beijing, China) as chromogen. Tissues were counterstained with hematoxylin.

The slides were washed between each step three times with PBS, Negative control was obtained by replacing the primary antibody with PBS. Adjacent normal squamous epithelium served as an internal positive control.

Evaluation of immunohistochemical staining

Tumor sections were scored by light microscopy by 3 independent observers (Chen H, Li H and Liu XS) without knowledge of the stage and patient profiles. Based on the previous immunohistochemical studies^[28], the membranous staining of cells were positively stained by the antibody. Calculating the percentage of positively stained cells evaluated for each tissue section after counting 100 cells at more than 5 high-power (×200) fields. The expression of E-cadherin and β -catenin were classified into 3 grades, as follows: -, If less than 10 % of the tumor cells were positively stained; +, If more than 90 % of the tumor cells were positively stained, the expression was judged to be positive; and \pm , between 10 % and 90 % of the tumor cells were evaluated as heterogeneous. The specimens graded + stand for normal expression, \pm and - were taken together and classified as reduced expression.

Statistical analysis

The χ^2 test and Spearman rank correlation coefficient analysis were used to assess the univariate association between the immunohistochemical status and the clinicopathological characteristics. The survival rate was calculated by life table and cumulative survival curves were constructed according to the Kaplan-Meier method, and differences in survival were estimated with the Log-rank test Cox proportional hazards model was used for multivariate survival analysis. A *P* value less than 0.05 was considered significant. All the statistical analyses were performed using the SPSS 10.0 V for Windows software.

RESULTS

Expression of E-cadherin and b-catenin in normal esophagus

Normal esophageal epithelium showed strong expression of E-cadherin and β -catenin at the membrane of cell and the intercellular junctions. Expression of these molecules was more marked in the prickle cell layer and para-basal cell layers. No or weak cytoplasmic staining of E-cadherin and no cytoplasmic staining of β -catenin were seen in normal esophageal epithelium. Esophageal glands and their duct also showed expression of these molecules at cell membranes, Whereas non-epithelial cells such as muscular tissue and infiltrating lymphocytes did not.

Expression of E-cadherin and b-catenin in esophageal carcinoma

Reduced homogenous and heterogeneous staining of E-cadherin and β -catenin were found in esophageal carcinoma (Figure 1). In well/moderately differentiated carcinomas, cancer cells from the tumor nest peripheries showed weaker expression of these molecules than those in the centers showing zonal differentiation (Figure 2). Although reduced expression and loss of them were always present in poorly differentiated carcinomas, some showed normal expression of these molecules in neoplastic nests. Reduced membranous expression of E-cadherin and β -catenin were found in 66.0 % (70/106) and 69.8 % (74/106), respectively.

Expression of E-cadherin and b-catenin and clinicopathologic variables

Significant inverse correlation existed between the intensity of E-cadherin expression and histologic grade, tumor size,

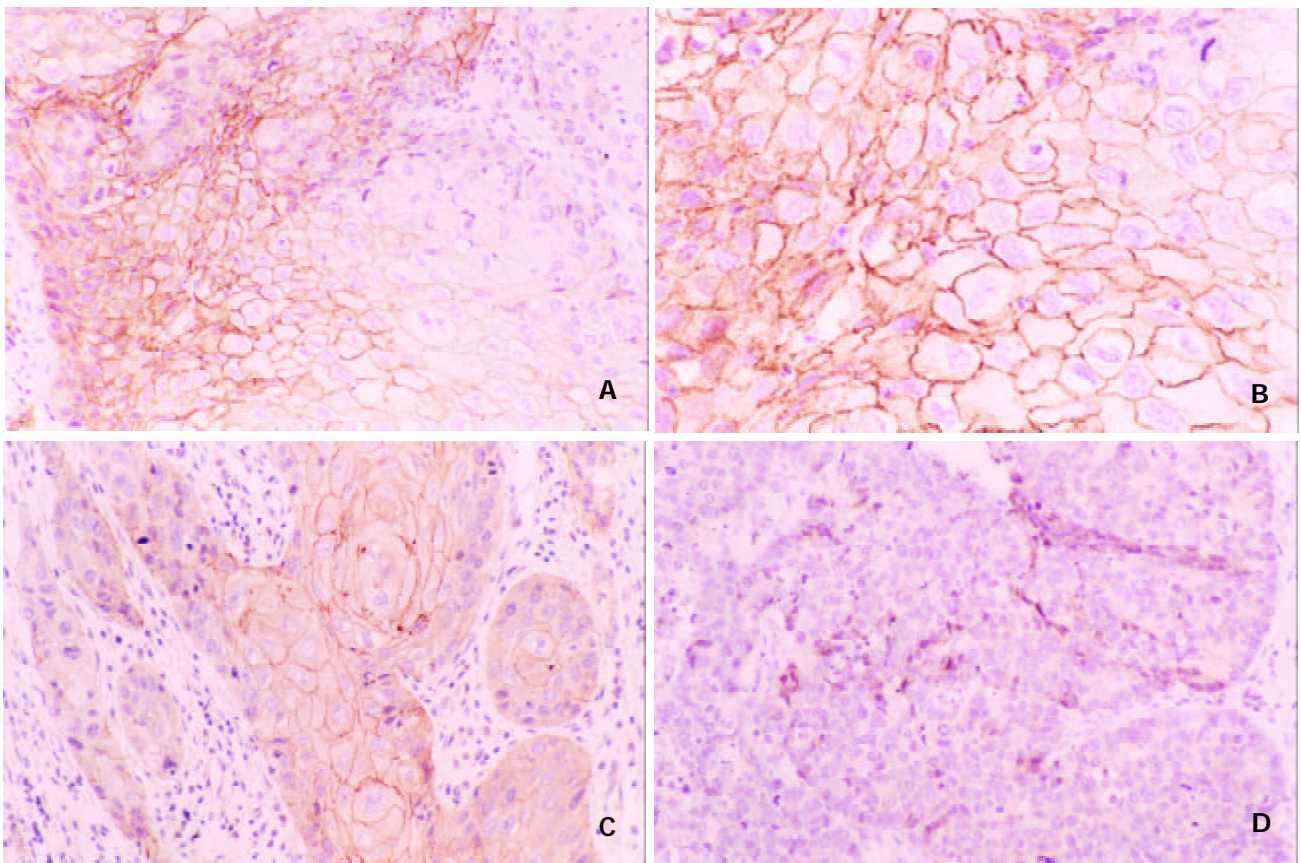


Figure 1 Expression of E-cadherin in esophageal squamous carcinoma tissue, brownish membrane and cytoplasm were shown in part of the tumor cells (A, B positive, C heterogeneous, D negative expression Original magnification $\times 200$; B, Original magnification $\times 400$).

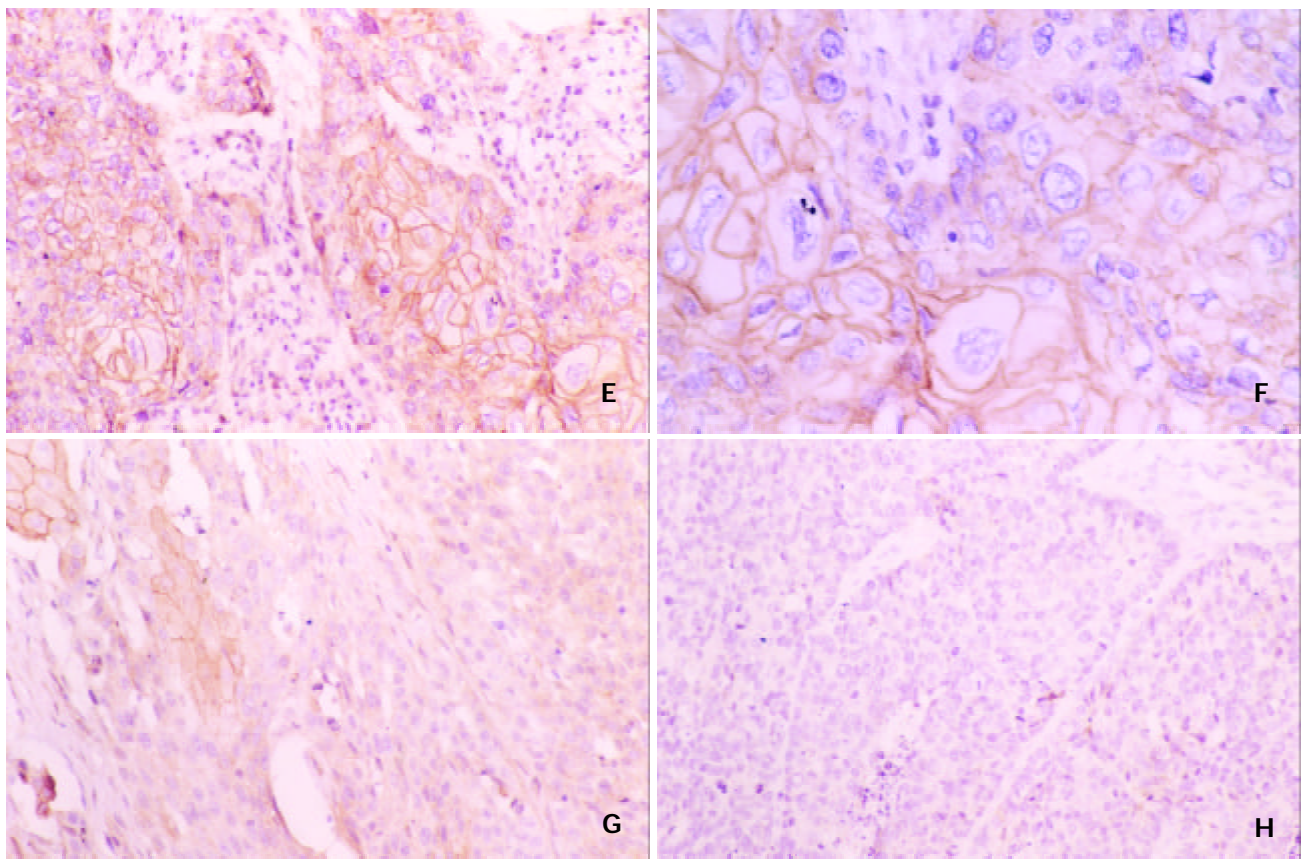


Figure 2 Expression of β -catenin in esophageal squamous carcinoma tissue, brownish membrane and cytoplasm were shown in part of the tumor cells in the centers showing zonal differentiation (E, F positive, G heterogeneous, H negative expression Original magnification; F, Original magnification $\times 400$).

clinical staging and venous invasiveness, No significant differences were seen in age, gender, location of tumor, growth pattern and invasion depth ($r_s=0.020\sim0.156$, $P=0.084\sim0.118$). Expression of β -catenin correlated significantly only with histologic grade, Whereas no differences were observed in age, gender, location of tumor, tumor size, clinical staging, growth pattern, venous invasiveness and invasion depth ($r_s=0.060\sim0.1569$, $P=0.541\sim0.104$), shown in Table 1. In carcinomas with lymph node metastasis, reduced expression of E-cadherin and β -catenin were seen in 76.59 % (36/47) and 72.34 % (34/47) versus 57.63 % (34/59) and 67.79 % (40/59) in carcinomas without lymph node metastasis, respectively. The staining of E-cadherin correlated only with lymph node status ($P=0.040$) and no significant differences for β -catenin.

Table 1 Relationships between expression of E-cadherin and β -catenin and clinicopathological parameters in patients with ESCC

Group	Total	E-cadherin			P	β -catenin			P
		+	\pm	-		+	\pm	-	
Histologic grade									
I	17	8	8	1		9	6	2	
II	69	25	33	11	0.001	21	28	20	0.014
III	20	3	7	10	-0.309	2	12	6	-0.238
Tumor size (cm)									
<3.0	10	6	2	2		0	5	5	
3.0-5.0	41	16	18	7		15	15	11	
5.0-7.0	44	11	24	9	0.054	12	24	8	0.213
≤ 7.0	11	3	4	4	-0.187	5	2	4	-0.212
Clinical staging									
I	2	2	0	0		0	2	0	
IIa	31	16	11	4		13	13	5	
IIb	10	2	5	3	0.013	3	2	5	0.124
III	60	15	31	14	-0.241	6	27	17	-0.150
IV	3	1	1	1		0	2	1	
Venous invasion									
Yes	27	5	14	8	0.042	6	12	9	0.237
No	79	31	34	14	-0.198	26	34	19	-0.116
Lymph node metastasis									
Yes	47	11	22	14	0.014	13	21	13	0.646
No	59	25	26	8	-0.239	19	25	15	-0.045

Relationships between E-cadherin and β -catenin

As summarized in Table 2, the expression of both E-cadherin and β -catenin were evaluated in consecutive sections. The correlation between E-cadherin and β -catenin was statistically significant ($P=0.005$). 17.92 % (19/106) of tumors were E-cadherin(+)/ β -catenin($\pm \sim -$), and 14.15 % (15/106) of tumors were E-cadherin($\pm \sim -$)/ β -catenin(+), statistically significant differences were observed in different expression of these molecules (Pearson $\chi^2=6.086$, $P=0.014$).

Table 2 Relationships between E-cadherin and β -catenin expression in ESCC

E-cadherin	Total	β -catenin		
		+	\pm	-
+	36	17	13	6
\pm	48	11	24	13
-	22	4	9	9
Total	106	32	46	28

$r_s=0.270$, $P=0.005$.

Expression of E-cadherin and β -catenin and survival

The median survival was 28.64 months and overall 1-, 3-, 5-year survival rates were 57.13 %, 34.89 % and 29.59 %, respectively. There obviously existed inverse correlation between intensity of E-cadherin protein and survival ($P=0.0532$), even in the group without receiving postoperative chemotherapy or radiotherapy ($P=0.0067$ and $P=0.0295$, respectively). Patients with loss of E-cadherin expression had lower survival at 1-, 3-, 5-year than those with expression tumors, and Patients with reduced E-cadherin expression had shorter disease-free survival than those with normal expression ($P=0.0278$). No significant correlation was apparent between abnormal expression of β -catenin and overall survival. But patients with low-expressing tumors for β -catenin and non-expressing tumors for E-cadherin/ β -catenin had shorter median survival period than those with normal expressing tumors ($P=0.0501$ and $P=0.0080$, respectively) in the group without receiving postoperative chemotherapy or radiotherapy ($P=0.0735$ and $P=0.0205$, respectively).

Expression of E-cadherin and survival stratified for tumor stage

In patients with stage I, IIa, IIb, the median survival for normal, heterogeneous and negative E-cadherin expressing groups were 106.59, 46.59 and 28.50 months, respectively. Statistically significance existed in different level of E-cadherin and overall survival ($P=0.0033$), Survival curves were shown in Figure 3, and disease-free survival ($P=0.0002$) in different E-cadherin expressing groups whose median survival were 78, 56, 32.00 and 14.00 months. In contrast, as for stage III or IV, no significance existed in different level of E-cadherin ($P=0.2152$ and $P=0.3397$, respectively). Survival curves were shown in Figure 4.

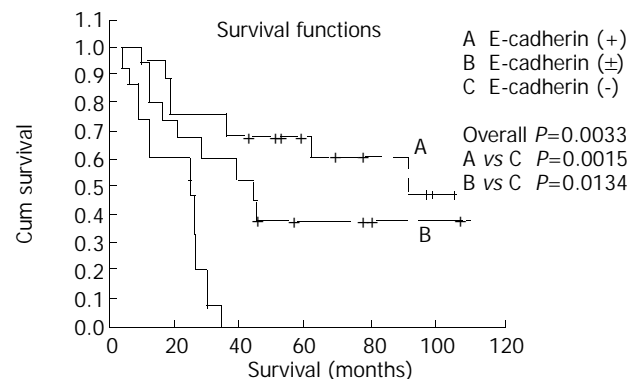


Figure 3 Kaplan-Meier survival curves for patients with stage I, II according to E-cadherin expression.

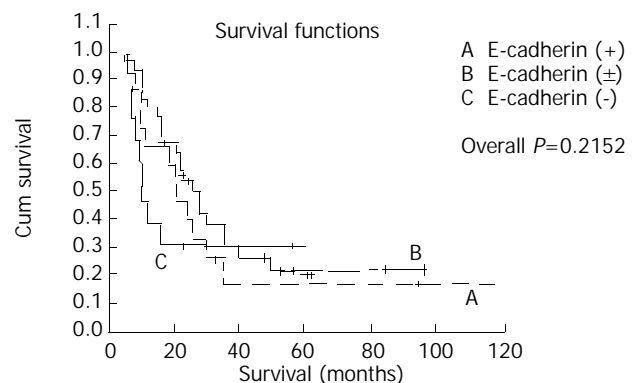


Figure 4 Kaplan-Meier survival curves for patients with stage III, IV according to E-cadherin expression.

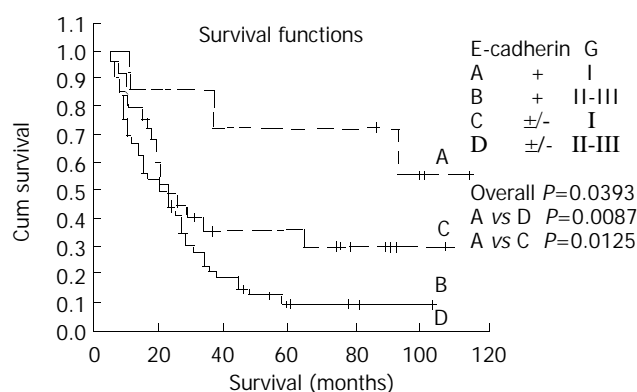
Expression of E-cadherin and survival stratified for histologic grade

Patients with diminished expression of E-cadherin and grade II or III had shorter survival period than those with normally

Table 3 Multivariate results in Cox proportional hazards analysis for patients with ESCC

Variables	Category(Value)	β	Wald	P Value	HR	95%CI
Overall survival (n=106)						
location (mid-thoracic)	No/Yes(0/1)	0.650	5.665	0.017	1.916	1.112~3.272
Lymph node metastasis	No/Yes(0/1)	0.599	5.893	0.015	1.821	1.1222.~953
Venous invasion	No/Yes(0/1)	1.147	18.633	<0.001	3.148	1.870~5.229
Clinical staging	I/II/III/IV (0/1/2/3)	0.420	8.475	0.004	1.521	1.147~2.018
E-cadherin	-/ \pm / $+$ (0/1/2)	-0.431	5.687	0.017	0.650	0.456~0.926
Disease-free survival (n=96)						
Gender	M/F(0/1)	0.675	4.786	0.029	1.965	1.073~3.598
Tumor size	Continue	0.179	4.302	0.038	1.196	1.010~1.417
Clinical staging	I/II/III/IV (0/1/2/3)	0.272	3.233	0.042	1.313	0.976~1.767
Location (mid-thoracic)	No/Yes(0/1)	0.615	4.111	0.043	1.849	1.021~3.349
Venous invasion	No/Yes(0/1)	0.982	9.797	0.002	2.671	1.444~4.942
E-cadherin	-/ \pm / $+$ (0/1/2)	-0.397	4.479	0.034	0.672	0.465~0.971

expressing ones and grade I, no significance existed between grade I and grade II or III with respect to different status of E-cadherin expression. In the patients with grade I, Statistically significant relationships existed between level of E-cadherin and overall survival ($P=0.0125$). The survival curves were shown in Figure 5.

**Figure 5** Kaplan-Meier survival curves for patients with ESCC stratified for histologic grade according to E-cadherin expression

Multivariate analysis of survival

Multivariate survival analysis was performed by means of the Cox proportional hazards model by entering the following covariates: age, gender, location of tumor, tumor size, invasion depth, venous invasiveness, histologic grade, clinical stage, lymph node status, E-cadherin and β -catenin expression. Covariates were selected in a stepwise fashion by using method of Backward: Wald. The significant prognostic factors influencing survival were location of tumor, venous invasiveness, clinical stage, lymph node status, E-cadherin expression. The results were shown in Table 3.

DISCUSSION

Previous studies reported that the reduction rate of E-cadherin expression was observed to be 18.2-87 % in specimens from the patients with ESCC^[28-34], While 66 % of ESCC examined showed reduced expression of E-cadherin in our investigation. This is not in accordance with references reported. It is our

logical thoughts that selection of the patients entering into the study, immunohistochemical method, antibody origination, tumor heterogeneity and differences in staining evaluation may be individually or in combination held responsible. As a marker associated with squamous cell differentiation^[35], the level of E-cadherin expression had inverse correlation with histologic grade. It suggested that normal function of E-cadherin molecule mediated cell-cell adherens junction to induce cell aggregates, which was consistent with histologic morphogenesis of tumor nest in well-differentiated tumors showed zonal differentiation. That phenomenon consists of a mechanical stretching and compression between adjacent cell and requires active contraction of the actin tethered to the cadherin intercellular contacts^[36]. But normal expression of E-cadherin was found in poorly-differentiated tumors, accounting for 15.0 % in our study. Several studies were available about this phenomenon, Nakanishi *et al* reported 14.58 % of the patients with poorly-differentiated ESCC also appeared normal expression of E-cadherin, of catenins (α , β and γ), so did 3.22 % of the patients with moderated or poorly-differentiated tumors from reports of Tamura *et al*^[29]. Then this showed simply reduced expression of E-cadherin was not independent factor impact on adherens junction. On the other hand normal function of adherens junction relate to cytoplasm protein expression and its normal function. Expression of E-cadherin was closely associated with size of tumor, lymph node metastases and venous invasion in our study. These were not identical to the results of Nakanishi *et al*, Tamura *et al*. However, diminished expression of E-cadherin facilitate tumor dedifferentiation, invasion and metastases, indeed, the tumor cells of solid tumor with high metastatic potentials are often focally dissociated at the invading fronts^[28,29,31]. Of particular interest is the finding in some studies in recent years that expression of E-cadherin might be used to predict micrometastasis in lymph node of the patients without signs of lymph node or distant metastases classified as N₀ and M₀ by routine histopathological methods^[22,37]. Based on these findings, in the present study, The relationship between reduced expression of E-cadherin and haematogenous metastasis in postoperative patients had also come under investigation. Hematogenous metastasis frequently occurred in the patients with reduced expression of E-cadherin, but multivariate analysis revealed the finding need further evaluation (data not shown). It seemed to accept that more intercellular adhesion

molecules such as integrins, selectins and immunoglobulin were involved in the process.

It appears to possess both irreversible and reversible mechanisms for inactivating the cell-cell adhesion system. Several studies revealed heterogeneous methylation patterns exhibit a remarkably unstable, allele-to-allele variability that, like the dynamic expression of E-cadherin during metastatic progression, can be modulated or selected for in relation to the tumor microenvironment^[38]. There have been several reports on E-cadherin gene mutations in human cancer^[16,18], however, mutations are rare in esophageal carcinoma, E-cadherin promoter hypermethylation is associated with decreased expression^[39,40], moreover, recent studies showed that, despite the frequent LOH of the E-cadherin locus, mutations in the E-cadherin gene are rare events and can not be held responsible for down regulation of E-cadherin observed in the majority of adenocarcinomas of the esophagus^[41]. Further studies demonstrated abnormal phosphorylation of cytoplasmic protein regulated by tyrosine kinases and tyrosine phosphatases affected expression of E-cadherin and its function^[42].

Significant difference in survival existed in patients with different level of E-cadherin protein and a trend towards better survival was found in patients having normal E-cadherin expression. But discrepancy resulted from studies on the kinds of tumors. Inada *et al* reported 5-year survival rate of the patients with ESCC ranged from 87.8 % in normal E-cadherin expression to 19.1 % in absent expression of E-cadherin^[30], but some coworkers did not acquire the same results^[32,33]. Nakanishi *et al* demonstrated no significant correlations between survival and reduced E-cadherin expression, however, in univariate analysis survival of the patients with reduced α -catenin expression was significantly shorter than that of those with normal expression, and the loss of α -catenin expression from cancer tissues might be attributable to loss of E-cadherin function, which reflected more serious dysfunction of the cadherin-mediated cell-cell adhesion system. In our study there obviously existed inverse correlation between the patients with reduced level of E-cadherin expression and survival, especially in tumors with stage I, II, and in group with absent expression of E-cadherin shorter survival period was observed. Multivariate analysis revealed E-cadherin expression was an independent factor impacted on prognosis of the patients with ESCC. These findings were consistent with the reports of Tamura *et al*, and recently a multicenter investigation supported this viewpoint^[34]. In view of the association between E-cadherin and histologic grade, furthermore, we analyzed and tried to elucidate whether these factors played different roles in combination or individually. Although several studies approved the discrepancy of survival could be partly explained by the histologic grade, owing to other clinicopathologic features and grading categories not to be precisely defined, the results of studies remain controversial. In our present investigation, no significance existed between grade I and grade II or III with respect to different E-cadherin status. But in group with grade I, survival of the patients with normal E-cadherin expression was statistically significantly higher than that of those with diminished one, suggesting an apparent difference in the effect of downregulation of E-cadherin between different histologic grade. Therefore, E-cadherin expression as an independent prognostic factor had more significance to predict prognosis for the patients at early stage and with similar histologic grade, might provide some suggestions for clinical treatments.

β -catenin played an important role in the interactions between cadherins and other transmembrane receptor proteins and regulated cellular differentiation and proliferation. Reduced and absent expression of β -catenin were also frequently in tumors might disrupt stability and integrity of the E-cadherin-catenin complex and disturb cellular adherens junction,

resulting in cell proliferation, migration, and invasion. Reduction of β -catenin expression was 73 % in ESCC from Nakanishi *et al* and 40.9 % from Ninomiya *et al*^[43]. Similarly, 69.8 % of patients with β -catenin expression were judged to be reduced in our study, whereas reduced expression of β -catenin significantly correlated only with the histologic grade. Also, an association between abnormal expression of E-cadherin and β -catenin was found, suggesting that loss of E-cadherin binding may cause a redistribution of β -catenin from the cell membrane to the cytoplasm.

It remains unclear that β -catenin expression is associated with lymph node status, invasion depth, tumor stage, hematogenous metastasis and histologic grade. Many believe as a member of oncogenes and signaling molecules, β -catenin plays an important role in tumor progression and carcinogenesis, and there exists relation with cytoplasmic protein such as α -, γ -catenin, p120^{cas}, APC^[23,24], Dsh, Tcf, Axin, β -Trcp, G12^[44], PP2A^[45], IQGAP1^[23] and Smad4^[46]. Since so intricate signaling network and multifunctional molecules are involved in regulating cellular function, it is difficult to explain abnormal expression of β -catenin and its functional abnormalities, thus negating correlation with clinicopathologic parameters^[47]. But undoubtedly β -catenin as a member of adhesion molecule should be imprudently considered in prognostic value of ESCC. To some extent absent expression of β -catenin reflects dysfunction of E-cadherin mediated cellular adherens junction, which may cause weak cell-cell adhesion and confer invasive properties on a tumor^[26,27,48].

To our knowledge, reduced β -catenin expression indicated poor prognosis in some kinds of tumor in addition to esophageal squamous cell carcinoma^[49,50]. We found that patients with low-expression tumors for β -catenin and non-expression tumors for E-cadherin/ β -catenin had shorter survival period than those with normally expressing ones. But in group with normal E-cadherin expression, no significant relation was found between β -catenin and prognosis. It was apparent that the prognostic value of β -catenin is lower than that of E-cadherin, this may be explained by their roles in the E-cadherin-catenin complex, E-cadherin influences redistribution and function of β -catenin, and γ -catenin might substitute for β -catenin as a component of the complex^[51], in other tumors several studies showed aberrant expression of β -catenin or γ -catenin does not necessarily lead to a nonfunctional complex^[52].

In conclusion, as a probable independent prognostic factor, it correlates with overall and disease free survival period, expression of E-cadherin but not β -catenin may predict prognosis in patients with ESCC, Further studies are needed to elucidate function of β -catenin by combining other cytoplasmic proteins.

REFERENCES

- 1 **Ikeda G**, Isaji S, Chandra B, Watanabe M, Kawarada Y. Prognostic significance of biologic factors in squamous cell carcinoma of the esophagus. *Cancer* 1999; **86**: 1396-1405
- 2 **Ohashi K**, Nemoto T, Nakamura K, Nemori R. Increased expression of matrix metalloproteinase 7 and 9 and membrane type 1-matrix metalloproteinase in esophageal squamous cell carcinomas. *Cancer* 2000; **88**: 2201-2209
- 3 **Miyazaki T**, Kato H, Shitara Y, Yoshikawa M, Tajima K, Masuda N, Shouji H, Tsukada K, Nakajima T, Kuwano H. Mutation and expression of the metastasis suppressor gene KAI1 in esophageal squamous cell carcinoma. *Cancer* 2000; **89**: 955-962
- 4 **Gu ZP**, Wang YJ, Li JG, Zhou YA. VEGF₁₆₅ antisense RNA suppresses oncogenic properties of human esophageal squamous cell carcinoma. *World J Gastroenterol* 2002; **8**: 44-48
- 5 **Xiao L**, Zhou HY, Luo ZC, Liu J. Telomeric associations of chromosomes in patients with esophageal squamous cell carcinomas. *World J Gastroenterol* 1998; **4**: 231-233

- 6 **Qiao GB**, Han CL, Jiang RC, Sun CS, Wang Y, Wang YJ. Overexpression of P53 and its risk factors in esophageal cancer in urban areas of Xi' an. *World J Gastroenterol* 1998; **4**: 57-60
- 7 **Li J**, Feng CW, Zhao ZG, Zhou Q, Wang LD. A preliminary study on ras protein expression in human esophageal cancer and precancerous lesions. *World J Gastroenterol* 2000; **6**: 278-280
- 8 **Shiozaki H**, Doki Y, Kawanishi K, Shamma A, Yano M, Inoue M, Monden M. Clinical application of malignancy potential grading as a prognostic factor of human esophageal cancers. *Surgery* 2000; **127**: 552-561
- 9 **Shimada Y**, Imamura M, Watanabe G, Uchida S, Harada H, Makino T, Kano M. Prognostic factors of oesophageal squamous cell carcinoma from the perspective of molecular biology. *Br J Cancer* 1999; **80**: 1281-1288
- 10 **Helliwell TR**. Molecular markers of metastasis in squamous carcinoma. *J pathol* 2001; **194**: 289-293
- 11 **Xu M**, Jin YL, Fu J, Huang H, Chen SZ, Qu P, Tian HM, Liu ZY, Zhang W. The abnormal expression of retinoic acid receptor- β , P53 and Ki67 protein in normal, premalignant and malignant esophageal tissues. *World J Gastroenterol* 2002; **8**: 200-202
- 12 **Hao MW**, Liang YR, Liu YF, Liu L, Wu MY, Yang HX. Transcription factor EGR-1 inhibits growth of hepatocellular carcinoma and esophageal carcinoma cell lines. *World J Gastroenterol* 2002; **8**: 203-207
- 13 **Wang AH**, Sun CS, Li LS, Huang JY, Chen QS. Relationship of tobacco smoking, CYP1A1, GSTM1 gene polymorphism and esophageal cancer in Xi' an. *World J Gastroenterol* 2002; **8**: 49-53
- 14 **Igarashi M**, Dhar DK, Kubota H, Yamamoto A, El-Assal O, Nagasue N. The prognostic significance of microvessel density and thymidine phosphorylase expression in squamous cell carcinoma of the esophagus. *Cancer* 1998; **82**: 1225-1232
- 15 **Huang S**, Li JY, Wu J, Meng L, Shou CC. Mycoplasma infections and different human carcinomas. *World J Gastroenterol* 2001; **7**: 266-269
- 16 **Hirohashi S**. Inactivation of the E-cadherin-mediate cell adhesion system in human cancers. *Am J Pathol* 1998; **153**: 333-339
- 17 **Ilyas M**, Tomlinson IP. The interactions of APC, E-cadherin and beta-catenin in tumour development and progression. *J Pathol* 1997; **182**:128-137
- 18 **Wijnhoven BP**, Dinjens WN, Pignatelli M. E-cadherin-catenin cell-cell adhesion complex and human cancer. *Br J Surg* 2000; **87**: 992-1005
- 19 **Yagi T**, Takeichi M. Cadherin superfamily genes: functions, genomic organization, and neurologic diversity. *Genes Dev* 2000; **14**: 1169-1180
- 20 **Ivanov DB**, Philippova MP, Tkachuk VA. Structure and Functions of Classical Cadherin. *Biochemistry (Mosc)* 2001; **66**: 1174-1186
- 21 **Sugio K**, Kase S, Sakada T, Yamazaki K, Yamaguchi M, Ondo K, Yano T. Micrometastasis in the bone marrow of patients with lung cancer associated with a reduced expression of E-cadherin and beta-catenin : risk assessment by immunohistochemistry. *Surgery* 2002; **131** (Suppl 1): S226-231
- 22 **Natsugoe S**, Mueller J, Stein HJ, Feith M, Hofler H, Siewert JR. Micrometastasis and tumor cell microinvolvement of lymph nodes from esophageal squamous cell carcinoma: frequency, associated tumor characteristics, and impact on prognosis. *Cancer* 1998; **83**: 858-866
- 23 **Polakis P**. Wnt signaling and cancer. *Genes Dev* 2000; **14**: 1837-1851
- 24 **Peifer M**, Polakis P. Wnt signaling in oncogenesis and embryogenesis—a look outside the nucleus. *Science* 2000; **287**: 1606-1609
- 25 **Dale TC**. Signal transduction by the Wnt family of ligands. *Biochem J* 1998; **329** (Pt 2): 209-223
- 26 **Aoki M**, Hecht A, Kruse U, Kemler R, Vogt PK. Nuclear endpoint of Wnt signaling: neoplastic transformation induced by transactivating lymphoid-enhancing factor 1. *Proc Natl Acad Sci USA* 1999; **96**: 139-144
- 27 **Hecht A**, Litterst CM, Huber O, Kemler R. Functional characterization of multiple transactivating elements in beta-catenin, some of which interact with the TATA-binding protein *in vitro*. *J Biol Chem* 1999; **274**: 18017-18025
- 28 **Nakanishi Y**, Ochiai A, Akimoto S, Kato H, Watanabe H, Tachimori Y, Yamamoto S, Hirohashi S. Expression of E-cadherin, alpha-catenin, beta-catenin and plakoglobin in esophageal carcinomas and its prognostic significance: immunohistochemical analysis of 96 lesions. *Oncology* 1997; **54**: 158-165
- 29 **Tamura S**, Shiozaki H, Miyata M, Kadowaki T, Inoue M, Matsui S, Iwazawa T, Takayama T, Takeichi M, Monden M. Decreased E-cadherin expression is associated with hematogenous recurrence and poor prognosis in patients with squamous cell carcinoma of the oesophagus. *Br J Surg* 1996; **83**: 1608-1614
- 30 **Inada S**, Koto T, Futami K, Arima S, Iwashita A. Evaluation of malignancy and the prognosis of esophageal cancer based on an immunohistochemical study (p53, E-cadherin, epidermal growth factor receptor). *Surg Today* 1999; **29**: 493-503
- 31 **de Castro J**, Gamallo C, Palacios J, Moreno Bueno G, Rodriguez N, Feliu J, Gonzatez Baron M. Beta-catenin expression pattern in primary oesophageal squamous cell carcinoma. Relationship with clinicopathologic features and clinical outcome. *Virchows Arch* 2000; **437**: 599-604
- 32 **Jian WG**, Darnton SJ, Jenner K, Billingham LJ, Matthews HR. Expression of E-cadherin in oesophageal carcinomas from the UK and China: disparities in prognostic significance. *J Clin Pathol* 1997; **50**: 640-644
- 33 **Pomp J**, Blom J, van Krimpen C, Zwinderman AH, Immerzeel JJ. E-cadherin expression in esophageal carcinoma treated with high-dose radiotherapy; correlation with pretreatment parameters and treatment outcome. *J Cancer Res Clin Oncol* 1999; **125**: 641-645
- 34 **Imamura M**. Prognostic significance of CyclinD1 and E-Cadherin in patients with esophageal squamous cell carcinoma: multinstitutional retrospective analysis. Research Committee on Malignancy of Esophageal Cancer, Japanese Society for Esophageal Diseases. *J Am Coll Surg* 2001; **192**: 708-718
- 35 **Wu H**, Song X, Xiao J, Hu F, Huang W, Lu D, Xue J, Jin L. Expression of E-cadherin is associated with squamous differentiation in squamous cell carcinomas. *Anticancer Res* 2000; **20**: 1385-1390
- 36 **Gottardi CJ**, Wong E, Gumbiner BM. E-cadherin Suppresses Cellular Transformation by inhibiting β -catenin signaling in an Adhesion independent Manner. *J Cell Biol* 2001; **153**: 1049-1059
- 37 **Matsumoto M**, Natsugoe S, Nakashima S, Sakamoto F, Okumura H, Sakita H, Baba M, Takao S, Aikou T. Clinical significance of lymph node micrometastasis of pN0 esophageal squamous cell carcinoma. *Cancer Lett* 2000; **153**: 189-197
- 38 **Graft JR**, Gabrielson E, Fujii H, Baylin SB, Herman JG. Thylation patterns of the E-cadherin 5' CpG island are unstable and reflect the dynamic, heterogeneous loss of E-cadherin expression during metastatic progression. *J Biol Chem* 2000; **275**: 2727-2732
- 39 **Si HX**, Tsao SW, Lam KY, Srivastava G, Liu Y, Wong YC, Shen ZY, Cheung AL. E-cadherin expression is commonly downregulated by CpG island hypermethylation in esophageal carcinoma cells. *Cancer Lett* 2001; **173**: 71-78
- 40 **Corn PG**, Heath EL, Heitmiller R, Fogt F, Forastiere AA, Herman JG, Wu TT. Frequent hypermethylation of the 5' CpG island of E-cadherin in esophageal adenocarcinoma. *Din Cancer Res* 2001; **7**: 2765-2769
- 41 **Wijnhoven BP**, de Both NJ, van Dekken H, Tilanus HW, Dinjens WNM. E-cadherin gene mutations are rare in adenocarcinomas of the oesophagus. *Br J Cancer* 1999; **80**: 1652-1657
- 42 **Muller T**, Choidas A, Reichmann E, Ullrich A. Phosphorylation and free pool of beta-catenin are regulated by tyrosine kinases and tyrosine phosphatases during epithelial cell migration. *J Biol Chem* 1999; **274**: 10173-10183
- 43 **Ninomiya I**, Endo Y, Fushida S, Sasagawa T, Miyashita T, Fujimura T, Nishimura G, Tani T, Hashimoto T, Yagi M, Shimizu K, Ohta T, Yonemura Y, Inoue M, Sasaki T, Miwa K. Alteration of beta-catenin expression in esophageal squamous-cell carcinoma. *Int J Cancer* 2000; **85**: 757-761
- 44 **Meigs TE**, Fields TA, McKee DD, Casey PJ. Interaction of Galpha 12 and Galpha 13 with the cytoplasmic domain of cadherin provides a mechanism for beta -catenin release. *Proc Natl Acad Sci USA* 2001; **98**: 519-524
- 45 **Seeling JM**, Miller JR, Gil R, Moon RT, White R, Virshup DM. Regulation of beta-catenin signaling by me B56 subunit of protein phosphatase 2A. *Science* 1999; **283**: 2089-2091

- 46 **Letamendia A**, Labbe E, Attisano L. Transcriptional regulation by Smads: crosstalk between the TGF-beta and Wnt pathways. *J Bone Joint Surg Am* 2001; **83** (Suppl 1 Pt 1): S31-39
- 47 **Kimura Y**, Shiozaki H, Doki Y, Yamamoto M, Utsunomiya T, Kawanishi K, Fukuchi N, Inoue M, Tsujinaka T, Monden M. Cytoplasmic beta-catenin in esophageal cancers. *Int J Cancer* 1999; **84**: 174-178
- 48 **Cui J**, Zhou XD, Liu YK, Tang ZY, Zile MH. Abnormal β -catenin gene expression with invasiveness of primary hepatocellular carcinoma in China. *World J Gastroenterol* 2001; **7**: 542-546
- 49 **Krishnadath KK**, Tilanus HW, van Blankenstein M, Hop WC, Kremers ED, Dinjens WN, Bosman FT. Reduced expression of the cadherin-catenin complex in oesophageal adenocarcinoma correlates with poor prognosis. *J Pathol* 1997; **182**: 331-338
- 50 **Huiping C**, Kristjansdottir S, Jonasson JG, Magnusson J, Egilsson V, Ingvarsson S. Alterations of E-cadherin and -catenin in gastric cancer. *BMC Cancer* 2001; **1**: 16
- 51 **Zhurinsky J**, Shtutman M, Ben-Ze'ev A. Plakoglobin and beta-catenin: protein interactions, regulation and biological roles. *J Cell Sci* 2000; **113** (Pt 18): 3127-3139
- 52 **Shimazui T**, Bringuier PP, van Berkel H, Ruijter E, Akaza H, Debruyne FM, Oosterwijk E, Schalken JA. Decreased expression of alpha-catenin is associated with poor prognosis of patients with localized renal cell carcinoma. *Int J Cancer* 1997; **74**: 523-528

Edited by Wu XN

TK gene combined with mIL-2 and mGM-CSF genes in treatment of gastric cancer

Shan-Yu Guo, Qin-Long Gu, Zheng-Gang Zhu, He-Qun Hong, Yan-Zhen Lin

Shan-Yu Guo, Department of Surgery, the Affiliated Ninth People's Hospital, Shanghai Second Medical University, Shanghai, 200011, China
Qin-Long Gu, Zheng-Gang Zhu, He-Qun Hong, Yan-Zhen Lin, Department of Surgery, Shanghai Institute of Digestive Surgery, the Affiliated Ruijin Hospital, Shanghai Second Medical University, Shanghai, 200025, China

Supported by Health Ministry Scientific and Research Foundation of China, No.98-1-312

Correspondence to: Dr. Shan-Yu Guo, Department of Surgery, the Affiliated Shanghai Ninth People's Hospital, Shanghai Second Medical University, Shanghai, 200011, China. doc.g@163.com

Telephone: +86-21-63138341 Ext 5136

Received: 2002-06-29 **Accepted:** 2002-08-29

Abstract

AIM: Cancer gene therapy has received more and more attentions in the recent decade. Various systems of gene therapy for cancer have been developed. One of the most promising choices is the suicide gene. The product of thymidine kinase (TK) gene can convert ganciclovir (GCV) to phosphorylated GCV, which inhibits the synthesis of cell DNA, and then induces the cells to death. Cytokines play an important role in anti-tumor immunity. This experiment was designed to combine the TK gene and mIL-2/mGM-CSF genes to treat gastric cancer, and was expected to produce a marked anti-tumor effect.

METHODS: TK gene was constructed into the retroviral vector pLxSN, and the mIL-2 and mGM-CSF genes were inserted into the eukaryotic expressing vector pIRES. The gastric cancer cells were transfected by retroviral serum that was harvested from the package cells. *In vitro* study, the transfected gastric cancer cells were maintained in the GCV-contained medium, to assay the cell killing effect and bystander effect. *In vivo* experiment, retroviral serum and cytokines plasmid were transfected into tumor-bearing mice, to observe the changes of tumor volumes and survival of the mice.

RESULTS: *In vitro* experiment, 20 % TK gene transduced cells could cause 70-80 % of total cells to death. *In vivo* results showed that there was no treatment effect in control group and TK/GCV could inhibit the tumor growth. The strongest anti-tumor effect was shown in TK+mIL-2+mGM-CSF group. The pathologic examination showed necrosis of the cancer in the treated groups.

CONCLUSION: TK/GCV can kill tumor cells and inhibit the tumor growth *in vivo*. IL-2 and GM-CSF strongly enhance the anti-tumor effect. Through the retrovirus and liposome methods, the suicide gene and cytokine genes are all expressed in the tissues.

Guo SY, Gu QL, Zhu ZG, Hong HQ, Lin YZ. TK gene combined with mIL-2 and mGM-CSF genes in treatment of gastric cancer. *World J Gastroenterol* 2003; 9(2): 233-237
<http://www.wjgnet.com/1007-9327/9/233.htm>

INTRODUCTION

Gastric cancer is a common malignancy in China. However, all the efforts of conventional treatments including extended resection, radiation and chemotherapy have a little influence on the improvement of its survival. In searching for a new way to the treatment of such a malignant disease, the gene therapy was introduced and displayed its promising. One of the landmark discoveries is the application of suicide gene to cancer cells. It converted a nontoxic prodrug into a cell-killing compound. The herpes simplex virus type I thymidine kinase (HSV-tk) and the *Escherichia coli* cytosine deaminase (CD) was popularly used as transfected suicide gene.

The expressed products of these genes are enzymes, which can convert the nontoxic anti-ancer drugs into toxic ones, and disrupt the synthesis of target DNA. The product of TK gene can phosphorylate the ganciclovir (GCV), and it was further phosphorylated by endogenous kinase that leads to the formation of cytotoxic ganciclovir triphosphate. Interestingly, neighbor tumor cells that do not express the suicide gene were also killed in the presence of prodrug. This phenomenon is called the "bystander effect"^[1-10].

Cytokines play important roles in the anti-tumor immune responses. IL-2 can activate the NK, LAK cells and CD8⁺ T lymphocytes. The activated CD8⁺ T lymphocytes can kill tumor cells directly. GM-CSF can promote the antigen presentation to macrophage and dendritic cells in the anti-tumor immune reaction^[11-14].

The aim of this study was to boost the anti-tumor effect to achieve long-term survival and tumor eradication in model by the combination of TK/GCV with IL-2 and GM-CSF.

MATERIALS AND METHODS

Materials

The retroviral vector pLxSN was purchased from the Genetech, the HSV-TK gene was provided by Dr. Bingya Liu. LacZ gene was purchased from Promega. MFC cell line was derived from the 615 murine carcinoma of proximal stomach, and obtained from the Drug Research Institute of Chinese Science Academy. PA317 cell and NIH3T3 cells were cultured in this laboratory. Ganciclovir was purchased from Shanghai Roche Company, DMEM from Gibco, and G 418 from Promega.

Methods

Vectors and cell lines The retroviral vector is pLxSN. TK gene was inserted into the multiple cloning site between EcoR I and BamH I, which was under the control of long terminal repeat (LTR), and the neomycin resistance gene was driven by an SV40 promoter. The report gene LacZ was inserted as same as TK gene. The murine IL-2 (Mil-2) and murine GM-CSF (mGM-CSF) were cloned from murine spleen tissue, and was confirmed by DNA sequencing. They were inserted into multiple cloning site of the pIRES vector through the EcoR I and BamH I, and driven by the cytomegalovirus (CMV) promoter.

MFC cells were maintained in DMEM (Dubecco's modified essential medium), supplemented with 10 % FBS (Hangzhou

Sijiqing Biotech Company), 2 mM L-glutamine, 100 units/ml penicillin and 100 ug/ml streptomycin. PA317 cell was used as the packaging cell, and NIH 3T3 cell was used to assay the virus titre.

Packaging cells transfection, clone selection and supernatant preparation The retrovirus plasmids containing TK and LacZ gene were transfected into the PA317 packaging cell line by lipofectamine (Gibco). Clones were isolated by G418 selection. After 48hs of lipofection, the media was replaced by the media contain G418 (600 ug/ml). The media was changed every 3 days. Most cells died after 2 weeks and the transfected cells survived. Culture and generate the selected anti-G418 cells. Collect virus suspension of four generations. To infect the NIH 3T3 cell with the virus suspension in different titres. Calculate the virus titres.

Infection of MFC gastric carcinoma cell line Infection was performed in suspension by a 30 minutes incubation of MFC cells with virus dilutions in 1 ml of PBS, supplemented with 4 ug/ml polybrene. To change the medium with DMEM which contained G418 48hs later, and repeated it every 3 days. Cells started to die after one week. The infected cells survived ultimately and formed cell clones.

In vitro experiment

1. *In vitro* sensitivity to GCV: Transfected MFC cells were planted in the 96 wells plate in 1×10^4 /well. The medium containing various concentration of GCV. Cells were cultured for 7 days, and the survival rate of cells was counted by MTT method. The result was calculated by the following formula,

$$\text{Survival rate} = \frac{\text{Value of experimental group} - \text{value of control group}}{\text{The max value} - \text{value of control group}} \times 100\%$$

2. *In vitro* evaluation of the bystander effect: The transfected MFC cells were mixed with untransfected MFC cells at varying ratios, and planted in 96 wells plate at a density of 1×10^4 /well. Cells were then cultured at 37 °C for 7 days in the present of 50 µg/ml GCV. The survival rate of cells was measured by MTT method.

In vivo experiments

The mouse MFC gastric cancer models were established by injecting of 5×10^5 cells (in 100 µl saline) into the flanks of 60 6-week-old female 615 mice (the Animal Laboratory of the Institute of Drugs, Chinese Academy of Science). Five days late, when tumors became palpable, the mice were randomized in a blinded manner into 5 groups: the control group, TK, TK/GCV, TK/GCV+mIL-2, TK/GCV+mGM-CSF, and TK/GCV+mIL-2+mGM-CSF.

The test supernatant containing retrovirus was injected into tumors, 100 µl/time, twice a week, for 2 weeks. The control group was injected with saline. The cytokine plasmids were transduced with liposome. The quantity of DNA was 50 µg/time/day and the volume ratio of DNA versus liposome was 5:1. The DNA/liposome mixture was injected for 4 consecutive days. Three days after the virus infection, the animals were treated with i.p. injection of GCV (500 ng/kg/d) or saline (control group). The treatment was maintained for 3 weeks. Measure the longest radius (A) and the shortest radius (B) of tumors at every 5 days. The tumor volumes were calculated in mm³ using the formula $1/2AB^2$.

In vivo expression of the transfected genes

RNA from tissues of mice receiving TK and cytokine genes were extracted and examined by RT-PCR and agarose gel electrophoresis.

All the primers were designed by ourselves. The forward primer of TK gene was 5' -GTGAATTCACAATGGCTT-CGTACCCCTGCCAT-3', and the reverse primer of TK gene was 5' -AGTGGATCCTCAGTTAGCTCCCCCATCTCC-

3'. The forward primer of mβ-actin was 5' -TAGCGGGGTCACCCACAC-3', and the reverse primer of mβ-actin was 5' -CTAGAAGCACTTGCGGTGCACG-3'.

The reaction condition of TK gene was denaturation in 95 °C for 1 minute, annealing in 60 °C for 1 minute, and extension in 72 °C for 3 minutes, for 39 cycles. The PCR conditions for β-actin were denaturation in 95 °C for 1 minute, annealing in 55 °C for 1 minute, and extension at 72 °C for 1 minute, for 39 cycles. The products of RT-PCR were analyzed by 1 % agarose gel electrophoresis and visualized by ethidium bromide staining.

To assess the expression of mIL-2 and mGM-CSF, the mRNA was extracted from the tumor surrounding tissues of mice and examined by RT-PCR. The forward primer of mIL-2 was 5' -TCGAATTCTGTACAGCATGCAGCTC-3', the reverse primer was 5' -TGGATCCGGTACATAGTTATTGAGGGC-3'. The forward primer of mGM-CSF was 5' -CGGAATTCATGTGGCTGCAGAAT-3', and the reverse primer was 5' -CGGAATTCTTCAGAGCTGGCCTG-3'. The reaction condition was denaturation in 95 °C for 1 minute, annealing in 55 °C for 55 seconds, and extension in 72 °C for 1 minute, for 30 cycles. The products were analyzed by 1 % agarose gel electrophoresis and visualized by ethidium bromide staining.

Histological analysis and immunohistochemical studies

Samples of tumor and surrounding tissues were fixed with formalin for 24 h, wax embedded. Sections were obtained with a microtome, and stained with haematoxylin-eosin for histological analysis. The frozen samples were fixed with cold acetone for 10 minutes and immunostain with specific antibodies using peroxidase method to detect the expression of CD3⁺, CD4⁺ and CD8⁺ in infiltrating cells. The sections were incubated for 15 minutes in phosphate buffered saline (PBS), 1 % bovine serum albumin (BSA), and then overnight at 4 with monoclonal antibodies diluted in PBS/1 % BSA.

Statistical analyses

The tumor volumes were performed using the variance analysis. $P < 0.05$ was considered to be statistically significant.

RESULTS

Plasmid transduction and virus supernatant collection

The TK gene retrovirus vector plasmid was transduced into packaging cells with lipofectamine and maintained for 5-7 days in culture medium containing G418 600 mg/ml, and many cells started to death. After cultured for 2-3 weeks, some adhesive cells formed cell clones contrasted with the dead cells.

The supernatants of every clone were collected and filtered after the cell clones were selected and expanded, the number of retroviral particles produced by the different cell clones was measured by NIH 3T3 cells. The maximum titer was 2×10^5 cfu/ml.

In vitro cytotoxicity and bystander-effect

After infected by the virus supernatant, many MFC cells began to die. Some adhesive cells immersed 3 weeks later, and formed cell clones.

MFC cells expressing TK gene were assayed for sensitivity to GCV. From the second day of culture with the medium containing GCV, the TK gene transfected cells began to die, and almost all the cells died at the seventh day. The untransfected cells in control group had no marked death.

The TK gene transfected MFC cells expressing marked bystander effect. A few transfected cells can cause many co-cultured cells to death combined with GCV (50 u/ml), Twenty percent of the TK gene transfected cells could kill 70-80 % of total cells (Figure 1).

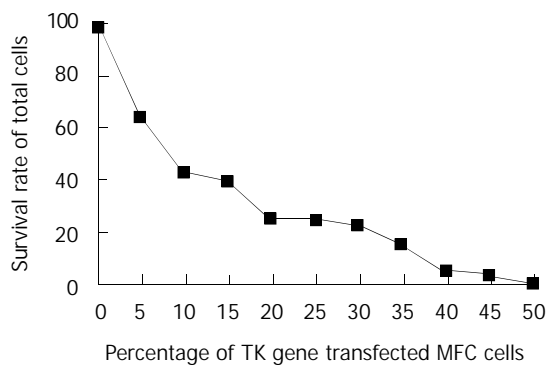


Figure 1 The bystander effect of TK transfected MFC cells.

In vivo experiment

In vivo analyses of TK/GCV and cytokines were performed in 615 mice implanted with the mouse carcinoma MFC cell line in proximal stomach. The retrovirus supernatant was injected into the tumors, and the cytokine genes were injected into the tumor surrounding tissues as indicated in the "materials and methods". There has no significant inhibition of tumor growth in control group although treated with peritoneum injection of GCV. The group of TK gene without use of GCV also had no inhibition effect on tumor growth. In the TK/GCV group, tumor growth was significantly suppressed ($P < 0.01$). In the animal groups treated with both TK/GCV and mIL-2 or mGM-CSF, there was a further significant reduction of the residual tumor size as compared to the group treated with TK/GCV ($P < 0.05$). There was further more decrease of tumor size in the group of TK/GCV combined with both cytokines. The tumors diminished in 7 mice of this group (Figure 2).

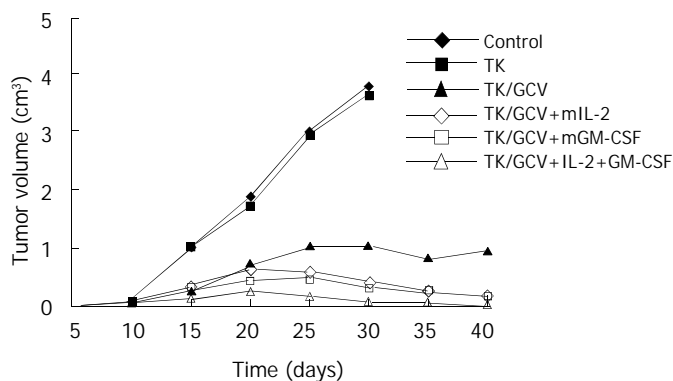


Figure 2 Compare of tumor volumes in every group.

Histological and immunohistochemical analyses

There were great many tumor cells with mitoses in the sections of control group. The TK/GCV group showed lots of necrotic cells, and some of them accompanied by bleeding. But active tumor cells could also be seen in this group. There was massive infiltration of inflammation cells surrounding the necrotic area of the tumor treated with TK + cytokine, but not in those area of animals treated with TK alone. Tumor cells diminished in most animals treated with TK/GCV+ mIL-2 + mGM-CSF. There were a few residue tumor tissues in part of these animals, but few mitoses phase can be seen, with great many of inflammatory cells.

Immunohistochemical analyses revealed that the infiltrates were mainly CD₈⁺ lymphocytes in the tumor boundary area of animals treated with TK+mIL-2 or TK+ mIL-2 + mGM-CSF. The number of CD₄⁺ lymphocytes was approximately equal in the TK + mGM-CSF and TK+mIL-2 + mGM-CSF groups.

In vivo expression of transfected genes

By RT-PCR analyses, TK gene and cytokine genes all can be expressed *in vivo* by virus transfection or liposome transduction.

DISCUSSION

Transfer suicide genes into tumors has emerged as an attractive gene therapy for the selective elimination of cancer cells. The suicide genes encode non-mammalian enzymes that can convert nontoxic prodrugs into cellular toxic metabolites. The most widely used suicide gene is HSV-tk, which confers prodrug GCV into phosphorylated GCV. The GCV monophosphate is further phosphorylated by cellular kinase, forming GCV triphosphate, which inhibits cellular DNA synthesis and lead to cell death. The "bystander effect" caused by TK gene can strongly enhance its killing capacity^[15-20]. Many researchers believe that necrosis of tumor cells is the mechanism of tumor killing effect caused by the metabolites of prodrugs, but the activated CTL can kill tumor cells as well. There also have many people think that apoptosis take an important role in the procession^[21-24]. In our studies, necrosis was shown in the prodrug used tumor tissues, some of them with bleeding. This might be the vascular endothelials transfected by suicide genes. *In vitro* experiment showed that 20 % gene transfected cells rendered 80 % of total cells to death. The mechanism of bystander effect has unclear. It has been hypothesized that the following factors may be concerned with the mechanism. (1) Gap junction: the toxic product of suicide gene was transferred from transfected cells into the surrounding untransfected ones^[25-27]. Studies demonstrated that the bystander effect of TK gene was via the gap junction. The converted phosphorylated GCV can get into the contact cells by gap junction, which needs the direct cell contact^[28-33]. (2) Apoptosis: the apoptotic acetes that released by the transfected cells engulfed by the surrounding cells^[34-37]. (3) Immune mechanism: tumor cells killed by TK/GCV can release tumor antigens. The tumor cell derived antigens were taken up by APCs (antigen presenting cells), and then presented to the CD₄⁺ T lymphocytes. It in turn activated tumor-specific CD₈⁺ cytolytic T cells. The immunohistochemistry shows tremendous aggregation of CD₄⁺ and CD₈⁺ lymphocytes surrounding the tumor tissue^[38-42].

Chen *et al* reported that cytokine gene IL-2 acted synergistically with the suicide gene to induce a systemic antitumor immunity. The immunity resulted in regression of local tumor and protection against distant site challenge of parental tumor cells. The antitumor immunity was attributed to IL-2 mediated activation and proliferation of CD₈⁺ CTLs^[43].

TK/GCV gene therapy led to death of the tumor cells. The tumor antigens were then available to the immune system, and might activate an anti-tumor immune response. The local expression of mGM-CSF enhanced the inflammatory response and antigen presentation. Expressed mIL-2 activated and enhanced the proliferation of T lymphocytes. Combination of mIL-2 with mGM-CSF can synergistically stimulate the anti-tumor immune response^[44-48].

The experimental results confirmed that TK/GCV gene therapy could kill tumor cells markedly. If combined with mIL-2 and mGM-CSF genes, they could boost the anti-tumor reaction, and produce powerful anti-tumor effects.

REFERENCES

- 1 **Roth JA**, Cristiano RJ. Gene therapy for cancer: What have we done and where are we going? *J Natl Cancer Inst* 1997; **89**: 21-39
- 2 **Huber BE**, Richards CA, Krenisky TA. Retroviral mediate gene therapy for the treatment of hepatocellular carcinoma: an innovative approach for cancer therapy. *Proc Natl Acad Sci USA* 1991; **88**: 8039-8043

- 3 **Freeman SM**, Abboud CN, Whartenby KA, Packman CH, Koeplin DS, Moolten FL, Abraham GN. The "bystander effect": tumor regression when a fraction of the tumor mass is genetically modified. *Cancer Res* 1993; **53**: 5274-5283
- 4 **Fick J**, Barker FG, Dazin P, Westphale EM, Beyer EC, Israel MA. The extent of heterocellular communication mediated by gap junctions is predictive of bystander tumor cytotoxicity *in vitro*. *Proc Natl Acad Sci USA* 1995; **92**: 11071-11075
- 5 **Gore ME**, Collins MK. Gene therapy for cancer. *Eur J Cancer* 1994; **30A**: 1047-1049
- 6 **Moolten FL**. Tumor chemosensitivity conferred by inserted herpes thymidine kinase genes; paradigm for a prospective cancer control strategy. *Cancer Res* 1986; **46**: 5276-5281
- 7 **Moolten FL**. Drug sensitivity ("suicide") genes for selective cancer chemotherapy. *Cancer Gene Ther* 1994; **1**: 279-287
- 8 **Mulligan RC**. The basic science of gene therapy. *Scienc* 1993; **260**: 926-932
- 9 **Marcel T**, Grausz JD. The TMC worldwide gene therapy enrollment report, end 1996. *Hum Gene Ther* 1997; **8**: 775-800
- 10 **Culver KW**, Ram Z, Wallbridge S, Ishii H, Oldfield EH, Blaese RM. *In vivo* gene transfect with retroviral vector producer cells for treatment of experimental brain tumors. *Science* 1992; **256**: 1550-1552
- 11 **Freeman SM**, Ramesh R, Marrogi AJ. Immune system in suicide gene therapy. *Lancet* 1997; **349**: 2-3
- 12 **Mahvi DM**, Burkholder JK, Turner J, Culp J, Malter JS, Sondel PM, Yang NS. Particle-mediated gene transfer of GM-CSF cDNA to tumor cells: implications for a clinically relevant tumor vaccine. *Hum Gene Ther* 1996; **7**: 1535-1543
- 13 **Kim TS**, Cohen EP. IL-2 secreting mouse fibroblasts transfected with genomic DNA from murine melanoma cells prolong the survival of mice with melanoma. *Cancer Res* 1994; **54**: 2531-2535
- 14 **Caio GW**, Gao J, Du P, Qi ZT, Kong XT. Construction of retroviral vectors to induce a strong expression of human class I interferon gene in human hepatocellular carcinoma cells *in vitro*. *China Natl J New Gastroenterol* 1997; **3**: 139-142
- 15 **Wei MX**, Bougnoux P, Beatrice SS, Peyrat MB, Lhuillery C, Salzman JL, Klatzmann D. Suicide gene therapy of chemically induced mammary tumor in rat: efficacy and distant bystander effect. *Cancer Res* 1998; **58**: 3529-3532
- 16 **Boucher PD**, Ruch RJ, Shewach DS. Differential ganciclovir-mediated cytotoxicity and bystander killing in human colon carcinoma cell lines expressing herpes simplex virus thymidine kinase. *Hum Gene Ther* 1998; **9**: 801-814
- 17 **Namba H**, Tagawa M, Iwadata Y, Kimura M, Sueyoshi K, Sakiyama S. Bystander effect-mediated therapy of experimental brain tumor by genetically engineered tumor cells. *Hum Gene Ther* 1998; **9**: 3-4
- 18 **Su H**, Lu R, Chang JC, Kan YW. Tissue-specific expression of herpes simplex virus thymidine kinase gene delivered by adeno-associated virus inhibits the growth of human hepatocellular carcinoma in athymic mice. *Proc Natl Acad Sci USA* 1997; **94**: 13891-13896
- 19 **Sturtz FG**, Waddell K, Shulok J, Chen X, Caruso M, Sanson M, Snodgrass HR, Platika D. Variable efficiency of the thymidine kinase/ganciclovir system in human glioblastoma cell lines: implications for gene therapy. *Hum Gene Ther* 1997; **8**: 1945-1953
- 20 **Chen CY**, Chang YN, Ryan P, Linscott M, McGarrity GJ, Chiang YL. Effect of herpes simplex virus thymidine kinase expression levels on ganciclovir-mediated cytotoxicity and the "bystander effect". *Hum Gene Ther* 1995; **6**: 1467-1476
- 21 **McMasters RA**, Saylor RL, Jones KE, Hendrix ME, Moyer MP, Drake RR. Lack of bystander killing in herpes simplex virus thymidine kinase-transduced colon cell lines due to deficient connexin43 gap junction formation. *Hum Gene Ther* 1998; **9**: 2253-2261
- 22 **Touraine RL**, Vahanian N, Ramsey WJ, Blaese RM. Enhancement of the herpes simplex virus thymidine kinase/ganciclovir bystander effect and its antitumor efficacy *in vivo* by pharmacologic manipulation of gap junctions. *Hum Gene Ther* 1998; **9**: 2385-2391
- 23 **Caruso M**, Panis Y, Gagandeep S, Houssin D, Salzman JL, Klatzmann D. Regression of established macroscopic liver metastases after *in situ* transduction of a suicide gene. *Proc Natl Acad Sci USA* 1993; **90**: 7024-7028
- 24 **Tanaka T**, Kanai F, Okabe S, Yoshida Y, Wakimoto H, Hamada H, Shiratori Y, Lan K H, Ishitobi M, Omata M. Adenovirus-mediated prodrug gene therapy for carcinoembryonic antigen-producing human gastric carcinoma cells *in vitro*. *Cancer Res* 1996; **56**: 1341-1345
- 25 **Mesnil M**, Piccoli C, Tiraby G, Wilecke K, Yamasak H. Bystander killing of cancer cells by herpes simplex virus thymidine kinase gene is mediated by connexins. *Proc Natl Acad Sci USA* 1996; **93**: 1831-1835
- 26 **Trinh QT**, Austin EA, Murray DM, Knick VC, Huber BE. Enzyme/prodrug gene therapy: comparison of CD/5-Fc versus TK/Gcv enzyme/prodrug systems in a human colorectal carcinoma cell line. *Cancer Res* 1995; **55**: 4808-4812
- 27 **Rogulski KR**, Kim JH, Kim SH, Freytag SO. Glioma cells transduced with an *E. Coli* CD/HSV-1TK fusion gene exhibit enhanced metabolic suicide and radiosensitivity. *Hum Gene Ther* 1997; **8**: 73-85
- 28 **Denning C**, Pitts JD. Bystander effects of different enzyme-prodrug systems for cancer gene therapy depend on different pathways for intercellular transfer of toxic metabolites, a factor that will govern clinical choice of appropriate regimes. *Hum Gene Ther* 1997; **8**: 1825-1835
- 29 **Yang L**, Chiang Y, Lenz HJ, Danenberg KD, Spears CP, Gordon EM, Anderson WF, Parekh D. Intercellular communication mediates the bystander effect during herpes simplex thymidine kinase/ganciclovir-based gene therapy of human gastrointestinal tumor cells. *Hum Gene Ther* 1998; **9**: 719-728
- 30 **Vile RG**, Nelson JA, Castleden S, Chong H, Hart IR. Systemic gene therapy of murine melanoma using tissue specific expression of the HSV-TK gene involved an immune component. *Cancer Res* 1994; **54**: 6228-6234
- 31 **Mullen CA**, Coale MM, Lowe R, Blaese RM. Tumor expressing the cytosine deaminase suicide gene can be eliminated *in vivo* with 5-FC and induce protective immunity to wild type tumor. *Cancer Res* 1994; **54**: 1503-1506
- 32 **Yang Y**, Nunes FA, Berencsi K, Furth EE, Gonczol E, Wilson JM. Cellular immunity to viral antigens limits E1-deleted adenovirus for gene therapy. *Proc Natl Acad Sci USA* 1994; **91**: 4407-4411
- 33 **Yang Y**, Li Q, Ertl HC, Wilson JM. Cellular and humoral immune responses to viral antigens create barriers to lung-directed gene therapy with recombinant adenoviruses. *J Virol* 1995; **69**: 2004-2015
- 34 **Mullen CA**, Kilstrup M, Blaese RM. Transfer of the bacterial gene for cytosine deaminase to mammalian cells confers lethal sensitivity to 5-fluorocytosine: a negative selective system. *Proc Natl Acad Sci USA* 1992; **89**: 33-37
- 35 **Huber BE**, Austin EA, Richards CA, Davis ST, Good SS. Metabolism of 5-fluorocytosine to 5-fluorouracil in human colorectal tumor cells transduced with the cytosine deaminase gene: significant antitumor effects when only a small percentage of tumor cells express cytosine deaminase. *Proc Natl Acad Sci USA* 1994; **91**: 8302-8306
- 36 **Consalvo M**, Mullen CA, Modesti A, Musiani P, Allione A, Cavallo F, Giovarelli M, Forni G. 5-Fluorocytosine-induced eradication of murine adenocarcinoma engineered to express the cytosine deaminase suicide gene regain host immune competence and leaves an efficient memory. *J Immunol* 1995; **154**: 5302-5312
- 37 **Plautz GE**, Yang ZY, Wu BY, Gao X, Huang L, Nabel GJ. Immunotherapy of malignancy by *in vivo* gene transfer into tumors. *Proc Natl Acad Sci USA* 1993; **90**: 4645-4649
- 38 **Ilsley DD**, Lee SH, Miller WH, Kuchta RD. A cyclic guanosine analogs inhibit DNA polymerase α , δ , and ϵ with very different potencies and have unique mechanisms of action. *Biochemistry* 1995; **34**: 2504-2510
- 39 **Ramesh R**, Marrogi AJ, Munshi A, Abboud CN, Freeman SM. *In vivo* analysis of the "bystander effect": a cytokine cascade. *Exp Hematol* 1996; **24**: 829-838
- 40 **Kianmanesh AR**, Perrin H, Panis Y, Fabre M, Nagy HJ, Houssin D, Klatzmann D. A "distant" bystander effect of suicide gene therapy: regression of nontransduced tumors together with a distant transduced tumor. *Hum Gene Ther* 1997; **8**: 1807-1814
- 41 **Wolff G**, Korner II, Schumacher A, Arnold W, Dorken B, Mapara MY. *Ex vivo* breast cancer cell purging by adenovirus-mediated

- cytosine deaminase gene transfer and short-term incubation with 5-fluorocytosine completely prevents tumor growth after transplantation. *Hum Gene Ther* 1998; **9**: 2277-2284
- 42 **Addison CL**, Braciak T, Ralston R, Muller WJ, Gaudie J, Graham FL. Intratumoral injection of an adenovirus expressing IL-2 induces regression and immunity in a murine breast cancer model. *Proc Natl Acad Sci USA* 1995; **92**: 8522-8526
- 43 **Chen SH**, Kosai K, Xu B, Khiem PN, Contant C, Finegold MJ, Woo SL. Combined suicide and cytokine gene therapy for hepatic metastasis of colon carcinoma: sustained antitumor immunity prolongs animal survival. *Cancer Res* 1996; **56**: 3758-3762
- 44 **Sobol RE**, Shawler DL, Carson C, Van Baveren C, Mercola D, Fakhrai H, Garrett MA, Barone R, Goldfarb P, Bartholomew RM, Brostoff S, Carlo DJ, Royston I, Gold DP. Interleukin 2 gene therapy of colotectal carcinoma with autologous irradiated tumor cells and genetically engineered fibroblasts: A phase I study. *Clin Cancer Res* 1999; **5**: 2359-2365
- 45 **Palu G**, Cavaggioni A, Calvi P, Franchin E, Pizzato M, Boschetto R, Parolin C, Chilosi M, Ferrini S, Zanusso A, Colombo F. Gene therapy of glioblastoma multiforme via combined expression of suicide and cytokine genes: a pilot study in humans. *Gene Ther* 1999; **6**: 330-337
- 46 **Gambotto A**, Tuting T, McVey DL, Kovesdi I, Tahara H, Lotze MT, Robbins PD. Induction of antitumor immunity by direct intratumoral injection of a recombinant adenovirus vector expressing interleukin-12. *Cancer Gene Ther* 1999; **6**: 45-53
- 47 **Saffran DC**, Horton HM, Yankauckas MA, Anderson D, Barnhart KM, Abai AM, Hobart P, Manthorpe M, Norman JA, Parker SE. Immunotherapy of established tumors in mice by intratumoral injection of IL-2 plasmid DNA: induction of CD8+ T-cell immunity. *Cancer Gene Ther* 1998; **5**: 321-330
- 48 **Shi FS**, Weber S, Gan J, Rakhmilevich AL, Mahvi DM. Granulocyte-macrophage colony-stimulating factor (GM-CSF) secreted by cDNA-transfected tumor cells induces a more potent antitumor response than exogenous GM-CSF. *Cancer Gene Ther* 1999; **6**: 81-88

Edited by Zhang JZ

Expression of 1A6 gene and its correlation with intestinal gastric carcinoma

Yi-Qiang Liu, Hong Zhao, Tao Ning, Yang Ke, Ji-You Li

Yi-Qiang Liu, Ji-You Li, Department of Pathology, Peking University school of Oncology, Beijing 100036, China

Hong Zhao, Tao Ning, Yang Ke, Laboratory of Genetics, Peking University school of Oncology, Beijing 100034, China

Supported by National Key Fundamental Research 973 Project, No1998051203 and National High Technology Research and Development Program of China (863 Program), No2001AA221121

Correspondence to: Prof. Ji-You Li, Department of Pathology, Peking University school of Oncology, Beijing 100036, China. lijyou@263.net and Prof. Yang Ke, Laboratory of Genetics, Peking University school of Oncology, Beijing 100034, China. keyang@mx.cei.gov.cn

Telephone: +86-10-88121122 Ext 2331

Received: 2002-08-13 **Accepted:** 2002-09-05

Abstract

AIM: To investigate the expression of 1A6 gene in the lesions during the development of intestinal gastric carcinoma.

METHODS: One hundred and thirty-six cases of intestinal metaplasia (IM) from surgical resections and biopsy were classified by mucous staining. Expression of 1A6 in all cases was detected using immunohistochemical S-P method.

RESULTS: The positive rates of 1A6 in normal and superficial gastritis (SG), severe atrophic gastritis (SAG), type I, II, III IM, dysplasia (Dys) and intestinal gastric carcinoma (IGC) were 12.2 %, 16.7 %, 7.1 %, 22.6 %, 47.8 %, 46.9 % and 60.8 %, respectively. A significant difference among type III IM and SG, SAG, type I and II IM was found ($P < 0.01$), the difference between type III and Dys, IGC being not significant.

CONCLUSION: As a new tumor-related gene, expression of 1A6 may be an effective parameter to predict the malignant transformation of precancerous lesion to gastric carcinoma.

Liu YQ, Zhao H, Ning T, Ke Y, Li JY. Expression of 1A6 gene and its correlation with intestinal gastric carcinoma. *World J Gastroenterol* 2003; 9(2): 238-241

<http://www.wjgnet.com/1007-9327/9/238.htm>

INTRODUCTION

Gastric cancer is a major health problem in the world^[1-3]. Clinical statistics have shown that 50 % of gastric cancer in China are intestinal type adenocarcinoma^[4]. The phenotypic events in intestinal gastric carcinoma have been well recognized as normal gastric mucosa, chronic superficial gastritis, severe atrophic gastritis, intestinal metaplasia, dysplasia, intramucosal ("early") carcinoma and invasive carcinoma^[5,6]. A considerable number of oncogenes and antioncogenes involved in this process have been described, such as c-met, p53, c-erbB-2, APC, PCNA, p16, akt etc^[7-12]. Unfortunately, they are not gastric carcinoma-specific. No significant progress has been made in the existing studies concerning special genotypic abnormalities in the premalignant

lesions of gastric carcinoma. 1A6 is a novel tumor-related gene. In this study, immunohistochemistry was used to detect the expression of 1A6 protein in IGC, its premalignant lesions and normal counterparts.

MATERIALS AND METHODS

Patients and specimens

Paraffin-embedded archival materials from surgical resections and biopsy performed during 1998 to 2001 in our department were retrieved. There were 92 cases of gastric carcinoma (62 men and 30 women; aged 29-81 years), among them 51 cases were IGC, and 41 cases were diffuse gastric carcinoma (DGC). The criterion for classifying gastric carcinoma was derived largely from the observations of Lauren^[13]. The 23 sarcoma patients consisted of 15 men and 8 women, their ages ranged from 20 to 81 years, the histopathologic types included malignant fibrohistiocytoma, leiomyosarcoma, liposarcoma, fibrosarcoma, malignant stromal tumor and malignant peripheral nerve sheath tumor. According to the updated Sydney system^[14] and the Padova International Classification for Gastric Dysplasia^[15], 198 cases from biopsy (109 men and 89 women; age ranged from 27-82 years) were divided into four groups: normal mucosal and chronic superficial gastritis (41 cases), severe atrophic gastritis without IM (24 cases), IM (136 cases) and dysplasia (32 cases).

Mucin histochemistry

We performed mucin histochemical studies on 136 cases of IM to classify them using HID/AB/PAS staining described previously^[16-19]. The variants fell into three main groups: type I (complete type) shows features of mature small intestinal epithelia, type II (incomplete small intestinal type) had features of both gastric and small intestinal epithelia, whereas type III (incomplete colonic type) has characteristics of large intestines. Neutral mucins appeared magenta in color (PAS positive), sialomucins, blue color (AB positive) and sulphomucins brown (HID positive), respectively. The criteria for classifying IM are given in Table 1.

Table 1 Classification of IM

	PAS	AB	HID
Type I	-	+	-
Type II	+	+	-
Type III	+	+	+

Immunohistochemical staining

To investigate the expression of 1A6 protein, we adopted the standard S-P immunohistochemical method^[20]. The 1A6 monoclonal antibody was provided by the Laboratory of Genetics, Beijing Institute of Cancer Research, its dilution was 1:500. The SP kit was provided by Beijing Zhongshan Biotechnology Company. All the slides were treated with PBS and were microwaved for antigen retrieval. 1A6 protein was located in nucleus. Only the samples with more than 10 % cells stained could be considered positive.

Statistical analysis

The difference of 1A6 protein expression among different lesions was analyzed by χ^2 square test. A *P* value of less than 0.05 was considered statistical significantly.

RESULTS

Expression of 1A6 protein in gastric carcinoma and sarcoma

The positive expression rate of 1A6 protein in all types of gastric carcinoma was 48.9 % (45/92). In contrast, 1A6 protein was negative in all cases of sarcoma (Figure 1). In comparison of IGC and DGC, there was significant difference ($P < 0.01$). In IGC, the positive rate was 60.8 % (31/51), whereas the positive rate in DGC was 34.1 % (14/41). Most positive cells showed a nuclear and plasmatic staining (Figure 2).

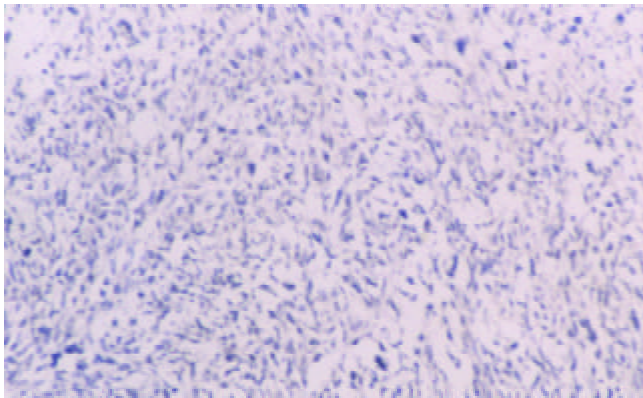


Figure 1 The expression of 1A6 protein in sarcoma. The cells were negative staining. Immunohistochemical stain, $\times 100$.

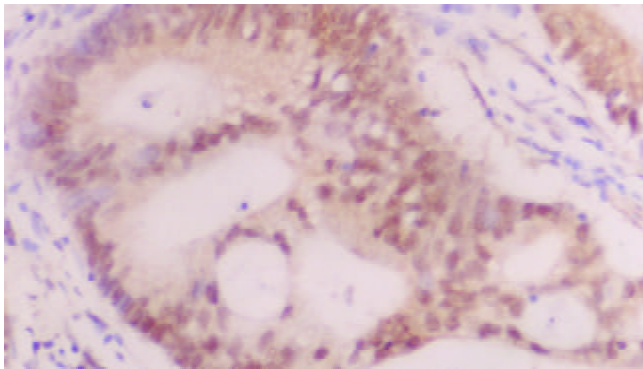


Figure 2 The expression of 1A6 protein in intestinal type gastric carcinoma. The tumor cells showed a nuclear staining. Immunohistochemical stain, $\times 400$.

Expression of 1A6 protein in intestinal metaplasia

According to the mucin histochemistry, there were 14 cases of type I IM, 53 cases of type II IM and 69 cases of type III IM. The expression of 1A6 protein in all kinds of IM is shown in Table 2 (Figures 3,4,5). The positive rate of type III was significantly higher than that of the other two types. A nuclear and plasmatic staining was also found in most positive cases (Figure 6).

Table 2 Expression of 1A6 protein in IM

	<i>n</i>	1A6(+) (%)	1A6(-) (%)
Type I	14	1 (7.1)	13(92.9)
Type II	53	12 (22.6)	41(77.4)
Type III	69	33 (47.8)	39(52.2) ^a

^a $P < 0.005$ ($\chi^2 = 7.965, 8.167$), vs type I IM, type II IM, respectively.

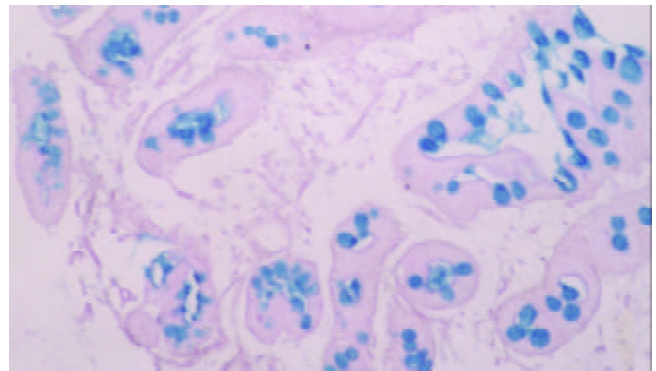


Figure 3 Type I intestinal metaplasia. The mucins in cells were stained blue. HID/AB/PAS stain, $\times 200$.

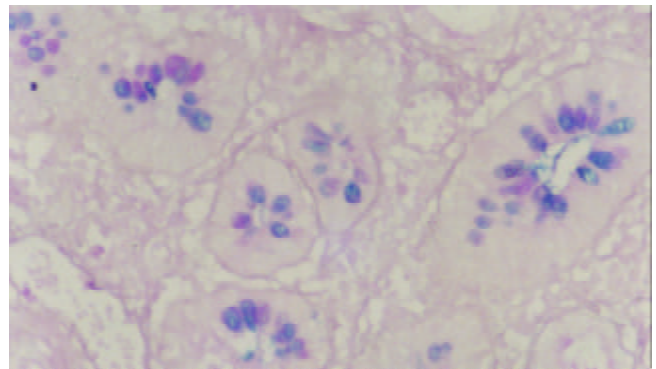


Figure 4 Type II intestinal metaplasia. The mucins in cells were stained blue and magenta. HID/AB/PAS stain, $\times 200$.

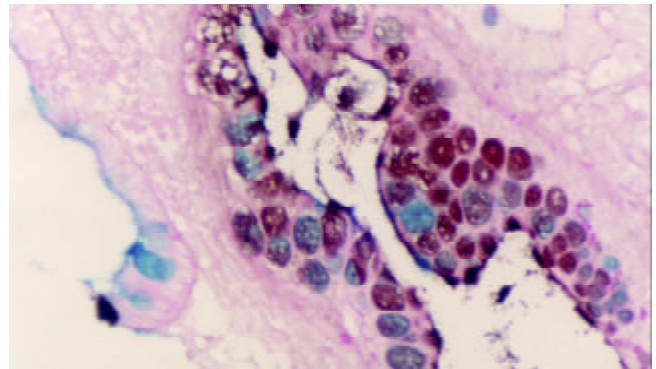


Figure 5 Type III intestinal metaplasia. The mucins in cells were stained blue and brown. HID/AB/PAS stain, $\times 200$.

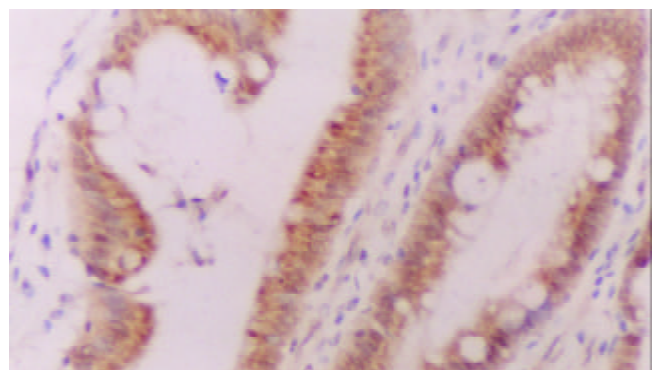


Figure 6 The expression of 1A6 protein in type III intestinal metaplasia. The metaplastic cells showed a nuclear and plasmatic staining. Immunohistochemical stain, $\times 200$.

Expression of 1A6 protein in normal mucosa and SG, SAG, type III IM, Dys and IGC

As the stomach mucosa changed from benign lesion to malignant tumor, the positive expression of 1A6 protein became higher and higher (Table 3). The positive rate of type III, Dys and IGC were higher than SG and SAG, the difference being statistically significant ($P < 0.01$). On the contrary, there were no significant differences among type III IM, Dys and IGC.

Table 3 Expression of 1A6 in different lesions of stomach

	<i>n</i>	1A6 + (%)
Normal mucosa and SG	41	5(12.2)
SAG	24	4(16.7)
Type III IM	69	33(47.8) ^a
Dys	32	15(46.9) ^b
IGC	51	31(60.8) ^c

^a $P < 0.01$ ($\chi^2 = 7.494$), vs normal mucosa and SG; ^b $P < 0.01$ ($\chi^2 = 10.067$), vs normal mucosa and SG; ^c $P < 0.01$ ($\chi^2 = 16.298$), vs normal mucosa and SG.

DISCUSSION

Recently, many investigations concerning intestinal metaplasia of stomach have been made in different aspects such as epidemiology, pathology and molecular biology^[21-23]. Although there were controversies about the phenotypic and genotypic events of IM, it has been widely accepted that the incomplete colonic type IM plays an important role in the histogenesis of gastric carcinoma and it is considered as the premalignant lesion of intestinal gastric carcinoma^[21, 24-28].

Gene 1A6 is a novel tumor-associated gene cloned from malignant cell line MC, which is an MNNG-treated human fetal gastric epithelial cell line. 1A6 is located in chromosome 12q23.2-23.3. Its cDNA is about 3kb. There are HEAT motif and nucleus-located sequence in 1A6 protein by molecular sequence analysis. 1A6 protein nucleus localization was further confirmed by immunofluorescence and immuno-electron microscopy. It was found in nucleole and heterochromatin. It suggested that 1A6 protein could interact with other proteins and may play a role as a nuclear transcription factor. Immunohistochemical studies in different tumors indicated that 1A6 was expressed not only in gastric carcinoma, but also in esophageal and breast cancers^[29-31].

As mentioned above, type III IM is thought to be the premalignant lesion of gastric carcinoma^[32-35]. In our study, the positive expression rate of 1A6 protein was very high in type III IM, which suggests that the overexpression of gene 1A6 maybe an early event in gastric malignant transformation. It can be an important index for predicting the carcinogenesis of stomach. How 1A6 protein functions in transformation of the intestinal metaplasia tissue into malignant tumor and the interaction between other oncogenes and antioncogenes need further investigation and the work is undergoing.

In this study, it was found that although the positive expression rate of 1A6 protein in DGC was much lower than that of IGC, one third of them were positive too. These results indicate that as gastric carcinoma, IGC and DGC may share some common characteristics, although their biological characteristics and etiological molecular mechanism are very different. In 23 cases of sarcoma, the positive rate was 0%, it is no doubt that 1A6 protein is epithelial-tumor-specific.

In this study, many positive cells showed both nuclear and plasmatic staining. There are three possibilities: (1) The synthesis of nuclear proteins takes place in cell plasma, and then transmit into the nucleus, the plasmatic positivity might

reflect the newly synthesized 1A6 protein. (2) Non-specific binding of 1A6 Ab with other plasmatic proteins. (3) Non-specific secondary Ab binding with the proteins in the plasma.

In conclusion, 1A6 is a new tumor-related gene, its expression may play an important role in the early stage of gastric carcinogenesis. The detection of 1A6 protein in the premalignant lesions of intestinal gastric carcinoma may be a very valuable index to predict the malignant transformation of these lesions.

REFERENCES

- Nie YZ**, He FT, Li ZK, Wu KC, Cao YX, Chen BJ, Fan DM. Identification of tumor associated single-chain Fv by panning and screening antibody phage library using tumor cells. *World J Gastroenterol* 2002; **8**: 619-623
- Deng DJ**. Progress of gastric cancer etiology: N-nitrosamides in the 1990s. *World J Gastroenterol* 2000; **6**: 613-618
- Chen GY**, Wang DR. The expression and clinical significance of CD44v in human gastric cancers. *World J Gastroenterol* 2000; **6**: 125-127
- Si JM**, Zhou W, Wu JG, Cao Q, Xiang Z, Jiang L, Lu W, Huang H. Establishment of an animal model of chronic atrophic gastritis and a study on the factors inducing atrophy. *Chin Med J* 2001; **114**: 1323-1325
- Correa P**. A human model of gastric carcinogenesis. *Cancer Res* 1988; **48**: 3554-3560
- Correa P**. Human gastric carcinogenesis: A multistep and multifactorial process-First american cancer society award lecture on cancer epidemiology and prevention. *Cancer Res* 1992; **52**: 6735-6740
- Correa P**, Shiao YH. Phenotypic and genotypic events in gastric carcinogenesis. *Cancer Res* 1994; **54**: 1941s-1943s
- Tahara E**. Molecular biology of gastric cancer. *World J Surg* 1995; **19**: 484-488
- Wu MS**, Shun CT, Lee WC, Chen CJ, Wang HP, Lee WJ, Sheu JC, Lin JT. Overexpression of p53 in different subtypes of intestinal metaplasia and gastric cancer. *Br J Cancer* 1998; **78**: 971-973
- Xu AG**, Li SG, Liu JH, Gan AH. Function of apoptosis and expression of the proteins Bcl-2, p53 and C-myc in the development of gastric cancer. *World J Gastroenterol* 2001; **7**: 403-406
- Ji F**, Peng QB, Zhan JB, Li YM. Study of differential polymerase chain reaction of C-erbB-2 oncogene amplification in gastric cancer. *World J Gastroenterol* 1999; **5**: 152-155
- He XS**, Su Q, Chen ZC, He XT, Long ZF, Ling H, Zhang LR. Expression, deletion and mutation of p16 gene in human gastric cancer. *World J Gastroenterol* 2001; **7**: 515-521
- Lauren P**. The two histologic main types of gastric carcinoma: diffuse and so-called intestinal type carcinoma. An attempt at a histoclinical classification. *Acta Pathol Microbiol Scand* 1965; **64**: 31-49
- Dixon MF**, Genta RM, Yardley JH, Correa P. Classification and grading of gastritis: the Updated Sydney System. *Am J Surg Pathol* 1996; **20**: 1161-1181
- Rugge M**, Correa P, Dixon MF, Hattori T, Leandro G, Lewin K, Diddell RH, Sipponen P, Watanabe H. Gastric dysplasia: the Padova International Classification. *Am J Surg Pathol* 2000; **24**: 167-176
- Jass JR**. Role of intestinal metaplasia in the histogenesis of gastric carcinoma. *J Clin Pathol* 1980; **33**: 801-810
- Xin Y**, Li XL, Wang YP, Zhang SM, Zheng HC, Wu DY, Zhang YC. Relationship between phenotypes of cell-function differentiation and pathobiological behavior of gastric carcinomas. *World J Gastroenterol* 2001; **7**: 53-59
- Byrne JP**, Bhatnagar S, Hamid B, Armstrong GR, Attwood SE. Comparative study of intestinal metaplasia and mucin staining at the cardia and esophagogastric junction in 225 symptomatic patients presenting for diagnostic open-access gastroscopy. *Am J Gastroenterol* 1999; **94**: 98-103
- Shaoul R**, Marcon P, Okada Y, Cutz E, Forstner G. The pathogenesis of duodenal gastric metaplasia: the role of local goblet cell transformation. *Gut* 2000; **46**: 632-638
- Taylor CR**, Kledzik G. Immunohistologic techniques in surgical pathology: A spectrum of "new" special stains. *Hum Pathol* 1981;

- 12: 590-596
- 21 **Stemmermann GN.** Intestinal metaplasia of the stomach: a status report. *Cancer* 1994; **74**: 556-564
- 22 **Yao YL, Xu B, Song YG, Zhang WD.** Overexpression of cyclin E in Mongolian gerbil with *Helicobacter pylori*-induced gastric precancerosis. *World J Gastroenterol* 2002; **8**: 60-63
- 23 **Stemmermann GN, Nomura AM, Kolonel LN, Goodman MT, Wilkens LR.** Gastric carcinoma: pathology findings in a multiethnic population. *Cancer* 2002; **95**: 744-750
- 24 **Sipponen P.** Gastric cancer: pathogenesis, risks, and prevention. *J Gastroenterol* 2002; **37** (Suppl): 39-44
- 25 **Leung WK, Yu L, Chan FK, To KF, Chan MW, Ebert MP, Ng EK, Chung SC, Malfertheiner P, Sung JJ.** Expression of trefoil peptides (TFF1, TFF2, and TFF3) in gastric carcinoma, intestinal metaplasia, and non-neoplastic gastric tissues. *J Pathol* 2002; **197**: 582-588
- 26 **Leung WK, Sung JJ.** Intestinal metaplasia and gastric carcinogenesis. *Aliment Pharmacol Ther* 2002; **16**: 1209-1216
- 27 **Takahashi H, Endo T, Yamashita K, Arimura Y, Yamamoto H, Sasaki S, Itoh F, Hirata K, Imamura A, Kondo M, Sato T, Imai K.** Mucin phenotype and microsatellite instability in early multiple gastric cancers. *Int J Cancer* 2002; **100**: 419-424
- 28 **Dixon MF.** Prospects for intervention in gastric carcinogenesis: reversibility of gastric atrophy and intestinal metaplasia. *Gut* 2001; **49**: 2-4
- 29 **Zhao H, Hagiwara K, Mcmenamin M, Ning T, Zheng SH, Harris CC, Ke Y.** Function study of a novel tumor-related gene 1A6. Poster, AACR 91st annual meeting
- 30 **Groves MR, Barford D.** Topological characteristics of helical proteins. *Curr Opin Struct Biol* 1999; **9**: 383-389
- 31 **Murzin AG, Patty L.** Sequence and topology: from sequence to structure to function. *Curr Opin Struct Biol* 1999; **9**: 359-363
- 32 **Palli D.** Epidemiology of gastric cancer: an evaluation of available evidence. *J Gastroenterol* 2000; **35** (Suppl 12): 84-89
- 33 **El-Zimaity HM, Ota H, Graham DY, Akamatsu T, Katsuyama T.** Patterns of gastric atrophy in intestinal type gastric carcinoma. *Cancer* 2002; **94**: 1428-1436
- 34 **Silva E, Teixeira A, David L, Carneiro F, Reis CA, Sobrinho-Simoes J, Serpa J, Veerman E, Bolscher J, Sobrinho-Simoes M.** Mucins as key molecules for the classification of intestinal metaplasia of the stomach. *Virchows Arch* 2002; **440**: 311-317
- 35 **van Rees BP, Saukkonen K, Ristimaki A, Polkowski W, Tytgat GN, Drilenburg P, Offerhaus GJ.** Cyclooxygenase-2 expression during carcinogenesis in the human stomach. *J Pathol* 2002; **196**: 171-179

Edited by Ma JY

The study of chemiluminescence in gastric and colonic carcinoma cell lines treated by anti-tumor drugs

Che Chen, Fu-Kun Liu, Xiao-Ping Qi, Jie-Shou Li

Che Chen, Fu-Kun Liu, Xiao-Ping Qi, Jie-Shou Li, Nanjing University School of Medicine, Department of General Surgery, Jinling Hospital, 305 Zhongshandong Road, Nanjing 210002, Jiangsu Province, China

Supported by the Natural Scientific Foundation of Jiangsu Province, No. BJ2000040

Correspondence to: Che Chen, Department of General Surgery, Jinling Hospital, 305 Zhongshandong Road, Nanjing 210002, China. drchenche@sohu.com

Telephone: +86-25-4826808-58005

Received: 2002-04-29 **Accepted:** 2002-09-05

Abstract

AIM: To study the influence of chemotherapy on proliferation activation of tumor cell by observing the change of chemiluminescence (CL) and cell cycle in various tumor cell lines after mitomycin C treated.

METHODS: BGC823 and LoVo cell lines were all cultured in RPMI-1640, and then were adjusted to a concentration of 1×10^5 cells/ml in fresh media and incubated for 24 h. Mitomycin C ($100 \text{ ng} \cdot \text{ml}^{-1}$) was added to each bottle. All indeses were examined after 24 h. No Mitomycin C was added in control group. Each group contained 8 samples. Flow cytometric analysis and luminol-dependent CL were used to investigate the effect of mitomycin C on two gastrointestinal carcinoma cell lines.

RESULTS: BGC823 and LoVo cell lines incubated with MMC for 24 h. We discovered that the emergence of peak of CL stimulated by PHA was postponed significantly (BGC823: 12.63 ± 3.21 vs 4.50 ± 1.04 , LoVo: 13.25 ± 2.96 vs 5.12 ± 1.36 , $P < 0.01$) and the peak intension of CL was reduced significantly (BGC823: 120.25 ± 16.61 vs 248.38 ± 29.17 , LoVo: 98.13 ± 10.49 vs 267.50 ± 18.56 , $P < 0.01$). The PI of cell lines was decreased significantly (BGC823: 51.87 ± 4.82 vs 25.44 ± 2.26 , LoVo: 47.11 ± 1.04 vs 24.23 ± 0.37 , $P < 0.01$) and the apoptotic fractions changed by contraries (BGC823: 26.25 ± 5.29 vs 9.83 ± 2.51 , LoVo: 33.50 ± 3.68 vs 9.63 ± 1.44 , $P < 0.01$).

CONCLUSION: CL can be used to measure activation of tumor cells. We discovered that the ground CL intensions of two cell lines were not high but increased rapidly after stimulation of PHA. The CL peak ranged from 4-5 minutes, and then decreased gradually. The results were not reported before. CL of tumor cell has close correlativity with the dynamics of cell cycle and can reflect the feature of oxidation metabolism and proliferation activation of tumor cell. So it can be used to observe the influence of chemotherapy drug on metabolism and proliferation activation of tumor cell and screen out chemotherapy drugs to which tumor cells are sensitive.

Chen C, Liu FK, Qi XP, Li JS. The study of chemiluminescence in gastric and colonic carcinoma cell lines treated by anti-tumor drugs. *World J Gastroenterol* 2003; 9(2): 242-245
<http://www.wjgnet.com/1007-9327/9/242.htm>

INTRODUCTION

Chemiluminescence (CL) is a natural phenomenon of creatures^[1]. As other cells, tumor cells also have the ability of CL. So the vigor of tumor cells could be measured by CL. At present, there were few reports about the CL of tumor cells^[2]. We used gastric and colonic carcinoma cell lines to study the CL of tumor cells and to investigate the dynamics of CL and the influence of drugs on CL.

MATERIALS AND METHODS

Cell line

BGC823 is a kind of human gastric carcinoma cell line^[3-5]; LoVo is a kind of human colonic carcinoma cell line^[6,7]. We bought them from Shanghai Cell Biology Institute of the Chinese Academy of Sciences.

Cell culture and mitomycin C treatment

Two cell lines were all cultured in RPMI-1640 (GIBCO) containing $100 \text{ g} \cdot \text{L}^{-1}$ newborn calf serum (Sijiqing, Hangzhou), penicillin ($100 \text{ U} \cdot \text{ml}^{-1}$), and streptomycin ($100 \text{ } \mu\text{g} \cdot \text{ml}^{-1}$). Log phase cells were adjusted to a concentration of 1×10^5 cells/ml in fresh media and incubated for 24 h. Mitomycin C ($100 \text{ ng} \cdot \text{ml}^{-1}$)^[8] was added to each bottle. All indeses were examined after 24 h. No Mitomycin C was added in control group. Each group contained 8 samples.

CL analysis

Media was removed and cells were washed in phenol red free D-Hank's solution three times and adjusted to a concentration of 1×10^3 cells $\cdot \text{ml}^{-1}$ in the same solution. Aliquots (0.1 ml) of this cell suspension were placed into a cuvette, to which 0.7 ml of phenol red free D-Hank's solution and 0.1 ml of luminol ($1 \text{ mmol} \cdot \text{L}^{-1}$) were added. All cuvettes were put into sample chamber of SHG-1 bio-luminometer (Shangli measure instrument factory). CL of tumor cell was measured using T-2 procedure, configuring measure times were 30 and interval was 60 seconds. At first background of CL was measured, then 0.1 ml of phaseolus vulgaris agglutinin (PHA, $4 \text{ mg} \cdot \text{L}^{-1}$) was added and shaken up rapidly. CL PHA stimulated was measured continuously for about 30 minutes. All assays were made at $37 \text{ }^\circ\text{C}$. After measurements completed, CL kinetics curve, peak value, peak time, slope function and integral were calculated using the computer. Unit of intension of CL was scintillation counting per minute^[9] (Figure 1).

Flow cytometric analysis

Cells were harvested and washed in D-Hank's solution three times and adjusted to a concentration of 1×10^6 cells $\cdot \text{ml}^{-1}$ in the same solution. The nuclei were stained with propidium iodide at a concentration of $50 \text{ } \mu\text{g} \cdot \text{ml}^{-1}$ and then filtered through $40 \text{ } \mu\text{m}$ nylon mesh before flow cytometric analysis^[10]. The nuclear DNA content was analyzed with a flow cytometer (Epics XL; Coulter Co. U.S.A); 1×10^6 cells were examined in each sample. The cell cycle distribution, i.e., G_0/G_1 , S, G_2/M were analyzed using a computer program (Multicycle). The mean coefficient of variation (CV) for the G_0/G_1 peak was less than 8.0 in all

cases^[11]. We assessed the proliferation index (PI) to evaluate the changes of cell cycle distribution caused by treatment of MMC.

$$PI = \frac{S+G_2M}{S+G_2M+G_0G_1} \times 100\%$$
 We used the fraction of subdiploid peak in front of DNA histograms as apoptotic fraction^[12].

Statistical analysis

Statistical analysis, i.e., one-way ANOVA, unpaired *t*-test, correlate analysis, was performed using SPSS 8.0. Data were presented as means ± standard deviation (S.D.). The level of significance was *P*<0.05.

RESULTS

CL analysis

Figure 1 and Table 1 show the time-course of CL change in control and treatment groups of BGC823. In control group a CL signal was noted almost immediately that peaked within 3-5 minutes and returned to baseline after about 10-15 min. In contrast treatment group cells responded slowly and the peak CL did not occur until after 11-18 min. The CL peak value in treatment group decreased significantly (*P*<0.01) when compared with control group. The same changes were detected in all two cell lines.

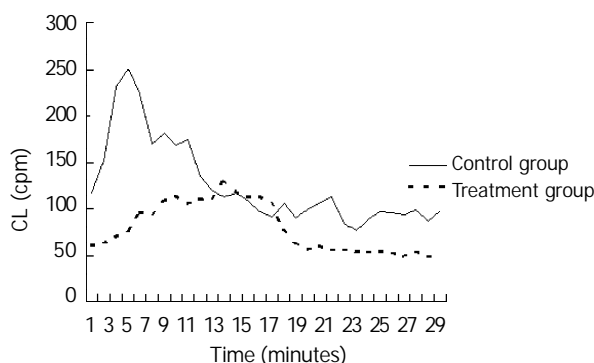


Figure 1 Time-course of CL change in control and treatment groups of BGC823.

Table 1 Effects of MMC treatment on CL of two cell lines

	BGC823 (n=8)		LoVo (n=8)	
	Control	Treatment	Control	Treatment
Peak value (cpm)	248.38±29.17	120.25±16.61 ^a	267.50±18.56	98.13±10.49 ^a
Peak time (minute)	4.50±1.04	12.63±3.21 ^a	5.12±1.36	13.25±2.96 ^a

^a*P*<0.01, vs control.

Flow cytometric analysis

The PI in treatment group decreased significantly and the apoptotic fraction increased significantly when compared with control group (*P*<0.01). There was no significant difference in the change of cell cycle contribution between two cell lines (Table 2).

Table 2 Effects of MMC treatment on cell cycle distribution of two cell lines

	BGC823		LoVo	
	Control	Treatment	Control	Treatment
PI (%)	51.87±4.82	25.44±2.26 ^a	47.11±1.04	24.23±0.37 ^a
Apoptosis (%)	9.83±2.51	26.25±5.29	9.63±1.44	33.50±3.68

^a*P*<0.01, vs control.

Correlations between CL and cell cycle distribution

There was positive correlation between CL and PI (BGC823: *r*=0.92, *P*<0.01; LoVo: *r*=0.90, *P*<0.01), and there was negative correlation between CL and apoptotic fraction (BGC823: *r*=-0.91, *P*<0.01; LoVo: *r*=-0.95, *P*<0.01) (Figures 2-5).

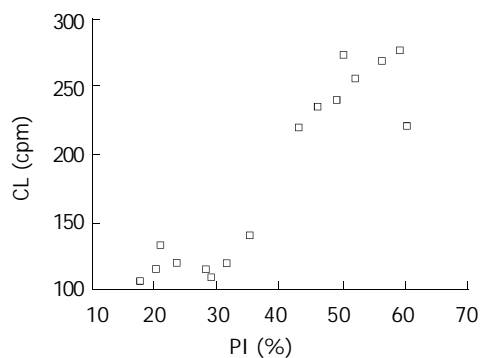


Figure 2 Correlations between CL and PI in BGC823.

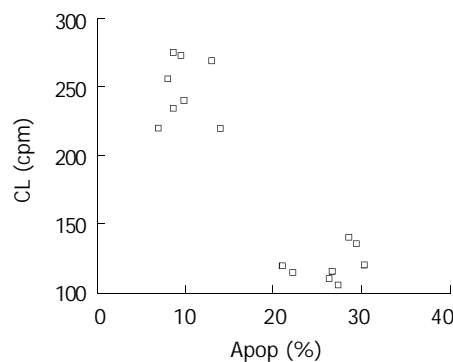


Figure 3 Correlations between CL and apoptotic fraction in BGC823.

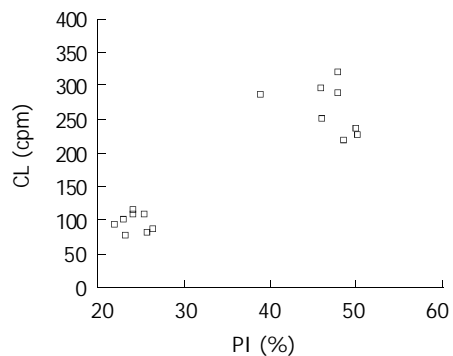


Figure 4 Correlations between CL and PI in LoVo.

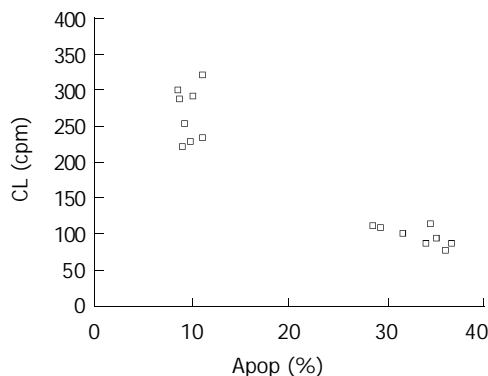


Figure 5 Correlations between CL and Apoptotic fraction in LoVo.

DISCUSSION

Oxygen radicals (OR) are intermediary products in the biochemical metabolism of cells, including O_2^- , H_2O_2 , OH^\cdot , 1O_2 , OCl^- and lipid peroxidation oxygen radical^[13]. They are produced mainly by aerobic respiration in mitochondrion and glycolysis^[14,15]. OR reacts to excitable substance in cells and produces CL ^[16]. So we can observe activation of cells by the measurement of CL ^[17,18].

In the present study, luminol-dependent chemiluminescence was used as a measure of CL of human gastric carcinoma cell line BGC823 and human colonic carcinoma cell line LoVo. We discovered that the ground CL intensions of two cell lines were not high but increased rapidly after stimulation of PHA. The CL peak ranged from 4-5 minutes, then decreased gradually. The results were not reported before.

Mitomycin C is a cycle-nonspecific anti-tumor agent. The mechanism of anti-cancer effect is its alkylation which makes DNA incorporation and DNA replication inhibition and single strand rupture. MMC affects mainly G1 and early S phases. However the influence of MMC on cell cycle *in vitro* may be different in different cells^[19-22]. MMC also up-regulated EpCAM and LewisY antigen expression in LoVo cell line^[23]. Cell cultures were growth arrested by exposure for 5 minutes to MMC^[24], and MMC retains its antiproliferative effect for at least 6 weeks^[25].

The CL of BGC823 and LoVo cell lines were decreased significantly after incubated with MMC for 24 hours. We also discovered that the peak of CL was postponed significantly and the peak intension of CL was reduced significantly after the stimulation of PHA. At the same time, the proliferation index (PI) was decreased significantly and apoptotic fractions changed by contraries^[26]. There was positive correlation between CL and PI, and there was negative correlation between CL and apoptotic fraction. These results revealed that the proliferation activation of tumor cell reduced, the apoptosis of cells increased and the reaction to stimulation of PHA weakened when the concentration of oxygen radicals in tumor cell decreased^[27-29]. So the decrease of concentration of oxygen radicals in low range depressed the mitochysis of tumor cell^[30] and prompted the apoptosis of tumor cell. These results also suggest the CL of cell can reflect change of proliferation activation of tumor cell treated by chemotherapy drugs.

In conclusion, the CL of tumor cell can reflect the feature of oxidation metabolism and proliferation activation of tumor cell, can be used to observe the influence of chemotherapy drug on metabolism and proliferation activation of tumor cell and screen out chemotherapy drugs to which tumor cells are sensitive. Compared with other methods cell chemiluminescence is more sensitive, more accurate, more rapid, less pollution and need fewer samples.

REFERENCES

- 1 **Li QG**. The physical chemistry principle of bioluminescence and chemiluminescence. In: Hu TX, eds. Luminescence analysis and medicine. Shanghai: East China Normal University Press 1990: 1-2
- 2 **Meyskens FL Jr**, Chau HV, Tohidian N, Buckmeier J. Luminol-enhanced chemiluminescent response of human melanocytes and melanoma cells to hydrogen peroxide stress. *Pigment Cell Res* 1997; **10**: 184-189
- 3 **Li QF**, Ouyang GL, Li CY, Hong SG. Effects of tachyplesin on the morphology and ultrastructure of human gastric carcinoma cell line BGC-823. *World J Gastroenterol* 2000; **6**: 676-680
- 4 **Liu S**, Wu Q, Chen ZM, Su WJ. The effect pathway of retinoic acid through regulation of retinoic acid receptor α in gastric cancer cells. *World J Gastroenterol* 2001; **7**: 662-666
- 5 **Li QF**, Ouyang GL, Li CY, Hong SG. Effects of tachyplesin on the morphology and ultrastructure of the human gastric carcinoma cell line BGC-823. *World J Gastroenterol* 2000; **6**(Suppl 3): 66

- 6 **Fan YF**, Huang ZH. Angiogenesis inhibitor TNP-470 suppresses growth of peritoneal disseminating foci of human colon cancer line Lov0. *World J Gastroenterol* 2002; **8**: 853-856
- 7 **Chen XX**, Lai MD, Zhang YL, Huang Q. Less cytotoxicity to combination therapy of 5-fluorouracil and cisplatin than 5-fluorouracil alone in human colon cancer cell lines. *World J Gastroenterol* 2002; **8**: 841-846
- 8 **Spraul CW**, Kaven C, Amann J, Lang GK, Lang GE. Effect of insulin-like growth factors 1 and 2, and glucose on the migration and proliferation of bovine retinal pigment epithelial cells *in vitro*. *Ophthalmic Res* 2000; **32**: 244-248
- 9 **Zheng RL**. Free radicals involvement in carcinogenesis. In: Zheng RL, eds. Advances in free radical life sciences. Vol. 6. Beijing: Atomic Energy Press 1998: 72-77
- 10 **Chen JP**, Lin C, Xu CP, Zhang XY, Wu M. The therapeutic effects of recombinant adenovirus RA538 on human gastric carcinoma cells *in vitro* and *in vivo*. *World J Gastroenterol* 2000; **6**: 855-860
- 11 **Han Y**, Han ZY, Zhou XM, Shi R, Zheng Y, Shi YQ, Miao JY, Pan BR, Fan DM. Expression and function of classical protein kinase C isoenzymes in gastric cancer cell line and its drug-resistant sublines. *World J Gastroenterol* 2002; **8**: 441-445
- 12 **Loo DT**, Rillema JR. Measurement of cell death. *Methods Cell Biol* 1998; **57**: 251-264
- 13 **Li JM**, Cai Q, Zhou H, Xiao GX. Effects of hydrogen peroxide on mitochondrial gene expression of intestinal epithelial cells. *World J Gastroenterol* 2002; **8**: 1117-1122
- 14 **Wu YL**, Sun B, Zhang XJ, Wang SN, He HY, Qiao MM, Zhong J, Xu JY. Growth inhibition and apoptosis induction of Sulindac on Human gastric cancer cells. *World J Gastroenterol* 2001; **7**: 796-800
- 15 **Li HL**, Chen DD, Li XH, Zhang HW, Lü YQ, Ye CL, Ren XD. Changes of NF- κ B, p53, Bcl-2 and caspase in apoptosis induced by JTE-522 in human gastric adenocarcinoma cell line AGS cells: role of reactive oxygen species. *World J Gastroenterol* 2002; **8**: 431-435
- 16 **Vidon DJ**, Donze S, Muller C, Entzmann A, Andre P. A simple chemiluminescence-based method for rapid enumeration of *Listeria* spp. microcolonies. *J Appl Microbiol* 2001; **90**: 988-993
- 17 **Mytar B**, Siedlar M, Woloszyn M, Ruggiero I, Pryjma J, Zembala M. Induction of reactive oxygen intermediates in human monocytes by tumour cells and their role in spontaneous monocyte cytotoxicity. *Br J Cancer* 1999; **79**: 737-743
- 18 **Shepard SL**, Noble AL, Filbey D, Hadley AG. Inhibition of the monocyte chemiluminescent response to anti-D-sensitized red cells by Fc gamma RI-blocking antibodies which ameliorate the severity of haemolytic disease of the newborn. *Vox Sang* 1996; **70**: 157-163
- 19 **Takahashi N**, Murayama T, Oda M, Miyakoshi M. Cell growth inhibition and DNA incorporation of mitomycin C in cell culture. *Ophthalmic Res* 1998; **30**: 120-125
- 20 **Machl AW**, Planitzer S, Kubies M. A novel, membrane receptor-based retroviral vector for Fanconi anemia group C gene therapy. *Gene Ther* 1997; **4**: 339-345
- 21 **Schlmeyer U**, Meister A, Beisker W, Wobus AM. Low mutagenic effects of mitomycin C in undifferentiated embryonic P19 cells are correlated with efficient cell cycle control. *Mutat Res* 1996; **354**: 103-112
- 22 **Clarke AA**, Philpott NJ, Gordon-Smith EC, Rutherford TR. The sensitivity of Fanconi anaemia group C cells to apoptosis induced by mitomycin C is due to oxygen radical generation, not DNA crosslinking. *Br J Haematol* 1997; **96**: 240-247
- 23 **Flieger D**, Hoff AS, Sauerbruch T, Schmidt-Wolf IG. Influence of cytokines, monoclonal antibodies and chemotherapeutic drugs on epithelial cell adhesion molecule (EpCAM) and LewisY antigen expression. *Clin Exp Immunol* 2001; **123**: 9-14
- 24 **Daniels JT**, Occleston NL, Crowston JG, Khaw PT. Effects of antimetabolite induced cellular growth arrest on fibroblast-fibroblast interactions. *Exp Eye Res* 1999; **69**: 117-127
- 25 **Woo E**, Tingey DP, Mackenzie G, Hooper P. Stability of the antiproliferative effect of mitomycin-C after reconstitution. *J Glaucoma* 1997; **6**: 33-36

- 26 **Tokunaga E**, Oda S, Fukushima M, Maehara Y, Sugimachi K. Differential growth inhibition by 5-fluorouracil in human colorectal carcinoma cell lines. *Eur J Cancer* 2000; **36**: 1998-2006
- 27 **Winters MD**, Schlinke TL, Joyce WA, Glore SR, Huycke MM. Prospective case-cohort study of intestinal colonization with enterococci that produce extracellular superoxide and the risk for colorectal adenomas or cancer. *Am J Gastroenterol* 1998; **93**: 2491-2500
- 28 **Edmiston KH**, Shoji Y, Mizoi T, Ford R, Nachman A, Jessup JM. Role of nitric oxide and superoxide anion in elimination of low metastatic human colorectal carcinomas by unstimulated hepatic sinusoidal endothelial cells. *Cancer Res* 1998; **58**: 1524-1531
- 29 **Izutani R**, Katoh M, Asano S, Ohyanagi H, Hirose K. Enhanced expression of manganese superoxide dismutase mRNA and increased TNFalpha mRNA expression by gastric mucosa in gastric cancer. *World J Surg* 1996; **20**: 228-233
- 30 **Burdon RH**. Superoxide and hydrogen peroxide in relation to mammalian cell proliferation. *Free Radic Biol Med* 1995; **18**: 775-794

Edited By Yuan HT

Association of cyclooxygenase-2 expression with *Hp-cagA* infection in gastric cancer

Xiao-Lin Guo, Li-Er Wang, Shu-Yan Du, Chen-Ling Fan, Li Li, Peng Wang, Yuan Yuan

Xiao-Lin Guo, Yuan Yuan, Cancer Institute, The First Hospital, China Medical University, Shenyang, 110001, Liaoning Province, China
Shu-Yan Du, Chen-Ling Fan, Li-Er Wang, Li Li, Peng Wang, Center Laboratory, The First Hospital, China Medical University, Shenyang, 110001, Liaoning Province, China
Supported by The National Basic Research Program (973) of China, No. G1998051203

Correspondence to: Dr. Yuan Yuan, Cancer institute, the First Hospital, China Medical University, Shenyang, 110001, Liaoning Province, China. yyuan@mail.cmu.edu.cn

Telephone: +86-24-23256666-6153

Received: 2002-04-18 **Accepted:** 2002-06-03

Abstract

AIM: To observe the expression of cyclooxygenase-2 (COX-2) and to investigate the association between COX-2 expression and infection with cytotoxic-associated gene A (*cagA*) positive strain *Helicobacter pylori* (*Hp*) in human gastric cancer, and subsequently to provide fresh ideas for the early prevention of gastric cancer.

METHODS: 32 Specimens of gastric cancer and corresponding adjacent normal gastric mucosa were obtained from patients who had undergone surgical operations of gastric cancer. All the samples including 1 case of stomach malignant lymphoma and 31 cases of gastric adenocarcinoma were confirmed by pathology diagnosis. The expression of COX-2 in 32 specimens of gastric cancer and corresponding adjacent normal gastric mucosa was quantitatively determined and analyzed with Flow Cytometry, and the levels of COX-2 protein were compared between specimens with *cagA*⁺ *Hp* infection and those without *cagA*⁺ *Hp* infection. The *cagA* gene in 32 specimens of gastric cancer was detected by polymerase chain reaction (PCR) method.

RESULTS: Twenty-seven of 32 (84 %) specimens of gastric cancer showed over-expression of COX-2, compared with the adjacent normal gastric mucosa. *cagA*⁺ gene were detected from 19 specimens of gastric cancer, but not from the other 13 specimens. The levels of COX-2 protein in 19 specimens of gastric cancer with *cagA*⁺ *Hp* infection (the number of positive cells was 73.82±18.2) were significantly higher than those in the 13 specimens without *cagA*⁺ *Hp* infection (the number of positive cells was 35.92±22.1).

CONCLUSION: COX-2 is overexpressed in gastric cancer and *cagA*⁺ *Hp* infection could up-regulate the expression of COX-2 in gastric cancer in human. There may also exist another way or channel to regulate the expression of COX-2 in gastric cancer in addition to *cagA*⁺ *Hp* infection. Therefore, applying COX-2 selective inhibitors could be an effective and promising way to prevent gastric cancer.

Guo XL, Wang LE, Du SY, Fan CL, Li L, Wang P, Yuan Y. Association of cyclooxygenase-2 expression with *Hp-cagA* infection in gastric cancer. *World J Gastroenterol* 2003; 9(2): 246-249
<http://www.wjgnet.com/1007-9327/9/246.htm>

INTRODUCTION

The mortality rate of gastric cancer still takes the first place in eastern Asia, particularly in China. So it is important to study the mechanism of gastric carcinogenesis and to explore the effective and reasonable methods for early prevention of gastric cancer, subsequently reducing the mortality rate of gastric cancer.

Epidemiological studies show that gastric cancer is closely linked to *Helicobacter pylori* (*Hp*) infection^[1-5], because the incidence of gastric cancer increases 4-9 times after *Hp* infection, and more than 60 % patients with gastric cancer had been infected with *Hp*^[6]. Recent studies indicate that infection with *cagA*⁺ *Hp* possesses a potent toxin and high risk for causing gastric cancer^[7, 8]. There is a close association between *cagA*⁺ *Hp* and precancerous stage, even gastric cancer^[9-12]. But the mechanism that how *cagA*⁺ *Hp* actually leads to gastric cancer still remains unclear.

Cyclooxygenase-2 (COX-2) is one isoform of COX enzyme family, which is the rate-limiting enzyme for prostaglandin H synthesis. It is an inducible enzyme, and normally absent in cells, but its expression is rapidly and transiently induced in response to growth factors, tumor promoters or cytokines^[13, 14]. Recent studies indicate that COX-2 not only involves in inflammatory responses but also relates to carcinogenesis. Since COX-2 is overexpressed in many tumors, such as colon-rectum cancer^[15-17], esophageal cancer^[18, 19] etc., it may play an important role in the development and progression of cancers^[20-22].

It is well documented that *Hp* infection can cause inflammation, and COX-2 is often involved in inflammatory responses and also related to carcinogenesis. However, it is not clear whether *cagA*⁺ *Hp* infection induces COX-2 expression and whether there is an association between them during gastric cancer development and progression.

To investigate the possible association between the COX-2 expression level and *cagA*⁺ *Hp* infection, in this study, Flow Cytometry technique was employed to quantitatively determine the expression level of COX-2 in specimens of gastric cancer and adjacent normal gastric mucosa and PCR method was used to amplify the *cagA* gene in specimens of gastric cancer.

MATERIALS AND METHODS

Materials

Specimens of gastric cancer and corresponding adjacent normal gastric mucosa were obtained from 32 patients who had undergone surgical operations of gastric cancer at the Department of Tumor Surgery of the first affiliated hospital of China Medical University. All samples including 1 case of stomach malignant lymphoma and 31 cases of gastric adenocarcinoma were confirmed by pathology diagnosis. The 32 patients were made up of 19 males and 13 females ranging in age from 46 to 73 years old.

Methods

Flow cytometry determination (1) Obtaining single cell solution: 0.5 cm³ specimen of gastric cancer and tissue of adjacent normal gastric mucosa were put on separate 400 pore cleaning copper nets on top of small cups, and the samples

were cut into very small chips and washed with 0.9 % NaCl, then single cell solution was collected and confirmed with microscope that over 90 % cells were single cells. (2) Permeabilizing cells: after being washed 2 times with PBS, the single cells were resuspended with 2 mL 1×FACS permeabilizing solution (Becton Dickson), and incubated at R.T. for 10 min before being washed 1 time with PBS containing 0.5 % bovine serum albumin. The cells were then divided in 2 flow cytometer tubes, and made sure the number of cells in each tube is 10^6 . (3) Immunofluorescence staining: COX-2 was indirectly immunofluorescence stained and 2 tubes were set for each specimens of gastric cancer and tissues of adjacent normal gastric mucosa. 1 tube of each set was stained with FITC (polyclonal anti-rabbit IgG Becton Dickson-Pharmingen company), which was a second fluorescent antibody, as a second antibody self contro l. 2 μ L anti-COX-2 rabbit polyclonal IgG (Santa Cruz Biotechnology, Inc.) were added to the other 1 tube of cells and mixed. The cells were incubated at R.T. for 30 min before being washed 1 time with PBS containing 0.5 % bovine serum albumin. 2 μ L secondary FITC antibody were then added and the cells were incubated in the dark at 2-8 °C for 30 min. After being washed 2 times with PBS, the cell pellet was resuspended in 500 μ L PBS for COX-2 detection by Flow Cytometer (FACScan Becton Dickson). (4) FACS detection and analysis: Laser excitation was at 488nm, the data was obtained and analyzed with Cell Quest multiple function software, and the fragment interference was eliminated by drawing a gate.

PCR amplification The template from specimen of gastric cancer was amplified by polymerase chain reaction. The *cagA-Hp* primers used were: upstream: 5' -GTG CCT GCT AGT TTG TCA GCG; and the downstream: 5' -TTG GAA ACC ACC TTT TGT ATT AGC. (obtained from Dr Berg, Washington University). PCR reaction: the 20 μ L reaction mixture including 5 μ L template, 2 μ L PCR buffer, 2 μ L dNTP, 2 μ L MgCl₂, 0.5 μ L upstream and 0.5 μ L downstream primers, 0.25 μ L Taq DNA polymerase and dH₂O was subjected to denaturation at 94 °C for 5 min; 35 cycles of 1 min at 94 °C, 1 min at 50 °C, 1 min at 72 °C; with a final extension at 72 °C for 10 min. The amplification reaction was proceeded in a PerkinElmer Cetus Thermocycler (PE-9600).

Assay of PCR production 10 μ L of reaction mixture were loaded to 1.5 % agarose gel containing 0.5 μ g/ml ethidium bromide for electrophoresis, the gel was then placed under ultraviolet ray for detection. The amplified *cagA* gene product was about 390 bp.

Statistical analysis

The expression of COX-2 protein in gastric cancer was analyzed by paired T test with Excel 2000; the association between the levels of COX-2 expression and *cagA-Hp* infection in gastric cancer was analyzed with T test between the two groups.

RESULTS

Expression of COX-2 protein in gastric cancer

27 cases of gastric cancer (in 32 cases) expressed high levels of COX-2 with an average of 67.51 % \pm 21.11 % positive cells and the range was between 30.36-98.56 % (Figure 1: A₁, A₂, A₃), in contrast, the corresponding 27 cases of adjacent normal gastric mucosa only showed a weak expression of COX-2 with an average of 12.41 % \pm 8.16 % positive cells and the range between 3.55-29.16 % (Figure 1: B₁, B₂, B₃). The percentage of positive cells in gastric cancer was significantly higher than that in the normal gastric mucosa beside cancers ($P < 0.001$). Out of the 5 remaining cases, 3 did not show the expression of COX-2 in both specimen of gastric cancer and adjacent normal gastric mucosa, whereas in the other 2 cases, the percentage

of positive cells in specimen of gastric cancer was not higher than that in the adjacent normal gastric mucosa. In total, 27 cases of 32 gastric cancer overexpressed COX-2 protein and the positive rate was 84.4 %.

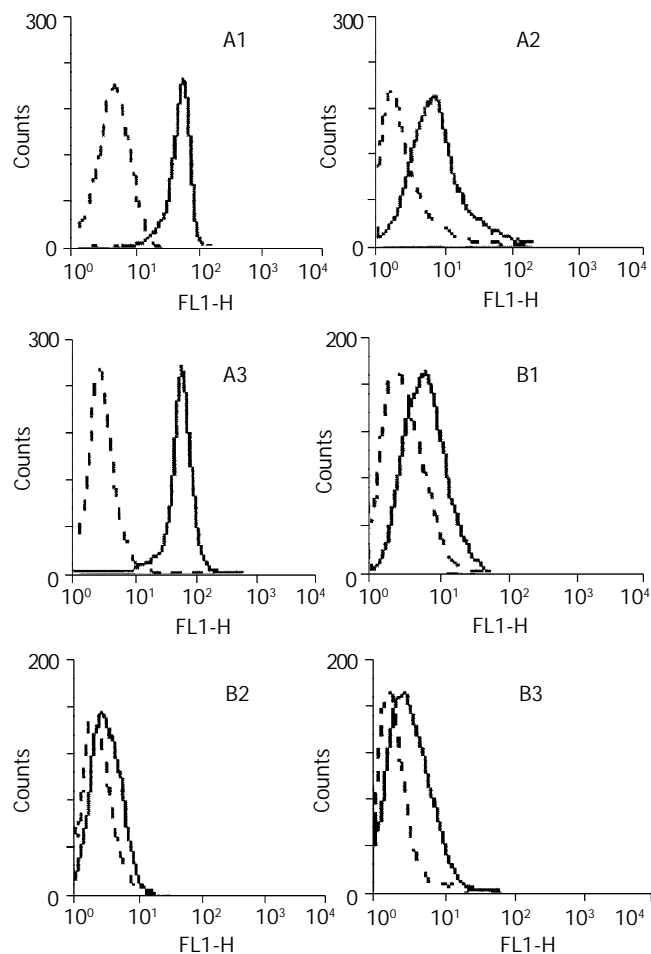


Figure 1 Analysis of COX-2 expressions in gastric cancer tissues and relevant adjacent normal gastric tissues by FACS. A₁, A₂, A₃: Gastric cancer tissues; B₁, B₂, B₃: Relevant adjacent normal gastric tissues. Dotted lines represent results generated with anti-rabbit-FITC; Solid lines represent results generated with rabbit-anti COX-2 and anti-rabbit-FITC.

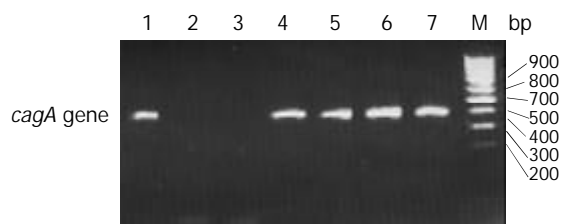


Figure 2 Agarose gel electrophoresis of PCR products of *cagA* gene in gastric cancer tissues. M: DNA marker; 1, 4, 5, 6 and 7: positive PCR products; 2 and 3: negative PCR products.

The association between the levels of COX-2 expression and *cagA-Hp* infection in gastric cancer

The *cagA⁺Hp* was detected in 19 out of 32 (59.3 %) gastric cancers (Figure 2). According to the *cagA* detection results, 32 cases of gastric cancer were then divided into two groups, the *cagA* positive group and *cagA* negative group, so that we could analyze the difference in the levels of COX-2 expression between the two groups. As shown in Table 1, the levels of COX-2 expression in *cagA* positive group were much higher than those in *cagA* negative group, and *cagA* gene was not

detected in the 5 cases with no obvious COX-2 expression. The results suggest that the expression of COX-2 is associated with the *cagA*⁺ *Hp* infection in gastric cancer and *cagA*⁺ *Hp* infection can up-regulate the expression of COX-2.

Table 1 The expression of COX-2 protein in gastric cancer

Grope	n	Cells expressed COX-2($\bar{x}\pm s$)%
Gastric cancer	32	67.51±21.11 ^a
Normal gastric mucosa	32	12.41±8.16
Gastric cancer with <i>cagA</i> ⁺ <i>Hp</i>	19	73.82±18.2 ^b
Gastric cancer without <i>cagA</i> ⁺ <i>Hp</i>	13	35.92±22.1

^a*P*<0.001 vs normal gastric mucosa; ^b*P*<0.001 vs without *cagA*⁺ *Hp* group.

DISCUSSION

Cyclooxygenases (COXs) are the key enzyme in arachidonate metabolism and catalyze the biosynthesis of prostaglandin H₂, which is the precursor for prostanoids. COX family consists of the classical COX-1 enzyme, which is constitutively expressed in many tissues, and involved in the homeostasis of various physiologic functions, and its isozyme COX-2, which was discovered in 1991^[13] and is involved in many inflammatory reactions with its expression rapidly induced by growth factors, tumor promoters or cytokines. Under normal conditions, COX-2 is absent in tissue cells. Since *Hp* infection causes inflammatory reaction, it may also induce the expression of COX-2. Romano and associates incubated MKN28 gastric mucosal cells with broth culture filtrates or bacterial suspensions from wild-type *Hp*, after 24 hours COX-2 mRNA levels increased by 5-fold and the synthesis of PGE₂, the main product of COXs, increased by 3-fold, whereas COX-1 mRNA levels remained unchanged^[23]. This effect was specifically related to *Hp* because it was not observed with *Escherichia coli*. This study indicates that *Hp* could induce the expression of COX-2 in gastric mucosal cells *in vitro*. However, whether *Hp* induces the expression of COX-2 *in vivo*, particularly in gastric cancer, and whether there is an association between *cagA*⁺ *Hp* infection and the expression of COX-2 still remain unclear. Our results showed that 27 out of 32 cases (84 %) of human gastric cancer expressed COX-2, which was similar to the status in colon-rectum cancer^[24], and indicated that the expression of COX-2 was closely associated with gastric cancer. The average percentage of cells that positively express COX-2 was 73.82 % in 19 cases of gastric cancer with *cagA*⁺ *Hp* infection; whereas it was 35.92 % in 13 cases of gastric cancer without *cagA*⁺ *Hp* infection. The levels of COX-2 expression in gastric cancer with *cagA*⁺ *Hp* infection were much higher than those without *cagA*⁺ *Hp* infection (*P*<0.001). 5 cases of gastric cancer did not show expression of COX-2 also were not detected for *cagA* gene PCR product. The result indicates that *cagA*⁺ *Hp* infection can up-regulate the expression of COX-2 in gastric cancer, and *cagA*⁺ *Hp* infection may play an important role during gastric carcinogenesis by mediating the expression of COX-2. McCarthy *et al*^[25] analyzed the COX-2 expression in gastric antral mucosa before and after eradication of *Hp* infection by immunohistochemistry and the results indicate that acute and chronic antral inflammation is associated with *Hp* as well as the expression of COX-2 protein in epithelial cells. The expression of COX-2 was reduced, but not eliminated, in the epithelium after successful eradication of *Hp*. Despite the reduction in COX-2 expression after *Hp* eradication, expression of COX-2 in epithelial cells remained and strongly correlated with the extent of the chronic inflammatory cell infiltration. This conclusion supports our

results that COX-2 was also expressed in some cases of gastric cancer without *cagA*⁺ *Hp* infection and that the expression of COX-2 in gastric cancer without *cagA*⁺ *Hp* infection is weaker than that with *cagA*⁺ *Hp* infection. Recent studies indicate that *Hp* can induce COX-2 expression in gastritis^[26-30], and COX-2 expression in gastric cancer with *Hp* infection has also been reported recently^[31,32], but most of the studies were conducted with immunohistochemistry, Western blot and RT-PCR methods^[26-32], and to quantitatively determinate COX-2 expression and to divide *Hp* into subtypes for analysis has seldom been reported so far.

Recently, evidence has been presented that COX-2 is induced in human colorectal cancers and in the polyps of mouse FAP models. When the COX-2 gene is inactivated in FAP model mice, both the number and size of polyps are reduced dramatically. In addition, selective inhibitors of COX-2 cause results similar to those caused by COX-2 gene knockout mutations. These genetic and pharmacological data open up the possibility of effectively treating human FAP and various human cancers with COX-2 selective inhibitors^[33-35].

The fact that COX-2 is overexpressed in gastric cancer and that the expression of COX-2 in gastric cancer infected by *cagA*⁺ *Hp* is much higher than that without *cagA*⁺ *Hp* infection indicates that *cagA*⁺ *Hp* infection up-regulate the expression of COX-2 in human gastric cancer, and the expression of COX-2 is closely associated with gastric cancer. But the fact that the specimens of gastric cancer without *cagA*⁺ *Hp* infection also express COX-2 at different levels implies that there may exist another way or channel to up-regulate the expression of COX-2 in gastric cancer besides *cagA* positive strain infection. Therefore, with the successful eradication of *Hp* infection, applying COX-2 selective inhibitors could be an effective and promising way to prevent gastric cancer.

REFERENCES

- 1 **Correa P.** A human model of gastric carcinogenesis. *Cancer Res* 1988; **48**: 3554-3560
- 2 **Tompkins LS,** Falkow S. The new path to preventing ulcers. *Science* 1995; **267**: 1621-1622
- 3 **Gao HJ,** Yu LZ, Bai JF, Peng YS, Sun G, Zhao HL, Miu K, Lu XZ, Zhang XY, Zhao ZQ. Multiple genetic alterations and behavior of cellular biology in gastric cancer and other gastric mucosal lesions: *H. pylori* infection, histological types and staging. *World J Gastroenterol* 2000; **6**: 848-854
- 4 **Zhuang XQ,** Lin SR. Research of *H. pylori* infection in precancerous gastric lesions. *World J Gastroenterol* 2000; **6**: 428-429
- 5 **Vandenplas Y.** *Helicobacter pylori* infection. *World J Gastroenterol* 2000; **6**: 20-31
- 6 **Quan J,** Fan XG. The progress of experiment for *Helicobacter pylori* infection and gastric carcinogenesis. *Shijie Huaren Xiaohua Zazhi* 1999; **7**: 1068-1069
- 7 **You WC,** Zhang L, Pan KF, Jiang J, Chang YS, Perez-Perez GI, Liu WD, Ma JL, Gail MH, Blaser MJ, Fraumeni JF, Xu GW. *Helicobacter pylori* prevalence and CagA status among children in two counties of China with high and low risks of gastric cancer. *Ann Epidemiol* 2001; **11**: 543-546
- 8 **Hirai M,** Azuma T, Ito S, Kato T, Kohli Y, Fujiki N. High Prevalence of neutralizing activity to *Helicobacter pylori* cytotoxin in serum of gastric carcinoma patient. *Int J Cancer* 1994; **56**: 56-60
- 9 **Zhang ZW,** Farthing MJ. Molecular mechanisms of *H. pylori* associated gastric carcinogenesis. *World J Gastroenterol* 1999; **5**: 369-374
- 10 **Blaser MJ,** Perez-Perez GI, Kleantous H, Cover TL, Peek RM, Chyou PH, Stemmermann GN, Nomura A. Infection with *Helicobacter pylori* strains possessing *cagA* is associated with an increased risk of developing adenocarcinoma of stomach. *Cancer Res* 1995; **55**: 2111-2115
- 11 **Perez-Perez GI,** Peek RM, Legath AJ, Heine PR, Graff LB. The role of CagA status in gastric and extragastric complications of *Helicobacter pylori*. *J Physiol Pharmacol* 1999; **50**: 833-845

- 12 **Guo XL**, Wang LE, Wang L, Dong M, Yuan Y. The significance of examination on serum *Hp-CagA* in high risk population in gastric cancer high rate area. *Shijie Huaren Xiaohua Zazhi* 2001; **9**: 13-14
- 13 **Xie WL**, Chipman JG, Robertson DL, Erikson RL, Simmons DL. Expression of a mitogen-responsive gene encoding prostaglandin synthase is regulated by mRNA splicing. *Proc Natl Acad Sci U S A* 1991; **88**: 2692-2696
- 14 **Kujubu DA**, Reddy ST, Fletcher BS, Herschman HR. Expression of the protein product of the prostaglandin synthase-2/*TIS10* gene in mitogen-stimulated Swiss 3T3 cells. *J Biol Chem* 1993; **268**: 5425-5430
- 15 **Kargman SL**, O' Neill GP, Vickers PJ, Evans JF, Mancini JA, Jothy S. Expression of prostaglandin G/H synthase-1 and -2 protein in human colon cancer. *Cancer Res* 1995; **55**: 2556-2559
- 16 **Sano H**, Kawahito Y, Wilder RL, Hashiramoto A, Mukai S, Asai K, Kimura S, Kato H, Kondo M, Hla T. Expression of cyclooxygenase-1 and -2 in human colorectal cancer. *Cancer Res* 1995; **55**: 3785-3789
- 17 **Kutchera W**, Jones DA, Matsunami N, Groden J, McIntyre TM, Zimmerman GA, White RL, Prescott SM. Prostaglandin H synthase 2 is expressed abnormally in human colon cancer: evidence for a transcriptional effect. *Proc Natl Acad Sci USA* 1996; **93**: 4816-4820
- 18 **Wilson KT**, Fu S, Ramanujam KS, Meltzer SJ. Increased expression of inducible nitric oxide synthase and cyclooxygenase-2 in Barrett's esophagus and associated adenocarcinomas. *Cancer Res* 1998; **58**: 2929-2934
- 19 **Zimmermann KC**, Sarbia M, Weber AA, Borchard F, Gabbert HE, Schror K. Cyclooxygenase-2 expression in human esophageal carcinoma. *Cancer Res* 1999; **59**: 198-204
- 20 **Van Rees BP**, Saukkonen K, Ristimaki A, Polkowski W, Tytgat GN, Drillenburger P, Offerhaus GJ. Cyclooxygenase-2 expression during carcinogenesis in the human stomach. *J Pathol* 2002; **196**: 171-179
- 21 **Alberts DS**. Reducing the risk of colorectal cancer by intervening in the process of carcinogenesis: a status report. *Cancer J* 2002; **8**: 208-221
- 22 **Zhang H**, Sun XF. Overexpression of cyclooxygenase-2 correlates with advanced stages of colorectal cancer. *Am J Gastroenterol* 2002; **97**: 1037-1041
- 23 **Romano M**, Ricci V, Memoli A, Tuccillo C, Di Popolo A, Acquaviva AM, Del Vecchio Blanco C, Bruni CB. *Helicobacter pylori* up-regulates cyclooxygenase-2 mRNA expression and prostaglandin E2 synthesis in MKN28 gastric mucosal cells *in vitro*. *J Biol Chem* 1998; **273**: 28560-28563
- 24 **Eberhart CE**, Coffey RJ, Radhika A, Giardiello FM, Ferrenl S, DuBois RN. Up-regulation of cyclooxygenase-2 gene expression in human colorectal adenomas and adenocarcinomas. *Gastroenterology* 1994; **107**: 1183-1188
- 25 **McCarthy CJ**, Crofford LJ, Greenson J, Scheiman JM. Cyclooxygenase-2 expression in gastric antral mucosa before and after eradication of *Helicobacter pylori* infection. *Am J Gastroenterol* 1999; **94**: 1218-1223
- 26 **Tatsuguchi A**, Sakamoto C, Wada K, Akamatsu T, Tsukui T, Miyake K, Futagami S, Kishida T, Fukuda Y, Yamanaka N, Kobayashi M. Localisation of cyclooxygenase 1 and cyclooxygenase 2 in *Helicobacter pylori* related gastritis and gastric ulcer tissues in humans. *Gut* 2000; **46**: 782-789
- 27 **Fu S**, Ramanujam KS, Wong A, Fantry GT, Drachenberg CB, James SP, Meltzer SJ, Wilson KT. Increased expression and cellular localization of inducible nitric oxide synthase and cyclooxygenase 2 in *Helicobacter pylori* gastritis. *Gastroenterology* 1999; **116**: 1319-1329
- 28 **Chan FK**, To KF, Ng YP, Lee TL, Cheng AS, Leung WK, Sung JJ. Expression and cellular localization of COX-1 and -2 in *Helicobacter pylori* gastritis. *Aliment Pharmacol Ther* 2001; **15**: 187-193
- 29 **Akhtar M**, Cheng Y, Magno RM, Ashktorab H, Smoot DT, Meltzer SJ, Wilson KT. Promoter methylation regulates *Helicobacter pylori*-stimulated cyclooxygenase-2 expression in gastric epithelial cells. *Cancer Res* 2001; **61**: 2399-2403
- 30 **Obonyo M**, Guiney DG, Harwood J, Fierer J, Cole SP. Role of gamma interferon in *Helicobacter pylori* induction of inflammatory mediators during murine infection. *Infect Immun* 2002; **70**: 3295-3299
- 31 **Yamagata R**, Shimoyama T, Fukuda S, Yoshimura T, Tanaka M, Munakata A. Cyclooxygenase-2 expression is increased in early intestinal-type gastric cancer and gastric mucosa with intestinal metaplasia. *Eur J Gastroenterol Hepatol* 2002; **14**: 359-363
- 32 **Walker MM**. Cyclooxygenase-2 expression in early gastric cancer, intestinal metaplasia and *Helicobacter pylori* infection. *Eur J Gastroenterol Hepatol* 2002; **14**: 347-349
- 33 **Dannenberg AJ**, Altorki NK, Boyle JO, Dang C, Howe LR, Weksler BB, Subbaramaiah K. Cyclo-oxygenase 2: a pharmacological target for the prevention of cancer. *Lancet Oncol* 2001; **2**: 544-551
- 34 **Blanke CD**. Celecoxib with chemotherapy in colorectal cancer. *Oncology* 2002; **16** (4 Suppl 3): 17-21
- 35 **Koki AT**, Masferrer JL. Celecoxib: a specific COX-2 inhibitor with anticancer properties. *Cancer Control* 2002; **9** (2 Suppl): 28-35

Expression of cyclooxygenase-2 and clinicopathologic features in human gastric adenocarcinoma

Ying-Wei Xue, Qi-Fan Zhang, Zhi-Bing Zhu, Qi Wang, Song-Bin Fu

Ying-Wei Xue, Qi-Fan Zhang, Zhi-Bing Zhu, Department of General Surgery, The Third Clinical Hospital, Harbin Medical University, Harbin 150040, Heilongjiang Province, China

Qi Wang, Song-Bin Fu, Laboratory of Medical Genetics and Department of Biology, College of Basic Medical Sciences, Harbin Medical University, Harbin 150086, Heilongjiang Province, China

Correspondence to: Dr. Ying-Wei Xue, Department of General Surgery, The Third Clinical Hospital, Harbin Medical University, Harbin 150040, Heilongjiang Province, China. lovezzb@sina.com.cn
Telephone: +86-451-6677580-2147

Received: 2002-08-06 **Accepted:** 2002-09-05

Abstract

AIM: To study the expression of cyclooxygenase-2 (COX-2) gene in gastric cancer and the relationship between COX-2 expression and clinicopathologic features of gastric cancer.

METHODS: With reference to the expression of β -actin gene, COX-2 mRNA level was examined in cancerous tissues and adjacent noncancerous mucosa from 33 patients by semiquantitative reverse transcription-polymerase chain reaction (RT-PCR). Quantitation of relative band Adj volume counts was performed using molecular Analyst for windows software. The COX-2 index was determined from the band Adj volume counts ratio of COX-2 to constitutively expressed actin.

RESULTS: The COX-2 index in gastric carcinoma was significantly higher than that in normal mucosa (0.5966 ± 0.2659 vs 0.2979 ± 0.171 , $u=5.4309$, $P<0.01$). Significantly higher expression of COX-2 mRNA was also observed in patients with lymph node involvement than that in those without (0.6775 ± 0.2486 vs 0.4105 ± 0.2182 , $t=2.9341$, $P<0.01$). Furthermore, the staging in the UICC TNM classification significantly correlated with COX-2 overexpression ($F=3.656$, $P<0.05$), the COX-2 index in stage III and IV was significantly higher than those in stage I and II ($q=3.2728$ and $q=3.4906$, $P<0.05$). The COX-2 index showed no correlation with patient's age, sex, blood group, tumor location, gross typing, depth of invasion, differentiation, and the greatest tumor dimension ($P>0.05$).

CONCLUSION: Expression of COX-2 mRNA in gastric carcinoma was significantly higher, which may enhance lymphatic metastasis in patients with gastric carcinoma. The staging in the UICC TNM classification was significantly correlated with COX-2 over-expression. COX-2 may contribute to progression of tumor in human gastric adenocarcinoma.

Xue YW, Zhang QF, Zhu ZB, Wang Q, Fu SB. Expression of cyclooxygenase-2 and clinicopathologic features in human gastric adenocarcinoma. *World J Gastroenterol* 2003; 9(2): 250-253
<http://www.wjgnet.com/1007-9327/9/250.htm>

INTRODUCTION

Cyclooxygenase-2 (COX-2) is a rate-limiting enzyme in

conversion of arachidonic acid to prostaglandins, also referred to as prostaglandin endoperoxide synthase (PGHS). Epidemiological and clinical results have suggested that non-steroidal anti-inflammatory drugs (NSAIDs) may reduce the risk of digestive tract carcinomas, including gastric and colon lesions. COX-2, which has been identified as being overexpressed in colorectal and gastric cancers, is one of the major targets of NSAIDs. Not only specific inhibitors of COX-2 significantly suppressed proliferation of gastric cancer cell lines^[1,2], but also a recent in-vitro study suggested that specific inhibitors of COX-2 significantly suppressed proliferation of gastric cancer xenografts in nude mice^[3]. This evidence supports the hypothesis that COX-2 is an important factor in the growth and development of gastric cancer. We used the semiquantitative reverse transcription-polymerase chain reaction (RT-PCR) to examine the expression of COX-2 mRNA in gastric cancerous tissues and adjacent noncancerous mucosa, and to study the relationship to the clinicopathologic features.

MATERIALS AND METHODS

Patients and samples

Thirty-three patients undergoing surgery for primary gastric cancer at the Third Clinical Hospital of Harbin Medical University from 2001 to 2002 were examined. Of these, 27 were male and 6 were female. The mean age was 58.6 years (range, 32-76). The clinicopathologic features showed in Table 1. Paired samples of cancer tissue and normal gastric mucosa (the distance to border of tumor is beyond 5 cm) were obtained from each patient at the time of surgery. The samples were immediately frozen in liquid nitrogen. All specimens were verified by the same pathologists.

Methods

Total RNA was isolated from 50-100 mg of the tissues according to the method of User Manual TRIzol reagent (Life Science) and was quantitated by reading absorbance at 260 nm. The total RNA solution was subjected to RT-PCR analysis using the TITANIUM™ one-step RT-PCR kit (CLONTECH Laboratories, Inc, USA). The total RNA specimens (1 μ g) were reverse transcribed and amplified in 25 μ l of reaction mixture, and the reaction conditions for COX-2 and β -actin was identical.

Oligonucleotide primers for COX-2 used were 5' -TGA AAC CCA CTC CAA ACA CAG-3' (sense) and 5' -TCA TCA GGC ACA GGA GGA AG-3' (antisense), the PCR product length was 232 bp; those for β -actin were 5' -GTT TGA GAC CTT CAA CAC CCC-3' (sense) and 5' -GTG GCC ATC TCT CTT GCT CGA AGT C-3' (antisense), the PCR product length was 320 bp. The RT-PCR procedures were as following: reverse transcription at 55 °C for 60 min, inactivation of reverse transcriptase at 94 °C for 5 min, amplification for 30 cycles of denaturation at 94 °C for 30 sec, annealing at 55 °C for 30 sec, and extension at 68 °C for 60 sec.

The PCR products were electrophoresed in 2 % agarose gels with 0.5 μ g/ml ethidium bromide and visualized under UV light. Quantitation of relative band volume counts was

performed using Molecular Analyst for windows software. To estimate COX-2 expression levels, a COX-2 index was designated as a band volume counts ratio of COX-2 to constitutively expressed β -actin, because β -actin mRNA is expressed constitutively in both the normal gastric mucosa and tumor tissues. The higher COX-2 index showed the higher expression level of COX-2 mRNA in tissues.

Statistical analysis

Statistical significance was calculated with the Students *t* test, Students *u* test, one-way ANOVA and Student-Newman-Keuls. $P < 0.05$ was selected as the statistically significant value. All results are shown as means \pm SE.

RESULTS

The total RNA was electrophoresed in 1 % agarose gels with 0.5 μ g/ml ethidium bromide and visualized under UV light, then showed three bands: 5s, 18s and 28s. The total RNA was quantitated by reading absorbance at 260 nm, and A260/280 that ranged from 1.7 to 2.0.

COX-2 mRNA and β -actin mRNA were amplified by RT-PCR, and their products length were 232bp and 320bp. The β -actin mRNA expressed constitutively in all tissues, including normal gastric mucosa and tumor tissues (Figure 1). COX-2 mRNA expressed in 29 of 33 (87.88 %) human gastric cancer specimens, over-expression was seen in 26 of 33 (78.79 %) cases (COX-2 index was 0.5966 ± 0.2659), and weak or negative COX-2 expression was seen in 25 of 33 (75.8 %) normal mucosa (COX-2 index was 0.2979 ± 0.171) (Figure 2). COX-2 index in gastric carcinoma was significantly higher than that in normal mucosa ($u = 5.4309$, $P < 0.01$). Significantly higher expression of COX-2 mRNA was also observed in patients with lymph node involvement than that in those without (0.6775 ± 0.2486 vs 0.4105 ± 0.2182 , $t = 2.9341$, $P < 0.01$). Furthermore, the staging in the UICC TNM classification (1985) significantly correlated with COX-2 overexpression ($F = 3.656$, $P < 0.05$), COX-2 index in stages III and IV was significantly higher than those in stages I and II ($q = 3.2728$ and $q = 3.4906$, $P < 0.05$). COX-2 index showed no correlation with patient's age, sex, blood group, tumor location, gross typing, depth of invasion, differentiation, and the greatest tumor dimension ($P > 0.05$, Table 1).

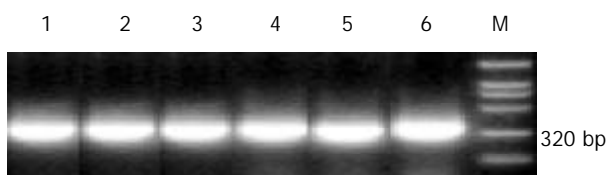


Figure 1 Representative β -actin mRNA expression in samples analyzed by RT-PCR. Lane M, molecular marker, from above down: 2 000, 1 000, 750, 500, 250, 100 bp.

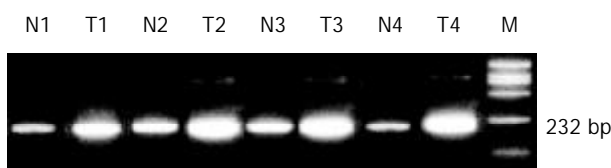


Figure 2 Representative COX-2 mRNA expression in gastric carcinoma tissues analyzed by RT-PCR. Lane M, molecular marker, from above down: 2 000, 1 000, 750, 500, 250, 100 bp. Lane N, noncancerous tissue; lane T, cancerous tissue.

Table 1 Clinicopathologic features in these patients and COX-2 index ($\bar{x} \pm s$)

Parameter	$\bar{x} \pm s$	P
Sex		
male (n=27)	0.5798 \pm 0.2754	NS ^a
female (n=6)	0.6722 \pm 0.2012	
Age (range)		
≤ 60 (n=16)	0.6144 \pm 0.2655	NS
> 60 (n=17)	0.5799 \pm 0.2651	
Blood group		
A type (n=10)	0.5928 \pm 0.2647	NS
B type (n=11)	0.6415 \pm 0.264	
O type (n=7)	0.5906 \pm 0.2614	
AB type (n=5)	0.6221 \pm 0.2551	
Greatest tumor dimension		
< 5 cm (n=11)	0.4929 \pm 0.2807	NS
≥ 5 cm (n=22)	0.6485 \pm 0.242	
Histopathologic type		
Middling differentiation (n=7)	0.5772 \pm 0.2645	NS
Low differentiation (n=9)	0.5563 \pm 0.249	
Middling and low differentiation (n=6)	0.4278 \pm 0.2911	
Signet-ring/mucous cell (n=11)	0.7341 \pm 0.186	
Gross type		
Borrmann I (n=8)	0.4897 \pm 0.28	NS
Borrmann II III (n=22)	0.6244 \pm 0.2672	
Borrmann IV (n=3)	0.6785 \pm 0.0443	
Depth of invasion ^b		
pT2 (n=10)	0.5198 \pm 0.2516	NS
pT3 (n=11)	0.5682 \pm 0.2526	
pT4 (n=12)	0.686 \pm 0.2633	
Lymph node ^b		
pN0 (n=10)	0.4105 \pm 0.2182	< 0.05
pN1 and pN2 (n=23)	0.6775 \pm 0.2486	
TNM stage ^b		
I and II (n=9)	0.4054 \pm 0.2275	< 0.05
III (n=13)	0.6561 \pm 0.2233	
IV (n=11)	0.6829 \pm 0.2631	
Tumor location		
Antrum (n=18)	0.5678 \pm 0.314	NS
Corpus (n=6)	0.6771 \pm 0.1488	
Cardiac orifice (n=9)	0.6006 \pm 0.203	

^aNS, not significant. ^bEach factor of pT, pN and TNM stage was determined according to the UICC TNM classification, published in 1985.

DISCUSSION

Two isoforms of COX have been identified: COX-1 expressed constitutively in a number of cell types, which take part in sustaining physiologic function of body; COX-2 is an inducing immediate-early gene, and human gastric mucosa normally expresses detectable levels of COX-2. COX-2 is induced by a variety of cytokines, hormones, and tumor promoters, leading to more PGs producing. Initial association of COX-2 with tumor has shown in studies for colorectal cancer, and then for other tumor^[4-10]. A series of studies confirmed that COX-2 levels elevated in colorectal carcinoma, and over-expression of COX-2 in colorectal cancer was associated with carcinogenesis, development^[11-17] and poor prognosis^[18, 19]. In recent years, a lot of researchers studied the association of COX-2 expression with gastric carcinoma^[20-26], but those conclusions were not identical, with a variety of causes.

In the current study, we found that elevated levels of COX-2 mRNA in human gastric adenocarcinoma tissues, and the COX-2 index in gastric carcinoma was significantly higher than that in normal mucosa ($u=5.4309$, $P<0.01$), which is identical to the data published^[20-26]. The mechanism of the COX-2 involved in the pathogenesis of tumor is that over-expression of COX-2 may promote PGs biosynthesis in gastric cancer cells, and PGs shows a potent immunosuppression effect by inhibiting the T-cell or natural killer cell activity^[27]. PGs thus provide a selective advantage for cancer cell survival; in addition, COX-2 can also suppress cell apoptosis^[28-32], prolong cell cycle G1^[33,34], and decrease level of cyclin D1^[35,36], which lead to that cells can not enter the cycle and proliferate continuously. Meantime, COX-2 enhances adhesion of cells^[37,38] and promotes tumor angiogenesis^[22,39], which may finally lead to the carcinogenesis and progression of the tumor.

Many researchers^[20-40] found that COX-2 mRNA expression in gastric carcinoma is correlated closely with depth of invasion, indicating that COX-2 is involved in the growth of the tumor. But, our studies did not find a correlation between COX-2 expression and the extent of primary tumor invasion. Our recent studies have found a correlation between the level of COX-2 expression and lymph node metastasis in patients with gastric carcinoma. Murata *et al*^[21] and Leung *et al*^[41] found that tumor with the overexpression of COX-2 protein by Western blot and immunohistochemical analysis was associated significantly with invasion into gastric wall lymphatic vessels as well as with metastasis to lymph nodes ($P<0.05$). Uefuji *et al*^[40] detected level of COX-2 mRNA expression by RT-PCR analysis, and the conclusion was in agreement with this study. We demonstrated that significantly higher expression of COX-2 mRNA was also observed in patients with lymph node involvement than that in those without ($t=2.9341$, $P<0.01$). It is suggested that COX-2 may influence lymphatic involvement by the way of increasing tumor invasiveness. Some studies have found that over-expression of COX-2 decreased the expression of both E-cadherin and the transforming growth factor- β receptor, which has been linked to enhancing tumorigenic potential and increasing tumor invasiveness^[37,38,42-45]. Meantime, the overexpression of the COX-2 promotes invasiveness in gastric cancer through the induction of metalloproteinase-2 and membrane-type metalloproteinase^[11,21,46].

Although several investigators^[20] reported that the COX-2 level was not associated with UICC TNM stage, but majority of them^[21,23] have reported a significant relation between the levels of COX-2 protein over-expression and UICC TNM stage. Our results are in agreement with previous ones. The COX-2 level in Stage III and IV was significantly higher than in Stage I and II ($q=3.2728$ and $q=3.4906$, $P<0.05$); but the difference of COX-2 level between Stages III and IV showed no statistical significance ($q=0.3702$, $P>0.05$). Consequently, we can infer that COX-2 may be independent or synergistic with other factors to promote growth of gastric cancer, and to enhance the lymph node metastasis and involvement. But, in advanced gastric cancer, when COX-2 expression is up-regulated to a certain level, COX-2 can not increase continuously, which suggests that there are some much more complicated mechanisms in the regulation of COX-2 expression.

In conclusion, COX-2 mRNA shows elevated expression in gastric carcinoma tissues, and the degree of COX-2 mRNA elevation is related to the lymphatic metastasis, UICC TNM stage, and poor prognosis. These findings suggest that COX-2 is involved in the carcinogenesis and growth of gastric carcinoma and that the inhibition of COX-2 activity may prove to have an important therapeutic benefit in the control of gastric carcinoma.

REFERENCES

- 1 **Sawaoka H**, Kawano S, Tsuji S, Tsujii M, Murata H, Hori M. Effects of NSAIDs on proliferation of gastric cancer cells *in vitro*: possible implication of cyclooxygenase-2 in cancer development. *J Clin Gastroenterol* 1998; **27**: S47-52
- 2 **Uefuji K**, Ichikura T, Shinomiya N, Mochizuki H. Induction of apoptosis by JTE-522, a specific cyclooxygenase-2 inhibitor, in human gastric cancer cell lines. *Anticancer Res* 2000; **20**: 4279-4284
- 3 **Sawaoka H**, Kawano S, Tsuji S, Tsujii M, Gunawan ES, Takei Y, Nagano K, Hori M. Cyclooxygenase-2 inhibitors suppress the growth of gastric cancer xenografts via induction of apoptosis in nude mice. *Am J Physiol* 1998; **274**: G1061-1067
- 4 **Wu QM**, Li SB, Wang Q, Wang SH, Li XB, Liu CZ. The expression of COX-2 in esophageal carcinoma and its relation to clinicopathologic characteristics. *Shijie Huaren Xiaohua Zazhi* 2001; **9**: 11-14
- 5 **Chan G**, Boyle JO, Yang EK, Zhang F, Sacks PG, Shah JP, Edelstein D, Soslow RA, Koki AT, Woerner BM, Masferrer JL, Dannenberg AJ. Cyclooxygenase-2 expression is up-regulated in squamous cell carcinoma of the head and neck. *Cancer Res* 1999; **59**: 991-994
- 6 **Tucker ON**, Dannenberg AJ, Yang EK, Zhang F, Teng L, Daly JM, Soslow RA, Masferrer JL, Woerner BM, Koki AT. Cyclooxygenase-2 expression is up-regulated in human pancreatic cancer. *Cancer Res* 1999; **59**: 987-990
- 7 **Zimmermann KC**, Sarbia M, Weber AA, Borchard F, Gabbert HE, Schror K. Cyclooxygenase-2 expression in human esophageal carcinoma. *Cancer Res* 1999; **59**: 198-204
- 8 **Wolff H**, Saukkonen K, Anttila S, Karjalainen A, Vainio H, Ristimaki A. Expression of cyclooxygenase-2 in human lung carcinoma. *Cancer Res* 1998; **58**: 4997-5001
- 9 **Jang BC**, Sanchez T, Schaefer HJ, Trifan OC, Liu CH, Creminon C, Huang CK, Hla T. Serum withdrawal-induced post-transcriptional stabilization of cyclooxygenase-2 mRNA in MDA-MB-231 mammary carcinoma cells requires the activity of the p38 stress-activated protein kinase. *JBC* 2000; **275**: 39507-39515
- 10 **Liu XL**, Fan DM. Protective effects of prostaglandin E1 on hepatocytes. *World J Gastroenterol* 2000; **6**: 326-329
- 11 **Chen WS**, Wei SJ, Liu JM, Hsiao M, Kou-Lin J, Yang WK. Tumor invasiveness and liver metastasis of colon cancer cells correlated with cyclooxygenase-2 (COX-2) expression and inhibited by a COX-2-selective inhibitor, etodolac. *Int J Cancer* 2001; **91**: 894-899
- 12 **Rao CV**, Indranie C, Simi B, Manning PT, Connor JR, Reddy BS. Chemopreventive properties of a selective inducible nitric oxide synthase inhibitor in colon carcinogenesis, administered alone or in combination with celecoxib, a selective cyclooxygenase-2 inhibitor. *Cancer Res* 2002; **62**: 165-170
- 13 **Oshima M**, Murai N, Kargman S, Arguello M, Luk P, Kwong E, Taketo MM, Evans JF. Chemoprevention of intestinal polyposis in the Apcdelta716 mouse by rofecoxib, a specific cyclooxygenase-2 inhibitor. *Cancer Res* 2001; **61**: 1733-1740
- 14 **Jacoby RF**, Seibert K, Cole CE, Kelloff G, Lubet RA. The cyclooxygenase-2 inhibitor celecoxib is a potent preventive and therapeutic agent in the min mouse model of adenomatous polyposis. *Cancer Res* 2000; **60**: 5040-5044
- 15 **Cianchi F**, Cortesini C, Bechi P, Fantappie O, Messerini L, Vannacci A, Sardi I, Baroni G, Boddi V, Mazzanti R, Masini E. Up-regulation of cyclooxygenase 2 gene expression correlates with tumor angiogenesis in human colorectal cancer. *Gastroenterology* 2001; **121**: 1339-1347
- 16 **Leahy KM**, Ornberg RL, Wang Y, Zweifel BS, Koki AT, Masferrer JL. Cyclooxygenase-2 inhibition by celecoxib reduces proliferation and induces apoptosis in angiogenic endothelial cells *in vivo*. *Cancer Res* 2002; **62**: 625-631
- 17 **Shen ZX**, Cao G, Sun J. Expression of COX-2 mRNA in colorectal carcinomas. *Shijie Huaren Xiaohua Zazhi* 2001; **9**: 1082-1084
- 18 **Sheehan KM**, Sheahan K, O' Donoghue DP, MacSweeney F, Conroy RM, Fitzgerald DJ, Murray FE. The relationship between cyclooxygenase-2 expression and colorectal cancer. *JAMA* 1999; **282**: 1254-1257
- 19 **Fosslien E**. Review: molecular pathology of cyclooxygenase-2 in cancer-induced angiogenesis. *Ann Clin Lab Sci* 2001; **31**: 325-348
- 20 **Ohno R**, Yoshinaga K, Fujita T, Hasegawa K, Iseki H, Tsunozaki H, Ichikawa W, Nihei Z, Sugihara K. Depth of invasion parallels increased cyclooxygenase-2 levels in patients with gastric

- carcinoma. *Cancer* 2001; **91**: 1876-1881
- 21 **Murata H**, Kawano S, Tsuji S, Tsuji M, Sawaoka H, Kimura Y, Shiozaki H, Hori M. Cyclooxygenase-2 overexpression enhances lymphatic invasion and metastasis in human gastric carcinoma. *Am J Gastroenterol* 1999; **94**: 451-455
- 22 **Uefuji K**, Ichikura T, Mochizuki H. Cyclooxygenase-2 expression is related to prostaglandin biosynthesis and angiogenesis in human gastric cancer. *Clin Cancer Res* 2000; **6**: 135-138
- 23 **Yamamoto H**, Itoh F, Fukushima H, Hinoda Y, Imai K. Overexpression of cyclooxygenase-2 protein is less frequent in gastric cancers with microsatellite instability. *Int J Cancer* 1999; **84**: 400-403
- 24 **Lim HY**, Joo HJ, Choi JH, Yi JW, Yang MS, Cho DY, Kim HS, Nam DK, Lee KB, Kim HC. Increased expression of cyclooxygenase-2 protein in human gastric carcinoma. *Clin Cancer Res* 2000; **6**: 519-525
- 25 **Saukkonen K**, Nieminen O, van Rees B, Vilkkii S, Harkonen M, Juhola M, Mecklin JP, Sipponen P, Ristimaki A. Expression of cyclooxygenase-2 in dysplasia of the stomach and in intestinal-type gastric adenocarcinoma. *Clin Cancer Res* 2001; **7**: 1923-1931
- 26 **Gao HJ**, Yu LZ, Sun L, Miao K, Bai JF, Zhang XY, Lu XZ, Zhao ZQ. Expression of COX-2 protein in gastric cancer tissue and accompanying tissue. *Shijie Huaren Xiaohua Zazhi* 2000; **8**: 578-579
- 27 **Kojima M**, Morisaki T, Uchiyama A, Doi F, Mibu R, Katano M, Tanaka M. Association of enhanced cyclooxygenase-2 expression with possible local immunosuppression in human colorectal carcinomas. *Ann Surg Oncol* 2001; **8**: 458-465
- 28 **Hsueh CT**, Chiu CF, Kelsen DP, Schwartz GK. Selective inhibition of cyclooxygenase-2 enhances mitomycin-C-induced apoptosis. *Cancer Chemother Pharmacol* 2000; **45**: 389-396
- 29 **Murakami A**, Takahashi D, Kinoshita T, Koshimizu K, Kim HW, Yoshihiro A, Nakamura Y, Jiwajinda S, Terao J, Ohigashi H. Zerumbone, a Southeast Asian ginger sesquiterpene, markedly suppresses free radical generation, proinflammatory protein production, and cancer cell proliferation accompanied by apoptosis: the alpha,beta-unsaturated carbonyl group is a prerequisite. *Carcinogenesis* 2002; **23**: 795-802
- 30 **Geloso MC**, Vercelli A, Corvino V, Repici M, Boca M, Haglid K, Zelano G, Michetti F. Cyclooxygenase-2 and caspase 3 expression in trimethyltin-induced apoptosis in the mouse hippocampus. *Exp Neurol* 2002; **175**: 152-160
- 31 **Waskewich C**, Blumenthal RD, Li H, Stein R, Goldenberg DM, Burton J. Celecoxib exhibits the greatest potency amongst cyclooxygenase (COX) inhibitors for growth inhibition of COX-2-negative hematopoietic and epithelial cell lines. *Cancer Res* 2002; **62**: 2029-2033
- 32 **Tian G**, Yu JP, Luo HS, Yu BP, Yue H, Li JY, Mei Q. Effect of nimesulide on proliferation and apoptosis of human hepatoma SMMC-7721 cells. *World J Gastroenterol* 2002; **8**: 483-487
- 33 **Trifan OC**, Smith RM, Thompson BD, Hla T. Overexpression of cyclooxygenase-2 induces cell cycle arrest. Evidence for a prostaglandin-independent mechanism. *J Biol Chem* 1999; **274**: 34141-34147
- 34 **Song S**, Xu XC. Effect of benzo[a]pyrene diol epoxide on expression of retinoic acid receptor-beta in immortalized esophageal epithelial cells and esophageal cancer cells. *Biochem Biophys Res Commun* 2001; **281**: 872-877
- 35 **Dihlmann S**, Siermann A, von Knebel Doeberitz M. The nonsteroidal anti-inflammatory drugs aspirin and indomethacin attenuate beta-catenin/TCF-4 signaling. *Oncogene* 2001; **20**: 645-653
- 36 **Bissonnette M**, Khare S, von Lintig FC, Wali RK, Nguyen L, Zhang Y, Hart J, Skarosi S, Varki N, Boss GR, Brasitus TA. Mutational and nonmutational activation of p21ras in rat colonic azoxymethane-induced tumors: effects on mitogen-activated protein kinase, cyclooxygenase-2, and cyclin D1. *Cancer Res* 2000; **60**: 4602-4609
- 37 **Zhang Z**, DuBois RN. Detection of differentially expressed genes in human colon carcinoma cells treated with a selective COX-2 inhibitor. *Oncogene* 2001; **20**: 4450-4456
- 38 **Rowland RG**. Macroscopic, microscopic and molecular observations of bladder cancer. *J Urol* 2001; **165**: 1480
- 39 **Seno H**, Oshima M, Ishikawa To, Oshima H, Takaku K, Chiba T, Narumiya S, Taketo MM. Cyclooxygenase 2- and prostaglandin E(2) receptor EP(2)-dependent angiogenesis in Apc(Delta716) mouse intestinal polyps. *Cancer Res* 2002; **62**: 506-511
- 40 **Uefuji K**, Ichikura T, Mochizuki H. Expression of cyclooxygenase-2 in human gastric adenomas and adenocarcinomas. *J Surg Oncol* 2001; **76**: 26-30
- 41 **Leung WK**, To KF, Ng YP, Lee TL, Lau JY, Chan FK, Ng EK, Chung SC, Sung JJ. Association between cyclooxygenase-2 overexpression and missense P53 mutations in gastric cancer. *Br J Cancer* 2001; **84**: 335-339
- 42 **Sheng H**, Shao J, O' Mahony CA, Lamps L, Albo D, Isakson PC, Berger DH, DuBois RN, Beauchamp RD. Transformation of intestinal epithelial cells by chronic TGF-beta 1 treatment results in downregulation of the type II TGF-beta receptor and induction of cyclooxygenase-2. *Oncogene* 1999; **18**: 855-867
- 43 **Saha D**, Datta PK, Sheng H, Morrow JD, Wada M, Moses HL, Beauchamp RD. Synergistic induction of cyclooxygenase-2 by transforming growth factor-beta1 and epidermal growth factor inhibits apoptosis in epithelial cells. *Neoplasia* 1999; **1**: 508-517
- 44 **O' Mahony CA**, Beauchamp RD, Albo D, Tsujii M, Sheng HM, Shao J, Dubois RN, Berger DH. Cyclooxygenase-2 alters transforming growth factor-beta 1 response during intestinal tumorigenesis. *Surgery* 1999; **126**: 364-370
- 45 **Shao J**, Sheng H, Aramandla R, Pereira MA, Lubet RA, Hawk E, Grogan L, Kirsch IR, Washington MK, Beauchamp RD, DuBois RN. Coordinate regulation of cyclooxygenase-2 and TGF-beta1 in replication error-positive colon cancer and azoxymethane-induced rat colonic tumors. *Carcinogenesis* 1999; **20**: 185-191
- 46 **Ji F**, Wang WL, Yang ZL, Li YM, Huang HD, Chen WD. Study on the expression of matrix metalloproteinase-2 mRNA in human gastric cancer. *World J Gastroenterol* 1999; **5**: 455-457

Endoscopic ultrasonography in preoperative staging of gastric cancer: determination of tumor invasion depth, nodal involvement and surgical resectability

Wei-Dong Xi, Cong Zhao, Guo-Sheng Ren

Wei-Dong Xi, Guo-Sheng Ren, Department of General Surgery, First Affiliated Hospital Chongqing University of Medical Sciences, Chongqing 400016, China

Cong Zhao, Division of Gastroenterology, the Third People's Hospital of Chengdu, Chengdu 610031, Sichuan Province, China

Correspondence to: Cong Zhao, Division of Gastroenterology, The Third People's Hospital of Chengdu, Chengdu 610031, Sichuan Province, China. czhao0050@sohu.com

Telephone: +86-28-86649831 Ext 50897 **Fax:** +86-28-86630055

Received: 2002-04-18 **Accepted:** 2002-08-23

Abstract

AIM: Current study was aimed to evaluate the usefulness of EUS in TNM staging of gastric cancer by comparing EUS preoperative staging with pathological findings, and the preliminary exploration of possible reasons for overstaging and understaging phenomenon was especially intended.

METHODS: A total of 35 patients with histologically confirmed gastric adenocarcinoma were referred to EUS and staged preoperatively by using the TNM system. The preoperative endosonographic results were compared with the histopathological staging.

RESULTS: The overall accuracy of EUS for determination of the T stage was 80.0 %, and for T1, T2, T3, and T4 was 100 %, 71.4 %, 87.5 % and 72.7 %, respectively. For N stage, EUS had the accuracy of 68.6 %, with sensitivity and specificity of 66.7 % and 73.7 %, respectively. Resectability was predicted with sensitivity and specificity of 87.5 % and 100 %, respectively.

CONCLUSION: EUS is an accurate staging modality in most cases, with a few exceptions of overstaging and understaging. Patients with gastric cancers can benefit from preoperative EUS staging for establishing individualized therapy. However, EUS criteria to differentiate benign from malignant nodes still need to be further defined by future studies.

Xi WD, Zhao C, Ren GS. Endoscopic ultrasonography in preoperative staging of gastric cancer: determination of tumor invasion depth, nodal involvement and surgical resectability. *World J Gastroenterol* 2003; 9(2): 254-257
<http://www.wjgnet.com/1007-9327/9/254.htm>

INTRODUCTION

Gastric cancer is one of the most encountered gastrointestinal malignancies. The overall 5-year survival rates are still not encouraging, although many advances in diagnostic modalities and therapeutic regimens have been achieved during last a few decades. The improvement of survival rates depends primarily on early detection and treatment of the tumor. Many large-scale clinical trials indicate that the majority of patients are in

advanced stage at time of diagnosis and the outcome is dismal. It has been well accepted that accurate preoperative staging is not only important for prediction of the prognosis, but also essential to establishment of individualized cancer therapy^[1]. The staging was previously made by analysis on the bases of clinical presentations, laboratory test results, and various imaging findings such as trans-abdominal B-mode Ultrasonography, computed tomography (CT) or magnetic resonance imaging (MRI). However, precise conclusion was often difficult to obtain due largely to limitations on or local unavailability of these techniques themselves^[2,3].

Endoscopic ultrasonography (EUS) was first introduced by a German doctor in the early 1980s and is now used worldwide. Without interference by abdominal fat, bones and gut gases, the probe can be placed in where is nearest to the target organ or tissue of interest and the more accurate imaging can be obtained. Because of the use of transducers of high frequency, it facilitates the early detection of minute lesions and the TNM staging of tumors^[4,5]. The ability of EUS to accurately visualize and differentiate the different layers of the gut wall makes it possible to determine the penetration depth of a gastrointestinal cancer more precisely. Simultaneously, the observation of the involvement of lymph nodes and other organs adjacent to the cancer within the range of EUS scanning can provide more detailed additional information to the disease. Currently, EUS is becoming one of the routine methods in staging of gastrointestinal cancers, including gastric carcinoma^[6-8]. Published data showed that the accuracy of T and N staging for gastric cancer is 78-92 % and 63-78 %, respectively^[9,10], being imperative in prognostic prediction and especially in decision-making regarding to individualized therapeutic regimens^[11,12].

It has been noticed that overstaging and understaging are the common problems encountered in current EUS practice, and accuracy for lymph node staging exhibits discrepancy between observers^[9,13]. Current study was aimed to evaluate the usefulness of EUS in TNM staging of gastric cancer by comparing EUS preoperative staging results with pathological findings, and the preliminary exploration of possible reasons for above-mentioned phenomenon was especially intended.

MATERIALS AND METHODS

Patients

Thirty-five patients with gastric cancer proven pathologically underwent EUS preoperative T and N staging, including 25 male, 10 female, aged 28-78 years with average of 61.7. Of them, 32 were treated surgically (two were found unresectable due to adjacent organ involvement). The diagnosis was reconfirmed and pathological TN staging made. Three cases were diagnosed T4N1M1 based on EUS, B ultrasound, and CT scanning findings and treated unsurgically. Therefore, 32 patients were finally enrolled in this study.

EUS examination procedures

A Pentax 3840T double-channeled video-gastroscope was

employed and Fujinon SP-701 radial scanning probes (with frequency of 7.5MHz, 12MHz, and 20MHz) introduced via one of the working channels. EUS preoperative staging for gastric cancer followed the TNM staging as of the Union Internationale Contre le Cancer (UICC)^[10]. Early cancer is clinically defined as the tumor confined to mucosa or submucosa regardless of lymph node metastasis^[14]. The extension of the cancer into muscularis propria is classified as the advanced. The judgment of local tumor invasion depth by EUS is according to the determination of the outmost involved layer of the gastric wall^[15]. Regional lymph node staging is classified as N0 (no lymph node involvement found) and N+ (perigastric lymph node metastasis confirmed). M refers to distant metastasis, defined as M0 and M1 (with or without distant metastasis).

RESULTS

EUS staging

EUS preoperative staging results were listed in Table 1.

Table 1 Accuracy of EUS preoperative T staging in 35 patients with gastric carcinoma

EUS stage	n	Pathologicstage				Accuracy of EUS (%)
		T1	T2	T3	T4	
T1	1	1	0	0	0	100
T2	7	1	5	1	0	71.4
T3	16	0	2	14	0	87.5
T4	8(3)	0	0	3	5(3)	72.7
Total	32(3)	2	7	18	5(3)	80.0

Surgical findings

Among 32 cases of the current study, cancer located in gastric atrium was found in 18 patients, gastric corpus in 9 and fundus in 5. Radical gastrectomy was performed in 15, total gastrectomy in 13, and palliative surgery in 2. Unresectable tumors were found in 2 patients. The sensitivity and specificity of EUS for predicting resectability were 87.5 % and 100 % respectively.

The comparison between EUS and pathologic T staging

By compared to the postoperative pathology, the overall accuracy of EUS T staging was 80.0 % (Table 1). Much attention should be paid to overstaging and understaging found in T2, T3, and T4. The assessment of tumor invasion in postoperative pathology was mostly consistent with preoperative EUS findings, except seven cases including 4 ulcerated type, 2 protruded type, and 1 flat type. Pathologically, the understaged one was due to micro-tumor invasion undetectable by EUS. The overstaged six cases were owing to local inflammatory reaction, edema, and fibrosis undifferentiable by EUS.

The comparison between EUS and pathologic N staging

The accuracy, sensitivity and specificity of EUS for N staging (Table 2) were 68.6 %, 66.7 %, and 73.3 %, respectively. However, 11 patients had inconsistent pathologic findings compared with EUS. Although four of them were diagnosed N+ by EUS during operation, the pathology confirmed inflammatory lymphadenopathy with no evidence of tumor metastasis. Lymph nodes susceptible of metastasis were not detected in 2 cases both by EUS during operation but confirmed

later pathologically. EUS-undetected lymph nodes in 3 cases were also diagnosed during operation and by postoperative pathology.

Table 2 Accuracy of EUS preoperative N staging in 35 patients with gastric carcinoma

EUS stage	n	Pathologic stage		Accuracy of EUS(%)
		N0	N+	
N0	20	14	6	70.0
N+	12(3)	5	7(3)	66.7
Total	32(3)	19	13(3)	68.6

(NOTES: three cases of T4N+ not surgically treated were included as being the correctly diagnosed).

DISCUSSION

Clinical experience with EUS used as an important preoperative staging tool for gastric cancer has been widely reported. On EUS imaging, early gastric cancer is visualized as hypo-echo masses invading the first, second, and third layers of the stomach, resulting in disruption, thickening, and irregularity of the layers involved. The fourth and fifth layers are often intact. Gastric cancer in advanced stage is usually accompanied by disruption of submucosa and muscularis propria, disappearance and replacement of the normal structures by hypo-echo mass as result of tumor invasion^[16-18]. Willis *et al*^[19] reported that overall accuracy of EUS for T, T1, T2, T3, and T4 staging was 78 %, 80 %, 63 %, 95 %, and 83 %, respectively. Regional lymph node staging was correctly conducted in 77 % of all 116 patients. Our results were similar to Willis' s, with 80.0 % and 68.6 % for T and N staging, respectively. Together with reports elsewhere, it is accepted that EUS is an accurate staging modality in most cases, with a few exceptions of overstaging and understaging. In our study, seven incorrectly staged patients consisted of ulcerated type in 4 cases, protruded type in 2, and flat type in 1. By careful examination and analysis, we found pathologically that reasons contributing to overstaging can be misinterpretation of necrotic tissue overlaying the ulcer surface, scars and fibrosis, inflammatory reaction in the peripheral structure of cancer, thickened gastric wall or ball-balloon alteration. Microscopic cancer invasion or focal destruction of a certain layer undetectable with lower-frequency ultrasound often results in understaging. In general, staging for elevated type may be more readily than that for ulcerated one, being with higher accuracy. To achieve the best visualization of the cancer and improve the diagnostic accuracy, high frequency probes (20MHz) may be more suitable for early cancer, while low frequency transducers (7.5 or 12MHz) for advanced ones^[20,21].

Lightdale^[22] and Zuccaro *et al*^[10] pointed out those lymph nodes of round shape, clear margin, and hypo-echo pattern similar to that of the primary tumor were more likely to be malignant. Heintz *et al*^[23] reported that the sensitivity and specificity could be 85 % and 45-85 % respectively if the followings were taken as the diagnostic criteria for malignant nodes: larger than 10 mm in diameter, heterogeneous echo pattern, and sharp border. EUS accuracy for N staging in this study was 68.6 %. Inaccuracy may be as the result of lack of reliable differential standard for benign and malignant nodes. The diameter, location, and the distance of lymph node to the primary lesion, and the endoscopists' expertise are important as well. Other factors affecting the accuracy may also include the frequency and penetration depth of the transducers used,

and intra-gastric substance. We recommend that based on our experience, visualization of lymph nodes by EUS should start with the site of primary tumor followed by gradual detection of each perigastric lymph node group. The differentiation of lymph nodes from other perigastric structures such as vessels on EUS imaging can be made by moving the probe forward and backward or using linear EUS equipped with color Doppler. Since many factors may influence the detection of nodes, negative EUS does not reliably indicate the absolute absence of nodal involvement and further assessment should be carried out to obtain definite diagnosis. EUS-guided fine needle aspiration (EUS-FNA) is now clinically available and has been accepted as the most reliable cytology for differentiation in this situation^[24,25].

The accurate preoperative staging for gastric cancer is very important in predicting prognosis and in determining individualized therapeutic regimens^[26-28]. Since EUS has its own limitations on accuracy of M staging, it must be emphasized here that precise staging results and proper management decision-making should rely on clinical presentations, laboratory tests and various imaging technologies. Nevertheless, EUS is undoubtedly superior to B ultrasound, CT, and conventional endoscopy in the assessment of primary tumor invasion depth and regional lymph node status^[4]. The therapeutic goals for gastric cancer should be set to maximally prolong the survival time, significantly improve the patient's quality of life, avoid any unnecessary procedure and any operation with no proven benefit, and also, reduce the economic burden on the patient. To achieve those, optimal therapy must be carefully individualized to meet the need of each patient based on precise TNM staging. Because early cancers confined to mucosa can be effectively managed by endoscopic resection and thus laparotomic surgery and its related complications can be avoided^[29-32], these lesions must be recognized clinically prior to the treatment decision-making. The very limited penetration depth of early tumors can be clearly displayed and reliably determined on EUS scanning especially when high-frequency probes are used, as reported by our team^[17]. Although surgery is still recommended as the first line therapy for T1-T3N1M0 cancer^[33], Rohde *et al.*^[10] found that 30 % of 1 420 gastric cancer patients undergoing surgery eventually had no curative results because of tumor invasion. For patients with T4 cancers, further investigation should be performed to determine whether there is any hope of surgical cure^[34,35]. Patients with cancer invading into adjacent organs such as the pancreas proven by EUS should not undergo radical management. For them, palliative surgery can be a treatment choice if digestive tract obstruction is present, and radiotherapy or chemotherapy may be instituted when indicated. Treatment plans for three patients initially considered as surgical candidates in this study were eventually amended because of the preoperative staging of T4N1M1. In these patients, the pancreas invasion, large vessel involvement and liver metastases were the major indicators against curative surgery, which were demonstrated clearly by EUS imaging (for pancreas and vessel involvement) and CT scanning (for liver metastases).

In summary, EUS is a useful study for accurate staging of gastric carcinoma. Its unique advantages make EUS become one of the reliable methods in guiding prediction of the prognosis and establishment of cancer therapy regimens, although not likely to replace other imaging modalities used to stage these patients. Further large-scale clinical trails and carefully planned investigations should be conducted to clarify those questions about the ability of EUS to differentiate tumor infiltration from fibrosis or inflammatory tissues, to detect microscopic invasions, and to discriminate the benign from malignant nodes.

REFERENCES

- 1 **Heyer T**, Frieling T, Haussinger D. How accurate is preoperative staging as a basis for treatment decisions in gastric carcinoma? *Schweiz Rundsch Med Prax* 1998; **87**: 443-446
- 2 **Miller FH**, Kochman ML, Talamonti MS, Ghahremani GG, Gore RM. Gastric cancer. Radiologic staging. *Radiol Clin North Am* 1997; **35**: 331-349
- 3 **Kuntz C**, Herfarth C. Imaging diagnosis for staging of gastric cancer. *Semin Surg Oncol* 1999; **17**: 96-102
- 4 **Zhang QL**. Present status and Prospect of Endoscopic ultrasonography. *Chin J Dig Endosc* 1998; **15**: 195-196
- 5 **Galetti G**, Fusaroli P. Endoscopic ultrasonography. *Endoscopy* 2001; **33**: 158-166
- 6 **Dittler HJ**, Siewert JR. Role of endoscopic ultrasonography in gastric carcinoma. *Endoscopy* 1993; **25**: 162-166
- 7 **Kelly S**, Harris KM, Berry E, Hutton J, Roderick P, Cullingworth J, Gathercole L, Smith MA. A systematic review of the staging performance of endoscopic ultrasound in gastro-oesophageal carcinoma. *Gut* 2001; **49**: 534-539
- 8 **Bergman JJ**, Fockens P. Endoscopic ultrasonography in patients with gastro-esophageal cancer. *Eur J Ultrasound* 1999; **10**: 127-138
- 9 **Rosch T**. Endosonographic staging of gastric cancer: a review of literature results. *Gastrointest Endosc Clin N Am* 1995; **5**: 549-557
- 10 **Zuccaro G**. Diagnosis and staging of gastric carcinoma by endoscopic ultrasonography. Chapter 13. Neoplasms of the digestive tract. Imaging, staging and management. Edited by Meyers AM. New York, USA. Lippincott Raven Publishers 1998: 137-142
- 11 **Wang JY**, Hsieh JS, Huang YS, Huang CJ, Hou MF, Huang TJ. Endoscopic ultrasonography for preoperative locoregional staging and assessment of resectability in gastric cancer. *Clin Imaging* 1998; **22**: 355-359
- 12 **Mancino G**, Bozzetti F, Schicchi A, Schiavo M, Spinelli P, Andreola S. Preoperative endoscopic ultrasonography in patients with gastric cancer. *Tumori* 2000; **86**: 139-141
- 13 **Meining A**, Dittler HJ, Wolf A, Lorenz R, Schusdziarra V, Siewert JR, Classen M, Hofler H, Rosch T. You get what you expect? A critical appraisal of imaging methodology in endosonographic cancer staging. *Gut* 2002; **50**: 599-603
- 14 **Matsumoto Y**, Yanai H, Tokiyama H, Nishiaki M, Higaki S, Okita K. Endoscopic ultrasonography for diagnosis of submucosal invasion in early gastric cancer. *J Gastroenterol* 2000; **35**: 326-331
- 15 **Yanai H**, Matsumoto Y, Harada T, Nishiaki M, Tokiyama H, Shigemitsu T, Tada M, Okita K. Endoscopic ultrasonography and endoscopy for staging depth of invasion in early gastric cancer: a pilot study. *Gastrointest Endosc* 1997; **46**: 212-216
- 16 **Zhao C**, Nong CY, Li H, Wu LP, Shi W, Qiu X. Evaluation of Endoscopic ultrasonography in differentiation of benign and malignant gastric ulcer. *Sichuan Yixue* 2001; **22**: 34-35
- 17 **Zhao C**, Shi W, Sun XB, Li H, Qiu X, Wu LP. The diagnosis of primary gastric cancer by Endoscopic ultrasonography and pathology: A case report. *Zhongguo Shiyong Neike Zazhi* 2001; **21**: 632
- 18 **Tsai TL**, Changchien CS, Hu TH, Hsiaw CM, Hsieh KC. Differentiation of benign and malignant gastric stromal tumors using endoscopic ultrasonography. *Chang Gung Med J* 2001; **24**: 167-173
- 19 **Willis S**, Truong S, Gribnitz S, Fass J, Schumpelick V. Endoscopic ultrasonography in the preoperative staging of gastric cancer: accuracy and impact on surgical therapy. *Surg Endosc* 2000; **14**: 951-954
- 20 **Yanai H**, Tada M, Karita M, Okita K. Diagnostic utility of 20-megahertz linear endoscopic ultrasonography in early gastric cancer. *Gastrointest Endosc* 1996; **44**: 29-33
- 21 **Okamura S**, Tsutsui A, Muguruma N, Ichikawa S, Sogabe M, Okita Y, Fukuda T, Hayashi S, Okahisa T, Shibata H, Ito S, Sano T. The utility and limitations of an ultrasonic miniprobe in the staging of gastric cancer. *J Med Invest* 1999; **46**: 49-53
- 22 **Lightdale CJ**, Mierop FV. Staging Gastric Cancer: The New York Experience. In: Dam JV, Sivak VM, eds. Gastrointestinal Endosonography. Chapter 18. W.B. Saunders 1999: 185-192
- 23 **Heintz A**, Mildenerger P, Georg H, Braunstein S, Jurginger TH. Endoscopic ultrasonography in the diagnosis of regional lymph nodes in esophageal and gastric cancer. *Endoscopy* 1993; **25**: 231-235
- 24 **Xi WD**, Ren GS, Zhao C. Clinical significance of endoscopic ultrasonography guided fine needle aspiration in upper digestive tract diseases. *Xiaohuabing Zhenduan He Zhiliao* 2002; **2**: 16-18

- 25 **Sun SY**, Wang MC, Wang CX, Li XL, Sun SY. The diagnosis of regional lymph nodes in upper digestive tract by EUS-FNA. *Shijie Huaren Xiaohua Zazhi* 2000; **8**: 1319-1320
- 26 **Songur Y**, Okai T, Watanabe H, Fujii T, Motoo Y, Sawabu N. Preoperative diagnosis of mucinous gastric adenocarcinoma by endoscopic ultrasonography. *Am J Gastroenterol* 1996; **91**: 1586-1590
- 27 **Guo W**, Zhang YL, Zhou DY, Zhang WD. The correlation of preoperative EUS staging and p53 gene mutation in gastric cancer. *Shijie Huaren Xiaohua Zazhi* 1999; **7**: 1094-1095
- 28 **Roukos DH**. Current advances and changes in treatment strategy may improve survival and quality of life in patients with potentially curable gastric cancer. *Ann Surg Oncol* 1999; **6**: 46-56
- 29 **Ohashi S**, Segawa K, Okamura S, Mitake M, Urano H, Shimodaira M, Takeda T, Kanamori S, Naito T, Takeda K, Itoh B, Goto H, Niwa Y, Hayakawa T. The utility of endoscopic ultrasonography and endoscopy in the endoscopic mucosal resection of early gastric cancer. *Gut* 1999; **45**: 599-604
- 30 **Kida M**, Tanabe S, Watanabe M, Kokutou M, Kondou I, Yamada Y, Sakaguchi T, Saigenji-K. Staging of gastric cancer with endoscopic ultrasonography and endoscopic mucosal resection. *Endoscopy* 1998; **30** (Suppl 1):A 64-68
- 31 **Wang JY**, Hsieh JS, Huang CJ, Hou MF, Huang TJ. Endoscopic ultrasonography for preoperative locoregional staging and assessment of resectability in gastric cancer. *Clin Imaging* 1998; **22**: 355-359
- 32 **Akahoshi K**, Chijiiwa Y, Hamada S, Sasaki I, Maruoka A, Kabemura T, Nawata H. Endoscopic ultrasonography: a promising method for assessing the prospects of endoscopic mucosal resection in early gastric cancer. *Endoscopy* 1997; **29**: 614-619
- 33 **Nakamura K**, Kamei T, Ohtomo N, Kinukawa N, Tanaka M. Gastric carcinoma confined to the muscularis propria: how can we detect, evaluate, and cure intermediate-stage carcinoma of the stomach? *Am J Gastroenterol* 1999; **94**: 2251-2255
- 34 **Feussner H**, Omote K, Fink U, Walker SJ, Siewert JR. Pretherapeutic laparoscopic staging in advanced gastric carcinoma. *Endoscopy* 1999; **31**: 342-347
- 35 **Fujino Y**, Nagata Y, Ogino K, Watahiki H. Evaluation of endoscopic ultrasonography as an indicator for surgical treatment of gastric cancer. *J Gastroenterol Hepatol* 1999; **14**: 540-546

Edited by Zhang JZ

Vascularity of hepatic VX2 tumors of rabbits: Assessment with conventional power Doppler US and contrast enhanced harmonic power Doppler US

Wen-Hua Du, Wei-Xiao Yang, Xiang Wang, Xiu-Qin Xiong, Yi Zhou, Tao Li

Wen-Hua Du, Wei-Xiao Yang, Xiang Wang, Xiu-Qin Xiong, Yi Zhou, Tao Li, Department of US, Daping Hospital & Research Institute of Surgery, the Third Military Medical University, Chongqing 400042, China
Supported by the National Science Foundation of China, No. 30070227
Correspondence to: Wen-Hua Du, Dept. of US, Daping Hospital & Research Institute of Surgery, the Third Military Medical University, Chongqing 400042, China. duwenhua001@163.net
Telephone: +86-23-68757441
Received: 2002-08-10 **Accepted:** 2002-09-05

Abstract

AIM: To investigate the characteristics of the vascularity of hepatic metastasis.

METHODS: Six New Zealand rabbits, weighing averagely 2.7 ± 0.4 kg, were selected and operated to establish hepatic VX2 tumor carrier model. Hepatic VX2 tumors were then imaged with conventional B mode US, second harmonic imaging (SHI), color Doppler flow imaging (CDFI), power Doppler imaging (PDI) and harmonic PDI by a transducer S8 connected to HP-5 500 ultrasound system. A kind of self made echo contrast agent was intravenously injected at a dose of 0.01 mL/kg through ear vein, and then the venous passage was cleaned with sterilized saline.

RESULTS: Totally, 6 hypoechoic lesions and 3 hyperechoic lesions were found in the six carrier rabbits with a mean size about 2.1 ± 0.4 cm under conventional B mode ultrasound, they were oval or round in shape with a clear outline or a hypoechoic halo at the margin of the lesions. Contrast agent could not change the echogenicity of the lesions under conventional B mode and SHI, however, it could greatly increase the flow sensitivity of the lesions under PDI and harmonic PDI. Nutrient artery of these metastatic lesions might also be well depicted under contrast enhanced PDI and harmonic PDI.

CONCLUSION: Our result suggested that contrast enhanced PDI, especially harmonic PDI, was a promised method in the detection of vascularity of hepatic tumor nodules.

Du WH, Yang WX, Wang X, Xiong XQ, Zhou Y, Li T. Vascularity of hepatic VX2 tumors of rabbits: Assessment with conventional power Doppler US and contrast enhanced harmonic power Doppler US. *World J Gastroenterol* 2003; 9(2): 258-261
<http://www.wjgnet.com/1007-9327/9/258.htm>

INTRODUCTION

Power Doppler ultrasonography (US) has been shown more sensitive than color Doppler US in the depiction of vascular flow in focal hepatic lesions, such as hepatocellular carcinoma (HCC), focal nodular hyperplasia (FNH) and metastasis (Mets). In addition, a wide variety of US contrast agents have been developed by using different gases and coating materials,

especially those called the third generation contrast agents manufactured through perfluorocarbon gases. These US contrast agents are promised to improve the quality of vascularity in Doppler studies, and its potential role in hepatic US has already been widely investigated. Researches have revealed that power Doppler US performed with the application of the contrast agent depicts more intratumoral vascularity in HCC than non-contrast power Doppler US does. Meanwhile, less knowledge is known about the vascularity of hepatic metastasis by harmonic power Doppler US. In this study, we intended to depict the characterization of the vascularity of hepatic Metastasis.

MATERIALS AND METHODS

Preparation of animal models

Six New Zealand rabbits weighing 2.6-3.2 kg, averagely 2.7 ± 0.4 kg were anaesthetized by Sumianxin (a product of the Changchun Argo-Pastoral University) at 0.2 mL/kg through intramuscular injection. Hairs in the abdominal region were moulted by 8 % sodium sulfide, then the region was cleaned by saline water. Median incision right beneath the metasternum was made to expose the right lobe of liver. A tunnel about 3cm deep at the lobe was established with an ophthalmic nipper. Viable VX2 tumor tissue masses about 2-3 mm³ were implanted into the tunnel, locally stanchd and then the each layer of abdominal wall was sutured accordingly. 2 or 3 weeks later, these rabbits were ready for the experiment. VX2 tumor is a kind of dermatological squamous cancer induced by Shope virus, viable VX2 tumor can be transplanted and generated through New Zealand rabbits, and therefore is used as simulate metastatic hepatic tumor models.

Preparation of echo contrast agent

Self made echo contrast agent was made from 5 % (g/L) human albumin and 40 % (g/L) Dextran in a ratio of 1:3 (v/v), the mixture was then underwent electromechanical sonication (Sonication machine JY92-2D was manufactured by Ninbo Xinzhi Research Institute) for 90 seconds under mechanical energy of 280W. During the sonication process, perfluoropropane gas was mixed into the mixture. Microbubbles manufactured in this way were counted by a Coulter counter, which concentration was about 1.6×10^9 bubbles/L with an average size 4.3 ± 2.1 μ m.

Equipments

A transducer S8 connected to HP-5 500 ultrasound system was used, which fundamental wave frequency was 3MHz and the second harmonic imaging was transmitted at frequency 3MHz receiving at frequency 6 MHz. Power Doppler imaging was tuned to PRF=2.2. During the whole process of experiment, the image depth, color gain and TGC should be kept constant.

Methods

Hepatic VX2 tumors were imaged with conventional B mode US, second harmonic imaging (SHI), color Doppler flow imaging (CDFI), power Doppler imaging (PDI) and harmonic PDI. Echo agent was intravenously injected at a dose of 0.01 mL/kg through ear vein, and then the venous passage was

cleaned with sterilized saline. All images were recorded realtimely by magnetic optics (MO), and they were analyzed further by at least two independent experienced sonographer.

RESULTS

Features of VX2 tumor under conventional and harmonic B mode US

Totally 6 hypoechoic lesions and 3 hyperechoic lesions were found in the six carrier rabbits with a mean size about 2.1 ± 0.4 cm under conventional B mode ultrasound, no even echoic lesions were found. They were oval or round in shape with a clear outline or a hypoechoic halo at the margin of the lesions. These images didn't seem to be improved by SHI. Contrast images under conventional B mode US also showed no improvement at all, meanwhile, SHI revealed a short duration of enhancement of the hepatic arteries and tumor lesions at the early phase, and, an enhancement of the liver parenchyma and an decreased echo at the later phase. A pronounced arterial enhancement was also found at one side of the lesion, which may be considered as the nutrient artery of the tumor. (Figures 1-3).

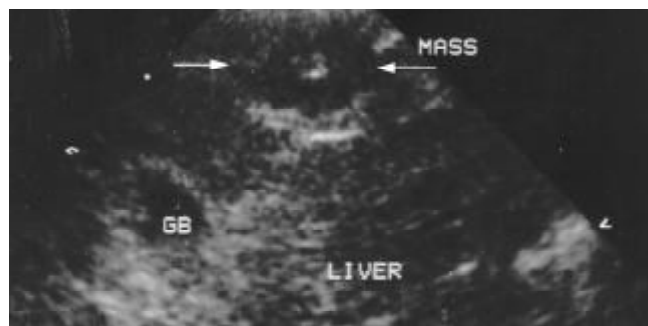


Figure 1 Image of VX2 tumor lesion under conventional B mode US. Arrow indicates the VX2 tumor lesion at the anterior part of the right lobe. It is oval and hypoechoic with a small hyperechoic scar at the center of the lesion.



Figure 2 Image of VX2 tumor lesion under conventional second harmonic imaging. Arrow indicates the same VX2 tumor lesion at the anterior part of the right lobe. The echogenicity of the lesion and the around liver parenchyma seem unchanged at all.



Figure 3 Contrast enhanced second harmonic image. It shows

the enhancement of the liver arteries in the parenchyma, arrows indicate the afferent artery and its branches.

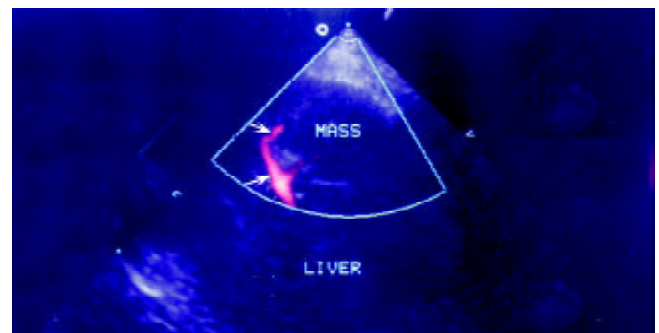


Figure 4 Conventional power Doppler image of the lesion. Arrows indicate the clear afferent blood flow signals of the lesion and its branches.



Figure 5 Contrast enhanced power Doppler image. It shows the enhancement of the afferent arteries in the lesion, arrow indicates especially the pronounced blooming artifacts around the artery and its branches.

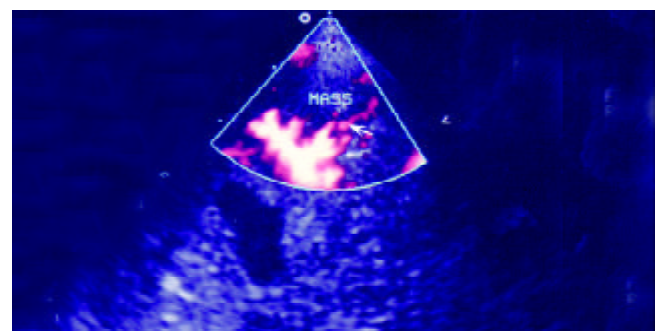


Figure 6 Contrast enhanced harmonic power Doppler image. It shows the enhancement of the afferent arteries in the lesion, arrow indicates the newly appeared intralesional blood signals and less blooming artefacts around the artery and its branches.



Figure 7 Contrast enhanced harmonic power Doppler image at a later stage. It shows the enhancement of the afferent arter-

ies in the lesion, where intralesional blood signals and rare blooming artefacts are observable around the artery and its branches.

Changes of intralesional blood flow under CDFI, PDI and harmonic PDI

Color Doppler flow imaging could only reveal a spot-like or short bar-like flow signals around the lesion, and rarely reveal intralesional flow signals (Figure 4). Contrast agent may increase CDFI signals, but not so ideally as we expected. PDI could reveal a clear bar-like flow signal at one side of the lesion, and relatively more signals around and inside the lesions as compared with CDFI (Figure 5). Contrast agent can increase PDI signals quite remarkably from the instant of injection of gas bubbles, and a short duration of blooming artifacts were clearly seen, then the intralesional blood flow signals and even its branches were well revealed (Figure 6). These phenomena may better demonstrated what had been revealed by contrast SHI described above. An interesting fact was shown when tumor lesion was imaged under contrast enhanced harmonic PDI. Under this situation, intralesional and perilesional blood flow was much clearer and blooming artifacts became less (Figure 7).

DISCUSSION

Ultrasound is the most common used imaging modality to scan for focal liver lesions. Populations at a high risk of developing either primary or secondary hepatic tumors are usually followed up with US examination performed every 6 months in order to detect malignant lesions at the early stage. Early detection of either primary or secondary malignancies may greatly enhance the possibilities of curative surgical operation or other ablation treatments. The major limitation of US in the detection of small tumor lesions is its sensitivity. However, the introduction of microbubble contrast agents and the development of contrast specific techniques have revealed many new prospects of US detection and characteristics of focal liver tumor lesions. Hepatic metastasis typically appears as multiple focal discrete but solid lesions, and occasionally appears diffuse infiltrate hepatic involvement. Metastasis^[1-5], under conventional B mode US, has a nonspecific appearance which shows hypoechoic, hyperechoic, or mixed echogenicity. The sensitivity for total tumor detection has been reported as 57 to 92 % with a specificity of 76-96 %^[6-8]. However, the reported sensitivity of US is only about 41 % for accurate detection in the total numbers of intrahepatic lesions^[9]. Color Doppler flow imaging and power Doppler imaging are often used in the differentiation of hepatocellular carcinoma and metastatic liver lesions. Tanaka *et al*^[11] had reported a description of vascular pattern on different hepatic malignancies using CDFI and PDI. In particular, the basket and vessels- within-the-tumor pattern were supposed to be characteristics of HCC, the spot pattern more frequently appeared in hemangioma, and the detour pattern was often seen in metastasis. PDI has already been demonstrated to be superior to conventional CDFI, particularly in depicting vessels in small tumors, and contrast enhanced PDI may even increase the sensitivity of HCC to as high as 100 % in comparison with the conventional techniques^[10-13]. While, metastatic liver lesions were usually considered as hypovascular. Choi *et al*^[8,21] had reported that most of the metastatic lesions were absent of flow signals under both CDFI and PDI. Another report revealed that in a series of 64 metastatic liver lesions 67 % appeared avascular, and only 32 % of these cases appeared intralesional flow signals in comparison to 76 % of HCC^[14-18].

In our study, conventional B mode US and CDFI results are in accord with other researches. However, contrast

enhanced second harmonic imaging and harmonic PDI in this study demonstrated that vascularity of metastasis might overlap with that of HCC. Although metastatic lesion may be considered as avascular under conventional ultrasonography, the introduction of new techniques such as SHI and pulse inversion harmonic imaging and the use of echo contrast agent may greatly increase the sensitivity in checking of perilesional and intralesional vasculature. Even the nutrient artery of the metastatic lesion could be clearly seen under these new techniques. Therefore, we should reconsider the differentiating criteria of HCC and metastasis, especially when lesions were all less than 3 cm. The major problems in the use of power Doppler were that the detected velocities were too slow in the tumor, there were too many blooming artifacts associated with microbubble injection, the duration of enhancement was short and the were motion artifacts resulted from respiration^[19-26]. Second harmonic imaging (SHI) US technique involves transmitting at frequency f and receiving at frequency $2f$, and contrast enhanced echoes could be therefore obtained at second harmonic frequency because of the non-linear motion of the gas bubbles when destroyed by high acoustic pressures^[27-29]. Thus, harmonic power Doppler US used in accord with contrast agent might provide vascular information in detail, and at the same time decreasing the artifacts associated with the contrast agent^[30-36]. Our findings confirmed that contrast enhanced harmonic PDI could reveal increased color sensitivity of vessels either inside the tumor lesion or in the surrounding liver parenchyma with less blooming artifacts. It was suggested that contrast enhanced harmonic PDI was convinced to be much more superior to conventional CDFI, PDI and contrast enhanced SHI.

REFERENCES

- 1 **Numata K**, Tanaka K, Mitsui K, Morimoto M, Inoue S, Yonezawa H. Flow characteristics of hepatic tumors at color Doppler sonography: correlation with arteriographic findings. *Am J Roentgenol* 1993; **160**: 515-521
- 2 **Choi BI**, Kim TK, Han JK, Kim AY, Seong CK, Park SJ. Vascularity of hepatocellular carcinoma: assessment with contrast-enhanced second harmonic versus conventional power Doppler US. *Radiology* 2000; **214**: 381-386
- 3 **Carter R**, Hemingway D, Cook TG, Pickard R, Poon FW, MacKillop JA, McArdle CS. A prospective study of six methods for detection of hepatic collateral metastases. *Ann Royal Coll Surg Engl* 1996; **78**: 27-30
- 4 **Machi J**, Isomoto H, Yamashita Y, Kurohiji T, Shirouzu K, Kakegawa T. Intraoperative ultrasonography in screening for liver metastases from colorectal cancer: comparative study accuracy with traditional procedures. *Surgery* 1987; **101**: 678-684
- 5 **Lundstedt C**, Ekberg H, Hederstrom E, Stridbek H, Torfason B, Transberg KG. Radiologic diagnosis of liver metastases in colorectal carcinoma. Prospective evaluation of the accuracy of angiography, ultrasonography, computed tomography and computed tomographic angiography. *Acta Radiol* 1987; **28**: 431-438
- 6 **Park SH**, Kim TK, Lee KH, Kim AY, Choi JI, Han JK, Choi BI. Quantitative comparison of tumor vascularity of hepatocellular carcinoma after intravenous contrast agent: conventional versus harmonic power Doppler US. *Abdom Imaging* 2001; **26**: 178-183
- 7 **Kim AY**, Choi BI, Kim TK, Han JK, Yun EJ, Lee KY, Han MC. Hepatocellular carcinoma: power Doppler US with a contrast agent: preliminary results. *Radiology* 1998; **209**: 135-140
- 8 **Choi BI**, Kim TK, Han JK, Chung JW, Park JH, Han MC. Power versus conventional color Doppler sonography: comparison in the depiction of vasculature in liver tumors. *Radiology* 1996; **200**: 55-58
- 9 **Kubota K**, Hisa N, Fujiwara Y, Fukumoto M, Yoshida D, Yoshida S. Evaluation of the intratumoral vasculature of hepatocellular carcinoma by power doppler sonography: advantages and disadvantages versus conventional color doppler sonography. *Abdom Imaging* 2000; **25**: 172-178

- 10 **Gaiani S**, Volpe L, Piscaglia F, Bolondi L. Vascularity of tumors and recent advances in Doppler ultrasound. *J Hepatol* 2001; **34**: 474-482
- 11 **Leen E**, McArdle CS. Ultrasound contrast agents in liver imaging. *Clin Radiol* 1996; **51** (Suppl 1): 35-39
- 12 Ramnarine K, Leen E, Oppo K. Improved characterization of focal liver tumors: dynamic power Doppler imaging using NC100100 echoenhancer. *Eur J Ultrasound* 2000; **11**: 95-104
- 13 **Solbiati L**, Tonolini M, Cova L, Goldberg SN. The role of contrast-enhanced ultrasound in the detection of focal liver lesions. *Eur Radiol* 2001; **11** (Suppl 3): E15-26
- 14 **Leen E**. The role of contrast-enhanced ultrasound in the characterisation of focal liver lesions. *Eur Radiol* 2001; **11** (Suppl 3): E27-34
- 15 **Blomley MJ**, Albrecht T, Cosgrove DO, Jayaram V, Butler-Barnes J, Echtersley R. Stimulated acoustic emission in liver parenchyma with Levovist. *Lancet* 1998; **351**: 568
- 16 **Blomley MJ**, Albrecht T, Cosgrove DO, Jayaram V, Eckersley RJ, Patel N, Taylor Robinson S, Bauer A, Schlieff R. Liver vascular transit time analyzed with dynamic hepatic venography with bolus injections of an US contrast agent: early experience in seven patients with metastases. *Radiology* 1998; **209**: 862-866
- 17 **Leen E**, Angerson WJ, Yamenitis S, Bongartz G, Blomley M, Del Maschio A, Summaria V, Maresca G, Pezzoli C, Llull JB. Multi-centre clinical study evaluating the efficacy of SonoVue (BR1), a new ultrasound contrast agent in Doppler investigation of focal hepatic lesions. *Eur J Radiol* 2002; **41**: 200-206
- 18 **Ding H**, Kudo M, Onda H, Suetomi Y, Minami Y, Maekawa K. Hepatocellular carcinoma: depiction of tumor parenchymal flow with intermittent harmonic power Doppler US during the early arterial phase in dual-display mode. *Radiology* 2001; **220**: 349-356
- 19 **Nisenbaum HJ**, Rowling SE. Ultrasound of focal hepatic lesions. *Semin Roentgenol* 1995; **30**: 324-346
- 20 **Zardi EM**, Uwechie V, Picardi A, Costantino S. Liver focal lesions and hepatocellular carcinoma in cirrhotic patients: from screening to diagnosis. *Clin Ter* 2001; **152**: 185-188
- 21 **Choi BI**, Kim TK, Han JK, Chung JW, Par JH, Han MC. Power versus conventional color Doppler sonography: comparison in the depiction of vasculature in liver tumors. *Radiology* 1996; **200**: 55-58
- 22 **Lencioni R**, Pinto F, Armilotta N, Bartolozzi C. Assessment of tumor vascularity in hepatocellular carcinoma: comparison of power Doppler US and color Doppler US. *Radiology* 1996; **201**: 353-358
- 23 **Hosoki T**, Mitomo M, Chor S, Miyahara N, Ohtani M, Morimoto K. Visualization of tumor vessels in hepatocellular carcinoma. Power Doppler compared with color Doppler and angiography. *Acta Radiol* 1997; **38**: 422-427
- 24 **Koito K**, Namieno T, Morita K. Differential diagnosis of small hepatocellular carcinoma and adenomatous hyperplasia with power Doppler sonography. *Am J Roentgenol* 1998; **170**: 157-161
- 25 **Lagalla R**, Caruso G, Finazzo M. Monitoring treatment response with color and power Doppler. *Eur J Radiol* 1998; **27** (Suppl 2): S149-156
- 26 **Kim AY**, Choi BI, Kim TK, Han JK, Yun EJ, Lee KY, Han MC. Hepatocellular carcinoma: power Doppler US with a contrast agent-preliminary results. *Radiology* 1998; **209**: 135-140
- 27 **Ohishi H**, Hirai T, Yamada R, Hirohashi S, Uchida H, Hashimoto H, Jibiki T, Takeuchi Y. Three-dimensional power Doppler sonography of tumor vascularity. *J Ultrasound Med* 1998; **17**: 619-622
- 28 **Hirashi T**, Ohishi H, Yamada R, Yoshimura H, Hirohashi S, Uchida H, Hashimoto H, Jibiki T, Takeuchi Y. Three-dimensional power Doppler sonography of tumor vascularity. *Radiat Med* 1998; **16**: 353-357
- 29 **Imamura M**, Shiratori Y, Shiina S, Sato S, Okudaira T, Teratani T, Kato N, Akahane M, Ohtomo K, Minami M, Omata M. Power Doppler sonography for hepatocellular carcinoma: factors affecting the power Doppler signals of the tumors. *Liver* 1998; **18**: 427-433
- 30 **Kawasaki T**, Itani T, Nakase H, Mimura J, Komori H, Sugimoto K. Power Doppler imaging of hepatic tumours: differential diagnosis between hepatocellular carcinoma and metastatic adenocarcinoma. *J Gastroenterol Hepatol* 1998; **13**: 1152-1160
- 31 **Hosten N**, Puls R, Lemke AJ, Steger W, Zendel W, Zwicker C, Felix R. Contrast-enhanced power Doppler sonography: improved detection of characteristic flow patterns in focal liver lesions. *J Clin Ultrasound* 1999; **27**: 107-115
- 32 **Chen RC**, Chen WT, Yang TH, Cheng NY, Wang CK, Liao LY, Wang CS, Chen PH. Assessment of vascularity in hepatic tumors: comparison of power Doppler sonography and intraarterial CO₂-enhanced sonography. *Am J Roentgenol* 2002; **178**: 67-73
- 33 **Cioni D**, Lecioni R, Rossi S, Garbagnati F, Donati F, Crocetti L, Bartolozzi C. Radiofrequency thermal ablation of hepatocellular carcinoma: using contrast-enhanced harmonic power doppler sonography to assess treatment outcome. *Am J Roentgenol* 2001; **177**: 783-788
- 34 **Meloni MF**, Goldberg SN, Livraghi T, Calliada F, Ricci P, Rossi M, Pallavicini D, Campani R. Hepatocellular carcinoma treated with radiofrequency ablation: comparison of pulse inversion contrast-enhanced harmonic sonography, contrast-enhanced power Doppler sonography, and helical CT. *Am J Roentgenol* 2001; **177**: 375-380
- 35 **Cedrone A**, Pompili M, Sallustio G, Lorenzelli GP, Gasbarrini G, Rapaccini GL. Comparison between color power Doppler ultrasound with echo-enhancer and spiral computed tomography in the evaluation of hepatocellular carcinoma vascularization before and after ablation procedures. *Am J Gastroenterol* 2001; **96**: 1854-1859
- 36 **Gaiani S**, Casali A, Serra C, Piscaglia F, Gramantieri L, Volpe L, Siringo S, Bolondi L. Assessment of vascular patterns of small liver mass lesions: value and limitation of the different Doppler ultrasound modalities. *Am J Gastroenterol* 2000; **95**: 3537-3546

Potent inhibition of angiogenesis and liver tumor growth by administration of an aerosol containing a transferrin-liposome-endostatin complex

Xi Li, Geng-Feng Fu, Yan-Rong Fan, Chan-Fu Shi, Xin-Juan Liu, Gen-Xing Xu, Jian-Jun Wang

Xi Li, Geng-Feng Fu, Gen-Xing Xu, Jian-Jun Wang, School of Life Science, Nanjing University, 22 Hankou Road, Nanjing 210093, Jiangsu Province, China

Yan-Rong Fan, Chan-Fu Shi, Xin-Juan Liu, Gen-Xing Xu, Nanjing Military Medical College of the Second Military Medical University, 2 Maqun Road, Nanjing 210049, Jiangsu Province, China
Supported by Jiangsu Natural Science Fund (China), BK20000001, the National Natural Science Foundation of China, 30070250 and the "985 Project" from Nanjing University

Correspondence to: Gen-Xing Xu, P.O.Box 4901, 2 Maqun Road, Nanjing 210049, Jiangsu Province, China. genxingx@yahoo.com.cn
Telephone: +86-25-4364753 **Fax:** +86-25-4350162

Received: 2002-07-31 **Accepted:** 2002-08-16

Abstract

AIM: To obtain an efficient delivery system for transporting endostatin gene to mouse liver tumor xenografts by administration of aerosol.

METHODS: Recombinant plasmid pcDNA3.0/endostatin containing human endostatin gene together with signal peptide from alkaline phosphatase were transferred into human umbilical vein endothelial cell (HUVEC) by transferrin (TF)-liposome-endostatin complex. Western blot was used to detect the expression of human endostatin in transfected HUVEC cells and its medium. After the tumor-bearing mice were administrated with TF-liposome-endostatin complex, the lung tissue was analyzed by immunohistochemical method for expression of endostatin and the tumors were treated with CD-31 antibody to detect the density of microvessels in tumor tissues. The inhibition of tumor growth was estimated by the weight of tumors from groups treated with different doses of TF-liposome-endostatin complex. DNA fragmentation assay was used to detect the apoptosis of the cells from primary liver tumor.

RESULTS: Western blot analysis and immunohistochemical method confirmed the expression of endostatin protein *in vitro* and *in vivo*. After the tumor sections were treated with CD-31 antibody, the positive reaction cells appeared brown while the negative cells were colorless. The positively stained area of the TF-liposome-endostatin treated group was significantly smaller ($P < 0.01$, $645.8 \pm 55.2 \mu\text{m}^2$) than that of the control group ($1\ 325.4 \pm 198.5 \mu\text{m}^2$). The data showed a significant inhibition of angiogenesis. After administration of TF-liposome-endostatin, comparing with the control group administrated with TF-liposome-pcDNA3.0, liver tumor growth in the mice treated with 50, 250 and 500 mg DNA/kg was inhibited by 36.6 %, 40.8 %, and 72.8 %, respectively ($P < 0.01$). And a typical DNA fragmentation of apoptosis was found in the cells from tumor tissues of the mice treated with TF-liposome-endostatin but none in the control group.

CONCLUSION: Endostatin gene could be efficiently transported into the mice with TF-liposome-DNA delivery

system by administration of aerosol. TF-liposome-mediated endostatin gene therapy strongly inhibited angiogenesis and the growth of mouse xenograft liver tumors. It also could promote the development of apoptosis of tumors without direct influence on tumor cells.

Li X, Fu GF, Fan YR, Shi CF, Liu XJ, Xu GX, Wang JJ. Potent inhibition of angiogenesis and liver tumor growth by administration of an aerosol containing a transferrin-liposome-endostatin complex. *World J Gastroenterol* 2003; 9(2): 262-266
<http://www.wjgnet.com/1007-9327/9/262.htm>

INTRODUCTION

Angiogenesis, the process of new blood vessel formation from existing vessels, is essential for tumor progression and metastasis^[1-7]. Tumor cells stimulate angiogenesis by secretion of angiogenic factors such as vascular endothelial growth factor (VEGF) and basic fibroblast growth factor (bFGF)^[8]. At the same time, tumor cells also produce anti-angiogenic factors, including angiostatin^[9] and endostatin^[10]. Tumor angiogenesis is dependent upon the local balance of these positive and negative regulators^[11]. Inhibition of angiogenesis has been shown to inhibit local tumor growth and metastasis^[12]. Systemic administration of endostatin in tumor-bearing mice has been shown to keep the primary tumors in a dormant state^[10], thereby preventing tumor metastasis.

Clinical trials involving angiostatin and endostatin require large quantities of recombinant proteins, which are difficult to produce. In addition, these proteins do not maintain their bioactivity and are hard to be administered systemically. Gene therapy with endostatin employing a viral delivery system has shown a high efficacy in inhibiting tumor growth and metastasis in mice^[13-15]. However, the safety issues in its usage make this approach less attractive in human clinical trials. Nonviral gene therapy with endostatin was reported^[16, 17], but the efficiency was rather low as compared with viral delivery systems. The use of a cationic liposome-mediated gene transfer system together with a transferrin ligand achieved high transfection efficiency upon delivery of the p53 gene in mice^[18]. In this study, we evaluated the effect of aerosol administration of TF-liposome-endostatin on liver tumor growth in mice. The results indicated that TF-liposome-mediated endostatin gene therapy strongly inhibited angiogenesis and the growth of mouse xenograft liver tumors.

MATERIALS AND METHODS

Plasmid construction

The endostatin gene was obtained by PCR from a human liver cDNA library (Clontech Co). Endostatin was digested with *EcoRI/XbaI* and cloned in the *EcoRI/XbaI* site of pcDNA3.0 (Invitrogen Co). The sequence encoding the signal peptide from alkaline phosphatase^[19] was inserted into the *HindIII/EcoRI* site upstream of endostatin and an epitope tag derived from influenza

virus hemagglutinin A (HA) was fused in the *EcoRI* site between the signal peptide and endostatin. Recombinant plasmid was purified by QIA prep spin miniprep kit (QIAGEN Co).

Preparation of liposomes

Dried lipid films were prepared by solubilizing stearylamine, phosphatidyl choline and cholesterol at a 2:7:1 molar ratio in chloroform and subsequent removal of the chloroform by evaporation^[20]. The films were hydrated for 10 min with sterile water at 60 °C and then vortexed to generate liposomes. After hydration, the liposomes were sonicated on ice and filtered (pore size 0.22 μm). The diameter of liposome was assessed under scanning electron microscopy.

Formation of the TF-liposome-plasmid complex and determination of the encapsulation coefficient

The TF-liposome-plasmid complexes were prepared using 10:1:1, 10:5:1, 10:10:1 or 10:20:1 (mg:nmol:mg) ratios of TF:liposome:DNA. Liposomes and TF were mixed and incubated for 20 min at room temperature. The purified plasmid was then added to the solution, mixed immediately and thoroughly, and incubated for a minimum of 20 min at room temperature. The encapsulation coefficient of the TF-liposome-plasmid complexes was determined by 7.5 g·L⁻¹ agarose electrophoresis. The complexes were dissociated with 4 g·L⁻¹ SDS.

Expression of endostatin in vitro

HUVEC cells were obtained from Shanghai Cellular Research Institute and maintained in 1640 medium supplemented with 100 mL·L⁻¹ fetal bovine serum. HUVEC cells were plated in six-well plates at 2.5×10⁵ cells/well, and transfected with TF-liposome-plasmid complex containing 2 μg of purified plasmid. The conditioned media were collected after 48 h and concentrated in a microconcentrator (Amicon Co). And the cells were harvested by centrifugation, mixed with sample buffer and treated with sonic. The samples were subjected to SDS-PAGE using 120 g·L⁻¹ polyacrylamide gels, followed by Western blot analysis. The primary monoclonal mouse-anti-HA antibody (Babco Co) was used at 1:1 000 dilution followed by goat anti-mouse IgG-HRP (Sino-American Biotechnology Co) at 1:50 dilution. The membrane was stained by DAB.

Treatment of tumor-bearing mice with TF-liposome-pcDNA3.0/endostatin complexes

BALB/c male and female mice (obtained from the Animal Center of Nanjing Medical University, China) weighing about 20 grams were used in this study. Mice were fed with a standard rodent diet. Hep5 mouse liver tumor^[21] (obtained from the Animal Center of Chinese Academy of Sciences in Shanghai, China) was minced thoroughly and cancer cells were obtained at a concentration of 5×10⁶ cells/mL. A total of 1×10⁶ tumor cells were inoculated under the skin of the right thigh for each mouse. After 72 h inoculation, the tumor-bearing mice were treated with the aerosol containing 50, 250 or 500 μg DNA/kg of TF-liposome-pcDNA3.0/endostatin complexes (in 100 μL) or 500 μg DNA/kg of TF-liposome-pcDNA3.0 vector complexes every 72 h, for a total of five administrations. After 72 h of the fifth administration, mice were sacrificed and tumors were excised and weighed. Inhibition of tumor growth was determined using the formula: (Tumor weight of control group - Tumor weight of treatment group)/tumor weight of control group ×100 %.

Detection of expression of endostatin in vivo

Lung tissues were harvested after sacrificing the mice and the

expression of endostatin was assayed by immunohistochemistry. They were then fixed in 40 g·L⁻¹ paraformaldehyde and frozen. The sections of 20 μm were cut and mounted on glass slides. The sections were subsequently treated with 0.1 mol·L⁻¹ PBS (pH 7.0) for 5 min, and methanol mixed with 3 mL·L⁻¹ H₂O₂ for 10 min. The sections were blocked with 10 g·L⁻¹ milk in PBS, incubated at 37 °C for 2 h with a 1:1 000 dilution of a monoclonal mouse anti-HA antibody, followed by 1 h incubation at 37 °C of 1:25 dilutions of goat-anti-mouse IgG-HRP. The sections were stained with 0.5 mL·L⁻¹ DAB mixed with 0.3 mL·L⁻¹ H₂O₂.

Immunohistochemistry

Mice were sacrificed after 18 days of treatment. Tumors were excised and fixed in 40 g·L⁻¹ paraformaldehyde. Tumor tissues were frozen, and 20 μm sections were cut and mounted on glass slides. Sections were treated as described above. The primary CD-31 monoclonal rat anti-mouse antibody (Pharmingen Co) was diluted 200 times. The secondary antibody was a 1:25 dilution of goat anti-rat IgG-HRP (Kirkegaard & Perry Laboratories Co). Sections were stained with DAB as described above.

DNA fragmentation assay

The tumor tissues were excised and homogenized thoroughly. Following centrifugation at 3 000×g at 4 °C for 5 min, the pellets were resuspended in a lysis buffer containing 10 mmol·L⁻¹ Tris-HCl buffer (pH8.0), 10 mmol·L⁻¹ EDTA, 10 g·L⁻¹ SDS, 20 mg·L⁻¹ DNase-free RNase and 200 mg·L⁻¹ of proteinase K. After overnight incubation at 37 °C, the DNA was purified by phenol/chloroform extraction, precipitated, and resuspended in TE buffer (pH 7.4). Ten mg DNA was subjected to electrophoresis on a 15 g·L⁻¹ agarose gel containing 0.5 mg·L⁻¹ ethidium bromide and visualized under UV light. Electrophoresis was carried out in TE buffer (pH 8.0) at 20V for 8 h.

RESULTS

Detection of liposome diameter and encapsulation coefficient of the TF-liposome-plasmid complex

Prepared liposomes were observed under scanning electron microscopy at 10 000 fold magnification. The mean diameter of the liposomes was about 180-220 nm. After formation of the TF-liposome-pcDNA3.0/endostatin complex, the encapsulation coefficient was determined by 7.5 g·L⁻¹ agarose gel electrophoresis (Figure 1). The results showed that the encapsulation coefficient rose with increased ratio of liposome:DNA. Moreover, at a TF:liposome:DNA ratio of 10:10:1 (mg/nmol/mg), the encapsulation coefficient was higher than 98 %.

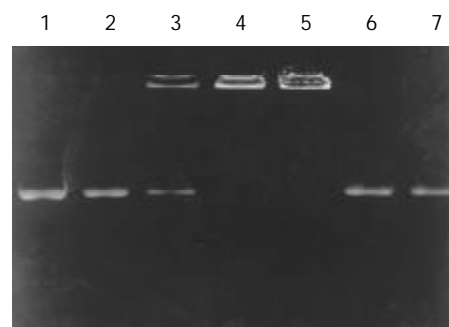


Figure 1 Determination of encapsulation coefficient. Lane 1: pure pcDNA3.0/endostatin plasmid, lanes 2-5: TF:liposome:DNA (mg:nmol:mg) at a ratio of 10:1:1, 10:5:1, 10:10:1 and 10:20:1. Lanes 6-7: complexes dissociated with 4 g·L⁻¹ SDS.

Expression of endostatin *in vitro* and *in vivo*

The *in vitro* expression of endostatin was detected by Western blot analysis. Distinct bands at around 22 kDa, the predicted molecular weight for the recombinant endostatin, were visualized in the supernatant and HUVEC cells transfected with pcDNA3.0/endostatin but not in the supernatant or HUVEC cells transfected with pcDNA3.0 (Figure 2). The *in vivo* expression of endostatin was detected by immunohistochemistry. After five administrations of the TF-liposome-pcDNA3.0/endostatin complex, the lung tissue was harvested and sectioned. Staining with an anti-HA antibody revealed positive cells containing endostatin in the sections of the treated group, whereas control sections were negative (Figure 3).

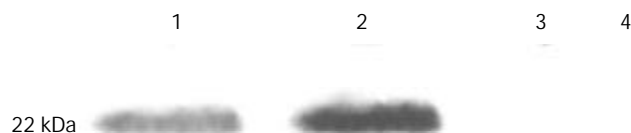


Figure 2 Expression of endostatin *in vitro*. Lane 1: HUVEC cells transfected with pcDNA3.0/endostatin; lane 2: supernatant of HUVEC cells transfected with pcDNA3.0/endostatin; lane 3: HUVEC cells transfected with pcDNA3.0; lane 4: supernatant of HUVEC cells transfected with pcDNA3.0.

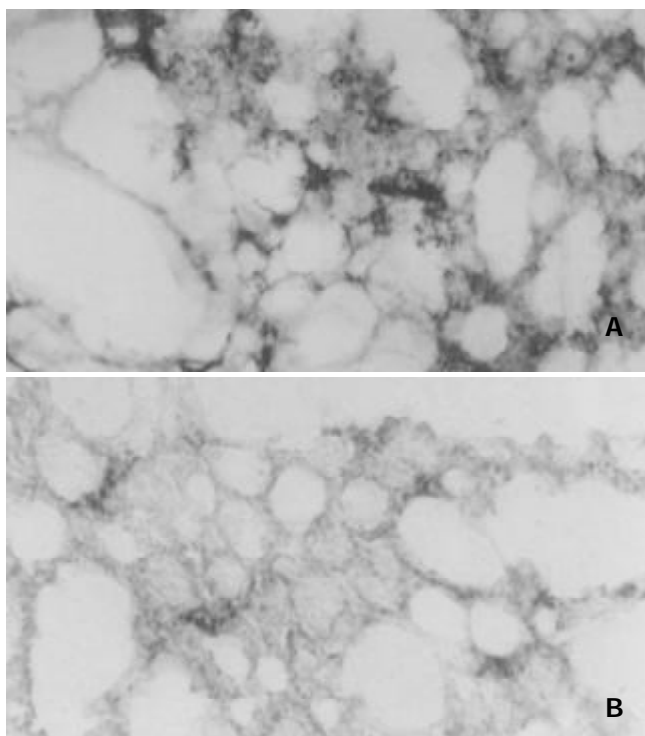


Figure 3 Expression of pcDNA3.0/endostatin *in vivo*. The lung tissue sections from mice treated with TF-liposome-pcDNA3.0/endostatin (A) and from mice treated with TF-liposome-pcDNA3.0 (B) were treated with anti-HA antibody.

Endostatin inhibits the growth of primary liver tumors

To determine the efficacy of the TF-liposome-endostatin complex on tumor growth, we treated tumor-bearing mice with aerosol containing the complex. Tumor growth in the mice treated with 50, 250 and 500 mg DNA/kg was inhibited by 36.6 %, 40.8 %, and 72.8 %, respectively ($P < 0.01$). We concluded that the growth of primary tumors was significantly suppressed by systemic therapy with TF-liposome-pcDNA3.0/endostatin in a dose-dependent manner (Figure 4).

Endostatin inhibits angiogenesis in primary tumors

Immunohistochemical analysis showed a potent inhibition of angiogenesis in the tumors treated with the TF-liposome-pcDNA3.0/endostatin complex. Blood vessels were counted in three areas of each tumor section. There were significantly ($P < 0.01$) less microvessels in the tumors of treated mice versus control mice after staining of the tumor tissues with a rat anti-mouse CD-31 monoclonal antibody (Figure 5).

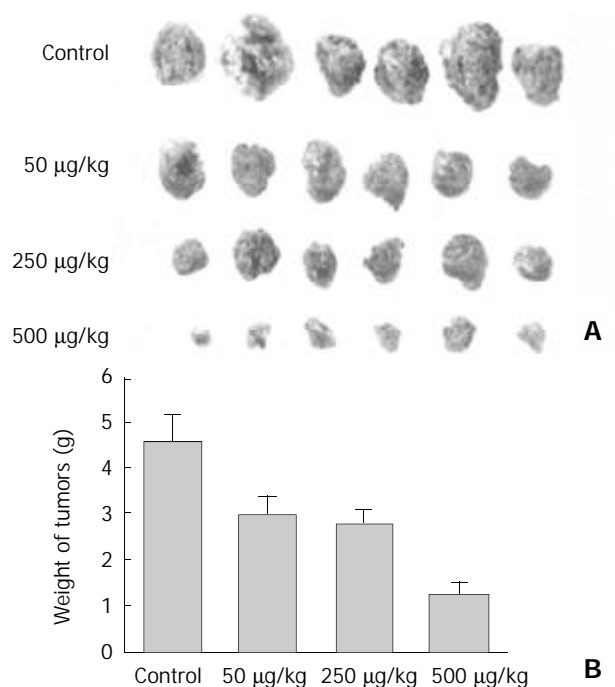


Figure 4 TF-liposome containing endostatin inhibits tumor growth. A: Tumors excised from mice treated with different doses of TF-liposome-pcDNA3.0/endostatin, or with TF-liposome-pcDNA3.0 (negative control). B: Tumor weight of mice treated with TF-liposome-pcDNA3.0/endostatin or TF-liposome-pcDNA3.0 vector. Each bar represents the mean \pm SD for six mice.

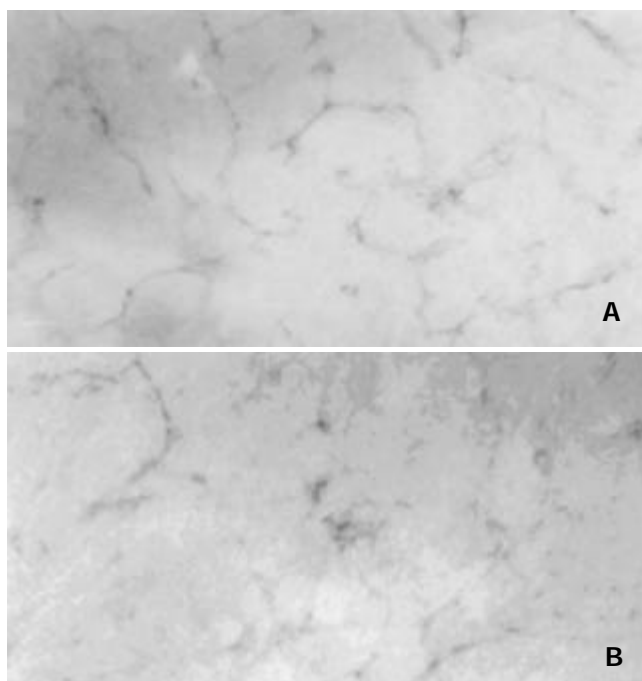


Figure 5 Reduced angiogenesis in TF-liposome-pcDNA3.0/endostatin treated tumors. Tumor sections from mice treated with TF-liposome-pcDNA3.0 (A) or treated with TF-liposome-

pcDNA3.0/endostatin (B) were stained with a CD-31 monoclonal antibody. CD-31-positive cells were brown whereas negative cells colorless in stain.

Quantitation of vessel density was determined under microscopy of the areas of brown (positive) and colorless (negative) staining at 432-fold magnification. One unit visual field encompassed 128×128 pixels. The positively stained area of the endostatin-treated group was significantly lower ($P < 0.01$, $645.8 \pm 55.2 \mu\text{m}^2$, mean \pm SD) than that of the control group ($1\,325.4 \pm 198.5 \mu\text{m}^2$, mean \pm SD), which showed that the TF-liposome-pcDNA3.0/endostatin complex blocked tumor angiogenesis, while the TF-liposome-pcDNA3.0 vector complex, as a negative control, did not block angiogenesis, which indicated that the inhibition of angiogenesis was caused by the introduced endostatin gene.

Induction of apoptosis in tumor cells by introduced endostatin gene

Fragmentation of cellular DNA represents a main change in the nuclei of cells undergoing apoptosis. Administration of the TF-liposome-pcDNA3.0/endostatin complex resulted in the typical DNA ladder pattern in apoptotic cells of tumor tissues (Figure 6). However, no DNA fragmentation could be detected in the tumor tissues from mice treated with the empty vector complex. The results showed that the introduced endostatin gene blocked angiogenesis accompanied by induction of apoptosis in liver tumors.

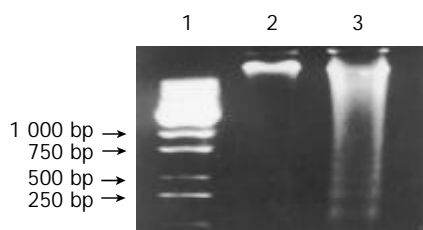


Figure 6 The introduced endostatin gene induces apoptosis in cells of tumor tissues. DNA was extracted from tumors and DNA fragmentation identified on a 15 g·L⁻¹ agarose gel. Lane 1: the DNA molecular weight marker; lane 2: DNA from mice treated with TF-liposome-pcDNA3.0 vector; lane 3: DNA from mice treated with TF-liposome-pcDNA3.0/endostatin.

DISCUSSION

Inhibition of angiogenesis has recently been acknowledged as a promising strategy to treat cancer. Endostatin, an endogenous angiogenesis inhibitor, specifically suppresses endothelial cell proliferation, thereby acting as a competitor for angiogenesis inducers secreted by tumor cells. The use of endostatin may serve as an attractive new strategy in cancer therapy^[22-25]. However, poor solubility of the endostatin protein together with a high effective dose hampered its widespread application, although high and continuous endostatin expression can be obtained by direct induction of the endostatin gene *in vivo*.

In recent years, great progress has been made in anti-cancer gene therapy and different gene delivery systems, based on retroviruses^[15,26,27], adenoviruses^[14,28] and liposomes have been used in animals. Liposomes are considered to provide a safer gene therapy delivery method, and can be administered intravenously, intramuscularly, intraperitoneally, or by intratracheal injection^[17,18,20,29]. We used a transferrin facilitated liposome delivery of the endostatin gene by aerosol administration in our experiments. This method provides several advantages: (1) Lung tissue and airways cover a large surface area, therefore the introduced gene can be expressed

efficiently in the lung. (2) TF enhances the efficiency of gene expression and transfection by facilitating the entry of DNA into the cells. (3) Recent liposome toxicity studies in the lungs of humans and several animal species show that liposomes cause no or minimal host inflammatory and immune responses^[30,31]. (4) Aerosol administration is convenient and can be performed repeatedly by the patients themselves.

In the TF-liposome-DNA mediated gene transfer system, transferrin facilitated the delivery of DNA by binding to its receptors. The liposomes along with the DNA were internalized by fusion with the plasma membrane and underwent receptor-mediated endocytosis. Following the internalization of the TF-liposome-DNA-TF receptor complex, transferrin may facilitate the escape of DNA from the endosome. So the transfection efficiency was improved by this transfer system^[18,32]. Indeed, the degree of inhibition of tumor growth (72.8 %) in our studies was greater than that reported by another group (49 %)^[17], who used liposomes alone to deliver the endostatin gene.

The potent antiangiogenic effect of endostatin can specifically inhibit the proliferation and migration of endothelial cells and subsequently promote the development of apoptosis and atrophy of tumors without direct influence on tumor cell or nonneoplastic cell growth^[33-35]. Our results demonstrated that typical DNA fragmentation was found in the nuclei of cells from tumor tissues of the mice treated with TF-liposome-pcDNA3.0/endostatin complexes, but not in the control group.

In conclusion, our results showed a strong inhibition of angiogenesis and tumor growth in mice after administration of the TF-liposome-endostatin plasmid complex. This suggests that TF-liposome-DNA complexes can be utilized as an efficient method for anti-angiogenic gene delivery to tumors in the gene therapy for cancers.

ACKNOWLEDGEMENTS

We would like to thank Drs. Sandra Liekens and Yan Chen from New York University School of Medicine for preparing this manuscript.

REFERENCES

- 1 **Folkman J**, Watson K, Ingber D, Hanahan D. Induction of angiogenesis during the transition from hyperplasia to neoplasia. *Nature* 1989; **339**: 58-62
- 2 **Perletti G**, Concaro P, Giardini R, Marras E, Piccinini F, Folkman J, Chen L. Antitumor activity of endostatin against carcinogen-induced rat primary mammary tumors. *Cancer Res* 2000; **60**: 1793-1796
- 3 **Dhanabal M**, Ramchandran R, Waterman MJF, Lu H, Knebelmann B, Segal M, Sukhatme VP. Endostatin induce endothelial cell apoptosis. *J Biol Chem* 1999; **274**: 11721-11726
- 4 **Jiang YF**, Yang ZH, Hu JQ. Recurrence or metastasis of HCC: predictors, early detection and experimental antiangiogenic therapy. *World J Gastroenterol* 2000; **6**: 61-65
- 5 **Hahnfeldt P**, Panigrahy D, Folkman J, Hlatky L. Tumor development under angiogenic signaling: a dynamical theory of tumor growth, treatment response and postvascular dormancy. *Cancer Res* 1999; **59**: 4770-4775
- 6 **Liu DH**, Zhang XY, Fan DM, Huang YX, Zhang JS, Huang WQ, Zhang YQ, Huang QS, Ma WY, Chai YB, Jin M. Expression of vascular endothelial growth factor and its role in oncogenesis of human gastric carcinoma. *World J Gastroenterol* 2001; **7**: 500-505
- 7 **Fan ZR**, Yang DH, Cui J, Qin HR, Huang CC. Expression of insulin like growth factor II and its receptor in hepatocellular carcinoma. *World J Gastroenterol* 2001; **7**: 285-288
- 8 **Folkman J**. Clinical applications of research on angiogenesis. *N Engl J Med* 1995; **333**: 1757-1763
- 9 **O'Reilly MS**, Holmgren L, Shing Y, Chen C, Rosenthal RA, Moses M, Lane WS, Cao Y, Sage EH, Folkman J. Angiostatin: a novel

- angiogenesis inhibitor that mediates the suppression of metastases by a Lewis lung carcinoma. *Cell* 1994; **79**: 315-328
- 10 **O' Reilly MS**, Boehm T, Shing Y, Fukai N, Vasios G, Lane WS, Flynn E, Birkhead JR, Olsen BR, Folkman J. Endostatin: an endogenous inhibitor of angiogenesis and tumor growth. *Cell* 1997; **88**: 277-285
 - 11 **Hanahan D**, Folkman J. Patterns and emerging mechanisms of the angiogenic switch during tumorigenesis. *Cell* 1996; **86**: 353-364
 - 12 **O' Reilly MS**, Holmgren L, Chen C, Folkman J. Angiostatin induces and sustains dormancy of human primary tumors in mice. *Natl Med* 1996; **2**: 689-692
 - 13 **Nguyen JT**, Wu P, Clouse ME, Hlatky L, Terwilliger EF. Adeno-associated virus-mediated delivery of antiangiogenic factors as an antitumor strategy. *Cancer Res* 1998; **58**: 5673-5677
 - 14 **Sauter BV**, Martinet O, Zhang WJ, Mandeli J, Woo SLC. Adenovirus-mediated gene transfer of endostatin *in vivo* results in high level of transgene expression and inhibition of tumor growth and metastases. *Proc Natl Acad Sci USA* 2000; **97**: 4802-4807
 - 15 **Wang X**, Liu FK, Li X, Li JS, Xu GX. Inhibitory effect of endostatin expressed by human liver carcinoma SMMC7721 on endothelial cell proliferation *in vitro*. *World J Gastroenterol* 2002; **8**: 253-257
 - 16 **Blezinger P**, Wang J, Gondo M, Quezada A, Mehrens D, French M, Singhal A, Sullivan S, Rolland A, Ralston R, Min W. Systemic inhibition of tumor growth and tumor metastases by intramuscular administration of the endostatin gene. *Nat Biotechnol* 1999; **17**: 343-348
 - 17 **Chen QR**, Kumar D, Stass SA, Mixson AJ. Liposomes complexed to plasmids encoding angiostatin and endostatin inhibit breast cancer in nude mice. *Cancer Res* 1999; **59**: 3308-3312
 - 18 **Xu L**, Pirolo KF, Tang WH, Rait A, Chang EH. Transferrin-liposome-mediated systemic p53 gene therapy in combination with radiation results in regression of human head and neck cancer xenografts. *Hum Gene Ther* 1999; **10**: 2941-2952
 - 19 **Kanamori T**, Mizushima S, Shimizu Y, Morishita H, Kubota H, Nii A, Ogino H, Nagase Y, Kisaragi M, Nobuhara M. Expression and excretion of human pancreatic secretory trypsin inhibitor in lipoprotein-deletion mutant of *Escherichia coli*. *Gene* 1988; **66**: 295-300
 - 20 **Lee ER**, Marshall J, Siegel CS, Jiang C, Yew NS, Nichols MR, Nietupski JB, Ziegler RJ, Lane MB, Wang KX. Detailed analysis of structures and formulations of cationic lipids for efficient gene transfer to the lung. *Hum Gene Ther* 1996; **7**: 1701-1717
 - 21 **Lin PF**. Antitumor effect of actinidia chinensis polysaccharide on murine tumor. *Zhonghua Zhongliu Zazhi* 1988; **10**: 441-444
 - 22 **Yoon SS**, Eto H, Lin CM, Nakamura H, Pawlik TM, Song SU, Tanabe KK. Mouse endostatin inhibits the formation of lung and liver metastases. *Cancer Res* 1999; **59**: 6251-6256
 - 23 **Yokoyama Y**, Dhanabal M, Griffioen AW, Sukhatme VP, Ramakrishnan S. Synergy between angiostatin and endostatin: inhibition of ovarian cancer growth. *Cancer Res* 2000; **60**: 2190-2196
 - 24 **Kim YM**, Jang JW, Lee OH, Yeon J, Choi EY, Kim EW, Lee ST, Kwon YG. Endostatin inhibits endothelial and tumor cellular invasion by blocking the activation and catalytic activity of matrix metalloproteinase. *Cancer Res* 2000; **60**: 5410-5413
 - 25 **Kuger EA**, Durat PH, Tsokos MG, Venzon DJ, Libutti SK, Dixon SC, Rudek MA, Pluda J, Allegra C, Figg WD. Endostatin inhibits microvessel formation in the ex vivo rat aortic ring angiogenesis assay. *Biochem and Biophys Res Commun* 2000; **268**: 183-191
 - 26 **Roth JA**, Nguyen D, Lawrence DD, Kemp BL, Carrasco CH, Ferson DZ, Hong WK, Komaki R, Lee JJ, Nesbitt JC, Pisters KM, Putnam JB, Schea R, Shin DM, Walsh GL, Dolormente MM, Han CI, Martin FD, Yen N, Xu K, Stephens LC, McDonnell TJ, Mukhopadhyay T, Cai D. Retrovirus-mediated wild-type p53 gene transfer to tumors of patients with lung cancer. *Nat Med* 1996; **2**: 985-991
 - 27 **Xiao B**, Jing B, Zhang YL, Zhou DY, Zhang WD. Tumor growth inhibition effect of hIL-6 on colon cancer cells transfected with the target gene by retroviral vector. *World J Gastroenterol* 2000; **6**: 89-92
 - 28 **Feldman AL**, Restifo NP, Alexander HR, Bartlett DL, Hwu P, Seth P, Libutti K. Antiangiogenic gene therapy of cancer utilizing a recombinant adenovirus to elevate systemic endostatin levels in mice. *Cancer Res* 2000; **60**: 1503-1506
 - 29 **Thurston G**, McLean JW, Rizen M, Baluk P, Haskell A, Murphy TJ, Hanahan D, McDonald DM. Cationic liposomes target angiogenic endothelial cells in tumors and chronic inflammation in mice. *J Clin Invest* 1998; **101**: 1401-1413
 - 30 **Nabel EG**, Gordon D, Yang ZY, Xu L, San H, Plautz GE, Wu BY, Gao X, Huang L, Nabel GJ. Gene transfer *in vivo* with DNA-liposome complexes: lack of autoimmunity and gonadal localization. *Hum Gene Ther* 1992; **3**: 649-656
 - 31 **Stewart MJ**, Plautz GE, Del Buono L, Yang ZY, Xu L, Gao X, Huang L, Nabel EG, Nabel GJ. Gene transfer *in vivo* with DNA-liposome complexes: safety and acute toxicity in mice. *Hum Gene Ther* 1992; **3**: 267-275
 - 32 **Xu L**, Pirolo KF, Chang EH. Transferrin-liposome-mediated p53 sensitization of squamous cell carcinoma of the head and neck to radiation *in vitro*. *Hum Gene Ther* 1997; **8**: 467-475
 - 33 **Berger AC**, Feldman AL, Gnant MFX, Kruger EA, Sim BKL, Hewitt S, Figg WD, Alexander HR, Libutti SK. The angiogenesis inhibitor, endostatin, does not affect murine cutaneous wound healing. *J Surg Res* 2000; **91**: 26-31
 - 34 **Sasaki T**, Fukai N, Mann K, Gohring W, Olsen BR, Timpl R. Structure, function and tissue forms of the C-terminal globular domain of collagen X VIII containing the angiogenesis inhibitor endostatin. *Embo J* 1998; **17**: 4249-4256
 - 35 **Dhanabal M**, Volk R, Ramchandran R, Simons M, Sukhatme VP. Cloning, expression, and *in vitro* activity of human endostatin. *Biochem and Biophys Res Commun* 1999; **258**: 345-352

Expression of IGF-II in early experimental hepatocellular carcinomas and its significance in early diagnosis

Zheng Wang, You-Bing Ruan, Yang Guan, Sheng-Hong Liu

Zheng Wang, You-Bing Ruan, Yang Guan, Department of Pathology, Tongji Medical College, Huazhong University of Science and Technology, Wuhan 430030, Hubei Province, China

Sheng-Hong Liu, Department of Histology and Embryology, Tongji Medical College, Huazhong University of Science and Technology, Wuhan 430030, Hubei Province, China

Supported by National Natural Science Foundation of China, No. 30070847

Correspondence to: Professor You-Bing Ruan, Department of Pathology, Tongji Medical College, 13 Hangkong Road, Wuhan 430030, Hubei province, China. ruanyb@public.wh.hb.cn

Telephone: +86-27-83692639 **Fax:** +86-27-83691794

Received: 2002-06-17 **Accepted:** 2002-08-09

Abstract

AIM: To investigate the serum level and expression of insulin growth factor II (IGF-II) in liver tissues of rats with early experimental hepatocellular carcinomas (HCC) and its significance in early diagnosis.

METHODS: Early experimental hepatocellular carcinomas were induced by diethylnitrosamine (DENa) in 180 male SD rats. Another 20 male SD rats served as control. The IGF-II serum level was measured by ELISA. Immunohistochemistry and electron microscopic immunohistochemistry were used to observe the expression of IGF-II in normal and tumor liver tissues and its ultrastructural location in malignant hepatocytes. The expressions of IGF-II in human hepatoma cell lines HepG2, SMMC7721 and human embryonic liver cell line L-02 were measured by immunocytochemistry. IGF-II mRNA level was studied by in situ hybridization.

RESULTS: IGF-II was expressed in the cytoplasm of both sinusoidal cells in paracancerous cirrhotic liver tissue and malignant hepatocytes in early experimental HCC tissues. Gold particles were seen on the rough endoplasmic reticulum and the mitochondrion in malignant hepatocytes. IGF-II was expressed in the human hepatoma cell lines. The mRNA level of IGF-II was higher in rat liver tumor tissue than in normal rat liver tissue. The serum IGF-II level of the early experimental HCC group was 34.67 ± 10.53 ng·ml⁻¹ and that of the control group was 11.75 ± 5.84 ng·ml⁻¹. The rank sum test was used for statistical analysis. There was a significant difference between the two groups ($P < 0.01$).

CONCLUSION: During the induction of early experimental HCC by DENa, IGF-II may promote hepatocytic proliferation via a paracrine mechanism in the pre-cancerous stage. When hepatocytes are transformed into malignant cells, they may secrete IGF-II and promote malignant cell proliferation by an autocrine mechanism. IGF-II may be a possible biological marker in the early diagnosis of HCC.

Wang Z, Ruan YB, Guan Y, Liu SH. Expression of IGF-II in early experimental hepatocellular carcinomas and its significance in early diagnosis. *World J Gastroenterol* 2003; 9(2): 267-270
<http://www.wjgnet.com/1007-9327/9/267.htm>

INTRODUCTION

IGF-II is a 67-amino-acid polypeptide growth factor which is mainly produced by liver cells and is crucial in normal fetal growth^[1-2]. The main researches about the relationship between IGF-II and HCC have been focused on: (1) the mechanism of IGF-II in the development of HCC^[3-6], (2) to decrease the expression of IGF-II searching the treatment methods for HCC^[7-9], and (3) its prognostic significance^[10]. Although IGF-II is believed to be implicated in normal and neoplastic liver growth, the mechanism of IGF-II in early hepatocellular carcinomas development and its significance in the early diagnosis of such cancer are unclear. So we used ELISA, immunohistochemistry, electron microscopic immunocytochemistry and in situ hybridization to search for possible answers to the questions.

MATERIALS AND METHODS

Animal model and tissue preparation

180 male SD rats were given DENa (diethylnitrosamine), once every week for 17 weeks in a dose of 70 mg/kg, to induce early experimental HCC. In the control group, 20 male SD rats were maintained on a standard laboratory diet and tap water. From the 4th week, 2 random experimental rats were sacrificed at the end of every week for pathological study of their livers. The remainder were killed at the 17th week for study. Sera were collected and stored at -70 °C. Liver tissues were fixed in 40 ml·L⁻¹ paraformaldehyde or 40 ml·L⁻¹ paraformaldehyde containing 5 ml·L⁻¹ glutaraldehyde for light and electron microscopic studies.

Cell lines culture

Human hepatoma cell lines HepG2 and SMMC7721, and human embryonic liver cell line L-02 (Wuhan University Cell Center) in PRMI 1640 (GIBCO), with 100 ml·L⁻¹ fetal calf serum (GIBCO), and 37 °C, 50 ml·L⁻¹ CO₂.

ELISA detection for the serum level of IGF-II

100 ul of goat anti-IGF-II polyclonal antibody (Santa Cruz Co.) (25 ug/ml in 0.1 mol/L NaHCO₃) was put into each well of a 96-well ELISA plate, and incubated for 36 hours at 4 °C. Nonspecific protein binding was blocked by 100 ul, 10 ml·L⁻¹ bovine serum albumin. Then 100 ul of sera of rat and recombinant human IGF-II (Pepro Tech Co.) were separately added to the wells, 1 hour at 37 °C. The 100 ul of Rabbit anti-IGF-II polyclonal antibody (Santa Cruz Co.) (1:200 dilution) was added to the wells, 1 hour at 37 °C. HRP-conjugated goat anti-rabbit immunoglobulin (Southern Biotech Co.) (1:2 000 dilution), 100 ul, 1 hour at 37 °C. Binding was developed with ortho-phenylene diamine. Absorbance was read at 490 nm. During the performance, washing the plate was according to the ELISA routine method.

Immunohistochemical detection for IGF-II expression in early experimental HCC tissues

Immunohistochemical detection was made using rabbit anti-IGF-II polyclonal antibody (Santa Cruz Co.) by SABC

technique. The experiment was performed following the manufacturer's recommendation of the SABC kit (Beijing Zhongshan Bioech Co.).

Immunocytochemical detection for IGF-II expression in human cell lines

Human hepatoma cell lines HepG2 and SMMC7721 and human embryonic cell line L-02 were cultivated to let them climb on coverslips, which then fixed in acetone at -20°C for 10 minutes. The antibody, SABC kit and experimental method were the same as those for the immunohistochemical detection.

Electron microscopic immunocytochemistry for IGF-II ultrastructural location in malignant hepatocytes

Early experimental HCC tissues were cut into 500 nm ultrathin sections, and the sections were etched in 10 % hydrogen peroxide solution for 10 minutes at room temperature. After the grids were drained, the sections were placed into 40 ml \cdot L⁻¹ BSA solution, and then were treated overnight at 4°C with rabbit anti-IGF-II polyclonal antibody (1:50 dilution). The sections were incubated with colloidal gold (5 nM) conjugated goat anti-rabbit IgG (Wuhan Best Co.) (1:40 dilution), 37°C , 10 minutes. The sections were examined with a transmission electron microscopy after counter staining. The solution for diluting antibody replacing the rabbit anti-IGF-II polyclonal antibody for those sections served as the negative control.

In situ hybridization detection for IGF-II mRNA level in early experimental HCC tissues

IGF-II in situ hybridization kit was purchased from the Wuhan Best Co. The experiment was conducted according to the manual of the kit.

Statistical analysis

SAS software and Rank Sum Test were used for statistical analysis.

RESULTS

Microscopic observation and histopathological examination

In the DENA group, the liver surfaces were covered with scattered small white nodules in the 4th week. In the 17th week, the diameter of the largest nodule was 8 mm. These rats were diagnosed as having early experimental hepatocellular carcinomas. The rat livers in the control group showed no pathological changes.

IGF-II serum level of early experimental HCC

The mean \pm standard deviation of IGF-II serum level was $34.67 \pm 10.53 \text{ ng} \cdot \text{ml}^{-1}$ in the DENA group and $11.75 \pm 5.84 \text{ ng} \cdot \text{ml}^{-1}$ in the control group. There was significant difference between the two groups ($P < 0.01$).

Expression of IGF-II in early experimental HCC tissues

Strong immunostaining of IGF-II was seen in the cytoplasm of sinusoidal cell in paracancerous cirrhotic tissues (Figure 1) and the malignant hepatocytes in HCC tissues. Only a few hepatocytes in paracancerous tissues had weakly positive expression. In the control group, however, the liver tissues showed no positive results.

Expression of IGF-II in human cell lines

Human hepatoma cell lines HepG2 and SMMC7721 and human embryonic liver cell line L-02 all expressed IGF-II. The positive immunolocalization of the three cell lines was in the cytoplasm. SMMC7721 cell line showed the most strongly positive immunostaining (Figure 2).

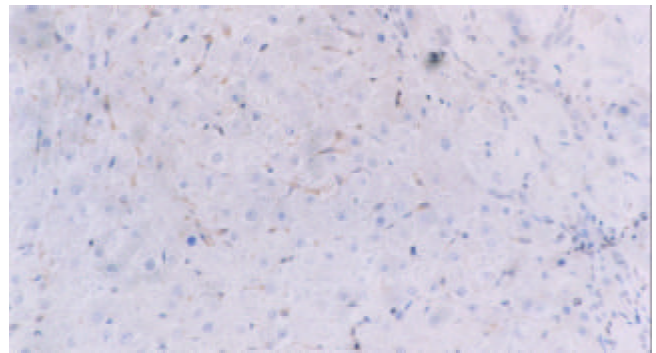


Figure 1 IGF-II expression in the cytoplasm of sinusoidal cells in the paracancerous cirrhotic tissues. Immunohistochemical staining, $\times 200$.

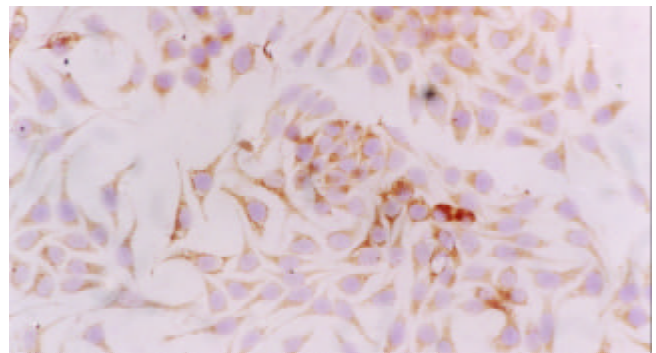


Figure 2 IGF-II expression in the cytoplasm of SMMC7721 cell line. Immunocytochemical staining, $\times 200$.

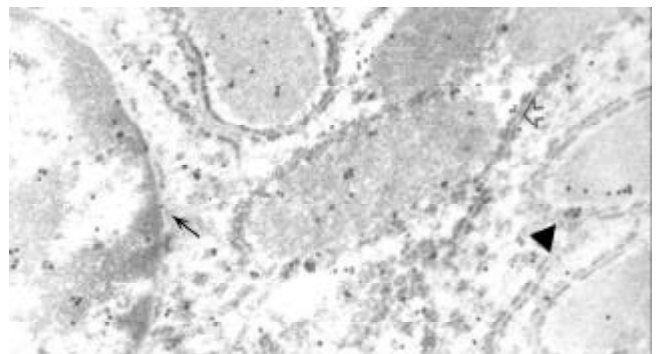


Figure 3 Colloidal gold particles in rough endoplasmic reticulum (||), mitochondrion (\blacktriangle), nucleus and paranuclear region (\leftarrow). Electron microscopic immunocytochemical staining for IGF-II, $\times 16\ 000$.

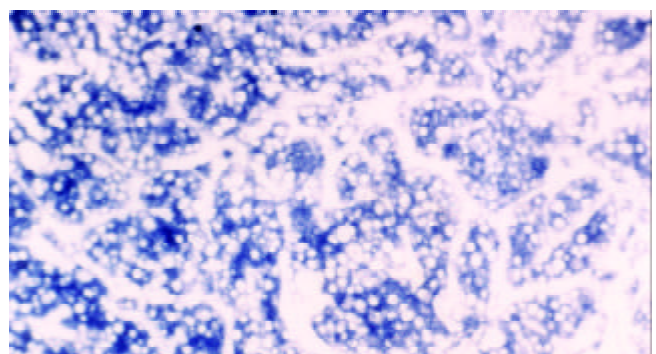


Figure 4 Expression of IGF-II mRNA in the cytoplasm of malignant hepatocytes. In situ hybridization, $\times 200$.

Ultrastructural localization of IGF-II in malignant hepatocytes of early experimental HCC tissues

Electron microscopic immunocytochemistry confirmed the light microscopic findings. Gold particles were seen in the rough endoplasmic reticulum, mitochondrion and the paranuclear region of malignant hepatocytes. A few gold particles were found in the nuclei of malignant hepatocytes (Figure 3). The negative control sections did not show positive results.

IGF-II mRNA level in early experimental HCC tissues

IGF-II mRNA was distributed in the cytoplasm of hepatocytes in the tissues of early experimental HCC, and IGF-II mRNA was overexpressed in HCC tissues (Figure 4).

DISCUSSION

Among the many growth factors, the insulin-like growth factor, transformation growth factor- α and hepatocyte growth factor are mostly strongly implicated in normal and neoplastic liver growth^[11-17]. IGF-II exerts its effect via two specific high affinity receptors, IGF1R and M6P/IGF2R, in paracrine and autocrine manner^[18-22]. IGF1R is a transmembrane glycoprotein which exists on the surface of hepatocytes with an intracellular tyrosine kinase domain. M6P/IGF2R is a single chain polypeptide associated with a G-protein signal pathway. In the present study, it has clearly been shown that: (1) the sinusoidal cells in paracancerous cirrhotic nodule tissues expressed IGF-II; (2) the malignant hepatocytes in rat early experimental HCC tissues expressed IGF-II. As we know that liver cirrhotic nodules are the pre-cancerous condition of HCC^[23], so it is clearly suggested that, in the pre-cancerous condition, IGF-II mediated hepatocyte proliferation mainly via IGF1R by a paracrine mechanism. However, after the hepatocytes were transformed into malignant cells, they could secrete IGF-II themselves, suggesting that IGF-II mediated malignant hepatocytes proliferation in an autocrine manner at that time and that M6P/IGF2R might be involved. Although several reports have shown that M6P/IGF2R protein and mRNA level were reduced and that the M6P/IGF2R gene had loss of heterozygosity in HCC^[24,25], Gomez-Angelats and Wada reported that no mutation was found in the M6P/IGF2R gene in the model of rat hepatocarcinogenesis and human HCC^[26,27]. By electron microscopic immunocytochemistry, we found that IGF-II existed in the mitochondria of malignant hepatocytes. M6P/IGF2R is a G-protein receptor which is closely related to mitochondrion. So we favor Gomez-Angelats' view that M6P/IGF-II was in an activated condition in the process of rat hepatocarcinogenesis.

Human hepatoma cell lines HepG2 and SMMC7721 expressed IGF-II strongly. This fact confirms the above postulate in another aspect, i.e., IGF-II could be secreted by malignant hepatocytes themselves and stimulate their proliferation via an autocrine mechanism. Human embryonic liver cell line L-02 expressed IGF-II too, suggesting that hepatoma cells may regain some embryonic development characteristics, like α -FP secretion.

α -FP is a diagnostic marker of HCC, but its significance in the early diagnosis of HCC is unclear and the positive rate is not high^[28-30]. In our research, the serum IGF-II level in the rat early experimental HCC group was significantly higher than that of the control group. IGF-II is a polypeptide hormone secreted by many organs of the fetus. After birth, however, it is mainly produced by liver cells^[31,32]. We may postulate that, in rat early experimental HCC, extrahepatic organs may regain the ability to secrete IGF-II and that their intrahepatic cells express IGF-II more strongly than those in normal condition^[33,35]. These might be the main reasons for the increase in serum IGF-II level. Hayakawa reported that the serum level of IGF-II was

significantly lower in primary hepatocellular carcinomas than in control^[36], but we haven't found any report on the serum IGF-II level in early HCC. So it is possible that serum IGF-II level increases temporarily in early HCC and then decreases gradually in the process of HCC development, IGF-II maybe a biological marker in the early diagnosis of HCC.

REFERENCES

- 1 **Kawamoto K**, Onodera H, Kan S, Kondo S, Imamura M. Possible paracrine mechanism of insulin-like growth factor-2 in the development of liver metastases from colorectal carcinomas. *Cancer* 1999; **85**: 18-25
- 2 **Hartmann W**, Waha A, Koch A, Albrecht S, Gray SG, Ekstrom TJ, von Schweinitz D, Pietsch T. Promoter-specific transcription of the IGF-2 gene: a novel rapid, non-radioactive and highly sensitive protocol for mRNA analysis. *Virchows Arch* 2001; **439**: 803-807
- 3 **Eriksson T**, Frisk T, Gray SG, von Schweinitz D, Pietsch T, Larsson C, Sandstedt B, Ekstrom TJ. Methylation changes in the human IGF-2 p3 promoter parallel IGF-2 expression in the primary tumor, established cell line, and xenograft of a human hepatoblastoma. *Exp Cell Res* 2001; **270**: 88-95
- 4 **Vernucci M**, Cerrato F, Besnard N, Casola S, Pedone PV, Bruni CB, Riccio A. The H19 endodermal enhancer is required for IGF-2 activation and tumor formation in experimental liver carcinogenesis. *Oncogene* 2000; **19**: 6376-6385
- 5 **Song BC**, Chung YH, Kim JA, Lee HC, Yoon HK, Sung KB, Yang SH, Yoo K, Lee YS, Suh DJ. Association between insulin-like growth factor-II and metastases after transcatheter arterial chemoembolization in patient with hepatocellular carcinomas: a prospective study. *Cancer* 2001; **91**: 2386-2393
- 6 **Bae SK**, Bae MH, Ahn MY, Son MJ, Lee YM, Bae MK, Lee OH, Park BC, Kim KW. Egr-1 mediates transcriptional activation of IGF-2 gene in response to hypoxia. *Cancer Res* 1999; **59**: 5989-5994
- 7 **Scharf JG**, Dombrowski F, Ramadori G. The IGF axis and hepatocarcinogenesis. *Mol Pathol* 2001; **54**: 138-144
- 8 **Huynh H**, Chow PK, Ooi LL, Soo KC. A possible role for insulin-like growth factor-binding protein-3 autocrine/paracrine loops in controlling hepatocellular carcinoma cell proliferation. *Cell Growth Differ* 2002; **13**: 115-122
- 9 **Zhang JY**, Zhu W, Imai H, Kiyosawa K, Chan EK, Tan EM. De novo humoral immune responses to cancer-associated autoantigens during transition from chronic liver disease to hepatocellular carcinoma. *Clin Exp Immunol* 2001; **125**: 3-9
- 10 **Barozzi C**, Ravaoli M, D'Errico A, Grazi GL, Poggioli G, Cavrini G, Mazziotti A, Grigioni WF. Relevance of biologic markers in colorectal carcinoma: a comparative study of a broad panel. *Cancer* 2002; **94**: 647-657
- 11 **Zhang N**, Siegel K, Odenthal M, Becker R, Oesch F, Dienes HP, Schirmacher P, Steinberg P. The role of insulin-like growth factor II in the malignant transformation of rat liver oval cells. *Hepatology* 1997; **25**: 900-905
- 12 **Chung YH**, Kim JA, Song BC, Lee GC, Koh MS, Lee YS, Lee SG, Suh DJ. Expression of transforming growth factor- α mRNA in liver of patients with chronic viral hepatitis and hepatocellular carcinoma. *Cancer* 2000; **89**: 977-982
- 13 **Nagata K**, Hirono S, Ido A, Kataoka H, Moriuchi A, Shimomura T, Hori T, Hayashi K, Koono M, Kitamura N, Tsubouchi H. Expression of hepatocyte growth factor activator and hepatocyte growth factor activator inhibitor type 1 in human hepatocellular carcinoma. *Biochem Biophys Res Comm* 2001; **289**: 205-211
- 14 **Tavian D**, Petro GD, Benetti A, Portolani N, Giulini SM, Barlati S. u-PA and c-MET mRNA expression is co-ordinately enhanced while hepatocyte growth factor mRNA is down-regulated in human hepatocellular carcinoma. *Int J Cancer* 2000; **87**: 644-649
- 15 **Schweinitz DV**, Faundez A, Teichmann B, Birnbaum T, Koch A, Hecker H, Gluer S, Fuchs J, Pietsch T. Hepatocyte growth-factor scatter factor can stimulate post-operative tumor-cell proliferation childhood hepatoblastoma. *Int J Cancer* 2000; **85**: 151-159
- 16 **Xie Q**, Liu KD, Hu MY, Zhou K. SF/HGF c-Met autocrine and paracrine promote metastasis of hepatocellular carcinoma. *World J Gastroenterol* 2001; **7**: 816-820
- 17 **Qin LX**, Tang ZY. The prognostic molecular markers in hepatocellular carcinoma. *World J Gastroenterol* 2002; **8**: 385-392

- 18 **Su Q**, Liu YF, Zhang JF, Zhang SX, Li DF, Yang JJ. Expression of insulin-like growth factor II in hepatitis B, Cirrhosis and hepatocellular Carcinoma: its relationship with hepatitis B virus antigen expression. *Hepatology* 1994; **19**: 788-799
- 19 **Costello M**, Baxter RC, Scott CD. Regulation of soluble insulin-like growth factor II/mannose 6-phosphate receptor in human serum: measurement by enzyme-linked immunosorbent assay. *J Clin Endocrinol Metab* 1999; **84**: 611-617
- 20 **Fan ZR**, Yang DH, Cui J, Qin HR, Huang CC. Expression of insulin like growth factor II and its receptor in hepatocellular carcinogenesis. *World J Gastroenterol* 2001; **7**: 285-288
- 21 **Scharf JG**, Ramadori G, Dombrowski F. Analysis of the IGF axis in preneoplastic hepatic foci and hepatocellular neoplasms developing after low-number pancreatic islet transplantation into the livers of streptozotocin diabetic rats. *Lab Invest* 2000; **80**: 1399-1411
- 22 **Fan ZR**, Yang DH, Qin HR, Huang CZ, Xu Z, Qu QL. Significance and expression of insulin-like growth factor II and its receptor in hepatocellular carcinogenesis. *Zhonghua Ganzangbing Zazhi* 2000; **8**: 84-86
- 23 **Mei MH**, Xu J, Shi QF, Yang JH, Chen Q, Qin LL. Clinical significance of serum intercellular adhesion molecule-1 detection in patients with hepatocellular carcinoma. *World J Gastroenterol* 2000; **6**: 408-410
- 24 **DeSouza AT**, Hankins GR, Washington MK, Orton TC, Jirtle RL. M6P/IGF-2R gene is mutated in human hepatocellular carcinomas with loss of heterozygosity. *Nat Genet* 1995; **11**: 447-449
- 25 **Yamada T**, De Souza AT, Finkelstein S, Jirtle RL. Loss of the gene encoding mannose6-phosphate/insulin-like growth factor II receptor is an early event in liver carcinogenesis. *Proc Natl Acad Sci* 1997; **94**: 10351-10355
- 26 **Gomez-Angelats M**, Teeguarden JG, Dragan YP, Pitot HC. Mutational analysis of three tumor suppressor genes in two models of rat hepatocarcinogenesis. *Mol Carcinog* 1999; **25**: 157-163
- 27 **Wada I**, Kanada H, Nomura K, Kato Y, Machinami R, Kitagawa T. Failure to detect genetic alteration of the mannose-6-phosphate/insulin-like growth factor 2 receptor(M6P/IGF2R)gene in hepatocellular carcinomas in Japan. *Hepatology* 1999; **29**: 1718-1721
- 28 **Zhai SH**, Liu JB, Liu YM, Zhang LL, Du ZP. Expression of HBsAg, HCV-Ag and AFP in liver cirrhosis and hepatocarcinoma. *Shijie Huaren Xiaohua Zazhi* 2000; **8**: 524-527
- 29 **Zhang L**, Li SN, Wang XN. CEA and AFP expression in human hepatoma cells transfected with antisense IGF-I gene. *World J Gastroenterol* 1998; **4**: 30-32
- 30 **Liu Y**, Zhang BH, Qian GX, Chen H, Wu MC. Detection of blood AFP mRNA in nude mice bearing human HCC using nested RT-PCR and its significance. *World J Gastroenterol* 1998; **4**: 268-270
- 31 **Kim KW**, Bae SK, Lee OH, Bae MH, Lee Mj, Park BC. Insulin-like growth factor II induced by hypoxia may contribute to angiogenesis of human hepatocellular carcinomas. *Cancer Res* 1998; **58**: 348-351
- 32 **Lin SB**, Hsieh SH, Hsu HL, Lai MY, Kan LS, Au LC. Antisense oligodeoxynucleotides of IGF-II selectively inhibit growth of human hepatoma cells overproducing IGF-II. *J Biochem* 1997; **122**: 717-722
- 33 **Fan ZR**, Yang DH, Tan HR. The expression and mutation of IGF-II gene in hepatocarcinoma and para-cancerous tissues. *Shijie Huaren Xiaohua Zazhi* 2000; **8**: 704-705
- 34 **Liang QM**, Zhou ZM, Yang DH, Xu Z. The expression of IGF-II and its receptor for proliferation of hepatocytes in liver tissue. *Shijie Huaren Xiaohua Zazhi* 2000; **8**: 545
- 35 **Ling CQ**, Qian Y, Zhao JA, Jin Y. The genes of C-myc, IGF-II and the expression of CyclinD1 in experimental liver carcinogenesis. *Shijie Huaren Xiaohua Zazhi* 2001; **9**: 1452-1453
- 36 **Hayakawa H**, Kondo T, Shibata T, Kitagawa M, Sakai Y, Kato K, Katada N, Sugimoto Y, Takeichi M, Yamamoto R, Kodaira N. Serum insulin-like growth factor II in chronic liver disease. *Dig Dis Sci* 1989; **34**: 338-342

Edited By Lu HM

Study on the mechanism of epidermal growth factor-induced proliferation of hepatoma cells

Bin-Wen Wu, Yuan Wu, Jia-Long Wang, Ju-Sheng Lin, Shu-Yu Yuan, Ai Li, Wu-Ren Cui

Bin-Wen Wu, Jia-Long Wang, Ju-Sheng Lin, Shu-Yu Yuan, Ai Li, Institute of Liver Disease, Tongji Hospital, Tongji Medical College, HuaZhong Sci.and Tech. University, Wuhan, 430030, HuBei Province, China

Yuan Wu, Shenzheng hospital, Beijing University, Shenzheng, Guangdong Province, China

Wu-Ren Cui, Department of Nuclear Medicine, Tongji Medical College, HuaZhong Sci.and Tech. University, WuHan, 430030, HuBei Province, China

Correspondence to: Jia-Long Wang, Institute of Liver Disease, Tongji Hospital, HuaZhong Sci.and Tech. University, 1095 JieFang AV., Wuhan, 430030, HuBei Province, China. whjllwang@163.net
Telephone: +86-27-83662578

Received: 2001-04-11 **Accepted:** 2002-03-18

Abstract

AIM: Many growth factors, such as epidermal growth factor (EGF), are associated with the carcinogenesis. EGF plays its role in the proliferation of hepatoma cells through binding with EGF receptor (EGFR) and a series of signal transduction. But the postreceptor pathway is still not clear. In the present experiment, we studied the effect of tyrosine kinase, protein kinase C, Na^+/H^+ exchange, calmodulin and voltage-dependent Ca^{2+} channel on EGF-induced hepatoma cell proliferation.

METHODS: Hepatoma cell line SMMC7721 was cultured in RPMI1640 serum-free medium. In order to study the effect of tyrosine kinase, protein kinase C, Na^+/H^+ exchange, calmodulin and voltage-dependent Ca^{2+} channel on human hepatoma cell proliferation induced by epidermal growth factor (EGF), DNA synthesis rate of hepatoma cells was measured by the method of ^3H -TdR incorporation.

RESULTS: EGF (10^{-9} M) stimulated the proliferation of hepatoma cells significantly (^3H -TdR incorporation was $1\ 880\pm 281$ cpm/well, $P<0.05$), and this effect was significantly inhibited by tyrosine kinase inhibitor genistein (^3H -TdR incorporation was 808 ± 209 cpm/well, $P<0.001$). Calmodulin inhibitor W-7, protein kinase C inhibitor H-7 and Na^+/H^+ exchange inhibitor amiloride individually had significant inhibiting effect on EGF-induced proliferation of hepatoma cells (^3H -TdR incorporation was 978 ± 87.3 cpm/well, $1\ 241\pm 147$ cpm/well, $1\ 380\pm 189$ cpm/well, respectively, $P<0.001$, $P<0.01$, $P<0.05$), but they all had no effect on the basal level proliferation of cultured hepatoma cells (^3H -TdR incorporation was $1\ 284\pm 260$ cpm/well, $1\ 179\pm 150$ cpm/well, $1\ 392\pm 152$ cpm/well, respectively, ^3H -TdR incorporation of the control was $1\ 353\pm 175$ cpm/well, $P>0.05$). Voltage-dependent Ca^{2+} channel inhibitor verapamil had no inhibition on EGF-induced proliferation of hepatoma cells (^3H -TdR incorporation was $1\ 637\pm 133$ cpm/well, $P>0.05$), it also had no effect on the basal level proliferation of cultured hepatoma cells (^3H -TdR incorporation was $1\ 196\pm 112$ cpm/well, $P>0.05$).

CONCLUSION: Our data suggest that tyrosine kinase, Ca^{2+} -calmodulin-dependent pathway, protein kinase C and Na^+/H^+

H^+ exchange play a critical role in EGF-induced proliferation of hepatoma cells and that the effect of EGF is independent of voltage-dependent Ca^{2+} channel.

Wu WB, Wu Y, Wang JL, Lin JS, Yuan SY, Li A, Cui WR. Study on the mechanism of epidermal growth factor-induced proliferation of hepatoma cells. *World J Gastroenterol* 2003; 9(2): 271-275
<http://www.wjgnet.com/1007-9327/9/271.htm>

INTRODUCTION

Most hepatocellular carcinoma (HCC) is associated with cirrhosis, a condition in which liver cell necrosis coexists with inflammation and hepatocellular regeneration. HCC arising in cirrhotic livers is exposed to a number of growth factors mediating hepatocellular regeneration. Epidermal growth factor (EGF) is one of them.

EGF is a single strand polypeptide composed of 53 amino acid and has implicated in the regulation of a wide variety of physiological and pathological processes including embryo genesis, growth, tissue repair, regeneration and neoplasia. EGF inhibits gastric acid secretion and has a cytoprotective effect on stomach tissue, EGF has been of clinical interest for the treatment of acid hypersecretion and the healing of ulcers. EGF has been implicated as a hepatotrophic factor during liver regeneration, has protective effect during hepatic damage through inducing the DNA synthesis of hepatic cells^[1-4]. EGF also induces DNA synthesis of hepatoma cells and promotes the occurrence and expansion of hepatoma^[5,6].

EGF exerts its biologic effects by binding with the EGF receptor (EGFR), a type of transmembrane glucoprotein with a molecule of 170kD. The primary structure of its intramembranous part is associated with the expression of oncogene erb-B. The intracellular part of EGFR has tyrosine kinase activity. EGFR is overexpressed in various carcinoma, such as hepatoma^[7-9], gastric carcinoma^[10-14], colon carcinoma^[15-20], lung carcinoma^[21-23] and prostatic carcinoma^[24-28], and also associated with the histologic types and invasiveness of the tumor^[29-32]. Many growth factors have the effect of promoting cells proliferation and malignant transformation by binding with EGFR such as EGF, heparin binding EGF (HB-EGF)^[33,34], transforming growth factor β (TGF- β)^[35,36] and hepatopointin^[37,38]. After the integration of HBV-X gene into hepatic cells, EGFR was activated and overexpressed, which induced liver carcinogenesis^[39].

In general, EGF induces tumor cell division and proliferation through a series of signal transduction by binding with EGF receptor (EGFR) and activating its tyrosine protein kinase and phosphorylating itself and its protein substrate^[40]. This postreceptor signal transduction is associated with phosphatidylinositol pathway^[41]. But the exact mechanism is still not clear.

In this report, we have characterized the anti-tumor activity of tyrosine kinase, calmodulin, protein kinase C, Na^+/H^+ exchange and voltage-dependent Ca^{2+} channel inhibitors. The SMMC7721 cell line cultured in serum-free medium was used in this study.

MATERIALS AND METHODS

Reagents

All chemicals were purchased from sigma chemical CO. (St. Louis, Mo. USA) unless otherwise stated. ^3H -TdR was purchased from the Institute of Nuclear Power of China. Verapamil, streptomycin, penicillin and 0.5 % hydrocortisone were clinical medicines.

Cell culture

SMMC7721 cells were stored in our laboratory and cultured in RPMI1640 serum-free medium. Briefly, SMMC7721 cells were grown in RPMI1640 supplemented with 5 $\mu\text{g}/\text{ml}$ transferrin, 20 $\mu\text{U}/\text{ml}$ insulin, 0.4 $\mu\text{g}/\text{ml}$ hydrocortisone and 100 $\mu\text{g}/\text{ml}$ streptomycin and penicillin.

Experiment program

Eleven groups were separated in the experiment: (1) control, (2) EGF (10^{-9}M), (3) W-7, (4) verapamil, (5) W-7+EGF, (6) verapamil+EGF, (7) genistein+EGF, (8) H-7, (9) H-7+EGF, (10) amiloride, (11) amiloride+EGF.

DNA synthesis rate of hepatoma cells

The DNA synthesis rates were measured by the method of ^3H -TdR incorporation. The hepatoma cells were seeded into 96 well plates at a density of $1 \times 10^4/\text{well}$ and incubated with serum-free RPMI1640. After 24 hours, fresh medium was changed, and reagents added. After incubation for 18 hours the medium was then replaced with fresh medium containing ^3H -TdR 0.5 $\mu\text{Ci}/\text{ml}$ for another 6 hours. The cells were finally lysed with 0.33 mol/L HCl, ^3H -TdR incorporation was determined with a β -counter.

Statistical analysis

Two-side *t* test was used to examine the significant difference between groups.

RESULTS

Effect of genistein on EGF-induced growth of hepatoma cells

Genistein is a tyrosine kinase inhibitor. EGF (10^{-9}M) stimulated the growth of hepatoma cells significantly compared with the control ($P < 0.05$). EGF-induced ^3H -TdR incorporation was reduced from $1\ 880 \pm 281$ cpm/well to 808 ± 209 cpm/well by genistein ($P < 0.001$, Figure 1).

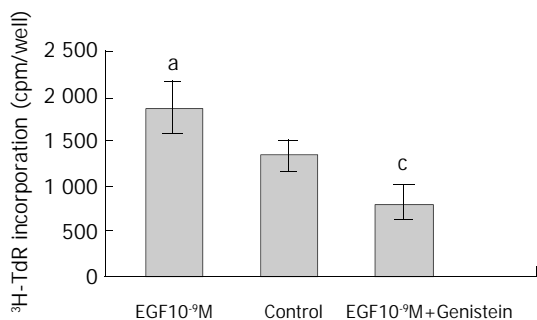


Figure 1 Effect of genistein on EGF-induced ^3H -TdR incorporation into hepatoma cells. $n=6$, $\bar{x} \pm s$ ^a $P < 0.05$, vs control; ^c $P < 0.001$, vs EGF 10^{-9}M .

Effect of W-7 on EGF-induced growth of hepatoma cells

W-7 is a calmodulin inhibitor. W-7 (25 $\mu\text{mol}/\text{L}$) alone had no effect on ^3H -TdR incorporation, the incorporation of W-7 group and control were $1\ 284 \pm 260$ cpm/well and $1\ 353 \pm 175$ cpm/well, respectively ($P > 0.05$). When W-7 was added with EGF

(10^{-9}M), the effect of EGF on the growth of hepatoma cells was inhibited significantly, the incorporation (978 ± 87.3 cpm/well) was significantly lower than that of EGF (10^{-9}M) group ($1\ 880 \pm 281$ cpm/well) ($P < 0.001$, Figure 2).

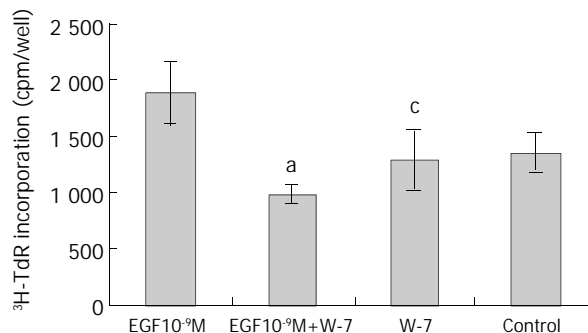


Figure 2 Effect of W-7 on EGF-induced ^3H -TdR incorporation into hepatoma cells. $n=6$, $\bar{x} \pm s$ ^a $P < 0.001$ vs W-7 group; ^c $P > 0.05$ vs control.

Effect of verapamil on EGF-induced growth of hepatoma cells

Verapamil is voltage-dependent Ca^{2+} channel inhibitor. As shown in Figure 3, verapamil (100 $\mu\text{mol}/\text{L}$) alone had no effect on ^3H -TdR incorporation, the incorporation of verapamil group and control were $1\ 196 \pm 112$ cpm/well and $1\ 353 \pm 175$ cpm/well, respectively ($P > 0.05$). When verapamil (100 $\mu\text{mol}/\text{L}$) was used with EGF (10^{-9}M), the incorporation was $1\ 637 \pm 133$ cpm/well, which was not significantly different from the incorporation with EGF (10^{-9}M) alone ($1\ 880 \pm 281$ cpm/well, $P > 0.05$).

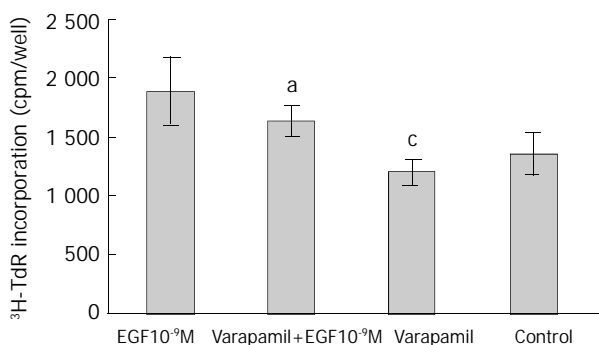


Figure 3 Effect of verapamil on EGF-induced ^3H -TdR incorporation into hepatoma cells. $n=6$, $\bar{x} \pm s$ ^a $P > 0.05$ vs EGF 10^{-9}M group; ^c $P > 0.05$ vs control.

Effect of H-7 on EGF-induced growth of hepatoma cells

H-7 is a specific inhibitor of protein kinase C. H-7 (50 $\mu\text{mol}/\text{L}$) alone had no effect on the basal level ^3H -TdR incorporation, the incorporation of H-7 group and control were $1\ 179 \pm 150$ cpm/well and $1\ 353 \pm 175$ cpm/well, respectively ($P > 0.05$). When H-7 was used together with EGF (10^{-9}M), the effect of EGF on the proliferation of hepatoma cells was inhibited significantly, the incorporation ($1\ 241 \pm 147$ cpm/well) was significantly lower than that of EGF group ($1\ 880 \pm 281$ cpm/well, $P < 0.01$) (Figure 4).

Effect of Na^+/H^+ exchange on EGF-induced growth of hepatoma cells

Amiloride is an inhibitor of Na^+/H^+ exchange. As shown in Figure 5, amiloride (0.1 mmol/L) alone had no effect on ^3H -TdR incorporation, the incorporation of amiloride group and control were $1\ 392 \pm 152$ cpm/well and $1\ 353 \pm 175$ cpm/well, respectively ($P > 0.05$). When amiloride (0.1 mmol/L) was used

with EGF (10^{-9} M), the effect of EGF on the proliferation of hepatoma cells was inhibited significantly, the incorporation ($1\,380 \pm 189$ cpm/well) was significantly lower than that of EGF group ($1\,880 \pm 281$ cpm/well, $P < 0.05$) (Figure 5).

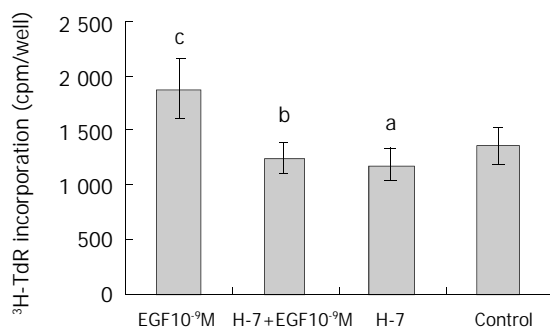


Figure 4 Effect of H-7 on EGF-induced $^3\text{H-TdR}$ incorporation into hepatoma cells. $n=6$, $\bar{x} \pm s$, $^a P > 0.05$ compared with control; $^b P < 0.01$ vs EGF 10^{-9} M group; $^c P < 0.05$ vs control.

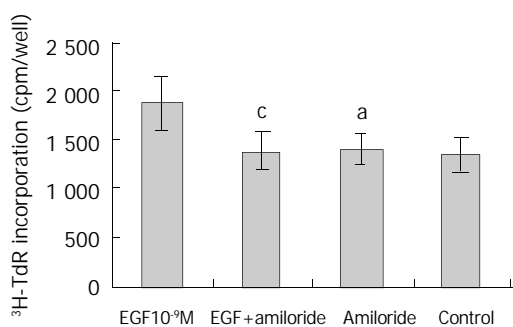


Figure 5 Effect of amiloride on EGF-induced $^3\text{H-TdR}$ incorporation into hepatoma cells. $n=6$, $\bar{x} \pm s$, $^a P > 0.05$ vs control; $^c P < 0.05$ vs EGF (10^{-9} M) group.

DISCUSSION

In this study, we demonstrated that EGF (10^{-9} M) had strong stimulation on the growth of hepatoma cells. It is well documented that EGF binds with the EGFR and activates the tyrosine kinase of the receptor. In this paper, the tyrosine kinase inhibitor genistein effectively blocked the growth of hepatoma cells induced by EGF.

Intracellular Ca^{2+} is one of critical factors maintaining the intracellular homeostasis. The concentration of Ca^{2+} in the cell plasma is about 10^{-7} mol/L, which is far lower than extracellular concentration of 10^{-3} mol/L. The enhancement of the intracellular Ca^{2+} concentration is achieved in two ways: one is the membrane depolarization, the other is the release from the intracellular stores intervened by phosphatidylinositol 1,4,5-triphosphate (IP_3). When the concentration of the intracellular Ca^{2+} rises to 5 folds above normal, the Ca^{2+} pump will be activated and put the Ca^{2+} out of the cell. Intracellular Ca^{2+} is the cofactor of many critical enzymes and functional proteins, and is an important intracellular messenger.

Studies demonstrate that in hepatoma cells EGF and other Ca^{2+} mobilizing hormones stimulate the rapid formation of IP_3 and a concomitant rise in cytosolic Ca^{2+} , apparently mobilized from intracellular stores^[42]. Ca^{2+} -binding protein regucalcin plays a role in the maintenance of intracellular Ca^{2+} homeostasis, and inhibits Ca^{2+} -activated DNA fragmentation. Regucalcin may play a physiological role in the control of over-proliferative cells^[43].

In this experiment, the calmodulin inhibitor W-7 was used

with EGF, and it significantly inhibited the growth of hepatoma cells induced by EGF, but it showed no effect on the growth of hepatoma cell when used alone. On the contrary, voltage-dependent Ca^{2+} channel inhibitor verapamil had no effect on the growth of hepatoma cells induced by EGF. It is suggested that Ca^{2+} -calmodulin-dependent pathway plays a critical role on the proliferation of hepatoma cells induced by EGF, and the effect of EGF is independent of voltage-dependent Ca^{2+} channel.

In the signal transduction pathway of phosphatidylinositol, activators bind with the cell surface receptor and activate phospholipase C (PLC)- β through G protein. PLC catalyzes dehydration of phosphatidylinositol 4,5-bisphosphate (PIP_2) into IP_3 and diglyceride (DG). IP_3 promotes the release of Ca^{2+} from endoplasmic reticulum. With the participation of Ca^{2+} , DG activates PKC, and PKC urges the phosphorylation of tyrosine which activates oncogene erb-B with productions of protein Erb-B2 and Erb-B3^[44]. In this study, PKC inhibitor H-7 used alone had no significant effect compared with control, but when used with EGF, it significantly inhibited the mitogenic effect of EGF on hepatoma cells. The result suggests the activation of PKC is an important link in the effect of EGF, and also implies that the effect of EGF is associated with phosphatidylinositol signaling pathway.

Intracellular pH (pHi) is another critical factor maintaining the intracellular homeostasis. At present, many studies found that pHi is associated with the pathogenesis of many diseases and mitosis of many kind of cells. Na^+/H^+ exchange is an important mechanism of pHi modulation. Activation of Na^+/H^+ exchange is the trigger of cellular protein and DNA synthesis, and is of fundamental importance for tumor growth. An increased influx of Na^+ through the stimulation of Na^+/H^+ exchange plays a key role during early phases of the cell cycle. Na^+/H^+ exchange messenger RNA expression may reach 10 times higher in HepG2 than in normal hepatocytes. EGF can increase baseline pHi in a dose-dependent manner. This effect was completely inhibited by pretreatment with amiloride^[45]. In this experiment, we found that Na^+/H^+ exchange inhibitor amiloride (0.1 mmol/L) alone showed no effect on the basal level $^3\text{H-TdR}$ incorporation of hepatoma cells. On the contrary, when it was used with EGF (10^{-9} M), the stimulatory effect of EGF was significantly inhibited. This suggests that the activation of Na^+/H^+ exchange may be one pathway of the effect of EGF.

Recent studies have shown that Ca^{2+} /calmodulin-dependent protein kinase IV was overexpressed in HCC with high activity and might be involved in the development of HCC^[46]. The effect of EGF on the hepatoma cells was associated with protein kinase C and calmodulin. Protein kinase C can activate Na^+/H^+ exchange. After the phosphorylation of EGFR, the proliferation signal was sent into the nucleus through STAT3 (signal transducers and activators of transcription 3)^[47]. The mechanism of this signal transduction is very complicated. It is connected with the activation of oncogene ras^[48,49], erb-B^[44], cyclinD1 and c-Myc^[50,51]. The effect of cell proliferation induced by EGF is associated with the MAPK (mitogen-activated protein kinase) pathway. The interactions between them demand more intensive studies.

In conclusion, our data suggest that PKC, calmodulin and Na^+/H^+ exchange could play a critical role in the growth of some hepatic tumors and that the inhibition of PKC, calmodulin or Na^+/H^+ exchange activity through pharmacological or genetic interventions, could theoretically be a useful strategy to reduce the growth rate of hepatocellular carcinoma.

REFERENCES

- 1 Diehl AM, Rai RM. Liver regeneration 3: Regulation of signal transduction during liver regeneration. *FASEB J* 1996; **10**: 215-227

- 2 **Fausto N**, Laird AD, Webber EM. Liver regeneration. 2. Role of growth factors and cytokines in hepatic regeneration. *FASEB J* 1995; **9**: 1527-1536
- 3 **Michalopoulos GK**, DeFrances MC. Liver regeneration. *Science* 1997; **276**: 60-66
- 4 **Yan JP**, Jia JB, Ma XH, Wu XR, Zhao YC, Han DW. Immunohistochemical study on expression of epidermal growth factor receptor at hepatocyte nuclei in experimental rat liver cirrhosis. *Huaren Xiaohua Zazhi* 1998; **6**: 15-16
- 5 **Kong YG**, Zhen J, Lu GJ, Xu SB, Chen YF. The effects of EGF on the growth of human hepatoma cells and the regulatory action of somatostatin on EGF receptors. *Zhonghua Xiaohua Zazhi* 1995; **15**: 129-132
- 6 **Hisaka T**, Yano H, Haramaki M, Utsunomiya I, Kojiro M. Expressions of epidermal growth factor family and its receptor in hepatocellular carcinoma cell lines: relationship to cell proliferation. *Int J Oncol* 1999; **14**: 453-460
- 7 **Moser GJ**, Wolf DC, Goldsworthy TL. Quantitative relationship between transforming growth factor-alpha and hepatic focal phenotype and progression in female mouse liver. *Toxicol Pathol* 1997; **25**: 275-283
- 8 **Kira S**, Nakanishi T, Suemori S, Kitamoto M, Watanabe Y, Kajiyama G. Expression of transforming growth factor alpha and epidermal growth factor receptor in human hepatocellular carcinoma. *Liver* 1997; **17**: 177-182
- 9 **DeCicco LA**, Kong J, Ringer DP. Carcinogen-induced alteration in liver epidermal growth factor receptor distribution during the promotion stage of hepatocarcinogenesis in rat. *Cancer Lett* 1997; **111**: 149-156
- 10 **Pelaez Bujan Mdel C**, Ruibal Morell A, Aza Gonzalez J. Gastric carcinoma: expression of c-erbB-2/neu oncoprotein, epidermal growth factor receptor, cathepsin D, progesterone receptor and tumor associated glycoprotein-72 in different histological types. *Rev Esp Enferm Dig* 1999; **91**: 826-837
- 11 **Koyama S**, Maruyama T, Adachi S. Expression of epidermal growth factor receptor and CD44 splicing variants sharing exons 6 and 9 on gastric and esophageal carcinomas: a two-color flow-cytometric analysis. *J Cancer Res Clin Oncol* 1999; **125**: 47-54
- 12 **Pai R**, Wyle FA, Cover TL, Itani RM, Domek MJ, Tarnawski AS. Helicobacter pylori culture supernatant interferes with epidermal growth factor-activated signal transduction in human gastric KATO III cells. *Am J Pathol* 1998; **152**: 1617-1624
- 13 **Wang HT**, Chen BW, Jia BQ. Roles of epidermal growth factor (EGF) and EGF receptor in gastric cancer. *Xin Xihuaqingxue Zazhi* 1997; **5**: 393-394
- 14 **Sanz-Ortega J**, Steinberg SM, Moro E, Saez M, Lopez JA, Sierra E, Sanz-Esponera J, Merino MJ. Comparative study of tumor angiogenesis and immunohistochemistry for p53, c-ErbB2, c-myc and EGFR as prognostic factors in gastric cancer. *Histol Histopathol* 2000; **15**: 455-462
- 15 **Baba I**, Shirasawa S, Iwamoto R, Okumura K, Tsunoda T, Nishioka M, Fukuyama K, Yamamoto K, Mekada E, Sasazuki T. Involvement of deregulated epiregulin expression in tumorigenesis *in vivo* through activated Ki-Ras signaling pathway in human colon cancer cells. *Cancer Res* 2000; **60**: 6886-6889
- 16 **Liu B**, Fang M, Schmidt M, Lu Y, Mendelsohn J, Fan Z. Induction of apoptosis and activation of the caspase cascade by anti-EGF receptor monoclonal antibodies in DiFi human colon cancer cells do not involve the c-jun N-terminal kinase activity. *Br J Cancer* 2000; **82**: 1991-1999
- 17 **Hao YR**, Ding GY, Chen PY, Geng JH. Effect of EGF receptor expression on cell proliferation in colorectal cancer. *Huaren Xiaohua Zazhi* 1998; **6**: 313-314
- 18 **Wang Q**, Wu JS, Gao DM, Lai DN, Ma QJ. Expression significance of epidermal growth factor receptor and transforming growth factor α mRNA in human colorectal carcinoma. *Shijie Huaren Xiaohua Zazhi* 1999; **7**: 590-592
- 19 **Porebska I**, Harlozinska A, Bojarowski T. Expression of the tyrosine kinase activity growth factor receptors (EGFR, ERB B2, ERB B3) in colorectal adenocarcinomas and adenomas. *Tumour Biol* 2000; **21**: 105-115
- 20 **Di Carlo A**, Mariano A, D' Alessandro V, Belli G, Romano G, Macchia V. Evaluation of epidermal growth factor receptor, carcinoembryonic antigen and Lewis carbohydrate antigens in human colorectal and liver neoplasias. *Oncol Rep* 2001; **8**: 387-392
- 21 **Reissmann PT**, Koga H, Figlin RA, Holmes EC, Slamon DJ. Amplification and overexpression of the cyclin D1 and epidermal growth factor receptor genes in non-small-cell lung cancer. Lung Cancer Study Group. *J Cancer Res Clin Oncol* 1999; **125**: 61-70
- 22 **Schneider J**, Presek P, Braun A, Bauer P, Konietzko N, Wiesner B, Woitowitz HJ. p53 protein, EGF receptor, and anti-p53 antibodies in serum from patients with occupationally derived lung cancer. *Br J Cancer* 1999; **80**: 1987-1994
- 23 **Lopez-Guerrero JA**, Bolufer-Gilabert P, Vera-Sempere FJ, Marugan de la Concha I, Barragan-Gonzalez E. C-erbB-2 expression and its relationship with ploidy, p53 abnormalities and epidermal growth factor receptor content in human non-small cell lung cancer. *Clin Chim Acta* 1999; **285**: 105-120
- 24 **Kumar VL**, Majumder PK, Kumar V. Observations on EGFR gene amplification and polymorphism in prostatic diseases. *Int Urol Nephrol* 2000; **32**: 73-75
- 25 **De Miguel P**, Royuela, Bethencourt R, Ruiz A, Fraile B, Paniagua R. Immunohistochemical comparative analysis of transforming growth factor alpha, epidermal growth factor, and epidermal growth factor receptor in normal, hyperplastic and neoplastic human prostates. *Cytokine* 1999; **11**: 722-727
- 26 **Richter F**, Huang HF, Li MT, Danielpour D, Wang SL, Irwin RJ Jr. Retinoid and androgen regulation of cell growth, epidermal growth factor and retinoic acid receptors in normal and carcinoma rat prostate cells. *Mol Cell Endocrinol* 1999; **153**: 29-38
- 27 **Sundareshan P**, Nagle RB, Bowden GT. EGF induces the expression of matrilysin in the human prostate adenocarcinoma cell line, LNCaP. *Prostate* 1999; **40**: 159-166
- 28 **Gil-Diez de Medina S**, Salomon L, Colombel M, Abbou CC, Bellot J, Thiery JP, Radvanyi F, Van der Kwast TH, Chopin DK. Modulation of cytokeratin subtype, EGF receptor, and androgen receptor expression during progression of prostate cancer. *Hum Pathol* 1998; **29**: 1005-1012
- 29 **Takita M**, Onda M, Tokunaga A. Immunohistochemical demonstration of angiogenic growth factors and EGF receptor in hepatic metastases and primary human gastric cancer. *Nippon Ika Daigaku Zasshi* 1998; **65**: 358-366
- 30 **Liu F**, Qi HL, Chen HL. Effects of all-trans retinoic acid and epidermal growth factor on the expression of nm23-H1 in human hepatocarcinoma cells. *J Cancer Res Clin Oncol* 2000; **126**: 85-90
- 31 **Parker C**, Roseman BJ, Bucana CD, Tsan R, Radinsky R. Preferential activation of the epidermal growth factor receptor in human colon carcinoma liver metastases in nude mice. *J Histochem Cytochem* 1998; **46**: 595-602
- 32 **De Jong KP**, Stellema R, Karrenbeld A, Koudstaal J, Gouw AS, Sluiter WJ, Peeters PM, Slooff MJ, De Vries EG. Clinical relevance of transforming growth factor alpha, epidermal growth factor receptor, p53, and Ki67 in colorectal liver metastases and corresponding primary tumors. *Hepatology* 1998; **28**: 971-979
- 33 **Kiso S**, Kawata S, Tamura S, Miyagawa J, Ito N, Tsushima H, Yamada A, Umeki S, Higashiyama S, Taniguchi N, Matsuzawa Y. Expression of heparin-binding epidermal growth factor-like growth factor in the hepatocytes of fibrotic rat liver during hepatocarcinogenesis. *J Gastroenterol Hepatol* 1999; **14**: 1203-1209
- 34 **Inui Y**, Higashiyama S, Kawata S, Tamura S, Miyagawa J, Taniguchi N, Matsuzawa Y. Expression of heparin-binding epidermal growth factor in human hepatocellular carcinoma. *Gastroenterology* 1994; **107**: 1799-1804
- 35 **Zhang J**, Wang WL, Li Q, Qiao Q. Expression and significance of transforming growth factor- α and its receptor in human primary hepatocellular carcinoma. *Shijie Huaren Xiaohua Zazhi* 1999; **7**: 939-942
- 36 **Harada K**, Shiota G, Kawasaki H. Transforming growth factor-alpha and epidermal growth factor receptor in chronic liver disease and hepatocellular carcinoma. *Liver* 1999; **19**: 318-325
- 37 **Wang G**, Yang X, Zhang Y, Wang Q, Chen H, Wei H, Xing G, Xie L, Hu Z, Zhang C, Fang D, Wu C, He F. Identification and characterization of receptor for mammalian hepatopoietin that is homologous to yeast ERV1. *J Biol Chem* 1999; **274**: 11469-11472
- 38 **Li Y**, Li M, Xing G, Hu Z, Wang Q, Dong C, Wei H, Fan G, Chen J, Yang X, Zhao S, Chen H, Guan K, Wu C, Zhang C, He F. Stimulation of the mitogen-activated protein kinase cascade and tyrosine phosphorylation of the epidermal growth factor receptor by hepatopoietin. *J Biol Chem* 2000; **275**: 37443-37447

- 39 **Miyaki M**, Sato C, Sakai K, Konishi M, Tanaka K, Muraoka M, Kikuchi-Yanoshita R, Nadaoka Y, Kanda H, Kitagawa T. Malignant transformation and EGFR activation of immortalized mouse liver epithelial cells caused by HBV enhancer-X from a human hepatocellular carcinoma. *Int J Cancer* 2000; **85**: 518-522
- 40 **Francavilla A**, Barone M, Azzarone A, Panella C, Giangaspero A. Cell regeneration in the pathobiology of liver carcinomas. *Ital J Gastroenterol* 1991; **23**: 589-593
- 41 **Hung WC**, Chuang LY, Tsai JH, Chang CC. Effects of epidermal growth factor on growth control and signal transduction pathways in different human hepatoma cell lines. *Biochem Mol Biol Int* 1993; **30**: 319-328
- 42 **Gilligan A**, Prentki M, Glennon C, Knowles BB. Epidermal growth factor-induced increases in inositol trisphosphates, inositol tetrakisphosphates, and cytosolic Ca^{2+} in a human hepatocellular carcinoma-derived cell line. *FEBS Lett* 1988; **233**: 41-46
- 43 **Nakajima M**, Murata T, Yamaguchi M. Expression of calcium-binding protein regucalcin mRNA in the cloned rat hepatoma cells (H4-II-E) is stimulated through Ca^{2+} signaling factors: involvement of protein kinase C. *Mol Cell Biochem* 1999; **198**: 101-107
- 44 **Emkey R**, Kahn CR. Cross-talk between phorbol ester-mediated signaling and tyrosine kinase proto-oncogenes. II. Comparison of phorbol ester and sphingomyelinase-induced phosphorylation of ErbB2 and ErbB3. *J Biol Chem* 1997; **272**: 31182-31189
- 45 **Strazzabosco M**, Poci C, Spirli C, Zsembery A, Granato A, Massimino ML, Crepaldi G. Intracellular pH regulation in Hep G2 cells: effects of epidermal growth factor, transforming growth factor-alpha, and insulin-like growth factor-II on Na^{+}/H^{+} exchange activity. *Hepatology* 1995; **22**: 588-597
- 46 **Tamura N**, Tai Y, Sugimoto K, Kobayashi R, Konishi R, Nishioka M, Masaki T, Nagahata S, Tokuda M. Enhanced expression and activation of Ca^{2+} /calmodulin-dependent protein kinase IV in hepatocellular carcinoma. *Cancer* 2000; **89**: 1910-1916
- 47 **Grandis JR**, Drenning SD, Chakraborty A, Zhou MY, Zeng Q, Pitt AS, Tweardy DJ. Requirement of Stat3 but not Stat1 activation for epidermal growth factor receptor-mediated cell growth *in vitro*. *J Clin Invest* 1998; **102**: 1385-1392
- 48 **Zheng XL**, Matsubara S, Diao C, Hollenberg MD, Wong NC. Epidermal growth factor induction of apolipoprotein A-I is mediated by the ras-map kinase cascade and sp1. *J Biol Chem* 2001; **276**: 13822-13829
- 49 **Wang Q**, Lin ZY, Feng XL. Alterations in metastatic properties of hepatocellular carcinoma cell following H-ras oncogene transfection. *World J Gastroenterol* 2001; **7**: 335-339
- 50 **Ramljak D**, Jones AB, Diwan BA, Perantoni AO, Hochadel JF, Anderson LM. Epidermal growth factor and transforming growth factor-alpha-associated overexpression of cyclin D1, Cdk4, and c-Myc during hepatocarcinogenesis in *Helicobacter hepaticus*-infected A/JCr mice. *Cancer Res* 1998; **58**: 3590-3597
- 51 **Niu ZS**, Li BK, Wang M. Expression of p53 and C-myc genes and its clinical relevance in the hepatocellular carcinomatous and pericarcinomatous tissues. *World J Gastroenterol* 2002; **8**: 822-826

Edited by Pang LH

The analysis of γ -glutamyl transpeptidase gene in different type liver tissues

Guo-Qing Han, Cheng-Yong Qin, Rong-Hua Shu

Guo-Qing Han, Cheng-Yong Qin, Rong-Hua Shu, The Center of Liver Diseases, Shandong Provincial Hospital, Clinical Medical College of Shandong University, Jinan 250021, China

Correspondence to: Dr. Guo-Qing Han, The Center of Liver Diseases, Shandong Provincial Hospital, Jinan 250021, China. hguoq@jn-public.sd.cninfo.net

Telephone: +86-531-7938911-2450

Received: 2002-09-13 **Accepted:** 2002-10-29

Abstract

AIM: To probe the value of γ -glutamyl transpeptidase (GGT) messenger RNA in monitoring canceration of liver cells and for early diagnosis of hepatocellular carcinoma (HCC), by researching the types of GGT messenger RNA (GGTmRNA) in liver tissues and peripheral blood of different hepatopathy.

METHODS: The three types of GGTmRNA (A, B, C) in liver tissues and peripheral blood from the patients with HCC, noncancerous hepatopathy, hepatic benign tumor, secondary carcinoma of liver, and healthy persons were detected by reverse-transcription polymerase chain reaction (RT-PCR).

RESULTS: (1) In normal liver tissues, type A was predominantly found (100.00 %), type B was not found, type C was found occasionally (25.00 %). (2) The distribution of types of GGTmRNA in liver tissues with acute hepatitis, chronic hepatitis, cirrhosis, alcoholic hepatopathy was similar as in normal liver tissues ($P>0.05$), but type B was found in 3 of 18 patients with chronic hepatitis (16.67 %), and also in 3 of 11 patients with cirrhosis (27.27 %). (3) There was no significant difference of types of GGTmRNA between liver tissues with hepatic benign tumor, secondary carcinoma of liver and normal liver tissues ($P>0.05$). (4) Type B was predominant in cancerous tissues with HCC (87.5 %), the prevalence of type B in cancerous tissues was significantly higher than that in normal liver tissues (0/12) ($P<0.05$), but the prevalence of type A in cancerous tissues (46.88 %) was significantly lower than that in normal liver tissues (100.00 %) ($P<0.05$), and the prevalence of type C (6.25 %) in cancerous was the same as that in normal liver tissues (25.00 %) ($P>0.05$). In noncancerous tissues of livers with HCC, the main types were type A and type B, the prevalence of type A (85.71 %, 90.48 %) and type C (14.29 %, 9.52 %) in noncancerous tissues of liver with HCC was similar as that in normal liver tissues (A: 100.00 %; C: 25.00 %) ($P>0.05$), but the prevalence of type B (80.95 %, 76.19 %) in noncancerous tissues of livers with HCC was significantly higher than that in normal liver tissues (0/12) ($P<0.05$). (5) The prevalence of type B (37.5 %) in peripheral blood with HCC was higher than that in normal person (0/12) ($P<0.05$). In peripheral blood, type B was found in 4 of 11 cases of HCC with serum AFP negative.

CONCLUSION: The shift of types of GGTmRNA from A to B in liver tissues may be closely related to the development of HCC, and the analysis of GGT gene may provide a useful tool for early diagnosis of HCC.

Han GQ, Qin CY, Shu RH. The analysis of γ -glutamyl transpeptidase gene in different type liver tissues. *World J Gastroenterol* 2003; 9(2): 276-280

<http://www.wjgnet.com/1007-9327/9/276.htm>

INTRODUCTION

HCC is one of common fatal malignant tumors^[1-5]. About 90 percent of tumors originated from liver are HCC^[6-10]. There are more than 250 000 patients of HCC in the world every year, 44.7 percent of these patients are Chinese^[11-15]. The pathogenic mechanism, early diagnosis, and efficient treatment of HCC are very important. Many studies concerning GGT in HCC have suggested that changes in hepatic GGT expression may be closely related to the development of HCC. It has been reported that HCC in humans expresses GGT enzymes with unique carbohydrate moieties compared with normal liver enzymes. The presence of the unique GGT isoform for HCC in patient sera was used as a marker for the diagnosis of HCC. However, the genomic changes in GGT relating to the development of HCC are not known, and genomic analysis of the specific GGT to HCC is also lacking. In this study, the specific primer sets for reverse-transcription polymerase chain reaction corresponding to the 5' -noncoding human GGTmRNA of fetal liver (type A), HepG2 cells (type B), and placenta (type C) were prepared. In order to clarify the type of GGTmRNA in human liver and the relationship between alterations in GGTmRNA expression and the development of HCC, we detected the types of GGTmRNA in normal liver tissues and diseased liver tissues with or without HCC.

MATERIALS AND METHODS

All cases were divided into 8 groups by type of diseases: (1) healthy control group 12 cases, male 9 cases, female 3 cases. (2) HCC group 32 cases, male 26 cases, female 6 cases, small sized HCC (size ≤ 3 cm) 8 cases, large sized HCC (size 3-10 cm) 16 cases, enormous sized HCC (size >10 cm) 8 cases. 11 HCC patients with serum alpha fetoprotein (AFP) negative, 21 HCC patients were treated with surgery. (3) Acute hepatitis group 15 cases, male 11 cases, female 4 cases, hepatitis A 4 cases, hepatitis B 3 cases, hepatitis E 5 cases, drug hepatitis 3 cases. (4) Chronic hepatitis group 18 cases, male 12 cases, female 6 cases, hepatitis B 14 cases, hepatitis C 4 cases. (5) Cirrhosis group 11 cases. The diagnosis of acute hepatitis, chronic hepatitis and cirrhosis meet the standard of National Academic Conference about infectious disease^[16]. (6) Alcoholic hepatopathy group 13 cases, male 13 cases. (7) Hepatic benign tumor group 10 cases, male 8 cases, female 2 cases, hepatic hemangioma 6 cases, hepatic cyst 4 cases. (8) Secondary carcinoma of liver 13 cases, male 8 cases, female 5 cases, primary carcinoma of stomach 4 cases, primary carcinoma of colon 4 cases, primary carcinoma of lung 2 cases, primary carcinoma of prostate 1 cases, primary carcinoma of ovary 2 cases.

Sample collection

Collection of liver tissues: Cancerous tissues, adjacent

paracancerous tissues (to the brim of carcinoma 3-5 cm) and distal cancerous tissues (to the brim of carcinoma >5 cm) were respectively obtained during surgery from 21 patients with HCC, and the cancerous tissues and noncancerous tissues were obtained by needle liver biopsy with help of ultrasound B from the other patients of HCC (11 cases). Liver tissues were obtained by needle liver biopsy in the other groups, non-tumor tissues were merely obtained in hepatic benign tumor and secondary carcinoma of liver. All the tissue specimens were immediately refrigerated by liquid nitrogen for 1 hour, and then were transferred to refrigerator at -80°C for future use.

Blood samples: peripheral blood was obtained from each person at morning before breakfast, anticoagulated by sodium citrate solution, and then peripheral blood mononuclear cells (PBMC) were separated from blood, total RNA was extracted from PBMC, cDNA was synthesized with reverse transcription, and then reserved in refrigerator at -80°C .

Total RNA extraction

Total RNA was extracted by using TRIzol (from TECH-LINE company) and the purity of RNA was tested with ultraviolet spectrophotometer of DAOJUN UR-2201.

Detection of the types of GGTmRNA by RT-PCR

cDNA was synthesized with RNA reverse transcriptase (M-MLV) and random primer (Oligodts). then cDNAs of GGTmRNA were amplified by PCR using polymerase and three different primer sets which were specific for the three GGTmRNA types. Nucleotide sequences of the primer sets to each type of GGTmRNAs are: type A sense 5' - CAC AGG GGA CAT ACA GTG AG-3', Antisense 5' - GAA ATA GCT GAA GCA CGC GC -3'; type B sense 5' - GGA TTC TCC CAG AGA TTG CC -3', antisense 5' - GAA GGT CAA GGG AGG TTA CC -3'; type C sense 5' - GCC CAG AAG TGA GAG CAG TT -3', antisense 5' - TCC AGA AAG CAG CTA GAG GG -3'. The condition of reaction: in advance denaturalization of 94°C for 3 min, and then PCR was performed with 30 cycles consisting of a denaturing step of 94°C 30 s, an annealing step of 58°C for 30 s and an elongation step of 72°C for 30 s. the final step at 72°C was extended to 8 min. The expected size of each PCR product is 308bp in type A, 300bp in type B, 386bp in type C. Products after gel electrophoresis by 1.3 % gelose were observed under ultraviolet radiation comparing with stander DNA.

Statistical analysis

The statistical software SPSS was used for statistical analysis, the level of significance was $P < 0.05$.

RESULTS

GGTmRNA in tissues

In normal liver tissues (12 cases), type A was the main type, it was found in all livers (100 %), type B was not found, type C was found in 3 cases, the GGTmRNA expression was monogenic (type A) in 9 livers and polygenic (type A + type C) in 3 cases (Table 1).

In liver tissues with acute hepatitis, chronic hepatitis, cirrhosis or alcoholic hepatopathy, type A was the main type (81.82-93.33 %), type C was found occasionally (13.33-23.08 %), the distribution of types of GGTmRNA was similar as in normal liver tissues ($P > 0.05$), type B was found in 3 cases with chronic hepatitis, 3 cases with cirrhosis, the prevalence of type B was higher than normal livers, but it was not significantly different ($P > 0.05$).

In 32 cancerous tissues with HCC, type B was the main type, it was found in 28 cases, the prevalence of type B in

cancerous tissues (87.5 %) was significantly higher than in normal livers ($P < 0.05$); type A was found in 15 cases, its prevalence in cancerous tissues (46.88 %) was lower than in normal livers ($P < 0.05$); the type C was not significantly different between cancerous tissues and normal liver tissues ($P > 0.05$). In 21 adjacent paracancerous tissues, 21 distal cancerous tissues and 11 noncancerous tissues, the main type was type A and B, the prevalence of type A (87.51 %, 90.48 %, 81.82 %) was similar as in normal livers ($P > 0.05$); however the prevalence of type B (80.95 %, 76.19 %, 72.73 %) was significantly higher than in normal liver tissues ($P < 0.05$); the prevalence of type C was similar as in normal livers ($P > 0.05$).

In nontumor tissues of livers with hepatic benign tumor and secondary carcinoma of liver, the distribution of GGTmRNA was similar as in normal livers ($P > 0.05$).

The relation between types of GGTmRNA and size of HCC: The prevalence of type A in cancerous tissues of larger sized HCC is lower than in that of smaller sized HCC, the monogenic pattern of type B tended to be found more frequently in larger sized HCC, but the difference was not significant ($P > 0.05$). Table 2.

Table 1 Incidence of Different GGTmRNA types in Livers of Each Group

Group	No. of Samples	Type of GGTmRNA		
		A (%)	B (%)	C (%)
1. Normal	12	12 (100%)	0	3 (25.00%)
2. Acute hepatitis	15	14 (93.33%)	1 (6.67%)	2 (13.33%)
3. Chronic hepatitis	18	16 (88.89%)	3 (16.67%)	4 (22.22%)
4. Cirrhosis	11	9 (81.82%)	3 (27.27%)	2 (18.18%)
5. Alcoholic hepatopathy	13	12 (92.31%)	1 (7.69%)	3 (23.08%)
6. Hepatic benign tumor	10	10 (100%)	0	1 (10.00%)
7. Secondary carcinoma of liver	13	11 (84.62%)	0	3 (23.08%)
8. HCC	32			
Cancerous tissues	32	15 (46.88%) ^a	28 (87.5%) ^a	2 (6.25%)
Adjacent Paracancerous tissues	21	18 (85.71%)	17 (80.95%) ^a	3 (14.29%)
Distal Cancerous tissues	21	19 (90.48%)	16 (76.19%) ^a	2 (9.52%)
Noncancerous tissues	11	9 (81.82%)	8 (72.73%) ^a	1 (9.09%)

^a $P < 0.05$ vs. normal liver.

Table 2 GGTmRNA and the size of HCC

	cases	Cancerous tissues type A	Cancerous tissues type B	Non cancerous tissues type B	Peripheral blood type B
Small sized HCC	8	5 (62.50%)	6 (75.00%)	5 (62.50%)	2 (25.00%)
Large sized HCC	16	7 (43.75%)	15 (93.75%)	14 (87.50%)	6 (37.50%)
Enormous sized HCC	8	3 (37.50%)	7 (87.50%)	7 (87.50%)	4 (50.00%)

GGTmRNA in peripheral blood

In peripheral blood of 32 patients with HCC, type A was found in 2 cases (6.25 %), type B was found in 12 cases, the prevalence of type B (37.5 %) was significantly higher than normal ($P < 0.05$), type C was found in 1 case (3.13 %). In peripheral blood of patients with acute hepatitis, type A was found in 2 cases. In chronic hepatitis group, type A was found in 1 case. Type B and C were not found in acute and chronic hepatitis group. In the other groups, GGTmRNA was not found. In 8 cases of small sized HCC, type B was found in 5 noncancerous tissues (62.5 %) and in peripheral blood of 2 cases (25 %). In the 8 cases, there were 3 patients with serum

AFP positive (37.5 %). Table 2.

In 21 cases of HCC with AFP positive, type B was found in peripheral blood of 8 cases (38.1 %). In 11 cases of HCC with AFP negative, type B was found in peripheral blood of 4 cases (36.36 %). Type B was not significantly different between them ($P>0.05$). Therefore the prevalence of type B in peripheral blood was not related to the prevalence of AFP.

DISCUSSION

Hepatocellular carcinoma is one of the common malignant tumor^[17-29], because of its severe malignance, quick development, early intrahepatic metastasis, mostly being combined with cirrhosis, frequent recurrence, the prognosis of HCC still remains dismal^[30-41]. By now, surgery is still the most efficient treatment for HCC, but about 70 percent of patients with HCC lost the opportunity of surgery, since they did not go to see a doctor until the tumor reached an advanced stage, and HCC reoccurred more frequently after surgery, on the other hand, HCC is not susceptible to radiotherapy, chemotherapy and other synthetic treatments^[42-44], so it is imperative to clarify the pathogenic mechanism of HCC and to find efficient methods for early diagnosis of HCC. The epidemiological studies suggested that the prevalence of HCC in patients with hepatopathy had been obviously increasing in China. At present, the pathogenic mechanisms of HCC are not well known, it is reported that the occurrence and evolvement HCC may be a process of polygenic and multiple steps, which related to polygenic expression, such as repair of DNA, signal transduction, cell cycle regulation etc^[45-52].

It is still difficult to monitor the canceration of liver cells in preneoplastic stage and early stage of HCC^[53]. If we could monitor the changes of the structure and function of some genes, we would find the patients with high risk of HCC, forecast the possibility of occurrence of HCC before cytological changes, and then we could prevent, make a diagnosis and give treatment on molecular level.

It has been reported that HCC synthesizes and secretes many proteins, polypeptides or isoenzymes such as AFP, GGT etc. they may be used as important marks for the diagnosis of HCC. GGT is closely relate to biotransformation, metabolism of nucleic acid, and the occurrence of carcinoma, it may be used as a mark for detection of bibulosity and the canceration of liver cells. In humans, the activity of GGT is at a very high level in embryo period, after birth it declines to a very low level quickly, HCC expresses a large amount of GGT and unique GGT isoenzyme. However, its mechanisms are not known. Human GGT gene is linked to a BCR gene-related segment that is located on band q11→qter of chromosome 22, maybe there is a family of GGT genes, it could suit for the various expressions of physiological aberrance and physiological state. Many studies concerning GGT complementary DNA (cDNA) sequences indicated that the cDNA sequences from fetal liver, HepG2 cells, and placenta showed identical open reading frame (ORF) consisting of 1707 nucleotide acids and GGT protein structure. The most significant difference among these cDNAs exists in the 5' -noncoding region^[54]. In the present study, polymorphisms of GGT mRNAs at the 5' -noncoding region from normal liver tissues and diseased liver tissues were analyzed with RT-PCR method.

In normal liver tissues, the main type of GGT mRNA was type A, the expression was monogenic in most cases (type A), but was polygenic in some cases (typeA+C).

In livers of acute hepatitis, chronic hepatitis, and cirrhosis, the distribution of types of GGT mRNA was nearly the same as in normal livers, but in livers of chronic hepatitis and cirrhosis, the prevalence of type B was higher than in normal livers ($P>0.05$).

In cancerous tissues with HCC, type B was predominant. In noncancerous tissues of livers with HCC, the main types were type A and B. The prevalence of type B was significantly higher in both cancerous and noncancerous tissues of livers with HCC than in normal livers and diseased livers without HCC. The prevalence of type A in cancerous tissues, but not in noncancerous tissues, was significantly lower than in normal livers and diseased livers without HCC. The prevalence of type A in noncancerous tissues of livers with HCC was similar as in livers without HCC. These results strongly suggest that the GGT mRNA expression in human liver may shift from type A to type B during the development of HCC. The prevalence of type B in noncancerous tissues of livers with HCC was significantly higher than in livers without HCC, and was similar as in cancerous tissues of livers with HCC. These suggest that the shift of the GGT mRNA may occur from the preneoplastic stage of hepatocytes. Type B was detected in livers of 3 cases with chronic active hepatitis and 3 cases with cirrhosis. It was not sure whether or not some liver cells in liver tissues of these 6 cases had developed to the preneoplastic stage or changed to cancerous cells, and whether or not these 6 patients would developed to HCC in the future. It need further follow-up study to answer these questions.

Among the patients of hepatic benign tumor and secondary carcinoma, the distribution of GGT mRNA in livers tissues but not tumor tissues was similar as that in normal livers. The results suggested that the shift from type A to type B did not exist in liver tissues with benign tumor and secondary carcinoma.

The serum level of GGT is mostly higher in patients with alcoholic hepatopathy, but the distribution of types of GGT mRNA in these liver tissues was similar as in normal liver tissues. This result suggested that alcohol did not induce the shift of GGT mRNA.

Studies about small sized HCC have been the important incident in the history of HCC in the past 20 years. Early diagnosis and treatment are the keys to increase survival rate and decrease recurrence rate. The detection of serum alpha-fetoprotein (AFP) is an important method for early diagnosis of HCC, especially in patients with high risk of HCC^[55,56]. However, the negative rate of AFP is higher in patients with small sized HCC. In present study, among the 8 patients with small sized HCC, type B was detected in noncancerous liver tissues of 5 patients, and in peripheral blood of 2 cases, however, AFP was positive in serum of only 2 patients. Moreover, in peripheral blood, type B of GGT mRNA was found in 4 of 11 HCC patients with AFP negative (36.36 %). These results suggested that the detection of unique type B of GGT mRNA may provide a useful tool for the diagnosis of the small sized HCC and HCC with AFP negative.

Since there are lots of RNA enzymes in blood plasma, RNA will be degraded by RNA enzymes as soon as it appears in plasma, so there are not dissociative GGT mRNAs in blood plasma in normal blood plasma. In this study, GGT mRNAs were not found in normal peripheral blood, however, among 32 cases of HCC, type B of GGT mRNA was found in peripheral blood of 12 cases (37.5 %). GGT mRNAs were not found in peripheral blood in other groups. So it may be inferred that cancerous cells exist in peripheral blood of this 12 patients. These results suggest that the shift of type of GGT mRNA are closely related to the development of HCC, and that analysis of GGT mRNA expression may provide a useful fool for early diagnosis of HCC.

REFERENCES

- 1 **Ma XD**, Sui YF, Wang WL. Expression of gap junction genes connexin32 and connexin43 and their proteins in hepatocellular

- carcinoma and normal liver tissues. *World J Gastroenterol* 2000; **6**: 66-69
- 2 **Wang Y**, Liu H, Zhao Q, Li X. Analysis of point mutation in site 1896 of HBV procore and its detection in the tissues and serum of HCC patients. *World J Gastroenterol* 2000; **6**: 395-397
 - 3 **Mei MH**, Xu J, Shi QF, Yang JH, Chen Q, Qin LL. Clinical significance of serum intercellular adhesion molecule detection on patients with hepatocellular carcinoma. *World J Gastroenterol* 2000; **6**: 408-410
 - 4 **Qin Y**, Li B, Tan YS, Sun ZL, Zuo FQ, Sun ZF. Polymorphism of p16INK4a gene and rare mutation of p15INK4b gene exon2 in primary hepatocellular carcinoma. *World J Gastroenterol* 2000; **6**: 411-414
 - 5 **Lin NF**, Tang J, Mohamed-Ishmael HS. Study on environmental etiology of high incidence areas of liver cancer in China. *World J Gastroenterol* 2000; **6**: 572-576
 - 6 **Tian DY**, Yang DF, Xia NS, Zhang ZG, Lei HB, Huang YC. The serological prevalence and risk factor analysis of hepatitis G virus infection in Hubei Province of China. *World J Gastroenterol* 2000; **6**: 585-587
 - 7 **Zhong DR**, Ji XL. Hepatic angiomyolipoma misdiagnosis as hepatocellular carcinoma: A report of 14 cases. *World J Gastroenterol* 2000; **6**: 608-612
 - 8 **Riordan SM**, Williams R. Transplantation of primary and reversibly immortalized human liver cells and other gene therapies in acute liver failure and decompensated chronic liver disease. *World J Gastroenterol* 2000; **6**: 636-642
 - 9 **Li Y**, Su JJ, Qin LL, Yang C, Luo D, Ban KC, Kensler TW, Roebuck BD. Chemopreventive effect of oltipraz on AFB1 induced hepatocarcinogenesis in tree shrew model. *World J Gastroenterol* 2000; **6**: 647-650
 - 10 **Xu HY**, Yang YL, Gao YY, Wu QL, Gao GQ. Effect of arsenic trioxide on human hepatoma cell line BEL7402 cultured *in vitro*. *World J Gastroenterol* 2000; **6**: 681-687
 - 11 **Zang GQ**, Zhou XQ, Yu H, Xie Q, Zhao GM, Wang B, Guo Q, Xiang YQ, Lia+o D. Effect of hepatocytic apoptosis induced by TNF-alpha on acute severe hepatitis in mouse models. *World J Gastroenterol* 2000; **6**: 688-692
 - 12 **Huang XF**, Wang CM, Dai XW, Li ZJ, Pan BR, Yu LB, Qian B, Fang L. Expression of chromogranin A and cathepsin D in human primary hepatocellular carcinoma. *World J Gastroenterol* 2000; **6**: 693-698
 - 13 **Xu HY**, Yang YL, Guan XL, Song G, Jiang AM, Shi LJ. Expression of regulating apoptosis gene and apoptosis index in primary liver cancer. *World J Gastroenterol* 2000; **6**: 721-724
 - 14 **Chen YP**, Liang WF, Zhang L, He HT, Luo KX. Transfusion transmitted virus infection in general populations and patients with various liver diseases in south China. *World J Gastroenterol* 2000; **6**: 738-741
 - 15 **Ma XD**, Sui YF, Wang WL. The expression of gap junction protein connexin32 in human hepatocellular carcinoma, cirrhotic and viral hepatitis liver tissues. *Aizheng* 1999; **18**: 133-135
 - 16 The prevention and cure project for virus hepatitis. *Zhonghua Ganzhangbing Zazhi* 2000; **8**: 324-329
 - 17 **Worman HJ**, Lin F, Mamiya N, Mustacchia PJ. Molecular biology and the diagnosis and treatment of liver diseases. *World J Gastroenterol* 1998; **4**: 185-191
 - 18 **Lee JH**, Ku JL, Park YJ, Lee KU, Kim WH, Park JG. Establishment and characterization of four human hepatocellular carcinoma cell lines containing hepatitis B virus DNA. *World J Gastroenterol* 1999; **5**: 289-295
 - 19 **He XX**, Wang JL. The current status and prospect in the gene therapy of liver cancer. *Huaren Xiaohua Zazhi* 1998; **6**: 158-159
 - 20 **Fu JM**, Yu XF, Shao YF. Telomerase and primary liver cancer. *Shijie Huaren Xiaohua Zazhi* 2000; **8**: 461-463
 - 21 **Zhai SH**, Liu JB, Liu YM, Zhang LL, Du ZP. Expression of HBsAg, HCV-Ag and AFP in liver cirrhosis and hepatocarcinoma. *Shijie Huaren Xiaohua Zazhi* 2000; **8**: 524-527
 - 22 **Su YH**, Zhu SN, Lu SL, Gu YH. HCV genotypes expression in hepatocellular carcinoma by reverse transcription in situ polymerase chain reaction. *Shijie Huaren Xiaohua Zazhi* 2000; **8**: 874-878
 - 23 **Tang YW**, Yao XX. Regulating effect of HCC cells on the activation of stellate cells. *Shijie Huaren Xiaohua Zazhi* 2001; **9**: 202-204
 - 24 **Cui J**, Yang DH, Qin HR. Mutation and clinical significance of c-fms oncogene in hepatocellular carcinoma. *Shijie Huaren Xiaohua Zazhi* 2001; **9**: 392-395
 - 25 **Cheng H**, Liu YF, Zhang HZ, Shen WA, Zhang SZ. Construction and expression of anti-HCC immunotoxin of sFv-TNF- α and GFP fusion proteins. *Shijie Huaren Xiaohua Zazhi* 2001; **9**: 640-644
 - 26 **Jiang YG**, Wang YM, Li QF. Expression significance of HLA-DR antigen and heat shock protein 70 in hepatocellular carcinoma. *Shijie Huaren Xiaohua Zazhi* 2001; **9**: 1139-1142
 - 27 **Wu MC**. The review of hepatology study in China. *Shijie Huaren Xiaohua Zazhi* 2000; **8**: 1201-1204
 - 28 **Meng ZH**, He ZP. Current situation of gene therapy studies in inhibition of liver cancer. *Shijie Huaren Xiaohua Zazhi* 1999; **7**: 350-352
 - 29 **Tang QY**, Yao DF, Liu YH, Meng XY, Yang SH, Wu XH, Wu W, Lu JX. Abnormal expression and methylation of γ -glutamyl transferase genes in human hepatoma tissue. *Zhonghua Xiaohua Zazhi* 1999; **19**: 168-171
 - 30 **Ning XY**, Yang DH. Study and progress on *in vivo* gene treatment of primary hepatocarcinoma. *Shijie Huaren Xiaohua Zazhi* 2000; **8**: 89-90
 - 31 **Tang ZY**, Sun FX, Tian J, Ye SL, Liu YK, Liu KD, Xue Q, Chen J, Xia JL, Qin LX, Sun SL, Wang L, Zhou J, Li Y, Ma ZC, Zhou XD, Wu ZQ, Lin ZY, Yang BH. Metastatic human hepatocellular carcinoma models in nude mice and cell line with metastatic potential. *World J Gastroenterol* 2001; **7**: 597-601
 - 32 **Wang WX**, Dong JY, Zhou SY, Li WL, Zhao Y. Modification of ricin and its hepatotoxicity and activity against hepatocellular cancer in mice. *World J Gastroenterol* 1998; **4**: 307-310
 - 33 **Wang ZX**, Hu GF, Wang HY, Wu MC. Expression of liver cancer associated gene HCCA3. *World J Gastroenterol* 2001; **7**: 821-825
 - 34 **Tang ZY**. Hepatocellular carcinoma-Cause, treatment and metastasis. *World J Gastroenterol* 2001; **7**: 445-454
 - 35 **Cui J**, Zhou XD, Liu YK, Tang ZY, Zile MH. Abnormal beta-catenin gene expression with invasiveness of primary hepatocellular carcinoma in China. *World J Gastroenterol* 2001; **7**: 542-546
 - 36 **Huang XF**, Wang CM, Dai XW, Li ZJ, Pan BR, Yu LB, Qian B, Fang L. Expressions of chromogranin A and cathepsin D in human primary hepatocellular carcinoma. *World J Gastroenterol* 2000; **6**: 693-698
 - 37 **Liang Y**, Lu B, Cui ZF, Li XD, Guo YJ, Lu YJ. The expression of Fas/FasL in hepatocellular carcinomas. *Shijie Huaren Xiaohua Zazhi* 2001; **9**: 1364-1368
 - 38 **Lee JH**, Ku JL, Park YJ, Lee KU, Kim WH, Park JG. Establishment and characterization of four human hepatocellular carcinoma cell lines containing hepatitis B virus DNA. *World J Gastroenterol* 1999; **5**: 289-295
 - 39 **Parks R**, Garden O. Liver resection for cancer. *World J Gastroenterol* 2001; **7**: 766-771
 - 40 **Xu HY**, Yang YL, Guan XL, Song G, Jiang AM, Shi LJ. Expression of regulating apoptosis gene and apoptosis index in primary liver cancer. *World J Gastroenterol* 2000; **6**: 721-724
 - 41 **Lin NF**, Tang J, Ismael HS. Study on environmental etiology of high incidence areas of liver cancer in China. *World J Gastroenterol* 2000; **6**: 572-576
 - 42 **Gao F**, Chen JY, Yu XL. Drug induce the apoptosis of hepatocellular cells. *Shijie Huaren Xiaohua Zazhi* 2001; **9**: 686-688
 - 43 **Zhang JK**, Chen HB, Sun JL, Zhou YQ. Effect of dendritic cells on LPAK cells induced at different times in killing hepatoma cells. *Shijie Huaren Xiaohua Zazhi* 1999; **7**: 673-675
 - 44 **Cao W**, Wang ZM, Liang ZH, Zhang HX, Wang YQ, Guan Y, Li WX, Pan BR. Effects of antiangiogenesis inhibitor TNP-470 with lipiodol in arterial embolization of liver cancer in rabbits. *Shijie Huaren Xiaohua Zazhi* 2000; **8**: 629-632
 - 45 **Lu B**, Dai YM. Abnormal cycle regulation of cells in the HCC. *Shijie Huaren Xiaohua Zazhi* 2001; **9**: 205-208
 - 46 **Wang Q**, Lin ZY, Feng XL. Alterations in metastatic properties of hepatocellular carcinoma cell following H-ras oncogene transfection. *World J Gastroenterol* 2001; **7**: 335-339
 - 47 **Xu DX**, Chen WS, Ye ZJ. The antisense gene of growth factor receptor reversing the malignant phenotype of human hepatoma cells. *Shijie Huaren Xiaohua Zazhi* 2001; **9**: 175-179
 - 48 **Yang JQ**, Yang LY, Zhu HC. Mitomycin C. Induced apoptosis of

- human hepatoma cell. *Shijie Huaren Xiaohua Zazhi* 2001; **9**: 268-272
- 49 **Li BA**, Wang HY, Chen ZJ, Wu MC. The association between signal-regulatory protein- α and hepatocellular carcinoma. *Zhonghua Yixue Zazhi* 1999; **79**: 268-270
- 50 **Zheng SX**, Li XG, Zhou LJ, Zhu XZ. Construction of pcDNA3/p16 plasmid and its inhibitory role in the proliferation of hepatoma cell line. *Shijie Huaren Xiaohua Zazhi* 2000; **8**: 49-51
- 51 **Lu DD**. The research progress of the relationship between DNA methyl and hepatocellular carcinoma. *Zhonghua Ganzangbing Zazhi* 1999; **7**: 251-252
- 52 **Yang DH**, Zhang MQ. Cell apoptosis and hepatocellular carcinoma. *Zhonghua Ganzangbing Zazhi* 1999; **7**: 123-124
- 53 **Yao DF**, Jiang DR, Wu XH, Zhu YS, Huang JF, Mong XY. Experimental study on value of carcino-embryonic gamma-glutamyl transferase isoenzymes for monitoring carcinogenesis of hepatocytes. *Zhonghua Ganzangbing Zazhi* 2000; **8**: 30-32
- 54 **Tsutsumi M**, Sakamuro D, Takada A. Detection of a unique γ -glutamyl transpeptidase messenger RNA species closely related to the development of hepatocellular carcinoma in humans: a new candidate for early diagnosis of hepatocellular carcinoma. *Hepatology* 1996; **23**: 1093-1097
- 55 **Zhou XP**, Chen WX. The image diagnosis of hepatocellular carcinoma. *Shijie Huaren Xiaohua Zazhi* 2000; **8**: 439-440
- 56 **Tian FZ**. Tumor markers of hepatocellular carcinoma. *Shijie Huaren Xiaohua Zazhi* 2000; **8**: 440-441

Edited by Ren SY

Effects of TNP-470 on proliferation and apoptosis in human colon cancer xenografts in nude mice

Zong-Hai Huang, Ying-Fang Fan, Hu Xia, Hao-Miao Feng, Fu-Xiang Tang

Zong-Hai Huang, Ying-Fang Fan, Hao-Miao Feng, Fu-Xiang Tang, Department of Surgery, Zhujiang Hospital, First Military Medical University, Guangzhou 510282, Guangdong Province, China
Hu Xia, Department of Respiratory Diseases, Zhujiang Hospital, First Military Medical University, Guangzhou 510282, Guangdong Province, China

Supported by the Natural Science Foundation of Guangdong Province, No.013072

Correspondence to: Dr. Zong-Hai Huang, Department of Surgery, Zhujiang Hospital, First Military Medical University, Guangzhou 510282, Guangdong Province, China. hghigh@gdvnet.com

Telephone: +86-20-61643211

Received: 2002-07-31 **Accepted:** 2002-08-27

Abstract

AIM: To study the effect of TNP-470 on cell growth, proliferation and apoptosis in human colon cancer xenografts in nude mice.

METHODS: Human colon cancer xenografts were transplanted into 20 nude mice. Mice were randomly divided into two groups. TNP-470 treated group received TNP-470 (30 mg/kg, s.c) every other day and the control group received a sham injection of same volume saline solution. They were sacrificed after 4 weeks and their tumors were processed for histological examination. The expression of proliferating cell nuclear antigen (PCNA) in tumors was detected using immunohistochemical method with image analysis, and apoptosis in tumor cells was measured by TdT-mediated biotinylated-dUTP nick end labeling (TUNEL) staining.

RESULTS: Comparing with controls, tumor growth was significantly inhibited in TNP-470 treated group, the inhibitory rate being 54.4 %. Expression of PCNA in tumors of TNP-470 treated group (PI 54.32±11.47) was significantly lower than that of control group (PI 88.54±12.36), $P < 0.01$. Apoptosis index (AI) of TNP-470 treated group (18.95±1.71) was significantly higher than that of control group (7.26±1.44), $P < 0.001$, typical morphological change of apoptosis in tumor cells was observed in TNP-470 treated group.

CONCLUSION: Besides the anti-angiogenic effects, TNP-470 can inhibit tumor growth by inhibiting the proliferation and inducing apoptosis of tumor cells.

Huang ZH, Fan YF, Xia F, Feng HM, Tang FX. Effects of TNP-470 on proliferation and apoptosis in human colon cancer xenografts in nude mice. *World J Gastroenterol* 2003; 9(2): 281-283
<http://www.wjgnet.com/1007-9327/9/281.htm>

INTRODUCTION

The worldwide incidence of colorectal cancer is estimated at 945 000 patients per year. Many of these patients present with metastases. The past decade has seen several extensive

investigations into advanced colorectal cancer. However, Most patients have limited improvement in long-term prognosis^[1]. Therefore, new therapeutic methods are needed to treat and improve the survival rate in colorectal cancer patients.

Tumors are always dependent on the development of an adequate blood supply through angiogenesis for growth at both primary and secondary sites, and colon cancer would not be an exception^[2-9]. The concept of anti-angiogenesis therapy was first proposed by Folkman^[10,11]. The implications of angiogenesis for tumor biology and therapy were investigated, and some anti-angiogenesis agents have been developed^[12-14]. TNP-470 is a potent angiogenesis inhibitor and an analogue of fimgallin, which is a natural antibiotic secreted by *Aspergillus fumigatus fresenius*^[15,16]. This agent shows a marked inhibitory effect on tumor growth and metastasis *in vivo*^[17-19]. Its target is not only the endothelial cells but also the cancer cells of the host, and the tumor is affected directly^[20-22]. In this study, we examined the inhibitory effect of TNP-470 on tumor growth of human colon cancer xenografts in nude mice. The expression of proliferating cell nuclear antigen (PCNA) in tumors was examined by immunohistochemical method and apoptotic cancer cells were measured by TUNEL assay.

MATERIALS AND METHODS

Drug and reagents

TNP-470 was a generous gift from Takeda Chemical Industries (Osaka, Japan). Its structure and characteristics have been reported. TNP-470 was suspended in a vehicle composed of 0.5 % ethanol plus 5 % gum Arabic in saline. RPMI 1640 and heat-inactivated fetal calf serum (FCS) were purchased from Gibco (Grand Island, NY).

Cell line

Human colon adenocarcinoma cell line Lovo was kindly provided by the Department of Pathology, Cancer Center, First Military Medical University (FIMMU). Cells were cultured in RPMI 1640 supplemented with 10 % FCS, and were maintained at 37 °C in 5 % CO₂. A single cell suspension of approximately 5×10⁶ cells in 0.5 mL of culture medium was inoculated subcutaneously in two Balb/c nude mice to make source tumors. These source tumors were excised when they grew to approximately 1 cm³, and then 2 to 3 mm³ of minced tumor tissue was implanted subcutaneously into the left axial region of the cervix of each balb/c nude mouse on day 0.

Animals

Female Balb/c nude mice were obtained from the Experimental Animal Center, FIMMU, and reared under specific pathogen-free conditions. Four-week-old mice weighing 17-22 g were used in the experiments. On day 1 after implantation, tumor-bearing nude mice were randomly divided into a control group ($n=10$) and a TNP-470 treated group ($n=10$). In the TNP-470 treated group, TNP-470 of 30 mg/kg was injected subcutaneously every other day from day 1 until sacrifice. In the control group, mice received a sham injection of the same volume of saline. The average tumor volumes and animal

weights in the treatment and control groups were almost equal at the beginning of treatment.

Tumor growth and animal weights

The tumor dimensions were measured every 3 days with a dial caliper. The tumor volumes were calculated with the formula width \times length \times 0.52. Mice were weighed every 3 days. The animals were painlessly killed on day 30. All animals were weighed before autopsy, at which time, the tumor weight and volume were obtained. The tumor volume was also expressed by the rate of the mean tumor volume in that treated animals to the mean tumor volume in that of control animals (T/S rate). Tumor tissues were resected and fixed intact with 10% formalin solution, and then cut into four-micrometer-thick sections for PCNA immunohistochemical assay and TUNEL staining.

Immunohistochemical detection of PCNA

Four-micrometer-thick sections were incubated with mouse monoclonal antibodies against PCNA (Gibco, Grand Island, NY) as the primary antibody, followed by biotinylated anti-mouse immunoglobulin and avidin-biotin complex. The PCNA indices were calculated with image analysis system as the percent rate of positively stain Lovo cell nuclei to the total of Lovo nuclei. A minimum of 500 cells was counted in triplicate^[23].

TUNEL staining detection of apoptotic Lovo cells

We stained tumor tissue sections with terminal deoxynucleotidyl transferase (TdT)-mediated dUTP nick end labeling (TUNEL) to identify apoptotic cells^[24]. Briefly, the sections (after being dewaxed in xylene and rehydrated in ethanol) were incubated with 20 μ g/L proteinase K at room temperature for 15 minutes. After quenching of endogenous peroxidase, sections were rinsed in TdT buffer (30 mM Tris, 140 mM sodium cacodylate, 1 mM cobalt chloride), pH 7.2, and incubated with TdT (Pharmacia Biotech, Piscataway, NJ, USA) 1:50 and biotinylated dUTP (Gibco, Grand Island, NY, USA) 1:50 in TdT buffer for 60 min at room temperature. Labeled nuclei were detected with DAB in PBS and counterstained with methyl green for 10 minutes and 5 minutes, respectively. The slides were then mounted and examined under light microscope. Negative controls were tissues processed with omission of the TdT reaction step. Cells were defined as apoptotic if the whole nuclear area of the cell labeled positively. The apoptotic cells and bodies were counted in 10 high-power fields, and this figure was divided by the number of cells in the high-power fields with image analysis system.

Statistical analysis

Data were expressed as mean \pm standard deviation. Comparison between two groups was made by the independent samples *t* test. $P < 0.05$ was considered statistically significant. All statistics were carried out using SPSS10.0 statistics software.

RESULTS

Antitumor effects

Before treatment, the mean tumor volumes in the two groups were approximately the same. The mean tumor volume and tumor weight of two groups at the end of the experiment are shown in Table 1. Tumor growth curve is illustrated in Figure 1. Significant inhibitory efficacy was obtained in TNP-470 treated group.

Proliferation and apoptosis of lovo cells

In PCNA immunohistochemical analysis and TUNEL staining, the number and extent of apoptotic cells were considerably increased and PCNA positive cells were decreased in the TNP-

470 treated group compared with those on the control group. The proliferation index and apoptosis rate of Lovo cells in two groups are shown in Table 2.

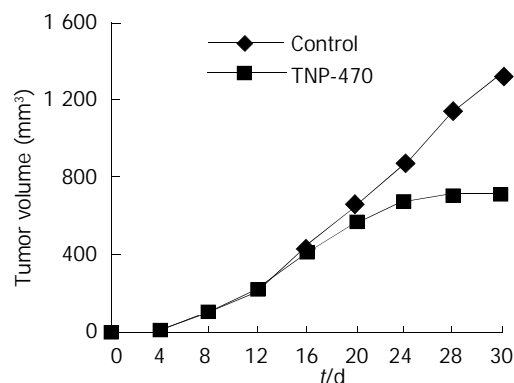


Figure 1 Tumor growth curve.

Table 1 Tumor weight and tumor volume in two groups ($\bar{x} \pm s$)

Group	n	Tumor weight (g)	Tumor volume(mm ³)	T/C(%)
Control	10	1.423 \pm 0.169	1345.24 \pm 38.46	100
TNP-470	10	0.830 \pm 0.123 ^a	731.66 \pm 40.42 ^b	54.4

^a $P < 0.05$; ^b $P < 0.01$, vs control.

Table 2 Proliferation index (PI) and apoptosis index (AI) in two groups ($\bar{x} \pm s$)

Group	n	PI (%)	AI(%)
Control	10	88.54 \pm 12.36	7.26 \pm 1.44
TNP-470	10	54.32 \pm 11.47 ^a	18.95 \pm 1.71 ^b

^a $P < 0.01$; ^b $P < 0.001$, vs control.

DISCUSSION

TNP-470 has been reported to be highly effective against a wide variety of tumors and metastases. This agent mainly exerts its anti-tumor effect by preventing tumor neovascularization^[25-27]. Angiogenesis is essential for the growth of solid tumors at primary and at secondary sites^[28]. It is thought that the new blood vessels in tumor are highly permeable and provide a route for cancer cells to enter the circulation^[29]. Therefore, anti-angiogenesis agents may have the potential to be clinically useful for the prevention of cancer progression.

TNP-470 is well described to antiproliferate the activity against endothelial cells and anti-angiogenic properties *in vivo*. In the recent study, TNP-470 was found to suppress DNA synthesis and cause an increased proportion of cells to go into the G0/G1 phase^[30-32]. A molecular target recently identified that TNP-470 is the mammalian protein MetAP-2. TNP-470 covalently attaching MetAP-2 in endothelial cells may prevent the myristylation of signaling components specific to cell cycle regulation of these cells, and inhibited the proliferation of endothelial cells^[33-35]. Other studies^[36,37] described that cell cycle inhibition by TNP-470 is mediated by p53 and p21^{WAF/CIP}.

TNP-470 has been reported to inhibit various tumor cell proliferation at concentrations much higher than those required to inhibit endothelial cells, yet the exact mechanisms underlying these effects are unclear. In contrast, there are reports that TNP-470 has no significant effect on primary tumors transplanted *s.c.*^[38]. These differences may arise because of organ-site-dependent differences in tumorigenesis and on cancer-cell properties. In addition, sensitivity to TNP-470 varied from tumors possibly due to the tumors' biological malignancy, the growth activity,

the metastasis rate, the adhesive activity to extracellular matrix and the production of VEGF^[10, 39, 40].

The antitumor activity of TNP-470 on a variety of tumors was evaluated *in vitro* and *in vivo*, but not in human colon cancer Lovo cells. In the present study, we found that TNP-470 inhibited the growth of human colon cancer cell line Lovo *in vivo* with an inhibitory rate (T/C) of 45.6% and no weight loss was observed. Another important discovery in the present study was that TNP-470 could inhibit the expression of PCNA in tumors and induce apoptosis of cancer cells *in vivo*. But mechanisms of effect are not clear. Further studies *in vitro* will be necessary.

In conclusion, the present *in vivo* results demonstrated that treatment with TNP-470 could be efficient to inhibit the growth of colon cancer. Further investigation on the mechanism of the apoptosis-inducing effect of TNP-470 will help understand the mechanisms of tumor growth and metastasis.

REFERENCES

- 1 **Shelton BK**. Introduction to colorectal cancer. *Semin Oncol Nurs* 2002; **18**: 2-12
- 2 **Ellis LM**, Liu W, Fan F, Jung YD, Reinmuth N, Stoeltzing O, Takeda A, Akagi M, Parikh AA, Ahmad S. Synopsis of angiogenesis inhibitors in oncology. *Oncology* 2002; **16**: 14-22
- 3 **Liu XP**, Song SB, Li G, Wang DJ, Wei LX. Correlations of microvessel quantitation in colorectal tumors and clinicopathology. *Shijie Huaren Xiaohua Zazhi* 1997; **7**: 37-39
- 4 **Jia L**, Chen TX, Sun JW, Na ZM, Zhang HH. Relationship between microvessel density and proliferating cell nuclear antigen and prognosis in colorectal cancer. *Shijie Huaren Xiaohua Zazhi* 2000; **8**: 74-76
- 5 **Fan YF**, Huang ZH. Progress in the studies of gene therapy for colorectal cancer. *Shijie Huaren Xiaohua Zazhi* 2001; **9**: 427-430
- 6 **Liu H**, Wu JS, Li LH, Yao X. The expression of Platelet-derived growth factor and angiogenesis in human colorectal carcinoma. *Shijie Huaren Xiaohua Zazhi* 2000; **8**: 661-664
- 7 **Wu J**, Fan DM. Neoplastic vascularization and vascular inhibitory treatment. *Shijie Huaren Xiaohua Zazhi* 2001; **9**: 316-321
- 8 **Fan YF**, Huang ZH. Angiogenesis inhibitor TNP-470 suppresses growth of peritoneal disseminating foci of human colon cancer line Lovo. *World J gastroenterol* 2002; **8**: 853-856
- 9 **Fan YF**, Huang ZH. Inhibitory effect of TNP-470 on colon ascites cancer in nude mice. *Shijie Huaren Xiaohua Zazhi* 2002; **10**: 770-773
- 10 **Kanai T**, Konno H, Tanaka T, Matsumoto K, Baba M, Nakamura S, Baba S. Effect of angiogenesis inhibitor TNP-470 on the progression of human gastric cancer xenotransplanted into nude mice. *Int J Cancer* 1997; **71**: 838-841
- 11 **Ribatti D**, Vacca A, Nico B, De Falco G, Giuseppe Montaldo P, Ponzoni M. Angiogenesis and anti-angiogenesis in neuroblastoma. *Eur J Cancer* 2002; **38**: 750-757
- 12 **Kieran MW**, Billett A. Antiangiogenesis therapy. Current and future agents. *Hematol Oncol Clin North Am* 2001; **15**: 835-851
- 13 **Tseng JE**, Glisson BS, Khuri FR, Shin DM, Myers JN, El-Naggar AK, Roach JS, Ginsberg LE, Thall PF, Wang X, Teddy S, Lawhorn KN, Zentgraf RE, Steinhaus GD, Pluda JM, Abbruzzese JL, Hong WK, Herbst RS. Phase II study of the antiangiogenesis agent thalidomide in recurrent or metastatic squamous cell carcinoma of the head and neck. *Cancer* 2001; **92**: 2364-2373
- 14 **Takahashi Y**, Mai M. Significance of angiogenesis and clinical application of anti-angiogenesis. *Nippon Geka Gakkai Zasshi* 2001; **102**: 381-384
- 15 **Miki T**, Nonomura N, Nozawa M, Harada Y, Nishimura K, Kojima Y, Takahara S, Okuyama A. Angiogenesis inhibitor TNP-470 inhibits growth and metastasis of a hormone-independent rat prostatic carcinoma cell line. *J Urol* 1998; **160**: 210-213
- 16 **Ogawa H**, Sato Y, Kondo M, Takahashi N, Oshima T, Sasaki F, Une Y, Nishihira J, Todo S. Combined treatment with TNP-470 and 5-fluorouracil effectively inhibits growth of murine colon cancer cells *in vitro* and liver metastasis *in vivo*. *Oncol Rep* 2000; **7**: 467-472
- 17 **Niwano M**, Arii S, Mori A, Ishigami S, Harada T, Mise M, Furutani M, Fujioka M, Imamura M. Inhibition of tumor growth and microvascular angiogenesis by the potent angiogenesis inhibitor, TNP-470, in rats. *Surg Today* 1998; **28**: 915-922
- 18 **Katzenstein HM**, Salwen HR, Nguyen NN, Meitar D, Cohn SL. Antiangiogenic therapy inhibits human neuroblastoma growth. *Med Pediatr Oncol* 2001; **36**: 190-193
- 19 **Liu B**, Lin Y, Yin H. Experimental study of the effect of angiogenesis inhibitor TNP-470 on the growth and metastasis of gastric cancer *in vivo*. *Zhonghua Zhongliu Zazhi* 1998; **20**: 34-36
- 20 **Farinelle S**, Malonne H, Chaboteaux C, Decaestecker C, Dedecker R, Gras T, Darro F, Fontaine J, Atassi G, Kiss R. Characterization of TNP-470-induced modifications to cell functions in HUVEC and cancer cells. *J Pharmacol Toxicol Methods* 2000; **43**: 15-24
- 21 **Sedlakova O**, Sedlak J, Hunakova L, Jakubikova J, Duraj J, Sulikova M, Chovancova J, Chorvath B. Angiogenesis inhibitor TNP-470: cytotoxic effects on human neoplastic cell lines. *Neoplasma* 1999; **46**: 283-289
- 22 **Mori J**, Haisa M, Naomoto Y, Takaoka M, Kimura M, Yamatsuji T, Notohara K, Tanaka N. Suppression of tumor growth and downregulation of platelet-derived endothelial cell growth factor/thymidine phosphorylase in tumor cells by angiogenesis inhibitor TNP-470. *Jpn J Cancer Res* 2000; **91**: 643-650
- 23 **Kato H**, Ishikura H, Kawarada Y, Furuya M, Kondo S, Kato H, Yoshiki T. Anti-angiogenic treatment for peritoneal dissemination of pancreas adenocarcinoma: a study using TNP-470. *Jpn J Cancer Res* 2001; **92**: 67-73
- 24 **Lopes De Faria JB**, Aikawa Da Silveira L. Increased renal cell proliferation in spontaneously hypertensive rats before the onset of hypertension. *Nephron* 2002; **91**: 170-172
- 25 **Takei H**, Lee ES, Cisneros A, Jordan VC. Effects of angiogenesis inhibitor TNP-470 on tamoxifen-stimulated MCF-7 breast tumors in nude mice. *Cancer Lett* 2000; **155**: 129-135
- 26 **Gleich LL**, Zimmerman N, Wang YO, Gluckman JL. Angiogenic inhibition for the treatment of head and neck cancer. *Anticancer Res* 1998; **18**: 2607-2609
- 27 **Ma J**, Pulfer S, Li S, Chu J, Reed K, Gallo JM. Pharmacodynamic-mediated reduction of temozolomide tumor concentrations by the angiogenesis inhibitor TNP-470. *Cancer Res* 2001; **61**: 5491-5498
- 28 **Li CY**, Shan S, Cao Y, Dewhirst MW. Role of incipient angiogenesis in cancer metastasis. *Cancer Metastasis Rev* 2000; **19**: 7-11
- 29 **Wyckoff JB**, Jones JG, Condeelis JS, Segall JE. A critical step in metastasis: *in vivo* analysis of intravasation at the primary tumor. *Cancer Res* 2000; **60**: 2504-2511
- 30 **Kruger EA**, Figg WD. TNP-470: an angiogenesis inhibitor in clinical development for cancer. *Expert Opin Investig Drugs* 2000; **9**: 1383-1396
- 31 **Taniguchi H**. Angiogenesis inhibitor (TNP-470: AGM-1470). *Nippon Rinsho* 2001; **59**: 678-682
- 32 **Kumeda SI**, Deguchi A, Toi M, Omura S, Umezawa K. Induction of G1 arrest and selective growth inhibition by lactacystin in human umbilical vein endothelial cells. *Anticancer Res* 1999; **19**: 3961-3968
- 33 **Wang J**, Lou P, Henkin J. Selective inhibition of endothelial cell proliferation by fumagillin is not due to differential expression of methionine aminopeptidases. *J Cell Biochem* 2000; **77**: 465-473
- 34 **Turk BE**, Griffith EC, Wolf S, Biemann K, Chang YH, Liu JO. Selective inhibition of amino-terminal methionine processing by TNP-470 and ovalicin in endothelial cells. *Chem Biol* 1999; **6**: 823-833
- 35 **Griffith EC**, Su Z, Niwayama S, Ramsay CA, Chang YH, Liu JO. Molecular recognition of angiogenesis inhibitors fumagillin and ovalicin by methionine aminopeptidase 2. *Proc Natl Acad Sci USA* 1998; **95**: 15183-15188
- 36 **Yeh JR**, Mohan R, Crews CM. The antiangiogenic agent TNP-470 requires p53 and p21CIP/WAF for endothelial cell growth arrest. *Proc Natl Acad Sci USA* 2000; **97**: 12782-12787
- 37 **Zhang Y**, Griffith EC, Sage J, Jacks T, Liu JO. Cell cycle inhibition by the anti-angiogenic agent TNP-470 is mediated by p53 and p21WAF1/CIP1. *Proc Natl Acad Sci USA* 2000; **97**: 6427-6432
- 38 **Sano J**, Sugiyama Y, Kunieda K, Sano B, Saji S. Therapeutic effect of TNP-470 on spontaneous liver metastasis of colon tumors in the rabbit. *Surg Today* 2000; **30**: 1100-1106
- 39 **Shishido T**, Yasoshima T, Denno R, Mukaiya M, Sato N, Hirata K. Inhibition of liver metastasis of human pancreatic carcinoma by angiogenesis inhibitor TNP-470 in combination with cisplatin. *Jpn J Cancer Res* 1998; **89**: 963-969
- 40 **Gasparini G**. The rationale and future potential of angiogenesis inhibitors in neoplasia. *Drugs* 1999; **58**: 17-38

Clinical characteristics and diagnosis of patients with hereditary nonpolyposis colorectal cancer

San-Jun Cai, Ye Xu, Guo-Xiang Cai, Peng Lian, Zu-Qing Guan, Shan-Jing Mo, Meng-Hong Sun, Qi Cai, Da-Ren Shi

San-Jun Cai, Ye Xu, Guo-Xiang Cai, Peng Lian, Zu-Qing Guan, Shan-Jing Mo, Department of Abdominal Surgery, Shanghai Cancer Hospital/Institute, Fudan University, Shanghai 200032, China
Meng-Hong Sun, Qi Cai, Da-Ren Shi, Department of Pathology, Shanghai Cancer Hospital/Institute, Fudan University, Shanghai 200032, China

Supported by Shanghai Medical Development Fund for Major Projects, No. 993025-I

Correspondence to: San-Jun Cai, Department of Abdominal Surgery, Shanghai Cancer Hospital/Institute, Fudan University, Shanghai 200032, China. sanjunc@online.sh.cn

Telephone: +86-21-64175590-2508

Received: 2002-08-15 **Accepted:** 2002-09-12

Abstract

AIM: To study the clinical characteristics of hereditary nonpolyposis colorectal cancer (HNPCC) in the Chinese population and discuss the identification and management of the patients with HNPCC.

METHODS: A series of 140 patients with colorectal cancers (CRC) and HNPCC associated tumors from 30 families fulfilling the Amsterdam criteria were analyzed.

RESULTS: A total of 118 patients had CRC. Average age at diagnosis of the first CRC was 45.7 years, 56.8 % and 23.4 % of the first CRC were located proximal to the splenic flexure and in the rectum respectively. Twenty-three (19.5 %) had synchronous and metachronous CRC. Twenty-seven patients were found to have extracolonic tumors. Gastric carcinoma was the most common tumor type in our series (44.4 %).

CONCLUSION: The frequency of HNPCC was 2.6 % in our series of patients. The main features are an excess of early onset with a propensity to involve the proximal colon, and high frequency of multiple foci. Management and surveillance for these patients should be different from sporadic CRC. Contrary to American and European reports, gastric cancer seems more frequent than endometrial cancer in Chinese. It is necessary to formulate a new HNPCC criterion for Chinese patients.

Cai SJ, Xu Y, Cai GX, Lian P, Guan ZQ, Mo SJ, Sun MH, Cai Q, Shi DR. Clinical characteristics and diagnosis of patients with hereditary nonpolyposis colorectal cancer. *World J Gastroenterol* 2003; 9(2): 284-287

<http://www.wjgnet.com/1007-9327/9/284.htm>

INTRODUCTION

Hereditary nonpolyposis colorectal cancer (HNPCC), also known as Lynch syndrome, is a distinct autosomal dominant syndrome. It accounts for 1-10 % of the total colorectal cancer population^[1-9]. On the basis of the absence or presence of extracolonic malignancies, it can be subdivided into Lynch syndrome I (hereditary site specific colorectal cancer) and

Lynch syndrome II (colorectal cancer in association with extracolonic cancer)^[10,11].

The criteria for clinical diagnosis of HNPCC were established by the International Collaborative Group on Hereditary Nonpolyposis Colorectal Cancer (ICG-HNPCC) in 1991. These criteria known as the "Amsterdam criteria" are as follows: (1) Histologically verified colorectal cancer in three or more relatives, one of whom is a first-degree relative of the other two; (2) Colorectal cancer involving at least two generations; (3) One or more colorectal cancers diagnosed below age of 50 years. In the present study, 30 Chinese HNPCC families fulfilling the Amsterdam criteria were studied.

MATERIALS AND METHODS

Materials

From September 1994 to December 2001, 30 Chinese HNPCC families that fulfilled the Amsterdam Criteria were registered at the Department of Abdominal Surgery in the Shanghai Cancer Hospital / Institute. Of the 30 identified patients, 8 were found to have colorectal cancer before October 1998 and 5 were diagnosed and treated from June 2000 to December 2001. From October 1998 to May 2000, we consecutively investigated 392 patients with colorectal cancer (CRC) for their detailed family history. The remaining 7 cases were diagnosed on follow-up in the clinic.

Methods

When the probands were verified, we investigated the more detailed family history of patients in the hospital or in the clinic through inquiry by telephone and mail. The tree of each family pedigree was drawn. And these HNPCC patients are being followed up.

RESULTS

Tumor frequency

From October 1998 to May 2000, we investigated 392 patients with CRC for their detailed family history and 10 families with the clinical features of HNPCC were identified, resulting in an overall incidence rate of 2.6 %. The 30 families included 14 Lynch type I families and 16 Lynch type II families. A total of 140 patients developed malignant tumors, 118 (65 males and 53 females) of whom had CRC. The median age at diagnosis of the first colorectal cancer was 45.7 years (range from 20 to 79 years). Eighty-eight patients (74.6 %) developed CRC below 50 years, including 10 patients (8.5 %) under 30 years of age, 56.8 % and 23.4 % of the first colorectal cancers were located in the colon proximal to spleen flexure and in rectum, respectively. Synchronous and metachronous colorectal cancer occurred in 23 (19.5 %) patients.

Extracolonic colorectal cancer

Twenty-seven extracolonic tumors were found, including 10 stomach cancers, 4 endometrial carcinomas, 3 esophageal cancer, 2 hepatic cancers, one renal carcinoma, one pancreatic cancer, one breast cancer, one laryngeal cancer, one lymphoma

and one leukemia. Gastric cancer is the most frequent extracolonic cancer in our series, accounting for 44.5 %.

Pathology of colorectal cancers

We reviewed the HE of 18 cases available. Five (27.8 %) cases of mucinous adenocarcinoma or signet cell type carcinoma were found. Four (22.2 %) tumors had lymphocyte infiltration.

DISCUSSION

Amsterdam criteria I was adopted to diagnose HNPCC in this study. As the widely accepted criteria for diagnosis of HNPCC, the Amsterdam criteria were established by the International Collaborative Group on Hereditary Nonpolyposis Colorectal Cancer (ICG-HNPCC). But as clinical criteria, the Amsterdam criteria are too restrictive, thus leading to a number of limitations: (1) The failure to acknowledge the contribution of endometrial cancer and other extracolonic cancer to the HNPCC diagnosis. (2) Small family size or poor documentation of disease and cause of death limits the identification of many affected families^[12]. (3) New mutations are not likely to be identified. Estimates of HNPCC frequency varied from country to country. On the one hand, a difference actually exists among different areas, ethnics, nationalities, etc. On the other hand, these studies were not based on uniform criteria. Amsterdam criteria I and II, Japanese criteria and other criteria for suspected HNPCC were used in different studies. According to the Amsterdam criteria, many population-based studies in foreign countries yielded the frequency at 1-10 %. In 1999, a national epidemiological research done in Italy indicated a frequency of HNPCC of 7 %^[13]. Nevertheless, suspected HNPCC cases were included in this study. The actual frequency of HNPCC will be lower than 7 % obviously with Amsterdam criteria I. Another study by Peel *et al.* showed that the frequency of HNPCC was nearly 1 %^[14]. In China, Bo Zhao reported that HNPCC accounted for 5.2 % of the Chinese population^[15]. However, this study included 11 HNPCC families fulfilling Amsterdam criteria I and 5 HNPCC families according to Japanese criteria. The actual frequency of HNPCC was 3.6 % excluding the 5 families fulfilling Japanese criteria. The frequency of HNPCC was found to be 2.6 % in our study, which agrees with previous studies.

To solve this problem, many investigators developed additional criteria, such as the Japanese criteria for HNPCC. They include class A, in which there are three or more colorectal cancers within first-degree relatives, and class B, in which there are two or more colorectal cancers within first degree relatives, and any of the following: (1) early onset of colorectal cancer (age <50years). (2) Right colon involvement, or (3) synchronous or metachronous colorectal and/or extracolonic cancers. Among our 392 patients, 24 families were found according to these criteria, accounting for 6.1 % of the total colorectal cancers. Compared with the Amsterdam criteria, the Japanese criteria are relatively looser, thus increasing the frequency for diagnosis of HNPCC. But there still remain some problems: (1) It does not give enough attention to extracolonic cancer in the diagnosis. (2) The early age of onset and transmissibility of HNPCC, which are the most striking characteristics of HNPCC, have not been emphasized. These weaknesses make it easy to diagnose sporadic colorectal cancers as HNPCC.

In 1998, new selection criteria for collaborative studies, called revised ICG-HNPCC or the Amsterdam criteria II, were proposed by ICG-HNPCC (The classic Amsterdam criteria were kept as Amsterdam criteria I). The new criteria include: (1) There should be at least three relatives with a histologically verified HNPCC-associated cancer (colorectal cancer, cancer of endometrium, small bowel, ureter, or renal pelvis), one of

whom is a first-degree relative of the other two. (2) At least two successive generations should be affected. (3) At least one should be diagnosed below 50 years of age. The new criteria raised the diagnostic value of some extracolonic cancers. Considering the risk of gastric and hepatic cancers is not high in the relatives, they excluded stomach cancer and hepatic cancer^[16], which were the most prevalent cancers in HNPCC families and in the general population of some Asian countries, including China, Korea, etc. The incidence of cancers of endometrium and small bowel is relatively lower than that of western countries. So the Amsterdam criteria II may be more applicable to western countries than to Asian countries. In our 392 consecutive colorectal cancer patients, except for the 10 families fulfilling the criteria I, no families met the Amsterdam criteria II. However, if we included other HNPCC-associated cancers in the criteria, 24 additional families would be found. Including the 10 families for criteria I, they accounted for 8.7 % of the 392 colorectal patients. We think that the specificity and sensitivity of the Amsterdam criteria II are not wholly suitable for the diagnosis of HNPCC in China. We have performed the detection of microsatellite instability, sequence analysis of mismatch repair genes and the detection of hMLH1 and hMSH2 protein on the probands of these 24 kindreds and 18 HNPCC patients. If we can detect the alteration of mismatch repair genes in these HNPCC families, we may include gastric and hepatic cancers in HNPCC related extracolonic tumors. Further epidemiological and genetic studies in China will advance our knowledge on HNPCC. The variance and similarity between Chinese and western countries should be evaluated. It is necessary to establish the Chinese criteria for HNPCC.

HNPCC is a syndrome that affects a distinct percentage of the total colorectal cancer population. It is characterized by the development of cancer at an early age^[17-19], predominance of proximal colonic cancer^[20-23], excess of multiple cancers^[24-27], an increased risk for selected extracolonic adenocarcinomas^[28], early occurrence of colonic adenomas^[16] and better prognosis^[29-31]. *In vitro* experiments showed that HNPCC is resistant to 5-Fluorouracil (5-FU), Cis-diaminedichloroplatinum (DDP) and Nitrogen mustard. By contrast, HNPCC is more sensitive to γrays. Identifying individuals afflicted with HNPCC has implications for early diagnosis, surgical management, chemotherapy, prognosis, follow-up, and surveillance of HNPCC patients and family members at risk. We have noticed that patients with HNPCC inherit a germline mutation in one of the genes responsible for repair of DNA mismatch errors^[32,33]. However, given the clinical unavailability for widespread application of gene test and the enormous cost for gene mutation hunting, selection of patients with HNPCC based on suspicious family history is still the most important approach^[34-36].

Early age of cancer onset is one of the most striking features about HNPCC. The average age to develop colorectal cancer was 45 years, 20 years earlier than the sporadic colorectal cancer. The study involving 43 HNPCC kindreds and 140 HNPCC patients by Bertario *et al* showed that the average age of onset was 49 years^[36]. Bo Zhao *et al* reported the mean age of cancer onset in 16 Chinese HNPCC families, which was 50.8 years in 68 patients^[15]. Another 13 HNPCC kindreds in China were reported by Sheng *et al* whose median age at diagnosis was 41 years. In Sheng's study, 68.75 % of the colorectal cancer developed below age of 50 years, and 90.63 % before 60 years of age^[37]. In the present study, the median age of onset of the first colorectal cancer was 45.7 years, with 74.6 % under age of 50 years and 8.5 % under 30 years of age.

Another important clinical characteristic of HNPCC is that the cancer is inclined to be located in the proximal colon. A Swedish national investigation in 2001 demonstrated the proportion of cancers located in the proximal colon was 51 %

of the total^[38]. Similar to the other reports, the colorectal cancer is more commonly found proximal to the splenic flexure (58.3 %) in our study. So a relatively young patient, especially younger than 50, with a proximal colon lesion is a clue to be noted. Special attention must be paid while inquiring into the family history. However, there were contrary reports. The percentage of cancers proximal to the splenic flexure was only 25 % in Peel's research^[14]. Given the early age of onset of the cancer and most of the tumor will develop in the proximal colon, we recommend that colonoscopy be performed for the family members with HNPCC and repeated annually or biannually thereafter from the age of 25 years. Flexible sigmoidoscopy is not an effective screening approach in this disease.

HNPCC also predisposes individuals to multiple synchronous and metachronous colon cancer. The prevalence rate of synchronous and metachronous colorectal cancer was about 35 %^[16]. Peel *et al* reported that 12.5 % of the patients had synchronous and metachronous cancers in the colon. Although the rate was not high, it was still higher than that of the patients without family cancer history and non-HNPCC cases with positive family cancer history, being 2.6 % and 5.9 % respectively. And the difference was statistically evident ($P=0.023$)^[14]. A domestic investigation in China showed the percentage of synchronous and metachronous colorectal cancers was 39.5 %. All of them developed within ten years after surgery and needed reoperations^[15]. In our series, 23 (19.5 %) of 118 patients presented with multiple cancers in the colorectum. The high incidence of multiple cancers implies that subtotal colectomy is an appropriate management when colon cancers are found in affected patients. It can reduce the chance of developing synchronous colorectal cancer and simplify the endoscopic examination^[39]. But considering the effect on the quality of life after subtotal colectomy and the psychological attack on the patients, we usually chose segmental resection for colorectal carcinoma and give intensive follow-up. Only when the patients were diagnosed with multiple cancers or adenomas at other segments, would subtotal colectomy be performed.

Individuals in HNPCC families had an increased risk of developing extracolonic carcinomas including endometrium, stomach, ovary, small intestine, pancreaticobiliary system, upper urological tract, and other sites. Fourteen Lynch type I families and 16 Lynch type II families were found in the 30 HNPCC families (0.88:1). There were 3 Lynch type I families and 13 Lynch type II families in a total of 16 HNPCC kindreds in Bo Zhao's study (0.23:1)^[15]. So extracolonic tumors are frequently seen in HNPCC patients and may contribute to the diagnosis of HNPCC. For this reason, extracolonic cancers were included in the Amsterdam criteria II. According to the reports of western countries, the endometrial and stomach cancers are the first and the second most common tumor in HNPCC, respectively. A study in Portugal revealed that endometrial carcinoma was most frequent in HNPCC extracolonic tumors, the prevalence among women patients even reached 25 %^[40]. In our series, of the 81 patients in the 16 Lynch syndrome II families, 27 developed extracolonic carcinomas. The three most common tumors were stomach cancer (12/27), endometrial carcinoma (4/27) and esophageal neoplasm (3/27). Different from the western countries, the incidence of stomach carcinoma was significantly higher than endometrial cancer ($P<0.05$). Bo Zhao *et al* in China reported 34 cases of extracolonic cancer in 16 HNPCC families. He also found stomach cancer was the most common extracolonic tumor in HNPCC (11 cases of stomach cancers) and endometrial cancer was less common (7 of 34) than gastric cancer^[15]. The difference in extracolonic tumor spectrum between China and western countries may lie in many aspects. The small size of our sample may be one of the reasons. Besides, different types of mutation or mutation loci and

interaction between environment, life style, ethnics and genotype may also contribute to the observed variation.

ACKNOWLEDGEMENTS

We are indebted to Professor Mo SJ for his critical advice for this study and assistance in collecting partial HNPCC cases. We also appreciate the help from Professor Shi DR for his pathological diagnosis and providing pathological data of patients.

REFERENCES

- Rodriguez-Bigas MA**, Boland CR, Hamilton SR, Henson DE, Jass JR, Khan PM, Lynch H, Perucho M, Smyrk T, Sobin L, Srivastava S. A national cancer institute workshop on hereditary nonpolyposis colorectal cancer syndrom: meeting highlights and Bethesda guidelines. *J Natl Cancer Inst* 1997; **89**: 1758-1762
- Ponz de Leon M**, Pedroni M, Benatti P, Percesepe A, Di Gregorio C, Foroni M, Rossi G, Genuardi M, Neri G, Leonardi F, Viel A, Capozzi E, Boiocchi M, Roncucci L. Hereditary colorectal cancer in the general population: from cancer registration to molecular diagnosis. *Gut* 1999; **45**: 32-38
- Debniak T**, Kurzawski G, Gorski B, Kladny J, Domagala W, Lubinski J. Value of pedigree/clinical data, immunohistochemistry and microsatellite instability analyses in reducing the cost of determining hMLH1 and hMSH2 gene mutations in patients with colorectal cancer. *Eur J Cancer* 2000; **36**: 49-54
- Midgley R**, Kerr D. Colorectal cancer. *Lancet* 1999; **353**: 391-399
- Katballe N**, Christensen M, Wikman FP, Orntoft TF, Laurberg S. Frequency of hereditary non-polyposis colorectal cancer in Danish colorectal cancer patients. *Gut* 2002; **50**: 43-51
- Aaltonen LA**, Salovaara R, Kristo P, Canzian F, Hemminki A, Peltomaki P, Chadwick RB, Kääriäinen H, Eskelinen M, Järvinen H, Mecklin JP, de la Chapelle A, Percesepe A, Ahtola H, Härkönen N, Julkunen R, Kangas E, Ojala S, Tulikoura J, Valkamo E. Incidence of hereditary nonpolyposis colorectal cancer and the feasibility of molecular screening for the disease. *New Engl J Med* 1998; **338**: 1481-1487
- Lynch HT**. Hereditary nonpolyposis colorectal cancer (HNPCC). *Cytogenet Cell Genet* 1999; **86**: 130-135
- Marra G**, Boland CR. Hereditary nonpolyposis colorectal cancer: the syndrome, the genes, and historical perspectives. *J Natl Cancer Inst* 1995; **87**: 1114-1125
- Raedle J**, Schaffner M, Esser N, Sahn S, Trojan J, Kriener S, Brieger A, Nier H, Bockhorn H, Berg PL, Frick B, Schafer I, Zeuzem S. Frequency of the amsterdam criteria in a regional german cohort of patients with colorectal cancer. *Z Gastroenterol* 2002; **40**: 561-568
- Bertolaccini L**, Olivero G. Hereditary non polyposis colorectal cancer (HNPCC). A clinical and genetic entity. *Minerva Chir* 2002; **57**: 63-72
- Muller A**, Fishel R. Mismatch repair and the hereditary non-polyposis colorectal cancer syndrome (HNPCC). *Cancer Invest* 2002; **20**: 102-109
- Gao SK**, Xu WH. Hereditary nonpolypoid colorectal cancer. *Huaren Xiaohua Zazhi* 1998; **6**: 70-71
- Gatta G**, Francisci S, Ponz-de-Leon M. The prevalence of colorectal cancer in Italy. *Tumor* 1999; **85**: 387-390
- Peel DJ**, Zogas A, Fox EA, Gildea M, Laham B, Clements E, Kolondner RD, Anton-Culver H. Characterization of hereditary nonpolyposis colorectal cancer families from a population-based series of cases. *J Natl Cancer Inst* 2000; **92**: 1517-1522
- Zhao B**, Wang ZJ, Xu YF, Wan YL, Li P, Huang YT. Report of 16 kindreds and one kindred with hMLH1 germline mutation. *World J Gastroenterol* 2002; **8**: 263-266
- Vasen HFA**, Watson P, Mecklin JP, Lynch HT. New clinical criteria for hereditary nonpolyposis colorectal cancer (HNPCC Lynch syndrome) proposed by the international collaborative group on HNPCC. *Gastroenterology* 1999; **116**: 1453-1456
- Wei SC**, Wang MH, Shieh MC, Wang CY, Wong JM. Clinical characteristics of Taiwanese hereditary non-polyposis colorectal cancer kindreds. *J Formos Med Assoc* 2002; **101**: 206-209
- Guillem JG**, Puig-La Calle J Jr, Cellini C, Murray M, Ng J, Fazzari M, Paty PB, Quan SH, Wong WD, Cohen AM. Varying features

- of early age-of-onset "sporadic" and hereditary nonpolyposis colorectal cancer patients. *Dis Colon Rectum* 1999; **42**: 36-42
- 19 **Song YM**, Zheng S. Analysis for phenotype of HNPCC in China. *World J Gastroenterol* 2002; **8**: 837-840
- 20 **Lynch HT**, Lynch JF. Hereditary nonpolyposis colorectal cancer. *Semin Surg Oncol* 2000; **18**: 305-313
- 21 **Bernstein IT**, Bisgaard ML, Myrholm T. Registration of hereditary non-polyposis colorectal cancer. *Ugeskr Laeger* 1999; **161**: 6174-6178
- 22 **Myrholm T**, Bisgaard ML, Bernstein I, Svendsen LB, Sondergaard JO, Bulow S. Hereditary non-polyposis colorectal cancer: clinical features and survival. Results from the Danish HNPCC register. *Scand J Gastroenterol* 1997; **32**: 572-576
- 23 **Ponz de Leon M**, Benatti P, Percesepe A, Rossi G, Viel A, Santarosa M, Pedroni M, Roncucci L. Clinical and molecular diagnosis of hereditary non-polyposis colorectal cancer: problems and pitfalls in an extended pedigree. *Ital J Gastroenterol Hepatol* 1999; **31**: 476-480
- 24 **Box JC**, Rodriguez-Bigas MA, Weber TK, Petrelli NJ. Clinical implications of multiple colorectal carcinomas in hereditary nonpolyposis colorectal carcinoma. *Dis Colon Rectum* 1999; **42**: 717-721
- 25 **Hemminki K**, Li XJ, Dong C. Second Primary Cancers after Sporadic and Familial Colorectal Cancer. *Cancer Epidemiol Biomarkers Prevent* 2001; **10**: 793-798
- 26 **Cai Q**, Sun MH, Lu HF, Zhang TM, Mo SJ, Xu Y, Cai SJ, Zhu XZ, Shi DR. Clinicopathological and molecular genetic analysis of 4 typical Chinese HNPCC families. *World J Gastroenterol* 2001; **7**: 805-810
- 27 **Fante R**, Roncucci L, Di Gregorio C, Tamassia MG, Losi L, Benatti P, Pedroni M, Percesepe A, De Pietri S, Ponz de Leon M. Frequency and clinical features of multiple tumors of the large bowel in the general population and in patients with hereditary colorectal carcinoma. *Cancer* 1996; **77**: 2013-2021
- 28 **Rodriguez-Bigas MA**, Vasen HF, Lynch HT, Watson P, Myrholm T, Jarvinen HJ, Mecklin JP, Macrae F, St John DJ, Bertario L, Fidalgo P, Madlensky L, Rozen P. Characteristics of small bowel carcinoma in hereditary nonpolyposis colorectal carcinoma. International Collaborative Group on HNPCC. *Cancer* 1998; **83**: 240-244
- 29 **Lynch HT**, Smyrk T. An update on Lynch syndrome. *Curr Opin Oncol* 1998; **10**: 349-356
- 30 **Edmonston TB**, Cuesta KH, Burkholder S, Barusevicius A, Rose D, Kovatich AJ, Boman B, Fry R, Fishel R, Palazzo JP. Colorectal carcinomas with high microsatellite instability: defining a distinct immunologic and molecular entity with respect to prognostic markers. *Hum Pathol* 2000; **31**: 1506-1514
- 31 **Tomoda H**, Baba H, Oshiro T. Clinical manifestations in patients with hereditary nonpolyposis colorectal cancer. *J Surg Oncol* 1996; **61**: 262-266
- 32 **Dieumegard B**, Grandjouan S, Sabourin JC, Bihan ML, Lefrere I, Bellefqih, Pignon J-P, Rougier P, Lasser P, Benard J, Couturier D, Paillerets BB. Extensive molecular screening for hereditary nonpolyposis colorectal cancer. *Br J Cancer* 2000; **82**: 871-880
- 33 **Peltomaki P**. Deficient DNA mismatch repair: a common etiologic factor for colon cancer. *Hum Mol Genet* 2001; **10**: 735-740
- 34 **Tinley ST**, Lynch HT. Integration of family history and medical management of patients with hereditary cancers. *Cancer* 1999; **86** (11 Suppl): 2525-2532
- 35 **Lynch HT**, Watson P. Multiple HNPCC tumors: ask the families. *Gut* 1998; **43**: 596-597
- 36 **Bertario L**, Russo A, Sala P, Eboli M, Radice P, Presciuttini S, Andreola S, Rodriguez-Bigas MA, Pizzetti P, Spinelli P. Survival of patients with hereditary colorectal cancer: comparison of HNPCC and colorectal cancer in FAP patients with sporadic colorectal cancer. *Int J Cancer* 1999; **80**: 183-187
- 37 **Sheng JQ**, Li SL, Mu H. Analysis of clinical phenotype of hereditary non-polyposis colorectal cancer. *Shijie Huaren Xiaohua Zazhi* 2002; **10**: 104-105
- 38 **Hemminki K**, Li X. Familial colorectal adenocarcinoma and hereditary nonpolyposis colorectal cancer: a nationwide epidemiological study from Sweden. *Br J Cancer* 2001; **84**: 969-974
- 39 **Lynch HT**, Smyrk T. Hereditary nonpolyposis cancer. *Cancer* 1996; **78**: 1149-1167
- 40 **Fidalgo P**, Almeida MR, West S, Gaspar C, Maia L, Wijnen J, Albuquerque C, Curtis A, Cravo M, Fodele R, Leitao CN, Burn J. Detection of mutations in mismatch repair genes in Portuguese families with hereditary non-polyposis colorectal cancer by a multi-method approach. *Eur J Hum Genet* 2000; **8**: 49-53

Angiography for diagnosis and treatment of colorectal cancer

Jin Gu, Zhao-Lai Ma, Ying Li, Ming Li, Guang-Wei Xu

Jin Gu, Ming Li, Guang-Wei Xu, Department of Surgery, Oncology School of Peking University, Beijing, Beijing 100036, China

Zhao-Lai Ma, Department of Surgery, the Third Hospital of Peking University, Beijing, 100083, China

Ying Li, Department of Surgery, Beijing Chaoyang Hospital, Beijing 100044, China

Correspondence to: Dr. Jin Gu, Department of Surgery, Oncology School of Peking University, 52 FuCheng Road, Beijing 100036, China. jingu_1999@yahoo.com

Telephone: +86-10-88141032 **Fax:** +86-10-88122437

Received: 2002-07-08 **Accepted:** 2002-07-27

Abstract

AIM: To evaluate the role of preoperative angiography in the diagnosis and treatment of colorectal cancer.

METHODS: The authors performed selective arterial cannulation by Seldinger's method in 47 patients to locate the primary cancer and to diagnose metastasis to the liver. Each patient was then given intra-arterial regional chemotherapy, and received 5-fluorouracil (5-Fu, 1 000 mg), mitomycin C (MMC, 20 mg), and cisplatinium (CDDP, 80 mg).

RESULTS: The location and shape of each tumor were observed, including metastatic tumors in the liver, in 42 of the 47 (89.4 %) patients. The site of the primary tumor was difficult to identify in 5 cases because the patients had a recurrence of cancer. Arterial chemotherapy was performed successfully in all patients. The authors recorded no partial or significant morbidity resulted from angiography. The only incident was bleeding from the artery puncture site in one patient, which was successfully stopped by general medication.

CONCLUSION: Preoperative selective arterial angiography can help the diagnosis and locate primary tumors and to detect liver metastasis. At the same time, regional arterial chemotherapy can be an important form of preoperative therapy.

Gu J, Ma ZL, Li Y, Li M, Xu GW. Angiography for diagnosis and treatment of colorectal cancer. *World J Gastroenterol* 2003; 9 (2): 288-290

<http://www.wjgnet.com/1007-9327/9/288.htm>

INTRODUCTION

Colorectal cancer is one of the three leading causes of worldwide cancer mortality^[1]. It is the second leading cause of cancer-related deaths in the Western world^[2]. Because of changes in life style and nutritional habits, the incidence of colorectal cancer is increasing in China. From 1972-1989, the incidence of colorectal cancer increased 85 % in men and 79 % in women. The average rate of increase in incidence was 4.2 % per year since 1970's. Of all cancers in China, colorectal cancer ranks the fifth in incidence. Although 80 % of patients initially can have the primary tumor completely resected, the cancer invades the serosa or involves the regional lymph nodes in

almost half of patients, predisposing them to a high risk of recurrence^[3]. Recurrent cancer of the large intestine is second in cancer-related deaths only to lung cancer^[4,5].

Colorectal cancers are detected mainly by endoscopic and radiological examination. However, endoscopy is unsuccessful in some patients who have a low tolerance for the procedure and in patients, especially elderly ones, who are physically unable to undergo a barium enema. In the United Kingdom a complete colonoscopic examination to the caecum is achieved in only 70 % of cases^[6].

Angiography has been used to define sites of gastrointestinal bleeding when endoscopy has been unsuccessful^[7]. To our knowledge, there have been no reports describing the significance of angiography to help diagnosis in colorectal cancer. Our present study assessed the clinical value of the angiography for colorectal cancer.

MATERIALS AND METHODS

Materials

Between Jan.1997 and Jan 1999, we enrolled in this study 47 consecutive patients (25 men, 22 women, age range, 37-81) with histologically or clinically proven colorectal cancer. All patients had normal cardiopulmonary, renal, and hepatic function. In addition, no patient had evidence of coagulopathy or had been previously treated with chemotherapy or any other anti-cancer treatment. Carcinoma was located in the rectum in 26 patients, in the sigmoid colon in 10, in the ascending colon in 7, in the descending colon in 1 and in the transverse colon in 3. Of the 47 tumors, 6 were classified on histologic study as mucinous adenocarcinoma and 41 were adenocarcinoma, of which 3 were poorly differentiated, 31 moderately to well differentiated, and 7 well differentiated. No case was defined as Dukes' s stage A; 3 were stage B1, 26 were stage B2, 13 were stage C, and 5 were stage D. Acute obstruction of the colon was seen in 6 patients, and 7 cases were postoperative recurrent tumor. In this group, 3 cases were colorectal cancer with hepatic metastases.

Methods

The groin was sterilized and prepared with local anesthesia. The abdominal aorta was catheterized through the femoral artery by Seldinger's method^[8].

In each patient, we selectively advanced the catheter into the vessel that supplied the tumor: the ileocolic artery for cancer of the ileoceum, right colic artery for cancer of the ascending colon, left colic artery for cancer of descending colon, sigmoid artery for cancer of the sigmoid colon, superior rectal artery and bilateral iliac arteries for cancers of the anus and most distal rectum^[9].

When these arteries could not be located, we placed the catheter into the superior mesenteric artery for the right half of the colon and the inferior mesenteric artery for the left half of the colon. Digital subtraction angiography (PHILIP INTEGRIS V 3 000, PHILIPS LTD, Holland) and the use of contrast dye of Ultravist 370 yielded a "Tumor flush" caused by the abnormal capillary mass of the tumor, which gave the exact location of the tumor. Then we infused chemotherapeutic agents into the tumor through the same artery; each patient received 5-fluorouracil (5-Fu 1 000 mg), mitomycin C (MMC,

20 mg), and cisplatinium (CDDP, 80 mg).

Both the hepatic and superior rectal arteries were cannulated in one patient who had rectal cancer with multiple liver metastases.

RESULTS

We performed a digital subtraction angiography procedure (DSA) in 47 patients with colorectal cancer. We were able to locate the exact tumor site in 42 of 47 (89.4 %) angiographic studies, including six patients with acute obstruction of the colon (Figures 1-3). The location of the primary tumor was difficult to identify in 5 cases because the patients had a recurrence of cancer and liver metastases that were found at the same time of the DSA during angiography. Regional chemotherapy for primary colorectal cancer was successfully completed in 47 patients, and 3 patients received chemotherapy for metastatic tumors in the liver at the same time (Figure 4).

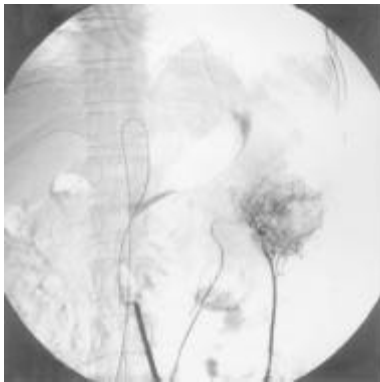


Figure 1 Detection of the tumor site by angiography. Carcinoma of the descending colon can be visualized.

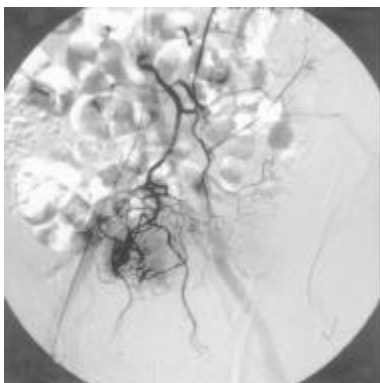


Figure 2 Detection of a tumor in the rectum by angiography.

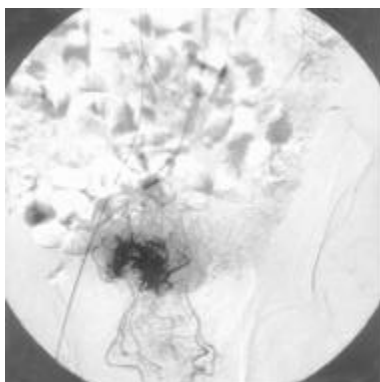


Figure 3 Angiography showing the tumor site in a patient with rectal carcinoma associated with liver metastasis.

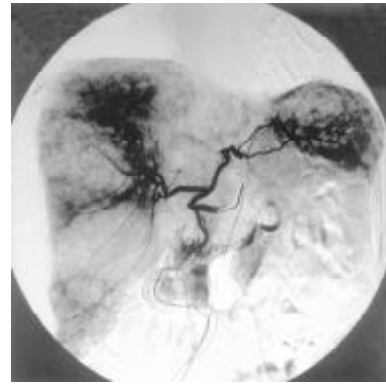


Figure 4 Angiography showing multiple liver metastases in the same patient as in Figure 3.

DISCUSSION

In patients with symptoms of colorectal cancer, flexible colonoscopy or barium enema are usually performed, for definitive diagnosis. Cathartics are usually necessary to prepare for the barium enema. However, if plain radiographs of the abdomen show a dilated colon and acute colonic obstruction is suspected, a barium enema (or water-soluble contrast study) may be obtained without preparation to define the location and nature of the obstructing lesion. Some patients, especially older patients, are not able to finish rolling on the table during the examination. Although flexible colonoscopy is the most accurate and complete examination for the large bowel, some patients cannot tolerate the procedure. In addition, technical limitations, such as the inability to evaluate the splenic or hepatic flexures or the cecum, compromise the diagnostic usefulness of colonoscopy. Furthermore, colonoscopy is contraindicated in patients with suspected perforation or obstruction of the large bowel^[10,11]. Angiography is a safe and accurate technique for localizing acute gastrointestinal hemorrhage^[12]. Since 1996, we have used angiography to diagnose colorectal cancer and to deliver regional chemotherapy^[13,14]. Our rate of locating tumors with is 89.4 %, and we have simultaneously detected cases of colorectal cancer with metastatic liver tumors using angiography. During this procedure, patients have been able to lie comfortably on the table, even those in pain with an acute bowel obstruction induced by colorectal cancer. We had difficulty to find the site of the tumor of recurrent colorectal cancer by angiography because the vessels supplied the tumor had been ligated during the last operation. Regional chemotherapy has been widely used to treat solid tumors^[15,16]. The rationale for arterial chemotherapy is that arterial administration allows for high local levels of the drug without corresponding systemic toxicity^[17-20]. After intraarterial infusion of 5-Fu, drug levels at the tumor site has been reported to be 9-to 69-fold higher than those obtained during intravenous administration^[21]. Few studies have been published on intraarterial chemotherapy in primary colorectal cancer. In our study, chemotherapeutic agents were infused after angiography into vessels supplying the colorectal cancer. As we were reporting short-term results (less than 3 years), we did not see a statistical survival benefit in this study.

Distant metastases develop in 10-15 % of patients despite complete resection of the primary colorectal tumor^[22]. Colorectal cancer commonly metastasizes through lymphatic pathways and portal venous vessels to the liver^[23-25]. Thus, hepatic arterial chemotherapy is an attractive treatment option for bilobar non-resectable liver metastases in patients in whom the liver is the sole site of distant disease and recurrence^[26-31]. Furthermore, angiography and intra-hepatic artery infusion chemotherapy may be used simultaneously we make it possible

to be finished at the same period.

Local recurrence and distant metastasis are the most common reasons for treatment failure after surgical resection for colorectal cancer. Local recurrence of rectal cancer, with extension through the wall and with regional lymph node involvement, occurs in 50 % of patients. In patients with unresectable lesions, pain and organ obstruction are distressing and potentially devastating symptoms^[32]. It was reported that intraarterial infusion of 5-Fu and MMC by percutaneous placement of an infusion catheter in the bilateral internal iliac arteries relieved the pain in 50 % of patients with unresectable, recurrent rectal cancer^[33]. In our study, one patient with recurrent cancer having severe pelvic pain underwent angiography for diagnosis and then received intraarterial chemotherapy in the bilateral internal iliac arteries. After treatment, the pain was relieved, and the bowels were more easily evacuated. We are not sure of the mechanism underlying these treatment effects.

REFERENCES

- Zhou CZ**, Peng ZH, Zhang F, Qiu GQ, He L. Loss of heterozygosity on long arm of chromosome 22 in sporadic colorectal carcinoma. *World J Gastroenterol* 2002; **8**: 668-673
- Santacroce L**, Buonfantino M, Santacroce S. Surgical treatment and prognostic factors in colon cancer. *J Chemother* 1997; **9**: 144-145
- Boring CC**, Squires TS, Tong T, Montgomery S. Cancer statistics, 1994. *CA Cancer J Clin* 1994; **44**: 7-26
- Kornmann M**, Link KH, Galuba I, Ott K, Schwabe W, Hausler P, Scholz P, Strater J, Polat S, Leibl B, Kettner E, Schlichting C, Baumann W, Schramm H, Hecker U, Ridwelski K, Vogt JH, Zerbian KU, Schutze F, Kreuser ED, Behnke D, Beger HG. Association of time to recurrence with thymidylate synthase and dihydropyrimidine dehydrogenase mRNA expression in stage II and III colorectal cancer. *J Gastrointest Surg* 2002; **6**: 331-337
- Obrand DI**, Gordon PH. Incidence and patterns of recurrence following curative resection for colorectal carcinoma. *Dis Colon Rectum* 1997; **40**: 15-24
- Makin GB**, Breen DJ, Monson JRT. The impact of new technology on surgery for colorectal cancer. *World J Gastroenterol* 2001; **7**: 612-621
- Jensen DM**. What to choose for diagnosis of bleeding colonic angiomias: colonoscopy, angiography, or helical computed tomography angiography? *Gastroenterology* 2000; **119**: 581-584
- Saito K**, Goto Y, Wakabayashi Y, Saito T, Abe K. Placing two parallel catheters by Seldinger's approach through the femoral artery for CT angiography and CT during arteriography: evaluation of efficacy and safety. *Nippon Igaku Hoshasen Gakkai Zasshi* 1998; **58**: 91-93
- Ho S**, Jackson J. The angiographic diagnosis of colonic carcinoma. *Clin Radiol* 1998; **53**: 345-349
- Nahas SC**, Oliveira Filho DE, Araujo SE, Lourencao JL, Sobrado Junior CW, Nahas CS, Habr-Gama A, Pinotti HW. Colonoscopy: indications, contraindications and complications. *Rev Hosp Clin Fac Med Sao Paulo* 1998; **53**: 91-99
- Han Y**, Uno Y, Munakata A. Does flexible small-diameter colonoscope reduce insertion pain during colonoscopy. *World J Gastroenterol* 2000; **6**: 659-663
- Velmahos GC**, Toutouzas KG, Vassiliu P, Sarkisyan G, Chan LS, Hanks SH, Berne TV, Demetriades D. A Prospective Study on the Safety and Efficacy of Angiographic Embolization for Pelvic and Visceral Injuries. *J Trauma* 2002; **53**: 303-308
- Gu J**, Peng Y, Ma Z. Long-term results of preoperative regional intraarterial chemotherapy against colorectal cancer. *Zhonghua Waike Zazhi* 2002; **40**: 404-406
- Gu J**, Ma Z, Ye Y, Xue WC, Qu J, Zhao YD, Yu YX, Leng XS, Zhu XG. Preoperative arterial infusion chemotherapy of colorectal carcinoma pathological and clinical effects. *Zhonghua Waike Zazhi* 1999; **37**: 333-335
- Tepper JE**, O'Connell M, Niedzwiecki D, Hollis DR, Benson AB 3rd, Cummings B, Gunderson LL, Macdonald JS, Martenson JA, Mayer RJ. Adjuvant therapy in rectal cancer: analysis of stage, sex, and local control-final report of intergroup 0114. *J Clin Oncol* 2002; **20**: 1744-1750
- Xu HB**, Zhang YJ, Wei WJ, Li WM, Tu XQ. Pancreatic tumor: DSA diagnosis and treatment. *World J Gastroenterol* 1998; **4**: 80-81
- Leslie A**, Steele RJ. Management of colorectal cancer. *Postgrad Med J* 2002; **78**: 473-478
- Kim R**, Yamaguchi Y, Toge T. Adjuvant therapy for colorectal carcinoma. *Anticancer Res* 2002; **22**: 2413-2418
- Graziano F**, Catalano V, Baldelli AM, Cascinu S. Prognostic biomarkers in resected colorectal cancer: implications for adjuvant chemotherapy. *Expert Rev Anticancer Ther* 2001; **1**: 247-257
- Tao HQ**, Zou SC. Effect of preoperative regional artery chemotherapy on proliferation and apoptosis of gastric carcinoma cells. *World J Gastroenterol* 2002; **8**: 451-454
- Liu LX**, Zhang WH, Jiang HC, Zhu AL, Wu LF, Qi SY, Piao DX. Arterial chemotherapy of 5-fluorouracil and mitomycin C in the treatment of liver metastases of colorectal cancer. *World J Gastroenterol* 2002; **8**: 663-667
- Obrand DI**, Gordon PH. Incidence and patterns of recurrence following curative resection for colorectal carcinoma. *Dis Colon Rectum* 1997; **40**: 15-24
- Fiorentini G**, Poddie DB, Cantore M, Giovanis P, Guadagni S, De Giorgi U, Cariello A, Dazzi C, Turci D. Locoregional therapy for liver metastases from colorectal cancer: the possibilities of intraarterial chemotherapy, and new hepatic-directed modalities. *Hepatogastroenterology* 2001; **48**: 305-312
- Yamaguchi A**, Taniguchi H, Kunishima S, Koh T, Yamagishi H. Correlation between angiographically assessed vascularity and blood flow in hepatic metastases in patients with colorectal carcinoma. *Cancer* 2000; **89**: 1236-1244
- Li XW**, Ding YQ, Cai JJ, Yang SQ, An LB, Qiao DF. Studies on mechanism of Sialy Lewis-X antigen in liver metastases of human colorectal carcinoma. *World J Gastroenterol* 2001; **7**: 425-430
- Fiorentini G**, Poddie DB, Giorgi UD, Guglielminetti D, Giovanis P, Leoni M, Latino W, Dazzi C, Cariello A, Turci D, Marangolo M. Global approach to hepatic metastases from colorectal cancer: indication and outcome of intra-arterial chemotherapy and other hepatic-directed treatments. *Med Oncol* 2000; **17**: 163-173
- Hladkyi OV**, Rodzaievs'kyi SO, Tur MO, Sorokin BV, Rozumii DO. The intra-arterial chemotherapy of tumorous lesions of the stomach, rectum and liver. *Lik Sprava* 1997; **2**: 86-90
- Sotsky TK**, Ravikumar TS. Cryotherapy in the treatment of liver metastases from colorectal cancer. *Semin Oncol* 2002; **29**: 183-191
- Zanon C**, Grosso M, Clara R, Alabiso O, Chiappino I, Miraglia S, Martinotti R, Bortolini M, Rizzo M, Gazzera C. Combined regional and systemic chemotherapy by a mini-invasive approach for the treatment of colorectal liver metastases. *Am J Clin Oncol* 2001; **24**: 354-359
- Kemeny N**, Fata F. Hepatic-arterial chemotherapy. *Lancet Oncol* 2001; **2**: 418-428
- Liu LX**, Zhang WH, Jiang HC, Zhu AL, Wu LF, Qi SY, Piao DX. Arterial chemotherapy of 5-fluorouracil and mitomycin C in the treatment of liver metastases of colorectal cancer. *World J Gastroenterol* 2002; **8**: 663-667
- Read TE**, Mutch MG, Chang BW, McNevin MS, Fleshman JW, Birnbaum EH, Fry RD, Caushaj PF, Kodner IJ. Locoregional recurrence and survival after curative resection of adenocarcinoma of the colon. *J Am Coll Surg* 2002; **195**: 33-40
- Tepper JE**, O'Connell M, Niedzwiecki D, Hollis DR, Benson AB 3rd, Cummings B, Gunderson LL, Macdonald JS, Martenson JA, Mayer RJ. Adjuvant therapy in rectal cancer: analysis of stage, sex, and local control-final report of intergroup 0114. *J Clin Oncol* 2002; **20**: 1744-1750

HCV replication in PBMC and its influence on interferon therapy

Guo-Zhong Gong, Li-Ying Lai, Yong-Fang Jiang, Yan He, Xian-Shi Su

Guo-Zhong Gong, Li-Ying Lai, Yong-Fang Jiang, Yan He, Xian-Shi Su, Center for Liver Diseases, Second Xiangya Hospital, Central South University, Changsha 410011, Hunan Province, China
Supported by National Natural Science Foundation of China, No. 3967067

Correspondence to: Dr. Guo-Zhong Gong, Center for Liver Diseases, Second Xiangya Hospital, Xiangya Medical School, Central South University, 86 Middle Renmin Street, Changsha 410011, Hunan Province, China. guozhong_gong@hotmail.com

Telephone: +86-731-5524222 Ext 2263 **Fax:** +86-731-5533525

Received: 2002-06-28 **Accepted:** 2002-09-16

Abstract

AIM: To study hepatic virus C (HCV) RNA and HCV protein expression in peripheral blood mononuclear cells (PBMCs) of patients with HCV infection, and explore the relationship between the HCV RNA in the PBMCs and response to interferon (IFN) therapy.

METHODS: Type-specific primers were designed and RT-nested PCR was used to detect the plus- and minus- strands of HCV RNA in PBMCs of 54 patients with HCV infection; Indirect immunofluorescence assay was applied to identify HCVNS5 protein expression in PBMCs; 6 month-, 3 MU-IFN regimen was administered to observe the responses to IFN in 35 chronic hepatitis C patients with different HCV RNA status in PBMCs.

RESULTS: HCV plus strand RNA was found in 10 of 19 (52.6 %) acute hepatitis C patients and 22 of 35 (62.9 %) chronic hepatitis C patients. HCV minus strand RNA was detected in 14 of 35 (40.0 %) chronic hepatitis C patients, but only one patient (5.3 %) with acute HCV infection was found to be minus HCV RNA positive. Though no HCV NS5 protein expression was found in the examined 10 cases of acute HCV infection, it was positive in 17 of 20 (85.0 %) chronic hepatitis C patients by indirect immunofluorescence assay. There are significant differences of positive rate of the minus-strand and HCVNS5 protein between acute and chronic hepatitis C groups ($u=2.07$, $P<0.05$ and $u=4.43$, $P<0.01$ respectively). The patients with minus-strand HCV RNA showed a significantly lower 6-month sustained response (SR-6) to IFN compared to those without minus-strand HCV RNA in PBMCs (biologically 14.3 % vs 42.8 %, $\chi^2=4.12$, $P<0.05$ and virologically 7.1 % vs 23.9 %, $\chi^2=4.24$, $P<0.05$).

CONCLUSION: HCV is capable of infecting and replicating in PBMCs, and HCVNS5 protein was expressed in PBMCs. The patients with minus strand HCV RNA in PBMCs showed a significantly lower 6-month sustained response to IFN, suggesting that minus-strand HCV RNA in PBMCs may be one of the factors influencing response to IFN therapy.

Gong GZ, Lai LY, Jiang YF, He Y, Su XS. HCV replication in PBMC and its influence on interferon therapy. *World J Gastroenterol* 2003; 9(2): 291-294

<http://www.wjgnet.com/1007-9327/9/291.htm>

INTRODUCTION

Hepatitis C virus (HCV), a single positive-strand RNA, belongs to the Flaviviridae family, and is the major cause of post-transfusion hepatitis. Infection with HCV usually results in chronic hepatitis, which may progress to cirrhosis and finally to hepatocellular carcinoma. The mechanisms responsible for the chronicity are unclear, one of which is supposed to be that HCV has the ability to escape the host immunity by mutations in genome. There are numerous genotypes of HCV worldwide, and genotype 1b is found to be responsible for the most cases of HCV infection in southern China^[1]. IFN has been a widely accepted drug for the treatment of patients with HCV infection for more than 10 years, and now combination of IFN with ribavirin becomes the choice of therapy^[3,4]. Reinfection of HCV after orthotopic liver transplantation has postulated that there exists extrahepatic sites suitable for HCV replication^[5,6]. The possible extrahepatic cells for HCV replication may be PBMC, cells in pancreas, adrenal gland, bone marrow and spleen, even in the cerebrospinal fluid^[2,7-9], among them, PBMCs have been the most controversial, in which the minus strand HCV RNA, a replicative intermediate of HCV, has been found. It still remains unclear whether HCV replication in PBMC is a factor influencing IFN therapy response. In this study, we not only detected the minus strand HCV RNA and HCVNS5 protein expression in PBMC of patients with hepatitis C, but also analyzed the relationship between minus strand HCV RNA in PBMC and IFN response.

MATERIALS AND METHODS

PBMC preparation

Blood samples were collected from 54 patients with hepatitis C virus infection from January of 1994 to January of 1998, all of them are positive for anti-HCV by ELISA (Sino-American Biotech. Company, China) and HCV RNA by RT-PCR (Sino-American Biotech. Company, China). PBMCs were separated from 10 mL of whole blood mixed with sodium citrate by density gradient centrifugation with ficoll-hypaque. The separated PBMCs were washed four times in 10 mL of RPMI-1640 and then frozen and stored at -70 °C until use.

Cellular total RNA extraction and RT-PCR

Total RNA of the PBMCs was extracted with an RNA isolation kit (Shanghai Huaxun Company, China) according to the manufacturer's instructions. Primers P1: 5' - CGCGCGACTAGGAAGACTTC-3' and P2: 5' - ATGTACCCCATGAGGTTCGGC-3' (as the external pair), and P3: 5' -AGGAAGACTTCCGAGCGCGGTC-3' and P4: 5' -GAGCCATCTGCC CACCCCA-3' (as the internal pair) for RT-PCR were designed according to Okamoto *et al*^[10]. 5 μ l of PBMC RNA and 1 μ l of P1 (for producing cDNA of minus HCV RNA) or 1 μ l of P2 (for producing cDNA of plus HCV RNA) were added to the reverse transcription system (Promega, USA). The reverse transcription system includes 10 \times buffer 2 μ l, 25 mmol/L MgCl₂ 4 μ l, RNasin 1 μ l, AMVRT 15 U, 10 mmol/L dNTP 2 μ l with a total volume of 20 μ l by adding ddH₂O. After incubation for 30 min at 42 °C, the synthesized HCV RNA cDNA was exposed at 95 °C for 30 min to destroy AMVRT. The first PCR was performed with the

above synthesized HCVRNA cDNA as a template. The external primers (P1 and P2) were added into the PCR reaction mix. After pre-denaturing for 5 min, the reaction mix denatured at 94 °C for 60sec, annealed at 55 °C for 60sec and extended at 72 °C for 90sec for 35 cycles. The second PCR was performed same as in the first PCR except the production of the first PCR was used as the template and with the internal primers (P3 and P4). A total volume of 7 μ l the second PCR product was loaded onto 2 % agarose gel containing 0.5 μ g/mL EB. After electrophoresis, the gel was placed under ultraviolet ray to analyze the results (Figure 1).

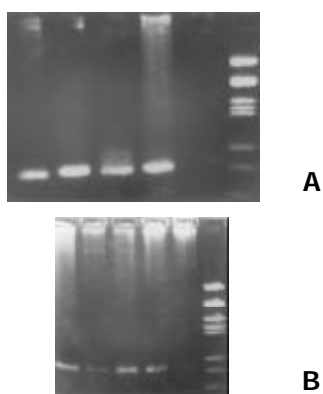


Figure 1 Analysis of HCVRNA plus-strand (A) and minus-strand (B). Lane 1, 2, 3, 4, 5: Serum Samples from the patients with hepatitis C. 144bp means plus of minus strand HCVRNA. Lane 6: DNA marker (pGEM-7 HindIII/EcoRI).

Immunofluorescence assay

After being separated, PBMCs were suspended (1×10^7 cell \cdot mL⁻¹) in RPMI-1640, dropped on to slides, and air dried. The slides were then fixed in acetone for 20 min at -20 °C, washed with PBS, and air-dried. Mouse anti-human HCV NS5 McAb (1:400, Virostat, U.S.A) was added onto the slides. After 30 min incubation at 37 °C, the slides were washed three times in PBS, and then isothiocyanate-conjugated rabbit anti-mouse IgG was added and incubated for 30 min. Slides were then washed and observed under microscope (Figure 2).

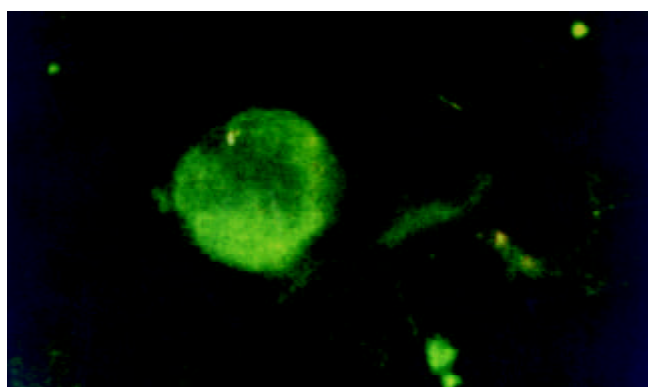


Figure 2 Indirect immunofluorescent assay for detection of HCV NS5A protein. HCV NS5A was stained in green and distributed mainly in the cytoplasm of PBMCs.

Treatment with IFN

Three MU of Interferon α -2b (Tianjing Hualida, China) was administered intramuscularly three times a week for 6 months. The efficacy of interferon therapy is defined biochemically as normalization of serum (adding full term of ALT here!!!) (ALT) and virologically as serum conversion of HCV RNA. End-treatment response (ETR) refers to the response to IFN

when the treatment ends, and the sustained response (SR) refers to the response after the ending of treatment, i.e., SR-6 means response at 6 months after the ending of treatment.

RESULTS

HCVRNA and HCVNS5 protein in PBMCs of patients with hepatitis C virus infection

HCV plus-strand RNA was found in 32 of 54 (59.26 %) patients with HCV infection, among them 10 of 19 (52.63 %) with acute hepatitis C and 22 of 35 (62.85 %) with chronic hepatitis C were positive respectively, and there is no statistically significant difference between the two groups. HCV minus-strand RNA was detected positive in 14 out of the 35 patients with chronic hepatitis C (14 of 35, 40 %) and 1 of 19 patients with acute hepatitis C and a significant difference was found between these two groups ($u=2.07$, $P<0.05$). Regarding to HCVNS5 expression in PBMCs of patients with hepatitis C, 17 out of 20 patients with chronic hepatitis C were found positive, but all the 10 patients with acute hepatitis C were found negative, and there is a remarkable statistically significant difference between the two groups ($u=4.43$, $P<0.01$. see Table 1).

Table 1 HCV plus and minus RNA and HCVNS5 in PBMCs

	HCVRNA		HCVNS5
	Plus	minus	positive
Acute hepatitis C	10/19 (52.6%)	1/19 (5.3%) ^b	0/10 (0%) ^d
Chronic hepatitis C	22/35 (62.9%)	14/35 (40.0%) ^b	17/20 (85%) ^d

^bComparison of the detection rates of HCV minus-RNA between acute and chronic hepatitis C, $u=2.07$, $P<0.05$;

^dComparison of the detection rates of HCV NS5 protein between acute and chronic hepatitis C, $u=4.43$, $P<0.01$.

The influence of HCV RNA status in PBMCs on therapy response to IFN

Six-month regimen with 3MU of IFN- α 2b was completed in 35 patients with chronic hepatitis C, and the biochemical and virological ETR and SR-6 were evaluated. There is a tendency to have a lower response to IFN treatment in the patients with plus-strand HCVRNA positive in PBMCs, although no statistically significant difference was found when compared with the negative group. The patients with minus-strand HCV RNA in PBMCs showed a significantly lower SR-6 to IFN therapy than those without HCV RNA minus-strand, both biochemically (SR-6: 14.3 % vs 42.8 %, $\chi^2=4.12$, $P<0.05$), and virologically (SR-6: 7.1 % vs 23.9 %, $\chi^2=4.24$, $P<0.05$) (Table 2).

Table 2 The influence of HCVRNA in PBMC on interferon response

	HCVRNA plus strand		HCVRNA minus strand	
	Positive	Negative	Positive	Negative
ETR (Biochemical)	13 (59.1%)	7 (53.7%)	8 (57.1%)	13 (61.9%)
ETR (Virological)	11 (50.0%)	9 (69.2%)	6 (42.9%)	12 (57.1%)
SR-6 (Biochemical)	8 (36.7%)	6 (46.2%)	2 (14.3%) ^a	9 (42.8%) ^a
SR-6 (Virological)	6 (27.3%)	5 (38.5%)	1 (7.1%) ^c	7 (33.3%) ^c

^aComparison of biochemical SR-6 between HCV minus-RNA positive and negative groups, $\chi^2=4.12$, $P<0.05$; ^cComparison of virological SR-6 between HCV minus-RNA positive and negative groups, $\chi^2=4.24$, $P<0.05$.

DISCUSSION

Extrahepatic HCV replication has long been a controversial topic since the finding of the high rate of re-infection of grafts after orthotopic liver transplantation in the patients with the end-stage HCV induced liver diseases. Whether PBMCs is suitable for HCV replication is still uncertain. The detection of the minus strand HCV RNA is thought to be reasonable for the discovery of HCV replication because the minus strand RNA is the replicative intermediate of HCV. In recent years, several reports on the detection of HCVRNA in PBMCs have been published^[12-14]. Cribier *et al* incubated PBMCs healthy donors with HCV positive sera, and detected HCV RNA plus-strand and minus-strand using RT-PCR and *in situ* hybridization^[15]. Our results showed that HCV RNA plus-strand were common in the PBMCs of patients, in both acute and chronic infection patients. This high rate of plus-strand HCV RNA is usually thought to be resulted from the contamination of plasma, therefore, minus-strand HCV RNA was explored in the PBMCs from hepatitis C patients, which indicates the replication of HCV in PBMCs. In acute HCV infection, HCV RNA minus-strand is rare in PBMCs, but in the chronic group, the minus-strand HCV RNA is not uncommon in the PBMCs (14 of 35, 40.0 %), which is similar to what Chang *et al* reported^[16]. The ratio of HCV RNA minus-strand detected in chronic hepatitis C is much higher than that in acute hepatitis C, suggesting that the replication of HCV in PBMCs may play an important role in the processes of chronicity, and the mechanism could be that HCV in PBMCs can escape from clearance resulting from host immunity, and make the infection of HCV persistent. On the other hand, the dysfunction of the HCV infected PBMCs leads to immune function decline or in disorder, and this becomes more difficult for the host to clear intrahepatic HCV, so that the injure of hepatocytes persists^[17]. Although minus-strand HCV RNA is the replicative form and not found in patient's serum or plasma, indicating that is a more convincing parameter for HCV replication, some authors are still arguing that the minus-strand HCV RNA in the blood cells including PBMC may be artifacts from self-priming or mispriming during PCR reaction^[18,19], or contamination or passive absorption by circulating virus^[20,21]. To overcome that point, the expression of HCV related proteins in extrahepatic cells has become the key point for the identification of HCV replication. Sansonno *et al*, found HCV exists and replicates mainly in plasma of PBMCs, and the viral proteins, such as core protein, NS3 were found to be expressed in PBMCs^[22]. Chen *et al*, analyzed the relationship between HCV core expression in PBMCs and the diseased state of hepatitis C patients and found that the core protein was more intensely expressed in the nucleus of PBMCs from advanced chronic hepatitis C patients than that from the moderate patients^[11]. We further performed an indirect immunofluorescent assay for HCVNS5 protein and its expression was found mainly in cytoplasm of PBMCs from patients with chronic hepatitis C. Our results indicate that HCV not only replicates but also produces its related protein in PBMCs.

IFN is known to possess both immunomodulatory and antiviral activities. It is tempting to postulate that IFN therapy may enhance the host immune response to promote the clearance of HCV infection. IFN is currently the only approved efficient drug for hepatitis C infection, and combined with ribavirin, its antiviral activity will be increased^[3,4,23]. Serum HCV load and the HCV subtypes have been considered as the major factors to influence the response to IFN therapy^[28,29]. Others influencing factors include the increased amount of Mx_A mRNA, the higher complexity of HCV quasispecies and the frequency of mutations in NS5A region^[30-33]. The extrahepatic HCV replication, especially in the PBMCs, acts

as a predictor for the response to IFN therapy needs to be explored. Omata *et al*, reported a prospective IFN study, in which most of patients treated with IFN obtained normalization of serum aminotransferase, whereas only 3 cases from the control showed such change ($P < 0.02$); serum hepatitis C virus RNA became undetectable in 10 of 11 treated cases, but in only 1 of 12 patients of control group. IFN prevents the progression of acute hepatitis C to chronicity by eradicating HCV. The response of patients with chronic hepatitis C to IFN treatment was significantly lower than that of patients with acute hepatitis C. That the detection ratio of HC VRNA minus in PBMC of chronic hepatitis C is significantly higher than that of acute hepatitis C suggests that the replication of HCV in PBMCs is an important factor influencing the response to IFN treatment^[24]. Löhr *et al*, reported that there was no relationship between HCVRNA minus-strand in PBMC and the response to IFN treatment^[25]. Others reported that the replication of HCVRNA in PBMC may be the source of relapse after IFN treatment in chronic hepatitis C^[26,27]. The different HCV quasispecies in liver or PBMC may response to IFN differently and the quasispecies in PBMCs should be considered to predictor in response to IFN therapy^[34-36]. Our results show the replication of HCV RNA in PBMC can influence the response to IFN. The patients with HCVRNA minus-strands in PBMC had a significantly lower 6-month sustained response to IFN, both biochemically and virologically, than those without minus-strand, suggesting HCV replication in PBMCs may be one reason for relapse after treatment with IFN.

REFERENCES

- 1 **Wang Y**, Okamoto H, Mishiro S. HCV genotypes in China. *Lancet* 1992; **339**: 1168
- 2 **Laskus T**, Radkowski M, Bednarska A, Wilkinson J, Adair D, Nowicki M, Nikolopoulou GB, Vargas H, Rakela J. Detection and analysis of hepatitis C virus sequences in cerebrospinal fluid. *J Virol* 2002; **76**: 10064-10068
- 3 **McHutchison JG**, Gordon SC, Schiff ER, Shiffman ML, Lee WM, Rustgi VK, Goodman ZD, Ling MH, Cort S, Albrecht JK. Interferon alfa2b alone or in combination with ribavirin as initial treatment for chronic hepatitis C. *N Engl J Med* 1998; **339**: 1485-1492
- 4 **Poynard T**, Marcellin P, Lee SS, Minuk K, Ideo G, Bain V, Heathcote J, Zeuzem S, Trepo C, Albrecht J. Randomised trial of interferon a2b plus ribavirin for 48 weeks or for 24 weeks versus interferon a2b plus placebo for 48 weeks for treatment of chronic infection with hepatitis C virus. *Lancet* 1998; **352**: 1426-1432
- 5 **Feray C**, Gigou M, Samuel D, Parasis J, Wilber J, David MF, Urdea MS, Reynes M, Brechot C, Bismuth H. The course of hepatitis C after liver transplantation. *Hepatology* 1994; **20**: 1137-1143
- 6 **Radkowski M**, Wang LF, Vargas HE, Rakela J, Laskus T. Detection of hepatitis C virus replication in peripheral blood mononuclear cells after orthotopic liver transplantation. *Transplantation* 1998; **5**: 664-666
- 7 **Schmidt MN**, Wu P, Brashear D, Klinzman D, Phillips MJ, LaBrecque DR, Stapleton JT. Effect of interferon therapy on hepatitis C virus RNA in whole blood, plasma, and peripheral blood mononuclear cells. *Hepatology* 1998; **28**: 1110-1116
- 8 **Laskus T**, Radkowski M, Wang LF, Vargas H, Rakela J. Search for hepatitis C virus extrahepatic replication sites in patients with acquired immunodeficiency syndrome: specific detection of negative-strand viral RNA in various tissues. *Hepatology* 1998; **28**: 1398-1401
- 9 **Cheng JL**, Liu BL, Zhang Y, Tong WB, Yan Z, Feng BF. Hepatitis C virus in human B lymphocytes transformed by Epstein-Barr virus in vitro by in situ reverse transcriptase-polymerase chain reaction. *World J Gastroenterol* 2001; **3**: 370-375
- 10 **Okamoto H**, Sugiyama Y, Okada S, Kurai K, Akahane Y, Sugai Y, Tanaka T, Sato K, Tsuda F, Miyakawa Y, Mayumi M. Typing Hepatitis C virus by polymerase Chain Reaction with type-specific primers: application to clinical surveys and tracing infectious sources. *J Gen Virol* 1992; **73**: 673-678

- 11 **Chen LB**, Chen PL, Fan GR, Li L, Liu CY. Localization of hepatitis C virus core protein in the nucleus of PBMCs of hepatitis C patients. *Zhonghua Shiyan He Linchuangbin Duxue Zazhi* 2002; **16**: 37-39
- 12 **Wang JT**, Sheu JC, Lin JT, Wang TH, Chen DS. Detection of replication form of HCVRNA in peripheral blood mononuclear cells. *J Infect Dis* 1992; **166**: 1167-1169
- 13 **Taliani G**, Badolato MC, Lecce R, Poliandri G, Bozza A, Duca F, Pasquazzi C, Clementi C, Furlan C, Bac CD. HCV RNA in PBMC: relation with response to IFN treatment. *J Med Virol* 1995; **47**: 16-22
- 14 **Zignego AL**, Carli MD, Monti M, Careccia G, Villa GL, Giannini C, D' Elios MM, Prete GD, Gentilini P. HCV infection of mononuclear cells from peripheral blood and liver infiltrates in chronically infected patients. *J Med Virol* 1995; **47**: 58-64
- 15 **Cribier B**, Schmitt C, Bingen A, Kirn A, Keller F. *In vitro* infection of peripheral blood mononuclear cells by HCV. *J of Gen Virol* 1995; **76**: 2485-2491
- 16 **Chang TT**, Yong KC, Yang YI, Lei HY, Wu HL. Hepatitis C virus RNA in PBMC: comparing acute and chronic hepatitis C virus infection. *Hepatology* 1996; **23**: 977-981
- 17 **Müller HM**, Pfaff E, Goeser T, Kallinowski B, Solbach C, Theilmann L. Peripheral blood leukocytes serve as a possible extrahepatic site for hepatitis C virus replication. *J Gen Virol* 1993; **74**: 669-676
- 18 **Mihm S**, Hartmann H, Ramadori G. A reevaluation of the association of hepatitis C virus replicative intermediates with peripheral blood cells including granulocytes by a tagged reverse transcriptase/polymerase chain reaction technique. *J Hepatol* 1996; **24**: 491-497
- 19 **Lerat H**, Berby F, Trabaud MA, Vidalin O, Major M, Trepo C, Inchauspe G. Specific detection of hepatitis C virus minus strand RNA in hematopoietic cells. *J Clin Invest* 1996; **97**: 845-851
- 20 **Agnello V**, Abel G, Elfahal M, Knight GB, Zhang QX. Hepatitis C virus and other Flaviviridae viruses enter cells via low density lipoprotein receptor. *PNAS* 1999; **96**: 12766-12771
- 21 **Meier V**, Mihm S, Wietzke-Braun P, Ramadori G. HCV-RNA positivity in peripheral blood mononuclear cells of patients with chronic HCV infection: does it really mean viral replication. *World J Gastroenterol* 2001; **2**: 228-232
- 22 **Sansonno D**, Lacobelli AR, Cornacchiolo V, Iodice G, Dammacco F. Detection of HCV proteins by immunofluorescence and HCVRNA genomic sequences by non-isotopic in situ hybridization in bone marrow cells and PBMC of chronically HCV infected patients. *Clin Exp Immunol* 1996; **103**: 414-421
- 23 **Da Silva LC**, Bassit L, Ono-Nita SK, Pinho JR, Nishiya A, Madruga CL, Carrilho. High rate of sustained response to consensus interferon plus ribavirin in chronic hepatitis C patients resistant to alpha-interferon and ribavirin: a pilot study. *J Gastroenterol* 2002; **37**: 732-736
- 24 **Omata M**, Yokosuka O, Takano S, Kato N, Hosoda K, Imazeki F, Tada M, Ito Y, Ohto M. Resolution of acute hepatitis C after therapy with natural beta interferon. *Lancet* 1991; **338**: 914-915
- 25 **Löhr HF**, Goergen B, Heyer KH. HCV replication in mononuclear cells stimulates anti-HCV secreting B cells and reflects non-responsiveness to interferon-alpha. *J Med Virol* 1995; **46**: 314-320
- 26 **Saleh MG**, Tibbs CJ, Koskinas J, Pereira LMMB, Bomford AB, Portmann BC, Mcfarlane IG, Williams R. Hepatic and extrahepatic HCV replication in relation to response to interferon therapy. *Hepatology* 1994; **20**: 1399-1404
- 27 **Manesis EK**, Papaioannou C, Gioustozi A, Kafiri G, Koskinas J, Hadziyannis SJ. Biochemical and virological outcome of patients with chronic hepatitis C treated with interferon alpha-2b for 6 or 12 months: A 4 year follow-up of 211 patients. *Hepatology* 1997; **26**: 734-739
- 28 **Torres B**, Martin JL, Caballero A, Villalobos M, Olea N. HCV in serum, peripheral blood mononuclear cells and lymphocyte subpopulations in C-hepatitis patients. *Hepatol Res* 2000; **18**: 141-151
- 29 **Knolle PA**, Kremp S, Hohler T, Krummenauer F, Schirmacher P, Gerken G. Viral and host factors in the predication of response to interferon-alpha therapy in chronic hepatitis C after long-term follow-up. *J Viral Hepat* 1998; **5**: 399-406
- 30 **Hino K**, Yamaguchi Y, Fujiwara D, Katoh Y, Korenaga M, Okazaki M, Okuda M, Okita K. Hepatitis C virus quasispecies and response to interferon therapy in patients with chronic hepatitis C: a prospective study. *J Viral Hepat* 2000; **7**: 36-42
- 31 **Antonelli G**, Simeoni E, Turrizian O, Tesoro R, Redaelli A, Roffi L, Antonelli L, Pistello M, Dianzani F. Correlation of interferon-induced expression of MxA mRNA in peripheral blood mononuclear cells with the response of patients with chronic active hepatitis C to IFN-alpha therapy. *J Interferon Cytokine Res* 1999; **19**: 243-251
- 32 **Schiappa DA**, Mittal C, Brown JA, Mika BP. Relationship of hepatitis C genotype 1 NS5A sequence mutations to early phase viral kinetics and interferon effectiveness. *J Infect Dis* 2002; **185**: 868-877
- 33 **Farci P**, Strazzeria R, Alter HJ, Farci S, Degioannis D, Coiana A, Peddis G, Usai F, Serra G, Chessa L, Diaz G, Balestrieri A, Purcell RH. Early changes in hepatitis C viral quasispecies during interferon therapy predict the therapeutic outcome. *Proc Natl Acad Sci U S A* 2002; **99**: 3081-3086
- 34 **Jiang J**, Zhang L, Gigou M. Compartmental distribution of hepatitis C virus quasispecies in mononuclear cells and liver. *Zhonghua Yixue Zazhi* 1998; **78**: 265-268
- 35 **Maggi F**, Fornai C, Morrica A, Vatteroni MI, Giorgi M, Marchi S, Ciccorossi P, Bendinelli M, Pistello M. Divergent evolution of hepatitis C virus in liver and peripheral blood mononuclear cells of infected patients. *J Med Virol* 1999; **57**: 57-63
- 36 **Kessler HH**, Pierer K, Santner BI, Vellimedu SK, Stelzl E, Marth E, Fickert P, Stauber RE. Evaluation of molecular parameters for routine assessment of viremia in patients with chronic hepatitis C who are undergoing antiviral therapy. *J Hum Virol* 1998; **1**: 341-349

Targeted ribonuclease can inhibit replication of hepatitis B virus

Jun Liu, Ying-Hui Li, Cai-Fang Xue, Jin Ding, Wei-Dong Gong, Ya Zhao, Yu-Xiao Huang

Jun Liu, Ying-Hui Li, Cai-Fang Xue, Jin Ding, Wei-Dong Gong, Ya Zhao, Yu-Xiao Huang, Department of Pathogenic Organism, Fourth Military Medical University, Xi'an 710033, Shaanxi Province, China

Supported by National Natural Science Foundation of China, No. 30100157, Medical Research Fund of PLA, No. 01MA184, and Innovation Project of FMMU, No. CX99005

Correspondence to: Dr. Jun Liu or Prof Cai-Fang Xue, Department of Pathogenic Organism, Fourth Military Medical University, Xi'an 710033, Shaanxi Province, China. etiology@fmmu.edu.cn

Received: 2002-07-17 **Accepted:** 2002-08-07

Abstract

AIM: To study the effect of a novel targeted ribonuclease (TN), the fusion protein of HBVc and human eosinophil-derived neurotoxin (hEDN), on the HBV replication *in vitro*.

METHODS: The gene encoding the targeted ribonuclease was cloned into pcDNA3.1 (-) to form recombinant eukaryotic expression vector p/TN. Control plasmids, including p/hEDN, p/HBVc, and p/TNmut in which a Lys113→Arg mutation was introduced by sequential PCR to eliminate the ribonuclease activity of hEDN, were also constructed. Liposome-mediated transfection of 2.2.15 cells by p/TN, p/TNmut, p/hEDN, p/HBVc, and pcDNA3.1 (-), or mock transfection was performed. After that, RT-PCR was used to verify the transgene expression. Morphology of the transfected cells was observed and MTT assay was performed to detect the cytotoxicity of transgene expression. Concentration of HBsAg in the supernatant of the transfected cells was measured using solid-phase radioimmunoassay.

RESULTS: Transgenes were successfully expressed in 2.2.15 cells. No obvious cytotoxic effect of transgene expression on 2.2.15 cells was found. The HBsAg concentration in the p/TN transfected cells was reduced by 58 % compared with that of mock transfected cells. No such an effect was found in all other controls.

CONCLUSION: The targeted ribonuclease can inhibit HBV replication *in vitro* while it has no cytotoxicity on host cells. The targeted ribonuclease may be used as a novel antiviral agent for human HBV infection.

Liu J, Li YH, Xue CF, Ding J, Gong WD, Zhao Y, Huang Y. Targeted ribonuclease can inhibit replication of hepatitis B virus. *World J Gastroenterol* 2003; 9(2): 295-299
<http://www.wjgnet.com/1007-9327/9/295.htm>

INTRODUCTION

Hepatitis B virus (HBV) infection is still a major health concern around the world. Globally, more than 350 million people are infected by HBV, and some of them will evolve into liver cirrhosis and hepatocellular carcinoma (HCC)^[1-3]. Although vaccination can elicit effective immunity in about 95 % of inoculated people, the non-responders to vaccination who may contact HBV infection in their life, the threat of escape mutants,

and the huge amount of currently infected people call for an effective treatment^[4-6]. Interferon- α (IFN- α) is the first choice for the treatment of chronic HBV infection. However, the sustained response rate to IFN- α treatment is only about 30 %^[7]. IFN- α can also cause many adverse effects, such as fatigue, fever, neutropenia, autoimmune disease, psychological problems, and so on^[8]. Nucleotide analogues such as lamivudine can inhibit replication of HBV *via* inhibiting the synthesis of minus-strand DNA of HBV, but cease of the treatment usually leads to relapse of the infection and drug-resistant virus variants have emerged^[9-11]. Antisense nucleotides and ribozymes have been reported to suppress HBV replication *in vitro*^[12-17]. However, up to now, antisense nucleotides and ribozymes can generally only moderately inhibit HBV replication intracellularly. In a word, the limited efficacy of current treatment for HBV infection justifies the search for new treatment strategy.

Capsid-targeted viral inactivation (CTVI), first proposed by Natsoulis and Boeke in 1991, is a conceptually powerful antiviral approach^[18]. The principle of CTVI is to construct a fusion protein of viral capsid protein and some degradative enzyme. The capsid part of the fusion protein serves to target the degradative enzyme to virions and the degradative enzyme can specifically destruct the component of the virions. The degradative enzymes used presently are nucleases though other enzymes such as lipases and proteinases can also be used in CTVI in principle. CTVI has been thoroughly investigated in the experimental treatment for retrovirus, such as Moloney murine leukemia virus (MMLV) and HIV, showing a promising prospect as an antiviral treatment^[19-26].

The replication of Hepadnavirus, including HBV, is unique in DNA virus in that it needs a RNA intermediate and a reverse transcription process^[1]. This 3.5 kb RNA intermediate contains all genetic information of HBV and is so called pregenomic RNA (pgRNA). The pgRNA is first translated to both the capsid, or core, protein (c protein) and the DNA polymerase protein (P protein). Then the pgRNA is bound first by P protein and cellular chaperones to form a complex which is then encapsidated by C protein^[27-29]. Inside the nucleocapsids, P protein catalyzes the synthesis of minus-strand DNA via reverse transcription and then the incomplete plus-strand DNA. The nucleocapsids containing minus- and plus-strand DNA can reenter nucleus or bud into endoplasmic reticulum and then be released via secretory pathway out of host cells^[30]. C-terminal 144-164 amino acids of C protein, rich in arginine, is necessary for pregenome encapsidation since particles formed by C mutant deleting this domain contain no pgRNA^[31].

The replication characteristic of HBV hints CTVI can also be applied to this malicious virus. Previously, we reported the construction of a fusion protein of HBV C protein and a ribonuclease, human eosinophil-derived neurotoxin (hEDN)^[32-34]. In this paper, we found that this fusion protein, which was named as targeted ribonuclease in this paper, could effectively inhibit the replication of HBV, while had no cytotoxicity on host cells.

MATERIALS AND METHODS

Cell culture

2.2.15 cell line, human hepatoblastoma Hep G2 cell line stably transfected by HBV genome^[35-37], was kindly provided by Dr.

Cheng (Chinese PLA 302 Hospital) and cultured in Dulbecco's modified Eagle's medium (DMEM, purchased from Gibco Life Technologies, Grand Island, NY) supplemented with 100 mL/L fetal calf serum (Sijiqing Biotech Company, Hangzhou).

Plasmid construction

Targeted ribonuclease eukaryotic expression plasmid p/TN (Figure 1) and control plasmids p/hEDN and p/HBVC were constructed with the method previously reported^[34]. Briefly, cDNA coding for hEDN or HBVC was amplified by RT-PCR from the total RNA isolated from HL60 cell line (kindly provided by Professor Boquan Jin, Department of Immunology, Fourth Military Medical University) or 2.2.15 cell line. Then, the PCR product was cloned into pUC18. After verification of the correctness of the open reading frames of the cloned hEDN and HBVC by sequencing, they were subcloned into pcDNA3.1 (-) (Gibco Life Technologies), to generate p/hEDN and p/HBVC, respectively, or they were ligated together by T4 ligase (Gibco Life Technologies) and the ligated DNA fragment was cloned into pcDNA3.1 (-) to form p/TN. To construct control plasmid p/TNmut in which the DNA fragment encoding hEDNmut (hEDN mutated for just one amino acid, Lys113→Arg, which eliminates the ribonuclease activity^[38]) substituted for hEDN in p/TN, sequential PCR was used to obtain hEDNmut-encoding DNA fragment (Figure 2).

For the first round of two separate PCR reactions, primers M1, N2 and M2, N1 (all synthesized by Sangon Company, Shanghai) were used, respectively, and pUC18/hEDN was used as template. The sequences of the primers are as follows:

N1: 5'-GCA GAA ACC AAA ATA CTT TCC T-3'
 N2: 5'-TCT GCA TCG CCG TTG ATA ATT-3'
 M1: 5'-GCG CGG ATC CAC CAT GAA ACC TCC ACA GTT TAC-3'

M2: 5'-GCG CGA GCT CGA TGA TTC TAT CCA GGT G-3'

The underlined nucleotides in N1 and N2 were used to introduce the mutation. The PCR products of the two reaction were mixed together. Two μ L of the mixture was used as the template, M1 and M2 were used as primers for the next round of PCR. The PCR product of this round amplification was cloned into pUC18 and sequenced for confirmation of the mutation. Then the hEDNmut gene was subcloned into p/TN to substitute hEDN gene to generate recombinant plasmid p/TNmut. pcDNA3.1(-)/GFP was generated by transferring green fluorescent protein (GFP) gene from pEGFP-N3 MCS (Clontech, Palo Alto, CA) into pcDNA3.1(-).

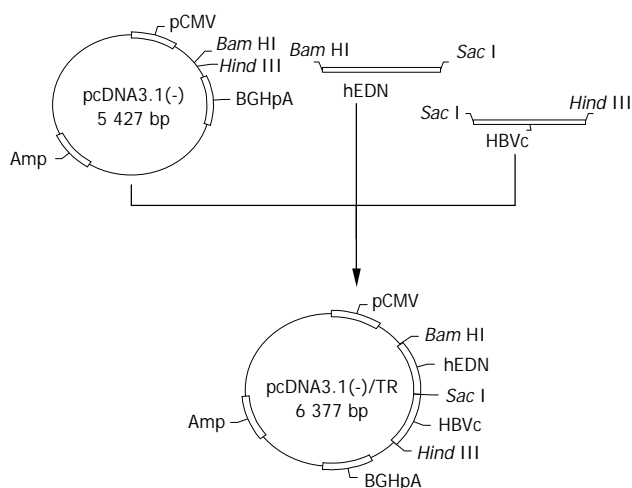


Figure 1 Construction of p/TN. cDNA coding for hEDN or HBVC was amplified by RT-PCR, ligated together, and then cloned into pcDNA3.1 (-) to form p/TN.

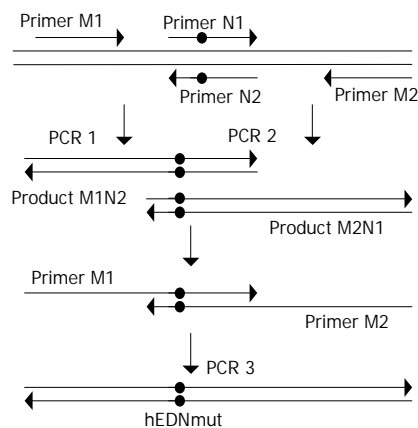


Figure 2 Generation of hEDNmut gene by sequential PCR. For PCR 1 and 2, pUC18/hEDN was used as template. Primers pair M1 and N2 were used in PCR 1 and N1 and M2 in PCR 2. For PCR 3, the mixture of PCR 1 and 2 product was used as template and M1 and M2 as primers. The black dots in the figure denote the nucleotides introducing the Lys113→Arg mutation which eliminates the ribonuclease activity.

Transfection

Twenty-four h before transfection, 2.2.15 cells were seeded into the culture plate at a density of 2×10^8 /L. LipofectamineTM 2000 reagent (Gibco Life Technologies) was used for the transfection of 2.2.15 cells by p/TN, p/TNmut, p/hEDN, p/HBVC, pcDNA3.1 (-), or mock solution (DMEM plus LipofectamineTM 2000 reagent containing no plasmid) according to the manufacturer's protocol. The amount of LipofectamineTM 2000 reagent (approximately 3.1 μ L/cm² surface area in this study) and the concentration of DNA (approximately 1 μ g/cm² surface area in this study) were first optimized in a preliminary transfection of 2.2.15 cells by pcDNA3.1(-)/GFP in which GFP gene was used as a reporter gene.

Confirmation of transgene expression by RT-PCR

Forty-eight h after the transfection, total RNA was isolated from transfected 2.2.15 cells using Trizol[®] reagent (Gibco Life Technologies) according to the manufacturer's protocol. One μ L of total RNA was used as template. RT-PCR was performed using SuperScriptTM One-step RT-PCR kit (Gibco Life Technologies) as recommended by the manufacturer. Forward primer was T7 promoter primer which is upstream to the multicloning site of pcDNA3.1 (-). Reverse primer was complementary to pcDNA3.1/BGH reverse priming site which is downstream to multicloning site of pcDNA3.1 (-). The sequences of the two primers are as follows:

Forward primer: 5'-TAA TAC GAC TCA CTA TAG GGA GA-3'

Reverse primer: 5'-TAG AAG GCA CAG TCG-3'

The condition of RT-PCR was: 50 °C 30 min, 94 °C 2 min, then 40 cycles at 94 °C 30 s, 60 °C 30 s, and 72 °C 2 min. To ensure that the amplified product was from RNA, but not DNA, a control was set up for each RT-PCR reaction, in which the reverse transcriptase was omitted.

Quantification of HBsAg in supernatant of cell culture

Forty-eight h after the transfection, the supernatant of the cell culture was collected, and HBsAg in the supernatant was quantified using the Solid Phase Radio-immunoassay Kit for Quantification of HBsAg (Beimian Dongya Biotech Institute, Beijing) according to the manufacturer's protocol. Briefly, 200 μ L of the supernatant was incubated with plastic bead coated by anti-HBs Ab at 45 °C for 1.5 h. After thorough washing, the bead with deionized water, 200 μ L of ¹²⁵I-labelled secondary antibody was added and incubated at room

temperature overnight. The bead was thoroughly washed, and cpm was measured. The concentration of HBsAg of each sample was obtained by comparing the cpm of each sample with a standard curve.

MTT assay

Forty-eight h after the transfection, 20 μ L of MTT solution (the concentration of MTT was 5 g/L) was added to each well and the culture plate was incubated at 37 °C for 4 h, then 150 μ L of DMSO was added to each well and the plate was shaken for 10 min. The A_{490} value of each well was obtained by an ELISA reader.

Statistical analysis

Variance analysis and Student's *t* test were used for data analysis. Differences were considered significant when $P < 0.05$.

RESULTS

Transgene expression in 2.2.15 cells

As shown in Figure 3, the results of the RT-PCR indicated that the transgenes were expressed in transfected 2.2.15 cells.

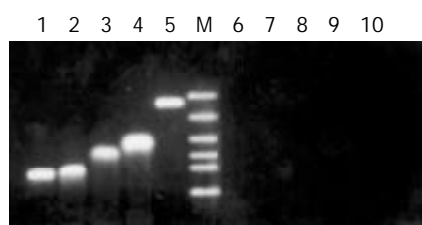


Figure 3 Confirmation of transgenes expression in transfected 2.2.15 cell line. Forty-eight h after the transfection, total RNA was isolated from transfected 2.2.15 cells and RT-PCR was performed to confirm the expression of transgenes. The RT-PCR products were then electrophoresed in 1.2 % agarose gel. Lanes 1-5 represent the RT-PCR results for total RNA isolated from 2.2.15 cells transfected by p/TN, p/TNmut, p/HBVC, p/hEDN, and pcDNA3.1 (-), respectively. Lanes 6-10 represent controls corresponding to lanes 1-5, respectively, in which reverse transcriptase was omitted in RT-PCR. M: DNA Marker (2000, 1000, 750, 500, 250, 100bp from top to bottom).

The effect of targeted ribonuclease on cell viability

The morphological alterations of the transfected 2.2.15 cells were observed under microscope. There were no discernible morphological differences of 2.2.15 cells transfected with p/TN, as compared with the controls (Figure 4). To further analyze the effect of targeted ribonuclease on cell viability, MTT assay was performed. The A_{490} value of 2.2.15 cells transfected with p/TN, p/hEDN, p/HBVC, p/TNmut, pcDNA3.1 (-), and mock transfection was 0.425 ± 0.065 , 0.465 ± 0.050 , 0.410 ± 0.075 , 0.438 ± 0.042 , 0.413 ± 0.063 , and 0.430 ± 0.065 , respectively ($\bar{x} \pm s$, $n=4$).

There were no significant differences between A_{490} value of 2.2.15 cells transfected with p/TN and those of controls ($P > 0.05$). Taken together, these results indicated that the targeted ribonuclease had no adverse effects on cell viability and proliferation.

Inhibition of HBV replication by targeted ribonuclease

As shown in Figure 5, the concentration of HBsAg in the supernatant of 2.2.15 cells transfected with p/TN was significantly lower than controls ($P < 0.05$), while that of 2.2.15 cells transfected with p/TNmut, p/hEDN, p/HBVC, pcDNA3.1 (-), or mock transfection did not significantly differ from each other ($P > 0.05$). Compared with that of mock transfected

2.2.15 cells, the concentration of HBsAg in the supernatant of 2.2.15 cells transfected with p/TN was decreased by 58 %.

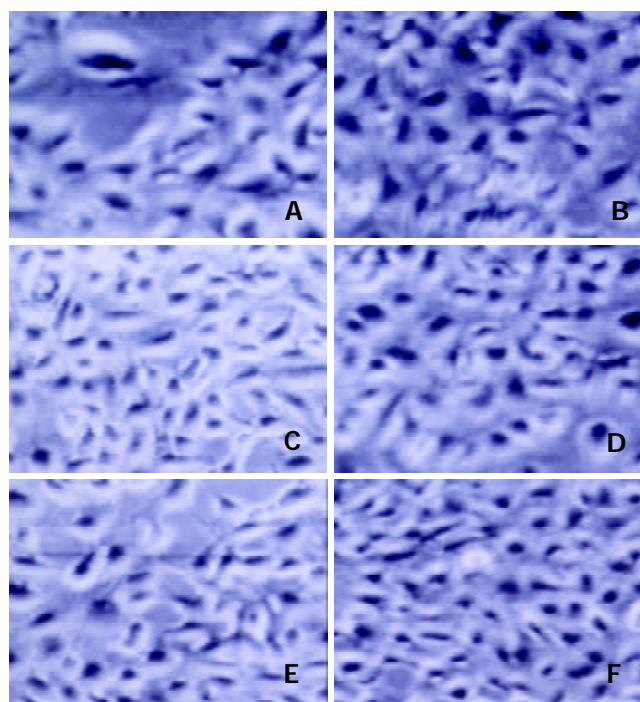


Figure 4 Morphology of 2.2.15 cells 48 h after transfection. A-F represent 2.2.15 cells transfected by p/TN, p/hEDN, p/HBVC, p/TNmut, pcDNA3.1 (-), or mock transfection, respectively. There were no discernible morphological differences of 2.2.15 cells transfected with p/TN, as compared with the controls.

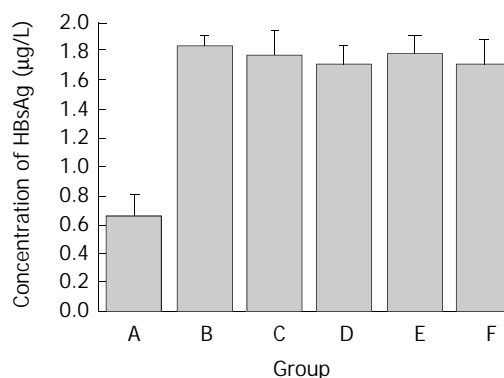


Figure 5 The HBsAg concentration in supernatants of transfected 2.2.15 cells. Groups A-F represent 2.2.15 cells transfected by p/TN, p/hEDN, p/HBVC, p/TNmut, pcDNA3.1 (-), or mock transfection, respectively. The concentration of HBsAg in the supernatant of 2.2.15 cells transfected with p/TN was decreased by 58 % as compared with that of mock transfected 2.2.15 cells.

DISCUSSION

Theoretically, CTVI has many advantages in the treatment of viral infection^[39]. First, CTVI is highly specific. This high specificity is conferred by the encapsidating capacity and self-assembly property of the viral capsid protein which is used as a targeting molecule in CTVI. Second, CTVI is highly efficient. The nuclease, which is used as an effector molecule in CTVI, is a protein enzyme, and its catalytic efficiency is higher than ribozyme. Third, escape mutants may rarely if not impossibly arise in case of CTVI since viral capsid proteins generally play important roles in virus assembly and infection. Fourth, while

ribozyme and antisense RNA can only be used clinically in the form of gene therapy, CTVI can be used in the form of either gene therapy or recombinant protein drug. The results of experimental research also indicate that CTVI is a promising antiviral strategy. Boeke *et al.* reported that the fusion protein of Gag of murine Moloney leukemia virus (MMLV) and staphylococcus nuclease could reduce the infection titer of MMLV by 20-60 %, while that of Gag and ribonuclease H1 of *E. coli* could inhibit the production of MMLV by 97-99 %^[21,24]. Recently, Schumann *et al.* tested the antiviral effect of CTVI *in vivo* using transgenic murine models^[26]. They found Gag-nuclease fusion protein could significantly inhibit MMLV replication, ameliorate the symptoms, and increase the life span up to 2.5 fold in transgenic mice. Furthermore, they found that the fusion protein was nontoxic for transgenic mice, confirming the previous *in vitro* cell culture results^[19-25]. In this report, we demonstrated that targeted ribonuclease constructed by us (the fusion protein of HBVc and hEDN) could reduce the concentration of HBsAg in the supernatant of the transfected 2.2.15 cells by 58 %. Although it is controversial that the decrease of HBsAg concentration is caused by some factors other than the inhibition of HBV replication by targeted ribonuclease, our results strongly disprove this argument. First, the fact that transfection of p/TN decreased HBsAg concentration in the supernatant while p/HBVc and p/TNmut, which are identical to p/TN except for only one amino acid mutation but lose ribonuclease activity, indicates that the reduction of HBsAg is dependent on the activity of the ribonuclease in the fusion protein targeted ribonuclease. Second, transfection of p/hEDN did not affect the HBsAg concentration, showing that the reduction of HBsAg relies on the existence of HBVc in the fusion protein. Our present results are most consistent with a model that the targeted ribonuclease encapsidates the pgRNA together with wild type capsid protein and then degrades it (also see below). This model has been corroborated by some recent research reports^[19-26, 40]. On the other hand, 58 % reduction of HBsAg in the supernatant of 2.2.15 cells caused by the targeted ribonuclease might be an underestimate for the inhibition of HBV replication since besides present in mature virions as envelope protein, a large amount of HBsAg was synthesized and secreted as 22 nm spherical and filamentous particles by 2.2.15 cells using 2.1kb HBV mRNA as transcript which, unlike pgRNA, can not be encapsidated and therefore may not be degraded by the targeted ribonuclease^[35,37]. Therefore, even if the targeted ribonuclease can strongly inhibit HBV replication, there might still be a large amount of HBsAg secreted extracellularly. The mechanism for the decrease of HBsAg concentration caused by the targeted ribonuclease might be as follows: the degradation of HBV pgRNA by targeted ribonuclease leads to the decrease of P and C protein of HBV since pgRNA also acts as mRNA for the translation of both proteins. The reduction of pgRNA, P and C protein will impair the assembly of viral capsid and then reduce the mature virions released from host cells. Further analysis including Northern and Southern blot is being performed in this laboratory to clarify the degree of inhibition on HBV replication by the targeted ribonuclease and to elucidate at what stage of HBV replication the targeted ribonuclease exerts its antiviral role.

In the process of this study, Beterams and Nassal reported their CTVI application for inhibition of HBV replication *in vitro*^[40]. Although both their research and ours used the same strategy against HBV replication and both used HBVc as the target molecule, the effector molecules adopted were different. Beterams *et al.* used staphylococcal nuclease (SN) and we used hEDN. Compared with SN, hEDN may be more suitable for the treatment of HBV infection in human beings because as a human-origin molecule, hEDN will not induce specific

immunity which may not only decrease the efficacy of CTVI but also induce immunopathological response. The difference of the effector molecules also means the targets of CTVI in the two studies were different. SN is generally believed to be active only extracellularly because it requires a high Ca^{2+} concentration present extracellularly but not intracellularly for its activity^[41]. Therefore, SN-capsid protein incorporated into the virion is only active in degrading the viral nucleic acids upon release of the virion from the cell into an extracellular milieu^[18-19, 21, 23, 25-26]. According to this scheme, the targeted SN in Beterams *et al.*'s study can only degrade the relaxed circular (RC) DNA of mature virion released from the cell. Although they suggested in their reports that targeted SN might be mildly activated intracellularly by somewhat unknown mechanism and then cut pgRNA and minus-strand DNA of HBV, their results showed targeted SN had no significant effect on pgRNA. In contrast, the effector molecule in our study, hEDN, is a ribonuclease. Therefore, the target molecule degraded by the targeted ribonuclease constructed by us is most probably HBV pgRNA, the only RNA stage in the replication of HBV. As stated above, this notion is also supported by our experimental results, since the ribonuclease activity of hEDN is necessary for the anti-HBV effect of targeted ribonuclease. Similarly, onconase, an amphibian ribonuclease was reported to inhibit HIV replication intracellularly by degrading HIV RNA^[42]. The degradation of HBV pgRNA will not only lead to less mature virions released from host cells, which means secreted viral particles had lower infectivity, but also inhibit the amplification of HBV closed circular DNA (cccDNA) which is downstream to pgRNA in HBV replication^[43]. This inhibition on HBV cccDNA amplification is of pivotal significance for the treatment of chronic HBV infection since the amplification of cccDNA, the template for all HBV transcripts, plays a major role in the persistence of HBV in infected hepatocytes^[1, 30].

In summary, we constructed a novel targeted ribonuclease which can specifically inhibit HBV replication but has no cytotoxicity for host cells. Our results raise the possibility of using the targeted ribonuclease as a therapeutic agent for human HBV infection. For this purpose, we are generating recombinant adenovirus vector carrying the targeted ribonuclease to test its antiviral efficacy in HBV murine model.

REFERENCES

- 1 **Ganem D**, Varmus HE. The molecular biology of the hepatitis B virus. *Annu Rev Biochem* 1987; **56**: 651-693
- 2 **Lau JY**, Wright TL. Molecular virology and pathogenesis of hepatitis B. *Lancet* 1993; **342**: 1335-1340
- 3 **Tang ZY**. Hepatocellular carcinoma. *World J Gastroenterol* 2001; **7**: 445-454
- 4 **Hoofnagle JH**. Therapy of viral hepatitis. *Digestion* 1998; **59**: 563-578
- 5 **Hilleman MR**. Overview of the pathogenesis, prophylaxis and therapeutic applications of viral hepatitis B, with focus on reduction to practical applications. *Vaccine* 2001; **19**: 1837-1848
- 6 **Francois G**, Kew M, Van Damme P, Mphahlele MJ, Meheus A. Mutant hepatitis B virus: a matter of academic interest only or a problem with far-reaching implications? *Vaccine* 2001; **19**: 3799-3815
- 7 **Wong DK**, Cheung AM, O'Rourke K, Naylor CD, Detsky AS, Heathcote J. Effect of alpha-interferon treatment in patients with hepatitis B e antigen-positive chronic hepatitis B: a meta-analysis. *Ann Intern Med* 1993; **119**: 312-323
- 8 **Hoofnagle JH**, di Bisceglie AM. Treatment of chronic viral hepatitis. *N Engl J Med* 1997; **336**: 347-356
- 9 **Nevens F**, Main J, Honkoop P, Tyrrell DL, Barber J, Sullivan MT, Fevery J, De Mau RA, Thomas HC. Lamivudine therapy for chronic hepatitis B: A six-month randomized dose-ranging study. *Gastroenterology* 1997; **113**: 1258-1263

- 10 **Tipples GA**, Ma MM, Fischer KP, Bain VG, Kneteman NM, Tyrrell DL. Mutation in HBV RNA-dependent DNA polymerase confers resistance to lamivudine *in vivo*. *Hepatology* 1996; **24**: 714-717
- 11 **Santantonio T**, Mazzola M, Iacovazzi T, Miglietta A, Guastadisegni A, Pastore G. Long-term follow-up of patients with anti-HBe/HBV DNA-positive chronic hepatitis B treated for 12 months with lamivudine. *J Hepatol* 2000; **32**: 300-306
- 12 **Tung FYT**, Bowen SW. Targeted inhibition of hepatitis B virus gene expression: a gene therapy approach. *Front Biosci* 1998; **3**: a11-a15
- 13 **Zhong S**, Wen SM, Zhang DF, Wang QL, Wang SQ, Ren H. Sequencing of PCR amplified HBV DNA pre-c and c regions in the 2.2.15 cells and antiviral action by targeted antisense oligonucleotide directed against sequence. *World J Gastroenterol* 1998; **4**: 434-436
- 14 **Song YH**, Lin JS, Liu NZ, Kong XJ, Xie N, Wang NX, Jin YX, Liang KH. Anti-HBV hairpin ribozyme-mediated cleavage of target RNA *in vitro*. *World J Gastroenterol* 2002; **8**: 91-94
- 15 **zu Putlitz J**, Wieland S, Blum HE, Wands JR. Antisense RNA complementary to Hepatitis B virus specifically inhibits viral replication. *Gastroenterology* 1998; **115**: 702-713
- 16 **zu Putlitz J**, Yu Q, Burke JM, Wands JR. Combinatorial screening and intracellular antiviral activity of hairpin ribozymes directed against Hepatitis B virus. *J Virol* 1999; **73**: 5381-5387
- 17 **Beck J**, Nassal M. Efficient hammerhead ribozyme-mediated cleavage of the structured hepatitis B virus encapsidation signal *in vitro* and in cell extracts, but not in intact cells. *Nucleic Acids Res* 1995; **23**: 4954-4962
- 18 **Natsoulis G**, Boeke JD. New antiviral strategy using capsid-nuclease fusion proteins. *Nature* 1991; **352**: 632-635
- 19 **Natsoulis G**, Seshiah P, Federspiel MJ, Rein A, Hughes SH, Boeke JD. Targeting of a nuclease to murine leukemia virus capsids inhibits viral multiplication. *Proc Natl Acad Sci USA* 1995; **92**: 364-368
- 20 **Melekhovets YF**, Joshi S. Fusion with an RNA binding domain to confer target RNA specificity to an RNase: design and engineering of Tat-RNase H that specifically recognizes and cleaves HIV-1 RNA *in vitro*. *Nucleic Acids Res* 1996; **24**: 1908-1912
- 21 **Schumann G**, Qin L, Rein A, Natsoulis G, Boeke JD. Therapeutic effect of Gag-nuclease fusion protein on retrovirus-infected cell cultures. *J Virol* 1996; **70**: 4329-4337
- 22 **VanBrocklin M**, Ferris AL, Hughes SH, Federspiel MJ. Expression of a murine leukemia virus Gag-*Escherichia coli* RNase HI fusion polyprotein significantly inhibits virus spread. *J Virol* 1997; **71**: 3312-3318
- 23 **Wu X**, Liu H, Xiao H, Kim J, Seshiah P, Natsoulis G, Boeke JD, Hahn BH, Kappes JC. Targeting foreign proteins to human immunodeficiency virus particles via fusion with Vpr and Vpx. *J Virol* 1995; **69**: 3389-3398
- 24 **Schumann G**, Cannon K, Ma WP, Crouch RJ, Boeke JD. Antiretroviral effect of a gag-RNase HI fusion gene. *Gene Ther* 1997; **4**: 593-599
- 25 **VanBrocklin M**, Federspiel MJ. Capsid-targeted viral inactivation can eliminate the production of infectious murine leukemia virus *in vitro*. *Virology* 2000; **267**: 111-123
- 26 **Schumann G**, Hermankova M, Cannon K, Mankowski JL, Boeke JD. Therapeutic effect of a Gag-nuclease fusion protein against retroviral infection *in vivo*. *J Virol* 2001; **75**: 7030-7041
- 27 **Hu J**, Toft DO, Seeger C. Hepadnavirus assembly and reverse transcription require a multi-component chaperone complex which is incorporated into nucleocapsids. *EMBO J* 1997; **16**: 59-68
- 28 **Junker-Niepmann M**, Bartenschlager R, Schaller H. A short cis-acting sequence is required for hepatitis B virus pregenome encapsidation and sufficient for packaging of foreign RNA. *EMBO J* 1990; **9**: 3389-3396
- 29 **Bartenschlager R**, Schaller H. Hepadnaviral assembly is initiated by polymerase binding to the encapsidation signal in the viral RNA genome. *EMBO J* 1992; **11**: 3413-3420
- 30 **Seeger C**, Mason WS. Hepatitis B virus biology. *Microbiol Mol Biol Rev* 2000; **64**: 51-68
- 31 **Nassal M**. The arginine-rich domain of the hepatitis B virus core protein is required for pregenome encapsidation and productive viral positive-strand DNA synthesis but not for virus assembly. *J Virol* 1992; **66**: 4107-4116
- 32 **Hamann KJ**, Barker RL, Loegering DA, Pease LR, Gleich GJ. Sequence of human eosinophil-derived neurotoxin cDNA: identity of deduced amino acid sequence with human nonsecretory ribonucleases. *Gene* 1989; **83**: 161-167
- 33 **Gleich GJ**, Loegering DA, Bell MP, Checkel JL, Ackerman SJ, McKean DJ. Biochemical and functional similarities between human eosinophil-derived neurotoxin and eosinophil Cationic protein: homology with ribonuclease. *Proc Natl Acad Sci USA* 1986; **83**: 3146-3150
- 34 **Li YH**, Liu J, Xue CF. Construction of HBV targeted ribonuclease and its expression in 2.2.15 cell line. *Xibao Yu Fenzi Mianyixue Zazhi* 2002; **18**: 217-220
- 35 **Sells MA**, Chen ML, Acs G. Production of hepatitis B virus particles in Hep G2 cells transfected with cloned hepatitis B virus DNA. *Proc Natl Acad Sci USA* 1987; **84**: 1005-1009
- 36 **Acs G**, Sells MA, Purcell RH, Price P, Engle R, Shapiro M, Popper H. Hepatitis B virus produced by transfected Hep G2 cells causes hepatitis in chimpanzees. *Proc Natl Acad Sci USA* 1987; **84**: 4641-4644
- 37 **Sells MA**, Zelent AZ, Shvartsman M, Acs G. Replicative intermediates of hepatitis B virus in Hep G2 cells that produce infectious virions. *J Virol* 1988; **62**: 2836-2844
- 38 **Rosenberg HF**, Dyer KD. Eosinophil cationic protein and eosinophil-derived neurotoxin. *J Biol Chem* 1995; **270**: 21539-21544
- 39 **Liu J**, Xue CF. Advances in the research of therapeutic ribonucleases. *Shengming Kexue* 2002; **14**: 139-140
- 40 **Beterams G**, Nassal M. Significant interference with hepatitis B virus replication by a core-nuclease fusion protein. *J Biol Chem* 2001; **276**: 8875-8883
- 41 **Tucker PW**, Hazen EE Jr, Cotton FA. Staphylococcal nuclease reviewed: a prototypic study in contemporary enzymology. I. Isolation; physical and enzymatic properties. *Mol Cell Biochem* 1978; **22**: 67-77
- 42 **Saxena SK**, Gravell M, Wu YN, Mikulski SM, Shogen K, Ardelt W, Youle RJ. Inhibition of HIV-1 production and selective degradation of viral RNA by an amphibian ribonuclease. *J Biol Chem* 1996; **271**: 20783-20788
- 43 **Tuttleman JS**, Pourcel C, Summers J. Formation of the pool of covalently closed circular viral DNA in hepadnavirus-infected cells. *Cell* 1986; **47**: 451-460

Interaction between hepatitis C virus core protein and translin protein- a possible molecular mechanism for hepatocellular carcinoma and lymphoma caused by hepatitis C virus

Ke Li, Lin Wang, Jun Cheng, Yin-Ying Lu, Ling-Xin Zhang, Jin-Song Mu, Yuan Hong, Yan Liu, Hui-Juan Duan, Gang Wang, Li Li, Ju-Mei Chen

Ke Li, Lin Wang, Jun Cheng, Yin-Ying Lu, Ling-Xin Zhang, Jin-Song Mu, Yuan Hong, Yan Liu, Hui-Juan Duan, Gang Wang, Li Li, Ju-Mei Chen, Jun Cheng Gene Therapy Research Center, Institute of Infectious Diseases The 302 Hospital of PLA, Beijing 100039, China

Supported partly by a grant from National Scientific Foundation of China, No.39970674

Correspondence to: Dr. Jun Cheng Gene Therapy Research Center, Institute of Infectious Diseases The 302 Hospital of PLA, Beijing 100039, China. cj@genetherapy.com.cn

Telephone: +86-10-66933392

Received: 2002-03-13 **Accepted:** 2002-04-20

Abstract

AIM: To investigate the interaction between hepatitis C virus core protein and translin protein and its role in the pathogenesis of hepatocellular carcinoma and lymphoma.

METHODS: With the components of the yeast two hybrid system 3, "bait" plasmids of HCV core the gene was constructed. After proving that hepatitis C virus core protein could be firmly expressed in AH109 yeast strains, yeast two-hybrid screening was performed by mating AH109 with Y187 that transformed with liver cDNA library plasmids - pACT2 and then plated on quadruple dropout (QDO) medium and then assayed for α -gal activity. Sequencing analysis of the genes of library plasmids in yeast colonies that could grow on QDO with α -gal activity was performed. The interaction between HCV core protein and the protein we obtained from positive colony was further confirmed by repeating yeast two - hybrid analysis and coimmunoprecipitation *in vitro*.

RESULTS: A gene from a positive colony was the gene of translin, a recombination hotspot binding protein. The interaction between HCV core protein and translin protein could be proved not only in yeast, but also *in vitro*.

CONCLUSION: The core protein of HCV can interact with translin protein. This can partly explain the molecular mechanism for hepatocellular carcinoma and lymphoma caused by HCV.

Li K, Wang L, Cheng J, Lu YY, Zhang LX, Mu JS, Hong Y, Liu Y, Duan HJ, Wang G, Li Li, Chen JM. Interaction between hepatitis C virus core protein and translin protein- a possible molecular mechanism for hepatocellular carcinoma and lymphoma caused by hepatitis C virus. *World J Gastroenterol* 2003; 9(2): 300-303 <http://www.wjgnet.com/1007-9327/9/300.htm>

INTRODUCTION

The core protein of hepatitis C virus (HCV) is the structural protein of the virus^[1-4]. However, some evidences suggested

that this protein has a pleiotropic nature. In addition to having a packaging function, the core protein has been shown to act *in trans* on the viral and cellular promoters and it is also capable of transformation of rat embryonic fibroblasts through cooperation with the *ras* oncogene. Previous studies showed that the core protein could interact with several proteins such as lymphotoxin- β Receptor, heterogeneous nuclear ribonucleoprotein K, RNA helicase^[5-8]. In order to understand the pathogenesis of HCV infection we examined the possibility that the HCV core protein interacts with cellular proteins.

MATERIALS AND METHODS

Material

Bacterial, yeast strains and Plasmids All yeast strains and plasmids for yeast two-hybrid experiments were obtained from Clontech (Palo Alto, Calif., USA) as components of the MATCHMAKER Two Hybrid System 3. Yeast strain AH109 (MAT α , *trp1-901*, *leu2-3,112*, *ura3-52*, *his3-200*, *gal4* Δ , *gal80* Δ , *LYS2::GAL1_{UAS}-GAL1_{TATA}-HIS3*, *GAL2_{UAS}-GAL2_{TATA}-ADE2 URA3::MEL1_{TATA}-lacZ MEL1*) containing pGBKT7-53, coding for DNA-BD/mouse p53 fusing protein and AH109 used for cloning of bait plasmids, yeast strain Y187 (MAT α *ura3-52*, *his3-200*, *Ade2-101*, *trp1-901*, *leu2-3, 112*, *gal4* Δ , *gal80* Δ , *met-*, *URA3::GAL1_{UAS}-GAL1_{TATA}-lacZ MEL1*) containing pTD1-1, in which pACT2 coding for AD/SV40 large T antigen fusing protein and Y187 used for cloning of library plasmids. Pretransformed cDNA liver cell library Y187. Bacterial strain DH5 α used for cloning of every shuttle plasmid. Yeast-*Escherichia coli* shuttle plasmids pGBKT7 DNA-BD cloning plasmid, pGADT7 AD cloning plasmid, pGBKT7-53 control plasmid, pGADT7, pGBKT7-Lam control plasmid, pCL1 plasmid from Clontech L.T.D Company(K1612-1). pGEM T vector from Promega Company, USA.

Chemical agents and cultural media Taq DNA polymerase purchased from MBI Company, T4 DNA ligase, EcoRI and BamHI restriction endonuclease from Takara. c-Myc monoclonal antibody secreted by 1-9E10.2 hybridoma (ATCC), goat anti-mouse IgG conjugated with horseradish peroxidase from Zhongshan Company,China. Lithium Acetate, semi-sulfate adenine, Acrylamide and N, N' -Bis-acrylamide from Sigma, TEMED from Boehringer Mannheim. Tryptone and yeast extracts from OXOID. X- α -Gal and Cultural media: YPDA, SD/-Trp SD/-Leu, SD/-Trp/-Leu, SD/-Trp/-Leu/-His, SD/-Trp/-Leu/-His/-Ade from Clontech L.T.D Company. protein-G agarose from Roche. RT-PCR kit and TNT[®]Coupled Reticulocyte Lysate Systems from Promega. [³⁵S]-methionine (.1 000 Ci/mmol; 10 mCi/ml) from Isotope company of china. Amplify Fluorographic Reagent (#NAMP100) from Amersham Life Sciences. Others from Sigma company.

Methods

Construction of "bait" plasmid and expression of HCV core protein Plasmid pGBKT7-core (Figure 1) containing full-

length HCV core gene was constructed by insertion of HCV core gene in-frame into EcoRI/BamHI site, which could direct expression of DNA binding domain, *c-myc* and core fusion protein. After the plasmid was transformed into yeast strain AH109 by using Lithium Acetate method^[9]. Western blotting was performed to confirm the expression of the fusion protein by using *c-myc* monoclonal antibody. Transformed AH109 was cultured on quadropole dropout media to exclude the auto-activity.

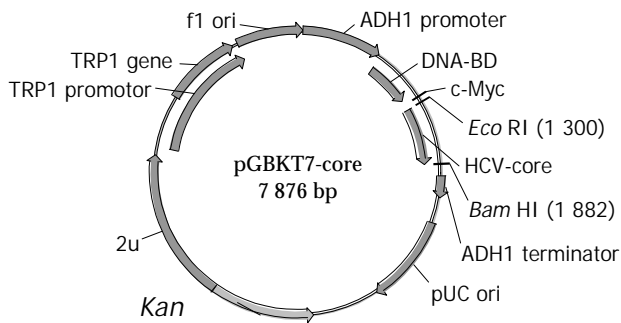


Figure 1 "bait" plasmid pGBKT7-core.

Two-hybrid library screening using yeast mating One large (2-3-mm), fresh (<2 months old) colony of AH109[bait] was inoculated into 50 ml of SD/-Trp and incubated at 30 °C overnight (16-24 hr) with shaking at 250-270 rpm. Then the cells were spinned down by centrifuging the entire 50-ml culture at 1 000×g for 5 min and supernatant Decanted the cell pellet was resuspended in the residual liquid by vortexing. The entire AH109[bait] culture and the 1-ml library were combined and cultured in a 2-L sterile flask and Add 45 ml of 2X YPDA/Kan was added and swirl gently. After 20 h mating, the cells were spinned down and resuspended then spreaded on -50 large (150-mm) plates, containing 200 ml of SD/-Ade/-His/-Leu/-Trp (QDO). After 6-18 days grew, the yeast colonies were transferred onto the plates containing X-a-Gal to check for expression of the MEL1 reporter gene (blue colonies).

Plasmid isolation from yeast and transforming *E.coli* with yeast plasmid Yeast plasmid was isolated with Lyticase method (provided by Clontech), and transformed into *E. coli* by using electroporation^[10], transformants were plated on ampicillin LB selection media, then, isolating plasmids from *E.coli* and sequencing analysis.

To confirm the true interaction in yeast To confirm the true protein-protein interaction and exclude false positives, the plasmids of positive colonies were transformed into yeast strain Y187, next mating experiments were carried out by mating with yeast strain AH109 containing pGBKT7-core or pGBKT7-Lam. After mating, the diploids yeast were plated on QDO covered with X-α-gal (Figure 2).

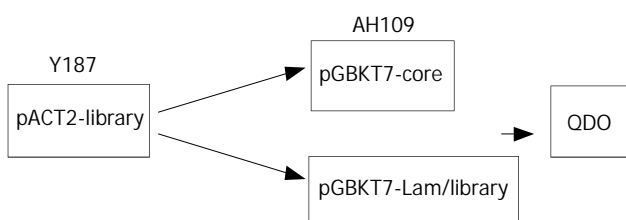


Figure 2 To confirm the interaction.

Bioinformatic analysis After sequencing the positive colonies, the sequences blasted with GenBank to analogize the function of the genes.

RT-PCR In order to clone the full-length gene, RT-PCRs were conducted by using PCR primers the designing based on the information of GenBank. The genes amplified by RT-PCR were ligated into yeast plasmid pGADT7.

In vitro translation Mixture of TNT[®]reticulocyte 25 μl, TNT[®]reactio buffer 2 μl, T7 TNT[®]RNA polymerase 1μl, amino acids mixture (minus methionine, 1 mM) 1μl, [³⁵S]methionine 2 μl, Rnasin[®]nuclease inhibitor (40u/μl) 1μl, DNA template (pGBKT7-core or pGADT7-library gene) (0.5 μg/μl) 2 μl, ddH₂O 50 μl, 30 °C incubated 90 minutes.

Coimmunoprecipitation The following reactants were combined in a 1.5-ml microcentrifuge tube on ice: Five μl *in vitro* translated bait protein, 5 μl *in vitro* translated library protein. The control only added 10 μl pGBKT7-core plasmid. The mixtures were incubated at 30 °C for 1 hr. Then, the following reagents added into the reaction tubes: 470 ml coimmunoprecipitation buffer (20 mM Tris-HCl (pH 7.5), 150 mM NaCl, 1 mM DTT, 5 μg/ml aprotinin, 0.5 mM PMSF, 0.1 % Tween 20), 10 μl Protein-G Agarose Beads, 10 μl c-Myc Monoclonal Antibody. Incubated at 4 for 2 hr with continuous rocking. The tubes were centrifuged at 14 000 rpm for 1-2 min. The supernatants were removed. 0.5 ml TBST added to the tubes. Rinse steps were repeated three times. 15 ml SDS-loading buffer were added. The samples was heated at 80 °C for 5 min. The tubes were placed on ice. Briefly centrifuged, and 10 μl loaded onto an SDS-PAGE minigel to begin the electrophoretic separation. After electrophoresis, the gel was transferred to a tray containing Gel Fixation Solution, and placed on a rotary shaker for 10 min at room temperature. Rinsed the gel with H₂O, then Amplify Fluorographic Reagent was added shaken for 20 min at room, then dried at 80 °C under constant vacuum. The gel was exposed to a X-ray film overnight at room temperature. The film was developed by using standard techniques.

RESULTS

Expression of the "bait" fusion protein

Yeast strain AH109 transformed with pGBKT7-core could stably express the fusion protein at high level (Figure 3) and could only grow on SD/-Trp medium and could not grow on QDO medium. Thus, the transformed yeast could be used for yeast hybrid analysis.

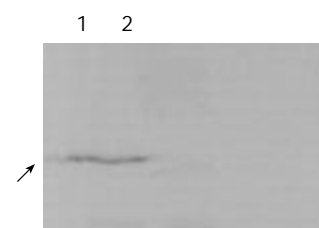


Figure 3 Western blotting showed the expression of HCV core protein in yeast (arrow indicated). lane 1 is HCV core protein and lane 2 is negative control.

RT-PCR experiments The yeast two hybrid analysis showed 30 blue colonies grew on QDO plates containing X-α-Gal. After confirming the true interaction in yeast, we isolated the plasmids from the blue colonies containing only pGBKT7-core and one library plasmid other than other plasmids. Sequencing the gene and blasted with the data from GenBank, a gene is translin. To further prove the interaction between HCV core protein and translin protein (Translin), a pair of primer were designed based on the gene of translin (Forward: 5' -GAA TTC ATG TCT GTG AGC GAG ATC TTC GTG G -3', down: 5' -GGA TCC CTA TTT TTC AAC ACA AGC

TGC TGC C-3'), up and down primers containing EcoRI and BamHI restriction endonuclease site, respectively. Total RNAs were prepared from HepG2, A 687bp fragment was amplified by using RT-PCR (Figure 4A). After cut by EcoRI/BamHI, the fragment was in-frame ligated into pGADT7 EcoRI/BamHI site (Figure 4B).

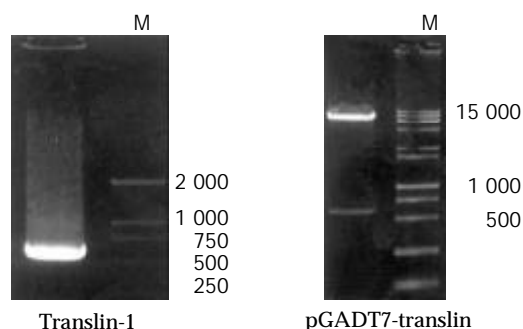


Figure 4 a 687bp fragment-translin, amplified by RT-PCR. (A) pGADT7-translin cut by EcoRI/BamHI (B).

In vitro coimmunoprecipitation

HCV core protein containing 192 aa, $M_r=20\ 968$, is smaller than Translin containing 228aa, $M_r=26\ 182$. Lane 1 showed two protein could interact with each other, lane 2 was only HCV core protein.(Figure 5).

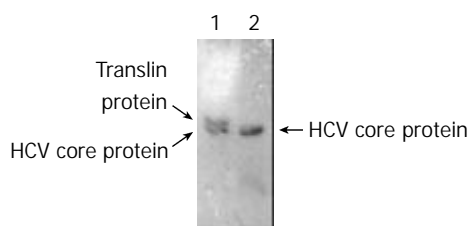


Figure 5 lane 1 HCV core protein and translin protein, lane 2 HCV core protein.

DISCUSSION

Hepatitis C virus infects an estimated 170 million persons worldwide and thus represents a viral pandemic. Progression to chronic disease occurs in the majority of HCV-infected persons^[11-17], and some patients can develop to hepatocellular carcinoma^[18] and lymphoma. Infection with the virus has become the main indication for liver transplantation. Although research advances have been impeded by the inability to grow HCV easily in culture, there have been some insights into pathogenesis of the infection and improvements in treatment options. The core protein of HCV is a multifunctional protein involved in several processes; it is phosphorylated and has both cytoplasmic and nuclear localization and thus it may play multiple roles in the viral life cycle^[3,4]. Several studies also suggested that it has regulatory roles for viral and cellular genes^[19,20] and possesses transformation activity. More recent studies revealed that the core protein can interact with tumor necrosis factor receptor-1, lymphotoxin β -R and viral envelope protein 1 (E1) and also forms a complex with apolipoprotein AII of the lipid droplet^[21]. A recent report showed that the HCV core protein can suppress the cisplatin- and c-Myc-mediated apoptotic effect, supporting its role in the establishment of persistent HCV infection^[22]. But there have reverse results that that the core protein also has the ability to enhance cell death triggered by LT- β R ligand or anti-Fas monoclonal antibody. Some research considered that the core protein of HCV can induce steatosis and hepatocellular carcinoma in transgenic mice^[23,24].

Thus, the molecular mechanism by which the HCV core protein and HCV induce hepatocellular carcinoma is not clear. Recent epidemical research indicated that a significant increase in the prevalence of HCV infection in a group of B-cell non-Hodgkin's lymphoma(NHL)^[25-29].

In this study, yeast two-hybrid system 3 based on the system originally designed by Fields and Song^[30] is developed by Bendixen^[31], which is commercially available from Clontech Company L.t.d. In this system, the promoters controlling *HIS3*, *ADE2*, and *MEL1* expression in AH109 have significantly fewer false positives and the simple mating protocol significantly reduces the labor and time involved in performing a two-hybrid library screening and improves the chances of finding rare protein-protein interactions and leads to more reproducible results.

The "bait" plasmid pGBKT7-core was transformed into yeast strain, After mating with liver cDNA library yeast strain Y187, the diploid yeast cells were plated on QDO media containing X- α -gal, 30 true positives were obtained. Sequencing analysis of isolated library plasmids, we find one of the genes is translin^[32] - a recombination hotspot binding protein. In order to further conform the interaction between the expressed protein and HCV core protein, we performed the experiment of coimmunoprecipitation of both proteins. A strong interaction between the HCV core protein and Translin protein *in vitro* was observed.

A number of studies have shown that chromosomal translocations either result in the activation of proto-oncogenes by joining them to immunoglobulin (Ig) or T-cell receptor genes or lead to the creation of tumor-specific fusion proteins. In man, such translocations consistently occur at particular sites in the genome. Translin protein, which specifically binds to the consensus sequences ATGCAG and GCCC (A/T) (G/C) (G/C) (A/T) found at the breakpoint junctions in many cases of chromosomal translocations, is a unique DNA binding protein^[33]. The nuclear translocation of translin protein only happened in the time when the cells were treated with mutagen. translin protein may be a typical DNA end binding protein, which is in contrast with one of the other DNA binding proteins, the Ku antigen, that initially binds to DNA ends and then moves to internal positions within the DNA molecule^[34]. Previous report showed that translin protein was not found in liver tumors. But in this study, we found the gene expressed in liver tumor cell HepG2 and in liver cDNA library. And the interaction between translin protein and HCV core protein not only existed in yeast, but also *in vitro*. The results suggested that translin protein may play a role in hepatocellular carcinoma. But there has had no report giving the evidence that the patients infected with HCV other than HBV have the chromosomal translocation, whether the hepatocellular carcinomas caused by infection of HCV have chromosomal translocation worthy of further studying.

The effects of translin protein on normal lymphocytes need the induction by some factors such as mutagens or biological factors (HCV infection). In lymphoproliferative disorder patients infected with HCV, some reports showed chromosomal translocation happened in B-cell^[35,36]. Therefore, our report indicated a molecular mechanism that the interaction between HCV core protein and translin protein may trigger the B-cell progressing into lymphoma in patients infected with HCV. How the interaction between the HCV core protein and translin protein causes chromosomal translocation or rather, causes lymphoma, more experiments are necessary to elucidate it.

REFERENCES

- 1 Harada S, Watanabe Y, La Monic N, Suzuki T, Katayama T,

- Takebe Y, Saito I, Miyamura T. Expression of processed core protein of hepatitis C virus in mammalian cells. *J Virol* 1991; **65**: 3015-3021
- 2 **Santolini E**, Migliaccio G, La Monica N. Biosynthesis and biochemical properties of the hepatitis C virus core protein. *J Virol* 1994; **68**: 3631-3641
- 3 **Lo SY**, Selby M, Tong M, Ou JH. Comparative studies of the core gene products of two different hepatitis C virus isolates: Two alternative forms determined by a single amino acid substitution. *Virology* 1994; **199**: 124-131
- 4 **Liu Q**, Tackney C, Bhat RA, Prince AM, Zhang P. Regulated processing of hepatitis C virus core protein is linked to subcellular localization. *J Virol* 1997; **71**: 657-662
- 5 **Yasui K**, Wakita T, Tsukiyama-Kohara K, Funahashi SI, Ichikawa M, Kajita T, Moradpour D, Wands JR, Kohara M. The native form and maturation process of hepatitis C virus core protein. *J Virol* 1998; **72**: 6048-6055
- 6 **Mamiya N**, Worman HJ. Hepatitis C virus core protein binds to a DEAD box RNA helicase. *J Biol Chem* 1999; **274**: 15751-15756
- 7 **You LR**, Chen CM, Yeh TS, Tsai TY, Mai RT, Lin CH, Lee YH. Hepatitis C virus core protein interacts with cellular putative RNA helicase. *J Virol* 1999; **73**: 2841-2853
- 8 **Chen CM**, You LR, Hwang LH, Lee YH. Direct interaction of hepatitis C virus core protein with the cellular lymphotoxin-beta receptor modulates the signal pathway of the lymphotoxin-beta receptor. *J Virol* 1997; **71**: 9417-9426
- 9 **Matsumoto M**, Hsieh TY, Zhu N, VanArsdale T, Hwang SB, Jeng KS, Gorbalenya AE, Lo SY, Ou JH, Ware CF, Lai MM. Hepatitis C virus core protein interacts with the cytoplasmic tail of lymphotoxin-beta receptor. *J Virol* 1997; **71**: 1301-1309
- 10 **Gietz D**, St.Jean A, Woods RA, Schiestl RH. Improved method for high efficiency transformation of intact yeast cells. *Nucleic Acids Res* 1992; **20**: 1425
- 11 **Yan ZY**, Wang HL. Short protocols in molecular biology. Beijing: Scientific press 1998: 23-24
- 12 **He YW**, Liu W, Zen LL, Xiong KJ, Luo DD. Effect of interferon in combination with ribavirin on the plus and minus strands of HCV RNA in patients with chronic hepatitis C. *China Natl J New Gastroenterol* 1996; **2**: 179-181
- 13 **Wei L**, Wang Y, Chen HS, Tao QM. Sequencing of hepatitis C virus cDNA with polymerase chain reaction directed sequencing. *China Natl J New Gastroenterol* 1997; **3**: 12-15
- 14 **Tang ZY**, Qi JY, Shen HX, Yang DL, Hao LJ. Short_ and long_ term effect of interferon therapy in chronic hepatitis C. *China Natl J New Gastroenterol* 1997; **3**: 77
- 15 **Zhou P**, Cai Q, Chen YC, Zhang MS, Guan J, Li XJ. Hepatitis C virus RNA detection in serum and peripheral blood mononuclear cells of patients with hepatitis C. *China Natl J New Gastroenterol* 1997; **3**: 108-110
- 16 **Assy N**, Minuk GY. A comparison between previous and present histologic assessments of chronic hepatitis C viral infections in humans. *World J Gastroenterol* 1999; **5**: 107-110
- 17 **Huang F**, Zhao GZ, Li Y. HCV genotypes in hepatitis C patients and their clinical significances. *World J Gastroenterol* 1999; **5**: 547-549
- 18 **Yan FM**, Chen AS, Hao F, Zhao XP, Gu CH, Zhao LB, Yang DL, Hao LJ. Hepatitis C virus may infect extrahepatic tissues in patients with hepatitis C. *World J Gastroenterol* 2000; **6**: 805-811
- 19 **Zhang LF**, Peng WW, Yao JL, Tang YH. Immunohistochemical detection of HCV infection in patients with hepatocellular carcinoma and other liver diseases. *World J Gastroenterol* 1998; **4**: 64-65
- 20 **Shih CM**, Chen CM, Chen SY, Lee YH. Modulation of the trans-suppression activity of hepatitis C virus core protein by phosphorylation. *J Virol* 1995; **69**: 1160-1171
- 21 **Cho JW**, Baek WK, Suh SI, Yang SH, Chang J, Sung YC, Suh MH. Hepatitis C virus core protein promotes cell proliferation through the upregulation of cyclin E expression levels. *Liver* 2001; **21**: 137-142
- 22 **Hahn CS**, Cho YG, Kang BS, Lester IM, Hahn YS. The HCV core protein acts as a positive regulator of fas-mediated apoptosis in a human lymphoblastoid T cell line. *Virology* 2000; **276**: 127-137
- 23 **Sabile A**, Perlemuter G, Bono F, Kohara K, Demaugre F, Kohara M, Matsuura Y, Miyamura T, Brechot C, Barba G. Hepatitis C virus core protein binds to apolipoprotein AII and its secretion is modulated by fibrates. *Hepatology* 1999; **30**: 1064-1076
- 24 **Ray RB**, Meyer K, Ray R. Suppression of apoptotic cell death by hepatitis C virus core protein. *Virology* 1996; **226**: 176-182
- 25 **Moriya K**, Fujie H, Shintani Y, Yotsuyanagi H, Tsutsumi T, Ishibashi K, Matsuura Y, Kimura S, Miyamura T, Koike K. The core protein of hepatitis C virus induces hepatocellular carcinoma in transgenic mice. *Nat Med* 1998; **4**: 1065-1067
- 26 **Moriya K**, Yotsuyanagi H, Shintani Y, Fujie H, Ishibashi K, Matsuura Y, Miyamura T, Koike K. Hepatitis C virus core protein induces hepatic steatosis in transgenic mice. *J Gen Virol* 1997; **78**: 1527-1531
- 27 **Ferri C**, La Civita L, Longombardo G, Cecchetti R, Giannini C, Zignego AL. Type C chronic hepatitis complicated by B-cell lymphoma. *Am J Gastroenterol* 1995; **90**: 2071-2072
- 28 **Ferri C**, Monti M, La Civita L, Careccia G, Mazzaro C, Longombardo G, Lombardini F, Greco F, Pasero G, Bombardieri S. Hepatitis C virus infection in non-Hodgkin' s B-cell lymphoma complicating mixed cryoglobulinaemia. *Eur J Clin Invest* 1994; **24**: 781-784
- 29 **Brind AM**, Watson JP, Burt A, Kestevan P, Wallis J, Proctor SJ, Bassendine MF. Non-Hodgkin' s lymphoma and hepatitis C virus infection. *Leuk Lymphoma* 1996; **21**: 127-130
- 30 **Pioltelli P**, Gargantini L, Cassi E, Santoleri L, Bellati G, Magliano EM, Morra E. Hepatitis C virus in non-Hodgkin' s lymphoma. A reappraisal after a prospective case-control study of 300 patients. Lombard Study Group of HCV-Lymphoma. *Am J Hematol* 2000; **64**: 95-100
- 31 **Suriawinata A**, Ye MQ, Emre S, Strauchen J, Thung SN. Hepatocellular carcinoma and non-Hodgkin lymphoma in a patient with chronic hepatitis C and cirrhosis. *Arch Pathol Lab Med* 2000; **124**: 1532-1534
- 32 **Fields S**, Song O. A novel genetic system to detect protein-protein interactions. *Nature* 1989; **340**: 245-246
- 33 **Bendixen C**, Gangloff S, Rothstein R. A yeast mating-selection scheme for detection of protein-protein interactions. *Nucleic Acids Res* 1994; **22**: 1778-1779
- 34 **Aoki K**, Suzuki K, Sugano T, Tasaka T, Nakahara K, Kuge O, Omori A, Kasai M. A novel gene, Translin, encodes a recombination hotspot binding protein associated with chromosomal translocations. *Nat Genet* 1995; **10**: 167-174
- 35 **Kasai M**, Matsuzaki T, Katayanagi K, Omori A, Maziarz RT, Strominger JL, Aoki K, Suzuki K. The translin ring specifically recognizes DNA ends at recombination hot spots in the human genome. *J Biol Chem* 1997; **272**: 11402-11407
- 36 **de Vries E**, van Driel W, Bergsma WG, Arnberg AC, van der Vliet PC. HeLa nuclear protein recognizing DNA termini and translocating on DNA forming a regular DNA-multimeric protein complex. *J Mol Biol* 1989; **208**: 65-78
- 37 **Zignego AL**, Giannelli F, Marrocchi ME, Mazzocca A, Ferri C, Giannini C, Monti M, Caini P, Villa GL, Laffi G, Gentilini P. T (14;18) translocation in chronic hepatitis C virus infection. *Hepatology* 2000; **31**: 474-479
- 38 **Zuckerman E**, Zuckerman T, Sahar D, Streichman S, Attias D, Sabo E, Yeshurun D, Rowe J. bcl-2 and immunoglobulin gene rearrangement in patients with hepatitis C virus infection. *Br J Haematol* 2001; **112**: 364-369

A novel hepatitis B virus mutant with A-to-G at nt551 in the surface antigen gene

Hua-Biao Chen, De-Xing Fang, Fa-Qing Li, Hui-Ying Jing, Wei-Guo Tan, Su-Qin Li

Hua-Biao Chen, De-Xing Fang, Fa-Qing Li, Hui-Ying Jing, Wei-Guo Tan, Su-Qin Li, Huadong Research Institute for Medical Biotechnics, Nanjing 210002, Jiangsu Province, China

Correspondence to: Hua-Biao Chen, Huadong Research Institute for Medical Biotechnics, Nanjing 210002, Jiangsu Province, China. chenhuabiao@hotmail.com

Telephone: +86-25-4542419 **Fax:** +86-25-4541183

Received: 2002-07-26 **Accepted:** 2002-08-16

Abstract

AIM: Hepatitis B surface antigen (HBsAg) mutant of hepatitis B virus (HBV) is one of the important factors that result in immune escape and cause failure of immunization. In this study we reported and characterized a novel HBV mutant with A-to-G at nt551 and intended to provide theoretical data for prevention of HBV infection in China.

METHODS: A methodology comprising polymerase chain reaction (PCR) amplifying, M13 bacteriophage cloning and nucleotide sequencing was used to analyze the sera of the pediatric patient who was hepatitis B (HB) immune failure. Expression plasmids containing the mutant S gene and a wild-type (*adr*) S gene were constructed respectively and the recombinant HBsAg were expressed in COS-7 cells under the regulation of SV40 early promoter. The recombinant proteins were investigated for their immunological reactivity with different monoclonal antibodies (mAb) against 'a' determinant and vaccine-raised human neutralizing antibodies.

RESULTS: It was found that there was a new point mutation at nt551 of the HBV (*adr*) genome from A to G, leading to a substitution of methionine (Met) to valine (Val) at position 133 in the 'a' determinant of HBsAg. Compared to the wild-type HBsAg, the binding activity of the mutant HBsAg to mAbs (A6, A11 and S17) and to vaccine-raised human anti-hepatitis B surface antibody (anti-HBs) decreased significantly.

CONCLUSION: According to the facts that the patient has been immunized with HB vaccine and that the serum is anti-HBs positive and HBsAg negative, and based on the nucleotide sequence analysis of the mutant HBV S gene and its alteration of antigenicity, the HBV is considered to be a new vaccine-induced immune escape mutant different from the known ones.

Chen HB, Fang DX, Li FQ, Jing HY, Tan WG, Li SQ. A novel hepatitis B virus mutant with A-to-G at nt551 in the surface antigen gene. *World J Gastroenterol* 2003; 9(2): 304-308
<http://www.wjgnet.com/1007-9327/9/304.htm>

INTRODUCTION

From late 1980's, there has been increasing number of reports on hepatitis B (HB) patients with atypical HBV serological markers. Analysis of HBV in those patients demonstrated

mutants^[1-6]. Mutations could be found within the C gene, S gene, P gene and X gene^[7,8]. HBsAg encoded by the S gene carries the common determinant 'a', as well as 'd' or 'y' and 'w' or 'r' subtype determinant, and is classified into four major subtypes, i.e. *adw*, *adr*, *ayw*, *ayr*. Two amino acid (aa) residues encoded by S gene at codon positions 122 and 160 have been postulated to determine the different antigenic subtypes^[9]. The most important S gene mutations are those affecting the antigenicity of HBsAg 'a' determinant (aa 124 to 147) to which the major immune-target of neutralizing polyclonal antibodies reacted. In this way, the HBsAg mutants can escape detection by current methods and influence the effect of HBV vaccines.

There have been several reports on HBV S gene mutants affecting amino acid positions 126, 129, 131, 141, 144 and 145 of HBsAg^[10-12]. In this report, we described a rare variant of HBV isolated from a pediatric patient whose serum was negative for HBsAg and positive for anti-HBs. Sequence analysis revealed the substitution at position 133 (Met to Val) in the 'a' determinant within S gene. Using a panel of three mAbs (A6, A11 and S17) against 'a' determinant and vaccine-raised anti-HBs, the recombinant mutant HBsAg showed less binding activity than the wild-type HBsAg. Taken together, the data we presented clearly demonstrated that the substitution results in antigenic alteration and may allow the mutant virus to escape the detection by standard HBsAg assays.

MATERIALS AND METHODS

Patient

The patient, male, 4 years old, was born to a HBV carrier mother. He had been immunized with HBV vaccine on a conventional 0-1-6 schedule, i.e., 3 injections of HBV vaccine were given at 0, 1 and 6 month (s) old respectively. The virus markers of his serum were anti-HBs positive, HBsAg negative and HBeAg positive, as well as positive for HBV DNA by PCR and high level of alanine transaminase (ALT) 200 IU·L⁻¹.

Extraction and amplification of HBs DNA

The viral DNA was extracted from the serum sample using the standard method. Briefly, 100 µl serum was treated with proteinase K, phenol and chloroform, and then DNA was precipitated with ethanol. The resulted DNA was resuspended in 20 µl didistilled water for later use. A nested PCR method^[13,14] was used to amplify HBV S gene fragment. The external primers were 5' -ACATACTCTGTGGAAGGC-3' (nt2 756 to nt2 773, forward) and 5' -TATCCCATGAAGTTAAGG-3' (nt884 to nt867, reverse). The internal primers were 5' -CGGGATCCATATTCTTGGGAACAAG-3' (nt2 826 to nt2 844, forward, underlined is a BamHI site) and 5' -CACTGCAGGGTTTAAATGTATACCCA-3' (nt839 to nt821, reverse, underlined is a PstI site). The PCR was carried out for 30 cycles, each cycle including 94 °C denaturation for 1 minute, 50 °C annealing for 1 minute and 72 °C chain elongation for 2 minutes.

Nucleotide and amino acid sequence analysis

The PCR-amplified HBV S gene fragments (about 1.2 kb) were

cleaned with a QIAquick spin column (Qiagen). The DNA was digested with both BamHI and PstI, and then ligated by T4 DNA ligase with M13mp18 RF DNA cut with the same restriction enzymes. The ligated DNA was used in the transformation of *E. coli* JM105 cells and the recombinant phages were recognized by loss of β -galactosidase activity in the culture plate containing X-gal and IPTG. The single-stranded recombinant DNA was prepared according to the standard protocol^[15]. The S gene sequence was determined on an ABI PRISM™ 377XL sequencer (PE Applied Biosystems, USA) and sequence analysis was performed using Release 6.70 of the PCGENE package (IntelliGenetics Co.). The HBsAg 'a' determinant coding regions of 48 defined HBV genotypes downloaded from National Center for Biotechnology Information (NCBI) were analyzed comparatively.

Construction of expression plasmids and transient protein expression

The process followed the reference^[16-18]. Briefly, the construction of recombinant wild-type and mutant HBsAg expression plasmids started with a plasmid pS300 which was constructed from pSP65 carrying the SV40 early promoter sequence, the preS/S gene and the poly (A) signal sequence of HBV. For construction of the major HBsAg expression plasmid, the preS1 and preS2 regions were deleted by restriction enzyme digestion. COS-7 cells were cultured in DMEM/HG medium supplemented with 5 % fetal calf serum, two million units/ml of ampicillin and one million units/ml of kanamycin under the condition of 5 % CO₂, 37 °C. The cells in 60-mm dishes were transfected with 10 μ g of the expression plasmids using calcium phosphate precipitation method. 72 hours later, the transfected cells were collected into 1.5-ml Eppendorf tubes, washed with 10 mM PBS (pH7.4) and resuspended with 500 μ l (for each dish) of 10 mM PBS (pH7.4). The cells were disrupted by freezing and thawing for 5 times, and then centrifuged at 8 000 rpm for 5 minutes. The supernatants contained the recombinant HBsAg proteins.

Recombinant HBsAg antigen immunoassay and epitope analysis

A solid phase radioimmunoassay (RIA) method was applied for detecting the binding activity of the expressed HBsAg with mAbs. In brief, polystyrene beads were coated with mAbs against different epitopes of HBsAg respectively and then incubated with the expressed HBsAg overnight at room temperature. The beads were washed thoroughly and incubated with ¹²⁵I-labeled anti-HBs (Beijing Atomic Energy Institute). Bound antibodies were detected as counts per minute (cpm) in LKB 1 272 gamma counter. To evaluate the reactivity of vaccine-raised human anti-HBs to recombinant wild-type HBsAg and mutant HBsAg, an enzyme-linked immunosorbent assay (ELISA) was established as follows^[19-21]: plates were coated with size filtrated and volume concentrated antigen from expression cell culture; Plasma from five HBV vaccinated individuals were pooled and serially diluted human anti-HBs was incubated in the plates at 37 °C for 90 minutes. Bound human IgG was detected by a second incubation with horseradish peroxidase (HRP) conjugated murine monoclonal anti-human IgG; The reactivity was determined by enzyme catalyzed OPD colour development and the results were expressed as absorbance units at 490 nm.

RESULTS

HBs variant nucleotide and amino acid sequence analysis

The HBs DNA sequence of the novel mutant was shown in Figure 1. The adenosine (A) at nt519 and the guanosine (G) at nt633 indicated that the mutant belonged to *adr* subtype^[22]. Sequence comparison between the mutant and 48 defined HBs genotypes revealed a new nucleotide mutation at nt551 from A to G, leading to the amino acid alteration at position 133 from Met to Val in the 'a' determinant. The mutant was first reported and its sequence data have been deposited with GenBank DNA databases under the accession number AF052576. The comparative analysis of HBsAg 'a' determinant coding regions of different HBV genotypes was shown in Figure 2.

DNA SEQUENCE 1203 BP; 254 A; 354 C; 265 G; 330 T; 0 OTHER

```

ATGGGAGGTT GGTCTTCCAA ACCTCGACAA GGCATGGGGA CGAATCTTTC TGTTCCCAAT 2907
CCTCTGGGAT TCTTTCCCGA TCACCAGTTG GACCCTGCGT TCGGAGCCAA CTCAAACAAT 2967
CCAGATTGGG ACTTCAACCC CAACAAGGAT CACTGGCCAG AGGCAAATCA GGTAGGAGCG 3027
GGAGCATTGG GCCAGGGTT CACCCACCA CACGGCGGTC TTTTGGGGTG GAGCCCTCAG 3087
GCTCAGGGCA TTTTGACAAC AGTGCCAGTA GCACCTCCTC CTGCCTCCAC CAATCGGCAG 3147
TCAGGAAGAC AGCCTACTCC CATCTCTCCA CCTCTAAGAG ACAGTCATCC TCAGGCCATG 3207
CAGTGGAACTC CACAACATT CCACCAAGCT CTGCCAGACC CCAGAGTGAG GGGCCTATAC 052
TTTCTGCTG GTGGCTCCAG TTCCGGAACA GTAACCCTG TTCCGACTAC TGCCTCACCC 112
ATATCGTCAA TCTTCTCGAG GACTGGGGAC CCTGCACCGA ACATGGAGAG CACAACATCA 172
GGATTCCTAG GACCCCTGCT CGTGTTACAG GCGGGGTTTT TCTTGTTGAC AAGAATCCTC 232
ACAATACCAC AGAGTCTAGA CTCGTGGTGG ACTTCTCTCA ATTTTCTAGG GGGAGCACCC 292
ACGTGTCCTG GCCAAAATTC GCAGTCCCCA ACCTCCAATC ACTACCAAC CTCTTGTCTC 352
CAAATTTGTC CTGGTTATCG TTGGATGTGT CTGCGGCGTT TTATCATATT CCTCTTCATC 412
CTGCTGCTAT GCCTCATCTT CTTGTTGGTT CTTCTGGACT ACCAAGGTAT GTTGCCCGTT 472
TGTCTCTAC TTCCAGGAAC ATCAACTACC AGCACGGGAC CATGCAAGAC CTGCACGATT 532
CCTGCTCAAG GAACCTCTGTG TTTCCCTCT TGTTGCTGTA CAAAACCTTC GGACGGAAAC 592
TGCACTTGTA TTCCATCCC ATCATCTGG GCTTTCGCAA GATTCTATG GGAGTGGGCC 652
TCAGTCCGTT TCTCCTGGCT CAGTTACTA GTGCCATTTG TTCAGTGGTT CGTAGGGCTT 712
TCCCCACTG TTTGGCTTTC AGTTATATGG ATGATGTGGT ATTGGGGGCC AAGTCTGTAC 772
AACATCTTGA GTCCTTTTTT ACCTCTATTA CCAATTTTCT TTTGTCTTTG GGTATACATT 832
TAA

```

835

Figure 1 The complete nucleotide sequence of the mutant S gene. The A-to-G mutation site at nt551 of HBV genome is in bold letter. The underlined are the EcoRI-like site, the initiation codon of HBsAg and the amino acid codon (ATG to GTG) respectively. The first C of the EcoRI-like site (GAACTC) is counted as nt1. The GenBank accession number of the sequence is AF052576.

The amino acid position on the 'a' determinant of

HBsAg

Gene names	124	133	137	139
(subtypes)	Cys	Met	Cys	Cys
147				
※HPBA11A (adr)	TGC ACGATTCTGCTCAAGGAACCTCT	ATG TTTCCCTCT	TGT	TGC TGT
ACAAAACCTTCGGACGGAAAC	TGC			
※HPBADRM (adr)	-----	-----	-----	-----
§ HPBCGADR (adr)	-----	-----	-----	-----
# HBVADR (adr)	-----	-----	-----	-----
§ HBVADR4 (adr)	-----	-----	-----	-----
※HPBB4HST1(adr)	-----	-----	-----	-----
§ HPBADR1CG(adr)	-----	-----	-----	-----
§ HPBADRA (adr)	-----	-----	-----	-----
§ HEHBVAYR (ayr)	-----	-----	-----	-----
※HPBC5HK02(ayw)	-----	-----	-----	-----
※HPBB5HK01(ayw)	-----	-----	-----	-----
※HPBC4HST2(adr)	-----	C-----	-----	-----
※HPBADRC (adr)	-----	C-----	-----	-----
※HPBCG (adr)	-----	-----	G-----	-----
※HPBC6T588(adr)	-----	C-----	-----	T-----
§ HPBADWZ (adw)	-----	C-----	A-----	A-----
※HPBADW3 (adw)	-----	C-----	A-----	A-----
# HBVP6CSX (adw)	-----	A-C-----	A-----	A-----
※HPBA2HYS2(adw)	-----	A-C-----	A-----	A-----
# HBVP4CSX (adw)	-----	A-C-----	A-----	A-----
# HBVCGWITY(adw)	-----	AGC-----	A-----	A-----
※HPBA3HMS2(adw)	-----	A-C-----	A-----	A---T-----
※HPBA1HKK2(adw)	-----	A-C-----	A-----	A---T-----
※HPBADW2 (adw)	-----	A-C-----	A-----	A---T-----
※HPBADW1 (adw)	-----	A-C-----	A-----	AT---T-----
# HVHEPB (ayw)	-----	C-----	C-A-----	A-----
§ HPBADWZCG(ayw)	-----	C-----	C-A-----	A-----
# HBVP3CSX (ayw)	-----	C-A-----	A-----	C-----
# HBVP6PCXX(ayw)	-----	C-A-----	A-----	C-----
# HBVP2CSX (ayw)	-----	C-----	A-----	C-----
# HBVAYWGEN(ayw)	-----	C-----	A-----	C-----
# HBVP5PCXX(ayw)	-----	C-----	A-----	C-----
# HBVP4PCXX(adr)	-----	C-----	A-----	C-----
§ HBU46935 (adr)	-----	CA-----	T-- A-----	A-----
§ HPBMUT (ayw)	-----	T-C-----	A-----	C-----
§ XXHEPAV (ayw)	-----	C-----	A-----	C-----
§ HBVAYWE (ayw)	-----	C-----	A-----	C-----
§ HPBAYW (ayw)	-----	T-C-A-----	A-----	C-----
§ HBVAYWC (ayw)	-----	C-----	A-----	C-----
# HBVAYWMCG(ayw)	-----	C-----	C-A-----	A-----
§ HPBADW2 (adw)	-----	C-----	A-----	C-----
§ HBVDNA (adw)	-----	C-----	A-----	C-----
§ HPBVCG (adw)	-----	C-----	T-- A-----	A-----
# HBVADW (adw)	-----	C-----	C-A-----	A-----
§ HBVADW2 (adw)	-----	C-----	C-A-----	A-----
# HBVXCPS (adw)	-----	C-----	C-A-----	A-----
§ HBVAYWCI (adw)	-----	C-----	C-A-----	A-----
§ HBVADW4A (adw)	-----	A-C---T---A-----	C-----	TCC---C-----

Figure 2 Comparative analysis of the HBsAg 'a' determinant coding regions of different HBV genomes. HBsAg 'a' determinant is a conformational epitope which has a special two-loop construction kept by the disulfide bonds between Cys124 and Cys137, Cys139 and Cys147, respectively. 48 HBV genome sequences were downloaded from National Center for Biotechnology Information (NCBI), USA (<http://www.ncbi.nlm.nih.gov>). "Gene names" are their names in the original gene databases. Here the ※ labeled ones are from DDBJ, the labeled are from EMBL, and the § labeled are from GenBank.

Recombinant HBsAg transient expression in COS-7 cell

The recombinant wild-type HBsAg and mutant HBsAg were expressed under the regulation of SV40 early promoter in COS-7 cells in a transient fashion. Only secreted HBsAg in culture supernatant was examined for expression. There was no obvious expression yield difference between the wild-type and mutant recombinant HBsAg based on protein silver staining on SDS-PAGE.

Immunoreactivity analysis

To compare the reactivity of recombinant wild-type HBsAg and mutant HBsAg to antibodies, the quantity of the antigens must be the same. Because both the wild-type and mutant HBV were known to be adr subtypes, an anti-‘d’ determinant mAb, S4 (Shanghai Institute of Biological Products), was used for the standardization of the HBsAg. After series of dilution and detection, both HBsAg preparations were adjusted to a protein concentration of 2.1 ng/ml. Three different anti-‘a’ determinant mAbs, A6, A11 and S17, were selected to characterize the binding activity of the expressed HBsAg. In the condition of the same concentration of HBsAg proteins determined by anti-‘d’ mAb, the reactivity of the mutant HBsAg to three anti-‘a’ mAbs were unexceptionally weaker than that of the wild-type HBsAg, as shown in Table 1. The recombinant wild-type and mutant HBsAg were also tested for their relative reactivity to vaccine-raised human anti-HBs. Clearly, pooled human HBV vaccinated antisera decreased its binding strength to the mutant HBsAg by about 5-fold by ELISA assay, as shown in Table 2. As control, the cell culture supernatant without recombinant plasmid transfection did not bind to human antisera in this assay. The results demonstrated that the Met-to-Val substitution at amino acid position 133 of HBsAg led to the antigenic alteration.

Table 1 Detection of immunoreactivity of the expressed HBsAg to anti-‘a’ monoclonal antibodies by radioimmunoassay^a

Anti-‘a’ monoclonal antibodies	Wild-type HBs (133Met)	Mutant HBs (133Val)
A6	1118 (5.82)	774 (3.93)
A11	932 (4.80)	744 (3.76)
S17	945 (4.87)	630 (3.14)

^aCounter per minute (cpm), the number in the parentheses is P/N value. According to the solid RIA kit producer’s recommendation, P/N=(sample cpm-background)/(negative control cpm-background). Untransfected cells were used as negative control, average cpm was 240. Blank polystyrene beads were used as background, average cpm was 58. P/N \geq 2.10 is considered to be positive reactivity. The more the P/N value, the stronger the reactivity.

Table 2 Immunoreactivity of vaccine-raised human anti-HBs to recombinant wild-type HBsAg and to recombinant mutant HBsAg in an ELISA assay

Plate coated with	Wild-type rHBsAg				Mutant rHBsAg				Control
Vaccine-raised anti-HBs	1:1	1:2	1:4	1:8	1:1	1:2	1:4	1:8	1:1
Absorbance at 490 nm	2.45	1.32	0.71	0.28	0.53	0.28	0.15	0.06	0.04

DISCUSSION

The hepatitis B virus has three envelope proteins, and the major envelope protein is S protein, consisting of 226 amino acids. A hydrophilic region in S protein (aa 124 to 147) is designated as ‘a’ determinant, an antigenic determinant common to all HBV subtypes. ‘a’ determinant is a conformational epitope

which is made up of a special two-loop structure kept by the disulfide bonds between Cys124 and Cys137, Cys139 and Cys147, respectively. This structure projects out from the surface of the HBV particle^[23]. The HBV DNA template is transcribed by cellular RNA polymerase to pregenomic RNA, which in turn is reverse transcribed to DNA by virus polymerase. This unique way of HBV replication means a significant tendency to mutation^[8,19]. On the other hand, the pressure of immunoprophylaxis with HB immunoglobulin and/or vaccines is another important cause to result in escape mutants^[23-28]. Up to date, in the reports about HBV vaccine-induced escape mutants, the most popular one is that with glycine to arginine at aa145 of HBsAg. The mutation decreased the binding activity of HBsAg to mAbs^[23,29]. There was another vaccine-induced escape mutant of HBV from an immunized child with anti-HBs positive. The aspartic acid at aa144 was substituted by an alanine in HBsAg, and anti-‘a’ monoclonal antibody assay showed the mutant HBsAg had weak reactivity^[12]. We also reported a different mutant of HBV with isoleucine at aa126 replaced by serine^[30]. It seemed that the Ser126 mutant was not an antibody-induced escape mutant since anti-HBs was not detected in the patient. Besides, the mutations, situated closely adjacent to the ‘a’ determinant, could also change the entire immunodominant region structure and therefore weaken the antigenicity even though no mutations were found within this ‘124-147’ region^[31]. Hence, the classical definition of the ‘a’ immunodominant region may need to be extended to require adjacent amino acids to support its conformation^[32-34].

In this report, we characterize a novel HBV mutant with A-to-G at nt551. The substitution of Met to Val at position 133 in the ‘a’ determinant of HBsAg results in the decrease of reactivity of the recombinant HBsAg to anti-‘a’ mAbs and vaccine-raised human anti-HBs. Since the major B-cell antigenic epitope resides in the group specific ‘a’ determinant region, which is reported to be conformational^[35], the data we presented clearly demonstrated that the mutation affects the conformation of the ‘a’ determinant and alters the antigenicity of HBsAg, leading to HBsAg escape from the detection by standard HBsAg assays. Our observations further indicate that the mutation in the HBV surface gene may lead to a considerable decrease of properly folded surface antigens which may render the virus particle less immunogenic in producing an effective neutralizing anti-HBs to clear the virus. According to the fact that the patient has been immunized with HBV vaccine and that the serum is anti-HBs positive and HBsAg negative, the HBV variant we report here is considered to be a new vaccine-induced immune escape mutant.

This antigenically divergent HBV mutant is important for both clinical and diagnostic reasons^[36,37]. Therefore, further studies using expressed mutant HBs proteins and accumulation of additional cases will be required for elucidation of the mechanism of the loss of antigenicity.

REFERENCES

- Cabrero M**, Bartolom J, Caramelo C, Barril G, Carreno V. Molecular analysis of hepatitis B virus DNA in serum and peripheral blood mononuclear cells from hepatitis B surface antigen-negative cases. *Hepatology* 2000; **32**: 116-123
- Grethe S**, Monazahian M, Bohme I, Thonssen R. Characterization of unusual escape variants of hepatitis B virus isolated from a hepatitis B surface antigen-negative subject. *J Virol* 1998; **72**: 7692-7696
- Bruce SA**, Murray K. Mutations of some critical amino acid residues in the hepatitis B virus surface antigen. *J Med Virol* 1995; **46**: 157-161
- Weinberger KM**, Zoulek G, Bauer T, Bohm S, Jilg W. A novel deletion mutant of hepatitis B virus surface antigen. *J Med Virol* 1999; **58**: 105-110

- 5 **Shinji T**, Koide N, Hanafusa T, Hada H, Oka T, Takayama N, Shiraha H, Nakamura M, Ujike K, Yumoto Y, Tsuji T. Point mutations in the S and pre-S2 genes observed in two hepatitis B virus carriers positive for antibody to hepatitis B surface antigen. *Hepatogastroenterology* 1998; **45**: 500-502
- 6 **Schories M**, Peters T, Rasenack J. Isolation, characterization and biological significance of hepatitis B virus mutants from serum of a patient with immunologically negative HBV infection. *J Hepatol* 2000; **33**: 799-811
- 7 **Brunetto MR**, Rodriguez UA, Bonino F. Hepatitis B virus mutants. *Intervirology* 1999; **42**: 69-80
- 8 **Carman WF**, Thomas HC. Genetic variation in hepatitis B virus. *Gastroenterology* 1992; **102**: 711-719
- 9 **Stirk HJ**, Thornton JM, Howard CR. A topological model for hepatitis B surface antigen. *Intervirology* 1992; **33**: 148-158
- 10 **Seddigh-Tonekaboni S**, Waters JA, Jeffers S, Gehrke R, Ofenloch B, Horsch A, Hess G, Thomas HC, Karayiannis P. Effect of variation in the common 'a' determinant on the antigenicity of hepatitis B surface antigen. *J Med Virol* 2000; **60**: 113-121
- 11 **Roznovsky L**, Harrison TJ, Fang ZL, Ling R, Lochman I, Orsagova I, Pliskova L. Unusual hepatitis B surface antigen variation in a child immunized against hepatitis B. *J Med Virol* 2000; **61**: 11-14
- 12 **Ni F**, Fang DX, Gan R, Li Z, Duan S, Xu Z. A new immune escape mutant of hepatitis B virus with an Asp to Ala substitution in aa144 of the envelope major protein. *Res Virol* 1995; **146**: 397-407
- 13 **Zhang SL**, Han XB, Yue YF. Relationship between HBV viremia level of pregnant women and intrauterine infection: nested PCR for detection of HBV DNA. *World J Gastroenterol* 1998; **4**: 61-63
- 14 **Dong J**, Cheng J, Wang Q, Wang G, Shi S, Liu Y, Xia X, Si C. Cloning and sequence analysis of truncated S gene from circulation of patients with chronic hepatitis B virus infection. *Zhonghua Ganzhangbing Zazhi* 2001; **9**: 163-165
- 15 **Sambrook J**, Fritsch EF, Maniatis T. Molecular Cloning: A Laboratory Manual. 2nd ed. New York: Cold Spring Harbor Laboratory Press 1990: 201-233
- 16 **Fang DX**, Li FQ, Tan WG, Chen HB, Jing HY, Li SQ, Lin HJ, Zhou ZX. Transient expression and antigenic characterization of HBsAg of HBV nt551 A to G mutant. *World J Gastroenterol* 1999; **5**: 73-74
- 17 **Gu B**, Ren H. Expression of HBsAg by using various eukaryotic expression vectors. *Zhonghua Ganzhangbing Zazhi* 1999; **7**: 98-100
- 18 **Jantet D**, Chemin I, Mandrand B, Zoulim F, Trepo C, Kay A. Characterization of two hepatitis B virus populations isolated from a hepatitis B surface antigen-negative patient. *Hepatology* 2002; **35**: 1215-1224
- 19 **Hasegawa K**, Huang J, Rogers SE, Blum HE, Liang TJ. Enhanced replication of a hepatitis B virus mutant associated with an epidemic of fulminant hepatitis. *J Virol* 1994; **68**: 1651-1659
- 20 **Gu B**, Ren H, Zhang D. Expression of recombinant inserting mutants of HBsAg in vitro and its antigenic analysis. *Zhonghua Yixue Zazhi* 1999; **79**: 139-142
- 21 **Cooreman MP**, van Roosma MH, te Morsche R, Sunnen CM, de Ven EM, Jansen JB, Tytgat GN, de Wit PL, Paulij WP. Characterization of the reactivity pattern of murine monoclonal antibodies against wild-type hepatitis B surface antigen to G145R and other naturally occurring 'a' loop escape mutations. *Hepatology* 1999; **30**: 1287-1292
- 22 **Okamoto H**, Imai M, Tsuda F, Tanaka T, Miyakama Y, Mayumi M. Point mutation in the S gene of hepatitis B virus for a *d/y* or *w/r* subtypic change in two blood donors carrying a surface antigen of compound subtype *adyr* or *adwr*. *J Virol* 1987; **61**: 3030-3034
- 23 **Carman WF**, Zanetti AR, Karayiannis P, Waters J, Manzillo G, Tanzi E *et al*. Vaccine-induced escape mutant of hepatitis B virus. *Lancet* 1990; **336**: 325-329
- 24 **Chiou HL**, Lee TS, Kuo J, Mau YC, Ho MS. Altered antigenicity of 'a' determinant variants of hepatitis B virus. *J Gen Virol* 1997; **78**: 2639-2645
- 25 **Karthigesu VD**, Allison LM, Ferguson M, Howard CR. A hepatitis B virus variant found in the sera of immunized children induces a conformational change in the HbaAg 'a' determinant. *J Med Virol* 1999; **58**: 346-352
- 26 **He JW**, LU Q, Zhu QR, Duan SC, Wen YM. Mutations in the 'a' determinant of hepatitis B surface antigen among Chinese infants receiving active postexposure hepatitis B immunization. *Vaccine* 1998; **16**: 170-173
- 27 **Cooreman MP**, Leroux-Roels G, Paulij WP. Vaccine- and hepatitis B immune globulin-induced escape mutations of hepatitis B virus surface antigen. *J Biomed Sci* 2001; **8**: 237-247
- 28 **Chen WN**, Oon CJ, Koh S. Horizontal transmission of a hepatitis B virus surface antigen mutant. *J Clin Microbiol* 2000; **38**: 938-939
- 29 **Heijntink RA**, van Bergen P, van Roosma MH, Sunnen CM, Paulij WP, Schalm SW, Osterhaus AD. Anti-HBs after hepatitis B immunization with plasma-derived and recombinant DNA-derived vaccines: binding to mutant HBsAg. *Vaccine* 2001; **19**: 3671-3680
- 30 **Fang DX**, Gan RB, Li ZP, Duan SC. A hepatitis B virus variant with an Ile to Ser mutation at aa126 of HbsAg. *Shengwu Hua Xueyu Shengwu Wuli Xuebao* 1996; **28**: 429-433
- 31 **Kfoury Baz EM**, Zheng J, Mazuruk K, Van Le A, Peterson DL. Characterization of a novel hepatitis B virus mutant: demonstration of mutation-induced hepatitis B virus surface antigen group specific 'a' determinant conformation change and its application in diagnostic assays. *Transfusion Medicine* 2001; **11**: 355-362
- 32 **Roznovsky L**, Harrison TJ, Fang ZL, Ling R, Lochman I, Orsagova I, Pliskova L. Unusual hepatitis B surface antigen variation in a child immunized against hepatitis B. *J Med Virol* 2000; **61**: 11-14
- 33 **Banerjee K**, Guptan RC, Bisht R, Sarin SK, Khandekar P. Identification of a novel surface mutant of hepatitis B virus in a seronegative chronic liver disease patient. *Virus Res* 1999; **65**: 103-109
- 34 **Ijaz S**, Torre F, Tedder RS, Williams R, Naoumov NV. Novel immunoassay for the detection of hepatitis B surface escape mutants and its application in liver transplant recipients. *J Med Virol* 2001; **63**: 210-216
- 35 **Koyanagi T**, Nakamuta M, Sakai H, Sugimoto R, Munechika E, Koto K, Iwamoto H, Kumazawa T, Mukaide M, Nawata H. Analysis of HBs antigen negative variant of hepatitis B virus: unique substitutions, Glu129 to Asp and Gly145 to Ala in the surface antigen gene. *Med Sci Monit* 2000; **6**: 1165-1169
- 36 **Rodriguez-Frias F**, Brti M, Jardi R, Vargas V, Quer J, Cotrina M, Martell M, Esteban R, Guardia J. Genetic alterations in the S gene of hepatitis B virus in patients with acute hepatitis B, chronic hepatitis B and hepatitis B liver cirrhosis before and after liver transplantation. *Liver* 1999; **19**: 177-182
- 37 **Coleman PF**, Chen YC, Mushahwar IK. Immunoassay detection of hepatitis B surface antigen mutants. *J Med Virol* 1999; **59**: 19-24

Evaluation of the string test for the detection of *Helicobacter pylori*

Rupert WL Leong, Ching C Lee, Thomas KW Ling, Wai K Leung, Joseph JY Sung

Rupert WL Leong, Department of Gastroenterology, University of New South Wales, Bankstown Hospital, Sydney, Australia

Ching C Lee, Thomas KW Ling, Department of Microbiology; Chinese University of Hong Kong, Prince of Wales Hospital, Shatin, Hong Kong, China

Wai K Leung, Joseph JY Sung, Department of Medicine & Therapeutics, Chinese University of Hong Kong, Prince of Wales Hospital, Shatin, Hong Kong, China

RWL Leong is partially supported by the Athelstan and Amy Saw Overseas Medical Research Fellowship from the University of Western Australia

Correspondence to: Professor Joseph JY Sung, Department of Medicine and Therapeutics, Prince of Wales Hospital, Shatin, N. T., Hong Kong, China. joesung@cuhk.edu.hk

Telephone: +852-26323132 **Fax:** +852-26467824

Received: 2002-08-24 **Accepted:** 2002-11-04

Abstract

AIM: *Helicobacter pylori* can be diagnosed by invasive or non-invasive tests but to obtain bacteria for culture and antibiotic susceptibility testing, an upper GI endoscopy is often required. The string test may be a minimally-invasive alternative method of obtaining *H. pylori* samples. This study evaluates the sensitivity and specificity of the string test in the diagnosis of *H. pylori* in comparison with endoscopic means of diagnosis.

METHODS: This was a prospective open comparative study of patients with dyspepsia with endoscopy-based tests as gold standard (defined as a positive CLO test and antral histology). Fasting patients swallowed the encapsulated-string (Enterotest Hp), which was withdrawn after 1 hour. The gastric juice from the string was plated onto *H. pylori*-selective media for culture. *Helicobacter pylori* was identified by typical colony morphology, gram stain and biochemical test results.

RESULTS: Thirty dyspeptic patients were recruited of whom 21 (70 %) were positive for *H. pylori* according to the gold standard. The sensitivity, specificity, positive predictive value, and negative predictive value for the string test were 38 %, 100 %, 100 % and 41 % respectively, and for endoscopic biopsies 81 %, 100 %, 100 %, 69 % respectively ($P=0.004$). Logistic regression showed that only abundant growth density from endoscopic biopsy cultures to be a predictor of a positive string test ($P=0.018$).

CONCLUSION: The string test is an alternative method to endoscopy in obtaining *H. pylori* but has a low sensitivity compared to endoscopic biopsies.

Leong RWL, Lee CC, Ling TKW, Leung WK, Sung JY. Evaluation of the string test for the detection of *Helicobacter pylori*. *World J Gastroenterol* 2003; 9(2): 309-311
<http://www.wjgnet.com/1007-9327/9/309.htm>

INTRODUCTION

The diagnosis of *H. pylori* can be made by invasive or non-invasive tests^[1]. While non-invasive methods offer distinct

advantages in terms of cost, ease-of-effort and comfort to patients, the retrieval of *H. pylori* for microscopy, culture, DNA analysis, cytotoxin profiling, strain identification and antibiotic susceptibility testing often require an endoscopy with gastric mucosal biopsies. With a rising incidence in antibiotic resistance, failed eradication therapy now occurs in up to 20 % of all patients^[2,3]. In this situation, obtaining *H. pylori* for antibiotic susceptibility testing may be necessary, with the goal of choosing an appropriate antibiotic regimen that will result in likely successful eradication of resistant organisms^[3,4]. In this regard, there is a growing need to develop a cost effective and minimally-invasive means of obtaining the bacteria for culture and antibiotic susceptibility testing^[4,5].

The string test consists of an encapsulated string that is swallowed and then later withdrawn orally along with gastric juice that may harbor *H. pylori*. It may be a method by which *H. pylori* can be obtained with minimal invasiveness. Studies have shown string test sensitivity as high as 78 % to 97 %^[4,6]. However these results are achieved in highly specialized centers with a dedicated team and expertise in the string test technique. The same high sensitivity may not be reproduced in a standard microbiology laboratory with less experience with this procedure. Other studies used PCR on the string test to improve the sensitivity through the detection of *H. pylori*-specific DNA^[7-10]. However this method does not obtain live *H. pylori* for culture and antibiotic susceptibility testing. We therefore evaluated the utility of the string test compared with endoscopy-based methods and more specifically the sensitivity and specificity of culture from the string compared with culture from endoscopic biopsies.

MATERIALS AND METHODS

Patient selection

Adult patients, 18-80 years of age, with dyspepsia were prospectively recruited from the Endoscopy Department of the Prince of Wales Hospital, prior to oesophagogastroduodenoscopy (OGD). Patients were excluded if they had previous *H. pylori* eradication therapy, recent use of antibiotics, histamine receptor antagonists or proton pump inhibitors within the 4 weeks prior to OGD, a previous endoscopy or diagnostic test for *H. pylori*, predominant reflux symptoms, or previous gastric surgery or gastric malignancy. Signed informed consent was obtained from every patient. The study was in accordance with the declaration of Helsinki.

String test

The string test protocol was based on that described by Samuels *et al*^[6]. The patients had fasted overnight prior to presentation. A 7 mm diameter gelatin capsule, which contained a 90 cm-long nylon string with a weighted end, was used for the string test (Enterotest HP, HDC Corporation, San Jose, CA, USA). A 20 cm-long portion of the string was pulled out from the capsule, and this proximal end was tapped to the patients' cheek to prevent the whole string from being swallowed. The capsule was then swallowed with up to 200 ml of water. The capsule dissolved within the gastric lumen releasing the string to absorb the gastric mucus. After an hour the string was retrieved orally. The proximal 30 cm of the string was cut using sterile scissors

and discarded. The distal gastric acid-impregnated string was flushed with 5 ml of normal saline to reduce contamination by naso- and oropharyngeal organisms, then placed into a sterile specimen bottle containing 3 ml of brain-heart-infusion broth (BHIB) and immediately sent for processing. Gastric juice was squeezed from the string and the juice and approximately 5 microliter aliquot was plated onto each of two different *H. pylori*-selective media-Skirrows agar (containing vancomycin 10 mg/L, trimethoprim 5 mg/L, polymixin B 2 500 IU/L) and Wilkins-Chalgren agar with Dent supplement (vancomycin 10 mg/L, trimethoprim 5 mg/L, cefsulodin 5 mg/L, amphotericin B 5 mg/L). The remaining BHIB/gastric juice was centrifuged at 14 000 rpm for 5 minutes. The supernatant was discarded and the concentrated pellet was resuspended in 200 microliter of BHIB and plated onto another set of the same 2 selective media. Therefore, every patient's string sample was inoculated onto 4 culture plates. The plates were incubated in micro-aerophilic conditions, (37 °C, 10 % carbon dioxide) and 95-100 % humidity. On day 3-4, suspected *H. pylori* colonies were identified and replated onto horse-blood agar and cultured for up to 7 more days. Formal identification was made by typical colony morphology, Gram stain, and positive biochemical test results (oxidase, catalase, and urease tests). Contaminants were gram stained but not formally identified.

Patients underwent OGD and had an antral biopsy taken for rapid urease test (CLO test, Tri-Med, Va, USA), and 2 antral and 2 body biopsies for histopathology, and 2 antral biopsies for culture. The gold standard for the presence of *H. pylori* was defined by a positive CLO test and antral histopathology. Growth of *H. pylori* from antral biopsies was graded as scant, moderate or abundant growth corresponding with the *H. pylori* colonies found in 1, 2 or=3 quadrants of the culture plate respectively. Antral specimens were examined with hematoxylin-eosin stain and Giemsa stain and examined by a pathologist unaware of the patient's *H. pylori* status. *Helicobacter pylori* seen on antral histology was graded according to the Sydney system as normal (no *H. pylori*), mild (focal bacteria), moderate (bacteria in several areas), or marked (abundance of bacteria in most glands)^[11].

Statistics

The Chi square test was used for comparison of categorical data and the Fisher's exact test was used when an expected variable was below 5 %. The McNemar test was used to detect the symmetry of the differences between the string test and other tests. A *P* value of <0.05 was considered significant.

RESULTS

Thirty-three patients were approached to participate in this study. One patient refused participation and 2 patients attempted to but could not swallow the string capsule due to gagging and dry retching. The remaining 30 patients (14 males and 16 females with mean age of 52 years, age range 19-77 years) had both the string test and the OGD. There were no complications from the string test or from the OGD, apart from minor transient discomfort or gagging on swallowing the string test and during withdrawal of the string.

Twenty-one out of 30 (70 %) patients had *H. pylori* infection based on the gold standard definition of a positive CLO test and antral histopathology. The string test detected *H. pylori* in only 8 patients and was negative in 22 patients. The sensitivity, specificity, positive predictive value and negative predictive value for the string test were 38 %, 100 %, 100 % and 41 % respectively. In comparison, the endoscopic biopsy culture method yielded a positive result in 17 patients with a sensitivity, specificity, positive predictive value and negative predictive value of 81 %, 100 %, 100 % and 69 %, respectively. (*P*=0.004).

Figure 1 illustrates this difference. The McNemar test showed that the string test result was significantly different to the gold standard (*P*<0.001), endoscopic biopsy culture (*P*=0.004), CLO test (*P*<0.001) and histopathology (*P*<0.001). The comparison between the string-test and with the OGD-based tests is presented in Tables 1 and 2.

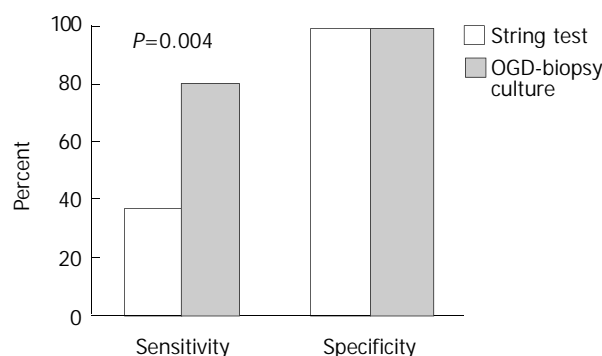


Figure 1 Comparison of the sensitivity and specificity of the culture results by the string test and from the endoscopic biopsies.

Table 1 Results of the 4 tests in detecting *Helicobacter pylori*

<i>Helicobacter pylori</i> status	CLO test	Histology	Antral biopsy culture	String test culture	Number of patients (n=30)
+	+	+	+	+	8*
+	+	+	+	-	9
+	+	+	-	-	4
-	-	+	-	-	1
-	-	-	-	-	8

+ denotes positive test; - denotes negative test. * one patient with a positive CLO test but the antral histopathology was not performed. He was counted as a positive case for this study.

Table 2 The sensitivity, specificity, positive predictive value, negative predictive value and the accuracy of the string test compared to endoscopy-based tests

	Sensitivity %	Specificity %	PPV %	NPV %	Accuracy %
CLO test	100	100	100	100	100
Antral histology	100	95	89	100	97
Antral biopsy culture	81	100	100	69	77
String test culture	38	100	100	41	57

The string test was more likely to be positive when there was also abundant growth of *H. pylori* from endoscopic biopsies, and less likely to be positive for moderate, scant or no growth (string test positive in 80 % and 16 % respectively, *P*=0.011, Table 3). However, the string test result was not statistically associated with the density of *H. pylori* organisms on antral histopathology (string test positive in 50 % of cases of marked density and 18 % of moderate or lower density, *P*=0.158, Table 4). Logistic regression showed that abundant growth from endoscopic biopsy cultures to be the only significant predictor of a positive string test (OR: 23.1, 95% CI: 1.71-310, *P*=0.018).

Overall on OGD, 18 (60 %) patients had endoscopic findings (5 patients with peptic ulcer disease and 13 patients with gastroduodenitis). The string test was positive in 4 out of 5 (80 %) patients with peptic ulcers, 3/13 (23 %) of patients with gastroduodenitis, and 1/12 (8 %) of patients with no pathology (*P*=0.009).

The concentrated Skirrow medium provided the best result

for the string test and grew *H. pylori* in all 8 patients who had a positive string test result. In contrast the Wilkins-Chalgren medium was positive in only 2 of these patients. Contamination of the plates with naso- and oropharyngeal organisms was the main reason for the low string test sensitivity, and occurred in 37/60 Wilkins-Chalgren plates, and 18/60 of the Skirrow plates. The contaminants were predominantly gram positive cocci and gram negative rods. A few plates had fungal contaminants. The plates with the concentrated BHIB were more likely to grow *H. pylori*, but also tended to have more contaminants. We attempted to reduce the load of oropharyngeal commensals by having the patients gargle their throats with water just prior to string extraction. However this did not improve the overall sensitivity of detecting *H. pylori* (data not presented). Contamination of the batch BHIB was excluded by the use of a fresh BHIB sample as a negative control. There was no growth of contaminants from this negative control. Also no contamination was reported from the antral biopsy cultures, which were also transported in BHIB.

Table 3 The results of the string test according to the growth rate of cultures from endoscopic biopsies

	Cultures of endoscopic biopsies and growth rate of <i>Helicobacter pylori</i>			
	Abundant	Moderate	Scant	No growth
String test negative (n=22)	1	2	6	13
String test positive (n=8)	4	1	3	0
Total	5	3	8	14

Table 4 The results of the string test according to the density of *Helicobacter pylori* on antral histology

	Antral histology and density of <i>Helicobacter pylori</i>			
	Marked	Moderate	Mild	None present
String test negative (n=22)	4	8	2	8
String test positive (n=8)	4	2	2	0
Total	8	10	4	8

DISCUSSION

The string test demonstrated only 38 % sensitivity in detecting *H. pylori* at our center contrasting previous results^[4,6]. In contrast, direct endoscopic mucosal biopsy cultures yielded a significantly higher sensitivity of 81 %. This low sensitivity of the string test could be attributable to either overgrowth of contaminants, or failure to collect sufficient *H. pylori* onto the string, or death of the organisms during handling.

To prevent oropharyngeal and nasopharyngeal organisms from overgrowing the culture plates require the use of *H. pylori*-selective media. We only used 2 types of *H. pylori* selective media (total of 4 plates per patient) whereas 3 types were used in Samuel's study^[6]. Samuel's study showed that there was no clear superiority of any one selective medium over another and that different strains of *H. pylori* may unpredictably preferentially grow in a certain medium and not the others. Therefore the use of all 3 media may improve the pick up rate^[6]. However, other experts have advocated on the use of only 2 types of selective plates for identifying *H. pylori*^[12].

Helicobacter pylori may have been successfully collected on the string but plate contaminants or improper handling may have resulted in the negative culture. PCR can be performed to detect *H. pylori*-specific DNA sequences and this may

increase the positive results. Previous studies have shown the high sensitivity of PCR-based string test^[7-10]. In one study the string test sensitivity increased from 37 % with culture to 93 % when PCR was utilized^[8]. However PCR testing is not a practical alternative in many centers and this will add to the overall cost of diagnosis. Also the main purpose of *H. pylori* culture in adults is to determine antibiotic susceptibility and this information is not determined by PCR.

The string test reported by Samuels *et al* with very high sensitivity rate of 97 % requires intensive laboratory methods, is labor-intensive, and requires the use of many culture plates. A vacuum hood was used when plating the selective media and this might reduce airborne contamination. String tests were processed immediately without refrigeration and this may improve the viability of the *H. pylori*. Six plates, instead of 4, were used and this may have also improved the yield of culture^[6]. Therefore, while the string test is an alternative method to an OGD for obtaining samples of *H. pylori*, the low sensitivity coupled with the demanding methodology may mean that it is not a realistic or possible option in many laboratories at present. Modifications of the methodology are required.

In conclusion, the string test is a minimally-invasive test to obtain *H. pylori*. As with other *H. pylori* culture techniques it has 100 % specificity but in contrast to previous studies, a low sensitivity was demonstrated. Despite the use of *H. pylori*-selective media, overgrowth of commensal organisms remains the major obstacle with this technique.

REFERENCES

- 1 **Vaira D**, Holton J, Menegatti M, Ricci C, Gatta L, Geminiani A, Miglioli M. Invasive and non-invasive tests for *Helicobacter pylori* infection. *Aliment Pharmacol Ther* 2000; **14** (Suppl 3): 13-22
- 2 **Gisbert JP**, Pajares JM. *Helicobacter pylori* therapy: first-line options and rescue regimen. *Dig Dis* 2001; **19**: 134-143
- 3 **Guslandi M**. Alternative antibacterial agents for *Helicobacter pylori* eradication. *Aliment Pharmacol Ther* 2001; **15**: 1543-1547
- 4 **Perez-Trallero E**, Montes M, Alcorta M, Zubillaga P, Telleria E. Non-endoscopic method to obtain *Helicobacter pylori* for culture. *Lancet* 1995; **345**: 622-623
- 5 **Perez-Trallero E**, Montes M, Larranaga M, Arenas JJ. How long for the routine *Helicobacter pylori* antimicrobial susceptibility testing? The usefulness of the string test to obtain *Helicobacter* for culture. *Am J Gastroenterol* 1999; **94**: 3075-3076
- 6 **Samuels AL**, Windsor HM, Ho GY, Goodwin LD, Marshall BJ. Culture of *Helicobacter pylori* from a gastric string may be an alternative to endoscopic biopsy. *J Clin Microbiol* 2000; **38**: 2438-2439
- 7 **Ferguson DA Jr**, Jiang C, Chi DS, Laffan JJ, Li C, Thomas E. Evaluation of two string tests for obtaining gastric juice for culture, nested-PCR detection, and combined single- and double-stranded conformational polymorphism discrimination of *Helicobacter pylori*. *Dig Dis Sci* 1999; **44**: 2056-2062
- 8 **Parejo R**, Garcia-Arata I, de Rafael L, Canton R, Olivares F, Boixeda D, Lorente Minarro M, Camarero H, Escobar y C. Usefulness of the enterotest method for the diagnosis of *Helicobacter pylori* infection in children. *Gut* 1998; **43** (Suppl 2): A74
- 9 **Roth DE**, Velapatino B, Gilman RH, Su WW, Berg DE, Cabrera L, Garcia E. A comparison of a string test-PCR assay and a stool antigen immunoassay (HpSA) for *Helicobacter pylori* screening in Peru. *Trans R Soc Trop Med Hyg* 2001; **95**: 398-399
- 10 **Dominguez-Bello MG**, Cienfuentes C, Romero R, Garcia P, Gomez I, Mago V, Reyes N, Gueneau de Novoa P. PCR detection of *Helicobacter pylori* in string-absorbed gastric juice. *FEMS Microbiol Lett* 2001; **198**: 15-16
- 11 **Dixon MF**, Genta RM, Yardley JM, Correa P. Classification and grading of gastritis. The updated Sydney system. *Am J Surg Pathol* 1996; **20**: 1161-1181
- 12 **Perez-Trallero E**, Montes M. String test for *Helicobacter pylori*. *J Clin Microbiol* 2000; **38**: 4303

Angiogenesis effect on rat liver after administration of expression vector encoding vascular endothelial growth factor D

Bao-Min Shi, Xiu-Yan Wang, Qing-Ling Mu, Tai-Huang Wu, Hong-Jun Liu, Zhen Yang

Bao-Min Shi, Qing-Ling Mu, Tai-Huang Wu, Hong-Jun Liu, Department of General Surgery, Shandong Provincial Hospital, Clinical College of Shandong University, Jinan 250021, Shandong Province, China

Xiu-Yan Wang, Department of Ultrasonography, Shandong Provincial Hospital, Clinical College of Shandong University, Jinan 250021, Shandong Province, China

Zhen Yang, Department of General Surgery, Tongji Hospital, Huazhong University of Science and Technology, Wuhan 430030, Hubei Province, China

Supported by the National Science Fund for Postdoctoral Fellows in China, No 2001.6; the Medical Science Found of Shandong Province, No. 2001CA1DBA10

Correspondence to: Dr. Bao-Min Shi, Department of General Surgery, Shandong Provincial Hospital, Clinical College of Shandong University, 324 Jingwu Road, Jinan 250021, Shandong Province, China. baomins@163.net

Telephone: +86-531-7938911-2363 **Fax:** +86-531-7937741

Received: 2002-07-12 **Accepted:** 2002-08-23

Abstract

AIM: To verify the expressing efficiency and angiogenesis effect after administration of expression vector encoding for vascular endothelial growth factor D in normal and ischemic rat liver.

METHODS: Ten female S-D rats were administrated with liver tissue dot injection of naked PCHO/hVEGF-D, 50 µg/dot, three dots for each. The same amount of physiological saline was used as control in the neighboring lobe. Fourteen S-D rats, using inflow occlusion of left lateral lobe, were divided into two groups, seven rats in each group. One was ischemic plasmid group, which received naked plasmid PCHO/hVEGF-D injection of 150 µg. The other received the equal amount of natural saline injection and designed as control. The expressions of hVEGF-D in mRNA and protein levels were identified by *in situ* hybridization and immunohistochemistry, respectively. Endothelial cells were labeled by the factor VIII immunohistochemically. The average number of perisinusoidal capillaries of each group was calculated and compared statistically 8 days after injection.

RESULTS: A large amount of hVEGF-D in mRNA level was found in both normal and ischemic plasmid groups and but none in their corresponding control groups. The protein of hVEGF was also highly expressed in both normal and ischemic plasmid groups than in the controls. The mean number of capillaries under microscopy (×200) of the plasmid group and control was 10.2 ± 2.78 vs 7.1 ± 2.02 ($P < 0.05$), and those of ischemic plasmid group and ischemic control were 7.43 ± 1.72 vs 4.71 ± 1.11 with statistical difference ($P < 0.05$).

CONCLUSION: The naked PCHO/hVEGF-D dot injection to normal, ischemic rat liver can produce comparatively high expression of hVEGF in both protein and mRNA levels, and prominently increase the number of new capillaries around hepatic sinuses. Therefore, it could be another ideal choice for the treatment of ischemic liver diseases.

Shi BM, Wang XY, Mu QL, Wu TH, Liu HJ, Yang Z. Angiogenesis effect on rat liver after administration of expression vector encoding vascular endothelial growth factor D. *World J Gastroenterol* 2003; 9(2): 312-315

<http://www.wjgnet.com/1007-9327/9/312.htm>

INTRODUCTION

Nowadays, the liver has become the most important target organ for gene therapy because of its unique structure and complex functions. Owing to its particular situation with respect to the blood circulation, the liver can serve as a secretory organ for the systemic delivery of therapeutic proteins. The liver parenchyma is readily accessible to large molecules such as DNA fragments or recombinant viruses present in the blood on account of its peculiar endothelium. Great progress has been achieved in various gene transfer protocols aimed at delivering genes to the normal or the pathologic liver in the last decade^[1,2].

Angiogenesis is a process of new blood vessel development from pre-existing vasculature. It plays an essential role in embryonic development, normal growth of tissues, wound healing, the female reproductive cycle, as well as a major role in many diseases. One of the most important growth and survival factors for endothelium is vascular endothelial growth factor (VEGF). VEGF induces angiogenesis and endothelial cell proliferation and it plays an important role in regulating vasculogenesis^[3-5]. Many previous studies also proved the antiangiogenic effect of VEGF antisense gene therapy for hepatic carcinoma and the killing effect of suppression of VEGF on gastric cancer cells^[6,7].

Most of the liver conditions were proved to be involved in the morphological and pathological changes of intra-hepatic vessels^[8-11]. Previous studies demonstrated that, when liver under the state of chronic inflammations, chronic necrosis and fibrosis, the density of microvessels were presumed to reduce probably due to the decreased expression of angiogenesis-related growth factors such as VEGF, insulin-like growth factor, and over expression of transforming growth factor beta, platelet-derived growth factor^[12-15]. The expression vector for VEGF has been used to treat various ischemic diseases both experimentally and clinically for nearly ten years^[16-20].

In order to verify the expression efficiency and angiogenesis effect after administration of expression vector for VEGF-D, we carried out experimental studies on normal and ischemic rat livers.

MATERIALS AND METHODS

Large scale preparations of plasmid

Eukaryotic expression plasmid PCHO/hVEGF-D was kindly presented by Prof. Miyuki Shimane (Chugai Institute, Japan). After transformation to E Coli DH5alpha, large scale plasmid was prepared, purified into TE at the concentration of 1 g/L, according to the instruction of Megaprep kit (Promega Co Ltd., German).

A 2.0 kb fragment was cut from PCHO/hVEGF-D by restriction enzymes, *EcoR I* and *BamH I*, as the probe for this hVEGF-D. The probe was labeled using randomly primed labeling method (Shanghai Sangon Co.Ltd, China).

Animal operations and groups

Studies on normal rat livers 10 healthy female Sprague-Dawley rats, weighing 200-220 g, were bought from the Experimental Animal Center of Tongji Medical University. After anaesthetized by pentobarbital ($40 \text{ mg} \cdot \text{kg}^{-1}$ intraperitoneally), all the rats were laparotomized and given liver tissue dot injection of naked PCHO/hVEGF-D, $50 \mu\text{g}/\text{dot}$, three dots for each. The same amount of NS (natural saline) was used as self-control in the neighboring lobe.

Study on ischemic rat liver Fourteen S-D rats, using inflow occlusion of left lateral lobe, were divided equally into two groups. One is study group, each received naked plasmid PCHO/hVEGF-D injection in the amount of $150 \mu\text{g}$ by dot injection as above. The other group received the equal amount of natural saline injection for each and designed as control.

All the rats were sacrificed 8 days after the operation and liver samples with injection were collected and fixed in 10 % neutral-buffered formalin, embedded in paraffin and cut into $4\text{--}6 \mu\text{m}$ sections.

Immunohistochemical method

The sections were deparaffinized, rehydrated, and treated with anti-VEGF antibody (Santa Cruz, Britain) and Factor VIII related antibody (Zymed, USA), their proteins were identified according to the instructions of SABC kit (Zhongshan Bio. Co. Beijing, China).

Positive rate was evaluated by Integral Score method from three aspects: positive cell distribution, intensity and pattern, as reported before^[21]. The positive integral scores of VEGF protein were compared between plasmid group and controls, ischemic group and ischemic controls.

Microvessel density was compared between groups. First choose three most abundant areas under microscopy $\times 100$, count effective vessels under microscopy $\times 200$ and calculated the average number in each group and compare their difference.

In situ hybridization

The investigation procedure was referred to related references^[22]. The *in situ* hybridization kit was purchased from Boshide Biological Technology Limited Company (Wuhan, China.). *In situ* hybridization was performed according to the manufacturer's instructions.

Statistical analysis

Student's *t* test was used for comparison of results among different groups. Values were expressed as means \pm SD. A *P* value of less than 0.05 was considered statistically significant.

RESULTS

Results in normal rat liver

A large amount of hVEGF-D mRNA was identified in plasmid group but none in control group. The hVEGF-D mRNA was located in the cytoplasm of hepatocytes, vascular endothelium, and some Kupffer cells. In the areas around vessels, there were relative more positive cells.

The protein of hVEGF was expressed in cytoplasm mainly in hepatocytes and some endothelial cells in both plasmid and control groups. The stain integral scores of plasmid group and control were 6.0 ± 1.63 and 3.7 ± 2.31 respectively. The difference between the two groups was significant (Student *t* test, $T=2.74 > 2.62$, $P < 0.05$) (Figure 1).

The mean numbers of capillaries under microscopy ($\times 200$) of the plasmid group and control were 10.2 ± 2.78 and 7.1 ± 2.02 , respectively, with very significant difference (paired Student *t* test, $T=3.59 > 3.25$, $P < 0.01$) (Figure 2).

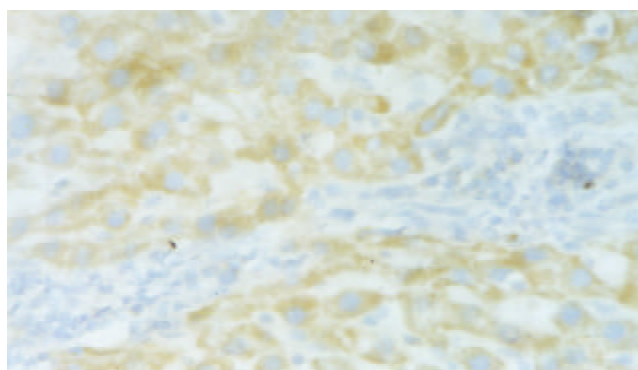


Figure 1 In situ hybridization in normal rat liver with PCHO/hVEGF-D injection, positive stained hepatocyte (hVEGF-D mRNA), $\times 200$.

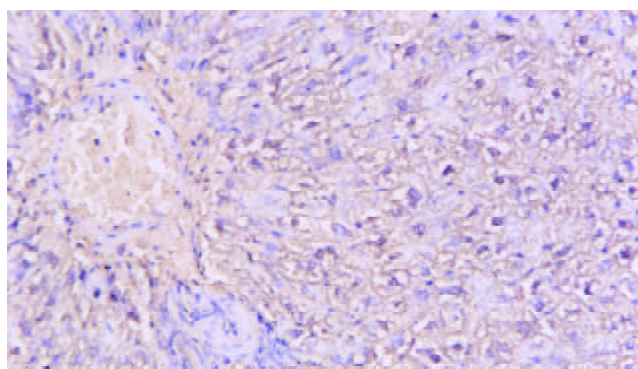


Figure 2 In situ hybridization, ischemic rat liver with injection of PCHO/hVEGF-D. Microscopy, positive stained hepatocytes (hVEGF-D mRNA), $\times 200$.

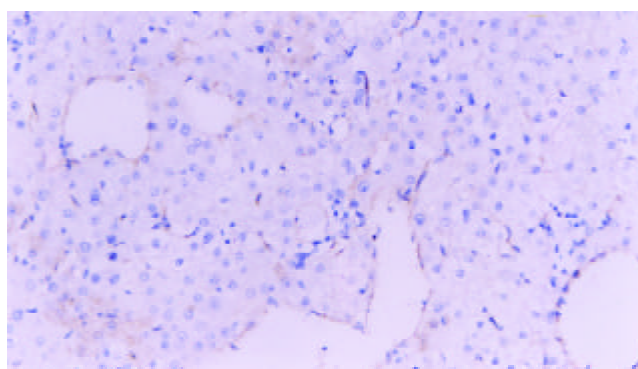


Figure 3 Immunohistochemistry. Normal rat liver vascular endothelial cells labeled by Factor VIII, $\times 200$.

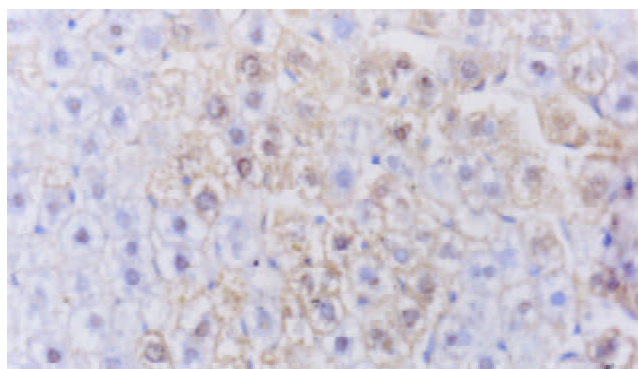


Figure 4 Immunohistochemistry. Normal rat liver injected by PCHO/hVEGF-D, VEGF protein stained positive hepatocytes, $\times 400$.

Results in ischemic rat livers

The mRNA of hVEGF-D was found in the study group, but none in the control. The positive cells and location were similar to the normal rat liver studies.

The average expression score of VEGF protein in plasmid group was higher than that of control ones (5.84 ± 1.72 vs 3.69 ± 1.53 , $P < 0.05$), (Figure 3). The average number of vessels under microscope ($\times 200$) was 7.43 ± 1.72 in plasmid group and 4.71 ± 1.11 in control group with statistical difference ($P < 0.05$).

DISCUSSION

VEGF-D (also known as c-fos-induced growth factor or FIGF) was first cloned by Yamada in 1997 from human lung cDNA library^[23]. It is 2 028bp long and encodes for 354 amino acid most closely related to VEGF-C^[23]. It shares structural homology and receptor specificity with VEGF-C, suggesting that VEGF-C and VEGF-D represent a subfamily of the VEGFs. VEGF-D is initially synthesized as a precursor protein containing unique N- and C-terminal propeptides in addition to a central receptor-binding VEGF homology domain (VHD). Similar to VEGF-C, VEGF-D binds, the cell surface receptor tyrosine kinases VEGF receptor 2 (VEGF R2/Flk-1/KDR) and VEGF R3 (Flt-4). VEGF R2 and VEGF R3 were localized in vascular and lymphatic endothelial cells and signal for angiogenesis and lymphangiogenesis^[24]. The gene for VEGF-D maps existed in the chromosome XP22.31 in human^[23].

Numerous techniques and approaches have been investigated for gene transfer to the liver. For the gene therapy of hepatic diseases in animal experiments, exogenous genes were usually delivered to the liver through the portal vein, bile duct injection and by direct liver injection^[25-30]. The most simple is direct DNA injection. More than 20 years ago, studies pioneered the use of DNA, either naked and complexed with calcium phosphate, for gene transfer to various organs including the liver^[31]. Dr. M Anner Hickman presented studies on the direct injection of plasmid DNA, which resulted in significant gene expression in the liver. The cats injected with a plasmid for a reporter gene were noted to exhibit peak expression of the gene 24-48 hours after intrahepatic injection. Residual reporter gene expression could be noted up to 6 weeks later^[32]. In our studies, 8 days after gene PCHO/hVEGF-D injection, VEGF proteins were markedly expressed in liver tissues.

The PCHO/hVEGF-D was specifically designed for mammal expression. It not only cloned the full length of VEGF-D cDNA, but also inserted a special promoter E α lpha. Therefore, it could have a relatively high expression efficiency. In our first part of studies, we tried to ascertain its expression efficiency *in vivo* with naked gene transfer. The result was the same as we anticipated, and the microvessel density of the injected tissue was promoted as an effect of VEGF protein.

Early in 1999, Marconcini L reported that Figf/Vegf-D was a potent angiogenic factor in rabbit cornea *in vivo* in a dose-dependent manner. *In vitro* Figf/Vegf-D induced tyrosine phosphorylation of VEGFR-2 and VEGFR-3 in primary human umbilical cord vein endothelial cells (HUVECs) and in an immortal cell line derived from Kaposi's sarcoma lesion (KS-IMM). The treatment of HUVECs with Figf/Vegf-D induced dose-dependent cell growth^[33]. Recently Byzova TV demonstrated *in vitro* that VEGF-D Delta N Delta C encoded by the adenovirus (Ad-VEGF-D Delta N Delta C) was capable of inducing endothelial cell proliferation and migration and that the latter response was primarily mediated by VEGF receptor-2. The proangiogenic effect of Ad-VEGF-D Delta N Delta C was evident as early as 5 days after injection into the rat cremaster muscle^[17].

From our studies in ischemic livers, naked plasmid PCHO/hVEGF-D direct injection could also produce a comparatively

high expression of hVEGF in both protein and mRNA levels, and prominently increased the number of new capillaries around hepatic sinuses.

In fact, absolute and relative ischemia of hepatic cells are very common in various situations such as chronic hepatitis, liver fibrosis or cirrhosis and portal thrombosis. Lots of previous studies on liver cirrhosis had already proved that the expression of VEGF was reduced and closely related to the state of liver function or portal hypertension degree^[9,10,12-15,34,35]. Assy N studied the serum VEGF levels between cirrhotic patients and normal controls. The results showed that the mean serum VEGF levels in all cirrhotic patients were significantly lower than those of healthy controls and acute hepatitis. These studies give much support for the angiogenesis treatment in chronic liver diseases^[12]. Therapeutic angiogenesis has already widely used to treat many ischemic diseases^[16,18-20]. By stimulating angiogenesis in liver by gene transfer method, hepatocytes would have more nutrition and oxygen and thus could preserve the liver function to some extent. Therefore, angiogenesis through gene transfer, by naked plasmid DNA PCHO/hVEGF-D injection, is a ideal method for the treatment of ischemic liver diseases especially for liver fibrosis and cirrhosis.

REFERENCES

- 1 **Ferry N**, Heard JM. Liver-directed gene transfer vectors. *Human Gene Therapy* 1998; **9**: 1975-1981
- 2 **Worman HJ**, Lin F, Mamiya N, Mustacchia PJ. Molecular biology and the diagnosis and treatment of liver diseases. *World J Gastroenterol* 1998; **4**: 185-191
- 3 **Ma XM**, Wang YL, Pan BR. The development of researches on VEGF. *Shijie Huaren Zazhi* 1999; **7**: 695-696
- 4 **Neufeld G**, Cohen T, Gengrinovitch S, Poltorak Z. Vascular endothelial growth factor (VEGF) and its receptors. *FASEB J* 1999; **13**: 9-22
- 5 **Clauss M**. Molecular biology of the VEGF and the VEGF receptor family. *Semin Thromb Hemost* 2000; **26**: 561-569
- 6 **Tang YC**, Li Y, Qian GX. Reduction of tumorigenicity of SMMC-7721 hepatoma cells by vascular endothelial growth factor antisense gene therapy. *World J Gastroenterol* 2001; **7**: 22-27
- 7 **Pan X**, Ke CW, Pan W, He X, Cao GW, Qi ZT. Killing effect on gastric cancer cells by DT/VEGF system. *Shijie Huaren Xiaohua Zazhi* 2000; **8**: 393-396
- 8 **Nakata M**, Nakamura K, Koda Y, Kaminou T, Ugami M, Kaneda K, Yamada R. Hemodynamics in the microvasculature of thioacetamide-induced cirrhotic rat livers. *Hepatogastroenterology* 2002; **49**: 652-656
- 9 **Yan JC**, Liu JH, Ma Y. Vascular obstruction in pathogenesis of hepatitis B fibrosis. *Xinxiaohuabingxue Zazhi* 1997; **5**: 647-649
- 10 **Assy N**, Paizi M, Gaitini D, Baruch Y, Spira G. Clinical implication of VEGF serum levels in cirrhotic patients with or without portal hypertension. *World J Gastroenterol* 1999; **5**: 296-300
- 11 **El-Assal ON**, Yamanoi A, Soda Y, Yamaguchi M, Igarashi M, Yamamoto A, Nabika T, Nagasue N. Clinical significance of microvessel density and vascular endothelial growth factor expression in hepatocellular carcinoma and surrounding liver: possible involvement of vascular endothelial growth factor in the angiogenesis of cirrhotic liver. *Hepatology* 1998; **27**: 1554-1562
- 12 **Akiyoshi F**, Sata M, Suzuki H, Uchimura Y, Mitsuyama K, Matsuo K, Tanikawa K. Serum vascular endothelial growth factor levels in various liver diseases. *Dig Dis Sci* 1998; **43**: 41-45
- 13 **Chen WB**, Yan JC, Ma Y, Shen YP. The relations between serum VEGF level and hepatic sinus lesions in patients with chronic hepatitis. *Shijie Huaren Xiaohua Zazhi* 2000; **8**: 1426-1427
- 14 **Wu W**, Zhang S, Wu YL, Ye J, Xi XP. Relationship between insulin-like growth factor I and liver function and number connection test. *Shijie Huaren Xiaohua Zazhi* 2001; **9**: 1391-1394
- 15 **Yan JC**, Chen WB, Ma Y, Shun XH. Expression of vascular endothelial growth factor in liver tissues of hepatitis B. *Shijie Huaren Xiaohua Zazhi* 1999; **7**: 837-840
- 16 **Vale PR**, Isner JM, Rosenfield K. Therapeutic angiogenesis in critical limb and myocardial ischemia. *J Interv Cardiol* 2001; **14**: 511-528

- 17 **Byzova TV**, Goldman CK, Jankau J, Chen J, Cabrera G, Achen MG, Stacker SA, Carnevale KA, Siemionow M, Deitcher SR, Dicorleto PE. Adenovirus encoding vascular endothelial growth factor-D induces tissue-specific vascular patterns *in vivo*. *Blood* 2002; **99**: 4434-4442
- 18 **Lee LY**, Patel SR, Hackett NR, Mack CA, Polce DR, El-Sawy T, Hachamovitch R, Zanzonico P, Sanborn TA, Parikh M, Isom OW, Crystal RG, Rosengart TK. Focal angiogen therapy using intramyocardial delivery of an adenovirus vector coding for vascular endothelial growth factor 121. *Ann Thorac Surg* 2000; **69**: 14-23
- 19 **Leotta E**, Patejunas G, Murphy G, Szokol J, McGregor L, Carbray J, Hamawy A, Winchester D, Hackett N, Crystal R, Rosengart T. Gene therapy with adenovirus-mediated myocardial transfer of vascular endothelial growth factor 121 improves cardiac performance in a pacing model of congestive heart failure. *J Thorac Cardiovasc Surg* 2002; **123**: 1101-1113
- 20 **Deodato B**, Arsic N, Zentilin L, Galeano M, Santoro D, Torre V, Altavilla D, Valdembrì D, Bussolino F, Squadrito F, Giacca M. Recombinant AAV vector encoding human VEGF165 enhances wound healing. *Gene Ther* 2002; **9**: 777-785
- 21 **Shiota G**, Okubo M, Noumi T, Noguchi N, Oyama K, Takano Y, Yashima K, Kishimoto Y, Kawasaki H. Cyclooxygenase-2 expression in hepatocellular carcinoma. *Hepato-Gastroenterology* 1999; **46**: 407-412
- 22 **Zhao GQ**, Xue L, Xu HY, Tang XM, Hu RD, Dong J. In situ hybridization assay of androgen receptor gene in hepatocarcinogenesis. *World J Gastroenterol* 1998; **4**: 503-505
- 23 **Yamada Y**, Nezu J, Shimane M, Hirata Y. Molecular cloning of a novel vascular endothelial growth factor, VEGF-D. *Genomics* 1997; **42**: 483-488
- 24 **Achen MG**, Jeltsch M, Kukk E, Makinen T, Vitali A, Wilks AF, Alitalo K, Stacker SA. Vascular endothelial growth factor D (VEGF-D) is a ligand for the tyrosine kinases VEGF receptor 2 (Flk1) and VEGF receptor 3 (Flt4). *Proc Natl Acad Sci USA* 1998; **95**: 548-553
- 25 **Dai WJ**, Jiang HC. Advances in gene therapy of liver cirrhosis: a review. *World J Gastroenterol* 2001; **7**: 1-8
- 26 **Shiratori Y**, Kanai F, Ohashi M, Omata M. Strategy of liver-directed gene therapy: present status and future prospects. *Liver* 1999; **19**: 265-274
- 27 **Yang CQ**, Wang JY, He BM, Liu JJ, Guo JS. Glyco-poly-L-lysine is better than liposomal delivery of exogenous genes to rat of liver. *World J Gastroenterol* 2000; **6**: 526-531
- 28 **Dubensky TW**, Campbell BA, Villarreal LP. Direct transfection of viral and plasmid DNA into the liver or spleen of mice. *Proc Natl Acad Sci USA* 1984; **81**: 7529-7533
- 29 **Malone RW**, Hickman MA, Lehmann-Bruinsma K, Sih TR, Walzem R, Carlson DM, Powell JS. Dexamethasone enhancement of gene expression after direct hepatic DNA injection. *J Biol Chem* 1994; **269**: 29903-29907
- 30 **Marconcini L**, Marchio S, Morbidelli L, Cartocci E, Albini A, Ziche M, Bussolino F, Oliviero S. c-fos-induced growth factor/vascular endothelial growth factor D induces angiogenesis *in vivo* and *in vitro*. *Proc Natl Acad Sci USA* 1999; **96**: 9671-9676
- 31 **De Godoy JL**, Malafosse R, Fabre M, Mehtali M, Houssin D, Soubrane O. *In vivo* hepatocyte retrovirus-mediated gene transfer through the rat biliary tract. *Human Gene Therapy* 1999; **10**: 249-257
- 32 **Yang CQ**, Wang JY, Fang JT, Liu JJ, Guo JS. A comparison between intravenous and peritoneal route on liver targeted uptake and expression of plasmid delivered by Glyco-poly-L-lysine. *World J Gastroenterol* 2000; **6**: 508-512
- 33 **Wang FS**, Wu ZZ. The development of gene therapy on liver fibrosis and cirrhosis. *Shijie Huaren Xiaohua Zazhi* 2000; **8**: 371-373
- 34 **Yan JC**, Chen WB, Ma Y, Xu CJ. Immunohistochemical study on hepatic vascular forming factors in liver fibrosis induced by CCl4 in rats. *Shijie Huaren Xiaohua Zazhi* 2000; **8**: 1238-1241
- 35 **Shi BM**, Wang X, Yang Z. Vascular endothelial growth factor and liver diseases. *Hepatogastroenterology* 2001; **48**: 1145-1148

Edited by Ma JY

Inhibition on the production of collagen type I, III of activated hepatic stellate cells by antisense TIMP-1 recombinant plasmid

Wen-Bin Liu, Chang-Qing Yang, Wei Jiang, Yi-Qing Wang, Jing-Sheng Guo, Bo-Ming He, Ji-Yao Wang

Wen-Bin Liu, Chang-Qing Yang, Wei Jiang, Yi-Qing Wang, Jing-Sheng Guo, Bo-Ming He, Ji-Yao Wang, Division of Gastroenterology, Zhongshan Hospital, Fudan University, Shanghai 200032, China

Supported by the National Natural Scientific Foundation of China, No. 39970339

Correspondence to: Professor Ji-Yao Wang, Division of Gastroenterology, Zhongshan Hospital, Fudan University, Shanghai 200032, China. jiyao_wang@hotmail.com

Telephone: +86-21-64041990 Ext 2420 Fax: +86-21-34160980

Received: 2002-09-14 Accepted: 2002-10-18

Abstract

AIM: To investigate the inhibition effects on the production of collagen type I, III secreted by activated rat hepatic stellate cells (rHSCs) by antisense tissue inhibitors of metalloproteinase 1 (TIMP-1) recombinant plasmid through elevating interstitial collagenase activity.

METHODS: rHSCs were extracted from normal rat liver by pronase and collagenase digestion and purified by centrifugal elutriation, and were cultured on plastic dishes until they were activated to a myofibroblastic phenotype after 7-10 days. RT-Nest-PCR and gene recombinant techniques were used to construct the rat antisense TIMP-1 recombinant plasmids which can express in eucaryotic cells. The recombinant plasmid and the pcDNA3 empty plasmid were transfected in rHSCs by Effectene (QIAGEN) separately. Cells were selected after growing in DMEM containing 400 µg/ml G418 for 2-3 weeks. Expression of exogenous gene was assessed by Northern blot, and expression of TIMP-1 in rHSCs was determined by Northern blot and Western blot. We tested the interstitial collagenase activity with FITC-labeled type I collagen as substrate. Ultimately, we quantified the type I, III collagen by Western blot.

RESULTS: The exogenous antisense TIMP-1 recombinant plasmid could be expressed in rHSCs well, which could block the expression of TIMP-1 greatly, the ratio of TIMP-1/GAPDH was 0.67, 2.41, and 2.97 separately at mRNA level ($P<0.05$); the ratio of TIMP-1/ β -actin was 0.31, 0.98 and 1.32 separately at protein level ($P<0.05$); It might elevate active and latent interstitial collagenase activity, the collagenase activity was 0.3049, 0.1411 and 0.1196 respectively. ($P<0.05$), which led to promotion the degradation of type I, III collagen, the ratio of collagen I/ β -actin was 0.63, 1.78 and 1.92 separately ($P<0.05$); and the ratio of collagen III/ β -actin was 0.59, 1.81 and 1.98 separately ($P<0.05$).

CONCLUSION: These data shows that the antisense TIMP-1 recombinant plasmid has the inhibitory effects on the production of type I, III collagens secreted by activated rHSCs in vitro. It could be a novel method to reverse hepatic fibrosis in the future.

Liu WB, Yang CQ, Jiang W, Wang YQ, Guo JS, He BM, Wang JY. Inhibition on the production of collagen type I, III of activated hepatic stellate cells by antisense TIMP-1 recombinant plasmid. *World J Gastroenterol* 2003; 9(2): 316-319

<http://www.wjgnet.com/1007-9327/9/316.htm>

INTRODUCTION

The incidence of liver fibrosis and cirrhosis is still high in China^[1-4], and fibrosis is the common pathological basis of chronic hepatic disease^[5]. Many factors inducing liver injury and inflammation may lead to hepatic fibrosis^[6,7]. At present, the common sense is that hepatic fibrosis could be reversed effectively when the right therapeutic strategy was applied^[8].

Recently, studies on the role of tissue inhibitors of metalloproteinases (TIMPs) in the process of hepatic fibrosis have attracted more attentions^[9-14]. Roeb *et al*^[15] reported that there were no expression of TIMP-3, 4 mRNA in normal and fibrotic liver tissues; the expression of TIMP-1, 2 mRNA could be detected in normal liver tissue at lower level^[15,16]. The expression of TIMP-1 increased greatly in liver tissues of experimental rat hepatic fibrosis models induced by CCl₄ or bile compared to TIMP-2^[15].

Hepatic stellate cells (HSCs) represent up to 15 % of the resident cells of the liver and play a pivotal role in hepatic fibrosis^[17]. In response to liver injury of any etiology, the normally quiescent HSC undergoes a progressive process of trans-differentiation into a proliferating myofibroblast-like activated HSC^[17]. Through increased secretion of extracellular matrix proteins and the tissue inhibitor of metalloproteinases (TIMP)-1, activated HSCs are responsible for deposition and accumulation of the majority of the excess extracellular matrix in the fibrotic liver^[18]. Furthermore, activated HSCs can contribute to the fibrogenic process through their ability to secrete and respond to a wide range of cytokines and growth factors^[19].

It had been considered that the antisense technique was used to inhibit the target genes and proteins expressed in experimental rat hepatic fibrosis. The main aim of our study is to try to block the gene and protein expression of TIMP-1 in rHSCs *in vitro* and investigate the effects of antisense-TIMP-1 recombinant plasmid on the production of collagen type I, III of activated rHSCs, so as to find out the possible mechanism of reversing hepatic fibrosis.

MATERIALS AND METHODS

Isolation and culture of rat hepatic stellate cells

rHSCs were isolated from normal male Sprague-Dawley rats (300±30 g) by sequential perfusion with Pronase and collagenase as previously described^[20]. rHSCs were separated and purified from the cell suspension by single-step density gradient centrifugation with gradient buffer (Ficoll and glycan 1.053, Pharmacia). The purity of cell was assessed by light microscopic appearance and vitamin A autofluorescence at 295nm. rHSCs were activated at day 7 after seeding on the plastic surface and became myofibroblast (MFB) phenotype.

The cells were cultured in Dulbecco's modified Eagle medium (DMEM, GIBCO U.S.A) containing 4 mM L-glutamine and 10 % fetal calf serum (GIBCO U.S.A). Additionally, all culture media were supplemented with penicillin (100 IU/ml) and streptomycin (100 µg/ml) respectively. They were maintained at 37 °C in an atmosphere of 5 % CO₂.

Transfection of rat hepatic myofibroblast cells

rHSCs were transfected 8 days after seeding with pcDNA3/antisense-TIMP-1 recombinant plasmid. Briefly, total RNAs were extracted from rat liver with Trizol (Life Tech, U.S.A) reagent. According to the full-length cDNA sequence that encoded rat TIMP-1, we designed special sense and antisense primers and obtained target sequence with the RT-NEST-PCR technique, which were linked into T4 vector with T4 DNA ligase. After transformation, selection, and appraisal with restriction enzymes EcoRI and XhoI, the resulting insert was subcloned into the plasmid pcDNA3 (Invitrogen CA) and sequenced (PE377 Auto sequencer). One day before transfection, cells were dispersed with trypsin-EDTA solution and counted, then the cells were pipetted into 6-well dishes at a density of 1×10⁴ cells per well so they would attain 70 % confluence the next day. Transfection was performed with the commercially available cationic liposome reagents Effectene (Qiagen, Germany), using pcDNA3/antisense-TIMP-1 recombinant plasmid (1.0 µg/well) and pcDNA3 empty plasmid, following essentially the instructions of the manufacturers. Transfecting cells were selected after growing in DMEM containing 400 µg/ml G418 for 2-3 weeks. Following selection, 10 drug-resistant (neo^r) clones of pcDNA3/antisense-TIMP-1 recombinant plasmid transfecting cells were picked randomly from different plates and studied after expansion; in the meantime, eight neo^r clones were picked from rMFB transfected with the pcDNA3 vector lacking the antisense sequences and eight non-transfected rMFB were studied as controls.

RNA isolation and Northern analysis for TIMP-1 and exogenous gene

The cells were rinsed with ice cold HBSS, the total RNAs were extracted from rMFBs with Trizol (Life Tech, Grand Island, NY) reagent. The concentration of RNA was determined by absorbance at 260 nm. For Northern analysis, 30 µg of total cellular RNAs were separated by electrophoresis in a 1 % denaturing agarose gel, transferred to a Hybond-N membrane (Amersham, UK) and fixed by baking for 2 h at 80 °C. The probe for pcDNA3 according to the special T7 promoter sequence (the probe sequence 5' - CAGAGGGATATCACTCAGCATAAT-3') and TIMP-1 cDNA probes were labeled with [α -³²P] dCTP (Amersham, UK) by random primer labeling method to detect exogenous gene and TIMP-1 expression. Blots were pre-hybridized for at least 3 h, and then hybridized for 20 h at 37 °C in a buffer containing 50 % formamide, 6×SSC, 5×Denhardt's solution [0.1 % Ficoll 400, 0.1 % BSA, 0.1 % polyvinylpyrrolidone], 5 mM EDTA, 0.5 % SDS, and 100 µg/ml sheared denatured herring sperm DNA (Roche, Germany). The filters were washed once at 55 °C for 20 minutes in a solution containing 2×SSC, 1 mM EDTA, and 0.1 % SDS, then twice at 50 °C for 20 minutes in a solution containing 0.4×SSC, 1 mM EDTA, and 0.1 % SDS. Autoradiographs were exposed to indicated times to Kodak films at -70 °C for 7 days. As an internal standard (loading control) the blots were re-hybridized with a GAPDH specific cDNA.

Western blotting for TIMP-1 and type collagen I, III

Rat TIMP-1 and collagen type I, III proteins in total cell extracts of transfected and non-transfected rMFBs were subjected to

Western-blot analyses. rMFB cells (1×10⁶) were pelleted by centrifugation, washed twice with ice-cold PBS, and lysed on ice in RIPA buffer [30 mM HEPES, 150 mM NaCl, 1 % Triton X-100, 0.1 % SDS and 1 % deoxycholic acid (pH 7.6)], with added proteinase inhibitors, pepstatin A (1.0 µg/ml), aprotinin (3.5 µg/ml), leupeptin (10 µg/ml) and 0.2 mM PMSF. Cell lysates were centrifuged at 3 000 g for 10 min at 4 °C, and BCA protein assay was performed. Protein samples (100 µg) were heated for 5 min at 100 °C and were separated on 12 % SDS-PAGE and transferred to PVDF membranes (Schleicher&Schuell Germany) in Tris-glycine buffer (pH 8.5) plus 20 % methanol. The membranes were blocked overnight in 5 % non-fat dried milk in Tris-buffer containing 0.1 % Tween-20 and then washed with Tris-buffer. The blots were incubated for 2 h at room temperature with mouse TIMP-1 monoclonal IgG (Oncogene) and rabbit anti-collagen type I, III diluted 1:500 in Tris-buffer. The blots were washed and then incubated with AP-conjugated secondary antibodies (Santa Cruz California U.S.A) at 1:2 000 dilution. The protein bands were visualized with BCIP/NBT (Wuhan, China) system. β -actin as the internal control.

Sample preparation and Enzyme assays

After transfection and selection, rMFBs were seeded into 6-well plates with 10⁵ cells/well and incubated for 2 weeks; the medium was changed twice a week. The media were harvested. Prior to assays, 225 µl of each medium was treated with 25 µl DTT(100mM) to give a final concentration of 10 mM for 30 min at 35 °C to inactivate endogenous collagenase inhibitors. Collagenase activity was determined by Type I Collagenase Activity Assay (Chemicon, Temecula CA). Briefly, the medium had been preincubated at room temperature for 30 min with APMA to obtain 1 mM final concentration to activate latent collagenase. The reaction mixture contained 50 µl (1 µg/µl) FITC-labeled type I collagen in a final volume of 100 µl, was further incubated at 37 °C for 3 h. The reaction was terminated by adding 200 µl enzyme stop reagent/extraction (0.05 M Tris-HCl pH9.5, ethanol containing NaCl, *o*-phenanthroline). After centrifugation at 4 000 rpm for 10 min, fluorescence in the supernatant was measured by Fluorometer (Hitachi Japan) at an excitation wavelength of 490 nm and an emission wavelength of 530nm. These experiments were performed in triplicate for each tissue sample.

One unit (U) of collagenase was defined as the amount of enzyme that hydrolyzed 1 µg of collagen substrate per min. The results shown in the figures were expressed as the mean with standard deviations of collagenase activity of samples.

Statistics

All values were expressed as mean \pm SD, ANOVA was used to determined the significance of differences among the three groups. A values of $P < 0.05$ was considered statistically significant.

RESULTS

Expression level of exogenous gene and TIMP-1 gene in rMFB

The exogenous gene expression could be detected in transfection groups (pcDNA3/antisense-TIMP-1 recombinant group and pcDNA3 empty vector group) by Northern blot, but not in non-transfected rMFB (Figure 1); the expression of TIMP-1 was much higher in pcDNA3 empty vector group and non-transfected rMFB control group than pcDNA3/antisense-TIMP-1 recombinant group at mRNA level (Figure 2), the ratio of TIMP-1/GAPDH was 0.67, 2.41, and 2.97 separately ($P < 0.05$); There was no significant difference ($P > 0.05$) between pcDNA3 empty vector group and non-transfected rMFB control group.

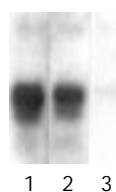


Figure 1 The expression of exogenous gene in rMFB detected by Northern blot after transfection and selection. 1: pcDNA3/antisense-TIMP-1 transfecting group; 2: pcDNA3 vector control group; 3: non-transfecting rMFB control group.

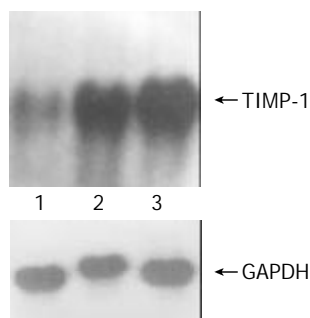


Figure 2 The expression of TIMP-1 mRNA in rMFB detected by Northern blot after transfection and selection. 1: pcDNA3/antisense-TIMP-1 transfecting group; 2: pcDNA3 vector control group; 3: non-transfecting rMFB control group.

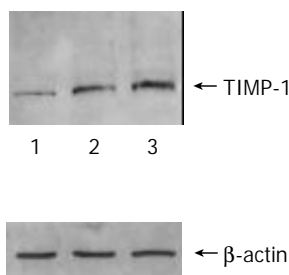


Figure 3 The expression of TIMP-1 protein level in rMFB detected by Western blot after transfection and selection. 1: pcDNA3/antisense-TIMP-1 transfecting group; 2: pcDNA3 vector control group; 3: non-transfecting rMFB control group.

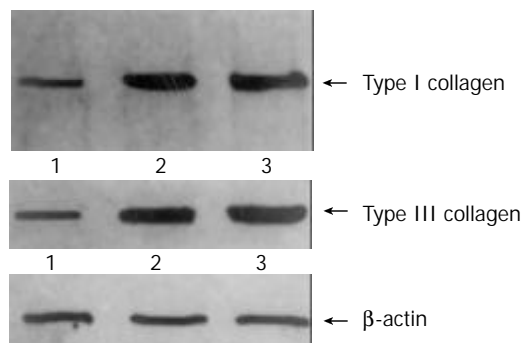


Figure 4 The expression of type I, III collagen in rMFB detected by Western blot after transfection and selection. 1: pcDNA3/antisense-TIMP-1 transfecting group; 2: pcDNA3 vector control group; 3: non-transfecting rMFB control group.

Antisense-TIMP-1 recombinant plasmid treated rMFB have reduced the content of TIMP-1 protein and type I, III collagen
The content of TIMP-1 protein and collagen type I, III in recombinant transfection group was lower than those of the

control groups ($P < 0.05$) as shown by the SDS-PAGE. (Figure 3,4). the ratio of TIMP-1/ β -actin was 0.31, 0.98 and 1.32 separately at protein level ($P < 0.05$); the ratio of collagen I/ β -actin was 0.63, 1.78 and 1.92 ($P < 0.05$); and the ratio of collagen III/ β -actin was 0.59, 1.81 and 1.98 ($P < 0.05$). Moreover, there was no significant difference ($P > 0.05$) between pcDNA3 empty vector group and non-transfected control group.

Collagenase activity of rMFB in response to antisense-TIMP-1 recombinant plasmid

The collagenolytic results were shown in Figure 5. Conditioned media from control groups showed low levels of collagenolytic activity; on the contrary, collagen degradation activity of the recombinant plasmid transfection group was significantly elevated, the collagenase activity was 0.3049, 0.1411 and 0.1196 respectively. ($P < 0.05$). Experiments were repeated twice separately.

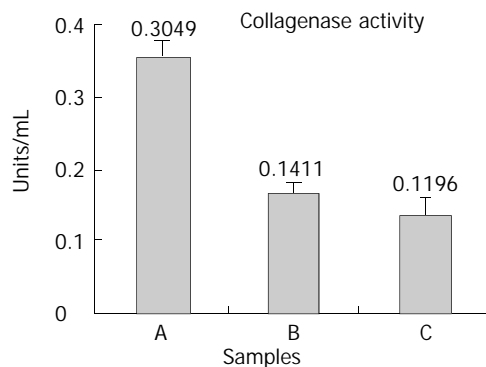


Figure 5 The enzymatic activity of MMP-1 in conditioned media from rMFB detected by Type I Collagenase Activity. Assay after transfection and selection. A: pcDNA3/antisense-TIMP-1 transfecting group; B: pcDNA3 vector control group; C: non-transfecting rMFB control group.

DISCUSSION

Liver fibrosis represents the final common pathological outcome for the majority of chronic liver insults^[21]. Pathological accumulation of extracellular matrix (ECM) in cases of liver fibrosis reflects imbalance of production and degradation of matrix proteins. At present, the common sense is that it is a reversible process. Matrix metalloproteinases (MMPs) are a family of secreted zinc proteases capable of degrading collagen and other ECM components. Recent studies suggest that MMPs may participate in pathological responses involved in liver fibrosis. Especially, interstitial collagenase (MMP-1) plays a key role in degrading collagen type I, III. (the main component of ECM). MMP-1 is tightly regulated by tissue inhibitors of matrix metalloproteinases I (TIMP-1).

Current evidence indicates that the central mediator of liver fibrosis is the hepatic stellate cell (HSC)^[18]. During fibrotic injury, these retinoid-rich perisinusoidal cells proliferate and undergo a phenotypic transformation to myofibroblast (MFB)-like cells, a process termed activation^[22]. Previous work has demonstrated that activated HSC can express TIMP-1, leading to the hypothesis that matrix degradation is inhibited during progressive fibrosis^[23]. This hypothesis is supported by findings that overexpression of TIMP-1 enhances experimental fibrosis^[24] and that spontaneous recovery from liver fibrosis is associated with a diminution of TIMP-1 expression and an increase in collagenase activity with consequent matrix degradation^[25]. Nucleic acid complemented with DNA/RNA of genome is called antisense nucleic acid, including antisense DNA, antisense RNA, and ribozyme^[26]. According to these theories, we designed a special antisense sequence which may complement with the mRNA of TIMP-1, constructing the rat

pcDNA3/antisense-TIMP-1 recombinant plasmid which can express in eucaryotic cells. After transfection and selection, we observed that the exogenous antisense-TIMP-1 recombinant plasmid could be expressed in rMFB well by Northern blot analysis. In order to evaluate the intervening or blocking effects on the expression of TIMP-1, Northern and Western blots were used. The results showed that antisense-TIMP-1 recombinant plasmid could block the expression of TIMP-1 greatly in rMFB compared to that of the control groups ($P < 0.05$); though the expression of TIMP-1 could not be blocked thoroughly, there maybe existed other factors which regulated the expression of TIMP-1.

We have chosen TIMP-1 as the target gene so as to elevate latent and active interstitial collagenase (MMP-1) activity in rMFB. In our study, we found that the enzymatic activity of MMP-1 in the pcDNA3/antisense-TIMP-1 recombinant transfecting group was 2-3 times higher than that in the control groups. However, the enzymatic activity was lower in the control groups ($P > 0.05$). These results were proven by FITC-labeled type I collagenase Activity Assay.

In healthy human liver, the collagen type I, III account for about 80 % of the total collagen of liver, while it rises up to more than 95 % in fibrotic livers. The collagen type I covers about 60-70 % of the total collagen of fibrotic liver, and type III was 20-30 %^[27-29]. Collagen I, III are the main target of MMP-1. MMP-1 has similar capacity of degrading collagen I, III. Therefore, collagen I, III are regarded as the important parameters to reflect the metabolism of collagen, and thus we can judge the therapeutic effect of the anti-fibrotic strategies of the liver^[30-32].

The content of collagen I, III was lower in the pcDNA3/antisense-TIMP-1 recombinant transfecting group than that in control groups ($P < 0.05$) determined by Western blotting. These data showed that this recombinant plasmid had stronger effects on increasing the degrading capacity of collagen I, III, decreasing the deposition of ECM, and reversing probably the hepatic fibrosis.

In conclusion, our experiment results have demonstrated that the pcDNA3/antisense-TIMP-1 recombinant has anti-hepatic fibrosis effect in vitro strongly through inhibiting the TIMP-1.

REFERENCES

- Huang ZG**, Zhai WR, Zhang YE, Zhang XR. Study of heteroserum-induced rat liver fibrosis model and its mechanism. *World J Gastroenterol* 1998; **4**: 206-209
- Jia JB**, Han DW, Xu RL, Gao F, Zhao LF, Zhao YC, Yan JP, Ma XH. Effect of endotoxin on fibronectin synthesis of rat primary cultured hepatocytes. *World J Gastroenterol* 1998; **4**: 329-331
- Du WD**, Zhang YE, Zhai WR, Zhou XM. Dynamic changes of type I, III and IV collagen synthesis and distribution of collagen-producing cells in carbon tetrachloride-induced rat liver fibrosis. *World J Gastroenterol* 1999; **5**: 397-403
- Cheng ML**, Wu YY, Huang KF, Luo TY, Ding YS, Lu YY, Liu RC, Wu J. Clinical study on the treatment of liver fibrosis due to hepatitis B by IFN- α 1 and traditional medicine preparation. *World J Gastroenterol* 1999; **5**: 267-269
- Friedman SL**. Seminars in medicine of the beth israel hosloital, boston. The cellular basis of hepatic fibrosis: mechanisms and treatment strategies. *N Engl J Med* 1993; **328**: 1828-1835
- Olaso E**, Friedman SL. Molecular regulation of hepatic fibrogenesis. *J Hepatol* 1998; **29**: 836-847
- Pinzari M**, Marra F, Carloni V. Signal transduction in hepatic stellate cells. *Liver* 1998; **18**: 2-13
- Brenner DA**. Signal transduction during liver regeneration. *J Gastroenterol Hepatol* 1998; **13** (Suppl): S93-95
- Torres L**, Garcia-Trevijano ER, Rodriguez JA, Carretero MV, Bustos M, Fernandez E, Eguinoa E, Mato JM, Avila MA. Induction of TIMP-1 expression in rat hepatic stellate cells and hepatocytes: a new role for homocysteine in liver fibrosis. *Biochim Biophys Acta* 1999; **1455**: 12-22
- George DK**, Ramm GA, Walker NI, Powell LW, Crawford DH. Elevated serum type IV collagen: a sensitive indicator of the presence of cirrhosis in haemochromatosis. *J Hepatol* 1999; **31**: 47-52
- Murawaki Y**, Ikuta Y, Idobe Y, Kawasaki H. Serum matrix metalloproteinase-1 in patients with chronic viral hepatitis. *J Gastroenterol Hepatol* 1999; **14**: 138-145
- Arthur MJ**, Iredale JP, Mann DA. Tissue inhibitors of metalloproteinases: role in liver fibrosis and alcoholic liver disease. *Alcohol Clin Exp Res* 1999; **23**: 940-943
- Sakaida I**, Uchida K, Hironaka K, Okita K. Prolyl 4-hydroxylase inhibitor (HOE 077) prevents TIMP-1 gene expression in rat liver fibrosis. *J Gastroenterol* 1999; **34**: 376-377
- Murawaki Y**, Ikuta Y, Kawasaki H. Clinical usefulness of serum tissue inhibitor of metalloproteinases (TIMP)-2 assay in patients with chronic liver disease in comparison with serum TIMP-1. *Clin Chim Acta* 1999; **281**: 109-120
- Roeb E**, Purucker E, Breuer B, Nguyen H, Heinrich PC, Rose-John S, Matern S. TIMP expression in toxic and cholestatic liver injury in rat. *J Hepatology* 1997; **27**: 535-544
- Geisler S**, Lichtinghagen R, Boker KH, Veh RW. Differential distribution of five members of the matrix metalloproteinase family and one inhibitor (TIMP-1) in human liver and skin. *Cell Tissue Res* 1997; **289**: 173-183
- Friedman SL**. Molecular regulation of hepatic fibrosis, an integrated cellular response to tissue injury. *J Biol Chem* 2000; **275**: 2247-2250
- Friedman SL**. Seminars in medicine of the Beth Israel Hospital, Boston. The cellular basis of hepatic fibrosis. mechanisms and treatment strategies. *N Engl J Med* 1993; **328**: 1828-1835
- Arthur MJ**, Mann DA, Iredale JP. Tissue inhibitors of metalloproteinases, hepatic stellate cells and liver fibrosis. *J Gastroenterol Hepatol* 1998; **13** (Suppl): S33-38
- Iredale JP**, Benyon RC, Arthur MJ, Ferris WF, Alcolado R, Winwood PJ, Clark N, Murphy G. Tissue inhibitor of metalloproteinase-1 messenger RNA expression is enhanced relative to interstitial collagenase messenger RNA in experimental liver injury and fibrosis. *Hepatology* 1996; **24**: 176-184
- Alcolado R**, Arthur MJ, Iredale JP. Pathogenesis of liver fibrosis. *Clin Sci (Lond)* 1997; **92**: 103-112
- Bachem MG**, Meyer D, Melchior R, Sell KM, Gressner AM. Activation of rat liver perisinusoidal lipocytes by transforming growth factors derived from myofibroblastlike cells. A potential mechanism of self-perpetuation in liver fibrogenesis. *J Clin Invest* 1992; **89**: 19-27
- Benyon RC**, Iredale JP, Goddard S, Winwood PJ, Arthur MJ. Expression of tissue inhibitor of metalloproteinases 1 and 2 is increased in fibrotic human liver. *Gastroenterology* 1996; **110**: 821-831
- Yoshiji H**, Kuriyama S, Miyamoto Y, Thorgeirsson UP, Gomez DE, Kawata M, Yoshii J, Ikenaka Y, Noguchi R, Tsujinoue H, Nakatani T, Thorgeirsson SS, Fukui H. Tissue inhibitor of metalloproteinases-1 promotes liver fibrosis development in a transgenic mouse model. *Hepatology* 2000; **32**: 1248-1254
- Iredale JP**, Benyon RC, Pickering J, McCullen M, Northrop M, Pawley S, Hovell C, Arthur MJ. Mechanisms of spontaneous resolution of rat liver fibrosis. Hepatic stellate cell apoptosis and reduced hepatic expression of metalloproteinase inhibitors. *J Clin Invest* 1998; **102**: 538-549
- Nie QH**, Cheng YQ, Xie YM, Zhou YX, Cao YZ. Inhibiting effect of antisense oligonucleotides phosphorothioate on gene expression of TIMP-1 in rat liver fibrosis. *World J Gastroenterol* 2001; **7**: 363-369
- Louis H**, Le Moine A, Quertinmont E, Peny MO, Geerts A, Goldman M, Le Moine O, Deviere J. Repeated concanavalin A challenge in mice induces an interleukin 10-producing phenotype and liver fibrosis. *Hepatology* 2000; **31**: 381-390
- Matrisian LM**. The matrix-degrading metalloproteinases. *Bioessays* 1992; **14**: 455-463
- Kovalovich K**, deAngelis RA, Li W, Furth EE, Ciliberto G, Taub R. Increased toxin induced liver injury and fibrosis in interleukin-6-deficient mice. *Hepatology* 2000; **31**: 149-159
- Tsukamoto H**, Matsuoka M, French SW. Experimental models of hepatic fibrosis: a review. *Semin Liver Dis* 1990; **10**: 56-65
- Arthur MJ**. Collagenases and liver fibrosis. *J Hepatol* 1995; **22**: S43-48
- Arthur MJ**. Degradation of matrix proteins in liver fibrosis. *Pathol Res Pract* 1994; **190**: 825-833

Effect of leflunomide on immunological liver injury in mice

Hong-Wei Yao, Jun Li, Yong Jin, Yun-Fang Zhang, Chang-Yu Li, Shu-Yun Xu

Hong-Wei Yao, Jun Li, Yong Jin, Yun-Fang Zhang, Chang-Yu Li, Shu-Yun Xu, Institute of Clinical Pharmacology, Anhui Medical University, Heifei 230032, Anhui Province, China; School of Pharmacy, Anhui Medical University, Heifei 230032, Anhui Province, China
Supported by Natural Science Foundations of Anhui Province, No. 98446733

Correspondence to: Prof. Jun Li, Institute of Clinical Pharmacology, Anhui Medical University; School of Pharmacy, Anhui Medical University, Heifei 230032, Anhui Province China. amuicplj@mail.hf.ah.cn
Telephone: +86-551-5161040 **Fax:** +86-551-5161040
Received: 2002-07-31 **Accepted:** 2002-09-12

Abstract

AIM: To study the effect of leflunomide on immunological liver injury (ILI) in mice.

METHODS: ILI was induced by tail vein injection of 2.5 mg *Bacillus Calmette-Guerin* (BCG), and 10 d later with 10 µg lipopolysaccharide (LPS) in 0.2 mL saline (BCG+LPS). The alanine aminotransferase (ALT), aspartate aminotransferase (AST), nitric oxide (NO) level in plasma and malondialdehyde (MDA), glutathione peroxidase (GSHpx) in liver homogenate were assayed by spectroscopy. The serum content of tumor necrosis factors-α (TNF-α) was determined by ELISA. Interleukin-1 (IL-1), interleukin-2 (IL-2) and Concanavalin A (ConA)-induced splenocyte proliferation response were determined by methods of ³H-infiltrated cell proliferation.

RESULTS: Leflunomide (4, 12, 36 mg·kg⁻¹) was found to significantly decrease the serum transaminase (ALT, AST) activity and MDA content in liver homogenate, and improve reduced GSHpx level of liver homogenate. Leflunomide (4, 12, 36 mg·kg⁻¹) significantly lowered TNF-α and NO level in serum, and IL-1 produced by intraperitoneal macrophages (PM_φ). Moreover, the decreased IL-2 production and ConA-induced splenocyte proliferation response were further inhibited.

CONCLUSION: These findings suggested that leflunomide had significant protective action on ILI in mice.

Yao HW, Li J, Jin Y, Zhang YF, Li CY, Xu SY. Effect of leflunomide on immunological liver injury in mice. *World J Gastroenterol* 2003; 9(2): 320-323

<http://www.wjgnet.com/1007-9327/9/320.htm>

INTRODUCTION

Earlier studies have identified leflunomide, an isoxazole derivative, as a unique immunomodulatory agent capable of treating rheumatoid arthritis, allograft and xenograft rejection, systemic lupus erythematosus, prostate carcinoma, and neuronal-glioma tumours, etc^[1-12]. Our studies indicated that leflunomide had significantly therapeutic effects on the secondary inflammation response of adjuvant arthritis (AA) in rats. Recent evidence suggested the anti-inflammatory and immunoregulatory effects of leflunomide were related to its ability to suppress IL-1 and TNF-α selectively over their

inhibitors in T lymphocyte/monocyte activation, and the activation of nuclear factor kappa B, a potent mediator of inflammation when stimulated by inflammatory agents^[13-16]. Jankovic reported that A₇₇₁₇₂₆, leflunomide's active metabolite, also had inhibitory effect on NO production and iNOS mRNA expression in IFN-γ+LPS-activated murine and rat primary fibroblast^[17, 18].

As we know, the activity of cytokines such as TNF-α, IL-1, IL-6, NO and T cell mediated immunity were closely related to the degree of liver injury caused by virus, endotoxin, ConA, and GalN^[19-21]. Thus, inhibition of proinflammatory cytokines and regulation of host immunity would be beneficial to alleviating liver injury.

Based on the immunological dysfunction in liver injury and leflunomide's immunomodulatory feature with high efficacy and low toxicity, we assumed that leflunomide might have therapeutic effect on ILI. To the best of our knowledge, however, there has been no report so far concerning the effect of leflunomide on ILI. In this study, therefore, we have clarified the therapeutic effect of leflunomide on ILI in mice.

MATERIALS AND METHODS

Animals and reagents

Male Kunming strain mice weighing 18-22 g were purchased from Animal Center of Anhui Medical University. Mice were allowed to take food and tap water *ad libitum*. Leflunomide was kindly donated by Cinkate Co., USA. ConA and LPS from *Escherichia coli* were purchased from Sigma Co., St. Louis, M, USA. 1, 1, 3, 3-tetraethoxypropane (TEP) and 5, 5'-dithiobis-(2-nitrobenzic acid) (DTNB) were purchased from FLUKA Co., Switzerland. BCG was purchased from Institute of Shanghai Biological Products.

Preparation of ILI^[22]

Each mouse was injected with 2.5 mg BCG (viable bacilli) in 0.2 mL saline via tail vein, and 10 d later with 10 µg LPS in 0.2 mL saline. At 0, 4, 8, and 12 h post-injection of LPS, animals received either leflunomide (4, 12, and 36 mg/kg, ig) or appropriate volume (25 mL/kg, ig) of vehicle (3 % prednisone). The mice were anesthetized with ether, then sacrificed by cervical dislocation 16 h after LPS injection and trunk blood was collected into heparinized tubes (50 U/mL) and centrifuged (1 500×g, 10 min, room temperature). Plasma was aspirated and stored at -70 °C until assayed as described below. The liver was also removed and stored at -70 °C until required.

Measurement of plasma ALT, AST, NO and TNF-α

Plasma ALT, and AST were determined using commercial kits produced by Institute of Shanghai Biological Products affiliated to the Ministry of Health. These activities are expressed as an international unit (U/L). Serum TNF-α and NO were measured using commercial kits produced by Sigma Co. and Beijing Biotinge-Tech., Co.Ltd, and their levels were expressed as pg·mL⁻¹ and µmol·L⁻¹ respectively.

Measurement of MDA and GSHpx in liver homogenate

Livers were thawed, weighed and homogenized with Tris-Hcl

buffer (5 mM containing 2 mM EDTA, pH 7.4). Homogenates were centrifuged (1 000×g, 10 min, room temperature) and the supernatant was used immediately for the assays of MDA and GSHpx. MDA was measured by the thiobarbituric acid method according to standard techniques (Gavino VG., 1981). The content of MDA was expressed as nmol per gram liver tissue. GSHpx was measured by the DTNB method, and its content was expressed as U per milligram protein.

Measurement of ConA induced splenocyte proliferation, IL-1 and IL-2

ConA induced splenocyte proliferation was determined according to the report by Yamamoto I in 1982. IL-1 and IL-2 were measured according to the reference (Liang JS, 1989; Ding GF, 1988).

Statistical analysis

Results were expressed by $\bar{x} \pm s$. Statistical significance of differences between groups were determined by ANOVA followed by Student's *t* test. *P* value of less than 0.05 was considered statistically significance.

RESULTS

Therapeutic effects of leflunomide on ILI induced by BCG+LPS in mice

Results are shown in Tables 1 and 2. ALT, AST, and NO in plasma and MDA content in liver homogenate were significantly increased after the interval injection of BCG and LPS. Meanwhile, the GSHpx level in liver homogenate was sharply decreased. Both leflunomide (12, 36 mg/kg) and prednisone (3 mg/kg) could not only significantly decrease ALT, AST, NO and MDA level, but evidently increase GSHpx in mice with ILI.

Table 1 Effects of leflunomide on serum ALT and AST activities induced by BCG+LPS in mice ($n=10$, $\bar{x} \pm s$)

Groups	Dose (mg·kg ⁻¹)	ALT (u·L ⁻¹)	AST (u·L ⁻¹)
Normal		32.1±5.6	35.8±6.4
Model		195.4±21.8 ^d	188.4±22.5 ^d
Leflunomide	4	181.5±19.5 ^d	175.2±18.1 ^d
	12	173.8±15.8 ^{ad}	166.5±15.7 ^{ad}
	36	121.8±11.5 ^{bd}	108.2±9.8 ^{bd}
Prednisone	3	81.5±7.8 ^{bd}	64.7±5.8 ^{bd}

^a*P*<0.05, ^b*P*<0.01 vs model group; ^d*P*<0.01 vs normal group.

Table 2 Effects of leflunomide on serum NO, MDA and GSHpx contents in liver homogenates induced by BCG+LPS in mice ($n=10$, $\bar{x} \pm s$)

Groups	Dose (mg·kg ⁻¹)	Plasma NO (μM)	Liver homogenates	
			MDA (nmol/g tissue)	GSHpx (μ/mg protein)
Normal		8.8±1.0	133.2±14.5	163.9±15.9
Model		74.5±10.1 ^d	395.9±23.6 ^d	62.5±8.8 ^d
Leflunomide	4	68.3±8.5 ^d	385.7±22.2 ^d	66.3±9.1 ^d
	12	60.7±7.1 ^{bd}	363.9±19.3 ^{bd}	87.1±9.9 ^{bd}
	36	55.3±6.2 ^{bd}	301.9±17.1 ^{bd}	95.1±10.7 ^{bd}
Prednisone	3	44.4±5.3 ^{bd}	272.0±15.7 ^{bd}	108.0±12.0 ^{bd}

^a*P*<0.05, ^b*P*<0.01 vs model group; ^d*P*<0.01 vs normal group.

Effects of leflunomide on TNF-α

As shown in Table 3, when the mice were first injected with BCG and then challenged with LPS, the level of TNF-α was elevated significantly. Leflunomide (4, 12, and 36 mg/kg) obviously decreased the increased TNF-α level in serum.

Table 3 Influences of leflunomide on serum TNF-α induced by BCG+LPS in mice ($n=8$, $\bar{x} \pm s$)

Groups	Dose (mg·kg ⁻¹)	TNF-α (pg·mL ⁻¹)
Normal	-	Under detection limit
Model	-	353.3±28.7 ^d
Leflunomide	4	305.0±31.4 ^{ad}
	12	240.0±31.1 ^{bd}
	36	140.0±31.1 ^{bd}
Prednisone	3	88.7±25.6 ^{bd}

^a*P*<0.05, ^b*P*<0.01 vs model group; ^d*P*<0.01 vs normal group.

Influence of leflunomide on IL-1

IL-1 excreted by PM_φ was significantly increased in the model group. As shown in Table 4, Leflunomide (4, 12, and 36 mg/kg) evidently inhibited PM_φ excreting too much IL-1.

Table 4 Influences of leflunomide *in vivo* on IL-1 and IL-2 production and splenocyte proliferation in mice induced by BCG+LPS. (unit:10³cpm) ($n=8$, $\bar{x} \pm s$)

Groups	Dose (mg·kg ⁻¹)	IL-1	IL-2	Splenocyte proliferation
Normal		11.2±2.40	13.3±1.76	17.5±2.26
Model		34.6±3.96 ^d	9.3±1.57 ^d	7.9±1.19 ^d
Leflunomide	4	29.6±3.71 ^{ad}	8.2±1.44 ^d	7.0±1.01 ^d
	12	18.9±3.28 ^{bd}	7.6±1.31 ^{ad}	6.4±0.95 ^{ad}
	36	16.6±3.08 ^{bd}	6.5±1.20 ^{bd}	5.2±0.87 ^{bd}
Prednisone	3	15.7±2.85 ^{bd}	5.0±1.12 ^{bd}	4.4±0.71 ^{bd}

^a*P*<0.05, ^b*P*<0.01 vs model group; ^d*P*<0.01 vs normal group.

Effect of leflunomide on IL-2 generation and ConA induced splenocyte proliferation

IL-2 and ConA induced splenocyte proliferation were significantly inhibited in the model group (Table 4). Leflunomide (4, 12, and 36 mg/kg) further inhibited IL-2 production and ConA induced splenocyte proliferation response.

DISCUSSION

It has been demonstrated that severe hepatitis could be induced by injecting a small dose of bacterial LPS into BCG-pretreated mice^[22]. In this article, ILI was successfully induced by BCG+LPS. On this basis, leflunomide (4, 12, and 36 mg/kg) could significantly lower the increased plasma transaminase level and MDA content in liver homogenate, meanwhile, GSHpx level rose significantly. All these indicated that leflunomide markedly protected ILI. Leflunomide significantly inhibited the generation of NO, TNF-α and IL-1 excreted by PM_φ, moreover, IL-2 production and ConA induced splenocyte proliferation was further inhibited by leflunomide. Therefore, the protective effects of leflunomide on ILI might be related with its function of balancing cytokine generation and modulating immune.

As it is known, TNF-α is one of the important mediators in liver injury. It has been demonstrated that liver injury induced by endotoxin was conducted by TNF-α, and the

activity of TNF- α was positively related with the extent of liver necrosis^[22-24]. However, TNF- α itself could not directly result in liver injury. The damaging degree of TNF- α on liver might be involved with infection, activity of Kupffer cell, and endogenous serine type protease, etc^[25-30]. TNF- α could act as the first factor of liver injury, its elevation would stimulate a number of proinflammatory mediators including NO, IL-1, IL-6, IL-8 and SIL-2R^[31-36], which further deteriorated the liver injury intoxicated by TNF. Therefore, although the TNF lever was low, liver was damaged significantly.

Leflunomide, an immunomodulatory reagent, is mainly aimed to inhibit the activity of dihydroorotate dehydrogenase (DHODH) involved in *de novo* pyrimidine biosynthesis. But at a higher concentration, it mainly inhibited protein tyrosine kinases initiating signaling^[1,13,14,37,38], and therefore could reduce the cell response to mitogen and cytokine. In the model of ILI induced by BCG+LPS, leflunomide could significantly lower the increased TNF- α level in serum, which agreed with the results of Smith's experiment that leflunomide significantly lowered the increased TNF level in joints from AA rats^[15,16,39]. As it is known, TNF mainly come from Kupffer cell in liver. In this article, leflunomide significantly inhibited TNF- α level in serum of ILI. It deserved further investigation on about whether it is related to leflunomide's effect of regulating the immunological dysfunction through inhibiting the growth and differentiation of Kupffer cell and production of TNF, thus, alleviating liver injury.

As reported in documents, the synthesis of NO was regulated by many immunological factors including TNF- α , IL-1, and IFN- γ , which is composed of a complicated web system, could act on hepatocytes, Kupffer cells and Ito in endotoxemia mice to increase the generation of NO^[31,32,35,40]. Likewise, LPS could also induce Ito cells to express iNOS and synthesis of a large amount of NO^[41,42]. According to our investigation, the effects of leflunomide to inhibit ILI might well be related with its function of decreasing the degeneration of NO.

Although IL-1 itself has no damage on liver, its elevation could stimulate many kinds of immunological and inflammatory cells to excrete cytokine including TNF- α , IFN- γ , IL-6, and IL-8, which mediate the inflammatory and immunological injury. Apart from these, IL-1, TNF- α , IFN- γ and LPS could act on hepatocyte to enhance the expression of iNOS mRNA in synergetic manner, and to increase the generation of NO, thus deteriorating the liver injury. Leflunomide significantly regulated abnormal IL-1 level excreted by PM ϕ in ILI mice *in vivo*, which agrees with Deage's investigation^[43] in effect of leflunomide on AA rats.

Suzuki found that splenectomy could modulate the excretion of inflammatory mediators, which prevented liver injury intoxicated by LPS after hepatectomy. In this study, we discovered that IL-2 production and ConA induced splenocyte proliferation were reduced in ILI induced by BCG+LPS. However, leflunomide further inhibited the production of IL-2 and ConA induced splenocyte proliferation response. Hoskin *et al*^[44] reported that leflunomide inhibited the T lymphatic cell growth and response to IL-2 and production of IL-2. Further studies are needed to elucidate the relationship between the protective effect of leflunomide on ILI and its inhibitory action on cellular immune function.

REFERENCES

- Sanders S**, Harisdangkul V. Leflunomide for the treatment of rheumatoid arthritis and autoimmunity. *Am J Med Sci* 2002; **323**: 190-193
- Wendling D**. Leflunomide in the treatment of rheumatoid arthritis. *Ann Med Interne* 2002; **153**: 21-24
- Aldred A**, Emery P. Leflunomide: a novel DMARD for the treatment of rheumatoid arthritis. *Expert Opin Pharmacother* 2001; **2**: 125-137
- Jakez-Ocampo J**, Richaud-Patin Y, Simon JA, Llorente L. Weekly dose of leflunomide for the treatment of refractory rheumatoid arthritis: an open pilot comparative study. *Joint Bone Spine* 2002; **69**: 307-311
- Williams JW**, Mital D, Chong A, Kottayil A, Millis M, Longstreth J, Huang W, Brady L, Jensik S, Anita C, Anita K, Michael M, James L, Wanyun H, Lynda B, Stephen J. Experiences with leflunomide in solid organ transplantation. *Transplantation* 2002; **73**: 358-366
- Jin MB**, Nakayama M, Ogata T, Fujita M, Mino K, Taniguchi M, Suzuki T, Shimamura T, Furukawa H, Todo S. A novel leflunomide derivative, FK778, for immunosuppression after kidney transplantation in dogs. *Surgery* 2002; **132**: 72-79
- Barthel HR**. Leflunomide for the treatment of systemic lupus erythematosus: comment on the article by McMurray. *Arthritis Rheum* 2001; **45**: 472
- Kessel A**, Toubi E. Leflunomide in systemic lupus erythematosus. *Harefuah* 2002; **141**: 355-357
- Remer CF**, Weisman MH, Wallace DJ. Benefits of leflunomide in systemic lupus erythematosus: a pilot observational study. *Lupus* 2001; **10**: 480-483
- Shawver LK**, Schwartz DP, Mann E, Chen H, Tsai J, Chu L, Taylorson L, Longhi M, Meredith S, Germain L, Jacobs JS, Tang C, Ullrich A, Berens ME, Hersh E, McMahan G, Hirth KP, Powell TJ. Inhibition of platelet-derived growth factor-mediated signal transduction and tumor growth by N-[4-(trifluoromethyl)phenyl]5-methylisoxazole-4-carboxamide. *Clin Cancer Res* 1997; **3**: 1167-1177
- Xu X**, Shen J, Mall JW, Myers JA, Huang W, Blinder L, Saclarides TJ, Williams JW, Chong ASF. *In vitro* and *in vivo* antitumor activity of a novel immunomodulatory drug, leflunomide: mechanisms of action. *Biochem Pharmacol* 1999; **58**: 1405-1413
- Huang M**, Wang Y, Collins M, Mitchell BS, Graves LM. A77 1726 induces differentiation of human myeloid leukemia K562 cells by depletion of intracellular CTP pools. *Mol Pharmacol* 2002; **62**: 463-472
- Herrmann ML**, Schleyerbach R, Kirschbaum BJ. Leflunomide: an immunomodulatory drug for the treatment of rheumatoid arthritis and other autoimmune diseases. *Immunopharmacology* 2000; **47**: 273-289
- Breedveld FC**, Dayer JM. Leflunomide: mode of action in the treatment of rheumatoid arthritis. *Ann Rheum Dis* 2000; **59**: 841-849
- Li WD**, Ran GX, Teng HL, Lin ZB. Dynamic effects of leflunomide on IL-1, IL-6, and TNF- α activity produced from peritoneal macrophages in adjuvant arthritis rats. *Acta Pharmacol Sin* 2002; **23**: 752-756
- Manna SK**, Mukhopadhyay A, Aggarwal BB. Leflunomide Suppresses TNF-Induced Cellular Responses: Effects on NF- κ B, Activator Protein-1, c-Jun N-Terminal Protein Kinase, and Apoptosis. *J Immunol* 2000; **165**: 5962-5969
- Jankovic V**, Samardzic T, Stosic-Grujicic S, Popadic D, Trajkovic V. Cell-specific inhibition of inducible nitric oxide synthase activation by leflunomide. *Cell Immunol* 2000; **199**: 73-80
- Trajkovic V**. Modulation of inducible nitric oxide synthase activation by immunosuppressive drugs. *Curr Drug Metab* 2001; **2**: 315-329
- Hoek JB**, Pastorino JG. Ethanol, oxidative stress, and cytokine-induced liver cell injury. *Alcohol* 2002; **27**: 63-68
- Sass G**, Koerber K, Tiegs G. TNF tolerance and cytotoxicity in the liver: the role of interleukin-1 β , inducible nitric oxide-synthase and heme oxygenase-1 in D-galactosamine-sensitized mice. *Inflamm Res* 2002; **51**: 229-235
- Trautwein C**, Rakemann T, Malek NP, Piumpe J, Tiegs G, Manns MP. Concanavalin A-induced liver injury triggers hepatocyte proliferation. *J Clin Invest* 1998; **101**: 1960-1969
- Wang GS**, Liu GT. Influences of Kupffer cell stimulation and suppression on immunological liver injury in mice. *Acta Pharmaceutica Sinica* 1997; **18**: 173-176
- Zhang XL**, Quan QZ, Sun ZQ, Wang YJ, Jiang XL, Wang D, LI WB. Protective effects of cyclosporine A on T-cell dependent ConA-induced liver injury in Kunming mice. *World J Gastroenterol*

- 2001; **7**: 569-571
- 24 **Zang GQ**, Zhou XQ, Yu H, Xie Q, Zhao GM, Wang B, Guo Q, Xiang YQ, Liao D. Effect of hepatocyte apoptosis induced by TNF- α on acute severe hepatitis in mouse models. *World J Gastroenterol* 2000; **6**: 688-692
- 25 **Enomoto N**, Ikejima K, Yamashina S, Hirose M, Shimizu H, Kitamura T, Takei Y, Sato And N, Thurman RG. Kupffer cell sensitization by alcohol involves increased permeability to gut-derived endotoxin. *Alcohol Clin Exp Res* 2001; **25** (Suppl): 51S-54S
- 26 **Enomoto N**, Yamashina S, Kono H, Schemmer P, Rivera CA, Enomoto A, Nishiura T, Nishimura T, Brenner DA, Thurman RG. Development of a new, simple rat model of early alcohol-induced liver injury based on sensitization of Kupffer cells. *Hepatology* 1999; **29**: 1680-1689
- 27 **Nagaki M**, Muto Y, Ohnishi H, Moriwaki H. Significance of tumor necrosis factor (TNF) and interleukin-1 (IL-1) in the pathogenesis of fulminant hepatitis: possible involvement of serine protease in TNF-mediated liver injury. *Gastroenterologia Japonica* 1991; **26**: 448-455
- 28 **Murr MM**, Yang J, Fier A, Kaylor P, Mastorides S, Norman JG. Pancreatic elastase induces liver injury by activating cytokine production within Kupffer cells via nuclear factor-Kappa B. *J Gastrointest Surg* 2002; **6**: 474-480
- 29 **McClain CJ**, Hill DB, Song Z, Deaciuc I, Barve S. Monocyte activation in alcoholic liver disease. *Alcohol* 2002; **27**: 53-61
- 30 **Hoebe KHN**, Witkamp RF, Fink-Gremmels J, Miert ASJPAM, Monshouwer M. Direct cell-to-cell contact between Kupffer cells and hepatocytes augments endotoxin-induced hepatic injury. *Am J Physiol Gastrointest Liver Physiol* 2001; **280**: G720-G728
- 31 **Muntane J**, Rodriguez FJ, Segado O, Quintero A, Lozano JM, Siendones E, Pedraza CA, Delgado M, O' Valle F, Garcia R, Montero JL, De La Mata M, Mino G. TNF-alpha dependent production of inducible nitric oxide is involved in PGE(1) protection against acute liver injury. *Gut* 2000; **47**: 553-562
- 32 **Nadler EP**, Dickinson EC, Beerstolz D, Alber SM, Watkins SC, Pratt DW, Ford HR. Scavenging nitric oxide reduces hepatocellular injury after endotoxin challenge. *Am J Physiol Gastrointest Liver Physiol* 2001; **281**: G173-G181
- 33 **Sopena B**, Fernandez-Rodriguez CM, Martinez Vazquez C, Mendez MX, de la Fuente J, Freire M, Arnillas E, Outon A. Serum levels of soluble interleukin-2 receptor in alcoholic patients. *An Med Interna* 1998; **15**: 189-193
- 34 **Tulek N**, Saglam SK, Saglam M, Turkyilmaz R, Yildiz M. Soluble interleukin-2 receptor and interleukin-10 levels in patients with chronic hepatitis B infection. *Hepatogastroenterology* 2000; **47**: 828-831
- 35 **Shiratori Y**, Ohmura K, Hikiba Y, Matsumura M, Nagura T, Okano K, Kamii K, Omata M. Hepatocyte nitric oxide production is induced by Kupffer cells. *Dig Dis Sci* 1998; **43**: 1737-1746
- 36 **Simeonova PP**, Gallucci RM, Hulderman T, Wilson R, Kommineni C, Rao M, Luster MI. The role of tumor necrosis factor-alpha in liver toxicity, inflammation, and fibrosis induced by carbon tetrachloride. *Toxicol Appl Pharmacol* 2001; **177**: 112-120
- 37 **Xu X**, Gong H, Blinder L, Shen J, Williams JW, Chong AS. Control of lymphoproliferative and autoimmune disease in MRL-lpr/lpr mice by brequinar sodium: mechanisms of action. *J Pharmacol Exp Ther* 1997; **283**: 869-875
- 38 **Elder RT**, Xu X, Williams JW, Gong H, Finnegan A, Chong AS. The immunosuppressive metabolite of leflunomide, A771726, affects murine T cells through two biochemical mechanisms. *J Immunol* 1997; **159**: 22-27
- 39 **Smith-Oliver T**, Noel LS, Stimpson SS, Yarnall DP, Connolly KM. Elevated levels of TNF in the joints of adjuvant arthritic rats. *Cytokine* 1993; **5**: 298-304
- 40 **Billiar TR**. The delicate balance of nitric oxide and superoxide in liver pathology. *Gastroenterology* 1995; **108**: 603-605
- 41 **Saibara T**, Ono M, Iwasaki S, Maeda T, Onishi S, Hayashi And Y, Enzan H. Effects of ethanol on L-arginine transport in rat Ito cells in relation to nitric oxide production. *Alcohol Clin Exp Res* 2001; **25** (Suppl): 39S-45S
- 42 **Rockey DC**, Chung JJ. Inducible nitric oxide synthase in rat hepatic lipocytes and the effect of nitric oxide on lipocyte contractility. *J Clin Invest* 1995; **95**: 1199-1206
- 43 **Deage V**, Burger D, Dayer JM. Exposure of T lymphocytes to leflunomide but not to dexamethasone favors the production by monocytic cells of interleukin-1 receptor antagonist and the tissue-inhibitor of metalloproteinases-1 over that of interleukin-1beta and metalloproteinases. *Eur Cytokine Netw* 1998; **9**: 663-668
- 44 **Hoskin DW**, Taylor RM, Makrigiannis AP, James H, Lee TD. Dose-dependent enhancing and inhibitory effects of A77 1726 (leflunomide) on cytotoxic T lymphocyte induction. *Int J Immunopharmacol* 1998; **20**: 505-513

Edited by Ma JY

Direct intrahepatic portacaval shunt: an experimental study

Jian-Jun Luo, Zhi-Ping Yan, Kang-Rong Zhou, Sheng Qian

Jian-Jun Luo, Zhi-Ping Yan, Kang-Rong Zhou, Sheng Qian,
Department of Radiology, Affiliated Zhongshan Hospital, Fudan
University Medical center, Shanghai 200032, China

Correspondence to: Dr. Jian-Jun Luo, Deartment of Radiology,
Zhongshan Hospital, Medical Center of Fundan University, 180
Fenglin Road, Shanghai 200032, China. luojj2001@yahoo.com

Telephone: +86-21-64041990 Ext 2533

Received: 2002-08-24 **Accepted:** 2002-10-12

Abstract

AIM: To determine the feasibility of creating direct intrahepatic portacaval shunt (DIPS) in swine with puncture under sonographic guidance.

METHODS: DIPS was created in 10 domestic swine under sonographic guidance. Liver function, blood ammonia level and portosystemic gradient (PSG) were compared before and after the procedure. Patency of shunt was followed by portography every 7 days after DIPS.

RESULTS: DIPS was successfully established in all 10 swine without any complications. One day after procedure the alanine aminotransferase (ALT), aspartate aminotransferase (AST), and blood ammonia level (BAL) of swine rose from 5.40 ± 0.69 , 16.00 ± 0.79 and 35.66 ± 4.10 to 34.20 ± 3.46 , 59.70 ± 2.22 and 66.94 ± 3.44 respectively. ($P < 0.05$). The PSG decreased from 0.59 ± 0.20 kPa to 0.24 ± 0.11 kPa after DIPS ($P < 0.05$). The shunt of 10 swine was kept patent from 7-28 days (median patency time was 14 days).

CONCLUSION: This initial experience demonstrated that creating intrahepatic portacaval shunt from retrohepatic segment of IVC to portal vein with puncture under sonographic guidance in swine is safe and feasible. Further studies are necessary to perform DIPS in cirrhosis patients.

Luo JJ, Yan ZP, Zhou KR, Qian S. Direct intrahepatic portacaval shunt: an experimental study. *World J Gastroenterol* 2003; 9 (2): 324-328

<http://www.wjgnet.com/1007-9327/9/324.htm>

INTRODUCTION

Since Röschl successfully created an intrahepatic shunt from hepatic vein to portal vein in a canine model in 1969, the transjugular intrahepatic portosystemic shunt (TIPS) procedure has been used increasingly in the management of portal hypertension and its complications^[1-12]. One of the main limitations of TIPS has been the high incidence of shunt malfunction. There is a wide range of shunt malfunction rates reported in the literature from 17-50 % within six months to 23-87 % within the first year^[11-21]. Many experimental and clinical studies^[4,15,23,26] demonstrated that stenosis of the outflow hepatic vein (HV) is the main problem to limit the long-term patency of TIPS and development of HV stenosis after TIPS placement will be minimized by the use of the largest HV (RHV or MHV). The inferior vane cava (IVC) is the largest vein in human being, whose diameter is far wider than that of HV.

Therefore, using IVC as the outflow vein might improve the patency of intrahepatic portosystemic shunt theoretically^[24-28]. To determine the feasibility and safety of creating DIPS in swine under a sonographic guidance, we carried out this study to provide a new route for clinical intrahepatic portosystemic shunt.

MATERIALS AND METHODS

Animals

10 domestic swine, 6-8 weeks old, each weighing 22-25 kg, were used for this study. All animals had a normal liver without portal hypertension.

Pre-procedural preparation

Before procedure, each animal underwent abdominal enhanced CT scan by bolus injection of 80 ml Iopamidol intravenously. The length, diameter and the extent of RHSIVC invested by hepatic parenchyma were measured. The anatomical relationship of the intrahepatic portal vein and RHSIVC was also carefully studied. Liver function and blood ammonia level were checked before procedure to serve as a baseline for further evaluating the damage to swine's liver function after DIPS.

Procedure

Each swine was anaesthetized with ketamine (20 mg/kg) and diazepam (5 mg/kg) intramuscularly. After right femoral vein cut down and dilated, a 10-F-diameter, 41-cm-long sheath (Cook Bloomington, U.S.A) was introduced into swine's IVC and pressure measurement was made. Then, RUPS-100 portal access set modified by increasing the primary curve was passed through the 10-F sheath and placed into swine's RHSIVC. Under sonographic guidance, the tip of modified RUPS set was wedged against the right anterior-lateral wall of the IVC just beneath the level of the portal vein (Figure 1). RUPS-100 set was advanced slightly and orientation of the tip was adjusted ceaselessly. When the posterior-lateral wall of intrahepatic portal vein became "pushed" on songraphy the 0.038-inch metal needle and 5-F teflon catheter of modified RUPS set was thrust toward portal vein. After metal needle removed the 5-F teflon catheter was pulled back slowly with intermittent aspiration. When blood can be freely aspirated 5 ml contrast medium was infused as test injection. If portal vein's access was confirmed a 0.035-inch guide wire was passed through the 5-F teflon catheter into the portal vein. Subsequently, a 5-F pigtail catheter was advanced over the guide wire into the portal vein. Then, portography was performed and the pressure of portal vein was measured. After 500 U/kg heparin was intravenously infused a 0.035-inch Amplatz super stiff guide wire was introduced into the portal vein and 5-F pigtail catheter was removed. A 6-mm-diameter, 8-cm-long angioplasty balloon catheter was advanced over the Amplatz guide wire and positioned in the tract between the RHSIVC and portal vein. The balloon was partially inflated and a spot radiography of the partially inflated balloon catheter was used as a road map guide for stent placement. The distal "waist" of the balloon served to mark the portal vein wall and the proximal "waist" marked the wall of the RHSIVC. The distance between the two "waists" is the length of the hepatic parenchymal tract between the portal vein and RHSIVC and is the minimum

length of the stent required to connecting these two structures. The balloon catheter was then fully inflated to predilate the tract. As the balloon was being deflated, the 10-F sheath was advanced over the balloon catheter into the portal vein. With use of the road map image as a guide, the shunt was lined by one or two home-made metal bare stents. Portography was performed immediately after stent placement and pressure measurements were also made. Finally, a 5-F pigtail catheter was retained in animal's IVC for follow-up portography and right femoral vein incision was sutured. No anticoagulant, antibiotics or antiplatelet therapy was administered after procedure. At termination of the study, the animals were sacrificed by overdose ketamine intravenously for pathological examination.

Follow-up

Cross-sectional abdominal contrast-enhanced CT scan was performed 3 days after DIPS to detect any puncture-related complications. Liver function and blood ammonia level were rechecked at 1, 7 and 14 days after procedure. Portography was performed through the 5-F pigtail catheter previously retained in animal's IVC every 7 days after DIPS to evaluate the patency of shunt till the shunt complete occlusion.

Statistical analysis

All measured values were expressed as mean \pm SD. Laboratory values and portosystemic gradient (PSG) before and after DIPS was compared using paired-samples *t* test. The patency of DIPS shunt was evaluated by Kaplan-Meier analysis. If *P* values <0.05 the difference was considered significant.

RESULTS

CT scan

On pre-procedure CT imaging the mean length and diameter of swine's RHSIVC was 47.28 ± 3.65 mm and 19.00 ± 2.24 mm respectively. About 85.83-100 % of swine's RHSIVC was completely invested by hepatic parenchyma (Figure 2). On the CT imaging obtained 3 days after DIPS no hematoma beneath the hepatic integument or intraperitoneal bleeding was revealed. All stents were accurately deployed in the shunt connecting the intrahepatic portal vein and RHSIVC. No thrombosis could be detected in the portal vein or IVC (Figure 3).

Portal vein puncture and stent deployment

The direct RHSIVC to portal vein puncture visualized with real-time ultrasound was successfully made in all 10 swine. 1-5 (mean 2.2) passes were required to complete the puncture. Mean length of the intraparenchymal tract from RHIVC to portal vein was 15.43 ± 3.36 mm. In 8 swine, the shunt linked right branch of portal vein and RHSIVC, in the remaining 2 animals the left branch of portal vein was connected. Mean angles between the axial of shunt and RHSIVC was $29.42 \pm 2.31^\circ$. Totally 14 stents were deployed in 10 animals' shunts. In No. 1 and 6 swine, first stent was deployed too far into the portal vein and a second stent was required to fully cover the tract. In No.2 and 8 swine, the first stent dislodged into animals' RHSIVC and a second stent was necessitated. All stents were dilated to 8 mm in diameter without any contraction. After stents deployment, immediate portography demonstrated rapid flow from portal vein to IVC through widely patent DIPS shunt and no obvious contrast-medium extravasation was observed. The post-procedure PSG was significantly lower than that of before (Table 1) (Figure 4, 5).

Follow-up

On follow-up, no procedure-related death occurred, every

animal grew well and no signs or symptoms of infection could be observed. The patency time of DIPS shunt varied from 7 days to 28 days (median patency time was 14 days) after procedure (Figure 6).

Table 1 Portosystemic Gradient before and after DIPS (kPa)

	Pressure of IVC		Pressure of Portal vein		PSG	
	Before	After	Before	After	Before	After
	1.28 \pm 0.28	1.41 \pm 0.28	1.86 \pm 0.21	1.57 \pm 0.17	0.59 \pm 0.20	0.24 \pm 0.11
<i>P</i> values	0.034		0.001		0.007	

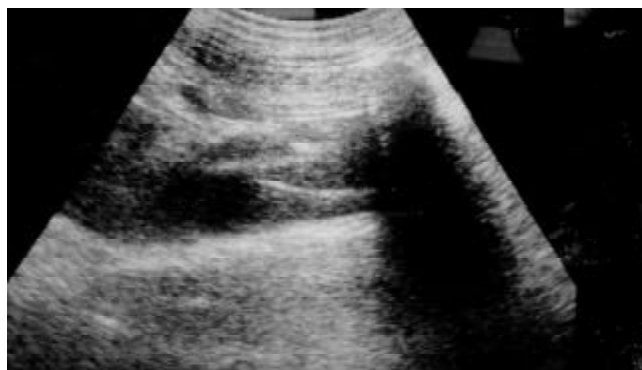


Figure 1 Intrahepatic portal vein, RHSIVC of swine and the modified RUPS-100 set wedging against the anterior-lateral wall of RHSIVC are clearly demonstrated on sonography.

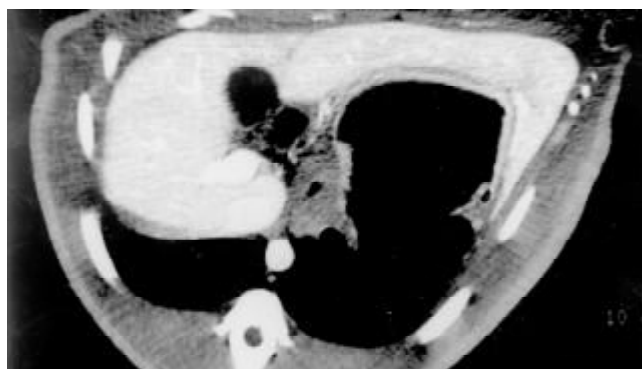


Figure 2 Sectional abdominal enhanced CT scan of swine before DIPS demonstrates the swine's intrahepatic portal vein and retrohepatic segment of IVC clearly.

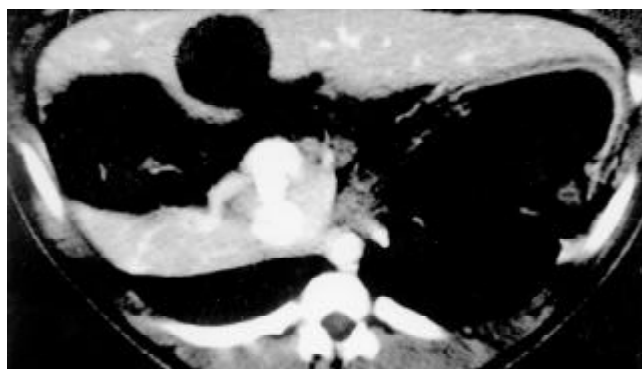


Figure 3 No hematoma beneath the hepatic integument or intraperitoneal bleeding is detected on sectional abdominal enhanced CT imaging of swine after DIPS. The self-expandable home-made stent is accurately deployed in the shunt connecting the intrahepatic portal vein and RHSIVC.



Figure 4 After intrahepatic portal vein successfully accessed via retrohepatic segment of IVC approach, portography was performed with a 5-F pigtail catheter. Swine's anterior and posterior branch of right portal vein is clearly demonstrated.

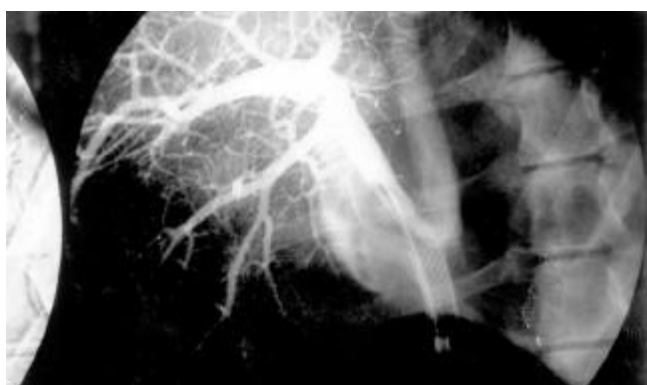


Figure 5 The DIPS shunt is lined by an 8 mm-diameter, 6 cm-long home-made metal bare stent. The stent is fully dilated and accurately connected the swine's RHSVIC and anterior branch of right portal vein. Swine's hepatic perfusion is well and animal's IVC was patent. No extravasation of contrast medium can be detected.

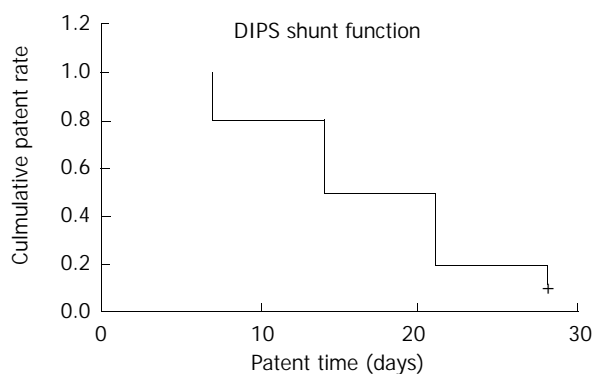


Figure 6 Median patency time of 10 DIPS shunt is 14 days. 7, 14, 21 and 28 days after DIPS procedure the cumulative patency rate of shunt is 100 %, 80 %, 50 % and 20 % respectively.

Laboratory examination

One and 7 days after DIPS, animal's alanine aminotransferase (ALT) and aspartate aminotransferase (AST) became significantly higher than the pre-DIPS values but the 7 day's values already became significantly lower than that of the first day after procedure. 14 days after DIPS, ALT and AST of swine returned to their normal pre-DIPS level. Animal's total bilirubin (TB) and combined bilirubin (CB) remained unchanged before and after DIPS. Swine's blood ammonia level increased significantly 1 day after procedure and returned to its baseline value at 7 days after DIPS (Table 2).

Table 2 Laboratory examination before DIPS, 1, 7 and 14 days after DIPS

Laboratory examination	Pre-DIPS	1d after DIPS	7d after DIPS	14d after DIPS
ALT (U/L)	5.40±0.69	34.20±3.46	18.0±2.11	5.80±0.66
AST(U/L)	16.00±0.79	59.70±2.22	23.90±0.90	17.60±0.75
TB(uoml/L)	1.86±0.20	1.94±0.23	2.16±0.17	2.10±0.17
CB(uoml/L)	0.66±0.10	0.86±0.14	0.95±0.12	0.88±0.19
BAL(uoml/L)	35.66±4.10	66.94±3.44	36.08±3.93	43.59±3.91

Note: Compared with the value of pre-DIPS the swine's ALT and AST rose significantly 1 and 7 days after DIPS. But 7 days' value had decreased significantly lower than that of first day after procedure. 14 days after DIPS the swine's ALT and AST returned to their baseline value of pre-DIPS. Swine's TB and CB kept no change before and after DIPS. Animal's blood ammonia level elevated significantly first day after DIPS. 7 days after procedure the animal's BAL returned to its baseline value of pre-DIPS and kept no significant change at 14 days after DIPS.

DISCUSSION

Direct intrahepatic portacaval shunt (DIPS) is to establish a low-resistant pathway between the intrahepatic portal vein and RHSVIC by diverting some of portal flow into IVC to achieve the goal of lowering the portal venous pressure. Compared with conventional TIPS, DIPS links RHSVIC rather than the hepatic vein. The diameter of RHSVIC is much wider than that of hepatic vein and the angle of DIPS shunt-to-IVC is more acute than that of TIPS shunt-to-hepatic vein. Thus, after DIPS the local hemodynamic change, a trigger factor of stenosis or occlusion of the outflow vein, may be less than that after TIPS and the patency time of DIPS may be longer than that of TIPS. In some cirrhosis patients, the hepatic vein drained into IVC with an approximate right angle or the level of intrahepatic portal vein might elevate too close to the level of hepatic vein owing to severe fibrosis of the liver. On these clinical situations, the RUPS-100 set can not be favorably introduced into the hepatic vein and puncture into portal vein is too difficult to be made^[24]. Moreover, to establish a portosystemic shunt in some portal hypertension patients with Budd-Chiari syndrome or hepatic venoocclusive disease the puncture into portal vein can but be made from IVC^[25,29]. Meanwhile, in some patients with previous TIPS shunt occlusion and no suitable hepatic vein could be supported a second parallel TIPS and DIPS seemed to be a rational choice^[30].

Local hematoma or pneumothorax resulted from mispunctures of the carotid artery or the trachea was considered as the serious complication of internal jugular vein puncture^[4,31,32]. Some authors^[31,32] pointed out that a previous TIPS procedure might interfere with the operative management of the subsequent orthotopic liver transplantation by deploying a stent into the suprahepatic portion of IVC, which often occurred at TIPS revision and a second parallel TIPS was established. To completely avoid these puncture-related complications and potential suboptimal stent placement of conventional TIPS we created this DIPS via a femoral vein's approach.

Anatomic construct of swine's liver and its post-trauma's histopathologic response are similar to those of human being^[35,36]. So DIPS can be created in pigs using techniques and equipment identical to that used in humans. The key step of successfully established DIPS is to select a suitable puncture site of IVC. In this study, the mean length of swine's RHSVIC was 47.28±3.65 mm and 85.83-100 % of RHSVIC was completely invested by hepatic parenchyma. These are the anatomic foundation of safely performing DIPS in swine. Mean diameter of swine's RHSVIC is 19.00±2.24 mm which is far

wider than the 10.10±1.58 mm-diameter of swine's hepatic vein. These results demonstrated using RHSIVC as the drain vein of DIPS in swine might improve the patency of intrahepatic portosystemic shunt theoretically.

Portal vein can not be precisely targeted under fluoroscopy. Thus, many major even fatal complications of conventional TIPS procedure are related to the "blind puncture" from hepatic vein into portal vein^[4,31,32]. Meanwhile, the bile duct injury and subsequent bile leak has been implicated as a cause of shunt thrombosis. Mucus in bile, not bile itself, is thought to be the thrombogenic factor of early shunt malfunction^[37,38]. Accordingly, using an effective guiding tool plays a most important role not only in creating DIPS safely but also in achieving a long-term patent shunt owing to improve the accuracy of puncture. We performed DIPS under sonographic guidance because of its free of X-ray and easy to perform. On sonography the location of intrahepatic portal vein and the tip of modified RUPS-100 placed in swine's RHSIVC can be clearly demonstrated. Only should we do is to adjust the angle of RUPS-100 set-to-IVC and advance the set slightly. When the left posterior-lateral wall of intrahepatic portal vein became "pushed", puncture was made. In our study, only 2.2 passes were required to accomplish the puncture, mean distance of puncture was only 15.43±3.36 mm and no puncture-related complications could be detected after procedure. These findings verified the effectiveness of real-time ultrasound to guide puncture in DIPS procedure. By using sonographic guidance to perform DIPS in cirrhosis patient attention should be paid to the interference brought by regenerated nodules, pneumatosis of bowel and ascites to the clarity of sonography. Portosystemic gradient (PSG) decreasing from 0.59±0.20 kPa to 0.24±0.11 kPa after procedure ($P<0.05$) verified the effectiveness of DIPS to decompress the portal venous pressure. After DIPS, the swine's ALT and AST increased significantly for a time but they finally returned to their normal pre-DIPS levels within two weeks after procedure. This exhibited the damage brought by DIPS to swine's liver function might just be temporary. Animal's TB and CB remained unchanged before and after DIPS. This implicated the injury of bile duct after DIPS is minor, which might attribute to the less number of passes required to complete the puncture and a short distance of intraparenchymal tract. Animal's blood ammonia level elevated significantly first day after DIPS. 7 days after procedure the animal's BAL returned to its baseline value before DIPS. This would be related to the swine used in this study without portal hypertension and portosystemic gradient quickly achieved a dynamic equilibrium after DIPS.

Our DIPS shunt kept patent from 7-28 days (median patency time was 14 days) which were shorter than the results published by Petersen *et al*^[26]. Except the breed disparity of animals between two studies some factors may be related to this despondent result. (1) All swine underwent DIPS without intubation and the respiratory movement of animals could not be well controlled. 4 stents' unprecisely deployment, 2 deployed far into the portal vein and 2 dislodged into animal's RHSIVC, were attributed to animal's irregular respiratory movement. (2) We created this DIPS via a femoral vein's approach. The direction of flow in shunt is opposite to the flow orientation in IVC. This might form whirlpool or turbulent flow at the outflow venous end of the stent and made it liable to injury from stress of the jet stream of blood. (3) Compared with the Palmaz stents used by Petersen, the high thrombogenicity of home-made stent may lead to early shunt malfunction. Finally, All swine used in this study have a normal liver without portal hypertension. After DIPS, the portosystemic gradient was decreased to 0.24±0.11 kPa which can not maintain the sufficient flow in shunt, using a "bare-stent" that can not effectively prevent the ingrowth of normal liver parenchyma and no anticoagulant

being administered were also related to this early stenosis or occlusion of shunt.

Our initial experience demonstrated creating direct intrahepatic portosystemic shunt in swine was safe and feasible. Carefully studying the anatomic relationship of intrahepatic portal vein and RHSIVC in cirrhosis patients and deploying a low-thrombogenic stent-graft in parenchymal track seem to be necessary for safely performing and achieving a long term patent DIPS in human being.

REFERENCES

- 1 **Teng GJ**, Bettmann MA, Hoopes PJ, Yang L. Comparison of a new stent and Wallstent for transjugular intrahepatic portosystemic shunt in a porcine model. *World J Gastroenterol* 2001; **7**: 74-79
- 2 **Schepke M**, Sauerbruch T. Transjugular portosystemic stent shunt in treatment of liver diseases. *World J Gastroenterol* 2001; **7**: 170-174
- 3 **Tripathi D**, Therapondos G, Jackson E, Redhead DN, Hayes PC. The role of the transjugular intrahepatic portosystemic stent shunt (TIPSS) in the management of bleeding gastric varices: clinical and haemodynamic correlations. *Gut* 2002; **51**: 270-274
- 4 **Rössle M**, Siegerstetter V, Huber M, Ochs A. The first decade of the transjugular intrahepatic portosystemic shunt (TIPS): state of the art. *Liver* 1998; **18**: 73-89
- 5 **LaBerge JM**, Ring EJ, Gordon RL, Ring EJ, Lake JR, Doherty MM, Somber KA, Roberts JP, Asher NL. Creation of transjugular intrahepatic portosystemic shunts with the wallstent endoprosthesis: results in 100 patients. *Radiology* 1993; **187**: 413-420
- 6 **Ugolotti U**, Larini P, Marcato C, Sacconi A, Puccianti F, Pedretti G. Is the tantalum strecker stent suitable for TIPS creation? short- and mid-term results in 20 consecutive patients. *Cardiovasc Intervent Radiol* 1997; **20**: 38-42
- 7 **Hirota S**, Ichikawa S, Matsumoto S, Motohara T, Fukuda T, Yoshikawa T. Interventional radiologic treatment for idiopathic portal hypertension. *Cardiovasc Intervent Radiol* 1999; **22**: 311-314
- 8 **Rösch J**, Keller FS. Transjugular intrahepatic portosystemic shunt: present status, comparison with endoscopic therapy and shunt surgery, and future perspectives. *World J Surg* 2001; **25**: 337-346
- 9 **Sanyal AJ**, Freedman AM, Luketic VA, Purdum PP, Shiffman ML, Tisnado J, Cole PE. Transjugular intrahepatic portosystemic shunts for patients with active variceal hemorrhage unresponsive to sclerotherapy. *Gastroenterology* 1996; **111**: 138-146
- 10 **Shiffman ML**, Jeffers L, Hoofnagle JH, Tralka TS. The role of transjugular intrahepatic portosystemic shunt for treatment of portal hypertension and its complications: a conference sponsored by the National Digestive Diseases Advisory Board. *Hepatology* 1995; **22**: 1591-1597
- 11 **Feu F**, García-Pagán JC, Bosch J, Luca A, Teres J, Escorsell A, Rodes J. Relation between portal pressure response to pharmacotherapy and risk of recurrent variceal haemorrhage in patients with cirrhosis. *Lancet* 1995; **346**: 1056-1059
- 12 **Haskal ZJ**. Improved patency of transjugular intrahepatic portosystemic shunts in humans: creation and revision with PTFE stent-grafts. *Radiology* 1999; **213**: 759-766
- 13 **Sterling KM**, Darcy MD. Stenosis of transjugular intrahepatic portosystemic shunts: presentation and management. *AJR* 1997; **168**: 239-244
- 14 **Lind CD**, Malisch TW, Chong WK, Richards WO, Pinson CW, Meranze SG, Mazer M. Incidence of shunt occlusion or stenosis following transjugular intrahepatic portosystemic shunt placement. *Gastroenterology* 1994; **106**: 1277-1283
- 15 **Ong JP**, Sands M, Younossi ZM. Transjugular intrahepatic portosystemic shunts (TIPS): A decade later. *J Clin Gastroenterol* 2000; **30**: 14-28
- 16 **Rössle M**, Haag K, Ochs A, Sellinger M, Nöldge G, Perarnau JM, Berger E, Blum V, Gabelmann A, Hauenstein K, Langer M, Gerok W. The transjugular intrahepatic portosystemic stent-shunt procedure for variceal bleeding. *N Engl J Med* 1994; **330**: 165-171
- 17 **Hausegger KA**, Sternthal HN, Klein GE, Karaic R, Stauber R, Zenker G. Transjugular intrahepatic portosystemic shunt: angiographic follow-up and secondary interventions. *Radiology* 1994; **191**: 177-181

- 18 **Laberge JM**, Somberg KA, Lake JR, Gordon RL, Kerlan RK, Ascher NL, Roberts JP, Simor MM, Doherty CA, Hahn J, Bacchetti P, Ring EJ. Two-year outcome following transjugular intrahepatic portosystemic shunt for variceal bleeding: results in 90 patients. *Gastroenterology* 1995; **108**: 1143-1151
- 19 **Latimer J**, Bawa SM, Rees CJ, Hudson M, Rose JDG. Patency and reintervention rates during routine TIPSS surveillance. *Cardiovasc Intervent Radiol* 1998; **21**: 234-239
- 20 **Jalan R**, Forrest EH, Stanley AJ, Redhead DN, Forbes J, Dillon JF, Macgilchrist AJ, Finlayson NDC, Hayes PC. A randomized trial comparing transjugular intrahepatic portosystemic stent-shunt with variceal band ligation in the prevention of rebleeding from esophageal varices. *Hepatology* 1997; **26**: 1115-1122
- 21 **Sauer P**, Theilmann L, Stremmel W, Benz C, Richter GM, Stiehl A. Transjugular intrahepatic portosystemic stent shunt versus sclerotherapy plus propranolol for variceal rebleeding. *Gastroenterology* 1997; **113**: 1623-1631
- 22 **Owens CA**, Bartolone C, Warner DL, Aizenstein R, Hibblen J, Yaghamai B, Wiley TE, Layden TJ. The inaccuracy of duplex ultrasonography in predicting patency of transjugular intrahepatic portosystemic shunts. *Gastroenterology* 1998; **114**: 975-980
- 23 **Murphy TP**, Beecham RP, Kim HM, Webb MS, Scola F. Long-term follow-up after TIPS: use of doppler velocity criteria for detecting elevation of the portosystemic gradient. *J Vasc Interv Radiol* 1998; **9**: 275-281
- 24 **Soares GM**, Murphy TP. Transcaval TIPS: indications and anatomic considerations. *J Vasc Interv Radiol* 1999; **10**: 1233-1238
- 25 **Huimin L**, Gansheng F, Jianyong Y, Ruming Z, Chuanshen Z. The anatomic study of imageology related to TIPS. *Chin J Radiol* 1998; **32**: 243-246
- 26 **Petersen B**, Uchida BT, Timmermans H, Keller FS, Rösch J. Intrahepatic us-guided direct intrahepatic portacaval shunt with a PTFE-covered stent-graft: feasibility study in swine and initial clinical results. *J Vasc Interv Radiol* 2001; **12**: 475-486
- 27 **Chang RW**, Shan-Quan S, Yen WW. An applied anatomical study of the ostia venae hepaticae and the retrohepatic segment of the inferior vena cava. *J Anat* 1989; **164**: 41-47 (abstract)
- 28 **Camargo AM**, Teixeira GG, Ortale JR. Anatomy of the ostia venae hepaticae and the retrohepatic segment of the inferior vena cava. *J Anat* 1996; **188**: 59-64
- 29 **Gasparini D**, Forno MD, Sponza M, Branca B, Tonintto P, Marzio A, Pirisi M. Transjugular intrahepatic portosystemic shunt by direct transcaval approach in patients with acute and hyperacute Budd-Chiari syndrome. *Eur J Gastroenterol Hepatol* 2002; **14**: 567-571
- 30 **Seong CK**, Kim YJ, Shin TB, Park HY, Kim TH, Kang DS. Transcaval TIPS in patients with failed revision of occluded previous TIPS. *Korean J Radiol* 2001; **2**: 204-209
- 31 **Helton WS**, Belshaw A, Althaus S, Park S, Coldwell D, Johansen K. Critical appraisal of the angiographic portacaval shunt (TIPS). *Am J Surg* 1993; **165**: 566-571
- 32 **Freedman AM**, Sanyal AJ, Tisnado J, Cole PE, Sbiffman ML, Luketic VA, Purdum PP, Darcy MD, Posner MP. Complications of transjugular intrahepatic portosystemic shunt: a comprehensive review. *Radiographics* 1993; **13**: 1185-1210
- 33 **Te HS**, Jeevanandam V, Millis JM, Cronin DC, Baker AL. Open cardiotomy for removal of migrating transjugular intrahepatic portosystemic shunt stent combined with liver transplantation. *Transplantation* 2001; **71**: 1000-1003
- 34 **Chui AKK**, Rao ARN, Waugh RC, Mayr M, Verran DJ, Koorey D, McCaughan GW, Ong J, Sheil AGR. Liver Transplantation in patients with transjugular intrahepatic portosystemic shunts. *Aust N Z J Surg* 2000; **70**: 493-495
- 35 **Nishimine K**, Saxon RR, Kichikawa K, Mendel-Hartvig J, Timmermans H, Shim HJ, Uchida BT, Barton R, Keller F, Rösch J. Improved transjugular intrahepatic portosystemic shunt patency with PTFE-covered stent-grafts: experimental results in swine. *Radiology* 1995; **196**: 341-347
- 36 **Haskal ZJ**, Davis A, McAllister A, Furth EE. PTFE-encapsulated endovascular stent-graft for transjugular intrahepatic portosystemic shunts: experimental evaluation. *Radiology* 1997; **205**: 682-688
- 37 **Mallery S**, Freeman ML, Peine CJ, Miller RP, Stanchfield WR. Biliary-shunt fistula following transjugular intrahepatic portosystemic shunt placement. *Gastroenterology* 1996; **111**: 1353-1357
- 38 **Saxon RR**, Mendel-Hartvig J, Corless CL, Rabkin J, Uchida BT, Nishimine K, Keller FS. Bile duct injury as a major cause of stenosis and occlusion in transjugular intrahepatic portosystemic shunts: comparative histopathologic analysis in humans and swine. *J Vasc Interv Radiol* 1996; **7**: 487-497

Edited by Zhang JZ

Effects of palmatine on potassium and calcium currents in isolated rat hepatocytes

Fang Wang, Hong-Yi Zhou, Lan Cheng, Gang Zhao, Ji Zhou, Li-Ying Fu, Wei-Xing Yao

Fang Wang, Hong-Yi Zhou, Lan Cheng, Ji Zhou, Li-Ying Fu, Wei-Xing Yao, Department of Pharmacology, Tongji Medical College of Huazhong University of Science and Technology, Wuhan 430030, Hubei Province China

Gang Zhao, Department of Pancreatic Surgery Center, Union Hospital, Tongji Medical College of Huazhong University of Science and Technology, Wuhan 430022, Hubei Province China

Correspondence to: Dr. Fang Wang, Department of Pharmacology, Tongji Medical College of Huazhong University of Science and Technology, Wuhan 430030, Hubei Province China. wangfang0322@yahoo.com.cn

Telephone: +86-27-83692033

Received: 2002-09-14 **Accepted:** 2002-10-17

Abstract

AIM: To study the effects of palmatine, a known inhibitor on delayed rectifier potassium current and L-type calcium current ($I_{Ca,L}$) in guinea pig ventricular myocytes, on the potassium and calcium currents in isolated rat hepatocytes.

METHODS: Tight-seal whole-cell patch-clamp techniques were performed to investigate the effects of palmatine on the delayed outward potassium currents (I_K), inward rectifier potassium current (I_{K1}) and Ca^{2+} release-activated Ca^{2+} current (I_{CRAC}) in enzymatically isolated rat hepatocytes.

RESULTS: Palmatine 0.3-100 μ M reduced I_K in a concentration-dependent manner with EC_{50} of 41.62 ± 10.11 μ M and n_H , 0.48 ± 0.07 ($n=8$). The effect of the drug was poorly reversible after washout. When the bath solution was changed to tetraethylammonium (TEA) 8 mM, I_K was inhibited. Palmatine 10 μ M and 100 μ M shifted the I-V curves of I_K downward, and the block of I_K was voltage-independent. Palmatine 0.3-100 μ M also inhibited I_{CRAC} in a concentration-dependent manner. The fitting parameters were as follows: $EC_{50}=51.19 \pm 15.18$ μ M, and $n_H=0.46 \pm 0.07$ ($n=8$). The peak value of I_{CRAC} in the I-V relationship was decreased by palmatine 10 μ M and 100 μ M. But the reverse potential of I_{CRAC} occurred at Voltage=0 mV in all cells. Palmatine 0.3-100 μ M failed to have any significant effect on either inward or outward components of I_{K1} at any membrane potential examined.

CONCLUSION: The inhibitory effects on I_K and I_{CRAC} could be one of the mechanisms that palmatine exerts protective effect on hepatocytes.

Wang F, Zhou HY, Cheng L, Zhao G, Zhou J, Fu LY, Yao WX. Effects of palmatine on potassium and calcium currents in isolated rat hepatocytes. *World J Gastroenterol* 2003; 9(2): 329-333 <http://www.wjgnet.com/1007-9327/9/329.htm>

INTRODUCTION

There are many natural drugs for liver diseases currently used in popular medicine. For example, quaternary protoberberine

alkaloids from *Flissitigma* and *Goniothalamus* have been used in popular medicine for hepatomegaly and hepatosplenomegaly^[1,2]. The uses of alkaloids from *Berberis aristata* for liver injury induced by chemical carcinogenesis and alkaloids from *Enantica* for disorders of bilirubin have also been reported^[3,4].

Palmatine, the protoberberine class of isoquinoline alkaloids, has been found in plants of various families, and mainly presents in the rhizomes of *Fibrarurea Tinctoria Lour.* These medicinal plants have been used as folk medicine in treatment of jaundice, dysentery, hypertension, inflammation and liver-related diseases^[5,6]. The previous studies have shown that palmatine could block the delayed rectifier potassium current and had inhibition effect on L-type calcium current ($I_{Ca,L}$) in guinea pig ventricular myocytes^[7-11]. Pauli *et al* reported a protoberberine alkaloids mixture from *Enantia chlorantha*, called Hepasor, containing palmatine, columbamine and jatrorrhizine prevented liver from chemically induced traumatization and also promoted the healing process in the hepatic injury models selected. Hepasor improved the blood flow and mitotic activity in thioacetamide-traumatized rat livers^[12]. However, the hepatoprotective mechanism of palmatine still remains unknown. And there are no data available to the relationship between ion currents in hepatocytes and the hepatoprotective effect of palmatine.

In the present study, we investigated the effects of palmatine on whole-cell currents recorded from isolated rat hepatocytes to explore its mechanisms against liver injury. We tried to develop not only an effective hepatoprotective agent but also a promising leading compound against liver injury while maintaining a low side-effect profile.

MATERIALS AND METHODS

Cell preparation

The rat hepatocytes were enzymatically isolated from Sprague Dawley (SD) rats of either sex (150 to 200 g) by slightly modified procedures described previously^[13-18]. Briefly, adult animals were anesthetized with an intraperitoneal injection of pentobarbital sodium (30 mg/kg) in strict accordance to the guidelines established by the Institutional Animal Care and Use Committee, which follow all applicable state and federal laws. The portal vein and the inferior vena cava were cannulated. The liver was initially perfused at a flow rate of 25 mL \cdot min⁻¹ with a constant-flow system with modified oxygenated Ca^{2+} , Mg^{2+} -free Hanks' solution containing (in mM): NaCl 137, KCl 5.4, NaH_2PO_4 0.5, Na_2HPO_4 0.58, $NaHCO_3$ 4.16 and Glucose 5.5 (pH 7.3) for several minutes, followed by perfusion with a Ca^{2+} , Mg^{2+} -free Hanks' solution containing collagenase (0.3 g \cdot L⁻¹; type I) for 10 min. The solutions were gassed with 100 % O_2 and warmed to 37 °C. After these perfusions, the liver was excised and then minced in Ca^{2+} , Mg^{2+} -free Hanks' solution at 0 °C. The cells were filtered through a 200 μ m nylon mesh, and washed three times by centrifugation at 50 g for 2 min. The cell pellets were resuspended in Kraft-bruhe (KB) solution containing (in mM): L-glutamic acid 70, KCl 130, taurine 15, KH_2PO_4 10, $MgCl_2$ 0.5, Glucose 11, 4-(2-hydroxyethyl)-1-piperazine-*N'*-2-ethanesulfonic acid (HEPES) 10 and ethylene glycol-bis (β -aminoethyl ether)-*N*,

N, N', N'-tetraacetic acid (EGTA) 0.5 (pH 7.4) that yielded approximately 85 % to 95 % viable hepatocytes. A small aliquot of the medium containing single cell was transferred into a 1 mL chamber mounted on the stage of an inverted microscope (XD-101_{2B}, Nanjing, China). The spherical, smooth cells were used for the whole-cell voltage-clamp studies. All experiments were performed at room temperature (20 to 22 °C).

Voltage-clamp recording

A programmable vertical puller (pp-83, Narishige, Japan) was used to pull the electrodes. The resistance of the capillary glass electrodes (GG-17, Nanjing, China) used was 2 to 4 MΩ when filled with internal solution. A patch-clamp amplifier (PC-II, Wuhan, China) was used to record whole-cell currents with four-pole Bessel filter set at 1 kHz, digitized at 5 kHz. The protocols for voltage clamp and data analysis were established with routines using software (pClamp 6.0, Wuhan, China) and data were stored on computer for subsequent analysis. Drug actions were measured only after steady-state-conditions were reached, which were judged by the amplitudes and time courses of currents remaining constant with further perfusion of drug.

Drugs and solutions

Palmitine hydrochloride was obtained from Zhonglian Pharmaceutical Company of China as base powders, dissolved in distilled water and made a stock solution at 0.1 M. Palmitine was added to bath solution for extracellular application. All drugs were from Sigma Chemical Co unless otherwise indicated.

With studies of I_K , the bath solution was a modified Tyrode's solution contained (in mM): NaCl 144, KCl 4.0, CaCl₂ 1.8, MgCl₂ 0.53, Na₂HPO₄ 0.33, HEPES 5 and Glucose 5.5 (pH 7.3). The patch pipette solution contained (in mM): KCl 130, K₂ATP 5.0, creatine phosphate 5.0 and HEPES 5.0 (pH 7.4).

For experiments on I_{K1} , both the bath solution and the pipette solution contained (in mM): KCl 7, MgCl₂ 2, EGTA 1, K-glutamate 130 and HEPES 10 (pH 7.4).

For I_{CRAC} recording, the bath solution was (in mM): NaCl 140, KCl 2.8, CaCl₂ 10, MgCl₂ 0.5, Glucose 11 and HEPES 10 (pH 7.4). The pipette solution used (in mM): K-glutamate 145, NaCl 8, MgCl₂ 1, MgATP 0.5, EGTA 10 and HEPES 10 (pH 7.2).

Statistics

All values are expressed as mean ± S.E.M and error bars were plotted as S.E.M. Student's *t* test was used to evaluate the statistical significance of differences between means. A value of $P < 0.05$ was considered to be statistically significant. Concentration-response curves were fitted by the Hill equation: Inhibition of current (%) = $100/[1+(EC_{50}/C)^{nH}]$

Where EC_{50} is the concentration of palmitine for half-maximum block, C is the concentration of palmitine, and n_H , the Hill coefficient.

RESULTS

Effects of palmitine on I_K

I_K was evoked in isolated rat hepatocytes by depolarizing pulse to +140 mV for 900 ms from a holding potential of -50 mV. The current at the end point of the test pulse was measured as the amplitude of I_K ^[19].

To better the concentration of palmitine necessary for half-maximal effect, six concentrations (0.3-100 μM) were studied. The percentage block of I_K was defined as $(I_{Control} - I_{palmitine})/I_{Control}$ and plotted as a function of logarithm [palmitine] in Figure 1B. At +140 mV, palmitine exerted a concentration-dependent inhibition of the current, which was poorly reversible after washout (Table 1). The data points are fitted according to the Hill equation with an EC_{50} for palmitine on I_K is 41.62 ± 10.11 μM

and n_H , 0.48 ± 0.07 ($n=8$). When the bath solution was changed to tetraethylammonium (TEA) 8 mM, I_K was inhibited.

Figure 1C shows the effects of palmitine 10 μM and 100 μM on the steady-state I-V relationship for I_K generated by applying 12 depolarizing pulses from +30 mV to +140 mV for 900 ms with a 10 mV increment from a holding potential of -50 mV. In the presence of palmitine 100 μM, the amplitude of I_K was significantly reduced from +70 mV through +140 mV ($n=8$, $P < 0.05$ or $P < 0.01$ vs control). The currents were inhibited in a voltage-independent manner at the potentials tested. For example, at +100 mV, I_K was reduced by palmitine 100 μM from 1319.52 ± 192.60 to 575.37 ± 133.29 pA (56.40 % reduction), and at +140 mV, current was reduced from 1861.42 ± 215.76 to 879.37 ± 172.30 pA (52.76 % reduction). The relative reductions of I_K were illustrated in Figure 1D. Currents after addition of 10 μM and 100 μM palmitine were normalized to currents under control conditions at a given voltage, and it can clearly be seen that the currents were inhibited to the same degree at all potentials tested.

Table 1 Effects of palmitine on I_K at a test potential of +140 mV and I_{CRAC} at -100 mV

Concentration (μM)	Inhibition of I_K (%)	Inhibition of I_{CRAC} (%)
0.3	3.36±1.96	3.81±0.40
1	11.04±3.03	10.19±2.03
3	23.97±4.62	21.42±3.22
10	36.75±5.12	37.39±3.95
30	49.58±7.98	47.50±4.38
100	55.40±8.97	52.10±5.98

Effects of palmitine on I_{K1}

Hyperpolarizing and depolarizing potentials over a range from -200 mV to +175 mV were applied from a holding level of 0 mV^[20]. The absolute value at the end of test pulse was measured as the amplitude of I_{K1} . Palmitine 0.3-100 μM failed to have any significant effect on either inward or outward components of I_{K1} at any membrane potential examined.

Effects of palmitine on I_{CRAC}

When the holding potential was 0 mV, and the cells were depolarized to -100 mV for 200 ms at a frequency of 0.2 Hz, the I_{CRAC} was evoked^[21]. As shown in Figure 2, I_{CRAC} also was blocked by palmitine in a concentration-dependent fashion, and the current was less sensitive to palmitine than I_K with an EC_{50} of 51.19 ± 15.18 μM and $n_H = 0.46 \pm 0.07$ ($n=8$). Table 1 also showed the effects of palmitine on I_{CRAC} at a test potential of -100 mV. Figure 2C showed the effects of palmitine on the steady-stated I-V relationships generated by applying a series depolarizing pulses from a holding potential of 0 mV to different membrane potentials (-100 mV to +80 mV) with a 20 mV increment. The peak value of I_{CRAC} in the I-V relationship was decreased by palmitine 10 μM and 100 μM ($n=8$, $P < 0.05$ or $P < 0.01$ vs control). But the reverse potential of I_{CRAC} occurred at voltage=0 mV in all cells.

DISCUSSION

In this study we have, for the first time, characterized the effects of palmitine on the hepatocyte I_K , I_{K1} and I_{CRAC} by patch-clamp techniques and demonstrated that palmitine effectively inhibited I_K and I_{CRAC} in isolated rat hepatocytes.

Membrane potential is important in regulating metabolic processes in the liver, including gluconeogenesis, amino acid transport, and the rate of uptake of bile salts^[22,23]. Changes in

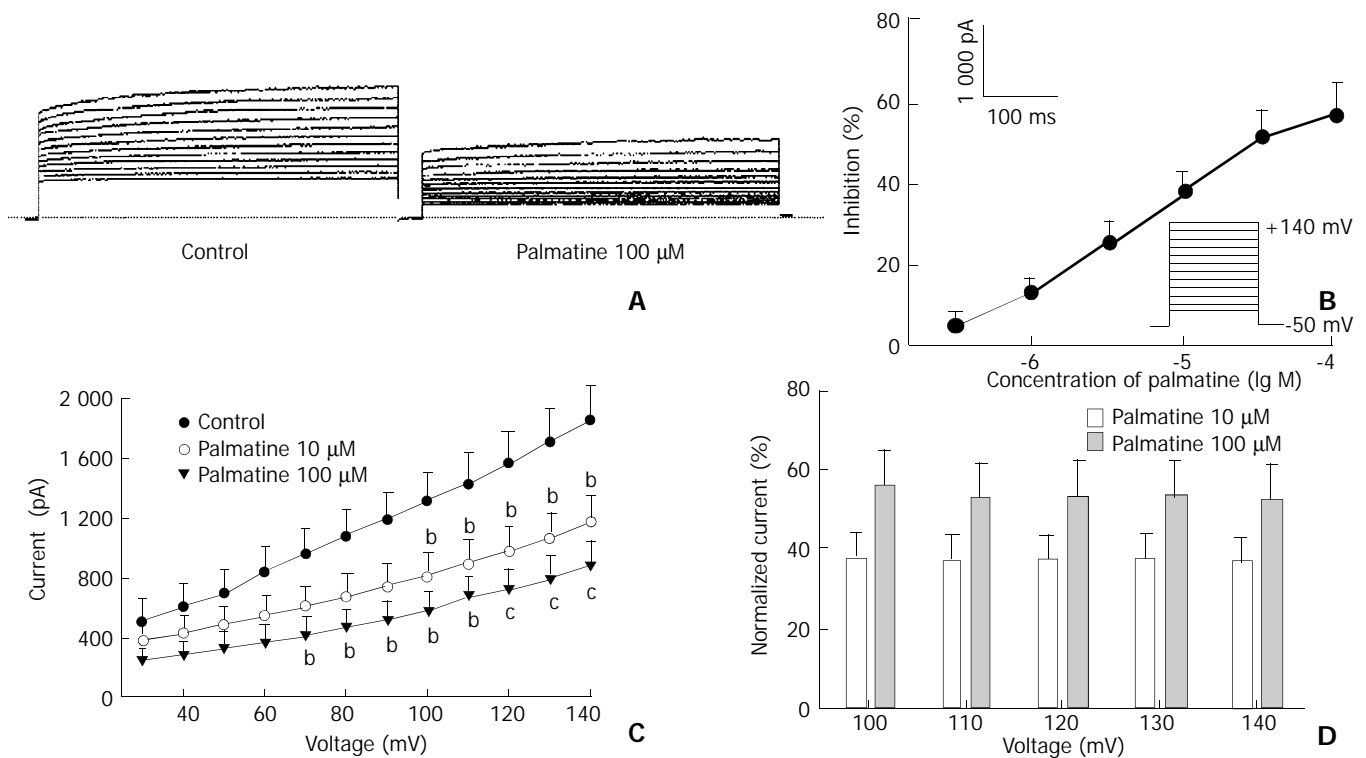


Figure 1 Effects of palmatine on I_K. (A) Family of I_K recorded with changes in the absent or present of palmatine 100 μM. Dotted line indicates zero current level. (B) Dose-response curve for the effects of palmatine on I_K. The data are mean values from *n*=8 cells. (C) I-V relationship of I_K under control (●) and palmatine 10 μM (○), 100 μM (●). The voltage steps used to elicit I_K are shown in the inset of panel (B). ^b*P*<0.05, ^c*P*<0.01 vs control (*n*=8). (D) Dependence of palmatine effects on test potential. The values for the mean percentage reductions in I_K induced by palmatine 10 μM (□) and 100 μM (■) are plotted against the corresponding test potential. No significant voltage-dependence was observed for the blocks induced by palmatine.

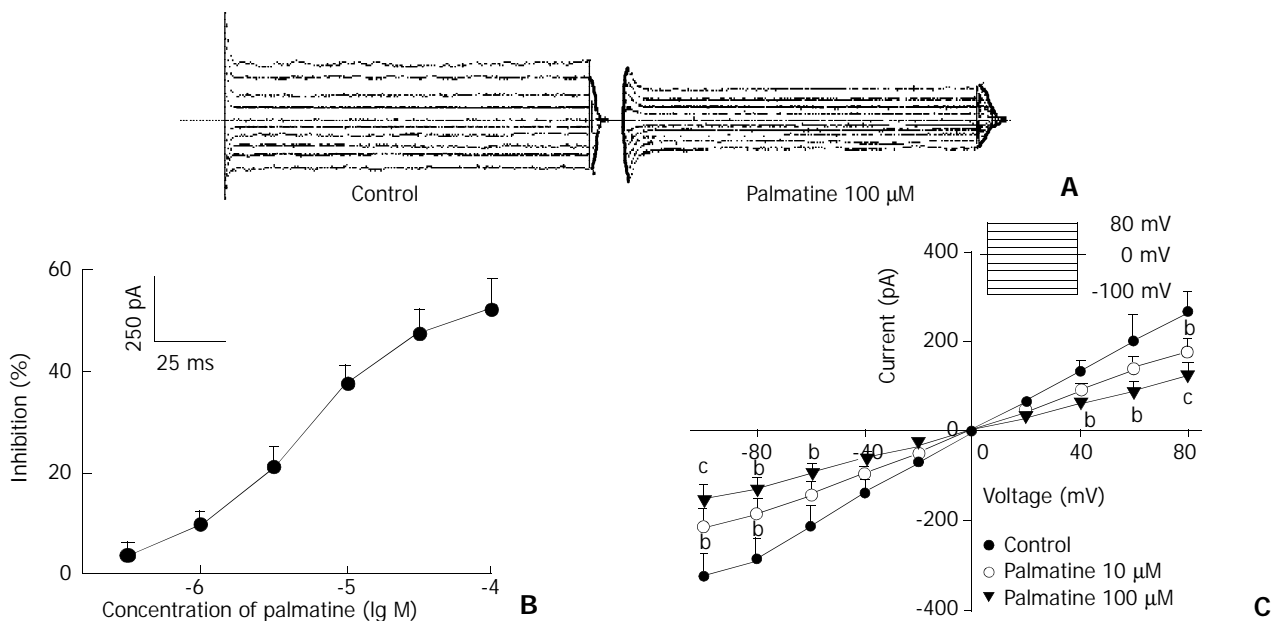


Figure 2 Effects of palmatine on I_{CRAC}. (A) Family of I_{CRAC} recorded with changes in the absent or present of palmatine 100 μM. Dotted line indicates zero current level. (B) Dose-response curve for effects of palmatine on I_{CRAC}. The data are mean values from *n*=8 cells. (C) I-V relationship of I_{CRAC} under control (●) and palmatine 10 μM (○), 100 μM (●). The voltage steps used to elicit I_K are shown in the inset of panel (B). ^b*P*<0.05, ^c*P*<0.01 vs control (*n*=8).

K⁺ permeability can affect the transmembrane potential. Transcellular bile acid transport is integrated in the regulation of intracellular pH, K⁺ homeostasis and membrane potential. Hepatocellular K⁺-depletion can result in inhibition of bile acid secretion despite rising intracellular concentration^[24-26].

During ischemia and hypoxia, hepatocellular volume and K⁺ conductance are increased. It was reported that the extracellular K⁺ increase would result in hyperpolarization and

hyperexcitability of cells. This would lead to cell death^[27-29]. Nietsch *et al* demonstrated membrane potential change by modulation of K⁺ channel activity might be involved in the mechanism of apoptosis in human hepatoma cells^[30,31]. The inhibition of K⁺ channels could delay hepatocyte apoptosis and death.

Calcium has been demonstrated to play an important role in hepatocyte damage. Elevation of intracellular Ca²⁺

concentration was associated with the development of cell damage and apoptosis^[32-35].

Recent developments suggest that an early disturbance in hepatocellular Ca^{2+} homeostasis might be involved in the hepatocellular damage induced by CCl_4 ^[36-38].

Hepatocytes as the nonexcitable cells are short of the voltage-dependent Ca^{2+} channels but possess plasma membrane Ca^{2+} channels that have a high selectivity for Ca^{2+} , and are activated by a decrease in the concentration of Ca^{2+} in intracellular stores, which named I_{CRAC} ^[39,40]. The gating of I_{CRAC} is independent of membrane voltage, there is, nevertheless, a strong dependence of Ca^{2+} influx on the driving force exerted by the membrane potential, ie, the influx rate increases with hyperpolarization and decreases with depolarization, which is different from cardiac myocytes that Ca^{2+} influx increases with depolarization and decreases with hyperpolarization^[41].

Palmitine inhibits I_{CRAC} with EC_{50} of 51.19 μM , which is higher than the EC_{50} of $\text{I}_{\text{Ca,L}}$ in cardiac myocytes^[42]. The differential drug sensitivity of the two currents also provides further support for the idea that I_{CRAC} is different from voltage-gated Ca^{2+} channel.

In conclusion, palmitine blocks K^+ channel and decreases the extracellular K^+ to regulate the metabolic processes in the liver. Palmitine also inhibits I_{CRAC} effectively and protects hepatocytes from calcium overload via the inhibition of I_{CRAC} . The inhibitory effects on I_{K} and I_{CRAC} may partly contribute to the hepatoprotective action of palmitine.

REFERENCES

- Virtanen P**, Lassila V, Njimi T, Mengata DE. Natural protoberberine alkaloids from *Enantia chlorantha*, palmitine, columbamine and jatrorrhizine for thioacetamide-traumatized rat liver. *Acta anat (basel)* 1988; **131**: 166-170
- Virtanen P**, Lassila V, Njimi T, Mengata DE. Regeneration of D-galactosamine-traumatized rat liver with natural protoberberine alkaloids from *Enantia chlorantha*. *Acta anat (basel)* 1988; **132**: 159-163
- Virtanen P**, Lassila V, Njimi T, Mengata DE. Effect of splenectomy on Hepasor treatment in allyl-alcohol-traumatized rat liver. *Acta anat (basel)* 1989; **134**: 301-304
- Anis KV**, Rajeshkumar NV, Kuttan R. Inhibition of chemical carcinogenesis by berberine in rats and mice. *J Pharm Pharmacol* 2001; **53**: 763-768
- Niu XW**, Zeng T, Qu AL, Kang HG, Dai SP, Yao WX, Jiang MX. Effects of 7-bromoethoxybenzene-tetrahydropalmitine on voltage-dependent currents in guinea pig ventricular myocytes. *Zhongguo Yaoli Xuebao* 1996; **17**: 227-229
- Chang YL**, Usami S, Hsieh MT, Jiang MJ. Effects of palmitine on isometric force and intracellular calcium levels of arterial smooth muscle. *Life Sci* 1999; **64**: 597-606
- Lau CW**, Yao XQ, Chen ZY, Ko WH, Huang Y. Cardiovascular actions of berberine. *Cardiovasc Drug Rev* 2001; **19**: 234-244
- Xu C**, Sun MZ, Li YR, Yang BF, Wang LJ, Li JM. Inhibitory effect of tetrahydropalmitine on calcium current in isolated cardiomyocyte of guinea pig. *Zhongguo Yaoli Xuebao* 1996; **17**: 329-331
- Li Y**, Fu LY, Yao WX, Xia GJ, Jiang MX. Effects of benzyltetrahydropalmitine on potassium currents in guinea pig and rat ventricular myocytes. *Acta Pharmacol Sin* 2002; **23**: 612-616
- Yang BF**, Zong XG, Wang G, Yao WX, Jiang MX. The mechanism of antiarrhythmic action of 7-bromoethoxybenzene-tetrahydropalmitine. *Yaoxue Xuebao* 1990; **25**: 481-484
- Li BX**, Yang BF, Zhou J, Xu CQ, Li YR. Inhibitory effects of berberine on I_{K1} , I_{K} , and HERG channels of cardiac myocytes. *Acta Pharmacol Sin* 2001; **22**: 125-131
- Virtanen P**, Lassila V, Soderstrom KO. Protoberberine alkaloids from *Enantia chlorantha* therapy of allyl-alcohol- and D-galactosamine-traumatized rats. *Pathobiology* 1993; **61**: 51-56
- Li D**, Sun J, Sun H. Bile salt induces apoptosis of hepatocytes: the mechanism of hepatic function injury during obstructive jaundice. *Zhonghua Waikexue* 1998; **36**: 624-626
- Serran H**, Musallam L, Haddad P. Comparative effects of UW and SLS solutions on concentrative proline uptake in cold preserved rat hepatocytes. *Therapie* 1999; **54**: 601-606
- Seglen PO**. Preparation of isolated rat liver cells. *Methods Cell Biol* 1976; **13**: 29-83
- Breit S**, Kolb HA, Häussinger D, Lang F. Effects of tetrabutylhydroperoxide on hepatocyte ion channels. *Cell Physiol Biochem* 1999; **9**: 133-138
- Zhang GL**, Wang YH, Teng HL, Lin ZB. Effects of aminoguanidine on nitric oxide production induced by inflammatory cytokines and endotoxin in cultured rat hepatocytes. *World J Gastroenterol* 2001; **7**: 331-334
- Wang YJ**, Li MD, Wang YM, Ding J, Nie QH. Simplified isolation and spheroidal aggregate culture of rat hepatocytes. *World J Gastroenterol* 1998; **4**: 74-76
- Li JM**, Cui GY, Liu DJ, Cui H, Chang TH, Wang YP, Zhang KY. Effects of N-methyl berbamine on delayed outward potassium current in isolated rat hepatocytes. *Zhongguo Yaoli Xuebao* 1998; **19**: 24-26
- Henderson RM**, Graf J, Boyer JL. Inward-rectifying potassium channels in rat hepatocytes. *Am J Physiol* 1989; **256**: G1028-G1035
- Cui GY**, Li JM, Cui H, Hao LY, Liu DJ, Zhang KY. Effects of calcium channel blockers on calcium release-activated calcium currents in rat hepatocytes. *Zhongguo Yaoli Xuebao* 1999; **20**: 415-418
- Bernardi P**, Azzone GF. Regulation of Ca^{2+} efflux in rat liver mitochondria. Role of membrane potential. *Eur J Biochem* 1983; **134**: 377-383
- Einarsson C**, Ellis E, Abrahamsson A, Ericzon BG, Bjrkhem I, Axelson M. Bile acid formation in primary human hepatocytes. *World J Gastroenterol* 2000; **6**: 522-525
- Devin A**, Espie P, Guerin B, Rigoulet M. Energetics of swelling in isolated hepatocytes: a comprehensive study. *Mol Cell Biochem* 1998; **184**: 107-121
- vom Dahl S**, Hallbrucker C, Lang F, Haussinger D. Regulation of cell volume in the perfused rat liver by hormones. *Biochem J* 1991; **280**: 105-109
- Kiss L**, Immke D, LoTurco J, Korn SJ. The interaction of Na^+ and K^+ in voltage-gated potassium channels. Evidence for cation binding sites of different affinity. *J Gen Physiol* 1998; **111**: 195-206
- Hill CE**, Jacques JE. Cholestatic effects of the K^+ channel blockers Ba^{2+} and TEA occur through different pathways in the rat liver. *Am J Physiol* 1999; **276**: G43-G48
- Hill CE**, Briggs MM, Liu J, Magtanong L. Cloning, Expression, and localization of a rat hepatocyte inwardly rectifying potassium channel. *Am J Physiol Gastrointest Liver Physiol* 2002; **282**: G233-G240
- Li L**, Jin NG, Piao L, Hong MY, Jin ZY, Li Y, Xu WX. Hyposmotic membrane stretch potentiated muscarinic receptor agonist-induced depolarization of membrane potential in guinea-pig gastric myocytes. *World J Gastroenterol* 2002; **8**: 724-727
- Nietsch HH**, Roe MW, Fiekers JF, Moore AL, Lidofsky SD. Activation of potassium and chloride channels by tumor necrosis factor- α role in liver cell death. *J Biol Chem* 2000; **275**: 20556-20561
- Kim JA**, Kang YS, Jung MW, Kang GH, Lee SH, Lee YS. Ca^{2+} influx mediates apoptosis induced by 4-aminopyridine, a K^+ channel blocker, in HepG₂ human hepatoblastoma cells. *Pharmacology* 2000; **60**: 74-81
- Crenesse D**, Hugues M, Ferre C, Poiree JC, Benoliel J, Dolisi C, Gugenheim J. Inhibition of calcium influx during hypoxia/reoxygenation in primary cultured rat hepatocytes. *Pharmacology* 1999; **58**: 160-170
- Isozaki H**, Fujii K, Nomura E, Hara H. Calcium concentration in hepatocytes during liver ischemia-reperfusion injury and the effects of diltiazem and citrate on perfused rat liver. *Eur J Gastroenterol Hepatol* 2000; **12**: 291-297
- Ueda T**, Takeyama Y, Hori Y, Takase K, Goshima M, Kuroda Y. Pancreatitis-associated ascitic fluid increases intracellular Ca^{2+} concentration on hepatocytes. *J Surg Res* 2000; **93**: 171-176
- Lafuente NG**. Calcium channel blockers and hepatotoxicity. *Am J Gastroenterol* 2000; **95**: 2145
- Hemmings SJ**, Pulga VB, Tran ST, Uwiera RR. Differential inhibitory effects of carbon tetrachloride on the hepatic plasma

- membrane, mitochondrial and endoplasmic reticular calcium transport systems: implications to hepatotoxicity. *Cell Biochem Funct* 2002; **20**: 47-59
- 37 **Recknagel RO**. A new direction in the study of carbon tetrachloride hepatotoxicity. *Life Sci* 1983; **33**: 401-408
- 38 **Huang ZS**, Wang ZW, Liu MP, Zhong SQ, Li QM, Rong XL. Protective effects of polydatin against CCl₄-induced injury to primarily cultured rat hepatocytes. *World J Gastroenterol* 1999; **5**: 41-44
- 39 **Takanashi H**, Sawanobori T, Kamisaka K, Maezawa H, Hiraoka M. Ca²⁺-activated K⁺ channel is present in guinea-pig but lacking in rat hepatocytes. *Jpn J Physiol* 1992; **42**: 415-430
- 40 **Rychkov G**, Brereton HM, Harland ML, Barritt GJ. Plasma membrane Ca²⁺ release-activated Ca²⁺ channels with a high selectivity of Ca²⁺ identified by patch-clamp recording in rat liver cells. *Hepatology* 2001; **33**: 938-947
- 41 **Gregory RB**, Rychkov G, Barritt GJ. Evidence that 2-aminoethyl diphenylborate is a novel inhibitor of store-operated Ca²⁺ channels in liver cells and acts through a mechanism which does not involve inositol trisphosphate receptors. *Biochem J* 2001; **354**: 285-290
- 42 **Huang K**, Dai GZ, Li XH, Fan Q, Cheng L, Feng YB, Xia GJ, Yao WX. Blocking L-calcium current by l-tetrahydropalmatine in single ventricular myocyte of guinea pigs. *Zhongguo Yaoli Xuebao* 1999; **20**: 907-911

Edited By Zhou YP

Localization of TRAIL/TRAILR in fetal pancreas

Li-Hua Chen, Xue-Song Liu, Wen-Yong Wang, Wei-Ning Han, Bo-Rong Pan, Bo-Quan Jin

Li-Hua Chen, Xue-Song Liu, Wei-Ning Han, Bo-Quan Jin, Department of Immunology, the Fourth Military Medical University, Xi' an 710032, Shaanxi Province, China

Wen-Yong Wang, Department of Pathology, the Fourth Military Medical University, Xi' an 710032, Shaanxi Province, China

Bo-Rong Pan, Oncology Center, Xijing Hospital, the Fourth Military Medical University, Xi' an 710032, Shaanxi Province, China

Supported by the grants of the National Key Basic Research Program of China, No. 2001CB510004

Correspondence to: Professor Bo-Quan Jin, 17 West Changle Road, Xi' an 710032, Shaanxi Province, China. immu_jin@fmmu.edu.cn

Telephone: +86-29-3374528 **Fax:** +86-29-3253816

Received: 2002-10-04 **Accepted:** 2002-11-04

Abstract

AIM: To observe the localization of TRAIL/TRAILR (DR4, DR5, DcR1, DcR2) in the fetal pancreas.

METHODS: Fetal pancreas of 32 weeks of pregnancy were obtained from induced abortions, embedded in paraffin, and 4- μ m sections were prepared. The localization of TRAIL/TRAILR in fetal pancreas was investigated by fluorescence immunohistochemical method combined with laser scanning confocal microscopy.

RESULTS: TRAIL immunoreactive cells were mainly located on the periphery of the pancreas islets. There were a few DcR1 and DcR2 positive cells whereas there were no immunoreactive cells of DR4 and DR5 in the pancreas islets. In the acini and the ducts of the exocrine pancreas there were no TRAIL/TRAILR immunoreactive cells.

CONCLUSION: This study not only describes the distribution of TRAIL/TRAILR in the fetal pancreas, but also provides a morphological basis for deducing the function of TRAIL/TRAILR in pancreas, suggesting that in normal pancreatic islets, the pancreatic cells are resistant towards apoptosis too.

Chen LH, Liu XS, Wang WY, Han WN, Pan BR, Jin BQ. Localization of TRAIL/TRAILR in fetal pancreas. *World J Gastroenterol* 2003; 9(2): 334-337

<http://www.wjgnet.com/1007-9327/9/334.htm>

INTRODUCTION

Being an important endocrinology organ, the pancreas plays an important role in many physical and pathological processes^[1-11]. The pancreatic islets could secrete not only the classical endocrinology substances such as insulin, glucagons, somatostatin and so on, but also could secrete some neuropeptides and cytokines^[12,13].

Tumor necrosis factor related apoptosis inducing ligand (TRAIL)/TRAILR is a group of molecules belong to TNFSF/TNFRSF identified from 1995 and displays very important biological function^[14-20]. Despite the widespread interest in TRAIL and its receptors to date, studies on TRAIL/TRAILR

are mostly stayed on mRNA level just for the lack of monoclonal antibodies. Fortunately, a series of antibodies against TRAIL/TRAILR system have been prepared and identified successfully by our department and Screation group recently and these provided a useful way to detect the expression of TRAIL/TRAILR in many organs and tissues^[21]. In this experiment, we detected the localization of TRAIL/TRAILR in fetal pancreas.

MATERIALS AND METHODS

Reagents

The mouse anti-human DR4, DR5, DcR1, and DcR2 antibodies and the rabbit anti-human TRAIL antibody were prepared in our department. Biotin conjugated horse anti-rabbit IgG, FITC conjugated goat anti-mouse IgG and Texas red-conjugated streptavidin were purchased from Sigma.

Preparation of tissue sections

Five fetal pancreas of 32-week pregnancy were surgically obtained. They were washed with physiological saline at 4 °C and a 6-mm³ piece was taken from each before fixed in Bouin' s solution overnight. Each piece was embedded in paraffin and 4- μ m sections were prepared.

Immunohistochemistry

Four-micrometer sections from fetal pancreas of 32-week pregnancy were employed in the fluorescent immunohistochemical analysis of TRAIL/TRAILR. Several dilutions of the antibody were tested to find the optimal staining concentration before the entire series was processed. The staining procedure was carried out as previous reports, without protease treatment^[22]. Briefly, the steps included: (1) the sections were deparaffinized in xylene, hydrated in ethanol, and washed in 0.01 mol/L PBS, then pretreated with 30 mL/L normal goat serum for 40 min and rinsed in 0.1 mol/L PBS; (2) incubation at 4 °C for 24 h in the primary antibodies, mouse anti-human DR4, DR5, DcR1 and DcR2 antibody (1:200 dilution, final concentration of 25 mg/L) was performed respectively, and then in rabbit anti-human TRAIL antibody (1:300 dilution in 10 mL/L BSA-PBS); (3) the secondary antibody, biotin-labeled horse anti-rabbit IgG (1:200 dilution), was incubated at room temperature for 1 h; (4) simultaneous incubation with 1:200 FITC conjugated goat anti-mouse IgG and Texas red-conjugated streptavidin (1:1 000 dilution) for 30 min. The sections were washed three times for 10 min each after incubation from steps 2 to 4, respectively, and were finally mounted in 50 g/L glycerin. The sections were examined with Bio-Rad 1024 LSCM. The specimens were excited with a laser beam at wavelengths of 568 nm (Texas Red) and 488 nm (FITC) and the emission light was focused through a pinhole aperture. The full field of view was scanned in square image formats of 512x512 pixels.

Controls

Primary antibodies were substituted by irrelevant antibodies and normal rabbit or goat serum as specific antibody control. PBS was substituted for primary antibody as negative control. Primary antibody was omitted as blank control.

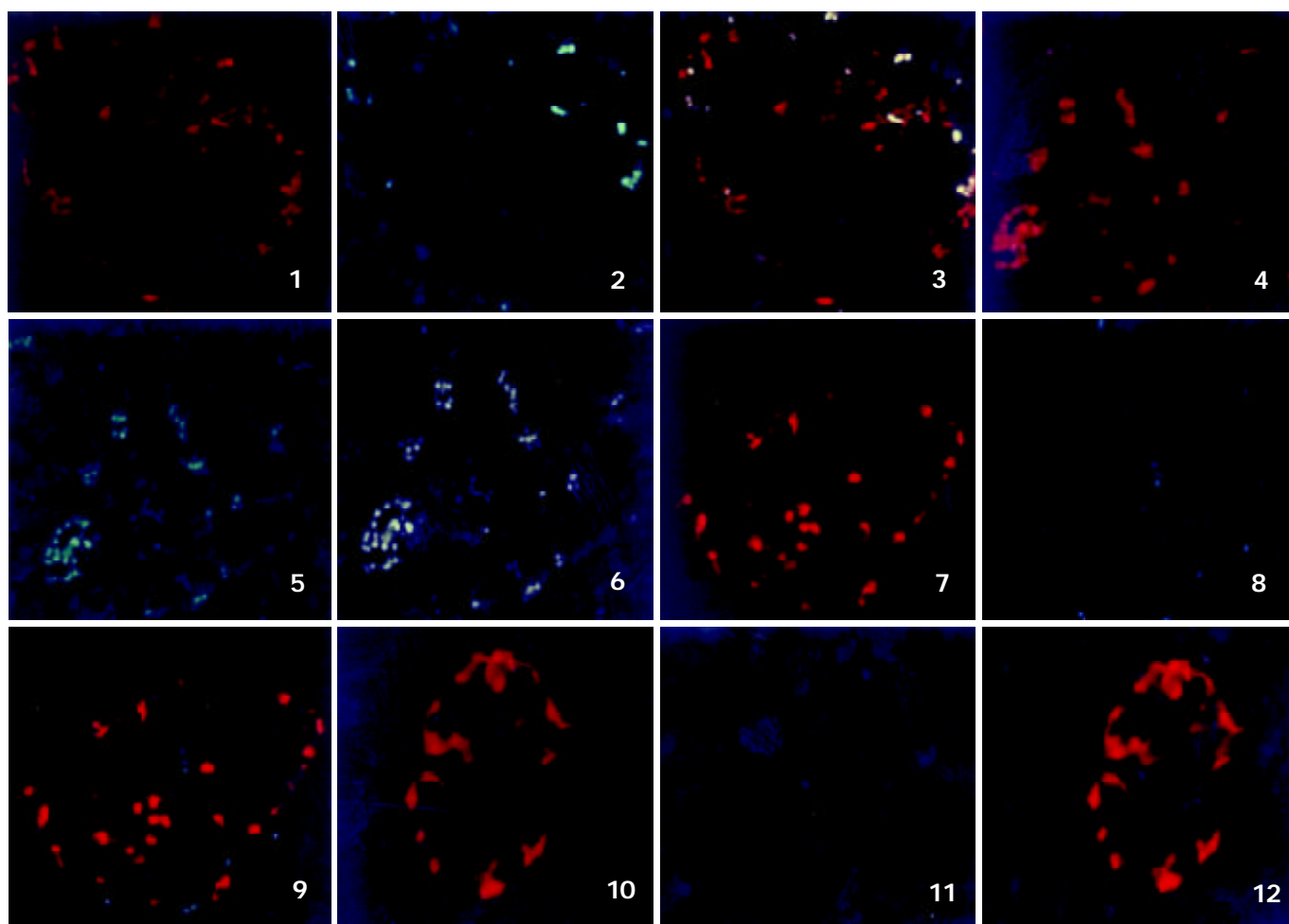


Figure 1, 4, 7, 10 Distribution of TRAIL in fetal pancreas. The positive reactivities are mainly distributed in membrane (red). TR-labelled $\times 400$.

Figure 2, 5, 8, 11 Localization of DcR1, DcR2, DR4 and DR5 respectively in fetal pancreas. There are a few DcR1 (Figure 2) and DcR2 (Figure 5) positive cells and the positive substances locate in membrane mainly (green). There is no DR4 (Figure 8) and DR5 (Figure 11) positive cells distributed in fetal pancreas. FITC-labelled $\times 400$.

Figure 3, 6, 9, 12 Coexpression of TRAIL/TRAILR in fetal pancreas. Some TRAIL positive cells coexpress with DcR1 or DcR2, whereas there is no coexpression of TRAIL and DR4, TRAIL and DR5 in fetal pancreas. The positive cells distribute in disperse (yellow). TR-labelled TRAIL, FITC-labelled TRAILR (DcR1, DcR2, DR4 and DR5) $\times 400$.

RESULTS

Localization of TRAIL in fetal pancreas

Fluorescent immunohistochemistry showed that TRAIL positive cells located on the periphery of pancreatic islets mainly. In the acini and the ducts of the exocrine pancreas there were no TRAIL immunoreactive cells. The positive cells distributed in disperse or patch pattern. The positive reactivity was mainly distributed in membrane and cytoplasm, while nuclei remained immunonegative (Figures 1, 4, 7 and 10).

Localization of TRAILR in fetal pancreas

Figures 2, 5, 8 and 11 showed the localization of DcR1, DcR2, DR4 and DR5 respectively in fetal pancreas. There were a few DcR1 (Figure 2) and DcR2 (Figure 5) positive cells and the positive reactivity located in membrane mainly (green). There was no DR4 (Figure 8) and DR5 (Figure 11) positive cells distributed in fetal pancreas.

Coexpression of TRAIL and TRAILR in fetal pancreas

Some TRAIL positive cells coexpressed with DcR1 or DcR2, whereas there was no coexpression of TRAIL and DR4, TRAIL and DR5 in fetal pancreas. All DcR1 and DcR2 immunoreactive cells showed TRAIL immunoreactivity (Figures 3, 6, 9 and 12).

DISCUSSION

Members of the TNF and TNF superfamilies of proteins are involved in the regulation of many important biological processes, including development, organogenesis, and innate and adaptive immunity^[23]. The TNF-related apoptosis-inducing ligand (TRAIL, also known as Apo-2L) is a newly identified TNF superfamily member with high homology to FasL. In the TRAIL/TRAILR system, control over apoptosis relies on differential display of receptors (TRAILR). These include DR4 (TRAIL-R1) and DR5 (TRICK2/ TRAIL-R2), which transduce apoptotic signals, as well as DcR1 (TRID/LIT/ TRAIL-R3) and DcR2 (TRUNDD/ TRAIL-R4), which lack functional death domains and act as decoys. Osteoprotegerin (OPG), a soluble decoy receptor for OPG/RANKL/ TRANCE, which is involved in osteoclast function, has also been reported to bind to TRAIL^[24-36].

There were some reports on the distribution of TRAIL/ TRAILR in human pancreas and pancreatic cancer. Liao *et al* found that TRAIL-R3 mRNA and protein expression were generally weak in pancreatic cancers and normal pancreatic tissues. In contrast, TRAIL-R4 mRNA and protein were expressed at moderate to high levels in human pancreatic cancer tissues, but demonstrated weak to negative expression in the normal pancreas by Northern blotting, Western blotting and

immunohistochemistry^[37]. Satoh *et al* detected the expression of TRAIL and its receptors other than osteoprotegerin in normal pancreatic tissues using RT-PCR^[38]. In our experiment, we found for the first time that in fetal pancreatic islets, there was strong distribution of TRAIL protein. The TRAIL immunoreactive substances mainly located on the membrane and cytoplasm with negative nuclei. Some TRAIL immunoreactive cells also showed DcR1 or DcR2 positive immunostaining, whereas there were no expression of DR4 and DR5 in fetal pancreas. Our results show some consistence with what Liao *et al* and Satoh *et al* have found.

We all know that pancreatic cancer is one of the most aggressive cancers, partly due to the general resistance of pancreatic cancer cells towards apoptosis. Ibrahim *et al* demonstrated that pancreatic carcinoma cells evaded the immune system in two mechanisms. One is the expression of nonfunctional receptors, decoy receptors, and molecules that block cell death, such as bcl2 and bcl-XL. The other is the expression of apoptosis-inducing ligands, such as TRAIL, that could induce cell death of immune cells^[39]. In our experiment, we found that in fetal pancreatic islets, some cells expressed TRAIL. At the same time, DcR1 and DcR2 also colocalized with TRAIL in some cells, but there was no expression of DR4 and DR5. Our findings suggest that in fetal pancreatic islets, the pancreatic cells are resistant towards apoptosis too. The characteristics of the fetal pancreas are consistent with those of pancreatic cancer.

It is well known that there are some kinds of cell types in human pancreatic islets such as A cells, B cells, D cells and PP cells. Although we found that TRAIL was located in some endocrine cells, we could not conclude which kind of cell types it existed in. This still needs to be clarified further.

REFERENCES

- Fu XY**, Wang HY, Tan L, Liu SQ, Cao HF, Wu MC. Overexpression of p28/gankyrin in human hepatocellular carcinoma and its clinical significance. *World J Gastroenterol* 2002; **8**: 638-643
- Kohut M**, Nowak A, Nowakowska-Duiawa E, Marek T. Presence and density of common bile duct microlithiasis in acute biliary pancreatitis. *World J Gastroenterol* 2002; **8**: 558-561
- Yu Y**, Yang WX, Wang H, Zhang WZ, Liu BH, Dong ZY. Characteristics and mechanism of enzyme secretion and increase in [Ca²⁺]_i in Saikosaponin(I) stimulated rat pancreatic acinar cells. *World J Gastroenterol* 2002; **8**: 524-527
- Zhou ZG**, Chen YD. Influencing factors of pancreatic microcirculatory impairment in acute pancreatitis. *World J Gastroenterol* 2002; **8**: 406-412
- Liu B**, Staren E, Iwamura T, Appert H, Howard J. Taxotere resistance in SUIT Taxotere resistance in pancreatic carcinoma cell line SUIT 2 and its sublines. *World J Gastroenterol* 2001; **7**: 855-859
- Ghaneh P**, Slavin J, Sutton R, Hartley M, Neoptolemos JP. Adjuvant therapy in pancreatic cancer. *World J Gastroenterol* 2001; **7**: 482-489
- Slavin J**, Ghaneh P, Sutton R, Hartley M, Rowlands P, Garvey C, Hughes M, Neoptolemos J. Management of necrotizing pancreatitis. *World J Gastroenterol* 2001; **7**: 476-481
- Fleischer F**, Dabew R, Goke B, Wagner AC. Stress kinase inhibition modulates acute experimental pancreatitis. *World J Gastroenterol* 2001; **7**: 259-265
- Guo XZ**, Friess H, Shao XD, Liu MP, Xia YT, Xu JH, Buchler MW. KAI1 gene is differently expressed in papillary and pancreatic cancer: influence on metastasis. *World J Gastroenterol* 2000; **6**: 866-871
- Pan QS**, Fang ZP, Huang FJ. Identification, localization and morphology of APUD cells in gastroenteropancreatic system of stomach-containing teleosts. *World J Gastroenterol* 2000; **6**: 842-847
- Yan FM**, Chen AS, Hao F, Zhao XP, Gu CH, Zhao LB, Yang DL, Hao LJ. Hepatitis C virus may infect extrahepatic tissues in patients with hepatitis C. *World J Gastroenterol* 2000; **6**: 805-811
- Adeghate E**, Ponery AS. The role of leucine-enkephalin on insulin and glucagon secretion from pancreatic tissue fragments of normal and diabetic rats. *Arch Physiol Biochem* 2001; **109**: 223-229
- Yang BM**, Demaine AG, Kingsnorth A. Chemokines MCP-1 and RANTES in isolated rat pancreatic acinar cells treated with CCK and ethanol *in vitro*. *Pancreas* 2000; **21**: 22-31
- Shetty S**, Gladden JB, Henson ES, Hu X, Villanueva J, Haney N, Gibson SB. Tumor necrosis factor-related apoptosis inducing ligand (TRAIL) up-regulates death receptor 5 (DR5) mediated by NFkappaB activation in epithelial derived cell lines. *Apoptosis* 2002; **7**: 413-420
- Petersen I**, Figenschau Y, Olsen E, Bakkelund W, Smedsrod B, Sveinbjornsson B. Tumor necrosis factor-related apoptosis-inducing ligand induces apoptosis in human articular chondrocytes *in vitro*. *Biochem Biophys Res Commun* 2002; **296**: 671
- Dorothee G**, Vergnon I, Menez J, Echchakir H, Grunenwald D, Kubin M, Chouaib S, Mami-Chouaib F. Tumor-infiltrating CD4+ T lymphocytes express APO2 ligand (APO2L)/TRAIL upon specific stimulation with autologous lung carcinoma cells: role of IFN-alpha on APO2L/TRAIL expression and-mediated cytotoxicity. *J Immunol* 2002; **169**: 809-817
- Guan B**, Yue P, Lotan R, Sun SY. Evidence that the human death receptor 4 is regulated by activator protein 1. *Oncogene* 2002; **21**: 3121-3129
- Eid MA**, Lewis RW, Abdel-Mageed AB, Kumar MV. Reduced response of prostate cancer cells to TRAIL is modulated by NFkappaB-mediated inhibition of caspases and Bid activation. *Int J Oncol* 2002; **21**: 111-117
- Xiang H**, Fox JA, Totpal K, Aikawa M, Dupree K, Sinicropi D, Lowe J, Escandon E. Enhanced tumor killing by Apo2L/TRAIL and CPT-11 co-treatment is associated with p21 cleavage and differential regulation of Apo2L/TRAIL ligand and its receptors. *Oncogene* 2002; **21**: 3611-3619
- Grataroli R**, Vindrieux D, Gougeon A, Benahmed M. Expression of tumor necrosis factor-alpha-related apoptosis-inducing ligand and its receptors in rat testis during development. *Biol Reprod* 2002; **66**: 1707-1715
- Simon AK**, Williams O, Mongkolsapaya J, Jin B, Xu XN, Walczak H, Sreaton GR. Tumor necrosis factor-related apoptosis-inducing ligand in T cell development: sensitivity of human thymocytes. *Proc Natl Acad Sci U S A* 2001; **98**: 5158-5163
- Huang XF**, Wang CM, Dai XW, Li ZJ, Pan BR, Yu LB, Qian B, Fang L. Expressions of chromogranin A and cathepsin D in human primary hepatocellular carcinoma. *World J Gastroenterol* 2000; **6**: 693-698
- Locksley RM**, Killeen N, Lenardo MJ. The TNF and TNF receptor superfamilies: integrating mammalian biology. *Cell* 2001; **104**: 487-501
- Evdokiou A**, Bouralexis S, Atkins GJ, Chai F, Hay S, Clayer M, Findlay DM. Chemotherapeutic agents sensitize osteogenic sarcoma cells, but not normal human bone cells, to Apo2L/TRAIL-induced apoptosis. *Int J Cancer* 2002; **99**: 491-504
- Zhang HG**, Xie J, Xu L, Yang P, Xu X, Sun S, Wang Y, Curiel DT, Hsu HC, Mountz JD. Hepatic DR5 induces apoptosis and limits adenovirus gene therapy product expression in the liver. *J Virol* 2002; **76**: 5692-5700
- He Q**, Lee DI, Rong R, Yu M, Luo X, Klein M, El-Deiry WS, Huang Y, Hussain A, Sheikh MS. Endoplasmic reticulum calcium pool depletion-induced apoptosis is coupled with activation of the death receptor 5 pathway. *Oncogene* 2002; **21**: 2623-2633
- Luciano F**, Ricci JE, Herrant M, Bertolotto C, Mari B, Cousin JL, Auberger P. T and B leukemic cell lines exhibit different requirements for cell death: correlation between caspase activation, DFF40/DFF45 expression, DNA fragmentation and apoptosis in T cell lines but not in Burkitt's lymphoma. *Leukemia* 2002; **16**: 700-707
- van Noesel MM**, van Bezouw S, Salomons GS, Voute PA, Pieters R, Baylin SB, Herman JG, Versteeg R. Tumor-specific down-regulation of the tumor necrosis factor-related apoptosis-inducing ligand decoy receptors DcR1 and DcR2 is associated with dense promoter hypermethylation. *Cancer Res* 2002; **62**: 2157-2161
- Lamothe B**, Aggarwal BB. Ectopic expression of Bcl-2 and Bcl-XL inhibits apoptosis induced by TNF-related apoptosis-inducing ligand (TRAIL) through suppression of caspases-8, 7, and 3

- and BID cleavage in human acute myelogenous leukemia cell line HL-60. *J Interferon Cytokine Res* 2002; **22**: 269-279
- 30 **Morrison BH**, Bauer JA, Hu J, Grane RW, Ozdemir AM, Chawla-Sarkar M, Gong B, Almasan A, Kalvakolanu DV, Lindner DJ. Inositol hexakisphosphate kinase 2 sensitizes ovarian carcinoma cells to multiple cancer therapeutics. *Oncogene* 2002; **21**: 1882-1889
- 31 **Nzeako UC**, Guicciardi ME, Yoon JH, Bronk SF, Gores GJ. COX-2 inhibits Fas-mediated apoptosis in cholangiocarcinoma cells. *Hepatology* 2002; **35**: 552-559
- 32 **Koyama S**, Koike N, Adachi S. Expression of TNF-related apoptosis-inducing ligand (TRAIL) and its receptors in gastric carcinoma and tumor-infiltrating lymphocytes: a possible mechanism of immune evasion of the tumor. *J Cancer Res Clin Oncol* 2002; **128**: 73-79
- 33 **Legembre P**, Moreau P, Daburon S, Moreau JF, Taupin JL. Potentiation of Fas-mediated apoptosis by an engineered glycosylphosphatidylinositol-linked Fas. *Cell Death Differ* 2002; **9**: 329-339
- 34 **Bretz JD**, Mezosi E, Giordano TJ, Gauger PG, Thompson NW, Baker JR Jr. Inflammatory cytokine regulation of TRAIL-mediated apoptosis in thyroid epithelial cells. *Cell Death Differ* 2002; **9**: 274-286
- 35 **Park SY**, Billiar TR, Seol DW. IFN-gamma inhibition of TRAIL-induced IAP-2 upregulation, a possible mechanism of IFN-gamma-enhanced TRAIL-induced apoptosis. *Biochem Biophys Res Commun* 2002; **291**: 233-236
- 36 **Odoux C**, Albers A, Amoscato AA, Lotze MT, Wong MK. TRAIL, FasL and a blocking anti-DR5 antibody augment paclitaxel-induced apoptosis in human non-small-cell lung cancer. *Int J Cancer* 2002; **97**: 458-465
- 37 **Liao Q**, Friess H, Kleeff J, Buchler MW. Differential expression of TRAIL-R3 and TRAIL-R4 in human pancreatic cancer. *Anti-cancer Res* 2001; **21**: 3153-3159
- 38 **Satoh K**, Kaneko K, Hirota M, Masamune A, Satoh A, Shimosegawa T. Tumor necrosis factor-related apoptosis-inducing ligand and its receptor expression and the pathway of apoptosis in human pancreatic cancer. *Pancreas* 2001; **23**: 251-258
- 39 **Ibrahim SM**, Ringel J, Schmidt C, Ringel B, Muller P, Koczan D, Thiesen HJ, Lohr M. Pancreatic adenocarcinoma cell lines show variable susceptibility to TRAIL-mediated cell death. *Pancreas* 2001; **23**: 72-79

Edited by Zhang JZ

Influence of platelet activating factor on expression of adhesion molecules in experimental pancreatitis

Hua Zhao, Ji-Wei Chen, Ya-Kui Zhou, Xue-Feng Zhou, Pei-Yun Li

Hua Zhao, Ji-Wei Chen, Ya-Kui Zhou, Xue-Feng Zhou, Department of general surgery, Zhongnan hospital, Wuhan University, Wuhan 430071, Hubei Province, China

Pei-Yun Li, Department of Pathology, Medical school, Wuhan University, Wuhan 430071, Hubei Province, China

Correspondence to: Dr. Hua Zhao, Department of general surgery, Zhongnan hospital, Wuhan University, Wuhan 430071, Hubei Province, China. jhonazao@yahoo.com.cn

Telephone: +86-27-87330104

Received: 2002-08-13 **Accepted:** 2002-09-02

Abstract

AIM: To determine whether Platelet activating factor (PAF) has a regulation role in the expression of adhesion molecules and accumulation of neutrophils in a murine model of acute pancreatitis.

METHODS: One hundred twenty-eight Kunming mice were divided into four groups. Group 1 received 0.1 ml saline s.c. every hour for three hours (sham). Group 2 received cerulein (50 µg/kg dose s.c.) every hour for three hours. Group 3 received AP and additional challenge of PAF (50 mg/kg in absolute ethanol) (AP/PAF). Group 4 received AP, plus therapeutic treatment with GAB (25 mg dose i.p.) immediately after the first challenge of cerulein (AP/GAB). Animals were sacrificed at 12 h after the first challenge of saline or cerulein. Adhesion molecules of pancreas were semi-quantified by SP methods. Standard assays were performed for serum amylase and myeloperoxidase activity (MPO) of pancreas. Histology of pancreas was scored in a blind manner. Water content of pancreas was also measured at the same time.

RESULTS: Control pancreata showed negligible adhesion molecule expression and neutrophil accumulation. There were evident adhesion molecules expression and neutrophil accumulation in AP and AP/PAF compared with sham ($P < 0.05$). AP/GAB had a lower level of adhesion molecules, neutrophils, and water content versus AP and AP/PAF ($P < 0.05$). Histology showed a trend toward improvement in AP/GAB, but did not reach statistical significance.

CONCLUSION: PAF can induce the expression of adhesion molecules that mediate neutrophil accumulation. The PAF antagonist reduces the expression of adhesion molecules and the severity of inflammation when given immediately after the induction of mild AP in mice. These results suggest that PAF antagonism may be useful in the treatment of mild pancreatitis after its clinical onset.

Zhao H, Chen JW, Zhou YK, Zhou XF, Li PY. Influence of platelet activating factor on expression of adhesion molecules in experimental pancreatitis. *World J Gastroenterol* 2003; 9(2):338-341
<http://www.wjgnet.com/1007-9327/9/338.htm>

INTRODUCTION

Acute pancreatitis (AP) was characterized as local and systemic

inflammatory reactions. Adhesion molecules play a pivotal role in neutrophil immigration and accumulation^[1]. Platelet activating factor (PAF) is a biologically active phospholipid which is thought to function as one of the proximal mediators in the inflammatory cascade of AP. However, the relationship between PAF and the expression of adhesion molecules in AP remains largely unknown, although Blackstone MO has ever speculated^[2].

The present study was conducted to determine whether PAF has a regulatory role in the expression of adhesion molecules and the accumulation of neutrophils. To examine this effect, a murine model of edematous pancreatitis was established by overdose administration of cerulein, as described by Tani *et al*^[3]. PAF and its antagonist (GAB) were also used in this experiment.

MATERIALS AND METHODS

Materials

Cerulein and PAF were purchased from Sigma Chemical Co. (St.Louis, Missouri). GAB (Ginkgolide AB) was a generous gift from associate professor Di-Qing Zhang in Guizhou University. MPO assay kit was purchased from Nanjing Jiancheng Bioengineering Co. Ltd. China. Rabbit anti-rat E-selectin polyclonal antibody and Rabbit anti-rat ICAM-1 polyclonal antibody were purchased from Boster Bioengineering Co. Ltd. China. SP assay kit was purchased from Maixin Bioengineering Co. Ltd. China. Cerulein was dissolved in normal saline at the concentration of 10 µg/ml. PAF was first dissolved in absolute ethanol, and then diluted with normal saline when it was to be used. GAB was dissolved in 30 % Dimethyl Sulfoxide (DMSO).

128 six-week-old Kunming mice, weighing 34-36 g each, were purchased from the experimental animal center of Wuhan University. The animals were randomly divided into 4 groups (described in methods) and fed standard laboratory chow. All animals were allowed to acclimatize for a minimum of 1 week prior to experimentation. Before the day of the experiment, animals were fasted overnight, but allowed free access to water.

Animals model

Acute pancreatitis was established in 32 mice (AP group) by subcutaneous injection of cerulein (50 µg/kg dose) every hour for three hours. Sham group (32 mice) received subcutaneous injection of normal saline every hour for three hours. AP/PAF group (32 mice) received subcutaneous injection of cerulein (50 µg/kg dose) every hour for three hours, plus PAF (50 µg/kg dose) injected peritoneally immediately after the first cerulein challenge. AP/GAB group (32 mice) received subcutaneous injection of cerulein (50 µg/kg dose) every hour for three hours, plus therapeutic treatment with GAB (25 mg/kg i.p.) immediately after the first cerulein challenge.

The animals were sacrificed at 12 h after the first cerulein challenge or saline injection. Some mice (eight in every group) were decapitated and the blood was collected in vials for the analysis of serum amylase. Pancreata were dissected. Some were weighted and grounded for the analysis of MPO, and the others were fixed with formalin for histological scoring and

immunohistochemical staining. Some left pancreatic tissues were dried and weighted.

MPO measurement

MPO assay of pancreas was performed according to the instructions of commercial kit.

Amylase

Serum amylase levels were measured using starch-iodine method.

Water content

Pancreas was dissected from its attachment and the fluid on its surface was dried with filter paper. Then the pancreas was placed in oven at a temperature of 90-92 °C for 10 hours. Water content = $(\text{Weight}_{\text{wet}} - \text{Weight}_{\text{dry}}) / \text{Weight}_{\text{wet}} \times 100\%$.

Histological grading

Pancreatic sections were stained with hematoxylin and eosin and graded in a blind manner by two investigators. Severity of pancreatitis was scored on a scale of 0 to 4 (normal to severity) in the categories (vacuolization, inflammation, edema) for a total score of 0 to 12, as described by J.Schmidt^[4].

Immunohistochemical staining

Pancreata were fixed in formalin for 12 h and then embedded in paraffin wax. Sections were cut at 4 μm in thickness and mounted on slides. They were deparaffinized by passing them through two changes of xylene and graded series of ethanol, followed by rinses in tap water and 0.01 mmol·l⁻¹ phosphate buffered saline (PBS), respectively. Endogenous peroxidase activity was quenched by treating the section with 3 % hydrogen peroxide for 10 minutes. Nonspecific binding was blocked by incubating sections in 1 % bovine albumin in PBS for 10 minutes, and then incubated for an hour in primary antibody (rabbit anti-E-selectin or rabbit anti-ICAM-1 polyclonal antibody). After rinsing in PBS, the sections were treated sequentially with biotinconjugated second antibody for 10 minutes and then with streptavidin-peroxidase for another 10 minutes with PBS rinsing after each step. Sections were stained subsequently with freshly prepared DAB reagent for 3 minutes, and terminated by rinsing in water. then the sections were immersed in hematoxylin for 3-5 minutes and 0.5 mmol·l⁻¹ HCl for 10 seconds. Finally, when passed through two changes of xylene and graded series of alcohol, the sections were covered with coverslip for light analysis. Every slice was counted on ten different fields by two investigators independently. Vessel stained brown was considered positive vessel. (-), score 0, means no positive vessel was observed. (+), score 1, means 1-2 positive vessels were observed. (++) , score 2, means 3-4 positive vessels were observed. (+++) , score 3, means more than 5 positive vessels were observed.

Statistical analysis

Numerical variables are reported as means ± SEM and compared between groups using *Newman-Keuls* method. Rank data are reported as means and analyzed with *Nemenyi* method. Difference with $P < 0.05$ are considered significant.

RESULTS

Expression of adhesion molecules

In control group there was no staining of E-selectin and ICAM-1 in pancreatic venules. Expression of the two adhesion molecules was eminent in AP and AP/PAF. But there was no difference between the two groups. AP/GAB has a lower level of E-selectin and ICAM-1 expression compared with AP (Table 1, Figures 1-4).

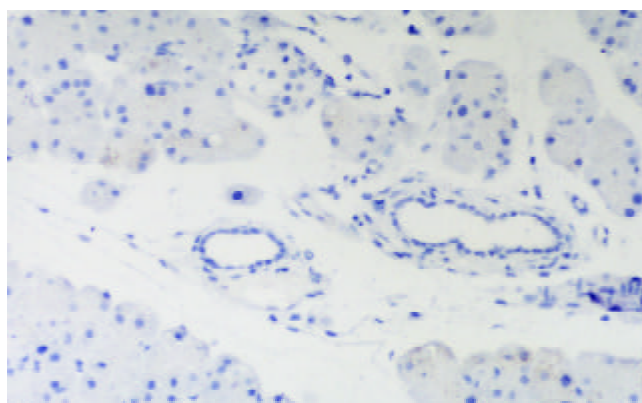


Figure 1 12 h, sham group showed negative expression of adhesion molecules. (×400).

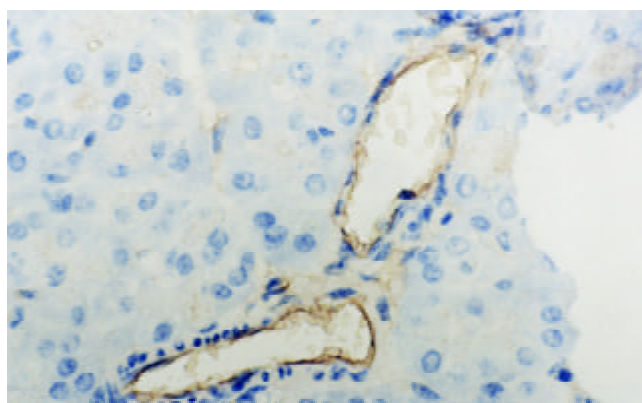


Figure 2 E-selectin was evident in AP at 12 h. (×400).

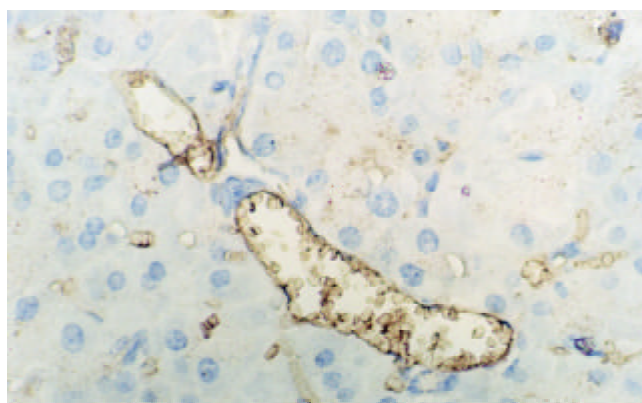


Figure 3 ICAM-1 was evident in AP at 12 h. (×400).

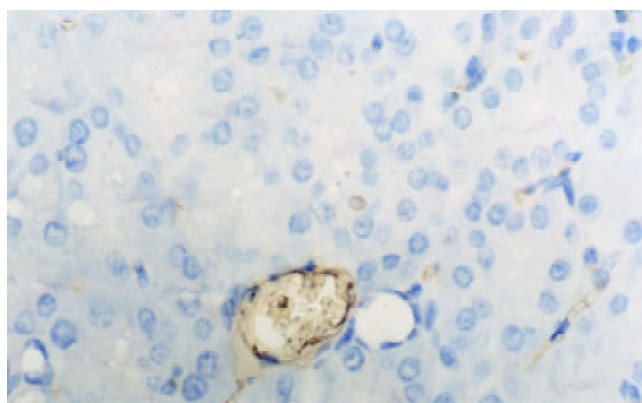


Figure 4 ICAM-1 expression in AP/GAB at 12 h. (×400).

Amylase and water content

Serum amylase levels and water content was used to evaluate the severity of pancreatic injury. Amylase rose at 12 h in AP and AP/PAF group against control group, but there was no difference between the two groups. GAB treatment significantly reduced the amylase level at 12 h ($P<0.05$). Water content reflects the extent of pancreatic edema. At 12 h AP and AP/PAF showed a higher level of water content against sham and AP/GAB. AP/GAB still has a higher level of water content than sham (Table 2).

MPO activity

Measurement of neutrophil accumulation by MPO activity revealed that AP and AP/PAF had an increase of MPO activity almost 10-fold greater than sham. AP/GAB showed significantly lower level of MPO Activity than AP ($P<0.05$). And this level did not return to the values seen in sham treated animals (Table 2).

Pancreatic histological analysis

Sham group was microscopically intact, with normal histological structure. Pancreatic lesions, such as edema, vacuolation and infiltration of PMN were found in AP, AP/PAF and AP/GAB. There was a trend toward improvement in histological parameters in AP/GAB, but it failed to reach statistical significance. (Data not shown).

Table 1 Expression of adhesion molecules in pancreas. ($\bar{x}\pm s$)

Group	E-selectin	ICAM-1
Sham	0	0
AP	2.1 ^a	2.3 ^a
AP/PAF	2.3 ^a	2.4 ^a
AP/GAB	1.1 ^b	1.1 ^b

^a $P<0.05$ vs sham, ^b $P<0.05$ vs AP.

Table 2 Measurement of amylase, MPO activity, water content. ($\bar{x}\pm s$).

Group	Amylase ($\times 10^3$ U/L)	MPO activity (AU/g)	Water content (%)
Sham	4.2 \pm 0.2	2.14 \pm 0.011	71.0 \pm 0.1
AP	22.1 \pm 2.7 ^a	2.213 \pm 0.035 ^a	81.0 \pm 0.2 ^a
AP/PAF	22.9 \pm 0.9 ^a	2.325 \pm 0.067 ^a	79.8 \pm 0.2 ^a
AP/GAB	10.9 \pm 0.8 ^{b,c}	0.795 \pm 0.004 ^{b,c}	75.3 \pm 0.1 ^{b,c}

^a $P<0.05$, ^b $P<0.05$ vs sham, ^c $P<0.05$ vs AP.

DISCUSSION

Platelet activating factor, 1-O-octadecyl-2-acetyl-Sn-glycero-3-phosphocholine, is a potent inflammatory mediator produced by endothelial cells, platelets, monocytes, neutrophils, and basophils. It has been widely studied that PAF played an important role in the pathogenesis of AP, and its local and systemic effects on AP have also been revealed. The systemic effects cause circulatory disturbances and multiple organ failure. Local effects include platelet aggregation, neutrophil accumulation, microvascular ischemia and increasing of capillary permeability^[5-7]. Moreover, PAF itself also can induce pancreatitis when injected in peritoneal or superior pancreaticoduodenal artery^[8-10].

Accordingly, treatment of experimental pancreatitis with PAF antagonist has consistently shown significant local and systemic protection to reduce inflammatory changes^[11-15]. But the mechanism of its protection has not been fully classified.

One kind of PAF antagonist, lexipafant, has been studied in clinical trials in acute pancreatitis. In phase II and phase III clinical studies lexipafant showed better protection against AP, although a phase III clinical trial in UK showed little protection in the treatment of severe acute pancreatitis^[16-18].

In vitro PAF can induce the expression of adhesion molecules^[19], there was little information whether PAF and its antagonist could regulate the expression of adhesion molecules in AP. So, we conducted this experiment to testify the hypothesis.

Leukocyte accumulation from circulating blood to the site of inflammation includes multiple steps involving different kind of adhesion molecules on the endothelial cell. There are four steps in the adhesion cascade: (1) tethering, (2) triggering, (3) firm adhesion and (4) diapedesis- and these steps must occur in ordered sequence. Tethering interactions are the first step in the adhesion cascade. The molecules involved in this reaction come from the selectin family, such as E-selectin and P-selectin. The firm-binding phase involves superimmunoglobulin family, such as ICAM-1 and VCAM-1. Both E-selectin and ICAM-1 have shown to be necessary for transendothelial migration of polymorphonuclear leukocytes^[20]. In AP, neutrophils and adhesion molecules elevate and play an important role^[21,22]. Treatment of severe acute pancreatitis with ICAM-1 monoclonal antibody reduces the severity of pancreatic and lung injury. The severity of AP is partially decreased in mice deficient in ICAM-1^[22].

In our study adhesion molecules were elevated in AP. But additional PAF challenge couldn't increase the expression of adhesion molecules. PAF antagonist (GAB) can reduce the expression of adhesion molecules and reduce the accumulation of neutrophils in pancreas in AP. The mechanism may be that internal PAF has enough capability to induce the expression of adhesion molecule, and exogenous PAF do not have accelerating ability to induce more expression of adhesion molecules. PAF antagonist may have different ways in AP to reduce the expression of adhesion molecules: (1) reduce the concentration of cytokines, such as TNF- α and IL-1 β ^[23,24]. (2) reduce oxidative stress in pancreas^[24,25]. (3) repress the activation of NF- κ B directly.

In conclusion, PAF plays an important role in the expression of adhesion molecules and accumulation of neutrophils in AP. PAF antagonist can be used early in mild AP. Further studies are necessary to determine whether PAF antagonist can prevent mild AP to transform into severe AP.

ACKNOWLEDGEMENT

We gratefully acknowledge associate Prof. Di-Qing Zhang for his precious PAF antagonist (GAB).

REFERENCES

- 1 **Albelda SM**, Smith CW, Ward PA. Adhesion molecules and inflammatory injury. *FASEB J* 1994; **8**: 504-512
- 2 **Blackstone MO**. ICAM-1-*incerulein*-induced pancreatitis. *Gastroenterology* 1999; **117**: 748-749
- 3 **Tani S**, Otsuki M, Itoh H, Fujii M, Nakamura T, Oka T, Baba S. Historic and biochemical alterations in experimental pancreatitis by supermaximal caerulein stimulation. *Int J Pancreatol* 1987; **2**: 337-348
- 4 **Schmidt J**, Lewandrowski K, Fernandez-del Castillo C, Mandavilli U, Compton CC, Warshaw AL, Rattner DW. Histopathologic correlation of serum amylase activity in acute experimental pancreatitis. *Dig Dis Sci* 1992; **37**: 1426-1433
- 5 **Johnson CD**. Platelet-activating factor and Platelet-activating factor antagonists in acute pancreatitis. *Dig Surg* 1999; **16**: 93-101
- 6 **Zhao LY**, Chen CY, Liang P, Chen LY. ICAM-1 and VCAM-1 expressions on benign gastric mucosa and gastric adenocarcinoma associated with *Helicobacter pylori* infection. *Shijie Huaren Xiaohua Zazhi* 2000; **8**: 279-281

- 7 **Zhao XY**, Xia SH. Platelet-activating factor and onset and treatment of acute pancreatitis. *Shijie Huaren Xiaohua Zazhi* 2001; **9**: 958-960
- 8 **Konturek SJ**, Dembinski A, Konturek PJ, Warzecha Z, Jaworek J, Gustaw P, Tomaszewska R, Stachura J. Role of platelet activating factor in pathogenesis of acute pancreatitis in rats. *Gut* 1992; **33**: 1268-1274
- 9 **Kald B**, Kald A, Ihse I, Tagesson C. Release of platelet-activating factor in acute experimental pancreatitis. *Pancreas* 1993; **8**: 440-442
- 10 **Emanuelli G**, Montrucchio G, Gaia E, Dughera L, Corvetti G, Gubetta L. Experimental pancreatitis induced by platelet activating factor in rabbits. *Am J Pathol* 1989; **134**: 315-326
- 11 **Werner J**, Z'graggen K, Fernandez-del-Castillo C, Lewandrowski KB, Compton CC, Warshaw AL. Specific therapy for local and systemic complications of acute pancreatitis with monoclonal antibodies against ICAM-1. *Ann Surg* 1999; **229**: 834-840
- 12 **Rau B**, Barer A, Eber S, Gansauge F, Poch B, Beger HG, Moller P. Anti-ICAM-1 antibody modulates last onset of acinar cell apoptosis and early necrosis in taurocholate-induced experimental acute pancreatitis. *Pancreas* 2001; **23**: 80-88
- 13 **Rau B**, Bauer A, Wang A, Gansauge F, Weidenbach H, Nevalainen T, Poch B, Beger HG, Nussler AK. Modulation of endogenous nitric oxide synthase in experimental acute pancreatitis: role of anti-ICAM-1 and oxygen free radical scavengers. *Ann Surg* 2001; **233**: 195-203
- 14 **Eibl G**, Buhr HJ, Foitzik T. Therapy for microcirculatory disorders in severe acute pancreatitis: what mediators should we block? *Intensive Care Med* 2002; **28**: 139-146
- 15 **Lundberg AH**, Fukatsu K, Gaber L, Callicutt S, Kotb M, Wilcox H, Kudsk K, Gaber AO. Blocking pulmonary ICAM-1 expression ameliorates lung injury in established diet-induced pancreatitis. *Ann Surg* 2001; **233**: 213-220
- 16 **Kingsnorth AN**, Galloway SW, Formela LJ. Randomized, double-blind, phase II trial of Lexipafant, a platelet-activating factor antagonist in human acute pancreatitis. *Br J Surg* 1995; **82**: 1414-1420
- 17 **McKay CJ**, Curran F, Sharples C, Baxter JN, Imrie CW. Prospective placebo-controlled randomized trial of Lexipafant in predicted severe acute pancreatitis. *Br J Surg* 1997; **84**: 1239-1243
- 18 **Johnson CD**, Kingsnorth AN, Imrie CW, McMahon MJ, Neoptolemos JP, McKay C, Toh SK, Skaife P, Leeder PC, Wilson P, Larvin M, Curtis LD. Double blind, randomized, placebo-controlled study of a PAF-antagonist, Lexipafant, in treatment and prevention of organ failure in predicted SAP. *Gut* 2001; **48**: 62-69
- 19 **Chihara J**, Maruyama I, Yasaba H, Yasukawa A, Yamamoto T, Kurachi D, Mouri T, Seguchi M, Nakajima S. Possible induction of intercellular adhesion molecule-1 (ICAM-1) expression on endothelial cells by platelet-activating factor (PAF). *J Lipid Mediat* 1992; **5**: 159-162
- 20 **Butcher EC**, Picker LJ. Lymphocyte homing and homeostasis. *Science* 1996; **272**: 60-66
- 21 **Zaninovic V**, Gukovskaya AS, Gukovsky I, Mouria M, Pandolfi SJ. Cerulein upregulates ICAM-1 in pancreatic acinar cells, which mediates neutrophil adhesion to these cells. *Am J Physiol Gastrointest Liver Physiol* 2000; **279**: G666-676
- 22 **Frossard JL**, Saluja A, Bhagat L, Lee HS, Bhatia M, Hofbauer B, Steer ML. The role of intercellular adhesion molecule 1 and neutrophils in acute pancreatitis and pancreatitis-associated lung injury. *Gastroenterology* 1999; **116**: 694-701
- 23 **Luscinskas FW**, Cybulsky MI, Kiely JM, Peckins CS, Davis VM, Gimbrone MA Jr. Cytokine-activated human endothelial monolayers support enhanced neutrophil transmigration via a mechanism involving both endothelial-leukocyte adhesion molecule-1 and intercellular adhesion molecule-1. *J Immunol* 1991; **146**: 1617-1625
- 24 **Lane JS**, Todd KE, Gloor B, Chandler CF, Kau AW, Ashley SW, Reber HA, McFadden DW. Platelet activating factor antagonism reduces the systemic inflammatory response in a murine model of acute pancreatitis. *J Surg Res* 2001; **99**: 365-370
- 25 **Wang WX**, Zhao HP, Shou NY, Yang CW. Role of oxygen free radical and other inflammatory mediators in acute necrotic pancreatitis. *World J Gastroenterol* 1998; **4** (Suppl 2): 59

Edited by Zhou YP

Co-expression of five genes in *E coli* for L-phenylalanine in *Brevibacterium flavum*

Yong-Qing Wu, Pei-Hong Jiang, Chang-Sheng Fan, Jian-Gang Wang, Liang Shang, Wei-Da Huang

Yong-Qing Wu, Chang-Sheng Fan, Jian-Gang Wang, Liang Shang, Department of Microbiology, School of Life Science, Fudan University, Shanghai 200433, China

Pei-Hong Jiang, Wei-Da Huang, Department of Biochemistry, School of Life Science, Fudan University, Shanghai 200433, China

Pei-Hong Jiang, equal contribution as the first author

Supported by the National Natural Science Foundation of China, No. 30070020

Correspondence to: Chang-Sheng Fan, Department of Microbiology, Fudan University, 220 Han Dan Road, Shanghai 200433, China. csfan@fudan.edu.cn

Telephone: +86-21-65642808 **Fax:** +86-21-55522773

Received: 2002-07-01 **Accepted:** 2002-07-26

Abstract

AIM: To study the effect of co-expression of *ppsA*, *pckA*, *aroG*, *pheA* and *tyrB* genes on the production of L-phenylalanine, and to construct a genetic engineering strain for L-phenylalanine.

METHODS: *ppsA* and *pckA* genes were amplified from genomic DNA of *E. coli* by polymerase chain reaction, and then introduced into shuttle vectors between *E. coli* and *Brevibacterium flavum* to generate constructs pJN2 and pJN5. pJN2 was generated by inserting *ppsA* and *pckA* genes into vector pCZ; whereas pJN5 was obtained by introducing *ppsA* and *pckA* genes into pCZ-GAB, which was originally constructed for co-expression of *aroG*, *pheA* and *tyrB* genes. The recombinant plasmids were then introduced into *B. flavum* by electroporation and the transformants were used for L-phenylalanine fermentation.

RESULTS: Compared with the original *B. flavum* cells, all the transformants were showed to have increased five enzyme activities specifically, and have enhanced L-phenylalanine biosynthesis ability variably. pJN5 transformant was observed to have the highest elevation of L-phenylalanine production by a 3.4-fold. Co-expression of *ppsA* and *pckA* increased activity of DAHP synthetase significantly.

CONCLUSION: Co-expression of *ppsA* and *pckA* genes in *B. flavum* could remarkably increase the expression of DAHP synthetase; Co-expression of *ppsA*, *pckA*, *aroG*, *pheA* and *tyrB* of *E. coli* in *B. flavum* was a feasible approach to construct a strain for phenylalanine production.

Wu YQ, Jiang PH, Fan CS, Wang JG, Shang L, Huang WD. Co-expression of five genes in *E coli* for L-phenylalanine in *Brevibacterium flavum*. *World J Gastroenterol* 2003; 9(2): 342-346

<http://www.wjgnet.com/1007-9327/9/342.htm>

INTRODUCTION

L-phenylalanine, one of the essential amino acids in human, is used as a major component of amino acid in infusion

clinically. For the past two decades, biosynthesis of L-phenylalanine has attracted more and more attentions due to the increasing demand of Aspartame, a dipeptide sweetener containing L-phenylalanine^[2,3].

Production of L-phenylalanine by microbes has clear advantages over chemical synthesis, e.g., the biological processes are more environmentally sound and utilize renewable resources^[4-8]. In bacteria, the biosynthesis of aromatic amino acids starts from condensation reaction of central carbon intermediates phosphoenolpyruvate (PEP) and erythrose-4-phosphate (E4P) to form 3-deoxy-D-arabino-heptulosonate-7-phosphate (DAHP), which is catalyzed by DAHP synthetase (DS)^[9,10]. DAHP is then converted to chorismate, the branch point of aromatic amino acid biosynthesis. L-phenylalanine is synthesized from chorismate by three continuous steps catalyzed by chorismate mutase (CM), prephenate dehydratase (PD) and aromatic-amino-acid transaminase (AT). In *E. coli*, *aroG* and *tyrB* genes encode DS and AT, respectively^[11-17], whereas CM and PD are encoded by a single gene *pheA*^[18-21].

Since the genes coding for amino acid biosynthesis are well characterized in *E. coli* and other microbes, it is possible to make metabolic pathway engineering via recombinant DNA approach to increase the productivity of phenylalanine in bacteria. As reported previously, introduction of a single gene *pheA* into *Corynebacterium glutamicum* resulted in a 35 % increase of L-phenylalanine production^[22]. In our previous work, co-expression of *aroG*, *pheA* and *tyrB* in *Brevibacterium lactofermentum* with pCZ-GAB gave a 2-fold increase in L-phenylalanine yield^[11]. On the other hand, elevation of intracellular levels of the precursor PEP is considered to be essential to channel more carbon flux into aromatic flux in order to get higher yield of L-phenylalanine. In *E. coli*, two enzymes are involved in the formation of PEP. PEP synthetase (PpsA) catalyzes the synthesis of PEP from pyruvate by transphosphorylation reaction^[23], whereas PEP carboxykinase (PckA) catalyzes the synthesis of PEP from oxaloacetate by decarboxylation reaction^[24-26]. PpsA and PckA are encoded by *ppsA* gene and *pckA* gene, respectively. Overexpression of *ppsA* gene in *E. coli* has been shown to elevate DAHP level by a 1.9-fold^[27]. PckA over-expression in *E. coli* cells showed a 20 % increase in molar conversion yields for L-phenylalanine production^[15].

In this study, the *ppsA* and *pckA* genes in *E. coli* were amplified from genomic DNA by polymerase chain reaction (PCR), and then introduced into a *B. flavum*-*E. coli* shuttle vector with *aroG*, both *pheA* and *tyrB* genes were used as operons. The constructs were transformed into *B. flavum* for L-phenylalanine fermentation, and the specific activities of each enzyme as well as the L-phenylalanine yield were measured.

MATERIALS AND METHODS

Bacterial strains and plasmids

All the strains and plasmids used in this study are listed in Table 1. *E. coli* XL1-Blue-G and *B. flavum* 311 are mutants resistant to phenylalanine analogue fluorophenylalanine. XL1-Blue-G was used as donor of *ppsA* and *pckA*.

Table 1 Bacterial strains and plasmids

Strain or plasmid	Relevant characteristics	Source or reference
<i>E. coli</i> XLI-Blue-G	Fp ^r (donor of <i>ppsA</i> , <i>pckA</i>)	Ref. 28
<i>E. coli</i> P2392	(strain for expression)	Stored by our lab
<i>B. flavum</i> 311	Nx ^r , Fp ^r (strain for expression and fermentation)	Stored by our lab
pλP _R	Ap ^r (<i>E. coli</i> expressing vector)	Ref. 28
pλP _R -pps	pλP _R inserted with <i>ppsA</i>	This study
pλP _R -pck	pλP _R inserted with <i>pckA</i>	This study
pλP _R -2p	pλP _R inserted with <i>ppsA</i> and <i>pckA</i> tandemly	This study
pSK-P _{BF}	pBluscript SK- inserted with promoter P _{BF}	Structured by our lab, unpublished
pCZ	Km ^r (<i>B. Flavum-E.coli</i> shuttle vector)	Stored by our lab
pCZ-GAB	pCZ inserted with tandem <i>aroG pheA tyrB</i>	Ref. 1
pJN2	pCZ inserted with tandem <i>ppsA pckA</i>	This study
pJN5	pCZ-GAB inserted with tandem <i>ppsA pckA</i>	This study

Fp^r, resistance to fluorophenylalanine; Nx^r, resistance to nalidixic acid; Ap^r, resistance to ampicillin; Km^r, resistance to kanamycin.

Media and growth conditions

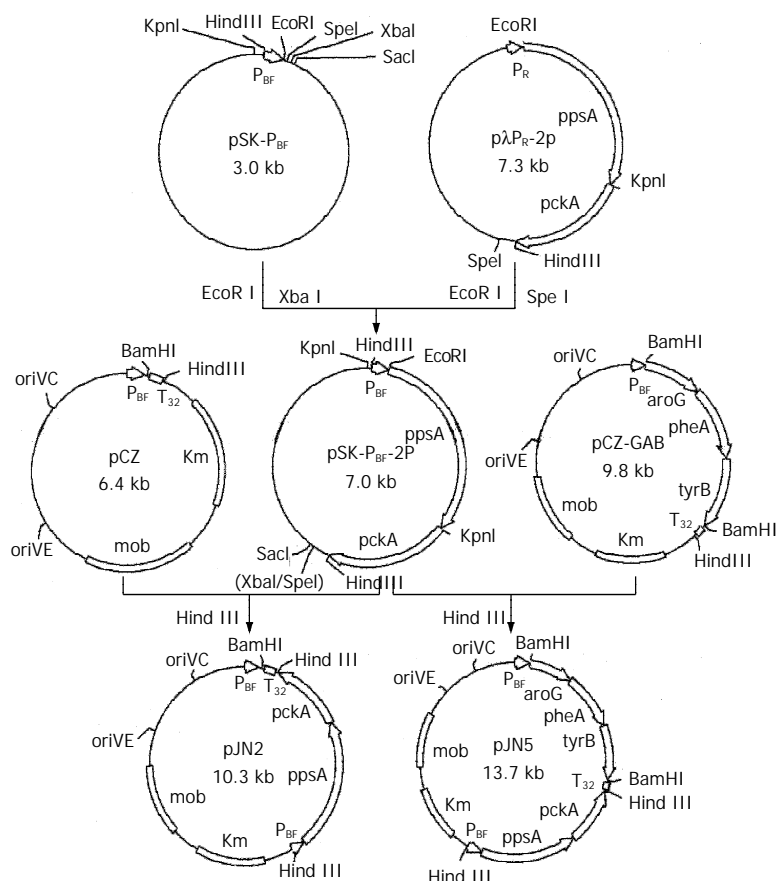
E. coli and transformants containing plasmid were grown at 37 °C in Luria-Bertani medium. *B. flavum* and plasmid-containing transformants were grown in complete medium at 31 °C for DNA manipulation and expression, and were grown in production medium for fermentation as described previously^[1]. Media were supplemented with the following antibiotics as required: fluorophenylalanine (1 mg/mL), nalidixic acid (10 µg/mL), ampicillin (100 µg/mL), kanamycin (20 µg/mL).

Construction of recombinant plasmids

Primers for amplification of *ppsA* gene were synthesized according to Ref. 29 with addition of restriction enzyme sites of *EcoRI* for forward primer (5' -GCATGAATTCGATGTCC AACAATGGCTCGTC-3') and *KpnI* for reverse primer (5' -GCATGGTACCGATTTCGATTGCGATGCAGGT-3'). Primers for amplification of *pckA* gene were designed according to Ref. 30 with addition of restriction enzyme sites of *KpnI* for forward primer (5' -GCATGGTACCATATTGG CTAAGGAGCAGTG-3') and *HindIII* for reverse primer (5' -TACGAAGCTTATCCAGCGAACCGTG-3'). The genes were amplified by PCR and cloned on pBlueScript II SK(+) and transferred on to expression vector pλP_R in a tandem arrangement as showed in Figure 1. The fragment containing tandem *ppsA* and *pckA* was then inserted into shuttle vector pCZ and pCZ-GAB to obtain pJN2 and pJN5.

Enzymatic activity assay

Crude lysates used for enzymatic activity assays were prepared as described previously^[11]. The total protein level was determined by the method of Bradford^[31]. PpsA activity was determined by method^[32] described with modification. In brief, each PpsA assay mixture contained 1.5 µmol/L pyruvate, 10 µmol/L ATP, 10 µmol/L MgCl₂, 100 µmol/L Tris-HCl (pH 8.0), and 200 µL crude lysates. The reaction was terminated by adding 0.3 mL 100 g/L TCA and 0.1 mL 1 g/L 2,4-dinitro phenylhydrazine, and was monitored by measuring the consumption of pyruvate at 520 nm. PckA activity was determined as publication^[33] with modification. In brief, each PckA assay mixture contained 10 µmol/L PEP, 50 µmol/L NaHCO₃, 4 µmol/L ADP, 80 µmol/L MgCl₂, 100 µmol/L Tris-HCl (pH 7.5), and 100 µL crude lysates. The reaction was terminated by adding 0.75 mL ethanol and 20 µL 20 g/L Fast

**Figure 1** Construction of recombinant plasmids

Violet B Salt, and was monitored at 520 nm. DS and AT activities were assayed as described previously^[28]. CM activity was determined as the method of Xia^[34]. PD activity was assayed as the method of Ref. 35.

Fermentation and analysis of phenylalanine

Fermentation of *B. flavum* 311 was carried out and the fermentation yields of L-phenylalanine were determined by the method of Ref. 1.

RESULTS

Expression of *ppsA* and *pckA* genes in transformed *E. coli* cells

The *ppsA* and *pckA* genes were amplified from *E. coli* genomic DNA by PCR and were then subsequently cloned onto pBluescript II SK(+) plasmid at corresponding restriction sites. Minor point mutations were detected on the amino acid sequences of PpsA and PckA protein as determined by DNA sequencing (data not shown). These two genes were expressed in *E. coli* to confirm its bioactivities.

The expression vectors were constructed based on vector $\rho\lambda P_R$ to either express a single gene or co-express the two genes as an operon. The constructs were transformed into in *E. coli* P2392 cells and the protein profiles of transformants were analyzed by SDS-PAGE (Figure 2). Distinct protein bands corresponding to the molecular weights of PpsA and PckA were detected on SDS-PAGE as shown in Figure 2. The relative specific activities of the transformants were also determined (Table 2). Independent expression of *ppsA* and *pckA* genes resulted in increase in specific enzymatic activities of the corresponding enzymes by 4.2- and 1.5-fold, respectively. Whereas in co-expression of *ppsA* and *pckA* genes, the increases in specific enzymatic activities were 2.1-fold and 1.3-fold, a slightly lower than that of independent expression. The results suggested that the two genes amplified by PCR had the normal enzymatic activities.

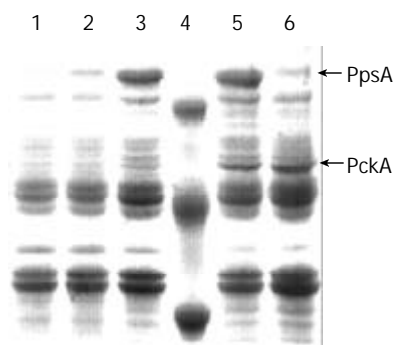


Figure 2 SDS-PAGE analysis of total proteins of *E. coli* P2392 cells harboring different recombinant plasmids. Lane 1, total protein of *E. coli* P2392 cells; lane 2, harboring $\rho\lambda P_R$; lane 3, harboring $\rho\lambda P_R$ -pps; lane 4, protein markers, lane 5, harboring $\rho\lambda P_R$ -2p; lane 6, harboring $\rho\lambda P_R$ -pck. Arrows indicate molecular weight of the protein markers and the positions of PpsA and PckA.

Table 2 The relative specific enzymatic activities in *E. coli* P2392 harboring different constructs

Strain/plasmid	Relative enzymatic activities		
	PpsA	PckA	DS
<i>E. coli</i> P2392/ $\rho\lambda P_R$	1	1	1
<i>E. coli</i> P2392/ $\rho\lambda P_R$ -pps	5.2	1.0	1.8
<i>E. coli</i> P2392/ $\rho\lambda P_R$ -pck	1.0	2.5	1.5
<i>E. coli</i> P2392/ $\rho\lambda P_R$ -2p	3.1	2.3	2.1

When we looked at the enzymatic activities of DS in different transformants, we found that either single-gene expression or co-expression of *ppsA* and *pckA* genes could induce elevated expression of DS by 0.5 to 1.1-fold.

Enzymatic activities in transformed *B. flavum* 311 cells

To attempt metabolite pathway engineering in *B. flavum*, a host strain for L-phenylalanine production, shuttle vectors pJN2 and pJN5 were constructed and introduced into *B. flavum* 311 cells by electroporation. The specific enzymatic activities were measured for each transformants as summarized in Table 3. For the pJN5-harboring transformant, all of the six specific enzymatic activities had increased. The pJN2-harboring transformant showed higher specific activities for PpsA and PckA than pJN5-harboring transformant as expected. Again, a significant increase in DS activity was observed, though *aroG* gene was not expressed by pJN2, which was very similar to the results of $\rho\lambda P_R$ -2p in *E. coli* P2392. Unexpectedly, all of the DS, AT and CM/PD enzymatic activities of pJN5-harboring transformant were higher than that of pCZ-GAB-harboring transformant, since the copy number of pJN5 in *G. flavum* transformant was lower than that of pCZ-GAB (data not shown).

Table 3 Relative specific enzymatic activities in *B. flavum* 311 harboring different constructs

Constructs	Relative specific enzymatic activities				
	PpsA	PckA	DS	CM/PD	AT
pCZ	1	1	1	1/1	1
pJN2	4.2	4.5	1.9	1.0/1.2	1.2
pCZ-GAB	0.9	1.1	4.2	4.1/2.2	4.7
pJN5	2.8	3.3	6.3	4.9/2.5	5.5

Phenylalanine production in transformed *B. flavum* 311 cells

To investigate the effect of enhanced enzymatic activities on L-phenylalanine production, the *B. flavum* 311 transformants harboring different constructs were subject to fermentation under conditions described in Materials and Methods, and the L-phenylalanine yield was determined. As shown in Table 4, pJN5-harboring transformant had a 2.4-fold increase in phenylalanine yield compared with the original *B. flavum* 311 cells, which had the highest phenylalanine yield among all the transformants. On the other hand, the effect of *ppsA* and *pckA* genes on L-phenylalanine yield was strictly limited with only a 0.3-fold increase. Phenylalanine yield of the pCZ-GAB-harboring transformant was almost equal to that of pJN5, implying that biosynthesis of L-phenylalanine was mainly determined by *aroG*, *tyrB* and *pheA* genes.

Table 4 Phenylalanine production of *B. flavum* harboring different constructs

Constructs	Yield (g/L)	Relative yield
None	1.64±0.27	1
pCZ	1.59±0.29	1
pJN2	2.04±0.25	1.3
pCZ-GAB	4.83±0.18	3.0
pJN5	5.39±0.32	3.4

DISCUSSION

The metabolic pathway engineering of microorganisms has been considered as the most promising approach to achieve high yield of fermentation products. Over-expressing of genes

playing important roles in biosynthesis pathway, and introducing of special genes isolated from other organisms by genetic manipulation, are major approaches for metabolic pathway engineering. Elevation of PpsA and PckA levels in bacterial cells usually leads to the accumulation of PEP, a limiting precursor of biosynthesis of L-phenylalanine. Therefore, over-expression of *ppsA* and *pckA* genes is expected to channel more carbon flux into aromatic flux. In this study, we amplified *ppsA* and *pckA* genes from *E. coli* genomic DNA, and successfully expressed the two genes together with other three genes in *B. flavum* to investigate the effect of over-expression of these genes on biosynthesis of L-phenylalanine. Our studies revealed that expression of *ppsA/pckA* genes both in *E. coli* and in *B. flavum* could not only significantly elevate the enzymatic activities of PpsA/PckA, but also remarkably increase the expression of DS, which plays a central role downstream PEP in the pathway of phenylalanine biosynthesis.

As shown in Table 4, introduction of pJN2, pCZ-GAB and pJN5 into *B. flavum* could increase the phenylalanine yield by 0.3-, 2.0- and 2.4-fold, respectively. The differences between pJN2 and the two others are significant. A reasonable conclusion from this result is that although *ppsA* and *pckA* genes are important for accumulating PEP, they are not crucial for phenylalanine yield. The net increase in phenylalanine yield by *ppsA* and *pckA* genes when other three genes (*aroG*, *pheA* and *tyrB*) are over-expressed, is 13 %. Though 13 % is not a big increase, but this makes a sense for industrial scale production of L-phenylalanine. These results demonstrated feasibility to increase the phenylalanine yield by over-expressing *ppsA* and *pckA* genes in microorganisms.

Recently it was reported that the disruption of *csrA* gene could increase gluconeogenesis and decrease glycolysis, and thus could in turn accumulate PEP^[36-41]. A strain in which the aromatic (shikimate) pathway had been optimized produced twofold more phenylalanine when *csrA* was disrupted. We have cloned this gene in this study and are trying to construct expression plasmid carrying *csrA* gene as well as other genes investigated. With further effort, metabolic pathway engineering will be finally applicable to the production of phenylalanine on a large scale.

REFERENCES

- 1 **Fan CS**, Jiang PH, Zeng XB, Wu YQ, Chen YQ, Huang WD. Phenylalanine biosynthesis in *Brevibacterium lactofermentum* using *Escherichia coli* genes *pheA*, *aroG* and *tyrB*. *Progress in Natural Science* 2001; **11**: 786-791
- 2 **Murata T**, Horinouchi S, Beppu T. Production of poly (L-aspartyl-L-phenylalanine) in *Escherichia coli*. *J Biotechnol* 1993; **28**: 301-312
- 3 **Tollefson L**, Barnard RJ. An analysis of FDA passive surveillance reports of seizures associated with consumption of aspartame. *J Am Diet Assoc* 1992; **92**: 598-601
- 4 **Petersen S**, Mack C, de Graaf AA, Riedel C, Eikmanns BJ, Sahn H. Metabolic consequences of altered phosphoenolpyruvate carboxykinase activity in *Corynebacterium glutamicum* reveal anaplerotic regulation mechanisms *in vivo*. *Metab Eng* 2001; **3**: 344-361
- 5 **Bongaerts J**, Kramer M, Muller U, Raeven L, Wubbolts M. Metabolic engineering for microbial production of aromatic amino acids and derived compounds. *Metab Eng* 2001; **3**: 289-300
- 6 **Yang YT**, Bennett GN, San KY. The effects of feed and intracellular pyruvate levels on the redistribution of metabolic fluxes in *Escherichia coli*. *Metab Eng* 2001; **3**: 115-123
- 7 **Delaunay S**, Uy D, Baucher MF, Engasser JM, Guyonvarch A, Goergen JL. Importance of phosphoenolpyruvate carboxylase of *Corynebacterium glutamicum* during the temperature triggered glutamic acid fermentation. *Metab Eng* 1999; **1**: 334-343
- 8 **Berry A**. Improving production of aromatic compounds in *Escherichia coli* by metabolic engineering. *Trends Biotechnol* 1996; **14**: 250-256
- 9 **Tatarko M**, Romeo T. Disruption of a global regulatory gene to enhance central carbon flux into phenylalanine biosynthesis in *Escherichia coli*. *Curr Microbiol* 2001; **43**: 26-32
- 10 **Gosset G**, Yong-Xiao J, Berry A. A direct comparison of approaches for increasing carbon flow to aromatic biosynthesis in *Escherichia coli*. *J Ind Microbiol* 1996; **17**: 47-52
- 11 **Kikuchi Y**, Tsujimoto K, Kurahashi O. Mutational analysis of the feedback sites of phenylalanine-sensitive 3-deoxy-D-arabinoheptulosonate-7-phosphate synthase of *Escherichia coli*. *Appl Environ Microbiol* 1997; **63**: 761-772
- 12 **Ger YM**, Chen SL, Chiang HJ, Shiuian D. A single Ser-180 mutation desensitizes feedback inhibition of the phenylalanine-sensitive 3-deoxy-D-arabinoheptulosonate 7-phosphate (DAHP) synthetase in *Escherichia coli*. *J Biochem (Tokyo)* 1994; **116**: 986-990
- 13 **Davies WD**, Pittard J, Davidson BE. Cloning of *aroG*, the gene coding for phospho-2-keto-3-deoxy-heptonate aldolase (*phe*), in *Escherichia coli* K-12, and subcloning of the *aroG* promoter and operator in a promoter-detecting plasmid. *Gene* 1985; **33**: 323-331
- 14 **Davies WD**, Davidson BE. The nucleotide sequence of *aroG*, the gene for 3-deoxy-D-arabinoheptulosonate-7-phosphate synthetase (*phe*) in *Escherichia coli* K12. *Nucleic Acids Res* 1982; **10**: 4045-4048
- 15 **Chao YP**, Lai ZJ, Chen P, Chern JT. Enhanced conversion rate of L-phenylalanine by coupling reactions of aminotransferases and phosphoenolpyruvate carboxykinase in *Escherichia coli* K-12. *Biotechnol Prog* 1999; **15**: 453-458
- 16 **Yang J**, Pittard J. Molecular analysis of the regulatory region of the *Escherichia coli* K-12 *tyrB* gene. *J Bacteriol* 1987; **169**: 4710-4715
- 17 **Fotheringham IG**, Dacey SA, Taylor PP, Smith TJ, Hunter MG, Finlay ME, Primrose SB, Parker DM, Edwards RM. The cloning and sequence analysis of the *aspC* and *tyrB* genes from *Escherichia coli* K12. Comparison of the primary structures of the aspartate aminotransferase and aromatic aminotransferase of *E. coli* with those of the pig aspartate aminotransferase isoenzymes. *Biochem J* 1986; **234**: 593-604
- 18 **Zhang S**, Wilson DB, Ganem B. Probing the catalytic mechanism of prephenate dehydratase by site-directed mutagenesis of the *Escherichia coli* P-protein dehydratase domain. *Biochemistry* 2000; **39**: 4722-4728
- 19 **Nelms J**, Edwards RM, Warwick J, Fotheringham I. Novel mutations in the *pheA* gene of *Escherichia coli* K-12 which result in highly feedback inhibition-resistant variants of chorismate mutase/prephenate dehydratase. *Appl Environ Microbiol* 1992; **58**: 2592-2598
- 20 **Gavini N**, Davidson BE. *pheA* mutants of *Escherichia coli* have a defective *pheA* attenuator. *J Biol Chem* 1990; **265**: 21532-21535
- 21 **Gowrishankar J**, Pittard J. Regulation of phenylalanine biosynthesis in *Escherichia coli* K-12: control of transcription of the *pheA* operon. *J Bacteriol* 1982; **150**: 1130-1137
- 22 **Ikeda M**, Ozaki A, Katsumata R. Phenylalanine production by metabolically engineered *Corynebacterium glutamicum* with the *pheA* gene of *Escherichia coli*. *Appl Microbiol Biotechnol* 1993; **39**: 318-323
- 23 **Oh MK**, Rohlin L, Kao KC, Liao JC. Global expression profiling of acetate-grown *Escherichia coli*. *J Biol Chem* 2002; **277**: 13175-13178
- 24 **Inui M**, Nakata K, Roh JH, Zahn K, Yukawa H. Molecular and functional characterization of the *Rhodospseudomonas palustris* no. 7 phosphoenolpyruvate carboxykinase gene. *J Bacteriol* 1999; **181**: 2689-2696
- 25 **Scovill WH**, Schreier HJ, Bayles KW. Identification and characterization of the *pckA* gene from *Staphylococcus aureus*. *J Bacteriol* 1996; **178**: 3362-3364
- 26 **Osteras M**, Driscoll BT, Finan TM. Molecular and expression analysis of the *Rhizobium meliloti* phosphoenolpyruvate carboxykinase (*pckA*) gene. *J Bacteriol* 1995; **177**: 1452-1460
- 27 **Pantalk R**, Liao JC. Engineering of *Escherichia coli* central metabolism for aromatic metabolite production with near theoretical yield. *Appl Environ Microbiol* 1994; **60**: 3903-3908
- 28 **Jiang PH**, Shi M, Qian ZK, Li NJ, Huang WD. Effect of F209S mutation of *Escherichia coli* *aroG* on resistance to phenylalanine feedback inhibition. *Shengwu Huaxue Yusheng Wuxuxi Xuebao* 2000; **32**: 441-444

- 29 **Niersbach M**, Kreuzaler F, Geerse RH, Postma PW, Hirsch HJ. Cloning and nucleotide sequence of the *Escherichia coli* K-12 *ppsA* gene, encoding PEP synthase. *Mol Gen Genet* 1992; **231**: 332-336
- 30 **Medina V**, Pontarollo R, Glaeske D, Tabel H, Goldie H. Sequence of the *pckA* gene of *Escherichia coli* K-12: relevance to genetic and allosteric regulation and homology of *E. coli* phosphoenolpyruvate carboxykinase with the enzymes from *Trypanosoma brucei* and *Saccharomyces cerevisiae*. *J Bacteriol* 1990; **172**: 7151-7156
- 31 **Bradford MM**. A rapid and sensitive method for the quantitation of microgram quantities of protein utilizing the principle of protein-dye binding. *Anal Biochem* 1976; **72**: 248-254
- 32 **Hutchins AM**, Holden JF, Adams MW. Phosphoenolpyruvate synthetase from the hyperthermophilic archaeon *Pyrococcus furiosus*. *J Bacteriol* 2001; **183**: 709-715
- 33 **Laivenieks M**, Vieille C, Zeikus JG. Cloning, sequencing, and overexpression of the *Anaerobiospirillum succiniciproducens* phosphoenolpyruvate carboxykinase (*pckA*) gene. *Appl Environ Microbiol* 1997; **63**: 2273-2280
- 34 **Xia T**, Zhao G, Jensen RA. Loss of allosteric control but retention of the bifunctional catalytic competence of a fusion protein formed by excision of 260 base pairs from the 3' terminus of *pheA* from *Erwinia herbicola*. *Appl Environ Microbiol* 1992; **58**: 2792-2798
- 35 **Zhang S**, Wilson DB, Ganem B. Probing the catalytic mechanism of prephenate dehydratase by site-directed mutagenesis of the *Escherichia coli* P-protein dehydratase domain. *Biochemistry* 2000; **39**: 4722-4728
- 36 **Baker CS**, Morozov I, Suzuki K, Romeo T, Babitzke P. CsrA regulates glycogen biosynthesis by preventing translation of *glgC* in *Escherichia coli*. *Mol Microbiol* 2002; **44**: 1599-1610
- 37 **Gudapaty S**, Suzuki K, Wang X, Babitzke P, Romeo T. Regulatory interactions of Csr components: the RNA binding protein CsrA activates *csrB* transcription in *Escherichia coli*. *J Bacteriol* 2001; **183**: 6017-6027
- 38 **Nogueira T**, Springer M. Post-transcriptional control by global regulators of gene expression in bacteria. *Curr Opin Microbiol* 2000; **3**: 154-158
- 39 **Wei B**, Shin S, LaPorte D, Wolfe AJ, Romeo T. Global regulatory mutations in *csrA* and *rpoS* cause severe central carbon stress in *Escherichia coli* in the presence of acetate. *J Bacteriol* 2000; **182**: 1632-1640
- 40 **Romeo T**. Global regulation by the small RNA-binding protein CsrA and the non-coding RNA molecule CsrB. *Mol Microbiol* 1998; **29**: 1321-1330
- 41 **Liu MY**, Romeo T. The global regulator CsrA of *Escherichia coli* is a specific mRNA-binding protein. *J Bacteriol* 1997; **179**: 4639-4642

Edited by Ren SY

Tri-iodothyronine supplement protects gut barrier in septic rats

Zhi-Li Yang, Lian-Yue Yang, Geng-Wen Huang, He-Li Liu

Zhi-Li Yang, Lian-Yue Yang, Geng-Wen Huang, He-Li Liu, Department of Surgery, Xiangya Hospital, Central South University, Changsha 410008, Hunan Province, China

Supported by the Scientific Research Fund of Chinese Ministry of Health, No.98-1-112

Correspondence to: Lian-Yue Yang, MD, Department of Surgery, Xiangya Hospital, Central South University, Changsha 410008, Hunan Province, China. damoyzl@163.net

Telephone: +86-731-4327326

Received: 2002-06-17 **Accepted:** 2002-07-19

Abstract

AIM: To investigate the role of tri-iodothyronine supplement in protecting gut barrier in septic rats.

METHODS: Twenty-two rats were randomized into three groups: sham group ($n=6$), sepsis group ($n=8$), and sepsis plus tri-iodothyronine (T_3) group ($n=8$). Septic rat model was established through cecal ligation and puncture (CLP). After 5 h, sham and sepsis groups received saline, and the remaining group received T_3 intraperitoneally. Twenty-one hrs After CLP, intestinal permeability and serum free T_3 and T_4 were measured with fluorescence spectrophotometer and by radioimmunoassay, respectively. Intestinal ultrastructure and histologic morphology were observed under transmission electron microscopy (TEM) and light microscopy, respectively.

RESULTS: After 21 h, septic symptoms and signs in sepsis plus T_3 group were milder than those in sepsis group. Serum FT_3 or FT_4 concentration in sepsis group was lower than that in sham group (1.59 ± 0.20 , 3.41 ± 2.14 pmol/L vs 3.44 ± 1.40 , 9.53 ± 3.39 pmol/L, $P<0.05$), and FT_3 concentration in sepsis plus T_3 group (3.40 ± 1.65 pmol/L, $P<0.05$) was corrected. Portal concentration of fluorescein isothiocyanate-dextran (FITC-D) in sepsis group (2.51 ± 0.56 mg/L) was higher than that in sham group (1.22 ± 0.21 mg/L) ($P<0.01$), and in sepsis plus T_3 group (1.68 ± 0.38 mg/L) it was decreased significantly ($P<0.01$). TEM and light microscopy showed that T_3 supplement preserved well ultrastructure and morphology of intestinal mucosa in septic rats.

CONCLUSION: Tri-iodothyronine supplement protects gut barrier in septic rats.

Yang ZL, Yang LY, Huang GW, Liu HL. Tri-iodothyronine supplement protects gut barrier in septic rats. *World J Gastroenterol* 2003; 9(2): 347-350
<http://www.wjgnet.com/1007-9327/9/347.htm>

INTRODUCTION

In recent years, laboratory and clinical researches have strongly shown that the gastrointestinal tract plays a pivotal role in the occurrence of sepsis and multiple organ dysfunction syndrome (MODS)^[1-4]. It is believed that gut barrier failure is a "trigger point" in sepsis and MODS, and some substances including intestinal trefoil factor^[5], glucagons-like peptide 2^[6-8] and glutamine^[9,10] may protect gut barrier, but we are still facing

either poor efficacy in clinical application or the challenge of translating the findings from the bench to the bedside. Therefore, it has become a breakthrough that may prevent MODS occurrence, improve septic prognosis and further seek for protective substances of gut barrier.

The "euthyroid sick syndrome, ESS" is defined as a decreased concentration of plasma tri-iodothyronine (T_3) with normal or low thyroxine (T_4), but serum thyroid-stimulating hormone concentration is normal^[11,12]. This syndrome is seen in states in which there are significant insults to the host including surgery, starvation, myocardial infarction, hypothermia and sepsis. In the study of ESS, it was reported that T_3 supplement may protect some organ functions^[13], such as pulmonary function during sepsis^[14], and donor myocardial function after transplantation^[15]. Recently, in sepsis, T_3 augmentation was shown by Chapital *et al* to increase the circulating antithrombin III levels, which is a critical material to prevent disseminated intravascular coagulation(DIC)^[16]. An earlier study revealed that hypothyroid hormone resulted in atrophy of intestinal epithelial cells, decreased mucosal DNA and protein contents, shortened the villi height, decreased the crypt depth and rates of utilization of glucose and glutamine, and consequently impaired the gut barrier^[17]. Based on these studies, we hypothesized that T_3 supplement may protect gut barrier in sepsis. This study was to investigate the relationship between T_3 and gut barrier in septic rats.

MATERIALS AND METHODS

Animals

Twenty-two adult male specific pathogen free (SPF) Sprague-Dawley rats weighing from 250 to 350 g were utilized in this investigation. The animals were purchased from Department of Animal Laboratory of Xiangya Medical College. Rats used in the present study were cared in accordance with the directory of Central South University Animal Care Unit, and the guidelines of the National Institutes of Health on welfare of laboratory animals.

Animal model

Rats were randomly divided into three groups: sham group ($n=6$), sepsis group ($n=8$), and sepsis plus T_3 group ($n=8$). Sepsis was induced by cecal ligation and puncture (CLP) as described by Wichterman *et al*^[18]. Under 3 % pentobarbital sodium anesthesia, a laparotomy was performed (the size of the incision was 2.0 cm), and the cecum was ligated just distally to the ileocecal valve to avoid any intestinal obstruction and was punctured across the intestine once with an 18 gauge needle. Punctured holes were placed 1-0 silk thread in case they were blocked up. The cecum was then returned to the peritoneal cavity and the abdomen was closed in two layers. Laparotomy in sham group was performed and the cecum was manipulated, but neither ligated nor punctured. All animals were resuscitated subcutaneously with 50 ml/kg body weight of normal saline at the completion of surgery. After 5 h, sepsis plus T_3 group were injected intraperitoneally with 1.5 ml/kg body weight of T_3 (0.01 g/L, Sigma), and sham group and sepsis group received 1.5ml/kg body weight of normal saline. All animals were anesthetized 21hrs post-CLP once more with

two-thirds of original dose, their intestinal permeability and serum free T_3 and T_4 were measured, intestinal ultrastructure and histologic morphology were observed.

Intestinal permeability measurement

Intestinal permeability was determined essentially according to the method described by Chen *et al*^[19]. A 20 cm segment of the ileum was dissected beginning at 3 cm ileum proximal to ileocecal valve with well protected superior mesenteric vessels. The bilateral end of the isolated ileum was clamped with rubber bands to prevent the leakage of fluorescein isothiocyanate-dextran (FITC-D). One ml of 0.1M phosphate buffer saline (PBS, pH7.2) containing 25 mg of FITC-D (MW4400, Sigma) was injected into the lumen. After 30 min, a blood sample (100 μ L) was taken by a puncture of the portal vein and immediately diluted with 1.9 ml of 50 Mm Tris(pH10.3) containing 150 mM chloride sodium. The diluted plasma was centrifuged at 3 000 \times g, 4 $^{\circ}$ C for 7 min. The supernatant was analyzed for FITC-D concentration with a Hitachi fluorescence spectrophotometer (F-2000) at an excitation wavelength of 480 nm and an emission wavelength of 520 nm. Standard curves for calculating the FITC-D concentration in the samples were obtained by diluting various amounts of FITC-D in a pool of rat plasma, then diluted and centrifuged in the same manner as the samples before measurement.

Transmission electron microscopy (TEM)

Segments of intestine were removed, small rings were cut from the intestine, and immediately fixed in 2.5 % glutaraldehyde for at least 24 hours, and counter-fixed in 2 % osmium tetroxide prepared in 0.1M phosphate buffer, pH7.4 for one hour. They were then dehydrated in graded series of ethanol and propylene oxide and embedded in Epon 812, Sections were cut, collected on copper grids, counter stained with uranyl acetate and lead citrate, and examined under a Hitachi H-600 electron microscope.

Histological assessment

A longitudinal 1 cm segment of intestine was removed and rinsed in normal saline, fixed in 10 % neutral formalin, and processed by conventional methods. The tissue was embedded in paraffin wax. Tissue sections (5 μ m) were stained with haematoxylin and eosin. Intestinal morphologic characteristics were evaluated under light microscopy.

Assay of serum free T_3 and T_4 (FT_3 , FT_4)

After 21hrs, 3 ml blood samples were collected from inferior vena cava, centrifuged at 1 500 \times g for 15 min. The supernatants were frozen at -20 $^{\circ}$ C for later FT_3 and FT_4 assay by radioimmunoassay (RIA).

Statistical analysis

Data were expressed as $\bar{x}\pm s$ and compared using one-way analysis of variance (ANOVA). The statistical analyses were made using the Statistical Package for the Social Science (SPSS10.0) software. Differences were considered as significant when the probability was less than 0.05.

RESULTS

All rats of sepsis group exhibited symptoms and signs of sepsis, including lethargy, piloerection, decreased grooming, and diarrhea. Above symptoms and signs of sepsis plus T_3 group were milder, and sham group were normal.

Serum FT_3 levels in sepsis group were decreased significantly compared with tri-iodothyronine treated rats at 21 hrs, sepsis plus T_3 rats had normal or slightly decreased FT_3 levels after CLP 21 hrs compared with sham operated rats,

and FT_4 levels in sepsis group were also much lower than those in sham operated rats (Table 1).

Table 1 Serum FT_3 and FT_4 concentrations measured by RIA ($\bar{x}\pm s$)

Groups	n	FT_3 (pmol/L)	FT_4 (pmol/L)
Sham	6	3.44 \pm 1.40 ^a	9.53 \pm 3.39 ^a
Sepsis	8	1.59 \pm 0.20	3.41 \pm 2.14
Sepsis plus T_3	8	3.40 \pm 1.65 ^a	6.37 \pm 4.45

^a $P < 0.05$ vs sepsis group.

Rats receiving normal saline after CLP showed a significant increase in intestinal permeability in comparison with sham group ($P < 0.01$), rats with administered T_3 after CLP showed a significant decrease in intestinal permeability in comparison with the sepsis plus normal saline group ($P < 0.01$) (Figure 1).

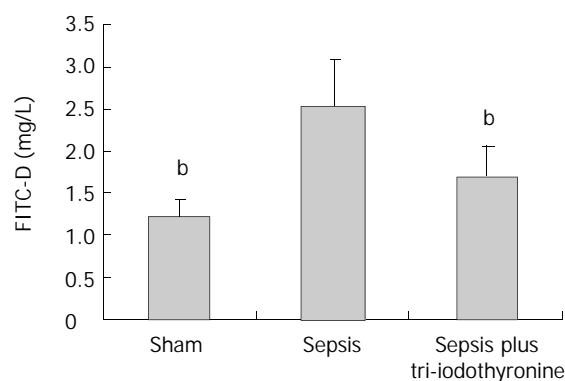


Figure 1 Effect of tri-iodothyronine on gut permeability. ^b $P < 0.01$ vs sepsis group.

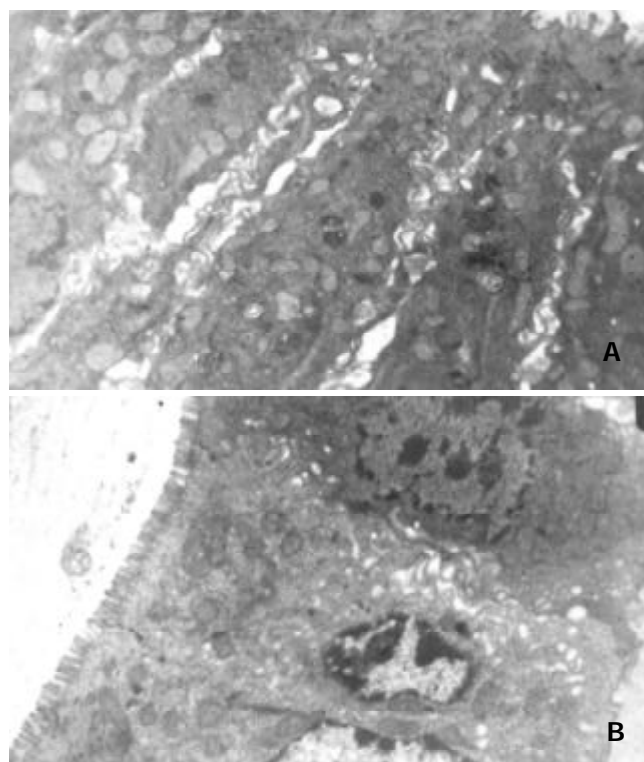


Figure 2 Transmission electron micrography of intestinal mucosal cells. (A) In sepsis group intestinal epithelial cells. (B) In sepsis plus T_3 group intestinal epithelial cells $\times 6 000$.

In sepsis group, the ultrastructure of intestinal epithelial cells showed that the microvilli were sharply reduced and deformed, and loss was patchy. The edema of the villi cells was more pronounced with the mitochondrias dropsy and vacuolar change, gaps of enterocytes were sharply widened, junctional complex among enterocytes were shortened and widened (Figure 2 A). In contrast, ultrastructure of sepsis plus T_3 group showed that the microvilli were dense and regular with a jagged and interlocking pattern among enterocytes and the mitochondrias were clear (Figure 2 B).

Under photomicrography, septic rats showed severe edema and sloughing of the villous tips compared with sham animals (Figure 3A and B). Rats with administered T_3 after CLP showed relatively normal villous tips without sloughing (Figure 3 C).

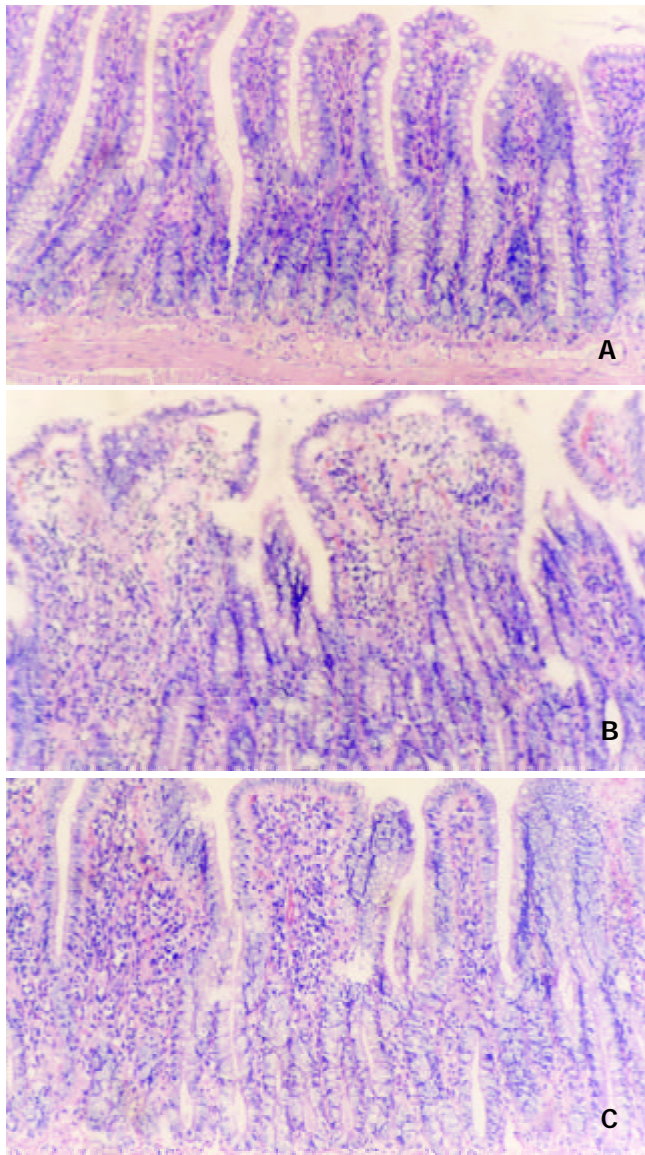


Figure 3 In sham rats, intestinal mucosal architecture is well preserved (A). Sepsis induced significantly edema of villous tips and sloughing of villous enterocytes (B). The tri-iodothyronine prevented the intestinal damages induced by sepsis (C). HE, $\times 100$.

DISCUSSION

For more than 3 decades, it has been known that the euthyroid sick syndrome exists probably in any severe illness, including starvation^[20], pulmonary tuberculosis^[21], sepsis^[22,23], surgery^[24,25], myocardial infarction^[26,27], bypass^[28] and bone marrow transplantation^[29]. The syndrome is also called low T_3 syndrome

or nonthyroidal illness, characterized by low serum T_3 levels, and serum free T_4 levels are commonly below normal, but may be normal or above normal. It is likely that mechanism of thyroid hormone suppression in these illness is multifactorial and may differ in different groups of patients, as for low serum T_3 levels in this syndrome, one important cause is a decreased generation of T_3 by type I iodothyronine deiodinase in the liver and a reduced degradation of r T_3 ^[30]. Subsequently, Nagaya *et al* demonstrated that in severe illness activated NF- κ B could inhibit T_3 -dependent induction of type I 5' - deiodinase mRNA and enzyme activity^[31]. In addition, the degree of low T_3 in circulation has been shown to correlate with the severity of the underlying disorders and the prognosis^[32]. Some authors believe that this is an abnormal state with decreased production rather than increased degradation, others content that this may be the body's adaptation to stress protecting the body against exaggerated catabolism. Hitherto, some T_3 supplementing studies suggested that the former might be more reasonable than the latter^[14-16,35].

In this study, we used cecum ligation and puncture (CLP) to establish classic animal model of sepsis. During the whole investigation, our septic models were coincident with the previous studies^[33,34]. An acute decrease in circulating levels of free T_3 and T_4 was seen after 21hrs CLP, T_3 supplement prevented the decrease in serum free T_3 concentration with sepsis. ESS was seen in our septic model. Moley *et al* showed in their study that absence of thyroid hormone abolished the hyperdynamic phase of sepsis, increased susceptibility to sepsis, and significantly increased the mortality in sepsis, and thyroxine replacement following thyroidectomy prevented the increased mortality from sepsis^[35]. In our research, T_3 supplement showed that septic symptoms and signs of the rats were abated to a certain extent. Thus, our data has confirmed that T_3 replacement in septic rats with ESS may be beneficial to the general condition of the patients.

The progression from sepsis to severe sepsis (sepsis with dysfunction of one organ) to multiple organ dysfunction syndrome and then to septic death requires escalation of treatment^[36]. During the course of the progression, gut barrier disruption is believed to be the "motor" of "irreversible" shock and multiple system organ failure^[37]. The critical cause is that translocation of bacteria and endotoxins contribute to the infection and injury of the body. Increased intestinal mucosal permeability is considered to be a quantitative index of injury or dysfunction of the intestinal mucosa barrier. The molecular probe FITC-D used in this study is considered to penetrate through a paracellular route toward portal vein via the tight junctions according to its size. Gut permeability indicated by FITC-D was coincident with the pathologic changes of injured gut in inflammation^[38]. Assay of FITC-D does not depend on systemic circulation and renal function compared with other probe molecule, and so application of FITC-D assay can indicate more exactly the gut permeability in this experimental model. Our data showed that T_3 administration significantly decreased gut permeability in septic rats. Photomicrography and TEM showed that T_3 supplement well preserved the ultrastructure and morphology of intestinal mucosa. Therefore, these data indicate that T_3 augmentation can protect from the structural and functional damages of gut barrier in septic rats. The proximate molecular mechanism by which T_3 regulates gut barrier in sepsis is not known. It is possible that T_3 administration is associated with protective substances synthesis of intestinal epithelial cells. Smith *et al* reported that administration of T_3 could induce expression of heme oxygenase-1 (HO-1) and stimulate activity of HO-1 in liver of thyroidectomized rats^[39]. HO-1 is a stress-associated protein whose expression is stimulated by hypoxia, and increases adaptive response of cells to hypoxia. Hypoxia inducible factor-1 (HIF-1) mediates transcriptional activation of HO-1 gene in

response to hypoxia^[40]. Our study showed that T₃ supplement increased expression of HIF-1 α in intestinal epithelial cells of septic rats (unpublished data). Thus, promoting adaptive response of cells to hypoxia may be one of approaches to improve gut barrier in sepsis by T₃.

In conclusion, thyroid hormone is one of the critical hormones in mammals and plays an indispensable role in development as well as in lipid, protein, and carbohydrate metabolism and energy generation. Our results demonstrate that tri-iodothyronine, active form of thyroid hormone, can protect gut barrier in septic rats. Obviously, biologic functions of thyroid hormone are expanded, and moreover, it may supply a novel method to protect from the injury of gut barrier in critic illness. It is of important theoretical significance and practical value to further investigate its protective mechanism.

ACKNOWLEDGEMENT

We are grateful to Professor Shi-Ling He and Professor Zhi-Qiang Xiao for their assistance in preparing this manuscript.

REFERENCES

- 1 **Moore FA**. Role of gastrointestinal tract in the postinjury multiple organ failure. *Am J Surg* 1999; **178**: 449-453
- 2 **Deitch EA**. Multiple organ failure: pathophysiology and potential future therapy. *Ann Surg* 1992; **216**: 117-134
- 3 **Wu CT**, Li ZL, Xiong DX. Relationship between enteric microecologic dysbiosis and bacterial translocation in acute necrotizing pancreatitis. *World J Gastroenterol* 1998; **4**: 242-245
- 4 **Yi JH**, Ni RY, Luo DO, Li SL. Intestinal flora translocation and overgrowth in upper gastrointestinal tract induced by hepatic failure. *World J Gastroenterol* 1999; **5**: 327-329
- 5 **Wong WM**, Poulosom R, Wright NA. Trefoil peptides. *Gut* 1999; **44**: 890-895
- 6 **Kouris GJ**, Liu Q, Rossi H, Djuricin G, Gattuso P, Nathan C, Weinstein RA, Prinz RA. The effect of glucagons-like peptide 2 on intestinal permeability and bacterial translocation in acute necrotizing pancreatitis. *Am J Surg* 2001; **181**: 571-575
- 7 **Wang FJ**, Zhao Y, Wang P, Wang SL, Liu J, Zhou X. Effects of glucagons-like peptide-2 on intestinal barrier function in severely burned rats. *Shijie Huaren Xiaohua Zazhi* 2002; **10**: 796-799
- 8 **Benjamin MA**, Mckay DM, Yang PC, Cameron H, Perdue MH. Glucagon-like peptide-2 enhances intestinal epithelial barrier function of both transcellular and paracellular pathways in the mouse. *Gut* 2000; **47**: 112-119
- 9 **Wischmeyer PE**, Kahana M, Wolfson R, Ren H, Mush MM, Chang EB. Glutamine reduces cytokine release, organ damage, and mortality in a rat model of endotoxemia. *Shock* 2001; **16**: 398-402
- 10 **Zhou X**, Li YX, Li N, Li JS. Effect of bowel rehabilitative therapy on structural adaptation of remnant small intestine: animal experiment. *World J Gastroenterol* 2001; **7**: 66-73
- 11 **Utiger RD**. Altered thyroid function in nonthyroidal illness and surgery: to treat or not to treat? *N Engl J Med* 1995; **333**: 1562-1563
- 12 **Yang LY**, Huang GW. Advance and development of sick syndrome of normal thyroid in surgical sever patients. *Zhongguo Shiyong Waikexue Zazhi* 2000; **20**: 114-115
- 13 **Liu JH**, Yang LY. Advance and development of research of protective mechanism of organ function by thyroxine. *Zhongguo Shiyong Waikexue Zazhi* 2001; **21**: 372-374
- 14 **Dulchavsky SA**, Bailey J. Triiodothyronine treatment maintains surfactant synthesis during sepsis. *Surgery* 1992; **112**: 475-479
- 15 **Jeevanandam V**, Todd B, Regillo T, Hellman S, Eldridge C, McClurken J. Reversal of donor myocardial dysfunction by triiodothyronine replacement therapy. *J Heart Lung Transplant* 1994; **13**: 681-687
- 16 **Chapital AD**, Hendrick SR, Lloyd L, Pieper D. The effects of triiodothyronine augmentation on antithrombin III levels in sepsis. *Am Surg* 2001; **67**: 253-255
- 17 **Ardawi MSM**, Jalalah SM. Effects of hypothyroidism on glucose and glutamine metabolism by the gut of the rat. *Clin Science* 1991; **81**: 347-355
- 18 **Wichterman KA**, Chaudry IH, Baue AE. Studies of peripheral glucose uptake during sepsis. *Arch Surg* 1979; **114**: 740-743
- 19 **Chen LW**, Hsu CM, Cha MC, Chen JS, Chen SC. Changes in gut mucosal nitric oxide synthase(NOS) activity after thermal injury and its relation with barrier failure. *Shock* 1999; **11**: 104-110
- 20 **Hennemann G**, Docter R, Krenning EP. Causes and effects of the low T₃ syndrome during caloric deprivation and non-thyroidal illness: an overview. *Acta Med Kaust* 1988; **15**: 42-45
- 21 **Chow CC**, Mak TW, Chan CH, Cockram CS. Euthyroid sick syndrome in pulmonary tuberculosis before and after treatment. *Ann Clin Biochem* 1995; **32**: 385-391
- 22 **Phillips RH**, Valente WA, Caplan ES, Connor TB, Wiswell JG. Circulating thyroid hormone changes in acute trauma: prognostic implications for clinical outcome. *J Trauma* 1984; **24**: 116-119
- 23 **Huang GW**, Yang LY, Yang JQ. Role of thyroid hormone in the protection of intestinal mucosal barrier of septic rats. *Zhonghua Shiyong Waikexue Zazhi* 2000; **17**: 531-532
- 24 **Cheren HJ**, Nellen HH, Barabejski FG, Chong MBA, Lifshitz GA. Thyroid function and abdominal surgery. A longitudinal study. *Arch Med Res* 1992; **23**: 143-147
- 25 **Yang LY**, Liu HL. Application of thyroxine in surgery. *Zhongguo Shiyong Waikexue Zazhi* 2001; **21**: 328-329
- 26 **Vardarli I**, Schmidt R, Wdowinski JM, Teuber J, Schwedes U, Usadel KH. The hypothalamo-hypophyseal thyroid axis, plasma protein concentrations and the hypophyseogonadal axis in low T₃ syndrome following acute myocardial infarct. *Klin Wochenschrift* 1987; **65**: 129-133
- 27 **Eber B**, Schumacher M, Langsteger W, Zweiker R, Fruhwald FM, Pokan R, Gasser R, Eber O, Klein W. Changes in thyroid hormone parameters after acute myocardial infarction. *Cardiology* 1995; **86**: 152-156
- 28 **Holland FW**, Brown PS, Weintraub BD, Clark RE. Cardiopulmonary by pass and thyroid function: a "euthyroid sick syndrome". *Ann Thorac Surg* 1991; **52**: 46-50
- 29 **Vexiau P**, Perez-Castiglioni P, Socie G, Devergie A, Toubert ME, Aracting S, Gluckman E. The "euthyroid sick syndrome": incidence, risk factors and prognostic value soon after allogeneic bone marrow transplantation. *Br J Hematol* 1993; **85**: 778-782
- 30 **DE Groot LJ**. Dangerous dogmas in medicine: the nonthyroidal illness syndrome. *J Clin Endocrinol Metab* 1999; **84**: 151-164
- 31 **Nagaya T**, Fujieda M, Otsuka G, Yang JP, Okamoto T, Seo H. A potential role of activated NF- κ B in the pathogenesis of euthyroid sick syndrome. *J Clin Invest* 2000; **106**: 393-402
- 32 **Yang LY**, Hu M, Huang YS. The relation of critic septic shock and peripheric metabolism malfunction of thyroxine. *Zhonghua Shiyong Waikexue Zazhi* 1990; **7**: 134-135
- 33 **Shieh P**, Zhou M, Orman DA, Chaudry IH, Wang P. Upregulation of inducible nitric oxide synthase and nitric oxide occurs later than the onset of the hyperdynamic response during sepsis. *Shock* 2000; **13**: 325-329
- 34 **Wang P**, Chaudry IH. Mechanism of hepatocellular dysfunction during hyperdynamic sepsis. *Am J Physiol* 1996; **270**: R927-938
- 35 **Moley JF**, Ohkawa M, Chaudry IH, Clemens MG, Baue AE. Hypothyroidism abolishes the hyperdynamic phase and increases susceptibility to sepsis. *J Surg Res* 1984; **36**: 265-273
- 36 **Tabrizi AR**, Zehnbaauer BA, Freeman BD, Buchman TG. Genetic markers in sepsis. *J Am Coll Surg* 2001; **192**: 106-117
- 37 **Antonsson JB**, Fiddian-Green RG. The role of the gut in shock and multiple system organ failure. *Eur J Surg* 1991; **157**: 3-12
- 38 **Travis S**, Menzies I. Intestinal permeability: functional assessment and significance. *Clin Sci* 1992; **82**: 471-488
- 39 **Smith TJ**, Drummand GS, Kourides IA, Kappas A. Thyroid hormone regulation of heme oxidation in the liver. *Proc Natl Acad Sci USA* 1982; **79**: 7537-7541
- 40 **Lee PJ**, Jiang BH, Chin BY, Iyer NV, Alam J, Semenza GL, Choi AMK. Hypoxia-inducible factor-1 mediates transcriptional activation of the heme oxygenase-1 gene in response to hypoxia. *J Bio Chem* 1997; **272**: 5375-5381

Effects of cholesterol on the phenotype of rabbit bile duct fibroblasts

Bao-Ying Chen, Jing-Guo Wei, Yao-Cheng Wang, Chun-Mei Wang, Jun Yu, Xiang-Xin Yang

Bao-Ying Chen, Jing-Guo Wei, Yao-Cheng Wang, Xiang-Xin Yang, Department of Radiology, Tangdu Hospital, Fourth Military Medical University, Xi'an 710038, Shannxi Province, China

Chun-Mei Wang, Electron Microscope Center, Fourth Military Medical University, Xi'an 710032, Shannxi Province, China

Jun Yu, Department of Physiology, Fourth Military Medical University, Xi'an 710032, Shannxi Province, China

Correspondence to: Jing-Guo Wei, Department of Radiology, Tangdu Hospital, Fourth Military Medical University, Xi'an 710038, Shannxi Province, China. chenbaoying2002@yahoo.com.cn

Received: 2002-10-08 **Accepted:** 2002-11-04

Abstract

AIM: To investigate how cholesterol (Ch) can affect the phenotype of bile duct fibroblasts of New Zealand rabbits.

METHODS: 16 rabbits were divided randomly into two groups: the control group and the experiment group. The rabbits in experiment group were fed with hypercholesterol diet for 8 weeks. Bile duct was dissociated from rabbits and prepared for transmission electron microscopy. The purified bile duct fibroblasts were cultured and divided randomly into three groups: control group, Ch middle concentration group (0.6 g/L), Ch high concentration group (1.2 g/L). After incubated for 72 h, the fibroblasts were made into specimens for transmission electron microscopy. The expression of α -actin in bile duct fibroblasts was measured by means of laser scanning confocal microscopy.

RESULTS: With the transmission electron microscopy, the normal bile duct fibroblasts were shuttle-shaped, and there were abundant rough endoplasmic reticulums (RER), but few mitochondria or microfilaments in cytoplasm. This is the typical phenotype of fibroblasts. Bile duct fibroblasts of hypercholesterolemic rabbits were observed. by the transmission electron microscopy Rough endoplasmic reticulums were significantly reduced, with a lot of microfilament bundles or stress fibers appeared in cytoplasm, especially under plasma membrane. Dense bodies were scattered within these bundles. Macula densas and discontinuous sarcolemma were found under plasma membrane. It suggested that the bile duct fibroblasts of hypercholesterolemic rabbits presented the phenotype of smooth muscle cell. The cultured bile duct fibroblasts also had typical phenotype of fibroblasts. After stimulated by middle concentration cholesterol (0.6 g/L) for 72 h, there appeared lots of microfilaments in cytoplasm, but without dense body, macula densa and discontinuous sarcolemma. Observed with confocal microscopy, there were many regular bundles of microfilaments in fibroblasts treated with middle concentration ch (0.6 g/L) and the expression of α -actin was significantly increased. The average fluorescence value of middle concentration group was $1\ 628\pm 189$ ($P<0.01$ vs control group). Microfilaments and the expression of α -actin were greatly decreased in fibroblasts of high concentration group (1.2 g/L). The average fluorescence value of high

concentration group was $1\ 427\pm 153$ ($P<0.05$ vs middle concentration group). There were a lower expression of α -actin and few microfilaments in bile duct fibroblasts of control group with an average fluorescence value of $1\ 224\pm 138$.

CONCLUSION: Cholesterol can make bile duct fibroblasts have the phenotypic characteristics of smooth muscle cell both *in vitro* and *in vivo* and this effect is more significant *in vivo*. The effect is probably associated with some other factors besides cholesterol.

Chen BY, Wei JG, Wang YC, Wang CM, Yu J, Yang XX. Effects of cholesterol on the phenotype of rabbit bile duct fibroblasts. *World J Gastroenterol* 2003; 9(2): 351-355

<http://www.wjgnet.com/1007-9327/9/351.htm>

INTRODUCTION

The disorder of cholesterol metabolism is an important cause of biliary diseases. Previous studies suggest that cholesterol can change the motility of cholecyst^[1,2], gallbladder contraction in the patients with cholecyst and in the animals with hypercholesterolemia decreases^[3-6]. Weak contraction may be a reason of cholesterol calculus. Researchers consider that cholesterol metabolism disorder has an effect on the structure and function of bile duct and sphincter of bile duct (SBD)^[7-10]. We found that cholesterol liposome (CL) affected not only the configuration and quantity of cytoskeleton in rabbit SBD smooth muscle cells but also the proliferation of cells^[11-15]. There are many fibroblasts in biliary system except that SBD is formed with smooth muscle cells^[16-18], but it is still unknown if cholesterol has any effect on bile duct fibroblasts and on the configuration variation of bile duct. Using cultured fibroblasts of bile duct, we studied the effect of cholesterol on the transformation of fibroblasts and its mechanism. We tried to find out the effect of fibroblast in bile duct remodeling.

MATERIALS AND METHODS

Materials

New Zealand immature rabbits aged 2-3 months and weighed 2.0-2.5 kg were provided by the Animal Center of the Fourth Military Medical University. Trysin (Gibco), DMEM medium (Gibco), fetal calf serum (Qinghu Institute of Foetus Bovine Utilization in Jinhua Zhejiang), water soluble cholesterol (Sigma), cholesterol (purity for analysis, Shanghai Chemical Co), antibody against α -actin (Gene Co), antibody of vimentin and desmin (Dako Co), ABC immunohistochemical kit (Vector Co), Fluo-3/AM (Molecular Probe Co), CO₂ incubator (Forma Scientific Co), IMT-2 inverted biological microscope (Olympus Co), YJ-875 ultra-clean operating boar (Suhang Experimental Animal Technology Development Co), LD4-2 centrifugal machine (Beijing Medical Centrifugal Machine Factory), JEM-2000EX transmission electron microscope (JEOL Co), and laser confocal scanning microscope (Bio-Rad MRC-1024) were commercially obtained.

Methods

Establishment of rabbit model with hypercholesterolemia

Sixteen pure breed New Zealand female rabbits were randomly divided into 2 groups ($n=8$). The rabbits in experiment group were fed with cholesterol at the dose of 10 g per day and 6 d per week for 8 weeks, the control rabbits were regularly fed. The rabbits with serum concentration of total cholesterol >10 mmol/L were considered to have hypercholesterolemia. It was normal that the serum concentration of total cholesterol ≤ 3.0 mmol/L. Before and during experiment, venous blood was used to measure the serum concentration of total cholesterol. Before experiment the rabbits with serum concentration of total cholesterol >3.0 mmol/L were rejected.

Transmission electron microscope (TEM) observation of the specimen of rabbit bile duct Rabbits of control and experiment group were killed by injecting 10 mL air through ear-margin vein. The bile ducts were removed quickly and milieu connective tissue of bile ducts was curetted carefully, then samples were put into 4 °C 30 mL/L glutaral for two hours, processed conventionally for TEM examination and observed by JEM-2000EX transmission electron microscope.

Culture of rabbit bile duct fibroblasts Bile ducts of the control rabbits were dissociated by the means of aseptic technique and broken by shears. The tissue was digested to become single cell suspension by trypsin (1.25 g/L). Cells were washed and resuspended with DMEM (containing 100 mL/L FCS) and incubated for 75-90 minutes. Then the cells were collected and transferred into culture bottles. The cells of 2-4 passages were used for experiments.

Identification of rabbit bile duct fibroblasts Three glass cover slips (18×18 mm) placed into each of 6 cm diameter culture dishes, then cell suspension was added and incubated for 48 h. The slips covered with cells were washed twice by PBS (pH 7.4). There slips were fixed by cold acetone for 15 (4 °C) minutes and were used for HE staining, another 3 slips were fixed for 20 minutes by citromint (40 g/L) for immunohistochemical ABC staining to exam vimentin and desmin expression.

Treatment of bile duct fibroblasts with cholesterol The cells of passage 2-4 were trypsinized and seeded in culture bottles or on glass cover slips in culture dishes, after overnight preincubation with cholesterol diluted with 20 g/L DMEM was added at the final concentration of 1.2 g/L (group of high concentration, HC) or 0.6 g/L (group of middle concentration, MC). The cells were exposed to cholesterol for 72h, then prepared for the studies with TEM and lasers caning confocal microscope (LSCM) respectively, the cells cultured without cholesterol were used as the control.

TEM and LSCM observation of rabbit bile duct fibroblasts

The cells grown in culture bottles and treated with 0.6 g/L of cholesterol were trypsinized, washed, fixed and then processed for TEM observation with a JEM-2000EX transmission electron microscope. The cells grown on cover slips and treated with 0.6 g/L or 1.2 g/L of cholesterol were fixed with cold acetone for 15 minutes (4 °C), washed three times with PBS and incubated for 30 minutes in normal caprine blood serum to block antibody nonspecific binding site. Rat anti rabbit α -actin antibody (1:50) diluted by BSA/NaN₃/PBS was added on the slips and the cells were incubated for 48 hours (4 °C). After the slips had been washed three times with PBS, FITC tagged caprine anti rat IgG (1:30) was added on the slips and the slips were incubated at room temperature for 3 hours. The amortization glycerin without fluorescence was used to seal slips. The slips were observed by LSCM. The excitation wavelength was of 488 nm. The software was provided by Bio-Rad Co. controled LSCM. The object glass for picture collection was Planneofluar 40×object glass. 7 % light filter was used. More than 200 cells in each group were scanned.

Statistical analyses

The data came into Kinetics-Imaga Scan Analysis program and were analyzed. Results were expressed as $\bar{x}\pm s$. Student's test or an analysis of variance (ANOVA) was performed to test the statistical significance as necessary, $P<0.05$ was regarded as significant.

RESULTS

Character and Identification of cultured rabbit bile duct fibroblasts

Under phase-contrast microscope, cultured rabbit bile duct fibroblasts showed shuttle-shaped or multiangular. Cytoplasm was clear and nucleus was large and ellipse. Nucleolus was obvious. Isolated bile duct fibroblasts were free of smooth muscle cell contamination as determined by positive staining with vimentin and negative staining with desmin by the means of immunocytochemical ABC staining.

TEM observation of rabbit bile duct and cultured rabbit bile duct fibroblasts

The normal bile duct fibroblasts were shuttle-shaped and there were abundant rough endoplasmic reticulum (RER), but few mitochondria and microfilament in cytoplasm. That was typical phenotype of fibroblasts (Figure 1). Rough endoplasmic reticulum (RER) was significantly reduced in the bile duct fibroblasts of hypercholesterolemic rabbits, but a lot of microfilament bundles or stress fibers appeared in cytoplasm, especially under plasma membrane. Dense bodies were scattered within these bundles. Macula densas and discontinuous sarcolemma were found under s plasma membrane. It suggested that the bile duct fibroblasts of hypercholesterolemic rabbits showed the phenotype of smooth muscle cell (Figure 2).

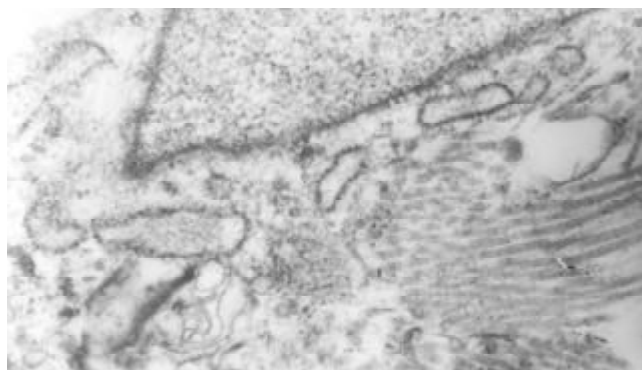


Figure 1 Bile duct fibroblasts of normal rabbit presented shuttle-shaped with abundant rough endoplasmic reticulum (RER), but few mitochondria and microfilament in cytoplasm.

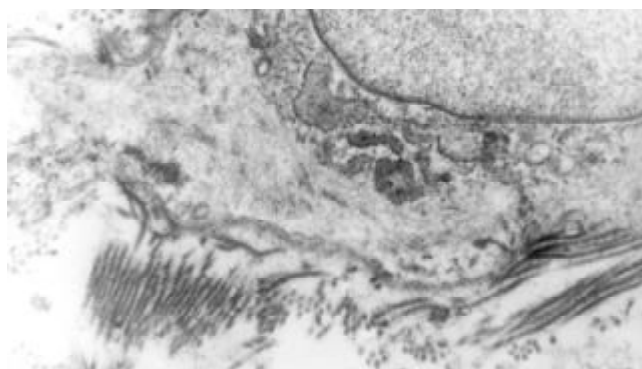


Figure 2 The bile duct fibroblasts of hypercholesterolemic rabbits showed the phenotype of smooth muscle cell. Rough endoplasmic reticulum (RER) was significantly reduced, but a

lot of microfilament bundles or stress fibers appeared in cytoplasm. Dense bodies were scattered within these bundles. Macula densas and discontinuous sarcolemma were found under splasma membrane.

In vitro experiment the cultured bile duct fibroblasts also had typical phenotype of fibroblasts (Figure 3). After stimulated by middle concentration cholesterol (0.6 g/L) for 72 h, there appeared lots of microfilament in cytoplasm, but without dense body. macula densa and discontinuous sarcolemma (Figure 4).

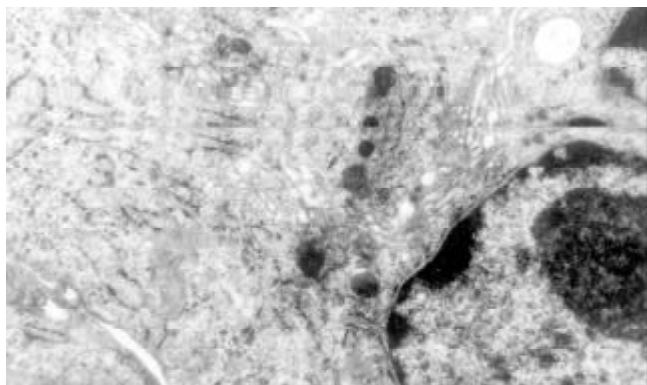


Figure 3 Cultured normal rabbit bile duct fibroblasts characterized typical phenotype of fibroblasts with abundant rough endoplasmic reticulum (RER) and Golgi bodies, but few mitochondria and microfilament.

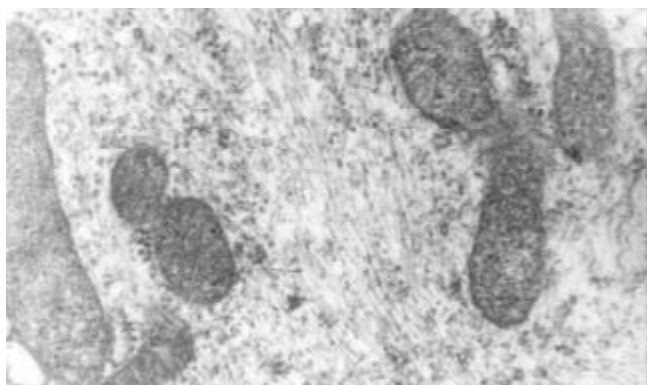


Figure 4 After stimulated by middle concentration cholesterol (0.6 g/L) for 72 h, the cultured bile duct fibroblasts showed some phenotype of fibroblasts, and there appeared lots of microfilament in cytoplasm, but without dense body, macula densa and discontinuous sarcolemma.

LSCM observation of cultured rabbit bile duct fibroblasts

Immunofluorescence display and LSCM were connected to measure the change of nucleic acid and protein in cells. The quantity of detected substance was expressed by average fluorescence value. There were many regular bundles of microfilament in fibroblasts treated with middle concentration cholesterol (0.6 g/L). Microfilament bundles were located along cytoplasmic extension (Figure 5). The expression of α -actin was significantly increased. The average fluorescence value of middle concentration group was 1628 ± 189 ($P < 0.01$ vs control group). The quantity of microfilaments and the expression of α -actin were greatly decreased in fibroblasts of high concentration cholesterol group (1.2 g/L). The average fluorescence value of high concentration group was 1427 ± 153 ($P < 0.05$ vs middle concentration group). There was a lower expression of α -actin and few microfilaments in bile duct fibroblasts of control group, the average fluorescence value was 1224 ± 138 (Figure 6).

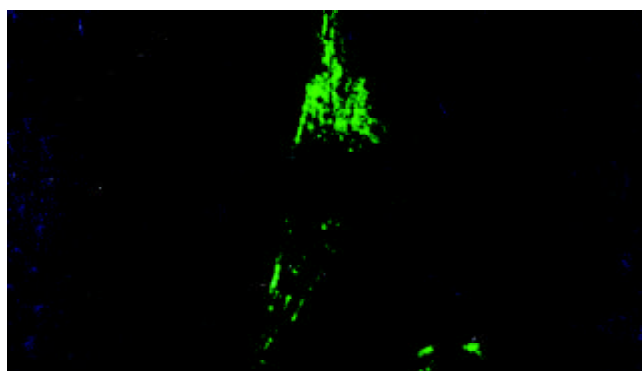


Figure 5 Effects of middle concentration cholesterol (0.6 g/L) on the cultured bile duct fibroblasts. There were many regular bundles of microfilament that were located along cytoplasmic extension.

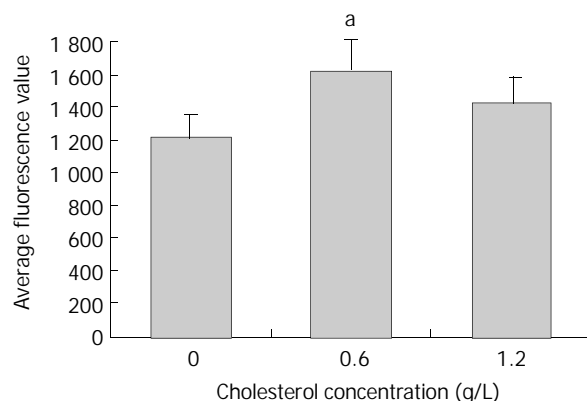


Figure 6 Effects of cholesterol on the α -actin expression of rabbit bile duct fibroblasts. Note ^a $P < 0.05$, vs control and high concentration group (1.2 g/L cholesterol).

DISCUSSION

Fibroblasts are derived from mesenchymal cell of embryo period. During the evolution of wound healing, fibroblasts can proliferate greatly by mitoses. At the same time fibroblasts can also synthesize and excrete collagen fibers and matrix components^[19-21]. With the stimulation of trauma and other agents, some mature fibroblasts can change into naive fibroblasts and their function can be recovered. These fibroblasts take part in the tissue damage plerosis. Hypoxia can, mediated by pulmonary arterial endothelial cells (PAECs) but not directly, induce phenotype modulation of human embryonic lung fibroblasts, namely transforming to smooth muscle cell-like cells. It suggests that the transformation of human embryonic lung fibroblasts is one of the reasons why nonmuscle lung arteriole becomes muscle arteriole^[22]. With the effects of many agents, fibroblasts will proliferate, accumulate or modulate phenotype. Fibroblasts can paracrine and autocrine many cytokines (such as bFGF, KGF). The cytokines can affect fibroblasts and other cells^[23]. Friedenstein A. Abdin M reported that fibroblasts can take part in heterotopic ossification under some pathologic conditions. Silent fibroblasts in the border of wound, adjusted by growth factors, can differentiate to contraction phenotype and have the special expression of α -SM actin. The cells are considered as myofibroblasts. The myofibroblasts can cause contraction of granulation tissue. It is thus clear that fibroblasts have multidifferentiation potential and take part in many kinds of physiological and pathologic responses. Fibroblasts have important effects on the occurrence and development of diseases.

Biliary system is the unique passage of bile ejection. It can modulate bile ejection and maintain normal pressure of biliary

system^[24-31]. The coordination of its anatomic structure and function makes it not only prevent regurgitation of duodenal fluid but also modulate and stabilize the pressure of bile duct^[32-38]. So the structural remodeling of biliary system and the derangement of motor function coordination can become one of basic reasons of biliary system diseases occurrence. There are a great deal of fibroblasts in bile duct system^[39]. At present, it is still unknown what are the effects of cholesterol on bile duct fibroblasts and whether cholesterol can change the configuration of bile duct^[40]. So we use hypercholesterolemia rabbit model and cultured rabbit bile duct fibroblasts to observe the effects of cholesterol on fibroblasts and the mechanism. Our results show that there are a lot of microfilament bundles, dense bodies, macula densa and discontinuous sarcolemma appeared in the bile duct fibroblasts of hypercholesterolemia rabbit. Bile duct fibroblasts present the phenotypic characters of smooth muscle cell. Vitro experiment show that lots of microfilament bundles are found in cultured bile duct fibroblasts treated by middle concentration cholesterol (0.6 g/L) but dense bodies and macula densa are not found. Laser confocal microscopy displays that the expression of α -actin in cultured bile duct fibroblasts treated by middle concentration cholesterol (0.6 g/L) and many regular bundles of microfilament are located along cytoplasmic extension.

Cholesterol is the major lipid structural component of mammal plasma membrane. It has important effects on maintaining plasmalemma normal behavior and function. It has been proved that cholesterol could alter smooth muscle membrane and cell function by changing the physical state of the membrane phospholipid bilayer, and therefore affect the function of integral membrane proteins, such as Ca^{2+} ^[41] and potassium channels, as well as transmembrane receptors^[42]. Excessive cholesterol incorporation decreased membrane fluidity and subsequently restricted optimal function of membrane proteins, such as receptor binding of ligands, receptor coupling with G proteins and activation of enzymes^[43]. Wei et al found the abnormalities in ultrastructure of SO in rabbits with hypercholesterolemia. Therefore, hypercholesterolemia might be one of causes of SOD. Meanwhile, the effect of cholesterol on gallbladder contractility has been interpreted by many authors, who found that the cholesterol incorporated into membrane can impair the cellular signal transduction and contractility as well. Thus, we think that cholesterol can affect signal transduction and in the end change the gene expression. In the 1950s caveolae were discovered. Now It has been proposed that caveolae are important in signal transduction, forming a platform on which different signaling components can congregate. and caveolae have been linked to cholesterol regulation: caveolin binds to cholesterol, its production is controlled by cholesterol. Simons^[44] found that caveolae are important for inhibiting certain signaling pathways that regulate cellular proliferation. Our experiment found that bile duct fibroblasts treated by middle concentration cholesterol presented the phenotypic characters of smooth muscle cell. We suppose that the mechanism may be that cholesterol can alter the biologic character of plasmalemma and affect signal transduction, which induces the gene expression. Whether the effects of cholesterol observed in this study were due to cytotoxicity, other authors reported that high concentration of cholesterol might have influence to cultured muscle cells. The similar procedures had been done by many reseachers, and the cholesterol was within the serum concentration range of hypercholesterolemia rabbit model. So, the cytotoxicity of cholesterol to cells in this study, if any, might be unconsiderable.

Epidemiological study shows that woman is the high-risk group of calculus and multiple birth procreation women are always accompanied with lipid metabolism disturbance. Du Fan confirmed that hypercholesterolemic rabbit presented the

functional disturbance of bile duct before the occurrence of cholelithiasis. It suggested that cholesterol does affect the function of bile duct. Fibroblasts have the potential of multidifferentiation and they can differentiate or transform after being activated. Fibroblasts can differentiate to myofibroblasts or transform to smooth muscle cells because there are some similarities of form and constitution between the two kinds of cells and fibroblasts. Our experiment detected that cultured rabbit bile duct fibroblasts treated with cholesterol presented some characters of smooth muscle cell. *In vivo* experiment shows that bile duct fibroblasts of hypercholesterolemic rabbits present more characters of smooth muscle cell. Therefore we can conclude that cholesterol does activate bile duct fibroblasts and induce fibroblasts to transform into smooth muscle cell. But the change is affected by multiple factors and is a multistage procedure. Although cholesterol is an important factor, only with the help of other factors, can it complete the procedure. The certain mechanism has not been elucidated yet. We suspect that the differentiation and transformation of bile duct fibroblasts have an important effect on the configuration remodeling of biliary system, which provides a pathway to research the occurrence, development and treatment of biliary system diseases.

REFERENCES

- 1 **Chen SZ**, Sha JP, Chen XC, Hou CC, Fu WH, Liu W. Dysrelaxation of Sphincter of Oddi in patients with bile reflux gastritis: study on effect of nifedipine on gallbladder emptying. *Shijie Huaren Xiaohua Zazhi* 1999; **7**: 1020-1023
- 2 **Li XP**, Ouyang KQ, Cai SX. The regulation of bile secretion and eduction. *Shijie Huaren Xiaohua Zazhi* 2001; **9**: 1066-1070
- 3 **Lammert F**, Sudfeld S, Busch N, Matern S. Cholesterol crystal binding of biliary immunoglobulin A: visualization by fluorescence light microscopy. *World J Gastroenterol* 2001; **7**: 198-202
- 4 **Lui P**, Chen DF. The separation and primary culture of canine gallbladder epithelium. *Shijie Huaren Xiaohua Zazhi* 2001; **9**: 99-100
- 5 **Zapata R**, Severin C, Manriquez M, Valdivieso V. Gallbladder motility and lithogenesis in obese patients during diet-induced weight loss. *Dig Dis Sci* 2000; **45**: 421-428
- 6 **Greaves RR**, O' Donnell LJ, Farthing MJ. Differential effect of prostaglandins on gallstone-free and gallstone-containing human gallbladder. *Dig Dis Sci* 2000; **45**: 2376-2381
- 7 **Wu PJ**. The motility and dysfunction of bile duct system. *Shijie Huaren Xiaohua Zazhi* 1999; **7**: 603-604
- 8 **Wei JG**, Wang YC, Du F, Yu HJ. Dynamic and ultrastructural study of sphincter of Oddi in early-stage cholelithiasis in rabbits with hypercholesterolemia. *World J Gastroenterol* 2000; **6**: 102-106
- 9 **Toouli J**. Biliary dyskinesia. *Curr Treat Options Gastroenterol* 2002; **5**: 285-291
- 10 **Yang CM**, Mao GP, Zhang XR, Zhang YH, Jian YP. The effects of ethanol on rabbit Oddi' s sphincter. *Shijie Huaren Xiaohua Zazhi* 2000; **8**: 87
- 11 **Zhang JS**, Wei JG, Wu JZ, Chen JY. Culture and morphologic observation of rabbit Oddi' s sphincter cells. *Shijie Huaren Xiaohua Zazhi* 1999; **7**: 316-319
- 12 **Abdel Salam OM**, Nada SA, Arbid MS. The effect of ginseng on bile-pancreatic secretion in the rat. increase in proteins and inhibition of total lipids and cholesterol secretion. *Pharmacol Res* 2002; **45**: 349-353
- 13 **Shen CM**, Mao SJ, Huang GS, Yang PC, Chu RM. Stimulation of smooth muscle cell proliferation by ox-LDL- and acetyl LDL-induced macrophage-derived foam cells. *Life Sci* 2001; **70**: 443-452
- 14 **Wang XJ**, Wei JG, Wang YC, Xu JK, Wu QZ, Wu DC, Yang XX. Effect of cholesterol liposome on contractility of rabbit Oddi' s sphincter smooth muscle cells. *Shijie Huaren Xiaohua Zazhi* 2000; **8**: 633-637
- 15 **Ishibashi Y**, Murakami G, Honma T, Sato TJ, Takahashi M. Morphometric study of the sphincter of oddi (hepatopancreatic) and configuration of the submucosal portion of the sphincteric muscle mass. *Clin Anat* 2000; **13**: 159-167

- 16 **Liashchenko SN.** The microsurgical anatomy of the major duodenal papilla and of the sphincter of the hepatopancreatic ampulla. *Morfologiya* 1999; **116**: 50-53
- 17 **Avisse C, Flament JB, Delattre JF.** Ampulla of Vater. Anatomic, embryologic, and surgical aspects. *Surg Clin North Am* 2000; **80**: 201-212
- 18 **Avisse C, Delattre JF, Flament JB.** The inguinofemoral area from a laparoscopic standpoint. History, anatomy, and surgical applications. *Surg Clin North Am* 2000; **80**: 35-48
- 19 **Laplante AF, Germain L, Auger FA, Moulin V.** Mechanisms of wound reepithelialization: hints from a tissue-engineered reconstructed skin to long-standing questions. *FASEB J* 2001; **15**: 2377-2389
- 20 **Yokohata K, Tanaka M.** Cyclic motility of the sphincter of Oddi. *J Hepatobiliary Pancreat Surg* 2000; **7**: 178-182
- 21 **Aymerich RR, Prakash C, Aliperti G.** Sphincter of oddi manometry: is it necessary to measure both biliary and pancreatic sphincter pressures? *Gastrointest Endosc* 2000; **52**: 183-186
- 22 **Delattre JF, Avisse C, Marcus C, Flament JB.** Functional anatomy of the gastroesophageal junction. *Surg Clin North Am* 2000; **80**: 241-260
- 23 **Li AJ, Liu JZ, Liu CY.** Anatomical and functional study of localization of originating neurons of the parasympathetic nerve to gallbladder in rabbit brain stem. *Chin J Physiol* 2002; **45**: 19-24
- 24 **Fang CH, Yang JZ, Kang HG.** A PCR study on *Hp* DNA of bile, mucosa and stone in gallstones patients and its relation to stone nuclear formation. *Shijie Huaren Xiaohua Zazhi* 1999; **7**: 233-235
- 25 **Gu SW, Luo KX, Zhang L, Wu AH, He HT, Weng JY.** Relationship between ductule proliferation and liver fibrosis of chronic liver disease. *Shijie Huaren Xiaohua Zazhi* 1999; **7**: 845-847
- 26 **Zhou LS, Shi JS, Wang ZR, Wang L.** Tumor necrosis factor α in gallbladder and gallstone. *Shijie Huaren Xiaohua Zazhi* 2000; **8**: 426-428
- 27 **Fang CH, Yang J.** A study on DNA of aerobic and anaerobic bacteria in bile, mucosa and stone in gallstone patients. *Shijie Huaren Xiaohua Zazhi* 2000; **8**: 66-68
- 28 **Li XP, Mao XZ.** Effect of estrogen, cholic acid loading and bile draining on hepatobiliary functions in rats. *Shijie Huaren Xiaohua Zazhi* 2000; **8**: 1009-1012
- 29 **He XS, Huang JF, Liang LJ, Lu MD, Cao XH.** Surgical resection for hepato portal bile duct cancer. *World J Gastroenterol* 1999; **5**: 128-131
- 30 **Huang ZQ, Zhou NX, Wang DD, Lu JG, Chen MY.** Changing trends of surgical treatment of hilar bile duct cancer: clinical and experimental perspectives. *World J Gastroenterol* 2000; **6**: 777-782
- 31 **Chen MY, Huang ZQ, Chen LZ, Gao YB, Peng RY, Wang DW.** Detection of hepatitis C virus NS5 protein and genome in Chinese carcinoma of the extrahepatic bile duct and its significance. *World J Gastroenterol* 2000; **6**: 800-804
- 32 **Yang HM, Wu J, Li JY, Zhou JL, He LJ, Xu XF.** Optic properties of bile liquid crystals in human body. *World J Gastroenterol* 2000; **6**: 248-251
- 33 **Craig A, Toouli J.** Sphincter of Oddi dysfunction: is there a role for medical therapy? *Curr Gastroenterol Rep* 2002; **4**: 172-176
- 34 **Nomura T, Shirai Y, Sandoh N, Nagakura S, Hatakeyama K.** Cholangiographic criteria for anomalous union of the pancreatic and biliary ducts. *Gastrointest Endosc* 2002; **55**: 204-208
- 35 **Baroni A, Gorga F, Baldi A, Perfetto B, Paoletti I, Russo A, Lembo L, Rossano F.** Histopathological features and modulation of type IV collagen expression induced by *Pseudomonas aeruginosa* lipopolysaccharide (LPS) and porins on mouse skin. *Histol Histopathol* 2001; **16**: 685-692
- 36 **Laukkarinen J, Koobi P, Kalliovalkama J, Sand J, Mattila J, Turjanmaa V, Porsti I, Nordback I.** Bile flow to the duodenum is reduced in hypothyreosis and enhanced in hyperthyreosis. *Neurogastroenterol Motil* 2002; **14**: 183-188
- 37 **Moulin V, Auger FA, Garrel D, Germain L.** Role of wound healing myofibroblasts on re-epithelialization of human skin. *Burns* 2000; **26**: 3-12
- 38 **Kupfahl C, Pink D, Friedrich K, Zurbrugg HR, Neuss M, Warnecke C, Fielitz J, Graf K, Fleck E, Regitz-Zagrosek V.** Angiotensin II directly increases transforming growth factor beta1 and osteopontin and indirectly affects collagen mRNA expression in the human heart. *Cardiovasc Res* 2000; **46**: 463-475
- 39 **Schnee JM, Hsueh WA.** Angiotensin II, adhesion, and cardiac fibrosis. *Cardiovasc Res* 2000; **46**: 264-268
- 40 **Chen BY, Wei JG, Wang YC, Yang XX, Qian JX, Yu J, Chen ZN, Xu J, Wu DC.** Effects of cholesterol on the proliferation of cultured rabbit bile duct fibroblasts. *Shijie Huaren Xiaohua Zazhi* 2002; **10**: 566-570
- 41 **Wang XJ, Wei JG, Wang CM, Wang YC, Wu QZ, Xu JK, Yang XX.** Effect of cholesterol liposomes on calcium mobilization in muscle cells from the rabbit sphincter of Oddi. *World J Gastroenterol* 2002; **8**: 144-149
- 42 **Xiao ZL, Chen Q, Biancani P, Behar J.** Abnormalities of gallbladder muscle associated with acute inflammation in guinea pigs. *Am J Physiol Gastrointest Liver Physiol* 2001; **281**: 490-497
- 43 **Razani B, Schlegel A, Lisanti MP.** Caveolin proteins in signaling, oncogenic transformation and muscular dystrophy. *J Cell Sci* 2000; **113**: 2103-2109
- 44 **Simons K, Toomre D.** Lipid rafts and signal transduction. *Nat Rev Mol Cell Biol* 2000; **1**: 31-39

The effect of famotidine on gastroesophageal and duodeno-gastro-esophageal refluxes in critically ill Patients

Ying Xin, Ning Dai, Lan Zhao, Jian-Guo Wang, Jian-Ming Si

Ying Xin, Ning Dai, Lan Zhao, Jian-Guo Wang, Department of Gastroenterology, Sir Run Run Shaw Hospital, Hangzhou 310016, Zhejiang Province, China

Jian-Ming Si, Zhejiang University, medical college, Hangzhou 310031, Zhejiang Province, China

Correspondence to: Dr. Ying Xin, Department of Gastroenterology, Sir Run Run Shaw Hospital, Hangzhou 310016, Zhejiang Province, China. xinying20012001@yahoo.com.cn

Telephone: +86-571-86994122

Received: 2002-06-14 **Accepted:** 2002-07-25

Abstract

AIM: To investigate the effect of famotidine on gastroesophageal reflux (GER) and duodeno-gastro-esophageal reflux (DGER) and to explore its possible mechanisms. To identify the relevant factors of the reflux.

METHODS: Nineteen critically ill patients were consecutively enrolled in the study. Dynamic 24 hours monitoring of GER and DGER before and after administration of famotidine was performed. The parameters of gastric residual volume, multiple organ disorder syndrome (MODS) score, acute physiology and chronic health evaluation II (APACHE II) score and PEEP were recorded. Paired *t* test; Wilcoxon signed ranks test and Univariate analysis with Spearman's rank correlation were applied to analyse the data.

RESULTS: Statistical significance of longest acid reflux, reflux time of pH<4 and fraction time of acid reflux was observed in ten critically ill patients before and after administration. *P* value is 0.037, 0.005, 0.005 respectively. Significance change of all bile reflux parameters was observed before and after administration. *P* value is 0.007, 0.024, 0.005, 0.007, 0.005. GER has positive correlation with APACHE II score and gastric residual volume with correlation coefficient of 0.720, 0.932 respectively.

CONCLUSION: GER and DGER are much improved after the administration of famotidine. GER is correlated with APACHE II score and gastric residual volume.

Xin Y, Dai N, Zhao L, Wang JG, Si JM. The effect of famotidine on gastroesophageal and duodeno-gastro-esophageal refluxes in critically ill patients. *World J Gastroenterol* 2003; 9(2): 356-358 <http://www.wjgnet.com/1007-9327/9/356.htm>

INTRODUCTION

The incidence of GER and DGER is relatively high in critically ill patients. It was reported that the incidence of DGER was 48% and that of GER 74%. GER and DGER are important causes of esophageal inflammation, ulcer, upper GI bleeding^[1], bronchospasm^[2] and aspiration pneumonia^[3]. In our study using 24 hours' acid and bile reflux monitoring, the effect of famotidine on GER and DGER was recorded and the relationship between reflux, gastric residual volume, positive

end expiratory pressure (PEEP), APACHE II and MODS scores were studied.

MATERIALS AND METHODS

General conditions

Clinical data: From June, 2001 to February, 2002 nineteen critically ill patients were enrolled including ten males and nine females with age ranging from thirty to seventy-five. Among them there were eleven cerebral trauma patients, four acute cerebrovascular accident, one intracranial neoplasm and three respiratory failure with lung infection. Criteria for enrollment were: fasting for at least 6 hours, on mechanical ventilator support, no enteral nutrition through nasogastric tube (NGT) before, and serum bilirubin level less than 2.0 mg/dl. Exclusion criteria included active gastrointestinal bleeding, esophageal and fundic varices, mechanical ileus, previous thoracic or abdominal radiotherapy, esophageal or gastric surgery, cholecystectomy, previous GERD or gastrointestinal dynamic disorders, esophageal or upper small intestinal Crohn's disease. Also excluded were patients receiving cisapride, erythromycin, atropine, theophylline, metoclopramide and acid suppressants within three days.

Drug and equipments

Famotidine (trade name of Xin Fa Ding, Shanghai Sine pharmaceutical company.), pH monitor of dynamical Digitrapper MK III and Bilitec 2000 all produced by Medtronic Syntectics Medical Company (Sweden).

Methods

The level of PEEP, the score of MODS and APACHE II (Knaus, 1985) were recorded on the day of study. The electrode of pH monitor was calibrated in buffers of pH 7.01 and 1.07. The Bilitec 2000 probe was calibrated in calibrating fluid. Then two probes were taped together and inserted into patients' stomach through nostril. Gastroesophageal junction was determined by pH gradient change. After exclusion of torsion by chest X-ray film the probes were taped to the patients' faces. During the study all patients were kept supine and received TPN nutritional support. All data was analysed by specific software provided by Medtronic Syntectics Medical Company. Pathologic acid reflux was defined as the fraction time of pH less than 4, greater than 4%^[4]. The pathologic bile reflux was defined as the fraction time of light absorption value more than 0.14, greater than 4%^[5]. MODS and APACHE II score was reevaluated on the second day. Acid and bile reflux monitoring were repeated after the administration of famotidine of 40 mg.iv.q12 h. On the third day nasogastric tube was inserted into the stomach and the gastric residual volume was recorded during the famotidine administration.

Ventilation associated pneumonia (VAP) (refer to informal guide for the diagnosis and treatment of nosocomial pneumonia set by CMA, pulmonary division in 1999) was also observed.

Statistics analysis

All results were expressed as $\bar{x} \pm s$ (M). Data were analyzed by

pair-matching *t* test, Wilcoxon signed rank test, Spearman's rank correlation.

RESULTS

Scoring

The ranges of PEEP, APACHE II and MODS were 5 mmHg to 15 mmHg, 10 to 26 points and 8 to 18 points respectively in nineteen critically ill patients. No significant differences were found in PEEP, APACHE II and MODS in ten patients before and after administration of famotidine.

Results of esophageal acid reflux

The parameters of acid reflux in ten patients were showed in Table 1. The incidence of pathological acid reflux before famotidine administration was 80 % (8/10) and 30 % (3/10) after famotidine administration. There were significant differences in longest reflux time, reflux time of pH less than 4 and fraction time of reflux.

Table 1 Acid reflux comparison before and after famotidine administration

	Before administration	After administration	<i>P</i> value
Reflux frequency	81.60±110.57 (49.50)	39.50±59.44(22.00)	0.059
Frequency of long reflux (>5 min)	13.90±13.08 (9.50)	7.60±9.79 (6.00)	0.052
Longest reflux time (min)	34.80±64.12 (12.00)	9.30±10.20 (7.50)	0.037
pH<4 reflux time (min)	146.80±293.46 (34.50)	27.10±45.68 (14.00)	0.005
pH<4 fraction time(%)	18.43±19.64 (11.43)	0.44±0.55(0.18)	0.005

Results of esophageal bile reflux

The parameters of bile reflux in ten patients were shown in Table 2. The incidence of pathological bile reflux before administration was 60 % (6/10) and 20 % (2/10) after famotidine administration. All the parameters were improved after famotidine administration.

Table 2 Bile reflux comparison before and after famotidine administration

	Before administration	After administration	<i>P</i> value
Reflux frequency	37.20±19.00 (34.50)	14.30±12.04 (11.50)	0.007
Frequency of long reflux (>5 min)	13.30±5.93 (13.50)	5.40±7.88(2.00)	0.024
Longest reflux time (min)	111.20±142.42 (18.00)	17.90±30.63 (5.50)	0.005
Absorption>0.14 reflux time (min)	308.00±413.02 (49.50)	32.60±49.40 (11.00)	0.007
Absorption>0.14 fraction time (%)	26.00±27.33 (15.30)	0.64±10.39 (0.29)	0.005

Esophageal mixed reflux

The incidence of mixed reflux in ten critical ill patients was 50 % (5/10) before famotidine administration and was 20 % (2/10) after famotidine administration. The total incidence of mixed reflux in nineteen patients was 36.84 % after the administration.

Correlation analysis

Before administration reflux time of pH<4 was positively related to APACHE II score with Pearson correlation coefficient of 0.72 (Figure 1). After administration fraction time of acid reflux and APACHE II score were positively related to gastric residual volume with Pearson correlation coefficient of 0.932 and 0.467 respectively (Figure 2,3).

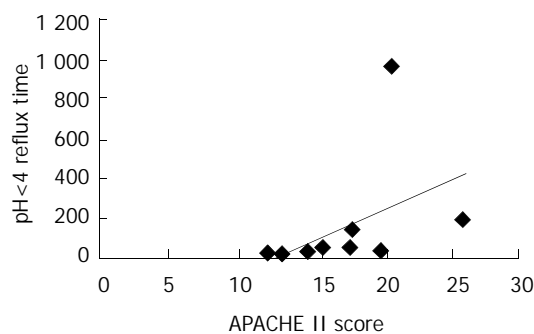


Figure 1 The relationship between pH<4 reflux time and APACHE II score before famotidine administration.

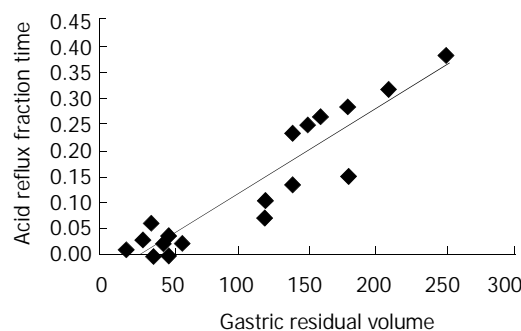


Figure 2 The relationship between acid reflux fraction time and gastric residual volume after famotidine administration.

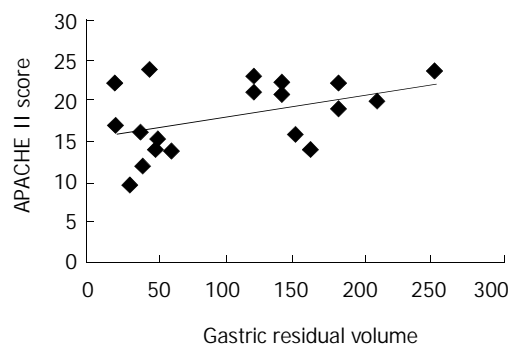


Figure 3 The relationship between APACHE II score and gastric residual volume.

Aspiration pneumonia and VAP

In our study no aspiration pneumonia and VAP were found.

DISCUSSION

The medical literatures reported that the incidence of GER and DGER could be 78.1 %^[6] and 48 %^[7] respectively in critically ill patients. Reasons for high reflux rate maybe due to the following: (1) Basic illnesses: Medical literature reported that acute or chronic cerebral injury could decrease lower esophageal sphincter pressure^[8] and delay the gastric emptying^[9] when accompanied with increased ICP. (2) Posture: Supine position is a high risk factor for GER and DGER. The incidence of GER increased from 12 % to 50 % when position was changed from semirecumbent to supine^[10]. (3) Mechanical ventilation: During ventilation swallowing hyperreflexia, inhibition of peristalsis and visceral hypoperfusion due to PEEP were observed^[11]. Similar study had not been reported in China. Researches reported that reflux of duodenal juice in gastroesophageal reflux disease was more common than pH

studies alone would suggest^[12] and the combined reflux of gastric and duodenal juices caused severe esophageal mucosal damage^[13]. We combined pH monitor with Bilited 2000^[14] to detect acid and bile reflux simultaneously. The pH step-up for electrode positioning was successfully carried out in nineteen critically ill patients^[15]. Our study showed before the administration of famotidine the incidence of pathological GER and DGER was 80 %, 60 % respectively which was in accordance with the medical literatures.

After famotidine administration acid and bile reflux were much improved. Famotidine is one of the most common drugs used in ICU. Venous injection of famotidine 40 mg twice per day would keep esophagus pH above 4 for twenty hours in our study. Parkman^[16] found increased antral phase III migrating motor complexes (MMCs) after administration of ranitidine, famotidine and omeprazole and especially in famotidine. Bortolotti noted the same finding^[17,18]. MMC III had the role of "street sweeper" in GI tract. Because of its powerful propulsion which can clean the duodenal contents reflux to stomach in the end of MMC II, MMC may have an anti-reflux role^[19]. Before MMC III there is a short duration of reversed peristalsis^[20] when MMC III is evoked by bile and pancreatic juice excretion and neutralization of acid in the duodenum^[21]. MMC III could be inhibited by continuous injection of acid in the duodenum. In conclusion famotidine improved GER through increasing gastric pH and improved DGER through increasing MMC III due to increased duodenal pH. Decreased gastric residual volume after acid inhibition may be one of the mechanisms.

In our study we also found that reflux time of pH<4 was positively correlated to APACHE II score (Figure 1). This suggests that GER and DGER occur more commonly when critical illness occurs and normal defense mechanisms are disturbed. It was reported that as part of scoring APACHE II Glasgow score was closely related to delayed gastric emptying^[22], which was consistent with our findings (Figure 3). We also found that gastric residual volume was positively related to fraction time of acid reflux (Figure 2). This may explain why famotidine may improve GER indirectly. Nasogastric tube, H₂ blocker^[23], sedatives^[24,25], muscle relaxant^[26] are known factors for ventilation associated pneumonia. But in our study there was no aspiration pneumonia or VAP. So famotidine may not increase the incidence of pneumonia. Furthermore by decreasing GER and DGER it may lessen the opportunity for aspiration. There is a need for further study in larger groups of patients to define more clearly this relationship.

REFERENCES

- Niederer C, Lubke H, Schumacher B, Strohmeyer G. Endoscopy in the intensive care unit. *Z Gastroenterol* 1994; **32**: 465-469
- Tomonaga T, Awad ZT, Filipi CJ, Hinder RA, Selima M, Tercero F Jr, Marsh RE, Shiino Y, Welch R. Symptom predictability of reflux-induced respiratory disease. *Dig Dis Sci* 2002; **47**: 9-14
- Saxe JM, Ledgerwood AM, Lucas CE, Lucas WF. Lower esophageal sphincter dysfunction precludes safe gastric feeding after head injury. *J Trauma* 1994; **37**: 581-584
- Richter JE, Bradley LA, Demeester TR, Wu WC. Normal 24-hr ambulatory esophageal pH values. Influence of study center, pH electrode, age and gender. *Dig Dis Sci* 1992; **37**: 849-856
- Vaezi MF, Richter JE. Role of acid and duodenogastric reflux in gastroesophageal reflux disease. *Gastroenterology* 1996; **111**: 1192-1199
- Gustafsson PM, Tibbling L. Gastro-oesophageal reflux and oesophageal dysfunction in children and adolescents with brain damage. *Acta Paediatr* 1994; **83**: 1081-1085
- Wilmer A, Tack J, Frans E, Dits H, Vanderschueren S, Gnemie A, Bobbaers H. Duodenogastric reflux and esophageal mucosal injury in mechanically ventilated patients. *Gastroenterology* 1999; **116**: 1293-1299
- Vane DW, Shiffler M, Grosfeld JL, Hall P, Angelides A, Weber TR, Fitzgerald JF. Reduced lower esophageal sphincter (LES) pressure after acute and chronic brain injury. *J Pediatr Surg* 1982; **17**: 960-964
- Kao CH, ChangLai SP, Chieng PU, Yen TC. Gastric emptying in head-injured patients. *Am J Gastroenterology* 1998; **93**: 1108-1112
- Ibanez J, Penafiel A, Raurich JM, Marse P, Jorda R, Mata F. Gastroesophageal reflux in intubated patients receiving enteral nutrition: effect of supine and semirecumbent position. *J Parenter Enter Nutr* 1992; **16**: 419-422
- Dive A, Moular M, Jonard P, Jamart J, Mahieu P. Gastrointestinal motility in mechanically ventilated critically ill patients: a manometric study. *Crit Care Med* 1994; **22**: 441-447
- Dai F, Gong J, Zhang R, Luo JY, Zhu YL, Wang XQ. Assessment of duodenogastric reflux by combined continuous intragastric pH and bilirubin monitoring. *World J Gastroenterol* 2002; **8**: 382-384
- Kauer WKH, Peters JH, DeMeester TR, Ireland AP, Bremner CG, Hagen JA. Mixed reflux of gastric and duodenal juices is more harmful to the esophagus than gastric juice alone. The need for surgical therapy re-emphasized. *Ann Surg* 1995; **222**: 525-533
- Bechi P, Pucciani F, Baldini F, Cosi F, Falciai R, Mazzanti R, Castagnoli A, Passeri A, Boscherini S. Long-term ambulatory enterogastric reflux monitoring. Validation of a new fiberoptic technique. *Dig Dis Sci* 1993; **38**: 1297-1306
- Klauser AG, Schindlbeck NE, Muller-Lissner SA. Esophageal 24-h pH monitoring: is prior manometry necessary for correct positioning of the electrode? *Am J Gastroenterol* 1990; **85**: 1463-1467
- Parkman HP, Urbain J-LC, Knight LC, Brown KL, Trate DM, Miller MA, Maurer AH, Fisher RS. Effect of gastric acid suppressants on human gastric motility. *Gut* 1998; **42**: 243-250
- Bortolotti M, Cucchiara S, Sarti P, Brunelli F, Del Campo L, Barbara L. Interdigestive gastroduodenal motility in patients with ulcer-like dyspepsia: effect of ranitidine. *Hepatogastroenterology* 1992; **39**: 31-33
- Bortolotti M, Pinotti R, Sarti P, Barbara L. Esophageal electromyography in scleroderma patients with functional dysphagia. *Am J Gastroenterol* 1989; **84**: 1497-1502
- Keane FB, Dimagno EP, Malagelada JR. Duodenogastric reflux in humans: its relationship to fasting antroduodenal motility and gastric, pancreatic, and biliary secretion. *Gastroenterology* 1981; **81**: 726-731
- Dalenback J, Abrahamson H, Bjornson E, Fandriks L, Mattsson A, Olbe L, Svennerholm A, Sjovall H. Human duodenogastric reflux, retroperistalsis, and MMC. *Am J Physiol* 1998; **275**: R762-769
- Woodtli W, Owyang C. Duodenal pH governs interdigestive motility in humans. *Am J Physiol* 1995; **268**: G146-152
- Acosta Escibano JA, Carrasco Moreno R, Fernandez Vivas M, Navarro Polo JN, Mas Serrano P, Sanchez Paya J, Caturla Such JJ. Gastric intolerance and hypertension intracranial pressure and their association with severity indexes in patients with severe head injury. *Nutr Hosp* 2001; **16**: 262-267
- Cook DJ, Reeve BK, Guyatt GH, Heyland DK, Griffith LE, Buckingham L, Tryba M. Stress ulcer prophylaxis in critically ill patients. Resolving discordant meta-analyses. *JAMA* 1996; **275**: 308-314
- Georges H, Leroy O, Guery B, Alfandari S, Beaucaire G. Predisposing factors for nosocomial pneumonia in patients receiving mechanical ventilation and requiring tracheotomy. *Chest* 2000; **118**: 767-774
- Kolbel CB, Rippel K, Klar H, Singer MV, van Ackern K, Fiedler F. Esophageal motility disorders in critically ill patients: a 24-hour manometric study. *Intensive Care Med* 2000; **26**: 1421-1427
- Schindler MB, Bohn DJ, Bryan AC. The effect of single-dose and continuous skeletal muscle paralysis on respiratory system compliance in paediatric intensive care patients. *Intensive Care Med* 1996; **22**: 486-491

Different alterations of cytochrome P450 3A4 isoform and its gene expression in livers of patients with chronic liver diseases

Li-Qun Yang, Shen-Jing Li, Yun-Fei Cao, Xiao-Bo Man, Wei-Feng Yu, Hong-Yang Wang, Meng-Chao Wu

Li-Qun Yang, Yun-Fei Cao, Wei-Feng Yu, Department of Anesthesiology, Eastern Hepatobiliary Surgery Hospital, the Second Military Medical University, Shanghai 200438, China

Shen-Jing Li, Xiao-Bo Man, Hong-Yang Wang, International Cooperation Laboratory on Signal Transduction, Eastern Hepatobiliary Surgery Institute, the Second Military Medical University, Shanghai 200438, China

Meng-Chao Wu, Department of Clinical Surgery, Eastern Hepatobiliary Surgery Hospital, the Second Military Medical University, Shanghai 200438, China

Supported by Military Medical Science Found of China, No.98Q050

Correspondence to: Dr. Wei-Feng Yu, Department of Anesthesiology, Eastern Hepatobiliary Surgery Hospital, the Second Military Medical University, Shanghai 200438, China. liqunyang@yahoo.com

Telephone: +86-21-25070783 **Fax:** +86-21-25070783

Received: 2002-09-13 **Accepted:** 2002-10-18

Abstract

AIM: To determine whether parenchymal cells or hepatic cytochrome P450 protein was changed in chronic liver diseases, and to compare the difference of CYP3A4 enzyme and its gene expression between patients with hepatic cirrhosis and obstructive jaundice, and to investigate the pharmacologic significance behind this difference.

METHODS: Liver samples were obtained from patients undergoing hepatic surgery with hepatic cirrhosis ($n=6$) and obstructive jaundice ($n=6$) and hepatic angioma (controls, $n=6$). CYP3A4 activity and protein were determined by Nash and western blotting using specific polyclonal antibody, respectively. Total hepatic RNA was extracted and CYP3A4cDNA probe was prepared according the method of random primer marking, and difference of cyp3a4 expression was compared among those patients by Northern blotting.

RESULTS: Compared to control group, the CYP3A4 activity and protein in liver tissue among patients with cirrhosis were evidently reduced. ($P<0.01$) Northern blot showed the same change in its mRNA levels. In contrast, the isoenzyme and its gene expression were not changed among patients with obstructive jaundice.

CONCLUSION: Hepatic levels of P450s and its CYP3A4 isoform activity were selectively changed in different chronic liver diseases. CYP3A4 isoenzyme and its activity declined among patients with hepatic cirrhosis as expression of cyp3a4 gene was significantly reduced. Liver's ability to eliminate many clinical therapeutic drug substrates would decline consequently. These findings may have practical implications for the use of drugs in patients with cirrhosis and emphasize the need to understand the metabolic fate of therapeutic compounds. Elucidation of the reasons for these different changes in hepatic CYP3A4 may provide insight into more fundamental aspects and mechanisms of impaired liver function.

Yang LQ, Li SJ, Cao YF, Man XB, Yu WF, Wang HY, Wu MC. Different alterations of cytochrome P450 3A4 isoform and its gene expression in livers of patients with chronic liver diseases. *World J Gastroenterol* 2003; 9(2): 359-363

<http://www.wjgnet.com/1007-9327/9/359.htm>

INTRODUCTION

Hepatic cytochrome P450 enzymes constitute a superfamily of hemoproteins which play a major role in the metabolism of endogenous compounds and in the detoxification of xenobiotic molecules, including anesthetics and carcinogens^[1-3]. About 200 CYPs have been found in the past 20 years, and many factors including age, gender, nutrition, hormone and general or local pathologic reaction affect CYPs, and the biotransformation of many clinical therapeutic drugs would be changed. P450 3A4 is one of the most important forms in human, mediating the metabolism of about 70 % of therapeutic drugs and endogenous compounds^[4-6].

Although the mechanism and consequences of regulation of P450s by drugs and chemicals have been intensively studied, the mechanisms by which P450s are changed by hepatic pathological factors still remained unclear^[7-11]. Hepatic cirrhosis and obstructive jaundice are most common chronic hepatobiliary diseases among Chinese people, the change of CYPs with cirrhosis and jaundice provided us fundamental knowledge about the effect of pathological factors on P450s^[12-15]. The aim of this study is to determine the alterations of CYP3A4 enzyme and its gene expression in patients with those chronic liver diseases, and to investigate the pharmacologic and clinical significance behind this alterations.

MATERIALS AND METHODS

Materials

pBS M13 CYP3A4 plasmid was kindly provided by Prof Ying-Nian Yu (*Zhe-jiang University, China*). Rabbit anti-human CYP3A4 polyclonal antibody was purchased from Chemicon (*San Diego, CA*); HRP tagged sheep anti-rabbit antibody was purchased from PharMingen (*Mannheim, Germany*); glucose 6-phosphoric acid, erythromycin, Lowry's phenol reagent, glucose 6-phosphoric transferase, acetic ammonium, acetyl-acetone, and NADP were purchased from Sigma Chemical (*St. Louis, MO*); and all other reagents used in this study were of analytical grade.

Source of human liver tissues and patient characters

Human liver samples (30-50 g) were taken from patients undergoing hepatic surgery. Patients had not receive medication of CYPs activator and inhibitor (rifampicin, dexamethasone, propofol, etc) before the surgery. None of the patients were habitual consumers of alcohol or other drugs. A total of 18 liver samples from 15 men and 3 women were used. They were all cases admitted from 2000 to 2001 in Eastern Hepatobiliary Surgery Hospital in Shanghai, China. Informed content was obtained from all patients for subsequent use of their specimen tissues. These specimens were immediately

dissected into small pieces under aseptic condition within half an hour, quickly frozen and preserved in liquid nitrogen before subsequent procedure. Patients' characters and liver function are shown in Table 1.

Table 1 Clinicopathological characteristics of patients studied and their Pugh class

Groups	Median Age (yrs)	Gender F/M	Smoking (n)	Ethanol (n)	Pugh Class A,B,C
C (n=6)	42(21-56)	2/4	2	1	A(6)
H (n=6)	38(28-61)	1/5	1	1	A(4),B(2)
O (n=6)	44(27-65)	0/6	1	2	B(6)

C: controls; H: hepatic cirrhosis; O: obstructive jaundice.

Preparation of microsomes

Liver tissues were subsequently homogenized in ice-cold 0.1 mol/L Tris-HCl buffer containing 1.15 % KCl(pH7.4) and to yield a liver homogenate tissue concentration of 0.33 g/ml. Microsomal fractions were prepared by differential ultracentrifugation. After tissue homogenization in 20 mM Tris-HCl buffer, pH 7.4, containing 0.15 M KCl, the microsomal fraction was isolated from the supernatant of a 20-min 9 000×g spin by ultracentrifugation. The microsomal precipitate was suspended in 100 mM potassium phosphate buffer, pH 7.4, and recentrifuged at 105 000×g for an additional 60 min. The final precipitate was suspended in 10 Mm Tris-HCl buffer (pH 7.4) containing 10 mM EDTA and 20 % (v/v) glycerol. Liver microsomal protein contents were determined following the methods of Lowry *et al*^[16], using bovine serum albumin as standard.

Microsomes P450s and CYP3A4 activity assays

CO-bound total cytochrome P450 content was determined by the method of Omura *et al*^[17]. Spectra were recorded using a Shimadzu UV-250 double-beam spectrophotometer. CYP3A4 specific activity was determined by N-demethylation of erythromycin using the Nash method as previously described^[18].

Immunoquantitation of CYP3A4 isoform protein by western blot analysis

Hepatic microsomal proteins were resolved by SDS-PAGE with vertical mini-gel electrophoresis equipment. Samples of liver microsomal protein (10 µg/lane) were denatured in 10 µl loading buffer (4 ml distilled water, 1 ml 0.5M Tris-HCl, pH 6.8, 0.8 ml glycerol, 1.6 ml 10 % w/v SDS, 0.4 ml mercaptoethanol, 0.05 ml 0.05 % w/v Pyronin Y) and were separated on a 10 % w/v resolving gel. Proteins were transferred from the polyacrylamide gel to the nitrocellulose sheets by an electrophoretic method, and probed with rabbit anti-human CYP3A4 polyclonal antibody (not cross-reactive with other rat P450s) according to supplied protocol. CYP3A4 protein was detected by secondary conjugation to the primary antibody by a HRP-linked sheep anti-rabbit second antibody using diaminobenzidine as substrate.

Northern blot analysis CYP3A4 mRNA

Total RNA was isolated from frozen human liver tissues by the acid guanidinium thiocyanate-phenol-chloroform one step extraction method as previously described^[19], 20 mg of RNA was size-fractionated on a 1.0 % agarose gel containing 2.2 mol/L formaldehyde, and then transferred into nitrocellulose membrane (BA85, Schleicher Schuell, Germany). The membrane was dried in a vacuum drying oven at 80 °C for 2 h and sealed in a plastic bag for use. CYP3A4 probe was cut

from pBS M13 CYP3A4 plasmid by Hand III. Hybridization was performed in the presence of the appropriate ³²P-labeled probes. The membrane was washed twice at room temperature in 2×SSC, 0.1 % SDS for 30 min, once at 65 °C in 1×SSC, 0.1 % SDS for 30 min and once at 65 °C in 0.1×SSC, 0.1 % SDS for 30 min. Membranes were then exposed to X-ray films (*Fujifilm, Tokyo, Japan*) at -70 °C for a week and analyzed by Phosphor Image (FLA 2000, Fujifilm, Japan). The difference of CYP3A4mRNA was compared among three groups.

Statistical analysis

Data was analyzed using the χ^2 test. A $P < 0.05$ was considered significant.

RESULTS

P450 and CYP3A4 activity changes in chronic liver diseases

As shown in Table 2, compared with controls, the hepatic microsome protein and total P450 content remained unchanged in the patients with hepatic cirrhosis and obstructive jaundice, but CYP3A4 activity in the liver tissue of patients with cirrhosis liver was evidently reduced. This change was not seen in the obstructive jaundice group.

Table 2 Microsomal protein, total P450 content and CYP3A4 content and its activity among three groups ($\bar{x} \pm s$)

	C	H	O
Microsome protein (g/L)	10.32±3.98	9.57±3.72	9.42±3.26
P450 content (nmol/mg protein)	0.99±0.16	0.94±0.151	0.89±0.18
CYP3A4 activity (nmol/min/mg protien)	3.01±0.74	1.78±0.653 ^a	2.89±0.65

^a $P < 0.01$ vs controls C: controls; H: hepatic cirrhosis; O: obstructive jaundice.

Change of CYP3A4 isoform protein

Hepatic CYP3A4 protein expression was shown in Figure 1 by western blot analysis. CYP3A4 protein in liver tissues was also reduced in the patients with cirrhosis liver, but in obstructive jaundice, there was no change of as compared with controls.

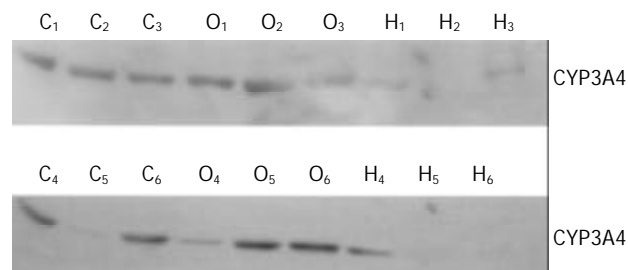


Figure 1 Western Blot analysis of CYP3A4 isoform protein among three groups, compared with controls (tagged by "C₁₋₆"). CYP3A4 protein content in liver tissues among patients with cirrhosis (tagged by "H₁₋₆") reduced. but in obstructive jaundice (tagged by "O₁₋₆"), There was no change of CYP3A4 protein expression.

Change of CYP3A4mRNA in chronic liver diseases

As shown in Figure 2, CYP3A4 probe was cut from pBS M13 CYP3A4 plasmid by Hand III, we got a 800 bp cDNA fragment as expected.

Northern blot analysis showed that CYP3A4 was expressed well in human liver tissues, which agreed with other reports^[20-23]. In patients with cirrhosis (shown in Figure 3), CYP3A4mRNA reduced significantly as compared with controls, but no change happened in the jaundice group.

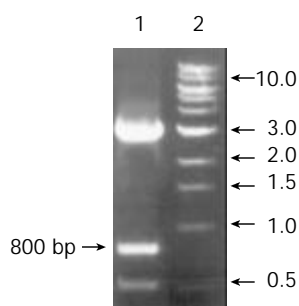


Figure 2 The results of substratum electrophoresis in pBS M13 CYP3A4 plasmid. Lane 1: pBS M13 CYP3A4 (Hind III), Lane 2: Marker (1kb DNA ladder).

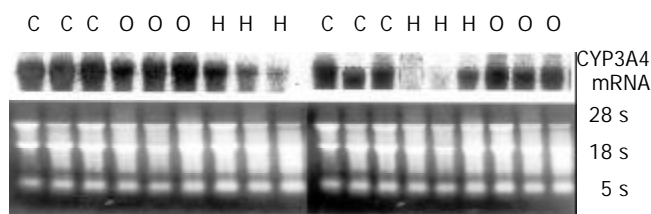


Figure 3 Northern blot analysis mRNA expression of CYP3A4 isoform in liver tissues among three groups. Total RNA was isolated without degradation and each bottom panel showed an equal amount of total RNA loading as indicated in 28 s and 18 s rRNA. CYP3A4mRNA was expressed well in human liver tissues, of patients with cirrhosis (tagged by "H"), CYP3A4mRNA was reduced significantly compared with control (tagged by "C"), but no decline happened in jaundice group (tagged by "O").

DISCUSSION

CYP3A appears to be one of the most important human enzymes as approximately 60 % of oxidised drugs are biotransformed. The isoforms of CYP3A in humans include 3A3, 3A4, 3A5 and 3A7, each of these enzymes shared at least 85 % amino acid sequence homology^[24]. CYP3A4 is the predominant isoform of CYP3A in adult humans. It can catalyse a remarkable number of metabolic processes including aliphatic oxidation, aromatic hydroxylation, N-dealkylation, O-demethylation, S-demethylation, oxidative deamination, sulfoxide formation, N-oxidation and N-hydroxylation. This usually produced inactivation and elimination of most pharmaceuticals. A number of drugs from a broad range of therapeutic categories are CYP3A4 substrates. The change of CYP3A4 isoform was the main reason for enhancement or reduction of drug elimination^[25-27].

In our studies, total P450 contents of 18 Chinese patients were obviously lower than results those reported about Caucasian. (1 pmol/mg vs 5-6 pmol/mg), and the activity of CYP3A4 isoform was also lower^[28-30]. Although CYP3A4 drug metabolizing activity varied widely among individuals, it had a unimodal population distribution and did not appear to be subject to genetic polymorphism as seen with other CYP isoforms (2D6, 2C9 and 2C19)^[31-34]. The wide inter races

variability was likely, in part, to be caused by ethnic or cultural differences, which might be related to an interaction between habit and diet. Therefore we could not draw any conclusion about the normal distribution character of CYPs in Chinese because of the limited sample number and experimental conditions. More detailed and complete studies should be performed for analysing the distribution of CYPs in Chinese in the near future^[35].

Most information on drug metabolism impairment at pathologic status has been obtained in rodent *in vivo* or *in vitro* models, and most of these studies have focused on the effects of IFNs and the major inflammatory cytokines, namely, IL-6, IL-1 and TNF α ^[36-39], but relatively few studies have examined the effect of liver disease on human CYP expression. Hepatic cirrhosis and obstructive jaundice are most common chronic hepatobiliary disease in Chinese, the change of CYPs with cirrhosis and jaundice can provide us basic knowledge about the effect of pathological factors on P450s. The present study demonstrated that, in patients with cirrhosis, CYP3A4-mediated erythromycin N-demethylation activity and 3A4 protein were significantly less than in controls, but the total P450 content and hepatic microsomal protein still remained unchanged. These results suggest that family ingredients of P450s have changed in the cirrhosis. That is, CYP family 1, 2 may enhance following with CYP3A reduced, since CYP1 and CYP2 families play a major role in biotransformation of most carcinogens, but few studies described whether high morbidity of hepatic cancer in cirrhosis is correlated with these changes of drug metabolic enzymes^[40].

Although many factors including age, gender, nutrition, hormone and general or local pathologic reaction affect drug elimination, the enzymatic activity as well as content of P450s is still a basic reason for change of drug metabolism, and the biotransformation of many clinical therapeutic drugs either enhanced or reduced^[41-43]. This study is for the first time to examine simultaneously in patients with liver diseases the hepatic P450 protein level, isoform activity as well as its mRNA expression. Significant correlations with CYP3A4 protein level, isoform activity and mRNA expression were observed, suggesting that with the decrease of CYP3A4 mRNA expression, RNA encoded CYP3A4 isoform protein reduced, which would cause the decrease of CYP3A4-mediated erythromycin N-demethylation activity. Since CYP3A4 is the predominant isoform of CYP3A in adult humans, the change of hepatic CYP3A4 activity will change the metabolism of most clinical therapeutic drugs. Firstly, a large number of intravenous anesthetic and sedative agents (including diazepam, midazolam, fentanyl, lidocaine, etc.) are substrates of CYP3A4 isoform, N-hydroxylation and N-dealkylation reactions of anesthetics reduced in cirrhosis patients will cause drug accumulation, oversedative and postoperative awake delay^[44,45]. Secondly, Amiodarone, quinidine, nifedipine, berhomine and Cyclosporin were also eliminated through CYP3A4, thus competitive inhibition should be noticed and avoided especially when more than one drugs must be administered in patients with cirrhosis. These findings are in agreement with pharmacokinetics studies that have shown reduced clearance of midazolam when combined with fentanyl in cirrhosis, but over-dosage condition of anti-irhythmia drugs had more clinical significance than that of other therapeutic drugs^[46,47]. Thirdly, as CYP3A4 also plays an important role in the biotransformation and detoxification of many endogenous substrates, reduction of CYP3A4 activity may result in inactivation disorder of endogenous substance including cholesterol, bile acid and sex steroids, thus causing more extensive physiopathologic changes in patients with cirrhosis, these changes, on contrary, will affect the drug metabolic enzymes^[48,49].

In summary, the present study demonstrated that, hepatic levels of individual P450s and its CYP3A4 isoform activity can selectively change in different chronic liver diseases. The hepatic microsome proteins and total P450 content remained unchanged in patients with hepatic cirrhosis and obstructive jaundice, but CYP3A4 activity and its protein level in liver tissue among patients with cirrhosis were evidently lowered. This change was not seen in obstructive jaundice group, and the cause of this change may be the lowered expression of CYP3A4 mRNA. These findings may have practical implications for the use of drugs in patients with liver diseases and emphasize the need to understand the metabolic fate of therapeutic compounds^[50,51]. Elucidation of the reasons for these different changes in hepatic P450s may provide insight into more fundamental aspects and mechanisms of impaired liver function in patients with chronic liver diseases.

REFERENCES

- Kostrubsky VE**, Ramachandran V, Venkataramanan R, Dorko K, Esplen JE, Zhang S, Sinclair JF, Wrighton SA, Strom SC. The use of human hepatocyte cultures to study the induction of cytochrome P-450. *Drug Metab Dispos* 1999; **27**: 887-894
- Nebert DW**, Nelson DR, Coon MJ, Estabrook RW, Feyereisen R, Fujii-Kuriyama Y, Gonzalez FJ, Guengerich FP, Gunsalus IC, Johnson EF. The P450 superfamily: update on new sequences, gene mapping, and recommended nomenclature. *DNA Cell Biol* 1991; **10**: 1-10
- Capdevila JH**, Harris RC, Falck JR. Microsomal cytochrome P450 and eicosanoid metabolism. *Cell Mol Life Sci* 2002; **59**: 780-789
- Guengerich FP**. Cytochrome P-450 3A4: regulation and role in drug metabolism. *Annu Rev Pharmacol Toxicol* 1999; **39**: 1-17
- Raucy JL**, Allen SW. Recent advances in P450 research. *Pharmacogenomics J* 2001; **1**: 178-186
- Zhu-Ge J**, Yu YN, Qian YL, Li X. Establishment of a transgenic cell line stably expressing human cytochrome P450 2C18 and identification of a CYP2C18 clone with exon 5 missing. *World J Gastroenterol* 2002; **8**: 888-892
- Goodwin B**, Redinbo MR, Kliewer SA. Regulation of cyp3a gene transcription by the pregnane x receptor. *Annu Rev Pharmacol Toxicol* 2002; **42**: 1-23
- Quattrochi LC**, Guzelian PS. Cyp3A regulation: from pharmacology to nuclear receptors. *Drug Metab Dispos* 2001; **29**: 615-622
- Waxman DJ**. P450 gene induction by structurally diverse xenochemicals: central role of nuclear receptors CAR, PXR, and PPAR. *Arch Biochem Biophys* 1999; **369**: 11-23
- Nicholson TE**, Renton KW. Modulation of cytochrome P450 by inflammation in astrocytes. *Brain Res* 1999; **827**: 12-18
- Dogra SC**, Whitelaw ML, May BK. Transcriptional activation of cytochrome P450 genes by different classes of chemical inducers. *Clin Exp Pharmacol Physiol* 1998; **25**: 1-9
- Lieber CS**. Ethanol metabolism, cirrhosis and alcoholism. *Clin Chim Acta* 1997; **257**: 59-84
- Paintaud G**, Bechtel Y, Brientini MP, Miguet JP, Bechtel PR. Effects of liver diseases on drug metabolism. *Therapie* 1996; **51**: 384-389
- Brockmoller J**, Roots I. Assessment of liver metabolic function. Clinical implications. *Clin Pharmacokinet* 1994; **27**: 216-248
- Murray M**. P450 enzymes. Inhibition mechanisms, genetic regulation and effects of liver disease. *Clin Pharmacokinet* 1992; **23**: 132-146
- Lowry OH**, Passonneau JV. Some recent refinements of quantitative histochemical analysis. *Curr Probl Clin Biochem* 1971; **3**: 63-84
- Omura T**. Forty years of cytochrome P450. *Biochem Biophys Res Commun* 1999; **266**: 690-698
- Hover CG**, Kulkarni AP. Lipoxigenase-mediated hydrogen peroxide-dependent N-demethylation of N, N-dimethylaniline and related compounds. *Chem Biol Interact* 2000; **124**: 191-203
- Chomczynski P**, Sacch N. Single-step method of RNA isolation by acid guanidinium thiocyanate-phenol-chloroform extraction. *Anal Biochem* 1987; **162**: 156-159
- Goodwin B**, Hodgson E, D'Costa DJ, Robertson GR, Liddle C. Transcriptional regulation of the human CYP3A4 gene by the constitutive androstane receptor. *Mol Pharmacol* 2002; **62**: 359-365
- Lin YS**, Dowling AL, Quigley SD, Farin FM, Zhang J, Lamba J, Schuetz EG, Thummel KE. Co-regulation of CYP3A4 and CYP3A5 and contribution to hepatic and intestinal midazolam metabolism. *Mol Pharmacol* 2002; **62**: 162-172
- Finnstrom N**, Thorn M, Loof L, Rane A. Independent patterns of cytochrome P450 gene expression in liver and blood in patients with suspected liver disease. *Eur J Clin Pharmacol* 2001; **57**: 403-409
- Rodriguez-Antona C**, Donato MT, Pareja E, Gomez-Lechon MJ, Castell JV. Cytochrome P-450 mRNA expression in human liver and its relationship with enzyme activity. *Arch Biochem Biophys* 2001; **393**: 308-315
- Mitra AK**, Patel J. Strategies to overcome simultaneous P-glycoprotein mediated efflux and CYP3A4 mediated metabolism of drugs. *Pharmacogenomics* 2001; **2**: 401-415
- de Wildt SN**, Kearns GL, Leeder JS, van den Anker JN. Cytochrome P450 3A: ontogeny and drug disposition. *Clin Pharmacokinet* 1999; **37**: 485-505
- Hakkola J**, Pelkonen O, Pasanen M, Raunio H. Xenobiotic-metabolizing cytochrome P450 enzymes in the human foeto-placental unit: role in intrauterine toxicity. *Crit Rev Toxicol* 1998; **28**: 35-72
- Inaba T**, Nebert DW, Burchell B, Watkins PB, Goldstein JA, Bertilsson L, Tucker GT. Pharmacogenetics in clinical pharmacology and toxicology. *Can J Physiol Pharmacol* 1995; **73**: 331-338
- El-Sankary W**, Bombail V, Gibson GG, Plant N. Glucocorticoid-Mediated Induction of CYP3A4 is Decreased by Disruption of a Protein: DNA Interaction Distinct from the Pregnane X Receptor Response Element. *Drug Metab Dispos* 2002; **30**: 1029-1034
- Hijazi Y**, Bouliou R. Contribution of CYP3A4, CYP2B6, and CYP2C9 Isoforms to N-Demethylation of Ketamine in Human Liver Microsomes. *Drug Metab Dispos* 2002; **30**: 853-858
- Shu Y**, Cheng ZN, Liu ZQ, Wang LS, Zhu B, Huang SL, Ouyang DS, Zhou HH. Interindividual variations in levels and activities of cytochrome P-450 in liver microsomes of Chinese subjects. *Acta Pharmacol Sin* 2001; **22**: 283-288
- Tenneze L**, Tarral E, Ducloux N, Funck-Brentano C. Pharmacokinetics and electrocardiographic effects of a new controlled-release form of flecainide acetate: Comparison with the standard form and influence of the CYP2D6 polymorphism. *Clin Pharmacol Ther* 2002; **72**: 112-122
- Cai L**, Yu SZ, Zhang ZF. Cytochrome P450 2E1 genetic polymorphism and gastric cancer in Changde, Fujian Province. *World J Gastroenterol* 2001; **7**: 792-795
- Zheng YX**, Chan P, Pan ZF, Shi NN, Wang ZX, Pan J, Liang HM, Niu Y, Zhou XR, He FS. Polymorphism of metabolic genes and susceptibility to occupational chronic manganese. *Biomarkers* 2002; **7**: 337-346
- Dahl ML**. Cytochrome p450 phenotyping/genotyping in patients receiving antipsychotics: useful aid to prescribing? *Clin Pharmacokinet* 2002; **41**: 453-470
- Bertilsson L**. Geographical/interracial differences in polymorphic drug oxidation. Current state of knowledge of cytochromes P450 (CYP) 2D6 and 2C19. *Clin Pharmacokinet* 1995; **29**: 192-209
- Renton KW**. Alteration of drug biotransformation and elimination during infection and inflammation. *Pharmacol Ther* 2001; **92**: 147-163
- Warren GW**, van Ess PJ, Watson AM, Mattson MP, Blouin RA. Cytochrome P450 and antioxidant activity in interleukin-6 knock-out mice after induction of the acute-phase response. *Interferon Cytokine Res* 2001; **21**: 821-826
- De Smet K**, Loyer P, Gilot D, Vercruyse A, Rogiers V, Guguen-Guillouzo C. Effects of epidermal growth factor on CYP inducibility by xenobiotics, DNA replication, and caspase activations in collagen I gel sandwich cultures of rat hepatocytes. *Biochem Pharmacol* 2001; **61**: 1293-1303
- Okamoto T**, Okabe S. Minimal effect of cytokine-independent hepatitis induced by anti-Fas antibodies on hepatic cytochrome P450 gene expression in mice. *Int J Mol Med* 2000; **6**: 459-462
- Shoda T**, Mitsumori K, Onodera H, Toyoda K, Uneyama C,

- Takada K, Hirose M. Liver tumor-promoting effect of beta-naphthoflavone, a strong CYP 1A1/2 inducer, and the relationship between CYP 1A1/2 induction and Cx32 decrease in its hepatocarcinogenesis in the rat. *Toxicol Pathol* 2000; **28**: 540-547
- 41 **Tanaka E**. Gender-related differences in pharmacokinetics and their clinical significance. *J Clin Pharm Ther* 1999; **24**: 339-346
- 42 **Morgan ET**, Sewer MB, Iber H, Gonzalez FJ, Lee YH, Tukey RH, Okino S, Vu T, Chen YH, Sidhu JS, Omiecinski CJ. Physiological and pathophysiological regulation of cytochrome P450. *Drug Metab Dispos* 1998; **26**: 1232-1240
- 43 **Imaoka S**, Funae Y. The physiological role of P450-derived arachidonic acid metabolites. *Nippon Yakurigaku Zasshi* 1998; **112**: 23-31
- 44 **Vuyk J**. Clinical interpretation of pharmacokinetic and pharmacodynamic propofol-opioid interactions. *Acta Anaesthesiol Belg* 2001; **52**: 445-451
- 45 **Oda Y**, Mizutani K, Hase I, Nakamoto T, Hamaoka N, Asada A. Fentanyl inhibits metabolism of midazolam: competitive inhibition of CYP3A4 *in vitro*. *Br J Anaesth* 1999; **82**: 900-903
- 46 **Nims RW**, Prough RA, Jones CR, Stockus DL, Dragnev KH, Thomas PE, Lubet RA. *In vivo* induction and *in vitro* inhibition of hepatic cytochrome P450 activity by the benzodiazepine anticonvulsants clonazepam and diazepam. *Drug Metab Dispos* 1997; **25**: 750-756
- 47 **Iribarne C**, Dreano Y, Bardou LG, Menez JF, Berthou F. Interaction of methadone with substrates of human hepatic cytochrome P450 3A4. *Toxicology* 1997; **117**: 13-23
- 48 **Ourlin JC**, Handschin C, Kaufmann M, Meyer UA. Link between cholesterol levels and phenobarbital induction of cytochromes P450. *Biochem Biophys Res Commun* 2002; **291**: 378-384
- 49 **Staudinger J**, Liu Y, Madan A, Habeebu S, Klaassen CD. Coordinate regulation of xenobiotic and bile acid homeostasis by pregnane X receptor. *Drug Metab Dispos* 2001; **29**: 1467-1472
- 50 **Hung DY**, Chang P, Cheung K, McWhinney B, Masci PP, Weiss M, Roberts MS. Cationic drug pharmacokinetics in diseased livers determined by fibrosis index, hepatic protein content, microsomal activity, and nature of drug. *J Pharmacol Exp Ther* 2002; **301**: 1079-1087
- 51 **Jaeschke H**, Gores GJ, Cederbaum AI, Hinson JA, Pessayre D, Lemasters JJ. Mechanisms of hepatotoxicity. *Toxicol Sci* 2002; **65**: 166-176

Edited by Ma JY

Changes in the level of serum liver enzymes after laparoscopic surgery

Min Tan, Feng-Feng Xu, Jun-Shen Peng, Dong-Ming Li, Liu-Hua Chen, Bao-Jun Lv, Zhen-Xian Zhao, Chen Huang, Chao-Xu Zheng

Min Tan, Feng-Feng Xu, Jun-Shen Peng, Dong-Ming Li, Liu-Hua Chen, Bao-Jun Lv, Zhen-Xian Zhao, Chen Huang, Chao-Xu Zheng, Department of General Surgery, the First Affiliated Hospital of Zhong Shan University, 58 Zhongshan 2 Road Guangzhou 510080, Guangdong Province China

Correspondence to: Dr Min Tan, Department of General Surgery, the First Affiliated Hospital of Sun Yat-sen University, 58 Zhongshan 2 Road Guangzhou 510080, Guangdong Province China. tommyt@vip.163.com
Telephone: +86-20-87766335 **Fax:** +86-20-87750632
Received: 2002-06-29 **Accepted:** 2002-07-24

Abstract

AIM: The purpose of this study was to investigate the effect of laparoscopic surgery on liver function in humans and the possible mechanisms behind such effect.

METHODS: Blood samples from 286 patients who underwent laparoscopic cholecystectomy (LC) and 40 patients who underwent open cholecystectomy (OC) were tested for liver function by measuring the level of serum alanine aminotransferase (ALT) and aspartate aminotransferase (AST) before and after the operations. The same tests were also applied to 18 laparoscopic colorectal cancer resection (LCR) patients and 23 open colorectal cancer resection (OCR) patients to determine whether CO₂ pneumoperitoneum could alter the serum liver enzymes.

RESULTS: The level of serum ALT and AST increased significantly during the first 48 hours post operations in both LC and LCR patients. However, no significant change of the serum liver enzymes was detected in both OC and OCR patients. As a result, there was statistically significant difference in change of both ALT and AST levels between LC and OC patients and LCR and OCR patients, respectively. By the 7th day post operation, the level of both enzymes returned to normal values in LC, OC and OCR patients except LCR patients whose enzymes remained at a higher level.

CONCLUSION: Transient elevation of hepatic transaminases occurred after laparoscopic surgery. The major causative factor seemed to be the CO₂ pneumoperitoneum. In most of the laparoscopic surgery patients, the transient elevation of serum liver enzymes showed no apparent clinical implications. However, if preoperative liver function was very poor, laparoscopic surgery may not be the best choice for the treatment of patients with certain abdominal diseases.

Tan M, Xu FF, Peng JS, Li DM, Chen LH, Lv BJ, Zhao ZX, Huang C, Zheng CX. Changes in the level of serum liver enzymes after laparoscopic surgery. *World J Gastroenterol* 2003; 9(2): 364-367
<http://www.wjgnet.com/1007-9327/9/364.htm>

INTRODUCTION

The introduction of laparoscopic surgery has profoundly

changed the way for the management of patients with both gallbladder disease and common bile duct stone, and the laparoscopic cholecystectomy (LC) has become the "gold standard" in the treatment of benign gallbladder diseases such as gallbladder stone and cholecystitis^[1-4]. However, little attention has been paid to effects on liver function by laparoscopic surgery. We noticed in clinical practice that, following laparoscopic surgery, the level of certain serum liver enzymes rose markedly in most patients who had shown normal preoperative liver function tests. This clinical observation raises several questions. Are these changes of any clinical significance? What is the mechanism responsible for these changes? Do other laparoscopic operations cause the same changes? To address these questions, we conducted a prospective study to compare changes in serum liver enzymes before and after operations between LC and open cholecystectomy (OC) and laparoscopic colorectal cancer resection (LCR) with open colorectal resection (OCR).

MATERIALS AND METHODS

A total of 286 patients (102 men and 184 women with mean age of 48.6 years and range of 21-89 years) underwent elective LC from February 2001 to April 2002. During the same period, 40 patients (18 men and 22 women with mean age of 51.2 years and range of 29-86 years) with symptomatic cholelithiasis, gallbladder stone or gallbladder polypus underwent OC and were included for the study. For comparison, 18 LCR (10 men and 8 women with mean age of 62.8 years and range of 43-85 years) and 23 OCR patients (16 men and 7 women with mean age of 61.6 years and range of 39-76 years) were also selected for the study. The LCR cases included 2 descending colon cancers, 7 sigmoid colon cancers and 9 rectal cancers. The OCR patients included 4 ascending colon cancers, 6 transverse colon cancers, 1 descending colon cancers, 6 sigmoid colon cancers and 6 rectal cancers.

All patients selected for the study had normal values of serum liver enzymes prior to the operations. The following patients were excluded from the study: those who had undergone endoscopic retrograde cholangiopancreatography (ERCP) and endoscopic sphincterotomy (EST) within one week before laparoscopic operation. The cases who developed complications such as bile duct injury, obstruction, infection, leakage and high fever by any reason were also excluded. All colorectal cancer patients included for the study had no evidence of cancer metastasis to liver by B-ultrasonic and CT scan.

Serum liver enzymes alanine amino transferase (ALT) and aspartate aminotransferase (AST) were measured before operations and 1, 2 and 7 days post operation to assess liver function except for LC patients. The LC patients were randomly divided into two groups before the operation, with group A of 143 LC patients tested for the liver function postoperatively on days 1 and 7 and group B of 143 patients tested for the liver function postoperatively on days 2 and 7. All LC and LCR patients received operation by one surgeon. The OC operations were performed by 3 surgeons from the same Division. The OCR operations were performed by the same team of surgical

staff. All patients received general anesthesia except OC patients who received local anesthesia. The operations on LC and LCR patients were performed with four-cannula technique. During laparoscopic surgery, the intra-abdominal pressure (IAP) was maintained at a range of 12-14 mmHg. Monopolar diathermy was used in LC and OC patients to dissect the gallbladder from the liver beds. Ultrasonic scissors and bipolar diathermy were used in LCR to dissect the mesenteric vessels.

All data were expressed as the mean \pm standard deviation. Student *t* test was used to analyse the difference in level of serum liver enzymes before and after LC, OC, LCR and OCR. The *P* value less than 0.05 was considered to be statistically significant.

RESULTS

Postoperative liver failure or mortality did not occur in any of the patients studied, and all the patients were hemodynamically stable during the perioperative period.

The level of serum ALT and AST increased significantly within 24-48 hours following operations in LC and LCR patients compared with those in OC and OCR patients (Table 1). In details, the mean pre- and post operation serum levels of ALT were respectively 23.3 U·L⁻¹ and 38.8 U·L⁻¹ in LC patients of group A (*P*<0.05), 21.5 U·L⁻¹ and 44.2 U·L⁻¹ in LC patients of group B (*P*<0.01), and 22.6 U·L⁻¹ and 45.7 U·L⁻¹ in LCR patients (*P*<0.01). In contrast, ALT only increased from a preoperative mean of 21.8 U·L⁻¹ to 28.2 U·L⁻¹ in OC patients (*P*>0.05) and from 22.2 U·L⁻¹ to 30.6 U·L⁻¹ in OCR patients (*P*>0.05). The degree of change in ALT following the operations was greater in LC patients than that in OC patients (*P*<0.05, D1), *P*<0.01, D2), so was the change between LCR and OCR patients (*P* <0.05, D1 and D7), *P*<0.01, D2).

Similar changes were observed in the mean value of serum AST. The AST increased significantly after operation in LC patients (from 28.4 to 41.5 U·L⁻¹, *P*<0.05, D1) and 27.1 up to 48.7 U·L⁻¹, *P*<0.01, D2) and LCR patients (from 27.3 to 40.7 U·L⁻¹, *P*<0.05, D1) and to 45.5 U·L⁻¹, *P*<0.01, D2). In OC and OCR patients, however, the AST showed only a small degree of increase (Table 1). The change of AST due to the operations was also greater in LC patients than that in OC patients (*P*<0.05, D1), *P*<0.01, D2), and so was the change between LCR and OCR (*P*<0.05, D1 and D7), *P*<0.01, D2).

Seven days following the operations, both enzymes returned to normal value in LC, OC and OCR patients except in LCR patients whose enzymes, although lower than day 2 level, remained higher (ALT 37.2 U·L⁻¹, D7, *P*<0.05) and AST 38.6 U·L⁻¹ (D7, *P*<0.05) (Table 1).

Table 1 Preoperative and postoperative level of serum liver enzymes

	<i>n</i>	Preoperation	D1	D2	D7
ALT					
LC(a)	143	23.3 \pm 11.6	38.8 \pm 15.2 ^{ac}		25.1 \pm 14.3
LC(b)	143	21.5 \pm 12.9		44.2 \pm 14.5 ^{bc}	26.3 \pm 11.7
OC	40	21.8 \pm 16.7	28.2 \pm 13.7	27.3 \pm 18.3	24.2 \pm 11.1
LCR	18	22.6 \pm 10.9	39.3 \pm 13.4 ^{ac}	45.7 \pm 17.2 ^{bd}	37.2 \pm 18.1 ^{ac}
OCR	23	22.2 \pm 17.3	29.6 \pm 11.8	30.6 \pm 15.5	27.1 \pm 11.2
AST					
LC(a)	143	28.4 \pm 20.2	41.5 \pm 24.7 ^{ac}		29.1 \pm 18.7
LC(b)	143	27.1 \pm 18.8		48.7 \pm 20.8 ^{bd}	29.6 \pm 15.4
OC	40	25.2 \pm 17.6	31.8 \pm 22.1	32.6 \pm 21.1	27.9 \pm 16.6
LCR	18	27.3 \pm 16.1	40.7 \pm 27.3 ^{ac}	45.5 \pm 22.2 ^{bc}	38.6 \pm 20.3 ^{ac}
OCR	23	26.8 \pm 19.5	30.2 \pm 25.1	32.9 \pm 24.6	28.5 \pm 18.6

n=cases, Preo-=Preoperative, ^a*P*<0.05, ^b*P*<0.01 vs Preo-; ^c*P*<0.05, ^d*P*<0.01 vs OC; ^e*P*<0.05, ^f*P*<0.01 vs OCR.

In this study, we also tested other liver function indice such as total bilirubin (TBIL), direct bilirubin (DBIL), alkaline phosphatase (ALP), lactic dehydrogenase (LDH), total protein (TP) and gamma glutamyl transferase (GGT) (data not shown). In general, TBIL and DBIL showed a slight increase within 24-48 hours following operation in some patients, but the changes were within normal range, and these values returned to preoperative levels. Other liver function test indice did not show significant alteration.

DISCUSSION

Changes in serum levels of liver enzymes in LC rather than OC patients had been reported before^[5-9]. In order to understand whether or not CO₂ pneumoperitoneum could cause these changes, we tested the liver function of patients who received LCR or OCR. Our present studies suggest that these transient postoperative hypertransaminases in LC and LCR patients might be attributed to the following possible factors.

The first factor of consideration was CO₂ pneumoperitoneum. Both LC and LCR patients were subject to CO₂ pneumoperitoneum during the operations and they showed significant changes in serum liver enzymes after operation. In contrast, both OC and OCR patients were under the operation conditions similar to those of LC and LCR patients except that they were not subject to CO₂ pneumoperitoneum and they showed no apparent change in the level of serum liver enzymes. This finding is consistent with other studies that showed similar changes in liver function clearance test after pneumoperitoneum^[10-16]. Because an intra-abdominal pressure (IAP) of 12-14 mmHg used in the present laparoscopic surgery was higher than the normal portal blood pressure of 7-10 mmHg, this operation might, therefore, reduce portal blood flow and cause alteration in liver function^[17-20]. On the other hand, the elevation and depression of IAP in a short time during laparoscopic operation might be causative as well. During laparoscopic procedure, the sudden alteration of IAP could cause the undulation of portal blood flow. This undulation and "re-irrigation" of organs blood flow may give rise to "ischemia and re-irrigation" damage of tissues and organs, especially the Kupffer and the endothelial cells of the hepatic sinusoids^[21]. The mesothelial cells were bulging up and the intercellular clefts thereby increased in size, and the underlying basal lamina became visible^[22]. During LC, an IAP of 8 mmHg was found to decrease the hepatic microcirculation significantly^[23,24]. Therefore, the elevation of IAP caused by CO₂ pneumoperitoneum may be the main reason behind these changes.

A second possible mechanism for alterations of serum liver enzymes after LC is the "squeeze" pressure effect on the liver. The traction of the gallbladder may free these enzymes into the blood stream. But in our study, 40 OC were performed with a small wound within 6 cm. There should be the same or more "squeeze" pressure effect on the liver in these patients, yet the change of serum liver enzymes was different between LC and OC patients. In addition, the same changes occurred in LCR patients. This mechanism remains to be determined in animal models.

The third possibility may be the local effect of prolonged use of diathermy to the liver surface and spread of heat to liver parenchyma. This hypothesis is supported by some other studies^[25-31]. However, similar type and intensity of diathermy were used in both OC and LC patients and it remains to be explained why the serum liver enzyme level increased in LCR patients whose focus was far from liver. While the thermal damage to liver by diathermy is generally recognized, there are no references available in the literature that compared the postoperative enzyme levels between cholecystectomies performed with and without the use of diathermy in humans.

In addition, transient liver dysfunction occurs in patients after some general anesthesia^[32-41]. This complication is associated with anesthesia-induced changes in splanchnic blood flow and oxygen consumption. However, the anesthesia-induced hepatic hypoperfusion may not be the cause of elevation of transaminases after LC and LCR as the same anesthesia protocols was used in our 23 OCR patients who did not show marked postoperative change in serum liver enzymes. It seems that the anesthesia could not acted exclusively to cause these changes. Other studies have also shown similar liver function test results in both LC and OC cases with general anesthesia^[42].

Another possible mechanism of alterations of serum liver enzymes that had been considered was the inadvertent clipping of the right branch of the hepatic artery or any other aberrant arterial branch supplying blood to the liver. When Calot's triangle has dense or cicatricial adhesion, the related arterial branch could be easily injured. This, however, should be followed by a massive increase in liver enzymes and usually has clinical implications^[43-45]. Nevertheless, the LCR hardly gave rise to any chance to injure the right branch of the hepatic artery, yet the LCR patients showed marked elevation of ALT and AST postoperatively. Therefore, arterial branch injury could be ruled out in almost LC patients.

In summary, our present studies demonstrated that transient elevation of hepatic transaminases could occur after laparoscopic procedures. These changes might be attributed to hepatocellular dysfunction secondary to one or combination of CO₂ pneumoperitoneum, diathermy, extruding liver, branch of the hepatic artery injured and general anesthesia. Based on our findings, the CO₂ pneumoperitoneum might be one of the main reasons for the change of serum liver enzymes. However, the transient elevation of hepatic transaminases showed no apparent clinical implication in most patients who received laparoscopic surgery according to follow-up observations and feedback from these patients. Nevertheless, these results indicate that, if the patient's preoperative liver function was very poor, laparoscopic surgery might not be the optimal choice for treating certain abdominal diseases^[46].

REFERENCES

- Cuschieri A.** Laparoscopic cholecystectomy. *J R Coll Surg Edinb* 1999; **44**: 187-192
- Himal HS.** Minimally invasive (laparoscopic) surgery. *Surg Endosc* 2002; **8**: 265-270
- Suter M, Meyer A.** A 10-year experience with the use of laparoscopic cholecystectomy for acute cholecystitis: is it safe? *Surg Endosc* 2001; **15**: 1187-1192
- Kiely JM, Brannigan AE, Foley E, Cheema S, O'Brien W, Delaney PV.** Day case laparoscopic cholecystectomy is feasible. *Ir J Med Sci* 2001; **170**: 98-99
- Giraud G, Brachet Contul R, Caccetta M, Morino M.** Gasless laparoscopy could avoid alterations in hepatic function. *Surg Endosc* 2001; **15**: 741-746
- Morino M, Giraud G, Festa V.** Alterations in hepatic function during laparoscopic surgery. An experimental clinical study. *Surg Endosc* 1998; **12**: 968-972
- Sala-Blanch X, Fontanals J, Martinez-Palli G, Taura P, Delgado S, Bosch J, Lacy AM, Visa J.** Effects of carbon dioxide vs helium pneumoperitoneum on hepatic blood flow. *Surg Endosc* 1998; **12**: 1121-1125
- Kotake Y, Takeda J, Matsumoto M, Tagawa M, Kikuchi H.** Sub-clinical hepatic dysfunction in laparoscopic cholecystectomy and laparoscopic colectomy. *Br J Anaesth* 2001; **87**: 774-777
- Andrei VE, Schein M, Margolis M, Rucinski JC, Wise L.** Liver enzymes are commonly elevated following laparoscopic cholecystectomy: is elevated intra-abdominal pressure the cause? *Dig Surg* 1998; **15**: 256-259
- Sato K, Kawamura T, Wakusawa R.** Hepatic blood flow and function in elderly patients undergoing laparoscopic cholecystectomy. *Anesth Analg* 2000; **90**: 1198-1202
- Takagi S.** Hepatic and portal vein blood flow during carbon dioxide pneumoperitoneum for laparoscopic hepatectomy. *Surg Endosc* 1998; **12**: 427-431
- Richter S, Olinger A, Hildebrandt U, Menger MD, Vollmar B.** Loss of physiologic hepatic blood flow control ("hepatic arterial buffer response") during CO₂-pneumoperitoneum in the rat. *Anesth Analg* 2001; **93**: 872-877
- Pemer A, Bugge K, Lyng KM, Schulze S, Kristensen PA, Bendtsen A.** Changes in plasma potassium concentration during carbon dioxide pneumoperitoneum. *Br J Anaesth* 1999; **82**: 137-139
- Tunon MJ, Gonzalez P, Jorquera F, Llorente A, Gonzalo-Orden M, Gonzalez-Gallego J.** Liver blood flow changes during laparoscopic surgery in pigs. A study of hepatic indocyanine green removal. *Surg Endosc* 1999; **13**: 668-672
- Klopfenstein CE, Morel DR, Clergue F, Pastor CM.** Effects of abdominal CO₂ insufflation and changes of position on hepatic blood flow in anesthetized pigs. *Am J Physiol* 1998; **275**: H900-905
- Schafer M, Sagesser H, Reichen J, Krahenbuhl L.** Alterations in hemodynamics and hepatic and splanchnic circulation during laparoscopy in rats. *Surg Endosc* 2001; **15**: 1197-1201
- Schmandra TC, Kim ZG, Gutt CN.** Effect of insufflation gas and intraabdominal pressure on portal venous flow during pneumoperitoneum in the rat. *Surg Endosc* 2001; **15**: 405-408
- Glantzounis GK, Tselepis AD, Tambaki AP, Trikalinos TA, Manataki AD, Galaris DA, Tsimoyiannis EC, Kappas AM.** Laparoscopic surgery-induced changes in oxidative stress markers in human plasma. *Surg Endosc* 2001; **15**: 1315-1319
- Tsugawa K, Hashizume M, Migou S, Tanoue K, Kishihara F, Kawanaka H, Sugimachi K.** The effect of carbon dioxide pneumoperitoneum on the portal hemodynamics in a portal-hypertensive rat model. *Surg Laparosc Endosc Percutan Tech* 1999; **9**: 338-347
- Bendet N, Morozov V, Lavi R, Panski M, Halevy A, Scapa E.** Does laparoscopic cholecystectomy influence peri-sinusoidal cell activity? *Hepatogastroenterology* 1999; **46**: 1603-1606
- Volz J, Koster S, Spacek Z, Paweletz N.** Characteristic alterations of the peritoneum after carbon dioxide pneumoperitoneum. *Surg Endosc* 1999; **13**: 611-614
- Gutt CN, Schmandra TC.** Portal venous flow during CO₂ pneumoperitoneum in the rat. *Surg Endosc* 1999; **13**: 902-905
- Jakimowicz J, Stultiens G, Smulders F.** Laparoscopic insufflation of the abdomen reduces portal venous flow. *Surg Endosc* 1998; **12**: 129-132
- Dessole S, Rubattu G, Capobianco G, Caredda S, Cherchi PL.** Utility of bipolar electrocautery scissors for abdominal hysterectomy. *Am J Obstet Gynecol* 2000; **183**: 396-399
- Raut V, Bhat N, Kinsella J, Toner JG, Sinnathuray AR, Stevenson M.** Bipolar scissors versus cold dissection tonsillectomy: a prospective, randomized, multi-unit study. *Laryngoscope* 2001; **111**: 2178-2182
- Tulikangas PK, Smith T, Falcone T, Boparai N, Walters MD.** Gross and histologic characteristics of laparoscopic injuries with four different energy sources. *Fertil Steril* 2001; **75**: 806-810
- Capelluto E, Champault G.** Variations in intraperitoneal temperature during laparoscopic cholecystectomy. *Ann Chir* 2000; **125**: 259-262
- Barrat C, Capelluto E, Champault G.** Intraperitoneal thermal variations during laparoscopic surgery. *Surg Endosc* 1999; **13**: 136-138
- Shamiyeh A, Schrenk P, Tulipan L, Vattay P, Bogner S, Wayand W.** A new bipolar feedback-controlled sealing system for closure of the cystic duct and artery. *Surg Endosc* 2002; **16**: 812-813
- Yang W, Benjamin IS, Sherwood R, Alexander B.** Correlation of endothelium-dependent and -independent vasodilatation with liver function tests during prolonged perfusion of the rat liver. *J Pharmacol Toxicol Methods* 1998; **40**: 227-234
- Berger M, Junemann K, Schramm H.** Danger of monopolar current in laparoscopic gallbladder surgery. *Zentralbl Chir* 2001; **126**: 591-595
- Scapa E, Pinhasov I, Eshchar J.** Does general anesthesia affect sinusoidal liver cells as measured by beta-N-acetyl hexosaminidase serum activity level? *Hepatogastroenterology* 1998; **45**: 1813-1815

- 33 **Shimamoto A**, Tanaka E, Mizuno D, Misawa S. Age- and sex-related changes in toluene metabolism by rat hepatic microsomes *in vitro*. *Res Commun Mol Pathol Pharmacol* 1999; **104**: 265-276
- 34 **Zamparelli M**, Eaton S, Quant PA, McEwan A, Spitz L, Pierro A. Analgesic doses of fentanyl impair oxidative metabolism of neonatal hepatocytes. *J Pediatr Surg* 1999; **34**: 260-263
- 35 **Tanaka E**, Yamazaki K, Misawa S. Update: the clinical importance of acetaminophen hepatotoxicity in non-alcoholic and alcoholic subjects. *J Clin Pharm Ther* 2000; **25**: 325-332
- 36 **Obata R**, Bito H, Ohmura M, Moriwaki G, Ikeuchi Y, Katoh T, Sato S. The effects of prolonged low-flow sevoflurane anesthesia on renal and hepatic function. *Anesth Analg* 2000; **91**: 1262-1268
- 37 **Ichinose K**, Yanagi F, Higashi K, Kozuma S, Akasaka T. Recurrent transient increases in liver enzymes specifically after isoflurane anesthesia. *Masui* 1999; **48**: 421-423
- 38 **Nishiyama T**, Yokoyama T, Hanaoka K. Liver function after sevoflurane or isoflurane anaesthesia in neurosurgical patients. *Can J Anaesth* 1998; **45**: 753-756
- 39 **McEwen MM**, Gleed RD, Ludders JW, Stokol T, Del Piero F, Erb HN. Hepatic effects of halothane and isoflurane anesthesia in goats. *J Am Vet Med Assoc* 2000; **217**: 1697-1700
- 40 **Darling JR**, Sharpe PC, Stiby EK, McAteer JA, Archbold GP, Milligan KR. Serum mitochondrial aspartate transaminase activity after isoflurane or halothane anaesthesia. *Br J Anaesth* 2000; **85**: 195-198
- 41 **Feierman DE**. The effect of paracetamol (acetaminophen) on fentanyl metabolism *in vitro*. *Acta Anaesthesiol Scand* 2000; **44**: 560-563
- 42 **Saber AA**, Laraja RD, Nalbandian HI, Pablos-Mendez A, Hanna K. Changes in liver function tests after laparoscopic cholecystectomy: not so rare, not always ominous. *Am Surg* 2000; **66**: 699-702
- 43 **Kayaalp C**, Nessar G, Kaman S, Akoglu M. Right liver necrosis: complication of laparoscopic cholecystectomy. *Hepatogastroenterology* 2001; **48**: 1727-1729
- 44 **Balsara KP**, Dubash C, Shah CR. Pseudoaneurysm of the hepatic artery along with common bile duct injury following laparoscopic cholecystectomy. A report of two cases. *Surg Endosc* 1998; **12**: 276-277
- 45 **Mathisen O**, Soreide O, Bergan A. Laparoscopic cholecystectomy: bile duct and vascular injuries: management and outcome. *Scand J Gastroenterol* 2002; **37**: 476-481
- 46 **Tsuboi S**, Kitano S, Yoshida T, Bandoh T, Ninomiya K, Baatar D. Effects of carbon dioxide pneumoperitoneum on hemodynamics in cirrhotic rats. *Surg Endosc* 2002; **3**[epub ahead of print]

Edited by Liu HX

Relationship between expression of E-cadherin-catenin complex and clinicopathologic characteristics of pancreatic cancer

Yu-Jun Li, Xiang-Rui Ji

Yu-Jun Li, Xiang-Rui Ji, Department of Pathology, the Affiliated Hospital of Medical College, Qingdao University, Qingdao 266003, Shandong Province, China

Correspondence to: Dr. Yu-Jun Li, the Affiliated Hospital of Medical College, Qingdao University, 16 Jiangsu Rd, Qingdao 266003, China. yunjun-li66@yahoo.com

Telephone: +86-532-2911533

Received: 2002-07-17 **Accepted:** 2002-09-12

Abstract

AIM: To investigate the expression of E-cadherin and alpha-catenin and beta-catenin in pancreatic carcinoma and its relationship with the clinicopathologic characteristics, and clarify the mechanism of invasion and metastasis of pancreatic cancer.

METHODS: The expression of E-cadherin and alpha-, beta-catenin was examined in 47 cases of infiltrative ductal adenocarcinoma of pancreas and 12 adult normal pancreatic tissues by immunohistochemical technique.

RESULTS: The immunoreactivity of E-cadherin and alpha-, beta-catenin was expressed by normal ductal and acinar cells with strong membranous staining at the intercellular border in 12 cases of adult normal pancreatic tissues. Abnormal expression of E-cadherin and alpha-, beta-catenin in 47 pancreatic carcinoma tissues was demonstrated in 53.2 %, 61.7 % and 68.1 %, respectively. Both abnormal expression of E-cadherin and alpha-catenin significantly correlated with differentiation, lymph node and liver metastases ($P < 0.05$, respectively), whereas aberrant beta-catenin expression only correlated with lymph node and liver metastases ($P < 0.001$). Abnormal E-cadherin and alpha-, beta-catenin expression was not associated with tumor size, invasion and survival time of patients ($P > 0.05$, all).

CONCLUSION: Pancreatic cancer likely occurs in case of E-cadherin-catenin complex genes mutations or deletions and abnormal expression of proteins, which significantly correlate with the biologic character of the tumor and lymph node and liver metastases. It is suggested that the abnormal E-cadherin-catenin complex expression plays an important role in the development and progression of tumor, and thus may become a new marker in pancreatic cancer metastasis.

Li YJ, Ji XR. Relationship between expression of E-cadherin-catenin complex and clinicopathologic characteristics of pancreatic cancer. *World J Gastroenterol* 2003; 9(2): 368-372 <http://www.wjgnet.com/1007-9327/9/368.htm>

INTRODUCTION

Pancreatic cancer is a highly malignant tumor, and is the fifth leading cause of death among the malignant diseases in Western societies, and its incidence has been increasing year by year. However, there is no valid diagnosis and treatment for this

disease. Only 15 % of patients can undergo resection, and the overall 5-year survival rate is about 10 %. One reason why the prognosis of pancreatic cancer is so poor is that many tumors remain silent until a late stage in the disease, and at the time of diagnosis 80-90 % of patients will have extensive invasion and metastasis^[1-5]. So studying the mechanism of invasion and metastasis of pancreatic cancer is double valued. A recent study demonstrated that the invasion and metastasis of tumors as a continuous process, include three steps: a reduced cell-cell adhesion, alterations in the interaction of the tumor cell with the extracellular matrix, and invasion into surrounding tissues including blood vessels and lymphduct; thus the first and critical step is that the tumor cells detach from the primary focus and re-adhere to metastatic position^[6-8]. E-cadherin is a transmembrane glycoprotein which maintains normal epithelial polarity and intercellular adhesion^[9]. It is almost present in all normal epithelial cell surface, and has been recognized as an important suppression gene^[10,11]. Catenins serve not only as associated cytoplasmic proteins of E-cadherin, but also as molecules of intracellular signal transduction^[12-15]. They link E-cadherin to the intracellular peptide segment to form E-cadherin-catenin complex, mediating homotypic cell-cell adhesion and playing an essential role in the control of epithelial cell architecture and differentiation^[10,11,16]. The abnormal structure and dysfunction of one or several molecules in E-cadherin-catenin complex correlate with tumorigenesis, differentiation, invasion, metastasis and prognosis^[17-20]. We detected the expression of E-cadherin and alpha-, beta-catenin in normal pancreas and pancreatic cancer by immunohistochemical technique, and investigated the action of abnormal expression of E-cadherin and alpha-, beta-catenin on invasion and metastasis of pancreatic cancer.

MATERIALS AND METHODS

Patients and specimens

Specimens of 47 pancreatic carcinoma collected between 1995 to 1999 were selected from the Department of Pathology, Affiliated Hospital of Medical College, Qingdao University. These included 29 male and 18 female patients with a mean age of 56.7 years (range 27-75 years). No patient received radiotherapy or chemotherapy before surgery. The tumor size was assessed by CT scan: smaller than 3 cm in 9 patients, 3-5 cm in 15 patients and larger than 5 cm in 23. Histologically, all cases were infiltrative ductal adenocarcinoma. According to the Modified Kloppel Histological Grading System^[21], there were 10 in grade I (well differentiated), 16 in grade II (moderately differentiated) and 21 in grade III (poorly differentiated). Based on the tumor being resected successfully or not, we divided 47 pancreatic carcinomas into two groups: non-invasion (17 cases) and invasion (30 cases). There were 19 cases with local lymph node metastasis, 12 cases with liver metastasis and 22 without metastasis. All patients were followed for more than 1 year; 9 patients survived more than 12 months and 38 patients died within 12 months. The 1-year survival rate was 19.1 %. 12 normal adult pancreatic tissues were obtained from healthy young men who died of traffic accident.

Immunohistochemistry

All specimens were fixed in 100 mL · L⁻¹ neutral buffered formalin for 24-48 h, paraffin-embedded, and cut into 4 μm thick sections for immunohistochemical staining. PicTure™ two-step method was used (Zmed, USA). Each step was practised according to the manual. The primary antibodies were E-cadherin monoclonal antibody (ready for use, Zmed, USA) and alpha-, beta-catenin monoclonal antibodies (diluted 1:100, Santa Cruz, USA), respectively. Before staining, the sections were pretreated with microwave (4 min × 4 at 900W) in 0.1 mol · L⁻¹ citrate buffer for antigen retrieval. DAB was used for chromogen. PBS was substituted for primary antibodies as negative control.

Evaluation of immunohistochemical staining

The slides were reviewed by two independent observers who had no knowledge of patients' outcome. The positive stainings of E-cadherin and alpha-, beta-catenin appeared in pale brown, and located in the cell membrane. Staining grade standard based on the method described by Jawhari *et al.*^[22]. 0 score: no expression; 1 score: expression in cytoplasm; 2 score: decreased expression; 3 score: expression at cell membrane, namely normal expression. A score of 0 to 2 was abnormal expression.

Statistical analysis

Statistical analysis was performed using the χ^2 test or Fisher's exact test. $P < 0.05$ was considered significant.

RESULTS

The expression of E-cadherin-catenin complex in normal pancreas and pancreatic carcinoma tissues

The immunoreactivity of E-cadherin and alpha-, beta-catenin was expressed by normal ductal and acinar cells with strong membranous staining at the intercellular border in 12 cases of adult normal pancreases (Figures 1). The rates of abnormal expression of E-cadherin and alpha-, beta-catenin in 47 pancreatic carcinoma tissue specimens were 53.2% (25/47), 61.7% (29/47) and 68.1% (32/47), respectively. The expression of E-cadherin-catenin complex in most cases was in cytoplasm, whereas membranous staining reduced or disappeared (Figures 2).

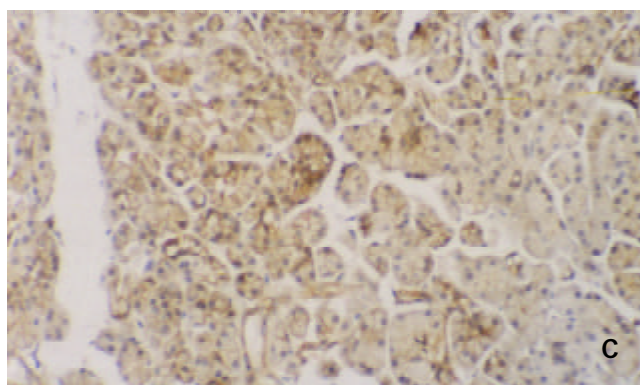
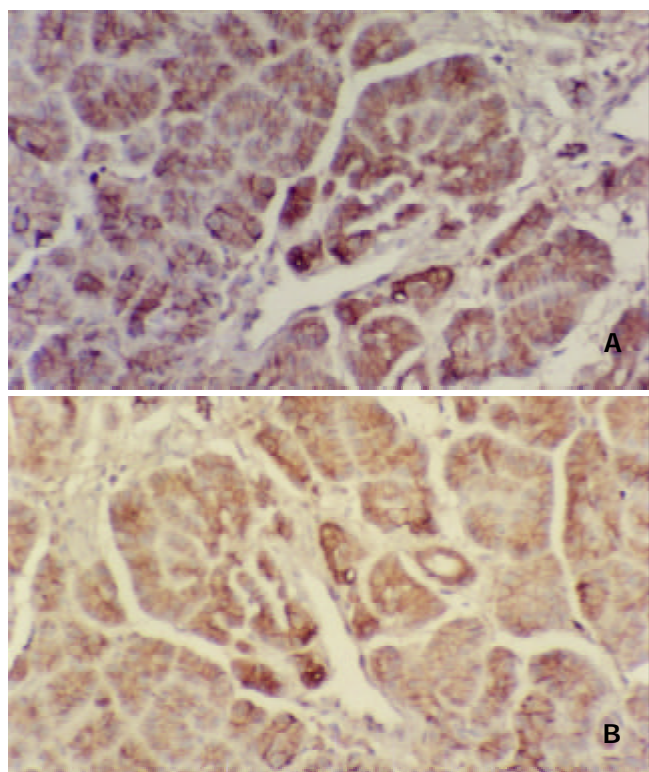


Figure 1 Immunohistochemical staining. A, B and C: The immunoreactivity of E-cadherin and alpha-, beta-catenin was expressed by normal ductal and acinar cells with strong membranous staining on the intercellular border in the same specimen. ×100.

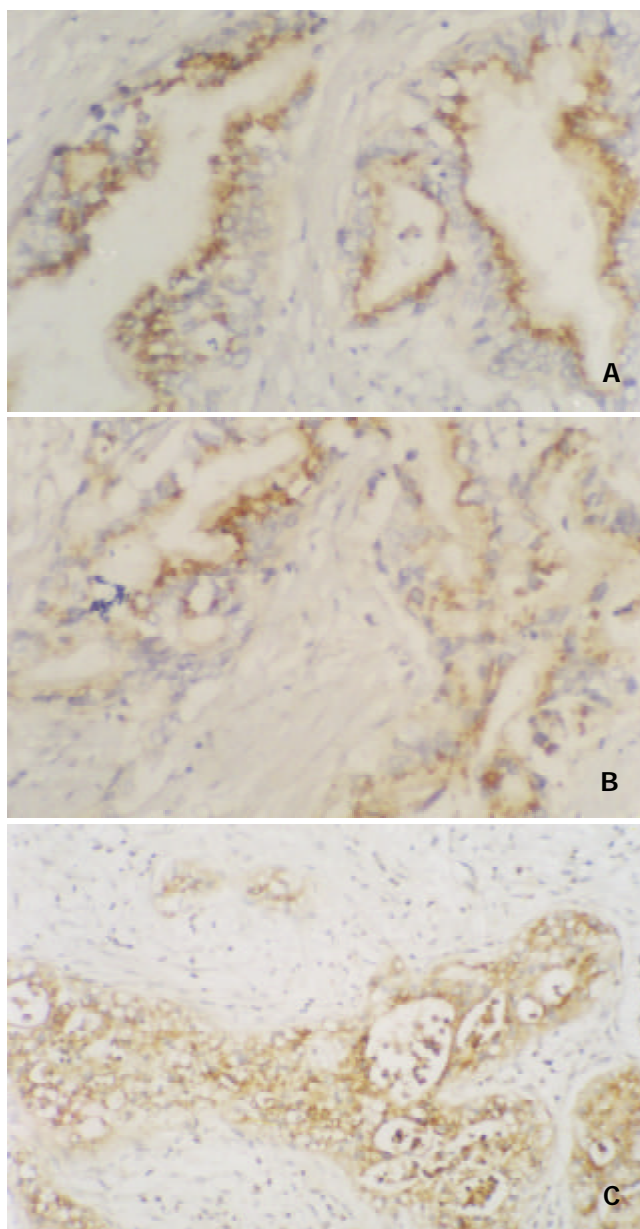


Figure 2 Immunohistochemical staining. A, B and C: E-cadherin and alpha-, beta-catenin expression mainly were in cytoplasm, whereas membranous staining reduced or disappeared in pancreatic cancer tissue. ×200.

The relationship between abnormal expression of E-cadherin-catenin complex and clinicopathologic characteristics of pancreatic cancer

The abnormal expression of E-cadherin and alpha-, beta-catenin was not associated with tumor size, invasion and survival time of patients ($P=0.12-0.926$, $P>0.05$, all). The significant difference of abnormal E-cadherin and alpha-catenin expression was seen between histological grade I, II and III ($\chi^2=12.02$, 7.74 ; $P=0.002$, 0.021 ; $P<0.01$, 0.05). The tumors with lymph node ($\chi^2=4.19$, 4.45 , 6.60 ; $P=0.0406$, 0.035 , 0.0102 ; $P<0.05$) and liver metastases ($P=0.0105$, 0.0005 , 0.0025 ; $P<0.05$, 0.01) showed a relatively higher frequency of abnormal expression of E-cadherin and alpha-, beta-catenin than those without metastasis (Table 1).

Table 1 The relationship between expression of E-cadherin-catenin complex and clinicopathologic characteristics of pancreatic cancer

Parameter	n	E-cadherin (%)		α -catenin(%)		β -catenin(%)	
		Normal	Abnormal	Normal	Abnormal	Normal	Abnormal
Mass size (cm)							
<3	9	5(55.6)	4(44.4)	4(44.4)	5(55.6)	3(33.3)	6(66.7)
3-5	15	7(46.7)	8(53.3)	5(33.3)	10(66.7)	4(26.7)	11(73.3)
>5	23	10(43.5)	13(56.5)	9(39.1)	14(60.9)	8(34.8)	15(65.2)
Histologic grade							
I	10	9(90.0)	1(10.0)	7(70.0)	3(30.0)	5(50.0)	5(50.0)
II	16	8(50.0)	8(50.0)	7(43.8)	9(56.2)	6(37.5)	10(62.5)
III	21	5(23.8)	16(76.2)	4(19.0)	17(81.0)	4(19.0)	17(81.0)
Invasive state							
Invasion	30	12(40.0)	18(60.0)	9(30.0)	21(70.0)	8(26.7)	22(73.3)
No invasion	17	10(58.8)	7(41.2)	9(52.9)	8(47.1)	7(41.2)	10(58.8)
Metastases	19	6(31.6)	13(68.4) ^a	5(26.3)	14(73.7) ^a	3(15.8)	16(84.2) ^a
Lymph node							
Liver	12	2(16.7)	10(83.3) ^a	0	12(100.0) ^b	0	12(100.0) ^b
No	22	14(63.6)	8(36.4)	13(59.1)	9(40.9)	12(54.5)	10(45.5)
Survival time (month)							
>12	9	6(66.7)	3(33.3)	5(55.6)	4(44.4)	4(44.4)	5(55.6)
≤12	38	16(42.1)	22(57.9)	13(34.2)	25(65.8)	11(28.9)	27(71.1)

^a $P<0.05$, vs no metastasis; ^b $P<0.01$, vs no metastasis.

DISCUSSION

E-cadherin-catenin complex is a major mediator of maintaining intercellular adhesion and epithelial integration^[16,19], and its down regulation may occur in several ways amongst which are gene mutations or deletions, transcriptional or posttranscriptional alterations, methylation of 5' CpG dinucleotides within the promoter region of E-cadherin, tyrosine phosphorylation of beta-catenin^[14, 23-26]. The abnormal structure and dysfunction of one or several molecules in E-cadherin-catenin complex correlate with the tumorigenesis, differentiation, invasion, metastasis and prognosis^[17-20]. Now the E-cadherin-catenin complex has been regarded as a suppressor of tumor invasion and metastasis, and its reduced expression has been observed in diverse types of human cancer and plays an important role in the process of tumor invasion and metastasis^[27-30]. Dai *et al*^[31] found that the positive rates of E-cadherin and alpha-catenin expression were 38.6 % and 28.6 % respectively and they were significantly reduced in gastric cancer with more prominent malignant phenotype, such

as tumor in stage III/IV with poor cell differentiation, invasion through serosa, lymph node and liver metastases, and peritoneal implantation of cancer cells. So they considered that down regulation of E-cadherin and/or alpha-catenin correlates with the degree of malignancy of gastric cancer and that examination of E-cadherin and alpha-catenin expression in gastric cancer helps evaluate the intensity of lymph node metastasis, TNM staging and prognosis. Joo *et al*^[32] reported that the immunoreactivity of E-cadherin and alpha-, beta-, and gamma-catenin was expressed by normal gastric epithelial cells with strong membranous staining at the intercellular border, and reduced expression of them occurred in a considerable proportion of both early and advanced cancer groups and correlated with the diffuse type of cancer with poor differentiation, but it was not related with depth of invasion or lymph node metastases.

Till now, there have been only a few articles about the relationship between expression of E-cadherin-catenin complex and biological behavior of pancreatic cancer, and the results were not consistent. Karayiannakis *et al*^[33,34] observed that in non-cancerous pancreatic cells E-cadherin, alpha-, beta- and gamma-catenin immunoreactivity was localized on the cell membrane, particularly at the intercellular junctions, but in 43 pancreatic carcinomas abnormal E-cadherin, alpha-, beta- and gamma-catenin expressions were found in 42 %, 37 %, 44 % and 40 %, respectively; moreover, E-cadherin, alpha-catenin and gamma-catenin expressions correlated with poor differentiation, disease stage and with lymph node and distant metastases, whereas aberrant beta-catenin expression only correlated with the presence of lymph node metastases. Some authors^[35-37] also reported that loss of E-cadherin played a causative role in peritoneal dissemination, invasion and metastasis of pancreatic carcinoma, and altered expression of adhesion molecules correlated with dedifferentiating change and aggressive biological behavior of pancreatic cancer. But Gunji *et al*^[38] concluded that reduced E-cadherin and alpha-catenin expression in primary pancreatic cancer had no significant predictive value regarding the presence of liver metastasis.

In this study, we found that the immunoreactivity of E-cadherin and alpha-, beta-catenin was expressed by normal ductal and acinar cells with strong membranous staining at the intercellular border in 12 cases of adult normal pancreases, but over 50 % pancreatic carcinomas showed abnormal expression of E-cadherin (53.2 %) and alpha-, beta-catenin (61.7 %, 68.1 %), and the three adhesion molecules in most cases were present in cytoplasm, whereas membranous staining was reduced or disappeared. The results pointed out that there was significant difference in protein level of E-cadherin-catenin complex expression between normal pancreas and pancreatic carcinoma tissues, and E-cadherin and alpha-, beta-catenin genes mutations or deletions likely were related with tumorigenesis of pancreas. Our data also demonstrated that both abnormal expression of E-cadherin and alpha-catenin significantly correlated with differentiation, lymph node and liver metastases ($P<0.05$, 0.01 , respectively), whereas aberrant beta-catenin expression only correlated with lymph node and liver metastases ($P<0.01$), and all 12 cases with liver metastasis showed abnormal expression of alpha-catenin and beta-catenin. It can be inferred from our findings that the changes of E-cadherin-catenin complex genes happen in early pancreatic carcinoma, and become more serious with the progression of tumor. Moreover, because of the gene inactivation and dysfunction of E-cadherin-catenin complex, carcinoma cells are "set free" for invasion and metastases. Therefore, these results suggest that abnormal change of E-cadherin and alpha-, beta-catenin plays a conjoint role in the development and progression of tumor, and combined examination of E-cadherin-catenin complex expression has very important

clinical value for evaluating the dedifferentiation, lymph node and liver metastases of pancreatic cancer.

Some authors reported^[39-42] that the level of E-cadherin-catenin complex expression could be regarded as a prognostic marker of tumors. Karayiannakis *et al.*^[33] also regarded that all three catenins and E-cadherin were associated with a poor prognosis of pancreatic cancer, but only E-cadherin and alpha-catenin were independent prognostic factors for cancer-specific survival. However, in this study our data showed the expression of E-cadherin and alpha-, beta-catenin had no significant relationship with survival time of patients ($P>0.05$), and was not associated with invasion and size of pancreatic cancer as well ($P>0.05$, all). Perhaps this was related to the criteria of invasion adopted in our research and different operative method and different postoperative therapy. All these factors can bring about influence on our results. A similar conclusion was reported in non-small cell lung cancer by Pirinen *et al.*^[43].

In summary, our findings suggested that the change of E-catenin complex genes and down regulation and abnormal distribution of their encoding proteins happened in the early phase of pancreatic carcinoma and finally the tumor completely lost E-cadherin and alpha-, beta-catenin, resulting in a loss of adhesive mechanism in maintaining intercellular attachment, a dedifferentiated state and an increased metastatic ability. This is a key link of metastatic mechanism of the late pancreatic cancer.

REFERENCES

- 1 **Wagman R**, Grann A. Adjuvant therapy for pancreatic cancer: current treatment approaches and future challenges. *Surg Clin North Am* 2001; **81**: 667-681
- 2 **Gebhardt C**, Meyer W, Reichel M, Wunsch PH. Prognostic factors in the operative treatment of ductal pancreatic carcinoma. *Langenbecks Arch Surg* 2000; **385**: 14-20
- 3 **Kayahara M**, Nagakawa T, Ohta T, Kitagawa H, Ueno K, Tajima H, Elnemr A, Miwa K. Analysis of paraaortic lymph node involvement in pancreatic carcinoma: a significant indication for surgery? *Cancer* 1999; **85**: 583-590
- 4 **Carr JA**, Ajlouni M, Wollner I, Wong D, Velanovich V. Adenocarcinoma of the head of the pancreas: effects of surgical and nonsurgical therapy on survival—a ten-year experience. *Am Surg* 1999; **65**: 1143-1149
- 5 **Benassai G**, Mastroianni M, Mosella F, Mosella G. Significance of lymph node metastases in the surgical management of pancreatic head carcinoma. *J Exp Clin Cancer Res* 1999; **18**: 23-28
- 6 **Beavon IR**. The E-cadherin-catenin complex in tumor metastasis: structure, function and regulation. *Eur J Cancer* 2000; **36**: 1607-1620
- 7 **Korn WM**. Moving toward and understanding of the metastatic process in hepatocellular carcinoma. *World J Gastroenterol* 2001; **7**: 777-778
- 8 **Stamenkovic I**. Matrix metalloproteinases in tumor invasion and metastasis. *Semin Cancer Biol* 2000; **10**: 415-433
- 9 **Bair EL**, Massey CP, Tran NL, Borchers AH, Heimark RL, Cress AE, Bowden GT. Integrin- and cadherin-mediated induction of the matrix metalloproteinase matrilysin in cocultures of malignant oral squamous cell carcinoma cells and dermal fibroblasts. *Exp Cell Res* 2001; **270**: 259-267
- 10 **Hirohashi S**. Inactivation of the E-cadherin-mediated cell adhesion system in human cancers. *Am J Pathol* 1998; **153**: 333-339
- 11 **Christofori G**, Semb H. The role of the cell-adhesion molecule E-cadherin as a tumor-suppressor gene. *Trends Biochem Sci* 1999; **24**: 73-76
- 12 **Van Aken E**, De Wever O, Correia da Rocha AS, Mareel M. Defective E-cadherin/catenin complexes in human cancer. *Virchows Arch* 2001; **439**: 725-751
- 13 **Wijnhoven BP**, Dinjens WN, Pignatelli M. E-cadherin-catenin cell-cell adhesion complex and human cancer. *Br J Surg* 2000; **87**: 992-1005
- 14 **Debruyne P**, Vermeulen S, Mareel M. The role of the E-cadherin/catenin complex in gastrointestinal cancer. *Acta Gastroenterol Belg* 1999; **62**: 393-402
- 15 **Behrens J**. Cadherins and catenins: role in signal transduction and tumour progression. *Cancer Metastasis Rev* 1999; **18**: 15-30
- 16 **El-Bahrawy MA**, Pignatelli M. E-cadherin and catenins: molecules with versatile roles in normal and neoplastic epithelial cell biology. *Microsc Res Tech* 1998; **43**: 224-232
- 17 **Bremnes RM**, Veve R, Hirsch FR, Franklin WA. The E-cadherin cell-cell adhesion complex and lung cancer invasion, metastasis, and prognosis. *Lung Cancer* 2002; **36**: 115-124
- 18 **Berx G**, Van Roy F. The E-cadherin/catenin complex: an important gatekeeper in breast cancer tumorigenesis and malignant progression. *Breast Cancer Res* 2001; **3**: 289-293
- 19 **Nollet F**, Berx G, van Roy F. The role of the E-cadherin/catenin complex in the development and progression of cancer. *Mol Cell Biol Res Commun* 1999; **2**: 77-85
- 20 **Kitagawa T**, Matsumoto K, Nagafuchi A, Tsukita S, Suzuki H. Co-expression of E-cadherin and alpha-catenin molecules in colorectal cancer. *Surg Today* 1999; **29**: 511-518
- 21 **Giulianotti PC**, Boggi U, Fornaciari G. Prognostic value of histological grading in ductal adenocarcinoma of the pancreas. *Int J Pancreatol* 1995; **17**: 279-289
- 22 **Jawhari A**, Jordan S, Poole S, Browne P, Pignatelli M, Farthing MJ. Abnormal immunoreactivity of the E-cadherin-catenin complex in gastric cancer: relationship with patient survival. *Gastroenterology* 1997; **112**: 46-54
- 23 **Hirohashi S**. Molecular aspects of adhesion-epigenetic mechanism for inactivation of the E-cadherin-mediated cell adhesion system in cancers. *Verh Dtsch Ges Pathol* 2000; **64**: 28-32
- 24 **Maeno Y**, Moroi S, Nagashima H, Noda T, Shiozaki H, Monden M. Alpha-catenin deficient F9 cells differentiate into signet ring cells. *Am J Pathol* 1999; **354**: 1323-1328
- 25 **Chalmers LJ**, Hofler H, Atkinson MJ. Mapping of a cadherin gene cluster to a region of chromosome 5 subject to frequent allelic loss in carcinoma. *Genomics* 1999; **57**: 160-163
- 26 **Li LC**, Chui RM, Sasaki M, Nakajima K, Perinchery G, Au HC, Nojima D, Carroll P, Dahiya R. A single nucleotide polymorphism in the E-cadherin gene promoter alters transcriptional activities. *Cancer Res* 2000; **60**: 873-876
- 27 **Maruyama K**, Ochiai A, Nakamura S, Baba S, Hirohashi S. Dysfunction of E-cadherin-catenin system in invasion and metastasis of colorectal cancer. *Nippon Geka Gakkai Zasshi* 1998; **99**: 402-408
- 28 **Mareel M**, van Roy F. The human E-cadherin/catenin complex: a potent invasion and tumor suppressor. *Verh K Acad Geneesk Belg* 1998; **60**: 576-598
- 29 **Tanakao M**, Kitajima Y, Edakuni G, Sato S, Miyazaki K. Abnormal expression of E-cadherin and beta-catenin may be a molecular marker of submucosal invasion and lymph node metastasis in early gastric cancer. *Br J Surg* 2002; **89**: 236-244
- 30 **Fujioka T**, Takebayashi Y, Kihana T, Kusanagi Y, Hamada K, Ochi H, Uchida T, Fukumoto M, Ito M. Expression of E-cadherin and beta-catenin in primary and peritoneal metastatic ovarian carcinoma. *Oncol Rep* 2001; **8**: 249-255
- 31 **Dai D**, Chen J, Xu H. The clinical significance of E-cadherin and alpha-catenin expression in human gastric cancer. *Zhonghua Zhongliu Zazhi* 2001; **23**: 35-38
- 32 **Joo YE**, Rew JS, Kim HS, Choi SH, Park CS, Kim SJ. Changes in the E-cadherin-catenin complex expression in early and advanced gastric cancers. *Digestion* 2001; **64**: 111-119
- 33 **Karayiannakis AJ**, Syrigos KN, Polychronidis A, Simopoulos C. Expression patterns of alpha-, beta- and gamma-catenin in pancreatic cancer: correlation with E-cadherin expression, pathological features and prognosis. *Anticancer Res* 2001; **21**: 4127-4134
- 34 **Karayiannakis AJ**, Syrigos KN, Chatzigianni E, Papanikolaou S, Alexiou D, Kalahanis N, Rosenberg T, Bastounis E. Aberrant E-cadherin expression associated with loss of differentiation and advanced stage in human pancreatic cancer. *Anticancer Res* 1998; **18**: 4177-4180
- 35 **Furuyama H**, Arii S, Mori A, Imamura M. Role of E-cadherin in peritoneal dissemination of the pancreatic cancer cell line, panc-1, through regulation of cell to cell contact. *Cancer Lett* 2000; **157**: 201-209
- 36 **Yonemasu H**, Takashima M, Nishiyama KI, Ueki T, Yao T, Tanaka M, Tsuneyoshi M. Phenotypical characteristics of undifferentiated carcinoma of the pancreas: a comparison with pan-

- creatic ductal adenocarcinoma and relevance of E-cadherin, alpha catenin and beta catenin expression. *Oncol Rep* 2001; **8**: 745-752
- 37 **Takao S**, Che X, Fukudome T, Natsugoe S, Ozawa M, Aikou T. Down-regulation of E-cadherin by antisense oligonucleotide enhances basement membrane invasion of pancreatic carcinoma cells. *Hum Cell* 2000; **13**: 15-21
- 38 **Gunji N**, Oda T, Todoroki T, Kanazawa N, Kawamoto T, Yuzawa K, Scarpa A, Fukao K. Pancreatic carcinoma: correlation between E-cadherin and alpha-catenin expression status and liver metastasis. *Cancer* 1998; **82**: 1649-1656
- 39 **Aaltomaa S**, Lipponen P, Ala-Opas M, Eskelinen M, Kosma VM. Alpha-catenin expression has prognostic value in local and locally advanced prostate cancer. *Br J Cancer* 1999; **80**: 477-482
- 40 **Inagawa S**, Itabashi M, Adachi S, Kawamoto T, Hori M, Shimazaki J, Yoshimi F, Fukao K. Expression and prognostic roles of beta-catenin in hepatocellular carcinoma: correlation with tumor progression and postoperative survival. *Clin Cancer Res* 2002; **8**: 450-456
- 41 **Bremnes RM**, Veve R, Gabrielson E, Hirsch FR, Baron A, Bemis L, Gemmill RM, Drabkin HA, Franklin WA. High-throughput tissue microarray analysis used to evaluate biology and prognostic significance of the E-cadherin pathway in non-small-cell lung cancer. *J Clin Oncol* 2002; **20**: 2417-2428
- 42 **Hugh TJ**, Dillon SA, Taylor BA, Pignatelli M, Poston GJ, Kinsella AR. Cadherin-catenin expression in primary colorectal cancer: a survival analysis. *Br J Cancer* 1999; **80**: 1046-1051
- 43 **Pirinen RT**, Hirvikoski P, Johansson RT, Hollmen S, Kosma VM. Reduced expression of alpha-catenin, beta-catenin, and gamma-catenin is associated with high cell proliferative activity and poor differentiation in non-small cell lung cancer. *J Clin Pathol* 2001; **54**: 391-395

Edited by Lu HM

Effects of time interval for hemofiltration on the prognosis of severe acute pancreatitis

En-Qiang Mao, Yao-Qing Tang, Sheng-Dao Zhang

En-Qiang Mao, Yao-Qing Tang, Sheng-Dao Zhang, Department of Surgery, Ruijin Hospital, Shanghai Second Medical University, Shanghai 200025, China

Correspondence to: En-Qiang Mao, Department of Surgery, Ruijin Hospital, Shanghai Second Medical University, Shanghai 200025, China. maocq@yeah.net

Telephone: +86-21-64370045 Ext 666014

Received: 2002-08-06 **Accepted:** 2002-10-18

Abstract

AIM: To evaluate the impact of time interval for hemofiltration (HF) on the prognosis of severe acute pancreatitis (SAP).

METHODS: Thirty-six consecutive patients with severe acute pancreatitis were included in the study. Atlanta classification system was applied for stratification. They were randomly divided into short veno-venous HF group (SVVH, Group 1, 20 patients); and long veno-venous HF group (LVVH, Group 2, 16 patients). In group 1, SVVH was stopped when the abdominal signs disappeared, and heart rate and breath rate were less than 90 beats/min and 20 times/min, respectively. HF was stopped if SVVH was continued, and when heart rate and breath rate were more than 90 beats/min and 20 times/min again (Group 2). Except that the time interval for HF was different, other parameters for HF were the same. And conservative curing rate, survival rate, cost for hospital stay and length of hospital stay were observed.

RESULTS: Time interval for HF in Group 1 (3.81 ± 1.3 hr) was shorter than that of in Group 2 (9.38 ± 2.9 hr), $P < 0.01$. Conservative curing rate (90 %) in Group 1 was much higher than that in Group 2 (56.3 %) ($P < 0.05$); but cost in Group 1 (RMB $56\,600 \pm 56\,400$ Yuan) was lower than that in Group 2 (RMB $137\,000 \pm 105\,000$ Yuan) ($P < 0.05$). And the survival rate (95 %) in Group 1 was higher than that in Group 2 (81.3 %) ($P < 0.25$); however, hospital stay in Group 1 (44.3 ± 41 days) was shorter than that in Group 2 (55.2 ± 39.5 days) ($P < 0.2$). So, the prognosis was not improved through the prolongation of time interval for HF, but side-effects were seen.

CONCLUSION: The prognosis was not further improved by LVVH in the treatment of SAP, with side-effects. Time interval for HF plays an important role in treatment of SAP in early stage. SVVH is thought to be superior to LVVH; and LVVH is superior to CVVH in early (72hrs) treatment of SAP.

Mao EQ, Tang YQ, Zhang SD. Effects of time interval for hemofiltration on the prognosis of severe acute pancreatitis. *World J Gastroenterol* 2003; 9(2): 373-376
<http://www.wjgnet.com/1007-9327/9/373.htm>

INTRODUCTION

Up to date, strategies of treatments of severe acute pancreatitis have been extensively developed, such as prolongation of operation^[1]; peritoneal lavage, blood purification^[2], and

continuous arterial infusion of protease inhibitor^[3], endothelin receptor antagonist to reduce capillary leakage^[4], and so on, in addition to intensive care. But the mortality of SAP is still about 15-25 %^[5]. So, how to further raise the survival rate is most difficult. A large amount of cytokines^[6] released from activated macrophages and other sites^[7] as well as cytokines cascades play an important role in deteriorating the disease^[8-11].

Clinical and experimental data suggest that hemofiltration might be of benefit for amelioration of severe systemic inflammatory response syndrome (SIRS) or multiple organ dysfunction^[12-16] and prevention of pancreatic necrosis^[17,18]. Our data^[17] showed that pancreatic necrosis was prevented, and the prognosis was ameliorated through short veno-venous hemofiltration (SVVH). However, it is reported that better efficacy was also obtained from continuous veno-venous hemofiltration (CVVH)^[2,19]. The aim of the present study is therefore to investigate the time-effect of hemofiltration, by prolonging the time interval for HF in order to observe its impact on clinical efficacy.

MATERIALS AND METHODS

Patients and groups

Patients Thirty-six consecutive patients with SAP admitted to Ruijin Hospital, Shanghai, China from April 1997 to May 2002, were included in the study. Prior to study, all patients themselves or their relatives had been informed in detail, and agreement was obtained. Atlanta classification system was applied for stratification of patients with SAP^[20]. Criteria for the study were APACHEII score more than 8, with dysfunction of one or more organs, within 72 hours after onset of the disease and no indication for operation temporarily. There were 25 men and 11 women, aged from 18 - 82 years. Etiologies included hyperlipidemia (26 cases) with significantly increased triglyceride and biliary disease (10 cases).

Groups The patients were divided randomly into short veno-venous hemofiltration group (Group 1, SVVH) and long veno-venous hemofiltration group (Group 2, LVVH). In Group 1, consisted of 20 patients, 16 men and 4 women; aged 52.4 ± 14.2 years, including 14 with hyperlipidemia, 1 with hyperlipidemia and alcoholic abuse, and 5 with biliary disease; In Group 2 was made up of 16 patients, 12 men and 4 women, aged 45.1 ± 9.2 years, including 11 patients with hyperlipidemia and 5 with biliary disease; and the time interval for HF ranged from 5-20 hours.

APACHEII scores were 13.9 ± 3.8 and 12.1 ± 4.2 in the two groups; and there was no difference ($P > 0.05$) before hemofiltration.

Methods

Hemofilters HF was performed using Diapact CRRT machine from B.Braun Co, Germany. And filters used for HF were polysulphone filters (Fresenius Medical Care, AV 600 S, with the cutoff of molecular weight of 30 KD); and extracorporeal lines were primed with one liter of heparinized saline (5 000 IU/L). Vascular access was obtained by two Gambro catheters inserted into each femoral vein. Low molecular weight heparin (Fragmin, 5 000/ampule) was administered at dose of 100-140 IU/kg, and bolus injection was made before HF.

Ultrafiltrate was replaced with substitute made according to electrolyte and blood glucose. Pre-dilution mode was used. Extracorporeal blood flow ranged from 250 to 360 ml/min. Ultrafiltrating rate was controlled within 50-300 ml/h.

Indication for stopping HF

In group 1, SVVH was stopped when the abdominal signs disappeared, and heart rate and breath rate were less than 90 beats/min and 20 times/min, respectively. HF was stopped if SVVH was continued when heart rate as well as breath rate were more than 90 beats/min and 20 times/min again (Group 2).

Follow-up

CT scanning was done every month; and intra-pancreatic as well as extra-pancreatic changes were analyzed.

Prognostic indices

Conservative curing rate, hospital stay, cost and survival rate were analyzed. The conservative cure referred to intra-pancreatic and extra-pancreatic lesions absorbed entirely and /or formed into pseudocyst without symptoms.

Statistical calculations

Data were reported as mean \pm standard deviation, and analyzed using Student's *t* and or *q* square.

RESULTS

Time interval

Time interval for HF was 3.81 ± 1.3 hrs in Group 1 and 9.38 ± 2.9 hrs in Group 2, $P < 0.05$.

Comparison of parameters of SVVH and LVVH

There was no difference in age, beginning time for HF, APACHEII scores before HF, substitute rate, blood flow and ultrafiltrate rate between the two groups, (Table 1).

There was significant difference in the amount of purified blood, ultrafiltrate, heparin, colloid, substitute and filters between the two groups, $P < 0.05$; and these indices were closely related to the time interval, (Table 1).

Table 1 Parameters of hemofiltration in two groups

Indices	Group 1 (≤ 5 h)	Group 2 (5-20 h)	P values
Number	20	16	
Age (years)	52.4 ± 14.2	45.1 ± 9.2	> 0.05
APACHEII before HF	13.9 ± 3.8	12.1 ± 4.2	> 0.05
Beginning time (hr)	45.9 ± 21.2	37.4 ± 12.5	> 0.05
Rate of substitute (ml/h)	2700 ± 500	2880 ± 300	> 0.05
Blood flow (ml/min)	200-250	250-360	> 0.05
Rate of ultrafiltrate(ml/h)	342.5 ± 251	240 ± 72	> 0.05
Time interval (hr)	3.81 ± 1.3	9.38 ± 2.9	< 0.01
Colloid volume (ml)	700 ± 258.2	1500 ± 852.9	< 0.01
The amount of heparin (IU)	7700 ± 2341.1	12000 ± 6000	< 0.01
Substitute volume(L)	9.5 ± 3.2	35.1 ± 16.5	< 0.01
Ultrafiltrate Volume(ml)	1040 ± 520	2400 ± 700	< 0.01
Filters	1.44 ± 0.73	2.75 ± 1.4	< 0.05

Prognosis

Conservative curing rate was more significantly increased in Group 1 than in Group 2, $P < 0.05$; but cost was significantly decreased, $P < 0.05$, (Table 2).

Survival rate was significantly higher in Group 1 than in Group 2, $P < 0.25$; but hospital stay was significantly shortened, $P < 0.2$.

Table 2 Indices of prognosis of severe acute pancreatitis

Indices	Group1 (≤ 5 h)	Group 2 (5-20 h)	P values
Number	20	16	
Conservative curing rate (%)	90 % (18/20)	56.3 % (9/16)	< 0.05
Survival rate (%)	95 % (19/20)	81.3 % (13/16)	< 0.25
Cost ($\times 10^4$ yuan)	5.66 ± 5.64	13.7 ± 10.5	< 0.05
Hospital stay (d)	44.3 ± 17.3	55.2 ± 29.5	< 0.2

DISCUSSION

Up to date, strategies have been used to target cytokines, such as cytokine anti-body, purification and transient transfection of human IL-10 gene. In term of neutralization of antibody, for example, Hughes^[8,9] reported that scores for pathology of pancreas were significantly improved by TNF α blockade. But, the method is only one antibody to one antigen to neutralize cytokine, and it is far from combating with complicated cytokines network. According to Grewal^[21] and Kingsnorth^[10], despite amelioration of ascites production by TNF α blockade, histologic evaluation scoring was not statistically different. And IL-1r antagonist only modified the changes in vital organs induced by SAP^[22], it did not affect the degree of local pancreatic insult. This method is controversial and has not been reported in clinical trial till now. Denham^[23] demonstrated that transient transfection of a human IL-10 gene decreased the severity of pancreatitis during acute inflammatory process. It is only an animal experiment, that blood purification^[14,18,24], such as plasmapheresis, hemadsorption, hemofiltration, can remove the mediators from circulation. Among them, hemofiltration is used widely in clinics.

In 1991, Blinzler reported that CVVH can be used to treat SAP at early stage^[18], although no organ failure happened. This is the earliest report of CVVH to blockade pancreatic necrosis. In 1994, Gehbart^[2] reported that CVVH was applied to 11 patients with most serious clinical course and multi-system failure. The overall lethality rate of the treated patients was 7.9 %. In 1998, Schmidt^[25] suggested that CVVH had been proven to be of no efficacy. In 1999, Yekebas^[19] performed animal experiment to investigate the effects of CVVH on SAP, showing that the survival time was significantly prolonged. In 2001, Pupelis^[26] applied that hemodialysis, hemofiltration, plasmapheresis, hemadsorption to SAP patients concomitant with organ failure, and achieved a good result.

These investigations have shown that CVVH is of benefit for treatment of SAP or multiple organ dysfunction secondary to SAP. We performed SVVH within 72 hours after onset of the disease, and obtained satisfactory clinical efficacy^[17]. The present study showed that survival rate in Group 1 was 95 %, which was much higher than that of 92 % from the 11 patients in Gehbart's report^[2]. Pupelis^[26] reported a survival rate of 80 % using CVVH and hemodialysis to treat SAP, which is the same as that of non-hemofiltration^[5]; and its conservative curing rate (38.2 %, 13/34) is much lower than ours (90 %, 18/20), ($\chi^2 = 13.8$, $P = 0.002$). Miller^[27] reported a survival rate of only 71.4 % (5/7) using CVVH to treat SAP. It is much lower than ours (95 %, 19/20), ($\chi^2 = 2.917$, $P = 0.088$). In the present study, the conservative curing rate, cost, hospital stay and survival rate were improved in SVVH group as compared with LVVH group. The conservative curing rate and cost were especially improved significantly ($P < 0.05$). Why is the efficacy decreased in LVVH group or CVVH group?

In the early stage of SAP, pro-inflammatory and anti-inflammatory cytokines are inter-related in a united entity under pathological state. Any of them which is over-produced or less-produced, will contribute to different pathophysiologic response, such as systemic inflammatory response syndrome (SIRS), compensatory anti-inflammatory response syndrome (CARS), Mixed antagonist response syndrome (MARS)^[28,29]. According to this assumption, pro-inflammatory and anti-inflammatory cytokines should be in a dynamic balance state through cytokines eliminated partly. The pro-inflammatory and anti-inflammatory level was modulated through 4h-SVVH^[17]; the former (TNF, IL-1, IL-8, IL-6 and sIL-2R) was decreased and the latter (IL-2, IL-10) was increased. Monocyte cytokine (TNF, IL-6, IL-8) production was increased in association with systemic complications in acute pancreatitis^[30]; and IL-10 prevented pancreatic necrosis^[31,32] as well as death in lethal necrotizing pancreatitis^[33]. SIRS was doomed to be interrupted and the severity of SAP was decreased significantly. This demonstrates that dynamic balance of pro- and anti-inflammatory cytokines is established at the pathological state. When T and B lymphocytes and monocytes are activated, membrane receptor of IL-2 would be expressed; and soluble receptor of IL-2 (sIL-2R) is liberated into circulation^[34] Simultaneously. sIL-2R can combine with IL-2; and if it is over produced, serum level of IL-2 will be decreased. It is reported that IL-2 production was decreased in acute pancreatitis^[35]. And IL-2 is the major factor that activated T and B lymphocytes and decreased infection rate^[36]. Therefore, over-produced sIL-2R may lead to decreased immune function. In clinical trial^[17], serum level of sIL-2R was decreased significantly through SVVH, however, serum concentration of IL-2 was increased, and the infection rate was decreased. At the same time, the time of infection occurrence was postponed, suggesting that immune function has been up-regulated. CVVH may contribute to immune-paralysis due to over-removed cytokines and inhibit the up-regulation of PMN phagocytosis capacity after intra-abdominal sepsis^[37]. Thus, dynamic balance obtained between pro-inflammatory cytokines and anti-inflammatory cytokines is imbalanced again. So, there is no difficulty in understanding increased infection and earlier operation in LVVH group.

During conservative treatment, two factors, immune function of body and optimal application of antibiotics, are important in the prevention of pancreatic infection. Ciprofloxacin and Metronidazole were infused to 36 patients on admission. If the body temperature was increased, carpenems plus fluconazole would be infused empirically. Simultaneously, body fluids were cultured. If the temperature was controlled, antibiotics were not stopped until the enteral nutrition had been fed for one week. On the contrary, antibiotics were changed according to the cultures. Given temperature was still abnormal through optimal antibiotics and strengthened immune function, and infection in other sites was excluded, drainage of infected necrotic pancreata should be performed. This demonstrated that pancreatic infection had not been controlled by intensive treatments from 48 to 72 hours.

In Group 1, pseudocysts were entirely absorbed from 2 months to 2 years in 15 patients, and 3 patients underwent jejuno-pseudocyst Roux-en-Y anastomosis or gastropseudocyst anastomosis. Seven patients underwent drainage within 20 to 30 days after onset of the disease in Group 2.

According to our clinical trial, once indices for cessation of hemofiltration were reached, it should be stopped immediately. Additionally, although indices for stopping HF has not been reached with more than 8 h-HF, hemofiltration should also be stopped as we seek other factors leading to the change of heart rate and breath rate, because they may be affected by other factors.

On admission, patients should be strictly estimated that whether he or she has the indication for SVVH. If he or she is below 70 years old, time is within 72 hours after onset of the disease and without billiary obstruction, it is wise to perform SVVH. It did not reach the peak of the disease until the time interval for abdominal pain was 72 hours. Within 72 hours, cascades of cytokines were blockaded easily, and vicious cycle was not formed between secondary chemokines released^[38] and cytokines. Thus, 72 hours should be emphasized heavily. And the earlier the hemofiltration began, the better the result was. Patients with ACST underwent operation, EST or nasobilliary catheter inserted to drain bile. SVVH could still be performed after these.

Although prognosis was improved through SVVH, it is only a new method in synthetical treatment strategies for SAP. It can not replace other measures. For example, Pixiao (a traditional Chinese medicine) is applied continuously to the whole abdomen after hemofiltration is stopped, and until it has no effects.

In summary, SVVH is superior to LVVH, and LVVH is better than CVVH in the treatment of SAP in early stage. Much more significant side-effects occurred due to longer time interval for HF.

REFERENCES

- 1 **Hartwig W**, Maksan SM, Foitzik T, Schmidt J, Herfarth C, Klar E. Reduction in mortality with delayed surgical therapy of severe acute pancreatitis. *J Gastrointest Surg* 2002; **6**: 481-487
- 2 **Gebhardt C**, Bodeker H, Blinzler L, Kraus D, Hergdt G. Changes in therapy of severe acute pancreatitis. *Chirurg* 1994; **65**: 33-40
- 3 **Yamauchi J**, Takeda K, Shibuya K, Sunamura M, Matsuno S. Continuous regional application of protease inhibitor in the treatment of acute pancreatitis. An experimental study using closed duodenal obstruction model in dogs. *Pancreatology* 2001; **1**: 662-667
- 4 **Eibl G**, Buhr HJ, Foitzik T. Therapy of microcirculatory disorders in severe acute pancreatitis: what mediators should we block? *Intensive Care Med* 2002; **28**: 139-146
- 5 **Bank S**, Singh P, Pooran N, Stark B. Evaluation of factors that have reduced mortality from acute pancreatitis over the past 20 years. *J Clin Gastroenterol* 2002; **35**: 50-60
- 6 **Norman J**. The role of cytokines in the pathogenesis of acute pancreatitis. *Am J Surg* 1998; **175**: 76-83
- 7 **Van Laethem**, Eskinazi R, Louis H, Richaert F, Bobberrecht P, Deviere. Multisystemic production of interleukin 10 limits the severity of acute pancreatitis in mice. *Gut* 1998; **43**: 408-413
- 8 **Hughes CB**, Grewal HP, Gaber LW, Kotb M, Mohey el-Din AB, Mann L, Gaber AO. Anti-TNF α therapy improves survival and ameliorates the pathophysiologic sequelae in acute pancreatitis in the rat. *Am J Surg* 1996; **171**: 274-280
- 9 **Hughes CB**, Gaber LW, Mohey el-Din AB, Kotb M, Mann L, Gaber AO. Inhibition of TNF improves survival in an experimental model of acute pancreatitis. *Am Surg* 1996; **62**: 8-13
- 10 **Kingsnorth A**. Role of cytokines and their inhibitors in acute pancreatitis. *Gut* 1997; **40**: 1-4
- 11 **Osman MO**, Gesser B, Mortensen JT, Matsushima K, Jensen SL, Larsen CG. Profiles of pro-inflammatory cytokines in the serum of rabbits after experimentally induced acute pancreatitis. *Cytokine* 2002; **17**: 53-59
- 12 **Oda S**, Hirasawa H, Shiga H, Nakanishi K, Matsuda K, Nakamura M. Continuous hemofiltration/hemodiafiltration in critical care. *Ther Apher* 2002; **6**: 193-198
- 13 **Gotloib L**, Barzilay E, Shustak A, Wais Z, Jaichenko J, Lev A. Hemofiltration in septic ARDS. The artificial kidney as an artificial endocrine lung. *Resuscitation* 1986; **13**: 123-132
- 14 **Gotloib L**, Shostak A, Lev A, Fudin R, Jaichenko J. Treatment of surgical and non-surgical septic multiple organ failure with bicarbonate hemodialysis and sequential hemofiltration. *Int Care Med* 1995; **21**: 104-111
- 15 **Barzilay E**, Kessler D, Berlot G, Gullo A, Geber D, Ben Zeev I. Use of extracorporeal supportive techniques as additional treatment for septic-induced multiple organ failure patients. *Crit Care*

- Med* 1989; **17**: 634-637
- 16 **Gomez A**, Wang R, Unruh H, Unruh H, Light RB, Bose D, Chau T, Correa E, Mink S. Hemofiltration reverses left ventricular dysfunction during sepsis in dogs. *Anesthesiology* 1990; **73**: 671-685
- 17 **Mao EQ**, TangYQ, Han TQ, Yuan ZR, Zhang SD. Effects of short veno-venous hemofiltration on severe acute pancreatitis. *Zhonghua Waike Zazhi* 1999; **37**: 141-143
- 18 **Blinzler L**, Hausßer J, Bodeker H, Zaune U, Martin E, Gebhardt C. Conservative treatment of severe necrotizing pancreatitis using early continuous veno-venous HF. In: Sieberth HG, Mann H, Stummvoll HK, eds. Continuous hemofiltration. *Contrib Nephrol* 1991; **93**: 234-236
- 19 **Yekebas EF**, Treede H, Knoefel WT, Bloechle C, Fink E, Izbicki JR. Influence of zero-balanced hemofiltration on the course of severe experimental pancreatitis in pigs. *Ann Surg* 1999; **229**: 514-522
- 20 **Bradley EL 3rd**. A clinically based classification system for acute pancreatitis. Summary of the international symposium on acute pancreatitis. Atlanta, Ga, September 11 through 13, 1992. *Arch Surg* 1993; **128**: 586-590
- 21 **Grewal HP**, Mohey el Din A, Gaber L, Kotb M, Gaber O. Amelioration of the physiologic and biochemical changes of acute pancreatitis using an anti-TNF α polyclonal antibody. *Am J Surg* 1994; **167**: 214-219
- 22 **Tanaka N**, Murata A, Uda K, Uda Ki, Toda H, Kato T, Hayashida H, Matsuura N, Mori T. Interleukin-1 receptor antagonist modifies the changes in vital organs induced by acute necrotic pancreatitis in a experimental model. *Crit Care Med* 1995; **23**: 901-908
- 23 **Denham W**, Denham D, Yang J, Carter G, Mackay S, Moldawer LL, Carey LC, Norman J. Transient human gene therapy. A novel cytokine regulatory strategy for experimental pancreatitis. *Ann Surg* 1998; **227**: 812-820
- 24 **Bellomo R**, Tipping P, Boyce N. Continuous veno-venous hemofiltration with dialysis removes cytokines from the circulation of septic patients. *Crit Care Med* 1993; **21**: 522-526
- 25 **Schmidt J**, Werner J. Acute pancreatitis: reliable and prospective conservative therapy. *Langenbecks Arch Chir Suppl Kongressbd* 1998; **115**: 434-438
- 26 **Pupelis G**, Austrums E, Snippe K. Blood purification methods for treatment of organ failure in patients with severe pancreatitis. *Zentralbl Chir* 2001; **126**: 780-784
- 27 **Miller BJ**, Henderson A, Strong RW, Fielding GA, DiMarco AM, O' Loughlin BS. Necrotizing pancreatitis: operating for life. *World J Surg* 1994; **18**: 906-911
- 28 **Davies MG**, Hagen PO. Systemic inflammatory response syndrome. *Br J Surg* 1997; **84**: 920-935
- 29 **Bone RC**. Sir Isaac Newton, Sepsis, Sirs and Cars. *Crit Care Med* 1996; **24**: 1125-1127
- 30 **McKay CJ**, Gallagher G, Brooks B, Imrie CW, Baxter JN. Increased monocyte cytokine production in association with systemic complications in acute pancreatitis. *Br J Surg* 1996; **83**: 919-923
- 31 **Van Laethem JL**, Marchant A, Delvaux A, Goldman M, Robberecht P, Velu T, Deviere J. Interleukin 10 prevents necrosis in murine experimental acute pancreatitis. *Gastroenterology* 1995; **108**: 1917-1922
- 32 **Rongione AJ**, Kusske AM, Kwan K, Ashley SW, Reber HA, Mcfadden DW. Interleukin-10 reduces the severity of acute pancreatitis in rats. *Gastroenterology* 1997; **112**: 960-967
- 33 **Kusske AM**, Rongione AJ, Ashley SW, Mcfadden DW, Reber HA. Interleukin-10 prevents death in lethal necrotizing pancreatitis in mice. *Surgery* 1996; **120**: 284-289
- 34 **Salomone T**, Boni P, Serra C, Morselli-Labate AM, Di Gioia AL, Romboli M, Guariento A. The soluble interleukin-2 receptor, peripheral blood, and reticulocyte fractions in acute pancreatitis. *Int J Pan* 1996; **20**: 197-203
- 35 **Curley P**, Nestor M, Collins K, Saporschetz I, Mendez M, Mannick JA, Rodrick M. Decreased Interleukin-2 production in murine acute pancreatitis: potential for immunomodulation. *Gastroenterology* 1996; **110**: 583-588
- 36 **Kusske AM**, Rongione AJ, Reber HA. Cytokine and acute pancreatitis. *Gastroenterology*, 1996; **110**: 639-642
- 37 **Discipio AW**, Burchard KW. Continuous Arteriovenous Hemofiltration attenuates polymorphonuclear leukocyte phagocytosis in porcine intra-abdominal sepsis. *Am J Surg* 1997; **173**: 174-180
- 38 **Grady T**, Liang P, Ernst SA, Logsdon CD. Chemokine gene expression in rat pancreatic acinar cells is an early event associated with acute pancreatitis. *Gastroenterology* 1997; **113**: 1966-1975

Edited by Ma JY

Expression of p57^{kip2}, Rb protein and PCNA and their relationships with clinicopathology in human pancreatic cancer

Hui Yue, Yan-Li Na, Xin-Li Feng, Shu-Ren Ma, Fu-Lin Song, Bo Yang

Hui Yue, Yan-Li Na, Xin-Li Feng, Shu-Ren Ma, Fu-Lin Song, Bo Yang, Department of Gastroenterology and Pathology, General Hospital of Shenyang Military Region, Shenyang 110016, Liaoning Province, China

Correspondence to: Dr. Hui Yue, Department of Gastroenterology, General Hospital of Shenyang Military Region, Shenyang 110016, Liaoning Province, China. yh12070430@sina.com

Telephone: +86-24-23056031 **Fax:** +86-24-83910176

Received: 2002-07-23 **Accepted:** 2002-08-23

Abstract

AIM: To investigate the effects of inhibiting factor of cell cycle regulation p57^{kip2}, retinoblastinoma protein (Rb protein) and proliferating cell nuclear antigen (PCNA) in the genesis and progression of human pancreatic cancer.

METHODS: The expression of p57^{kip2}, Rb protein and PCNA in tumor tissues and adjacent tissues of 32 patients with pancreatic cancer was detected with SP immunohistochemical technique.

RESULTS: p57^{kip2} protein positive-expression rate in tumor tissues of pancreatic cancer was 46.9 %, which was lower than that in adjacent pancreatic tissues (75.0 %) ($\chi^2=5.317$, $P<0.05$), p57^{kip2} protein positive-expression correlated significantly with tumor cell differentiation (well-differentiation versus moderate or low-differentiation, $P<0.05$) but did not correlate significantly with lymph node metastasis (lymph node metastasis versus non-lymph node metastasis, $P>0.05$); Rb gene protein positive-expression rate in tumor tissues was 50.0 %, which was also lower than that in adjacent pancreatic tissues (78.1 %) ($\chi^2=5.497$, $P<0.05$); PCNA positive-expression rate was 71.9 %, being higher than that in adjacent pancreatic tissues (43.8 %) ($\chi^2=5.189$, $P<0.05$), PCNA positive-expression also correlated significantly with tumor cell differentiation and lymph node metastasis (well-differentiation versus moderate or low-differentiation, lymph node metastasis versus non-lymph node metastasis, $P<0.05$). Rb protein positive-expression rate in the tumor tissues of p57^{kip2} protein positive-expression group was 53.3 %; and Rb protein positive-expression rate in the tumor tissues of p57^{kip2} protein negative-expression group was 47.1 %. There was no significant relationship between the two groups ($r=0.16507$, $P>0.05$).

CONCLUSION: The decreased expression of p57^{kip2}, Rb protein or over-expression of PCNA protein might contribute to the genesis or progression of pancreatic cancer, p57^{kip2}, Rb protein and PCNA may play an important role in genesis and progression of pancreatic cancer.

Yue H, Na YL, Feng XL, Ma SR, Song FL, Yang B. Expression of p57^{kip2}, Rb protein and PCNA and their relationships with clinicopathology in human pancreatic cancer. *World J Gastroenterol* 2003; 9(2): 377-380

<http://www.wjgnet.com/1007-9327/9/377.htm>

INTRODUCTION

The abnormality of mammalian cell cycle regulation is an important cause of cell over-proliferation and oncogenesis^[1]. Orderly progression of the cell cycle is controlled by a family of cyclins and cyclin-dependent kinase (CDKs) which are restrictively counterbalanced by CDK inhibitors(CDKIs)^[2].

Two distinct families of CDKIs, the INK4 and CIP/KIP families which regulate the the activity of the cyclin-CDK complexes, have been described^[3]. The CIP/KIP family, including p21, p27 and p57 proteins, harbors homologous CDK binding domains or fuction of cyclin-CDK complexes and makes cell cycle to arrest in G₁ phase. Retinoblastinoma protein (Rb protein) is one of the tumor suppressor proteins and affects the progression of G₁ phase of cell cycle. The expression of proliferating cell nuclear antigen (PCNA) is obviously associated with cell proliferation. The relationships between p57^{kip2} protein and pancreatic cancer has not been reported in China. In this study, the expression of p57^{kip2}, Rb and PCNA protein in the tissues of pancreatic cancer were detected with immunohistochemical technique to investigate the effects of inhibiting proteins of cell cycle regulation p57^{kip2}, Rb protein and PCNA in the genesis and progression of human pancreatic cancer.

MATERIALS AND METHODS

Patients and tumor samples

Thirty-two specimens of primary human pancreatic cancer collected at pancreatic resection performed in the Hepatobiliary Department of General Hospital of Shenyang Military Region and the First Clinical College, China Medical University were studied. Of the patients, 20 (62.5 %) were male and 12 (37.5 %) were female. The mean age was 59.5 years (range, 26-72 years). Nineteen (59.4 %) were well-differentiated pancreatic cancer, thirteen (40.6 %) were moderate or low-differentiated pancreatic cancer. Twelve (37.5 %) had lymph node metastasis. All the patients were confirmed by clinicopathological diagnosis. Tumor tissues and adjacent tissues were obtained from the thirty-two specimens of primary human pancreatic cancer and were fixed in 100 mL/L buffered formalin, processed routinely and embedded in paraffin. In each case, all available hematoxylin and eosin-stained sections were reviewed, and representative blocks were chosen for further studies.

Immunohistochemical study

Four micrometer-thick sections from the formalin-fixed paraffin-embedded tissues were placed on the poly-L-lysine-coated slide for immunohistochemistry. The expression of p57^{kip2}, Rb protein and PCNA were assessed by SP immunohistochemical method using an anti-human p57^{kip2} monoclonal antibody (57P06), anti-human Rb protein monoclonal antibody (1F8), anti-human PCNA monoclonal antibody (PC10) and UltraSensitive™ S-P kit (kit-9720). The deparaffinized sections were boiled in the EDTA buffer at high temperature and high pressure for antigen retrieval and incubated with each antibody at 4 °C overnight. Immunohistochemical staining for these proteins was then performed according to the UltraSensitive™ S-P kit manual.

All the reagents were supplied by Maixin-Bio Co. Fuzhou, China. The cells with brown-yellow granules in the nuclei or cytoplasm were taken as positive cells. Five hundred cells on each slide were counted. The slides were distinguished as negative (-), positive (+), strong positive (++) and strongest positive (+++) when the count of positive cells were less than 10 %, ranging from 10-25 %, ranged from 25-50 %, and more than 50 % respectively for p57^{kip2} and Rb proteins. The slides were distinguished as negative (-), and positive (+) when the count of positive cells were less than 50 % and exceeded 50 % for PCNA respectively.

Statistical analysis

The Chi-square test and Fisher exact test of SAS system statistical software (Release 6.12) were adopted. $P < 0.05$ was considered as the significant level.

RESULTS

Expression of p57^{kip2} protein

p57^{kip2} protein was located in the nuclei or cytoplasm of normal pancreatic cells and positive pancreatic cancer cells with brown-yellow granules (Figure 1). p57^{kip2} protein positive-expression rate in tumor tissues of pancreatic cancer was 46.9 %, which was lower than that (75.0 %) in adjacent pancreatic tissues ($\chi^2 = 5.317$, $P < 0.05$, Table 1). p57^{kip2} protein positive-expression rate in the moderate or low differentiated group was 23.1 %, being lower than that (63.2 %) in the well differentiated group ($\chi^2 = 4.979$, $P < 0.05$, Table 1). p57^{kip2} protein positive-expression rate in the lymph node metastasis group was 25.0 %, which was lower than that (60.0 %) in the non-lymph node metastasis group ($P > 0.05$, Table 1).

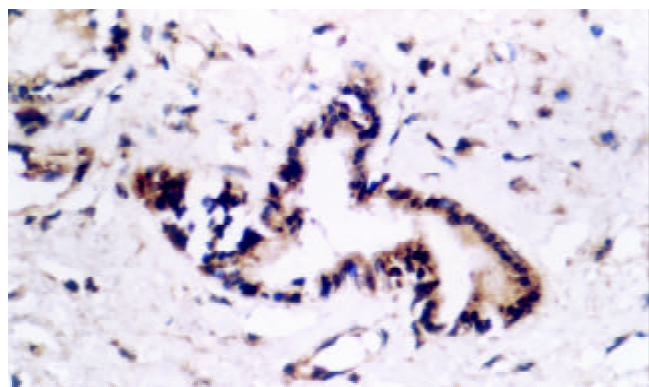


Figure 1 Expression of p57^{kip2} in tumor tissues of pancreatic cancer. SP×400.

Table 1 Expression of p57^{kip2} protein in pancreatic cancer tissues

Characteristics	p57 ^{kip2} protein expression				Rate (%)
	-	+	++	+++	
Tumor tissues	17	11	3	1	46.9 ^a
Adjacent tissues	8	13	6	5	75.0 ^a
Well-differentiated	7	9	2	1	63.2 ^b
Moderate or low-differentiated	10	2	1	0	23.1 ^b
Lymph node metastasis	9	2	1	0	25.0 ^c
Non- lymph node metastasis	8	9	2	1	60.0 ^c

^a $P < 0.05$, ^b $P < 0.05$, ^c $P > 0.05$.

Expression of Rb protein

Rb protein was located in the nuclei or cytoplasm of normal pancreatic cells and positive pancreatic cancer cells with brown-

yellow granules (Figure 2). Rb protein positive-expression rate in tumor tissues of pancreatic cancer was 50.0 %, which was lower than that (78.1 %) in adjacent pancreatic tissues ($\chi^2 = 5.497$, $P < 0.05$, Table 2). Rb protein positive-expression rate in the moderate or low differentiated group of pancreatic cancer was 46.2 %, being lower than that (52.6 %) in the well differentiation ($P > 0.05$, Table 2). Rb protein positive-expression rate in the lymph node metastasis group was 33.3 %, which was lower than that (60.0 %) in the non-lymph node metastasis group ($P > 0.05$, Table 2).

Table 2 Expression of Rb protein in pancreatic cancer tissues

Characteristics	Rb protein expression				Rate(%)
	-	+	++	+++	
Tumor tissues	16	10	2	4	50.0 ^a
Adjacent tissues	7	12	8	5	78.1 ^a
Well differentiated	9	4	2	4	52.6 ^b
Moderate or low-differentiated	7	6	0	0	46.2 ^b
Lymph node metastasis	8	3	1	0	33.3 ^c
Non- lymph node metastasis	8	7	1	4	60.0 ^c

^a $P < 0.05$, ^b $P > 0.05$, ^c $P > 0.05$.

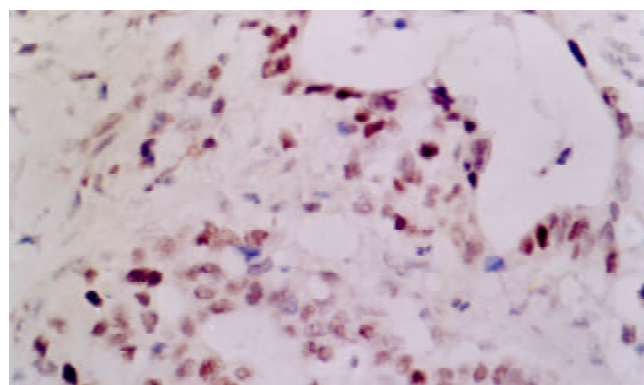


Figure 2 Expression of Rb protein in tumor tissue of pancreatic cancer. SP×400.

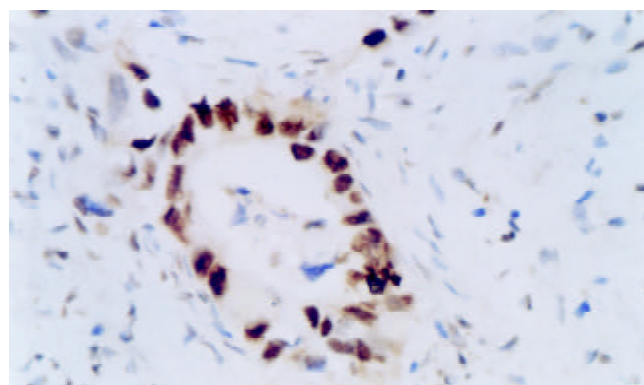


Figure 3 Expression of PCNA protein of tumor tissue in pancreatic cancer. SP×400.

Expression of PCNA protein

PCNA protein was located in the nuclei of normal pancreatic cells and positive pancreatic cancer cells with brown-yellow granules (Figure 3). PCNA protein positive-expression rate in tumor tissues of pancreatic cancer was 71.9 %, which was higher than that (43.8 %) in adjacent pancreatic tissues ($\chi^2 = 5.189$, $P < 0.05$, Table 3). PCNA protein positive-expression rate in the moderate or low differentiated group of pancreatic cancer was

92.3 %, which was higher than that (57.9 %) in the well differentiated group ($\chi^2=4.522$, $P<0.05$, Table 3). PCNA protein positive-expression rate in the lymph node metastasis group of pancreatic cancer was 100.0 %, which was higher than that (55.0 %) in the non-lymph node metastasis group ($\chi^2=7.513$, $P<0.05$, Table 3).

Table 3 Expression of PCNA protein in pancreatic cancer tissues

Characteristics	PCNA protein expression		
	-	+	Rate (%)
Tumor tissue	9	23	71.9 ^a
Adjacent tissue	18	14	43.8 ^a
Well-differentiation	8	11	57.9 ^b
Moderate or low-differentiation	1	12	92.3 ^b
Lymph node metastasis	0	12	100.0 ^c
Non- Lymph node metastasis	9	11	55.0 ^c

^a $P<0.05$, ^b $P<0.05$, ^c $P<0.05$.

Relationships of expression between p57^{kip2} and Rb protein

Rb protein positive-expression rate in the tumor tissues of p57^{kip2} protein positive-expression group was 53.3 %; and Rb protein positive-expression rate in the tumor tissues of p57^{kip2} protein negative-expression group was 47.1 %. There was no significant relationships between the two groups ($r=0.16507$, $P>0.05$, Table 4).

Table 4 Relationships between p57^{kip2} and Rb protein in pancreatic cancer

p57 ^{kip2}	Rb -expression				Rate(%)
	-	+	++	+++	
-	9	6	0	2	47.1
+	6	3	1	1	53.3
++	1	1	0	1	
+++		0	0	1	0

DISCUSSION

The question on cell cycle regulation is a hot issue of oncological research at present. The studies in recent years showed G1 phase regulation was a complex procedures which multiple cell factors took part in and abnormality of cell cycle regulation significantly correlated with the genesis and progression of tumors^[4-7]. p57^{kip2} gene was located in chromosome 11p15.5, and p57^{kip2} protein was a cell cycle inhibitor with molecular weight of 57kD which was included in the CIP/KIP family and similar to p21, p27 protein in functions^[8,9]. Lee *et al*^[10] suggested that the tumor suppressor mechanism of p57^{kip2} protein may be integrated with cyclin-CDK complexes and made cell cycle to arrest in the G₁ phase. Kondon *et al*^[11] considered that paternal alleles of p57^{kip2} were imprinted, maternal alleles of p57^{kip2} were expressed in the normal status, Loss of imprinting and imprinting mistakes of p57^{kip2} led to decrease at level of gene expression in the tumors. Matsumoto *et al*^[12] reported that p57^{kip2} protein positive-expression rate was 43.3±3.2 % with immunohistochemical technique in 92 patients with esophageal squamous cell carcinoma. The author considered that this was the first immunohistochemical study to characterize p57^{kip2} expression in non-neoplastic esophageal epithelium and esophageal squamous cell carcinoma in the year 2000. From then on, a few of studies about p57^{kip2} protein expression in human colorectal carcinoma, epithelial ovarian tumor, hepatocellular

carcinoma, neoplastic thyroid tissues, extrahepatic bile duct carcinoma and intrahepatic cholangiocellular carcinoma have been reported^[13-20], but the relationship between p57^{kip2} protein expression and pancreatic carcinoma was less reported^[21]. In this study, We found that p57^{kip2} protein positive-expression rate in tumor tissues of pancreatic cancer was significantly lower than that in adjacent tissues; the worse cancer cell differentiated, the lower expression of p57^{kip2} in tumor tissue was, and there was no correlation between the reduced expression of p57^{kip2} and lymph node metastasis. The results suggested that reduced expression of p57^{kip2} correlated with genesis and malignant degree of pancreatic cancer. Rb gene was the first isolated and detected tumor suppressor gene, and was an important factor in regulating system of G₁ phase as well. Inactivity of Rb protein was associated with liver carcinoma, small cell lung carcinoma, gastric cancer and pancreatic cancer apart from retinoblastoma^[22-25]. The results in this study showed Rb protein positive-expression rate in tumor tissues was significantly lower than that in adjacent tissues, which suggested reduced expression or loss of p57^{kip2} protein correlated with genesis of pancreatic cancer. The lower expression of p57^{kip2} protein decreased, the higher malignant degree and lymph node metastasis increased, but there was no significant difference between two groups possibly because of the limited cases of pancreatic cancer. PCNA was δ -assistant factor of DNA synthetase, took part in DNA biological synthesis and regulated cell cycle and cell proliferation by tetramer with cyclin, CDK and p21. Over-expression of PCNA was associated with a variety of tumors of digestive system^[26-35]. The results in this study showed PCNA protein positive-expression rate in tumor tissues was higher than that in adjacent tissues of pancreatic cancer, PCNA protein positive-expression rate in the moderate or low differentiated group was higher than that in the well differentiated group. PCNA protein positive-expression rate in the lymph node metastasis group was higher than that in the non-lymph node metastasis group. these suggested that over-expression of PCNA was associated with the genesis and progression of pancreatic cancer, and malignant proliferating status of pancreatic cancer determined by expression of PCNA was of an practical value. our results suggested that cell proliferative activity was high for the negative or reduced expression of p57^{kip2} and Rb protein, furthermore, p57^{kip2}, Rb protein played a suppressor role in cell proliferation. There was no significant difference in Rb protein positive-expression rate between p57^{kip2} positive-expression group and p57^{kip2} negative-expression group, suggesting there was no significant correlation in tumor suppression between p57^{kip2} protein and Rb protein.

In summary, our findings in p57^{kip2}, Rb and PCNA expression at the protein level suggested that loss of p57^{kip2}, Rb protein expression or over-expression of PCNA protein may contribute to the genesis or progression of pancreatic cancer, p57^{kip2}, Rb and PCNA proteins might play a regulating role in different pathways of cell cycle.

REFERENCES

- 1 **Kamb A**, Gruis NA, Weaver-Feldhaus J, Liu Q, Harshman K, Tavitgian SV, Stockent E, Day RS 3rd, Johson BE, Skolnick MH. A cell cycle regulator potentially involved in genesis of many tumor types. *Science* 1994; **264**: 436-440
- 2 **Grana X**, Reddy EP. Cell cycle control in mammalian cells: role of cyclins, cyclin dependent kinase(CDKs), growth suppressor and cyclin dependent kinase inhibitors(CDKIs). *Oncogene* 1995; **11**: 211-219
- 3 **Sherr CJ**. G₁ phase progression: cyclins on cue. *Cell* 1994; **79**: 551-555
- 4 **Sherr CJ**. Cancer cell cycles. *Science* 1996; **274**: 1672-1677
- 5 **Kamb A**. Cell-cycle regulators and cancer. *Trends Genet* 1995; **11**: 136-140

- 6 **Hunter T**, Pines J. Cyclins and cancer II: CyclinD and CDK inhibitors come of age. *Cell* 1994; **79**: 573-582
- 7 **Clurman BE**, Roberts JM. Cell cycle and cancer. *J Natl Cancer Inst* 1995; **87**: 1499-1501
- 8 **Matsuoka S**, Edwards MC, Bai C, Parker S, Zhang P, Baldini A, Harper JW, Elledge SJ. p57^{kip2} a structurally distinct member of the p21CIP1 Cdk inhibitor family, is a candidate tumor suppressor gene. *Genes Dev* 1995; **9**: 650-662
- 9 **Orlow I**, Iavarone A, Crider-Miller SJ, Bonilla F, Latres E, Lee MH, Gerald WL, Massague J, Weissman BE, Cordon-Cardo C. Cyclin-dependent kinase inhibitor p57^{kip2} in soft tissue sarcomas and Wilms tumor. *Cancer Res* 1996; **56**: 1219-1221
- 10 **Lee MH**, Reynisdottir I, Massague J. Cloning of p57^{kip2}, a cyclin dependent kinase inhibitor with unique domain structure and tissue distribution. *Genes Dev* 1995; **9**: 639-649
- 11 **Kondo M**, Matsuoka S, Uchida K, Osada H, Nagatake M, Takagi K, Harper JW, Takahashi T, Elledge SJ, Takahashi T. Selective maternal allele loss in human lung cancers of the maternally expressed p57^{kip2} gene at 11p15.5. *Oncogen* 1996; **12**: 1365-1368
- 12 **Matsumoto M**, Furihata M, Ohtsuki Y, Sasaguri S, Ogoshi S. Immunohistochemical characterization of p57^{kip2} expression in human esophageal squamous cell carcinoma. *Anticancer Res* 2000; **20**: 1947-1952
- 13 **Noura S**, Yamamoto H, Sekimoto M, Takemasa I, Miyake Y, Ikenaga M, Matsuura N, Monden M. Expression of second class of KIP protein p57KIP2 in human colorectal carcinoma. *Int J Oncol* 2001; **19**: 39-47
- 14 **Ito Y**, Takeda T, Sakon M, Tsujimoto M, Monden M, Matsuura N. Expression of p57/Kip2 protein in hepatocellular carcinoma. *Oncology* 2001; **61**: 221-225
- 15 **Nakai S**, Masaki T, Shiratori Y, Ohgi T, Morishita A, Kurokohchi K, Watanabe S, Kuriyama S. Expression of p57(KIP2) in hepatocellular carcinoma: relationship between tumor differentiation and patient survival. *Int J Oncol* 2002; **20**: 769-775
- 16 **Schwarze SR**, Shi Y, Fu VX, Watson PA, Jarrard DF. Role of cyclin-dependent kinase inhibitors in the growth arrest at senescence in human prostate epithelial and uroepithelial cells. *Oncogene* 2001; **20**: 8184-8192
- 17 **Ito Y**, Yoshida H, Nakano K, Kobayashi K, Yokozawa T, Hirai K, Matsuzuka F, Matsuura N, Kuma K, Miyauchi A. Expression of p57/Kip2 protein in normal and neoplastic thyroid tissues. *Int J Mol Med* 2002; **9**: 373-376
- 18 **Rosenberg E**, Demopoulos RI, Zeleniuch-Jacquotte A, Yee H, Sorich J, Speyer JL, Newcomb EW. Expression of cell cycle regulators p57(KIP2), cyclin D1, and cyclin E in epithelial ovarian tumors and survival. *Hum Pathol* 2001; **32**: 808-813
- 19 **Ito Y**, Takeda T, Sasaki Y, Sakon M, Yamada T, Ishiguro S, Imaoka S, Tsujimoto M, Monden M, Matsuura N. Expression of p57/Kip2 protein in extrahepatic bile duct carcinoma and intrahepatic cholangiocellular carcinoma. *Liver* 2002; **22**: 145-149
- 20 **Lee MH**, Yang HY. Negative regulators of cyclin-dependent kinases and their roles in cancers. *Cell Mol Life Sci* 2001; **58**: 1907-1922
- 21 **Ito Y**, Takeda T, Wakasa K, Tsujimoto M, Matsuura N. Expression of p57/Kip2 protein in pancreatic adenocarcinoma. *Pancreas* 2001; **23**: 246-250
- 22 **Zhou Y**, Gao SS, Li YX, Fan ZM, Zhao X, Qi YJ, Wei JP, Zou JX, Liu G, Jiao LH, Bai YM, Wang LD. Tumor suppressor gene p16 and Rb expression in gastric cardia precancerous lesions from subjects at a high incidence area in northern China. *World J Gastroenterol* 2002; **8**: 423-425
- 23 **Hilgers W**, Rosty C, Hahn SA. Molecular pathogenesis of pancreatic cancer. *Hematol Oncol Clin North Am* 2002; **16**: 17-35
- 24 **Gerdes B**, Ramaswamy A, Ziegler A, Lang SA, Kersting M, Baumann R, Wild A, Moll R, Rothmund M, Bartsch DK. p16INK4a is a prognostic marker in resected ductal pancreatic cancer: an analysis of p16INK4a, p53, MDM2, an Rb. *Ann Surg* 2002; **235**: 51-59
- 25 **Sunamura M**, Motoi F, Oonuma M, Hoshida T, Matsuno S. Gene therapy for pancreatic cancer. *Gan To Kagaku Ryoho* 2002; **29**: 398-404
- 26 **Zhuang XQ**, Lai RQ, Shun GH, Wang XH, Yuan SZ. Prognostic significance of expression of p53 protein and PCNA in human colorectal carcinoma. *Shijie Huaren Xiaohua Zazhi* 1999; **7**: 616
- 27 **Zheng XX**, Wang XZ, Lin GZ, Wang P. Expression of C-erbB-2 gene production and PCNA in human colorectal carcinoma and clinical significance. *Shijie Huaren Xiaohua Zazhi* 1999; **7**: 274
- 28 **Xu QW**, Li YS, Zhu HG. Relationships between expression of p53 protein, PCNA, CEA and lymph node metastasis in human colorectal carcinoma. *Shijie Huaren Xiaohua Zazhi* 1998; **6**: 244-246
- 29 **Feng XH**, Liu K, Wang ZH, Zhou SY, Tang XP. Significance and expression of PCNA in human esophageal squamous cell carcinoma. *Shijie Huaren Xiaohua Zazhi* 1999; **7**: 190
- 30 **Zhao GM**, Zhao WX, He RZ, Shu W, Zhang LJ. Expression of p53, PCNA and local non-cell immunology in human esophageal carcinoma. *Shijie Huaren Xiaohua Zazhi* 2001; **9**: 714-715
- 31 **Yie H**, Feng ZZ, Liu YF, Yuan ZH. Relationships between expression of P53, P21, nm23, PCNA and prognostic factors in hepatocellular carcinoma. *Shijie Huaren Xiaohua Zazhi* 1999; **7**: 160
- 32 **Shen XB**, Zhao XM, Hu JG, Jin XP, Wang J. Significance of cell apoptosis and expression of PCNA in gastric cancer. *Shijie Huaren Xiaohua Zazhi* 2000; **8**: 1050-1052
- 33 **Gao MX**, Zhang NZ, Ji CX. Relationship between receptor and PCNA. *Shijie Huaren Xiaohua Zazhi* 2000; **8**: 1117-1120
- 34 **Sato T**, Konishi K, Kimura H, Maeda K, Yabushita K, Tsuji M, Miwa A. Evaluation of PCNA, p53, K-ras and LOH in endocrine pancreas tumors. *Hepatogastroenterology* 2000; **47**: 875-879
- 35 **Niijima M**, Yamaguchi T, Ishihara T, Hara T, Kato K, Kondo F, Saisho H. Immunohistochemical analysis and in situ hybridization of cyclooxygenase-2 expression in intraductal papillary-mucinous tumors of the pancreas. *Cancer* 2002; **94**: 1565-1573
- 36 **Terada T**, Ohta T, Kitamura Y, Ashida K, Matsunaga Y. Cell proliferative activity in intraductal papillary-mucinous neoplasms and invasive ductal adenocarcinomas of the pancreas: an immunohistochemical study. *Arch Pathol Lab Med* 1998; **122**: 42-46

One-stage urethral reconstruction using colonic mucosa graft: an experimental and clinical study

Yue-Min Xu, Yong Qiao, Ying-Long Sa, Jiong Zhang, Hui-Zhen Zhang, Xin-Ru Zhang, Deng-Long Wu, Rong Chen

Yue-Min Xu, Yong Qiao, Ying-Long Sa, Jiong Zhang, Xin-Ru Zhang, Deng-Long Wu, Rong Chen, Department of Urology, Sixth People's Hospital, Jiao Tong University of Shanghai, Shanghai 200233, China

Hui-Zhen Zhang, Department of Pathology, Sixth People's Hospital, Jiao Tong University of Shanghai, Shanghai 200233, China

Supported by the Shanghai Health Science Development Foundation, No.2000429

Correspondence to: Yue-Min Xu, M.D., Ph.D., Chief of Department of Urology, Sixth People's Hospital, Jiao Tong University of Shanghai, Shanghai 200233, China. sshospy@public.sta.net.cn

Telephone: +86-21-64369181 Ext 8382 **Fax:** +86-21-67647129

Received: 2002-08-03 **Accepted:** 2002-08-27

Abstract

AIM: To investigate the possibility of urethral reconstruction with a free colonic mucosa graft and to present our preliminary experience with urethral substitution using a free graft of colonic mucosa for treatment of 7 patients with complex urethral stricture of a long segment.

METHODS: Ten female dogs underwent a procedure in which the urethral mucosa was totally removed and replaced with a free graft of colonic mucosa. A urodynamic study was performed before the operation and sacrifice. The dogs were sacrificed 8 to 16 weeks after the operation for histological examination of urethra. Besides, 7 patients with complex urethral stricture of a long segment were treated by urethroplasty with the use of a colonic mucosal graft. The cases had undergone an average of 3 previous unsuccessful repairs. Urethral reconstruction with a free graft of colonic mucosa ranged from 10 to 17 cm (mean 13.1 cm). Follow-up included urethrography, urethroscopy and uroflowmetry.

RESULTS: Urethral stricture developed in 1 dog. The results of urodynamic studies showed that the difference in the maximum urethral pressure between the pre-operation and pre-sacrifice in the remaining 9 dogs was not of significance ($P>0.05$). Histological examination revealed that the colonic free mucosa survived inside the urethral lumen of the 10 experimental dogs. Plicae surface and unilaminar cylindrical epithelium of the colonic mucosa was observed in dogs sacrificed 8 weeks after the operation. The plicae surface and unilaminar cylindrical epithelium of the colonic mucosa was not observed, and metaplastic transitional epithelium covered a large proportion of the urethral mucosa in dogs sacrificed 12 weeks after the operation. Clinically, the patients were followed up for 3-18 months postoperatively (mean 8.5 months). Meatal stenosis was developed in 1 patient 3 months postoperatively and needed reoperation. The patient was voiding very well with urinary peak flow 28.7 ml/s during the follow-up of 9 months after reoperation. The other patients were voiding well with urinary peak flow greater than 15 ml/s. Urethrogram revealed a patent urethra with an adequate lumen with no significant graft sacculation. Neither necrosis of neourethral mucosa nor stenosis at the

anastomosis sites has been observed on urethroscopy in 4 patients over 6 months after operation.

CONCLUSION: Urethral mucosa can be replaced by colonic mucosa without damaging the continence mechanism in female dogs. Colonic mucosa graft urethral substitution is a feasible procedure for the treatment of complex urethral stricture of a long segment. The technique may be considered when more conventional options have failed or are contraindicated.

Xu YM, Qiao Y, Sa YL, Zhang J, Zhang HZ, Zhang XR, Wu DL, Chen R. One-stage urethral reconstruction using colonic mucosa graft: an experimental and clinical study. *World J Gastroenterol* 2003; 9(2): 381-384

<http://www.wjgnet.com/1007-9327/9/381.htm>

INTRODUCTION

In most instances, primary reconstruction for urethral strictures can be accomplished with local penile or preputial skin and buccal or bladder mucosa^[1-11]. However, in patients with complex, long-segment urethral strictures and significant scar tissue formation after the failure of previous anterior urethroplasty still present an operative challenge. The key is to obtain a suitable substitute for urethral reconstruction.

From the viewpoint of postoperative quality of life, neobladder construction is superior to urinary diversion in patients who have to undergo cystectomy for bladder cancer. However, in patients having cystectomy as definitive treatment for bladder cancer, the overall risk of urethral recurrence of transitional cell carcinoma is between 0.7 % and 18 %^[16]. The urethral recurrence of bladder cancer would be reduced, if the urethral mucosa can be replaced by another mucosa without damaging urethral sphincter function. We explored the feasibility of urethral reconstruction with a free graft of colonic mucosa for the treatment of complicated long segment strictures or reducing urethral recurrence of bladder cancer in patients who have to undergo cystectomy for bladder cancer and neobladder construction. We investigated colonic mucosa as a novel substitute for urethral reconstruction in 10 dogs before performing the operation in 7 patients with severe lengthy urethral stricture.

MATERIALS AND METHODS

Animal experimental study

Ten adult mongrel female dogs, weighing 14.5 Kg to 28 Kg, were used for the experiment. Under intravenous pentobarbital anesthesia, the dogs were first used for urodynamic studies and then underwent a procedure in which urethral mucosa was replaced with a free graft of colonic mucosa. With a partial resection of the pubic symphysis, the urethra was incised longitudinally at its full length on the ventral side and the urethral mucosa was totally removed. The sigmoid colon was exposed and 8-10 cm. in length colectomy was performed. The digestive connection was immediately restored by an end-

to-end anastomosis. A mucosa graft was harvested from the resected colon. After tailoring the mucosa graft, excess submucosal tissue, fat or muscle was carefully dissected away to optimize subsequent vascularization. The free graft was tubularized over a 14 Fr catheter with one layer of 5-zero polyglactin running sutures. The proximal end of the graft was sutured to the edge of the bladder neck mucosa and the distal end to the external meatus with interrupted 5-zero polyglactin suture. The urethral muscle layer was then closed with one layer of 4-zero polyglactin interrupted sutures. The urethral catheter was left indwelling to provide bladder drainage for 7 to 10 days after the operation. Ampicillin (2 gm. per day) was given intravenously for 5 days after the operation.

Postoperatively, the urinary stream and external meatus were observed periodically. To determine the influence of the longitudinal urethral incision on urethral continence mechanism, Urodynamic study was carried out again 8 to 16 weeks (8 weeks 2, 12 weeks 6 and 16 weeks 2) after the operation. The data from the urodynamic study were statistically analyzed by *t* test. After the urodynamic study, the dogs were sacrificed for histological examination of the urethra.

Clinical study

Between September 2000 and April 2002, 7 men aged 18 to 58 years (median 39.5) with complex lengthy urethral stricture underwent urethral reconstruction with a free colonic mucosa graft. The etiology of the urethral stricture was trauma and urethritis in 5 patients, perineal hypospadias in 2. All patients had a history of extensive urethral stricture disease for 1.5 to 9 years (median age 3.5 years) and had undergone an average of 3 previous unsuccessful repairs (1-5 times) or repeated urethral dilation. The urethral stricture was 10 to 17 cm long (median 13.1 cm). 5 patients underwent a procedure of suprapubic cystostomy because of severe urethral stricture or *atresia*. 2 patient presented with strangury cause by severe urethral stricture. Uroflowmetry examination showed the urinary peak flow was 1 ml/s. Retrograde urethrogram demonstrated multiple urethral strictures and pseudopath (Figure 1).

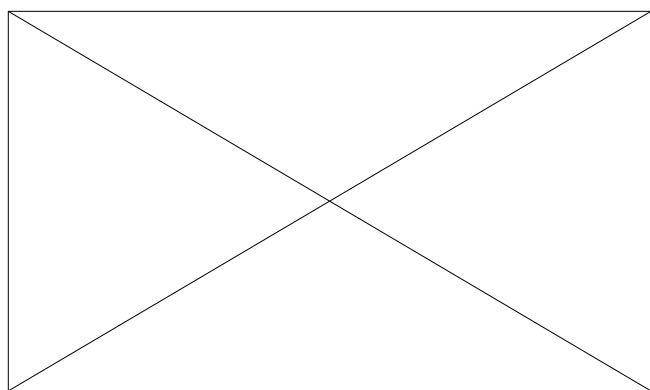


Figure 1 Retrograde urethrogram. Small arrows indicate stricture, and big arrow indicates stricture and pseudopath.

Urethral reconstruction was performed with the patients under general anesthesia. Strictured or atretic urethra and scar tissue were excised and the penis was straightened. The urethra defected 10 to 17 cm in length. 10 to 15 cm long sigmoid colon with its blood pedicle was isolated from the intestinal tract. The digestive connection was immediately restored by an end-to-end anastomosis. A full thickness mucosal graft was harvested from the isolated colon and the isolated colon was resected afterward. After tailoring the mucosa graft, excess submucosal tissue, fat or muscle was carefully dissected away to optimize subsequent vascularization. An unstretched colonic

mucosa, 10 to 17 cm in length and 2.5-3 cm in width, was tubularized over an 18 to 22 F fenestrated silicone stent with interrupted 5-zero polyglactin suture to create a neourethra (Figure 2A). An end-to-end anastomosis was performed between normal urethra and neourethra with interrupted 5-zero polyglactin suture in 4 patients (Figure 2B). In the remaining 3 patients one end of neourethra was anastomosed with proximal normal urethra and the other end of the neourethra was through the glanular tunnel to form new meatus. The penis was wrapped with soft, elastic, and roller bandage incorporating the traction suture into the dressing. Strips of elastic adhesive were placed over this to keep the penis in the erect position.

The bladder drainage was through the suprapubic catheter and the urethral silicone stent was left indwelling for 14 days. The patients underwent urethrography, urethroscopy and uroflowmetry 3 months after operation.

RESULTS

Animal experimental study

Nine dogs were able to void normally after removal of the catheter and the external meatus were dry whenever examined before urination. Urodynamic studies showed that the maximum urethral pressure ranged from 34-70 cmH₂O (56.5±11.05, mean±S.D.) before the operation and ranged from 43-82 cmH₂O (51.75±13.36, mean ±S.D.) before sacrifice. There was no significant difference in the maximum urethral pressure between pre-operation and pre-sacrifice (*t*=1.22, *P*=0.26). These findings indicated that the dogs were continent in the usual state. The one remaining dog was not voiding well and had a thin urinary stream. A urodynamic study was not done in this dog postoperatively.

At sacrifice, the colonic mucosa-replaced urethra was macroscopically normal in 9 dogs. No necrosis or erosion was observed on the urethra epithelium in these dogs (Figure 3). In the other 1 dog, a slightly distended bladder was observed; 3 stones, soybean in size, were found in the bladder and a urethral stricture of 1 cm in length developed at the bladder neck.

Histological examination of the urethras showed that the colonic mucosa graft survived inside the urethral lumen. Plicae surface and unilaminar cylindrical epithelium of the colonic mucosa was observed in dogs sacrificed 8 weeks after the operation (Figure 4). The plicae surface and unilaminar cylindrical epithelium of colonic mucosa was not observed in dogs sacrificed at 12 weeks postoperatively. Metaplastic transitional epithelium covered a large proportion of the urethral mucosa and some degree of atrophy of the colonic crypts were seen in dogs sacrificed at 12 weeks after the operation (Figure 5). In the dog with the urethral stricture, the submucosal layer was thickened with inflammatory cell infiltration at the site of the stricture.

Clinical study

The patients were followed up for 3-18 months postoperatively (mean 8.5 months). Meatal stenosis was developed in 1 patient 3 months postoperatively and needed reoperation. 9 months later the patient returned to the hospital and the new urethra was found to be most satisfactory. Uroflowmetry examination showed the urinary peak flow was 28.7 ml/s. Hyperplasia of the verumontanum was observed during urethroscopy and transurethral colliculectomy carried out in 1 patient over 14 months after operation. Uroflowmetry examination showed the urinary peak flow was 46.5 ml/s postoperatively. The other patients were voiding well with urinary peak flow greater than 15 ml/s (from 16 to 27.8 ml/s) (Figure 6A). Urethrogram revealed a patent urethra with an adequate lumen with no significant graft sacculcation (Figure 6B). Neither necrosis of neourethral mucosa nor stenosis at the anastomosis sites has been observed on urethroscopy in 4 patients over 6 months after operation.

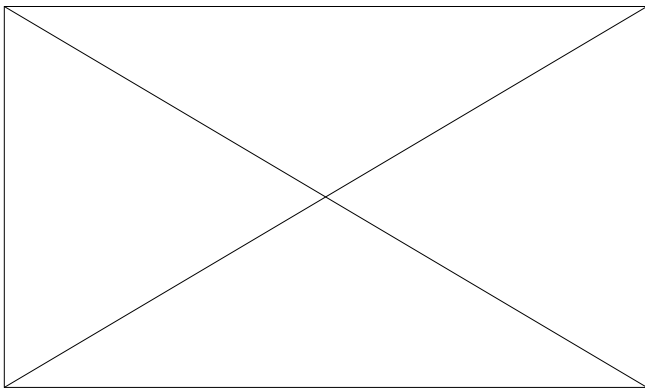


Figure 2A A tubularized free colonic mucosa over 22 F fenestrated silicone tube.

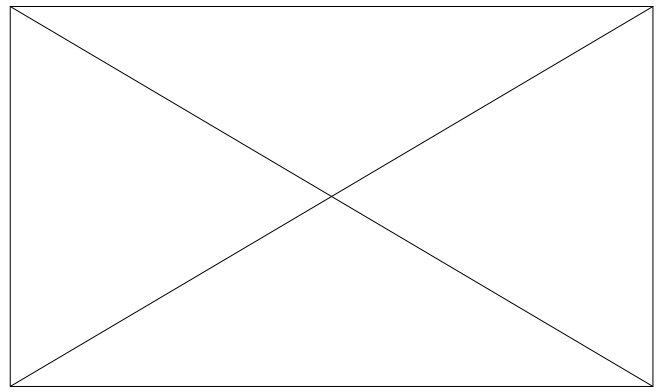


Figure 5 Longitudinal section of urethra. Arrowhead indicates urinary epithelium, arrows indicate atrophic glandular body (Hematoxylin and eosin stain, $\times 100$).

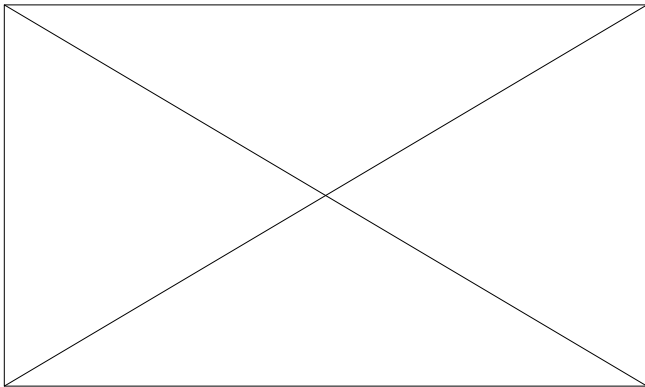


Figure 2B Reconstructive urethra with colonic mucosa.

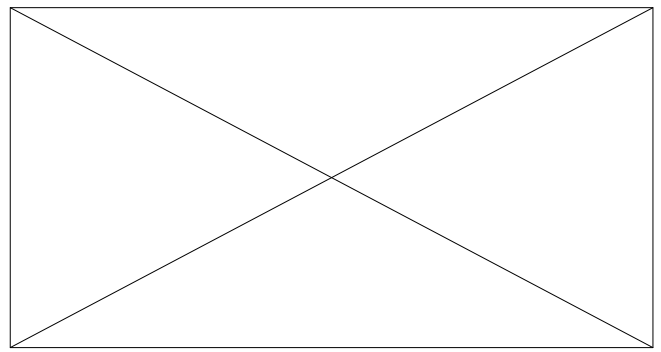


Figure 6A Patient have good urinary streams.

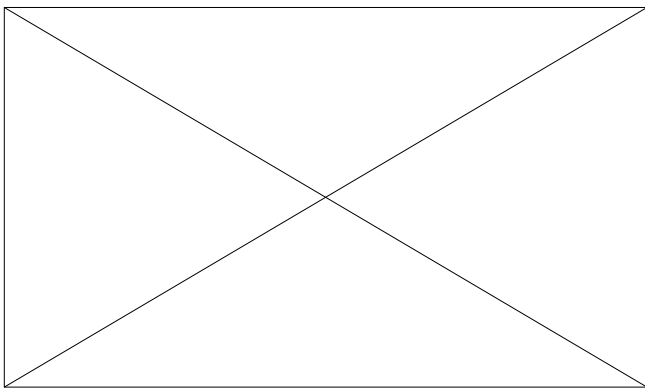


Figure 3 Colonic mucosa-replaced urethra is macroscopically difficult to distinguish from bladder mucosa.

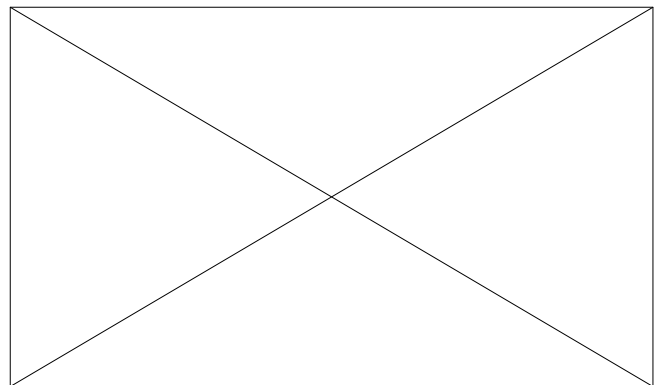


Figure 6B Cystourethrography reveals patent neourethra.

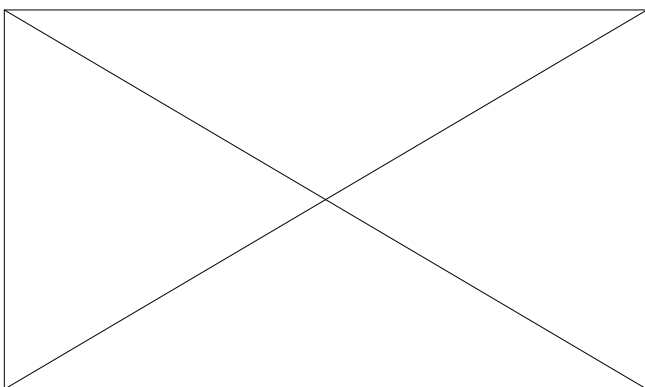


Figure 4 Cross-section of urethra. Urethral wall is lined by the glandular epithelium (Hematoxylin and eosin stain, $\times 100$).

DISCUSSION

Up to now, a variety of tissues have been used for urethral reconstruction, including full thickness skin graft, free bladder or buccal mucosa and pedicled flaps^[5-10,13-15]. In 1996, Iziuka *et al*^[17] reported on the total replacement of urethra mucosa with oral mucosa in a dog model, with the intention of reducing the recurrence rate of urethral cancer in bladder cancer patients requiring radical cystoprostatectomy. However, substituting buccal mucosa in total urethral reconstruction is difficult in humans, and it may not be useful for the treatment of complicated long segment urethral strictures because of limited material. The use of bladder mucosa may also be difficult in cases with a previous bladder operation, chronic cystitis or even long-term suprapubic cystostomy.

Recently, Bales *et al*^[12] reported a novel technique to urethral reconstruction using tailored jejunal free tissue transfer

to reconstruct the anterior urethra in 2 patients with complex urethral stricture. The patients have good urinary streams and are able to void in the standing position. However, the technique is time-consuming and surgeon must have experienced with microvascular anastomosis.

The appendix mucosa as a graft in urethroplasty was used by Lexer in 1911 for the treatment of hypospadias^[18]. The result was difficult to interpret as no complete histological examination or follow-up had originally been attempted. In fact, the appendix may not be available consequent to a previous appendectomy; it also may not be useful for the treatment of complicated long length urethral strictures because of inappropriate size and fibrous obstruction^[19]. Leuret *et al*^[18] studied the histology of the colonic mucosa as a graft for urethral construction in Spague-Dawley rats. They found that the glandular epithelium of colonic mucosa had been transformed into a typical urothelium 6 weeks to 3 months after operation. In our study, although plicate surface and unilaminar cylindrical epithelium of colonic mucosa was observed in dogs sacrificed 8 weeks after the operation (Figure 4), the plicate surface mucosa and unilaminar cylindrical epithelium were not observed in dogs sacrificed 12 weeks postoperatively. Metaplastic transitional epithelium covered a large proportion of the urethral mucosa and some degree of atrophy of the colonic crypts were seen in those dogs (Figure 5). This is similar to results published by Leuret *et al*.

In these experiments, urethral stricture developed at the anastomotic site between the colonic mucosa and bladder neck mucosa in one dog. This may be related to a catheter dropping early; urine leakage from the anastomotic site probably caused an inflammatory reaction leading to stricture. Whether a longitudinal incision of the urethra will damage sphincteric function is worthy of consideration. To measure urine leakage, a 10-minute pad test was performed once a month in the investigation of Iiziuka *et al*^[17]. There was no significant difference in the weight increase of the pad among the control, sham-operated and mucosa-replaced dogs. In our study, 9 dogs were able to void normally after removal the catheter and the external meatus was dry whenever examined before urination. Data from urodynamic study showed no significant difference in maximum urethral pressure pre-operation and pre-sacrifice ($P>0.05$), indicate that a longitudinal incision of the urethra does not damage sphincter function in female dogs.

Colonic mucosa graft urethral reconstruction is a one-stage urethroplasty for the treatment of complex urethral lengthy stricture. The key to a successful transplantation of the colonic mucosa, as with any free graft, depends on whether the neovascularization is established. The following conditions are necessary for the success: (1) scar tissue was excised as long as possible and the bed to receive the graft must be well vascularized, (2) an ischemia time of the colonic mucosa should be short as far as possible, (3) to avoid wound infection and sterile urine should be ensured. The clinical results of our patients are satisfactory. They have a functioning urethra of good caliber throughout the entire length (Figure 6A,B). Uroflowmetry examination showed the maximum flow rate was greater than 15 ml/s. Being more invasive than the use of other types of grafts, the technique may have limited applications in the practice of urethroplasty. However, we believe that colonic mucosa graft should be used in patients with complex lengthy urethral stricture after the failure of previous anterior urethroplasty and penial skin and /or bladder mucosa are not available. The technique has opened up a new way for the treatment of complex lengthy urethral stricture.

In summary

Our study indicates that urethral mucosa can be replaced with colonic mucosa and this technique can provide rich material for urethroplasty. The colonic mucosa is easy to harvest; the colonic mucosal graft is elastic and shows only a slight tendency to retract. The technique is particularly useful for the treatment of complicated long segment strictures (>10 cm in length) or reducing urethral recurrence of bladder cancer in patients who undergo cystectomy for bladder cancer and neobladder construction.

REFERENCES

- 1 **Andrich DE**, Mundy AR. Urethral strictures and their surgical treatment. *BJ Urol* 2000; **86**: 571-580
- 2 **Kessler TM**, Fisch M, Heitz M, Olianias R, Schreiter F. Patient satisfaction with the outcome of surgery for urethral stricture. *J Urol* 2002; **167**: 2507-2511
- 3 **Santucci RA**, Mario LA, McAninch JW. Anastomotic urethroplasty for bulbar urethral stricture: analysis of 168 patients. *J Urol* 2002; **167**: 1715-1719
- 4 **Joseph JV**, Andrich DE, Leach CJ, Mundy AR. Urethroplasty for refractory anterior urethral stricture. *J Urol* 2002; **167**: 127-129
- 5 **Palminteri E**, Lazzeri M, Guazzoni G, Turini D, Barbagli G. New 2-stage buccal mucosal graft urethroplasty. *J Urol* 2002; **167**: 130-132
- 6 **Kane CJ**, Tarman GJ, Summerton DJ, Buchmann CE, Ward JF, O'Reilly KJ, Ruiz H, Thresher JB, Zorn B, Smith C, Morey AF. Multi-institutional experience with buccal mucosa onlay urethroplasty for bulbar urethral reconstruction. *J Urol* 2002; **167**: 1314-1317
- 7 **Meneghini A**, Cacciola A, Cavarretta L, Abatangelo G, Ferrarrese P, Tasca A. Bulbar urethral stricture repair with buccal mucosa graft urethroplasty. *Eur Urol* 2001; **39**: 264-267
- 8 **Greenwell TJ**, Venn SN, Mundy AR. Changing practice in anterior urethroplasty. *Br J Urol* 1999; **83**: 631-635
- 9 **Hemal AK**, Dorairajan LN, Gupta NP. Posttraumatic complete and partial loss of urethra with pelvic fracture in girls: an appraisal of management. *J Urol* 2000; **163**: 282-287
- 10 **McAninch JW**, Morey AF. Penile circular fasciocutaneous skin flap in 1-stage reconstruction of complex anterior urethral stricture. *J Urol* 1998; **159**: 1209-1213
- 11 **Al-Ali M**, Al-Hajaj R. Johanson's staged urethroplasty revisited in the salvage treatment of 68 complex urethral stricture patients: presentation of total urethroplasty. *Eur Urol* 2001; **39**: 268-271
- 12 **Bales GT**, Kuznetsov DD, Kim HL, Gottlieb LJ. Urethral substitution using an intestinal free flap: a novel approach. *J Urol* 2002; **168**: 182-184
- 13 **Pansadoro V**, Emiliozzi P, Gaffi M, Scarpone P. Buccal mucosa urethroplasty for the treatment of bulbar urethral stricture. *J Urol* 1999; **161**: 1501-1503
- 14 **El-Sherbiny MT**, Abol-Enein H, Dawaba MS, Ghoneim MA. Treatment of urethral defects: skin, buccal or bladder mucosa, tube or patch? An experimental study in dogs. *J Urol* 2002; **167**: 2225-2228
- 15 **Wadhwa SN**, Chahal R, Hemal AK, Gupta NP, Dogra PN, Seth A. Management of obliterative posttraumatic posterior urethral strictures after failed initial urethroplasty. *J Urol* 1998; **159**: 1898-1902
- 16 **Freeman JA**, Esrig D, Stein JP, Skinner DG. Management of the patient with bladder cancer. *Urol Clin North Am* 1994; **21**: 645-651
- 17 **Iiziuka K**, Muraishi O, Maejima T, Kitami Y, Xu YM, Watanabe K, Ogawa A. Total replacement of urethral mucosa with oral mucosa in dogs. *J Urol* 1996; **156**: 498-501
- 18 **Leuret T**, Gobet F, Dallaserre M, Mitrofanoff P. Use of a digestive mucosal graft in urethroplasty. An experimental study-prospective utilization of the appendix mucosa. *Eur Urol* 1995; **27**: 58-61
- 19 **Leibovitch I**, Avigad I, Nativ O, Goldwasser B. The frequency of histopathological abnormalities in incidental appendectomy in urological patients: the implications for incorporation of the appendix in urinary tract reconstruction. *J Urol* 1992; **148**: 41-43

Hepatocellular carcinoma with obstructive jaundice: diagnosis, treatment and prognosis

Lun-Xiu Qin, Zhao-You Tang

Lun-Xiu Qin, Zhao-You Tang, Liver Cancer Institute and Zhongshan Hospital, Fudan University, Shanghai, China
Correspondence to: Zhao-You Tang, M.D., Professor & Chairman, Liver Cancer Institute, Fudan University, 136 Yi Xue Yuan Road, Shanghai 200032, China. zytang@srcap.stc.sh.cn
Telephone: +86-21-64037181 **Fax:** +86-21-64037181
Received: 2002-10-09 **Accepted:** 2002-11-25

HCC is generally dismal, but is better than those HCC patients who have jaundice caused by hepatic insufficiency.

Qin LX, Tang ZY. Hepatocellular carcinoma with obstructive jaundice: diagnosis, treatment and prognosis. *World J Gastroenterol* 2003; 9(3): 385-391
<http://www.wjgnet.com/1007-9327/9/385.htm>

Abstract

Obstructive jaundice as the main clinical feature is uncommon in patients with hepatocellular carcinoma (HCC). Only 1-12 % of HCC patients manifest obstructive jaundice as the initial complaint. Such cases are clinically classified as "icteric type hepatoma", or "cholestatic type of HCC". Identification of this group of patients is important, because surgical treatment may be beneficial. HCC may involve the biliary tract in several different ways: tumor thrombosis, hemobilia, tumor compression, and diffuse tumor infiltration. Bile duct thrombosis (BDT) is one of the main causes for obstructive jaundice, and the previously reported incidence is 1.2-9 %. BDT might be benign, malignant, or a combination of both. Benign thrombi could be blood clots, pus, or sludge. Malignant thrombi could be primary intrabiliary malignant tumors, HCC with invasion to bile ducts, or metastatic cancer with bile duct invasion. The common clinical features of this type of HCC include: high level of serum AFP; history of cholangitis with dilation of intrahepatic bile duct; aggravating jaundice and rapidly developing into liver dysfunction. It is usually difficult to make diagnosis before operation, because of the low incidence rate, ignorant of this disease, and the difficulty for the imaging diagnosis to find the BDT preoperatively. Despite recent remarkable improvements in the imaging tools for diagnosis of HCC, such cases are still incorrectly diagnosed as cholangiocarcinoma or choledocholithiasis. Ultrasonography (US) and CT are helpful in showing hepatic tumors and dilated intrahepatic and /or extrahepatic ducts containing dense material corresponding to tumor debris. Direct cholangiography including percutaneous transhepatic cholangiography (PTC) and endoscopic retrograde cholangiopancreatography (ERCP) remains the standard procedure to delineate the presence and level of biliary obstruction. Magnetic resonance cholangiopancreatography (MRCP) is superior to ERCP in interpreting the cause and depicting the anatomical extent of the perihilar obstructive jaundice, and is particularly distinctive in cases associated with tight biliary stenosis and along segmental biliary stricture. Choledochoscopy and bile duct brushing cytology could be alternative useful techniques in the differentiating obstructions due to intraluminal mass, infiltrating ductal lesions or extrinsic mass compression applicable before and after duct exploration. Jaundice is not necessarily a contraindication for surgery. Most patients will have satisfactory palliation and occasional cure if appropriate procedures are selected and carried out safely, which can result in long-term resolution of symptoms and occasional long-term survival. However, the prognosis of icteric type

INTRODUCTION

Jaundice presents in 19 % to 40 % of patients with hepatocellular carcinoma (HCC) at the time of diagnosis and usually occurs in later stages. In most situations, it is due to diffuse tumor infiltration of liver parenchyma, hilar invasion, or progressive terminal liver failure (advanced underlying cirrhosis)^[1]. Obstructive jaundice as the main presenting clinical feature is uncommon. Only 1-12 % of HCC patients manifest obstructive jaundice as the initial complaint^[2]. Identification of this group of patients is clinically important, because surgical treatment may be beneficial.

Mallory *et al.* described the first such case in 1947, in which HCC invaded the cystic duct and gave rise to obstructive jaundice caused by hemobilia from the tumor thrombi^[3]. Thereafter, there have been few and scattered reports of such presentations of HCC in English literatures^[4-11]. In 1975, Lin *et al.* clinically classified such cases as "icteric type hepatoma", which manifested as obstructive jaundice in the early stage before the tumor became discernible or palpable^[12]. Okuda classified these patients as "cholestatic type of HCC"^[13].

Thrombus in bile duct (BDT) is one of the main reasons of obstructive jaundice. The incidence was 1.2-9 % in previous report^[4,12-15]. Huang *et al.* collected the cases from the newly diagnosed HCC patients of the admission registration database, and found the incidence of this type HCC was only 0.53 %^[16]. Variation in the biological behavior of HCC may partly account for the difference in incidence. It is reported that the incidence is increasing in patients with HCC, and transcatheter arterial chemoembolization (TACE) therapy could increase the possibility of common bile duct obstruction of tumor thrombi^[17].

PATHOLOGICAL FEATURES

HCC may involve the biliary tract in several different ways: tumor thrombi, hemobilia, tumor compression, and diffuse tumor infiltration. Infrequently, jaundice may also result from the external compression on the major bile ducts by direct tumor encasement or by the metastatic lymphadenopathy at the porta hepatis^[18,19].

BDT might be benign, malignant, or a combination of both. Benign thrombi could be blood clots, pus, or sludge. Malignant thrombi could be primary intrabiliary malignant tumors, HCC with invasion to bile ducts, or metastatic cancer with bile duct invasion. HCC invasion into bile duct may be due to one of the three mechanisms: (1) a distal tumor may grow continuously until it fills the entire extrahepatic biliary system; (2) a fragment of necrotic tumor may separate from the proximal intraductal growth, migrate to the distal common bile

duct and cause an obstruction; (3) hemorrhage from the tumor may partially or completely fill the biliary tract with tumor-containing blood clots^[4, 14-16, 20, 21]. In this type of HCC, blood clots are inevitably mixed with fresh tumor debris. However, Shimoji *et al.* reported one case suspected recurrent HCC during the choledochotomy after left hepatectomy for HCC, no HCC was detected by either macroscopic or intra-operative ultrasonographic examination. The course of hemobilia thus remained unclear until the autopsy was performed. Hemorrhage from a ruptured branch of the portal vein into the intrahepatic bile duct, filling the entire common bile duct with solid casts of blood, is uncommon. The hemorrhage into intrahepatic bile duct may be secondary to a portal vein rupture from: (1) a rupture of the engorged or variceal proximal portal vein leading directly into the intrahepatic duct; (2) necrosis of a cirrhotic liver nodule adjacent to both the intrahepatic bile duct and the vein; or (3) either cholangitis or an abscess in the proximal intrahepatic bile duct. Despite the remarkable recent improvements in various diagnostic modalities, hemobilia is still often incorrectly diagnosed as biliary tract carcinoma or stones. The etiologic diagnosis of jaundice in patients with cirrhosis, either with or without HCC, is thus of great clinical importance^[22].

Fragments of tumor in the bile duct, as described by Edmondson and Steiner, are usually fragile, fleshy, and grayish-white, having the appearance of chicken fat^[23]. BDT often grows faster than the primary cancer. The parenchymal tumor could be not continuous with the extrahepatic bile duct tumor. The bile duct tumor might attach to the mucosa of the bile duct with a thin stalk, without invasive growth into the submucosa^[24]. Most of the primary tumors are pathologically confirmed as HCC, however, the growth of mixed type of liver cancer (HCC and cholangiocarcinoma) into the common bile duct (CBD) has also been found, which may differ from the underlying mechanism of the development of icteric type HCC^[25].

In most cases, hepatic tumors can not be palpated from the liver surface because they are deep-seated and small, or because the liver is cirrhotic^[12, 18, 21, 26]. Intraductal HCC growth is mostly caused by direct invasion from the primary lesion and occasionally from an adjacent massive tumor thrombus in the portal vein^[27]. Icteric type HCC may occur even with no primary detectable lesion^[21, 28]. Most primary lesions of icteric type HCC patients are grossly infiltrative type or mixed infiltrative and nodular type. Usually, no tumor capsule formation could be found in the primary tumors. The infiltrative nature of this particular type of HCC may in part explain their invasion of the biliary tree and portal veins early in their growth without regard to tumor size or type^[19, 29].

CLINICAL MANIFESTATION AND DIAGNOSIS

Clinical features

The common clinical features of this type of HCC include: high level of serum AFP; the history of cholangitis with dilation of intrahepatic bile duct; aggravating jaundice and rapidly developing into liver dysfunction. It is usually difficult to make diagnosis before operation, because of the low incidence rate, ignorant of this disease, and the difficulty for the imaging diagnosis to find the BDT preoperatively.

Just as other types of HCC, no specific symptoms could be found in the early stage. Only when intraductal tumor growth occurs in the common hepatic duct and/or the common bile duct does obstructive jaundice become a clinical concern. Hemobilia due to intraductal tumor growth is occasionally observed.

Besides jaundice, right upper quadrant pain is one of the major presenting features. In cirrhotic patients, unexplained hemobilia could be the initial complaint without any

manifestation of primary tumor, which can reveal a small, potentially curable, HCC that has spread to the biliary tree^[30]. Sometimes, this kind of patient is manifested as acute pancreatitis^[31].

The serum total bilirubin level can rise very rapidly and correlates well with ALP and GGT levels^[16, 32]. It is important to evaluate carefully when dealing with patients with intrabiliary tumor thrombi, even though they may show negative for viral hepatitis infection.

There are still difficulties and challenging problems in differential diagnosis of this type of HCC. The presence of an elevated AFP level and positive HBV markers are helpful to establish the diagnosis. The absence of these findings, especially with no primary hepatic tumor being detected, a variety of other diagnoses will be entertained. Despite remarkable recent improvements in the imaging tools for diagnosis of HCC, such cases were still incorrectly diagnosed as cholangiocarcinoma or choledocholithiasis^[4, 14-16, 21, 33, 34]. Ultrasonography (US) and CT are helpful in showing hepatic tumors and dilated intrahepatic and/or extrahepatic ducts containing dense material corresponding to tumor debris.

Ultrasonography (US)

Abdominal US is valuable as an initial investigation and for differentiation of patients with these presentations. Using US, it is able to suspect patients with icteric type HCC, even before other diagnostic strategies. Dilatation of proximal biliary tracts developed inevitably with time. Distension of the gallbladder was occasionally seen if the thrombus was located below the common hepatic duct (CHD). Tumor thrombi of bile duct could be easily identified on US as low-, iso-, or high-echogenic masses. At times, vascular signals could be detected on a Color Doppler sonography (CDS). Regarding biliary tract tumor thrombi, icteric type HCC should be strongly suspected whenever liver tumors exist. Moreover, pathological proof of thrombi can be obtained with an US-guided approach.

CDS is a non-invasive method in liver hemodynamic studies. Because HCC is known to be a hypervascular tumor, CDS is useful in detection of blood flow in HCC and helpful in differentiating it from other liver tumors. For the detection of tumor vascularity, spectral Doppler sonography guided by CDS is shown to be useful in the differential diagnosis of liver tumors. It is also useful in detection of blood flow within portal vein thrombosis in liver cirrhosis. It is a useful method for differentiating malignant from benign portal vein thrombi in liver cirrhosis, with 45-90 % sensitivity and 95-100 % specificity^[35]. Wang *et al.* found blood flow in bile duct tumor thrombi in 7 of 8 patients (87.5 %) with HCC and bile duct infiltration. Power Doppler sonography, a technique based on the integrated power of the Doppler spectrum, is more sensitive than CDS in depicting vascular flow in HCC. Its utility in detection of vascularity of bile duct tumor thrombi in patients with HCC might be more sensitive than that of CDS^[36].

Endoscopic sonography could show a tumor thrombus with central echogenicity and a "nodule-in-nodule" pattern, could provide more accurate evidence for the correct diagnosis^[37].

Computed tomography (CT)

Although CT is useful in patients with obstructive biliary disease, axial CT is not an effective method of demonstrating biliary anatomy. Because of the cross-sectional orientation of the CT images, the anatomy is fragmented and CT alone is less accurate in providing information of complex anatomic relationships. 3D CT cholangiography demonstrated the dilated bile ducts but could not depict nondilated peripheral bile ducts not seen on 2D axial images. On 3D CT cholangiography with miniIP, grades for anatomic details of biliary system were over

grade 4: visualization up to third-order branches. 3D CT cholangiography with miniIP determined the cause and level of all patients. Grades for anatomic visualization of the biliary tree corrected with an attenuation difference between bile ducts and enhanced hepatic parenchyma. Therefore, maximal hepatic parenchymal enhancement is one of the most important factors for 3D cholangiography with miniIP. Appropriate dilatation of the biliary tree is also necessary to extract pixels of bile ducts for 3D cholangiography. Focal disruptions of peripheral bile ducts were in all patients. However, the limitation of resolution in demonstrating a normal size of bile duct and focal disruption do not interfere with the determination of the level of obstruction, contiguity of ducts between different hepatic segments, and the presence or absence of isolated hepatic segment. 3D CT cholangiography correctly show the presence of biliary obstruction. Moreover, there is complete agreement between 3D CT cholangiography and PTC in the determination of obstruction level and cause in all patients. Spiral CT cholangiographic findings were also in agreement with those of direct cholangiography with regard to the site and extent of obstruction^[38].

Direct cholangiography

Although sonography and CT are sensitive in detecting biliary tract obstruction, direct cholangiography including percutaneous transhepatic cholangiography (PTC) and endoscopic retrograde cholangiopancreatography (ERCP) remains the standard procedure to delineate the presence and level of biliary obstruction. Nevertheless, direct cholangiography is operator dependant and invasive, with a higher complication rate in patients (up to 9 %) with obstructive jaundice^[39,40]. The complications, such as pancreatitis, sepsis, hemobilia, and bower proliferation, can be life threatening and can delay or even diminish the chance of managing the primary disease. ERCP and PTC are useful in the diagnosis of intrabiliary thrombi, and intraductal filling defects resulting in partial or complete obstruction and ductal dilatation are shown in 70 % of bile invasion by HCC. However, these cholangiographic features are not diagnostic for bile duct invasion by HCC; therefore, ERC and PTC are limited in their usefulness for characterization of BDT.

Magnetic resonance cholangiopancreatography (MRCP)

The MR features of intraductal tumors, bile duct obstruction with an associated hepatic mass or localized intrahepatic duct dilatation within wedge-shaped areas, indicated intraductal tumor extension. The enhancement of intraductal masses on dynamic MR images shows an extension of HCC rather than blood clots. MR cholangiography is recently shown to be superior to ERCP in detecting the presence of biliary obstruction, but it is relatively ineffective for interpretation of icteric-type HCC.

MRCP was introduced in 1991 by Wallner *et al*^[41]. It is an absolutely noninvasive imaging modality, allowing demonstration of the biliopancreatic system by means of data acquisition and images post-processing reconstruction presenting at the coronal planes similar to conventional cholangiography. It requires neither contrast medium injection, nor biliary endoscopic intervention; therefore, it completely avoids the formidable complications inherent to conventional cholangiographic examinations. Both primary liver tumors and dilatation of biliary system could be demonstrated in MRCP. Recent studies have demonstrated that MRCP can accurately depict abnormalities in the hepatobiliary system, and claimed a high accuracy in depicting various biliary and pancreatic disease entities, with reported sensitivities approaching 90-95 % for biliary and pancreatic ductal dilation and stricture^[42].

Presence of intraluminal soft tissue at the bile duct, and enhancement of the intraluminal soft tissue in the arterial phase are two typical features of HCC with tumor thrombi in bile duct. Sometimes, the simultaneous presence of an intraluminal tumor in the portal trunk and CHD could be found in this type of patients. Three different MRCP features could be found: (a) an oval defect in the hilar bile duct(s) with dilated intrahepatic ducts. A bulky intraluminal-filling defect resulting from either tumor fragments or blood clots obstructing the major bile duct is the most common cholangiographic finding of icteric type HCC. This feature has been reported in about 70 % of this type of patients. It most frequently occurs in the hepatic or common bile ducts, causing partial or complete obstruction. The bile ducts containing tumor fragments are visualized because the impacted tumor appears dark on MRCP and there is no surrounding bile. A comparison of direct cholangiography with MRCP showed that the non-visualized bile duct in type I MRCP corresponded well in size, contour, and location to the intraluminal filling defect on conventional cholangiography; (b) dilated intrahepatic ducts with missing major bile ducts, and (c) localized stricture of the hilar bile duct(s). It is an unusual cholangiographic feature of icteric-type HCC, and an incidence of 9-15 % has been reported. The stricture is short, smooth, and confined to the porta hepatis, in contrast to the multiple, long segmental dilatations and "rat-tail" stricture seen in cholangiocarcinoma. The localized stricture is probably the result of bile duct encasement by the large infiltrative tumor in the caudate lobe and hepatic hilum and the enlarged hilar lymph nodes. However, it may be very difficult to differentiate from hilar cholangiocarcinoma or cystic duct cancer in a patient presenting with type III MRCP, because of the very similar cholangiographic appearance. Other imaging modalities are required for additional information about the extent of the tumor, the extraluminal tumor compression, and the presence of enlarged lymph nodes. The presence of one or more of the following features in multiplanar MRI and MRCP help to identify this rare, specific type of HCC: (a) the presence of an intraluminal tumor in both the portal trunk and the common hepatic duct, (b) enhancement of the intraluminal tumor in the CHD on the arterial phase, (c) type I MRCP feature, and (d) hemobilia, blood clot within the gallbladder, and/or type II MRCP feature^[29, 42-45].

Both ERCP and MRCP are excellent for confirming the presence of malignant perihilar biliary obstruction that has been suggested by sonography and CT. Nevertheless, MRCP is obviously superior to ERCP in interpreting the cause and depicting the anatomical extent of the perihilar obstructive jaundice. It is particularly distinctive in cases associated with tight biliary stenosis and along segmental biliary stricture. For this kind of patients, an undue pressure and retention of contrast medium imposed on a diseased biliary tree might deteriorate the pre-existing biliary tract infection. Therefore, the amount of injected contrast agents given is below the optimal dose needed to appropriately visualize the biliary tree cephalad to the lesion site. Complementary PTC is warranted to remedy this problem. Certainly, the procedure-related risk increases synergically. Furthermore, in cases with separate biliary obstruction, detailed opacification of the intrahepatic biliary system may have necessitated multiple PTC sessions before the MRCP era. For deeply jaundiced patients with renal insufficiency, an iodinated contrast material is particularly dangerous; whereas MRCP is also satisfactorily delineate the dilated biliary system irrespective to the serum bilirubin level and renal function. In addition, the nonopacified area on the direct cholangiography, such as a sequestered bile duct or gallbladder as a result of tumor invasion, can be depicted clearly by MRCP.

Icteric type HCC represents the most difficult disease entity to correctly diagnose using either MRCP or ERCP. The

characteristic cholangiographic feature of bile duct involvement by a ruptured HCC is a large expanding intraluminal filling defect with an irregularly lobulated outline and ground-glass radiolucency of the filling defects, which may be smooth or irregular, usually seen in the common hepatic duct^[14,44,45]. The differential diagnoses of this type of cholangiography include papillary type cholangiocarcinoma, intraductal polyps or mucin-hypersecreting intrahepatic biliary neoplasm. It still relies on other information, such as the presence of liver cirrhosis, hepatitis markers, tumor markers (AFP, CEA), the fluctuation of jaundice, and hemobilia. The presence of an encapsulated mass with a central scar or internal fat may also be helpful to diagnose icteric HCC. MRCP and direct cholangiography provide the equivalent diagnosis information that segmental bile ducts are not visualized and the CHD is partially opacified because of migrating tumor thrombi. Furthermore, by means of T2-weighted axial and coronal plane of MR images, tumor thrombi that ruptured from the primary tumor into both intrahepatic and extrahepatic bile ducts could be perfectly depicted. This novel diagnostic modality makes the diagnosis of icteric HCC more straightforward and certain than ever before^[46].

Choledochoscopy

Choledochoscopy is an alternative diagnostic technique applicable before and after duct exploration. Choledochoscopy can differentiate obstructions resulting from intraluminal mass, infiltrating ductal lesions or extrinsic mass compression. Yamakawa first introduced intra-operative fiber optic choledochoscopy (IOC), using an improved fiberoptic choledochoscope, in 1976. Chen *et al.*^[47] used IOC to visualize the nature of obstruction of the bile duct.

Characteristic cholangiographic findings of HCC invading into the bile duct include intraluminal expanding hilar mass density. Jan *et al.* found the main choledochoscopic findings were a yellowish intraluminal nodular mass and tumor thrombus in the CBD. These features may allow differential diagnosis from hilar papillary type cholangiocarcinoma^[44].

Bile duct brushing cytology

Bile duct brushing cytology is another useful technique in the diagnosis of malignant biliary strictures. In HCC with obstructive jaundice due to invasion of the biliary tract, a striking feature of the brushing is the prominent capillary vascular pattern associated with the tumor cells. This is a cytologic feature that has been noted in fine-needle aspirates of HCC as well, and is distinct from the expected findings in adenocarcinoma^[48].

TREATMENT STRATEGIES

Surgical treatment

Jaundice is not necessarily a harbinger of advanced disease and a contraindication for surgery. Patients with primary liver cancer and jaundice due to migrated tumor fragments in the bile duct may benefit from surgical resection. Most patients will have satisfactory palliation and occasional cure if the appropriate procedures are selected and carried out safely, which can result in long-term resolution of symptoms and occasional long-term survival.

The goals of operative intervention are biliary decompression with removal of tumor debris or tumor-containing blood clots, and, if possible, curative resection of the hepatic tumor. The commonly used operative methods are lobectomy (including the primary tumor and the tumor thrombi in bile duct), hepatectomy plus thrombectomy, choledochotomy with T-tube drainage alone, internal biliary stenting, or biliary diversion. The ideal treatment of these patients is hepatic resections^[18,33,34,49-51].

“Curative” resection is possible in some patients with obstructive jaundice. The overall survival of patients with HCC with obstructive jaundice might be similar to those patients who present with no clinical detectable jaundice, and is much better than those with jaundice due to hepatic insufficiency^[52].

There are numerous techniques that can be employed for biliary decompression and drainage^[26]. The decision to perform what kind of operations or interventions should be based on the nature and location of the main tumor mass, severity of the symptoms, associated neoplastic strictures, the patient's overall status, and the experience of the surgeon. Wang *et al.* reported 10 cases with gross evidence of tumor thrombi in the bile duct were treated with different resection methods and interventions. Eight out of the 10 patients underwent exploratory laparotomy (right lobectomy with extrahepatic bile duct resection in 2 cases, right lobectomy with tumor thrombectomy in 2 cases, left lobectomy and caudate lobectomy with extra-hepatic bile duct resection in 2 cases including T-tube drainage in 1 case and biopsy only with post-operative internal biliary stent in 1 case). Survival time of these patients was 39 months (still alive); 38 months (still alive); 8 months (died); 8 months (died); 8 months (still alive); 1 month (still alive); 14 months (died); 8 months (died), respectively. Of the 2 non-surgical cases, 1 underwent PTBD only and the other had endoscopic removal of the thrombi. Their survival time was 18 days (died) and 24 months (still alive with recurrence), respectively. The 4 cases, with right lobectomy or left lobectomy including extrahepatic bile duct resection, had relatively long-term disease-free survival (39 months, 38 months, 8 months and 1 month after operation, respectively). However, there were no differences in survival between the partial hepatectomy procedure with removal of tumor thrombi and the simple drainage procedure without tumor resection. So, they suggested that, for the improvement of survival, it was necessary to perform major hepatic resection with removal of the extrahepatic bile duct. If hepatic resection could not be accomplished with bile duct resection due to limited liver function, non-surgical modalities should be considered instead of surgery because there was no difference in prognosis between the 2 groups^[53]. Hu *et al.* reviewed 18 patients with obstructive jaundice by tumor emboli from HCC during a 15-year period of time. Types of surgical procedures were choledochotomy with T-tube drainage alone in 9 patients, choledochotomy with T-tube drainage followed by hepatectomy in six, and T-tube drainage followed by TACE in the remaining three patients. The mean survival time for 9 patients with external drainage alone was 4.5 months. For the 3 patients with T-tube drainage and TACE, the mean survival time was 11 months. Six patients who had undergone hepatectomy had a better postoperative survival time, with 1 surviving for more than 3 years and another alive for 70 months, without evidence of recurrence at the moment^[54]. Tantawi *et al.* reported 5 patients underwent liver resection associated with biliary exploration, clearance and T-tube drainage, 4 of them received major hepatectomy. All of the patients survived more than 1 year with a median survival of 29 months. There were 2 long-term survivors without recurrence at 29 and 80 months^[51].

Intraoperative identification of the nature and location of intraluminal biliary obstruction is crucial for the initial assessment and planning of operative strategy. In this respect, IOC, cholangiography, and intraoperative US are important adjuncts to formal common bile duct exploration. Direct endoscopic visualization of bile ducts will facilitate differentiation of neoplastic stricture from filling defects demonstrated in cholangiograms. Removal of gross tumor debris as much as possible from the luminal of the bile duct through manual extraction and irrigation is one of the key procedures to the prognosis. This can often be verified at the end of the procedure either by repeated cholangioscopy or

cholangiography. Using intra-operative US on the surface of the liver, small or deeply seated tumor and intrahepatic metastasis can be found and an adequate tumor resection margin can be marked out accurately. IOC reveals the characteristic finding of an intraluminal yellowish nodular mass in patients with malignant obstruction of the bile duct due to HCC. Liver resection with a free margin of the involved hepatic duct can be achieved by a choledochoscopically guided operation^[14].

It is not difficult to remove such tumor casts at operation in most cases. However, active hemorrhage occurred during operation in some cases, possibly because of the continuity of the intraductal tumor debris with the main intrahepatic tumor. Suturing, electrocauterization, compression, Pringle's maneuver, or hepatic arterial ligation usually can achieve hemostasis. When noncalculous material is found to be obstructing the extrahepatic ducts, even no obvious primary hepatic tumor was found, tumor embolus must be considered and the material sent routinely for pathological evaluation.

The role of preoperative biliary drainage (PBD) before liver resection in the presence of obstructive jaundice remains controversial. Cherqui *et al.* found major liver resections without PBD were safe in most patients with obstructive jaundice. Recovery of hepatic synthetic function was identical to that of no jaundiced patients. Transfusion requirements and incidence of postoperative complications, especially bile leaks and subphrenic collections are higher in jaundiced patients. Whether PBD could improve these results remains to be determined^[55]. Teda *et al.* thought a combination of biliary drainage and subsequent TAE is a recommended pre-operative strategy for the successful surgical treatment of Icteric type HCC. Nine of the 10 patients achieved sufficient reduction of the jaundice preoperatively. After the evaluation of liver function, 8 patients underwent hepatectomy without any appreciable morbidity or mortality. The median survival time of the resected cases was 18 months^[56].

Non-surgical treatments

Although successfully resected cases of Icteric type HCC have been reported, most of this type of patients are inoperable^[49-52,57]. The alternative treatment strategy is palliative in intent, including palliative treatment for the tumor and thrombi, and alleviating the jaundice. Palliative treatment strategies, including TACE and/or radiotherapy (R/T) show a beneficial effect in improving the survival.

Biliary drainage is usually used as the initial treatment because of overt cholangitis. Early and effective biliary drainage (percutaneous transhepatic biliary drainage, PTBD) might be necessary in this group of patients with limited hepatic function to prove the prognosis^[58].

To some extent, for icteric type HCC patients with poor and complicated conditions, the palliative strategies are chosen based on experience. In icteric type HCC patients with sufficient reserved liver function, TACE is effective and should be tried as a first choice of therapy^[59]. The median survival time among those eight patients who received palliative treatment was 13.4 months (a range of 8-26 months), which was significantly longer than for the other two patients without treatment (2 and 4 months).

External beam radiation therapy may be beneficial in some patients with unresectable icteric-type HCC. Also, US-guided localized radiotherapy, particularly on the critically located CBD and CHD thrombi, could be effective^[60,61]. Huang *et al.* demonstrated that radiotherapy could be an effective adjuvant strategy in those who showed limited response to TACE or those who had poor liver reserve function. The median survival time of those 8 patients receiving palliative treatment (TACE

alone, or radiotherapy alone, or in combination) was longer than that the other two patients without treatment (13.4 months vs. 3 months)^[16]. When combined with other conventional therapies (such as TACE), radiation therapy may play an important role in the treatment of HCC^[62].

Endoscopic biliary drainage (EBD) for unresectable HCC associated with obstructive jaundice remains controversial because of the short survival of these patients. Some reports suggest EBD is one of the most effective treatments for patients with unresectable malignant biliary stenosis, and even for patients with obstructive jaundice caused by liver metastasis. However, EBD is often difficult in HCC patients with obstructive jaundice and may fail because of proximal biliary obstructive at the hilum, underlying liver cirrhosis, and a poor hepatic functional reserve. Consequently, it is not a commonly used procedure in patients with advanced inoperable HCC and obstructive jaundice, and the indications for EBD in these patients are also controversial because of their short survival^[63].

ERCP can be both diagnostic and therapeutic. Biliary stenting can relieve jaundice and allow further chemotherapy, but at additional expense and potential morbidity. Martin *et al.* retrospectively analyzed 26 patients with HCC and jaundice undergoing ERCP after CT or US, and found in selected patients, stenting could safely relieve jaundice and allow subsequent chemotherapy. CT or US accurately predicted lesions that responded to stenting. ERCP and stenting provided no benefit in the absence of biliary dilation on CT or US^[64]. Placement of metallic stents is the procedure of choice for palliation of malignant biliary obstruction. Stents show a favorable patency rate with regard to patient survival. In patients with hilar obstruction, the clinical efficacy of metallic stents is superior to that in patients with CBD obstruction^[65]. In the palliative treatment of HCC patients, a large stent may be necessary, as used in reports of HCC successfully treated by metal stents, if the hepatic functional reserve is not too poor^[66,67].

EBD is more effective for palliation in the patients with obstructive jaundice caused by tumor fragments and/or blood clots or with tumor protruding into the CBD lumen than in the patients who mainly have tumor invasion. So it is important to understand the causes of obstruction on cholangiograms before performing EBD. And it is difficult in most patients with direct tumor invasion involving both hepatic ducts, and multiple tumors in both lobes. It is important to determine the site, extent, and nature of the obstruction, as well as liver function and the presence of portal thrombus, before performing EBD. In patients with tumor involvement of both the right and left intrahepatic ducts, EBD should be avoided because of the low successful drainage rate and short survival. In HCC patients with obstructive jaundice, considering the progression of hepatic insufficiency, it is important to achieve complete drainage at the first stenting procedure. In patients with CBD bifurcation tumors, drainage of both lobes should be achieved, if possible. However, attempted drainage of all obstructed liver segments may cause cholangitis or sepsis if it is unsuccessful^[68,69].

The combination of palliative methods may relieve jaundice, ensure a good quality of life and possibly prolong survival of this type of HCC patients. Lauffer *et al.* reported 1 case received combination treatment with surgical segment III drainage, TACE and radioembolization with Yttrium-90 resin particles and endoscopic stenting was performed. With these combined procedures, relief of jaundice and a survival time of 32 months could be achieved^[70].

PROGNOSIS

The prognosis of icteric type HCC patients is generally dismal, but is better than those HCC patients who have jaundice caused by hepatic insufficiency. Cholangitis secondary to tumor

obstruction is found to be the major cause of death in these patients.

The prognosis of this type of HCC patients is closely related to the stage of disease, the location and extension of tumor thrombi in bile duct. In 1994, Ueda *et al.* classified HCC with BDT into 4 types. Type I: BDT located in the secondary branch of the biliary tree. Type II: BDT extending to the first branch of the biliary tree. Type III: BDT extending to the common hepatic duct (CHD) (IIIa); an implanted tumor growing in the CHD (IIIb). Type IV: floating tumor debris from the ruptured tumor in the CBD^[71]. They also found that the patients with type I, IIIb and IV of BDT had a relative better prognosis than other types.

Different therapies also influence the prognosis of this type of patients. Lau *et al.* reported that patients who received curative liver resection had a much better survival rate than those without resection (with a median survival of 25.3 vs. 2.1 months, respectively)^[72]. Huang *et al.* studied 9 patients who had a patent portal vein and reported that the mean survival of 4 patients with curative resection was 35.8 months, but that of the 5 patients with palliative treatment was only 4.5 months. Thus, the ideal treatment for HCC associated with obstructive jaundice is to reduce the jaundice with preoperatively and perform hepatic resection, but the prognosis of patients who are inoperable is extremely poor^[73]. Kojiro *et al.* reported that 2 of their patients died 40-60 days after the development of obstructive jaundice^[4]. In a study of 49 HCC patients with obstructive jaundice, Lau *et al.* reported that 9 patients received curative resection, 35 had biliary stents, and 5 had supportive treatment, and the overall survival of these patients was similar to that of HCC patients without jaundice. They concluded that good palliation and occasional cure were possible with proper treatment^[52]. For biliary drainage in patients with unresectable HCC, the mean survival time of patients with only EBD was 3.9 months^[29], and the patients with external drainage alone was 4.5 months^[54].

CONCLUSIONS

Obstructive jaundice as the main presenting clinical feature of HCC is uncommon. The prognosis of this type of HCC is generally dismal, but is better than those HCC patients who have jaundice caused by hepatic insufficiency. Jaundice is not necessarily a harbinger of advanced disease and a contraindication for surgery. Patients with primary liver cancer and obstructive jaundice due to migrated tumor fragments in the bile duct may benefit from surgical resection. Most patients will have satisfactory palliation and occasional cure if appropriate procedures are selected and carried out safely, which can result in long-term resolution of symptoms and occasional long-term survival.

REFERENCES

- 1 **Becker FF.** Hepatoma-nature's model tumor. A review. *Am J Pathol* 1974; **74**: 179-210
- 2 **Kew MC, Paterson AC.** Unusual presentations of hepatocellular carcinoma. *Trop Gastroenterol* 1985; **6**: 10-22
- 3 **Mallory TB, Castleman B, Parris EE.** Case records of the Massachusetts General Hospital. *N Eng J Med* 1947; **237**: 673-676
- 4 **Kojiro M, Kawabata K, Kawano Y, Shirai F, Takemoto N, Nakashima T.** Hepatocellular carcinoma presenting as intrabiliary duct tumor growth. A clinicopathological study of 24 cases. *Cancer* 1982; **49**: 2144-2147
- 5 **Ishikawa I, Kobayashi K, Odajima S, Takada A, Takeuchi J.** Primary hepatic cancer with recurrent episodes of obstructive jaundice and distended gall bladder. A case report and review of the literature. *Am J Gastroenterol* 1973; **60**: 496-503
- 6 **Ihde DC, Sherlock P, Winawer SJ, Fortner JG.** Clinical manifestation of hepatoma. A review of 6 years' experience at a cancer hospital. *Am J Med* 1974; **56**: 83-91
- 7 **Roslyn JJ, Kuchenbecker S, Longmire WP Jr, Tompkins RK.** Float-

- ing tumor debris. *Arch Surg* 1984; **119**: 1312-1315
- 8 **Okuda K, Kubo Y, Okazaki N, Arishima T, Hashimoto M.** Clinical aspects of intrahepatic bile duct carcinoma including hilar carcinoma. *Cancer* 1977; **39**: 232-246
- 9 **Wang JH, Wang LY, Lin ZY, Chen SC, Kang SC, Chuang WL, Lu SN, Hsieh MY, Tsai JF, Chang WY.** Doppler sonography of common hepatic duct tumor invasion in hepatocellular carcinoma: report of two cases. *J Ultrasound Med* 1995; **14**: 471-474
- 10 **Juroco S, Kim H.** Extrahepatic biliary obstruction by hepatocellular carcinoma. *Am J Gastroenterol* 1980; **74**: 176-178
- 11 **Terada T, Nakanuma Y, Kawai K.** Small hepatocellular carcinoma presenting as intrabiliary pedunculated polyp and obstructive jaundice. *J Clin Gastroenterol* 1989; **11**: 578-583
- 12 **Lin TY, Chen KM, Chen YR, Lin WS, Wang TH, Sung JL.** Icteric type hepatoma. *Med Chir Dig* 1975; **4**: 267-270
- 13 **Okuda K.** Clinical aspects of hepatocellular carcinoma: analysis of 134 cases. In: Okuda K, Peters RL, eds. *Hepatocellular carcinoma*. New York: John Wiley 1976: 387-436
- 14 **Jan YY, Chen MF.** Obstructive jaundice secondary to hepatocellular carcinoma rupture into the common bile duct: choledochoscopic findings. *Hepatogastroenterology* 1999; **46**: 157-161
- 15 **Lau WY, Leung JW, Li AK.** Management of hepatocellular carcinoma presenting as obstructive jaundice. *Am J Surg* 1990; **160**: 280-282
- 16 **Huang JF, Wang LY, Lin ZY, Chen SC, Hsieh MY, Chuang WL, Yu MY, Lu SN, Wang JH, Yeung KW, Chang WY.** Incidence and clinical outcome of icteric type hepatocellular carcinoma. *J Gastroenterol Hepatol* 2002; **17**: 190-195
- 17 **Spahr L, Frossard JL, Felley C, Brundler MA, Majno PE, Hadengue A.** Biliary migration of hepatocellular carcinoma fragment after transcatheter arterial chemoembolization therapy. *Eur J Gastroenterol Hepatol* 2000; **12**: 243-244
- 18 **VanSonnenberg E, Ferrucci JT.** Bile duct obstruction in hepatocellular carcinoma (hepatoma)-clinical and cholangiographic characteristics. Reports of 6 cases and review of the literature. *Radiology* 1979; **130**: 7-13
- 19 **Soyer P, Laissy JP, Bluemke DA, Sibert A, Menu Y.** Bile duct involvement in hepatocellular carcinoma: MR demonstration. *Abdom Imaging* 1995; **20**: 118-121
- 20 **Afroudakis A, Bhuta SM, Ranganath KA, Kaplowitz N.** Obstructive jaundice caused by hepatocellular carcinoma. *Dig Dis* 1978; **23**: 609-617
- 21 **Buckmaster MJ, Schwartz RW, Carnahan GE, Strodel WE.** Hepatocellular carcinoma embolus to the common hepatic duct with no detectable primary hepatic tumor. *Am Surg* 1994; **60**: 699-702
- 22 **Shimoji H, Shiraishi M, Hiroyasu S, Isa T, Kusano T, Muto Y.** Common bile duct blood clot: an unusual cause of ductal filling defects for calculi. *J Gastroenterol* 1999; **34**: 420-423
- 23 **Edmondson HA, Steiner PE.** Primary carcinoma of the liver, study of case among 43900 necropsies. *Cancer* 1954; **7**: 462-502
- 24 **Narita R, Oto T, Mimura Y, Ono M, Abe S, Tabaru A, Yoshikawa I, Tanimoto A, Otsuki M.** Biliary obstruction caused by intrabiliary transplantation from hepatocellular carcinoma. *J Gastroenterol* 2002; **37**: 55-58
- 25 **Saito M, Hige S, Takeda H, Tomaru U, Shibata M, Asaka M.** Combined hepatocellular carcinoma and cholangiocarcinoma growing into the common bile duct. *J Gastroenterol* 2001; **36**: 842-847
- 26 **Kuroyanagi Y, Sawada M, Hidemura R, Aoki S, Kato H.** Common bile duct obstruction by hepatoma. *Am J Surg* 1977; **133**: 233-235
- 27 **Kojiro M, Nakashima T.** Pathology of hepatocellular carcinoma. In: Okuda K, Ishak KG, eds. *Neoplasms of the Liver*. Tokyo: Springer Verlag 1987: 81-107
- 28 **Cho HG, Chung JP, Lee KS, Chon CY, Kang JK, Park IS, Kim KW, Chi HS, Kim H.** Extrahepatic bile duct hepatocellular carcinoma without primary hepatic parenchymal lesions-a case report. *Korean J Intern Med* 1996; **11**: 169-174
- 29 **Tseng JH, Hung CF, Ng KK, Wan YL, Yeh TS, Chiu CT.** Icteric-type hepatoma: magnetic resonance imaging and magnetic resonance cholangiographic features. *Abdom Imaging* 2001; **26**: 171-177
- 30 **Cajot O, Descamps C, Navez B, Lacreman D, Druez P.** Hemobilia disclosing very small hepatocellular carcinoma ruptured into the biliary ducts. *Gastroenterol Clin Biol* 1997; **21**: 426-429
- 31 **Tseng LJ, Jao YT, Mo LR.** Acute pancreatitis caused by hemobilia secondary to hepatoma with bile duct invasion. *Gastrointest Endosc* 2002; **55**: 240-241

- 32 **Lai ST**, Lam KT, Lee KC. Biliary tract invasion and obstruction by hepatocellular carcinoma: report of five cases. *Postgrad Me J* 1992; **68**: 961-963
- 33 **Tsuzuki T**, Ogata Y, Iida S, Dasajima M, Takahashi S. Hepatoma with obstructive jaundice due to the migration of a tumor mass in the biliary tract: report of a successful resection. *Surgery* 1979; **85**: 593-598
- 34 **Matzen P**, Malchow-Moller A, Brun B, Gronvall S, Haubek A, Henrksen JH. Ultrasonography, computed tomography and cholescintigraphy in suspected obstruction jaundice. A prospective comparative study. *Gastroenterology* 1983; **84**: 1492-1497
- 35 **Dodd GD III**, Mernel DS, Baron RL, Eichner L, Santiguida LA. Portal vein thrombosis in patients with cirrhosis: does sonographic detection of intrathrombus flow allow differentiation of benign and malignant thrombus? *Am J Roentgenol* 1995; **165**: 573-577
- 36 **Wang JH**, Chen TM, Tung HD, Lee CM, Changchien CS, Lu SN. Color Doppler sonography of bile duct tumor thrombi in hepatocellular carcinoma. *J Ultrasound Med* 2002; **21**: 767-772
- 37 **Lee YC**, Wang HP, Huang SP, Chang YT, Wu CT, Yang CS, Wu MS, Lin JT. Obstructive jaundice caused by hepatocellular carcinoma: Detection by endoscopic sonography. *J Clin Ultrasound* 2001; **29**: 363-366
- 38 **Park SJ**, Han JK, Kim TK, Choi BI. Three-dimensional spiral CT cholangiography with minimum intensity projection in patients with suspected obstructive biliary disease: comparison with percutaneous transhepatic cholangiography. *Abdom Imaging* 2001; **26**: 281-286
- 39 **Harbin WP**, Mueller PR, Ferrucci JT. Transhepatic cholangiography: complications and use pattern of the fine needle technique. *Radiology* 1980; **135**: 15-22
- 40 **Zimmon DS**, Falkenstein DB, Riccobono C, Aaron B. Complications of endoscopic retrograde cholangiopancreatography. Analysis of 300 consecutive cases. *Gastroenterology* 1975; **69**: 303-309
- 41 **Wallner BK**, Schumacher KA, Weidenmaier W, Friedrich JM. Dilated biliary tract: evaluation with MR cholangiography with a T2-weighted contrast-enhanced fast sequence. *Radiology* 1991; **181**: 805-808
- 42 **Fulcher AS**, Turner MA, Capps GW, Zfass AM, Baker KM. Half-Fourier RARE MR cholangiopancreatography: experience in 300 subjects. *Radiology* 1998; **207**: 21-32
- 43 **Barish MA**, Yucel EK, Soto JA, Chuttani R, Ferrucci JT. MR cholangiopancreatography: efficacy of three-dimensional turbo spin-echo technique. *Am J Roentgenol* 1995; **165**: 295-300
- 44 **Wu CS**, Wu SS, Chen PC, Chiu CT, Lin SM, Jan YY, Hung CF. Cholangiography of icteric type hepatoma. *Am J Gastroenterol* 1994; **89**: 774-777
- 45 **Lee NW**, Wong KP, Siu KF, Wong J. Cholangiography in hepatocellular carcinoma with obstructive jaundice. *Clin Radiol* 1984; **35**: 119-123
- 46 **Yeh TS**, Jan YY, Tseng JH, Chiu CT, Chen TC, Hwang TL, Chen MF. Malignant perihilar biliary obstruction: magnetic resonance cholangiopancreatographic findings. *Am J Gastroenterol* 2000; **95**: 432-440
- 47 **Chen MF**, Jan YY, Wang CS, Jeng LB, Hwang TL. Intraoperative fiberoptic choledochoscopy for malignant biliary tract obstruction. *Gastrointest Endosc* 1989; **35**: 545-547
- 48 **Dusenbery D**. Biliary stricture due to hepatocellular carcinoma: diagnosis by bile duct brushing cytology. *Diagn Cytopathol* 1997; **16**: 55-56
- 49 **Chen MF**, Jan YY, Jeng LB, Hwang TL, Wang CS, Chen SC. Obstructive jaundice secondary to ruptured hepatocellular carcinoma into the common bile duct. *Cancer* 1994; **73**: 1336-1340
- 50 **Jan YY**, Chen MF, Chen TJ. Long term survival after obstruction of the common bile duct by ductal hepatocellular carcinoma. *Eur J Surg* 1995; **161**: 771-774
- 51 **Tantawi B**, Cherqui D, Tran van Nhie J, Kracht M, Fagniez PL. Surgery for biliary obstruction by tumour thrombus in primary liver cancer. *Br J Surg* 1996; **83**: 1522-1525
- 52 **Lau W**, Leung K, Leung TW, Liew CT, Chan MS, Yu SC, Li AK. A logical approach to hepatocellular carcinoma presenting with jaundice. *Ann Surg* 1997; **225**: 281-285
- 53 **Wang HJ**, Kim JH, Kim JH, Kim WH, Kim MW. Hepatocellular carcinoma with tumor thrombi in the bile duct. *Hepatogastroenterology* 1999; **46**: 2495-2499
- 54 **Hu J**, Pi Z, Yu MY, Li Y, Xiong S. Obstructive jaundice caused by tumor emboli from hepatocellular carcinoma. *Am Surg* 1999; **65**: 406-410
- 55 **Cherqui D**, Benoist S, Malassagne B, Humeres R, Rodriguez V, Fagniez PL. Major liver resection for carcinoma in jaundiced patients without preoperative biliary drainage. *Arch Surg* 2000; **135**: 302-308
- 56 **Tada K**, Kubota K, Sano K, Noie T, Kosuge T, Takayama T, Makuuchi M. Surgery of icteric-type hepatoma after biliary drainage and transcatheter arterial embolization. *Hepatogastroenterology* 1999; **46**: 843-848
- 57 **Chen CL**, Huang SM, Chien CH, Chang TT, Yu CY, Lee JC. Successful resection of a minute icteric hepatocellular carcinoma-case report. *Hepatogastroenterology* 1994; **41**: 503-505
- 58 **Lee JW**, Han JK, Kim TK, Choi BI, Park SH, Ko YH, Yoon CJ, Yeon KM. Obstructive jaundice in hepatocellular carcinoma: response after percutaneous transhepatic biliary drainage and prognostic factors. *Cardiovasc Intervent Radiol* 2002; **25**: 176-179
- 59 **Takagi H**, Yamada S, Abe T, Uehara M, Takezawa J, Nagamine T, Ichikawa K, Kobayashi S, Katakai S. A case report of transcatheter arterial embolization of cholestatic type of hepatoma. *Gastroenterol Jpn* 1989; **24**: 315-319
- 60 **Chen SC**, Lian SL, Chang WY. The effect of external radiotherapy in treatment of portal vein invasion in hepatocellular carcinoma. *Cancer Chem Pharm* 1994; **33**: S124-127
- 61 **Chen SC**, Lian SL, Chuang WL, Hsieh MY, Wang LY, Chang WY, Ho YH. Radiotherapy in the treatment of hepatocellular carcinoma and its metastases. *Cancer Chemother Pharmacol* 1992; **31**: S103-105
- 62 **Sung KF**, Tsang NM, Tseng JH, Yeh CT. Effective relief of obstructive jaundice in a patient with nonresectable icteric-type hepatocellular carcinoma by external beam radiation therapy: case report. *Chang Gung Med J* 2001; **24**: 114-118
- 63 **Matsueda K**, Yamamoto H, Umeoka F, Ueki T, Matsumura T, Tezen T, Doi I. Effectiveness of endoscopic biliary drainage for unresectable hepatocellular carcinoma associated with obstructive jaundice. *J Gastroenterol* 2001; **36**: 173-180
- 64 **Martin JA**, Slivka A, Rabinovitz M, Carr BI, Wilson J, Silverman WB. ERCP and stent therapy for progressive jaundice in hepatocellular carcinoma: which patients benefit, which patients don't? *Dig Dis Sci* 1999; **44**: 1298-1302
- 65 **Lee BH**, Choe DH, Lee JH, Kim KH, Chin SY. Metallic stents in malignant biliary obstruction: prospective long-term clinical results. *Am J Roentgenol* 1997; **168**: 741-745
- 66 **Okazaki M**, Mizuta A, Hamada N, Kawamura N, Nakao K, Kikuchi T, Osada T. Hepatocellular carcinoma with obstructive jaundice successfully treated with a self-expandable metallic stent. *J Gastroenterol* 1998; **33**: 886-890
- 67 **Yoshioka T**, Uchida H, Kitano S, Makutari S, Maeda M, Taoka T, Ohishi H. Long-term palliative treatment of hepatocellular carcinoma extending into the portal vein and bile duct by chemoembolization and metallic stenting. *Cardiovasc Intervent Radiol* 1997; **20**: 390-393
- 68 **Polydorou AA**, Cairns SR, Dowsett JF, Hatfield ARW, Salmon PR, Cotton PB, Russell RC. Palliation of proximal malignant biliary obstruction by endoscopic endoprosthesis insertion. *Gut* 1991; **32**: 685-689
- 69 **Ducreux M**, Liguory CI, Lefebvre JF, Ink O, Choury A, Fritsch J, Bonnel D, Derhy S, Etienne JP. Management of malignant hilar biliary obstruction by endoscopy: results and prognostic factors. *Dig Dis Sci* 1992; **37**: 778-783
- 70 **Lauffer JM**, Mai G, Berchtold D, Curti CG, Triller J, Baer HU. Multidisciplinary approach to palliation of obstructive jaundice caused by a central hepatocellular carcinoma. *Dig Surg* 1999; **16**: 531-536
- 71 **Ueda M**, Takeuchi T, Takayasu T, Takahashi K, Okamoto S, Tanaka A, Morimoto T, Mori K, Yamaoka Y. Classification and surgical treatment of hepatocellular carcinoma (HCC) with bile duct thrombi. *Hepatogastroenterology* 1994; **41**: 349-354
- 72 **Lau WY**, Leung KL, Leung TW, Ho S, Chan M, Liew CK, Leung N, Johnson P, Li AK. Obstructive jaundice secondary to hepatocellular carcinoma. *Surg Oncol* 1995; **4**: 303-308
- 73 **Huang GT**, Sheu JC, Lee HS, Lai MY, Wang TH, Chen DS. Icteric type hepatocellular carcinoma: revisited 20 years later. *J Gastroenterol* 1998; **33**: 53-56

Analysis of gene expression profile induced by EMP-1 in esophageal cancer cells using cDNA Microarray

Hai-Tao Wang, Jian-Ping Kong, Fang Ding, Xiu-Qin Wang, Ming-Rong Wang, Lian-Xin Liu, Min Wu, Zhi-Hua Liu

Hai-Tao Wang, Jian-Ping Kong, Fang Ding, Xiu-Qin Wang, Ming-Rong Wang, Lian-Xin Liu, Min Wu, Zhi-Hua Liu, National Laboratory of Molecular Oncology, Cancer Institute, Chinese Academy of Medical Science and Peking Union Medical College, Beijing 100021, China

Supported by China Key Program on Basic Research (G1998051021) and the Chinese Hi-Tech R&D program (2001AA231310).

Correspondence to: Dr. Zhi-Hua Liu, National Laboratory of Molecular Oncology, Cancer Institute, Chinese Academy of Medical Science and Peking Union Medical College, Beijing 100021, China. liuzh@pubem.cicams.ac.cn

Telephone: +86-10-67723789 **Fax:** +86-10-67715058

Received: 2002-06-20 **Accepted:** 2002-08-09

Abstract

AIM: To obtain human esophageal cancer cell EC9706 stably expressed epithelial membrane protein-1 (EMP-1) with integrated eukaryotic plasmid harboring the open reading frame (ORF) of human EMP-1, and then to study the mechanism by which EMP-1 exerts its diverse cellular action on cell proliferation and altered gene profile by exploring the effect of EMP-1.

METHODS: The authors first constructed pcDNA3.1/myc-his expression vector harboring the ORF of EMP-1 and then transfected it into human esophageal carcinoma cell line EC9706. The positive clones were analyzed by Western blot and RT-PCR. Moreover, the cell growth curve was observed and the cell cycle was checked by FACS technique. Using cDNA microarray technology, the authors compared the gene expression pattern in positive clones with control. To confirm the gene expression profile, semi-quantitative RT-PCR was carried out for 4 of the randomly picked differentially expressed genes. For those differentially expressed genes, classification was performed according to their function and cellular component.

RESULTS: Human EMP-1 gene can be stably expressed in EC9706 cell line transfected with human EMP-1. The authors found the cell growth decreased, among which S phase was arrested and G1 phase was prolonged in the transfected positive clones. By cDNA microarray analysis, 35 genes showed an over 2.0 fold change in expression level after transfection, with 28 genes being consistently up-regulated and 7 genes being down-regulated. Among the classified genes, almost half of the induced genes (13 out of 28 genes) were related to cell signaling, cell communication and particularly to adhesion.

CONCLUSION: Overexpression of human EMP-1 gene can inhibit the proliferation of EC9706 cell with S phase arrested and G1 phase prolonged. The cDNA microarray analysis suggested that EMP-1 may be one of regulators involved in cell signaling, cell communication and adhesion regulators.

Wang HT, Kong JP, Ding F, Wang XQ, Wang MR, Liu LX, Wu M, Liu ZH. Analysis of gene expression profile induced by EMP-1 in esophageal cancer cells using cDNA Microarray. *World J Gastroenterol* 2003; 9(3): 392-398

<http://www.wjgnet.com/1007-9327/9/392.htm>

INTRODUCTION

EMP-1 is a member of the PMP22 family with the similarity in structure. Since EMP-1 was first found by Taylor, it has been isolated independently from human, mouse and rabbit and received many different designations, such as TMP (tumor membrane Protein), PAP (Progression Associated Protein), CL-20 and B4B^[1]. All tissues expressing EMP-1 mRNA contain 2.76-kb EMP-1 transcripts. In some regions of the gastrointestinal tract, including the fundus, ileum, cecum, and colon, however, additional transcripts of approximately 1.7 kb hybridize with the EMP-1 cDNA^[2]. The 2.76-kb EMP-1 cDNA contains five exons about 0.2kb, 0.12kb, 0.1kb, 0.14kb, and 2.2 kb and four introns about 15kb, 1.9kb, 0.1kb, and 0.7 kb in length respectively. EMP-1 has been mapped to chromosome 12p12 by fluorescence in situ hybridization^[3]. EMP-1 is encoded by a single-copy gene with the positions of introns exactly conserved between EMP-1 and PMP22, corroborating the hypothesis that EMP-1 belongs to the PMP22 family^[4]. EMP-1 transcript is expressed at high levels in heart, placenta, lung, skeletal muscle, kidney, spleen, colon prostate, ovary, testicle, small intestine and thymus in human^[5].

EMP-1 was selected from a series of differential expressed genes obtained from cDNA microarray analysis of expression profiles of esophageal cancer in our previous work. EMP-1 expression was 6 fold down-regulated in esophageal cancer lower than in normal tissue. EMP-1 is highly up-regulated during squamous cell differentiation and in certain tumors, and a role in tumorigenesis has been proposed^[6]. Moreover, The overexpression of PMP22 leads to an apoptotic-like phenotype in NIH3T3 growing cells^[7] and delays serum-forskolin-stimulated entry of resting Schwann cells from G1 into the S+G2/M phase in Schwann cell^[8]. Transient expression of EMP-1 specifically inhibited cellular proliferation by more than 50 %^[9]. Preliminary data suggested that EMP-1 was involved in growth control in esophageal cancer cell line EC9706. However, whether there is a similar effect of EMP-1 expression on the cell cycle of epithelial cells remains to be determined and little is known about the function of EMP-1 in growth control in esophageal cancer cell line EC9706.

To elucidate the effect of EMP-1 on EC9706 cell, the open reading frame (ORF) of human EMP-1 was cloned into pcDNA3.1/myc-his, a eukaryotic expression vector. EC9706 was transfected with the integrated plasmid containing EMP-1 to enforce expression of the exogenous EMP-1. Western blotting and RT-PCR were used to analyze positive clones. The cell growth curve was observed and the cell cycle was checked by FACS method. However, the mechanism by which EMP-1 may exert its activity remains unclear. Because the differentiation of mammalian cells is associated with changes in gene expression that is primarily controlled at the level of transcription, we tested the expression alteration with cDNA microarray technology to address the question of which genes are influenced by EMP-1 gene overexpression.

MATERIALS AND METHODS

Sample collection

Fifteen pairs of esophageal tumors and matched adjacent

normal mucosa were obtained at surgery. Samples were frozen in liquid nitrogen until RNA was extracted.

Cell lines and cell culture

Esophageal carcinoma cell line EC9706 was established in our laboratory. The cell lines were maintained in M199 medium with 15 % FBS and cultured at 37 °C in 5 % CO₂.

The eukaryotic plasmid vector pcDNA3.1-myc-his (-) C

An *Xho*I and *Hind*III fragment ORF of EMP-1 was cloned into the pcDNA3.1/myc-his vector. The correct construct sequence was confirmed by DNA sequencing.

Atlas human cancer cDNA expression array

Atlas Human Cancer cDNA Expression Array (Clontech) was used to analyze EMP-1-induced gene expression which included over 588 genes on the nylon membrane.

Isolation of RNA and semi-quantitative RT-PCR

Paired esophageal cancer tissues and adjacent normal mucosa tissues (-100 mg) were homogenized mechanically in 1 ml of TRIzol reagent (Life Technologies, Inc.), and cell pellets were harvested to isolate the total RNA. According to the manufacturer's protocol (Life Technologies, Inc.). First-strand cDNA was synthesized from 5 µg of total RNA using Superscript II reverse transcriptase (Life Technologies, Inc.) and OligodT12-18 primers following the company's protocol. The same amount of cDNAs was subsequently used for PCR amplification. PCR reaction was performed in 25 µl buffer containing 1 µl cDNA, dATP, dCTP, dGTP, dTTP each 0.2 mmol/L, 1×PCR buffer, 1.5 mmol/l MgCl₂ and 1.5U Taq DNA polymerase (GIBCO). The primers for GAPDH are 5' -ACC ACA GTC CAT GCC ATC AC-3' and 5' -TCC ACC ACC CTG TTG CTG TA-3'; EMP-1 5' -GGA TCA GGG CTC CTA GGC TCA-3' and 5' -GGT GGC TTG CCC TCA ACA TT-3'; the primer for the ORF of EMP-1 is 5' -ATC TTT GTG GTC CAC ATC GCT-3' and 5' -CTT CTC CAT GGT GAA GAG CT-3'; Primers for four random selected genes were respectively designed for human CDK inhibitor p19INK4d, 5' -TCC ATG ACG CAG CCC GCA CT-3' and 5' -TCT CTG CAG TGC CAG CTC CA-3'; Human tissue-type plasminogen activator (t-PA), 5' -AGT GCA TTT TCC CAG ATA CT-3' and 5' -TTT GTG GTC CTG TTT CCA AAG-3'; Human interleukin-6, 5' -AGG CACTGG CAG AAA ACA AC-3' and 5' -TCC AAG AAA TGA TCT GGC TC-3'; Human alpha-1 type XI collagen (COL11A1), 5' -TCC TGT TTG TTT TCT TGG CT-3' and 5' -TTA TGA TTT TCA AAG CTT TTG T-3'. The amplification was performed with one denaturing cycle of 5 min at 95 °C, then 94 °C for 40s, 55 °C for 40s, 72 °C for 40 s for 25-27 cycles, and one final extension of 7 min at 72 °C. RT-PCR products were analyzed on 1.2 % agarose gel. The number of cycles and melting temperature was adjusted depending on the genes amplified.

In vitro transfection and cell culture

According to the manufacturer's instructions (Invitrogen), the day before transfection, seed 3×10⁶ EC9706 cells in 3 ml of the 15 % serum complete growth medium. Combine diluted DNA with diluted Lipofectamine™ Reagent. For each transfection, add 0.8 ml of medium without serum to the tube containing the complexes. Incubate the cells with the complexes for 5 hours at 37 °C in a CO₂ incubator. Following incubation, add 3 ml of growth medium containing 30 % serum without removing the transfection mixture. Add G418 after 3 days and select monoclonal cell to a fresh bottle and keep on culturing with G418 (1 mg/ml). The positive clones together with the negative parental vector without EMP-1 and EC9706

Cells (3×10⁵ in 2 ml) were seeded and incubated at 37 °C in 5 % CO₂ with G418 (1 mg/ml). Cells were harvested and then quantitated every 24 hours.

Flow cytometry assay

Flow cytometry was performed to assess the cell cycle alteration. Trypsinized adherent and floating cells were collected, washed twice with cold PBS, and resuspended in PBS containing 0.1 % Triton X-100 and 0.1 % RNase for 5 min at room temperature. The samples were then stained with propidium iodide (0.1 mg/ml), filtered through a 300-µm-pore-size nylon mesh, and analyzed in a cell sorter (Coulter, epics® elite ESP)^[10].

Western blotting analysis

Cells were rinsed twice with PBS, and protein preparation was performed according to the manufacturer's instruction (Santa Cruz). Protein concentration in homogenates was determined using a BSA-Protein assay (Hyclone) employing bovine serum albumin as the standard. The extracted proteins (20 µg) were subjected to 15 % polyacrylamide gel electrophoresis in the presence of sodium dodecyl sulfate under reducing conditions, and then transferred onto poly (vinylidene difluoride) (PVDF) membranes (Hybond-P). Mouse monoclonal anti-human hexad-HIS antibodies (Santa Cruz; final dilution 1:1 000) were used as the primary antibody, and horseradish peroxidase-labeled anti-mouse immunoglobulin (Santa Cruz; final dilution 1:1 500) was used as the secondary reagent. Detection was performed using an ECL system (Amersham-Pharmacia).

cDNA microarray analysis

Total RNA was extracted by TRIzol from positive clone 2 cells and the parental vector without cDNA insert pcDNA3.1-myc-his (-) C cells as negative control. Poly (A) RNA was purified using an Oligotex-dT30 mRNA purification kit (TAKARA). One µg of highly purified poly (A) RNA from the negative control and cell clone 2 was performed for cDNA microarray analysis. The mRNA was reverse transcribed with ³³P-dATP (Amersham). The paired reactions were purified with a TE-30 column (Clontech, Palo Alto, CA). The radioactive labeled probe was then applied to the array for hybridization at 68 °C for 12 hours. After hybridization, the membrane was washed with buffer of decreasing ionic strength. The X-ray film was scanned at a resolution of 16-bit. AtlasImage software (version1.01a, Clontech) was used for image analysis. The area surrounding each element image was used to calculate a local background, which was then subtracted from the total element signal. Background subtracted element signals are used to calculate intensity ratios. The average of the resulting total intensity signal gives a ratio that is used to balance or normalize the signals. Then semi-quantitative RT-PCR analysis of 4 randomly selected genes confirms the microarray results.

RESULTS

Differential expression of EMP-1 judged by RT-PCR

RT-PCR was used to detect the EMP-1 gene expression in the pair of esophageal cancer (C) and normal mucosa (N). We checked 15 pairs of esophageal cancer and its adjacent normal tissue and found the expression of EMP-1 was higher in normal tissue than that in cancer tissue in 14 pairs, and lower in only 1 pair (Figure 1).

Selection of positive transfectant clone by RT-PCR

Since the expression of EMP-1 should be up-regulated after transfection, RT-PCR was used to analyze the positive clones and the parental vector as negative control. The clones 1, 2, 3,

4, 5, 6, 8 and 10 showed a comparable increased expression of EMP-1 (Figure 2).

Expression of EMP-1 in positive clones detected by western blotting

Since the vector carrying 6xHis peptide as a selective marker, it can be detected by anti-His monoclonal antibody with Western blot. Hexad-His peptide has been expressed in host cell clone 1, clone 2, clone 3, clone 5, clone 6 and clone 8, however, EMP-1 protein was not identified in clone 4 which was highly expressed in transcriptional level for unknown reasons (Figure 3).

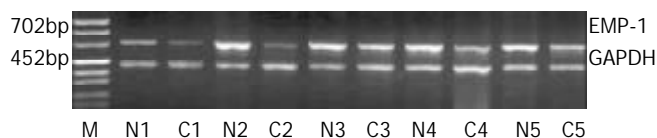


Figure 1 Different expression of EMP-1 detected in matched pairs of esophageal cancer tissue. The upper band represents EMP-1 (702 bp); the lower band represents GAPDH (452 bp). The expression of EMP-1 is higher in normal (N) tissue than its cancer (C) tissue. RT-PCR for GAPDH was used as equal loading control.

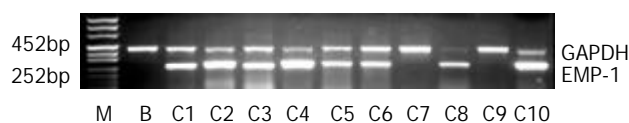


Figure 2 Different expression of EMP-1 cell clones transfected with pcDNA3.1-EMP-1-myc-his (-) C vector and the parental vector without cDNA insert pcDNA3.1myc-his (-) C cells as negative control. Clones 1, 2, 3, 4, 5, 6, 8 and 10 showed the increased expression of EMP-1. RT-PCR for GAPDH was used as equal loading control. B represents the parental vector as negative control.

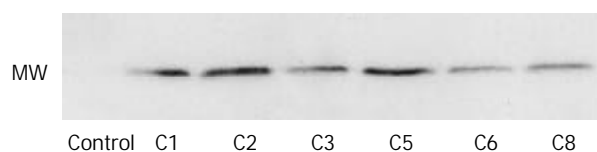


Figure 3 Western blotting check the expression of EMP-1 after transfected into the EC9706 cell with anti-HIS monoclonal antibody. His peptide has been expressed successfully in host cell clones (C1, C2, C3, C5, C6 and C8.). Control represents the negative control.

The growth curve of positive clone and the parental vector without the cDNA insert as negative control

The cell proliferation rate had been observed and the cells displayed a decreased proliferation rate in clone 1, clone 2, clone 3, clone 5, clone 6, clone 8 and clone 10, especially in clone 2. The proliferation rates of clone 4, clone 7, and clone 9 are close to that of negative control. The expression of EMP-1 in clone 1, clone 2, clone 3, clone 6 and clone 8 was up-regulated in both RNA and protein levels by RT-PCR and Western blot, respectively, and a reduced ability to proliferate was as shown in these clones (Figure 4).

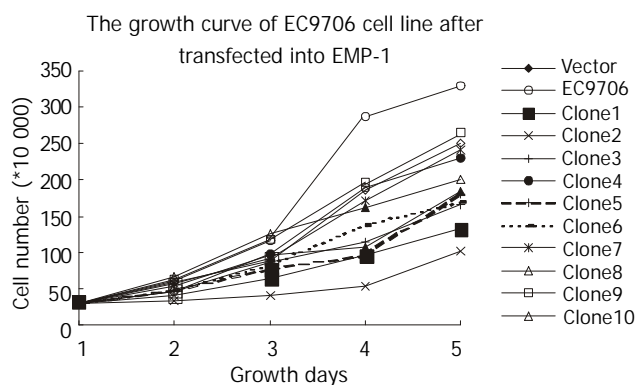


Figure 4 The growth curve of EC9706 cell line after transfected into EMP-1. The clones 1, 2, 3, 5, 6, 8 and 10 slow down obviously, and the clones 4, 7 and 9 are close to the vector control. Vector represents the negative control.

Flow cytometry analysis

Five of ten clones showed similar results after flow cytometry analysis. The percentages of cells in G1 and S phases of clone 1, clone 2, clone 3, clone 6 and clone 8 were 66.6 %, 17.9 %; 64.0 %, 30.2 %; 63.8 %, 29.1 %; 60.9 %, 34.6 %; and 69.5 %, 24.2 %; respectively. The percentage of cells in G1 and S phases of negative control were 52.2 % and 41.7 %, respectively. Comparing the cells transfected with cDNA insert and the negative control, we found that S phase was arrested and G1 phase was prolonged. Then cell clone 2 was used as a representative because its proliferation has been inhibited obviously (Figure 5).

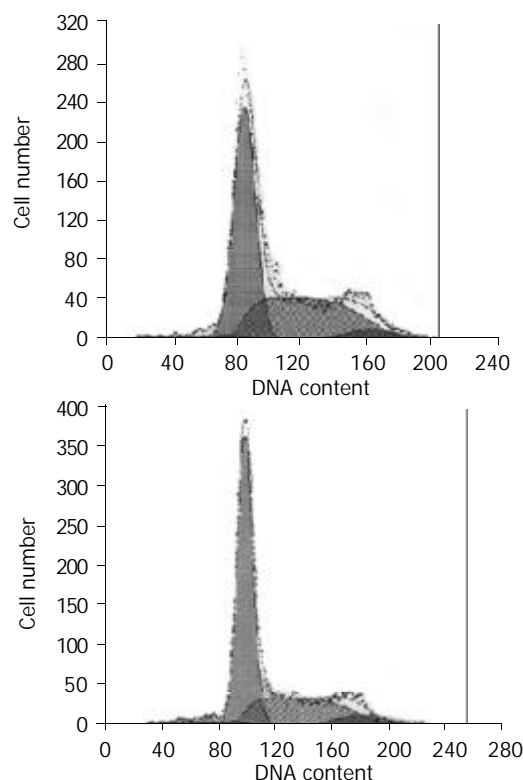


Figure 5 Flow cytometric analysis of cell cycle of negative control (left) and cell clone 2 (right). The percentages of negative cells and the clone 2 cells in G₁, G₂ and S phase are 52.2 %, 6.2 %, 41.7 %; 64 %, 5.8 % and 30.2 %, respectively.

cDNA microarray results of the parental vector pcDNA3.1/myc-his and EMP-1 transfected cell

By cDNA microarray analysis, 35 genes showed an over 2.0-fold change in expression level after transfection, with 28 genes

being consistently up-regulated and 7 genes being down-regulated in clone 2 cells (Figure 6).

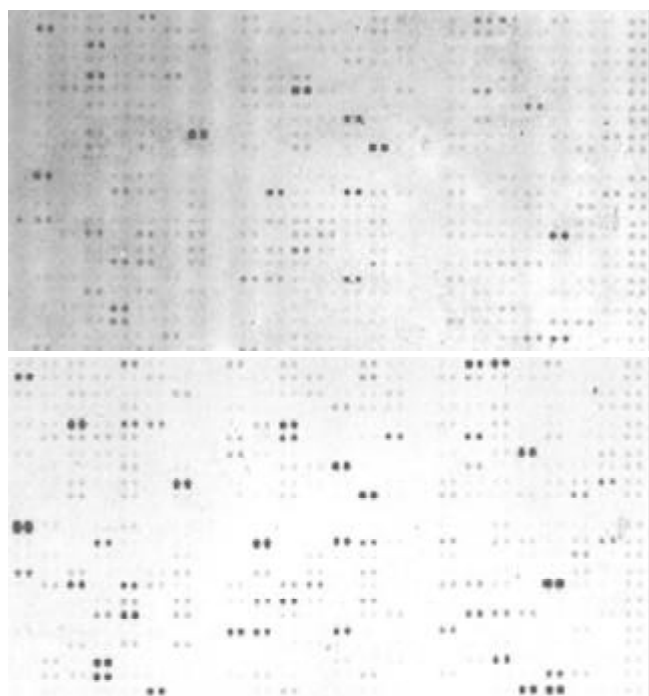


Figure 6 cDNA microarray analysis of parental negative control expression (left) and the EMP-1 transfected cell clone 2 (Right). 35 genes show an over 2.0-fold change in expression level after transfection, with 28 genes being consistently up-regulated and 7 genes being down-regulated.

RT-PCR validation of the microarray results

To confirm the gene expression profile, semi-quantitative RT-PCR was carried out for 4 randomly selected differentially expressed genes. As a result, the expression of these 4 genes was similar with the microarray analysis (Figure 7).

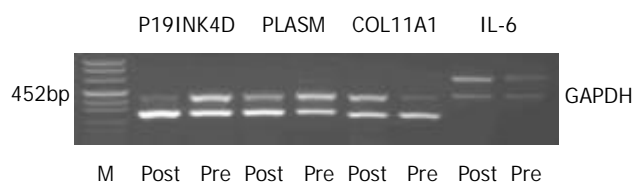


Figure 7 Verification of up-regulated and down-regulated gene expression in EC9706 induced by overexpression of EMP-1. Interleukin-6, plasminogen and P19INK4D increased their expression and COL11A1 decreased its expression. Pre represents the sample not transfected with the vector carried with the ORF of EMP-1, and post represents the sample transfected with EMP-1. RT-PCR for GAPDH was used as equal loading control.

Gene expression profile induced by overexpression of EMP-1

In further analysis of the data from this study provided an insight into the alteration in the EMP-1 induced genes. Because these 588 genes are cancer associated genes and include almost all aspects involved in carcinogenesis and development of tumor and can be the representative of tumor, these data provide an independent and relatively unbiased estimate of the EMP-1 induced expression profile. In general, genes that expression were was more than 2.0-fold were informative and valuable (Table 1).

DISCUSSION

In our previous work on the expression profile of esophageal cancer, we found that the expression of EMP-1 was 6 fold down-regulated in esophageal cancer than that in its adjacent normal mucosa. This study was designed to determine the diverse cellular action of EMP-1 by enforcing its expression in EC9706. Human EMP-1 gene can be stably expressed by EC9706 cell line transfected with human EMP-1. As a result, the cell proliferation was inhibited, S phase was arrested and G1 phase was prolonged after EMP-1 overexpression in EC9706 cells, which is similar to the action of PMP22 in Schwann cells^[8]. We then analyzed EMP-1 induced gene expression using AtlasTM human cancer cDNA expression microarray composed of 588 genes, 35 genes showed an over 2.0- fold change in expression level, in which 28 genes were consistently up-regulated and 7 genes were down-regulated. Among the classified genes, almost half of the induced genes (13 out of 28 genes) were related to cell signaling, communication and adhesion, which indicated that EMP-1 may be one of the cell signaling, communication and adhesion regulators (Table 2).

Table 2 Summary of genes regulated by EMP-1

Major category	Sub category	Up-regulated	Down-regulated
Cell division	General	1	
	DNA synthesis/replication	1	
	Apoptosis	2	
	Cell cycle	1	4
	Chromosome structure	1	
	Total	6	4
Cell signaling or cell communication and adhesion	Cell adhesion		
	Channels/transport protein		
	Effectors/modulators		
	Extracellular Communication	1	
	Hormones/growth factors	4	1
	Intracellular transducers	2	
	Protein modification	3	
	Receptors	3	2
	Total	13	3
	Cell structure/motility	General	
Cytoskeletal		3	
Extracellular matrix Proteins		2	
Microtubule-associated proteins/motors			
Total	5		
Cell/organism defense	General		
	Homeostasis		
	Immunology	1	
Total	1		
Gene/protein expression	RNA synthesis	1	
	protein synthesis		
Total	1		
Metabolism	General		
	Amino acid		
	Cofactors		
	Energy/TCA cycle	2	
	Lipid		
	Nucleotide		
	Protein modification		
	Sugar/glycolysis		
	Transport		
	Total	2	
	Unclassified	1	
	Total	1	

Table 1 Genes whose expression was altered more than 2.0-fold

Genes up-regulated by EMP-1				
Coordinate	Gene Name	Ratio	Category	Sub Category
A3i	Cyclin-dependent kinase 4 inhibitor 2D	2.04	Cell division	Cell-cycle regulators
A7d	Cytokeratin 1	2.26	Cell structure	Intermediate Filament Proteins
B3i	Caspase 9	4.11	Cell division	Cell-apoptosis
B7b	Chromatin assembly factor 1 p48 subunit	2.93	Cell division	Chromosome structure
B7j	Abelson-related gene	4.49	Tumor Suppressors	Oncogenes & Suppressors
C2e	DNA damage-inducible transcript 3	2.80	Cell division	Apoptosis-Associated Proteins
C2j	Ras associated with diabetes protein 1	2.47	Cell signaling	Intracellular transducers
C3e	UV excision repair protein RAD23	5.15	Cell division	DNA synthesis/replication
C4b	Wingless-related MMTV integration 5a	3.09	Cell Adhesion	Extracellular Communication Proteins
C4k	Dishevelled homolog 1-like protein	4.13	Cell signaling	Intracellular Transducers
C7m	Retinoic acid receptor beta	5.47	Cell division	Death Receptors
D3e	Vitronectin (VTN);	2.36	Cell structure	Extracellular Matrix Proteins
D4j	Integrin beta 7 (ITGB7)	2.27	Cell Adhesion	Matrix Adhesion Receptors
D4k	Integrin beta 8 (ITGB8)	2.45	Cell Adhesion	Cell-Cell Adhesion Receptors
D5g	Ezrin; cytovillin 2; villin 2 (VIL2)	3.06	Tumor Suppressors	Oncogenes & Tumor Suppressors
D6l	Caveolin 1	3.29	Metabolism	GTP/GDP Exchangers
E1h	Matrix metalloproteinase 11 (MMP11)	4.64	Cell structure	Extracellular matrix Proteins
E1m	Matrix metalloproteinase 16 (MMP16)	3.06	Protein modification	Metalloproteinases
E2b	Tissue inhibitor of metalloproteinase 1	3.82	Protein modification	Protease Inhibitors
E2h	Tissue-type plasminogen activator	4.39	Protein modification	Serine Proteases
E5b	RHO GDP-dissociation inhibitor 1	2.42	Metabolism	GTP/GDP Exchangers
E5h	Cadherin 5 (CDH5);	2.64	Cell Adhesion	Cell-Cell Adhesion Receptors
F1h	Bone morphogenetic protein 2A (BMP2A)	12.45	Cell communication	Cytokines
F3j	Early growth response protein 1	16.06	RNA synthesis	Transcription Activators & Repressors
F4l	Interleukin 6 (IL6)	4.28	Cell communication	Interleukins & Interferons
F5e	Interleukin 13 (IL13)	2.62	Cell communication	Interleukins & Interferons
F5k	Interferon gamma (IFN-gamma; IFNG)	6.04	Cell communication	Interleukins & Interferons
F5l	Leukocyte interferon-inducible peptide	2.73	Unclassified	Functionally Unclassified Proteins
A1j	Cell division cycle 25 homolog A	0.35	Cell division	Cell-cycle regulators
2m	Cyclin D2 (CCND2)	0.34	Cell division	Cell-cycle regulators
A2n	G1/S-specific cyclin D3 (CCND3)	0.30	Cell division	Cell-cycle regulators
A3k	Polo-like kinase (PLK)	0.47	Cell division	Cell Cycle-Regulating Kinases
D1m	Collagen VI alpha 2 subunit (COL6A2)	0.32	Cell communication	Extracellular Matrix Proteins
D2b	Collagen XI alpha 1 subunit (COL11A1)	0.17	Cell communication	Extracellular Matrix Proteins
D7e	Vascular endothelial growth factor C	0.11	Cell communication	Growth Factors,

cDNA microarray analysis offers the opportunity to monitor changes in gene expression across the entire set of expressed genes in cells. These 588 known genes are classified on the basis of the biological function of the encoded protein, using a modified version of a previously established classification scheme^[11,12]. The classification scheme was composed of six major functional categories and several minor functional categories within the major categories. As shown in Table 2, 34 genes were classified as known function genes, and one gene was categorized as unclassified.

Interestingly, the largest categories (13 out of 28 genes) of EMP-1-induced genes are those involved in cell signaling (Table 1), cell adhesion and cell-cell communication, which included integrin beta 7 (ITGB7), integrin beta 8 (ITGB8) and cadherin 5 (CDH5). These results indicated that EMP-1 might be related with cell adhesion and cell-cell communication.

Cadherin-5 and the alpha E beta 7 integrin mediated heterotypic adhesive interactions between epithelial cells and intraepithelial lymphocytes *in vitro*^[13]. Integrin beta 7 (ITGB7) and integrin beta 8 (ITGB8) are heterodimeric (alpha/beta) transmembrane receptors for extracellular matrix (ECM) ligands. The beta subunit of integrins are considered important for regulation of stimulated cell adhesion and adhesion-dependent signal transduction. Through interactions with molecular partners at cell junctions, they provide a connection between the ECM and the cytoskeleton and regulate many aspects of cell behaviors. Integrins play an important role in lymphocyte adhesion to cellular and extracellular components of their microenvironment^[14]. Cadherin 5 was also induced by EMP-1 in our microarray analysis. It is generally accepted that cadherins are a group of cell adhesion molecules located at intercellular junctions, and they play an important role in

embryogenesis and morphogenesis in animals and humans due to their adhesive and cell-signaling functions. Disturbances of the expression or function of cadherins and their associated proteins are crucial for the initiation and development of many pathological states. Cadherin 5 is an epithelium-specific cadherin that is required for the development and maintenance of the normal function of all epithelial cells in tissues. The loss or down-regulation of cadherin 5 is a key event in the process of tumour invasion and metastasis^[15]. Cadherin 5 has the major role in intercellular adhesion in esophageal mucosa^[16]. Appropriate cadherin expression reflects the differentiation of squamous cell carcinoma^[17]. These results support the putative function of EMP-1, which was a potential maker of differentiation^[18] and was related to cell proliferation, differentiation, regulation and cell death^[3].

In addition, the second largest categories of EMP-1-induced genes were those involved in cell division, Such as cyclin-dependent kinase 4 inhibitor 2D, DNA damage-inducible transcript 3, and retinoic acid receptor beta. The up-regulated cyclin-dependent kinase 4 inhibitor 2D and the down-regulated genes in this categories including cell division cycle 25 homolog A^[19] and cyclin D2 (CCND2) and cyclin D3 (CCND3)^[20] affect the cell cycle collaboratively. These support our finding that the inhibition of cell proliferation after overexpression of EMP-1 associates with the induction of S phase arrested and the prolonged G1 phase with flow cytometric assay.

Retinoic acid receptors beta (RAR- β) is another up-regulated gene induced by EMP-1. It is well established that retinoids can modulate epithelial cell growth, differentiation, and apoptosis *in vitro* and *in vivo* by binding to specific nuclear retinoid receptors, which include RAR- β ^[21]. Retinoids can prevent abnormal squamous cell differentiation in nonkeratinizing tissues physiologically. Retinoids can also reverse squamous cell metaplasia, which develops during vitamin A deficiency^[22]. The expression of RAR-beta varied along with the differentiation level of esophageal cancer. RAR-beta mRNA was expressed in 62.7 % (42/67), 55.1 % (43/78) and 29.2 % (7/24) of well, moderated and poorly differentiated SSCs, respectively^[23]. Retinoic acid, which inhibits squamous cell differentiation with RAR-beta involved in, represses EMP-1 expression in normal human bronchial epithelial cells^[4]. EMP-1 is one of down-regulation of a cluster of squamous cell differentiation marker genes^[18] and RAR- β may be involved in this process.

Some genes associated with the intracellular signaling pathway, such as dishevelled homolog 1-like protein and ras associated with diabetes protein 1, were induced by EMP-1 overexpression (Table 1).

A study addressing the relationship between EMP-1 and these cell adhesion and cell-cell communication proteins has not, to our knowledge, previously been reported. The presumed protein structure of EMP-1 also supports its function in cell signaling, cell adhesion and communication. The predicted EMP-1 polypeptide of 157 amino acid residues has a calculated molecular weight of approximately 18 kDa, and bioinformatics analysis reveals that amino acid residues 1-28, 64-89, 95-117, and 134-157 represent four hydrophobic, potentially membrane-spanning domains. Computer-predicted structural domains of EMP-1 are partially mirrored by the exon/intron structure of EMP-1. Most interestingly, exon 4, which covers the potential second transmembrane domain, a small intracellular loop, and half of the third transmembrane domain, encodes the most highly conserved regions between the EMP-1 and PMP22 proteins indicating some shared functional significance for this module in the PMP22 family. Because of the small size of the intracellular loops, it appears unlikely that they are involved in specific interaction with intracellular proteins and therefore in intracellular signaling. In contrast,

the extracellular loops would be able to interact with other molecules and could have functional significance. Furthermore, the first hydrophilic region of PMP22/EMPs, between the first and second hydrophobic domains, forms an extracellular loop that contains one or more consensus sequences that can be N-linked glycosylated *in vitro*, a structure which has been implicated in cell-cell recognition and adhesion processes^[4,24].

In conclusion, the study of the gene expression changes sustains cellular finding that the inhibition of cell proliferation after enforcing expression of EMP-1 associates with the induction of S phase shorten and the prolonged G1 phase. The expression profile and localization of EMP-1 suggests a role in cell signaling, adhesion and communication. This is the first demonstration of global gene expression analysis of esophageal cancer cell line EC9706 transfectant with EMP-1, and these results provides a new insight in the study of the relationship between EMP-1 and esophageal cancer.

REFERENCES

- Gnirke AU**, Weidle UH. Investigation of prevalence and regulation of expression of progression associated protein (PAP). *Anti-cancer Res* 1998; **18**: 4363-4369
- Taylor V**, Welcher AA, Program AEST, Suter U. Epithelial membrane protein-1, peripheral myelin protein 22, and lens membrane protein 20 define a novel gene family. *J Biol Chem* 1995; **270**: 28824-28833
- Chen Y**, Medvedev A, Ruzanov P, Marvin KW, Jetten AM. cDNA cloning, genomic structure, and chromosome mapping of the human epithelial membrane protein CL-20 gene (EMP1), a member of the PMP22 family. *Genomics* 1997; **41**: 40-48
- Lobsiger CS**, Magyar JP, Taylor V, Wulf P, Welcher AA, Program AE, Suter U. Identification and characterization of a cDNA and the structural gene encoding the mouse epithelial membrane protein-1. *Genomics* 1996; **36**: 379-387
- Taylor V**, Suter U. Epithelial membrane protein-2 and epithelial membrane protein-3: two novel members of the peripheral myelin protein 22 gene family. *Gene* 1996; **175**: 115-120
- Jetten AM**, Suter U. The peripheral myelin protein 22 and epithelial membrane protein family. *Prog Nucleic Acid Res Mol Biol* 2000; **64**: 97-129
- Fabbretti E**, Edomi P, Brancolini C, Schneider C. Apoptotic phenotype induced by overexpression of wild-type gas3/PMP22: its relation to the demyelinating peripheral neuropathy CMT1A. *Genes Dev* 1995; **9**: 1846-1856
- Zoidl G**, Blass-Kampmann S, D'Urso D, Schmalenbach C, Muller HW. Retroviral-mediated gene transfer of the peripheral myelin protein PMP22 in Schwann cells: modulation of cell growth. *EMBO J* 1995; **14**: 1122-1128
- Ruegg CL**, Wu HY, Fagnoni FF, Engleman EG, Laus R. B4B, a novel growth-arrest gene, is expressed by a subset of progenitor/pre-B lymphocytes negative for cytoplasmic mu-chain. *J Immunol* 1996; **157**: 72-80
- Kadowaki Y**, Fujiwara T, Fukazawa T, Shao J, Yasuda T, Itoshima T, Kagawa S, Hudson LG, Roth JA, Tanaka N. Induction of differentiation-dependent apoptosis in human esophageal squamous cell carcinoma by adenovirus-mediated p21sdi1 gene transfer. *Clin Cancer Res* 1999; **5**: 4233-4241
- Adams MD**, Kerlavage AR, Fleischmann RD, Fuldner RA, Bult CJ, Lee NH, Kirkness EF, Weinstock KG, Gocayne JD, White O. Initial assessment of human gene diversity and expression patterns based upon 83 million nucleotides of cDNA sequence. *Nature* 1995; **377**: 3-174
- Naiki T**, Nagaki M, Shidoji Y, Kojima H, Imose M, Kato T, Ohishi N, Yagi K, Moriwaki H. Analysis of gene expression profile induced by hepatocyte nuclear factor 4alpha in hepatoma cells using an oligonucleotide microarray. *J Biol Chem* 2002; **277**: 14011-14019
- Ceppek KL**, Shaw SK, Parker CM, Russell GJ, Morrow JS, Rimm DL, Brenner MB. Adhesion between epithelial cells and T lymphocytes mediated by E-cadherin and the alpha E beta 7 integrin. *Nature* 1994; **372**: 190-193
- Poinat P**, De Arcangelis A, Sookhareea S, Zhu X, Hedgecock EM,

- Labouesse M, Georges-Labouesse E. A conserved interaction between beta1 integrin/PAT-3 and nck-interacting kinase/MIG-15 that mediates commissural axon navigation in *C. elegans*. *Curr Biol* 2002; **12**: 622-631
- 15 **Nachtigal P**, Gojova A, Semecky V. The role of epithelial and vascular-endothelial cadherin in the differentiation and maintenance of tissue integrity. *Acta Medica (Hradec Kralove)* 2001; **44**:83-87
- 16 **Bailey T**, Biddlestone L, Shepherd N, Barr H, Warner P, Jankowski J. Altered cadherin and catenin complexes in the Barrett's esophagus-dysplasia-adenocarcinoma sequence: correlation with disease progression and dedifferentiation. *Am J Pathol* 1998; **152**: 135-144
- 17 **Sanders DS**, Bruton R, Darnton SJ, Casson AG, Hanson I, Williams HK, Jankowski J. Sequential changes in cadherin-catenin expression associated with the progression and heterogeneity of primary oesophageal squamous carcinoma. *Int J Cancer* 1998; **79**: 573-579
- 18 **Hippo Y**, Yashiro M, Ishii M, Taniguchi H, Tsutsumi S, Hirakawa K, Kodama T, Aburatani H. Differential gene expression profiles of scirrhous gastric cancer cells with high metastatic potential to peritoneum or lymph nodes. *Cancer Res* 2001; **61**: 889-895
- 19 **Wang Z**, Wang M, Lazo JS, Carr BI. Identification of Epidermal Growth Factor Receptor as a Target of Cdc25A Protein Phosphatase. *J Biol Chem* 2002; **277**: 19470-19475
- 20 **Buschges R**, Weber RG, Actor B, Lichter P, Collins VP, Reifenberger G. Amplification and expression of cyclin D genes (CCND1, CCND2 and CCND3) in human malignant gliomas. *Brain Pathol* 1999; **9**: 435-442
- 21 **De Luca LM**. Retinoids and their receptors in differentiation, embryogenesis, and neoplasia. *FASEB J* 1991; **5**: 2924-2933
- 22 **Chambon P**. A decade of molecular biology of retinoid acid receptors. *FASEB J* 1996; **10**: 940-954
- 23 **Xu M**, Jin YL, Fu J, Huang H, Chen SZ, Qu P, Tian HM, Liu ZY, Zhang W. The abnormal expression of retinoic acid receptor-beta, p 53 and Ki67 protein in normal, premalignant and malignant esophageal tissues. *World J Gastroenterol* 2002; **8**: 200-202
- 24 **Schachner M**, Martini R. Glycans and the modulation of neural-recognition molecule function. *Trends Neurosci* 1995; **18**: 183-191

Edited by Zhang JZ

Peptidergic innervation of human esophageal and cardiac carcinoma

Shuang-Hong Lü, Yan Zhou, Hai-Ping Que, Shao-Jun Liu

Shuang-Hong Lü, Yan Zhou, Hai-Ping Que, Shao-Jun Liu,
Department of Neurobiology, Institute of Basic Medical Sciences,
Academy of Military Medical Sciences, Beijing 100850, China
Supported by the National Natural Science Foundation of China,
No. 39870315

Correspondence to: Dr. Shao-Jun Liu, Department of Neurobiology,
Institute of Basic Medical Sciences, Academy of Military Medical
Sciences, Beijing 100850, China. liusj@nic.bmi.ac.cn
Telephone: +86-10-66932379 **Fax:** +86-10-68213039
Received: 2002-08-15 **Accepted:** 2002-10-18

Abstract

AIM: To investigate the distribution of neuropeptide-immunoreactive nerve fibers in esophageal and cardiac carcinoma as well as their relationship with tumor cells so as to explore if there is nerve innervation in esophageal and cardiac carcinoma.

METHODS: Esophageal and cardiac carcinoma specimens were collected from surgical operation. One part of them were fixed immediately with 4 % paraformaldehyde and then cut with a cryostat into 40- μ m-thick sections to perform immunohistochemical analysis. Antibodies of ten kinds of neuropeptide including calcitonin gene-related peptide (CGRP), galanin (GAL), substance P (SP), etc. were used for immunostaining of nerve fibers. The other part of the tumor specimens were cut into little blocks (1 mm³) and co-cultured with chick embryo dorsal root ganglia (DRG) to investigate if the tumor blocks could induce the neurons of DRG to extend processes, so as to probe into the possible reasons for the nerve fibers growing into tumors.

RESULTS: Substantial amounts of neuropeptide including GAL-, NPY-, SP-immunoreactive nerve bundles and scattered nerve fibers were distributed in esophageal and cardiac carcinomas. The scattered nerve fibers waved their way among tumor cells and contacted with tumor cells closely. Some of them even encircled tumor cells. There were many varicosities aligned on the nerve fibers like beads. They were also closely related to tumor cells. In the co-culture group, about 63 % and 67 % of DRG co-cultured with esophageal and cardiac tumor blocks respectively extended enormous processes, especially on the side adjacent to the tumor, whereas in the control group (without tumor blocks), no processes grew out.

CONCLUSION: Esophageal and cardiac carcinomas may be innervated by peptidergic nerve fibers, and they can induce neurons of DRG to extend processes *in vitro*.

Lü SH, Zhou Y, Que HP, Liu SJ. Peptidergic innervation of human esophageal and cardiac carcinoma. *World J Gastroenterol* 2003; 9(3): 399-403

<http://www.wjgnet.com/1007-9327/9/399.htm>

INTRODUCTION

The problem about the innervation of tumors was noticed as

early as 50 years ago. Though many authors at that time studied this problem and some obtained affirmative results, the ultimate conclusion made by authoritative pathologist^[1] was that there was no innervation in tumor. And this theory was been generally accepted since then.

However, because of the involvement of mental factors in the genesis and development of tumors, the studies on the relationship between nerve and tumor never stopped. Some authors^[2,3] claimed their findings of nerve fibers in tumors, and some others^[4] studied the perineural invasion by carcinoma cells. In our previous investigations, we also observed many scattered nerve fibers in meningioma and cardiac cancer, which was closely related to tumor cells. In addition, accumulated data^[5-7] show that neuropeptides are involved in the regulation of the growth of tumors. Considering these new advancements, we decided to study the distribution of neuropeptide-containing nerve fibers in esophageal and cardiac carcinomas as well as their relationship with tumors so as to find some new proofs about tumor innervation.

MATERIALS AND METHODS

Reagents

Antibodies of ten kinds of neuropeptide were obtained from Sigma, Chemicon or Bohringmanham Companies. Their working dilutions are listed in Table 1. ABC kit was obtained from Vector Company.

Table 1 Antibodies of neuropeptides and their work dilution

Antibody	Working dilution
CGRP	1:8 000
GAL	1:8 000
SP	1:5 000
NT	1:4 000
SOM	1:8 000
CCK	1:4 000
L-ENK	1:5 000
Dyn	1:4 000
NPY	1:6 000
M-ENK	1:6 000

CGRP: Calcitonin gene-related peptide, GAL: Galanin, SP: Substance P, NT: Neurotensin, SOM: Somatostatin, CCK: Cholecystokinin, L-ENK: Leu-enkephalin, Dyn: Dynorphine, NPY: Neuropeptide Y, M-ENK: Met-enkephalin.

Specimens

The surgical tumor specimens were collected from the Affiliated Cancer Hospital of Beijing University and the General Hospital of People's Liberation Army. Clinical and pathological diagnoses confirmed that the esophageal carcinoma specimens were squamous cell carcinomas and cardiac carcinoma specimens were adenocarcinomas. In our preliminary investigations, we found that the probability to find neuropeptide immunoreactive nerve fibers was decreased in large tumors, only tumors with diameter under 3 cm were selected for the present study. Totally, 16 cases of esophageal carcinoma and 13 cardiac carcinoma specimens were used.

After rinsed in saline, one part of the tissue were fixed immediately by immersing in 4 % paraformaldehyde in 0.01 M PBS (pH 7.4) for 10 hrs at 4 °C and then in PBS containing 30 % sucrose to stay overnight. The specimens were then cut with a cryostat (JUNG 2700, America) into 40- μ m-thick sections for immunohistochemical analysis. The other part of the specimens were collected into DMEM containing 1 000U/ml penicillin and streptomycin for co-culture experiment.

Immunohistochemistry

Immunohistochemical reactions were carried out according to the avidin-biotinylated peroxidase complex method (ABC) as previously reported^[8]. Briefly, the tumor sections were incubated at room temperature for 30 min in 1.2 % H₂O₂ (v/v) solution to quench endogenous peroxidase activity. After washed with PBS for 10 min \times 3, they were incubated with 0.3 % Triton X-100 and then moved into antibodies of neuropeptides (diluted by PBS containing 1 % BSA) for 24-48 hrs at 4 °C. The sections were then incubated in biotin-conjugated IgG (diluted in PBS, 1:200) for 2.5hrs at room temperature and washed for 30 min by three changes of PBS, followed by incubation with the streptavidin-peroxidase complex for 2.5 hrs. The reaction product was detected with 3'-diaminobenzidine tetrahydrochloride (DAB, Sigma). Nerve fibers containing the neuropeptides were identified by the presence of dark black color. Thereafter, part of the sections were counterstained with neutral red and dehydrated in graded ethanol before mounted.

Negative controls were made either by omitting the specific neuropeptide antibodies or by replacing them with non-immune goat serum to assess the nonspecific adsorption of secondary antibodies.

Co-culture of tumor blocks with DRG

Tumor blocks were co-cultured with DRG according to the method of reference^[9]. Totally, 10 specimens of the esophageal and cardiac carcinoma respectively were used for co-culture. DRG were isolated from E8-10 chick embryo (obtained from Chinese Academy of Agricultural & Science) and seeded into 24-well plate coated with poly-L-lysine 30 min before co-culture. Tumor specimens were cut into 1 mm³ blocks to co-culture with DRG at a distance of 1.5-2 mm. Each well had one tumor block and one ganglion. Each specimen was co-cultured for 12 wells. They were then incubated at 37 °C with 7.5 % CO₂ for 4hrs to attach. After that, DMEM without any serum was added into the wells. In the control group, DRG were cultured without tumor blocks in the same medium as in the experimental group. There were 10 wells of DRG cultured as control for each case of tumor specimens. The co-cultures were observed under a phase-contrast microscope (IX70, OLYMPUS) 24hrs later and the DRG with processes outgrowth were counted for statistical analysis.

Statistical analysis

The completely randomized design *t* test was used to analyze for statistical significance. The *P* values less than 0.05 were considered as significantly different.

RESULTS

Distribution of neuropeptide-immunoreactive nerve fibers in tumor and their relationship with tumor cells

Under light microscope, substantial amounts of many kinds of neuropeptide-immunoreactive nerve bundles and scattered nerve fibers were observed in both esophageal and cardiac carcinomas. Many of them were distributed around blood vessels and in the connective tissues. But more importantly, a lot of scattered nerve fibers were distributed among tumor cells

(Figures 1-6). In this study, only those areas with neuropeptide immunoreactive nerve fibers scattered among tumor cells were specified as positive. Distribution of positive nerve fibers in tumor was scored as 0 to 3+. The tumor sections with >2/3 positive area were scored as +++, 1/3-2/3 positive area were ++ and <1/3 positive area were + (Table 2). The frequency of neuropeptides-containing nerve fibers varied among individual tumor specimens. In some cases, the positive nerve fibers were numerous around blood vessels and in the parenchyma, while in others there were only a few fibers running along blood vessels. Relatively, in tumors with good differentiation, the frequency of positive nerve fibers was a little higher than in those with poor differentiation. To a great extent, the distribution pattern and frequency were similar in esophageal and cardiac carcinomas. GAL- and NPY-immunoreactive nerve fibers were numerous in the parenchyma in the both carcinomas, whereas CCK- and SOM-immunoreactive nerve fibers were scarce. No NT-immunoreactive nerve fibers could be detected. In the sections of the negative control group, no immunoreactive nerve fibers were observed.

Table 2 Distribution of neuropeptide-immunoreactive nerve fibers in tumors

Antibodies	Cardiac cancer (n=13)			Esophageal cancer (n=16)		
	+++	++	+	+++	++	+
CGRP	0	2	2	0	2	2
GAL	2	6	4	3	7	4
SP	1	5	1	2	5	5
NT	0	0	0	0	0	0
SOM	0	3	3	0	3	6
CCK	0	0	1	0	0	3
L-ENK	1	3	1	0	3	7
Dyn	2	3	5	0	8	1
NPY	2	5	3	1	6	6
M-ENK	3	3	2	0	5	7

The scattered nerve fibers were mainly derived from either the nerve bundles or the connective tissues around (Figure 1). Wherever they came from, they had a common distribution pattern of extending toward the inside of the parenchyma of tumors. Most of the nerve fibers had varicosities aligned on them like beads (Figures 2, 5). Nerve fibers and their varicosities waved their way among tumor cells. Sometimes they were found entering into tumor convergently from the connective tissue around (Figures 3, 4), or extending fine branches into the nest formed by carcinoma cells (Figure 6). They contacted with tumor cells closely; some of them even encircled tumor cells (Figure 2).

Outgrowth of processes of DRG in co-cultured group

After incubation for 24-48hr, most of the DRG in the co-culture group extended their processes longer than their diameter (Table 3, Figure 7). Interestingly, the processes were distributed around DRG asymmetrically (Figure 7). On the sides adjacent to tumor blocks, they were dense and long, whereas on the opposite sides, they were sparse and short, or no processes at all. In the control group, no DRG extended their processes.

Table 3 Outgrowth of processes of DRG co-cultured with tumor blocks

Tumor group	DRG with processes (n)	DRG without processes (n)	Rate of DRG with processes (x \pm s)
Esophageal	49	28	0.63 \pm 0.10 ^a
Cardiac	60	29	0.67 \pm 0.09 ^a
Control	0	63	0

^a*P*<0.0001 vs the control group

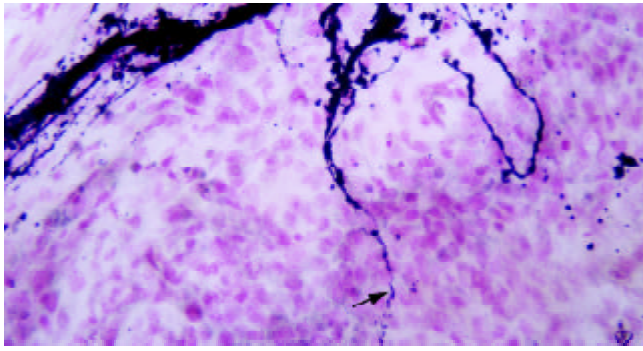


Figure 1 GAL-immunostaining of esophageal carcinoma. Scattered nerve fibers (arrows) branched almost vertically from nerve bundles in connective tissue and entered into tumor parenchyma $\times 250$.

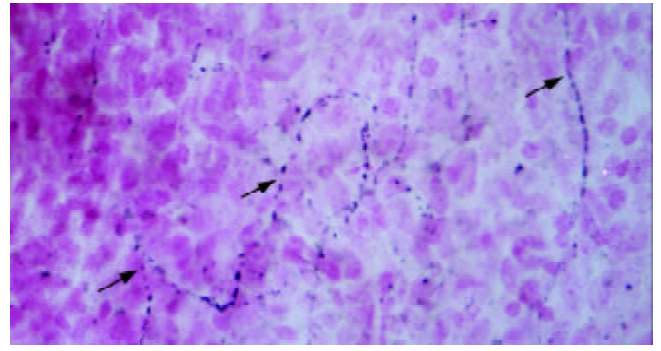


Figure 5 Section of Cardiac adenocarcinoma immunostained for GAL. Many immunoreactive nerve fibers with beads-like varicosities distributed in the parenchyma of tumor $\times 500$.

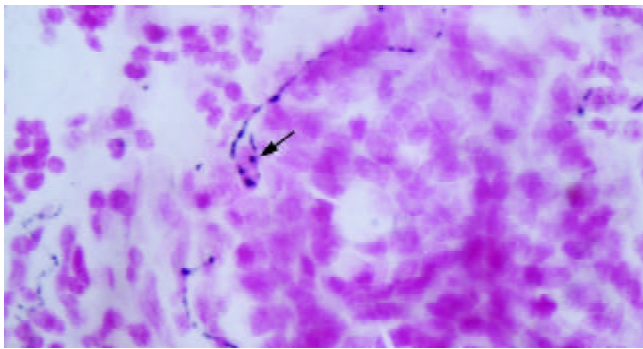


Figure 2 L-ENK-immunoreactive nerve fibers in esophageal carcinoma. The fine nerve fiber (arrow) with varicosities on it encircled a tumor cell and contacted with it closely $\times 500$.

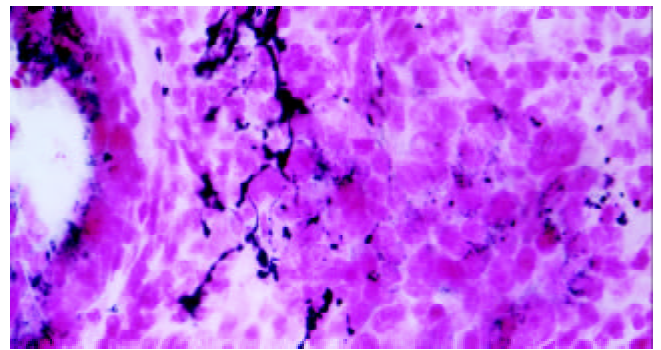


Figure 6 GAL-immunoreactive nerve fibers extended into nestlike cancerous tissue formed by cardiac adenocarcinoma cells. The scattered nerve fibers contacted with tumor cells closely $\times 500$.

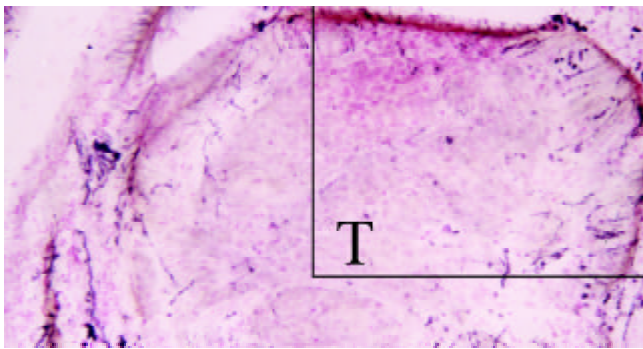


Figure 3 GAL-immunostaining of esophageal carcinoma. Many nerve fibers entered into a nestlike cancerous tissue (T) convergently from collective tissue around it. The structure on the top right corner was amplified in Figure 4 $\times 125$.

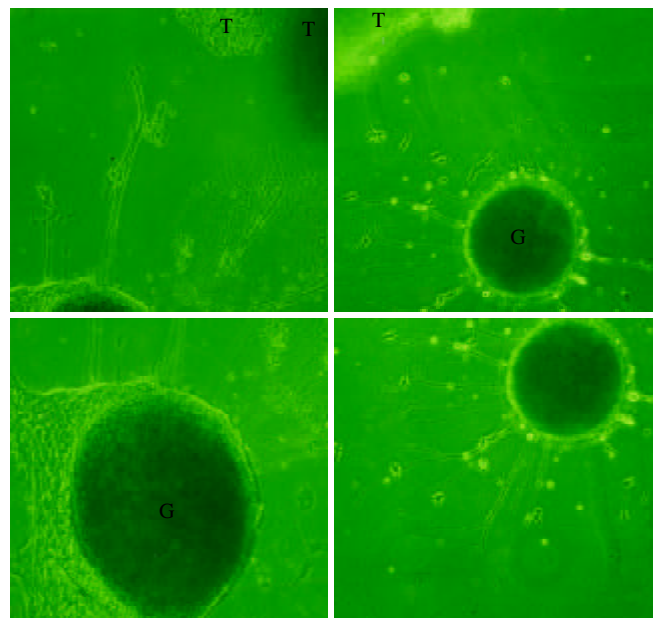


Figure 7 Montage photographs showing the effects of esophageal (a) and cardiac (b) carcinoma tissue block (T) on co-cultured DRG (G). On the side adjacent to tumor, DRG extending long and dense processes whereas on the opposite side, the processes are sparse and short (b), or no processes at all (a) $\times 125$.

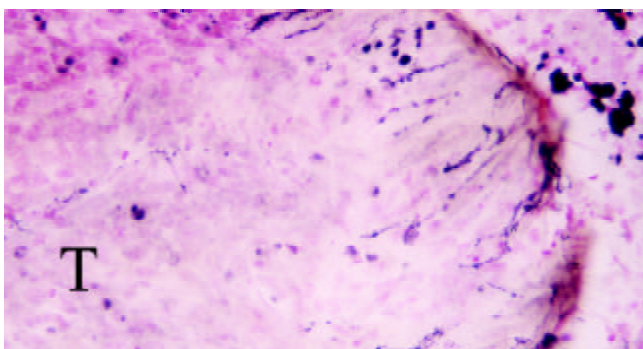


Figure 4 Higher magnification of the part on the top right in Fig.3. GAL-immunoreactive nerve fibers entered into esophageal carcinoma from peripheral areas $\times 250$.

DISCUSSION

Previous studies^[10-12] have shown that the esophagus is richly supplied with neuropeptidergic nerves. In the present study, the neuropeptide-immunoreactive nerves fibers in the

esophageal and cardiac carcinomas seem to have roughly the same topographic distribution as those in the normal digestive tract in that GAL-, NPY-, ENK- and SP-containing nerves fibers predominate in esophagus and stomach, whereas SOM-, NT-containing nerves fibers predominate in intestine^[13]. These neuropeptides have very important functions^[14-16] on the physiological activities of digestive system such as the motility, secretion, etc. Recently, there are more and more evidences showing that neuropeptides can also affect the growth and differentiation of tumors^[17-20]. But since there are endocrine cells in gastrointestinal wall, it is difficult to distinguish if the neuropeptides come from endocrine cells or nerve terminals^[21-22]. Therefore, to some extent, the findings of scattered neuropeptides-containing nerve fibers in tumor will help us understand the mechanisms of neuropeptides affecting tumors.

On the other hand, the findings about the distributions of nerve fibers in esophageal and cardiac carcinomas and their close relationship with tumor cells provided a new viewpoint about the innervation of tumors. In a previous report^[2], the single adrenergic and NPY-containing nerve fibers were found distributed in the parenchyma of human parathyroid adenomas, but most of them were located in the perivascular space. And no detailed descriptions of their relationship with tumor cells are available. With regard to the perineural invasion by carcinomas^[3,4], it was usually considered to be one of the important routes of tumor dissemination and could not be called innervation. In 2001, some German researchers^[23] observed nerve fibers within an adenoma of the ciliary body epithelium of the eye. Under a transmission electron microscope, a small number of fine unmyelinated nerve fibers were found containing clear and dense core vesicles in tumors. Recently, they examined the exophytic tumors of the urinary bladder and human choroidal melanoma^[24,25], and also found irregularly distributed fine nerve strands comprised of axons; hence they concluded that tumors may be innervated. In this regard, they happened to have the same view with us. In this study, we found many scattered nerve fibers not only around blood vessels, but also in the parenchyma of tumors and among tumor cells. Although we did not find specific structure of synapse under electron microscope, these scattered nerve fibers with their beads-like varicosities attached with tumor cells so closely that we can reasonably deduce that they must have important effects on tumor cells, because varicosities are considered containing vesicles and can form synapse-like structures, and will release neuropeptides or other neurotransmitters in their vesicles when stimulated properly. These results suggest that esophageal and cardiac carcinomas may be innervated by peptidergic nerve fibers. Together with previous studies, we suggest that it is necessary to investigate the validity of the old theory about the innervation of tumor.

Why do we get the results that the previously published data did not? We think we have the following advantages: (1) we used frozen sections to facilitate the preservation of the antigen; (2) we used immunohistochemical ABC method to examine the immunoreactive nerve fibers, which is more sensitive than old methods. (3) Neuropeptides-containing nerve fibers are widely distributed in digestive tract from esophagus to the anal sphincter, which provide the possibility for nerve fibers to grow into tumors.

In order to understand how the nerve fibers grow into tumors, we performed co-culture experiment to investigate if tumors had the ability to induce neurons to extend their processes. Our results affirmed this possibility. The neurons of DRG extended processes and the processes on the side adjacent to tumor blocks were dense and long, suggesting that the esophageal and cardiac carcinoma tissues may secrete neurotrophic factors, which are important for the extending of neuronal processes. The SDS electrophoresis (data not shown)

of the tumor-conditioned medium confirmed this assumption and demonstrated that one of them was NGF. Many kinds of tumors have been found secrete NGF, BDNF, NT-3, etc^[26-28]. NGF high-affinity receptor TrkA was also found to exist in esophageal carcinoma^[29]. Therefore, it is possible that these neurotrophic factors in esophageal and cardiac carcinoma tissues act on the neurons in enteric nervous system and induce their fibers to grow into tumors. Or they may exert their neurotrophic functions by helping the injured nerve trunks in tumors regenerate and sprout new nerve fibers. These nerve fibers would extend along with the direction of the diffusion of the neurotrophic factors^[30] and therefore enter into the tumors.

The functional role of these neuropeptide-containing nerve fibers in esophageal and cardiac carcinoma is not clear. The morphological observation indicated that nerve fibers and their varicosities were in close contact with the tumor cells. This would suggest a role of nerve terminals in the regulation of tumor growth and/or differentiation, which is consistent with the function of neuropeptides on tumors. This might partly explain why mental factors could affect the tumorigenesis and tumor development.

REFERENCES

- 1 **Willis RA**. The spread of the tumors in the human. 3rd ed. *London: Butterworths* 1973: 121-125
- 2 **Luts L**, Bergenfelz A, Alumets J, Sundler F. Peptide-containing nerve fibres in normal human parathyroid glands and in human parathyroid adenomas. *Eur J Endocrinol* 1995; **133**: 543-551
- 3 **Stack PS**. Lymphomatous involvement of peripheral nerves: clinical and pathologic features. *South Med J* 1991; **84**: 512-514
- 4 **Takubo K**, Takai A, Yamashita K, Yoshimatsu N, Kitano M, Sasajima K, Fujita K. Light and electron microscopic studies of perineural invasion by esophageal carcinoma. *J Natl Cancer Inst* 1985; **74**: 987-993
- 5 **Iishi H**, Tatsuta M, Baba M, Uehara H, Nakaizumi A. Protection by galanin against gastric carcinogenesis induced by N-Methyl-N'-nitro-N-nitrosoguanidine in wistar rats. *Cancer Res* 1994; **54**: 3167-3170
- 6 **Evers BM**, Parekh D, Townsend CM Jr, Thompson JC. Somatostatin and analogues in the treatment of cancer. *Ann Surg* 1991; **213**: 190-198
- 7 **Tallett A**, Chilvers ER, Hannah S, Dransfield I, Lawson MF, Haslett C, Sethi T. Inhibition of neuropeptide-stimulated tyrosine phosphorylation and tyrosine kinase activity stimulates apoptosis in small cell lung cancer cells. *Cancer Res* 1996; **56**: 4255-4263
- 8 **Hsu SM**, Raine L, Fanger H. Use of avidin-biotin-peroxidase complex (ABC) in immunoperoxidase techniques: a comparison between ABC and unlabeled antibody (PAP) procedures. *J Histochem Cytochem* 1981; **29**: 577-580
- 9 **Eranko O**, Lahtinen T. Attraction of nerve fiber outgrowth from sympathetic ganglia to heart auricles in tissue culture. *Acta Physiol Scand* 1978; **103**: 394-403
- 10 **Uddman R**, Alumets J, Hakanson R, Sundler F, Wallis B. Peptidergic (enkephalin) innervation of the mammalian esophagus. *Gastroenterology* 1980; **78**: 732-737
- 11 **Wattchow DA**, Furness JB, Costa M, O'Brien PE, Peacock M. Distributions of neuropeptides in the human esophagus. *Gastroenterology* 1987; **93**: 1363-1371
- 12 **Singaram C**, Sengupta A, Sweet MA, Sugarbaker DJ, Goyal RK. Nitrinergic and peptidergic innervation of the human oesophagus. *Gut* 1994; **35**: 1690-1696
- 13 **Yamashita Y**, Pedersen JH, Hansen CP. Distribution of neurotensin-like immunoreactivities in porcine and human gut. *Scand J Gastroenterol* 1990; **25**: 481-488
- 14 **Chiba T**, Taminato T, Kadowaki S, Inoue Y, Mori K, Seino Y, Abe H, Chihara K, Matsukura S, Fujita T, Goto Y. Effects of various gastrointestinal peptides on gastric release. *Endocrinology* 1980; **106**: 145-149
- 15 **Johnson LR**. Physiology of the Gastrointestinal Tract. 2nd ed. *New York: Raven Press* 1987: 41-65
- 16 **Aggestrup S**, Uddman R, Jensen SL, Hakanson R, Sundler F,

- Schaffalitzky de Muckadell O, Emson P. Regulatory peptides in lower esophageal sphincter of pig and man. *Dig Dis Sci* 1986; **31**: 1370-1375
- 17 **Baldwin GS**, Shulkes A. Gastrin as an autocrine growth factor in colorectal carcinoma: implications for therapy. *World J Gastroenterol* 1998; **4**: 461-463
- 18 **Camby I**, Salmon I, Bourdel E, Nagy N, Danguy A, Brotchi J, Pasteels JL, Martinez J, Kiss R. Neurotensin-mediated effects on astrocytic tumor cell proliferation. *Neuropeptides* 1996; **30**: 133-139
- 19 **Nakaizumi A**, Uehara H, Baba M, Iishi H, Tatsuta M. Enhancement by neurotensin of hepatocarcinogenesis by N-nitrosomorpholine in Sprague-Dawley rats. *Cancer Lett* 1996; **110**: 57-61
- 20 **Seufferlein T**, Rozengurt E. Galanin, neurotensin, and phorbol esters rapidly stimulate activation of mitogen-activated protein kinase in small cell lung cancer cells. *Cancer Res* 1996; **56**: 5758-5764
- 21 **Johnson LR**. Physiology of the Gastrointestinal Tract. 2nd ed. *New York: Raven Press* 1987: 111-129
- 22 **Furness JB**, Young HM, Pompolo S, Bornstein JC, Kunze WA, McConalogue K. Plurichemical transmission and chemical coding of neurons in the digestive tract. *Gastroenterology* 1995; **108**: 554-563
- 23 **Seifert P**, Spitznas M. Tumours may be innervated. *Virchows Arch* 2001; **438**: 228-231
- 24 **Seifert P**, Benedic M, Effert P. Nerve fibers in tumors of the human urinary bladder. *Virchows Arch* 2002; **440**: 291-297
- 25 **Seifert P**, Spitznas M. Axons in human choroidal melanoma suggest the participation of nerves in the control of these tumors. *Am J Ophthalmol* 2002; **133**: 711-713
- 26 **MacGrogan D**, Saint-Andre JP, Dicoeu E. Expression of nerve growth factor and nerve growth factor receptor genes in human tissues and in prostatic adenocarcinoma cell lines. *J Neurochem* 1992; **59**: 1381-1391
- 27 **Ohta T**, Numata M, Tsukioka Y, Futagami F, Kayahara M, Kitagawa H, Nagakawa T, Yamamoto M, Wakayama T, Kitamura Y, Terada T, Nakanuma Y. Neurotrophin-3 expression in human pancreatic cancers. *J Pathol* 1997; **181**: 405-412
- 28 **Descamps S**, Lebourhis X, Delehedde M, Boilly B, Hondermarck H. Nerve growth factor is mitogenic for cancerous but not normal human breast epithelial cells. *J Biol Chem* 1998; **273**: 16659-16662
- 29 **Koizumi H**, Morita M, Mikami S, Shibayama E, Uchikoshi T. Immunohistochemical analysis of TrkA neurotrophin receptor expression in human non-neuronal carcinomas. *Pathol Int* 1998; **48**: 93-101
- 30 **Tessier-Lavigne M**, Goodman CS. The molecular biology of axon guidance. *Science* 1996; **274**: 1123-1133

Edited by Ma JY

Expression of MUC1 in esophageal squamous-cell carcinoma and its relationship with prognosis of patients from Linzhou city, a high incidence area of northern China

Zi-Bo Song, Shan-Shan Gao, Xin-Na Yi, Yan-Jie Li, Qi-Ming Wang, Ze-Hao Zhuang, Li-Dong Wang

Zi-Bo Song, Institute of Medical Genetics, People's Hospital of Henan Province, 450003, Henan Province, China

Shan-Shan Gao, Xin-Na Yi, Yan-Jie Li, Qi-Ming Wang, Ze-Hao Zhuang, Li-Dong Wang, Laboratory for Cancer Research, Medical College of Zhengzhou University, Zhengzhou 450052, Henan Province, China

Supported by National Outstanding Young Scientist Award of China, NO. 30025016; NCI CA65871 (U.S.A.)

Correspondence to: Zi-Bo Song, Institute of Medical Genetics, People's Hospital of Henan Province, 450003, Henan Province, China. zbsong@sohu.com

Telephone: +86-371-5580463

Received: 2002-10-30 **Accepted:** 2002-11-19

Abstract

AIM: To further characterize the possible relationship between the molecular changes and prognosis of ESC and to elucidate the possible mechanisms involved.

METHODS: 114 specimens of ESC were collected from Linzhou city, and all patients were followed up for more than 5 years after resection. Histopathological analysis and immunohistochemical staining (ABC) were employed to detect the alteration of MUC1.

RESULTS: The positive immunostaining rate for MUC1 was 79 % (90/114), and the high-expression rate was 63 % (72/114). The mean survival periods (months) of those with high- and low-expression rates of MUC1 were 41 (95 % CI: 35, 47) and 52 (95 % CI: 45, 59), respectively. Patients in the low-expression group obviously survived longer than those in high-expression group, and the difference was significant ($P < 0.05$). The expression of MUC1 protein in the esophageal carcinoma specimens with metastasis was stronger than those without metastasis, the difference was also significant ($P < 0.05$). The stepwise multivariate analysis showed that "differentiation", "expression of MUC1" and "TNM staging" were the most important factors affecting the prognosis of esophageal carcinoma patients ($P < 0.05$).

CONCLUSION: A good correlation between the alteration of MUC1 and the regional lymph node metastasis was observed. Furthermore, high-expression of MUC1 was associated with poor prognosis for esophageal cancer patients. These results indicated that MUC1 is a promising biomarker for predicting lymph node metastasis and prognosis in esophageal cancer.

Song ZB, Gao SS, Yi XN, Li YJ, Wang QM, Zhuang ZH, Wang LD. Expression of MUC1 in esophageal squamous-cell carcinoma and its relationship with prognosis of patients from Linzhou city, a high incidence area of northern China. *World J Gastroenterol* 2003; 9(3): 404-407

<http://www.wjgnet.com/1007-9327/9/404.htm>

INTRODUCTION

Esophageal squamous-cell carcinoma (ESC) is one of the most common malignant diseases in northern China, and Linzhou city (formerly Linxian) had being the highest incidence area^[1,2]. The five-year survival rate for early esophageal cancer patients is more than 90 %. However, for the patients at late or advanced stage, the five year survival rate is only 10-15 %^[1,2]. So far, the conventional traditional prognostic markers, such as cancer stage based on metastasis and pathological grade are still used to evaluate the prognosis of esophageal cancer patients. But, it has been well recognized that there is discordance between the conventional prognosis biomarkers and the actual prognosis. For example the patients with well differentiated cancer may have a worse prognosis than those with poorly differentiated ones, indicating the limitation of those markers for predicating.

With the development of molecular biotechnology, many new measurements have been applied in cancer prognosis research. Studies on ESC prognosis have been expanded in recent years; however, the molecular mechanisms involved in prognosis of esophageal cancer, especially the survival analysis on whom from high-incidence area of esophageal carcinoma was very limited. We followed up the ESC patients from Linzhou city and determined the alteration of MUC1 expression and its relationship to the prognosis, to further characterize the possible relationship between them so as to elucidate the possible mechanisms of ESC carcinogenesis, and to determine the alteration of MUC1 and prognosis with histopathological and immunohistochemical methods.

MATERIALS AND METHODS

Patients

One hundred and fourteen patients with ESC, who had undergone esophagectomy at the Esophageal Carcinoma Hospital of Linzhou City between 1993 and 1996 were enrolled in this study. All the patients were local residents of Linzhou city and had not received radiation therapy or chemotherapy prior to the surgery. There were 67 men and 49 women. The mean age was 53.5 ± 8.1 (range 37-72) years for males and 53.6 ± 7.8 (range 40-69) years for females, respectively. All specimens were confirmed by pathology as ESC.

Follow-up

All patients were followed up until March 2001, at which the patients had survived for more than 5 years or died within that period after surgical treatment. 57 patients survived less than 5 years died of recurrence or metastasis.

Tissues processing

All tumor specimens were fixed with formalin and embedded with paraffin. Each block was sectioned serially at 5 μ m, one of which was stained with hematoxylin and eosin for histopathological analysis by two pathologists and the others were used for immunostaining.

Histopathological analysis

Histopathological diagnoses were made according to the previously established criteria^[3].

Immunohistochemical staining

Anti-MUC1 antibody was a mouse monoclonal anti-serum directed at a hexapeptide in the tandem repeat region of the protein core of MUC1 (clone Ma552; Novocastra, Burlingame, CA), which was kindly provided by Dr. Yongqin Li (College of Medicine, Harvard University). The avidin-biotin-peroxidase complex (ABC) method was used for MUC1 immunostaining. In brief, after dewaxing, quenching endogenous peroxidase activity with 3 % H₂O₂, and blocking cross-reactivity with normal serum (Vectastain Elite Kit; Vector, Burlingame, CA), the tissues were incubated overnight at 4 °C with primary antibodies (1:400 for MUC1). Location of the primary antibodies was achieved by subsequent use of a biotinylated anti-primary antibody, an avidin-biotin complex conjugated to horseradish peroxidase, and 3',5'-diaminobenzidine (Vectastain Elite Kit). Normal serum blocking and omission of the primary antibody were used as negative controls.

Evaluation of immunostaining

Clear cytoplasm and cell membrane staining was the criterion for a positive reaction. The staining was graded by the percentage of positively stained neoplastic cells as follows: -, <5 %; +, 5-50 %; ++, >50 % of the neoplastic cells stained. For statistical analysis, the examined cases were divided into 2 groups: the low-expression group, composed of the “-” and “+” groups (less than 50 % of neoplastic cells stained) and the high-expression group, the “++” group (over 50 % of the neoplastic cells stained)^[4].

Statistical analysis

Chi-squared test was performed to evaluate the relevance of regional lymph node metastasis and expression of MUC1 protein, Kaplan-Meier was used for survival analysis, and multivariate analysis for screening prognostic factors. The significant difference was considered when the *P* value was less than 0.05.

RESULTS

Results of follow up

Among the follow up of 114 ESC patients followed up, 33 % (33/114) survived 5 years, 50 % (57/114) died within 5 years after surgical treatment and 17 % (20/114) cases were censored during the follow-up.

Expression of MUC1 and its relationship with survival of ESC

Among the 114 surgically resected ESC specimens examined, the positive immunostaining for MUC1 was observed in 90 cases (78.9 %), and high-expression was seen in 72 cases (63.2 %) and low-expression was in 42 cases (36.8 %). The mean survival period (months) and 95 % confidence interval of esophageal carcinoma patients with high- and low-expression of MUC1 were 41(35, 47) and 52(45, 59), respectively. Patients in the low-expression group obviously survived longer than those in high-expression group, and the difference was significant (*P*<0.05, Table 1 and Figure 1).

Relationship between the expression of MUC1 and regional lymph node metastasis

According to the status of the regional lymph nodes with or without metastasis, all specimens were divided into two groups, with metastasis and without metastasis. The expression of

MUC1 protein in the ESC specimens with metastasis was obviously stronger than those without metastasis, and the difference was significant (*P*<0.05, Table 2).

Table 1 Survival analysis of high-expression and low-expression of MUC1 in ESC

Expression of MUC1	No. of specimens examined	No. of death	Mean survival period (month) x (95% CI*)
Low-expression	42	17	52(45, 59)
High-expression	72	40	41(35, 47)
Total	114	57	

*: Confidence Interval; Log-rank: $\chi^2=5.11, P=0.0238$.

Table 2 Relationship between the expression of MUC1 and regional lymph node metastasis

Group	No. of specimens examined	Expression of MUC1 protein			
		- n(%)	+ n(%)	++ n(%)	+++ n(%)
Without metastasis	77	19(24.7)	29(37.7)	7(9.1)	22(28.5)
With Metastasis	37	0(0)	4(10.8)	5(13.5)	28(75.7)
Total	114	19	33	12	50

Chi-squared test: $\chi^2=27.4693, P<0.05$.

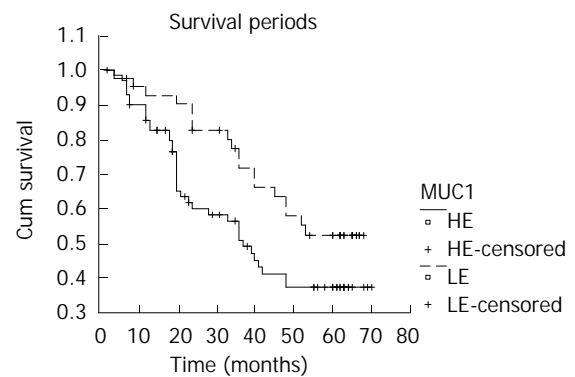


Figure 1 Comparison of survival period between high-expression and low-expression of MUC1 in ESC. HE: High-expression; LE: Low-expression.

Cox model analysis

Ten parameters, including sex, age, invading depth, regional lymph node metastasis, metastasis of other organs, TNM stage, differentiation and MUC1, were used as independent variables, survival periods of ESC patients were used as dependent variables, and all variables were ranked into Cox model analysis (Table 3). The stepwise multivariate analysis showed that “differentiation”, “expression of MUC1” and “TNM staging”, were the most important factors affecting the prognosis of ESC patients (*P*<0.05), RR values for each parameter were 2.2382, 1.9409 and 1.8621, respectively (Table 4).

Table 3 All factors employed by Cox regression model

Factors	Variable
Sex	X1 0=male, 1=female
Age	X2 0=<45 years, 1=45~55 years, 2=>55 years
Invading depth	X3 0=lamina propria or submucosa, 1=muscularis propria, 2=adventitia, 3=adjacent structures
Regional lymph node metastasis	X4 0=no, 1=yes
Distant metastasis	X5 0=no, 1=yes
TNM stage	X6 0=0, 1=I, 2=II, 3=III, 4=IV
Differentiation	X7 0=high, 2=moderate, 3=low
Expression of MUC1	X8 0=low, 1=high

Table 4 Results of Cox model stepwise regression analysis

Variable	Parameter Estimated	Standard error	R	RR
X6	0.6217	0.1549	0.1717	1.8621
X7	0.8057	0.1961	0.1763	2.2382
X8	0.6632	0.3075	0.0311	1.9409

DISCUSSION

Both patients and doctors monitored the patients' survival period after surgery. So far, it is still controversial about evaluating. Our study on the expression of MUC1 in ESC tissues showed that the patients in the low-expression group obviously survived longer than those in high-expression group, and the difference was significant ($P < 0.05$). It is therefore indicated that detection of expression of MUC1 may be of value in assessing the prognosis of ESC patients.

The epithelial mucin coded by the MUC1 gene is a transmembrane molecule, which is expressed in most glandular epithelial cells. The molecule was first identified in human milk, as a large molecular weight glycoprotein rich in serine, threonine and proline carrying a high percentage of *O*-linked carbohydrate^[5]. MUC1 is widely expressed by normal glandular epithelial cells, and the expression is dramatically increased when the cells become malignant^[6,7], and its relationship with the prognosis of several carcinomas have been already reported^[4, 8-11]. Changes in the expression levels of MUC1 have also been described in esophageal lesions^[12]. Our finding showed that MUC1 was expressed in all surgical specimens with lymph node metastasis. Its high-expression rate reached 89 %, and was significantly different from the specimens without lymph node metastasis ($P < 0.05$). The lymph node and lymphatic vessel invasion has been reported as poor prognosis factor^[13, 14].

Mucins are heavily glycosylated glycoproteins that have protective and lubricating functions^[15, 16]. MUC1 expressed in tumors may function as an anti-adhesion molecule, which inhibits cell-cell adhesion, inducing a release of cells from tumor nests. Thus, MUC1 expression may be related to invasion or metastasis of carcinoma cells^[17-19]. MUC1 can down-regulate the expression of E-cadherin, which is a calcium-dependent adhesion molecule, functioning in the cell-cell adhesion, while the low-expression of E-cadherin increased the invading ability of tumor cells^[20-22]. Our previous studies found that MUC1 was expressed in 50 primary ESC cells and the metastasized cancer cells of the matched lymph nodes. In addition, it was found that the coincidence of positive immunostaining between primary tumor and its matching lymph node was observed in 28 cases (56.0 %), while the coincidence of negative immunostaining was observed only in 2 cases (1.0 %)^[23]. It therefore indicated that the expression of MUC1 might play an important role in the invasion or metastasis of ESC cells, which might be one of the mechanisms involving in poor prognosis. But a discordant view was held by Japanese authors who argued that the expression of MUC1 was not significantly associated with metastasis of human esophageal carcinomas^[24]. Further study is still necessary.

Considering the complexity in cancer, it is difficult to define it useful prognostic and predictive factors^[25-28]. In the present study, we use multivariate analytic method for screening the prognostic factors in combination with clinical data. The stepwise multivariate analysis shows that "differentiation", "expression of MUC1" and "TNM staging" are the most important factors affecting the prognosis of ESC patients ($P < 0.05$), our findings also indicate that high expression of MUC1 is related to poor prognosis of ESC.

REFERENCES

- 1 **Yang CS.** Research on esophageal cancer in China: a review. *Cancer Res* 1980; **40**: 2633-2644
- 2 **Lu JB, Yang WX, Zu SK, Chang QL, Sun XB, Lu WQ, Quan PL, Qin YM.** Cancer mortality and mortality trends in Henan, China, 1974-1985. *Cancer Detect Prev* 1988; **13**: 167-173
- 3 **Wang LD, Shi ST, Zhou Q, Goldstein S, Hong JY, Shao P, Qiu SL, Yang CS.** Changes in P53 and cyclin D1 protein levels and cell proliferation in different stages of human esophageal and gastric cardia carcinomas. *Int J Cancer* 1994; **59**: 514-519
- 4 **Sagara M, Yonezawa S, Nagata K, Tezuka Y, Natsugoe S, Xing PX, McKenzie I FC, Aikou T, Sato E.** Expression of MUCIN 1 (MUC1) in esophageal squamous-cell carcinoma: its relationship with prognosis. *Int J Cancer* 1999; **84**: 251-257
- 5 **Taylor-Papadimitriou J, Burchell J, Miles DW, Dalziel M.** MUC1 and cancer. *Biochimica Biophysica Acta* 1999; **1455**: 301-313
- 6 **Hirasawa Y, Kohno N, Yokoyama A, Kondo K, Hiwada K, Miyake M.** Natural autoantibody to MUC1 is a prognostic indicator for non-small cell lung cancer. *Am J Respir Crit Care Med* 2000; **161**: 589-594
- 7 **Baldus SE, Zirbes TK, Glossmann J, Fromm S, Hanisch FG, Monig SP, Schroder W, Schneider PM, Flucke U, Karsten U, Thiele J, Holscher AH, Dienes HP.** Immunoreactivity of monoclonal antibody BW835 represents a marker of progression and prognosis in early gastric cancer. *Oncology* 2001; **61**: 147-155
- 8 **Xu Y, Kimura N, Yoshida R, Lin H, Yoshinaga K.** Immunohistochemical study of Muc1, Muc2 and human gastric mucin in breast carcinoma: relationship with prognostic factors. *Oncol Rep* 2001; **8**: 1177-1182
- 9 **Lee HS, Lee HK, Kim HS, Yang HK, Kim YI, Kim WH.** MUC1, MUC2, MUC5AC, and MUC6 expressions in gastric carcinoma: their roles as prognostic indicators. *Cancer* 2001; **92**: 1427-1434
- 10 **Kraus S, Abel PD, Nachtmann C, Linsenmann HJ, Weidner W, Stamp GW, Chaudhary KS, Mitchell SE, Franke FE, Lalani el-N.** MUC1 mucin and trefoil factor 1 protein expression in renal cell carcinoma: correlation with prognosis. *Hum Pathol* 2002; **33**: 60-67
- 11 **Kashiwagi H, Kijima H, Dowaki S, Ohtani Y, Tobita K, Yamazaki H, Nakamura M, Ueyama Y, Tanaka M, Inokuchi S, Makuuchi H.** MUC1 and MUC2 expression in human gallbladder carcinoma: a clinicopathological study and relationship with prognosis. *Oncol Rep* 2001; **8**: 485-489
- 12 **Guillem P, Billeret V, Buisine MP, Flejou JF, Lecomte-Houcke M, Degand P, Aubert JP, Triboulet JP, Porchet N.** Mucin gene expression and cell differentiation in human normal, premalignant and malignant esophagus. *Int J Cancer* 2000; **88**: 856-861
- 13 **Brucher BL, Stein HJ, Werner M, Siewert JR.** Lymphatic vessel invasion is an independent prognostic factor in patients with a primary resected tumor with esophageal squamous cell carcinoma. *Cancer* 2001; **92**: 2228-2233
- 14 **Eloubeidi MA, Desmond R, Arguedas MR, Reed CE, Wilcox CM.** Prognostic factors for the survival of patients with esophageal carcinoma in the U.S: the importance of tumor length and lymph node status. *Cancer* 2002; **95**: 1434-1443
- 15 **Jarrard JA, Linnoila RH, Lee H, Steinberg SM, Witschi H, Szabo E.** MUC1 is a novel marker for the type II Pneumocyte lineage during lung carcinogenesis. *Cancer Research* 1998; **58**: 5582-5589
- 16 **Reis CA, David L, Correa P, Carneiro F, Bolos C, Garcia E, Mandel U, Clausen H, Sobrinho-Simoes M.** Intestinal metaplasia of Human stomach displays distinct patterns of mucin (MUC1, MUC2, MUC5AC, and MUC6) expression. *Cancer Research* 1999; **59**: 1003-1007
- 17 **Kam JL, Regimbald LH, Hilgers JH, Hoffman P, Krantz MJ, Longenecker BM, Hugh JC.** MUC1 synthetic peptide inhibition of intercellular adhesion molecule-1 and MUC1 binding requires six tandem repeats. *Cancer Res* 1998; **58**: 5577-5581
- 18 **Takao S, Uchikura K, Yonezawa S, Shinchi H, Aikou T.** Mucin core protein expression in extrahepatic bile duct carcinoma is associated with metastases to the liver and poor prognosis. *Cancer* 1999; **86**: 1966-1975
- 19 **Kimura H, Konishi K, Arakawa H, Oonishi I, Kaji M, Maeda K, Yabushita K, Tsuji M, Miwa A.** Number of lymph node metastases influences survival in patients with thoracic esophageal carcinoma: therapeutic value of radiation treatment for

- recurrence. *Dis Esophagus* 1999; **12**: 205-208
- 20 **Kondo K**, Kohno N, Yokoyama A, Hiwada K. Decreased MUC1 expression induces E-cadherin-mediated cell adhesion of breast cancer cell lines. *Cancer Res* 1998; **58**: 2014-2019
- 21 **Wesseling J**, van der Valk SW, Hilkens J. A mechanism for inhibition of E-cadherin-mediated cell-cell adhesion by the membrane-associated mucin episialin/MUC1. *Mol Biol Cell* 1996; **7**: 565-577
- 22 **Si HX**, Tsao SW, Lam KY, Srivastava G, Liu Y, Wong YC, Shen ZY, Cheung AL. E-cadherin Expression is commonly downregulated by CpG island hypermethylation in esophageal carcinoma cells. *Cancer Lett* 2001; **173**: 71-78
- 23 **Zhuang ZH**, Wang LD, Gao SS, Fan ZM, Song ZB, Qi YJ, Li YJ, Li JX. Expression of MUC1 in esophageal and gastric cardiac carcinoma tissues from high-incidence area for esophageal cancer in Henan. *Zhennzhou Daxue Xuebao* 2002; **37**: 774-777
- 24 **Kijima H**, Chino O, Oshiba G, Tanaka H, Kenmochi T, Kise Y, Shimada H, Abe Y, Tokunaga T, Yamazaki H, Nakamura M, Tanaka M, Makuuchi, H, Ueyama Y. Immunohistochemical MUC1 (DF3 Antigen) expression of human esophageal squamous cell carcinoma. *Anticancer Research* 2001; **21**: 1285-1290
- 25 **Hall PA**, Goings JJ. Predicting the future: a critical appraisal of cancer prognosis studies. *Histopathology* 1999; **35**: 489-494
- 26 **Song ZB**, Gao SS, Wang LD, Li JL, Fan ZM, Guo HQ, Yi XN. Correlation between p53, PCNA and the prognosis of esophageal carcinoma from the subjects in high-incidence area. *Henan Yixue Yanjiu* 2002; **11**: 97-100
- 27 **Xiong XD**, Xu LY, Shen ZY, Cai WJ, Luo JM, Han YL, Li EM. Identification of differentially expressed proteins between human esophageal immortalized and carcinomatous cell lines by two-dimensional electrophoresis and MALDI-TOF-mass spectrometry. *World J Gastroenterol* 2002; **8**: 777-781
- 28 **Zeng WJ**, Liu GY, Xu J, Zhou XD, Zhang YE, Zhang N. Pathological characteristics, PCNA labeling index and DNA index in prognostic evaluation of patients with moderately differentiated hepatocellular carcinoma. *World J Gastroenterol* 2002; **8**: 1040-1044

Edited by Ma JY

Resveratrol induces apoptosis in human esophageal carcinoma cells

Hai-Bo Zhou, Yun Yan, Ya-Ni Sun, Ju-Ren Zhu

Hai-Bo Zhou, Ju-Ren Zhu, Department Of Gastroenterology, Shandong Provincial Hospital, Jinan 250052, Shandong Province, China

Yun Yan, Ya-Ni Sun, People's Hospital of WeiFang, WeiFang 261041, Shandong Province, China

Correspondence to: Dr. Hai-Bo Zhou, Department Of Gastroenterology, Shandong Provincial Hospital, Jinan 250052, Shandong Province, China. zhouhbyy@fm365.com.cn

Telephone: +86-531-2603194

Received: 2002-10-08 **Accepted:** 2002-11-13

Abstract

AIM: To investigate the apoptosis in esophageal cancer cells induced by resveratrol, and the relation between this apoptosis and expression of Bcl-2 and Bax.

METHODS: In *in vitro* experiments, MTT assay was used to determine the cell growth inhibitory rate. Transmission electron microscope and TUNEL staining method were used to quantitatively and qualitatively detect the apoptosis status of esophageal cancer cell line EC-9706 before and after the resveratrol treatment. Immunohistochemical staining was used to detect the expression of apoptosis-regulated gene Bcl-2 and Bax.

RESULTS: Resveratrol inhibited the growth of esophageal cancer cell line EC-9706 in a dose-and time-dependent manner. Resveratrol induced EC-9706 cells to undergo apoptosis with typically apoptotic characteristics, including morphological changes of chromatin condensation, chromatin crescent formation, nucleus fragmentation and apoptotic body formation. TUNEL assay showed that after the treatment of EC-9706 cells with resveratrol (10 mmol·L⁻¹) for 24 to 96 hours, the AIs were apparently increased with treated time ($P<0.05$). Immunohistochemical staining showed that after the treatment of EC-9706 cells with resveratrol (10 mmol·L⁻¹) for 24 to 96 hours, the PRs of Bcl-2 proteins were apparently reduced with treated time ($P<0.05$) and the PRs of Bax proteins were apparently increased with treated time ($P<0.05$).

CONCLUSION: Resveratrol is able to induce the apoptosis in esophageal cancer. This apoptosis may be mediated by down-regulating the apoptosis-regulated gene Bcl-2 and up-regulating the expression of apoptosis-regulated gene bax.

Zhou HB, Yan Y, Sun YN, Zhu JR. Resveratrol induces apoptosis in human esophageal carcinoma cells. *World J Gastroenterol* 2003; 9(3): 408-411

<http://www.wjgnet.com/1007-9327/9/408.htm>

INTRODUCTION

The Bcl-2 family plays a crucial role in the control of apoptosis. The family includes a number of proteins which have homologous amino acid sequence, including anti-apoptotic members such as Bcl-2 and Bcl-x_L, as well as pro-apoptotic members including Bax and Bad. In *in vitro* experiments, overexpression of Bcl-2 has been shown to inhibit apoptosis,

but overexpression of Bax has been shown to promote apoptosis.

Resveratrol, a phytoalexin found in grapes, fruits, and root extracts of the weed *Polygonum cuspidatum*, is an important constituent of Chinese folk medicine. Indirect evidence suggests that the presence of resveratrol in white and rose wine may be helpful to reduce risks of coronary heart disease which would be achieved by moderate wine consumption. This effect has been attributed to the inhibition of platelet aggregation and coagulation, in addition to the antioxidant and anti-inflammatory activity of resveratrol. Moreover, a recent report shows that resveratrol is a potent cancer chemopreventive agent in three major stages of carcinogenesis. The anti-tumor activity of resveratrol might be related to induce the apoptosis of tumor cells but the precise mechanism of antitumor activity is not well understood.

MATERIALS AND METHODS

Materials

Resveratrol and MTT were obtained from Sigma Chemical Co. Ltd. *In situ* cell detection kit, anti-Bcl-2 monoclonal antibody and anti-Bax monoclonal antibody were purchased from Beijing Zhongshan biotechnology Co. Ltd. Stock solution of resveratrol was made in dimethylsulfoxide (DMSO) at a concentration of 100 mmol·L⁻¹. Working dilutions were directly made in the cell culture medium. Human esophageal carcinoma cell line EC-9706 was obtained from Professor Ming-Rong Wang in Chinese Scientific Academy.

Methods

Cell culture EC-9706 cells were incubated in RPMI 1640 supplemented with 100 ml·L⁻¹ fetal bovine serum, 100 kU·L⁻¹ penicillin, 100 mg·L⁻¹ streptomycin and 2 mmol·L⁻¹ L-glutamine under 50 ml·L⁻¹ CO₂ in a humidified incubator at 37 °C. EC-9706 cells were incubated for different time periods in the presence of resveratrol at 0.1, 1, 10 and 100 mmol·L⁻¹.

MTT assay 1×10⁵ cells/well in a 96-well plate after incubation for 24 hours were treated with different concentrations of resveratrol (0.1, 1, 10, 100 mmol·L⁻¹) for 24, 48, 72, 96 hours respectively. 10 μL of 5 g·L⁻¹ of MTT was added to the medium in three wells at every dose and incubated for 4 hours at 37 °C. Culture media were discarded followed by adding 0.2 ml DMSO and vibrating for 10 minutes. The absorbance (OD) was measured at 570 nm using a microplate reader. The cell growth inhibitory rate was calculated as follows: [(OD of control group - OD of experimental group)/(OD of control group - OD of blank group)]×100 %.

Transmission electron microscopy Cells treated with 10 mmol·L⁻¹ resveratrol were harvested after incubation for 24 hours. Subsequently the cells were fixed in 4 % glutaral and immersed with Epon 821, imbedded for 72 hours at 60 °C, the cells were prepared into ultrathin section (60 nm) and stained with uranyl acetate and lead citrate. Cell morphology was observed by transmission electron microscopy.

TUNEL assay Apoptosis of EC-9706 cells was evaluated by using an *in situ* cell detection kit. The cells were treated in the presence or absence of 10 mmol·L⁻¹ resveratrol for 24 to 96 hours and fixed in ice-colded 80 % ethanol for up to 24 hours, treated with proteinase K and then 0.3 % H₂O₂, labeled with fluorescein dUTP in a humid box for 1 hour at 37 °C. The cells

were then combined with POD-Horseradish peroxidase, colorized with DAB and counterstained with methyl green. Controls were received the same management except the labeling of omission of fluorescein dUTP. Cells were visualized with light microscope. The apoptotic index (AI) was calculated as follows: $AI = (\text{Number of apoptotic cells} / \text{Total number}) \times 100\%$.

Immunohistochemical staining Immunohistochemical staining was done by an avidinbiotin technique. EC-9706 cells treated in the presence or absence of $10 \text{ mmol} \cdot \text{L}^{-1}$ resveratrol for 24 to 96 hours were grown six-well glass slides and were fixed by acetone. After washing in PBS, the cells were incubated in 0.3% H_2O_2 solution at room temperature for 5 minutes. The cells were then incubated with anti-Bcl-2 or anti-Bax monoclonal antibody at a 1:300 dilution at 4°C overnight. After washing in PBS, the second antibody, biotinylated antirat Ig G, was added and the cells were incubated at room temperature for 1 hour. After washing in PBS, ABC compound was added and then incubated at room temperature for 10 minutes. DAB was used as the chromagen. After ten minutes, the brown color signifying the presence of antigen bound to antibodies was detected by light microscopy and photographed at $\times 200$. Controls were managed the same as the experimental group except the incubation of the primary antibody. The positive rate (PR) was calculated as follows: $PR = (\text{Number of positive cells} / \text{Total number}) \times 100\%$.

Statistical analysis

Datas were analyzed by the paired two-tailed Student *t* test, and significance was considered when $P < 0.05$.

RESULTS

MTT assay

EC-9706 cells were exposed to increasing concentrations ($0.1 \text{ mmol} \cdot \text{L}^{-1}$ to $100 \text{ mmol} \cdot \text{L}^{-1}$) of resveratrol for 24 to 96 hours, respectively. EC-9706 cells showed the mortality in a dose- and time-dependent manner. The data were summarised in Table 1.

Table 1 The inhibitory effect of resveratrol on EC-9706 cells

Time(h)	Inhibitory rate(%)				
	RPMI-1640	Resveratrol ($\text{mmol} \cdot \text{L}^{-1}$)			
		0.1	1	10	100
24	0.0	9.2 ^a	18.4 ^b	21.8 ^b	34.4 ^b
48	0.0	17.1 ^b	21.3 ^b	36.7 ^b	45.5 ^b
72	0.0	23.9 ^b	37.5 ^b	48.6 ^b	59.9 ^b
96	0.0	36.6 ^b	45.7 ^b	56.6 ^b	88.8 ^b

^a $P < 0.01$, ^b $P < 0.001$ vs the control group.

Morphological changes

After treatment of EC-9706 cells with resveratrol ($10 \text{ mmol} \cdot \text{L}^{-1}$) for 24 hours, some cells appeared apoptotic characteristics including chromatin condensation, appearance of chromatin crescent, nucleus fragmentation and of formation apoptotic body which could be seen by transmission electron microscope.

TUNEL assay

Apoptotic cell death was determined by TUNEL assay according to the manufacture's instructions. Positive staining located in the nucleus (Figure 1). After treatment with resveratrol ($10 \text{ mmol} \cdot \text{L}^{-1}$) for 24 to 96 hours, AIs were apparently increased with treated time ($P < 0.05$) (Table 2).

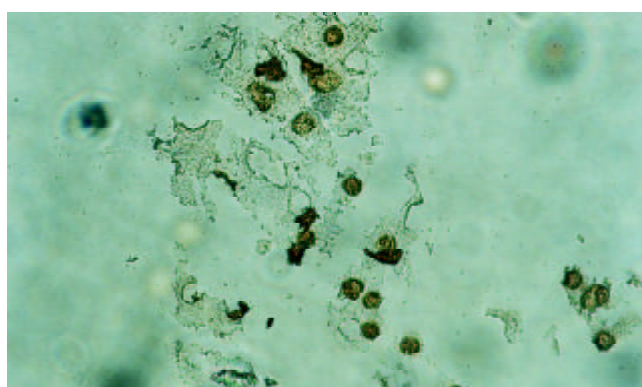


Figure 1 TUNEL assay of apoptotic cells induced by resveratrol with ($\times 200$).

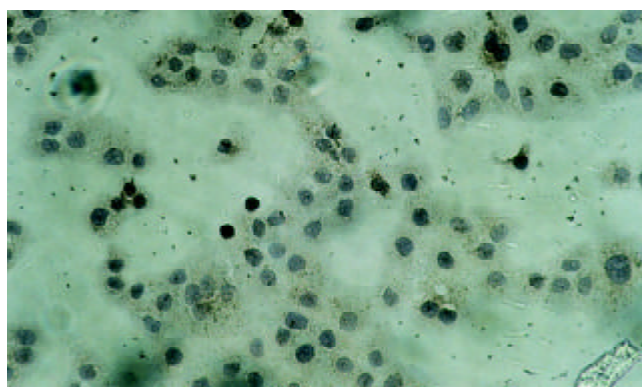


Figure 2 Immunohistochemical staining of the expression of Bcl-2 ($\times 200$).

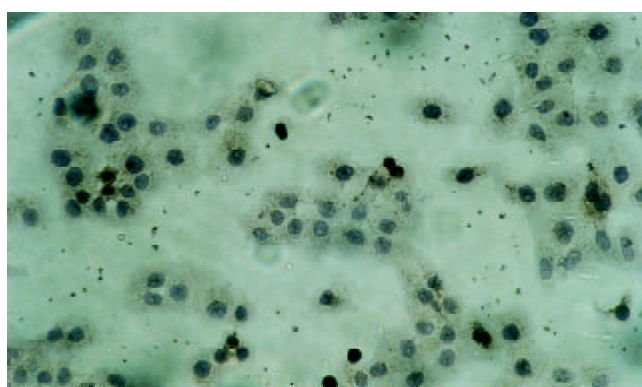


Figure 3 Immunohistochemical staining of the expression of Bax ($\times 200$).

Table 2 Apoptotic Index (AI) of treated EC-9706 cells by resveratrol

Time(h)	AI(%)
0	1.46 \pm 2.51
24	4.96 \pm 2.67 ^a
48	16.64 \pm 1.87 ^a
72	27.94 \pm 3.32 ^b
96	37.46 \pm 3.96 ^b

^a $P < 0.05$, ^b $P < 0.01$ vs the control group.

Expression of Bcl-2 proteins

Positive staining located in the cytoplasm (Figure 2). After treatment with resveratrol ($10 \text{ mmol} \cdot \text{L}^{-1}$) for 24 to 96 hours, PRs of Bcl-2 proteins were apparently reduced with treated

time ($P < 0.05$) (Table 3). This suggested that resveratrol could down-regulate the expression of Bcl-2.

Expression of bax proteins

Positive staining located in the cytoplasm (Figure 3). After treatment with resveratrol ($10 \text{ mmol} \cdot \text{L}^{-1}$) for 24 to 96 hours, PRs of Bax proteins were apparently increased with treated time ($P < 0.05$) (Table 4). This suggested that resveratrol could up-regulate the expression of Bax.

Table 3 Positive rate of Bcl-2 on treated EC-9706 cells by resveratrol

Time (h)	PR(%)
0	35.64±3.95
24	20.50±2.79 ^a
48	10.76±2.46 ^a
72	6.82±1.78 ^b
96	3.88±1.24 ^b

^a $P < 0.05$, ^b $P < 0.01$ vs the control group.

Table 4 Positive rate of Bax on treated EC-9706 cells by resveratrol

Time(h)	PR(%)
0	10.66±2.26
24	19.68±2.67 ^a
48	30.77±3.76 ^a
72	41.56±6.14 ^a
96	59.96±5.34 ^a

^a $P < 0.01$ vs the control group.

DISCUSSION

Currently, only few chemotherapeutic drugs take effect in the treatment of human primary esophageal carcinoma and it clearly need to look for new anti-esophageal carcinoma drugs. Resveratrol, a polyphenol found in various fruits and vegetables and is rich in grapes. The root extracts of the weed *Polygonum cuspidatum*, an important constituent of Chinese folk medicine, is also an ample source of resveratrol^[1,2]. Several studies in last several years have shown that resveratrol have cardioprotective and chemopreventive effects^[3-5]. This constituent may account for the reduced risk of coronary heart disease in humans which may be achieved by moderate wine consumption^[6]. Resveratrol is able to inhibit the growth of a wide variety of tumor cells, including leukemic, prostate, breast and hepatic cells^[7-11]. The anti-tumor activity of resveratrol might be related to the induction of tumor apoptosis of tumor cells^[12-22].

The Bcl-2 family plays a crucial role in the control of apoptosis. The family includes a number of proteins which have homologous amino acid sequences, including anti-apoptotic members such as Bcl-2 and Bcl-x_L, as well as pro-apoptotic members including Bax and Bad^[23-26]. Overexpression of Bax has the effect of promoting the cell death^[27-31]. Conversely, Overexpression of antiapoptotic proteins such as Bcl-2 will repress the function of Bax^[32-36]. Thus, the ratio of Bcl-2 / Bax appears to be a critical determinant of a cell's threshold for undergoing apoptosis^[37].

In this study resveratrol could reduce Bcl-2 expression and improve Bcl-2 expression. The ratio of Bcl-2 /Bax was decreased when EC-9706 cells were treated with resveratrol. The decreased ratio could triggered the apoptosis of EC-9706 cells.

Our results demonstrated resveratrol is able to induce the apoptosis in esophageal cancer. This apoptosis may be

mediated by down-regulating the expression of apoptosis-regulated gene Bcl-2 and up-regulating the expression of apoptosis-regulated gene Bax. Resveratrol may be potentially used as a chemotherapeutic drug in the anti-esophageal carcinoma chemotherapy.

REFERENCES

- 1 **Yoon S**, Kim Y, Ghim S, Song B, Bae Y. Inhibition of protein kinase CKII activity by resveratrol, a natural compound in red wine and grapes. *Life Sci* 2002; **71**: 2145
- 2 **Gao X**, Xu YX, Divine G, Janakiraman N, Chapman RA, Gautam SC. Disparate *in vitro* and *in vivo* antileukemic effects of resveratrol, a natural polyphenolic compound found in grapes. *J Nutr* 2002; **132**: 2076-2081
- 3 **Bhat KP**, Pezzuto JM. Cancer chemopreventive activity of resveratrol. *Ann N Y Acad Sci* 2002; **957**: 210-229
- 4 **Kuwajerwala N**, Cifuentes E, Gautam S, Menon M, Barrack ER, Reddy GP. Resveratrol induces prostate cancer cell entry into S phase and inhibits DNA synthesis. *Cancer Res* 2002; **62**: 2488-2492
- 5 **Joe AK**, Liu H, Suzui M, Vural ME, Xiao D, Weinstein IB. Resveratrol induces growth inhibition, S-phase arrest, apoptosis, and changes in biomarker expression in several human cancer cell lines. *Clin Cancer Res* 2002; **8**: 893-903
- 6 **Wang Z**, Zou J, Huang Y, Cao K, Xu Y, Wu JM. Effect of resveratrol on platelet aggregation *in vivo* and *in vitro*. *Chin Med J (Engl)* 2002; **115**: 378-380
- 7 **Fery-Dumazet H**, Garnier O, Mamani-Matsuda M, Vercauteren J, Belloc F, Billiard C, Dupouy M, Thiolat D, Kolb JP, Marit G, Reiffers J, Mossalayi MD. Resveratrol inhibits the growth and induces the apoptosis of both normal and leukemic hematopoietic cells. *Carcinogenesis* 2002; **23**: 1327-1333
- 8 **Kampa M**, Hatzoglou A, Notas G, Damianaki A, Bakogeorgou E, Gemetzi C, Kouroumalis E, Martin PM, Castanas E. Wine antioxidant polyphenols inhibit the proliferation of human prostate cancer cell lines. *Nutr Cancer* 2000; **37**: 223-233
- 9 **Bove K**, Lincoln DW, Tsan MF. Effect of resveratrol on growth of 4T1 breast cancer cells *in vitro* and *in vivo*. *Biochem Biophys Res Commun* 2002; **291**: 1001-1005
- 10 **Tian XM**, Zhang ZX. The anticancer activity of resveratrol on implanted tumor of HepG2 in nude mice. *Shijie Huaren Xiaohua Zazhi* 2001; **9**: 161-164
- 11 **Sun ZJ**, Pan CE, Liu HS, Wang GJ. Anti-hepatoma activity of resveratrol *in vitro*. *World J Gastroenterol* 2002; **8**: 79-81
- 12 **Pervaiz S**. Resveratrol-from the bottle to the bedside? *Leuk Lymphoma* 2001; **40**: 491-498
- 13 **Dorrie J**, Gerauer H, Wachter Y, Zunino SJ. Resveratrol induces extensive apoptosis by depolarizing mitochondrial membranes and activating caspase-9 in acute lymphoblastic leukemia cells. *Cancer Res* 2001; **61**: 4731-4739
- 14 **She QB**, Bode AM, Ma WY, Chen NY, Dong Z. Resveratrol-induced activation of p53 and apoptosis is mediated by extracellular-signal-regulated protein kinases and p38 kinase. *Cancer Res* 2001; **61**: 1604-1610
- 15 **Tsan MF**, White JE, Maheshwari JG, Bremner TA, Sacco J. Resveratrol induces Fas signaling-independent apoptosis in THP-1 human monocytic leukemia cells. *Br J Haematol* 2000; **109**: 405-412
- 16 **Szende B**, Tyihak E, Kiraly-Veghely Z. Dose-dependent effect of resveratrol on proliferation and apoptosis in endothelial and tumor cell cultures. *Exp Mol Med* 2000; **32**: 88-92
- 17 **Bernhard D**, Tinhofer I, Tonko M, Hubl H, Ausserlechner MJ, Greil R, Kofler R, Csordas A. Resveratrol causes arrest in the S-phase prior to Fas-independent apoptosis in CEM-C7H2 acute leukemia cells. *Cell Death Differ* 2000; **7**: 834-842
- 18 **Mouria M**, Gukovskaya AS, Jung Y, Buechler P, Hines OJ, Reber HA, Pandolfi SJ. Food-derived polyphenols inhibit pancreatic cancer growth through mitochondrial cytochrome C release and apoptosis. *Int J Cancer* 2002; **98**: 761-769
- 19 **Shih A**, Davis FB, Lin HY, Davis PJ. Resveratrol induces apoptosis in thyroid cancer cell lines via a MAPK- and p53-dependent mechanism. *J Clin Endocrinol Metab* 2002; **87**: 1223-1232
- 20 **Mahyar-Roemer M**, Katsen A, Mestres P, Roemer K. Resveratrol induces colon tumor cell apoptosis independently of p53 and precede by epithelial differentiation, mitochondrial proliferation

- and membrane potential collapse. *Int J Cancer* 2001; **94**: 615-622
- 21 **Lin HY**, Shih A, Davis FB, Tang HY, Martino LJ, Bennett JA, Davis PJ. Resveratrol induced serine phosphorylation of p53 causes apoptosis in a mutant p53 prostate cancer cell line. *J Urol* 2002; **168**: 748-755
- 22 **She QB**, Huang C, Zhang Y, Dong Z. Involvement of c-jun NH (2)-terminal kinases in resveratrol-induced activation of p53 and apoptosis. *Mol Carcinog* 2002; **33**: 244-250
- 23 **Konopleva M**, Konoplev S, Hu W, Zaritskey AY, Afanasiev BV, Andreeff M. Stromal cells prevent apoptosis of AML cells by up-regulation of anti-apoptotic proteins. *Leukemia* 2002; **16**: 1713-1724
- 24 **Van Der Woude CJ**, Jansen PL, Tiebosch AT, Beuving A, Homan M, Kleibeuker JH, Moshage H. Expression of apoptosis-related proteins in Barrett's metaplasia-dysplasia-carcinoma sequence: A switch to a more resistant phenotype. *Hum Pathol* 2002; **33**: 686-692
- 25 **Panaretakis T**, Pokrovskaja K, Shoshan MC, Grandier D. Activation of Bak, Bax and BH3-only proteins in the apoptotic response to doxorubicin. *J Biol Chem* 2002; [epub ahead of print]
- 26 **Bellosillo B**, Villamor N, Lopez-Guillermo A, Marce S, Bosch F, Campo E, Montserrat E, Colomer D. Spontaneous and drug-induced apoptosis is mediated by conformational changes of Bax and Bak in B-cell chronic lymphocytic leukemia. *Blood* 2002; **100**: 1810-1816
- 27 **Matter-Reissmann UB**, Forte P, Schneider MK, Filgueira L, Groscurth P, Seebach JD. Xenogeneic human NK cytotoxicity against porcine endothelial cells is perforin/granzyme B dependent and not inhibited by Bcl-2 overexpression. *Xenotransplantation* 2002; **9**: 325-337
- 28 **Lanzi C**, Cassinelli G, Cuccuru G, Supino R, Zuco V, Ferlini C, Scambia G, Zunino F. Cell cycle checkpoint efficiency and cellular response to paclitaxel in prostate cancer cells. *Prostate* 2001; **48**: 254-264
- 29 **Mertens HJ**, Heineman MJ, Evers JL. The expression of apoptosis-related proteins bcl-2 and ki67 in endometrium of ovulatory menstrual cycles. *Gynecol Obstet Invest* 2002; **53**: 224-230
- 30 **Mehta U**, Kang BP, Bansal G, Bansal MP. Studies of apoptosis and bcl-2 in experimental atherosclerosis in rabbit and influence of selenium supplementation. *Gen Physiol Biophys* 2002; **21**: 15-29
- 31 **Chang W**, Yang K, Chuang H, Jan J, Shaio M. Glutamine protects activated human T cells from apoptosis by up-regulating glutathione and bcl-2 levels. *Clin Immunol* 2002; **104**: 151
- 32 **Chen GG**, Lai PB, Hu X, Lam IK, Chak EC, Chun YS, Lau WY. Negative correlation between the ratio of Bax to Bcl-2 and the size of tumor treated by culture supernatants from Kupffer cells. *Clin Exp Metastasis* 2002; **19**: 457-464
- 33 **Usuda J**, Chiu SM, Azizuddin K, Xue LY, Lam M, Nieminen AL, Oleinick NL. Promotion of photodynamic therapy-induced apoptosis by the mitochondrial protein Smac/DIABLO: dependence on Bax. *Photochem Photobiol* 2002; **76**: 217-223
- 34 **Sun F**, Akazawa S, Sugahara K, Kamihira S, Kawasaki E, Eguchi K, Koji T. Apoptosis in normal rat embryo tissues during early organogenesis: the possible involvement of Bax and Bcl-2. *Arch Histol Cytol* 2002; **65**: 145-157
- 35 **Jang M**, Shin M, Shin H, Kim K, Park H, Kim E, Kim C. Alcohol induces apoptosis in TM3 mouse Leydig cells via bax-dependent caspase-3 activation. *Eur J Pharmacol* 2002; **449**: 39
- 36 **Tilli CM**, Stavast-Koey AJ, Ramaekers FC, Neumann HA. Bax expression and growth behavior of basal cell carcinomas. *J Cutan Pathol* 2002; **29**: 79-87
- 37 **Pettersson F**, Dalgleish AG, Bissonnette RP, Colston KW. Retinoids cause apoptosis in pancreatic cancer cells via activation of RAR-gamma and altered expression of Bcl-2/Bax. *Br J Cancer* 2002; **87**: 555-561

Edited by Xu XQ

HLA-DRB1 allele polymorphisms in genetic susceptibility to esophageal carcinoma

Jun Lin, Chang-Sheng Deng, Jie Sun, Xian-Gong Zheng, Xing Huang, Yan Zhou, Ping Xiong, Ya-Ping Wang

Jun Lin, Chang-Sheng Deng, Jie Sun, Xian-Gong Zheng, Xing Huang, Yan Zhou, Department of Gastroenterology, Zhongnan Hospital, Wuhan University, Wuhan 430071, Hubei Province, China
Ping Xiong, Department of Immunology, Tongji Medical College of Huazhong University of Science and Technology, Wuhan 430030, Hubei Province, China

Ya-Ping Wang, State Key Lab, Institute of Hydrobiology, The Chinese Academy of Sciences, Wuhan 430077, Hubei Province, China
Correspondence to: Dr Jun Lin, Department of Gastroenterology, Zhongnan Hospital, Wuhan University, Wuhan 430071, Hubei Province, China. linjun64@yahoo.com.cn

Telephone: +86-27-87335914 **Fax:** +86-27-87307622

Received: 2001-07-19 **Accepted:** 2001-08-27

Abstract

AIM: To probe into the genetic susceptibility of HLA-DRB1 alleles to esophageal carcinoma in Han Chinese in Hubei Province.

METHODS: HLA-DRB1 allele polymorphisms were typed by polymerase chain reaction with sequence-specific primers (PCR-SSP) in 42 unrelated patients with esophageal cancer and 136 unrelated normal control subjects and the associated HLA-DRB1 allele was measured by nucleotide sequence analysis with PCR. SAS software was used in statistics.

RESULTS: Allele frequency (AF) of HLA-DRB1*0901 was significantly higher in esophageal carcinoma patients than that in the normal controls (0.2500 vs 0.1397, $P=0.028$, the odds ratio 2.053, etiologic fraction 0.1282). After analyzed the allele nucleotide sequence of HLA-DRB1*0901 which approaches to the corresponded exon 2 sequence of the allele in genebank. There was no association between patients and controls in the rested HLA-DRB1 alleles.

CONCLUSION: HLA-DRB1*0901 allele is more common in the patients with esophageal carcinoma than in the healthy controls, which is positively associated with the patients of Hubei Han Chinese. Individuals carrying HLA-DRB1*0901 may be susceptible to esophageal carcinoma.

Lin J, Deng CS, Sun J, Zheng XG, Huang X, Zhou Y, Xiong P, Wang YP. HLA-DRB1 allele polymorphisms in genetic susceptibility to esophageal carcinoma. *World J Gastroenterol* 2003; 9(3): 412-416

<http://www.wjgnet.com/1007-9327/9/412.htm>

INTRODUCTION

The major histocompatibility complex (MHC) refers to as human leukocyte antigen (HLA). The loss of HLA antigens by neoplastic cells is considered important for tumor growth and metastasis^[1-3]. Since tumor neoantigens on the surface of aberrant cells are recognized by T-cells only in the context of the HLA "self" antigens, loss of the HLA antigens may allow the tumors to escape immunosurveillance^[4]. HLA system is a

kind of genetic marker of human being, and the most complicated human genetic polymorphic system with hereditary features of haplotype inheritance and allele polymorphism and linkage disequilibrium. It played an important role in the event of antigen recognition and presentation, immune response and modulation, destroying foreign antigen targeted cells. The alleles of the HLA system control a variety of immune functions and influence the susceptibility to more than 40 diseases, many of which have an autoimmune component^[5-17], esophageal cancer is a complex, probably multifactorial disease^[18-41]. Association of a particular HLA allele with a disease implies that the frequency of the allele is different in the patient population as compared with that of an ethnically matched control population. However, there has been no report on the association between HLA alleles and esophageal carcinoma.

In this study, we used polymerase chain reaction with sequence-specific primers (PCR-SSP) and DNA sequence analysis techniques on HLA-DRB1 alleles typing to investigate the genetic susceptibility of HLA allele polymorphisms in esophageal carcinoma of Hubei Han Chinese. This may be beneficial to the early prevention and surveillance, thus setting up gene therapy basis for esophageal carcinoma.

MATERIALS AND METHODS

Subjects

Included in our study were healthy controls and patients with esophageal carcinoma. The control group consists of one hundred and thirty-six unrelated donors or healthy individuals by physical examination, including 62 men and 74 women, ranging 22-48 years, in age, with a mean of 36±6 years. The esophageal carcinoma group includes forty-two unrelated patients with esophageal squamous cell carcinoma, 35 men and 7 women, ranging in age 41-80 years, with a mean age of 60±5 years, who were evaluated endoscopically and surgically. And all were tested by histopathology at Zhongnan Hospital of Wuhan University, between August 1998 and June 1999.

DNA extraction

Genomic DNA was isolated from leukocytes obtained from anticoagulated peripheral blood of patients and controls using the salting-out procedure^[5,42,43], or QIAamp Blood Kit (QIAGEN GmbH, Germany) with which DNA was obtained through solid phase affinity columns.

HLA-DRB1 alleles PCR-SSP typing

For HLA-DRB1 "low resolution" typing by PCR-SSP, 23 separate PCR reactions were performed for each sample. PCR-SSP typed system: each PCR reaction mixture contained 2-4 allele- or group-specific -DRB1 primers and the internal positive control primer pair. Allele sequence specific primers (2pmol), designed on the basis of published sequences^[43-45], were used in multiple amplification reaction. HLA-DRB1 alleles PCR-SSP typed system consisted of 60 ng genomic DNA, 0.5 U *Taq* DNA polymerase (Ampli Taq[®] DNA polymerase, Roche Diagnostic System, Inc. USA), 20 μmol

each deoxyadenosine triphosphate (dATP), deoxycytidine triphosphate (dCTP), deoxyguanosine triphosphate (dGTP), deoxythymidine triphosphate (dTTP), 10 mmol/L Tris-HCl pH8.3, 50 mmol·L⁻¹ KCl (kalium chloride), 1.5 mmol·L⁻¹ MgCl₂ (magnesium chloride). PCR amplifications were carried out in PTC-100 thermal cycler (MJ Research, Inc, USA) according to the method of Olerup *et al.*^[5,42,43]. Initial denaturation was made at 94 °C for 5 min; with 30 cycles each consisting of denaturation at 94 °C for 30 s, annealing at 65 °C for 1 min and extension at 72 °C for 1 min. The HLA-DRB1 alleles typed visualization of amplification was observed using medium resolution PCR-SSP products by 20 g·L⁻¹ gels agarose(Boehringer Mannheim GmbH, Germany) electrophoresis. The gels were run for 20 min at 15 V·cm⁻¹ in 0.5xTBE buffer and visualized using UV illumination and keeping file copies in computer.

Positive control, false negative allele

The most common form of individual PCR reaction failure is where random individual reactions fail to produce allele or control bands. This occurred on average in 1 % of all PCR-SSP amplification. In each PCR reaction, a pair primers were included which specifically amplify the exon 2 of HLA-DRB1 alleles. These two primers matched non-allelic sequences and thus functioned as an internal positive amplification control. We used human growth hormone gene as a intra-positive control, in which primer^[5] is 5' -primer, 21 mer, 5' GCC TTC CCA ACC ATT CCC TTA 3' , Tm64 °C; 3' -primer, 22 mer, 5' TCA CGG ATT TCT GTT GTG TTT C 3' , terminal concentration 0.15 μmol·L⁻¹, product 429 base pair (bp) fragment. Control failure is not a problem if the genotype obtained is heterozygous for all alleles and the type is unequivocal. Homozygous samples, in which the control failed, normally would require typing with a new DNA sample once

again. Individual false negative allele amplifications where the control amplification worked but an expected allele was not amplified, did occur, the same be required repeated typing.

DNA sequence analysis of PCR-SSP products

Specific PCR-SSP products of amplification were obtained from agarose gels electrophoresis, then purified with glassmilk kit (Clontech Laboratories, Inc, USA), and the base sequence was examined by PCR sequence analysis with ABI prism 310 (Perkin-Elmer, USA) with the addition of a terminal deoxytransferase extension step at the end of the chain termination reaction.

Statistical analysis

SAS (6.12 for Win), including χ^2 analysis or Fisher's Exact Test, was used to compare the allele frequency (AF) of HLA-DRB1 between the patients with esophageal carcinoma and the controls.

RESULTS

HLA-DRB1*0901 was present at increased frequency in patients with esophageal squamous cell carcinoma, 0.2500 vs 0.1397, $P=0.028$, odds ratio 2.053, etiologic fraction 0.1282 (Table 1). The rested HLA-DRB1 alleles frequencies showed no significant difference in comparison between patients and the controls, i.e., there was positive association between HLA-DRB1*0901 and the patients of Hubei Hans. The HLA-DRB1*0901 nucleotide sequence, was analyzed in this study, approaches to the corresponded exon 2 of the allele sequence in genebank. Esophageal carcinoma was associated with HLA genotype: individuals carrying HLA-DRB1*0901 may be susceptibilitive to esophageal carcinoma in Hubei Hans.

Table 1 HLA-DRB1 allele frequencies in esophageal cancer patients of Hubei Han Chinese

HLA-DRB1 alleles	Control group			Esophageal cancer group			P
	N1	AF($n_1=272$)	PF($n_2=136$)%	N2	AF($n_1=84$)	PF($n_2=42$)%	
0101-2	13	0.0478	9.5588	2	0.0238	4.7619	>0.05
0103	0	0.0000	0.0000	0	0.0000	0.0000	
150X	46	0.1691	32.3529	9	0.1071	21.4286	>0.05
160X	9	0.0331	6.6176	3	0.0356	7.1429	>0.05
0301	19	0.0699	13.9706	6	0.0714	14.2857	>0.05
0302	2	0.0074	1.4706	0	0.0000	0.0000	>0.05
040X	30	0.1103	20.5882	12	0.1429	26.1905	>0.05
0701-2	13	0.0478	9.5588	3	0.0357	7.1429	>0.05
080X	22	0.0809	15.4412	4	0.0476	9.5238	>0.05
0901	38	0.1397	26.4706	21	0.2500	45.2400	0.028*
1001	11	0.0404	7.3529	2	0.0238	4.7619	>0.05
110X	18	0.0662	12.5000	7	0.0833	16.6667	>0.05
120X	17	0.0625	12.5000	11	0.1310	26.1905	>0.05
1301-2	15	0.0551	11.0294	1	0.0119	2.3810	>0.05
1303-4	4	0.0147	2.9412	0	0.0000	0.0000	>0.05
1305	1	0.0037	0.7353	0	0.0000	0.0000	>0.05
1305-6	0	0.0000	0.0000	0	0.0000	0.0000	
140X	15	0.0551	11.0294	3	0.0357	0.0357	>0.05

AF: allele frequency, PF: phenotype frequency;

P: Fisher's exact test (2-tail) or χ^2 , compared with the control with AF;

*Odds ratio=2.053, etiologic fraction=0.12820.

DISCUSSION

Familial aggregation of esophageal cancer is common. There is an approximate increase in abnormal chromosome ratio of this cancerous relatives as compared with the general population, although the inheritance patterns clearly fit no simple Mendelian patterns. However, the illness may exist in the same family at a higher frequency than expected by chance alone^[5,24-27]. This suggests that there may be an internal environment susceptible to malignant and a genetic component in the patients' families, which supports the concept that heredity may play an important role in the pathogenesis of esophageal cancer^[2, 9, 46-53].

Major histocompatibility complex (MHC) is a genetic name describing alleles encoding antigens first discovered because they determine in a major way the fate of a graft, i.e., histocompatibility. In many species, the MHC has an additional name such as HLA for humans, H-2 for mice, SLA for swine, etc. The HLA alleles are located in a 3 500-4 000 kilobase region of chromosome 6; and the allele encoding β 2-microglobulin, a related protein in the system, is on chromosome 15. The major classes of HLA alleles are class I (HLA-A, -B, and -C) and class II (HLA-DR, -DQ, and -DP). Between the class I and II alleles, there are many other alleles, some with immune-related functions that could also be associated with diseases, tumor necrosis factor A and B genes being among them. Class II HLA presents peptides derived from extracellular antigens. The HLA polymorphism appears to be responsible for variations in the immune response of different individuals to different antigens, and may contribute to the susceptibility to diseases and autoimmune disorders^[5,15-17]. The loss of HLA antigens by neoplastic cells is considered important to tumor growth and metastasis, and for tumor escape immune surveillance. HLA class I molecules are required for the presentation of tumor neoantigens to cytotoxic T-lymphocytes. There is evidence that tumor cells with reduced expression or lack of such antigens could evade an immune response and selected for tumor progression. It can be considered that either extensive abnormalities in the regulation of the HLA alleles occurred or substantial chromosomal damage took place in the short arm of chromosome 6, where the human HLA allele complex is located. It was demonstrated that oncogenes may suppress the expression of HLA class I alleles, such as the activation of oncogenes or the inactivation of suppressor genes^[50,54-56]. The data presented here demonstrate that HLA-DRB1*0901 AF increased in the patients with esophageal cancer compared with that in healthy controls (0.2500 vs 0.1397, $P=0.028$, OR=2.053, EF=0.1282), but none of the rested HLA-DRB1 alleles occurred at markedly altered frequency between the patients and the normal individuals we investigated, indicating that HLA-DRB1*0901 is positively associated with esophageal cancer.

The nucleotide sequence of HLA-DRB1*0901 allele which was measured in our research approaches to the corresponded exon 2 gene sequence of genebank^[44,45]. The AF of HLA-DRB1*0901 was also increased in both Japanese patients with lung cancer and prostate cancer. It is the allele that is associated with genetic susceptibility of various tumors, but why? It was entirely unclear up to now. Pathogenesis of genetic association may be linkage disequilibrium (nonrandom association) and/or changing in the recognized procession of the specific antigen.

It is still controversial whether or not HLA antigen expression in carcinomas correlates with the development of carcinoma and prognosis. The immune responses involving HLA antigens expressed on carcinoma cells are thought to play an important role in eliminating mutated cells or suppressing carcinoma progression^[51-53,57-59]. As reported in some studies, the reduced expression of HLA antigens in malignant tissues

has been proposed as a mechanism whereby tumor-associated proteins cannot be presented in the T cells, therefore the tumor cell proliferates are unperturbed by the immune system and carcinomas protect themselves from hosts' immunosurveillance. There is a possibility that HLA allele genetic association and expression on carcinoma may provide a clue to the understanding of the therapeutic mechanisms of biological response modifiers or immunotherapy which may cut through the induction of HLA antigens on carcinoma cells^[56,60-63]. The cells of a given individual may express HLA alleles, which altered binding to tumor peptides, thereby leading to a modified immune response to the tumor. Identification of the mechanism associating HLA-DRB1*0901 with esophageal cancer could ultimately help target individuals most likely to benefit from cancer screening and prevention programs, and could facilitate novel therapeutic strategies for cancer immunoprevention.

REFERENCES

- 1 **Geertsens R**, Hofbauer G, Kamarashev J, Yue FY, Dummer R. Immune escape mechanisms in malignant melanoma. *Int J Mol Med* 1999; **3**: 49-57
- 2 **Jimenez P**, Canton J, Concha A, Cabrera T, Fernandez M, Real LM, Garcia A, Serrano A, Garrido F, Ruiz-Cabello F. Microsatellite instability analysis in tumors with different mechanisms for total loss of HLA expression. *Cancer Immunol Immunother* 2000; **48**: 684-690
- 3 **Ramal LM**, Maleno I, Cabrera T, Collado A, Ferron A, Lopez-Nevot MA, Garrido F. Molecular strategies to define HLA haplotype loss in microdissected tumor cells. *Hum Immunol* 2000; **61**: 1001-1012
- 4 **Facoetti A**, Capelli E, Nano R. HLA class I molecules expression: evaluation of different immunocytochemical methods in malignant lesions. *Anticancer Res* 2001; **21**: 2435-2440
- 5 **Lin J**, Deng CS, Sun J, Zhou Y, Xiong P, Wang YP. Study on the genetic susceptibility of HLA-DQB1 alleles in esophageal cancer of Hubei Chinese Hans. *Shijie Huaren Xiaohua Zazhi* 2000; **8**: 965-968
- 6 **Noble A**. Review article: molecular signals and genetic reprogramming in peripheral T-cell differentiation. *Immunology* 2000; **101**: 289-299
- 7 **Douek DC**, Altmann DM. T-cell apoptosis and differential human leucocyte antigen class II expression in human thymus. *Immunology* 2000; **99**: 249-256
- 8 **Boyton RJ**, Lohmann T, Londei M, Kalbacher H, Halder T, Frater AJ, Douek DC, Leslie DG, Flavell RA, Altmann DM. Glutamic acid decarboxylase T lymphocyte responses associated with susceptibility or resistance to type I diabetes: analysis in disease discordant human twins, non-obese diabetic mice and HLA-DQ transgenic mice. *Int Immunol* 1998; **10**: 1765-1776
- 9 **Koriyama C**, Shinkura R, Hamasaki Y, Fujiyoshi T, Eizuru Y, Tokunaga M. Human leukocyte antigens related to Epstein-Barr virus-associated gastric carcinoma in Japanese patients. *Eur J Cancer Prev* 2001; **10**: 69-75
- 10 **Chatzipetrou MA**, Tarassi KE, Konstadoulakis MM, Pappas HE, Zafirellis KD, Athanassiades TE, Papadopoulos SA, Panousopoulos DG, Golematis BC, Papasteriades CA. Human leukocyte antigens as genetic markers in colorectal carcinoma. *Dis Colon Rectum* 1999; **42**: 66-70
- 11 **Ishigami S**, Aikou T, Natsugoe S, Hokita S, Iwashige H, Tokushige M, Sonoda S. Prognostic value of HLA-DR expression and dendritic cell infiltration in gastric cancer. *Oncology* 1998; **55**: 65-69
- 12 **Zamani M**, Cassiman JJ. Reevaluation of the importance of polymorphic HLA class II alleles and amino acids in the susceptibility of individuals of different populations to type I diabetes. *Am J Med Genet* 1998; **76**: 183-194
- 13 **Hanifi Moghaddam P**, de Knijf P, Roep BO, Van der Auwera B, Naipal A, Goris F, Schuit F, Giphart MJ. Genetic structure of IDDM1: two separate regions in the major histocompatibility complex contribute to susceptibility or protection. Belgian Diabetes Registry. *Diabetes* 1998; **47**: 263-269
- 14 **Rigby AS**, MacGregor AJ, Thomson G. HLA haplotype sharing

- in rheumatoid arthritis sibships: risk estimates subdivided by proband genotype. *Genet Epidemiol* 1998; **15**: 403-418
- 15 **Azuma T**, Ito S, Sato F, Yamazaki Y, Miyaji H, Ito Y, Suto H, Kuriyama M, Kato T, Kohli Y. The role of the HLA-DQA1 gene in resistance to atrophic gastritis and gastric adenocarcinoma induced by *Helicobacter pylori* infection. *Cancer* 1998; **82**: 1013-1018
- 16 **Zavaglia C**, Martinetti M, Silini E, Bottelli R, Daielli C, Asti M, Airoldi A, Salvaneschi L, Mondelli MU, Ideo G. Association between HLA class II alleles and protection from or susceptibility to chronic hepatitis C. *J Hepatol* 1998; **28**: 1-7
- 17 **Weinshenker BG**, Santrach P, Bissonet AS, McDonnell SK, Schaid D, Moore SB, Rodriguez M. Major histocompatibility complex class II alleles and the course and outcome of MS: a population-based study. *Neurology* 1998; **51**: 742-747
- 18 **Wu MY**, Chen MH, Liang YR, Meng GZ, Yang HX, Zhuang CX. Experimental and clinicopathologic study on the relationship between transcription factor Egr-1 and esophageal carcinoma. *World J Gastroenterol* 2001; **7**: 490-495
- 19 **Kawaguchi H**, Ohno S, Araki K, Miyazaki M, Saeki H, Watanabe M, Tanaka S, Sugimachi K. p⁵³ polymorphism in human papillomavirus-associated esophageal cancer. *Cancer Res* 2000; **60**: 2753-2755
- 20 **Wijnhoven BP**, Nollet F, De Both NJ, Tilanus HW, Dinjens WN. Genetic alteration involving exon 3 of the β -catenin gene does not play a role in adenocarcinomas of the esophagus. *Int J Cancer* 2000; **86**: 533-537
- 21 **Takubo K**, Nakamura K, Sawabe M, Arai T, Esaki Y, Miyashita M, Mafune K, Tanaka Y, Sasajima K. Primary undifferentiated small cell carcinoma of the esophagus. *Hum Pathol* 1999; **30**: 216-221
- 22 **Fong LY**, Pegg AE, Magee PN. α -difluoromethylornithine inhibits *N*-nitrosomethylbenzylamine-induced esophageal carcinogenesis in zinc-deficient rats: effects on esophageal cell proliferation and apoptosis. *Cancer Res* 1998; **58**: 5380-5388
- 23 **Arber N**, Gammon MD, Hibshoosh H, Britton JA, Zhang Y, Schonberg JB, Roterdam H, Fabian I, Holt PR, Weinstein IB. Overexpression of cyclin D1 occurs in both squamous carcinomas and adenocarcinomas of the esophagus and in adenocarcinomas of the stomach. *Hum Pathol* 1999; **30**: 1087-1092
- 24 **Van Lieshout EM**, Roelofs HM, Dekker S, Mulder CJ, Wobbes T, Jansen JB, Peters WH. Polymorphic expression of the glutathione S-transferase P1 gene and its susceptibility to Barrett's esophagus and esophageal carcinoma. *Cancer Res* 1999; **59**: 586-589
- 25 **Zou JX**, Wang LD, Shi ST, Yang GY, Xue ZH, Gao SS, Li YX, Yang CS. p53 gene mutations in multifocal esophageal precancerous and cancerous lesions in patients with esophageal cancer in high-risk northern China. *Shijie Huaren Xiaohua Zazhi* 1999; **7**: 280-284
- 26 **Liu J**, Su Q, Zhang W. Relationship between HPV-E6 p53 protein and esophageal squamous cell carcinoma. *Shijie Huaren Xiaohua Zazhi* 2000; **8**: 494-496
- 27 **Qin HY**, Shu Q, Wang D, Ma QF. Study on genetic polymorphisms of DDC gene VNTR in esophageal cancer. *Shijie Huaren Xiaohua Zazhi* 2000; **8**: 782-785
- 28 **Mori M**, Mimori K, Shiraiishi T, Alder H, Inoue H, Tanaka Y, Sugimachi K, Huebner K, Croce CM. Altered expression of Fhit in carcinoma and precarcinomatous lesion of the esophagus. *Cancer Res* 2000; **60**: 1177-1182
- 29 **Dolan K**, Garde J, Walker SJ, Sutton R, Gosney J, Field JK. LOH at the sites of the *DCC*, *APC*, and *TP53* tumor suppressor genes occurs in Barrett's metaplasia and dysplasia adjacent to adenocarcinoma of the esophagus. *Hum Pathol* 1999; **30**: 1508-1514
- 30 **Zur Hausen A**, Sarbia M, Heep H, Willers R, Gabbert HE. Retinoblastoma-protein (p16) expression and prognosis in squamous-cell carcinomas of the esophagus. *Int J Cancer* 1999; **84**: 618-622
- 31 **Shen ZY**, Shen J, Li QS, Chen CY, Chen JY, Zeng Y. Morphological and functional changes of mitochondria in apoptotic esophageal carcinoma cells induced by arsenic trioxide. *World J Gastroenterol* 2002; **8**: 31-35
- 32 **Xu CT**, Yan XJ. p53 anti-cancer gene and digestive system neoplasms. *Shijie Huaren Xiaohua Zazhi* 1999; **7**: 77-79
- 33 **Gu HP**, Shang PZ, Su H, Li ZG. Association of CD15 antigen expression with cathepsin D in esophageal carcinoma tissues. *Shijie Huaren Xiaohua Zazhi* 2000; **8**: 259-261
- 34 **Liu J**, Chen SL, Zhang W, Su Q. P31^{WAF1} gene expression with P53 mutation in esophageal carcinoma. *Shijie Huaren Xiaohua Zazhi* 2000; **8**: 1350-1353
- 35 **Tan LJ**, Jiang W, Zhang W, Zhang XR, Qiu DH. Fas/FasL expression of esophageal squamous cell carcinoma, dysplasia tissues and normal mucosa. *Shijie Huaren Xiaohua Zazhi* 2001; **9**: 15-19
- 36 **Wang LD**, Chen H, Guo LM. Alterations of tumor suppressor gene system p53-Rb and human esophageal carcinogenesis. *Shijie Huaren Xiaohua Zazhi* 2001; **9**: 367-371
- 37 **Gao F**, Yi J, Shi GY, Li H, Shi XG, Tang XM. The sensitivity of digestive tract tumor cells to As₂O₃ is associated with the inherent cellular level of reactive oxygen species. *World J Gastroenterol* 2002; **8**: 36-39
- 38 **Shen ZY**, Shen WY, Chen MH, Shen J, Cai WJ, Yi Z. Nitric oxide and calcium ions in apoptotic esophageal carcinoma cells induced by arsenite. *World J Gastroenterol* 2002; **8**: 40-43
- 39 **Gu ZP**, Wang YJ, Li JG, Zhou YA. VEGF₁₆₅ antisense RNA suppresses oncogenic properties of human esophageal squamous cell carcinoma. *World J Gastroenterol* 2002; **8**: 44-48
- 40 **Wang LD**, Zhou Q, Wei JP, Yang WC, Zhao X, Wang LX, Zou JX, Gao SS, Li YX, Yang CS. Apoptosis and its relationship with cell proliferation, p53, Waf1p21, bcl-2 and c-myc in esophageal carcinogenesis studied with a high-risk population in northern China. *World J Gastroenterol* 1998; **4**: 287-293
- 41 **Zhang LJ**, Chen KN, Xu GW, Xing HP, Shi XT. Congenital expression of *mdr-1* gene in tissues of carcinoma and its relation with patho-morphology and prognosis. *World J Gastroenterol* 1999; **5**: 53-56
- 42 **Carter AS**, Bunce M, Cerundolo L, Welsh KI, Morris PJ, Fuggle SV. Detection of microchimerism after allogeneic blood transfusion using nested polymerase chain reaction amplification with sequence-specific primers (PCR-SSP): a cautionary tale. *Blood* 1998; **92**: 683-689
- 43 **Carter AS**, Cerundolo L, Bunce M, Koo DD, Welsh KI, Morris PJ, Fuggle SV. Nested polymerase chain reaction with sequence-specific primers typing for HLA-A, -B, and -C alleles: detection of microchimerism in DR-matched individuals. *Blood* 1999; **94**: 1471-1477
- 44 **Schreuder GM**, Hurley CK, Marsh SG, Lau M, Maiers M, Kollman C, Noren HJ. The HLA Dictionary 2001: a summary of HLA-A, -B, -C, -DRB1/3/4/5, -DQB1 alleles and their association with serologically defined HLA-A, -B, -C, -DR and -DQ antigens. *Tissue Antigens* 2001; **58**: 109-140
- 45 **Marsh SG**. HLA class II region sequences, 1998. *Tissue Antigens* 1998; **51**: 467-507
- 46 **Xu M**, Jin YL, Fu J, Huang H, Chen SZ, Qu P, Tian HM, Liu ZY, Zhang W. The abnormal expression of retinoic acid receptor- β , p53 and Ki67 protein in normal, premalignant and malignant esophageal tissues. *World J Gastroenterol* 2002; **8**: 200-202
- 47 **Zhou Y**, Gao SS, Li YX, Fan ZM, Zhao X, Qi YJ, Wei JP, Zou JX, Liu G, Jiao LH, Bai YM, Wang LD. Tumor suppressor gene p16 and Rb expression in gastric cardia precancerous lesions from subjects at a high incidence area in northern China. *World J Gastroenterol* 2002; **8**: 423-425
- 48 **Xiong XD**, Xu LY, Shen ZY, Cai WJ, Luo JM, Han YL, Li EM. Identification of differentially expressed proteins between human esophageal immortalized and carcinomatous cell lines by two-dimensional electrophoresis and MALDI-TOF-mass spectrometry. *World J Gastroenterol* 2002; **8**: 777-781
- 49 **Qin LX**. Chromosomal aberrations related to metastasis of human solid tumors. *World J Gastroenterol* 2002; **8**: 769-776
- 50 **Wang AH**, Sun CS, Li LS, Huang JY, Chen QS. Relationship of tobacco smoking, CYP1A1, GSTM1 gene polymorphism and esophageal cancer in Xi'an. *World J Gastroenterol* 2002; **8**: 49-53
- 51 **Bustin SA**, Li SR, Phillips S, Dorudi S. Expression of HLA class II in colorectal cancer: evidence for enhanced immunogenicity of microsatellite-instability-positive tumours. *Tumour Biol* 2001; **22**: 294-298
- 52 **Hombach A**, Heuser C, Marquardt T, Wiczarkowicz A, Gronck V, Pohl C, Abken H. CD4+ T cells engrafted with a recombinant immunoreceptor efficiently lyse target cells in a MHC antigen- and Fas-independent fashion. *J Immunol* 2001; **167**: 1090-1096
- 53 **Iguchi C**, Nio Y, Takeda H, Yamasawa K, Hirahara N, Toga T,

- Itakura M, Tamura K. Plant polysaccharide PSK: cytostatic effects on growth and invasion; modulating effect on the expression of HLA and adhesion molecules on human gastric and colonic tumor cell surface. *Anticancer Res* 2001; **21**: 1007-1013
- 54 **Kim C**, Matsumura M, Saijo K, Ohno T. *In vitro* induction of HLA-A2402-restricted and carcinoembryonic antigen-specific cytotoxic T lymphocytes on fixed autologous peripheral blood cells. *Cancer Immunol Immunother* 1998; **47**: 90-96
- 55 **Savoie CJ**, Kamikawaji N, Sudo T, Furuse M, Shirasawa S, Tana T, Sasazuki T. MHC class I bound peptides of a colon carcinoma cell line, a Ki-ras gene-targeted progeny cell line and a B cell line. *Cancer Lett* 1998; **123**: 193-197
- 56 **Tanaka H**, Tsunoda T, Nukaya I, Sette A, Matsuda K, Umamo Y, Yamaue H, Takesako K, Tanimura H. Mapping the HLA-A24-restricted T-cell epitope peptide from a tumour-associated antigen HER2/neu: possible immunotherapy for colorectal carcinomas. *Br J Cancer* 2001; **84**: 94-99
- 57 **Wang RF**, Johnston SL, Zeng G, Topalian SL, Schwartzentruber DJ, Rosenberg SA. A breast and melanoma-shared tumor antigen: T cell response to antigenic peptides translated from different reading frames. *J Immunol* 1998; **161**: 3598-3606
- 58 **Nagorsen D**, Keilholz U, Rivoltini L, Schmittel A, Letsch A, Asemussen AM, Berger G, Buhr HJ, Thiel E, Scheibenbogen C. Natural T-cell response against MHC class I epitopes of epithelial cell adhesion molecule, her-2/neu, and carcinoembryonic antigen in patients with colorectal cancer. *Cancer Res* 2000; **60**: 4850-4854
- 59 **Sato N**, Nabeta Y, Kondo H, Sahara H, Hirohashi Y, Kashiwagi K, Kanaseki T, Sato Y, Rong S, Hirai I, Kamiguchi K, Tamura Y, Matsuura A, Takahashi S, Torigoe T, Ikeda H. Human CD8 and CD4 T cell epitopes of epithelial cancer antigens. *Cancer Chemother Pharmacol* 2000; **46** (Suppl): S86-90
- 60 **Nabeta Y**, Sahara H, Suzuki K, Kondo H, Nagata M, Hirohashi Y, Sato Y, Wada Y, Sato T, Wada T, Yamashita T, Kikuchi K, Sato N. Induction of cytotoxic T lymphocytes from peripheral blood of human histocompatibility antigen (HLA)-A31(+) gastric cancer patients by *in vitro* stimulation with antigenic peptide of signet ring cell carcinoma. *Jpn J Cancer Res* 2000; **91**: 616-621
- 61 **Schirle M**, Keilholz W, Weber B, Gouttefangeas C, Dumrese T, Becker HD, Stevanovic S, Rammensee HG. Identification of tumor-associated MHC class I ligands by a novel T cell-independent approach. *Eur J Immunol* 2000; **30**: 2216-2225
- 62 **Novellino PS**, Trejo YG, Beviacqua M, Bordenave RH, Rumi LS. Regulation of HLA-DR antigen in monocytes from colorectal cancer patients by *in vitro* treatment with human recombinant interferon-gamma. *J Invest Allergol Clin Immunol* 2000; **10**: 90-93
- 63 **Novellino PS**, Trejo YG, Beviacqua M, Bordenave RH, Rumi LS. Cisplatin containing chemotherapy influences HLA-DR expression on monocytes from cancer patients. *J Exp Clin Cancer Res* 1999; **18**: 481-484

Edited by Ma JY

Difference of gene expression profiles between esophageal carcinoma and its pericancerous epithelium by gene chip

Shen-Hua Xu, Li-Juan Qian, Han-Zhou Mou, Chi-Hong Zhu, Xing-Ming Zhou, Xiang-Lin Liu, Yong Chen, Wen-Yu Bao

Shen-Hua Xu, Li-Juan Qian, Han-Zhou Mou, Chi-Hong Zhu, Xiang-Lin Liu, Zhejiang Cancer Research Institute, Hangzhou 310022, China

Xing-Ming Zhou, Department of Surgical, Zhejiang Cancer Hospital, Hangzhou 310022, Zhejiang, China

Yong Chen, Wen-Yu Bao, United Gene Scientific Tech. (Group) Company Limited, Shanghai 200092, China

Supported by Zhejiang Medical and Health Science Foundation No. 2002A023

Correspondence to: Dr. Shen-Hua Xu, Zhejiang Cancer Research Institute, No.38 Guangji Road, banshan Hangzhou 310022, Zhejiang, China. xsh1947@LoL365.com

Telephone: +86-571-8144401-263 **Fax:** +86-571-8145807

Received: 2002-07-31 **Accepted:** 2002-09-20

Abstract

AIM: To study the difference of gene expression between esophageal carcinoma and its pericancerous epithelium and to screen novel associated genes in the early stage of esophageal carcinogenesis by cDNA microarray.

METHODS: Total RNA was extracted with the original single step way from esophageal carcinoma, its pericancerous epithelial tissue and normal esophageal epithelium far from the tumor. The cDNA retro-transcribed from equal quantity of mRNA was labeled with Cy5 and Cy3 fluorescence functioning as probes. The mixed probes were hybridized with two pieces of BioDoor 4 096 double dot human whole gene chip. Fluorescence signals were scanned by ScanArray 3 000 laser scanner and farther analyzed by ImaGene 3.0 software with the digital computer.

RESULTS: (1) A total of 135 genes were screened out, in which 85 and 50 genes whose the gene expression levels (fluorescence intensity) in esophageal carcinoma were more than 2 times and less than 0.5 times respectively compared with the normal esophageal epithelium. (2) There were also total 31 genes, among then 27 and 4 whose expressions in pericancerous tissue were 2-fold up-regulated and 0.5-fold down-regulated respectively compared with normal esophageal epithelium. (3) There were 13 genes appeared simultaneously in both pericancerous epithelium and esophageal carcinoma, while another 18 genes existed in pericancerous epithelium only.

CONCLUSION: With the parallel comparison among these three gene profiles, it was shown that (1). A total of 135 genes, Whose expression difference manifested as fluorescence intensity were more than 2 times between esophageal carcinoma and normal esophageal epithelium, were probably related to the occurrence and development of the esophageal carcinoma. (2). The 31 genes showing expression difference more than 2 times between pericancerous and normal esophageal epithelium might be relate to the promotion of esophageal pericancerosis and its progress. The present study illustrated that by using the gene chip to detect the difference of gene expression profiles

might be of benefit to the gene diagnosis, treatment and prevention of esophageal carcinoma.

Xu SH, Qian LJ, Mou HZ, Zhu CH, Zhou XM, Liu XL, Chen Y, Bao WY. Difference of gene expression profiles between esophageal carcinoma and its pericancerous epithelium by gene chip. *World J Gastroenterol* 2003; 9(3): 417-422

<http://www.wjgnet.com/1007-9327/9/417.htm>

INTRODUCTION

The differentially expressed genes in different specimens may be detected with parallel analysis by gene chips which has greatly improved the traditional experiment in that only a single or several genes expression can be observed for each test. More and more cDNA microarray methods are applied nowadays in the study of gene expression. In this paper, gene chip technique was used to analysis the difference of gene expression patterns between the esophageal carcinoma, its pericancerous tissue and normal epithelium of esophagus, in order to explore the tumor-associated gene-clusters and their functions in the process of occurrence and development of esophageal carcinoma, which will be helpful to understand comprehensively the molecular mechanism of cell transformation and provide molecular markers and target genes for clinical diagnosis, prevention, susceptibility forecast and treatment of esophageal carcinoma.

MATERIALS AND METHODS

Materials

All the tissue specimens including esophageal carcinoma, its pericancerous epithelium and normal epithelium of esophagus that serves as control were taken from 11 patients being operated in our hospital from July 17 to September 7,2000. For each sample, one part was cut to be frozen in liquid nitrogen immediately after surgical resection, and the other part was used for histopathological examination to ensure all the pericancerous and control esophageal epithelia without cancer cells but with their corresponding histological appearance. The clinical and pathological data of these patients were show in Table 1.

Methods

Chip preparation Four thousand and ninety six target cDNA clones used in cDNA chip were provided by United Gene Ltd. and cooperative fellows. These genes were amplified with PCR using universal primers and then purified with standard method. The quality of PCR was monitored by agarose electrophoresis. The obtained genes were dissolved in 3×SSC spotting solution and then spotted on silylated slides (Telechem. Inc) by Cartesian 7 500 spotting Robotics (Cartesian, Inc). Each target gene was dotted twice. After spotting, the slides were hydrated (2 h) and dried (0.5 h, room temperature.). The samples were cross-linked with UV light and treated with 0.2 % SDS, H₂O and 0.2 % NaNBH₄ for 10 min respectively. Then the slides were dried in cold condition and ready for use.

Probe preparation Total sample RNA was extracted by single step method^[1]. Briefly, after taking out from liquid Nitrogen specimens were ground completely into tiny powder while

adding liquid Nitrogen in ceramic mortar and then homogenized in D solution plus 1 % mercaptoethanol. After centrifugation, the supernatant was extracted with phenol: chloroform (1:1), NaAC and acidic phenol: chloroform (5:1) respectively. The aqueous phase was precipitated by equal volume of isopropanol and centrifuged. The precipitate was dissolved with Millie-Q H₂O. After further purification by LiCl precipitating method obtained RNA sample was demonstrated, good in quality with UV analysis and electrophoresis. mRNAs were isolated and purified with Oligotex mRNA Midi Kit (Quagen, Inc.). The fluorescent-labeled cDNA probe was prepared through retro-transcription, referring to the method of Schena^[2]. The probes from normal epithelium were labeled with Cy3-dUTP, while those from cancer tissue and pericancerous epithelium with Cy5-dUTP respectively. The probes were mixed (Cy3-dUTP control + Cy5-dUTP esophageal carcinoma, Cy3-dUTP control + Cy5-dUTP pericancerous epithelium) and precipitated by ethanol, and then resolved in 20 μ l hybridization solution (5 \times SSC + 0.2 % SDS). **Hybridization and washing** Probes and chip were denatured respectively in 95 °C bath for 5 min, then the probes were added on the chip. They were hybridized in sealed chamber at 60 °C for 15 - 17 h and washed in turn with solutions of 2 \times SSC + 0.2 % SDS, 0.1 \times SSC + 0.2 % SDS and 0.1 % SSC 10 min each, then dried at room temperature.

Fluorescent scanning and results analysis The chip was read by Scan Array 3 000 Scanner (General Scanning Inc). The overall intensities of Cy3 and Cy5 were normalized and corrected by a coefficient according to the ratios of the located 40 housekeeping genes. The acquired image was further analyzed by ImeGene 3.0 Software with digital computer to obtain the intensities of fluorescent signals and the Cy3/Cy5 ratio. The data were taken on an average of the two repeated spots. The differentially expressed gene were defined as: (1) The absolute value of the Cy5/Cy3 natural logarithm was more than 0.69 (the variation of gene expression was more than 2-fold). (2) Either Cy3 or Cy5 signal value was required for more than 600. (3) The PCR results were satisfactory.

RESULTS

Scatter-plot of hybridization signals on gene chip

The scatter plot that was plotted with Cy3 and Cy5 fluorescent signal values displayed a quite disperses pattern in distribution. Most of spots gathered around a 45° diagonal line, in which blue spots represented the area where the signal intensities varied between 0.5 to 2- fold compared with that of the control. Some red spots distributed beyond or far from 45° diagonal line were indicated the existence of abnormal gene expression in esophageal carcinoma and in pericancerous epithelium. Their signal intensities were 2 times more than that of the control. (Figure 1 A and B).

Results and gene expression pattern by scanning analysis

The fluorescent scanning profile of gene expression was showed in Figure 2 A and B.

cDNA probes that labeled with Cy3 from control epithelium and that labeled with Cy5 from esophageal carcinoma or that labeled with Cy5 from pericancerous epithelium were hybridized through microarray. Hybridization results were obtained in parallel by comparing with these sample gene expression patterns demonstrated. In carcinoma tissues, A total of 41 genes were found having expression variations more than three times from the normal control, the up-and down-regulated genes were 28 and 13 respectively (Table 2). There were also 135 genes that manifested expression variations more than two times from the control and the up-and down-regulated genes were 85 and 50 respectively. Besides, there were nine genes found in the esophageal carcinoma having not been

recorded in genbank. Their functions remain to be studied.

In pericancerous epithelia there were 31 genes found having expression variations more than two times from the control, the up-and down-regulated genes were 27 and 4 respectively. These genes might be divided into 16 groups (Table 3) according to their functions.

There were 13 genes appeared simultaneously in both pericancerous epithelium and esophageal carcinoma, while another 18 genes were found in pericancerous epithelium only (Table 4).

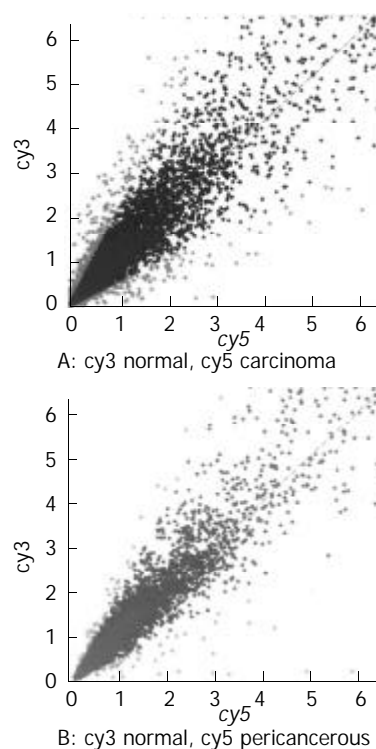


Figure 1 The scatter plots of gene expression pattern. (A) Carcinoma; (B) Pericancerous epithelium.

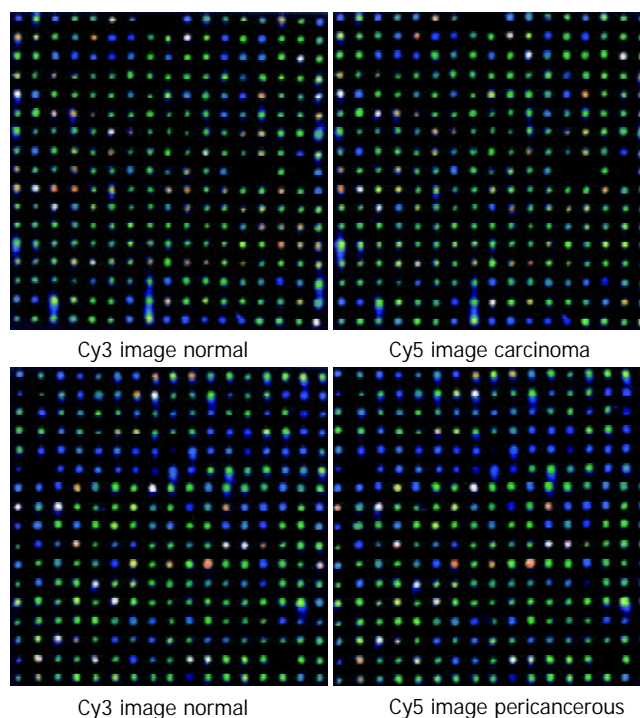


Figure 2 Scanning results of hybridizing signals on gene chip. (A) Carcinoma and the control epithelium; (B) Pericancerous and the control epithelium.

Table 1 Clinical and pathological data of 11 cases with esophageal carcinoma

No. of in-P	Name	Sex	Age	Pathological diagnosis	Lymph metastasis	Clinical stage
106811	Xu_	F	65	Middle esophageal, marrow type, well-middle d. Scc, exterior layer invasion with tumor embolus	0/18	II
106850	Xu_	F	58	Middle esophageal, marrow type, Poor d. Scc with Exterior layer invasion	1/8	III
106839	Yu_	M	60	Middle-inferior esophageal, marrow type, well-middle d. Scc, exterior layer invasion with tumor embolus	0/26	II
107001	Zhou_	M	53	Middle esophageal, ulcer type, middle d. Scc, Exterior layer invasion with tumor embolus	4/19	III
107151	Wang_	M	42	Middle-up esophageal, marrow type, middle d. Scc with exterior layer invasion	0/8	II
107326	Gu_	M	51	Middle- inferior esophageal, marrow type, Middle-Poor d. Scc with exterior layer invasion	2/14	III
107546	Zhao_	F	63	Middle- inferior esophageal, ulcer type, well-Middle d. Scc with shallow muscle layer invasion	0/15	II
107564	Lu_	M	61	Middle- inferior esophageal, marrow type, Middle d. Scc with deep muscle layer invasion	1/32	III
107146	Chen_	F	65	Superior esophageal, ulcer type, well d. Scc with exterior layer invasion	0/17	II
107527	Xu_	M	49	Inferior esophageal, ulcer type, middle d. Scc with shallow muscle layer invasion	1/18	III
107531	Guan_	M	56	Middle esophageal, marrow type, middle d. Scc with deep muscle layer invasion	0/26	II

d.: differentiated Scc: squamous cell carcinoma.

Table 2 Genes with expression difference > 3 or < 0.33 on average ratio between esophageal carcinoma and normal epithelium

Genbank-ID	Fcf	Gene name	R1	R2	AR
hsu67963		Human lysophospholipase homolog(HU-K5)mRNA, complete cds.	0.11	0.16	0.14
Hslimdp	8	H.sapiens mRNA for ZNF185 gene.	0.15	0.23	0.19
4505166			0.13	0.26	0.19
d87451	15	Human mRNA for KIAA0262gene,complete cds	0.13	0.31	0.22
hsy15409	11	Homo sapiens mRNA for putative glucose 6-phosphate translocase.	0.28	0.23	0.25
hsu16996	12	Human protein tyrosine phosphatase mRNA, complete cds.	0.31	0.26	0.29
hsu30255	12	Human phosphogluconate dehydrogenase (hPGDH) gene, complete cds.	0.29	0.30	0.29
4504714			0.47	0.16	0.31
ab002349	15	Human mRNA for KIAA0351 gene, complete cds.	0.14	0.50	0.32
humpai2	13	Human placental plasminogen activator inhibitor mRNA, complete cds.	0.28	0.35	0.32
hsu73824		Human p97 mRNA, complete cds.	0.30	0.34	0.32
hsa132270	2	Homo sapiens mRNA for integral type I protein p24B (p26).	0.31	0.34	0.33
Humorfkg1f	11	Human mRNA for KIAA0058 gene,complete cds.	0.31	0.36	0.33
s74452	3	Cyclin B1{promoter region}[human,cervical carcinoma cell line, HeLa cells,Genomic, 351 nt].	3.21	2.79	3.00
hspros27	10	H.sapiens PROS-27 mRNA.	3.29	2.85	3.07
Hstrr	10	Human mRNA for transferrin receptor.	2.70	3.48	3.09
Humprion	15	Homo sapiens mRNA for prion protein, complete cds.	3.07	3.19	3.13
hshr21spa	13	H.sapiens mRNA for protein involved in DNA double-strand break repair.	2.29	4.01	3.15
AB00109S14	11	Homo sapiens gene for H-cadherin, exon 14 and complete cds.	2.95	3.50	3.23
hsranbp1	11	H.sapiens mRNA for RanBP1.	3.98	2.57	3.27
Hsxprf	8	Homo sapiens mRNA for putative transcription factor XPRF.	3.35	3.38	3.37
humcd3621	11	Human antigen CD36 (clone 21) mRNA, complete cds.	3.28	3.54	3.41
Humsparc	5	Human SPARC/osteonectin mRNA, complete cds.	2.87	3.96	3.42
Humhcmap3	5	Human gene for hepatitis C-associated microtubular aggregate protein p44, exon 4.	3.72	3.30	3.51
Humprofii	5	Human profilin II mRNA, complete cds.	3.07	4.07	3.57
5729755			2.35	4.88	3.61
Hsrnasmg	13	H.sapiens mRNA for Sm protein G.	2.91	4.57	3.74
Humpgc	5	Human chondroitin sulfate proteoglycan core protein mRNA, 3' end.	3.67	3.91	3.79
hstop2a10	8	Homo sapiens topoisomerase II alpha (TOP2A) gene,exons 34 and 35,and complete cds.	4.02	3.76	3.89
hsu09559	14	Human Rch1 (RCH1) mRNA, complete cds.	3.75	4.03	3.89
humcol1a42		Human alpha-1 collagen type IV gene, exon 52.	4.37	3.69	4.03
hsinta6r	11	Human mRNA for integrin alpha 6.	3.28	5.43	4.35
d86983	15	Human mRNA for KIAA0230 gene, partial cds.	4.71	4.84	4.78
hsu26555		Human versican V2 core protein precursor splice-variant mRNA, complete cds.	6.93	5.91	6.42
hspgp95	13	Human mRNA for protein gene product (PGP) 9.5.	5.66	7.54	6.60
af052124	15	Homo sapiens clone 23810 osteopontin mRNA, complete cds.	11.77	4.63	8.20
Humcolva		Human alpha-2 type V collagen gene, 3' end.	7.64	10.17	8.91
humca1xia	15	Human alpha-1 type XI collagen (COL11A1) mRNA, complete cds.	6.75	12.07	9.41
Hscalbr11		Human mRNA for 27-kDa calbindin.	6.72	12.17	9.45
hsu50078	8	Human guanine nucleotide exchange factor p532 mRNA, complete cds.	12.28	17.11	14.70
Hsop	5	Human mRNA for osteopontin.	20.23	20.22	20.23

Fcf: function classification average ratio >3: up regulation average ratio <0.33: down regulation; R1: the first ratio; R2: the second ratio; AR: R1+R2 average ratio.

Table 3 Function classification for genes showing expression differences in esophageal carcinoma and pericancerous epithelium that were >2 or <0.5 fold from the control tissue

Gene function classification	Carcinoma/normal			Pericancerous/normal		
	N	>2	<0.5	N	> 2	<0.5
1 Proto-oncogenes and tumor suppression genes	2	1	1	0	0	0
2 Cell signals and transducing proteins	3	2	1	3	3	0
3 Cell cycle proteins	6	5	1	0	0	0
4 Extra-pressure reaction proteins	1	0	1	0	0	0
5 Cell regulatory proteins	7	7	0	3	3	0
6 Cell apoptosis related proteins	1	1	0	1	0	1
7 DNA synthesis, repair and recombinant proteins	3	3	0	0	0	0
8 DNA binding, transcription and its factor	6	4	2	1	1	0
9 Cell receptors	0	0	0	0	0	0
10 Cell surface antigen and adhesion proteins	10	8	2	4	4	0
11 Ion-channel and transporters	24	14	10	2	2	0
12 Metabolism-related proteins	21	10	11	6	4	2
13 Protein synthesis-related genes	14	7	7	2	1	1
14 Development-related genes	1	1	0	2	2	0
15 Other genes	27	18	9	7	7	0
16 New genes	9	4	5	0	0	0
Total	135	85	50	31	27	4

Table 4 Genes showing expression difference between the esophageal carcinoma and pericancerous epithelium

Genbank-ID	Fcf	Gene name	PR	TR
Hscalbr	11	Human mRNA for 27-kDa calbindin.	2.91	9.45
af052124	15	Homo sapiens clone 23810 osteopontin mRNA, complete cds.	5.34	8.20
Hsinta6r	11	Human mRNA for integrin alpha 6.	2.93	4.35
Humprofii	5	Human profilin II mRNA, complete cds.	2.50	3.57
Humhcamap3	5	Human gene for hepatitis C-associated microtubular aggregate protein p44, exon 4.	2.79	3.51
hum927a	10	Human interferon-inducible protein 9-27 mRNA, complete cds.	2.43	2.92
Hstrr	10	Human mRNA for transferrin receptor.	3.76	3.09
hsu50078	8	Human guanine nucleotide exchange factor p532 mRNA, complete cds.	18.7	14.7
Humtfr	10	Human transferrin receptor mRNA, complete cds.	3.51	2.81
hsu30255	12	Human phosphogluconate dehydrogenase(hPGDH)gene, complete cds.	0.48	0.29
hsu05684	2	Homo sapiens dihydrodiol dehydrogenase mRNA, complete cds.	3.75	2.31
Hsop	5	Human mRNA for osteopontin.	37.1	20.2
Hspgp95	13	Human mRNA for protein gene product (PGP) 9.5.	19.4	6.60
hsu46571	13	Human tetratricopeptide repeat protein (tpr2) mRNA, complete cds.	0.41	
Humrsc390	6	Human mRNA for KIAA0018gene, complete cds.	0.44	
hcox4gn	12	Homo sapiens hypothetical protein (COX4AL) gene, partial cds, and cytochromec oxidase subunit IV precursor (COX4) gene, complete cds.	0.47	
d79997		Human mRNA for KIAA0175 gene, complete cds.	2.05	
ab01755s10	15	Homo sapiens IGSF4 gene, exon 10 and complete cds.	2.06	
Hsnov	15	H.sapiens mRNA for novel gene in Xq28 region.	2.09	
hsifi56r		Human mRNA for 56-KDa protein induced by interferon.	2.1	
af054182	12	Homo sapiens mitochondrial processing peptidase beta-subunit mRNA, complete cds.	2.11	
af131818	15	Homo sapiens clone 25237mRNA sequence.	2.19	
af035301	2	Homo sapiens clone 23876 neuronal olfactomedin-related ER localized protein mRNA, partial cds.	2.28	
Humorfi	14	Homo sapiens (clone S240ii117/zap112) mRNA, complete cds.	2.26	
af038660	12	Homo sapiens chromosome 1p33-p34 beta-1,4-galactosyltransferase mRNA, complete cds.	2.32	
d88687	12	Homo sapiens mRNA for KM-102-derived reductase-like factor,complete cds.	2.51	
hsu05598	12	Human dihydrodiol dehydrogenase mRNA, complete cds.	3.07	
Humalcam	10	Homo sapiens CD6 ligand (ALCAM) mRNA, complete cds.	3.07	
hsu79299	2	Human neuronal olfactomedin-related ER localized protein mRNA,partial cds.	3.33	
ab003476	14	Homo sapiens mRNA for gravin, complete cds. 3.65		
af100757	15	Homo sapiens COP9 complex subunit 4 mRNA, complete cds. 5.96		

Fcf: function classification; TR: esophageal carcinoma average ratio; PR: pericancerous epithelium average ratio.

DISCUSSION

Because of the occult characteristic esophageal carcinoma, one of the most common malignant tumors in China, is difficult to be diagnosed for a size of <2 cm tumor mass by using CT and ultrasound. At present, almost most of the clinical cases are in the late stage, with a five years survival rate of about 30 % only. It is therefore necessary to explore new and efficacious diagnostic method to detect esophageal carcinoma at the early stage.

The carcinogenesis is a process caused by abnormal expression of tumor-associated genes or inactivation of tumor suppression genes or both. Clarifying the gene expression differences between the malignant and normal tissue is therefore the key procedure for the cancer control study. With the advances of molecular biological techniques, gene chip has been used to detect gene expression difference in various specimens by parallel analysis on a large scale^[2-29]. Some papers have also been published about the studying human esophageal carcinoma by using gene chips^[30-35]. However, a investigation on the difference of gene expression profiles between esophageal carcinoma and its paracancerous epithelium by gene chip has not been reported yet.

In the present study the gene chip technique was employed to analyze the difference of gene expression patterns in esophageal carcinoma and its paracancerous epithelium as well as their normal control. The results showed that: (1) There were 135 genes with expression levels marked as fluorescence intensity of more than 2 times or less than 0.5 times in esophageal carcinoma compared with the normal esophageal epithelium. It suggested these genes might well be related to the occurrence and development of the esophageal carcinoma.

Xu *et al*^[2] reported that the protein tyrosine phosphatase (PTPase) the high and low metastatic human ovarian cancer cell lines were down-regulated with a varied degree (0.64 and 0.27 respectively). PTPase was associated with the cell signaling control, energy metabolism, proliferation and the promotion of MHC-I antigen expression, mediated by numerous hormones (such as epidermal growth factor, insulin, insulin-like growth factor 1 and so on). The down-regulated PTPase would decrease the antigen expression on the cell surface, and result in the malignant cell escaping from the immune surveillance. In the present study, the enzyme was also down-regulated (0.29) in the esophageal carcinoma.

We found expression levels that of a variety of adhesion protein genes such as collagen protein type IV (8.9), integrin (4.45), calbindin protein (9.45) were increased, which coincided with Yanagawa *et al*^[16], Mori *et al*^[24], Hippo *et al*^[25] and Kan *et al*^[33] reported papers, inclusive of colorectal, gastric and esophageal carcinomas. The increased adhesion protein expression might associate with the invasiveness and metastasis of cancer cells.

It has been demonstrated that in proliferous cells the activity of topoisomerase II (TopoII) was rapidly increased from S phase to the end of G2/M stage, which meant that the enzyme might relate to the malignant transformation of the tumor cells. Varis *et al*^[22] and Hu *et al*^[34] reported that TopoII expression levels was obviously up-regulated in human gastric cancer and esophageal squamous cell carcinoma. In our study the TopoII expression was up-regulated as well (3.89).

Cell cycle-protein B₁ was also found up-regulated in esophageal carcinoma as Hu *et al*^[34] have reported, which might indicate that the malignant cells were in an abnormal proliferative state.

(2) There were 31 genes with expression levels marked as fluorescence intensity of more than 2 times or less than 0.5 times in pericancerous epithelium compared with normal control. Although an abnormal appearance of pericancerous epithelium was not found in the pathological examination, the

gene expression however indicated that there were thirteen genes expressed both in esophageal carcinoma and in pericancerous epithelium. Among these, the expression levels of 6 up-regulated genes in pericancerous epithelium were less than that of the corresponding genes in esophageal carcinoma and as for the other 6 up-regulated and 1 down-regulated genes, the expression levels in the former was higher than that in the latter. There were 18 genes appeared only in pericancerous epithelium, which suggested that these genes were probable related to the promotion and progression of carcinogenesis at the early stage of esophageal carcinoma.

The application of gene chip technique was a revolution of research method in life science. Our experiment illustrated that the detection of gene expression difference between malignant and normal tissue by gene chip might provide a new direction for diagnosis, therapy and prevention of human esophageal carcinoma.

REFERENCES

- 1 **Peng XL**, Yuan HY, Xie Y, Wang HH. Experimental technique of gene engineering. *HuNa Sci Tech Issue Ag Second* 1998: 197-199
- 2 **Xu SH**, Mou HZ, Lu GQ, Zhu CH, Yang ZY, Gao YL, Lou HK, Liu XL, Chen Y, Yang W. Gene expression profile difference in high and low metastatic human ovarian cancer cell lines by gene chip. *Chin Med J (Engl)* 2002; **115**: 36-41
- 3 **Wang K**, Gan L, Jeffery E, Gayle M, Gown AM, Skelly M, Nelson PS, Ng WV, Schummer M, Hood L, Mulligan J. Monitoring gene expression profile changes in ovarian carcinomas using cDNA microarra. *Gene* 1999; **229**: 101-108
- 4 **Furey TS**, Cristianini N, Duffy N, Bednarski DW, Schummer M, Haussler D. Support vector machine classification and validation of cancer tissue samples using microarray expression data. *Bioinformatics* 2000; **16**: 906-914
- 5 **Ono K**, Tanaka T, Tsunoda T, Kitahara O, Kihara C, Okamoto A, Ochiai K, Takagi T, Nakamura Y. Identification by cDNA microarray of genes involved in ovarian carcinogenesis. *Cancer Res* 2000; **60**: 5007-5011
- 6 **Zou TT**, Selaru FM, Xu Y, Shustova V, Yin J, Mori Y, Shibata D, Sato F, Wang S, Olaru A, Deacu E, Liu TC, Abraham JM, Meltzer SJ. Application of cDNA microarrays to generate a molecular taxonomy capable of distinguishing between colon cancer and normal colon. *Oncogene* 2002; **21**: 4855-4862
- 7 **Lin YM**, Furukawa Y, Tsunoda T, Yue CT, Yang KC, Nakamura Y. Molecular diagnosis of colorectal tumors by expression profiles of 50 genes expressed differentially in adenomas and carcinomas. *Oncogene* 2002; **21**: 4120-4128
- 8 **Sepulveda AR**, Tao H, Carloni E, Sepulveda J, Graham DY, Peterson LE. Screening of gene expression profiles in gastric epithelial cells induced by *Helicobacter pylori* using microarray analysis. *Aliment Pharmacol Ther* 2002; **16** (Suppl 2): 145-157
- 9 **Zhou Y**, Gwadry FG, Reinhold WC, Miller LD, Smith LH, Scherf U, Liu ET, Kohn KW, Pommier Y, Weinstein JN. Transcriptional regulation of mitotic genes by camptothecin-induced DNA damage: microarray analysis of dose- and time-dependent effects. *Cancer Res* 2002; **62**: 1688-1695
- 10 **Iizaka M**, Furukawa Y, Tsunoda T, Akashi H, Ogawa M, Nakamura Y. Expression profile analysis of colon cancer cells in response to sulindac or aspirin. *Biochem Biophys Res Commun* 2002; **292**: 498-512
- 11 **Nguyen DV**, Rocke DM. Tumor classification by partial least squares using microarray gene expression data. *Bioinformatics* 2002; **18**: 39-50
- 12 **Nakeff A**, Sahay N, Pisano M, Subramanian B. Painting with a molecular brush: genomic/proteomic interfacing to define the drug action profile of novel solid-tumor selective anticancer agents. *Cytometry* 2002; **47**: 72-79
- 13 **Takahashi Y**, Nagata T, Ishii Y, Ikarashi M, Ishikawa K, Asai S. Up-regulation of vitamin D3 up-regulated protein 1 gene in response to 5-fluorouracil in colon carcinoma SW620. *Oncol Rep* 2002; **9**: 75-79
- 14 **Hegde P**, Qi R, Gaspard R, Abernathy K, Dharap S, Earle-Hughes

- J, Gay C, Nwokekeh NU, Chen T, Saeed AI, Sharov V, Lee NH, Yeatman TJ, Quackenbush J. Identification of tumor markers in models of human colorectal cancer using a 19,200-element complementary DNA microarray. *Cancer Res* 2001; **61**: 7792-7797
- 15 **Fujita M**, Furukawa Y, Tsunoda T, Tanaka T, Ogawa M, Nakamura Y. Up-regulation of the ectodermal-neural cortex 1 (ENC1) gene, a downstream target of the beta-catenin/T-cell factor complex, in colorectal carcinomas. *Cancer Res* 2001; **61**: 7722-7726
- 16 **Yanagawa R**, Furukawa Y, Tsunoda T, Kitahara O, Kameyama M, Murata K, Ishikawa O, Nakamura Y. Genome-wide screening of genes showing altered expression in liver metastases of human colorectal cancers by cDNA microarray. *Neoplasia* 2001; **3**: 395-401
- 17 **Pinheiro NA**, Caballero OL, Soares F, Reis LF, Simpson AJ. Significant overexpression of oligophrenin-1 in colorectal tumors detected by cDNA microarray analysis. *Cancer Lett* 2001; **172**: 67-73
- 18 **Takemasa I**, Higuchi H, Yamamoto H, Sekimoto M, Tomita N, Nakamori S, Matoba R, Monden M, Matsubara K. Construction of preferential cDNA microarray specialized for human colorectal carcinoma: molecular sketch of colorectal cancer. *Biochem Biophys Res Commun* 2001; **285**: 1244-1249
- 19 **Gupta RA**, Brockman JA, Sarraf P, Willson TM, DuBois RN. Target genes of peroxisome proliferator-activated receptor gamma in colorectal cancer cells. *J Biol Chem* 2001; **276**: 29681-29687
- 20 **Kitahara O**, Furukawa Y, Tanaka T, Kihara C, Ono K, Yanagawa R, Nita ME, Takagi T, Nakamura Y, Tsunoda T. Alterations of gene expression during colorectal carcinogenesis revealed by cDNA microarrays after laser-capture microdissection of tumor tissues and normal epithelia. *Cancer Res* 2001; **61**: 3544-3549
- 21 **Suzuki H**, Gabrielson E, Chen W, Anbazhagan R, van Engeland M, Weijenberg MP, Herman JG, Baylin SB. A genomic screen for genes upregulated by demethylation and histone deacetylase inhibition in human colorectal cancer. *Nat Genet* 2002; **31**: 141-149
- 22 **Varis A**, Wolf M, Monni O, Vakkari ML, Kokkola A, Moskaluk C, Frierson H Jr, Powell SM, Knuutila S, Kallioniemi A, El-Rifai W. Targets of gene amplification and overexpression at 17q in gastric cancer. *Cancer Res* 2002; **62**: 2625-2629
- 23 **Selaru FM**, Xu Y, Yin J, Zou T, Liu TC, Mori Y, Abraham JM, Sato F, Wang S, Twigg C, Olaru A, Shustova V, Leytin A, Hytiroglou P, Shibata D, Harpaz N, Meltzer SJ. Artificial neural networks distinguish among subtypes of neoplastic colorectal lesions. *Gastroenterology* 2002; **122**: 606-613
- 24 **Mori M**, Mimori K, Yoshikawa Y, Shibuta K, Utsunomiya T, Sadanaga N, Tanaka F, Matsuyama A, Inoue H, Sugimachi K. Analysis of the gene-expression profile regarding the progression of human gastric carcinoma. *Surgery* 2002; **131**(Suppl 1): S39-47
- 25 **Hippo Y**, Taniguchi H, Tsutsumi S, Machida N, Chong JM, Fukayama M, Kodama T, Aburatani H. Global gene expression analysis of gastric cancer by oligonucleotide microarrays. *Cancer Res* 2002; **62**: 233-240
- 26 **Maeda S**, Otsuka M, Hirata Y, Mitsuno Y, Yoshida H, Shiratori Y, Masuho Y, Muramatsu M, Seki N, Omata M. cDNA microarray analysis of *Helicobacter pylori*-mediated alteration of gene expression in gastric cancer cells. *Biochem Biophys Res Commun* 2001; **284**: 443-449
- 27 **Kudoh K**, Ramanna M, Ravatn R, Elkahoul AG, Bittner ML, Meltzer PS, Trent JM, Dalton WS, Chin KV. Monitoring the expression profiles of doxorubicin-induced and doxorubicin-resistant cancer cells by cDNA microarray. *Cancer Res* 2000; **60**: 4161-4166
- 28 **Sgroi DC**, Teng S, Robinson G, LeVangie R, Hudson JR, Elkahoul AG. *In vivo* gene expression profile analysis of human breast cancer progression. *Cancer Res* 1999; **59**: 5656-5661
- 29 **Pollack JR**, Perou CM, Alizadeh AA, Eisen MB, Pergamenschikov A, Williams CF, Jeffrey SS, Botstein D, Brown PO. Genome-wide analysis of DNA copy-number changes using cDNA microarrays. *Nat Genet* 1999; **23**: 41-46
- 30 **Xu Y**, Selaru FM, Yin J, Zou TT, Shustova V, Mori Y, Sato F, Liu TC, Olaru A, Wang S, Kimos MC, Perry K, Desai K, Greenwald BD, Krasna MJ, Shibata D, Abraham JM, Meltzer SJ. Artificial neural networks and gene filtering distinguish between global gene expression profiles of Barrett's esophagus and esophageal cancer. *Cancer Res* 2002; **62**: 3493-3497
- 31 **Selaru FM**, Zou T, Xu Y, Shustova V, Yin J, Mori Y, Sato F, Wang S, Olaru A, Shibata D, Greenwald BD, Krasna MJ, Abraham JM, Meltzer SJ. Global gene expression profiling in Barrett's esophagus and esophageal cancer: a comparative analysis using cDNA microarrays. *Oncogene* 2002; **21**: 475-478
- 32 **Kihara C**, Tsunoda T, Tanaka T, Yamana H, Furukawa Y, Ono K, Kitahara O, Zembutsu H, Yanagawa R, Hirata K, Takagi T, Nakamura Y. Prediction of sensitivity of esophageal tumors to adjuvant chemotherapy by cDNA microarray analysis of gene-expression profiles. *Cancer Res* 2001; **61**: 6474-6479
- 33 **Kan T**, Shimada Y, Sato F, Maeda M, Kawabe A, Kaganoi J, Itami A, Yamasaki S, Imamura M. Gene expression profiling in human esophageal cancers using cDNA microarray. *Biochem Biophys Res Commun* 2001; **286**: 792-801
- 34 **Hu YC**, Lam KY, Law S, Wong J, Srivastava G. Identification of differentially expressed genes in esophageal squamous cell carcinoma (ESCC) by cDNA expression array: overexpression of Fra-1, Neogenin, Id-1, and CDC25B genes in ESCC. *Clin Cancer Res* 2001; **7**: 2213-2221
- 35 **Lu J**, Liu Z, Xiong M, Wang Q, Wang X, Yang G, Zhao L, Qiu Z, Zhou C, Wu M. Gene expression profile changes in initiation and progression of squamous cell carcinoma of esophagus. *Int J Cancer* 2001; **91**: 288-294

Methylation and mutation analysis of p16 gene in gastric cancer

Yi Ding, Xiao-Ping Le, Qin-Xian Zhang, Peng Du

Yi Ding, Xiao-Ping Le, Qin-Xian Zhang, Molecular Cell Biology Research Center, Medical College of Zhengzhou University; Zhengzhou 450052, Henan Province, China

Peng Du, Henan Key Lab. of Molecular Medicine, Zhengzhou 450052, Henan Province, China

Supported by the National Natural Science Foundation of China, No. 39170440

Correspondence to: Pro. Qin-Xian Zhang, Molecular Cell Biology Research Center, Medical College of Zhengzhou University; 40 Daxue Road, Zhengzhou 450052, Henan Province, China. qxz53@zzu.edu.cn

Telephone: +86-371-6977002 **Fax:** +86-371-6977002

Received: 2002-10-22 **Accepted:** 2002-11-18

Abstract

AIM: To study methylation, frequencies of homozygous deletion and mutation of p16 gene in gastric carcinoma.

METHODS: The methylation pattern in exon 1 and exon 2 of p16 gene was studied with polymerase chain reaction (PCR), using methylation sensitive restriction endonuclease HpaII and methylation insensitive restriction endonuclease MspI. PCR technique was used to detect homozygous deletions of exon 1 and exon 2 of p16 gene and single strand conformation polymorphism (SSCP) technique was used to detect the mutation of the gene.

RESULTS: Hypermethylation changes in exon 1 and exon 2 of p16 gene were observed in 25 % and 45 % of 20 gastric cancer tissues, respectively, while no methylation abnormality was found in normal tissues. The homozygous deletion frequency of exon 1 and exon 2 of p16 gene in 20 gastric cancer tissues was 20 % and 10 %, respectively. No mutation was found in exon 1 of p16 gene, while abnormal single strands were found in 2 (10 %) cases in exon 2 as detected by SSCP.

CONCLUSION: The results suggest that hypermethylation and abnormality of p16 gene may play a key role in the progress of gastric cancer. Hypermethylation of exon 2 of p16 gene may have effects on the carcinogenesis of gastric mucosa and may be a later event.

Ding Y, Le XP, Zhang QX, Du P. Methylation and mutation analysis of p16 gene in gastric cancer. *World J Gastroenterol* 2003; 9(3): 423-426

<http://www.wjgnet.com/1007-9327/9/423.htm>

INTRODUCTION

DNA methylation abnormality could influence gene transcription directly, and it could also cause the abnormal gene expression through the C→T mutation induced by deamination of 5' methyl cytosine (5 mC)^[1]. In the eukaryote, 5 mC mainly appears in the CpG sequence of genome, and it is the site in which p16 gene mutation occurs frequently^[2]. Highly frequent homozygous deletion, mutation and abnormal methylation of p16 gene exhibit in many kinds of carcinoma^[3-9]. In China, studies on p16 gene methylation abnormality and

deletion, mutation in gastric carcinoma have scarcely been reported. In this paper, restriction endonuclease-polymerase chain reaction (PCR) and single strand conformation polymorphism (SSCP) techniques were used to detect the CpG methylation and mutation in exon 1 and 2 of p16 gene. The biological significance of p16 gene and its methylation abnormality in the development and progress of gastric carcinoma were discussed.

MATERIALS AND METHODS

Specimens

20 specimens of gastric carcinoma and their corresponding adjacent normal-appearing gastric tissue were collected from the First and Second Affiliated Hospital of Medical College of Zhengzhou University and frozen in liquid nitrogen in 30 min. All the specimens were pathologically diagnosed and without radio or chemical therapy before operation.

Analysis of methylation

Tissue DNA was extracted by normal phenol-chloroform method. DNA samples were treated with HpaII and MspI. Primers were synthesized by Shanghai Cell Biology Research Institute of China Scientific Institute and purified with PAGE. The primers of p16 exon 1 (E1): 5' -GAA GAA AGA GGA GGG GCT G-3' ; 5' -GCG CTA CCT GAT TCC AAT TC-3' ; the primers of exon 2 (E2): 5' -CAC AAG CTT CCT TTC CGT CAT G-3' , 5' -TCT GAG CTT TGG AAG CTC TCA GG -3' . The length of amplified fragments was 336bp and 424bp respectively. The parameter of PCR cycle was: 92 °C 60 s, 60 °C (renaturing temperature of E2 was 58.5 °C) 60 s, 71 °C 90 s. After 24 cycles, the reaction system was thermal retarded at 71 °C for 10 min. 8 µl of PCR products were electrophoresized on 20 g/L agarose gel. After the electrophoresis, the gel was visualized under ultraviolet and photographed.

PCR-SSCP

The primers were the same as mentioned above. The parameter of PCR cycle was: 91.5 °C 60 s, 61.5 °C (E1) or 59.5 °C (E2) 60 s, 70.5 °C 90 s. After 30 cycles, the reaction system was thermal retarded at 70.5 °C for 10 min. PCR products were electrophoresized on 20 g/L agarose gel and stained with ethidium bromide. SSCP was taken on the 80 g/L undenatured polyacrylamide gel. After denaturing at 95 °C for 5 min, the samples were ice bathed immediately for 5 to 10 min and electrophorized under constant voltage 160 V for 4-6 h. After electrophoresis the gel was removed and silver stained.

Statistic analysis

Data were analyzed using Fisher's exact test of probabilities with SPSS 10.0 statistic software.

RESULTS

Methylation analysis of DNA

HpaII is a methylation sensitive restriction endonuclease, when methylation occurs at the second C in the CCGG target sequence, HpaII can not recognize the target site. However,

Msp I is isoenzyme of HpaII, and can recognize the target site whether or not methylation occurs at the second C in the CCGG target sequence. The exon 1 and 2 of p16 gene include 2 and 4 5' -CCGG-3' sites. If methylation occurs, HpaII can not identify the target sequence, the specific patterns would appear after PCR products are electrophoresed (336bp or 424bp) (Figure 1). If no specific bands were amplified by PCR, then no methylation alteration at second C in 5' -CCGG-3' sequence is indicated (Figure 2).



Figure 1 Methylation analysis of p16 gene exon 1 (abnormality). 1: DNA marker; 2: negative control; 3-5 carcinoma tissue; (3: without enzyme treatment, 4: Hpa II treatment, 5: Msp I treatment); 6-8 normal tissue (6: without enzyme treatment, 7: Hpa II treatment, 8: MspI treatment).

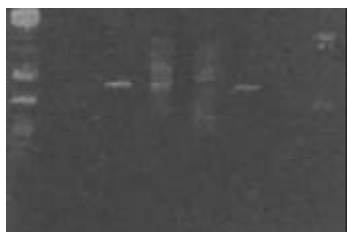


Figure 2 Methylation analysis of p16 gene exon 1 (no abnormality). 1: DNA marker; 2: negative control; 3-5 carcinoma tissue (3: without enzyme treatment, 4: Hpa II treatment, 5: MspI treatment); 6-8 normal tissue (6: without enzyme treatment, 7: Hpa II treatment, 8: MspI treatment).



Figure 3 PCR of p16 gene exon 1 of gastric carcinoma tissue. 1: Marker; 3: negative control; 2-8: 336bp of E1 PCR.



Figure 4 PCR of p16 gene exon 2 of gastric carcinoma tissue. 1: Marker; 2-8: 424bp of E2 PCR; 3: deletion.

Homozygous deletion analysis

After agarose electrophoresis of PCR products, if no amplified products were found at the sites corresponding to 336bp or 424bp, then homozygous deletion of E1 or E2 could be

determined. In gastric carcinoma tissues, 4 cases (20 %) of E1 deletion and 2 cases (10 %) of E2 deletion were found. The 6 cases with homozygous deletion included 1 with well differentiated and 5 with moderately or poorly differentiated gastric carcinoma tissues (Figure 3 and 4).

PCR-SSCP analysis

Mobility shift is defined when abnormal bands appear or the position of bands alter. No abnormal alteration was found at E1 of p16 gene (Figure 5). At E2, abnormal single strand of mobility shift exhibited in 2 (10 %) cases, in 1 of which (IIIa stage, poorly differentiated adenocarcinoma) mobility shift occurred in both carcinoma and adjacent carcinoma tissues (Figure 6).

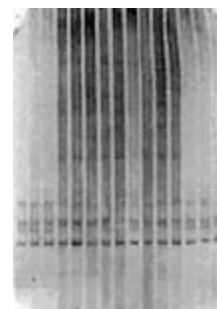


Figure 5 PCR-SSCP of p16 gene exon 1 (no abnormality).

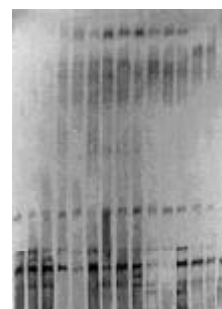


Figure 6 PCR-SSCP of p16 gene exon 1. Abnormal single strand occurred in 2, 3 lane (adjacent carcinoma and carcinoma tissue) and 9 lane (carcinoma tissue).

DISCUSSION

Methylation of p16 gene

In the process of multistage canceration, abnormality of gene expression may be controlled by genetic mechanism and epigenetic mechanism. Epigenetic mechanism is indicated by methylation alteration at 5 mC which cause gene expression abnormality without change in the DNA sequence and product of gene expression, and is a key mechanism causing genomic instability and canceration. Hypermethylation at CpG induces abnormality of DNA conformation stability which may influence the binding of specific protein and DNA regulating sequence, and cause gene silence. Inability to transcribe the tumor suppressor genes resulted in dysfunction of the genes and induced the development of carcinoma^[10, 11].

Regional hypermethylation plays an important role in the alteration of gene expression in human carcinoma and in the progression of carcinoma. In the present paper, methylation at CpG in exons 1 and 2 of p16 gene in gastric carcinoma tissues was detected by treatment of methylation sensitive restriction endonuclease combined with PCR technique. The results showed that abnormal methylation was present in 5 and 9 of 20 cancer tissues, respectively, but no abnormality was found in corresponding adjacent normal gastric mucosa, suggesting

an association between methylation of p16 gene and gastric carcinogenesis. Homozygous deletion of p16 gene occurred, to some extent, in many kinds of human carcinoma cells. However, gene mutation rarely occurred and the frequency of homozygous deletion was low in primary carcinoma. It is interesting that in some human carcinoma without site mutation or homozygous deletion, for example, in the pulmonary cancer cell line in oat cell type, the frequency of remethylation at p16 CpG island is 78 % resulting in the loss of p16 gene transcription activity. The same phenomena exists in mammary, prostate, gastric and colon carcinomas, especially in the colon carcinoma with the frequency of methylation being high as 92 %. In the cells of colon carcinoma without homozygous deletion, methylation occurs at both alleles of p16 gene, and is related to its entire deactivation^[1]. Based on the fact that the alteration of methylation of p16 gene and other genes occur in many kinds of carcinomas lacking of mutation and deletion, methylation might be a key mechanism of deactivation of tumor suppressor genes in primary carcinoma. Expression of p16 gene in gastric carcinoma is decreased significantly^[12-22]. However, the frequency of mutation and deletion of p16 gene is low, suggesting that abnormal methylation might be a key mechanism in alteration of the gene expression in gastric carcinoma.

The results in the present study showed that abnormal methylation mainly appeared in poorly differentiated gastric carcinoma. Two cases with methylation in both exons were poorly differentiated and progressive gastric carcinoma. Hypermethylation of exon 2 mainly exhibited in the cases of late stage of gastric carcinoma, suggesting that hypermethylation of exon 2 is related to the differentiated degree and the clinical progression of gastric carcinoma, and thus might be a late event. Kampster *et al.*^[23], reported in their study on methylation of p16 gene in esophagus carcinoma that alteration of methylation at exon 2 was obviously related to clinical stage and progression of carcinoma, and a correlation existed between hypermethylation of exon 1 and no gene expression. Yi *et al.*^[24] reported that methylation of p16 gene in colorectal cancer was obviously related to the Duke's stage. Methylation of p16 gene was increased gradually with the progression of carcinoma, and could induce detectable alteration and consequence to late stage which may be related to clinical stage of gastric carcinoma.

Deletion and mutation of p16 gene

Deletion and mutation of p16 gene are also important mechanisms responsible for the dysfunction of tumor suppressor genes. Abnormality in 9p21-22 of chromosome has been reported in many kinds of carcinoma cells, and p16 gene is an important gene located in this region. By analysis of the sites adjacent to p16 gene, simultaneous mini-deletions (<200bp) of p16 allele were found in many carcinomas, and homozygous deletion of p16 gene has been testified in many kinds of primary carcinoma^[25-27]. Lu *et al.*^[28], detected that the deletion of E1 of p16 gene in 16.4 % of gastric carcinoma tissues, Wu *et al.*^[29], reported a rate of 10 % (6/60). Different deletion rates of p16 gene in gastric carcinoma were reported by the other investigators^[30-32]. In the present study, deletion of E1 and E2 was detected in 20 % and 10 %, respectively, of 20 cases gastric carcinoma cases, but amplified products appeared in corresponding normal gastric mucosa tissues.

Mutation of p16 gene mainly includes nonsense, missense, and frame shift mutation. The frequency of mutation is significantly lower than deletion with 70-90 % being present on E2^[2]. Mutation of p16 gene in gastric carcinoma is rare, but the frequency is much higher than the natural mutation (10-6~10-4) of general genes, thus, it is conceivable that mutation of p16 gene might be involved in the development and

progression of gastric carcinoma. In the present study, mutation of p16 gene E2 was detected in 2 cases of gastric carcinoma tissues, and no E1 mutation was found. Both the gastric carcinoma cases with mutation were progressive gastric carcinoma. One of them exhibited mobility shift in both carcinoma and adjacent carcinoma tissues, and belonged to IIIa stage and poorly differentiated adenocarcinoma, suggesting that p16 gene mutation might be a late event in the process of gastric carcinoma. It has been reported that the mutation site of p16 gene is the same as that of p53 gene, i.e. at CpG. It is believed that mutation is induced by nucleotide methylation^[2]. It is suggested that mutation of p16 gene might be the consequence of the DNA genomic insatibility, and gradually causes the canceration.

REFERENCES

- 1 **Yskoob J**, Fan XG, Hu GL, Zhang Z. DNA methylation and carcinogenesis in digestive neoplasms. *World J Gastroenterol* 1998; **4**: 174-177
- 2 **Pollock PM**, Pearson JV, Hayward NK. Compilation of somatic mutation of the CDKN2 gene in human cancers: non random distribution of base substitutions. *Genes Chromosomes Cancers* 1996; **15**: 77-88
- 3 **Hayashi K**, Metzger R, Salonga D, Danenberg K, Leichman LP, Fink U, Sendler A, Kelsen D, Schwartz GK, Groshen S, Lenz HJ, Danenberg PV. High frequency of simultaneous loss of p16 and p16 beta gene expression in squamous cell carcinoma of the esophagus but not in adenocarcinoma of the esophagus or stomach. *Oncogene* 1997; **15**: 1481-1488
- 4 **Song ZY**, Xu RZ, Qian KD, Tang XQ, Zhao XY, Lin M. Abnormal expression of p16/CDKN2 gene in human gastric carcinoma. *Xin Xiaohua Bingxue Zazhi* 1997; **5**: 139-140
- 5 **Igaki H**, Sasaki H, Tachimori Y, Kato H, Watanabe H, Kimura T, Harada Y, Sugimura T, Terada M. Mutation frequency of the p16/CDK2 gene in primary cancer in the upper digestive tract. *Cancer Res* 1995; **55**: 3421-3423
- 6 **Okamoto A**, Hussain SP, Hagiwara K, Spillare EA, Rusin MR, Demetrick DJ, Serrano M, Hannon GJ, Shiseki M, Zariwala M. Mutations in the p16INK4/MTS1/CNKN2, p15INK4B/MTS2, and p18 genes in primary and metastatic lung cancer. *Cancer Res* 1995; **55**: 1448-1451
- 7 **Mori T**, Miura K, Aoki T, Nishihira T, Mori S, Nakamura Y. Frequent somatic mutation of the MTS1/CDK4I (multiple tumor suppressor/cyclin-dependent kinase 4 inhibitor) gene in esophageal squamous cell carcinoma. *Cancer Res* 1994; **54**: 3396-3397
- 8 **Gonzalez-Zulueta M**, Bender CM, Yang AS, Nguyen T, Beart RW, Van Tornout JM, Jones PA. Methylation of the 5' CpG island of the p16/CDK2 tumor suppressor gene in normal and transformed human tissues correlates with gene silencing. *Cancer Res* 1995; **55**: 4531-4535
- 9 **Zhang J**, Lai MD, Chen J. Methylation status of p16 gene in colorectal carcinoma and normal colonic mucosa. *World J Gastroenterol* 1999; **5**: 451-454
- 10 **Issa JP**, Ottaviano YL, Celano P, Hamilton SR, Davidson NE, Baylin SB. Methylation of oestrogen receptor CpG island links aging and neoplasia in human colon. *Nat Genet* 1994; **7**: 536-540
- 11 **Zingg JM**, Jones PA. Genetic and epigenetic aspects of DNA methylation on genome expression, evolution, mutation and carcinogenesis. *Carcinogenesis* 1997; **18**: 869-882
- 12 **Wang B**, Shi LC, Zhang WB, Xiao CM, Wu JF, Dong YM. Expression of tumor suppressor gene p16 in gastric cancer and precancerous lesions. *Shijie Huaren Xiaohua Zazhi* 2001; **9**: 39-42
- 13 **Zhou Y**, Gao SS, Li YX, Fang ZM, Zhao X, Qi YJ, Wei JP, Zou JX, Liu G, Jiao LH, Bai YM, Wang LD. Tumor suppressor gene p16 and Rb expression in gastric cardia precancerous lesions from subjects at a high incidence area in northern China. *World J Gastroenterol* 2002; **8**: 423-425
- 14 **He XS**, Su Q, Chen ZC, He XT, Long ZF, Ling H, Zhang LR. Expression, deletion and mutation of p16 gene in human gastric cancer. *World J Gastroenterol* 2001; **7**: 515-521
- 15 **Wei TY**, Wei MX, Yang SM. Expression of cyclin D1 P16 and Rb protein in gastric cancer. *Shijie Huaren Xiaohua Zazhi* 2000; **8**: 234-235

- 16 **Zhu ZY**, Tian X, Wang X, Yang XL. Mutation of p16 and APC gene in gastric cancer. *Shijie Huaren Xiaohua Zazhi* 2000; **8**: 1418-1419
- 17 **Yang SM**, Yang LS, Li L, Deng LY, Wang CY, Yuan XB, Shen XD. Methylation of MTS1/P16 gene and expression of P16 protein in gastric cancer. *Shijie Huaren Xiaohua Zazhi* 2000; **8**: 1427-1429
- 18 **Zhao Y**, Zhang XY, Shi XJ, Hu PZ, Zhang CS, Ma FC. Expression of P16, P53 and proliferating cell nuclear antigen in gastric cancer. *Shijie Huaren Xiaohua Zazhi* 1999; **7**: 246-248
- 19 **Li GX**, Li GQ, Zhao CZ, Xu GL. Relationship between telomerase hTRT and the expression of tumor suppressor gene p53 and p16. *Shijie Huaren Xiaohua Zazhi* 2002; **10**: 591-593
- 20 **Jiang YX**, Zhao MY, Geng M, Chao YC, Wang XY. Expression of P16, cerB-2 protein in gastric tumor. *Shijie Huaren Xiaohua Zazhi* 2002; **10**: 1050-1051
- 21 **Yang ZL**, Li YG, Huang YF, Wang QW. Expression of cyclin D1, CDK4, P16 and Rb in gastric cancer. *Shijie Huaren Xiaohua Zazhi* 2000; **8**: 362-363
- 22 **Wang GT**. Progression in the study on gastric precancerous lesions and its reversion. *Shijie Huaren Xiaohua Zazhi* 2000; **8**: 1-4
- 23 **Kempster S**, Phillips WA, Baidur-Hudson S, Thomas RJ, Dow C, Rockman SP. Methylation of exon 2 of p16 is associated with late stage oesophageal cancer. *Cancer Lett* 2000; **150**: 57-62
- 24 **Yi J**, Wang ZW, Cang H, Chen YY, Zhao R, Yu BM, Tang XM. P16 gene methylation in colorectal cancers associated with Duke's staging. *World J Gastroenterol* 2001; **7**: 722-725
- 25 **Hui AM**, Shi YZ, Li X, Takayama T, Makuuchi M. Loss of p16 (INK4) protein, alone and together with loss of retinoblastoma protein, correlate with hepatocellular carcinoma progression. *Cancer Lett* 2000; **154**: 93-99
- 26 **Lin SC**, Chang KW, Chang CS, Liu TY, Tzeng YS, Yang FS, Wong YK. Alteration of p16/MTS1 gene in oral squamous cell carcinomas from Taiwanese. *J Oral Pathol Med* 2000; **29**: 159-166
- 27 **Liggett WH Jr**, Sidransky D. Role of the p16 tumor suppressor gene in cancer. *J Clinical Oncol* 1998; **16**: 1197-1206
- 28 **Lu YY**, Gao CF, Cui JQ. Deletion and down-regulation of mts1/p16 gene in human gastric cancer. *Zhonghua Zhongliu Zazhi* 1996; **18**: 189-191
- 29 **Wu MS**, Shun CT, Sheu JC, Wang HP, Wang JT, Lee WJ, Chen CJ, Wang TH, Lin JT. Overexpression of mutant p53 and c-erbB-2 proteins and mutations of the p15 and p16 genes in human gastric carcinoma: with respect to histological subtypes and stages. *J Gastroenterol Hepatol* 1998; **13**: 305-310
- 30 **Jiang HX**, Liu ZM, Zhuang YQ, Yang DH, Jiang YQ, Li JQ. Homologous deletion of p16 gene in human gastric carcinoma. *Huaren Xiaohua Zazhi* 1998; **6**: 934-935
- 31 **Lee YY**, Kang SH, Seo JY, Jung CW, Lee KU, Choe KJ, Kim BK, Kim NK, Koeffler HP, Bang YJ. Alterations of p16INK4A and p15INK4B genes in gastric carcinomas. *Cancer* 1997; **15**: 1889-1896
- 32 **Tang SH**, Luo HS. Aberration of p16 gene and p18 gene in gastric carcinoma. *Shijie Huaren Xiaohua Zazhi* 2001; **9**: 91-92

Edited by Xia HHX

Relationship between the expression of human telomerase reverse transcriptase gene and cell cycle regulators in gastric cancer and its significance

Jin-Chen Shao, Ji-Feng Wu, Dao-Bin Wang, Rong Qin, Hong Zhang

Jin-Chen Shao, Ji-Feng Wu, Dao-Bin Wang, Rong Qin, Hong Zhang, Department of Pathology, Anhui Medical University, Hefei, 230032, Anhui Province, China

Jin-Chen Shao, Department of Pathology, Shanghai Chest Hospital, 241 HuaiHaiXi Rd, Shanghai 200030, China

Supported by Science and Technology Fund, Governmental Department of Education, Anhui Province, No.99j10091

Correspondence to: Professor Ji-Feng Wu, Department of Pathology, Anhui Medical University, Hefei, 230032, Anhui Province, China. jifengwu@mail.hf.ah.cn

Telephone: +86-551-5161130

Received: 2002-09-13 **Accepted:** 2002-10-29

Abstract

AIM: To investigate the expression of human telomerase reverse transcriptase gene (hTERT) in gastric cancer (GC) and its relevance with cell cycle regulators including P16INK4, cyclin and P53.

METHODS: In situ hybridization (ISH) for hTERT mRNA was performed in 53 cases of gastric cancer and adjacent cancerous tissues. Immunohistochemical staining (S-P method) for hTERT protein, P16INK4, cyclinD1 and P53 was performed in 53 cases of GC and adjacent cancerous tissues.

RESULTS: Of 53 cases of GC, the expression of hTERT mRNA and hTERT protein was significantly higher than the expression of hTERT mRNA and hTERT protein in adjacent cancerous tissues ($P < 0.01$), the positive rates of hTERT mRNA and hTERT protein were 79.2 % and 88.6 %. There was a statistical difference of the expression of hTERT protein among well differentiated adenocarcinoma, poorly differentiated adenocarcinoma and mucoid carcinoma. And there was a highly significant positive correlation between the expression of hTERT mRNA and hTERT protein ($r = 0.625$, $P < 0.01$). However, the expression of hTERT mRNA and its protein in GC were not related with other clinicopathological parameters including gender, age, location and size of neoplasm, invasion depth, lymph node metastasis and clinical stage. There was a significant positive correlation between the expression of hTERT mRNA and cyclinD1 protein ($r = 0.350$, $P < 0.01$). There was a significant positive correlation between the expression of cyclinD1 protein and hTERT protein ($r = 0.549$, $P < 0.01$), so was between P53 and hTERT protein ($r = 0.319$, $P < 0.05$).

CONCLUSION: The expression of hTERT gene is correlated significantly to the specific defects of cell cycle on G1/S check point; telomerase activity may depend on cell cycle in gastric cancer and it is available to clarify the molecular mechanism of telomerase activity regulation. The expression of hTERT mRNA and hTERT protein in GC is significantly different from the expression of hTERT mRNA and hTERT protein in adjacent cancerous tissue which indicates that these targets are correlated closely to the occurrence of GC and can provide important morphologic index for diagnosis of GC.

Shao JC, Wu JF, Wang DB, Qin R, Zhang H. Relationship between the expression of human telomerase reverse transcriptase gene and cell cycle regulators in gastric cancer and its significance. *World J Gastroenterol* 2003; 9(3): 427-431

<http://www.wjgnet.com/1007-9327/9/427.htm>

INTRODUCTION

Telomerase activity is absent in most normal somatic cells, but has been detected in the tissues of vast majority of human malignant neoplasm by a highly sensitive method of Trap-PCR assay, and the positive of telomerase activity is 85 %. Currently, it may be the broadest-spectrum molecular marker of malignant neoplasm^[1]. Human telomerase is composed of human telomerase RNA (hTR), human telomerase reverse transcriptase (hTERT/hTRT) as well as human telomerase catalytic subunit, hEst2) and human telomerase associated protein (TP) which connects two subunit concerned above^[2-5]. High level hTERT expression has been detected in primary carcinoma, cancer cell lines and tissues which express telomerase activity. There is a consistent correlation between hTERT and telomerase activity. Meanwhile, we can't detect hEst2/hTERT in cell lines whose telomerase activity is negative and in well differentiated tissues^[6-8]. Therefore, Meyserson proposed that the expression of hEst2/hTERT mRNA is a critical step in cell immortalization and tumorigenesis^[3].

It has been reported in telomere-telomerase hypothesis that the senescence process of human cell can be divided into two stages, one is the mortality stage 1 (M1), another is the mortality stage 2 (M2). When telomerase shortens to a critical length 2kb-4kb, the stability of chromosome will be damaged and the cells enter the senescence stage that is M1. At this stage, DNA breaks with activation of P53-dependent or-independent DNA damage pathways, and the DNA damage can also induce products of CDK3 inhibitors such as p21, p27 and lead to the G1 block and eventual death^[9]. If certain tumor suppressor genes PRb, P53 or P16 are inactivated and are deprived of normal function, cells will prolong their life span, but usually not to immortalization. Then telomere further decreases to M2 stage. Most cells will die at this stage, but rare cells will survive and become immortalized because of the up-regulation or re-activation of telomerase activity which restores the telomere function and the stability of chromosome^[10]. Thus, telomere length and activation of telomerase closely correlate to life span of cells. Zhux *et al* demonstrated that the level of telomerase activity varies with different phases of cell cycle^[11]. In this study, we chose hTERT which could represent telomerase activity and markers around the G1/S check point of cell cycle such as P16, cyclinD1, P53 to reveal the interaction between hTERT gene and regulation of cell cycle and to investigate the role of these indexes in the oncogenesis and development of gastric cancer by in situ hybridization method and immunohistochemistry technique.

MATERIALS AND METHODS

Tissue specimens

Tissue specimens of gastric cancer were obtained from the first affiliated hospital of Anhui Medical University from October 1994 to October 1997. No patient had been treated with anti-neoplasm therapy before surgical removal. 53 patients (42 males, 11 females, from 23 to 73 years old, median age 55 years) were as follows: 22 cases of poorly differentiated adenocarcinoma, 26 cases of well differentiated adenocarcinoma (including 18 cases of tubular adenocarcinoma, 8 papillary adenocarcinoma), 5 cases of mucoid carcinoma (including 4 cases of mucinous adenocarcinoma, 1 case of signet-ring cell carcinoma). 53 cases of adjacent cancerous tissues were taken as controls. All specimens were fixed in 10 % formalin, embedded in paraffin, cut in serial 4 μ m sections and adhered to slides treated by poly-L-Lysine and 0.1 % DEPC.

Reagents

hTERT ISH detection kit was purchased from Boster Biological Technology Ltd. The probe labeled by digoxin is made of three sequences of oligonucleotide of hTERT: (1) 5' -AGTCAGGCTG GGCCT CAGAG AGCTG AGTAG GAAGG-3'; (2) 5' -GCATG TACGG CTGGA GGTCT GTCAA GGTAAGACG-3'; (3) 5' -TGCAC ACCGT CTGGA GGCTG TTCAC CTGCA AATCC-3'.

Rabbit polyclonal antibodies against hTERT and P16INK4, monoclonal mouse antibodies against cyclinD1 and P53, and S-P immunohistochemical kit were purchased from Beijing Zhongshan Biological Technology Ltd.

In situ hybridization

The specimens were deparaffinized and rehydrated through a graded series of ethanol, and endogenous peroxidase was blocked by using 3 % hydrogen peroxide for 10 min. After washed with distilled water treated by 0.1 % DEPC three times at 5 min each, the slides were digested with pepsin diluted by 3 % citric acid at 37 °C for 15-20 min. 20 μ l reagent of pre-hybridization was added to each slide at 37 °C for 2 hours, then 20 μ l of probe was hybridized to each slide at 42 °C for 16-20 hours. After hybridization, each slide was washed with 2 \times SSC twice at 37 °C for 20 min each, then again with 0.2 \times SSC twice at 37 °C for 10 min each. Blocking reagent was dropped to the slides and incubated for 30 min, then the mouse anti-digoxin antibody labeled by biotin was added at 37 °C for 60 min. After washed with 0.5M PBS thrice at 2 min each, the slides were incubated with strept-avidin-biotin complex (SABC) for 20 min at 37 °C, then washed with 0.5M PBS four times at 5 min each. At last, chromogen DAB was added to visualize the reaction products of peroxidase, then the slides were counterstained for nuclei by haematoxylin stain. A negative control was prepared according to the above steps with the probe substituted by 2 \times SSC, a positive control showed positive always in repeated experiments. The positive signals of hTERT mRNA expression were stained with brown-yellow color located in cytoplasm and/or nucleus. The percentage of positive cells was determined by 10 areas at high power fields (\times 400) and graded as follows: negative (-); mildly positive (+), the percentage of positive staining was less than 25 %, moderately positive (++) , the percentage of positive staining was less than 25-50 %; strongly positive (+++), the percentage of positive staining was more than 50 %.

Immunohistochemistry

Immunohistochemical staining was performed by S-P method, anti-hTERT antibody was diluted into 1:100, anti-P16INK4 1:50, anti-cyclinD1 1:50. anti-P53 antibody was the reagent ready to use. A negative control was dyed according to the above

method with the primary antibody substituted by animal serum. The positive standard of hTERT protein expression was stained with the brown-yellow color in cell plasma, P53 positive expression was stained in nucleus, the expression of P16 and cyclinD1 was stained in nucleus and(or) cytoplasm. A semi-quantitative evaluation was used to determine positive expression of positive cell by viewing 10 areas at high power field (\times 400)^[12]: negative(-), cells were stained less than 10 %; mildly positive (+), cells were stained in 11-25 %; moderately positive (++) , cells were stained in 26-50 %; strongly positive (+++), cells were stained over 50 %. And we regarded the last three grades as positive.

Statistical analyses

The data was copied down by Excel and analyzed by SPSS version 10.0. The χ^2 test or Fisher's exact test ($n < 5$) was used for statistical analysis, Spearman rank correlation was performed for correlation analysis.

RESULTS

Expression of hTERTmRNA and hTERT protein

The positive signals of hTERTmRNA were brownish-yellow stains located in cytoplasm and/or nucleus (Figure 1,2). There was barely hTERTmRNA expression in adjacent cancerous tissues, only a few positive cells in dysplasia and intestinal metaplasia of adjacent cancerous tissues. Positive expression of hTERTmRNA was detected in 42 of 53(79.2 %) of GC, but only 8 of 53(15.1 %) of adjacent cancerous tissues. The expression of hTERTmRNA of GC was significantly higher than those of the adjacent cancerous tissues ($P < 0.01$) (Table1).

Table 1 Expression of hTERTmRNA in histologic pattern of gastric cancer and adjacent cancerous tissue

Groups	n	hTERTmRNA				Positive(%)	P
		(-)	(+)	(++)	(+++)		
WD	26	5	12	7	2	80.8	0.067 ^a
PD	22	3	11	8	0	83.4	
Mucoid GC	5	3	1	1	0	40.0	
Adjacent	53	45	6	2	0	15.1	<0.01 ^b

^a: comparison among groups of GC; ^b: comparison between adjacent cancerous tissue and GC. WD: well differentiated adenocarcinoma; PD: poorly differentiated adenocarcinoma.

The positive signals of hTERT protein were brownish-yellow stains located in cytoplasm and the strength of coloration was directly proportional to positive percentage (Figure 3, 4). There was barely hTERT protein expression in adjacent cancerous tissues, but a few positive cells in dysplasia and intestinal metaplasia of adjacent cancerous tissues. Positive expression of hTERT protein was detected in 47 of 43(88.6 %) of GC, but 13 of 53(24.5 %) of adjacent cancerous tissues, so there was significant difference between GC and adjacent cancerous tissues ($P < 0.01$). There was statistical difference of the expression of hTERT protein among groups of different histologic patterns. Further comparison showed no significant difference between well differentiated adenocarcinoma and poorly differentiated adenocarcinoma, but there was statistical difference between mucoid carcinoma and well differentiated adenocarcinoma, so was mucoid carcinoma and poorly differentiated adenocarcinoma (Table2). And there was a highly significant positive correlation between the expression of hTERTmRNA and its protein ($r = 0.625$, $P < 0.01$).

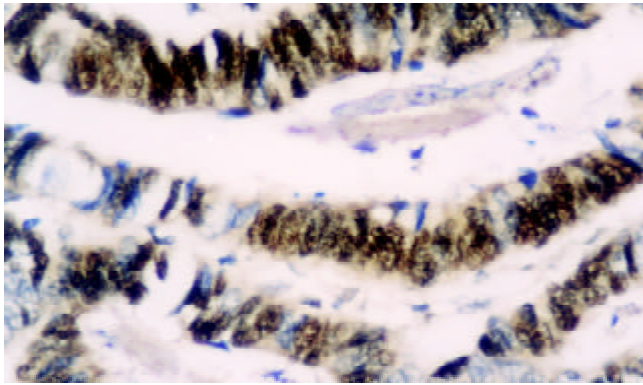


Figure 1 The expression of hTERTmRNA is strongly positive in tubular adenocarcinoma. ISH×400.

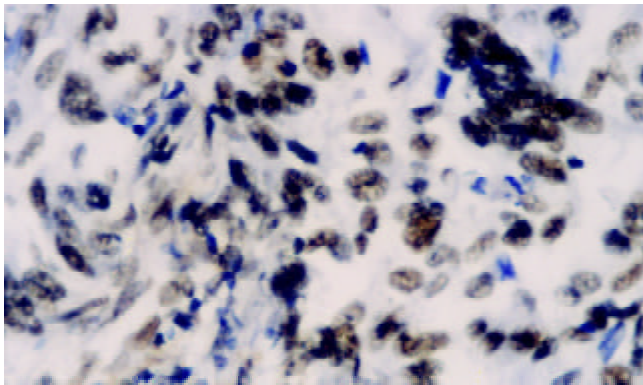


Figure 2 The expression of hTERTmRNA is moderately positive in poorly differentiated adenocarcinoma. ISH×400.

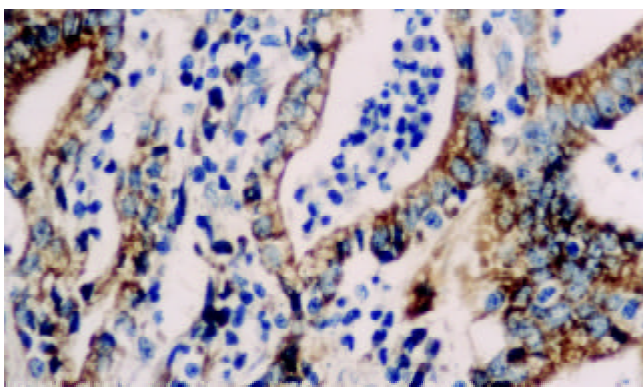


Figure 3 The expression of hTERT protein is strongly positive in papillary adenocarcinoma. S-P×400.

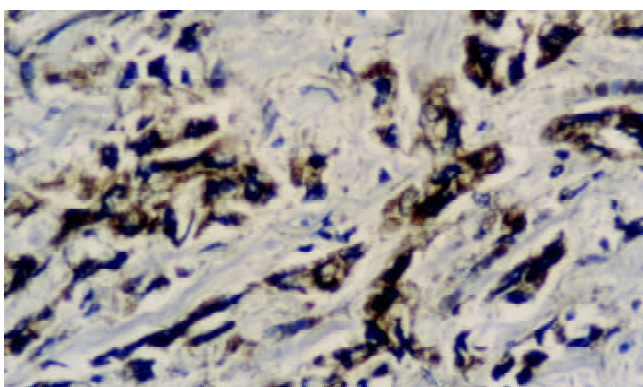


Figure 4 The expression of hTERT protein is moderately positive in poor differentiated adenocarcinoma. S-P×400.

Table 2 Expression of hTERT protein in histologic pattern of gastric cancer and adjacent cancerous tissue

Groups	n	hTERT protein				Positive(%)	P
		(-)	(+)	(++)	(+++)		
WD	26	1	6	15	4	96.2	<0.01 ^a
PD	22	2	9	10	1	90.9	
Mucoid GC	5	3	2	0	0	40.0	
Adjacent	53	40	11	2	0	24.5	<0.01 ^b

^a: comparison among groups of GC; ^b: comparison between adjacent cancerous tissue and GC.

We grouped the 53 cases of cancer patients who had complete clinical data as gender, age, tumor location and size, lymph node metastasis, invasion depth and clinical staging, and found that the expression of hTERTmRNA and its protein in GC was not related with clinicopathological parameters concerned above (Table 3).

Table 3 Relationship between the expression of hTERTmRNA, hTERT protein and clinicopathological parameters in gastric cancer

Parameters	n	hTERTmRNA positive (%)	P	hTERT protein positive(%)	P
Gender					
Male	42	35 (83.3)	0.309	39 (92.9)	0.180
Female	11	7 (63.6)		8 (72.7)	
Age(years)					
<55	25	18 (72.0)	0.219	20 (80.0)	0.147
≥55	28	24 (85.7)		27 (96.4)	
Tumor size(cm)					
< 5	24	20 (83.3)	0.735	22 (91.7)	0.678
≥5	29	22 (75.9)		25 (86.2)	
Tumor location					
Cardia	26	23 (88.5)	0.128	24 (92.3)	0.529
Body	16	10 (62.5)		13 (81.3)	
Antrum	11	9 (81.8)		10 (90.9)	
Lymph node metastasis					
Absent	25	18 (72.0)	0.219	20 (80.0)	0.089
Present	28	24 (85.7)		27 (96.4)	
Invasion depth					
Not invading serosa	8	7 (87.5)	0.879	7 (87.5)	1.000
Invading serosa	45	35 (77.8)		40 (88.9)	
Clinical stage					
I and II	47	37 (78.7)	1.000	41 (87.2)	0.806
III and IV	6	5 (83.3)		6 (100.0)	

Correlation between hTERTmRNA, hTERT protein and cell cycle regulators

The positive percentage of P16INK4 expression was 60.3 % (32/53) of GC, but 88.6 % (47/53) of the adjacent cancerous tissues; the positive percentage of cyclinD1 overexpression was 69.8 % (37/53) of GC, but 5.7 % (3/53) of adjacent cancerous tissues; the positive expression of P53 was 32 of 53 (60.4 %) of GC, but none of adjacent tissues. We analyzed relationship between hTERTmRNA, hTERT protein and cell cycle regulators through Spearman rank correlation. There was a significant positive correlation between the expression of hTERT mRNA and cyclinD1 protein ($r=0.350$, $P<0.01$), and a significant positive correlation between the expression of cyclinD1 protein and hTERT protein ($r=0.549$, $P<0.01$), so was P53 and hTERT protein ($r=0.319$, $P<0.05$). The expression of

P16INK4 didn't correlate with hTERTmRNA and hTERT protein, but the tumor tissues of the group with negative P16INK4 in combination with cyclinD1 overexpression had the strongest positive stains of hTERTmRNA, and the hTERTmRNA overexpression of this group was 79 % (10/13). However, the hTERTmRNA overexpression of the group with positive P16INK4 in combination with low-expression of cyclinD1 was 37.5 % (3/8), but there was no significant difference between the two groups ($P>0.05$).

DISCUSSION

Current studies have proposed that activation of telomerase is a critical step in tumorigenesis of gastric cancer. Jong *et al* observed telomerase activity in 25 of 27 primary GC and found the up-regulation of hTERTmRNA expression in 26 of 26 GC tissues by RT-PCR analysis^[6]. Hiyama *et al* had detected telomerase activity in 66 samples of primary GC and found that the positive percentage was 85 %, but 6 % in the adjacent cancerous tissues^[13]. In our study, we detected the expression of hTERT gene in 53 GC specimens by ISH and immunohistochemistry, and found that positive percentage of hTERTmRNA and hTERT protein was 79.2 % and 88.6 % respectively in GC, and was 15.1 % and 24.5 % in the adjacent cancerous tissues. Meanwhile, the index of hTERT could be located for observation and determined semiquantitatively. So it provided an important morphological marker for detection of GC. It is reported that telomerase activity is associated with histological differentiation and malignant grade of tumor^[14,15]. However, telomerase activity doesn't correlate with age, gender, tumor stage and histological differentiation of gastric cancer^[16-19]. In our present study of GC, the expression of hTERTmRNA and hTERT protein was not associated with clinicopathological parameters including gender, age, tumor size, location, lymph node metastasis, invasion depth and clinical staging. There was statistical difference of hTERT protein only between mucoid carcinoma and well differentiated adenocarcinoma, poorly differentiated adenocarcinoma, but our cases of mucoid carcinoma were few. Therefore, we considered that the expression of hTERT gene might be associated with gastric carcinogenesis, but not involved in differentiation and biological property of the tumor. Mild expression of hTERTmRNA and hTERT protein in dysplasia and intestinal metaplasia of adjacent cancerous tissues showed that the expression of hTERT gene might be presented in precancerous lesions or diseases, and the positive cells may be precancerous cells, but it was needed to do further studies to demonstrate the precise significance of this phenomenon.

There are several checkpoints of different function during cell cycle including G1/S checkpoint, S checkpoint and G2/M checkpoint. G1/S checkpoint that is the PRb pathway is especially important to ensure completion of cell cycle events on schedule and to prevent abnormal cells from proliferation to carcinogenesis^[20]. At the end of G1 stage, cyclinD1 combined with CDK4/6 is responsible for the phosphorylation of PRB to release an important transcription factor -E2F, which initiates DNA synthesis and drives the cells through G1/S checkpoint. There are two vital inhibitory pathways of G1/S checkpoint, one is that P16INK4 competitively combines with CDK4 against cyclinD1 to suppress CDK4 activity^[21,22], the other is that P53 initiates P21 gene to express P21 protein combined with cyclinD1/CDK4 and to inhibit the activity of cyclinD1/CDK4 when DNA is damaged^[23-29]. The two pathways both abolish phosphorylation of PRb, and cell cycle arrests at G1 phase. It is reported at the M1/M2 model of telomere-telomerase hypothesis that a cell can't obtain immortality until it passes through M1/M2stage. When the activity of tumor suppressor proteins such as P53, PRb,

P16INK4 are absent, the cells can prolong their life by passing through M1 stage, thus there will provide more chances of activating telomerase for those cells to pass through M2 and obtain immortality^[30-33].

There were a few studies about relationship between P16INK4 and telomerase. In the studies of human keratinocytes and mesothelial cells, Dickson *et al* proposed that the expression of hTERT and loss of P16INK4 were two prerequisites for cell immortalization and carcinogenesis^[34]. Landberg *et al* reported that though down-regulation of P16INK4 was not related to telomerase activity, tumors with low P16INK4 had demonstrated to have high activity of telomerase; down-regulation of P16INK4 alone was insufficient to activation of telomerase, and it was necessary in combination with other cell cycle defects such as overexpression of cyclinD1 or cyclinE^[35]. In our study of GC, the expression of P16INK4 was not associated with hTERTmRNA and hTERT protein, but there were two strong positive cases of hTERTmRNA which were absence of P16INK4 expression. So it was coordinate with studies in breast cancer of Landberg. CyclinD1 and P16INK4 locating in up-stream of PRb regulated phosphorylation of PRb and combined with CDK competitively, and the function of the two regulators was just contrary. During the progress of carcinogenesis, the abnormal expression of the two was in cooperation. Absence of P16INK4 and overexpression of cyclinD1 always occurred at the same time in studies of telomerase. In the investigation of development of UVB-induced tumors in SKH-1 hairless mice, Balasubramanian *et al* found that telomerase activity increased persistently after exposure to UVB, meanwhile, the expression of cyclinD1 and cyclinE was up-regulated when combined with CDK4, CDK2, and the expression of P16INK4, P21WAF1 and P27KIP1 all changed significantly between tumor and normal epidermis^[36]. It was reported that the over expression of cyclinD1 protein was associated with high telomerase level in the studies of breast cancer, and tumors with cyclinD1 or E overexpression in combination with low P16INK4 and normal PRb demonstrated high activity of telomerase^[35]. In our study, there was positive correlation between cyclinD1 protein and hTERTmRNA, hTERT protein, the strongest expression of hTERTmRNA existed in the tumor sample which presented the absence of P16INK4 and overexpression of cyclinD1 at the same time. Our data demonstrated that cyclinD1 protein was highly correlated with the expression of hTERT gene. The mechanism may be that the overexpression of cyclinD1 protein accelerates the phosphorylation of PRb and elevates the proliferation rate of abnormal cells, then cell cycle loses regulation. Activated telomerase drives cells to pass through M2 stage to tumorigenesis. If in combination with inactivation of tumor suppressor genes such as the loss of P16INK4, it is especially helpful for activation of telomerase and quickening the pace of carcinogenesis. Therefore, the overexpression of cyclinD1 represents a cell cycle defect correlated with telomerase activity closely. Li *et al* reported that telomerase activity was inhibited lately in human breast cancer cells after introducing recombinant human P53 to them, and this experiment indicated that activity of telomerase might be regulated by P53 *in vivo* and the down-regulation of P53 might increase the telomerase activity^[37]. In our study, the expression of P53 positively correlated with hTERT protein; the result demonstrated that P53 regulated the telomerase, and it prompted that when the pathway of P53-P21WAF1 was inactive, abnormal cells devoid of braking mechanism and passing through G1/S checkpoint to S stage at which telomerase activity increases giving cells the chance to pass through M2 and achieving immortality that produces specific tumor phenotype.

Our data shows that the expression of hTERT gene is correlated significantly to the specific defects of cell cycle in

G1/S checkpoint, which proposes that telomerase activity may depend on cell cycle in gastric cancer and thus helps to clarify the molecular mechanism of telomerase activity regulation.

REFERENCES

- 1 **Hiyama E**, Kodama T, Shinbara K, Iwao T, Itoh M, Hiyama K, Shay JW, Matsuura Y, Yokoyama T. Telomerase activity is detected in pancreatic cancer but not in benign tumors. *Cancer Res* 1997; **57**: 326-331
- 2 **Feng J**, Funk WD, Wang SS, Weinrich SL, Avilion AA, Chiu CP, Adams RR, Chang E, Allsopp RC, Yu J, Li S, West MD, Harely CB, Andrews WH, Greider CW, Villeponteau B. The RNA component of human telomerase. *Science* 1995; **269**: 1236-1241
- 3 **Meyerson M**, Counter CM, Eaton EN, Ellisen LW, Steiner P, Caddle SD, Ziaugra L, Beijersbergen RL, Davidoff MJ, Liu Q, Bacchetti S, Haber DA, Weinberg RA. hEST2, the putative human telomerase catalytic subunit gene, is up-regulated in tumor cells and during immortalization. *Cell* 1997; **90**: 785-795
- 4 **Smith S**, Giriati I, Schmitt A, de Lange T. Tankyrase, a poly(ADP-ribose) polymerase at human telomerase. *Science* 1998; **282**: 1484-1487
- 5 **Harrington L**, McPhail T, Mar V, Zhou W, Oulton R, Bass MB, Arruda I, Robinson MO. A mammalian telomerase-associated protein. *Science* 1997; **275**: 973-977
- 6 **Jong HS**, Park YI, Kim S, Sohn JH, Kang SH, Song SH, Bang YI, Kim NK. Up-regulation of human telomerase catalytic subunit during gastric carcinogenesis. *Cancer* 1999; **86**: 559-565
- 7 **Meyerson M**. Telomerase enzyme activation and human cell immortalization. *Toxicol Lett* 1998; **102-103**: 41-45
- 8 **Takakura M**, Kyo S, Kanaya T, Tanaka M, Inoue M. Expression of human telomerase subunits and correlation with telomerase activity in cervical cancer. *Cancer Res* 1998; **58**: 1558-1561
- 9 **Vaziri H**, Benchimol S. From telomere loss to P53 induction and activation of a DNA-damage pathway at senescence: the telomere loss/DNA damage model of cell aging. *Exp Gerontol* 1996; **31**: 295-301
- 10 **Rogan EM**, Bryan TM, Hukku B, Maclean K, Chang AC, Moy EL, Englezou A, Warneford SG, Dalla-Pozza L, Reddel RR. Alterations in P53 and P16INK4 expression and telomere length during spontaneous immortalization of Li-Fraumeni syndrome fibroblasts. *Mol Cell Biol* 1995; **15**: 4745-4753
- 11 **Zhu X**, Kumar R, Mandal M, Sharma N, Sharma HW, Dhingra U, Sokoloski JA, Hsiao R, Narayanan R. Cell cycle-dependent modulation of telomerase activity in tumor cells. *Proc Natl Acad Sci USA* 1996; **93**: 6091-6095
- 12 **Barnes DM**, Dublin EA, Fisher CJ, Levison DA, Millis RR. Immunohistochemical detection of p53 protein in mammary carcinoma: an important new independent indicator of prognosis? *Hum Pathol* 1993; **24**: 469-476
- 13 **Hiyama E**, Yokoyama T, Tatsumoto N, Hiyama K, Imamura Y, Murakami Y, Kodama T, Piatyszek MA, Shay JW, Matsuura Y. Telomerase activity in gastric cancer. *Cancer Res* 1995; **55**: 3258-3262
- 14 **Sharma HW**, Sokoloski JA, Perez JR, Maltese JY, Sartorelli AC, Stein CA, Nichols G, Khaled Z, Telang NT, Narayanan R. Differentiation of immortal cells inhibits telomerase activity. *Proc Natl Acad Sci USA* 1995; **92**: 12343-12346
- 15 **Yuan X**, Zhang B, Ying J, Jin Y, Hou L. Expression of telomerase gene in human tumor tissues. *Zhonghua Binglixue Zazhi* 2000; **29**: 16-19
- 16 **Ahn MJ**, Noh YH, Lee YS, Lee JH, Chung TJ, Kim IS, Choi IY, Kim SH, Lee JS, Lee KH. Telomerase activity and its clinicopathological significance in gastric cancer. *Eur J Cancer* 1997; **33**: 1309-1313
- 17 **Yang SM**, Fang DC, Luo YH, Lu R, Yang JL, Liu WW. The Detection of telomerase activity and subunit in different lesions of gastric mucosa. *Aizheng* 2001; **20**: 23-27
- 18 **Zhan WH**, Ma JP, Peng JS, Gao JS, Cai SR, Wang JP, Zheng ZQ, Wang L. Telomerase activity in gastric cancer and its clinical implications. *World J Gastroenterol* 1999; **5**: 316-319
- 19 **Yao XX**, Yin L, Sun ZC. The expression of hTERT mRNA and cellular immunity in gastric cancer and precancerosis. *World J Gastroenterol* 2002; **8**: 586-590
- 20 **Clurman BE**, Roberts JM. Cell cycle and cancer. *J Natl Cancer Inst* 1995; **87**: 1499-1501
- 21 **Kamb A**, Gruis NA, Weaver-Feldhaus J, Liu Q, Harshman K, Tavtigian SV, Stockert E, Day RS 3rd, Johnson BE, Skolnick MH. A cell cycle regulator potentially involved in genesis of many tumor types. *Science* 1994; **264**: 436-440
- 22 **Serrano M**, Hannon GJ, Beach D. A new regulatory motif in cell-cycle control causing specific inhibition of cyclin D/CDK4. *Nature* 1993; **366**: 704-707
- 23 **Harper JW**, Adami GR, Wei N, Keyomarsi K, Elledge SJ. The p21 Cdk-interacting protein Cip1 is a potent inhibitor of G1 cyclin-dependent kinases. *Cell* 1993; **75**: 805-816
- 24 **el-Deiry WS**, Tokino T, Velculescu VE, Levy DB, Parsons R, Trent JM, Lin D, Mercer WE, Kinzler KW, Vogelstein B. WAF1, a potential mediator of p53 tumor suppression. *Cell* 1993; **75**: 817-825
- 25 **Deng C**, Zhang P, Harper JW, Elledge SJ, Leder P. Mice lacking p21CIP1/WAF1 undergo normal development, but are defective in G1 checkpoint control. *Cell* 1995; **82**: 675-684
- 26 **Somasundaram K**, Zhang H, Zeng YX, Houvras Y, Peng Y, Zhang H, Wu GS, Licht JD, Weber BL, El-Deiry WS. Arrest of the cell cycle by the tumour-suppressor BRCA1 requires the CDK-inhibitor p21WAF1/Cip1. *Nature* 1997; **389**: 187-190
- 27 **Liu Y**, Martindale JL, Gorospe M, Holbrook NJ. Regulation of p21WAF1/CIP1 expression through mitogen-activated protein kinase signaling pathway. *Cancer Res* 1996; **56**: 31-35
- 28 **Marchetti A**, Doglioni C, Barbareschi M, Buttitta F, Pellegrini S, Bertacca G, Chella A, Merlo G, Angeletti CA, Dalla Palma P, Bevilacqua G. p21 RNA and protein expression in non-small cell lung carcinomas: evidence of p53-independent expression and association with tumoral differentiation. *Oncogene* 1996; **12**: 1319-1324
- 29 **Greenblatt MS**, Bennett WP, Hollstein M, Harris CC. Mutations in the P53 tumor suppressor gene: clues to cancer etiology and molecular pathogenesis. *Cancer Res* 1994; **54**: 4855-4878
- 30 **Sherr CJ**. Cancer cell cycles. *Science* 1996; **274**: 1672-1677
- 31 **Herman JG**, Merlo A, Mao L, Lapidus RG, Issa JP, Davidson NE, Sidransky D, Baylin SB. Inactivation of the CDKN2/p16/MTS1 gene is frequently associated with aberrant DNA methylation in all common human cancers. *Cancer Res* 1995; **55**: 4525-4530
- 32 **Velculescu VE**, El-Deiry WS. Biological and clinical importance of the p53 tumor suppressor gene. *Clin Chem* 1996; **42**: 858-868
- 33 **Cho Y**, Gorina S, Jeffrey PD, Pavletich NP. Crystal structure of a p53 tumor suppressor-DNA complex: understanding tumorigenic mutations. *Science* 1994; **265**: 346-355
- 34 **Dickson MA**, Hahn WC, Ino Y, Ronfard V, Wu JY, Weinberg RA, Louis DN, Li FP, Rheinwald JG. Human keratinocytes that express hTERT and also bypass a P16(INK4a)-enforced mechanism that limits life span become immortal yet retain normal growth and differentiation characteristics. *Mol Cell Biol* 2000; **20**: 1436-1447
- 35 **Landberg G**, Nielsen NH, Nilsson P, Emdin SO, Cajander J, Roos G. Telomerase activity is associated with cell cycle deregulation in human breast cancer. *Cancer Res* 1997; **57**: 549-554
- 36 **Balasubramanian S**, Kim KH, Ahmad N, Mukhtar H. Activation of telomerase and its association with G1-phase of the cell cycle during UVB-induced skin tumorigenesis in SKH-1 hairless mouse. *Oncogene* 1999; **18**: 1297-1302
- 37 **Li H**, Cao Y, Berndt MC, Funder JW, Liu JP. Molecular interactions between telomerase and the tumor suppressor protein P53 *in vitro*. *Oncogene* 1999; **18**: 6785-6794

Prospective cohort study of comprehensive prevention to gastric cancer

Hai-Qiang Guo, Peng Guan, Hai-Long Shi, Xuan Zhang, Bao-Sen Zhou, Yuan Yuan

Hai-Qiang Guo, Peng Guan, Hai-Long Shi, Xuan Zhang, Bao-Sen Zhou, Department of Epidemiology, College of Public Health, China Medical University, Shenyang 110001, Liaoning Province, China
Yuan Yuan, Cancer Institute, The First Clinical Hospital, China Medical University, Shenyang 110001, Liaoning Province, China
Supported by National Ninth Five-year Study Program for Taking Key Scientific Problems, No.96-906-01-04, and National Tenth Five-year Study Program for Taking Key Scientific Problems, No. 2001BA703B06(B)

Correspondence to: Prof. Yuan Yuan, Cancer Institute, The First Clinical Hospital, China Medical University, Shenyang 110001, Liaoning Province, China. yyuan@mail.cmu.edu.cn

Telephone: +86-24-23256666-6292

Received: 2002-07-17 **Accepted:** 2002-11-04

Abstract

AIM: To evaluate the preliminary effects of comprehensive prevention of gastric cancer in Zhuanghe County epidemiologically.

METHODS: Stratified sampling and cluster sampling were applied to define the intervention group and the control group. The prospective cohort study was used for evaluating the effect of preventing gastric cancer. The relative risk (RR) and attributable risk percent (AR %) of intervention on gastric cancer death were calculated. Potential years of life lost (PLYL) of the disease was analyzed, and the RR and AR % of PLYL were calculated. Survival analysis was applied among the screened patients.

RESULTS: In the first 4 years after intervening, the relative risk (RR) of intervention on death was 0.5059 (95 % CI: 0.3462~0.7392, $P < 0.05$) with significance statistically. AR % of the intervention on death was 49.41 %. The RR of intervention on cumulative PLYL was 0.6778 (95 % CI: 0.5604~0.8198, $P < 0.05$) with statistic significance. AR % of the intervention on cumulative PLYL was 30.32 %. The four-year survival rate of the screened patients was 0.6751 (95 % CI: 0.5298~0.9047).

CONCLUSION: The initiative intervention results showed that the intervention approach used in the trial was effective, it reduced mortality and increased survival rate, and alleviated the adverse effect of gastric cancer on the health and life of screened population.

Guo HQ, Guan P, Shi HL, Zhang X, Zhou BS, Yuan Y. Prospective cohort study of comprehensive prevention to gastric cancer. *World J Gastroenterol* 2003; 9(3): 432-436
<http://www.wjgnet.com/1007-9327/9/432.htm>

INTRODUCTION

Gastric cancer is one of the most common malignant tumor, its prevalence in 1999 was 138.60×10^{-5} according to the report of WHO^[1], however, its prevalence (300.87×10^{-5}) and mortality

(29.31×10^{-5}) are even higher in China^[1]. The incidence of gastric cancer has been declining globally during the recent decades, but not in China^[2]. It was believed that the main reasons of the declining were prevention and diagnosis, but not therapy^[3]. Most studies show that the incidence of gastric cancer is related to dietary factors, infection of helicobacter pylori(Hp), etc.^[4-9]. If these relative factors were eliminated or decreased, the incidence and mortality of gastric cancer would be lowered., thus gastric cancer could be prevented^[10-13]. So it is very important to find an effective comprehensive preventive method for gastric cancer.

Zhuanghe is a county in Liaoning Province with total population of approximate 900 000, locates along the seaside of the Huanghai Sea. The previous survey showed that the incidence of gastric cancer in this county was higher than the average level of other areas. In 1994, the mortality rate was 49.55×10^{-5} in male, and 22.23×10^{-5} in female. The population in Zhuanghe County has been surveyed in census and studied for 18 years by the Stomach Investigation Group of China Medical University because of higher incidence and mortality of gastric cancer. A series of comprehensive preventive approaches have been applied since 1997, including primary and secondary prevention. The goal was to explore a series of comprehensive preventive approaches to reduce the incidence and the mortality of gastric cancer. The initiative effect of intervention approaches by epidemiological study was evaluated in this paper.

MATERIALS AND METHODS

Definition of sample

Stratified sampling and cluster sampling were applied to define the intervention group and the control group. Each village in this county was stratified into two groups according to location geographically close seaside or not, then the sampled villages were defined by cluster sampling in the two groups, and the number of the sampled villages in each group was proportional to its location stratification. All individuals of the sampled villages were used as the samples.

Sixteen villages were sampled as the intervention group, other 14 villages were used as the control based on location, economic level, and proportion of population in each intervention village. 63 133 persons from 30 villages, 16 870 in the intervention group, and 14 900 in the control group were observed, respectively. The age and sex were proportional in each group.

Intervention approaches

The design of the intervention was as the following (Figure 1). **Common approaches in intervention and control group** Knowledge of prevention and treatment of gastric cancer, especially dietary habits was provided for all residents through broadcasting, video, brochures and face-to-face conversation. **Approaches in intervention groups** Initially 3 033 persons were selected as suspected high risk population from intervention villages according to the epidemiological survey and clinical symptoms. Persons who had the family history of

gastric cancer, and/or were over 35 years old and had history of gastric illness, or had obvious symptoms of gastric illness were grouped as suspected high risk population, from which 1781 persons were further detected and grouped as high risk population of gastric cancer^[16-18], and were treated with antibiotics, Chinese herb medicine, and nutritional therapy, based on X-ray, HP detected, and gastroscopic and pathological examination^[19-21]. Patients with gastric cancer screened from the high risk population were treated promptly.

The whole process of screening and treatment was performed under strict quality control. Twenty five percent of intervened individuals were randomly selected and checked for the compliance to medication by interviewing with individuals and their family and measuring the metabolites of medicine in urine, results showed that the compliance rate was 96.6 %. The screening and surveying were initiated in 1997 and had been processed successfully since then.

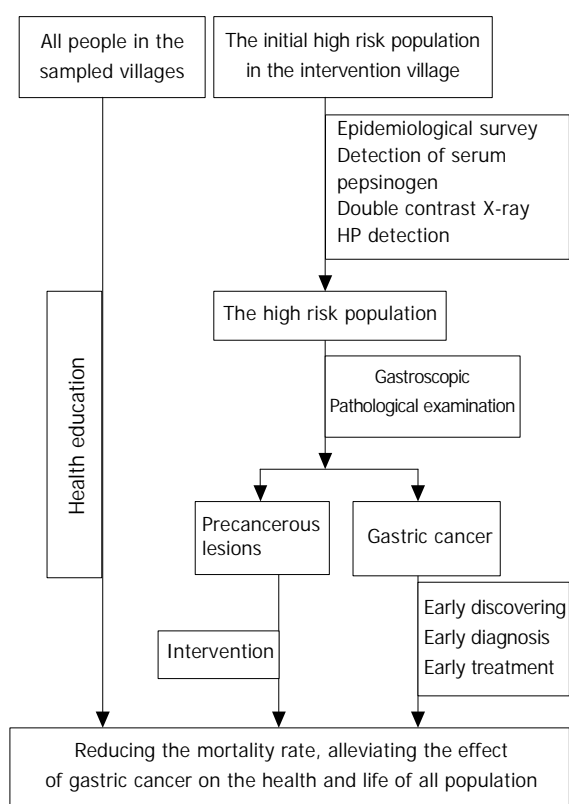


Figure 1 The intervention trial sketch.

Analysis of data

The prospective cohort study was applied to observe the samples. The cause of all death including gastric cancer from 1996 to 2000 were documented in both intervention group and control groups. The screened patients with gastric cancer were observed and reported annually.

The relative risk (RR) and attributable risk percent (AR %) of intervention on death of gastric cancer, potential years of life lost (PLYL) of the disease, and the RR and AR % of PYLL were calculated. The survival rate of all the screened patients with gastric cancer was evaluated.

The maximum expectancy method was adopted to calculate PYLL^[22].

$$PYLL = \sum a_i d_i, a_i = L - x - 0.5$$

L: the upper limit age, evaluated at 70.

x: the middle value of age interval.

a_i: the residual years from age interval (i~i+1) to the maximum expect age (L).

d: the death number of age interval (i~i+1) from the disease. PYLL= (PYLL/N)*1000‰.

N: the number of total observed population or person-years.

Life-table method and product-limit method^[23] were applied to analyze the survival rate of all the screened patients with gastric cancer.

$$S(t) = \prod (1 - d_i/n_i)$$

n_i: the adjusted population at the beginning of the period i.

d_i: the death number of the period i.

RESULT AND ANALYSIS

General

The composition of the sample is shown in Table 1.

Table 1 Composition of the samples

	Male	Female	Total
Intervention group	26 922	26 256	53 178
Control group	23 840	23 924	47 788
Total	50 762	50 204	100 966

During the first screening in 1997, 32 patients with gastric cancer were diagnosed, in which 18 patients were early gastric cancer, and 14 were advanced gastric cancer. The incidence of cancer in the screened group was 1.80 % (32/1781). In addition, 1 306 persons were detected having other gastric diseases. The screening rate of all gastric diseases was 75.13 % (1 338/1 781), therefore the screening method was very effective. From 1998 to 1999, 12 patients with gastric cancer were detected, in which 7 patients were early gastric cancer, and 5 were advanced gastric cancer.

Mortality of gastric cancer

The mortality rate of gastric cancer in Zhuanghe from 1996 to 2000 was between 45.21×10⁻⁵~63.29×10⁻⁵, the annual rate was 53.24×10⁻⁵ (person· year)⁻¹, whose 95 % CI is 44.57×10⁻⁵-61.91×10⁻⁵, which is higher than the average rate in China (29.31×10⁻⁵). The rate in male was 75.11×10⁻⁵ (95 % CI: 60.60×10⁻⁵-89.61×10⁻⁵), and in female was 30.08×10⁻⁵ (95 % CI: 20.98×10⁻⁵-39.18×10⁻⁵). The death from gastric cancer was 8.25 % of all death from any reasons, and 38.94 % of all carcinoma deaths, which were higher than that of the national average level (P<0.05)^[24-26].

The annual mortality rate of gastric cancer in Zhuanghe was shown in Figure 2. The alterations of mortality from 1996 to 2000 were not statistically significant.

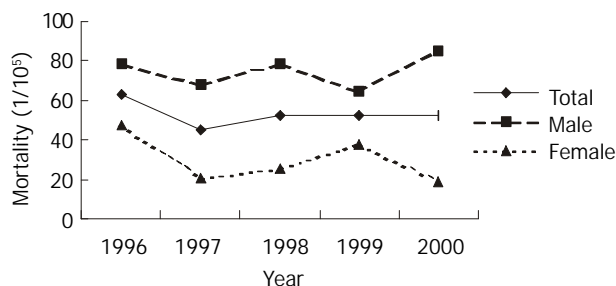


Figure 2 Mortality of gastric cancer in Zhuanghe County from 1996 to 2000.

The annual mortality rates of gastric cancer in intervention groups were shown in Figure 3. The rates in the period from 1997 to 2000 were lower than that in 1996 with no significance by Poison test^[27] (P>0.05 except that in male in 2000. In

contrast, the average mortality rate (34.97×10^{-5}) in intervention groups during post-intervention period (1997-2000) was lower significantly than that (59.31×10^{-5}) in pre-intervention period (1996) (one-sided test, $\chi^2=2.930, P<0.05$). However, no statistical decrease of mortality was found in control groups (Figure 4).

The tendency of descending in mortality of gastric cancer was observed (Figure 3). The linear correlation analysis is shown in Table 2. No obvious alteration in the mortality of gastric cancer in control group from 1996 to 2000 was observed.

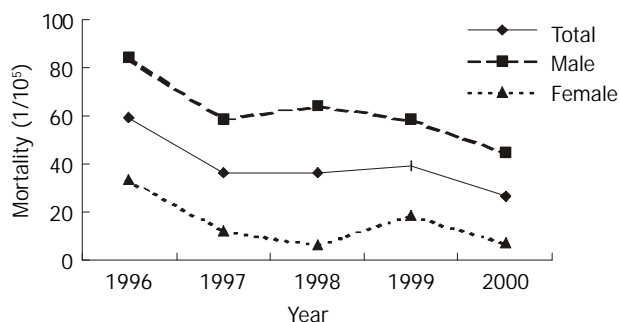


Figure 3 Mortality of gastric cancer in intervention groups from 1996 to 2000.

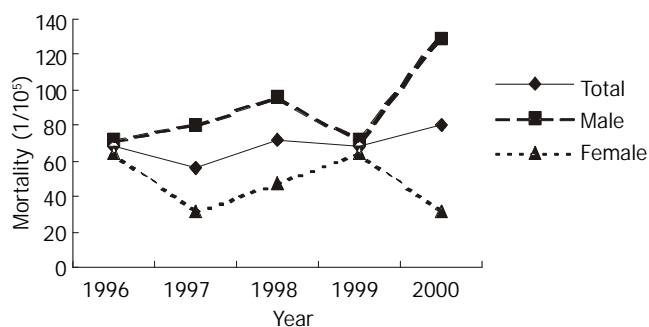


Figure 4 Mortality of gastric cancer in control groups from 1996 to 2000.

Table 2 Linear correlation in gender of gastric cancer mortality in intervention groups

Group	r	F	P
Male	0.8688	9.2369	0.0559
Female	0.6690	2.4308	0.2169
Total	0.8148	5.9256	0.0930

The difference of the mortality rate of gastric cancer between the intervention group and the control group in 1996 was not significant ($\chi^2=0.0283, P>0.05$). The annual average rates between the intervention group and the control group from 1997 to 2000 differed significantly ($\chi^2=5.873, P<0.05$) (Figure 5).

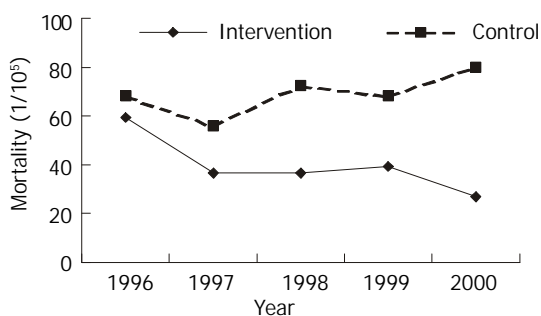


Figure 5 Mortality rate in intervention and control groups from 1996 to 2000.

Relative risk analysis

One hundred and ten patients in both groups had died from gastric cancer since the beginning the trial in 1997. The cumulative mortality rate (CMR) was 34.97×10^{-5} in intervention villages, and 69.13×10^{-5} in control villages. The relative risk (RR) of intervention was 0.5059 (95 % CI: 0.3462~0.7392, $P<0.05$) with statistic significance. The attributable risk percent of the intervention was 49.41 %, which indicated that intervention reduced gastric cancer death by 49.41 % of all population. All these data showed that the intervention approaches can reduce the death of gastric cancer.

Table 3 Cumulative mortality rate and relative risk

	Total person-year	Death No.	CMR (10 ⁻⁵)	RR	RR 95%CI	AR%
Control	99 816	69	69.13			
Intervention	117 234	41	34.97	0.5059	0.3462~0.7392	49.41

Potential years of life lost in gastric cancer

From 1996 to 2000, the potential years of life lost (PYLL) of gastric cancer were 731 person-years, and the PYLL was 3.07 ‰ which meant the lost years of 1 000 people from gastric cancer were 3.07 every year. In the intervention group, the PYLL was 300 person-years, and the PYLL was 2.89 ‰. The PYLL of the control group was 431 person-years, and the PYLL was 3.94 ‰ (Figure 6). The PYLL in intervention group in 1996 and 1998 was not significantly different from that in control group ($\chi^2=1.3948, 0.2074, P>0.05$), and the differences in 1997, 1999 and 2000 were statistically significant ($\chi^2=5.0603, 73.2124, 11.4119, P<0.05$). Difference of the total PYLL from 1997 to 1999 between the intervention group and the control group was significant ($\chi^2=16.1527, P<0.01$).

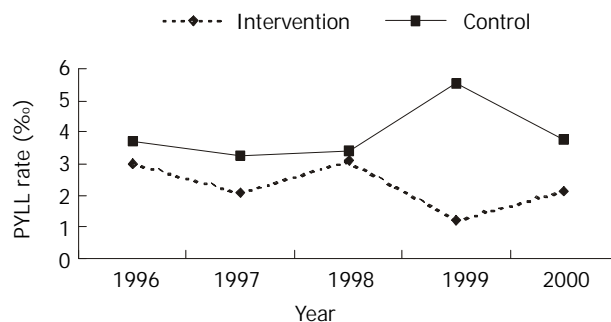


Figure 6 PYLL in intervention group and control group from 1996 to 2000.

The RR of intervention to cumulative PYLL was 0.6778 (95 % CI: 0.5604~0.8198, $P<0.05$), which was statistically significant. The AR % of the intervention to cumulative PYLL was 30.32 %, which showed that the intervention decreased PYLL of gastric cancer by 30.32 % of all population.

Table 4 PYLL and its RR

	Total person-year	PYLL	PYLL (%)	RR	RR 95%CI	AR%
Control	87 757	272	3.10			
Intervention	103 191	223	2.16	0.6778	0.5604~0.8198	30.32

Survival analysis

During the 4-year observation after intervening, 32 patients with gastric cancer were detected by screening, of which 9 patients died. The annual survival rates were shown in Table 5.

Table 5 Annual survival rate and its 95 % CI

Year	Survival rate	Standard error	95 % CI of survival rate
1-	0.8305	0.0691	0.6951, 0.9659
2-	0.7173	0.0852	0.5503, 0.8842
3-	0.7173	0.0852	0.5503, 0.8842
4-	0.6751	0.0956	0.5298, 0.9047

The one-year and three-year survival rate of the screened patients with cancer was 0.8305 (95 % CI: 0.6951~0.9659), and 0.7173 (95 % CI: 0.5503~0.8842), respectively, which are higher than those in Changde County of Fujian Province^[28]. In this study, all screened patients were not operated due to some reasons; otherwise, the survival rate would be higher.

DISCUSSION

All intervention approaches were based on the following studies: (1) Many epidemiological and histological studies showed gastric cancer is related with infection of *Helicobacter pylori*, which cause excessive hyperplasia and reduction of apoptosis of gastric epithelium. These cellular dynamic changes lead to injury of DNA and the generation of gastric cancer cell clone^[29-33]. (2) Garlic oil can inhibit malignant proliferation of cancer cells, and induce their differentiation. The mechanism is likely to adjust the expression of oncogene. Garlic oil can restrain and reverse experimental gastric cancer and precancerous lesions^[34,35]. (3) Surveys showed that cancer is correlated with precancerous lesions. Not all precancerous lesions will develop to cancers, but the generation of cancers may be prevented if the precancerous lesions are cared and cured early^[36,37].

It was reported that gastric cancer was related with high-salt diet and preserved-food diet^[14,15,38,39]. These dietary habits are extremely common in Zhuanghe County, and may be the main cause of gastric cancer^[40]. Accordingly, health education for applying and maintaining right dietary habits was stressed in intervention and control groups.

The analysis of the mortality and PYLLs was focused on all the population instead of a single patient in evaluating the initiative effects of comprehensive preventive approaches. The intervention can reduce the mortality rate of patients with gastric cancer and alleviate the effect of gastric cancer on the health and life of all population. The analysis of PYLL endues the death with weight according to the age of the death, and age standardized mortality rate is applied, so this method reflects the "early death" and the "deferred death". At the initial period of prevention, the decrease of the mortality may not be obvious, but the time on the mortality may be deferred, that is, the survival time of the patients may be prolonged due to early discovering, early diagnosis, and early treatment. It is more suitable to analyze and evaluate the initial effect of comprehensive prevention and treatment of gastric cancer than mortality analysis. Analysis of survival is based on patients with gastric cancer rather than the whole population, and thus it reflects whether the approaches have prolonged the life of patients with gastric cancer.

The results of the survey show that although local mortality rate of gastric cancer in Zhuanghe County is still higher than that of national level in China, the initial outcome of the intervention indicates that the intervention approaches used in the trial are effective, as these approaches have prolonged the screened patients' life, reduced the mortality rate, and alleviated the adverse effect of gastric cancer on the health and life of all population screened. Because effect of chemical intervention effect is behind of the approaches, the initial outcome showed

in this article is mostly due to secondary prevention, that is early discovering, early diagnosis and early treatment.

REFERENCES

- 1 <http://www.who.int/whr/1999/en/report.htm>: The World Health Report 1999 of WHO
- 2 **Li LM**. Epidemiology. 4th ed. Beijing: People's Medical Publishing House, 2000: 86-89
- 3 **Vutuc C**, Waldhoer T, Haidinger G, Ahmad F, Micksche M. The burden of cancer in Austria. *Eur J Cancer Prev* 1999; **8**: 49-55
- 4 **Inoue M**, Tajima K, Kobayashi S, Suzuki T, Matsuura A, Nakamura T, Shirai M, Nakamura S, Inuzuka K, Tominaga S. Protective factor against from atrophic gastritis to gastric cancer -data from a cohort study in Japan. *Int J Cancer* 1996; **66**: 309-314
- 5 **Forman D**, Newell DG, Fullerton F, Yarnell JWG, Stacey AR, Wald N, Sitas F. Association between infection with *Helicobacter pylori* and risk of gastric cancer: evidence from a prospective investigation. *BMJ* 1991; **302**: 1302-1305
- 6 **Correa P**. Human gastric carcinogenesis: a multistep and multifactorial process-First American Cancer Society Award Lecture on Cancer Epidemiology and Prevention. *Cancer Res* 1992; **52**: 6735-6740
- 7 **Chyou PH**, Nomura AM, Hankin JH, Stemmermann GN. A case-cohort study of diet and stomach cancer. *Cancer Res* 1990; **50**: 7501-7504
- 8 **Lee JK**, Park BJ, Yoo KY, Ahn YO. Dietary factors and stomach cancer: a case-control study in Korea. *Int J Epidemiol* 1995; **24**: 33-41
- 9 **Tredaniel J**, Boffetta P, Buiatti E, Saracci R, Hirsch A. Tobacco smoking and gastric cancer: review and meta-analysis. *Int J Cancer* 1997; **72**: 565-573
- 10 **Harris A**. Treatment of *Helicobacter pylori*. *World J Gastroenterol* 2001; **7**: 303-307
- 11 **Wang DX**, Fang DC, Li W, Du QX, Liu WW. A study on relationship between infection of *Helicobacter pylori* and inactivation of antioncogenes in cancer and pre-cancerous lesion. *Shijie Huaren Xiaohua Zazhi* 2001; **9**: 984-987
- 12 **Zhao AG**, Zhao HL, Jin XJ, Yang JK, Tang LD. Effects of Chinese Jianpi herbs on cell apoptosis and related gene expression in human gastric cancer grafted onto nude mice. *World J Gastroenterol* 2002; **8**: 792-796
- 13 **Lao SX**, Chen GX. The traditional Chinese medicine study of precancerous lesions of gastric cancer. *Shijie Huaren Xiaohua Zazhi* 2002; **10**: 1117-1120
- 14 **Kato I**, Tominaga S, Ito Y, Kobayashi S, Yoshii Y, Matsuura A, Kameya A, Kano T. A comparative case-control analysis of stomach cancer and atrophic gastritis. *Cancer Res* 1990; **50**: 6559-6564
- 15 **Beno I**, Sigmundova V. Nitrates and nitrites in gastric juice in chronic gastritis. *Bratisl Lek Listy* 1993; **94**: 531-535
- 16 **Sun LP**, Yuan Y. Determinations of plasma pepsinogen levels and its application to diagnosis and treatment of gastric cancer. *Shijie Huaren Xiaohua Zazhi* 2001; **9**: 1174-1176
- 17 **Hou P**, Tu ZX, Xu GM, Gong YF, Ji XH, Li ZS. *Helicobacter pylori* vacA genotypes and cagA status and their relationship to associated diseases. *World J Gastroenterol* 2000; **6**: 605-607
- 18 **Xiao XD**, Liu WZ. Treatment to infection of *Helicobacter pylori*. *Shijie Huaren Xiaohua Zazhi* 1999; **7**: 3-4
- 19 **Wang W**, Xia T, Zhang ZH. Effects of Yiweicongji Herbs on chronic atrophic gastritis and precancerous conditions. *Shijie Huaren Xiaohua Zazhi* 1999; **7**: 541-542
- 20 **Yao YL**, Zhang WD. Relationship between *Helicobacter pylori* and gastric cancer. *Shijie Huaren Xiaohua Zazhi* 2001; **9**: 1045-1049
- 21 **Shan ZW**. Present situation of study on infection of *Helicobacter pylori* and expectation of its treatment of the traditional Chinese medicine. *Shijie Huaren Xiaohua Zazhi* 1998; **6**: 553-554
- 22 **Ram F**, Dhar M. A modified procedure for calculating person years of life lost. *Janasamkhyā* 1992; **10**: 1-12
- 23 **Zhao ZT**. Research Method and Application of Epidemiology. 1st ed. Beijing: Science Publishing house, 2000:543-545
- 24 **Health Statistical Information Center**. The Annual Data of National Health in 1996. Beijing: Ministry of health China, 1997: 308-310
- 25 **Health Statistical Information Center**. The Annual Data of Na-

- tional Health in 1997. Beijing: Ministry of health China, 1998: 308-310
- 26 **Health Statistical Information Center.** The Annual Data of National Health in 1998. Beijing: Ministry of health China, 1999: 308-310
- 27 **Jin PH.** Medical Statistics. 1st ed. Shanghai: Publishing House of Shanghai Medical University 1993: 349, 203
- 28 **Chen JG,** Li WG, Liu B, Ye BF, Pan HB, Li SK, Chen DL. An epidemiological study on features of the distribution of cancer of some common sites. *Zhonghua Liuxingbingxue Zazhi* 1986; **7**: 193-199
- 29 **McNamara D,** O' Morain C. *Helicobacter pylori* and gastric cancer. *Ital J Gastroenterol Hepatol* 1998; **30** (Suppl): S294-298
- 30 **Sud R,** Wells D, Talbot IC, Delhanty JD. Genetic alterations in gastric cancers from British patients. *Cancer Genet Cytogenet* 2001; **126**: 111-119
- 31 **Chung YJ,** Park SW, Song JM, Lee KY, Seo EJ, Choi SW, Rhyu MG. Evidence of genetic progression in human gastric cancers with microsatellite instability. *Oncogene* 1997; **15**: 1719-1726
- 32 **Xia HX,** Fan XG, Talley NJ. Clarithromycin resistance in *Helicobacter pylori* and its clinical relevance. *World J Gastroenterol* 1999; **5**: 263-266
- 33 **Que FG,** Gores GJ. Cell death by apoptosis: basic concepts and disease relevance for the gastroenterologist. *Gastroenterology* 1996; **110**: 1238-1243
- 34 **Li XG,** Xie JY, Lu YY. Suppressive action of garlic oil on growth and differentiation of human gastric cancer cell line BGC-823. *Shijie Huaren Xiaohua Zazhi* 1998; **6**: 10-12
- 35 **Su Q,** Luo ZY, Teng H, Yin WD, Li YQ, He XE. Effect of garlic and garlic-green tea mixture on serum lipids in MNG-1-induced experimental gastric cancer and precancerous lesion. *Shijie Huaren Xiaohua Zazhi* 1998; **6**: 112-113
- 36 **Bajtai A,** Hidvegi J. The role of gastric mucosal dysplasia in the development of gastric cancer. *Pathol Oncol Res* 1998; **4**: 297-300
- 37 **You WC,** Zhang L, Gail MH, Li JY, Chang YS, Blot WJ, Zhao CL, Liu WD, Li HQ, Ma JL, Hu YR, Bravo JC, Correa P, Xu GW, Fraumeni JF Jr. Precancerous lesions in two counties of China with contrasting gastric cancer risk. *Int J Epidemiol* 1998; **27**: 945-948
- 38 **Tominaga K,** Koyama Y, Sasagawa M, Hiroki M, Nagai M. A case-control study of stomach cancer and its genesis in relation to alcohol consumption, smoking, and familial cancer history. *Jpn J Cancer Res* 1991; **82**: 974-979
- 39 **Pisani P,** Oliver WE, Parkin DM, Alvarez N, Vivas J. Case-control study of gastric cancer screening in Venezuela. *Br J Cancer* 1994; **69**: 1102-1105
- 40 **Yuan Y,** Gong W, Xu RT, Wang XJ, Gao H, Dong M, Wu HQ, Wang L, Wang MX, Song XJ, Wang FC, Jiang H, Song LY, Li X, Zhou BS, Zhang YC. Census Report of gastric cancer in Zhuanghe County, a high-risk area of gastric cancer. *Shijie Huaren Xiaohua Zazhi* 1998; **6**(Suppl 7): 478

Edited by Ren SY

Studies on microsatellite instability in p16 gene and expression of hMSH2 mRNA in human gastric cancer tissues

Qin-Xian Zhang, Yi Ding, Xiao-Ping Le, Peng Du

Qin-Xian Zhang, Yi Ding, Xiao-Ping Le, Molecular Cell Biology Research Center, Medical College of Zhengzhou University; Zhengzhou 450052, Henan Province, China

Peng Du, Henan Key Lab. of Molecular Medicine, Zhengzhou 450052, Henan Province, China

Supported by the National Natural Science Foundation of China, No. 39170440

Correspondence to: Pro. Qin-Xian Zhang, Molecular Cell Biology Research Center, Medical College of Zhengzhou University; 40 Daxue Lu, Zhengzhou 450052, Henan Province, China. qxz53@zzu.edu.cn

Telephone: +86-371-6977002 **Fax:** +86-371-6977002

Received: 2002-09-13 **Accepted:** 2002-10-29

Abstract

AIM: To detect the loss of heterozygosity (LOH) frequency of microsatellite sites D9s171, D9s1604 of p16 gene and expression of hMSH2 mRNA in various differentiated types of gastric cancer, adjacent cancer tissues and normal gastric mucosa.

METHODS: LOH was detected by polymerase chain reaction (PCR)-denaturing polyacrylamide gel electrophoresis-silver staining. The expression of hMSH2 mRNA was examined with *in situ* hybridization.

RESULTS: The frequency rate of LOH was significantly higher in gastric cancers than that in adjacent cancer tissues ($P=0.032$). No significant difference was noted among various differentiated types and various clinical stages of gastric cancers. The significantly reduced expression of hMSH2 mRNA positive signal cells exhibited in gastric cancers, in comparison with that in the adjacent cancer tissues and normal gastric mucosa, respectively ($P=0.001$). No significant difference was noted among various clinical stages of gastric cancers ($P>0.05$). The difference of positive signal cells in poorly differentiated cancers and those in well and moderately differentiated cancers were significant ($P<0.001$).

CONCLUSION: The frequencies of LOH in two microsatellite sites, D9s171 and D9s1604, in p16 genome were associated with development of gastric cancer and no significant correlation was demonstrated between the LOH frequency and the cell differentiated types of tumor cells or clinical stages. There was a positive relationship between the expression of hMSH2 mRNA and the differentiated types of gastric cancer.

Zhang QX, Ding Y, Le XP, Du P. Studies on microsatellite instability in p16 gene and expression of hMSH2 mRNA in human gastric cancer tissues. *World J Gastroenterol* 2003; 9(3): 437-441 <http://www.wjgnet.com/1007-9327/9/437.htm>

INTRODUCTION

Microsatellite instability (MI) occurs frequently adjacent to the loci of tumor suppressor genes^[1]. The defects of mismatch

repair (MMR) gene are closely related to the occurrence of MI and abnormality of genes^[2,3]. Expression of p16 gene was significantly reduced in gastric cancer^[4-12] and was associated with the progression and metastasis^[13,14]. The relationship between the MI of p16 gene in the gastric cancer and adjacent cancer tissue and the abnormal expression of MMR gene has rarely been reported. In this paper, two microsatellite loci, D9s171 and D9s1604 located at the upstream of p16 gene, were selected to study the loss of heterozygosity (LOH) of 9p21-22 region in gastric cancer tissues. The expression of hMSH2 mRNA in gastric cancer, adjacent cancer and normal gastric tissues was detected by *in situ* hybridization with hMSH2 oligonucleotide probe.

MATERIALS AND METHODS

Specimens

All the specimens were collected from the First and Second Affiliated Hospital of Medical College of Zhengzhou University and the People Hospital of Henan Province.

Specimens used to extract DNA: Specimens of gastric cancer tissue, adjacent cancer tissue and normal gastric mucosa were from each of 20 patients with gastric cancer. Of 20 patients, there were 4 cases with well differentiated and 16 moderately and poorly differentiated gastric cancer tissue. All specimens were used for isolation of DNA.

Specimens used *in situ* hybridization: gastric cancer specimens in 27 cases (including 20 cases gastric cancer specimens, with no history of radio- or chemotherapy preoperatively), adjacent cancer tissue specimens in 10 cases and normal gastric tissue specimens in 19 cases were used *in situ* hybridization. All the specimens were diagnosed pathologically (well differentiated in 5 cases, moderately 9 and poorly differentiated cancer 13). According to the PTNM of International Alliance of Anticancer in 1987, the specimens were divided into 4 clinical stages, the number in stage I, II, III and IV was 5, 10, 9 and 3, respectively.

Detection of microsatellite instability

The tissue DNA was extracted by routine phenol-chloroform method. The primers were synthesized by Shanghai Cell Biology Research Institute of China Scientific Institute and purified with PAGE. The sequence of primer was as follows, D9s171: 5' AGCTAAGTGAACCTCATCTCTGTCT3', 5' ACCCTAGCACTGATGGTATAGTCT3', and the length of amplified fragment was 159-177bp; D9s1604: 5' CCTGGGTCTCCAATTTGTCA3', 5' AGCACATGACACTGTGTGTG3', and the length of amplified fragment was 172-196bp. The annealing temperature of PCR was 60 °C and 50 °C, respectively. The PCR products were electrophoresized on 80 g/L denatured polyacrylamide gel under constant voltage of 30 V/cm. The gel was stained with silver staining after electrophoresis.

In situ hybridization

Digoxigenin-labeled hMSH2 oligonucleotide probe and BCIP/NBT staining system were used to demonstrate the expression

of hMSN2 mRNA. Control consisted of specimens pretreated with 0.05 g/L RNase A at 37 °C for 30 min, and specimens hybridized with hybridization buffer without probe.

Analysis of results

Compared with that of normal gastric mucosa removed from the same case, if the band of the identical allele disappeared or its intensity reduced over 50 %, the result was defined as LOH positive. Specimens *in situ* hybridization observed under microscope, the cells with cytoplasm containing bluish violet granules were determined as positive signal cells. Five fields in each specimen were checked randomly.

Statistic analysis

Data of electrophoretic specimens were analyzed using Fisher's exact test of probabilities with SPSS 10.0 statistic software. Correlative analysis were decided by using paired χ^2 test for numerical samples and $P < 0.05$ was considered as significant difference. *In situ* hybridization specimens were treated using one way analysis of variance and $P < 0.05$ was considered as different significantly.

RESULTS

Results of LOH at D9s171 and D9s 1604 of p16 gene in gastric cancer and adjacent cancer tissues (Figure 1 and 2)

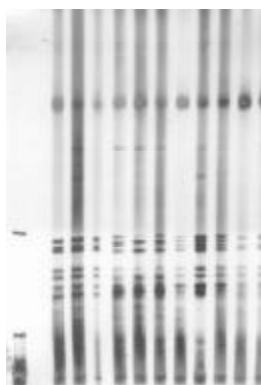


Figure 1 LOH of D9s171 in gastric cancer. Left 1: Marker Left 6: LOH(+).

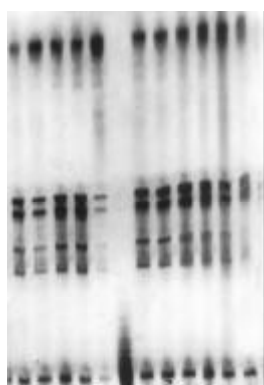


Figure 2 LOH of D9s1604 in gastric cancer. Left 6: LOH(+).

The number of LOH at D9s171 and D9s1604 in cancer tissues in 20 cases was 3 and 10, respectively, and that in adjacent cancer tissues was 2 and 4, respectively. There was no significant difference between the ratio of LOH at the two microsatellite loci. However, the combined ratio of LOH at the two microsatellite loci in gastric cancer tissues was obviously higher than that in adjacent cancer tissue ($P < 0.05$) (Table 1).

Table 1 LOH at D9s171 and D9s 1604 in gastric cancer and adjacent cancer tissue

	LOH(+)	LOH(-)	Total
Gastric cancer tissue	13	7	20
Adjacent cancer tissue	6	14	20
Total	19	21	40

^a $P < 0.05$ vs adjacent cancer tissue.

Relationship between the ratio of LOH and the differentiated type and clinical stage of gastric cancer

The difference of incidence of LOH at D9s1604 in well differentiated adenocarcinoma (1/4) and that in moderately and poorly differentiated cancer (10/16) was not significant ($P > 0.05$). The proportion of LOH in early stage and progressive stage of cancer was 50 % (4/8) and 58.2 (7/12), respectively.

Relationship between the LOH occurred at D9s171 and at D9s1604 in gastric cancer and adjacent cancer tissues

The incidence of LOH at D9s171 and D9s1604 were showed in Table 2. Analysis by paired χ^2 test for numerical sample showed that an intrinsic relation exhibits between them.

Table 2 Relation between LOH occurred at D9s171 and at D9s1604 in gastric cancer

D9s1604	D9s171		Total
	+	-	
+	4	10	14
-	1	25	26
Total	5	35	40

+: LOH (+); -: LOH (-); ^a $P < 0.05$ vs LOH (-).

Expression of hMSH2 mRNA in normal gastric mucosa, gastric cancer and adjacent cancer tissues

The *in situ* hybridization positive signals of hMSH2 mRNA appeared as bluish violet granules distributed in the cytoplasm. No positive signals were found in nucleus. There were round or irregular granules in positive cells in normal gastric tissues. The number of positive signal cells increased from the superficial to deep layer of mucosa. A few positive signal cells scattered in the submucosa and no positive signal cells in muscular layer (Figure 3). Expression of hMSH2 mRNA in gastric cancer and adjacent cancer tissues was significantly decreased than that in normal gastric tissues (Table 3). The positive signal cells mainly scattered in the deep layer of mucosa. No positive signal cells were found in the submucosa and muscular layer (Figure 4, 5).

Table 3 hMSH2 mRNA in the normal gastric mucosa, gastric cancer and adjacent cancer tissue ($\bar{x} \pm s$) (*In situ* hybridization)

	<i>n</i>	No. of positive cases (ratio)	No. of positive cells in each scope
Normal gastric mucosa	19	13(68.4 %)	175.8±26.4 ^a
Adjacent cancer tissue	10	6(60 %)	99.7±16.8 ^b
Gastric cancer tissue	27	20(74.1%)	42.1±25.9 ^c

^a $P < 0.01$ vs adjacent cancer tissue; ^b $P < 0.01$ vs gastric cancer tissue.

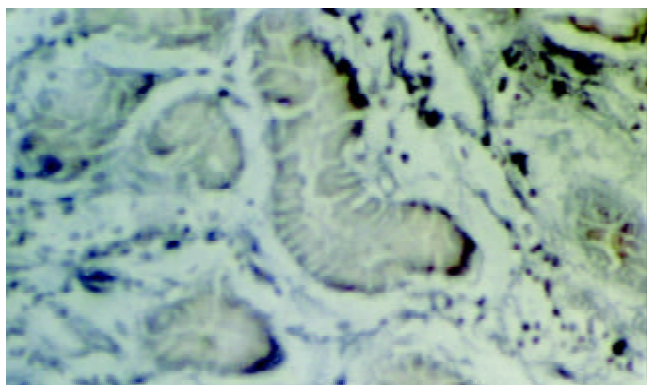


Figure 3 hMSH2 in normal gastric mucosa (×1000).

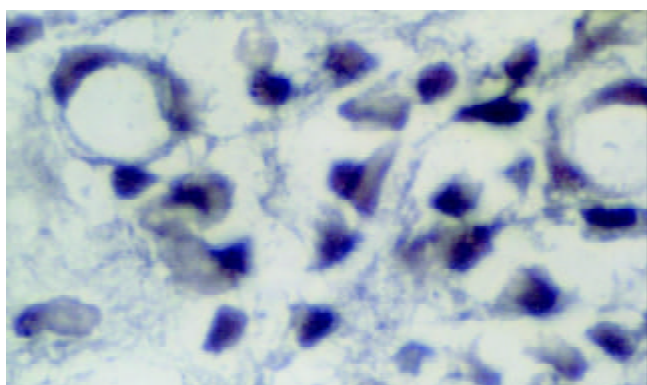


Figure 4 hMSH2 in adjacent gastric cancer tissue (×1000).

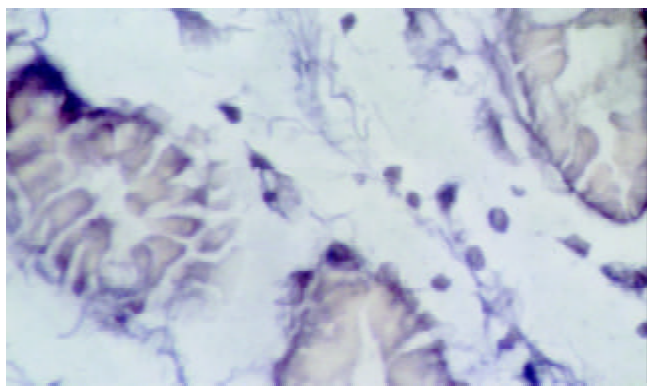


Figure 5 hMSH2 in gastric cancer tissue (×1000).

Expression of hMSH2 mRNA in various clinical stage of gastric cancer

Compared with that in the normal gastric tissue, the expression of hMSH2 mRNA in gastric cancer tissues was reduced significantly. However, there was no obvious difference in the number of positive cells among the various clinical stages of gastric cancer ($P>0.05$) (Table 4).

Table 4 hMSH2 mRNA in various clinical stage gastric cancer (In situ hybridization)

Clinical stage	n	No. of positive cases	No. of positive cells	F value	P value
I	5	4	62.8±25.4	2.495	0.097
II	10	8	46.3±24.4		
III	9	6	32.3±22.3		
IV	3	2	13.5±3.5		

Expression of hMSH2 mRNA in various differentiated types of gastric cancer

Compared with that in the normal gastric tissue, the expression of hMSH2 mRNA in gastric cancer tissue was decreased significantly ($P>0.05$). The number of positive signal cells differed among various differentiated types of gastric cancer. In poorly differentiated cancer tissue, the positive signal cells scattered in the middle and lower parts of mucosa, and the number of positive signal cells was smallest (Figure 6). There was a significant difference between the number of positive signal cells in the poorly differentiated gastric cancer tissue and that in the moderately and well differentiated gastric cancer tissue (Figure 7, 8).

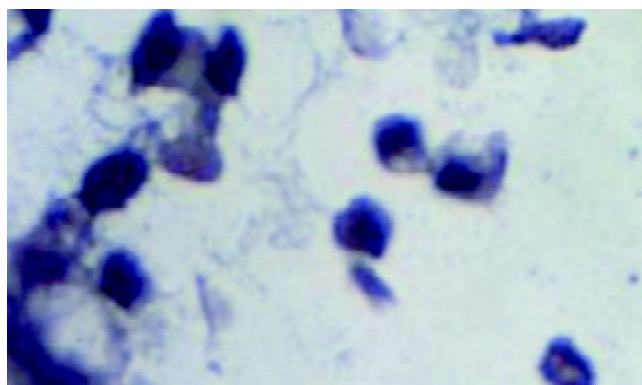


Figure 6 hMSH2 in poorly differentiated gastric cancer (×1000).

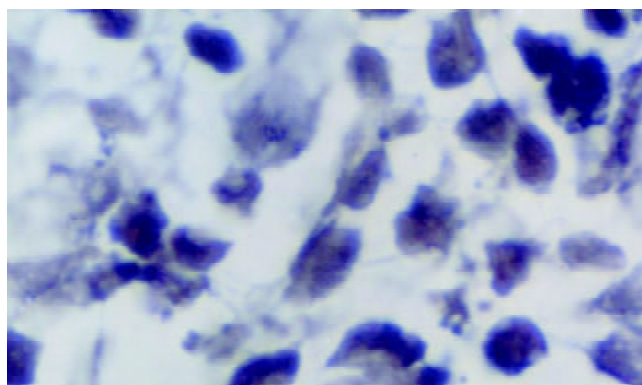


Figure 7 hMSH2 in moderately differentiated gastric cancer (×1000).

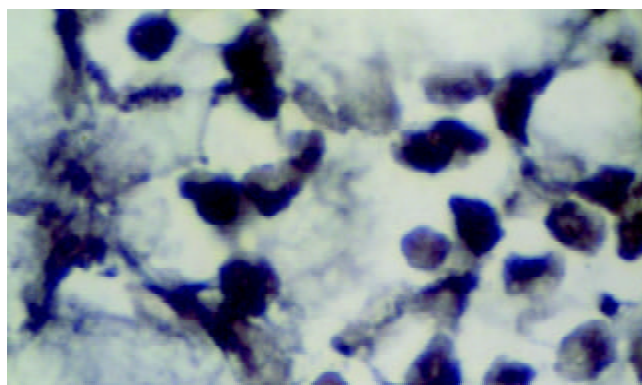


Figure 8 hMSH2 in well differentiated gastric cancer (×1000).

Negative reaction was showed in situ hybridization assay in control specimen.

DISCUSSION

Microsatellite instability of p16 gene

Microsatellite DNA is a genome-wide simple repeat sequence. Its normal length is shorter than 350bp, and the number of repeating is less than 60. The number of repeat unit of MI varied with individuals or tissues even in same body^[15]. MI varied in different kinds of cancer^[16-19]. In the gastric cancer tissues, MI was a frequent event, and the average frequency of MI was reported in different papers to be 33.9 %, 32.1 % and 25 %, respectively^[20-22]. The results showed that the LOH frequency of D9s171 and D9s1604 microsatellite loci, located at upstream of p16 gene, were 15 % and 50 %, respectively. The LOH frequency in well differentiated gastric cancer tissue was lower than that in the moderately and poorly differentiated gastric cancer tissue without significant difference ($P>0.05$). The relation of MI and the differentiation degree of gastric cancer has been not known clearly^[23,24].

It was showed that MI occurred at early stage of malignancy and gradually caused the formation of cancer^[25,26]. The results in this study showed that the LOH of microsatellite loci exhibited 50 % frequency at the early stage of gastric cancer, which suggested that the alteration of these loci might activate specific oncogenes and deactivate tumor suppressor genes, therefore, cause the development and progress of cancer. The alteration of microsatellite DNA normally appears as LOH. If LOH occurs frequently at the same locus of one chromosome in the tumor, the site of occurring LOH usually is the location of tumor suppressor gene^[27]. Through the analysis of the loci adjacent to p16 gene, small losses (<200bp) of p16 gene could be found in many kinds of cancer, which might be one of deactivation mechanisms of p16 gene. In this paper, two microsatellite loci were selected to demonstrate MI, D9s171 located at the site between the upstream of p16 gene and an adjacent tumor suppressor gene p15, D9s1604 located at the site between the exon 1 α and exon 1 β of p16 gene. LOH was detected at both D9s171 and D9s1604, and correlation between the occurrence of MI at the D9s171 and at the D9s1604 was existed, which suggested that occurrence of MI at the two loci might be related molecular event.

Expression of hMSH2 mRNA

Mismatch repair gene superfamily belongs to housekeeping genes, and is able to correct unmatched or mismatched bases in the process of DNA replication and DNA damage repairing, and control the accuracy of replication and recombination. Up to date, 6 human mismatch repair genes have been found, including 3 homologous of bacterial MutS (hMSH2, hMSH6 and hMSH3) and 3 homologous of bacterial MutL (hMSH1, hPMS1 and hPMS2). Loss of hMSH2 protein existed in the colonic and other cancer^[28-33] and genetic alterations in hMSH2 was observed in gastric cancer cell line^[34]. Loss of hMSH2 protein in the cancer tissue indicated that hMSH2 peptide or its coding mRNA was at an instable state. The number of the positive signal cells of hMSH2 mRNA in normal gastric mucosa, in adjacent cancer tissue, and in gastric cancer tissue was 175.8 \pm 26.4, 99.7 \pm 16.8 and 42.1 \pm 25.9, respectively. The number of positive signal cells was decreased significantly in adjacent cancer and gastric cancer tissue ($P<0.01$) No significant difference was found in the number of the positive signal cells of hMSH2 mRNA at various clinical stages in gastric cancer. A correlation might exist between the instability of gene expression and the development of gastric cancer. Tumor development is a multi-step process of somatic cell mutation and clonal amplification. With the hMSH2 (or other mismatch repair genes) mutation and the cell proliferation, the instability of genome occurred, and then the mutator acted selectively at the mutated site, caused enlargement of genome

instability in deepness and wideness, the accumulation of oncogene mutation was accelerated and caused the formation of tumor finally^[35].

Expression of hMSH2 protein in 115 bladder cancers was studied with immunohistochemistry^[36] and showed that low expression of hMSH2 protein exhibited in 25 % cases and complete loss in 2 cases. A closely correlation existed between the decrease of hMSH2 mRNA and the recurrence of poorly differentiated cancer. The results in this work showed that expression of hMSH2 mRNA significantly decreased in gastric cancer tissues, especially in moderately and poorly differentiated cancer ($P<0.05$). The results suggested that low expression of hMSH2 mRNA in poorly differentiated cancer might be related to the metastasis and prognosis of cancer. The lower the gastric cancer was differentiated, the more unstable the gene expression was. As the ratio of DNA mismatch increased, the instability of genome enhanced, tumor became more invasive and the prognosis got worse.

REFERENCES

- 1 **Yamamoto H**, Sawai H, Perucho M. Frameshift somatic mutation in gastrointestinal cancer of the microsatellite mutator phenotype. *Cancer Res* 1997; **57**: 4420-4426
- 2 **Fleisher AS**, Esteller M, Wang S, Tamura G, Suzuki H, Yin J, Zou TT, Abraham JM, Kong D, Smolinski KN, Shi YQ, Rhyu MG, Powell SM, James SP, Wilson KT, Herman JG, Meltzer SJ. Hypermethylation of the hMLH1 gene promoter in human gastric cancers with microsatellite instability. *Cancer Res* 1999; **59**: 1090-1095
- 3 **Kang YJ**, Wang LN, Zhang ZK. Microsatellite instability and DNA mismatch repair system. *Shijie Huaren Xiaohua Zazhi* 2000; **8**: 1139-1140
- 4 **Wang B**, Shi LC, Zhang WB, Xiao CM, Wu JF, Dong YM. Expression of tumor suppressor gene p16 in gastric cancer and precancerous lesions. *Shijie Huaren Xiaohua Zazhi* 2001; **9**: 39-42
- 5 **Zhou Y**, Gao SS, Li YX, Fan ZM, Zhao X, Qi YJ, Wei JP, Zou JX, Liu G, Jiao LH, Bai YM, Wang LD. Tumor suppressor gene p16 and Rb expression in gastric cardia precancerous lesions from subjects at a high incidence area in northern China. *World J Gastroenterol* 2002; **8**: 423-425
- 6 **He XS**, Su Q, Chen ZC, He XT, Long ZF, Ling H, Zhang LR. Expression, deletion and mutation of p16 gene in human gastric cancer. *World J Gastroenterol* 2001; **7**: 515-521
- 7 **Wei TY**, Wei MX, Yang SM. Expression of cyclin D1 P16 and Rb protein in gastric cancer. *Shijie Huaren Xiaohua Zazhi* 2000; **8**: 234-235
- 8 **Zhu ZY**, Tian X, Wang X, Yang XL. Mutation of p16 and APC gene in gastric cancer. *Shijie Huaren Xiaohua Zazhi* 2000; **8**: 1418-1419
- 9 **Yang SM**, Yang LS, Li L, Deng LY, Wang CY, Yuan XB, Shen XD. Methylation of MTS1/P16 gene and expression of P16 protein in gastric cancer. *Shijie Huaren Xiaohua Zazhi* 2000; **8**: 1427-1429
- 10 **Zhao Y**, Zhang XY, Shi XJ, Hu PZ, Zhang CS, Ma FC. Expression of P16, P53 and proliferating cell nuclear antigen in gastric cancer. *Shijie Huaren Xiaohua Zazhi* 1999; **7**: 246-248
- 11 **Li GX**, Li GQ, Zhao CZ, Xu GL. Relationship between telomerase hTERT and the expression of tumor suppressor gene p53 and p16. *Shijie Huaren Xiaohua Zazhi* 2002; **10**: 591-593
- 12 **Jiang YX**, Zhao MY, Geng M, Chao YC, Wang XY. Expression of P16, cerB-2 protein in gastric tumor. *Shijie Huaren Xiaohua Zazhi* 2002; **10**: 1050-1051
- 13 **Yang ZL**, Li YG, Huang YF, Wang QW. Expression of cyclin D1, CDK4, P16 and Rbin gastric cancer. *Shijie Huaren Xiaohua Zazhi* 2000; **8**: 362-363
- 14 **Wang GT**. Progression in the study on gastric precancerous lesions and its reversion. *Shijie Huaren Xiaohua Zazhi* 2000; **8**: 1-4
- 15 **Ji XL**. Microsatellite instability: New point in gene study. *Shijie Huaren Xiaohua Zazhi* 1999; **7**: 372-374
- 16 **Spanakis NE**, Gorgoulis V, Mariatos G, Zacharatos P, Kotsinas A, Garinis G, Trigidou R, Karameris A, Tsimare-Papastamatiou H, Kouloukousa M, Manolis EN, Kittas C. Aberrant p16 expression is correlated with homozygous deletions at the 9p21-23 chro-

- mosome region in non-small cell lung cancers. *Anticancer Res* 1999; **19**: 1893-1899
- 17 **Niederacher D**, Yan HY, An HY, Bender HG, Beckmann MW. CDKN2A gene inactivation in epithelial sporadic ovarian cancer. *Br J Cancer* 1999; **80**: 1920-1926
- 18 **Li M**, Zhang ZF, Reuter VE, Cordon-Cardo C. Chromosome 3 allelic losses and microsatellite alterations in transitional cell cancer of the urinary bladder. *Am J Pathol* 1996; **149**: 229-235
- 19 **Ionov Y**, Peinado MA, Malkhosyan S, Shibata D, Perucho M. Ubiquitous somatic mutations in simple repeated sequences reveal a new mechanism for colonic carcinogenesis. *Nature* 1993; **363**: 558-561
- 20 **Wang Y**, Ke Y, Ning T, Feng L, Lu G, Liu WEZ. Studies of microsatellite instability in Chinese gastric cancer tissue. *Zhonghua Yixue Yichanxue Zazhi* 1998; **15**: 155-157
- 21 **Fang DC**, Zhou XD, Luo YH, Wang DX, Lu R, Yang SM, Liu WW. Microsatellite instability and the loss of heterologous of tumor suppressor gene in gastric cancer. *Shijie Huaren Xiaohua Zazhi* 1999; **7**: 479-481
- 22 **Fang DC**, Luo YH, Yang SM, Li XA, Ling XL, Fang L. Mutation analysis of APC gene in gastric cancer with microsatellite instability. *World J Gastroenterol* 2002; **8**: 787-791
- 23 **Han HJ**, Yanagisawa A, Kato Y, Park JG, Nakamura Y. Genetic instability in pancreatic cancer and poorly differentiated type of gastric cancer. *Cancer Res* 1993; **53**: 5087-5089
- 24 **Lin JT**, Wu MS, Shun CT, Lee WJ, Wang JT, Wang TH, Sheu JC. Microsatellite instability in gastric cancer with special references to histopathology and cancer stages. *Eur J Cancer* 1995; **31A**: 1879-1882
- 25 **Wirtz HC**, Muller W, Noguchi T, Scheven M, Ruschoff J, Hommel G, Gabbert HE. Prognostic value and clinicopathological profile of microsatellite instability in gastric cancer. *Clin Cancer Res* 1998; **4**: 1749-1754
- 26 **Kim JJ**, Baek MJ, Kim L, Kim NG, Lee YC, Song SY, Noh SH, Kim H. Accumulated frameshift mutations at coding nucleotide repeats during the progression of gastric cancer with microsatellite instability. *Lab Invest* 1999; **79**: 1113-1120
- 27 **Weissenbach J**, Gyapay G, Dib C, Vignal A, Morissette J, Millasseau P, Vaysseix G, Lathrop M. A second generation linkage map of the human genome. *Nature* 1992; **359**: 794-801
- 28 **Jass JR**, Iino H, Ruszkiewicz A, Painter D, Solomon MJ, Koorey DJ, Cohn D, Furlong KL, Walsh MD, Palazzo J, Edmonston TB, Fishel R, Young J, Leggett BA. Neoplastic progression occurs through mutator pathways in hyperplastic polyposis of colorectum. *Gut* 2000; **47**: 43-49
- 29 **Borresen AL**, Lothe RA, Meling GI, Lystad S, Morrison P, Lipford J, Kane MF, Rognum TO, Kolodner RD. Somatic mutation in the hMSH2 gene in microsatellite unstable colorectal cancers. *Hum Mol Genet* 1995; **4**: 2065-2072
- 30 **Bock N**, Meden H, Regenbrecht M, Junemann B, Wangerin J, Marx D. Expression of the mismatch repair protein hMSH2 in cancer in situ and invasive cancer of the breast. *Anticancer Res* 2000; **20**: 119-124
- 31 **Leach FS**, Hsieh JT, Molberg K, Saboorian MH, McConnell JD, Sagalowsky AI. Expression of the human mismatch repair gene hMSH2: a potential marker for urothelial malignancy. *Cancer* 2000; **88**: 2333-2341
- 32 **Parc YR**, Halling KC, Burgart LJ, McDonnell SK, Schaid DJ, Thibodeau SN, Halling AC. Microsatellite instability and hMLH1/hMSH2 expression in young endometrial cancer patients: associations with family history and histopathology. *Int J Cancer* 2000; **86**: 60-66
- 33 **Chen HC**, Bhattacharyya N, Wang L, Recupero AJ, Klein EA, Harter ML, Banerjee S. Defective DNA repair genes in a primary culture of human renal cell cancer. *J Cancer Res Clin Oncol* 2000; **126**: 185-190
- 34 **Shin KH**, Park JG. Microsatellite instability is associated with genetic alteration but not with low levels of expression of the human mismatch repair proteins hMSH2 and hMLH1. *Eur J Cancer* 2000; **36**: 925-931
- 35 **Perucho M**. Microsatellite instability: the mutator that mutates the other mutator. *Nat Med* 1996; **2**: 630-631
- 36 **Jin TX**, Furihata M, Yamasaki I, Kamada M, Liang SB, Ohtsuki Y, Shuin T. Human mismatch repair gene (hMSH2) product expression in relation to recurrence of transitional cell cancer of the urinary bladder. *Cancer* 1999; **85**: 478-484

Paclitaxel induces apoptosis in human gastric carcinoma cells

Hai-Bo Zhou, Ju-Ren Zhu

Hai-Bo Zhou, Ju-Ren Zhu, Department Of Gastroenterology, Shandong Provincial Hospital, Jinan 250052, Shandong Province, China

Correspondence to: Dr. Hai-Bo Zhou, Department Of Gastroenterology, Shandong Provincial Hospital, Jinan 250052, Shandong Province, China. zhouhbyy@fm365.com.cn

Telephone: +86-531-2603194

Received: 2002-08-03 **Accepted:** 2002-11-21

Abstract

AIM: To investigate the apoptosis in gastric cancer cells induced by paclitaxel, and the relation between this apoptosis and expression of Bcl-2 and Bax.

METHODS: In *in vitro* experiments, MTT assay was used to determine the cell growth inhibitory rate. Transmission electron microscope and TUNEL staining method were used to quantitatively and qualitatively detect the apoptosis status of gastric cancer cell line SGC-7901 before and after the paclitaxel treatment. Immunohistochemical staining was used to detect the expression of apoptosis-regulated gene Bcl-2 and Bax.

RESULTS: Paclitaxel inhibited the growth of gastric cancer cell line SGC-7901 in a dose- and time-dependent manner. Paclitaxel induced SGC-7901 cells to undergo apoptosis with typically apoptotic characteristics, including morphological changes of chromatin condensation, chromatin crescent formation, nucleus fragmentation and apoptotic body formation. Paclitaxel could reduce the expression of apoptosis-regulated gene Bcl-2, and improve the expression of apoptosis-regulated gene Bax.

CONCLUSION: Paclitaxel is able to induce the apoptosis in gastric cancer. This apoptosis may be mediated by down-expression of apoptosis-regulated gene Bcl-2 and up-expression of apoptosis-regulated gene Bax.

Zhou HB, Zhu JR. Paclitaxel induces apoptosis in human gastric carcinoma cells. *World J Gastroenterol* 2003; 9(3): 442-445
<http://www.wjgnet.com/1007-9327/9/442.htm>

INTRODUCTION

Apoptosis is a form of cell death characterized by active cellular suicide during T-cell clonal deletion, embryogenesis, and DNA damage. Apoptotic cell death is often associated with distinctive characteristics, such as nuclear fragmentation, cytoplasmic blebbing, and internucleosomal fragmentation of DNA. Whether a cell committed to apoptosis partly depends upon the balance between proteins that mediate cell death, such as Bax, and proteins that promote cell viability, such as Bcl-2 or Bcl-xl. Overexpression of Bax has been shown to accelerate the cell death. Overexpression of antiapoptotic proteins such as Bcl-2 represses the death function of Bax. Thus, the ratio of Bcl-2 to Bax appears to be a critical determinant of a cell's threshold for undergoing apoptosis.

Microtubule inhibitors such as paclitaxel can increase tubulin polymerization, tubulin bundling, and cell cycle arrest.

Paclitaxel have been proven to induce apoptosis in many cancers. In order to study the mechanism of paclitaxel induces apoptosis of SGC-7901 gastric cancer cells, MTT assay was used to determine the cell growth inhibitory rate. Transmission electron microscope and TUNEL staining method were used to quantitatively and qualitatively detect the apoptosis status of gastric cancer cell line SGC-7901 before and after the paclitaxel treatment. Immunohistochemical staining was used to detect the expression of apoptosis-regulated gene Bcl-2 and Bax.

We report here the results of our findings showing paclitaxel inhibited the growth of gastric cancer cell line SGC-7901 in a dose- and time-dependent manner. Paclitaxel induced SGC-7901 cells to undergo apoptosis with typically apoptotic characteristics, including morphological changes of chromatin condensation, chromatin crescent formation, nucleus fragmentation and apoptotic body formation. Paclitaxel reduces Bcl-2 expression and improves Bax expression on SGC-7901 cells.

MATERIALS AND METHODS

Materials

Paclitaxel was obtained from Xiehe Pharmaceutical Factory in Beijing. MTT was obtained from Sigma Chemical Co. Ltd. Anti-Bcl-2 monoclonal antibody and anti-Bax monoclonal antibody were purchased from Beijing Zhongshan biotechnology Co. Ltd.

Methods

Cell culture Human gastric carcinoma cell line SGC-7901 was obtained from laboratory in Shandong Provincial Hospital and maintained in RPMI 1640 supplemented with 100 ml·L⁻¹ fetal bovine serum, 100 kU·L⁻¹ penicillin, 100 mg·L⁻¹ streptomycin and 2 μmol·L⁻¹ L-glutamine under 50 ml·L⁻¹ CO₂ in a humidified incubator at 37 °C. SGC-7901 cells were incubated for different time periods in the presence of paclitaxel at 0.001, 0.01, 0.1, 1 μmol·L⁻¹.

MTT assay 1×10⁵ cells/well in a 96-well plate after 24 hours incubation were treated with increasing concentrations of paclitaxel (0.001 μmol·L⁻¹ to 1 μmol·L⁻¹) for 24 to 96 hours. 10 μL of 5 g·L⁻¹ of MTT was added to the cells in every well and incubated for 4 hours at 37 °C. Culture media were discarded followed by addition of 0.2 ml of DMSO and vibration for 10 minutes. The absorbance (OD) was measured at 570 nm using a microplate reader. The cell growth inhibitory rate was calculated as follows: (OD of control group - OD of experimental group) / (OD of control group - OD of blank group) × 100 %.

Transmission electron microscopy The cells treated with 0.1 μmol·L⁻¹ paclitaxel were trypsinized and harvested after 24 hours. Subsequently the cells were fixed in 4 % glutaral and immersed with Epon 821, imbedded in capsules and converged for 72 hours at 60 °C, the cells were prepared into ultrathin section (60 nm) and stained with uranyl acetate and lead citrate. Cell morphology was examined by transmission electron microscopy.

TUNEL assay Apoptosis of SGC-7901 cells was evaluated by using an *in situ* cell detection kit (Beijing Zhongshan biotechnology Co. Ltd). The cells were treated in the presence or absence of 0.1 μmol·L⁻¹ paclitaxel for 24 to 96 hours and fixed in ice-cold 80 % ethanol for up to 24 hours, treated with proteinase K and then 0.3 % H₂O₂, labeled with fluorescein

dUTP in a humid box for 1 hour at 37 °C. The cells were then combined with POD-Horseradish peroxidase, colorized with DAB. Controls consisted of omission of fluorescein dUTP. Cells were visualized with light microscope. The Apoptotic Index (AI) was calculated as follows: $AI = (\text{Number of apoptotic cells} / \text{Total number}) \times 100\%$.

Immunohistochemical staining Immunohistochemical staining was accomplished utilizing an avidinbiotin technique. SGC-7901 cells treated in the presence or absence of 0.1 $\mu\text{mol} \cdot \text{L}^{-1}$ paclitaxel for 24 to 96 hours were grown on six-well glass slides and fixed in acetone. After washing in PBS, the cells were incubated in 0.3% H_2O_2 solution at room temperature for 5 minutes. The cells then were incubated with anti-Bcl-2 or anti-Bax at a 1:300 dilution at 4 °C overnight. Following washing in PBS, the second antibody, biotinylated antirat Ig G, was added and the cells were incubated at room temperature for 1 hour. After washing in PBS, ABC compound was added and then incubated at room temperature for 10 minutes. DAB was used as the chromagen. After ten minutes, the brown color signifying the presence of antigen bound to antibodies was detected by light microscopy and photographed at $\times 200$. Controls consisted of omission of the primary antibody. The Positive Rate (PR) was calculated as follows: $PR = (\text{Number of positive cells} / \text{Total number}) \times 100\%$.

Statistical analysis

Data were analyzed employing the paired two-tailed Student *t* test, and significance was assumed at $P < 0.05$.

RESULTS

MTT assay

SGC-7901 cells were exposed to increasing concentrations (0.001 $\mu\text{mol} \cdot \text{L}^{-1}$ to 1 $\mu\text{mol} \cdot \text{L}^{-1}$) of commercially available paclitaxel for 24 to 96 hours. Our results show a dose- and time-dependent increase in tumor cell mortality. The data were summarised in Table 1.

Table 1 The inhibitory effect of paclitaxel on SGC-7901 cells (inhibitory rate, %)

Time(h)	RPMI-1640	Paclitaxel ($\text{mmol} \cdot \text{L}^{-1}$)			
		0.1	1	10	100
24	0.0	9.6 ^b	18.8 ^d	22.8 ^d	34.3 ^d
48	0.0	17.5 ^d	21.6 ^d	36.4 ^d	45.4 ^d
72	0.0	23.8 ^d	37.3 ^d	47.6 ^d	58.9 ^d
96	0.0	35.6 ^d	44.7 ^d	57.6 ^d	87.8 ^d

^b $P < 0.01$, ^d $P < 0.001$ vs the control group.

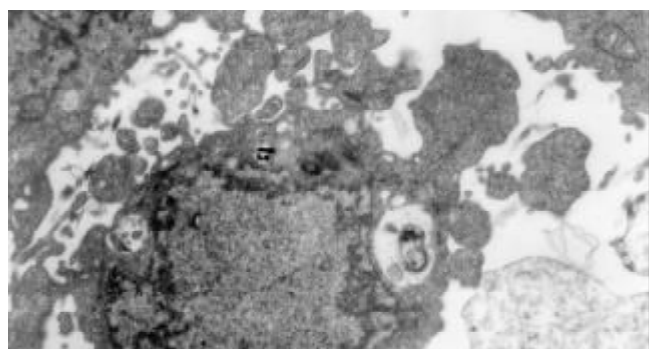


Figure 1 Paclitaxel-induced apoptosis in SGC-7901 cells with Transmission Electron Microscope Apoptotic cell with chromatin condensation, chromatin crescent formation, nucleus fragmentation ($\times 4000$).

Morphological changes

After treatment of SGC-7901 cells with paclitaxel (0.1 $\mu\text{mol} \cdot \text{L}^{-1}$) for 24 hours, some cells appeared apoptotic characteristics including chromatin condensation, chromatin crescent formation, nucleus fragmentation and apoptotic body formation were seen by transmission electron microscope (Figure 1).

TUNEL assay

Positive staining located in the nucleus (Figure 2). The results showed after treatment of SGC-7901 cells with paclitaxel (0.1 $\mu\text{mol} \cdot \text{L}^{-1}$) for 24 to 96 hours, the AIs were apparently increased with treat time ($P < 0.05$) (Table 2).



Figure 2 Apoptotic cells induced by paclitaxel with TUNEL assay ($\times 200$)

Table 2 Apoptotic Index (AI) of treated SGC-7901 cells by paclitaxel

Time(h)	AI(%)
0	1.43 \pm 2.42
24	4.89 \pm 2.63 ^b
48	16.34 \pm 1.85 ^b
72	27.86 \pm 3.23 ^d
96	36.49 \pm 3.95 ^d

^b $P < 0.05$, ^d $P < 0.01$ vs the control group.

Expression of Bcl-2 proteins

Positive staining located in the cytoplasm. The results showed after treatment of SGC-7901 cells with paclitaxel (0.1 $\mu\text{mol} \cdot \text{L}^{-1}$) for 24 to 96 hours, the PRs of Bcl-2 proteins were apparently reduced with treat time ($P < 0.05$) (Table 3). This suggested paclitaxel could reduce Bcl-2 expression.

Table 3 Positive Rate of Bcl-2 on treated SGC-7901 cells by paclitaxel

Time(h)	PT(%)
0	35.44 \pm 3.86
24	20.50 \pm 2.71 ^b
48	10.66 \pm 2.36 ^b
72	6.78 \pm 1.65 ^d
96	3.98 \pm 1.34 ^d

^b $P < 0.05$, ^d $P < 0.01$ vs the control group.

Expression of bax proteins

Positive staining located in the cytoplasm. The results showed after treatment of SGC-7901 cells with paclitaxel (0.1 $\mu\text{mol} \cdot \text{L}^{-1}$) for 24 to 96 hours, the PRs of Bax proteins were apparently improved with treat time ($P < 0.05$) (Table 4). This suggested paclitaxel could improve Bcl-2 expression.

Table 4 Positive Rate of Bax on treated SGC-7901 cells by paclitaxel

Time(h)	PT(%)
0	10.27±2.19
24	19.68±2.64 ^b
48	30.57±3.76 ^b
72	41.28±6.14 ^b
96	59.98±6.25 ^b

^b $P < 0.05$ vs the control group.

DISCUSSION

Apoptosis is a form of cell death characterized by active cellular suicide during T-cell clonal deletion, embryogenesis, and DNA damage. Apoptotic cell death is often associated with distinctive characteristics, such as nuclear fragmentation, cytoplasmic blebbing, and internucleosomal fragmentation of DNA^[1-6]. The Bcl-2 family plays a central role in the control of apoptosis. The family includes a number of proteins which have amino acid sequence homology, including anti-apoptotic members such as Bcl-2 and Bcl-x_L, as well as pro-apoptotic members including Bax and Bad^[7-10]. Overexpression of Bax has been shown to accelerate the cell death^[11-15]. Conversely, Overexpression of antiapoptotic proteins such as Bcl-2 represses the death function of Bax^[16-20]. Thus, the ratio of Bcl-2 to Bax appears to be a critical determinant of a cell's threshold for undergoing apoptosis^[21].

Microtubule inhibitors such as paclitaxel can increase tubulin polymerization, tubulin bundling, and cell cycle arrest^[22-24]. Paclitaxel have been proven to induce apoptosis in many cancers^[25-37]. In order to study the mechanism of paclitaxel induces apoptosis of SGC-7901 gastric cancer cells, MTT assay was used to determine the cell growth inhibitory rate. Transmission electron microscope and TUNEL staining method were used to quantitatively and qualitatively detect the apoptosis status of SGC-7901 gastric cancer cell before and after the paclitaxel treatment. Immunohistochemical staining was used to detect the expression of apoptosis-regulated gene Bcl-2 and Bax.

In the present study, MTT assay was used to observe the effect of paclitaxel on the growth of SGC-7901 gastric carcinoma cells *in vitro*, indicating that the drug could inhibit the the growth of gastric carcinoma cells. Our results show a dose- and time-dependent increase in tumor cell mortality. Its concentration- and time-effect relationships were significant. TUNEL assay showed after treatment of SGC-7901 cells with paclitaxel (0.1 $\mu\text{mol} \cdot \text{L}^{-1}$) for 24 to 96 hours, the AIs were apparently increased with treat time ($P < 0.05$). Immunohistochemical staining was used to detect the expression of Bcl-2 proteins and Bax proteins. The results showed after treatment of SGC-7901 cells with paclitaxel (0.1 $\mu\text{mol} \cdot \text{L}^{-1}$) for 24 to 96 hours, the PRs of Bcl-2 proteins were apparently reduced with treat time ($P < 0.05$), but the PRs of Bax proteins were apparently improved with treat time ($P < 0.05$). These suggested paclitaxel could reduce Bcl-2 expression and improve Bcl-2 expression. The ratio of Bcl-2 to Bax was decreased. The decreased ratio could trigger the apoptosis of SGC-7901 cells.

The research in our laboratory demonstrated paclitaxel is able to induce the apoptosis in gastric cancer. This apoptosis may be mediated by down-expression of apoptosis-regulated gene Bcl-2 and up-expression of apoptosis-regulated gene Bax. The mechanism of Paclitaxel as a chemotherapeutic drug in anti-gastric carcinoma chemotherapy should be further studied.

REFERENCES

- 1 **Manygoats KR**, Yazzie M, Stearns DM. Ultrastructural damage in chromium picolinate-treated cells: a TEM study. *J Biol Inorg Chem* 2002; **7**: 791-798
- 2 **Gu Y**, Zeng S, Qiu P, Peng D, Yan G. Apoptosis of bovine trabecular meshwork cells induced by dexamethasone. *Chung Hua Yen Ko Tsa Chih* 2002; **38**: 302-304
- 3 **Fidzianska A**. Suicide muscle cell programme-apoptosis. Ultrastructural study. *Folia Neuropathol* 2002; **40**: 27-32
- 4 **Narayanan S**, Stewart GC, Chengappa MM, Willard L, Shuman W, Wilkerson M, Nagaraja TG. Fusobacterium necrophorum Leukotoxin Induces Activation and Apoptosis of Bovine Leukocytes. *Infect Immun* 2002; **70**: 4609-4620
- 5 **Dini L**, Pagliara P, Carla EC. Phagocytosis of apoptotic cells by liver: a morphological study. *Microsc Res Tech* 2002; **57**: 530-540
- 6 **Mathiasen IS**, Sergeev IN, Bastholm L, Elling F, Norman AW, Jaattela M. Calcium and calpain as key mediators of apoptosis-like death induced by vitamin D compounds in breast cancer cells. *J Biol Chem* 2002; **277**: 30738-30745
- 7 **Konopleva M**, Konoplev S, Hu W, Zaritsky AY, Afanasiev BV, Andreeff M. Stromal cells prevent apoptosis of AML cells by up-regulation of anti-apoptotic proteins. *Leukemia* 2002; **16**: 1713-1724
- 8 **Van Der Woude CJ**, Jansen PL, Tiebosch AT, Beuving A, Homan M, Kleibeuker JH, Moshage H. Expression of apoptosis-related proteins in Barrett's metaplasia-dysplasia-carcinoma sequence: A switch to a more resistant phenotype. *Hum Pathol* 2002; **33**: 686-692
- 9 **Panaretakis T**, Pokrovskaja K, Shoshan MC, Grandier D. Activation of Bak, Bax and BH3-only proteins in the apoptotic response to doxorubicin. *J Biol Chem* 2002; [epub ahead of print]
- 10 **Bellosillo B**, Villamor N, Lopez-Guillermo A, Marce S, Bosch F, Campo E, Montserrat E, Colomer D. Spontaneous and drug-induced apoptosis is mediated by conformational changes of Bax and Bak in B-cell chronic lymphocytic leukemia. *Blood* 2002; **100**: 1810-1816
- 11 **Matter-Reissmann UB**, Forte P, Schneider MK, Filgueira L, Groscurth P, Seebach JD. Xenogeneic human NK cytotoxicity against porcine endothelial cells is perforin/granzyme B dependent and not inhibited by Bcl-2 overexpression. *Xenotransplantation* 2002; **9**: 325-337
- 12 **Lanzi C**, Cassinelli G, Cuccuru G, Supino R, Zuco V, Ferlini C, Scambia G, Zunino F. Cell cycle checkpoint efficiency and cellular response to paclitaxel in prostate cancer cells. *Prostate* 2001; **48**: 254-264
- 13 **Mertens HJ**, Heineman MJ, Evers JL. The expression of apoptosis-related proteins bcl-2 and ki67 in endometrium of ovulatory menstrual cycles. *Gynecol Obstet Invest* 2002; **53**: 224-230
- 14 **Mehta U**, Kang BP, Bansal G, Bansal MP. Studies of apoptosis and bcl-2 in experimental atherosclerosis in rabbit and influence of selenium supplementation. *Gen Physiol Biophys* 2002; **21**: 15-29
- 15 **Chang W**, Yang K, Chuang H, Jan J, Shaio M. Glutamine protects activated human T cells from apoptosis by up-regulating glutathione and bcl-2 levels. *Clin Immunol* 2002; **104**: 151
- 16 **Chen GG**, Lai PB, Hu X, Lam IK, Chak EC, Chun YS, Lau WY. Negative correlation between the ratio of Bax to Bcl-2 and the size of tumor treated by culture supernatants from Kupffer cells. *Clin Exp Metastasis* 2002; **19**: 457-464
- 17 **Usuda J**, Chiu SM, Azizuddin K, Xue LY, Lam M, Nieminen AL, Oleinick NL. Promotion of photodynamic therapy-induced apoptosis by the mitochondrial protein Smac/DIABLO: dependence on Bax. *Photochem Photobiol* 2002; **76**: 217-223
- 18 **Sun F**, Akazawa S, Sugahara K, Kamihira S, Kawasaki E, Eguchi K, Koji T. Apoptosis in normal rat embryo tissues during early organogenesis: the possible involvement of Bax and Bcl-2. *Arch Histol Cytol* 2002; **65**: 145-157
- 19 **Jang M**, Shin M, Shin H, Kim K, Park H, Kim E, Kim C. Alcohol induces apoptosis in TM3 mouse Leydig cells via bax-dependent caspase-3 activation. *Eur J Pharmacol* 2002; **449**: 39
- 20 **Tilli CM**, Stavast-Koey AJ, Ramaekers FC, Neumann HA. Bax expression and growth behavior of basal cell carcinomas. *J Cutan Pathol* 2002; **29**: 79-87
- 21 **Pettersson F**, Dalgleish AG, Bissonnette RP, Colston KW. Retinoids cause apoptosis in pancreatic cancer cells via activation of RAR-gamma and altered expression of Bcl-2/Bax. *Br J*

- Cancer* 2002; **87**: 555-561
- 22 **Demaria S**, Volm MD, Shapiro RL, Yee HT, Oratz R, Formenti SC, Muggia F, Symmans WF. Development of tumor-infiltrating lymphocytes in breast cancer after neoadjuvant paclitaxel chemotherapy. *Clin Cancer Res* 2001; **7**: 3025-3030
- 23 **Oyaizu H**, Adachi Y, Okumura T, Okigaki M, Oyaizu N, Taketani S, Ikebukuro K, Fukuhara S, Ikehara S. Proteasome inhibitor 1 enhances paclitaxel-induced apoptosis in human lung adenocarcinoma cell line. *Oncol Rep* 2001; **8**: 825-829
- 24 **Charles AG**, Han TY, Liu YY, Hansen N, Giuliano AE, Cabot MC. Taxol-induced ceramide generation and apoptosis in human breast cancer cells. *Cancer Chemother Pharmacol* 2001; **47**: 444-450
- 25 **Zhou J**, Gupta K, Yao J, Ye K, Panda D, Giannakakou P, Joshi HC. Paclitaxel-resistant human ovarian cancer cells undergo c-Jun NH2-terminal kinase-mediated apoptosis in response to noscaphine. *J Biol Chem* 2002; [epub ahead of print]
- 26 **Li Y**, Shi T, Zhao W. The mechanism of docetaxel-induced apoptosis in human lung cancer cells. *Zhonghua Zhongliu Zazhi* 2000; **22**: 208-211
- 27 **Fowler CA**, Perks CM, Newcomb PV, Savage PB, Farndon JR, Holly JM. Insulin-like growth factor binding protein-3 (IGFBP-3) potentiates paclitaxel-induced apoptosis in human breast cancer cells. *Int J Cancer* 2000; **88**: 448-453
- 28 **Makino K**, Yu D, Hung MC. Transcriptional upregulation and activation of p55Cdc via p34 (cdc2) in Taxol-induced apoptosis. *Oncogene* 2001; **20**: 2537-2543
- 29 **Yu C**, Wang S, Dent P, Grant S. Sequence-dependent potentiation of paclitaxel-mediated apoptosis in human leukemia cells by inhibitors of the mitogen-activated protein kinase/ mitogen-activated protein kinase pathway. *Mol Pharmacol* 2001; **60**: 143-154
- 30 **Cheng SC**, Luo D, Xie Y. Taxol induced Bcl-2 protein phosphorylation in human hepatocellular carcinoma QGY-7703 cell line. *Cell Biol Int* 2001; **25**: 261-265
- 31 **Odoux C**, Albers A, Amoscato AA, Lotze MT, Wong MK. TRAIL, FasL and a blocking anti-DR5 antibody augment paclitaxel-induced apoptosis in human non-small-cell lung cancer. *Int J Cancer* 2002; **97**: 458-465
- 32 **Huisman C**, Ferreira CG, Broker LE, Rodriguez JA, Smit EF, Postmus PE, Kruyt FA, Giaccone G. Paclitaxel triggers cell death primarily via caspase-independent routes in the non-small cell lung cancer cell line NCI-H460. *Clin Cancer Res* 2002; **8**: 596-606
- 33 **Hu L**, Hofmann J, Lu Y, Mills GB, Jaffe RB. Inhibition of phosphatidylinositol 3'-kinase increases efficacy of paclitaxel in *in vitro* and *in vivo* ovarian cancer models. *Cancer Res* 2002; **62**: 1087-1092
- 34 **Carre M**, Carles G, Andre N, Douillard S, Ciccolini J, Briand C, Braguer D. Involvement of microtubules and mitochondria in the antagonism of arsenic trioxide on paclitaxel-induced apoptosis. *Biochem Pharmacol* 2002; **63**: 1831-1842
- 35 **Peng WD**, Zhang J, Hui HX, Xu YM, Zhu F, Yang AG, Wang CJ. Upregulation of bax Gene Expression Promotes Paclitaxel-induced Apoptosis in Esophageal Carcinoma Cells. *Shengwu Huaxue Yusheng Wuwuli Xuebao (Shanghai)* 2000; **32**: 356-358
- 36 **Bacus SS**, Gudkov AV, Lowe M, Lyass L, Yung Y, Komarov AP, Keyomarsi K, Yarden Y, Seger R. Taxol-induced apoptosis depends on MAP kinase pathways (ERK and p38) and is independent of p53. *Oncogene* 2001; **20**: 147-155
- 37 **Qin YC**, Qi YQ, Si JL, Lin J, Zhu JR, Liu JY. Paclitaxel induces apoptosis in human gastric cancer cells and influences on the activity of telomerase *in vitro*. *Shijie Huaren Xiaohua Zazhi* 2001; **9**: 1086-1087

Edited by Ren SY

Protective effect of ascorbic acid in experimental gastric cancer: reduction of oxidative stress

Claudia P.M.S.Oliveira, Paulo Kassab, Fabio P. Lopasso, Heraldo P. Souza, Mariano Janiszewski, Francisco R. M. Laurindo, Kioshi Iriya, Antonio A. Laudanna

Claudia P.M.S.Oliveira, Paulo Kassab, Fabio P.Lopasso, Antonio A. Laudanna, Department of Gastroenterology of Medical School of University of São Paulo (USP), São Paulo, Brazil

Heraldo P. Souza, Mariano Janiszewski, Department of Emergency Medicine of Medical School of University of São Paulo (USP), São Paulo, Brazil

Francisco R. M. Laurindo, Heart Institute of Medical School of University of São Paulo (USP), São Paulo, Brazil

Kioshi Iriya, Department of Pathology of Medical School of University of São Paulo (USP), São Paulo, Brazil

Correspondence to: Claudia P.M.S.Oliveira, M.D., Department of Gastroenterology School of Med. of University of São Paulo, Av. Dr Enéas de Carvalho Aguiar n° 255, Instituto Central 9th Floor, 9159, 05403000 São Paulo, Brazil. mauclaud@uol.com.br

Telephone: +55-11-30696447 **Fax:** +55-11-3082-7599

Received: 2002-03-13 **Accepted:** 2002-04-06

Abstract

AIM: Oxidative stress participates in the cell carcinogenesis by inducing DNA mutations. Our aim was to assess whether ascorbic acid, an antioxidant, could have a role in preventing ROS (Reactive Oxygen Species) generation in experimental gastric carcinoma in a rat model.

METHODS: Experimental gastric cancer was induced in twelve Wistar male rats (weighting 250-350 g) by profound duodeno-gastric reflux through split gastrojejunostomy. The rats were allocated to the following groups: Group I ($n=6$) was the control; Group II ($n=6$) which was maintained with daily intake of tap water with Vitamin C (30 mg/Kg). After 6 or 12 months, samples of gastric tumor or non tumor mucosa were taken from the anastomosis of both groups. Oxidative stress was measured by superoxide quantification through lucigenin-amplified chemiluminescence base and by staining with Nitrobluetetrazolium. The histopathologic confirmation of adenocarcinoma was made by eosin-hematoxylin method.

RESULTS: The intestinal type of gastric adenocarcinoma was microscopically identified in all animals of group I whereas only 3 rats of group II showed an adenocarcinoma without macroscopic evidence of them. The cancers were located in the anastomosis in all cases. Basal luminescence from tumor gastric tissue generated 38.4 ± 6.8 count per minute/mg/ $\times 10^6$ (mean \pm SD) and 14.9 ± 4.0 count per minute/mg/ $\times 10^6$, respectively, in group I and II animals ($P < 0.05$). The Nitrobluetetrazolium method showed intense staining in tumor tissues but not in non neoplastic mucosa.

CONCLUSION: Experimental gastric tumors seem to produce more reactive oxygen species than non neoplastic gastric tissue. The reduction of oxidative stress and gastric tumor incidence in rats were induced by the intake of ascorbic acid. Therefore, it may have a role in the prevention of gastric carcinoma.

Oliveira CPMS, Kassab P, Lopasso FP, Souza HP, Janiszewski M, Laurindo FRM, Iriya K, Laudanna AA. Protective effect of ascorbic acid in experimental gastric cancer: reduction of oxidative stress. *World J Gastroenterol* 2003; 9(3): 446-448

<http://www.wjgnet.com/1007-9327/9/446.htm>

INTRODUCTION

The pathogenesis of human gastric cancer is a multistep and multifactorial process^[1]. The complex of cellular and molecular changes can be mediated by a diversity of endogenous and environmental agents that include free radicals, *H. pylori* infection^[2, 3] bile reflux, intake of diets high salt and low consumption of fruits and vegetables^[1]. Free radicals or reactive oxygen species (ROS) are low molecular weight metabolites reactive enough to damage essential biological molecules. The inability of the cell to scavenge ROS, overproduced by failure of the antioxidant systems, induced lesions in macromolecules such as DNA, proteins and lipids of cytosolic membranes. The release of ROS inside the nuclear membranes of the cell can damage the DNA, and there it induces mutations^[8,9] which is one of bases of the carcinogenesis^[4]. There are several mechanisms that could explain the relationships between the cell oxidative stress and the growth of tumors, such as proto-oncogene expression, generation of genotoxic products like 8-hydroxynonenal and conversion of procarcinogens to carcinogens^[4].

Epidemiologic studies has shown that vitamin C dietary intake decreases the risk for gastric tumor development^[5, 6]. Both antioxidant property and the ability to react with nitrite make vitamin C a putative candidate agent in the prevention of N-nitroso compound generation^[5,7,8]. There were a number reports on the role of the ROS as the first step in cancer induction, but there were few on ROS generation in tumor tissue and on the possible properties of vitamin C in protecting the cell against tumor transformation using an intragastric bile reflux rat model. The objectives of this work were to determine what is the oxidative stress involvement in experimental gastric carcinogenesis induced by intragastric bile reflux and what are the effects of the ascorbic acid on ROS generation in this model.

MATERIALS AND METHODS

The animal experiments were carried out in accordance to the Institute of Experimental Animals of School of Medicine, University of São Paulo Guidelines for Care and Use of Laboratory Animals.

Study groups

Wistar male rats (weighting 250-350 g) were submitted to the surgical procedure and were randomly allocated into two groups: Group I ($n=6$) was the control animals; Group II ($n=6$) was animals with daily oral administration (7 days per week) of Vitamin C (30 mg/Kg body weight) tap water solution. The total amount of vitamin C for 4 animals, in each cage, was dissolved in the total minimal volume of water intake that was previously measured for each animal. All rats were maintained in light and dark alternatively each phase for 12 h.

Surgical procedures

Experimental gastric cancer was induced by profound duodeno-gastric reflux in twelve Wistar rats underwent split gastrojejunostomy. The jejunum was divided at 5 cm distant from duodeno-jejunal angle. The afferent loop was anastomosed to the gastric body whereas the efferent jejunal loop was anastomosed in pre-pyloric antrum. The animals were killed at 6th month after the surgical procedure according with the appearance of weight loss, intestinal obstruction, ascites, anemia and visible abdominal mass. When these signs did not appear, the animals were killed at the 12th month after the operation. Just after killing, three fragments of 5 mm² each, were taken from the gastric tumor and from the gastric mucosa without tumor, at the same place on the anastomosis.

Lucigenin-amplified chemiluminescence assays

Each fragment was immersed in Krebs-HEPES buffer composition in mmol/L: NaCl 118.3; KCl 4.69; CaCl₂ 1.87; MgSO₄ 1.20; KH₂PO₄ 1.03; NaHCO₃ 25.0; Glucose 11.1; Na-HEPES 20.0) at 37 °C, strictly maintained at pH 7.40, for at least 15 min. The gastric fragments were rapidly transferred to a counter vial, under light protection, and immersed in 2.0 mL of a solution of Krebs-HEPES buffer and 0.10 mol/L lucigenin (Sigma Chemicals). This lucigenin concentration was chosen because, instead of higher concentration ranges, it has been shown to reflect superoxide generation by tissues. Each fragment was counted for 10 min in a luminometer (Berthold Multi Biolumat). Vials containing the buffer and lucigenin alone were counted and these blank values were subtracted from the signals obtained from the tissue fragments. The counts were normalized for the dry weight of each fragment. The results were expressed as counts per min per mg. In some experiments the gastric fragments were hold for 45 min in a solution of superoxide dismutase (100 kU/L) before and during the counts. NADH (0.1 mol/L) or NADPH (0.1 mol/L) were added to the counter vials in some experiments.

Histochemistry with nitrobluetrazolium

Nitrobluetrazolium (NBT) is a yellow dye that, under double reduction, generates insoluble bluish/black diformazan precipitates that are visible by light microscopy. NBT can be reduced directly by superoxide radicals, but it can also work as an electron acceptor during diaphorase enzyme activity. The gastric fragments (tumoral or not) were prepared as above, and immersed in a solution containing NBT (1.25 mg/mL), bovine serum albumin (17 mg/mL), NADH (0.1 mmol/L) and NADPH (0.1 mmol/L) for 30 minutes. The fragments were, then, fixed in 4 % buffered formalin, pH=7.40, for 24 hours. Afterwards, these specimens were then, embedded in paraffin, cut into 10 micra-thick slices and examined by light microscopy, without additional staining.

Hystology

The fragments previously fixed in 100 mL/L formalin, were dehydrated though increasing concentration of alcohol solutions, soaked in paraffin, cut into 5 mm -thick slices, stained with hematoxilin-eosin (HE) and examined by light microscopy.

Statistical analysis

The data are expressed as mean \pm SEM. The values of differences between groups were compared using the Student test. *P* critical value of 0.05 was chosen to identified significant different means.

RESULTS

Each of the six rats of Group I at 6th month after surgery had

two advanced gastric tumor (Figure 1A), each one on the side of gastric mucosa of both afferent and efferent anastomosis. The rats of Group II had no signs of gastric tumor. However, in three of them, an early well differentiated intestinal adenocarcinoma of the anastomosis was microscopically detected (Figures 1B). The stromal tissue of these tumors had plenty inflammatory cells. The three other rats had epithelial inflammation and intestinal metaplasia in the same place of the macroscopic tumors in the another three animals. The well differentiated patterns of tumors were similar in both groups.

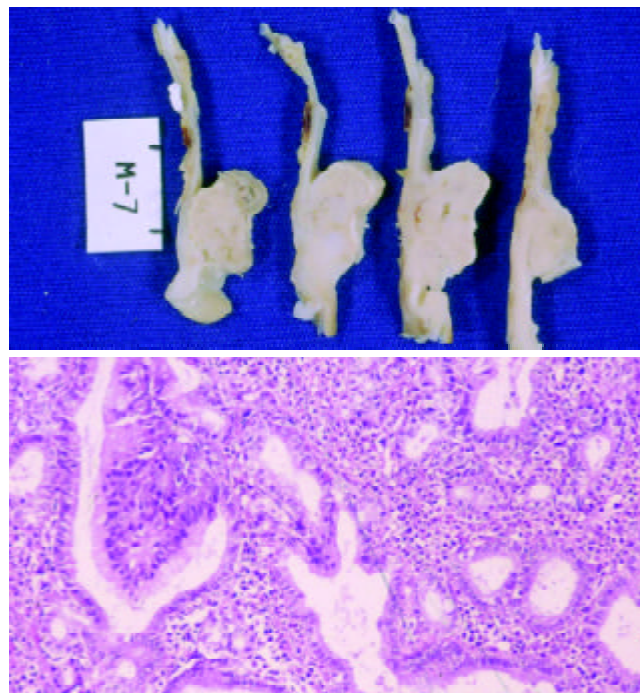


Figure 1 A. Microscopic appearance of the gastric tumor (Note the tubular pattern with variability of glomerular size, rudimentary papillary and nuclear atipia); B. Macroscopic appearance.

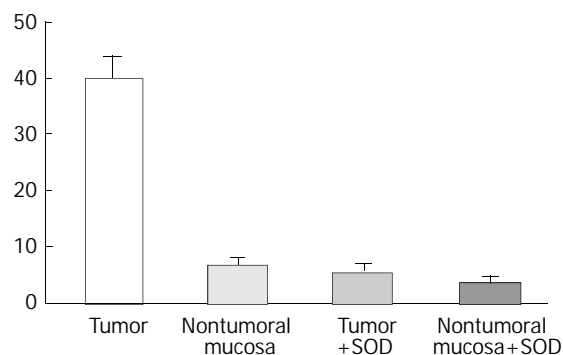


Figure 2 Lucigenin amplified-luminescence (count per minute $\times 10^6$). Basal Luminescence in the tumor and non tumoral mucosa. The addition of SOD (100 kU/L) to the substrate decreases the amplified-luminescence in visible tumoral mucosa and non tumoral gastric mucosa of rats.

The values of basal luminescence were higher in Group I (38.4 ± 6.8 count per minute/per mg $\times 10^6$) than in Group II (14.9 ± 4.0) ($P < 0.05$). The addition of NADPH to the substrate increased the luminescence in the non visible tumor tissue of the rats of Group II more than tumor tissues of Group I. Addition of NADH, however, increased the luminescence production by tumors and non tumorous mucosa. The luminescence generation after addition of superoxide dismutase

(SOD) was reduced in about 80 % and 30 % respectively, in the tumors and in non tumor gastric mucosa (Figure 2). Histochemical features produced by NBT showed insoluble bluish/black diformazan precipitates, visible with light microscopy in tumor tissue but not in the non tumoral tissues.

DISCUSSION

The choice of this experimental design was based on our previous studies which demonstrated that the appearance of gastric cancer was evident in these models at least after the 6th month of the surgical procedure. Gastric carcinogenesis is a multifactorial event. Endogenous and environmental stimuli are involved like *H. pylori* infection and gastric accumulation of N-nitroso compounds^[9-11]. Indeed there are evidences that oxidative stress participates in the carcinogenic cell transformation induced by DNA mutations^[1,4]. Studies on populations at high risk to gastrointestinal cancer have shown that dietary antioxidants are able to reduce the prevalence rates of cancer and, therefore, seem to protect them against the carcinogenesis in the stomach^[12,13]. In our rat model of profound duodeno-gastric reflux induced gastric adenocarcinomas within a 6-12 month period after the surgical procedure without antioxidant therapy. On the contrary, in animals with daily intake of vitamin C during the postoperative period, no obvious signs of gastric tumor were detected after 12 months. Though, in three of them, microscopic early gastric adenocarcinoma was found. Interestingly, the other three rats of this group remained without gastric carcinoma for as long as twelve months after the potential carcinogenic surgical procedure. So, vitamin C seems to have a breaking role on the carcinogenic process in the gastric mucosa under chronic and intense duodenal-gastric reflux. Probably this action might be due to its antioxidant properties and the ability to react with nitrites, preventing the formation of gastric N-nitroso compounds.

The lucigenin-amplified luminescence method showed that the generation of ROS was higher in gastric neoplastic than in non neoplastic tissue. Macroscopic tumor in the rats of group I produced more luminescence than gastric tissue in the rats of group II without any visible tumor. These features suggest that increased ROS activity participates in gastric carcinogenesis during the development to the most advanced stages of the cancer. Indeed, the presence of ROS in non tumorous mucosa during the presence of cancer in the anastomosis suggests that is not possible to preclude the primary effect of the reflux that might induce cancer during the early stage of carcinogenic process. The use of an antioxidant agent, such as vitamin C, can reduce the ROS generation and, thus tumor cell transformation. Recent studies have suggested that the gastric concentration of ascorbic acid is decreased in *H.pylori* infected patients^[2,3], especially, in patients who had intestinal metaplasia and serious and extensive gastritis. This fact could be associated with the gastric carcinogenic mechanism. On the other hand, intragastric bile reflux seems to induce intestinal metaplasia in humans, but only in the presence of *H.pylori* gastritis^[14]. In our previous studies using rats without *H.pylori* infection, metaplasia had preceded the appearance of gastric adenocarcinoma. In the present study a relationship between intragastric bile reflux and oxidative stress could be observed. The use of vitamin C reduced the ROS generation that might have had a role in the tumoral cell transformation. The addition of NADPH induces superoxide generation by action of NADPH oxidase produced by activated neutrophils present in inflammatory tissues. The ROS generation in group I seems to be produced by the tumor and not by the inflammatory activity because: (1) there was no increase of luminescence when it was added to phorbol myristate acetate and (2) the luminescent response to NADH addition was higher than NADPH addition.

However, in group II, the addition of NADPH increased the luminescent activity more than it did after the NADH addition. These observations are relevant, because, in gastric tissue with visible tumors, superoxide generation might be related to gastric adenocarcinoma but not to the inflammatory process. Notwithstanding, when the gastric tissue without visible tumors was exposed to NADPH, there was an increase in the luminescence measures, in spite of the inflammation present in the tissue samples. A relationship was also established between histochemical data and superoxide generation. Moreover, the addition of a superoxide blocker (superoxide dismutase) to the substrate of tumor tissues caused a 80 % reduction of the luminescence generation.

As previously reported, the present study confirms the relationship between gastric superoxide anion generation and gastric carcinogenesis of the intestinal type, in rats. Vitamin C also seems to have a protective role in the cell mutagenic factors by a retarding action upon the growth of gastric tumors. This putative protection may be explained by the reduction of oxidative stress in gastric tissue. Consequently, vitamin C could be used in further therapeutic approaches.

REFERENCES

- 1 **Correa P.** A New Paradigm For Human Gastric Carcinogenesis. *J Clin Gastroenterol* 2000; **30**: 381-385
- 2 **Reed PI,** Vitamin C. *Helicobacter pylori* Infection and Gastric Carcinogenesis. *Int J Vitam Nutr Res* 1999; **69**: 220-227
- 3 **Zhang ZW,** Patchett SE, Perrett D, Katelaris PH, Domizio P, Farthing MJG. The relation between gastric vitamin C concentrations, mucosa histology, and Cag A seropositivity in the human stomach. *Gut* 1998; **43**: 322-326
- 4 **Farinati F,** Cardin R, Degan P, Rugge M, Di Mario F. Oxidative DNA damage accumulation in gastric carcinogenesis. *Gut* 1998; **42**: 351-356
- 5 **Correa P,** Malcom G, Schmidt B, Fontham E, Ruiz B, Bravo JC, Bravo LE, Zarama G, Realpe JL. Antioxidants micronutrients and gastric cancer. *Aliment Pharmacol Ther* 1998; **12** (Suppl1): 73-82
- 6 **Tsubono Y,** Tsugane S, Gey KF. Plasma antioxidant vitamins and carotenoid in five Japanese populations with varied mortality from gastric cancer. *Nutr Cancer* 1999; **34**: 56-61
- 7 **Mowat C,** Carswell A, Wirz A, McColl KE. Omeprazole and dietary nitrate independently affect levels of vitamin C and nitrite in gastric juice. *Gastroenterology* 1999; **116**: 813-822
- 8 **Dabrowska-Ufniaz E,** Dzieniszewski J, Jaroz M, Wartanowicz M. Vitamin C concentration in gastric juice in patients with pre-cancerous lesions of the stomach and gastric cancer. *Med Sci Monit* 2002; **8**: CR96-103
- 9 **You WC,** Zhang L, Gail MH, Chang YS, Liu WD, Ma JL, Li JY, Jin ML, Hu YR, Yang CS, Blaser MJ, Correa P, Blot WJ, Fraumeni JF Jr, Xu GW. Gastric dysplasia and gastric cancer: *Helicobacter pylori*, serum vitamin C, and other risk factors. *J Natl Cancer Inst* 2000; **92**: 1607-1612
- 10 **Yamaguchi N,** Kakizoe T. Synergistic interaction between *Helicobacter pylori* gastritis and diet in gastric cancer. *Lancet Oncol* 2001; **2**: 88-94
- 11 **Zhang ZW,** Abdullahi M, Farthing MJ. Effect of physiological concentrations of vitamin C on gastric cancer cells and *Helicobacter pylori*. *Gut* 2002; **50**: 165-169
- 12 **Jacobs EJ,** Connell CJ, McCullough ML, Chao A, Jonas CR, Rodriguez C, Calle EE, Thun MJ. Vitamin C, vitamin E, and multivitamin supplement use and stomach cancer mortality in the Cancer Prevention Study II cohort. *Cancer Epidemiol Biomarkers Prev* 2002; **11**: 35-41
- 13 **Correa P,** Fontham ET, Bravo JC, Bravo LE, Ruiz B, Zarama G, Realpe JL, Malcom GT, Li D, Johnson WD, Mera R. Chemoprevention of gastric dysplasia: randomized trial of antioxidant supplements and anti-*helicobacter pylori* therapy. *J Natl Cancer Inst* 2000; **92**: 1881-1888
- 14 **Dixon MF.** Prospects for intervention in gastric carcinogenesis: reversibility of gastric atrophy and intestinal metaplasia. *Gut* 2001; **49**: 2-4

The microcell mediated transfer of human chromosome 8 into highly metastatic rat liver cancer cell line C5F

Hu Liu, Sheng-Long Ye, Jiong Yang, Zhao-You Tang, Yin-Kun Liu, Lun-Xiu Qin, Shuang-Jian Qiu, Rui-Xia Sun

Hu Liu, Sheng-Long Ye, Jiong Yang, Zhao-You Tang, Yin-Kun Liu, Lun-Xiu Qin, Shuang-Jian Qiu, Rui-Xia Sun, Liver Cancer Institute, Zhong Shan Hospital, Fudan University, Shanghai 200032, China

Supported by The State Key Basic Research Program, No.G1998051200 and National Scientific Foundation of China, No. 30271459

Correspondence to: Sheng-Long Ye, Professor, Liver Cancer Institute, Zhong Shan Hospital, Fudan University, Shanghai 200032, China. slye@shmu.edu.cn

Telephone: +86-21-64041990-2150 **Fax:** +86-21-64037181

Received: 2002-10-05 **Accepted:** 2002-11-04

Abstract

AIM: Our previous research on the surgical samples of primary liver cancer with CGH showed that the loss of human chromosome 8p had correlation with the metastatic phenotype of liver cancer. In order to seek the functional evidence that there could be a metastasis suppressor gene (s) for liver cancer on human chromosome 8, we tried to transfer normal human chromosome 8 into rat liver cancer cell line C5F, which had high metastatic potential to lung.

METHODS: Human chromosome 8 randomly marked with neo gene was introduced into C5F cell line by MMCT and positive microcell hybrids were screened by double selections of G418 and HAT. Single cell isolation cloning was applied to clone microcell hybrids. Finally, STS-PCR and WCP-FISH were used to confirm the introduction.

RESULTS: Microcell hybrids resistant to HAT and G418 were obtained and 15 clones were obtained by single-cell isolation cloning. STS-PCR and WCP-FISH proved that human chromosome 8 had been successfully introduced into rat liver cancer cell line C5F. STS-PCR detected a random loss in the chromosome introduced and WCP-FISH found a consistent recombination of the introduced human chromosome with the rat chromosome.

CONCLUSION: The successful introduction of human chromosome 8 into highly metastatic rat liver cancer cell line builds the basis for seeking functional evidence of a metastasis suppressor gene for liver cancer harboring on human chromosome 8 and its subsequent cloning.

Liu H, Ye SL, Yang J, Tang ZY, Liu YK, Qin LX, Qiu SJ, Sun RX. The microcell mediated transfer of human chromosome 8 into highly metastatic rat liver cancer cell line C5F. *World J Gastroenterol* 2003; 9(3): 449-453

<http://www.wjgnet.com/1007-9327/9/449.htm>

INTRODUCTION

With the practice of diagnosis of primary liver cancer at early stage, surgical resection of small hepatocellular carcinoma (HCC) and other improvements in medical diagnosis, imaging, nonsurgical therapies, etc, important progresses have been

made toward the control of liver cancer. For example, surgical resection of small HCC has resulted in a marked increase in 5-year survival rate from 20-30 % to 40-60 %. In our institute, the 5-year survival rate of 963 patients with small HCC (≤ 5 cm) resection was 65.1 %. However, recurrence and metastasis still remain to be major challenges for clinical workers^[1-3]. The main obstacle to control of metastasis for liver cancer is the lack of sensitive predictive biomarkers and novel molecular targets for biotherapies^[4,5]. The discovery of metastasis suppressor genes for liver cancer will undoubtedly be of vital importance to the prognostic diagnosis and intervention therapy for overcoming the metastasis of liver cancer.

Our previous study suggested that there may harbor metastasis suppressor genes on human chromosome 8p^[6]. To seek functional evidence for this possibility, we tried to introduce the normal human chromosome 8 into the highly metastatic rat liver cancer cell line C5F^[3] through microcell mediated chromosome transfer (MMCT). The positive microcell hybrids were screened through drug selection and confirmed by sequence tagged sites- polymerase chain reaction (STS-PCR) and whole chromosome painting-fluorescence in situ hybridization (WCP-FISH).

MATERIALS AND METHODS

Cell lines

The highly metastatic rat liver cancer cell line C5F^[7] was generously provided by Dr.Kumiko Ogawa (the First Department of Pathology, Nagoya City University, Nagoya, Japan). The cells were maintained in Dulbecco's modified Eagle's medium (DMEM) supplemented with 10 % fetal bovine serum (FBS). The human chromosome 8 donor cell line A9 (neo8) was purchased from Japanese Collection of Research Bioresources (JCRB) Cell Bank, Osaka, Japan. A9 (neo8) is a mouse fibroblast cell line that contains a human chromosome 8. The human chromosome 8 was randomly marked with neo resistant gene. The A9 (neo8) cells were cultured in DMEM containing 10 % FBS and 800 $\mu\text{g} \cdot \text{mL}^{-1}$ geneticin (G418).

Reagents and instruments

Colcemid, cytochalasin B, phytohemagglutinin A (PHA), polyethylene glycol (PEG, MW1 300~1 600, Hybrid-Max[®]) and Dimethylsulfoxide (DMSO, Hybrid-Max[®]) were purchased from Sigma, USA. DMEM high glucose, 100 \times HAT (10 mM hypoxanthin, 40 μM aminopterin, 1.6 mM thymidine) and G418 were ordered from Life Technologies, GIBCO BRL, USA. Isopore[™] polycarbonate membranes were purchased from Millipore, USA. WCP paint DNA probes for chromosome 8 (SpectrumGreen[™]) were purchased from Vysis Inc, IL, USA. Primers were ordered from Sangon Biotechnology Company, Shanghai, China. Taq polymerase, dNTP and 100bp DNA ladder marker were the products of Sino-America Biotechnology Company, China. Fetal bovine serum (FBS, define) and Bovine Calf Serum (BCS) were purchased from Hyclone, USA. PE-2400 thermocycler was the product of Perkin-Elmer Company, USA. The high speed Hitachi himac CR21G centrifuge was the product of Hitachi, Japan. Cyto

Vision™ Chromosome Analysis System (Cytovision™ Image Analysis Workstations, USA) was the product of Applied Imaging, USA.

MMCT^[8-10]

Micronucleation of A9(neo8) A9(neo8) cells were seeded in six straight-neck T25 flasks respectively. Colcemid was added to the culture to the final concentration of 0.05 $\mu\text{g}\cdot\text{mL}^{-1}$ when the cells reached confluence of 80 %. The cells were subsequently incubated at 37 °C in 50 mL $\cdot\text{L}^{-1}$ CO₂ incubator for 40-48 h.

Enucleation and filtration Media was removed from culture and cells were washed twice with PBS. The flasks were filled to the neck with DMEM containing 20 $\mu\text{g}\cdot\text{mL}^{-1}$ cytochalasin B which had been prewarmed at 37 °C. Flasks were sealed with parafilm, and then put into a R12A3 rotor (fixed-angle 28°) to centrifuge at 7 500 \times g at 36 °C for 75 min. Pellets were collected and resuspended with DMEM. Suspension was serially filtered through 8 μm , 5 μm and 5 μm polycarbonate membranes. Microcells were observed and counted on hemacytometer under microscope. Microcells were collected again by centrifuging at 2 000 \times g at 4 °C for 20 min and thereafter resuspended with 2 mL of DMEM with 100 $\mu\text{g}\cdot\text{mL}^{-1}$ PHA-P.

Microcell fusion & drug selection of microcell hybrids The recipient cell line C5F was trypsinized to make single cell suspension and counted on a hemacytometer for its cell density. C5F cells equivalent to 1/10 of microcells were taken and washed twice with PBS to get rid of remnant serum and thereby collected by centrifugation and resuspended with the PHA-P solution containing the microcells. The mixture was incubated at 37 °C for 15 min and subsequently centrifuged at 2 000 \times g for 15 min. Supernatant was removed as much as possible. Microcells were fused with the recipient cells for 30-60 s with 1 mL of 50 % PEG, 10 % DMSO in DMEM. Fusion reaction was terminated immediately by adding 10 mL of DMEM containing 5 % DMSO to remove the PEG medium. Pellets were resuspended with DMEM supplemented with 10 % FBS. The culture was recovered at 37 °C for 48 h and replaced with selective media of 1 \times HAT and 800 $\mu\text{g}\cdot\text{mL}^{-1}$ G418. The selective medium was refreshed twice per week.

Single cell Isolation cloning^[11]

Viable cells in selective media of G418 and HAT were trypsinized to make single cell suspension. Cell density was examined on a hemacytometer. Fifty to one hundred cells were added into a P100 culture plate with serum free DMEM. Single cells were picked up with a P20 pipette under microscope in laminar flow. It was assured that there was only one cell in view under a low-power objective to exclude the possibility of aspirating more than one cell each time. The opening of tip was pointed by the side of the selected cell and 5 μL media was aspirated each time. The single cell could be seen disappear into the tip under the low magnification microscope. Single cells were added to 96-well cell culture plate containing 0.1 mL of selective media (DMEM supplemented with 20 % FBS containing 1 \times HAT and 800 $\mu\text{g}\cdot\text{mL}^{-1}$ G418) in each well. After about 10 days, clones that are actively proliferating were picked up and transferred to a 24-well plate. After about 7 days, cells were transferred again to T25 flask. When cells reached large quantity, they were frozen down in liquid nitrogen to keep in stock.

Genomic DNA extraction from cell lines^[12]

About 1 \times 10⁶ cultured cells were harvested by trypsinization and centrifugation, into which 0.5 mL of cell lysis buffer (100 mmol $\cdot\text{L}^{-1}$ NaCl, 1 mmol $\cdot\text{L}^{-1}$ EDTA, 0.5 % SDS, 50 mmol $\cdot\text{L}^{-1}$ Tris-HCl, pH 8.0) and 10 μL of Proteinase K (2 g $\cdot\text{L}^{-1}$) were

added. The mixture was incubated at 37 °C in water bath for 6 h. Genomic DNA was extracted with phenol and chloroform, precipitated with ethanol, dissolved with 20 μL of sterile dd-H₂O, quantitated by spectrophotometer, diluted to 10 $\mu\text{g}\cdot\mu\text{L}^{-1}$ with sterile dd-H₂O, and finally aliquoted and stored at -20 °C.

STS-PCR^[13,14]

A human STS, D8S277, which located at 8p23.3-p22, was randomly chosen to confirm the result of MMCT. Primers were designed according to the published sequences on NCBI UniSTS database (<http://www.ncbi.nlm.nih.gov/genome/sts/>). Forward primer: CCAGGTGAGTTTATCAATTCCTGAG; reverse primer: TGAGAGGT CTGAGT GAC ATCCG. PCR product size: 148-180 (bp). PCR reaction solution (10 mmol $\cdot\text{L}^{-1}$ Tris, 50 mmol $\cdot\text{L}^{-1}$ KCl, 2 mmol $\cdot\text{L}^{-1}$ MgCl₂, 0.001 % Gelatin, 200 mmol $\cdot\text{L}^{-1}$ dNTPs, 0.5 mmol $\cdot\text{L}^{-1}$ primers and 2U of *Taq* polymerase) was added into 50 ng of DNA template for each sample respectively. PCR program was run as: 94 °C 2 min, 1 cycle; 95 °C 40 s 60 °C 40 s 72 °C 40 s, 35 cycles in all; 72 °C 4 min, 1 cycle; keep at 4 °C. Results were checked on 2 % agarose gel electrophoresis stained with ethidium bromide.

Chromosome slide preparation^[15]

Microcell hybrids at logarithmic phase were treated with colcemid at a final concentration of 0.02 $\mu\text{g}\cdot\text{mL}^{-1}$ for 45 to 60 min at 37 °C and trypsinized subsequently to make single cell suspension. Cells were pelleted and then exposed to 5 mL of hypotonic solution (0.075 M KCl) by incubating for 10 to 15 min at 37 °C in a water bath. Chromosomes were repetitively fixed with methanol: glacial acetic acid (3:1, volume ratio) for 3 times, and finally resuspended with 0.5-1 mL of fixative. Three to four drops were dropped evenly on a cold wet slide, which was allowed to dry later. It was examined under low magnification phase objective (10 \times or 16 \times) to check the cell density and spread of metaphase chromosomes.

WCP-FISH^[16]

WCP-FISH was performed according to the protocol provided by Vysis Inc (IL, USA). Briefly chromosome slides were immersed in denaturation solution (700 mL $\cdot\text{L}^{-1}$ formamide/2 \times SSC) at 73 \pm 1 °C in water bath for 5 min and subsequently dehydrated serially in 700 mL $\cdot\text{L}^{-1}$, 850 mL $\cdot\text{L}^{-1}$ and 1 000 mL $\cdot\text{L}^{-1}$ ethanol and dried at 45 °C-50 °C. The WCP probe mix (7 μL of WCP hybridization buffer, 2 μL of purified H₂O and 1 μL of WCP paint DNA probe for human chromosome 8 Spectrum Green™) was incubated at 73 \pm 1 °C in water bath for 5 min and placed at 45 °C~50 °C ready for use. The probe mix was applied to the target area and coverslip was immediately applied which was sealed with rubber cement. Slides were placed in a prewarmed humidified box, which were put into a 37 °C incubator for 16 h. Coverslips were removed from slides, which were immediately immersed in 0.4 \times SSC/3 mL $\cdot\text{L}^{-1}$ NP-40 prewarmed to 73 \pm 1 °C agitating for 1-3 s. Slides were removed after 2 min and immersed into 2 \times SSC/1 mL $\cdot\text{L}^{-1}$ NP-40 at ambient temperature agitating for 1-3 s and removed after 5 s to 1 min. Slides were air dried in darkness. 10 μL of DAPI counterstain was applied to the target area of slide and coverslip was applied. Slides were viewed using DAPI/Green Vysis filter set on an optimally performing fluorescence microscope and images were captured using CytoVision™ Chromosome Analysis System (Applied Imaging).

RESULTS

Selective screening of microcell hybrids and single cell isolation cloning

Three to four weeks after MMCT, viable floating cells were

observed among dead cells in selective media containing G418 and HAT. Figure 1. The viable cells had good refraction and round shape while the dead cells had poor refraction and morphologic shrinkage.

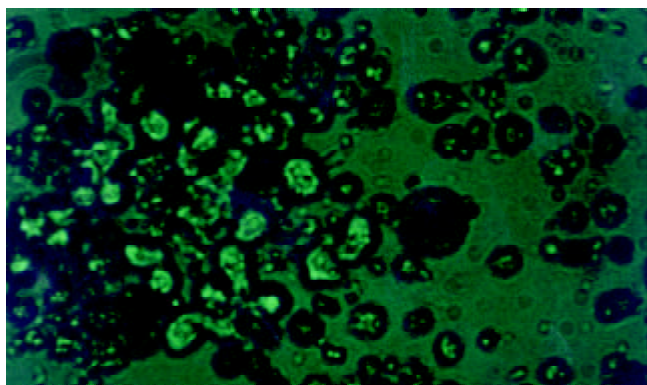


Figure 1 Double selection of microcell hybrids in HAT and G418 (10×25 magnification).

Fifteen microcell hybrid clones were obtained by single cell isolation cloning, which were named neo8/C5F-1~15 respectively. It took about 4 weeks for the progress of enlargement culture serially from 96- to 24-well cell culture plate and finally to T25 flask. Feeder cells are proven unnecessary for the single cell isolation cloning of C5F microcell hybrids. Figure 2 showed the microcell hybrid clone obtained in 96-well plate containing selective media of HAT (1×) and G418 (800 µg·mL⁻¹) one week after single cell isolation.



Figure 2 Single-cell isolation cloning in 96-well cell culture plate (10×25 magnification).

STS-PCR

The chromosome donor cell line A9 (neo8) was taken as positive control and the recipient cell line C5F as negative control. DNA extracted from A9 (neo8), C5F and microcell hybrids was used as template. PCR was performed with the primers for D8S277, which is a unique STS located on human chromosome 8p23.3-p22. PCR products, when checked on 2 % agarose gel electrophoresis, were found of the same length with those reported in UniSTS database of NCBI. Figure 3 showed that neo8/C5F-3 had the deletion of D8S277.

WCP-FISH

WCP-FISH was performed using whole chromosome painting DNA probe for human chromosome 8 (WCP 8 probe SpectrumGreen™, Vysis) to confirm its presence. Figure 4 (a and b) showed that the human chromosome 8 had been successfully introduced into rat liver cancer cell line. Meanwhile, the recombination of human chromosome 8 with rat chromosome could be observed clearly by comparing the

probe with its DAPI counterstain image. This recombination was found to be consistent in different metaphase cells.

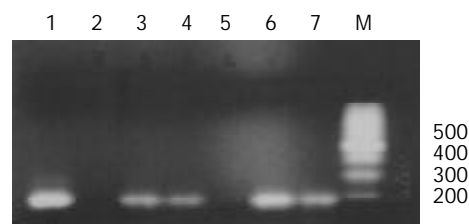


Figure 3 STS-PCR Amplification of D8S277. 1: chromosome donor cell line A9(neo8); 2: recipient cell line C5F; 3-7: microcell hybrids neo8/C5F-1-5; M: 100bp ladders.

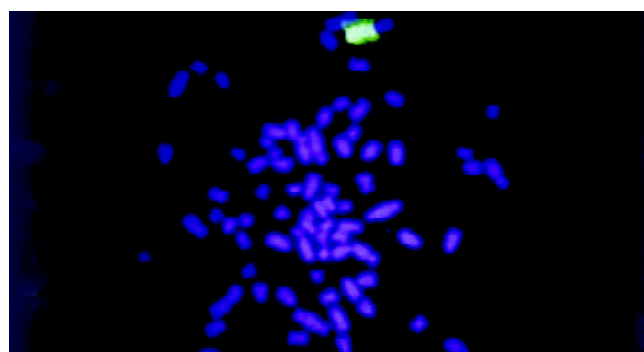


Figure 4a WCP-FISH analysis of neo8/C5F microcell hybrids.

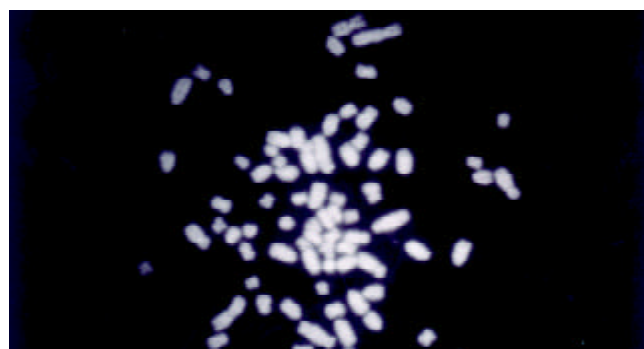


Figure 4b WCP-FISH of neo8/C5F microcell hybrids DAPI counterstain.

DISCUSSION

Metastasis is a major problem puzzling both specialists of cancer biology and of clinical oncology. Thousands of cancer patients die of it each year while clinicians can do little to deal with it. The main reason is that the molecular mechanisms of metastasis have not been totally clarified yet. Researchers fascinated by metastasis hope that the discovery of metastasis suppressor genes could shed light on the solution of this problem, while hitherto few of them have been discovered^[17,18].

Metastasis suppressor genes suppress the formation of spontaneous, macroscopic metastases without affecting the growth rate of the primary cancer. Until presently, only five genes, nm23, KAI1, KISS1, MKK4 and BrMS1, have been proved to meet this criteria^[17,18]. Despite the first metastasis suppressor gene nm23 was discovered by subtractive hybridization, most of encoding regions of metastasis suppressor genes have been discovered with the methodology of MMCT^[18], which is thought to be the methodology particularly suitable for the functional localization of metastasis suppressor genes^[19]. MMCT is established on somatic cell

hybrid. Before MMCT was introduced, researchers had found that somatic cell fusion of metastatic cell line with normal cells could change its metastatic phenotype^[20]. Microcells that contain only one single human chromosome are obtained by the micronucleation and enucleation of human monochromosome donor cells, which include only one intact human chromosome labeled with selective markers such as the neo gene. The target monochromosomes are thereby introduced into recipient cells through the fusion of microcells with recipient cells and the cloning screening of microcell hybrids based on drug resistance conferred. Due to unknown reasons, the introduced chromosome is unstable and random loss or recombination can occur, which result in a series of microcell hybrid clones with different regions of the target chromosome. In this study, the human chromosome 8 introduced into C5F was found to not only have random loss by STS-PCR but also have recombined with rat chromosome by FISH. Those clones in all are called human monochromosome somatic cell panel^[21]. In order to judge which region on the target chromosome harbors the gene of deserved function, spontaneous metastasis assay will be performed with these microcell hybrids. Based on the comparison of changes of metastatic phenotype and different chromosome regions each microcell hybrid contains, the target gene can be narrowed down to specific chromosome region.

Most of current researches for the discovery of metastasis suppressor genes focused on the functional localization of metastasis suppressor genes for prostate cancer, melanoma and breast cancer^[19, 22-31]. However, there hasn't been any report of such work on liver cancer. Our previous study on the surgical samples of primary liver cancer through comparative genomic hybridization (CGH) showed that the loss of the short arm of human chromosome 8 had correlation with metastasis, which suggested that there could be metastasis suppressor gene(s) on chromosome 8p^[6]. This discovery made our present research work imperative. In this study, the highly metastatic rat liver cancer cell line C5F, whose incidence of subcutaneous tumorigenicity is 100 % and that of lung metastasis is 89 %, was chosen as the recipient. The genetic background of rat facilitated STS-PCR screening of the regions remained on the chromosome introduced, as STS is a unique genetic marker different between species. One STS on human chromosome 8p23.3-22, D8S277, was chosen to confirm the introduction of human chromosome with the genomic DNA of microcell hybrids as templates. The results indicated that the microcell hybrids contained the STS specific for human chromosome 8, which could be taken as a proof for the successful chromosome transfer. Meanwhile some clones had deletions of STS, which showed that random losses of regions on human chromosome had occurred. This phenomenon built the basis for construction of human monochromosome panel. The target chromosome was randomly labeled with the G418 resistance gene, neo, which facilitated the selection of positive microcell hybrid clones. In the mean time, the chromosome donor cell line A9 is hypoxanthine-guanine phosphoribosyl transferase (HGPRT) deficient. Therefore A9 can't survive in the media with HAT. Double selections of G418 and HAT were applied in this study to exclude the fake clones from either chromosome donor cell line or recipient cell line. Based on the acquisition of drug resistance, we can reasonably infer that the target chromosome has been transferred into C5F. The results of FISH provide the most direct evidence for the successful chromosome transfer. Recombination between human chromosome and rat chromosome was also observed in different metaphase cells, which showed that the recombination had been stabilized. The introduction of human chromosome can cause transient genetic instability, but with the selection the genetic change will become stable, which is the foundation for further analysis.

All in all, the human chromosome 8 has been successfully transferred into the highly metastatic rat liver cancer cell line C5F, which builds solid basis for future researches on the discovery of metastasis suppressor genes for liver cancer.

ACKNOWLEDGEMENTS

We are much grateful to Dr. Kumiko Ogawa (First Department of Pathology, Nagoaya City University, Japan) for his generous offer of C5F cell line, Prof. Hong-Xuan Lin (Plant Physiology and Ecology Institute, Chinese Academy of Science, Shanghai, China) for his warmhearted provision and assistance in the usage of Hitachi high speed centrifuge and Dr. M.Z.Zdzienicka and Wouter Wiegant (Leiden University Medical College, Netherland) for kindly providing us the detailed protocol of MMCT.

REFERENCES

- 1 **Tang ZY.** Hepatocellular carcinoma- cause, treatment and metastasis. *World J Gastroenterol* 2001; **7**: 445-454
- 2 **Tang ZY.** Hepatocellular carcinoma. *J Gastroenterol Hepatol* 2000; **15** (Suppl): G1-G7
- 3 **Tang ZY, Yu YQ, Zhou XD, Ma ZC, Wu ZQ.** Progress and prospects in hepatocellular carcinoma surgery. *Ann Chir* 1998; **52**: 558-563
- 4 **Qin LX, Tang ZY.** The prognostic significance of clinical and pathological features in hepatocellular carcinoma. *World J Gastroenterol* 2002; **8**: 193-199
- 5 **Qin LX, Tang ZY.** The prognostic molecular markers in hepatocellular carcinoma. *World J Gastroenterol* 2002; **8**: 385-392
- 6 **Qin LX, Tang ZY, Sham JS, Ma ZC, Ye SL, Zhou XD, Wu ZQ, Trent JM, Guan XY.** The association of chromosome 8p deletion and tumor metastasis in human hepatocellular carcinoma. *Cancer Res* 1999; **59**: 5662-5665
- 7 **Ogawa K, Nakanishi H, Takeshita F, Futakuchi M, Asamoto M, Imaida K, Tatematsu M, Shirai T.** Establishment of rat hepatocellular carcinoma cell lines with differing metastatic potential in nude mice. *Int J Cancer* 2001; **91**: 797-802
- 8 **Fournier RE.** A general high-efficiency procedure for production of microcell hybrids. *Proc Natl Acad Sci U S A* 1981; **78**: 6349-6353
- 9 **McNeill CA, Brown RL.** Genetic manipulation by means of microcell-mediated transfer of normal human chromosomes into recipient mouse cells. *Proc Natl Acad Sci U S A* 1980; **77**: 5394-5398
- 10 **Kraakman-van der Zwet M, Overkamp WJ, Jaspers NG, Natarajan AT, Lohman PH, Zdzienicka MZ.** Complementation of chromosomal aberrations in AT/NBS hybrids: inadequacy of RDS as an endpoint in complementation studies with immortal NBS cells. *Mutation Res* 2001; **485**: 177-185
- 11 **Cowell JK.** Single-cell Isolation Cloning. Human Chromosome Principles and techniques, Verma RS and Babu A eds. 2nded. *McGraw-Hill Inc USA* 1995: 37-38
- 12 **Sambrook J, Russell DW.** Molecular cloning: A laboratory manual. 3rded. *New York: Cold Spring Harbor Laboratory Press* 2000: 542-545
- 13 **Schuler GD.** Electronic PCR: bridging the gap between genome mapping and genome sequencing. *Trends Biotechnol* 1998; **16**: 456-459
- 14 **Nelson DL.** Applications of polymerase chain reaction methods in genome mapping. *Curr Opin Genet Dev* 1991; **1**: 62-68
- 15 **Verma RS, Babu A.** Human Chromosome Principles and techniques. 2nded. *McGraw-Hill Inc USA* 1995: 12-13
- 16 **Jenkins RB, Le Beau MM, Kraker WJ, Borell TJ, Stalboerger PG, Davis EM, Penland L, Fernald A, Espinosa R 3rd, Schaid DJ.** Fluorescence *in situ* hybridization: a sensitive method for trisomy 8 detection in bone marrow specimens. *Blood* 1992; **79**: 3307-3315
- 17 **Welch DR, Rinker-Schaeffer CW.** What defines a useful marker of metastasis in human cancer? *J Natl Cancer Inst* 1999; **91**: 1351-1353
- 18 **Yoshida BA, Sokoloff MM, Welch DR, Rinker-Schaeffer CW.** Metastasis-suppressor genes: a review and perspective on an emerging field. *J Natl Cancer Inst* 2000; **92**: 1717-1730

- 19 **Mashimo T**, Watabe M, Cuthbert AP, Newbold RF, Rinker-Schaeffer CW, Helfer E, Watabe K. Human chromosome 16 suppresses metastasis but not tumorigenesis in rat prostatic tumor cells. *Cancer Res* 1998; **58**: 4572-4576
- 20 **Ramshaw IA**, Carlsen S, Wang HC, Badenoch-Jones P. The use of cell fusion to analyze factors involved in tumor cell metastasis. *Int J Cancer* 1983; **32**: 471-478
- 21 **Overhauser J**. Somatic Cell Hybrid Mapping Panels: Resources for Mapping Disease Genes. In: Human Genome Methods, Adolph KW ed. *CRC Press LLC USA* 1998: 258-264
- 22 **Dong JT**, Lamb PW, Rinker-Schaeffer CW, Vukanovic J, Ichikawa T, Isaacs JT, Barrett JC. KAI1, a metastasis suppressor gene for prostate cancer on human chromosome 11p11.2. *Science* 1995; **268**: 884-886
- 23 **Chekmareva MA**, Hollowell CM, Smith RC, Davis EM, LeBeau MM, Rinker-Schaeffer CW. Localization of prostate cancer metastasis suppressor activity on human chromosome 17. *Prostate* 1997; **33**: 271-280
- 24 **Nihei N**, Kouprina N, Larionov V, Oshima J, Martin GM, Ichikawa T, Barrett JC. Functional evidence for a metastasis suppressor gene for rat prostate cancer within a 60-kilobase region on human chromosome 8p21-p12. *Cancer Res* 2002; **62**: 367-370
- 25 **Ichikawa T**, Ichikawa Y, Dong J, Hawkins AL, Griffin CA, Isaacs WB, Oshimura M, Barrett JC, Isaacs JT. Localization of metastasis suppressor gene(s) for prostatic cancer to the short arm of human chromosome 11. *Cancer Res* 1992; **52**: 3486-3490
- 26 **Yoshida BA**, Dubauskas Z, Chekmareva MA, Christiano TR, Stadler WM, Rinker-Schaeffer CW. Mitogen-activated protein kinase kinase 4/stress-activated protein/Erk kinase 1 (MKK4/SEK1), a prostate cancer metastasis suppressor gene encoded by human chromosome 17. *Cancer Res* 1999; **59**: 5483-5487
- 27 **Miele ME**, Jewett MD, Goldberg SF, Hyatt DL, Morelli C, Gualandi F, Rimessi P, Hicks DJ, Weissman BE, Barbanti-Brodano G, Welch DR. A human melanoma metastasis-suppressor locus maps to 6q16.3-q23. *Int J Cancer* 2000; **86**: 524-528
- 28 **Lee JH**, Miele ME, Hicks DJ, Phillips KK, Trent JM, Weissman BE, Welch DR. KiSS-1, a novel human malignant melanoma metastasis-suppressor gene. *J Natl Cancer Inst* 1996; **88**: 1731-1737
- 29 **Mashimo T**, Goodarzi G, Watabe M, Cuthbert AP, Newbold RF, Pai SK, Hirota S, Hosobe S, Miura K, Bandyopadhyay S, Gross SC, Watabe K. Localization of a novel tumor metastasis suppressor region on the short arm of human chromosome 2. *Genes Chromosomes Cancer* 2000; **28**: 285-293
- 30 **Goodarzi G**, Mashimo T, Watabe M, Cuthbert AP, Newbold RF, Pai SK, Hirota S, Hosobe S, Miura K, Bandyopadhyay S, Gross SC, Balaji KC, Watabe K. Identification of tumor metastasis suppressor region on the short arm of human chromosome 20. *Genes Chromosomes Cancer* 2001; **32**: 33-42
- 31 **Seraj MJ**, Samant RS, Verderame MF, Welch DR. Functional evidence for a novel human breast carcinoma metastasis suppressor, BRMS1, encoded at chromosome 11q13. *Cancer Res* 2000; **60**: 2764-2769

Edited by Zhang J

Effects of tachyplesin on the regulation of cell cycle in human hepatocarcinoma SMMC-7721 cells

Qi-Fu Li, Gao-Liang Ouyang, Xuan-Xian Peng, Shui-Gen Hong

Qi-Fu Li, Xuan-Xian Peng, The Key Laboratory of China Education Ministry for Cell Biology and Tumor Cell Engineering, School of Life Sciences, Xiamen University, Xiamen 361005, Fujian Province, China
Gao-Liang Ouyang, Shui-Gen Hong, Laboratory of Cell Biology, School of Life Sciences, Xiamen University, Xiamen 361005, Fujian Province, China

Supported by the National Natural Science Foundation of China, No. 30170724

Correspondence to: Dr. Qi-Fu Li, The Key Laboratory of China Education Ministry for Cell Biology and Tumor Cell Engineering, School of Life Sciences, Xiamen University, Xiamen 361005, Fujian Province, China. chifulee@163.net

Telephone: +86-592-2183619 **Fax:** +86-592-2186392

Received: 2002-08-26 **Accepted:** 2002-10-29

Abstract

AIM: To investigate the effects of tachyplesin on the cell cycle regulation in human hepatocarcinoma cells.

METHODS: Effects of tachyplesin on the cell cycle in human hepatocarcinoma SMMC-7721 cells were assayed with flow cytometry. The protein levels of p53, p16, cyclin D1 and CDK4 were assayed by immunocytochemistry. The mRNA levels of p21^{WAF1/CIP1} and c-myc genes were examined with *in situ* hybridization assay.

RESULTS: After tachyplesin treatment, the cell cycle arrested at G₀/G₁ phase, the protein levels of mutant p53, cyclin D1 and CDK4 and the mRNA level of c-myc gene were decreased, whereas the levels of p16 protein and p21^{WAF1/CIP1} mRNA increased.

CONCLUSION: Tachyplesin might arrest the cell at G₀/G₁ phase by upregulating the levels of p16 protein and p21^{WAF1/CIP1} mRNA and downregulating the levels of mutant p53, cyclin D1 and CDK4 proteins and c-myc mRNA, and induce the differentiation of human hepatocarcinoma cells.

Li QF, Ouyang GL, Peng XX, Hong SG. Effects of tachyplesin on the regulation of cell cycle in human hepatocarcinoma SMMC-7721 cells. *World J Gastroenterol* 2003; 9(3): 454-458

<http://www.wjgnet.com/1007-9327/9/454.htm>

INTRODUCTION

A variety of anticancer agents with distinctive effects have been used for treatment of malignant tumors. These agents generally induce tumor cell necrosis and apoptosis as well as differentiation. Today, induction of differentiation is a new strategy in cancer therapy^[1-6]. A number of recent experiments have showed that cell-cycle-arrest may be necessary for cell differentiation. The current knowledge of cell cycle regulation have revealed that the progression of the cell cycle is governed mainly by the activation and deactivation of cyclin-dependent kinases (CDKs). In order for cell cycle arrest to differentiation, it is necessary either to downregulate positive regulation of

CDKs, such as cyclins, or to activate negative regulators of CDKs, such as CDK inhibitors (CKIs)^[7].

It had revealed that tachyplesin, a low molecular weight peptide, could alter the morphological and ultrastructural characteristics, inhibit the proliferation and induce the differentiation of human gastric carcinoma cells and hepatocarcinoma cells^[8,9]. In this paper, we investigate the effects of tachyplesin on the regulation of cell cycle in human hepatocarcinoma SMMC-7721 cells.

MATERIALS AND METHODS

Reagents

Tachyplesin was isolated from acid extracts of Chinese horseshoe crab (*Tachyplesus tridentatus*) hemocytes as described by Nakamura^[10] with minor modification. RPMI-1640 medium were obtained from Gibco. Fetal calf serum was supplied by Si-Ji-Qing Biotechnology Co. (Hangzhou, China). Mouse anti-human p53, p16, cyclin D1 monoclonal antibodies and rabbit anti-human CDK4 antibody were purchased from Santa Cruz. Immunocytochemistry detection kit and *in situ* hybridization kit were provided by Beijing Zhongshan Biotechnology Co.

Cell culture and treatment

SMMC-7721 cells, provided by the Institute of Biochemistry and Cell Biology, Shanghai Institute of Biological Sciences, Chinese Academy of Sciences, were maintained in RPMI-1640 medium supplemented with 20 % heat-inactivated fetal calf serum, 100 units/mL penicillin, 100 mg/L streptomycin and 50 mg/L kanamycin at 37 °C, 5 % CO₂ in air atmosphere. SMMC-7721 cells were treated with culture medium containing 3.0 mg/L tachyplesin after being seeded for 24 hours.

Flow cytometry assay

SMMC-7721 cells and the cells treated with 3.0 mg/L tachyplesin for 2, 4 or 6 days were collected, rinsed in 0.1 M PBS, resuspended and fixed in 70 % ethanol at 4 °C overnight. Cells were centrifuged, resuspended in 100 mg/L RNase A at 37 °C for 30 min and in 50 mg/L propidium iodide at 4 °C for 30 min. Cell cycle was analyzed by flow cytometry.

Immunohistochemistry analysis

SMMC-7721 cells and the cells treated with 3.0 mg/L tachyplesin for 5 days were seeded in little penicillin bottles with coverslips for 48 hours respectively. The cells grown on coverslips were fixed with cold acetone for 10 min, rinsed twice in PBS for 15 min, immersed in 3 % hydrogen peroxide for 10 min, washed with distilled water and PBS for 15 min, blocked with 10 % normal goat serum for 10 min at room temperature, and incubated with primary antibodies at 4 °C overnight. After incubation with primary antibodies, coverslips were rinsed twice in PBS for 15 min, incubated with biotin-labeled secondary antibody at 37 °C for 10 min, rinsed twice in PBS for 15 min, and then incubated in streptavidin-peroxidase at 37 °C for 10 min. The antigen-antibody complex was visualized with diaminobenzidine (DAB) substrate. Negative controls were incubated in the absence of primary antibodies.

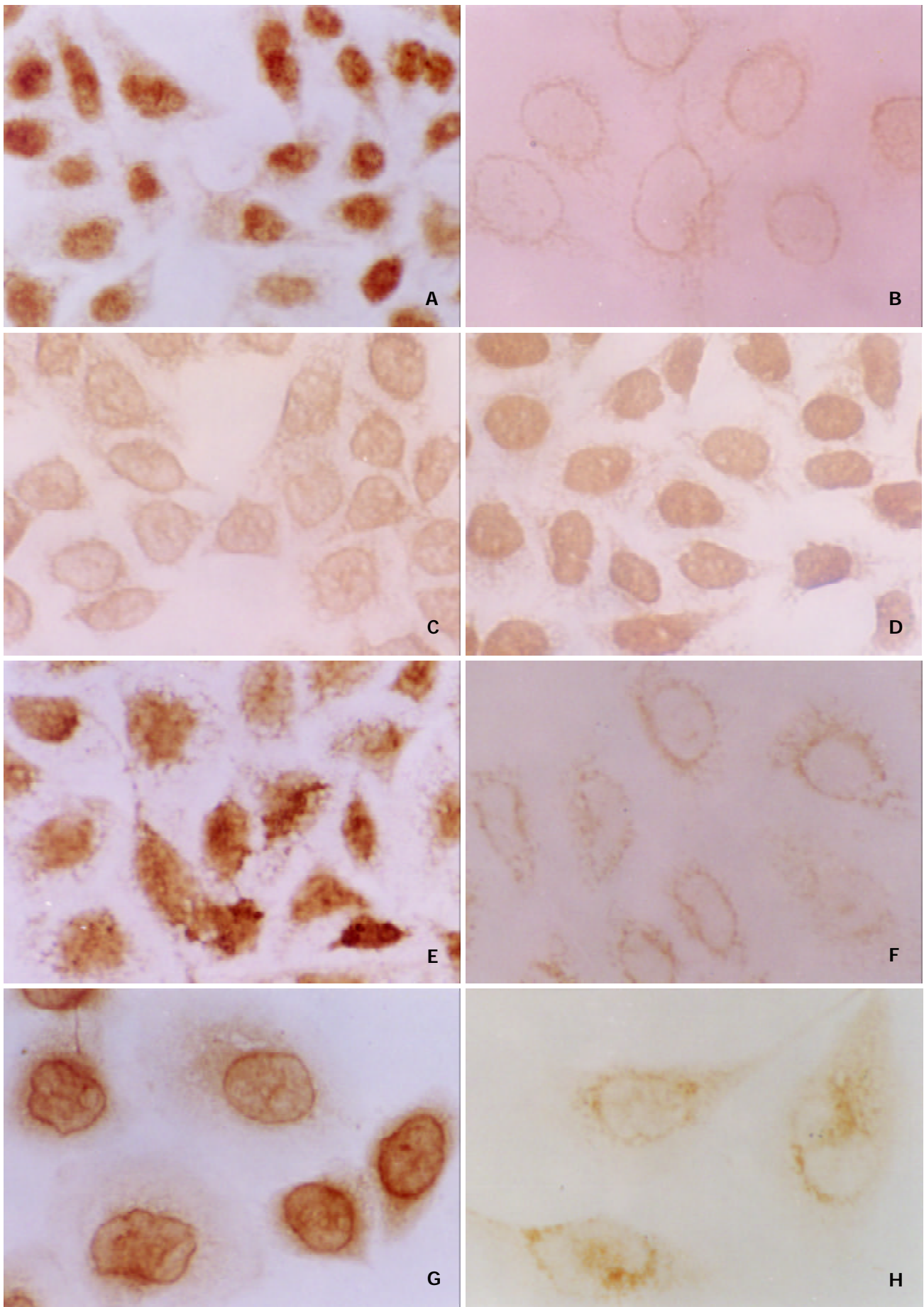


Figure 1 Immunocytochemistry analysis of the effects of tachyplestin on the protein levels of mutant p53, p16, cyclin D1, CDK4 in SMMC-7721 cells ($\times 536$). The protein levels of mutant p53 (**A**), cyclin D1 (**E**), CDK4 (**G**) were high in SMMC-7721 cells while the levels of mutant p53 (**B**), cyclin D1 (**F**), CDK4 (**H**) were decreased by tachyplestin. The level of p16 protein was low in SMMC-7721 cells (**C**) while high in the tachyplestin-treated cells (**D**).

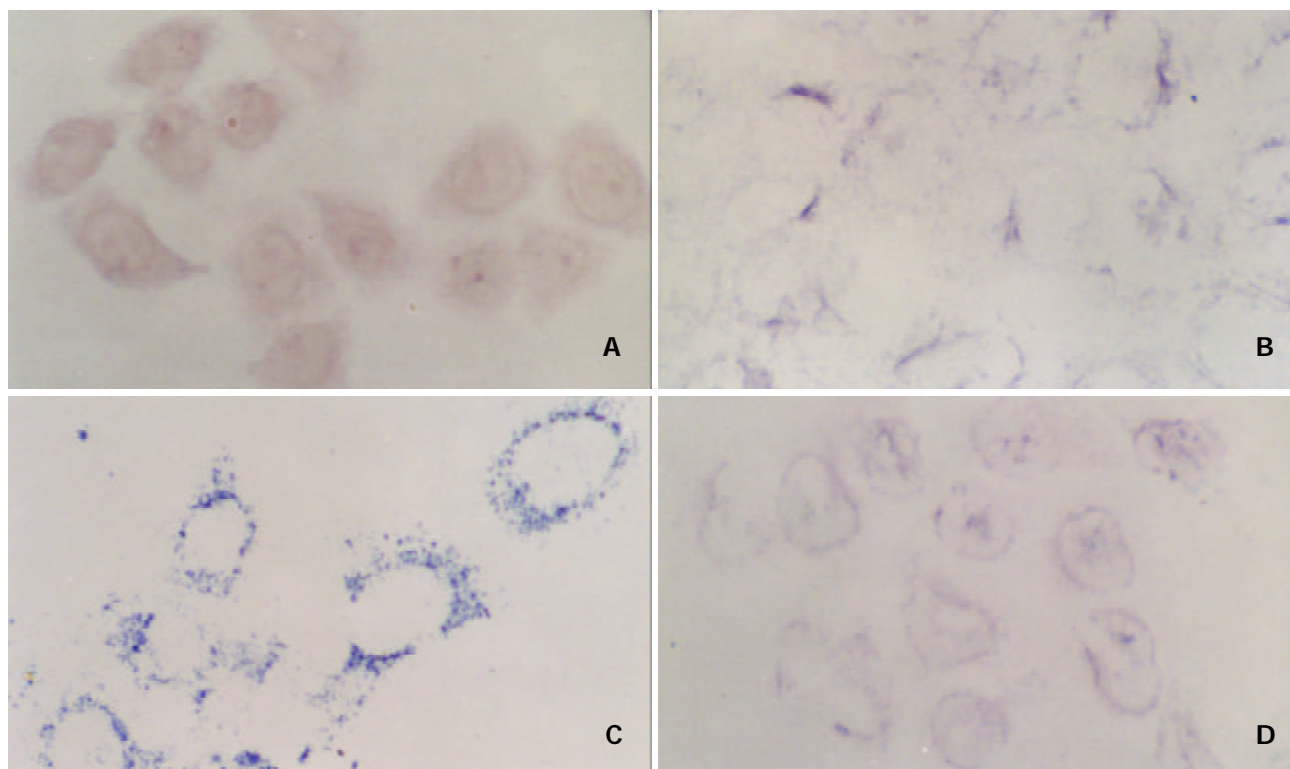


Figure 2 *In situ* hybridization analysis of p21^{WAF1/CIP1} and c-myc mRNA in untreated and tachyplesin-treated SMMC-7721 cells ($\times 536$). The level of p21^{WAF1/CIP1} mRNA was low in SMMC-7721 cells (A) but high in the tachyplesin-treated cells (B). High level of c-myc mRNA was observed in SMMC-7721 cells (C) while the level of c-myc mRNA in the tachyplesin-treated cells down-regulated (D).

In situ hybridization

SMMC-7721 cells and the cells treated with 3.0 mg/L tachyplesin for 5 days were seeded in little penicillin bottles with coverslips for 48 hours respectively. *In situ* hybridization procedure was carried out as described by Spector^[11] with minor modifications. The coverslips were rinsed twice in PBS, prefixed with methanol/acetone (1:1, v/v) for 10 min, incubated in 0.1 M HCl for 10 min, rinsed in 0.01 M PBS for 5 min $\times 2$, and incubated in 25 mg/L proteinase K at 37 °C for 20 min and in 0.2 % glycine in PBS for 5 min $\times 3$. They were postfixed in 4 % paraformaldehyde for 10 min, dehydrated, and air dried. The prehybridization was conducted at room temperature for 1 hour, followed by hybridization in a humid chamber at 42 °C for 16-22 hours. The hybridization solution contained prehybridization solution and 1.0 μ g/mL digoxigenin-labeled p21^{WAF1/CIP1} cRNA or c-myc cRNA probe. Coverslips were rinsed in 2 \times SSC at 37 °C for 15 min $\times 2$, in 1 \times SSC for 5 min $\times 2$, in 0.5 \times SSC for 5 min $\times 2$, in 0.2 \times SSC for 5 min $\times 2$, washed with Buffer I (100 mM Tris-HCl buffer, 150 mM NaCl, pH7.5) for 5 min, and incubated with Blocking buffer (2 % horse serum and 0.3 % Triton X-100 in Buffer I) for 1 hour, and then incubated at 37 °C for 1 hour in alkaline phosphatase-conjugated anti-digoxigenin antibody diluted 1:500 in Blocking buffer, then rinsed in Buffer I for 15 min $\times 3$, and equilibrated in Buffer II (100 mM Tris-HCl buffer, 100 mM NaCl, 50 mM MgCl₂, pH9.5). The alkaline phosphatase reaction was conducted by incubation with NBT/BCIP solution for 20-30 min. The reaction was stopped with Buffer III (10 mM Tris-HCl buffer, 1 mM EDTA, pH8.0). The coverslips were then dehydrated in alcohol, cleared in xylene, and mounted on gelatin. The negative controls were processed without labeled probes.

RESULTS

Effects of tachyplesin on the cell cycle distribution of SMMC-7721 cells

Cell cycle kinetics of SMMC-7721 cells was analyzed by flow

cytometry. As demonstrated in Table 1, 3.0 mg/L tachyplesin could induce an accumulation of the cells at G₀/G₁ phase on day 2, 4, 6, respectively. Compared with control group, the amount of cells at G₀/G₁ phase increased from 48.2 % to 65.6 %, while the quantity of cells in S phase decreased from 48.0 % to 24.8 % after being treated with tachyplesin for 6 days. This indicated that tachyplesin could arrest the SMMC-7721 cells at G₀/G₁ phase.

Table 1 Effects of 3.0 mg/L tachyplesin on the cell cycle kinetics of SMMC-7721 cells

	SMMC-7721	Tachyplesin 2 d	Tachyplesin 4 d	Tachyplesin 6 d
G ₀ /G ₁	48.2 %	66.5 %	61.8 %	65.6 %
S	48.0 %	29.7 %	34.8 %	24.8 %
G ₂ /M	3.8 %	3.8 %	3.4 %	9.6 %

Effects of tachyplesin on p53, p16 protein levels in SMMC-7721 cells

It has revealed that p53 protein detected by immunohistochemistry is mutant p53. Immunohistochemistry showed that the level of mutant p53 protein was high in the nucleus and cytoplasm of SMMC-7721 cells. However, very low level of mutant p53 protein in the tachyplesin-treated cells was observed (Figure 1A and B). p16 protein was distributed mainly in the nucleolus of SMMC-7721 cells in low level while the level of immunohistochemical reaction was very high in the tachyplesin-treated cells (Figure 1C and D).

Effects of tachyplesin on cyclin D1, CDK4 protein levels in SMMC-7721 cells

As shown in Figure 1E and F, the level of cyclin D1 protein was high in the nucleolus and cytoplasm of untreated cells while it was very weak in the cells treated with tachyplesin. It also revealed that exposure of SMMC-7721 cells to tachyplesin resulted in an obvious decrease of CDK4 protein level (Figure 1G and H).

Effects of tachyplesin on p21^{WAF1/CIP1}, c-myc mRNA levels in SMMC-7721 cells

To investigate the effects of tachyplesin on the expression of tumor suppressor gene and oncogene associated with the G₀/G₁ arrest, the levels of p21^{WAF1/CIP1} and c-myc mRNA were also detected. *In situ* hybridization assay showed that the level of p21^{WAF1/CIP1} mRNA was low in the nuclear and cytoplasm of the untreated cells while it was high in the cytoplasm around the nucleolus in the cells treated with tachyplesin (Figure 2A and B). And high level of c-myc mRNA was observed in the cytoplasm of SMMC-7721 cells. However, the level of c-myc mRNA was down-regulated in the tachyplesin-treated cells (Figure 2 C and D).

DISCUSSION

In multi-cellular organism, the balance among cell proliferation, cell differentiation and cell death maintains a constant cell number. Cell proliferation depends on the cell's growth and division cycles, which are governed by periodic assembly of the core cell cycle clock, composed of cyclins and cyclin-dependent kinases (CDKs)^[7,12]. Distinct cyclins associate and activate different CDKs throughout the cell cycle. The activity of cyclin/CDK complexes is modulated by both activating and inhibiting phosphorylation of the CDKs, and by binding to cyclin-dependent kinases inhibitors (CKIs). In higher eukaryotic cells, signals that arrest the cycle usually act at a G₁ checkpoint. The G₁ checkpoint can be viewed as a master checkpoint of the mammalian cell cycle^[7,13]. Regulation of the G₁ phase of the cell cycle is extremely complicated and involves many different families of cyclins, CDKs and CKIs. In eukaryotes, D-cyclins (D1, D2, and D3) bind CDK4/6 to wire external signals to the cell cycle and regulate progression through mid-G₁. cyclin E binds CDK2 in late G₁ and its activity is rate-limiting for progression from G₁ to S phase^[14]. The p16 tumor suppressor belongs to the INK4 family of CKIs. p16 specifically inhibit CDK4/6 by preventing binding of the activating cyclin subunits. p21^{WAF1/CIP1}, one CKI of CIP/KIP family, unlike p16, binds to a number of cyclin/CDK complexes such as cyclin D1/CDK4, cyclin E/CDK2 and cyclin A/CDK2, inhibits kinases activities and induces cell cycle arrest and cell differentiation^[7,15-17].

In addition, some other genes are associated with G₁ checkpoint. It is known that wild-type p53 gene has anti-proliferation, anti-transforming and inducing apoptosis activities. Growth arrest induced by wild-type p53 blocks cells prior to or near the checkpoint in late G₁ phase. Mutations of p53 are observed with a high incidence in most cancer^[18,19]. One of the phenotype effects of mutant p53 protein is called dominant-negative effect, which mutant p53 can override the normal inhibitory function of wild-type p53. In the meantime, c-myc gene, an early-response gene necessary for cell cycle progression (G₁-S transition), also plays an essential role in the regulation of the cell cycle and differentiation^[20-24].

As revealed by many experiments, the regulation of G₁/S checkpoint was abnormal in tumor cells. G₀/G₁ arrest was a common phenomenon in the cells undergoing induction of differentiation. And many differentiation inducers could arrest tumor cells in G₀/G₁ phase and alter the expression of cell cycle regulators^[25-31]. Our results showed that tachyplesin could down-regulate the levels of mutant p53, cyclin D1, CDK4 proteins and c-myc mRNA, up-regulate the levels of p16 protein and p21^{WAF1/CIP1} mRNA in SMMC-7721 cells, and arrest the cell in G₀/G₁ phase as other inducers on tumor cells. Taken together, the results indicated that tachyplesin might decrease the kinase activity of cyclin D1/CDK4 complex by decreasing the expression of mutant p53 protein and increasing the levels of p16 and p21^{WAF1/CIP1}, and suppress the phosphorylation of

retinoblastoma (Rb) protein and downregulate the level of c-myc mRNA, which cause a decrease of the cell in S phase significantly and arrest most of the cells at G₀/G₁ phase, and induce the cells to terminal differentiation as other inducers.

REFERENCES

- 1 **Yoneda K**, Yamamoto T, Ueta E, Osaki T. Induction of cyclin-dependent kinase inhibitor p21 in vesnarinone-induced differentiation of squamous cell carcinoma cells. *Cancer Lett* 1998; **133**: 35-45
- 2 **Lo Coco F**, Zelent A, Kimchi A, Carducci M, Gore SD, Waxman S. Progress in differentiation induction as a treatment for acute promyelocytic leukemia and beyond. *Cancer Res* 2002; **62**: 5618-5621
- 3 **Wang Z**, Sun G, Shen Z, Chen S, Chen Z. Differentiation therapy for acute promyelocytic leukemia with all-trans retinoic acid: 10-year experience of its clinical application. *Chin Med J* 1999; **112**: 963-967
- 4 **Leszczyniecka M**, Roberts T, Dent P, Grant S, Fisher PB. Differentiation therapy of human cancer: basic science and clinical applications. *Pharmacol Ther* 2001; **90**: 105-156
- 5 **Hansen LA**, Sigman CC, Andreola F, Ross SA, Kelloff GJ, De Luca LM. Retinoids in chemoprevention and differentiation therapy. *Carcinogenesis* 2000; **21**: 1271-1279
- 6 **Gali-Muhtasib H**, Bakkar N. Modulating cell cycle: current applications and prospects for future drug development. *Curr Cancer Drug Targets* 2002; **2**: 309-336
- 7 **Donjerkovic D**, Scott DW. Regulation of the G₁ phase of the mammalian cell cycle. *Cell Res* 2000; **10**: 1-16
- 8 **Li QF**, Ouyang GL, Li CY, Hong SG. Effects of tachyplesin on the morphology and ultrastructure of human gastric carcinoma cell line BGC-823. *World J Gastroenterol* 2000; **6**: 676-680
- 9 **Ouyang GL**, Li QF, Peng XX, Liu QR, Hong SG. Effects of tachyplesin on proliferation and differentiation of human hepatocellular carcinoma SMMC-7721 cells. *World J Gastroenterol* 2002; **8**: 1053-1058
- 10 **Nakamura T**, Furunaka H, Miyata T, Tokunaga F, Muta T, Iwanaga S, Niwa M, Takao T, Shimonishi Y. Tachyplesin, a class of antimicrobial peptide from the hemocytes of the horseshoe crab (*Tachypus tridentatus*), isolation and chemical structure. *J Biol Chem* 1988; **263**: 16709-16713
- 11 **Spector DL**, Goldman RD, Leinwand LA. Cells A Laboratory Manual. Cold Spring Harbor Laboratory Press 1998
- 12 **Steinman RA**. Cell cycle regulators and hematopoiesis. *Oncogene* 2002; **21**: 3403-3413
- 13 **Wang J**, Barsky LW, Shum CH, Jong A, Weinberg KI, Collins SJ, Triche TJ, Wu L. Retinoid-induced G₁ arrest and differentiation activation are associated with a switch to cyclin-dependent kinase-activating kinase hypophosphorylation of retinoic acid receptor alpha. *J Biol Chem* 2002; **277**: 43369-43376
- 14 **Agami R**, Bernards R. Convergence of mitogenic and DNA damage signaling in the G₁ phase of the cell cycle. *Cancer Lett* 2002; **177**: 111-118
- 15 **Harada K**, Ogden GR. An overview of the cell cycle arrest protein, p21^{WAF1}. *Oral Oncol* 2000; **36**: 3-7
- 16 **Gartel AL**, Tyner AL. The growth-regulatory role of p21 (WAF1/CIP1). *Prog Mol Subcell Biol* 1998; **20**: 43-71
- 17 **Boulaire J**, Fotedar A, Fotedar R. The functions of the cdk-cyclin kinase inhibitor p21^{WAF1}. *Pathol Biol* 2000; **48**: 190-202
- 18 **Lin D**, Shields MT, Ullrich SJ, Appella E, Mercer WE. Growth arrest induced by wild-type p53 protein blocks cells prior to or near the restriction point in late G₁ phase. *Proc Natl Acad Sci USA* 1992; **89**: 9210-9214
- 19 **Liu MC**, Gelmann EP. P53 gene mutations: case study of a clinical marker for solid tumors. *Semin Oncol* 2002; **29**: 246-257
- 20 **Bartova E**, Kozubek S, Kozubek M, Jirsova P, Lukasova E, Skalnikova M, Cafourkova A, Koutna I. Nuclear topography of the c-myc gene in human leukemic cells. *Gene* 2000; **244**: 1-11
- 21 **He Y**, Zhang J, Zhang J, Yuan Y. The role of c-myc in regulating mdr-1 gene expression in tumor cell line KB. *Chin Med J* 2000; **113**: 848-851
- 22 **Jiang N**, Zhan F, Cao L, Yao K, Li G. c-myc gene inactivation during inducing of nasopharyngeal carcinoma cells with retinoic

- acid. *Chin Med J* 2000; **113**: 823-826
- 23 **Obaya AJ**, Kottenko I, Cole MD, Sedivy JM. The proto-oncogene c-myc acts through the cyclin-dependent kinase (Cdk) inhibitor p27(Kip1) to facilitate the activation of Cdk4/6 and early G(1) phase progression. *J Biol Chem* 2002; **277**: 31263-31269
- 24 **Boxer LM**, Dang CV. Translocations involving c-myc and c-myc function. *Oncogene* 2001; **20**: 5595-5610
- 25 **Chen RC**, Su JH, Ouyang GL, Cai KX, Li JQ, Xie XG. Induction of differentiation in human hepatocarcinoma cells by Isoverbasoside. *Planta Med* 2002; **68**: 370-372
- 26 **Yuan SL**, Huang RM, Wang XI, Song Y, Huang GQ. Reversing effect of Tanshinone on malignant phenotypes of human hepatocarcinoma cell line. *World J Gastroenterol* 1998; **4**: 317-319
- 27 **Kiyokama H**, Richon VM, Rifkind RA, Marks PA. Suppression of cyclin-dependent kinase 4 during induced differentiation of erythroleukemia cells. *Mol Cell Biol* 1994; **14**: 7195-7203
- 28 **Spinella MJ**, Freemantle SJ, Sekula D, Chang JH, Christie AJ, Dmitrovsky E. Retinoic acid promotes ubiquitination and proteolysis of cyclin D1 during induced tumor cell differentiation. *J Biol Chem* 1999; **274**: 22013-22018
- 29 **Bergh G**, Telleus A, Fritzon A, Kornfalt S, Johnson E, Gullberg U. Forced expression of the cyclin-dependent kinase inhibitor p16^{INK4A} in leukemic U-937 cells reveals dissociation between cell cycle and differentiation. *Exp Hematol* 2001; **29**: 1382-1391
- 30 **Hyman T**, Rothmann C, Heller A, Malik Z, Salzberg S. Structural characterization of erythroid and megakaryocytic differentiation in Friend erythroleukemia cells. *Exp Hematol* 2001; **29**: 563-571
- 31 **Zhang LP**, Jiang JK, Tam JW, Zhang Y, Liu XS, Xu XR, Liu BZ, He YJ. Effects of matrine on proliferation and differentiation in K-562 cells. *Leuk Res* 2001; **25**: 793-800

Edited by Ren SY

Detection of HBV, PCNA and GST-p in hepatocellular carcinoma and chronic liver diseases

Li-Juan Shen, Hua-Xian Zhang, Zong-Ji Zhang, Jin-Yun Li, Ming-Qin Chen, Wei-Bo Yang, Run Huang

Li-Juan Shen, Hua-Xian Zhang, Zong-Ji Zhang, Run Huang,
Department of Pathology, Kunming Medical College, Kunming 650031, Yunnan Province, China

Jin-Yun Li, Department of Pathology, the Second Affiliated Hospital, Kunming Medical College, Kunming 650032, Yunnan Province, China

Ming-Qin Chen, the Third Affiliated Hospital, Kunming Medical College, Kunming 650032, Yunnan Province, China

Wei-Bo Yang, Department of infectious diseases, the First Affiliated Hospital, Kunming Medical College, Kunming 650032, Yunnan Province, China

Supported by Natural Science Foundation of Yunnan Province, China, NO.2000C0058M and Scientific Research Foundation of the Education Department of Yunnan Province, NO.0011010

Correspondence to: Li-Juan Shen, Department of Pathology, Kunming Medical College, Kunming 650031, Yunnan Province, China. wycslj@public.km.yn.cn

Telephone: +86-871-5338845 **Fax:** +86-871-5173299

Received: 2002-07-27 **Accepted:** 2002-08-23

Abstract

AIM: To investigate the change of HBV DNA, PCNA and GST- π in chronic liver disease and hepatocellular carcinoma (HCC).

METHODS: Hepatitis B surface antigen (HBsAg), proliferating cell nuclear antigen (PCNA) and glutathione S-transferases (GST- π) were detected by immunohistochemical staining and HBV DNA was detected by *in situ* hybridization (ISH) in formalin-fixed and paraffin-embedded sections with a total of 111 specimens of chronic hepatitis, liver cirrhosis, paratumorous tissue, HCC and normal liver tissue.

RESULTS: The positive rates of HBsAg and HBVDNA were 62.5 % (15/24) and 75.0 % (12/16) in chronic hepatitis, 64.0 % (16/25) and 83.3 % (15/18) in liver cirrhosis, 72.7 % (16/22) and 85.7 % (12/14) in the paratumorous tissue and 45.0 % (14/31) and 64.3 % (9/14) in HCC. The positive HBVDNA granules in chronic hepatitis, liver cirrhosis and the paratumorous tissue were more intense than that in HCC. The positive rates of PCNA and GST- π were 34.8 % (8/23) and 25.0 % (4/16) in chronic hepatitis, 73.7 % (14/19) and 17.6 % (3/17) in liver cirrhosis, 86.7 % (13/15) and 53.3 % (8/15) in the paratumorous tissue, 100 % (15/15) and 60.0 % (9/15) in HCC, respectively, and the positive rate of GST- π in the paratumorous tissue was significantly higher than that in the liver cirrhosis without tumor ($P < 0.05$), but same as that in HCC ($P > 0.05$).

CONCLUSION: The HBV infection may increase expression of PCNA and GST- π . The paratumorous cirrhosis may be a sequential lesion of precancerous cirrhosis around HCC.

Shen LJ, Zhang HX, Zhang ZJ, Li JY, Chen MQ, Yang WB, Huang R. Detection of HBV, PCNA and GST- π in hepatocellular carcinoma and chronic liver diseases. *World J Gastroenterol* 2003; 9(3): 459-462

<http://www.wjgnet.com/1007-9327/9/459.htm>

INTRODUCTION

Proliferating cell nuclear antigen (PCNA) is an auxiliary protein of DNA polymerase and is thought to play an important role in the elongation or replication of the DNA chain. It accumulated in the nucleus during the G-1 and S stages of the cell cycle and the percentage of PCNA-positive cell is correlated with the proliferative activity and the prognosis of various malignant tumors^[1-5]. Glutathione S-transferases (GST- π) is closely related with cancer and is increased in blood and tissues of cancer patients, it is now recognized as a tumor marker^[6, 7]. We have detected hepatitis B surface antigen (HBsAg), PCNA and GST- π by immunohistochemical staining and hepatitis B virus DNA (HBV DNA) by *in situ* hybridization (ISH) in patients with chronic hepatitis, liver cirrhosis, the paratumorous tissue, hepatocellular carcinoma (HCC) and normal liver tissue, to see whether there are any changes of HBV, PCNA and GST- π in the above diseases.

MATERIALS AND METHODS

Materials

Specimens *obtained* from surgical resection, autopsy and needle aspiration biopsy of livers from 1965 to 2001 were fixed in 10 % formalin, embedded in paraffin sections, and stained by routine HE. They were divided into 5 groups: Normal liver tissues used as controls ($n=9$); Chronic hepatitis ($n=24$); liver cirrhosis ($n=25$); The paratumorous tissue ($n=22$); HCC ($n=31$). All specimens were examined by two pathologists. The diagnosis of hepatitis was according to the standard of Xi'an Conference in 2000^[8].

Immunohistochemical staining

Immunohistochemistry S-P method was used to detect HBsAg, PCNA and GST- π . Mouse monoclonal antibody to human HBsAg (ZMHB5), PCNA (PC10), GST- π (353-10) and Immunostaining S-P Kit were purchased from Fuzhou Maxim Biotechnical Company. The main steps were as follows: (1) The tissues were treated with endogenous peroxidase blocking solution at room temperature for 10 minutes and then incubated in normal nonimmune serum at room temperature for 10 minutes. (2) The mouse anti HBsAg, PCNA or GST- π antibody were added to adjacent tissue sections respectively and incubated overnight at 4 °C. (3) Biotin-conjugated second antibody was added to the sections and incubated at room temperature for 10 minutes. (4) S-P complex was added at room temperature for 10 minutes and then DAB was used for the color reaction. The tissue sections were washed with PBS (0.01M, pH 7.4) between each step. Positive and negative controls were simultaneously used to ensure specificity and reliability of the staining process. A positive section was taken as positive control. In negative control, PBS was used to replace the first antibody. The positive result showed brown coloration in the cytoplasm or /and the nucleus and was graded as follows: <10 %-, 10-30 % +, 31-50 % ++, >50 % +++^[9].

In situ hybridization (ISH)

In situ hybridization was used for detection of HBV DNA.

The HBV DNA probed with biotin-labeled and ISH-kit were purchased from Fuzhou Maxim Biotechnical Company. The main steps were as follows: (1) Baked the slides at 60-80 °C for 1 hour till overnight. (2) Deparaffinized by xylene and graded alcohols. (3) Dried at 37 °C for 5 min. (4) Added proteinase K at 37 °C for 10-15 min. (5) Enhancer wash buffer for 5 min. (6) Dehydrated the slides by graded alcohols. (7) Dried at 37 °C for 5 min. (8) Added biotin-labeled probe with coverslip. (9) Denatured at 95 °C for 8-10 min. (10) Hybridized at 37 °C for 1-2 hours in humidity chamber. (11) Soaked off coverslips in PBS. (12) Hybridization wash at 37 °C for 10 min. (13) Protein block at 37 °C for 20 min. (14) Conjugated at 37 °C for 20 min. (15) PBS rinsed enhancer wash buffer for 5 min. (16) The substrate (NBT/BCIP) showed coloration at room temperature for 10-40 min, or till the coloration developed became complete. (17) Distilled water washed for 2-3 times. (18) The slides were counterstained using nuclear fast red. The positive and negative controls were concomitantly used to ensure the specificity and reliability of the staining with a known HBVDNA positive tissue section, the normal liver tissues and hybridization liquids without probe were served as controls. The positive result showed blue coloration in the cytoplasm or/and in the nucleus.

RESULTS

Detection of HBsAg and HBV DNA

HBsAg and HBVDNA were widely expressed in chronic hepatitis, liver cirrhosis, paratumorous tissue cirrhosis and HCC (Table 1). The positive rates of HBsAg and HBVDNA were highest in the paratumorous tissue.

Table 1 Detection of hepatitis B virus, PCNA and GST- π in hepatocellular carcinoma and chronic liver diseases

Group	HBsAg ^a	HBVDNA ^b	PCNA ^c	GST- π ^d
1. Normal liver tissue	0/9 (0)	0/9 (0)	0/5 (0)	0/5 (0)
2. Chronic hepatitis	15/24 (62.5)	12/16 (75.0)	8/23 (34.8)	4/16 (25.0)
3. Liver cirrhosis	16/25 (64.0)	15/18 (83.3)	14/19 (73.7)	3/17 (17.6)
4. Paratumorous tissue	16/22 (72.7)	12/14 (85.7)	13/15 (86.7)	8/15 (53.3)
5. HCC	14/31 (45.2)	9/14 (64.3)	15/15 (100)	9/15 (60.0)

HCC: hepatocellular carcinoma; HBsAg: Hepatitis B surface antigen; HBVDNA: hepatitis B virus DNA; PCNA: proliferating cell nuclear antigen; GST- π : glutathione S-transferases. ^a $P < 0.05$, 5 vs 4, $P < 0.01$, 1 vs 4; ^b $P < 0.01$, 1 vs 4; ^c $P < 0.01$, 1 vs 4, 2 vs 4; ^d $P < 0.05$, 3 vs 4, $P < 0.01$, 1 vs 4.

The expression of HBsAg was seen in the cytoplasm (Figure 1). HBVDNA was detected in the cytoplasm and in the nucleus. HBVDNA positive granules in chronic hepatitis, liver cirrhosis and the paratumorous tissue were more intense than that in HCC. HBVDNA positive granules in HCC was mainly expressed in the nucleus but the signals were much weaker (Figure 2).

Detection of PCNA and GST- π

PCNA and GST- π were widely expressed in chronic hepatitis, liver cirrhosis, paratumorous tissue and HCC, the positive rates of PCNA and GST- π increased evidently in the paratumorous tissue and HCC (Figure 3-4). The positive rate of GST- π in paratumorous tissue (53.3 %) was significantly higher than that in cirrhosis without tumor (17.6 %) ($P < 0.05$, $\chi^2 = 6.58$).

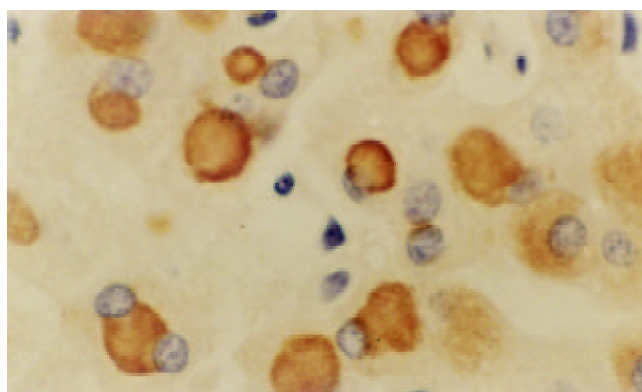


Figure 1 HBsAg was expressed at cytoplasm in chronic hepatitis. $\times 400$.

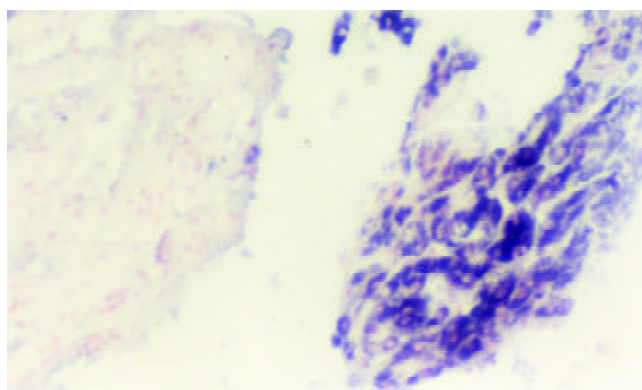


Figure 2 HBV DNA was rich in paratumorous tissue (right) and less in HCC (left). $\times 100$.

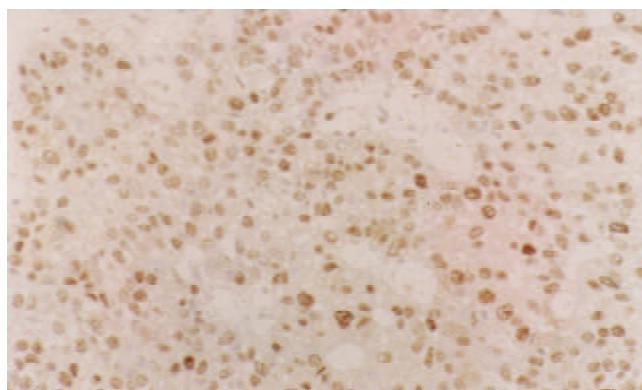


Figure 3 PCNA was expressed in nuclei of HCC. $\times 100$.

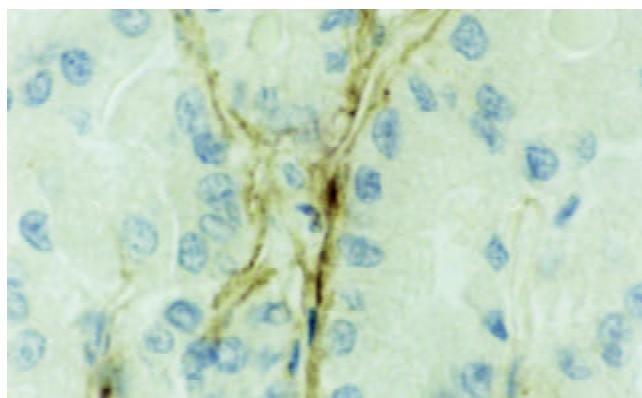


Figure 4 GST- π was expressed on cell membranes of HCC. $\times 400$.

DISCUSSION

HCC is one of the most common malignant tumors in China. In recent decades, the incidence of HCC has been found to be increasing and HCC came ranks the second in cancer mortality since 1990s^[10]. Most of patients with HCC were associated with HBV^[11-15]. The relative risk of HBV carrier developing HCC approaches 200:1, which is the highest relative risks known for HCC^[16]. we have found that there are higher positive rates of HBsAg and HBV DNA in chronic hepatitis, liver cirrhosis, paratumorous tissue and HCC, but the highest positive rate in the paratumorous tissue, supports the view of HBV as the main cause of HCC in China. The positive rate of HBV DNA in HCC was 64.3 %, mainly expressed in nuclei, HBV DNA positive granules were less and weakly stained, perhaps because most of the HBV DNA had been integrated into the genome of HCC tissue. The positive rates of HBV DNA were 85.7 % in the paratumorous tissue, which was mainly expressed in the cytoplasm, HBV DNA positive granules were more intense, because HBV DNA was mainly in the free form and in an active replicative state. Our results were similar to those of most researchers^[17]. The carcinogenesis of HCC was related to integration of HBV DNA into the genome with rearrangement of the chromosome. The integration of viral gene often occurred in the earlier stage of HCC. The integration of HBV might lead to the structural abnormality of the chromosome, which enhanced the transcription of oncogene and lost the its suppressor function, resulting in malignant transformation of hepatic cells by reverse activation of the X gene of HBV^[18]. HBV DNA was integrated into the genome randomly. The integrated HVB DNA was not complete, there were some defect in the virus genome which caused the weaking of HBV DNA hybridization signal in the nuclei of HCC^[19]. The integrated HVB DNA in the hepatic cells could bring about abnormal expression of the gene and abnormal synthesis of protein so that the growth of HCC and the differentiation and regulation of the hepatic cells became out of control. PCNA is a better marker for assessment of cellular proliferative activity, the poorer the differentiation of the cancer, the stronger the proliferative activity and the higher positive rate of PCNA^[20-21]. When the carcinogenesis initiated, the shape and structure of the cells did not have much changes, but the function and the metabolism enzymes had already been abnormal. The expression of GST- π might increase abnormally in the course of the carcinogenesis of many tumors. This change occurred much more earlier than that of the morphology^[22,23]. Our study demonstrated that PCNA and GST- π were all expressed in chronic hepatitis (34.8 % and 25.0 %), liver cirrhosis (73.7 % and 17.6 %), the paratumorous tissue (86.7 % and 53.3 %) and HCC (100 % and 60.0 %). But the positive rates of PCNA and GST- π increased significantly in the paratumorous tissue and in the HCC. These results demonstrated that repeated degeneration, necrosis and hyperplasia occurred in the chronic HBV hepatitis, because of the increase of cell proliferation and the integration of viral genome, caused disturbed proteins synthesis abnormality in metabolism enzymes. It might be a gradual developmental process from quantitation to qualitation change. The paratumorous tissue differs essentially from cirrhosis without tumor, it is rather a precancerous lesion^[24-28], which already has some characteristics of fetal liver or HCC with earlier expression AFP and AFPmRNA^[29,30], also with increased expression of PCNA and GST- π ^[31-39].

REFERENCES

- Zeng WJ**, Liu GY, Xu J, Zhou XD, Zhang YE, Zhang N. Pathological characteristics, PCNA labeling index and DNA index in prognostic evaluation of patients with moderately differentiated hepatocellular carcinoma. *World J Gastroenterol* 2002; **8**: 1040-1044
- Kong XB**, Liang LJ, Huang JF. A Study of correlation between apoptosis, expression of p21 protein and PCNA and the clinical prognosis in hepatocellular carcinoma. *Aizheng J* 1999; **18**: 426-429
- Huang Y**, Cai SM, Yu SY, Shi DR, Zhang GL, Wang HY, Lu HF. Significance of c-erbB-2 and PCNA expression in adenocarcinoma of uterine cervix. *Zhonghua Zhongliu Zazhi* 1997; **19**: 150-152
- Wang D**, Shi JQ. Immunohistochemical detection of proliferating cell nuclear antigen in hepatocellular carcinoma. *Aizheng J* 1996; **15**: 112-114
- Zhang XL**, Shi JQ, Wang XD, Wang D. Quantitative study of proliferative activity of human hepatocellular cancerous cells and cancer-adjacent hepatocytes. *Dishan Junyi Daxue Xuebao* 1996; **18**: 36-39
- Li CH**, Guo YJ, Ye XS, Tang XF. Advances in study of molecular biology of tumors. The first edition. *Beijing, Milit Med Publ House* 1996: 103-115
- Chen LY**, Zhang S, Lin H, Wang XY. Significance of expression of GST- π in gastric carcinomas. *Linchuang Yu Shiyan Binglixue Zazhi* 1999; **15**: 221-223
- Branch association of infectious disease, parasitic disease and hepatic disease under Chinese Medical Association. The prevention and treatment regime of virus hepatitis. *Zhonghua Ganzhangbing Zazhi* 2000; **8**: 324-329
- Qin LX**, Tang ZY, Ma ZC, Wu ZQ, Zhou XD, Ye QH, Ji Y, Huang LW, Jia HL, Sun HC, Wang L. P53 immunohistochemical scoring: an independent prognostic marker for patients after hepatocellular carcinoma resection. *World J Gastroenterol* 2002; **8**: 459-463
- Tang ZY**. Hepatocellular carcinoma—cause, treatment and metastasis. *World J Gastroenterol* 2001; **7**: 445-454
- Kao JH**. Hepatitis B viral genotypes: clinical relevance and molecular characteristics. *J Gastroenterol Hepatol* 2002; **17**: 643-650
- Okuda K**. Hepatocellular carcinoma. *J Hepatol* 2000; **32** (Suppl 1): 225-237
- Jin Y**, Abe K, Sato Y, Aita K, Irie H, Shiga J. Hepatitis B and C virus infection and p53 mutation in human hepatocellular carcinoma in Harbin, Heilongjian Province, China. *Hepatol Res* 2002; **24**: 379-384
- Evans AA**, Chen G, Ross EA, Shen FM, Lin WY, London WT. Eight-year follow-up of the 90,000-person Haimen cohort: I. Hepatocellular carcinoma mortality, risk factors, and gender differences. *Cancer Epidemiol Biomarkers Prev* 2002; **11**: 369-376
- Ding X**, Mizokami M, Yao G, Xu B, Orito E, Ueda R, Nakanishi M. Hepatitis B virus genotype distribution among chronic hepatitis B virus carriers in Shanghai, China. *Intervirology* 2001; **44**: 43-47
- Yu MC**, Yuan JM, Govindarajan S, Ross RK. Epidemiology of hepatocellular carcinoma. *Can J Gastroenterol* 2000; **14**: 703-709
- Yuan FP**, Huang PS, Gao MQ, Gong HS. Expression of transforming growth factor α and its relationship with HBV infection in hepatocellular carcinoma. *Zhonghua Binglixue Zazhi* 1999; **28**: 35-38
- Wang XZ**, Chen XC, Yang YH, Chen ZX, Huang YH, Tao QM. Expression of HbxAg and Fas/FasL in patients with hepatocellular carcinoma. *Aizheng J* 2001; **20**: 41-44
- Zhang LN**, Cao YL, Song J, Ma CH, Liou SX, Suen WS. The correlation between integration of HBV X,S,Pre-S,C gene and the expression of oncogenes/tumor suppressor gene in primary hepatocellular carcinoma. *Zhonghua Ganzhangbing Zazhi* 1999; **7**: 138-139
- Hino N**, Higashi T, Nouse K, Nakatsukasa H, Urabe Y, Kinugasa N, Yoshida K, Ashida K, Ohguchi S, Tsuji T. Proliferating cell nuclear antigen and grade of malignancy in small hepatocellular carcinoma—evaluation in US-guided specimens. *Hepatogastroenterology* 1997; **44**: 245-250
- Ikeguchi M**, Sato N, Hirooka Y, Kaibara N. Computerized nuclear morphometry of hepatocellular carcinoma and its relation to proliferative activity. *J Surg Oncol* 1998; **68**: 225-230
- Qi CH**, Guo SC, Li H, Li CH. Expression of GST- π in gastric carcinoma and precancerous lesions. *Zhonghua Binglixue Zazhi* 1995; **24**: 53-54
- Nie KR**, Li CH, Zhu YJ, Zhang XM, Huang GJ, Zhang DW, Zhang RG. Immunohistochemical study of GST- π in lung cancer.

- Zhonghua Jiehe He Huxi Zazhi* 1993; **16**: 141-143
- 24 **Shen LJ**, Zhang ZJ, Ou YM, Zhang HX, Huang R, He Y, Wang MJ, Xu GS. Computer morphometric analysis of human hepatocellular carcinoma and the related lesion. *Zhongguo Zuzhihuaxue Yu Xibaohuaxue Zazhi* 1997; **6**: 53-56
- 25 **Shen LJ**, Zhang ZJ, Ou YM, Zhang HX, Huang R, He Y, Wang MJ, Xu GS. Computed morphometric analysis and expression of alpha fetoprotein in hepatocellular carcinoma and its related lesion. *World J Gastroenterol* 2000; **6**: 415-416
- 26 **Shen LJ**, Zhang ZJ, Zhang HX, Ou YM, Huang R, Yang WB. Computer morphometric analysis and detection by immunohistochemistry and in situ hybridization in hepatocellular carcinoma and the related lesion. *Zhonghua Ganzangbing Zazhi* 2001; **9**: 278, 290
- 27 **Shen LJ**, Zhang ZJ, Zhang HX, Yang WB, Huang R. Expression of GST- π and HBV infection in hepatocellular carcinoma. *Aizheng J* 2002; **21**: 29-32
- 28 **Shen LJ**, Zhang ZJ, Zhang HX, Yang WB, Huang R. Expression of Alpha fetoprotein and its relationship with HBV infection. *Shiyong Aizheng Zazhi* 2002; **17**: 162-163,166
- 29 **Zhang JZ**. Carcinogenesis and expression of alpha fetoprotein in experimental hepatocarcinoma. *Linchuang Yu Shiyang Binglixue Zazhi* 1999; **15**: 224-226
- 30 **He P**, Liu BB, Ye SL, Tang ZY. Analysis of AFPmRNA in human hepatoma and paratumorous tissue. *Zhongguo Zhongliu Shengwu Zhiliao Zazhi* 1998; **5**: 163-166
- 31 **Su Q**, Benner A, Hofmann WJ, Otto G, Pichlmayr R, Bannasch P. Human hepatic preneoplasia: phenotypes and proliferation kinetics of foci and nodules of altered hepatocytes and their relationship to liver cell dysplasia. *Virchows Arch* 1997; **431**: 391-406
- 32 **Zhong S**, Tang MW, Yeo W, Liu C, Lo YM, Johnson PJ. Silencing of GSTP1 gene by CpG island DNA hypermethylation in HBV-associated hepatocellular carcinomas. *Clin Cancer Res* 2002; **8**: 1087-1092
- 33 **Nishikawa T**, Wanibuchi H, Ogawa M, Kinoshita A, Hiroi T, Funae Y, Kishida H, Nakae D, Fukushima S. Promoting effects of monomethylarsonic acid, dimethylarsinic acid and trimethylarsine oxide on induction of rat liver preneoplastic glutathione s-transferase placental form positive foci: a possible reactive oxygen species mechanism. *Int J Cancer* 2002; **100**: 136-139
- 34 **Sawaki M**, Hattori A, Tsuzuki N, Sugawara N, Enomoto K, Sawada N, Mori M. Chronic liver injury promotes hepatocarcinogenesis of the LEC rat. *Carcinogenesis* 1998; **19**: 331-335
- 35 **Marwoto W**, Miskad UA, Siregar NC, Gani RA, Boedihusodo U, Nurdjanah S, Suwarso, Watadianto Boedi P, Hasan HA, Akbar N, Noer HM, Hayashi Y. Immunohistochemical study of p53 and AFP in hepatocellular carcinomas, a comparison between Indonesian and Japanese cases. *Kobe J Med Sci* 2000; **46**: 217-229
- 36 **Feng Z**, He R, Lu Z, Ling Y. Expression of ras oncogene p21 product and proliferating cell nuclear antigen in liver cirrhosis and the correlation with liver cell dysplasia. *Zhonghua Ganzangbing Zazhi* 2000; **8**: 343-345
- 37 **Zhao M**, Zimmermann A. Liver cell dysplasia: reactivities for c-met protein, Rb protein, E-cadherin and transforming growth factor-beta 1 in comparison with hepatocellular carcinomas. *Histol Histopathol* 1998; **13**: 657-670
- 38 **Tiniakos DG**, Brunt EM. Proliferating cell nuclear antigen and Ki-67 labeling in hepatocellular nodules: a comparative study. *Liver* 1999; **19**: 58-68
- 39 **Mise K**, Tashiro S, Yogita S, Wada D, Harada M, Fukuda Y, Miyake H, Isikawa M, Izumi K, Sano N. Assessment of the biological malignancy of hepatocellular carcinomas: relationship to clinicopathological factors and prognosis. *Clin Cancer Res* 1998; **4**: 1475-1482

Edited by Wu XN

A novel HBV antisense RNA gene delivery system targeting hepatocellular carcinoma

Chun-Hong Ma, Wen-Sheng Sun, Pei-Kun Tian, Li-Fen Gao, Su-Xia Liu, Xiao-Yan Wang, Li-Ning Zhang, Ying-Lin Cao, Li-Hui Han, Xiao-Hong Liang

Chun-Hong Ma, Wen-Sheng Sun, Li-Fen Gao, Su-Xia Liu, Xiao-Yan Wang, Li-Ning Zhang, Ying-Lin Cao, Li-Hui Han, Xiao-Hong Liang, Institute of Immunology, Medical College of Shandong University, Jinan 250012, Shandong Province, China

Pei-Kun Tian, National Laboratory for Oncogenes and Related Genes, Shanghai Cancer Institute, Shanghai 200032, China

Supported by the National Natural Science Foundation Community, No. 39970333

Correspondence to: Prof Wen-Sheng Sun, Institute of Immunology, Medical College of Shandong University, Jinan 250012, Shandong Province, China. sunwenshengsws@yahoo.com

Telephone: +86-531-8382038

Received: 2002-07-18 **Accepted:** 2002-09-04

Abstract

AIM: To construct a novel HBV antisense RNA delivery system targeting hepatocellular carcinoma and study its inhibitory effect *in vitro* and *in vivo*.

METHODS: GE7, a 16-peptide specific to EGFR, and HA20, a homologue of N-terminus of haemagglutinin of influenza viral envelope protein, were synthesized and conjugated with polylysine. The above conjugates were organized into the pEBAF-as-preS2, a hepatocarcinoma specific HBV antisense expression vector, to construct a novel HBV antisense RNA delivery system, named AFP-enhancing 4-element complex. Hepatocellular carcinoma HepG2.2.15 cells was used to assay the *in vitro* inhibition of the complex on HBV. Expression of HBV antigen was assayed by ELISA. BALB/c nude mice bearing HepG2.2.15 cells were injected with AFP-enhancing 4-element complex. The expression of HBV antisense RNA was examined by RT-PCR and the size of tumor in nude mice were measured.

RESULTS: The AFP-enhancing 4-element complex was constructed and DNA was completely trapped at the slot with no DNA migration when the ratio of polypeptide to plasmid was 1:1. The expression of HBsAg and HBeAg of HepG2.2.15 cells was greatly decreased after being transfected by AFP-enhancing 4-element complex. The inhibitory rates were 33.4 % and 58.5 % respectively. RT-PCR showed HBV antisense RNA expressed specifically in liver tumor cells of tumor-bearing nude mice. After 4 injections of AFP-enhancing 4-element complex containing 0.2 µg DNA, the diameter of the tumor was 0.995 cm±0.35, which was significantly smaller than that of the control groups (2.215 cm±0.25, $P < 0.05$).

CONCLUSION: AFP-enhancing 4-element complex could deliver HBV antisense RNA targeting on hepatocarcinoma and inhibit both HBV and liver tumor cells *in vitro* and *in vivo*.

Ma CH, Sun WS, Tian PK, Gao LF, Liu SX, Wang XY, Zhang LN, Cao YL, Han LH, Liang XH. A novel HBV antisense RNA gene delivery system targeting hepatocellular carcinoma. *World J Gastroenterol* 2003; 9(3): 463-467

<http://www.wjgnet.com/1007-9327/9/463.htm>

INTRODUCTION

A major hurdle in most current gene therapy lies in how to transfer genes to target tissues efficiently and how to obtain therapeutic expression of target genes. The targeting efficacy of gene transfection and expression directly determines whether the gene therapy has high efficiency and whether it is harmful to normal tissues. Therefore, how to enhance the targeting efficacy of gene delivery has become a problem to be solved urgently^[1-4].

At present, various gene delivery methods have been used in gene therapy^[5-8]. Among them, there are two important methods to achieve tumor-targeting gene therapy: one is receptor-mediated gene delivery; another is the construction of tumor-targeting gene expression vector which utilizes tumor-specific transcription regulatory sequence^[9-12]. However, either of them, if used singly, can not really accomplish the tumor-targeting gene therapy.

This paper reported a novel HBV antisense RNA delivery system targeting on hepatocarcinoma cells, named AFP enhancing 4-element complex. This complex includes four elements: (1) recombinant EB virus vector, pEBAF-as-preS2, in which antisense preS2 gene was cloned under the control of human α -fetoprotein (AFP) promoter and enhancer, enabled preS2 antisense RNA to be expressed specifically in AFP-positive cells; (2) ligand oligopeptide GE7, synthesized according to the putative binding region of epidermal growth factor (EGF) to its receptor (EGFR), could transfer DNA specifically to EGFR positive cells; (3) HA20, a homologue of N-terminus of haemagglutinin of Influenza envelope protein, was synthesized as endosome-releasing oligopeptide (EROP); (4) polylysine was polycation peptides (PCP) which could interact with pEBAF-as-preS2 DNA to form a complex after conjugation with GE7 and HA20. Both *in vitro* and *in vivo* studies indicated that preS2 antisense RNA could be expressed strictly and specifically in hepatocarcinoma cells after being transfected by this complex. This study implicated the great therapeutic potential of AFP-enhancing 4-element complex for HBV-associated hepatocellular carcinoma.

MATERIALS AND METHODS

Cells and cultures

Hepatocellular carcinoma cell line HepG2.2.15 integrated with whole HBV gene not only can accomplish the transcription and translation of HBV, but also may produce Dane's particles. This cell line, provided by BeiJing Institute of Medicine and Biology, was cultured in the MEM medium containing 10 % FCS and 380 µg/ml G418. The human hepatocellular carcinoma cell line BEL7402 was cultured in the DMEM medium with 10 % FCS. The human umbilical vein endothelial cell line ECV304 contributed by Chinese Academy of Military Medical science was cultured in the DMEM medium, containing 10 % FCS and diantibiotics. The medium mentioned above were purchased from Hyclone Co. American, serum from GIBCO Co.

Animals

BALB/C nude mice, male, 5-6 weeks of age, were purchased

from experimental animal center of TongJi medical college, Central China Science and Technology University, WuHan. 1×10^7 HepG2.2.15 cells were transplanted subcutaneously into nude mice and were ready for use when the tumor size reached about 0.5 cm in diameter.

Plasmid

HBV preS2 gene (3 203-3 340) was cloned reversely downward 5.5 kb of AFP promoter and enhancer to construct hepatocarcinoma specific preS2 antisense RNA expression vector, pEBAF-as-preS2 (Figure 1) which could express antisense RNA against preS2 in AFP-positive cells. (published elsewhere).

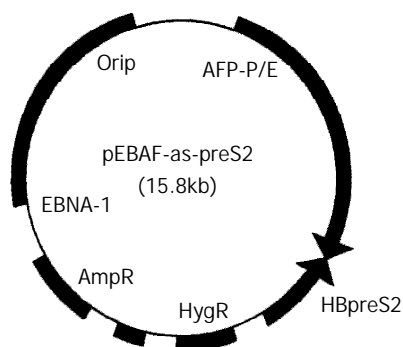


Figure 1 Physical map of pEBAF-as-preS2. hepatocarcinoma specific preS2 antisense RNA expression vector, pEBAF-as-preS2 was constructed by inserting HBV preS2 gene (3203-3340) reversely downward the AFP promoter and enhancer (AFP-P/E) of plasmid pEBAF which contains the key element of EB virus duplication (Ori P and EBNA-1).

Synthesis of GE7-PL and HA20-PL^[13]

GE7, a 16-peptide specific to EGFR, and HA20, a homologue of N-terminus of haemagglutinin of influenza viral envelope protein, were synthesized by National Laboratory for Oncogene and Related Genes, Shanghai Cancer Institute. GE7 and HA20 were conjugated with polylysine (PL) respectively (GE7-PL and HA20-PL).

Preparation of AFP-enhancing 4-element complex

pEBAF-as-preS2 DNA, GE7-PL and HA20-PL conjugates were respectively mixed dropwise into 10 μ l of deionized water in different ratios. The mixture was incubated at 25 $^{\circ}$ C for 30 min. A mixture containing 0.2 μ g plasmid DNA was analyzed on 1 % agarose gel electrophoresis to examine the retardation of DNA migration, in order to determine the optimal ratio. According to the optimal ratio of DNA to conjugates based on above experiment, the plasmid DNA was mixed dropwise to the conjugates of GE7-PL and HA20-PL and reacted at 25 $^{\circ}$ C for 30 min. Examine the retardation of DNA by 1 % agarose gel electrophoresis. Then the complex could be used for gene transfection.

In vitro gene transfer by 4-element complex

5×10^4 cells were seeded into 0.5 ml medium in each well of a 24 well plate. After cell density reached a confluence of 60 %, the medium was removed and replaced with 0.5 ml of complete medium containing 4-element complex in a quantity equivalent to 0.2 μ g DNA. Cells were cultured at 37 $^{\circ}$ C and incubated with 5 % CO₂ overnight, then replaced with fresh complete MEM medium without 4-element complex and cultured at 37 $^{\circ}$ C with 5 % CO₂. 3 days after, the supernatant was collected to detect the HBV antigen. Non-transfected HepG2.2.15 cells were used as negative control.

Detection of virus antigens

According to the protocol of antigen detection kit (Lizhu Co. ShenZhen, China), the concentration of HBsAg and HBeAg in the supernatant were detected by ELISA. The results were illustrated with P/N value (P/N=sample A/negative control A; A stands for the amount of light absorbent).

In vivo gene transfection by AFP-enhancing 4-element complex

AFP-enhancing 4-element complex containing 0.2 μ g DNA were injected into a tail vein of nude mice bearing 0.5 cm tumor. Animals were sacrificed 3 days after injection, then the tumor, liver, spleen, kidney, stomach were dissected and used for extracting the total RNA.

Extraction of total RNA

Total RNA was extracted from 5 mm³ fresh mice tissues according to the protocol of TRIZOL kit. Products were quantitated by Biophotometer (Eppendorf Co.).

Primer design

According to the sequence described by Ono *et al* in 1986^[14], the primers were designed to amplify HBpreS2 gene: forward (S2P1): 5' GCTCTAGACTCAGGCCATGCATG3'; reverse (S2P2): 5' GCTCTAGATGGTGAGTGATTGGAGGT3'. The primers for β -actin, a housekeeping gene, were designed simultaneously (forward: 5' AACTGTGCCCA 3'; reverse: 5' ATGATGGAGTTGAAGGTAGTTTCGTGGAT3'). All of these oligonucleotide primers were synthesized by Shanghai Biology and Engineering Company.

RT-PCR

Reverse transcription was performed in 20 μ l volume including: 1 μ g of total RNA, 4 μ l of 5 \times buffer, 20 nmol dNTP, 20 Units of RNase inhibitor and 200 Units of Moloney murine leukemia virus (M-MLV) reverse transcriptase. The reverse transcription reaction was performed at 42 $^{\circ}$ C for 1hr. The products were denatured at 70 $^{\circ}$ C for 10 min and then preserved at 4 $^{\circ}$ C. cDNA was used as templates for the amplification of preS2 with primers S2P1 and S2P2. PCR was carried out in 25 μ l volume with 1 μ l of cDNA, 2.5 μ l of 10 \times buffer, 0.3 mmol Mg⁺⁺, 5nmol/L dNTP, 3 Units of *Taq* polymerase, 10 nmol/L primers (forward and reverse). Reaction conditions were: 94 $^{\circ}$ C for 5 min, then 35 cycles at 94 $^{\circ}$ C for 40 sec, 50 $^{\circ}$ C for 40 sec, 72 $^{\circ}$ C for 50 sec, followed by a final extension period of 7 min at 72 $^{\circ}$ C.

In vivo tumor-inhibitory experiments

100 μ l AFP-enhancing 4-element complex containing 0.2 μ g pEBAF-as-preS2 DNA were injected into tumors of nude mice bearing hepatocarcinoma cells HepG2.2.15, once each week for 4 weeks and physiological salt solution was injected likewise in the control group. The diameters of tumors were measured every 3 days. Animals were sacrificed 1 week after the final injection. Tumor tissues were dissected and their diameters were measured.

RESULTS

Construction of AFP-enhancing 4-element complex

Polypeptide and plasmid were mixed in different ratios. According to the results of 1 % agarose gel electrophoresis, DNA was completely trapped at the slot with no DNA migration when the ratio was 1:1 (Figure 2). This is the optimal ratio of polypeptide to pEBAF-as-preS2 plasmid DNA.

Extraction of total RNA

Total RNA from all biopsies were analysed by Biophotometer

(Eppendorf Co.). The ratios of A260 to A280 were all between 1.8 to 2.0. Using above total RNA as templates, RT-PCR were performed with primers for β -actin gene. A band of about 300bp in size was obtained in agarose gel electrophoresis (Figure 3A), proving that RNA was qualified for RT-PCR.

Hepatocarcinoma directed expression of antisense RNA mediated by AFP-enhancing 4-element complex

RT-PCR was carried out with specific primers (S2P1, S2P2) for HBpreS2 gene. 2 % gel electrophoresis demonstrated that the products of amplification could be detected only in tumor tissues of animals injected with AFP-enhancing 4-element complex. No specific bands could be tested in other tissues, especially in the epithelial cells of stomach mucosa and spermatid. (Figure 3B).

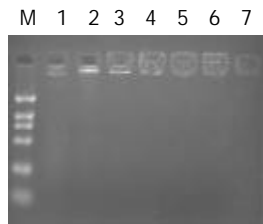


Figure 2 Construction of AFP-enhancing 4-element complex. 0.2 μ g plasmid DNA was independently mixed dropwise with various quantity of polypeptide conjugation for 30 min at room temperature, and then the mixture was analyzed with 1 % agarose gel electrophoresis. Fig 2 showed the DNA retardation of different complex mixed with DNA and peptide in different ratios. The ratio of DNA and peptide in Lane 1 to 7 is 0, 1/1, 1/2, 1/2.5, 1/3, 1/3.5, 1/4. M indicates DNA marker.

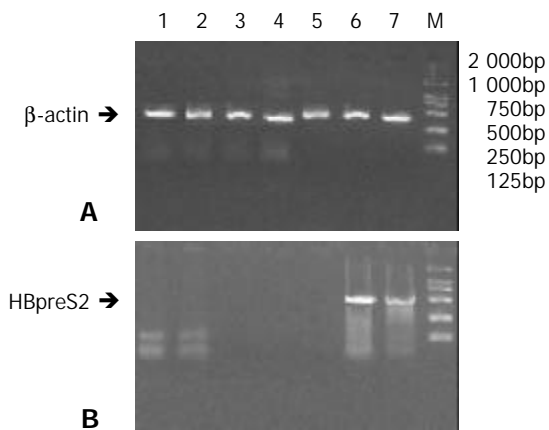


Figure 3 RT-PCR of tissues in nude mice treated AFP-enhancing 4-element complex. Total RNAs of different tissues of Nude mice bearing hepatocarcinoma were extracted 3 days after treatment with AFP-enhancing 4-element complex and then RT-PCR was performed; the expression of HBV preS2 gene was analyzed. A. RT-PCR of beta-actin. (bands 1 to 7 stand for the PCR products of spermatid, stomach, liver, spleen, heart, and tumors, M stands for the DNA marker); B. RT-PCR of HBV preS2 gene.

Inhibitory effects of AFP-enhancing 4-element complex on expression of HBV antigen in hepatocarcinoma cells

In order to correct the results, the supernatants of cell cultures in all groups were collected before transfection, marked as P/N-0hr. The final results were calculated according to the following formula: antigen secretion of cells transfected with AFP-enhancing 4-element (tested)=[P/N of tested]/([P/N-0hr of tested] \times [P/N-0hr of control]). HBsAg and HBeAg expressions of

HepG2.2.15 were lowered prominently after transfection with AFP-enhancing 4-element complex. The inhibitory rates were 33.4 % and 58.5 % respectively (Figure 4).

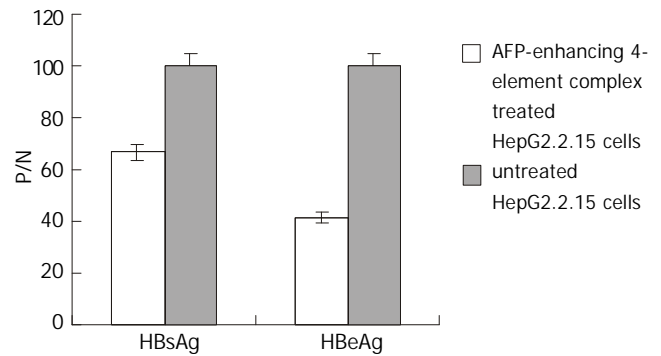


Figure 4 Effect of AFP-enhancing 4-element complex on HBV gene expression in HepG2.2.15 cells.

In vivo inhibitory effects of AFP-enhancing 4-element complex on growth of hepatocellular carcinoma in nude mice

After 4 injections of AFP-enhancing 4-element complex containing 0.2 μ g DNA, the diameter of tumor tissue was 0.995 cm \pm 0.35, which was significantly smaller than that of the control groups (2.215 cm \pm 0.25, $P < 0.05$).

DISCUSSION

Hepatocellular carcinoma (HCC), especially HBV-associated HCC, is one of the most common malignant tumor in China. At present, there's still no efficient therapy methods^[15-26]. Antisense nucleic acid, blocking the target gene and inhibiting its expression at the molecular level, has potential antiviral and antitumor effects^[27-31]. In recent years, great interests have been focusing on such novel gene therapy. Compared with synthesized antisense DNA, antisense RNA could be expressed constantly *in vivo*, so that it has long-term antiviral effects. Thus, antisense RNA is an ideal choice in gene therapy for HBV^[32-34].

There are three crucial factors to determine the efficacy of antisense gene therapy^[35]: whether the target gene plays a crucial role in tumorigenesis, whether it could be transfected uniquely to target cells, and whether it could be expressed efficiently and specifically in those target cells. In this research, according to the characteristics of HBV-associated HCC, we selected preS2 which might play an important role in the pathogenetic target site to be blocked. Moreover, in order to express preS2 antisense RNA strictly targeting on liver tumor cells, virus expression vector containing hepatocarcinoma-specific regulatory sequences (AFP promoter and enhancer) and EROP (HA20) combined with receptor mediated gene delivery system was prepared.

The protein encoded by preS2 gene plays an important role in the infection as well as malignant transformation of HBV^[36,37]. In a previous research, we have proved that synthesized antisense oligodeoxynucleotids (asON) against translation initiation region (3' 203-3' 219) of HBpreS2 has the strongest inhibitory effect on the expression of HBV antigen in HepG2.2.15 cells *in vitro*^[38]. In addition, AS5, designed by Putlitz^[33] in this region, could efficiently inhibit the viral replication and the expression of HBV antigen. In this paper, preS2 gene (3' 203-3' 240nt) was selected as target site for blocking by antisense RNA. Inhibitory experiments *in vitro* had demonstrated that a block of preS2 gene (3' 203-3' 240) could efficiently inhibited the expression of HBV antigen in HepG 2.2.15 cells. The inhibitory rates of the expression of HBsAg and HBeAg were 33.4 % and 58.5 % respectively.

The receptor-mediated gene delivery system transfers genes into the target cells by endocytosis via specific receptor. In 1998, Tian, Gu *et al* (Shanghai Cancer Institute)^[13] established a novel high-efficiency receptor-mediated gene delivery system in which GE7 targeted on EGFR were used to transfer genes to tumor cells, and HA20 was synthesized as an EROP to enable the exogenous genes to escape from the lysosome. These properties guaranteed this system to have a significant potential in gene therapy.

However, the expression of EGFR is not limited to tumor cells. We have demonstrated that green fluorescence protein (GFP) reporter gene could be also expressed in the epithelial cells of stomach mucosa and spermatid after being transfected with 4-element complex *in vivo* (published elsewhere).

For this reason, hepatocarcinoma tissue-specific antisense RNA expression vector under the control of AFP promoter was used to conjugate with GE7-PL and HA20-PL to construct an AFP-enhancing 4-element complex. As a specific marker for primary hepatocellular carcinoma, alpha fetal protein (AFP) possesses a high-targetable transcription-regulatory sequence which could be regulated precisely^[39]. Therefore, it could direct the therapeutic gene to be specifically expressed in AFP-positive hepatocellular carcinoma cells. Using human AFP incis element (promoter and enhancer) to control the expression of antisense RNA could not only enhance the high efficacy, but also possesses the targetability to hepatocellular carcinoma cells. Results showed that preS2 antisense RNA was only examined in tumor tissues of nude mice injected with AFP-enhancing 4-element complex but could not be examined in the epithelial cells of stomach mucosa and spermatid either. Moreover, the growth of hepatocellular carcinoma in nude mice could be thwarted distinctively by being injected with AFP-enhancing 4-element complex at a dose equivalent of 0.2 µg DNA per mouse each time for 4 times.

In summary, this experiment showed that AFP-enhancing 4-element complex could deliver preS2 antisense RNA targeted on hepatoma cells and inhibited both HBV gene expression *in vitro* and tumor growth *in vivo*. All these results indicated the therapeutic potential of AFP-enhancing 4-element complex for HBV related HCC.

REFERENCES

- Mah C**, Fraithe TJ Jr, Zolotukhin I, Song S, Flotte TR, Dobson J, Batick C, Byrne BJ. Improved Method of Recombinant AAV2 Delivery for Systemic Targeted Gene Therapy. *Mol Ther* 2002; **6**: 106-112
- Zhang Y**, Zhu C, Pardridge WM. Antisense gene therapy of brain cancer with an artificial virus gene delivery system. *Mol Ther* 2002; **6**: 67-72
- Ghosh SS**, Takahashi M, Thummala NR, Parashar B, Roy Chowdhury N, Roy Chowdhury J. Liver-directed gene therapy: Promises, problems and prospects at the turn of the century. *J Hepatol* 2000; **32** (Suppl 1): 238-252
- Lalwani AK**, Jero J, Mhatre AN. Current issues in cochlear gene transfer. *Audiol Neurootol* 2002; **7**: 146-151
- Walther W**, Stein U, Fichtner I, Voss C, Schmidt T, Schleaf M, Nellessen T, Schlag PM. Intratumoral low-volume jet-injection for efficient nonviral gene transfer. *Mol Biotechnol* 2002; **21**: 105-115
- Oupicky D**, Ogris M, Seymour LW. Development of long-circulating polyelectrolyte complexes for systemic delivery of genes. *J Drug Target* 2002; **10**: 93-98
- Richardso P**, Kren BT, Steer CJ. *In vivo* application of non-viral vectors to the liver. *J Drug Target* 2002; **10**: 123-131
- Yaghamai R**, Cutting GR. Optimized regulation of gene expression using artificial transcription factors. *Mol Ther* 2002; **5**: 685-694
- Wu GY**, Wilson JM, Shalaby F, Grossman M, Shafritz DA, Wu CH. Receptor mediated gene delivery in vivo. partial correction of genetic analbuminemia in nagase rats. *J Biol Chem* 1991; **266**: 14338-14342
- Huber BE**, Richards CA, Krenitsky TA. Retroviral mediated gene therapy for the treatment of hepatocellular carcinoma: an innovative approach for cancer therapy. *Proc Natl Acad Sci USA* 1991; **88**: 8039-8043
- Sato Y**, Tanaka K, Lee G, Kanegae Y, Sakai Y, Kaneko S, Nakabayashi H, Tamaoki T, Saito I. Enhanced and specific gene expression via tissue-specific production of cre-recombinase using adenovirus vector. *Biochem Biophys Res Commun* 1998; **244**: 455-462
- Brand K**, Loser P, Arnold W, Bartels T, Strauss M. Tumor cell-specific transgene expression prevents liver toxicity of the adeno-HSVtk/GCV approach. *Gene Ther* 1998; **5**: 1363-1371
- Tian PK**, Ren SJ, Ren CC, Teng QS, Qu SM, Yao M, Gu JR. A novel receptor-targeted gene delivery system for gene therapy. *Zhongguo Kexue (Series C)* 1998; **28**: 554-558
- Ono Y**, Onda H, Sasaada R, Igarashi K, Sugino Y, Nishiola K. The complete nucleotide sequences of the cloned hepatitis B virus DNA; subtype adr and adw. *Nucleic Acids Research* 1983; **11**: 1747-1757
- Maddrey WC**. Hepatitis B: an important public health issue. *J Med Virol* 2000; **61**: 362-366
- Lau GK**. Hepatitis B infection in China. *Clin Liver Dis* 2001; **5**: 361-379
- Merican I**, Guan R, Amarapura D, Alexander MJ, Chutaputti A, Chien RN, Hasnain SS, Leung N, Lesmana L, Phiet PH, Sjalfoellah Noer HM, Sollano J, Sun HS, Xu DZ. Chronic hepatitis B virus infection in Asian countries. *J Gastroenterol Hepatol* 2000; **15**: 1356-1361
- Zhuang L**, You J, Tang BZ, Ding SY, Yan KH, Peng D, Zhang YM, Zhang L. Preliminary results of Thymosin-α1 versus interferon-α-treatment in patient with HBeAg negative and serum HBV DNA positive chronic hepatitis B. *World J Gastroenterol* 2001; **7**: 407-410
- Xie Q**, Guo Q, Zhou XQ, Gu RY. Effect of adenine arabinoside monophosphate coupled to lactosaminated human serum albumin on duck hepatitis B virus. *Shijie Huaren Xiaohua Zazhi* 1999; **7**: 125-126
- Li J**, Tang B. Effect on replication of hepatitis B virus by Chinese traditional medicine. *Shijie Huaren Xiaohua Zazhi* 2000; **8**: 945-946
- Xu CT**, Pan BR. Current status of gene therapy in gastroenterology. *World J Gastroenterol* 1998; **4**: 85-89
- Xu KC**, Wei BH, Yao XX, Zhang WD. Recently therapy for chronic hepatitis B virus by combined traditional Chinese and Western medicine. *Shijie Huaren Xiaohua Zazhi* 1999; **7**: 970-974
- Lau GK**. Use of immunomodulatory therapy (other than interferon) for the treatment of chronic hepatitis B virus infection. *J Gastroenterol Hepatol* 2000; **15** (Suppl): E46-52
- Guan R**. Interferon monotherapy in chronic hepatitis B. *J Gastroenterol Hepatol* 2000; **15** (Suppl): E34-40
- Torresi J**, Locarnini S. Antiviral chemotherapy for the treatment of hepatitis B virus infections. *Gastroenterology* 2000; **118** (2 Suppl 1): S83-103
- Doo E**, Liang TJ. Molecular anatomy and pathophysiologic implications of drug resistance in hepatitis B virus infection. *Gastroenterology* 2001; **120**: 1000-1008
- Feng RH**, Zhu ZG, Li JF, Liu BY, Yan M, Yin HR, Lin YZ. Inhibition of human telomerase in MKN-45 cell line by antisense hTR expression vector induces cell apoptosis and growth arrest. *World J Gastroenterol* 2002; **8**: 436-440
- Nie QH**, Cheng YQ, Xie YM, Zhou YX, Cao YZ. Inhibiting effect of antisense oligonucleotides phosphorothioate on gene expression of TIMP-1 in rat liver fibrosis. *World J Gastroenterol* 2001; **7**: 363-369
- Wang XW**, Yuan JH, Zhang RG, Guo LX, Xie Y, Xie H. Antihepatoma effect of alpha-fetoprotein antisense phosphorothioate oligodeoxyribonucleotides in vitro and in mice. *World J Gastroenterol* 2001; **7**: 345-351
- Yatabe N**, Kyo S, Kondo S, Kanaya T, Wang Z, Maida Y, Takakura M, Nakamura M, Tanaka M, Inoue M. 2-5A antisense therapy directed against human telomerase RNA inhibits telomerase activity and induces apoptosis without telomere impairment in cervical cancer cells. *Cancer Gene Ther* 2002; **9**: 624-630
- Yang S**, Fang D, Liu A, Yang J, Luo Y, Lu R, Liu W. Reversing malignant phenotypes of liver cancer cell lines with antisense gene to human telomerase reverse transcriptase. *Zhonghua*

- Ganzangbing Zazhi* 2002; **10**: 97-99
- 32 **Wu J**, Gerber MA. Gerber. The inhibitory effects of antisense RNA on hepatitis B virus surface antigen synthesis. *J General Virol* 1997; **78**: 641-647
- 33 **zu Putlitz J**, Wieland S, Blum HE, Wands JR. Antisense RNA complementary to hepatitis B virus specifically inhibits viral replication. *Gastroenterology* 1998; **115**: 702-713
- 34 **Arteaga CL**, Holt JT. Tissue-targeted antisense c-fos retroviral vector inhibits established breast cancer xenografts in nude mice. *Cancer Res* 1996; **56**: 1098-1103
- 35 **Wang S**, Dolnick BJ. Quantitative evaluation of intracellular sense: antisense RNA hybrid duplexes. *Nucleic Acids Res* 1993; **21**: 4383-4391
- 36 **Neurath AR**, Strick N, Sproul P. Search for hepatitis B virus cell receptors reveals binding sites for interleukin 6 on the virus envelope protein. *J Exe Med* 1992; **175**: 461-469
- 37 **Alka S**, Hemlata D, Vaishali C, Shahid J, Kumar PS. Hepatitis B virus surface (S) transactivator with DNA-binding properties. *J Med Virol* 2000; **61**: 1-10
- 38 **Ma CH**, Sun WS, Liu SX, Ding PF, Zhang LN, Cao YL, Song J. Comparison of the anti-HBV effect of various antisense oligodeoxynucleotides. *Zhonghua Weisheng Wuwue Yu Mianyixue Zazhi* 2000; **20**: 12-14
- 39 **Watanabe K**, Saito A, Tamaoki T. Cell-specific enhances activity in far upstream region of the human alpha-fetoprotein gene. *J Biol Chem* 1987; **262**: 4812-4818

Edited by Lu HM

Is the expression of γ -glutamyl transpeptidase messenger RNA an indicator of biological behavior in recurrent hepatocellular carcinoma?

I-Shyan Sheen, Kuo-Shyang Jeng, Yi-Chun Tsai

I-Shyan Sheen, Liver Research Unit, Chang Gung Memorial Hospital, Taipei, Taiwan, China

Kuo-Shyang Jeng, Departments of Surgery, Mackay Memorial Hospital, Taipei, Taiwan and Mackay Junior School of Nursing, Taipei, Taiwan, China

Yi-Chun Tsai, Medical Research, Mackay Memorial Hospital, Taipei, Taiwan, China

Supported by grants from the Department of Health, National Science Council, Executive Yuan, Taiwan. NSC 87-2314-B-195-003

Correspondence to: Kuo-Shyang Jeng, M.D., F.A.C.S. Department of Surgery, Mackay Memorial Hospital, No. 92, Sec 2, Chung-San North Road, Taipei, Taiwan, China. issheen.jks@msa.hinet.net

Telephone: +886-2-25433535 **Fax:** +886-2-27065704

Received: 2002-10-04 **Accepted:** 2002-11-04

Abstract

AIM: To investigate the correlation between gamma-glutamyl transpeptidase (γ -GTP) expression in the primary HCC and post-resection recurrence and its biological behaviors.

METHODS: Forty consecutive patients having curative resection for HCC were included in this study. The primers for reverse-transcription polymerase chain reaction (RT-PCR) were corresponding to the 5'-noncoding human γ -GTP mRNA of fetal liver (type A), HepG2 cells (type B), and placenta (type C). Both the cancer and non-cancerous tissues of the resected liver were analyzed. The correlations between the expression of γ -GTP and the clinicopathological variables and outcomes (recurrence and survival) were studied.

RESULTS: Those with type B γ -GTP mRNA in cancer had significant higher recurrence rate than those without it (63.6 % vs 14.3 %). Both those with type B in cancer and in non-cancer died significantly more than those without it (45.5 % vs 0 % and 53.6 % vs 0 %, respectively). By multivariate analysis, the significant predictors of recurrence included high serum AFP ($P=0.0108$), vascular permeation ($P=0.0084$), and type B γ -GTP mRNA in non-cancerous liver ($P=0.0107$). The significant predictors of post-recurrence death included high serum AFP ($P=0.0141$), vascular permeation ($P=0.0130$), and daughter nodules ($P=0.0053$). As to the manifestations (recurrent number, recurrent extent, segments, extra-hepatic metastasis, and death) in recurrent patients, there were no statistical significant differences between those with type B in the primary tumor and those without it. The difference between those with type B in non-cancerous liver and those without it also was not significant.

CONCLUSION: Patients of HCC with type B γ -GTP mRNA both in cancer and in non-cancerous tissue had a worse outcome, earlier recurrence, and more post-recurrence death.

Sheen IS, Jeng KS, Tsai YC. Is the expression of γ -glutamyl transpeptidase messenger RNA an indicator of biological behavior in recurrent hepatocellular carcinoma? *World J Gastroenterol* 2003; 9(3): 468-473

<http://www.wjgnet.com/1007-9327/9/468.htm>

INTRODUCTION

Hepatocellular carcinoma (HCC) is one of the leading malignant tumors with a poor prognosis in areas of high hepatitis B and C prevalence. During the last 10 years, efforts have been made worldwide toward earlier detection and safer surgical resection of HCC. However, despite these recent diagnostic and therapeutic advances, postoperative recurrence is still common^[1-4]. How to predict recurrence before resection is a challenging problem for surgeons. Certain characteristics related to HCC recurrence have been reported widely and variably in the literatures^[1-14]. γ -glutamyl transpeptidase (γ -GTP) is an important enzyme catalyzing hydrolysis of glutathione and transfer of the γ -glutamyl residue and is widely distributed in mammalian tissues^[15-23]. The enzyme has been used as an important marker enzyme for some neoplasms, HCC and preneoplastic lesions of the liver^[24-31]. According to Tsutumi's study, changes in the expression of hepatic γ -GTP mRNA may be related to the development of HCC^[24]. The aim of this study is to elucidate the role of the expression of γ -GTP in both cancerous and non-cancerous liver tissues of primary lesion in the prediction of HCC recurrence.

MATERIALS AND METHODS

Patients and tumor samples

Forty patients with HCC who underwent curative hepatectomy at the Department of Surgery, Mackay Memorial Hospital from January 1997 to June 1998, whose tissue specimens histopathologically found to have no degeneration or necrosis, were included in this study. Freshly resected specimens were used. Clinical details were available from medical records on all patients (Table 1). The mean age of patients was 52.4 ± 16.6 years (range 16-82) with a male to female ratio of 26:14. The operations included major resections (12 partial lobectomies, 18 lobectomies and 5 extended lobectomies) and minor resections (4 segmentectomies and 1 subsegmentectomy). After the resection, all patients were followed up at out-patient-clinic receiving regular clinical assessment, periodic abdominal ultrasonography (every 2 to 3 months during the first 5 years, then every 4 to 6 months thereafter) to detect tumor recurrence, serum alpha-fetoprotein (AFP) and liver biochemistry (every 2 months during the first 2 years, then every 4 months during the following 3 years, and every 6 months thereafter). Abdominal computed tomography was also done (every 6 months during the first year, then every year). Liver specimens were stored at -80°C until RNA extraction.

Patients in the control group included 5 healthy volunteers, 5 individuals with chronic active hepatitis without HCC and 5

individuals with liver cirrhosis without HCC. All received liver biopsies for γ -GTP mRNA study during exploratory laparotomy.

Table 1 Demography

Characteristics	Total (n=40)
Age (years)	52.4±16.6 [16-78]
Male 26 (65%)	
Liver cirrhosis	33 (82.5%)
Child-Pugh class A:B	32:8 (80%:20%)
Tumor size	
Small (<3 cm)	6 (15.0%)
Median (3-10 cm)	23 (57.5%)
Large (>10 cm)	11 (27.5%)
HBsAg (+)	22 (55.0%)
Anti-HCV (+)	15 (37.5%)
AFP	
Below 20 μ g/L	17 (42.5%)
Over 1000 μ g/L	14 (35.0%)
Capsule	
Complete	18 (45.0%)
Incomplete or absent	22 (55.0%)
Edmondson-Steiner grade	
I & II	19 (47.5%)
III & IV	21 (52.5%)
Vascular permeation	17 (42.5%)
Satellite formation	19 (47.5%)
Multiple HCC	13 (32.5%)
Major resection	32 (80.0%)
Minor resection	8 (20.0%)

Reverse transcription-polymerase chain reaction

For HCC liver specimens, both nucleotide probes to each type of γ -GTP mRNA were shown in Table 2. To rule out any false positive, cancerous and non-cancerous tissue were studied for the expression of γ -GTP mRNA, respectively. For the resected specimens, the non-cancerous tissue was taken at least 1.0 cm far from HCC. For control group, only non-cancerous liver tissue was studied.

Table 2 Nucleotide sequences of the primer sets and specific oligonucleotide probes to each type of γ -GTP 5'-noncoding mRNA

Type of γ -GTP mRNA or	Primers probes	Nucleotide sequences
Primer sets		
A type	Sense	5'-CAC AGG GGA CAT ACA GTG AG-3'
	Antisense	5'-GAA ATA GCT GAA GCA CGC GC-3'
B type	Sense	5'-GGA TTC TCC CAG AGA TTG CC-3'
	Antisense	5'-GAA GGT CAA GGG AGG TTA CC-3'
C type	Sense	5'-GCC CAG AAG TGA GAG CAG TT-3'
	Antisense	5'-TCC AGA AAG CAG CTA GAG GG-3'
Oligonucleotide probes		
A type		5'-GGG CAG GGC TTG GTG AAT GGT AGC TGT GAT TAT CAT CAT G-3'
B type		5'-CGC AGG ATG GTG TGC GAG GAC CCC GAG CTG GTG TTC CAG GC-3'
C type		5'-ATA GAG ACA CCG ATT CCT GGA GGT CCA AAG AGC CTC AGG A-3'

Total RNA was extracted from the homogenized liver specimens by the method of Chomocynsky *et al.*^[32]. cDNA of γ -GTP mRNAs were amplified by reverse-transcription polymerase chain reaction (RT-PCR) using three different primer sets, which were specific for the three types. Six oligonucleotides, designed from cDNA sequences of γ -GTP at the 5'-noncoding region of human fetal liver, human placenta, and HepG2 cells were synthesized for use as the primers in PCR. The expected size of each PCR product was 308 bp in fetal liver (type A), 300 bp in Hep G2 (type B), and 386 bp in placenta (type C). The existence of intron sequences between each PCR primer set was confirmed by human γ -GTP genomic cloning and partial sequencing. The primer sets for type A, type B, and type C were corresponded to the sequences on γ -GTP cDNA from fetal liver, Hep G2 cells and placenta, respectively. An aliquot of the amplified γ -GTP cDNA fragments was analyzed on a 1 % agarose gel and transferred onto a Hybond-N membrane. The amplified γ -GTP cDNA were hybridized on Southern blots with oligonucleotide probes which were specific for each type of γ -GTP mRNA.

As the probes for type A, type B, and type C, 3 oligonucleotides were synthesized and were labeled at their 3' end using fluorescein d-UTR. The hybridized bands were reacted with HRP-labeled anti-fluorescein antibody and visualized on film using the ECL 3'-oligolabelling and detection systems of Amersham Life Science (Buckinghamshire, England), according to the instruction manual.

Parameters

The difference of γ -GTP expression in diverse clinicopathologic parameters were evaluated. Parameters included the presence of liver cirrhosis (confirmed by the operative findings and also by the pathology examination of the specimen), hepatitis B surface antigen (HBsAg), hepatitis C virus infection (anti-HCV), Child-Pugh classification of liver reverse (class A vs B), serum alpha-fetoprotein (AFP, <20 ng/ml vs 20-1 000 ng/ml vs >1 000 ng/ml) titer, tumor size (<3 cm, 3-10 cm, >10 cm), cell differentiation grade (Edmondson-Steiner grade I-II vs III-IV), encapsulation (complete, infiltration by HCC or absent) and vascular permeation (including vascular invasion and/or tumor thrombi within the portal vein or hepatic vein), daughter nodules or satellite nodules, multi-centric HCC and clinical evidence of recurrence, recurrence free interval, survival and death. The expression of γ -GTP mRNA of both cancerous tissue and non-cancerous tissue of the liver from resected specimens were compared with the above parameters by both univariate (UV) and multivariate (MV) analysis, respectively.

Statistical analysis

Statistical program (BMDP), Student's *t*-test or Mann-Whitney U test for continuous variables, χ^2 test of Fisher's exact test for categorical variables, and logistic regression and COX proportional hazards model for multivariate analysis were used. *P* value <0.05 was considered as a significant difference.

RESULTS

The types of γ -GTP mRNAs in livers obtained from 15 control patients were shown in Table 3. The γ -GTP mRNA expression was monogenic in 13 patients and polygenic in 2 patients. Type A was found in all patients (100 %), type B was found in one patient (6.7 %) and type C was found in one patient (6.7 %). In those with HCC, from the cancerous portion of the livers, the distribution of the type of γ -GTP mRNA was one (2.5 %) case of type A (monogenic), 24 (60.0 %) cases of type B (monogenic), 15 (37.5 %) cases of both type A and B (polygenic), and none of type C. From their non-cancerous portion of the livers, the distribution of the type of γ -GTP

mRNA was 12 (30.0 %) cases of type A (monogenic), 16 (40 %) cases of type B (monogenic), 12 (30 %) cases of type A and type B (polygenic) and none of type C (Table 3). Among those with HCC, the frequency of type A with type B (polygenic) or type B (monogenic) was 97.5 % in cancerous tissues and 70.0 % in non-cancerous tissues.

Table 3 Frequency of γ -GTP mRNA in liver

Tissues	mRNA types (%)				
	A	A+B	B	A+B or B	C
HCC					
Cancerous	1 (2.5)	15 (37.5)	24 (60.0)	39 (97.5)	0 (0)
Non-Cancerous	12 (30.0)	12 (30.0)	16 (40.0)	28 (70.0)	0 (0)
	A	B	C		
Control	15 (100.0)	1 (6.7)	1 (6.7)		

The correlation between those with type B and type B with type A in cancerous tissue and non-cancerous tissue and patients' characteristics were shown in Table 4. Gender, positivity of HBsAg, and Chlid-Pugh class A or B showed no statistically significant differences between the presence and the absence of type B and type B with type A γ -GTP mRNA.

Table 4 Correlation between type B γ -GTP mRNA and clinical parameters

Parameters	Cases	Type B/A+B(%)	
		HCC liver	Non HCC liver
Male	26	23 (88.5)	20 (76.9)
Female	14	10 (71.4)	8 (43.9)
HBsAg (+)	22	19 (86.4)	17 (60.7)
(-)	18	14 (77.8)	11 (39.3)
HCV (+)	15	14 (93.3)	14 (93.3) ^b
(-)	25	19 (76.0)	14 (56.0) ^b
Child A	32	25 (75.8)	21 (65.6)
Child B	8	8 (100.0)	7 (87.5)
AFP (ng/ml) <20	17	11 (64.7) ^a	9 (32.1) ^c
=20	23	22 (95.6) ^a	19 (82.6) ^c

Denotes: ^a $P=0.0295$; ^b $P=0.0151$; ^c $P=0.0430$.

From the univariate analysis, in cancerous portion of HCC livers, a significant correlation was found between type B and type B with type A expression of γ -GTP mRNA and high serum AFP level ($P=0.0295$). In non-cancerous portion of HCC livers, a significant correlation was found between type B and type B with A expression of γ -GTP mRNA and positivity of HCV antibody ($P=0.0151$) and high serum AFP level ($P=0.0430$).

The correlations between the types of γ -GTP mRNA expression and pathological parameters were shown in Table 5. From the univariate analysis, in cancerous portion of HCC livers, a significant correlation was found between type B and type B with type A γ -GTP mRNA and the presence of daughter nodules ($P=0.0089$).

In non-cancerous portion of HCC livers, a significant correlation was found between type B and type B with type A and the Edmondson-Steiner grade I and II vs III and IV ($P=0.0226$), the absence of tumor capsule ($P=0.0014$), the presence of vascular permeation ($P=0.0042$) and the presence of daughter nodules ($P=0.0012$). In both cancerous and non-cancerous livers, no statistically significant difference was

shown between type B and type B with type A and the presence of liver cirrhosis, tumor size and multi-centric HCC.

From outcome point of view, among those 39 patients whose cancerous liver with type B or type B with A γ -GTP mRNA, 21 patients (53.8 %) had recurrence (Table 6). As for the other patients without type B and B with A did not have had recurrence. The difference was statistically significant ($P=0.0328$). Among the former, 15 patients (38.5) died. Among the latter, no patient died. The difference was also statistically significant ($P=0.0328$). The death was related to tumor recurrence.

Table 5 Correlation between types of γ -GTP mRNA and pathological parameters

Parameters	Cases	Type B/A+B(%)	
		HCC liver	Non HCC liver
Cirrhosis (+)	33	27 (81.8)	22 (66.7)
	(-)	7	6 (85.7)
Size < 3 cm	6	6 (100.0)	4 (66.7)
	3-10 cm	11	7 (63.6)
	=10 cm	23	20 (86.9)
Differentiated grade I/II	19	14 (73.7)	10 (52.6) ^b
	III/IV	21	19 (90.5)
Complete capsule (+)	18	13 (72.2)	8 (44.4) ^c
	(-)	22	20 (90.9)
Vascular permeation (+)	17	16 (94.1)	16 (94.1) ^d
	(-)	23	17 (73.9)
Daughter nodules (+)	19	19 (100.0) ^a	18 (94.7) ^e
	(-)	21	14 (66.7) ^a
Multi-centric (+)	13	12 (92.3)	12 (92.3)
	(-)	27	21 (77.8)

Denotes: ^a $P=0.0089$; ^b $P=0.0226$; ^c $P=0.0014$; ^d $P=0.0042$; ^e $P=0.0012$.

Table 6 Correlation between γ -GTP mRNA and their outcome

γ -GTP mRNA	Cases	Recurrence (%)	Death (%)	
Type B in HCC liver	(+)	33	21 (63.6) ^a	15 (45.5) ^b
	(-)	7	1 (14.3) ^a	0 (0) ^b
Type B in non-HCC liver	(+)	28	22 (78.6) ^c	15 (53.6) ^d
	(-)	12	0 (0) ^c	0 (0) ^d

Denotes: ^a $P=0.0328$; ^b $P=0.0328$; ^c $P<0.0001$; ^d $P=0.0011$

Among 28 patients whose non-cancerous liver tissue was type B or type B with type A, 22 patients (78.6 %) had recurrence. Among the other 12 patients without type B or type B with type A, no patient had recurrence. The difference had statistical significance ($P<0.0001$). Among the former, 15 patients (53.6 %) died, while among the latter, no patient died. The difference had statistical significance ($P=0.0011$).

The correlations between the parameters and recurrence were shown in Table 7. In UV analysis, statistically significant difference was found in high serum AFP ($P=0.0001$), large size ($P=0.0213$), differentiation grade (III and IV) ($P=0.0049$), absence of complete capsule ($P=0.001$), vascular permeation ($P<0.0001$), presence of daughter nodules ($P=0.0003$), type B (including type B and type B with type A) in cancerous liver ($P=0.0094$) and type B in non-cancerous (including type B and type B with type A) liver ($P=0.0003$). In MV analysis, only AFP ($P=0.0108$), vascular permeation ($P=0.0048$), and type B γ -GTP mRNA in non-cancerous liver had significant difference ($P=0.0107$).

Table 7 Significant factors in recurrence and death

Parameters	Recurrence		Death	
	UV	MV	UV	MV
Sex	n.s.	n.s.	n.s.	n.s.
Age	n.s.	n.s.	n.s.	n.s.
Child-Pugh's classification: A vs. B	n.s.	n.s.	n.s.	n.s.
HBsAg (+)	n.s.	n.s.	0.0166	n.s.
HCV (+)	n.s.	n.s.	n.s.	n.s.
AFP<20 vs. 20-1000	0.0001	0.0108	0.0006	0.0141
γ -GTP mRNA (+)	n.s.	n.s.	n.s.	n.s.
Pathology of HCC:				
Size: <3 cm vs. 3-10 cm	0.0213	n.s.	0.0080	n.s.
Cirrhosis	n.s.	n.s.	n.s.	n.s.
Edmondson-Steiner grade				
Complete capsule (+)	0.0001	n.s.	0.0007	n.s.
Vascular permeation (+)	<0.0001	0.0084	<0.0001	0.0130
Daughter nodules (+)	0.0003	n.s.	0.0001	0.0053
Multicentric (+)	0.0549	n.s.	0.0550	n.s.
Type B γ -GTP mRNA in HCC liver	0.0094	n.s.	0.0119	n.s.
Type B γ -GTP mRNA in non-HCC liver	0.0003	0.0107	0.0046	n.s.

Denotes: n.s.=not significant.

Significant factors relevant to post-recurrence survival in univariate analysis included negative HBsAg ($P=0.0166$), low serum AFP level ($P=0.0006$), small tumor size ($P=0.0080$), complete capsule ($P=0.0007$), absence of vascular permeation ($P<0.0001$), absence of daughter nodules ($P=0.0001$), absence of multi-centric HCC ($P=0.550$), absence of type B γ -GTP mRNA in cancerous tissue ($P=0.0119$) or non-cancerous tissue of HCC liver ($P=0.0046$). However, in MV analysis, only serum AFP ($P=0.0141$), vascular permeation ($P=0.0130$) and daughter nodules ($P=0.0053$) had significant difference.

DISCUSSION

γ -glutamyl transpeptidase (γ -GTP) is a plasma membrane-bound enzyme which has major importance in the metabolism of glutathione^[33,34]. Stark *et al* mentioned that metabolism of glutathione by γ -GTP in pre-neoplastic liver foci may initiate an oxidative process leading to a radical-rich environment and result in oxidative damage^[25]. Such damage may contribute to foci progress to malignancy. It has been reported that HCC of rat and human both expresses γ -GTP enzymes with unique carbohydrate moieties compared with normal liver enzymes^[20,24,28,35]. The presence of the unique γ -GTP isoform for HCC in patient serum had been used as a marker for the diagnosis of HCC^[28]. γ -GTP was used as an important marker enzyme for chemically induced HCC, because it is present in both primary HCC and pre-neoplastic lesions of the liver or some other liver diseases^[24-27,30,31,36-40]. It has been recently used as a response indicator in the treatment of hepatitis^[41].

Experimentally, Mallory bodies develop in mice treated chronically with griseofulvin, and HCC is also found in these animals^[42]. In hepatocytes developing Mallory bodies, histologically detectable γ -GTP activity was observed from the early stage of development. These results strongly suggested that changes in γ -GTP in livers may be closely related to the phenotypical expression of carcinogenesis of hepatocytes.

Furthermore, many previous studies concerning γ -GTP in HCC strongly suggest that changes in hepatic γ -GTP expression may closely related to the development of HCC. However, its mechanisms are not well known, and the reports of genomic analysis on the specific γ -GTP to HCC is not common.

Recently, human γ -GTP complementary DNA (cDNA) sequences from fetal liver, placenta, and HepG2 cells have been published. These cDNA sequences showed identical GGT protein structure. The most significant difference among these cDNAs exists in the 5'-noncoding region, suggesting that (1) human γ -GTP mRNA might be regulated by alternative-splicing mechanisms in this region, or (2) they are derived from different γ -GTP genes. Pawlak *et al* reported that at least four different γ -GTP genes or pseudogenes are present in human genome^[16]. However, pathophysiological roles of the genetic polymorphisms of γ -GTP genes are not well known. In Tsutsumi's study, polymorphisms of γ -GTP mRNAs at the 5'-noncoding region were analyzed.

The results obtained in placenta, fetal liver and Hep G2 cells indicate that the system used in the study is specific to define three types of γ -GTP mRNA^[24]. Differences of γ -GTP in tissues have been attributed to sialic acid contents^[15]. In normal liver, the main type of γ -GTP mRNA was type A^[24]. The expression was monogenic in most cases and polygenic in some cases. In the polygenic cases, type C was found commonly and type B was found occasionally. According to Tsutsumi's report, in cases with liver diseases but not HCC, the distribution of the of γ -GTP mRNA was nearly the same as in normal livers^[24]. Our results are similar with the above. On the other hand, the main type of γ -GTP mRNA in cancerous tissue was type B. In Tsutsumi's series, type B was found in all cases, and in more than half of the cases, only type B was detected^[24]. In our series, type B was found in 60 % of patients and the combination of type A with type B and only type B are detected in 97.5 %. Tsutsumi reported that in non-cancerous tissues from livers with HCC, the main types of γ -GTP mRNA were type A and B^[24]. Both types were found in all cases, except for one case in which type B was not detected. In this study, type B was found in 40 % of patients and both type B with Type A and type B were detected in 70 % of patients. The prevalence of type B was significantly higher in both cancerous and non-cancerous tissues of liver with HCC than that in livers without HCC. The prevalence of type A in cancerous tissues, but not in non-cancerous tissues, was significantly lower than that in livers without HCC. These results strongly suggested that the γ -GTP mRNA expression in the human liver may shift from type A to type B during the development of HCC. The high prevalence of type B in non-cancerous tissues of livers with HCC suggested that the shift of the γ -GTP mRNA may occur from the preneoplastic stage of hepatocytes. The shift of mRNA expression may occur early in the development of recurrence or even in pre-neoplastic stage. Based on that, we used the shift of the γ -GTP mRNA as a tool to predict the recurrence of HCC during the follow-up after resection of primary lesion of HCC.

The high recurrence rate after resection is one of the main factors in the poor outcome for HCC patients^[1-6]. Tumor recurrence limits the long-term survival. However, tumor recurrence is well correlated with tumor invasiveness. From the literatures, tumor invasiveness may be determined from high serum AFP, hepatitis vascular permeation, the grade of cell differentiation, infiltration or absence of capsule, size, coexisting cirrhosis, presence of daughter nodules, and multiple lesions^[1-14]. Our study suggested that the presence of type B (Hepa G cells) in both HCC tissue and non-cancerous liver tissue of resected HCC specimens was closely related to some invasiveness parameters of HCC. The presence of type B γ -GTP mRNA in cancerous tissue was correlated statistically with high serum level of AFP, daughter nodules, post-resection recurrence and post-recurrence survival. Whereas, the presence of type B γ -GTP mRNA in non-cancerous liver tissue was correlated significantly with hepatitis C infection, high serum level of AFP, Edmondson-Steiner grade III and IV of cellular

differentiation, absence of infiltration of capsule, vascular permeation, daughter nodules, post-resection recurrence and postrecurrence survival.

The presence of type B γ -GTP mRNA which is detected from non-cancerous portion of liver tissue of the resected HCC specimens may be considered as its presence in the remnant liver of the patients who had received resection. High level of serum AFP had been considered as a poor prognostic index^[5]. According to our study, it was correlated well with the presence of type B γ -GTP mRNA in both cancerous tissue and non-cancerous tissue. It was also correlated statistically significantly with tumor recurrence and survival.

More hepatitis C infection, but not hepatitis B infection was found in the presence of type γ -GTP mRNA in the remnant liver. It was also corresponded with a higher recurrence and less survival. Some literature has also mentioned that the prognosis of hepatitis C infection is worse^[1,11]. Vascular permeation, indicating tumor invasiveness, consists of either tumor invasion of the hepatic vein, portal vein and/or hepatic artery, or tumor thrombi within the vessels. It may be detected preoperatively by ultrasonography, arteriography or portography, intraoperatively by ultrasonography or direct observation, or postoperatively by pathological examination of surgical specimens. Vascular permeation is the most consistent significant prognostic factor of postoperative tumor recurrence^[2, 3, 8-10, 11-13]. In univariate analysis, the presence of type B the prognosis in the remnant liver is significantly related to vascular permeation and in the COX model, patients with vascular permeation had significantly more recurrence and less survival.

Whether the grade of differentiation of HCC is a determinant of recurrence after resection has been debated for a long time^[1, 2, 9, 11]. The histological differentiation of the HCCs in this study correlated significantly with γ -GTP, and the presence of type B γ -GTP mRNA increased with increasing dedifferentiation. Our findings are consistent with that shift to type B γ -GTP mRNA in the remnant liver may be associated with the progression of HCC as an event in hepatocarcinogenesis.

The exact mechanism of capsular formation is not known. A tumor capsule may act as a barricade preventing the spread of cancer cells and has a positive role in the prognosis of HCC^[2, 5, 7, 8, 10, 13]. The invaded capsule was regarded as incomplete in our series. We found that the expression of type B γ -GTP mRNA in the remnant liver was higher in patients with no capsule and incomplete capsule. Multifocal HCCs are also a controversial issue. Some consider them an early metastasis via the portal vein but some consider them multicentric. The former is a poor prognostic factor but the latter might not be. Without the aid of molecular biology, it is difficult to differentiate daughter nodules, intrahepatic metastatic nodules and multicentric HCC^[14]. In the present study, we selected daughter or satellite nodules according to the criteria of the Liver Cancer Study Group of Japan. As for the evaluation of prognosis after recurrence, some authors reported that the most significant factor affecting the survival time of patients with intrahepatic recurrence was the number of tumor nodules at the time of recurrence^[1, 2, 4, 8, 9, 12]. In our study, those with the presence of daughter nodules showed a higher presence of type B γ -GTP mRNA in both remnant liver and the original resected HCC tissues.

Tumor size has been emphasized as one of the significant prognostic factors because vascular invasion and daughter lesions may increasingly develop as the tumor grows^[2-5, 8, 11-13]. In our study, no correlation between the presence of type B γ -GTP mRNA and tumor size was found. In addition, tumor size also had no correlation with recurrence or survival in our patients. From our experience, some large HCCs were the result

of expansive growth and had slow intraportal or distant spread. Our studies showed tumor invasiveness and prognosis was correlated with the presence of HCV infection, high serum level of AFP, vascular permeation, the grade of cell differentiation, infiltration or absence of capsule and daughter nodules. They were also all associated with the expression of type level mRNA in the remnant liver. Among them, serum AFP level and daughter nodules were associated with the presence of type B in HCC tissues. It suggested that the shift of type A to type B of γ -GTP mRNA in the liver tissues were strongly related to the development of HCC, including the progression of preneoplastic tissue and the potential of post-resection recurrence, the invasiveness of HCC and less survival of the patients. It was recommended that the expression of γ -GTP mRNA in both cancerous tissue and non-cancerous tissue of the resected HCC specimens may play a significant role in predicting the prognosis of HCC in patients after resection.

REFERENCES

- 1 **Ikedo K**, Saitoh S, Tsubota A, Arase Y, Chayama K, Kumada H, Watanabe G, Tsurumaru M. Risk factors for tumor recurrence and prognosis after curative resection of hepatocellular carcinoma. *Cancer* 1993; **71**: 19-25
- 2 **Arii S**, Tanaka J, Yamazoe Y, Minematsu S, Morino T, Fujita K, Maetani S, Tobe T. Predictive factors for intrahepatic recurrence of hepatocellular carcinoma after partial hepatectomy. *Cancer* 1992; **69**: 913-919
- 3 **Shirabe K**, Kanematsut T, Matsumata T, Adachi E, Akazawa K, Sugimachi K. Factors linked to early recurrence of small hepatocellular carcinoma after hepatectomy: univariate and multivariate analysis. *Hepatology* 1991; **14**: 802-805
- 4 **Jow SC**, Chiu JH, Chau GY, Loong CC, Lui WY. Risk factors linked to tumor recurrence of human hepatocellular carcinoma after hepatic resection. *Hepatology* 1992; **16**: 1367-1371
- 5 **Nagao T**, Inoue S, Goto S, Mizuta T, Omori Y, Kawano N, Morioka Y. Hepatic resection for hepatocellular carcinoma. *Ann Surg* 1987; **205**: 33-40
- 6 **Sasaki Y**, Imaoka S, Masutani S, Ohashi I, Ishikawa O, Koyama H, Iwanaga T. Influence of coexisting cirrhosis on long-term prognosis after surgery in patients with hepatocellular carcinoma. *Surgery* 1992; **112**: 515-521
- 7 **Lai EC**, Ng IO, Ng MM, Lok AS, Tam PC, Fan ST, Choi TK, Wong J. Long-term results of resection for large hepatocellular carcinoma: a multivariate analysis of clinicopathological features. *Hepatology* 1990; **11**: 815-818
- 8 **Anonymous**. Primary liver cancer in apan-clinicopathologic features and results of surgical treatment. Liver cancer study group of Japan. *Ann Surg* 1990; **211**: 277-287
- 9 **Hsu HC**, Sheu JC, Lin YH, Chen DS, Lee CS, Hwang LY, Beasley RP. Prognostic histologic features of resected small hepatocellular carcinoma (HCC) in Taiwan. *Cancer* 1985; **56**: 672-680
- 10 **el-Assal ON**, Yamanoi A, Soda Y, Yamaguchi M, Yu L, Nagasue N. Proposal of invasiveness score to predict recurrence and survival after curative hepatic resection for hepatocellular carcinoma. *Surgery* 1997; **122**: 571-572
- 11 **Haratake J**, Takeda S, Kasai T, Nakano S, Tokui N. Predictable factors for estimating prognosis of patients after resection of hepatocellular carcinoma. *Cancer* 1993; **72**: 1178-1183
- 12 **Yamanaka N**, Okamoto E. Conditions favoring long-term survival after hepatectomy for hepatocellular carcinomas. *Cancer Chem Pharm* 1989; **23** (Suppl): S83-S86
- 13 **Vauthey JN**, Vauthey JN, Klimstra D, Franceschi D, Tao Y, Fortner J, Blumgart L, Brennan M. Factors affecting long-term outcome after hepatic resection for hepatocellular carcinoma. *Am J Surg* 1995; **169**: 28-35
- 14 **Nakano S**, Haratake J, Okamoto K, Takeda S. Investigation of resected multinodular hepatocellular carcinoma: assessment of unicentric or multicentric genesis from histological and prognosis viewpoint. *Am J Gastroenterol* 1994; **9**: 189-193
- 15 **Pawlak A**, Cohen EH, Octave JN, Schweickhardt R, Wu SJ, Bulle F, Chikhi N, Baik JH, Siegrist S, Guellaen G. An alternatively processed mRNA specific for gamma-glutamyl transpeptidase

- in human tissues. *J Biol* 1990; **265**: 3256-3262
- 16 **Pawlak A**, Wu SJ, Bulle F, Suzuki A, Chikhi N, Ferry N, Baik JH, Siegrist S, Guellaen G. Different gamma-glutamyl transpeptidase mRNAs are expressed in human liver and kidney. *Biochem Biophys Res Communications* 1989; **164**: 912-918
- 17 **Das ND**, Shichi H. Tissue difference in gamma-glutamyl transpeptidase attributed to sialic acid content. *Life Sciences* 1979; **25**: 1821-1827
- 18 **Kottgen E**, Reutter W, Gerok W. Two different gamma-glutamyl transpeptidase during development of liver and small intestine: a fetal and an adult glycoprotein. *Biochem Biophys Res Communications* 1976; **72**: 61-66
- 19 **Rajpert-De Meyts E**, Heisterkamp N, Groffen J. Cloning and nucleotide sequence of human gamma-glutamyl transpeptidase. *Proc Natl Acad Sci USA* 1988; **85**: 8840-8844
- 20 **Hudson EA**, Munks RJ, Manson MM. Characterization of transcriptional regulation of gamma-glutamyl transpeptidase in rat liver involving both positive and negative regulatory elements. *Mol Carcinog* 1997; **20**: 376-388
- 21 **Brouillet A**, Holic N, Chobert MN, Laperche Y. The gamma-glutamyl transpeptidase gene is transcribed from a different promoter in rat hepatocytes and biliary cells. *AM J Pathol* 1998; **152**: 1039-1048
- 22 **Hanigan MH**, Frierson HF Jr, Brown JE, Lovell MA, Taylor PT. Human ovarian tumors express gamma-glutamyl transpeptidase. *Cancer Res* 1994; **54**: 286-290
- 23 **Wetmore LA**, Gerard C, Drazen JM. Human lung expresses unique gamma-glutamyl transpeptidase transcripts. *Proc Natl Acad Sci USA* 1993; **90**: 7461-7465
- 24 **Tsutsumi M**, Sakamuro D, Takada A, Zang SC, Furukawa T, Taniguchi N. Detection of a unique gamma-glutamyl transpeptidase messenger RNA species closely related to the development of hepatocellular carcinoma in humans: a new candidate for early diagnosis of hepatocellular carcinoma. *Hepatology* 1996; **23**: 1093-1097
- 25 **Stark AA**, Russell JJ, Langenbach R, Pagano DA, Zeiger E, Huberman E. Localization of oxidative damage by a glutathione-gamma-glutamyl transpeptidase system in preneoplastic lesions in sections of livers from carcinogen-treated rats. *Carcinogenesis* 1994; **15**: 343-348
- 26 **Tsuchiya S**, Yamazaki T, Camba EM, Morita T, Matsue H, Yoshida Y, Sato K. Comparison of the peptide and saccharide moieties of gamma-glutamyl transpeptidase isolated from neoplastic and non-neoplastic human liver tissue. *Clin Chem Acta* 1985; **152**: 17-26
- 27 **Toya D**, Sawabu N, Ozaki K, Wakabayashi T, Nakagen M, Hattori N. Purification of gamma-glutamyltranspeptidase (gamma-GTP) from human hepatocellular carcinoma (HCC), and comparison of gamma-GTP with the enzyme from human kidney. *Ann N Y Acad Sci* 1983; **417**: 86-96
- 28 **Taniguchi N**, House S, Kuzumaki N, Yokosawa N, Yamagiwa S, Iizuka S, Makita A, Sekiya C. A monoclonal antibody against gamma-glutamyltransferase from human primary hepatoma: its use in enzyme-linked immunosorbent assay of sera of cancer patients. *JNCI* 1985; **75**: 841-847
- 29 **Doodspeed DC**, Dunn TJ, Miller CD, Pitot HC. Gamma-glutamyl transpeptidase transpeptidase cDNA: comparison of hepatoma and kidney mRNA in the human and rat. *Gene* 1989; **76**: 1-9
- 30 **Carter JH**, Richmond RE, Carter HW, Potter CL, Daniel FB, DeAngelo AB. Quantitative image cytometry of hepatocytes expressing gamma-glutamyl transpeptidase and glutathione S-transferase in diethylnitrosamine-initiated rats treated with phenobarbital and/or phthalate esters. *J Histochem Cytochem* 1992; **40**: 1105-1115
- 31 **Gallagher BC**, Rudolph DB, Hinton BT, Hanigan MH. Differential induction of gamma-glutamyl transpeptidase in primary cultures of rat and mouse hepatocytes parallels induction during hepatocarcinogenesis. *Carcinogenesis* 1998; **19**: 1251-1255
- 32 **Chomczynski P**, Sacchi N. Single-step method of RNA isolation by acid guanidinium thiocyanate-phenol-chloroform extraction. *Ann Biochem* 1987; **162**: 156-159
- 33 **Sakamuro D**, Yamazoe M, Matsuda Y, Kangawa K, Taniguchi N, Matsuo H, Yoshikawa H, Ogasawara N. The primary structure of human gamma-glutamyl transpeptidase. *Gene* 1988; **73**: 1-9
- 34 **Hochwald SN**, Harriossn LE, Rose DM, Anderson M, Burt ME. Gamma-glutamyl transpeptidase mediation of tumor glutathione utilization *in vivo*. *J Natl Cancer Inst* 1996; **88**: 193-197
- 35 **Habib GM**, Rajagopalan S, Godwin AK, Lebovitz RM, Lieberman MW. The same gamma-glutamyl transpeptidase RNA species is expressed in fetal liver, hepatic carcinomas, and rasT24-transformed rat liver epithelial cells. *Mol Carcinog* 1992; **5**: 75-80
- 36 **Okuyama K**. Separation and identification of serum gamma-glutamyl transpeptidase isoenzymes by wheat germ agglutinin affinity electrophoresis: a basic analysis and its clinical application to various liver diseases. *Keio J Med* 1993; **42**: 149-156
- 37 **Seckin P**, Alptekin N, Kocak-Toker N, Uysal M, Aykac-Toker G. Hepatic gamma-glutamyl cysteine synthetase and gamma-glutamyl transpeptidase activities in galactosamine-treated rats. *Res Commun Mol pathol Pharmacol* 1995; **87**: 237-240
- 38 **Kitten O**, Ferry N. Mature hepatocytes actively divide and express gamma-glutamyl transpeptidase after D-galactosamine liver injury. *Liver* 1998; **18**: 398-404
- 39 **Colombatto P**, Randone A, Civitico G, Monti Gorin J, Dolci L, Medaina N, Oliveri F, Verme G, Marchiaro G, Pagni R, Karayiannis P, Thomas HC, Hess G, Bonino F, Brunetto MR. Hepatitis G virus RNA in the serum of patients with elevated gamma-glutamyl transpeptidase and alkaline phosphatase-a specific liver disease. *J Viral Hepatitis* 1996; **3**: 301-306
- 40 **Griffiths SA**, Good VM, Gordon LA, Hudson EA, Barrett MC, Munks RJ, Manson MM. Characterization of a promoter for gamma-glutamyl transpeptidase activated in rat liver in response to aflatoxin b1 and ethoxyquin. *Mol Carcinog* 1995; **14**: 251-262
- 41 **Van Thiel DH**, Friedlander L, Malloy P, Wright HI, Gurakar A, Faggiuoli S, Irish W. gamma-Glutamyl transpeptidase as a response predictor when using alpha-interferon to treat hepatitis C. *Hepato Gastroenterol* 1995; **42**: 888-892
- 42 **French SW**. The Mallory body: Structure, composition, and pathogenesis. *Hepatology* 1981; **1**: 76-83

Hepatocyte transformation and tumor development induced by hepatitis C virus NS3 c-terminal deleted protein

Qiong-Qiong He, Rui-Xue Cheng, Yi Sun, De-Yun Feng, Zhu-Chu Chen, Hui Zheng

Qiong-Qiong He, Rui-Xue Cheng, Yi Sun, De-Yun Feng, Hui Zheng, Department of Pathology, Xiangya School of Medicine, Central South University, Changsha 410078, Hunan Province, China
Zhu-Chu Chen, Cancer Research Institute, Central South University, Changsha 410078, Hunan Province, China

Supported by the Health Ministry Science Foundation of China, No.98-1-110

Correspondence to: Pro. Rui-Xue Cheng, Department of Pathology, Xiangya School of Medicine, Central South University, Changsha 410078, Hunan Province, China. chengrx@cs.hn.cn

Telephone: +86-731-2650410

Received: 2002-06-24 **Accepted:** 2002-07-11

Abstract

AIM: To study the effect of hepatitis C virus nonstructural protein 3 c-terminal deleted protein (HCV NS3-5') on hepatocyte transformation and tumor development.

METHODS: QSG7701 cells were transfected with plasmid pRcHCNS3-5' (expressing HCV NS3 c-terminal deleted protein) by lipofectamine and selected in G418. The expression of HCV NS3 gene and protein was determined by PCR and immunohistochemistry respectively. Biological behavior of transfected cells was observed through cell proliferation assay, anchorage-independent growth and tumor development in nude mice. The expression of HCV NS3 and *c-myc* proteins in the induced tumor was evaluated by immunohistochemistry.

RESULTS: HCV NS3 was strongly expressed in QSG7701 cells transfected with plasmid pRcHCNS3-5' and the positive signal was located in cytoplasm. Cell proliferation assay showed that the population doubling time in pRcHCNS3-5' transfected cells was much shorter than that in pRcCMV and non-transfected cells (24 h, 26 h, 28 h respectively). The cloning ratio of cells transfected with pRcHCNS3-5', pRcCMV and non-transfected cells was 33 %, 1.46 %, 1.11 %, respectively, the former one was higher than that in the rest two groups ($P < 0.01$). Tumor development was seen in nude mice inoculated with pRcHCNS3-5' transfected cells after 15 days. HE staining showed its feature of hepatocarcinoma, and immunohistochemistry confirmed the expressions of HCV NS3 and *c-myc* proteins in tumor tissue. The positive control group inoculated with HepG2 also showed tumor development, while no tumor developed in the nude mice injected with pRcCMV and non-transfected cells after 40 days.

CONCLUSION: 1. HCV NS3 c-terminal deleted protein has transforming and oncogenic potential. 2. Human liver cell line QSG7701 may be used as a good model to study HCV NS3 pathogenesis.

He QQ, Cheng RX, Sun Y, Feng DY, Chen ZC, Zheng H. Hepatocyte transformation and tumor development induced by hepatitis C virus NS3 c-terminal deleted protein. *World J Gastroenterol* 2003; 9(3): 474-478

<http://www.wjgnet.com/1007-9327/9/474.htm>

INTRODUCTION

HCV infection is a major worldwide health problem. Persistent infection with HCV is a critical risk for the development of hepatocellular carcinoma (HCC)^[1-3]. It has been reported that the Core protein, NS3, NS4B, and NS5A have oncogenic potential^[2, 4-6]. HCV NS3 protein (nucleotide 3 420 to 5 312 with 631 amino acid residues) is a multi-functional viral protein. In addition to serine proteinase activity, which is located in the one-third of the NS3 protein at the N-terminal end, helicase and nucleotide triphosphatase activities are identified in the c-terminal half of the NS3 protein^[7]. HCV NS3 that plays a key role in the life cycle of virus and interacts with host cellular protein has been one of hot spots in recent research. We found that the NIH3T3 cell has stronger telomerase activity after transfected with HCV NS3 plasmid, indicating that HCV NS3 may be an important part in the hepatocarcinogenesis^[8]. Most studies on NS proteins have been carried out by expression of single or multiple NS proteins in cultured none hepatocyte, despite the fact that HCV is a hepacivirus. In order to reflect the relation between HCV NS3 and host cell transformation more clearly, here we tried to transfect human liver cell line QSG7701 with eukaryotic cell plasmid pRcHCNS3-5' (expressing NS3 c-terminal deleted protein), and then inoculated nude mice with transfected cells to investigate its biological behaviors and carcinogenesis.

MATERIALS AND METHODS

Materials

Hepatocyte cell line QSG7701 was got from Shanghai Institute of Cell Biology, Chinese Academe of Sciences (CAS) and HepG2 cell line was got from Cell Center of Central South University. Nude mice (BALB/cA-nude) were got from Shanghai Laboratorial Animal Center, CAS. The plasmid pRcHCNS3-5' (expressing HCV NS3 c-terminal deleted protein) was the kind gift from professor Takegami^[9]. Non-expressive plasmid pRcCMV was purchased from Sigma Com USA. LipofectaminTM reagent, G418 and Dulbecco's modified Eagle medium (DMEM) were products of GIBCO BRL (Germany). *Xba*I, buffer and PCR kit, marker were bought from Sino-American Biotechnology INC (Shanghai, P.R.China). Anti-HCV NS3 protein MAb, anti-c-myc protein MAb and S-P detection kit were purchased from Boshide Com (Wuhan, P. R.China) and Maxim Biotech INC (Fuzhou, P.R.China), respectively. New-born calf serum was got from Sijiqing Bioengineering Ltd. (Hangzhou, P.R.China). PCR primers for amplifying HCVNS3-5' gene were synthesized at Shanghai Sangon Com (Shanghai, P.R.China).

Methods

Experimental groups Group 1: QSG7701 parental cells; Group 2: QSG7701 transfected with blank plasmid pRcCMV; Group 3: QSG7701 transfected with plasmid pRcHCNS3-5'; Group 4: HepG2 cell line used as positive control.

Cell culture Cell lines were maintained in DMEM with 10 % heat-inactivated new-born calf serum, 100 unit/ml penicillin and 100 unit/ml streptomycin at 37 °C in a humidified atmosphere of 5 % CO₂.

Preparation, purification and identification of plasmids pRcHCNS3-5' and pRcCMV Plasmids pRcCMV and pRcHCNS3-5' were transferred into competent *E coli* JM109 respectively. JM109 was cultured to amplify the two plasmids. Little plasmids were prepared from JM109 to identify the specificity of the plasmids. The plasmid pRcHCNS3-5' was digested with *Xba*I, resolved with agarose gel electrophoresis, and stained with ethidium bromide (EB). As shown in Figure 1, the electrophoresis analysis revealed the major 886bp fragment of the plasmid pRcHCNS3-5' as being expected. Then the plasmids were massively extracted and purified for transfecting QSG7701 cells.

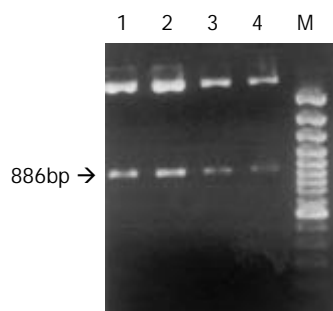


Figure 1 pRcHCNS3-5' digested with *Xba*I. Lane M:DNA marker (Generuler™ 100bpDNA). Lane: 1, 2, 3, 4 plasmid pRcHCNS3-5' with 886bp fragment. (×100).

Transfection of QSG7701 cells with plasmids pRcHCNS3-5' and pRcCMV QSG7701 cells were transfected with the plasmids pRcHCNS3-5' and pRcCMV, respectively according to the instruction of Lipofectamine reagent. Cells were seeded into selection medium containing 400 µg/ml G418 until G418-resistant clones were obtained, and then cells were maintained in G418 with concentration of 200 µg/ml (Figure 2). QSG7701 parental cells were used for the parallel control. To detect cDNA in stable transfectants, total genomic DNA was extracted according to standard methods and subjected to PCR and agarose gel electrophoresis analysis. The primers for amplifying HCVNS3-5' gene were based on published sequences^[9]. PCR conditions were 35 cycles of three steps (94 °C 30 sec, 57 °C 30 sec, 72 °C 40 sec) and then 72 °C 5 min in a 50 µl reaction mixture containing 5 µl 10×buffer, 5 µl 2 mM dNTPs, 0.5 µl of each primer (25 pmol/µl), 1 µl (100 ng)DNA, 0.5 ul 5U/µl Taq DNA polymerase, and 37.5 µl distilled water. PCR products were subjected to electrophoresis on a 0.8 % agarose gel, visualized by EB staining. As shown in Figure 3, 257bp fragment was specifically amplified from DNA of the QSG7701 cells transfected with plasmid pRcHCNS3-5', but no fragment was amplified from DNA of the pRcCMV transfected cells and parental cells.



Figure 2 Colony formation of pRcHCNS3-5' transfected QSG7701 cells in G418 (×100).

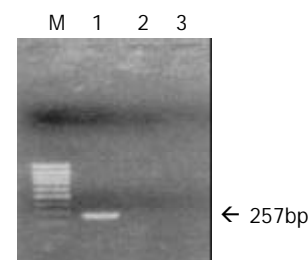


Figure 3 PCR analysis of DNA from QSG7701 transfected with pRcHCNS3-5' and pRcCMV; Lane M: 100bp marker; Lane 1: pRcHCNS3-5' transfected cells; Lane 2: pRcCMV transfected cells; Lane 3: QSG parental cells.

Immunohistochemistry S-P method was used to detect the expression of HCV NS3 protein in parental QSG7701 cells and QSG7701 cells transfected with plasmid pRcHCNS3-5', pRcCMV. PBS substituting Mabs was used as blank control. HCC expressing HCV NS3 protein was used as positive control. **Cell proliferation assay** QSG parental cells and cells transfected with pRcHCNS3-5', pRcCMV (6×10^4 cells per well) were seeded in 24-well plates and counted daily with a haemocytometer respectively. Experiment was lasted for 7 days and was repeated three times.

Anchorage-independent growth Cells were suspended at a density of 2×10^3 /ml containing 0.3 % granulated agar. The mixture was added over a layer of 0.7 % agar in medium. After 4 weeks, the morphology of transfected cells was analysed microscopically. Colonies including more than 50 cells were scored. Experiment was repeated three times.

Tumor development in athymic nude mice 12 nude mice (BALB/cA-nude, females, 4-6 weeks, 18-22 g) were divided into 4 groups of 3 nude mice each and inoculated subcutaneously in the right flank with pRcHCNS3-5', pRcCMV and parental cells (1×10^7 cells in 0.2 ml of phosphate-buffered saline) and monitored for tumor development. HepG2 cells were used as the positive control. Tumor size and animal weight were measured weekly. The nude mice were sacrificed and the tumors were removed 40 days after inoculating. Tumor tissue was fixed by 10 % formalin, embedded with paraffin wax, sliced successively 5 µm per section and stained by HE. Immunohistochemistry S-P method was used to detect the expressions of HCV NS3 protein and *c-myc* protein in tumor tissue.

Statistical analysis

F test was used. *P* value of less than 0.05 was considered as statistically significant.

RESULTS

HCV NS3 protein expression in QSG7701 cells transfected with plasmid pRcHCNS3-5'

Immunohistochemical staining showed that QSG7701 cells transfected with pRcHCNS3-5' strongly expressed HCV NS3 protein. The positive signal was in cytoplasm (Figure 4). The positive signal was also found in the positive control group, but not in the blank and negative control groups.

Cell proliferation assay

The population doubling time in cells transfected with pRcHCNS3-5' (12 h) was much shorter than that in those transfected with pRcCMV and parental QSG7701 cells (26 h, 28 h respectively). (Figure 5).

Anchorage-independent growth

The cloning efficiencies in pRcHCNS3-5', pRcCMV

transfected cells and parental cells were 33 %, 1.46 %, 1.11 %, respectively ($P < 0.01$, the former vs the rest two).

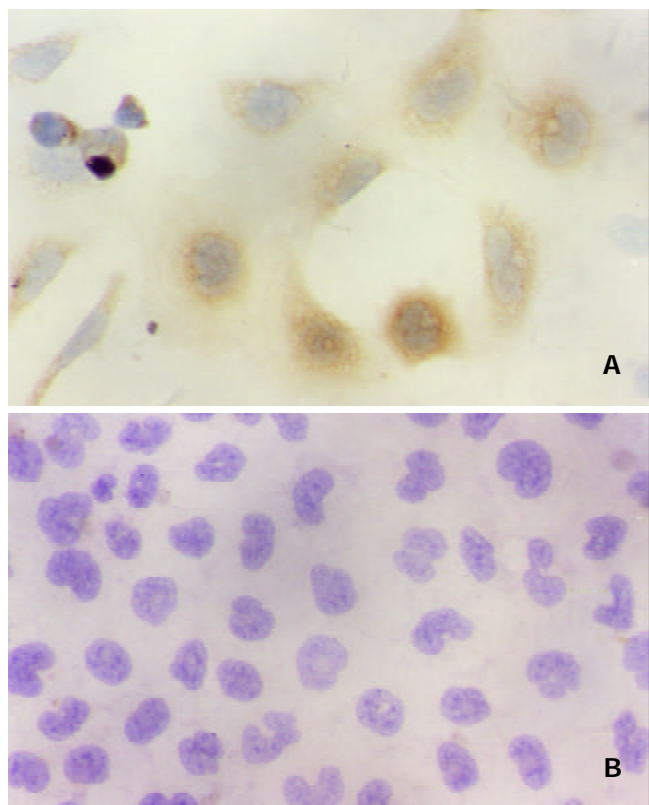


Figure 4 Immunohistochemistry analysis (S-P) of HCV NS3 protein expression in pRcHCNS3-5' transfected cells (up) and the negative control without positive signal (down) ($\times 400$).

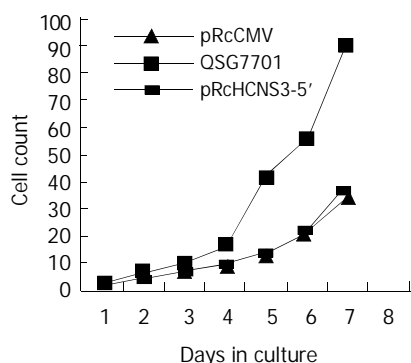


Figure 5 Proliferation rate of cells transfected with pRcHCNS3-5', pRcCMV and parental QSG7701 cells.

Tumor development in nude mice

In the nude mice inoculated with pRcHCNS3-5' transfected cells, the first evidence of well-defined and distinct subcutaneous tumors appeared on day 15. The mean tumor size and weight on day 40 were 3.08 cm³ and 3.13 g, respectively. The HepG2 cells, as positive control, also induced tumor in the nude mice. But no tumor developed in the mice inoculated with pRcCMV and non-transfected QSG7701 cells until 40 days after inoculating (Figure 6). Macroscopically, the tumors induced by pRcHCNS3-5' showed irregular yellow-brown node and appeared to be encapsulated. Central necrosis could be seen on the cut surface. Microscopically, the tumor cells exhibited similarity to hepatocyte except for heterogenesis and they arranged as trabecular with intervening sinusoids. Cancer cell nests with abundance granular necrosis were separated by fibrous tissue (Figure 7a, 7b). They showed the

histologically feature of hepatocellular carcinoma. Immunohistochemical staining showed that tumor tissue expressed HCV NS3 protein and *c-myc* protein. The positive signal was located in cytoplasm (Figure 7c, 7d).

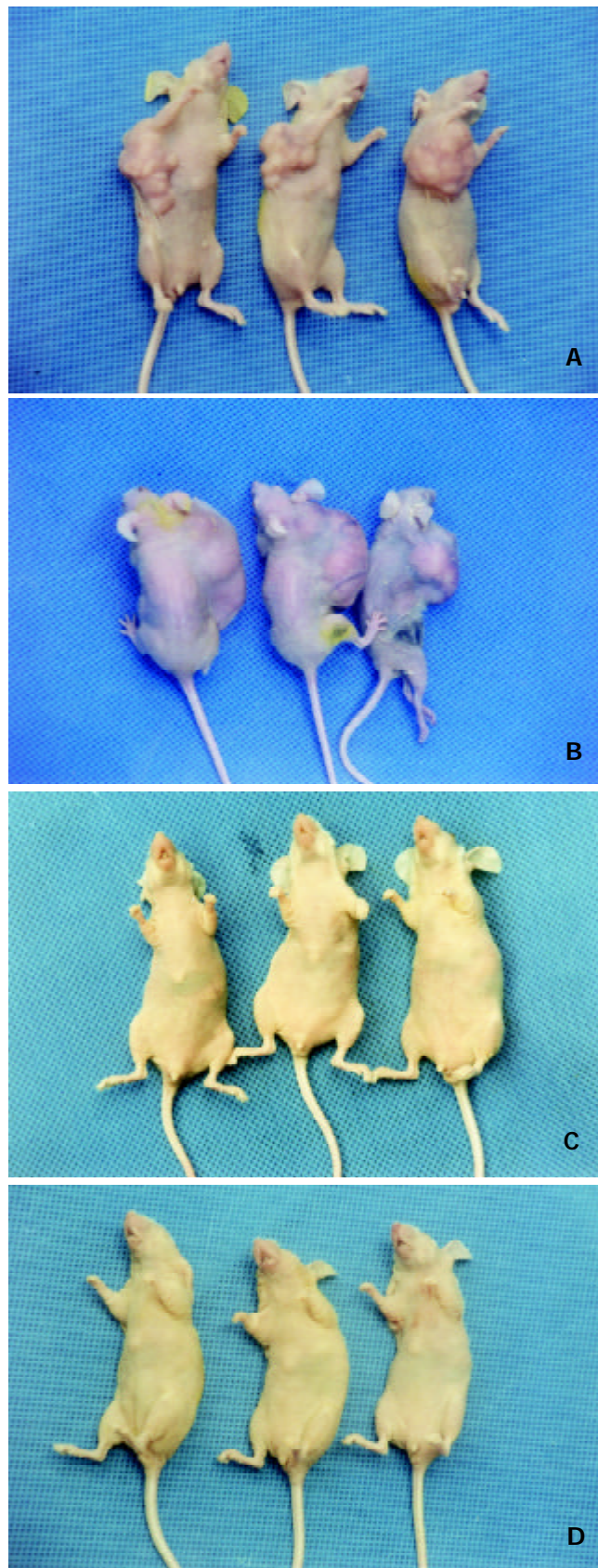


Figure 6 Tumor development in nude mice, 6a, 6b, 6c and 6d show inoculated with pRcHCNS3-5' transfected QSG7701 cells, HepG2 cells, QSG7701 cells transfected with pRcCMV and parental QSG7701 cells, respectively.

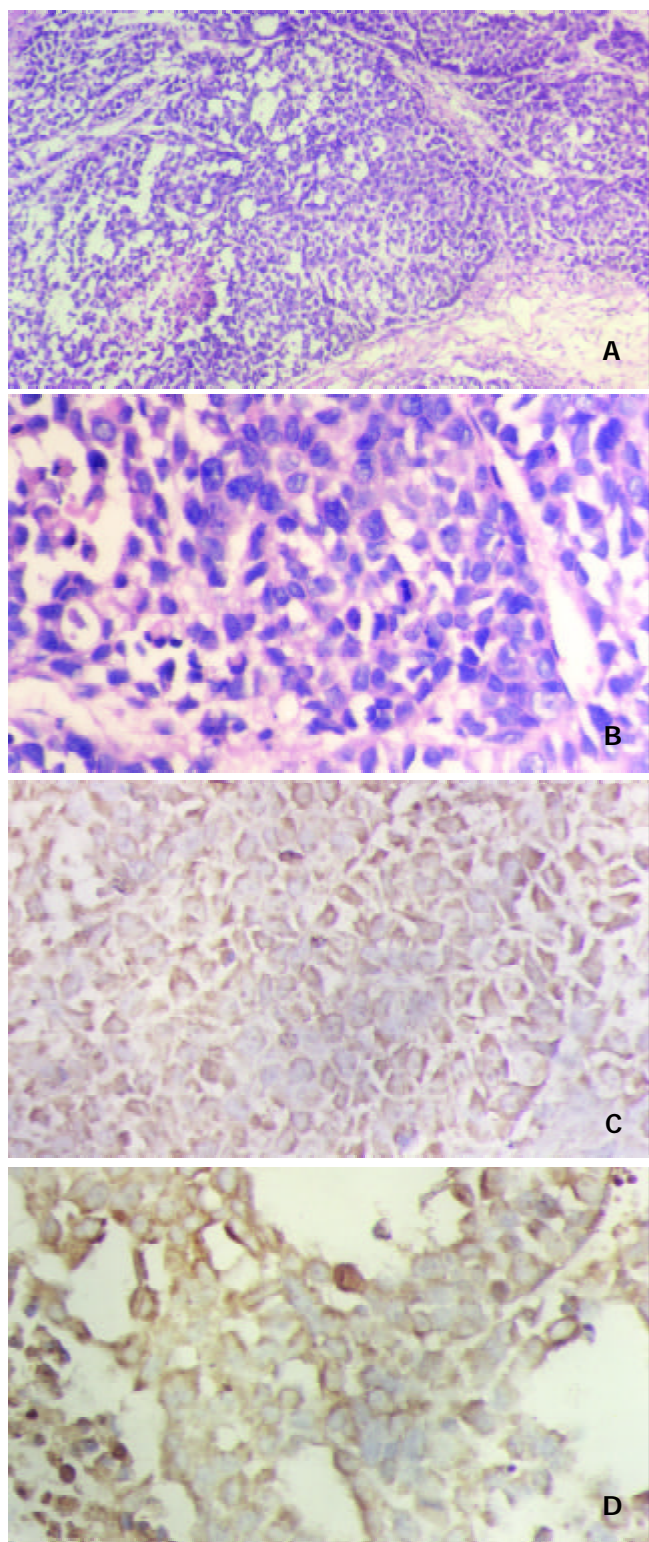


Figure 7 pRcHCNS3-5' induced hepatocellular carcinoma (7a HE \times 100, 7b HE \times 400), HCV NS3 (7c) and *c-myc* (7d) protein expressing in the tumor tissue by immunohistochemistry (S-P), the positive signals are both in cytoplasm (\times 400).

DISCUSSION

It has been reported that persistent infection with HCV is associated with HCC, and HCV replication and protein expression can be observed in HCC tissue^[1, 10-11], although the pathogenesis of HCV infection-associated HCC is still unknown. HCV, as a RNA virus without any RT activity, is replicated in the cytoplasm and does not integrate with host genome like HBV. Furthermore, unlike EBV or HPV, the HCV genome itself, does not contain any known oncogene. Most

studies indicate that the interaction between the HCV protein and liver cell gene/protein has been involved in hepatocarcinogenesis. Zemel *et al* reported significant mutations of amino acids that occur at the catalytic domain of the NS3 serine protease gene isolated from HCC tissue will affect the activity and substrate specificity of serine protease^[12]. Sakamuro^[9] and Zemel^[2] *et al* founded that HCV NS3 could transform NIH3T3 cell and non-tumorigenic rat fibroblast (RF) cell respectively. HCV NS3 can suppress actinomycin D induced apoptosis^[13], inhibit cAMP-dependent protein kinase^[14] and repress P53 function^[15-17]. But the cell lines used by most researchers were not based on HCV natural host cell-hepatocyte. Here non-tumorigenic human liver cell line QSG7701 was used in our study. QSG7701 cells that were immortally normal hepatocytes came from liver tissue 6 cm far from HCC and their karyotype number was 57^[18]. QSG7701 cells with normal hepatocyte phenotype were stably transfected with an expression vector containing cDNA for NS3 proteinase activity. The transfected cells grew rapidly, showed anchorage -independent growth in soft agar and induced significant tumor formation in nude mice. Our study firstly showed that the protease-coding gene of HCV induced malignant transformation of nontumorigenic human liver cells. Moreover injecting pRcHCNS3-5' transfected cells into nude mice led to significant tumor formation. The tumor obtained from the nude mice showed the histologically feature of hepatocellular carcinoma. The results suggest the involvement of proteinase activity of HCV NS3 N terminal peptide in cellular transforming and oncogenic potential.

Current studies show that HCV NS3 may be directly involved in hepatocarcinogenesis by disturbing the regulation of cell proliferation. But the mechanism of carcinogenesis is still perplexing. Carcinogenesis, including HCC, is the result of the abnormal proliferation of cancer cells. It is reported that various oncogenic products are related to functional abnormalities of intracellular signal transduction pathway, which have been proved to be one of the proliferative mechanism of cancer cells. Great progress has been made that HCV proteins regulate signal transduction in the recent studies. Ras/Raf/MAPK pathway is regarded to have close relation to HCV associated HCC.

Constitutive activation of the Ras/Raf/MAPK pathway is important for the transformation of mammalian cells^[19,20]. Indeed, studies have demonstrated that HCC development and progression is associated with the activation of Ras/Raf/MAPK pathway in humans and rodents^[21,22]. Our lab also found that MAPK activity is higher in HCC than that in the adjacent noncancerous lesions, suggesting a progression of HCC through Ras/Raf/MAPK activation^[23]. Recently, the development of anticancer drugs that target signaling proteins of MAPK pathway has been a major goal in the cancer treatment^[24,25]. There are several reports concerning the relationship between HCV protein and Ras/Raf/MAPK signal transduction pathway. For example, some evidences suggest that HCV C protein directly or indirectly activates Ras/Raf/MAPK signal transduction pathway elements (including Raf-1, ERK, MEK, Elk, SRE, AP-1) in different cells such as HepG2, CCL13, COS7, MCF-7, BALB/3T3 and NIH3T3^[26-31]. Borowski *et al* reported an arginine-rich domain located in the NS3 region (residues1487 to 1500 of HCV polyprotein) which strongly resembles the autoinhibitory sequence of the PKA R subunit. It binds to the C subunit of PKA and inhibits the translocation of C subunit into nucleus. Consequently, PKA functions are arrested^[32]. Marshall identified that specific sites between Ras and Raf-1 are essential to plasma membrane localization and Raf activation. The formation of Ras/Raf-1 complex is negatively regulated by PKA through phosphorylation of Raf-1 N terminal serine 43, which is believed to cause an N-terminal cap structure to cover the Ras docking site which ultimately leads to inhibit Raf-1 activation^[33,34]. HCV NS3 may activate Raf-1 by interfering the function of PKA. We

previously demonstrated that HCV NS3 N-terminal peptide (residues 1020-1295) positively regulates ERK1/2 phosphorylation. Because the N terminal peptide of HCV NS3 used in our study does not include the arginine-rich domain. We preclude that either HCV NS3 interacts with PKA through other domain or HCV NS3 involves in Ras/Raf/MAPK signal transduction pathway through other targets. Nuclear transcriptional factors *c-myc* as a target factor regulated by downstream of the MAPK cascade may increased when MAPK is activated. Overexpression of *c-myc* in tumor tissue of nude mice was detected which was consistent with other's report^[35]. It is supposed that HCV NS3 may be involved in hepatocarcinogenesis through Ras/Raf/MAPK/*c-myc* signal transduction.

ACKNOWLEDGEMENT

We thank professor Takegami for his generous gift of plasmid pRcHCNS3-5'.

REFERENCES

- 1 **Li L**, Wang WL, Yu XX, Zhen JY. Detection of hepatitis C virus RNA in the tissue of hepatocellular carcinoma by multiple detection system. *Zhonghua Shiyian He Linchuangbing Duxue Zazhi* 2000; **14**: 47-52
- 2 **Zemel R**, Gerechet S, Greif H, Bachmatove L, Birk Y, Golan-Goldhirsh A, Kunin M, Berdichevsky Y, Benhar I, Tur-Kaspa R. Cell transformation induced by hepatitis C virus NS3 serine protease. *J Viral Hepat* 2001; **8**: 96-102
- 3 **Koike K**, Tsutsumi T, Fujie H, Shintani Y, Kyoji M. Molecular mechanism of viral hepatocarcinogenesis. *Oncology* 2002; **62**(Suppl 1): 29-37
- 4 **Park JS**, Yang JM, Min MK. Hepatitis C virus nonstructural protein NS4B transforms NIH3T3 cells in cooperation with the Haras oncogene. *Biochem Biophys Res Commun* 2000; **267**: 581-587
- 5 **Ghosh AK**, Steele R, Meyer K, Ray R, Ray RB. Hepatitis C virus NS5A protein modulates cell cycle regulatory genes and promotes cell growth. *J Gen Virol* 1999; **80**: 1179-1183
- 6 **Moriya K**, Fujie H, Shintani Y, Yotsuyanagi H, Tsutsumi T, Ishibashi K, Matsuura Y, Kimura S, Miyamura T, Koike K. The core protein of hepatitis C virus induces hepatocellular carcinoma in transgenic mice. *Nat Med* 1998; **4**: 1065-1067
- 7 **Kato N**. Molecular virology of hepatitis C virus. *Acta Med Okayama* 2001; **55**: 133-159
- 8 **Feng D**, Cheng R, Ouyang X, Zheng H, Tsutomu T. Hepatitis C virus nonstructural protein NS (3) and telomerase activity. *Chin Med J* 2002; **115**: 597-602
- 9 **Sakamuro D**, Furukawa T, Takegami T. Hepatitis C virus nonstructural protein NS3 transforms NIH 3T3 cells. *J Virol* 1995; **69**: 3893-3896
- 10 **Yang JM**, Wang RQ, Bu BG, Zhou ZC, Fang DC, Luo YH. Effect of HCV infection on expression of several cancer-associated gene products in HCC. *World J Gastroenterol* 1999; **5**: 25-27
- 11 **Ohishi M**, Sakisaka S, Harada M, Koga H, Taniguchi E, Kawaguchi T, Sasatomi K, Sata M, Kurohiji T, Tanikawa K. Detection of hepatitis-C virus and hepatitis-C virus replication in hepatocellular carcinoma by *in situ* hybridization. *Scand J Gastroenterol* 1999; **34**: 432-438
- 12 **Zemel R**, Kazatsker A, Greif F, Ben-Ari Z, Greif H, Almog O, Tur-Kaspa R. Mutations at vicinity of catalytic sites of hepatitis C virus NS3 serine protease gene isolated from hepatocellular carcinoma tissue. *Dig Dis Sci* 2000; **45**: 2199-2202
- 13 **Fujita T**, Ishido S, Muramatsu S, Itoh M, Hotta H. Suppression of actinomycin D-induced apoptosis by the NS3 protein of hepatitis C virus. *Biochem Biophys Res Commun* 1996; **229**: 825-831
- 14 **Borowski P**, Heiland M, Oehlmann K, Becker B, Kornetzky L, Feucht H, Laufs R. Non-structural protein 3 of hepatitis C virus inhibits phosphorylation mediated by cAMP-dependent protein kinase. *Eur J Biochem* 1996; **237**: 611-618
- 15 **Okada F**, Shiraki T, Maekawa M, Sato S. A p53 polymorphism associated with increased risk of hepatitis C virus infection. *Cancer Lett* 2001; **172**: 137-142
- 16 **Kwon HJ**, Jung EY, Ahn JY, Lee MN, Jang KL. P53-dependent transcriptional repression of p21(waf1) by hepatitis C virus NS3. *J Gen Virol* 2001; **82**: 2235-2241
- 17 **Feng DY**, Chen RX, Peng Y, Zheng H, Yan YH. Effect of HCV NS (3) protein on p53 protein expression in hep atocarcinogenesis. *World J Gastroenterol* 1999; **5**: 45-46
- 18 **Zhu DH**, Wang JB. The culture of HCC host hepatocyte QSG7701 cell line and as compared with hepatocarcinoma cell. *Zhongliu Fangzhi Yanjiu* 1979; **5**: 7-9
- 19 **Pinkas J**, Leder P. MEK1 signaling mediates transformation and metastasis of EpH4 mammary epithelial cells independent of an epithelial to mesenchymal transition. *Cancer Res* 2002; **62**: 4781-4790
- 20 **Hamad NM**, Elconin JH, Karnoub AE, Bai W, Rich JN, Abraham RT, Der CJ, Counter CM. Distinct requirements for Ras oncogenesis in human versus mouse cells. *Genes Dev* 2002; **16**: 2045-2057
- 21 **Zhu J**, Leng X, Dong N, Liu Y, Li G, Du R. Expression of mitogen-activated protein kinase and its upstream regulated signal in human hepatocellular carcinoma. *Zhonghua Waikexue Zazhi* 2002; **40**: 1-16
- 22 **Ostrowski J**, Woszczyński M, Kowalczyk P, Wocial T, Hennig E, Trzeciak L, Janik P, Bomsztyk K. Increased activity of MAP, p70S6 and p90rs kinases is associated with AP-1 activation in spontaneous liver tumours, but not in adjacent tissue in mice. *Br J Cancer* 2000; **82**: 1041-1050
- 23 **Feng DY**, Zheng H, Tan Y, Cheng RX. Effect of phosphorylation of MAPK and Stat3 and expression of c-fos and c-jun proteins on hepatocarcinogenesis and their clinical significance. *World J Gastroenterol* 2001; **7**: 33-36
- 24 **Shapiro P**. Ras-MAP kinase signaling pathways and control of cell proliferation: relevance to cancer therapy. *Crit Rev Clin Lab Sci* 2002; **39**: 285-330
- 25 **Sebolt-Leopold JS**. Development of anticancer drugs targeting the MAP kinase pathway. *Oncogene* 2000; **19**: 6594-6599
- 26 **Aoki H**, Hayashi J, Moriyama M, Arakawa Y, Hino O. Hepatitis C virus core protein interacts with 14-3-3 protein and activates the kinase Raf-1. *J Virol* 2000; **74**: 1736-1741
- 27 **Giambartolomei S**, Covone F, Levrero M, Balsano C. Sustained activation of the Raf/MEK/Erk pathway in response to EGF in stable cell lines expressing the Hepatitis C Virus (HCV) core protein. *Oncogene* 2001; **20**: 2606-2610
- 28 **Tsuchihara K**, Hijikata M, Fukuda K, Kuroki T, Yamamoto N, Shimotohno K. Hepatitis C virus core protein regulates cell growth and signal transduction pathway transmitting growth stimuli. *Virology* 1999; **258**: 100-107
- 29 **Fukuda K**, Tsuchihara K, Hijikata M, Nishiguchi S, Kuroki T, Shimotohno K. Hepatitis C virus core protein enhances the activation of the transcription factor, Elk1, in response to mitogenic stimuli. *Hepatology* 2001; **33**: 159-165
- 30 **Kato N**, Yoshida H, Kioko Ono-Nita S, Kato J, Goto T, Otsuka M, Lan K, Matsushima K, Shiratori Y, Omata M. Activation of intracellular signaling by hepatitis B and C viruses: C-viral core is the most potent signal inducer. *Hepatology* 2000; **32**: 405-412
- 31 **Shrivastava A**, Manna SK, Ray R, Aggarwal BB. Ectopic expression of hepatitis C virus core protein differentially regulates nuclear transcription factors. *J Virol* 1998; **72**: 9722-9728
- 32 **Borowski P**, Heiland M, Feucht H, Laufs R. Characterisation of non-structural protein 3 of hepatitis C virus as modulator of protein phosphorylation mediated by PKA and PKC: evidences for action on the level of substrate and enzyme. *Arch Virol* 1999; **144**: 687-701
- 33 **Marshall M**. Interactions between Ras and Raf: key regulatory proteins in cellular transformation. *Mol Reprod Dev* 1995; **42**: 493-499
- 34 **Hafner S**, Adler HS, Mischak H, Janosch P, Heidecker G, Wolfman A, Pippig S, Lohse M, Ueffing M, Kolch W. Mechanism of inhibition of Raf-1 by protein kinase A. *Mol Cell Biol* 1994; **14**: 6696-6703
- 35 **Fang Y**, Huang B, Liang Q, Li H, Huang C. Clinical significance of *c-myc* oncogene amplification in primary hepatocellular carcinoma by interphase fluorescence *in situ* hybridization. *Zhonghua Binglixue Zazhi* 2001; **30**: 180-182

Antitumor immunopreventive and immunotherapeutic effect in mice induced by hybrid vaccine of dendritic cells and hepatocarcinoma *in vivo*

Jin-Kun Zhang, Jun Li, Juan Zhang, Hai-Bin Chen, Su-Biao Chen

Jin-Kun Zhang, Jun Li, Juan Zhang, Hai-Bin Chen, Su-Biao Chen, Cancer Pathology Laboratory, Shantou University Medical College, Shantou 515031, Guangdong Province, China

Supported by the Natural Science Foundation of Guangdong Province, China, No. 980180; the Woman Science and Technology Workers Association of Guangdong Province, China, No.2001001

Correspondence to: Prof. Jin Kun Zhang, Tutor of Doctor, Cancer Pathology Laboratory, Shantou University Medical College, 22 Xinlinglu, Shantou 515031, Guangdong Province, China. jkzhang@stu.edu.cn

Telephone: +86-754-8900443 **Fax:** +86-754-8557562

Received: 2002-07-20 **Accepted:** 2002-10-12

Abstract

AIM: To develop a tumor vaccine by fusion of H22 hepatocarcinoma cells and DC, and to study its protective and therapeutic effect against H22 cell.

METHODS: H22-DC vaccine was produced by PEG fusion of H22 and DC induced by cytokine released from splenic mononuclear cells, sorted by CD11c magnetic microbead marker. It was injected through the tail vein of the mice and the H₂₂-DC oncogenesis was detected in the liver, spleen and lung. In order to study the therapeutic and protective effect of H₂₂-DC against tumor H₂₂, two groups were divided: immune group and therapeutic group. Immune group was further divided into P, D, HD and H subgroups, immunized by PBS, DC, H₂₂-DC and inactivated H₂₂, respectively, and attacked by H₂₂ cell. The tumor size, tumor weight, mice survival time and tumor latent period were recorded and statistically analyzed; Therapeutic group was divided into three subgroups of P, D and HD, and attacked by H₂₂, then treated with PBS, DC, and H₂₂-DC, respectively. Pathology and flow cytometry were also applied to study the mechanism how the H₂₂-DC vaccine attacked on the H₂₂ cell.

RESULTS: 1. No oncogenesis was found in spleen, lung and liver after H22-DC injection. 2. Hybrid vaccine immunized mice had strongest CTL activity. 3. In the immune group, latent period was longer in HD subgroup than that in P, H and D subgroup; and tumor size and weight were smaller in HD subgroup than that in P, H and D subgroup. 4. In therapeutic group, tumor size was smaller in HD subgroup than that in P, D subgroup.

CONCLUSION: 1. H22-DC tumor vaccine is safe without oncogenesis *in vivo*. 2. Hybrid vaccine can stimulate potent specific CTL activity against H22. 3. H22-DC vaccine has distinctive prophylactic effect on tumor H22 and can inhibit the tumor growth.

Zhang JK, Li J, Zhang J, Chen HB, Chen SB. Antitumor immunopreventive and immunotherapeutic effect in mice induced by hybrid vaccine of dendritic cells and hepatocarcinoma *in vivo*. *World J Gastroenterol* 2003; 9(3): 479-484
<http://www.wjgnet.com/1007-9327/9/479.htm>

INTRODUCTION

Tumor cells have low antigenicity and high antigen modulatory ability, by which tumor associated antigen or tumor specific antigen can't be efficiently presented to T cells and tumor specific killing T cell can't be efficiently activated^[1-5]. Furthermore, as one of antigen presenting cells (APC), tumor cells are anergy to T cells because of their deficiency of costimulator. Dendritic cells (DC), as a potent professional APC, not only express MHC molecules and costimulators to present tumor antigen and activate tumor specific T cells, but also can directly activate NK cell to kill MHC molecule negative tumor cell in nonspecific immunity. So much attention was paid to DC for its potential application in antitumor immunity^[6-10]. Hepatocarcinoma is a high malignant tumor, so it is an important assignment to find a suitable way to kill the hepatocarcinoma. Our previous work showed that hybrid vaccine could kill tumor cell *in vitro*^[11-16]. In this report, we tried to find a way to apply the DC in the prevention and therapy of hepatocarcinoma.

MATERIALS AND METHODS

Materials

Tumor cell line H₂₂ cell line, constructed by Dalian medical university from the mouse ascite, was heterogeneous cells with higher declination to spread by lymph vessel.

Animal BALB/c mice were bought from laboratory animal center of antibiotic industrial institute in Sichuan china. All mice were male, specific pathogen free animals, with age of 6-8 weeks and weight of 15-20 g.

Main reagents Metrizamide was product of Amresco Company. Mini MACS cell sorter and CD11c MicroBeads marked antibody were products of Miltenyi Biotec GmbH Company. rmGM-CSF (granulocyte-macrophage colony-stimulating factor) was a product of R & D company. Polyethylene glycol (PEG) was purchased from Sigma Chemical Company. MTT solution was a product of Amresco Company.

Methods

Culture of tumor cells H₂₂ cell was incubated in double-layer agarose culture medium (upper layer 0.3 %, base layer 0.6 %) with concentration of 5×10⁵/L and cultured for 10 days. Single colony was selected and transferred to culture flask for expanding culture. Cells of the logarithmic stage were collected and conserved in frozen conditions for later use. 0.1 ml 1×10⁷ H₂₂ cells were incubated subcutaneously at the right armpit, carcinogenesis *in vivo* was observed.

Isolation of DC from spleen Spleen of mice was grinded it into cell suspension, they were lysed by NH₄Cl, centrifugated by metrizamide gradient solution. Cells in the interface were collected, and cultured routinely by complete culture medium RPMI 1640 at 100 % humidity, 37 °C, 50 mL·L⁻¹ CO₂ for 3 hours, then the suspended cells were removed and continued to be cultured for another 16hours, the non-adherent cells were collected, and adjusted to the concentration of 1×10⁹/L, then

cultured in the complete medium with 200 mL·L⁻¹ NCS and rmGM-CSF (500 ng/L) for 5-7days^[17].

Fusion of DCs and H₂₂ DCs and H₂₂ were washed by PBS for 3 times, then the mixture of these two kinds of cells (DCs: H₂₂=1:1) were centrifugated to remove the upper liquid gently and completely, the cell droplet was loosen by shaking, 500 mL·L⁻¹ PEG was added in the droplet in 37 °C water bath to fuse for 1 min, and simultaneously the tube was shook gently. D-hanks solution was added to terminate the fusion process for 5 min in 37 °C water bath, the upper liquid was removed by centrifugation, and the cell droplet was collected. the cell availability and number of fusion cells was detected by trypan blue staining.

Screening and determination of hybrid cell The fusion cells were marked by CD11c antibody, and sorted by Mini MACS to remove the CD11c- cells and the CD11c⁺ cells were collected and they were cultured in RPMI complete medium with rmGM-CSF (500 ng/L) and 200 mL·L⁻¹ NCS for 2-3 weeks^[18].

Carcinogenic effect of hybrid vacciney *in vivo* Mice were divided into five groups of HD1group, HD2 group, D group, H group and P group. 0.1 ml hybrid vaccine was injected into tail veil of mice in the HD1group, mice in the other group were injected at right armpit subcutaneously with 0.1 ml 1-2×10⁷/ml vaccine, H₂₂ cells+DC, H₂₂ cells and PBS, respectively. And, 14 days later, tissues of the injection site, spleen, liver and lung were isolated, the tumor weight was compared.

Analysis of the CTL activity 20 mice were classified to four groups of HD group, D group, H group and P group, each group had 5 mice. Mice were injected with 0.1 ml hybrid vaccine, DC, heat inactivated H₂₂ and PBS at the concentration of 1×10¹⁰-2×10¹⁰/L, twice every three days. All the mice were killed at 10 days after the last immunization and the spleen lymphocytes were separated and cultured under condition of complete medium with IL-2 (1×10⁵u/L) and 100 mL·L⁻¹ FCS at saturated humidity, 37 °C, 50 mL·L⁻¹ CO₂ to induce the CTL. CTL and H₂₂ was mixed at 5:1 and 10:1 effector/target rate, respectively. In addition, there were a CTL control group, a H₂₂ control group and a culture medium control group. All specimens had 3 parallel wells on a 96-well culture plate. All were cultured under conditions of saturated humidity 37 °C, 50 mL·L⁻¹ CO₂ for 48 hours. MTT method was used to detect the CTL cytotoxicity against H₂₂. Chief process was as below: adding 5 g/L MTT solution 20 ul in each well for 4 hour before the detection, then it was centrifugated to remove the free MTT; 150 ul DMSO was added to the cell droplet for 10 min to solve the MTT. Bio-Rad 350-uv automatic enzyme linker detector is used to detect the OD value at 570 wavelength^[19]. All were repeated for 4 times.

Protective effect of hybrid vaccine against H₂₂ 40 BALB/c mice were randomly divided into HD, D, H and P subgroups, ten mice in each subgroup, immunized by 0.1 mL hybrid vaccine, DC, heat inactivated H₂₂ and PBS, respectively, at concentration of 1×10⁹/L, two times every three days by tail veil. Three days after the last immunization, all mice were injected by 1×10⁶ H₂₂ at the right armpit subcutaneously. The mice weight, tumor formation, tumor size and day of mice death were recorded. 5 mice were randomly chose and killed on day 14, tumor tissue, lung tissue, liver tissue and lymph node of neck and armpit were sampled for routine paraffin embedded slice and HE staining. Other mice were kept observation for 50 days.

Therapeutic effect of hybrid vaccine against H₂₂ 30 BALB/c mice were randomly divided into HD, D and P subgroups, ten mice in each subgroup. All mice was injected with H₂₂ tumor cell 1×10⁶ subcutaneously at right armpit. 3 days later, tumor was formed in all mice which demonstrated the successful construction of tumor model. Mice in different

groups were treated with 0.1 mL hybrid vaccine, DC, and PBS, respectively, at the concentration of 1×10⁹/L, two times every three days, by the tail veil. The tumor weight and size were recorded each day. 5 mice were randomly chose and killed on day 14; pathological changes were observed in tumor tissue. The other mice were kept on feeding for 50 days.

Statistical analysis

Data were analyzed by the method of ANOVA (SPSS 10.0 software).

RESULTS

Culture of tumor cell

H₂₂ grew *in vitro* in a suspended manner, single or integrated, its double proliferation time was 24 hours. H₂₂ cell can grow to form colony composed of hundreds of cells in 5-6 days, thousands cells in ten days on agarose cultured medium.

Incubation of 1×10⁶ H₂₂ at right armpit subcutaneously *in vivo* can successfully induce tumor in all mice. Tumor grew aggressively to invade the surrounding tissue, tumor appeared necrosis when tissue bulk were big enough, even gangrenous impairment appeared on skin when tissue diameter was beyond 30 mm. Tumor tissue had integrated cell with few intercellular materials, had no funicular structure of normal liver. Tumor cells had distinctive cellular pleomorphism, nuclear pleomorphism, nuclear hyperchromatism and increased nuclear: cytoplasmic ratio (Figure 1).

Morphology of spleen DC

DC was round and irregular with sharp and long, or blunt cell extension. Induced by rmGM-CSF for 5-7days, DC grew into a colony; outer cell of it had much extension. Sorted by Microbead marked CD11c, most of them were CD11c⁺.

Carcinogenesis of Hybrid vaccine *in vivo*

No carcinogenesis appeared after hybrid vaccine was injected subcutaneously for 60 days, while H₂₂ was injected, tumor appeared in 100 % mice at site of injection. There was significant in tumor weight between the HD and H₂₂ subgroup ($P<0.01$). 1×10⁶ hybrid vaccine was injected by tail veil, the mice's spleen, lung and liver were sampled after 14 days, three slices were sectioned for each organ, no carcinogenesis appeared (Figure 2-3).

Activity of spleen CTL

CTL activity of mice in HD subgroup was significantly higher than that of D, H and P subgroup (Figure 4).

The protective effect *in vivo* hybrid vaccine against H₂₂ in different subgroup

Observation of carcinogenesis Mice of different subgroups in protective group were injected with H₂₂ cells, the tumor latent time ranked as P<H<D<HD subgroup ($P<0.05$). This demonstrated that the HD subgroup had delayed tumor latent time (Figure 5A); tumor size and tumor weight ranked as HD<D<H<P subgroup ($P<0.05$) (Figure 5B, C), which showed that mice in the HD subgroup had the lowest tumor size and tumor weight, and the D subgroup had secondly lowest tumor size and tumor weight. Survival time among different subgroups had no significant difference ($P>0.05$) (Figure 5D).

Pathology of different subgroups Macroscopic structure showed the tumor tissue was hard and adherenced to the surrounding tissue. Cutting face of tumor tissue was gray and diffused dot-like brown. Microscopic structure showed that tumor had dot like or sheet like necrosis (Figure 6A, B, C, D).

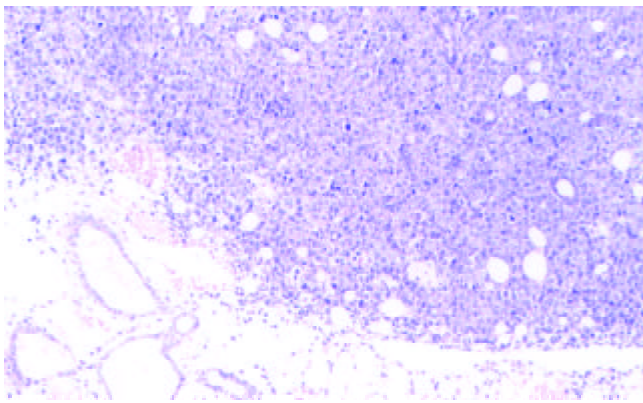


Figure 1 Tumor tissue after 14 d subcutaneous incubation. HE, 3.3×10.

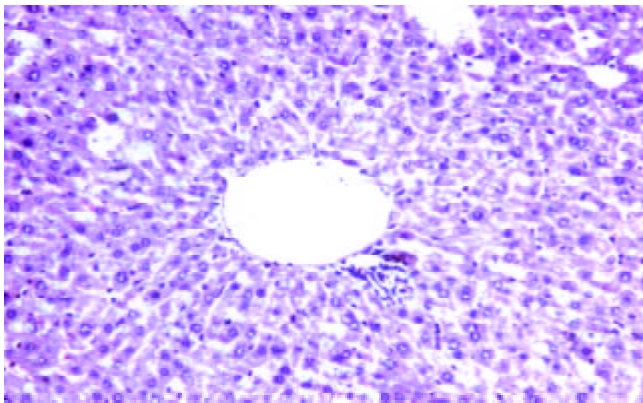


Figure 2 Liver tissue of 14 d after hybrid vaccine injection by tail vein HE, 3.3×20.

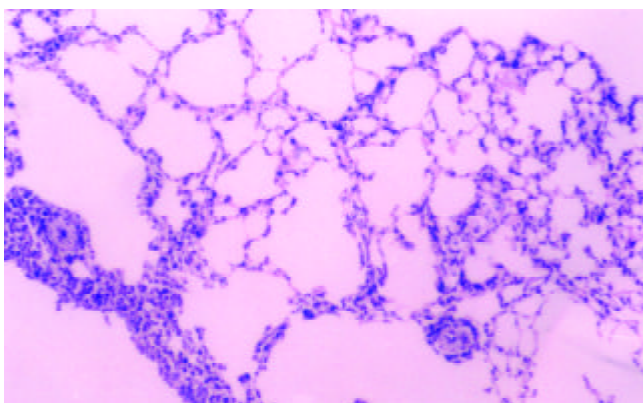


Figure 3 Lung tissue of 14 d after hybrid vaccine injection by tail vein HE, 3.3×20.

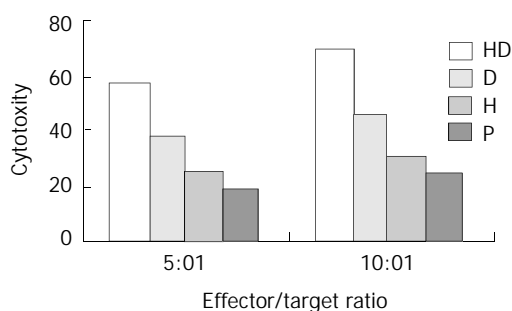


Figure 4 CTL activity of different subgroup at different effector/target ratio.

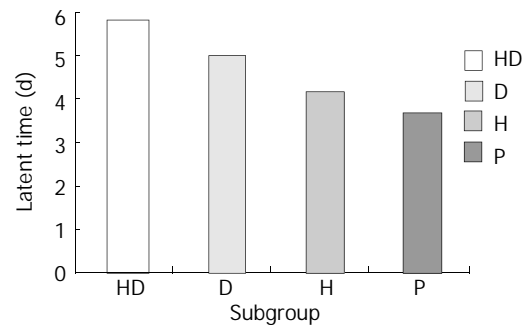


Figure 5A Comparison of latent time among different subgroups.

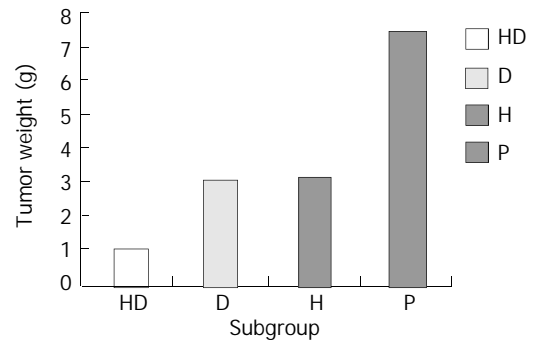


Figure 5B Comparison of tumor weight among different subgroups.

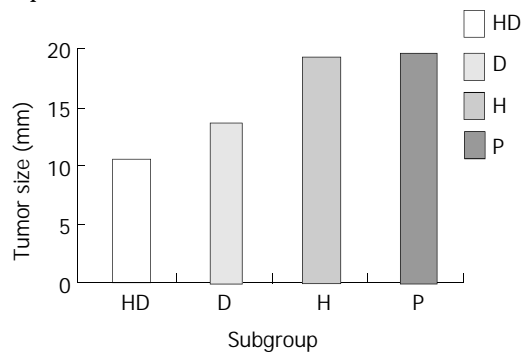


Figure 5C Comparison of tumor size among different subgroups.

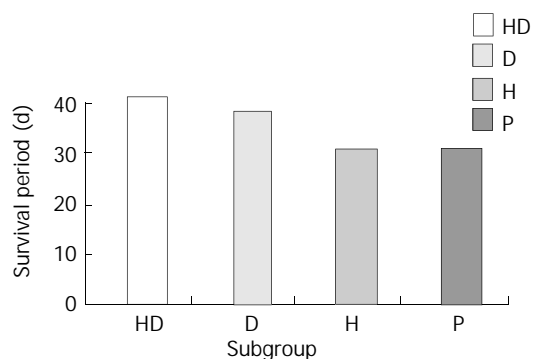


Figure 5D Comparison of survival period among different subgroups.

Therapeutic effect of hybrid vaccine against H_{22}

Inhibitory effect of hybrid vaccine in carcinogenesis Treated with hybrid vaccine, DC and PBS, tumor size in different subgroups ranked as HD<D<P ($P<0.05$) (Figure 7). Survival time and tumor weight had no significant difference among the different subgroups in therapeutic group.

Pathology of different subgroups Macroscopic structure

showed the tumor tissue was hard and can't separate with surrounding tissue easily. Cutting face of tumor tissue is gray and diffuse dot-like brown. Microscopic structure showed tumor has dot like or sheet like necrosis (Figure 8A, B, C).

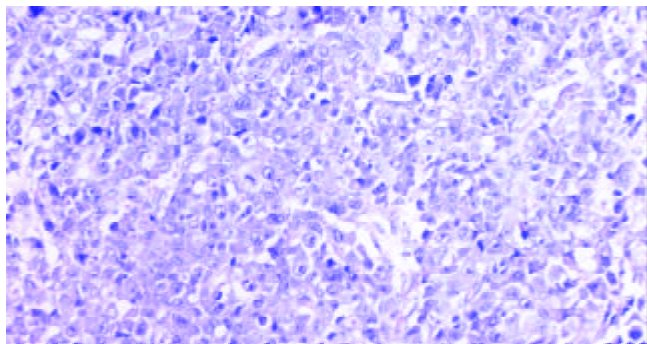


Figure 6A There isn't obvious necrosis in tumor tissue of 14 d in protective group P subgroup. HE, 3.3×20.

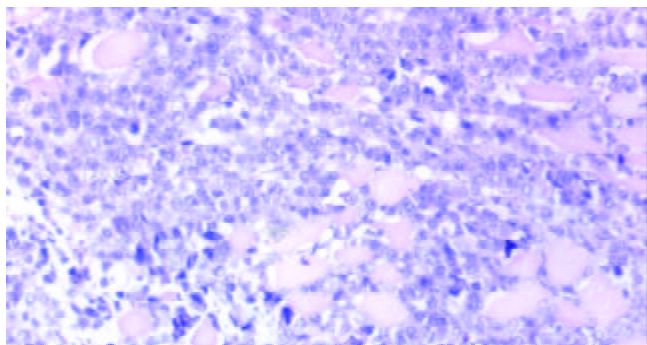


Figure 6B There is dot like necrosis in tumor tissue of 14 d in protective group H subgroup. HE, 3.3×20.

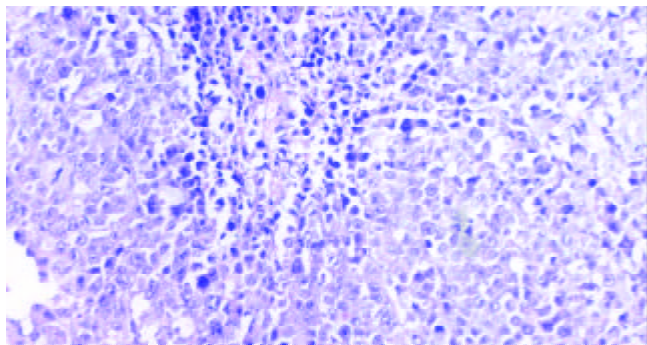


Figure 6C There is sheet like necrosis in tumor tissue of 14 d in protective group D subgroup. HE, 3.3×20.

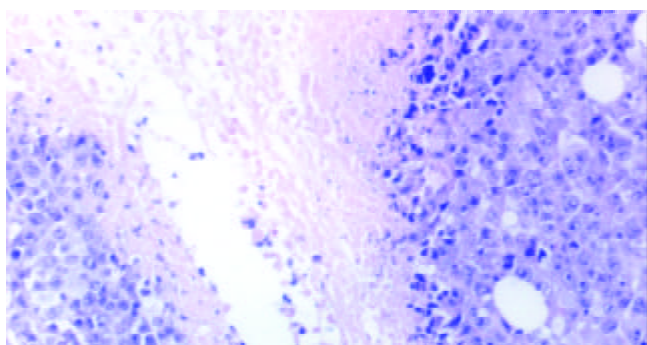


Figure 6D There is extensive necrosis in tumor tissue of 14 d in protective group HD subgroup. HE, 3.3×20.

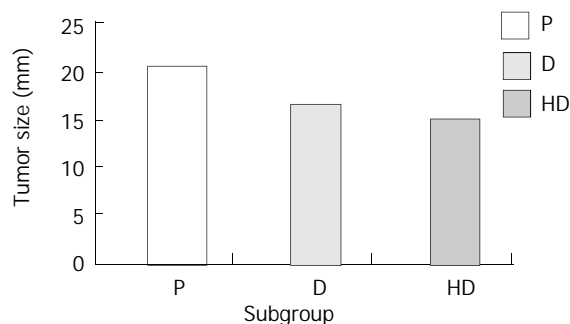


Figure 7 Comparison of tumor size on day 14 among different subgroups of therapeutic group.

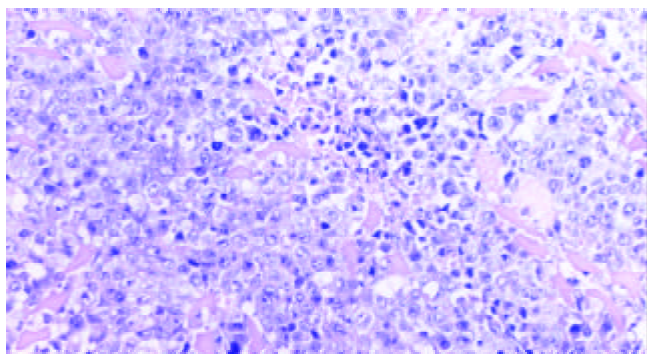


Figure 8A There is dot or sheet like necrosis in tumor tissue of 14d in therapeutic group P subgroup. HE, 20×3.3.

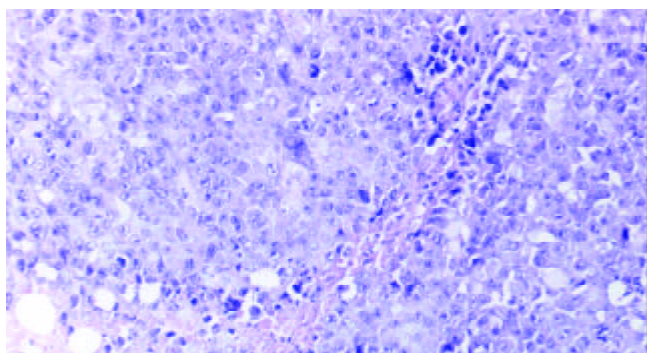


Figure 8B There is sheet like necrosis in tumor tissue of 14 d in therapeutic group D subgroup. HE, 20×3.3.

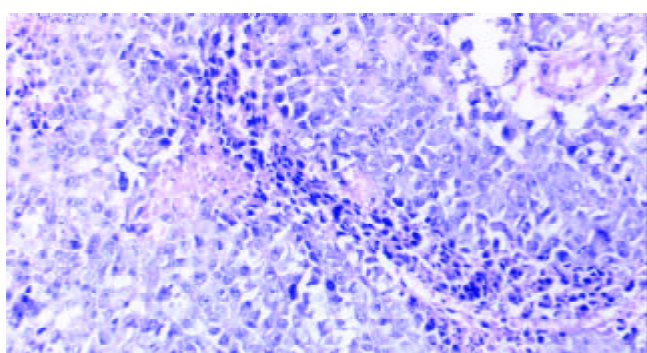


Figure 8C There is sheet like necrosis in tumor tissue of 14 d in therapeutic group HD subgroup. HE, 20×3.3.

DISCUSSION

H₂₂ ascite hepatocarcinoma has strong invasion and spreading declination by lymph vessel. In this report, H₂₂ cells had 100 %

carcinogenesis effect on BALB/c mice, which was consistent with other report^[19]. H₂₂ cells grow quickly *in vitro*, which can be easily used to construct the tumor animal model, and express low level of MHC molecule. So H₂₂ cells are suitable for DC antitumor research.

In this report, DC was separated through centrifugation by metrizamide; the maturation of DC was induced by cytokine of rmGM-CSF; DC and H₂₂ were fused through PEG, they were marked by CD11c, and sorted by Mini MACS. By above process, the hybrid vaccine was successfully constructed^[15,17,19,20]. The methods were simple and easily operated. Hybrid Vaccine, injected subcutaneously, has no tumor formation at local tissue, and injected by tail vein, it also has no carcinogenesis in the liver, lung and spleen, so it loses the carcinogenic effect of H₂₂ cells, and is safe to develop tumor vaccine *in vivo*.

In the protective group, different subgroups had different tumor latent time, and different interval between the H₂₂ incubation and tumor formation. The HD subgroup had the longest tumor latent time; the D subgroup had the second longest tumor latent time. The results showed that the hybrid vaccine and DC could delay the tumor carcinogenesis. The HD subgroup had the lowest tumor size and tumor weight, the D subgroup had the second lowest tumor size and tumor weight. The results showed that hybrid vaccine had the strongest anti-tumor effect. Hybrid vaccine could express some DC characteristics such as membrane molecule MHC-I, II molecule and costimulator, secrete some cell factors which can stimulate the T cell expansion, capture and present endogenous tumor associated antigens derived from parents H₂₂ cells, so it can efficiently stimulate the immune response^[21-25]. There were similar results in other research reports on hybrid vaccines of DC with MC38, NS1, B16 melanoma, RMA-s lymphoma and renal carcinoma^[26-35].

Mice immunized by hybrid vaccine could induce the tumor specific memory T cells, which could quickly be activated and expanded when they contact with tumor antigen again. When CD40 which was expressed by memory T cell integrated with CD40L of DC, it could stimulate DC to secrete high level of IL-12, and to enhance the expression of ICAM-1, CD80 and CD86. The activated DC could stimulate the proliferation of T cells and secretion of IFN- γ of T cells^[36-39]. It was reported that IFN- γ gene modified H₂₂ cells could enhance the antigenicity and the expression of MHC-II molecule from 10 % to 19 %; TNF gene modified H₂₂ cell also could enhance the MHC-I molecule expression in different clones with different transfection methods which was enhanced to 28.39 % and 35.78 % in two clones which had the highest expression of MHC-I; GM-CSF gene modified H₂₂ had lower oncogenicity *in vivo*, the possible mechanism attributed to the enhanced MHC expression^[40-44].

Hybrid vaccine also takes part in nonspecific immunity; it can directly activate NK cells to kill MHC-tumor cells. Some reports demonstrated DC could produce large number of INF- γ , which can inhibit the virus replication and stimulate the NK and macrophages^[45-47]. In this report, the hybrid vaccine antitumor function perhaps attributed to both adaptive and inborn immunity.

In the therapeutic group, tumor size in the HD subgroup was significantly lower than that in other subgroups after treated for 14 days, which showed that H₂₂-DC could inhibit the tumor growth. Some reported the similar effect. For example, after breast cancer cells hybridised with CD14⁺ derived DC, ³H incorporation assay showed that hybrid cell can stimulate the proliferation T cells, while only tumor cell, DC and mixture of DC and tumor cell have no such effect^[48-55].

From above, it is concluded that hybrid vaccine acquired the function of parents cell such as antigen presenting function of DC and T stimulating ability and capture the tumor derived

antigen. Hybrid vaccine has the protective and therapeutic effect against H₂₂. This research can provide some evidence for the clinical application of tumor vaccine.

REFERENCES

- Cohen PA**, Peng L, Kjaergaard J, Plautz GE, Finke JH, Koski GK, Czerniecki BJ, Shu S. T cell adoptive therapy of tumors: mechanisms of improved therapeutic performance. *Crit Rev Immunol* 2001; **21**: 215-248
- Nawrocki S**, Wysocki PJ, Mackiewicz A. Genetically modified tumour vaccines: an obstacle race to break host tolerance to cancer. *Expert Opin Biol Ther* 2001; **1**: 193-204
- Azuma I**, Seya T. Development of immunoadjuvants for immunotherapy of cancer. *Int Immunopharmacol* 2001; **1**: 1249-1259
- Smyth MJ**, Godfrey DI, Trapani JA. A fresh look at tumor immunosurveillance and immunotherapy. *Nat Immunol* 2001; **2**: 293-299
- Renner C**, Kubuschok B, Trumper L, Pfreundschuh M. Clinical approaches to vaccination in oncology. *Ann Hematol* 2001; **80**: 255-266
- Nishioka Y**, Hua W, Nishimura N, Sone S. Genetic modification of dendritic cells and its application for cancer immunotherapy. *J Med Invest* 2002; **49**: 7-17
- Gunzer M**, Grabbe S. Dendritic cells in cancer immunotherapy. *Crit Rev Immunol* 2001; **21**: 133-145
- Brossart P**, Wirths S, Brugger W, Kanz L. Dendritic cells in cancer vaccines. *Exp Hematol* 2001; **29**: 1247-1255
- Meidenbauer N**, Andreesen R, Mackensen A. Dendritic cells for specific cancer immunotherapy. *Biol Chem* 2001; **382**: 507-520
- Bhardwaj N**. Processing and presentation of antigens by dendritic cells: implications for vaccines. *Trends Mol Med* 2001; **7**: 388-394
- Sun JL**, Zhang JK, Chen HB, Chen JD, Qiu YQ. Promoting effects of dendritic cells on LPAK cells killing human hepatoma cells. *Zhongguo Zhongliu Lingchuang yu Kangfu* 1998; **5**: 16-18
- Zhang JK**, Chen HB, Sun JL, Zhou YQ. Effect of dendritic cells on LPAK cells induced at different times in killing hepatoma cells. *Shijie Huaren Xiaohua Zazhi* 1999; **7**: 673-675
- Zhang JK**, Sun JL, Chen HB, Zhou YQ. Influence of granulocyte macrophage colony stimulating factor and tumor necrosis factor upon the anti hepatoma activities of human dendritic cells. *World J Gastroenterol* 2000; **6**: 718-720
- Sun JL**, Zhang JK, Chen JD, Chen HB, Chew YQ, Chen JX. *In vitro* study on the morphology of human blood dendritic cells and LPAK cells inducing apoptosis of the hepatoma cell line. *Chinese Medical Journal* 2001; **114**: 600-605
- Zhang J**, Zhang JK, Zhuo SH, Chen HB. Effect of a cancer vaccine prepared by fusions of hepatocarcinoma cells with dendritic cells. *World J Gastroenterol* 2001; **7**: 690-694
- Zhang JK**, Li J, Chen HB, Sun JL, Qu YJ, Lu JJ. Antitumor activities of human dendritic cells derived from peripheral and cord blood. *World J Gastroenterol* 2002; **8**: 87-90
- Chen HB**, Zhang JK, Huang ZL, Sun JL, Zhou YQ. Effects of cytokines on dendritic cells against human hepatoma cells. *Shijie Huaren Xiaohua Zazhi* 1999; **7**: 191-193
- Sun JL**, Zhang JK, Chen HB, Zhou YQ. Morphology of cultured human peripheral blood dendritic cells and their antitumor activity. *Zhongguo Zuzhihuaxue Yu Xibaoxue Zazhi* 1999; **8**: 28-31
- Zhang JK**, Chen HB, Sun JL, Zhou YQ. Effect of dendritic cells on LPAK cells induced at different times in killing hepatoma cells. *Shijie Huaren Xiaohua Zazhi* 1999; **7**: 673-675
- Zhang JK**, Sun JL, Chen HB, Zhou YQ. Ultrastructural comparison of apoptosis of human hepatoma cells and lak cells. *Huaren Xiaohua Zazhi* 1998; **6**: 877-879
- Hart I**, Colaco C. Fusion induces tumor or rejection. *Nature* 1997; **388**: 626-627
- van Schooten WC**, Strang G, Palathumpat V. Biological properties of dendritic cells: implications to their use in the treatment of cancer. *Mol Med Today* 1997; **3**: 254-260
- Kolb HJ**, Holler E. Adoptive immunotherapy with donor lymphocyte transfusions. *Curr Opin Oncol* 1997; **9**: 139-145
- Mayordomo JI**, Zorina T, Storkus WJ, Zitvogel L, Garcia Prats

- MD, DeLeo AB, Lotze MT. Bone marrow derived dendritic cells serve as potent adjuvants for peptide based antitumor vaccines. *Stem Cells* 1997; **15**: 94-103
- 25 **Slingluff CL Jr.** Tumor antigens and tumor vaccines: peptides as immunogens. *Semin Surg Oncol* 1996; **12**: 446-453
- 26 **Scott Taylor TH.** Pettengell R, Clarke I, Stuhler G, La Barthe MC, Walden P, Dalglish AG. Human tumour and dendritic cell hybrids generated by electrofusion: potential for cancer vaccines. *Biochim Biophys Acta* 2000; **1500**: 265-279
- 27 **Gong J,** Avigan D, Chen D, Wu Z, Koido S, Kashiwaba M, Kufe D. Activation of antitumor cytotoxic T lymphocytes by fusions of human dendritic cells and breast carcinoma cells. *Proc Natl Acad Sci USA* 2000; **97**: 2715-2718
- 28 **Cao X,** Zhang W, Wang J, Zhang M, Huang X, Hamada H, Chen W. Therapy of established tumour with a hybrid cellular vaccine generated by using granulocyte macrophage colony stimulating factor genetically modified dendritic cells. *Immunology* 1999; **97**: 616-625
- 29 **Wang J,** Saffold S, Cao X, Krauss J, Chen W. Eliciting T cell immunity against poorly immunogenic tumors by immunization with dendritic cell tumor fusion vaccines. *J Immunol* 1998; **161**: 5516-5524
- 30 **Celluzzi CM,** Falo LD Jr. Physical interaction between dendritic cells and tumor cells results in an immunogen that induces protective and therapeutic tumor rejection. *J Immunol* 1998; **160**: 3081-3085
- 31 **Lespagnard L,** Mettens P, Verheyden AM, Tasiaux N, Thielemans K, van Meirvenne S, Geldhof A, De Baetselier P, Urbain J, Leo O, Moser M. Dendritic cells fused with mastocytoma cells elicit therapeutic antitumor immunity. *Int J Cancer* 1998; **76**: 250-258
- 32 **Grosjean I,** Caux C, Bella C, Berger I, Wild F, Banchereau J, Kaiserlian D. Measles virus infects human dendritic cells and blocks their allostimulatory properties for CD4+ T cells. *J Exp Med* 1997; **186**: 801-812
- 33 **Gong J,** Apostolopoulos V, Chen D, Chen H, Koido S, Gendler SJ, McKenzie IF, Kufe D. Selection and characterization of MUC1 specific CD8+ T cells from MUC1 transgenic mice immunized with dendritic carcinoma fusion cells. *Immunology* 2000; **101**: 316-324
- 34 **Gong J,** Nikrui N, Chen D, Koido S, Wu Z, Tanaka Y, Cannistra S, Avigan D, Kufe D. Fusions of human ovarian carcinoma cells with autologous or allogeneic dendritic cells induce antitumor immunity. *J Immunol* 2000; **165**: 1705-1711
- 35 **Holmes LM,** Li J, Sticca RP, Wagner TE, Wei Y. A rapid, novel strategy to induce tumor cell specific cytotoxic T lymphocyte responses using instant dendritomas. *J Immunother* 2001; **24**: 122-129
- 36 **Akasaki Y,** Kikuchi T, Homma S, Abe T, Kofe D, Ohno T. Antitumor effect of immunizations with fusions of dendritic and glioma cells in a mouse brain tumor model. *J Immunother Antitumor* 2001; **24**: 106-113
- 37 **Tuting T,** Storkus WJ, Lotze MT. Gene based strategies for the immunotherapy of cancer. *J Mol Med* 1997; **75**: 478-491
- 38 **Gong J,** Chen D, Kashiwaba M, Kufe D. Induction of antitumor activity by immunization with fusions of dendritic and carcinoma cells. *Nat Med* 1997; **3**: 558-561
- 39 **Gluckman JC,** Canque B, Chapuis F, Rosenzweig M. *In vitro* generation of human dendritic cells and cell therapy. *Cytokines Cell Mol Ther* 1997; **3**: 187-196
- 40 **Asher AL,** Mule JJ, Kasid A, Restifo NP, Salo JC, Reichert CM, Jaffe G, Fendly B, Kriegler M, Rosenberg SA. Murine tumor cells transduced with the gene for tumor necrosis factor alpha. Evidence for paracrine immune effects of tumor necrosis factor against tumors. *J Immunol* 1991; **146**: 3227-3234
- 41 **Porgador A,** Tzehoval E, Vadai E, Feldman M, Eisenbach L. Immunotherapy via gene therapy: comparison of the effects of tumor cells transduced with the interleukin 2, interleukin 6, or interferon gamma genes. *J Immunother* 1993; **14**: 191-201
- 42 **Zhang LH,** Pan JP, Yao HP, Sun WJ, Xia DJ, Wang QQ, He L, Wang J, Cao X. Intrasplenic transplantation of IL 18 gene modified hepatocytes: an effective approach to reverse hepatic fibrosis in schistosomiasis through induction of dominant Th1 response. *Gene Ther* 2001; **8**: 1333-1342
- 43 **Lu Y,** Yamauchi N, Koshita Y, Fujiwara H, Sato Y, Fujii S, Takahashi M, Sato T, Kato J, Yamagishi H, Niitsu Y. Administration of sub-tumor regression dosage of TNF alpha to mice with pre existing parental tumors augments the vaccination effect of TNF gene modified tumor through the induction of MHC class I molecule. *Gene Ther* 2001; **8**: 499-507
- 44 **van Slooten ML,** Storm G, Zoepfel A, Kupcu Z, Boerman O, Crommelin DJ, Wagner E, Kircheis R. Liposomes containing interferon gamma as adjuvant in tumor cell vaccines. *Pharm Res* 2000; **17**: 42-48
- 45 **Homma S,** Toda G, Gong J, Kufe D, Ohno T. Preventive antitumor activity against hepatocellular carcinoma (HCC) induced by immunization with fusions of dendritic cells and HCC cells in mice. *J Gastroenterol* 2001; **36**: 764-771
- 46 **Treon SP,** Raje N, Anderson KC. Immunotherapeutic strategies for the treatment of plasma cell malignancies. *Semin Oncol* 2000; **27**: 598-613
- 47 **Orentas RJ,** Schauer D, Bin Q, Johnson BD. Electrofusion of a weakly immunogenic neuroblastoma with dendritic cells produces a tumor vaccine. *Cell Immunol* 2001; **213**: 4-13
- 48 **Tanaka Y,** Koido S, Chen D, Gendler SJ, Kufe D, Gong J. Vaccination with allogeneic dendritic cells fused to carcinoma cells induces antitumor immunity in MUC1 transgenic mice. *Clin Immunol* 2001; **101**: 192-200
- 49 **Scanlan MJ,** Jager D. Challenges to the development of antigen specific breast cancer vaccines. *Breast Cancer Res* 2001; **3**: 95-98
- 50 **Brugger W,** Brossart P, Scheding S, Stuhler G, Heinrich K, Reichardt V, Grunebach F, Buhring HJ, Kanz L. Approaches to dendritic cell based immunotherapy after peripheral blood stem cell transplantation. *Ann NY Acad Sci* 1999; **872**: 363-371
- 51 **Jager E,** Jager D, Knuth A. Strategies for the development of vaccines to treat breast cancer. *Recent Results Cancer Res* 1998; **152**: 94-102
- 52 **Steinman RM.** Dendritic cells and immune based therapies. *Exp Hematol* 1996; **24**: 859-862
- 53 **Chen CH,** Wu TC. Experimental vaccine strategies for cancer immunotherapy. *J Biomed Sci* 1998; **5**: 231-252
- 54 **Hermans IF,** Moroni-Rawson P, Ronchese F, Ritchie DS. The emerging role of the dendritic cell in novel cancer therapies. *N Z Med J* 1998; **111**: 111-113
- 55 **Engleman EG.** Dendritic cells: potential role in cancer therapy. *Cytotechnology* 1997; **25**: 1-8

Photodynamic inhibitory effects of three perylenequinones on human colorectal carcinoma cell line and primate embryonic stem cell line

Lan Ma, Hong Tai, Cong Li, Yu Zhang, Ze-Hua Wang, Wei-Zhi Ji

Lan Ma, Tai Hong, Graduate School of the Chinese Academy of Sciences, Beijing 100871, China

Lan Ma, Yu Zhang, Ze-Hua Wang, Monoclonal Antibody Biotechnology Center, Yunnan University, Kunming 650091, Yunnan Province, China

Tai Hong, The First People's Hospital of Yunnan Province, Kunming 650032, Yunnan, China

Cong Li, Chemistry, Yunnan University, Kunming 650091, Yunnan Province, China

Lan Ma, Tai Hong, Wei-Zhi Ji, Kunming Institute of Zoology, Chinese Academy of Science, Kunming 650223, Yunnan Province, China

Supported by National Natural Science Foundation of China, No. 980174, Natural Scientific Foundation of Yunnan Province, No. C0106M

Correspondence to: Wei-Zhi Ji, Kunming Institute of Zoology, Chinese Academy of Science, Kunming 650223, Yunnan, China. wji@mail.kiz.ac.cn

Telephone: +86-871-5139413 **Fax:** +86-871-5139413

Received: 2002-07-04 **Accepted:** 2002-07-27

Abstract

AIM: To investigate the photodynamic inhibitory effects of Elsinochrome A (EA), Hypocrellin A (HA) and Hypocrellin B (HB) on human colorectal carcinoma Hce-8693 cells and rhesus monkey embryonic stem R366.4 cells, via inducing apoptosis.

METHODS: EA, HA and HB were extracted from metabolites of *Hypomyces* (Fr) Tul.Sp. R366.4 cells or Hce-8693 cells were cultured with different concentrations of EA, HA or HB respectively, irradiated and incubated with fresh medium for 2 h. Cell cycle analysis was performed by flow cytometry (FCM). Data were expressed as means \pm SD and analysis of variance and Student's *t*-test for individual comparisons.

RESULTS: The photodynamic bioactivity of EA was first reported in this study. After irradiation for 5 min, 6 min, 10 min or 20 min, photoactivated EA at lower concentrations, which were 10^{-7} Mol/L, 10^{-6} Mol/L, 10^{-5} Mol/L respectively, had no cytotoxic effects on R366.4 ES cells. Whereas, all of the three perylenequinones could induce apoptosis with a dose-dependent manner when Hce-8693 cells were incubated with photoactivated EA, HA and HB respectively. When Hce-8693 cells were incubated with EA at 10^{-6} Mol/L and irradiated 5 min, 6 min, 10 min and 20 min respectively, the rates of EA-induced apoptosis were 0, 0, 13.4 % and 40.5 %. While the rates of HA-induced apoptosis were 29.5 %, 32.0 %, 40.2 % and 22.6 %. And the rates of HB-induced apoptosis were 0, 0, 0 and 13.7 % respectively. Meanwhile, after 10^{-5} Mol/L treatment, the rates of EA-induced apoptosis were 32.7 %, 19.3 %, 26.4 % and 52.7 %, the rates of HA-induced apoptosis were 47.2 %, 39.1 %, 45.2 % and 56.6 %, and the rates of HB-induced apoptosis were 0, 0, 20.0 % and 13.9 % respectively.

CONCLUSION: EA, HA and HB have significant anti-cancer activity. The order of photodynamic inhibitory effects on tumor cells would be approximately HA>EA>HB. The molecular mechanisms of apoptosis may not be induced by reactive oxygen species and are worth further investigation.

Ma L, Tai H, Li C, Zhang Y, Wang ZH, Ji WZ. Photodynamic inhibitory effects of three perylenequinones on human colorectal carcinoma cell line and primate embryonic stem cell line. *World J Gastroenterol* 2003; 9(3): 485-490

<http://www.wjgnet.com/1007-9327/9/485.htm>

INTRODUCTION

Perylenequinones are a type of photosensitive pigments widespread in nature, which have been isolated from fungi, as well as other organisms^[1-5]. These lipid-soluble 4,9-dihydroxy-3, 10-perylenequinone derivatives are efficient producers of singlet oxygen (1O_2) in visible light^[6-11]. Due to their excellent photosensitive properties, they are expected to be developed as new phototherapeutic medicines^[8,12-17]. Among them, Elsinochrome A (EA) was first reported in 1966 by Chen CT *et al.*, who isolated EA from *Elsinoe* spp. I^[1-2]. And Meille SV *et al.* reported the structure of EA^[18]. Since then, there are no more related reports about EA. Hypocrellins are well-known photosensitizers, including hypocrellin A (HA) and hypocrellin B (HB), isolated from natural fungus sacs of *Hypocrella bambusae* growing in north western region of Yunnan Province in China^[19]. Hypocrellins were potent inhibitors of protein kinase C (PKC)^[20], and could inactivate some types of viruses in the presence of visible light and oxygen. These processes appeared to be mediated predominately by 1O_2 . This was further supported by the extremely high quantum yield of 1O_2 generation by hypocrellin^[21-23]s. Many investigations demonstrated that hypocrellins had a strong photodynamic effect on tumours^[24] and impressive antiviral activity against human immunodeficiency virus type 1 (HIV-1)^[25]. Recently, it has been reported that hypocrellin can photosensitize apoptotic cell death^[26]. The above investigations collectively provide a compelling rationale for the development of hypocrellin and its derivatives as PDT photosensitizers.

Our group has recently isolated a filamentous fungal strain from western region of Yunnan Province in China and identified it as *Ascomycetes Hypocreales Hypocreaceae Hypomyces* (Fr) Tul.sp based on the taxonomic study. *Hypomyces* (Fr) Tul.Sp. was found for the first time to produce Elsinochrome A (EA), Hypocrellin A (HA) and Hypocrellin B (HB), under solid-phase fermentation conditions. Colorectal cancer is common in China. Since EA and Hypocrellins could be a potential tumor photopreventive and phototherapeutic agents, it is worthwhile to investigate the photodynamic effects of these photosensitizers. In this study, we examined the relative potency of EA, HA and HB against two cell lines, human colorectal carcinoma Hce-8693 cells and rhesus monkey embryonic stem (ES) R366.4 cells, and attempted to correlate anticancer activity with chemical structure and quantum yield of 1O_2 .

MATERIALS AND METHODS

Synthesis

The fungal metabolites were isolated from solid-substrate fermentation cultures of *Hypomyces* (Fr) Tul.Sp. and evaporated to dryness. The powder of *Hypomyces* (Fr) Tul.Sp. was extracted with acetone at room temperature and then evaporated to dryness in vacuo. The recrystallized crude product was purified by silica gel column chromatography with a mixed solvent of petroleum ether:EtOAc:EtOH (4:2:1). The purified crystallized products were characterized with element analysis measurement (PE 2 400), UV-visible spectrophotometry (PE UV/V is Lambda Bio), fluorescence spectra instruments (Hitachi-850), FT-IR (PE 1 000), ¹H, ¹³C-nuclear magnetic resonance (Bruker AM-400). The results were consistent with literature data.

Each of the above products was dissolved respectively in dimethylsulfoxide (DMSO) at 1 M and stored at 4 °C in dark conditions. Under these conditions the solutions were stable for 2 months. The stock solutions were diluted 10³ to 10⁷ fold and in the final experimental conditions, the final DMSO concentration (0.1 %) did not affect the viability of the culture cells, as demonstrated in control experiments.

Cell lines

Rhesus monkey embryonic stem cell line R366.4 was kindly provided by Dr James A Thomson (The Wisconsin Regional Primate Research Center, University of Wisconsin, US). Cells were plated in mouse embryonic fibroblasts (previously exposed to 3 000 rads γ -radiation) in medium consisting of 85 % Dulbecco's Modified Eagle medium (4 500 mg of glucose per liter, with L-glutamine, without sodium pyruvate; GIBCO) with 15 % fetal bovine serum (HyClone), 1 \times 10⁻⁷ Mol/L 2-mercaptoethanol (Sigma) and 1 % nonessential amino acid stock (GIBCO). Human colorectal carcinoma Hce-8693 cells were obtained from ATCC. The cell lines Hce-8693 were maintained in Dulbecco's Modified Eagle medium (GIBCO) supplemented with 10 % new born calf serum (HyClone). All cell lines were grown at 37 °C under a water-saturated sterile atmosphere containing 5 % CO₂ (Forma Scientific Incubator). All cell manipulations in the presence of EA, HA and HB were performed under subdued light conditions.

Light irradiation

Cells incubated with EA, HA and HB were irradiated with a water-cooled 1 300 W tungsten-bromine lamp. All cells proliferated as monolayers attached to the plastic bottom of the plate which was completely transparent for the excitation light. Temperature recorded in tissue culture plate did not exceed room temperature during the irradiation period. Immediately after irradiation, cells were rinsed three times with PBS and grown in a fresh medium for 2 hours.

Flow cytometry

Cells were incubated with various doses of EA, HA or HB, irradiated, incubated for additional 2 h and then harvested, washed with phosphate-buffered saline (PBS) three times and fixed with 700 mL · L⁻¹ ethanol at 4 °C overnight. Fixed cells were washed three times with PBS and stained with 800 μ L propidium iodide and 200 μ L deoxyribonuclease-free ribonuclease A in PBS. The fluorescence intensity of propidium iodide-stained nuclei was detected with flow cytometer (EPICS-XL, Coulter, USA) and 10 000 cells were analyzed with Multicycle software.

Photocytotoxicity studies in R366.4 cell lines

R366.4 cells growing in sub-confluent culture were used to assess photocytotoxic effects of EA via flow cytometric assays. Graded doses of EA (1 \times 10⁻⁷ Mol/L, 1 \times 10⁻⁶ Mol/L, 1 \times 10⁻⁵ Mol/L, 1 \times 10⁻⁴ Mol/L, 1 \times 10⁻³ Mol/L) dissolved in DMSO were mixed

into the medium overlying 5.0 \times 10⁴ cells in 6-well plates. Following 2 h incubation, the cells were irradiated for 5 min, 6 min, 10 min and 20 min respectively (or not in case of darkness). After the drug-containing medium was removed, the cells were washed with phosphate-buffered saline (PBS) three times and the fresh ES culture medium was put on the cells prior to incubation for 2 h at 37 °C in saturated humidified air with 5 % CO₂. Finally, the cell proliferation was determined by flow cytometric assay.

Inhibitory effect of EA, HA and HB on the proliferation of Hce-8693 cells by inducing apoptosis

Hce-8693 cells growing in confluent culture were used to assess inhibitory effects of EA, HA and HB via flow cytometric assays. For each compound, graded doses (1 \times 10⁻⁶ Mol/L, 1 \times 10⁻⁵ Mol/L, 1 \times 10⁻⁴ Mol/L, 1 \times 10⁻³ Mol/L) dissolved in DMSO were mixed into the medium overlying 5.0 \times 10⁴ cells in 6-well plates. Following 2 h incubation, the cells were irradiated for 5 min, 6 min, 10 min and 20 min respectively (or not in case of darkness). After the drug-containing medium was removed, the cells were washed with phosphate-buffered saline (PBS) three times and the fresh culture medium was put on the cells prior to an incubation for 2 h at 37 °C in saturated humidified air with 5 % CO₂. Finally, the cell proliferation was determined by flow cytometric assay.

Statistical analysis

Student's *t* test was used to assess statistical significance of differences. If *P* < 0.01, the difference was considered very significant.

RESULTS

Synthesis

The structures of the compounds are shown in Figure 1, and their relevant photochemical properties are summarized in Table 1.

Table 1 The photochemical properties of the perylenequinones

Structure	UV λ_{\max} (log ϵ)*	λ_{\max} (log ϵ)*	$\phi \cdot ^1O_2$
EA	459(1.60), 528(0.84), 568(1.04)	460(3.78), 531(3.13), 571(3.60)	0.94
HA	468(1.88), 542(0.83), 582(0.90)	417(5.51), 542(1.02), 582(7.70)	0.83
HB	470(0.27), 540(0.12), 583(0.13)	471(4.39), 543(3.01), 583(3.36)	0.76

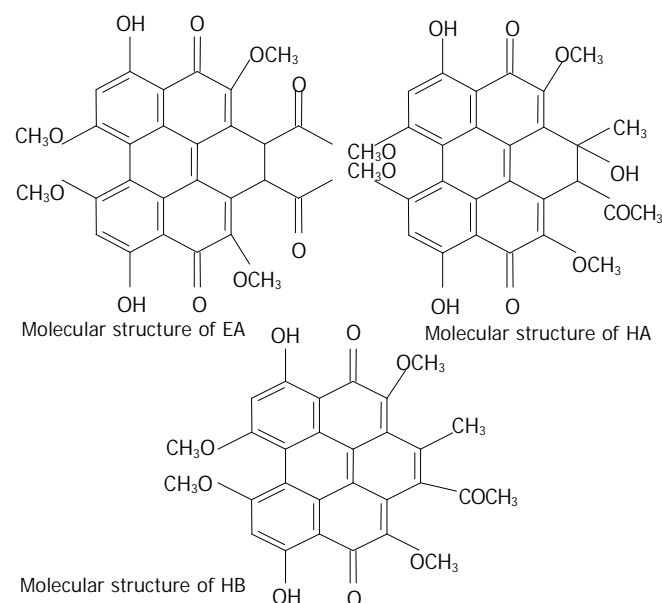


Figure 1 Structures of the three perylenequinones for photo-dynamic activity.

Photodependent cytotoxicity studies in R366.4 cell lines

Embryonic stem (ES) cells are derived from preimplantation embryos, have a normal karyotype, and are capable of indefinite, undifferentiated proliferation^[27]. Recently, *in vitro* mouse ES cell culture method has been used to test mutagenic, cytotoxic and embryotoxic effects of chemical substances^[28-30]. In this study, rhesus monkey ES R366.4 cells were first used to measure the photocytotoxicity of EA by judging the apoptosis of ES cells. After treated the R366.4 ES cells with EA at various concentrations, with or without light irradiation, the rate of apoptosis obtained by FCM were shown in Table 2 and Figure 2. The data illustrated that photoactivated EA had no cytotoxic effects on the R366.4 ES cells at low concentrations, which were 10⁻⁷ Mol/L, 10⁻⁶ Mol/L, 10⁻⁵ Mol/L respectively. Whereas, all of photoactivated EA at higher concentrations (10⁻⁴ Mol/L and 10⁻³ Mol/L respectively) exhibited a potent cytotoxic effects on R366.4 cells. In general, no large differences in the photodependent cytotoxic effects of EA were found between the different irradiation time. In the case of the photocytotoxic EA no cytotoxic effect was observed in dark conditions.

Table 2 EA-induced apoptosis in R366.4 ES cells with FCM assay (means ±SD, n=3)

Group	Rate of apoptosis/%			
	5 min	6 min	10 min	20 min
Control	0	0	0	0
10 ⁻⁷ Mol/L	0	0	0	0
10 ⁻⁶ Mol/L	0	0	0	0
10 ⁻⁵ Mol/L	0	0	0	0
10 ⁻⁴ Mol/L	48.8±4.50 ^b	50.3±4.14 ^b	52.1±2.35 ^b	50.5±3.68 ^b
10 ⁻³ Mol/L	54.9±2.99 ^b	53.4±4.01 ^b	52.4±3.50 ^b	50.2±4.93 ^b

^bP<0.01, vs EA control.

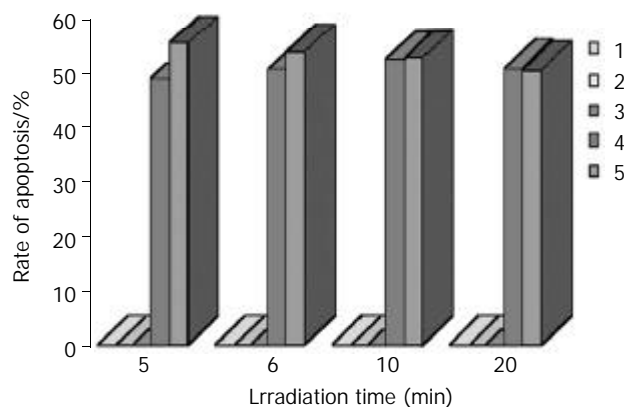


Figure 2 Photodependent cytotoxic effects of EA on R366.4 ES cells at various concentrations: (1) 10⁻⁷ Mol/L, (2) 10⁻⁶ Mol/L, (3) 10⁻⁵ Mol/L, (4) 10⁻⁴ Mol/L, (5) 10⁻³ Mol/L respectively. Results are means ± SD of three independent experiments.

Inhibitory effect of EA on the proliferation of Hce-8693 cells by inducing apoptosis

In order to investigate the antiproliferative effect of EA, Hce-8693 cells were incubated with different concentrations of EA under dark conditions and subjected 2 hours to different irradiation time (5, 6, 10 and 20 min respectively). The cells were then further incubated for an additional 2 hours in the dark without photosensitizer and measured via FCM assay. The rates of apoptosis induced by EA are shown in Table 3 and Figure 3. For each irradiation time, the data showed that there was dose-dependent relationship between EA doses and

rate of Hce-8693 cell apoptosis. On the contrary, no large differences in the antiproliferative effect of the photoactivated EA was found between the different irradiation time.

Table 3 Hce-8693 cell apoptosis induced by photoactivated EA (means ±SD, n=3)

Group	Rate of apoptosis/%			
	10 ⁻⁶ Mol/L	10 ⁻⁵ Mol/L	10 ⁻⁴ Mol/L	10 ⁻³ Mol/L
Control	0	0	0	0
5 min	0	32.7±7.56 ^b	53.6±6.62 ^b	63.4±10.24 ^b
6 min	0	19.3±4.16 ^b	32.8±7.38 ^b	55.5±7.00 ^b
10 min	13.4±3.25 ^b	26.4±4.89 ^b	31.3±5.39 ^b	44.9±5.46 ^b
20 min	40.5±8.58 ^b	52.7±11.82 ^b	65.2±11.22 ^b	68.0±5.93 ^b

^bP<0.01, vs EA control.

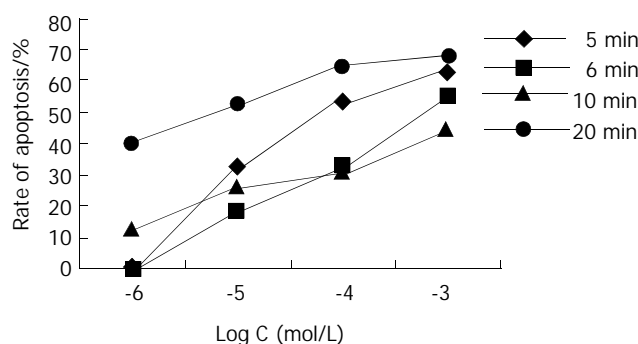


Figure 3 Dose-dependent relationship between EA doses and rate of Hce-8693 cell apoptosis. Cells were incubated for 2 h with 1×10⁻⁶ Mol/L, 1×10⁻⁵ Mol/L, 1×10⁻⁴ Mol/L, 1×10⁻³ Mol/L EA photosensitizer respectively and then irradiated. Results are means ± SD of three independent experiments.

Inhibitory effect of HA on the proliferation of Hce-8693 cells by inducing apoptosis

In order to investigate the antiproliferative effect of HA, Hce-8693 cells were incubated with different concentrations of HA under dark conditions and subjected 2 hours to different irradiation time (5, 6, 10 and 20 min respectively). The cells were then further incubated for additional 2 hours in the dark without photosensitizer and measured via FCM assay. The rates of apoptosis induced by HA were shown in Table 4 and Figure 4. For each irradiation time, the data showed that there was dose-dependent relationship between HA doses and rates of Hce-8693 cell apoptosis. On the contrary, no large differences in the antiproliferative effect of the photoactivated HA was found between the different irradiation time.

Table 4 Hce-8693 cell apoptosis induced by photoactivated HA (means ± SD, n=3)

Ggroup	Rate of apoptosis/%			
	10 ⁻⁶ Mol/L	10 ⁻⁵ Mol/L	10 ⁻⁴ Mol/L	10 ⁻³ Mol/L
Control	0	0	0	0
5 min	29.5±2.29 ^b	47.2±8.79 ^b	48.4±4.66 ^b	58.8±8.40 ^b
6 min	32.0±5.64 ^b	39.1±6.41 ^b	43.2±8.84 ^b	66.4±8.02 ^b
10 min	40.2±6.23 ^b	45.2±8.40 ^b	45.5±8.38 ^b	53.4±8.77 ^b
20 min	22.6±3.39 ^b	56.6±3.86 ^b	62.8±4.23 ^b	68.4±8.85 ^b

^bP<0.01, vs HA control.

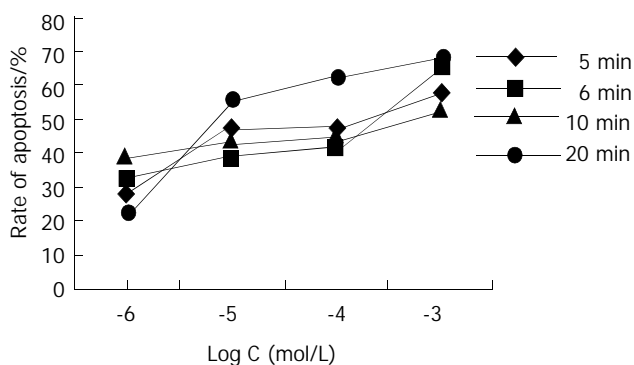


Figure 4 Dose-dependent relationship between HA doses and rate of Hce-8693 cell apoptosis. Cells were incubated for 2 h with 1×10^{-6} Mol/L, 1×10^{-5} Mol/L, 1×10^{-4} Mol/L, 1×10^{-3} Mol/L HA photosensitizer respectively and then irradiated. Results are means \pm SD of three independent experiments.

Inhibitory effect of HB on the proliferation of Hce-8693 cells by inducing apoptosis

In order to investigate the antiproliferative effect of HB, Hce-8693 cells were incubated with different concentrations of HB under dark conditions and subjected 2 hours to different irradiation time (5, 6, 10 and 20 min respectively). The cells were then further incubated for additional 2 hours in the dark without photosensitizer and measured via FCM assay. The rates of apoptosis induced by HB were shown in Table 5 and Figure 5. For each irradiation time, the data showed that there was dose-dependent relationship between HB doses and rate of Hce-8693 cell apoptosis. On the contrary, no large differences in the antiproliferative effect of the photoactivated HB was found between the different irradiation time.

Table 5 Hce-8693 cell apoptosis induced by photoactivated HB (means \pm SD, $n=3$)

Group	Rate of apoptosis/%			
	10^{-6} Mol/L	10^{-5} Mol/L	10^{-4} Mol/L	10^{-3} Mol/L
Control	0	0	0	0
5 min	0	0	28.1 \pm 6.21 ^b	64.8 \pm 11.78 ^b
6 min	0	0	17.3 \pm 3.68 ^b	32.0 \pm 7.57 ^b
10 min	0	20.0 \pm 4.21 ^b	20.5 \pm 4.57 ^b	71.0 \pm 10.57 ^b
20 min	13.7 \pm 3.02 ^b	13.9 \pm 2.87 ^b	19.1 \pm 4.06 ^b	29.4 \pm 6.56 ^b

^b $P < 0.01$, vs HB control.

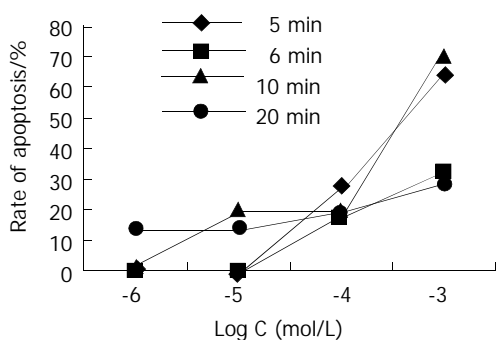


Figure 5 Dose-dependent relationship between HB doses and rate of Hce-8693 cell apoptosis. Cells were incubated for 2 h with 1×10^{-6} Mol/L, 1×10^{-5} Mol/L, 1×10^{-4} Mol/L, 1×10^{-3} Mol/L HB photosensitizer respectively and then irradiated. Results were means \pm SD of three independent experiments.

Inhibitory effect of EA, HA and HB on the proliferation of Hce-8693 cells by inducing apoptosis

From the results of photodependent cytotoxicity studies in R366.4 cell lines, it seemed that photoactivated EA had no cytotoxic effects at 10^{-6} Mol/L and 10^{-5} Mol/L concentrations. On the contrary, EA, HA and HB exhibited more or less antiproliferative effects on human Hce-8693 cells at this range of concentrations. Thus, the photodynamic effects of the photosensitizers could be compared from the rate of apoptosis (Table 6). The order of efficiency would be approximately HA>EA>HB (Figure 6).

Table 6 Comparison of antiproliferative effects of EA, HA and HB

Group	Rate of apoptosis/%					
	10^{-6} Mol/L			10^{-5} Mol/L		
	HA	EA	HB	HA	EA	HB
5 min	0	0	0	47.2 \pm 8.79	32.7 \pm 7.56	0
6 min	32.0 \pm 5.64	0	0	39.1 \pm 6.41	19.3 \pm 4.16	0
10 min	40.2 \pm 6.23	13.4 \pm 3.25	0	45.2 \pm 8.40	26.4 \pm 4.89	20.0 \pm 4.21
20 min	22.6 \pm 3.39	40.5 \pm 8.58	13.7 \pm 3.02	56.6 \pm 3.86	52.7 \pm 11.82	13.9 \pm 2.87

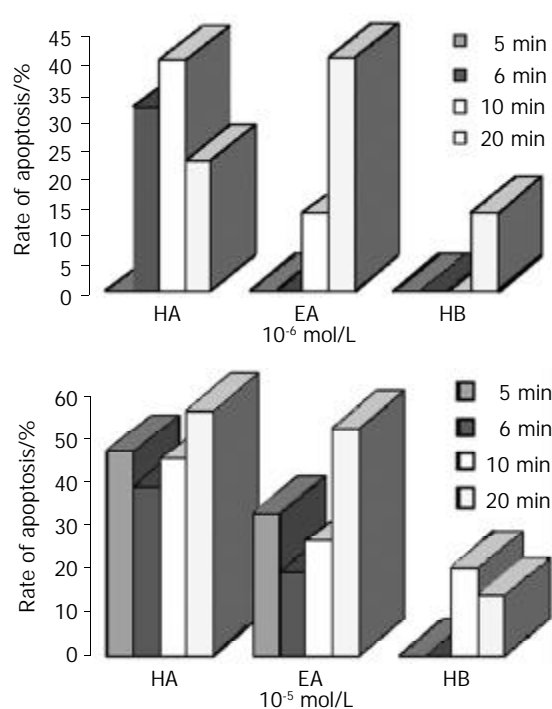


Figure 6 (a)-(b) illustrated the different antiproliferative effects of photoactivated HA, EA and HB on human Hce-8693 cells.

DISCUSSION

Photodynamic therapy (PDT) is a medical treatment based on the use of a sensitizer to promote photoinduced damage to biological molecules including lipids, proteins and DNA^[31,32]. It can be used to eradicate early localized tumours and for palliation of more advanced disease when metastasis has occurred. This treatment modality involves the use of light in combination with a photosensitizing compound. Following excitation of photosensitizers to long-lived excited singlet and/or triplet states, the tumour is destroyed either by reactive oxygen species (Type II mechanism) and/or by radical products (Type I mechanism)^[33-37].

Hypocrellins are efficient singlet oxygen generators during

photochemical reactions and may also exert photosensitization via radical mechanisms, which may confer a degree of independence from classical oxygen-dependent photochemical mechanisms. This feature is important in the context of impaired radiosensitivity and chemosensitivity of hypoxic human tumour cells. However, the precise mode of action of these molecules at the cellular level is not clear and seems to go far beyond Type I and Type II photoprocesses^[38-42]. An additional mechanism involving protons released in the excited state and leading to cellular pH drop has also been proposed for the related pigments hypocrellin and hypericin^[43].

Apoptosis is a complex and programmed process which is regulated by a variety of factors. Recently, it has been reported that hypocrellins and their derivatives can photosensitize apoptotic cell death^[44,45]. However, the molecular mechanisms of tumor cell apoptosis induction by Hypocrellin A and B are poorly understood. The antiproliferative actions of hypocrellin may be due, in part, to the ability of hypocrellin A to induce reactive oxygen species (Type II mechanism)^[46,47]. In addition, hypocrellin A-mediated apoptosis is increased when antisense bcl-2 retrovirus vector is transfected into human gastric adenocarcinoma MGC803 cells^[48]. And also, Ali *et al.* reported that caspase-3 and hydrogen peroxide may play an important role in HA and HB-induced apoptosis^[49,50].

According to the photochemical properties, the quantum yields of EA, HA and HB are 0.94, 0.83, 0.76 respectively. From the results of inhibitory effect of EA, HA and HB on the proliferation of Hce-8693 cells, it seems that the order of efficiency would be approximately HA>EA>HB. In this way, the molecular mechanisms of Hce-8693 cell apoptosis induction by EA, HA and HB may not be induced by reactive oxygen species (Type II mechanism). It is also noteworthy that photoactivated EA, HA and HB can selectively inhibit the growth of human colorectal carcinoma cells but not rhesus monkey embryonic stem R366.4 cells at lower concentrations. Thus, the molecular mechanisms of apoptosis induced by photoactivated EA, HA and HB are worth further investigation.

REFERENCES

- 1 **Chen CT**, Nakanishi K, Natori S. Biosynthesis of elsinochrome A, the perylenequinone from *Elsinoe* spp. I. *Chem Pharm Bull (Tokyo)* 1966; **14**: 1434-1437
- 2 **Weisgraber KH**, Weiss U. Pigments of *Elsinoe* species. VI. A simple synthesis of a related perylenequinone. *J Chem Soc [Perkin 1]* 1972; **1**: 83-88
- 3 **Stack ME**, Mazzola EP, Page SW, Pohland AE, Highet RJ, Tempesta MS, Corley DG. Mutagenic perylenequinone metabolites of *Alternaria alternata*: altertoxins I, II, and III. *J Nat Prod* 1986; **49**: 866-871
- 4 **Davis VM**, Stack ME. Mutagenicity of stemphytoxin III, a metabolite of *Alternaria alternata*. *Appl Environ Microbiol* 1991; **57**: 180-182
- 5 **Xu S**, Chen S, Zhang M, Shen T. A novel method for the preparation of amino-substituted hypocrellin B. *Bioorg Med Chem Lett* 2001; **11**: 2045-2047
- 6 **Ma JS**, Yan F, Wang CQ, An JY. Hypocrellin-A sensitized photooxidation of bilirubin. *Photochem Photobiol* 1989; **50**: 827-830
- 7 **Miller GG**, Brown K, Ballangrud AM, Barajas O, Xiao Z, Tulip J, Lown JW, Leithoff JM, Allalunis-Turner MJ, Mehta RD, Moore RB. Preclinical assessment of hypocrellin B and hypocrellin B derivatives as sensitizers for photodynamic therapy of cancer: progress update. *Photochem Photobiol* 1997; **65**: 714-722
- 8 **He YY**, An JY, Jiang LJ. Glycoconjugated hypocrellin: synthesis of [(beta-D-glucosyl)ethylthyl]hypocrellins and photosensitized generation of singlet oxygen. *Biochim Biophys Acta* 1999; **1472**: 232-239
- 9 **Daub ME**, Ehrenshaft M. The photoactivated cercospora toxin: contributions to plant disease and fundamental biology. *Annu Rev Phytopathol* 2000; **38**: 461-490
- 10 **Yu C**, Chen S, Zhang M, Shen T. Spectroscopic studies and photodynamic actions of hypocrellin B in liposomes. *Photochem Photobiol* 2001; **73**: 482-488
- 11 **Ververidis P**, Davrazou F, Diallinas G, Georgakopoulos D, Kanellis AK, Panopoulos N. A novel putative reductase (Cpd1p) and the multidrug exporter Snp2p are involved in resistance to cercosporin and other singlet oxygen-generating photosensitizers in *Saccharomyces cerevisiae*. *Curr Genet* 2001; **39**: 127-136
- 12 **Wang SS**, Mathes C, Thompson SH. Membrane toxicity of the protein kinase C inhibitor calphostin A by a free-radical mechanism. *Neurosci Lett* 1993; **157**: 25-28
- 13 **Gamou S**, Shimizu N. Calphostin-C stimulates epidermal growth factor receptor phosphorylation and internalization via light-dependent mechanism. *J Cell Physiol* 1994; **158**: 151-159
- 14 **Pedron T**, Girard R, Inoue K, Charon D, Chaby R. Lipopolysaccharide and the glycoside ring of staurosporine induce CD14 expression on bone marrow granulocytes by different mechanisms. *Mol Pharmacol* 1997; **52**: 692-700
- 15 **Dubauskas Z**, Beck TP, Chmura SJ, Kovar DA, Kadkhodaiian MM, Shrivastav M, Chung T, Stadler WM, Rinker-Schaeffer CW. Activated calphostin C cytotoxicity is independent of p53 status and *in vivo* metastatic potential. *Clin Cancer Res* 1998; **4**: 2391-2398
- 16 **Chen CL**, Chen H, Zhu DM, Uckun FM. Quantitative high-performance liquid chromatography-based detection method for calphostin C, a naturally occurring perylenequinone with potent antileukemic activity. *J Chromatogr B Biomed Sci Appl* 1999; **724**: 157-162
- 17 **Chen CL**, Tai HL, Zhu DM, Uckun FM. Pharmacokinetic features and metabolism of calphostin C, a naturally occurring perylenequinone with antileukemic activity. *Pharm Res* 1999; **16**: 1003-1009
- 18 **Meille SV**, Malpezzi L, Allegra G, Nasini G, Weiss U. Structure of elsinochrome A: a perylenequinone metabolite. *Acta Crystallogr C* 1989; **45**: 628-632
- 19 **Ma JS**, Yan F, Wang CQ, An JY. Hypocrellin-A sensitized photooxidation of bilirubin. *Photochem Photobiol* 1989; **50**: 827-830
- 20 **Diwu Z**, Zimmermann J, Meyer T, Lown JW. Design, synthesis and investigation of mechanisms of action of novel protein kinase C inhibitors: perylenequinonoid pigments. *Biochem Pharmacol* 1994; **47**: 373-385
- 21 **Fehr MJ**, Carpenter SL, Wannemuehler Y, Petrich JW. Roles of oxygen and photoinduced acidification in the light-dependent antiviral activity of hypocrellin A. *Biochemistry* 1995; **34**: 15845-15848
- 22 **Hirayama J**, Ikebuchi K, Abe H, Kwon KW, Ohnishi Y, Horiuchi M, Shinagawa M, Ikuta K, Kamo N, Sekiguchi S. Photoinactivation of virus infectivity by hypocrellin A. *Photochem Photobiol* 1997; **66**: 697-700
- 23 **Park J**, English DS, Wannemuehler Y, Carpenter S, Petrich JW. The role of oxygen in the antiviral activity of hypericin and hypocrellin. *Photochem Photobiol* 1998; **68**: 593-597
- 24 **Diwu Z**. Novel therapeutic and diagnostic applications of hypocrellins and hypericins. *Photochem Photobiol* 1995; **61**: 529-539
- 25 **Hudson JB**, Zhou J, Chen J, Harris L, Yip L, Towers GH. Hypocrellin, from *Hypocrella bambusa*, is phototoxic to human immunodeficiency virus. *Photochem Photobiol* 1994; **60**: 253-255
- 26 **Zhang J**, Cao EH, Li JF, Zhang TC, Ma WJ. Photodynamic effects of hypocrellin A on three human malignant cell lines by inducing apoptotic cell death. *J Photochem Photobiol B* 1998; **43**: 106-111
- 27 **Thomson JA**, Kalishman J, Golos TG, Durning M, Harris CP, Becker RA, Hearn JP. Isolation of a primate embryonic stem cell line. *PNAS* 1995; **92**: 7844-7848
- 28 **Schleger C**, Krebsfaenger N, Kalkuhl A, Bader R, Singer T. Innovative cell culture methods in drug development. *ALTEX* 2001; **18**: 5-8
- 29 **Rohwedel J**, Guan K, Hegert C, Wobus AM. Embryonic stem cells as an *in vitro* model for mutagenicity, cytotoxicity and embryotoxicity studies: present state and future prospects. *Toxicol in vitro* 2001; **15**: 741-753
- 30 **Genschow E**, Spielmann H, Scholz G, Seiler A, Brown N, Piersma A, Brady M, Clemann N, Huuskonen H, Paillard F, Bremer S, Becker K. The ECVAM international validation study on *in vitro* embryotoxicity tests: results of the definitive phase and evaluation of prediction models. *Altern Lab Anim* 2002; **30**: 151-176

- 31 **Xu Y**, Zhao H, Zhang Z. Raman spectroscopic study of microcosmic and photosensitive damage on the liposomes of the mixed phospholipids sensitized by hypocrellin and its derivatives. *J Photochem Photobiol B* 1998; **43**: 41-46
- 32 **He YY**, Jiang LJ. Photosensitized damage to calf thymus DNA by a hypocrellin derivative: mechanisms under aerobic and anaerobic conditions. *Biochim Biophys Acta* 2000; **1523**: 29-36
- 33 **Fu NW**. Advances in research on photosensitizers. *Shengli Kexue Jinzhan* 1992; **23**: 36-40
- 34 **Estey EP**, Brown K, Diwu Z, Liu J, Lown JW, Miller GG, Moore RB, Tulip J, McPhee MS. Hypocrellins as photosensitizers for photodynamic therapy: a screening evaluation and pharmacokinetic study. *Cancer Chemother Pharmacol* 1996; **37**: 343-350
- 35 **Diwu ZJ**, Haugland RP, Liu J, Lown JW, Miller GG, Moore RB, Brown K, Tulip J, McPhee MS. Photosensitization by anticancer agents 21: new perylene- and aminonaphthoquinones. *Free Radic Biol Med* 1996; **20**: 589-593
- 36 **Wang ZJ**, He YY, Huang CG, Huang JS, Huang YC, An JY, Gu Y, Jiang LJ. Pharmacokinetics, tissue distribution and photodynamic therapy efficacy of liposomal-delivered hypocrellin A, a potential photosensitizer for tumor therapy. *Photochem Photobiol* 1999; **70**: 773-780
- 37 **Wu T**, Xu S, Shen J, Song A, Chen S, Zhang M, Shen T. New potential photodynamic therapeutic anti-cancer agents: synthesis and characterization of demethoxy amino-substituted hypocrellins. *Anticancer Drug Des* 2000; **15**: 287-293
- 38 **Nenghui W**, Zhiyi Z. Relationship between photosensitizing activities and chemical structure of hypocrellin A and B. *J Photochem Photobiol B* 1992; **14**: 207-217
- 39 Yuying H, Jingyi A, Lijin J. Effect of structural modifications on photosensitizing activities of hypocrellin dyes: EPR and spectrophotometric studies. *Free Radic Biol Med* 1999; **26**: 1146-1157
- 40 **Datta A**, Smirnov AV, Wen J, Chumanov G, Petrich JW. Multidimensional reaction coordinate for the excited-state H-atom transfer in perylene quinones: importance of the 7-membered ring in hypocrellins A and B. *Photochem Photobiol* 2000; **71**: 166-172
- 41 **Wu T**, Shen J, Song A, Chen S, Zhang M, Shen T. Photodynamic action of amino substituted hypocrellins: EPR studies on the photogenerations of active oxygen and free radical species. *J Photochem Photobiol B* 2000; **57**: 14-21
- 42 **Xu S**, Shen J, Chen S, Zhang M, Shen T. Active oxygen species ($^1\text{O}_2$, O_2^{*-}) generation in the system of TiO_2 colloid sensitized by hypocrellin B. *J Photochem Photobiol B* 2002; **67**: 64-70
- 43 **Chaloupka R**, Sureau F, Kocisova E, Petrich JW. Hypocrellin A photosensitization involves an intracellular pH decrease in 3T3 cells. *Photochem Photobiol* 1998; **68**: 44-50
- 44 **Ali SM**, Chee SK, Yuen GY, Olivo M. Hypericin and hypocrellin induced apoptosis in human mucosal carcinoma cells. *J Photochem Photobiol B* 2001; **65**: 59-73
- 45 **Ali SM**, Olivo M, Yuen GY, Chee SK. Photodynamic-induced apoptosis of human nasopharyngeal carcinoma cells using Hypocrellins. *Int J Oncol* 2001; **19**: 633-643
- 46 **Ma J**, Jiang L. Photogeneration of singlet oxygen ($^1\text{O}_2$) and free radicals (Sens^- , O_2^{*-}) by tetra-brominated hypocrellin B derivative. *Free Radic Res* 2001; **35**: 767-777
- 47 **Wu T**, Xu S, Shen J, Chen S, Zhang M, Shen T. EPR investigation of the free radicals generated during the photosensitization of TiO_2 colloid by hypocrellin B. *Free Radic Res* 2001; **35**: 137-143
- 48 **Zhang WG**, Ma LP, Wang SW, Zhang ZY, Cao GD. Antisense bcl-2 retrovirus vector increases the sensitivity of a human gastric adenocarcinoma cell line to photodynamic therapy. *Photochem Photobiol* 1999; **69**: 582-586
- 49 **Ali SM**, Chee SK, Yuen GY, Olivo M. Hypocrellins and Hypericin induced apoptosis in human tumor cells: A possible role of hydrogen peroxide. *Int J Mol Med* 2002; **9**: 461-472
- 50 **Ali SM**, Chee SK, Yuen GY, Olivo M. Photodynamic therapy induced Fas-mediated apoptosis in human carcinoma cells. *Int J Mol Med* 2002; **9**: 257-270

Edited by Xu JY

Expression and significance of PTEN, hypoxia-inducible factor-1 alpha in colorectal adenoma and adenocarcinoma

Ying-An Jiang, Li-Fang Fan, Chong-Qing Jiang, You-Yuan Zhang, He-Sheng Luo, Zhi-Jiao Tang, Dong Xia, Ming Wang

Ying-An Jiang, He-Sheng Luo, Department of Gastroenterology, Renming Hospital of Wuhan University, Wuhan 430060, Hubei Province, China

Li-Fang Fan, Zhi-Jiao Tang, Dong Xia, Ming Wang, Department of Pathology, Medical College of Wuhan University, Wuhan 430071, Hubei Province, China

Chong-Qing Jiang, Department of Surgery, Zhongnan Hospital of Wuhan University, Wuhan 430071, Hubei Province, China

You-Yuan Zhang, Department of Pathology, Central Hospital of Huangshi City, Huangshi 435000, Hubei Province, China

Correspondence to: Ying-An Jiang, Central Hospital of Huangshi City, 43 Wuhan Road, Huangshi 435000, Hubei Province, China. hszxyy@public.hs.hb.cn

Telephone: +86-714-6283783 **Fax:** +86-714-6233931

Received: 2002-11-12 **Accepted:** 2003-01-09

Abstract

AIM: To investigate the expression and significance of PTEN, hypoxia-inducible factor-1 alpha (HIF-1 α), and targeting gene VEGF during colorectal carcinogenesis.

METHODS: Total 71 cases colorectal neoplasms (9 cases of colorectal adenoma and 62 colorectal adenocarcinoma) were formalin fixed and paraffin-embedded, and all specimens were evaluated for PTEN mRNA, HIF-1 α mRNA and VEGF protein expression. PTEN mRNA, HIF-1 α mRNA were detected by *in situ* hybridization. VEGF protein was identified by citrate-microwave SP immunohistochemical method.

RESULTS: There were significant differences in PTEN, HIF-1 α and VEGF expression between colorectal adenomas and colorectal adenocarcinoma ($P < 0.05$). The level of PTEN expression decreased as the pathologic stage increased. Conversely, HIF-1 α and VEGF expression increased with the Dukes stage as follows: stage A (0.1029 \pm 0.0457: 0.1207 \pm 0.0436), stage B (0.1656 \pm 0.0329: 0.1572 \pm 0.0514), and stage C+D (0.2335 \pm 0.0748: 0.2219 \pm 0.0803). For PTEN expression, there was a significant difference among Dukes stage A, B, and C+D, and the level of PTEN expression was found to be significant higher in Dukes stage A or B than that of Dukes stage C or D. For HIF-1 α expression, there was a significant difference between Dukes stage A and B, and the level of HIF-1 α expression was found to be significantly higher in Dukes stage C+D than that of Dukes stage A or B. The VEGF expression had similar results as HIF-1 α expression. In colorectal adenocarcinoma, decreased levels of PTEN were significantly associated with increased expression of HIF-1 α mRNA ($r = -0.36$, $P < 0.05$) and VEGF protein ($r = -0.48$, $P < 0.05$) respectively. The levels of HIF-1 were positively correlated with VEGF expression ($r = 0.71$, $P < 0.01$).

CONCLUSION: Loss of PTEN expression and increased levels of HIF-1 α and VEGF may play an important role in carcinogenesis and progression of colorectal adenocarcinoma.

Jiang YA, Fan LF, Jiang CQ, Zhang YY, Luo HS, Tang ZJ, Xia D, Wang M. Expression and significance of PTEN, hypoxia-inducible factor-1 alpha in colorectal adenoma and adenocarcinoma. *World J Gastroenterol* 2003; 9(3): 491-494

<http://www.wjgnet.com/1007-9327/9/491.htm>

INTRODUCTION

So far, the mechanism of colorectal oncogenesis is not fully understood. Recent studies^[1-6] have reported on the association of a tumor suppressor gene PTEN with the oncogeneses of several type cancer and cancer cell lines and on PTEN playing an important role in the tumor progression and metastases. Moreover, hypoxia-inducible Factor-1 alpha (HIF-1 α) is a transcription factor identified as being activated by hypoxia, and plays a central role in tumor angiogenesis^[7-19]. Therefore, this study was undertaken to investigate the expression and relationship between PTEN and HIF-1 α and VEGF in colorectal carcinogenesis.

MATERIALS AND METHODS

Materials

The specimens of colorectal cancer were surgically obtained from 71 patients at the Hospital of Wuhan University between 1996 and 1997, and 71 patients were catalogued by histological subtypes as follows: 62 cases of colorectal adenocarcinoma (17 cases in Dukes stage A, 18 stage B, 20 stage C and 7 stage D) and 9 patients of colorectal adenoma (5 cases of tubulovillous adenoma, 2 tubular adenoma and 2 villous adenoma).

Antibodies and reagents

A rabbit VEGF polyclonal antibody was purchased from Neomark International Corporation (Taipei, Taiwan), PTEN mRNA, HIF-1 α mRNA *in situ* hybridization and immunohistochemical repairase were purchased from Boster Corporation (Wuhan, China), and S-P reagent was purchased from Maixin Corporation (Fuzhou, China).

Immunohistochemical technique

Sections were dewaxed in xylene, taken thorough ethanol, and then incubated with 3 % hydrogen peroxide to block endogenous peroxidase activity. Sections then were repaired by repairase for 10 minutes, and the procedure of immunohistochemical determination was performed according to the manufacturer's instruction. A rabbit polyclonal antibody was a dilution of 1:50.

In situ hybridization

Frozen sections were cut onto slides, briefly air-dried, and stored at -80 °C. Prior to use they were fixed in 4 % paraformaldehyde in PBS for 20 min, washed in PBS, and treated with proteinase K (0.0005 %) in 0.1 M Tris/0.05 M EDTA, pH 8.0 for 5 min at 37 °C. Slides were rinsed in 0.2 M glycine in water, postfixed in 4 % paraformaldehyde/0.1 M NaOH/0.1 M NaAc for 5 min, rinsed in 0.1 M triethanolamine

(TEA), pH 8.0 for 3 min, acetylated for 10 min in 0.25 % acetic anhydride/0.1 M TEA, pH 8.8, washed in 2×SSC, and dehydrated. RNA probe was then hybridized to the sections at 60 °C for 16 hrs in 50 % formamide/10 % dextran sulfate/0.15 M NaCl/1×Denhardt's solution/0.01 M Tris·Cl, pH 8.0/0.01 M DTT with 0.5 mg/ml tRNA. Sections from each tumor were always hybridized to sense probes as a control for specificity. The slides were next rinsed in 4×SSC and incubated at 37 °C for 30 min with 0.1 mg/ml RNaseA in 0.5 M NaCl/0.01 M Tris·Cl, pH 8.0/1 mM EDTA. They were then desalted, dehydrated through graded ethanols, and coated with emulsion. Following exposure at 4 °C for 5 days, emulsion was developed and fixed, and sections were stained with hematoxylin and eosin. To analyse image scanning, we obtained value of absorbance.

Statistical analysis

All results were expressed as the means \pm SD. Statistical analyses, including the Chi-square test and correlated Spearman test, were carried out with the software package SPSS10.0. A *P* value of <0.05 was considered statistically significant.

RESULTS

Characteristics of PTEN and HIF-1 α expression in colorectal adenoma and adenocarcinoma

PTEN mRNA and HIF-1 α mRNA expression was brown granular, and localized in cytoplasm of tumor cells (Figures 1, 2). HIF-1 α mRNA expression was mainly localized in cytoplasm of tumor cells, frequently observed in margin of tumor necrotic zones. VEGF expression was mainly localized in cytoplasm of tumor cells, also observed in endothelial cell of blood vessel (Figure 3). Expression of PTEN mRNA, HIF-1 α mRNA and VEGF protein was detected in 7, 4 and 3 cases of 9 colorectal adenomas respectively. PTEN mRNA expression was significantly higher (*P*<0.05) in adenomas than that in adenocarcinoma, but HIF-1 α mRNA expression was significantly lower (*P*<0.05) in adenomas than that in adenocarcinoma. There was a significant difference (*P*<0.05) in VEGF expression between colorectal adenomas and adenocarcinoma.

Correlation between PENT, HIF-1 α , VEGF expressions and dukes stages of colorectal adenocarcinoma

Table 1 shows the correlation between PENT, HIF-1 α , VEGF expression and Dukes stages of colorectal adenocarcinoma. For PTEN expression, there was a significant difference among Dukes stage A, B, C and D, and the level of PTEN expression was found to be significant higher in Dukes stage A or B than that in Dukes stage C+D. For HIF-1 α expression, there was a significant difference between Dukes stage A and Dukes stage B, and the level of HIF-1 α expression was found to be significantly higher in Dukes stage C+D than that in Dukes stage A or B. VEGF expression had same results as HIF-1 α expression.

Table 1 Correlation between expressions of PENT, HIF-1 α , VEGF and Dukes stages of colorectal adenocarcinoma

Dukes stage	<i>n</i>	PTEN($\bar{x}\pm s$)	HIF-1 ($\bar{x}\pm s$)	VEGF($\bar{x}\pm s$)
A	17	0.1782 \pm 0.0271 ^{ab}	0.1029 \pm 0.0457 ^{ac}	0.1207 \pm 0.0436 ^{ac}
B	18	0.1583 \pm 0.0397 ^b	0.1656 \pm 0.0329 ^c	0.1772 \pm 0.0514 ^c
C+D	27	0.1470 \pm 0.0524	0.2335 \pm 0.0748	0.2219 \pm 0.0803

^a*P*<0.05, vs Dukes stage B; ^b*P*<0.05, vs Dukes stage C+D; ^c*P*<0.01, vs Dukes stage C+D.

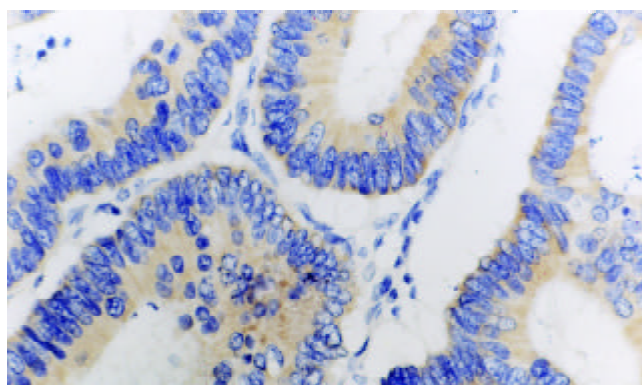


Figure 1 PTEN expression was observed in the cytoplasm of rectal tubular adenoma. Immunostaining, S-P method. \times 400.

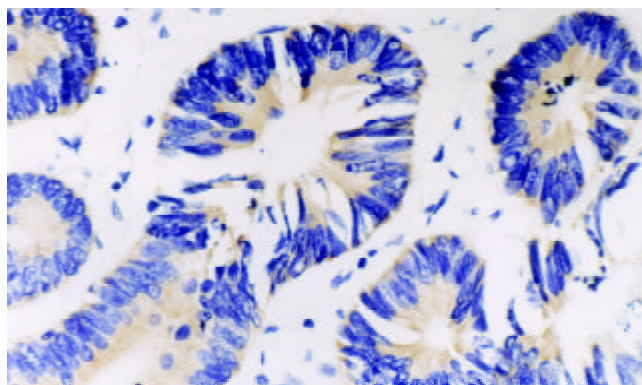


Figure 2 HIF-1 α expression was observed in rectal tubular adenoma. Immunostaining, S-P method. \times 400.

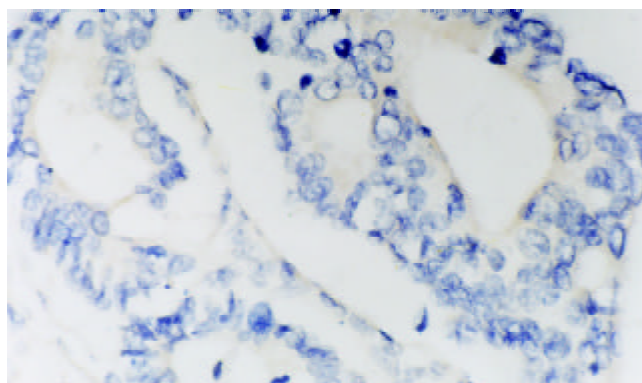


Figure 3 Sigmoid carcinoma shows infiltration into the deep muscular layer, intermeditated differentiation, in which VEGF expression was observed. Immunostaining, S-P method. \times 400.

Correlation between colorectal adenoma and adenocarcinoma in PTEN, HIF-1 α and VEGF expression

The Spearman analysis showed that the level of PTEN was significantly associated with HIF-1 α expression (*r*=-0.36, *P*<0.05) and with VEGF protein expression (*r*=-0.68, *P*<0.05) respectively. The level of HIF-1 α was correlated with VEGF expression (*r*=0.72, *P*<0.01).

DISCUSSION

PTEN (phosphatase and Tensin homologue deleted on chromosome 10) or MMAC1 (mutated in multiple advanced cancers 1) was recently reported to undergo frequent genetic alterations, including mutations and deletions in multiple advanced cancers^[20-22]. PTEN located at chromosome 10q23.3

encodes a dual-specificity phosphatase that negatively regulates the phosphoinositol-3-kinase (PI3K)/Akt (protein kinase B) pathway and mediates cell cycle arrest and apoptosis^[23]. PTEN protein contains sequence motifs with significant homology to the catalytic domain of protein phosphatases and to the cytoskeletal protein, tensin, and auxilin^[24]. PTEN mutations and deletions were observed in a number of glioma, prostate, kidney and breast carcinoma cell lines or tumor specimens^[25-27]. Recently, Shin *et al.*^[28] screened the PTEN gene in 32 colorectal cancers (8 cell lines and 24 tissues), displaying microsatellite instability (MSI) and six frameshift mutations. We observed that PTEN mRNA decreased as the pathological stage increased, and was significantly associated with VEGF protein expression ($r=-0.68$, $P<0.05$) in colorectal adenoma and adenocarcinoma. These findings suggested that PTEN alteration was possibly involved in the tumor progression and formation of metastasis, and the roles of PTEN in tumor progression and metastasis may be correlated with VEGF expression. Hwang *et al.*^[29] observed that PTEN inhibited the tumorigenicity of B16F10 melanoma cells, and their results suggested that PTEN inhibited tumorigenicity and metastasis through regulating VEGF expression. Jiang *et al.*^[30] found that the overexpression of PTEN inhibited angiogenesis in chicken embryos, and that the PTEN overexpression inhibited the VEGF expression through the PI 3-kinase or Akt dependent pathway. Our results also indicated that PTEN played an important role by inhibiting VEGF expression in colorectal oncogenesis.

HIF-1 is a BHLH-PAS transcription factor that plays an essential role in O₂ homeostasis^[31-34]. HIF-1 is a heterodimer composed of HIF-1 α and HIF-1 β subunits^[31]. HIF-1 β (also known as the aryl hydrocarbon receptor nuclear translocator) is a common subunit of multiple BHLH-PAS proteins, whereas HIF-1 α is the unique, O₂-regulated subunit that determines HIF-1 activity^[35,36]. HIF-1 α activates the transcription of genes encoding transferrin, VEGF, endothelin-1 and inducible nitric oxide synthase, which are implicated in vasodilation, neovascularization, and tumor metastasis^[36,37]. Many studies had identified that HIF-1 α protein was overexpressed in multiple types of human cancer including lung, prostate, breast, and colon carcinomas, even in preneoplastic and premalignant lesions^[38-42]. More importantly, Birner *et al.*^[43] found that the overexpression of HIF-1 α is an important marker in precancerous lesion such as early-stage cervical cancer, cervical intra-epithelial neoplasia III, early stage lymph node-negative breast cancer. We also found that the levels of HIF-1 α mRNA increased gradually as the pathologic stage increased, and were statistically significantly associated with VEGF expression. The same alterations were observed in other tumor tissues. Our findings further identified that HIF-1 α and VEGF played an important role in the tumor angiogenesis and formations of metastases. In this study, we found that HIF-1 α mRNA and VEGF were overexpressed in 4 and 3 cases of colorectal adenomas respectively, and suggested that cell hypoxia occurred prior to carcinogenesis, and persisted to subsequent progression. Generally, these data suggested that HIF-1 α overexpression may be an early stage of carcinogenesis and it occurred prior to angiogenesis or invasion which morphologically confirmed. In this study, the expression of HIF-1 α mRNA and VEGF was significantly higher in the tissues of Dukes stage C/D of colorectal adenocarcinoma than those in Dukes stage A/B, indicating that HIF was involved in the tumor invasion and formation of metastasis. Thus, we believe that the HIF-1 α mRNA and VEGF overexpression is a strong independent prognostic marker in colorectal tumor.

That HIF-1 expression was activated and regulated by EGFR, HER2, and IGF1R through PI3K/Akt/FRAP (FKBP-rapamycin-associated protein) pathway had been identified, and a tumor suppressor gene PTEN regulated the HIF-1 α

expression and transcription activation by inhibiting PI3K/Akt/FRAP pathway^[44,45]. The loss of wild-type PTEN resulted in HIF-1 α overexpression, and contributed to the formations of tumor angiogenesis in human prostate cancer and glioma. Our findings that the levels of HIF-1 α were negatively correlated with VEGF expression and the level of PTEN were positively correlated with VEGF expression had further identified that loss of PTEN expression and increased levels of HIF-1 α and VEGF may play an important role in carcinogenesis and progression of colorectal carcinoma.

REFERENCES

- Teng DH**, Hu R, Lin H, Davis T, Iliev D, Frye C, Swedlund B, Hansen KL, Vinson VL, Gumpfer KL, Ellis L, EI-Naggar A, Frazier M, Jasser S, Langford LA, Lee J, Mills GB, Pershouse MA, Pollack RE, Tornos C, Troncso P, Yung WK, Fujii G, Berson A, Steck PA. MMAC1/PTEN mutations in primary tumor specimens and tumor cell lines. *Cancer Res* 1997; **57**: 5221-5225
- Tsuchiya KD**, Wiesner G, Cassidy SB, Limwongse C, Boyle JT, Schwartz S. Deletion 10q23.2-q23.33 in a patient with gastrointestinal juvenile polyposis and other features of a Cowden-like syndrome. *Genes Chromosomes Cancer* 1998; **21**: 113-118
- Tsao H**, Zhang X, Benoit E, Haluska FG. Identification of PTEN/MMAC1 alterations in uncultured melanomas and melanoma cell lines. *Oncogene* 1998; **16**: 3397-3402
- Yang L**, Kuang LG, Zheng HC, Li JY, Wu DY, Zhang SM, Xin Y. PTEN encoding product: a marker for tumorigenesis an progression of gastric carcinoma. *World J Gastroenterol* 2003; **9**: 35-39
- Wen S**, Stolarov J, Myers MP, Su JD, Wigler MH, Tonks NK, Durden DL. PTEN controls tumor-induced angiogenesis. *Proc Natl Acad Sci U S A* 2001; **98**: 4622-4627
- Poetsch M**, Dittberner T, Woencckhans C. PTEN/MMAC1 in malignant melanoma and its importance for tumor progression. *Cancer Genet Cytogenet* 2001; **125**: 21-26
- Semenza GL**, Agani F, Booth G, Forsythe J, Iyer N, Jiang BH, Leung S, Roe R, Wiener C, Yu A. Structural and functional analysis of hypoxia-inducible factor 1. *Kidney Int* 1997; **51**: 553-555
- Maxwell PH**, Dachs GU, Gleadle JM, Nicholls LG, Harris AL, Stratford IJ, Hankinson O, Pugh CW, Ratcliffe PJ. Hypoxia-inducible factor-1 modulates gene expression in solid tumors and influences both angiogenesis and tumor growth. *Proc Natl Acad Sci U S A* 1997; **94**: 8104-8109
- Minet E**, Michel G, Remacle J, Michiels C. Role of HIF-1 as a transcription factor involved in embryonic development, cancer progression and apoptosis (review). *Int J Mol Med* 2000; **5**: 253-259
- Zagzag D**, Zhong H, Scalzitti JM, Laughner E, Simons JW, Semenza GL. Expression of hypoxia-inducible factor 1 α in brain tumors: association with angiogenesis, invasion, and progression. *Cancer* 2000; **88**: 2606-2618
- Sondergaard KL**, Hilton DA, Penney M, Ollerenshaw M, Demaine AG. Expression of hypoxia-inducible factor 1 α in tumours of patients with glioblastoma. *Neuropathol Appl Neurobiol* 2002; **28**: 210-217
- Talks KL**, Turley H, Gatter KC, Maxwell PH, Pugh CW, Ratcliffe PJ, Harris AL. The expression and distribution of the hypoxia-inducible factors HIF-1 α and HIF-2 α in normal human tissues, cancers, and tumor-associated macrophages. *Am J Pathol* 2000; **157**: 411-421
- Bos R**, Zhong H, Hanrahan CF, Mommers EC, Semenza GL, Pinedo HM, Abeloff MD, Simons JW, van Diest PJ, van der Wall E. Levels of hypoxia-inducible factor-1 α during breast carcinogenesis. *J Natl Cancer Inst* 2001; **93**: 309-314
- Zhong H**, Hanrahan C, van der Poel H, Simons JW. Hypoxia-inducible factor 1 α and 1 β proteins share common signaling pathways in human prostate cancer cells. *Biochem Biophys Res Commun* 2001; **284**: 352-356
- Nakayama K**, Kanzaki A, Hata K, Katabuchi H, Okamura H, Miyazaki K, Fukumoto M, Takebayashi Y. Hypoxia-inducible factor 1 α (HIF-1 α) gene expression in human ovarian carcinoma. *Cancer Lett* 2002; **176**: 215-223
- Semenza GL**. Involvement of hypoxia-inducible factor 1 in human cancer. *Intern Med* 2002; **41**: 79-83

- 17 **Koukourakis MI**, Giatromanolaki A, Sivridis E, Simopoulos C, Turley H, Talks K, Gatter KC, Harris AL. Hypoxia-inducible factor (HIF1A and HIF2A), angiogenesis, and chemoradiotherapy outcome of squamous cell head-and-neck cancer. *Int J Radiat Oncol Biol Phys* 2002; **53**: 1192-1202
- 18 **Ryan HE**, Poloni M, McNulty W, Elson D, Gassmann M, Arbeit JM, Johnson RS. Hypoxia-inducible factor-1 α is a positive factor in solid tumor growth. *Cancer Res* 2000; **60**: 4010-4015
- 19 **Semenza GL**. HIF-1 and tumor progression: pathophysiology and therapeutics. *Trends Mol Med* 2002; **8** (Suppl): S62-67
- 20 **Chang JG**, Chen YJ, Peng LI, Wang NM, Kao MC, Yang TY, Chang CP, Tsai CH. Mutation analysis of the PTEN/MMAC1 gene in cancers of the digestive tract. *Eur J Cancer* 1999; **35**: 647-651
- 21 **Guanti G**, Resta N, Simone C, Cariola F, Demma I, Fiorente P, Gentile M. Involvement of PTEN mutations in the genetic pathways of colorectal carcinogenesis. *Hum Mol Genet* 2000; **9**: 283-287
- 22 **Steck PA**, Pershouse MA, Jasser SA, Yung WK, Lin H, Ligon AH, Langford LA, Baumgard ML, Hattier T, Davis T, Frye C, Hu R, Swedlund B, Teng DH, Tavtigian SV. Identification of a candidate tumour suppressor gene, MMAC1, at chromosome 10q23.3 that is mutated in multiple advanced cancers. *Nat Genet* 1997; **15**: 356-362
- 23 **Zhou XP**, Loukola A, Salovaara R, Nystrom-Lahti M, Peltomaki P, de la Chapelle A, Aaltonen LA, Eng C. PTEN mutational spectra, expression levels, and subcellular localization in microsatellite stable and unstable colorectal cancers. *Am J Pathol* 2002; **161**: 439-447
- 24 **Steck PA**, Pershouse MA, Jasser SA, Yung WK, Lin H, Ligon AH, Langford LA, Baumgard ML, Hattier T, Davis T, Frye C, Hu R, Swedlund B, Teng DH, Tavtigian SV. Identification of a candidate tumour suppressor gene, MMAC1, at chromosome 10q23.3 that is mutated in multiple advanced cancers. *Nat Genet* 1997; **15**: 356-362
- 25 **Koul D**, Shen R, Garyali A, Ke LD, Liu TJ, Yung WK. MMAC/PTEN tumor suppressor gene regulates vascular endothelial growth factor-mediated angiogenesis in prostate cancer. *Int J Oncol* 2002; **21**: 469-475
- 26 **Velickovic M**, Delahunt B, McIver B, Grebe SK. Intragenic PTEN/MMAC1 loss of heterozygosity in conventional (clear-cell) renal cell carcinoma is associated with poor patient prognosis. *Mod Pathol* 2002; **15**: 479-485
- 27 **Harima Y**, Sawada S, Nagata K, Sougawa M, Ostapenko V, Ohnishi T. Mutation of the PTEN gene in advanced cervical cancer correlated with tumor progression and poor outcome after radiotherapy. *Int J Oncol* 2001; **18**: 493-497
- 28 **Shin KH**, Park YJ, Park JG. PTEN gene mutations in colorectal cancers displaying microsatellite instability. *Cancer Lett* 2001; **174**: 189-194
- 29 **Hwang PH**, Yi HK, Kim DS, Nam SY, Kim JS, Lee DY. Suppression of tumorigenicity and metastasis in B16F10 cells by PTEN/MMAC1/TEP1 gene. *Cancer Lett* 2001; **172**: 83-91
- 30 **Jiang BH**, Zheng JZ, Aoki M, Vogt PK. Phosphatidylinositol 3-kinase signaling mediates angiogenesis and expression of vascular endothelial growth factor in endothelial cells. *Proc Natl Acad Sci U S A* 2000; **97**: 1749-1753
- 31 **Wang GL**, Jiang BH, Rue EA, Semenza GL. Hypoxia-inducible factor 1 is a basic-helix-loop-helix-PAS heterodimer regulated by cellular O₂ tension. *Proc Natl Acad Sci U S A* 1995; **92**: 5510-5514
- 32 **Iyer NV**, Kotch LE, Agani F, Leung SW, Laughner E, Wenger RH, Gassmann M, Gearhart JD, Lawler AM, Yu AY, Semenza GL. Cellular and developmental control of O₂ homeostasis by hypoxia-inducible factor 1 α 1pha. *Genes Dev* 1998; **12**: 149-162
- 33 **Ryan HE**, Lo J, Johnson RS. HIF-1 α 1pha is required for solid tumor formation and embryonic vascularization. *EMBO J* 1998; **17**: 3005-3015
- 34 **Carmeliet P**, Dor Y, Herbert JM, Fukumura D, Brusselmans K, Dewerchin M, Neeman M, Bono F, Abramovitch R, Maxwell P, Koch CJ, Ratcliffe P, Moons L, Jain RK, Collen D, Keshet E, Keshet E. Role of HIF-1 α 1pha in hypoxia-mediated apoptosis, cell proliferation and tumour angiogenesis. *Nature* 1998; **394**: 485-490
- 35 **Jiang BH**, Semenza GL, Bauer C, Marti HH. Hypoxia-inducible factor 1 levels vary exponentially over a physiologically relevant range of O₂ tension. *Am J Physiol* 1996; **271**: C1172-1180
- 36 **Semenza GL**. Regulation of mammalian O₂ homeostasis by hypoxia-inducible factor 1. *Annu Rev Cell Dev Biol* 1999; **15**: 551-578
- 37 **Kerbek RS**. New targets, drugs, and approaches for the treatment cancer: an overview. *Cancer Metastasis Rev* 1998; **17**: 145-147
- 38 **Giatromanolaki A**, Koukourakis MI, Sivridis E, Turley H, Talks K, Pezzella F, Gatter KC, Harris AL. Relation of hypoxia inducible factor 1 α and 2 α 1pha in operable non-small cell lung cancer to angiogenic/molecular profile of tumours and survival. *Br J Cancer* 2001; **85**: 881-890
- 39 **Saramaki OR**, Savinainen KJ, Nupponen NN, Bratt O, Visakorpi T. Amplification of hypoxia-inducible factor 1 α 1pha gene in prostate cancer. *Cancer Genet Cytogenet* 2001; **128**: 31-34
- 40 **Schindl M**, Schoppmann SF, Samonigg H, Hausmaninger H, Kwasny W, Gnant M, Jakesz R, Kubista E, Birner P, Oberhuber G. Overexpression of Hypoxia-inducible Factor 1 α 1pha Is Associated with an Unfavorable Prognosis in Lymph Node-positive Breast Cancer. *Clin Cancer Res* 2002; **8**: 1831-1837
- 41 **Welsh SJ**, Bellamy WT, Briehl MM, Powis G. The redox protein thioredoxin-1 (Trx-1) increases hypoxia-inducible factor 1 α 1pha protein expression: Trx-1 overexpression results in increased vascular endothelial growth factor production and enhanced tumor angiogenesis. *Cancer Res* 2002; **62**: 5089-5095
- 42 **Zhong H**, De Marzo AM, Laughner E, Lim M, Hilton DA, Zagzag D, Buechler P, Isaacs WB, Semenza GL, Simons JW. Overexpression of hypoxia-inducible factor 1 α 1pha in common human cancers and their metastases. *Cancer Res* 1999; **59**: 5830-5835
- 43 **Birner P**, Schindl M, Obermair A, Plank C, Breitenecker G, Oberhuber G. Overexpression of hypoxia-inducible factor 1 α 1pha is a marker for an unfavorable prognosis in early-stage invasive cervical cancer. *Cancer Res* 2000; **60**: 4693-4696
- 44 **Laughner E**, Taghavi P, Chiles K, Mahon PC, Semenza GL. HER2 (neu) signaling increase the rate of hypoxia-inducible factor 1 α 1pha (HIF-1 α 1pha) synthesis: novel mechanism for HIF-1-mediated vascular endothelial growth factor expression. *Mol Cell Biol* 2001; **21**: 3995-4004
- 45 **Zhong H**, Chiles K, Feldser D, Laughner E, Hanrahan C, Georgescu MM, Simons JW, Semenza GL. Modulation of hypoxia-inducible factor 1 α 1pha expression by the epidermal growth factor/phosphatidylinositol 3-kinase/PTEN/AKT/FRAP pathway in human prostate cancer cells: implications for tumor angiogenesis and therapeutics. *Cancer Res* 2000; **60**: 1541-1545

Edited by Zhang JZ

Application of autologous tumor cell vaccine and NDV vaccine in treatment of tumors of digestive tract

Wei Liang, Hui Wang, Tie-Mie Sun, Wen-Qing Yao, Li-Li Chen, Yu Jin, Chun-Ling Li, Fan-Juan Meng

Wei Liang, Tie-Mie Sun, Wen-Qing Yao, Li-Li Chen, Yu Jin, Chun-Ling Li, Fan-Juan Meng, Liaoning Provincial Tumor Research Institute, Shenyang 110042, Liaoning Province, China

Hui Wang, Department of Coloproctology Surgery of Liaoning Tumor Hospital, Shenyang 110042, Liaoning Province, China

Supported by Scientific Foundation of Liaoning Province, No. 895215

Correspondence to: Wen-Qing Yao, Liaoning Provincial Tumor Research Institute, 44 xiaohedian Road, Dadong District, Shenyang 110042, Liaoning Province, China. yaowenq@mail.sy.ln.cn

Telephone: +86-24-24324202

Received: 2002-08-03 **Accepted:** 2002-09-12

Abstract

AIM: To treat patients with stage I-IV malignant tumors of digestive tract using autologous tumor cell vaccine and NDV (Newcastle disease virus) vaccine, and observe the survival period and curative effect.

METHODS: 335 patients with malignant tumors of digestive tract were treated with autologous tumor cell vaccine and NDV vaccine. The autologous tumor cell vaccine received were assigned for long-term survival observation. While these failed to obtain the autologous tumor tissue were given with NDV vaccine for a received short-term observation on curative effect.

RESULTS: The colorectal cancer patients treated with autologous tumor cell vaccine were divided into two groups: the controlled group (subjected to resection alone) ($n=257$), the vaccine group (subjected to both resection and immunotherapy) ($n=310$). 25 patients treated with NDV immunotherapy were all at stage IV without having resection. In postoperation adjuvant therapy patients, the 5, 6 and 7-year survival rates were 66.51 %, 60.52 %, 56.50 % respectively; whereas in patients with resection alone, only 45.57 %, 44.76 % and 43.42 % respectively. The average survival period was 5.13 years (resection alone group 4.15 years), the median survival period was over 7 years (resection alone group 4.46 years). There were significant differences between the two groups. The patients treated with resection plus vaccine were measured delayed-type hypersensitivity (DTH) reactions after vaccination, (indurative scope >5 mm). The magnitude of DTH was related to the prognosis. The 5-year survival rate was 80 % for those with indurations greater than 5 mm, compared with 30 % for those with indurations less than 5 mm. The 1-year survival rate was 96 % for 25 patients treated with NDV immunotherapy. The total effective rate (CR+PR) was 24.00 % in NDV immunotherapy; complete remission (CR) in 1 case (4.00 %), partial remission (PR) in 5 cases (20.00 %), stabilized in 16 cases (64.00 %), progression (PD) in 1 case (4.00 %). After NDV vaccine immunotherapy, the number of NK cell increased and immune function improved obviously.

CONCLUSION: The autologous tumor cell vaccine and NDV vaccine can prolong the patients' life. NDV vaccine is notably

effective for short-term with promotion of quality of life and can be used whenever necessary with good prospects.

Liang W, Wang H, Sun TM, Yao WQ, Chen LL, Jin Y, Li CL, Meng FJ. Application of autologous tumor cell vaccine and NDV vaccine in treatment of tumors of digestive tract. *World J Gastroenterol* 2003; 9(3): 495-498

<http://www.wjgnet.com/1007-9327/9/495.htm>

INTRODUCTION

Malignant tumors of digestive tract is common. It is difficult to improve the survival rate only by resection plus radiotherapy and chemotherapy. This study reported 335 patients treated with autologous tumor cell vaccine and NDV vaccine. 310 of 335 patients with colorectal cancer of stages I-IV received autologous tumor cell vaccine postoperatively and the controlled group (resection alone) constituted 257 patients. The duration of follow-up was 7 years. There were statistically significant differences in the survival rate, the median survival period and the mean survival period between the two groups and the controlled group. The 1-year survival rate was 96 % for 25 late cancer patients treated with NDV vaccine. This study provided a basis for the clinical application of autologous tumor cell vaccine and NDV vaccine^[1,2,5,6,24,25,26,30].

MATERIALS AND METHODS

Clinical data

Those receiving autologous tumor cell vaccine is consisted of 567 patients with colorectal cancer in 1993-1995 with a further follow-up of 7-year. 25 patients with late cancer were given NDV vaccine from June, 2001 to June, 2002: 15 men, 10 women; 41 to 83-year-old, mean age 62.3 years, they were all at stage IV patients and were followed up for 1-year. 310 postoperative patients treated with autologous tumor cell vaccine consisted of 204 men and 106 women range from 19 to 79 years, mean age 55.8 years: 136 patients having Miles operation, 98 colonic operation, including 74 anterior resection and 2 partial resection. The resection alone group (controlled group) consisted of 257 patients: 155 men, 102 women; age ranged 18 to 77 years of age, mean age 55.1 years; among these, 120 patients had Miles operation, 78 colonic operation, 59 anterior resection. The DTH reactions were observed in 20 patients treated with immunotherapy after resections. Among these 20 all were stage II, III colorectal cancer among them 10 were male and 10 female age ranged 35 to 65 years, mean age 52.7 years. The follow-up results were shown in Table 1, 2 and 4. The TNM stages were shown in Table 3.

Preparation of autologous tumor cell vaccine

Material and reagent Tumor tissue specimen ($\phi \geq 1$ cm), element for injection (Da Lian Jin Gang Pharmaceutical Factory), mitomycin C, 25 % glutaraldehyde (E merk), RPMI 1640 complete culture media.

Method The tumor tissue obtained under sterile conditions was placed in a sterile container and sent to the lab in two

hours. Prepare the suspended tumor cell solution by routine methods. Then add mitomycin C and elemene 0.3 mg/ml. placed in 37 °C incubator (0.5 h). heated at 42 °C for 30 min. centrifuged, washed, and fixed in 0.0625 % glutaraldehyde (10 min). After washing out the fixation solution, the sterile suspended autologous tumor cell solution ($\geq 10^7$ /ml) was then prepared for use.

Immune procedure First Vaccination: The Patients treated received first vaccination a week after surgical resection, once a week for four weeks.

Intensive immunotherapy: Began at 1 to 2 months intervals after the first vaccination.

Method of injection: The vaccine was injected in three adjacent sites each 3-5 an apact on the anterior arm or deltoid region. one 0.2 ml intradermally and two 0.4 ml hypodamically.

DTH test: Prior to the vaccination and two weeks after vaccination, skin test was performed. For the controllis distilled water was used. DTH reaction was concided position when the indention was at 72 hours >5 mm (+), 6-10 mm (++) .

Table 1 Follow-up results of survival status for colorectal cancer patients with resection plus autologous tumor cell vaccine from 1993 to 2000

Year	n	Survival period							
		0	1	2	3	4	5	6	7
1993-2000	50	50	50	44	39	35	31	31	29
1994-2000	133	133	125	104	94	90	85	75	
1995-2000	127	127	126	116	106	98	93		
Total	310	310	301	264	239	223	209	106	

Table 2 Follow-up results of survival status for colorectal cancer patients with resection alone from 1993 to 2000

Year	n	Survival period							
		0	1	2	3	4	5	6	7
1993-2000	73	73	71	60	54	41	35	34	33
1994-2000	94	94	85	68	56	47	43	43	
1995-2000	90	90	84	69	57	50	47		
Total	257	257	240	197	167	138	125	77	33

Table 3 TNF staging in colorectal cancer patients with resection plus vaccine group and resection alone group

Treatment	n	TNF stages			
		I	II	III	IV
Resection plus vaccine	310	46(14.8%)	121(39%)	80(25.8%)	63(20.3%)
Resection alone	257	55(21.4%)	94(36.6%)	66(25.7%)	42(16.3%)
Total	567	101	215	146	105

Statistical analysis

Using SPSS computer program, analyses were performed by *t*-test for the mean value between the two groups by life table and logrank test for survival rate, by graphical method and linear inner insert method for the median survival period and by Kaplan-Meier method for the mean survival period.

Preparation of NDV vaccine

Primary fluid of NDV La Sota IV weak toxicant stem was vaccinated in chick embryo chorioallantoic cavity. SPF fertilized egg was placed in the 37 °C incubator. On day 10, injecting 0.2 ml NDV diluted with 0.5 % LH into the

chorioallantoic cavity in sterile conditions, sealed it with wax, and obtained the virus after 72 hours in 37 °C incubator. Before getting the virus, placed the chick embryo overnight at 4 °C refrigerator. Then removed the eggshell in air chamber, opened the egg membrane and aspirated the chorioallantoic fluid containing virus by sterile technique. The fluid was centrifuged for 30 minutes at low speed (2 800 r/min, 800 g) to get rid of the sediment. The supernatants of NDV was centrifuged 60 minutes at low temperature and high speed (4 °C, 30 000 r/min, 90 000 g) and the viruses were precipitated. Resuspended the virus sediment by pH7.2, 0.1 mol/L PBS, assayed the hemagglutinin unit (Hu) of NDV by 0.5 % fresh chick erythrocyte suspended solution and then diluted to 1:1 280 Hu/ml. The solution was packed into ampoules separately and stored at -20 °C. Unfreeze it before using.

Immune procedure

Injected 1-2 ml in three sites intradermally at deltoid muscle region, once every three days. Three times constituted one course, and the injections also could be given continually.

Immune function assay

Prior to and after the immunotherapy, assayed the NK, CD₃⁺, CD₄⁺, CD₈⁺, CD₄⁺/CD₈⁺ by flow cytometry.

RESULTS

Table 4 Comparison of yearly survival rates of resected colorectal cancer patients in vaccination group and controll group

Treatment method	n	*Yearly survival rates (%±s \bar{x})						
		1	2	3	4	5	6	7
Vaccination group	310	97.05 ±0.97	84.35 ±2.10	76.42 ±3.23	71.12 ±3.43	66.51 ±3.84	60.52 ±4.57	56.50 ±6.52
Controll group	257	93.16 ±1.60	74.83 ±2.51	62.50 ±2.06	50.58 ±1.99	45.57 ±1.32	44.76 ±0.81	43.42 ±1.32

*Life table χ^2 test $P < 0.005$ of the two groups.

By life table method, the 7-year survival rate of the vaccination group was 56.5 % and the median survival period was approximately 50 %. Hence by graphical method the median survival period was over 7 years, whereas by linear inner insert method, the median survival period of the controll group was 4.46 years. The average survival period of vaccination group was 5.13±0.60 years where that of the controlled group 4.15±0.60 years (Table 5).

Table 5 Comparison of median survival period, mean survival period of resected colorectal cancer patients of vaccination group and controlled group

Treatment method	n	Median survival period (year)	Mean survival period (year)
Resection plus vaccination group	310	>7 ^a	5.13±0.60 ^b
Resection alone group	257	4.46	4.15±0.60

^b $P < 0.01$ vs resection alone group.

The positive rate of DTH reactions in resection plus vaccine group was over 90 % whereas in resection alone group all negative. Most active immunotherapy for patients succeeded (Table 6). The remission rate of late digestive tract carcinoma treated with NDV vaccine (Table 7,9). The charge of immune function pre- and post-NDV vaccine therapy (Table 8).

Table 6 Comparison of five-year survival rate, survival period of resected colorectal cancer patients in vaccination group with positive and negative DTH reaction

DTH reactions	<i>n</i>	5-year survival cases	Survival rate ^b	^a Survival period ($\bar{x}\pm s$)
Positive group	10	8	80 %	4.7±0.67
Negative group	10	3	30 %	3.5±1.80

χ^2 test ^a $P<0.05$, ^b $P<0.01$ vs negative group.

Table 7 The remission rate of late cancer of digestive tract carcinoma treated with NDV vaccine

Types of disease	<i>n</i>	CR(%)	PR(%)	SD(%)	PD(%)	CR+PR(%)
Colorectal cancer	13	1	3	8	0	4
Stomach cancer	6	0	0	5	0	0
Liver cancer	4	0	2	1	0	2
Pancreatic head cancer	1	0	0	1	1	0
Gall bladder cancer	1	0	0	1	0	0
Total	25	1(4.00%)	5(20.00%)	16(64.00%)	1(4.00%)	6(24.00%)

Table 8 Immunologic function prior to and after NDV vaccination therapy

Item	<i>n</i>	Before therapy ($\bar{x}\pm s$)	After therapy ($\bar{x}\pm s$)	<i>P</i>
NK	10	24.65±7.21	36.58±11.87	<0.05
CD ₃ ⁺	10	67.15±2.43	71.12±2.86	<0.01
CD ₄ ⁺	10	38.23±3.01	41.62±2.71	<0.01
CD ₈ ⁺	10	30.55±1.21	29.84±2.43	>0.05
CD ₄ ⁺ /CD ₈ ⁺	10	1.23±0.12	1.41±0.13	<0.05

Table 9 Comparison of treatment courses and therapeutic effect of colorectal cancer patients with NDV immunotherapy

Group	<i>n</i>	CR	PR	SD	PD	CR+PR
1 Course	6	0	0	5	1	0
>2 Courses	7	1	3	3	0	4

$\chi^2=10$, $P<0.01$.

DISCUSSION

The major treatments of malignant tumors of digestive tract malignant tumor postoperatively are radiotherapy and chemotherapy. However, it is very difficult to improve the 5-year survival rate. We treated these patients with autologous tumor cell vaccine and NDV vaccine and made a 7-year follow-up survey of postoperative patients with autologous tumor cell vaccine. The 5, 6, 7-year survival rate are 66.51 %, 60.52 %, 56.50 %, respectively, whereas they were only 45.57 %, 44.76 % and 43.42 % respectively in resection plus radiotherapy or chemotherapy group. The survival rate increased by 20.94 %, 15.76 %, 13.08 %. The increase of amplitude arrived at 46.00 %, 35.20 % and 30.12 % respectively. This indicated autologous tumor cell vaccine could really increase the long-term survival rate of colorectal cancer patients^[7,9,10].

The median survival period increased more obviously: for over 7-year in vaccination group but only 4.46 years in resection alone group, it increased by over 2.5 years. The amplitude of increase was 57 %. The mean survival period was 5.13 years in vaccination group yet only 4.15 years in

resection alone group, an increase of 1 year in average.

The DTH reaction in postoperative colorectal cancer patients showed positive reaction two weeks after the immunotherapy in over 90 %, but negative before therapy. The 5-year survival rate was 80 % in the positive response group, and the 30 % in negative response group, the difference was significant. It demonstrated that active specific immunotherapy by autologous tumor cell vaccine could yield positive DTH reaction in resected colorectal cancer patients. The 5-year survival rate increased obviously as a result of augmented antitumor immunity after immunotherapy^[2,3,7]. We conclude that most of the patients who are treated with active specific immunization lead to a specific antitumor effect. Our vaccine is effective in prevention of tumor progression. The protection achieved can be augmented by serial vaccinations and can be maintained for a long period of time^[4-20].

With booming of biotherapy lately, more attention have been paid to NDV vaccine. Many reports from abroad showed some effectiveness of NDV in malignant tumor of digestive tract and malignant melanoma^[21-23, 27-29] with few adverse effects. After transfection NDV, immune response could be induced with production of cytokines and triggering of active tumor vaccine reaction. In the 1950s, people tried to treat malignant tumor with virus and discovered that much virus had greater killing effect on tumor cells than on normal cells. For example, NDV-73-T could infect all kinds of human tumor cells, with intracellular replication, elicit cell fusion and multinuclear body, and the tumor cells die eventually. NDV had selective killing effect on tumor cells, but not the normal cells. Despite there were many reports about the antitumor effect of NDV^[27-36], yet long-term observation on the use of NDV was scarce, especially about its side effects. The NDV vaccine given to 25 patients in our study were 2-6 courses, some of them 8 courses. The duration of continuous injection was over 3 months, no significant side effects were found. We compared the effectiveness of one course and two course in 13 colorectal cancer patients. See Table 9, the curative effect of the latter was superior to that of the former. A few patients had flu-like symptoms, such as fatigue, low-grade fever, soreness of joints, which disappeared in 1-2 days. Now we had treated 80 patients bearing all kinds of late malignant tumor with NDV vaccine. We found that the curative effects on urinary bladder cancer and colorectal cancer were notable. Take for instance, one bladder cancer patient developed a 2.0×2.0 cm tumor in the right wall of his bladder, having hematuria and 2.5×2.7 cm hypodermic metastatic nodule over his left thigh. After four courses of NDV immunotherapy, the mass in the bladder wall and the metastatic nodule over his left thigh regressed, hematuria also ceased. One colon cancer patient had a 3.0×3.5 cm cauliflower-like tumor on the left wall of the rectum, about 4 cm away from the anus, having hematochezia. After four courses of NDV vaccine, the mass in the rectum regressed and hematochezia ceased. Another patient with primary liver cancer, measuring 5.5×7.2 cm before the NDV therapy, after three courses, the mass decreased somewhat to 5.5×5.3 cm and the backache ameliorated. NDV injection can remit patients in a late gastric cancer impending to death with extensive peritoneal and pelvic metastasis, anuria, comatous and maintained his life only by intravenous nutrients and renal dialysis. After 12 days of large doses of NDV vaccination, the patient became conscious and could urinate by himself, with stoppage of dialysis, and could eat a little, the survival period prolonged to 30 days. As from Table 8, we could see that NDV could improve the immune functions by activating the lymphocytes. The preliminary use of NDV showed a new therapeutic approach to the treatment of late malignant tumors, especially for those who were unable to obtain the autologous tumor tissue. After NDV vaccination, the curative efficacy

occurs rapidly and long-term observation is undertaken. From this study we can expect that the NDV vaccine has a good prospect.

REFERENCES

- Mimori K, Mori M. Recent advances in the diagnosis and treatment of colorectal cancers. *Nippon Geka Gakkai Zasshi* 2002; **103**: 468-471
- Indar A, Maxwell-Armstrong CA, Durrant LG, Carmichael J, Scholefield JH. Current concepts in immunotherapy for the treatment of colorectal cancer. *J R Coll Surg Edinb* 2002; **47**: 458-474
- de Kleijn EM, Punt CJ. Biological therapy of colorectal cancer. *Eur J Cancer* 2002; **38**: 1016-1022
- Miyagi Y, Imai N, Sasatomi T, Yamada A, Mine T, Katagiri K, Nakagawa M, Muto A, Okouchi S, Isomoto H, Shirouzu K, Yamana H, Itoh K. Induction of cellular immune responses to tumor cells and peptides in colorectal cancer patients by vaccination with SART3 peptides. *Clin Cancer Res* 2001; **7**: 3950-3962
- Bartnes K. Tumor antigens presented to T helper lymphocyte-critical components of the cancer vaccine. *Tidsskr Nor Laegeforen* 2001; **121**: 2941-2945
- Zou SC, Qiu HS, Zhang CW, Tao HQ. A clinical and long-term follow-up study of peri-operative sequential triple therapy for gastric cancer. *World J Gastroenterol* 2000; **6**: 284-286
- Saeterdal I, Bjrheim J, Lislrud K, Gjertsen MK, Bukholm IK, Olsen OC, Nesland JM, Eriksen JA, Moller M, Lindblom A, Gaudernack G. Frameshift-mutation-derived peptides as tumor-specific antigens in inherited and spontaneous colorectal cancer. *Proc Natl Acad Sci U S A* 2001; **98**: 13255-13260
- Harris JE, Ryan L, Hoover HC Jr, Stuart RK, Oken MM, Benson AB 3rd, Mansour E, Haller D G, Manola J, Hanna MG Jr. Adjuvant active specific immunotherapy for stage II and III colon cancer with an autologous tumor cell vaccine: Eastern Cooperative Oncology Group Study E5283. *J Clin Oncol* 2000; **18**: 148-157
- Zeh HJ, Stavely-O'Carroll K, Choti MA. Vaccines for colorectal cancer. *Trends Mol Med* 2001; **7**: 307-313
- Habal N, Gupta RK, Bilchik AJ, Yee R, Leopoldo Z, Ye W, Elashoff RM, Morton DL. CancerVax, an allogeneic tumor cell vaccine, induces specific humoral and cellular immune responses in advanced colon cancer. *Ann Surg Oncol* 2001; **8**: 389-401
- Maxwell-Armstrong CA, Durrant LG, Buckley TJ, Scholefield JH, Robins RA, Fielding K, Monson JR, Guillou P, Calvert H, Carmichael J, Hardcastle JD. Randomized double-blind phase II survival study comparing immunization with the anti-idiotypic monoclonal antibody 105AD7 against placebo in advanced colorectal cancer. *Br J Cancer* 2001; **84**: 1433-1436
- Tartaglia J, Bonnet MC, Berinstein N, Barber B, Klein M, Moingeon P. Therapeutic vaccines against melanoma and colorectal cancer. *Vaccine* 2001; **19**: 2571-2575
- Safa MM, Foon KA. Adjuvant immunotherapy for melanoma and colorectal cancers. *Semin Oncol* 2001; **28**: 68-92
- Foon KA. Immunotherapy for colorectal cancer. *Curr Oncol Rep* 2001; **3**: 116-126
- Smith AM, Justin T, Michaeli D, Watson SA. Phase I/II study of G17-DT, an anti-gastrin immunogen in advanced colorectal cancer. *Clin Cancer Res* 2000; **6**: 4719-4724
- Rains N, Cannan RJ, Chen W, Stubbs RS. Development of a dendritic cell (DC)-based vaccine for patients with advanced colorectal cancer. *Hepatogastroenterology* 2001; **48**: 347-351
- Woodlock TJ, Sahasrabudhe DM, Marquis DM, Greene D, Pandya KJ, McCune CS. Active specific immunotherapy for metastatic colorectal carcinoma: phase I study of an allogeneic cell vaccine plus low-dose interleukin-1 alpha. *J Immunother* 1999; **22**: 251-259
- Suh KW, Piantadosi S, Yazdi HA, Pardoll DM, Brem H, Choti MA. Treatment of liver metastases from colon carcinoma with autologous tumor vaccine expressing granulocyte-macrophage colony-stimulating factor. *J Surg Oncol* 1999; **72**: 218-224
- Yamana H, Itoh K. Specific immunotherapy with cancer vaccines. *Gann To Kagaku Ryoho* 2000; **27**: 1477-1488
- Chen W, Rains N, Young D, Stubbs RS. Dendritic cell-based cancer immunotherapy: potential for treatment of colorectal cancer? *J Gastroenterol Hepatol* 2000; **15**: 698-705
- Yip D, Strickland AH, Karapetis CS, Hawkins CA, Harper PG. Immunomodulation therapy in colorectal carcinoma. *Cancer Treat Rev* 2000; **26**: 169-190
- Pecora AL, Rizvi N, Cohen GI, Meropol NJ, Serman D, Marshall JL, Goldberg S, Gross P, O'Neil JD, Groene WS, Roberts MS, Rabin H, Bamat MK, Lorence RM. Phase I trial of intravenous administration of PV701, an oncolytic virus in patients with advanced solid cancers. *J Clin Oncol* 2002; **20**: 2251-2266
- Schneider T, Gerhards R, Kirches E, Firsching R. Preliminary results of active specific immunization with modified tumor cell vaccine in glioblastoma multiforme. *J Neurooncol* 2001; **53**: 39-46
- Schirmacher V. Anti-tumor vaccination. *Zentralbl Chir* 2000; **125** (Suppl 1): 33-36
- Zorn U, Duensing S, Langkopf F, Anastassiou G, Kirchner H, Hadam M, Knuver-Hopf J, Atzpodien J. Active specific immunotherapy of renal cell carcinoma: cellular and humoral immune responses. *Cancer Biother Radiopharm* 1997; **12**: 157-165
- Sonoda K, Sakaguchi M, Okamura H, Yokogawa K, Tokunaga E, Tokiyoshi S, Kawaguchi Y, Hirai K. Development of an effective polyvalent vaccine against both Marek's and Newcastle diseases based on recombinant Marek's disease virus type 1 in commercial chickens with maternal antibodies. *J Virol* 2000; **74**: 3217-3226
- Schirmacher V, Haas C, Bonifer R, Ahlert T, Gerhards R, Ertel C. Human tumor cell modification by virus infection: an efficient and safe way to produce cancer vaccine with pleiotropic immune stimulatory properties when using Newcastle disease virus. *Gene Ther* 1999; **6**: 63-73
- Csatary LK, Moss RW, Beuth J, Torocsik B, Szeberenyi J, Bakacs T. Beneficial treatment of patients with advanced cancer using a Newcastle disease virus vaccine (MTH-68/H). *Anticancer Res* 1999; **19**: 635-638
- Batliwalla FM, Bateman BA, Serrano D, Murray D, Macphail S, Maino VC, Ansel JC, Gregersen PK, Armstrong CA. A 15-year follow-up of AJCC stage III malignant melanoma patients treated postsurgically with Newcastle disease virus (NDV) oncolysate and determination of alterations in the CD8 T cell repertoire. *Mol Med* 1998; **4**: 783-794
- Puangsab A, Lorence RM, Reichard KW, Peeples ME, Walter RJ. Newcastle disease virus therapy of human tumor xenografts: antitumor effects of local or systemic administration. *Cancer Lett* 2001; **172**: 27-36
- Schirmacher V, Griesbach A, Ahlert T. Antitumor effects of Newcastle disease virus in vivo: local versus systemic effects. *Int J Oncol* 2001; **18**: 945-952
- Zhang JK, Sun JL, Chen HB, Zeng Y, Qu YJ. Influence of granulocyte macrophage colony stimulating factor and tumor necrosis factor on anti-hepatoma activities of human dendritic cells. *World J Gastroenterol* 2000; **6**: 718-720
- Termeer CC, Schirmacher V, Brocker EB, Becker JC. Newcastle disease virus infection induces B7-1/B7-2-independent T-cell costimulatory activity in human melanoma cells. *Cancer Gene Ther* 2000; **7**: 316-323
- Schirmacher V, Bai L, Umansky V, Yu L, Xing Y, Qian Z. Newcastle disease virus activates macrophages for anti-tumor activity. *Int J Oncol* 2000; **16**: 363-373
- Haas C, Ertel C, Gerhards R, Schirmacher V. Introduction of adhesive and costimulatory immune functions into tumor cells by infection with Newcastle Disease Virus. *Int J Oncol* 1998; **13**: 1105-1115
- King DJ. A comparison of the onset of protection induced by Newcastle disease virus strain B1 and a fowl poxvirus recombinant Newcastle disease vaccine to a viscerotropic velogenic Newcastle disease virus challenge. *Avian Dis* 1999; **43**: 745-755

Full-length genome of wild-type hepatitis A virus (DL3) isolated in China

Guo-Dong Liu, Ning-Zhu Hu, Yun-Zhang Hu

Guo-Dong Liu, Ning-Zhu Hu, Yun-Zhang Hu, Department of Vaccine Research, Institute of Medical Biology, Chinese Academy of Medical Sciences, Peking Union of Medical College, Kunming 650118, Yunnan Province, China

Correspondence to: Yun-Zhang Hu, Department of Vaccine Research, Institute of Medical Biology, Chinese Academy of Medical Sciences, 379 Jiaoling Road, Kunming 650118, Yunnan Province, China. huyunz@21cn.com

Telephone: +86-871-8335334 **Fax:** +86-871-8334483

Received: 2002-10-09 **Accepted:** 2002-11-08

Abstract

AIM: To characterize the genome of an wild-type HAV isolate (DL3) in China.

METHODS: A stool specimen was collected from hepatitis A patient from Dalian, China. HAV (DL3) was isolated and viral RNA was extracted. The genome of DL3 was amplified by reverse transcription and polymerase chain reaction (RT-PCR), followed by cloning into pGEM-T vector. The positive colonies were selected and sequenced. The full-length genome of DL3 was analyzed and compared with other wild-type HAV isolates.

RESULTS: The genome of DL3 was 7 476 nucleotides (nt) in size, containing 732-nt 5' untranslated region (UTR), 6 681-nt open reading frame (ORF) which encoded a polyprotein of 2 227 amino acids (aa), and 63-nt 3' UTR. The base composition was 28.96 % A (2 165), 16.08 % C (1 202), 22.11 % G (1 653) and 32.85% U (2 456). Genomic comparisons with wild-type HAV isolates revealed that DL3 had the highest identity of 97.5 % for nt (185 differences) with AH1, the lowest identity of 85.7 % (1 066 differences) with SLF88. The highest identity of 99.2 % for amino acid (18 differences) appeared among DL3, AH2 and FH3, and the lowest identity of 96.8 % (72 differences) between DL3 and SLF88. Based upon comparisons of the VP1/2A junction and the VP1 amino terminus, DL3 was classified as subgenotype IA. Phylogenetic analysis showed that DL3 was closest to the isolates in Japan.

CONCLUSION: The sequence comparison and phylogenetic analysis revealed that DL3 is most similar to the isolates in Japan, suggesting the epidemiological link of hepatitis A happened in China and Japan.

Liu GD, Hu NZ, Hu YZ. Full-length genome of wild-type hepatitis A virus (DL3) isolated in China. *World J Gastroenterol* 2003; 9 (3): 499-504

<http://www.wjgnet.com/1007-9327/9/499.htm>

INTRODUCTION

Hepatitis A virus (HAV) is an important human pathogen causing hepatitis, with a higher incidence in developing countries than that in developed countries. Direct person-to-person spread by the fecal/oral route is the most important means of transmission of hepatitis A, and infection with HAV

can cause sporadic and epidemic acute hepatitis in humans^[1,2]. Although improvements in sanitation have led to a significant reduction in the endemicity of hepatitis A virus infection, hepatitis A is still the most common viral hepatitis infection and a cause of substantial morbidity in China.

HAV is classified as one of two members of the genus *Hepatitisvirus* within the family *Picornaviridae*^[3,4]. HAV virion is a naked, spherical particle with a diameter of 27-32 nm. The virion consists of a genome of a linear, single-stranded, 7.5-kb positive-sense RNA and of a protein shell made up of three major proteins, VP1- VP3^[1,5]. The genome can be divided into a long 5' terminal untranslated region (5' UTR) of about 735 nucleotides, a large open reading frame encoding a polyprotein of 2 227 amino acids, a short 3' UTR with a polyA tail. The HAV polyprotein is co- and posttranslationally cleaved into smaller structural proteins (VP1, VP2, VP3 and a putative VP4) and nonstructural proteins (2A, 2B, 2C, 3A, 3B, 3C and 3D) by the virus-encoding proteinase^[6].

Human isolates of HAV possess a single serotype, and monoclonal antibodies raised to various isolates of human HAV have failed to distinguish between individual isolates. However, the nucleotide sequencing of selected genome regions that encode the putative VP1/2A junction region of wild-type HAV isolates present in human specimens has demonstrated significant sequence heterogeneity^[7]. Using this approach, HAV isolates could be differentiated into seven unique genotypes based upon the sequence of the VP1/2A junction region. A genotype is defined as a group of viruses that differed from each other by no more than 15 %, and a subgenotype as a group of viruses with >92.5 % nucleotide sequence identity^[7].

Until now, complete nucleotide sequences of eleven different human wild-type HAV isolates and partial nucleotide sequences of wild-type isolates or cell-adaptative variants of HAV have been reported^[8-19]. These isolates were isolated from hepatitis A epidemic of diverse geographic origin, including partial sequence of the isolates from fulminant hepatitis A in Shanghai in 1988^[7]. But the complete nucleotide sequence of genome of the isolate from China remains unknown. In order to elucidate the genetic characteristics and molecular epidemiology and evolution of wild-type HAV in China, we determined the complete nucleotide sequence of genome of an acute HAV isolate (DL3) from Dalian, and compared the complete genome sequences and deduced amino acid sequence of isolate DL3 with those of other eleven wild-type HAV isolates. There are significant differences and identities among the twelve independent isolates.

MATERIALS AND METHODS

Virus sample

Wild-type human HAV isolate DL3 was recovered from stool specimens stored at -70 °C from an patient with acute hepatitis A, infected during an outbreak at Dalian, Liaoning Province, and was named as DL3. HAV contained in stool were identified by ELISA, immune precipitation and immune electron microscopy. The concentrated and purified HAV for RT-PCR were prepared by chloroform extraction for three times from 10 % of stool supernatant, followed by discontinuous sucrose/glycerol density gradient ultracentrifugation^[20].

cDNA synthesis and cloning

Antigen-capture RT-PCR was used to prepare cDNA of DL3 genome^[21], with some modifications. Sterile 0.5-ml conical tube (Eppendorf) was coated with 100 µl of human anti-HAV IgG diluted 1:1 000 in 50 mM sodium carbonate buffer (pH 9.6). After 4 h of incubation at 37 °C, the unbound IgG was removed, and 150 µl of 1 % bovine serum albumin (Sigma) diluted in the buffer was added. After 1 h at 37 °C, the tube was washed three times with 300 µl of PBS (pH 7.4) containing 0.05 % Tween 80. Purified HAV (100 µl) was added, and the preparation was incubated overnight at 4 °C. The tube was washed six times with 500 µl of a 40 mM Tris (pH 8.4) -40 mM KCL-7 mM MgCl₂ solution. Then 100 µl of water was added and tube was heated to 95 °C for 5 min to disrupt captured viruses and melt any secondary structures within the viral RNA. The first strand cDNA was synthesized using Superscript™ First-Strand Synthesis System for RT-PCR kit (Gibco, Life Technologies), following the instruction by manufacturer. Oligo (dT)₁₈ was used as primer. The partial sequencing showed that subgenotype of isolate from Shanghai in 1988 was IA^[7], the oligonucleotide primers (Table 1) corresponding to the nucleotide sequence of wild-type HAV isolate GBM^[16] were designed to produce subgenomic overlapping HAV fragments with an average length of about 1 000bp which cover the entire HAV genome. The clones of different fragments were performed by PCR in a mixture (50 µl) including 5 µl 10×LA PCR buffer, 8 µl 2.5mM dNTPs, 2 µl template of RT-PCR products, 300 nM positive-sense primer, 300 nM negative-sense primer and 2.5U *Taq* DNA polymerase (TaKaRa). The reaction mixture was subjected to 95 °C for 5 min, then 30 automated cycles of denaturation at 95 °C for 30 sec, annealing at 50 °C for 30 sec, and extension at 72 °C for 1 min or 1 min 30 sec. After the PCR products were recovered and purified, the fragments were ligated into pGEM®-T Vector (Promega). The resulting products were transformed into competent *E. coli* DH5α cells. Three ampicillin-resistant clones were picked out for each fragment. The size of inserts in positive clones was estimated with restriction enzyme site at either side of the inserted fragment. Rapid plasmid preparations were made with the Wizard plasmid purification kit (Promega).

Table 1 The primers used for amplification of DL3 genomic RNA

Clones	Primers	Sequences
A (0.8kb)	5' RACE RT-primer	5-(P)GCAGAATGAATC-3
	5' RACE A1	5-AGTCCGTTGATAGGACTGAG-3
	5' RACE S1	5-TGTTCTTCCTCAATATCTGCC-3
	5' RACE A2	5-TTCTAAGAAGACTCAGGGGG-3
	5' RACE S2	5-CTGAAAATTCCTTGTGGCC-3
B (0.5kb)	B1	5-GCTGAGGTAAGTCAAGGATGC-3
	B2	5-AGGATAAACAGTCAAGGATGC-3
C (1.1kb)	C1	5-ACATATGCAAGATTGGCATTG-3
	C2	5-ATCCATAGCATGATAAAGAGG-3
D (1.0kb)	D1	5-CCTGGATTCTGACTCC-3
	D2	5-CAGTGGATAACATGGCATTG-3
E (1.1kb)	E1	5-TCTGTCACAGAACAATCAGAG-3
	E2	5-AATCCCTGAACAAATGCTCC-3
F (1.2kb)	F1	5-TCCAGAATGATGGAGCTGAG-3
	F2	5-CTTCGACAAGCACTCCAAG-3
G (1.2kb)	G1	5-AGTTCCTTAGTAATGACAGTTG-3
	G2	5-GCCATTGGATCAATCTCAGC-3
H (1.1kb)	H1	5-AAGTGGAAATTTCTCAGTGTTC-3
	H2	5-GTCCAATCAAGTCAAGATTATC-3
I (0.5kb)	I1	5-GATTCTCTGTTATGGAGATG-3
	I2	5-TTTTTTTTTTTTTTTTTTATT-3

DNA sequencing and analysis

Sequencing strategy of genome of DL3 was showed in Figure 1. Oligonucleotide primers specific for HAV and primers corresponding to the T7/SP6 promoter region of pGEM®-T Vector were used to sequence the inserted and identified HAV fragment. A *Taq* DyeDeoxy Terminator Cycle sequencing kit and a 377 DNA sequencer (Perkin Elmer) were used to determine nucleotide sequences. To eliminate the possibility of errors in the sequence due to *Taq* polymerase for PCR, at least three clones of each amplified fragment, derived from two individual PCR products, were sequenced. Also to correctly determine the sequence of extreme 5' terminus of HAV genome, a 5' RACE reaction^[22] was used to obtain the a cDNA fragment from 5' UTR of genome with 5' -Full RACE Core Set (TaKaRa). Analysis, alignment and translation in the amino acids of the obtained nucleotide sequences were done using the sequence analysis program OMEGA2.0 (Oxford Molecular).

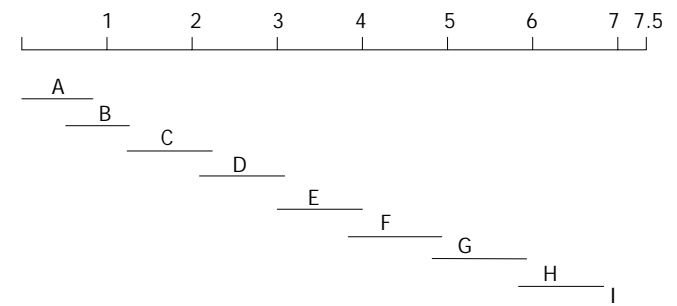


Figure 1 Sequencing strategy of genome of DL3.

Phylogenetic analysis

Multiple alignments of genome sequences of twelve HAV isolates were done using the Clustal W Program^[23]. Phylogenetic tree was calculated from genomes to determine the association of DL3 with other eleven wild-type HAV isolates with Vector NTI Suite6.0 software using the Neighbor Joining method^[24].

Reference isolates

The accession numbers of the sequences included in the analysis were as follows: LA, K02990; HM175, M14707; MBB, M20273; GBM, X75215; AH1: AB020564; AH2: AB020564 AB020565; AH3: AB020564 AB020566; FH1: AB020567; FH2: AB020568; FH3: AB020569; SLF88, AY032861.

RESULTS

Complete nucleotide sequence of DL3 genome and deduced amino acids

The Complete nucleotide sequence of DL3 has been deposited into GenBank under the accession no. AF512536.

The genome was 7 476-nucleotide long and encoded a polyprotein of 2 227 amino acids. The genome contained a 5' UTR of 732 nucleotides that was two nucleotides shorter than that of HAV HM175/WT. The long open reading frame coding for polyprotein was started at base 733 by codon AUG and terminated at base 7 416 by codon UGA followed by a second stop codon (UAA) 7 nucleotides downstream. The 3' UTR consisted of 63 nucleotides. The base composition was 28.96 % A (2165), 16.08 % C (1 202), 22.11 % G (1 653) and 32.85 % U (2 456). The G+C content is 38.19 %.

The 5' UTR contained three main pyrimidine-rich tracts. The first region, near the 5' terminus (nucleotide99- 138), had

a 92.3 % pyrimidine content. The second region (nucleotide 204- 250) had a 83 % pyrimidine content. The third tract (nucleotide 711- 725) with a 93.9 % pyrimidine content lay immediately before the initiation codon. The 5' UTR had a G+C content of 46.29 % which is higher than that of the genome.

Comparisons with other isolates

The complete nucleotide sequence and deduced amino acid

sequences of HAV DL3 have been compared with those of reported wild-type isolates (Table 2, Table3). DL3 had the highest identity of 97.5 % for nt (185 differences) with AH1, but the highest identity of 99.2 % for amino acid (18 differences) with AH2 and FH3. DL3 shared the lowest identities of 85.7 % for nucleotide (1 066 differences) and 96.8 % for amino acid (72 differences) with SLF88. Most of the changes were nucleotide transitions.

Table 2 Nucleotide identities of full-length genomes between DL3 and reference isolates

	Numbers of nucleotide differences/identity										
	AH1	AH2	AH3	FH1	FH2	FH3	GBM	LA	HM175	MBB	SLF88
Full	185/97.5	263/96.5	307/95.9	282/96.2	200/97.3	199/97.3	323/95.7	344/95.4	642/91.4	659/91.2	1066/85.7
5' NTR	15/98.0	29/96.0	25/96.6	16/97.8	13/98.2	13/98.2	18/97.4	14/98.1	38/94.8	50/93.1	84/88.5
VP4	1/98.6	2/97.1	4/94.2	2/97.1	2/97.1	2/97.1	3/95.7	2/97.1	7/89.9	7/89.9	8/88.4
VP2	15/97.7	25/96.2	28/95.8	24/96.4	18/97.3	24/96.4	39/94.1	28/95.8	58/91.3	58/91.3	98/85.3
VP3	15/98.0	25/96.6	28/96.2	27/96.3	13/98.2	23/96.9	35/95.3	40/94.6	67/90.9	63/91.5	114/84.6
VP1	23/97.2	27/96.7	25/97.0	23/97.2	22/97.3	13/98.4	30/96.4	44/94.6	76/90.8	78/90.5	124/84.9
2A	5/97.7	10/95.3	11/94.8	9/95.8	3/98.6	9/95.8	9/95.8	12/94.4	17/92.0	14/93.4	27/87.3
2B	13/98.3	26/96.5	29/96.1	46/93.9	18/97.6	28/96.3	33/95.6	37/95.1	75/90.0	73/90.3	99/86.9
2C	30/97.0	42/95.8	42/95.8	44/95.6	35/96.5	35/96.5	52/94.8	55/94.5	114/88.7	120/88.1	152/84.9
3A	1/99.5	4/98.2	4/98.2	9/95.9	4/98.2	3/98.6	13/94.1	8/96.4	14/93.7	18/91.9	23/89.6
3B	1/98.6	1/98.6	2/97.1	3/95.7	3/95.7	0	2/97.1	3/95.7	6/91.3	7/89.9	12/82.6
3C	14/97.9	20/97.0	24/96.3	25/96.2	16/97.6	21/96.8	30/95.4	27/95.9	56/91.5	50/92.4	98/85.1
3D	51/96.5	51/96.5	84/94.3	53/96.4	52/96.5	27/98.2	57/96.1	64/95.6	113/92.3	114/92.2	209/85.8
3' NTR	1/98.4	1/98.4	1/98.4	1/98.4	1/98.4	1/98.4	2/96.8	10/84.4	1/98.4	7/88.9	18/71.4

Table 3 Amino acid identities of full-length genomes between DL3 and reference isolates

	Numbers of amino acid differences/identity										
	AH1	AH2	AH3	FH1	FH2	FH3	GBM	LA	HM175	MBB	SLF88
Full	21/99.1	18/99.2	36/98.4	28/98.7	21/99.1	18/99.2	36/98.4	34/98.5	35/98.4	49/97.8	72/96.8
VP4	1/95.7	1/95.7	1/95.7	1/95.7	1/95.7	1/95.7	1/95.7	1/95.7	1/95.7	1/95.7	2/91.3
VP2	0	0	0	1/99.5	0	0	1/99.5	0	2/99.1	2/99.1	1/99.5
VP3	1/99.6	1/99.6	1/99.6	2/99.2	1/99.6	1/99.6	1/99.6	1/99.6	2/99.2	2/99.2	4/98.4
VP1	0	0	0	1/99.6	0	1/99.6	2/99.3	13/95.3	1/99.6	2/99.3	2/99.3
2A	1/98.6	1/98.6	1/98.6	1/98.6	1/98.6	0	1/98.6	0	1/98.6	2/97.2	1/98.6
2B	2/99.2	2/99.2	3/98.8	5/98.0	5/98.0	5/98.0	3/98.8	4/98.4	4/98.4	6/97.6	6/97.6
2C	6/98.2	5/98.5	4/98.8	6/98.2	5/98.5	4/98.8	7/97.9	5/98.5	11/96.7	17/94.9	14/95.8
3A	0	1/98.6	1/98.6	1/98.6	0	0	5/93.2	1/98.6	1/98.6	3/95.9	1/98.6
3B	0	0	0	0	0	0	1/95.7	0	0	0	0
3C	2/99.1	2/99.1	3/98.6	2/99.1	2/99.1	2/99.1	3/98.6	2/99.1	2/99.1	2/99.1	8/96.3
3D	8/98.4	5/99.0	22/95.5	8/98.4	6/98.8	4/99.2	11/97.8	7/98.6	10/98.0	12/97.5	33/93.3

5' Untranslated region

The 5' UTR of HAV forms conserved and highly ordered secondary structure and plays an important role in controlling viral translation^[25, 26]. Comparisons with eleven other isolates in 5' UTR showed that DL3 shared the lowest identity of 88.5 % (84 nucleotide changes) with SLF88, the highest identity of 98.2 % (13 nucleotide changes) with FH2 and FH3. There were a G deletion at position 28 and a T deletion at position 102 compared with HM175 and MBB. In contrast to the comparison with complete nucleotide sequence, identities of 5' UTR for DL3 with other isolates were higher than that of complete genomes except the identity with AH2, which suggested that the 5' UTR of HAV was conserved. In contrast to ribosomes scanning from the capped 5' ends of the majority of cellular mRNA, the long and highly structured 5' UTR of HAV mediated the binding of ribosomal subunits internally at internal ribosome entry site (IRES) of nucleotide 324 to nucleotide 692 (base position was corresponding to HM175/WT) that directed cap-independent initiation of viral translation at correct AUG codon^[25, 26]. In this region DL3 shared higher identities of 97.9 %, 98.4 %, 99.2 %, 98.6 %, 98.6 %, 95.9 %, 95.4 % and 94.9 % with AH2, FH1, FH2, FH3, LA, HM175, MBB and SLF88 than that in whole 5' UTR. But DL3 was identical to SLF88 between nucleotide 223 to nucleotide 371 (base position is corresponding to HM175/WT). The result suggested higher conservative and importance of common secondary structure of IRES in initiation of viral translation.

Coding region

The open reading frame of HAV RNA encoding a large polyprotein with 2 227 amino acids was divided into P1, P2 and P3 region. The P1 region encodes structural or capsid proteins, VP4, VP2, VP3 and VP1. The P2 and P3 region encoded nonstructural proteins, 2A, 2B, and 2C, and 3A, 3B, 3C and 3D, respectively. In coding region, the amino acid differences for the structural and nonstructural proteins of twelve isolates are showed in Table 3. In contrast to the high heterogeneous of nucleotide sequences, the amino acid sequences were highly conserved among twelve wild-type isolates. Comparisons within the coding region (6 681 nucleotides) of DL3 and SLF88 yielded 964 nucleotide changes (14.4 % difference), resulting in only 72 amino acid substitutions (3.2 % difference). In comparison with eleven isolates, DL3 had the highest identity (99.2 %) of amino acids with AH2 and FH3, lowest identity (96.8 %) with SLF88.

P1 region, the structural protein region of HAV, consisted of 2 295 nucleotides and encodes 765-amino acid polypeptide which was processed into four structural proteins, VP4, VP2, VP3 and VP1. The capsid protein of HAV consisted of VP1, VP2 and VP3. The presence of a fourth protein VP4 has been described repeatedly, but the reported apparent molecular weights (7- 14kD) contrasted sharply with those predicted from nucleic acid sequence data (1.5 or 2.3kD). Conclusive physical identification of VP4 was still unavailable. The alignment of amino acid sequence indicated that no amino acid mutation of polyprotein of DL3 occurred at cleavage site of VP4/VP2, VP2/VP3, VP3/VP1, implying the importance of conserved cleavage sites in entire viral structure. In VP4 DL3 shared lowest amino acid sequence identities with other isolates in structural region, 91.3 % identity with SLF88, 95.7 % identity with other ten wild-type isolates. DL3 had a unique amino acid mutation (S to A) at position 4 different from all the other isolates. In VP2 region amino acid sequences were highly conserved. There was 100 % identity between DL3 and AH1, AH2, AH3, FH2, FH3 and LA. And even for DL3 and SLF88, the identity was also up to 99.5 %. In VP3 region DL3 had another unique amino acid mutation (K to R) at position 47 different from all the other isolates. It had been reported that

VP1 had the most amino acid diversity of the capsid proteins^[16]. But it was not the case for DL3. In VP1 region there was 100 % amino acid sequence identity between DL3 and AH1, AH2, AH3 and FH2. The highest difference was between DL3 and LA (13 amino acid differences, 95.3 % identity), just because one amino acid was inserted into the LA between amino acids 540-548, at which a cluster of 8 amino acids was altered due to 3 changes in the open reading frame resulting from the insertion of 3 nucleotides.

The HAV P2 region encoded nonstructural proteins 2A, 2B and 2C. The proposed 2A region encoded for 71 amino acids, but the exact function of 2A was not yet determined. Recent study revealed that 2A protein might participate in virion morphogenesis^[27]. 2B and 2C proteins were found to have 251 and 335 amino acids residues, respectively. Both proteins playing important roles in the replication of viral RNA were considered significant in host-dependent adaptation since many mutations had been detected in both regions of adapted variants^[28]. HAV 2C protein was considered to have helicase and NTPase activities. With some variants, multiple mutations in P2 contributed to enhance viral replication with 5' UTR and P3 proteins and to express the cytopathic phenotype^[29]. In 2A, 2B and 2C proteins, 2C protein was the most variable between twelve isolates, DL3 shared the lowest identity of 94.9 % (17 amino acid differences) with MBB and the highest identity of 98.8 % with AH3 and FH3 (only 4 amino acid differences). In contrast, 2B was more conservable. The 99.2 % identities of DL3 with AH1 and AH2 and the 98.8 % identities of DL3 with AH3 and GBM revealed high conservation of 2B protein among wild-type viruses. It has been reported that a little more amino acid substitutions seemed to be found in FH than in AH in 2B region^[18]. This research also showed that more amino acid substitutions were found in FH than that in AH when compared with DL3, suggesting the possible association between the severity of hepatitis A and amino acid substitutions in 2B region.

The HAV P3 region encoded 3A, 3B, 3C and 3D proteins with 74, 23, 219 and 489 amino acids, respectively. 3A functioned as pre-Vpg, 3B was a genome-linked viral protein (Vpg), 3C was the sole protease for HAV protein processing. The recombinant HAV 3C prepared in *E. coli* catalyzed the putative cleavage sites and released mature or intermediate proteins, VP0, VP3, VP1-2A, VP1, 2A, 2B, 2BC, 2C, 3ABC, 3AB, 3C and 3D^[30-34]. 3D was an RNA-dependent RNA polymerase. By comparison, 3B protein showed highest amino acid sequence homology, with 100 % identities among eleven isolates except 95.7 % identity between DL3 and GBM. Compared with 3D proteins, 3C protein showed higher amino acid sequence identities in all twelve isolates. In this protein, DL3 shared the 96.3 % identity with SLF88, 98.6 % with AH3 and GBM, and the highest identity 99.1 % with the other eight isolates. The comparison indicated that high conservation of 3C protein in wild-type HAV played an important role in the replication of virus. 3D among isolates of genotype I showed no significant variation. But the 3D polymerase of SLF88 showed low identity with that of DL3, with only 93.3 % identity (33 amino acid differences). GBM showed a little higher variability among the eleven reference isolates in P3 region, especially for 3A and 3D. The identities for these two proteins between DL3 and GBM were 93.2 % (5 amino acid differences) and 97.8 % (11 amino acid differences), respectively. Even for 3B, GBM had 1 amino acid difference with DL3.

3' Untranslated region

The 3' UTR of DL3 was 63-nucleotide long, the same as those of 9 isolates, 1 nucleotide less than that of LA, and 14 nucleotides more than that of SLF88. All twelve isolates had two stop codons, separated by 6 nucleotides. The 3' UTR

exhibited the great identity in nucleotide sequence between DL3 and isolates from Japan, GBM and HM175, with only 1 or 2 nucleotide difference. But for DL3 and the other 3 isolates, identities were lower, especially 71.4% between DL3 and SLF88.

Subgenotype classification

Alignment analysis of 168 nucleotides in VP1/2A (nucleotide 3 024- 3 191) of DL3 with other eleven wild-type isolates revealed that DL3 had >92.5 % identities with six Japanese isolates, LA and GBM (IA subgenotype), <92.5 % identity with HM175 (IB subgenotype), and only 83.9 % identity with SLF88 (the newly determined isolate of genotype VII). According to these comparison, DL3 was classified as subgenotype IA. Something strange was that comparison of the same region between DL3 and MBB showed 94 % identity, suggesting DL3 to be subgenotype IB. To solve this paradox, the VP1 amino terminus (nucleotide 2 208- 2 468) of DL3 was compared with isolate MBB. The result showed DL3 belonged to subgenotype IA.

Phylogenetic relationships

Phylogenetic relations of various HAV wild-type isolates were analyzed on the genomes of twelve isolates (Figure 2). The result showed that twelve wild-type isolates formed four main subclusters, subcluster I contained DL3, AH1, FH2 and FH3, subcluster II contained AH2 and AH3, subcluster III contained LA and GBM, and subcluster IV contained MBB and HM175. Subcluster I, II, III and FH1 composed of subgenotype IA cluster. SLF88 located near this cluster. By this phylogenetic analysis DL3 isolate showed closer phylogenetic affiliation to AH1 and FH2. Besides, the comparison of full-length genome of nine isolates showed DL3 had higher identity with AH1 and FH2 than those with GBM, LA, HM175, MBB and SLF88. The analysis suggested that phylogenetic relations of various HAV wild-type isolates correlated with geographical region.

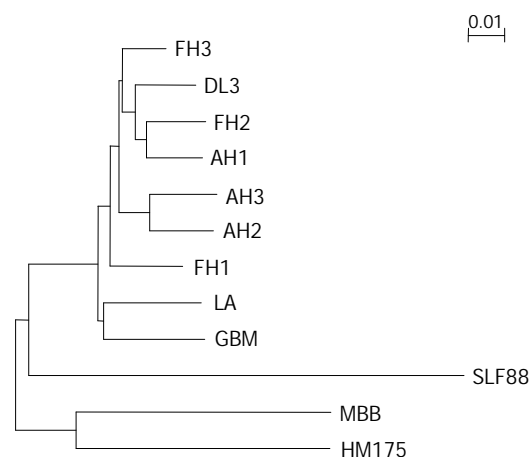


Figure 2 Phylogenetic relations of DL3 full-length genome to those of other HAV.

DISCUSSION

Although hepatitis A remains a disease of major public health importance in China, the study on the genome of wild-type HAV isolate in China has not been reported. Here, we analyzed the full-length genome of a wild-type HAV isolate DL3 in China. The genome sequence of DL3 contained 7 476 nucleotides, dividing into three regions, 732-nucleotide 5' UTR, 6 681-nucleotide ORF coding for a polyprotein of 2 227 amino acid, 63-nucleotide 3' UTR.

Sequence comparisons of genomes showed DL3 shared the highest nucleotide identity (97.5 %) with AH1 and amino

acid identity (99.2 %) with AH2 and FH3, and lowest nucleotide identity (85.7 %) and amino acid identity (96.8 %) with SLF88. But the nucleotide sequence and amino acid sequence differences were not evenly distributed along the genome in all isolates. The 5' UTR region showed high conservatism, and even SLF88 is 88.5 % identical to DL3, an identity higher than that of full-length genome. This suggests the importance of this region for HAV. The 3' UTR region showed high identities between DL3 and other isolates of genotype I. When compared with SLF88, DL3 had high divergence of 28.6 % with SLF88, which lead to 18 nucleotide changes, including 14 deletions and 4 mutations. Although the exact function of 3' UTR is unknown, several studies have revealed that sequence elements within the 3' UTR are expected to play an important role in initiation and regulation of synthesis of HAV RNA^[35, 36]. The high heterogeneity between DL3 and SLF88 in the 3' UTR may suggest the difference of the replicating characteristics between DL3 and SLF88.

In structural region, the highest difference (13 amino acid differences, between DL3 and LA) existed in VP1. But this high divergence was due to 1 amino acid insertion into LA. For DL3 and other eleven isolates, high homology was observed, and the high variability of VP1 reported early was not observed. In nonstructural region the majority of amino acid identities between DL3 and other eleven isolates appeared in 3B and 3C proteins, implying that both proteins play important roles in the replication of virus and the processing of polyprotein. Differences between DL3 and other isolates of subgenotype IA in 2C region were a little more than those in 2B region. But differences between DL3 and other isolates of subgenotype IB or SLF88 in 2C region were much more than those in 2B region. SLF88 had 33 amino acid mutations with DL3 in 3D, suggesting the polymerase of SLF88 may have different efficiency compared with DL3.

Based on the higher nucleotide sequence identities of DL3 with AH1 and FH2 in the whole 7 476-nucleotide genome (97.5 % and 97.3, respectively), 732-nucleotide 5' UTR region (98.0 % and 98.2 %, respectively), 63-nucleotide 3' UTR region (98.4 % for both), 168-nucleotide region of subgenotype classification (98.2 %), 6681-nucleotide ORF (97.5 % and 97.2 %, respectively), DL3 is found to be in phylogenesis closest to AH1 and FH2. So we proposed that DL3, AH1 and FH2 probably represent different isolates of the same strain. Moreover, it is noteworthy that Japan where AH1 and FH2 were isolated geographically close to China, where DL3 was isolated. The phylogenetic affiliation and geographical closure suggested the epidemiological link of hepatitis A happened in Dalian and Japan.

By comparison of VP1/2A junction, genotypes were defined by at least 15 %, and subgenotypes differed by at least 7.5 %. According to this, we defined DL3 as subgenotype IA by comparisons with isolates HM175, AH1, AH2, AH3, FH1, FH2 and FH3. Interestingly, comparisons of this region with isolate MBB showed DL3 to be subgenotype IB. To solve this paradox, the VP1 amino terminus of DL3 was compared with isolate MBB. The comparison showed DL3 belonged to subgenotype IA. This suggests that it may not be so accurate to define a genotype only by comparison of VP1/2A junction. And the more accurate result may be achieved by comparison of more nucleic acid fragments.

REFERENCES

- 1 **Lemon SM.** Type A hepatitis: new developments in an old disease. *N Engl J Med* 1985; **313**: 1059-1067
- 2 **Cuthbert JA.** Hepatitis A: old and new. *Clin Microbiol Rev* 2001; **14**: 38-58
- 3 **Minor PD.** Picornaviridae. In Francki RIB, Fauquet CM, Kundson

- DL, Brown F, eds. Archives of Virology, Supplement 2. New York: Springer-Verlag 1991: 320-326
- 4 **Marvil P**, Knowles NJ, Mockett APA, Britton P, Brown TDK, Cavanagh D. Avian encephalomyelitis virus is a picornavirus and is most closely related to hepatitis A virus. *J Gen Virol* 1999; **80**: 653-662
 - 5 **Weitz M**, Siegl G. Hepatitis A virus: structure and molecular virology. In: Zuckerman AJ, Thomas HC. Viral hepatitis. 2nd edition. London: Churchill Livingstone 2001: 15-27
 - 6 **Totsuka A**, Moritsugu Y. Hepatitis A virus proteins. *Intervirology* 1999; **42**: 63-68
 - 7 **Robertson BH**, Jansen RW, Khanna B, Totsuka A, Nainan OV, Siegl G, Widell A, Margolis HS, Isomura S, Ito K, Ishizu T, Moritsugu Y, Lemon SM. Genetic relatedness of hepatitis A virus strains recovered from different geographical regions. *J Gen Virol* 1992; **73**: 1365-1377
 - 8 **Ticehurst JR**, Racaniello VR, Baroudy BM, Baltimore D, Purcell RH, Feinstone SM. Molecular cloning and characterization of hepatitis A virus cDNA. *Proc Natl Acad Sci USA* 1983; **80**: 5885-5889
 - 9 **Linemeyer DL**, Menke JG, Martin-Gallardo A, Hughes JV, Young A, Mitra SW. Molecular cloning and partial sequencing of hepatitis A viral cDNA. *J Virol* 1985; **54**: 247-255
 - 10 **Najarian R**, Caput D, Gee W, Potter SJ, Renard A, Merryweather J, Van Nest G, Dina D. Primary structure and gene organization of human hepatitis A virus. *Proc Natl Acad Sci USA* 1985; **82**: 2627-2631
 - 11 **Venuti A**, Di Russo C, Del Grosso N, Patti A-M, Ruggeri F, Stasio RP, Martiniello GM, Pagnotti P, Degener AM, Midulla M, Pana A, Perez-Bercoff R. Isolation and molecular cloning of a fast-growing isolate of human hepatitis A virus from its double-stranded replicative form. *J Virol* 1985; **56**: 579-588
 - 12 **Robertson BH**, Brown VK, Bradley DW. Nucleic acid sequence of the VP1 region of attenuated MS-1 hepatitis A virus. *Virus Res* 1987; **8**: 309-316
 - 13 **Cohen JJ**, Ticehurst JR, Purcell RH, Buckler-White A, Baroudy BM. Complete nucleotide sequence of wild-type hepatitis A virus: Comparison of different isolates of hepatitis A virus and other picornaviruses. *J Virol* 1987; **61**: 50-59
 - 14 **Paul AV**, Tada H, von der Helm K, Wissel T, Kiehn R, Wimmer E, Deinhardt F. The entire nucleotide sequence of the genome of human hepatitis A virus (isolate MBB). *Virus Res* 1987; **8**: 153-171
 - 15 **Khanna B**, Spelbring JE, Innis BL, Robertson BH. Characterization of a genetic variant of human hepatitis A virus. *J Med Virol* 1992; **36**: 118-124
 - 16 **Graff J**, Normann A, Feinstone SM, Flehmig B. Nucleotide sequence of wild-type hepatitis A virus GBM in comparison with two cell culture-adapted variants. *J Virol* 1994; **68**: 548-554
 - 17 **Beneduce F**, Pisani G, Divizia M, Pana A, Morace G. Complete nucleotide sequence of a cytopathic hepatitis A virus isolate isolated in Italy. *Virus Res* 1995; **36**: 299-309
 - 18 **Fujiwara K**, Yokosuka O, Fukai K, Imazeki F, Saisho H, Omata M. Analysis of full-length hepatitis A virus genome in sera from patients with fulminant and self-limited acute type A hepatitis. *J Hepatol* 2001; **35**: 112-119
 - 19 **Ching KZ**, Nakano T, Chapman LE, Demby A, Robertson BH. Genetic characterization of wild-type genotype VII hepatitis A virus. *J Gen Virol* 2002; **83**: 53-60
 - 20 **Bishop NE**, Hugo DL, Borovec SV, Anderson DA. Rapid and efficient purification of hepatitis A virus from cell culture. *J Virol Med* 1994; **47**: 203-216
 - 21 **Jansen RW**, Siegl G, Lemon SM. Molecular epidemiology of human hepatitis A virus defined by an antigen-capture polymerase chain reaction method. *Proc Natl Acad Sci USA* 1990; **87**: 2867-2871
 - 22 **Frohman MA**, Dush MK, Martin GR. Rapid production of full-length cDNAs from rare transcripts: amplification using a single gene-specific oligonucleotide primer. *Proc Natl Acad Sci USA* 1988; **85**: 8998-9002
 - 23 **Thompson JD**, Higgins DG, Gibson TJ. Clustal W: improving the sensitivity of progressive multiple sequence alignment through sequence weighting, position-specific gap penalties and weight matrix choice. *Nucleic Acids Res* 1994; **22**: 4673-4680
 - 24 **Saitou N**, Nei M. The neighbor-joining method: a new method for reconstructing phylogenetic trees. *Mol Biol Evol* 1987; **4**: 406-425
 - 25 **Brown EA**, Day SP, Jansen RW, Lemon SM. The 5' nontranslated region of hepatitis A virus RNA: secondary structure and elements required for translation *in vitro*. *J Virol* 1991; **65**: 5828-5838
 - 26 **Brown EA**, Zajac AJ, Lemon SM. *In vitro* characterization of an internal ribosome entry site (IRES) present within the 5' nontranslated region of hepatitis A virus RNA: comparison with the IRES of encephalomyocarditis virus. *J Virol* 1994; **68**: 1066-1074
 - 27 **Cohen L**, Benichou D, Martin A. Analysis of deletion mutants indicated that the 2A polypeptide of hepatitis A virus participates in virion morphogenesis. *J Virol* 2002; **76**: 7495-7505
 - 28 **Emerson SU**, Huang YK, Purcell RH. 2B and 2C mutations are essential but mutations throughout the genome of HAV contribute to adaptation to cell culture. *Virology* 1993; **194**: 475-480
 - 29 **Zhang H**, Chao SF, Ping LH, Grace K, Clarke B, Lemon SM. An infectious cDNA clone of a cytopathic hepatitis A virus: genomic regions associated with rapid replication and cytopathic effect. *Virology* 1995; **212**: 686-697
 - 30 **Schultheiss T**, Kusov YY, Gauss-Muller V. Proteinase 3C of hepatitis A virus (HAV) cleaves the HAV polyprotein P2-P3 at all sites including VP1/2A and 2A/2B. *Virology* 1994; **198**: 275-281
 - 31 **Schultheiss T**, Sommergruber W, Kusov Y, Gauss-Muller V. Cleavage specificity of purified recombinant hepatitis A virus 3C proteinase on natural substrates. *J Virol* 1995; **69**: 1727-1733
 - 32 **Probst C**, Jecht M, Gauss-Muller V. Processing of proteinase precursors and their effect on hepatitis A virus particle formation. *J Virol* 1998; **72**: 8013-8020
 - 33 **Harmon SA**, Updike W, Jia XY, Summers DF, Ehrenfeld E. Polyprotein processing in cis and in trans by hepatitis A virus 3C protease cloned and expressed in Escherichia coli. *J Virol* 1992; **66**: 5242-5247
 - 34 **Malcolm BA**, Chin SM, Jewell DA, Stratton-Thomas JR, Thudium KB, Ralston R, Rosenberg S. Expression and characterization of recombinant hepatitis A virus 3C proteinase. *Biochemistry* 1992; **31**: 3358-3363
 - 35 **Nuesch JP**, Weitz M, Siegl G. Proteins specifically binding to the 3' untranslated region of hepatitis A virus RNA in persistently infected cells. *Arch Virol* 1993; **128**: 65-79
 - 36 **Kusov Y**, Weitz M, Dollenmeier G, Gauss-Muller V, Siegl G. RNA-protein interactions at the 3' end of the hepatitis A virus RNA. *J Virol* 1996; **70**: 1890-1897

Glucose intolerance in Chinese patients with chronic hepatitis C

Liang-Kung Chen, Shinn-Jang Hwang, Shih-Tzer Tsai, Jiing-Chyuan Luo, Shou-Dong Lee, Full-Young Chang

Liang-Kung Chen, Shinn-Jang Hwang, Department of Family Medicine, Department of Medicine, Taipei Veterans General Hospital and National Yang-Ming University School of Medicine, Taipei, Taiwan, China

Shinn-Jang Hwang, Jiing-Chyuan Luo, Shou-Dong Lee, Full-Young Chang, Division of Gastroenterology, Department of Medicine, Taipei Veterans General Hospital and National Yang-Ming University School of Medicine, Taipei, Taiwan, China

Shih-Tzer Tsai, Division of Endocrinology and Metabolism, Department of Medicine, Taipei Veterans General Hospital and National Yang-Ming University School of Medicine, Taipei, Taiwan, China

Correspondence to: Shinn-Jang Hwang, M.D., F.A.C.G., Department of Family Medicine, Taipei Veterans General Hospital, No. 201, Shih-Pai Road Sec 2, Taipei, 11217, Taiwan, China. sjhwang@vghtpe.gov.tw
Telephone: +886-2-28757460 **Fax:** +886-2-28737901

Received: 2002-07-31 **Accepted:** 2002-11-04

Abstract

AIM: To investigate the prevalence and the risk factors of glucose intolerance in Chinese patients with chronic hepatitis C and to evaluate the relationship between interferon (IFN) treatment and glucose intolerance in these patients.

METHODS: Prospective cross-sectional study was done to evaluate the prevalence of glucose intolerance in Chinese patients with chronic hepatitis C virus (HCV) infection from the outpatient clinic of Department of Family Medicine, Taipei Veterans General Hospital. Chronic hepatitis C was defined as persistent presence of anti-HCV and persistent elevation of liver transaminase for at least 1.5 folds for at least 6 months. Moreover, patients were further categorized into normal fasting glucose and glucose intolerance (diabetes mellitus (DM) and impaired fasting glucose) according to the diagnostic criteria of American Diabetic Association.

RESULTS: Totally, 359 Chinese patients with chronic hepatitis C were enrolled (212 males and 147 females, mean age = 58.1 ± 13.0 years). One hundred and twenty-three patients (34.3 %) had received various forms of IFN treatment. One hundred and twenty-five patients (34.6 %) had glucose intolerance, including 99 patients (27.6 %) with DM and 26 patients (7.0 %) with impaired fasting glucose. In comparison with those with normal fasting glucose levels, patients with chronic hepatitis C with glucose intolerance were significantly older, had a significantly higher body mass index, and they were more likely to suffer from obesity, to have family history of diabetes and to have had previous IFN treatment. Stepwise multivariate logistic regression revealed significantly that age ≥ 57 years, obesity, previous history of IFN treatment and the presence of family history of diabetes were independent risk factors associated with the presence of glucose intolerance in chronic hepatitis C patients.

CONCLUSION: In conclusion, 34.6 % of Chinese patients with chronic hepatitis C had glucose intolerance. Chronic hepatitis C patients who were older in age, obese, had previous IFN treatment history and had family history of

diabetes were prone to develop glucose intolerance. To our knowledge, this is the first population-based report to confirm that interferon treatment to be an independent risk factor to develop glucose intolerance.

Chen LK, Hwang SJ, Tsai ST, Luo JC, Lee SD, Chang FY. Glucose intolerance in Chinese patients with chronic hepatitis C. *World J Gastroenterol* 2003; 9(3): 505-508

<http://www.wjgnet.com/1007-9327/9/505.htm>

INTRODUCTION

Hepatitis C virus (HCV) infection has become a common worldwide medical problem. Patients with chronic HCV infection may develop various extrahepatic manifestations including cryoglobulinemia, the presence of serum autoantibodies, glomerulonephritis, sialoadenitis and porphyria cutaneous tarda^[1-3]. The association of chronic HCV infection and diabetes mellitus (DM) was first reported by Alison *et al.* in 1994^[4]. Based on case-control studies, the prevalence of DM had been reported in 21 % to 50 % of patients with chronic HCV infection, which was significantly higher than that in the general population or among patients with other diseases^[4-7]. Population surveys from western countries also demonstrated that chronic HCV infection was associated with a high incidence of DM^[5,7]. In addition, the prevalence of anti-HCV was significantly higher in patients with DM than in the general population^[8,9].

The cause of a higher prevalence of DM in patients with chronic HCV infection remains unclear. Altered glucose metabolism has been well documented in patients with chronic liver diseases, especially in patients with liver cirrhosis^[10]. However, patients with HCV-related liver cirrhosis is associated with a significantly higher prevalence of DM than those cirrhotic patients with other etiologies^[1]. Furthermore, recipients of HCV-related liver transplantation were more likely to develop post-transplantation DM when compared to recipients with other etiologies^[6,11]. Therefore, HCV infection *per se* plays an important role in the pathogenesis of DM in patients with chronic HCV infection. Yet, analysis in previous studies rarely considered the confounding factors associated with DM development such as age, obesity and diabetic family history.

Interferon (IFN) has been widely used in the treatment of patients with chronic hepatitis C^[12-16]. Development of DM has also been reported as an adverse effect of IFN- α treatment in patients with chronic hepatitis C^[17,18]. In addition, exacerbation of previous diabetic control has been reported in chronic hepatitis B patients who received IFN- α treatment^[19]. The mechanism of IFN-related DM development or exacerbation of glycemic control remains unclear.

According to the American Diabetic Association (ADA) criteria, DM is diagnosed as repeated fasting plasma glucose ≥ 26 mg/dL, and impaired fasting glucose (IFG) is defined as the fasting plasma glucose >110 mg/dL and <126 mg/dL^[20]. Patients with IFG were reported to be prone to develop DM^[21]. Previous studies focused on the relationship of chronic HCV infection and DM. Patients with IFG were rarely evaluated. The purpose of this study was to evaluate the prevalence of

glucose intolerance (DM and IFG) in Chinese patients with chronic hepatitis C in Taiwan. In addition, risk factors associated with DM development such as age, body mass index (BMI), diabetic family history in first-degree relatives and previous IFN treatment were also evaluated to clarify the possible role of chronic HCV infection in association with the development of DM.

MATERIALS AND METHODS

Demographic data

From July 1999 to June 2001, we conducted a cross-sectional study by enrolling and following patients who were previously or newly diagnosed as chronic hepatitis C in the Office Clinics of Taipei Veterans General Hospital in Taipei, Taiwan. The diagnosis of chronic hepatitis C was based on the presence of serum anti-HCV with or without histological confirmation. At least twice for more than 6 months, all patients had elevated serum alanine aminotransferase levels 1.5-fold above the upper limit of the normal value (>60 U/L). Patients who had positive serum hepatitis B surface antigens and chronic liver diseases were excluded.

According to the ADA diagnostic criterias, diagnosis of DM was established according to the documentation of DM in previous medical records and/or repeated fasting plasma glucose ≥ 126 mmol/L (126 mg/dL), and IFG was diagnosed with a FPG >110 mg/dL and <126 mg/dL^[20]. In this study, both patients with DM and IFG were categorized together as having glucose intolerance to compare them with patients with normal glucose tolerance.

The BMI and family history of DM were recorded for each patient during enrollment. The BMI was expressed as the body weight (in kilograms) divided by the square of the body length (in meter). The family history of diabetes was obtained from the patients themselves and was recorded as positive if their first-degree relatives had DM. Obesity was defined when BMI was >27 Kg/m² in males and >25 Kg/m² in females^[22]. Liver cirrhosis was diagnosed by either liver histology or by characteristic findings in abdominal sonography, computed tomography, celiac angiography and/or the presence of esophageal varices and ascites.

IFN treatment

We recorded details of patients who received IFN treatment, including various regimens of IFN α -2a, IFN α -2b, consensus IFN, subcutaneous injections three times a week, and long-acting pegylated IFN α -2a subcutaneous injections once a week with or without oral ribavirin for either 24 weeks or 48 weeks^[23-26].

Biochemical data

Series of biochemical tests including serum alanine aminotransferase and fasting plasma glucose were measured by using an autoanalyzer (Hitachi sequential multiple autoanalyzer; Model 736, Tokyo, Japan). Antibodies to HCV were measured by using a second-generation enzyme immunoassay containing both structural and non-structural antigens (EverNew, Taipei, Taiwan). Hepatitis B surface antigens were measured by using a radioimmunoassay (Abbott Laboratories, Chicago, IL, USA).

Statistical analysis

Data in the text and tables are expressed as mean \pm standard deviation (mean \pm S.D.). Results were compared between groups depending on the type of data analyzed using the Chi-squared test, Student *t*-test or Mann-Whitney *U*-test. Stepwise multivariate logistic regression (SPSS 10.0, Chicago, IL, USA)

was performed to evaluate the predictive variables associated with the presence of glucose intolerance in patients with chronic hepatitis C. For all tests, results with *P* values less than 0.05 were considered statistically significant.

RESULTS

General data of patients

Totally, 359 patients (212 males and 147 females) were enrolled in this study and completed their follow-up investigations in the Office Clinic for more than six months. The mean age of all patients was 58.1 ± 13.0 years old (ranging from 22 to 85 years old). Among these patients, 112 (31.2 %) had a previous history of blood transfusion. Patients without a transfusion history had a past history of undisposable needle injections. None of these patients were intravenous drug abusers or under regular hemodialysis. Among all patients, 66 (18.4 %) of them had a family history of diabetes. The mean BMI of all patients was 24.0 ± 3.5 Kg/m². Eighty-seven (24.2 %) patients were obese. One hundred and fifty patients had received a percutaneous liver biopsy. Clinical and histology-diagnosed liver cirrhosis was identified in 75 patients (20.9 %). One hundred and twenty-three patients (34.3 %) had a prior history of IFN treatment with a mean duration of 3.3 years (ranging from 0.5 to 7 years) from completion of IFN treatment till enrollment.

Results of glucose intolerance

Among the 359 patients, 125 patients (34.6 %) had glucose intolerance, including 99 patients (27.6 %) with DM, and 26 patients (7.0 %) with IFG. The remaining 234 patients had normal fasting glucose. None of the 125 patients with glucose intolerance were diagnosed as type 1 DM. The mean age of chronic hepatitis C patients with glucose intolerance was significantly older than the age of those with normal fasting glucose (61.1 ± 11.2 vs 56.6 ± 13.6 years; $P=0.001$). The mean BMI of chronic hepatitis C patients with glucose intolerance was significantly higher than that of those with normal fasting glucose (24.5 ± 3.7 vs 23.7 ± 3.2 Kg/m², $P=0.024$). Thirty-eight of the 125 (30.4 %) patients with glucose intolerance were obese, which was significantly higher than those with normal fasting glucose (53/235, 22.6 %, $P=0.02$). Chronic hepatitis C patients with glucose intolerance had a significantly higher rate of diabetic family history than those with normal fasting glucose (29.6 % vs 12.8 %, $P<0.001$, Table 1).

Table 1 Comparisons of demographic data between chronic hepatitis C patients with glucose intolerance* and normal fasting glucose

	Patients with glucose intolerance (n=125)	Patients with normal fasting glucose (n=234)	P value
Age	61.1 \pm 11.2	56.6 \pm 13.6	0.001
Sex (male:female)	47:78	99:135	0.452
Body mass index (Kg/m ²)	24.5 \pm 3.7	23.7 \pm 3.2	0.024
Family history of DM (+:-)	37:88	30:204	<0.001
Obesity (+:-)	38:87	49:185	0.046
Liver cirrhosis (+:-)	28:97	47:187	0.706
Previous interferon treatment (+:-)	51:74	66:168	0.021

Denotes: Data were expressed as mean \pm S.D. * Patients with glucose intolerance included patients with diabetes mellitus and impaired fasting glucose by the diagnostic criteria of the American Diabetic Association.

Data of IFN treatment

One hundred and seventeen patients (32.6 %) had a previous history of IFN treatment. Among these 117 patients, 44 patients were treated with consensus IFN 3 µg ($n=14$), 9 µg ($n=17$) or 15 µg ($n=13$) for 24 weeks, 29 patients were treated with IFN α -2b 3 million units (MU) three times a week for 24 weeks, 4 patients were treated with IFN α -2a 6 MU three times a week for 12 weeks followed by 3 MU three times a week for 36 weeks, and 7 patients were treated with IFN α -2b 3 MU three times a week for 48 weeks along with oral ribavirin (1 000 mg/day for patients who weighed less than 75 Kg, and 1 200 mg/day for those who weighed more than 75 Kg).

Twenty-seven patients were treated with pegylated IFN α -2a 180 µg once a week for 48 weeks, and 19 of them also received oral ribavirin treatment. Six patients received pegylated IFN α -2a 180 µg once a week and oral ribavirin for 24 weeks. In patients who had a previous history of IFN treatment, 42.7 % (50/117) were glucose intolerant, which was significantly higher than the 30.2 % (73/242) of those without a history of IFN treatment ($P=0.021$). Fifty-one patients out of a total of 125 patients (40.8 %) with glucose intolerance had a past history of IFN treatment, which was significantly higher than the 66 patients out of 234 patients (28.2 %) with normal fasting glucose ($P=0.021$). There was no significant difference in gender and in relation to the presence of cirrhosis between the two groups (Table 1).

Dependent variable associated with glucose intolerance

Age, gender, BMI, family history of diabetes, the presence of liver cirrhosis and previous IFN treatment were identified as independent variables in a logistic regression analysis with the glucose intolerance as the dependent variable. Continuous variables were transformed into categorical variables with the cut-off determined by the Receiver Operating Characteristic curve. Stepwise multivariate logistic regression analysis revealed that age ≥ 57 years, the presence of family history of diabetes, obesity and previous IFN treatment were significant as independent predictive variables associated with the presence of glucose intolerance in patients with chronic hepatitis C (Table 2).

Table 2 Significant predictive variables of glucose intolerance in chronic hepatitis C patients using stepwise multivariate logistic regression analysis

	Coefficient	Odds ratio	95% CI	P value
Age ≥ 57 years	1.251	3.50	2.06-5.92	<0.001
Diabetic family history	1.289	3.64	2.00-6.57	<0.001
Obesity	0.576	1.78	1.05-3.03	0.034
Previous interferon treatment	0.803	2.23	1.34-3.72	0.002

Denotes: CI: confidence interval.

DISCUSSION

The close relationship between DM and chronic HCV infection had been reported in several previous studies although the exact pathogenesis remains unclear^[4,11]. The age-adjusted population-based prevalence of type 2 DM and IFG in Taiwan was 5.9 % and 15.7 %, respectively^[27-30]. According to our results, the prevalence of DM and IFG in patients with chronic hepatitis C was 27.6 % and 7.0 %, respectively. The prevalence of glucose intolerance (DM and IFG) was significantly higher than the age-matched normal population in Taiwan.

An altered glucose metabolism had been reported in patients with chronic liver diseases and liver cirrhosis^[11]. However,

patients with HCV-related chronic hepatitis and liver cirrhosis demonstrated a stronger correlation than those patients with other etiologies^[5,6,11]. Patients with a viral infection alone such as cytomegalovirus, Coxsackie virus and mumps were reported to develop DM, but most of the reported cases were type 1 DM^[31-33]. The pathogenesis of HCV-related DM remains mysterious.

Although the close relationship between DM and chronic HCV infection has been noted, the risk factors of DM including age, sex, the presence of family history of diabetes, BMI, liver cirrhosis, and previous history of IFN treatment has not been well investigated in previous case-control studies. In the general population, male gender, older age, obesity and the presence of family history of diabetes were well recognized as significant risk factors for the development of DM. According to our results, all these risk factors except the male gender remained independent risk factors associated with the presence of DM in chronic hepatitis C patients. These findings indicated that multiple factors may contribute to the development of DM in patients with chronic hepatitis C.

Of particular interest, our results showed significantly that previous IFN treatment was an independent risk factor for the development of glucose intolerance in patients with chronic hepatitis C. IFN had been widely used in the treatment of patients with chronic hepatitis C^[12-16]. Development of DM or the exacerbation of previously stable glycemic control in diabetic patients had been reported as drug side effects in chronic hepatitis C patients who were receiving IFN treatment, but the mechanism of this phenomenon remains unknown^[17-19]. The presence of islet cell autoantibodies had ever been reported in a chronic hepatitis C patient during IFN treatment^[34]. Fabris *et al* reported that the development of DM during IFN treatment was resulted from the amplification of previously existing autoimmunity against pancreatic β cells^[35]. However, a report contradicting these findings was published later^[36].

Koivisto *et al* also postulated that impaired glucose tolerance was found in healthy volunteers who received IFN treatment, and this phenomenon may have resulted from the development of insulin resistance through the complex interaction between insulin and its counter-regulatory hormones^[37]. However, by using a minimal model, IFN- α injection was reported to ameliorate the glucose tolerance in diabetic and non-diabetic patients with chronic HCV infection^[38]. Our results showed that previous IFN therapy can be used significantly as an independent variable to predict the development of glucose intolerance in patients with chronic hepatitis C. Patients enrolled in our study received various forms of IFN with different dosages and durations. Therefore, further evaluations are needed to clarify the enigmatic association between IFN treatment and DM development in patients with chronic hepatitis C.

In conclusion, 34.6 % of patients with chronic hepatitis C were glucose intolerant. Chronic hepatitis C patients who were older in age, were obese, and had a previous history of IFN treatment as well as a family history of diabetes were prone to develop glucose intolerance. To our best knowledge, this is the first population-based report to confirm that interferon treatment to be an independent risk factor to develop glucose intolerance.

ACKNOWLEDGEMENTS

This study was supported by a grant (NSC) from National Science Council, Taiwan. The authors wish to thank Miss Wei-Lin Chen for her assistance in blood collection, and Miss Rei-Hwa Lu for her laboratory assistance.

REFERENCES

- 1 **Gumber SC**, Chopra S. Hepatitis C: a multifaceted disease. *Ann Intern Med* 1995; **123**: 615-620

- 2 **Hwang SJ**, Lee SD, Li CP, Lu RH, Chan CY, Wu JC. Clinical study of cryoglobulinemia in Chinese patients with chronic hepatitis C. *J Gastroenterol Hepatol* 1997; **12**: 513-517
- 3 **Luo JC**, Hwang SJ, Li CP, Lu RH, Chan CY, Wu JC, Chang FY, Lee SD. Clinical significance of serum auto-antibodies in Chinese patients with chronic hepatitis C: negative role of serum viral titre and genotype. *J Gastroenterol Hepatol* 1998; **13**: 475-479
- 4 **Allison ME**, Wreghitt T, Palmer CR, Alexander GJ. Evidence for a link between hepatitis C virus infection and diabetes mellitus in a cirrhotic population. *J Hepatol* 1994; **21**: 1135-1139
- 5 **Caronia S**, Taylor K, Pagliaro L, Carr C, Palazzo U, Petrik J, O'Rahilly S, Shore S, Tom BD, Alexander GJ. Further evidence for an association between non-insulin-dependent diabetes mellitus and chronic hepatitis C virus infection. *Hepatology* 1999; **30**: 1059-1063
- 6 **Knobler H**, Stagnaro-Green A, Wallenstein S, Schwartz M, Roman SH. Higher incidence of diabetes in liver transplant recipients with hepatitis C. *J Clin Gastroenterol* 1998; **26**: 30-33
- 7 **Mason AL**, Lau JY, Hoang N, Qian K, Alexander GJ, Xu L, Guo L, Jacob S, Regenstein FG, Zimmerman R, Everhart JE, Wasserfall C, Maclaren NK, Perrillo RP. Association of diabetes mellitus and chronic hepatitis C virus infection. *Hepatology* 1999; **29**: 328-333
- 8 **Ozyilkkan E**, Erbas T, Simsek H, Telatar F, Kayhan B, Telatar H. Increased prevalence of hepatitis C virus antibodies in patients with diabetes mellitus. *J Intern Med* 1994; **235**: 283-284
- 9 **Simo R**, Jardi R, Hernandez C, Mesa J, Genesca J. High prevalence of hepatitis C virus infection in diabetic patients. *Diabetes Care* 1996; **19**: 998-1000
- 10 **Kingston ME**, Ali MA, Atiyeh M, Donnelly RJ. Diabetes mellitus in chronic active hepatitis and cirrhosis. *Gastroenterology* 1984; **87**: 688-694
- 11 **Bigam DL**, Pennington JJ, Carpentier A, Wanless IR, Hemming AW, Croxford R, Greig PD, Lilly LB, Heathcote JE, Levy GA, Cattral MS. Hepatitis C-related cirrhosis: a predictor of diabetes after liver transplantation. *Hepatology* 2000; **32**: 87-90
- 12 **Carithers RL Jr**, Emerson SS. Therapy of hepatitis C: meta-analysis of interferon alfa-2b trials. *Hepatology* 1997; **26** (Suppl 1): 83S-88S
- 13 **Poynard T**, Leroy V, Cohard M, Thevenot T, Mathurin P, Opolon P, Zarski JP. Meta-analysis of interferon randomized trials in the treatment of viral hepatitis C: effects of dose and duration. *Hepatology* 1996; **24**: 778-789
- 14 **Farrell GC**. Therapy of hepatitis C: interferon alfa-n1 trials. *Hepatology* 1997; **26**(Suppl 1): 96S-100S
- 15 **Poynard T**, Marcellin P, Lee SS, Niederau C, Minuk GS, Ideo G, Bain V, Heathcote J, Zeuzem S, Trepo C, Albrecht J. Randomized trial of interferon alfa-2b plus ribavirin for 48 weeks or 24 weeks versus alfa-2b plus placebo for 48 weeks for treatment of chronic hepatitis C virus. *Lancet* 1998; **352**: 1426-1432
- 16 **McHutchison JG**, Gordon SC, Schiff ER, Shiffman ML, Lee WM, Rustgi VK, Goodman ZD, Ling MH, Cort S, Albrecht JK. Interferon alfa-2b alone or in combination with ribavirin as initial treatment for chronic hepatitis C. *N Engl J Med* 1998; **339**: 1485-1492
- 17 **Okanoue T**, Sakamoto S, Itoh Y, Minami M, Yasui K, Sakamoto M, Nishioji K, Katagishi T, Nakagawa Y, Tada H, Sawa Y, Mizuno M, Kagawa K, Kashima K. Side effects of high-dose interferon therapy for chronic hepatitis C. *J Hepatol* 1996; **25**: 383-391
- 18 **Fattovich G**, Giustina G, Favarato S, Ruol A. A survey of adverse events in 11,241 patients with chronic viral hepatitis treated with alpha interferon. *J Hepatol* 1996; **24**: 38-47
- 19 **Lopes EP**, Oliveira PM, Silva AE, Ferraz ML, Costa CH, Miranda W, Dib SA. Exacerbation of type 2 diabetes mellitus during interferon alfa therapy for chronic hepatitis B. *Lancet* 1994; **343**: 224
- 20 **The Expert Committee of the Diagnosis and Classification of Diabetes Mellitus**. Report of the expert committee on the diagnosis and classification of diabetes mellitus. *Diabetes Care* 1997; **20**: 1183-1197
- 21 **Tsai ST**, Li CL, Chen CH, Chou P. Community-based epidemiological study of glucose tolerance in Kin-Chen, Kinmen: support for a new intermediate classification. *J Clin Epidemiol* 2000; **53**: 505-510
- 22 **National Diabetes Data Group**. Classification and diagnosis of diabetes mellitus and other categories of glucose intolerance. *Diabetes* 1979; **28**: 1039-1057
- 23 **Hwang SJ**, Chan CY, Lu RH, Wu JC, Lee SD. Randomized controlled trial of recombinant interferon-alpha 2b in the treatment of Chinese patients with chronic hepatitis C. *J Interferon Cytokine Res* 1995; **15**: 611-666
- 24 **Hwang SJ**, Lee SD, Chan CY, Lu RH, Chang FY. A randomized, double-blind controlled trial of consensus interferon in the treatment of Chinese patients with chronic hepatitis C. *Am J Gastroenterol* 1999; **94**: 2496-2500
- 25 **Hwang S**, Lee S, Chu C, Lu R, Chang F. An open-label trial of consensus interferon 15 microg in the treatment of Chinese patients with chronic hepatitis C. *Hepatol Res* 2001; **19**: 284-293
- 26 **Zeuzem S**, Feinman SV, Rasenack J, Heathcote EJ, Lai MY, Gane E, O'Grady J, Reichen J, Diago M, Lin A, Hoffman J, Brunda MJ. Peginterferon alfa-2a in patients with chronic hepatitis C. *N Engl J Med* 2000; **343**: 1666-1672
- 27 **Tai TY**, Yang CL, Chang CJ. Epidemiology of diabetes mellitus among adults in Taiwan, ROC. *J Med Assoc Thailand* 1987; **70** (Suppl 2): 42-48
- 28 **Lin JD**, Shieh WB, Huang MJ, Huang HS. Diabetes mellitus and hypertension based on the family history and 2-h postprandial blood sugar in the Ann-Lo district (northern Taiwan). *Diabetes Res Clin Pract* 1993; **20**: 75-85
- 29 **Lu FH**, Yang YC, Wu JS, Wu CH, Chang CJ. A population-based study of the prevalence and associated factors of diabetes in southern Taiwan. *Diabet Med* 1998; **15**: 564-572
- 30 **Chang C**, Lu F, Yang YC, Wu JS, Wu TJ, Chen MS, Chuang LM, Tai TY. Epidemiologic study of type 2 diabetes in Taiwan. *Diabetes Res Clin Pract* 2000; **50** (Suppl 2): S49-S59
- 31 **Forrest JM**, Menser MA, Burgress JA. High frequency of diabetes mellitus in young adults with congenital rubella. *Lancet* 1971; **2**: 332-334
- 32 **King ML**, Shaikh A, Bidwell D, Voller A, Banatvala JE. Cocksackie-B-virus-specific IgM responses in children with insulin-dependent (juvenile onset; type I) diabetes mellitus. *Lancet* 1983; **1**: 1397-1399
- 33 **Pak CY**, Eun HM, McArthur RG, Yoon JW. Association of cytomegalovirus infection with autoimmune type 1 diabetes. *Lancet* 1988; **2**: 1-4
- 34 **Campbell S**, McLaren EH, Danesh BJ. Rapidly reversible increase in insulin requirement with interferon. *Brit Med J* 1996; **313**: 92
- 35 **Fabris P**, Betterle C, Greggio NA, Zanchetta R, Bosi E, Biasin MR, de Lalla F. Insulin-dependent diabetes mellitus during alpha-interferon therapy for chronic viral hepatitis. *J Hepatol* 1998; **28**: 514-517
- 36 **Betterle C**, Fabris P, Zanchetta R, Pedini B, Tositti G, Bosi E, de Lalla F. Autoimmunity against pancreatic islets and other tissues before and after interferon- α therapy in patients with hepatitis C virus chronic infection. *Diabetes Care* 2000; **23**: 1177-1181
- 37 **Koivisto VA**, Cantell K, Pelkonen R. Effect of interferon on glucose tolerance and insulin sensitivity. *Diabetes* 1989; **38**: 641-647
- 38 **Konrad T**, Vicini P, Zeuzem S, Toffolo G, Breim D, Lormann J, Herrmann G, Wittmann D, Lenz T, Kusterer K, Teuber G, Cobelli C, Usadel KH. Interferon- α improves glucose tolerance in diabetic and non-diabetic patients with HCV-infected liver disease. *Exp Clin Endocrinol Diabetes* 1999; **107**: 343-349

A mutation specific polymerase chain reaction for detecting hepatitis B virus genome mutations at nt551

Chun-Ling Ma, De-Xing Fang, Hua-Biao Chen, Fa-Qing Li, Hui-Ying Jin, Su-Qin Li, Wei-Guo Tan

Chun-Ling Ma, De-Xing Fang, Hua-Biao Chen, Fa-Qing Li, Hui-Ying Jin, Su-Qin Li, Wei-Guo Tan, Huadong Research Institute for Medical Biotechnics, Nanjing 210002, Jiangsu Province, China
Supported by the Natural Science Foundation of Jiangsu Province, No. BJ2000039

Correspondence to: Chun-Ling Ma, Huadong Research Institute for Medical Biotechnics, Nanjing 210002, China. mchunling@hotmail.com

Telephone: +86-25-4542419 **Fax:** +86-25-4541183

Received: 2002-06-08 **Accepted:** 2002-07-11

Abstract

AIM: The hepatitis B surface antigen (HBsAg) is considered to be one of the best markers for the diagnosis of acute and chronic HBV infection. But in some patients, this antigen cannot be detected by routine serological assays despite the presence of virus. One of the most important explanations for the lack of detectable HBsAg is that mutations which occur within the "a" determinant of HBV S gene can alter expression of HBsAg and lead to changes of antigenicity and immunogenicity of HBsAg accordingly. As a result, these mutants cannot be detected by diagnosis assays. Thus, it is essential to find out specific and sensitive methods to test the new mutants and further investigate their distribution. This study is to establish a method to investigate the distribution of the HBsAg mutant at nt551.

METHODS: A mutation specific polymerase chain reaction (msPCR) was established for amplifying HBV DNA with a mutation at nt551. Four sets of primer pairs, P551A-PPS, P551G-PPS, P551C-PPS and P551T-PPS, with the same sequences except for one base at 3' terminus were designed and synthesized according to the known HBV genome sequences and the popular HBV subtypes, adr and adw, in China. At the basis of regular PCR method, we explored the specific conditions for amplifying HBV DNAs with a mutation at nt551 by regulating annealing temperature and the concentration of these primers. 126 serum samples from patients of hepatitis B were collected, among which 16 were positive for HBV S DNA in the nested PCR amplification. These 16 HBV S DNAs were detected by using the msPCR method.

RESULTS: When the annealing temperature was raised to 71 °C, nt551A and nt551G were amplified specifically by P551A-PPS and P551G-PPS; At 72 °C and 5 pmole of the primers (each) in reaction of 25 µl volume, nt551C and nt551T were amplified specifically by P551C-PPS and P551T-PPS. 16 of HBV S gene fragments were characterized by using this method. 14 of them were positive for nt551A, one was positive for nt551G, and the other one was positive for nt551T. The results were confirmed by nucleotide sequencing.

CONCLUSION: The mutation specific polymerase chain reaction is a specific and sensitive method for detecting the mutations of HBV genome at nt551.

Ma CL, Fang DX, Chen HB, Li FQ, Jin HY, Li SQ, Tan WG. A mutation specific polymerase chain reaction for detecting hepatitis B virus genome mutations at nt551. *World J Gastroenterol* 2003; 9(3): 509-512

<http://www.wjgnet.com/1007-9327/9/509.htm>

INTRODUCTION

Hepatitis B virus (HBV) is a hepatotropic DNA virus, in the reverse transcription process of DNA replication, the HBV DNA template is transcribed by cellular RNA polymerase to pregenomic RNA, which is reverse transcribed to DNA by viral polymerase, and a consequence of the unique way of HBV replication is a significant tendency of mutation^[1-3]. Substitution, deletion and frame-shift by insertion or deletion of short sequence were found in four open reading frames^[4-7]. The diversity is also shown in different serological subtypes such as adr, adw, ayr and ayw, which have a common "a" determinant. It is well known that "a" determinant is the common antigenic epitopes of all subtypes of HBsAg. A large antigenic area of "a" determinant is now called the major hydrophilic region (MHR). Mutations within MHR of HBsAg have been considered to be associated with vaccine failure and chronic infection^[1,2,6,8]. These mutations have been reported repeatedly since Carman found the first case of immune escape mutants in 1990^[9]. The point mutation reported most commonly in immunized children causes a substitution of Arg for Gly at position 145 of HBsAg^[1,3,8,9]. Other reports about substitutions in HBsAg such as 120, 121, 126, 129, 131, 133, 141, 144 were found repeatedly^[8-12]. These findings of HBV immune escape mutants have caused attention from scientists all over the world in recent years. Immune escape of HBV mutants was best known to be associated with HBV genome itself, but the immune pressure was considered to be one of the most important factors that result in escape mutants^[13-17].

The immune escape variants could influence the effect of HBV vaccine, it was argued that the components of mutant HBsAg should be considered to be added in the HBV vaccine in the future^[3,13,17,18]. However, in order to achieve this aim, it is needed to confirm first the mutants that are the big problems among hepatitis B patients. At present, it is very important to find out new escape mutants and further investigate their distribution. Specific and sensitive assays are essential for investigating the distribution of mutants. To detect the mutant HBV DNA, mutation specific polymerase chain reaction (msPCR) is a potential method. Our lab had discovered a mutation at nt551 A-to-G of HBV genome, resulting in the alteration at aa133 Met to Val of HBsAg, from a four-year-old hepatitis B patient^[12,3]. To investigate the distribution of mutants with a mutation at nt551 among the hepatitis B patients in China, a msPCR method was established according to HBV DNA sequences and the main popular subtypes, adr and adw.

MATERIALS AND METHODS

Materials

Collection of serum samples 126 of serum samples were

provided by Department of Laboratory Diagnosis, Nanjing Jinling Hospital. The viral markers were tested by using the enzyme immune assay (EIA) methodology. All of the samples were positive for anti-HBs and negative for HBsAg. The ALT level was considered to be abnormal to all of them.

Methods

Extraction of HBV genome DNAs DNAs was isolated and purified from 100 μ L of serum samples. Proteinase K (20 mg/ml) and SDS (10 %) were added into 100 μ L of sera and their concentrations in reaction were 2.5 mg/ml and 0.5 %, respectively. After a brief vortex, the mixture was heated at 70 $^{\circ}$ C for 3 hours. Then the same volume of phenol: chloroform was added to the mixture to extract DNA. The DNA pellet was obtained with 100 % ethanol precipitation, and was washed with 70 % ethanol. The dried DNA pellet was then resuspended in 20 μ L of H₂O and stored at -20 $^{\circ}$ C. All of 126 sera were prepared in this way.

Amplification of HBV S DNAs The amplification of HBV S gene was carried out by using the nested PCR method. In the first-round PCR, the 50 μ L reaction solution including 5 μ L DNA template and 40 pmole (each) of the first-round primers. The mixture was heated to 94 $^{\circ}$ C for 5 min, followed by 30 PCR cycles consisting of 94 $^{\circ}$ C for 30 s, 55 $^{\circ}$ C for 30 s and 72 $^{\circ}$ C for 60 s in a thermal cycler. And then 1.25 μ L of the first-round PCR product served as the template for the second-round of PCR amplification which consisting of the same cycles except that the annealing temperature was raised to 65 $^{\circ}$ C. Positive PCR product, a DNA band of 1.2kb as expected, was detected on agarose gel electrophoresis. After amplification, we achieved 16 HBV S DNAs.

The primers for the nested PCR were designed according to the known HBV genome sequences and the main popular subtypes, adr and adw, in China, as follows:

The primers for first-round:

P1' : 5' ACATCATCTGTGGAAGGC 3', nt2756-nt2773, the upstream primer;

P6' : 5' TATCCCATGAAGTTAAGG 3', nt884-nt867, the downstream primer;

The primers for second-round:

PEC: 5' CGGAATTCACCATATTCTTGGGAACAAG 3', nt2 823-nt2 844, the upstream primer;

PPS: 5' GCTGCAGGTTTAAATGTATACCCAAAGAC 3', nt838-nt816, the downstream primer;

An EcoRI or a Pst I sites was originally added at 5' -end respectively for cloning purpose.

Amplification of HBV DNA fragments for control To achieve the HBV DNA fragment with an A at nt551, the wild-type HBV S DNA as template was amplified by using the primer pair P551A-PPS under the condition of regular PCR. The HBsAg mutant with a G at nt551 as template was amplified by using the primer pair P551G-PPS to achieve the HBV DNA fragment with a G at nt551. The HBV DNA fragment with a C or T at nt551 was achieved by using introducing mutation in a PCR. The PCR primer sequences were as follows:

P551A: 5' TCCTGCTCAAGGAACCTCTA 3', nt532-nt551, upstream primer;

P551G: 5' TCCTGCTCAAGGAACCTCTG 3', nt532-nt551, upstream primer;

P551C: 5' TCCTGCTCAAGGAACCTCTC 3', nt532-nt551, upstream primer;

P551T: 5' TCCTGCTCAAGGAACCTCTT 3', nt532-nt551, upstream primer;

PPS: See the above.

P551C-PPS and P551T-PPS were used respectively to amplify HBV DNA fragments with a C or T at nt551, which are 314 bp long. Additionally, two upstream primers had been designed respectively by introducing mutation in order to

achieve the controls of HBV DNA with a C or T at nt551.

P551CM: TCCTGCTCAAGGAACCTCTCTGTTC, nt532-nt557;

P551TM: TCCTGCTCAAGGAACCTCTTTGTTC, nt532-nt557.

Establishment of msPCR In order to amplify HBV DNA specifically, the annealing temperature of PCR was regulated according to the T_m. The reaction volume of PCR was 25 μ L. The PCR reaction was carried out by using P551A-PPS, P551G-PPS, P551C-PPS and P551T-PPS as primer pairs to amplify HBV S DNA templates with an A, G, C, or T at nt551, respectively.

Application of msPCR Under the condition of the msPCR method, the 16 of samples which were positive for HBV S DNA as templates were amplified by using P551A-PPS, P551G-PPS, P551C-PPS and P551T-PPS as primer pairs respectively.

HBV S DNA sequencing In order to confirm the validity of the msPCR, the purified PCR products of HBV S gene fragments from selected samples according to the results of msPCR, NO.2, NO.5, NO.8 and NO.57 were sequenced by using the primer PPS.

RESULTS

HBV DNA fragments for control

The HBV S DNA with an A, G, C or T at nt551 was amplified respectively for control. This result is shown in Figure 1.

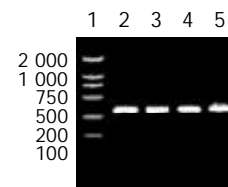


Figure 1 Amplification of Control HBV DNA. Lane 1: DNA Marker; Lane 2: HBV DNA with an A at nt551 amplified by P551A-PPS; Lane 3: HBV DNA with a G at nt551 amplified by P551G-PPS; Lane 4: HBV DNA with a C at nt551 amplified by P551CM-PPS; Lane 5: HBV DNA with a T at nt551 amplified by P551TM-PPS. The amplified DNA fragments are 314 bp long.



Figure 2 Establishment of the msPCR for nt551A and nt51G. Lane 1: DNA Marker; Lane 2-5: P551A-PPS amplified HBV DNAs of control (nt551A in Lane 2, nt551G in Lane 3, nt551C in Lane 4, nt551T in Lane 5). Lane 6-9: P551G-PPS amplified HBV DNAs of control (nt551A in Lane 6, nt551G in Lane 7, nt551C in Lane 8, nt551T in Lane 9).

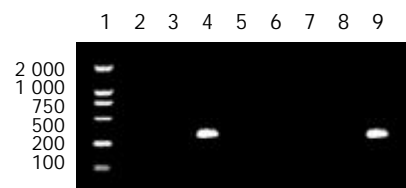


Figure 3 Establishment of the msPCR for nt551C and nt551T. Lane 1: DNA Marker; Lane 2-5: P551C-PPS amplified HBV DNAs of control (nt551A in Lane 2, nt551G in Lane 3, nt551C in Lane 4, nt551T in Lane 5). Lane 6-9: P551T-PPS amplified HBV DNAs of control (nt551A in Lane 6, nt551G in Lane 7, nt551C in Lane 8, nt551T in Lane 9).

- of HBs antigen negative variant of hepatitis B virus: unique substitutions, Glu129 to Asp and Gly145 to Ala in the surface antigen gene. *Med Sci Monit* 2000; **6**: 1165-1169
- 2 **Brunetto MR**, Rodriguez UA, Bonino F. Hepatitis B virus mutants. *Intervirology* 1999; **42**: 69-80
- 3 **Kfoury Baz EM**, Zheng J, Mazuruk K, Van Le A, Peterson DL. Characterization of a novel hepatitis B virus mutants demonstration of mutation-induced hepatitis B virus surface antigen group specific "a" determinant conformation change and its application in diagnosis assays. *Transfus Med* 2001; **11**: 355-362
- 4 **Dong J**, Cheng J, Wang Q, Huangfu J, Shi S, Zhang G, Li L, Si C. The study on heterogeneity of hepatitis B virus. *Zhonghua Yixue Zazhi* 2002; **82**: 81-85
- 5 **Kreutz C**. Molecular, immunological and clinical properties mutated hepatitis B viruses. *J Cell Mol Med* 2002; **6**: 113-143
- 6 **Zhong S**, Chan JY, Yeo W, Tam JS, Johnson PJ. Hepatitis B envelope protein mutants in human hepatocellular carcinoma tissues. *J Viral Hepat* 1999; **6**: 195-202
- 7 **Weinberger KM**, Zoulek G, Bauer T, Bohm S, Jilg W. A novel deletion mutant of hepatitis B virus surface antigen. *J Med Virol* 1999; **58**: 105-110
- 8 **Roznovsky L**, Harrison TJ, Fang ZL, Ling R, Lochman I, Orsagova I, Pliskova L. Unusual hepatitis B surface antigen variation in a child immunised against hepatitis B. *J Med Virol* 2000; **61**: 11-14
- 9 **Carman WF**, Zanetti AR, Karayiannis P, Waters J, Tanzi E, Zuckerman AJ, Thomas HC. Vaccine-induced escape mutant of hepatitis B virus. *Lancet* 1990; **336**: 325-329
- 10 **Yang X**, Lei J, Zhang Y, Luo H, Huang L, Zheng Y, Tang X. A novel stop codon mutation in S gene: the molecular basis of a patient with cryptogenic cirrhosis. *Zhonghua Yixue Zazhi* 2002; **82**: 400-402
- 11 **Zhu Q**, Lu Q, Xiong S, Yu H, Duan S. Hepatitis B virus S gene mutants in infants infection despite immunoprophylaxis. *Chin Med J* 2001; **114**: 352-354
- 12 **Fang DX**, Li FQ, Tan WG, Chen HB, Jin HY, Li SQ, Lin HJ, Zhou ZX. Transient expression and antigenic characterization of HBsAg of HBV nt551 A to G mutant. *World J Gastroenterol* 1999; **5**: 73-74
- 13 **Santantonio T**, Gunther S, Sterneck M, Rendina M, Messner M, Launois B, Francavilla A, Pastore G, Will H. Liver graft infection by HBV S-gene mutants in transplant patients receiving long-term HBIG prophylaxis. *Hepatogastroenterology* 1999; **46**: 1848-1854
- 14 **Rodriguez-Frias F**, Buti M, Jardi R, Vargas V, Quer J, Cotrina M, Martell M, Esteban R, Guardia J. Genetic alterations in the S gene of hepatitis B virus in patients with acute hepatitis B, chronic hepatitis B and hepatitis B liver cirrhosis before and after liver transplantation. *Liver* 1999; **19**: 177-182
- 15 **He C**, Nomura F, Itoga S, Isobe K, Nakai T. Prevalence of vaccine-induced escape mutants of hepatitis B virus in the adult population in Chinese prospective study in 176 restaurant employees. *J Gastroenterol Hepatol* 2001; **16**: 1373-1377
- 16 **Cooreman MP**, Leroux-Roels G, Paulij WP. Vaccine-and hepatitis B immune globulin-induced escape mutations of hepatitis B virus surface antigen. *J Biomed Sci* 2001; **8**: 237-247
- 17 **Komatsu H**, Fujisawa T, Sogo T, Isozaki A, Inui A, Kobata M, Ogawa Y. Acute self-limiting hepatitis B after immunoprophylaxis failure in an infant. *J Med Virol* 2002; **66**: 28-33
- 18 **Heijtink RA**, Van Bergen P, Van Roosmalen MH, Paulij WP, Schalm SW, Osterhaus AD. Anti-HBs after hepatitis B immunization with plasma-derived and recombinant DNA-derived vaccines: binding to mutant HBsAg. *Vaccine* 2001; **19**: 3671-3680
- 19 **Francois G**, Kew M, van Damme P, Mphahlele MJ, Meheus A. Mutants hepatitis B viruses: a matter of academic interest only or a problem with far-reaching implications? *Vaccine* 2001; **19**: 3799-3815
- 20 **Burda MR**, Gunther S, Dandri M, Will H, Petersen J. Structural and functional heterogeneity of nature occurring hepatitis B virus variants. *Antiviral Res* 2001; **52**: 125-138
- 21 **Coleman PF**, Chen YC, Mushahwar IK. Immunoassay detection of hepatitis B surface antigen mutants. *J Med Virol* 1999; **59**: 19-24
- 22 **Torresi J**, Earnest-Silveira L, Civitico G, Walters TE, Lewin SR, Fyfe J, Locarnini SA, Manns M, Trautwein C, Bock TC. Restoration of replication phenotype of lamivudine-resistant hepatitis B virus mutants by compensatory changes in the "fingers" subdomain of the viral polymerase selected as a consequence of mutations in the overlapping S gene. *Virology* 2002; **299**: 88
- 23 **Cooreman MP**, van Roosmalen MH, te Morsche R, Sunnen CM, Ven EM, Jansen JB, Tytgat GN, de Wit PL, Paulij WP. Characterization of the reactivity pattern of monoclonal antibodies against wild-type hepatitis surface antigen to G145R and other naturally occurring a loop escape mutations. *Hepatology* 1999; **30**: 1287-1292
- 24 **Wu L**, Yuan ZH, Liu F, Waters JA, Wen YM. Comparing the immunogenicity of hepatitis B virus gene variants by DNA immunization. *Viral Immunol* 2001; **14**: 359-367
- 25 **Owiredu WK**, Kramvis A, Kew MC. Molecular analysis of hepatitis B virus genomes isolated from black African patients with fulminant hepatitis B. *J Med Virol* 2001; **65**: 485-492
- 26 **Banerjee K**, Guptan RC, Bisht R, Sarin SK, Khandekar P. Identification of a novel surface mutant of hepatitis B virus in a seronegative chronic liver disease patient. *Virus Res* 1999; **65**: 103-109
- 27 **Chen WN**, Oon CJ. Hepatitis B virus surface antigen (HBsAg) mutants in Singapore adults and vaccinated children with high anti-hepatitis B virus antibody levels but negative for HBsAg. *J Clin Microbiol* 2000; **38**: 2793-2794
- 28 **Oon CJ**, Chen WN, Goo KS, Goh KT. Intra-familial evidence of horizontal transmission hepatitis B virus surface antigen mutant G145R. *J Infect* 2000; **41**: 260-264
- 29 **Chen WN**, Oon CJ, Koh S. Horizontal transmission of a hepatitis B virus surface antigen mutant. *J Clin Microbiol* 2000; **38**: 938-939
- 30 **Schories M**, Peter T, Rasenack J. Isolation, characterization and biological significance of hepatitis B virus mutants from some of a patient with immunologically negative HBV infection. *J Hepatol* 2000; **33**: 799-811
- 31 **Weinberger KM**, Bauer T, Bohm S, Jilg W. High genetic variability of the group-specific adeterminant of hepatitis B virus surface antigen (HBsAg) and the corresponding fragment of the viral polymerase in chronic virus carriers lacking detectable HBsAg in serum. *J Gen Virol* 2000; **81**(Pt 5): 1165-1174
- 32 **Chen WN**, Oon CJ, Moh MC. Detection of hepatitis B virus surface antigen mutants in paraffin-embedded hepatocellular carcinoma tissues. *Virus Genes* 2000; **20**: 263-267
- 33 **Ijaz S**, Torre F, Tedder RS, Williams R, Naoumov NV. Novel immunoassay for the detection of hepatitis surface escape mutants and its application in transplant recipients. *J Med Virol* 2001; **63**: 210-216
- 34 **Jolivet-Reynaud C**, Lesenechal M, O'Donnell B, Becquart L, Foussadier A, Forge F, Battail-Poirot N, Carman W, Jolivet M. Localization of hepatitis B surface antigen epitopes present on variants and specifically recognised by anti-hepatitis B surface antigen monoclonal antibodies. *J Med Virol* 2001; **65**: 241-249
- 35 **Worman HJ**, Feng L, Mamiya N. Molecular biology and the diagnosis and treatment of liver diseases. *World J Gastroenterol* 1998; **4**: 185-191
- 36 **Wu DY**, Ugozzoli L, Pal BK, Wallace RB. Allele-specific enzymatic amplification of β -globin genomic DNA for diagnosis of sickle cell anemia. *Proc Natl Acad Sci USA* 1989; **86**: 2757-2760

Expression of RNase H of human hepatitis B virus polymerase in *Escherichia coli*

Hong Cheng, Hui-Zhong Zhang, Wan-An Shen, Yan-Fang Liu, Fu-Cheng Ma

Hong Cheng, Yan-Fang Liu, Fu-Cheng Ma, Department of Pathology, Xijing Hospital, Fourth Military Medical University, Xi'an 710033, Shaanxi Province, China

Hui-Zhong Zhang, Wan-An Shen, Orthopedics Oncology Institute of Chinese PLA, Fourth Military Medical University, Tangdu Hospital, Xi'an 710038, Shaanxi Province, China

Correspondence to: Dr. Hong Cheng, Department of Pathology, Xijing Hospital, Fourth Military Medical University, Xi'an 710033, Shaanxi Province, China. nelson@fmmu.edu.cn

Telephone: +86-29-3375497

Received: 2002-10-17 **Accepted:** 2002-11-16

Abstract

AIM: To amplify HBV-RNase H gene fragment and expression of RNase H for further use in the studies of HBV associated liver diseases.

METHODS: The encoding gene of HBV-RNase H was separately amplified for the first half and second half (H1 and H2) by PCR from full length HBV gene and cloned into pT7Blue-T vector. Clones were first screened by digestion with *Xba*I and *Hind* III enzyme for the correct size, and analyzed further by DNA sequencing. The RNase H1 and H2 fragments isolated from *Xba*I and *Hind* III digestion products of pT7 Blue-RNase H plasmid were ligated to the GSTag expressing vectors separately, and expressed in *E. coli* BL21. The expressed proteins were checked by PAGE gel and Western blot.

RESULTS: Both H1 and H2 nucleotide sequences consisting of known genes and proteins, in correct size, were further confirmed by Western blot to be the GST and RNase H1 or H2 fusion proteins.

CONCLUSION: The successful cloning and expression of HBV-RNase H will contribute to further research and application in HBV-associated diseases.

Cheng H, Zhang HZ, Shen WA, Liu YF, Ma FC. Expression of RNase H of human hepatitis B virus polymerase in *Escherichia coli*. *World J Gastroenterol* 2003; 9(3): 513-515
<http://www.wjgnet.com/1007-9327/9/513.htm>

INTRODUCTION

Human hepatitis B virus (HBV) infection has a wide range of clinical outcomes, from self-limited silent or acute infection to fulminant hepatitis. It has been estimated that over 300 million cases of chronic HBV infection exist globally^[1]. In China, nearly 100 million people have a persistent infection with HBV, who are at risk of developing chronic hepatitis leading to liver cirrhosis and hepatocellular carcinoma^[2-6]. Significant advances have been made during the last few years in the treatment of chronic hepatitis B^[7-13]. Several new antiviral agents have been shown to be safe and effective in inhibiting HBV replication^[14-20]. However, it has remained refractory to

the treatment since not all patients respond properly and still there is no breakthrough results in therapeutic vaccine^[21-23]. The increase of chronic hepatitis and hepatocellular carcinoma associated with the HBV infection has become a worldwide medical problem.

HBV replication is accomplished by its own polymerase. Hepadnavirus polymerases are multifunctional enzymes that play critical roles during the viral life cycle^[24]. Ribonuclease H (RNase H), the HBV RNaseH domain of HBV polymerase, is one of the four domains (Terminal, Spacer, Reverse Transcriptase and RNase H) encoded by HBV polymerase gene. With 480 bp in full length and encoding a 16ku protein which is responsible for degrading RNA from RNA-DNA intermediate, HBV-RNase H plays a pivotal role in the HBV life cycle. Although the rest of HBV encoded antigen rather than RNase H has been studied in detail^[25-30], there is less paper about HBV-RNase H which is intimately related with HBV replication. To explore the potential use of HBV-RNase H in the diagnosis and treatment of HBV associated liver diseases, we cloned and expressed RNase H of the HBV polymerase.

MATERIALS AND METHODS

Materials

pTKHH2 plasmid containing the full length HBV genomic DNA of subtype adw2 was kindly provided by Dr. Lingxun Duan in Thomas Jefferson University (Philadelphia PA). The primers with restriction enzyme site *Xba*I at 5' end and *Hind* III at 3' end used to amplify HBV-RNase H gene was synthesized in Gibco Inc. pT7Blue cloning vector, DH5 α competent cells, GSTag expression vector and anti-GST antibody were products of Novagen Inc.

Plasmid construction^[31,32]

Two pairs of primers were used in PCR reactions to amplify the first half (H1 1-240) and the second half (H2 241-480) fragments of RNase H gene from pTKHH2 plasmid (P1: 5' - TTCTAGACCGCCAGGTCTGTGCCAAGTG-3', P2: 5' - AAG CTTACCAGTTGGCAGCACAGCCTAG-3' for H1; and P3: 5' - TTCTAGACA TCCTGCGCGGGACGTCCTTTG-3', P4: 5' -AAGCTTAATGCGGTGGTCTCCA TGCG-3' for H2). The amplified H1 and H2 fragments were purified on a 15 g/L low-melting agarose gel, utilizing the PCR purification system (Promega Inc). The purified PCR products were directly ligated into the pT7 Blue-T vector respectively. After transformation of the *Escherichia coli* strain DH5 α , recombinants were selected on x-Gal plates. Ten white colonies were selected for miniprep and the insert evaluation was by enzyme digestion and DNA sequencing. The plasmids with proper inserts were recut with *Xba*I and *Hind* III enzyme and ligated into pGSTag vector. The pGSTag containing H1 or H2 fragment were transformed into BL21 *Escherichia coli* strain and propagated in LB medium.

Expression^[33] and identification of HBV-RNaseH

Picked the recombinant colonies and grew them overnight at 37 °C in 3 mL of LB medium. Removed 1 mL culture and

inoculated into 100 mL of fresh LB medium and grew at 37 °C to an A600 of 0.6. Added 100 mmol/L IPTG to the bacterial culture to a final concentration of 0.3 mmol/L and incubated the culture for an additional 3–4 h. Pelletized the cells by centrifuging at 12 000 g for 3 min and resuspending the bacterial pellet in 3 mL lysis buffer. After the bacteria lysed by ultrasonic machine, the fusion proteins were purified with glutathione Sepharose 4B column and identified by PAGE gel stained with Coomassie blue and further confirmed by Western blot.

RESULTS

Recombinant expression vectors of pGSTag containing Cloned HBV RNase H1 and H2 fragments were identified by restriction enzyme digestion and DNA sequencing and the results showed that the inserted DNA fragment were expected known sequences. The expressed proteins could be seen in Coomassie blue stained PAGE gel with 34 ku band (Figure 1) which were further confirmed by Western blot as GST and HBV RNase H fusion protein.

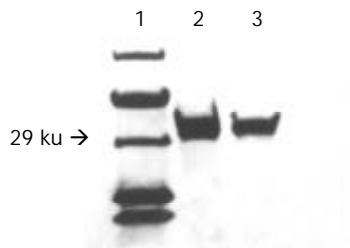


Figure 1 PAGE Electrophoresis stained with Coomassie brilliant blue light. 1: Protein MW standards; 2: RNaseH1 protein (34 ku); 3: RNaseH2 protein (34 ku).

DISCUSSION

Genome replication of hepadnavirus proceeds by reverse transcription from a viral pregenomic RNA template by a virally encoded polymerase, a polypeptide of 90 to 97 ku^[34]. The genome of all hepadnaviruses has the open reading frame, the polymerase gene, and the product or products of this polymerase gene are involved in multiple functions of the viral life cycle. These functions include a priming activity which initiates minus-strand DNA synthesis, a polymerase activity which synthesizes DNA by using either RNA or DNA templates (reverse transcriptase), a nuclease activity which degrades the RNA strand of RNA-DNA hybrids (RNase H), and involvement in packaging the RNA pregenome into nucleocapsids^[35].

Molecular genetic studies have revealed that the human HBV polymerase protein, a polypeptide of about 94 ku, which plays a critical role in the HBV life cycle, contains four domains. These are the 5' -terminal protein (TP), spacer, RNA reverse transcriptase (RT)/DNA polymerase, and RNase H, respectively, from the amino (N) to carboxy (C) terminus^[36-42]. All of the TP and RT and RNase H, rather than spacer protein, play an important role in the process of HBV replication. The RNase H, as it functions in all other retrovirus, can degrade the RNA of DNA-RNA hybrid which plays a role in optimizing the priming of minus-strand DNA synthesis^[43]. We had constructed an expression vector containing full length of HBV RNase H DNA and we failed to propagate the transformed bacteria, which might be caused by the toxic effect of RNase H activation as Lee Yi reported^[44] earlier. So we redesigned two pairs of primers to clone and expressed with two separate fragments of the RNase H. The successfully expressed RNase H and its function which will be performed in our next experiment will

contribute to further generating anti-RNase H antibody producing hybridoma cells for the purpose of HBV related liver diseases gene therapy. It has been confirmed that RNase H can be used as a marker to reflect the low level virus replication without other positive markers^[45], so to investigate and analyze the results of anti-HBV RNase H might be able to provide a new marker for the early diagnosis of HBV infection and to assess the effects of clinical therapy of HBV infection diseases.

REFERENCES

- 1 **Pramoolsinsup C.** Management of viral hepatitis B. *J Gastroenterol Hepatol* 2002; **17** (Suppl): S125-145
- 2 **Wang PZ,** Zhang ZW, Zhou YX, Bai XF. Quantitative PCR detection of HBV-DNA in patients with chronic hepatitis B and its significance. *Shijie Huaren Xiaohua Zazhi* 2000; **8**: 755-758
- 3 **Shi H,** Wang FS. Host factors in chronicity of hepatitis B virus infection and their significances clinic alh. *Shijie Huaren Xiaohua Zazhi* 2001; **9**: 66-69
- 4 **Wang Y,** Liu H, Zhou Q, Li X. Analysis of point mutation in site 1896 of HBV precore and its detection in the tissues and serum of HCC patients. *World J Gastroenterol* 2000; **6**: 395-397
- 5 **Li Y,** Su JJ, Qin LL, Yang C, Luo D, Ban KC, Kensler TW, Roe-buck BD. Chemopreventive effect of oltipraz on AFB1-induced hepatocarcinogenesis in tree shrew model. *World J Gastroenterol* 2000; **6**: 647-650
- 6 **De Clercq E.** Highlights in the development of new antiviral agents. *Mini Rev Med Chem* 2002; **2**: 163-175
- 7 **Du DW,** Zhou YX, Feng ZH, Li GY, Yao ZQ. Study on immunization of anti-subcutaneous transplanting tumor induced by gene vaccine. *Shijie Huaren Xiaohua Zazhi* 1999; **7**: 955-957
- 8 **Du DW,** Zhou YX, Feng ZH, Yao ZQ, Li GY. Immune responses to interleukin 12 and hepatitis B gene vaccine in H2 d mice. *Shijie Huaren Xiaohua Zazhi* 2000; **8**: 128-130
- 9 **Wang QC,** Zhou YX, Yao ZQ, Feng ZH. Effects of DNA vector constructs and different genes on the induction of immune responses by HBV DNA based vaccine. *Shijie Huaren Xiaohua Zazhi* 2000; **8**: 289-291
- 10 **Huang ZH,** Zhuang H, Lu S, Guo RH, Xu GM, Cai J, Zhu WF. Humoral and cellular immunogenicity of DNA vaccine based on hepatitis B core gene in rhesus monkeys. *World J Gastroenterol* 2001; **7**: 102-106
- 11 **Liu HB,** Meng ZD, Ma JC, Han CQ, Zhang YL, Xing ZC, Zhang YW, Liu YZ, Cao HL. A 12-year cohort study on the efficacy of plasma-derived hepatitis B vaccine in rural newborns. *World J Gastroenterol* 2000; **6**: 381-383
- 12 **Li H,** Wang L, Wang SS, Gong J, Zeng XJ, Li RC, Nong Y, Huang YK, Chen XR, Huang ZN. Research on optimal immunization strategies for hepatitis B in different endemic areas in China. *World J Gastroenterol* 2000; **6**: 392-394
- 13 **Zeng XJ,** Yang GH, Liao SS, Chen AP, Tan J, Huang ZJ, Li H. Survey of coverage, strategy and cost of hepatitis B vaccination in rural and urban areas of China. *World J Gastroenterol* 1999; **5**: 320-323
- 14 **Liu P,** Hu YY, Liu C, Zhu DY, Xue HM, Xu ZQ, Xu LM, Liu CH, Gu HT, Zhang ZQ. Clinical observation of salvianolic acid B in treatment of liver fibrosis in chronic hepatitis B. *World J Gastroenterol* 2002; **8**: 679-685
- 15 **Jin J,** Yang JY, Liu J, Kong YY, Wang Y, Li GD. DNA immunization with fusion genes encoding different regions of hepatitis C virus E2 fused to the gene for hepatitis B surface antigen elicited immune responses to both HCV and HBV. *World J Gastroenterol* 2002; **8**: 505-510
- 16 **Guan XJ,** Guan XJ, Wu YZ, Jia ZC, Shi TD, Tang Y. Construction and characterization of an experimental ISCOMS-based hepatitis B polypeptide vaccine. *World J Gastroenterol* 2002; **8**: 294-297
- 17 **Hussain M,** Lok AS. Mutations in the hepatitis B virus polymerase gene associated with antiviral treatment for hepatitis B. *J Viral Hepat* 1999; **6**: 183-194
- 18 **Stuyver L,** Van Geyt C, De Gendt S, Van Reybroeck G, Zoulim F, Leroux-Roels G, Rossau R. Line probe assay for monitoring drug resistance in hepatitis B virus-infected patients during antiviral therapy. *J Clin Microbiol* 2000; **8**: 702-707

- 19 **Liu P**, Liu C, Xu LM, Xue HM, Liu CH, Zhang ZQ. Effects of Fuzheng Huayu 319 recipe on liver fibrosis in chronic hepatitis B. *World J Gastroenterol* 1998; **4**: 348-353
- 20 **Zoulim F**. Detection of hepatitis B virus resistance to antivirals. *J Clin Virol* 2001; **21**: 243-253
- 21 **Honorati MC**, Facchini A. Immune response against HBsAg vaccine. *World J Gastroenterol* 1998; **4**: 464-466
- 22 **Li H**, Li RC, Liao SS, Yang JY, Zeng XJ, Wang SS. Persistence of hepatitis B vaccine immune protection and response to hepatitis B booster immunization. *World J Gastroenterol* 1998; **4**: 493-496
- 23 **Gao FG**, Sun WS, Cao YL, Zhang LN, Song J, Li HF, Yan SK. HBx DNA probe preparation and its application in study of hepatocarcinogenesis. *World J Gastroenterol* 1998; **4**: 320-322
- 24 **Zu Pudlitz J**, Lanford RE, Carlson RI, Notvall L, de la Monte SM, Wands JR. Properties of monoclonal antibodies directed against hepatitis B virus polymerase protein. *J Virol* 1999; **73**: 4188-4196
- 25 **Lin X**, Yuan ZH, Wu L, Ding JP, Wen YM. A single amino acid in the reverse transcriptase domain of hepatitis B virus affects virus replication efficiency. *J Virol* 2001; **75**: 11827-11833
- 26 **Lott L**, Beames B, Notvall L, Lanford RE. Interaction between hepatitis B virus core protein and reverse transcriptase. *J Virol* 2000; **74**: 11479-11489
- 27 **Laras A**, Koskinas J, Hadziyannis SJ. *In vivo* suppression of precore mRNA synthesis is associated with mutations in the hepatitis B virus core promoter. *Virology* 2002; **295**: 86-96
- 28 **Laras A**, Koskinas J, Avgidis K, Hadziyannis SJ. Incidence and clinical significance of hepatitis B virus precore gene translation initiation mutations in e antigen-negative patients. *J Viral Hepat* 1998; **5**: 241-248
- 29 **Stuyver LJ**, Locarnini SA, Lok A, Richman DD, Carman WF, Dienstag JL, Schinazi RF. Nomenclature for antiviral-resistant human hepatitis B virus mutations in the polymerase region. *Hepatology* 2001; **33**: 751-757
- 30 **Kim Y**, Hong YB, Jung G. Hepatitis B virus: DNA polymerase activity of deletion mutants. *Biochem Mol Biol Int* 1999; **47**: 301-308
- 31 **Cheng H**, Liu YF, Zhang HZ, Zhang SZ. Construction and expression of anti-HCC immunotoxin of sFv-TNF- α and GFP fusion proteins. *Shijie Huaren Xiaohua Zazhi* 2001; **9**: 640-644
- 32 **Cheng H**, Liu YF, Zhang HZ, Shen WA. Construction of the recombinant retroviral vector encoding anti-HCC single-chain bifunctional antibody and establishment of a stable virus producing PA317 cell line. *Shijie Huaren Xiaohua Zazhi* 2000; **8**: 708-709
- 33 **Lee YI**, Hong YB, Kim Y, Rho HM, Jung G. RNase H activity of human hepatitis B virus polymerase expressed in *Escherichia coli*. *Biochem Biophys Res Commun* 1997; **233**: 401-407
- 34 **Li Z**, Tyrrell DL. Expression of an enzymatically active polymerase of human hepatitis B virus in an coupled transcription-translation system. *Biochem Cell Biol* 1999; **77**: 119-126
- 35 **Chen KL**, Chen CM, Shih CM, Huang HL, Lee YH, Chang C, Lo SJ. Hepatitis B viral polymerase fusion proteins are biologically active and can interact with the hepatitis C virus core protein *in vivo*. *J Biomed Sci* 2001; **8**: 492-503
- 36 **Villamil FG**. Hepatitis B: Progress in the last 15 years. *Liver Transpl* 2002; **8**(10 Suppl 1): S59-66
- 37 **Chen Y**, Marion PL. Amino acids essential for RNaseH activity of hepadnaviruses are also required for efficient elongation of minus-strand viral DNA. *J Virol* 1996; **70**: 6151-6156
- 38 **Lok AS**, Hussain M, Cursano C, Margotti M, Gramenzi A, Grazi GL, Jovine E, Benardi M, Andreone P. Evolution of hepatitis B virus polymerase gene mutations in hepatitis B e antigen-negative patients receiving lamivudine therapy. *Hepatology* 2000; **32**: 1145-1153
- 39 **Torresi J**. The virological and clinical significance of mutations in the overlapping envelope and polymerase genes of hepatitis B virus. *J Clin Virol* 2002; **25**: 97
- 40 **Cerritelli SM**, Fedoroff OY, Reid BR, Crouch RJ. A common 40 amino acid motif in eukaryotic Rnases H1 and caulimovirus ORF VI proteins binds to duplex RNAs. *Nucleic Acids Res* 1998; **26**: 1834-1840
- 41 **Wakil SM**, Kazim SN, Khan LA, Raisuddin S, Parvez MK, Guptan RC, Thakur V, Hasnain SE, Sarin SK. Prevalence and profile of mutations associated with lamivudine therapy in Indian patients with chronic hepatitis B in the surface and polymerase genes of hepatitis B virus. *J Med Virol* 2002; **68**: 311-318
- 42 **Kim Y**, Hong YB, Jung G. Hepatitis B virus: DNA polymerase activity of deletion mutants. *Biochem Mol Biol Int* 1999; **47**: 301-308
- 43 **Li Z**, Tyrrell DL. Expression of an enzymatically active polymerase of human hepatitis B virus in an coupled transcription-translation system. *Biochem Cell Biol* 1999; **77**: 119-126
- 44 **Kim Y**, Jung G. Active human hepatitis B viral polymerase expressed in rabbit reticulocyte lysate system. *Virus Genes* 1999; **19**: 123-130
- 45 **Yuki N**, Hayashi N, Kasahara A, Katayama K, Ueda K, Fusamoto H, Kamada T. Detection of antibodies against the polymerase gene product in hepatitis B virus infection. *Hepatology* 1990; **12**: 193-198

Virulence of water-induced coccoid *Helicobacter pylori* and its experimental infection in mice

Fei-Fei She, Jian-Yin Lin, Jun-Yan Liu, Cheng Huang, Dong-Hui Su

Fei-Fei She, Department of Microbiology, Medical College of Wuhan University, Wuhan 234007, Hubei Province, China & Department of Microbiology, Fujian Medical University, Fuzhou 350004, Fujian Province, China

Jian-Yin Lin, Department of Molecular Medicine, Fujian Medical University, Fuzhou 350004, Fujian Province, China

Jun-Yan Liu, Department of Microbiology, Medical College of Wuhan University, Wuhan 234007, Hubei Province, China

Cheng Huang, Department of Microbiology, Fujian Medical University, Fuzhou 350004, Fujian Province, China

Dong-Hui Su, Department of Immunology, Fujian Medical University, Fuzhou 350004, Fujian Province, China

Supported by the Natural Science Fundation of Fujian Province, China, No. C95031

Correspondence to: Fei-Fei She, Department of Microbiology, Fujian Medical University, Fuzhou 350004, Fujian Province, China. cyslff@163.net

Telephone: +86-591-3569309

Received: 2002-09-14 **Accepted:** 2002-10-17

Abstract

AIM: To explore the virulence and the infectivity of coccoid *Helicobacter pylori* (*H. pylori*) transformed from spiral form by exposure to sterile tap water.

METHODS: Three strains of *H. pylori*, isolated from gastric biopsy specimens of confirmed peptic ulcer, were converted from spiral into coccoid form by exposure to sterile tap water. Both spiral and coccoid forms of *H. pylori* were tested for the urease activity, and the adherence to Hep-2 cells. The presence of flagella was examined under electron microscopy. In the experimental animal infection, the spiral and coccoid forms of *H. pylori* originated from the same strain F49 were inoculated intragastrically into BALB/c mice respectively four times at a 3-day interval. Half of the mice from each group were sacrificed at Day 21 and Day 28 after the last inoculation. Histology and *H. pylori* colonization were detected by urease test of gastric mucosa, cultures of *H. pylori*, and electron microscopy and so on.

RESULTS: The urease activity and the ability of adherence to Hep-2 cells were found to be lower in coccoid *H. pylori* than that in its spiral form. For example, the transformation in strain F₄₄ led to a significant decrease of the adherence rate and adherence index from 70.0±5.3 % to 30.2±3.5 % ($P<0.01$), and from 2.6±0.4 to 0.86±0.3 ($P<0.01$), respectively. The flagella of coccoid *H. pylori* were observed under electron microscope. In the experimental infection in mice, the positive rate of gastric mucosa urease test was 93.8 % (15/16) in the group infected by spiral *H. pylori* and 50 % (8/16) in the group infected by coccoid *H. pylori*, and the estimated coccoid *H. pylori* colony number was 1.75 vs 0.56. The positive rates of *H. pylori* culture were 87.5 % (14/16) in spiral *H. pylori* group and 68.8 % (11/16) in coccoid *H. pylori* group. There was no significant difference in either urease test or bacterial culture rate between the groups examined at Day 21 and Day 28 after inoculation.

Electron microscopic examination of the samples taken from both groups showed the adherence of *H. pylori* in spiral, bacillary and coccoid shapes to the epithelial cells of gastric wall. Histological examination showed the occurrence of gastric mucosal injury as indicated by various degrees of erosion, ulcer, and inflammatory cell infiltration. Mucosal injury was slighter in the mice infected by coccoid *H. pylori*. No positive result was obtained in the control group that received intragastrical administration of sterile tap water.

CONCLUSION: Although the virulence of coccoid *H. pylori* induced by water decrease, coccoid *H. pylori* still remains a considerable urease activity and the adhering ability to epithelial cells. Furthermore, the flagella, an important component responsible for bacterial movement and infection, were still observed as a cellular structure of coccoid *H. pylori* under electron microscope. The coccoid *H. pylori* induced by water is capable of colonizing in gastric mucosa and causing gastritis in mice.

She FF, Lin JY, Liu JY, Huang C, Su DH. Virulence of water-induced coccoid *Helicobacter pylori* and its experimental infection in mice. *World J Gastroenterol* 2003; 9(3): 516-520 <http://www.wjgnet.com/1007-9327/9/516.htm>

INTRODUCTION

Helicobacter pylori has been recognized as an important pathogen that causes chronic gastritis and peptic ulcer and likely as a risk factor associated with gastric carcinoma^[1-9]. *H. pylori* infection is endemic. In despite of more than 10 years of intensive research, the precise mode and route of *H. pylori* transmission remain elusive. Four routes including fecal-oral, oral-oral, gastro-oral and iatrogenic transmission have been postulated^[10-13]. The association between water consumption and *H. pylori* infection indicates that *H. pylori* may be transmitted through a waterborne route^[14-16]. *H. pylori* exists in two forms: the spiral form and the coccoid form. Coccoid *H. pylori* is non-culturable but alive^[17-20]. Some researches have shown that *H. pylori* can survive water microcosms in coccoid form^[20,21]. The coccoid *H. pylori* in water has therefore been suspected to contribute an important part to the transmission of the bacteria. However, the virulence and infectivity of coccoid *H. pylori* in water has not been studied. To explore the pathogenicity of the coccoid *H. pylori* in water, three strains of spiral *H. pylori* were treated by prolonged exposure to sterile tap water and examined for the presence of flagella under electron microscopy and tested for their urease activity and their adherence to Hep-2 cells. A strain was inoculated into the BALB/c mice. The gastric mucosal samples were taken to assess the bacterial *in vivo* colonization and pathological effects by means of urease test, bacterial culture, electron microscopy, and light microscopy.

MATERIALS AND METHODS

Animals

Female BALB/c mice were purchased from Shanghai

Experimental Animal Center, Chinese Academy of Sciences and raised under SPF conditions. Those of 8 weeks old, weighing 20-22 g were used for bacterial inoculation. Sterile food and tap water were given ad libitum.

Cells

Human epithelial cell line Hep-2 cells were maintained in 1 640 medium supplemented with 10 % fetal calf serum, 200 IU/ml penicillin and 50 µg/ml streptomycin at 37 °C in 5 % CO₂-95 % air, and re-cultivated twice a week.

Bacterial strains

Three strains (F44, F45 and F49) of *H.pylori* were isolated in this laboratory from gastric biopsy specimens of confirmed peptic ulcer patients. The isolates were spiral in shape, positive for catalase, oxidase, urease, and *cagA* and *vacA* gene. Stock cultures were maintained in defatted milk at -80 °C.

H. pylori cultivation and coccoid form induction

The stored strains of *H.pylori* were cultured on Brucella agar with 5 % sheep blood at 37 °C for 2-3 d under microaerophilic conditions (5 % O₂; 10 % CO₂; 85 % N₂). After being subcultured, the bacteria were harvested and suspended in sterile tap water and the suspensions were incubated at 4 °C for a few days (about 3-4 d) until 100 % transformation to coccoid form was achieved and confirmed under light microscopy. The transformed bacteria were inoculated on the Brucella agar media supplemented with 5 % sheep blood for reversion trial culture. The stock suspensions were stored at 4 °C until use.

Electron microscopy

H. pylori flagella were examined under A Hu-12A transmission electron microscope. To prepare the bacterial samples, *H. pylori* suspensions were centrifuged, and the pellets were embedded in Epoxy 618. The ultra-thin sections were cut and negatively stained by 1 % phosphotungstic acid.

Assessment of cell adherence

Hep-2 cells were grown to confluence on glass coverslips in culture flask, and 0.5 ml of the suspension of *H.pylori* (10⁸ cfu/ml) was added to culture medium (5 ml) for an additional 3.5 h culture at 37 °C in 5 % CO₂-95 % air. Cultures on the coverslips were washed and stained with Wright-Giemsa. One hundred Hep-2 cells were examined under light microscope for the counts of both the cells adhered by bacteria and the bacteria adhering to each cell. The adherence rate and adherence index were then calculated by the formula (described in the Results).

Animal infection experiment

Forty-two BALB/c mice were randomly divided into 3 groups. By oral gavage, groups 1 and 2 (16 mice each) were given 0.4 ml (10⁹ cfu/ml) of suspensions of F49 strain spiral *H.pylori* and coccoid *H.pylori* (in water for 40 days), respectively, four times at a 3-day interval. The control group (10 mice) received 0.4 ml sterile tap water. At Day 21 and 28 after inoculation, half of the mice from each group were sacrificed, respectively. Before killing, the mice were fasted for 36 hours with free access to water. At sacrifice, stomachs were removed, opened and washed with sterile saline and longitudinally divided into 3 sections in same size, which were used respectively for fast urease test and bacterial culture, electron microscopy, and histological examination.

Urease activity assay

Urease activity fast assay kit was purchased from Sanqiang

Company (Sanming, Fujian). The assays were made according to the manufacturer's instructions. Diluted *H. pylori* cultures (10¹⁰ cfu/ml, 5 µ), or tissue fragments (3×3 mm) obtained from the pylorus part of one-third of the mouse gastric mucosa were added to the test wells to react with the commercial reagents. To evaluate the urease activity, the colors developed in the assay were scored into five grades (++++, +++, ++, + and -) for bacterial cultures and four grades (+++, ++, + and -) for tissue fragments.

Bacterial examination

After collected for urease assay, the remaining one-third gastric mucosa samples were grounded into homogenate, daubed on Brucella agar with 5 % sheep blood, and incubated at 37 °C for 3-4 d under microaerophilic conditions. Colonies were taken and identified under light microscopy, urease activity test and *cagA* gene amplification by PCR. In addition, two samples from groups 1 and 2 respectively, which were bacteriologic positive and trimmed to 1 mm³, were embedded in Epoxy 618, then the ultra-thin sections were cut, stained by uranyl acetate and lead citrate and examined under a Hu-12A transmission electron microscope.

Light microscopic histological examination

The gastric mucosal samples were embedded in paraffin, cut in 5 µm sections, stained with hematoxylin-eosin, and examined under light microscope.

Statistical analysis

Data was analyzed using the Student *t* test. The statistically significant difference was suggested by a value of *P*<0.05, and the very significant difference by *P*<0.01.

RESULTS

In vitro virulence of water-induced coccoid *H.pylori*

Flagella Three strains (F44, F45 and F49) of *H.pylori* were seen under light microscope in a typical spiral shape before their exposure to water. After 3-4 d incubation in sterile tap water at 4 °C, no spiral but only coccoid shaped bacteria were observed. Reversion trial showed that water-induced coccoid *H. pylori* failed to grow on Brucella agar supplemented with 5 % sheep blood. Electron microscopy showed that the flagella remained a part of the bacterial cell structure (Figure 1).

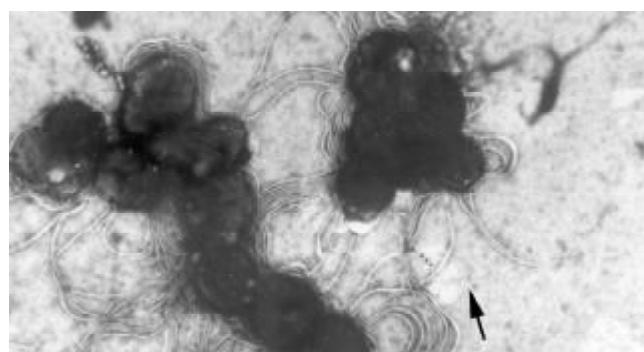


Figure 1 The flagella of coccoid *H.pylori* under transmission electron microscope ×6 000.

Urease activity Table 1 shows the urease activity assayed for three strains (F44, F45 and F49) of *H.pylori* both in spiral form (normal culture) and the respective coccoid form (subjected to water treatment). Strong urease activity (++++) was confirmed in the spiral *H. pylori* of all the three strains tested. The urease activity of the water-induced *H. pylori*, i.e., the

cocoid form of these three strains, significantly reduced, but still existed on a detective level (+ to ++).

Table 1 Urease activity of *H. pylori*

Strain	Urease activity	
	Spiral form	Cocoid form
F44	++++	+
F45	++++	++
F49	++++	+

Adhering ability All the three strains of *H. pylori* in both spiral form and water-induced cocoid form were tested for their adhering ability to Hep-2 cells. According to the following formula, the rate and the index of adherence were calculated. The rate of adherence=the amount of cell adherenced by bacteria/100×100 %;

The index of adherence=the amount of bactria adhering to cells/100;

Five groups of each 100 Hep-2 cells were counted for the number of cells adhered by bacteria and the total number of bacteria adhering to the cells. The percentages of cells adhered by bacteria (adherence rate) and the average bacteria number (adherence index) adhered to each cell are presented in Table 2. The adherence was observed in all groups tested. Student *t* test showed a very significant difference between the spiral and cocoid forms of *H. pylori* in either adherence rate or adherence index.

Table 2 Adherence of *H.pylori* to Hep-2 cells

	Adherence rate (%) ^a			Adherence index ^b (Bacteria numbers per cell)		
	F44	F45	F49	F44	F45	F49
	Spiral form	70.0±5.3	73.0±5.1	72.6±4.5	2.6±0.4	3.1±0.5
Cocoid form	30.2±3.5	35.7±4.1	31.4±4.0	0.86±0.3	0.91±0.3	0.88±0.4
<i>t</i> value	12.3	11.2	12.8	7.2	7.8	7.4
<i>P</i>	<0.01	<0.01	<0.01	<0.01	<0.01	<0.01

^aAdherence rate=amount of cells adhered by bacteria/100×100 %; ^bAdherence index=total amount of bacteria adhering to 100 cells/100; Five groups of 100 cells on the same coverslip were counted for the bacteria adhered. Data are presented as mean ±SD. *t* and *P* values were obtained using Student *t* test.

Cocoid *H. pylori* infection in mice

Bacterial colonization *H.pylori* colonization in the gastric mucosa of inoculated mice was determined by the urease assay and bacterial culture of the of tissue samples. The bacterial cultures were found to be characteristic of spiral *H.pylori* as proved by the spiral shaped structure under light microscope, the positive urease activity, and the positive amplification of *cagA* gene fragments (data not shown). Data shown in Table 3 were the rates of positive findings in each group of mice. The positive rates of urease test of gastric mucosa, which was infected by spiral *H.pylori* and cocoid *H.pylori*, were 93.8 % (15/16) and 50 % (8/16), respectively. The positive rates of cultures of *H.pylori* were 87.5 % (14/16) and 68.8 % (11/16) respectively. Neither urease assay nor bacterial culture was found positive in the mice of the control group. Sampling at Day 21 and Day 28 after inoculation found almost no difference in both tests. In the semi-quantitative study, the color development in fast urease assay was scored. The colors distinguished at grades -, +, ++, and +++, which were associated with the existence of the *H. pylori* in 0, 1-10, 11-30, and >30 per microscope filed, respectively, according to the guide of

test kit, were accordingly assigned by 0, 1, 2, and 3 point(s). Table 4 presents the number of mice scored at the same points in this assay and the average points of each group. Again, the score in group 1 was much higher than in group 2 (1.75 vs 0.56), while the score in control group was zero. In addition, electron microscopy showed the adherence of bacteria to the gastric mucosal samples taken from both group 1 and group 2 (Figure 2A and B). These bacteria were in spiral, bacillary or cocoid shapes, and some of them had invaded into the gastric epithelial cells. No similar bacterium adherence and invasion was observed in the samples from control group.

Table 3 Tests of bacteria in gastric mucosa samples

Group	Total no.	Fast urease test			Culture of bacterial		
		Positive/total		Positive rate(%)	Positive/total		Positive rate(%)
		D21	D28		D21	D28	
1	16	7/8	8/8	93.8	7/8	7/8	87.5
2	16	4/8	4/8	50.0	5/8	6/8	68.8
Control	10	0/5	0/5	0	0/5	0/5	0

Group 1 was inoculated with spiral *H. pylori*, group 2 was inoculated with water-induced cocoid *H. pylori*, and control group received sterile tap water.

Table 4 Scores for urease tests of tissue samples

Groups	Color development				Urease activity (mean score)
	-	+	++	+++	
1	1 ^a	5	7	3	1.75 ^b
2	8	7	1	0	0.56
Control	10	0	0	0	0

^aNumbers of mice; ^bRefers to text for scoring and calculation.

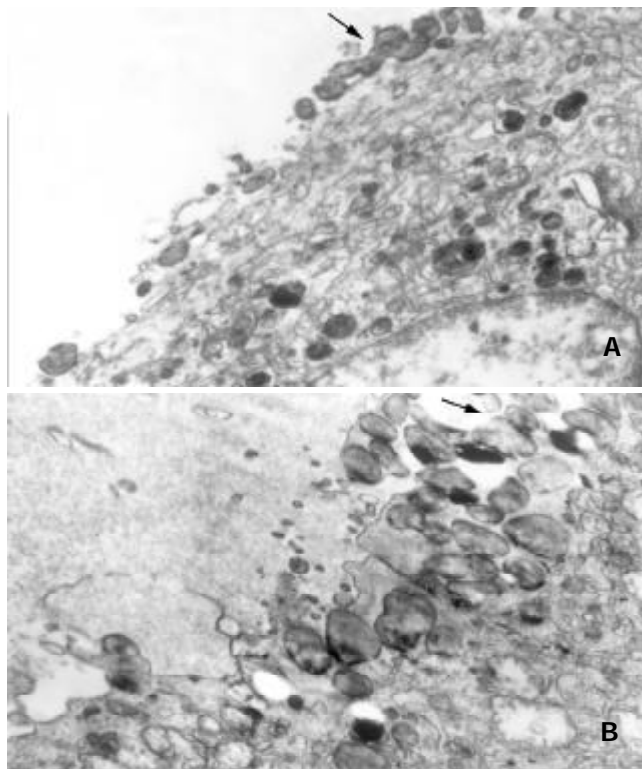


Figure 2 *H.pylori* colonization in mouse stomach under transmission electron microscope. A. infection of spiral *Hp.* ×7 000; B. infection of cocoid *Hp.* ×9 000.

Histopathological alteration Inflammatory pathological features were observed in both group 1 and group 2 samples under light microscope (Table 5 and Figure 3). Fifteen mice of group 1 and ten mice of group 2 developed inflammatory cell infiltration and different degrees of erosion or ulcer. The frequency and intensity of the erosion in group 1 was higher than in group 2. Two out of sixteen mice in group 1 even developed mucosal ulcers. Mucosal injury was slighter in the mice infected by coccoid *H.pylori*. None of these features was found in the control group.

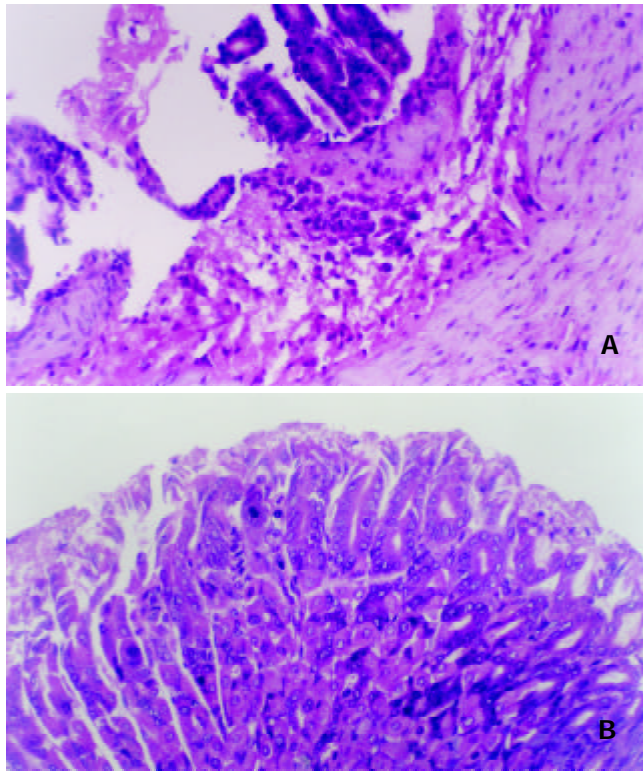


Figure 3 Light microscopy for gastric mucosa of mice. H&E×200. A. infection of spiral *Hp*; B. infection of coccoid *Hp*.

Table 5 Pathological alterations of gastric mucosa from mice

Group	Histopathological event (no. of mice)				Total
	Normal	Gentle erosion	Deep erosion	Ulcer	
1	1	7	6	2	16
2	6	9	1	0	16
Control	10	0	0	0	10

DISCUSSION

Increasing reports showed that *H. pylori* had been detected from water by immunomagnetic separation, bacterial culture or polymerase chain reaction (PCR) technique^[22-27] and that consumption of water was closely related to *H.pylori* infection^[14-16]. Water borne route is therefore thought to be an important route of *H. pylori* transmission. *H.pylori* has been found to be able to convert from spiral form to coccoid form under certain adverse circumstances such as increased oxygen tension, extended incubation and exposure to antibiotics or water^[17,28-32]. Some researches suggested that *H. pylori* in coccoid form can survive the water for a long time. However, it remains unknown whether coccoid *H. pylori* can attack and colonize in stomach., resulting in the diseases of digestive system. Going deep inside to the behavior of coccoid *H. pylori*

will thus be very beneficial to our understandings on the transmission of *H. pylori* infection and its association with many severe human diseases like gastritis, ulcer and peptic carcinomas.

The putative pathogenic determinants of *H.pylori* have been divided into two major groups^[35]: maintenance factors, which allow the bacterium to colonize and remain within the host, and virulence factors, which contribute to the pathogenetic effects of the bacterium. Flagella, urease activity and adherence to epithelial cells of *H.pylori* are important maintenance factors^[34-37]. If coccoid *H.pylori* in water remains infective, they must possess maintenance factors in order to colonize and remain in stomach. In this study, it is shown that both urease activity and adherence to Hep-2 cells of coccoid *H. pylori* decreased as compared with the spiral forms, suggesting a reduction of virulence related to colonization of *H.pylori* when the transformation to coccoid form occurs. However, as shown by the microbial assays, coccoid *H.pylori* induced by water still remains a considerable urease activity and the adhering ability to epithelial cells. Furthermore, the flagella, an important component responsible for bacterial movement and infection, were still observed as a cellular structure of coccoid *H.pylori* under electron microscope. This adds to the potential of *in vivo* infection of the coccoid *H.pylori* induced by water.

In the animal experiments described here, some mice (10/16) inoculated with water-induced coccoid *H.pylori* developed significant pathological changes such as mucosal erosion and inflammatory cell infiltration in gastrical mucosa, as were shown by histopathological examinations. The evidences of the coccoid *H.pylori* being the pathogen of the mucosal injury were further provided by bacteriological examinations. In this aspect, a 50 % positive rate and a considerable intensity of urease test were detected in the mucosal samples of mice inoculated with water-induced coccoid *H.pylori*, and the positive *H.pylori* cultures of these samples reached a percentage of 68.8 %. In addition, electron microscopy for these samples showed the presence of spiral bacteria in gastric mucosa. All these findings reveal the ability of water-induced coccoid *H. pylori* in their colonization on mouse gastric wall and their injury to the mucosal tissues.

It might be reasonably queried whether there still exists an undetectable trace amount of spiral *H.pylori* among the huge quantity of their coccoid variance, which could be intrinsically responsible for the virulence and infectivity of the bacteria in some studies including ours. The facts that the bacteria were kept in in-nutritious water for up to 40 days and that the water-treated bacteria were assayed for *in vitro* virulence in real time, eliminated the possibility of an expansion of the spiral population or in-water reversion of the coccoid variance to its spiral origins. The failure of the trial reversion in supplemented Brucella medium further supported the concept of a direct virulence of the coccoid *H. pylori*. Now that the spiral shaped bacteria were observed in the mucosal tissues of mice inoculated with coccoid *H. pylori*, it seemed that the reversion took place *in vivo*. However, whether the reversion is a key precondition for the infection remains unclear. In despite of our ignorance in the process and mechanisms of the inter-transformation of *H.pylori*, conclusions can be drawn from our current study that water-induced coccoid form of *H.pylori* remains virulent and infective to gastric wall in mice. Water borne route transmission of *H.pylori* needs more attention.

REFERENCES

- 1 Gao GL, Pan BR, Yang SF, SongG, Xu XQ, Liu Y. The value of *Helicobacter pylori* in gastro-duodenal diseases. *Xin Xiaohuabingxue Zazhi* 1994; 2: 232-233

- 2 **Li ZX**, Zhang WD, Zhou DY, Zhang YL, Guo XP, Yang HT. Relationship between *Helicobacter pylori* and duodenal ulcer. *Xin Xiaohuabingxue Zazhi* 1996; **4**: 153-155
- 3 **Liu WZ**, Zheng X, Shi Y, Dong QJ, Xiao SD. Effect of *Helicobacter pylori* infection on gastric epithelial proliferation in progression from normal mucosa to gastric carcinoma. *World J Gastroenterol* 1998; **4**: 246-248
- 4 **Blaser MJ**, Perez-Perez GI, Kleanthous H, Cover TL, Peek RM, Chyou PH, Stemmermann GN, Nomura A. Infection with *Helicobacter pylori* strains possessing cagA is associated with an increased risk of developing adenocarcinoma of the stomach. *Cancer* 1995; **55**: 2111-2115
- 5 **Lu XL**, Qian KD, Tang XQ, Zhu YL, Du Q. Detection of *H.pylori* DNA in gastric epithelial cells by in situ hybridization. *World J Gastroenterol* 2002; **8**: 305-307
- 6 **Liu WZ**, Zheng X, Shi Y, Dong QJ, Xiao SD. Effect of *Helicobacter pylori* infection on gastric epithelial proliferation in progression from normal mucosa to gastric carcinoma. *World J Gastroenterol* 1998; **4**: 246-248
- 7 **Wang RT**, Wang T, Chen K, Wang JY, Zhang JP, Lin SR, Zhu YM, Zhang WM, Cao YX, Zhu CW, Yu H, Cong YJ, Zheng S, Wu BQ. *Helicobacter pylori* infection and gastric cancer: evidence from a retrospective cohort study and nested case-control study in China. *World J Gastroenterol* 2002; **8**: 1103-1107
- 8 **Xue FB**, Xu YY, Wan Y, Pan BR, Ren J, Fan DM. Association of *H. pylori* infection with gastric carcinoma: a Meta analysis. *World J Gastroenterol* 2001; **7**: 801-804
- 9 **Cai L**, Yu SZ, Zhang ZF. *Helicobacter pylori* infection and risk of gastric cancer in Changde County, Fujian Province, China. *World J Gastroenterol* 2000; **6**: 374-376
- 10 **Song Q**, Spahr A, Schmid RM, Adler G, Bode G. *Helicobacter pylori* in the oral cavity: high prevalence and great DNA diversity. *Dig Dis Sci* 2000; **45**: 2162-2167
- 11 **Yoshimatsu T**, Shirai M, Nagata K, Okita K, Nakazawa T. Transmission of *Helicobacter pylori* from challenged to nonchallenged nude mice kept in a single cage. *Dig Dis Sci*, 2000; **45**: 1747-1753
- 12 **Leung WK**, Siu KL, Kwok CK, Chan SY, Sung R, Sung JJ. Isolation of *Helicobacter pylori* from vomitus in children and its implication in gastro-oral transmission. *Am J Gastroenterol* 1999; **94**: 2881-2884
- 13 **Liu WZ**, Xiao SD, Jiang SJ, Li RR, Pang ZJ. Seroprevalence of *Helicobacter pylori* infection in medical staff in Shanghai. *Scand J Gastroenterol* 1996; **31**: 749-752
- 14 **Baker KH**, Hegarty JP. Presence of *Helicobacter pylori* in drinking water is associated with clinical infection. *Scand J Infect Dis* 2001; **33**: 744-746
- 15 **Klein PD**, Graham DY, Gaillour A, Opekun AR, Smith EO. Water source as risk factor for *H.pylori* infection in Peruvian children. *Lancet* 1991; **337**: 1503-1506
- 16 **Bunn JE**, MacKay WG, Thomas JE, Reid DC, Weaver LT. Detection of *Helicobacter pylori* DNA in drinking water biofilms: implications for transmission in early life. *Lett Appl Microbiol* 2002; **34**: 450-454
- 17 **Bode G**, Mauch F, Malfertheiner P. The coccoid forms of *Helicobacter pylori*. Criteria for their viability. *Epidemiol Infect* 1993; **111**: 483-490
- 18 **Cellini L**, Allocati N, Di Campli E, Dainelli B. *Helicobacter pylori*: A fickle germ. *Microbiol Immunol* 1994; **38**: 25-30
- 19 **Benaissa M**, Babin P, Quellard N, Pezennec L, Cenatiempo Y, Fauchere JL. Changes in *Helicobacter pylori* ultrastructure and antigens during conversion from the bacillary to the coccoid form. *Infect Immun* 1996; **64**: 2331-2335
- 20 **Shahamat M**, Mai U, Paszko-Kolva C, Kessel M, Colwell RR. Use of autoradiography to assess viability of *Helicobacter pylori* in water. *Appl Environ Microbiol* 1993; **59**: 1231-1235
- 21 **Mizoguchi H**, Fujioka T, Nasu M. Evidence for viability of coccoid forms of *Helicobacter pylori*. *J Gastroenterol* 1999; **34** (Suppl 11): 32-36
- 22 **Winiiecka-Krusnell J**, Wreiber K, von Euler A, Engstrand L, Linder E. Free-living amoebae promote growth and survival of *Helicobacter pylori*. *Scand J Infect Dis* 2002; **34**: 253-256
- 23 **Lu Y**, Redlinger TE, Avitia R, Galindo A, Goodman K. Isolation and genotyping of *Helicobacter pylori* from untreated municipal wastewater. *Appl Environ Microbiol* 2002; **68**: 1436-1439
- 24 **Mazari-Hiriart M**, Lopez-Vidal Y, Castillo-Rojas G, Ponce de Leon S, Cravioto A. *Helicobacter pylori* and other enteric bacteria in freshwater environments in Mexico City. *Arch Med Res* 2001; **32**: 458-467
- 25 **Horiuchi T**, Ohkusa T, Watanabe M, Kobayashi D, Miwa H, Eishi Y. *Helicobacter pylori* DNA in drinking water in Japan. *Microbiol Immunol* 2001; **45**: 515-519
- 26 **Mazari-Hiriart M**, Lopez-Vidal Y, Calva JJ. *Helicobacter pylori* in water systems for human use in Mexico City. *Water Sci Technol* 2001; **43**: 93-98
- 27 **Hegarty JP**, Dowd MT, Baker KH. Occurrence of *Helicobacter pylori* in surface water in the United States. *J Appl Microbiol* 1999; **87**: 697-701
- 28 **Catrenich CE**, Makin KM. Characterization of the morphologic conversion of *Helicobacter pylori* from bacillary to coccoid forms. *Scand J Gastroenterol* 1991; **181** (Suppl): 58-64
- 29 **Cellini L**, Allocati N, Angelucci D, Iezzi T, Di Campli E, Marzio L, Dainelli B. Coccoid *Helicobacter pylori* not culturable *in vitro* reverts in mice. *Microbiol Immunol* 1994; **38**: 843-850
- 30 **Costa K**, Bacher G, Allmaier G, Dominguez-Bello MG, Engstrand L, Falk P, de Pedro MA, Garcia-del Portillo F. The morphological transition of *Helicobacter pylori* cells from spiral to coccoid is preceded by a substantial modification of the cell wall. *J Bacteriol* 1999; **181**: 3710-3715
- 31 **Xu ZM**, Zhou DY, Pan LJ, Song S. Transformation and reversion of *Helicobacter pylori* *in vitro*. *Shijie Huaren Xiaohua Zazhi* 1999; **7**: 215-217
- 32 **Shirai M**, Kakada J, Shibata K, Morshed MG, Matsushita T, Nakazawa T. Accumulation of polyphosphate granules in *Helicobacter pylori* cell under anaerobic conditions. *J Med Microbiol* 2000; **49**: 513-519
- 33 **Dunn BE**, Cohen H, Blaser MJ. *Helicobacter pylori*. *Clin Microbiol Rev* 1997; **10**: 720-741
- 34 **Eaton KA**, Brooks CL, Morgan DR, Krakowka S. Essential role of urease in pathogenesis of gastritis induced by *Helicobacter pylori* in gnotobiotic piglets. *Infect Immun* 1991; **59**: 2470-2475
- 35 **Smoot DT**, Mobley HL, Chippendale GR, Lewison JF, Resau JH. *Helicobacter pylori* urease activity is toxic to human gastric epithelial cells. *Infect Immun* 1990; **58**: 1992-1994
- 36 **Boren T**, Falk P, Roth KA, Larson G, Normark S. Attachment of *Helicobacter pylori* to human gastric epithelium mediated by blood group antigens. *Science* 1993; **262**: 1892-1895
- 37 **Ottmann KM**, Lowenthal AC. *Helicobacter pylori* uses motility for initial colonization and to attain robust infection. *Infect Immun* 2002; **70**: 1984-1990

Overexpression of *c-fos* in *Helicobacter pylori*-induced gastric precancerosis of Mongolian gerbil

Yong-Li Yang, Bo Xu, Yu-Gang Song, Wan-Dai Zhang

Yong-Li Yang, Yu-Gang Song, Wan-Dai Zhang, Institute of Gastrointestinal Diseases, Nanfang Hospital, First Military Medical University, Guangzhou 510515, Guangdong Province, China

Bo Xu, Department of Orthopedics, Nanfang Hospital, First Military Medical University, Guangzhou 510515, Guangdong Province, China

Correspondence to: Dr. Yong-Li Yao, Institute of Gastrointestinal Diseases, Nanfang Hospital, First Military Medical University, Guangzhou 510515, Guangdong Province, China. xbyyl@fimmu.edu.cn

Telephone: +86-20-85141547 **Fax:** +86-20-87208770

Received: 2001-09-26 **Accepted:** 2001-11-06

Abstract

AIM: To explore dysregulation of *c-fos* in several human malignancies, and to further investigate the role of *c-fos* in *Helicobacter pylori* (*H. pylori*)-induced gastric precancerosis.

METHODS: Four-week-old male Mongolian gerbils were employed in the study. 0.5 mL 1×10^8 cfu \cdot L⁻¹ suspension of *H. pylori* NCTC 11 637 in Brucella broth were inoculated orally into 20 Mongolian gerbils. Another 20 gerbils were inoculated with Brucella broth as controls. 10 of the infected gerbils and 10 of the non-infected control gerbils were sacrificed at 25 and 45 weeks after infection. The stomach of each gerbil was removed and opened for macroscopic observation. The expression of *c-fos* was analyzed by RT-PCR and immunohistochemical studies in *H. pylori*-induced gastric precancerosis of Mongolian gerbil. Half of each gastric antrum mucosa was dissected for RNA isolation and RT-PCR. β -actin was used as the housekeeping gene and amplified with *c-fos* as contrast. PCR products of *c-fos* were analyzed by gel image system and the level of *c-fos* was reflected with the ratio of *c-fos*/ β -actin. The immunostaining for *c-fos* was conducted using monoclonal antibody of *c-fos* and the StreptAvidin-Biotin-enzyme Complex kit.

RESULTS: *H. pylori* was constantly found in all infected animals in this study. After infection of *H. Pylori* for 25 weeks, ulcers were observed in the antral and the body of stomach of 60 % infected animals (6/10). Histological examination showed that all animals developed severe inflammation, especially in the area close to ulcers, and multifocal lymphoid follicles appeared in the lamina propria and submucosa. After infection of *H. Pylori* for 45 weeks, severe atrophic gastritis in all infected animals, intestinal metaplasia in 80 % infected animals (8/10) and dysplasia in 60 % infected animals (6/10) could be observed. *C-fos* mRNA levels were significantly higher after infection of *H. pylori* for 25 weeks (1.84 ± 0.79), and for 45 weeks (1.59 ± 0.37) than those in control-animals (0.74 ± 0.22 , $P < 0.01$). *C-fos* mRNA levels were increased 2.5-fold by 25th week ($P < 0.01$) and 2.1-fold by 45th week ($P < 0.01$) in precancerosis induced by *H. pylori*, when compared with normal gastric epithelium of Mongolian gerbil. Immunohistochemical staining revealed exclusive nuclear staining of *c-fos*. Furthermore, there was a sequential increase in *c-fos* positive cells from normal epithelium to precancerosis.

CONCLUSION: The study suggested that overexpression of *c-fos* occurs relatively early in gastric tumorigenesis in this precancerosis model induced by *H. pylori*.

Yang YL, Xu B, Song YG, Zhang WD. Overexpression of *c-fos* in *Helicobacter pylori*-induced gastric precancerosis of Mongolian gerbil. *World J Gastroenterol* 2003; 9(3): 521-524
<http://www.wjgnet.com/1007-9327/9/521.htm>

INTRODUCTION

H. pylori, a gram-negative spiral bacterium first isolated in 1982 from a patient with chronic active gastritis, is responsible for a large portion of chronic gastritis and nearly all duodenal ulcers, most gastric ulcers, and probably an increased risk of gastric adenocarcinoma^[1-9]. More than 50 % of the adult population are infected with *H. pylori* in developing countries as well as in developed countries. Gastric cancer is a major health problem^[10] and remains the second most common cancer in the world^[11]. Although epidemiological studies have indicated that *H. pylori* infection plays a crucial role in human gastric carcinogenesis^[12-25], there is no direct proof that *H. pylori* is actually associated with gastric carcinogenesis^[26]. The purpose of this study was to elucidate the relationship between *H. pylori* infection and gastric carcinogenesis by using an animal model of long-term *H. pylori* infection, and to explore the role played by *c-fos* in gastric tumorigenesis.

MATERIALS AND METHODS

Animals treatment

Four-week-old specific pathogen-free male Mongolian gerbils weighing 20 ± 5 g were employed in this study. They were housed in individual metabolic cages in a temperature conditioned room 23 ± 2 °C with a 12 h light-dark cycle, allowed to access to standard rat chow (provided by Experimental Animal Center, First Military Medical University) and water ad libitum, and acclimatized to the surrounding for 7 days prior to the experiments. *H. pylori* (NCTC 11 637) was obtained from American Type Culture Collection and cultured on Brucella agar plates containing 70 mL \cdot L⁻¹ goat blood in a microaerobic condition (volume fraction, N₂: 85 %, O₂: 5 %, CO₂: 10 %, in aerobic globe box) at 37 °C for 3 days. The strain was identified by morphology, Gram's stain, urease production and so on.

Experimental protocol

0.5 mL 1×10^8 cfu \cdot L⁻¹ suspension of *H. pylori* NCTC 11 637 in Brucella broth were inoculated orally into 20 Mongolian gerbils for 14 days continuously which had been fasted overnight. Another 20 gerbils were inoculated with Brucella broth as controls. 10 of the infected gerbils and 10 of the non-infected control gerbils were sacrificed after infection for 25 and 45 weeks, respectively. The stomach of each animal was removed and opened for macroscopic observation. Half of each gastric antrum mucosa were dissected for RNA isolation. The rest of the stomach samples were used for histological examination,

which were fixed with neutral-buffered 100 mL · L⁻¹ formalin and processed by standard methods that embedded in paraffin, sectioned and stained with haematoxylin for analyzing histological changes. Giemsa stain for detecting for *H. pylori* and Alcian blue (AB)/PAS stain for examining intestinal metaplasia.

RNA isolation and RT-PCR analysis

Using Tripure isolation reagent (Boehringer Mannheim, Germany), total cellular RNA was isolated from previously frozen tissues according to the manufacturer's instruction. All RNA samples were analyzed for integrity of 18s and 28s rRNA by ethidium bromide staining of 0.5 µg RNA resolved by electrophoresis on 12 g · L⁻¹ agarose-formaldehyde gels. RT-PCR analysis was performed as follows. RNA was incubated at 60 °C for 10 min and chilled to 4 °C immediately before being reverse transcribed. 1 µg of total RNA was reversely transcribed using antisense primers in a volume of 20 µl for 40 min at 50 °C, containing 200 U MMLV reverse transcriptase, 1×buffer RT, 1 MU · L⁻¹ Rnasin, 0.5 mmol · L⁻¹ dNTPs of dATP, dGTP, dCTP and dTTP and each antisense primers including *c-fos* and β -actin at 0.2 µmol · L⁻¹. The samples were heated to 99 °C for 5 min to terminate the reverse transcription reaction. By using a Perkin-Elmer DNA Thermocycler 4 800 (Perkin-Elmer, Norwalk, CT), 5 µl cDNA mixture obtained from the reverse transcription reaction was then amplified for *c-fos* and β -actin. β -actin was used as the housekeeping gene and amplified with *c-fos* as control. The amplification reaction mixture consisted of 10×buffer 5 µl, 0.2 mmol · L⁻¹ dNTPs of dATP, dGTP, dCTP and dTTP, 2.5 U Taq DNA polymerase, and sense and antisense primers at 0.2 µmol · L⁻¹ in a final volume of 50 µl. The reaction mixture was first heated at 94 °C for 2 min and amplification was carried out for 29 cycles at 94 °C for 0.5 min, 58 °C for 1 min, 70 °C for 1.5 min, followed by an incubation for 7 min at 70 °C. The amplification cycles was previously determined to keep amplification in the linear range to avoid the "plateau effect" associated with increased PCR cycles. The PCR primers were as following: *c-fos*, sense 5' -CAC GAC CAT GAT GTT CTC GG-3' and antisense 5' -AGT AGA TTG GCA ATC TCG GT-3'; β -actin, sense 5' -CCA AGG CCA ACC GCG AGA AGA TGA C-3' and antisense 5' -AGG GTA CAT GGT GGT GCC GCC AGA C-3'. PCR products of *c-fos* and β -actin had 348 bp and 587 bp, respectively. PCR products were run on a 15 g · L⁻¹ agarose gel in 0.5×TBE buffer and then analyzed by gel image analysis system. The level of *c-fos* was reflected with the ratio of *c-fos*/ β -actin.

Immunohistochemical staining

Four micrometers paraffin-embedded tissue sections were deparaffinized and rehydrated. Endogenous peroxidase activity was ablated with 10 mL · L⁻¹ hydrogen peroxide in methanol. The immunostaining for *c-fos* was conducted using the StreptAvidin-Biotin-enzyme Complex kit (Boster, Wuhan). Immunostaining by replacing primary antibody with PBS was also conducted as a negative control. The staining was evaluated semiquantitatively on the basis of the percentage of positive cells, and classified as follows^[27]: diffusely positive (+++) when positive cells accounted for more than 70 % of the total cells, partially positive (++) when positive cells were 35-70 %, partially positive (+) when positive cells accounted for 5-35 %, and negative (-) when positive cells accounted for less than 5 %.

Statistical analysis

Experimental results were analyzed with Chi-square Tests and K-Related Samples Test by SPSS software. Statistical significance was determined at $P < 0.05$.

RESULTS

Histopathological findings

H. pylori was detected in gastric antrum and gastric body of all infected animals in this study, and more in gastric antrum than that in gastric body. After infection of *H. Pylori* for 25 weeks, ulcers were observed in the gastric antrum and gastric body in 60 % infected animals (6/10). Histological examination showed that all infected animals developed severe inflammation, especially in the area close to ulcers; multifocal lymphoid follicles appeared in the lamina propria and submucosa; and there were mild atrophic gastritis in all infected animals. After infection of *H. Pylori* for 45 weeks, severe atrophic gastritis in all infected animals, intestinal metaplasia in 80 % infected animals (8/10) and dysplasia in 60 % infected animals (6/10) could be observed. Those metaplastic glands appeared more atypical than the surrounding nonmetaplastic and hyperplastic glands. Severe atrophic gastritis, intestinal metaplasia and dysplasia were gastric precancerosis. In the uninfected animals, there were no significant changes throughout the study.

Analysis of *c-fos* mRNA expression

There was *c-fos* mRNA expression in gastric antrum mucosa of control-animals. *C-fos* mRNA levels were significantly higher after infection of *H. pylori* for 25 weeks (1.84 ± 0.79), and for 45 weeks (1.59 ± 0.37) than that in control-animals (0.74 ± 0.22 , $P < 0.01$); *C-fos* mRNA levels were increased 2.5-fold in 25 weeks ($P < 0.01$) and 2.1-fold in 45 weeks ($P < 0.01$) in precancerosis induced by *H. pylori*, when compared with control gastric epithelium of Mongolian gerbil (Figure 1-4).

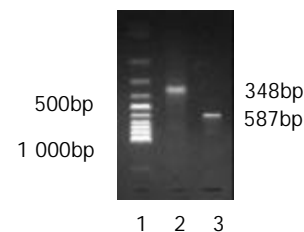


Figure 1 RT-PCR products. Lane 1 PCR marker; Lane 2 *c-fos*; Lane 3 β -actin.

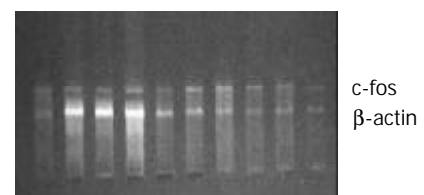


Figure 2 RT-PCR analysis of *c-fos* mRNA levels using β -actin as internal control. Total RNA was first reverse transcribed into cDNA and then amplified by PCR in control.

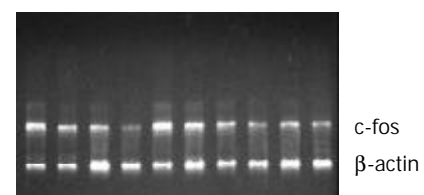


Figure 3 RT-PCR analysis of *c-fos* mRNA levels using β -actin as internal control after *H. pylori* infection for 25 weeks.

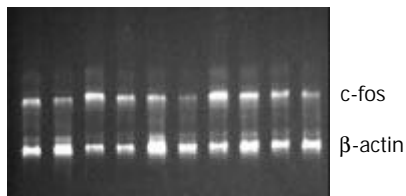


Figure 4 RT-PCR analysis of *c-fos* mRNA levels using β -actin as internal control after *H. pylori* infection for 45 weeks.

Immunohistochemical analysis of *c-fos* protein expression

Immunohistochemical analysis was performed to examine whether increased *c-fos* mRNA expression were accompanied by increased expression of *c-fos* protein. *C-fos* protein expression lied in nuclei (Figure 5). *C-fos* protein expression was evaluated significantly ($P < 0.01$) in precancerosis induced by *H. pylori* for 45 weeks, when compared with control gastric epithelium of Mongolian gerbil (Table 1).

Table 1 Expression of *c-fos* by Immunohistochemical staining

Group	n	c-fos				Positive/%
		-	+	++	+++	
Control	10	10	0	0	0	0
Inf 25 weeks	10	8	2	0	0	20
Time 45 weeks	10	6	4	0	0	40 ^a

^a $P < 0.01$, vs Control.

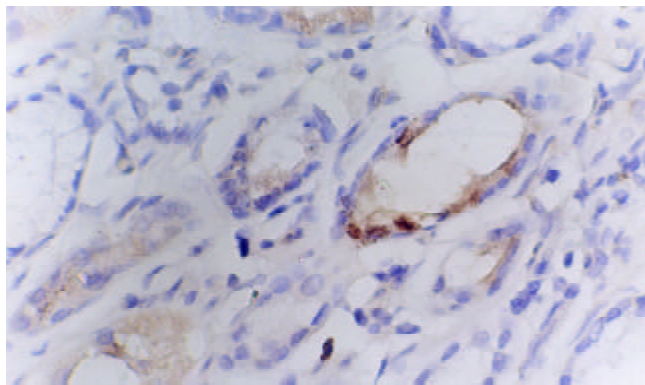


Figure 5 Expression of *c-fos* after *H. pylori* infection for 25 weeks, immunohistochemistry staining ($\times 400$).

DISCUSSION

H. pylori infection is now known as a major cause of acute and chronic active gastritis, peptic ulcer disease and atrophic gastritis and is also considered as a risk factor in the incidence of gastric adenocarcinoma and mucosa-associated lymphoma^[1-8]. Chronic colonization of the human stomach by the gram-negative spiral bacterium *H. pylori* is associated with the development of cancer in the distal portion of the stomach. Although there is no direct proof that *H. pylori* is actually associated with gastric carcinogenesis, epidemiological studies have indicated that *H. pylori* infection plays an important role in human gastric carcinogenesis. Because of this strong epidemiological association, *H. pylori* is classified as a definite carcinogen (group I) by the International Agency for Research on Cancer (IRAC), a branch of the World Health Organization (WHO). Many animals infected with human *H. pylori* have already been studied to determine the pathogenetic background, but none

of the models studied mimics human *H. pylori* infection and subsequent pathology. Recently, two experiments were conducted in Japan that demonstrated that chronic *H. pylori*-infection models of Mongolian gerbils would develop gastric carcinoma. These results will be extremely helpful to elucidate the mechanism of gastric carcinogenesis due to *H. pylori* infection^[9-26]. Apoptosis, a programmed cell death, was ignored, just like *H. pylori*, only to reappear recently. However, the number of current publications dealing with apoptosis of *H. pylori* has increased exponentially. Although gastric epithelial apoptosis is a programmed physiological event in the superficial aspect of the mucosa and is important for healthy cell turnover, *H. pylori* infection reportedly promotes such a cell death sequence^[27,28]. Because apoptosis regulates the cycle of cell turnover in balance with proliferation, dysregulation of apoptosis or proliferation evoked by *H. pylori* colonization would be linked to the gastric carcinogenesis^[29-31].

C-fos is an immediate early response gene, and *c-fos* protein is an important transcription-factor of nuclei^[32-39]. Oncogene *c-fos* is also a kind of effect protein of the karyomitosis signal, which can trigger and regulate the transcription of the genes related with proliferation. Besides, *c-fos* can also regulate its own gene expression with a positive feedback and promote the mitosis and proliferation of the cells. Because *c-fos* can regulate cell proliferation and cell apoptosis, its abnormal expression might induce cell turnover and carcinogenesis^[40-46]. Previous studies have showed that the expression of oncogene *c-fos* is closely related to cellular multiplication and differentiation. The amplification and over-expression of *c-fos* gene are associated with malignancy and tumorigenicity of cells. Recently, some studies suggested that oncogene *c-fos* was amplified in the primary tumor DNA^[47-49]. Shirin *et al* tested the hypothesis that *H. pylori* might inhibit cell growth and cell cycle progression by inhibiting signaling pathways that mediate the transactivation of the serum-response element in the *c-fos* promoter^[27].

In this study, mRNA level of *c-fos* was measured by quantitative RT-PCR analysis in Mongolian gerbil gastric antrum mucosa to explore dysregulation of *c-fos* in malignancies and to further investigate the role of *c-fos* in *H. pylori*-induced gastric precancerosis. In addition, the expression and localization of its protein product was analyzed by immunohistochemical staining. *C-fos* mRNA levels were significantly increased in precancerosis induced by *H. pylori*, when compared with normal gastric epithelium of Mongolian gerbil. Immunohistochemical staining revealed exclusive nuclear staining of *c-fos*. Furthermore, there was a sequential increase in *c-fos* positive cells from normal epithelium to precancerosis. This study indicates that the expression of *c-fos* mRNA and protein is increased from normal epithelium to precancerosis. The dysregulation of *c-fos* expression occurs relatively early in gastric tumorigenesis in this model and may participate in tumor progression. These findings suggest that *H. pylori*-induced gastric precancerosis is associated with dysregulation of gastric epithelial cell cycle. Further studies are needed to delineate the mechanism of those alterations.

REFERENCES

- 1 **Tabata H**, Fuchigami T, Kobayashi H, Sakai Y, Nakanshi M, Tomioka K, Nakamura S, Fujishima M. *Helicobacter pylori* and mucosal atrophy in patients with gastric cancer: a special study regarding the methods for detecting *Helicobacter pylori*. *Dig Dis Sci* 1999; **44**: 2027-2034
- 2 **Meining AG**, Bayerdorffer E, Stolte M. *Helicobacter pylori* gastritis of the gastric cancer phenotype in relatives of gastric carcinoma patients. *Eur J Gastroenterol Hepatol* 1999; **11**: 717-720
- 3 **Yamaoka Y**, Kodama T, Kashima K, Graham DY. Antibody against *Helicobacter pylori* Cag A and Vac A and the risk for gas-

- tric cancer. *J Clin Pathol* 1999; **52**: 215-218
- 4 **Danesh J**. *Helicobacter pylori* infection and gastric cancer: systematic review of the epidemiological studies. *Aliment Pharmacol Ther* 1999; **13**: 851-885
- 5 **Harris RA**, Owens DK, Witherell H, Parsonnet J. *Helicobacter pylori* and gastric cancer: what are the benefits of screening only for the Cag A phenotype of *H. pylori*? *Helicobacter* 1999; **4**: 69-76
- 6 **Hansen S**, Melby KK, Aase S, Jellum E, Vollset SE. *Helicobacter pylori* infection and risk of cardia cancer and non-cardia gastric cancer. A nested case-control study. *Scand J Gastroenterol* 1999; **34**: 353-360
- 7 **Scheiman JM**, Cutler AF. *Helicobacter pylori* and gastric cancer. *Am J Med* 1999; **106**: 222-226
- 8 **Kuipers EJ**. Review article: exploring the link between *Helicobacter pylori* and gastric cancer. *Aliment Pharmacol Ther* 1999; **13**: 3-11
- 9 **Alexander GA**, Arng MC. Association of *Helicobacter pylori* infection with gastric cancer. *Mil Med* 2000; **165**: 21-27
- 10 **Zhuang XQ**, Lin SR. Study on the relationship between *Helicobacter pylori* and gastric cancer. *Shijie Huaren Xiaohua Zazhi* 2000; **9**: 206-207
- 11 **Vandenplas Y**. *Helicobacter pylori* infection. *World J Gastroenterol* 2000; **6**: 20-31
- 12 **Pan KF**, Liu WD, Ma JL, Zhou T, Zhang L, Chang YS, You WC. Infection of *Helicobacter pylori* in children and mode of transmission in a high-risk area of gastric cancer. *Shijie Huaren Xiaohua Zazhi* 1998; **6**: 42-44
- 13 **Zhang L**, Jiang J, Pan KF, Liu WD, Ma JL, Zhou T, Perez GT, Blaser MJ, Chang YS, You WC. Infection of *Helicobacter pylori* with cag A strain in a high-risk area of gastric cancer. *Shijie Huaren Xiaohua Zazhi* 1998; **6**: 40-41
- 14 **Zhuang XQ**, Lin SR. Study on *Helicobacter pylori* infection in gastric cancer and precancerosis. *Shijie Huaren Xiaohua Zazhi* 2000; **8**: 710-711
- 15 **Hu PJ**. *Helicobacter pylori* and gastric cancer. *Shijie Huaren Xiaohua Zazhi* 1999; **7**: 1-2
- 16 **Huang XQ**. *Helicobacter pylori* infection and gastrointestinal hormones: a review. *World J Gastroenterol* 2000; **6**: 783-788
- 17 **Shang SH**, Zheng JW. Treatment on *Helicobacter pylori*-induced diseases. *Shijie Huaren Xiaohua Zazhi* 2000; **8**: 556-557
- 18 **Wang XH**, Zhang WD, Zhang YL, Zeng JZ, Sun Y. Relationship between *Hp* infection and oncogene and tumor suppressor gene expression in gastric cancer and precancerosis. *Shijie Huaren Xiaohua Zazhi* 1998; **6**: 516-518
- 19 **Ye GA**, Zhang WD, Liu LM, Shi L, Xu ZM, Chen Y, Zhou DY. *Hp vac A* gene and chronic gastritis. *Shijie Huaren Xiaohua Zazhi* 2001; **9**: 593-594
- 20 **Quan J**, Fan XG. Experimental studies on *Helicobacter pylori* and gastric cancer. *Shijie Huaren Xiaohua Zazhi* 1999; **7**: 1068-1069
- 21 **Lu SY**, Pan XZ, Peng XW, Shi ZL, Lin L, Chen MH. Effect of *Hp* infection on gastric epithelial cell kinetics in stomach diseases. *Shijie Huaren Xiaohua Zazhi* 2000; **8**: 386-388
- 22 **Xiao SD**. *Helicobacter pylori* and gastric cancer. *Shijie Huaren Xiaohua Zazhi* 1998; **6**: 4
- 23 **Harry XH**. Association between *Helicobacter pylori* and gastric cancer: current knowledge and future research. *World J Gastroenterol* 1998; **4**: 93-96
- 24 **Zu Y**, Shu J, Yang CM, Zhong ZF, Dai HY, Wang X, Qin GM. Study on *Helicobacter pylori* infection and risk of gastric cancer. *Shijie Huaren Xiaohua Zazhi* 1998; **6**: 367-368
- 25 **Cai L**, Yu SZ, Zhang ZF. *Helicobacter pylori* infection and risk of gastric cancer in Changle County, Fujian Province, China. *World J Gastroenterol* 2000; **6**: 374-376
- 26 **Shimizu M**, Nikaido T, Toki T, Shiozawa T, Fujii S. Clear cell carcinoma has an expression pattern of cell cycle regulatory molecules that is unique among ovarian adenocarcinomas. *Cancer* 1999; **85**: 669-677
- 27 **Shirin H**, Sordillo EM, Oh SH, Yamamoto H, Delohery T, Weinstein B, Moss SF. *Helicobacter pylori* inhibits the G1 to S transition in AGS gastric epithelial cell. *Cancer Res* 1999; **59**: 2277-2281
- 28 **Gao H**, Wang JY, Shen XZ, Liu JJ. Effect of *Helicobacter pylori* infection on gastric epithelial cell proliferation. *World J Gastroenterol* 2000; **6**: 442-444
- 29 **Hidekazu SU**, Hiromasa IS. Role of apoptosis in *Helicobacter pylori*-associated gastric mucosal injury. *J Gastroenterol Hepatol* 2000; **15**: D46-D54
- 30 **Zhuang XQ**, Lin SR. Research of *Helicobacter pylori* infection in precancerous gastric lesions. *World J Gastroenterol* 2000; **6**: 428-429
- 31 **Gu JZ**, Hou TW, Wang XX. Study on precancerous gastric lesions induced by *Helicobacter pylori*. *Shijie Huaren Xiaohua Zazhi* 2001; **9**: 111
- 32 **Tischmeyer W**, Grimm R. Activation of immediate early genes and memory formation. *Cell Mol Life Sci* 1999; **55**: 564-574
- 33 **Lennartsson J**, Blume Jensen P, Hermanson M, Ponten E, Carlberg M, Ronnstrand L. Phosphorylation of Shc by Src family kinases is necessary for stem cell factor receptor/c-kit mediated activation of the Ras/MAP kinase pathway and c-fos induction. *Oncogene* 1999; **18**: 5546-5553
- 34 **Trauth JA**, Seidler FJ, McCook EC, Slotkin TA. Persistent c-fos induction by nicotine in developing rat brain regions: interaction with hypoxia. *Pediatr Res* 1999; **45**: 38-45
- 35 **Duan R**, Porter W, Samudio I, Vyhidal C, Kladd M, Safe S. Transcriptional activation of c-fos protooncogene by 17beta-estradiol: mechanism of aryl hydrocarbon receptor-mediated inhibition. *Mol Endocrinol* 1999; **13**: 1511-1521
- 36 **Morrissey JJ**, Raney S, Heasley E, Rathinavelu P, Dauphinee M, Fallon JH. IRIDIUM exposure increase c-fos expression in the mouse brain only at levels which likely result in tissue heating. *Neuroscience* 1999; **92**: 1539-1546
- 37 **Hasebe T**, Imoto S, Sasaki S, Tsubono Y, Mukai K. Proliferative activity and tumor angiogenesis is closely correlated to stromal cellularity of fibroadenoma: proposal fibroadenoma, cellular variant. *Pathol Int* 1999; **49**: 435-443
- 38 **Whong WZ**, Gao HG, Zhou G, Ong T. Genetic alterations of cancer-related genes in glass fiber-induced transformed cells. *J Toxicol Environ Health* 1999; **56**: 397-404
- 39 **Chen W**, Dong Z, Valcic S, Timmermann BN, Bowden GT. Inhibition of ultraviolet B-induced c-fos gene expression and p38 mitogen-activated protein kinase activation by (-)-epigallocatechin gallate in a human keratinocyte cell line. *Mol Carcinog* 1999; **24**: 79-84
- 40 **Aigner A**, Juhl H, Malerczyk C, Tkybusch A, Benz CC, Czubyko F. Expression of a truncated 100 kDa HER2 splice variant acts as an endogenous inhibitor of tumor cell proliferation. *Oncogene* 2001; **20**: 2101-2111
- 41 **Mitsuno Y**, Yoshida H, Maeda S, Ogura K, Hirata Y, Kawabe T, Shiratori Y, Omata M. *Helicobacter pylori* induced transactivation of SRE and AP-1 through the ERK signaling pathway in gastric cancer cells. *Gut* 2001; **49**: 18-22
- 42 **He SW**, Shen KQ, He YJ, Xie B, Zhao YM. Regulatory effect and mechanism of gastrin and antagonists on colorectal carcinoma. *World J Gastroenterol* 1999; **5**: 408-416
- 43 **Yuan SL**, Huang RM, Wang XJ, Song Y, Huang GQ. Reversing effect of Tanshinone on malignant phenotypes of human hepatocarcinoma cell line. *World J Gastroenterol* 1998; **4**: 317-319
- 44 **YH**, Hu DR, Nie QH, Liu GD, Tan ZX. Study on activation and c-fos, c-jun expression of in vitro cultured human hepatic stellate cells. *Shijie Huaren Xiaohua Zazhi* 2000; **8**: 299-301
- 45 **Jiang LX**, Fu XB, Sun TZ, Yang YH, Gu XM. Relationship between oncogene c-jun activation and fibrobl. *Shijie Huaren Xiaohua Zazhi* 1999; **7**: 498-500
- 46 **Chen BW**, Wang HT, Liu ZX, Jia BQ, Ma QJ. Effect of exogenous EGF on proto-oncogene expression in experimental gastric ulcers. *Shijie Huaren Xiaohua Zazhi* 1999; **7**: 504-506
- 47 **Chai Y**, Chipitsyna G, Cui J, Liao B, Liu S, Aysola K, Yezdani M, Reddy ES, Rao VN. C-fos oncogene regulator Elk-1 interacts with BRCA1 splice variants BRCA1a/1b and enhances BRCA1a/1b-mediated growth suppression in breast cancer cells. *Oncogene* 2001; **20**: 1357-1367
- 48 **Ma KS**, Zhang FS, He ZP, Wanf SG, Zhong JH. Effect of CCK on cell apoptosis of bile duct neoplasms. *Shijie Huaren Xiaohua Zazhi* 2000; **8**: 1312-1313
- 49 **Salmi A**, Carpen O, Rutanen E. The association between c-fos and c-jun expression and estrogen and progesterone receptors is lost in human endometrial cancer. *Tumour Biol* 1999; **20**: 202-211

L-forms of *H. pylori*

Ke-Xia Wang, Chao-Pin Li, Yu-Bao Cui, Ye Tian, Qing-Gui Yang

Ke-Xia Wang, Chao-Pin Li, Yu-Bao Cui, Ye Tian, Qing-Gui Yang,
School of Medicine, Anhui University of Science & Technology
Huainan 232001, Anhui Province, China

Correspondence to: Dr. Chao-Pin Li, Department of Etiology and
Immunology, School of Medicine, Anhui University of Science and
Technology Huainan 232001, Anhui Province, China. cpli@aust.edu.cn

Telephone: +86-554-6658770 **Fax:** +86-554-6662469

Received: 2002-09-14 **Accepted:** 2002-10-17

Abstract

AIM: To study the occurrence of L-forms of *H. pylori* infection in patients with peptic ulcers and its association with possible changes of cellular immune function in the patients.

METHODS: Endoscopic biopsy specimens of gastric antrum and gastric corpus were taken from 228 patients with peptic ulcers and inoculated into Skirrow selective medium for *H. pylori* vegetative forms and special medium for *H. pylori* L-forms, followed by bacterial isolation and identification. And peripheral venous blood of the patients was taken to detect the percentage of CD3⁺, CD4⁺ and CD8⁺ with biotin-streptavidin (BSA) and the level of IL-2, IL-6 and IL-8 with ELISA.

RESULTS: (1) The detection rates of *H. pylori* L-forms and vegetative forms in the patients were 50.88 % (116/228) and 64.91 % (148/228) respectively, and the co-infection rate of *H. pylori* L-forms and vegetative forms was 78.38 % (116/148). To be more exact, the detection rates of *H. pylori* L-forms in male and female patients were 57.04 % (77/135) and 41.94 % (39/93) respectively, and statistics found significant difference between them ($P < 0.05$). Furthermore, the detection rates of *H. pylori* L-forms in patients aged 14 years-, 30 years-, 40 years- and 50 years- were 31.91 % (15/47), 42.86 % (24/56), 56.94 % (41/72) and 67.92 % (36/53) respectively, and there was significant difference between them ($P < 0.01$). (2) The percentages of CD3⁺, CD4⁺, CD8⁺, the ratio of CD4⁺/CD8⁺, and the level of IL-2, IL-6, IL-8 in *H. pylori*-positive patients were (52.59±5.44) %, (35.51±5.74) %, (27.77±8.64) %, (1.56±0.51), (2.66±0.47) mg/L, (108.62±5.85) ng/L and (115.79±7.18) ng/L respectively, compared with those in *H. pylori*-negative patients, the percentages of CD3⁺, CD4⁺ and the ratio of CD4⁺/CD8⁺ decreased, but the level of IL-2, IL-6 increased, and the difference was significant ($P < 0.001$ - $P < 0.01$). Moreover, the percentages of CD3⁺, CD4⁺, CD8⁺, the ratio of CD4⁺/CD8⁺, and the level of IL-2, IL-6, IL-8 in the patients with mixed infection of both *H. pylori* L-forms and vegetative forms were (51.69±5.28) %, (34.75±5.89) %, (27.15±7.45) %, (1.48±0.47), (2.16±0.38) mg/L, (119.45±5.44) ng/L and (123.64±6.24) ng/L respectively, compared with those in patients with simple infection of *H. pylori* vegetative forms, the percentage of CD4⁺, the ratio of CD4⁺/CD8⁺ and the level of IL-2 increased, but the level of IL-6 and IL-8 decreased, statistical difference was found between them ($P < 0.001$ - $P < 0.05$).

CONCLUSION: L-forms variation often occurs in patients with peptic ulcers who are infected by *H. pylori*, which is

commonly found in male patients and related to ages. The L-forms variation of *H. pylori* can be an important factor causing disorder of cellular immune function in the patients with peptic ulcers who are infected by *H. pylori*.

Wang KX, Li CP, Cui YB, Tian Y, Yang QG. L-forms of *H. pylori*. *World J Gastroenterol* 2003; 9(3): 525-528
<http://www.wjgnet.com/1007-9327/9/525.htm>

INTRODUCTION

Helicobacter pylori (*H. pylori*) is one of the commonest bacteria causing chronic infection, which infects more than 50 % of the human population, and is associated with a range of pathology, such as chronic gastritis, peptic ulcer and gastric cancer^[1-5]. And infection of *Helicobacter pylori* is life-long that elicits a marked host inflammatory response. However, natural infection fails to yield protective immunity^[6].

H. pylori is a gram-negative, spiral and microaerophilic bacterium that colonizes the gastric epithelium of humans^[7]. It causes chronic gastritis and, together with non-steroidal anti-inflammatory drugs, is considered as the most frequent etiologic agent of peptic ulcer^[8-10]. After long-term treatment with antibiotic, cell walls deficiency of *H. pylori* vegetative forms occurs and *H. pylori* L-forms comes into being^[11,12]. Whether in animal experiments or clinical studies, damages induced by *H. pylori* were reported to be associated with Th1 cell-mediated immune response^[13-15].

In order to confirm the occurrence of L-forms variation of *H. pylori* vegetative forms and its association with possible changes of cellular immune function in the patients, gastric mucosa biopsy specimens were taken from 228 patients with peptic ulcers randomly enrolled in this study to isolate and identify *H. pylori* vegetative forms and L-forms, and T lymphocyte subsets and the level of IL-2, IL-6 and IL-8 of the patients were detected at the same time.

MATERIALS AND METHODS

Materials

Patients A total of 228 patients with peptic ulcer (gastric ulcers 66, duodenal ulcers 132, and complex ulcers of gastric and duodenal 30) diagnosed in our affiliated hospital from August, 2000 to April 2002 were involved in this study. All of them were except aged from 14 to 67 years, 135 male and 93 female, other were eliminated for presence of other diseases.

Reagents *H. pylori* L-forms solid medium designed by Jia JH was served in this study. Based on broth culture medium, the medium consisted of peptone 1 %, tryptone 1 %, glucose 0.1 %, yeast powder 0.2 %, D-methionine 0.02 %, NaCl 1.5 %, MgSO₄·7H₂O, 15mM, agar 0.8 % and Caprine plasma 15 % with the inducer of carbenicillin and made into pour plate. BSA reagent for T lymphocyte subsets was provided by Jin' an Medical Laboratory Institute in Shanghai, Separating medium for Lymphocyte was supplied by The Second Biochemical Reagent Factory in Shanghai (batch No. 011215), and the test kit for IL-6 (batch No. 1006-32), IL8 (batch No.1008-25), IL-2 (batch No.1002-21) was offered by Besancon Company in France.

Methods

We used gastric antral and corporal biopsies for bacterial culture, blood samples for detection of T lymphocyte subsets and IL-2, IL-6, IL-8.

Bacteriological examination Endoscopic biopsies of gastric antrum and gastric corpus were taken from 228 patients with peptic ulcers and inoculated into Skirrow selective medium for *H. pylori* vegetative forms and special medium for *H. pylori* L-forms. Then the plates were incubated at 37 °C under microaerobic conditions (5 % O₂, 8 % H₂, 7 % CO₂ and 80 % N₂) for 72 hours. Based on the results of Gram staining, cell morphology and positive reaction for urease, oxidase and immunoenzyme staining, the identification was carried out.

Detection of cellular immune function To investigate the possible changes of cellular immune function in *H. pylori*-infected individuals, including the patients infected by *H. pylori* L-forms and vegetative forms, the level of CD3+, CD4+, CD8+, CD4+/CD8+ and IL-2, IL-6, IL-8 in peripheral blood of *H. pylori*-positive individuals were tested with biotin-streptavidin (BSA) method. Firstly, the peripheral venous blood of the subjects was taken, anticoagulated with heparin, and diluted with fluid free of Ca²⁺, Mg²⁺. Secondly, peripheral blood mononuclear cells were separated with lymphocytes separating medium, cleaned, and the number of cells was adjusted to (1-3)×10⁹/L of which 10 μl was taken and smeared in an acid-proof varnish circle on the surface of the slides. When it dried naturally, McAb of anti-CD3+, anti-CD4+ and anti-CD8+ and sheep anti-guineapig IgG, SA-HRP was added into the circle. After development with DAB, the slides were observed under microscope. Only brown cytomembrane staining was regarded as positive, otherwise, as negative specimen. A total of 200 cells were counted, and the positive percentages of cells were analyzed respectively. In addition, the level of IL-2, IL-6 and IL-8 were detected by ELLISA following the procedure detailed in the product description.

Statistical analysis

Data were expressed as mean ± standard deviation. And multiple comparison tests were performed with χ^2 test and *t*-test.

RESULTS

Bacteriological examination By endoscopic biopsy of gastric mucosa, 116 out of all the 228 patients were detected to be positive for both *H. pylori* vegetative forms and L-forms, and 32 (14.04 %) to be positive for vegetative forms only. The detection rates of *H. pylori* L-forms and vegetative forms were 50.88 % (116/228) and 64.91 % (148/228) respectively. "Fried Egg" colonies grew in the special medium for *H. pylori* L-forms after induction with carbenicillin. And the morphology of *H. pylori* L-forms was highly variably seen on the smears under microscopy, such as spheroid, coccoid form, big body, elementary body, long filament body.

Relationship between infection of *H. pylori* L-forms and gender as well as age of the patients with peptic ulcer The detection rates of *H. pylori* L-forms and vegetative forms in the patients were 50.88 % (116/228) and 64.91 % (148/228) respectively, and among the vegetative forms of *H. pylori*-positive patients, it was 78.38 % (116/148) which was the co-infection rate of L-forms of *H. pylori*. To be more exact, the detection rates of *H. pylori* L-forms in male and female patients were 57.04 % (77/135) and 41.94 % (39/93) respectively, and with statistically significant difference between them (*P*<0.05). In addition, the detection rate of *H. pylori* L-forms was associated with age. The detailed results were shown in Table 1.

Detection of cellular immune function Compared with the percentages of CD3+, CD4+, CD8+, the ratio of CD4+/CD8+, and the level of IL-2, IL-6, IL-8 in *H. pylori*-negative patients,

the percentages of CD3+, CD4+ and the ratio of CD4+/CD8+ decreased in *H. pylori*-positive patients, but the level of IL-2, IL-6 increased. And compared with the percentages of CD3+, CD4+, CD8+, the ratio of CD4+/CD8+, and the level of IL-2, IL-6, IL-8 in the patients only infected by vegetative forms of *H. pylori*, the percentage of CD4+, the ratio of CD4+/CD8+ and the level of IL-2 increased in the patients not only infected by L-forms of *H. pylori* but also the vegetative forms, but the level of IL-6 and IL-8 decreased, statistical difference was found between them (*P*<0.001-*P*<0.05). All of these were shown in Table 2 and Table 3.

Table 1 Relationship between *H. pylori* L-forms and gender as well as ages of the patients with peptic ulcer (*n*, %)

Age	Male		Female		Total	
	<i>n</i>	Detection Rate (%)	<i>n</i>	Detection Rate (%)	<i>n</i>	Detection Rate (%)
14~	28	9 (32.14)	19	6 (31.58)	47	15 (31.91) ^b
30~	36	13 (36.11)	20	11 (55.00)	56	24 (42.86) ^b
40~	42	28 (66.67)	30	13 (43.33)	72	41 (56.94) ^b
50~	29	27 (93.10)	24	9 (37.50)	53	36 (67.92) ^b
Total	135	77 (57.04) ^a	93	39 (41.94) ^a	228	116 (50.88)

^a*P*<0.05, $\chi^2=5.02$; ^b*P*<0.01, $\chi^2=15.43$.

Table 2 Detection of the T lymphocyte subsets in 228 patients with peptic ulcers

Group	<i>n</i>	CD3+ (%)	CD4+ (%)	CD8+ (%)	CD4+/CD8+ (%)
Hp(-)	80	65.72±9.38 ^c	46.33±4.86 ^d	29.83±7.39	1.74±0.34 ^e
Hp(+)	148	52.59±5.44 ^c	35.51±5.74 ^d	27.77±8.64	1.56±0.51 ^e
Hp(+)&Hp-L(-)	32	55.87±6.23	38.27±6.43 ^f	30.04±11.84	1.86±0.58
Hp(+)&Hp-L(+)	116	51.69±5.28	34.75±5.89 ^f	27.15±7.45	1.48±0.47 [*]
Total	228	57.20±6.43	39.31±5.18	28.49±7.86	1.61±0.466

^c*P*<0.001, *t*=13.38; ^d*P*<0.001, *t*=14.31; ^e*P*<0.01, *t*=2.82; ^f*P*<0.01, *t*=2.93; ^{*}*P*<0.05, *t*=2.65.

Table 3 Detection of IL-2, IL-6, IL-8 in patients with peptic ulcers

Group	<i>n</i>	IL-2 (mg/L)	IL-6 (ng/L)	IL-8 (ng/L)
Hp(-)	80	7.24±0.65 ^h	40.82±3.15 ⁱ	52.35±3.63 ^j
Hp(+)	148	2.66±0.47 ^h	108.62±5.85 ⁱ	115.79±7.18 ^j
Hp(+)&Hp-L(-)	32	4.49±0.57 ^k	69.35±6.51 ⁱ	87.33±8.45 ^m
Hp(+)&Hp-L(+)	116	2.16±0.38 ^k	119.45±5.44 ⁱ	123.64±6.24 ^m
Total	228	4.27±0.52	84.83±4.73	93.53±5.68

^h*P*<0.001, *t*=61.14; ⁱ*P*<0.001, *t*=96.32; ^j*P*<0.001, *t*=74.03; ^k*P*<0.001, *t*=27.30; ^l*P*<0.001, *t*=43.95; ^m*P*<0.001, *t*=26.86.

DISCUSSION

Helicobacter pylori is a gram-negative, spiral-shaped, microaerophilic bacterium that colonizes the human gastric epithelium but not cleared by the host immune response, which can be found in approximately 50 % of the world's population, and which plays a causative role in peptic ulcer and perhaps gastric cancer. As a matter of fact, it results in a release of various bacterial and host dependent cytotoxic substances including ammonia, platelet activating factor, cytotoxins and lipopolysaccharides as well as cytokines such as interleukins (IL)-1-12, tumor necrosis factor alpha (TNF-alpha), interferon

gamma (INF-gamma) and reactive oxygen species^[16-22]. Although the mucus layer is the major reservoir of *H. pylori* *in vivo*, a growing body of evidence suggests that *H. pylori* can persist in multiple intracellular sites^[23]. And primary gastritis, duodenitis, peptic ulcer are no longer considered to be disorders of the balance of secretion of acid and immune responses of the gastric mucosa, but it is thought to be caused by *Helicobacter pylori* infection. Moreover, the chronic inflammatory response associated with natural infection can contribute to tissue damage and the pathogenesis of gastroduodenal disease^[24-27]. In 1994, the connection of *H. pylori* to stomach cancer became so certain that the World Health Organization International Agency for Research in Cancer (IARC) classified it as a class I carcinogen. So *H. pylori* became the first bacteria to be connected with carcinogenesis^[28-30].

Recurrence of *H. pylori* infection after successful dual or triple therapy is fairly common, and gastroduodenal disease, gender, and gastritis activity seem to affect relapse of infection^[31,32]. Many scholars believed that pleomorphic variation of the *H. pylori* is a crucial factor to the occurrence and development of gastric malignant tumor, and some detailed it to L-forms variation of *H. pylori* that played an important role in prolongation and relapse of peptic ulcer as well as chronic gastritis.

In this study, gastric mucosal biopsy specimens from 228 patients with peptic ulcers were inoculated into Skirrow selective blood plate for *H. pylori* vegetative forms and special plate for *H. pylori* L-forms. The experimental results showed that 116 patients were infected with both *H. pylori* L-forms and vegetative forms, but 32 patients were infected with *H. pylori* only. This indicated that L-form variation of *H. pylori* is common in patients with peptic ulcers related to *H. pylori*. Under circumstances of gastric juice, bile, antibiotic and other factors either *in vitro* or *in vivo*, many bacteria could come into pleomorphic variation^[33-36]. For example, in penicillin-susceptible bacteria, penicillin causes growth of a small fraction of cells as wall-deficient forms if an appropriate osmo protection is provided (unstable L-forms). According to some scholar's reports, *H. pylori* vegetative forms could turn into *H. pylori* L-forms in the treatment of peptic ulcer with antibacterial, so co-infection of *H. pylori* L-forms and vegetative forms yields in some patients with *H. pylori*. Following the loss of cell walls, the L-forms lose certain components of antigen and become less antigenic, and with increase of charge of the bacteria surface, which make it more adhesive when cultivating in a liquid L-form medium. Moreover, when condition is available, L-forms can revert to typical vegetative forms, which may be an important factor leading to deterioration and relapse of infection^[33]. That is to say *H. pylori* L-forms possess more adhesiveness, invasiveness and risky. Therefore, co-infection of *H. pylori* vegetative forms in extracellular and L-forms in intracellular can result in chronic damage to the host cells.

In this study, the detection rates of *H. pylori* L-forms in male and female were 57.04 % (77/135) and 41.94 % (39/93), which were significantly different. This may be related to some male habits, such as smoking, drinking, irregular diet, which might damage gastric mucosa and change the gastric internal environment^[37-39]. In addition, *H. pylori* L-forms infection could occur in different age groups and the positive rate of *H. pylori* L-forms seemed to be related to the patients' ages, as opportunities of infection increase with time due to age, smoking, exposure to antibacterial agents, eating habit, etc.

In recent years, cellular immune function of the patients with *H. pylori* has been discussed very frequently. Rather than providing protection, the chronic inflammatory response associated with natural infection can contribute to tissue damages and pathogenesis of gastroduodenal disease, including atrophic gastritis, peptic ulcer, and gastric cancer. These

immune responses are likely to attribute to a subset of T helper lymphocyte, so-called Th1 cells, that enhance cell-mediated immunity and induce damage to the gastric epithelium^[13-15]. To investigate the reason for Th1 immune response caused by *H. pylori* based on the variation of L forms, detection of T lymphocyte subsets and the level of IL-2, IL-6, IL-8 in peripheral blood of the patients were performed. The results showed that in 148 *H. pylori*-positive patients, CD3+, CD4+, CD4+/CD8 and IL-2 decreased, IL-6 and IL-8 increased, which were significantly different from those in *H. pylori*-negative ($P < 0.001$, $P < 0.01$). It indicated that *H. pylori* infection might weaken the immune function of the host and cause a predominant Th1 cellular response.

The results showed that among the 148 patients with *H. pylori* vegetative forms, 116 were co-infected with *H. pylori* L-forms. That is to say, only 32 patients were found with *H. pylori* vegetative forms only. Therefore, the roles of *H. pylori* L-forms in the change of immune function of the patients with peptic ulcers are worthy of great awareness. Compared the T lymphocyte subsets and the levels of IL-2, IL-6, IL-8 in patients with *H. pylori* vegetative forms only and co-infection of *H. pylori* vegetative forms and L-forms, the percentage of CD4+, CD4+/CD8 and the level of IL-2 in the patients with co-infection were lower than those with vegetative forms infection only, but the level of IL-6 and IL-8 was higher. As a conclusion, *H. pylori* L-forms infection is related to disorder of the immune function of the host, and may be one of the crucial factors causing Th1 immune response. When infesting in the host cell, *H. pylori* L-forms may be a pronounced inducer for Th1-type CD4 (+) T cell response and decrease the percentage of CD4+ and the ratio of CD4+/CD8. Active CD4+-T cell may also inhibit the activation of Th1 cells cytokine, and the outcome of IL-2 is a risk factor of cellular immune response.

In addition, in this study, the levels of IL-6 and IL-8 in peripheral blood of the patients increased significantly, which is likely to be associated with ulceration inflammation, blood macrophage stimulation and active secretion by the neutrophils and vascular endothelial cells. Once attached to the gastric epithelial cells, *H. pylori* incites an immune response characterized by the increased pro-inflammatory cytokine of IL-8, IL-12 and TNF-alpha. Activated inflammatory and immunologically competent cells as neutrophils, lymphocytes, monocytes, could release cytokine as IL-6, IL-8 and IFN-gamma. As a result, the level of IL-6 and IL-8 in serum of the patients increased^[40].

To sum up, vegetative forms of *H. pylori*'s susceptibly turning into L-forms is because of antibacterial agent and alteration of gastric environment in patients with peptic ulcers, and it is common for patients to be co-infected by both *H. pylori* vegetative forms and L-forms. Once *H. pylori* L-forms occurs, the morphology and microstructure of the organisms change, to be exact, the cell walls of the L-forms are partly or completely lost, the charge of the bacteria surface increases, and the adherence and invasiveness of the bacteria become more powerful. All of these make the pathogen invading into intracellular compartment Mac easily, which can be an important factor causing disordered cellular immune function in the patients with peptic ulcers infected by *H. pylori*.

REFERENCES

- 1 **Vandenplas Y.** *Helicobacter pylori* infection. *World J Gastroenterol* 2000; **6**: 20-31
- 2 **Pineros DM,** Riveros SC, Marin JD, Ricardo O, Diaz OO. *Helicobacter pylori* in gastric cancer and peptic ulcer disease in a Colombian population. Strain heterogeneity and antibody profiles. *Helicobacter* 2001; **6**: 199-206
- 3 **Kotloff KL,** Sztein MB, Wasserman SS, Losonsky GA, DiLorenzo SC, Walker RI. Safety and immunogenicity of oral inactivated

- whole-cell *Helicobacter pylori* vaccine with adjuvant among volunteers with or without subclinical infection. *Infect Immun* 2001; **69**: 3581-3590
- 4 **Brigic E**, Hodzic L, Zildzic M. *Helicobacter pylori* and gastroduodenal disease in our patients: 2-year experience. *Med Arh* 2000; **54**: 313-316
- 5 **Nguyen TN**, Barkun AN, Fallone CA. Host determinants of *Helicobacter pylori* infection and its clinical outcome. *Helicobacter* 1999; **4**: 185-197
- 6 **Ernst PB**, Pappo J. T-cell-mediated mucosal immunity in the absence of antibody: lessons from *Helicobacter pylori* infection. *Acta Odontol Scand* 2001; **59**: 216-221
- 7 **Oyedeji KS**, Smith SI, Arigbabu AO, Coker AO, Ndububa DA, Agbakwuru EA, Atoyebi OA. Use of direct Gram stain of stomach biopsy as a rapid screening method for detection of *Helicobacter pylori* from peptic ulcer and gastritis patients. *J Basic Microbiol* 2002; **42**: 121-125
- 8 **Ballesteros-Amozurrutia MA**. Peptic ulcer and *Helicobacter pylori*. Results and consequences of its eradication. *Rev Gastroenterol Mex* 2000; **65**: 41-49
- 9 **McCull KE**, Gillen D, El-Omar E. The role of gastrin in ulcer pathogenesis. *Baillieres Best Pract Res Clin Gastroenterol* 2000; **14**: 13-26
- 10 **Vergara M**, Calvet X, Roque M. *Helicobacter pylori* is a risk factor for peptic ulcer disease in cirrhotic patients. A meta-analysis. *Eur J Gastroenterol Hepatol* 2002; **14**: 717-722
- 11 **Schmidtke LM**, Carson J. Induction, characterization and pathogenicity in rainbow trout *Oncorhynchus mykiss* (Walbaum) of *Lactococcus garvieae* L-forms. *Vet Microbiol* 1999; **69**: 287-300
- 12 **Rakovskaia IV**. Role of works of S. V. Prozorovskii in solving problems of persistence of wall-free forms of microorganisms. *Vestn Ross Akad Med Nauk* 2001; **11**: 5-8
- 13 **Ihan A**, Tepes B, Gubina M. Diminished Th1-type cytokine production in gastric mucosa T-lymphocytes after *H. pylori* eradication in duodenal ulcer patients. *Pflugers Arch* 2000; **440**: 89-90
- 14 **Londono-Arcila P**, Freeman D, Kleanthous H, O'Dowd AM, Lewis S, Turner AK, Rees EL, Tibbitts TJ, Greenwood J, Monath TP, Darsley MJ. Attenuated *Salmonella enterica* Serovar Typhi expressing urease effectively immunizes mice against *Helicobacter pylori* challenge as part of a heterologous mucosal priming-parenteral boosting vaccination regimen. *Infect Immun* 2002; **70**: 5096-5106
- 15 **Kusters JG**, Scand J. Recent developments in *Helicobacter pylori* vaccination. *Gastroenterol Suppl* 2001; **234**: 15-21
- 16 **Stassi G**, Arena A, Speranza A, Iannello D, Mastroeni P. Different modulation by live or killed *Helicobacter pylori* on cytokine production from peripheral blood mononuclear cells. *New Microbiol* 2002; **25**: 247-252
- 17 **Amjad M**, Kazmi SU, Qureshi SM, Reza-ul Karim M. Inhibitory effect of IL-4 on the production of IL-1 beta and TNF-alpha by gastric mononuclear cells of *Helicobacter pylori* infected patients. *Ir J Med Sci* 2001; **170**: 112-116
- 18 **Han FC**, Yan XJ, Su CZ. Expression of the CagA gene of *H.pylori* and application of its product. *World J Gastroenterol* 2000; **6**: 122-124
- 19 **Olbe L**, Fandriks L, Thoreson AC, Svennerholm AM, Hamlet A. When is *H.pylori* a cause of duodenal ulcer? Hypersecretion of gastric acid, active duodenitis and reduced bicarbonate secretion are links in the chain. *Lakartidningen* 2000; **97**: 5910-5913
- 20 **Konturek PC**, Bielanski W, Konturek SJ, Hahn EG. *Helicobacter pylori* associated gastric pathology. *J Physiol Pharmacol* 1999; **50**: 695-710
- 21 **Ji KY**, Hu FL. Progress on *Helicobacter pylori* and cytokine. *Shijie Huaren Xiaohua Zazhi* 2002; **10**: 503-508
- 22 **Guillemin K**, Salama NR, Tompkins LS, Falkow S. Cag pathogenicity island-specific responses of gastric epithelial cells to *Helicobacter pylori* infection. *Proc Natl Acad Sci* 2002; **99**: 15136-15141
- 23 **Allen LA**. Intracellular niches for extracellular bacteria: lessons from *Helicobacter pylori*. *J Leukoc Biol* 1999; **66**: 753-756
- 24 **Innocenti M**, Thoreson AC, Ferrero RL, Stromberg E, Bolin I, Eriksson L, Svennerholm AM, Quiding-Jarbrink M. *Helicobacter pylori*-induced activation of human endothelial cells. *Infect Immun* 2002; **70**: 4581-4590
- 25 **Al-Muhtaseb MH**, Abu-Khalaf AM, Aughsteeen AA. Ultrastructural study of the gastric mucosa and *Helicobacter pylori* in duodenal ulcer patients. *Saudi Med J* 2000; **21**: 569-573
- 26 **Di Leo A**, Messa C, Russo F, Linsalata M, Amati L, Caradonna L, Pece S, Pellegrino NM, Caccavo D, Antonaci S, Jirillo E. *Helicobacter pylori* infection and host cell responses. *Immunopharmacol Immunotoxicol* 1999; **21**: 803-846
- 27 **Naito Y**, Yoshikawa T. Molecular and cellular mechanisms involved in *Helicobacter pylori*-induced inflammation and oxidative stress (1,2). *Free Radic Biol Med* 2002; **33**: 323-326
- 28 **Zhang WD**, Xu ZM. Status and cognition of studies on *Helicobacter pylori*. *Shijie Huaren Xiaohua Zazhi* 2000; **8**: 1084-1088
- 29 **Pineros DM**, Riveros SC, Marin JD, Ricardo O, Diaz OO. *Helicobacter pylori* in gastric cancer and peptic ulcer disease in a Colombian population. Strain heterogeneity and antibody profiles. *Helicobacter* 2001; **6**: 199-206
- 30 **Mielhke S**, Kirsch C, Dragosics B, Gschwantler M, Oberhuber G, Antos D, Dite P, Lauter J, Labenz J, Leodolter A, Malfratherer P, Neubauer A, Ehninger G, Stolte M, Bayerdorffer E. *Helicobacter pylori* and gastric cancer: current status of the Austrian Czech German gastric cancer prevention trial (PRISMA Study). *World J Gastroenterol* 2001; **7**: 243-247
- 31 **Zullo A**, Rinaldi V, Hassan C, Taggi F, Giustini M, Winn S, Castagna G, Attili AF. Clinical and histologic predictors of *Helicobacter pylori* infection recurrence. *J Clin Gastroenterol* 2000; **31**: 38-41
- 32 **Ihan A**, Tepez B, Gubina M, Malovrh T, Kopitar A. Diminished interferon-gamma production in gastric mucosa T lymphocytes after *H. pylori* eradication in duodenal ulcer patients. *Hepatogastroenterology* 1999; **46**: 1740-1745
- 33 **Xu ZM**, Zhou DY, Pan LJ, Song S. Transformation and reversion of *Helicobacter pylori* in vitro. *Shijie Huaren Xiaohua Zazhi* 1999; **7**: 215-217
- 34 **Wen M**, Zhang Y, Yamada N, Matsuhisa T, Matsukura N, Sugisaki Y. An evaluative system for the response of antibacterial therapy: based on the morphological change of *Helicobacter pylori* and mucosal inflammation. *Pathol Int* 1999; **49**: 332-337
- 35 **Khin MM**, Hua JS, Ng HC, Wadstrom T, Bow H. Agglutination of *Helicobacter pylori* coccoids by lectins. *World J Gastroenterol* 2000; **6**: 202-209
- 36 **She FF**, Su DH, Lin JY, Zhou LY. Virulence and potential pathogenicity of coccoid *Helicobacter pylori* induced by antibiotics. *World J Gastroenterol* 2001; **7**: 254-258
- 37 **Brenner H**, Bode G, Adler G, Hoffmeister A, Koenig W, Rothenbacher D. Alcohol as a gastric disinfectant? The complex relationship between alcohol consumption and current *Helicobacter pylori* infection. *Epidemiology* 2001; **12**: 209-214
- 38 **Parasher G**, Eastwood GL. Smoking and peptic ulcer in the *Helicobacter pylori* era. *Eur J Gastroenterol Hepatol* 2000; **12**: 843-853
- 39 **Guarner J**, Mohar A. The association between *Helicobacter pylori* and gastric neoplasia. Epidemiologic evidence. *Rev Gastroenterol Mex* 2000; **65**: 20-24
- 40 **Ohara T**, Arakawa T, Higuchi K, Kaneda K. Overexpression of co-stimulatory molecules in peripheral mononuclear cells of *Helicobacter pylori*-positive peptic ulcer patients. *Eur J Gastroenterol Hepatol* 2001; **13**: 11-18

Inhibitive effect of cordyceps sinensis on experimental hepatic fibrosis and its possible mechanism

Yu-Kan Liu, Wei Shen

Yu-Kan Liu, Wei Shen, Department of Gastroenterology, the Second affiliated hospital, Chongqing University of Medical Sciences, Chongqing 400010, China

Correspondence to: Wei Shen, Department of Gastroenterology, the Second affiliated hospital, Chongqing University of Medical Sciences, Chongqing 400010, China. shenwei2002932@sohu.com

Telephone: +86-23-63849076-2323 **Fax:** +86-23-63849076

Received: 2002-07-08 **Accepted:** 2002-10-21

Abstract

AIM: To investigate the inhibitive effect and its possible mechanism of Cordyceps Sinensis (CS) on CCl₄-plus ethanol-induced hepatic fibrogenesis in experimental rats.

METHODS: Rats were randomly allocated into a normal control group, a model control group and a CS group. The latter two groups were administered with CCl₄ and ethanol solution at the beginning of the experiment to induce hepatic fibrosis. The CS group was also treated with CS 10 days after the beginning of CCl₄ and ethanol administration. All control groups were given corresponding placebo at the same time. At the end of the 9th week, rats in each group were humanely sacrificed. Blood and tissue specimens were taken. Biochemical, radioimmunological, immunohistochemical and molecular biological examinations were used to determine the level change of ALT, AST, HA, LN content in serum and TGFβ₁, PDGF, collagen I and III expression in tissue at either protein or mRNA level or both of them.

RESULTS: As compared with the model control group, serum ALT, AST, HA, and LN content levels were markedly dropped in CS group (86.0±34.4 vs 224.3±178.9, 146.7±60.2 vs 272.6±130.1, 202.0±79.3 vs 316.5±94.1 and 50.4±3.0 vs 59.7±9.8, respectively, $P<0.05$). Tissue expression of TGFβ₁ and its mRNA, collagen I mRNA were also markedly decreased (0.2±0.14 vs 1.73±1.40, 1.68±0.47 vs 3.17±1.17, 1.10±0.84 vs 2.64±1.40, respectively, $P<0.05$). More dramatical drop could be seen in PDGF expression (0.87±0.43 vs 1.91±0.74, $P<0.01$). Although there was no statistical significance, it was still strongly suggested that collagen III mRNA expression was also decreased in CS group as compared with model control group (0.36±0.27 vs 0.95±0.65, $P=0.0615$). In this experiment, no significant change could be found in PDGF mRNA expression between two groups (0.35±0.34 vs 0.70±0.46, $P>0.05$).

CONCLUSION: Cordyceps sinensis could inhibit hepatic fibrogenesis derived from chronic liver injury, retard the development of cirrhosis, and notably ameliorate the liver function. Its possible mechanism involves inhibiting TGFβ₁ expression, and thereby, down regulating PDGF expression, preventing HSC activation and deposition of procollagen I and III.

Liu YK, Shen W. Inhibitive effect of cordyceps sinensis on experimental hepatic fibrosis and its possible mechanism. *World J Gastroenterol* 2003; 9(3): 529-533
<http://www.wjgnet.com/1007-9327/9/529.htm>

INTRODUCTION

The incidence rate of chronic in China is high, which afflicts the patients by progressively developing into irreversible cirrhosis^[1,2]. Hepatic fibrosis is the intermediate and crucial stage of this process, characterized by reversibility. If treated properly in this stage, cirrhosis could be successfully prevented^[3].

Clinical observation and experimental data suggested that liver fibrosis could be reabsorbed under certain conditions. Chinese herbs, well known for their definite effectiveness, cheap prices and negligible side effects, have particular advantages in therapeutic research of hepatic fibrogenesis. Several herbs were suggested recently by some reports to have preventive effect on hepatic fibrosis^[4-12], and cordyceps sinensis (CS) is one of them^[4,5]. However, its exact effectiveness and detailed mechanisms have not been elaborated. In this study, we established the animal model of chronic liver injury-hepatic fibrosis-cirrhosis, intervened with CS, and observed its inhibitive effect. An array of indexes in protein and mRNA levels was established in order to thoroughly investigate its possible mechanism.

MATERIALS AND METHODS

Animals

Male Wistar rats weighing between 200 g and 300 g were obtained from Experimental Animal Center of Chongqing University of Medical Science, China. The rats were housed 3 or 4 per cage and subjected to 12-day/12-night cycle with unrestricted access to basic food. All animals were treated humanely according to the national guideline for the care of animals in the country.

Preparation for CS suspension

CS was purchased from Bao Ding Pharmaceutical Company, China.

The CS and double-distilled water were mixed in proportion of 1:3 and subject to full vibration.

Reagents

TGFβ₁, PDGF, procollagen I and III RNA probe and detection kit for *in-situ* hybridization were purchased from Boster Biologic Technology Company, China. Anti-TGFβ₁ monoclonal antibody, anti-PDGF multiclonal antibody and its detection kit for immunohistochemical assay were purchased from Santa Cluz biologic technology Company, USA. Serum ALT, AST, HA, and LN examinations were performed by the Laboratory Department of Chong Qing University of Medical Sciences, China.

Establishment of animal model: carbon tetrachloride (CCL₄)-plus-ethanol induced hepatic fibrosis

Sixty-six male Wista rats were randomly assigned to a normal control group, a model control group and a CS group. At the beginning of the experiment, rats in model control group and CS group were subjected to hypodermic injection of (40 % in bean oil) at a dose of 0.3 ml/100 g of body weight twice a week. Besides, rats in these two groups also received 5 %

ethanol solution as the only fluid to drink. Rats in normal control group received hypodermic injection of bean oil at the same dose and frequency as the other two groups and received water ad libitum. Ten days after the CCL₄ administration (for 3 times), CS group was given CS suspension orally at a dose of 1 ml/100 g body weight daily. In the meantime, three rats in model control group were randomly sacrificed to evaluate the liver histological change at this moment while other rats along with rats in normal control group were given saline orally at a dose of 1 ml/100 g body weight daily. All the administrations lasted 9 weeks.

Collection of specimens

At the end of the 9th week, rats in each group were humanely sacrificed by amobarbital sodium anesthesia. Midline laparotomy was performed. Livers were excised and blood was collected through cardiopuncture.

Histological grading

Liver tissues were fixed in formalin and embedded in paraffin blocks according to standard procedures (glass slide was cleaned with 95 % ethanol, treated with APES solution and air dried.) four to six micron thick tissue sections were cut using microtome and applied to slides; And deparafinized in xylenes using three changes for 5 minutes each. Hydrate sections gradually passed through graded alcohols: washing in 100 % ethanol twice, then 95 % ethanol twice for 10 minutes each; and washing in deodorized water for 1 minute. Hemotoxylin and eosin (HE) staining was performed according to the standard procedure.

Fibro-proliferation degree of liver sections were graded numerically based on the criterion described below: grade 0: normal liver; grade 1: few collagen fibrils extend from the central vein and portal tract; grade 2: collagen fibrils extension are obvious but do not encompass the whole lobule; grade 3: collagen fibrils extend and encompass the whole lobule; grade 4: collagen fibrils extend and separate lobule into pseudo-lobule, but mainly shaped in square form; and grade 5: pseudo-lobule shaped mainly in circle form.

Two pathologists who had no knowledge of their sources and each other's assessment examined stained slide independently.

Immunohistochemistry

Liver tissues were fixed in formalin and embedded in paraffin blocks according to standard procedures. Glass slide was cleaned with 95 % ethanol, treated with subbing solution and air-dried. Tissue sections of 4-6 micron thick were cut using microtome and applied to slides; and deparafinized in xylenes using three changes for 5 minutes each. Hydrate sections gradually through graded alcohols: washing in 100 % ethanol twice, then 95 % ethanol twice for 10 minutes each; and washing in deionized water for 1 minutes. Incubate sections for 15 minutes in 0.1 % pepsin at room temperature to expose the antigen masked by formalin fixation and paraffin embedding. Incubate sections with 3 % H₂O₂ and normal non-immunal goat serum for 10 minutes respectively to inactivate endogeneous peroxidase and biotin; incubate sections with primary antibody overnight at 4 °C. Optimal antibody concentration was determined previously. Wash with three changes of PBS for 5 minutes each. Incubate for 20 minutes with biotin-conjugated secondary antibody and avidin biotin enzyme reagent respectively. Wash with three changes of PBS for 5 minutes each. Incubate in peroxidase substrate for 5 minutes, after that dehydrate through alcohols and xylenes. Immediately add 1-2 drops of permanent mounting medium and covered with glass coverlip.

In situ hybridization

The sequence of RNA probe is as follows:

1. TGFβ₁mRNA
 - (1) 5' -CGTTT CACCA GCTCC ATGTC GATGG TGTTG CAGGT-3'
 - (2) 5' -CTTGA TTITA ATCTC TGCAA GCGCA GCTCT GCACG-3'
 - (3) 5' -TTGGT ATCCA GGGCT CTCCG GTGCC GTGAG CTGTG-3'
2. PDGF mRNA
 - (1) 5' -CTCGG CTTCC TCGGC CAGAA CATGG GCGAG GTATC-3'
 - (2) 5' -AACCT CACCT GGACT TCTTT CAATT TTGGC TTCTT-3'
 - (3) 5' -TTGCA CTCGG CGATC ATGGC CGGCT CAGCA ATGGT-3'
 - (4) 5' -GGCTC CAAGG GTCTC CTTCA GTGCC GTCTT GTCAT-3'
3. Col-I mRNA
 - (1) 5' -CACAG ATCAC GTCAT CGCAC AACAC CTTGC CGTTG-3'
 - (2) 5' -AGCTT CACCG GGACG ACCAG CTTCA CCAGG AGATC-3'
 - (3) 5' -TCACT CCTTC TACAT TATAT TCAAA CTGGC PGCCA-3'
4. Col-III mRNA
 - (1) 5' -ATTAA CAGAC TTGAG TGAAG TCATA ATCTC ATCGG-3'
 - (2) 5' -AGAAT ACAAT CTGTG TTTCT GACCA GGTGA GGTAG-3'
 - (3) 5' -GAAGG AGGAG AATCC CGTGG CATGC CAATG AATCT-3'

In situ hybridization was performed as described elsewhere. Briefly, formalin-fixed and paraffin-embedded liver section slides were pretreated by incubation with 0.1 % pepsin, 3 % H₂O₂ and normal non-immunal bovine serum for 10-15 minutes respectively to expose signals masked by formalin fixation and paraffin embedding and inactivate endogeneous peroxidase and biotin. Antisense RNA probe was then added to the sections and incubated together in humidified chamber overnight at 37 °C. After washing with three changes of 2×standard saline citrate (SSC) and 0.2×SSC for 10 minutes each, the sections were subject to incubation with biotin-conjugated secondary antibody and avidin biotin enzyme reagent respectively. Wash with three changes of PBS for 5 minutes each, incubate in peroxidase substrate for 20 minutes, and dehydrate through alcohols and xylenes. One to two drops of permanent mounting medium were immediately added and covered with glass coverlip.

Semiquantitative image analysis

Computer morphometry (CM-2000B Medical Image Analysis Software, Beijing Medical Software Company, China) was used to quantify the optical density of the signal generated by the immunohistochemical and *in situ* hybridization examination. The exact method is described as follows: The video image was generated with a video camera and digitalized for image analysis at 256 gray levels. An optical threshold and filter combination was set to select positive stains. The structure of interest was discriminated automatically by computer and measured for its optical intensity and total area. Staining index was obtained by multiplying the quantified number of optical intensity and total area.

Statistical analysis

Data were analyzed with SAS software. Quantitative data were presented as means ±SD and were compared using *t* test procedure. Frequency data were compared using NPAR1WAY procedure.

RESULTS

CS inhibits fibril deposition and ameliorates liver function of chronic hepatitis

After 10 days (3 times) of CCL₄ administration, rats suffered hepatocyte lipid degeneration, narcosis, and inflammatory cells infiltration, which fulfilled the diagnostic standard for chronic hepatitis.

Specimens from model control group showed apparent formation of fibrotic septa, encompassing regenerated hepatocytes into pseudo-lobules. Regenerated hepatocytes

underwent severe lipraoid degeneration. Specimens from CS group showed only slight fibrogenesis without pseudo-lobule formation.

Although statistical analysis failed to present any significant disparity between quantitative data of histological grading of the two groups, it still indicated that fibrogenesis of CS group was much less severe than that of model control group (Table 1). Compared with model control group, serum contents of HA and LN in CS group were markedly decreased ($P < 0.05$), which indicates from another perspective that CS could inhibit hepatic fibrogenesis (Table 2).

Serum contents of ALT and AST in model control group were significantly elevated compared with both normal control and CS groups. However, there was no significant statistical difference between normal control and CS groups ($P > 0.05$), which showed that CS could notably ameliorate liver function (Table 2).

CS reduces procollagen I and III mRNA synthesis

Procollagen I and III mRNA synthesis level in liver tissues were determined by *in situ* hybridization and quantified by computer image analyzing system. Positive staining could only be seen at central vein and periportal areas in normal control group. As the model control and CS groups, positive stains were distributed mainly along fibrotic septa other than central vein and periportal areas.

Compared with model control group, staining index of CS group remarkably dropped ($P < 0.05$), which suggested that procollagen I mRNA synthesis was strongly inhibited by CS treatment. On the part of procollagen III, despite that there was no significant difference between the two groups, it was also reasonably suggested that CS could inhibit the synthesis of procollagen III mRNA on the consideration of P value (0.0695) (Table 3).

CS reduces TGF β_1 expression

TGF β_1 expression in protein and mRNA level were determined by immunohistochemistry and *in situ* hybridization, respectively. Positive stains were quantified with computer image analyzing system. For the sections of normal control group, positive staining of TGF β_1 and its mRNA was found at central vein and periportal areas. In the sections of model control group and CS group, positive staining could be seen at interstitial cells, inflammatory cells, impaired hepatocytes as well as normal hepatocytes. Fibrotic septa were only slightly stained. TGF β_1 mRNA positive stain distribution was not completely consistent with that of TGF β_1 . More stain was found at fibrotic septa and less at impaired and normal hepatocytes.

Compared with model control group, the staining index of both TGF β_1 and TGF β_1 mRNA in CS group was markedly decreased ($P < 0.05$, respectively), indicating that CS could inhibit TGF β_1 mRNA transcription and, thereby, reducing the TGF β_1 expression (Table 3).

CS reduces PDGF expression

PDGF expression in protein and mRNA level was determined, like TGF β_1 , by immunohistochemistry and *in situ* hybridization respectively. Positive staining was quantified with computer image analyzing system. For the sections of normal control group, positive stains of PDGF and its mRNA could be seen at central vein and periportal areas. In the sections of model control group and CS group, positive stains mainly appeared at fibrotic septa.

PDGF expression in CS group dropped dramatically compared with model control group ($P < 0.01$). But for PDGF mRNA, there was no significant difference by statistical analysis. In spite of this, the means of two groups still suggested difference. To make sure of this, further studies are needed (Table 3).

Table 1 Histological grading

Group	Grade						
	0	1	2	3	4	5	6
Normal	7						
Model		3	1	2	2	2 ^a	
CS		4	5 ^{ab}				

^a $P < 0.05$ vs normal control group, ^b $P < 0.05$ vs model control group.

Table 2 Serum content of HA, LN, ALT and AST ($\bar{x} \pm s$)

Groups	HA ($\mu\text{g/L}$)	LN ($\mu\text{g/L}$)	ALT (U/L)	AST(U/L)
Normal	142.4 \pm 51.0	41.6 \pm 2.2	63.6 \pm 11.9	108.6 \pm 27.7
Model	316.5 \pm 94.1 ^a	59.7 \pm 9.8 ^a	224.3 \pm 178.9 ^a	272.6 \pm 130.1 ^a
CS	202.0 \pm 79.3 ^{ab}	50.4 \pm 3.0 ^{ab}	86.0 \pm 34.4 ^b	146.7 \pm 60.2 ^b

^a $P < 0.05$ vs normal control group, ^b $P < 0.05$ vs model control group.

Table 3 Staining index of procollagen I, III mRNA, TGF β_1 , TGF β_1 mRNA, PDGF and PDGF mRNA in liver tissues ($\bar{x} \pm s$)

Groups	Procoll mRNA	ProcollIII mRNA	TGF β_1	TGF β_1 mRNA	PDGF	PDGF mRNA
Model	2.64 \pm 1.40	0.95 \pm 0.65	1.73 \pm 1.40	3.17 \pm 1.17	1.91 \pm 0.74	0.70 \pm 0.46
CS	1.10 \pm 0.84 ^a	0.36 \pm 0.27 ^c	0.2 \pm 0.14 ^a	1.68 \pm 0.47 ^a	0.87 \pm 0.43 ^b	0.35 \pm 0.34 ^c

^a $P < 0.05$, ^b $P < 0.01$, and ^c $P > 0.05$, vs model control group.

DISCUSSION

In this study, we demonstrated that CS could inhibit hepatic fibrogenesis and retard the development of cirrhosis by evaluating histological grading and serum contents of HA and LN. Its possible mechanism involves inhibiting the synthesis of TGF β_1 mRNA and thereby downregulating the expression of TGF β_1 and PDGF, reducing the deposition of collagen I and III.

CS is a type of traditional Chinese tonic that has already been demonstrated by modern pharmacological researches to have extensively positive effect on a few systems of human body^[13-19]. Recently, some reports suggested that this herb might also have preventive effect on hepatic fibrosis^[4,5]. But the real effect and mechanisms have not been elaborated. This study was designed to evaluate its exact effect on hepatic fibrosis and to investigate its possible mechanism.

Various kinds of chronic liver injury widely spread all over the world and afflicted patients greatly. Effective ways to inhibit fibrogenesis and prevent the development of cirrhosis are of great clinical and academic significance. Although many new agents were being tested, no satisfactory agent with ascertained effectiveness and negligible side effects has appeared as yet. Traditional Chinese herbs were well known for their cheap prices and negligible side effects. Exploration in this area is promising.

We started to treat the rats with CS after 10 days of CCL4 administration. Pathological evaluation showed that rats suffered chronic liver injury in this moment. CS treatment based on this disorder presented its inhibitive effect on preventing the development of cirrhosis. HA and LN are good serum markers of hepatic fibrogenesis^[20]. In this study, serum contents of HA and LN in CS group markedly dropped compared with model control group, which indicates that CS could successfully prevent hepatic fibrogenesis. Histological grading also supported this conclusion.

To address the ways in which this herb yielded in a

significant reduction in fibrosis, we investigated the effect of CS treatment in the expression of TGF β ₁ as well as its mRNA. Overexpression of this cytokine was associated closely with fibrogenesis in many ways^[21-25]. It can promote HSC to synthesize collagen I and III, and simultaneously inhibit their decomposition by upregulating the expression of Tissue Inhibitor of Metalproteinase (TIMP), which neutralize the activity of Matrix Metalproteinase (MMP)^[26-28], an important degrading enzyme of collagen I and III. In addition, TGF β ₁ could also indirectly promote the HSC proliferation by enhancing the expression of PDGF and its receptor^[21]. One strategy in the development of antifibrotic drug is the exploration of TGF β ₁ inhibitors^[21]. Because TGF β ₁ expression was regulated by diverse factors in transcription, post-transcription, secretion and releasing levels, the expression of its protein and mRNA varied considerably^[22]. Consequently, analyses in two levels were indispensable. In this study, we determined the expression of this cytokine by immunohistochemistry and *in situ* hybridization to investigate the effect of CS on TGF β ₁ expression in the both levels. The results showed that both TGF β ₁ and its mRNA expression remarkably decreased in CS group, indicating that CS could downregulate the expression of this important cytokine, which possibly contributed to the reduction of fibrosis.

PDGF is another important cytokine that influences the development of fibrosis. According to the previous reports^[29-33], it is the most potent HSC-proliferation promoter, which plays an important role in fibrogenesis. In spite of its earlier identification and isolation, few pharmacological studies observed the effect of the potential agents on this cytokine. In this study, we initially observed the change of this cytokine responding to CS treatment. Compared with model control group, PDGF expression level in protein of CS group dramatically dropped, indicating that CS could inhibit the PDGF expression. Statistical analysis showed no significant difference of PDGFmRNA expression between the two groups. Whether CS exerts inhibitive effect on PDGF expression in mRNA or directly in protein still remains unclear. Further studies are needed to elucidate the detailed mechanisms.

Pathological feature of hepatic fibrosis is the excessive deposition of ECM components^[34-36]. As the medium of parenchyma cells, constancy of ECM component is essential to the maintenance of liver function. Changes of proportion of ECM components, and the change of their quantities, cause the damage of hepatocytes and the deterioration of liver function. Syntheses of Collagen I and III increase greatly when fibrogenesis occurs, which are mainly responsible for the adverse effects brought about by ECM. As a result, Collagen I and III overshadow other components and become the most important ECM in the development of fibrosis. After nine weeks of CS treatment, expression of procollagen I and III decreased. On one hand, this result further manifests that CS has inhibitive effects on fibrosis; on the other hand, it might be one of the possible explanations for the amelioration of liver function.

CS is a cheap and widely available herb that is well tolerated and has been used for centuries in traditional Chinese medicine without any side effect reported. In this study, we demonstrated that, administered at the stage of chronic hepatitis, CS could successfully inhibit hepatic fibrogenesis and retard the development of cirrhosis. Moreover, it can strikingly ameliorate the liver function. Therefore, we suggest that this herb should serve as a promising antifibrotic agent and deserves further investigations.

REFERENCES

- Lamireau T**, Desmouliere A, Bioulac-Sage P, Rosenbaum J. Mechanisms of hepatic fibrogenesis. *Arch Pediatr* 2002; **9**: 392-405
- Brenner DA**, Waterboer T, Sung Kyu Choi, Lindquist JN, Stefanovic B, Burchardt E, Yamauchi M, Gillan A, Rippe RA. New aspects of hepatic fibrosis. *J Hepatol* 2000; **32** (Suppl 1): 32-38
- Riley TR 3rd**, Bhatti AM. Preventive strategies in chronic liver disease: part II. Cirrhosis. *Am Fam Physician* 2001; **64**: 1735-1740
- Liu YK**, Shen W. Effect of Cordyceps sinensis on hepatocytic proliferation of experimental hepatic fibrosis in rats. *Shijie Huaren Xiaohua Zazhi* 2002; **10**: 388-391
- Ma X**, Qiu DK, Xu J, Zeng MD. Effects of Cordyceps polysaccharides in patients with chronic hepatitis C. *Huaren Xiaohua Zazhi* 1998; **6**: 582-584
- Yang Q**, Yan YC, Gao YX. Inhibitory effect of Quxianruangan Capsulae on liver fibrosis in rats and chronic hepatitis patients. *Shijie Huaren Xiaohua Zazhi* 2001; **9**: 1246-1249
- You H**, Wang B, Wang T. Proliferation and apoptosis of hepatic stellate cells and effects of compound 861 on liver fibrosis. *Zhonghua Ganzhangbing Zazhi* 2000; **8**: 78-80
- Nan JX**, Park EJ, Kim YC, Ko G, Sohn DH. Scutellaria baicalensis inhibits liver fibrosis induced by bile duct ligation or carbon tetrachloride in rats. *J Pharm Pharmacol* 2002; **54**: 555-563
- Wang QC**, Shen DL, Zhang CD, Xu LZ, Nie QH, Xie YM, Zhou YX. Effect of Rangsuoipiwan in expression of tissue inhibitor of metalloproteinase-1/2 in rat liver fibrosis. *Shijie Huaren Xiaohua Zazhi* 2001; **9**: 379-382
- Shen M**, Chen Y, Qiu DK, Xiong WJ. Effects of recombinant augmenter of liver regeneration protein, danshen and oxymatrine on rat fibroblasts. *Shijie Huaren Xiaohua Zazhi* 2001; **9**: 1129-1133
- Wang XL**, Liu P, Liu CH, Liu C. Effects of coordination of FZHY decoction on functions of hepatocytes and hepatic satellite cells. *Shijie Huaren Xiaohua Zazhi* 2001; **7**: 663-665
- Yao XX**, Tang YW, Yao DM, Xiu HM. Effect of yigan decoction on the expression of type I, III collagen proteins in experimental hepatic fibrosis in rats. *Shijie Huaren Xiaohua Zazhi* 2001; **9**: 263-267
- Nakamura K**, Yamaguchi Y, Kagota S, Shinozuka K, Kunitomo M. Activation of in vivo Kupffer cell function by oral administration of Cordyceps sinensis in rats. *Jpn J Pharmacol* 1999; **79**: 505-508
- Huang BM**, Hsu CC, Tsai SJ, Sheu CC, Leu SF. Effects of Cordyceps sinensis on testosterone production in normal mouse Leydig cells. *Life Sci* 2001; **69**: 2593-2602
- Chiou WF**, Chang PC, Chou CJ, Chen CF. Protein constituent contributes to the hypotensive and vasorelaxant activities of Cordyceps sinensis. *Life Sci* 2000; **66**: 1369-1376
- Yamaguchi Y**, Kagota S, Nakamura K, Shinozuka K, Kunitomo M. Antioxidant activity of the extracts from fruiting bodies of cultured Cordyceps sinensis. *Phytother Res* 2000; **14**: 647-649
- Huang BM**, Ju SY, Wu CS, Chuang WJ, Sheu CC, Leu SF. Cordyceps sinensis and its fractions stimulate MA-10 mouse Leydig tumor cell steroidogenesis. *J Androl* 2001; **22**: 831-837
- Dai G**, Bao T, Xu C, Cooper R, Zhu JS. CordyMax Cs-4 improves steady-state bioenergy status in mouse liver. *J Altern Complement Med* 2001; **7**: 231-240
- Yang LY**, Chen A, Kuo YC, Lin CY. Efficacy of a pure compound H1-A extracted from Cordyceps sinensis on autoimmune disease of MRL lpr/lpr mice. *J Lab Clin Med* 1999; **134**: 492-500
- Li BS**, Wang J, Zhen YJ, Liu JX, Wei MX, Sun SQ, Wang SQ. Experimental study on serum fibrosis markers and liver tissue pathology and hepatic fibrosis in immuno-damaged rats. *Shijie Huaren Xiaohua Zazhi* 1999; **7**: 1031-1034
- Bissell DM**. Chronic liver injury, TGF-beta, and cancer. *Exp Mol Med* 2001; **33**: 179-190
- Friedman SL**. Cytokines and fibrogenesis. *Semin Liver Dis* 1999; **19**: 129-140
- Chen WX**, Li YM, Yu CH, Cai WM, Zheng M, Chen F. Quantitative analysis of transforming growth factor beta 1 mRNA in patients with alcoholic liver disease. *World J Gastroenterol* 2002; **8**: 379-381
- Gressner AM**, Weiskirchen R, Breitkopf K, Dooley S. Roles of TGF-beta in hepatic fibrosis. *Front Biosci* 2002; **7**: d793-807
- Lewindon PJ**, Pereira TN, Hoskins AC, Bridle KR, Williamson RM, Shepherd RW, Ramm GA. The role of hepatic stellate cells and transforming growth factor-beta (1) in cystic fibrosis liver disease. *Am J Pathol* 2002; **160**: 1705-1715
- Eichler W**, Friedrichs U, Thies A, Tratz C, Wiedemann P. Modu-

- lation of Matrix Metalloproteinase and TIMP-1 Expression by Cytokines in Human RPE Cells. *Invest Ophthalmol Vis Sci* 2002; **43**: 2767-2773
- 27 **Britton RS**, Bacon BR. Intracellular signaling pathways in stellate cell activation. *Alcohol Clin Exp Res* 1999; **23**: 922-925
- 28 **Li D**, Friedman SL. Liver fibrogenesis and the role of hepatic stellate cells: new insights and prospects for therapy. *J Gastroenterol Hepatol* 1999; **14**: 618-633
- 29 **Kuter DJ**. Future directions with platelet growth factors. *Semin Hematol* 2000; **37** (2 Suppl 4): 41-49
- 30 **Pinzani M**. Pdgf and signal transduction in hepatic stellate cells. *Front Biosci* 2002; **7**: D1720-1726
- 31 **Isbrucker RA**, Peterson TC. Platelet-derived growth factor and pentoxifylline modulation of collagen synthesis in myofibroblasts. *Toxicol Appl Pharmacol* 1998; **149**: 120-126
- 32 **Fibbi G**, Pucci M, Grappone C, Pellegrini G, Salzano R, Casini A, Milani S, Del Rosso M. Functions of the fibrinolytic system in human Ito cells and its control by basic fibroblast and platelet-derived growth factor. *Hepatology* 1999; **29**: 868-878
- 33 **Yuan N**, Wang P, Wang X, Wang Z. Expression and significance of platelet derived growth factor and its receptor in liver tissues of patients with liver fibrosis. *Zhonghua Ganzangbing Zazhi* 2002; **10**: 58-60
- 34 **Benyon RC**, Arthur MJ. Extracellular matrix degradation and the role of hepatic stellate cells. *Semin Liver Dis* 2001; **21**: 373-384
- 35 **Neubauer K**, Saile B, Ramadori G. Liver fibrosis and altered matrix synthesis. *Can J Gastroenterol* 2001; **15**: 187-193
- 36 **Schuppan D**, Ruehl M, Somasundaram R, Hahn EG. Matrix as a modulator of hepatic fibrogenesis. *Semin Liver Dis* 2001; **21**: 351-72

Edited by Ma JY

Effect of cisapride on intestinal bacterial and endotoxin translocation in cirrhosis

Shun-Cai Zhang, Wei Wang, Wei-Ying Ren, Bo-Ming He, Kang Zhou, Wu-Nan Zhu

Shun-Cai Zhang, Wei-Ying Ren, Bo-Ming He, Kang Zhou, Wu-Nan Zhu, Department of Gastroenterology, Zhongshan Hospital, Fudan University, Shanghai, 200032, China

Wei Wang, Institute of Materia Medica, Chinese Academy of Science, Shanghai, 200032, China

Supported by the National Natural Science Foundation No.30070340

Correspondence to: Dr. Shun-Cai Zhang, Department of Gastroenterology, Zhongshan Hospital, Fudan University, 180 Fenglin Road, Shanghai 200032, China. zhangsc.zshospital.@net

Telephone: +86-21-64041990-2424

Received: 2002-06-11 **Accepted:** 2002-07-19

Abstract

AIM: To investigate the effects of cisapride on intestinal bacterial overgrowth (IBO), bacterial and endotoxin translocation, intestinal transit and permeability in cirrhotic rats.

METHODS: All animals were assessed with variables including bacterial and endotoxin translocation, intestinal bacterial overgrowth, intestinal transit and permeability. Bacterial translocation (BT) was assessed by bacterial culture of MLN, liver and spleen, IBO by a jejunal bacterial count of the specific organism, intestinal permeability by determination of the 24-hour urinary ^{99m}Tc -DTPA excretion and intestinal transit by measurement of the distribution of ^{51}Cr in the intestine.

RESULTS: Bacterial translocation (BT) and IBO was found in 48 % and 80 % cirrhotic rats respectively and none in control rats. Urinary excretion of ^{99m}Tc -DTPA in cirrhotic rats with BT (22.2 ± 7.8) was greater than those without BT (10.5 ± 2.9). Intestinal transit (geometric center ratio) was significantly delayed in cirrhotic rats (0.31 ± 0.06) and further more delayed in cirrhotic rats with BT (0.24 ± 0.06) than those without BT (0.38 ± 0.11). Cirrhotic rats with IBO had significantly higher rates of intestinal bacterial and endotoxin translocation, slower intestinal transit time and higher intestinal permeability than those without IBO. It was also found that BT was closely associated with IBO and the injury of intestinal barrier. Compared with the placebo group, cisapride-treated rats had lower rates of bacterial/endotoxin translocation and IBO, which was closely associated with increased intestinal transit and improved intestinal permeability by cisapride.

CONCLUSION: These results indicate that endotoxin and bacterial translocation in cirrhotic rats may be attributed to IBO and increased intestinal permeability. Cisapride that accelerates intestinal transit and improve intestinal permeability might be helpful in preventing intestinal bacterial and endotoxin translocation.

Zhang SC, Wang W, Ren WY, He BM, Zhou K, Zhu WN. Effect of cisapride on intestinal bacterial and endotoxin translocation in cirrhosis. *World J Gastroenterol* 2003; 9(3): 534-538
<http://www.wjgnet.com/1007-9327/9/534.htm>

INTRODUCTION

Cirrhotic patients have an increasing susceptibility to bacterial infection, such as spontaneous bacterial peritonitis (SBP) and bacteremia, which are mainly caused by aerobic gram-negative organism of enteric origin^[1,2]. Bacteria of enteric origin crossing the intestinal barrier to the mesenteric lymph nodes (MLN), a phenomenon known as bacterial translocation (BT) has recently been documented to occur commonly in cirrhotic rats compared to normal rats. BT has also been reported to be involved in the development of SBP in experimental models of ascitic cirrhosis^[3-5]. The major mechanisms concerning bacterial translocation are deficiencies in local host immune defense, increased permeability of gut barrier and intestinal bacterial overgrowth (IBO). Certain pathological conditions such as shock, sepsis, trauma, burns, intestinal radiation, antibiotic overdose, malnutrition and immuno-suppression are closely related to BT and endotoxemia^[6-8]. Although it has been showed that several mechanisms are involved in development of BT in liver cirrhosis^[9-13], the increased intestinal permeability and IBO due to intestinal mucous membrane congestion and edema attributed to portal hypertension are considered the most important^[13,14]. However, so far there have been not satisfied methods for prevention and treatment of intestinal endotoxemia. Strategies to reduce the intestinal bacterial translocation (BT) and endotoxemia in patients and experimental models of cirrhosis have mainly focused on the selective intestinal decontamination^[15,16]. In this way the effectiveness of alternative antibiotics might be decreased with time because of the selection of resistant bacterial strains that could subsequently colonize the gut and become a potential source of infection, especially in patients with long-time prophylactic treatment. So nonantibiotic drugs are needed to be evaluated in the treatment and prevention of bacterial and endotoxin translocation in cirrhosis and decided whether or not to be applied to the clinical practice^[17].

Cisapride is a 5-HT₄ agonist that can accelerate the movement of the intestine. Many studies have reported that the intestinal bacterial and endotoxin translocation were closely related to IBO and intestinal hypomotility.

In this study we intend to study the effect of cisapride on intestinal transit and the permeability of gut barrier, two factors that are closely associated with intestinal bacterial and endotoxin translocation in cirrhotic rats.

MATERIALS AND METHODS

One hundred and sixty male Sprague-Dawley rats weighing 180-200 g were included in the study. Animals were caged in a controlled room temperature of 21 °C with a 12-hour light/dark cycle and fed standard rat diet with water *ad libitum*. The study was in accordance with guideline for animal research and was approved by the ethical and research committee of the hospital.

Cirrhotic animal model

Cirrhosis was induced in one hundred and thirty-five rats by subcutaneous injection of 50 % CCl₄-olive oil solution twice

a week at an initial dose of 0.6 ml/100 g. Subsequent dosage was adjusted with body weight changes at a dose of 0.3 ml/100 g for 12 weeks. Seventy rats died during the induction of cirrhosis with a mortality of 50 % on average. At last sixty-five cirrhotic rats were used for further study.

Experimental design

25 rats were assigned as healthy controls (group 1). 65 cirrhotic rats were further divided into three groups. Group 2, which included 25 cirrhotic animals without any treatment, was used to study various parameter changes in cirrhosis. Group 3 was consisted of 20 cirrhotic animals with intragastric administration of cisapride suspension for two weeks and used to determine whether cisapride had effects on BT, endotoxemia, IBO, intestinal transit and intestinal permeability. Another 20 cirrhotic animals receiving equal volume of saline to cisapride suspension were named group 4 and used as cirrhotic controls.

Determination of parameters

Animals were fasted for 8 hours before killed. All experimental procedures were performed in sterile conditions. The animals were anesthetized by injection of 2 % pento-barbital sodium into abdominal cavity at a dose of 25–40 mg/kg. At the first day of experiment the rats were fed 5 μ ci of ^{99m}Tc -diethylenetriamine pentaacetic acid (^{99m}Tc -DTPA) (dissolved in 2 ml water) and housed individually in metabolic cages to collect 24-hour urine for further analysis. At the second day, after another 8-hour fasting animals were given 2 ml water containing 2 μ ci of ^{51}Cr through a gastric tube. Thirty minutes later animals were anesthetized and undergone a laparotomy under strict aseptic conditions. After small intestine was ligated at both ends MLN, liver, spleen and intestine were carefully removed out of the cavity. Blood samples were taken from the inferior vena cava.

Intestinal permeability

Intestinal permeability was determined by the 24-hour urinary excretion of ^{99m}Tc -DTPA. Results were expressed as fractional excretion of the radioactive substance. ^{99m}Tc -DTPA was a macromolecule and rarely absorbed into bloodstream through intestinal mucous membrane. When the intestinal permeability was increased as a result of intestinal mucous membrane injury, The absorption of DTPA into blood stream and thus excretion from urine would be increased. Therefore, increased excretion of DTPA from urine was assumed to be reliable index of intestinal permeability^[18, 19].

Intestinal transit

Measurement of intestinal transit by determining the distribution of ^{51}Cr in the intestine was performed in all animals^[20–22]. Special care was taken to prevent movement of intestinal contents in experimental procedures. After separated from the mesentery intestine was removed out of the abdominal cavity, put longitudinally in a moist container and then divided by the ligation of threads into 5-cm segments from orad to aborad. The radioactivity of every segment was measured with gamma-scintillation. Intestinal transit was expressed as the geometric center of ^{51}Cr distribution within the intestine and was calculated as the sum of the products of the fraction of the total administered dose of radioactivity per segment and the segment number. The geometric center were divided by the total number of segments of each rat to correct the difference in the length of intestine and finally expressed as geometric center ratio, which was regarded to be the most accurate method for measurement of intestinal transit.

BT studies

BT from the intestinal lumen was defined on the basis of

positive culture of MLNs (particularly those draining lymph from ileum and cecum), liver, spleen and blood and excluding the infection from other possible sources. All the samples were immediately stored at $-70\text{ }^{\circ}\text{C}$ until detection. MLNs, liver and spleen were washed free of blood with sterile saline solutions (SS) and made 10 % tissue-slurry (1 g tissue plus 10 ml sterile SS), then immediately cultured in agar-blood medium plates.

IBO studies

IBO was defined as a jejunal bacterial count of the specific organism that was more than the mean plus two standard deviations of the same organism count in control rats. For the determination of IBO, 0.1 ml of jejunal contents were obtained under aseptic conditions by needle puncture. Then 20 μ l of samples that were diluted 100 or 1 000 folds respectively were cultured in blood-agar plates. After an incubation period of 24–48 hours, the number of colony-forming units (CFUs) was counted. Moreover, the composition of the isolated flora was determined with standard identification techniques. The results were expressed as CFU/ml of jejunal contents.

Determination of serum endotoxin

All the blood specimens for the endotoxin determination were stored in endotoxin-free tubes. The serum was separated by 8 000 g 10 min. Serum level of endotoxin was determined by limulus ameobatic lysate (LAL) test with LAL kits (purchased from Shanghai medical-chemical institute).

Statistical analysis

Data are presented as means \pm SD or proportions as required. Comparisons of quantitative variables among groups were made with the 1-way ANOVA or its corresponding nonparametric test as required. The χ^2 test was used for comparing proportion. The Spearman or Pearson test was used for correlation analyses when appropriate. A *P* value of <0.05 was considered statistically significant.

RESULTS

BT was found in 12 of 25 (48 %) cirrhotic rats and none in control rats (Table 1, $P < 0.01$). IBO was present in 20 of 25 cirrhotic rats (80 %) and none in the control rats. All the 12 cirrhotic rats with BT and 63 % of 13 cirrhotic rats without BT were found having IBO (Table 2). The translocated bacteria were *Escherichia coli* in 10 cirrhotic rats and *Klebsiella P.* and *Enterococcus* in other two rats respectively. The same organism was always found at the same time both in BT and IBO. (Table 3).

BT was observed in 11 of the 20 rats with IBO and in only one of the five rats without IBO (55 % vs 20 %, $P < 0.05$) (Figure 1). Endotoxin level was measured in the blood of inferior vena cava of all animals and higher endotoxin level was found in cirrhotic rats. Animals with BT or IBO have higher blood endotoxin level than that without. Intestinal transit was significantly delayed in cirrhotic rats and much more delayed in that with BT. This may result from IBO because cirrhotic rats with IBO have more delayed intestinal transit than that without.

Urinary ^{99m}Tc -DTPA excretion was greatly increased in cirrhotic rats than that of their controls. Although the urinary ^{99m}Tc -DTPA excretion in cirrhotic rats with IBO was more than that without the difference was not significant. Similarly urinary ^{99m}Tc -DTPA excretion in cirrhotic rats with BT was more than that without. All of these showed that severer impairment of mucous membrane barrier that had occurred in cirrhotic rats, which might be the key factor to promote occurrence of BT.

The mortality of rats was similar in both cisapride and placebo-treated animals. BT was present in 1 of the 20 cirrhotic rats treated with cisapride and in 11 of the 20 rats receiving placebo (5 % vs 58 %, $P < 0.01$). IBO incidence in cirrhotic rats

receiving cisapride suspension was lower than that treated with placebo. Lower serum endotoxin level and faster intestinal transit was found in cirrhotic rats with cisapride treatment than that in the placebo group. (Table 4) Intestinal permeability as showed by the urinary ^{99m}Tc -DTPA excretion was reduced significantly after cisapride treatment.

Table 1 Characteristics of control and cirrhotic rats

	Control rats	Cirrhotic rats
Number of animal	25	25
IBO(%)	0	20/25(80%) ^b
Total jejunal bacteria contents (CFU/ml)	0.54±0.18	1.59±0.48 ^b
Bacterial translocation(%)	0	12/25(48%) ^b
Endotoxin level(pg/ml)	0.11±0.058	0.648±0.134 ^b
Intestinal transit (geometric center ratio)	0.49±0.08	0.31±0.06 ^a
Intestinal permeability (%urinary excretion of ^{99m}Tc -DTPA)	1.62±0.8	16.1±7.6 ^b

^b*P*<0.01 vs control rats; ^a*P*<0.05 vs control rats.

Table 2 Characteristics of Cirrhotic rats with and without BT

	Cirrhotic rats with BT	Cirrhotic rats without BT
Number of animal	12	13
IBO(%)	100%	63% ^a
Total jejunal bacteria contents (CFU/ml)	2.61±0.56	0.65±0.12 ^b
Endotoxin level(pg/ml)	0.873±0.137	0.440±0.108 ^b
Intestinal transit (geometric center ratio)	0.24±0.06	0.38±0.11 ^a
Intestinal permeability (%urinary excretion of ^{99m}Tc -DTPA)	22.2±7.8	10.5±2.9 ^b

^b*P*<0.01 vs cirrhotic rats with BT; ^a*P*<0.05 vs cirrhotic rats with BT.

Table 3 Bacterial species cultured from mesenteric lymph nodes, liver, spleen, peripheral blood and overgrowth in the jejunum

No.	Mesenteric lymph nodes	Liver	Spleen	Blood	Intestinal bacterial overgrowth
1	E.coli	E.coli	E.coli	-	E.coli
2	E.coli	E.coli	E.coli	E.coli	E.coli
3	E.coli	E.coli	E.coli	E.coli	E.coli
4	E.coli	E.coli	E.coli	E.coli	E.coli
5	-	E.coli	-	-	E.coli
6	E.coli	E.coli	-	-	E.coli
	Ps. aeruginosa	-	-	-	Ps. aeruginosa
7	E.coli	-	E.coli	-	E.coli
8	P klebsiella	-	-	-	P klebsiella
9	E.coli	E.coli	-	-	E.coli
	P. mirabilis	-	-	-	P. mirabilis
10	-	E.coli	E.coli	-	E.coli
11	P enterococcus	-	SP	-	P enterococcus
	E.coli	-	enterococcus	-	E.coli
12	E.coli	-	-	E.coli	E.coli

Abbreviations: E. coli, Escherichia coli; P. mirabilis, Proteus mirabilis; Ps. Aeruginosa, Pseudomonas aeruginosa, P klebsiella: Pneumonia Klebsiella.

Table 4 Effect of cisapride on BT, IBO, serum endotoxin level, intestinal transit and intestinal permeability of cirrhotic rats

	Placebo	Cisapride
Number of animal	20	20
Bacterial translocation (%)	11/20(55%)	2/20(10%) ^b
IBO(%)	16/20(80%)	3/20(15%) ^b
Total jejunal bacteria contents (CFU/ml)	1.60±0.42	0.60±0.58 ^a
Endotoxin level(pg/ml)	0.721±0.123	0.148±0.079 ^b
Intestinal transit (geometric center ratio)	0.33±0.08	0.68±0.16 ^b
Intestinal permeability (%urinary excretion of ^{99m}Tc -DTPA)	17.2±5.98	12.2±5.28 ^a

^b*P*<0.01 vs placebo; ^a*P*<0.05 vs placebo.

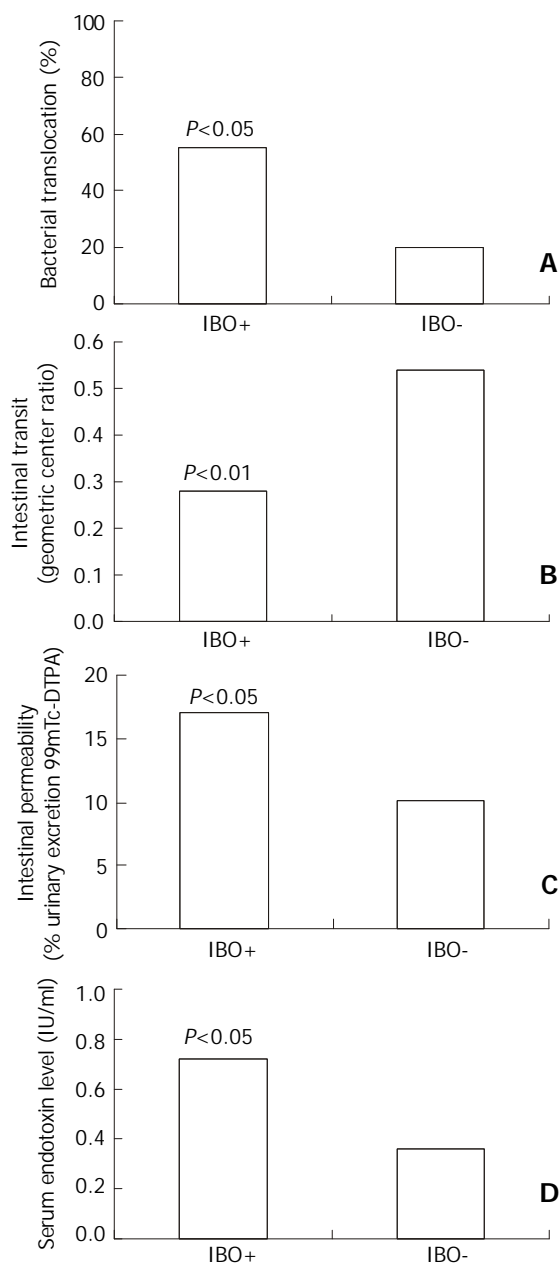


Figure 1 Bacterial translocation, intestinal transit, intestinal permeability and serum endotoxin level in cirrhotic rats with and without IBO (IBO+, IBO-, respectively). Cirrhotic rats with IBO have a higher incidence of BT (A), slower intestinal transit (B), higher intestinal permeability (C) and higher serum endotoxin level (D) than that of cirrhotic rats without IBO.

DISCUSSION

Many studies have shown a high susceptibility to bacterial infection among cirrhotic patients. In recent years, IBO and BT have been suggested to be involved in the pathogenesis of gut-origin bacterial infections, such as SBP, in animal with cirrhosis^[21-23]. Although the phenomenon of BT has been recognized for more than a century, the precise mechanism of BT remains to be elucidated. IBO is postulated to be one of the major factors of BT. Guarner *et al*^[24,25] have shown that the intestinal aerobic bacterial count in cecal stool is significantly increased in CCl₄ induced cirrhotic rats with BT as compared with without and the prevalence of SBP was found to be significantly higher in cirrhotic patients with IBO than in those without. Reilly JA and Perez-Paramo M have reported that the incidence of IBO was significantly higher in cirrhotic patients with SBP than in those without^[21,22]. Pardo *et al*^[26] have observed that jejunal IBO were significantly higher in ascitic cirrhotic rats with BT than in those without, for a specific organism BT was always associated with its IBO, which suggests that the IBO favors the development of BT in experimental cirrhosis. In this experimental study, we have observed a direct relationship between the IBO and BT, which also suggests that IBO is one of the major mechanisms that promote BT in experimental models. However, The fact that not all cirrhotic rats with IBO developed BT suggested that other factors may play an important role in development of BT. It had been reported that impairment of gut barrier was a necessary process in the development of BT. Our result that higher value of urinary excretion of ^{99m}Tc-DTPA was seen in BT rats other than in that without was also suggested that the impairment of gut barrier was an important factor in promoting BT.

The mechanisms of gut barrier impairment were not completely elucidated. Some putative mechanisms have been proposed from animal and clinical studies. Portal hypertension in liver cirrhosis may be the most attractive factor in the impairment of gut barrier^[26,27]. However, many studies have showed that poor linear relationship existed between the severity of high portal pressure and the impairment in intestinal permeability and that there was lack of improvement in permeability after reducing portal pressure^[21]. It was possible that increased intra-luminal endotoxin level resulted from IBO played a contributory role in the damage to the gut barrier^[21]. Our results of reduced incidence of IBO and improved intestinal permeability after cisapride treatment have shown the effect of endotoxin on the impairment of gut barrier.

Prevention of IBO was dependent on normal intestinal motility. Intestinal hypomotility was a main cause of IBO in cirrhotic animals^[21,22, 24,25]. This was supported by the delayed intestinal transit in cirrhotic animals with IBO and by the lower incidence of IBO in cirrhotic animals treated with cisapride, a drug that shortens bowel transit time.

During physiological processes, endotoxin is released from the bowel and detoxified by Kupffer cells and hepatocytes. High levels of endotoxin have been noted in cirrhotic patients. A number of previous studies have been shown that the plasma endotoxin level may be potentially helpful in the diagnosis of bacterial infection in patients with cirrhosis^[27]. Recently a study revealed that increased levels of endotoxin indicated the occurrence of gram-negative bacterial infection^[28,29]. In this study, we observed that the serum endotoxin level of the cirrhotic rats, especially those with IBO and BT, was much higher than that of healthy rats. The results suggested that endotoxemia caused by enteric bacteria was common in experimental cirrhosis and positively correlated with IBO and BT.

Several circumstances in cirrhosis could predispose a patient to IBO, such as alcohol abuse, malnutrition, hypochlorhydria,

decreased intraluminal immunoglobulin A or bile salts in the intestine, and disturbances of the small intestinal motility^[6-8,12]. Among which, prolonged intestinal transit, as a consequence of altered intestinal motility seems to play a major role in the development of IBO. Altered small intestinal motility was described in patients with cirrhosis^[8,30,31]. Pardo and his associates^[26] have recently found that alterations in small intestinal motility could result in a prolonged intestinal transit time in cirrhotic patients, which might facilitate the appearance of IBO and the 10-day treatment with prokinetic drug resulted in a marked reduction in jejunal bacterial content and BT in cirrhotic rats^[21], which was coincide with our present study. In addition, and even more important, the prokinetic drug treatment was associated with a dramatic reduction in serum endotoxin level. Although the exact mechanisms by which the prokinetic drug reduce the incidence of BT, endotoxemia and IBO could not be completely elucidated on the basis of the present study, the observations that the serum endotoxin level was positively correlated with jejunal bacterial overgrowth, and that the prokinetic drug administration reduce not only IBO and BT but also endotoxin level, suggested that the beneficial effects of prokinetic drug may be due to the increasing of bowel movement and the promoting of intestinal bacterial and endotoxin elimination, which has been shown by shortened intestinal transit time in cisapride-treated group. Moreover, the administration of prokinetic drug could improve intestinal permeability in cirrhotic rats, which also suggested that increased intestinal permeability in cirrhotic rats was partially due to the damage of intestinal mucous membrane by bacteria overgrowth and high concentrations because cisapride has no direct protective effect on intestinal mucous membrane. In fact, it has been reported that prolonged the OCT could be significantly recovered in cirrhotic patients after cisapride therapy. These results suggested that the beneficial effect of the prokinetic drug on endotoxemia may be due to increasing the abolition of intestinal bacteria through the prokinetic effect. Unfortunately cisapride has lethal side-effect and has been prohibited to be used in treatment of disturbance of intestinal function in human. However, new prokinetic drugs have been available in the market and showed with similar effect on intestinal movement as cisapride. Therefore oral administration of prokinetic drugs might be beneficial to liver diseases by reducing absorption of endotoxin, a substance that is toxic to hepatocytes and could aggravate liver diseases.

In conclusion, the results of our experimental study indicated that the administration of prokinetic drug to cirrhotic rats resulted in a reduction of endotoxemia and BT incidence, which was accompanied by a marked decrease of IBO, reduced intestinal transit time and intestinal permeability. These findings suggested the beneficial effects of prokinetic drug on the prophylaxis of gut origin infection in cirrhosis, which should be taken as an adjuvant or alternative therapy to the selective intestinal decontamination with antibiotics.

REFERENCES

- 1 **Caly WR**, Strauss E. A prospective study of bacterial infections in patients with cirrhosis. *J Hepatol* 1993; **18**: 353-358
- 2 **Bauer TM**, Steinbruckner B, Brinkmann FE, Ditzen AK, Schwacha H, Aponte JJ, Pelz K, Kist M, Blum HE. Small intestinal bacterial overgrowth in patients with cirrhosis: prevalence and relation with spontaneous bacterial peritonitis. *Am J Gastroenterol* 2001; **96**: 2962-2967
- 3 **Llovet JM**, Bartoli R, March F, Planas R, Vinado B, Cabre E, Arnal J, Coll P, Ausina V, Gassull MA. Translocated intestinal bacteria cause spontaneous bacterial peritonitis in cirrhotic rats: molecular epidemiologic evidence. *J Hepatol* 1998; **28**: 307-313
- 4 **Llovet JM**, Bartoli R, Planas R, Vinado B, Perez J, Cabre E, Arnal J, Ojanguren I, Ausina V, Gassull MA. Selective intestinal decon-

- tamination with norfloxacin reduces bacterial translocation in ascitic cirrhotic rats exposed to hemorrhagic shock. *Hepatology* 1996; **23**: 781-787
- 5 **Garcia-Tsao G**, Lee FY, Barden GE, Cartun R, West AB. Bacterial translocation to mesenteric lymph nodes is increased in cirrhotic rats with ascites. *Gastroenterology* 1995; **108**: 1835-1841
- 6 **Casafont F**, Sanchez E, Martin L, Aguero J, Romero FP. Influence of malnutrition on the prevalence of bacterial translocation and bacterial spontaneous bacterial peritonitis in experimental cirrhosis in rats. *Hepatology* 1997; **25**: 1334-1337
- 7 **Plummer JL**, Ossowicz CJ, Whibley C, Ilsley AH, Hall PD. Influence of intestinal flora on the development of fibrosis and cirrhosis in rat model. *J Gastroenterol Hepatol* 2000; **15**: 1307-1311
- 8 **Jackson GD**, Dai Y, Sewell WA. Bile mediates intestinal pathology in endotoxemia in rats. *Infect Immun* 2000; **68**: 4714-4719
- 9 **Madrid AM**, Cumsille F, Defilippi C. Altered small bowel motility in patients with liver cirrhosis depends on severity of liver disease. *Dig Dis Sci* 1997; **42**: 738-742
- 10 **Chang CS**, Chen GH, Lien HC, Yeh HZ. Small intestine dysmotility and bacterial overgrowth in cirrhotic patients with spontaneous bacterial peritonitis. *Hepatology* 1998; **28**: 1187-1190
- 11 **Achord JL**. Mortality associated with spontaneous bacterial peritonitis. *J Clin Gastroenterol* 2001; **33**: 295-298
- 12 **Ramachandran A**, Balasubramania KA. Intestinal dysfunction in liver cirrhosis: its role in spontaneous bacterial peritonitis. *J Gastroenterol Hepatol* 2001; **16**: 607-612
- 13 **Garcia-Tsao G**, Albillos A, Barden GE, West AB. Bacterial translocation in acute and chronic portal hypertension. *Hepatology* 1993; **17**: 1081-1085
- 14 **Veal N**, Auduberteau H, Lemarie C, Oberti F, Cales P. Effects of octreotide on intestinal transit and bacterial translocation in conscious rats with portal hypertension and liver fibrosis. *Dig Dis Sci* 2001; **46**: 2367-2373
- 15 **Runyon BA**, Borzio M, Young S, Squier SU, Guarner C, Runyon MA. Effect of selective bowel decontamination with norfloxacin on spontaneous bacterial peritonitis translocation and survival in an animal model of cirrhosis. *Hepatology* 1995; **21**: 1719-1724
- 16 **Guarner C**, Runyon BA, Heck M, Young S, Sheikh MY. Effect of long-term trimethoprim-sulfamethoxazole prophylaxis on ascites formation, bacterial translocation, spontaneous bacterial peritonitis and survival in cirrhotic rats. *Dig Dis Sci* 1999; **44**: 1957-1962
- 17 **Nanji AA**, Khettry U, Sadrzadeh SM. Lactobacillus feeding reduces endotoxemia and severity of experimental alcoholic liver (disease). *Proc Soc Exp Biol Med* 1994; **205**: 243-247
- 18 **Bjarnason I**, Macpherson A, Hollander D. Intestinal permeability: an overview. *Gastroenterology* 1995; **108**: 1566-1581
- 19 **Campillo B**, Pernet P, Bories PN, Richardet JP, Devanlay M, Aussel C. Intestinal permeability in liver cirrhosis: relationship with severe septic complications. *Eur J Gastroenterol Hepatol* 1999; **11**: 755-759
- 20 **Miller MS**, Galligan JJ, Burks TF. Accurate measurement of intestinal transit in the rat. *J Pharmacol Methods* 1981; **6**: 211-217
- 21 **Reilly JA Jr**, Quigley EM, Forst CF, Rikkens LF. Small intestinal transit in the portal hypertensive rat. *Gastroenterology* 1991; **100**: 670-674
- 22 **Perez-Paramo M**, Munoz J, Albillos A, Freile I, Portero F, Santos M, Ortiz-Berrocal J. Effect of propranolol on the factors promoting bacterial translocation in cirrhotic rats with ascites. *Hepatology* 2000; **31**: 43-48
- 23 **Llovet JM**, Bartoli R, Planas R, Cabre E, Jimenez M, Urban A, Ojanguen I, Arnal J, Gassull MA. Bacterial translocation in cirrhotic rats. Its role in the development of spontaneous bacterial peritonitis. *Gut* 1994; **35**: 1648-1652
- 24 **Guarner C**, Soriano G. Spontaneous bacterial peritonitis. *Semin Liver Dis* 1997; **17**: 203-217
- 25 **Guarner C**, Runyon BA, Young S, Heck M, Sheikh MY. Intestinal bacterial overgrowth and bacterial translocation in cirrhotic rats with ascites. *J Hepatol* 1997; **26**: 1372-1378
- 26 **Pardo A**, Bartoli R, Lorenzo-Zuniga V, Planas R, Vinado B, Riba J, Cabre E, Santos J, Luque T, Ausina V, Gassull MA. Effect of cisapride on intestinal bacterial overgrowth and bacterial translocation in cirrhosis. *Hepatology* 2000; **31**: 858-863
- 27 **Cirera I**, Bauer TM, Navasa M, Vila J, Grande L, Taura P, Fuster J, Garcia-Valdecasas JC, Lacy A, Suarez MJ, Rimola A, Rodes J. Bacterial translocation of enteric organisms in patients with cirrhosis. *J Hepatol* 2001; **34**: 32-37
- 28 **Kuo CH**, Changchien CS, Yang CY, Sheen IS, Liaw YF. Bacteremia in patients with cirrhosis of the liver. *Liver* 1991; **11**: 334-339
- 29 **Chan CC**, Hwang SJ, Lee FY, Wang SS, Chang FY, Li CP, Chu CJ, Lu RH, Lee SD. Prognostic value of plasma endotoxin levels in patients with cirrhosis. *Scand J Gastroenterology* 1997; **32**: 942-946
- 30 **Madrid AM**, Hurtado C, Venegas M, Cumsille F, Defilippi C. Long-Term treatment with cisapride and antibiotics in liver cirrhosis: effect on small intestinal motility, bacterial overgrowth, and liver function. *Am J Gastroenterol* 2001; **96**: 1251-1255
- 31 **Madrid AM**, Brahm J, Antezana C, Gonzalez-Koch A, Defilippi C, Pimentel C, Oksenberg D, Defilippi C. Small bowel motility in primary biliary cirrhosis. *Am J Gastroenterol* 1998; **93**: 2436-2440

Effects of transmitters and interleukin-10 on rat hepatic fibrosis induced by CCl₄

Xiao-Zhong Wang, Li-Juan Zhang, Dan Li, Yue-Hong Huang, Zhi-Xin Chen, Bin Li

Xiao-Zhong Wang, Li-Juan Zhang, Dan Li, Yue-Hong Huang, Zhi-Xin Chen, Bin Li, Department of Gastroenterology, The Affiliated Union Hospital, Fujian Medical University, Fuzhou, 350001, Fujian Province, China

Supported by Natural Science Foundation of Fujian Province, No. C96042

Correspondence to: Xiao-Zhong Wang, Department of Gastroenterology, The Affiliated Union Hospital, Fujian Medical University, Fuzhou, 350001, Fujian Province, China. drwangxz@public6.fz.fj.cn

Telephone: +86-591-3357896 Ext 8482

Received: 2002-07-31 **Accepted:** 2002-10-12

Abstract

AIM: To study the effects of transmitters ET, AgII, PGI₂, CGRP and GG on experimental rat hepatic fibrosis and the antifibrogenic effects of IL-10.

METHODS: One hundred SD rats were randomly divided into 3 groups: control group (N): intraperitoneal injection with saline 2 ml·kg⁻¹ twice a week; the fibrogenesis group (C): intraperitoneal injection with 50 % CCl₄ 2 ml·kg⁻¹ twice a week; IL-10 treated group (E): besides same dosage of CCl₄ given, intraperitoneal injection with IL-10 4 ug·kg⁻¹ from the third week. In the fifth, the seventh and the ninth week, rats in three groups were selected randomly to collect plasma and liver tissues. The levels of ET, AgII, PGI₂, CGRP and GG were assayed by radioimmunoassay (RIA). The liver fibrosis was observed with silver staining.

RESULTS: The hepatic fibrosis was developed with the increase of the injection frequency of CCl₄. The ET, AgII, PGI₂, CGRP and GG levels in serum of group N were 71.84±60.2 ng·L⁻¹, 76.21±33.3 ng·L⁻¹, 313.03±101.71 ng·L⁻¹, 61.97±21.4 ng·L⁻¹ and 33.62±14.37 ng·L⁻¹, respectively; the levels of them in serum of group C were 523.30±129.3 ng·L⁻¹, 127.24±50.0 ng·L⁻¹, 648.91±357.29 ng·L⁻¹, 127.15±62.0 ng·L⁻¹ and 85.26±51.83 ng·L⁻¹, respectively; the levels of them in serum of group E were 452.52±99.5 ng·L⁻¹, 90.60±44.7 ng·L⁻¹, 475.57±179.70 ng·L⁻¹, 102.2±29.7 ng·L⁻¹ and 38.05±19.94 ng·L⁻¹, respectively. The histological examination showed that the degrees of the rats liver fibrosis in group E were lower than those in group C.

CONCLUSION: The transmitters ET, AgII, PGI₂, CGRP and GG play a significant role in the rat hepatic fibrosis induced by CCl₄. IL-10 has the antagonistic action on these transmitters and can relieve the degree of the liver fibrosis.

Wang XZ, Zhang LJ, Li D, Huang YH, Chen ZX, Li B. Effects of transmitters and interleukin-10 on rat hepatic fibrosis induced by CCl₄. *World J Gastroenterol* 2003; 9(3): 539-543
<http://www.wjgnet.com/1007-9327/9/539.htm>

INTRODUCTION

Hepatic fibrosis is a disease which is characterized by an

increase of type I and type III collagens, proteoglycans fibronectin and hyaluronic acid in extracellular matrix (ECM) deposition^[1-9]. It is an inevitable phase during the formation of liver cirrhosis, which is an irreversible stage of several liver pathological changes^[10-12]. So it is important for how to prevent and cure hepatic fibrosis, i.e. antifibrogenetic treatment. Transmitters play an important role in the portal hypertension which is associated with the fibrosis^[13,14]. In our study, the transmitters endothelin (ET), angiotensin II (Ag II), prostacyclin (PGI₂), calcitonin-gene related peptide (CGRP) and glucagon (GG) were selected to explore their effects on hepatic fibrosis induced by CCl₄ and the antifibrogenesis effect of interleukin-10 (IL-10) was explored as well.

MATERIALS AND METHODS

Animals

One hundred clean SD rats weighing 140-180 g were randomly divided into 3 groups. The control group (group N) included 24 rats; the fibrogenesis group (group C) included 40 rats and the IL-10 treated group (group E) included 36 rats, respectively. All the rats were breeding in the routine condition (room temperature 22±2 °C, humidity 55±5 %, lighting 12hrs per day, to drink tap water and eat in any time when they needed, animal food was provided by BK company in shanghai.).

Establishment of the fibrosis model

Rats in group N were injected intraperitoneally with saline 2 ml·kg⁻¹ twice a week. Rats in group C and group E were injected intraperitoneally with 50 % CCl₄ 2 ml·kg⁻¹ twice a week^[15]. From the third week, rats in group E were injected intraperitoneally with IL-10 4 ug·kg⁻¹ (dissolved in saline)^[16] 20 minutes before they were injected with CCl₄. All injections were performed in Monday and Thursday, rats' body weight was recorded before the injection. In the fifth week, 3 rats in group C and 2 rats in group E died, in the seventh week, total 8 rats in group C and 4 rats in group E died, in the ninth week, total 10 rats in group C, 6 rats in group E and 3 rats in group N died. In 5,7,9 weeks, 10 rats of group C and E and 7 rats in the control group were selected randomly to collect their plasma and liver tissue samples.

Assessment of samples

The blood samples were added into the tubes with 30 µl 10 % EDTA and 40 µl trasylol in ice bath, the tubes were centrifuged at 3 000 rpm for 10 minutes at 4 °C, then the plasma was frozen for the assessment. The plasma levels of ET, Ag II, PGI₂, CGRP and GG were assayed by radioimmunoassay (RIA, kits provided by EastAsia Immune-technology Institute, Beijing). Each plasma sample was taken 100 µl into the tube, then 200 µl buffer and 100 µl antiserum were added into each sample, they were agitated and incubated for 24 hour at 4 °C; then 100 µl ¹²⁵I-marked serum was added, agitated and incubated for 24 hour at 4 °C; also 500 µl precipitation was added, after incubation for 20 min at room temperature, the tubes were centrifuged at 3 500 rpm for 25 min at 4 °C, the upper layer was carefully removed, the cpm account was measured using γ

radioimmuno-counter. The blank control and the standard control was measured respectively at the same time. The liver tissue was made of paraffin section with silver staining.

Statistical analysis

All data were expressed as $\bar{x} \pm s$, *t* test was used for comparison between groups.

RESULTS

Plasma levels of ET, AgII, 6-K-PGF_{1α}, CGRP and GG

The plasma levels of ET, AgII, 6-K-PGF_{1α}, CGRP and GG in group C were higher than those in the control (*P*<0.05). After the intervention of IL-10, the levels of them were decreased, and had no difference with group N (*P*>0.05). Furthermore, their levels were increased with the development of hepatic fibrosis.

Table 1 Plasma levels of ET, AgII, 6-K-PGF_{1α}, CGRP and GG in fibrosis and normal rats (ng·L⁻¹)

<i>n</i>	ET	AgII	6-K-PGF _{1α}	CGRP	GG
N 21	71.84±60.2	76.21±33.3	313.03±101.71	61.97±21.4	33.62±14.37
C ^a 30	523.30±129.3	127.24±50.0	648.91±357.29	127.15±62.0	85.26±51.83
E ^b 30	452.52±99.5	90.60±44.7	475.57±179.70	102.2±29.7	38.05±19.94

^a*P*<0.05 vs group N, ^b*P*<0.05 vs group N.

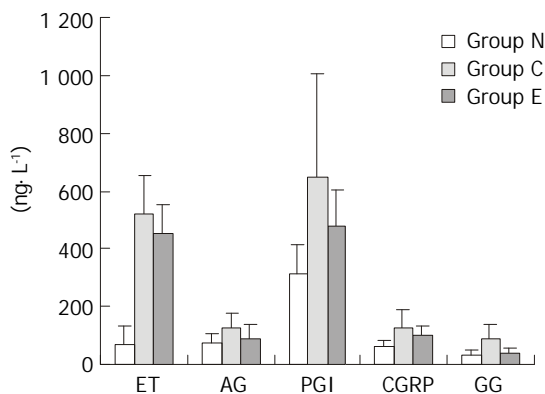


Figure 1 Plasma levels of ET, AgII, 6-K-PGF_{1α}, CGRP and GG in fibrosis and normal rats.

Table 1 and Figure 1 showed that after the treatment of CCl₄, the plasma levels of ET, AgII, 6-K-PGF_{1α}, CGRP and GG were increased, their levels were significantly higher than those in the normal controls (*P*<0.05). After treated with IL-10, their levels were obviously decreased, and there was no significant difference with those in the normal controls. It was showed that when the effective treatment was applied in the fibrosis rats, the levels of these transmitters showed the descending trend. It suggested that the levels of those transmitters were increased in liver fibrosis and they might play important pathogenic roles during the development of liver fibrosis.

Table 2 Plasma levels of ET, AgII, 6-K-PGF_{1α}, CGRP and GG in fibrosis rats (ng·L⁻¹)

Week	<i>n</i>	ET	AgII	6-K-PGF _{1α}	CGRP	GG
No.5	10	421.48±52.3	105.73±36.3	323.15±76.2	88.68±23.2	54.48±18.9
No.7	10	489.80±87.7	131.42±18.9	684.98±214.0	118.14±24.3	55.77±19.2
No.9	10	658.61±102.3	144.58±72.2	1081.61±294.3	174.65±87.7	141.66±50.8

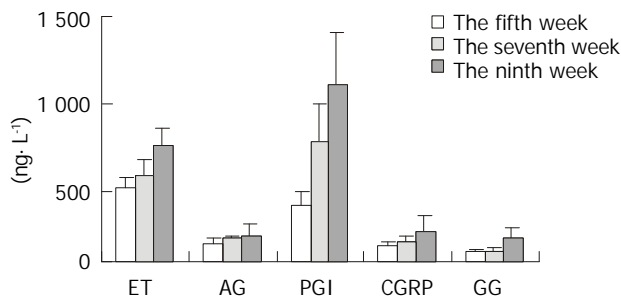


Figure 2 Plasma levels of ET, AgII, 6-K-PGF_{1α}, CGRP and GG in fibrosis rats.

Table 2 and Figure 2 showed that the levels of ET, AgII, 6-K-PGF_{1α}, CGRP and GG were gradually increased and associated with the increase of CCl₄-treated frequency, especially in the ninth week (*P*<0.05). It suggested that there was close relation between the levels of the transmitters and the degrees of liver fibrosis.

Pathological assay

The histological feature showed that liver of control rats had no appreciable alterations (Figure 3). The degree of liver fibrosis in group C was up-going with the increases of the treatment frequency of CCl₄. In the fifth week, few reticular fiber deposited in the periportal tissue space. In the seventh week, the reticular fiber extended with hepatic plate but the full delimitation was not formed, while in the ninth week the integrity fibrous septum was developed in the interlobular septum, sometimes pseudolobular could be seen (Figure 4,5,6). The degrees of inflammation of hepatocytes were decreased evidently in the seventh week after the treatment of IL-10, in the ninth week, the reticular fiber in the interlobular septum was limited remarkably, no pseudolobular could be seen (Figure 7).

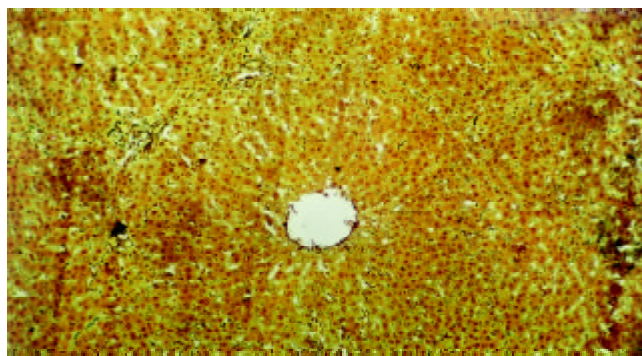


Figure 3 The liver of normal rat (silver staining, ×100).

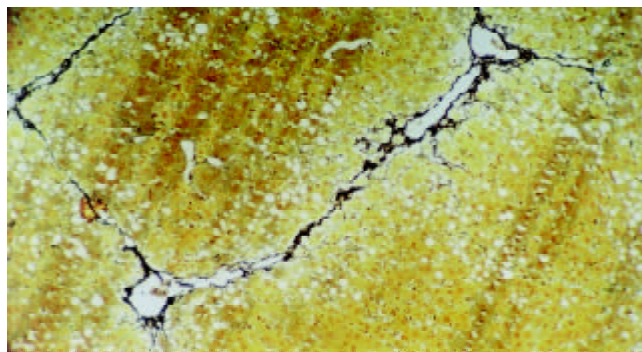


Figure 4 The liver of the rat in group C (the fifth week, silver staining, ×100).

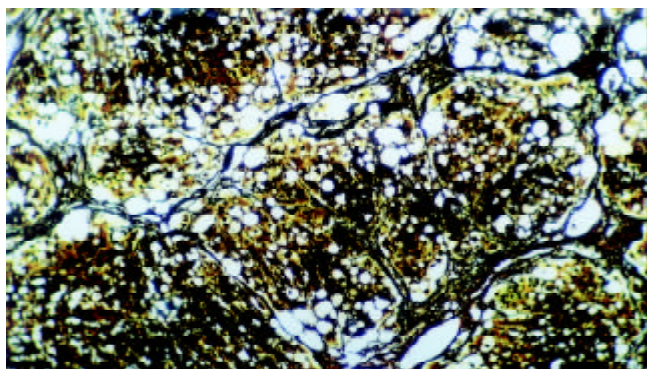


Figure 5 The liver of the rat in group C (the seventh week, silver staining, $\times 100$).

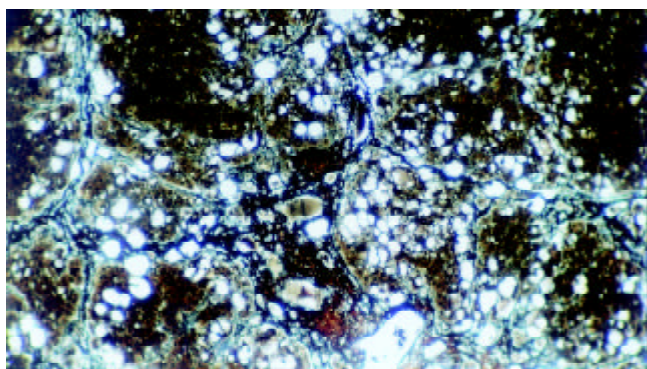


Figure 6 The liver of the rat in group C (the ninth week, silver staining, $\times 100$).

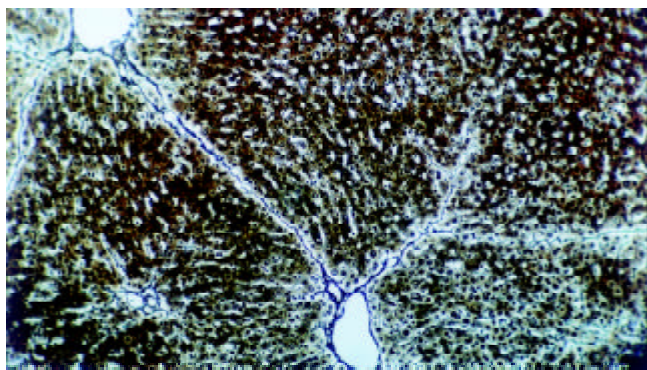


Figure 7 The liver of the rat in group E (the ninth week, silver staining, $\times 100$).

DISCUSSION

Endothelins are a family of polypeptides consisting of 21-amino acids^[17-19]. ET-1 is initially noted for its powerful vasoconstrictor properties^[20-24]. It is markedly overexpressed in different cellular elements in cirrhotic liver tissue, and particularly in sinusoidal endothelial cells and hepatic stellate cells (HSCs) in their activated phenotype located in the sinusoids of the regenerating nodules and at the edges of fibrous septa^[25]. It plays an important role in the regulation of hepatic vascular tone. They elicit biological responses via the ET_A and ET_B receptors. ET-1 induces contraction, proliferation, and collagen synthesis of HSCs *in vitro*, which may be mediated *via* the ET_A receptors^[26]. ET-1 is able to increase [Ca²⁺]_i in a dose-dependent fashion in HSCs, which results from both intracellular release of Ca²⁺ and extracellular Ca²⁺ influx via a dihydropyridine-insensitive pathway. ET-1-induced contractility of HSCs is maintained through all stages of

activation and is independent of the absolute number of ET_A-binding sites if a threshold level of expression is maintained. It has been shown that ET-1 could act as a cell growth promoter *via* the ET_A receptor to promote the proliferation of smooth muscle cell. Also, ET-1 is able to elicit MAPK (mitogen-activated protein kinase) activity in human HSCs with time-course and dose-response kinetics similar to those reported in mesangial cells through the ET_A receptor. Recent studies have shown that the ETR antagonist modifies the development of portal hypertension in carbon tetrachloride treated rats^[27,28]. Some studies suggest that ET has two effects on HSC^[29]. ET can inhibit the contraction and collagen synthesis in cells that have more ET_B receptors than ET_A receptors; it indicates that ET could restrict the development of liver fibrosis. The difference is linked to the active, contractile HSC phenotype. The cellular sites of action of AgII within the hepatic vasculature are incompletely defined; recent studies have shown that HSCs may be a potential cell target for the AgII actions in the hepatic vasculature^[30]. Two different types of AgII receptors have been described. The AT1 receptors are present in most mesenchymal cells and mediate most of the biological effects of AgII. The AT2 receptors are mainly found in fetal cells, but their physiological role is not completely understood. AgII receptors (AT1 subtype) exist in many cells, including the human HSC^[31], the activated HSCs may be an important target of the AgII in the hepatic vasculature^[32]. The binding of AgII to AT1 receptor induces contraction and proliferation^[33,34]. AgII causes a marked increase in [Ca²⁺]_i and cell contraction, which largely depends on the entrance of Ca²⁺ through L-type Ca²⁺ channels. In recent years, much attention has been focused on the growth-promoting effects of AgII and it has been found that AgII is also a mitogenic factor for activated HSCs through an MAPK- dependent pathway. So we could hypothesis that AgII plays a role in the proliferation of HSCs and in the progression of liver fibrosis. The inflammation may be the initial fibrogenic event. PGI₂, a potent vasodilator produced by the splanchnic endothelium, would account for much of the observed hyperemia^[35]. Cyclooxygenase blockade reverses the splanchnic hyperemia^[36]. The mechanism for the increase of portal PGI₂ remains unknown. Some have suggested of increase that blood pressure alone will increase the production of PGI₂. Theoretically, damage to any type of liver cell membrane can serve as a source of AA metabolites that initiate fibrosis. In the intact liver, the most probable target cells are the nonparenchymal cells such as endothelial cells. The inflammation may be the initial fibrogenic event. The inflammation involving the release of arachidonic acid (AA) from phospholipids by activation of phospholipase A₂ in damaged cell membranes and formation of bioactive AA metabolites (prostaglandins, thromboxane A₂ and leukotrienes) by way of 5' lipoxygenase pathway is one of the earliest biochemical events in hepatic fibrosis. The concentration of 6-keto-PGF₁ α , the stable metabolite of PGI₂, represents the plasma level of PGI₂. The enhanced production of 6-keto-PGF₁ α increases the TGF- β ₁ gene expression by way of enhancing degranulation of platelets and inflammatory cells which are rich source of the fibrotic cytokine TGF- β ₁^[37]. As we all know, TGF- β ₁ can promote the synthesis and deposition of ECM and inhibit the degradation of ECM^[38,39]. CGRP is a highly potent vasodilator and is widely distributed in nerve fibers with relation to vascular structures^[40]. The circulating CGRP is elevated in liver cirrhosis^[41,42], but little information is known about CGRP in these patients^[43]. Some authors have reported that CGRP could inhibit the lipid peroxidation on the liver, which antagonists the effects of ET^[44]. So it is a protector in the liver fibrosis. Whether the CGRP has effects on the activation of HSC and the synthesis of collagen is not clarified. GG is a stress hormone whose release is stimulated by

catecholamines, cortisol, and growth hormone^[45]. GG plays an important role in the formation of portal hypertension^[46]. The present studies show that plasma GG levels are elevated in cirrhotic patients with portal hypertension. It is also clearly demonstrated that plasma GG levels is increased with the progression of cirrhosis. In addition, positive correlations has been found between plasma GG levels and Pugh's score or liver functions. In our study the increase of GG was associated with the failure of GG's degradation in liver and the hyperexcretion of pancreas. IL-10 is a potent anti-inflammatory cytokine that inhibits the synthesis of pro-inflammatory cytokines by T helper type 1 cells. It is produced locally in the liver and acts in an autocrine or paracrine way. IL-10 can inhibit a range of macrophage effector functions, including nitric oxide and reactive oxygen intermediate production, MHC class II antigen expression, and eicosanoid synthesis. IL-10 can down-regulate expression of adhesion molecules, ICAM-1 and B7, on human monocytes, and also the nuclear transcription factor, nuclear factor κ B. It is able to inhibit chemokine synthesis in T cells, neutrophils, and fibroblasts. Moreover, proinflammatory cytokines synthesis by a wide range of cells, particularly monocytes and macrophages, is profoundly inhibited by IL-10^[47]. Previous reports indicated that IL-10 had a role in the remodeling of the extracellular matrix^[48]. *In vitro*, IL-10 down regulates collagen type I while up regulates metalloproteinase gene expression. It also has antifibrogenic properties by down regulating profibrogenic cytokines, like TGF- β_1 and TNF- α ^[47,49]. Nelson *et al* had treated 24 patients with chronic hepatitis C with IL-10, they found that IL-10 normalized serum ALT levels, decreased hepatic inflammation, reduced liver fibrosis and was well tolerated in patients^[16].

After that treatment of IL-10, all of the transmitters decreased. Therefore, transmitters play important roles in rat hepatic fibrosis induced by CCl₄. IL-10 decreases the levels of these transmitters so it has antifibrogenesis effect.

REFERENCES

- Nie QH, Cheng YQ, Xie YM, Zhou YX, Bai XG, Cao YZ. Methodologic research on TIMP-1, TIMP-2 detection as a new diagnostic index for hepatic fibrosis and its significance. *World J Gastroenterol* 2002; **8**: 282-287
- Nie QH, Cheng YQ, Xie YM, Zhou YX, Cao YZ. Inhibiting effect of antisense oligonucleotides phosphorothioate on gene expression of TIMP-1 in rat liver fibrosis. *World J Gastroenterol* 2001; **7**: 363-369
- Weng HL, Cai WM, Liu RH. Animal experiment and clinical study of effect of gamma-interferon on hepatic fibrosis. *World J Gastroenterol* 2001; **7**: 42-48
- Sun DL, Sun SQ, Li TZ, Lu XL. Serologic study on extracellular matrix metabolism in patients with viral liver cirrhosis. *Shijie Huaren Xiaohua Zazhi* 1999; **7**: 55-56
- Chen PS, Zhai WR, Zhang YE, Zhang JS. The effects of hypoxia on hepatic stellate cell generate collagen and matrix metalloproteinase. *Shijie Huaren Xiaohua Zazhi* 2000; **8**: 586-587
- Liu SR, Gu HD, Li DG, Lu HM. A comparative study of fat storing cells and hepatocytes in collagen synthesis and collagen gene expression. *Xin Xiaohua Bingxue Zazhi* 1997; **15**: 761-762
- Wu J, Zern MA. Hepatic stellate cells: a target for the treatment of liver fibrosis. *J Gastroenterol* 2000; 665-672
- Jiang HQ, Zhang XL. Mechanism of liver fibrosis. *Shijie Huaren Xiaohua Zazhi* 2000; **8**: 687-689
- Wang YJ, Sun ZQ, Quan QZ, Yu JJ. Fat-storing cells and liver fibrosis. *Chin J New Gastroenterol* 1996; **2**: 58-60
- Missale G, Ferrari C, Fiaccadori F. Cytokine mediators in acute inflammation and chronic course of viral hepatitis. *Ann Ital Med Int* 1995; **10**: 14-18
- Wang YJ, Sun ZQ. The cytology and molecular biology investigate advance in liver fibrosis. *Xin Xiaohua Bingxue Zazhi* 1994; **2**: 244-246
- Wang FS, Wu ZZ. Current situation in studies of gene therapy for liver cirrhosis and liver fibrosis. *Shijie Huaren Xiaohua Zazhi* 2000; **8**: 371-373
- Zhang LJ, Wang XZ. Liquid substance and portal hypertension. *Shijie Huaren Xiaohua Zazhi* 2000; **8**: 1280-1281
- Zhang LJ, Wang XZ, Huang YH, Chen ZX. The effects of CGRP, AgII and ET on the liver fibrosis rats. *Shijie Huaren Xiaohua Zazhi* 2001; **9**: 457-459
- Takahara T, Kojima T, Miyabayashi C, Inoue K, Sasaki H, Muragaki Y, Ooshima A. Collagen production in fat-storing cells after carbon tetrachloride intoxication in the rat. Immunoelectron microscopic observation of type I, type III collagens and prolyl hydroxylase. *Lab Invest* 1988; **59**: 509-521
- Nelson DR, Lauwers GY, Lau JY, Davis GL. Interleukin 10 treatment reduces fibrosis in patients with chronic hepatitis C: a pilot trial of interferon nonresponders. *Gastroenterology* 2000; **118**: 655-660
- Zhang Y, Ren XL. Endothelin, nitric oxide and liver cirrhosis. *Chin J New Gastroenterol* 1996; **4**: 40-41
- Cheng RC, Jin XL. The changes of plasma endothelin level in the patient with discompensation liver cirrhosis. *Xin Xiaohua Bingxue Zazhi* 1995; **3**: 110-111
- Li XR, Wu JS, He ZS, Ma QJ. The contents of endothelin in portal vein and peripheral blood of patients with portal hypertension of liver cirrhosis. *Shijie Huaren Xiaohua Zazhi* 1998; **6**: 827
- Liu F, Li JX, Li CM, Leng XS. Plasma endothelin in patients with endotoxemia and dynamic comparison between vasoconstrictor and vasodilator in cirrhotic patients. *World J Gastroenterol* 2001; **7**: 126-127
- Liu BH, Chen HS, Zhou JH, Xiao N. Effects of endotoxin on endothelin receptor in hepatic and intestinal tissues after endotoxemia in rats. *World J Gastroenterol* 2000; **6**: 298-300
- Zhang ZY, Ren XL, Yao XX. Effects of endothelin and nitric oxide in hemodynamics disturbance of cirrhosis. *Shijie Huaren Xiaohua Zazhi* 1998; **6**: 588-590
- Chen S, Liu B, Cai XM, Gu CH. Clinical significance of changes of endothelin and nitric oxide levels in peripheral blood of patients with severe hepatitis. *Shijie Huaren Xiaohua Zazhi* 1999; **7**: 122-124
- Chen YK. The significance of changes of endothelin in patients with severe hepatitis. *Shijie Huaren Xiaohua Zazhi* 1998; **6**: 157
- Pinzani M, Milani S, De Franco R, Grappone C, Caligiuri A, Gentilini A, Tosti-Guerra C, Maggi M, Failli P, Ruocco C, Gentilini P. Endothelin-1 is overexpressed in human cirrhotic liver and exerts multiple effects on activated hepatic stellate cells. *Gastroenterology* 1996; **110**: 534-548
- Reinehr RM, Kubitz R, Peters-Regehr T, Bode JG, Haussinger D. Activation of rat hepatic stellate cells in culture is associated with increased sensitivity to endothelin-1. *Hepatology* 1998; **28**: 1566-1577
- Sogni P, Moreau R, Gomola A, Gadano A, Cailmail S, Calmus Y, Clozel M, Lebrec D. Beneficial hemodynamic effects of bosentan, a mixed ET_A and ET_B receptor antagonist, in portal hypertensive rats. *Hepatology* 1998; **28**: 655-659
- Cho JJ, Hoher B, Herbst H, Jia JD, Ruehl M, Hahn EG, Riecken EO, Schuppan D. An oral endothelin-A receptor antagonist blocks collagen synthesis and deposition in advanced rat liver fibrosis. *Gastroenterology* 2000; **118**: 1169-1176
- Rockey D. Endothelin in hepatic fibrosis-friend or foe? *Hepatology* 1996; **23**: 1698-1700
- Schneider AW, Kald F, Klein CP. Effect of Losartan, an Angiotensin II receptor antagonist, on portal pressure in cirrhosis. *Hepatology* 1999; **29**: 334-339
- Wei HS, Lu HM, Li DG, Zhan YT, Wang ZR, Huang X, Cheng JL, Xu QF. The regulatory role of AT1 receptor on activated HSCs in hepatic fibrogenesis: effects of RAS inhibitors on hepatic fibrosis induced by CCl₄. *World J Gastroenterol* 2000; **6**: 824-828
- Wei HS, Li DG, Lu HM, Zhan YT, Wang ZR, Huang X, Zhang J, Cheng JL, Xu QF. Effects of AT1 receptor antagonist, losartan, on rat hepatic fibrosis induced by CCl₄. *World J Gastroenterol* 2000; **6**: 540-545
- Bataler R, Gines P, Nicolas JM, Gorbis MN, Garcia-Ramallo E, Gasull X, Bosch J, Arroyo V, Rodes J. Angiotensin II induces contraction and proliferation of human hepatic stellate cells. *Gastro*

- enterology* 2000; **118**: 1149-1156
- 34 **Gorbig MN**, Gines P, Bataller R, Nicolas JM, Garcia-Ramalli E, Tobias E, Titos E, Rey MJ, Claria J, Arroyo V, Rodes J. Artial nareuretic peptides angagonizes endothelin-induced calcium increased and cell contraction in culture human hepatic stellate cells. *Heaptology* 1999; **30**: 501-509
- 35 **Garcia-Pagan JC**, Bosch J, Rodes J. The role of vasoactive mediators in portal hypertension. *Semin Gastrointest Dis* 1995; **6**: 140-147
- 36 **Yue QL**, Zhang XK, Zhang XR. The changes of contents of nitrix oxide and prostaglandine in gastric mucosa and plasma of rats with portal hypertensive gastropathy. *Shijie Huaren Xiaohua Zazhi* 1999; **7**: 547
- 37 **Geraci JP**, Mariano MS. Radiation hepatology of the rat: association of the production of prostacyclin with radiation-induced hepatic fibrosis. *Radiat Res* 1996; **145**: 93-97
- 38 **de Bleser PJ**, Niki T, Rogiers V, Geerts A. Transforming growth factor-beta gene expression in normal and fibrotic rat liver. *J Hepatol* 1997; **26**: 886-893
- 39 **Sun ZQ**, Wang YJ. The regulate effect of soluble cytokines on liver fibrosis. *Xin Xiaohua Bingxue Zazhi* 1994; **2**: 163-164
- 40 **Schifter S**. Expression of the calcitonin gene family in medullary thyroid carcinoma. *Peptides* 1997; **18**: 307-317
- 41 **Wang X**, Wen QS, Huang YX, Zhong YX, Chu YQ, Wang QL. The effects of calcitonin gene-related peptide on portal vein pressure of rats with liver cirrhosis. *Shijie Huaren Xiaohua Zazhi* 1998; **6**: 933
- 42 **Liu CQ**, Pu J, Li ZX, Liu XF, Zhao YT. The changes of plasma peptides in the patients with liver cirrhosis. *Shijie Huaren Xiaohua Zazhi* 1999; **7**: 1089
- 43 **Henriksen JH**, Schifter S, Moller S, Bendrsen F. Increased circulating calcitonin in cirrhosis. Relation to severity of disease and calcitonin gene-related peptide. *Metabolism* 2000; **49**: 47-52
- 44 **Moller S**, Bendtsen F, Schifter S, Henriksen JH. Relation of calcitonin gene-related peptide to systemic vasodilatation and central hypovolemia in cirrhosis. *Scand J Gastroenterol* 1996; **31**: 928-933
- 45 **Johnson TJ**, Quigley EM, Adrian TE, Jin G, Rikkers L. Glucagon, stress, and portal hypertension Plasma glucagon levels and portal hypertension in relation to anesthesia and surgical stress. *Dig Dis Sci* 1995; **40**: 1816-1823
- 46 **Greco AV**, Crucitti F, Ghirlanda G, Manna R, Altomonte L, Rebuzzi AG, Bertoli A. Insulin and glucagon concentrations in portal and peripheral veins in patients with hepatic cirrhosis. *Diabetologia* 1979; **17**: 23-28
- 47 **Kovalovich K**, DeAngelis RA, Li W, Furth EE, Ciliberto G, Taub R. Increased toxin-induced liver injury and fibrosis in interleukin-6-deficient mice. *Hepatology* 2000; **31**: 149-159
- 48 **Thompson K**, Maltby J, Fallowfield J, McAulay M, Millward-Sadler H, Sheron N. Interleukin-10 expression and function in experimental murine liver inflammation and fibrosis. *Hepatology* 1998; **28**: 1597-1606
- 49 **Louis H**, Laethem JL, Wu W, Quertinmont E, Degraef C, Van Den Berg K, Demols A, Goldman M, Moine OL, Geerts A, Deviere J. Interleukin-10 controls neutrophilic infiltration, hepatocyte proliferation, and liver fibrosis induced by carbon tetrachloride in mice. *Hepatology* 1998; **28**: 1607-1615

Edited by Xu XQ

A selective tropism of transfused oval cells for liver

Jian-Zhi Chen, Hai Hong, Jin Xiang, Ling Xue, Guo-Qiang Zhao

Jian-Zhi Chen, Hai Hong, Jin Xiang, Ling Xue, Guo-Qiang Zhao,
Department of Pathology, Medical School of Sun Yat-Sen University,
Guangzhou 510080, Guangdong Province, China

Supported by the National Natural Science Foundation of China,
No. 39570348 and 30170473

Correspondence to: Prof. Dr. Guo-Qiang Zhao, Department of
Pathology, Medical School of Sun Yat-Sen University, 74
Zhongshan 2nd Rd., Guangzhou 510080, Guangdong Province,
China. gqzhao@gzsums.edu.cn

Telephone: +86-20-87330743 **Fax:** +86-20-87331679

Received: 2002-06-22 **Accepted:** 2002-07-12

Abstract

AIM: To explore the biological behaviors of hepatic oval cells after transfused into the circulation of experimental animals.

METHODS: Oval cells from male SD rat were transfused into the circulation of a female rat which were treated by a 2-AAF/CCl₄ program, through caudal vein. Sex-determining gene *sry* which located on Y chromosome was examined by PCR and in situ hybridization technique in liver, kidney and spleen of the experimental animals, respectively.

RESULTS: The results of the cell-transplant experiment showed that the *sry* gene was detectable only in the liver but not in spleen and kidney of the experimental rats, and no signals could be detected in the control animals. It can be also morphologically proved that some exogenous cells had migrated into the parenchyma of the liver and settled there.

CONCLUSION: The result means that there are exogenous cells located in the liver of the experimental animal and the localization is specific to the liver. This indicates that some "signal molecules" must exist in the circulation of the rats treated by 2-AAF/CCl₄. These "signal molecules" might play an important role in specific localization and differentiation of transfused oval cells.

Chen JZ, Hong H, Xiang J, Xue L, Zhao GQ. A selective tropism of transfused oval cells for liver. *World J Gastroenterol* 2003; 9 (3): 544-546

<http://www.wjgnet.com/1007-9327/9/544.htm>

INTRODUCTION

Hepatic oval cells were first described by Opie in 1944 and named as oval cells first by Farber in 1956^[1,2]. Oval cells could be seen at the early stage of hepatocarcinogenesis induced by chemicals in animal and in the liver of human suffering from chronic hepatitis, cirrhosis and other chronic liver diseases^[3-8]. The emergence of oval cells was considered initially to be related to hepatocarcinogenesis. Oval cell was once believed to be a progenitor cell of carcinoma in liver^[9-11]. Recently, more and more evidences showed that oval cell may be a potential stem cell in liver and it could differentiate into hepatocyte and epithelial cell of bile duct in certain conditions^[12,13]. It is believed now that the potential stem cells existing in liver might

play a role in the repair of damaged liver. However, when and how oval cells could be activated still remains unclear. Our aim in this study is to explore the biological behavior of hepatic oval cells after transfused into the circulation of rat for interpreting possible activating mechanisms of hepatic stem cells.

MATERIALS AND METHODS

Culture of oval cells

Hepatic oval cells were isolated from SD male rats and a cell line of OC3 was established by Dr. Xue in our group^[14]. Oval cells were cultivated under a routine condition (37 °C, 5 % CO₂). The cells were collected and suspended in a solution of RPMI-1640 (Gibco BRL) without serum on the day of transfusion experiment, on standby.

Establishment of animal model and transfusion of oval cells

SD female rats, weighing 100-150 g, were used for the establishment of an animal model of liver-damaging. The model was made by means of a 2-AAF/CCl₄ program according to Petersen^[31]. In the experimental group, 2-acetylaminofluorene (2-AAF, Sigma), 2.5 g·L⁻¹ in earthnut oil, was administered to stomach of rats everyday for 14 days. On the 7th day of 2-AAF administering, a Ld50 dose of CCl₄ was given by intraperitoneal injection. Then, the suspended oval cells (5×10⁶ cells per rat) were transfused into the circulation of the rats through caudal vein in 24 hours after CCl₄ injection. In the control group, 1 ml earthnut oil per day was administered to stomach of rats instead of 2-AAF, and without CCl₄ injection, the other treatments was the same as in the experimental group. The animals were sacrificed on the 7th day after transfusion of oval cells. The liver, kidney and spleen of the rats were picked out, respectively and frozen rapidly in liquid nitrogen. The frozen tissues were kept in -80 °C refrigerator.

Isolation of DNA

DNA was extracted from the frozen tissues of liver, kidney and spleen respectively according to the protocol of our laboratory. DNA samples were kept in -80 °C refrigerator.

Primers selection of sry gene

The primers selection was according to the DNA sequence of rat *sry* gene from GenBank Database (Accession No.: AJ222688): *Sry*F17: 5' -catctctgacttctctggtgcaa-3', *Sry*R16: 5' -atgctgggattctgtgagcc-3'. The PCR product was 241 bp in length, corresponding to the sequence between 273-514 of rat *sry* gene.

PCR reactions

The DNA samples from liver, kidney and spleen in each experimental group were used as a template in PCR reactions. The reaction cocktails (containing 1 µg Template DNA, 0.125 m mol·L⁻¹ dNTPs, 0.4 µmol·L⁻¹ *sry* F17 primer, 0.4 µmol·L⁻¹ *sry* R16 primer, 1×PCR buffer, 2.5 m mol·L⁻¹ MgCl₂, 1 U Taq-polymerase, add H₂O to 50 µL of total volume) were run on GeneAmp® PCR System 9 600 (AB) with a program combination of Prog. 1 (95 °C, 5 min), Prog. 2 (95 °C, 50 sec; 56 °C, 50 sec; 72 °C, 60 sec; 30 cycles) and Prog. 3 (95 °C, 50 sec; 56 °C, 50 sec; 72 °C, 60 sec). The PCR products were

electrophoresed in 1.2 % agarose, stained with ethidium bromide and photographed.

In situ hybridization

In situ hybridization was carried out according to the protocol described by Zhao^[15]. A DNA probe complementary to rat *sry* gene was labeled with digoxigenin by means of PCR reactions. The sections of liver from rats transfused with oval cells were selected for *in situ* hybridization assay. After deparaffin and rehydrate, the sections were fixed in 4 % paraformaldehyde again. The hybridization (2×SSC, 500 mL·L⁻¹ formamide, 1×Denhardt's solution, 0.5 g·L⁻¹ dextran sulfate, 60 µg·L⁻¹ DIG-Probe) was carried out at 37 °C over night. The hybrids were then revealed by an alkaline phosphatase-conjugated anti-digoxigenin antibody and detected with the detection system of Boehringer Mannheim.

RESULTS

Sry gene was located in Y chromosome and used as a marker of transfused oval cells in female animal. The results of the cell-transplant experiment showed that the *sry* gene was detectable only in the liver but not in the spleen and the kidney of the rats treated by 2-AAF/CCl₄ program, and no signals could be detected in the control animals, neither liver nor spleen and kidney. The distribution of PCR signals of *sry* gene in experimental groups can be seen in Figure 1 and Table 1. On the section of *in situ* hybridization, a cluster of cells with *sry* gene marker could be seen in the parenchyma of the liver of a female rat undergoing oval cell-transplantation (Figure 2A). It was distinguished between sections in the negative and positive controls (Figure 2B and Figure 2C). This result meant that some exogenous cells had migrated into the parenchyma of the liver and settled there.

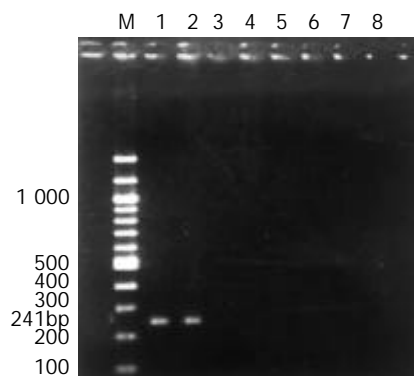


Figure 1 PCR signals of *sry* gene in experimental groups. (M. 100 bp DNA marker; 1. Liver(M): liver of male rat as a positive control; 2. Liver(E): liver of female rat in experimental group; 3. Spleen(E): spleen of female rat in experimental group; 4. Kidney(E): kidney of female rat in experimental group; 5. Liver (C): liver of female rat in control group; 6. Spleen(C): spleen of female rat in control group; 7. Kidney(C): kidney of female rat in control group; 8. Liver(F): liver of female rat negative control).

Table 1 Distribution of PCR signals of *sry* gene in experimental groups

	Liver (M)	Liver (E)	Spleen (E)	Kidney (E)	Liver (C)	Spleen (C)	Kidney (C)	Liver (F)
<i>Sry</i>	+	+	-	-	-	-	-	-

Note: Liver(M): liver of male rat as a positive control; Liver(E): liver of female rat in experimental group; Spleen(E): spleen of female rat in experimental group; Kidney(E): kidney of female

rat in experimental group; Liver(C): liver of female rat in control group; Spleen(C): spleen of female rat in control group; Kidney(C): kidney of female rat in control group; Liver(F): liver of female rat negative control.

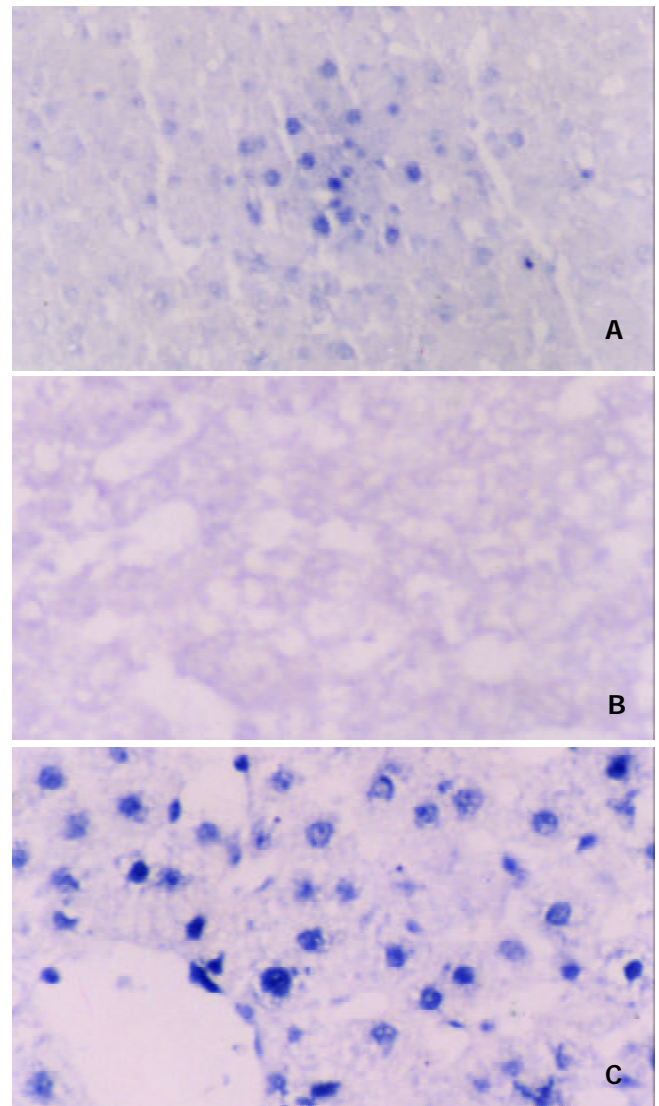


Figure 2 *In situ* hybridization assay of *sry* gene in liver. A. Experimental group, Liver of female rat undergoing oval cell-transplanting. A cluster of cells with *sry* gene marker could be seen in the parenchyma of liver. B. Negative control group, liver of normal female rat. No hybridization signals could be seen. C. Positive control group, liver of normal male rat. Each cell with distinct hybridization signals.

DISCUSSION

As we know, liver has a powerful capacity of regeneration. In general, the injured liver can regenerate itself by self-replication of hepatocyte. So, it is believed that hepatocytes themselves are the functional stem cells of the liver^[16]. Oval cell is now recognized as a potential stem cell existing in liver. But they cannot be seen in normal status. The emergence of oval cells occurs only in a special status in which the liver is damaged severely and the capacity of regeneration of hepatocyte is restrained^[17-20]. At the past, oval cell was believed as a progenitor cell of carcinoma in liver^[9-11,21], because it was often seen at the early stage of hepatocarcinogenesis induced by chemicals^[22-26]. Recently, more and more evidences showed that oval cell could differentiate toward hepatocyte and epithelial cell of bile duct^[12,13,27-30]. So it was guessed that the emergence of oval cells might be relevant to the repair of

damaged liver, and under special conditions the injured liver might produce and release some "signal molecules" which might play an important role in the activation of stem cell. In this study, an animal model of liver-damaging was established by a 2-AAF/CCl₄ program according to Petersen^[31], the capacity of regeneration of hepatocyte was first impaired by 2-AAF and then the liver was damaged severely by CCl₄. In this status the damaged liver might produce a signal of "distress call" to initiate the activation of stem cell. Our results of cell transplantation showed that the *sry* gene was detectable only in the liver but not in the spleen and the kidney of the rats treated by 2-AAF/CCl₄ program, and no signals could be detected in the control animals, neither liver nor spleen and kidney. The results of in situ hybridization also showed that some exogenous cells had migrated into the parenchyma of the liver and settled there. It means that the transfused oval cells have a selective tropism for liver and the driver force might come from the injured liver. All evidences revealed that some "signal molecules" might exist in the circulation of the rats treated by 2-AAF/CCl₄ and the "signal molecules" might be produced and released from the damaged liver. The "signal molecules" might play an important role in the initiation of the activation of stem cell. Further identifying and isolation of these "signal molecules" would be significative for achieving activation and directional inducement of hepatic stem cells.

REFERENCES

- Opie EL.** The pathogenesis of tumors of the liver produced by butter yellow. *J Exp Med* 1944; **80**: 231-246
- Farber E.** Similarities in the sequence of early histologic changes induced in the livers of rats by ethionine, 2-acetylaminofluorene and 3'-methyl-4-dimethylaminoazobenzene. *Cancer Res* 1956; **16**: 142-148
- De Vos R, Desmet V.** Ultrastructural characteristics of novel epithelial cell types identified in human pathologic liver specimens with chronic ductular reaction. *Am J Pathol* 1992; **140**: 1441-1450
- Crosby HA, Hubscher S, Fabris L, Joplin R, Sell S, Kelly D, Strain AJ.** Immunolocalization of putative human liver progenitor cells in livers from patients with end-stage primary biliary cirrhosis and sclerosing cholangitis using the monoclonal antibody OV-6. *Am J Pathol* 1998; **152**: 771-779
- Theise ND, Saxena R, Portmann BC, Thung SN, Yee H, Chiriboga L, Kumar A, Crawford JM.** The canals of Hering and hepatic stem cells in humans. *Hepatology* 1999; **30**: 1425-1433
- Lowes KN, Brennan BA, Yeoh GC, Olynyk JK.** Oval cell numbers in human chronic liver diseases are directly related to disease severity. *Am J Pathol* 1999; **154**: 537-541
- Malhi H, Irani AN, Gagandeep S, Gupta S.** Isolation of human progenitor liver epithelial cells with extensive replication capacity and differentiation into mature hepatocytes. *J Cell Sci* 2002; **115**: 2679-2688
- Ma X, Qiu DK, Peng YS.** Immunohistochemical study of hepatic oval cells in human chronic viral hepatitis. *World J Gastroenterol* 2001; **7**: 238-242
- Goyette M, Faris R, Braun L, Hixson D, Fausto N.** Expression of hepatocyte and oval cell antigens in hepatocellular carcinomas produced by oncogene-transfected liver epithelial cells. *Cancer Res* 1990; **50**: 4809-4817
- Faris RA, Monfils BA, Dunsford HA, Hixson DC.** Antigenic relationship between oval cells and a subpopulation of hepatic foci, nodules and carcinomas induced by the "resistant hepatocyte" model system. *Cancer Res* 1991; **51**: 1308-1317
- Sirica AE, Mathis GA, Sano N, Elmore LW.** Isolation, culture, and transplantation of intrahepatic biliary epithelial cells and oval cells. *Pathobiology* 1990; **58**: 44-64
- Golding M, Sarraf CE, Lalani EN, Anilkumar TV, Edwards RJ, Nagy P, Thorgeirsson SS, Alison MR.** Oval cell differentiation into hepatocytes in the acetylaminofluorene-treated regenerating rat liver. *Hepatology* 1995; **22**: 1243-1253
- Alison M, Golding M, Lalani EN, Nagy P, Thorgeirsson S, Sarraf C.** Wholesale hepatocytic differentiation in the rat from ductular oval cells, the progeny of biliary stem cells. *J Hepatol* 1997; **26**: 343-352
- Xue L, Wen J, Zhao G.** The characteristics and significance of oncogenes expression in oval cells cultivated *in vitro*. *Zhonghua Binglixue Zazhi* 1998; **27**: 191-193
- Zhao GQ, Xue L, Xu HY, Tang XM, Hu RD, Dong J.** *In situ* hybridization assay of androgen receptor gene in hepatocarcinogenesis. *World J Gastroenterol* 1998; **4**: 503-505
- Forbes S, Vig P, Poulosom R, Thomas H, Alison M.** Hepatic stem cells. *J Pathol* 2002; **197**: 510-518
- Gournay J, Auvigne I, Pichard V, Ligeza C, Bralet MP, Ferry N.** *In vivo* cell lineage analysis during chemical hepatocarcinogenesis in rats using retroviral-mediated gene transfer: evidence for dedifferentiation of mature hepatocytes. *Lab Invest* 2002; **82**: 781-788
- Yin L, Lynch D, Ilic Z, Sell S.** Proliferation and differentiation of ductular progenitor cells and littoral cells during the regeneration of the rat liver to CCl₄/2-AAF injury. *Histol Histopathol* 2002; **17**: 65-81
- Faris RA, Konkin T, Halpert G.** Liver stem cells: a potential source of hepatocytes for the treatment of human liver disease. *Artif Organs* 2001; **25**: 513-521
- Petersen BE.** Hepatic "stem" cells: coming full circle. *Blood Cells Mol Dis* 2001; **27**: 590-600
- Liao G, Chen J, Ding L.** Relationship between oval cells and preneoplastic lesions induced by 2-acetylaminofluorene in rat liver. *Zhonghua Binglixue Zazhi* 1998; **27**: 87-90
- Shinozuka H, Lombardi B, Sell S, Iammarino RM.** Early histological and functional alterations of ethionine liver carcinogenesis in rats fed a choline-deficient diet. *Cancer Res* 1978; **38**: 1092-1098
- Sell S, Hunt JM, Knoll BJ, Dunsford HA.** Cellular events during hepatocarcinogenesis in rats and the question of premalignancy. *Adv Cancer Res* 1987; **48**: 37-111
- Novikoff PM, Ikeda T, Hixson DC, Yam A.** Characterizations of and interactions between bile ductule cells and hepatocytes in early stages of rat hepatocarcinogenesis induced by ethionine. *Am J Pathol* 1991; **139**: 1351-1368
- Gera N, Bhatia A, Sood SK.** Light & electron microscopy of proliferating oval cells during early chemical hepatocarcinogenesis. *Indian J Med Res* 1991; **94**: 200-205
- Evarts RP, Nakatsukasa H, Marsden ER, Hsia CC, Dunsford HA, Thorgeirsson SS.** Cellular and molecular changes in the early stages of chemical hepatocarcinogenesis in the rat. *Cancer Res* 1990; **50**: 3439-3444
- Yoon BI, Jung SY, Hur K, Lee JH, Joo KH, Lee YS, Kim DY.** Differentiation of hamster liver oval cell following *Clonorchis sinensis* infection. *J Vet Med Sci* 2000; **62**: 1303-1310
- Factor VM, Radaeva SA, Thorgeirsson SS.** Origin and fate of oval cells in dipin-induced hepatocarcinogenesis in the mouse. *Am J Pathol* 1994; **145**: 409-422
- Alpini G, Aragona E, Dabeva M, Salvi R, Shafritz DA, Tavoloni N.** Distribution of albumin and alpha-fetoprotein mRNAs in normal, hyperplastic, and preneoplastic rat liver. *Am J Pathol* 1992; **141**: 623-632
- Nagy P, Bisgaard HC, Thorgeirsson SS.** Expression of hepatic transcription factors during liver development and oval cell differentiation. *J Cell Biol* 1994; **126**: 223-233
- Petersen BE, Bowen WC, Patrene KD, Mars WM, Sullivan AK, Murase N, Boggs SS, Greenberger JS, Goff JP.** Bone marrow as a potential source of hepatic oval cells. *Science* 1999; **284**: 1168-1170

Comparative study in the effect of C-type natriuretic peptide on gastric motility in various animals

Hui-Shu Guo, Zheng Jin, Zheng-Yuan Jin, Zhe-Hao Li, Yi-Feng Cui, Zuo-Yu Wang, Wen-Xie Xu

Hui-Shu Guo, Zheng Jin, Zheng-Yuan Jin, Yi-Feng Cui, Zuo-Yu Wang, Wen-Xie Xu, Department of Physiology, Yanbian University College of Medicine, Yanji 133000, Jilin Province China
Wen-Xie Xu, Zhe-Hao Li, Center of experiment, Affiliated Hospital of Yanbian University College of Medicine, Yanji 133000, Jilin Province China

Supported by the National Natural Science Foundation of China, No. 30160028

Correspondence to: Dr. Wen-Xie Xu, Department of Physiology, Yanbian University College of Medicine, Juzi 121, Yanji 133000, Jilin Province China. wenxiexu@ybu.edu.cn

Telephone: +86-433-2660586 **Fax:** +86-433-2659795

Received: 2002-10-17 **Accepted:** 2002-11-14

Abstract

AIM: To investigate the effect of natriuretic peptides on gastric motility in various animals, and the effect of C-type natriuretic peptide (CNP) on spontaneous contraction of gastric smooth muscle in rat, guinea-pig and human in vitro was compared.

METHODS: Spontaneous contraction of gastric smooth muscle was recorded by four channel physiograph.

RESULTS: In the guinea-pig and rat gastric antral circular smooth muscle, CNP markedly decreased the amplitude of spontaneous contraction but it didn't affect the frequency, however, the contractile activity was completely inhibited by CNP in gastric antral longitudinal smooth muscle. In the human gastric antral circular and longitudinal smooth muscle, CNP completely inhibited spontaneous contraction. In the circular smooth muscle of guinea-pig and rat gastric fundus, CNP obviously decreased the amplitude of spontaneous contraction but it didn't affect the frequency, however, the contractile activity was completely inhibited by CNP in smooth muscle of fundus longitudinal. In the circular and longitudinal smooth muscle of guinea-pig gastric body, CNP at first induced a relaxation and then an increase in amplitude of spontaneous contraction (rebound contraction), but the frequency was not changed. After the circular smooth muscle of gastric body was pretreated with atropine, an M receptor blocker, the rebound contraction was abolished; In circular and longitudinal smooth muscle of rat gastric body, CNP induced a transient and slight relaxation and successively followed by the recovery in amplitude of spontaneous contraction but it also didn't affect the frequency. After the smooth muscle was pretreated with atropine, the transient and slight relaxation was replaced by long term and complete inhibition; The percentage of CNP-induced inhibition was 76.77 ± 6.21 % (fundus), 67.21 ± 5.32 % (body) and 58.23 ± 6.21 % (antral) in the gastric circular muscle, however, the inhibitory percentage was 100 ± 0.00 % (fundus), 68.66 ± 3.55 % (body) and 100 ± 0.00 % (antrum) in the gastric longitudinal smooth muscle of guinea-pigs; In the rat, the percentage of CNP-induced inhibition was 95.87 ± 4.12 % (fundus), 94.91 ± 5.08 % (body) and 66.32 ± 7.32 % (antrum) in the gastric circular smooth muscle, but in the longitudinal smooth muscle, CNP completely inhibited the spontaneous

contraction. Using LY83583, a guanylate cyclase inhibitor, and zaparinast as a phosphoesterase inhibitor to inhibit the generation of cGMP, the effect of CNP on the spontaneous contraction was markedly weakened by LY83583, however, the inhibitory effect was enhanced by zaparinast.

CONCLUSION: (1) CNP can obviously inhibit the spontaneous contraction of gastric antral circular and longitudinal smooth muscle in the rat, guinea-pig and human. The order of inhibitory potency is human >rat> guinea-pig. (2) In the same animals, the inhibitory effect of CNP on spontaneous contraction is the most powerful in fundus and the weakest in antrum, in the same position, the inhibitory effect on the circular smooth muscle is more powerful than that on longitudinal smooth muscle. (3) The inhibitory effect of CNP on spontaneous contraction in the gastric smooth muscle is mediated by a cGMP dependent pathway.

Guo HS, Jin Z, Jin ZY, Li ZH, Cui YF, Wang ZY, Xu WX. Comparative study in the effect of C-type natriuretic peptide on gastric motility in various animals. *World J Gastroenterol* 2003; 9(3): 547-552 <http://www.wjgnet.com/1007-9327/9/547.htm>

INTRODUCTION

Since atrial natriuretic peptide (ANP) was isolated from atrium by de Bold *et al* in 1981^[1], brain natriuretic peptide (BNP), C-type natriuretic peptide (CNP), dendroaspis (DNP), micrurus natriuretic peptide (MNP) and ventricular natriuretic peptide (VNP) were successively found. They distribute in all over the body not only in the heart. Among the natriuretic peptides (NP) family, the most studies were focused on ANP, BNP and CNP. The NP family has function of natriuresis-diuresis, vasorelaxation and is able to lower blood pressure and to keep electrolyte homeostasis and so on. CNP was originally found in the central nervous system of the porcine, but it has recently been found in many other systems. In adult mice, the highest CNP expression was detected in the uterus and ovaries, which exceeded the CNP concentrations of the forebrain and brainstem. In contrast, neonatal mice showed highest CNP-mRNA levels in forebrain and brainstem but with lower levels in the skin, tongue, heart, lung, thymus, skeletal muscle, liver, kidney, stomach, and skull^[2]. In the rat, generation and secretion of CNP was demonstrated not only in endothelium but also in vascular smooth muscle cells^[3], and natriuretic peptides gene was expressed^[4] in human coronary arteries. CNP exhibits many functions besides natriuresis-diuresis; for instance, CNP inhibits the growth of vascular smooth muscle cells in the rat^[5] and in has many functions including anti-thrombus and anti-proliferation against vascular smooth muscle cells and myofibroblasts in addition to vasodilation in rabbit^[6,7].

The study on the relationship between CNP and gastrointestinal function has recently become the hot spot. In 1991, Komatsu *et al*^[8] demonstrated that CNP also existed in gastrointestinal and three kinds of NPR receptors was found in both mucosa and muscle tissues of the antrum in the rat by Gower *et al*^[9] in 2000. The study on CNP in gastrointestinal

tract was mainly focused on physiological functions of absorption, secretion and intestinal motility^[10-12]. But few studies reported the regulation of natriuretic peptides on gastric smooth muscles motility. Therefore in the present study, the effect of CNP on spontaneous contraction of gastric smooth muscles in different positions of various animals were investigated.

MATERIALS AND METHODS

Sample preparation

Wista rats (provided by Experimental Animal Center of Yanbian University medical college) of either sex weighing 250±50 g and EWG/B guinea-pigs (provided by Experimental Animal Center of Jilin University medical college) of either sex weighing 300±50 g were euthanized by lethal dose of intravenous pentobarbital sodium (50 mg/kg). The abdomen of each rat was opened along the midline and stomach was removed and placed in a pre-oxygenated Tyrode's solution at room temperature. The mucous layer was removed. Strips (about 2.0×15.0 mm) of gastric antral circular smooth muscle were prepared by cutting along the vertical direction of the longer axis of the stomach and strips of gastric antral longitudinal smooth muscle were prepared by cutting along the longer axis of the stomach. Muscle strips were placed in a chamber. One end of the strip was fixed on the lid of the chamber through glass claw, the other end was attached to an isometric force transducer (TD-112S, JAPAN) to record the contraction. The chamber (2 mL volume) was constantly perfused with pre-oxygenated Tyrode's solution at 1 mL/min. Temperature was maintained at 37.0±0.5 °C by a water bath thermostat (WC/09-05, Chongqing, China). The muscle strips were incubated for at least 40 min before experiments were started. The samples of human stomach were offered by Affiliated Hospital of Yanbian University College of Medicine (As the sample of human gastric was limited, only the gastric antral of human was sampled).

Drugs and solution

Tyrode solution containing (mmol·L⁻¹) 147 NaCl, 4 KCl, 1.05 MgCl₂·6H₂O, 0.42 CaCl₂·2H₂O, 1.81 Na₂PO₄·2H₂O, and 5.5 mM glucose was used. Its pH was adjusted to 7.35 by NaOH. C-type natriuretic peptide and LY83583 was diluted to 10⁻⁷ mol·L⁻¹. And, Zaprinast was diluted to 10⁻⁶ mol·L⁻¹. All drugs above were purchased from Sigma (USA).

Data analysis

All data was expressed as means ± SD. Statistical significance was evaluated by a *t*-test. Differences were considered to be significant when *P* value was less than 0.05.

RESULTS

Effect of CNP on the spontaneous contraction of the gastric antral smooth muscle in various animals

Different concentrations of CNP obviously inhibited spontaneous contraction in a dose-dependent manner and the percentage of inhibition was 22.8±7.2 %, 44.9±7.6 %, 69.1±12.9 % and 98.2±4.7 % at the concentrations of 1×10⁻⁸ mol·L⁻¹, 3×10⁻⁸ mol·L⁻¹, 1×10⁻⁷ mol·L⁻¹ and 1×10⁻⁶ mol·L⁻¹ respectively (Figure 1, *n*=7). The middle dose of CNP 10⁻⁷ mol·L⁻¹ was used in following all experiments.

The amplitude of spontaneous contraction in gastric antral circular smooth muscles of guinea-pigs and rats was significantly decreased by CNP and the percentage of inhibition was 58.23±6.21 % and 66.32±7.32 % respectively, however, the frequency was not influenced by CNP (Figure 2A and Figure 2C, Table 1.). The spontaneous contraction of the longitudinal smooth muscle was entirely inhibited by CNP in guinea-pigs and rats (Figure 2B and Figure 2D, Table 1). In the human gastric

antrum both circular and longitudinal smooth muscles, the spontaneous contraction was also completely inhibited by CNP (Figure 2E and Figure 2F, Table 1).

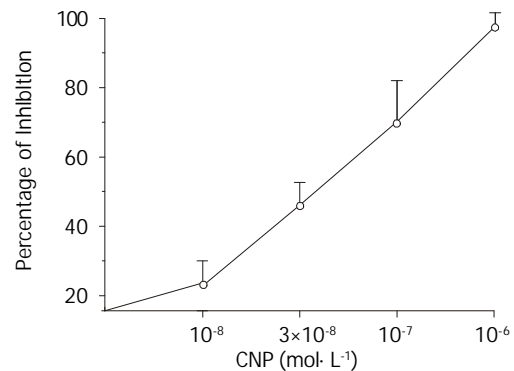


Figure 1 Response of CNP on spontaneous contraction of gastric circular muscle in rats with different concentration.

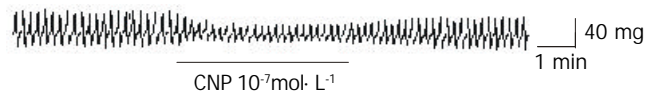


Figure 2A Effect of CNP on spontaneous contraction in gastric antral circular smooth muscle in guinea-pig.



Figure 2B Effect of CNP on spontaneous contraction in gastric antral longitudinal smooth muscle in guinea-pig.



Figure 2C Effect of CNP on spontaneous contraction in gastric antral circular smooth muscle in rat.

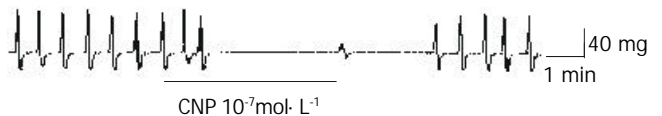


Figure 2D Effect of CNP on spontaneous contraction in gastric antral longitudinal smooth muscle in rat.

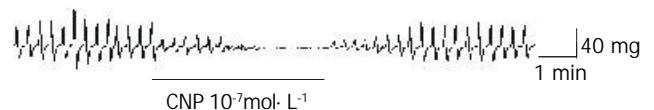


Figure 2E Effect of CNP on spontaneous contraction in gastric antral circular smooth muscle in human.

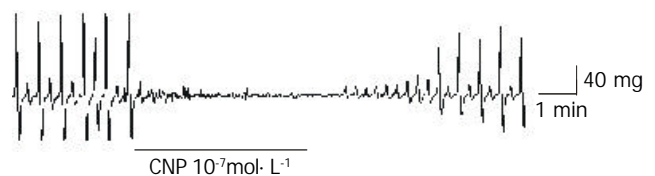


Figure 2F Effect of CNP on spontaneous contraction in gastric antral longitudinal smooth muscle in human.

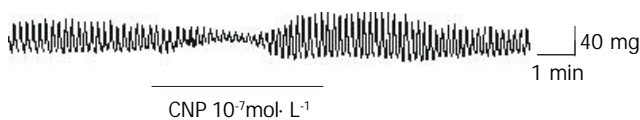
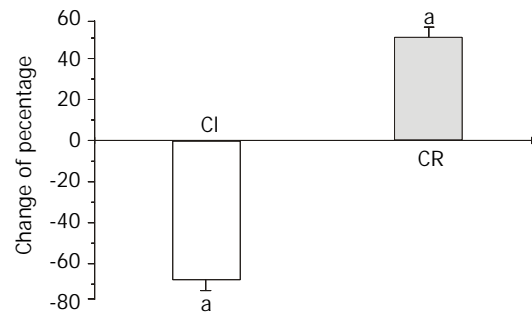
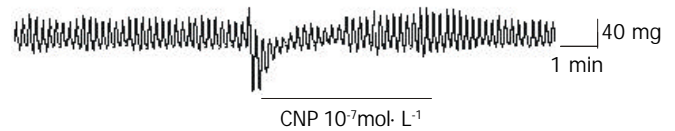
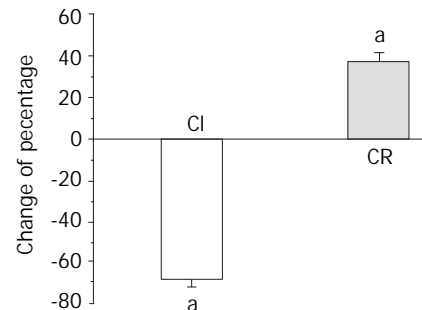
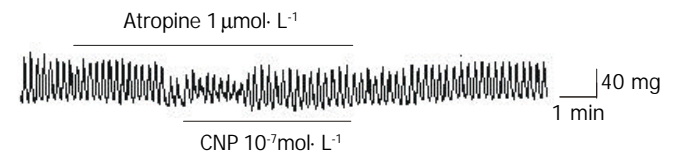
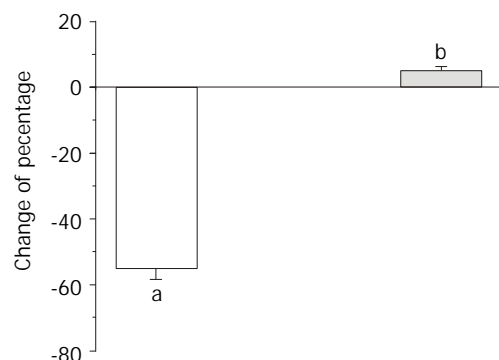
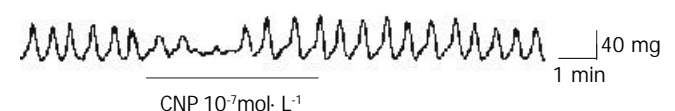
Table 1 Effect of CNP on spontaneous contraction of gastric antral smooth muscle in various animals ($\bar{x}\pm s$)

Species	n	Change of strip motility	
		Amplitude (%)	Frequency (%)
Guinea-pig(C)	6	-58.23±6.21 ^{a,d}	-10.81±3.14
Guinea-pig(L)	6	-100.00±0.00 ^a	-100.00±0.00 ^a
Rat(C)	8	-66.32±7.32 ^{a,b,e}	-10.76±3.21
Rat(L)	8	-100.00±0.00 ^a	-100.00±0.00 ^a
Human(C)	4	-100.00±0.00 ^{a,c}	-100.00±0.00 ^a
Human(L)	4	-100.00±0.00 ^a	-100.00±0.00 ^a

C: circular muscle; L: longitudinal muscle. ^a $P<0.01$ vs pretreatment; ^b $P<0.05$ vs Guinea-pig (C) group; ^c $P<0.01$ vs Guinea-pig (C) group and Rat (C) group; ^d $P<0.01$ vs Guinea-pig (L) group; ^e $P<0.01$ vs Rat (L) group.

Effect of CNP on the spontaneous contraction of the gastric body smooth muscle in various animals

CNP-induced response in the gastric body smooth muscle was different from the response in gastric antral smooth muscle in guinea-pigs and rats. In circular and longitudinal smooth muscles of guinea-pig gastric body, CNP first induced a relaxation and successively an increase in the amplitude of spontaneous contraction (rebound contraction), but the frequency was not changed (Figure 3A and C). After the gastric body circular smooth muscle was pretreated with atropine, an M receptor blocker, the rebound contraction was abolished (Figure 3E). In the circular smooth muscle of guinea-pig body, the percentage of inhibition was 67.21±5.32 % and the percentage of increase was 50.22±4.67 % (Figure 3B). However, in the longitudinal smooth muscle of guinea-pig body, the percentage of inhibition was 68.66±3.55 % and the percentage of increase was 38.91±4.08 % (Figure 3D). The frequency was not affected by CNP in the circular and longitudinal smooth muscles of gastric body of the guinea-pig and the pre-and post treat frequency were 6.44±0.64, 6.48±0.67 (circular smooth muscle); 6.53±0.34, 6.55±0.29 (longitudinal smooth muscle) respectively. After treated with atropine, the percentages of CNP-induced inhibition and increase were 55.33±3.23 % and 5.12±1.19 % respectively in the gastric body circular smooth muscle of the guinea-pig (Figure 3F). In the circular and longitudinal smooth muscles of rat gastric body, CNP induced a transient and a slight relaxation and it was followed by the recovery in an amplitude of spontaneous contraction, but the frequency was not affected by CNP (Figure 4A and C). The percentage of inhibition was 94.91±5.08 % in the circular smooth muscle of gastric body and 94.34±5.65 % in the longitudinal smooth muscle of gastric body (Figure 4B and D) respectively. After the smooth muscle was treated with atropine, the transient and slight relaxation was replaced by long term and complete inhibition. After treated with atropine, the inhibitory duration of contractile activity was lengthened from 1.3±0.21 min to 4.88±0.34 min and the rebound contraction disappeared in the gastric body circular smooth muscles of the rat (Figure 4A and E).

**Figure 3A** Effect of CNP on spontaneous contraction in gastric body circular smooth muscle in guinea-pig.**Figure 3B** Effect of CNP on spontaneous contraction in gastric body circular smooth muscle in guinea-pig. ^a $P<0.01$ vs pretreatment.**Figure 3C** Effect of CNP on spontaneous contraction in gastric body longitudinal smooth muscle in guinea-pig.**Figure 3D** Effect of CNP on spontaneous contraction in gastric body longitudinal smooth muscle in guinea-pig. ^a $P<0.01$ vs pretreatment.**Figure 3E** Effect of Atropine on CNP-induced spontaneous contraction in gastric body circular smooth muscle in guinea-pig.**Figure 3F** Effect of Atropine on CNP-induced spontaneous contraction in gastric body circular smooth muscle in guinea-pig. ^a $P<0.01$ vs pretreatment; ^b $P>0.05$ vs pretreatment.**Figure 4A** Effect of CNP on spontaneous contraction in gastric body circular smooth muscle in rat.

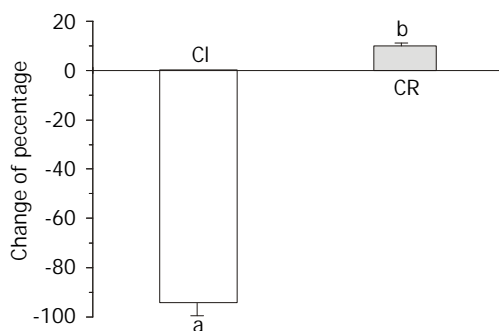


Figure 4B Effect of CNP on spontaneous contraction in gastric body circular smooth muscle in rat. ^a $P < 0.01$ vs pretreatment; ^b $P > 0.05$ vs pretreatment.

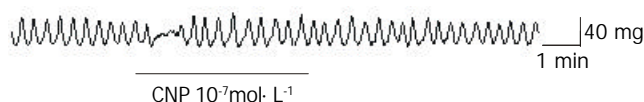


Figure 4C Effect of CNP on spontaneous contraction in gastric body longitudinal smooth muscle in rat.

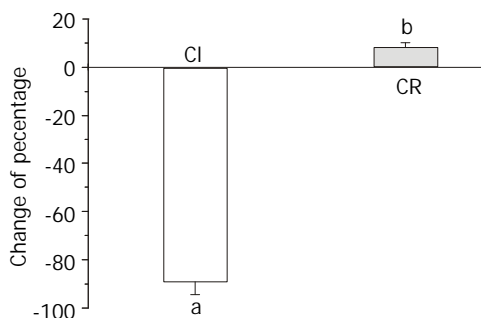


Figure 4D Effect of CNP on spontaneous contraction in gastric body longitudinal smooth muscle in rat. ^a $P < 0.01$ vs pretreatment; ^b $P > 0.05$ vs pretreatment.

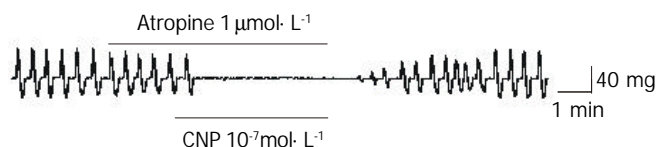


Figure 4E Effect of Atropine on CNP-induced spontaneous contraction in gastric body circular smooth muscle in rat.

Effect of CNP on the spontaneous contraction of the gastric fundus smooth muscle in various animals

CNP diminished the amplitude of the gastric fundus circular smooth muscles of guinea-pigs and rats, and the percentage of inhibition was $76.77 \pm 6.21\%$ and $95.87 \pm 4.12\%$, respectively (Figure 5A and B, Table 2). However, the frequency of spontaneous contraction was not affected by CNP in the g circular smooth muscles of gastric fundus of guinea-pigs and rats (Table 2). The spontaneous contraction of gastric fundus longitudinal smooth muscles of guinea-pigs and rats was completely inhibited (Figure 5C and Figure 5D, Table 2).

Effect of CNP on the spontaneous contraction of gastric smooth muscles in different positions of the same animal

The contractile amplitude was decreased by CNP in the gastric fundus, body and antral circular smooth muscles of the guinea-pig and the percentages of inhibition were $76.77 \pm 6.21\%$, $67.21 \pm 5.32\%$ and $58.23 \pm 6.21\%$ respectively. However, the percentages of inhibition in longitudinal smooth muscle were

$100 \pm 0.00\%$, $68.66 \pm 3.55\%$ and $100 \pm 0.00\%$ respectively (Figure 6A). The contractile amplitude was decreased by CNP in the gastric fundus, body and antral circular smooth muscles of the rat and the percentages of inhibition were $95.87 \pm 4.12\%$, $94.91 \pm 5.08\%$ and $66.32 \pm 7.32\%$, respectively. However, the percentages of inhibition in the longitudinal smooth muscles were $100 \pm 0.00\%$, $94.34 \pm 5.65\%$ and $100 \pm 0.00\%$ (Figure 6B) respectively.

Table 2 Effect of CNP on spontaneous contraction of gastric fundus smooth muscle in various animals ($\bar{x} \pm s$)

Species	n	Change of strip motility	
		Amplitude/%	Frequency/%
Guinea-pig (C)	6	$-76.77 \pm 6.21^{a,b}$	-12.21 ± 3.23
Guinea-pig (L)	6	-100.00 ± 0.00^a	-100.00 ± 0.003^a
Rat (C)	8	$-95.87 \pm 4.12^{a,c,e}$	-94.81 ± 5.19^c
Rat (L)	8	-100.00 ± 0.00^a	-100.00 ± 0.00^a

C: circular muscle; L: longitudinal muscle; ^a $P < 0.01$ vs pretreatment; ^b $P < 0.01$ vs Guinea-pig (L) group; ^c $P < 0.01$ vs Guinea-pig (C) group; ^e $P < 0.01$ vs Rat (L) group.



Figure 5A Effect of CNP on spontaneous contraction in gastric fundus circular smooth muscle in guinea-pig.



Figure 5B Effect of CNP on spontaneous contraction in gastric fundus circular smooth muscle in rat.

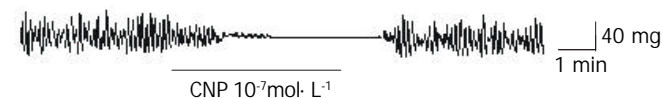


Figure 5C Effect of CNP on spontaneous contraction in gastric fundus longitudinal smooth muscle in guinea-pig.



Figure 5D Effect of CNP on spontaneous contraction in gastric fundus longitudinal smooth muscle in rat.

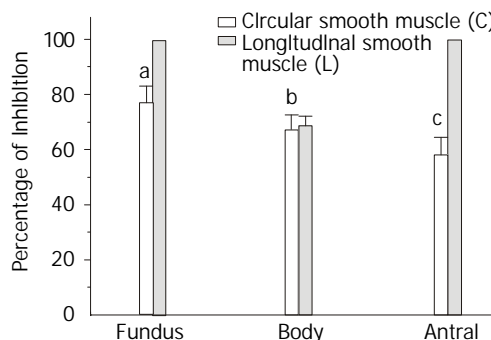


Figure 6A Effect of CNP on spontaneous contraction of different position in guinea-pig. ^a $P < 0.05$ vs Body (C) group and Antral

(C) group; ^a $P < 0.01$ vs Fundus(L) group; ^b $P < 0.01$ vs Fundus(L) group and Antral(L) group; ^c $P < 0.05$ vs Body(C) group; ^c $P < 0.01$ vs Antral(L) group.

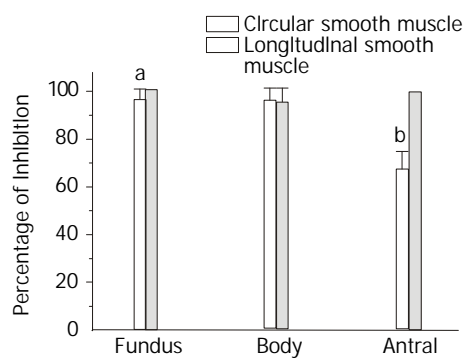


Figure 6B Effect of CNP on spontaneous contraction of different position in rat. ^a $P < 0.01$ vs Antral (C) group; ^b $P < 0.05$ vs Antral (L) group.

Effect of LY83583 and Zaparinast on CNP-induced inhibition in the gastric antral circular smooth muscle

After the gastric antral circular smooth muscle was treated by LY83583 10^{-7} mol·L⁻¹ and zaparinast (10^{-7} mol·L⁻¹) for 15 min to regulate the generation of cGMP, the effect of CNP on gastric motility was observed in the gastric antral circular smooth muscle of the rat. LY83583 markedly diminished the inhibitory effect of CNP on the spontaneous contraction, however, zaparinast enhanced the inhibitory effect of CNP on the spontaneous contraction (Table 3).

Table 3 Effect of LY83583 and Zaparinast on CNP-induced inhibition in gastric circular smooth muscle of rat ($\bar{x} \pm s$)

Group	n	Percentage of inhibition (%)
CNP1	5	63.61±3.68
CNP1+LY	5	54.15±2.97 ^a
CNP2	5	65.67±3.17
CNP2+Zap	5	77.67±5.86 ^b

^a $P < 0.05$ vs CNP1 group; ^a $P < 0.05$ vs CNP2 group.

DISCUSSION

In the present study, the effects of CNP on the spontaneous contraction of gastric smooth muscles in the rat, guinea-pig and human were comparatively investigated. The results indicated that CNP markedly inhibited the spontaneous contraction of gastric antral circular smooth muscles in these three kinds of animals and the order of inhibitory potency was human >rat> guinea-pig; CNP inhibited the contractile activity of gastric fundus circular and longitudinal smooth muscles in the rat and guinea-pig and this response was more obvious in the rat than that in guinea-pig; The effects of CNP on gastric body circular and longitudinal smooth muscles had double-phase, in which CNP first induced a relaxation and then an increase in the amplitude of the spontaneous contraction (rebound contraction) in the rat and guinea-pig. The response was more distinct in the guinea-pig than that in the rat and it disappeared after pretreating with atropine. In the same animal, the CNP-induced inhibition was the most potent in the gastric fundus and the weakest in the gastric antrum, and the inhibition was more obvious in the longitudinal smooth muscle than that in the circular smooth muscle. Using LY83583, a guanylate cyclase inhibitor, and zaparinast as phosphoesterase inhibitor to regulate the generation of cGMP, the effect of CNP on spontaneous contraction was markedly diminished by

LY83583. However, the inhibitory effect was enhanced by zaparinast. It was similar to the result observed in intestinal smooth muscle by Murthy *et al*^[13].

Since CNP was isolated from the central nerve system^[14], previous studies indicated that as a neurotransmitter, CNP exerted functions in the central nervous system^[15] and participated in the regulation of physiological functions in many other systems. CNP was successively found in the cardiovascular system^[16,17], respiratory system^[18], urinary system^[19], reproductive system^[2] and sense system^[20]. Since Komatsu *et al*^[8] found CNP in the gastrointestinal tracts of humans and rats, there were more and more studies on the relationship between CNP and the gastrointestinal tract. But the study on physiological functions of CNP in gastrointestinal tract was mainly focused on absorption, secretion and intestinal motility^[10-12]. Serial studies on natriuretic peptides regulating gastric smooth muscles motility were not reported. In this study, the effect of CNP on gastric motility in various animals, in different positions and in different smooth muscles of the same position of the same animal was comparatively investigated.

In various animals, the effects of CNP on the gastric motility of antrum and fundus smooth muscles presented species diversity. The order of inhibitory potency in gastric antrum was human >rat> guinea-pig, and in gastric fundus, the order was rat > guinea-pig. Analyzing this from the animal characters, It was presumed that either the distribution of the CNP receptor in gastric smooth muscle of three kinds of animals was different or the sensitivity of CNP to CNP receptor in different animal was diverse.

In different positions of the same animal, the effect of CNP on gastric motility exhibited positional diversity. CNP-induced inhibition was the most potent in gastric fundus and the weakest in gastric antrum. The responses may be related to the structure and function of the stomach. It was thought that the muscle layer was the thickest in the gastric antrum and the thinnest in the gastric fundus, and the gastric antrum played an important role in gastric emptying while gastric fundus was related to receptive relaxation. It indicated that the contractile function of the gastric antrum was more potent than the function of gastric fundus. In the same position of the same animal, the inhibition was more obvious in longitudinal smooth muscles than that in circular smooth muscles. The reason was probably that the distribution of CNP receptors showed diversity.

It is well known that NP and NO system are all cGMP-generation system. They play a very important role in regulation of multiple physiological functions. To investigate the mechanism of CNP-induced inhibition, LY83583, a kind of inhibitor of guanylate cyclase, and zaparinast, a phosphoesterase inhibitor were used for observing the effect of CNP on gastric motility in gastric antral circular smooth muscle of the rats. LY83583 markedly diminished the inhibitory effect of CNP on the spontaneous contraction, however, zaparinast enhanced the inhibitory effect of CNP on the spontaneous contraction. It indicated that CNP-induced inhibition on the spontaneous contraction in the gastric smooth muscle *via the cGMP* dependent pathway. Previous studies also supported the theory, for example, CNP dilated the vascular smooth muscle^[21] and relaxed the bronchus smooth muscle^[22] *via cGMP* dependent pathway.

In this present study, the CNP-induced response on spontaneous contraction of the gastric body showed double-phase, in which CNP first induced a relaxation and then inducing rebound contractions in rats and guinea-pigs. The response was more distinct in guinea-pigs than that in rat and it disappeared after pretreated with atropine. The results indicated that cholinergic M receptor participated in this CNP-induced rebound contraction of gastric body smooth muscle in guinea-pigs and rats. Previous studies also indicated that

vagus nerve regulated many functions of NP, for example, ANP promoted gastric acid secretion^[23], ANP, BNP and CNP could all induce bradycardia^[24] and BNP and CNP could enhance vagus-induced response of slowing heart rate^[25]. Then, it was suggested that CNP may facilitate the cholinergic nerve activity in gastric smooth muscles.

CNP may participate in the regulation of gastric motility as gastrointestinal hormone or neurotransmitter. CNP-induced inhibition has species diversity and position diversity in gastric smooth muscles. CNP-induced inhibition on gastric motility may be related to the increase of intracellular cGMP.

REFERENCES

- De Bold AJ**, Borenstein HB, Veress AT, Sonnenberg H. A rapid and potent natriuretic response to intravenous injection of atrial myocardial extracts in rats. *J Am Soc Nephrol* 2001; **12**: 403-409
- Stepan H**, Leitner E, Bader M, Walther T. Organ-specific mRNA distribution of C-type natriuretic peptide in neonatal and adult mice. *Regul Pept* 2000; **95**: 81-85
- Woodard GE**, Rosado JA, Brown J. Expression and control of C-type natriuretic peptide in rat vascular smooth muscle cells. *Am J Physiol Regul Integr Comp Physiol* 2002; **282**: R156-165
- Casco VH**, Veinot JP, Kuroski de Bold ML, Masters RG, Stevenson MM, de Bold AJ. Natriuretic peptide system gene expression in human coronary arteries. *J Histochem Cytochem* 2002; **50**: 799-809
- Furuya M**, Yoshida M, Hayashi Y, Ohnuma N, Minamino N, Kangawa K, Matsuo H. C-type natriuretic peptide is a growth inhibitor of rat vascular smooth muscle cells. *Biochem Biophys Res Commun* 1991; **177**: 927-931
- Wang X**, Xue L, Tong L. Influence of vasoactive peptides on homocysteine-induced proliferation of cultured rabbit vascular smooth muscle cell. *Zhonghua Yixue Zazhi* 1999; **79**: 411-413
- Ohno N**, Itoh H, Ikeda T, Ueyama K, Yamahara K, Doi K, Yamashita J, Inoue M, Masatsugu K, Sawada N, Fukunaga Y, Sakaguchi S, Sone M, Yurugi T, Kook H, Komeda M, Nakao K. Accelerated reendothelialization with suppressed thrombogenic property and neointimal hyperplasia of rabbit jugular vein grafts by adenovirus-mediated gene transfer of C-type natriuretic peptide. *Circulation* 2002; **105**: 1623-1626
- Komatsu Y**, Nakao K, Suga S, Ogawa Y, Mukoyama M, Arai H, Shirakami G, Hosoda K, Nakagawa O, Hama N. C-type natriuretic peptide (CNP) in rats and humans. *Endocrinology* 1991; **129**: 1104-1106
- Gower WR Jr**, Salhab KF, Foulis WL, Pillai N, Bundy JR, Vesely DL, Fabri PJ, Dietz JR. Regulation of atrial natriuretic peptide gene expression in gastric antrum by fasting. *Am J Physiol Regul Integr Comp Physiol* 2000; **278**: R770-780
- Vuolteenaho O**, Arjamaa O, Vakkuri O, Maksniemi T, Nikkila L, Kangas J, Puurunen J, Ruskoaho H, Leppaluoto J. Atrial natriuretic peptide (ANP) in rat gastrointestinal tract. *FEBS Lett* 1988; **233**: 79-82
- Brockway PD**, Hardin JA, Gall DG. Intestinal secretory response to atrial natriuretic peptide during postnatal development in the rabbit. *Biol Neonate* 1996; **69**: 60-66
- Akiho H**, Chijiwa Y, Okabe H, Harada N, Nawata H. Interaction between atrial natriuretic peptide and vasoactive intestinal peptide in guinea pig cecal smooth muscle. *Gastroenterology* 1995; **109**: 1105-1112
- Murthy KS**, Teng B, Jin J, Makhoulf GM. G protein-dependent activation of smooth muscle eNOS via natriuretic peptide clearance receptor. *Am J Physiol* 1998; **275**: C1409-1416
- Sudoh T**, Minamino N, Kangawa K, Matsuo H. C-type natriuretic peptide (CNP): A new member of natriuretic peptide family identified in porcine brain. *Biochem Biophys Res* 1990; **168**: 863-870
- Minerds KL**, Donald JA. Natriuretic peptide receptors in the central vasculature of the toad, *Bufo marinus*. *Comp Biochem Physiol A Mol Integr Physiol* 2001; **128**: 259-268
- Doyle DD**, Upshaw-Earley J, Bell EL, Palfrey HC. Natriuretic peptide receptor-B in adult rat ventricle is predominantly confined to the nonmyocyte population. *Am J Physiol Heart Circ Physiol* 2002; **282**: H2117-2123
- Wright RS**, Wei CM, Kim CH, Kinoshita M, Matsuda Y, Aarhus LL, Burnett JC Jr, Miller WL. C-type natriuretic peptide-mediated coronary vasodilation: role of the coronary nitric oxide and particulate guanylate cyclase systems. *J Am Coll Cardiol* 1996; **28**: 1031-1038
- Nakanishi K**, Tajima F, Itoh H, Nakata Y, Hama N, Nakagawa O, Nakao K, Kawai T, Torikata C, Suga T, Takishima K, Aurues T, Ikeda T. Expression of C-type natriuretic peptide during development of rat lung. *Am J Physiol* 1999; **277**: L996-L1002
- Meier SK**, Toop T, Donald JA. Distribution and characterization of natriuretic peptide receptors in the kidney of the toad, *Bufo marinus*. *Gen Comp Endocrinol* 1999; **115**: 244-253
- Suzuki M**, Kitanishi T, Kitano H, Yazawa Y, Kitajima K, Takeda T, Tokunaga Y, Maeda T, Kimura H, Tooyama I. C-type natriuretic peptide-like immunoreactivity in the rat inner ear. *Hear Res* 2000; **139**: 51-58
- Wennberg PW**, Miller VM, Rabelink T, Burnett JC Jr. Further attenuation of endothelium-dependent relaxation imparted by natriuretic peptide receptor antagonism. *Am J Physiol* 1999; **277**: H1618-1621
- Borges A**, de Villarreal SS, Winand NJ, de Becembeg IL, Alfonso MJ, de Alfonso RG. Molecular and biochemical characterization of a CNP-sensitive guanylyl cyclase in bovine tracheal smooth muscle. *Am J Respir Cell Mol Biol* 2001; **25**: 98-103
- Puurunen J**, Ruskoaho H. Vagal-dependent stimulation of gastric acid secretion by intracerebroventricularly administered atrial natriuretic peptide in anaesthetized rats. *Eur J Pharmacol* 1987; **141**: 493-495
- Thomas CJ**, May CN, Sharma AD, Woods RL. ANP, BNP, and CNP enhance bradycardic responses to cardiopulmonary chemoreceptor activation in conscious sheep. *Am J Physiol Regul Integr Comp Physiol* 2001; **280**: R282-288
- Herring N**, Zaman JA, Paterson DJ. Natriuretic peptides like NO facilitate cardiac vagal neurotransmission and bradycardia via a cGMP pathway. *Am J Physiol Heart Circ Physiol* 2001; **281**: H2318-2327

Edited by Xu XQ

Significance of changes of gastrointestinal peptides in blood and ileum of experimental spleen deficiency rats

Li-Sheng Li, Rui-Yao Qu, Wei Wang, Hua Guo

Li-Sheng Li, Rui-Yao Qu, Wei Wang, Hua Guo, Department of Physiology, Capital University of Medical Sciences, 100054, Beijing, China

Supported by the Traditional Chinese Medicine-Drug Science and Technology Development Foundation, Beijing City (1999-2000)

Correspondence to: Li-Sheng Li, Department of Physiology, Capital University of Medical Sciences, 100054, Beijing, China. lls@sohu.com

Telephone: +86-10-63051492

Received: 2002-09-13 **Accepted:** 2002-10-31

Abstract

AIM: To explore the mechanism of spleen deficiency (SD) by studying the relationship of gastro-intestinal peptides level and ileal electro-mechanical activity of SD rats and cold restrain rats.

METHODS: (1) spleen deficiency (SD) model was established by feeding Houpu:Zhishi: Dahuang in the ratio of 3:3:2, 3 ml/time, for 42 days. (2) The cold restrain stress model: Animals were restrained on grille and placed in a cool water at 18 °C for 3 h. (3) Substance P (SP) and vasoactive intestinal peptide (VIP) levels in all layers of initial part of ileum and blood in rats were measured by radioimmunoassays (RIA) while changes of electric activity and motility in ileum of rats were recorded with electrode and strain gauge.

RESULTS: SP levels in ileum and blood of experimental SD rats were significantly higher than that of the control groups (9.89±5.65 vs 1.22±1.18, $P<0.005$, in ileum; 22.7±3.95 vs 6.60±1.47, $P<0.001$, in blood) while the VIP levels of the SD rats were significantly lower than that of the controls (3.50±2.01 vs 9.10±4.91, $P<0.05$, in ileum; 229.8±62.4 vs 560.4±151.3, $P<0.001$, in blood). As compared with the controls, the average frequency of slow electric waves (21.3±0.96 vs 18.2±2.28, $P<0.05$) and motility (21.5±0.58 vs 18±2.65, $P<0.005$) of SD rats increased obviously and the frequency of fast waves of SD rat also increased. In spontaneous recovery cases, SP levels recovered significantly (compared with the SD groups, 2.99±0.62 vs 9.89±5.65, $P<0.001$, in ileum; 14.4±4.22 vs 22.7±3.95, $P<0.001$, in blood) but did not drop to normal. After the SD rats treated with Chinese herbs (Jiawei Sijun zi Tang), SP improved (compared with SD cases, 2.20±1.25 vs 9.89±5.65, ($P<0.001$), in ileum; 10.7±1.88 vs 22.7±3.95, ($P<0.001$), in blood) and VIP in blood also improved (compared with SD rats, 485.7±229.0 vs 229.8±62.4, $P<0.01$) while the amplitude of motility decreased apparently (compared with the SD rats, 0.64±0.096 vs 0.89±0.15, $P<0.01$). The ileal SP levels of cool stress didn't change while the ileal VIP levels of cool stress became significantly lower than that of the control groups (2.87±0.87 vs 9.10±4.91, $P<0.01$). The blood SP levels of cool stress were significantly higher (15.60±1.83 vs 6.60±1.47, $P<0.001$) whereas the blood VIP levels of cool stress were significantly lower than that of the control group (153.4±70.46 vs 560.4±151.30, $P<0.001$).

CONCLUSION: Changes of SP and VIP levels in initial part

of ileum and blood of SD rats and cool stress rats may be closely related to the gastrointestinal motility disorders presented in SD and cool stress rats. the Chinese herbs (Jiawei Sijun zi Tang) currently used have partially therapeutic effect.

Li LS, Qu RY, Wang W, Guo H. Significance of changes of gastrointestinal peptides in blood and ileum of experimental spleen deficiency rats. *World J Gastroenterol* 2003; 9(3): 553-556
<http://www.wjgnet.com/1007-9327/9/553.htm>

INTRODUCTION

It was well known that Spleen-Stomach theory is an important constituent of the theoretical basis of traditional Chinese Medicine. The spleen here is not synonymous with the spleen in western medicine anatomically, physiologically or pathophysiologically^[1-3]. Conceptually, Spleen-Stomach theory is a comprehensive one. It mainly involves the digestive system, its vegetative nervous system, immunologic function, hemopoiesis, muscle metabolism, endocrine function, hepatic metabolic function, protein, nucleotide, energy, water and salt metabolism.

In recent years, the field of gastrointestinal hormones has expanded at a dazzling speed. The successful isolation of some gastrointestinal hormones and development of sensitive assays for their detection have led to many unexpected findings^[4]. Gastrointestinal hormones as regulatory peptides appear to be major components of bodily integration and have important regulatory actions on physiological function of gastrointestinal tract^[5-17]. Some studies indicated that spleen deficiency syndrome (SDS) was closely related with gastrointestinal hormones^[18-21].

But up to now, the mechanisms of the relationship between gastrointestinal peptides levels and gastrointestinal functional disorder in SD still remain unclear^[22-31]. We tried to explore the relationship between SDS and gastrointestinal hormones by measuring SP and VIP, and by using electrode and highly sensitive strain sensor to record alterations of ileum activity and ileum motility in SD and cool stress rats.

MATERIALS AND METHODS

Experimental animals

Healthy adult male Wistar rats (provided by Experimental Animal center, capital university of medical sciences), weighing 0.12-0.17 kg were used in this study. They were caged in an air conditioned room (23±2 °C).

Sijunzi decoction (SJZD), composed of ginseng, Atractylodes, Poria, Glycyrrhiza, It was prepared by routine method of decocting the crude herbal medicine twice. The filtered medication was preserved in refrigerator at 4 °C.

Fifty rats were randomly divided into five groups: (1) control group: The rats were fed standard rat chow and water ad libium. (2) experimental SD model group. by feeding Houpu: Zhishi: Dahuang (3:3:2), 3 ml/time, 42 day. (3) Spontaneous recovery group. (4) SJZD treated group. (5) cold stress group: rats were restrained on grille and placed in cool water at 18 °C for 3 h.

Table 3 Changes of electric-mechanical activity in ileum ($\bar{x}\pm s$)

	Main frequency (time/min)		Average frequency (time/min)		Amplitude (time/min)	
	Slow wave	Motility	Slow wave	Motility	Slow wave	Motility
Control group	17.5±2.05	18.5±1.7	18.2±2.28	18±2.65	0.30±0.26	0.43±0.31
SD group	17.4±0.79	18.0±0.69	21.3±0.96 ^b	21.5±0.58 ^a	0.31±0.24	0.89±0.15 ^b
Spontaneous recovery group	16.8±7.8	16.8±1.3	20.5±5.5	19.1±4.85	0.25±0.103	0.77±0.65
Treated group	13.8±3.92	16.1±3.36	20.0±4.04	19.0±3.61	0.14±0.015	0.64±0.096 ^c
Cool stress group	16.5±2.67	15.7±1.1	15.2±2.01	16±2.17	0.27±0.11	0.33±0.12

^a $P<0.005$, vs control group; ^b $P<0.05$, vs control group; ^c $P<0.01$, vs SD group.

Measurements

Radioimmunoassay (RIA) of SP and VIP in these samples was conducted with kits purchased from Beijing HaiKerui Biological technique center. The concentrations of SP, VIP were measured with radioimmunoassay kits. Under anesthesia, the abdomen was opened and the samples were taken as follows: (1) Blood samples of 5-6 ml from the heart were collected in tubes, the plasma was immediately separated by centrifugation, then was frozen and stored at -20 °C until analysis. (2) The initial part of ileal tissue were removed, rinsed and weighed, then were put into a tube with boiling water. The tube was plunged into vigorous boiling water for 3 minutes, then it was cooled down and homogenized for 10 minutes. After centrifugation at 3 000 r/min for 5 minutes, the supernatant was collected and stored at -20 °C until assay.

All groups fasted for 18 h before operating, anesthetized by 20 % urethane, the abdomen was opened, then the silver electrodes and strain gauge were implanted on the initial part of ileum. The changes of electric slow wave and motility of ileum were recorded. Electrode wires were passed through the abdominal muscle and fixed on the skin. All data were handled by a two-channel physiological recorder and a computer.

The cold restrain stress model: Animals were restrained on grille and placed in a cool water at 18 °C for 3 h.

Statistical analysis

Data were expressed as mean \pm standard deviation. Experimental results were analyzed by *t* tests was determined $P<0.05$ was considered statistically significant.

RESULTS

To assess the changes of gut peptides of gastrointestinal functional disorder in SD rats and cold restraint rats, we measured the plasma levels of SP and VIP and those in the initial part of the ileum. SP levels in ileum and blood of experimental SD rats were significantly higher than those of the control groups ($P<0.005$, in ileum; $P<0.001$, in blood) while the VIP levels of the SD rats were significantly lower than those of the controls ($P<0.05$ in ileum, $P<0.001$, in blood). In spontaneous recovery cases, SP levels recovered significantly (compared with the SD groups, $P<0.001$) and did not drop to normal. After the SD rats were treated with Chinese herbs (Jiawei Sijun Zi Tang), SP was improved (compared with SD cases, $P<0.001$) and VIP in blood was also improved (compared with SD rats, $P<0.01$). SP levels in ileum of cool stress didn't change while the VIP levels were significantly lower than that of the controls groups ($P<0.01$). SP levels in blood of cool stress were significantly higher ($P<0.001$) while the VIP levels were significantly lower than that of the control groups ($P<0.001$), Table 1-2.

As compared with the controls, average frequency of slow electric waves ($P<0.05$) and motility ($P<0.05$) of SD rats

increased obviously while the amplitude of motility decreased apparently ($P<0.05$), Table 3.

Table 1 Changes of SP and VIP in plasma ($\bar{x}\pm s$, $\mu\text{g}\cdot\text{L}^{-1}$)

Group	<i>n</i>	SP	VIP
Control group	7	6.60±1.47	560.40±151.30
SD group	8	22.7±3.95 ^a	229.8±62.4 ^a
Spontaneous recovery group	7	14.4±4.22 ^c	332.7±119.1
Treated group	7	10.7±1.88 ^b	485.7±229.0 ^c
Cool stress group	7	15.60±1.83 ^a	153.4±70.46 ^a

^a $P<0.001$, vs control group; ^b $P<0.001$, vs SD group; ^c $P<0.01$, vs SD group.

Table 2 Changes of SP and VIP in ileum ($W_B/\mu\text{g}\cdot\text{mg}^{-1}$, $\bar{x}\pm s$)

Group	<i>n</i>	SP	VIP
Control group	7	1.22±1.18	9.10±4.91
SD group	8	9.89±5.65 ^a	3.50±2.01 ^c
Spontaneous recovery group	7	2.99±0.62 ^b	4.11±0.83
Treated group	7	2.20±1.25 ^b	4.48±1.14
Cool stress group	7	0.57±0.51	2.87±0.87 ^c

^a $P<0.005$, vs control group; ^b $P<0.001$, vs SD group; ^c $P<0.01$, vs control group.

DISCUSSION

Spleen is one of the five solid organs, which in Traditional Chinese Medicine (TCM), does not completely match the organ designated in western medicine from the standpoint of structure, location and function. It has the functions of digesting food, absorbing and transporting nutrients to the body tissues. The spleen also serves to control the blood and to keep the blood circulating within the vessels, and takes part in the regulation of fluid metabolism^[32-38]. Spleen-Stomach theory forms the basis of diagnostic approach and treatment of Spleen-Stomach disease, Spleen deficiency syndrome is a multisystem and multiorgan functional impairment, but mainly manifest as digestive tract disturbance. Experimental researches on animal model and clinical studies on spleen deficiency syndrome have yielded fruitful results in this field which lead to a better understanding of its mechanism and help open a new avenue for treatment of diseases relevant to Spleen deficiency^[21,39-47]. The Spleen stomach has various physiologic functions. such as: Spleen governs transport and transformation, Spleen-stomach transforms food into nutrients which are the sources of Qi and blood. Stomach governs down-bearing function and spleen governs up-bearing which signify the motility, secretory, assimilative, absorptive and dispersing functions of upper

digestive tract, among which, gut hormones are involved^[20,48-50]. Dysfunction of up-and down-bearing function of spleen-stomach can cause gastrointestinal disturbances and various spleen deficiency syndromes^[1,2,19,20,51,52].

SP and VIP are both important gut Peptides, SP and VIP partly distributed in the mucosa of gastric antrum, the mucosa of the jejunum, ileum. And the central nervous system SP has a wide range of biological actions. In the intestine, VIP markedly stimulates intestinal secretion of electrolytes and hence of water. Its other actions include relaxation of intestinal smooth muscle; sphincters; dilation of peripheral blood vessels; and inhibition of gastric acid secretion.

Our previous studies included: The use of electrode and highly sensitive sensor to record alteration of gut electric activity and motility. To explore the potential role of gut peptides in spleen deficiency (SD), we studied immunoreactive Substance P, VIP, Calcitonin Gene Related Peptide (CGRP) levels in gastric antrum, duodenum and jejunal tissues in experimental SD rats by radioimmunoassays (RIA). The study suggested that motion frequency of several regions in SD rats was lower than that of control and treatment groups, respectively ($P<0.05$). The minimal amplitude of electric activity was also lower than that of control and treatment respectively ($P<0.05$). Correlation between motion frequency and its total amplitude index was different from various regions, the time of MMC was obviously less than that of the control, and the amplitude of motility was significantly higher than that of the control. The SP, VIP levels in antrum of SD rats were obviously less than that of the control, whereas, the SP and VIP levels in duodenum of SD rats were obviously higher than that of control ($P<0.05$), but in jejunum only SP levels increased obviously than that of the control ($P<0.05$). The VIP level in duodenum of SD rats was significantly less than that of treatment group ($P<0.05$), but VIP level of treatment group was higher than that of the control ($P<0.05$). As to CGRP level in antrum and small intestine, there was no obvious difference among the 3 groups.

The present study reveals changes SP and VIP in ileum of SD rats and cool stress rat. All these data imply that changes of SP and VIP levels in the antrum and the small intestine of SD rats may be closely related with the dysmotility of gastrointestinal, malabsorption and diarrhea. The Chinese herb (si junzi Tang) is capable of improving the spleen deficiency significantly and gastrointestinal electro-mechanical activity.

REFERENCES

- Gao R**, Li L, Lu Z. Clinical observation on 300 cases of angina pectoris treated by the spleen-stomach regulating method. *J Tradit Chin Med* 1998; **18**: 87-90
- Wu XN**. Current concept of Spleen-Stomach theory and Spleen deficiency syndrome in TCM. *World J Gastroenterol* 1998; **4**: 2-6
- Straus E**. Gastrointestinal hormones. *Mt Sinai J Med* 2000; **67**: 54-57
- Bierkamp C**, Kowalski-Chauvel A, Dehez S, Fourmy D, Pradayrol L, Seva C. Gastrin mediated cholecystokinin-2 receptor activation induces loss of cell adhesion and scattering in epithelial MDCK cells. *Oncogene* 2002; **21**: 7656-7670
- Patten GS**, Head RJ, Abeywardena MY, McMurchie EJ. An apparatus to assay opioid activity in the infused lumen of the intact isolated guinea pig ileum. *J Pharmacol Toxicol Methods* 2001; **45**: 39-46
- De Man JG**, Moreels TG, De Winter BY, Bogers JJ, Van Marck EA, Herman AG, Pelckmans PA. Disturbance of the prejunctional modulation of cholinergic neurotransmission during chronic granulomatous inflammation of the mouse ileum. *Br J Pharmacol* 2001; **133**: 695-707
- Wise RM**, Bass P, Oaks JA. Myoelectric response of the small intestine to the oral presence of the tapeworm *Hymenolepis diminuta*. *J Parasitol* 2001; **87**: 1255-1259
- Stebbing M**, Johnson P, Vremec M, Bornstein J. Role of alpha(2)-adrenoceptors in the sympathetic inhibition of motility reflexes of guinea-pig ileum. *J Physiol* 2001; **534**(Pt. 2): 465-478
- Shafik A**, El-Sibai O, Ahmed A. Study of the mechanism underlying the difference in motility between the large and small intestine: the "single" and "multiple" pacemaker theory. *Front Biosci* 2001; **6**: B1-5
- Soderholm JD**, Perdue MH. Stress and gastrointestinal tract. II. Stress and intestinal barrier function. *Am J Physiol Gastrointest Liver Physiol* 2001; **280**: G7-G13
- Bayer S**, Raul F, Boehm N, Klein A, Angel F. Modulatory effects of polyamines and GABA on rat ileal motility *in vitro*. *Gastroenterol Clin Biol* 1999; **23**: 824-831
- Chang IY**, Glasgow NJ, Takayama I, Horiguchi K, Sanders KM, Ward SM. Loss of interstitial cells of Cajal and development of electrical dysfunction in murine small bowel obstruction. *J Physiol* 2001; **536**(Pt 2): 555-568
- Shibata C**, Murr MM, Balsiger B, Anding WJ, Sarr MG. Contractile activity of circular smooth muscle in rats one year after small bowel transplantation: differing adaptive response of the jejunum and ileum to denervation. *J Gastrointest Surg* 1998; **2**: 463-472
- Pfefferkorn MD**, Fitzgerald JF, Croffie JM, Gupta SK, Caffrey HM. Direct measurement of pancreatic enzymes: a comparison of secretagogues. *Dig Dis Sci* 2002; **47**: 2211-2216
- Takeuchi T**, Fujita A, Roumy M, Zajac JM, Hata F. Effect of 1DMe, a neuropeptide FF analog, on acetylcholine release from myenteric plexus of guinea pig ileum. *Jpn J Pharmacol* 2001; **86**: 417-422
- Marinovich M**, Viviani B, Capra V, Corsini E, Anselmi L, D'Agostino G, Di Nucci A, Binaglia M, Tonini M, Galli CL. Facilitation of acetylcholine signaling by the dithiocarbamate fungicide propineb. *Chem Res Toxicol* 2002; **15**: 26-32
- Venkova K**, Sutkowski-Markmann DM, Greenwood-Van Meerveld B. Peripheral activity of a new NK1 receptor antagonist TAK-637 in the gastrointestinal tract. *J Pharmacol Exp Ther* 2002; **300**: 1046-1052
- Yin G**, Zhang W, Li G. Therapeutic effect of weikangfu on gastric precancerous disorder with spleen deficiency syndrome and its effect of gastric mucosal zinc, copper, cyclic adenosine monophosphate, superoxide dismutase, lipid peroxide and 3H-TdR lymphocyte conversion test. *Zhongguo Zhongxiyi Jiehe Zazhi* 2000; **20**: 176-179
- Ren P**, Huang X, Zhang L. Effect of sijnunzi decoction on gastric emptying rate in rat model of spleen deficiency syndrome. *Zhongguo Zhongxiyi Jiehe Zazhi* 2000; **20**: 596-598
- Yin G**, Zhang W, Xu F. Effect of Weikangfu granule on ultrastructure of gastric mucosa in patients of precancerosis with spleen deficiency syndrome. *Zhongguo Zhongxiyi Jiehe Zazhi* 2000; **20**: 667-670
- Xu L**. Twenty-seven cases of spleen-qi deficiency syndrome treated by heat-producing needling at zusanli. *J Tradit Chin Med* 2000; **20**: 40-41
- Hockerfelt U**, Franzen L, Kjorell U, Forsgren S. Parallel increase in substance P and VIP in rat duodenum in response to irradiation. *Peptides* 2000; **21**: 271-281
- Fujimiya M**, Inui A. Peptidergic regulation of gastrointestinal motility in rodents. *Peptides* 2000; **21**: 1565-1582
- Chang FY**, Doong ML, Chen TS, Lee SD, Wang PS. Vasoactive intestinal polypeptide appears to be one of the mediators in misoprostol-enhanced small intestinal transit in rats. *J Gastroenterol Hepatol* 2000; **15**: 1120-1124
- Huang X**, Ren P, Wen AD, Wang LL, Zhang L, Gao F. Pharmacokinetics of traditional Chinese syndrome and recipe: a hypothesis and its verification (I). *World J Gastroenterol* 2000; **6**: 384-391
- Pei WF**, Xu GS, Sun Y, Zhu SL, Zhang DQ. Protective effect of electroacupuncture and moxibustion on gastric mucosal damage and its relation with nitric oxide in rats. *World J Gastroenterol* 2000; **6**: 424-427
- Zhang XC**, Gao RF, Li BQ, Ma LS, Mei LX, Wu YZ, Liu FQ, Liao ZL. Clinical and experimental study of therapeutic effect of Weixibaonizhuan pills on gastric precancerous lesions. *World J Gastroenterol* 1998; **4**: 24-27
- Xu CT**, Pan BR. Current status of gene therapy in gastroenterology. *World J Gastroenterol* 1998; **4**: 85-89

- 29 **Xu CT**, Pan BR. Current medical therapy for ulcerative colitis. *World J Gastroenterol* 1999; **5**: 64-72
- 30 **Yuan HY**, Li Y, Yang GL, Bei DJ, Wang K. Study on the causes of local recurrence of rectal cancer after curative resection: analysis of 213 cases. *World J Gastroenterol* 1998; **4**: 527-529
- 31 **Yamamoto H**, Umeda M, Mizoguchi H, Kato S, Takeuchi K. Protective effect of Irsogladine on monochloramine induced gastric mucosal lesions in rats: a comparative study with rebamipide. *World J Gastroenterol* 1999; **5**: 477-482
- 32 **Yin G**, Zhang W, He X. Histo-cytopathological study on gastric mucosa of spleen deficiency syndrome. *Zhongguo Zhongxiyi Jiehe Zazhi* 1999; **19**: 660-663
- 33 **Zhu L**, Yang ZC, Li A, Cheng DC. Reduced gastric acid production in burn shock period and its significance in the prevention and treatment of acute gastric mucosal lesions. *World J Gastroenterol* 2000; **6**: 84-88
- 34 **Zheng TZ**, Li W, Qu SY, Ma YM, Ding YH, Wei YL. Effects of Dangshen on isolated gastric muscle strips in rats. *World J Gastroenterol* 1998; **4**: 354-356
- 35 **Li W**, Zheng TZ, Qu SY. Effect of cholecystokinin and secretin on contractile activity of isolated gastric muscle strips in guinea pigs. *World J Gastroenterol* 2000; **6**: 93-95
- 36 **Shen XZ**, Koo MWL, Cho CH. Sleep deprivation increase the expression of inducible heat shock protein 70 in rat gastric mucosa. *World J Gastroenterol* 2001; **7**: 496-499
- 37 **Peng X**, Feng JB, Wang SL. Distribution of nitric oxide synthase in stomach wall in rats. *World J Gastroenterol* 1999; **5**: 92
- 38 **Peng X**, Feng JB, Yan H, Zhao Y, Wang SL. Distribution of nitric oxide synthase in stomach myenteric plexus of rats. *World J Gastroenterol* 2001; **7**: 852-854
- 39 **Li L**, Jin NG, Piao L, Hong MY, Jin ZY, Li Y, Xu WX. Hyposmotic membrane stretch potentiated muscarinic receptor agonist-induced depolarization of membrane potential in guinea-pig gastric myocytes. *World J Gastroenterol* 2002; **8**: 724-727
- 40 **Yang WY**, Liang R, Che JX. Clinical study on relation between spleen-qi deficiency syndrome and the pancreatic exocrine function. *Zhongguo Zhongxiyi Jiehe Zazhi* 1996; **16**: 414-416
- 41 **Zhang M**, Zhang Z, Xia T. Effect of sijunzi decoction on serum soluble intercellular adhesive molecule-1, interleukin-15 and monocyte antibody-dependent cell-mediated cytotoxicity in patients of spleen-deficiency. *Zhongguo Zhongxiyi Jiehe Zazhi* 1999; **19**: 270-272
- 42 **Xu MY**, Lu HM, Wang SZ, Shi WY, Wang XC, Yang DX, Yang CX, Yang LZ. Effect of devazepide reversed antagonism of CCK-8 against morphine on electrical and mechanical activities of rat duodenum *in vitro*. *World J Gastroenterol* 1998; **4**: 524-526
- 43 **Lin Z**, Chen JD, Schirmer BD, McCallum RW. Postprandial response of gastric slow waves: correlation of serosal recordings with the electrogastrogram. *Dig Dis Sci* 2000; **45**: 645-651
- 44 **Xu D**, Shen Z, Wang W. Immunoregulation of Youguiyin, Sijunzitang, Taohong Siwutang in treating patients with deficiency of kidney, spleen and blood stasis syndrome. *Zhongguo Zhongxiyi Jiehe Zazhi* 1999; **19**: 712-714
- 45 **Wang ZS**, Cheung JY, Gao SK, Chen JD. Spati-temporal nonlinear modeling of gastric myoelectrical activity. *Methods Inf Med* 2000; **39**: 186-190
- 46 **Tabor S**, Thor PJ, Pitala A, Laskiewicz J. Value of electrogastrographic parameters in evaluation of gastric myoelectrical activity. *Folia Med Cracov* 1999; **40**: 27-42
- 47 **Abo M**, Kono T, Wang Z, Chen JD. Impairment of gastric and jejunal myoelectrical activity during rectal distension in dogs. *Dig Dis Sci* 2000; **45**: 1731-1736
- 48 **Lin X**, Hayes J, Peters LJ, Chen JD. Entrainment of intestinal slow waves with electrical stimulation using intraluminal electrodes. *Ann Biomed Eng* 2000; **28**: 582-587
- 49 **Lin X**, Peters LJ, Hayes J, Chen JD. Entrainment of small intestinal slow waves with electrical stimulation in dogs. *Dig Dis Sci* 2000; **45**: 652-656
- 50 **Abo M**, Liang J, Qian L, Chen JD. Distension-induced myoelectrical dysrhythmia and effect of intestinal pacing in dogs. *Dig Dis Sci* 2000; **45**: 129-135
- 51 **Zeng J**, Dai X, Yang J. 159 sterility patients of yang-deficiency of spleen and kidney treated by shouwu huanjing capsule. *Zhongguo Zhongxiyi Jiehe Zazhi* 1998; **18**: 477-479
- 52 **Muth ER**, Koch KL, Stern RM. Significance of autonomic nervous system activity functional dyspepsia. *Dig Dis Sic* 2000; **45**: 854-863

Edited by Wu XN

Effect of pinaverium bromide on stress-induced colonic smooth muscle contractility disorder in rats

Yun Dai, Jian-Xiang Liu, Jun-Xia Li, Yun-Feng Xu

Yun Dai, Jian-Xiang Liu, Jun-Xia Li, Department of Gastroenterology, First Hospital of Peking University, Beijing 100034, China

Yun-Feng Xu, The Center Laboratory, First Hospital of Peking University, Beijing 100034, China

Correspondence to: Yun Dai, P.O. Box 97-242 Beijing 100016, China. caolanzi@263.net

Telephone: +86-10-66171122-2301

Received: 2002-09-14 **Accepted:** 2002-10-18

Abstract

AIM: To investigate the effect of pinaverium bromide, a L-type calcium channel blocker with selectivity for the gastrointestinal tract on contractile activity of colonic circular smooth muscle in normal or cold-restraint stressed rats and its possible mechanism.

METHODS: Cold-restraint stress was conducted on rats to increase fecal pellets output. Each isolated colonic circular muscle strip was suspended in a tissue chamber containing warm oxygenated Tyrode-Ringer solution. The contractile response to ACh or KCl was measured isometrically on ink-writing recorder. Incubated muscle in different concentrations of pinaverium and the effects of pinaverium were investigated on ACh or KCl-induced contraction. Colon smooth muscle cells were cultured from rats and $[Ca^{2+}]_i$ was measured in cell suspension using the Ca^{2+} fluorescent dye fura-2/AM.

RESULTS: During stress, rats fecal pellet output increased 61 % ($P < 0.01$). Stimulated with ACh or KCl, the muscle contractility was higher in stress than that in control. Pinaverium inhibited the increment of $[Ca^{2+}]_i$ and the muscle contraction in response to ACh or KCl in a dose dependent manner. A significant inhibition of pinaverium to ACh or KCl induced $[Ca^{2+}]_i$ increment was observed at 10^{-6} mol/L. The IC_{50} values for inhibition of ACh induced contraction for the stress and control group were 1.66×10^{-6} mol/L and 0.91×10^{-6} mol/L, respectively. The IC_{50} values for inhibition of KCl induced contraction for the stress and control group were 8.13×10^{-7} mol/L and 3.80×10^{-7} mol/L, respectively.

CONCLUSION: Increase in $[Ca^{2+}]_i$ of smooth muscle cells is directly related to the generation of contraction force in colon. L-type Ca^{2+} channels represent the main route of Ca^{2+} entry. Pinaverium inhibits the calcium influx through L-type channels; decreases the contractile response to many kinds of agonists and regulates the stress-induced colon hypermotility.

Dai Y, Liu JX, Li JX, Xu YF. Effect of pinaverium bromide on stress-induced colonic smooth muscle contractility disorder in rats. *World J Gastroenterol* 2003; 9(3): 557-561
<http://www.wjgnet.com/1007-9327/9/557.htm>

INTRODUCTION

Irritable bowel syndrome (IBS) is a common functional

gastrointestinal disorder in which abdominal pain is associated with changes of bowel habit and abdominal distension^[1,35]. The pathophysiological mechanisms for IBS are not clear and therefore the therapy is usually empirical. Abnormal contraction of intestinal smooth muscle may be important in producing the main IBS symptoms^[2-5,43], thus, modifying the contractility is often the major aim in the treatment of IBS^[6,7]. Pinaverium bromide, a L-type calcium channel blocker with selectivity for the gastrointestinal tract, effectively relieves pain, diarrhea and intestinal discomfort, provides good therapeutic efficacies without significant adverse effects on IBS patients^[8-10].

To evaluate the rational use of calcium channel blockers in colonic motor activity affecting the contraction of smooth muscle and to explore the physiopathology in such functional bowel disorders, we conducted cold-restraint stress on rats to induce fecal pellet output increased, investigated changes in contractility of circular muscle isolated from stressed colon treated with or without pinaverium. In addition, to further clarify the mechanism in the action of pinaverium we cultured colonic smooth muscle cells from rats, analyzed the influence of pinaverium on the free cytoplasmic Ca^{2+} concentration ($[Ca^{2+}]_i$). The circular muscle was chosen because it was the musculature predominantly responsible for propulsive contractile activity.

MATERIALS AND METHODS

Animal model

Male Wister rats, weighing 250-300 g, were housed in individual cages and provided with standard rodent chow and tap water for at least one week prior to the experiment. Room temperature was maintained at 25-28 °C. Rats were deprived of food but not water for 24 h before testing. Rats were studied for 2 h in normal living cages at room temperature (control, no stressed animals) or in wire-mesh restraining cylinders (5.5 cm in diameter × 18.5 cm in length) placed in a cold (4-6 °C) environment (cold-restraint stressed animals). The quality of fecal pellets expelled by each animal was measured after 2 h.

Recording of contractile responses to the stimulation of agonist

Each animal was killed by cervical dislocation, and the segments of distal colon (4 cm from anus) were removed. Circular smooth muscle strips (2 mm × 8 mm) were prepared by separating the mucosa and serosa from the muscle layers.

Muscle strips were mounted in individual tissue baths containing warm (37 °C) oxygenated (95 % O_2 and 5 % CO_2) Tyrode-Ringer solution (pH 7.4, composition in mmol/L: 137 NaCl, 5.4 KCl, 0.5 $MgCl_2$, 1.8 $CaCl_2$, 11.9 $NaHCO_3$, 0.4 NaH_2PO_4 , 5 Glucose) and attached to an isometric force transducer. The contractile activity was detected as change of tension, which was generated by circular muscle^[39-41]; the contractile response was measured isometrically on ink-writing recorder and the data were expressed as milli-Newton per square millimeter (mN/mm²).

Muscle strips from the control and stressed rats were randomly stimulated by ACh (10^{-5} mol/L) or KCl (60 mmol/L).

To investigate the effect of pinaverium bromide on muscle contractility, each muscle strip was stimulated by ACh or KCl twice before and twice after introduction of pinaverium (10^{-7} - 3×10^{-5} mol/L) following at least a 15 min equilibration period for each concentration of the blocker in Tyrode-Ringer solution. For a single strip, up to three different concentrations of pinaverium were applied cumulatively. Mean values obtained before and after the treatment of the blocker were compared. The contractile response to pinaverium was expressed as the percent of decreased response in the control recorded immediately before exposure to the calcium channel blocker.

Isolation and culture of colonic smooth muscle cells

Smooth muscle cells were isolated from the colon of rats by two consecutive digestions with collagenase respectively, following the method previously described^[11]. Briefly, after peeling off the serosal and mucosal layers, muscle tissues were minced into small pieces of 2 to 3 mm² and incubated in culture medium A (pH7.4, composition in mmol/L: 25 HEPES, 120 NaCl, 4 KCl, 2 CaCl₂, 0.6 MgSO₄, 2.6 KH₂PO₄ and 14 glucose) containing 0.1 % collagenase, 0.1 % BSA, and 0.01 % soybean trypsin inhibitor for 40 min at 31 °C, the culture medium was filtered through a nylon mesh. The filtrate, which contained isolated cells, was diluted with enzyme-free culture medium A and centrifuged at 150 g for 5 min. The cell pellet was then diluted in PBS. The remaining tissue from the first incubation was reincubated in culture medium A for 30 min at 31 °C and fragments were dispersed into single cells by passages in and out the inverted wide end of a 5-ml pipette. The acquired cell suspension was filtered through a nylon mesh (500 μm). Isolated cells from the two incubations were pooled and counted. Freshly isolated colonic muscle cells were resuspended in DMEM medium with high glucose (12 mmol/L), sodium pyruvate (1 mmol/L), 10 % heat-inactivated fetal bovine serum and antibiotics (100 UI/mL penicillin G, 100 UI/mL streptomycin, 50 μg/mL gentamicin and 3 μg/mL amphotericin B). Cells were plated in sterile flasks at a density of 5×10^4 cells/mL and incubated at 37 °C in a humidified atmosphere with 5 % CO₂. Culture medium was exchanged every 3 d. Only those cells that were cultured for 14 to 17 days were used for subsequent studies.

Measurement of [Ca²⁺]_i in colonic smooth muscle cells

After the cultured cells were digested with 0.125 % trypsin, [Ca²⁺]_i was measured in cell suspension (10^6 cells/ml) using the Ca²⁺ fluorescent dye fura-2/AM as described by Shi *et al*.^[11] Muscle cells were suspended in a modified HEPES buffer containing (in mmol/L) 10 HEPES, 125 NaCl, 5 KCl, 1 CaCl₂, 0.5 MgSO₄ and 5 glucose, and were incubated with 5 μmol/L fura-2/AM for 30 min at 37 °C. The fura-2/AM treated samples were diluted, centrifuged twice, and suspended in 1.5 ml solution with the same composition for immediate measurement of [Ca²⁺]_i. Fluorescence was measured at 510nm with excitation wavelengths alternating between 340nm and 380nm. Autofluorescence value of unloaded cells was subtracted from the fluorescence value of fura-2/AM treated cells. The [Ca²⁺]_i was calculated from the fluorescence ratio ($R = F_{340}/F_{380}$), $[Ca^{2+}]_i = K_d \cdot (R - R_{min}) / (R_{max} - R)$. The dissociation constant (K_d) of 224 nmol/L was used for fura-2/AM. The maximum and minimum fluorescence value were determined after adding 10 % Triton-X100 and 5 mmol/L EGTA, respectively, in each sample.

To investigate the effect of pinaverium bromide on [Ca²⁺]_i, cells were incubated for 20 min in HEPES buffer containing pinaverium (10^{-7} - 10^{-5} mol/L) before the stimulation of agonists.

Statistical analysis

All values were expressed as $\bar{x} \pm s$. Statistical analysis was done

by one-way analysis of variance and the Student's *t*-test for unpaired observations. $P < 0.05$ was considered statistically significant.

RESULTS

Defecation during stress

Cold-restraint stress significantly increased fecal pellet output. During 2 h, there were 2.40 ± 1.23 fecal pellets in the stressed rats vs 1.49 ± 1.04 in the control ($n=45$ each, $P < 0.001$). In addition, stressed rats showed a higher incidence of poorly formed fecal pellets, which appeared to contain more fluid.

After the cold-restraint stress for 2 hours, there was no gastric ulcers in rats, and the histological examination on the colon showed that no inflammatory responses (erosion, ulcer, edema, petechia, *etc.*) were found.

Effect of stress on colonic contractility

In the Tyrode-Ringer solution, ACh or KCl induced colonic circular muscle contraction and produced increase in force. Contractility of muscle in the stress group was significantly higher than that in control group ($P < 0.05$) (Table 1).

Table 1 Contractile response to ACh and KCl in colonic circular muscle (mN/mm², $\bar{x} \pm s$)

	ACh (10^{-5} mol/L)	KCl (60 mmol/L)
Control	71.56 ± 19.36 ($n=8$)	73.85 ± 13.08 ($n=9$)
Stress	109.66 ± 34.42^a ($n=8$)	119.54 ± 19.06^a ($n=8$)

^a $P < 0.05$, vs control.

Effect of Pinaverium on smooth muscle contractility

Pinaverium bromide inhibited the contractile response to ACh or KCl in the control and stressed colonic circular muscle in a dose dependent manner. The IC₅₀ value for inhibition of 10^{-5} mol/L ACh induced contraction in the stress group was 1.66×10^{-6} mol/L, and in the control was 0.91×10^{-6} mol/L. Effects of pinaverium on stressed colon were not significantly different from that in the control except for the effects of 3×10^{-6} mol/L and 10^{-5} mol/L. The inhibitory response at the maximum concentration of 3×10^{-5} mol/L pinaverium was 99.57 ± 0.62 % ($n=8$) and 98.24 ± 1.92 % ($n=7$), respectively, in the stress and the control group there was no significant difference between them ($P > 0.05$). Concentration-response curve was shown in Figure 1.

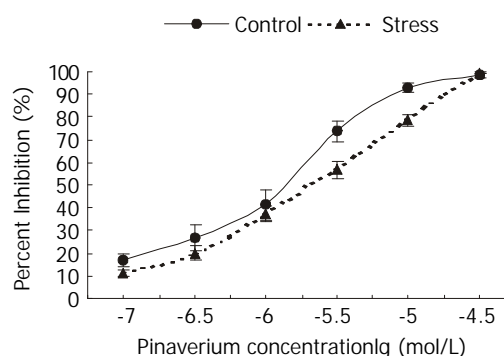


Figure 1 Effect of pinaverium on ACh-induced colonic circular muscle contraction. ^a $P < 0.05$, vs control.

The IC₅₀ values for the inhibition of 60 mmol/L KCl induced contraction in the stress group and control group were 8.13×10^{-7} mol/L, and 3.80×10^{-7} mol/L, respectively. Effects of pinaverium on stressed colon were significantly different from

that in the control at 3×10^{-7} mol/L and 10^{-6} mol/L. The inhibitory response of pinaverium at 3×10^{-5} mol/L was 99.68 ± 0.44 % and 99.54 ± 0.65 %, respectively, in the stress and the control group there was no significant difference between them ($P > 0.05$). It was shown in Figure 2.

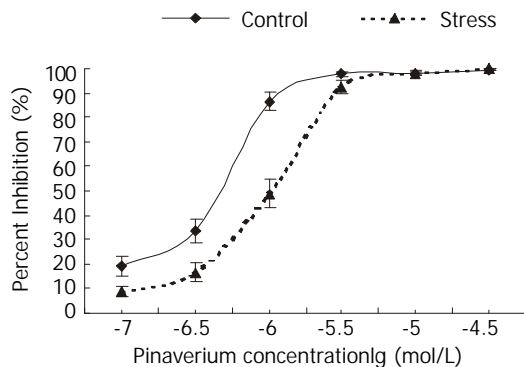


Figure 2 Effect of pinaverium on KCl-induced colonic circular muscle contraction. ^a $P < 0.05$, vs control.

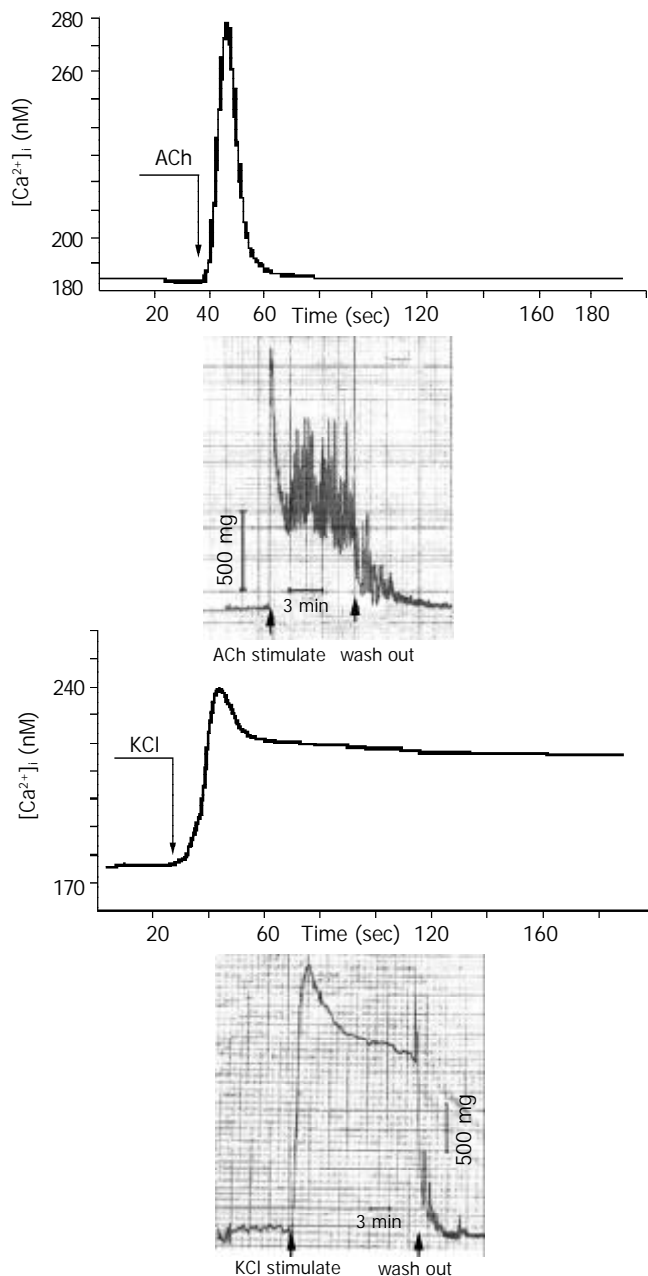


Figure 3 Effect of ACh and KCl on $[Ca^{2+}]_i$ and contraction of colonic smooth muscle.

Effect of Pinaverium on $[Ca^{2+}]_i$

ACh at 10^{-5} mol/L evoked a rapid increase in $[Ca^{2+}]_i$ that reached a peak in 10–15 s (Figure 3A). Similarly, 60 mmol/L KCl increased $[Ca^{2+}]_i$ in colonic muscle cells, the peak $[Ca^{2+}]_i$ was reached at 15–20 s (Figure 3B). Figure 3 also showed that the force of contraction in colonic muscle had no linear relationship with $[Ca^{2+}]_i$, and both velocity and amplitude of $[Ca^{2+}]_i$ increment in contraction were directly related to the force generation.

Pinaverium inhibited the increment of $[Ca^{2+}]_i$ in response to ACh or KCl in a dose dependent manner. A significant inhibition to 10^{-5} mol/L ACh or 60 mM KCl was observed at 10^{-6} mol/L pinaverium, as expressed in Table 2.

Table 2 Effect of pinaverium bromide on the increment of $[Ca^{2+}]_i$ ($\Delta [Ca^{2+}]_i$) in response to ACh and KCl (nmol/L, $\bar{x} \pm s$)

Concentration of pinaverium (mol/L)	ACh (10^{-5} mol/L) (n=7)	KCl (60 mmol/L) (n=6)
0	94.78 ± 15.99	64.61 ± 8.06
10^{-7}	83.57 ± 13.54	55.73 ± 17.39
10^{-6}	34.73 ± 13.98^a	41.71 ± 1.61^a
10^{-5}	27.09 ± 5.64^a	40.34 ± 10.96^a

Figures in this table are the increment of $[Ca^{2+}]_i$ in response to ACh and KCl. $\Delta [Ca^{2+}]_i = [Ca^{2+}]_i \text{After (ACh, KCl) stimulated} - [Ca^{2+}]_i \text{Before (ACh, KCl) stimulated}$. ^a $P < 0.05$, vs pinaverium 0 mmol/L.

DISCUSSION

Different types of stresses play important roles in the onset and modulation of IBS symptoms^[12–18]. Our results showed that cold-restraint stress significantly increased fecal pellet output in rats; which appeared to be the results of an increased colonic motility. There was no gastric ulcer or histological changes on the colon in the model of stressed rats, so it was an appropriate animal model to investigate the functional intestinal dysmotility such as IBS. In vitro studies using colonic smooth muscle strips obtained from rats showed that stress was accompanied by an increase in the contractility of muscle, it may be the reason for the colonic dysmotility.

Abnormal contraction of intestinal smooth muscle may be important in the pathology of IBS symptoms, thus, modifying the contractility is often the major aim in treating IBS^[6,7,19]. A new approach to such disorder is based on the fact that Ca^{2+} is involved in the mechanism of excitation-contraction coupling, which directly or indirectly controls the contractility of smooth muscle^[44]. $[Ca^{2+}]_i$ regulates the contractile state of smooth muscle; increase of $[Ca^{2+}]_i$ is the primary stimulus for contraction^[20–22]. Elevation of $[Ca^{2+}]_i$ in contraction is accomplished by Ca^{2+} entry from extracellular and/or intracellular release of Ca^{2+} from sarcoplasmic reticulum. Between these two Ca^{2+} mobilization pathways, Ca^{2+} influx from extracellular plays a major role in the contraction of colonic smooth muscle^[23–29,34]. L-type voltage-dependent Ca^{2+} channel represents the main route of entry of inward Ca^{2+} current that is gated by potential in smooth muscle cells, particularly in the gastrointestinal tract. Thus, activation of Ca^{2+} channel represents the final ‘common path’ of all mechanisms that regulate muscle contractility^[32,36]. So important are these mechanisms in regulating $[Ca^{2+}]_i$ and the contractile state of smooth muscle that minor defects in function can greatly affect the mechanical activity of colon^[11,30,31,33].

In this study, we investigated the contractile response to KCl and ACh in colonic circular smooth muscle in rats. KCl can induce depolarization of the plasma membrane, activate the voltage-dependent Ca^{2+} channel (dihydropyridine-sensitive L-type Ca^{2+} channel), which results in increase of $[Ca^{2+}]_i$ and

force generation. ACh is one of the most important neurotransmitters in gastrointestinal. ACh can activate Muscarinic M_2 receptors, then non-selective cation channels (NSCC) will be opened. The amount of Ca^{2+} entry through NSCC is controversial, but these channels yield depolarization that activates L-type Ca^{2+} channels, Ca^{2+} entering cells^[25].

We found that the force of contraction in colonic muscle was related nonlinearly to $[Ca^{2+}]_i$; however both velocity and amplitude of $[Ca^{2+}]_i$ increment in muscle cells were directly related to the force generation. Pinaverium bromide is a L-type calcium channel blocker with selectivity for the gastrointestinal used in the treatment of IBS^[37,38,42]. Our work demonstrated that pinaverium inhibited both neurohormonal (ACh) and depolarization (KCl)-induced increment of $[Ca^{2+}]_i$ and contraction of colonic circular muscle in a dose dependent manner. The contractile responses were almost completely blocked at the maximum concentration of 3×10^{-5} mol/L pinaverium, which indicated that repaid influx of Ca^{2+} through L-type calcium channels played a major role in contractions of colon. Pinaverium acted on colonic muscle, and reduced the plateau phase of slow wave, thereby inhibited influx of Ca^{2+} , abolished the accompanying contractile activity^[32]. In normal Ca^{2+} -contain buffer, the contractile responses to ACh and KCl were significantly increased in stress group than those in control group which indicated that more the contractile response was depended on extracellular Ca^{2+} in the stress state and that influx of Ca^{2+} through the cell membrane was increased.

The IC_{50} values (deduced from the concentration-response curves) for inhibition of ACh or KCl induced contraction in the stress group were higher than those in the control group, indicated that increased contractility of stressed colon may in part be due to the increased Ca^{2+} influx through the L-type channels.

Our experiments in insolated circular smooth muscle from rats demonstrated that alterations of the muscle calcium-handling properties was responsible for the increased contractility in colon. However, the precise contribution of these pathways in the intact conscious state can only be speculated. The colonic circular muscle of rat can generate three distinct types of contractions: rhythmic phasic contractions, giant migrating contractions and tone. The amplitudes, durations and motility functions of these contractions differ widely. Because Ca^{2+} is a critical second messenger in the contraction of these cells and the amplitude and duration of cell contraction are correlated with $[Ca^{2+}]_i$, it is likely that the three types of contractions would utilize Ca^{2+} sources differently. The increase of Ca^{2+} influx through L-type channels may be the reason why colonic smooth muscle exhibits hypermotility during stress.

Our study shows that increase of $[Ca^{2+}]_i$ in smooth muscle cells is directly related to the generation of contraction force in colon. L-type Ca^{2+} channels represent the main route of Ca^{2+} entry. Colonic circular muscle hypermotility in rats induced by cold-restraint stress is the result of an increased influx of extracellular Ca^{2+} through L-type Ca^{2+} channels. These studies provide a rationale for the use of pinaverium bromide in the treatment of colonic motor disorders (such as IBS) where excessive contraction need to be suppressed.

REFERENCES

- Janssen HA**, Muris JW, Knotterus JA. The clinical course and prognostic determinants of the irritable bowel syndrom: a literature review. *Scand J Gastroenterol* 1998; **33**: 561-567
- Camilleri M**. Motor function in irritable bowel syndrom. *Can J Gastroenterol* 1999; **13**: 8A-11A
- Ringel Y**, Sperber AD, Drossman DA. Irritable bowel syndrome. *Annu Rev Med* 2001; **52**: 319-338
- Drossman DA**. Review article: an integrated approach to the irritable bowel syndrome. *Aliment Pharmacol Ther* 1999; **13**: 3-14
- Collins SM**. Peripheral mechanisms of symptom generation in irritable bowel syndrome. *Can J Gastroenterol* 2001; **15**: 14B-16B
- Camilleri M**. Review article: clinical evidence to support current therapies of irritable bowel syndrome. *Aliment Pharmacol Ther* 1999; **13**: 48-53
- Camilleri M**. Management of the irritable bowel syndrome. *Gastroenterology* 2001; **120**: 652-668
- Lu CL**, Chen CY, Chang FY, Chang SS, Kang LJ, Lu RH, Lee SD. Effect of a calcium channel blocker and antispasmodic in diarrhoea-predominant irritable bowel syndrome. *J Gastroenterol Hepatol* 2000; **15**: 925-930
- Bouchoucha M**, Faye A, Devroede G, Arzac M. Effect of oral pinaverium bromide on colonic response to food in irritable bowel syndrome patients. *Biomed Pharmacother* 2000; **54**: 381-387
- Scarpignato C**, Pelosini I. Management of irritable bowel syndrome: novel approaches to the pharmacology of gut motility. *Can J Gastroenterol* 1999; **13**: 50A-65A
- Shi XZ**, Sarna SK. Impairment of Ca^{2+} mobilization in circular muscle cells of the inflamed colon. *Am J Physiol Gastrointest Liver Physiol* 2000; **278**: G234-242
- Mayer EA**, Naliboff BD, Chang L, Coutinho SV. Stress and the Gastrointestinal Tract V. Stress and irritable bowel syndrome. *Am J Physiol Gastrointest Liver Physiol* 2001; **280**: G519-524
- Plourde V**. Stress-induced changes in the gastrointestinal motor system. *Can J Gastroenterol* 1999; **13**: 26A-31A
- Delvaux MM**. Stress and visceral perception. *Can J Gastroenterol* 1999; **13**: 32A-36A
- Bennett EJ**, Tennant CC, Piesse C, Badcock CA, Kellow JE. Level of chronic life stress predicts clinical outcome in irritable bowel syndrome. *Gut* 1998; **43**: 256-261
- Tache Y**, Martinez V, Million M, Rivier J. Corticotropin-releasing factor and the brain-gut motor response to stress. *Can J Gastroenterol* 1999; **13**: 18A-25A
- Drossman DA**, Creed FH, Olden KW, Svedlund J, Toner BB, Whitehead WE. Psychosocial aspects of the functional gastrointestinal disorders. *Gut* 1999; **45**: II25-II30
- Aziz Q**, Thompson DG. Brain-gut axis in health and disease. *Gastroenterology* 1998; **114**: 559-578
- De Schryver AMP**, Samsom M. New developments in the treatment of irritable bowel syndrome. *Scand J Gastroenterol* 2000; **35**: 38-42
- Li JX**, Liu XG, Xie PY, Gu Q, Li J, Zhang Y, Tang CS. The regulation of calcium in the movement of colonic smooth muscle in wrap restraint stress rats. *Zhonghua Neike Zazhi* 2000; **39**: 588-591
- Sanders KM**. Invited review: mechanisms of calcium handling in smooth muscles. *J Appl Physiol* 2001; **91**: 1438-1449
- Bolton TB**, Prestwich SA, Zholos AV, Gordienko DV. Excitation-contraction coupling in gastrointestinal and other smooth muscles. *Annu Rev Physiol* 1999; **61**: 85-115
- Gibson A**, McFadzean I, Wallace P, Wayman CP. Capacitative Ca^{2+} entry and the regulation of smooth muscle tone. *Trends Pharmacol Sci* 1998; **19**: 266-269
- McCarron JG**, Flynn ERM, Bradley KN, Muir TC. Two Ca^{2+} entry pathways mediate $InsP_3$ -sensitive store refilling in guinea-pig colonic smooth muscle. *J Physiol* 2000; **525**(Pt 1): 113-124
- Eglen RM**. Muscarinic receptor and gastrointestinal tract smooth muscle function. *Life Sci* 2001; **68**: 2573-2578
- Bolton TB**, Gordienko DV. Confocal imaging of calcium release events in single smooth muscle cells. *Acta Physiol Scand* 1998; **164**: 567-575
- Young SH**, Ennes HS, McRoberts JA, Chaban VV, Dea SK, Mayer EA. Calcium waves in colonic myocytes produced by mechanical and receptor-mediated stimulation. *Am J Physiol* 1999; **276**: G1204-1212
- Petkov GV**, Boev KK. Control of the phasic and tonic contractions of guinea pig stomach by a ryanodine-sensitive Ca^{2+} store. *Eur J Pharmacol* 1999; **367**: 335-341
- Henkel CC**, Asbun J, Ceballos G, Castillo MC, Castillo EF. Relationship between extra and intracellular sources of calcium and the contractile effect of thiopental in rat aorta. *Can J Physiol Pharmacol* 2001; **79**: 407-414
- Mule F**, Serio R. Increased calcium influx is responsible for the sustained mechanical tone in colon from dystrophic (mdx) mice. *Gastroenterology* 2001; **120**: 1430-1437

- 31 **Sarna SK.** *In vivo* signal-transduction pathways to stimulate phasic contractions in normal and inflamed ileum. *Am J Physiol* 1998; **274**: G618-625
- 32 **Boyer JC,** Magous R, Christen MO, Balmes JL, Bali JP. Contraction of human colonic circular smooth muscle cells is inhibited by the calcium channel blocker pinaverium bromide. *Cell Calcium* 2001; **29**: 429-438
- 33 **Khan I.** Molecular basis of altered contractility in experimental colitis: expression of L-type calcium channel. *Dig Dis Sci* 1999; **44**: 1525-1530
- 34 **Niu WX,** Qin XY, Lu YQ, Shi NC, Wang CP. Role of intracellular calcium in contraction of internal anal sphincter. *World J Gastroenterol* 1999; **5**: 183-184
- 35 **Leahy A,** Epstein O. Non-pharmacological treatments in the irritable bowel syndrome. *World J Gastroenterol* 2001; **7**: 313-316
- 36 **Morel N,** Buryi V, Feron O, Gomez JP, Christen MO, Godfraind T. The action of calcium channel blockers on recombinant L-type calcium channel alpha1-subunits. *Br J Pharmacol* 1998; **125**: 1005-1012
- 37 **Jayanthi V,** Malathi S, Ramathilakam B, Dinakaran N, Balasubramanian V, Mathew S. Role of pinaverium bromide in south Indian patients with irritable bowel syndrome. *J Assoc Physicians India* 1998; **46**: 369-371
- 38 **Poynard T,** Regimbeau C, Benhamou Y. Meta-analysis of smooth muscle relaxants in the treatment of irritable bowel syndrome. *Aliment Pharmacol Ther* 2001; **15**: 355-361
- 39 **Xie DP,** Li W, Qu SY, Zheng TZ, Yang YL, Ding YH, Wei YL, Chen LB. Effect of areca on contraction of colonic muscle strips in rats. *World J Gastroenterol* 2002; **8**: 350-352
- 40 **Li W,** Zheng TZ, Qu SY. Effect of cholecystokinin and secretin on contractile activity of isolated gastric muscle strips in guinea pigs. *World J Gastroenterol* 2000; **6**: 93-95
- 41 **Zheng TZ,** Li W, Qu SY, Ma YM, Ding YH, Wei YL. Effects of Dangshen on isolated gastric muscle strips in rats. *World J Gastroenterol* 1998; **4**: 354-356
- 42 **Villanueva A,** Dominguez-Munoz JE, Mearin F. Update in the therapeutic management of irritable bowel syndrome. *Dig Dis* 2001; **19**: 244-250
- 43 **Cole SJ,** Duncan HD, Claydon AH, Austin D, Bowling TE, Silk DB. Distal colonic motor activity in four subgroups of patients with irritable bowel syndrome. *Dig Dis Sci* 2002; **47**: 345-355
- 44 **Wang XJ,** Wei JG, Wang CM, Wang YC, Wu QZ, Xu JK, Yang XX. Effect of cholesterol liposomes on calcium mobilization in muscle cells from the rabbit sphincter of Oddi. *World J Gastroenterol* 2002; **8**: 144-149

Edited by Xu XQ

Role of mitochondrial dysfunction in hydrogen peroxide-induced apoptosis of intestinal epithelial cells

Jian-Ming Li, Hong Zhou, Qian Cai, Guang-Xia Xiao

Jian-Ming Li, Hong Zhou, Qian Cai, Guang-Xia Xiao, Institute of Burn Research, Southwest Hospital, Third Military Medical University, Chongqing 400038, China

Supported by the Special Funds for Major State Basic Research of China, No.G1999054202

Correspondence to: Professor Hong Zhou, Institute of Burn Research, Southwest Hospital, Third Military Medical University, Chongqing 400038, China. zhouh64@mail.tmmu.com.cn

Received: 2002-01-11 **Accepted:** 2002-03-05

Abstract

AIM: To study the role of mitochondrial dysfunction in hydrogen peroxide-induced apoptosis of intestinal epithelial cells.

METHODS: Hydrogen peroxide-induced apoptosis of human intestinal epithelial cell line SW-480 was established. Cell apoptosis was determined by Annexin-V and PI double-stained flow cytometry and DNA gel electrophoresis. Morphological changes were examined with light and electron microscopy. For other observations, mitochondrial function, cytochrome c release, mitochondrial translocation and membrane potential were determined simultaneously.

RESULTS: Percentage of apoptotic cells induced with 400 $\mu\text{mol/L}$ hydrogen peroxide increased significantly at 1 h or 3 h after stimulation and recovered rapidly. Meanwhile percentage of apoptotic cells induced with 4 mmol/L hydrogen peroxide increased with time. In accordance with these changes, we observed decreased mitochondrial function in 400 $\mu\text{mol/L}$ H_2O_2 -stimulated cells at 1 h or 3 h and in 4 mmol/L H_2O_2 -stimulated cells at times examined. Correspondingly, swelling cristae and vacuole-like mitochondria were noted. Release of cytochrome c, decreased mitochondrial membrane potential and mitochondrial translocation were also found to be the early signs of apoptosis.

CONCLUSION: Dysfunctional mitochondria play a role in the apoptosis of SW-480 cell line induced by hydrogen peroxide.

Li JM, Zhou H, Cai Q, Xiao GX. Role of mitochondrial dysfunction in hydrogen peroxide-induced apoptosis of intestinal epithelial cells. *World J Gastroenterol* 2003; 9(3): 562-567
<http://www.wjgnet.com/1007-9327/9/562.htm>

INTRODUCTION

Hidden injuries of gut during the early stage of severe burn may contribute to early translocation of bacteria or its endotoxin. Although the mechanisms of gut barrier dysfunction postburn are unclear^[1-10], evidences recently indicate that apoptosis of intestinal epithelial cells after thermal injury may be one of possible factors leading to gut barrier dysfunction^[11,12]. Apoptosis of intestinal epithelial cells induced by excessive reactive oxygen

species released by activated polymorphonuclear leukocytes and vascular endothelia cells plays a role in the pathogenesis of dysfunction of intestinal mucosa. Besides, the role of mitochondrion in the development of apoptosis has been emphasized recently^[13]. We have found that differential expression of mitochondrial genes encoding cytochrome c oxidase and ATPase was involved in apoptosis of intestinal epithelial cells by affecting activities of cytochrome c oxidase and ATPase^[14]. So mitochondrial dysfunction may contribute to the apoptosis of intestinal epithelial cells. In the present study, possible relationship between mitochondrial dysfunction and apoptosis was studied in hydrogen peroxide-induced apoptosis model of SW-480 cells.

MATERIALS AND METHODS

Cell line and culture

Human intestinal epithelial cell line SW-480 stored routinely in our laboratory was cultured in RPMI1640 supplemented with 10 % (V/V) heat-inactivated newborn calf serum (Hyclone), 100 units/ml of penicillin, 0.1 mg/ml streptomycin and 2 mM l-glutamine at 37 °C in a humidified 5 % CO_2 incubator. Confluent cells were prepared for further studies.

Treatment

Experimental cells were treated with 4 mmol/L or 400 $\mu\text{mol/L}$ hydrogen peroxide. Cells without stimulation by hydrogen peroxide were prepared as control.

Transmission electron microscopy

Samples were fixed, embedded and sectioned routinely. Ultrastructural changes of mitochondria were observed with transmission electron microscopy.

Assessment of apoptosis by Annexin-V and PI double-staining flow cytometry

Annexin-V and PI double staining kit (Roche) was used to assess apoptosis in hydrogen peroxide-stimulated SW-480 cells. Ten thousands of cells were counted, and data acquisition and analysis were performed in a Becton Dickinson FACS-can flow cytometer using the CellQuest software.

DNA fragmentation analysis

The DNA fragmentation pattern (DNA ladder) was demonstrated by agarose gel electrophoresis described previously^[15].

Determination of cytochrome c release by cell immunocytochemistry

Cells were grown on glass cover slips. After treated with 4 mmol/L or 400 $\mu\text{mol/L}$ hydrogen peroxide, samples were fixed in 10 % neutral formaldehyde solution for 30 min with PBS rinsing for several times. Then, cells were stained by overnight incubation with 100-fold diluted rabbit anti-human cytochrome c polyclonal antibody (Oncogene) at 4 °C, followed by extensive washing with phosphate-buffered saline and a 30 min incubation with biotin-binding goat anti-rabbit antibody. After another 30 min incubation with horseradish peroxidase conjugated ovalbumin, the specimens were colorized and photographed.

MTT assay

Mitochondrial function was assessed by MTT (3, (4,5-dimethylthiazol-2-yl) 2, 5-diphenyltetrazolium bromide) assay as described previously^[16]. Cells were cultured in 96-well plates 5 000 cells for each well at 37 °C in a humidified 5 % CO₂ incubator. Confluent cells were prepared for further studies. After treated with hydrogen peroxides and washed with phosphate-buffered saline, cells were incubated with MTT (2 µg/ml, Sigma) and RPMI1640 medium without serum at 37 °C for 1 h and dissolved with dimethyl sulphoxide. The absorbance at 570nm, which represented the total mitochondrial function, was recorded.

Measurement of mitochondrial membrane potential

Cells were grown on glass cover slips. After treated with 4 mmol/L or 400 µmol/L hydrogen peroxide, cells were incubated with Rhodamine 123 (1 µmol/L, Molecular probe) and RPMI1640 medium without serum at 37 °C for 30 min, fluorescence intensity was determined by confocal microscope (Leica) with fixed parameters, cells in three random-selected visual fields from each group were scanned and analysed.

Mitochondrial translocation assay

As described previously, cells were seeded in chambered cover slips and preincubated overnight at 37 °C in a humidified 5 % CO₂ air incubator. After the cells were treated with hydrogen peroxide, mitochondria were stained with Rhodamine 123 for 30 min at 37 °C before analysis. The distribution of mitochondria was analyzed with a Zeiss TSTN confocal microscope^[17].

Statistical analysis

Data were summarized as mean ±SD. Student's *t* test was used for multiple comparisons between groups. *P* values less than 0.05 were considered to be statistically significant.

RESULTS

Effects of hydrogen peroxide on apoptosis of SW-480 cells

Percentage of apoptotic cells induced with 400 µmol/L hydrogen peroxide increased significantly at 1 h or 3 h after stimulation and recovered rapidly. Meanwhile percentage of apoptotic cells induced with 4 mmol/L hydrogen peroxide increased with the time, which indicated that the irreversible changes had taken place (Table 1).

Table 1 Percentage of apoptotic cells induced with hydrogen peroxide at different time after stimulation

Group	0 h	1 h	3 h	6 h	12 h	24 h
400 µmol/L	10.93±0.63	19.47±0.36 ^a	19.81±1.82 ^a	12.32±1.67	13.61±1.24	12.72±0.72
4 mmol/L	10.93±0.63	20.84±1.47 ^a	32.25±1.37 ^a	39.48±4.26 ^a	57.91±9.82 ^a	69.05±11.62 ^a

^a*P*<0.05 vs preceding time point (0 h).

Table 2 MTT absorbance (570nm) of SW-480 cells stimulated by hydrogen peroxide

Group	1 h	3 h	6 h	12 h	24 h
Control	1.971±0.101	1.996±0.013	1.867±0.008	2.087±0.126	2.189±0.178
4mmol/L	0.864±0.116 ^a	0.756±0.023 ^a	0.612±0.006 ^a	0.518±0.035 ^a	0.373±0.043 ^a
400mmol/L	1.588±0.005	1.277±0.300 ^a	1.778±0.098	1.599±0.214	1.899±0.031
200mmol/L	1.626±0.262	1.914±0.046	1.941±0.032	1.787±0.033	1.962±0.149
100mmol/L	1.683±0.070	1.973±0.048	1.933±0.094	1.901±0.097	2.079±0.081
50mmol/L	1.865±0.122	1.974±0.080	2.077±0.077	1.876±0.053	1.922±0.048

^a*P*<0.05 vs control at corresponding time point.

DNA fragmentation analysis

DNA ladder in both 4 mmol/L and 400 µmol/L H₂O₂-stimulated groups were clearly observed by DNA fragmentation assay at 1h or 3h after stimulation (Figure 1).

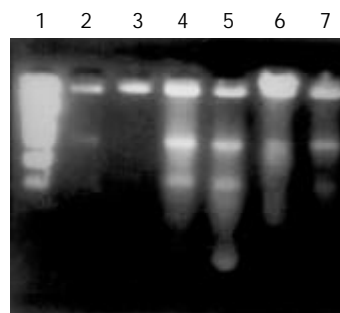


Figure 1 Hydrogen peroxide induced apoptosis of SW-480 cells. 1: PBR322/Hinf I (75, 154, 220, 221, 298, 344, 396, 504, 517, 1632); 2, 3: cells from normal control; 4: 4 mmol/L H₂O₂-stimulated cells (1 h); 5: 4 mmol/L H₂O₂-stimulated cells (3h); 6: 400 µmol/L H₂O₂-stimulated cells (1 h) 7: 400 µmol/L H₂O₂-stimulated cells (3 h).

MTT assay

The MTT assay is based on the conversion of MTT (light yellow) to formazan (blue) by the mitochondrial enzyme succinate dehydrogenase and has been widely used as an indicator of cellular respiration and viability^[3]. We observed decreased mitochondrial function in 400 µmol/L H₂O₂-stimulated cells at 1 h or 3 h after stimulation and in 4 mmol/L H₂O₂-stimulated cells at times examined (Table 2). Interestingly, these changes were in accordance with the apoptosis induced by hydrogen peroxide.

Ultrastructural changes of mitochondria

Swelling cristae and vacuole-like mitochondria were found in hydrogen peroxide -treated cells.

Translocation of mitochondria

Mitochondria were observed to be evolved from an originally scattered, bipolar and nearly symmetric distribution to the asymmetric clustered state in the majority of cells treated with H₂O₂ (Figure 2).

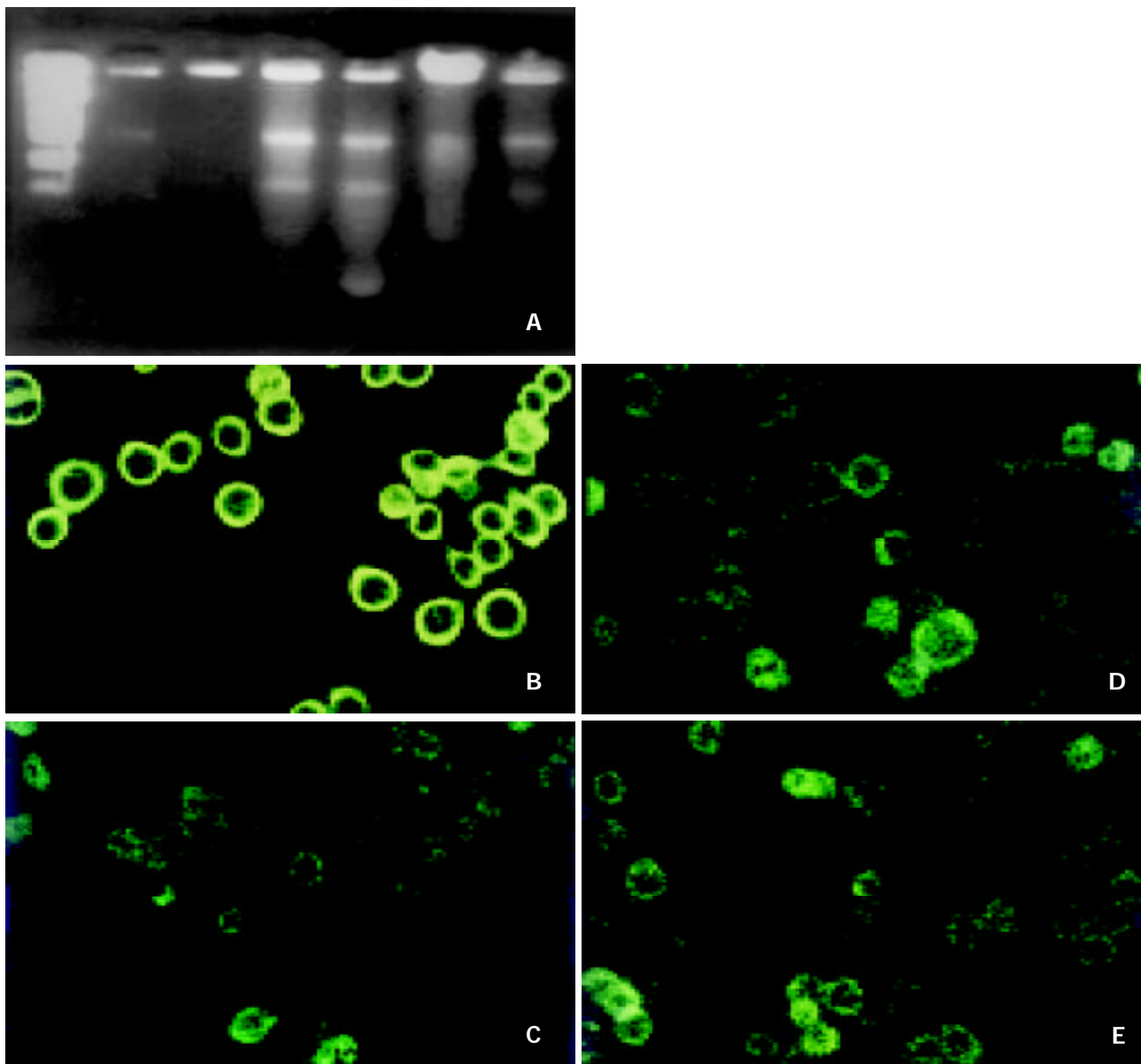


Figure 3a Changes of mitochondrial membrane potential induced by hydrogen peroxide. (A) cells from normal control; (B) 400 μmol/L H₂O₂-stimulated cells (1 h); (C) 400 μmol/L H₂O₂-stimulated cells (3 h); (D) 4 mmol/L H₂O₂-stimulated cells (1h); (E) 4 mmol/L H₂O₂-stimulated cells (3 h).

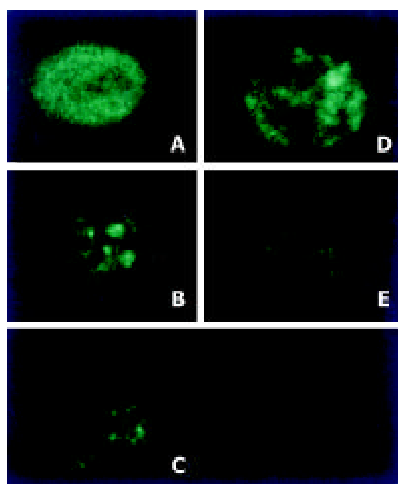


Figure 2 Hydrogen peroxide induced translocation of mitochondria. (A) cells from normal control; (B) 400 μmol/L H₂O₂-stimulated cells (1 h); (C) 400 μmol/L H₂O₂-stimulated cells (3 h); (D) 4 mmol/L H₂O₂-stimulated cells (1 h); (E) 4 mmol/L H₂O₂-stimulated cells (3 h).

Changes of mitochondrial membrane potential induced by hydrogen peroxide

Decreased mitochondrial membrane potential was observed in cells at 3 h after 400 μmol/L H₂O₂ stimulation and at 1h after 4 mmol/L H₂O₂ treatment (Figure 3a, 3b).

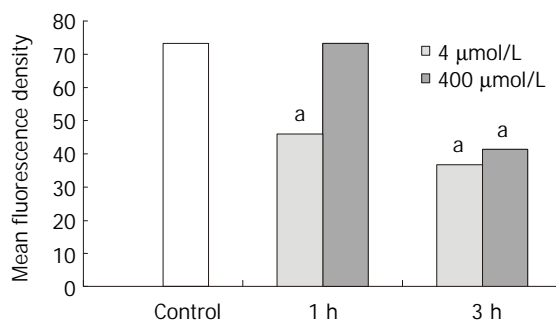


Figure 3b Effects of hydrogen peroxide on mitochondrial membrane potential of SW-480 cells (*P<0.05 vs control).

Cytochrome c Release

Cytochrome c release could be found in both 400mmol/L and 4mmol/L H₂O₂-stimulated cells 30 min after stimulation by immunocytochemistry assay (Figure 4).

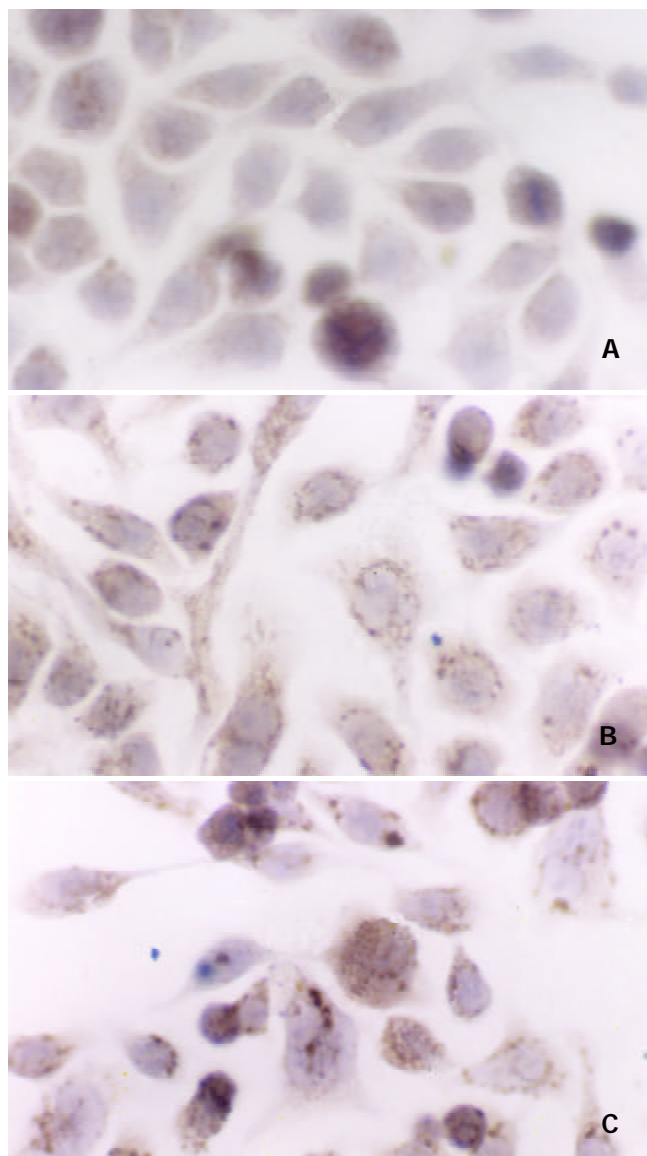


Figure 4 Cytochrome c release in SW-480 cells induced by hydrogen peroxide (S-P×400). A: control cells, B: 400 μmol/L H₂O₂-treated cells (30 min), C: 4 mmol/L H₂O₂-treated cells (30 min).

DISCUSSION

Metabolism of intestinal mucosal epithelium is so active that it is very sensitive to changes of energy supplies in normal conditions^[11]. Many researches have demonstrated that gut is a sensitive organ to be injured postburn^[18-22]. Intestinal mucosal injury can be caused by excessive reactive oxygen species (ROS) released by polymorphonuclear leukocytes and vascular endothelial cells, which is also involved in translocation of intestinal bacteria and its endotoxin.

Our results showed that hydrogen peroxide could lead to injuries of intestinal epithelial cells in the concentration of both 400 μmol/L and 4 mmol/L. From the results of DNA ladders and flow cytometry, apoptosis could be considered one of the main mechanisms for the injury. This indicated that the *in vitro* model of hydrogen peroxide-stimulated SW-480 cells used in the present study could be used to investigate mitochondrial dysfunction in apoptosis of intestinal epithelial cells, and it

also might be helpful to study the role of mitochondria in ROS-induced injuries of intestinal epithelial cells and to clarify mechanism of gut barrier dysfunction.

Role of mitochondria in the pathogenesis of apoptosis has been well defined^[23-27]. Mitochondria, a kind of organelle controlling growing, breeding and dying of eukaryocyte, perform their functions by production of ATP, production of ROS, ROS are also known as signals regulating gene expression and triggering of cell death^[28,29]. Many stimulators like ROS, Ca²⁺ and cytokines could activate caspases by inducing cytochrome c release.

Our results showed that the apoptotic cells were characterized with swelling or vacuole-like mitochondria. It was considered previously that the apoptotic cells manifested condensed chromatin but intact mitochondria. Now much more evidences found that significant changes of mitochondria such as swelling, megamitochondria^[30], mitochondrial pyknosis and disrupted out-membrane have been taken place in many apoptosis models^[31]. Mitochondrial pyknosis was characterized with decreased size and condensed matrix of mitochondria. In apoptotic model of sympathetic neuron triggered by nerve growth factor (NGF) deprivation, the transition from normal to condensed morphology could be reversible following readdition of NGF to the neuron culture^[25]. In addition, the mitochondrial distribution within cells was profoundly affected during apoptosis. Mitochondria were normally dispersed throughout the entire cell. However, during the apoptosis triggered by tumor necrosis factor (TNF-α) a perinuclear clustering of mitochondria could be observed. Both mitochondrial condensation and perinuclear clustering occurred following production of the Bcl-2-related proapoptotic protein Bax in many cell types^[25].

Evidence showed that the spatial distribution of mitochondria evolved from an originally scattered, bipolar or nearly symmetric distribution to an asymmetric, clustered distribution in the majority of the cells within 1 h of treatment of L929 cells with TNF^[17]. Study also indicated that hydrogen peroxide could not lead to the mitochondrial translocation as TNF did^[17]. Interestingly, we found that hydrogen peroxide could induce mitochondrial translocation and massive aggregation by confocal microscopy and 3-D reconstruction technique, which was accompanied by decrease of mitochondrial membrane potential. So our results suggested that mitochondrial translocation may play a role in reactive oxygen species (ROS)-induced injuries of intestinal epithelial cells. As some researches proposed, the condensation of mitochondria may play roles in the inducing of cytochrome c release, generating high ATP levels in energy dependent apoptotic events and facilitating the translocation of mitochondrial proteins to the nucleus. Its mechanism is still uncertain.

The mitochondrial transmembrane potential has been found to be decreased in many apoptosis models, which indicates the opening of a large conductance channel known as the mitochondrial PT pore^[32-36]. PT pore opening results in a volume dysregulation of mitochondria due to the hyperosmolality of the matrix, which causes the matrix space to be expanded. Because the mitochondrial inner membrane with its folded cristae possesses a larger surface area than the outer membrane, this matrix volume expansion can eventually cause the outer membrane rupture, releasing caspase-activating proteins located within the intermembrane space into the cytosol.

We observed that hydrogen peroxide could result in the collapse of mitochondrial membrane potential, if we related it with the release of cytochrome c, we may get the conclusion that hydrogen peroxide caused the release of cytochrome c from mitochondria to cytosol followed by the increased permeability mitochondrial membrane and the opening of mitochondrial

PT pore, which initiated cascade reaction of apoptosis events. This idea has been confirmed by some studies^[37,38].

Recent progress in studies on apoptosis has revealed that cytochrome c is a pro-apoptotic factor^[39]. It is released from its places on the outer surface of the inner mitochondrial membrane at early steps of apoptosis and, combining with some cytosolic proteins, activates conversion of the latent apoptosis-promoting protease pro-caspase-9 to its active form^[39]. Our results also indicated that cytochrome c was released early in hydrogen peroxide-stimulated SW-480 cells.

Our results found that the morphological and functional changes of mitochondria appeared in SW-480 cells treated with hydrogen peroxide and correlated with development of cell apoptosis. Decreased mitochondrial membrane potential or early release of cytochrome c would be the early signs of apoptosis, which suggested mitochondrial dysfunction might be the key event in the development of apoptosis. We also observed mitochondrial translocation, which was reported in TNF-stimulated L929 cells but not in hydrogen peroxide-stimulated cells^[33]. Mitochondrial translocation suggested that cytoskeleton be involved in apoptosis induced by hydrogen peroxide.

Many researches indicated that oxidative stress led to mutation of mitochondrial genes^[40-50]. Researches showed that there are some links between mitochondrial dysfunction and injuries of mitochondrial DNA or abnormal expression of mitochondrial genes in hydrogen peroxide-stimulated vascular endothelial cells and smooth muscle cells^[50]. Our results also indicated that mitochondrial genes were involved in apoptosis of SW-480 cells. Injuries of mitochondrial genes may contribute to early mitochondrial dysfunction. Relationship between response of mitochondrial genes and dysfunctional mitochondria would be the next problem to be answered.

REFERENCES

- Zuo GQ**, Gong JP, Liu CA, Li SW, Wu XC, Yang K, Li Y. Expression of lipopolysaccharide binding protein and its receptor CD14 in experimental alcoholic liver disease. *World J Gastroenterol* 2001; **7**: 836-840
- Meng AH**, Ling YL, Zhang XP, Zhao XY, Zhang JL. CCK-8 inhibits expression of TNF-alpha in the spleen of endotoxic shock rats and signal transduction mechanism of p38 MAPK. *World J Gastroenterol* 2002; **8**: 139-143
- Wu RQ**, Xu YX, Song XH, Chen LJ, Meng XJ. Relationship between cytokine mRNA expression and organ damage following cecal ligation and puncture. *World J Gastroenterol* 2002; **8**: 131-134
- Li SW**, Gong JP, Wu CX, Shi YJ, Liu CA. Lipopolysaccharide induced synthesis of CD14 proteins and its gene expression in hepatocytes during endotoxemia. *World J Gastroenterol* 2002; **8**: 124-127
- Yu PW**, Xiao GX, Qin XX, Zhou LX, Wang ZQ. The effects of PAF antagonist on intestinal mucosal microcirculation after burn in rats. *World J Gastroenterol* 2000; **6**: 906-908
- Qin RY**, Zou SQ, Wu ZD, Qiu FZ. Influence of splanchnic vascular infusion on the content of endotoxins in plasma and the translocation of intestinal bacteria in rats with acute hemorrhage necrosis pancreatitis. *World J Gastroenterol* 2000; **6**: 577-580
- Wang QG**, He LY, Chen YW, Hu SL. Enzymohistochemical study on burn effect on rat intestinal NOS. *World J Gastroenterol* 2000; **6**: 421-423
- Fu XB**, Yang YH, Sun TZ, Gu XM, Jiang LX, Sun XQ, Sheng ZY. Effect of intestinal ischemia-reperfusion on expressions of endogenous basic fibroblast growth factor and transforming growth factor betain lung and its relation with lung repair. *World J Gastroenterol* 2000; **6**: 353-355
- Fu WL**, Xiao GX, Yue XL, Hua C, Lei MP. Tracing method study of bacterial translocation *in vivo*. *World J Gastroenterol* 2000; **6**: 153-155
- Yang YH**, Fu XB, Sun TZ, Jiang LX, Gu XM. bFGF and TGFbeta expression in rat kidneys after ischemic/ reperfusional gut injury and its relationship with tissue repair. *World J Gastroenterol* 2000; **6**: 147-149
- Ramzy PI**, Wolf SE, Irtun O, Hart DW, Thompson JC, Herndon DN. Gut epithelial apoptosis after severe burn: effects of gut hypoperfusion. *J Am Coll Surg* 2000; **190**: 281-287
- Wolf SE**, Ikeda H, Matin S, Debroy MA, Rajaraman S, Herndon DN, Thompson JC. Cutaneous burn increases apoptosis in the gut epithelium of mice. *J Am Coll Surg* 1999; **188**: 10-16
- Green DR**, Reed JC. Mitochondria and apoptosis. *Science* 1998; **281**: 1309-1312
- Li JM**, Cai Q, Zhou H, Xiao GX. Effects of hydrogen peroxide on mitochondrial gene expression of intestinal epithelial cells. *World J Gastroenterol* 2002; **8**: 1117-1122
- Zhang C**, Cai Y, Adachi MT, Oshiro S, Aso T, Kaufman RJ, Kitajima S. Homocysteine induces programmed cell death in human vascular endothelial cells through activation of the unfolded protein response. *J Biol Chem* 2001; **276**: 35867-35874
- Salazar JJ**, Van Houten B. Preferential mitochondrial DNA injury caused by glucose oxidase as a steady generator of hydrogen peroxide in human fibroblasts. *Mutation Res* 1997; **385**: 139-149
- De Vos K**, Goossens V, Boone E, Vercammen D, Vancompernelle K, Vandenabeele P, Haegeman G, Fiers W, Grooten J. The 55-kDa tumor necrosis factor receptor induces clustering of mitochondria through its membrane-proximal region. *J Biol Chem* 1998; **273**: 9673-9680
- Cone JB**, Wallace BH, Lubansky HJ, Caldwell FT. Manipulation of the inflammatory response to burn injury. *J Trauma* 1997; **43**: 41-45
- Dries DJ**, Lorenz K, Kovacs EJ. Differential neutrophil traffic in gut and lung after scald injury. *J Burn Care Rehabil* 2001; **22**: 203-209
- Jeschke MG**, Debroy MA, Wolf SE, Rajaraman S, Thompson JC. Burn and starvation increase programmed cell death in small bowel epithelial cells. *Dig Dis Sci* 2000; **45**: 415-420
- Eaves Pyles T**, Alexander JW. Rapid and prolonged impairment of gut barrier function after thermal injury in mice. *Shock* 1998; **9**: 95-100
- Baskaran H**, Yarmush ML, Berthiaume F. Dynamics of tissue neutrophil sequestration after cutaneous burns in rats. *J Surg Res* 2000; **93**: 88-96
- Hengartner MO**. Apoptosis: DNA destroyers. *Nature* 2001; **412**: 27-29
- Hengartner MO**. The biochemistry of apoptosis. *Nature* 2000; **407**: 770-776
- Desagher S**, Martinou JC. Mitochondria as the central control point of apoptosis. *Trends Cell Biol* 2000; **10**: 369-377
- Petit PX**, Susin SA, Zamzami N, Mignotte B, Kroemer G. Mitochondria and programmed cell death: back to the future. *FEBS Letters* 1996; **396**: 7-13
- Finkel E**. The mitochondrion: is it central to apoptosis? *Science* 2001; **292**: 624-626
- Kluck RM**, Bossy Wetzel E, Green DR, Newmeyer DD. The release of cytochrome C from mitochondria: a primary site for Bcl2 regulation of apoptosis. *Science* 1997; **275**: 1132-1136
- Susin SA**, Zamzami N, Castedo M, Hirsch T, Marchetti P, Macho A, Daugas E, Geuskens M, Kroemer G. Bcl-2 inhibits the mitochondrial release of an apoptogenic protease. *J Exp Med* 1996; **184**: 1331-1341
- Wakabayashi T**. Structural changes of mitochondria related to apoptosis: swelling and megamitochondria formation. *Acta Biochim Pol* 1999; **46**: 223-237
- Frey TG**, Mannella CA. The internal structure of mitochondria. *Trends Biochem Sci* 2000; **25**: 319-324
- Hirsch T**, Marzo I, Kroemer G. Role of the mitochondrial permeability transition pore in apoptosis. *Biosci Rep* 1997; **17**: 67-76
- Zamzami N**, Hirsch T, Dallaporta B, Petit PX, Kroemer G. Mitochondrial implication in accidental and programmed cell death: apoptosis and necrosis. *J Bioenerg Biomembr* 1997; **29**: 185-193
- Kroemer G**. Mitochondrial control of apoptosis: an overview. *Biochem Soc Symp* 1999; **66**: 1-15
- Ravagnan L**, Marzo I, Costantini P, Susin SA, Zamzami N, Petit PX, Hirsch F, Goubern M, Poupon MF, Miccoli L, Xie Z, Reed JC, Kroemer G. Lomidamine triggers apoptosis via a direct, Bcl-2-inhibited effect on the mitochondrial permeability transition

- pore. *Oncogene* 1999; **18**: 2537-2546
- 36 **Larochette N**, Decaudin D, Jacotot E, Brenner C, Marzo I, Susin SA, Zamzami N, Xie Z, Reed J, Kroemer G. Arsenite induces apoptosis via a direct effect on the mitochondrial permeability transition pore. *Exp Cell Res* 1999; **249**: 413-421
- 37 **Anuradha CD**, Kanno S, Hirano S. Oxidative damage to mitochondria is a preliminary step to caspase-3 activation in fluoride-induced apoptosis in HL-60 cells. *Free Radic Biol Med* 2001; **31**: 367-373
- 38 **Smaili SS**, Hsu YT, Sanders KM, Russell JT, Youle RJ. Bax translocation to mitochondria subsequent to a rapid loss of mitochondrial membrane potential. *Cell Death Differ* 2001; **8**: 909-920
- 39 **Skulachev VP**. Cytochrome c in the apoptotic and antioxidant cascades. *FEBS Lett* 1998; **423**: 275-280
- 40 **Simon DK**, Lin MT, Ahn CH, Liu GJ, Gibson GE, Beal MF, Johns DR. Low mutational burden of individual acquired mitochondrial DNA mutations in brain. *Genomics* 2001; **73**: 113-116
- 41 **Wallace DC**. A mitochondrial paradigm for degenerative diseases and ageing. *Novartis Found Symp* 2001; **235**: 247-263
- 42 **Chang SW**, Zhang D, Chung HD, Zassenhaus HP. The frequency of point mutations in mitochondrial DNA is elevated in the Alzheimer's brain. *Biochem Biophys Res Commun* 2000; **273**: 203-208
- 43 **Esposito LA**, Melov S, Panov A, Cottrell BA, Wallace DC. Mitochondrial disease in mouse results in increased oxidative stress. *Proc Natl Acad Sci USA* 1999; **96**: 4820-4825
- 44 **Lu CY**, Lee HC, Fahn HJ, Wei YH. Oxidative damage elicited by imbalance of free radical scavenging enzymes is associated with large-scale mtDNA deletions in aging human skin. *Mutat Res* 1999; **423**: 11-21
- 45 **Bhat HK**, Hiatt WR, Hoppel CL, Brass EP. Skeletal muscle mitochondrial DNA injury in patients with unilateral peripheral arterial disease. *Circulation* 1999; **99**: 807-812
- 46 **Swerdlow RH**, Parks JK, Cassarino DS, Shilling AT, Bennett JP, Harrison MB, Parker WD. Characterization of cybrid cell lines containing mtDNA from Huntington's disease patients. *Biochem Biophys Res Commun* 1999; **261**: 701-704
- 47 **Wei YH**. Oxidative stress and mitochondrial DNA mutations in human aging. *Proc Soc Exp Biol Med* 1998; **217**: 53-63
- 48 **Ide T**, Tsutsui H, Hayashidani S, Kang D, Suematsu N, Nakamura K, Utsumi H, Hamasaki N, Takeshita A. Mitochondrial DNA damage and dysfunction associated with oxidative stress in failing hearts after myocardial infarction. *Circ Res* 2001; **88**: 529-535
- 49 **Swerdlow RH**, Parks JK, Davis JN, Cassarino DS, Trimmer PA, Currie LJ, Dougherty J, Bridges WS, Bennett JP, Wooten GF, Parker WD. Matrilineal inheritance of complex I dysfunction in a multigenerational Parkinson's disease family. *Ann Neurol* 1998; **44**: 873-881
- 50 **Ballinger SW**, Patterson C, Yan CN, Doan R, Burow DL, Young CG, Yakes FM, Van Houten B, Ballinger CA, Freeman BA, Runge MS. Hydrogen peroxide and peroxynitrite induced mitochondrial DNA damage and dysfunction in vascular endothelial and smooth muscle cells. *Circ Res* 2000; **86**: 960-966

Edited by Zhu L

Combined therapy of allantoin, metronidazole, dexamethasone on the prevention of intra-abdominal adhesion in dogs and its quantitative analysis

Xiao-Chen Wang, Chang-Qing Gui, Qing-Shan Zheng

Xiao-Chen Wang, Qing-Shan Zheng, Anhui Provincial Center for Drug Clinical Evaluation & Yijishan Hospital of Wanan Medical Collage, Wuhu 241001, Anhui Province, China

Chang-Qing Gui, Department of Pharmacology, Wanan Medical Collage, Wuhu 241001, Anhui Province, China

Correspondence to: Dr. Qing-Shan Zheng, Anhui Provincial Center for Drug Clinical Evaluation & Yijishan Hospital of Wanan Medical Collage, 93 TuanJieDong Lu, Wuhu 241001, Anhui Province, China. editorys@mail.wh.ah.cn

Telephone: +86-553-573-8350 **Fax:** +86-553-573-8350

Received: 2002-10-30 **Accepted:** 2002-11-19

Abstract

AIM: To observe the preventive effects of combined therapy of AMD (allantoin, metronidazole and dexamethasone in combination) on intra-abdominal adhesion in dogs.

METHODS: 20 dogs of both sexes were used in this study. After laparotomy under anesthesia, 2 cm section of cecal end was clamped and ligated, then 1 cm cecum section was cut and another 1 cm was kept. The cecum stump was closed with purse-string suture. Both parietal and visceral peritonea were stripped for an area of about 3×4 cm². Before the skin closure, the animals were divided into two groups randomly. The abdominal cavities in Group AMD (*n*=10) were rinsed by 200 ml of AMD solution, and with 50 ml left, whereas the control (*n*=10) received the equal volume of normal saline. After 7 d, the degree of intra-abdominal adhesions was evaluated by using the score method of ultrasonography and traditional dissection.

RESULTS: Compared with the control, both the ultrasonography and traditional dissection scores in Group AMD were significantly decreased that marked as 2.0±1.25 vs 3.3±0.82 and 1.91±0.83 vs 3.3±0.82 respectively (*P*<0.01).

CONCLUSION: The combined therapy of AMD is an effective way to prevent intra-abdominal adhesion, and ultrasonography is an useful tool to diagnose intra-abdominal adhesion.

Wang XC, Gui CQ, Zheng QS. Combined therapy of allantoin, metronidazole, dexamethasone on the prevention of intra-abdominal adhesion in dogs and its quantitative analysis. *World J Gastroenterol* 2003; 9(3): 568-571

<http://www.wjgnet.com/1007-9327/9/568.htm>

INTRODUCTION

Intra-abdominal adhesions are almost inevitable to some extent after major abdominal surgery. Weibel and Majno reviewed 289 subjects at post-mortem who had had previous laparotomies, and 67 % of the patients showed adhesions; after multiple operations, the incidence rose to 93 %^[1]. However, there has been little advances in the treatment and prevention

of this complication in recent years. Numerous attempts with agents and surgical techniques often obtain conflicting results^[2,3]. The cause may be mainly, at least partly, due to multi-factor in the adhesion etiology and multi-pathway in the adhesion mechanism^[4-6], which made the adhesions difficult to be prevented by using a single drug or certain measures. Besides, the evaluation of intra-abdominal adhesion was based classically on traditional dissection method, which was impossible to be applied to the clinical settings. In this study, we employed a new reproducible animal model of intra-abdominal adhesion caused by multi-factors, and a new evaluation method by ultrasonography to assess the effects of combined AMD (allantoin, metronidazole and dexamethasone in combination) therapy.

MATERIALS AND METHODS

Materials

Allantoin (Alt) powder with the purity of 99.6 % was obtained from Jiangsu Huanghai Pharmaceutical Factory. Metronidazole (Met) powder was from Tianjing Hebei Pharmaceutical Factory with the purity of 99.85 %. Dexamethasone (Dex) powder was purchased from Roussel Uclaf Co and the purity is 99.6 %. They were dissolved and mixed with 5 % GS, the ratio of Alt:Met:Dex is 50:32:1. The HEWLETT-PACKARD Sonos-2000 Color Ultrasonic Doppler Method Diagnostic Equipment was employed in this study, using a real-time sonolayer SSA-270A ultrasound scanner (Toshiba, Tokyo, Japan) and a 3.5 MHz sector transducer.

Experimental animal

20 adult healthy dogs of both sexes, weighing from 7 to 10 kg were purchased from the Animal Center of Wannan Medical College.

Animal models

The experiment was carried out in clean but not sterile condition. Under 3 % sodium pentobarbital anesthesia (1 ml/kg iv), following shaving and skin disinfecting, the laparotomy was performed through a 5 cm, vertical, midline incision. 2 cm section from the cecal end was clamped and ligated, 1 cm of the section was cut, and the other 1 cm from the ligated site was kept. The cecum stump was closed with the purse-string suture. Then a 3×4 cm² patch of parietal peritoneum corresponding to the cecal was carefully stripped. In addition, both sides of peritoneum along the abdomen incision were scraped for an area of about 3×4 cm². Before skin closure of abdomen, the animals were randomly divided into 2 groups. The abdominal cavity in Group AMD were rinsed by 200 ml of AMD solution and with 50 ml left, whereas the control received the equal volume of normal saline. All the animals were fasted for 8 hours after operation.

Adhesion assessment by ultrasonography

At the seventh day after operation, all the dogs were reanesthetized. Selecting the skin point corresponding to the

appendix, 1 000 ml of normal saline was instilled into the abdominal cavity with a 12G needle to improve the acoustic window^[7]. The whole abdomen was divided into four areas artificially by a horizon through navel and a vertical line through xiphoid (Figure 1), the number and density of adhesion sites were graded on the basis of ultrasonographic findings (Table 1).

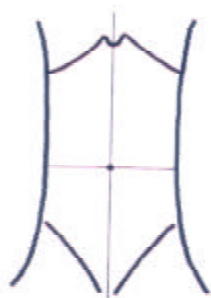


Figure 1 Abridged general view of dog abdomen subregion.

Table 1 Adhesion assessment by ultrasonography

Score	Description
1	Echogenic bands in one area
2	Echogenic bands in two areas
3	Echogenic bands in three areas or alveolate echogenic bands in one area
4	Massive agglutinating adhesion or adhesion between viscera and abdominal wall

Adhesion assessment by traditional dissection

After ultrasonic examination, the dogs were sacrificed and an autopsy examination was carried out with the attention to the number, density and site of the adhesion formation, which was scored by a modified scale by Swolin^[8,9] (Table 2). The highest score for each dog was taken to be further processed.

Table 2 Adhesion assessment by traditional dissection

Score	Description
1	Filmy connections separated spontaneously
2	Firm adhesions separated by gravity
3	Firm adhesions by traction
4	Dense adhesions requiring sharp dissection

Statistical analysis

Quantitative results were expressed as mean \pm SD. Statistical analysis was performed using Student's *t* test. $P < 0.05$ was considered statistically significant.

RESULTS

One week postoperation animals in control group developed strip or round adhesions (Figure 2), attached either to the closed peritoneal defect or to the midline scar, or connected between the bowels. All the control animals had positive sonographic findings. Transabdominal sonogram clearly showed echogenic bands floating in the abdominal cavity like mice-tails (Figure 3). In more serious subjects, the adhesions were so dense that the sonogram showed alveolate echogenic masses (Figure 4); Some adhesions were formed between the organs in abdominal cavity (Figure 5). All the sonographic positive findings were proved to be the adhesion formation in laparotomy. The adhesion formed in Group AMD was significantly decreased compared with the control group as shown by both ultrasonography and

traditional dissection score that marked as 2.0 ± 1.25 vs 3.3 ± 0.82 and 1.91 ± 0.83 vs 3.3 ± 0.82 respectively ($P < 0.01$).

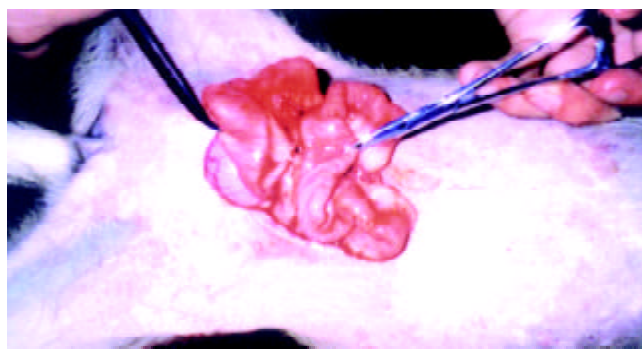


Figure 2 Adhesions between the bowels of animal in control group.



Figure 3A Transabdominal sonogram showed the adhesions between bowels, the adhesion looks like a mouse tail, and the score is 1.



Figure 3B Transabdominal sonogram showed massive agglutinating adhesion between bowels, and the score is 3.

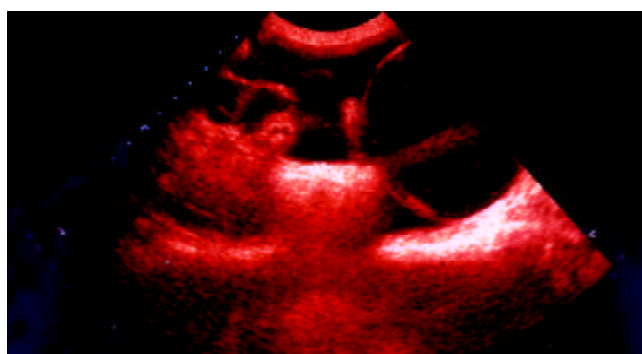


Figure 3C Transabdominal sonogram showed the adhesions between bladder and bowels, and the score is 4.

DISCUSSION

Because of the high incidence of intra-abdominal adhesion formation postoperation, plenty of investigations have been made for the past decades; However, up to the present, satisfactory results have not been achieved yet, which reflected such a fact that there still existed some obstacles waiting to be overcome.

The animal model of intra-abdominal adhesion was such a problem. Traditionally, the model was made mainly on mice, rats and rabbits by a series of America, British investigators in different means^[10-12]; however, these small animals were quite different from human beings in phylogenesis, metabolism reactivity and so on. In addition, such model making laid much stress on mechanical trauma, many important factors, such as tissue ischemia, infection, inflammation and exudation^[13-16] were severely neglected, which made the experimental results inconsistent with clinical settings. In the present, study a novel dog model of intra-abdominal adhesion caused by multi-factors was employed, which might reflect really the complexity of etiology and the nature of intra-abdominal adhesion formation.

There are a large number of substances used to combat adhesion formation at present^[17-26], however, because of the multi-factors in the adhesion etiology and multi-pathways in the adhesion mechanism, the single use one or two of these agents could not turn out satisfactory results. Besides, the majority of these agents have been proven to be too toxic to be used^[27-29].

The formation of intra-abdominal adhesion has been attributed to the local depression of plasminogen activator activity (PAA) for more than 3 decades^[30-33]. This deficit permits the deposited fibrin on peritoneal surface to form fibrous adhesion. In this study, we used the combined AMD composed of allantoin, metronidazole and dexamethasone, which was proven to play a role of anti-inflammation, anti-bacteria and anti-exudation by prohibiting the fibrin rich exudate into the abdominal cavity and increasing the activity of endogenous tissue plasminogen activator, to prevent intra-abdominal adhesion postoperation. According to our pilot study, the best proportion of these three drugs was 50:32:1, which made the effectiveness of the combination reinforced, whereas the toxicity didn't increase^[34]. As for the impairment of the combination on wound healing, it was too slight to be noticed, for the intra-abdominal adhesion formed mainly in 6 hours postoperation, after that, the wound healing began to occur while the effect of the combination was gradually disappeared.

Intra-abdominal adhesion failed to be detected by routine ultrasonography. Lee *et al* identified instilling normal saline into abdominal cavity could diagnose the female pelvic lesions^[7], we employed this method to perform an assessment for the intra-abdominal adhesion. It was demonstrated that this method was visible and accurate, the score of intra-abdominal adhesion was well in agreement with that done by the laparotomy. The most notable finding of sonography in the examination of intra-abdominal adhesion was the mouse-tail appearance, which was believed as the sign of adhesion band. In conclusion, we suggested that the combined AMD might be an effective way to prevent intra-abdominal adhesion, and the ultrasonography an useful tool to diagnose intra-abdominal adhesion, and their applications might be valuable to the clinical settings.

REFERENCES

- 1 **Lower AM**, Hawthorn RJ, Ellis H, O' Brien F, Buchan S, Crowe AM. The impact of adhesions on hospital readmissions over ten years after 8849 open gynaecological operations: an assessment from the Surgical and Clinical Adhesions Research Study. *BJOG* 2000; **107**: 855-862
- 2 **Jacobi CA**, Sterzel A, Braumann C, Halle E, Stosslein R, Krahenbuhl L, Muller JM. The impact of conventional and laparoscopic colon resection (CO₂ or helium) on intraperitoneal adhesion formation in a rat peritonitis model. *Surg Endosc* 2001; **15**: 380-386
- 3 **Farmer L**, Ayoub M, Warejcka D, Southerland S, Freeman A, Solis M. Adhesion formation after intraperitoneal and extraperitoneal implantation of polypropylene mesh. *Am Surg* 1998; **64**: 144-146
- 4 **Tulandi T**. Introduction-prevention of adhesion formation: the journey continues. *Hum Reprod Update* 2001; **7**: 545-546
- 5 **Dijkstra FR**, Nieuwenhuijzen M, Reijnen MM, van Goor H. Recent clinical developments in pathophysiology, epidemiology, diagnosis and treatment of intra-abdominal adhesions. *Gastroenterol Suppl* 2000; **232**: 52-59
- 6 **Thompson J**. Pathogenesis and prevention of adhesion formation. *Dig Surg* 1998; **15**: 153-157
- 7 **Li GJ**, Zhou YC, Wu J. A preliminary application of normal saline instilling abdomen cavity in diagnosis of female pelvic lesions. *Zhongguo Chaosheng Yixue Zazhi* 2000; **16**: 535-538
- 8 **Gul A**, Kotan C, Dilek I, Gul T, Tas A, Berktaş M. Effects of methylene blue, indigo carmine solution and autologous erythrocyte suspension on formation of adhesions after injection into rats. *J Reprod Fertil* 2000; **120**: 225-229
- 9 **Tran HS**, Chrzanowski FA Jr, Puc MM, Patel NG, Geldziler B, Malli D, Ramsamooj R, Hewitt CW, DelRossi AJ. An *in vivo* evaluation of a chondroitin sulfate solution to prevent postoperative intraperitoneal adhesion formation. *J Surg Res* 2000; **88**: 78-87
- 10 **Yesildaglar N**, Koninckx PR. Adhesion formation in intubated rabbits increases with high insufflation pressure during endoscopic surgery. *Hum Reprod* 2000; **15**: 687-691
- 11 **Mueller PO**, Hay WP, Harmon B, Amoroso L. Evaluation of a bioresorbable hyaluronate-carboxymethylcellulose membrane for prevention of experimentally induced abdominal adhesions in horses. *Vet Surg* 2000; **29**: 48-53
- 12 **Toosie K**, Gallego K, Stabile BE, Schaber B, French S, de Virgilio C. Fibrin glue reduces intra-abdominal adhesions to synthetic mesh in a rat ventral hernia model. *Am Surg* 2000; **66**: 41-45
- 13 **Sjosten AC**, Ellis H, Edelstam GA. Post-operative consequences of glove powder used pre-operatively in the vagina in the rabbit model. *Sjosten AC. Hum Reprod* 2000; **15**: 1573-1577
- 14 **van den Tol MP**, Haverlag R, van Rossen ME, Bonthuis F, Marquet RL, Jeekel J. Glove powder promotes adhesion formation and facilitates tumour cell adhesion and growth. *Br J Surg* 2001; **88**: 1258-1263
- 15 **Qiu G**, Wang C, Smith R, Harrison K, Yin K. Role of IFN-gamma in bacterial containment in a model of intra-abdominal sepsis. *Shock* 2001; **16**: 425-429
- 16 **Halverson AL**, Barrett WL, Bhanot P, Phillips JE, Iglesias AR, Jacobs LK, Sackier JM. Intraabdominal adhesion formation after preperitoneal dissection in the murine model. *Surg Endosc* 1999; **13**: 14-16
- 17 **Reijnen MM**, de Man BM, Hendriks T, Postma VA, Meis JF, van Goor H. Hyaluronic acid-based agents do not affect anastomotic strength in the rat colon, in either the presence or absence of bacterial peritonitis. *Br J Surg* 2000; **87**: 1222-1228
- 18 **Verco SJ**, Peers EM, Brown CB, Rodgers KE, Roda N, diZerega G. Development of a novel glucose polymer solution (icodextrin) for adhesion prevention: pre-clinical studies. *Hum Reprod* 2000; **15**: 1764-1772
- 19 **Szabo A**, Haj M, Waxman I, Eitan A. Evaluation of seprafilm and amniotic membrane as adhesion prophylaxis in mesh repair of abdominal wall hernia in rats. *Eur Surg Res* 2000; **32**: 125-128
- 20 **Ghellai AM**, Stucchi AF, Chegini N, Ma C, Andry CD, Kaseta JM, Burns JW, Skinner KC, Becker JM. Role of transforming growth factor beta-1 in peritonitis-induced adhesions. *Gastrointest Surg* 2000; **4**: 316-323
- 21 **Kramer K**, Senninger N, Herbst H, Probst W. Effective prevention of adhesions with hyaluronate. *Arch Surg* 2002; **137**: 278-282
- 22 **Cubukcu A**, Alponat A, Gonullu NN. Mitomycin-C prevents reformation of intra-abdominal adhesions after adhesiolysis. *Surgery* 2002; **131**: 81-84
- 23 **Reijnen MM**, Skrabut EM, Postma VA, Burns JW, van Goor H. Polyanionic polysaccharides reduce intra-abdominal adhesion and abscess formation in a rat peritonitis model. *J Surg Res* 2001;

- 101:** 248-253
- 24 **Vela AR**, Littleton JC, O' Leary JP. The effects of minidose heparin and low molecular weight heparin on peritonitis in the rat. *Am Surg* 1999; **65**: 473-477
- 25 **Ozogul Y**, Baykal A, Onat D, Renda N, Sayek I. An experimental study of the effect of aprotinin on intestinal adhesion formation. *Am J Surg* 1998; **175**: 137-141
- 26 **Gul A**, Kotan C, Dilek I, Gul T, Tas A, Berktaş M. Effects of methylene blue, indigo carmine solution and autologous erythrocyte suspension on formation of adhesion after injection into rat. *J Reprod Fertil* 2000; **120**: 225-229
- 27 **Trickett JP**, Rainsbury RM, Green R. Paradoxical outcome after use of hyaluronate barrier to prevent intra-abdominal adhesions. *J R Soc Med* 2001; **94**: 183-184
- 28 **Reijnen MM**, de Man BM, Hendriks T, Postma VA, Meis JF, Van Goor H. Hyaluronic acid-based agents do not affect anastomotic strength in the rat colon, in either the presence or absence of bacterial peritonitis. *Br J Surg* 2000; **87**: 1222-1228
- 29 **Haverlag R**, van Rossen ME, van den Tol MP, Bonthuis F, Marquet RL, Jeekel J. Hyaluronate-based coating solution for prevention of surgical adhesions has no major effect on adhesion and growth of intraperitoneal tumour cells. *Eur J Surg* 1999; **165**: 791-795
- 30 **Edelstam G**, Lecander I, Larsson B, Astedt B. Fibrinolysis in the peritoneal fluid during adhesions, endometriosis and ongoing pelvic inflammatory disease. *Inflammation* 1998; **22**: 341-351
- 31 **Cheong YC**, Laird SM, Li TC, Shelton JB, Ledger WL, Cooke ID. Peritoneal healing and adhesion formation/reformation. *Hum Reprod Update* 2001; **7**: 556-566
- 32 **Cao TS**, Liu RH, Sun XM. Experimental study of the effect of methylene blue combined with aprotinin on intraperitoneal adhesion. *Zhongguo Weichang Waikē Zazhi* 2000; **3**: 238-239
- 33 **Gimbel ML**, Chelius D, Hunt TK, Spencer EM. A novel approach to reducing postoperative intraperitoneal adhesion through the inhibition of insulinlike growth factor I activity. *Arch Surg* 2001; **136**: 311-317
- 34 **Zheng QS**, Gui CQ, Sun RY, Wang M. A novel animal model of intra-abdominal adhesion and quantitative evaluation with related indices. *Zhongguo Linchuang Yaolixue Yu Zhilixue Zazhi* 2000; **5**: 101-104

Edited by Zhu L

Preparation and identification of anti-transforming growth factor b1 U1 small nuclear RNA chimeric ribozyme *in vitro*

Ju-Sheng Lin, Yu-Hu Song, Xin-Juan Kong, Bin Li, Nan-Zhi Liu, Xiao-Li Wu, You-Xin Jin

Ju-Sheng Lin, Yu-Hu Song, Xin-Juan Kong, Nan-Zhi Liu, Xiao-Li Wu, Institute of Liver Diseases, Tongji Hospital, Tongji Medical College, Huazhong University of Science and Technology, Wuhan 430030, Hubei Province, China

Bin Li, You-Xin Jin, State Key Laboratory of Molecular Biology, Institute of Biochemistry and Cell Biology, Shanghai Institutes for Biological Sciences, Chinese Academy of Sciences, Shanghai 200031, China

JS Lin and YH Song contributed equally to this study

Supported by the grant from Chinese Academy of Sciences, No. KSCX2-2-204

Correspondence to: Dr. You-Xin Jin, State Key Laboratory of Molecular Biology, Institute of Biochemistry and Cell Biology, Shanghai Institutes for Biological Sciences, Chinese Academy of Sciences, Shanghai 200031, China. yxjin@sunm.shnc.ac.cn

Telephone: +86-21-64315030-5221

Received: 2002-09-13 **Accepted:** 2002-10-18

Abstract

AIM: To study the preparation and cleavage activity of anti-transforming growth factor (TGF) β 1 U1 small nuclear (sn) RNA chimeric hammerhead ribozymes *in vitro*.

METHODS: TGF β 1 partial gene fragment was cloned into T-vector at the downstream of T7 promoter. 32 p-labeled TGF β 1 partial transcripts as target RNA were transcribed *in vitro* and purified by denaturing polyacrylamide gel electrophoresis (PAGE). Anti-TGF β 1 ribozymes were designed by computer, then synthetic ribozyme fragments were cloned into the U1 ribozyme vector pZeoU1EcoSpe containing U1 snRNA promoter/enhancer and terminator. 32 p-labeled U1 snRNA chimeric ribozyme transcripts were gel-purified, incubated with target-RNAs at different conditions and autoradiographed after running denaturing PAGE.

RESULTS: Active U1snRNA chimeric ribozyme (U1Rz803) had the best cleavage activity at 50 °C; at 37 °C, it was active, $K_m=34.48$ nmol/L, $K_{cat}=0.14$ min $^{-1}$; while the point mutant ribozyme U1Rz803_m had no cleavage activity, so these indicated the design of U1Rz803 was correct.

CONCLUSION: U1Rz803 prepared in this study possessed the perfect specific catalytic cleavage activity. These results indicate U1 snRNA chimeric ribozyme U1Rz803 may suppress the expression of TGF β 1 *in vivo*, therefore it may provide a new avenue for the treatment of liver fibrosis in the future.

Lin JS, Song YH, Kong XJ, Li B, Liu NZ, Wu XL, Jin YX. Preparation and identification of anti-transforming growth factor β 1 U1 small nuclear RNA chimeric ribozyme *in vitro*. *World J Gastroenterol* 2003; 9(3): 572-577

<http://www.wjgnet.com/1007-9327/9/572.htm>

INTRODUCTION

The incidence of liver cirrhosis is still high all over the world, especially in China^[1-6]. Cirrhotic livers are characterized by

extensive fibrosis throughout the entire hepatic parenchyma^[7-12]. Many factors inducing liver injury and inflammation will lead to chronic liver disease, and hepatic fibrosis^[13-22].

TGF β 1 is an important cytokine in the regulation of the production, degradation, accumulation of extracellular matrix proteins, and that it may play a pivotal role in the fibroproliferative changes that follow tissue damage in many vital organs and tissues, including liver, lung, kidney, skin, heart, and arterial walls^[7,23-27]. In the past decade dramatic advances have been made in the understanding of cellular and molecular mechanisms underlying liver fibrogenesis, it is thought that TGF β 1 is of crucial importance in rat hepatic fibrosis *in vivo*^[7,28-34]. Inhibition of TGF β can not only prevent liver fibrosis, but also preserve organ function^[30]. So TGF β 1 has been thought to be an ideal target molecule to prevent the progression of liver fibrosis.

Ribozymes are a class of small catalytic RNA molecules that recognize specific substrate RNA molecules by their complementary nucleotide sequence, cleaving the substrate RNA as an endoribonuclease at enzymatic rates^[35-38]. In the last years ribozyme-mediated inhibition of gene expression in intact cells have been tested many times, but some of them were largely unsuccessful^[39-42]. Factors that contributed to ribozyme efficacy in transfected cell are expression level, stability against rapid degradation, correct folding for exposure to target, and subcellular localization of ribozyme and target. U1 snRNA is a highly expressed stable small RNA (164 nucleotides) involved in both spliceosome and catalytic processing during pre-mRNA splicing. U1small nuclear RNA expression cassette can provide an excellent vehicle for ribozyme delivery and expression in intact cell because of stability, nuclear localization, highly efficient expression^[43-45].

Because TGF β 1 plays a crucial role in liver fibrosis, in this study we designed ribozymes directed against TGF β 1 by computer, then cloned them into U1 snRNA chimeric ribozyme vector, it had been proven that it could cleave target RNA efficiently *in vitro* through the cleavage reaction, so it indicated that it might suppress intracellular TGF β 1 expression, which would provide a new avenue in treatment of liver fibrosis.

MATERIALS AND METHODS

Materials

HSC-T6 cell line is a kind gift from Dr. Scott L. Friedman (Dept of Medicine and Division of Liver Diseases, Mount Sinai School of Medicine). pZeoU1EcoSpe was provided by Dr. Harry C. Dietz (Department of Pediatrics, Medicine and Molecular Biology & Genetics, Johns Hopkins University School of Medicine). pGEM-T vector kit, transcription kit were purchased from Promega Company. Trizol kit, DMEM were purchased from Gibco BRL Company. The PCR primers and ribozyme fragments were synthesized in the Beckman oligo-1 000 DNA synthesizer. Zeocin was purchased from Invitrogen Company. Newborn calf serum was purchased from Hyclone Company. RT-PCR kit, RNase inhibitor, restriction endonucleases, and T4 DNA ligase were purchased from Takara Company. α 32 P UTP was purchased from Beijing Ya-Hui Company.

Methods

Construction of target RNA *in vitro* Total RNA was extracted using Trizol Kit (GIBCO BRL) from cultured HSC-T6 cell, an immortalized rat hepatic stellate cells line (HSC), exhibited an activated phenotype^[46,47]. The upstream primer P1 (5' - GAATTCATTCAGGACTATCAC CTACC-3') in the untranslated region and the downstream primer P2 (5' - AAGCTTTTCTGGT AGAGTTCTACGTG -3') in the open reading frame were selected to amplify a 651-base pair fragment corresponding to bases 279 to 930 of the rat TGF beta 1^[48]. The extracted RNA was reversely transcribed and polymerase chain reaction (PCR) amplified using a pair of primers in one step reverse transcriptase (RT) PCR kit. The PCR products were analyzed and purified on 1 % (w/v) agarose gels. Purified PCR products were ligated into pGEM-T vector. DNA sequencing results showed that the PCR-amplified fragments were cloned into the molecular cloning sites of pGEM-T vector at the downstream of T7 promoter as pTGFβ1. Target RNA was prepared through *in vitro* transcription of PCR-amplified products of pTGFβ1, which contained T7 promoter at the upstream of upper primer. The sequence of the primers for transcription was GAATTCTAATACGACTCACTATAGGGAGGCGGACTACTACGCCAA and TTCTGGTAGAG TTCTACGTG; **TAATACGACTCACTATAG GG** represents T7 promoter. Then PCR product was analyzed and purified by 1 % (w/v) agarose gels electrophoresis as the template for transcription. *In vitro* transcription was carried out at 37 °C for 90 min in a 40 μL final volume containing 40 mmol/L of Tris·HCl (pH 7.5), 5 mmol/L of DTT, 2 mmol/L of spermidine, 8 mmol/L of MgCl₂, 0.25 mmol/L of ATP, GTP,CTP, 0.05 mmol/L of UTP, 20 μCi alpha ³²p-UTP, 80 U T₇ RNA polymerase and 2 μg purified PCR product. Target RNA was purified by 6 % denaturing gel electrophoresis through cutting off the

autoradiograph bands and soaking in NES (0.5 mol/L NH₄Ac, 0.1 mol/L EDTA, 0.1 % SDS pH 5.4) at 42 °C overnight. the products were precipitated by ethanol, washed twice by 75 % ethanol, dissolved in DEPC H₂O and reserved under -20 °C.

Construction of recombinant plasmid for ribozyme pZeoU1EcoSpe contained the pZeoSV plasmid DNA modified by excising the SV40 promoter, SV40 polyadenylation site, and polylinker at the *Bam*HI sites. In constructing the pZeoU1 EcoSpe, a U1 snRNA expression cassette in pUC13^[49, 50] was excised with *Bam*HI digestion and ligated into the *Bam*HI sites of the modified pZeoSV. Two rounds of site-directed mutagenesis were then performed to change 4 nt flanking the Sm protein binding site of U1 snRNA, creating unique *Eco*RI and *Spe*I restriction sites. The 5' -flanking region of the inserted U1 snRNA expression cassette possessed a promoter/enhancer comparable in strength with the SV40 early promoter^[51]. The ribozymes for TGFβ1 were designed according to the computer software pcFOLD compiled by professor Zuker (Canadian Academy of Science). The homologous possibility with the gene of rat was excluded by consulting with RNA sequence of rat cells from NCBI Genbank. The enclosed vector pZeoU1EcoSpe was cut by *Eco*RI and *Spe*I restriction enzymes and purified by 1 % (w/v) agarose gels electrophoresis. The synthesized oligonucleotides of ribozyme were mixed with equal molar amounts together, then were cloned into the *Eco*RI/*Spe*I sites of pZeoU1EcoSpe to create pU1Rz803. pZeoU1EcoSpe and the reconstruction could be confirmed by DNA sequencing (Figure 1). The oligonucleotides of Rz803 were 5' AATTACATATATACT (G/A)ATGAGTCCGTGAGGACGAAACTGTGT3' and 5' CTAGACACAGTTTCGTCCTCACGGACTCAT(C/T)AGTATATATGT3' ; G and C for activated ribozyme, A and T for inactivated ribozyme.

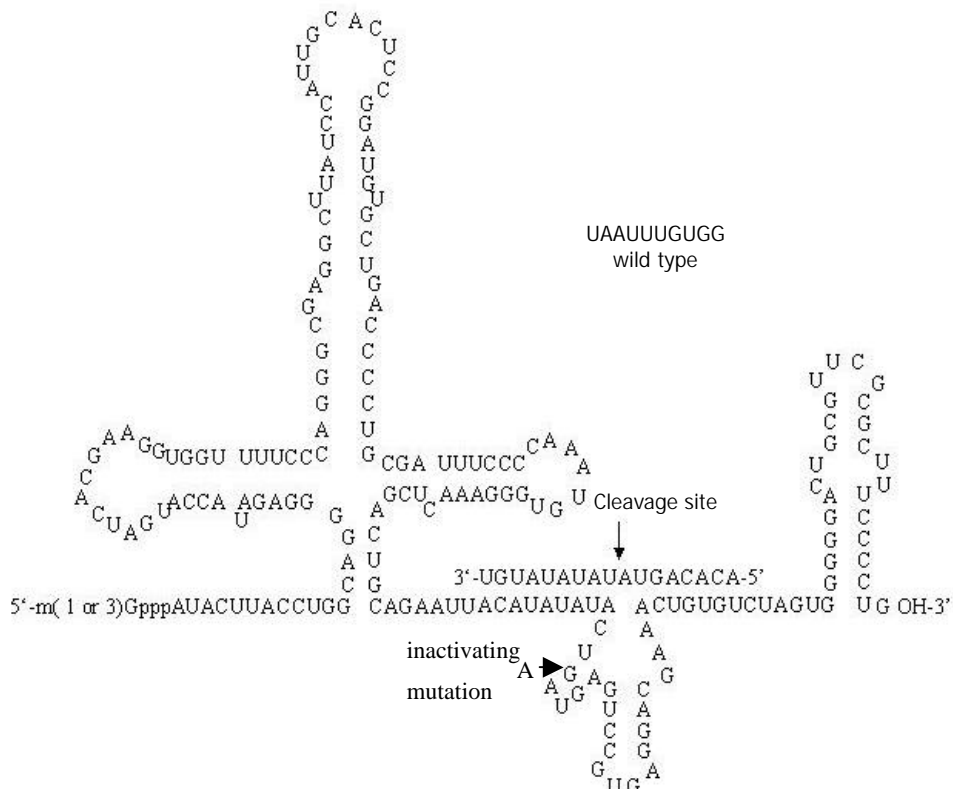


Figure 1 Sequence and predicted structure of U1 snRNA chimeric ribozymes. arrows represent cleavage site and inactivating mutation.

Preparation of ribozymes *in vitro* The templates used for transcription of U1 snRNA chimeric ribozymes were obtained by PCR amplification of pU1Rz803. The primers used for transcription were as follows: upstream primer: 5'-GAATTCTAATACGACTCACTATAGGG GATACTTACC TGGCAGGGGA-3'; downstream primer: 5'-CAGGGGAAAGCGCGAACGCA-3'; **TAATACGA CTAATAGGG** represented T7 promoter. The purification of PCR products was the same as that of the template for target RNA. *In vitro* transcription and purification of ribozyme were done as described above.

***In vitro* cleavage reaction of U1Rz803 and U1Rz803_m** U1Rz803, U1Rz803_m and target RNA were quantified by measuring their radioactivity cpm in 1 μ L solution. The cleavage reaction was carried out in 5 μ L solution containing 50 mmol/L Tris·HCl (pH7.5), 20 mmol/L MgCl₂. The molar ratio between ribozyme and target RNA could be estimated according to the cpm value combined with the U number in their RNAs. The initial experiment was: (I) Ribozyme (R): Substrate (S)=1:1(mol/L) ratio, 37 °C, 120 min; (II) the condition as (I), R:S=1:5 (mol/L) ratio, 37 °C, 120 min; (III) the condition as (I), U1Rz803 was incubated with target RNA at different temperatures and at different times. 1 μ L loading buffer (0.25 % Bromophenol Blue, 0.25 % Xylene cyanol FF, 20 mmol/L EDTA and saturated Urea) was added to stop the reaction. The result could be analyzed after running a 6 % denaturing polyacrylamide gel electrophoresis. The cleavage efficiency [CE] was calculated from Bq values of the bands of substrate (S) and products (P) which were cut off from denaturing PAGE. $CE=[P/(P+S)] \cdot 100\%$.

Kinetics studies of the reaction The procedure was described by Uhlenbeck^[52]. The Michaelis constant (K_m) and K_{cat} were determined for the ribozyme by performing multiple turnover kinetics experiments. The volume of kinetics reaction is 15 μ L. Ribozyme concentration was held constant at 5 nmol/L and substrate concentrations ranged from 10 nmol/l to 160 nmol/L. The cleavage reaction was done in the same buffer as described above at 37 °C for 20 minutes. The results were analyzed as above. K_m and K_{cat} were calculated by Lineweaver-Burke method (double- reciprocal plot).

RESULTS

Identification of transcription of target RNA and ribozyme

The length of target RNA transcribed from PCR-amplified template should be 220 nt. In this study the ribozymes were embedded into U1 snRNA, but stem-loop structures of U1 snRNA were maintained. Therefore, the transcripts of PCR-amplified template included U1 snRNA and ribozyme, the transcripts of U1snRNA chimeric ribozyme should be 205 nt. These results (Figure 2) were inconsistent with our design and proven to be correct.

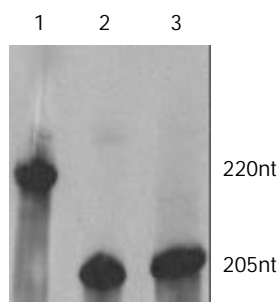


Figure 2 *In vitro* transcripts of target RNA and U1snRNA chimeric ribozymes. 1: transcript of target RNA (220 nt), 2: transcripts of U1Rz803(205 nt), 3: transcripts of U1Rz803_m (205 nt).

In vitro cleavage reaction of U1Rz803 and U1Rz803_m

The cleavage result showed that U1Rz803 was capable of cleaving target RNA *in vitro*. It could cleave target RNA (220 nt) efficiently and exactly to produce two fragments 93 nt/127 nt. while U1Rz803_m showed no *in vitro* cleavage efficacy after 120 min (Figure 3), even at R:S=5:1 (data not shown). At a 1:1 U1Rz803-to-S molar ratio, the cleavage efficiency (CE) was calculated under the condition of 37 °C and 120-minute reaction time, CE=51.36 %. At a 1:5 U1Rz803-to-S molar ratio, CE=27.81 %. This result indicated that the cleavage efficiency increased with increase of ribozyme concentration. The temperature and time would affect the cleavage efficiency.

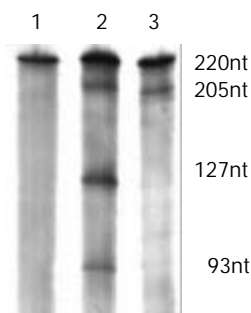


Figure 3 Cleavage of U1Rz803 and U1Rz803_m *in vitro*. 1: Target RNA, 2: target RNA incubated with U1Rz803, 3: target RNA incubated with U1Rz803_m. The ribozymes (205 nt) were shown in this figure because the transcripts were incorporated into alpha ³²P-UTP in the preparation of ribozymes.

Cleavage activity of U1Rz803 *in vitro*

Temperature course When the ratio of U1Rz803 to target RNA was 1:1(molar ratio), the reaction mixture were incubated at different temperature for 90 minutes. The optimal temperature was 50 °C, the cleavage efficacy increased at higher temperatures ranging from 0 °C to 50 °C, but when the temperature was above 50 °C, the cleavage efficacy decreased because the combination of ribozyme and target RNA was weakened (Figure 4).

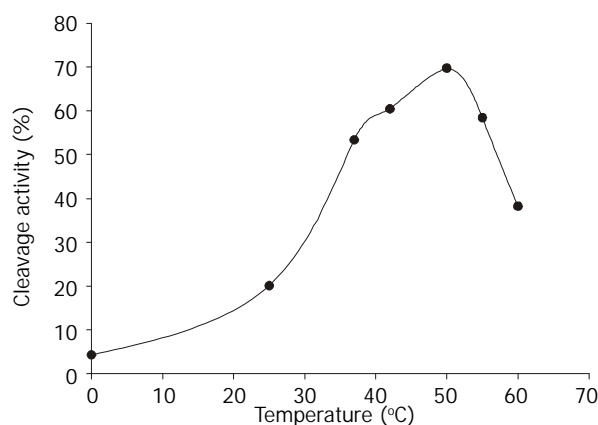


Figure 4 Temperature curve of the cleavage reactions of U1Rz803 prepared *in vitro*.

Time course The cleavage mixture (Rz:substrate=1:5 mol·L⁻¹) were incubated at 37 °C for different times, it was shown that the reaction product increased with increase in incubation time and it was linear within 60 min, CE_{max}=27.81% (Figure 5).

The kinetics of cleavage reaction Under the condition of 37 °C and 20-minute reaction time the cleavage efficiency was calculated at R:S=1:2, 1:4, 1:8, 1:16 and 1:32 (mol/L)ratio. K_m and K_{cat} were obtained by the Lineweaver-Burke method (Figure 6) $K_m=34.48$ nmol/L, $K_{cat}=0.14$ min⁻¹.

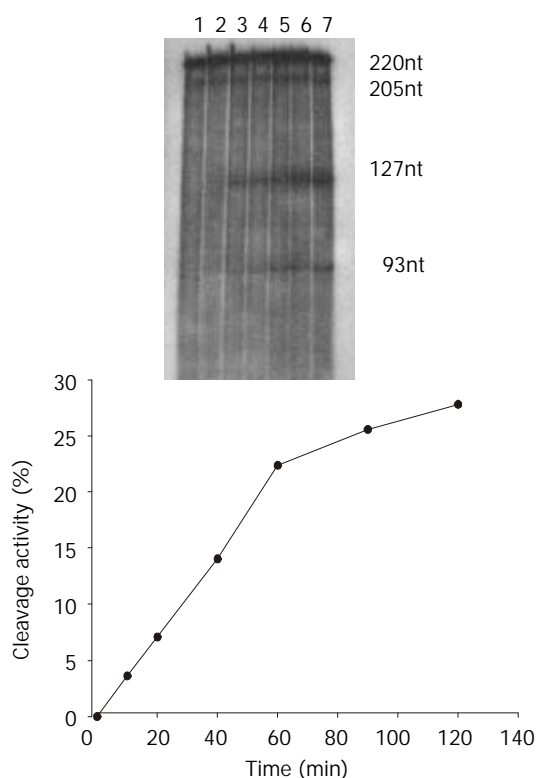


Figure 5 Time course. (A) Specific cleavage of target RNA by U1Rz803 *in vitro* at 37 °C for different times. Lane 1: substrate control; lane 2 : incubated for 10 min; lane 3: 20 min; lane 4: 40 min; lane 5: 60 min; lane 6: 90 min; lane 7: 120 min. (B) Time course of cleavage reactions of U1Rz803 prepared *in vitro*.

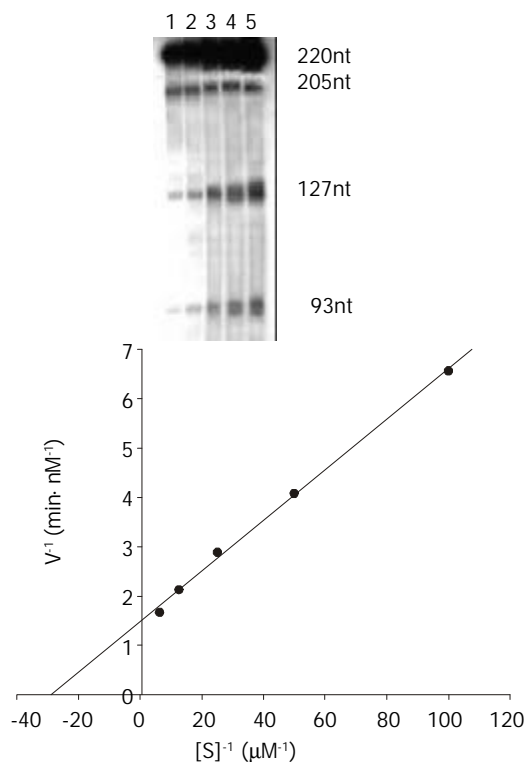


Figure 6 The kinetic of cleavage reaction for U1Rz803. (A) Specific cleavage of target RNA by U1Rz803 for the kinetic of U1Rz803 *in vitro*. U1Rz803 concentration was 5 nmol·L⁻¹, substrate concentration was 10, 20, 40, 80, 160 nmol·L⁻¹ from left to right. (B) Lineweaver-Burk kinetic plots of cleavage reaction for U1Rz803 *in vitro*. U1Rz803 concentration was 5 nmol·L⁻¹, substrate concentration was 160, 80, 40, 20, 10 nmol·L⁻¹ for each dot from left to right. Reactions were performed at 37 °C for 20 minutes.

DISCUSSION

Hepatic fibrosis is a common response to chronic liver injury from many causes, including alcohol, persistent viral infection and hereditary metal overload. To date, reversing the causative agent is the only effective therapy to stop or even reverse the liver fibrosis, but the efficacy is limited. Therefore, the development of effective antifibrotic therapies represents a challenge for modern hepatology. With the knowledge on molecular mechanism underlying pathological fibrosis expanding, there are many antifibrotic therapies based on sound biological mechanisms have been carried out. Ueki *et al* injected a mix of a haemagglutinating virus of Japan (HVJ) liposomes and a plasmid containing the complementary DNA for human hepatocyte growth factor (HGF) into the gluteus muscle of rats treated with dimethylnitrosamine (DMN), a model of persistent liver fibrosis, that could produce the resolution of fibrosis in the cirrhotic liver^[32], but tumorigenicity found in transgenic mice overexpressing HGF^[53] and repetitive *in vivo* transfection are two disadvantages. Qi and Nakamura *et al* prevent liver fibrosis from blockade of TGF beta signal by adenovirus-mediated local expression of a dominant negative type II TGF-beta receptor in the liver of rats treated with DMN, this intervention not only suppressed fibrosis, but also facilitated hepatocyte regeneration, however prolonged period of blocking TGF beta signal could result in unfavorable consequences, such as the inflammation and tissue necrosis^[30,33]. Because TGF β 1 plays a crucial role in liver fibrosis and no report on anti-TGF β 1 ribozyme-mediated cleavage of target RNA for the treatment of liver fibrosis has been published, in this study we designed ribozyme targeting against TGF β 1 and cloned the ribozyme genes into U1 ribozyme vector, prepared U1 snRNA chimeric ribozymes and identified the cleavage activity of ribozymes *in vitro*.

In the previous study on cleavage activity of U1 snRNA chimeric ribozyme *in vitro*, ribozymes were prepared through the transcription of synthesized ribozyme genes containing T7/SP6 promoter, the transcripts only included ribozyme^[43]; but ribozyme structure induced by the secondary structure of long flanking sequences would affect ribozyme's turnover ratio and/or binding activity as the results of less accurate hybridization and less cleavage. In this study we prepared ribozyme by the PCR-amplified templates. The transcripts included U1 snRNA and ribozyme. Compared with the previous study, it may reflect the cleavage activity of U1Rz803 more accurately *in vivo*. From our study, we found that the cleavage activity of U1sn RNA chimeric ribozyme was inferior to that of non-modified ribozyme, the result was not shown in this paper. Trimethylguanosine 5' cap, stable stem-loop structures at both end, high GC content of 3' loop in the structure of U1 snRNA confer resistance to exonucleases *in vivo*^[54]. The hypermethylation of the 5' cap structure and Sm binding site enable U1 snRNA to accumulate in the nucleoplasm, these make U1 snRNA an effective vector for efficient expression and delivery of ribozyme in the nuclear compartment *in vivo*. The transcripts of ribozyme labeled by isotope not only provided convenience for us to isolate ribozyme by cutting off autoradiograph bands, but the transcripts were qualified more accurately than non-labeled transcripts of ribozymes. In this study K_m and K_{cat} of U1Rz803 were measured at 37 °C, not at optimal temperature. Because the ribozyme is used *in vivo* and the temperature *in vivo* is constant at 37 °C, these results may reflect cleavage activity of U1Rz803 in physiological condition.

Ribozymes have all the properties of antisense RNA with the additional feature of catalytic cleavage. To separate antisense from cleavage effect, we created inactive ribozymes by substituting an essential nucleotide of the catalytic core with

an inactive one. The cleavage reaction revealed that U1Rz803 possessed the perfect cleavage activity, while U1Rz803_m possessed no catalytic activity. It can be used as control to exclude antisense effect of ribozyme *in vivo* in order that it is proven that the activity of U1Rz803 is due to catalytic cleavage *in vivo*. The kinetics of U1Rz803 showed that U1Rz803 possessed perfect specific ability of cleaving the TGFβ1 transcripts *in vitro*. These results made U1Rz803 to be worthy of being studied in intact cell and be developed as a nucleic acid drug in the future. However the *in vitro* result cannot completely reflect *in vivo* performance. The secondary and tertiary structure formed by the total TGF beta 1 mRNA transcript in the cell, the subcellular compartment which the ribozyme and target are located in, degradation of ribozyme, the complexes which are formed by ribozyme and ribonucleoprotein within cell and gene delivery system affect expression of ribozyme and cleavage activity of ribozyme. So *in vivo* effect of the ribozyme should be investigated as soon as possible. Experimental analysis of activity of the anti-TGF beta1 ribozyme in HSC-T6 cell is in progress.

ACKNOWLEDGEMENTS

We thanks Mr. F Xu, Mr. G Jiang, Mr. XL Chen, Mr. J Jia, Mr. ZW Wang and Miss W Li for their kind help.

REFERENCES

- Zhu YH**, Hu DR, Nie QH, Liu GD, Tan ZX. Study on activation and c-fos, c-jun expression of *in vitro* cultured human hepatic stellate cells. *Shijie Huaren Xiaohua Zazhi* 2000; **8**: 299-302
- Du WD**, Zhang YE, Zhai WR, Zhou XM. Dynamic changes of type I, III and IV collagen synthesis and distribution of collagen-producing cells in carbon tetrachloride-induced rat liver fibrosis. *World J Gastroenterol* 1999; **5**: 397-403
- Huang ZG**, Zhai WR, Zhang YE, Zhang XR. Study of heteroserum-induced rat liver fibrosis model and its mechanism. *World J Gastroenterol* 1998; **4**: 206-209
- Jia JB**, Han DW, Xu RL, Gao F, Zhao LF, Zhao YC, Yan JP, Ma XH. Effect of endotoxin on fibronectin synthesis of rat primary cultured hepatocytes. *World J Gastroenterol* 1998; **4**: 329-331
- Cheng ML**, Wu YY, Huang KF, Luo TY, Ding YS, Lu YY, Liu RC, Wu J. Clinical study on the treatment of liver fibrosis due to hepatitis B by IFN-α1 and traditional medicine preparation. *World J Gastroenterol* 1999; **5**: 267-269
- Nie QH**, Cheng YQ, Xie YM, Zhou YX, Cao YZ. Inhibiting effect of antisense oligonucleotides phosphorothioate on gene expression of TIMP-1 in rat liver fibrosis. *World J Gastroenterol* 2001; **7**: 363-369
- Friedman SL**. The cellular basis of hepatic fibrosis: mechanism and treatment strategies. *N Engl J Med* 1993; **328**: 1828-1835
- Wang X**, Chen YX, Xu CF, Zhao GN, Huang YX, Wang QL. Relationship between tumor necrosis factor-α and liver fibrosis. *Huaren Xiaohua Zazhi* 1998; **6**: 106-108
- Xu LX**, Xie XC, Jin R, Ji ZH, Wu ZZ, Wang ZS. Effect of selenium in rat experimental liver fibrosis. *Huaren Xiaohua Zazhi* 1998; **6**: 133-135
- Li DG**, Lu HM, Chen YW. Studies on anti-liver fibrosis of tetradrine. *Shijie Huaren Xiaohua Zazhi* 1999; **7**: 171-172
- Wu YA**, Kong XT. Anti-hepatic fibrosis effect of pentoxifylling. *Shijie Huaren Xiaohua Zazhi* 1999; **7**: 265-266
- Liu F**, Liu JX, Cao ZC, Li BS, Zhao CY, Kong L, Zhen Z. Relationship between TGF-β1, serum indexes of liver fibrosis and hepatic-tissue pathology in patients with chronic liver diseases. *Shijie Huaren Xiaohua Zazhi* 1999; **7**: 519-521
- Gu SW**, Luo KX, Zhang L, Wu AH, He HT, Weng JY. Relationship between ductular proliferation and liver fibrosis of chronic liver disease. *Shijie Huaren Xiaohua Zazhi* 1999; **7**: 845-847
- Li BS**, Wang J, Zhen YJ, Liu JX, Wei MX, Sun SQ, Wang SQ. Experimental study on serum fibrosis markers and liver tissue pathology and hepatic fibrosis in immuno damaged rats. *Shijie Huaren Xiaohua Zazhi* 1999; **7**: 1031-1034
- Wang Y**, Gao Y, Huang YQ, Yu JL, Fang SG. Gelatinase a proenzyme expression in the process of experimental liver fibrosis. *Shijie Huaren Xiaohua Zazhi* 2000; **8**: 165-167
- Wang FS**, Wu ZZ. Current situation in studies of gene therapy for liver cirrhosis and liver fibrosis. *Shijie Huaren Xiaohua Zazhi* 2000; **8**: 371-373
- Wang GQ**, Kong XT. Action of cell factor and decorin in tissue fibrosis. *Shijie Huaren Xiaohua Zazhi* 2000; **8**: 458-460
- Liu F**, Wang XM, Liu JX, Wei MX. Relationship between serum TGF-β1 of chronic hepatitis B and hepatic tissue pathology and hepatic fibrosis quantification. *Shijie Huaren Xiaohua Zazhi* 2000; **8**: 528-531
- Li JC**, Ding SP, Xu J. Regulating effect of Chinese herbal medicine on the peritoneal lymphatic stomata in enhancing ascites absorption of experimental hepatofibrotic mice. *World J Gastroenterol* 2002; **8**: 333-337
- Olaso E**, Friedman SL. Molecular regulation of hepatic fibrogenesis. *J Hepatol* 1998; **29**: 836-842
- Pinari M**, Marra F, Carloni V. Signal transduction in hepatic stellate cells. *Liver* 1998; **18**: 2-13
- Alcolado R**, Arthur MIP, Iredale JP. Pathogenesis of liver fibrosis. *Clin Sci* 1997; **92**: 103-112
- Massague J**. The transforming growth factor-beta family. *Annu Rev Cell Biol* 1990; **6**: 597-641
- Sporn MB**, Robert AB. Transforming growth factor-beta: recent progress and new challenges. *J Cell Biol* 1992; **119**: 1017-1021
- Border WA**, Noble NA. Transforming growth factor-beta in tissue fibrosis. *N Engl J Med* 1994; **331**: 1286-1292
- Heldin CH**, Miyazono K, ten Dijke P. TGF-beta signaling from cell membrane to nucleus through SMAD proteins. *Nature* 1997; **390**: 465-471
- Miyazono K**. TGF-beta receptors and signal transduction. *Int J Hematol* 1997; **65**: 97-104
- Friedman SL**. Molecular regulation of hepatic fibrosis, an integrated cellular response to tissue injury. *J Biol Chem* 2000; **275**: 2247-2250
- Bissell DM**, Roulot D, George J. Transforming Growth factor and liver. *Hepatology* 2001; **34**: 859-867
- Qi Z**, Atsuchi N, Ooshima A, Takeshita A, Ueno H. Blockade of type beta transforming growth factor signaling preventing liver fibrosis and dysfunction in the rat. *Proc Natl Acad Sci* 1999; **96**: 2345-2349
- Sanderson N**, Factor V, Nagy P, Kopp J, Kondaiah P, Wakefield L, Roberts AB, Sporn MB, Thorgeirsson SS. Hepatic expression of mature transforming growth factor beta 1 in transgenic mice results in multiple tissue lesions. *Proc Natl Acad Sci* 1995; **92**: 2572-2576
- Ueki T**, Kaneda Y, Tsutsui H, Nakanishi K, Sawa Y, Morishita R, Matsumoto K, Nakamura T, Takahashi H, Okamoto E, Fujimoto J. Hepatocyte growth factor gene therapy of liver cirrhosis in rats. *Nat Med* 1999; **5**: 226-230
- Nakamura T**, Sakata R, Ueno T, Sata M, Ueno H. Inhibition of transforming growth factor beta prevents progression of liver fibrosis and enhances hepatocyte regeneration in dimethylnitrosamine-treated rats. *Hepatology* 2000; **32**: 247-255
- Ueno H**, Sakamoto T, Nakamura T, Qi Z, Atsuchi N, Takeshita A, Shimizu K, Ohashi H. A soluble transforming growth factor beta receptor expressed in muscle prevents liver fibrogenesis and dysfunction in rats. *Hum Gene Ther* 2000; **11**: 33-42
- Persidis A**. Ribozyme therapeutics. *Nat Biotechnol* 1997; **15**: 921-922
- Gibson SA**, Shillito EJ. Ribozymes. Their functions and strategies for their use. *Mol Biotechnol* 1997; **7**: 125-137
- James HA**, Gibson I. The therapeutic potential of ribozymes. *Blood* 1998; **91**: 371-382
- Muotri AR**, da Veiga Pereira L, dos Reis Vasques L, Menck CF. Ribozymes and the anti-gene therapy: how a catalytic RNA can be used to inhibit gene function. *Gene* 1999; **237**: 303-310
- von Weizsacker F**, Blum HE, Wands JR. Cleavage of hepatitis B virus RNA by three ribozymes transcribed from a single DNA template. *Biochem Biophys Res Commun* 1992; **189**: 743-748
- Beck J**, Nassal M. Efficient hammerhead ribozyme-mediated cleavage of the structured hepatitis B virus encapsidation signal *in vitro* and in cell extracts, but not in intact cells. *Nucleic Acids Res* 1995; **23**: 4954-4962

- 41 **Xu RH**, Liu J, Zhou XQ, Xie Q, Jin YX, Yu H, Liao D. Activity identification of anti-caspase-3 mRNA hammerhead ribozyme in both cell-free condition and BRL-3A cells. *Chin Med J* 2001; **114**: 606-611
- 42 **Xu RH**, Liu J, Xu F, Jiang G, Xie Q, Zhou XQ, Jin YX, Wang DB. Activity identification of chimeric anti-caspase-3 mRNA hammerhead ribozyme *in vitro* and *in vivo*. *Science China(C)* 2001; **44**: 618-627
- 43 **Liu R**, Li W, Karin NJ, Bergh JJ, Adler-Storthz K, Farach-Carson MC. Ribozyme ablation demonstrates that the cardiac subtype of the voltage-sensitive calcium channel is the molecular transducer of 1, 25-dihydroxyvitamin D(3)-stimulated calcium influx in osteoblastic cells. *J Biol Chem* 2000; **275**: 8711-8718
- 44 **Montgomery RA**, Dietz HC. Inhibition of fibrillin 1 expression using U1 snRNA as a vehicle for the presentation of antisense targeting sequence. *Hum Mol Genet* 1997; **6**: 519-525
- 45 **Michienzi A**, Prislei S, Bozzoni I. U1 small nuclear RNA chimeric ribozymes with substrate specificity for the Rev pre-mRNA of human immunodeficiency virus. *Proc Natl Acad Sci* 1996; **93**: 7219-7224
- 46 **Vogel S**, Piantedosi R, Frank J, Lalazar A, Rockey DC, Friedman SL, Blaner WS. An immortalized rat liver stellate cell line (HSC-T6): a new cell model for the study of retinoid metabolism *in vitro*. *J Lipid Res* 2000; **41**: 882-893
- 47 **Kim Y**, Ratziu V, Choi SG, Lalazar A, Theiss G, Dang Q, Kim SJ, Friedman SL. Transcriptional activation of transforming growth factor beta1 and its receptors by the Kruppel-like factor Zf9/core promoter-binding protein and Sp1. Potential mechanisms for autocrine fibrogenesis in response to injury. *J Biol Chem* 1998; **273**: 33750-33758
- 48 **Qian SW**, Kondaiah P, Roberts AB, Sporn MB. cDNA cloning by PCR of rat transforming growth factor beta-1. *Nucleic Acids Res* 1990; **18**: 3059
- 49 **Manser T**, Gesteland RF. Characterization of small nuclear RNA U1 gene candidates and pseudogenes from the human genome. *J Mol Appl Genet* 1981; **1**: 117-125
- 50 **Zhuang Y**, Weiner AM. A compensatory base change in U1 snRNA suppresses a 5' splice site mutation. *Cell* 1986; **46**: 827-835
- 51 **Skuzeski JM**, Lund E, Murphy JT, Steinberg TH, Burgess RR, Dahlberg JE. Synthesis of human U1 RNA. II. Identification of two regions of the promoter essential for transcription initiation at position +1. *J Biol Chem* 1984; **259**: 8345-8352
- 52 **Uhlenbeck OC**. A small catalytic oligoribonucleotide. *Nature* 1987; **328**: 596-600
- 53 **Takayama H**, LaRochelle WJ, Sharp R, Otsuka T, Kriebel P, Anver M, Aaronson SA, Merlino G. Diverse tumorigenesis associated with aberrant development in mice overexpressing hepatocyte growth factor/scatter factor. *Proc Natl Acad Sci* 1997; **94**: 701-706
- 54 **Green MR**. Biochemical mechanisms of constitutive and regulated pre-mRNA splicing. *Annu Rev Cell Biol* 1991; **7**: 559-599

Edited by Wu XN

Analysis of spontaneous, gamma ray- and ethylnitrosourea-induced hprt mutants in HL-60 cells with multiplex PCR

Sheng-Xue Liu, Jia Cao, Hui An, Hua-Min Shun, Lu-Jun Yang, Yong Liu

Sheng-Xue Liu, Jia Cao, Hui An, Hua-Min Shun, Lu-Jun Yang, Yong Liu, Department of Health Toxicology, Preventive Medical College, Third Military Medical University, Chongqing 400038, China
Supported by the National Natural Science Foundation of China, No.39970650

Correspondence to: Dr. Jia Cao, Preventive Medical College, Third Military Medical University, Chongqing 400038, China. caoqq@yahoo.com

Telephone: +86-23-68752271 **Fax:** +86-23-68752277

Received: 2002-10-09 **Accepted:** 2002-11-09

Abstract

AIM: To explore the molecular spectra and mechanism of human hypoxanthine guanine phosphoribosyl transferase (hprt) gene mutation induced by ethylnitrosourea (ENU) and ^{60}Co γ -rays.

METHODS: Independent human promyelocytic leukemia cells (HL-60) mutants at the hprt locus were isolated from untreated, ethylnitrosourea (ENU) and ^{60}Co γ -ray-exposed cells, respectively, and verified by two-way screening. The genetic changes underlying the mutation were determined by multiplex polymerase chain reaction (PCR) amplification and electrophoresis technique.

RESULTS: With dosage increased, survival rate of plated cell reduced (in the group with dosage of ENU with 100-200 $\mu\text{g}/\text{ml}$, $P < 0.01$; in the group with dosage of ^{60}Co γ -ray with 2-4 Gy, $P < 0.05$) and mutational frequency increased (in the group of ENU 12.5-200.0 $\mu\text{g}/\text{ml}$, $P < 0.05$; in the group of ^{60}Co γ -ray with 1-4 Gy, $P < 0.05$) significantly. In the 13 spontaneous mutants analyzed, 92.3 % of mutant clones did not show any change in number or size of exon, a single exon was lost in 7.7 %, and no evidence indicated total gene deletion occurred in nine hprt exons. However, deletions were found in 79.7 % of ENU-induced mutations (62.5-89.4 %, $P < 0.01$) and in 61.7 % of gamma-ray-induced mutations (28.6-76.5 %, $P < 0.01$). There were deletion mutations in all 9 exons of hprt gene and the most of induced mutations were chain deletion with multiplex exons (97.9 % in gamma-ray-induced mutants, 88.1 % in ENU-induced mutants).

CONCLUSION: The spectra of spontaneous mutations differs completely from that induced by EUN or ^{60}Co γ -ray. Although both ENU and γ -ray can cause destruction of genetic structure, mechanism of mutagenesis between them may be different.

Liu SX, Cao J, An H, Shun HM, Yang LJ, Liu Y. Analysis of spontaneous, gamma ray- and ethylnitrosourea-induced hprt mutants in HL-60 cells with multiplex PCR. *World J Gastroenterol* 2003; 9(3): 578-583

<http://www.wjgnet.com/1007-9327/9/578.htm>

INTRODUCTION

Many developments in molecular biology, especially,

polymerase chain reaction (PCR) have made procedure of mutation analysis relatively simple^[1,2]. Classically, Southern hybridization was the primary method for the molecular analysis of deletion mutations. However, southern analysis not only is time-consuming but also provides incomplete results due to the limited resolution of each exon and possible cross-hybridization with pseudogenes. Therefore, using PCR to amplify each individual exon of the hprt gene provides a powerful alternative method to southern analysis^[3]. PCR has been used for the analysis of various mutations in human and Chinese hamster cells. These and other studies of the hprt locus in various mammalian cells have shown a wide spectrum of structural aberrations in the hprt gene, which are induced by physical and chemical mutagens^[4-7]. Ionizing radiation induces deletion mutations and results in genetic alterations, which can be detected by Southern analysis^[8]. Such detectable genetic alterations have been found infrequently after exposure to ultraviolet (UV) light, ethyl methane sulfonate (EMS), ICR-191 and N-ethyl-N-nitrosourea (ENU)^[9-11]. Thus, while conventional missense mutagens induce predominantly point mutations, ionizing radiation induces both point and deletion mutations.

As a part of our ongoing effort to analyze the nature and spectrum of mutations induced by various types of physical and chemical mutagens, we adopted the multiplex PCR technique for the initial screening of deletion mutants. In this paper, we have characterized the molecular nature of mutations induced by γ -ray and ENU at the hprt locus of human promyelocytic leukemia cells.

MATERIALS AND METHODS

Cell culture

HL-60 is a human acute promyelocytic leukemia cell line described earlier by Collins *et al.* HL-60 cells were maintained as an asynchronous, exponentially growing population in RPMI 1640 medium (Sigma, St. Louis, USA) supplemented with 10 % fetal bovine serum (SJK, Hangzhou, China), 100 U/ml penicillin (Sigma), 100 $\mu\text{g}/\text{ml}$ streptomycin (Sigma), and 2 mM L-glutamine (Gibco, Carlsbad, USA) at 37 °C in an atmosphere of 5 % CO_2 . Preexisting hprt mutants that cannot live in thymidine (Sigma; HAT culture medium) were removed by incubating cells in complete medium supplemented with 10^{-6} M aminopterin (Gibco), 10^{-4} M hypoxanthine (Sigma) and 10^{-5} M HAT culture medium for 24 hours, then the medium was replaced with complete medium containing 10^{-5} M thymidine and 10^{-4} M hypoxanthine and cultured for 48 hours. Following removal this medium, the cells were incubated in normal medium for 7-10 days.

Cytotoxicity

For measuring the cytotoxicity of γ -ray and ENU (Tokyo, Japan), exponentially growing HL-60 cells were treated with different doses of γ -ray and ENU. Initial cell number inoculated was 5.0×10^6 . Sterile distilled water was used as negative control. After incubation, the cells were harvested and washed twice with D-Hank's medium at 37 °C, counted and diluted in normal culture medium and transferred to 96 microwell plates (Gibco),

one single cell was inoculated in 200 μ l medium per well. After incubating for 7 days, colonies per well were counted and the plating efficiency (PE) was calculated with equation:

$$PE = \frac{-\ln(\text{Number of negative well/Number of all wells})}{\text{Number of cells per well}}$$

Mutation experiments

After expression of gene mutations (8 days) HL-60 cells were added in the 96-well microtiter plates to ensure one cell was inoculated per well. After incubating for 7 days, wells with colony formation were counted as positive wells for cloning efficiency (CE). Meanwhile, cells were added in other 96 microwell plates to ensure that each well received 1×10^4 cells in 200 μ l medium containing 1 μ g/ml 6-thioguanine (6-TG; Sigma). After incubating for 8 days, positive wells were counted and mutant frequency (MF) was calculated. Three plates were used for CE and MF in each treatment.

$$MF = \frac{-\ln(\text{Number of negative wells/Number of all wells})}{\text{Number of cells per well} \times CE}$$

Screening, extension and DNA isolation

A single positive clone was transferred from the 96-well plate to a 24-microwell plate (Gibco) with 1 ml screening medium containing 2 μ g/ml 6-TG in each well and cultured for additional 1-2 days. Then, 10^3 cells was transferred to each well in a new 24-microwell plate in HAT culture medium and cultured for 1-3 days. If the cells in a well were obviously dead, the cloned cells of the well were identified as mutated clones and the remaining cloned cells in the 24-microwell were transferred into culture bottles for extension expression. DNA isolation and purification from wild-type cells and hprt-mutated cells was performed with conventional method.

Design, synthesis and appraisal of primers

Eight pairs of oligonucleotide primers were designed by computer software with a minor modification of the literature^[12]. The synthesis and appraisal of the 8 pairs of primers were completed by different laboratories of Beckman Company in Beijing, Cybersyn B. J. in American and the Institute of Cellular Biology of Chinese Academy of Science in Shanghai.

Sequence of 8 pairs of oligonucleotide primers was showed in Table 1. Exons 7 and 8 were amplified simultaneously with same primers, because they are only 163 bp apart. All primers except the exon 1 specific ones enabled amplification of the corresponding exons in the multiplex PCR. It was, however, difficult to include exon 1 primers within the remaining set of all primers without having a spurious synthesis of non-specific signal. In our pre-experiments with several primer pairs in one PCR reaction it was difficult to control and optimize the reaction conditions. In addition, insertions and deletions within exons could occur, therefore we restricted the number of primer pairs in a single PCR reaction in order to confirm the distances among of PCR products based on molecular weights. So, false-negative or false-positive rate was reduced. Following some preliminary experiments, 8 pairs of primers of exons were divided into 3 groups, group one was multiplex PCR including exons 2, 5, 6 and 7/8, group two included exons 3, 4, and 9; in group three, exon 1 was amplified separately. Multiplex PCR method was used to analyze 119 mutants.

PCR analysis

For amplification of hprt exons, 0.5-2.0 μ l of genomic DNA (36-50 ng) was mixed with 50 pmol of each primer in 50 μ l containing 50 mM KCl, 10 mM Tris-HCl (pH8.8), 0.3-1.05

mM MgCl₂, 0.2 mM dNTPs and 2.5 U of Amplitaq DNA polymerase (Shenggong, Shanghai, China). After initial denaturation of the template DNA at 98 $^{\circ}$ C for 7 min, a total of 40 PCR cycles were performed with denaturation at 94 $^{\circ}$ C for 1.5 min, annealing at 52 $^{\circ}$ C for 1.5 min and extension at 72 $^{\circ}$ C for 2.0 min. Exon 1 was synthesized individually with a modified condition: a total of 30 PCR cycles were performed with denaturation at 95 $^{\circ}$ C for 0.5 min, annealing at 64 $^{\circ}$ C for 1.0 min and extension at 72 $^{\circ}$ C for 1 min. The last cycle was extension at 72 $^{\circ}$ C for 7 min. The PCR product (10 μ l) was used for analysis by 3 % agarose gel or by using polyacrylamide gel electrophoresis (Figure 1).

Table 1 Oligonucleotide primers in multiplex PCR of the human HPRT locus

Exons	Primers sequence (5' -3')	Fragment size (bp)
1	F TGG GAC GTC TGG TCC AAG GAT TCA R CCG AAC CCG GGA AAC TGG CCG CCC	626
2	F CCT GAT ATG CTC TCA TTG AAA CA R GCT GCT GAT GTT TGA AAT TAA CAC	211
3	F GTT TAA TGA CTA AGA GGT GTT TG R GAA AAC CTA GTG TTG CCA CAT AA	311
4	F GTG TGT GTA CAT AAG GAT ATA CA R TTC TTC CCT TTC AAG ATA CAT AC	165
5	F GGA AAT ACC GTT TTA TTC ATT GT R GTG CAT ACT AAG TTA GAA AGG TC	125
6	F GTG ACT CTG AAT TTA AAG CTA TG R CTG TGT CAA AAT GTC ATA CAT AC	150
7/8	F GTC TCT CTG TAT GTT ATA TGT CAC R TGC GTG TTT TGA AAA ATG AGT GAG	379
9	F GCT ATT CTT GCC TTT CAT TTC AG R CAA ACT CAA CTT GAA CTC TCA TC	136

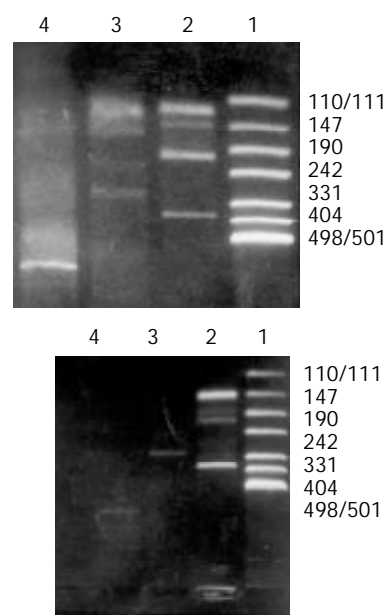


Figure 1 Detection of deletion mutation in human hprt gene by multiplex PCR. (A) PCR products from normal cells; (B) PCR products from one hprt mutant. (1) PUC Mix Marker; (2) Exons 2,5,6,7/8; (3) Exons 3,4,9; (4) Exon 1.

Statistics

All data were analyzed by student's *t* test and total rate test. The statistical difference $P < 0.05$ was considered as significant and $P < 0.01$ as very significant.

RESULTS

Cytotoxicity and mutagenicity of γ -rays and ENU

The HL-60 cells plating efficiency (PE) gradually decreased with increasing concentrations of ENU. There was a significant difference from the control of PE at concentrations above 100.0 $\mu\text{g/ml}$ of ENU. A linear increase of the mutation frequency (MF) with increasing concentration of ENU was found. At 12.5-200.0 $\mu\text{g/ml}$ ENU, MF was 3.5-20.8 times higher than that in the control cultures. The cytotoxicity and mutagenicity of γ -rays were similar to ones of ENU. The HL-60 cells PE gradually decreased with increasing doses of γ -rays. There was a significant difference of PE at doses above 2.0 Gy of γ -rays in comparison with the control. A linear increase of the MF with increasing doses of γ -rays was found. At 1.0-4.0 Gy γ -rays, MF was 3.6-14.2 times higher than that in the control cultures (Table 2).

Table 2 Cytotoxicity and mutagenicity of γ -rays and ENU in HL-60 cells

Type	Dose	PE(%)	CE(%)	MF($\times 10^{-6}$)
Control ($\mu\text{g/ml}$)	0.0	93.01	86.64	5.13
ENU ($\mu\text{g/ml}$)	12.5	75.92	85.91	17.73 ^a
	25.0	70.67	78.62	31.18 ^b
	50.0	61.45	82.67	64.45 ^b
	100.0	45.77 ^b	83.91	82.61 ^b
	200.0	25.63 ^b	67.02	106.70 ^b
γ -ray (Gy)	0.5	91.63	146.0 ^b	12.30
	1.0	69.31	186.0 ^b	18.30 ^b
	2.0	55.34 ^a	108.2	23.20 ^a
	4.0	39.94 ^b	69.0	73.00 ^b

^a $P < 0.05$ vs control group, ^b $P < 0.01$ vs control group.

Multiplex PCR analysis

Analysis of multiplex PCR was done in 13 spontaneous mutants, 59 ENU-induced and 47 γ -rays-induced *hprt* mutants. Forty-two mutants (35.3 %) of 119 mutants analyzed were found to exhibit no abnormal band in any of the 9 exons, which indicated that these mutants had point mutation without exon deletion or insertion. In 47 of 119 mutants, less than 8 bands were existed for each locus, and showed partial deletions of exons. The remaining 30 mutants had no PCR products, which meant that all exons studied were deleted. Of all mutants analyzed, 64.7 % (77/119) had partial or complete deletions.

Molecular spectrum of *HPRT* gene

Spontaneously derived, γ -rays- and ENU-induced mutants at the *hprt* locus were showed in Table 3. The electrophoresis patterns of mutants mainly consisted of three types: "normal pattern" including point mutations, total deletion and partial deletion. γ -rays- (1.0-4.0 Gy) and ENU-induced (12.5-200.0 $\mu\text{g/ml}$) mutant cells showed mutation spectra that were significantly different from the spectra of spontaneous mutations. Total exon deletion did not exist in any spontaneous mutants but in γ -rays- and ENU-induced mutants. The proportions of deletion mutations were quite different between spontaneous mutants and induced mutants, and similar change of γ -rays- and ENU-induced mutants occurred at the *hprt* locus. Over 60 % deletion mutations were found in these two kind of induced mutants while only 7.7 % deletions were found in spontaneous mutants. The proportion of the "normal pattern" in spontaneous mutants and induced mutants were 92.3 % and less than 40 %, respectively. The clearer dose-response relationship was seen in induction of partial- and whole-deletion mutation than in induction of mutants including and kind of mutations.

Analysis of deletion breakpoints

Distribution of the deletions in the 9 exons of the *hprt* gene found in the 119 mutants analyzed (Table 4). Deletion mutations were found in all 9 exons of the *hprt* gene, but number of single exon deletion was very small. Most of γ -rays- (59.6 %) and ENU-induced (67.8 %) mutations were chain deletion with multiple exons.

Table 3 Summary of multiplex PCR analysis of THH-induced *HPRT* mutants in HL-60 cells

Categories of mutation	Number analyzed	Number showing PCR changes		Percentage deleted	Number showing no change
		Complete deletion	Partial deletion		
Spontaneous	13	0	1/13 (7.7%)	7.7%	12/13 (92.3%)
ENU ($\mu\text{g/ml}$)	12.5	1/8 (12.5%)	4/8 (50.0%) ^a	62.5% ^b	3/8 (37.5%) ^a
	25.0	2/10 (20.0%)	5/10 (50.0%) ^a	70.0% ^b	3/10 (30.0%) ^b
	50.0	2/10 (20.0%)	6/10 (60.0%) ^b	80.0% ^b	2/10 (20.0%) ^b
	100.0	4/12 (33.3%) ^a	6/12 (50.0%) ^a	83.3% ^b	2/12 (16.7%) ^b
	200.0	7/19 (36.8%) ^a	10/19 (52.6%) ^a	89.4% ^b	2/19 (10.6%) ^b
γ -rays (Gy)	0.5	1/7 (14.3%)	1/7 (14.3%)	28.6%	5/7 (71.4%)
	1.0	3/13 (23.1%)	5/13 (38.5%)	61.5% ^b	5/13 (38.5%) ^b
	2.0	3/10 (30.0%) ^a	3/10 (30.0%)	60.0% ^b	4/10 (40.0%) ^b
	4.0	7/17 (41.2%) ^b	6/17 (35.3%)	76.5% ^b	4/17 (23.5%) ^b

^a $P < 0.05$ vs control group, ^b $P < 0.01$ vs control group.

Table 4 Schematic diagram of the distribution of deletion within nine exons of the human HPRT gene

	Types of exons deletion									Mutation clones	
	1	2	3	4	5	6	7/8	9	Number	Percent (%)	
Spontaneous mutants									12	92.3	
					– ^a				1	7.7	
ENU-induced mutants									12	20.3	
	–								3	5.1	
			–						2	3.4	
				–	–				4	6.8	
					–				2	3.4	
			–					–	1	1.7	
	–	–	–						2	3.4	
		–	–	–					2	3.4	
				–	–	–	–		2	3.4	
						–	–	–	1	1.7	
	–	–	–	–	–	–	–	–	1	1.7	
				–	–	–	–	–	3	5.1	
		–	–	–	–	–	–	–	1	1.7	
	–	–	–	–	–	–	–	–	16	27.1	
				–	–			–	1	1.7	
	–				–	–	–		1	1.7	
		–			–				2	3.4	
			–			–	–		2	3.4	
					–	–			1	1.7	
r-rays-induced mutants									18	38.3	
			–						1	2.1	
	–	–							1	2.1	
			–	–					2	4.3	
	–	–	–						2	4.3	
						–	–	–	1	2.1	
	–	–	–	–					1	2.1	
					–	–	–	–	3	6.4	
	–	–	–	–	–	–	–	–	1	2.1	
				–	–	–	–	–	1	2.1	
		–	–	–	–	–	–	–	2	4.3	
	–	–	–	–	–	–	–	–	14	29.8	

^adeletion of a exon.

DISCUSSION

The X-linked HPRT gene is the most extensively examined mammalian locus for mutagenesis studies^[13-15]. The enzyme is part of the purine salvage pathway, catalyzing the reaction of 5-phosphoribosyl, 1-pyrophosphate with either hypoxanthine or guanine to form precursors that are recycled for use in DNA synthesis. As exploited in mutation analysis, this pathway leads to the killing of wild-type cells exposed to the toxic base analogue 6-TG^[16-18]. Toxicity and mutagenesis of γ -ray and ENU were characterized in HPRT locus forward mutation test, and found that reverse relationship between them was existed. γ -ray and ENU could serve a dual purpose to clone efficiency of HL-60 cell, which have association with dosages.

DNA hybridization used to be a main method in mutation analysis of HPRT gene, and recently PCR has been used in studies of gene mutation, and improved the precision of mutation analysis^[19-21]. HPRT gene mutations were studied with multiplex PCR method. As it was difficult to control and

optimize the reaction conditions in our preliminary study, insertions and deletions within exons could occur, the number of primer pairs in a single PCR reaction was restricted in order to confirm the distances among of PCR products according to their molecular weights, consequently false-negative or false-positive rate were reduced. Therefore, eight pairs of primers were divided into 3 groups: one multiplex PCR included exons 2, 5, 6 and 7/8, second one included exons 3, 4 and 9, and in third one, exon 1 was amplified separately.

ENU is a direct-acting alkylating agent that produces similar ratios of well-characterized ethyl adducts in DNA in solution, in prokaryotes, in cultured mammalian cells, and in various tissues of rats and mice *in vivo*^[22-24]. Several O-ethyl-adducts, including O⁶-ethylguanine, O⁴-ethylthymine, and O²-ethylthymine, have been shown to direct mispairing of bases during DNA replication *in vitro*^[25,26], and the results of site-directed mutations are consistent with the types of base substitutions observed in assays of ENU mutation specificity^[27].

Furthermore, ENU was used as the model agent for developing the *in vivo* hprt mutation assays in mouse, rat, and monkey and for defining the age-dependent relationships between chemical exposure, DNA adduction, and phenotypic expression of hprt mutations in T cells of exposed mice^[28,29].

Ionizing radiation may exert a carcinogenic stimulus, even at low levels of exposure. Such biological effects have been extensively studied. Observed mutation frequencies of γ -ray-induced mutation in HL-60 cells were similar to the results reported previously for X-irradiated human fibroblasts^[30-32]. Our results support the general observation that the majority of ionizing-radiation-induced mutations at the hprt locus are large deletions, about 60 % of mutants of γ -irradiated HL-60 cells exhibited large deletions (1.0-4.0 Gy). These results suggest that the size of genetic alteration appears to be dependent on doses. It is now thought that hprt gene mutations unlikely results from block of transcription and the initial damage leads to irreversible DNA loss.

No obvious differences among the absolute numbers of mutants in all 9 exons of hprt gene were found, meaning that there were no clear "hot spots". However, some reports showed the preferential localization of deletion breakpoints at or toward the 3' end of the hprt gene^[33-35]. Our results suggested that 9 exons of hprt gene are not well distributed, so the controversy might be due to different methods rather than results. As deletion breakpoints are mapped and sequenced more precisely, it may be helpful in clarifying the mechanisms of induced deletion.

REFERENCES

- Mognato M**, Ferraro P, Canova S, Sordi G, Russo A, Cherubini R, Celotti L. Analysis of mutational effects at the HPRT locus in human G(o) phase lymphocytes irradiated *in vitro* with r rays. *Mut Res* 2001; **474**: 147-158
- Schwartz JL**, Rotmensch J, Sun J, An J, Xu Z, Yu Y, Hsie AW. Multiplex polymerase chain reaction-based deletion analysis of spontaneous, gamma ray- and alpha-induced hprt mutants of CHO-K1 cells. *Mutagenesis* 1994; **9**: 537-540
- Park MS**, Hanks T, Jaberaboansari A, Chen DJ. Molecular analysis of gamma-ray-induced mutations at the hprt locus in primary human skin fibroblasts by multiplex polymerase chain reaction. *Rad Res* 1995; **141**: 11-18
- Ward JB**, Abdel-Rahman SZ, Henderson RF, Stock TH, Morandi M, Rosenblatt JJ, Ammenheuser MM. Assessment of butadiene exposure in synthetic rubber manufacturing workers in Texas using frequencies of hprt mutant lymphocytes as a biomarker. *Chemico-Biological Interactions* 2001; **135-136**: 465-483
- Jones IM**, Thomas CB, Haag K, Pleshonov P, Vorobstova I, Tureva L, Nelson DO. Total gene deletions and mutant frequency of the HPRT gene as indicators of radiation exposure in Chernobyl liquidators. *Mut Res* 1999; **431**: 233-246
- Mognato M**, Graziani M, Celotti L. Analysis of point mutations in HPRT mutant T-lymphocytes derived from coke-oven workers. *Mut Res* 1999; **431**: 271-278
- Dennog C**, Gedik C, Wood S, Speit G. Analysis of oxidative DNA damage and HPRT mutations in human after hyperbaric oxygen treatment. *Mut Res* 1999; **431**: 351-359
- Suzuki K**, Hei TK. Mutation induction in gamma-irradiated primary human bronchial epithelial cells and molecular analysis of the HPRT mutants. *Mut Res* 1996; **349**: 33-41
- Kiefer J**, Schreiber A, Guterath F, Koch S, Schmidt P. Mutation induction by different types of radiation at the Hprt locus. *Mut Res* 1999; **431**: 429-448
- Krause G**, Garganta F, Vrieling H, Scherer G. Spontaneous and chemically induced point mutations in HPRT cDNA of the metabolically competent human lymphoblastoid cell line, MCL-5. *Mut Res* 1999; **431**: 417-428
- Walker VE**, Jones IM, Crippen TL, Meng Q, Walker DM, Bauer MJ, Reilly AA, Tates AD, Nakamura J, Upton PB, Skopek TR. Relationships between exposure, cell loss and proliferation, and manifestation of Hprt mutant T cells following treatment of preweanling, weanling, and adult male mice with N-ethyl-N-nitrosourea. *Mut Res* 1999; **431**: 371-388
- Wei SJ**, Chang RL, Cui XX, Merkler KA, Wong CQ, Yagi H, Jerina DM, Conney AH. Dose-dependent differences in the mutational profiles of (-)-(1R, 2S, 3S, 4R)-3,4-dihydroxy-1,2-epoxy-1,2,3,4-tetrahydrobenzo [c]phenanthrene and its less carcinogenic enantiomer. *Cancer Res* 1996; **56**: 3695-3703
- Jie YM**, Jia C. Chromosomal composition of micronuclei in mouse NIH3T3 cells treated with acrylamide, extract of Tripterygium hypoglaucom (level) hutch, mitomycin C and colchicines, detected by multicolor FISH with centromeric and telomeric DNA probes. *Mutagenesis* 2001; **16**: 145-149
- Meng Q**, Henderson RF, Long LY, Blair L, Walker DM, Upton PB, Swenberg JA, Walker VE. Mutagenicity at the Hprt locus in T cells of female mice following inhalation exposures to low levels of 1, 3-butadiene. *Chemico-Biological Interactions* 2001; **135-136**: 343-361
- Barnett YA**, Warnock CA, Gillespie ES, Barnett CR, Livingstone MB. Effect of dietary intake and lifestyle factors on *in vivo* mutant frequency at the HPRT gene locus in healthy human subjects. *Mut Res* 1999; **431**: 305-315
- Aidoo A**, Morris SM, Casciano DA. Development and utilization of the rat lymphocyte hprt mutation assay. *Mut Res* 1997; **387**: 69-88
- Loucas BD**, Cornforth MN. Postirradiation growth in HAT medium fails to eliminate the delayed appearance of 6-thioguanine-resistant clones in EJ30 human epithelial cells. *Rad Res* 1998; **149**: 171-178
- Recio L**, Steen AM, Pluta LJ, Meyer KG, Saranko CJ. Mutational spectrum of 1, 3-butadiene and metabolites 1,2-epoxybutene and 1,2,3,4-diepoxybutane to assess mutagenic mechanisms. *Chemico-Biological Interactions* 2001; **135-136**: 325-341
- Evans HH**, Demarini DM. Ionizing radiation-induced mutagenesis: radiation studies in Neurospora predictive for results in mammalian cells. *Mut Res* 1999; **437**: 135-150
- da Costa GG**, Manjanatha MG, Marques MM, Beland FA. Induction of lacI mutations in Big Blue rats treated with tamoxifen and α -hydroxytamoxifen. *Cancer Letters* 2002; **176**: 37-45
- Turner SD**, Wijnhoven SW, Tinwell H, Lashford LS, Rafferty JA, Ashby J, Vrieling H, Fairbairn LJ. Assays to predict the genotoxicity of the chromosomal mutagen etoposide-focussing on the best assay. *Mut Res* 2001; **493**: 139-147
- van Delft JH**, Bergmans A, van Dam FJ, Tates AD, Howard L, Winton DJ, Baan RA. Gene-mutation assays in λ lacZ transgenic mice: comparison of lacZ with endogenous genes in splenocytes and small intestinal epithelium. *Mut Res* 1998; **415**: 85-96
- Laws GM**, Skopek TR, Reddy MV, Storer RD, Glaab WE. Detection of DNA adducts using a quantitative long PCR technique and the fluorogenic 5' nuclease assay (TaqMan). *Mut Res* 2001; **484**: 3-18
- Sankaranarayanan K**. Ionizing radiation and genetic risks X. The potential "disease phenotypes" of radiation-induced genetic damage in humans: perspectives from human molecular biology and radiation genetics. *Mut Res* 1999; **429**: 45-83
- Cosentino L**, Heddl JA. Differential mutation of transgenic and endogenous loci *in vivo*. *Mut Res* 2000; **454**: 1-10
- Dobrovolsky VN**, Casciano DA, Heflich RH. Tk⁺ mouse model for detecting *in vivo* mutation in an endogenous, autosomal gene. *Mut Res* 1999; **423**: 125-136
- Tates AD**, van Dam FJ, Natarajan AT, van Teylingen CM, de Zwart FA, Zwinderman AH, van Sittert NJ, Nilsen A, Nilsen OG, Zahlsen K, Magnusson AL, Tornqvist M. Measurement of HPRT mutations in splenic lymphocytes and haemoglobin adducts in erythrocytes of Lewis rats exposed to ethylene oxide. *Mut Res* 1999; **431**: 397-415
- Casciano DA**, Aidoo A, Chen T, Mittelstaedt RA, Manjanatha MG, Heflich RH. Hprt mutant frequency and molecular analysis of Hprt mutations in rats treated with mutagenic carcinogens. *Mut Res* 1999; **431**: 389-395
- Hageman GJ**, Sterum RH. Niacin poly(ADP-ribose) polymerase-1 and genomic stability. *Mut Res* 2001; **475**: 45-56
- Sprung CN**, Wang YP, Miller DL, Giannini DD, Dhananjaya N, Bodell WJ. Induction of lacI mutations in Big Blue Rat-2 cells treated with 1-(2-hydroxyethyl)-1-nitrosourea: a model system

- for the analysis of mutagenic potential of the hydroxyethyl adducts produced by 1, 3-bis (2-chloroethyl)-1-nitrosourea. *Mut Res* 2001; **484**: 77-86
- 31 **Mills AA**, Bradley A. From mouse to man: generating megabase chromosome rearrangements. *Trends Genetics* 2001; **17**: 331-339
- 32 **Waldren C**, Vannais D, Drabek R, Gustafson D, Kraemer S, Lenarczyk M, Kronenberg A, Hei T, Ueno A. Analysis of mutant quantity and quality in human-hamster hybrid A₁ and A₁-179 cells exposed to ¹³⁷Cs-gamma or HZE-Fe ions. *Adv Space Res* 1998; **22**: 579-585
- 33 **Branda RF**, Lafayette AR, O' Neill JP, Nicklas JA. The effect of folate deficiency on the hprt mutational spectrum in Chinese hamster ovary cells treated with monofunctional alkylating agents. *Mut Res* 1999; **427**: 79-87
- 34 **Mittelstaedt RA**, Smith BA, Chen T, Beland FA, Heflich RH. Sequence specificity of Hprt lymphocyte mutation in rats fed the hepatocarcinogen 2-acetylaminofluorene. *Mut Res* 1999; **431**: 167-173
- 35 **Pluth JM**, O' Neill JP, Nicklas JA, Albertini RJ. Molecular bases of HPRT mutations in malathion-treated human T-lymphocytes. *Mut Res* 1998; **397**: 137-148

Edited by Ren SY

A mouse model of severe acute pancreatitis induced with caerulein and lipopolysaccharide

Shi-Ping Ding, Ji-Cheng Li, Chang Jin

Shi-Ping Ding, Ji-Cheng Li, Chang Jin, Department of Lymphology, Department of Histology and Embryology, Medical College of Zhejiang University, Hangzhou 310031, Zhejiang Province, China

Correspondence to: Dr. Ji-Cheng Li, Department of Lymphology, Department of Histology and Embryology, Medical College of Zhejiang University, Hangzhou 310031, Zhejiang Province, China. lijc@mail.hz.zj.cn

Telephone: +86-571-87217139 **Fax:** +86-571-87217139

Received: 2002-09-13 **Accepted:** 2002-10-17

Abstract

AIM: To establish a non-traumatic, easy to induce and reproducible mouse model of severe acute pancreatitis (SAP) induced with caerulein and lipopolysaccharide (LPS).

METHODS: Thirty-two healthy mature NIH female mice were selected and divided at random into four groups (each of 8 mice), i.e., the control group (NS group), the caerulein group (Cn group), the lipopolysaccharide group (LPS group), and the caerulein+LPS group (Cn+LPS group). Mice were injected intraperitoneally with caerulein only, or LPS only, and caerulein and LPS in combination. All the animals were then killed by neck dislocation three hours after the last intraperitoneal injection. The pancreas and exo-pancreatic organs were then carefully removed for microscopic examination. And the pancreatic acinus was further observed under transmission electron microscope (TEM). Pancreatic weight, serum amylase, serum nitric oxide (NO) concentration, superoxide dismutase (SOD) and malondialdehyde (MDA) concentration of the pancreas were assayed respectively.

RESULTS: (1) NS animals displayed normal pancreatic structure both in the exocrine and endocrine. In the LPS group, the pancreas was slightly edematous, with the infiltration of a few inflammatory cells and the necrosis of the adjacent fat tissues. All the animals of the Cn group showed distinct signs of a mild edematous pancreatitis characterized by interstitial edema, infiltration of neutrophil and mononuclear cells, but without obvious parenchyma necrosis and hemorrhage. In contrast, the Cn+LPS group showed more diffuse focal areas of nonviable pancreatic and hemorrhage as well as systemic organ dysfunction. According to Schmidt's criteria, the pancreatic histologic score showed that there existed significant difference in the Cn+LPS group in the interstitial edema, inflammatory infiltration, parenchyma necrosis and parenchyma hemorrhage in comparison with those of the Cn group, LPS group and NS group ($P<0.01$ or $P<0.05$). (2) The ultrastructure of acinar cells was seriously damaged in the Cn+LPS group. Chromatin margination of nuclei was present, the number and volume of vacuoles greatly increased. Zymogen granules (ZGs) were greatly decreased in number and endoplasmic reticulum exhibited whorls. The swollen mitochondria appeared, the crista of which was decreased in number or disappeared. (3) Pancreatic weight and serum amylase levels in the Cn

+LPS was significantly higher than those of the NS group and the LPS group respectively ($P<0.01$ or $P<0.05$). However, the pancreatic wet weight and serum amylase concentration showed no significant difference between the Cn+LPS group and the Cn group. (4) NO concentration in the Cn+LPS group was significantly higher than that of NS group, LPS group and Cn group ($P<0.05$ or $P<0.01$). (5) The SOD and MDA concentration of the pancreas in the Cn+LPS group were significantly higher than those of NS, LPS and Cn groups ($P<0.05$ or $P<0.01$).

CONCLUSION: The mouse model of severe acute pancreatitis could be induced with caerulein and LPS, which could be non-traumatic and easy to induce, reproducible with the same pathological characteristics as those of SAP in human, and could be used in the research on the mechanism of human SAP.

Ding SP, Li JC, Jin C. A mouse model of severe acute pancreatitis induced with caerulein and lipopolysaccharide. *World J Gastroenterol* 2003; 9(3): 584-589

<http://www.wjgnet.com/1007-9327/9/584.htm>

INTRODUCTION

Severe acute pancreatitis (SAP) is characterized by local pancreatic necrosis as well as systemic organ failure and is still associated with a higher morbidity and mortality despite continuing improvements in critical care^[1-9]. Several animal models have been developed for studying the mechanism, recovery, prognosis and treatment of human SAP^[10-12]. However, these methods such as retrograde pancreatic duct injection, intraductal infusion of sodium taurocholate, closed duodenal loop, pancreatic duct obstruction are so invasive and complex in operation that the mortality of the animals was high^[10-12]. The aim of this study is to establish a SAP animal model induced with caerulein and lipopolysaccharide (LPS), which is non-traumatic, convenient and easy to practise, and reproducible and with the same histopathologic characteristics as those of SAP in human.

MATERIALS AND METHODS

Chemicals

Caerulein and LPS (*Escherichia coli* 0111:B4) were purchased from Sigma Chemical Co. (St. Louis, MO, USA). Assay kits for serum amylase, NO, SOD and MDA concentration were from Nanjing Jiancheng Biological Products Institute (Nanjing, China). Other reagents used were of analytic grade.

Animal and grouping

Thirty-two healthy mature NIH female mice, weighing 22.0-28.0 g, provided by Experimental Animal Center of Zhejiang Academy of Medical Sciences, were selected and divided at random into four groups (each of 8 mice), i.e. the control group (NS group), the caerulein group (Cn group), the

lipopolysaccharides group (LPS group), the caerulein + lipopolysaccharides group (Cn+LPS group).

Establishment of the model of severe acute pancreatitis

All the female NIH mice were fed with a standard diet and fasted for 18 hours before induction of pancreatitis. They received water ad libitum during the experiments. In the NS group, the animals were injected intraperitoneally by normal saline at a dose of 50 ml/kg at a 1 h interval six times. In the Cn group, acute pancreatitis was induced by six intraperitoneal injections of caerulein administered at a dose of 50 µg/kg at a 1 h interval. This pancreatitis was mild, and all animals survived. In the LPS group, the animals were injected intraperitoneally with normal saline (50 ml/kg) six times every one hour prior to the intraperitoneal infusion of LPS (10 mg/kg). In the Cn + LPS group, the mice were induced by LPS challenge after induction of mild pancreatitis, i.e., the mice received intraperitoneal injections of 10 mg/kg LPS immediately after the sixth caerulein injection. Three hours later, all the animals were killed by neck dislocation and the pancreas was carefully dissected from its attachment to the stomach, duodenum and spleen. Fat and tissue excess were trimmed away. The pancreas was rinsed with saline, blotted on paper and weighed. And then, one part was fixed and embedded in paraffin wax for histological analysis; the other part was immediately frozen in liquid nitrogen and stored at -78 °C until the measurement of SOD and MDA concentration. And the liver, kidney and lung were also carefully removed. Blood samples were obtained from femoral artery and were stored at -78 °C until use.

Histological examination

For histological examination, the pancreas was fixed in 10 % formaldehyde for 24 hours, embedded in paraffin, and stained with haematoxylin and eosin. According to Schmidt's standard^[13], a pathologist who was blinded to the treatment protocol scored the tissues for edema, inflammatory infiltration, parenchymal necrosis, and hemorrhage in 20 fields. Grading for edema was scaled as: 0, absent or rare; 1, edema in the interlobular space; 2, edema in the intralobular space; and 3, the isolated-island shape of pancreatic acinus. Inflammation was scored as: 0, absent; 1, mild; 2, moderate; and 3, severe. The parenchyma necrosis was as follows: 0, absent; 1, focal (<5 %); 2, and/or sublobular (<20 %); 3, and/or lobular (>20 %). The parenchyma hemorrhage was scored as: 0, absent; 1, mild; 2, moderate and 3, severe. Liver, kidney and lung sections were similarly stained and assessed for histological changes.

Separate experiment was performed to observe the changes of the pancreas. Pancreatic tissues were double fixed in 2.5 % glutaraldehyde and 1 % osmic acid for 2 hours, then stained with 2 % acetic acid U rapidly, dehydrated in a graded series of alcohol and acetone, embedded in Epon 812 and cut with Leica Ultracut UCT ultramicrotome. Specimens were double stained by acetic acid U and lead citrate fluid and examined with Philips Tecnai 10 TEM operated at 80Kv.

Measurement of serum amylase, NO concentration, SOD and MDA concentration of the pancreas

Serum amylase and NO concentration were assayed according to I-starch chromatometry and a copper-coated cadmium reduction method respectively. The pancreas was isolated and was made homogenate. SOD and MDA concentration of the pancreas were measured by the xanthine oxidase method and the sulfo-barbituric acid method respectively.

Statistical analyse

Data were expressed as means ± SD and analyzed by two-tailed Student's *t* test.

RESULTS

Histological examination

Microscopic examination NS animals displayed normal pancreatic histology both in the exocrine and endocrine. In the LPS group, the pancreas was slightly edematous (Figure 1), with the infiltration of a few inflammatory cells and the necrosis of the adjacent fat tissues. The animals of the Cn group treated with caerulein, showed distinct signs of a mild edematous pancreatitis characterized by interstitial edema (Figure 2), infiltration of neutrophil and mononuclear cells, but without obvious parenchyma necrosis and hemorrhage. The organs, except for the pancreas, showed normal histological characteristics. However, the animals of the Cn+LPS group, which was induced with caerulein and aggravated by subsequent LPS injection, showed the features of a severe form of acute pancreatitis characterized by expansion of interlobular and intralobular spaces caused by moderate to severe interstitial edema, extensive infiltration with inflammatory cells, more diffuse focal areas of nonviable pancreatic parenchyma (Figure 3). Necrosis of peripancreatic fat was also a distinct feature in these animals. In addition, renal cells were swollen (Figure 4A); the lobules of liver was disorganized, with the vacuolization of liver cells (Figure 4B) and a lot of erythrocyte and inflammatory cells also infiltrated in the cavity of pulmonary alveolus (Figure 4C).

According to Schmidt's criteria, the histological score showed that there existed significant difference in the Cn+LPS group in the interstitial edema, inflammatory infiltration, parenchyma necrosis and parenchyma hemorrhage as compared with those of the Cn group, the LPS group and the NS group ($P < 0.01$ or $P < 0.05$) (Table 1).

Table 1 Comparison of the pancreas lesion between groups ($n=8$)

Groups	Interstitial edema	Inflammatory infiltration	Parenchyma necrosis	Parenchyma hemorrhage
NS	0.0	0.0	0.0	0.0
Cn	1.95±0.26 ^b	1.12±0.22 ^{bc}	0.63±0.09 ^{bd}	0
LPS	0.25±0.03 ^{ad}	0.25±0.43 ^{bd}	0	0
Cn+LPS	2.75±0.43 ^{bc}	2.88±0.33 ^{bc}	2.75±0.33 ^{bd}	1.25±0.26 ^{bd}

^a $P < 0.05$, ^b $P < 0.01$, vs NS group; ^c $P < 0.05$, ^d $P < 0.01$, vs Cn group.

Electron microscope examination of the pancreatic acinus

The ultrastructure of acinar cells was normal in the NS group. In the cytoplasm of the acinar cells, a plenty of rough endoplasmic reticulum (RER) and ribosome and a great deal of ZGs appeared. After LPS stimulation, a few cytoplasmic vacuoles formed in acinar cells (Figure 5). In the Cn group, a few cytoplasmic vacuoles in acinar cells also appeared, and ZGs were decreased in number. The RER and the mitochondria was slightly swollen (Figure 6). However, in the Cn+LPS group, the morphological alterations of mouse pancreatic acinar cells were observed under transmission electron microscope. Chromatin margination of nuclei was present (Figure 7A), the number of vacuoles greatly increased and their volume also greatly increased (Figure 7B). ZGs were greatly decreased in number and endoplasmic reticulum exhibited whorls (Figure 7C). The swollen mitochondria appeared, the crista of which was decreased or disappeared (Figure 7D).

Comparison of pancreatic weight and serum amylase

Subsequent experiment showed that pancreatic weight and serum amylase in the Cn +LPS and the Cn group were significantly higher than those in the NS group and the LPS group respectively ($P < 0.01$ or $P < 0.05$). However, the pancreatic wet weight and serum amylase showed no significant difference between the Cn+LPS and the Cn groups (Table 2).

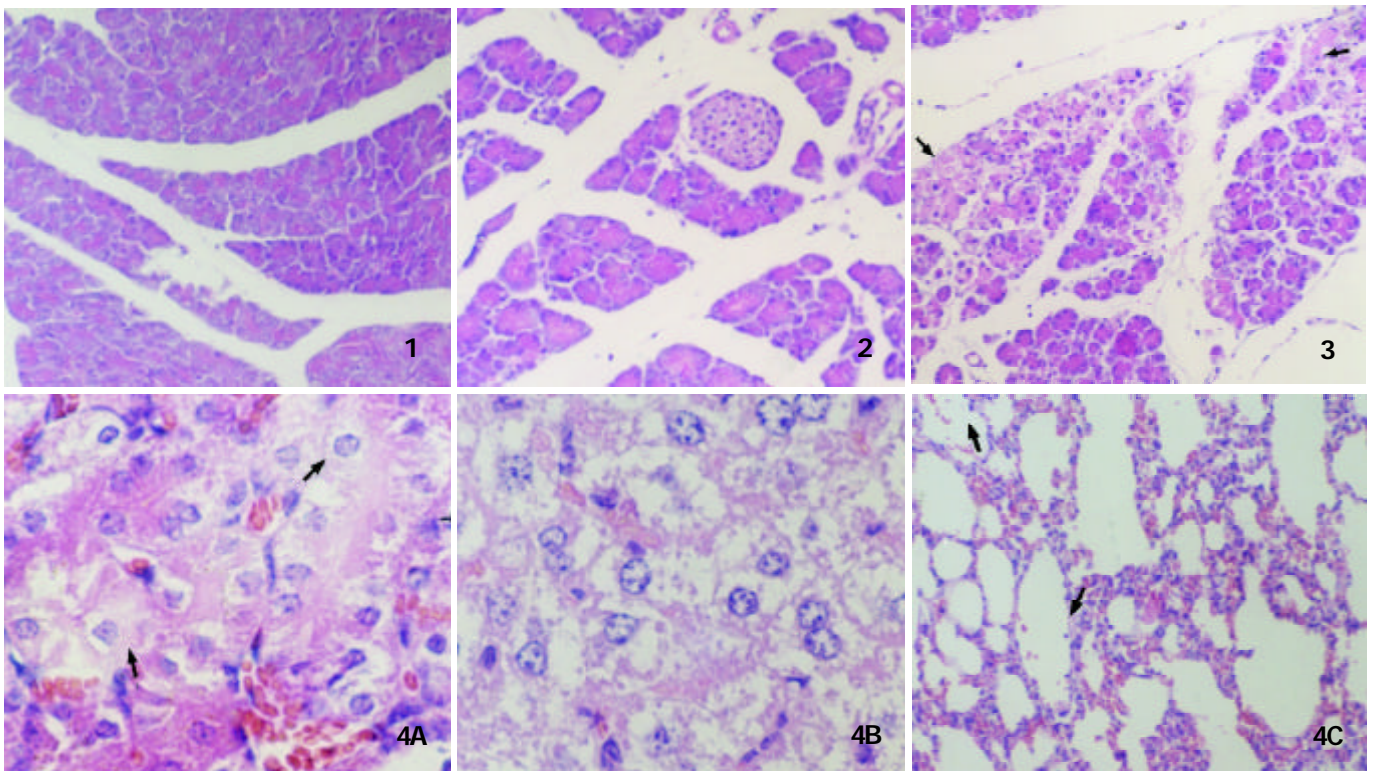


Figure 1 In the LPS group, the pancreas was slightly edematous. $\times 100$.

Figure 2 Microscopic section of the pancreas from the Cn group, showing the features of acute edematous pancreatitis notably interstitial edema. $\times 100$.

Figure 3 In the Cn+LPS group, more diffuse focal areas of nonviable pancreatic parenchyma appeared obviously. $\times 100$.

Figure 4 The histological change of the exo-pancreatic organs in the Cn+LPS group. A: Renal cells were swollen; $\times 100$; B: The vacuolization of liver cells; $\times 400$; C: A lot of erythrocyte and inflammatory cells also infiltrated in the cavity of pulmonary alveolus. $\times 100$.

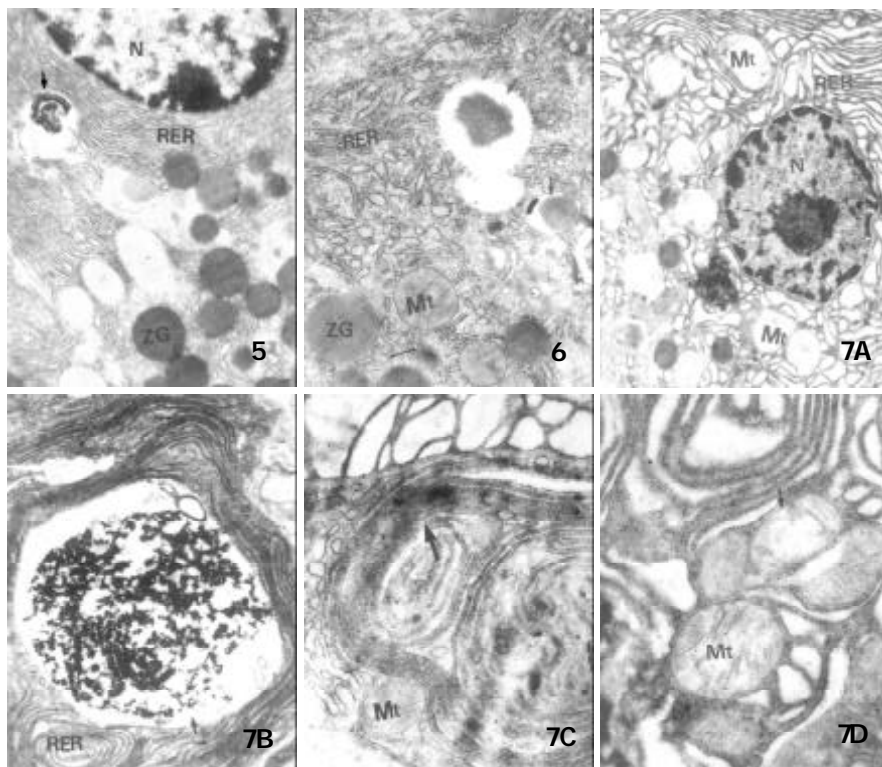


Figure 5 A few cytoplasmic vacuoles formed in acinar cells in the LPS group. $\times 10\ 000$.

Figure 6 In the Cn group, a few cytoplasmic vacuoles in acinar cell appeared, and ZGs were decreased in number. The RER and the mitochondria was slightly swollen. $\times 10\ 000$.

Figure 7 The ultrastructure change of the pancreatic acinus in the Cn+LPS group. A: Chromatin margination of nuclei was present, the swollen mitochondria appeared; $\times 7\ 000$; B: the number of vacuoles greatly increased and their volume also greatly increased; $\times 7\ 000$; C: the endoplasmic reticulum exhibited whorls; $\times 14\ 000$; D: The crista of mitochondria was decreased or disappeared. $\times 20\ 000$.

Table 2 Comparison of pancreatic wet weight and serum amylase between groups ($\bar{x}\pm s$)

Groups	Pancreatic weight (mg)	Serum amylase (U/L)
NS	247.70 \pm 30.20	1861.35 \pm 303.36
Cn	337.20 \pm 50.90 ^{bc}	11042.32 \pm 528.03 ^{bd}
LPS	290.10 \pm 39.70 ^a	2385.50 \pm 73.60 ^b
Cn+LPS	380.00 \pm 32.00 ^{bc}	10031.70 \pm 906.19 ^{bd}

^a P <0.05, ^b P <0.01, vs NS group; ^c P <0.05, ^d P <0.01, vs LPS group.

Comparison of NO concentration

There was significant difference in the concentration of NO among the groups (Figure 8). The results showed that the concentration of NO in the Cn+LPS group was significantly higher than that in the NS, LPS and Cn groups (P <0.01).

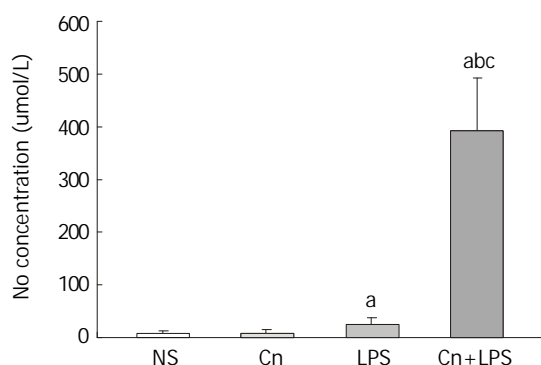


Figure 8 Comparison of NO concentration between groups ($\bar{x}\pm s$) ($n=8$). ^a P <0.01, vs NS group; ^b P <0.01, vs LPS group; ^c P <0.05, vs Cn group.

SOD and MDA concentration of the pancreas

The concentration of SOD and MDA in the pancreas showed significant difference between groups (Table 3). SOD concentration of the pancreas in the Cn+LPS group decreased significantly as compared with that of the NS, LPS and Cn groups. However, MDA concentration of the pancreas in the Cn+LPS group increased significantly compared with that of the NS, LPS and Cn groups.

Table 3 Comparison of SOD and MDA concentration between groups ($\bar{x}\pm s$) ($n=8$)

Groups	SOD concentration (NU/mgprot)	MDA concentration (nmol/mgprot)
NS	151.67 \pm 10.74	0.74 \pm 0.34
Cn	135.73 \pm 10.87 ^a	0.79 \pm 0.31
LPS	136.05 \pm 17.25 ^a	0.97 \pm 0.29
Cn+LPS	85.13 \pm 11.19 ^{bcd}	1.22 \pm 0.24 ^{bd}

^a P <0.05, ^b P <0.01, vs NS group; ^c P <0.01, vs LPS group; ^d P <0.01, vs Cn group.

DISCUSSION

Acute pancreatitis may be classified histologically as interstitial edematous or necrotizing according to the inflammatory changes in the pancreatic parenchyma^[14-19]. As for a mild edematous form, the pancreas observed under light microscope showed interstitial edema, interstitial hyperemia and inflammatory cell infiltration and occasionally punctate fat necrosis, but without obvious parenchyma necrosis and hemorrhage^[20-24]. However, a severe necrotizing form is characterized by extensively coagulative necrosis and

hemorrhage as well as systemic organ dysfunction^[25-34]. In the present study, the results showed that the animals of the Cn group, which was treated with caerulein only, showed distinct signs of a mild edematous pancreatitis, indicating that the pancreatic weight and serum amylase became gradually higher than those of the NS group and the LPS group. The microscopic examination showed interstitial edema and inflammatory cell infiltration in the pancreas, and slight parenchyma necrosis and hemorrhage. And the organs except the pancreas, had a normal histological feature. Furthermore, transmission electron microscopic observation of the acinus cells displayed a few cytoplasmic vacuoles in acinar cell, and ZGs were found decreased in number and the RER and the mitochondrion were slightly swollen. In the LPS group which was treated with LPS only, serum amylase and pancreatic weight had an increasing tendency, but the pancreas showed interstitial edema and the formation of a few vacuoles in the cytoplasm of the acinar cells. LPS could not induce acute pancreatitis, which further confirmed Jaworek's findings^[35]. In the Cn+LPS group, which was induced by caerulein and aggravated by subsequent LPS injection, the level of serum amylase and pancreatic weight increased and the pancreas became edematous and the inflammatory cells infiltrated and necrosis and hemorrhage appeared obviously in the pancreas, the ultrastructure of the acinus was destroyed, the organs except the pancreas was lesioned to a different extent. Moreover, in the histological score, there existed significant difference in the Cn+LPS group in the interstitial edema (2.75 \pm 0.43), inflammatory infiltration (2.88 \pm 0.33), parenchyma necrosis (2.75 \pm 0.33) and parenchyma hemorrhage (1.25 \pm 0.26) in comparison with those of caerulein only (1.95 \pm 0.26; 1.12 \pm 0.22; 0.63 \pm 0.09; 0), those of LPS only (0.25 \pm 0.03; 0.25 \pm 0.43; 0; 0) and the NS group (0; 0; 0; 0) (P <0.01 or P <0.05). It is thus clear that, when induced with caerulein and LPS in combination, the pancreas was destroyed so severely as to result in inflammatory reaction in the body and systemic organ dysfunction. Moreover, the model induced with caerulein and LPS was almost stable under the condition of duplications. Therefore, the mouse model induced with caerulein and LPS was non-traumatic, convenient, easily replicating and bearing the same histological changes as those of human SAP.

Caerulein is a kind of ten-peptide substances, the analog of cholecystokinin, and possesses different biological activities^[36,37]. Caerulein can stimulate the acinar cells to excrete a large amount of digestive enzyme and pancreatic fluid, resulting in a mild edematous pancreatitis characterized by a higher serum amylase level, interstitial edema, leukocyte infiltration and the vacuolation of acinar cells^[36,37]. LPS is a kind of endotoxin, which could activate the mononuclear cell system to release cytokines to switch on systemic inflammation reaction^[38]. Clinically, the endotoxin level was related to the severity of the illness. Therefore, the mechanism to develop severe acute pancreatitis and organ failure with caerulein and LPS might be that caerulein could activate the pancreatin to destroy the pancreas, and detonate inflammatory cells to release inflammation mediators and subsequently LPS challenged the reaction of inflammation medium, thus developing local pancreatitis into severe inflammation reaction in the body^[39-50].

Recent evidence indicated that these cytokines from the inflamed pancreas can activate the production of the inducible nitric oxide (NO) synthase, resulting in overproduction of NO, which acts as a key final cellular and intercellular mediator^[51-53]. In this study, the concentration of NO was significantly higher in the Cn+LPS group, as compared with that of caerulein alone or LPS alone (P <0.01). NO as an endothelium-derived relaxing factor (EDRF) and a highly reactive free radical, is produced from the amino acid L-arginine by a family of isoenzymes, the nitric oxide synthases (NOS). Two broad groups can be

identified: constitutive (cNOS) and inducible (iNOS). cNOS is present predominantly as a normal constituent of healthy endothelial cells (endothelial isoform, eNOS) and synthesizes NO in small amounts in response to physical or receptor stimulation. iNOS is not a normal cellular constituent, but can be expressed in a wide variety of cells and generates large amounts of NO in a sustained and largely uncontrolled manner. Excessive production of NO causes vasodilatation and hypotension that is refractory to vasoconstriction, together with increased microvascular permeability and extravascular third spacing. The physiological inability to correct these adverse responses results in end organ hypoperfusion, oedema, initiation of anaerobic metabolism, and end organ dysfunction. Moreover, the reaction of NO with superoxide causes the formation of peroxynitrite, which is a powerful oxidant and cytotoxic agent and may play an important role in the cellular damage associated with the overproduction of NO. The spontaneous reaction of peroxynitrite with proteins makes the nitration of tyrosine residues to form nitrotyrosine, which is a specific nitration product of peroxynitrite and a marker for peroxynitrite induced oxidative tissue damage. It is thus evident that the increase of NO concentration is related to the lesion of pancreas and other organs. In addition, the concentration of SOD as an antioxidant significantly lowered and that of MDA as the lipid peroxide significantly increased, which further indicated that the free radical reaction and oxidation response could be intensified with caerulein and LPS so that a mild edematous form could change subsequently into a severe necrotizing form.

REFERENCES

- 1 **Baron TH**, Morgan DE. Acute necrotizing pancreatitis. *N Engl J Med* 1999; **340**: 1412-1417
- 2 **Pastor CM**, Frossard JL. Are genetically modified mice useful for the understanding of acute pancreatitis. *FASEB J* 2001; **15**: 893-897
- 3 **Lecesne R**, Taourel P, Bret PM, Atri M, Reinhold C. Acute pancreatitis: Interobserver agreement and correlation of CT and MR cholangiopancreatography with outcome. *Radiology* 1999; **211**: 727-735
- 4 **Slavin J**, Ghaneh P, Sutton R, Hartley M, Rowlands P, Garvey C, Hughes M, Neoptolemos J. Management of necrotizing pancreatitis. *World J Gastroenterol* 2001; **7**: 476-481
- 5 **Wu XN**. Treatment revisited and factors affecting prognosis of severe acute pancreatitis. *World J Gastroenterol* 2000; **6**: 633-635
- 6 **Qi QH**, Guo LM. The surgical treatment of acute pancreatitis. *Shijie Huaren Xiaohua Zazhi* 2001; **9**: 416-417
- 7 **Yu CG**, Chen LD, Zhang ZH. Severe acute pancreatitis and infection of pancreas. *Shijie Huaren Xiaohua Zazhi* 2001; **9**: 689-693
- 8 **Zhao M**, Chen RF. Pathogenesis of acute lung injury induced by acute necrotizing pancreatitis. *Shijie Huaren Xiaohua Zazhi* 2001; **9**: 954-957
- 9 **Chen QP**. Enteral nutrition and acute pancreatitis. *World J Gastroenterol* 2001; **7**: 185-192
- 10 **Shang ZM**, Wang BE, Zhang SW, Ci XL. The establishment of the rat model of severe acute pancreatitis. *Shijie Huaren Xiaohua Zazhi* 2000; **8**: 921
- 11 **Tashiro M**, Schafer C, Yao H, Ernst SA, Williams JA. Arginine induced acute pancreatitis alters the actin cytoskeleton and increases heat shock protein expression in rat pancreatic acinar cells. *Gut* 2001; **49**: 241-250
- 12 **Wu WK**. The pathogenesis of acute pancreatitis. *Shijie Huaren Xiaohua Zazhi* 2001; **9**: 410-411
- 13 **Shimizu T**, Shiratori K, Sawada T, Kobayashi M, Hayashi N, Saotome H, Keith JC. Recombinant human interleukin-11 decrease severity of acute necrotizing pancreatitis in mice. *Pancreas* 2000; **21**: 134-140
- 14 **Li JC**. Discussion on the conception of severe acute pancreatitis. *Shijie Huaren Xiaohua Zazhi* 1999; **7**: 1072-1073
- 15 **Wu XN**. Current concept of pathogenesis of severe acute pancreatitis. *World J Gastroenterol* 2000; **6**: 32-36
- 16 **Pezzilli R**, Mancini F. Assessment of severity of acute pancreatitis: a comparison between old and most recent modalities used to evaluate this perennial problem. *World J Gastroenterol* 1999; **5**: 283-285
- 17 **Uhl W**, Buchler MW, Malferteiner P, Beger HG, Adler G, Gaus W. The german pancreatitis study group. A randomized, double blind, multicentre trial of octreotide in moderate to severe acute pancreatitis. *Gut* 1999; **45**: 97-104
- 18 **Hartwig W**, Careter EA, Jimenez RE, Werner J, Fischman AJ, Castillo CF, Warshaw AL. Chemotactic peptide uptake in acute pancreatitis: correlation with tissue accumulation of leukocytes. *J Appl Physiol* 1999; **87**: 743-749
- 19 **Pezzilli R**, Morselli-labate AM, Miniero R, Barakat B, Fiocchi M, Cappelletti O. Simultaneous serum assays of lipase and interleukin-6 for early diagnosis and prognosis of acute pancreatitis. *Clin Chem* 1999; **45**: 1762-1767
- 20 **Zhou ZG**, Chen YD. Influencing factors of pancreatic microcirculatory impairment in acute pancreatitis. *World J Gastroenterol* 2002; **8**: 406-412
- 21 **Chen DL**, Wang WZ, Wang JY. Epidermal growth factor prevents gut atrophy and maintains intestinal integrity in rats with acute pancreatitis. *World J Gastroenterol* 2000; **6**: 762-765
- 22 **Kohut M**, Nowak A, Nowakowska-Dulawa E, Marek T. Presence and density of common bile duct microlithiasis in acute biliary pancreatitis. *World J Gastroenterol* 2002; **8**: 558-561
- 23 **Fleischer F**, Dabew R, Goke B, Wagner AC. Stress kinase inhibition modulates acute experimental pancreatitis. *World J Gastroenterol* 2001; **7**: 259-265
- 24 **Tiscomia OM**, Hamamura S, de Lehmann ES, Otero G, Waisman H, Tiscomia-Wasserman P, Bank S. Biliary acute pancreatitis: a review. *World J Gastroenterol* 2000; **6**: 157-168
- 25 **Frossard JL**, Hadengue A, Pastor CM. New serum markers for the detection of severe acute pancreatitis in humans. *Am J Respir Crit Care Med* 2001; **164**: 162-170
- 26 **Hamano H**, Kawa S, Horiuchi A, Unno H, Furuya N, Akamatsu T, Fukushima M, Nikaido T, Nakayama K, Usuda N, Kiyosawa K. High serum IgG₄ concentrations in patients with sclerosing pancreatitis. *N Engl J Med* 2001; **344**: 732-738
- 27 **Kyriakides C**, Jasleen J, Wang Y, Moore FD, Ashley SW, Hechtman HB. Neutrophils, not complement, mediate the mortality of experimental hemorrhagic pancreatitis. *Pancreas* 2001; **22**: 40-46
- 28 **Luo Y**, Yuan CX, Peng YL, Wei PL, Zhang ZD, Jiang JM, Dai L, Hu YK. Can ultrasound predict the severity of acute pancreatitis early by observing acute fluid collection. *World J Gastroenterol* 2001; **7**: 293-295
- 29 **Wu JX**, Xu JY, Yuan YZ. Effect of emodin and sandostatin on metabolism of eicosanoids in acute necrotizing pancreatitis. *World J Gastroenterol* 2000; **6**: 293-294
- 30 **Qin RY**, Zou SQ, Wu ZD, Qiu FZ. Influence of splanchnic vascular infusion on the content of endotoxins in plasma and the translocation of intestinal bacteria in rats with acute hemorrhage necrosis pancreatitis. *World J Gastroenterol* 2000; **6**: 577-580
- 31 **Yuan YZ**, Gong ZH, Lou KX, Tu SP, Zhai ZK, Xu JY. Involvement of apoptosis of alveolar epithelial cells in acute pancreatitis-associated lung injury. *World J Gastroenterol* 2000; **6**: 920-924
- 32 **Sun XQ**, Fu XB, Zhang R, Lu Y, Deng Q, Jiang XG, Sheng ZY. Relationship between plasma D(-) - lactate and intestinal damage after severe injuries in rats. *World J Gastroenterol* 2001; **7**: 555-558
- 33 **Zhang WZ**, Han TQ, Tang YQ, Zhang SD. Rapid detection of sepsis complicating acute necrotizing pancreatitis using polymerase chain reaction. *World J Gastroenterol* 2001; **7**: 289-292
- 34 **Xia Q**, Jiang JM, Gong X, Chen GY, Li L, Huang ZW. Experimental study of Tong Xia purgative method in ameliorating lung injury in acute necrotizing pancreatitis. *World J Gastroenterol* 2000; **6**: 115-118
- 35 **Jaworek J**, Jachimczak B, Tomaszewska R, Konturek PC, Pawlik WW, Sendur R, Hahn EG, Stachura J, Konturek SJ. Protective action of lipopolysaccharides in rat caerulein-induced pancreatitis: role of nitric oxide. *Digestion* 2000; **62**: 1-13
- 36 **Wagner ACC**, Mazzucchelli L, Miller M, Camoratto AM, Goke B. CER-1347 inhibits caerulein-induced rat pancreatitis JNK activation and ameliorates caerulein pancreatitis. *Am J Physiol Gastrointest Liver Physiol* 2000; **278**: G165-G172

- 37 **Frossard JL**, Bhagat L, Lee HS, Hietaranta AJ, Singh VP, Song AM, Steer ML, Saluja AK. Both thermal and non-thermal stress protect against caerulein induced pancreatitis and prevent trypsinogen activation in the pancreas. *Gut* 2002; **50**: 78-83
- 38 **Vaccaro MI**, Calvo EL, Suburo AM, Sordelli DO, Lanosa G, Iovanna JL. Lipopolysaccharide directly affects pancreatic acinar cell: implications on acute pancreatitis pathophysiology. *Dig Dis Sci* 2000; **45**: 915-926
- 39 **Xia SH**, Zhao XY, Guo P, Da SP. Hemocirculatory disorder in dogs with severe acute pancreatitis and intervention of platelet activating factor antagonist. *Shijie Huaren Xiaohua Zazhi* 2001; **9**: 550-554
- 40 **Yin Y**, Gao NR, Li ZL. Protective effects of ulinostatin on acute lung injury induced by acute necrotizing pancreatitis in rats. *Shijie Huaren Xiaohua Zazhi* 2002; **10**: 558-561
- 41 **Chen H**, Li F, Cheng YF, Sun JB. Pathogenic role of neutrophils in evolution of acute pancreatitis in rats. *Shijie Huaren Xiaohua Zazhi* 2001; **9**: 776-779
- 42 **Yuan YZ**, Lou KX, Gong ZH, Tu SP, Zhai ZK, Xu JY. Effects and mechanisms of emodin on pancreatic tissue EGF expression in acute pancreatitis in rats. *Shijie Huaren Xiaohua Zazhi* 2001; **9**: 127-130
- 43 **Wu K**, Wang BX, Wang XP. Effects of clostridium butyricum on bacterial translocation in rats with acute necrotizing pancreatitis. *Shijie Huaren Xiaohua Zazhi* 2000; **8**: 883-886
- 44 **Gong ZH**, Yuan YZ, Lou KX, Tu SP, Zhai ZK, Xu JY. Effects and mechanisms of somatostatin analogues on apoptosis of pancreatic acinar cells in acute pancreatitis in mice. *Shijie Huaren Xiaohua Zazhi* 1999; **7**: 964-966
- 45 **Wang CH**, Qian KD, Zhu YL, Tang XQ. The significance of TNF and IL-6 level in the patients with acute pancreatitis. *Shijie Huaren Xiaohua Zazhi* 2001; **9**: 1434
- 46 **Okabe A**, Hirota M, Nozawa F, Shibata M, Nakano S, Ogawa M. Altered cytokine response in rat acute pancreatitis complicated with endotoxemia. *Pancreas* 2001; **22**: 32-39
- 47 **Vaquero E**, Gukovsky I, Zaninovic V, Gukovskaya AS, Pandolfi SJ. Localized pancreatic NF- κ B activation and inflammatory response in taurocholate-induced pancreatitis. *Am J Physiol Gastrointest Liver Physiol* 2001; **280**: G1197-G1208
- 48 **Mayer J**, Rau B, Gansauge F, Beger HG. Inflammatory mediators in human acute pancreatitis: clinical and pathophysiological implications. *Gut* 2000; **47**: 546-552
- 49 **Saluja AK**, Bhagat L, Lee HS, Bhatia M, Frossard JL, Steer ML. Secretagogue-induced digestive enzyme activation and cell injury in rat pancreatic acini. *Am J Physiol* 1999; **276**: G835-G842
- 50 **Matsumura N**, Ochi K, Ichimura M, Mizushima T, Harada H, Harada M. Study on free radicals and pancreatic fibrosis-pancreatic fibrosis induced by repeated injections of superoxide dismutase inhibitor. *Pancreas* 2001; **22**: 53-57
- 51 **Simsek I**, Refik M, Yasar M, Ozyurt M, Saglamkaya U, Deveci S, Comert B, Basustaoglu A, Kocabalkan F. Inhibition of inducible nitric oxide synthase reduces bacterial translocation in a rat model of acute pancreatitis. *Pancreas* 2001; **23**: 296-301
- 52 **Gomez-Cambronero L**, Camps B, de La Asuncion JG, Cerda M, Pellin A, Pallardo FV, Calvete J, Sweiry JH, Mann GE, Vina J, Sastre J. Pentoxifylline ameliorates cerulein-induced pancreatitis in rats: role of glutathione and nitric oxide. *J Pharmacol Exp Ther* 2000; **293**: 670-676
- 53 **Schulz HU**, Niederau C, Klonowski Stumpe H, Halangk W, Luthen R, Lippert H. Oxidative stress in acute pancreatitis. *Hepatogastroenterology* 1999; **46**: 2736-2750

Edited by Ma JY

In situ detection of TGF betas, TGF beta receptor II mRNA and telomerase activity in rat cholangiocarcinogenesis

Jian-Ping Lu, Jian-Qun Mao, Ming-Sheng Li, Shi-Lun Lu, Xi-Qi Hu, Shi-Neng Zhu, Shintaro Nomura

Jian-Ping Lu, Department of Pathology, Medical Center of Fudan University (Former Shanghai Medical University), Shanghai 200032, China. Max-Planck-Institute for Cell Biology, Ladenburg 68526, Germany

Jian-Qun Mao, Ming-Sheng Li, Shi-Lun Lu, Xi-Qi Hu, Shi-Neng Zhu, Department of Pathology, Medical Center of Fudan University, (Former Shanghai Medical University), Shanghai 200032, China

Shintaro Nomura, Department of Pathology, Osaka University, School of Medicine, Fukita 565, Japan

Supported by China National Natural Science Foundation, No. 30070846/C03031904

Correspondence to: Jian-Ping Lu, Ph.D. Max-Planck-Institute for Cell Biology, Ladenburg 68526, Germany. lu_jp@hotmail.com

Telephone: +49-6203-106-208 **Fax:** +49-6203-106-122

Received: 2002-10-09 **Accepted:** 2002-11-04

Abstract

AIM: Initial report on the *in situ* examination of the mRNA expression of transforming growth factor betas (TGFβs), TGFβ type II receptor (TβRII) and telomerase activity in the experimental rat liver tissue during cholangiocarcinogenesis.

METHODS: Rat liver cholangiocarcinogenesis was induced by 3'-methyl 4-dimethylazobenzene (3' Me-DAB). *In situ* hybridization was used to examine the TGFβs and TGFβ type II receptor (TβRII) mRNA, *in situ* TRAP was used to check the telomerase activity in the tissue samples.

RESULTS: There was no TGFβs, TβRII mRNA expression or telomerase activity in the control rat cholangiocytes. The expression of TGFβ1, TβRII was increased in regenerative, hyperplastic, dysplastic cholangiocytes and cholangiocarcinoma (CC) cells. The expression of TGFβ2 mRNA was observed in only a part of hyperplastic, dysplastic cholangiocytes. TGFβ3 expression was very weak, only in hyperplastic lesion. There was positive telomerase activity in the regenerative, hyperplastic, dysplastic cholangiocytes, and CC cells. Stroma fibroblasts of these lesions also showed positive TGFβs, TβRII mRNA expression and telomerase activity.

CONCLUSION: There were TGFβs, TβRII expression and telomerase activity in hyperplastic, dysplastic cholangiocytes, cholangiocarcinoma cells as well as in stroma fibroblasts during cholangiocarcinogenesis. Their expression or activity is important in cholangiocarcinogenesis and stroma formation.

Lu JP, Mao JQ, Li MS, Lu SL, Hu XQ, Zhu SN, Nomura S. In situ detection of TGF betas, TGF beta receptor II mRNA and telomerase activity in rat cholangiocarcinogenesis. *World J Gastroenterol* 2003; 9(3): 590-594

<http://www.wjgnet.com/1007-9327/9/590.htm>

INTRODUCTION

Transforming growth factor beta (TGFβ)-TGFβ receptor (TβR) signaling system is important in growth regulating

carcinogenesis and cancer progression^[1,2]. Lacks of the expression of TGFβ and/or TβR, mutation of the related genes were reported in human and animal malignancies^[3-5]. These abnormalities were considered to be the cause of interruption of the growth signal from the TGFβ to the cell nuclear, resulting in the uncontrolled growth of the involved cells. While there are reports on the efficacy of TGFβ which supported that TGFβ was involved in cancer invasion and metastasis^[1,2,6].

Hepatocellular carcinoma (HC) and intrahepatic cholangiocarcinoma (CC) are two most common types of liver carcinoma^[7,8]. Though there are reports on their expression in HC^[9,10], few reports dealt with the expression of TGFβs and/or TβR in CC. Bile ducts had increased expression of TGFβ1 in inflammatory or obstructive lesions^[11]. TGFβ1 was detected in small amount of cancer cells among 25 of 30 CC cases^[12]. The expression and significance of TGFβs and their receptors during cholangiocarcinogenesis are poorly understood. Stroma fibrosis is one of the characteristics of CC^[7,8], but the mechanism of excessive stroma formation is not clear.

Telomerase is a key enzyme in the maintenance of the telomeric DNA length^[13]. Telomerase is undetectable in most normal somatic tissues. Its activity was reported in most cancer cell lines as well as cancer tissues from human and experimental animals^[13,14]. mRNA of telomerase and telomerase-associated protein were detected in CC and its preneoplastic lesions^[15]. It is not clear in which stage the telomerase is activated during cholangiocarcinogenesis.

Liver carcinogenesis was induced by feeding rats with 0.05 % 3'-methyl 4-dimethylazobenzene (3' Me-DAB) in maize flour. The model showed progressive changes from degeneration, necrosis, to cholangiocyte hyperplasia, dysplasia and CC^[16]. We found obviously increased expression of TGFβ and TGFβ type II receptor (TβRII) mRNA and telomerase activity in the proliferative, dysplastic cholangiocytes, CC cells as well as stroma fibroblasts. Here we report these findings and discuss their significance.

MATERIALS AND METHODS

Animals and reagents

Male Wistar rats ($n=100$, weighing 65 ± 10 g) and foods were purchased from the Shanghai Experimental Animal Center of Chinese Academy of Science. All rats received humane care.

3' Me-DAB was purchased from the Tokyo Kasai Co. Ltd. (Tokyo, Japan Cat. 0207). DIG RNA labeling kit (Cat. No. 1175025), DIG nucleic acid detecting kit (Cat. No. 1175041), and Telomerase PCR ELISA kit (Cat. No. 1854666) were bought from Roche, Germany. Mouse anti-proliferating cell nuclear antigen (PCNA), goat anti-vimentin and biotinylated secondary antibodies were purchased from DAKO. ABC Kit was the product of Vector.

Alcian blue (8GS) was the product of Chroma. Sirius red (F3B) was from Sigma. All other reagents were of analytical or molecular biology research grade from Sigma, Merck or Shanghai Analytical Chemical Co.

Experimental design

The rats were divided into Experimental ($n=60$) and Control

($n=40$) Groups randomly and fed with common compound food and tap water during the first week of adaptation. Maize flour containing 0.05 % 3' Me-DAB was prescribed to the Experimental Group rats for 12 weeks to induce liver cancer. The Control Group rats were fed with maize flour only for the 12-week-period. Common compound food was given to all rats after the period. The rats were sacrificed under anesthetization from 4-week to the end of 22-week since 3' Me-DAB feeding.

The liver tissues with macroscopic lesions were sampled. Samples from half of the lesions were fixed in 4 % buffered paraformaldehyde, embedded in paraffin for routine H.E, histochemical staining, immunohistochemistry and *in situ* hybridization. Samples from residual half of the lesions were embedded in OCT compounds, snap frozen, and cryostat section for histochemical staining and *in situ* TRAP reaction. H.E. alcian blue, PAS and sirius red staining were undertaken. The liver lesions were classified into not obvious, hyperplastic or cholangial proliferative, dysplastic proliferative foci and cancer^[7, 8, 14]. The cholangial property of the cells in the lesion was confirmed by positive mucin staining with either serum albumin mRNA expression, or cytoplasmic glycogen.

In situ hybridization

Plasmids containing cDNAs of TGF β 1, 2, 3; T β RII and serum albumin (SA) were proliferated in *E. Coli*. The plasmids were extracted, purified and linearized with specified endonucleases (Table 1). Anti-sense and sense cRNAs were then made and labeled with digoxigenin *in vitro*^[17].

Paraffin embedded tissue samples were sectioned (5 μ m). The sections were deparaffinized in serial xylene and alcohol solvents, transferred into 100 mM PBS (pH7.4) and digested with proteinase K. The sections were pretreated with 4 % buffered paraformaldehyde, PBS, 200 mM HCl, 100 mM TEA-HCl buffer (pH8.0), 100 mM TEA·0.25 % anhydrous acetate, PBS and further dehydrated with serial alcohol. Pre-warmed hybridization solution containing digoxigenin labeled probe was dropped on the pretreated sections, covered with parafilm and incubated in wet chamber for 15 hours at 50 °C. After hybridization, the sections were washed in 5 \times SSC, 2 \times SSC with 50 % formamide and TNE solutions. Non-hybridized probe was digested with RNase A. Digoxigenin labeled probe was detected with alkaline phosphatase labeled anti-digoxigenin antibody and visualized with NBT-BCIP substrate^[17, 18]. Some of the sections were further counterstained with eosin, alcian blue, and /or hematoxylin.

Addition of SA anti-sense probe was used as positive control, sense probes were used as negative controls.

Table 1 Probes and plasmids

Probe	Vector	Endonuclease and cRNA (-)	promotor cRNA (+)	Length of cDNA
T β RII	pBluescript II KS(-)	EcoRI T3	Hind III T7	485bp
TGF β 1	pBluescript II KS(-)	XhoI T3	Hind III T7	400bp
TGF β 2	pGEM 3ZF(-)	HindIII T7	EcoRI SP6	500bp
TGF β 3	pGEM 3ZF(-)	BamHI T7	EcoRI SP6	280bp
SA	pBluescript II KS(-)	HindIII T3	EcoRI T7	620bp

In situ TRAP

Liver tissues embedded in O.C.T. compounds were sectioned (10 μ m), air-dried shortly for further processing. The *in situ* TRAP was performed as reported^[14, 19]. Briefly, the elongation and PCR mixture was dropped onto cryostat sections and incubated in wet chamber for 30 min at 30 °C. Telomerase was inactivated at 94 °C for 5 min. The elongated telomere

sequence was amplified within GeneAmp *in situ* PCR System 1000 (Perkin-Elmer Co. Foster City, CA 94404) for 30 cycles. Each cycle included: 94 °C for 30 sec, 50 °C for 30 sec, 72 °C for 20 sec. Last cycle was followed by 72 °C for 10 min. The sections were then washed with washing buffer and fixed with 4 % buffered paraformaldehyde.

The sections were further treated with digoxigenin labeled probes, peroxidase labeled anti-digoxigenin antibody and coloration substrate to show the products of amplification. The reaction products were directly photographed before the addition of stop solution. Negative controls included: elongation after inactivation of telomerase, no probe, no antibody or substrate only control.

Immunohistochemical and histochemical reactions

Paraffin sections were routinely deparaffinized and transferred to PBS. PCNA affinity to antibody was recovered by microwave oven treatment of the sections in 10mM TAE. Immunohistochemical detection of PCNA and vimentin was performed following routine procedure^[20].

Alcian blue and sirius red staining were undertaken on paraffin sections. PAS staining was carried out on paraffin as well as frozen sections.

The experiment was undertaken on at least 6 rats from different period of carcinogenesis with lesions of regeneration, hyperplasia, dysplasia and carcinoma foci separately. The experiments on the same sample were duplicated to ensure the results.

RESULTS

The Control Group rats showed no obvious pathologic changes. There was no detectable expression of TGF β 1, 2, 3, T β RII mRNA in the cholangiocytes and bile duct cells from the control rat liver. There was a zonal expression of SA in hepatocytes, stronger at zone 1 and weaker at zone 3. Neither telomerase activity, nor PCNA reaction was detected in the cholangiocytes and bile duct cells. The stellate cells of the sinus were positive to vimentin.

There were successive histological changes in the liver tissue samples in Experimental Group rats: from degeneration and necrosis, regeneration and proliferation, hyperplasia and dysplasia, to carcinoma.

At the early stage, there were massive degeneration and necrosis of the liver tissue samples. No TGF β 1, 2, 3, T β RII expression or telomerase were detected in the degenerative and necrotic liver tissue samples.

Later, regeneration and proliferation of cholangiocytes and hepatocytes were observed. Early in the regenerative and proliferative lesion, there were epithelial cells with edematous stroma. The epithelial cells were scattered in small clusters or forming cell cords, sometimes with lumen in the cords. When the cells differentiate toward cholangiocytes, the cytoplasm of the cells became basophilic without SA or glycogen. There was mucus accumulation in the cytoplasm or in some of the lumens. These cells showed positive TGF β 1 mRNA expression (Figure 1-2). Telomerase activity and PCNA positive nucleus appeared in these epithelial cells.

The proliferation of cholangiocytes continued but the edema of the stroma reduced with time, while vimentin positive fibroblast proliferation appeared in stroma followed by deposition of collagen. At this stage, the cholangiocytes and fibroblasts expressed high level of TGF β 1, 2 and T β RII mRNA (Figure 3-4). These cells were also positive to PCNA and telomerase reactions (Figure 7). TGF β 3 can also be detected transiently in some cholangiocytes. The lesion developed into cholangiocyte hyperplasia with stroma fibrosis (Figure 4, 7).

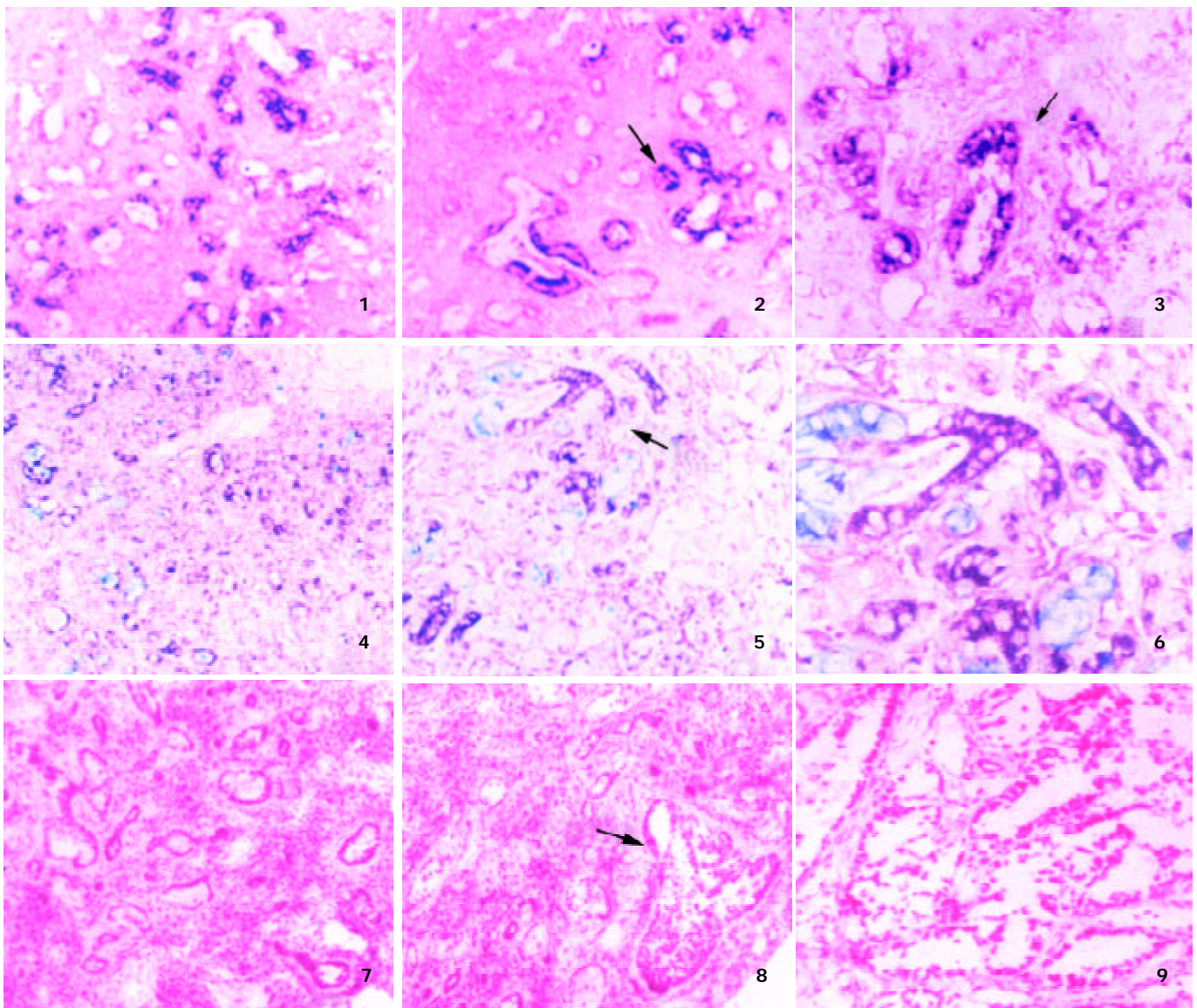


Figure 1-6 *In situ* hybridization showed the mRNA localization (NBT-BCIP purple colored) of TGFβ1 (Figure 1, 2), TGFβ2 (Figure 3), TβR II (Figure 4-6). Figure 1-3 counterstained with eosin; Figure 4-6 counterstained with alcian blue and eosin.

Figure 7-9 *In situ* TRAP shows telomerase activity of the hyperplastic (Figure 7), dysplastic cholangiocytes (Figure 8) and cholangiocarcinoma (Figure 9) in rat liver tissue. Hyperplastic epithelial cells in the stroma form clusters, cords, and ducts (Figure 1, 4, 7). There was mucin formation in some of the ducts (Figure 4) indicating they were cholangiocytes. The hyperplastic cholangiocytes showed TGFβ1, TβR II mRNA expression. (Figure 1, 4). There was telomerase activity in their nuclei (Figure 7). Proliferative cholangiocytes forming duct structures. Some of them had structural and cellular atypia indicating cholangial dysplasia or cholangiocarcinoma in hyperplastic lesion (Figure 2, 3, 5, 6, 8). The expression of TGFβ1, 2, (Figure 2, 3), TβR II (Figure 4-6) and mucin formation in the hyperplastic and dysplastic ducts were uneven (Figure 2-3, 5-6). In Cholangial dysplasia foci and cholangiocarcinoma, there was telomerase activity in the nuclei of cancer cells and stroma fibroblasts (Figure 8-9). (Figure 1, 4, 7, 8×100; Figure 2, 3, 5, 9×200; Figure 6×400).

Later, the cholangiocytes in some areas disappeared with the maturation of fibroblasts to fibrocytes and increased deposition of collagen forming a “burnt-out” picture.

In other areas, the cholangiocytes kept growing with atypical cell morphology, forming irregular cellular clusters, and abortive tubular or glandular structures, indicating cholangiocyte dysplasia. Some of them may accompany with CC. The dysplasia was first found in the liver tissues after 12 weeks of 3' Me-DAB treatment. Small foci of CC appeared in the liver lesion at the 16th to 20th week of experiment.

There was mucin in the cytoplasm of the dysplastic cholangiocytes, CC cells or in the lumen formed in the cell clusters. The expressions of TGFβ1 and TβRII mRNA in the dysplastic cholangiocytes and CC cells differed greatly from negative to strong positive among different cells and different cell clusters (Figure 2, 5, 6). TGFβ2 mRNA expression was

also uneven in the dysplastic lesions (Figure 3). TGFβ3 expression was undetectable. Most of the dysplastic cholangiocytes and cancer cells showed telomerase activity (Figure 8-9). Strong PCNA positive reaction was observed in the hyperplastic, dysplastic cholangiocytes and CC. The stroma was abundant with proliferative fibroblasts (PCNA and vimentin positive) and collagen deposition. The fibroblasts had positive TGFβ1, TβRII mRNA expression and telomerase activity.

DISCUSSION

The liver tissues from our carcinogenesis model had lesions from cholangiocyte hyperplasia, dysplasia to CC with positive mucin staining with neither albumin mRNA, nor glucagon in the cytoplasm.

TGF β is well known for its effects on fibroblasts which can induce formation of stroma^[1,2,21]. But there is no report on the expression of T β R during experimental cholangiocarcinogenesis. We observed the expression of TGF β 1 and T β R II expression in the fibroblasts of regenerative, dysplastic cholangiocyte lesions and in CC. There was increased fibrous stroma formation around the fibroblasts and fibrocytes. These results supported the function of TGF β -T β R II system in the excessive stroma formation in these lesions.

Present experiment showed that there was no TGF β 1, 2, 3 and T β R II expression in normal bile duct cells. TGF β 1, 2, 3 and T β R II mRNA expression was detected in the repairing and proliferative cholangiocytes. In the dysplastic cholangiocytes and CC cells, their expression varied from negative to strong positive. TGF β 1 protein was also detected in experimental rat and human CC cells^[21-23]. TGF β 1 can suppress the proliferation of epithelium, prevent epithelial carcinogenesis^[1,2]. On the other hand, there are reports that TGF β can not inhibit the cancer growth or even accelerate the cancer invasion^[2, 6]. TGF β can suppress the growth of the normal bile duct cell but not the CC cells^[12]. Transgenic mouse with TGF β 1 over expression accelerates hepatocarcinogenesis^[24]. Dominant-negative T β R II mice had accelerated carcinogenesis^[25]. Our results showed that TGF β and T β R II expression accompanied with the cholangiocarcinogenesis procedure.

Cancer progress is related to the reaction between cancer cells and its stroma^[26]. Treatment of Ras-transformed mammary epithelial cells with TGF-beta results in resistant to growth inhibition by TGF-beta. These cells start to secrete TGF-beta, leading to maintenance of the invasive phenotype. The action is dependent on epithelial-stromal interaction^[27]. Our results showed that there was TGF β 1 and T β R II expression in the dysplastic cholangiocytes, CC cells and stroma fibroblasts. Thus, the paracrine and autocrine functions of TGF β 1 are important in supporting the process of cholangiocarcinogenesis.

The expression of TGF β 2 mRNA was only detected in part of hyperplastic, dysplastic cholangiocytes. TGF β 3 mRNA was only weakly positive in some hyperplastic cholangiocytes. There is few reports on the expression of TGF β 2, 3 mRNA in the process of cholangiocarcinogenesis. Their role may be transient.

Phase of telomerase activation during cholangiocarcinogenesis is not specified. Present experiment showed that normal bile duct cells were telomerase negative. There was telomerase activity in the regenerative, hyperplastic, and dysplastic cholangiocytes as well as CC cells. The activation of telomerase occurred in the early stage of cholangio-carcinogenesis. There were also reports on the positive hTR and TP1 mRNA expression in intrahepatic biliary dysplasia^[28]. Increased telomerase activity was reported in dysplastic hepatocytes during hepatocellular carcinogenesis^[29].

The expression of TERT can induce resistance to TGF β growth inhibition^[30]. This may be another reason for the hyperplastic, dysplastic cholangiocytes and CC cells escaping from TGF β -T β R growth suppression in our cholangiocarcinogenesis model.

The telomerase activity is a marker of immortalized or malignant cells^[13,14,31]. In present experiment, telomerase was positive in the proliferating cells no matter they were parenchyma or stroma cells. The phenomenon was observed in other liver proliferative lesions^[14, 32]. So that telomerase activation was also a good marker of cell in proliferation.

In summary, this is the first report on the *in situ* detection of TGF β 1, 2, 3, T β R II mRNA and telomerase activity during rat cholangiocarcinogenesis. There is TGF β 1, 2, 3, T β R II mRNA and telomerase activity in the hyperplastic, dysplastic cholangiocytes, CC cells as well as stroma fibroblasts. There is gradual increase of the fibrous stroma (fibrosis) during the

development of CC. It is considered that the expression of TGF β 1, 2, 3, T β R II and telomerase activation has important implication in cholangiocarcinogenesis and cancer stroma formation.

REFERENCES

- 1 **Heldin CH**, Miyazono K, Dijke PT. TGF-signaling from cell membrane to nucleus through SMAD proteins. *Nature*1997; **390**: 465-471
- 2 **Derynck R**, Akhurst RJ, Balmain A. TGF-signaling in tumor suppression and cancer progression. *Nature Genetics* 2001; **29**: 117-129
- 3 **Francis-Thickpenny KM**, Richardson DM, Eel CC, Love DR, Winship IM, Baguley BC, Chenevix-Trench G, Shelling AN. Analysis of the TGF β functional pathway in epithelial ovarian carcinoma. *Brit J Cancer* 2001; **85**: 687-691
- 4 **Jonson T**, Albrechtsson E, Axelson J, Heidenblad M, Gorunova L, Johansson B, Hoglund M. Altered expression of TGF β receptors and mitogenic effects of TGF β in pancreatic carcinomas. *Int J Oncol* 2001; **19**: 71-81
- 5 **Paterson IC**, Matthews JB, Huntley S, Robinson CM, Fahey M, Parkinson EK, Prime SS. Decreased expression of TGF-beta cell surface receptors during progression of human oral squamous cell carcinoma. *J Pathol* 2001; **193**: 458-467
- 6 **Xiong B**, Yuan HY, Hu MB, Zhang F, Wei ZZ, Gong LL, Yang GL. Transforming growth factor- β 1 in invasion and metastasis in colorectal cancer. *World J Gastroenterol* 2002; **8**: 674-678
- 7 **Ishak KG**, Anthony PP, Sobin LH. Histological Typing of Tumours of the Liver. WHO International Histological Classification of Tumours. Berlin: Springer Verlag, 1994
- 8 **Barwick WK**, Rosai J. Liver. In Rosai J ed. Ackerman's Surgical Pathology 7th ed. Mosby CO. St Louis. 1989: 675-735
- 9 **Rossmannith W**, Schulte-Hermann R. Biology of transforming growth factor beta in hepatocarcinogenesis. *Microsc Res Tech* 2001; **52**: 430-436
- 10 **Sasaki Y**, Tsujiuchi T, Murata N, Tsutsumi M, Konishi Y. Alterations of the transforming growth factor-beta signaling pathway in hepatocellular carcinomas induced endogenously and exogenously in rats. *Jpn J Cancer Res* 2001; **92**: 16-22
- 11 **Su WC**, Shiesh SC, Liu HS, Chen CY, Chow NH, Lin XZ. Expression of oncogene products HER2/Neu and Ras and fibrosis-related growth factors bFGF, TGF-beta, and PDGF in bile from biliary malignancies and inflammatory disorders. *Dig Dis Sci* 2001; **46**: 1387-1392
- 12 **Yokomuro S**, Tsuji H, Lunz JG, Sakamoto T, Ezure T, Murase N, Demetris AJ. Growth control of human biliary epithelial cells by interleukin 6, hepatocyte growth factor, transforming growth factor beta1, and activin A: comparison of a cholangiocarcinoma cell line with primary cultures of non-neoplastic biliary epithelial cells. *Hepatology* 2000; **32**: 26-35
- 13 **Holt SE**, Shay JW. Role of telomerase in cellular proliferation and cancer. *J Cell Physiol* 1999; **180**: 10-18
- 14 **Lu JP**, Zhu SN, Song BP, Mao JQ, Li MS, Hayashi K. In situ detection of telomerase activity in hepatic carcinogenesis of rats. *J Shanghai Med Univ* 1999; **26**: 413-416
- 15 **Ozaki S**, Harada K, Sanzen T, Watanabe K, Tsui W, Nakanuma Y. In situ nucleic acid detection of human telomerase in intrahepatic cholangiocarcinoma and its preneoplastic lesion. *Hepatology* 1999; **30**: 914-919
- 16 **Yuan ST**, Hu XQ, Lu JP, Hayashi K, Zhai WR, Zhang YE. Changes of integrin expression in rat hepatocarcinogenesis induced by 3' Me-DAB. *World J Gastroenterol* 2000; **6**: 231-233
- 17 **Wada K**, Nomura S, Mori E, Kitamura Y, Nishizawa Y, Miyake A, Terada N. Changes in levels of mRNAs of transforming growth factor (TGF)-beta1, -beta2, -beta3, TGF-beta type II receptor and sulfated glycoprotein-2 during apoptosis of mouse uterine epithelium. *J Steroid Biochem Mol Biol* 1996; **59**: 367-375
- 18 **Lu JP**. Non-isotopic in situ hybridization technique. *Nanhai Publication* 1996; Haikou, China
- 19 **Lu JP**, Zhu SN, Song BP, Mao JQ, Lu SL. In situ telomerase repeat amplification protocol (TRAP) detecting telomerase activity in human hepatocellular carcinoma. *Acta Histochem Cytochem* 1999; **32**: 477-480
- 20 **Lu JP**, Hayashi K. Transferrin receptor distribution and iron deposition in the hepatic lobule of iron-overloaded rats. *Pathol Int* 1995; **45**: 202-206

- 21 **Mao JQ**, Lu JP, Zhu SN, Li MS, Lu SL, Hayashi K, Nomura S. The significance of TGF β - and its receptor on the difference of stroma formation in experimental rat hepatocellular carcinoma and cholangiocarcinoma. *Chinese Hepatol* 2001; **6**: 23-25
- 22 **Nakatsukasa H**, Everts RP, Hsia CC, Marsden E, Thorgeirsson SS. Expression of transforming growth factor-beta 1 during chemical hepatocarcinogenesis in the rat. *Lab Invest* 1991; **65**: 511-517
- 23 **Vogelbruch M**, Wellmann A, Maschek H, Schafer MK, Flemming P, Georgii A. Transforming growth factor beta 1 in human liver tumors. *Verh Dtsch Ges Pathol* 1995; **79**: 132-136
- 24 **Factor VM**, Kao CY, Santoni-Rugiu E, Woitach JT, Jensen MR, Thorgeirsson SS. Constitutive expression of mature transforming growth factor beta1 in the liver accelerates hepatocarcinogenesis in transgenic mice. *Cancer Res* 1997; **57**: 2089-2095
- 25 **Kanzler S**, Meyer E, Lohse AW, Schirmacher P, Henninger J, Galle PR, Blessing M. Hepatocellular expression of a dominant-negative mutant TGF-beta type II receptor accelerates chemically induced hepatocarcinogenesis. *Oncogene* 2001; **20**: 5015-5024
- 26 **Lu JP**, Hayashi K. Myofibroblasts and stroma difference between cholangiocarcinoma and hepatocellular carcinoma. *Arch Histopathol D* 1996; **3**: 55-62
- 27 **Oft M**, Peli J, Rudaz C, Schwarz H, Beug H, Reichmann E. TGF-beta1 and Ha-Ras collaborate in modulating the phenotypic plasticity and invasiveness of epithelial tumor cells. *Genes Dev* 1996; **10**: 2462-2477
- 28 **Shimonishi T**, Sasaki M, Nakanuma Y. Precancerous lesions of intrahepatic cholangiocarcinoma. *J Hepatobil Pancreat Surg* 2000; **7**: 542-550
- 29 **Hytioglou P**, Kotoula V, Thung SN, Tsokos M, Fiel MI, Papadimitriou CS. Telomerase activity in precancerous hepatic nodules. *Cancer* 1998; **82**: 1831-1838
- 30 **Stampfer MR**, Garbe J, Levine G, Lichtsteiner S, Vasserot AP, Yaswen P. Expression of the telomerase catalytic subunit, hTERT, induces resistance to transforming growth factor beta growth inhibition in p16INK4A (-) human mammary epithelial cells. *Proc Natl Acad Sci USA* 2001; **98**: 4498-4503
- 31 **Qin LX**, Tang ZY. The prognostic molecular markers in hepatocellular carcinoma. *World J Gastroenterol* 2002; **8**: 385-392
- 32 **Ogami M**, Ikura Y, Nishiguchi S, Kuroki T, Ueda M, Sakurai M. Quantitative analysis and in situ localization of human telomerase RNA in chronic liver disease and hepatocellular carcinoma. *Lab Invest* 1999; **79**: 15-26

Edited by Xu XQ

Postoperative endoscopic surveillance of human living-donor small bowel transplantations

Jie Ding, Chang-Cun Guo, Cai-Ning Li, An-Hua Sun, Xue-Gang Guo, Ji-Yan Miao, Bo-Rong Pan

Jie Ding, Chang-Cun Guo, Cai-Ning Li, An-Hua Sun, Xue-Gang Guo, Ji-Yan Miao, Institute of Digestive Disease, Xijing Hospital, Fourth Military Medical University, Xi'an 710032, Shaanxi Province, China

Bo-Rong Pan, Oncology Center, Xijing Hospital, 127 Changle West Road, Xi'an 710032, China

Correspondence to: Prof. Jie Ding, Institute of Digestive Disease, Xijing Hospital, Fourth Military Medical University, Xi'an 710032, Shaanxi Province, China. charlson_cole@yahoo.com

Telephone: +86-29-3375230

Received: 2002-08-24 **Accepted:** 2002-10-20

Abstract

AIM: To determine the significance of endoscopic surveillance in the diagnosis of acute rejection after human living-donor small bowel transplantations.

METHODS: Endoscopic surveillance was performed through the ileostomy after human living-donor small bowel transplantations. The intestinal mucosa was observed and biopsies were performed for pathological observations.

RESULTS: Acute rejection was diagnosed in time by endoscopic surveillance. The endoscopic and pathological manifestations of acute rejection were described.

CONCLUSION: Endoscopic surveillance and biopsy are reliable methods to diagnose the acute rejection after human living-donor small bowel transplantations.

Ding J, Guo CC, Li CN, Sun AH, Guo XG, Miao JY. Postoperative endoscopic surveillance of human living-donor small bowel transplantations. *World J Gastroenterol* 2003; 9(3): 595-598 <http://www.wjgnet.com/1007-9327/9/595.htm>

INTRODUCTION

Prompt and accurate diagnosis of acute rejection is a key element to ensure the success of human small intestinal transplantation. However due to the limited cases of successful human small intestinal transplantations, little is available for the prompt and accurate diagnosis of acute rejection after the operations. Here we reported the postoperative endoscopic surveillance of acute rejection in 2 cases of human living-donor small bowel transplantations performed in our hospital. We also discussed the significance of endoscopic surveillance and pathological examination of the mucosal biopsy specimen in the diagnosis of acute rejections in this paper.

MATERIALS AND METHODS

Case material

Patient 1, Male, 18 years old, underwent enterectomy because of small bowel necrosis after volvulus with the residual jejunum being only 49 cm in length, had more than 10 defecations in a day with the content being undigested foods, suffered from

severe malnutrition, and was diagnosed as short bowel syndrome. Living-donor small bowel transplantation was performed on the patient on May 20 1999. The donor was his father. The donor and the recipient were ABO compatible (both O type) and their HLA and HLA-DR antigen were semi-compatible. The lymphocytotoxic cross matching test showed reaction <10%. A 150 cm segment of terminal ileum 20 cm away from the ileocecal valve was removed from the donor. The distal end of graft ileum was anastomosed to the distal end of the recipient ileum. Ileostomy was performed at the terminal end of the graft ileum.

Patient 2, Male, 15 years old, underwent resection of the most part of the small bowel and part of the cecum because of necrosis due to cecum hernia trap. The residual jejunum was only 10 cm in length. The patient defecated shortly after eating. Content of the defecations was undigested food. After 1 year and a half of parenteral nutrition, the patient developed mild liver dysfunction and was diagnosed as short bowel syndrome. Living-donor small bowel transplantation was performed on the patient on Jan 6 2001. The donor was his mother (47 years old). Both the donor and the recipient have a B type in ABO blood type. Their HLA and HLA-DR were semi-compatible. Lymphocytotoxic cross matching test showed <10% reaction. A 160 cm segment of terminal ileum 20 cm away from the ileocecal valve was removed from the donor. The distal end of graft ileum was anastomosed to the distal end of the recipient ileum. Ileostomy was performed at the terminal end of the graft ileum.

Both patients were given immunosuppressors FK506, MMF and MP together with antibiotics, anticoagulant and nutrition support. Patient 1 developed acute rejection after 67 days after operation. After implosion therapy, the rejection was taken under control, and so far, the patient has survived healthily for 30 months. Patient 2 developed acute rejection after 20 days of the operation, which was controlled after implosion therapy. However acute rejection reoccurred after 80 days of the operation together with severe infection. And the patient died after 5 months of the operation.

Methods

Endoscopic surveillance through the ileostomy was started at 15 days after operation for the patient 1, and 2 days after operation for the patient 2. Endoscopy was performed when discharge from the ileostomy increased or at the case of hemorrhage or other abnormalities. Patients took no food in 12 h before the endoscopic examination, and 1 000 ml 5% glucose saline was orally taken by the patients to clear the bowels. An Olympus GIF-XQ230 gastroscope was inserted through the ileostomy into the graft bowels for examination. And for a control observation, the gastroscope was extended to pass through the stoma to observe autologous small intestine or colon. Mucosal biopsies were performed at the graft bowels and the autologous small intestine or colon. Then the pathological and microbiological examinations of biopsy specimens were done.

RESULTS

During the 48 days after the operation, 8 times of endoscopic

examinations were performed on patient 1. Biopsies were performed at the same time for pathological examinations. No signs of rejection or infection were seen. After 60 days of the operation, discharge from the ileostomy was increased, and it went up to 1 200 ml at the 66th day. At the 66th day, endoscopy examination was performed, and it was found that the segments of graft bowel 20-35 cm, 40-60 cm and 70-90 cm away from the ileostomy had hyperemia and edema in the mucosa displaying a strong reflection; light yellow mucus was seen on the mucosal surface; patches of mucosal hemorrhage and erosion were also observed; besides, there were several oval-shaped (0.3-0.6 cm in diameter) and linear ulcers (paralleling with the mucosal folds) in the graft bowel; the ulcers were covered with white coat (Figure 1-4). The intestinal wall was quite fragile and easy to bleed. There was much hemorrhage in the biopsy sites after the biopsy. The vermiculation of the graft became weak. The residual autologous small bowel showed no signs of hyperemia, edema, erosion or ulceration. Pathological examination of the biopsy specimen revealed that there were local erosions in the mucosa; some parts of the epithelia showed atrophy in a shape of short column; the goblet cells decreased in size or just disappeared; edema was found universally in the lamina propria; there were infiltrations of neutrophils, plasma cells and lymphocytes in the lamina propria and the muscularis mucosa; there was an increase of the number of neutrophils in the blood vessels. Microbiological examination found no abnormalities. The residual autologous bowel was normal as confirmed by pathological examination in the biopsy specimen. The patient was diagnosed as acute rejection and was treated accordingly. After 3 days of treatment, endoscopic examination was performed, and it was found that the hyperemia and edema abated a lot, the erosions healed up; the ulcers decreased in size and depth and were partly scarred over (Figure 5). Follow-up by endoscopic and pathological examinations detected no lesions thereafter.



Figure 1 Rejection in the graft bowel 40 cm away from the ileostomy.



Figure 2 In the rejection of patient 1, we can see the linear ulcer paralleling with the mucosal plica.

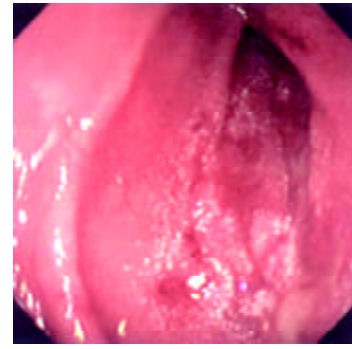


Figure 3 Rejection in the graft segment 50 cm away from the stoma of patient 1.



Figure 4 Rejection in the graft bowel 70 cm away from the stoma in patient 1.

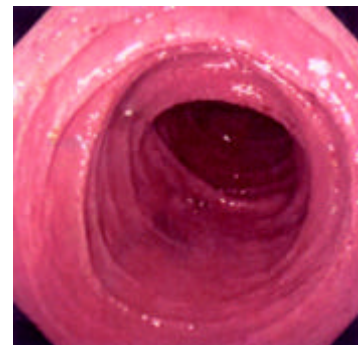


Figure 5 The mucosal edema abated and erosions healed 3 days after treatment. (patient 1).

Endoscopic examinations were performed during the time from the 2nd day to the 17th day after the transplantation. No signs of rejection were detected. However, on day 20 the discharge from the ileostomy increased up to 1 000 ml. Endoscopy was performed on day 22. It was found that: there was severe mucosal hyperemia and edema in the distal end of the graft bowel; patches of hemorrhage and erosions could be seen; a 0.6×1.2 cm oval-shaped longitudinal ulcer was seen 30 cm away from the ileostomy in the graft bowel. The ulcer was shallow and had a flat base with gray coat covering it. The autologous bowel was normal. On day 26, endoscopy was performed again and found that the ulcer was enlarged and deepened with edge raised. Circular broken plica was seen (Figure 6). Pathological examination of the specimen from the lesions suggested that there was acute rejection. No significant changes were seen in the microbiological examination. The autologous bowel showed normal pathological features. After 9 days of anti-rejection treatment, the ulcer became smaller and shallower with no coat on it and showed partial healing (Figure 8). On day 80 after transplantation, the discharge from

the ileostomy increased again. Endoscopy was performed and found that there were multiple lesions of hyperemia and edema in the graft bowel (showing strong reflection under the gastroscope); a great deal of white yellow mucus was seen on the lesions; the bowel lumen at the lesion sites became narrower; and the vermiculation of the graft bowel became weak; in the graft bowel, there were spots or patches of hemorrhage, superficial erosions, and deep round or oval ulcers varying from 0.8-2.0 cm in diameter; the edges of the ulcers showed severe hyperemia and edema. Pathological examination showed that there were ulcerations in the graft bowel; obvious edema could be seen in the lamina propria; the lamina propria and the muscularis mucosa had severe infiltration of neutrophils and lymphocytes. The patient was therefore diagnosed as severe acute rejection. Anti-rejection therapy had no effect on the patient. Follow-up by endoscopies witnessed the enlargement and deepening of the previous ulcers and the formation of new ulcers on the premise of mucosal edema and erosion (Figure 9). Ulcerative hemorrhage was also found.



Figure 6 Longitudinal oval- shaped shallow ulcers could be seen in the rejection 30 cm away from the stoma in patient 2.



Figure 7 Part of the shallow ulcers 30 cm away from the stoma was healed after patient 2 was treated for 9 days.



Figure 8 80 d after operation, severe rejection was seen 10 cm away from the ileostomy of the patient 2.



Figure 9 In patient 2, new ulcers formed 109 days after operation, and severe edema could be seen in the mucosa.

DISCUSSION

The significance of endoscopic surveillance

The difficulty of small bowel transplantation lies mainly in the high immunogenicity of the organ. The small bowel is rich in lymphocytes and dendritic cells (DC), especially in the Peyer's patches, lamina propria and the mesenteric nodes. The DC cells have been reported of great importance in the host's rejection to liver graft^[1]. All of the mentioned features of small bowel present a formidable challenge to small bowel transplantation. The major impediment to success of small bowel transplantation is the rejection, which will lead to failure if it is severe. Even though there have been some improvements in the technique of small bowel transplantation, both in human^[2] and animal model^[3], the rejection remains the major cause of failure in transplantation. Therefore, prompt and accurate diagnosis and treatment of rejection is the crux for successful transplantation. Pathological examinations of the mucosal biopsy specimen of the graft serve as the most important and fundamental method in current clinical diagnosis of rejection, for it can well show the characteristics of the rejection and its degree. The biopsy specimen can be openly taken through the stoma or under the endoscopic surveillance. However, typical lesions can not be easily taken by open biopsy, and erosions and ulcerations are often induced near the stoma due to repeated biopsies. Endoscopic surveillance has a good view of the mucosa of the graft bowel and biopsy specimen can be taken precisely at the lesion sites. Now it has been accepted as the most reliable conventional method for surveillance.

Living small bowel transplantation has high tissue compatibility and can reduce the frequency of rejection or its severity. Novel immunosuppressor agents such as FK506 can effectively suppress rejection after transplantation. Living-donor small bowel transplantation was first reported by Deltz *et al*^[4]. Since then, there have been several reports of living small bowel transplantations reported, and most of the transplantations in 1990's were successful^[5]. Compared with cadaveric bowel transplantation, living-donor small bowel transplantation has a lower rate of rejection and infection^[6]. But acute rejection is not uncommon in living small bowel transplantation^[7,8], and if the rejection is severe, it can cause loss of the graft or death of the patients. So, the surveillance, prevention and treatment of the rejection should be paid attention to all the time after the small bowel transplantation. Some indices of enteral function and biochemistry and immunology have been used in immune surveillance after small bowel transplantation in experimental animal, but most of them are under investigation and show no values of clinical practice. The recognition and diagnosis of the rejection are mainly depended on clinical observation, endoscopy and pathological examination. Rejection has no clinical characteristics for diagnosis; the biopsy specimen is not always a mirror of the

situation of rejection; and for definite diagnosis of rejection, the specimen should cover all the layers of the intestinal wall, but the biopsy can easily cause severe complications such as perforation. Therefore, endoscopic examination is the most important method for posttransplant surveillance and diagnosis of rejection.

Method and time for Endoscopy surveillance

Most of the living-donor small bowel transplantations were staged operations, and there was an ileostomy often left for postoperative observation. The graft bowel and the discharge could be observed directly through the ileostomy. And the stoma also provided a passage for the endoscopic surveillance and mucosal biopsy. The endoscopy plays an important role in the assessment of the graft bowel, and in 1999, Kato *et al*^[9] reported the first case of using zoom videoendoscope to evaluate graft bowel mucosa in human intestine transplantation. This method was further proved to be effective to determine the severity of acute cellular rejection and to be able to minimize the times of biopsies^[10]. In this report, with a gastroscopy, we successfully performed endoscopic examinations and mucosa biopsies for 39 times through the stoma in these 2 patients. No complications were observed, which suggested that endoscopy and biopsy are safe and convenient methods for the surveillance of the graft bowel. As for the timing of the endoscopic surveillance, the frequency of endoscopy should be generally 1 or 2 times every week during the first 3 months after the operation. Rejections and other complications of small bowel transplantation such as hemorrhage and thrombosis in mesentery occur most often during the initially several days after the transplantation. So we consider that it is proper to perform endoscopic examination everyday in the first 3 days, and afterwards, the frequency of endoscopy be reduced to once every 2 or 3 days and the intervals between two endoscopies can be prolonged gradually in the following 2 or 3 weeks. Emergency endoscopic examinations should be taken in case of intestinal bleeding and increased discharge from the stoma, etc. As results shown by the study of Sigurdsson and his colleagues, the endoscopy was sensitive enough to diagnose only 63 % of the rejections^[8]. We think it necessary to perform biopsies at the same time. As the rejections have a high anatomic variability in the graft bowel^[11], we recommend that the specimen should be taken at multiple sites in the graft bowel, and residual autologous small should bowel be sampled for the control. If necessary, the specimen should undergo microbiological examination to exclude lesions caused by infection.

Clinical features of acute rejection and its endoscopic manifestations

Acute rejections in human small bowel transplantation often occur early after operation, especially during the first 30 days^[12], but also may happen late beyond the first year after transplantation. Generally, clinical features of rejection show as fever, nausea, vomiting, abdominal pain, diarrhea and increased discharge from the stoma. Under endoscopic observation, mucosal hyperemia and edema, fragile intestine wall, erosion, ulceration and hypoperistalsis can be found. Uleration always suggests the onset of acute rejection. Pathological changes vary with the severity of the rejection. At the early stage, microvillus may become blunt, the goblet cell may disappear, and there may be infiltration of inflammatory cells. And then, there may be crypt inflammation, increased apoptotic cells, and in cases of severe rejection, they

can be mucosa hemorrhage, patchy mucosal exfoliation and formation of small abscesses.

When the discharge from the stoma increased in the 2 patients taking small bowel transplantation in our hospital, the manifestations mentioned above were observed by endoscopic surveillance. Combining the endoscopic and pathological findings together, the acute rejection was diagnosed. After the pulse therapy, the lesions of acute rejection abated or disappeared, which confirmed the diagnosis of acute rejection. Endoscopic surveillance is significant for diagnosing rejection and determining the outcomes of corresponding treatment. According to our experience, when there are mucosal hyperemia, edema, hemorrhage and erosions, they should be regarded them as precautions for rejection; if there are ulcers, it often means the onsets of rejections, in addition to the pathological findings, a prompt diagnosis is warranted; improved situations of the patients and healing ulcers suggests the validity of anti-rejection therapy, while no amelioration, enlargement and deepening of ulcers, hemorrhage or formation of new ulcers are indicators of invalidity of anti-rejection treatment and progress of rejection.

So far, there are no standard criteria for the diagnosis of rejection after human small transplantation, and little is known about the endoscopic characteristics of rejection and pathological changes. But more detailed standard of endoscopic surveillance and pathological examinations will be set with more cases of human small bowel transplantation performed.

REFERENCES

- 1 **Xu MQ**, Yao ZX. Functional changes of dendritic cells derived from allogeneic partial liver graft undergoing acute rejection in rats. *World J Gastroenterol* 2003; **9**: 141-147
- 2 **Zhang WJ**, Liu DG, Ye QF, Sha B, Zhen FJ, Guo H, Xia SS. Combined small bowel and reduced auxiliary liver transplantation: case report. *World J Gastroenterol* 2002; **8**: 956-960
- 3 **Wu XT**, Li JS, Zhao XF, Zhuang W, Feng XL. Modified techniques of heterotopic total small intestinal transplantation in rats. *World J Gastroenterol* 2002; **8**: 758-762
- 4 **Deltz E**, Schroeder P, Gundlach M, Hansmann ML, Leimenstoll G. Successful clinical small-bowel transplantation. *Transplant Proc* 1990; **22**: 2501
- 5 **Margreiter R**. Living-donor pancreas and small-bowel transplantation. *Langenbecks Arch Surg* 1999; **384**: 544-549
- 6 **Cicalese L**, Rastellini C, Sileri P, Abcarian H, Benedetti E. Segmental living related small bowel transplantation in adults. *J Gastrointest Surg* 2001; **5**: 168-172
- 7 **Uemoto S**, Fujimoto Y, Inomata Y, Egawa H, Asonuma K, Pollard S, Tanaka K. Living-related small bowel transplantation: the first case in Japan. *Pediatr Transplant* 1998; **2**: 40-44
- 8 **Sigurdsson L**, Reyes J, Putnam PE, del Rosario JF, Di Lorenzo C, Orenstein SR, Todo S, Kocoshis SA. Endoscopies in pediatric small intestinal transplant recipients: five years experience. *Am J Gastroenterol* 1998; **93**: 207-211
- 9 **Kato T**, O'Brien CB, Nishida S, Hoppe H, Gasser M, Berho M, Rodriguez MJ, Ruiz P, Tzakis AG. The first case report of the use of a zoom videoendoscope for the evaluation of small bowel graft mucosa in a human after intestinal transplantation. *Gastrointest Endosc* 1999; **50**: 257-261
- 10 **Sasaki T**, Hasegawa T, Nakai H, Kimura T, Okada A, Musiaki S, Doi R. Zoom endoscopic evaluation of rejection in living-related small bowel transplantation. *Transplantation* 2002; **73**: 560-564
- 11 **Sigurdsson L**, Reyes J, Todo S, Putnam PE, Kocoshis SA. Anatomic variability of rejection in intestinal allografts after pediatric intestinal transplantation. *J Pediatr Gastroenterol Nutr* 1998; **27**: 403-406
- 12 **Sudan DL**, Kaufman S, Horslen S, Fox I, Shaw Jr BW, Langnas A. Incidence, Timing, and Histologic Grade of Acute Rejection in Small Bowel Transplant Recipients. *Transplant Proc* 2000; **32**: 1199

The effects of the formula of amino acids enriched BCAA on nutritional support in traumatic patients

Xin-Ying Wang, Ning Li, Jun Gu, Wei-Qin Li, Jie-Shou Li

Xin-Ying Wang, Ning Li, Jun Gu, Wei-Qin Li, Jie-Shou Li, Medical School of Nanjing University, Research Institute of General Surgery, Jinling Hospital, Nanjing 210002, Jiangsu Province, China
Supported by the Natural Science Foundation of Jiangsu Province, China (No. BQ 2000014), and the Tenth Five-year Medicine Research Foundation in the CPLA (No. 01Z011)

Correspondence to: Xin-Ying Wang, Research Institute of General Surgery, Jinling Hospital, 305 East Zhongshan Road, Nanjing 210002, Jiangsu Province, China. wxinying@263.net

Telephone: +86-25-4826808-58066 **Fax:** +86-25-4803956

Received: 2002-08-13 **Accepted:** 2002-09-16

Abstract

AIM: To investigate the formula of amino acid enriched BCAA on nutritional support in traumatic patients after operation.

METHODS: 40 adult patients after moderate or large abdominal operations were enrolled in a prospective, randomly and single-blind-controlled study, and received total parenteral nutrition (TPN) with either formula of amino acid (AA group, 20 cases) or formula of amino acid enriched BCAA (BCAA group, 20 cases). From the second day after operation, total parenteral nutrition was infused to the patients in both groups with equal calorie and equal nitrogen by central or peripheral vein during more than 12 hours per day for 6 days. Meanwhile, nitrogen balance was assayed by collecting 24 hours urine for 6 days. The markers of protein metabolism were investigated such as amino acid patterns, levels of total protein, albumin, prealbumin, transferrin and fibronectin in serum.

RESULTS: The positive nitrogen balance in BCAA group occurred two days earlier than that in AA group. The serum levels of total protein and albumin in BCAA group were increased more obviously than that in AA group. The concentration of valine was notably increased and the concentration of arginine was markedly decreased in BCAA group after the formula of amino acids enriched BCAA transfusion.

CONCLUSION: The formula of amino acid enriched BCAA may normalize the levels of serum amino acids, reduce the proteolysis, increase the synthesis of protein, improve the nutritional status of traumatic patients after operation.

Wang XY, Li N, Gu J, Li WQ, Li JS. The effects of the formula of amino acids enriched BCAA on nutritional support in traumatic patients. *World J Gastroenterol* 2003; 9(3): 599-602
<http://www.wjgnet.com/1007-9327/9/599.htm>

INTRODUCTION

Hypermetabolism and increased catabolism can be observed in traumatic patients after operation, which may result in severe disturbance of sugar, lipid and protein metabolism^[1-4], accompanied with the changes on the levels of amino acids in serum^[5,6]. How to adjust the formula of amino acids to improve

the metabolism is an interesting project. There has been no data about formula of amino acid which is fit for nutritional support of patients after trauma yet^[7-11]. The purpose of our study was to investigate the effects of the formula of amino acids enriched BCAA on nutritional support in traumatic patients after operation.

MATERIALS AND METHODS

Subjects

40 adult patients after moderate or large abdominal operations who needed total parenteral nutrition (TPN) for more than 6 days were enrolled in a prospective, randomly and single-blind-controlled study from multiple centers during the period from March 2000 to November 2000. The patients (21 males and 19 females) weighed 45-71 kg and were 20-70 years old without metabolic diseases, malnutrition and dysfunction of liver and kidney. The change of weight in each patient was less than 10 % of that before disease. The patients were divided into two groups in random order, the control group (AA group) supplemented with the formula of amino acid (BCAA 22.8 %) and the study group (BCAA group) with the formula of amino acid enriched BCAA (BCAA 35.9 %).

Experiment protocols

TPN was infused with equal nitrogen and calorie through peripheral or central vein during more than 12 hours per day for 6 days, and began on the 2nd day after operation. The formula included nitrogen (0.2 g·kg⁻¹·d⁻¹), non-protein calorie (NPC, 25 kcal·kg⁻¹·d⁻¹), the ratio of NPC to N (125/1), the ratio of lipid to sugar (1/1-3/2).

Collection of samples

Serum samples from all patients were collected on the day before operation and on the 7th day after operation. The amino acid pattern, total protein, albumin, prealbumin, transferrin and fibronectin in serum were detected.

Urine samples: 24-hour urine samples (total volume of urine from 6 am on the first day to 6 am on the second day) of 40 patients were collected from the day before operation to the 7th day after operation to analyze nitrogen balance.

Assays of amino acids, proteins and nitrogen balance

The amino acid pattern in serum was analyzed by the system of high liquid phase amino acid analysis (BECKMAN, USA): 126AA, 166 monitor, 232 reactor, 507 autoloader, golden data station. The total protein (TP) and albumin in serum were respectively detected by the automatic biochemistry analyzer. The serum prealbumin, transferrin, fibronectin were monitored with anti-Pa, anti-Tf, anti-Fn immuno-diffusion board. (Yuhuan reagent Co.) The nitrogen balance was analyzed with the method of Kjeldahl to get the data of nitrogen content in urine.

Statistical analysis

All data were expressed as mean±SD. Comparisons between two groups were performed using an unpaired Student's *t* test. Differences were considered statistically significant when *P*<0.05.

Table 1 The comparability of patients' age, sex and operation

Group	Case	Age(y)	Sex (M/F)	Weigh before operation(kg)	Colectomy	Enterectomy	Miles	Rectal cancer anterior-rectal resection	Abormal trauma	Digestive tract tumor resection
AA	20	20-75	9/11	59.58±12.28	9	4	2	1	1	3
BCAA	20	20-75	12/8	60.38±9.83	7	5	0	2	5	1

Table 2 The changes of prealbumin, fibronectin and transferrin in two groups

	Group	Case	Before transfusion $\bar{x}\pm s$	After transfusion $\bar{x}\pm s$	Difference $\bar{x}\pm s$	P value
Prealbumin (g/L)	I	20	0.467±0.294	0.449±0.305	-0.018±0.091	0.305
	II	20	0.296±0.239	0.297±0.250	0.001±0.048	
Fibronectin (g/L)	I	20	2.200±0.752	2.112±0.789	-0.085±0.344	0.128
	II	20	2.201±0.792	2.345±1.052	0.144±0.735	
Transferrin (g/L)	I	20	0.316±0.171	0.335±0.179	0.019±0.211	0.970
	II	20	0.276±0.107	0.296±0.524	0.018±0.116	

I: AA group (the formula of amino acids); II: BCAA group (the formula of amino acids enriched BCAA).

Table 3 The changes of the amino acid pattern in serum after infusion

	Group	Case	Before infusion $\bar{x}\pm s$	After infusion $\bar{x}\pm s$	P value	Difference $\bar{x}\pm s$	P value
Asparagic acid(umol/L)	I	20	0.0748±0.0672	0.0942±0.0789	0.2580	0.0194±0.0638	0.8728
	II	20	0.0633±0.0413	0.0797±0.0558	0.0999	0.0164±0.0360	
Threonine (umol/L)	I	20	0.1973±0.1554	0.2829±0.2147	0.0354	0.0856±0.1424	0.2415
	II	20	0.1549±0.0863	0.3154±0.2331	0.0065	0.1601±0.1943	
Serine (umol/L)	I	20	0.2320±0.1455	0.2600±0.1701	0.4696	0.0279±0.1456	0.5872
	II	20	0.1981±0.1305	0.2518±0.1576	0.0759	0.0537±0.1086	
Glutacid (umol/L)	I	20	0.2619±0.2755	0.2829±0.2146	0.8237	0.0209±0.3574	0.3334
	II	20	0.2718±0.2409	0.4212±0.3217	0.1275	0.1493±0.3570	
Glycine (umol/L)	I	20	0.3844±0.2695	0.5402±0.3608	0.0173	0.1558±0.2237	0.9325
	II	20	0.3722±0.2207	0.5193±0.3565	0.1028	0.1471±0.3265	
Alanine (umol/L)	I	20	0.5067±0.3043	0.5737±0.4167	0.5325	0.0669±0.4053	0.1322
	II	20	0.4382±0.2862	0.7291±0.5371	0.0111	0.2908±0.3849	
Valine (umol/L)	I	20	0.2959±0.2188	0.2722±0.2168	0.6596	-0.0237±0.2038	0.0264
	II	20	0.2601±0.1494	0.4599±0.3765	0.0249	0.1999±0.3082	
Cysteine (umol/L)	I	20	0.0138±0.0180	0.0209±0.0182	0.1043	0.0057±0.0127	0.9373
	II	20	0.0300±0.0202	0.0350±0.0244	0.5238	0.0050±0.0296	
Methionine (umol/L)	I	20	0.0472±0.0361	0.0590±0.0498	0.3292	0.0118±0.0452	0.4447
	II	20	0.0282±0.0222	0.0516±0.0440	0.0253	0.0234±0.0362	
Isoleucine (umol/L)	I	20	0.1030±0.0728	0.1298±0.0874	0.1973	0.0268±0.0766	0.7457
	II	20	0.0825±0.0586	0.1181±0.0914	0.0730	0.0356±0.0711	
Leucine (umol/L)	I	20	0.2368±0.1699	0.2496±0.1694	0.7556	0.0128±0.1557	0.3377
	II	20	0.1770±0.1113	0.2399±0.1674	0.0698	0.0629±0.1242	
Tyrosine (umol/L)	I	20	0.0774±0.0511	0.0787±0.0631	0.9380	0.0014±0.0659	0.7263
	II	20	0.0584±0.0378	0.0677±0.0528	0.5343	0.0093±0.0563	
Phenylalanine (umol/L)	I	20	0.0897±0.0960	0.1572±0.1323	0.0289	0.0675±0.1074	0.9835
	II	20	0.0736±0.0518	0.1418±0.1277	0.0138	0.0683±0.0939	
Lysine (umol/L)	I	20	0.1888±0.1780	0.2311±0.1984	0.3706	0.0422±0.1767	0.6928
	II	20	0.1124±0.1226	0.1836±0.2403	0.2280	0.0712±0.2187	
Histidine (umol/L)	I	20	0.2517±0.1691	0.2885±0.2054	0.2654	0.0368±0.1227	0.2958
	II	20	0.1907±0.1041	0.2756±0.1778	0.0196	0.0850±0.1249	
Arginine (umol/L)	I	20	0.1214±0.2102	0.2534±0.5048	0.1584	0.1320±0.3433	0.0412
	II	20	0.2038±0.4115	0.0480±0.0678	0.1459	-0.1559±0.3921	
BCAA (umol/L)	I	20	0.6358±0.4556	0.6516±0.4014	0.8631	0.0158±0.3494	0.0785
	II	20	0.5196±0.3128	0.8180±0.6279	0.0325	0.2984±0.4869	

I: AA group (the formula of amino acids); II: BCAA group (the formula of amino acids enriched BCAA).

RESULTS

General clinical data

The age, sex, weight diagnosis and operation of patients were presented in Table 1, and showed the data comparable in both groups.

Nitrogen balance

As shown in Figure 1, the negative nitrogen balance was observed from all patients in both groups after operation, which was significantly improved after TPN infusion. The positive nitrogen balance in study group occurred on the third day after operation, which was earlier two days than that in the control group. On the sixth day after operation, the nitrogen balance in the study group is obviously better than that in the control group ($P<0.05$).

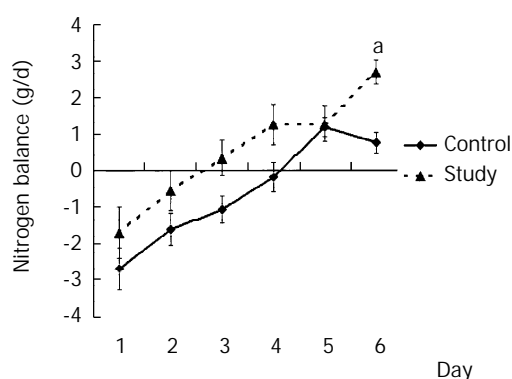


Figure 1 Nitrogen balance after infusion in two groups. ^a $P<0.05$ vs the control group.

Serum levels of prealbumin, fibronectin, and transferrin

The serum levels of prealbumin, fibronectin, and transferrin have no significant difference between two groups (Table 2).

Serum levels of albumin and total protein

There is significant difference before and after study in the serum levels of albumin and total protein of two groups. As shown in Figure 2, contrast to the study group, the serum levels of total protein and albumin decreased greatly in the control group after operation ($P<0.05$).

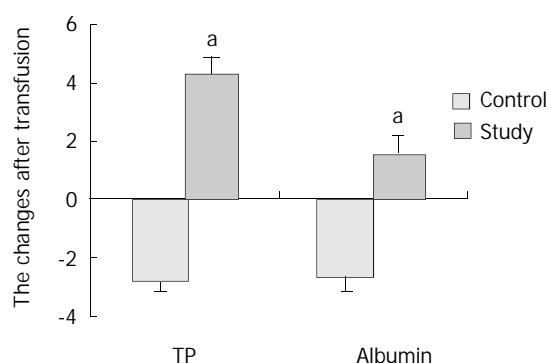


Figure 2 The changes of total protein and albumin after infusion in two groups. ^a $P<0.05$ vs the control group.

The change in the pattern of serum amino acid

The concentration of valine was notably increased ($P=0.02642$) and that of arginine was markedly decreased ($P=0.0412$) in the study group after the formula of amino acids enriched BCAA infusion when compared with the control group. In the study group, the concentrations of valine, threonine, alanine,

methionine, histidine, phenylalanine and BCAA are higher after infusion than those before transfusion ($P<0.05$). In the control group, the concentrations of glycine, histine and phenylalanine are higher after infusion than those before infusion ($P<0.05$). (Table 3).

DISCUSSION

The trauma caused by moderate or large operation may result in disturbance of glucose, lipid and protein metabolism including hypermetabolism and increased catabolism, which may lead to acute protein malnutrition, decline of immunological function and dysfunction of multiple organs^[12-16]. It was reported that the supplement of the special amino acids such as arginine, BCAA and glutamine would improve recovery of patients^[17-24]. Our present study was to observe the effect of the formula of amino acids enriched BCAA on patients after trauma.

In this study, we began to supplement the application of the formula of amino acid enriched BCAA on day 2 after operation to correct patients' hypermetabolism, to normalize the pattern of plasma amino acid concentrations and to improve recovery of patients. BCAA(valine, leucine, isoleucine) can be used as the substrate for energy and glyconeogenesis and as the muscle protein regulator. BCAA can increase the intake of energy by means of oxidization into energy in the tissues without aggrandizing the burden of the liver. As glyconeogenesis substrate, BCAA can also be oxidized in body and produce much energy by the mechanism of circulation between oxidation and alanine synthesis^[25-28]. The valine, leucine and isoleucine per gram molecular can produce 42, 43 and 32 gram molecular ATP respectively, which can supply a lot of energy to the body. The character as the source of energy for these 3 amino acids is that their first carbon can be oxidized and produce phosphate of high energy without glutamic acid, which is helpful for the decline of mechanism of producing energy with glutamic acid during trauma and stress. Because BCAA is mainly metabolized in muscle, the application of the formula of amino acid enriched BCAA can decrease the decompose of visceral protein such as muscle and liver proteins, prevent the loss of amino acids from muscle, correct negative balance, improve protein synthesis and regulate serum amino acids. In addition our results demonstrated the effect was dependent on the dose of BCAA.

Under the stress of trauma, the decompose of muscle protein seriously increases and produces a lot of free amino acids^[29-33], and hyperphenylalaninaemia appears. The ratio of phenylalanine to tyrosine (phe/tyr) rises and the ratio of BCAA to aromatic amino acid (AAA) descends after trauma because of the dysfunction of liver^[34, 35]. The low dose of phenylalanine and the high dose of BCAA in the formula of amino acid enriched BCAA can also improve the pattern of serum amino acids after trauma.

In summary, the nitrogen balance, the synthesis of acute phase proteins and visceral proteins and the pattern of serum amino acid concentrations were measured and compared with two groups after six days of TPN after trauma. Our results demonstrated that the formula of amino acid enriched BCAA could normalize of serum amino acid levels, reduce proteolysis, increase protein synthesis and improve nitrogen balance.

REFERENCES

- 1 **Liang LJ**, Yin XY, Luo SM, Zheng JF, Lu MD, Huang JF. A study of the ameliorating effects of carnitine on hepatic steatosis induced by total parenteral nutrition in rats. *World J Gastroenterol* 1999; **5**: 312-315
- 2 **Wu YA**, Lu B, Liu J, Li J, Chen JR, Hu SX. Consequence alimentary reconstruction in nutritional status after total gastrectomy for gastric cancer. *World J Gastroenterol* 1999; **5**: 34-37

- 3 **Cui XL**, Iwasa M, Iwasa Y, Ogoshi S. Arginine-supplemented diet decreases expression of inflammatory cytokines and improves survival in burned rats. *JPEN* 2000; **24**: 89-96
- 4 **Mansoor O**, Cayol M, Gachon P, Boirie Y, Schoeffler P, Obled C, Beaufriere B. Albumin and fibrinogen syntheses increase while muscle protein synthesis decreases in head-injured patients. *Am J Physiol* 1997; **273**: E898-902
- 5 **Vente JP**, von Meyenfeldt MF, van Eijk HM, van Berlo CL, Gouma DJ, van der Linden CJ, Soeters PB. Plasma-amino acid profiles in sepsis and stress. *Ann Surg* 1989; **209**: 57-62
- 6 **Wu Y**, Chai JK, Li JY, Diao L. The change in plasma concentration of free amino acids during early postburn stage in severely scalded rats. *Zhonghua Shaoshang Zazhi* 2001; **17**: 215-218
- 7 **Klein S**, Kinney J, Jeejeebhoy K, Alpers D, Hellerstein M, Murray M, Twomey P. Nutrition support in clinical practice: review of published data and recommendations for future research directions. *Am J Clin Nutr* 1997; **66**: 683-706
- 8 **Cao WX**, Cheng QM, Fei XF, Li SF, Yin HR, Lin YZ. A study of preoperation methionine-depleting parenteral nutrition plus chemotherapy in gastric cancer patients. *World J Gastroenterol* 2000; **6**: 255-258
- 9 **Chen QP**. Enteral nutrition and acute pancreatitis. *World J Gastroenterol* 2001; **7**: 185-192
- 10 **Pei WF**, Xu GS, Sun Y, Zhu SL, Zhang DQ. Protective effect of electroacupuncture and moxibustion on gastric mucosal damage and its relation with nitric oxide in rats. *World J Gastroenterol* 2000; **6**: 424-427
- 11 **Boctor DL**, Pillo-Blocka F, McCrindle BW. Nutrition after cardiac surgery for infants with congenital heart disease. *Nutritim Clinical Practice* 1999; **14**: 111-115
- 12 **Antonio J**, Sanders MS, Ehler LA, Uelmen J, Raether JB, Stout JR. Effects of exercise training and amino-acid supplementation on body composition and physical performance in untrained women. *Nutrition* 2000; **16**: 1043-1046
- 13 **Wang SJ**, Wen DG, Zhang J, Man X, Liu H. Intensify standardized therapy for esophageal and stomach cancer in tumor hospitals. *World J Gastroenterol* 2001; **7**: 80-82
- 14 **Dionigi P**, Alessiani M, Ferrazi A. Irreversible intestinal failure, nutrition support, and small bowel transplantation. *Nutrition* 2001; **17**: 747-750
- 15 **Zhou HP**, Wang X, Zhang NZ. Early apoptosis in intestinal and diffuse gastric carcinomas. *World J Gastroenterol* 2000; **6**: 898-901
- 16 **Zhou ZW**, Wan DS, Chen G, Chen YB, Pan ZZ. Primary malignant tumor of the small intestine. *World J Gastroenterol* 1999; **5**: 273-276
- 17 **Freund HR**, Hanani M. The metabolic role of branched-chain amino acids. *Nutrition* 2002; **18**: 287-288
- 18 **Garcia-de-Lorenzo A**, Ortiz-Leyba C, Planas M, Montejo JC, Nunez R, Ordonez FJ, Aragon C, Jimenez FJ. Parenteral administration of different amounts of branch-chain amino acids in septic patients: clinical and metabolic aspects. *Crit Care Med* 1997; **25**: 418-424
- 19 **James JH**. Branched chain amino acids in hepatic encephalopathy. *Am J Surg* 2002; **183**: 424-429
- 20 **Bassit RA**, Sawada LA, Bacurau RFP, Navarro F, Martins E, Santos RVT, Caperuto EC, Rogeri P, Rosa LFBPC. Branched-chain amino acid supplementation and the immune response of long-distance athletes. *Nutrition* 2002; **18**: 376-379
- 21 **Bruins MJ**, Soeters PB, Lamers WH, Deutz NE. L-arginine supplementation in pigs decreases liver protein turnover and increases hindquarter protein turnover both during and after endotoxemia. *Am J Clin Nutr* 2002; **75**: 1031-1044
- 22 **Yin L**, Li JS, Guo AQ, Liu FK, Liu FN. The prospective study of metabolic support with individual amino acids after trauma. *Chinese J Surg* 1992; **30**: 659-662
- 23 **Apovian CM**. Nutritional assessment in the elderly: facing up to the challenges of developing new tools for clinical assessment. *Nutrition* 2001; **17**: 62-63
- 24 **Harper AE**, Yoshimura NN. Protein quality, amino acid balance, utilization, and evaluation of diets containing amino acids as therapeutic agents. *Nutrition* 1993; **9**: 460-469
- 25 **Holecck M**. Relation between glutamine, branched-chain amino acids, and protein metabolism. *Nutrition* 2002; **18**: 130-133
- 26 **Kouzetsova L**, Bijlsma PB, van Leeuwen PAM, Groot JA, Houdijk APJ. Glutamine reduces phorbol-12,13-dibutyrate-induced macromolecular hyperpermeability in HT-29Cl.19A intestinal cells. *JPEN* 1999; **23**: 136-139
- 27 **Khan J**, Iiboshi Y, Cui L, Wasa M, Sando K, Takagi Y, Okada A. Alanyl-glutamine-supplemented parenteral nutrition increases luminal mucus gel and decreases permeability in the rat small intestine. *JPEN* 1999; **23**: 24-31
- 28 **Kudsk KA**, Wu Y, Fukatsu K, Zarzaur BL, Johnson CD, Wang R, Hanna MK. Glutamine-enriched total parenteral nutrition maintains intestinal interleukin-4 and mucosal immunoglobulin A levels. *JPEN* 2000; **24**: 270-274
- 29 **Bush JA**, Wu G, Suryawan A, Nguyen HV, Davis TA. Somatotropin-induced amino acid conservation in pigs involves differential regulation of liver and gut urea cycle enzyme activity. *J Nutr* 2002; **132**: 59-67
- 30 **Meadows GG**, Zhang H, Ge X. Specific amino acid deficiency alters the expression of genes in human melanoma and other tumor cell lines. *J Nutr* 2001; **131**: 3047S-3050S
- 31 **Ratheiser KM**, Pesola GR, Campbell RG, Matthews DE. Epinephrine transiently increases amino acid disappearance to lower amino acid levels in humans. *JPEN* 1999; **23**: 279-287
- 32 **Baggott JE**. Metabolism of methionine derived from deuterated serine infused in a human. *Am J Clin Nutr* 2001; **74**: 701-703
- 33 **Klassen P**, Furst P, Schulz C, Mazariegos M, Solomons NW. Plasma free amino acid concentrations in healthy Guatemalan adults and in patients with classic dengue. *Am J Clin Nutr* 2001; **73**: 647-652
- 34 **Roberts SA**, Thorpe JM, Ball RO, Pencharz PB. Tyrosine requirement of healthy men receiving a fixed phenylalanine intake determined by using indicator amino acid oxidation. *Am J Clin Nutr* 2001; **73**: 276-282
- 35 **de Jonge WJ**, Marescau B, Hooge RD, de Deyn PP, Hallemeesch MM, Deutz NEP, Ruijter JM, Lamers WH. Overexpression of arginase alters circulating and tissue amino acids and guanidino compounds and affects neuromotor behavior in mice. *J Nutr* 2001; **131**: 2732-2740

Adhesive small bowel obstruction: How long can patients tolerate conservative treatment?

Shou-Chuan Shih, Kuo-Shyang Jeng, Shee-Chan Lin, Chin-Roa Kao, Sun-Yen Chou, Horng-Yuan Wang, Wen-Hsiung Chang, Cheng-Hsin Chu, Tsang-En Wang

Shou-Chuan Shih, Shee-Chan Lin, Chin-Roa Kao, Sun-Yen Chou, Horng-Yuan Wang, Wen-Hsiung Chang, Cheng-Hsin Chu, Tsang-En Wang. Gastroenterology Section, Department of Internal Medicine, Mackay Memorial Hospital, Taipei, Taiwan
Kuo-Shyang Jeng. General Surgery Section, Department of Surgery, Mackay Memorial Hospital, Taipei, Taiwan, China
Shou-Chuan Shih, Mackay Junior School of Nursing, Taipei, Taiwan, China

Correspondence to: Dr. Shou-Chuan Shih, Gastroenterology Section, Department of Internal Medicine, Mackay Memorial Hospital and Mackay Junior College of Nursing, No. 92, section 2, Chang-San North Road, Taipei, Taiwan, China. sschuan@ms2.mmh.org.tw
Telephone: +886-2-25433534 **Fax:** +886-2-27752142
Received: 2002-08-17 **Accepted:** 2002-08-19

Abstract

AIM: To evaluate how long patients with small bowel obstruction caused by postoperative adhesions can tolerate conservative treatment.

METHODS: The records of patients with small bowel obstruction due to postoperative adhesions were retrospectively reviewed. Data collected included the number of admissions, type of management for each admission, duration of conservative treatment, number of repeat laparotomies, and operative findings.

RESULTS: One hundred fifty-five patients with this condition from January 1999 to December 2001, for a total of 293 admissions were enrolled in this study. Medical treatment alone was given in 220 admissions, and repeat laparotomy was performed in 73 admissions. The period of observation in patients managed medically ranged from 2 to 12 days (average: 6.9 days), while for those who underwent surgery, the range was 1 to 14 days (average 5.4 days). At surgery, adhesions were the only finding in 46 cases, while there were intestinal complications in 27, or 9.2 % of all 293 admissions. Fever and leukocytosis greater than 15 000/mm³ were prediction of intestinal complications.

CONCLUSION: With closely monitoring, most patients with small bowel obstruction due to postoperative adhesions could tolerate supportive treatment and recover well averagely within 1 week, although some patients require more than 10 days of observation.

Shih SC, Jeng KS, Lin SC, Kao CR, Chou SY, Wang HY, Chang WH, Chu CH, Wang TE. Adhesive small bowel obstruction: How long can patients tolerate conservative treatment? *World J Gastroenterol* 2003; 9(3): 603-605
<http://www.wjgnet.com/1007-9327/9/603.htm>

INTRODUCTION

Postoperative adhesions are a frequently encountered problem.

They are the most common cause of small bowel obstruction in adults^[1-3]. Clinically, the obstruction may progress to life-threatening complications or follow a more benign course. There is debate about the optimal treatment: surgical or medical management. Some authors have emphasized the importance of early operation for any attack of bowel obstruction because of the possibility of serious sequelae with delayed treatment^[4-6]. However, there is no question that the problem is remitted spontaneously in a significant number of patients, who therefore need not require reoperation^[7-9]. We undertook this retrospective study to evaluate how long patients may safely be treated conservatively, as well as what factors might suggest the need for surgical intervention.

MATERIALS AND METHODS

General data

Cases of small bowel obstruction caused by postoperative adhesions were got from the computerized medical records from January 1999 to December 2001 at Mackay Memorial Hospital, Taipei, Taiwan. The diagnostic criterias for adhesive small bowel obstruction included: (1) history of previous laparotomy (defined as initial laparotomy); (2) clinical features of mechanical ileus, such as vomiting, abdominal pain, abdominal distention and obstipation; (3) obvious evidence of small bowel obstruction on plain x-ray of the abdomen; and (4) exclusion of other organic lesions by radiological contrast study. In patients with a past history of cancer leading to the initial laparotomy or recurrence was ruled out by meticulous examinations (tumor markers, ultrasonography and radiology including CT scan, depending on types of malignancy). Other clinical findings recorded included the presence or absence of fever, tachycardia, rebound tenderness (peritoneal signs), leukocytosis, and elevation of serum amylase and alkaline phosphatase, as well as assessment of the progress and severity of the small bowel obstruction. The diseases or organs accounting for the initial laparotomy in each patient were recorded. The entire medical record for each patient was examined to see how many hospitalizations they had had in the past for adhesion-related small bowel obstruction. The interval between the initial laparotomy and any subsequent admissions were also noted. The management given, medical (conservative) or surgical (re-laparotomy), was recorded, as well as length of stay for each admission and the duration of observation before the final outcome (either resolution with conservative treatment or surgery). Medical management might include any or all of the following: no oral intake; decompression by nasogastric intubation; intravenous fluids, with electrolytes and nutrition as needed; administration of parenteral antibiotics when leukocytosis was present; and regular abdominal x-rays (usually daily). For patients treated surgically, the location of adhesions and the presence or absence of local or systemic complications were identified. Simple obstruction was defined as the presence of adhesions alone, while complicated obstruction included the presence of gangrene and/or strangulation.

RESULTS

During the study period, 155 patients were admitted with the diagnosis of adhesion-related small bowel obstruction. The male to female ratio was 75 to 80, and the age ranged from 18 to 80 years old. The organs involved in the initial laparotomies were the female genital organs in 36 cases (including incidental appendectomy in 5 cases); appendix in 27 cases; colon and rectum in 25 cases (including appendectomy in 3); stomach and duodenum in 19 cases; small bowel in 14 cases; gallbladder, biliary tract and pancreas in 13 cases; and others (including soft tissue trauma, kidney, and spleen) in 21 (Table 1).

Table 1 Initial laparotomy

Organs/types	Number of cases
OB-GYN	36 (5 ^a)
Appendix	27
Colon/Rectum	25 (3 ^a)
Stomach/Duodenum	19
Small intestine	14
Gallbladder/bile duct/pancreas	13
Others (spleen, trauma, etc)	21
Total	155

^awith incidental appendectomy.

The 155 patients had had a total of 293 admissions, with 1 patient being admitted 11 times. The interval between initial laparotomy and subsequent admissions varied widely. The shortest was 2 weeks, while the longest approached 30 years. Of the 293 admissions, medical management alone was used during 220 (75.1 %) admissions. The duration of observation until resolution of bowel obstruction ranged from 2 to 12 days (average 6.9 days, Table 2).

Table 2 Duration of observation in adhesive small bowel obstruction

Duration of observation (days)	Medical treatment: (n=220)	Simple obstruction (n=46)	Complicated obstruction (n=27)
	Admissions	Admissions	Admissions
1	0	2	4
2	15	3	5
3	18	5	3
4	20	6	5
5	26	4	3
6	25	8	2
7	30	6	1
8	19	2	2
9	18	3	1
10	15	2	1
11	19	1	0
12	15	2	0
13	0	1	0
14	0	1	0

Average duration: medical 6.9 days; all re-laparotomy 5.4 days, simple 6.1 days, complicated 4.1 days.

There were 73 admissions in which repeat laparotomy were performed to treat the obstruction (including twice in 2 patients and 3 times in 1 patient). The duration of observation prior to surgery ranged from several hours to 14 days (average 5.4 days, Table 2). At surgery, there was simple obstruction in 46

cases, and there was complicated obstruction in the other 27 (9.2 % of all admissions). The average preoperative observation period was shorter in complicated obstruction than that in simple obstruction (4.1 vs 6.1 days). The comparison of preoperative characteristics in simple and complicated obstruction was shown in Table 3. The site of initial laparotomy did not seem to influence the presence or absence of complications (for easy comparison, the types of initial laparotomies were simply divided into upper and lower abdomen, Table 3). In patients with complicated obstruction, fever was present in 18 (67 %) cases and leukocytosis (greater than 15 000/cu mm) in 20 (74 %) cases. None of the patients with simple obstruction had these findings. No patients in our series died.

Table 3 Comparison of simple and complicated obstruction

	Simple (n=46)	Complicated (n= 27)
Initial laparotomy site		
Upper abdomen	17 (37%)	9 (33%)
Lower abdomen	29 (63%)	18 (67%)
Preoperative clinical findings		
Rebound tenderness	29 (63%)	25 (93%)
Fever >38 °C	0 (0%)	18 (67%)
Tachycardia	15 (33%)	20 (74%)
Leukocytosis>15 000/cumm	0 (0%)	20 (74%)
↑ Hematocrit/ ↑ BUN	20 (43%)	24 (89%)
↑ Serum amylase	2 (4.3%)	10 (37%)
↑ Alkaline phosphatase	3 (6.5%)	7(26%)
Metabolic acidosis	0 (0%)	4 (15%)

DISCUSSION

Formation of adhesions after transperitoneal operation may be both beneficial and deleterious^[10-13]. On one hand, adhesions may localize suture line leakage or isolate an inflammatory process, thus preventing more widespread disease. On the other hand, they may contribute to morbidity, with obstruction being the major serious complication. Small bowel obstruction due to postoperative adhesions develops in 6 % to 11 % of all patients undergoing laparotomy^[9]. It may occur at any time after the initial laparotomy and result in frequent re-admissions in subsequent years^[14, 15]. In our study, adhesive small bowel obstruction followed initial laparotomy in as few as 2 weeks to as long as nearly 30 years. While it may follow any type of laparotomy, it occurs most commonly after manipulation of the lower abdomen and pelvic cavity (appendix, gynecological organs and rectum, Table 1)^[16-18].

There is continuing debating about the ideal approach to patients with adhesive small bowel obstruction^[6, 9]. The process leading to obstruction is dynamic one with twisting and untwisting of bowel segments trapped by adhesions^[12, 13]. There are as yet no totally reliable clinical predictors to differentiate episodes that will resolve spontaneously from those that will require surgery. Even with the imminent onset of bowel strangulation, signs indicating this serious condition, such as fever, leukocytosis and peritoneal signs, are not always present^[14, 19]. This makes determining how long to try conservative management prior to opting for repeat surgery difficult.

In the literature, the incidence of spontaneous recovery with conservative management ranges from 20 % to 60 %^[7, 8, 14]. Some authors recommend only a limited observation period of 24 to 48 hours^[4, 5], but others suggest a longer period is safe, although the recommended upper limit is 5 days^[20, 21]. However, in our experience, an average of 6.9 days was required for spontaneous resolution. The longest period, in 15 cases, was

12 days (Table 2). In all these cases, the patients recovered without any sequelae. This suggested that laparotomy could safely be delayed longer than recommended in the literature. Had we operated in all cases after 5 days, 141 of the 220 patients who eventually had spontaneous remission would have required surgery?

Why conservative treatment may be extended in some patients but not in others probably depends on individual variables. In reports recommending earlier surgical intervention, most of the patients who finally developed bowel complications in fact already had signs of more serious obstruction on initial presentation^[4-6]. In our series, the surgically treated patients had a shorter observation time on average, 5.4 days vs 6.9 days for those who resolved spontaneously (Table 2). This suggested that these patients had relatively early onset of signs suggestive of complications. In reported series in which conservative treatment is recommended, most patients who finally recovered spontaneously had no apparent toxic signs throughout the hospital course^[14, 20, 21]. In our experience with reoperation, in only 27 of 73 procedures were actual intestinal complications. It's conceivable that some among the other 46 might have recovered spontaneously had we observed them longer. In fact, none of these 46 episodes were characterized by fever or leukocytosis. The patients chose to undergo surgical intervention mainly because they became inpatient with medical treatment.

Although episodes of small bowel obstruction can be managed conservatively, the adhesions remain. So the possibility of recurrence still exists^[12, 15]. Unfortunately, reoperating to excise the adhesions (adhesiolysis) is not clearly beneficial, since the repeat surgical procedure itself may cause more adhesions^[22]. In addition, the average cost of an admission with surgery is much higher than that of an admission with only medical treatment^[23, 24]. Surgery is thus not a panacea for this condition, and the decision to perform it should only be made after all factors are carefully considered. Certainly, the presence of peritoneal signs, fever, and leukocytosis suggest the need for early surgery. In the absence of these signs, watchful waiting is reasonable.

In conclusion, the actual incidence of serious complications in patients with small bowel obstruction due to postoperative adhesions is low. Most patients can be managed medically. With closely monitoring and in the absence of signs suggestive of complications, an observation period even longer than 10 days before proceeding to surgical intervention appears to be safe.

REFERENCES

- Füzün M**, Kaymak MFE, Harmancıođlu Ö, Astarıcıođlu K. Principal causes of mechanical bowel obstruction in surgically treated adults in Western Turkey. *Br J Surg* 1991; **78**: 202-203
- Lee SH**, Ong ETL. Changing pattern of intestinal obstruction in Malaysia: a review of 100 consecutive cases. *Br J Surg* 1991; **78**: 181-182
- McEntee G**, Pender GMD, Mulvin D, McCullough M, Naeeder S, Farah S, Badurdeen MS, Ferraro V, Cham C, Gillham N, Matthews P. Current spectrum of intestinal obstruction. *Br J Surg* 1987; **74**: 976-980
- Otamiri T**, Sjødahl R, Ihse I. Intestinal obstruction with strangulation of the small bowel. *Acta Chir Scand* 1987; **153**: 307-310
- Sosa J**, Gardner B. Management of patients diagnosed as acute intestinal obstruction secondary to adhesions. *Am Surg* 1993; **59**: 125-128
- Mucha PJ**. Small bowel obstruction. *Surg Clin North Am* 1987; **67**: 597-620
- Wolfson PJ**, Bauer JJ, Gelernt IM, Krel I, Aufses AH Jr. Use of the long tube in the management of patients with small-intestinal obstruction due to adhesions. *Arch Surg* 1985; **120**: 1001-1006
- Brolin RE**, Krasna MJ, Mast BA. Use of tubes and radiographs in the management of small bowel obstruction. *Ann Surg* 1987; **206**: 126-133
- Bass KN**, Jones B, Bulkley GB. Current management of small-bowel obstruction. *Adv Surg* 1997; **31**: 1-34
- Scott-Coombes DM**, Whawell SA, Thompson JN. The operative peritoneal fibrinolytic response to abdominal operation. *Eur J Surg* 1995; **161**: 395-399
- Holmdahl L**, Eriksson E, Eriksson BI, Risberg B. Depression of peritoneal fibrinolysis during operation is a local response to trauma. *Surgery* 1998; **123**: 539-544
- Holmdahl L**, Risberg B. Adhesions: prevention and complications in general surgery. *Eur J Surg* 1997; **163**: 169-174
- Dijkstra FR**, Nieuwenhuijzen M, Reijnen MMPJ, Goor van H. Recent clinical developments in pathophysiology, epidemiology, diagnosis and treatment of intra-abdominal adhesions. *Scand J Gastroenterol* 2000; **232**(Suppl): 52-59
- Tanphiphat C**, Chittmitrapap S, Prasopsunti K. Adhesive small bowel obstruction: a review of 321 cases in a Thai hospital. *Am J Surg* 1987; **145**: 283-287
- Ellis H**, Moran BI, Thompson JN, Parker MC, Wilson MS, Menzies D, McGuire A, Lower AM, Hawthorn RJS, O'Brien F, Buchan S, Crowe AM. Adhesion-related hospital readmissions after abdominal and pelvic surgery: a retrospective cohort study. *Lancet* 1999; **353**: 1476-1480
- Monk BJ**, Berman ML, Montz FJ. Adhesions after extensive gynecologic surgery: clinical significance, etiology and prevention. *Am J Obstet Gynecol* 1994; **170**: 1396-1403
- Al-Took S**, Platt R, Tulandi T. Adhesion-related small-bowel obstruction after gynecologic operations. *Am J Obstet Gynecol* 1999; **180**: 313-315
- Nieuwenhuijzen M**, Reijnen MMPJ, Kuijpers JHC, Goor van H. Small bowel obstruction after total or subtotal colectomy: a 10-year retrospective review. *Br J Surg* 1998; **85**: 1242-1245
- Sarr MG**, Bulkley GB, Zuidema GD. Preoperative recognition of intestinal strangulation obstruction: Prospective evaluation of diagnostic capability. *Am J Surg* 1983; **145**: 176-181
- Hall RI**. Adhesive obstruction of the small intestine: a retrospective review. *Br J Clin Pract* 1984; **38**: 89-92
- Seror D**, Feigin E, Szold A, Allweis TM, Carmon M, Nissan S, Freund HR. How conservatively can postoperative small bowel obstruction be treated? *Am J Surg* 1993; **165**: 121-126
- Ellis H**. The clinical significance of adhesions: focus on intestinal obstruction. *Eur J Surg* 1997; **577**(Suppl): 5-9
- Menzies D**, Parker M, Hoare R, Knight A. Small bowel obstruction due to postoperative adhesions: treatment patterns and associated costs in 110 hospital admissions. *Ann R Coll Surg Engl* 2001; **83**: 40-46
- Ray NF**, Denton WG, Thamer M, Henderson SC, Perry S. Abdominal adhesiolysis: inpatient care and expenditures in the United States in 1994. *J Am Coll Surg* 1998; **186**: 1-9

Decision making in right-sided diverticulitis

Li-Rung Shyung, Shee-Chan Lin, Shou-Chuan Shih, Chin-Roa Kao, Sun-Yen Chou

Li-Rung Shyung, Shee-Chan Lin, Shou-Chuan Shih, Chin-Roa Kao, Sun-Yen Chou, Division of Gastroenterology, Department of Internal Medicine, Mackay Memorial Hospital, Taipei, Taiwan, China
Correspondence to: Dr. Li-Rung Shyung, Division of Gastroenterology, Department of Internal, Medicine, Mackay Memorial Hospital, 92, Section 2, Chungshan North Road, Taipei, Taiwan, China. luke.skywalk@msa.hinet.net

Telephone: +886-922988910

Received: 2002-11-29 **Accepted:** 2002-12-22

Abstract

AIM: To evaluate systematically our nine-year experience in treating right-sided diverticulitis of the colon, and to explore its clinical and radiological relationship.

METHODS: The clinical and radiological data of 40 patients with colonic diverticulitis treated in Mackay Memorial Hospital, Taipei, from 1993 through 2002 were reviewed retrospectively.

RESULTS: The average age of the patients with right-sided diverticulitis was 53.1 years, which was 11.6 years younger than that of the patients with left-sided diverticulitis. The preoperative diagnosis of appendicitis was made in 8 of 13 right-sided diverticulitis patients. Nine (69 %) had right lower quadrant abdominal pain for more than 48 hours, and ten patients (77 %) presented with fever. CT findings suggesting acute right-sided diverticulitis including thickening of the intestinal wall and pericolonic inflammation were present in five patients.

CONCLUSION: Right-sided diverticulitis is easily confused with acute appendicitis because it occurs at a somewhat younger age than that in left-sided diverticulitis. Barium enema and CT are helpful for the early diagnosis of right-sided diverticulitis. While clearly not required in the majority of patients with right lower quadrant abdominal pain, barium enema and CT may be helpful in making the decision with a clinical history or physical examinations atypical of acute appendicitis.

Shyung LR, Lin SC, Shih SC, Kao CR, Chou SY. Decision making in right-sided diverticulitis. *World J Gastroenterol* 2003; 9(3): 606-608

<http://www.wjgnet.com/1007-9327/9/606.htm>

INTRODUCTION

Diverticular disease was almost unknown in 1990, but has become the commonest affliction of the colon in Western countries^[1] which was regarded as a deficient disease of Western civilization. The right-sided diverticulitis is more common than left-sided diverticulitis in Far-eastern countries. In a study of 105 patients in Taiwan, China, the incidence of right-sided diverticulosis was 60 %^[2]. The distinction between right-sided diverticulitis and acute appendicitis is often difficult at the time of presentation^[3]. The condition is frequently misdiagnosed and has often been mistreated. During the past nine years, we have treated 13 cases of right-sided diverticulitis

at the Mackay Memorial Medical Center, our experience in relation to the clinical and radiological manifestations was reviewed.

MATERIALS AND METHODS

General data

The pathological reports of medical records at the Mackay Memorial Medical Center were reviewed from January 1993 to June 2002. During this period, there were 40 patients with colonic diverticulitis treated at our institution, we retrospectively reviewed their presentation, diagnostic studies, management and pathology. Colonic diverticulitis was stratified into two groups according to the distribution of diverticula: (1) right-sided diverticulitis with diverticula in the cecum, ascending colon and proximal transverse colon; (2) left-sided diverticulitis with diverticula in the sigmoid and/or descending colon. Clinical details of these patients were shown in Table 1. Presenting symptoms and signs of right-sided diverticulitis patients were shown in Table 2.

Table 1 General data of right-sided and left-sided diverticulitis

	Right-sided diverticulitis	Left-sided diverticulitis
Number	13	27
Male/Female	10/3	20/7
Age (yr)		
Mean±SD	53.15±9.86	64.74±11.28
Range	40-70	44-83
Median	50	68

Table 2 Presenting symptoms and signs (13 cases of total number)

Initial features	Cases number (%)
RLQ abdominal pain for >2 days	9(69)
Nausea/vomiting	2(15)
Diarrhea	2(15)
Leukocytosis	9(69)
Fever	10(77)
Anorexia	1(8)

Statistical analysis

Statistical comparison was performed using Student's *t* test. All analyses were performed with the Stastical Package for the Social Science (SPSS) for windows (Version 10.0) software. The results were considered to be statistically significant at a value of $P<0.05$.

RESULTS

The incidence of right-sided diverticulitis was 33 % in our treated patients. There was no difference between right-sided diverticulitis patients and left-sided diverticulitis patients as regarding to male: female ratio. The age of patients with right-sided diverticulitis was younger than those with left-sided diverticulitis ($P=0.003$, Table1).

Details of their presenting symptoms and signs were shown

in Table 2. The primary complaints among all patients were right lower quadrant abdominal pain for more than two days prior to admission. Nausea and/or vomiting were reported in two patients (15 %) and diarrhea was present in two patients (15 %), but only one of the 13 exhibited anorexia. Ten patients had a fever of more than 37 °C and all of these also had a leukocytosis. The preoperative diagnosis was appendicitis in 8 of the 13 patients in our series. Four patients had performed preoperative barium enemas. In one patient a 4 cm×4.5 cm diverticulum of the proximal transverse colon was identified. In the other three, the barium enema was interpreted as showing a right-sided colonic mass (Figure 1). Six patients had CT scans, of which five correctly diagnosed diverticulitis of the cecum. Diverticulitis of the right colon was correctly diagnosed preoperatively in one patient in whom marked wall thickening of the cecum with classic target appearance was demonstrated (Figure 2). Diverticula was found in one patient. There was no evidence of contrast extravasation in any of the six patients.



Figure 1 Barium contrast roentgenogram demonstrated a right-sided colonic mass. (black arrow head).

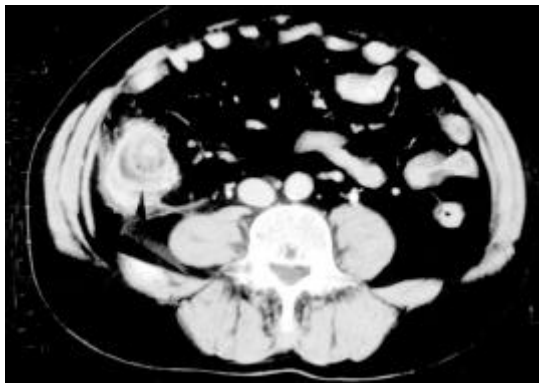


Figure 2 Acute diverticulitis of cecum in 50-year-old man. CT scan clearly showed enhancement of thickened diverticular wall and preservation of wall enhancement pattern of cecum as hyperattenuating inner layer, thickened middle layer of low attenuation, and outer high-attenuation layer (black arrow head).

DISCUSSION

The preoperative distinction between right-sided diverticulitis and appendicitis is extremely difficult to discern based on clinical presentation alone^[4]. In our study, a misdiagnosis of appendicitis was made in 8 of the 13 patients preoperatively which is common in all other reported series^[3-5]. The majority of patients will still undergo laparotomy. The surgeon must make a diagnosis based on operative findings. Hidden diverticula pose a diagnostic dilemma since at laparotomy it may be difficult to distinguish the inflamed mass from Crohn's

disease, malignant lesions of the right colon, a perforated foreign body or even tuberculosis^[3].

Patients with right-sided diverticulitis tend to be younger than those with left-sided diverticulitis^[5]. We compared the age distribution of right-sided diverticulitis and left-sided diverticulitis patients in this study (Table 1).

Clinically, in contrast to appendicitis, relative long history of right lower quadrant abdominal pain, relative lack of systemic toxic signs and low frequency of nausea/vomiting may be helpful in correctly diagnosing right-sided diverticulitis^[2]. The symptoms of right-sided diverticulitis usually begin and remain localized in the right lower quadrant, rather than originating in the epigastrium^[6]. Appendicitis patients typically experience the classic migration of pain to the right lower quadrant at later stage which caused by the stimulation of the visceral afferent nerve fibers that enter the spinal cord at thoracic levels T8 through T10. Nine of our patients presented more than 48 hours after the onset of symptoms (69 %). Eleven of our patients (85 %) had neither nausea, vomiting, nor diarrhea. This absence of vomiting has been noted by others^[7-9].

About one third of patients in this series were right-sided diverticulitis, which differed from other reports in Far-eastern countries^[10-12]. This bias was due to our review was obtained from pathological database of medical records from our hospital, in which some uncomplicated right-sided diverticulitis cases were excluded. Right-sided diverticulitis tends to have a more benign course than that which occurs on the left^[13]. So this differential probably carries little significance, despite our own findings. Diverticular disease is considered as a fiber deficient disease in Western Countries^[1], so duty of the profession is to point the way of prevention of white flour, both brown and white sugar, confectionery, and foods or drinks which contain unnaturally concentrated carbohydrates. But some Eastern racial groups have a higher incidence of right-sided diverticulitis despite a high fiber intake. These findings were coincident to a study from China where about 62 % of right-sided diverticular disease despite a good fiber intake^[14].

Contrast enema studies are the most accurate way to find out the colonic diverticula^[15]. However, because of the risks of extravasation of barium from the perforation in the patients with acute right-sided diverticulitis, barium enema examination should be generally be avoided in patients with suspected acute right-sided diverticulitis and localized peritoneal signs. Criteria for the diagnosis of right-sided diverticulitis include extravasation of barium, narrowed lumen or thickened mucosa, and mass effect^[15]. In our series, barium enema studies were done in four patients who presented a cecal mass in three patients.

In contrast to the barium enema, CT scan demonstrates both the intraluminal and extracolonic manifestations of acute right-sided diverticulitis^[16]. Criteria of CT scan for the diagnosis of right-sided diverticulitis include colonic wall thickening, pericolic fat infiltration (streaky fat), pericolic or distant abscesses, and extraluminal air. In this series, CT scans were obtained preoperatively in six patients with right-sided diverticulitis. CT findings suggesting right-sided diverticulitis were present in five patients. A recent study found that pericolic lymph nodes adjacent to the focal area of colonic thickening are more commonly seen in patients with colonic cancer. Pericolic inflammatory changes are more commonly seen in right-sided diverticulitis^[17]. CT may be helpful for the evaluation of patients with atypical symptoms of acute appendicitis or those who have undergone an appendectomy. Right-sided diverticulitis occurs with greater frequency in Asians. This condition is easily confused with acute appendicitis, since it occurs at a somewhat younger age than those with left-sided diverticulitis. If diagnosed preoperatively, uncomplicated right-sided diverticulitis can be managed conservatively with antibiotic therapy.

REFERENCES

- 1 **Painter NS**, Burkitt DP. Diverticular disease of the colon: a deficient disease of Western civilization. *BMJ* 1971; **2**: 450-454
- 2 **Chiu JH**, Lin JT, Lin JK, Leu SY, Liang CL, Wang FM. Diverticular disease of the colon. *J Surg Asso* 1987; **20**: 102-108
- 3 **Gouge TH**, Coppa GF, Eng K, Ranson JHC, Localio SA. Management of diverticulitis of ascending colon. 10 years' experience. *Am J Surg* 1983; **145**: 387-391
- 4 **Markham NI**, Li AKC. Diverticulitis of the right colon- experience from Hong Kong. *Gut* 1992; **33**: 547-549
- 5 **Fischer MG**, Farkas AM. Diverticulitis of the cecum and ascending colon. *Dis Colon Rectum* 1984; **27**: 454-458
- 6 **Birnbaum BA**, Wilson SR. Appendicitis at the millennium. *Radiology* 2000; **215**: 337-348
- 7 **Arrington P**, Judd C. Cecal diverticulitis. *Am J Surg* 1981; **142**: 56-60
- 8 **Asch M**, Markowitz A. Cecal diverticulitis; report of 16 cases and a review of the literature. *Surgery* 1969; **65**: 906-910
- 9 **Schuler JG**, Bayley J. Diverticulitis of the cecum. *Surg Gynecol Obstet* 1983; **156**: 743-748
- 10 **Wang CH**, Chou LC. The incidence of the diverticular diseases of the colon in T.S.G.H., Taiwan, China. *J Surg Asso* 1979; **12**: 260-266
- 11 **Sugihara K**, Muto T, Morioka Y, Asano A, Yamamota T. Diverticular disease of the colon in Japan. A review of 615 cases. *Dis Colon Rectum* 1984; **27**: 531-537
- 12 **Vajrabukka T**, Saksornchai K, Jimakorn P. Diverticular disease of the colon in a Far-eastern community. *Dis Colon Rectum* 1980; **23**: 151-154
- 13 **Ferzoco LB**, Raptopoulos V, Silen W. Current concepts: acute Diverticulitis. *N Engl J Med* 1998; **338**: 1521-1526
- 14 **Pan G**, Liu T, Chen M, Chang H. Diverticular disease of the colon in China. *Chin Med J* 1984; **97**: 391-394
- 15 **Beranbaum SL**, Zausner J, Lane B. Diverticular disease of the right colon. *AJR* 1972; **115**: 334-348
- 16 **Crist DW**, Fishman EK, Scatarige JC, Cameron JL. Acute diverticulitis of the cecum and ascending colon diagnosed by computed tomography. *Surg Gynecol Obstet* 1988; **166**: 99-102
- 17 **Macari M**, Balthazar EJ. CT of bowel wall thickening: significance and pitfalls of interpretation. *AJR* 2001; **176**: 1105-1116

Edited by Xu XQ

Esophageal ulceration complicating doxycycline therapy

Mohammad A. Al-Mofarreh, Ibrahim A. Al Mofleh

Mohammad A. Al-Mofarreh, Consultant Physician & Gastroenterologist, Poly Clinic, College of Medicine, King Saud University, Riyadh, Saudi Arabia

Ibrahim A. Al Mofleh, Professor of Medicine, College of Medicine, King Saud University, Riyadh

Correspondence to: Prof. Ibrahim A. Al Mofleh, Gastroenterology Div. & Endoscopy Unit, College of Medicine, King Saud University, P.O. Box 2925 (59), Riyadh 11461, Saudi Arabia. iamofleh@yahoo.com

Telephone: +966-1-4671215 **Fax:** +966-1-4671217

Received: 2002-06-27 **Accepted:** 2002-07-27

Abstract

AIM: To report present state of iatrogenic drug-induced esophageal injury (DIEI) induced by medications in a private clinic.

METHODS: Iatrogenic drug-induced esophageal injury (DIEI) induced by medications has been more frequently reported. In a private clinic we encountered 36 cases of esophageal ulcerations complicating doxycycline therapy in a mainly younger Saudi population (median age 29 years).

RESULTS: The most frequent presenting symptoms were odynophagia, retrosternal burning pain and dysphagia (94 %, 75 % and 56 %, respectively). The diagnosis was according to medical history and confirmed by endoscopy in all patients. Beside withdrawal of doxycycline, when feasible, all patients were treated with a proton-pump inhibitor (PPI) and a prokinetic. Thirty patients who reported to the clinic after treatment were improved within 1-7 (median 1.7) days.

CONCLUSION: Esophageal ulceration has to be suspected in younger patients with odynophagia, retrosternal burning pain and/or dysphagia during the treatment with doxycycline.

Al-Mofarreh MA, Al Mofleh IA. Esophageal ulceration complicating doxycycline therapy. *World J Gastroenterol* 2003; 9(3): 609-611

<http://www.wjgnet.com/1007-9327/9/609.htm>

INTRODUCTION

Three decades after the first report of drug-induced esophageal injury (DIEI) induced by potassium therapy^[1], approximately 1 000 cases of DIEI caused by almost 100 different drugs, have been reported in the world literature. Antibiotics have contributed to almost 50 % and doxycycline alone to 27 % of all cases^[2].

The reported DIEI approximate incidence of 4/100 000 is probably underestimated. The actual incidence is apparently much higher for increase of drugs prescription, and they are not all reported^[2,3]. History has been considered sufficient for assuming a clinical diagnosis^[4,5]. Retrosternal pain, sudden odynophagia with or without dysphagia is suspicious of the diagnosis^[2]. History of medication, time of drug intake and amount of concurrent fluid ingested are important^[6,7]. Upper gastrointestinal endoscopy is almost always abnormal and it has been considered as the method of choice to confirm DIEI^[2].

The clinical course is usually uneventful and DIEI may heal after withdrawal of the offending drugs^[5-8].

MATERIALS AND METHODS

General data of patients

In a retrospective analysis of upper gastrointestinal (UGI)-endoscopies performed at Dr. Al Mofarreh's Polyclinic over a period of 9 years, 36 patients who had doxycycline-induced esophageal ulcerations were included in this study. Another seven patients, who had typical symptoms, but had no endoscopy, no ulcer on endoscopy or the offending medication was unknown, were not included.

Methods

The patients were asked history of recent drug intake, the mode, timing of medication and the concurrent amount of fluid ingested.

Endoscopy was performed after a 12 hours fasting using Pentax EPM 3000, EG 2901 videoscope after a local anesthesia with 10 % xylocain spray or 2 % xylocain viscous (Astra, Sweden). Hard print photo documentation was performed in all patients with a color video printer (UP-5000 P, Sony). The number of ulcers, their size, depth and localization at the esophagus were documented.

Patients were treated with withdrawal of doxycycline, when feasible, along with proton-pump inhibitors (PPI) and prokinetics and were requested to report within seven days of management initiation to give feedback on their response of treatment.

RESULTS

Over a period of nine years (from July 1992 to June 2001), 36 patients who complained with sudden odynophagia (34 cases, 94 %), retrosternal burning pain (27 cases, 75 %) and/or dysphagia (20 cases, 56 %) after ingestion of doxycycline capsules, underwent UGI-endoscopy and were found to have esophageal ulcerations. Their age ranged from 12 to 72 (Median: 29) years old and 22 were males. Endoscopy was performed within an average of six days after the onset of symptoms. The median number of ulcers was two (range: 1-9) and one patient had multiple ulcers spread all over the esophagus. The ulcers were localized at the mid, upper and lower esophagus in 24, 6 and 5 patients, respectively. In one patient, the ulcers were scattered all over the esophagus. The ulcers were variable in size, shape and depth (Figure 1-4). No bleeding or significant strictures were encountered in these patients and none of the patients had a pre-existing esophageal disorder. Along with withdrawal of doxycycline when feasible, all patients were treated with PPI and prokinetics. All thirty patients, who reported for follow up, were improved within 1-7 (Median 1.7) days including three patients continued on doxycycline to treat brucellosis.

DISCUSSION

Approximately 100 types of drugs have been incriminated in the etiology of around 1 000 cases of DIEI. The precise mechanism is not well explained. However multiple factors,

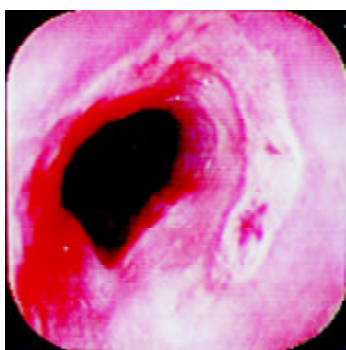


Figure 1 Superficial linear, semicircular esophageal ulcer with partially uncovered eroded mucosa.

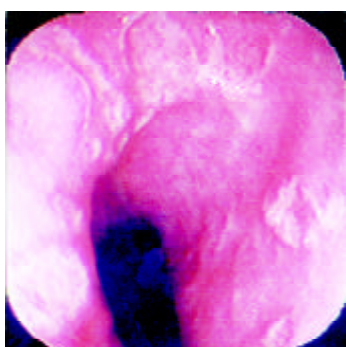


Figure 2 Multiple, variable sized crater-like mid-esophageal ulcer positioned in almost a circular pattern.

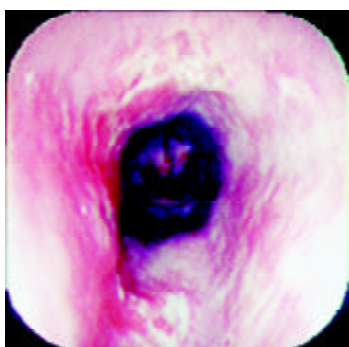


Figure 3 Anterior and posterior superficial mucosal ulcerations.



Figure 4 Deep, butterfly-like mid-esophageal ulceration partially extending in a semi-circular fashion and inducing mild narrowing of the lumen.

including the increasing age, decreased esophageal peristalsis and external compression are predisposing to DIEI^[2]. Furthermore, drugs that have a large size and sticky surface are retained longer in the esophagus^[2,7,9]. A clinical and

experimental study has shown that doxycycline capsules remain three times longer in the esophagus than doxycycline tablets^[10].

Elderly patients are more prone to develop DIEI due to their altered esophageal motility and decreased saliva production. In addition, they more frequently suffer of cardiac disease, require more cardiovascular medication and remain longer in a recumbent position^[7,11,12]. In younger patients, DIEI is mainly caused by antibiotics^[2,5,6]. In our study, majority of patients were young and the only incriminated drug was doxycycline. All patients took doxycycline capsules and shared the same risk factor of taking the medication at bed time with a little amount of fluid. None of these patients suffered from a cardiac or a pre-existing esophageal disease.

The mechanism of esophageal mucosal injury induced by doxycycline capsules may be explained by their acidic effect, gelatinous sticky capsules, increased mucosal concentration and intracellular toxicity^[2,13,14]. The presence of hiatal hernia in patients receiving indomethacin or doxycycline is associated with an increased risk of developing DIEI. The relative risk is 3.96^[15]. The symptoms of DIEI, usually, manifest few hours up to ten days after exposure in form of chest pain, odynophagia and dysphagia, ranked according to their frequency^[7]. In our series, odynophagia, retrosternal burning pain and dysphagia were the commonest symptoms and occurred in 94 %, 80 % and 54 % of patients, respectively.

Although the typical history is sufficient to establish the diagnosis, endoscopy remains the method of choice for detecting DIEI^[3]. Findings on endoscopic biopsies material are non specific^[6,16].

Despite the absence of a significant stricture, dysphagia occurred more frequently in our population compared to other series^[7].

The ulcer varied in size, depth and number. We have previously reported discrete, confluent, linear broad band-formed and butterfly-shaped ulcers partially covered with pseudomembranes. Ulcers were also noted on the opposite site with normal surrounding mucosa^[6]. The majority (66 %) of ulcers were at the mid-esophagus. The presence of mid-esophageal ulceration may raise the possibility of DIEI^[5,6,17,18]. The presence of intact pills or their residues are also important clues for the diagnosis of DIEI^[19].

In agreement with other authors, the main step of treatment in our patients was the withdrawal of the offending drug, however we feel doxycycline treatment could be continued when required with emphasis on patients education in regarding to timing of medication and required amount of fluid^[6]. In addition, patients received a PPIs along with a prokinetics. The value of antacids, anti-secretory drug and PPIs remain questionable in patients without gastroesophageal reflux^[5,7,10]. Apart from sucralfate, no data from the literature have suggested the benefit of acid suppression^[2]. Patients who develop complications in form of hemorrhage or chronic stricture and with unsuccessful surgical intervention require endoscopic management^[3,21].

In the majority of patient, DIEI symptoms resolved within one week (median time: 1.7 days). However, one patient went to the clinic with symptoms persisting over one month following a course of doxycycline and endoscopy revealed esophageal ulcerations. His symptoms were improved soon after initiation of treatment with a PPI and a prokinetic drug and ulcer healing was confirmed by endoscopy. Also the three patients continued with doxycycline to treat brucellosis improved. This observation supported continuation of doxycycline therapy when required and patients education was considered not only as a preventive, but also as a therapeutic measure.

Protracted courses up to six weeks and severe symptoms have also been reported^[22]. Furthermore, severe non-typical

symptoms in form of intractable hiccups have been described after the first dose of doxycycline inducing a lower esophageal ulcer at the gastric junction. The patients' symptoms have been resolved with the medication of omeprazole and sucralfate^[23].

Doxycycline was the only offending drug in this study. A sudden onset of odynophagia, retrosternal pain and/or dysphagia in a healthy individual give a strong evidence of drug induced esophageal injury and necessitate a careful exploration of drug history. Endoscopy is important to determine the type, size, site and depth of injury. Discontinuation of the offending drug, when feasible, is the first step of management acid suppressing agents and prokinetics may be proved helpful. In patients at risk, education and use of alternative medication are important preventive measures.

REFERENCES

- 1 **Pemberton J.** Esophageal obstruction and ulceration caused by oral potassium therapy. *Br Heart J* 1970; **32**: 267-268
- 2 **Kikendall JW.** Pill esophagitis. *J Clin Gastroenterol* 1999; **28**: 298-305
- 3 **Jaspersen D.** Drug-induced esophageal disorders: pathogenesis, incidence, prevention and management. *Drug Safety* 2000; **22**: 237-249
- 4 **Ramirez RA,** Valladares G, Barreda CC. Esophageal ulcers induced by doxycycline: evaluation of 4 cases. *Acta Gastroenterol Latinoam* 1981; **11**: 309-313
- 5 **Bott S,** Prakash C, McCallum RW. Medication-induced esophageal injury. Survey of the literature. *Am J Gastroenterol* 1987; **82**: 758-763
- 6 **Al Mofarreh MA,** Al Mofleh IA. Doxycycline-induced esophageal ulcerations. *Saudi J Gastroenterol* 1998; **4**: 20-24
- 7 **Boyce HW.** Drug-induced esophageal damage: diseases of medical progress. *Gastrointest Endoscopy* 1998; **47**: 547-550
- 8 **Mason SJ,** O' Meara TF. Drug-induced esophagitis. *J Clin Gastroenterol* 1981; **3**: 115-120
- 9 **Hey H,** Jorgensen F, Sorensen K, Hasselbach H, Wamberg T. Esophageal transit of six commonly used tablets and capsules. *BMJ* 1982; **285**: 1717-1719
- 10 **Carlborg B,** Densert O, Lindqvist C. Tetracycline-induced esophageal ulcers. A clinical and experimental study. *Laryngoscope* 1983; **93**:184-187
- 11 **Bohane TD,** Perralt J, Fowler RS. Esophagitis and esophageal obstruction from quinidine tablets in association with left atrial enlargement. *Aust Peadiatr J* 1978; **14**: 191-192
- 12 **Boyce HW.** Dysphagia after open heart surgery. *Hosp Prac* 1985; **20**: 40-50
- 13 **Bonavina L,** DeMeester TR, McChesney L, Schwizer W, Albertucci M, Bailey RT. Drug-induced esophageal stricture. *Ann Surg* 1987; **206**: 173-183
- 14 **Giger M,** Sonnenberg A, Brandli H, Singeisen M, Guller R, Blum AL. Das tetracyclin-ulkurs der speiserohre. *Dtsch Med Wochenschr* 1978; **103**: 1038-1040
- 15 **Alvartez JF,** Kulkarni SG, Bhatia SJ, Desai SA, Dhawan PS. Prospective evaluation of medication-induced esophageal injury and its relation to esophageal function. *Indian J Gastroenterol* 1999; **18**: 115-117
- 16 **Abraham SC,** Cruz-Correra M, Lee LA, Yardly JH, Wu TT. Alendronate-associated esophageal injury: Pathologic and endoscopic features. *Mod Pathology* 1999; **12**: 1152-1157
- 17 **Kikendall JW,** Friedman AC, Oyewole MA. Pill-induced esophageal injury. Case reports and review of the medical literature. *Dig Dis Sci* 1983; **28**: 174-182
- 18 **Castell DO.** "Pills esophagitis" The case of alendronate. *N Engl J Med* 1996; **335**: 1058-1059
- 19 **O' Meara TF.** A new endoscopic finding of tetracycline-induced esophageal ulcers. *Gastrointest Endosc* 1980; **26**: 106-107
- 20 **De Groen PC,** Lubbe DF, Hirsch LJ. Esophagitis associated with the use of alendronate. *N Engl J Med* 1996; **335**: 1016-1021
- 21 **Kikendall JW.** Pill-induced esophageal injury. *Gastroenterol Clin N Am* 1991; **20**: 835-846
- 22 **Tankurt IE,** Akbaylar H, Yenicerioglu Y, Simsek I, Gonen O. Severe long-lasting symptoms from doxycycline-induced esophageal injury. *Endoscopy* 1995; **27**: 626
- 23 **Tzianetas I,** Habal F, Keystone JS. Short report: Severe hiccups secondary to doxycycline-induced esophagitis during treatment of malaria. *Am J Trop Med Hyg* 1996; **54**: 203-204

Edited by Xu XQ

Endosonography with linear array instead of endoscopic retrograde cholangiography as the diagnostic tool in patients with moderate suspicion of common bile duct stones

Maciej Kohut, Andrzej Nowak, Ewa Nowakowska-Duława, Tomasz Marek, Roman Kaczor

Maciej Kohut, Andrzej Nowak, Ewa Nowakowska-Duława, Tomasz Marek, Roman Kaczor, Gastroenterology Department of Silesian Medical Academy, Katowice, Poland

Correspondence to: Maciej Kohut, Department of Gastroenterology, Silesian Academy of Medicine, Medyków 14 40-752 Katowice, Poland. maciej.2250177@pharmanet.com.pl

Telephone: +48-32-7894401 **Fax:** +48-32-2523119

Received: 2002-03-11 **Accepted:** 2002-05-20

Abstract

AIM: To evaluate the diagnostic efficiency of endoscopic ultrasound (EUS) as the main imaging modality in patients with moderate suspicion of common bile duct stones (CBDS).

METHODS: 55 patients with moderate clinical suspicion of CBDS were prospectively included to the study and evaluated with EUS. This study was done in single blind method in the clinical and biochemical data of patients. EUS was done with echo-endoscope Pentax FG 32-UA ($f=5-7.5$ MHz) and Hitachi EUB 405 ultrasound machine. Patients diagnosed with CBDS by EUS were excluded from this study and treated with ERC. All the other patients were included to the follow up study obtained by mail every 6 months for clinical evaluation (need of ERC or surgery).

RESULTS: CBDS was found in 4 patients by EUS. Diagnosis was confirmed in all cases on ERC. The remaining 51 patients without CBDS on EUS were followed up for 6-26 months (meanly 13 months) There were: 40 women, 42 cholecystectomized patients, aged: 55 (mean). Biochemical values (mean values) were as follows: bilirubin: $14.9 \mu\text{mol} \cdot \text{L}^{-1}$, alkaline phosphatase: $95 \text{ IU} \cdot \text{L}^{-1}$, $\gamma\text{-GTP}$: $131 \text{ IU} \cdot \text{L}^{-1}$, ALT: $50 \text{ IU} \cdot \text{L}^{-1}$, AST: $49 \text{ IU} \cdot \text{L}^{-1}$. Only 1 patient was lost for follow up. In the remaining 50 patients with follow up, there was only 1 (2 %) patient with persistent biliary symptoms in whom CBDS was finally diagnosed by ERC with ES. All other patients remained symptoms free on follow up and did not require ERC or biliary surgery.

CONCLUSION: Vast majority of patients with moderate suspicion of CBDS and no stones on EUS with linear array can avoid invasive evaluation of biliary tree with ERC.

Kohut M, Nowak A, Nowakowska-Duława E, Marek T, Kaczor R. Endosonography with linear array instead of endoscopic retrograde cholangiography as the diagnostic tool in patients with moderate suspicion of common bile duct stones. *World J Gastroenterol* 2003; 9(3): 612-614

<http://www.wjgnet.com/1007-9327/9/612.htm>

INTRODUCTION

Common bile duct stones mostly come from the gallbladder. Spontaneous passage of bile duct stones to the duodenum is

quite often. Both facts make the presence of bile duct stones a very dynamic state. Precise diagnosis of presence bile duct stones with the minimal invasive method is eagerly awaited and important for the optimal treatment. The clinical suspicion of choledocholithiasis is often difficult to verify. The “gold standard” for bile duct stones diagnosis is still endoscopic retrograde cholangiography (ERC) with endoscopic sphincterotomy (ES) and surgical choledochotomy with choledochoscopy^[1]. Surgical exploration is reserved after failed endoscopic access to the biliary tree. Unfortunately, ERC carries possibility of serious complications. Acute iatrogenic pancreatitis is the most frequent. The need for pre-cut technique during ERC in some patients with difficult access to the papilla exposes the patient to the additional risk of bleeding from the papilla or perforation of the intestine.

The necessity for less invasive imaging modality of biliary tree is obvious. Several imaging modalities including magnetic resonance (MRI), spiral computerised tomography (spiral CT) and EUS are currently under evaluation.

According to several authors - sensitivity, specificity and accuracy of EUS with radial scanning transducer in the diagnosis of bile duct stones are almost the same as the ERC and are described between 84-100 %, 76-100 % and 90-99 %, respectively^[2-11]. The results of EUS with sector scanning transducer in this setting are similar^[12-14]. The sector scanning instruments are cheaper compared with radial scanning instruments. Fine needle aspiration (FNA) monitored under direct ultrasound visual control and Doppler scanning of vessels are additional advantages of sector scanning EUS.

There is only one communication describing the use of EUS (with radial scanning) with intention to replace diagnostic ERC in patients with moderate suspicion of CBDS^[15]. This study of Napoleon *et al.* was neither prospective nor controlled study^[15]. No data about the implementation of EUS with linear array with such intention exist. Thus, a prospective evaluation of the usefulness of EUS with linear array in the evaluation of patients with moderate suspicion of CBDS with intention to avoid ERC or biliary surgery was undertaken.

MATERIALS AND METHODS

Patients

The material comprised of 55 patients with moderate suspicion of bile duct stones treated from January 1996 to March 1997 in the Department of Gastroenterology Silesian Medical Academy. The project of the study was accepted by the Ethical Committee of the Silesian Medical Academy. Informed consent was obtained from every patient.

Inclusion criteria were as stated as follows: 1. clinical suspicion of bile duct stones - biliary colics at present or during the last 6 months prior to the admission. 2. abnormal results of the following biochemical serum tests (at least two times) - bilirubin, transaminases, alkaline phosphatase, γ -glutamylotranspeptidase - at present or in the last 6 months. 3. enlarged bile ducts on conventional ultrasound (US) - at present or in the last 6 months. Bile ducts were evaluated as enlarged

when the diameter of common bile duct exceeded 7 mm in cases with gallbladder *in situ* or 9 mm in post - cholecystectomy cases. 4. patient's data available during follow up (at least 6 months).

Exclusion criterias were as follows: 1. suspicion of bile duct stones on conventional ultrasound. 2. suspicion of biliary or pancreatic malignancy on CT scans. 3. present acute biliary pancreatitis - such patients were directly sent to ERC. 4. present acute cholangitis - treated as acute biliary pancreatitis.

In patients enrolled to the study, case history and a set of mentioned above blood biochemical indexes were collected. In following, conventional ultrasound (US) and EUS as initial imaging methods were performed. Examiners (US, EUS) knew nothing of a patient except for that the patient was suspected for bile duct stones.

In the case of CBDS on US and /or EUS, the patient was sent to ERC and excluded from the follow up study (4 cases). In the case of normal appearance of biliary tree on EUS, the decision to abandon ERC was made and the patient was enrolled to the follow up study (51 cases). The follow up program consisted of postal inquires every three months. We asked the following questions: 1. Did you experience any biliary symptoms - postprandial colics in upper right quadrant of the abdomen? 2. Did you notice any changes in the colour of stools (whitish stools), urine (dark urine) or skin (jaundice) during or after any colic? 3. Did you undergo any investigation in order to evaluate biliary tree (US, ERCP, biliary surgery)?

In the case of recurrence of biliary symptoms during follow up, the patient was admitted to our Gastroenterology Department again. ERC was performed on the in-patient basis. Only patients who completed at least 6 months follow up program were finally evaluated (mean follow up time - 13 months). Demographic and clinical data of patients were shown in Table 1-3.

Table 1 Demographics data of patients (*n*=51)

Age, [years]	
$x \pm s$	55 (± 13)
Minimum	21
Maximum	85
Sex, [Females (%): Males (%)]	40 (78 %): 11 (22 %)
Cholecystectomized cases (%)	42 (82 %)

Table 2 Previous history of patients (up to 6 months prior to hospitalisation) (*n*=51)

Disease	Cases (%)
Acute biliary pancreatitis	4 (8 %)
Acute cholecystitis	2 (4 %)
Obstructive jaundice	7 (14 %)

Table 3 Biochemical values of patients before EUS (*n*=51)

Parameter	Cases (*)	Cases with abnormal results (%)
Alkaline phosphatase	45	6 (13%) 95 \pm 70 IU·L ⁻¹
γ -GTP	43	9 (21%) 131 \pm 175 IU·L ⁻¹
ALT	45	6 (13%) 48 \pm 64 IU·L ⁻¹
AST	32	3 (9%) 51 \pm 84 IU·L ⁻¹
Bilirubin	46	1 (2%) 149.6 \pm 100.5 μ mol·L ⁻¹

(*) some biochemical results unavailable in several cases

(*) Normal levels of liver enzymes in our lab:

- Alkaline phosphatase	<110	IU·L ⁻¹
- γ -GTP	<65	IU·L ⁻¹
- ALT	<40	IU·L ⁻¹
- AST	<40	IU·L ⁻¹
- Bilirubin	<17	μ mol·L ⁻¹

EUS

Endoscopic ultrasonography was performed with linear array scanning echoendoscope (Pentax FG 32 UA equipped with HITACHI 405 EUB ultrasonography machine). All EUS procedures were done by the same endosonographer with the experience of 400 EUS examinations (MK). Conscious sedation was achieved with midazolam given intravenously (mean 3,0 mg; range 1-7 mg) in one third patients. In the other two thirds patients midazolam was given orally (7,5 mg) 1,5-2 hours prior to the procedure. Patients were monitored by an anaesthesiologist with the use of ECG monitor and pulsoximetry. Topical pharyngeal anaesthesia with xylocain was used in all patients. EUS was performed with water filling balloon method, starting from the second portion of the duodenum in retrograde direction. EUS was considered positive for the diagnosis of choledocholithiasis if single or multiple hyperechoic structures within biliary tree with acoustic shadowing were found. Patients were diagnosed as stones free in the absence of findings described above. In several cases, antispasmodic agent (Buscopan) was used to control duodenal motility. EUS time was recorded (mean 18 minutes; range 9-37).

RESULTS

EUS was performed successfully with no complications in all 51 cases which were enrolled to the follow up program. Results of EUS showing no stones in the biliary tree in 51 cases could be confirmed in 49 cases during the follow up (96 %). The follow up lasted at least 6 months. The mean follow up time was 13 months (range 6-26 months). Only three patients were followed up for 6 months, the remaining cases were followed up longer. One patient was lost for follow up (2 % of all cases). Another one patient complained of persistent biliary colics on follow up. He was admitted again 3 months after his initial evaluation, as he was found to have complaints on the first postal inquiry. No patients with biliary symptoms were revealed during next postal inquires. In the symptomatic patients, ERC was carried out during the second admission and a single 7 mm stone was found in common bile duct (Figure 1). The stone was extracted after endoscopic sphincterotomy and the patient was discharged without complaints 2 days later.



Figure 1 Common bile duct stone EUS with linear array.

DISCUSSION

According to Cotton, who classified patients before planned cholecystectomy, one can distinguish three groups of patients with different levels of suspicion of CBDS^[16,17]. First group of cases with high risk of CBDS (80-90 %) is characterised by the enlargement over 10 mm of the diameter of common bile duct on US, obstructive jaundice (bilirubin over 20 μ mol·L⁻¹ with the elevation of alkaline phosphatase (3 times above upper limit of the normal value) and the history of acute biliary pancreatitis or acute cholangitis in the last few days. ERC with its possibility of therapeutic intervention should be the diagnostic

tool of first choice in case of strong suspicion of CBDS^[18]. The delay in therapeutic ERC due to the implementation of other imaging tests such EUS, MRI or CT is even unethical in patients with biliary obstruction (cholangitis, acute biliary pancreatitis). However, in case of uncertain reason of obstructive jaundice EUS, MRI or CT can be used to explain the etiology of the jaundice^[7]. Second group of patients, classified as the low risk group (approximately 2 % of cases have CBDS), consists of patients with no relevant case history, normal biochemical values and no abnormalities of biliary tree on US. Preoperative US and intraoperative cholangiography is proposed as the proper approach to the problem of possible CBDS^[16,17]. The third group of patients with moderate risk of CBDS is characterised by suspected (but not documented) acute biliary pancreatitis or obstructive cholangitis in the past, some elevation of alkaline phosphatase level and the diameter of common bile duct between 7 and 10 mm on US.

It is still debatable in the approach to patients with low risk for common bile duct stones. Some authors propose ERC before, after or even during the cholecystectomy^[6,16,19-25]. Spiral CT is proposed as the reliable imaging test for biliary tree evaluation^[9]. MRI is also considered as the possible choice^[26]. One can also learn from the literature that ERC is the only proposal in previously cholecystectomised cases^[16]. However cholecystectomised patients with suspected CBDS are usually old, and ERC can be thought to be even more aggressive approach, that in non cholecystectomised population of patients suspected for biliary lithiasis.

It is well known that EUS with either radial or sector scanning transducers is a powerful tool in the evaluation of patients suspected for biliary tree lithiasis^[2-14]. EUS is as reliable as ERC in the diagnosis of choledocholithiasis.

On the other hand, literatures showing that EUS can really replace ERC in patients with moderate risk of CBDS are curiously few. The only one paper dealing with that problem was appeared in an abstract form only by Napoleon *et al.*^[15]. Napoleon *et al.* described the results of a follow up of 238 patients suspected for CBDS and negative EUS (with radial scanning) results. In his group 58 cases were cholecystectomised (24 %). Fourteen cases (6 %) were lost on follow up (median 490 days). ERC was needed due to persistent biliary symptoms (12 %) in 28 cases. However ERC was judged as useful in only 6 cases (3 %). One patient with CBDS, three patients with ampullary sclerosis and two cases with biliary tumors were found on ERC^[15]. The authors concluded that patients suspected for CBDS and negative EUS had a very low risk to need ERC during follow up. They added that EUS but not ERC was the best imaging method in case of moderate suspicion of CBDS^[15].

Our result supported these findings that EUS can be successfully used in older, previously cholecystectomised patients, as our group consisted predominantly of such cases. In conclusion, that EUS with sector scanning transducer (as shown previously for EUS with radial transducers) can be used as the main diagnostic test in patients with moderate risk of CBDS. A large proportion of these patients can avoid ERC or surgical bile ducts exploration in case of negative EUS results.

REFERENCES

- Pitt HA.** Role of open choledochotomy in the treatment of choledocholithiasis. *Am J Surg* 1993; **165**: 483-486
- Amouyal G,** Amouyal P, Levy P. Value of endoscopic ultrasonography in the diagnosis of idiopathic acute pancreatitis. *Gastroenterology* 1994; **105**: 283
- Amouyal P,** Amouyal G, Levy P, Tuzet S, Palazzo L, Vilgrain V, Gayet B, Belghiti J, Fekete F, Bernards P. Diagnosis of choledocholithiasis by endoscopic ultrasonography. *Gastroenterology* 1994; **106**: 1062-1067
- Canto M,** Chak A, Stellato T, Sivak MV. Endoscopic ultrasonography vs cholangiography for extrahepatic biliary stones: a prospective study in pre- and post-cholecystectomy pts. *Gastrointest Endosc* 1998; **47**: 439-448
- Denis B,** Bas V, Goudot C, Frederic M, Bigard M, Gaucher P. Accuracy of endoscopic ultrasonography in the diagnosis of common bile duct stones. *Gastroenterology* 1993; **104**: 358
- Edmuntowicz S,** Aliperti G, Middleton W. Preliminary experience using endoscopic ultrasonography in the diagnosis of choledocholithiasis. *Endoscopy* 1992; **24**: 774-778
- Giovannini M,** Roche J, Lapuelle J, Rabbia J, Hoballah H, Rinaldi Y, Dancour M, Pauwells A, Ley G. Multicenter evaluation of EUS using a curved array transducer for assesment of unexplained cholestasis. Result in 121 cases. *Digestive Diseases Week San Francisco* 1996; **339**
- Napoleon B,** Pujal B, Pouchon T, Keriven O, Soquet J. Prospective study of the accuracy of endoscopic ultrasonography for the diagnosis bile duct stones. *Endoscopy* 1994; **26**: 238
- Polkowski M,** Palucki J, Regula J, Tilszer A, Butruk E. Helical CT cholangiography versus endosonography for suspected bile duct stones-a prospective blinded study in non-jaundiced patients. *Gut* 1999; **45**: 744-749
- Prat F,** Amouyal G, Amouyal P, Pelletier G, Fritsch J, Choury AD, Buffet C, Etienne JP. Prospective controlled study of endoscopic ultrasonography and endoscopic retrograde cholangiography in patients with suspected common bile duct lithiasis. *Lancet* 1996; **346**: 75-79
- Sugiyama M,** Atomi Y. Endoscopic ultrasonography for diagnosing choledocholithiasis: a prospective comparative study with ultrasonography and tomography. *Gastrointest Endosc* 1997; **45**: 143-146
- Lachter J,** Eshef R, Shiller M, Levy A, Sussa A, Yassin K. Linear EUS for bile duct stones. *Gastrointest Endosc* 2000; **51**: 51-54
- Quirk D,** Kesley P, Schapiro R, Brugge W. The use of linear-array ultrasonography in the detection of common bile duct stones. *Gastrointest Endosc* 1997; **45**: 178
- Kohut M,** Nowakowska-Dulawa E, Marek T, Kaczor R, Nowak A. Accuracy of linear endoscopic ultrasonography in the evaluation of patients with suspected common bile duct stones. *Endoscopy* 2002; **34**: 299-303
- Napoleon B,** Keriven-Soquet O, Pujol B, Soquet JC, Ponchon T. Does normal endoscopic ultrasound really avoid ERCP in patients with suspicion of bile duct stone? Study in 238 patients. *Gastrointest Endosc* 1996; **43**: 426
- Cotton PB,** Baillie J, Pappers T, Meyers W. Laparoscopic cholecystectomy and the biliary endoscopist. *Gastrointest Endosc* 1991; **37**: 94-97
- Cotton PB.** ERCP and laparoscopic cholecystectomy. *Am J Surg* 1993; **165**: 474-478
- Palazzo L.** Which test for common bile duct stones? Endoscopic and intraductal ultrasonography. *Endoscopy* 1997; **29**: 655-665
- Deslandres E,** Gagner M, Pomp A, Rheault M, Leduc R, Clermont R, Gratton J, Bernard EJ. Intraoperative endoscopic sphincterotomy for common bile duct stones during laparoscopic cholecystectomy. *Gastrointest Endosc* 1993; **39**: 54-58
- Dion Y,** Ratelle R, Morin J, Gravel D. Common bile duct exploration: the place of laparoscopic choledochotomy. *Surg Laparosc Endosc* 1994; **6**: 419-424
- Miller R,** Kimmelstiel F, Winkler W. Management of common bile duct stones in the era of laparoscopic cholecystectomy. *Am J Surg* 1995; **169**: 273-276
- Neuhaus H,** Feussner H, Ungeheuer A, Hoffman W, Classen M. Prospective evaluation of the use of ERCP prior to laparoscopic cholecystectomy. *Endoscopy* 1992; **24**: 745-749
- Rieger R,** Sulzbacher H, Woisetchlaeger R, Schrenk P, Wayand. Selective use of ERCP in patients undergoing laparoscopic cholecystectomy. *World J Surg* 1994; **18**: 900-905
- Shim CS,** Joo JH, Park CW, Kim YS, Lee JM, Lee MS, Hwang SG. Effectiveness of endoscopic ultrasonography in the diagnosis of choledocholithiasis prior to laparoscopic cholecystectomy. *Endoscopy* 1995; **27**: 428-432
- Widdison A,** Longstaff A, Armstrong A. Combined laparoscopic and endoscopic treatment of gallstones and bile duct stones: a prospective study. *Br J Surg* 1994; **81**: 595-597
- de Ledinghen V,** Lecesne R, Raymond JM. EUS or magnetic resonance cholangiography? A prospective controlled study. *Gastrointest Endosc* 1999; **49**: 26-31

Crohn's disease and risk of fracture: does thyroid disease play a role?

Nakechand Pooran, Pankaj Singh, Simmy Bank

Nakechand Pooran, Pankaj Singh, Simmy Bank, Division of Gastroenterology Albert Einstein College of Medicine - Long Island Jewish Medical Center, New Hyde Park, New York, USA

Correspondence to: Simmy Bank, M.D., FRCP, Division of Gastroenterology, Long Island Jewish Medical Center, New Hyde Park, NY 11040, USA. simmybank@lij.edu

Telephone: +1-718-4704692 **Fax:** +1-718-3430128

Received: 2002-10-05 **Accepted:** 2002-11-04

Abstract

AIM: To assess the role of thyroid disease as a risk for fractures in Crohn's patients.

METHODS: A cross-sectional study was conducted from 1998 to 2000. The study group consisted of 210 patients with Crohn's disease. A group of 206 patients without inflammatory bowel disease served as controls. Primary outcome was thyroid disorder. Secondary outcomes included use of steroids, immunosuppressive medications, surgery and incidence of fracture.

RESULTS: The prevalence of hyperthyroidism was similar in both groups. However, the prevalence of hypothyroidism was lower in Crohn's patients (3.8 % vs 8.2 %, $P=0.05$). Within the Crohn's group, the use of immunosuppressive agents (0 % vs 11 %), steroid usage (12.5 % vs 37 %), small bowel surgery (12.5 % vs 28 %) and large bowel surgery (12.5 % vs 27 %) were lower in the hypothyroid subset as compared to the euthyroid subset. Seven (3.4 %) Crohn's patients suffered fracture, all of whom were euthyroid.

CONCLUSION: Thyroid disorder was not found to be associated with Crohn's disease and was not found to increase the risk for fractures. Therefore, screening for thyroid disease is not a necessary component in the management of Crohn's disease.

Pooran N, Singh P, Bank S. Crohn's disease and risk of fracture: does thyroid disease play a role? *World J Gastroenterol* 2003; 9(3): 615-618

<http://www.wjgnet.com/1007-9327/9/615.htm>

INTRODUCTION

Recent studies have shown that patients with Crohn's disease have decreased bone density^[1,2] that predisposes to an increased risk of fracture^[3,4]. A chronic inflammatory state with the release of inflammatory cytokines, steroid usage and malnutrition is the proposed mechanism. The co-existence of other medical conditions, which are independently associated with osteoporosis, will further increase the risk of fracture in patients with Crohn's disease. Thyroid disorder is associated with changes in bone metabolism and is an important cause of osteoporosis^[5-7]. Thyroid disorder has also been reported in patients with underlying inflammatory bowel disease (IBD)^[8-12]. One study showed altered thyroid physiology and anatomy in

patients with IBD^[9] and suggests that it may be important to investigate the association between thyroid disorders and Crohn's disease. If patients with Crohn's disease have a higher prevalence of thyroid disease, then screening and treatment of the thyroid disease may reduce the risk of fractures in the Crohn's disease population. Secondly, it has been reported that the presence of hyperthyroidism makes the treatment of inflammatory bowel disease more difficult^[10,13] and, therefore, correcting the thyroid disorder may have an impact on treatment response.

We compared the prevalence of hypothyroidism and hyperthyroidism in patients with Crohn's disease and those without Crohn's disease. To investigate whether co-existing thyroid dysfunction has an impact on the treatment of Crohn's disease, we compared the use of immunosuppressive medications and surgical procedures for the underlying Crohn's disease in patients with and without co-existing thyroid dysfunction.

MATERIALS AND METHODS

Study design and subjects

A retrospective cross-sectional study was conducted at this hospital from 1998 to 2000. The study group included 210 patients with Crohn's disease admitted to the hospital or referred to the endoscopy suite for endoscopic procedures. A control group comprised of 206 consecutive patients who did not have inflammatory bowel disease and who were referred for either screening colonoscopy or esophagogastroduodenoscopy (EGD).

Data collection

Medical records of patients were reviewed to extract information regarding their baseline demographic information, diagnosis and extent of Crohn's disease, presence of thyroid disease and use of either steroid or immunosuppressive agents. The diagnosis of Crohn's disease was made either endoscopically or radiographically. A history of other medical diagnoses (e.g. rheumatoid arthritis, chronic obstructive pulmonary disease) where the potential use of steroids or immunosuppressive agents may be a confounding factor was also recorded. Sample size was calculated based on a reference value of 1 % of thyroid dysfunction in the general population. To detect the difference of 5 % between the two groups with power of 0.8 and a two sided alpha error of 0.05, more than 200 patients were required in both the groups.

Outcome

The primary outcome was the presence of hypothyroidism or hyperthyroidism. Secondary outcomes included the use of immunosuppressive medications and surgery for the Crohn's disease. Thyroid disorder was considered present if the patient had a prior diagnosis of thyroid disorder and was taking thyroid medication (thyroxine, propylthiouracil, methimazole) or had an abnormal thyroid stimulating hormone (TSH) level.

Statistical analysis

Descriptive statistics were reported as proportions, means \pm

standard deviation or median and range. Comparison between groups was done using the Pearson chi-square test for categorical variable (or the Fisher exact test if appropriate) and two-sided student *t*-test for continuous variables (SPSS for Windows, release 10.0, Chicago, IL). $P < 0.05$ was considered significant.

RESULTS

Demographic and clinical characteristics

There were 210 patients with Crohn's disease and 206 controls. The two groups were matched for age (49.24 yr. vs 48.58 yr., $P = 0.68$), sex (88 males/122 females vs 91 males/133 females, $P = 0.29$), and race (153 whites/1 black/34 others vs 118 whites/14 blacks/36 others, $P = 0.34$). The groups differed in body mass index (24.35 kg/m² vs 27.46 kg/m², $P = 0.001$). (Table 1).

Table 1 Comparison of baseline characteristics and thyroid status in patients with Crohn's disease and control group

	Case (n=210)	Control (n=206)	P
Age (years)	49.24±13.71	48.58±18.43	0.68
Sex (M/F)	88/122	91/113	0.29
Body Mass Index (kg/cm ²)	24.35	27.46	0.001
Race (white/black/others)	153/1/34	118/14/36	0.34
Steroid use	75 (35.7%)	None	–
Immunosuppressive therapy	22 (10.4%)	None	–
Hypothyroidism	8 (3.8%)	17 (8.2%)	0.05
Hyperthyroidism	2 (0.01%)	None	0.25

Primary outcome - thyroid dysfunction

In the Crohn's group there were 8 (3.8 %) cases of hypothyroidism and 2 (0.01 %) cases of hyperthyroidism. The control population had 17 (8.2 %) cases of hypothyroidism and 0 (0 %) case of hyperthyroidism. The difference in hypothyroidism showed borderline significance ($P = 0.05$) while hyperthyroidism was not significant ($P = 0.25$) (Figure 1).

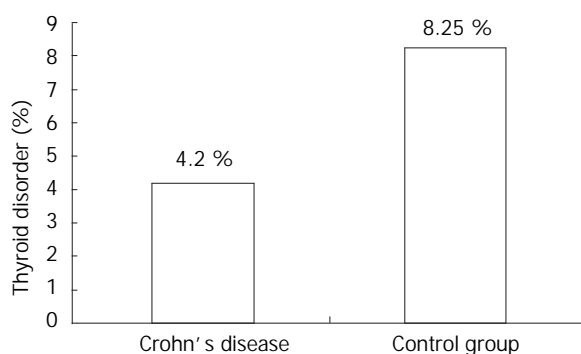


Figure 1 Bar graph showing the prevalence of thyroid disorder in patients with Crohn's disease and in the control group.

Secondary outcome - use of immunosuppressives and surgery

Patients with Crohn's disease were divided into those with hypothyroidism and those without any thyroid disorder. There was clinically higher use of immunosuppressive agents (0 % vs 11 %, $P = 0.59$), steroid usage (12.5 % vs 37 %, $P = 0.15$), small bowel surgery (12.5 % vs 28 %, $P = 0.34$) and large bowel surgery (12.5 % vs 27 %, $P = 0.38$) in Crohn's patients with hypothyroidism in comparison to those who were euthyroid. This difference however, was not statistically significant. (Table 2, Figure 2).

Table 2 Comparison of medical and surgical treatment in patients with hypothyroidism and euthyroidism in Crohn's disease

	Hypothyroidism (n=8)	Euthyroid (n=201)	P
Immunosuppressive medications	None	22 (11%)	0.59
Steroid use	1 (12.5%)	74 (37%)	0.15
Small bowel surgery	1 (12.5%)	56 (28%)	0.34
Large bowel surgery	1 (12.5%)	54 (27%)	0.38

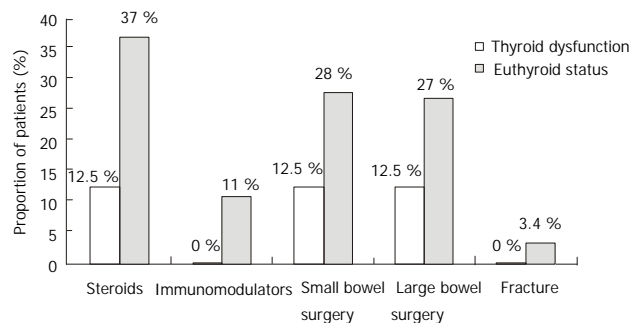


Figure 2 Bar graph showing the usage of steroids, immunosuppressive agents, small bowel surgery, large bowel surgery and fractures in Crohn's patients with thyroid disorder and those without thyroid disorder.

DISCUSSION

Crohn's disease is a chronic illness that is associated with a lower bone mineral density and a higher incidence of fracture^[1-4]. This results in increased morbidity and mortality. Thyroid disorder may potentiate the risk of fracture. The purpose of this study was to investigate whether thyroid disorder contributed to this adverse event and if present, whether thyroid disorder has an impact on the management of Crohn's disease. We did not find a higher prevalence of thyroid disease in our Crohn's population when compared to a control group. In fact, the prevalence of hypothyroidism was less in the Crohn's group. Sub-group analysis of the Crohn's group showed that there was lower usage of steroids, immunosuppressive medications and surgery in those who were also hypothyroid when compared to those who were euthyroid. There were 7 (3.4 %) fractures in the Crohn's population. All of the fractures occurred in those who were euthyroid.

The prophylactic use of a bisphosphonate has been shown to increase the bone mineral density in patients with Crohn's disease^[14]. However, the beneficial effect in lowering the incidence of fracture has not been reported. Due to the lack of an effective prophylactic medication, it becomes important to identify and treat any other co-existing illness that can enhance bone loss and increase the risk of fracture. One common disease that is linked to Crohn's and has an impact on bone metabolism is thyroid disease^[8-12].

In our study, we did not find a difference in the prevalence of thyroid disease between patients with Crohn's disease and our controls. These findings are consistent with two prior studies^[8,12]. Snook *et al*^[8] found a higher prevalence of thyroid disorder in patient with ulcerative colitis, but not Crohn's disease, when comparing patients with IBD to the general population. Hammer *et al*^[12] also found a higher prevalence of thyroid disorder in the ulcerative colitis subset of their IBD population when compared to the general population. The lack of association of clinical thyroid disorder and Crohn's disease is contradicted by the objective findings of Jenerot *et al*^[9]. They showed that patients with IBD had a 35 % higher thyroid

volume and were three times more likely to have an enlarged thyroid. Their finding of thyroid enlargement may be secondary to iodine deficiency, which has been reported in Crohn's disease and is unrelated to functional derangement of the thyroid^[15]. When we subdivided our thyroid disorder into hyperthyroid and hypothyroid, we did not find a difference in the prevalence of hyperthyroid between those with Crohn's disease and controls. Surprisingly, we found a lower prevalence of hypothyroidism in the Crohn's group as compared to controls.

Finding no difference in the prevalence of hyperthyroidism between patients with Crohn's disease and controls has clinical significance. Hyperthyroidism is associated with accelerated bone turnover and shortening of the normal bone remodeling cycle^[6,7]. This results in increased bone metabolism and osteoporosis. Since patients with Crohn's disease do not have a higher prevalence of hyperthyroidism, an elevation of thyroxine levels cannot be the basis for the increased osteoporosis seen in this group of patients. Factors such as chronic inflammation, prolonged steroid usage and malnutrition are the more likely etiological agents for osteoporosis^[16]. Thus, evaluating patients with Crohn's disease for hyperthyroidism should be done on clinical grounds and not as a screening procedure.

Our finding of a lower prevalence of hypothyroidism in our Crohn's population as compared to our controls is similar to those of Hammer *et al.*^[12]. It is possible that since both Crohn's disease and thyroid disorder have a possible autoimmune etiology, treating Crohn's disease with corticosteroids and immune modulating agents may prevent the manifestation of an autoimmune thyroid disorder. The difference in prevalence of hypothyroidism may also be the result of a higher than expected prevalence of hypothyroidism in our control group. The prevalence of hypothyroidism in population based studies varies from 0.5 % to 5 %^[17-19], however, we had an 8 % prevalence of hypothyroidism in our controls. This higher prevalence of hypothyroidism may be explained by the availability of third generation assays for thyroid stimulating hormone (TSH) and increased frequency of screening for thyroid disorder, leading to detection of sub-clinical disease. There is also the possibility of a selection bias in the control group. The controls included people who underwent screening colonoscopy. Those persons are more likely to be health conscious and, therefore, are more likely to visit a physician; thus, this would result in increased screening for thyroid disease as compared to the general population. In addition, the control group had a higher body mass index (BMI) as compared to the Crohn's group. BMI can act as a confounding factor as it is related to both hypothyroidism and reflux symptoms. Hypothyroidism is associated with weight gain^[18,19]. Patients who have a higher BMI are more likely to have reflux symptoms^[20,21] and thus, are more likely to undergo EGD than the general population. Since our controls included patients having EGD, it is possible that our controls contained a higher percentage of people who are hypothyroid. This may be a theoretical concern as a recent, well design; prospective study^[22] did not show an association between obesity and reflux symptoms.

There are concerns that the presence of thyroid disease may have an impact on the management of IBD. Moreover, there are case reports that suggest that thyroid disease needs to be treated in order to successfully treat IBD^[10,13]. We subdivided our Crohn's disease population into those who are euthyroid and those who had thyroid disease. The two groups were compared with regard to steroid usage, use of immune modulating agents, surgery for the management of Crohn's and rate of fracture. There was a higher rate of steroid usage, use of immune modulating agents, and both small and large

bowel surgeries in patients who were euthyroid. For instance, there were seven fractures in the Crohn's group, all of which occurred in patients who were euthyroid. The differences, though clinically significant, were not statistically significant. This is probably due to a small sample size. A larger prospective, controlled study is needed to evaluate this issue. Hypothyroidism is known to decrease metabolism and slow physiological functions. The presence of hypothyroidism may act as endogenous disease modification in patients with Crohn's disease.

Our study was limited by retrospective data collection. This makes it difficult to evaluate and compare disease severity index and extent of disease between Crohn's disease patients who are euthyroid and those who had a thyroid disorder present. It also makes it difficult to establish a temporal relationship between thyroid disease and Crohn's disease. Our results are based on the assumption that patients who were characterized as euthyroid are actually euthyroid. Symptoms may not suggest thyroid disease when it is mild and are often atypical in the elderly^[23-25]. Thus, it is possible that we missed patients with subclinical thyroid disease.

In conclusion, patients with Crohn's disease do not have a higher prevalence of thyroid disease than the general population and, therefore, routine screening for thyroid disease is not a necessary component in the management of Crohn's disease. However, it is apparent that thyroid disease has a significant clinical impact on the course of Crohn's disease, which needs to be studied in a prospective manner.

ACKNOWLEDGEMENT

The authors thank S.D. Rampertab, M.D. for her critical comments on the manuscript.

REFERENCES

- 1 **Silvennoinen JA**, Karttunen TJ, Niemela SE, Manelius JJ, Lehtola JK. A controlled study of bone mineral density in patients with inflammatory bowel disease. *Gut* 1995; **37**: 71-76
- 2 **Andreassen H**, Rungby J, Dahlerup JF, Mosekilde L. Inflammatory bowel disease and osteoporosis. *Scand J Gastroenterol* 1997; **32**: 1247-1255
- 3 **Vestergaard P**, Krogh K, Rejnmark L, Laurberg S, Mosekilde L. Fracture risk is increased in Crohn's disease, but not in ulcerative colitis. *Gut* 2000; **46**: 176-181
- 4 **Bernstein CN**, Blanchard JF, Leslie W, Wajda A, Yu BN. The incidence of fracture among patients with inflammatory bowel disease. A population-based cohort study. *Ann Int Med* 2000; **133**: 759-799
- 5 **Greenspan SL**, Greenspan FS. The effect of thyroid hormone on skeletal integrity. *Ann Int Med* 1999; **130**: 750-758
- 6 **Mosekilde L**, Eriksen EF, Charles P. Effects of thyroid hormone on bone and mineral metabolism. *Endo Metabol Clin NA* 1990; **19**: 35-63
- 7 **Ross DS**. Hyperthyroidism, thyroid hormone therapy, and bone. *Thyroid* 1994; **4**: 319-326
- 8 **Snook JA**, de Silva HJ, Jewell DP. The association of autoimmune disorders with inflammatory bowel disease. *Q J Med* 1989; **72**: 835-840
- 9 **Jarnerot G**, Kagedal B, von Schenck A, Trulove SC. The thyroid in ulcerative colitis and Crohn's disease. V. Triiodothyronine. Effect of corticosteroids and influence of severe disease. *Acta Med Scand* 1976; **199**: 229-232
- 10 **Bonapace ES**, Srinivasan R. Simultaneous occurrence of inflammatory bowel disease and thyroid disease. *Am J Gastroenterol* 2001; **96**: 1925-1926
- 11 **Bianchi GP**, Marchesini G, Gurli C, Zoli M. Thyroid involvement in patients with active inflammatory bowel diseases. *Ital J Gastroenterol* 1995; **27**: 291-295
- 12 **Hammer B**, Ashurst P, Naish J. Diseases associated with ulcerative colitis and Crohn's disease. *Gut* 1968; **9**: 17-21

- 13 **Modebe O**. Autoimmune thyroid disease with ulcerative colitis. *Post Med J* 1986; **62**: 475-476
- 14 **Haderslev KV**, Tjellesen L, Sorensen HA, Staun M. Alendronate increases lumbar spine bone mineral density in patients with Crohn's disease. *Gastroenterol* 2000; **119**: 866-869
- 15 **Janerot G**. The thyroid in ulcerative colitis and Crohn's disease I. Thyroid radioiodide uptake and urinary iodine excretion. *Acta Med Scand* 1975; **197**: 95
- 16 **Andreassen H**, Rungby J, Dahlerup JF, Mosekilde L. Inflammatory bowel disease and osteoporosis. *Scand J Gastroenterol* 1997; **32**: 1247-1255
- 17 **Sawin CT**, Castelli WP, Hershman JM, McNamara P, Bacharach P. The aging thyroid. Thyroid deficiency in the framingham study. *Arch Int Med* 1985; **145**: 1386-1388
- 18 **Dale J**, Daykin J, Holder R, Sheppard MC, Franklyn JA. Weight gain following treatment of hyperthyroidism. *Clin Endo* 2001; **55**: 233-239
- 19 **Pinkney JH**, Goodrick SJ, Katz J, Johnson AB, Mohamed-Ali V, Coppack SW. Leptin and the pituitary-thyroid axis: a comparative study in obese, hypothyroid and hyperthyroid subjects. *Clin Endo* 1998; **49**: 572-583
- 20 **Wajed SA**, Streets CG, Bremner CG, DeMeester TR. Elevated body mass disrupts the barrier to gastroesophageal Reflux. *Arch Surg* 2001; **136**: 1014-1018
- 21 **Wilson LJ**, Ma W, Hirschowitz BI. Association of obesity with hiatal hernia and esophagitis. *Am J Gastroenterol* 1999; **94**: 2840-2844
- 22 **Langergren J**, Bergstrom R, Nyren O. No relation between body mass and gastro-oesophageal reflux symptoms in a swedish population based study. *Gut* 2000; **47**: 26-29
- 23 **Evered DC**, Ormston BJ, Smith PA, Hall R, Bird T. Grades of hypothyroidism. *Brit Med J* 1973; **1**: 657-662
- 24 **Wenzel KW**, Meinhold H, Raffenberg M, Adlkofer F, Schleusener H. Classification of hypothyroidism in evaluating patients after radioiodine therapy by serum cholesterol, T3-uptake, total T4. *Eur J Clin Invest* 1974; **4**: 141-148
- 25 **Bahemuka M**, Hodkinson HM. Screening for hypothyroidism in elderly patients. *Brit Med J* 1975; **2**: 601-603

Edited by Xu XQ

Elevated serum values of procollagen III peptide (PIIIP) in patients with ulcerative colitis who will develop pseudopolyps

Žarko Babić, Vjekoslav Jagić, Zvonko Petrović, Ante Bilić, Kapetanović Dinko, Goranka Kubat, Rosana Troskot, Mira Vukelić

Žarko Babić, Ante Bilić, Rosana Troskot, Division of Hepatogastroenterology, Department of Medicine, Sveti Duh General Hospital, Zagreb, Croatia

Vjekoslav Jagić Department of Laboratory Biochemistry Diagnosis, Sveti Duh General Hospital, Zagreb, Croatia

Zvonko Petrović Department of Pathology, Sveti Duh General Hospital, Zagreb, Croatia

Kapetanović Dinko, Goranka Kubat, Mira Vukelić Department of Radiology, Sveti Duh General Hospital, Zagreb, Croatia

Correspondence to: Assist. Professor Žarko Babić, M.D., Ph.D Fabkovićaeva 3, HR-10000 Zagreb, Croatia. zarko.babic@zg.hinet.hr

Telephone: +385-1-3712111 **Fax:** +385-1-3745550

Received: 2002-07-12 **Accepted:** 2002-07-29

Abstract

AIM: To assess the impact of procollagen III peptide as a marker of collagenesis in the development of pseudopolyps in patients with ulcerative colitis.

METHODS: Development of pseudopolyps was monitored in 25 patients with ulcerative colitis classified according to Powell-Tuck index as mild ($n=12$) or moderate ($n=13$) form of disease. Patients with a mild form of disease were treated with oral mesalazine medication (2-4 g/day) and local mesalazine preparation (suppository). Patients with a moderate form of disease received oral mesalazine medication (2-4 g/day), local mesalazine preparation (suppository) and local methylprednisolone at an initial dose of 60 mg/day, followed by dose tapering. How many significant variables (previously determined by analysis of variance) were elevated in the groups with and without pseudopolyp development was observed. ROC analysis for calculation of new index was made.

RESULTS: Serum values of procollagen III peptide (PIIIP), C-reactive protein (CRP) and C4 complement component (C4) were statistically significantly lower in the group of patients free from pseudopolyp development than those who developed one or more pseudopolyps (0.45 ± 0.12 vs 1.42 ± 0.70 , $P<0.0027$; 7.6 ± 4.7 vs 17.8 ± 9.17 , $P<0.035$; and 0.46 ± 0.11 vs 0.34 ± 0.16 , $P<0.068$, respectively) at endoscopic controls with pathohistologically samples during 13 months. There were no statistically significant differences in the values of C3, ceruloplasmin and IgM between the two groups ($P>0.05$). Discrimination function analysis yielded highest standardized cannon coefficients for PIIIP (0.876), CRP (0.104), C3 (-0.534) and C4 (0.184) ($P<0.036$). The elevation in two of three laboratory variables (PIIIP, CRP and C4) reached sensitivity of 93 % and specificity of 90 % in the development of pseudopolyps.

CONCLUSION: It is proposed that an increase in two of the three laboratory parameters (PIIIP, CRP and C4) could improve the accuracy of prediction of the development of pseudopolyps. When using PIIIP, CRP and C4 on decision

making, the positive predictive value and accuracy were 90 % and 92 %, respectively.

Babić Ž, Jagić V, Petrović Z, Bilić A, Dinko K, Kubat G, Troskot R, Vukelić M. Elevated serum values of procollagen III peptide (PIIIP) in patients with ulcerative colitis who will develop pseudopolyps. *World J Gastroenterol* 2003; 9(3): 619-621 <http://www.wjgnet.com/1007-9327/9/619.htm>

INTRODUCTION

The role of procollagen and of its metabolites and enzymes involved in the synthesis and degradation of procollagen during the development of ulcerative colitis has already been investigated in a number of studies^[1-6]. Higher levels of procollagen transcripts have been reported in patients with ulcerative colitis as compared with healthy subjects^[4], pointing to an enhanced *de novo* synthesis of all types of collagen in patients with ulcerative colitis^[1,3,4]. Also, the expression of collagenase has been demonstrated to be higher in patients with ulcerative colitis than in normal subjects^[4]. These patients showed hyperexpression of procollagen III RNA transcripts. The elevated level of procollagen messenger RNA correlated with the rate of inflammatory infiltrations^[1,3,4], represented by inflammatory polyps (pseudopolyps). In the process of healing inflammatory desctructed mucosa is changed with the reparatory process^[1-9].

The development of pseudopolyps sometimes is seen in the stage of disease remission^[7,8]. The presence of procollagen and other materials is necessary for polyp formation^[1,9]. The measurement of procollagen may be helpful in the determination of the patient who will develop pseudopolyp formation. Insight to literature of the last 20 years, there were no studies into the predictive value of procollagen III peptide (PIIIP) for polyp development in patients with ulcerative colitis. The aim of the study was to assess the role of PIIIP as a marker of collagen synthesis in the development of pseudopolyps in patients with ulcerative colitis.

MATERIALS AND METHODS

Patients

Twenty-five patients with ulcerative colitis^[7], 11 men with median age of 34 years (aged 30-45) and 14 women with median age 35 years (aged 29-47), were included in the study. Only newly detected patients were enrolled in the study, thus to exclude the effect of previous therapy on collagen formation^[1-7]. Thus the patients were classified according to Powell-Tuck index^[7,8] for disease severity into the groups with mild ($n=12$) and moderate ($n=13$) form of disease. Mild form of disease had no system symptoms, had less then 4 stools over 24 hours. This form of disease was without significant rectal bleeding, had no signs of anemia, had normal body temperature, normal puls rate and had sedimentation rate under 30 mm per hour. Moderate form of disease had 4-6 diarrhoic stools per day, crampy abdominal pain, elevated body

temperature, increased pulse rate, tachycardia, anemia, elevated sedimentation over 30 mm per hour and extraintestinal symptoms (arthritis). Severe form of disease with more than 6 diarrhoic stools per day, more rectal bleeding and severe intestinal and extraintestinal complications, *etc.* were not included in the study, while the therapy for this form of disease can influence to the collagen formation^[1-12].

The course of disease was monitored clinically, endoscopically and histologically. The development of pseudopolyps was observed by using endoscopy^[1,7,9-12]. The formation of intraluminal mucosal enlargement with one or more polyps in former or newly inflamed mucosa was observed. Histological criteria for inflammatory polyps (pseudopolyps) were: only the finding of a diffuse colitis with nonspecific inflammation, no granulomas, and involved rectum would be consistent with ulcerative colitis; however, even in cases that the patient might still have some other form of diffuse colitis and the diagnosis of ulcerative colitis is only established by exclusion of all other causes^[13]. The criteria for the diagnosis of epithelial dysplasia and its distinction from the inflammatory and reparative^[14,15] lesions and neoplasms^[16] that regularly occur in these patients have been established.

Clinical and endoscopic controls were done once monthly during 12 months (12 times), and then once after six months again, what meant totally 13 controls^[7].

Laboratory measurements and new index calculation

PIIIP was measured by using RIA-gnost PIIIP method (Berhingwerke). CRP, C3, C4, IgM and ceruloplasmin were measured by using Turbox Immunonephelometry method (Orion diagnostics).

The significant laboratory variables were determined by using analysis of variance. The contribution of each variable was determined by using the discriminant canonical function on Statistica 5.0 software.

The indexes from three most significant variables were calculated by using ROC analysis. How many significant variables were elevated above laboratory reference values for each patient in two groups (with and without pseudopolyps) was observed. ROC analysis was used to determine the sensitivity, specificity, accuracy and positive predictive value of our new index.

Therapy

The patients with a mild form of disease were treated with oral mesalazine medication (2-4 g/day) and local mesalazine preparation (suppository)^[7]. The patients with a moderate form of disease received oral mesalazine medication (2-4 g/day), local mesalazine preparation (suppository) and oral methylprednisolone at an initial dose of 60 mg/day followed by methylprednisolone dose tapering^[7]. Severe form of disease was excluded with Powell-Tuck index, while therapy for severe form of disease can influence on inflammatory polyps formation^[1-7].

RESULTS

In the group of patients without pseudopolyp development ($n=15$), the levels of PIIIP, C-reactive protein (CRP) and C4 complement component (C4) were statistically significantly lower than those in the group of patients developing pseudopolyps (0.45 ± 0.12 vs 1.42 ± 0.70 , $P<0.0027$; 7.6 ± 4.7 vs 17.8 ± 9.17 , $P<0.035$; and 0.46 ± 0.11 vs 0.34 ± 0.16 , $P<0.068$, respectively). Other parameters, i.e. C3 complement component (C3), ceruloplasmin and IgM, showed no statistically significant differences between the groups of patients with and without pseudopolyp development. Analysis of the discriminative canonical function yielded highest

standardized canonical coefficients for PIIIP (0.876), CRP (0.104), C3 (-0.534) and C4 (0.184) ($P<0.036$), which were then used for subsequent data analysis.

The use of PIIIP, CRP and C4 levels showed that an increase in two of these three laboratory parameters improved the accuracy of prediction of pseudopolyp development. When using PIIIP, CRP and C4 (ROC analysis) on decision making sensitivity was 93 % and specificity 90 %, the positive predictive value and accuracy were 90% and 92%, respectively.

DISCUSSION

In ulcerative colitis patients, inflammatory mucosal destruction is changed by regenerative process (inflammatory polyps (pseudopolyps))^[1-7,13-16]. Collagen is a constituent of connective tissue, thus also of polyps^[1]. In inflammatory bowel diseases, elevated levels of collagen I, III and V are found^[1-3]. Serum level of PIIIP was found to be higher in patients with ulcerative colitis and liver damage, then in patients without liver damage^[9]. Collagenase is regulated by the processes involved in the collagen synthesis (N-terminal propeptide of type III procollagen and C-terminal propeptide of type I procollagen) and degradation (C-terminal telopeptide of type I collagen)^[1]. Degradation of collagens is highly regulated by a cascade of matrix metalloproteases and their tissue inhibitors taken by endoscopic biopsies in patients with inflammatory bowel disease^[8]. The histological severity degree of acute inflammation was correlated well with the expression of metalloproteases gene^[8].

Collagenase can be influenced by glucocorticoid therapy, therefore only newly detected patients were enrolled in the study^[1]. The effect of glucocorticoids on collagenase and collagen degradation has not yet been fully clarified, however, a number of speculative theories have been proposed^[1,3,5,6,9,17]. So, that was the reason why we did not include severe forms of disease in the study, while there was a lot of factors that could have influence on the synthesis of collagen and therefore lead to misinterpretation of results (we tried to succeed "a homogenous sample" according to collagenesis). We found no data about any study predicting pseudopolyps development in patients with inflammatory bowel disease. The development of pseudopolyps is sometimes seen in disease relapses, but not strongly^[1].

Many studies have tackled the issue of predicting disease relapse, however, little has been reported on predicting remission of the disease and none using PIIIP^[1,8,18-22].

The levels of interleukin-1, a potent CRP stimulus, were also monitored^[23]. Serum levels of interleukin-1 receptor antagonist (IL-1ra) may also be an index of ulcerative colitis activity, being low in disease remission^[24]. This parameter may be useful in the differential diagnosis against other IBDs. A group of authors from Aachen prefer the level of interleukin-6 to CRP^[25]. In the present study, CRP levels were among those that, used in combination with other parameters, improved the accuracy of predicting pseudopolyp development, probably pointing not only to inflammation expression but also to the cellular reparatory potential.

The levels of total sialic acid remained increased after the therapy, especially in patients with poor response to therapy with 5-aminosalicylic acid and corticosteroids, while the levels of CRP were normalized after three weeks in most of the patients, irrespective of their therapeutic response^[26].

Endoscopic monitoring of IBD activity should be supplemented by the noninvasive measurement of the levels of alpha₁-antitrypsin in stool and serum albumin^[27], the more so, Moran *et al* recommend them as routine markers of the disease endoscopic activity^[28].

The levels of immunoglobulin proved helpful in the

assessment of intestinal resorption, however, in spite of previous belief, had no practical clinical relevance in the determination of disease activity^[29,30]. The results of our study were consistent with these concepts. So, only the values of C4 complement component could be used for subsequent evaluation, and these only in combination with other parameters. Neither were the values of ceruloplasmin as an early inflammation reactant useful for further analysis.

According to Schmoud *et al.*, age is an unfavorable prognostic factor for disease relapse in patients with inflammatory bowel disease (IBD)^[31]. Therefore, the patients included in our study were matched by both sex and age, thus to minimize the impact of these factors on study results.

In the present study, we used the ever more popular method including a combination of factors, providing more accurate information on the real state than each of the factors alone. The role of procollagen should be investigated in a larger sample. Studies with tissue collagen determined before and after therapy may also be expected to yield interesting results. In addition, studies in more severe forms of the disease would be highly interesting, although it might be difficult to differentiate between the collagenase involved in the connective tissue formation in the intestinal wall and the collagenase formed by systemic stimulation of other tissues due to the disease severity^[1,2,6,8,9].

In conclusion, based on the study results, it is proposed that elevation in two of the three laboratory parameters (PIIP, CRP and C4) can improve the prediction of the development of pseudopolyps in patients with ulcerative colitis. When PIIP, CRP and C4 are used in the assessment of pseudopolyp development, the positive predictive value and accuracy were as high as 90 % and 93 %, respectively.

REFERENCES

- Kjeldsen J**, Schaffalitzky OBM, Junker P. Seromarkers of collagen I and III metabolism in active Crohn's disease. Relation to disease activity and response to therapy. *Gut* 1995; **37**: 805-810
- Graham MF**, Diegelmann RF, Elson CO, Lindblad WJ, Gitschalk N, Gay S, Adam J. Collagen content and types in the intestinal strictures of Crohn's disease. *Gastroenterology* 1988; **94**: 257-265
- Matthes H**, Herbst H, Schuppan D, Stallmach A, Milani S, Stein H, Riecken EO. Cellular localisation of procollagen gene transcripts in inflammatory bowel disease. *Gastroenterology* 1992; **102**: 431-442
- Matthes H**, Stallmach A, Matthes B, Herbst H, Schuppan D, Riecken ED. Indications for different collagen metabolism in Crohn's disease and ulcerative colitis. *Med Clin* 1993; **88**: 185-192
- Berg S**, Brodin B, Hesselvik F, Laurent TC, Maller R. Elevated levels of plasma hyaluronan in septicaemia. *Scand J Clin Lab Invest* 1998; **48**: 727-732
- Kaushner I**. The phenomenon of the acute phase response. *Ann NY Acad Sci* 1982; **389**: 39-48
- Rutgeerts P**. Medical therapy of inflammatory bowel disease. *Digestion* 1998; **59**: 453-469
- von Lampe B**, Barthel B, Coupland SE, Riecken EO, Rosewicz S. Differential expression of matrix metalloproteinases and their tissue inhibitors in colon mucosa of patients with inflammatory bowel disease. *Gut* 2000; **47**: 12-14
- Lidenius MH**, Risteli LT, Risteli JP, Taskinsen EI, Kellokumpu IH, Hockerstedt KA. Serum aminoterminal propeptide of type III procollagen (S-PIIP) and hepatobiliary dysfunction in patients with ulcerative colitis. *Scand J Clin Lab Invest* 1997; **57**: 297-305
- Walmsley RS**, Ayres RCS, Pounder RE, Allan RN. A simple clinical activity index. *Gut* 1998; **43**: 29-32
- Stallmach A**, Schuppan D, Riese HH, Matthes H, Riecken ED. Increased collagen type III synthesis by fibroblasts isolated from strictures of patients from Crohn's disease. *Gastroenterology* 1992; **102**: 1920-1929
- Modigliani R**. Definition of patient groups: remission. In: Campieri M, Bianchi-Poro G, Fiocchi G, Scholmerich J. eds. Clinical challenges in inflammatory bowel disease- diagnosis, prognosis and treatment. Dordrecht, Boston, London: *Kluwer Academic Publishers* 1998: 85-94
- Goldman H**. Interpretation of large intestinal mucosal biopsy specimens. *Hum Pathol* 1994; **25**: 1150-1159
- Riddell RH**, Goldman H, Ransohoff DF. Dysplasia in inflammatory bowel disease: Standardized classification with provisional clinical applications. *Hum Pathol* 1983; **14**: 931-968
- Pascal RR**. Consistency in the terminology of colorectal dysplasia. *Hum Pathol* 1988; **19**: 1249-1250
- Pascal RR**. Dysplasia and early carcinoma in inflammatory bowel disease and colorectal adenomas. *Hum Pathol* 1994; **25**: 1160-1171
- Dionne S**, Ruemmele M, Seidman EG. Immunopathogenesis of inflammatory bowel disease: role of cytokines and immune cell-enterocyte interactions. In: Bistran BR, Walker-Smith JA. editors. *2nd Nestle Nutrition Workshop Series Clinical & Performance Programme* 1999: 41-62
- Mahmud N**, Stinson J, O'Connell MA, Mantle TJ, Keeling PW, Feely J, Weir DG, Kellehr D. Microalbuminuria in inflammatory bowel disease. *Gut* 1994; **11**: 1599-1604
- Nielsen OH**, Langholz E, Hendel J, Brynskov J. Circulating soluble intercellular adhesion molecule-1 (sICAM-1) in active inflammatory bowel disease. *Dig Dis Sci* 1994; **39**: 1918-1923
- Rowe FA**, Camilleri M, Forstrom LA, Batts KP, Mullan BP, Thomforde GMDunn W, Zinsmeister AR. A pilot study of splenic and whole body retention of autologous radiolabeled leukocytes in the assessment of severity in inflammatory colitis. *Am J Gastroenterol* 1995; **90**: 1771-1775
- Weldon MJ**, Masoomi AM, Britten AJ, Gene J, Finlaysen CJ, Joseph AE, Maxwell MD. Quantification of inflammatory bowel disease activity using technetium-99m HMPAO labelled leucocyte single photon emission computerised tomography (SPECT). *Gut* 1995; **36**: 243-250
- Patel RT**, Bain I, Youngs D, Keighely MR. Cytokine production in pouchitis is similar to that in ulcerative colitis. *Dis Colon Rectum* 1995; **38**: 831-837
- Mazlam MZ**, Hodgson HJ. Interrelations between interleukin-6, interleukin-1 beta, plasma C-reactive protein values, and *in vitro* C-reactive protein generation in patients with inflammatory bowel disease. *Gut* 1994; **35**: 77-83
- Propst A**, Propst T, Herold M, Vogel W, Judmaier G. Interleukin-1 receptor antagonist in differential diagnosis of inflammatory bowel disease. *Eur J Gastroenterol Hepatol* 1995; **11**: 1031-1036
- Hotkamp W**, Stollberg T, Reis HE. Serum interleukin-6 related to disease activity but not disease specificity in inflammatory bowel disease. *J Clin Gastroenterol* 1995; **20**: 123-126
- Ricci G**, D' Ambrosi A, Resca D, Masotti M, Alvisi V. Comparison of serum total sialic acid, C-reactive protein, alpha 1-acid glycoprotein and beta 2-microglobulin in patients with non-malignant bowel disease. *Biomed Pharmacother* 1995; **49**: 259-262
- Lindgren S**, Floren CH, Lindgren T, Starck M, Stewnius J, Nassberger L. Low prevalence of anti-neutrophil cytoplasmic antibodies in ulcerative colitis patients with long-term remission. *Eur J Gastroenterol Hepatol* 1995; **7**: 563-568
- Moran A**, Jones A, Asquith P. Laboratory markers of colonoscopic activity in ulcerative colitis and Crohn's colitis. *Scand J Gastroenterol* 1995; **30**: 356-360
- Ivanov AF**, Eroshkina TD, Fomin SA, Musin II, Chirkin VV. The effect of hemosorption on the glycoprotein concentration of the blood serum in inflammatory diseases of the large intestine. *Ter Arkh* 1995; **67**: 36-39
- Philipsen EK**, Bondesen S, Andersen J, Larsen S. Serum immunoglobulin G subclasses in patients with ulcerative colitis and Crohn's disease of different disease activity. *Scand J Gastroenterol* 1995; **30**: 50-53
- Sahmoud T**, Hocht-Boes G, Modigliani R, Bitoun A, Colombel JF, Soule JC, Florent C, Gendre JP, Lerebours E, Sylvester R, Mary JY. Identifying patients with a high risk of relapse in quiescent Crohn's disease. The GETAID groups. The groupe d' Etudes therapeutiques des affectious inflammatoires digestives. *Gut* 1995; **37**: 811-818

Synthesis of endotoxin receptor CD14 protein in Kupffer cells and its role in alcohol-induced liver disease

Li-Li Dai, Jian-Ping Gong, Guo-Qing Zuo, Chuan-Xin Wu, Yu-Jun Shi, Xu-Hong Li, Yong Peng, Wu Deng, Sheng-Wei Li, Chang-An Liu

Li-Li Dai, Guo-Qing Zuo, Department of Digestive Disease, the Second College of Clinical Medicine & the Second Affiliated Hospital of Chongqing University of Medical Science, 74 Linjiang Road, Chongqing 400010, China

Jian-Ping Gong, Chuan-Xin Wu, Yu-Jun Shi, Xu-Hong Li, Yong Peng, Wu Deng, Sheng-Wei Li, Chang-An Liu, Department of General Surgery, the Second College of Clinical Medicine & the Second Affiliated Hospital of Chongqing University of Medical Science, 74 Linjiang Road, Chongqing 400010, China

Supported by the National Natural Science Foundation of China, No.39970719, 30170919

Correspondence to: Dr Jian-Ping Gong, Department of General Surgery, the Second College of Clinical Medicine & the Second Affiliated Hospital of Chongqing University of Medical Science, 74 Linjiang Road, Chongqing 400010, China. gongjianping11@hotmail.com

Telephone: +86-23-63766701 **Fax:** +86-23-63822815

Received: 2002-06-24 **Accepted:** 2002-07-22

Abstract

AIM: To observe the synthesis of endotoxin receptor CD14 protein and its mRNA expression in Kupffer cells (KCs), and evaluate the role of CD14 in the pathogenesis of liver injury in rats with alcohol-induced liver disease (ALD).

METHODS: Twenty-eight Wistar rats were divided into two groups: ethanol-fed group and control group. Ethanol-fed group was fed ethanol (dose of 5g·12g·kg·d⁻¹) and control group received dextrose instead of ethanol. Two groups were sacrificed at 4 wk and 8 wk, respectively. KCs were isolated and the synthesis of CD14 protein and its mRNA expression in KCs were determined by flow cytometric analysis (FCM) or the reverse transcription polymerase chain reaction (RT-PCR) analysis. The levels of plasma endotoxin and alanine transaminase (ALT) were measured by Limulus Amebocyte Lysate assay and standard enzymatic procedures respectively, and the levels of plasma tumor necrosis factor (TNF)- α and interleukin (IL)-6 were both determined by ELISA. The liver pathology change was observed under light and electric microscopy.

RESULTS: In ethanol-fed group, the percentages of FITC-CD14 positive cells were 76.23 % and 89.42 % at 4 wk and 8 wk, respectively. Compared with control group (4.45 % and 5.38 %), the difference was significant ($P < 0.05$). The expressions of CD14 mRNA were 7.56 \pm 1.02 and 8.74 \pm 1.37 at 4 wk and 8 wk, respectively, which were significantly higher compared with the control group (1.77 \pm 0.21 and 1.98 \pm 0.23) ($P < 0.05$). Plasma endotoxin levels at 4 wk and 8 wk increased significantly in ethanol-fed group (129 \pm 21 ng·L⁻¹ and 187 \pm 35 ng·L⁻¹) than those in control rats (48 \pm 9 ng·L⁻¹ and 53 \pm 11 ng·L⁻¹) ($P < 0.05$). Mean values of plasma ALT levels increased dramatically in ethanol-fed rats (112 \pm 15 IU/L and 147 \pm 22 IU/L) than those in the control animals (31 \pm 12 IU/L and 33 \pm 9 IU/L) ($P < 0.05$). In ethanol-fed rats, the levels of TNF- α were 326 \pm 42 ng·L⁻¹ and 402 \pm 51 ng·L⁻¹ at 4 wk and 8 wk, respectively which were significantly higher than those

in control group (86 \pm 12 ng·L⁻¹ and 97 \pm 13 ng·L⁻¹) ($P < 0.05$). The levels of IL-6 were 387 \pm 46 ng·L⁻¹ and 413 \pm 51 ng·L⁻¹, which were also higher than control group (78 \pm 11 ng·L⁻¹ and 73 \pm 10 ng·L⁻¹) ($P < 0.05$). In liver section from ethanol-fed rats, there were marked pathological changes including steatosis, cell infiltration and necrosis. No marked pathological changes were seen in control group.

CONCLUSION: Ethanol administration led to a significant synthesis of endotoxin receptor CD14 protein and its gene expression in KCs, which maybe result in the pathological changes of liver tissue and hepatic functional damages.

Dai LL, Gong JP, Zuo GQ, Wu CX, Shi YJ, Li XH, Peng Y, Deng W, Li SW, Liu CA. Synthesis of endotoxin receptor CD14 protein in Kupffer cells and its role in alcohol-induced liver disease. *World J Gastroenterol* 2003; 9(3): 622-626

<http://www.wjgnet.com/1007-9327/9/622.htm>

INTRODUCTION

Our previous studies have shown that the ethanol-fed rats or rats with endotoxemia had higher endotoxin levels in plasma, increased lipopolysaccharide (LPS) receptor CD14 in the liver, and more serious liver injury compared with control rats^[1-6]. But it was unclear where CD14 came from. Accordingly, the purpose of this study is to determine whether Kupffer cells (KCs) synthesize CD14 protein and express its mRNA, and evaluate the role of CD14 protein in alcohol-induced liver disease (ALD).

MATERIALS AND METHODS

Animals and treatments

Twenty-eight adult female Wistar rats weighing 180 g to 220 g were fed *ad libitum* a liquid diet. Animals were divided into two groups: ethanol liquid diet group (ethanol-fed group) and liquid diet group (control group). The rats of ethanol-fed group were fed ethanol, and control group received the same diet but with isocaloric amounts of dextrose instead of ethanol. In ethanol-fed group, the initial dose is 5 g·kg⁻¹·d⁻¹ and the concentration of ethanol within the diet increased up to 12 g·kg⁻¹·d⁻¹ gradually in 8 weeks. All diets were prepared fresh daily. All the animals were anesthetized with sodium pentobarbital (30 mg·kg⁻¹ intraperitoneally) and sacrificed at 4 wk and 8 wk, respectively. Blood was withdrawn from the portal vein and stored at -70 °C before use.

KCs isolation

KCs were isolated with the in situ collagenase perfusion technique, modified as described previously^[7,8]. In brief, the livers were removed after a portal vein perfusion with Hanks' balanced salt solution (HBSS) and the homogenate was digested in a solution of 0.5 g·L⁻¹ collagenase (Type IV, Sigma). The digest was washed thoroughly and plated on plastic dishes in RPMI medium containing 50 mL·L⁻¹ fetal calf serum (FCS).

After 3 h incubation at 37 °C in O₂ and CO₂ (0.95/0.05), nonadherent cells were removed with pipet. The adherent cells were collected with a rubber policeman. KCs purity exceeded 90 % as assessed by light microscopy, and viability was typically greater than 92 % as determined by trypan blue exclusion assay.

Flow cytometric analysis (FCM)

Synthesis of CD14 protein in KCs was examined by FCM^[2,3]. In brief, KCs were incubated with the anti-CD14 polyclonal antibody (0.1 mg·L⁻¹) for 30 mins after washing, cells were incubated with goat anti-rabbit immunoglobulin G labeled with FITC for 30 min, after being washed for three times, and 10 000 cells were analyzed by FCM (Coulter, USA). The percentage and mean fluorescence intensity (MFI) of CD14-positive cells were taken as the indexes.

RNA isolation and complementary DNA synthesis

Total RNA was isolated from KCs with the TRIZOL Reagent (Life Technologies, USA). The quality of RNA was controlled by the intactness of ribosomal RNA bands. 0.5 mg of each intact total RNA samples was reverse-transcribed to complementary DNA (cDNA) with the reverse transcription polymerase chain reaction (RT-PCR) kit (Roche, USA). cDNA was stored at -70 °C until polymerase chain reaction (PCR) analysis.

Determination of CD14 mRNA by RT-PCR

The PCR primers used were CD14: sense (5'-CTCAACCTAGAGCCGTTTCT-3'), anti-sense (5'-CAGGATTGTCAGACAGGTCT-3'); β-actin: sense (5'-ACCACAGCTGAGAGGAAATCG-3'), antisense (5'-AGAGGTCTTACGGATGTCAACG-3'). The sizes of the amplified PCR products were 267 bp for CD14, and 281 bp for β-actin. The reaction conditions for amplification were as below: denaturation at 93 °C for 1 min, annealing at 57 °C for 2 min, and extension at 71 °C for 1 min for 30 cycles. The PCR products were electrophoresed in 20 g·L⁻¹ agarose gels, and the gels were ethidium bromide stained and video photographed on an ultraviolet transilluminator, and the results were showed with the relative absorbance (Ar: relative optical density, ROD).

Blood endotoxin & ALT

To determinate the endotoxin, blood was collected into pyrogen-free tubes containing heparin. Plasma was immediately separated at 4 °C by centrifugation at 200 g for 8 minutes and stored in pyrogen-free tubes at -70 °C. Plasma endotoxin levels were measured within a week using the Limulus Amebocyte Lysate assay. Serum alanine transaminase (ALT) was measured by standard enzymatic procedures.

Bioassay for cytokines production in plasma

The levels of TNF-α and IL-6 in plasma were determined with enzyme-linked immunosorbent assay (ELISA) kits according to the manufacture's instructions and guidelines (Biosource International, Camarillo, CA).

Liver pathology

Liver samples from left liver lobes were fixed with 100 ml·L⁻¹ buffered formalin or 25 g·L⁻¹ glutaraldehyde immediately. For optical microscope, the tissue blocks were embedded in paraffin, and stained with hematoxylin and eosin (HE). For electronic microscope, the tissue blocks were embedded in Epon 618 resin and ultrathin sections were stained with uranyl acetate and lead citrate. A H-2000 transmission electron microscope was employed.

Statistical analysis

All results were expressed as $\bar{x} \pm s_x$. Statistical differences between means were determined using Student's *t* test. A *P* value of ≤ 0.05 was considered significant.

RESULTS

Binding of FITC to KCs

To confirm the synthesis of CD14 protein in KCs, we examined the binding of FITC to the cells. The percentages of FITC-CD14 positive cells at 4 wk and 8 wk were 4.45 % and 5.38 % in control group, respectively. While in ethanol-fed group, the mean fluorescence intensity (MFI) dramatically increased, the numbers of FITC-CD14 positive cells were 76.23 % and 89.42 % at 4 wk and 8 wk, respectively. There was significant difference when compared to control group ($P < 0.05$).

Expression of CD14 mRNA in KCs

CD14 mRNA expression in both groups KCs was determined with RT-PCR. In control group, there was no significant expression at the level of CD14 mRNA at 4 wk and 8 wk, respectively. However, it was significantly higher in ethanol-fed rats compared with control group ($P < 0.05$, Figure 1).

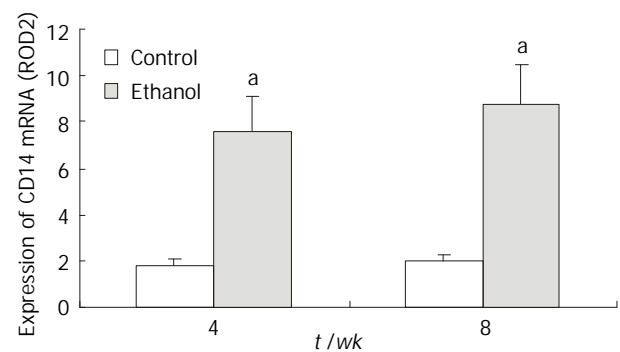


Figure 1 Expression of CD14 mRNA in KCs. ^a $P < 0.05$ vs controls.

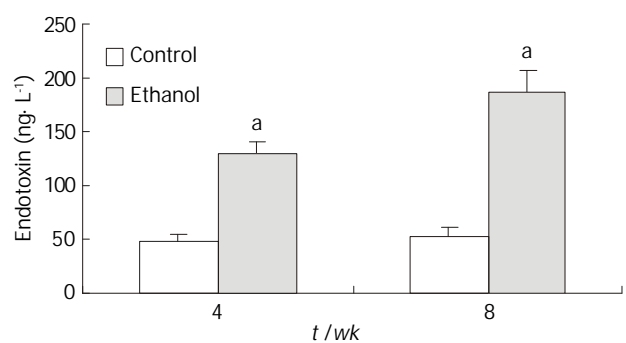


Figure 2 Changes of endotoxin levels. ^a $P < 0.05$, vs controls.

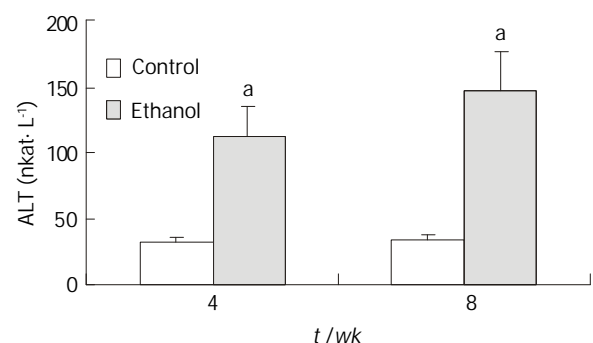


Figure 3 Changes of serum alanine transaminase levels. ^a $P < 0.05$, vs controls.

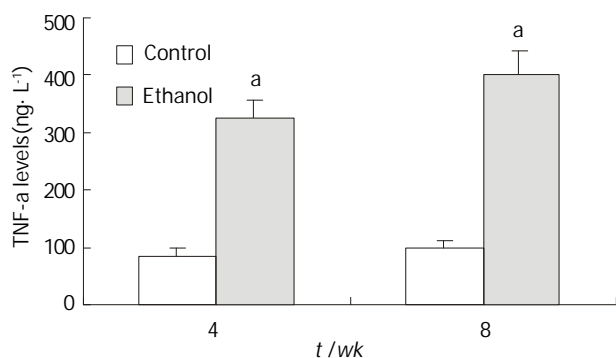


Figure 4 Changes of TNF- α concentrations. ^a $P < 0.05$ vs controls.

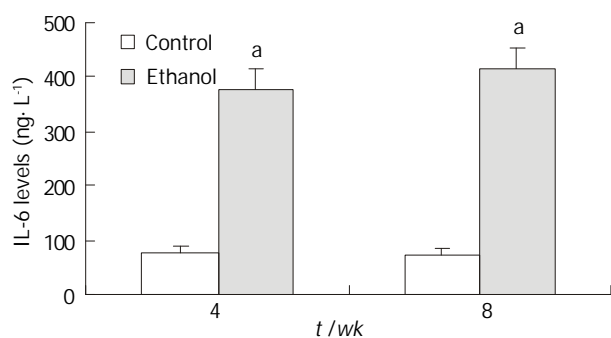


Figure 5 Changes of IL-6 concentrations. ^a $P < 0.05$ vs controls.

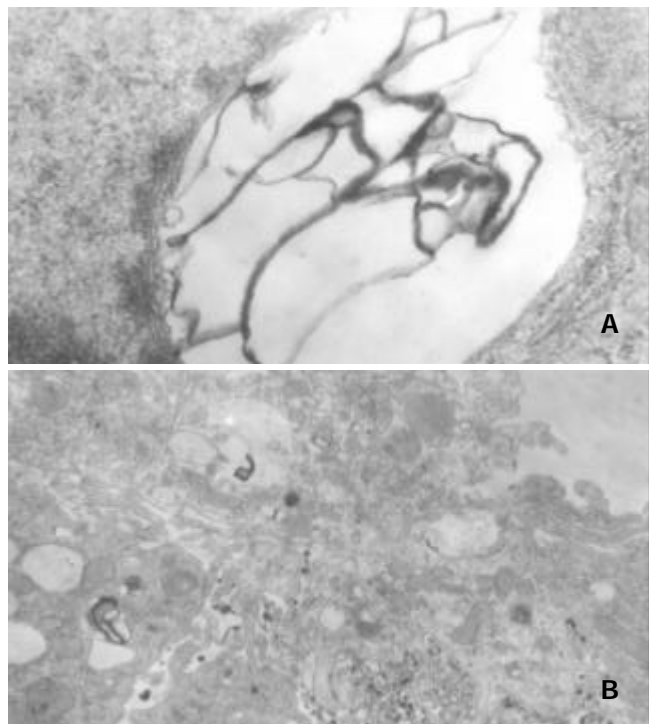


Figure 6 Ethanol-fed rats. A: Huge focal cytoplasmic degeneration in the cytoplasm of hepatocyte TEM $\times 30\,000$; B: Many focal cytoplasmic degeneration and myelin figures in the cytoplasm of KC TEM $\times 15\,000$.

Blood endotoxin and ALT levels

Plasma endotoxin levels in ethanol-fed rats increased significantly by ethanol to values of (129 ± 21) ng \cdot L⁻¹ at 4 wk and (187 ± 35) ng \cdot L⁻¹ at 8 wk, the levels of endotoxin were about 2-fold and 3-fold higher than the values of control rats [(48 ± 9) ng \cdot L⁻¹ and (53 ± 11) ng \cdot L⁻¹] ($P < 0.05$, Figure 2). Mean values for ALT in the control animals were (31 ± 12) nkat \cdot L⁻¹ and

(33 ± 9) nkat \cdot L⁻¹ at 4 wk and 8 wk, respectively. Plasma ALT levels were increased dramatically to (112 ± 15) nkat \cdot L⁻¹ and (147 ± 22) nkat \cdot L⁻¹ in ethanol-fed rats after 4 wk and 8 wk, respectively ($P < 0.05$, Figure 3).

Cytokines production in plasma

In ethanol-fed group, the plasma concentrations of TNF- α and IL-6 at 4 wk and 8 wk were 326 ± 42 ng \cdot L⁻¹, 402 ± 51 ng \cdot L⁻¹, 387 ± 46 ng \cdot L⁻¹, and 413 ± 51 ng \cdot L⁻¹, respectively, which were higher than those in control group (86 ± 12 ng \cdot L⁻¹, 97 ± 13 ng \cdot L⁻¹, 78 ± 11 ng \cdot L⁻¹, and 73 ± 10 ng \cdot L⁻¹) ($P < 0.05$, Figure 4 and Figure 5).

Pathological changes

No pathological changes in the liver were observed in the control rats at 4 wk or 8 wk. However, in liver section from rats after 4 wk on ethanol liquid diet, steatosis in both microvesicular and macrovesicular was observed. Few inflammation but accumulation of blood cells in the sinusoidal lining was observed. In liver section from rats after 8 wk on ethanol diet, marked pathological changes (steatosis, cell infiltration and necrosis), KCs proliferation and hypertrophy were detected. Under electron microscopy, huge focal cytoplasmic degeneration and necrosis could be seen in hepatocytes of ethanol-fed rats (Figure 6A). KCs hypertrophy and their surface projections increased as well as, and the phagocytic vacuoles or electron dense phagosomes, Focal cytoplasmic degeneration and many myelin figures in their cytoplasm could also be seen (Figure 6B).

DISCUSSION

Many studies have documented that liver disease could result from the dose- and time-dependent consumption of alcohol^[1,9,10]. However, the mechanisms remain unclear. There appears to be increasing evidences that ethanol toxicity maybe associated with increased levels of endotoxin in plasma^[9, 11-16]. Endotoxin or LPS is believed to exert many of its effects on the liver injury via interacting with LBP and CD14^[17-23]. LBP and CD14 are clearly implicated in the molecular and cellular basis of the interaction between endotoxin and monocytes/macrophages. LBP in serum can recognize and bind LPS to form LPS-LBP complexes and activate cells through CD14 receptor on the membrane of these cells, initiate a process leading to the release of cytokines (e.g., tumor necrosis factor- α and interleukines), prostanoids, and other soluble mediators^[9,10,24-29]. The release of these mediators is considered to be an early key step in the pathogenesis of liver disease because they trigger inflammatory events in the liver and alter the parenchymal homeostasis, ultimately initiate liver injury^[30-34]. But, it is not clear where CD14 in liver comes from.

The major goal of this study is to observe the synthesis of CD14 protein and its mRNA expression in KCs in ethanol-fed rats and evaluate the its role in ALD. It was found that endotoxin levels in the plasma of rats treated with ethanol were increased significantly when compared with control animals. The increase in CD14 mRNA levels in the ethanol-fed rats is correlated to inflammation degree and necrosis in the liver of these animals, which developed fatty liver, necrosis, and inflammation. Control rats showed no liver pathological changes. In the present study, we found the severity of pathological changes in ethanol-fed rats was accompanied with the increase in CD14 mRNA in KCs and serum ALT. A similar pattern of changes was observed by Yin *et al*^[12]. They found that blood endotoxin and hepatic CD14 mRNA and protein were increased by ethanol. Therefore, the sensitivity (vulnerability) of rat liver to alcohol-induced injury is directly related to CD14 expression in the liver, leading to the increased production of TNF- α , free radicals, interleukins and other

cytokines^[35-39]. The marked increase in the synthesis of CD14 protein suggests a new mechanism by which alcohol enhanced the LPS-mediated cytokine signaling by the liver macrophages, thus promoting the interaction between alcohol and endotoxins in the development of liver injury^[40-43].

It has been well established that the Liver is the main source of acute reaction protein^[1-6, 8]. However, the mechanism by which the synthesis of CD14 protein and its mRNA expression in the liver increased is thus as yet unclear. It is reported that the synthesis of CD14 protein and its gene expression occurred mainly in monocytes/macrophages, including the cells that reside in the liver (KCs) and these may represent recruitment of inflammatory cells, for example, infiltrating mononuclear cells or macrophages that have high expression of CD14 gene and CD14 protein^[44-48]. The increased CD14 protein may promote monocytes/macrophages response to low level of endotoxin, and lead to NF- κ B activation and production of pro-inflammatory cytokines, which play an important role in alcoholic liver injury^[49-53].

In summary, our results show that ethanol administration led to a significant increase of CD14 protein synthesis and its mRNA expression in KCs when compared with the control rats. The synthesis of CD14 protein and its gene expression may result in greater sensitivity of hepatocytes to endotoxin and lead to the pathological changes of liver tissue and liver functional injury.

REFERENCES

- Zuo GQ**, Gong JP, Liuo CH, Li SW, Wu CX, Yang K, Li Y. Expression of lipopolysaccharide binding protein and its receptor CD14 in experimental alcoholic liver disease. *World J Gastroenterol* 2001; **7**: 836-840
- Li SW**, Gong JP, Wu CX, Shi YJ, Liu CA. Lipopolysaccharide induced synthesis of CD14 protein and its gene expression in hepatocytes during endotoxemia. *World J Gastroenterol* 2002; **8**: 124-127
- Han DW**. Intestinal endotoxemia as a pathogenetic mechanism in liver failure. *World J Gastroenterol* 2002; **8**: 961-965
- Li SW**, Wu CX, Shi YJ, Liu CA. Lipopolysaccharide upregulates expression of CD14 gene and CD14 proteins of hepatocytes in rats. *Zhonghua Ganzangbing Zazhi* 2001; **9**: 103-105
- Gong JP**, Liu CA, Wu CX, Li SW, Shi YJ, Yang K, Li Y, Li XH. Liver sinusoidal endothelial cell injury by neutrophils in rats with acute obstructive cholangitis. *World J Gastroenterol* 2002; **8**: 342-345
- Gong JP**, Han BL. Role of CD14 in activation of Kupffer cell induced by lipopolysaccharide. *Shijie Huaren Xiaohua Zazhi* 1999; **7**: 875-877
- Gong JP**, Han BL. Isolation, culture and identification of liver cells. *Shijie Huaren Xiaohua Zazhi* 1999; **7**: 417-419
- Gong JP**, Wu CX, Liu CA, Li SW, Shi YJ, Yang K, Li Y, Li XH. Intestinal damage mediated by Kupffer cells in rats with endotoxemia. *World J Gastroenterol* 2002; **8**: 923-927
- Jarvelainen HA**, Fang C, Ingelman-Sundberg M, Lindros KO. Effect of chronic coadministration of endotoxin and ethanol on rat liver pathology and proinflammatory and anti-inflammatory cytokines. *Hepatology* 1999; **29**: 1503-1510
- Mathurin P**, Deng QG, Keshavarzian A, Choudhary S, Holmes EW, Tsukamoto H. Exacerbation of alcoholic liver injury by eneral endotoxin in rats. *Hepatology* 2000; **32**: 1008-1017
- Lin H**, Lu M, Zhang YX, Wang BY, Fu BY. Induction of a rat model of alcoholic liver disease. *Shijie Huaren Xiaohua Zazhi* 2001; **9**: 24-28
- Yin M**, Ikejima K, Wheeler MD, Bradford BU, Seabra V, Forman DT, Sato N, Thurman RG. Estrogen is involved in early alcohol-induced liver injury in a rat enteral feeding model. *Hepatology* 2000; **31**: 117-123
- Kono H**, Rusyn I, Yin M, Gabele E, Yamashina S, Dikalova A, Kadiiska MB, Connor HD, Mason RP, Segal BH, Bradford BU, Holland SM, Thurman RG. NADPH oxidase-derived free radicals are key oxidants in alcohol-induced liver disease. *J Clin Invest* 2000; **106**: 867-872
- French SW**. Intra gastric ethanol infusion model for cellular and molecular studies of alcoholic liver disease. *J Biomed Sci* 2001; **8**: 20-27
- Enomoto N**, Ikejima K, Yamashina S, Enomoto A, Nishiura T, Nishimura T, Brenner DA, Schemmer P, Bradford BU, Rivera CA, Zhong Z, Thurman RG. Kupffer cell-derived prostaglandin E₂ is involved in alcohol-induced fat accumulation in rat liver. *Am J Physiol* 2000; **279**: G100-G106
- Bautista AP**. Impact of alcohol on the ability of Kupffer cells to produce chemokines and its role in alcoholic liver disease. *J Gastroenterol Hepatol* 2000; **15**: 349-356
- Wu RQ**, Xu YX, Song XH, Chen LJ, Meng XJ. Adhesion molecule and proinflammatory cytokine gene expression in hepatic sinusoidal endothelial cells following cecal ligation and puncture. *World J Gastroenterol* 2001; **7**: 128-130
- Ling YL**, Meng AH, Zhao XY, Shan BE, Zhang JL, Zhang XP. Effect of cholecystokinin on cytokines during endotoxic shock in rats. *World J Gastroenterol* 2001; **7**: 667-671
- Hiki N**, Berger D, Mimura Y, Frick J, Dentener MA, Buurman WA, Seidelmann M, Kaminishi M, Beger HG. Release of endotoxin-binding protein during major elective surgery: role of soluble CD14 in phagocytic activation. *World J Surg* 2000; **24**: 499-506
- Gutsmann T**, Muller M, Carroll SF, Mackenzie RC, Wiese A, Seydel U. Dual role of lipopolysaccharide (LPS)-binding protein in neutralization of LPS and enhancement of LPS-induced activation of mononuclear cells. *Infect Immun* 2001; **69**: 6942-6950
- Heumann D**, Adachi Y, Le Roy D, Ohno N, Yadomae T, Glauser MP, Calandra T. Role of plasma, lipopolysaccharide-binding protein, and CD14 in response of mouse peritoneal exudates macrophages to endotoxin. *Infect Immun* 2001; **69**: 378-385
- Scott MG**, Vreugdenhil ACE, Buurman WA, Hancock REW, Gold MR. Cutting edge: cationic antimicrobial peptides block the binding of lipopolysaccharide (LPS) to LPS binding protein. *J Immunol* 2000; **164**: 549-553
- Kono H**, Wheeler MD, Rusyn I, Lin M, Seabra V, Rivera CA, Bradford BU, Forman DT, Thurman RG. Gender differences in early alcohol-induced liver injury: role of CD14, NF- κ B, and TNF- α . *Am J Physiol Gastrointest Liver Physiol* 2000; **278**: G652-G661
- Lin E**, Calvano SE, Lowry SF. Inflammatory cytokines and cell response in surgery. *Surgery* 2000; **127**: 117-126
- Wang LS**, Zhu HM, Zhou DY, Wang YL, Zhang WD. Influence of whole peptidoglycan of *bjfdobacterium* on cytotoxic effectors produced by mouse peritoneal macrophages. *World J Gastroenterol* 2001; **7**: 440-443
- Bai XY**, Jia XH, Cheng LZ, Qu YD. Influence of IFN α -2b and BCG on the release of TNF and IL-1 by Kupffer cells in rats with hepatoma. *World J Gastroenterol* 2001; **7**: 419-421
- Asea A**, Kraeft SK, Hurt-Jones EA, Stevenson MA, Chen LB, Finberg RW, Koo GC, Calderwood SK. HSP70 stimulates cytokine production through a CD14-dependant pathway, demonstrating its dual role as a chaperone and cytokine. *Nature Med* 2000; **6**: 435-442
- McCaughan GW**, Gorrell MD, Bishop GA, Abbott CA, Shackel NA, McGunness PH, Levy MT, Sharland AF, Bowen DG, Yu D, Slaitini L, Church WB, Napoli J. Molecular pathogenesis of liver disease: an approach to hepatic inflammation, cirrhosis and liver transplant tolerance. *Im ol Rev* 2000; **174**: 172-191
- Hedin KE**, Kaczynski JA, Gibson MR, Urrutia R, Minn R. Transcription factors in cell biology, surgery, and transplantation. *Surg Research Rev* 2000; **128**: 1-5
- Bone-Larson CL**, Simpson KJ, Colletti LM, Lukacs NW, Chen SC, Lira S, Kunkel SL, Hogaboam CM. The role of chemokines in the immunopathology of the liver. *Immunol Rev* 2000; **177**: 8-20
- Marlin M**, Katz J, Vogel SN, Michalek SM. Differential induction of endotoxin tolerance by lipopolysaccharides derived from *porphyromonas gingivalis* and *Escherichia coli*. *J Immunol* 2001; **167**: 5278-5285
- Enomoto N**, Yamashina S, Kono H, Schemmer P, Rivera CA, Enomoto A, Nishiura T, Nishimura T, Brenner DA, Thurman RG. Development of a new, simple rat model of early alcohol-induced liver injury based on sensitization of Kupffer cells. *Hepatology* 1999; **29**: 1680-1689
- Ikejima K**, Enomoto N, Seabra V, Ikejima A, Brenner DA, Thurman RG. Pronase destroys the lipopolysaccharide receptor

- CD14 on Kupffer cells. *Am J Physiol Gastrointest Liver Physiol* 1999; **276**: G591-G598
- 34 **Jarvelainen HA**, Orpana A, Perola M, Savolainen VT, Karhunen PJ, Lindros KO. Promoter polymorphism of the CD14 endotoxin receptor gene as a risk factor for alcoholic liver disease. *Hepatology* 2001; **33**: 1148-1153
- 35 **Shoham S**, Huang C, Chen JM, Golenbock DT, Levitz SM. Toll-like receptor 4 mediates intracellular signaling without TNF- α release in response to cryptococcus neoformans polysaccharide capsule. *J Immunol* 2001; **166**: 4620-4626
- 36 **Kimmings AN**, van Deventer SJH, Obertop H, Rauws EAJ, Huijbregtse K, Gouma DJ. Endotoxin, cytokines, and endotoxin binding proteins in obstructive jaundice and after preoperative biliary drainage. *Gut* 2000; **46**: 725-731
- 37 **Guo XW**, Dudman NP. Homocysteine induces expressions of adhesive molecules on leukocytes in whole blood. *Chin Med J* 2001; **114**: 1235-1239
- 38 **LeVan TD**, Bloom JW, Bailey TJ, Karp CL, Halonen M, Martinez FD, Vercelli D. A common single nucleotide polymorphism in the CD14 promoter decreases the affinity of Sp protein binding and enhances transcriptional activity. *J Immunol* 2001; **167**: 5838-5844
- 39 **Nanbo A**, Nishimura H, Muta T, Nagasawa S. Lipopolysaccharide stimulates HepG2 human hepatoma cells in the presence of lipopolysaccharide-binding protein via CD14. *Eur J Biochem* 1999; **260**: 183-191
- 40 **Gordon H**. Detection of alcoholic liver disease. *World J Gastroenterol* 2001; **7**: 297-302
- 41 **Macdonald GA**, Bridle KR, Ward PJ, Walker NI, Houghlum K, George DK, Smith JL, Powell LW, Crawford DH, Ramm GA. Lipid peroxidation in hepatic steatosis in humans is associated with hepatic fibrosis and occurs predominately in acinar zone 3. *J Gastroenterol Hepatol* 2001; **16**: 599-606
- 42 **Calne RY**. Immunological tolerance-the liver effect. *Immunol Rev* 2000; **174**: 280-282
- 43 **Uesugi T**, Froh M, Arteel GE, Bradford BU, Thurman RG. Toll-like receptor 4 is involved in the mechanism of early alcohol-induced liver injury in mice. *Hepatology* 2001; **34**: 101-108
- 44 **Heinrich JM**, Bernheiden M, Minigo G, Yang KK, Schutt C, Mannel DN, Jack RS. The essential of lipopolysaccharide-binding protein in protection of mice against a peritoneal *salmonella* infection involves the rapid induction of an inflammatory response. *J Immunol* 2001; **167**: 1624-1628
- 45 **Neilsen PO**, Zimmerman GA, McIntyre TM. *Escherichia coli* braun lipoprotein induces a lipopolysaccharide-like endotoxic response from primary human endothelial cells. *J Immunol* 2001; **167**: 5231-5239
- 46 **Jersmann HPA**, Hii CST, Hodge GL, Ferrante A. Synthesis and surface expression of CD14 by human endothelial cells. *Infect Immun* 2001; **69**: 479-485
- 47 **Funda DP**, Tuckova L, Farre MA, Iwase T, Moro I, Tlaskalova-Hogenova H. CD14 is expressed and released as soluble CD14 by human intestinal epithelial cells in vitro: lipopolysaccharide activation of epithelial cells revisited. *Infect Immun* 2001; **69**: 3772-3781
- 48 **Le Roy D**, Padova FD, Adachi Y, Glauser MP, Calandra T, Heumann D. Critical role of lipopolysaccharide-binding protein and CD14 in immune responses against gram-negative bacteria. *J Immunol* 2001; **167**: 2759-2765
- 49 **Perera PY**, Mayadas TN, Takeuchi O, Akira S, Zaks-Zilberman M, Goyert SM, Vogel SN. CD11b/CD18 acts in concert with CD14 and Toll-like receptor (TLR) 4 to elicit full lipopolysaccharide and taxol-inducible gene expression. *J Immunol* 2001; **166**: 574-581
- 50 **Gong JP**, Liu CA, Wu CX, Li SW, Shi YJ, Li XH. Nuclear factor κ B activity in patients with acute severe cholangitis. *World J Gastroenterol* 2002; **8**: 346-349
- 51 **Medvebev AE**, Henneke P, Schromm A, Lien E, Ingalls R, Fenton MJ, Golenbock DT, Vogel SN. Induction of tolerance to lipopolysaccharide and mycobacterial components in Chinese hamster ovary/CD14 cells is not affected by overexpression of Toll-like receptor 2 or 4. *J Immunol* 2001; **167**: 2257-2267
- 52 **Jiang Q**, Akashi S, Miyake K, Petty HR. Cutting Edge: Lipopolysaccharide induces physical proximity between CD14 and Toll-like receptor 4 (TLR4) prior to nuclear translocation of NF- κ B. *J Immunol* 2000; **165**: 3541-3544
- 53 **Jarvelainen HA**, Fang C, Ingelman-Sundberg M, Lukkari TA, Sippel H, Lindros KO. Kupffer cell inactivation alleviates ethanol-induced steatosis and CYP2E1 induction but not inflammatory responses in rat liver. *J Hepatol* 2000; **32**: 900-910

Concomitant hepatocellular adenoma and adenomatous hyperplasia in a patient without cirrhosis

Chuan-Yuan Hsu, Cheng-Hsin Chu, Shee-Chan Lin, Fee-Shih Yang, Tsen-Long Yang, Kuo-Ming Chang

Chuan-Yuan Hsu, Cheng-Hsin Chu, Shee-Chan Lin, Department of Hepatology & Gastroenterology, Mackay Memorial Hospital, Taipei, Taiwan, China

Fee-Shih Yang, Department of Radiology, Mackay Memorial Hospital, Taipei, Taiwan, China

Tsen-Long Yang, Department of Surgery, Mackay Memorial Hospital, Taipei, Taiwan, China

Kuo-Ming Chang, Department of Pathology, Mackay Memorial Hospital, Taipei, Taiwan, China

Correspondence to: Dr. Chuan-Yuan Hsu, Department of Hepatology & Gastroenterology, Mackay Memorial Hospital, No. 92, Chung-Shan N. Road 2 Section, 104 Chung-Shan Area, Taipei, Taiwan, China. erichsu@msl.mmh.org.tw

Telephone: +886-2-25433535

Received: 2002-11-29 **Accepted:** 2002-12-22

Abstract

AIM: Hepatocellular adenoma (HCA) and adenomatous hyperplasia (AH) are rare benign tumors of the liver. HCA is usually found in women who use oral contraceptives. AH usually occurs in patients with liver cirrhosis. Both tumors have potential for malignant transformation.

METHODS: We described a male adult with chronic liver disease (CLD) who had been known to be a hepatitis B carrier (HBV) for years. He was found to have a space-occupying lesion with a suspicion of hepatocellular carcinoma (HCC) by abdominal ultrasonography. His α -fetoprotein (AFP) was normal. Angiographic findings were consistent with the diagnosis of HCC, he wished to avoid an operation, was treated with transcatheter hepatic arterial embolization.

RESULTS: He subsequently consented to surgery, and a right lobectomy was performed. The liver pathology disclosed HCA with nuclear dysplasia and post-embolization effects. In addition, there were multiple small foci of AH with nuclear dysplasia in the resected liver. Although he had some focal areas of cirrhosis-like change or post-embolization effect, the AH was associated only with normal liver tissue.

CONCLUSION: This case confirms that HCA and AH may resemble HCC on imaging studies, and that AH may occur in CLD in the absence of cirrhotic change.

Hsu CY, Chu CH, Lin SC, Yang FS, Yang TL, Chang KM. Concomitant hepatocellular adenoma and adenomatous hyperplasia in a patient without cirrhosis. *World J Gastroenterol* 2003; 9(3): 627-630

<http://www.wjgnet.com/1007-9327/9/627.htm>

INTRODUCTION

Benign hepatic tumors, such as hepatocellular adenoma (HCA) and adenomatous hyperplasia (AH), result from a variety of neoplastic and regenerative proliferative processes. HCA is an uncommon benign tumor of the liver most frequently

occurring in women with long-standing contraceptive steroid use^[1-4, 10, 11]. It usually regresses after discontinuation of contraceptives^[5, 6]. HCA in men has usually been found in association with glycogen storage disease, diabetes, and the use of androgen and anabolic steroids^[7, 10, 11]. HCA is usually solitary, but multiple adenomas have been described, ranging from two nodules to multiple or disseminated lesions of various size. The latter is termed hepatic adenomatosis^[8-10]. Patients may present with a palpable mass over the right upper quadrant. Although most cases are asymptomatic and detected only incidentally, HCA may rupture and lead to life-threatening hemorrhage^[12]. Malignant transformation of HCA is rare, but it may be very difficult to distinguish a benign tumor from a well-differentiated hepatocellular carcinoma (HCC) clinically^[10].

Edmondson first reported adenomatous hyperplasia (AH) of the liver in 1974. He defined it as a regenerative overgrowth with limited growth potential^[13]. AH is the term most commonly used in Japan, while researchers in the United States and Europe call it a macroregenerative nodule (MRN). At the recommendation of the International Working Party Consensus Conference, the terminology for these dysplastic nodules has been standardized^[10]. Based on characterization of cytological and architectural atypia, AH is generally classified as type I MRN (or ordinary AH) and type II MRN (or atypical AH)^[14, 30]. The lesions are usually associated with liver cirrhosis^[14]. The size of AH varies from 5 mm to 10 mm in different series^[10], but a huge AH lesion of 10 cm in diameter has been reported^[29]. AH probably represents one type of malignant precursor^[30]. However, the distinction of AH from well-differentiated HCC, particularly in samples obtained by needle biopsy, can be quite difficult, if not impossible^[10]. Despite several cases reported in the literature, AH remains a poorly understood disease of unknown etiology.

We reported a case with infrequent presentation of both HCA and multiple AH lesions in HBV-related chronic liver disease.

MATERIALS AND METHODS

Case report

A 30-year-old Asian man had been known to be a hepatitis B virus (HBV) carrier for many years. His younger brother had died of HBV-related HCC about 1 year ago. Therefore, he came to the outpatient department (OPD) of Mackay Memorial Hospital (a tertiary referral center) for evaluation of his liver condition. Nine years previously, he had undergone laparotomy at another hospital for a ruptured appendix. He had no history of smoking or alcohol consumption, and he denied use of any medications or exogenous hormones. His alanine aminotransferase (ALT) was 40 U/L (normal: 5-30 U/L), hepatitis B surface antigen (HBsAg) was positive; "e" antigen of hepatitis B (HBeAg) was negative, and AFP 3.33 ng/ml (normal < 6.00 ng/ml). Abdominal sonography demonstrated (a) a space-occupying lesion consistent with HCC, (b) chronic liver disease (CLD), and (c) a gall bladder polyp without stone. The space-occupying hypoechoic lesion, measuring about 24×22 mm in size, was located in the right lobe of the liver (Figure 1).

Because of the abnormal sonographic findings, he was admitted for further assessment and management.

On physical examination, he had no hepatosplenomegaly or abdominal tenderness. In admission, not only the routine hemogram of blood cells and differential count, platelet count, but also prothrombin and activated partial thromboplastin time were normal. The urinalysis and stool for occult blood were negative findings. Biochemistry of blood glucose, protein, albumin, alkaline-phosphatase, aspartate aminotransferase (AST), ALT, total cholesterol, triglycerides, blood urea nitrogen, uric acid, creatinine, potassium, sodium, chloride, and CA19-9 were all normal. The total bilirubin was mildly elevated (1.4 mg/dl, normal range: 0.2-1.3 mg/dl), but the direct bilirubin was normal. The chest X-ray and electrocardiogram were unremarkable. No liver tumor was seen on computed tomography (CT) with or without contrast (Figure 2). On the 6th hospital day, he underwent hepatic angiography that revealed multiple tumor stains in the right lobe of the liver, strongly suggestive of HCC (Figure 3). Given the fact that this patient was hesitant to undergo operation and that there were multiple angiographic lesions, these tumors were embolized with 6 cubic centimetres lipiodol, 6 cubic centimetres lipodox, gelfoam pieces and cephalosporin. The patient subsequently consented to surgery. Indocyanine green (ICG) was 3 % (normal: 0-10 %).



Figure 1 A hypoechoic lesion in the right lobe of the liver, segment S6, 24×22 mm in diameter (asterisks).

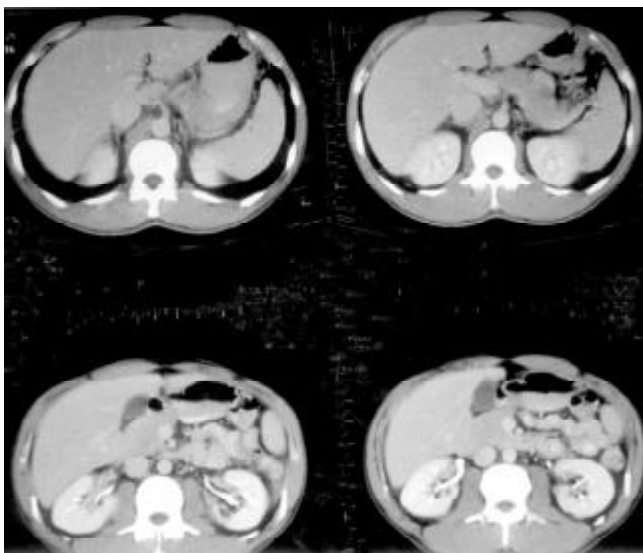


Figure 2 No evidence of hepatocellular tumor seen on upper abdominal CT with contrast.



Figure 3 On angiography, there was an oval hypervascular lesion (black arrows) and multiple scattered tiny hypervascular spots in the right lobe of the liver (white arrows).

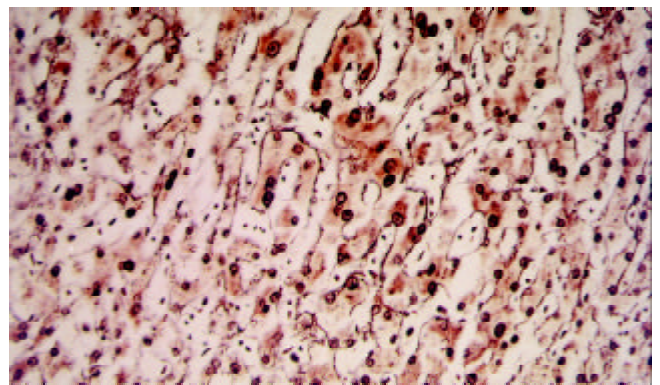


Figure 4 Slightly disarrayed hepatocytes with nuclear dysplasia were found. Besides one-to-two layer reticulin stain, not consistent with HCC, was present. (Reticulin stain, ×250).

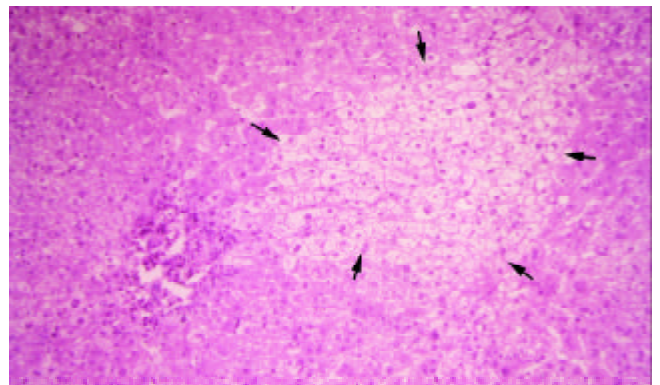


Figure 5 An oval-shape nodule (black arrows) which consisted of disarrayed hepatocytes with nuclear change and clear change in the cytoplasm was surrounded by normal liver tissue. (H&E stain, ×125).

On the 17th hospital day, he underwent total right hepatic lobectomy and cholecystectomy. Grossly on the cut section, there was an easily identifiable, well-defined solitary nodule, 2 cm in the greatest dimension, darker than the surrounding hepatic tissue with a central stellate dark red appearance. The hepatic tissue elsewhere has several 2-4 mm, fairly well-defined dark gray spots. And three areas of subcapsular hemorrhage, the largest 1 cm in diameter, were noted. The surgical margins appeared to be free of tumor involvement.

Microscopically, the main nodule was composed of hepatocytes much larger than the normal cells, with frequent nuclear dysplasia but no apparent increase of nucleus-to-

cytoplasm ratio or mitoses. The arrangement of the hepatocytes in the nodule was disturbed (partially collapsed), which was thought to represent an ischemic-degenerative effect of embolization. However, there was not yet frank infarction except for a focal area in the stellate scar-like lesion in the center. Reticulin staining demonstrated a one-to-two layer arrangement with slight disarray, inconsistent with the appearance of HCC (Figure 4). No biliary ductules were found at the periphery of the stellate area. There was preservation of Kupffer's cells. The lesion was fairly well demarcated from the surrounding normal liver tissue, but it lacked a capsule. The overall appearance indicated a liver cell adenoma post-embolization.

The small gray spots had slightly disarrayed hepatocytes with occasional nuclear dysplasia and clear changes in the cytoplasm, which were arranged in one-to-two-layer thin cords. They had preserved reticulin fibers, in contrast to HCC, and thus were consistent with AH (Figure 5). Excluding the aforementioned lesions, the remaining hepatic tissue was fairly normal except for focal areas with chronic inflammation in the portal triads with bridging fibrosis and possible early cirrhosis. However, post-embolization effect may be considered. The GB was found to have cholesterol polyps.

The patient recovered from surgery uneventfully. He was discharged and followed in the OPD. The other viral markers including HCV and HDV were negative by immunoassay.

DISCUSSION

In regions where HBV is hyper-epidemic, there is a corresponding increase in the incidence of HCC compared to areas with less HBV disease. HBV carriers are more likely than HBV-free individuals to develop HCC. Therefore, in Taiwan, China, with its high prevalence of HBV carriage and incidence of HCC, an HBV carrier presenting with a hepatic mass requires careful evaluation. Therefore, benign lesions must be precisely differentiated from malignant masses.

HCA is a rare benign tumor with a variable sonographic appearance. Cherqui *et al* reported that, of 6 cases, 4 tumors were hyperechoic, 3 hypoechoic, and 1 isoechoic^[15]. Welch *et al* reported that 4 of 13 tumors had mixed echogenicity and 1 was hypoechogenic^[16]. C.H. Hung *et al* reported the appearance of 12 lesions, 1 with isoechoic, 4 with hypoechogenicity, 3 with hyperechogenicity, and the remaining with mixed echogenicity^[7]. The CT scan features of HCA are also very nonspecific. Mathieu *et al* reported 22 cases with 27 tumors that were hyperdense and 5 with hypodense tumors on dynamic CT^[17]. Cherqui *et al* described 3 lesions in 2 of 6 patients had a hyperdense area corresponding to recent hemorrhage, while the others didn't^[15]. Welch *et al* stated that, of 13 cases, 6 tumors were hypodense and 1 was hyperdense^[16]. Magnetic resonance imaging (MRI) may be used, but it is not always helpful in distinguishing HCA from other liver tumor^[11]. Scintigraphy or radionuclide imaging provides a functional assessment of the liver but is helpless for anatomic imaging. Therefore, abdominal sonography, contrast-enhanced CT or MRI are all limited in their ability to discriminate HCA from HCC. However, they do provide helpful information on the size, number, and tumor location, particularly in relation to vascular structures and the biliary tract. It is very important to assess preoperatively.

Angiographic findings may also vary. Kerlin *et al* demonstrated hypervascular tumors in all 15 patients examined, but 7 also had areas of hypovascularity^[1]. Welch *et al* described 9 of 13 cases with hypervascular lesions that also contained small hypovascular area^[16]. As with the other imaging studies, the specificity of angiography is too low to provide a definitive diagnosis, but is helpful in assessing anatomy prior to resection.

Some researchers have suggested using percutaneous fine-needle biopsy^[18], but we are reluctant to do so. HCA is a hypervascular lesion, with a significant risk of hemorrhage if a large-caliber needle is used^[19,21]. Second, if the lesion turns out to be malignant, there is a risk of tumor seeding along the needle track^[19,20]. Third, a small sample obtained with a small-bore needle may not be adequate for a histological diagnosis^[21]. Finally, lesions with malignant transformation within an adenoma could be missed, leading to a false-negative biopsy result. Therefore, we did not feel that percutaneous biopsy was appropriate in our patient.

In most reports, AH is considered to begin with small nodules in a cirrhotic liver, progressing to a larger nodule, and then rapidly transforming into a malignant lesion. Hence, AH is thought to be an early stage in hepatocarcinogenesis, especially when the AH is atypical^[14,30]. While differentiation between malignancy and AH is clinically important, it is also quite difficult. Nomura *et al* reported 4 cases, 2 of which were hypoechogenic and 3 of which had a hyperechoic focus in an area of hypoechoic change; all 4 lesions were missed on CT, and only 1 was detected at angiography^[22]. Again, some authors advise fine-needle biopsy. However, AH is a small liver tumor, usually less than 2 cm in diameter^[10]. An adequate biopsy specimen should be at least 2.5 cm in diameter^[23]. Given the relatively low chance of benefit, it is not worth the risk of biopsy in cases having small area of AH is suspected. Thus, as with HCA, imaging studies are helpful for screening but not for definitive diagnosis of AC, and biopsy is probably not helpful.

AH usually occurs in the presence of liver cirrhosis^[10,24,25]. Nevertheless, Gindhart *et al* reported a case of AH of the liver arising spontaneously in an 82-year-old woman without cirrhosis^[26]. Terada *et al* described another case of AH in a patient with chronic active hepatitis^[27]. Theise *et al* incidentally found a small HCC arising in AH in a patient with chronic hepatitis C infection but without cirrhosis^[28]. Furuya *et al* reviewed 345 autopsy cases of chronic liver disease and found one case of AH in a noncirrhotic liver^[25]. In this case, aside from the HCA and AH, most of the liver tissue was normal, except for focal areas of early cirrhosis. The AH lesions all occurred in areas with normal liver tissue, not in conjunction with the focal cirrhosis. AH thus apparently can occur in CLD, not only in patients with cirrhosis. It may represent a malignant precursor in either condition.

In conclusion, this case confirms the difficulty noted in the literature of distinguishing HCA and AH from malignant hepatoma using clinical criteria alone, i.e., history, physical examination, imaging study or biopsy. Surgical intervention for diagnosis, therefore, is undoubtedly required. If that is not possible, very close follow up is recommended. Consideration of the diagnosis of AH should not be limited to patients with liver cirrhosis, since it may occur in CLD of varying etiology, such as HBV. Further research is needed to establish methods for early differentiation of small HCC and benign liver tumors. Until such methods are available, an aggressive, invasive approach is most likely necessary.

ACKNOWLEDGEMENT

Thank Dr. MJ Buttrey for revise elaborately.

REFERENCES

- 1 **Kerlin P**, Davis GL, McGill DB, Weiland LH, Adson MA, Sheedy PF II. Hepatic adenoma and focal nodular hyperplasia: clinical, pathologic, and radiologic features. *Gastroenterology* 1983; **84**: 994-1002
- 2 **Nichols III FC**, van Heerden JA, Weiland LH. Benign liver tumors. *Surg Clin North Am* 1989; **69**: 297-314
- 3 **Edmondson HA**, Henderson B, Benton B. Liver cell adenomas

- associated with the use of oral contraceptives. *N Engl J Med* 1976; **294**: 470-472
- 4 **Thomas R**, Kirsten F, Klaus G, Benno R. Liver tumours in women on oral contraceptives. *The Lancet* 1994; **344**: 1568-1569
 - 5 **Edmondson HA**, Reynolds TB, Henderson B, Benton B. Regression of liver cell adenoma associated with oral contraceptives. *Ann Intern Med* 1977; **86**: 180-182
 - 6 **Kawakatsu M**, Vilgrain V, Erlinger S, Nahum H. Disappearance of liver cell adenoma: CT and MRI imaging. *Abdom Imaging* 1997; **22**: 274-276
 - 7 **Hung CH**, Changchien CS, Lu SN, Eng HL, Wang JH, Lee CM, Hsu CC, Tung HD. Sonographic features of hepatic adenomas with pathologic correlation. *Abdom Imaging* 2001; **26**: 500-506
 - 8 **Flejou JF**, Barge J, Menu Y, Degott C, Bismuth H, Potet F, Benhamou JP. Liver adenomatosis. An entity distinct from liver adenoma? *Gastroenterology* 1985; **89**: 1132-1138
 - 9 **Chiche L**, Dao T, Salamé E, Galais MP, Bouvard N, Schmutz G, Rousselot P, Bioulac-Sage P, Ségol P, Gignoux M. Liver adenomatosis: reappraisal, diagnosis, and surgical management: eight new cases and review of the literature. *Ann Surg* 2000; **231**: 74-81
 - 10 **Elizabeth M**. Brunt. Benign tumors of the liver. *Clin Liver Dis* 2001; **5**: 1-15
 - 11 **Patricia J**. Mergo, Pablo R. Ros. Benign lesions of the liver. *Radiol Clin North Am* 1998; **36**: 319-331
 - 12 **Ann Simpson Fulcher**, Richard Keith Sterling. Hepatic neoplasms: computed tomography and magnetic resonance features. *J Clin Gastroenterol* 2002; **34**: 463-471
 - 13 **Edmondson HA**. Benign epithelial tumors and tumor-like lesions of the liver. In: Okuda K, Peters RL, eds. *Hepatocellular carcinoma*. New York: John Wiley & Sons 1976: 309-330
 - 14 **Hytiroglou P**, Theise ND, Schwartz M, Mor E, Miller C, Thung SN. Macroregenerative nodules in a series of adult cirrhotic liver explants: Issues of classification and nomenclature. *Hepatology* 1995; **21**: 703-708
 - 15 **Cherqui D**, Rahmouni A, Charlotte F, Boulahdour H, Métreau JM, Meignan M, Fagniez PL, Zafrani ES, Mathieu D, Dhumeaux D. Management of focal nodular hyperplasia and hepatocellular adenoma in young women: A series of 41 patients with clinical, radiological and pathological correlations. *Hepatology* 1995; **22**: 1674-1681
 - 16 **Welch TJ**, Sheedy PF II, Johnson CM, Stephens DH, Charboneau JW, Brown ML, May GR, Adson MA, McGill DB. Focal nodular hyperplasia and hepatic adenoma: comparison of angiography, CT, US and scintigraphy. *Radiology* 1985; **156**: 593-595
 - 17 **Mathieu D**, Bruneton JN, Drouillard J, Pointreau CC, Vasile N. Hepatic adenomas and focal nodular hyperplasia: dynamic CT study. *Radiology* 1986; **160**: 53-58
 - 18 **Levy I**, Greig PD, Gallinger S, Langer B, Sherman M. Resection of hepatocellular carcinoma without preoperative tumor biopsy. *Ann Surg* 2001; **234**: 206-209
 - 19 **Smith EH**. Complications of percutaneous abdominal fine-needle biopsy. *Radiology* 1991; **178**: 253-258
 - 20 **Nakamuta M**, Tanabe Y, Ohashi M, Yoshida K, Hiroshige K, Nawata H. Transabdominal seeding of hepatocellular carcinoma after fine-needle aspiration biopsy. *J Clin Ultrasound* 1993; **21**: 551-556
 - 21 **Moulton JS**, Moore PT. Coaxial percutaneous biopsy technique with automated biopsy devices: value in improving accuracy and negative predictive value. *Radiology* 1993; **186**: 515-522
 - 22 **Nomura Y**, Matsuda Y, Yabuuchi I, Nishioka M, Tarui S. Hepatocellular carcinoma in adenomatous hyperplasia: detection with contrast-enhanced US with carbon dioxide microbubbles. *Radiology* 1993; **187**: 353-356
 - 23 **Caturelli E**, Giacobbe A, Facciorusso D. Percutaneous biopsy in diffuse liver disease: increasing diagnostic yield and decreasing complication rate by routine ultrasound assessment of puncture site. *Am J Gastroenterol* 1996; **91**: 1318-1321
 - 24 **Terada T**, Terasaki S, Nakanuma Y. A clinicopathologic study of adenomatous hyperplasia of the liver in 209 consecutive cirrhotic livers examined by autopsy. *Cancer* 1993; **72**: 1551-1556
 - 25 **Furuya K**, Nakamura M, Yamamoto Y, Toge K, Otsuka H. Macroregenerative nodule of the liver. A clinicopathologic study of 345 autopsy cases of chronic liver disease. *Cancer* 1988; **61**: 99-105
 - 26 **Gindhart TD**, Cimisi RJ, Mosenthal WT. Adenomatous hyperplasia of the liver. *Arch Pathol Lab Med* 1979; **103**: 34-37
 - 27 **Terada T**, Kitani S, Ueda K, Nakanuma Y, Kitagawa K, Masuda S. Adenomatous hyperplasia of the liver resembling focal nodular hyperplasia in patients with chronic liver disease. *Virchows Arch A Pathol Anat Histopathol* 1993; **422**: 247-452
 - 28 **Theise ND**, Lapook JD, Thung SN. A macroregenerative nodule containing multiple foci of hepatocellular carcinoma in a noncirrhotic liver. *Hepatology* 1993; **17**: 993-996
 - 29 **Chen LK**, Chang FC, Lai CR, Luo JC, Tsai ST, Hwang SJ. Huge adenomatous hyperplasia of the liver. *J Clin Gastroenterol* 2002; **34**: 272-274
 - 30 **Orsatti G**, Theise ND, Thung SN, Paronetto F. DNA image cytometric analysis of macroregenerative nodules (adenomatous hyperplasia) of the liver: Evidence in support of their preneoplastic nature. *Hepatology* 1993; **17**: 621-627

Edited by Xu XQ

Successful rescuing a pregnant woman with severe hepatitis E infection and postpartum massive hemorrhage

Zhan-Sheng Jia, Yu-Mei Xie, Guo-Wu Yin, Jun-Rong Di, Wei-Pin Guo, Chang-Xing Huang, Xue-Fang Bai

Zhan-Sheng Jia, Yu-Mei Xie, Jun-Rong Di, Chang-Xing Huang, Xue-Fang Bai, Center of Diagnosis and Treatment for Infectious Diseases of PLA, Tangdu Hospital, Fourth Military Medical University, Xi'an 730038, Shaanxi Province

Guo-Wu Yin, Department of Obstetrics and Gynecology, Tangdu Hospital, Fourth Military Medical University, Xi'an 730038, Shaanxi Province

Wei-Pin Guo, Department of Intervention, Tangdu Hospital, Fourth Military Medical University, Xi'an 730038, Shaanxi Province

Correspondence to: Dr. Zhan-Sheng Jia, Center of Diagnosis and Treatment for Infectious Diseases of PLA, Tangdu Hospital, 1 Xinsi Road, Baqiao District, Xi'an 710038, Shaanxi Province, China. jiazsh@fmmu.edu.cn

Telephone: +86-29-3377742 **Fax:** +86-29-3537377

Received: 2002-10-30 **Accepted:** 2002-11-19

Abstract

AIM: To sum up the experience of the successful therapy for the severe hepatitis of pregnant woman with postpartum massive hemorrhage.

METHODS: The advanced therapeutic methods including the bilateral uterine artery embolism, hemodialysis and artificial liver support therapy were performed with comprehensive medical treatments and the course of the successful rescuing the patient was analyzed.

RESULTS: Through the hospitalization of about two months the patient and her neonatus had gotten the best of care in our department and pediatric department separately. Both of them were discharged in good condition.

CONCLUSION: The key points for a successful therapy of the pregnant woman with severe hepatitis are termination of the pregnancy and the control of their various complications. It was suggested that the proper combination of these measures of modern therapy would race against time for renewing of hepatic and renal functions.

Jia ZS, Xie YM, Guo WP, Di JR, Yin GW, Huang CX, Bai XF. Successful rescuing a pregnant woman with severe hepatitis E infection and postpartum massive hemorrhage. *World J Gastroenterol* 2003; 9(3): 631-632

<http://www.wjgnet.com/1007-9327/9/631.htm>

INTRODUCTION

Hepatitis E infection is the most common cause of severe hepatitis in pregnancy, being seriously dangerous for both maternal and fetal life with a mortality rate of 58 %, even up to 100 % if a postpartum massive hemorrhage occurs^[1-4]. A pregnant woman with severe hepatitis E infection complicated with postpartum massive hemorrhage and fulminant hepatic and acute renal failure is presented in this report. With the comprehensive medical treatments in an intensive care setting and three advanced therapeutic measures including bilateral

uterine artery embolism, hemodialysis and artificial liver support therapy, a satisfactory outcome of both the mother and child was achieved.

CASE REPORT

A 24-year-old pregnant woman was admitted to our hospital in May 11th 2002 and presented with a 31-week pregnancy and an 11-day history of asthenia, abdominal distention with deep jaundice. On examination she had a blood pressure of 20/12 kPa, peripheral and facial puffiness, icteric sclera and xanthochromia. The fetal heart rate was 140 beats/min. Laboratory findings showed a normal white blood cell count and a decreased platelet counts ($76 \times 10^9/L$) with a hemoglobin level of 102 g/L. Liver function tests were obvious abnormal (albumin 25.9 g/L, bilirubin 579 $\mu\text{mol/L}$, alanine transaminase 158 IU/L). Prothrombin time activity (PTA) was 21.5 %. The markers of hepatitis virus showed negative for hepatitis A, C and D, positive for anti-HB surface and anti-HE (IgM). So a diagnosis of fulminant hepatic failure of pregnancy (FHFP) with hepatitis E infection was made.

A further clinical course gave a risk signal for the maternal and fetal life. After admission, the gravid woman in the intensive care unit was treated by catharsis with lactulose in order to terminate the pregnancy. With the regular uterine contraction and colporrhagia that appeared as parturient signals, she was immediately sent to the childbearing ward for parturition. After the childbirth of a 1 300 g-weight male baby who was sent to the pediatric care ward, the patient developed postpartum massive hemorrhage. Her blood pressure dropped to 10.7-6.67/6.67-4.0 kPa, at a minimum falling to 0/0 kPa. With the drug hemostasis, such as uterotonics, thromboplasin, and p-amino-merthyl beozic acid, her colporrhagia could not be stopped. The total of her hemorrhage was about 3 500 ml, and she was on the verge of death. Therefore, it was decided to perform the bilateral uterine artery embolism by the method of intervention. As a result, her colporrhagia was effectively controlled. At the same time fresh blood was transfused together with albumin, and her blood pressure rose up to 15.5/11.5 kPa with the normal vital signs.

After a dangerous delivery the patient underwent a clinical course of exacerbation with hepatic encephalopathy, hepatic renal syndrome, bacterial infection of puerperium and disseminated intravascular coagulation (DIC). The parturient presented fever (to 39.8 °C), oliguria (<400 ml/d) and confusion. The physical signs included severe edema of the whole body, intensive stasis of blood under subcutaneous layer of the abdominal wall and bilateral groin, and huge amount of hemorrhagic ascites. Laboratory study showed that the white blood cell count was $28.8 \times 10^9/L$, N 0.89, Hb $49 \times 10^9/L$, serum creatinine 583.3 $\mu\text{mol/L}$, blood urea nitrogen 24.2 $\mu\text{mol/L}$, blood NH_3 164 $\mu\text{mol/L}$. The tests for DIC revealed thrombocytopenia ($42 \times 10^9/L$), prolonged prothrombin time (PT 32.8 seconds, normal range from 11 to 14 seconds) and active partial thromboplastin time (APTT 88.5 seconds, normal range from 25 to 36 seconds), and hypofibrinogenemia (0.23 g/L).

It was the key time to rescue her hepatic and renal function. The comprehensive medical treatments including diuresis,

hemostasis (antifibrinolytic agents and prothrombin complex) was used with antibiotics for controlling infection and a large number of albumin for improving hypoproteinemia, and in the meanwhile twice hemodialysis for getting rid of the toxic metabolite and the much abundance of her body water were performed. And so the renal and coagulative functions were effectively improved with the increase of her urine volume and the reduction of her whole body edema. However, the improvement of her hepatic function was not significant, total bilirubin remaining at 468 $\mu\text{mol/L}$. Therefore, it was decided that the artificial liver support therapy, an advanced therapeutic approach, was carried out and then the patient got better in her liver function and clinical syndromes with a good appetite. Through the hospitalization of about two months the patient and her neonatus had gotten the best of care in our department and pediatric department separately. Both of them were discharged in good condition.

DISCUSSION

Viral hepatitis during pregnancy is common in China^[5-13]. It is one of the most dangerous conditions with a high mortality both for the mother and her fetus, particularly when fulminant hepatic failure occurred^[2,3]. Severe hepatitis is the main cause of FHF in terms of the trimester of gestation^[4]. The pregnant woman with severe hepatitis presents frequently hypodynamia, deep jaundice, coma, hypoproteinemia and sometime acute renal failure^[5]. The patient in this report had a 31-week pregnancy developed severe hepatic dysfunction with deep jaundice (TB 579.9 $\mu\text{mol/L}$, PTA 21.5%), and a positive anti-HE-IgM in her serum, therefore severe hepatitis of pregnancy with HEV infection was diagnosed. It was reported that there were many viruses causing severe hepatitis of pregnancy, but HEV and HBV were frequent, especially HEV infection. The mortality rate was highest (56 %) among HEV infected FHF cases during the third trimester of pregnancy^[4, 14].

Intensive care facilities and an early diagnosis are essential for the management of pregnant patient with severe liver disease^[1,2,14]. The key points for a successful therapy of them are termination of the pregnancy on the proper time and the control of their various complications. It was reported that the severe hepatitis of pregnant woman was with a high mortality rate, even up to 100 % if a postpartum massive hemorrhage and hepatic renal syndrome occur. In this case she presented the very severe hepatic dysfunction and coagulative dysfunctions, and complicated with postpartum massive hemorrhage, bacterial infection, hepatic encephalopathy and hepatic renal syndrome meanwhile or continuously. Therefore the treatments of her were usually very difficult and contradictory.

We considered that the key points of the successful rescuing the patient were on the proper time to adopt three important therapeutic measures. The first was to perform decisively on proper time the bilateral uterine artery embolism by the intervention that is an advanced method with a smaller damage in comparison of the complete hysterectomy and effectively stopped the postpartum massive hemorrhage. The second was to use twice hemodialysis by which removed the toxic metabolite and the abundance of water and the proper comprehensive medical treatments for the improvement of her

renal and coagulative function. The third was to carry out in time the artificial liver support therapy that provides a temporary liver support and promotes the spontaneous liver regeneration in the patient with the remove of toxic metabolic products and the decrease of total bilirubin^[15-18]. It was suggested that the proper combination of these measures of modern therapy would race against time for renewing of hepatic and renal functions, and therefore a better outcome of treatment was anticipated.

REFERENCES

- 1 **Jaiswal SP**, Jain AK, Naik G, Soni N, Chitnis DS. Viral hepatitis during pregnancy. *Int J Gynaecol Obstet* 2001; **72**: 103-108
- 2 **Tank PD**, Nandanwar YS, Mayadeo NM. Outcome of pregnancy with severe liver disease. *Int J Gynaecol Obstet* 2002; **76**: 27-31
- 3 **Yang W**, Shen Z, Peng G, Chen Y, Jiang S, Kang S, Wu J. Acute fatty liver of pregnancy: diagnosis and management of 8 cases. *Chin Med J (Engl)* 2000; **113**: 540-543
- 4 **Hussaini SH**, Skidmore SJ, Richardson P, Sherratt LM, Cooper BT, O'Grady JG. Severe hepatitis E infection during pregnancy. *J Viral Hepat* 1997; **4**: 51-54
- 5 **Yan J**, Chen LL, Luo YH, Mao YF, He M. High frequencies of HGV and TTV infections in blood donors in Hangzhou. *World J Gastroenterol* 2001; **7**: 637-641
- 6 **Yan J**, Ma JY, Pan BR, Ma LS. Study on hepatitis B virus in China. *Shijie Huaren Xiaohua Zazhi* 2001; **9**: 611-616
- 7 **Yuan JM**, Govindarajan S, Gao YT, Ross RK, Yu MC. Prospective evaluation of infection with hepatitis G virus in relation to hepatocellular carcinoma in Shanghai, China. *J Infect Dis* 2000; **182**: 1300-1303
- 8 **Wen YM**. Laboratory diagnosis of viral hepatitis in China: the present and the future. *Clin Chem Lab Med* 2001; **39**: 1183-1189
- 9 **Wang XZ**, Jiang XR, Chen XC, Chen ZX, Li D, Lin JY, Tao QM. Seek protein which can interact with hepatitis B virus X protein from human liver cDNA library by yeast two-hybrid system. *World J Gastroenterol* 2002; **8**: 95-98
- 10 **Wei J**, Wang YQ, Lu ZM, Li GD, Wang Y, Zhang ZC. Detection of anti-preS1 antibodies for recovery of hepatitis B patient by immunoassay. *World J Gastroenterol* 2002; **8**: 276-281
- 11 **Zhang Z**, Wang J, Jiang L. Epidemiological characteristics and risk factors of hepatitis E in Taiyuan. *Zhonghua Yufang Yixue Zazhi* 1997; **31**: 144-146
- 12 **Wu C**, Tao Q. Comparison between homologies of E2/NS1 gene from genotype III Chinese isolates of hepatitis C virus and that from reported isolates. *Chin Med J (Engl)* 1998; **111**: 807-809
- 13 **Guo XC**, Wu YQ. A review: progress of prevention and control on viral hepatitis in China. *Biomed Environ Sci* 1999; **12**: 227-232
- 14 **Luo KX**, Zhang L, Wang SS, Nie J, Yang SC, Liu DX, Liang WF, He HT, Lu Q. An outbreak of enterically transmitted non-A, non-E viral hepatitis. *J Viral Hepat* 1999; **6**: 59-64
- 15 **Hamid SS**, Jafri SM, Khan H, Shah H, Abbas Z, Fields H. Fulminant hepatic failure in pregnant women: acute fatty liver or acute viral hepatitis? *J Hepatol* 1996; **25**: 20-27
- 16 **Strain AJ**, Neuberger JM. A bioartificial liver-state of the art. *Science* 2002; **295**: 1005-1009
- 17 **Nyberg SL**, Hay EJ, Ramin KD, Rosen CB. Successful pregnancy after porcine bioartificial liver treatment and liver transplantation for fulminant hepatic failure. *Liver Transpl* 2002; **8**: 169-170
- 18 **Morsiani E**, Pazzi P, Puviani AC, Brogli M, Valieri L, Gorini P, Scoletta P, Marangoni E, Ragazzi R, Azzena G, Frazzoli E, Di Luca D, Cassai E, Lombardi G, Cavallari A, Faenza S, Pasetto A, Girardis M, Jovine E, Pinna AD. Early experiences with a porcine hepatocyte-based bioartificial liver in acute hepatic failure patients. *Int J Artif Organs* 2002; **25**: 192-202

Large pedunculated antral hyperplastic gastric polyp traversed the bulbous causing outlet obstruction and iron deficiency anemia: endoscopic removal

Murat Alper, Yusuf Akcan, Olcay Belenli

Murat Alper, Olcay Belenli, Departments of Pathology, University of Abant izzet Baysal, Düzce Medical Faculty, Turkey

Yusuf Akcan, Departments of Gastroenterology, University of Abant izzet Baysal, Düzce Medical Faculty, Turkey

Correspondence to: Dr. Murat Alper, Düzce Tıp Fakültesi Patoloji Ana Bilim Dalı, Konuralp/Düzce, Turkey. malper@ibuduzce-tip.edu.tr

Telephone: +90 380-541 42 13 **Fax:** +90 380-541 42 13

Received: 2002-04-18 **Accepted:** 2002-06-11

Abstract

We present here a large (3 cm) hyperplastic gastric polyp prolapsed into duodenum and caused outlet obstruction and iron deficiency anemia in 60 years old male patient. Endoscopic removal was performed successfully.

Alper M, Akcan Y, Belenli O. Large pedunculated antral hyperplastic gastric polyp traversed the bulbous causing outlet obstruction and iron deficiency anemia: endoscopic removal. *World J Gastroenterol* 2003; 9(3): 633-634

<http://www.wjgnet.com/1007-9327/9/633.htm>

INTRODUCTION

In the literature, it is rarely to see the patients with gastric outlet obstruction due to prolapsing gastric polyps^[1]. Inflammatory fibroid polyp of the gastrointestinal tract is the type most frequently reported^[2]. We present here a large (3 cm) hyperplastic gastric polyp prolapsed into duodenum and caused outlet obstruction and iron deficiency anemia in 60 years old male patient. Endoscopic removal was performed successfully.

CASE

A 60 years old man was admitted to hospital due to severe fatigue, intermittent nausea and vomiting. Undigested food might have been seen in the vomitus. His hemoglobin was 7.6 gr/dl, MCV: 65 and serum iron level: 35 (low); iron binding capacity: 450 (high). All of aforementioned laboratory results indicated that the patient was suffering from iron deficiency anemia. Lower GIS barium enema examination and fiber sigmoidoscopy revealed no pathologic change. In upper endoscopy, initially we saw pyloric canal partially obstructed by a smooth surfaced pili-like structure. When passed to bulbous we observed a large polypoid mass. The biopsies taken were reported as hyperplastic gastric polyp. After re-evaluation of the endoscopic appearance by a second upper endoscopy, we thought that the pili-like structure traversing the pyloric canal might be a stalk of a polyp. Upon dragging the polyp with a controlled force, we were able to bring the polyp back to stomach. It was a pedunculated large antral polyp with a small area eroded on it, which was a possible explanation for blood loss. The polypectomy and removal was performed successfully in toto. The gross appearance (Figure 1) and microscopic examination (Figure 2) revealed a large

hyperplastic polyp with no malignant component in any part. The patient who was regarded cured is under periodic endoscopic followed up. Clinically we transfused two bags of blood and later continued with iron supplementation therapy. Now, the patient is quite well with hemoglobin level of 13.5 gr/dl and has no signs of gastric outlet obstruction, freely consumes a normal diet.

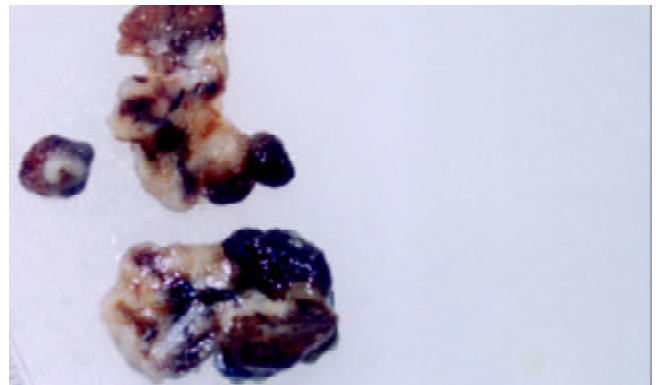


Figure 1 The macroscopic appearance of the polyp.

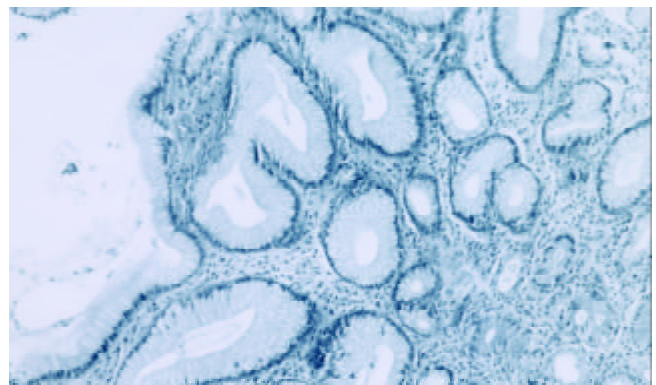


Figure 2 Hyperplastic polyp showing polypoid architecture, foveolar hyperplasia, mild inflammation, and edema. (H&E×200).

DISCUSSION

Histologically, hyperplastic polyp is characterised by a markedly elongated foveolar region: the underlying glands are usually mucous glands. There is a marked lamina propria edema and inflammatory cell infiltration. The frequency of hyperplastic gastric polyps is reported between 1.3 % and 28.3 % in different series of upper gastrointestinal polypectomy^[3,4]. Malignant transformation for hyperplastic polyps is small but the risk may be little bit higher if the polyp is more than 2 cm^[5]. Among the gastric polyps causing outlet obstruction, fibroid polyps are relatively more frequent. Sporadic case reports with other histologic types are

encountered like submucous lipoma^[6]. To the best of our knowledge, there is no hyperplastic gastric polyp with a size of 3 cm originated in the antrum, crossed through the pylorus and captured in the bulbus. Rösch *et al*, by now, reported one case of hyperplastic polyp in duodenum formed as a heterotopia of gastric mucosa^[7]. But it was different from our case clinically and with respect to place of formation. In our patient, a 3-cm pediculated polyp had formed in antrum, passed through the pylorus while it was small. Later, it presumably enlarged in bulbus so much that it was unable to go back to the stomach. We think so because we hardly take back it to the stomach through pylorus.

Gastric polyps may intussusept to duodenum causing gastric outlet obstruction. If the prolapsed polyp contains a functional antral mucosa over it, that mucosa may keep secreting gastrin due to being placed in the alkaline media of duodenum. In turn this hypergastrinemia may lead to erosion of the prolapsed polyp and blood loss^[8]. Such an assumption could be valid in our case too.

Consequently, large prolapsed polyps can be dragged into stomach by easing the polypectomy procedure with a controlled force, instead of performing it in bulbus, which is a narrower space than stomach.

REFERENCES

- 1 **Kumar A**, Quick AU, Carr-Locke DL. Prolapsing gastric polyp, an unusual cause of gastric outlet obstruction: a review of the pathology and management of gastric polyps. *Endoscopy* 1996; **28**: 452-455
- 2 **Johnstone JM**, Morson BC. Inflammatory fibroid polyp of the gastrointestinal tract. *Histopathology* 1978; **2**: 349-361
- 3 **Möckel W**. Hyperplasiogenic gastric polyps and stomach cancer. Endoscopic findings of early stomach cancer in 3 out of 42 biopsies of hyperplasiogenic polyps. *Fortschr Med* 1984; **102**: 635-638
- 4 **Stolte M**, Sticht T, Eidt S, Ebert D, Finkenzeller G. Frequency, location, and age and sex distribution of various types of gastric polyp. *Endoscopy* 1994; **26**: 659-665
- 5 **Gschwantler M**, Pulgram T, Feichtenschlager T, Brownstone E, Gabriel C, Bibus B, Weiss W. Gastric carcinoma arising from a hyperplasiogenic polyp with a diameter of less than 2 centimetres. *Z Gastroenterol* 1995; **33**: 610-612
- 6 **Kallie NR**, Peters JA. Submucous lipoma of the stomach: a case report. *Can J Surg* 1976; **19**: 42-45
- 7 **Rösch W**, Höer PW. Hyperplasiogenic polyp in the duodenum. *Endoscopy* 1983; **15**: 117-118
- 8 **Brooks GS**, Frost ES, Wesselhoeft C. Prolapsed hyperplastic gastric polyp causing gastric outlet obstruction, hypergastrinemia, and hematemesis in an infant. *J Pediatr Surg* 1992; **27**: 1537-1538

Edited by Zhang JZ

Preventive treatments for recurrence after curative resection of hepatocellular carcinoma - A literature review of randomized control trials

Hui-Chuan Sun, Zhao-You Tang

Hui-Chuan Sun, Zhao-You Tang, Liver Cancer Institute and Zhong Shan Hospital, Fudan University, Shanghai 200032, China

Correspondence to: Hui-Chuan Sun, MD, Associate Professor of Surgery, Liver Cancer Institute and Zhong Shan Hospital, Fudan University, 136 Yi Xue Yuan Road, Shanghai 200032, China. sunhc@zshospital.com

Telephone: +86-21-64041990 Ext 3056 **Fax:** +86-21-64037181

Received: 2002-09-13 **Accepted:** 2002-10-17

Abstract

To review the inhibitory effect of preventive approaches on recurrence after operation in patients with hepatocellular carcinoma (HCC), we summarized all available publications reporting randomized control trial indexed in PubMed. The treatment approaches presented above included pre-operative transcatheter arterial chemoembolization (TACE), post-operative TACE, systemic or locoregional chemotherapy, immunotherapy, Interferons and acyclic retinoic acid. Although no standard treatment has been established, several approaches presented promising results, which were both effective and tolerable in post-operative patients. Pre-operative TACE was not effective on prolonging survivals, while post-operative TACE was shown with both disease-free survival and overall survival benefits in some papers, however, it was also questioned by others. Systemic chemotherapy was generally not effective on prolonging survival but also poorly tolerated for its significant toxicities. Adoptive immunotherapy using LAK cells was proved to be beneficial to patients' survival in a recent paper. Interferon α and Interferon β can inhibit recurrence in HCC patients with HCV infection background, though the mechanism is not fully understood. Acyclic retinoic acid was shown to decrease multi-centric recurrence after operation, which was reported by only one group. In conclusion, several adjuvant approaches have been studied for their efficacy on recurrence in HCC patients in randomized control trials; however, multi-centric randomized control trial is still needed for further evaluation on their efficacy and systemic or local toxicities; in addition, new adjuvant treatment should be investigated to provide more effective and tolerable methods for the patients with HCC after operation.

Sun HC, Tang ZY. Preventive treatments for recurrence after curative resection of hepatocellular carcinoma - A literature review of randomized control trials. *World J Gastroenterol* 2003; 9(4): 635-640

<http://www.wjgnet.com/1007-9327/9/635.htm>

INTRODUCTION

Over the last two decades, the surgical techniques and peri-operative care have been improved, and the operative death (within 30 days after operation) decreased to 2.5 %^[1], the 5-year overall survival after curative resection of hepatocellular

carcinoma (HCC) increased to 25 %^[1] or 46.7 %^[2]. However, HCC is far from a curable disease because of high recurrence rate, the 5-year recurrence rate after curative resection was 38 %^[1] and 61.5 %^[2], the 5-year disease-free survival was 16 %^[3] or 38.6 %^[4] after curative resection of HCC, and the recurrence resulted in most deaths after resection^[5].

People have tried a number of approaches to prevent recurrence, however, only a few of them were designed as randomized control trial (RCT), which provide evidence-based results for those treatment modalities. In this paper, the authors summarized those results from randomized control trials, attempting to find a more suitable treatment modality for prevention of recurrence.

IMPORTANT ISSUES RELATED TO EVALUATION OF EFFICACY OF PREVENTION

It is difficult to compare the results among different RCTs because of different study settings and patient collection; therefore, several important issues should be addressed in evaluation of efficacy of prevention of HCC recurrence.

The definition of "curative resection"

The most important issue is the definition of "curative resection" of HCC, because, the definition will greatly affect the recurrence rate. There is no consensus on this definition in the literature. Some authors described it as "complete removal of tumor tissues"^[6]; others prefer to "complete removal of tumor tissues plus a clear resection margin ≥ 1 cm on pathological examination"^[7]. And some authors used a strict criterion, in which negative findings by angiography followed by Lipiodol-CT and ultrasound one or two months after resection were also included^[8]. The 1 year disease-free survival was 43.0 % by the first criteria^[6], and 59.1 % by the second^[7], and 69 % by the third^[8]. The different definitions of curative resection and their results are listed in Table 1.

Bias in patient collection

The clinicopathological characteristics of patients enrolled in a study also influence the results. For example, tumor size, which was regarded as the age of tumor, affects the recurrence rates and survival after operation, thereafter, has great impact on the results (Table 1).

Origins of recurrence

The origin of recurrence can be divided into two sources, uni-centric and multi-centric origins^[9], which could be discriminated by genetic markers, such as HBV integration sites^[9,10] or p53 mutation types^[11]. Uni-centric origin can also be named as intrahepatic metastatic recurrence or residual tumor, which means metastatic lesion spread from the primary main tumor, and left in the remnant liver. However, multi-centric recurrence is a newly developed lesion in the cirrhotic background. Generally two kinds of recurrences can be roughly divided according to the time of appearance. Twelve months^[12] or 3-years^[13] were set as a parameter to distinguish them by

different authors. A study may be needed to clarify the percentage of uni-centric and multi-centric recurrence by different set point.

Most preventive procedures are targeting the metastatic recurrence, which are used to control the residual tumor cells in the liver. Therefore, 1, 2, 3-year disease-free survival or recurrence rates are used to evaluate the efficacy of preventive procedures targeting metastatic recurrence; however, if a preventive procedure is targeting the multi-centric origin recurrence, 3 or 5-year disease-free survival or recurrence rate should be noticed.

Table 1 showed the overall survival and disease free survival are better when the tumor size decreases, and when a stricter criteria for curative resection was applied. Therefore, when evaluating a preventive treatment targeting residual tumors, it is suggested that a subgroup of patient with more invasive HCC should be enrolled. On the other hand, a subgroup of patient with less invasive HCC or selected by stricter criteria for curative resection should be recruited to investigate a preventive treatment targeting secondary HCC appearance.

LITERATURE REVIEWS OF RANDOMIZED CONTROL TRIALS (RCT) TO PREVENT RECURRENCE OF HCC

Pre-operative or post-operative TACE

TACE has been used to control the growth of HCC for a long time^[17]. Pre-operative and post-operative TACE were investigated by RCT to clarify if it reduced the recurrence rate after curative resection of HCC (Table 2).

Wu *et al* have studied the effect of pre-operative TACE (preTACE) on resectability and curability in management of huge resectable HCC. Although preTACE induced tumor shrinkage as expected, the shrinkage of tumor didn't result in an easy operation, on the contrary, the preTACE group had a longer operative time, more blood loss, more extra-hepatic metastasis, higher possibility of invading adjacent organs by tumors and removal of adjacent organs; furthermore, the disease-free survival (DFS) in preTACE group was not statistically different with that in the control group, the overall survival (OS) was even worse than that in control group. The author suggested that preTACE delayed the resection, which may leave tumor more time to develop intra-hepatic or distant metastasis; in addition, preTACE can't eliminate tumor cells completely, therefore, preTACE for resectable huge HCC was not recommended^[16].

In another study by Yamasaki *et al*, the efficacy of preTACE on small HCC was tested. The results confirmed that preTACE induced necrosis in tumor, but the results demonstrated again that it didn't improve the DFS, because preTACE was not capable to inhibit the intrahepatic micrometastatic lesions and tumor thrombus in microvessel^[17].

The first RCT study on post-operative TACE (postTACE) was reported by Izumi *et al* in 1994. The authors enrolled 50 patients after curative resection of HCC with blood vessel involvement or intra-hepatic spreadings. The results showed that both DFS rate and DFS time were higher in postTACE group than those in control group. However, 1 and 3-year OS rates were similar in both groups (58.8 % vs 63.5 %; 30.5 % vs

Table 1 The important issues related to evaluation of efficacy of prevention of recurrence

Authors	Average tumor size	Definition of curative resection			1 year RR	1 year DFS	1 year OS
		Complete removal in operation	Negative in histology on surgical margin	Negative in post-operative exams			
Kubo ^[144]	2.6 cm	Yes	No	Yes	25% ^a	NA	92%
Lau ^[77]	3.8 cm	Yes	Yes	No	NA	59.1%	86.4%
Tang ^[155]	<5 cm, complete tumor capsule, without portal vein involvement	Yes	Yes	No	6.5%	NA	NA
Poon ^[12]	>5 cm ^a	Yes	No	No	46%	NA	55.5%
Izumi ^[6]	>5 cm ^a	Yes	No	No	51.7%	43.0%	81.0%
Lai ^[8]	10.4 cm	Yes	No	Yes	20-30%	69.0%	75%*

RR: recurrence rate; DFS: disease free survival; OS: overall survival; NA: data not available.

^aestimated according to the authors' paper.

Table 2 Summary of RCTs to evaluate the efficacy of pre- and post-operative TACE on prevention of recurrence

Authors	Tumor factors	Treatment protocol	Sample size (Tx/Ctl)	Observation time	DFS (Tx vs Ctl)	OS (Tx vs Ctl)	Conclusions
Wu ^[18]	>10 cm; resectable	Pre-operative TACE	52 (24/28)	2-10 years	3-year 39% vs 46% ^a	3-year 31% vs 62% ^a	Harmful
Yamasaki ^[19] Izumi ^[6]	2-5 cm; Single With vessel involvement or intrahepatic spreading	Pre-operative TACE Post-operative TACE, once L 3ml/m ² +A 20mg/m ² +M 10mg/m ² +G or: L 2ml/m ² +A+M	97 (50/47) 50 (23/27)	4-6.6 years 28.7 Months (median)	39.1% vs 31.1% 3-year 32% vs 11.7%	NA 3-year 56.6% vs 53.4%	Not effective Postpone recurrence, but change over all survival
Lai ^[8]	Negative in lipiodol CT, angiography and ultrasound one month after operation	Post-operative TACE, 3 times L 10ml+C 10mg+EA(40mg/m ² iv×8)	66 (30/36)	Median 28.3 months	3-year 18% vs 48%	3-year 65% vs 67% ^a	Harmful
Lau ^[7]	Surgical margin ≥1 cm	Post-operative TACE I ¹²⁵ Lipiodol	43 (21/22)	14.1-69.7 months	3-year 74.5% vs 36%	3-year 84.4% vs 46.3%	Beneficial

L: lipiodol; M: mitomycin; A: adriamycin, G: gelfoam; C: cis-platin; Tx: treatment; Ctl: control; DFS: disease free survival; OS: overall survival.

^aestimated according to the figure in authors' paper.

33.9 %, $P=0.7647$), the median survival time in postTACE was shorter than that in the control group (644.5 ± 129.4 days vs 759.9 ± 137.5 day, $P<0.05$). The authors concluded that postTACE may postpone but not eliminate the recurrence (60.9% vs 81.5% , $P=0.106$)^[6].

In another RCT reported by Lau *et al.*, the authors used ¹³¹I-Lipiodol instead of conventional Lipiodol. The result showed that postTACE improved DFS and OS, decreased recurrence without major side-effects^[7]. This is the only one RCT reporting a positive result for postTACE treatment. The authors suggested more effective agents should be used in postTACE.

However, in Lai *et al.*'s study of postTACE, although the preventive treatment protocol was more aggressive than Izumi's study, the result was even worse. The recurrence rate and extrahepatic metastasis rate were higher in postTACE group (recurrence rate: 23/30 vs 17/36, $P=0.01$) extrahepatic metastasis rate: 11/30 vs 5/36, $P=0.03$); 3-year DFS in postTACE group was lower than that in the control group (18 % vs 48 %, $P=0.04$). The OS in postTACE group was worse than that in the control group, especially in the first two years, but the difference was not statistically significant. Therefore, the authors concluded postTACE is harmful to patients after curative resection of HCC^[8].

The reason of why conflicting results came from different RCTs is the selection of patients. Lai *et al.*'s group of patients was selected by a highly rigorous standard; the rationale of preventive treatment was not solid enough to protect this group of patient with interventional treatment like postTACE. However, in Izumi and Lau's studies, the authors selected a group of patients with more possibility of recurrence (invasive cancer or large cancer), so the results turned out to be effective.

In summary, preTACE is not helpful in terms of decreasing recurrence after resection of resectable HCC. PostTACE is only beneficial to the patients with invasive HCC, but not effective or even harmful to the patients after a "real" curative resection.

Systemic or locoregional chemotherapy

Systemic chemotherapy is generally not effective in most cases with HCC^[18], only a few papers showed a favorable results of systemic chemotherapy^[19]. Here is a summary of RCTs studying post-operative systemic and locoregional chemotherapy (Table 3).

Yamamoto *et al.* studied systemic chemotherapy using HCFU 200 mg bid as a adjuvant treatment for the patients after curative resection of HCC. The result showed that systemic chemotherapy was effective in a subgroup of patients with mild cirrhosis and good liver function, but not effective in a subgroup of patients with severe cirrhosis and poor liver function. The authors discussed that systemic chemotherapy inhibited the growth of micro-metastatic lesions existing before operation or multi-centric carcinogenesis after operation, but jeopardized liver function as well, which resulted a negative effect on both OS and DFS, especially in patients with poor liver function reserve^[20].

Kohno *et al.* studied the result of an aggressive treatment combining systemic and one course of transcatheter arterial chemotherapy (TAC). There was no obvious side-effect of this treatment. However, the results showed this combination treatment did not improve the 3 and 5-year OS and DFS compared with the control group with UFT treatment alone, and another control group without any specific treatment^[21].

Ono *et al.*'s treatment protocol was even more aggressive with combining systemic and multiple courses of TAC, however, the result was still negative. Furthermore, very aggressive protocol was intolerable to most enrolled patients, and too many cases withdrew from this study^[22].

Ueno *et al.*'s study showed multiple courses of TAC improved DFS after curative resection of HCC. The flaw of this study is too small sample size^[23].

A recent meta-analysis also showed that systemic chemotherapy was not effective or even harmful as an adjuvant treatment in patients after resection of HCC^[24]. Another meta-analysis showed that TAE (transcatheter arterial embolization) improved OS after resection of HCC compared with TAC, and no evidence showing TACE was more effective than TAE^[25], which implied a very limited benefit of locoregional chemotherapy introduced by TACE overtopping TAE alone.

From the above data, it is suggested that systemic or locoregional chemotherapy didn't inhibit the recurrence, and the tolerance was another important factor influencing the results.

Post-operative adoptive immunotherapy

Post-operative active or adoptive immunotherapy became a very attractive cancer treatment modality in early 1990s

Table 3 Summary of locoregional or systemic chemotherapy for prevention of recurrence

Authors	Entry criteria	Treatment protocol	Sample size (Tx/Ctl)	Observation time	DFS (Tx vs Ctl)	OS (Tx vs Ctl)	Conclusions
Yamamoto ^[20]	Liver cancer study group of japan for UICC stage II HCC ^a	HCFU 200mg, bid	67(32/35)	6-10 years	Stage I ^b cirrhosis 62% vs 32% Stage II cirrhosis 0% vs 0% ^c	Stage I cirrhosis 79% vs 70% Stage II cirrhosis 59% vs 57% ^c	Beneficial only to patients with Stage I liver dys function Not effective
Kohno ^[21]	NA	UFT 300mg, qd vs UFT 300mg, qd+A (ia, 40mg/m ² , once)	88 (40/48)	NA	3-year 37% vs 32%	NA	Not effective
Ono ^[22]	NA	A 40mg/m ² ia and 40mg/m ² iv every 3 months for 2 years, and HCFU 300mg qd for 2 years	56 (29/27)	24 months	NA	NA	Not effective, with poor tolerance
Ueno ^[23]	NA	CDDP 50-80mg and MMC 10mg ia, 2-3 times	21 (11/10)	>1 year	70% vs 20% ^c	NA	Beneficial

NA: not available; A: adriamycin or Epirubicin; ia: intraarterially; iv: intravenously; DFS: disease free survival; OS: overall survival.
^a complete excision of a solitary tumor, less than 5 cm in diameter, with a tumor capsule and no vascular invasion to the first or second branches of the portal vein, or for other stage II tumors, complete removal with a surgical margin from the tumor edge of more than 1 cm;

^bsee the original paper;

^cestimated according to the figure in authors' paper.

because of a series of successful animal experiments^[26]; however, it turned out to be not so effective as expected in a number of clinical trials^[27-29]. At the same time, several clinical trials have been set up to test the effect of adoptive immunotherapy on recurrence in patients with HCC in early 1990s. The followings are a summary of these RCTs (Table 4).

Une *et al*'s study compared the effect of locoregional chemotherapy with locoregional chemotherapy plus systemic immunotherapy on recurrence after curative resection of HCC. The results showed that locoregional chemotherapy plus systemic immunotherapy decreased recurrence rate^[30]. However, Kawata *et al*, reported from the same institution and used almost identical treatment settings, demonstrated immunochemotherapy didn't present any survival benefit to the patients, although in a subgroup of patients with negative surgical margin (≥ 1 cm), the immunochemotherapy group had a better disease-free survival rate than the chemotherapy group^[31]. The reason of the difference might come from the different observation time.

Lygidakis *et al* employed a protocol combining pre-operative and post-operative locoregional chemotherapy with systemic immunotherapy to prevent post-operative recurrence in HCC patients. The results showed this protocol decreased recurrence^[32].

In Takayama's study, which had a more than 5-year observation time, presented a clear survival benefit from adoptive immunotherapy in terms of DFS but not OS. To explain the reason of that, the authors discussed that adoptive immunotherapy may eliminate the micrometastatic lesion in the remnant liver, but can't prevent multicentric recurrence; the second reason was, during a longer time of observation, the treatment choice for recurrence was not totally dependent

on doctors' presetting, therefore different treatment modalities may affect the long term results^[1].

In general, the immunotherapy may inhibit recurrence in patients after resection of HCC, especially in the first several years after operation, with a good tolerance. However, it needs more randomized control trial to confirm, and more powerful agents need to be discovered.

Post-operative Interferon (IFN) treatment

The rationale of post-operative IFN treatment came from the several findings in HCV related HCC. First, a lower incidence of HCC was observed in many studies when IFN was used to clear HCV viremia^[33]; second, recurrence after curative resection of HCC developed from multicentric origin, which was closely related to the HCC viremia status^[14]. Third, IFN had anti-cancer effect on the early stage tumors, like micrometastatic lesions^[34]. The following is the summary of post-operative IFN treatment (Table 5).

Ikeda *et al*^[35]s results showed that, although the recurrence curve increased similarly in both groups in the first two years, but it remained the same in treatment group after that, which suggested that the effect of IFN β on prevention of recurrence was not through direct inhibition of tumor cells per se, but depended on the clearance of HCV viremia, implying the mechanism of IFN α is through inhibition of multicentric recurrence. However, in Kubo *et al*'s study, the decrease of recurrence rate was associated with neither clearance of HCV nor normalization of serum ALT level, the actual reason was unknown, but the authors suggested that it might depend on direct antitumor effects or inhibition of carcinogenesis by HCV. Therefore, the mechanism of IFN's effect on recurrence remains to be investigated further^[14,36]. Recently, our data

Table 4 A summary of RCT results of adoptive immunotherapy to prevent recurrence

Authors	Entry criteria	Treatment protocol	Sample size (Tx/Ctl)	Observation time	DFS Tx vs Ctl	OS Tx vs Ctl	Conclusions
Une ^[30]	NA	A ia vs A+LAK and IL2 ia	24(12/12)	NA	50% vs 8.3%	NA	Beneficial
Kawata ^[31]	NA	A ia vs A +IL2+LAK ia	24(12/12)	NA	NS	NA	Not beneficial
Lygidakis ^[32]	NA	No Tx vs Chemoimmunotherapy	40(20/20)	NA	Recurrence: 0/18 vs 7/17	NA	Beneficial
Takayama ^[1]	Completely remove; histologically negative in surgical margin	LAK IV at the 2 nd , 3 rd , 4 th , 12 th , 24 th week after operation	155 (76/79)	>5 years	3-year 48% vs 33% 5 year 37% vs 22%	5-year 68% vs 62%	Beneficial

ia: intra-arterially; iv: intravenously; NA: not available; NS: not significant; DFS: disease free survival; OS: overall survival; Tx: treatment; Ctl: control; LAK: lymphokine activated killer cells; NA: not available.

Table 5 Summary of RCTs of Interferon treatment

Authors	Entry criteria	Tx protocol	Sample size	Observation time	DFS Tx vs Ctl	OS Tx vs Ctl	Conclusions
Ikeda ^[35]	Complete remove by resection or PEI	IFN β 6MU im biw \times 36 months	20(10/10)	2-34.6 months	1 year 0% vs 62.5%	NA	Beneficial
Kubo ^[14,36]	Complete remove, negative in CT scan 3-4 weeks after operation	IFN α 6MU biw \times 2 weeks then tiw \times 14 weeks then biw \times 88 weeks	30(15/15)	1817 days (Tx) and 1487 (Ctl)	Recurrence 9/15 vs 13/15 P=0.041	NA	Beneficial

Table 6 Summary of RCTs of acyclic retinoic acid

Authors	Entry criteria	Tx protocol	Sample size	Observation time	Recurrence Tx vs Ctl	OS Tx vs Ctl	Conclusions
Muto ^[37,38]	Complete removal by resection or PEI, negative in postoperative Ultrasound or CT	ARA 300mg, bid	89(44/45)	62 months (Median)	27% vs 49% (P=0.04)	6 year 74% vs 46%	Beneficial

Tx: treatment; Ctl: control; OS: overall survival.

suggested anti-angiogenesis instead of the anti-proliferation property of IFN α involving in antitumor effect in animal models, and it may act through regulation of VEGF expression. A randomized control trial in HBV related HCC patients after curative resection was also conducted to test the effect of IFN α on recurrence in the authors' institution, the interim results showed that long-term IFN α treatment improved disease-free survival of patients through direct antitumor effect, which was not associated with serum conversion of HBeAg.

Acyclic retinoid acid

Retinoid acid is an inducer of differentiation. All-trans retinoic acid has been successfully used to treat a subtype of leukemia. Muto *et al* reported a serial results in patients with HCV-related HCC treated by post-operative acyclic retinoic acid (ARA), and showed long term ARA treatment improvement in OS and DFS^[37,38]. A further study revealed the mechanism of ARA treatment was through inhibition of second primary liver cancer by deletion of a latent clonal hepatoma cells^[39] (Table 6).

SUMMARY

A number of preventive treatment protocols to inhibiting recurrence after curative resection of HCC have been evaluated by RCT. Although no standard treatment has been proven to be effective to all patients, several approaches presented promising results, which were both effective and tolerable in post-operative patients. Generally systemic and locoregional chemotherapy or combined with embolization was not as effective as expected, meanwhile the side-effects, such as downstaging of liver function was noticed in this treatment; however, biological treatment approaches showed a better outcome, but need more evidence before being accepted widely.

REFERENCES

- Takayama T**, Sekine T, Makuuchi M, Yamasaki S, Kosuge T, Yamamoto J, Shimada K, Sakamoto M, Hirohashi S, Ohashi Y, Kakizoe T. Adoptive immunotherapy to lower postsurgical recurrence rates of hepatocellular carcinoma: a randomised trial. *Lancet* 2000; **356**: 802-807
- Tang ZY**, Yu YQ, Zhou XD, Ma ZC, Wu ZQ. Progress and prospects in hepatocellular carcinoma surgery. *Ann Chir* 1998; **52**: 558-563
- Poon RTP**, Fan ST, Lo CM, Ng IOL, Liu CL, Lam CM, Wong J. Improving survival results after resection of hepatocellular carcinoma: a prospective study of 377 patients over 10 years. *Ann Surg* 2001; **234**: 63-70
- Qin LX**, Tang ZY. The prognostic molecular markers in hepatocellular carcinoma. *World J Gastroenterol* 2002; **8**: 385-392
- Ikeda K**, Saitoh S, Tsubota A, Arase Y, Chayama K, Kumada H, Watanabe G, Tsurumaru M. Risk factors for tumor recurrence and prognosis after curative resection of hepatocellular carcinoma. *Cancer* 1993; **71**: 19-25
- Izumi R**, Shimizu K, Iyobe T, Ii T, Yagi M, Matsui O, Nonomura A, Miyazaki I. Postoperative adjuvant hepatic arterial infusion of Lipiodol containing anticancer drugs in patients with hepatocellular carcinoma. *Hepatology* 1994; **20**: 295-301
- Lau WY**, Leung TW, Ho SKW, Chan M, Machin D, Lau J, Chan ATC, Yeo W, Mok TSK, Yu SC, Leung NW, Johnson PJ. Adjuvant intra-arterial lipiodol iodine-131 for resectable hepatocellular carcinoma: a prospective randomised trial. *Lancet* 1999; **353**: 797-801
- Lai ECS**, Lo CM, Fan ST, Liu CL, Wong J. Postoperative adjuvant chemotherapy after curative resection of hepatocellular carcinoma: a randomized controlled trial. *Arch Surg* 1998; **133**: 183-188
- Sakon M**, Nagano H, Nakamori S, Dono K, Umeshita K, Murakami T, Nakamura H, Monden M. Intrahepatic recurrences of hepatocellular carcinoma after hepatectomy: analysis based on tumor hemodynamics. *Arch Surg* 2002; **137**: 94-99
- Yamamoto T**, Kajino K, Kudo M, Sasaki Y, Arakawa Y, Hino O. Determination of the clonal origin of multiple human hepatocellular carcinomas by cloning and polymerase chain reaction of the integrated hepatitis B virus DNA. *Hepatology* 1999; **29**: 1446-1452
- He B**, Tang ZY, Liu KD, Zhou G. Analysis of the cellular origin of hepatocellular carcinoma by p53 genotype. *J Cancer Res Clin Oncol* 1996; **122**: 763-766
- Poon RTP**, Fan ST, Ng IOL, Lo CM, Liu CL, Wong J. Different risk factors and prognosis for early and late intrahepatic recurrence after resection of hepatocellular carcinoma. *Cancer* 2000; **89**: 500-507
- Sugimoto R**, Okuda K, Tanaka M, Aoyagi S, Kojiro M. Metachronous multicentric occurrence of hepatocellular carcinoma after surgical treatment - clinicopathological comparison with recurrence due to metastasis. *Oncol Rep* 1999; **6**: 1303-1308
- Kubo S**, Nishiguchi S, Hirohashi K, Tanaka H, Shuto T, Yamazaki O, Shiomi S, Tamori A, Oka H, Igawa S, Kuroki T, Kinoshita H. Effects of long-term postoperative interferon-alpha therapy on intrahepatic recurrence after resection of hepatitis C virus-related hepatocellular carcinoma. A randomized, controlled trial. *Ann Intern Med* 2001; **134**: 963-967
- Tang ZY**, Yu YQ, Zhou XD. An important approach to prolonging survival further after radical resection of AFP positive hepatocellular carcinoma. *J Exp Clin Cancer Res* 1984; **4**: 359-366
- Wu CC**, Ho YZ, Ho WL, Wu TC, Liu TJ, P' Eng FK. Preoperative transcatheter arterial chemoembolization for resectable large hepatocellular carcinoma: a reappraisal. *Br J Surg* 1995; **82**: 122-126
- Yamasaki S**, Hasegawa H, Kinoshita H, Furukawa M, Imaoka S, Takasaki K, Kakumoto Y, Saitu H, Yamada R, Oosaki Y, Arii S, Okamoto E, Monden M, Ryu M, Kusano S, Kanematsu T, Ikeda K, Yamamoto M, Saoshiro T, Tsuzuki T. A prospective randomized trial of the preventive effect of pre-operative transcatheter arterial embolization against recurrence of hepatocellular carcinoma. *Jpn J Cancer Res* 1996; **87**: 206-211
- Alsowmely AM**, Hodgson HJF. Non-surgical treatment of hepatocellular carcinoma. *Aliment Pharmacol Ther* 2002; **16**: 1-15
- Clavien PA**, Selzner N, Morse M, Selzner M, Paulson E. Downstaging of hepatocellular carcinoma and liver metastases from colorectal cancer by selective intra-arterial chemotherapy. *Surgery* 2002; **131**: 433-442
- Yamamoto M**, Arii S, Sugahara K, Tobe T. Adjuvant oral chemotherapy to prevent recurrence after curative resection for hepatocellular carcinoma. *Br J Surg* 1996; **83**: 336-340
- Kohno H**, Nagasue N, Hayashi T, Yamanoi A, Uchida M, Ono T, Yukaya H, Kimura N, Nakamura T. Postoperative adjuvant chemotherapy after radical hepatic resection for hepatocellular carcinoma (HCC). *Hepatogastroenterology* 1996; **43**: 1405-1409
- Ono T**, Nagasue N, Kohno H, Hayashi T, Uchida M, Yukaya H, Yamanoi A. Adjuvant chemotherapy with epirubicin and carmofur after radical resection of hepatocellular carcinoma: a prospective randomized study. *Semin Oncol* 1997; **24**(2Suppl 6): S618-S625
- Ueno S**, Tanabe G, Yoshida A, Yoshidome S, Takao S, Aikou T. Postoperative prediction of and strategy for metastatic recurrent hepatocellular carcinoma according to histologic activity of hepatitis. *Cancer* 1999; **86**: 248-254
- Ono T**, Yamanoi A, Nazmy El Assal O, Kohno H, Nagasue N. Adjuvant chemotherapy after resection of hepatocellular carcinoma causes deterioration of long-term prognosis in cirrhotic patients: metaanalysis of three randomized controlled trials. *Cancer* 2001; **91**: 2378-2385
- Camma C**, Schepis F, Orlando A, Albanese M, Shahied L, Trevisani F, Andreone P, Craxi A, Cottone M. Transarterial chemoembolization for unresectable hepatocellular carcinoma: meta-analysis of randomized controlled trials. *Radiology* 2002; **224**: 47-54
- Rosenberg SA**. Adoptive immunotherapy for cancer. *Sci Am* 1990; **262**: 62-69
- Hermans J**, Bonenkamp JJ, Boon MC, Bunt AM, Ohyama S, Sasako M, Van de Velde CJ. Adjuvant therapy after curative resection for gastric cancer: meta-analysis of randomized trials. *J Clin Oncol* 1993; **11**: 1441-1447
- Huncharek M**, Caubet JF, McGarry R. Single-agent DTIC versus

- combination chemotherapy with or without immunotherapy in metastatic melanoma: a meta-analysis of 3273 patients from 20 randomized trials. *Melanoma Res* 2001; **11**: 75-81
- 29 **Hanna MG Jr**, Hoover HC Jr, Vermorken JB, Harris JE, Pinedo HM. Adjuvant active specific immunotherapy of stage II and stage III colon cancer with an autologous tumor cell vaccine: first randomized phase III trials show promise. *Vaccine* 2001; **19**: 2576-2582
- 30 **Une Y**, Kawata A, Uchino J. Adopted immunochemotherapy using IL-2 and spleen LAK cell-randomized study. *Nippon Geka Gakkai Zasshi* 1991; **92**: 1330-1333
- 31 **Kawata A**, Une Y, Hosokawa M, Wakizaka Y, Namieno T, Uchino J, Kobayashi H. Adjuvant chemoimmunotherapy for hepatocellular carcinoma patients. Adriamycin, interleukin-2, and lymphokine-activated killer cells versus adriamycin alone. *Am J Clin Oncol* 1995; **18**: 257-262
- 32 **Lygidakis NJ**, Pothoulakis J, Konstantinidou AE, Spanos H. Hepatocellular carcinoma: surgical resection versus surgical resection combined with pre- and post-operative locoregional immunotherapy-chemotherapy. A prospective randomized study. *Anticancer Res* 1995; **15**: 543-550
- 33 **Camma C**, Giunta M, Andreone P, Craxi A. Interferon and prevention of hepatocellular carcinoma in viral cirrhosis: an evidence-based approach. *J Hepatol* 2001; **34**: 593-602
- 34 **Jonasch E**, Haluska FG. Interferon in oncological practice: review of interferon biology, clinical applications, and toxicities. *Oncologist* 2001; **6**: 34-55
- 35 **Ikeda K**, Arase Y, Saitoh S, Kobayashi M, Suzuki Y, Suzuki F, Tsubota A, Chayama K, Murashima N, Kumada H. Interferon beta prevents recurrence of hepatocellular carcinoma after complete resection or ablation of the primary tumor-A prospective randomized study of hepatitis C virus-related liver cancer. *Hepatology* 2000; **32**: 228-232
- 36 **Kubo S**, Nishiguchi S, Hirohashi K, Tanaka H, Shuto T, Kinoshita H. Randomized clinical trial of long-term outcome after resection of hepatitis C virus-related hepatocellular carcinoma by postoperative interferon therapy. *Br J Surg* 2002; **89**: 418-422
- 37 **Muto Y**, Moriwaki H, Ninomiya M, Adachi S, Saito A, Takasaki KT, Tanaka T, Tsurumi K, Okuno M, Tomita E, Nakamura T, Kojima T. Prevention of second primary tumors by an acyclic retinoid, polyprenoic acid, in patients with hepatocellular carcinoma. Hepatoma Prevention Study Group. *N Engl J Med* 1996; **334**: 1561-1567
- 38 **Muto Y**, Saito A. Prevention of second primary tumors by an acyclic retinoid in patients with hepatocellular carcinoma. *N Engl J Med* 1999; **340**: 1046-1047
- 39 **Moriwaki H**, Yasuda I, Shiratori Y, Uematsu T, Okuno M, Muto Y. Deletion of serum lectin-reactive alpha-fetoprotein by acyclic retinoid: a potent biomarker in the chemoprevention of second primary hepatoma. *Clin Cancer Res* 1997; **3**: 727-731

Edited by Wu XN

Current status and prospects of studies on human genetic alleles associated with hepatitis B virus infection

Fu-Sheng Wang

Fu-Sheng Wang, Division of Biological Engineering, Beijing Institute of Infectious Diseases, 100 Xi Si-Huan-Zhong Road, Beijing 100039, China

Supported by Key project grant from Natural Science Foundation of Beijing Municipal Government No: 7011005

Correspondence to: Dr. Fu-Sheng Wang, Professor of Medicine, Division of Bioengineering, Beijing Institute of Infectious Diseases, 100 Xi Si-Huan-Zhong Road, Beijing 100039, China. fswang@public.bta.net.cn

Telephone: +86-10-63831870 **Fax:** +86-10-63831870

Received: 2002-11-26 **Accepted:** 2002-12-18

Abstract

Chronic hepatitis B virus (HBV) infection can cause a broad spectrum diseases, including from asymptomatic HBV carriers or cryptic hepatitis, to acute hepatitis, chronic hepatitis, Liver cirrhosis and primary hepatocellular carcinoma. The variable pattern and clinical outcome of the infection were mainly determined by virological itself factors, host immunological factors and genetic factors as well as the experimental factors. Among the human genetic factors, major candidate or identified genes involved in the process of HBV infection fall into the following categories: (1) genes that mediate the processes of viral entry into hepatocytes, including genes involved in viral binding, fusion with cellular membrane and transportation in target cells; (2) genes that modulate or control the immune response to HBV infection; (3) genes that participate in the pathological alterations in liver tissue; (4) genes involved in the development of liver cirrhosis and hepatocellular carcinoma associated with chronic HBV infection, including genes related to mother-to-infant transmission of HBV infection; and (5) those that contribute to resistance to antiviral therapies. Most of the reports of human genes associated with HBV infection have currently focused on HLA associations. For example, some investigators reported the association of the HLA class II alleles such as DRB1*1302 or HLA-DR13 or DQA1*0501-DQB1*0301-DQB1*1102 haplotypes with acute and/or chronic hepatitis B virus infection, respectively. Several pro-inflammatory cytokines such as Th1 cytokines (including IL-2 and IFN- γ) and TNF- α have been identified to participate the process of viral clearance and host immune response to HBV. In contrast, the Th2 cytokine IL-10 serves as a potent inhibitor of Th1 effector cells in HBV diseases. The MBP polymorphisms in its encoding region were found to be involved in chronic infection. Thus, reports from various laboratories have shown some inconsistencies with regard to the effects of host genetic factors on HBV clearance and persistence. Since genetic interactions are complex, it is unlikely that a single allelic variant is responsible for HBV resistance or susceptibility. However, the collective influence of several single nucleotide polymorphisms (SNPs) or haplotype (s) may underlie the natural combinational or synergistic protection against HBV. The future study including the multi-cohort collaboration will be needed to clarify these preliminary associations and identify other potential candidate genes. The ongoing study of the distributions and functions of the implicated allele polymorphisms will not only provide insight

into the pathogenesis of HBV infection, but may also provide a novel rationale for new methods of diagnosis and therapeutic strategies.

Wang FS. Current status and prospects of studies on human genetic alleles associated with hepatitis B virus infection. *World J Gastroenterol* 2003; 9(4): 641-644

<http://www.wjgnet.com/1007-9327/9/641.htm>

INTRODUCTION

Chronic hepatitis B virus (HBV) infection is one of the most common infectious diseases and leads to high morbidity and mortality due to the development of liver cirrhosis (LC) and hepatocellular carcinomas (HCC). It is estimated that HBV is present in a reservoir of more than 130 million chronic carriers, representing more than 10 % of Chinese population^[1]. In particular, more than 23 million of Chinese HBV-infected subjects clinically manifest liver damage with abnormally elevated ALT levels and HBV active replication. Generally, exposure to HBV can cause a broad spectrum ranging from no infection to different clinical conditions^[2]. What produces the individual or ethnic differences in infection, severity, and outcome? The reasons for this variation in the natural history of HBV infection are not fully understood, but are environmental factors and the following: (1) *Virological factors* such as viral load, genotype, and genetic divergence due to viral gene mutations. HBV mutates very rapidly and uses high genetic variability as an effective mechanism for escaping the host immune response^[3]. (2) *Immunological factors* including the innate and adaptive immune responses against viral infection, which play important roles in modulating both the antiviral immune response and host susceptibility to HBV. The rapid mutations in HBV epitopes recognized by HBV-specific CTLs may cause both humoral and cell-mediated virus-specific immune responses to quickly lose their ability to efficiently control the virus^[4,5]. (3) The *host genetic factors* are believed to be responsible for clinical outcomes of many infectious diseases^[6-9].

In the last decade, the virological and immunological factors of HBV have been extensively studied, but the examination of the relationship between host genetics and HBV resistance is still in its infancy^[10-12]. Therefore, this review focuses on the recent progress in study of human genetic alleles associated with chronic HBV infection, and discuss the unanswered questions and future directions in this field.

HOST GENETIC FACTORS INVOLVED IN HBV INFECTION

HBV-infected subjects generally fall into one of the following clinical types: (1) asymptomatic HBV carriers and cryptic hepatitis; (2) acute hepatitis; (3) chronic hepatitis; (4) liver cirrhosis with or without decompensated liver failure; and (5) primary hepatocellular carcinoma associated with HBV infection^[2,13]. However, the pattern and clinical outcome of the infection are highly variable. Why is this? Previous epidemiological investigation in humans suggests that there is

a strong genetic component to affect the individual susceptibility to infectious pathogens^[14-16], although to date, no single allele has not been clearly associated with HBV persistence or disease severity. However, the following reflects individual and ethnic differences in response to HBV infection.

- (1) Infection with the same HBV virus has been found to cause various clinical outcomes in patients. In adults suffering from primary HBV infection, 90-95 % of the subjects can successfully clarify the virus through self-limiting hepatitis and only 5-10 % of adults become chronic HBV carriers^[17]. Among the chronically infected subjects, 20-30 % lead to liver cirrhosis and -5 % develop hepatocellular carcinoma through a long-term disease progression. Of teen-ager subjects that acquire HBV infection from either perinatal or horizontal transmission, more than 90 % develop chronic infection. In China, mother-to-child transmission of HBV was once a common source of chronic infection.
- (2) The long-term follow-up studies indicate that some individuals in high-risk groups (e.g. spouses in HBV-infected families) never develop the disease. This suggest the existence of an individual-specific resistance to HBV infection^[1,3].
- (3) There is a different incidence and infection rate among global ethnic groups. HBV infection is significantly endemic in Asia and Africa, and there is a significantly higher incidence of chronic HBV infection in Chinese compared to Caucasians^[18].
- (4) In clinic, HBV-infected individuals may display complete, partial or no response to interferon- α or Lamivudine antiviral therapy alone or in combination.
- (5) Around 85 % of healthy subjects can produce the efficient protective anti-HBsAg antibody upon the HBV vaccination, while remaining fail.

The above-mentioned data suggests that the knowledge of understanding human genetic factors may provide critical clues not only to the ethnic diversity of HBV infection, but also to the issue of disparity in therapeutic response^[19]. The human genome project has indicated that there are approximately thirty-five thousand genes in the human genome. Many of these alleles contain polymorphisms such as single nucleotide polymorphisms (SNPs) within the encoding or flanking regions. It is estimated that there are 3.5 million SNPs within human genome and there are likely to explain much of the genetic diversity of individuals and ethnic groups^[13]. If a specific SNP version is associated with a favorable outcome and low risk of progression of HBV infection and liver disease, the allele may be considered an 'HBV resistant' allele. Conversely, a version of the SNP that confers an unwanted HBV phenotype (quick disease progression or high risk of severe infection) may be called a 'HBV susceptible' allele. Current research is focusing on the hunt and identification for these alleles.

SELECTION OF CANDIDATE ALLELES

Two strategies are currently used in the study involving genetic markers associated with disease phenotypes. The *candidate gene method* is the typing of markers located near genes that could be chemically related to the disease in question^[20]. Conversely, a genome-wide search scans markers throughout the whole genome in search of chromosomal regions that could be associated with disease susceptibility or resistance. The choice of candidate genes for the first method is strongly determined by the function (or putative function) of the gene and its possible role in the host response to HBV infection and disease progression. Major genes involved in the process of HBV infection can be identified by characterizing host response to HBV exposure such as clinical response, biological response (intensity of infection), and immunological response (levels

of antibodies, cytokines or cell-mediated response against HBV)^[10]. These biological processes may then suggest genes of interest for screening. Many of the candidate genes fall into the following categories: (1) genes that mediate the processes of viral entry into hepatocytes, including genes involved in viral binding, fusion with cellular membrane and transportation in target cells; (2) genes that modulate or control the immune response to HBV infection; (3) genes that participate in the pathological alterations in liver tissue; (4) genes involved in the development of liver cirrhosis and hepatocellular carcinoma associated with chronic HBV infection, including genes related to mother-to-infant transmission of HBV infection; and (5) those that contribute to resistance to antiviral therapies^[19,20]. This study is still in its early stages, and much more remains to be done on candidate genes, including the clarification of sequence, identification of mutant SNPs, functional evaluation of SNPs, and evaluation of their association with diseases.

ADVANCES ASSOCIATED WITH INDIVIDUAL GENETIC SUSCEPTIBILITY TO HBV INFECTION

Some candidate gene work has been completed at this time. Since both chemokine receptor and HLA genes play critical roles in host immune response to viral infection, they are among the first HBV candidate genes screened.

HLA class I and II alleles

The genes for HLA class I (HLA-A, -B, and -C) and class II (HLA-DRB1, -DQA1, -DQB1, -DPA1, and -DPB1) are located on the short arm of chromosome 6. As the primary modulator of host immune response, the HLA molecules present foreign antigens to both the CD4+ T lymphocytes and the CD8+ cytolytic T cells, leading to both humoral and cell-mediated immune response. The majority of the human genetic studies associated with HBV infection has focused on HLA associations^[21]. Thursz et al investigated a large cohort of pediatric patients from Gambia and identified the association of the HLA class II allele DRB1*1302 with a self-limiting course of acute hepatitis B^[23,24]. Hohler *et al*^[17], confirmed the effect of DRB1*1302 in Gambian adults that seemed to clear the HBV infection *in vivo*. Thio *et al*^[25] examined the DQA1*0501, DQB1*0301 and DQA1-DQB1 haplotypes and found the haplotype cluster of DQA1*0501-DQB1*0301-DQB1*1102 had a significant association with viral persistence. However, Zavaglia *et al* reported that no correlation could be observed between the clearance of HBV or HCV virus and HLA phenotypes^[22]. Recently, Diepolder *et al* reported that HLA-DR13 allele is less frequent in patients with chronic hepatitis B than in healthy controls or subjects with a self-limiting hepatitis B^[26]. Additional study has confirmed a strong association between the HLA class II allele DR13 and a self-limiting course of acute HBV infection. Rapid progression to chronic hepatitis B is rare in these patients, suggesting that patients with HLA-DR13 can mount a more vigorous CD+ T cell response to HBV core antigen during acute HBV infection. The beneficial effect of HLA-DR13 allele on the outcome of HBV infection may either be the result of more proficient antigen presentation by the HLA-DR13 molecules themselves or of a linked polymorphism in a neighboring immunoregulatory gene. To date, no associations between HLA class I alleles and the viral persistence or disease progression in HBV-infected patients was found, though class I molecule mediates the cytotoxic T lymphocyte (CTL) response through the cytolytic and noncytolytic mechanisms^[13]. Future studies have to investigate whether one of these polymorphisms or a yet unidentified immunoregulatory gene is possibly associated with a more successful immune response against HBV^[27].

Cytokine and chemokines

Since individual variation in cytokine release is predominantly caused by polymorphisms near or within the genes^[28,29], heterogeneity of the candidate gene in HBV-infected patients serves as a probable biomarker for influence the disease phenotypes. Several pro-inflammatory cytokines such as Th1 cytokines (including IL-2 and IFN- γ) and tumor necrosis factor-alpha (TNF- α) have been identified as participating in the viral clearance and the host immune response to HBV. In contrast, the Th2 cytokine IL-10 serves as a potent inhibitor of Th1 effector cells^[30].

Tumor necrosis factor (TNF)- α is an important cytokine involved in noncytotoxic antiviral mechanisms^[31]. This gene is located within the class III region of the MHC complex and has five polymorphisms in its promoter region, located at positions -1031(T/C), -863(C/A), -857(C/T), -308(G/A) and -238(G/A) respectively [negative numbers represent number of bases upstream from the transcription initiation site]^[32,33]. Miyazoe *et al* reported the TNF- α gene promoter polymorphisms were not linked to disease progression in HBV carriers in Japan^[34], however both Hohler^[35,36] found that the two polymorphisms such as -308(G/A) and -238(G/A) were significantly associated with HBV or HCV persistence in patients. It is thought that the polymorphism influences the expression of TNF- α , which may block HBV gene expression. Similar to TNF- α , IFN- γ clears HBV *in vivo* by a noncytolytic effect. Hoffmann *et al*^[18], showed that the Asian population contains more IFN- γ genotypes that result in low expression than do Caucasian populations, which suggests the possibility of an association between low IFN- γ expression in the highly HBV-susceptible Asian population.

The promoter region of IL-10 gene contains three SNPs at position -1082 (A/G), -819 (T/C), and -592 (A/C), which may assort into three different haplotypes^[37]. Miyazoe *et al* analyzed the distributions of TNF- α and IL-10 promoter SNPs in Japanese HBV-infected patients and found that the -819T and -592A wild-type alleles in the IL-10 gene promoter were significantly more common in asymptomatic carriers than in patients with chronic progressive liver diseases^[32], suggesting that inheritance of the IL-10 gene promoter polymorphisms is relevant to progression in chronic HBV infection, perhaps due to decreased IL-10 production induced by -819T and -592A haplotype allele.

Mannose binding protein (MBP)

MBP is a calcium-dependent opsonin that plays an important role in innate immunity by activating the classical complement pathway and phagocytosis. There are three identified polymorphisms in the MBP gene encoding region (in codons 54, 57 and 52), leading to low serum concentrations and thus abolishing its ability to affect host immunity because of an opsonic defect. The middle surface protein of HBV viral envelope contains a mannose-rich oligosaccharide to which MBP could potentially bind. Thomas *et al* showed that 27 % of Caucasian patients chronically infected with HBV were homozygous or heterozygous for the codon 52 mutant allele whereas only 11 % of patients with acute infection and 4 % of controls carried the wild type allele, which suggests that the codon 52 mutant gene has been associated with persistence of HBV infection^[38]. The higher frequency of the codon 52 mutation among the HBV patients than among controls is probably consistent with the fact that the mutation leads to the failure of opsonisation and phagocytosis of HBV. Yuen *et al*^[39], reported that the codon 54 mutation was associated with symptomatic persistent viral infection in Chinese patients. In German Caucasians and Gambians, these MBP polymorphisms were not associated with chronic infection^[40].

Vitamin D receptor, cytochrome P450 and Complement four associated with HBV infection

The active form of vitamin D is an immunomodulatory hormone that inhibits the Th1 response and activates the Th2 immune reaction. Bellamy *et al.* studied two known Vitamin D receptor gene polymorphisms in Gambian HBV-infected patients and found that the tt genotype of one polymorphism was associated with viral clearance^[41].

Thus far, reports from various laboratories have shown some inconsistencies with regard to the effects of host genetic factors on HBV clearance and persistence. This ambiguity may be attributable to one or more of the following reasons: (1) a complex interaction between the virus and host multiple alleles; (2) the ethnic differences in the studied groups; (3) an association with a gene in linkage disequilibrium with an HLA allele. Therefore, a global multicenter studies may be needed to integrate the genetic data and the clinical data for fully clarification of underlying immunogenetic pathogenesis of HBV infection. In addition, further candidate genes must be identified and screened for associated polymorphisms.

PROSPECT FOR STUDY OF HBV RESISTANCE ALLELES

A growing body of evidence related to the genetic effects on infectious diseases has shown only a fraction of the total picture. The most successful example is the identification of CCR5 delta32 allele in HIV-1 infection^[8,42]. Since genetic interactions are complex, it is unlikely that a single allelic variant is responsible for HBV resistance or susceptibility^[43]. However, the collective influence of several SNPs or haplotype(s) may exert the natural combinational or synergistic protection against HBV. Recently developed genetic epidemiology strategies and dense genome-wide search, together with the growing availability of candidate alleles and sequence information supply a basic platform for identifying genes associated in HBV infection. These investigations will depend on the interactions of many different factors including the viral phenotypes, population traits, accurate measurement of environmental factors, and previous knowledge. Genetic resistance to HBV-induced persistent hepatitis is likely to involve a complex array of host genetic effects involving multiple variants and haplotypes. Because of this, future study including the multicohort collaboration will be needed to clarify these preliminary associations and identify other potential candidate genes^[20]. In addition, it will be necessary to functionally characterize the identified associated genes, such as versions of HLA molecules and MBP, and see whether the mutations have functional significance in terms of individual susceptibility to HBV infection. The ongoing study of the distributions and functions of the implicated allele polymorphisms will not only provide insight into the pathogenesis of HBV infection, but may also provide a novel rationale for new methods of diagnosis and therapeutic strategies^[44].

REFERENCES

- 1 **Gu CH, Luo KX.** Hepatitis B: Basic biology and clinical science. Second edition. Beijing, People's Medical Publishing House 2001: 1-6
- 2 **Iino S.** Natural history of hepatitis B and C virus infections. *Oncology* 2002; **62**(Suppl 1): 18-23
- 3 **Luo KX.** Hepatitis B: Basic biology and clinical science. Second edition. Beijing, People's Medical Publishing House 2001: 56-70
- 4 **Ferrari C.** Hepatitis B virus immunopathogenesis. *Annu Rev Immunol* 1995; **13**: 29-60
- 5 **Guidotti LG, Chisari FV.** Noncytolytic control of viral infections by the innate and adaptive immune response. *Annu Rev Immunol* 2001; **19**: 65-91
- 6 **Abel L, Dessein AJ.** The impact of host genetics on susceptibility

- to human infectious diseases. *Curr Opin Immunol* 1997; **9**: 509-516
- 7 **McNicholl J**. Host genes and infectious diseases. *Emerg Infect Dis* 1998; **4**: 423-426
- 8 **McNicholl JM**, Cuenco KT. Host genes and infectious diseases. HIV, other pathogens, and a public health perspective. *Am J Prev Med* 1999; **16**: 141-154
- 9 **McGuire W**, Hill AV, Allsopp CE, Greenwood BM, Kwiatkowski D. Variation in the TNF-alpha promoter region associated with susceptibility to cerebral malaria. *Nature* 1994; **371**: 508-510
- 10 **Dean M**, Carrington M, O' Brien SJ. Balanced polymorphism selected by genetic versus infectious human disease. *Annu Rev Genomics Hum Genet* 2002; **3**: 263-292
- 11 **Hill AV**. Host genetics of infectious diseases: old and new approaches converge. *Emerg Infect Dis* 1998; **4**: 695-697
- 12 **Hill AV**. The immunogenetics of human infectious diseases. *Annu Rev Immunol* 1998; **16**: 593-617
- 13 **Thio CL**, Thomas D L, Carrington M. Chronic viral hepatitis and the human genome. *Hepatology* 2000; **31**: 819-827
- 14 **Kwiatkowski D**. Genetic dissection of the molecular pathogenesis of severe infection. *Intensive Care Med* 2000; **26**(Suppl 1): S89-97
- 15 **Weatherall D**, Clegg J, Kwiatkowski D. The role of genomics in studying genetic susceptibility to infectious disease. *Genome Research* 1997; **7**: 967-973
- 16 **Powell EE**, Edwards-Smith CJ, Hay JL, Clouston AD, Crawford DH, Shorthouse C, Purdie DM, Jonsson JR. Host genetic factors influence disease progression in chronic hepatitis C. *Hepatology* 2000; **31**: 828-833
- 17 **Hohler T**, Gerken G, Notghi A, Lubjuhn R, Taheri H, Protzer U, Lohr HF, Schneider PM, Meyer zum Buschenfelde KH, Rittner C. HLA-DRB1*1301 and *1302 protect against chronic hepatitis B. *J Hepatol* 1997; **26**: 503-507
- 18 **Hoffmann SC**, Stanley EM, Cox ED, DiMercurio BS, Koziol DE, Harlan DM, Kirk AD, Blair PJ. Ethnicity greatly influences cytokine gene polymorphism distribution. *Am J Transplant* 2002; **2**: 560-567
- 19 **Knolle PA**, Kremp S, Hohler T, Krummenauer F, Schirmacher P, Gerken G. Viral and host factors in the prediction of response to interferon-alpha therapy in chronic hepatitis C after long-term follow-up. *J Viral Hepat* 1998; **5**: 399-406
- 20 **Abel L**, Dessein AJ. Genetic epidemiology of infectious diseases in humans: design of population-based studies. *Emerg Infect Dis* 1998; **4**: 593-603
- 21 **Almarri A**, Batchelor JR. HLA and hepatitis B infection. *Lancet* 1999; **344**: 1194-1195
- 22 **Zavaglia C**, Bortolon C, Ferrioli G, Rho A, Mondazzi L, Bottelli R, Ghessi A, Gelosa F, Iamoni G, Ideo G. HLA typing in chronic type B, D and C hepatitis. *J Hepatol* 1996; **24**: 658-665
- 23 **Thursz MR**, Kwiatkowski D, Allsopp CE, Greenwood BM, Thomas HC, Hill AV. Association between an MHC class II allele and clearance of hepatitis B virus in the Gambia. *N Engl J Med* 1995; **332**: 1065-1069
- 24 **Thursz MR**. Host genetic factors influencing the outcome of hepatitis. *J Viral Hepat* 1997; **4**: 215-220
- 25 **Thio CL**, Carrington M, Marti D, O' Brien SJ, Vlahov D, Nelson KE, Astemborski JA, Thomas DL. Class II of HLA alleles and hepatitis B Virus persistence African Americans. *J Infect Dis* 1999; **179**: 1004-1006
- 26 **Diepolder HM**, Jung MC, Keller E, Schraut W, Gerlach JT, Gruner N, Zachoval R, Hoffmann RM, Schirren CA, Scholz S, Pape GR. A vigorous virus-specific CD4+ T cell response may contribute to the association of HLA-DR13 with viral clearance in hepatitis B. *Clin Exp Immunol* 1998; **113**: 244-251
- 27 **Ahn SH**, Han KH, Park JY, Lee CK, Kang SW, Chon CY, Kim YS, Park K, Kim DK, Moon YM. Association between hepatitis B virus infection and HLA-DR type in Korea. *Hepatology* 2000; **31**: 1371-1373
- 28 **Westendorp RG**, Langermans JA, Huizinga TW, Verweij CL, Sturk A. Genetic influence on cytokine production in meningococcal disease. *Lancet* 1997; **349**: 1912-1913
- 29 **van Deventer SJ**. Cytokine and cytokine receptor polymorphisms in infectious disease. *Intensive Care Med* 2000; **26**(Suppl 1): S98-102
- 30 **Fiorentino DF**, Zlotnik A, Vieira P, Mosmann TR, Howard M, Moore KW, O' Garra A. IL-10 acts on the antigen-presenting cell to inhibit cytokine production by Th1 cells. *J Immunol* 1991; **146**: 3444-3451
- 31 **Knight JC**, Kwiatkowski D. Inherited variability of tumor necrosis factor production and susceptibility to infectious disease. *Proc Assoc Am Physicians* 1999; **111**: 290-298
- 32 **Hajeer AH**, Hutchinson IV. TNF-alpha gene polymorphism: clinical and biological implications. *Microsc Res Tech* 2000; **50**: 216-228
- 33 **Higuchi T**, Seki N, Kamizono S, Yamada A, Kimura A, Kato H, Itoh K. Polymorphism of the 5' -flanking region of the human tumor necrosis factor (TNF)-alpha gene in Japanese. *Tissue Antigens* 1998; **51**: 605-612
- 34 **Miyazoe S**, Hamasaki K, Nakata K, Kajiyama Y, Kitajima K, Nakao K, Daikoku M, Yatsushiro H, Koga M, Yano M, Eguchi K. Influence of interleukin-10 gene promoter polymorphisms on disease progression in patients chronically infected with hepatitis B virus. *Am J Gastroenterol* 2002; **97**: 2086-2092
- 35 **Hohler T**, Kruger A, Gerken G, Schneider PM, Meyer zum Buschenfelde KH, Rittner C. A tumor necrosis factor-alpha (TNF-alpha) promoter polymorphism is associated with chronic hepatitis B infection. *Clin Exp Immunol* 1998; **111**: 579-582
- 36 **Hohler T**, Kruger A, Gerken G, Schneider PM, Meyer zum Buschenfelde KH, Rittner C. Tumor necrosis factor alpha promoter polymorphism at position -238 is associated with chronic active hepatitis C infection. *J Med Virol* 1998; **54**: 173-177
- 37 **Edwards-Smith CJ**, Jonsson JR, Purdie DM, Bansal A, Shorthouse C, Powell EE. Interleukin-10 promoter polymorphism predicts initial response of chronic hepatitis C to interferon alfa. *Hepatology* 1999; **30**: 526-530
- 38 **Thomas HC**, Foster GR, Sumiya M, McIntosh D, Jack DL, Turner MW, Summerfield JA. Mutation of gene of mannose-binding protein associated with chronic hepatitis B viral infection. *Lancet* 1996; **348**: 1417-1419
- 39 Yuen MF, Lau CS, Lau YL, Wong WM, Cheng CC, Lai CL. Mannose binding lectin gene mutations are associated with progression of liver disease in chronic hepatitis B infection. *Hepatology* 1999; **29**: 1248-1251
- 40 **Hohler T**, Wunschel M, Gerken G, Schneider PM, Meyer zum Buschenfelde KH, Rittner C. No association between mannose-binding lectin alleles and susceptibility to chronic hepatitis B Virus infection in German patients. *Exp Clin Immunogenet* 1998; **15**: 130-133
- 41 **Bellamy R**, Hill AV. Genetic susceptibility to mycobacteria and other infectious pathogens in humans. *Curr Opin Immunol* 1998; **10**: 483-487
- 42 **Dean M**, Carrington M, Winkler C, Huttley GA, Smith MW, Allikmets R, Goedert JJ, Buchbinder SP, Vittinghoff E, Gomperts E, Donfield S, Vlahov D, Kaslow R, Saah A, Rinaldo C, Detels R, O' Brien SJ. Genetic restriction of HIV-1 infection and progression to AIDS by a deletion allele of the CKR5 structural gene. Hemophilia Growth and Development Study, Multicenter AIDS Cohort Study, Multicenter Hemophilia Cohort Study, San Francisco City Cohort, ALIVE Study. *Science* 1996; **273**: 1856-1862
- 43 **Griffiths PD**. Interactions between viral and human genes. *Rev Med Virol* 2002; **12**: 197-199
- 44 **Dean M**, Carrington M, O' Brien SJ. Balanced polymorphism selected by genetic versus infectious human disease. *Annu Rev Genomics Hum Genet* 2002; **3**: 263-292

Translocation of annexin I from cellular membrane to the nuclear membrane in human esophageal squamous cell carcinoma

Yu Liu, Hui-Xin Wang, Ning Lu, You-Sheng Mao, Fang Liu, Ying Wang, Hai-Rong Zhang, Kun Wang, Min Wu, Xiao-Hang Zhao

Yu Liu, Hui-Xin Wang, Fang Liu, Ying Wang, Min Wu, Xiao-Hang Zhao, National Laboratory of Molecular Oncology, Cancer Institute and Hospital, Chinese Academy of Medical Sciences & Peking Union Medical College, Beijing 100021, China

Ning Lu, Department of Pathology, Cancer Institute and Hospital, Chinese Academy of Medical Sciences & Peking Union Medical College, Beijing 100021, China

You-Sheng Mao, Department of Pectoral Surgery, Cancer Institute and Hospital, Chinese Academy of Medical Sciences & Peking Union Medical College, Beijing 100021, China

Hai-Rong Zhang, Kun Wang, Beijing Yanjing Hospital, Beijing 100037, China

Supported by the Major State Basic Research Development Program of China, No.G1998051205; the National Hi-Tech R & D Program of China, No.2001AA227091; the National Natural Science Foundation of China, No. 39990570 (Major Program) and No. 30171049 (General Program), and the National Science Fund for Distinguished Young Scholars (No.30225045)

Correspondence to: Dr. Xiao-Hang Zhao, National Lab. of Molecular Oncology, Cancer Institute and Hospital, Chinese Academy of Medical Sciences & Peking Union Medical College, Beijing P. O. Box 2258, Beijing 100021, China. zhaoxh@pubem.cicams.ac.cn

Telephone: +86-10-67709015 **Fax:** +86-10-67709015

Received: 2002-12-25 **Accepted:** 2003-01-05

Abstract

AIM: To investigate the alteration of the annexin I subcellular localization in esophageal squamous cell carcinoma (ESCC) and the correlation between the translocation and the tumorigenesis of ESCC.

METHODS: The protein localization of annexin I was detected in both human ESCC tissues and cell line via the indirect immunofluorescence strategy.

RESULTS: In the normal esophageal epithelia the annexin I was mainly located on the plasma membrane and formed a consecutive typical trammels net. Annexin I protein also expressed dispersively in cytoplasm and the nuclei without specific localization on the nuclear membrane. In esophageal cancer annexin I decreased very sharply with scattered disappearance on the cellular membrane, however it translocated and highly expressed on the nuclear membrane, which was never found in normal esophageal epithelia. In cultured esophageal cancer cell line annexin I protein was also focused on the nuclear membrane, which was consistent with the result from esophageal cancer tissues.

CONCLUSION: This observation suggests that the translocation of annexin I protein in ESCC may correlate with the tumorigenesis of the esophageal cancer.

Liu Y, Wang HX, Lu N, Mao YS, Liu F, Wang Y, Zhang HR, Wang K, Wu M, Zhao XH. Translocation of annexin I from cellular membrane to the nuclear membrane in human esophageal squamous cell carcinoma. *World J Gastroenterol* 2003; 9(4): 645-649

<http://www.wjgnet.com/1007-9327/9/645.htm>

INTRODUCTION

Annexin I is a member of annexins, an evolutionary conserved multigene family, which are calcium and phospholipid-binding proteins. Annexins consist of a conserved C-terminal domain that confers calcium-dependent phospholipid binding and a variable N-terminal domain that is responsible for the specific properties of each annexin I^[1,2]. As a steroid-regulated protein annexin I has been found to participate in the cell differentiation and anti-inflammatory effects^[3,4]. It is also a major substrate of EGF receptor, which related to endocytic trafficking and sorting of EGFR in multivesicular endosomes^[5]. The annexin I modulates the signal transduction through MAPK/ERK pathway and, specifically, inhibits the activities of phospholipase A2^[6,7]. Recent studies describe increased expression of annexin I in human hepatocellular carcinoma but it is absent in several types of carcinomas, such as human esophageal cancer and prostatic neoplasm^[8,9]. We have found that annexin I is clearly lost in ESCC, a kind of major diseases and the 4th killer of malignant tumors in China, and it seems that the annexin I protein plays an important role in the carcinogenesis.

It is well known that the protein subcellular localization is a very important way to better understand protein functions. The alteration of protein subcellular localizations and the membrane trafficking will facilitate the specific cellular functions as well as signal transduction. To detect the subcellular localizations of annexin I in both normal epithelia and ESCC mucosa will give us some clues to address the functions of annexin I in malignant tumors.

MATERIALS AND METHODS

Materials

Tissues specimens The esophageal specimens used for immunohistochemical (IHC) staining were obtained from patients who presented to the Cancer Hospital of Chinese Academy of Medical Sciences, Beijing, China and were diagnosed as esophageal squamous cell carcinoma without chemotherapy and radiotherapy by two senior pathologists. After surgical resections the specimens were fixed in 70 % ethanol or 40 mg·L⁻¹ neutral formalin and embedded in paraffin.

Cell line Human ESCC cell line, EC0156 was generated in our laboratory from an ESCC tissue.

Antibodies Commercial available antibodies included annexin I monoclonal antibody (Santa Cruz Biotechnology Inc., Santa Cruz, CA, USA), goat anti-mouse TRITC and goat anti-mouse FITC antibodies (Jackson ImmunoResearch Laboratories, Inc., West Grove, PA, USA). All other reagents were of analytical grade.

Methods

Cell cultures The human esophageal cancer cell line EC0156 was cultured in Dulbecco's modified Eagle's medium (DMEM) with 10 % fetal bovine serum and antibiotics (penicillin and streptomycin) at 37 °C in a humidified atmosphere with 5 % CO₂.

Indirect immunofluorescence staining^[10] For immunostaining, EC0156 cells were grown on glass-coverslips at 80 % confluence and fixed in 4 % paraformaldehyde in 100 mmol·L⁻¹

PBS (pH=7.4) for 15 min at room temperature. After three washes with the buffer (25 mmol·L⁻¹ HEPES, 1 mmol·L⁻¹ CaCl₂, 1 mmol·L⁻¹ MgCl₂ and 10 g·L⁻¹ BSA), the paraffin embedded tissue sections were deparaffinized and hydrated through xylenes and graded alcohol series, and then rinsed for 5 min in water. The fixed cells and deparaffinized tissue sections were incubated in blocking solution (0.1 % horse serum and 0.06 % Triton-X 100 in PBS) for 1 hour to decrease the non-specific binding of the antibodies and to improve the penetration of the antibodies through membranes. The blocking solution was also used for diluting the primary and secondary antibodies. After 1 hour, the blocking solution was changed for the primary antibody solution (anti-annexin I monoclonal antibody was diluted to 1:200 and PBS was used as negative control) and the cells were incubated at 4 °C overnight. After three washes, cells and tissues were incubated with the fluorescence-labeled secondary antibodies (1:300 diluted goat anti-mouse TRITC or the goat anti-mouse FITC) for 30 min at room temperature.

This was followed by a last washing step (3×5 min, in PBS), then the cells were rinsed with distilled water, air dried and mounted on glass slides using Cytoseal 60 mounting medium (Stephens Scientific). Cells were then analyzed and images were obtained with a fluorescence microscope (Olympus BX51, OLYMPUS OPTICAL CO., LTD., Japan).

RESULTS

Localization of annexin I in normal esophageal epithelia

Annexin I protein was mostly located on the cell membrane in a granular pattern and some of them on the nucleus and cytoplasm as well through immunofluorescence staining in the normal esophagus epithelia (Figure 1. d, e, f and g). Consecutively and symmetrically expressed annexin protein on the cellular membrane makes typical trammel net. Annexin I also expressed in the cytoplasm and nuclei dispersively without specific localization on the nuclear membrane.

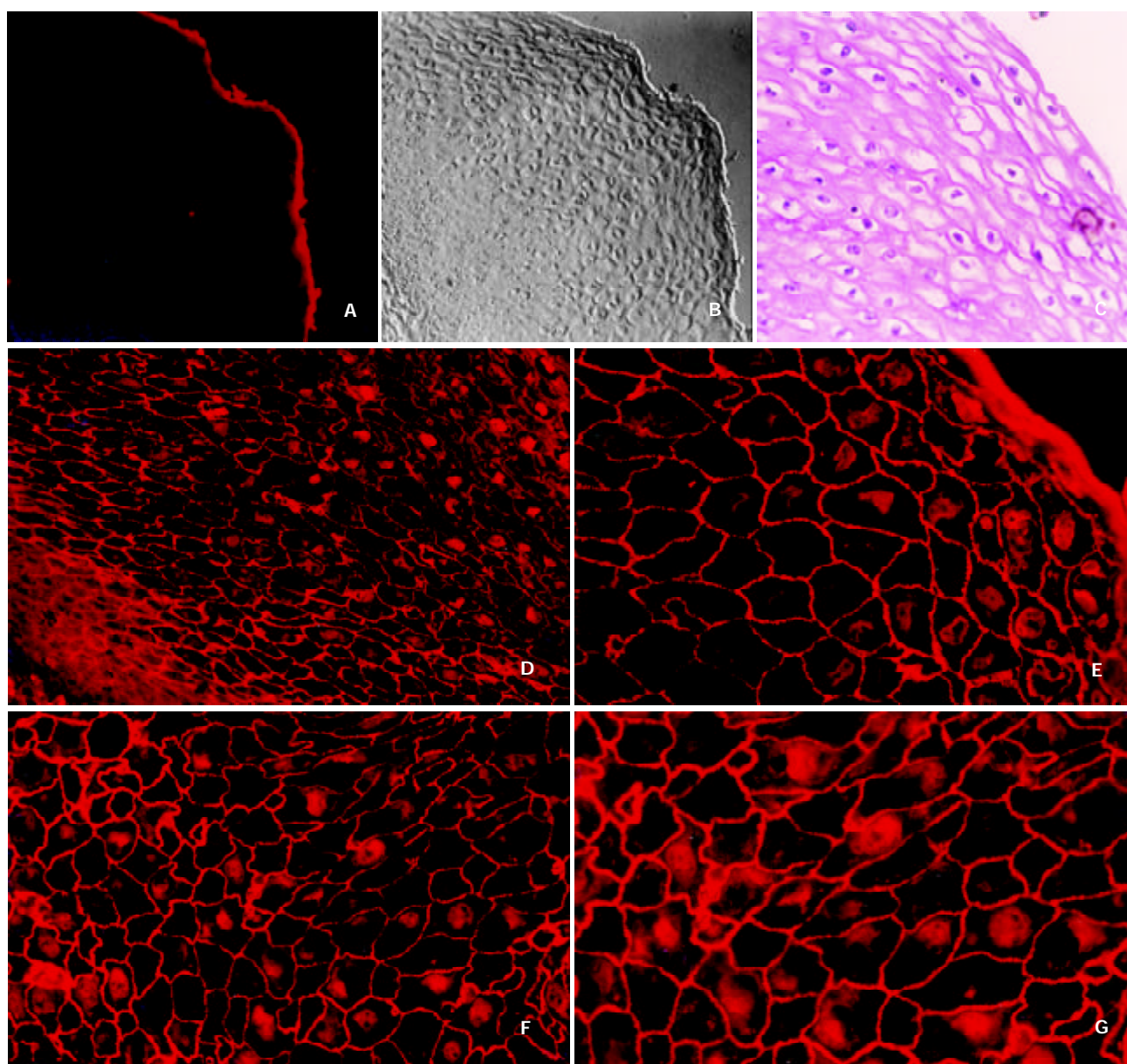


Figure 1 The localization of annexin I in normal esophageal epithelium. The normal esophageal epithelia on the paraffin-embedded tissues were detected with anti-annexin I monoclonal antibody and imaged with TRITC-conjugated goat anti-mouse antibody, and then observed under a fluorescence microscope (a, d, e, f and g). PBS was used as a negative control (a 50×), the tissue section was viewed under a Nomarski interference-contrast microscopy (b 50×) and the additional H & E staining was also performed (c 200×). The localization of annexin I protein in normal esophageal epithelium was shown from d to g (d 200×; e 400×; f 400× and g 400×). The orientation of the bottom left corner was the basal membrane of the esophageal mucosa.

Translocation of annexin I protein in ESCC

Figure 2 (c, d, e and f) showed clearly that the beautiful trammel net of annexin I protein on the esophageal epithelia had been broken and the holes of the net had been fused each other on the ESCC cellular membrane. The expression of annexin I on the cellular membrane decreased very sharply with unequal

distribution or scattered disappearance. In the meantime, we also found the nuclear membrane localization of annexin I protein had appeared and increased very obviously (shown by the yellow arrows), which has never been found in normal esophageal epithelia. However, the expression of annexin I in nuclear plasma had been decreased distinctly.

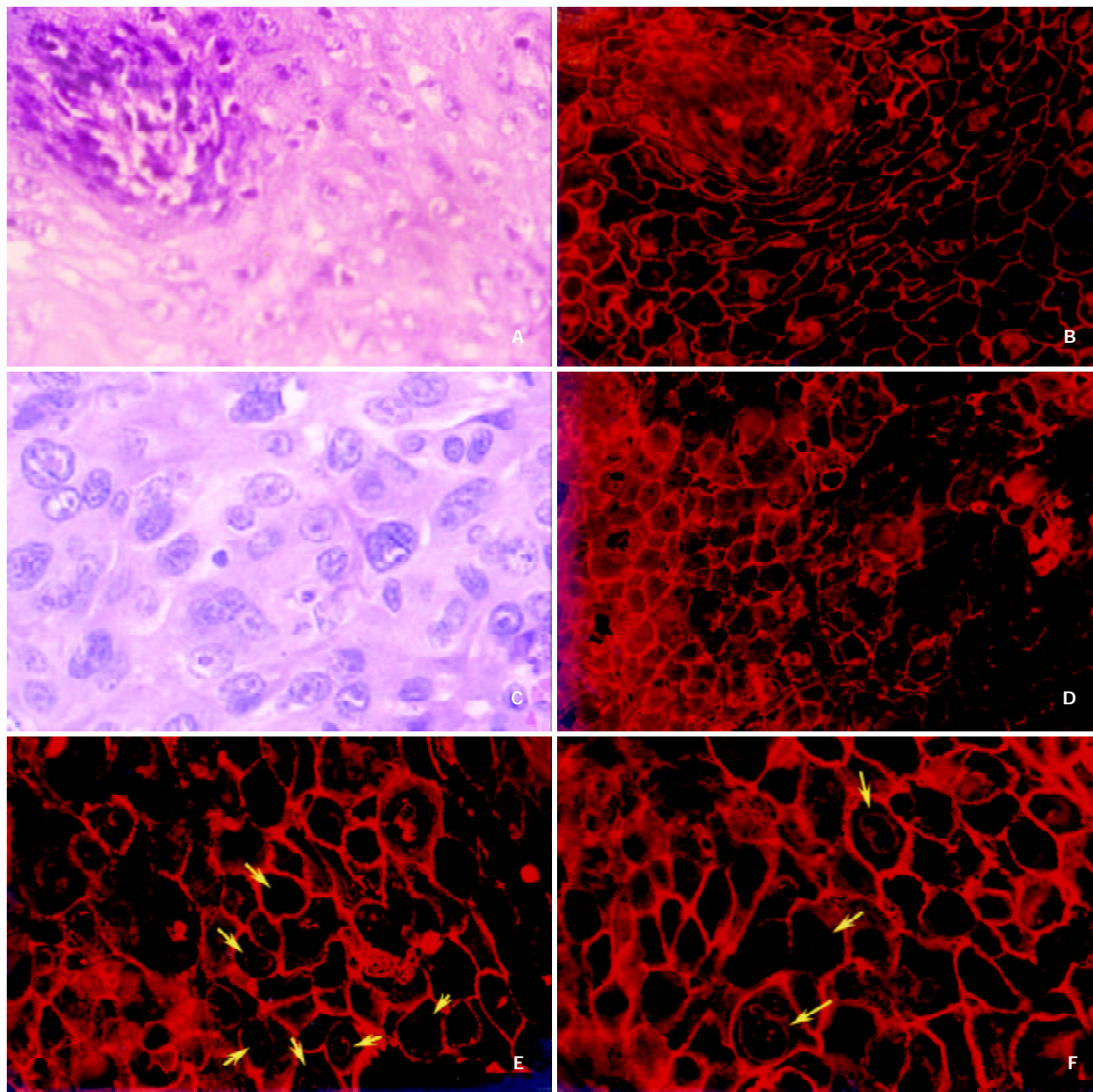


Figure 2 The translocation of annexin I protein in ESCC. Paraffin-embedded tissue sections of ESCC were detected with anti-annexin I antibody and annexin I protein was labeled by TRITC-conjugated secondary antibody. The fluorescence image was visualized under a fluorescence microscope (Olympus BX51, Japan). An H & E staining was performed (a 200 \times ; c 400 \times). A hyperplasia of esophageal epithelia were shown in Figure 2 (a and b, b 200 \times) and there were basal papillae displaying boundary area of the epithelium, which consecutively expressed annexin I formed the typical trammel net on the cellular membrane. Annexin I protein was decreased sharply and translocated from cellular membrane to the nuclear membrane (d 200 \times ; e 400 \times ; f 400 \times). The yellow arrows showed the nuclear membrane localization of annexin I in ESCC and all of the materials were from a same ESCC case.

Nuclear membrane localization of annexin I on ESCC cell line

In order to further confirm the localization of annexin I protein in ESCC, a human esophageal cancer cell line, EC0156 was used to inspect the distributions of annexin I by indirect immunofluorescence staining. Annexin I protein was distinctly

focused on the nuclear membrane (Figure 3, indicated by red arrows) of the EC0156 cells and it was consistent with what we saw in esophageal cancer tissues. On the cell line, annexin I proteins were also expressed on cytoplasm, cellular membrane and nuclear plasma as well.

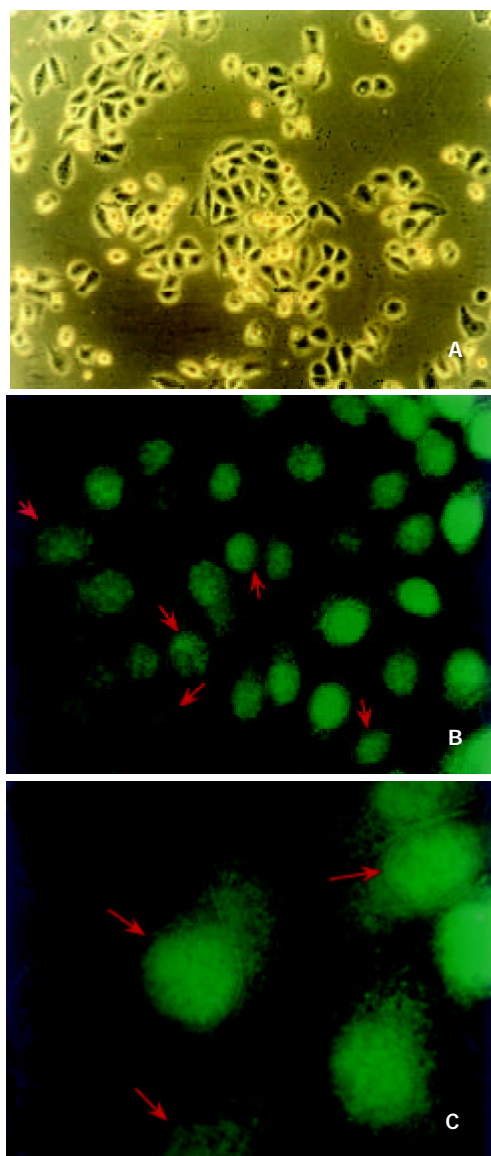


Figure 3 The localization of annexin I in ESCC cell line. EC0156 cells were grown on glass coverslips at 80 % confluence, detected with the anti-annexin I monoclonal antibody and visualized by FITC-conjugated secondary antibody under the fluorescence microscope. EC0156 cells were cultured in DMEM medium and photomicrographed under a phase-contrast microscope (a 100 \times). Annexin I was observed by fluorescence microscope (b 400 \times and c 1 000 \times). The red arrows showed that annexin I protein was also located on nuclear membranes in EC0156 cells.

DISCUSSION

Annexin I protein belongs to a family of calcium-dependent phospholipid-binding proteins whose functions are presumed to participate in various membrane related events including membrane fusion in exocytosis and endocytosis as well as membrane organization. Previously studies have reported that in human epidermis annexin I was stained in a granular pattern in the monolayer but in an envelope pattern in the stratified keratinocytes^[11]. The subcellular localization of annexins in rat was mainly found in the cytoplasm and nucleus of the mesangial cells^[12], and in cytoplasm of mast cells^[13]. By the localization of annexin I, II, VI and XIII in epithelial cells of intestinal, hepatic and pancreatic tissues of the rabbit, Massey-Harroche *et al*^[14] showed that the basolateral domain of polarized cells appears to be the main site where annexins are located, and annexins may therefore be involved in the

important cellular events occurring at this level. It suggests that the different localizations of annexin I contribute to its versatile functions.

Recently it has been found that annexin I is drastically down-regulated in esophageal cancer and assumed that it may play a key role in the tumorigenesis of ESCC^[8,15,16]. To gain the insight into the localization of annexin I, its relationship with the processing of esophageal cancer and the possible functions of this protein, we investigated the subcellular localization of annexin I in ESCC cell line, normal and cancer esophageal epithelia by indirect immunofluorescence strategy. It was found that annexin I was mainly located on the membrane of the normal esophageal epithelia in granular pattern and formed a typical trammel net between the esophageal epithelia. Annexin I also expressed dispersively in the nuclei and cytoplasm without specific localization on the nuclear membrane. However, on the cellular membrane of ESCC the beautiful trammel net of annexin I had been broken and the holes on the net had been fused together. The expression of annexin I on the cellular membrane and nuclear plasma decreased very sharply, and the protein distributed unequally with scattered disappearance. Meanwhile, the nuclear membrane localization of annexin I had been appeared and increased obviously, which was never been found in normal esophageal epithelia. Additionally the distribution of annexin I on the human esophageal cancer cell line, EC0156 was also distinctly focused on the nuclear membrane. This finding suggests that the translocation of the subcellular localization of annexin I may be correlated with the tumorigenesis of ESCC. An IHC analysis of annexin I in ductal epithelial cells of various human breast tissues indicated that this annexin was not demonstrable in both the ductal luminal cells of normal breast and benign tumors, but was generally expressed in various types of breast cancer. Therefore it is most likely involved in an early stage of human breast cancer development. Annexin I expression might also correlate with breast cancer progress^[17].

Annexin I appeared to be cleaved by neutrophil elastase at the N-terminal portion between Val-36 and Ser-37 to yield a 33 kDa protein. Cleavage of the N-terminal portion of annexin I was accompanied by a marked change in the annexin I isoelectric point (pI) value (from 6.0 to 8.5-9.0) and greatly diminished its functional activities. The findings demonstrate that annexin I degradation in epithelial lining fluid is closely related to lung inflammation^[18].

The mechanisms of annexin I localization are a complexity. A study showed calcium induced translocation of annexin I into subcellular organelles and secretory vesicles in human neutrophils, which suggested annexin I might contribute to the secretory process in neutrophils^[19]. Other studies also showed that dexamethasone and IL-6 could affect the localization of annexin I. In A549 human adenocarcinoma cell line dexamethasone could inhibit EGF-stimulated cytosolic PLA2 activation and arachidonic acid release. Annexin I participated in this regulated pathway. Dexamethasone induced annexin I phosphorylation and translocation mediated by glucocorticoids receptor, then brought about a competition between annexin I and Grb2 leading to a failure of recruitment of signaling factors to EGFR^[6]. In U937 cells dexamethasone also caused translocation of annexin I from the intracellular compartment to the cell membrane^[20]. Solito *et al* reported that induction of annexin I protein and its translocation to the cell membrane were stimulated by interleukin 6 and a unique 30 bp region of the annexin I promoter, which was critical for the responsiveness of the reporter gene to IL-6 and dexamethasone. IL-6 stimulation was mediated by a C/EBP beta-like transcriptional factor. Annexin I might participate in host defence system as a new acute class II phase protein^[21].

Another study showed that stresses, treatment of A549 and

Hela cells with heat, hydrogen peroxide or arsenate, resulted in the translocation of annexin I from cytoplasm to nucleus and perinuclear region. There were different intracellular distributions of annexins in macrophage-like cells in phagocytosis, and reactions to hydrogen peroxide and sodium arsenate^[22].

In summary, we have first detected the translocation of annexin I from cellular membrane to nuclear membrane in ESCC cells. It seems that the subcellular localizations of annexin I are closely related to its functions and the alterations are most likely involved in the tumorigenesis of ESCC, especially at the early stage. More investigations are doing to further clarify the mechanisms of annexin I subcellular-localization changes during tumorigenesis of human ESCC.

REFERENCES

- Kourie JI**, Wood HB. Biophysical and molecular properties of annexin-formed channels. *Prog Biophys Mol Biol* 2000; **73**: 91-134
- Rosengarth A**, Wintergalen A, Galla HJ, Hinz HJ, Gerke V. Ca²⁺-independent interaction of annexin I with phospholipid monolayers. *FEBS Lett* 1998; **438**: 279-284
- Solito E**, de Coupade C, Parente L, Flower RJ, Russo-Marie F. Human annexin I is highly expressed during the differentiation of the epithelial cell line A 549: involvement of nuclear factor interleukin 6 in phorbol ester induction of annexin I. *Cell Growth Differ* 1998; **9**: 327-336
- Perretti M**. Lipocortin 1 and chemokine modulation of granulocyte and monocyte accumulation in experimental inflammation. *Gen Pharmacol* 1998; **31**: 545-552
- Futter CE**, Felder S, Schlessinger J, Ullrich A, Hopkins CR. Annexin I is phosphorylated in the multivesicular body during the processing of the epidermal growth factor receptor. *J Cell Biol* 1993; **120**: 77-83
- Alldrige LC**, Harris HJ, Plevin R, Hannon R, Bryant CE. The annexin protein lipocortin 1 regulates the MAPK/ERK pathway. *J Biol Chem* 1999; **274**: 37620-37628
- Croxtall JD**, Choudhury Q, Newman S, Flower RJ. Lipocortin 1 and the control of cPLA2 activity in A549 cells. Glucocorticoids block EGF stimulation of cPLA2 phosphorylation. *Biochem Pharmacol* 1996; **52**: 351-356
- Paweletz CP**, Ornstein DK, Roth MJ, Bichsel VE, Gillespie JW, Calvert VS, Vocke CD, Hewitt SM, Duray PH, Herring J, Wang QH, Hu N, Linehan WM, Taylor PR, Liotta LA, Emmert-Buck MR, Petricoin EF 3rd. Loss of annexin I correlates with early onset of tumorigenesis in esophageal and prostate carcinoma. *Cancer Res* 2000; **60**: 6293-6297
- Masaki T**, Tokuda M, Ohnishi M, Watanabe S, Fujimura T, Miyamoto K, Itano T, Matsui H, Arima K, Shirai M, Maeba T, Sogawa K, Konishi R, Taniguchi K, Hatanaka Y, Hatase O, Nishioka M. Enhanced expression of the protein kinase substrate annexin in human hepatocellular carcinoma. *Hepatology* 1996; **24**: 72-81
- Zhao X**, Varnai P, Tuymetova G, Balla A, Toth ZE, Oker-Blom C, Roder J, Jeromin A, Balla T. Interaction of neuronal calcium sensor-1 (NCS-1) with phosphatidylinositol 4-kinase beta stimulates lipid kinase activity and affects membrane trafficking in COS-7 cells. *J Biol Chem* 2001; **276**: 40183-40189
- Ma AS**, Ozers LJ. Annexins I and II show differences in subcellular localization and differentiation-related changes in human epidermal keratinocytes. *Arch Dermatol Res* 1996; **288**: 596-603
- Vervoordeldonk MJ**, Schalkwijk CG, Vishwanath BS, Aarsman AJ, van den Bosch H. Levels and localization of group II phospholipase A2 and annexin I in interleukin- and dexamethasone-treated rat mesangial cells: evidence against annexin mediation of the dexamethasone-induced inhibition of group II phospholipases A2. *Biochim Biophys Acta*. 1994; **1224**: 541-550
- Oliani SM**, Christian HC, Manston J, Flower RJ, Perretti M. An immunocytochemical and *in situ* hybridization analysis of annexin 1 expression in rat mast cells: modulation by inflammation and dexamethasone. *Lab Invest* 2000; **80**: 1429-1438
- Massey-Harroche D**, Mayran N, Maroux S. Polarized localizations of annexins I, II, VI and XIII in epithelial cells of intestinal, hepatic and pancreatic tissues. *J Cell Sci* 1998; **111**: 3007-3015
- Zhou G**, Li H, DeCamp D, Chen S, Shu H, Gong Y, Flaig M, Gillespie JW, Hu N, Taylor PR, Emmert-Buck MR, Liotta LA, Petricoin EF 3rd, Zhao Y. 2D Differential in-gel electrophoresis for the identification of esophageal scans cell cancer-specific protein markers. *Mol Cell Proteomics* 2002; **1**: 117-124
- Emmert-Buck MR**, Gillespie JW, Paweletz CP, Ornstein DK, Basrur V, Appella E, Wang QH, Huang J, Hu N, Taylor P, Petricoin EF 3rd. An approach to proteomic analysis of human tumors. *Mol Carcinog* 2000; **27**: 158-165
- Ahn SH**, Sawada H, Ro JY, Nicolson GL. Differential expression of annexin I in human mammary ductal epithelial cells in normal and benign and malignant breast tissues. *Clin Exp Metastasis* 1997; **15**: 151-156
- Tsao FH**, Meyer KC, Chen X, Rosenthal NS, Hu J. Degradation of annexin I in bronchoalveolar lavage fluid from patients with cystic fibrosis. *Am J Respir Cell Mol Biol* 1998; **18**: 120-128
- Sjolin C**, Stendahl O, Dahlgren C. Calcium-induced translocation of annexins to subcellular organelles of human neutrophils. *Biochem J* 1994; **300**: 325-330
- Solito E**, Nuti S, Parente L. Dexamethasone-induced translocation of lipocortin (annexin) 1 to the cell membrane of U-937 cells. *Br J Pharmacol* 1994; **112**: 347-348
- Solito E**, de Coupade C, Parente L, Flower RJ, Russo-Marie F. IL-6 stimulates annexin 1 expression and translocation and suggests a new biological role as class II acute phase protein. *Cytokine* 1998; **10**: 514-521
- Rhee HJ**, Kim GY, Huh JW, Kim SW, Na DS. Annexin I is a stress protein induced by heat, oxidative stress and a sulfhydryl-reactive agent. *Eur J Biochem* 2000; **267**: 3220-3225

Edited by Zhang JZ

Loss of clusterin both in serum and tissue correlates with the tumorigenesis of esophageal squamous cell carcinoma via proteomics approaches

Li-Yong Zhang, Wan-Tao Ying, You-Sheng Mao, Hong-Zhi He, Yu Liu, Hui-Xin Wang, Fang Liu, Kun Wang, De-Chao Zhang, Ying Wang, Min Wu, Xiao-Hong Qian, Xiao-Hang Zhao

Li-Yong Zhang, Hong-Zhi He, Yu Liu, Hui-Xin Wang, Fang Liu, Ying Wang, Min Wu, Xiao-Hang Zhao, National Laboratory of Molecular Oncology, Cancer Institute and Hospital, Chinese Academy of Medical Sciences & Peking Union Medical College, Beijing 100021, Beijing, China

You-Sheng Mao, De-Chao Zhang, Department of Pectoral Surgery, Cancer Institute and Hospital, Chinese Academy of Medical Sciences & Peking Union Medical College, Beijing 100021, Beijing, China
Wan-Tao Ying, Xiao-Hong Qian, Department of Genomics and Proteomics, Beijing Institute of Radiation Medicine, Beijing 100850, China

Kun Wang, Beijing Yanjing Hospital, Beijing 100037, China
Supported by the Major State Basic Research Development Program of China, No.G19980512 and No.2001CB510201; the National Hi-Tech R & D Program of China, No.2001AA227091 and No.2001AA233061; National Natural Science Foundation of China, No.39990570, No.30171049, 30225045 and No.39990600

Correspondence to: Dr. Xiao-Hang Zhao, National Laboratory of Molecular Oncology, Cancer Institute and Hospital, Chinese Academy of Medical Sciences & Peking Union Medical College, Beijing 100021, Beijing, China. zhaoxh@pubem.cicams.ac.cn

Telephone: +86-10-67709015 **Fax:** +86-10-67709015
Dr. Xiao-Hong Qian, Department of Genomics and Proteomics, Beijing Institute of Radiation Medicine, Beijing 100850, China. qianxh@nic.bmi.ac.cn

Telephone: +86-10-68279585 **Fax:** +86-10-68279585

Received: 2002-11-26 **Accepted:** 2002-12-18

Abstract

AIM: To identify the differentially secreted proteins or polypeptides associated with tumorigenesis of esophageal squamous cell carcinoma (ESCC) from serum and to find potential tumor secreted biomarkers.

METHODS: Proteins from human ESCC tissue and its matched adjacent normal tissue; pre-surgery and post-surgery serum; and pre-surgery and normal control serum were separated by two-dimensional electrophoresis (2-DE) to identify differentially expressed proteins. The silver-stained 2-DE were scanned with digital ImageScanner and analyzed with ImageMaster 2D Elite 3.10 software. A cluster of protein spots differentially expressed were selected and identified with matrix-assisted laser desorption/ionization time-of-flight mass spectrometry (MALDI-TOF-MS). One of the differentially expressed proteins, clusterin, was down-regulated in cancer tissue and pre-surgery serum, but it was reversed in post-surgery serum. The results were confirmed by semi-quantitative reverse-transcription (RT)-PCR and western blot.

RESULTS: Comparisons of the protein spots identified on the 2-DE maps from human matched sera showed that some proteins were differentially expressed, with most of them showing no differences in composition, shape or density. Being analyzed by MALDI-TOF-MS and database searching, clusterin was differentially expressed and down-regulated

in both cancer tissue and pre-surgery serum compared with their counterparts. The results were also validated by RT-PCR and western blot.

CONCLUSION: The differentially expressed clusterin may play a key role during tumorigenesis of ESCC. The 2DE-MS based proteomic approach is one of the powerful tools for discovery of secreted markers from peripheral.

Zhang LY, Ying WT, Mao YS, He HZ, Liu Y, Wang HX, Liu F, Wang K, Zhang DC, Wang Y, Wu M, Qian XH, Zhao XH. Loss of clusterin both in serum and tissue correlates with the tumorigenesis of esophageal squamous cell carcinoma via proteomics approaches. *World J Gastroenterol* 2003; 9(4): 650-654
<http://www.wjgnet.com/1007-9327/9/650.htm>

INTRODUCTION

Esophageal squamous cell carcinoma (ESCC), the major histological form of esophageal cancer, is one of the most common malignant tumors in China especially in the north part of the country. Human ESCC carcinogenesis is a multistage process involving multifactorial etiology and genetic-environment interactions^[1-3]. Patients with ESCC have a poor prognosis, with 5-year survival rates of less than 10 %, because of the rapid spread and of the cancer associated malnutrition due to dysphagia and cachexia^[4]. The molecular mechanisms that underlie the tumor formation and progression are still not completely perspicuous, although several progresses based on alterations of gene expression^[5] and deregulated proteins, such as annexin I^[6] and tumor rejection antigen^[7] in esophageal cancer via proteomic approaches have been reported recently. Discovery of new markers to discriminate tumorigenic from normal cells, as well as the different stage is critical important for early detection and diagnosis of ESCC. The success of the Human Genome Project and the initiation of human proteome are strongly facilitating these efforts as tremendous information of genes and proteins are currently available^[8,9]. It would be possible to undertake comprehensive profiling of tumor at the proteomics level to identify protein alterations that are unpredictable at either the genomics or transcriptomics levels^[10]. However there is no comprehensive study of esophageal cancer protein profiling or protein expression patterns have been generated, especially the tumor-associated serum protein biomarkers. To identify specific protein tumor markers both in serum and tissue by proteomics approaches is a currently critical issue^[8,11,12].

Tumor associated proteins as well as post-translational modifications can be identified via proteomic methodologies. In the present study, we used the 2-DE/mass spectrometry (MS)-based proteomic analysis to profile the proteins in serum of ESCC patients. We analyzed 17 pairs of patient-matched pre- and post-surgery as well as normal and tumor sera from ESCC patients to discover the alterations of expression profiling. We first found the clusterin is loss in both serum and tissue of ESCC.

MATERIALS AND METHODS

Specimens and preparation

The esophageal specimens were from patients diagnosed with esophageal cancer by the pathologists in Cancer Hospital of Chinese Academy of Medical Sciences (CAMS) (Beijing, China). The study was approved by the Institutional Review Board of Cancer Institute of CAMS. The pre-surgery serum were obtained from the first physical examination after the patients presented to the hospital, ESCC tumor tissues were obtained immediately after surgical resection and the post-surgery serum were obtained from the matched patients during the day 8 to day 10 after surgery. Sera described in Table 1, were centrifuged at 3 000 g at 4 °C for 15 min. Both tissue and serum samples were snap-frozen in liquid nitrogen immediately and then stored at -80 °C. The tissues were homogenized in five volumes of lysis buffer [8M urea, 4 % CHAPS, 2 % Pharmalyte, pH 3-10, 10 mM DTT] and centrifuged at 12 000 g at 4 °C for 40 minutes. The supernatant was removed and protein concentration was determined using the Bradford assay.

Table 1 The matched sera for 2-DE

No. of matched-sera	Gender	Age	Histopathological diagnosis
M51Q-M51H	M	59	MDSCC
M88Q-M88H	F	56	MDSCC
M88Q-M88H	M	62	MDSCC
M92Q-M92H	M	65	MDSCC
M93Q-M93H	M	65	MDSCC
M141Q-Nor86	F	62	MDSCC
M149Q-Nor67	M	67	PDSCC
M151Q-Nor24	M	64	MDSCC
M156Q-Nor87	F	70	PDSCC
M160Q-Nor15	M	68	MDSCC
M162Q-Nor34	M	72	MDSCC
M168Q-Nor16	M	70	MDSCC
M180Q-Nor66	F	65	HDSCC
M180Q-Nor10	F	65	HDSCC
M181Q-Nor97	M	57	MDSCC
M192Q-Nor36	M	68	MDSCC
M193Q-Nor19	F	66	HDSCC

The abbreviations used are: Q, pre-surgery; H, post-surgery; Nor, age and gender matched normal serum; MDSCC, moderate differentiated squamous Cell Carcinoma; PDSCC, poorly differentiated squamous Cell Carcinoma; HDSCC, Highly Differentiated squamous Cell Carcinoma.

Reagents

Electrophoresis reagents including acrylamide solution (40 %), N, N-methylenebisacrylamide, N, N, N', N'-tetramethylethylenediamine, tris base, glycine, SDS, DTT, CHAPS, Immobiline Drystrips, IPG buffer, IPG cover fluid, LMW protein marker were from Amersham Pharmacia Biotechnology Inc. (Uppsala, Sweden); Iodoacetamide was from Acros (New Jersey, USA); Sequence grade Trypsin was from Washington Biochemical Corporation; Trifluoroacetic acid (TFA) was from Fluka (Switzerland); Trizol™ Reagent and Transcriptase SuperScript II™ were from Gibco BRL; PVDF membrane was from Bio-Rad; Taq DNA polymerase and dNTPs were from TaKaRa; All other reagents were of analytical grade.

Analytical 2-DE

All sera or cell lysates were quantitated by Bradford assay. 2-DE was performed by standard procedures as described^[8,12] using precast IPG strips (pH3-10 linear, 18 cm, Amersham Pharmacia Biotechnology Inc.) in the first dimension,

isoelectric focusing (IEF). Briefly, 180 µg proteins were diluted to a total volume of 350 µl with the buffer [8 M urea, 2 % CHAPS, 0.5 % IPG buffer 3-10, 20 mM DTT and a trace of bromophenol blue]. After loaded on IPG strips, IEF was carried out according to the following protocol: 6 hours of rehydration at 0 V; 6 hours at 30 V; 1 hour at 500 V; 1 hour at 1 000 V and 5 hours at 8 000 V. The current was limited to 50 µA per gel. After IEF separation, the strips were immediately equilibrated 2×15 min with equilibration solution [50 mM Tris-HCl, pH6.8, 6 M urea, 30 % glycerol and 2 % SDS]. 20 mM DTT was included in the first equilibration solution, and 2 % (w/v) iodoacetamide was added in the second equilibration step to alkylate thiols. SDS-polyacrylamide gel electrophoresis (PAGE) was performed using 1 mm thick, 13 % SDS-PAGE gels. The strips were held in place with 0.5 % agarose dissolved in SDS/Tris running buffer and electrophoresis was carried out at constant power (2.5 W/gel for 40 min and 15 W/gel for 6 hours) and temperature (20 °C) using Ettan Dalt II system (Amersham Pharmacia Biotechnology Inc.). Gels were stained with silver nitrate according to the instructions of the silver-staining kit (Amersham Pharmacia Biotechnology Inc.).

Gel scanning and image analysis

Silver stained 2-DE gels were scanned with ImageScanner and analyzed including spots detection, quantification and normalization with ImageMaster 2D Elite 3.10 (Amersham Pharmacia Biotechnology Inc.). Statistical analysis was performed using SPSS statistical software late.

In-gel protein digestion

Individual protein spot was excised from the gel by Ettan Spot Picker (Amersham Pharmacia Biotechnology Inc.), destained with the solution [15 mM potassium ferricyanide, 50 mM sodium thiosulfate] and washed till opaque and colorless with 25 mM ammonium bicarbonate/50 % acetonitrile. After dried with vacuum concentrator (SpeedVac Plus, USA) the gel was rehydrated with 3-10 µl trypsin solution (10 ng/µl) at 4 °C for 30 min and then incubated at 37 °C overnight. Tryptic peptides were eluted and dried on SpeedVac vacuum concentrator.

Protein identification by MALDI mass spectrometry

Digested peptides were dissolved with 0.5 % TFA, with saturated CHCA solution in 0.1 % TFA/50 % acetic acid as matrix and analyzed by M@LDI R (Micromass, Manchester, UK). Spectrum acquisition was externally calibrated with lock mass 2465.199 Da and internally calibrated with autodigested peaks of trypsin (MH⁺: 2211.105 Da). The protein identification was performed by searching protein databases of Swiss-prot/trEMBL (<http://www.expasy.ch/tools/peptide.html>) and Mascot (<http://www.matrixscience.com/>). The error for peptide mass was set as 50 ppm and possible missed cleavage of trypsin was set as 1. The proteins with more than 4 matched peptides were thought significant.

RT-PCR

Total RNAs were isolated from esophageal cancer tissues using TRIzol reagent (Gibco BRL) according to the manufactures' instructions. First strand cDNA was reversely transcribed from 5 µg total RNAs using SuperScript II kit (Life Technologies) at 42 °C for 50 min. Clusterin was amplified by the primers (left: 5' ACCTCACGCAAGGCGAAGAC3', right: 5' TCTCACTCCTCCCGGTGCTT3') and a product with 232bp was generated.

Western blot

Total cells or tissues were lysated with the buffer [1 % SDS, 10 Mm Tris-Cl, pH 7.6, 20 µg/ml aprotinin, 20 µg/ml leupeptin

and 1 mM AEBSF]. The protein concentrations were determined using Bradford method. Five micrograms of protein were separated on 12 % of SDS-PAGE gels and transferred to PVDF membranes. After blocked with 10 % non-fat milk, the membranes were incubated with anti-clusterin monoclonal antibody (Santa Cruz Biotechnology Inc.) (1:1 000 dilution) at 4 °C overnight. After washing for three times the membranes were incubated with rabbit anti-mouse IgG at room temperature for 1 hour. The signals were developed with the ECL kit (Amersham Pharmacia Biotechnology Inc.) and using anti- α -tubulin antibody (Santa Cruz Biotechnology Inc.) as an internal control.

RESULTS

Clusterin was identified down-regulated in pre-surgery serum

A proteomic approach was used to determine the differentiated proteins profiling between the pre-surgery and post-surgery sera of ESCC. The proteins from five pairs of matched sera from pre- and post-surgery of ESCC patients were separated by 2DE. Figure 1 illustrates the proteomic profilings of the pre- and post-surgery sera from same individual and more than 600 proteins and polypeptides were detected on each gel. The matched rate of the five pairs gel was more than 87.2 % and the spots localized in pI 3-10 with the molecular mass range around 20-200 kDa. All the identified spots can be considered as abundant proteins since they are detectable with Coomassie Blue staining on the preparative 2-DE gel. After computer analysis for spots detection, background subtraction and volume normalization, we were able to identify 20 spots (corresponding to 5 different proteins) from the tryptic digestion via MALDI-TOF-MS analysis. The isoforms of clusterin were identified from 8 spots as multi-peptides components, which were dramatically down-regulated in tumor sera (Figure 2 A and Figure 3).

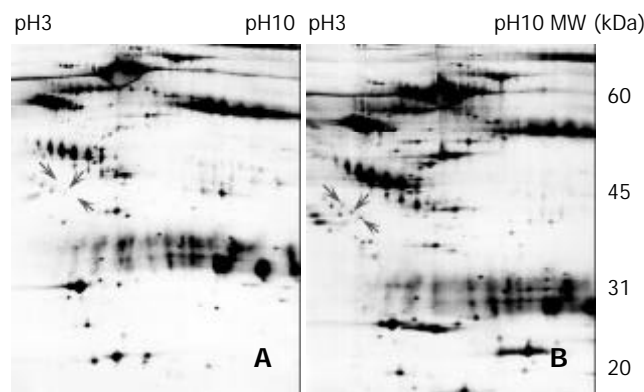


Figure 1 2-DE profiles of the pre- and post-surgery matched esophageal cancer sera from a same individual. One hundred and eighty microgram of protein was separated by 2-DE (IEF at pH 3-10, 13 % of SDS-PAGE) and stained by silver staining. LMW markers were from Amersham Pharmacia. (A) pre-surgery serum, (B) matched post-surgery serum.

Proteomic determination of esophageal cancer serum

We asked the question whether the loss of clusterin was induced by surgical attacks? In order to get rid of the interferences of the human immunoresponse after routine surgery, we additionally selected and matched 12 pairs of pre-surgery sera with the healthy sera from the same age and gender individuals who had no any surgical attacks and infections recently. We ran 2-DE profiling again between the two groups. Comparison with the healthy reference sera, clusterin proteins were also identified as more than four times lower in esophageal cancer serum after statistical analysis (Figure 2B).

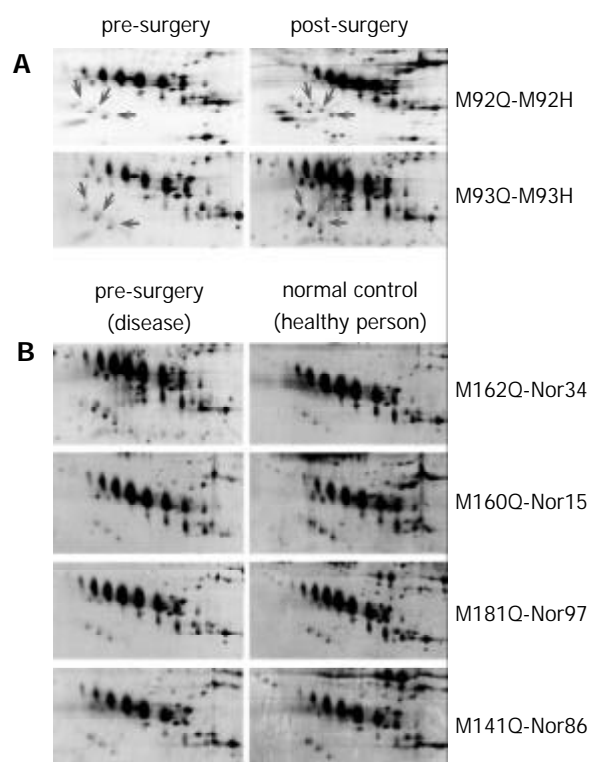


Figure 2 Representative regions of 2-DE patterns of more matched esophageal cancer sera. One hundred and eighty microgram of protein was separated by 2-DE (IEF at pH 3-10, SDS-PAGE 13 %) and stained by silver staining. LMW markers were from Amersham Pharmacia. (A) pre-surgery sera vs post-surgery sera, (B) pre-surgery sera vs normal control sera.

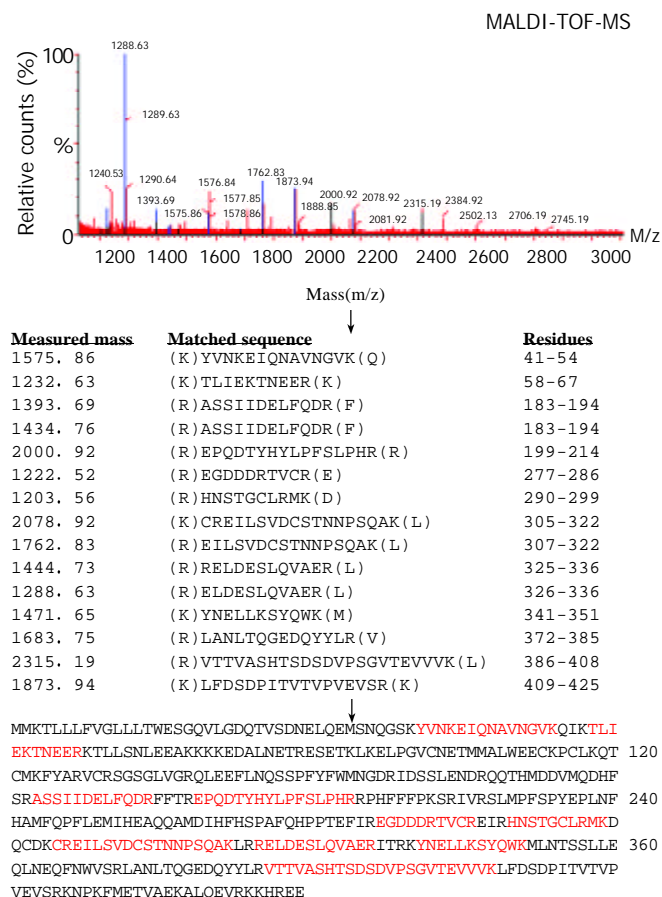


Figure 3 The spectra of MALDI-TOF-MS obtained from one of the differentiated polypeptide spots matched with the tryptic peptide sequences of clusterin (characters in red).

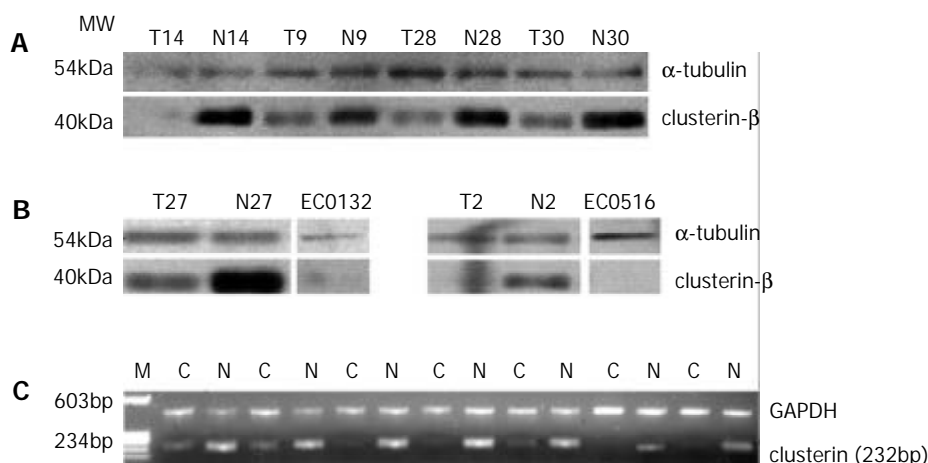


Figure 4 (A) Western blot analysis of clusterin proteins expressed in patient-matched normal and tumor epithelium; (B) Western blot analysis of clusterin proteins expressed in two kinds of esophageal squamous cell carcinoma, EC0132 and EC0516. Alpha-tubulin was used as a loading control. (C) Expression analysis of clusterin in patient-matched esophageal cancer tissues by semi-quantitative RT-PCR. GAPDH was used as an internal control.

Loss of clusterin in tumor epithelium

Immunoblot analysis of clusterin expressed in patient-matched normal and tumor epithelium from different ESCC individuals, whose sera had been found with low level of clusterin was performed. Using a commercially available antibody, clusterin has also been found down-regulated at different ESCC tissues (20/24), but absent in two kinds of cell lines of esophageal squamous cell carcinoma, EC1 and EC2 (Figure 4A, B). At the transcriptional level, clusterin was also found lower-expressed in 88 % of esophageal cancer tissues (22/25) by semi-quantitative RT-PCR (Figure 4C). The findings of tumor tissue and cell lines were consistent with the findings of ESCC serum.

DISCUSSION

To identify the differentially secreted proteins or polypeptides associated with tumorigenesis of esophageal squamous cell carcinoma, we carried out differentially proteomic analysis of human serum in two groups. First we compared the pre- and post-surgery sera of ESCC patient to identify the differentiated proteins from the same individuals. Second, the sera from the disease (pre-surgery) and age- and gender-matched healthy populations (normal control) had been analyzed through 2DE-MS strategy. There were 3 protein spots quantitatively changed between the two groups and were identified as clusterin, which was completely loss or dramatically down-regulated in pre-surgery serum of esophageal cancer compared with the post-surgery and the healthy controls. In addition, clusterin was also lost or decreased in tumor cell lines and tissues. Clusterin has never been known to be associated with esophageal cancer. This study reports identified clusterin as a candidate protein of a tumor-associated serum marker in esophageal squamous cell carcinoma via proteomic approaches for the first time.

Clusterin, so-called the testosterone-repressed prostate message-2^[13], sulfated glycoprotein 2, complement-associated protein SP-40, complement cytolysis inhibitor, a 80 kDa heterodimeric highly conserved secreted glycoprotein expressed in a wide variety of tissues and was found in all human fluids. It responses to a number of diverse stimuli, including hormone ablation and has been attributed functions in several diverse physiological processes such as sperm maturation, lipid transportation, complement inhibition, tissue remodeling, membrane recycling, cell adhesion and cell-substratum interactions, stabilization of stressed proteins in a folding-competent state and promotion or inhibition of apoptosis^[14-16].

Clusterin gene is differentially regulated by cytokines, growth factors and stress- inducing agents, while another defining prominent and intriguing clusterin feature is its upregulation in many severe physiological disturbances states and in several neurodegenerative conditions mostly related to advanced aging^[17-22]. Active cell death (ACD) in hormone-dependent tissues such as the prostate and mammary gland is readily induced by hormone ablation and by treatment with anti-androgens or anti-estrogens, calcium channel agonists and TGF beta^[23]. Clusterin has been found up-regulated in several cases of *in vivo* cancer progression and tumor formation such as human prostate carcinomas^[18,24], renal cell carcinoma (RCC)^[25,26], breast carcinoma^[17], ovarian cancer^[22], glioblastoma, testicular tumor cells, the normal and cancerous endometrium, hemangioma^[21], anaplastic large-cell lymphomas^[20], transitional cell carcinoma (TCC) of the bladder^[27], as well as hepatoma cells. Clusterin, on the other hand, is a membrane-stabilizing protein that appears to be involved in limiting the autophagic lysis of epithelial cells during apoptosis. Recent studies have shown the clusterin expression mediates antiapoptotic activity against a wide variety of stimuli^[28] and using antisense oligonucleotides of clusterin, also could enhance androgen sensitivity and chemosensitivity in prostate cancer therapy^[29]. On the other hand, it has recently been shown that decreased synthesis and delayed processing of clusterin in testicular germ cell tumors, colorectal cancer^[16,30] and human polycystic kidneys cells^[31,32]. However, there is no definitive biochemical evidence to support a specific function for clusterin except for its role in the modulation of the immune system and the functional roles of clusterin are still enigmatic.

A robust antigen capture assay for the measurement of serum clusterin concentrations has been developed and validated for increased clusterin expression, and alterations in serum clusterin levels associated with a number of disease states^[33]. Whether the decrease of clusterin in pre-surgery serum is a predictor of ESCC progression and prognosis, still need more efforts to address and the molecular mechanisms of clusterin implicated in tumorigenesis needs to be elucidated.

REFERENCES

- 1 **Zhang WH**, Bailey-Wilson JE, Li WD, Wang XQ, Zhang CL, Mao XZ, Liu ZH, Zhou CN, Wu M. Segregation analysis of esophageal cancer in a moderately high-incidence area of norther China. *Am J Hum Genet* 2000; **67**: 110-119
- 2 **Wang DX**, Li W. Advances on pathogenesis of esophageal cancer. *Shijie Huaren Xiaohua Zazhi* 2000; **8**: 1029-1030

- 3 **Hu SP**, Yang HS, Shen ZY. Study on etiology of esophageal carcinoma: retrospect and prospect. *Zhongguo Aizheng Zazhi* 2001; **11**: 171-174
- 4 **Oka M**, Yamamoto K, Takahashi M, Hakozaki M, Abe T, Iizuka N, Hazama S, Hirazawa K, Hayashi H, Tangoku A, Hirose K, Ishihara T, Suzuki T. Relationship between serum levels of interleukin 6, various disease parameters and malnutrition in patients with esophageal squamous cell carcinoma. *Cancer Res* 1996; **56**: 2776-2780
- 5 **Lu J**, Liu Z, Xiong M, Wang Q, Wang X, Yang G, Zhao L, Qiu Z, Zhou C, Wu M. Gene expression profile changes in initiation and progression of squamous cell carcinoma of esophagus. *Int J Cancer* 2001; **91**: 288-294
- 6 **Paweletz CP**, Ornstein DK, Roth MJ, Bichsel VE, Gillespie JW, Calvert VS, Vocke CD, Hewitt SM, Duray PH, Herring J, Wang QH, Hu N, Linehan WM, Taylor PR, Liotta LA, Emmert-Buck MR, Petricoin EF 3rd. Loss of annexin I correlates with early onset of tumorigenesis in esophageal and prostate carcinoma. *Cancer Res* 2000; **60**: 6293-6297
- 7 **Zhou G**, Li H, DeCamp D, Chen S, Shu H, Gong Y, Flaig M, Gillespie JW, Hu N, Taylor PR, Emmert-Buck MR, Liotta LA, Petricoin EF 3rd, Zhao Y. 2D differential in-gel electrophoresis for the identification of esophageal scans cell cancer-specific protein markers. *Mol Cell Proteomics* 2002; **1**: 117-124
- 8 **Xiong XD**, Xu LY, Shen ZY, Cai WJ, Luo JM, Han YL, Li EM. Identification of differentially expressed proteins between human esophageal immortalized and carcinomatous cell lines by two-dimensional electrophoresis and MALDI-TOF-mass spectrometry. *World J Gastroenterol* 2002; **8**: 777-781
- 9 **Li F**, Guan YJ, Chen ZC. Proteomics in cancer research. *Shengwu Huaxue Yu Shengwu Wuli Jinzhan* 2001; **28**: 164-167
- 10 **Wang H**, Hanash SM. Contributions of proteome profiling to the molecular analysis of cancer. *Technology in Cancer Research & Treatment* 2002; **1**: 1-8
- 11 **Vercoutter-Edouart AS**, Lemoine J, Louis H, Boilly B, Nurcombe V, Revillion F, Peyrat JP, Hondermarck H. Proteomic analysis reveals that 14-3-3 sigma is down-regulated in human breast cancer cells. *Cancer Res* 2001; **61**: 76-80
- 12 **Zhan XQ**, Chen ZC, Guan YJ, Li C, He CM, Liang SP, Xie JY, Chen P. Analysis of human lung squamous carcinoma cell line NCI-H520 proteome by two-dimensional electrophoresis and MALDI-TOF-mass spectrometry. *Ai Zheng* 2001; **20**: 575-582
- 13 **Parczyk K**, Pilarsky C, Rachel U, Koch-Brandt C. Gp80 (clusterin; TRPM-2) mRNA level is enhanced in human renal clear cell carcinomas. *J Cancer Res Clin Oncol* 1994; **120**: 186-188
- 14 **Trougakos IP**, Gonos ES. Clusterin/Apolipoprotein J in human aging and cancer. *Int J Biochem Cell Biol* 2002; **34**: 1430-1448
- 15 **Jones SE**, Jomary C. Clusterin. *Int J Biochem Cell Biol* 2002; **34**: 427-431
- 16 **Yang CR**, Leskov K, Hosley-Eberlein K, Criswell T, Pink JJ, Kinsella TJ, Boothman DA. Nuclear clusterin/XIP8, an x-ray-induced Ku70-binding protein that signals cell death. *Proc Natl Acad Sci USA* 2000; **97**: 5907-5912
- 17 **Redondo M**, Villar E, Torres-Munoz J, Tellez T, Morell M, Petito CK. Overexpression of clusterin in human breast carcinoma. *Am J Pathol* 2000; **157**: 393-399
- 18 **Behrens P**, Jeske W, Wernert N, Wellmann A. Downregulation of clusterin expression in testicular germ cell tumours. *Pathobiology* 2001; **69**: 19-23
- 19 **Tobe T**, Minoshima S, Yamase S, Choi NH, Tomita M, Shimizu N. Assignment of a human serum glycoprotein SP-40, 40 gene (CLI) to chromosome 8. *Cytogenet Cell Genet* 1991; **57**: 193-195
- 20 **Wellmann A**, Thieblemont C, Pittaluga S, Sakai A, Jaffe ES, Siebert P, Raffeld M. Detection of differentially expressed genes in lymphomas using cDNA arrays: identification of as a new diagnostic marker for anaplastic large-cell lymphomas. *Blood* 2000; **91**: 398-404
- 21 **Hasan Q**, Ruger BM, Tan ST, Gush J, Davis PF. Clusterin/apo J expression during the development of hemangioma. *Hum Pathol* 2000; **31**: 691-697
- 22 **Hough CD**, Cho KR, Zonderman AB, Schwartz DR, Morin PJ. Coordinately up-regulated genes in ovarian cancer. *Cancer Res* 2001; **61**: 3869-3876
- 23 **Tenniswood MP**, Guenette RS, Lakins J, Mooibroek M, Wong P, Welsh JE. Active cell death in hormone-dependent tissues. *Cancer Metastasis Rev* 1992; **11**: 197-220
- 24 **Kadomatsu K**, Anzano MA, Slayter MV, Winokur TS, Smith JM, Sporn MB. Expression of sulfated glycoprotein 2 is associated with carcinogenesis induced by N-nitroso-N-methylurea in rat prostate and seminal vesicle. *Cancer Res* 1993; **53**: 1480-1483
- 25 **Miyake H**, Gleave ME, Arakawa S, Kamidono S, Hara I. Introducing the clusterin gene into human renal cell carcinoma cells enhances their metastatic potential. *J Urol* 2002; **167**: 2203-2208
- 26 **Hara I**, Miyake H, Gleave ME, Kamidono S. Introduction of clusterin gene into human renal cell carcinoma cells enhances their resistance to cytotoxic chemotherapy through inhibition of apoptosis both *in vitro* and *in vivo*. *Jpn J Cancer Res* 2001; **92**: 1220-1224
- 27 **Welsh J**. Induction of apoptosis in breast cancer cells in response to vitamin D and antiestrogens. *Biochem Cell Biol* 1994; **72**: 537-545
- 28 **Viard I**, Wehrli P, Jornot L, Bullani R, Vechietti JL, Schifferli JA, Tschopp J, French LE. Clusterin gene expression mediates resistance to apoptotic cell death induced by heat shock and oxidative stress. *J Invest Dermatol* 1999; **112**: 290-296
- 29 **Zellweger T**, Miyake H, Cooper S, Chi K, Conklin BS, Monia BP, Gleave ME. Antitumor activity of antisense clusterin oligonucleotides is improved *in vitro* and *in vivo* by incorporation of 2'-O-(2-methoxy)ethyl chemistry. *J Pharmacol Exp Ther* 2001; **298**: 934-940
- 30 **Yamori T**, Kimura H, Stewart K, Ota DM, Cleary KR, Irimura T. Differential production of high molecular weight sulfated glycoproteins in normal colonic mucosa, primary colon carcinoma and metastasis. *Cancer Res* 1987; **47**: 2741-2747
- 31 **Longo VD**, Viola KL, Klein WL, Finch CE. Reversible inactivation of superoxide-sensitive aconitase in Abeta1-42- treated neuronal cell lines. *J Neurochem* 2000; **75**: 1977-1985
- 32 **Zellweger T**, Chi K, Miyake H, Adomat H, Kiyama S, Skov K, Gleave ME. Enhanced radiation sensitivity in prostate cancer by inhibition of the cell survival protein clusterin. *Clin Cancer Res* 2002; **8**: 3276-3284
- 33 **Morrissey C**, Lakins J, Moquin A, Hussain M, Tenniswood M. An antigen capture assay for the measurement of serum clusterin concentrations. *J Biochem Biophys Methods* 2001; **48**: 13-21

Mutation and methylation of hMLH1 in gastric carcinomas with microsatellite instability

Dian-Chun Fang, Rong-Quan Wang, Shi-Ming Yang, Jian-Ming Yang, Hai-Feng Liu, Gui-Yong Peng, Tian-Li Xiao, Yuan-Hui Luo

Dian-Chun Fang, Rong-Quan Wang, Shi-Ming Yang, Jian-Ming Yang, Hai-Feng Liu, Gui-Yong Peng, Tian-Li Xiao, Yuan-Hui Luo, Department of Gastroenterology, Southwest Hospital, Third Military Medical University, Chongqing, 400038, China
Supported by the National Natural Science Foundation of China, No. 30070043, and "10.5" Scientific Research Foundation of Chinese PLA, No. 01Z075

Correspondence to: Dian-Chun Fang, M.D., Ph.D. Southwest Hospital, Third Military Medical University, Chongqing 400038, China. fangdianchun@hotmail.com

Telephone: +86-23-68754624 **Fax:** +86-23-68754124

Received: 2002-10-09 **Accepted:** 2002-11-14

Abstract

AIM: To appraise the correlation of mutation and methylation of hMSH1 with microsatellite instability (MSI) in gastric cancers.

METHODS: Mutation of hMLH1 was detected by Two-dimensional electrophoresis (Two-D) and DNA sequencing; Methylation of hMLH1 promoter was measured with methylation-specific PCR; MSI was analyzed by PCR-based methods.

RESULTS: Sixty-eight cases of sporadic gastric carcinoma were studied for mutation and methylation of hMLH1 promoter and MSI. Three mutations were found, two of them were caused by a single bp substitution and one was caused by a 2 bp substitution, which displayed similar Two-D band pattern. Methylation of hMLH1 promoter was detected in 11(16.2 %) gastric cancer. By using five MSI markers, MSI in at least one locus was detected in 17/68(25 %) of the tumors analyzed. Three hMLH1 mutations were all detected in MSI-H (≥ 2 loci, $n=8$), but no mutation was found in MSI-L (only one locus, $n=9$) or MSS (tumor lacking MSI or stable, $n=51$). Methylation frequency of hMLH1 in MSI-H (87.5 %, 7/8) was significantly higher than that in MSI-L (11.1 %, 1/9) or MSS (5.9 %, 3/51) ($P<0.01-0.001$), but no difference was found between MSI-L and MSS ($P>0.05$).

CONCLUSION: Both mutation and methylation of hMLH1 are involved in the MSI pathway but not related to the LOH pathway in gastric carcinogenesis.

Fang DC, Wang RQ, Yang SM, Yang JM, Liu HF, Peng GY, Xiao TL, Luo YH. Mutation and methylation of hMLH1 in gastric carcinomas with microsatellite instability. *World J Gastroenterol* 2003; 9(4): 655-659

<http://www.wjgnet.com/1007-9327/9/655.htm>

INTRODUCTION

Our previous studies indicated that genetic instability may play an important role in gastric carcinogenesis^[1]. There are at least two distinct genetic instabilities in gastric tumorigenesis: one is the chromosomal instability (or suppressor pathway) and the other is microsatellite instability (or MSI pathway). In the

former, perhaps including tumors with low-frequency MSI (MSI-L) as well as microsatellite stable (MSS), accumulation of loss of tumor suppressor genes such as p53, Rb, APC, MCC and DCC play an important role in their carcinogenesis; whereas in the latter, consisting of a small subset of gastric cancer with high-frequency MSI (MSI-H), defective repair of mismatched bases results in an increased mutation rate at the nucleotide level, and the consequent widespread MSI^[2-4].

Mismatch repair is required for the cell to accurately copy its genome during cellular proliferation. Deficiencies of this system result in mutation rates 100-fold greater than those observed in normal cells^[5]. MSI is a hallmark of mismatch repair gene (MMR)-deficient cancers. MSI in tumors from patients with hereditary non-polyposis colorectal cancer (HNPCC) is caused by germline mutations in MMR genes, principally hMSH2 and hMLH1^[6-10]. In contrast, somatic mutations in MMR genes are relatively rare in sporadic MSI+ colon cancers^[9,11]. Rather, the majority of negative mutation, MSI+ cases involve hypermethylation of the hMLH1 promoter and subsequent lack of expression of hMLH1^[12-16]. The details of the mechanisms of this epigenetic gene silencing remain to be elucidated in gastric cancer. The aim of this study was to define the mutation and methylation of hMLH1 in gastric carcinomas with MSI.

MATERIALS AND METHODS

Tissue samples

Sixty-eight cancer and corresponding normal tissues were obtained from surgically resected gastric carcinoma in our hospital. Each specimen was frozen immediately and stored at -80°C until analyzed. A 5 μm section was cut from each tissue and stained with hematoxylin/eosin in order to ascertain whether the cancer cells in the tissues were predominant or not. Genomic DNA was isolated by standard proteinase-K digestion and phenol-chloroform extraction protocols. Of the 68 patients with gastric cancer, 45 were men and 23 were women with an age range of 30-76 years (a mean of 56.2 years at diagnosis). None of the patients included in the present series had a family history suggestive of HNPCC or had received chemotherapy or radiation therapy.

hMLH1 mutation analysis

PCR and heteroduplexing Primer pairs for long-chain and short-chain PCR and GC-clamped primers used were shown in Table 1^[17]. PCR reactions were carried out in 50 μl reactions in thin-walled tubes in a Perkin-Elmer 2 400 thermocycler. A total of 200-400 ng of genomic DNA, varying concentrations of each primer, and the LA PCR kit (TaKaRa, Otsu, Shiga, Japan) were used for long PCR. Final concentrations of each LA PCR primer pair were as follows: hMLH1-4F and hMLH1-4R, 0.16 μM each; hMLH5-10F and hMLH5-10R, 0.125 μM each; hMLH11-13F and hMLH11-13R, 0.094 μM each; and hMLH14-19F and hMLH14-19R, 0.125 μM each. The reactions were carried out according to the manufacturer's instructions. In brief, the conditions were as follows: a hot start of 94°C for 2 min, with the addition of Taq Pol in between,

followed by eight cycles of 98 °C×20 sec, 69 °C×1 min (with decrements of 0.5 °C/cycle), and 68 °C×12 min; six cycles of 96 °C×20 sec, and 68 °C×12 min; 16 cycles of 96 °C×20 sec, and 68 °C×12 min (with increments of 15 sec/cycle), and finally a chain extension of 72 °C for 10 min.

Table 1 Primer information for long and short PCR for HMLH1

A. Primer pairs for long-distance PCR

Exons 1-4

MLH1-4F GCG.GCT.AAG.CTA.CAG.CTG.AAG.GAA.GAA.CGT.GA^a
MLH1-4R GGC.GAG.ACA.GGA.TTA.CTC.TGA.GAC.CTA.GGC.CC

Product size=10.8kb

Exons5-10

MLH5-10F GCG.CCC.CTT.GGG.ATT.AGT.ATC.TAT.CTC.TCT.ACT.GG
MLH5-10R GCG.CTC.ATC.TCT.TTC.AAA.GAG.GAG.AGC.CTG

Product size=10.5kb

Exons11-13

MLH11-13F CGG.CTT.TTT.CTC.CCC.CTC.CCA.CTA.TCT.AAG.G
MLH11-13R GGG.TTA.GTA.AAG.GAA.GAG.GAG.CTT.GCC.C

Product size=8.7kb

Exons14-19

MLH14-19F GGT.GCT.TTG.GTC.AAT.GAA.GTG.GGG.TTG.GTA.G
MLH14-19R GCG.CGC.GTA.TGT.TGG.TAC.ACT.TTG.TAT.ATC.ACA.C

Product size=10.5kb

B. Primer pairs for short PCR

Exon	Clamp ^b	Product size	T _m ^c	Primer sequence
1	5 40	258	64.13	GCA.CTT.CCG.TTG.AGC.ATC CCG.TTA.AGT.CGT.AGC.CCT
2	40	187	38.14	ATA.AAT.TAT.TTT.CTG.TTT CAT.CCT.GCT.ACT.TTG.AGG
3	40 2	237	32.22	GGA.AAA.TGA.GTA.ACA.TGA TGT.CAT.CAC.AGG.AGG.ATA
4	2 40	218	36.26	ACC.CAG.CAG.TGA.GTT.TT GCC.CAA.AAT.ACA.TTT.CAG
5	40	170	30.19	ATA.TTA.ATT.TGT.TAT.ATT CAA.TTT.ACT.CTC.CCA.TGT
6	40	228	35.58	TTT.CAA.GTA.CTT.CTA.TGA ACT.TTG.TAG.ACA.AAT.CTC
7	40	194	30.88	GAC.ATC.TAG.TGT.GTG.TTT CCC.CTT.TTT.TCT.TTT.CAT
8	5 50	213	42.21	GAC.AAT.AAA.TCC.TTG.TGT AAG.ATT.TTT.TTA.TAT.AGG
9	40	249	33.73	TTT.GAG.TTT.TGA.GTA.TTT TGG.GTG.TTT.CCT.GTG.AGT
10	50	240	41.47	CAC.CCC.TCA.GGA.CAG.TTT ACA.TCT.GTT.CCT.TGT.GAG
11.1	50	145	40.58	AGG.TAA.TTG.TTC.TCT.CTT GAA.GTG.AAC.TTC.ATG.CTT
11.2	40 2	224	60.81	TCC.CAA.GAA.TGT.GGA.TGT AAA.GGC.CCC.AGA.GAA.GTA
12.1	40	184	44.53	TTT.TTT.TTT.TTT.TAA.TAC.A AAT.CTG.TAC.GAA.CCA.TCT
12.2	8 40	366	53.23	TGG.AAG.TAG.TGA.TAA.GGT TGT.ACT.TTT.CCC.AAA.AGG
13	40	272	49.06	ATC.TGC.ACT.TCC.TTT.TCT AAA.ACC.TTG.GCA.GTT.GAG
14	45 5	235	48.94	TAC.TTA.CCT.GTT.TTT.TGG GTA.GTA.GCT.CTG.CTT.GTT
15	40	179	29.97	CAG.CTT.TTC.CTT.AAA.GTC CAG.TTG.AAA.TGT.CAG.AAG
16	40	261	47.56	CTT.GCT.CCT.TCA.TGT.TCT.TG AGA.AGT.ATA.AGA.ATG.GCT.GTC
17	40	199	47.01	ATT.ATT.TCT.TGT.TCC.CTT AAT.GCT.TAG.TAT.CTG.CCT
18	45	215	46.67	CCT.ATT.TTG.AGG.TAT.TGA.AT GCC.AGT.GTG.CAT.CAC.CA
19	40	282	43.43	TGT.TGG.GAT.GCA.AAC.AGG ATC.CCA.CAG.TGC.ATA.AAT

^aUnderlined nucleotides represented nucleotides added to

modify the melting temperatures of the primers. ^bGClampsm are: 50clamp,CGC.CCG.CCG.CCG.CCC.GCC.GCG.CCC.CGC.GCC.CGT.CCC.GCC.GCC.CCC.GCC.CG; 45 GC clamp, CGC.CCG.CCG.CCG.CCC.CGC.CCC.GTC.CCG.CCG.CCC.CCG.CCC.GGC.CCG; 40 clamp, CGC.CCGCCG.CGC.CCC.CCG.CCC.GGC.CCG.CCG.CCC.CCG.CCC.G; 8 clamp, CGT.CCC.GC; 5 clamp, GCG. CG; 2 clamp,CG; ^cTM is given in %UF.

After checking and visualizing the long PCR products on a 0.8 % agarose gel, 1µl of the long PCR amplicons was used as template for subsequent extensive multiplex short PCR. The short PCR was performed in two multiplex groups of 11 and 10 amplicons, respectively. The final concentrations of each primer were shown in Table 2. The final concentrations of the PCR mix included 1×PCR buffer, 7 mM MgCl₂, and 0.25 mM each dNTP. Cycling conditions included a hot start of 3 min at 94 °C with the Taq Pol added after 2 min, followed by five cycles of 94 °C×1 min, 52 °C×45 sec (decrements of 1 °C/cycle), and 72 °C×1 min; 15 cycles of 94 °C×1 min, 48 °C×45 sec, and 72 °C×1 min, 30 sec (with increments of 2 sec/cycle); 15 cycles of 94 °C×1 min, 38 °C×45 sec, and 72 °C×1 min 30 sec. Each PCR reaction was terminated with a round of heteroduplexing: 72 °C×10 min, 98 °C×10 min, 45 °C×30 min, and finally 37 °C×30 min. Each tube reaction was directly mixed with 1/10 volume of 10×loading buffer, 6.5 µl of multiplex group I and 8.5 µl of multiplex group II were loaded onto a slab gel for size separation.

Table 2 Multiplex groups for short PCR

Multiplex group I		Multiplex group II	
Exon	Final concentration	Exon	Final concentration
11.1	0.375 µM	5	1.5 µM
15	0.5 µM	2	1.25 µM
12.1	0.375 µM	7	1.75 µM
17	0.5 µM	4	1.625 µM
8	0.375 µM	11.2	0.5 µM
18	1.25 µM	6	1.625 µM
14	1.25 µM	9	1.5 µM
3	0.625 µM	1	1.25 µM
10	0.625 µM	13	1.625 µM
16	1.0 µM	12.2	0.325 µM
19	1.75 µM		

Two-dimensional electrophoresis For two-dimensional electrophoresis, the DGGE instrument was from CBS Scientific Co. (Solana Beach, CA. Amplicons from each of the two multiplex reactions were mixed and subjected to electrophoresis in 0.5×TAE (Tris-Acetate EDTA). A 10 % polyacrylamide, 0.75 mm thick slab gel was used, the amplicons were fractionated at 140V for 7.5hr at 50 °C. The separation pattern was detected by SYBR green staining and UV-transillumination of the slab gel. The 120-to 420-bp region in the middle of each lane was quickly cut out and applied to a 1mm thick DGGE gel.

The DGGE gel was prepared as a 1 mm thick slab gel with a 10-6.5 % reverse polyacrylamide gradient containing 25-70 % urea/formamide (UF) and 3-9 % glycerol gradients. Electrophoresis was carried out for 16 hr at 56 °C and 90-110V. After electrophoresis, the gels were stained with SYBR-green I and II for 30 min. The DGGE band patterns were detected and documented with a gel documentation system (Oncor, Gaithersburg, MD).

Sequence analysis Amplicons were prepared by PCR such that a standard M13 primer site was incorporated at one end. These products were sequenced on an ABI 377 sequencer (Foster

City, CA) with kits containing Taq FS DNA polymerase and dye primer technology, as recommended by the manufacturer.

hMLH1 methylation analysis

DNA methylation patterns in the CpG islands of *hMLH1* gene were determined by Methylation-specific PCR (MSP) as described^[18]. The primer sequences of *hMLH1* for unmethylated reaction were 5' -TTTGTAGTAGATGTTTATTAGGGTTGT-3' (sense) and 5' -ACCACCTCAT CATAACTACCCACA-3' (antisense), and for methylated reaction were 5' -ACGTAGACGTTTATT AGGGTCGC-3' (sense) and 5' -CCTCATCGTAACTACC CGCG-3' (antisense).

MSI detection

MSI analyses included five microsatellite markers: BAT25, BAT26, BAT40, D2S123, and D5S346. PCR was performed as previous described^[11]. MSI was defined as the presence of band shift in the tumor DNA that was not present in the corresponding normal DNA. Based on the number of mutated MSI markers in each tumor, carcinomas were characterized as MSI-H if they manifested instability in two or more markers, MSI-L if unstable in only one marker, and MSS if they showed no instability in any marker^[19,20].

Statistical analysis

Chi-square test with Yates' correction were used. A *P* value <0.05 was considered significant.

RESULTS

MSI in gastric cancer

Alterations of electrophoretic patterns of PCR products of five microsatellite markers were compared between the tumor and the normal DNA in each patient (Figure 1). MSI affecting at least one locus was observed in 17 (25 %) of 68 tumors, among which eight (11.8 %) were MSI-H, nine (13.2 %) were MSI-L, and fifty-one (75 %) were MSS.

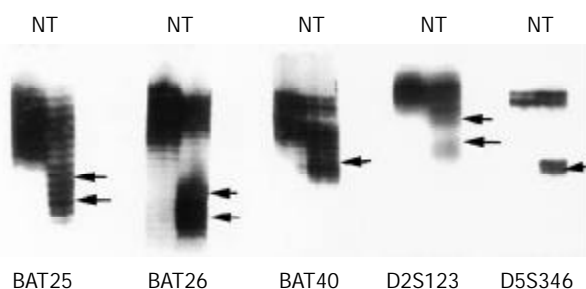


Figure 1 MSI in gastric cancer using 5 microsatellite loci (BAT-25, BAT-26, BAT-40, D2S123, and D5S346). Arrows indicate variant conformers. N: normal DNA pattern; T: tumor specimens containing variant conformers representing MSI.

hMLH1 mutation and MSI

Mutations and sequence alteration in various exons manifested as the four-spot pattern denoting a heterozygous variant (Figure 2). We found three mutations in 68 (4.4 %) gastric cancer by DNA sequencing. Two mutations were caused by a single bp substitution (exon 8 at codon 226, CGG→CTG, Arg→Leu; exon 9 at codon 252, TCA→TTA, Ser→Phe); One identical change was caused by a 2 bp substitution (exon 12 at codon 409, CAG→CGT, Gln→Arg), which displayed similar DGGE band pattern. A comparison of MSI status with *hMLH1* mutation was shown in Table 3. Three *hMLH1* mutations were all detected in MSI-H, but no mutation was found in MSI-L or MSS.

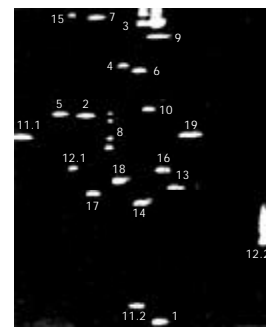


Figure 2 Detection of mismatching repair gene *hMLH1* mutation in gastric cancer by two-dimensional DNA electrophoresis. Four-band pattern was observed at exon 8.

Table 3 The relevance of MSI and *hMLH1* mutation

MSI Status	No. of cases	<i>hMLH1</i> mutation
MSI-H	8	3
MSI-L	9	0
MSS	51	0

hMLH1 methylation status and MSI

To examine methylation of promoter region of *hMLH1*, we adapted MSP for the 5' CpG islands in this gene. The region chosen spanned the area of greatest CpG density immediately 5' to the transcription starting site, in an area previously studied for methylation changes^[15]. In gastric mucosal samples without cancer, only unmethylated *hMLH1* genes were present. Eleven of 68 (16.2 %) gastric cancers exhibited prominent methylation, which always had both methylated and nonmethylated *hMLH1* genes (Figure 3). A comparison of MSI status with *hMLH1* methylation status was shown in Table 4. Seven of 8 (87.5 %) cancers with MSI-H exhibited prominent methylation, whereas methylated *hMLH1* gene was only found in 1/9 (11.1 %) gastric cancer with MSI-L and 3/51 (5.9 %) with MSS, suggesting that *hMLH1* methylation was more correlated with gastric cancers with MSI-H than that with MSI-L or with MSS (*P*<0.01-0.001).

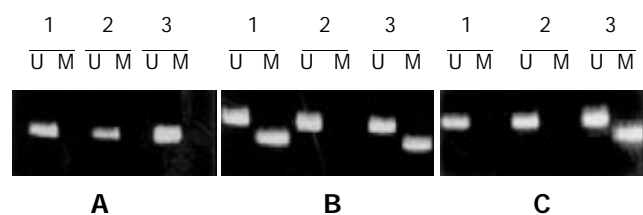


Figure 3 Methylation of *hMLH1* in gastric cancer. A: No methylation was found in normal mucosa; B: Methylation of *hMLH1* in MSI-H gastric cancer. Cases 1, 3 showed both hypermethylation and unmethylation; C: Methylation of *hMLH1* in MSI-L gastric cancer. Case 3 showed both hypermethylation and unmethylation; U: Unmethylation; M: methylation.

Table 4 The relevance of methylation of *hMLH1* and MSI

MSI status	Unmethylated	Hypermethylation(%)
MSI-H	1	7(87.5)
MSI-L	8	1(11.1) ^b
MSS	48	3(5.9) ^d

^b*P*<0.01; ^d*P*<0.001 vs MSI-H group.

DISCUSSION

A significant portion of gastric cancers exhibit defective DNA mismatch repair, manifested as MSI. There is now evidence that MSI cancer comprises distinctive MSI-H and MSI-L categories^[21-23]. MSI-H cancers are distinguished clinicopathologically and in their spectrum of genetic alterations from cancers showing MSI-L and MSS cancers^[24-34]. Our previous studies indicated that MSI-H gastric cancers often showed lower frequency of LOH in APC, MCC and DCC genes than do MSI-L and MSS cancers^[1]. In the present study, all three hMLH1 mutations were detected in MSI-H, but no mutation was found in those showing MSI-L or MSS. This result further indicates that hMLH1 is mutational target in MSI-H tumor cells and supported the notion that MSI-H tumors identified an alternative pathway of tumorigenesis that had been proposed by Vogelstein and co-workers^[35].

Human cancers with MSI-H phenotype develop due to defects in DNA mismatch repair genes. Silencing of a DNA mismatch repair gene, hMLH1 gene, by promoter hypermethylation is a frequent cause of MSI-H phenotype^[36-42]. In this study, 11 (16.2 %) of 68 gastric cancers exhibited prominent hMLH1 methylation, which is similar to previous studies^[36]. It has been reported that MSI-H is related to methylation of the hMLH1 promoter but not hMSH1 mutations in sporadic gastric carcinomas^[43]. It was also found that MSI-L gastric carcinomas share the hMLH1 methylation status of MSI-H carcinomas but not their clinicopathological profile^[44]. In this study, 7/8 (87.5 %) cancers with MSI-H exhibited prominent methylation of the hMLH1 promoter, suggesting that methylation of the hMLH1 promoter is correlated with MSI-H gastric cancer. The frequency of methylation in MSI-H cancers is significantly higher than that in cancers with MSI-L and MSS, however no difference was found between cancers with MSI-L and MSS, indicating that MSI-H tumors identify a different methylation pathway from cancers with MSI-L and MSS, and MSI-L cancers involves the same methylation pathway as MSS tumors. This finding is in agreement with our recently published data on molecular pathway in the gastric carcinogenesis^[2].

It has been found that colorectal cancer cell lines only had methylated hMLH1 genes, but had absent unmethylated hMLH1 genes^[45]. In the present study, unlike the situation with the cell lines, however, the primary MSI+ gastric cancers always had both methylated and nonmethylated hMLH1 genes. It is likely that a significant fraction of the unmethylated genes is derived from the non-neoplastic cells (stromal, inflammatory, vascular, etc.), which are invariably present within the primary tumors but are not found in cultured cell lines. It has been reported that methylation of the hMLH1 promoter correlates with lack of expression of hMLH1 in sporadic colon tumors and mismatch repair-defective human tumor cell lines^[13], whereas demethylation of hMLH1 promoter results in reexpression of hMLH1 in tumor cells tested. Not only was the protein expressed, but MMR activity was restored. DNA methylation is a fundamental feature of the genomes and the control of their functions therefore it is a candidate for pharmacological manipulation that might have important therapeutic advantage.

REFERENCES

- 1 **Fang DC**, Jass JR, Wang DX, Zhou XD, Luo YH, Young J. Infrequent loss of heterozygosity of APC/MCC and DCC genes in gastric cancer showing DNA microsatellite instability. *J Clin Pathol* 1999; **52**: 504-508
- 2 **Fang DC**, Yang SM, Zhou XD, Wang DX, Luo YH. Telomere erosion is independent of microsatellite instability but related to loss of heterozygosity in gastric cancer. *World J Gastroenterol* 2001; **7**: 522-526
- 3 **Martins C**, Kedda MA, Kew MC. Characterization of six tumor suppressor genes and microsatellite instability in hepatocellular carcinoma in southern African blacks. *World J Gastroenterol* 1999; **5**: 470-476
- 4 **Wu BP**, Zhang YL, Zhou DY, Gao CF, Lai ZS. Microsatellite instability, MMR gene expression and proliferation kinetics in colorectal cancer with familial predisposition. *World J Gastroenterol* 2000; **6**: 902-905
- 5 **Thomas DC**, Umar A, Kunkel TA. Microsatellite instability and mismatch repair defects in cancer. *Mutat Res* 1996; **350**: 201-205
- 6 **Peltomaki P**. Microsatellite instability and hereditary non-polyposis colon cancer. *J Pathol* 1995; **176**: 329-330
- 7 **Cai Q**, Sun MH, Lu HF, Zhang TM, Mo SJ, Xu Y, Cai SJ, Zhu XZ, Shi DR. Clinicopathological and molecular genetic analysis of 4 typical Chinese HNPCC families. *World J Gastroenterol* 2001; **7**: 805-810
- 8 **Modrich P**. Mismatch repair, genetic stability, and cancer. *Science* 1994; **266**: 1959-1960
- 9 **Papadopoulos N**, Lindblom A. Molecular basis of HNPCC: mutations of MMR genes. *Hum Mutat* 1997; **10**: 89-99
- 10 **Zhao B**, Wang ZJ, Xu YF, Wan YL, Li P, Huang YT. Report of 16 kindreds and one kindred with hMLH1 germline mutation. *World J Gastroenterol* 2002; **8**: 263-266
- 11 **Aaltonen LA**, Peltomaki P, Leach FS, Sistonen P, Pylkkanen L, Mecklin JP, Jarvinen H, Powell SM, Jen J, Hamilton SR. Clues to the pathogenesis of familial colorectal cancer. *Science* 1993; **260**: 812-816
- 12 **Miyakura Y**, Sugano K, Konishi F, Ichikawa A, Maekawa M, Shitoh K, Igarashi S, Kotake K, Koyama Y, Nagai H. Extensive methylation of hMLH1 promoter region predominates in proximal colon cancer with microsatellite instability. *Gastroenterology* 2001; **121**: 1300-1309
- 13 **Kane MF**, Loda M, Gaida GM, Lipman J, Mishra R, Goldman H, Jessup JM, Kolodner R. Methylation of the hMLH1 promoter correlates with lack of expression of hMLH1 in sporadic colon tumors and mismatch repair-defective human tumor cell lines. *Cancer Research* 1997; **57**: 808-811
- 14 **Garinis GA**, Patrinos GP, Spanakis NE, Menounos PG. DNA hypermethylation: when tumour suppressor genes go silent. *Hum Genet* 2002; **111**: 115-127
- 15 **Jones PA**. DNA methylation and cancer. *Oncogene* 2002; **21**: 5358-5360
- 16 **Ehrlich M**. DNA methylation in cancer: too much, but also too little. *Oncogene* 2002; **21**: 5400-5413
- 17 **Wu Y**, Nystrom-Lahti M, Osinga J, Looman MW, Peltomaki P, Aaltonen LA, de la Chapelle A, Hofstra RM, Buys CH. MSH2 and MLH1 mutations in sporadic replication error-positive colorectal carcinoma as assessed by two-dimensional DNA electrophoresis. *Genes Chromosomes Cancer* 1997; **18**: 269-278
- 18 **Herman JG**, Graff JR, Myohanen S, Nelkin BD, Baylin SB. Methylation-specific PCR: A novel PCR assay for methylation status of CpG islands. *Proc Natl Acad Sci USA* 1996; **93**: 9821-9826
- 19 **Boland CR**, Thibodeau SN, Hamilton SR, Sidransky D, Eshleman JR, Burt RW, Meltzer SJ, Rodriguez-Bigas MA, Fodde R, Ranzani GN, Srivastava S. A national cancer institute workshop on microsatellite instability for cancer detection and familial predisposition: Development of international criteria for the determination of microsatellite instability in colorectal cancer. *Cancer Res* 1998; **58**: 5248-5257
- 20 **Sood AK**, Holmes R, Hendrix MJ, Buller RE. Application of the national cancer institute international criteria for determination of microsatellite instability in ovarian cancer. *Cancer Res* 2001; **61**: 4371-4374
- 21 **Jass JR**, Biden KG, Cummings MC, Simms LA, Walsh M, Schoch E, Meltzer SJ, Wright C, Searle J, Young J, Leggett BA. Characterization of a subtype of colorectal cancer combining features of the suppressor and mild mutator pathways. *J Clin Pathol* 1999; **52**: 455-460
- 22 **Wahlberg SS**, Schmeits J, Thomas G, Loda M, Garber J, Syngal S, Kolodner RD, Fox E. Evaluation of microsatellite instability and immunohistochemistry for the prediction of germ-line MSH2 and MLH1 mutations in hereditary nonpolyposis colon cancer families. *Cancer Res* 2002; **62**: 3485-3492
- 23 **Kambara T**, Matsubara N, Nakagawa H, Notohara K, Nagasaka

- T, Yoshino T, Isozaki H, Sharp GB, Shimizu K, Jass J, Tanaka N. High frequency of low-level microsatellite instability in early colorectal cancer. *Cancer Res* 2001; **61**: 7743-7746
- 24 **Miyoshi E**, Haruma K, Hiyama T, Tanaka S, Yoshihara M, Shimamoto F, Chayama K. Microsatellite instability is a genetic marker for the development of multiple gastric cancers. *Int J Cancer* 2001; **95**: 350-353
- 25 **Yamamoto H**, Min Y, Itoh F, Imsumran A, Horiuchi S, Yoshida M, Iku S, Fukushima H, Imai K. Differential involvement of the hypermethylator phenotype in hereditary and sporadic colorectal cancers with high-frequency microsatellite instability. *Genes Chromosomes Cancer* 2002; **33**: 322-325
- 26 **Halford S**, Sasieni P, Rowan A, Wasan H, Bodmer W, Talbot I, Hawkins N, Ward R, Tomlinson I. Low-level microsatellite instability occurs in most colorectal cancers and is a nonrandomly distributed quantitative trait. *Cancer Res* 2002; **62**: 53-57
- 27 **Young J**, Simms LA, Biden KG, Wynter C, Whitehall V, Karamatic R, George J, Goldblatt J, Walpole I, Robin SA, Borten MM, Stitz R, Searle J, McKeone D, Fraser L, Purdie DR, Podger K, Price R, Buttenshaw R, Walsh MD, Barker M, Leggett BA, Jass JR. Features of colorectal cancers with high-level microsatellite instability occurring in familial and sporadic settings: parallel pathways of tumorigenesis. *Am J Pathol* 2001; **159**: 2107-2116
- 28 **Lee JH**, Abraham SC, Kim HS, Nam JH, Choi C, Lee MC, Park CS, Juhng SW, Rashid A, Hamilton SR, Wu TT. Inverse relationship between APC gene mutation in gastric adenomas and development of adenocarcinoma. *Am J Pathol* 2002; **161**: 611-618
- 29 **Duval A**, Hamelin R. Genetic instability in human mismatch repair deficient cancers. *Ann Genet* 2002; **45**: 71-75
- 30 **Moran A**, Iniesta P, de Juan C, Gonzalez-Quevedo R, Sanchez-Prnate A, Diaz-Rubio E, Ramon Y, Cajal S, Torres A, Balibrea JL, Benito M. Stromelysin-1 promoter mutations impair gelatinase B activation in high microsatellite instability sporadic colorectal tumors. *Cancer Res* 2002; **62**: 3855-3860
- 31 **Peiro G**, Diebold J, Lohse P, Ruebsamen H, Lohse P, Baretton GB, Lohrs U. Microsatellite instability, loss of heterozygosity, and loss of hMLH1 and hMSH2 protein expression in endometrial carcinoma. *Hum Pathol* 2002; **33**: 347-354
- 32 **Wu CW**, Chen GD, Jiang KC, Li AF, Chi CW, Lo SS, Chen JY. A genome-wide study of microsatellite instability in advanced gastric carcinoma. *Cancer* 2001; **92**: 92-101
- 33 **Ogata S**, Tamura G, Endoh Y, Sakata K, Ohmura K, Motoyama T. Microsatellite alterations and target gene mutations in the early stages of multiple gastric cancer. *J Pathol* 2001; **194**: 334-340
- 34 **Tamura G**, Sato K, Akiyama S, Tsuchiya T, Endoh Y, Usuba O, Kimura W, Nishizuka S, Motoyama T. Molecular characterization of undifferentiated-type gastric carcinoma. *Lab Invest* 2001; **81**: 593-598
- 35 **Vogelstein B**, Fearon ER, Hamilton SR, Kern SE, Preisinger AC, Leppert M, Nakamura Y, White R, Smits AM, Bos JL. Genetic alterations during colorectal tumor development. *N Engl J Med* 1988; **319**: 525-532
- 36 **Fleisher AS**, Esteller M, Tamura G, Rashid A, Stine OC, Yin J, Zou TT, Abraham JM, Kong D, Nishizuka S, James SP, Wilson KT, Herman JG, Meltzer SJ. Hypermethylation of the hMLH1 gene promoter is associated with microsatellite instability in early human gastric neoplasia. *Oncogene* 2001; **20**: 329-335
- 37 **Murata H**, Khattar NH, Kang Y, Gu L, Li GM. Genetic and epigenetic modification of mismatch repair genes hMSH2 and hMLH1 in sporadic breast cancer with microsatellite instability. *Oncogene* 2002; **21**: 5696-5703
- 38 **Norrie MW**, Hawkins NJ, Todd AV, Meagher AP, O' Connor TW, Ward RL. The role of hMLH1 methylation in the development of synchronous sporadic colorectal carcinomas. *Dis Colon Rectum* 2002; **45**: 674-680
- 39 **Sakata K**, Tamura G, Endoh Y, Ohmura K, Ogata S, Motoyama T. Hypermethylation of the hMLH1 gene promoter in solitary and multiple gastric cancers with microsatellite instability. *Br J Cancer* 2002; **86**: 564-567
- 40 **Baranovskaya S**, Soto JL, Perucho M, Malkhosyan SR. Functional significance of concomitant inactivation of hMLH1 and hMSH6 in tumor cells of the microsatellite mutator phenotype. *Proc Natl Acad Sci U S A* 2001; **98**: 15107-15112
- 41 **Deng G**, Peng E, Gum J, Terdiman J, Sleisenger M, Kim YS. Methylation of hMLH1 promoter correlates with the gene silencing with a region-specific manner in colorectal cancer. *Br J Cancer* 2002; **86**: 574-579
- 42 **Hawkins N**, Norrie M, Cheong K, Mokany E, Ku SL, Meagher A, O' Connor T, Ward R. CpG island methylation in sporadic colorectal cancers and its relationship to microsatellite instability. *Gastroenterology* 2002; **122**: 1376-1387
- 43 **Bevilacqua RA**, Simpson AJ. Methylation of the hMLH1 promoter but no hMLH1 mutations in sporadic gastric carcinomas with high-level microsatellite instability. *Int J Cancer* 2000; **87**: 200-203
- 44 **Pinto M**, Oliveira C, Machado JC, Cirnes L, Tavares J, Carneiro F, Hamelin R, Hofstra R, Seruca R, Sobrinho-Simoes M. MSI-L gastric carcinomas share the hMLH1 methylation status of MSI-H carcinomas but not their clinicopathological profile. *Lab Invest* 2000; **80**: 1915-1925
- 45 **Herman JG**, Umar A, Polyak K, Graff JR, Ahuja N, Issa JP, Markowitz S, Willson JK, Hamilton SR, Kinzler KW, Kane MF, Kolodner RD, Vogelstein B, Kunkel TA, Baylin SB. Incidence and functional consequences of hMLH1 promoter hypermethylation in colorectal carcinoma. *Proc Natl Acad Sci USA* 1998; **95**: 6870-6875
- 46 **Machover D**, Zittoun J, Saffroy R, Broet P, Giraudier S, Magnaldo T, Goldschmidt E, Debuire B, Orrico M, Tan Y, Mishal Z, Chevallier O, Tonetti C, Jouault H, Ulusakarya A, Tanguy ML, Metzger G, Hoffman RM. Treatment of cancer cells with methioninase produces DNA hypomethylation and increases DNA synthesis. *Cancer Res* 2002; **62**: 4685-4689
- 47 **Nichol K**, Pearson AC. CpG methylation modifies the genetic stability of cloned repeat sequences. *Genome Res* 2002; **12**: 1246-1256
- 48 **Karpf AR**, Jones DA. Reactivating the expression of methylation silenced genes in human cancer. *Oncogene* 2002; **21**: 5496-5503
- 49 **Christman JK**. 5-Azacytidine and 5-aza-2'-deoxycytidine as inhibitors of DNA methylation: mechanistic studies and their implications for cancer therapy. *Oncogene* 2002; **21**: 5483-5495

Tributylin inhibits human gastric cancer SGC-7901 cell growth by inducing apoptosis and DNA synthesis arrest

Jun Yan, Yong-Hua Xu

Jun Yan, Yong-Hua Xu, Lab of Molecular and Cellular Oncology and Lab of Molecular Cell Biology, Institute of Biochemistry and Cell Biology, Shanghai Institutes for Biological Sciences, Chinese Academy of Sciences, Shanghai 200031, China

Supported by the Major State Basic Research (973) Program of China, (G1999053905) and National Natural Science Foundation of China, No. 30170207

Correspondence to: Dr. Yong-Hua Xu, Lab of Molecular and Cellular Oncology, Institute of Biochemistry and Cell Biology, Shanghai Institutes for Biological Sciences, Chinese Academy of Sciences, 320 Yue Yang Road, Shanghai 200031, China. yhxu@sunm.shnc.ac.cn

Telephone: +86-21-54921361 **Fax:** +86-21-54921361

Received: 2002-10-09 **Accepted:** 2002-11-04

Abstract

AIM: To evaluate the effects of tributyrin, a pro-drug of natural butyrate and a neutral short-chain fatty acid triglyceride, on the growth inhibition of human gastric cancer SGC-7901 cell.

METHODS: Human gastric cancer SGC-7901 cells were exposed to tributyrin at 0.5, 1, 2, 5, 10 and 50 mmol·L⁻¹ for 24-72 h. MTT assay was applied to detect the cell proliferation. [³H]-TdR uptake was measured to determine DNA synthesis. Apoptotic morphology was observed by electron microscopy and Hoechst-33258 staining. Flow cytometry and terminal deoxynucleotidyl transferase-mediated dUTP nick end labeling (TUNEL) assay were performed to detect tributyrin-triggered apoptosis. The expressions of PARP, Bcl-2 and Bax were examined by Western blot assay.

RESULTS: Tributyrin could initiate growth inhibition of SGC-7901 cell in a dose- and time-dependent manner. [³H]-TdR uptake by SGC-7901 cells was reduced to 33.6 % after 48 h treatment with 2 mmol·L⁻¹ tributyrin, compared with the control (*P*<0.05). Apoptotic morphology was detected by TUNEL assay. Flow cytometry revealed that tributyrin could induce apoptosis of SGC-7901 cells in dose-dependent manner. After 48 hours incubation with tributyrin at 2 mmol·L⁻¹, the level of Bcl-2 protein was lowered, and the level of Bax protein was increased in SGC-7901, accompanied by PARP cleavage.

CONCLUSION: Tributyrin could inhibit the growth of gastric cancer cells effectively *in vitro* by inhibiting DNA synthesis and inducing apoptosis, which was associated with the down-regulated Bcl-2 expression and the up-regulated Bax expression. Therefore, tributyrin might be a promising chemopreventive and chemotherapeutic agent against human gastric carcinogenesis.

Yan J, Xu YH. Tributyrin inhibits human gastric cancer SGC-7901 cell growth by inducing apoptosis and DNA synthesis arrest. *World J Gastroenterol* 2003; 9(4): 660-664

<http://www.wjgnet.com/1007-9327/9/660.htm>

INTRODUCTION

Gastric cancer is one of the most common causes of

malignancy-related death worldwide. In China, the annual average mortality rate of gastric carcinoma is as high as 16 per 100 thousand^[1]. Environmental factors, diet that is high in salts and low in fresh fruit and vegetables are regarded as the risk of stomach cancer^[2-6]. Although plenty of advances have been made in the gastrointestinal medicine, the inability to diagnose early and treat effectively of the gastric cancer remains an unsolved problem for clinicians^[7-23].

Chemoprevention and chemotherapy including the use of natural products, synthetic compounds or dietary substances are promising ways to stop or reverse the process of carcinogenesis^[24]. Large number of minor dietary components has been found to inhibit carcinogenesis at various stages^[25]. Tributyrin is a neutral short-chain fatty acid triglyceride existed in some spice plants at low levels in nature^[26], and has been approved as a food additive in the United States^[27]. Tributyrin is also a pro-drug of natural butyrate synthesized by the bacterial fermentation of various complex carbohydrates unabsorbed in the digestive tract^[28] and has been reported bearing anti-tumor effect on neoplastic cells^[27, 29, 30] as well as inhibiting proliferation and stimulating differentiation in multiple cancer cell lines. Most importantly, tributyrin is more lipophilic compared with the butyrate and can be metabolized by the intracellular lipases, progressively releasing therapeutically effective butyrate directly in the cell^[26, 31]. However, the underlying mechanisms of tributyrin against different types of tumor remain to be understood and so far, the effect of tributyrin on gastric cancer cells has not been reported yet.

In this study, we are trying to evaluate the ability of tributyrin to inhibit cell proliferation, arrest DNA synthesis and induce apoptosis in human gastric cancer SGC-7901 cells and go further into some apoptosis-related events in these processes.

MATERIALS AND METHODS

Cell lines and reagents

Human gastric cancer cell line SGC-7901 was provided by the Cell Bank of Shanghai Institute of Cell Biology, Chinese Academy of Sciences (Shanghai, China). Cells were cultured in Dulbecco's Modified Eagle Medium (DMEM; Life Technologies Inc., Grand Island, NY) supplemented with 10 % fetal calf serum (FCS; Life Technologies Inc., Rockville, MD), penicillin (100 kU·L⁻¹) and streptomycin (0.1 g·L⁻¹) at 37 °C in a 5 % CO₂-95 % air atmosphere. Antibodies against Bax, Bcl-2, PARP, and Actin were obtained from Santa Cruz. Other chemicals used in the study were purchased from Sigma Chemical Co (St. Louis, MO, USA). *In situ* cell death detection kit was purchased from Roche Diagnostics. [³H]-TdR was obtained from Amersham Company.

Assessment of cell proliferation

MTT assay was conducted to determine the cell proliferation. SGC-7901 cells were seeded in a 96-well plate (1×10⁴·well⁻¹) as described previously^[32]. In brief, after 24 h incubation cells were treated with tributyrin for three days and untreated cells served as a control. Prior to the determination, 5 μL of the 2.5 g·L⁻¹ stock solution of 3-[4,5-dimethylthiazolyl]-2,5-diphenyl-

tetrazolium bromide (MTT) was added to each well. After 4 h incubation, the culture media were discarded followed by addition of 100 μL of DMSO to each well and vibration for 10 min. The absorbance (A) was measured at 492nm with a microplate reader. The percentage of viable cells was calculated as follows: (A of experimental group/A of control group) $\times 100\%$.

^3H -TdR incorporation

The cells were treated with 2 $\text{mmol}\cdot\text{L}^{-1}$ Tributyrin for the indicated time as described previously^[33]. 74kBq of ^3H -TdR were added to cells 3 h before the end of the culture. Cells were then washed with ice-cold PBS and 5 % trichloroacetic acid and lysed in 0.25 $\text{mol}\cdot\text{L}^{-1}$ NaOH. The lysates were neutralized with 3 $\text{mol}\cdot\text{L}^{-1}$ HCl and ^3H -TdR uptake was measured with Beckman LS5000 TD liquid scintillation counter.

Transmission electron microscopy

The cultured cells treated with 2 $\text{mmol}\cdot\text{L}^{-1}$ tributyrin for 48 h were trypsinized and harvested, respectively. Subsequently the cells were immersed with Epon 821, embedded in capsules and converged at 60 $^{\circ}\text{C}$ for 72 h, then they were prepared into ultrathin section (60 nm) and stained with uranyl acetate and lead citrate. Cell ultrastructure was examined by transmission electron microscopy.

Morphological change of apoptosis

The morphological changes of cell apoptosis were determined under fluorescence microscope. Briefly, the experimental cells were pelleted and fixed in 200 $\text{ml}\cdot\text{L}^{-1}$ ethanol/phosphate-buffered saline (PBS), stained with 5 $\text{mg}\cdot\text{L}^{-1}$ Hoechst-33258 for 10min at room temperature, then visualized under fluorescence microscope.

TUNEL assay

Apoptosis of SGC-7901 cells was analyzed by using *in situ* cell death detection kit. The method is essentially based on the terminal deoxynucleotidyl transferase-mediated dUTP nick end labeling (TUNEL) technique. In brief, after cells were treated with or without tributyrin for the indicated time, they were fixed overnight in 100 $\text{g}\cdot\text{L}^{-1}$ formaldehyde, then treated with proteinase K and H_2O_2 , labeled with fluorescein dUTP in a humid box at 37 $^{\circ}\text{C}$ for 1 h and visualized under fluorescence microscope. The cells without addition of TdT enzyme were used as negative control.

Flow cytometry

After harvested, the experimental cells were washed with PBS twice and fixed with 700 $\text{mL}\cdot\text{L}^{-1}$ ethanol at 4 $^{\circ}\text{C}$ overnight. The fixed cells were washed twice with PBS and stained with 800 μL propidium iodide and 200 μL deoxyribonulcase-free ribonuclease A in PBS. The fluorescence density of propidium iodide-stained nuclei was determined by flow cytometry.

Western blot analysis

The experimental cells were lysed in lysis buffer [25 $\text{mmol}\cdot\text{L}^{-1}$ HEPES, 1.5 % Triton X-100, 1 % sodium deoxycholate, 0.1 % SDS, 0.5 $\text{mol}\cdot\text{L}^{-1}$ NaCl, 5 $\text{mmol}\cdot\text{L}^{-1}$ EDTA, 50 $\text{mmol}\cdot\text{L}^{-1}$ NaF, 0.1 $\text{mmol}\cdot\text{L}^{-1}$ sodium vanadate, 1 $\text{mmol}\cdot\text{L}^{-1}$ phenylmethylsulfonyl fluoride (PMSF), and 0.1 $\text{g}\cdot\text{L}^{-1}$ leupeptin (pH7.8)] at 4 $^{\circ}\text{C}$ with sonication. The lysates were centrifuged at 15 000 g for 15 min at 4 $^{\circ}\text{C}$ and the proteins were separated on SDS-PAGE, transferred to nitrocellulose filter and incubated with antibodies against Bcl-2, Bax, PARP, and Actin, respectively. Then the membrane was incubated with peroxidase-conjugated secondary antibodies. Detection was performed with enhanced chemiluminescence reagent.

Statistical analysis

Student's *t* test was used to assess statistical significance of differences. If $P < 0.05$, the difference was considered statistically significant.

RESULTS

Inhibition of human gastric cancer SGC-7901 cell proliferation by tributyrin

The experimental SGC-7901 cells were treated with various concentrations of tributyrin for 1-3 days and the cell viability was determined as described above by MTT assay. As shown in Figure 1, tributyrin could inhibit the growth of gastric cancer cells in a dose- and time-dependent manner. Cell growth was suppressed by 24.9 %, 36.6 %, 50.3 %, 60.6 %, 84.1 % and 91.3 % after 72 h treatment with tributyrin at 0.5, 1, 2, 5, 10 and 50 $\text{mmol}\cdot\text{L}^{-1}$, respectively. It was noted that tributyrin at 50 $\text{mmol}\cdot\text{L}^{-1}$ had an inhibitory effect of more than 90 % on the tumor cell growth after 48-72 h treatment. The IC_{50} value of tributyrin for SGC-7901 cell at 72 h was 2 $\text{mmol}\cdot\text{L}^{-1}$.

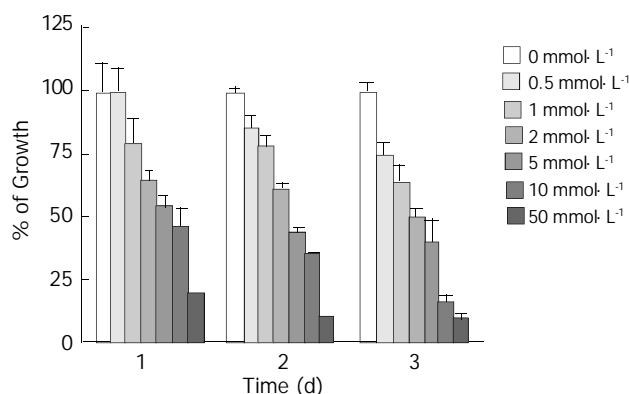


Figure 1 Effect of tributyrin on cell growth in SGC-7901 cells. The cells were treated with various concentrations of tributyrin for 24, 48 and 72 h. The antiproliferative effect was measured by MTT assay. Results were expressed as the means \pm SD from three independent determinations.

DNA synthesis arrest by tributyrin

Since the IC_{50} value of tributyrin was 2 $\text{mmol}\cdot\text{L}^{-1}$, the concentration was used for the following assay. Tributyrin inhibited the ^3H -TdR uptake by SGC-7901 cells in a time-dependent manner. Compared with the control, the DNA synthesis of tumor cells was significantly reduced by 66.4 %, 92.2 % and 90.1 % after 48 h, 72 h and 96 h treatment with tributyrin, respectively, ($P < 0.05$, Figure 2).

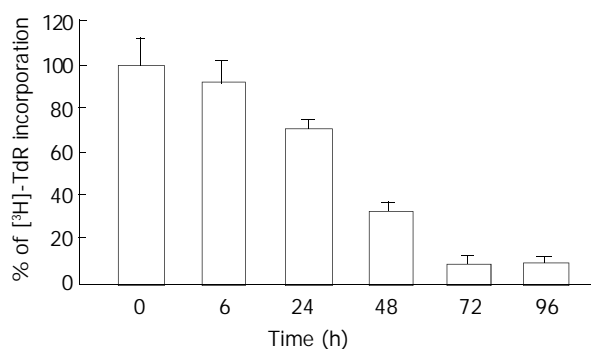


Figure 2 Inhibitory effect of tributyrin on DNA synthesis incorporated with ^3H -TdR. With the concentration of 2 $\text{mmol}\cdot\text{L}^{-1}$, tributyrin inhibited the ^3H -TdR uptake by SGC-7901 cells in a time-dependent manner. Results were expressed as means \pm SD from three independent determinations.

Tributyryn induction of apoptosis

Morphological changes After 48 h of exposure to tributyrin, gastric cancer cells began to show morphologic features of apoptosis, which manifested as cell shrinkage, chromatin condensation and nuclear pyknosis, *etc* by transmission electron microscopy (Figure 3). The tributyrin-treated SGC-7901 cells labeled with Hoechst-33258 also showed apoptotic features including nuclear shrinkage or fragmentation by fluorescence microscopy (Figure 4).

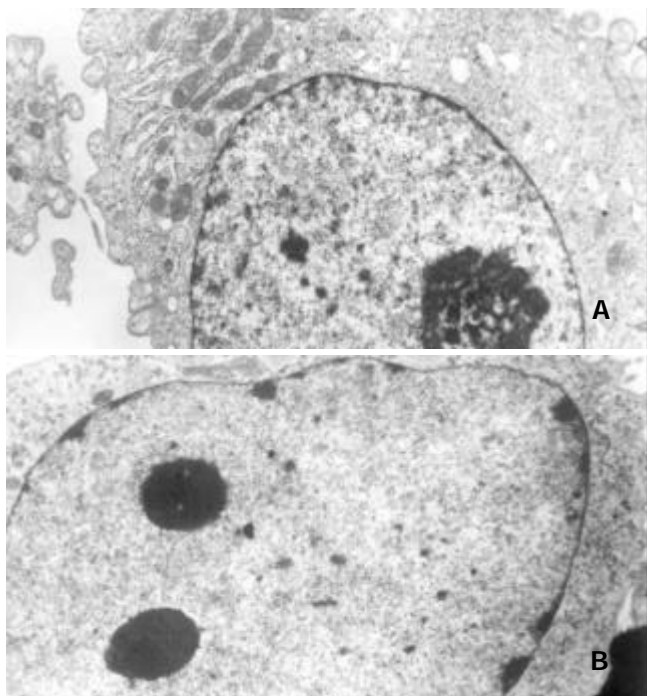


Figure 3 Ultrastructural changes of the gastric cancer cells treated with $2 \text{ mmol} \cdot \text{L}^{-1}$ tributyrin for 48 h. (A) The control SGC-7901 cell; (B) the experimental cell showing early changes of apoptosis in which nuclear chromatin condensation and cell shrinkage were observed (B).

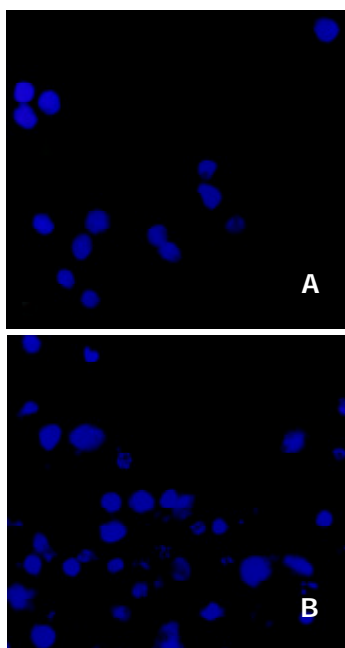


Figure 4 Tributyryn-induced apoptosis in SGC-7901 cells stained with Hoechst-33258. A: the control SGC-7901 cells; B: the experimental cells showing nuclear shrinkage or fragmentation.

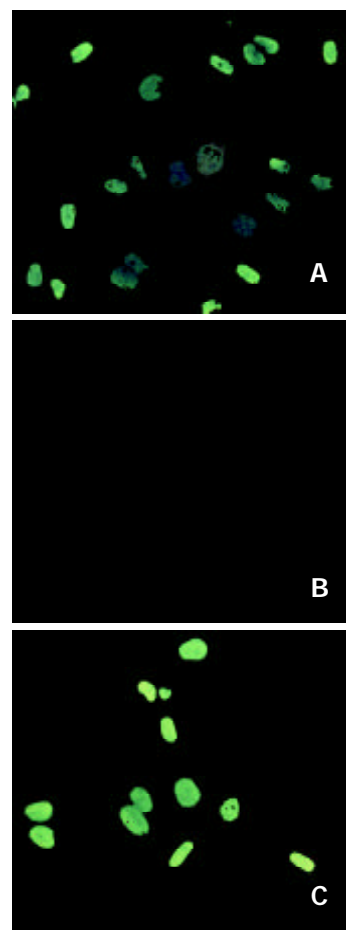


Figure 5 Tributyryn-induced apoptosis by TUNEL assay. A: the positive control cells; B: the negative control cells; C: the experimental cells treated with tributyrin at $2 \text{ mmol} \cdot \text{L}^{-1}$ for 2 days.

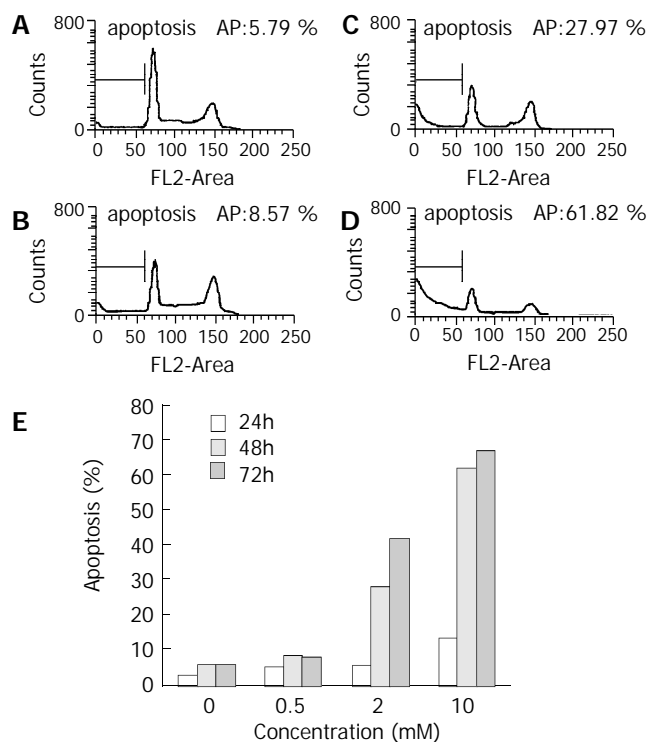


Figure 6 Tributyryn-induced apoptosis in SGC-7901 cells by flow cytometry. (A) The control cells, (B)-(D) The experimental cells treated with tributyrin at 0.5, 2 and $10 \text{ mmol} \cdot \text{L}^{-1}$ respectively for 48 h. (E) Apoptosis rates in SGC-7901 cells treated with 0.5, 2 and $10 \text{ mmol} \cdot \text{L}^{-1}$ or without tributyrin for the indicated times.

TUNEL assay

The TUNEL assay revealed that tributyrin could induce the apoptosis of SGC-7901 cells, while the negative control did not show any signs of fluorescence signals (Figure 5).

Flow cytometry

Cell cycle analysis in SGC-7901 cells treated with tributyrin revealed that a sub-G₁ apoptotic peak appeared (Figure 6). The apoptosis rate in tributyrin-treated tumor cells was increased in a time- and dose-dependent manner. When treated with 2 mmol·L⁻¹ tributyrin for 72 h, the experimental SGC-7901 cells showed a 41.5 % of apoptosis.

Differential expression of Bcl-2 and Bax protein and PARP cleavage in tributyrin-treated cells

After treated with indicated concentrations of tributyrin for 48 h, the expression of Bcl-2 protein was markedly decreased while that of Bax displayed an increased trend. PARP cleavage in the experimental cells appeared at 0.5 mmol·L⁻¹ and was obvious at 2 mmol·L⁻¹ of tributyrin treatment for 48 h (Figure 7).

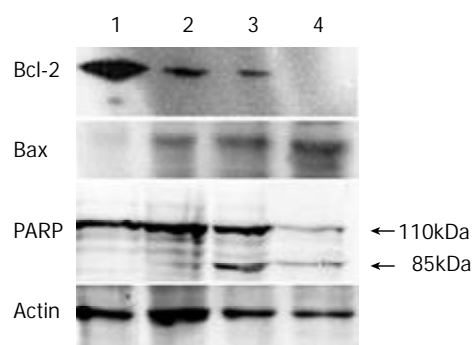


Figure 7 The expression of Bcl-2, Bax protein and PARP cleavage in tributyrin-treated SGC-7901 cells. (1) The control cells; (2)-(4) The experimental cells treated with tributyrin for 48 h at 0.5, 2 and 10 mmol·L⁻¹, respectively.

DISCUSSION

It has been reported tributyrin, a substance that naturally exists in some foods, was a potent agent against various malignancies, including colon and pancreas carcinomas, and that 1 mmol of tributyrin could result in an inhibitory effect comparable with 3 mmol of butyrate^[32,33]. The high lipophilic property and the long duration in blood made tributyrin a promising anti-tumor agent. However, the effects of tributyrin on gastric cancer cells have not been reported.

The present study demonstrated that tributyrin could inhibit the growth of human gastric cancer SGC-7901 cells in a dose- and time-dependent manner, which might be caused by DNA synthesis arrest as shown in our experiment via preventing SGC-7901 cells from progressing into S-phase and ultimately blocking the cell proliferation. The inhibition of DNA synthesis was more than 90 % when SGC-7901 cells were treated with tributyrin at 2 mmol·L⁻¹ for 48-72 h.

Besides DNA synthesis arrest, the induced cell death was another major reason for the cell growth inhibition. Apoptosis, also called programmed cell death, is a natural process of cell suicide which plays a critical role in the development and homeostasis of metazoans^[34,35]. Our results that tributyrin could induce apoptosis in SGC-7901 cells revealed by the typical apoptotic alterations, including the morphological changes by electron microscopy, positive Hoechst-33258 staining, DNA fragmentation by TUNEL assay and apoptotic sub-G₁ peak by flow cytometry.

Apoptosis is a complex process regulated by a variety of factors^[36-39]. The members of the Bcl-2 family are important regulators in the apoptotic pathway with individual members that can suppress (eg Bcl-2, Bcl-x_l) or promote (eg Bax, Bad) apoptosis. As an oncogene-derived protein, Bcl-2 confers a negative control in the pathway of cellular suicide machinery, whereas Bax, a Bcl-2-homologous protein, promotes cell death by competing with Bcl-2. Introduction of Bcl-2 into most eukaryotic cells has been reported to be able to protect the recipient cell from a wide variety of stress applications that lead to cell death^[40,41]. In the present study, we observed that the expression of Bcl-2 was reduced and that of Bax was up-regulated, indicating the reduced ratio of Bcl-2/Bax might serve as a mechanism of SGC-7901 cells apoptosis induced by tributyrin. Its subsequent event might be the release of cytochrome c and caspase-3 activation. On the other hand, the cleavage of PARP, one of caspase-3 downstream target^[42], was also observed in the experimental SGC-7901 cells with the increase of tributyrin concentrations. However, PARP could also be cleaved through a parallel caspase-3 independent pathway. Therefore, the exact mechanism underlying the apoptosis of SGC-7901 cells needed to be further investigated.

In summary, we have demonstrated that tributyrin, an oral analogue of butyrate, could induce DNA synthesis arrest and apoptosis in human gastric cancer SGC-7901 cells in vitro. The effect was dose- and time-dependent. The apoptotic mechanism of the SGC-7901 cells induced by tributyrin was at least via the reduction of Bcl-2/Bax ratio. These data suggested that further evaluation of tributyrin, a promising anti-tumor agent, for the treatment gastric cancer was warranted.

ACKNOWLEDGEMENT

We thank Dr. Rugang Zhang from Institute of Biochemistry and Cell Biology, Shanghai Institutes for Biological Sciences, Chinese Academy of Sciences, for his helpful suggestion.

REFERENCES

- 1 **Xue FB**, Xu YY, Wan Y, Pan BR, Ren J, Fan DM. Association of *H. pylori* Infection with gastric carcinoma: a Meta analysis. *World J Gastroenterol* 2001; **7**: 801-804
- 2 **Sugie S**, Okamoto K, Watanabe T, Tanaka T, Mori H. Suppressive effect of irsogladine maleate on N-methyl-N-nitro-N-nitrosoguanidine (MNNG)-initiated and glyoxal-promoted gastric carcinogenesis in rats. *Toxicology* 2001; **166**: 53-61
- 3 **Palli D**, Russo A, Saieva C, Salvini S, Amorosi A, Decarli A. Dietary and familial determinants of 10-year survival among patients with gastric carcinoma. *Cancer* 2000; **89**: 1205-1213
- 4 **Mathew A**, Gangadharan P, Varghese C, Nair MK. Diet and stomach cancer: a case-control study in South India. *Eur J Cancer Prev* 2000; **9**: 89-97
- 5 **Palli D**. Epidemiology of gastric cancer: an evaluation of available evidence. *J Gastroenterol* 2000; **35**(Suppl 12): 84-89
- 6 **Palli D**, Russo A, Ottini L, Masala G, Saieva C, Amorosi A, Cama A, D'Amico C, Falchetti M, Palmirotta R, Decarli A, Costantini RM, Fraumeni JF Jr. Red meat, family history, and increased risk of gastric cancer with microsatellite instability. *Cancer Res* 2001; **61**: 5415-5419
- 7 **Skoropad V**, Berdov B, Zagrebina V. Concentrated preoperative radiotherapy for resectable gastric cancer: 20-years follow-up of a randomized trial. *J Surg Oncol* 2002; **80**: 72-78
- 8 **Yao XX**, Yin L, Sun ZC. The expression of hTERT mRNA and cellular immunity in gastric cancer and precancerosis. *World J Gastroenterol* 2002; **8**: 586-590
- 9 **Fahy JW**, Haristoy X, Dolan PM, Kensler TW, Scholtus I, Stephenson KK, Talalay P, Lozniewski A. Sulforaphane inhibits extracellular, intracellular, and antibiotic-resistant strains of *Helicobacter pylori* and prevents benzo[a]pyrene-induced stomach tumors. *Proc Natl Acad Sci U S A* 2002; **99**: 7610-7615
- 10 **Martin RC 2nd**, Jaques DP, Brennan MF, Karpel M. Extended

- local resection for advanced gastric cancer: increased survival versus increased morbidity. *Ann Surg* 2002; **236**: 159-165
- 11 **Yu WL**, Huang ZH. Progress in studies on gene therapy for gastric cancer. *Shijie Huaren Xiaohua Zazhi* 1999; **7**: 887-889
- 12 **Chen GY**, Wang DR. The expression and clinical significance of CD44v in human gastric cancers. *World J Gastroenterol* 2000; **6**: 125-127
- 13 **Wang RQ**, Fang DC, Liu WW. MUC2 gene expression in gastric cancer and preneoplastic lesion tissues. *Shijie Huaren Xiaohua Zazhi* 2000; **8**: 285-288
- 14 **Guo YQ**, Zhu ZH, Li JF. Flow cytometric analysis of apoptosis and proliferation in gastric cancer and precancerous lesion. *Shijie Huaren Xiaohua Zazhi* 2000; **8**: 983-987
- 15 **Chen SY**, Wang JY, Ji Y, Zhang XD, Zhu CW. Effects of *Helicobacter pylori* and protein kinase C on gene mutation in gastric cancer and precancerous lesions. *Shijie Huaren Xiaohua Zazhi* 2001; **9**: 302-307
- 16 **Xu AG**, Li SG, Liu JH, Gan AH. Function of apoptosis and expression of the proteins Bcl-2, p53 and C-myc in the development of gastric cancer. *World J Gastroenterol* 2001; **7**: 403-406
- 17 **Zhou HP**, Wang X, Zhang NZ. Early apoptosis in intestinal and diffuse gastric carcinomas. *World J Gastroenterol* 2000; **6**: 898-901
- 18 **Zhang FX**, Zhang XY, Fan DM, Deng ZY, Yan Y, Wu HP, Fan JJ. Antisense telomerase RNA induced human gastric cancer cell apoptosis. *World J Gastroenterol* 2000; **6**: 430-432
- 19 **Gu QL**, Li NL, Zhu ZG, Yin HR, Lin YZ. A study on arsenic trioxide inducing *in vitro* apoptosis of gastric cancer cell lines. *World J Gastroenterol* 2000; **6**: 435-437
- 20 **Wu K**, Shan YJ, Zhao Y, Yu JW, Liu BH. Inhibitory effects of RRR-alpha-tocopheryl succinate on benzo(a)pyrene (B(a)P) induced forestomach carcinogenesis in female mice. *World J Gastroenterol* 2001; **7**: 60-65
- 21 **Jung YD**, Mansfield PF, Akagi M, Takeda A, Liu W, Bucana CD, Hicklin DJ, Ellis LM. Effects of combination anti-vascular endothelial growth factor receptor and anti-epidermal growth factor receptor therapies on the growth of gastric cancer in a nude mouse model. *Eur J Cancer* 2002; **38**: 1133-1140
- 22 **Cui RT**, Cai G, Yin ZB, Cheng Y, Yang QH, Tian T. Transretinoic acid inhibits rats gastric epithelial dysplasia induced by N-methyl-N-nitro-N-nitrosoguanidine: influences on cell apoptosis and expression of its regulatory genes. *World J Gastroenterol* 2001; **7**: 394-398
- 23 **Gonzalez CA**, Sala N, Capella G. Genetic susceptibility and gastric cancer risk. *Int J Cancer* 2002; **100**: 249-260
- 24 **Morse MA**, Stoner GD. Cancer chemoprevention: Principles and prospects. *Carcinogenesis* 1993; **14**: 1737-1746
- 25 **Wattenberg LW**. Inhibition of carcinogenesis by minor dietary constituents. *Cancer Res* 1992; **52**(Suppl 7): S2024-S2029
- 26 **Bach A**, Metais P. Fats with short and medium chains. Physiological, biochemical, nutritional and therapeutic aspects. *Ann Nutr Alim* 1970; **24**: 75-144
- 27 **Heerdt BG**, Houston MA, Anthony GM, Augenlicht LH. Initiation of growth arrest and apoptosis of MCF-7 mammary carcinoma cells by tributyrin, a triglyceride analogue of the short-chain fatty acid butyrate, is associated with mitochondrial activity. *Cancer Res* 1999; **59**: 1584-1591
- 28 **Scheppach W**. Effects of short chain fatty acids on gut morphology and function. *Gut* 1994; **35**: S35-38
- 29 **Schroder C**, Eckert K, Maurer HR. Tributyrin induces growth inhibitory and differentiating effects on HT-29 colon cancer cells *in vitro*. *Int J Oncol* 1998; **13**: 1335-1340
- 30 **Maier S**, Reich E, Martin R, Bachem M, Altug V, Hautmann RE, Gschwend JE. Tributyrin induces differentiation, growth arrest and apoptosis in androgen-sensitive and androgen-resistant human prostate cancer cell lines. *Int J Cancer* 2000; **88**: 245-251
- 31 **Egorin MJ**, Yuan ZM, Sentz DL, Plaisance K, Eiseman JL. Plasma pharmacokinetics of butyrate after intravenous administration of sodium butyrate or oral administration of tributyrin or sodium butyrate to mice and rats. *Cancer Chemother Pharmacol* 1999; **43**: 445-453
- 32 **Ying H**, Yu Y, Xu Y. Cloning and characterization of F-LANA, upregulated in human liver cancer. *Biochem Biophys Res Comm* 2001; **286**: 394-400
- 33 **Clarke KO**, Feinman R, Harrison LE. Tributyrin, an oral butyrate analogue, induces apoptosis through the activation of caspase-3. *Cancer Lett* 2001; **171**: 57-65
- 34 **Green DR**, Reed JC. Mitochondria and apoptosis. *Science* 1998; **281**: 1309-1312
- 35 **Ashkenazi A**, Dixit VM. Apoptosis control by death and decoy receptors. *Curr Opin Cell Biol* 1999; **11**: 255-260
- 36 **Adams JM**, Cory S. The Bcl-2 protein family: arbiters of cell survival. *Science* 1998; **281**: 1322-1326
- 37 **Li HL**, Chen DD, Li XH, Zhang HW, Lu JH, Ren XD, Wang CC. JTE-522-induced apoptosis in human gastric adenocarcinoma [correction of adenocarcinoma] cell line AGS cells by caspase activation accompanying cytochrome C release, membrane translocation of Bax and loss of mitochondrial membrane potential. *World J Gastroenterol* 2002; **8**: 217-223
- 38 **Fan XQ**, Guo YJ. Apoptosis in oncology. *Cell Res* 2001; **11**: 1-7
- 39 **Yuan RW**, Ding Q, Jiang HY, Qin XF, Zou SQ, Xia SS. Bcl-2, P53 protein expression and apoptosis in pancreatic cancer. *Shijie Huaren Xiaohua Zazhi* 1999; **7**: 851-854
- 40 **Basu A**, Haldar S. The relationship between Bcl2, Bax and p53: consequences for cell cycle progression and cell death. *Mol Hum Reprod* 1998; **4**: 1099-1109
- 41 **Chang YC**, Xu YH. Expression of Bcl-2 inhibited Fas-mediated apoptosis in human hepatocellular carcinoma BEL-7404 cells. *Cell Res* 2000; **10**: 233-242
- 42 **Tewari M**, Quan LT, O'Rourke K, Desnoyers S, Zeng Z, Beidler DR, Poirier GG, Salvesen GS, Dixit VM. Yama/ CPP32b, a mammalian homolog of CED-3, is a CrmA-inhibitable protease that cleaves the death substrate poly(ADP-ribose) polymerase. *Cell* 1995; **81**: 801-809

Expression of estrogen receptor and estrogen receptor messenger RNA in gastric carcinoma tissues

Xin-Han Zhao, Shan-Zhi Gu, Shan-Xi Liu, Bo-Rong Pan

Xin-Han Zhao, Shan-Zhi Gu, Shan-Xi Liu, Department of Medical Oncology, First Hospital of Xi'an Jiaotong University, Xi'an 710061, Shaanxi Province, China

Bo-Rong Pan, Department of Oncology, Xijing Hospital, Fourth Military Medical University, Xi'an 710032, Shaanxi Province, China
Supported by the First Hospital Scientific Foundation of Xi'an Jiaotong University, No.95012

Correspondence to: Dr. Xin-Han Zhao, Department of Medical Oncology, First Hospital of Xi'an Jiaotong University, Xi'an 710061, Shaanxi Province, China. zhixinhan@pub.xaonline.com

Telephone: +86-29-5324136 **Fax:** +86-29-5275472

Received: 2002-12-22 **Accepted:** 2003-01-16

Abstract

AIM: To study estrogen receptor (ER) and estrogen receptor messenger RNA (ERmRNA) expression in gastric carcinoma tissues and to investigate their association with the pathologic types of gastric carcinoma.

METHODS: The expression of ER and ERmRNA in gastric carcinoma tissues (15 males and 15 females, 42-70 years old) was detected by immunohistochemistry and *in situ* hybridization, respectively.

RESULTS: The positive rate of ER (immunohistochemistry) was 33.3 % in males and 46.7 % in females. In Borrmann IV gastric carcinoma ER positive rate was greater than that in other pathologic types, and in poorly differentiated adenocarcinoma and signet ring cell carcinoma the positive rates were greater than those in other histological types of both males and females ($P < 0.05$). The ER was more highly expressed in diffused gastric carcinoma than in non-diffused gastric carcinoma ($P < 0.05$). The ER positive rate was also related to regional lymph nodes metastases ($P < 0.05$), and was significantly higher in females above 55 years old, and higher in males under 55 years old ($P < 0.05$). The ERmRNA (*in situ* hybridization) positive rate was 73.3 % in males and 86.7 % in females. The ERmRNA positive rates were almost the same in Borrmann I, II, III and IV gastric carcinoma ($P > 0.05$). ERmRNA was expressed in all tubular adenocarcinoma, poorly differentiated adenocarcinoma and signet ring cell carcinoma ($P < 0.05$). The ERmRNA positive rate was related to both regional lymph nodes metastases and gastric carcinoma growth patterns, and was higher in both sexes above 55 years old but without statistical significance ($P > 0.05$). The positive rate of ERmRNA expression by *in situ* hybridization was higher than that of ER expression by immunohistochemistry ($P < 0.05$).

CONCLUSION: ERmRNA expression is related to the pathological behaviors of gastric carcinoma, which might help to predict the prognosis and predict the effectiveness of endocrine therapy for gastric carcinoma.

Zhao XH, Gu SZ, Liu SX, Pan BR. Expression of estrogen receptor and estrogen receptor messenger RNA in gastric carcinoma tissues. *World J Gastroenterol* 2003; 9(4): 665-669
<http://www.wjgnet.com/1007-9327/9/665.htm>

INTRODUCTION

Gastric carcinoma is the most common cause of cancer mortality in China^[1-6] and is responsible for approximately 160 000 deaths annually. During the last 10 years, there has been no improvement in survival after the diagnosis of gastric cancer with an overall 5-year survival rate of 20 %. Surgery remains the primary treatment of choice. However, the disease is often advanced at first presentation, and only 30-40 % of patients undergoing surgery will have a curative resection. The failure of surgery on the disease has led to the use of chemotherapy and radiotherapy as adjuvant or palliative means, but their value is limited because of toxicity and lack of efficacy^[7-12]. Since Jensen discovered the existence of estrogen receptor (ER) in the cytoplasm of human mammary cancer cells in 1960, many researchers have also discovered the presence of ER in some gastric cancer cells, suggesting that these cells can be controlled and regulated by sex hormones. From this we can infer that some cases of gastric cancer are hormone-dependent tumor, and this has stimulated the use of the anti-estrogen compound in its treatment. In this study, the expression of ER, ERmRNA in gastric cancer tissues was examined by immunohistochemistry and *in situ* hybridization, respectively, and the association of their expression and clinical significance at molecular pathological level was also investigated.

MATERIALS AND METHODS

Specimens

Thirty specimens of gastric cancer tissue were collected from The General Surgical Department and The Tumor Surgical Department of the First hospital of Xi'an Jiaotong University. All the cases were pathologically proved to be gastric carcinoma. Of the patients, 15 were females and 15 males. Their age ranged from 42 to 70 and the average age was 58.4. Pathologically 2 cases were papillary adenocarcinoma, 12 tubular adenocarcinoma, 13 poorly differentiated adenocarcinoma, and 3 signet ring cell carcinoma. According to Borrmann classification, 6 cases were type I, 8 type II, 8 type III and another 8 type IV.

ERmRNA *in situ* Hybridization

The slides were treated with 3-amino propyltri-ethoxy saline (APES) and with polylysine. The slides were deparaffinized, hydrated and treated with 30 mL/L H₂O₂ at room temperature for 10 minutes to eliminate the endogenous peroxidase. The slides were incubated with freshly diluted protease K (1:1 000 with 0.01 mol/L Tris buffer saline (TBS)) at 37 °C for 5 to 15 minutes. After being washed with distilled water three times, the slides were treated with 2 g/L glycine for 5 minutes, washed with PBS for 5 minutes, fixed with 40 g/L polymethanol for 30 minutes, and washed again with PBS for 5 minutes, dehydrated with gradient alcohol, and then washed with DEPC, treated with digoxin-labeled probe in 90-100 °C water for 5 to 10 minutes, and then taken out and immediately put in shattered ice for 5 minutes. After the slides became dry in the air, 10 µL *in situ* hybridization solution containing digoxin-labeled probe was added onto each slide,

and the hybridization was conducted in a humidified box for 20 hours. The slides were then washed twice with $2\times$ SSC at 20-30 °C for 5 minutes and with $1\times$ SSC at 37 °C for 10 minutes, incubated with mouse anti-digoxin at 20-37 °C for 30 minutes and washed with 0.5 mol/L PBS three times, each for 2 minutes. The slides were then incubated with anti-mouse biotin IgG at 20-37 °C for 20 minutes, washed with 0.5 mol/L PBS three times, each for 2 minutes and again incubated with SABC at 20-37 °C for 20 minutes, washed with 0.5 mol/L PBS four times, each for 5 minutes. The color reaction was developed with the addition of DAB, and the slides were counter-stained with hematoxylin and sealed with xylene.

Negative control: No estrogen receptor probe in the hybridization solution. The slides showed color directly without any solution added. Hybridization solution was replaced by reserve hybridization solution containing no probe.

Positive control: The specimens from 3 women with mammary cancer and 3 with ovarian cancer, all under 45 years old, were collected and treated in the same way as in the gastric cancer specimens.

ER Immunohistochemistry

Consecutive 5 μ m thick sections were stained with HE and by immunohistochemistry separately. The deparaffinized sections were washed with PBS three times, soaked in 30 mL/L hydrogen dioxide solution for 10 minutes to eliminate the endogenous peroxidase, washed with PBS three times, digested with 10 g/L trypsin for 15 minutes (37 °C), washed with PBS three times, heated to 95 °C in pH 6.0 citric acid buffer solution for 10 minutes before cooled down to room temperature, and then washed three times with PBS, and then blocked with serum (45 °C). The sections were then incubated with the first antibody (1:50) over night, washed three times with PBS, incubated with biotin-labeled secondary antibody and then washed with PBS. The sections were finally incubated with streptavidin biotin peroxidase complex, the color reaction was developed with the addition of DAB, and the sections were counter-stained with hematoxylin and sealed transparently.

Positive cells from *in situ* hybridization appeared yellow and the positive stain was mainly located in the nuclei and cytoplasm around the nuclei. Immunohistochemically positive cells appeared brown yellow and the positive stain was located in the cytoplasm. The average positive rate in every case was calculated in 5 high-power fields. When 10 % or more of the cancer cells were stained positive in a labeled slice, it was defined as ER or ERmRNA positive.

Statistical analysis

All data were analyzed with SPSS 8.0 statistical software (including the accurate four square table probability method and similar χ^2 test) and $P < 0.05$ was considered to have statistical significance.

RESULTS

Immunohistochemically stained positive cells looked brown yellow in cytoplasm. The distribution of ER positive cells and the intensity of positive reaction were uneven (Figure 1). The smooth muscle cells and the lymphocytes in the interstice and the mucosa membrane beside the cancer tissue appeared negative. The positively expressed ERmRNA were mainly located in cytoplasm and nuclei of cancer cells, next to the interstice (Figure 2). The number of positive cells was different in different fields. It was greater in some fields, with 34 positive cells in a high power field, but in other fields, the positive cells were scarce or absent. There were weakly hybridized

positive signals in interstitial smooth muscle cells and lymphocytes. The tissue beside the cancer appeared negative.

ER positive gastric cancer tissues both in men and women were more common in Borrmann type IV, histologically it was more common in poorly differentiated adenocarcinoma and signet ring cell carcinoma ($P < 0.05$). ERmRNA positive cells were found in Borrmann type I, II, III and IV ($P > 0.05$). ERmRNA expression was also found in tubular adenocarcinoma, poorly differentiated adenocarcinoma and signet ring cells ($P < 0.05$, Table 1).

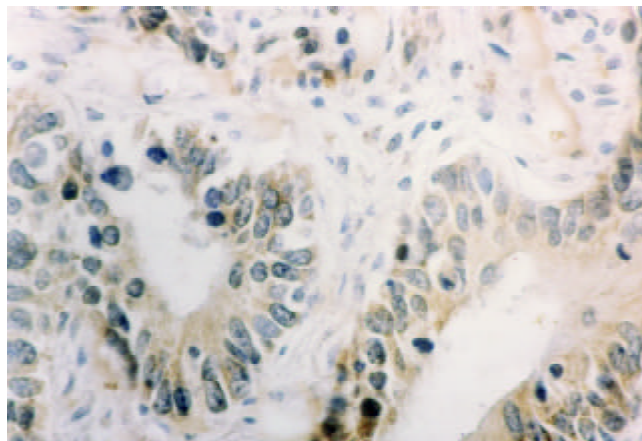


Figure 1 ER positive expression in gastric carcinoma tissue SABC $\times 400$.

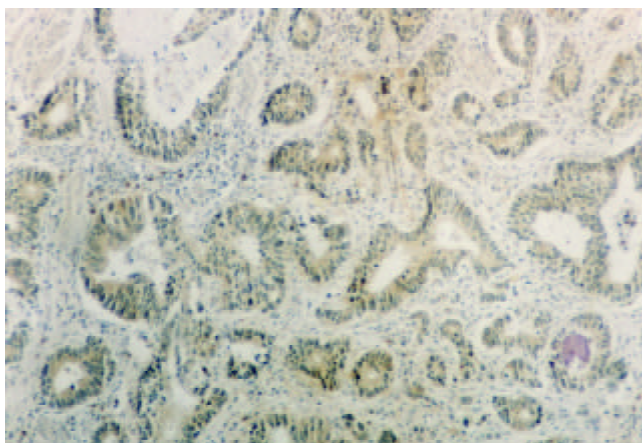


Figure 2 ER mRNA positive expression in gastric carcinoma tissue *in situ* hybridization $\times 100$.

ER expression had a high positive rate in females above 55 years old and in males under 55 years old ($P < 0.05$). And ERmRNA expression had a high positive rate in both males and females above 55 years old ($P > 0.05$, Table 1).

Diffusely growing gastric cancer had a high ER positive rate ($P < 0.05$). Both the diffusely and non-diffusely growing gastric cancers had a high positive expression rate of ERmRNA ($P > 0.05$, Table 1). The increase of ER positive rate is associated with the increase of the involved regional lymph nodes including the upper and lower parts of pylorus, the greater and lesser curvatures of the stomach and the lymph nodes on both sides of cardia ($P < 0.05$). There seemed to be a tendency that the increase of ERmRNA positive rate is associated with the increase of the number of the involved lymph nodes ($P > 0.05$, Table 1).

To compare the immunohistochemistry results with *in situ* hybridization results, ER positive rate was 40.0 % (M/F: 33.3 % vs 46.7 %), and ERmRNA positive rate was 80.0 % (M/F: 73.3 % vs 86.7 %, $P < 0.05$, Table 1).

Table 1 Relationship between ER, ERmRNA expression and pathology in gastric cancer

Pathology	Male					Female					Total				
	n	ER(+)	%	ERmRNA(+)	%	n	ER(+)	%	ERmRNA(+)	%	n	ER(+)	%	ERmRNA(+)	%
Borrmann I	3	1	33.3	1	33.3	3	0	0	2	66.7	6	1	16.7	3	50.0
II	4	1	25.0	3	75.0	4	2	50.0	3	75.0	8	3	37.5	6	75.0
III	4	1	25.0	3	75.0	4	2	50.0	4	100.0	8	3	37.5	7	87.5
IV	4	2	50.0	4	100.0	4	3	75.0	4	100.0	8	5	62.5	8	100.0
Papillary	1	0	0	0	0	1	0	0	0	0	2	0	0	0	0
Tubular	6	0	0	4	66.7	6	1	16.7	5	88.3	12	1	8.3	10	83.3
Poorly differentiated	7	4	57.1	6	85.7	6	4	66.7	6	100.0	13	8	61.5	11	84.6
Signet ring cell	1	1	100.0	1	100.0	2	2	100.0	2	100.0	3	3	100.0	3	100.0
Nondiffused	9	2	22.2	6	66.7	5	1	20.0	4	80.0	14	3	21.4	10	71.4
Diffused	6	3	50.0	5	83.3	10	6	60.0	9	90.0	16	9	56.3	14	87.5
Lymph node 0	3	0	0	1	33.3	4	0	0	3	75.0	7	0	0	4	57.1
Involvement ≤3	4	1	25.0	3	75.0	5	3	60.0	4	80.0	9	4	44.4	7	77.8
4~6	6	2	33.3	5	83.3	5	3	60.0	5	100.0	11	5	45.5	10	90.9
>6	2	2	100.0	2	100.0	1	1	100.0	1	100.0	3	3	100.0	3	100.0
Age ≤55	6	3	50.0	4	66.7	9	3	33.3	7	77.8	15	6	40.0	11	73.3
>55	9	2	22.2	7	77.8	6	4	66.7	6	100.0	15	6	40.0	13	86.7
Total	15	5	33.3	11	73.3	15	7	46.7	13	86.7	30	12	40.0	24	80.0

DISCUSSION

In 1960 Jensen reported for the first time that after injecting a physiological dose of $^3\text{H-E}_2$ into the hypoderm of a young mouse, the amount of $^3\text{H-E}_2$ found in the tissues of uterus, vagina and other parts was far greater than that found in blood plasma. This proved for the first time that ER protein was present in the tissues of uterus and vagina. When estrogen enters target cells, it first combines with its receptor in cytoplasm, then forms a compound of receptor protein-estradiol which then enters cell nucleus, binds to the chromatin and affects the transcription of DNA. To sexual and non-sexual target organs, estrogen may be a hormone promoting splitting. There are proved documents that gastric cancer cells have sex hormone receptors and may be controlled and regulated by sex hormones, suggesting that gastric cancer in some cases is hormone-dependent tumor, but the molecular mechanisms underlying carcinogenesis are still largely unknown^[13-17]. A lot of documents have proved that molecular biology plays an important role in the development and metastasis of some cancers, such as endometrial adenocarcinoma^[18-20], lung cancer^[21], breast cancer^[22-37], apocrine carcinoma^[38], leukemia^[39] and prostate cancer^[40,41]. But there are very few studies on the ERmRNA expression in gastric cancer tissues.

With ER examination on the specimens of ten primary gastric cancer patients (6 men and 4 women), Tokunaga discovered that 2 cases were ER(+) and the patients were women with histological undifferentiated cancer. Yanzuoshaner used the PAP method to analyze 140 specimens of primary gastric cancer after operation. The results showed that 23 cases were ER(+) (16.4%), 6 cases were ER(±) (4.3%), 111 cases were ER(-) (79.3%). Recently, a new estrogen receptor, called estrogen receptor beta, has been found to be expressed in various tissues including normal gastrointestinal tract, the effect of estrogen in stomach cancer, as well as in normal stomach, might be mediated by ER beta, and the role of ER beta might differ by the subtype of stomach adenocarcinoma, specifically signet ring cell adenocarcinomas. But the conclusions needed

more evidence to support^[13]. Takano *et al* reported the expression of estrogen receptor-alpha and ER-beta mRNAs in human gastric cancers, and the results showed that the expression of estrogen receptor-alpha and ER-beta mRNAs were changed in 20 cases (49%) and unchanged in 21 cases (51%). The incidences of lymph node metastasis and liver metastasis were significantly higher in changed cases than in unchanged cases^[14]. One fourth gastric cancers were ER positive compared with breast cancers, and gastric cancer nuclear receptors were also smaller than that of breast cancers in number^[22,23]. Of 95 cases of male patients with gastric cancers, 12 were ER(+) (12.6%), of 45 cases of female patients 10 were ER(+) (22.2%), 11.5% of men under 50 years old were ER(+) and 14.5% of men above 50 years old were ER(+). There was no marked difference between them, most of the ER(+) cases were Borrmann II, and most cases of the histological type were undifferentiated^[15-16].

Our results of the present study showed that ER positive rate was 40.0% and ER-mRNA positive rate was 80.0% in gastric cancers. ER(+) was related to lymph node metastasis and gastric cancer growth patterns. Furthermore, we also discovered that the positive rates of gastric cancer ER, ERmRNA were higher in female than in male. Thus we can conclude that female gastric cancer patients are more easily affected by estrogen than male gastric cancer patients. Our results are similar to the results reported by other scholars.

Many foreign researchers think that compared with other methods in examining ER protein, the molecular hybridizations in examining ERmRNA has a higher sensitivity^[13-17]. By using Northern hybridization method Hankin found that the ERmRNA positive rate of breast cancer was 87.0%. But by using the $^3\text{H-estradiol}$ method to examine ER protein the positive rate was only 46.0%. The two methods showed a marked difference. In our study, the immunohistochemical examination showed that the high expression of ER protein was most common in poorly differentiated adenocarcinoma and signet ring cell carcinoma. *In situ* hybridization showed

that ERmRNA had a high positive expression rate, which was also found in tubular adenocarcinoma and poorly differentiated adenocarcinoma of histological type. What is more noteworthy is that in 13 cases of ER(-) gastric cancer tissues *in situ* hybridization examination showed that ERmRNA was (+). The reason may be that *in situ* hybridization probe could hybridize with mRNA which directs the synthesis of protein of irregular quality lacking function. The protein may lack the epitope that can be identified by the ER monoclonal antibody, and there may be defects present in ER protein synthesis after transcription. ERmRNA positive signal was also present in interstitial smooth muscle cells and lymphocytes, which suggests that estrogen can regulate not only epithelial cells but also interstitial cells.

We speculate that ERmRNA expression has greater value than ER protein expression in clinical application because of the high sensitivity of *in situ* hybridization and the strong ERmRNA expression in gastric cancer, which can be used to judge the prognosis of tumor and predict the effectiveness of endocrine therapy for gastric cancer.

REFERENCES

- Zhou Y**, Gao SS, Li YX, Fan ZM, Zhao X, Qi YJ, Wei JP, Zou JX, Liu G, Jiao LH, Bai YM, Wang LD. Tumor suppressor gene p16 and Rb expression in gastric cardia precancerous lesions from subjects at a high incidence area in northern China. *World J Gastroenterol* 2002; **8**: 423-425
- Cai L**, Yu SZ, Zhan ZF. Cytochrome p450 2E1 genetic polymorphism and gastric cancer in Changde, Fujian Province. *World J Gastroenterol* 2001; **7**: 792-795
- Su M**, Lu SM, Tian DP, Zhao H, Li XY, Li DR, Zheng ZC. Relationship between ABO blood groups and carcinoma of esophagus and cardia in Chaoshan inhabitants of China. *World J Gastroenterol* 2001; **7**: 657-661
- Cai L**, Yu SZ, Zhang ZF. Glutathione S-transferases M1, T1 genotypes and the risk of gastric cancer: a case-control study. *World J Gastroenterol* 2001; **7**: 506-509
- Xin Y**, Li XL, Wang YP, Zhang SM, Zheng HC, Wu DY, Zhang YC. Relationship between phenotypes of cell-function differentiation and pathobiological behavior of gastric carcinomas. *World J Gastroenterol* 2001; **7**: 53-59
- Wang RT**, Wang T, Chen K, Wang JY, Zhang JP, Lin SR, Zhu YM, Zhang WM, Cao YX, Zhu CW, Yu H, Cong YJ, Zheng S, Wu BQ. *Helicobacter pylori* infection and gastric cancer: evidence from a retrospective cohort study and nested case-control study in China. *World J Gastroenterol* 2002; **8**: 1103-1107
- Song ZJ**, Gong P, Wu YE. Relationship between the expression of iNOS, VEGF, tumor angiogenesis and gastric cancer. *World J Gastroenterol* 2002; **8**: 591-595
- Tao HQ**, Zou SC. Effect of preoperative regional artery chemotherapy on proliferation and apoptosis of gastric carcinoma cells. *World J Gastroenterol* 2002; **8**: 451-454
- Xao HB**, Co WX, Yin HR, Lin YZ, Ye SH. Influence of L-methionine-deprived total parenteral nutrition with 5-fluorouracil on gastric cancer and host metabolism. *World J Gastroenterol* 2001; **7**: 698-701
- Ma ZF**, Wang ZY, Zhang JR, Gong P, Chen HL. Carcinogenic potential of duodenal reflux juice from patients with long-standing postgastrectomy. *World J Gastroenterol* 2001; **7**: 376-380
- Miehlke S**, Kirsch C, Dragosics B, Gschwantler M, Oberhuber G, Antos D, Dite P, Lauter J, Labenz J, Leodolter A, Malfertheiner P, Neubauer A, Ehninger G, Stolte M, Bayerdorffer E. *Helicobacter pylori* and gastric cancer: current status of the Austrain Czech German gastric cancer prevention trial (PRISMA Study). *World J Gastroenterol* 2001; **7**: 243-247
- Wu K**, Shan YJ, Zhao Y, Yu JW, Liu BH. Inhibitory effects of RRR-alpha-tocophery1 succinate on benzo (a) pyrene (B(a)P)-induced forestomach carcinogenesis in female mice. *World J Gastroenterol* 2001; **7**: 60-65
- Matsuyama S**, Ohkura Y, Eguchi H, Kobayashi Y, Akagi K, Uchida K, Nakachi K, Gustafsson JA, Hayashi S. Estrogen receptor beta is expressed in human stomach adenocarcinoma. *J Cancer Res Clin Oncol* 2002; **128**: 319-324
- Takano N**, Iizuka N, Hazama S, Yoshino S, Tangoku A, Oka M. Expression of estrogen receptor-alpha and -beta mRNAs in human gastric cancer. *Cancer Lett* 2002; **176**: 129-135
- Tot T**. The role of cytokeratins 20 and 7 and estrogen receptor analysis in separation of metastatic lobular carcinoma of the breast and metastatic signet ring cell carcinoma of the gastrointestinal tract. *Apmis* 2000; **108**: 467-472
- Goldstein NS**, Long A, Kuan SF, Hart J. Colon signet ring cell adenocarcinoma: immunohistochemical characterization and comparison with gastric and typical colon adenocarcinomas. *Appl Immunohistochem Mol Morphol* 2000; **8**: 183-188
- Messa C**, Russo F, Pricci M, Di Leo A. Epidermal growth factor and 17beta-estradiol effects on proliferation of a human gastric cancer cell line (AGS). *Scand J Gastroenterol* 2000; **35**: 753-758
- Robertson JA**, Farnell Y, Lindahl LS, Ing NH. Estradiol up-regulates estrogen receptor messenger ribonucleic acid in endometrial carcinoma (Ishikawa) cells by stabilizing the message. *J Mol Endocrinol* 2002; **29**: 125-135
- Cobellis L**, Reis FM, Driul L, Vultaggio G, Ferretti I, Villa E, Petraglia F. Estrogen receptor alpha mRNA variant lacking exon 5 is coexpressed with the wild-type in endometrial adenocarcinoma. *Eur J Obstet Gynecol Reprod Biol* 2002; **102**: 92-95
- Horvath G**, Leser G, Hahlin M, Henriksson M. Exon deletions and variants of human estrogen receptor mRNA in endometrial hyperplasia and adenocarcinoma. *Int J Gynecol Cancer* 2000; **10**: 128-136
- Mollerup S**, Jorgensen K, Berge G, Haugen A. Expression of estrogen receptors alpha and beta in human lung tissue and cell lines. *Lung Cancer* 2002; **37**: 153-159
- Chearskul S**, Bhothisuwan K, Churintrapun M, Semprasert N, Onreabroi S. Estrogen receptor-alpha mRNA in primary breast cancer: relationship to estrogen and progesterone receptor proteins and other prognostic factors. *Asian Pac J Allergy Immunol* 2002; **20**: 13-21
- Zhao H**, Hart LL, Keller U, Holth LT, Davie JR. Characterization of stably transfected fusion protein GFP-estrogen receptor-alpha in MCF-7 human breast cancer cells. *J Cell Biochem* 2002; **86**: 365-375
- Bouras T**, Southey MC, Chang AC, Reddel RR, Willhite D, Glynn R, Henderson MA, Armes JE, Venter DJ. Stanniocalcin 2 is an estrogen-responsive gene coexpressed with the estrogen receptor in human breast cancer. *Cancer Res* 2002; **62**: 1289-1295
- Zheng WQ**, Lu J, Zheng JM, Hu FX, Ni CR. Variation of ER status between primary and metastatic breast cancer and relationship to p53 expression. *Steroids* 2001; **66**: 905-910
- Otto AM**, Schubert S, Netzker R. Changes in the expression and binding properties of the estrogen receptor in MCF-7 breast cancer cells during growth inhibition by tamoxifen and cisplatin. *Cancer Chemother Pharmacol* 2001; **48**: 305-311
- Yang X**, Phillips DL, Ferguson AT, Nelson WG, Herman JG, Davidson NE. Synergistic activation of functional estrogen receptor(ER)-alpha by DNA methyltransferase and histone deacetylase inhibition in human ER-alpha-negative breast cancer cells. *Cancer Res* 2001; **61**: 7025-7029
- Lacroix M**, Querton G, Hennebert P, Larsimont D, Leclercq G. Estrogen receptor analysis in primary breast tumors by ligand-binding assay, immunocytochemical assay, and northern blot: a comparison. *Breast Cancer Res Treat* 2001; **67**: 263-271
- Diel P**, Olf S, Schmidt S, Michna H. Molecular identification of potential selective estrogen receptor modulator(SERM) like properties of phytoestrogen in the human breast cancer cell line MCF-7. *Planta Med* 2001; **67**: 510-514
- Brouillet JP**, Dujardin MA, Chalbos D, Rey JM, Grenier J, Lamy PJ, Maudelonde T, Pujol P. Analysis of the potential contribution of estrogen receptor (ER) beta in ER cytosolic assay of breast cancer. *Int J Cancer* 2001; **95**: 205-208
- Fasco MJ**, Keyomarsi K, Arcaro KF, Gierthy JF. Expression of an estrogen receptor alpha variant protein in cell lines and tumors. *Mol Cell Endocrinol* 2000; **166**: 156-169
- Yang X**, Ferguson AT, Nass SJ, Phillips DL, Butash KA, Wang SM, Herman JG, Davidson NE. Transcriptional activation of estrogen receptor alpha in human breast cancer cells by histone deacetylase inhibition. *Cancer Res* 2000; **60**: 6890-6894

- 33 **Koduri S**, Poola I. Quantitation of alternatively spliced estrogen receptor alpha mRNAs as separate gene populations. *Steroids* 2001; **66**: 17-23
- 34 **Omoto Y**, Iwase H, Iwata H, Hara Y, Toyama T, Ando Y, Kobayashi S. Expression of estrogen receptor alpha exon 5 and 7 deletion variant in human breast cancers. *Breast Cancer* 2000; **7**: 27-31
- 35 **Anandappa SY**, Sibson R, Platt-Higgins A, Winstanley JH, Rudland PS, Barraclough R. Variant estrogen receptor alpha mRNAs in human breast cancer specimens. *Int J Cancer* 2000; **88**: 209-216
- 36 **Shao ZM**, Shen ZZ, Fontana JA, Barsky SH. Genistein' s "ER-dependent and independent" actions are mediated through ER pathways in ER-positive breast carcinoma cell lines. *Anticancer Res* 2000; **20**: 2409-2416
- 37 **Koduri S**, Fuqua SA, Poola I. Alterations in the estrogen receptor alpha mRNA in the breast tumors of African American women. *J Cancer Res Clin Oncol* 2000; **126**: 291-297
- 38 **Bratthauer GL**, Lininger RA, Man YG, Tavassoli FA. Androgen and estrogen receptor mRNA status in apocrine carcinomas. *Diagn Mol Pathol* 2002; **11**: 113-118
- 39 **Cutolo M**, Carruba G, Villaggio B, Coviello DA, Dayer JM, Campisi I, Miele M, Stefano R, Castagnetta LA. Phorbol diester 12-O-tetradecanoylphorbol 13-acetate(TPA)up-regulates the expression of estrogen receptors in human THP-1 leukemia cells. *J Cell Biochem* 2001; **83**: 390-400
- 40 **Maruyama S**, Fujimoto N, Asano K, Ito A, Usui T. Expression of estrogen receptor alpha and beta mRNAs in prostate cancers treated with leuprorelin acetate. *Eur Urol* 2000; **38**: 635-639
- 41 **Li LC**, Chui R, Nakajima K, Oh BR, Au HC, Dahiya R. Frequent methylation of estrogen receptor in prostate cancer: correlation with tumor progression. *Cancer Res* 2000; **60**: 702-706

Edited by Pang LH

Effects of astragali radix on the growth of different cancer cell lines

Jiang Lin, Hui-Fang Dong, JJ Oppenheim, OM Howard

Jiang Lin, Department of Gastroenterology, Shuguang Hospital, Shanghai University of Traditional Chinese Medicine, Shanghai 200021, China

Hui-Fang Dong, JJ Oppenheim, OM Howard, Laboratory of Molecular Immunoregulation, National Cancer Institute, Frederick, MD 21702, USA

Correspondence to: Dr. Jiang Lin, Department of Gastroenterology, Shuguang Hospital, Shanghai University of Traditional Chinese Medicine, Shanghai, 200021, China. lin_jiang@hotmail.com

Telephone: +86-21-53821650-292

Received: 2002-04-12 **Accepted:** 2002-05-08

Abstract

AIM: To investigate the inhibitory effect of a Chinese herb medicine Astragali radix (AR) on growth of different cancer cell lines.

METHODS: To observe the in vitro effects of AR on tumor cell proliferation by trypan blue exclusion, MTS method and tritium thymidine incorporation assay. Apoptosis was detected by DNA ladder method.

RESULTS: The inhibition rates of AR on the cell respiration of AGS, KATOIII, HT29, MDA231, MEL7 and MEL14 were 68.25 %, 62.36 %, 22.8 %, 27.69 %, 2.85 % and 5.14 % respectively at the concentration of 100 ug/ml; it inhibited AGS DNA synthesis by 87.33 % at the concentration of 50 ug/ml. The inhibitory effect on AGS was time- and dose-dependent. AR did not induce apoptosis in AGS cells.

CONCLUSION: AR specifically inhibits gastric cancer cells growth in vitro and the mechanism is mainly cytostatic but not cytotoxic or inducing apoptosis.

Lin J, Dong HF, Oppenheim JJ, Howard OM. Effects of astragali radix on the growth of different cancer cell lines. *World J Gastroenterol* 2003; 9(4): 670-673

<http://www.wjgnet.com/1007-9327/9/670.htm>

INTRODUCTION

Astragali radix (AR) is the dried root of *Astragalus membranaceus* Bge. Var. *mongholicus* and is used as a tonic in the traditional Chinese medicine. It has been used extensively as an adjuvant^[1,2] in cancer treatment and as a phytochemical immune modulator. Kurashige *et al.* reported that AR lowered the incidence of urinary bladder carcinoma in N-butyl-N'-butanolnitrosoamine treated mice by activating the cytotoxicity of lymphocytes and increasing the production of IL-2 and IFN- γ ^[3]. Lau's study showed that it also restored the chemiluminescent oxidative burst activity of murine splenic macrophage suppressed by renal cell carcinoma^[4]. Wang's research suggested that an extract of AR had the synergetic effect with IL-2 in activating LAK cells, resulting in reducing the dosage of IL-2 and the associated toxicity^[5]. In addition, AR also could promote the proliferation of B cell and the production of immunoglobulin^[6] and has a bidirectional modulating effect on T cells. It was reported that it could reduce

the suppressive activity of Ts in post-burn mice^[7] and also increase Th cell activity in immunodepressed mice^[8].

However, there was no report on whether AR affects tumor cells growth directly. In this paper, we studied the effect of an aqueous extract of AR on the growth of different cancer cell lines.

MATERIALS AND METHODS

Cell lines and culture conditions

Human gastric cancer cell lines AGS and KATO-III were purchased from the American Type Culture Collection. AGS is a cell line of moderately-poorly differentiated adenocarcinoma and KATO-III is a cell line of signet ring carcinoma. HT29 is a cell line of colon cancer and MDA231 is a breast cancer cell line, both of them were kindly provided by Dr. Bill Murphy. Mel7 and Mel14 are melanoma cell lines, which were gifted by Dr. D. Schadendorf. All the cells were cultured in RPMI1640 medium supplemented with 10 % FBS, 100 U/ml penicillin, 100 μ g/ml streptomycin and Glutamine (GIBCO BRL, Life Technologies, Grand Island, NY, USA) in a humidified atmosphere of 95 % air with 5 % CO₂ at 37 °C as a monolayer.

Preparation of herbal extract

AR was purchased from Da Xing Chinese herbal medicines store in DC, USA. The aqueous extract was prepared by the Natural Product Branch of National Cancer Institute. 8 grams of aqueous extract was dissolved in 100 ml distilled water and centrifuged at 4 000 rpm for 20 min. The supernatant was passed through a 0.22 μ m filter (Corning, Costar, NY, USA) and reached a final concentration of 80 mg/ml. The solution was aliquoted and stored at -20 °C for future use.

AR treatment

The herbal treatment was modified from the anti-cancer drug screening program of natural product branch in NCI^[9]. Cells were harvested by trypsinization when they were confluent. 1×10^4 and 3×10^5 cells were seeded in each of the 96-well and 6-well plates respectively and cultured in RPMI 1640 medium supplemented with 5 % FBS for 24 hours. Then different concentrations of AR were added in each well to attain a series of different concentrations (1, 12.5, 25, 50 and 100 μ g/ml) and incubated for 48 hours for further measurements.

MTS assay

Cell growth was measured by MTS assay. The Cell Titer 96 Aqueous Non-Radioactive Cell Proliferation Assay Kit was purchased from Promega, WI, USA. Briefly, MTS and PMS were mixed at the ratio of 20:1 immediately before being added to the samples. 20 μ l of MTS/PMS solution was added to each of the 96-well plate and incubated at 37 °C in a humidified 5 % CO₂ atmosphere for 3 hours. The absorbance was read at 490 nm using Bio-Tek's Power Wave x reader-assay system (BIO-TEK Instruments INC, VT, USA). Each sample was triplicated.

³H-thymidine incorporation assay

Cell DNA synthesis was measured by ³H-thymidine incorporation assay. At the end of herbal treatment, 1 μ Ci of ³H-thymidine was added in each well of a 96-well plate. Then the plate was incubated at 37 °C in a humidified 5 % CO₂

atmosphere for 4 hours and stored at -70°C overnight. On the second day, the frozen plate was thawed at 37°C and the DNA was transferred to the filtermat using multi-channel cell collector. The filtermat was washed with distilled water thrice and 95 % alcohol once. 4.5 ml Betaplate Scint was added to the filtermat and read the filtermat with liquid scintillation and luminescence counter (Perkin Elmer Wallac Inc. MD, USA). Each sample was quadruplicated.

Cell viability assay

Cells were cultured and treated in 6-well plate. At the end of the treatment, the cells were collected by trypsinization and counted with 1 % Trypan-blue. Each sample was triplicated.

DNA ladder analysis

DNA ladder was measured as described previously^[10] with some modification. Briefly, 1×10^6 cells in 0.5 ml were lysed in 1 ml DNA lysis buffer containing 1 M Tris-HCl, 0.2 M EDTA, 4 M NaCl, 20 % SDS and 400 $\mu\text{g}/\text{ml}$ proteinase K) and incubated at 37°C overnight. DNA was extracted in Phase LockGel eppendorf (Eppendorf Scientific Inc. NY, USA) with an equal volume of phenol/choloroform/isoamyl alcohol (25:24:1) and precipitated with 2 volumes of ice-cold 100 % ethanol and 1/10 volume of 3 M sodium acetate at -70°C for 1 hr. DNA was collected, washed with ice-cold 70 % ethanol once and dried in air. Then DNA was dissolved in TE buffer containing 10 $\mu\text{g}/\text{ml}$ RNase I and incubated at 37°C for 1 hr. Equal amounts of DNA (10 $\mu\text{g}/\text{well}$) were electrophoresed in 1.8 % agarose gels impregnated with ethidium bromide (0.1 $\mu\text{g}/\text{ml}$) for 2 hr at 70 V. DNA fragments were visualized by UV transillumination.

Statistical analysis

The inhibition rate was calculated by the following formula: inhibition rate (%) = $(\text{OD}/\text{CPM}_{\text{control}} - \text{OD}/\text{CPM}_{\text{test}}) / \text{OD}/\text{CPM}_{\text{control}} \times 100\%$. Student's *t*-test was used to compare the results. All *P* values were described by two-tailed analysis. $P < 0.05$ was considered statistically significant.

RESULTS

Growth inhibiting effect of AR on different cancer cell lines

Figure 1 illustrated the inhibiting effects of AR on the proliferation of 6 tumor cell lines, including AGS, KATOIII, HT29, MDA231, MEL7 and MEL14, measured by MTS method. It was found that after 48 hours incubation, 100 $\mu\text{g}/\text{ml}$ of AR had greater inhibiting effect on gastric tumor cell lines of AGS and KATOIII than the other cancer cell lines. It inhibited the growth of AGS and KATOIII by 68.25 % and 62.36 % respectively, compared to only 22.8 %, 27.69 %, 2.85 % and 5.14 % reduction in cell growth of HT29, MDA231, MEL7 and MEL14. It appeared to be selectively inhibiting the growth of gastric cancer cell line.

Effect of AR on AGS viability

Whether the inhibitory effect of AR on AGS growth was cytotoxic was determined by the trypan blue measurement. Figure 2 showed the viable cell numbers of AGS treated with different concentrations of AR. In the range from 1 to 50 $\mu\text{g}/\text{ml}$, AR had a dose-dependent inhibiting effect on AGS growth and almost completely inhibited the AGS growth at the concentration of 50 $\mu\text{g}/\text{ml}$, of which the cell number of the test group was very close to the cell number seeded at the beginning of the test and few cells were stained blue. However, at the concentration of 100 $\mu\text{g}/\text{ml}$, AR showed cytotoxicity on AGS, of which the cell number was lower than the initial cell number.

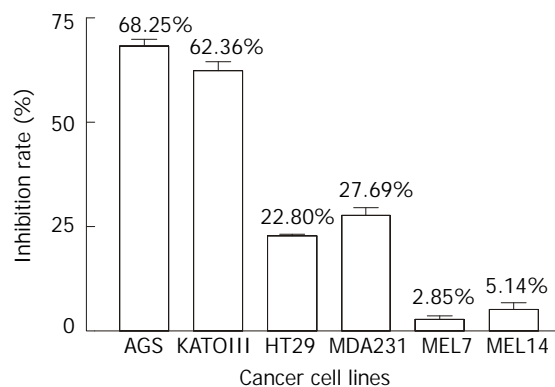


Figure 1 Effect of AR on the growth of 6 cancer cell lines. Cells were treated with AR at the concentration of 100 $\mu\text{g}/\text{ml}$ for 48 hrs and cell growth was measured with MTS method.

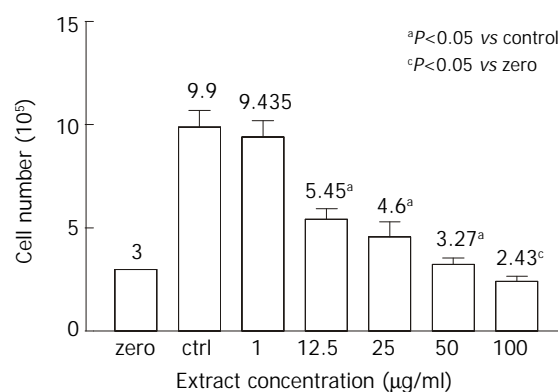


Figure 2 Effect of AR on AGS viability. AGS cells were treated with different concentrations of AR for 48 hrs and cell viability was measured with trypan blue. At or below the concentration of 50 $\mu\text{g}/\text{ml}$, AR was not cytotoxic to AGS cells. But at the concentration of 100 $\mu\text{g}/\text{ml}$, it showed cytotoxicity on AGS.

Dose-dependent and time-dependent effects of AR on AGS growth

The dose-dependent and time-dependent effects of AR on AGS growth were observed by MTS assay. AGS cells were treated with different concentrations of AR for 48 hours. Figure 3 showed that the inhibitory effect of AR on AGS was proportional to the extract concentrations. In the time-course experiment, AGS cells were treated with 50 $\mu\text{g}/\text{ml}$ of AR and incubated for 6, 12, 24 and 48 hours respectively. In Figure 4, it was found that AR began to inhibit the cell growth significantly at the 12th hour and the effect was also improved linearly while prolonging the incubation time.

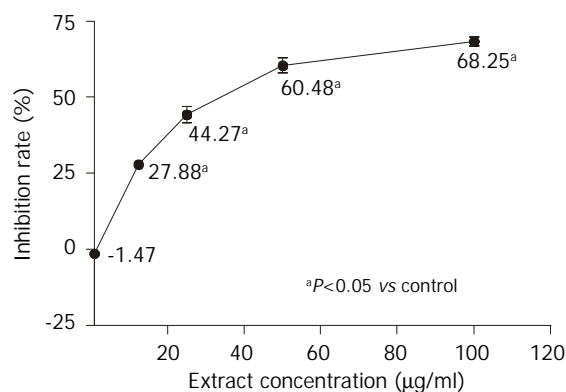


Figure 3 Dose-dependent effect of AR on AGS growth. AGS cells were treated with a serial of diluted concentrations (1, 12.5, 25, 50 and 100 $\mu\text{g}/\text{ml}$) of AR for 48 hrs and cell growth was measured with MTS method. The inhibition effect of AR was improved accompanied by increase of concentration.

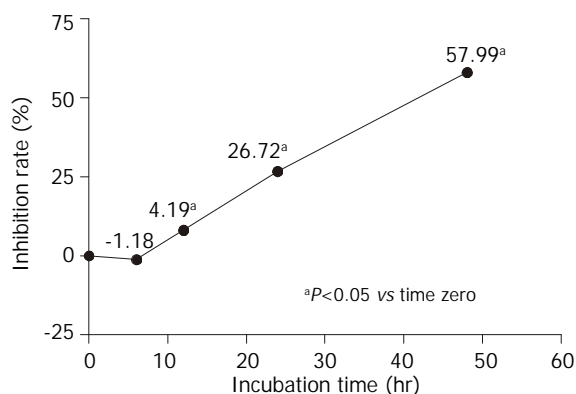


Figure 4 Time-dependent effect of AR on AGS growth. AGS cells were treated with 50 $\mu\text{g}/\text{ml}$ of AR for 6, 12, 24 and 48 hrs. The cell growth was measured by MTS method. The inhibition effect of AR on AGS growth was enhanced with incubation time.

Effect of AR on AGS DNA synthesis

Tritium-labeled thymidine incorporation assay was used to evaluate the effect of AR on AGS DNA synthesis. AGS cells were treated with different concentrations of AR for 48 hours. Figure 5 demonstrated that AR could significantly inhibit the DNA synthesis of AGS. It was also observed that the inhibiting effect of AR increased sharply from the concentrations of 1 $\mu\text{g}/\text{ml}$ to 25 $\mu\text{g}/\text{ml}$ and it increased slowly from then on.

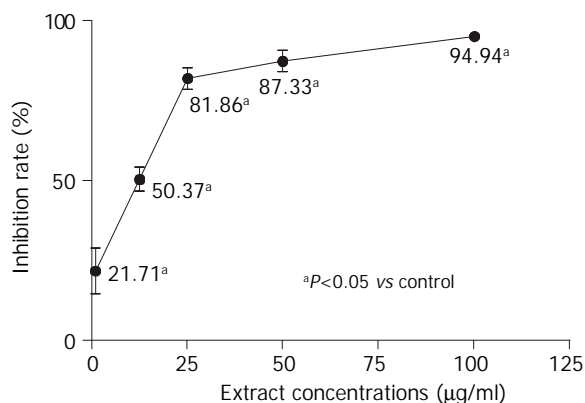


Figure 5 Effect of AR on DNA synthesis of AGS. AGS cells were treated with a serial of diluted concentrations (1, 12.5, 25, 50 and 100 $\mu\text{g}/\text{ml}$) of AR for 48 hrs and cell growth was measured with tritium labeled thymidine incorporation assay. AR started to inhibit the DNA synthesis of AGS at 1 $\mu\text{g}/\text{ml}$ and the inhibiting effect was dose-dependent.

Effect of AR on AGS apoptosis

DNA fragmentation method was used to observe whether apoptosis was induced in AGS by AR. AGS cells were treated with different concentrations of AR for 48 hours. However, there was no DNA ladder appeared in the electrophoresis gel. So the herbal extract had no effect on AGS apoptosis.

DISCUSSION

AR is a tonic herbal medicine which is used as an adjuvant extensively in the treatment of various cancers, such as lung cancer, digestive tract cancers, renal cancer, bladder cancer^[1,2,11], melanoma and AIDS^[12]. It had been reported that it could improve the host immune function suppressed by tumors and relieve the marrow suppression induced by chemotherapeutic agents so that it could make the patients more tolerant to chemotherapeutic therapy. Although there were some studies showing that AR could inhibit the tumor growth *in vivo*, the anti-cancer effect was testified through activating the activity of Th, LAK and macrophages and promoting the production

of IL-2 and IFN- γ . However, whether it has direct inhibition effect on tumors cells has not been elucidated yet.

In this study, 6 different cancer cell lines were used to test the inhibitory effect of AR. After 48 hours incubation, AR inhibited the gastric cancer cell lines of AGS and KATOIII growth by 68.25 % and 62.36 %, compared to the inhibition rates of colon cancer cell line HT29, breast cancer cell line MDA231 and melanoma cell lines of Mel7 and Mel14 which were 22.8 %, 27.69 %, 2.85 % and 5.14 % respectively, suggesting that AR has anti-cancer effect on gastric cancer cell lines. To fully confirm this, many other kinds of cancer cell lines should be tested in order to determine the specificity of the effect. AGS and KATOIII are two different gastric cancer cell lines. AGS is a moderately-poorly differentiated adenocarcinoma cell line while KATOIII is a cell line of signet ring cell carcinoma, but AR has almost the same inhibitory effect on both cell lines.

Many herbal extracts can inhibit cell growth *in vitro* through their cytotoxic effect^[13-16]. We determined whether the inhibitory effect of AR was due to cytotoxicity. In order to clarify this question, we measured the cell growth with trypan blue exclusion method. The initial cell number was 300 000/well and in the untreated wells the cell number reached 990 000/well after 48 hours incubation. The cell number in testing group treated with 1 $\mu\text{g}/\text{ml}$ of AR was 943 500/well ($P>0.05$, vs control group). However, the cell numbers of the other testing groups treated with AR from the concentrations of 12.5 $\mu\text{g}/\text{ml}$ to 100 $\mu\text{g}/\text{ml}$ were significantly lower than that of the control group and but higher than the initial cell number except for the testing group treated with 100 $\mu\text{g}/\text{ml}$ AR, whose cell number was only 243 000/well ($P=0.017$, compared to the initial cell number). Few cells stained trypan blue could be seen in the testing groups treated with AR at the concentration lower than 100 $\mu\text{g}/\text{ml}$. So the inhibition effect of AR at the concentrations of 50 $\mu\text{g}/\text{ml}$ or below was not cytotoxic while AR is cytotoxic to AGS cell at the concentration of 100 $\mu\text{g}/\text{ml}$. Further studies showed that the inhibition effect of AR on AGS was dose- and time-dependent. The maximal concentration without cytotoxicity was around 50 $\mu\text{g}/\text{ml}$ and the corresponding inhibition rate was 60.48 %. AR came into effect at the 12th hour and reached its peak at the 48th hour.

One characteristic of the tumor cells is that their rapid proliferations are accompanied by DNA synthesis and cellular replication. Tritium labeled thymidine incorporation assay reflects the cellular DNA synthesis. Our results showed that the DNA synthesis of AGS was significantly inhibited by AR. The inhibition rate increased sharply from 21.71 % to 81.86 % at the concentrations ranging from 1 $\mu\text{g}/\text{ml}$ to 25 $\mu\text{g}/\text{ml}$, then it reached a plateau. So AR might suppress AGS cell growth through inhibition of DNA synthesis. The inhibition rates of AGS cell growth expressed by MTS method and tritium labeled thymidine incorporation assay were different. The latter was higher than the former. This may be attributed to that MTS and tritium labeled thymidine incorporation assay were two different indirect measurements used in cell growth evaluation. MTS reflects the cell growth at the level of cell respiration while tritium labeled thymidine incorporation assay at the level of DNA synthesis. When the cellular DNA synthesis is suppressed, the cells might be in an inactive status in which the cells could still respire. So the inhibition rate of cell growth expressed by MTS is lower than that expressed by tritium labeled thymidine incorporation assay.

Apoptosis is a kind of programming cell death whose impairment may induce cell immortality and carcinogenesis^[17]. Some agents such as aspirin, indomethacin and arsenic trioxide^[10,18] and some herbs such as Anemarrhena asphodeloides Bunge, Albizzia Lucidior I. Nielsen and Paeoniae radix^[19-21] were reported to have the ability of inducing apoptosis in gastric

cancer cells and inhibiting their growth. However, apoptosis could not be observed in AGS cells treated with AR. Combined with the results of trypan blue experiment that there were few cells, which were treated with AR, stained blue, the inhibition effect of AR on AGS is not through the mechanism of cytotoxic or apoptosis.

The aqueous and organic extracts of AR were used in this study. But the organic extract had no effect on AGS growth (data not shown). So the effective anti-cancer components are in the aqueous extract. Polysaccharide^[22], astragaloside^[23], and flavonoids^[24] have been found in AR. Some studies showed that the polysaccharides and flavonoids from other herbs had the anti-tumor efficiency *in vitro* and *in vivo*^[25-29]. But up to now, there has no evidence showing that these compounds from AR have anti-cancer activity *in vitro*. Hence, further studies are required. Selenium toxicity has been confirmed in the livestock consuming plants of the genus *Astragalus* and selenium was reported to have the carcinostatic activity in the animals^[30,31]. So selenium might play a critical role in AR inhibiting AGS growth.

In conclusion, the inhibitory effect of AR on the growth of gastric cancer cell line of AGS is mainly cytostatic.

REFERENCES

- 1 **Cha RJ**, Zeng DW, Chang QS. Non-surgical treatment of small cell lung cancer with chemo-radio-immunotherapy and traditional Chinese medicine. *Zhonghua Neike Zazhi* 1994; **33**: 462-466
- 2 **Li NQ**. Clinical and experimental study on shen-qi injection with chemotherapy in the treatment of malignant tumor of digestive tract. *Zhongguo Zhongxiyi Jiehe Zazhi* 1992; **12**: 588-592
- 3 **Kurashige S**, Akuzawa Y, Endo F. Effects of astragali radix extract on carcinogenesis, cytokine production, and cytotoxicity in mice treated with a carcinogen, N-butyl-N'-butanolnitrosoamine. *Cancer Invest* 1997; **17**: 30-35
- 4 **Lau BH**, Ruckle HC, Botolazzo T, Lui PD. Chinese medicinal herbs inhibit growth of murine renal cell carcinoma. *Cancer Biother* 1994; **9**: 153-161
- 5 **Wang Y**, Qian XJ, Hadley HR, Lau BH. Phytochemicals potentiate interleukin-2 generated lymphokine-activated killer cell cytotoxicity against murine renal cell carcinoma. *Mol Biother* 1992; **4**: 143-146
- 6 **Yoshida Y**, Wang MQ, Liu JN, Shan BE, Yamashita U. Immunomodulating activity of Chinese medicinal herbs and *Oldenlandia diffusa* in particular. *Int J Immunopharmacol* 1997; **19**: 359-370
- 7 **Liang H**, Zhang Y, Geng B. The effect of astragalus polysaccharides (APS) on cell mediated immunity (CMI) in burned mice. *Zhonghua Zhengxing Shaoshang Waike Zazhi* 1994; **10**: 138-141
- 8 **Zhao KS**, Mancini C, Doria G. Enhancement of the immune response in mice by *Astragalus membranaceus* extracts. *Immunopharmacology* 1990; **20**: 225-233
- 9 **Alley MC**, Scudiero DA, Monks PA, Hursey ML, Czenwinski MJ, Fine DL, Abbott BJ, Mayo JG, Shoemaker RH, Boyd MR. Feasibility of drug screening with panels of human tumor cell lines using a microculture tetrazolium assay. *Cancer Research* 1988; **48**: 589-601
- 10 **Jiang XH**, Wong BCY, Yuen ST, Jiang SH, Cho CH, La KC, Lin MCM, Kung HF, Lam SK. Arsenic trioxide induces apoptosis in human gastric cancer cells through up-regulation of p53 and activation of caspase-3. *Int J Cancer* 2001; **91**: 173-179
- 11 **Rittenhouse JR**, Lui PD, Lau BH. Chinese medicinal herbs reverse macrophage suppression induced by urological tumors. *J Urol* 1991; **146**: 486-490
- 12 **Chu DT**, Lin JR, Wong W. The *in vitro* potentiation of LAK cell cytotoxicity in cancer and AIDS patients induced by F3-a fractionated extract of *Astragalus membranaceus*. *Zhonghua Zhongliu Zazhi* 1994; **16**: 167-171
- 13 **Chen SB**, Gao GY, Li YS, Yu SC, Xiao PG. Cytotoxic constituents from *Aquilegia ecalcarata*. *Planta Med* 2002; **68**: 554-556
- 14 **Wang S**, Zhang YJ, Chen RY, Yu DQ. Goniolactones A-F, six new styrylpyrone derivatives from the roots of *Goniolthalmus cheliensis*. *J Nat Prod* 2002; **65**: 835-841
- 15 **Fan CQ**, Sun HF, Chen SN, Yue JM, Lin ZW, Sun HD. Triterpene saponins from *Graniotome furcata*. *Nat Prod Lett* 2002; **16**: 161-166
- 16 **Li J**, Liang N, Mo L, Zhang X, He C. Comparison of the cytotoxicity of five constituents from *Pteris semipinnata* L. *in vitro* and the analysis of their structure-activity relationships. *Yaoxue Xuebao* 1998; **33**: 641-644
- 17 **Willie AH**, Bellamy CO, Bubb VJ, Clarke AR, Corbet S, Curtis L, Harrison DJ, Hooper ML, Toft N, Webb S, Bird CC. Apoptosis and carcinogenesis. *Br J Cancer* 1999; **80** (Suppl 1): 34-37
- 18 **Zhou XM**, Wong BCY, Fan XM, Zhang HB, Lin MCM, Kung HF, Fan DM, Lam SK. Non-steroidal anti-inflammatory drugs induce apoptosis in gastric cancer cells through up-regulation of bax and bak. *Carcinogenesis* 2001; **22**: 1393-1397
- 19 **Takeda Y**, Togashi H, Matsuo T, Shinzawa H, Takeda Y, Takahashi T. Growth inhibition and apoptosis of gastric cancer cell lines by *Anemarrhena asphodeloides bunge*. *J Gastroenterol* 2001; **36**: 79-90
- 20 **Cai B**, Zhang HF, Zhang DY, Cui CB, Li WX. Apoptosis-inducing activity of extract from Chinese herb, *Albizia Lucidior* I. Nielsen. *Aizheng* 2002; **21**: 373-378
- 21 **Lee SM**, Li ML, Tse YC, Leung SC, Lee MM, Tsui SK, Fung KP, Lee CY, Waye MM. *Paenoniae Radix*, a Chinese herbal extract, inhibit hepatoma cells growth by inducing apoptosis in a p53 independent pathway. *Life Sci* 2002; **71**: 2267-2277
- 22 **Zheng Z**, Liu D, Song C, Cheng C, Hu Z. Studies on chemical constituents and immunological function activity of hairy root of *Astragalus membranaceus*. *Chin J Biotechnol* 1998; **14**: 93-97
- 23 **Hirotsani M**, Zhou Y, Rui H, Furuya T. Cycloartane triterpene glycosides from the hairy root cultures of *Astragalus membranaceus*. *Phytochemistry* 1994; **37**: 1403-1407
- 24 **Lin LZ**, He XG, Lindenmairer M, Nolan G, Yang J, Cleary M, Qiu SX, Cordell GA. Liquid chromatography-electrospray ionization mass spectrometry study of the flavonoids of the roots of *Astragalus mongholicus* and *A. membranaceus*. *J Chromatogr A* 2000; **876**: 87-95
- 25 **Lu X**, Su M, Li Y, Zeng L, Liu X, Li J, Zheng B, Wang S. Effect of *Acanthopanax giraldii* Harms Var. *Hispidium* Hoo polysaccharides on the human gastric cancer cell line SGC-7901 and its possible mechanism. *Chin Med J (Engl)* 2002; **115**: 716-721
- 26 **Wang SY**, Hus ML, Hus HC, Tzeng CH, Lee SS, Shiao MS, Ho CK. The anti-tumor effect of *Ganoderma lucidum* is mediated by cytokines released from activated macrophages and T lymphocytes. *Int J Cancer* 1997; **70**: 699-705
- 27 **Wang HB**, Zheng QY. Effects of *Phytolacca acinosa* polysaccharides I with different schedules on its antitumor efficiency in tumor bearing mice and production of IL-1, IL-2, IL-6, TNF, CSF activity in normal mice. *Immunopharmacol Immunotoxicol* 1997; **19**: 197-213
- 28 **Chang WH**, Chen CH, Lu FJ. Different effects of baicalein, baicalin and wogonin on mitochondrial function, glutathione content and cell cycle progression in human hepatoma cell lines. *Planta Med* 2002; **68**: 128-132
- 29 **Zheng GQ**. Cytotoxic terpenoids and flavonoids from *Artemisia annua*. *Planta Med* 1994; **60**: 54-57
- 30 **Spallholz JE**. On the nature of selenium toxicity and carcinostatic activity. *Free Radic Bio Med* 1994; **17**: 45-64
- 31 **Harrison PR**, Lanfear J, Wu L, Fleming J, McGarry L, Blower L. Chemopreventive and growth inhibitory effects of selenium. *Biomed Environ Sci* 1997; **10**: 235-245

Correlation between expression of cyclooxygenase-2 and angiogenesis in human gastric adenocarcinoma

Hong-Xia Li, Xin-Ming Chang, Zheng-Jun Song, Shui-Xiang He

Hong-Xia Li, Xin-Ming Chang, Zheng-Jun Song, Shui-Xiang He,
Department of gastroenterology, First Affiliated Hospital of Xi'an Jiaotong University, Xi'an 710061, Shaanxi Province, China

Correspondence to: Dr. Hong-Xia Li, Department of Gastroenterology, First Affiliated Hospital of Xi'an Jiaotong University, Xi'an 710061, Shaanxi Province, China. hx1105sina.com

Telephone: +86-29-5324101

Received: 2002-10-09 **Accepted:** 2002-11-09

Abstract

AIM: To evaluate the expression of cyclooxygenase (COX-2) and the relationship with tumor angiogenesis and advancement in gastric adenocarcinoma.

METHODS: Immunohistochemical stain was used for detecting the expression of COX-2 in 45 resected specimens of gastric adenocarcinoma; the monoclonal antibody against CD34 was used for displaying vascular endothelial cells, and microvascular density (MVD) was detected by counting of CD34-positive vascular endothelial cells. Paracancerous tissues were examined as control.

RESULTS: Immunohistological staining with COX-2-specific polyclonal antibody showed cytoplasmic staining in the cancer cells, some atypical hyperplasia and intestinal metaplasia, as well as angiogenic vasculature present within the tumors and preexisting vasculature adjacent to cancer lesions. The rate of expression of COX-2 and MVD index in gastric cancers were significantly increased, compared with those in the paracancerous tissues (77.78 vs 33.33 %, 58.13±19.99 vs 24.02±10.28, $P<0.01$, $P<0.05$, respectively). In 36 gastric carcinoma specimens with lymph node metastasis, the rate of COX-2 expression and MVD were higher than those in the specimens without metastasis (86.11 vs 44.44 %, 58.60±18.24 vs 43.54±15.05, $P<0.05$, $P<0.05$, respectively). The rate of COX-2 expression and MVD in the specimens with invasive serosa were significantly higher than those in the specimens without invasion to serosa (87.88 vs 50.0 %, 57.01±18.79 vs 42.35±14.65, $P<0.05$, $P<0.05$). Moreover, MVD in COX-2-positive specimens was higher than that in COX-2-negative specimens (61.29±14.31 vs 45.38±12.42, $P<0.05$). COX-2 expression was positively correlated with MVD ($r=0.63$, $P<0.05$).

CONCLUSION: COX-2 expression might correlate with the occurrence and advancement of gastric carcinoma and is involved in tumor angiogenesis in gastric carcinoma. It is likely that COX-2 by inducing angiogenesis can be one of mechanisms which promotes invasion and metastasis of gastric carcinoma. It may become a new therapeutic target for anti-angiogenesis.

Li HX, Chang XM, Song ZJ, He SX. Correlation between expression of cyclooxygenase-2 and angiogenesis in human gastric adenocarcinoma. *World J Gastroenterol* 2003; 9(4): 674-677
<http://www.wjgnet.com/1007-9327/9/674.htm>

INTRODUCTION

COX is a key enzyme in the conversion of arachidonic acid to prostaglandin, and two isoforms of COX, namely COX-1 and COX-2, have been identified^[1,2]. COX-1 is constitutively expressed in many tissues and is considered to be involved in various physiological functions, whereas COX-2 is induced by pathological stimuli, such as inflammation, various growth factors and cytokines produced by tumor cells^[1-3].

Epidemiologic studies showed that nonsteroidal anti-inflammatory drugs (NSAIDs), known to inhibit COX, could reduce the incidence rate and mortality from digestive tract carcinomas^[4-10]. In rodent models of FAP, a genetic disease leading to colonic carcinoma, blockade of COX-2, suppresses intestinal polyp formation^[11]. Increased COX-2 expression has been reported in colorectal, pancreatic, hepatocellular and other cancers^[12-20]. Taken together, these data provide strong evidence for the importance of COX-2 in oncogenesis.

It has been reported that tumor angiogenesis play an important role in tumor growth, invasion and metastasis^[21-25]. We investigated the expression of COX-2, MVD in human gastric cancer. The aim of this study was to determine the relationship between COX-2 and tumor angiogenesis, and the development, progression of gastric cancer. The further understanding of oncogenesis might provide a new approach to tumor therapy.

MATERIALS AND METHODS

Materials

45 patients with gastric adenocarcinomas confirmed pathologically underwent gastrectomy in our hospital from January 2000 to October 2001. From these subjects, gastric tumor and paracancerous tissues (more than 5 cm away from the lesion) were obtained from resected specimen. Among them, 35 were male, and 10 female, with a mean age of 57.51±10.73 (33 to 78). Patients who had received radiotherapy or chemotherapy before gastrectomy were excluded. Histologically, they were classified by the WHO criteria, 5 were highly differentiated adenocarcinoma, 10 moderately-differentiated, 27 poorly-differentiated, 3 undifferentiated. As regards to the size of cancer, 20 were <5 cm, 25 ≥5 cm. 33 tumors invaded to the serosa and 12 tumors not. 36 cases had local lymph node metastasis.

Reagents and methods

Antibody against COX-2 was purchased from Santa Cruz Biotechnology, Inc; antibody against CD34 and ready to use SP immunohistochemical reagent box were purchased from Fijian Maixin CO, Ltd. Formalin-fixed, paraffin-embedded surgical specimens from 45 cases of gastric carcinoma were available and sliced sequentially with a thickness of 4 μm. The slices carrying the detected antigen were dyed with SP immunohistochemical staining method, and those in the control group were dyed according to the above method, with the first antibody substituted by PBS.

Statistical methods

The data were presented as $\bar{x}\pm s$; numerical variable by χ^2 test;

enumeration data by *t* test; COX-2 relationship with MVD by spearman rank correlation test (depending on the quantitative index of COX-2 and MVD).

RESULTS

The cytoplasm of the gastric cancer cells stained with brown granules were identified to be COX-2 positive. Only nuclei stained blue were identified to be COX-2 negative. COX-2 expression was scored semi-quantitatively according to the density and the percentage of positivity into score 0, 1, 2, 3. A minimum of 10 high power view were used to assess COX-2 expression level. If the sum of two scores was 1-3, the slice would be considered as low-expression of COX-2. If 4-6, it would be considered as high-expression of COX-2. Vascular endothelial cells were considered CD34-positive if their cytoplasm stained brown or brownish yellow. The microvessels were counted according to the number of single endothelial cell or endothelial cell cluster showing brownish yellow granules in the cytoplasm. The slices were observed first microscopically under the low power ($\times 40$), then selected the most dense area of microvessels was selected to be observed under high power ($\times 200$, the surface area of every visual field was 0.785 mm^2), and the number of microvessels in 3 visual field were counted and took the average as MVD of this specimen^[26].

COX-2, MVD expression and distribution

77.78 % (35/45) cases of gastric carcinomas showed COX-2 positive expression while high-expression was detected in 22 cases, low-expression in 13. 33.33 % (15/45) cases of paracancerous tissues showed COX-2 positive expression while high-expression was only detected in 3 cases. The rate and density of COX-2 expression in cancerous tissues were significantly higher than in paracancerous tissues ($\chi^2=18$, $\chi^2=6.09$, $P<0.005$, $P<0.05$, respectively). The positive COX-2 staining was mainly diffusely located as brownish yellow stained granules in the cytoplasm. Immunohistological analysis revealed cytoplasmic staining in the neoplastic cells (Figure 1), atypical hyperplasia and intestinal metaplasia. In addition, COX-2 was also detected in the angiogenic vasculature present within the tumors and preexisting vasculature adjacent to cancer lesions (Figure 2). In contrast, normal epithelium or stroma occasionally showed weak staining pattern or didn't.

The mean MVD in gastric carcinoma was significantly higher than that in para-cancerous tissues (58.13 ± 19.99 , 24.02 ± 10.28 , $t=10.18$, $P<0.001$). The positive expression of CD34 was mainly presented as brownish yellow or brownish granules in the cytoplasm of vascular endothelial cell (Figure 3). New blood vessels in the cancerous lesions had no regular contour and were not evenly distributed.

The relationship between the rate of COX-2 expression and MVD

The result showed that MVD (61.29 ± 14.31) in the COX-2-positive gastric cancerous tissues was higher than that (45.38 ± 12.43) in the COX-2-negative one ($t=5.64$, $P<0.001$). The expression of COX-2 was positively correlated with MVD ($r=0.63$, $P<0.05$).

The relationship between the expression of COX-2, MVD and pathological features of gastric carcinoma

In Table 1, the associations between COX-2, MVD expression and the pathological features were shown. Both COX-2 and MVD were not correlated with tumor size, tumor histological type. However, there was correlation between COX-2, MVD and depth of invasion and lymph-node metastasis of gastric carcinoma respectively.

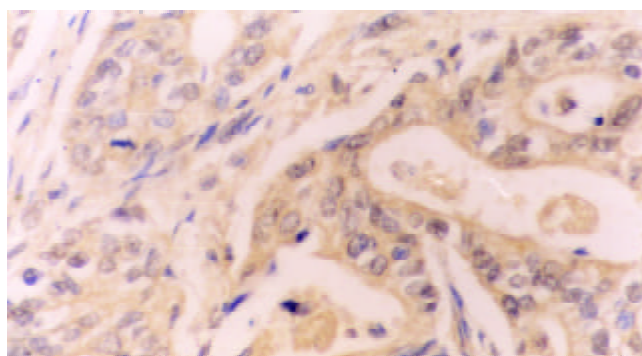


Figure 1 COX-2 expression in gastric adenocarcinoma.

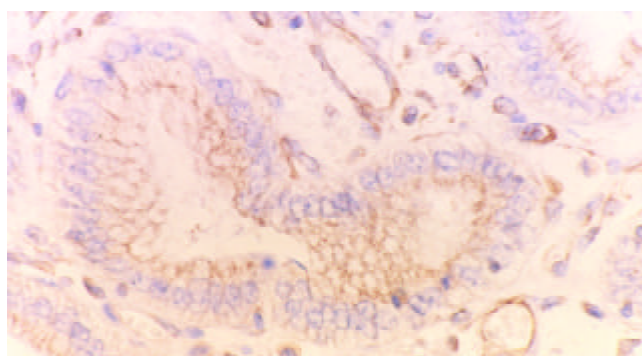


Figure 2 COX-2 expression was also detected in the vasculature within gastric adenocarcinoma.

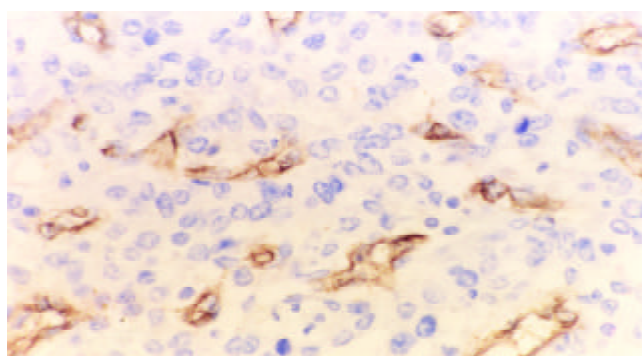


Figure 3 CD₃₄ expression in the cytoplasm of vascular endothelial cell within gastric adenocarcinoma.

Table 1 The relationship between COX-2, MVD and pathological features of gastric carcinoma

Pathological characteristics	Positive COX-2(%)	MVD $\bar{x} \pm s$	Total
Tumor size			
<5 cm	15(75.0)	60.64 \pm 18.55	20
\geq 5 cm	20(80.0)	55.68 \pm 17.98	25
Depth of invasion			
Invading serosa	29(87.88) ^a	57.01 \pm 18.79 ^c	33
No invasion to serosa	6(50.0)	42.35 \pm 14.65	12
Degree of differentiation			
Well differentiated	12(80.0)	52.45 \pm 17.67	30
Poorly differentiated	23(76.67)	57.32 \pm 18.20	15
Lymph-node metastasis			
Positive	31(86.11) ^b	58.60 \pm 18.24 ^d	36
negative	4(44.44)	43.54 \pm 15.05	9

Note: well differentiated cancer cells include highly and moderately differentiated ones; poorly differentiated cancer

cells include poorly differentiated and undifferentiated ones. ^a $P < 0.05$ ($\chi^2 = 5.23$), vs the rate of COX-2 expression in gastric carcinomas not invading serosa; ^b $P < 0.05$ ($\chi^2 = 5.08$), vs the rate of COX-2 expression in gastric carcinoma without lymph-node metastasis; ^c $P < 0.05$ ($t = 2.44$), vs MVD in gastric carcinomas not invading serosa; ^d $P < 0.05$ ($t = 2.28$), vs MVD in gastric carcinomas without lymph-node metastasis.

DISCUSSION

Human gastric mucosa normally expresses no detectable levels of COX-2 protein^[27,28]. In the current study, we found that the rate of COX-2 expression in gastric cancer was significantly increased, compared with that in the paracancerous tissues, the expression of COX-2 showed cytoplasmic staining, not only in cancerous cells but also in precancerous lesion such as atypical hyperplasia and intestinal metaplasia. A similar pattern of COX-2 expression has previously been found in human gastric cancer^[29-34]. The above data demonstrated that COX-2 was up-regulated in human gastric cancer, suggesting COX-2 may play an important role in occurrence of gastric cancer, being a relatively early event in the carcinogenesis of stomach.

Here, we also analyzed the relationship between COX-2 expression and clinical pathological features in gastric carcinoma. It was shown that the rate of COX-2 expression was correlated closely with the depth of tumor invasion, indicating COX-2 may contribute to invasive growth of gastric carcinoma. The rate of COX-2 expression of gastric carcinoma with lymph-node metastasis was higher than that without suggesting the increase of its expression in gastric cancer tissue can promote lymph-node metastasis. It seemed more likely that COX-2 probably heightened viability and increased infiltrative potential of gastric cancer. The mechanism was not clear. Tsujii concluded that overexpression of the COX-2 gene as a result of transfection promoted invasiveness in wild type human colon carcinoma cell lines through the induction of metalloproteinase-2 and membrane-type metalloproteinase^[35]. Rat intestinal epithelial cells that overexpressed COX-2 protein were found to be resistant to butyrate-induced apoptosis and had elevated bcl-2 protein expression and decrease expression of both E-cadherin and the transforming growth factor- β receptor^[36]. Each of these changes has been linked to enhanced tumorigenic potential and increased tumor invasiveness. Therefore, the above data further indicated that COX-2 might play an important role in gastric tumorigenesis and tumor progression.

Recently the relation of COX-2 and tumor angiogenesis is emphasized. One of the mechanisms by which PGE₂ supports tumor growth is by inducing the angiogenesis necessary to supply oxygen and nutrients to tumors >2 mm in diameter^[37,38]. Masferrer^[39] reported that SC-236, a COX-2-selective inhibitor, was effective in reducing angiogenesis driven by bFGF in the matriel rat model, whereas SC-560, a COX-1-selective inhibitor was ineffective. He also observed COX-2 expression in newly formed blood vessels within tumors grown in animals, whereas under normal physiological conditions the quiescent vasculature expressed only the COX-1 enzyme, indicating COX-2-derived prostaglandins contributed to tumor angiogenesis^[40]. In our study, COX-2 expression was also detected in the angiogenic vasculature present within the tumors and preexisting vasculature adjacent to cancer lesions, suggesting COX-2 may induce newly formed blood vessels to sustain tumor cell viability and growth. COX-2 was also expressed within atypical hyperplasia, intestinal metaplasia and neovasculature in the paracancerous tissue, indicating COX-2 may promote precancerous lesion to cancer by new blood vessel formation.

MVD is a reliable index of tumor angiogenesis^[41]. We found that the MVD in COX-2 positive tumors was significantly

higher than that in COX-2 negative tumors, MVD in gastric carcinoma was higher than that in paracancerous tissues, suggesting its distribution was similar to the pattern of COX-2 in gastric carcinoma. A close correlation was present between MVD and COX-2 ($P < 0.01$), indicating COX-2 was closely related to tumor angiogenesis further, and may be one of important factors involved in gastric carcinoma angiogenesis. In addition, MVD in the specimens with lymph node metastasis was significantly higher than that without and it was also correlated closely with the depth of tumor invasion, suggesting that tumor angiogenesis in gastric carcinomas might result in cancer cells entering blood circulation, and the lymph node metastasis could be promoted when the gastric cancer cells invade lymphatic vessels. Both COX-2 and MVD were associated with the depth of invasion and lymph-node metastasis, suggesting the effect of COX-2 on angiogenesis can promote metastatic potential as well as tumor invasiveness. Therefore, inducing tumor angiogenesis may be one of mechanisms which COX-2 promotes the development and metastasis of gastric cancer.

In conclusion, COX-2 expression in gastric adenocarcinoma was higher than that in the paracancerous tissues, and was related to lymph node metastasis and the depth of invasion, suggesting COX-2 might correlate with the occurrence and advancement of gastric carcinoma; COX-2 expression in gastric carcinoma was closely related to MVD, suggesting COX-2 might be involved in tumor angiogenesis in gastric carcinoma, it is likely that COX-2 inducing angiogenesis may be one of mechanisms which COX-2 promotes the invasion, metastasis of tumor in gastric carcinoma. These findings suggest that COX-2 may be a new therapeutic target for anti-angiogenesis.

REFERENCES

- 1 **Williams CS**, DuBois RN. Prostaglandin endoperoxide synthase: why two isoforms? *Am J Physiol* 1996; **270**: G393-G400
- 2 **Eberhart CE**, Dubois RN. Eicosanoids and the gastrointestinal tract. *Gastroenterology* 1995; **109**: 285-301
- 3 **DuBois RN**, Awad J, Morrow J, Roberts LJ 2nd, Bishop P. Regulation of eicosanoid production and mitogenesis in rat intestinal epithelial cells by transforming growth factor-alpha and phorbol ester. *J Clin Invest* 1994; **93**: 493-498
- 4 **Farrow DC**, Vaughan TL, Hansten PD, Stanford JL, Risch HA, Gammon MD, Chow WH, Dubrow R, Ahsan H, Mayne ST, Schoenberg JB, West AB, Rotterdam H, Fraumeni JF Jr, Blot WJ. Use of aspirin and other nonsteroidal antiinflammatory drugs and risk of esophageal and gastric cancer. *Cancer Epidemiol Biomarkers Prev* 1998; **7**: 97-102
- 5 **Garcia-Rodriguez LA**, Huerta-Alvarez C. Reduced risk of colorectal cancer among long-term users of aspirin and nonsteroidal antiinflammatory drugs. *Epidemiology* 2001; **12**: 88-93
- 6 **Morgan G**. Non-steroidal anti-inflammatory drugs and the chemoprevention of colorectal and nonaspirin oesophageal cancers. *Gut* 1996; **38**: 646-648
- 7 **Reeves MJ**, Newcomb PA, Trentham-Dietz A, Storer BE, Remington PL. Nonsteroidal anti-inflammatory drug use and protection against colorectal cancer in women. *Cancer Epidemiol Biomarkers Prev* 1996; **5**: 955-960
- 8 **Thun MJ**. NSAID use and decreased risk of gastrointestinal cancers. *Gastroenterol Clin North Amer* 1996; **25**: 333-348
- 9 **Funkhouser EM**, Sharp GB. Aspirin and reduced risk of esophageal carcinoma. *Cancer* 1995; **76**: 1116-1119
- 10 **Zhuang ZH**, Wang LD. NSAID and digestive tract carcinomas. *Shijie Huaren Xiaohua Zazhi* 2001; **9**: 1050-1053
- 11 **Oshima M**, Dinchuk JE, Kargman SL, Oshima H, Hancock B, Kwong E, Trzaskos JM, Evans JF, Taketo MM. Suppression of intestinal polyposis in Apc delta716 knockout mice by inhibition of cyclooxygenase 2(COX-2). *Cell* 1996; **87**: 803-809
- 12 **Tsujii M**, Kawano S, DuBois RN. Cyclooxygenase-2 expression in human colon cancer cells increase metastatic potential. *Proc*

- Natl Acad Sci USA* 1997; **94**: 3336-3340
- 13 **Chan G**, Boyle JO, Yang EK, Zhang F, Sacks PG, Shah JP, Edelstein D, Soslow RA, Koki AT, Woerner BM, Masferrer JL, Dannenberg AJ. Cyclooxygenase-2 expression is up-regulated in squamous cell carcinoma of the head and neck. *Cancer Res* 1999; **59**: 991-994
 - 14 **Tucker ON**, Dannenberg AJ, Yang EK, Zhang F, Teng L, Daly JM, Soslow RA, Masferrer JL, Woerner BM, Koki AT, Fahey TJ. Cyclooxygenase-2 expression is up-regulated in human pancreatic cancer. *Cancer Res* 1999; **59**: 987-990
 - 15 **Zimmermann KC**, Sarbia M, Weber AA, Borchard F, Gabbert HE, Schrör K. Cyclooxygenase-2 expression in human esophageal carcinoma. *Cancer Res* 1999; **59**: 198-204
 - 16 **Shiota G**, Okubo M, Noumi T, Noguchi N, Oyama K, Takano Y, Yashima K, Kishimoto Y, Kawasaki H. Cyclooxygenase-2 expression in hepatocellular carcinoma. *Hepatogastroenterology* 1999; **46**: 407-412
 - 17 **Shirahama T**, Sakakura C. Overexpression of cyclooxygenase-2 in squamous cell carcinoma of the urinary bladder. *Clin Cancer Res* 2001; **7**: 558-561
 - 18 **Soslow RA**, Dannenberg AJ, Rush D, Woerner BM, Khan KN, Masferrer J, Koki AT. COX-2 is expressed in human pulmonary, colonic, and mammary tumors. *Cancer* 2000; **89**: 2637-2645
 - 19 **Wu QM**, Li SB, Wang Q, Wang DH, Li XB, Liu CZ. The expression of COX-2 in esophageal carcinoma and its relation to clinicopathologic characteristics. *Shijie Huaren Xiaohua Zazhi* 2001; **9**: 11-14
 - 20 **Qiu DK**, Ma X, Peng YS, Chen XY. Significance of cyclooxygenase-2 expression in human primary hepatocellular carcinoma. *World J Gastroenterol* 2002; **8**: 815-817
 - 21 **Che X**, Hokita S, Natsugoe S, Tanabe G, Baba M, Takao S, Aikou T. Tumor angiogenesis related to growth pattern and lymph node metastasis in early gastric cancer. *Chin Med J* 1998; **111**: 1090-1093
 - 22 **Shimoyama S**, Kaminishi M. Increased angiogenin expression in gastric cancer correlated with cancer progression. *J Cancer Res Clin Oncol* 2000; **126**: 468-474
 - 23 **Yoshikawa T**, Yanoma S, Tsuburaya A, Kobayashi O, Sairenji M, Motohashi H, Noguchi Y. Angiogenesis inhibitor, TNP-470, suppresses growth of peritoneal disseminating foci. *Hepatogastroenterology* 2000; **47**: 298-302
 - 24 **Xiangming C**, Hokita S, Natsugoe S, Tanabe G, Baba M, Takao S, Kuroshima K, Aikou T. Angiogenesis as an unfavorable factor related to lymph node metastasis in early gastric cancer. *Ann Surg Oncol* 1998; **5**: 585-589
 - 25 **Maehara Y**, Hasuda S, Abe T, Oki E, Kakeji Y, Ohno S, Sugimachi K. Tumor angiogenesis and micrometastasis in bone marrow of patients with early gastric cancer. *Clin Cancer Res* 1998; **4**: 2129-2134
 - 26 **Weidner N**, Folkman J, Pozza F, Bevilacqua P, Allred EN, Moore DH, Meli Gasparini G. Tumor angiogenesis: a new significant and independent prognostic indicator in early state breast carcinoma. *J Natl Cancer Inst* 1992; **84**: 1875-1887
 - 27 **Mizuno H**, Sakamoto C, Matsuda K, Wada K, Uchida T, Noguchi H, Akamatsu T, Kasuga M. Induction of cyclooxygenase 2 in gastric mucosal lesions and its inhibition by the specific antagonist delays healing in mice. *Gastroenterology* 1997; **112**: 389-397
 - 28 **Kargman S**, Charleson S, Cartwright M, Frank J, Riendeau D, Mancini J, Evans J, O' Neill G. Characterization of prostaglandin G/H synthase 1 and 2 in rat, dog, monkey and human gastrointestinal tracts. *Gastroenterology* 1996; **111**: 445-454
 - 29 **Uefujik K**, Ichikura T, Mochizuki H, Shinomiya N. Expression of cyclooxygenase-2 protein in gastric adenocarcinoma. *J Surg Oncol* 1998; **69**: 168-172
 - 30 **Ratnasinghe D**, Tangrea JA, Roth MJ, Dawsey SM, Anver M, Kasprzak BA, Hu N, Wang QH, Taylor PR. Expression of cyclooxygenase-2 in human adenocarcinomas of the gastric cardia and corpus. *Oncol Rep* 1999; **6**: 965-968
 - 31 **Lim HY**, Joo HJ, Choi JH, Yi JW, Yang MS, Cho DY, Kim H, Nam DK, Lee KB, Kim HC. Increased expression of cyclooxygenase-2 protein human gastric carcinoma. *Chin Cancer Res* 2000; **6**: 519-525
 - 32 **van Rees BP**, Saukkonen K, Ristimäki A, Polkowski W, Tytgat GN, Drillenburger P, Offerhaus GJ. Cyclooxygenase-2 expression during carcinogenesis in the human stomach. *J Pathol* 2002; **196**: 171-179
 - 33 **Ohon R**, Yoshinaga K, Fujita T, Hasegawa K, Iseki H, Tsunozaki H, Ichikawa W, Nihei Z, Sugihara K. Depth of invasion parallels increased cyclooxygenase-2 levels in patients with gastric carcinoma. *Cancer* 2001; **91**: 1876-1881
 - 34 **Xue YW**, Zhang QF, Zhu ZB, Wang Q, Fu SB. Expression of cyclooxygenase-2 and clinicopathologic features in human gastric adenocarcinoma. *World J Gastroenterol* 2003; **9**: 250-253
 - 35 **Murata H**, Kawano S, Tsuji S, Tsuji M, Sawaoka H, Kimura Y, Shiozaki H, Hori M. Cyclooxygenase-2 overexpressing enhances lymphatic invasion and metastasis in human gastric carcinoma. *Am J Gastroenterology* 1999; **94**: 451-455
 - 36 **Tsujii M**, DuBois RN. Alterations in cellular adhesion and apoptosis in epithelial cells overexpressing prostaglandin endoperoxide synthase-2. *Cell* 1995; **83**: 493-501
 - 37 **Form DM**, Auerbach R. PGE2 and angiogenesis. *Proc Soc Exp Biol Med* 1983; **172**: 214-218
 - 38 **Hanahan D**, Folkman J. Patterns and emerging mechanisms of the angiogenic switch during tumorigenesis. *Cell* 1996; **86**: 353-364
 - 39 **Masferrer JL**, Koki A, Seibert K. COX-2 inhibitors. A new class of antiangiogenic agents. *Ann N Y Acad Sci* 1999; **889**: 84-86
 - 40 **Masferrer JL**, Leahy KM, Koki AT, Zweifel BS, Settle SL, Woerner BM, Edwards DA, Flickinger AG, Moore RJ, Seibert K. Antiangiogenic and antitumor activities of cyclooxygenase-2 inhibitors. *Cancer Res* 2000; **60**: 1306-1311
 - 41 **Fukumura D**, Jain RK. Role of nitric oxide in angiogenesis and microcirculation in tumors. *Cancer Metastasis Rev* 1998; **17**: 77-89

Expression, purification and serological analysis of hepatocellular carcinoma associated antigen HCA587 in insect cells

Bing Li, Hong-Yan Wu, Xiao-Ping Qian, Yan Li, Wei-Feng Chen

Bing Li, Hong-Yan Wu, Xiao-Ping Qian, Yan Li, Wei-Feng Chen, Immunology Department of Peking University Health Science Center, Beijing, 100083, China

Supported by National "973" foundation, No. G1999053904 and "863" foundation, No. 2001AA215411

Correspondence to: Dr. Wei-Feng Chen, Immunology Department of Peking University Health Science Center, 38 Xueyuan Road, Beijing, 100083, China. wfchen@public.bta.net.cn

Telephone: +86-10-62091155 **Fax:** +86-10-62091436

Received: 2002-12-08 **Accepted:** 2003-01-02

Abstract

AIM: In order to assess hepatocellular carcinoma associated antigen HCA587 as a potential target for immunotherapy, the Bac-to-Bac expression system was used to express recombinant protein HCA587 in insect cells.

METHODS: The cDNA encoding HCA587 gene was cloned into donor vector pFasBacHtb and recombinant pFasBac Htb-587 was transformed into competent cells DH10Bac. Recombinant Bacmid-587 was transfected into Sf9 insect cells using CELLFECTIN, Recombinant HCA587 protein was produced in Sf9 insect cells after infection with recombinant baculovirus, and was purified using Ni-NTA resin. Sera from HCC patients were also screened using recombinant protein HCA587.

RESULTS: The molecular weight of the recombinant protein HCA587 expressed in insect cells was approximately 43kd. Western blot results proved the recombinant protein HCA587 had the similar antigenicity with its native counterpart. Serological analysis told that the rate of seroreactivity to HCA587 was not high in HCC patients.

CONCLUSION: The recombinant protein HCA587 was successfully expressed and purified using Bac-to-Bac expression system. It paved the way for generation of specific antibody and investigation of immunohistochemical analysis and immune responses of HCC in the future.

Li B, Wu HY, Qian XP, Li Y, Chen WF. Expression, purification and serological analysis of hepatocellular carcinoma associated antigen HCA587 in insect cells. *World J Gastroenterol* 2003; 9 (4): 678-682

<http://www.wjgnet.com/1007-9327/9/678.htm>

INTRODUCTION

The recent developments in the molecular characterization of human tumors and a better understanding of tumor immunology have led to the identification of different kinds of tumor-associated antigens^[1-5]. Of these antigens, Cancer/testis antigens (CT antigens) have played important roles as targets for cancer vaccine development because of their characteristic expression pattern in cancer and testis^[6-9]. Many promising results have been achieved in tumor immunotherapy

using peptides derived from CT antigens^[10-13]. Identifying new CT antigens and evaluating their possible application in the clinic have become a hot spot in this field.

Since hepatocellular carcinoma (HCC) is one of the most pernicious cancers in China, we have adopted serological analysis of recombinant cDNA expression library (SEREX) method and successfully identified a number of novel HCC genes encoding immunogenic proteins. Of these, hepatocellular carcinoma associated antigen HCA587 was identified as one novel CT antigen which was predominantly expressed in HCC and other types of cancers, but not in normal tissues except testis^[14]. Studies on HCA587 may play important roles in transformation, metastasis, diagnosis and immunotherapy of HCC.

The bac-to-bac baculovirus expression system is an eukaryotic gene expression system which allows the rapid and efficient generation of recombinant baculovirus DNAs by site-specific transposition in *E.coli*, rather than homologous recombinant in insect cells^[15,16]. High level heterologous gene expression are often achieved compared to other eukaryotic expression systems, and most of the expressed proteins were shown to have the similar functions as their authentic counterparts. In the present studies, we utilized the Bac-to-Bac system to express the recombinant protein HCA587 in *Spodoptera frugiperda* (sf9) cell lines. The HCA587 protein was then purified using Ni-NTA resin, and the anti-HCA587 antibodies were screened in sera from 81 HCC patients.

MATERIALS AND METHODS

Expression system, insect cells and sera

The Gibco BRL BAC-TO-BAC Baculovirus expression system consists of the transposing vector pFasBacHtb, CELLFECTIN reagent and Max Efficiency DH10Bac competent cells which contain Bacmid (baculovirus shuttle vector plasmid) and helper plasmid to be used to generate recombinant Bacmids. Sf9 insect cells were cultured at 27 °C in SF-900 SFM (Cell culture media and reagents were Gibco BRL brand). All sera of HCC were collected from Peking University teaching hospitals with the agreements of HCC patients.

Amplification and DNA sequencing of gene HCA587

The oligonucleotide primers specific for gene HCA587 were designed and synthesized by Sangon biotechnology company (P1: 5' ATCGGATCCCCTCCCGTTCCAGGCGT 3', P2: 5' ACTAAGCTTTCACCTCAGAAAAGGAGAC 3'). The cDNA produced from normal testis was amplified as template. The PCR products were cloned into pGEM-T-easy vector and sequenced with T7 and SP6 primers by the dideoxy chain termination method using the BigDye Terminator cycle sequencing kit and an ABI PRISM automated DAN sequencer.

Construction of pFasBac Htb-587 plasmid

pFasBac Htb donor plasmid and pGEM-T-easy-587 were prepared by digesting with restriction enzymes BamHI and HindIII. The fragments of interests were purified and recovered from gel using clontech DNA purification system. After ligated

by T4 DNA ligase, the ligation mixture were transformed into DH5 α competent cells. The recombinant plasmid pFasBac HTb-587 was identified by restriction endonuclease digestion.

Generation of recombinant bacmid DNA

Recombinant pFasBac HTb-587 plasmids were transformed into Max Efficiency DH10Bac competent cells, and the gene of interest was transposed into Bacmid through lacZ gene disruption. White clones, containing the recombinant Bacmids were selected on Luria agar plates with 50 μ g/ml kanamycin, 7 μ g/ml gentamicin, 10 μ g/ml tetracycline, 100 μ g/ml Bluo-gal, and 40 μ g/ml IPTG. After 36 h incubation at 37 °C, High-molecular-weight DNA was isolated from the overnight cultures as described in the manual. PCR analysis was used to verify successful transposition to the recombinant Bacmid with M13/pUC primes.

Transfection of Sf9 cells with recombinant bacmid-587

The minipreparations of recombinant Bacmid DNA were transfected into Sf9 insect cells using CELLFECTIN reagent. For each transfection, 9 \times 10⁵ cells were seeded in a 6-well plate and allowed to attach for at least 1 h. The Lipid reagent and Bacmid DNA were diluted separately into 100 μ l of SF-900 SFM without antibiotics, then combined to form lipid-DNA complexes. The lipid-DNA complexes were diluted to 1 ml with SFM and laid over the washed Sf9 cells. The cells were incubated for 5 h at 27 °C, rinsed, and incubated for another 72 h. Recombinant baculovirus were harvested from supernatant and titrated by viral plaque assay. The expression of recombinant protein HCA587 was analyzed by western blot.

Expression and purification of HCA587 from Sf9 insect cells

The recombinant baculovirus were amplified from the suspension cultures of Sf9 cells at MOI of 0.1. We analyzed the effects of several factors in various combinations on the level of protein expression, the factors were: adherent or suspension cultures in different densities; multiplicity of infection (MOI) and recombinant virus replication time. Since the expressed recombinant protein contained 6 \times histidine tag at N-terminal, it was purified using Ni-NTA resin conveniently according to the manufacturer's instructions. SDS-PAGE was performed to analyze the purified protein from the infected cells.

Serological analysis of recombinant HCA587 protein

To analyze the anti-HCA587 antibody in sera of patients, Western blot method was used to screen the reactivity of recombinant HCA587 to sera from 81 HCC patients. The serum was diluted 1/250 as primary antibody, and rabbit-anti-human IgG, conjugated to AP, were used as secondary antibodies. In this assay, the negative control was the serum from healthy volunteers.

RESULTS

Identification of recombinant pFasBacHTb-587 and Bacmid-587

The fragments of gene HCA587 were amplified by PCR using specific primers (Figure 1) and sequenced to ensure the correctness of the ORF. Restriction endonuclease digestion was performed to verify the correct insertion of the gene HCA587 in the recombinant pFasBacHTb-587. The gel electrophoresis in 1 % agarose showed 1.2kb of HCA587 and 4.8kb of pFasBacHTb donor plasmid (Figure 2).

The Bacmid DNA is >135kb. Verification of the insertion of the gene HCA587 in recombinant Bacmid-587 is difficult using classical restriction endonuclease digestion analysis. So PCR was used to confirm the recombinant Bacmid-587. The

pUC/M13 amplification primers are directed at sequences on either side of the mini-attTn7 site with the lacZ α -complementation region of the Bacmid. Amplification products from transposition of recombinant bacmid-587 generated a band of 3.5kb (lane1,2) while amplification of the non-recombinant Bacmid plasmid generated a 300bp band (lane3,4) (Figure 3).

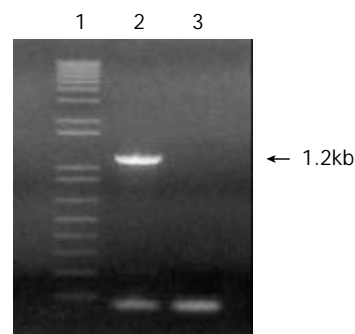


Figure 1 PCR amplified products of HCA587. (Lanes 1: 1 kb DNA marker; lane2: 1.2 kb fragment of HCA587; lane3: negative control).

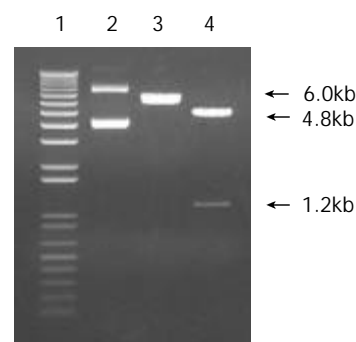


Figure 2 Recombinant pFasBac Htb-587 vector digested by BamHI and HindIII. (Lanes 1: 1kb DNA marker; lane2: recombinant plasmid; lane3: digested by BamHI; lane4: digested by BamHI+HindIII).

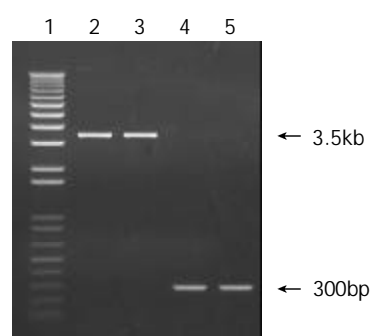


Figure 3 PCR identification of recombinant Bacmid-587. (lane 1: DNA marker; lane 2-3: recombinant Bacmid-587; lane 4-5: blank bacmid).

Transfection of Sf9 cells and amplification of recombinant virus

Recombinant Bacmid-587 was isolated from overnight cultures and transfected into insect cells sf9 with CELLFECTIN reagents. Infected and uninfected sf9 cells can be distinguished by morphology. Uninfected cells continued to divide and form a confluent monolayer while infected cells stopped dividing and enlarged (data not shown).

The Bacmid-587 transfected cells were collected and

analyzed for recombinant protein expression by western blot. Figure 4 showed a specific expressed protein band at 43kd as expected, while no specific band appeared in Sf9 cells without transfection (lane 3). Viral plaque assay showed the viral titer could reach 5×10^8 pfu/ml after amplifying the primary virus in Sf9 suspension cell culture.

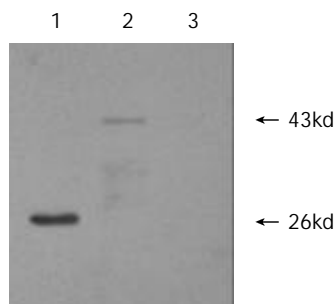


Figure 4 Western blot analysis of recombinant protein expression in sf9 insect cells after transfection. (lane 1: positive control; lane2: Sf9 cell transfected with bacmid-587; lane 3: blank Sf9 cells).

SDS-PAGE analysis of purified HCA587 protein

The optimal conditions varies to express different proteins. Recombinant HCA587 protein was expressed at the highest level when 1×10^6 Sf9 cells/ml were infected with an MOI of 5 and harvested after 96 h of replication. After purification with chromatography using Ni-NTA resin, the purified protein, infected and uninfected Sf9 cells were lysed directly in SDS-loading buffer and boiled for 5 min. All samples were cleared by centrifugation and analyzed on 12.5 % acrylamide gels, which was stained by Coomassie blue and scanned by a densitometer to visualize the purity of purified protein. Figure 5 showed that the recombinant protein with 43kd was more than 90 % purity.

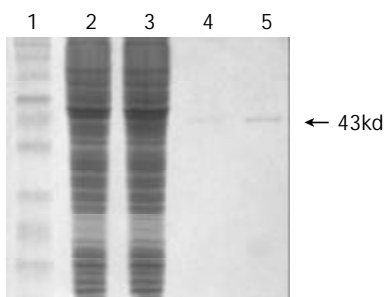


Figure 5 SDS-PAGE analysis of recombinant HCA587. (lane 1: protein marker; lane2: sf9 lysate; lane3: infected sf9 lysate; lane4-5: purified HCA587 protein).

Identification of antigenicity of the recombinant protein HCA587

In order to know if the recombinant protein HCA587 has the similar antigenicity with its native counterpart, the serum containing antibodies which recognize native HCA587 was used as primary antibody in western blot analysis. Figure 6 showed that the recombinant protein HCA587 was able to react with the specific antibody in serum (lane 2) while no reactivity was seen in negative control (lane 3), indicating it's similar functions with natural counterpart.

Reactivity of allogeneic HCC sera to recombinant protein HCA587

To determine the anti-HCA587 antibody produced in HCC patients, Sera collected from 81 allogeneic HCC patients were

screened to test their reactivities with the recombinant protein HCA587 expressed from Sf9 insect cells. The positive frequency of antibody response in HCC patients was not high, with only 2 positive of 81 patients (Figure 7, negative results not shown). This low late of serological reactivities was also shown in other CT antigens^[24].

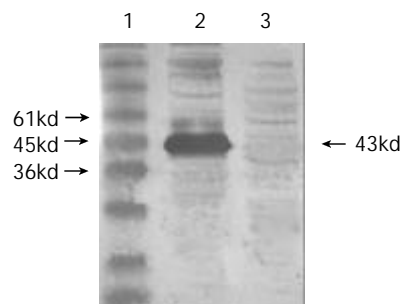


Figure 6 Western blot of recombinant HCA587 reacting with positive serum. (lane 1: protein marker; lane 2: positive serum of HCC; lane 3: negative control).

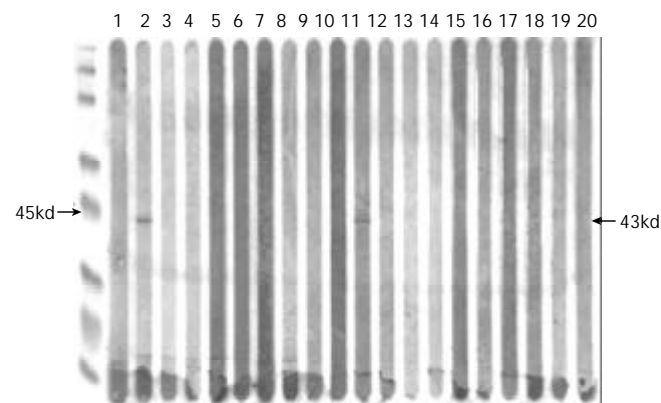


Figure 7 Serological analysis of HCC patients with recombinant protein HCA587. (lane 2 and 11: positive; others: negative; left: protein marker).

DISCUSSION

HCA587 was one of the SEREX-defined CT antigens identified from HCC patients^[14]. The protein of HCA587 was immunogenic and capable of inducing an antibody response as it was cloned by serologic method from the sera of HCC patients. In view that the SEREX-defined NY-ESO-1 can induce a CTL response and CTL-defined MAGE-1 has also been identified by SEREX^[17,18], this suggests that HCA587, as a CT antigen, may possibly contain both B and T epitopes and can elicit CTL responses. Because CTLs represent a major arm of the immune response against cancer, the elicitation of a specific CTL response against tumor Ags is one of the main aims of current immunotherapy trial. Therefore, it is crucial to define CD8⁺ T cell epitopes in HCA587 protein, which may determine its potential vaccine candidates for HCC immunotherapy. In addition, the mRNA expression rate of CT antigens can reach 70 % (14/20) in liver cancer tissues from HCC patients but not in normal liver tissue or cirrhosis, indicating its potential functions in tumorigenesis^[14]. Current knowledge about this expression pattern is mainly based on RT-PCR analysis, not based on protein levels^[19-21]. So immunohistochemical analysis of HCA587 antigen expression in HCC tissues is very necessary. Expression and purification of HCA587 protein makes both CTL-mediated responses and immunohistochemical study become possible.

Bac-to-Bac baculovirus expression system was developed which allows rapid and efficient generation of recombinant baculovirus. With this system, recombinant virus DNA isolated from selected colonies is not mixed with parental virus which eliminate the need for multiple rounds of plaque purification. High-titer virus are produced from the initial transfection too. These features reduce the time to identify and purify recombinant virus from 4 to 6 weeks to 7 to 9 days. In the present study, The cDNAs of the HCA587 were subcloned into pFasBacHTb donor vector at the BamHI and HindIII sites. The recombinant bacmid-587 was constructed by transposing a mini-Tn7 element from a pFasBacHTb donor plasmid to the mini-attTn7 attachment site on the bacmid when the Tn7 transposition functions are provided in *trans* by a helper plasmid in DH10Bac competent cells. After transfecting the recombinant bacmid-587 to Sf9 cells, we successfully expressed and purified the recombinant protein HCA587 which contained 333 amino acids with 6 his tags at its N-termini, which makes the purification procedure more convenient with its high affinity to Ni-NTA resin^[22,23].

Western blot analysis showed that the recombinant protein HCA587 has the similar immunological reactivity with its natural counterpart (Figure 6). It was used as antigen to screen the generation of anti-HCA587 antibody in serum from HCC patients. The results proved that HCC patients was able to develop humoral immune response to HCA587 antigen, but the frequency is not high (2/81). This low rate of seroreactivity to allogeneic sera is similar to some other CT antigens, either defined by a CD8⁺ CTL response (MAGE-1)^[24] or by SEREX (SSX-2)^[25]. In a survey of humoral responses of cancer patients against recombinant tumor antigens, it was indeed shown that seroreactivity to MAGE gene products is uncommon, and sera from 234 cancer patients showed antibodies to MAGE-1 in 3, to MAGE-3 in 2, and to SSX-2 in 1 patient^[24]. Since many members of MAGE family have been shown to be recognized by CTL from cancer patients^[26-30], it would be important to investigate possible HCA587 epitopes recognized by CD8⁺ and CD4⁺ cells. In conclusion, our experiments pave the way for further study of HCA587 for the development of tumor vaccine and clinical tumor diagnosis.

REFERENCES

- Schultze JL**, Vonderheide RH. From cancer genomics to cancer immunotherapy: toward second-generation tumor antigens. *Trends in immunology* 2001; **22**: 516-523
- Krackhardt AM**, Witzens M, Harig S, Hodi FS, Zauls AJ, Chessia M, Barrett P, Gribben JG. Identification of tumor-associated antigens in chronic lymphocytic leukemia by SEREX. *Blood* 2002; **100**: 2123-2131
- Chomez P**, De Backer O, Bertrand M, De Plaen E, Boon T, Lucas S. An overview of the MAGE gene family with the identification of all human members of the family. *Cancer research* 2001; **61**: 5544-5551
- Offringa R**, van der Burg SH, Ossendorp F, Toes RE, Melief CJ. Design and evaluation of antigen-specific vaccination strategies against cancer. *Current opin Immunol* 2000; **12**: 576-582
- Perico ME**, Mezzanzanica D, Luison E, Alberti P, Panza L, Russo G, Canevari S. Development of a new vaccine formulation that enhances the immunogenicity of tumor-associated antigen CaMBr1. *Cancer Immunol Immunother* 2000; **49**: 296-304
- Jager D**, Jager E, Knuth A. Immune responses to tumor antigens: implications for antigen specific immunotherapy of cancer. *J Clin Pathol* 2001; **54**: 669-674
- Scanlan MJ**, Gure AO, Jungbluth AA, Old LJ, Chen YT. Cancer/testis antigens: an expanding family of targets for cancer immunotherapy. *Immunol Rev* 2002; **188**: 22-32
- Gure AO**, Stockert E, Arden KC, Boyer AD, Viars CS, Scanlan MJ, Old LJ, Chen YT. CT10: a new cancer testis(CT) antigen homologous to CT7 and the mage family, identified by RDA. *Int J Cancer* 2000; **85**: 726-732
- Tureci O**, Sahin U, Zwick C, Koslowski M, Seitz G, Pfreundschuh M. Identification of a meiosis-specific protein as a member of the class of cancer/testis antigens. *Proc Natl Acad Sci USA* 1998; **95**: 5211-5216
- Thurner B**, Haendle I, Roder C, Dieckmann D, Keikavoussi P, Jonuleit H, Bender A, Maczek C, Schreiner D, von den Driesch P, Brocker EB, Steinman RM, Enk A, Kampgen E, Schuler G. Vaccination with Mage-3A1 peptide-pulsed mature, monocyte-derived dendritic cells expands specific cytotoxic T cells and induces regression of some metastases in advanced stage IV melanoma. *J EXP Med* 1999; **190**: 1669-1678
- Marchand M**, van Baren N, Weynants P, Brichard V, Dreno B, Tessier MH, Rankin E, Parmiani G, Arienti F, Humblet Y, Bourlond A, Vanwijck R, Lienard D, Beauduin M, Dietrich PY, Russo V, Kerger J, Masucci G, Jager E, De Greve J, Atzpodien J, Brasseur F, Coulie PG, van der Bruggen P, Boon T. Tumor regressions observed in patients with metastatic melanoma treated with an antigen peptide encoded by gene Mage-3 and presented by HLA-A1. *Int J Cancer* 1999; **80**: 219-230
- Fujie T**, Tahara K, Tanaka F, Mori M, Takesako K, Akiyoshi T. A mage-1-encoded HLA-A24-binding synthetic peptide induces specific anti-tumor cytotoxic T lymphocytes. *Int J Cancer* 1999; **80**: 169-172
- Ayyoub M**, Stevanovic S, Sahin U, Guillaume P, Servis C, Rimoldi D, Valmori D, Romero P, Cerottini JC, Rammensee HG, Pfreundschuh M, Speiser D, Levy F. Proteasome-assisted identification of a SSX-2-derived epitope recognized by tumor-reactive CTL infiltrating metastatic melanoma. *J Immunol* 2002; **168**: 1717-1722
- Wang Y**, Han KJ, Pang XW, Vaughan HA, Qu W, Dong XY, Peng JR, Zhao HT, Rui JA, Leng XS, Cebon J, Burgess AW, Chen WF. Large scale identification of human hepatocellular carcinoma-associated antigens by autoantibodies. *J Immunol* 2002; **169**: 1102-1109
- Schmidt M**, Olejnik AK, Stepien K, Olejnik AM, Butowska W, Grajek W, Warchol JB, Gozdzicka-Jozefiak A. Production of human papillomavirus type 16 early proteins in Bac-To-Bac Expression System (GibcoBRL). *Folia Histochem Cytobiol* 2001; **39**: 125-126
- Joshua MN**, Qi Y, Fu HY, Yong XH. Comparison of the biological activities of human immunodeficiency virus 1 P24 and GP41 expressed in *Spodoptera frugiperda* cells by use of bac-to-bac system. *Acta Virol* 2000; **44**: 125-130
- Jager E**, Nagata Y, Gnjjatic S, Wada H, Stockert E, Karbach J, Dunbar PR, Lee SY, Jungbluth A, Jager D, Arand M, Ritter G, Cerundolo V, Dupont B, Chen YT, Old LJ, Knuth A. Monitoring CD8 T cell responses to NY-ESO-1: correlation of humoral and cellular immune responses. *PNAS* 2000; **97**: 4760-4765
- Chen YT**, Gure AO, Tsang S, Stockert E, Jager E, Knuth A, Old LJ. Identification of multiple cancer/testis antigens by allogenic antibody screening of a melanoma-cell line library. *PNAS* 1998; **95**: 6919-6923
- Scanlan MJ**, Gordon CM, Williamson B, Lee SY, Chen YT, Stockert E, Jungbluth A, Ritter G, Jager D, Jager E, Knuth A, Old LJ. Identification of cancer/testis genes by database mining and mRNA expression analysis. *Int J Cancer* 2002; **98**: 485-492
- Zendman AJ**, van Kraats AA, den Hollander AI, Weidle UH, Ruiter DJ, van Muijen GN. Characterization of XAGE-1b, a short major transcript of cancer/testis-associated gene XAGE-1, induced in melanoma metastasis. *Int J Cancer* 2002; **97**: 195-204
- Scanlan MJ**, Altorki NK, Gure AO, Williamson B, Jungbluth A, Chen YT, Old LJ. Expression of cancer-testis antigens in lung cancer: definition of bromodomain testis-specific gene (BRDT) as a new CT gene, CT9. *Cancer Let* 2000; **150**: 155-164
- Nakajima M**, Hirakata M, Nittoh T, Ishihara K, Ohuchi K. Expression and purification of recombinant rat eosinophil-associated ribonucleases, homologues of human eosinophil cationic protein and eosinophil-derived neurotoxin, and their characterization. *Int Arch Allergy Immunol* 2001; **125**: 241-249
- Jungbluth AA**, Chen YT, Busam KJ, Coplan K, Kolb D, Iversen K, Williamson B, Van Landeghem FK. CT7 (MAGE-C1) antigen expression in normal and neoplastic tissues. *Int J Cancer* 2002; **99**: 839-845
- Stockert E**, Jager E, Chen YT, Scanlan MJ, Gout I, Karbach J, Arand

- M, Knuth A, Old LJ. A survey of the humoral immune response of cancer patients to a panel of human tumor antigens. *J Exp Med* 1998; **187**: 1349-1354
- 25 **Sahin U**, Tureci O, Pfreundschuh M. Serological identification of human tumor antigens. *Curr Opin Immunol* 1997; **9**: 709-716
- 26 **Oiso M**, Eura M, Katsura F, Takiguchi M, Sobao Y, Masuyama K, Nakashima M, Itoh K, Ishikawa T. A newly identified MAGE-3-derived epitope recognized by HLA-A24-restricted cytotoxic T lymphocytes. *Int J Cancer* 1999; **81**: 387-394
- 27 **Serrano A**, Lethe B, Delroisse JM, Lurquin C, De Plaen E, Brasseur F, Rimoldi D, Boon T. Quantitative evaluation of the expression of MAGE genes in tumors by limiting dilution of cDNA libraries. *Int J Cancer* 1999; **83**: 664-669
- 28 **Schultz ES**, Chapiro J, Lurquin C, Claverol S, Burlet-Schiltz O, Warnier G, Russo V, Morel S, Levy F, Boon T, Van den Eynde BJ, van der Bruggen P. The production of a new MAGE-3 peptide presented to cytolytic T lymphocytes by HLA-B40 requires the immunoproteasome. *J Exp Med* 2002; **195**: 391-399
- 29 **Chaux P**, Luiten R, Demotte N, Vantomme V, Stroobant V, Traversari C, Russo V, Schultz E, Cornelis GR, Boon T, Van der Bruggen P. Identification of five MAGE-A1 epitopes recognized by cytolytic T lymphocytes obtained by *in vitro* stimulation with dendritic cells transduced with MAGE-A1. *J Immunol* 1999; **163**: 2928-2936
- 30 **Graff-Dubois S**, Faure O, Gross DA, Alves P, Scardino A, Chouaib S, Lemonnier FA, Kosmatopoulos K. Generation of CTL recognizing an HLA-A*0201-restricted epitope shared by MAGE-A1, -A2, -A3, -A4, -A6, -A10, and -A12 tumor antigens: implication in a broad-spectrum tumor immunotherapy. *J Immunol* 2002; **169**: 575-580

Edited by Ren SY

Gene expression profiles of hepatoma cell line HLE

Lian-Xin Liu, Zhi-Hua Liu, Hong-Chi Jiang, Wei-Hui Zhang, Shu-Yi Qi, Jie Hu, Xiu-Qin Wang, Min Wu

Lian-Xin Liu, Hong-Chi Jiang, Wei-Hui Zhang, Department of Surgery, the First Clinical College, Harbin Medical University, Harbin 150001, Heilongjiang Province, China

Lian-Xin Liu, Zhi-Hua Liu, Xiu-Qin Wang, Min Wu, National Laboratory of Molecular Oncology, Department of Cell Biology, Cancer Institute, Chinese Academy of Medical Science & Peking Union Medical College, Beijing 100021, China

Shu-Yi Qi, Jie Hu, Department of VIP, the First Clinical College, Harbin Medical University, Harbin 150001, Heilongjiang Province, China

Supported by China Key Program on Basic Research, No.Z-19-01-01-02; Chinese Climbing Project, No.18; Youth Natural Scientific Foundation of Heilongjiang Province and Harbin, No.QC01C11

Correspondence to: Dr. Lian-Xin Liu, Department of Surgery, the First Clinical College of Harbin Medical University, No.23 Youzheng Street, Nangang District, Harbin 150001, China. liulianxin@sohu.com

Telephone: +86-451-3668999 **Fax:** +86-451-3670428

Received: 2002-10-17 **Accepted:** 2002-12-16

Abstract

AIM: To investigate the global gene expression of cancer related genes in hepatoma cell line HLE using Atlas Human Cancer Array membranes with 588 well-characterized human genes related with cancer and tumor biology.

METHODS: Hybridization of cDNA blotting membrane was performed with ³²P-labeled cDNA probes synthesized from RNA isolated from Human hepatoma cell line HLE and non-cirrhotic normal liver which was liver transplantation donor. AtlasImage, a software specific to array, was used to analyze the result. The expression pattern of some genes identified by Atlas arrays hybridization was confirmed by reverse transcription polymerase chain reaction (RT-PCR) in 24 pairs of specimens and Northern blot of 4 pairs of specimens.

RESULTS: The differential expression of cell cycle/growth regulator in hepatocellular carcinoma (HCC) showed a stronger tendency toward cell proliferation with more than 1.5-fold up-regulation of Cyclin C, ERK5, ERK6, E2F-3, TFDP-2 and CK4. The anti-apoptotic factors such as Akt-1 were up-regulated, whereas the promotive genes of apoptosis such as ABL2 were down-regulated. Among oncogene/tumors suppressors, SKY was down-regulated. Some genes such as Integrin beta 8, Integrin beta 7, DNA-PK, CSPCP, byglycan, Tenacin and DNA Topo were up-regulated. A number of genes, including LAR, MEK1, eps15, TDGF1, ARHGDI A were down-regulated. In general, expression of the cancer progression genes was up-regulated, while expression of anti-cancer progression genes was down-regulated. These differentially expressed genes tested with RT-PCR were in consistent with cDNA array findings.

CONCLUSION: Investigation of these genes in HCC is helpful in disclosing molecular mechanism of pathogenesis and progression of HCC. For the first time few genes were discovered in HCC. Further study is required for the precise relationship between the altered genes and their correlation with the pathogenesis of HCC.

Liu LX, Liu ZH, Jiang HC, Zhang WH, Qi SY, Hu J, Wang XQ, Wu M. Gene expression profiles of hepatoma cell line HLE. *World J Gastroenterol* 2003; 9(4): 683-687

<http://www.wjgnet.com/1007-9327/9/683.htm>

INTRODUCTION

Hepatocellular carcinoma (HCC) is one of the most common malignant tumors and ranks the eighth in incidence of human cancer in Asia, Africa and South Europe, and causes an estimated 1 million deaths annually. The molecular mechanism underlying HCC is currently unknown^[1-15]. Tumor development and progression involves a cascade of genetic alterations. Techniques frequently used in study of gene expression, such as RT-PCR, differential display PCR and Northern blot analysis, have their limitations including requirement of large amounts of RNA, time-consuming, and limited number of genes being tested simultaneously. Hence, analysis of expression profiles of a large number of genes in hepatoma cell line is an essential step toward clarifying the detailed mechanisms of hepatocarcinogenesis and discovering target molecules for the development of novel therapeutic drugs.

DNA microarray enables investigators to study the gene expression profile and gene activation in thousands of genes and sequences^[16-25]. In this study, we used cDNA expression microarray containing 588 genes related to carcinoma to analyze genes that are differentially expressed in human Hepatoma cell line HLE.

MATERIALS AND METHODS

Tissues and specimens

Four normal liver tissues without cirrhosis and 24 pairs of primary HCC and corresponding noncancerous liver tissues without cirrhosis were obtained with informed consent from patients who underwent liver transplantation and hepatectomy at the First Clinical College of Harbin Medical University. Histopathological identification was confirmed by the same pathologist. These specimens were immediately frozen in liquid nitrogen once obtained.

Cell culture

The HCC cell line HLE, epithelial-like cells, established from HCC patient in 1975 by Dr Dor was used in this study. HLE was cultured in RPMI1640 (Sigma, Saint Louis, USA) media containing 10 % fetal bovine serum, 1 % penicillin and streptomycin in a 37 °C incubator. Cells were harvested at 70-80 % confluence.

RNA isolation and purification

Total RNA of normal liver tissues was obtained by extracting frozen tissues in Trizol (Life Technologies Inc., Gaithersburg, MD) according to the manufacturer's instructions. Normal liver were made in spices and homogenized in Trizol solution (1 ml/100 mg). Trizol was added into the bottles cultured with HLE, after washed with cold PBS. The concentration of RNA was assessed by absorbency at 260nm using a Nucleic Acid and Protein Analyzer (BECKMAN 470, USA).

cDNA microarray membrane

Atlas human cancer cDNA expression array (7742-1) was purchased from Clontech Laboratories Inc (Palo Alto, USA). The membrane contained 10 ng of each gene-specific cDNA from 588 known genes and 9 housekeeping genes. The cancer-related genes analyzed in this study were divided into six different groups according to its function.

cDNA synthesis, labeling and purification

Total RNA was reverse-transcribed into cDNA and labeled with α -³²P dCTP using Superscript™ Preamplification system for First Strand cDNA Synthesis Kit (Life Technologies, Gaithersburg, MD) following the manufacture's instructions. The labeled first strand cDNA probes were purified by Spin 200 column (Clontech, Palo Alto, CA) to remove the unincorporated nucleotides.

Membrane hybridization and exposure

Different probes were added to tubes containing Atlas human cancer cDNA expression array, which were pre-hybridized at 68 °C for 2 hr, and hybridization was performed at 68 °C for 18 hr in rolling bottles. The membranes were washed strictly and exposed to X-ray films (Fuji Films, Tokyo, Japan) at -70 °C for 1-3 days.

Image and analysis

The images were scanned with Fluor-S MultiImager (Bio-Rad, Hercules, CA) and analyzed with AtlasImage analysis software Version 1.01a (Clontech, Palo Alto, CA). Human glyceraldehyde-3-phosphate dehydrogenase (*GAPDH*) was selected for normalization because its expression was constant in cancer array hybridization system. The normalized intensity of each spot representing a unique gene expression level was acquired. Genes were considered to be up-regulated when the intensity ratio was ≥ 1.5 or the difference was $\geq 10\ 000$ between the expressions of HLE and normal liver tissues.

Semi-quantitative RT-PCR

To confirm the cDNA array results, semi-quantitative RT-PCR of 24 pairs of HCC tissues and normal liver tissues was performed for two genes (*TFDP2*, *E2F3*) displaying expression alterations. Twenty-five ml reaction mixture was performed under the following conditions: denaturation at 95 °C (3 min); 24 cycles of 94 °C (30 s), 60 °C (30 s) and 72 °C (45 s); then 72 °C extension (3 min). *GAPDH* were used as an internal reference in each PCR reaction. The 5 ml RT-PCR product was analyzed by electrophoresis on a 1.5% agarose gel.

Primer were as follows: *GAPDH*, forward primer 5' - ACCACAGTCCATGCCATCAC-3' and reverse primer 5' - TCCACCACCCTGTTGCTGTA-3'; *TFDP2*, forward primer 5' - GGAGTCAGGCAAATGCTCTC-3' and reverse primer 5' - GCTAAGGCCACTTCTGCATC-3'; *E2F3*, forward primer 5' - TTATGACTGCGTGAGCCTTAG-3' and reverse primer 5' - AGAGCCACAACAAAGAACA-3'.

Northern blot

RNAs of HCC and normal liver tissues were electrophoresed in a 1.5% agarose gel containing 2.2M formaldehyde, and then transferred onto a nylon membrane (Zeta-Probe, Bio-Rad, USA) by capillary action. RNA was permanently attached to the membrane by UV illumination for 150 s (GS Gene Linker, Bio-Rad, USA). The hybridization probe was obtained by PCR. The primers were as follows: β -actin, forward primer 5' - CGTCTGGACCTGGCTGGCCGGGACC-3' and reverse primer 5' - CTAGAAGCATTTGCGGTGGACGATG-3'; *TFDP2*, forward primer 5' - GGAGTCAGGCAAATGCTCTC-3' and reverse primer 5' - CTGCCCTCAGTATCCCTCAC-3'; *E2F3*,

forward primer 5' - AAGAGCAGGAGCAGAGAGATG-3' and reverse primer 5' - TTTGACAGGCCTTGACACTG-3'. α -³²P-labeled cDNA probes were synthesized using Primer-a-Gen random labeling Kit (Promega, USA). Hybridization was performed overnight in rolling bottles containing 8 ml of hybridization buffer. The membranes were washed and exposed to X-ray films (Fuji Films, Tokyo, Japan) at -70 °C for 24-48 h.

RESULTS

Atlas human cancer cDNA microarray expression profile

Using a cDNA expression microarray technique we established the expression profile of 588 genes selected from different areas in human hepatoma cell line HLE and normal liver tissues (Figure 1A, 1B). No signals were visible in the blank spots and negative control spots indicating that the Atlas human cancer array hybridization was highly specific. The intensity for housekeeping genes was similar at the same time indicating that the results were credible. *GAPDH* was used to normalize the intensities. The comparison results analyzed by AtlasImage software showed that there were 30 genes changed, 22 up-regulated and 8 down-regulated in Hepatoma cell line HLE versus normal liver tissues. In the test, the ratio one over the other ≥ 1.5 or the difference between two $\geq 10\ 000$ was considered as up-regulated genes (Table 1).

Table 1 Genes differentially expressed between hepatoma cell line HLE and normal liver tissues generated by AtlasImage software (Version 1.01a)

Gene	Ratio	Difference	Protein/gene
F6k	0.361	-7908	TDGF1 + TDGF2 + TDGF3
B7g	0.412	-9606	SKY (DTK) (TYRO3) (RSE)
A5b	0.484	-8262	ERK activator kinase 1; MAPK/ERK kinase 1 (MEK1)
C5f	0.487	-8154	Epidermal growth factor receptor substrate (eps15)
E5b	0.504	-14946	Rho GDP-dissociation inhibitor 1
D6c	0.662	-10998	Semaphorin E
B7j	0.664	-12474	Tyrosine-protein kinase ABL2; tyrosine kinase ARG (ABLL)
F5l	0.732	-12132	Leukocyte interferon-inducible peptide
B2g	1.237	10252	TRAF-interacting protein (TRIP)
B3h	1.241	10508	Caspase-8 precursor; MACH; FLICE; (CAP4) (CASP8)
D5f	1.363	12000	CD9
C7l	1.381	14882	Retinoic acid receptor gamma
A3i	1.387	14088	CDK inhibitor p19INK4d
C7m	1.401	13224	Retinoid X receptor beta (RXR-beta)
C6n	1.444	11820	Sex gene
D3e	1.52	17176	Vitronectin precursor; serum spreading factor;
D4b	1.61	16212	Integrin alpha8
D2n	1.692	19718	TENASCIN-R
C1a	1.804	15096	DNA-dependent protein kinase (DNA-PK)
A4j	2.008	17856	Extracellular signal-regulated kinase 6 (ERK6) (ERK5)
D1b	2.038	20026	Byglycan
A7d	2.06	18522	Type II cytoskeletal 11 keratin; cytokeratin 1 (K1; CK 1);
A2k	2.061	18084	Cyclin C G1/S-specific
D4j	2.178	27156	Integrin beta7
D4k	2.252	28122	Integrin beta8
A7g	2.257	13428	Type II cytoskeletal 4 keratin; cytokeratin 4 (K4; CK4)
D1a	2.31	29184	Cartilage-specific proteoglycan core protein (CSPCP); aggrecan1
A5i	2.418	10668	E2F-3
B4d	2.474	11814	Akt1; rac protein kinase alpha; protein kinase B; c-Akt
A5l	4.256	37824	DP2 dimerization partner of E2F

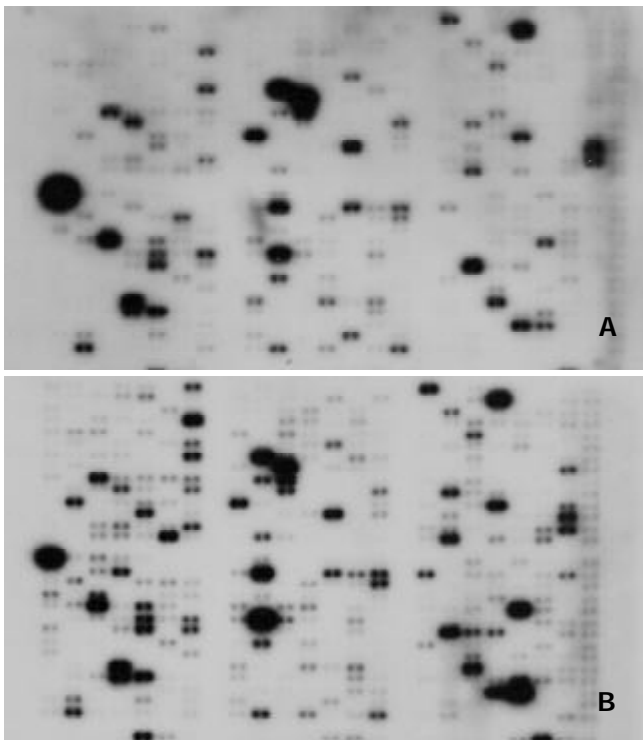


Figure 1 Parallel analyses of gene expression profiles in human hepatoma cell line HLE and normal liver tissues. Atlas human cancer cDNA expression array (Clontech, USA) was hybridized with ^{32}P -labeled cDNA probes in normal liver tissues (A) and human hepatoma cell line HLE (B).

Semi-quantitative RT-PCR

Twenty four paired tissues were performed for RT-PCR to verify accuracy and universality of the hybridization data. The RT-PCR results for 2 genes were consistent with hybridization data after normalization. Among the 24 paired tissues, the RT-PCR results of 2 genes were identical to the microarray results and the constituency was TFDP2 17/24, E2F3 16/24, respectively (Figure 2).

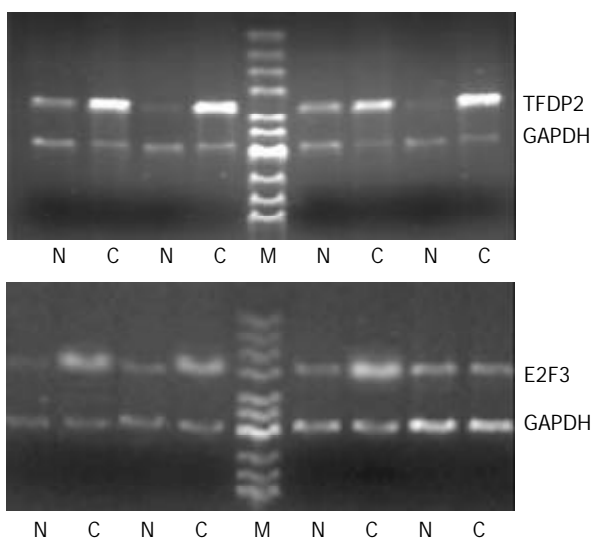


Figure 2 Partial semi-quantitative RT-PCR for 2 genes in 24 paired tissues. A total of 10 μl RT-PCR products were electrophoresed on 2% agarose gel containing ethidium bromide. GAPDH was used as an internal control. (RT-PCR, reverse transcription polymerase chain reaction; N, adjacent normal liver tissue; C, human hepatocellular carcinoma tissue; GAPDH, glyceraldehyde-s-phosphate dehydrogenase; M, pUC Mix Maker).

Northern blot

Northern blot of four paired tissues were performed and verified the accuracy of the microarray. Among the 4 paired tissues, the northern blot results of 4 genes further meant that the Atlas human cancer cDNA microarray data were believable and comparable (Figure 3).

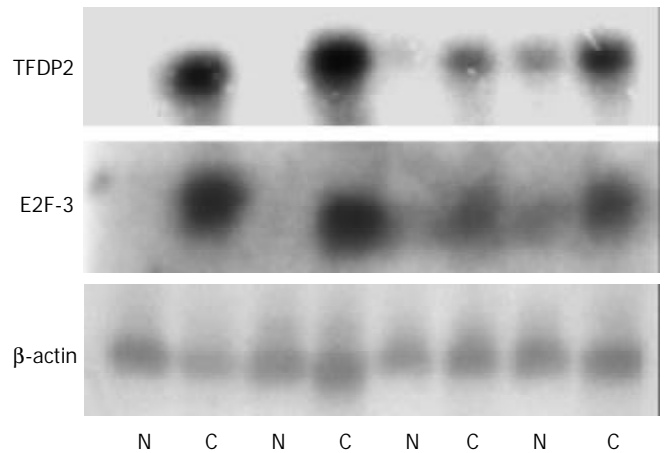


Figure 3 Northern blot analysis of 2 genes to confirm the Atlas human cancer cDNA expression array. Four paired cases were used to determine these genes expression patterns. Twenty μg RNA was analyzed on a 1.2% denaturing agarose gel and transferred onto a nylon membrane. ^{32}P -labeled cDNA probes for these genes were hybridized to the RNA-blotting membranes. After stringent washes, membranes were exposed to X-ray film overnight at -70°C . The same membranes were rehybridized with human β -actin for an RNA loading control (N, adjacent normal liver tissue; C, human HCC tissue).

DISCUSSION

In this study, we explored the gene expression profiles in human hepatoma cell line HLE and normal liver tissues using Atlas human cancer array. cDNA array technology was used to examine simultaneously the expression of specific genes on a single hybridization. Although human genome projects have generated a large-scale sequence data for millions of genes, the biological functions of such genes remain to be deciphered. It is very important to define differential gene expression profiles of tumors and normal tissues before understanding the functional significance of specific gene products. Thus a systematic approach for examining large number of genes simultaneously is required. Microarray techniques have been developed in this conditions^[23]. The gene expression profiles obtained from microarray technique was first reported in 1995^[16]. It might be useful for tumor classification, elucidation of key factor in tumors, and identification of genes^[24-27].

Several genes related to cell cycle regulators, growth regulators were abundantly up-regulated in our HCC samples. E2F-3 is a transcription factor that plays an important role during the cell cycle of proliferating cells, its products are rate limiting for initiation of DNA replication^[28]. E2F-3 is able to activate transcription of E2F-responsive genes in a manner depending upon the presence of at least one functional E2F binding site^[29,30]. TFDP2 gene is a member of the TFDP genes family of transcription factors. TFDP2 protein can form heterodimers with E2F family proteins in vivo. The E2F-TFDP transcription factors are major regulators of genes that are required for the progression of S-phase and they play a critical role in cell cycle regulation and differentiation^[29]. TFDP2 may play a major role in modulating the function of E2F in cell cycle regulation and oncogenesis. The retinoblastoma tumor suppressor protein has been shown to induce growth arrest by

binding to E2F-TFDP and repressing its activity^[31]. The up-regulation of E2F-3 and TFDP2 may play an important role in HCC cell proliferation.

Protein kinase B (PKB)/Akt is a growth-factor-regulated serine/threonine kinase which contains a pleckstrin homology domain^[32]. Activated PKB/Akt provides a survival signal that protects cells from apoptosis induced by various stresses, and also mediates a number of metabolic effects of insulin^[33]. The up-regulation of Akt1 may have a great help for tumor cell to survive from apoptosis.

In our study, genes related to DNA repair and recombination was up-regulated in HLE, which indicates that the generative ability of tumor cell was stronger than that of normal hepatocytes. DNA-dependent protein kinase (DNA-PK) is a nuclear protein serine/threonine kinase that is activated by DNA double strand breaks (DSBs). It is a component of the DNA DSB repair apparatus, and cells deficient in DNA-PK are hypersensitive to ionizing radiation and radio-mimetic drugs^[34]. DNA-PK may have roles in controlling transcription, apoptosis, and the length of telomeric chromosomal ends. The DNA-PK complex is regulated in a cell cycle-dependent manner, with peaks of activity found at the G₁/early S phase and again at the G₂ phase in wild-type cells^[35].

Integrins are a major family of cell adhesion molecules involved in cell-cell and cell-extracellular matrix interactions. Integrins are suggested to be involved in many different biological processes such as growth, differentiation, migration, and cell death. The integrin alpha 8 beta 1 has been reported to bind to fibronectin, vitronectin, tenascin-C and osteopontin in cell adhesion or neurite outgrowth assays^[36,37]. Integrins are heterodimeric cell adhesion proteins connecting the extracellular matrix to the cytoskeleton and transmitting signals in both directions^[38]. The up-regulation of Integrin may play a role in HCC metastasis.

In conclusion, our study demonstrates the cDNA array is a powerful tool to explore gene expression profiles in cancer. The genes described in this study provide valuable resources not only for basic research, such as molecular mechanism of carcinogenesis, progression and prognosis, but also for clinical application, such as development of new diagnostic markers, identification of therapeutic intervention in human HCC.

REFERENCES

- Schafer DF**, Sorrell MF. Hepatocellular carcinoma. *Lancet* 1999; **353**: 1253-1257
- Qin LX**, Tang ZY. The prognostic molecular markers in hepatocellular carcinoma. *World J Gastroenterol* 2002; **8**: 385-392
- Wu W**, Lin XB, Qian JM, Ji ZL, Jiang Z. Ultrasonic aspiration hepatectomy for 136 patients with hepatocellular carcinoma. *World J Gastroenterol* 2002; **8**: 763-765
- Tang ZY**, Sun FX, Tian J, Ye SL, Liu YK, Liu KD, Xue Q, Chen J, Xia JL, Qin LX, Sun SL, Wang L, Zhou J, Li Y, Ma ZC, Zhou XD, Wu ZQ, Lin ZY, Yang BH. Metastatic human hepatocellular carcinoma models in nude mice and cell line with metastatic potential. *World J Gastroenterol* 2001; **7**: 597-601
- Liu LX**, Jiang HC, Piao DX. Radiofrequency ablation of liver cancers. *World J Gastroenterol* 2002; **8**: 393-399
- Rabe C**, Pilz T, Klostermann C, Berna M, Schild HH, Sauerbruch T, Caselmann WH. Clinical characteristics and outcome of a cohort of 101 patients with hepatocellular carcinoma. *World J Gastroenterol* 2001; **7**: 208-215
- Tang ZY**. Hepatocellular carcinoma-cause, treatment and metastasis. *World J Gastroenterol* 2001; **7**: 445-454
- Zhao WH**, Ma ZM, Zhou XR, Feng YZ, Fang BS. Prediction of recurrence and prognosis in patients with hepatocellular carcinoma after resection by use of CLIP score. *World J Gastroenterol* 2002; **8**: 237-242
- Jiang HC**, Liu LX, Piao DX, Xu J, Zheng M, Zhu AL, Qi SY, Zhang WH, Wu LF. Clinical short-term results of radiofrequency ablation in liver cancers. *World J Gastroenterol* 2002; **8**: 624-630
- Yip D**, Findlay M, Boyer M, Tattersall MH. Hepatocellular carcinoma in central Sydney: a 10-year review of patients seen in a medical oncology department. *World J Gastroenterol* 1999; **5**: 483-487
- Chen MS**, Li JQ, Zhang YQ, Lu LX, Zhang WZ, Yuan YF, Guo YP, Lin XJ, Li GH. High-dose iodized oil transcatheter arterial chemoembolization for patients with large hepatocellular carcinoma. *World J Gastroenterol* 2002; **8**: 74-78
- Zhang WH**, Zhu SN, Lu SL, Huang YL, Zhao P. Three-dimensional image of hepatocellular carcinoma under confocal laser scanning microscope. *World J Gastroenterol* 2000; **6**: 344-347
- Jiang YF**, Yang ZH, Hu JQ. Recurrence or metastasis of HCC: predictors, early detection and experimental antiangiogenic therapy. *World J Gastroenterol* 2000; **6**: 61-65
- Sithinamsuwan P**, Piratvisuth T, Tanomkiat W, Apakupakul N, Tongyoo S. Review of 336 patients with hepatocellular carcinoma at Songklanagarind Hospital. *World J Gastroenterol* 2000; **6**: 339-343
- Fan J**, Wu ZQ, Tang ZY, Zhou J, Qiu SJ, Ma ZC, Zhou XD, Ye SL. Multimodality treatment in hepatocellular carcinoma patients with tumor thrombi in portal vein. *World J Gastroenterol* 2001; **7**: 28-32
- Schena M**, Shalon D, Davis RW, Brown PO. Quantitative monitoring of gene expression patterns with a complementary DNA microarray. *Science* 1995; **270**: 467-470
- DeRisi J**, Penland L, Brown PO, Bittner ML, Meltzer PS, Ray M, Chen Y, Su YA, Trent JM. Use of a cDNA microarray to analyse gene expression patterns in human cancer. *Nat Genet* 1996; **14**: 457-460
- Liu LX**, Liu ZH, Jiang HC, Qu X, Zhang WH, Wu LF, Zhu AL, Wang XQ, Wu M. Profiling of differentially expressed genes in human Gastric carcinoma by cDNA expression array. *World J Gastroenterol* 2002; **8**: 580-585
- Wang K**, Gan L, Jeffery E, Gayle M, Gown AM, Skelly M, Nelson PS, Ng WV, Schummer M, Hood L, Mulligan J. Monitoring gene expression profile changes in ovarian carcinomas using cDNA microarray. *Gene* 1999; **229**: 101-108
- Ross DT**, Scherf U, Eisen MB, Perou CM, Rees C, Spellman P, Iyer V, Jeffrey SS, Van de Rijn M, Waltham M, Pergamenschikov A, Lee JC, Lashkari D, Shalon D, Myers TG, Weinstein JN, Botstein D, Brown PO. Systematic variation in gene expression patterns in human cancer cell lines. *Nat Genet* 2000; **24**: 227-235
- Khan J**, Simon R, Bittner M, Chen Y, Leighton SB, Pohida T, Smith PD, Jiang Y, Gooden GC, Trent JM, Meltzer PS. Gene expression profiling of alveolar rhabdomyosarcoma with cDNA microarrays. *Cancer Res* 1998; **58**: 5009-5013
- Lu J**, Liu Z, Xiong M, Wang Q, Wang X, Yang G, Zhao L, Qiu Z, Zhou C, Wu M. Gene expression profile changes in initiation and progression of squamous cell carcinoma of esophagus. *Int J Cancer* 2001; **91**: 288-294
- Kallioniemi OP**. Biochip technologies in cancer research. *Ann Med* 2001; **33**: 142-147
- Liu LX**, Jiang HC, Liu ZH, Zhou J, Zhang WH, Zhu AL, Wang XQ, Wu M. Intergrin gene expression profiles of human hepatocellular carcinoma. *World J Gastroenterol* 2002; **8**: 631-637
- Khan J**, Saal LH, Bittner ML, Chen Y, Trent JM, Meltzer PS. Expression profiling in cancer using cDNA microarrays. *Electrophoresis* 1999; **20**: 223-229
- Hu YC**, Lam KY, Law S, Wong J, Srivastava G. Identification of differentially expressed genes in esophageal squamous cell carcinoma (ESCC) by cDNA expression array: overexpression of Fra-1, Neogenin, Id-1, and CDC25B genes in ESCC. *Clin Cancer Res* 2001; **7**: 2213-2221
- Selaru FM**, Zou T, Xu Y, Shustova V, Yin J, Mori Y, Sato F, Wang S, Oлару A, Shibata D, Greenwald BD, Krasna MJ, Abraham JM, Meltzer SJ. Global gene expression profiling in Barrett's esophagus and esophageal cancer: a comparative analysis using cDNA microarrays. *Oncogene* 2002; **21**: 475-478
- Leone G**, DeGregori J, Yan Z, Jakoi L, Ishida S, Williams RS, Nevins JR. E2F3 activity is regulated during the cell cycle and is required for the induction of S phase. *Genes Dev* 1998; **12**: 2120-2130
- Moberg K**, Starz MA, Lees JA. E2F-4 switches from p130 to p107

- and pRB in response to cell cycle reentry. *Mol Cell Biol* 1996; **16**: 1436-1449
- 30 **Zhang Y**, Chellappan SP. Cloning and characterization of human DP2, a novel dimerization partner of E2F. *Oncogene* 1995; **10**: 2085-2093
- 31 **Zhang Y**, Venkatraj VS, Fischer SG, Warburton D, Chellappan SP. Genomic cloning and chromosomal assignment of the E2F dimerization partner TFDP gene family. *Genomics* 1997; **39**: 95-98
- 32 **Downward J**. Mechanisms and consequences of activation of protein kinase B/Akt. *Curr Opin Cell Biol* 1998; **10**: 10262-10267
- 33 **Alessi DR**, Cohen P. Mechanism of activation and function of protein kinase B. *Curr Opin Genet Dev* 1998; **8**: 55-62
- 34 **Jackson SP**. DNA-dependent protein kinase. *Int J Biochem Cell Biol* 1997; **29**: 935-938
- 35 **Lee SE**, Mitchell RA, Cheng A, Hendrickson EA. Evidence for DNA-PK-dependent and -independent DNA double-strand break repair pathways in mammalian cells as a function of the cell cycle. *Mol Cell Biol* 1997; **17**: 1425-1433
- 36 **Denda S**, Reichardt LF, Muller U. Identification of osteopontin as a novel ligand for the integrin alpha8 beta1 and potential roles for this integrin-ligand interaction in kidney morphogenesis. *Mol Biol Cell* 1998; **9**: 1425-1435
- 37 **Denda S**, Muller U, Crossin KL, Erickson HP, Reichardt LF. Utilization of a soluble integrin-alkaline phosphatase chimera to characterize integrin alpha 8 beta 1 receptor interactions with tenascin: murine alpha 8 beta 1 binds to the RGD site in tenascin-C fragments, but not to native tenascin-C. *Biochemistry* 1998; **37**: 5464-5474
- 38 **Fogarty FJ**, Akiyama SK, Yamada KM, Mosher DF. Inhibition of binding of fibronectin to matrix assembly sites by anti-integrin (alpha 5 beta 1) antibodies. *J Cell Biol* 1990; **111**: 699-708

Edited by Ren SY

Construction of a regulable gene therapy vector targeting for hepatocellular carcinoma

Shao-Ying Lu, Yan-Fang Sui, Zeng-Shan Li, Cheng-En Pan, Jing Ye, Wen-Yong Wang

Shao-Ying Lu, Cheng-En Pan, Department of General Surgery, First Hospital of Xi'an Jiaotong University, Xi'an 710061, Shaanxi Province, China

Yan-Fang Sui, Zeng-Shan Li, Cheng-En Pan, Jing Ye, Wen-Yong Wang, Department of Pathology, Fourth Military Medical University, Xi'an 710032, Shaanxi Province, China

Supported by Natural Scientific Foundation of China, No. 30271474
Correspondence to: Professor Yan-Fang Sui, Department of Pathology, Fourth Military Medical University, Xi'an 710032, China. suiyanf@fmmu.edu.cn

Telephone: +86-29-3374541-211 **Fax:** +86-29-3374597

Received: 2002-10-08 **Accepted:** 2002-12-07

Abstract

AIM: To construct a gene modified hepatocellular carcinoma (HCC) specific EGFP expression vector regulated by abbreviated cis-acting element of AFP gene.

METHODS: The minimal essential DNA segments of AFP gene enhancer and promoter were synthesized through PCR from Genome DNA of HepG2 cells. Gene fragments were then cloned into the multiple cloning site of non-promoter EGFP vector pEGFP-1. Recombinant plasmid was transferred into positive or negative AFP cell lines by means of lipofectamine. The expression of EGFP was tested by fluorescence microscope and flow cytometry. The effect of all-trans retinoic acid (ATRA) on the expression of EGFP was tested in different concentrations.

RESULTS: By the methods of restriction digestion and sequence analyses we confirmed that the length, position and orientation of inserted genes of cis-acting element of AFP were all correct. The transcription of EGFP was under the control of AFP cis-acting element. The expressing EGFP can only be detected in AFP producing hepatoma cells. The expression rate of EGFP in G418 screened cell line was $34.9 \pm 4.1\%$. 48 h after adding $1 \times 10^{-7} \text{M}$ retinoic acid, EGFP expression rate was $14.7 \pm 3.5\%$. The activity of AFP gene promoter was significantly suppressed by addition of $1 \times 10^{-7} \text{M}$ retinoic acid ($P < 0.05$, $P = 0.003$, $t = 6.488$).

CONCLUSION: This recombinant expression vector can be used as a gene therapy vector for HCC. The expression of tumor killing gene will be confined within the site of tumor and the activity of which can be regulated by retinoic acid.

Lu SY, Sui YF, Li ZS, Pan CE, Ye J, Wang WY. Construction of a regulable gene therapy vector targeting for hepatocellular carcinoma. *World J Gastroenterol* 2003; 9(4): 688-691
<http://www.wjgnet.com/1007-9327/9/688.htm>

INTRODUCTION

Hepatocellular carcinoma (HCC) is one of the most common tumors worldwide, especially in several areas of Asia and Africa. It is the cause of death of around 1 000 000 people

annually. Although many new methods appeared as palliative protocols in the past 30 years, patient survival after onset of symptoms remained dismal^[1-3]. Surgical treatment such as resection or orthotopic liver transplantation is potentially curative only for patients with small and localized HCC^[4]. Transfer of therapeutic genes to tumor mass or to the peritumoral tissues provides a promising new approach for cancer therapy^[5-8]. Both viral and non-viral vectors were used to transfer genetic material to the interior of target cells^[9]. Experiments demonstrate that tissue and transcriptional targeting expression of transgenes in tumor cells not only improves the outcome of treatment, but also reduces systemic toxicity^[10]. This results in a much higher therapeutic index. Alpha-fetoprotein (AFP) is over expressed in about 70 % of HCC cases^[11]. Several groups have used AFP promoter or/and enhancer to control foreign gene expression in different vectors^[12, 13]. We constructed a gene modified AFP cis-acting element using the minimal essential DNA segments of AFP gene enhancer and promoter. Specific transcription activity of this element and its response to the addition of ATRA were tested using reporter gene vector pEGFP-1.

MATERIALS AND METHODS

Reagents

Reagents were obtained as follows: EX Taq DNA Polymerase, DNA Ligation Kit Ver.2, restriction endonuclease (TakaRa Biotechnology (Dalian) Co. Ltd.); DNA isolation and Purification kit (ShangHai ShunHua Biotechnology Ltd.); Lipofectamine™ 2000 (Invitrogen); IPTG, X-gal, DNA maker (Sino-American Biotechnology Company); Dulbecco's Modified Eagle Media: high glucose, with L-glutamine (DMEM) and G418 (GibcoBRL); all-trans retinoic acid, ATRA (Sigma).

Plasmids

pBluescript II ks(+) vector was preserved in our laboratory. The reporter gene vector pEGFP-1 was purchased from Clontech. This vector encoded a red-shifted variant of wild-type green fluorescent protein (GFP), which had been optimized for brighter fluorescence and higher expression in mammalian cells. This vector was also a non-promoter EGFP vector which could be used to monitor transcription from different promoters and promoter/enhancer combinations inserted into the MCS located in upstream of the EGFP coding sequence.

Cell lines

HepG2 and SMMC-7721 are human hepatoma cell lines produce or do not produce AFP. HeLa is human cervical cancer cell line, all Cell lines were cultured in Dulbecco's modified Eagle's medium, high glucose content, containing 10 % heat-inactivated fetal calf serum, 100 units/ml penicillin, 100 µg/ml streptomycin, 0.292 mg/ml glutamine. The cell lines were incubated in a humidified 5 % CO₂ and 95 % air incubator at 37 °C.

Polymerase chain reaction (PCR)

The primer sequences used for PCR were used as reported^[14, 15].

For PCR amplification, genomic DNA were extracted from 1×10^6 HepG2 cells and digested by *EcoR I/Xho I*. PCR was performed in a total volume of 50 μ l consisting of 1 μ M each primer, 200 μ M each dNTP, 5 μ L 10 \times polymerase reaction buffer, and 1.25U EX Taq DNA Polymerase with 1 μ L digested DNA. The samples were heated to 94 $^{\circ}$ C for 5 min followed by amplification for 30 cycles of 30s at 94 $^{\circ}$ C, 50s at 55 $^{\circ}$ C, and 1 min at 72 $^{\circ}$ C. After the last cycle, a final extension step was done at 72 $^{\circ}$ C for 7 min. Then 10 μ l of each PCR product was analyzed by 1 % agarose gel (containing 0.5 μ g/mL EB) electrophoresis. After which the amplified PCR products were purified from agarose gel according to DNA purification kit description. The abbreviated gene fragments of AFP enhancer (e) and promoter (p) were subcloned into pBluescript II ks(+). The positive clones were selected from the transfected DH5 α and performed as described in reference^[16]. The constructed plasmids (designated as ks-e, ks-p) were identified by restriction enzyme analysis. DNA sequences were verified by DNA Sequencing Core Facility in Bioasia (Shanghai) Biotechnology Company.

Construction and identification of expressing vector pEGFP-1-EP

Gene fragments of AFP enhancer (e) and promoter (p) were released by *EcoR I-Sal I*, and *Sal I-BamH I* double digestions respectively, and inserted into the *EcoR I- BamH I* sites of pEGFP-1. The Recombinant was identified by restriction endonuclease digestion. The restriction maps of pEGFP-1-EP were shown in Figure 1.

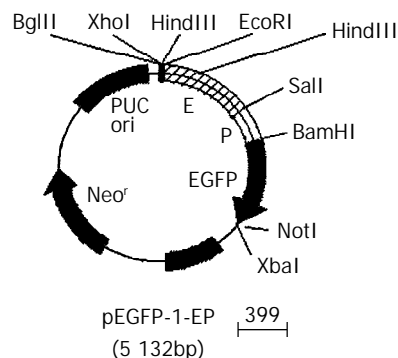


Figure 1 Gene map of pEGFP-1-EP.

Transient EGFP expression

18 hours before transfection, 2×10^5 HepG2, SMMC-7721 and Hela cells were plated into 12-well culture plates. At the bottom of each well, a sterilized coverslip was placed in advance. When the plated cells were 90 to 95 % confluence, transfection was performed with 1 μ g of DNA (pEGFP-1 or pEGFP-1-EP) per dish, using LipofectamineTM 2000 reagent according to the manufacturer's instruction. 48 h after transfection, the cells were washed twice with cold PBS (0.01M) and fixed with 4 % paraformaldehyde for 30 min at room temperature. Coverslips were then mounted directly onto a glass slide with a tiny drop of 50 % glycerol in PBS (9.1 mM Na₂HPO₄/1.7 mM NaH₂PO₄/50 mM NaCl, pH 7.4). Fluorescent images were captured at 490nm using a Nikon Eclipse E1000 microscope attached to a MicroMax camera (Princeton Instruments, Trenton, NJ).

Effect of all-trans retinoic acid (ATRA) on the expression of EGFP

A similar transfection procedure was performed to transfect vector pEGFP-1-EP for stable EGFP expression. After 48 h of transfection, the cells were passaged at a 1:4 dilution into fresh medium. The next day, selective medium (G418 400 μ g/mL)

was added to the cells for screening of stable lines of transfected cells. After culturing for an additional 2 weeks in G418, cells expressing EGFP fluorescence were selected using a fluorescence-activated cell sorter. The EGFP-positive cells were maintained in growth medium supplemented with 400 μ g/mL G418. For RA regulation studies, stably transfected cells were plated on 12-well dishes at 1×10^5 cells/well in growth medium with G418, incubated overnight, then changed into the medium with or without all-trans retinoic acid (1×10^{-7} M, 2.5×10^{-7} M, 1×10^{-6} M ATRA) (without G418). The expression rate of EGFP fluorescence was measured by flow cytometry (ETITE ESP, COULTER Company) 48 h later. The green fluorescence was analyzed through a 530-nm/30-nm band pass filter after illumination with the 488-nm line of an argon ion laser.

Statistical analysis

All experiments were performed three times in triplicate, the data were presented as the mean \pm SEM, and compared by Student's *t* test.

RESULTS

PCR amplification and DNA sequencing of gene modified AFP enhancer and promoter

Electrophoretic result of PCR products showed that the size of amplified DNA fragments was consistent with design. Through PCR amplification of AFP promoter we obtained two gene fragments (0.3kb, 0.5kb). The 0.3kb fragment was what we expected, the 0.5kb one was nonspecific amplification (Figure 2). PCR products were subcloned into pBluescript II ks(+) vector. The DNA Sequencing results confirmed that DNA sequence of both fragments was correct.

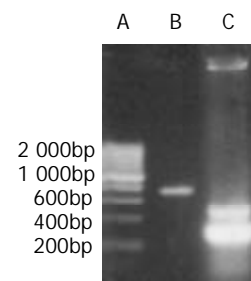


Figure 2 PCR result of gene segments. A. 200bp DNA marker; B. enhancer of AFP; C. promoter of AFP.

Gene modified AFP cis-acting element was successfully inserted into the MCS of pEGFP-1

Recombined AFP cis-acting element was 1 035 bp with *EcoR I* and *BamH I* restriction site on each side. The size of pEGFP-1 was 4.2 kb, which had *BglIII* and *Hind III* sites in the 3' -side of MCS. The expressing vector pEGFP-1-EP was digested by *BglIII/Sal I/BamH I*, and *Xho I/BamH I*, and *Hind III* respectively. 0.73 bp-0.31bp, and 1.03bp, and 0.27 bp DNA fragments appeared (Figure 3). This result meant that the size, direction of cis-acting element were correct and the construction of expressing vector was successful.

Specific expression of EGFP in AFP positive hepatoma

Three cell lines were transfected with plasmid pEGFP-1 and pEGFP-1-EP simultaneously. The expression of EGFP could only be detected in HepG2 cells (AFP positive) transfected with pEGFP-1-EP (Figure 4). The transient expression rate of EGFP in HepG2 was 16 %. Hela cell and SMMC-7721 cell (AFP negative) did not express EGFP. The HepG2 cell transfected with pEGFP-1 also did not express EGFP. So we

could conclude that gene modified cis-acting element retained specific transcription activity in AFP positive cells.

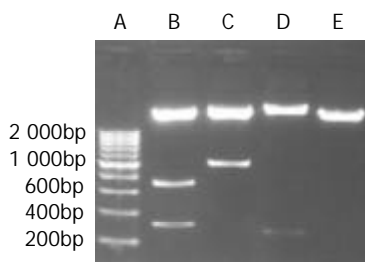


Figure 3 Enzyme digestion analysis of the recombinant expression vector. A. 200bp DNA marker; B. pEGFP-1-EP (*Bgl*III, *Sal* I, *Bam*H I); C. pEGFP-1-EP (*Xho* I, *Bam*H I); D. pEGFP-1-EP (*Hind* III); E. pEGFP-1 (*Eco*R I, *Bam*H I).

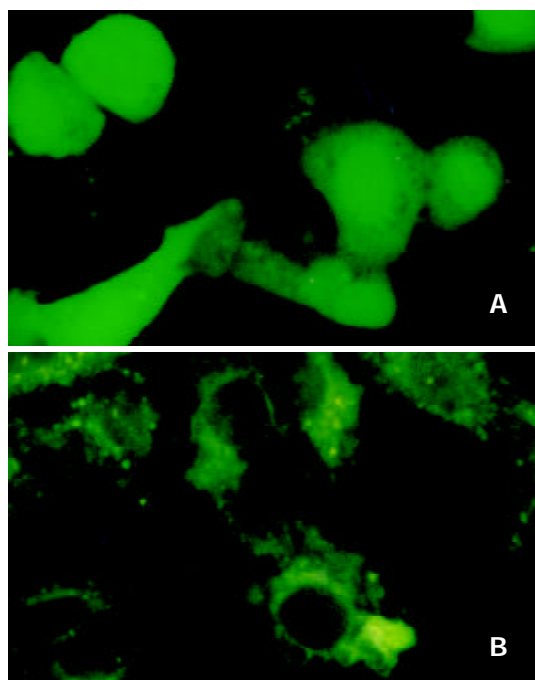


Figure 4 Transient expression of EGFP. A. EGFP expressing in HepG2; B. EGFP do not express in Hela cells.

The expressing of EGFP can be suppressed by the adding of ATRA
EGFP-expressing HepG2 cell line was obtained through two weeks screening by adding G418 into the culture medium. These cells were then cultured in the medium with or without retinoic acid for 48 h and measured by flow cytometry. The expression rate of EGFP was $34.9 \pm 4.1\%$ in cells without retinoic acid and $14.7 \pm 3.5\%$, $13.5 \pm 2.7\%$, $12.1 \pm 3.9\%$ in cells adding $1 \times 10^{-7}M$, $2.5 \times 10^{-7}M$, $1 \times 10^{-6}M$ retinoic acid (Figure 5). Transcription activity of modified AFP cis-acting element was suppressed by adding either concentration of retinoic acid ($P < 0.05$).

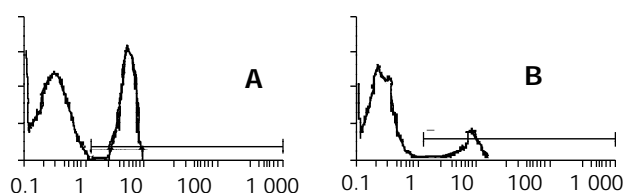


Figure 5 The expression of EGFP suppressed by ATRA. A. stable expression of EGFP in HepG2; B. expression of EGFP suppressed by $2.5 \times 10^{-7}M$ ATRA.

DISCUSSION

There are numerous gene therapy strategies that have been applied to the treatment of HCC. They include gene replacement (e.g. tumor suppressor genes), antisense strategies, drug sensitization (suicide genes), genetic immunotherapy (cytokines, costimulatory molecules, polynucleotide vaccination), and interventions to interfere with the biology of the tumor growth (antiangiogenesis)^[17-19]. But HCC frequently occurs in patients with liver cirrhosis, the potentially toxic effects of gene transfer may have marked deleterious consequences, so the targeted gene transfer or the specific expression of transfected genes to hepatoma cells is vital for gene therapy of HCC.

A practical system to ensure tumor-restricted expression of the transgenes is the use of tumor-specific promoters. Since elevated levels of AFP have been observed in about 70 % of hepatocellular carcinomas^[20], using AFP transcriptional sequence to achieve hepatocellular carcinoma specific gene expression is an ideal way. Arbuthnot *et al*^[21, 22] demonstrated that retroviral and adenoviral vectors containing the lacZ reporter gene under the control of AFP regulatory sequences resulted in the specific expression of the lacZ gene only in HCC cells with AFP expression. Similar results were reported by Kanai *et al*^[23], who demonstrated that expression of the herpes simplex virus thymidine kinase (HSV-tk) gene by adenovirus from AFP promoter/enhancer induced the cells to be sensitive to ganciclovir (GCV) in the AFP-producing cells. But The AFP gene has a large and complex transcription control region which is located within a region from -7.6 kb to the transcription starting site. It contains the promoter, the enhancer, and the silencer that contain specific binding sequences for the transcription factors and provide precisely regulated AFP gene transcription^[24, 25]. Most investigators have used human AFP 5' -flanking region that including the all the *trans*- and *cis*-acting elements from AFP 5' -flanking sequences^[24, 26-29] as a hepatoma specific regulation element. Although this sequences can achieve sufficient cytotoxicity in AFP-producing hepatoma cells, but also induce a killing effect on hepatic stem cells that also express AFP and appear in the injured liver, thus resulting in damage of the hepatic reserve and a poor prognosis for patients with HCC. On the other hand, the package capacity of most gene therapy vectors is very small, which cannot accommodate the whole transcriptional sequence of AFP in the construct. The activity of promoter alone is too weak to be used in targeting gene therapy. In this study, we subcloned the minimal essential enhancer region (-4.0 to -3.3) and 0.3 kb minimal promoter of human AFP gene, and constructed abbreviated HCC specific cis-acting element. The expressing of the report gene (EGFP) was detected in AFP-producing hepatoma cells (HepG2), and none in non-AFP-producing hepatoma (SMMC-7721) and nonhepatoma cells (Hela). So this minimal cis-acting element well conserved the specific transcription characteristic of AFP 5' -flanking sequences. This element is very small (1.0 kb) and fits to the package capacity of most conventional gene therapy vectors.

The expression of AFP is under the control of retinoic acid which both activates and represses AFP expression in different cell lines^[30, 31]. Within the AFP gene regulatory region three elements determining sensitivity for retinoic acid have been revealed. One of them is localized in promoter (-139/-127 bp) and overlaps with other transcription factor binding sites^[31]. The influence of retinoic acid on AFP gene expression can be carried out both by means of HNF induction and through the hormone-receptor complex binding to the corresponding sites in AFP regulatory elements^[32]. Activation of the AFP gene by RA had been reported in McA-RH8994 and F9 cell lines^[30, 31], while AFP was down-regulated by RA in the human hepatoma cell line Hep3B. How can RA regulate the expression of AFP

in HepG2 human hepatoma cell line is rarely reported. In this study we established an EGFP-expressing HepG2 cell line, the expressing of EGFP is under the control of modified cis-acting element of AFP. When treated with ATRA, we found that the transcription activity of AFP cis-acting element could be significantly suppressed by 1×10^{-7} M ATRA. So when we use this transcription element as a regulator of anti-tumor gene the cytotoxicity effects on target cell can be controlled by RA within the expected range. This is very important when a gene therapy vector is applied clinically.

There are restriction sites in the upstream or downstream of EGFP in the expressing vector pEGFP-1-EP, through which we can replace EGFP with any tumor-killing gene. So this vector can be used as a gene therapy vector targeting for hepatocellular carcinoma. The transcription activity of hepatocellular carcinoma specific promoter can be controlled by the adding of ATRA.

REFERENCES

- Badvie S.** Hepatocellular carcinoma. *Postgrad Med J* 2000; **76**: 4-11
- Llovet JM, Mas X, Aponte JJ, Fuster J, Navasa M, Christensen E, Rodes J, Bruix J.** Cost effectiveness of adjuvant therapy for hepatocellular carcinoma during the waiting list for liver transplantation. *Gut* 2002; **50**: 123-128
- Tang ZY.** Hepatocellular carcinoma-cause, treatment and metastasis. *World J Gastroenterol* 2001; **7**: 445-454
- Schöniger-Hekele M, Müller C, Kutilek M, Oesterreicher C, Ferenci P, Gangl A.** Hepatocellular carcinoma in Central Europe: prognostic features and survival. *Gut* 2001; **48**: 103-109
- Narvaiza I, Mazzolini G, Barajas M, Duarte M, Zaratiegui M, Qian C, Melero I, Prieto J.** Intratumoral coinjection of two adenoviruses, one encoding the chemokine IFN- γ -inducible protein-10 and another encoding IL-12, results in marked antitumoral synergy. *J Immunol* 2000; **164**: 3112-3122
- Ruiz J, Qian C, Drozdik M, Prieto J.** Gene therapy of viral hepatitis and hepatocellular carcinoma. *J Viral Hepat* 1999; **6**: 17-34
- Kuriyama S, Nakatani T, Masui K, Sakamoto T, Tominaga K, Yoshikawa M, Fukui H, Ikenaka K, Tsujii T.** Evaluation of prodrugs ability to induce effective ablation of cells transduced with viral thymidine kinase gene. *Anticancer Res* 1996; **16**: 2623-2628
- Schmitz V, Qian C, Ruiz J, Sangro B, Melero I, Mazzolini G, Narvaiza I, Prieto J.** Gene therapy for liver diseases: recent strategies for treatment of viral hepatitis and liver malignancies. *Gut* 2002; **50**: 130-135
- Qian C, Idoate M, Bilbao R, Sangro B, Bruna O, Vazquez J, Prieto J.** Gene transfer and therapy with adenoviral vector in rats with diethylnitrosamine-induced hepatocellular carcinoma. *Hum Gene Ther* 1997; **8**: 349-358
- Uto H, Ido A, Hori T, Hirono S, Hayashi K, Tamaoki T, Tsubouchi H.** Hepatoma-specific gene therapy through retrovirus-mediated and targeted gene transfer using an adenovirus carrying the ecotropic receptor gene. *Biochem Biophys Res Commun* 1999; **265**: 550-555
- Chen XP, Zhao H, Zhao XP.** Alternation of AFP-mRNA level detected in blood circulation during liver resection for HCC and its significance. *World J Gastroenterol* 2002; **8**: 818-821
- Dachs GU, Dougherty GJ, Stratford IJ, Chaplin DJ.** Targeting gene therapy to cancer: a review. *Oncol Res* 1997; **9**: 313-325
- Kanai F.** Transcriptional targeted gene therapy for hepatocellular carcinoma by adenovirus vector. *Mol Biotechnol* 2001; **18**: 243-250
- Su H, Chang JC, Xu SM, Kan YW.** Selective killing of AFP-positive hepatocellular carcinoma cells by adeno-associated virus transfer of the herpes simplex virus thymidine kinase gene. *Hum Gene Ther* 1996; **7**: 463-470
- Ido A, Uto H, Moriuchi A, Nagata K, Onaga Y, Onaga M, Hori T, Hirono S, Hayashi K, Tamaoki T, Tsubouchi H.** Gene therapy targeting for hepatocellular carcinoma: selective and enhanced suicide gene expression regulated by a hypoxia-inducible enhancer linked to a human alpha-fetoprotein promoter. *Cancer Res* 2001; **61**: 3016-3021
- Sambrook J, Fritsch EF, Maniatis T.** Molecular Cloning: A Laboratory Manual, 2nd ed. Cold Spring Harbor Laboratory Press, New York, 1989
- Ueki T, Nakata K, Mawatari F, Tsuruta S, Ido A, Ishikawa H, Nakao K, Kato Y, Ishii N, Eguchi K.** Retrovirus-mediated gene therapy for human hepatocellular carcinoma transplanted in athymic mice. *Int J Mol Med* 1998; **1**: 671-675
- Barajas M, Mazzolini G, Genove G, Bilbao R, Narvaiza I, Schmitz V, Sangro B, Melero I, Qian C, Prieto J.** Gene therapy of orthotopic hepatocellular carcinoma in rats using adenovirus coding for interleukin-12. *Hepatology* 2001; **33**: 52-61
- Brunda MJ, Luistro L, Warriar RR, Wright RB, Hubbard BR, Murphy M, Wolf SF, Gately MK.** Antitumor and antimetastatic activity of interleukin 12 against murine tumors. *J Exp Med* 1993; **178**: 1223-1230
- Sato Y, Nakata K, Kato Y, Shima M, Ishii N, Koji T, Taketa K, Endo Y, Nagataki S.** Early recognition of hepatocellular carcinoma based on altered profiles of α -fetoprotein. *N Engl J Med* 1993; **328**: 1802-1806
- Arbuthnot P, Bralet MP, Thomassin H, Danan JL, Brechot C, Ferry N.** Hepatoma cell-specific expression of a retrovirally transferred gene is achieved by alpha-fetoprotein but not insulin-like growth factor II regulatory sequences. *Hepatology* 1995; **22**: 1788-1796
- Arbuthnot PB, Bralet MP, Le Jossic C, Dedieu JF, Perricaudet M, Brechot C, Ferry N.** *In vitro* and *in vivo* hepatoma cell-specific expression of a gene transferred with an adenoviral vector. *Hum Gene Ther* 1996; **7**: 1503-1514
- Kanai F, Shiratori Y, Yoshida Y, Wakimoto H, Hamada H, Kanegae Y, Saito I, Nakabayashi H, Tamaoki T, Tanaka T, Lan KH, Kato N, Shiina S, Omata M.** Gene therapy for alpha-fetoprotein-producing human hepatoma cells by adenovirus-mediated transfer of the herpes simplex virus thymidine kinase gene. *Hepatology* 1996; **23**: 1359-1368
- Nakabayashi H, Watanabe K, Saito A, Otsuru A, Sawadaishi K, Tamaoki T.** Transcriptional regulation of alpha-fetoprotein expression by dexamethasone in human hepatoma cells. *J Biol Chem* 1989; **264**: 266-271
- Watanabe K, Saito A, Tamaoki T.** Cell-specific enhancer activity in a far upstream region of the human alpha-fetoprotein gene. *J Biol Chem* 1987; **262**: 4812-4818
- Ishikawa H, Nakata K, Mawatari F, Ueki T, Tsuruta S, Ido A, Nakao K, Kato Y, Ishii N, Eguchi K.** Retrovirus-mediated gene therapy for hepatocellular carcinoma with reversely oriented therapeutic gene expression regulated by alpha-fetoprotein enhancer/promoter. *Biochem Biophys Res Commun* 2001; **287**: 1034-1040
- Kaneko S, Hallenbeck P, Kotani T, Nakabayashi H, McGarrity G, Tamaoki T, Anderson WF, Chiang YL.** Adenovirus-mediated gene therapy of hepatocellular carcinoma using cancer-specific gene expression. *Cancer Res* 1995; **55**: 5283-5287
- Wills KN, Huang WM, Harris MP, Machemer T, Maneval DC, Gregory RJ.** Gene therapy for hepatocellular carcinoma: chemosensitivity conferred by adenovirus-mediated transfer of the HSV-1 thymidine kinase gene. *Cancer Gene Ther* 1995; **2**: 191-197
- Igarashi T, Suzuki S, Takahashi M, Tamaoki T, Shimada T.** A novel strategy of cell targeting based on tissue-specific expression of the ecotropic retrovirus receptor gene. *Hum Gene Ther* 1998; **9**: 2691-2698
- Li C, Locker J, Wan YJ.** RXR-mediated regulation of the alpha-fetoprotein gene through an upstream element. *DNA Cell Biol* 1996; **15**: 955-963
- Liu Y, Chen H, Dong JM, Chiu JF.** Cis-acting elements in 5' flanking region of rat alpha-fetoprotein mediating retinoic acid responsiveness. *Biochem Biophys Res Commun* 1994; **205**: 700-705
- Magge TR, Cai Y, El-Houseini ME, Locker J, Wan YJ.** Retinoic acid mediates down-regulation of the alpha-fetoprotein gene through decreased expression of hepatocyte nuclear factors. *J Biol Chem* 1998; **273**: 30024-30032

Codon 249 mutation in exon 7 of p53 gene in plasma DNA: maybe a new early diagnostic marker of hepatocellular carcinoma in Qidong risk area, China

Xing-Hua Huang, Lu-Hong Sun, Dong-Dong Lu, Yan Sun, Li-Jie Ma, Xi-Ran Zhang, Jian Huang, Long Yu

Xing-Hua Huang, Li-Jie Ma, Long Yu, The State Key Laboratory of Genetic Engineering, Fudan University, 200433, Shanghai, China
Lu-Hong Sun, Dong-Dong Lu, Xi-Ran Zhang, School of life sciences, Nanjing Normal University, Nanjing 210097, Jiangsu Province, China
Xing-Hua Huang, Yan Sun, Jian Huang, Qidong Liver Cancer Institute, Qidong 226200, Jiangsu Province, China

Correspondence to: Long Yu, The State Key Laboratory of Genetic Engineering, Fudan University, 200433, Shanghai, China. longyu@fudan.edu.cn

Telephone: +86-21-65643954 **Fax:** +86-21-65643250

Received: 2002-08-02 **Accepted:** 2002-08-27

Abstract

AIM: One of the characteristics of hepatocellular carcinoma (HCC) in Qidong area is the selective mutation resulting in a serine substitution at codon 249 of the p53 gene (1, 20), and it has been identified as a "hotspot" mutation in hepatocellular carcinomas occurring in populations exposed to aflatoxin and with high prevalence of hepatitis B virus carriers (2, 3, 9, 10, 16, 24). We evaluated in this paper whether this "hotspot" mutation could be detected in cell-free DNA circulating in plasma of patients with hepatocellular carcinoma and cirrhosis in Qidong, China, and tried to illustrate the significance of the detection of this molecular biomarker.

METHODS: We collected blood samples from 25 hepatocellular carcinoma patients, 20 cirrhotic patients and 30 healthy controls in Qidong area. DNA was extracted and purified from 200 µl of plasma from each sample. The 249^{Ser} p53 mutation was detected by restriction digestion analysis and direct sequencing of exon-7 PCR products.

RESULTS: We found in exon 7 of p53 gene G→T transversion at the third base of codon 249 resulting 249^{Arg}→249^{Ser} mutation in 10/25 (40 %) hepatocellular carcinoma cases, 4/20 (20 %) cirrhotics, and 2/30 (7 %) healthy controls. The adjusted odds ratio for having the mutation was 22.1 (95 % CI, 3.2~91.7) for HCC cases compared to controls.

CONCLUSION: These data show that the 249^{Ser} p53 mutation in plasma is strongly associated with hepatocellular carcinoma in Qidong patients. We found this mutation was also detected, although it was at a much lower frequency, in plasma DNA of Qidong cirrhotics and healthy controls; We consider that these findings, together with the usual method of HCC diagnosis, will give more information in early diagnosis of HCC, and 249^{Ser} p53 mutation should be developed to a new early diagnostic marker for HCC.

Huang XH, Sun LH, Lu DD, Sun Y, Ma LJ, Zhang XR, Huang J, Yu L. Codon 249 mutation in exon 7 of p53 gene in plasma DNA: maybe a new early diagnostic marker of hepatocellular carcinoma in Qidong risk area, China. *World J Gastroenterol* 2003; 9(4): 692-695

<http://www.wjgnet.com/1007-9327/9/692.htm>

INTRODUCTION

Qidong is a high risk area of hepatocellular carcinoma (HCC), chiefly due to chronic hepatitis B virus (HBV) infection, and exposure to AFB1^[1,2]. HCC is a major cause of cancer death in this area. Epidemiological and experimental evidence show that hepatitis B virus (HBV) and dietary exposure to aflatoxin B1 (AFB1) contribute to hepatocarcinogenesis^[3-9]. About 10-15 % of the Qidong populations are chronically infected with HBV (LU. PX *et al.*, 1991). An analysis of individual biomarkers of aflatoxin exposure in Qidong (Daxing country) has shown 99 % (791/792) of individuals with detectable serum aflatoxin-albumin adducts (Zhu YR *et al.*, 1999).

p53 mutations have been identified in several human cancers^[10-12]. A selective G to T transversion mutation at codon 249 (AGG→AGT, arginine to serine) of the p53 gene has been identified as a "hotspot" mutation for HCC in Qidong area^[13-16]. Data from Qidong Liver Cancer Institute have suggested that this mutation in HCC is strongly associated with exposure to AFB1^[13]. Recent research in Gambia^[17] has shown that in some human cancers, circulating tumor DNA can be successfully retrieved from plasma or serum and used as a surrogate material to analyze for genetic alterations present in the original tumor^[18-20]. We adopted this approach to evaluate the presence of 249^{Ser} p53 mutation in plasma from HCC cases, cirrhotic patients and healthy controls, and this mutation could be regarded as a new biomarker in HCC earlier diagnosis.

MATERIALS AND METHODS

Subjects and specimens

Blood samples from 25 cases of HCC, 20 cirrhotic patients and 30 healthy controls were collected in Qidong Liver Cancer Institute. The definition for 25 cases of HCC included compatible clinical and ultrasonographic findings and serum AFP levels. The ultrasonographic data were most important. 20 Cirrhotic patients were included as an additional referent group for evaluation of factors associated with progression to HCC. The diagnosis of cirrhosis was also based on compatible clinical history and by ultrasonographic method. 30 cases of controls were recruited from the outpatient clinics among individuals with no history or clinical findings suggestive of liver disease, and have the same distributions of age, gender and recruitment site with the HCC and cirrhotic cases.

DNA extraction

Blood samples anticoagulated with EDTA were processed immediately after collection, plasma was transferred to a plain tube and stored at -70 °C at Qidong Liver Cancer Institute. AFP and HBV serological testing was performed using standard laboratory kits. A 500 µl aliquot of plasma was shipped in liquid nitrogen to the state key laboratory of genetic engineering, Fudan University (Shanghai), for 249 Ser testing. DNA was extracted from 200 µl of plasma using a QiAamp blood kit (Qiagen Company) according to the manufacturer's protocol. The purified DNA was eluted from silica column with 50 µl of Nuclease-Free Water.

PCR

Primers used for PCR amplification synthesized by Sangon company (Shanghai) were as follows: p1 (up) (5' -ctt gcc aca ggt ctc ccc aa-3'), p2 (down) (5' -agg ggt cag cgg caa gca ga-3'). The expected size of the product was 254 bp, and this fragment was located in the exon 7 of p53 gene.

Using TaKaRa PCR kit, the 25 μ l reaction included 18.3 μ l ddH₂O, 2.5 μ l 10 \times buffer, 1 μ l dNTPs, 0.5 μ l primer 1, 0.5 μ l primer 2, 0.2 μ l Taq DNA polymerase, 2 μ l DNA templates. The thermo-cycling conditions were 94 $^{\circ}$ C for 5 min, and 40 cycles of 94 $^{\circ}$ C for 30 sec, 60 $^{\circ}$ C for 30 sec, 72 $^{\circ}$ C for 30 sec, and finally 72 $^{\circ}$ C for 10 min in a Peltier Thermal Cycler (PTC 200). The amplification products (254 bp) were visualized by staining with ethidium bromide, after electrophoresis on 2 % agarose gel.

Purification of PCR products

To obtain enough amounts of DNA fragments for further testing, 1 μ l of PCR product of each sample was picked up as template to have another PCR reaction with the same amplifying condition. The PCR products were then purified with 3S PCR Product Purification Kit (Biocolor Biological Science & Technology Co., Ltd) to eliminate some impurities such as dNTPs, primers, polymerase, and mineral oil.

Mutation detection by restriction analysis

The 254 bp of purified DNA fragment, which is derived from exon 7 of p53 gene, was submitted to restriction enzyme *Hae* III (New England Biolabs Company) digestion. The restriction enzyme digestion reaction system was as follows: 1 μ l *Hae* III, 2 μ l 10 \times buffer2, 5 μ l DNA fragment, 12 μ l ddH₂O (20 μ l total volume). These reaction systems were submitted to 37 $^{\circ}$ C water incubation for 4 hours. Enzyme *Hae* III cleaves a GG/CC sequence at codons 249-250, generating 92bp, 66bp and several small fragments from the 254 bp purified DNA product of the PCR reaction. If there is a mutation at codon 249-250 resulting in an uncleaved, 158bp fragment, and this feature will be distinguished from that of normal samples on 2 % agarose gel stained with ethidium bromide. Absence of the band at 254 bp (full-length PCR products) provides a control for complete digestion of the PCR product. In our protocol, we also arrange positive (with 249 mutation) and negative (wild-type) controls. The presence of the uncleaved 158 bp fragment indicates that there are mutations in the corresponding samples, and DNA fragments of these special samples were analyzed by automated DNA sequencing (ABI 377) using BigDye Terminator Cycle Sequencing Ready Reaction Kit (PE company).

Statistical analysis

Pearson's chi-square and Fisher's exact test were used to assess statistical significance of frequency tables of independent variables and 249 Ser mutations as a dichotomous variable. Multivariable logistic regression analysis was performed to estimate odds ratios (OR) along with 95 % confidence intervals (CI) to estimate the risk of mutation among the different study groups considering age, gender, recruitment site, and hepatitis B surface antigen status as potential confounders.

RESULTS

The characteristics of the 75 subjects from Qidong were evaluated in the study (Table 1).

HCC cases, cirrhosis cases and controls from Qidong were of similar age and gender distribution. 84 % of HCC cases, 65 % of cirrhotics and 13 % of controls were positive for hepatitis B surface antigen (HBsAg), a marker of chronic infection with HBV ($P < 0.001$ for difference between groups).

80 % of HCC cases, 70 % of cirrhotics and 0 % of controls were positive for serum alpha-fetoprotein positive (AFP > 100 ng/ml).

Table 1 Characteristics of study participants from Qidong

	Hepatocellular carcinomas	Cirrhotics	Controls
	(25)	(20)	(30)
Age (average [range], in years)	49 (27-70)	39 (25-65)	45 (19-87)
Number of males (%)	20 (80)	17 (85)	25 (83)
Hepatitis B surface antigen positive (%)	21 (84)	13 (65)	4 (13)
Serum alpha-fetoprotein positive (%)	20 (80)	14 (70)	0 (0)

The electrophoresis on 2 % agarose gel shows that the 254 bp specific DNA fragments amplified between p1 and p2 are at the appropriate location according to the DNA molecular weight markers (Figure 1).

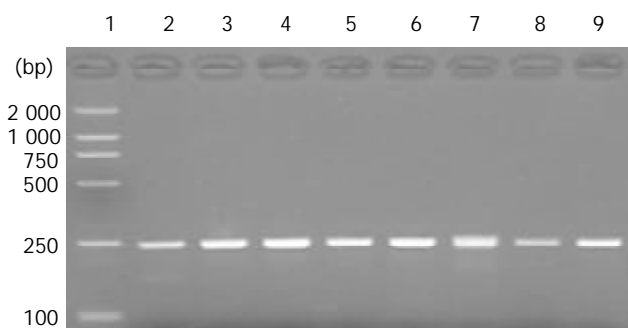


Figure 1 The electrophoresis map of PCR products. Lane 1: DNA molecular weight markers. Lane 2-9: PCR products of partial samples.

DNA fragment from each sample was digested with restriction enzyme *Hae* III. Presence of undigested 158 bp fragments on 2 % agarose gel indicates that there is a point mutation in the *Hae* III recognition site (Figure 2).

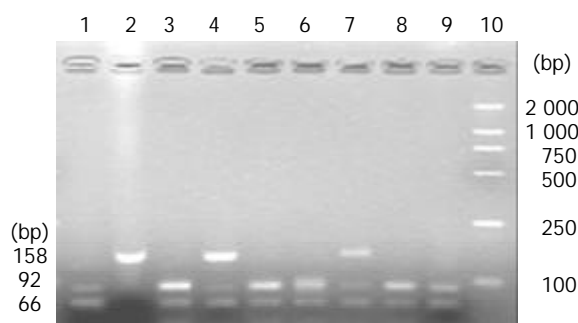


Figure 2 Mutation at codon 249 was identified by restriction digestion. Lane 1: negative control, Lane 2: positive control, Lane 3-9: HCC samples, Lane 10: DNA molecular weight markers.

p53 exon 7 fragments from normal controls (wild type) and mutation (identified by restriction digestion) HCC cases were sequenced (Figure 3).

We found in this paper 16 of 75 subjects from Qidong have 249^{ser} p53 mutation, including ten of 25 HCC cases, four of 20 cirrhotic patients, and two of 30 controls, giving a prevalence of 40 %, 20 % and 7 %, respectively ($P < 0.001$ for difference between groups) (Table 2).

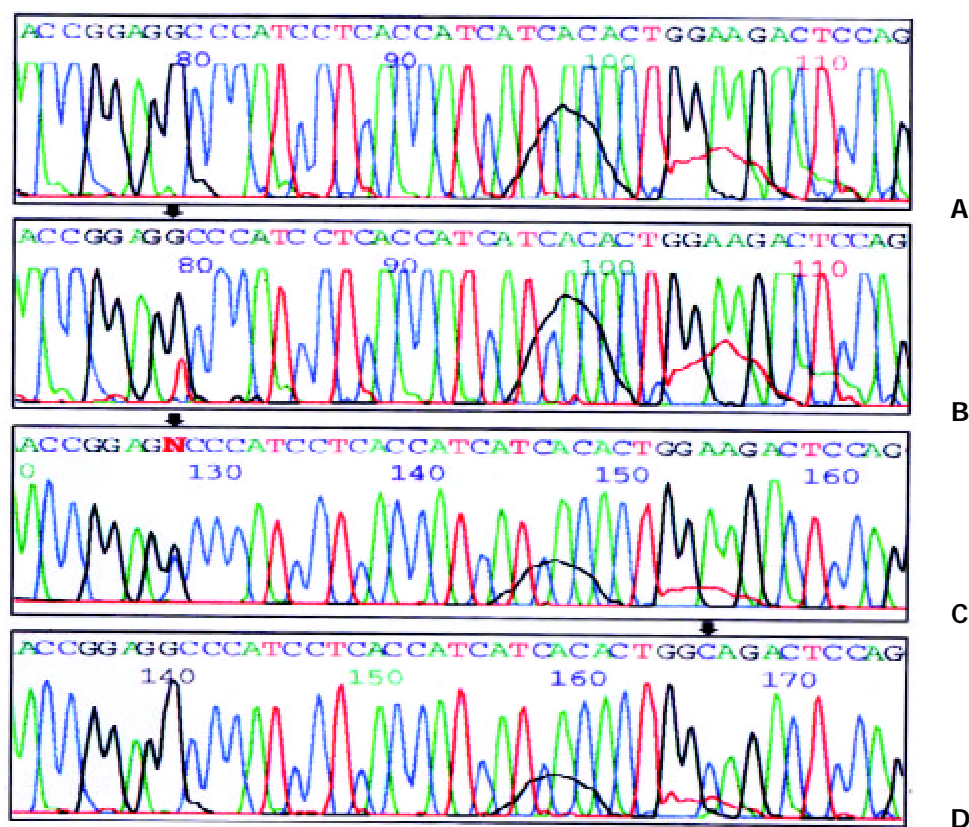


Figure 3 Sequencing results (partial electropherogram). A: Wild type sequence shows codon 249 AGG; B: Mutation sequence shows codon 249 AGG→AGT transversion; C: Mutation sequence shows codon 249 AGG→AGC transversion; D: A→C transversion at the second base of codon 258.

Table 2 Prevalence and adjusted odds ratios for plasma 249^{Ser} p53 mutations by subject groups from Qidong

	Controls ^a	Cirrhotics	Hepatocellular carcinomas
	(30)	(20)	(25)
No. positive (%)	2 (7)	4 (20)	10 (40)
OR (95% CI)	1.0	5 (0.6, 29.3)	22.1 (3.2, 91.7)

^aEstimated odds ratios (OR) and 95 % confidence intervals (CI) were adjusted for age, gender, recruitment site and hepatitis B surface antigen status, using controls as the referent group.

DISCUSSION

In the People's Republic of China, HCC accounts for over 250 000 deaths annually with an incidence rate in some areas of the country approaching 150 cases/100 000/year. Mutations in the p53 tumor suppressor gene have been identified in a majority of human cancers^[21], especially in HCC^[2,22]. The most striking example of a specific mutation in the p53 gene is a G→T transversion in the third base of codon 249, which has been detected in 10-70 % of HCCs from area with a high exposure to AFB1^[6,23-25], where this mutation is absent from HCC in regions with negligible exposure to AFB1^[13,26,27].

Jackson *et al.* reported that a high percentage of the tumors from Qidong had G→T mutation at the third base of codon 249 of the p53 gene than tumors from Shanghai (46.7 % compared with 30 %) ^[10,28]. The mutation frequency corresponds to exposure to aflatoxins because these areas have high and intermediate exposure levels, respectively. A recent report by Kirk *et al.* reported for the first time the detection of codon 249 p53 mutation in the plasma of liver tumor patients from Gambia. DNA circulating in the serum or plasma can be successfully retrieved and used as surrogate material to analyze

for genetic alterations present in the original tumor^[10,29]. Although the mechanisms accounting the presence of this circulating DNA are uncertain, there is some evidence that the DNA, of up to 21 Kb, are released from the tumor as a glyconucleoprotein complex, and may protect the DNA from degradation by nucleases. Although we don't understand the relationship between the release of tumor DNA into the plasma and necrosis of the tumor, apoptosis or other selective cellular processes, we considered from our experimental data that plasma or serum may be used as a source of tumor-specific DNA^[30,31].

We reported the presence of 249^{Ser} p53 mutations in DNA circulating in the plasma of Qidong population at high risk for HCC, chronic HBV infection and exposure to the carcinogen AFB1. We found in this paper 16 of 75 subjects from Qidong had 249^{Ser} p53 mutation, including ten of 25 HCC cases, four of 20 cirrhotic patients, and two of 30 controls (Table 2). It is interesting that we found in one HCC case a G→C transversion at the third base of codon 249 instead of G→T transversion, although both of AGC and AGT coded serine. The 249^{Ser} p53 "hotspot" mutation was detected in 40 % of HCC cases, and a much lower prevalence was observed in cirrhotic patients (20 %) and in controls (7 %) ($P < 0.001$ for difference between groups). Additionally, we found in another HCC case A→C transversion at the second base of codon 258. We checked the exon 7 of p53 gene using NCBI Blast, and found none of the ESTs could support this point mutation. Is it a SNP or a point mutation associated with AFB1 exposure? It is to be studied. Although we didn't check the 249^{Ser} p53 mutations in the corresponding tissues, we can draw a conclusion from these data that p53 mutation frequency of these different groups provided the strong relationship between cirrhosis and the future development of HCC^[32]. This mutation may be regarded as an early detection marker or a prognostic molecular marker in HCC^[33,34]. The detection of 249^{Ser} DNA may be useful as a

maker of neoplastic development, and the presence of the mutation in healthy subjects may reflect chronic exposure to high levels of AFB1^[35].

Besides the detection of serum aflatoxin-albumin adducts, we can also use plasma 249^{ser} p53 mutation as a marker of aflatoxin exposure in epidemiological studies. It is expected in Qidong area that the detection of p53 mutation in plasma DNA could be developed into a usual method to estimate the development of HCC, and this mutation could be regarded as an early diagnostic marker of hepatocellular carcinoma.

REFERENCES

- Jackson PE**, Groopman JD. Aflatoxin and liver cancer. *Baillieres Best Pract Res Clin Gastroenterol* 1999; **13**: 545-555
- Hsia CC**, Kleiner DE Jr, Axiotis CA, Di Bisceglie A, Nomura AM, Stemmermann GN, Tabor E. Mutations of p53 gene in hepatocellular carcinoma: roles of hepatitis B virus and aflatoxin contamination in the diet. *J Natl Cancer Inst* 1992; **84**: 1638-1641
- Lunn RM**, Zhang YJ, Wang LY, Chen CJ, Lee PH, Lee CS, Tsai WY, Santella RM. p53 mutations, chronic hepatitis B virus infection, and aflatoxin exposure in hepatocellular carcinoma in Taiwan. *Cancer Res* 1997; **57**: 3471-3477
- Park US**, Su JJ, Ban KC, Qin L, Lee EH, Lee YI. Mutations in the p53 tumor suppressor gene in tree shrew hepatocellular carcinoma associated with hepatitis B virus infection and intake of aflatoxin B1. *Gene* 2000; **251**: 73-80
- Lee YI**, Lee S, Das GC, Park US, Park SM, Lee YI. Activation of the insulin-like growth factor II transcription by aflatoxin B1 induced p53 mutant 249 is caused by activation of transcription complexes; implications for a gain-of-function during the formation of hepatocellular carcinoma. *Oncogene* 2000; **19**: 3717-3726
- Wang JS**, Huang T, Su J, Liang F, Wei Z, Liang Y, Luo H, Kuang SY, Qian GS, Sun G, He X, Kensler TW, Groopman JD. Hepatocellular carcinoma and aflatoxin exposure in Zhuqing Village, Fusui County, People's Republic of China. *Cancer Epidemiol Biomarkers Prev* 2001; **10**: 143-146
- Smela ME**, Hamm ML, Henderson PT, Harris CM, Harris TM, Essigmann JM. The aflatoxin B(1) formamidopyrimidine adduct plays a major role in causing the types of mutations observed in human hepatocellular carcinoma. *Proc Natl Acad Sci U S A* 2002; **99**: 6655-6660
- Zhang F**, Zhu Y, Sun Z. Universal presence of HBVx gene and its close association with hotspot mutation of p53 gene in hepatocellular carcinoma of prevalent area in China. *Zhonghua Zhongliu Zazhi* 1998; **20**: 18-21
- Zhu M**, Dai Y, Zhan R. HBxAg enhanced p53 protein accumulation in hepatoma cells. *Zhonghua Binglixue Zazhi* 1999; **28**: 31-34
- Jackson PE**, Qian GS, Friesen MD, Zhu YR, Lu P, Wang JB, Wu Y, Kensler TW, Vogelstein B, Groopman JD. Specific p53 mutations detected in plasma and tumors of hepatocellular carcinoma patients by electrospray ionization mass spectrometry. *Cancer Res* 2001; **61**: 33-35
- Pfeifer GP**, Denissenko MF, Olivier M, Tretyakova N, Hecht SS, Hainaut P. Tobacco smoke carcinogens, DNA damage and p53 mutations in smoking-associated cancers. *Oncogene* 2002; **21**: 7435-7451
- Niu ZS**, Li BK, Wang M. Expression of p53 and C-myc genes and its clinical relevance in the hepatocellular carcinomatous and pericarcinomatous tissues. *World J Gastroenterol* 2002; **8**: 822-826
- Hsu IC**, Metcalf RA, Sun T, Welsh JA, Wang NJ, Harris CC. Mutational hotspot in the p53 gene in human hepatocellular carcinoma. *Nature* 1991; **350**: 427-428
- Li D**, Cao Y, He L, Wang N J, Gu JR. Aberrations of p53 gene in human hepatocellular carcinoma from China. *Carcinogenesis* 1993; **14**: 169-173
- Fujimoto Y**, Hampton LL, Wirth PJ, Wang NJ, Xie JP, Thorgeirsson SS. Alterations of tumor suppressor genes and allelic losses in human hepatocellular carcinomas in China. *Cancer Res* 1994; **54**: 281-285
- Deng ZL**, Ma Y. Aflatoxin sufferer and p53 gene mutation in hepatocellular carcinoma. *World J Gastroenterol* 1998; **4**: 28-29
- Kirk GD**, Camus-Randon AM, Mendy M, Goedert JJ, Merle P, Trepo C, Brecht C, Hainaut P, Montesano R. 249 Ser- p53 mutations in plasma DNA of patients with hepatocellular carcinoma from the Gambia. *J Natl Cancer Inst* 2000; **92**: 148-153
- Wong IH**, Lo YM, Zhang J, Liew CT, Ng MH, Wong N, Lai PB, Lau WY, Hjelm NM, Johnson PJ. Detection of aberrant p16 methylation in the plasma and serum of liver cancer patients. *Cancer Res* 1999; **59**: 71-73
- Chen XQ**, Stroun M, Magnenat JL, Nicod LP, Kurt AM, Lyautey J, Lederrey C, Anker P. Microsatellite alterations in plasma DNA of small cell lung cancer patients. *Nat Med* 1996; **2**: 1033-1035
- Nawroz H**, Koch W, Anker P, Stroun M, Sidransky D. Microsatellite alterations in serum DNA of head and neck cancer patients. *Nat Med* 1996; **2**: 1035-1037
- Martins C**, Kedda MA, Kew MC. Characterization of six tumor suppressor genes and microsatellite instability in hepatocellular carcinoma in southern African blacks. *World J Gastroenterol* 1999; **5**: 470-476
- Jiang W**, Lu Q, Pan G. p53 gene mutation in hepatocellular carcinoma. *Zhonghua Waikexue Zazhi* 1998; **36**: 531-532
- Yang M**, Zhou H, Kong RY, Fong WF, Ren LQ, Liao XH, Wang Y, Zhuang W, Yang S. Mutations at codon 249 of p53 gene in human hepatocellular carcinomas from Tongan, China. *Mutat Res* 1997; **381**: 25-29
- Shimizu Y**, Zhu JJ, Han F, Ishikawa T, Oda H. Different frequencies of p53 codon-249 hot-spot mutations in hepatocellular carcinomas in Jiangsu province of China. *Int J Cancer* 1999; **82**: 187-190
- Ming L**, Yuan B, Thorgeirsson SS. Characteristics of high frequency 249 codon mutation of p53 gene in hepatocellular carcinoma in prevalent area of China. *Zhonghua Zhongliu Zazhi* 1999; **21**: 122-124
- Qian GS**, Ross RK, Yu MC, Yuan JM, Gao YT, Henderson BE, Wogan GN, Groopman JD. A follow-up study of urinary markers of aflatoxin exposure and liver cancer risk in Shanghai, People's Republic of China. *Cancer Epidemiol Biomarkers Prev* 1994; **3**: 3-10
- Liu H**, Wang Y, Zhou Q, Gui SY, Li X. The point mutation of p53 gene exon7 in hepatocellular carcinoma from Anhui Province, a non HCC prevalent area in China. *World J Gastroenterol* 2002; **8**: 480-482
- Qian GS**, Kuang SY, He X, Groopman JD, Jackson PE. Sensitivity of electrospray ionization mass spectrometry detection of codon 249 mutations in the p53 gene compared with RFLP. *Cancer Epidemiol Biomarkers Prev* 2002; **11**: 1126-1129
- Anker P**, Lefort F, Vasioukhin V, Lyautey J, Lederrey C, Chen XQ, Stroun M, Mulcahy HE, Farthing MJ. K-ras mutations are found in DNA extracted from the plasma of patients with colorectal cancer. *Gastroenterology* 1997; **112**: 1114-1120
- Stroun M**, Anker P, Beljanski M, Henri J, Lederrey C, Ojha M, Maurice PA. Presence of RNA in the nucleoprotein complex spontaneously released by human lymphocytes and frog auricles in culture. *Cancer Res* 1978; **38**: 3546-3554
- Goessl C**, Heicappell R, Munker R, Anker P, Stroun M, Krause H, Muller M, Miller K. Microsatellite analysis of plasma DNA from patients with clear cell renal carcinoma. *Cancer Res* 1998; **58**: 4728-4732
- Minouchi K**, Kaneko S, Kobayashi K. Mutation of p53 gene in regenerative nodules in cirrhotic liver. *J Hepatol* 2002; **37**: 231-239
- Qin LX**, Tang ZY. The prognostic molecular markers in hepatocellular carcinoma. *World J Gastroenterol* 2002; **8**: 385-392
- Qin LX**, Tang ZY, Ma ZC, Wu ZQ, Zhou XD, Ye QH, Ji Y, Huang LW, Jia HL, Sun HC, Wang L. P53 immunohistochemical scoring: an independent prognostic marker for patients after hepatocellular carcinoma resection. *World J Gastroenterol* 2002; **8**: 459-463
- Makarananda K**, Pengpan U, Srisakulthong M, Yoovathaworn K, Sriwatanakul K. Monitoring of aflatoxin exposure by biomarkers. *J Toxicol Sci* 1998; **23**: 155-159

Docetaxel inhibits SMMC-7721 human hepatocellular carcinoma cells growth and induces apoptosis

Chang-Xin Geng, Zhao-Chong Zeng, Ji-Yao Wang

Chang-Xin Geng, Ji-Yao Wang, Department of Gastroenterology, Zhongshan Hospital, Fudan University, Shanghai 200032, China

Zhao-Chong Zeng, Department of Radiation Oncology, Zhongshan Hospital, Fudan University, Shanghai 200032, China

Correspondence to: Prof. Ji-Yao Wang, Director of Department of Gastroenterology, Zhongshan Hospital, Fudan University, Shanghai 200032, China. jiyao_wang@hotmail.com

Telephone: +86-21-64041990-2420 **Fax:** +86-21-34160980

Received: 2002-08-06 **Accepted:** 2002-09-03

Abstract

AIM: To investigate the in vitro anti-hepatocellular carcinoma (HCC) activity of docetaxel against SMMC-7721 HCC cells and its possible mechanism.

METHODS: The HCC cells were given different concentrations of docetaxel and their growth was measured by colony forming assay. Cell cycle and apoptosis were analyzed by flow cytometry and fluorescence microscopy (acridine orange/ethidium bromide double staining, AO/EB), as well as electronic microscopy. The SMMC-7721 HCC cell reactive oxygen species (ROS) and glutathione (GSH) were measured after given docetaxel.

RESULTS: Docetaxel inhibited the hepatocellular carcinoma cells growth in a concentration dependent manner with $IC_{50} 5 \times 10^{-10}$ M. Marked cell apoptosis and G2/M phase arrest were observed after treatment with docetaxel $\geq 10^{-8}$ M. Docetaxel promoted SMMC-7721 HCC cells ROS generation and GSH deletion.

CONCLUSION: Docetaxel suppressed the growth of SMMC-7721 HCC cells in vitro by causing apoptosis and G2/M phase arrest of the human hepatoma cells, and ROS and GSH may play a key role in the inhibition of growth and induction of apoptosis.

Geng CX, Zeng ZC, Wang JY. Docetaxel inhibits SMMC-7721 human hepatocellular carcinoma cells growth and induces apoptosis. *World J Gastroenterol* 2003; 9(4): 696-700
<http://www.wjgnet.com/1007-9327/9/696.htm>

INTRODUCTION

Docetaxel is a new taxoid structurally similar to paclitaxel, a semisynthetic product of a renewable resource, the needles of the European yew, *Taxus baccata* L. In comparison to paclitaxel, docetaxel is more potent as an inhibitor of microtubule depolymerization^[1]. Docetaxel has shown an active effect against cancers^[2-5]. Current studies have shown that docetaxel combined with other chemotherapeutic drugs has higher anticancer efficacy and reduced side effects in patients with breast, pancreatic, gastric, urothelial carcinomas^[6-9]. But there is limited data about that in hepatocellular carcinoma and thus needs further investigation. Human hepatocellular carcinoma (HCC) is one of the major causes of death worldwide^[10-12], and

surgical resection is the only curative therapy^[13]. However it has limitations for patients with multiple type or metastatic tumors. Searching for effective chemotherapeutic agents is important to improve the survival rate of patients with advanced or recurrent HCC after surgical treatment. HCC is usually insensitive to chemotherapeutic drugs currently used in clinical setting, and there is thus an urgent need for the evaluation of new active drugs against HCC. HCC is well known for its expression of multidrug resistance (MDR) gene and its poor response to chemotherapeutic agents, but it has been found that docetaxel is effective in treating mice bearing xenografts of MDR protein positive human tumors^[14], also a low efflux of docetaxel from tumor cells being observed^[15]. These results suggest that docetaxel may be effective in the treatment of HCC. But the related information is limited and the mechanism of docetaxel remains to be elucidated. This study is to investigate its growth inhibition and induction of apoptosis effect and the mechanism in human SMMC-7721 hepatocellular cell line, and to provide the theoretical basis for clinical application in patients with HCC.

MATERIALS AND METHODS

Reagents

Docetaxel (Rhône-Poulenc Rorer Pharmaceuticals Inc.) was stored as 100 μ M stock solution in absolute ethanol at -80°C . This solution was further diluted in the medium and used in the cell culture immediately before each experiment.

Cell cultures

Human hepatocellular carcinoma SMMC-7721 cell line was obtained from Liver Cancer Institute of Fudan University. The cells were cultured in flasks with RPMI1640 (Gibco BRL, Grand Island, NY) medium supplemented with 100 IU/ml penicillin, 100 μ g/ml streptomycin and 10 % new born bovine serum (Hyclone, Logan, UT) and maintained at 37°C in humidified atmosphere containing 5 % CO_2 .

Colony forming assay

Exponential growth phase SMMC-7721 cells were seeded in 60 mm culture plate (Corning, NY) at a density of 200 cells/plate, after 24hr, the media was discarded and replaced with equal volume of fresh media containing different doses of docetaxel (0, 10^{-11} , 10^{-10} , 10^{-9} , 10^{-8} , 10^{-7} , 10^{-6} M). 24hr later docetaxel containing media was again discarded and replaced by media without containing docetaxel. The cells were cultured continually for 9 days. The colonies were fixed with 95 % ethanol and stained with Giemsa, and manually counted. Colonies ≥ 50 cells were considered survivors. All experiments were conducted in triplicate.

Flow cytometric analysis of DNA content after docetaxel treatment

After exponential growth phase SMMC-7721 cells were treated with different doses of docetaxel (0, 10^{-11} , 10^{-10} , 10^{-9} , 10^{-8} , 10^{-7} , 10^{-6} M) for 24hr and harvested with 0.25 % trypsin and resuspended in RPMI1640 media. 1×10^6 cells was centrifuged at 300 g for 5 minutes and then washed once with PBS. The cell pellets were added with 100 % precooled ethanol at 4°C

for 4hr, centrifuged at 300 g for 5 minutes and then washed once, resuspended with PBS (1×10^6 cells/ml). The cells were added 500 u Rnase, incubated at 37 °C for 30 minutes, washed with PBS. 1×10^6 cells were stained with 50 µg/ml PI for 20 minutes in the dark. The DNA content of each cell was measured using a Becton Dickinson FACSCalibur flow cytometer and analyzed with ModFit LT software (San Jose, CA).

Morphological study with fluorescence microscope

Exponential growth phase SMMC-7721 cells were treated with 10nM docetaxel for 24hr and 48hr and harvested with 0.25 % trypsin and resuspended in RPMI1640 medium. 1×10^6 cells were washed once and resuspended with PBS. 25 µl of the cells suspension was mixed with 1 µl of dye mixture containing AO 100 µg/ml and EB 100 µg/ml in PBS^[16]. The cells were visualized immediately under a fluorescence microscope, the peak excitation wave length was 490 nm.

Transmission electron microscopic observation

After exponential growth phase SMMC-7721 cells treated with 10nM docetaxel for 24hr and 48hr, they were fixed in Karnovsky solution, followed by cacodylate buffer for ultrastructural examination. The cells were postfixed in 1 % osmium tetroxide and dehydrated for staining with uranyl acetate and lead citrate. Thin sections were observed under electron microscope.

ROS measurement

After exponential growth phase SMMC-7721 cells were treated with different doses of docetaxel (0.25 nM, 0.5 nM, 10 nM) for 24hr, the cells were incubated with 2', 7' -dichlorofluorescein diacetate (DCF/DA; 5 µM; Sigma) at 37 °C for 50 minutes to estimate the ROS level. The cells were harvested and detected immediately for fluorescence intensity detection on Becton Dickinson FACSCalibur flow cytometer and data were acquired and analyzed using FACS/CELLQuest software (San Jose, CA) on a Power Macintosh 7600/120 computer (Apple Computers, Cupertino, CA)^[17], three independent experiments were repeated in each drug treated group and the control group was not given docetaxel but incubated with DCF/DA. All experiments were conducted in triplicate.

Determination of intracellular GSH content

The determination of intracellular GSH content was conducted according to Shen *et al*^[18] with modification. Briefly after logarithmic growth phase SMMC-7721 cells ($\geq 10^6$) were

treated with different doses of docetaxel (0.25 nM, 0.5 nM, 10 nM) for 24hr, harvested by trypsination, washed, resuspended in PBS and counted under phase contrast microscope. The cells suspension was centrifuged at 300 g for 5 minutes, the cell pellets were added 0.75 ml distilled water and 0.25 ml thioisallylic acid to precipitate the protein. After centrifugation at 12 000 g for 5 minutes at 4 °C, the supernatant was used for GSH assay. The control group was not given docetaxel. All experiments were conducted in triplicate.

Statistical analysis

The intracellular GSH content was expressed as mean \pm SD. Their differences between drug treated groups and the control group were analyzed with Student's *t*-test.

RESULTS

Effect of docetaxel on SMMC-7721 cells growth inhibition

The colony forming ability decreased gradually with increasing dose of docetaxel treatment, when the docetaxel concentration was increased to 10^{-8} M, the colony forming inhibition rate attained 100 % with $IC_{50} 5 \times 10^{-10}$ M (0.5 nM) (Figure 1).

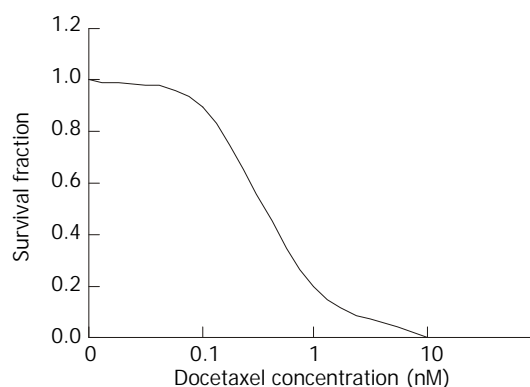


Figure 1 The survival fraction of SMMC-7721 cells treated with docetaxel for 24hr.

Effect on of docetaxel cell cycle and apoptosis of SMMC-7721 cells

As demonstrated in Figure 2, docetaxel induced a marked apoptosis at 10^{-8} M for 24hr, and caused cells G2/M phase arrest mainly at 10^{-7} M and 10^{-6} M, at 10^{-6} M the G2/M phase cells accounted for 96.1 %.

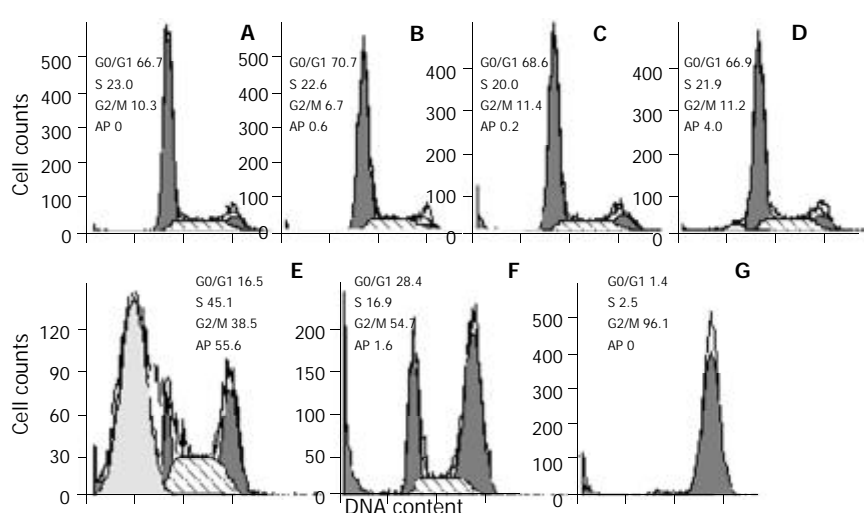


Figure 2 Cell cycle changes and apoptosis induction in SMMC-7721 cells treated with docetaxel for 24hr. Cells were treated with docetaxel at 0M(A), 10^{-11} M(B), 10^{-10} M(C), 10^{-9} M(D), 10^{-8} M(E), 10^{-7} M(F), 10^{-6} M(G). A marked apoptosis was induced at 10^{-8} M, and a peaked G2/M phase accumulation was caused at 10^{-6} M. Ap:apoptosis.

Morphological observation with fluorescence microscope

After the SMMC-7721 cells were given 10^{-8} M docetaxel for 24hr, the early apoptotic cells could be observed: because of their cells membrane integrity, the cells were stained green with AO, the nuclei exhibited bright condensed chromatin or fragmented, some cells blebbed. After the cells being treated for 48hr, some late apoptotic cells could be observed: Since their cell membrane lost integrity, they were stained red with EB, the apoptotic bodies could be seen clearly. On the contrary, the untreated cells did not show these apoptotic characteristics (Figure 3).

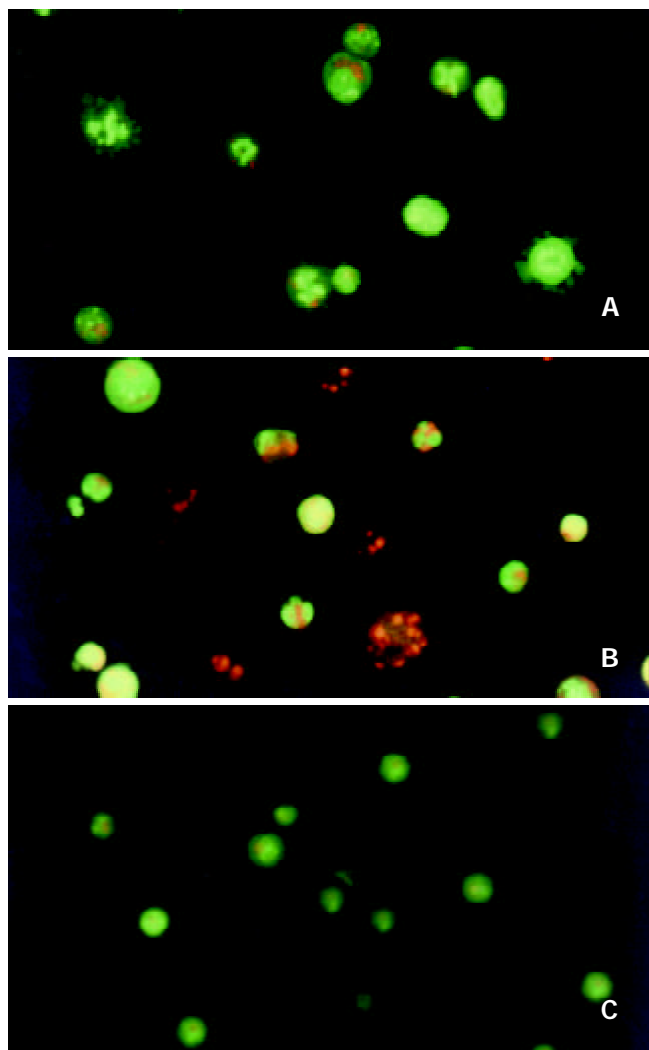


Figure 3 Morphological study with fluorescence microscope. After the SMMC-7721 cells were given 10^{-8} M docetaxel for 24hr (A), the cells were stained green with AO, the nuclei exhibited bright condensed chromatin or fragmented, some cells blebbed. After being treated for 48hr (B), cells were stained red with EB, the apoptotic bodies could be seen clearly. On the contrary, the untreated cells (C) did not show these apoptotic characteristics.

Transmission electron microscopic observation

After treatment with 10^{-8} M docetaxel for 24hr, the chromatin of some SMMC-7721 cells was located along the nuclear edges or formed irregularly shaped crescents at the nuclear edges, or became condensed or fragmented; Some cells nuclear membrane became irregular; The vacuole in some cytoplasm could be observed (Figure 4).

Effect of docetaxel on intracellular ROS

As demonstrated in Figure 5, The SMMC-7721 cells ROS level (corresponding to the fluorescence intensity) increased after

treatment with 0.25 nM, 0.5 nM, 10 nM docetaxel. In comparison with the control group, the ROS level increased by 1.69, 1.78 and 1.80 times respectively.

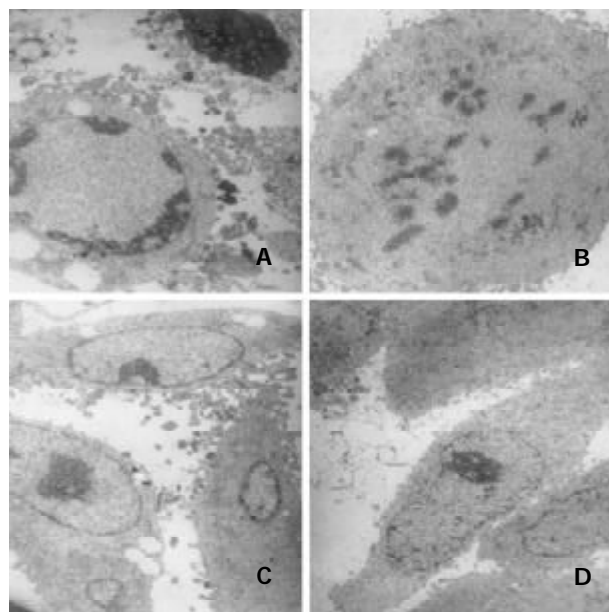


Figure 4 Transmission electron microscopic observation. After treatment with 10^{-8} M docetaxel for 24hr, the chromatin of some SMMC-7721 cells was located along the nuclear edges or formed irregularly shaped crescents at the nuclear edges (A, C), or became condensed or fragmented (A, B); The vacuole could be observed in some cytoplasm (A, C).

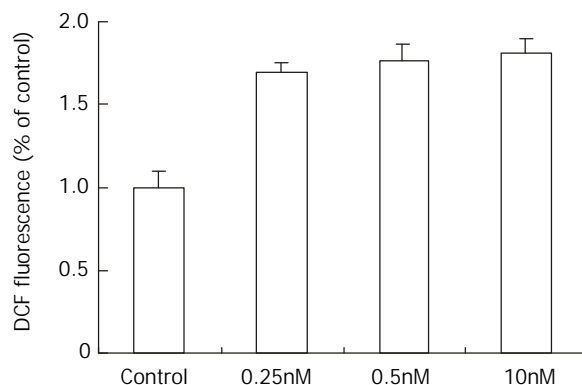


Figure 5 The effect of docetaxel on the formation of ROS in SMMC-7721 cells. Data are from three independent experiments.

Effect of docetaxel on intracellular GSH

The control group intracellular GSH content was 11.6 ± 1.1 fmol/cell, after treatment with docetaxel 0.25 nM, 0.5 nM, 10 nM for 24hr, the SMMC-7721 cells GSH decreased to 4.7 ± 0.7 fmol/cell, 3.0 ± 0.5 fmol/cell, 1.0 ± 0.1 fmol/cell respectively, there was a significant difference between the drug treated groups and the control group ($P < 0.05$).

DISCUSSION

In the present study, we used colony forming assay to observe the effect of docetaxel on the growth of the human hepatocellular carcinoma SMMC-7721 cells in vitro, indicating that docetaxel can inhibit the SMMC-7721 cells growth and in concentration dependent manners, at 10^{-8} M the survival fraction decreased to 0 (Figure 1). A previous study demonstrated that docetaxel showed cytotoxic effect on other human hepatoma cell lines^[17], together with this report, our result suggests that

the growth-inhibiting effect of docetaxel may be a general phenomenon for human hepatocellular carcinoma cells. Also the flow cytometry showed that docetaxel causes SMMC-7721 cells apoptosis at a low dose (10^{-8} M), which was confirmed by fluorescence microscope, transmission electron microscope, and at 10^{-7} M, 10^{-6} M induced a marked G2/M phase arrest without apparent apoptosis, this phenomenon seems to suggest that docetaxel can induce apoptosis independent of G2/M phase arrest in SMMC-7721 cells.

In order to elucidate the mechanisms of the anti-hepatocellular carcinoma action of docetaxel, we examined its possible effect on cell cycle kinetics of SMMC-7721 cells. As demonstrated in Figure 2, following treatment with docetaxel for 24hr, the G2/M phase cells increased with docetaxel doses increasing from 10^{-8} M, at 10^{-6} M the G2/M phase cells accounted for 96.1 %. This result indicates that high dose of docetaxel blocks cell cycle at G2/M phase, disturbs mitosis and inhibits SMMC-7721 cells growth. In this clinical setting, such information may be useful for liver carcinoma therapy with docetaxel and other cytotoxic drugs which affect cell cycle progression.

According to Figure 1, docetaxel could inhibit SMMC-7721 cells at very low doses, the IC_{50} is 5×10^{-10} M. This dose of docetaxel had no significant effect on the cell apoptosis or cell cycle progression, which was confirmed by flow cytometry. In order to elucidate the mechanism underlying this phenomenon, the intracellular ROS and GSH were further investigated in this study. Our results indicated that docetaxel both at $1/2IC_{50}$, IC_{50} and apoptosis-inducing dose (10nM) could cause significantly increased ROS levels (Figure 5) and significantly decreased GSH, compared with those of the control.

It has been reported that tumor cells have persistently higher levels of ROS^[19]. The relationship between ROS and apoptosis, cell growth inhibition has been broadly investigated. ROS has been found to regulate translocation of NF- κ B^[20] as well as translocation of p53 and the p53-mediated apoptosis pathway^[21,22]. Also it has been found that induction of apoptosis was accompanied with the generation of intracellular ROS prior to the activation of caspase-3^[23] and down-regulation of Bcl-2^[24]. Simizu *et al.* reported that some anticancer agents, including vinblastin and camptothecin, induced cells apoptosis with the generation of ROS^[25]. Recently it was reported that arsenic trioxide and l-S,R-buthionine sulfoximine (BSO) combination treatment enhanced hepatocellular carcinoma cells apoptosis through increased production of ROS^[26]. Also it was reported ROS played a mediatory role in the synergistic interaction between 1, 25-dihydroxyvitamin D (3) and anticancer cytokines^[27], modulation of the ROS production intra and extracellularly may influence the cell survival during oxidative insults^[28].

Accordingly, we speculate that docetaxel-induced high level ROS may be involved in the growth inhibition and apoptosis of SMMC-7721 cells.

In order to confirm the SMMC-7721 cells redox status after docetaxel treatment, the intracellular GSH content was also investigated. Our result demonstrated that the intracellular GSH decreased significantly ($P < 0.05$) after both $1/2IC_{50}$, IC_{50} and apoptosis-inducing dose docetaxel treatment, compared with that of the control group. This indicates that the decrease of GSH may be involved in the SMMC-7721 cells growth inhibition and apoptosis caused by docetaxel. Liu *et al.* found *Salvia miltiorrhiza* inhibited human hepatoma HepG2 cells growth and induced apoptosis involving in intracellular GSH deletion^[29], early studies have also demonstrated that the onset of apoptosis was associated with a fall of intracellular GSH in different cellular systems^[30]. And GSH could significantly reduce apoptosis mediated by a monoclonal antibody directed to Fas antigen, and apoptosis could be nearly completely

prevented by GSH^[31]. GSH is an important cellular thiol which is regarded as the major determinant of the intracellular redox potential, on the other hand, apoptosis may be regulated by the redox status within the cells^[32]. Loss of GSH was shown to be tightly coupled with a number of down-stream events in apoptosis, in caspase activation and events in chromatin^[33], and GSH depletion may act as a link between oxidative stress and ceramide-mediated apoptosis^[34]. Also it was found that decreased cells proliferation associated with decreased levels of intracellular GSH, and blockade of GSH synthesis enhanced ROS production and suppressed cells proliferation^[35], cells with compromised cellular GSH were susceptible to redox imbalance-induced inhibition of proliferation^[36].

In summary, the present study demonstrates that docetaxel has profound effects on SMMC-7721 hepatocellular carcinoma cells in vitro. It reduces the proliferation of these cells, causes changes in their morphology, and induces cell death by apoptosis. It leads to ROS generation and GSH deletion, subsequently results in redox imbalance in SMMC-7721 cells, and it is speculated that the redox imbalance caused by docetaxel may play an important role in the growth inhibition and induction of apoptosis of SMMC-7721 cells. As far as we know, there is few report concerning the redox imbalance and docetaxel. Our results not only provide the basis for further in vivo and clinical research in hepatocellular carcinoma, but also contribute to understanding of the pharmacology of docetaxel further.

REFERENCES

- Gueritte-Voegelein F**, Guenard D, Lavelle F, Le Goff MT, Mangatal L, Potier P. Relationships between the structure of taxol analogues and their antimetabolic activity. *J Med Chem* 1991; **34**: 992-998
- Donnellan P**, Armstrong J, Rowan S, Fennelly D, Lynch V, McDonnell T, McDonnell T, McNicholas W, Crown J. New chemotherapy combination with docetaxel in the treatment of patients with non-small cell lung cancer. *Semin Oncol* 1998; **25**: 20-23
- Coleman RE**, Howell A, Eggleton SP, Maling SJ, Miles DW. Phase II study of docetaxel in patients with liver metastases from breast cancer. *Ann Oncol* 2000; **11**: 541-546
- Papakostas P**, Kouroussis C, Androulakis N, Samelis G, Aravantinos G, Kalbakis K, Sarra E, Souglakos J, Kakolyris S, Georgoulas V. First-line chemotherapy with docetaxel for unresectable or metastatic carcinoma of the biliary tract. A multicentre phase II study. *Eur J Cancer* 2001; **37**: 1833-1838
- Glisson BS**, Murphy BA, Frenette G, Khuri FR, Forastiere AA. Phase II Trial of docetaxel and cisplatin combination chemotherapy in patients with squamous cell carcinoma of the head and neck. *J Clin Oncol* 2002; **20**: 1593-1599
- Wenzel C**, Locker GJ, Schmidinger M, Rudas M, Taucher S, Gnant MF, Jakesz R, Steger GG. Combined analysis of two phase II trials in patients with primary and advanced breast cancer with epidoxorubicin and docetaxel plus granulocyte colony stimulating factor. *Anticancer Drugs* 2002; **13**: 67-74
- Cascinu S**, Graziano F, Barni S, Labianca R, Comella G, Casaretti R, Frontini L, Catalano V, Baldelli AM, Catalano G. A phase II study of sequential chemotherapy with docetaxel after the weekly PELF regimen in advanced gastric cancer. A report from the Italian group for the study of digestive tract cancer. *Br J Cancer* 2001; **84**: 470-474
- Ryan DP**, Kulke MH, Fuchs CS, Grossbard ML, Grossman SR, Morgan JA, Earle CC, Shivdasani R, Kim H, Mayer RJ, Clark JW. A Phase II study of gemcitabine and docetaxel in patients with metastatic pancreatic carcinoma. *Cancer* 2002; **94**: 97-103
- Sinibaldi VJ**, Carducci MA, Moore-Cooper S, Laufer M, Zahurak M, Eisenberger MA. Phase II evaluation of docetaxel plus one-day oral estramustine phosphate in the treatment of patients with androgen independent prostate carcinoma. *Cancer* 2002; **94**: 1457-1465
- Wu MC**. Clinical research advances in primary liver cancer. *World J Gastroenterol* 1998; **4**: 471-474

- 11 **Yip D**, Findlay M, Boyer M, Tattersall MH. Hepatocellular carcinoma in central Sydney: a 10-year review of patients seen in a medical oncology department. *World J Gastroenterol* 1999; **5**: 483-487
- 12 **Schmid R**. Prospect of gastroenterology and hepatology in the next century. *World J Gastroenterol* 1999; **5**: 185-190
- 13 **Qin LX**, Tang ZY. The prognostic significance of clinical and pathological features in hepatocellular carcinoma. *World J Gastroenterol* 2002; **8**: 193-199
- 14 **Vanhoefter U**, Cao S, Harstrick A, Seeber S, Rustum YM. Comparative antitumor efficacy of docetaxel and paclitaxel in nude mice bearing human tumor xenografts that overexpress the multidrug resistance protein (MRP). *Ann Oncol* 1997; **8**: 1221-1228
- 15 **Lavelle F**, Bissery MC, Combeau C, Riou JF, Vrignaud P, Andre S. Preclinical evaluation of docetaxel (Taxotere). *Semin Oncol* 1995; **22**: 3-16
- 16 **McGahon AJ**, Martin SJ, Bissonnette RP, Mahboubi A, Shi Y, Mogil RJ, Nishioka WK, Green DR. The end of the (cell) line: methods for the study of apoptosis *in vitro*. *Methods Cell Biol* 1995; **46**: 153-185
- 17 **Lin HL**, Liu TY, Chau GY, Lui WY, Chi CW. Comparison of 2-methoxyestradiol-induced, docetaxel-induced, and paclitaxel-induced apoptosis in hepatoma cells and its correlation with reactive oxygen species. *Cancer* 2000; **89**: 983-994
- 18 **Shen HM**, Yang CF, Ong CN. Sodium selenite-induced oxidative stress and apoptosis in human hepatoma HepG2 cells. *Int J Cancer* 1999; **81**: 820-828
- 19 **Toyokuni S**, Okamoto K, Yodoi J, Hiai H. Persistent oxidative stress in cancer. *FEBS Lett* 1995; **358**: 1-3
- 20 **Kheradmand F**, Werner E, Tremble P, Symons M, Werb Z. Role of Rac1 and oxygen radicals in collagenase-1 expression induced by cell shape change. *Science* 1998; **280**: 898-902
- 21 **Takenaka K**, Moriguchi T, Nishida E. Activation of the protein kinase p38 in the spindle assembly checkpoint and mitotic arrest. *Science* 1998; **280**: 599-602
- 22 **Martinez JD**, Pennington ME, Craven MT, Wartens RL, Cress AE. Free radicals generated by ionizing radiation signal nuclear translocation of p53. *Cell Growth Diff* 1997; **8**: 941-949
- 23 **Ueda S**, Nakamura H, Masutani H, Sasada T, Takabayashi A, Yamaoka Y, Yodoi J. Baicalin induces apoptosis via mitochondrial pathway as prooxidant. *Mol Immunol* 2002; **38**: 781-791
- 24 **Li HL**, Chen DD, Li XH, Zhang HW, Lu YQ, Ye CL, Ren XD. Changes of NF- κ B, p53, Bcl-2 and caspase in apoptosis induced by JTE-522 in human gastric adenocarcinoma cell line AGS cells: role of reactive oxygen species. *World J Gastroenterol* 2002; **8**: 431-435
- 25 **Simizu S**, Takada M, Umezawa K, Imoto M. Requirement of caspase-3 (like) protease-mediated hydrogen peroxide production for apoptosis induced by various anticancer drugs. *J Biol Chem* 1998; **273**: 26900-26907
- 26 **Kito M**, Akao Y, Ohishi N, Yagi K, Nozawa Y. Arsenic trioxide-induced apoptosis and its enhancement by buthionine sulfoximine in hepatocellular carcinoma cell lines. *Biochem Biophys Res Commun* 2002; **291**: 861-867
- 27 **Koren R**, Rocker D, Kotestiano O, Liberman UA, Ravid A. Synergistic anticancer activity of 1, 25-dihydroxy vitamin D(3) and immune cytokines: the involvement of reactive oxygen species. *J Steroid Biochem Mol Biol* 2000; **73**: 105-112
- 28 **Teramoto S**, Tomita T, Matsui H, Ohga E, Matsuse T, Ouchi Y. Hydrogen peroxide-induced apoptosis and necrosis in human lung fibroblasts: protective roles of glutathione. *Jpn J Pharmacol* 1999; **79**: 33-40
- 29 **Liu J**, Shen HM, Ong CN. Salvia miltiorrhiza inhibits cell growth and induces apoptosis in human hepatoma HepG2 cells. *Cancer Letters* 2000; **153**: 85-93
- 30 **Hall AG**. The role of glutathione in the regulation of apoptosis. *Eur J Clin Invest* 1999; **29**: 238-245
- 31 **Wedi B**, Straede J, Wieland B, Kapp A. Eosinophil apoptosis is mediated by stimulators of cellular oxidative metabolisms and inhibited by antioxidants: involvement of a thiol-sensitive redox regulation in eosinophil cell death. *Blood* 1999; **94**: 2365-2373
- 32 **Watson RW**, Rotstein OD, Nathens AB, Dackiw AP, Marshall JC. Thiol-mediated redox regulation of neutrophil apoptosis. *Surgery* 1996; **120**: 150-157
- 33 **Van den Dobbelsteen DJ**, Nobel CS, Schlegel J, Cotgreave IA, Orrenius S, Slater AF. Rapid and specific efflux of reduced glutathione during apoptosis induced by anti-Fas/APO-1 antibody. *J Biol Chem* 1996; **271**: 15420-15427
- 34 **Lavrentiadou SN**, Chan C, Kawcak T, Ravid T, Tsaba A, van der Vliet A, Rasooly R, Goldkorn T. Ceramide-mediated apoptosis in lung epithelial cells is regulated by glutathione. *Am J Respir Cell Mol Biol* 2001; **25**: 676-684
- 35 **Chang WK**, Yang KD, Shaio MF. Lymphocyte proliferation modulated by glutamine: involved in the endogenous redox reaction. *Clin Exp Immunol* 1999; **117**: 482-488
- 36 **Noda T**, Iwakiri R, Fujimoto K, Aw TY. Induction of mild intracellular redox imbalance inhibits proliferation of CaCo-2 cells. *FASEB J* 2001; **15**: 2131-2139

Edited by Wu XN

Experimental study on ultrasound-guided intratumoral injection of "Star-99" in treatment of hepatocellular carcinoma of nude mice

Li-Wu Lin, Xiao-Dong Lin, Yi-Mi He, Shang-Da Gao, En-Sheng Xue

Li-Wu Lin, Xiao-Dong Lin, Yi-Mi He, Shang-Da Gao, En-Sheng Xue, Department of Ultrasound, Union Hospital of Fujian Medical University, Fuzhou 350001, Fujian Province, China

Correspondence to: Dr. Li-Wu Lin, Department of Ultrasound, Union Hospital of Fujian Medical University, Fuzhou 350001, Fujian Province, China. lxdghl@163.net

Telephone: +86-591-3357896-8352

Received: 2002-08-06 **Accepted:** 2002-09-04

Abstract

AIM: To investigate the anti-cancer effect and the immunological mechanism of ultrasound-guided intratumoral injection of Chinese medicine "Star-99" in hepatocellular carcinoma (HCC) of nude mice.

METHODS: Twenty-eight human hepatocellular carcinoma SMMC-7721 transplanted nude mice, 14 of hypodermically implanted and 14 of orthotopic liver transplanted, were randomly divided into three groups of which 14 mice with Star-99, and 7 with ethanol and saline respectively. Ten days after the transplantation the medicines were injected into the tumors of all the nude mice once every 5 days. After 4 injections the nude mice were killed. The diameters of three dimension of the tumors were measured by high frequency ultrasound before and after the treatment and the tumor growth indexes* (TGI) were calculated. Radioimmunoassay was used to detect the serum levels of interleukin-2 (IL-2) and tumor necrosis factor (TNF)-alpha. The tumor tissues were sent for flow cytometry (FCM) DNA analysis. Apoptotic cells were visualized by TUNEL assay. All the experiments were carried out by double blind method.

RESULTS: The TGI of Star-99 group (0.076 ± 0.024) was markedly lower than that of the saline group (4.654 ± 1.283) ($P < 0.01$). It also seemed to be lower than that of the ethanol group (0.082 ± 0.028), but not significantly different ($P > 0.05$). Serum levels of IL-2 and TNF- α were markedly higher than those of ethanol group and saline groups ($P < 0.05$). The mean apoptotic index (AI: percentage of TUNEL signal positive cells) in Star-99 group ($48.98 \pm 5.09\%$) was significantly higher than that of the ethanol group ($11.95 \pm 2.24\%$) and the saline group ($10.48 \pm 3.85\%$) ($P < 0.01$). FCM DNA analysis showed that the appearance rate of the apoptosis peak in Star-99 group was 92.9%, markedly higher than that of the ethanol group (14.3%) and the saline group (0.0%) ($P < 0.01$). Correlation ($r = 0.499$, $P < 0.05$) was found between AI and serum level of TNF- α .

CONCLUSION: Star-99 has an effect on the elevation of the serum levels of IL-2 and TNF- α . It indicates that Star-99 has the function of enhancing the cellular immunity and inducing cancer cell apoptosis. The correlation between AI and serum level of TNF- α indicates that the elevation of the serum of TNF- α induced by Star-99 may be an important factor in the promotion of the hepatic cancer cell apoptosis. Star-99 has strong effects on the inhibition and destruction

of cancer cells. Its curative effect is as good as ethanol. Its major mechanisms can be as follows: (1) it increases the serum levels of IL-2 and TNF- α and triggers cellular immunity. (2) It can induce cancer cells apoptosis, the effective mechanism of the Star-99 is different from that of the ethanol. The mechanisms of triggering the immunologic function of the organism and inducing cell apoptosis are, of particular significance. This study will provide a new pathway of drug administration and an experimental basis for the treatment of HCC with Chinese herbal, and the study of Star-99 in the treatment of tumor is of profound significance with good prospects.

Lin LW, Lin XD, He YM, Gao SD, Xue ES. Experimental study on ultrasound-guided intratumoral injection of "Star-99" in treatment of hepatocellular carcinoma of nude mice. *World J Gastroenterol* 2003; 9(4): 701-705

<http://www.wjgnet.com/1007-9327/9/701.htm>

INTRODUCTION

The ultrasound-guided percutaneous intratumoral injection with ethanol, in treatment of hepatocellular carcinoma (HCC), has been widely used in the clinic in recent years since the report by the Japanese scholars (1983)^[1-3]. Yet there are certain limitations in this treatment that lead us to search for newer drug that we have been studied for many years. In 1999, we discovered that the compound Chinese medicine "Star-99" had anti-cancer effect. In order to probe the effective mechanism of the ultrasound-guided intratumoral injection of HCC with Star-99, we detected the serum levels of interleukin-2 (IL-2) and tumor necrosis factor (TNF)-alpha, and conducted FCM DNA analysis and TUNEL assay to observe the phenomenon of apoptosis and to appraise the biological effect of Star-99.

MATERIALS AND METHODS

Experimental animal

For the experiment, we used 28 BALB/CA nude mice, which were 5-8 weeks old, provided by the Medical Experimental Animal Unit of Anti-cancer Center of Xia Men University, China. The average weight of the nude mice was 18 ± 2.1 grams. The mice were raised in the layer drift shelves under aseptic condition. The cages, cushion, drinking water and standard forage were provided by Shanghai Bikai Company periodically.

Animal model production of human HCC

Human HCC SMMC-7721 cellular cultural suspension was centrifuged and the supernatant was removed. Then the cellular cultural liquid was added to make up 5×10^7 cells per milliliter. Subcutaneous injection was taken in the back of a nude mouse with 0.2 ml liquid. When the tumor grew to 1 cm in diameter, part of it was taken out under the aseptic condition and cut into small pieces in the size of $0.2 \times 0.2 \times 0.2$ cm, which were transplanted subcutaneously at the back of other nude mice with a canula needle and underwent passages from generation to generation. The nude mice, under general anesthesia with

sodium pentothal injected intraperitoneally. The process was as follows: The abdomen of the mouse was incised 1 cm in length deep to peritoneum on the linea alba below the xiphoid process. The liver was squeezed out, a piece of tumor was embedded into the liver with canula needle, the needle aperture was blocked with gelatin sponge to stop bleeding, then the liver was sent back into the abdomen, the peritoneum and skin were sutured and the process of orthotopic liver transplantation was completed.

Experimental method

Twenty-eight human HCC transplanted nude mice, including 14 implanted hypodermically and the other 14 with liver transplanted orthotopically, were randomly divided into three groups: the Star-99 group containing 14 nude mice, the ethanol group and the saline group containing 7 nude mice each. The three dimensional diameters of the tumor were measured by high frequency ultrasound (Aloka 5500 with 10MHz probe) after 10 days transplantation of HCC. Then 0.1 ml Star-99, ethanol and saline were respectively injected into the center of the tumor with No.5 needle. The nude mice were killed after being injected every 5 days for a total of 4 injections in each mouse. The three dimensional diameters of the tumor were measured again before the mice were killed. Mice blood was obtained from the eye socket, and the sera were separated by low velocity centrifugation. The Radioimmunoassay (RIA) kit was purchased from Beijing East Asian Institute of Immunology. Sn-682 Radioimmunoassay γ counting apparatus was used to detect the serum levels of IL-2 and TNF- α . The apoptotic cells were visualized by terminal deoxynucleotidyl transferase (TdT)-mediated dUTP nick end labelling (TUNEL). The TUNEL kit (POD) was purchased from Roche Molecular Biochemicals. The assay performance followed the technical manual and the references^[4-7]. It was TUNEL positive when the nucleolus appeared evidently brown granule. Ten high power fields were observed in each slide and at least 1 000 positive cells were calculated at random. The cellular suspension made by fresh tumor tissues was analyzed by FCM DNA. The appearance rates of the heteroploidy peak and apoptosis peak were analyzed. Double blind method was applied in this experiment.

Observation indexes

The tumor growth index (TGI) was calculated by the formula: volume of tumor (after treatment-before treatment) / volume of tumor (before treatment). The serum levels of IL-2 and TNF- α were determined. The apoptotic index (AI: percentage of TUNEL signal positive cells) were calculated as the TUNEL-positive cells / the total number of cancer cells \times 100 %. The appearance rates of the heteroploidy peak and apoptosis peak of the tumor tissue were analyzed by FCM DNA. The correlation coefficient between AI and serum levels of TNF- α was calculated.

Statistics method

The results were expressed as the mean \pm SD. The data were analyzed by one-way ANOVA with Student's *t* test, chi-square test and liner regression analysis. Value of $P < 0.05$ was considered significant.

RESULTS

The tumor growth index

Table 1 showed that the growth index of Star-99 group was markedly lower than that of the saline group ($P < 0.01$). It was also lower than that of the ethanol group, but there was no significant difference between them ($P > 0.05$).

Table 1 Comparison of the growth index of Star-99, ethanol and saline groups

Groups	<i>n</i>	\bar{x}	SD	<i>P</i>
Star-99 (A)	14	0.076	± 0.024	A, B >0.05
Ethanol (B)	7	0.082	± 0.028	B, C <0.01
Saline (C)	7	4.654	± 1.283	A, C <0.01

The serum levels of IL-2 and TNF- α after treatment

Table 2 showed that the serum levels of IL-2 and TNF- α in the Star-99 group were 6.63 ± 1.39 ng/ml and 3.98 ± 1.05 ng/ml, markedly higher than those of the ethanol and the saline groups ($P < 0.05$).

Table 2 Comparison of the serum levels of IL-2 and TNF- α after treatment in the three groups

Groups	<i>n</i>	IL-2 (ng/ml)	TNF- α (ng/ml)	<i>P</i>
Star-99 (A)	14	6.63 ± 1.39	3.98 ± 1.05	A:B <0.05
Ethanol (B)	7	4.22 ± 1.23	2.95 ± 1.01	A:C <0.05
Saline (C)	7	4.51 ± 0.84	2.84 ± 1.05	B:C >0.05

The apoptotic index of Star-99, ethanol and saline groups after treatment

Table 3 showed that the AI in Star-99 group (48.98 ± 5.09 %) was significantly higher than that of the ethanol group (11.95 ± 2.24 %) and the saline group (10.48 ± 3.85 %) ($P < 0.01$), (Figure 1).

Table 3 Comparison of the apoptotic index of Star-99, ethanol and saline groups after treatment

Groups	<i>n</i>	AI (%)	<i>P</i>
Star-99 (A)	14	48.98 ± 5.09	A:B <0.01
Ethanol (B)	7	11.95 ± 2.24	B:C >0.05
Saline (C)	7	10.48 ± 3.85	A:C <0.01

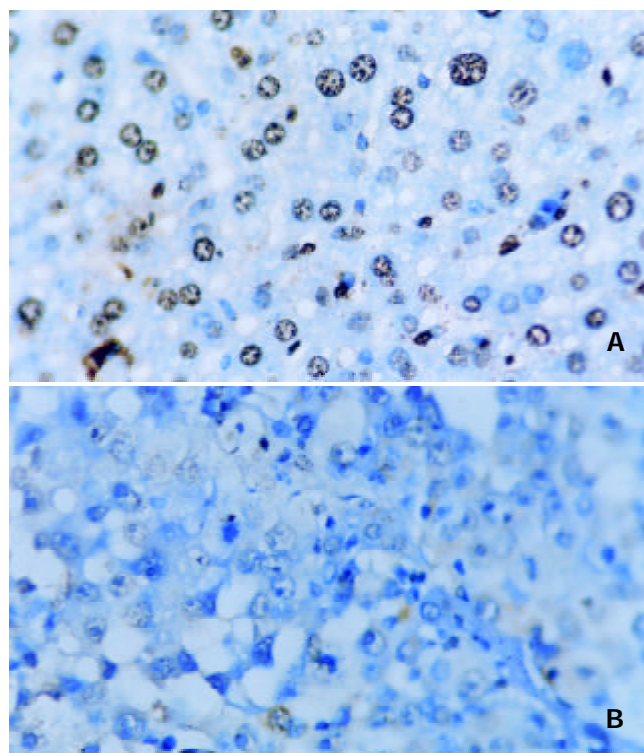


Figure 1 TUNEL marker (Nucleolus with brown granule indicated positive). A: Star-99 group; B: saline group; $\times 400$.

FCM DNA analysis

Table 4 showed the results of FCM DNA analysis of the tumor tissues of the three groups. The appearance rate of the heteroploidy peak after the treatment was 57.1 % in the saline group (Figure 2), markedly higher than that of the ethanol group (0.0 %) and the Star-99 group (7.1 %) ($P<0.01$). Another remarkable characteristic was that 92.9 % of the Star-99 group appeared apoptosis peaks formed by the cells in the sub G_1 period (Figure 3), markedly higher than that of the ethanol group and the saline group, which were 14.3 % (1/7) and 0.0 (0/7), respectively ($P<0.01$).

Table 4 Comparison of the appearance rates of the heteroploidy and apoptosis peak after treatment in the three groups

Groups	n	Heteroploidy peak (%)	P	Apoptosis peak (%)	P
Star-99 (A)	14	7.1 (1/14)	A:B>0.05	92.9 (13/14)	A:B<0.01
Ethanol (B)	7	0.0 (0/7)	B:C<0.05	14.3 (1/7)	B:C>0.05
Saline (C)	7	57.1 (4/7)	A:C<0.05	0.0 (0/7)	A:C<0.01

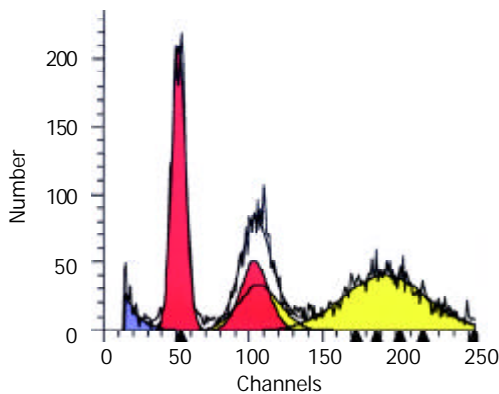


Figure 2 FCM DNA analysis showed the hereroploidy peak in the saline group. (Yellow peak).

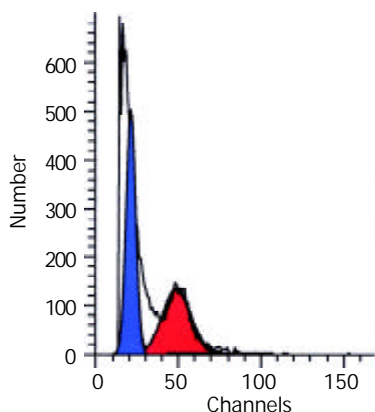


Figure 3 FCM DNA analysis showed the apoptosis peak in the Star-99 group. (Blue peak).

The relationship between HCC apoptosis and serum levels of TNF- α

There was close relationship between HCC apoptosis and serum level of TNF- α . Significant correlation ($r=0.499$, $P<0.05$) was found between AI and serum levels of TNF- α .

DISCUSSION

At present, many kinds of ultrasound-guided interventional therapy have been practiced by clinicians such as laser^[8,9], microwave^[10-13], radio frequency^[14-19] and high energy focus

ultrasound^[20,21] since 1990s. The efficacy are as good as that of surgical resection^[2, 22-24]. Early In 1985, the American National Cancer Institute considered biotherapy as the fourth modality in cancer treatment as it attacked the tumor cells directly; furthermore, it stimulates the immune system of the host. The present study provided a new avenue to combat the tumor from immunologic point of view. As shown in this experiment, the Star-99 has marked effect on the growth restraint of the tumor, the effectiveness is more or less equivalent to that of the ethanol.

The two important cytokines IL-2 and TNF- α can be used as biological response modifiers (BRM). IL-2 can enhance the activity of lymphocyte and the killing effect of CTL, NK and LAK cells, induce secretion of cytokine. The serum level of IL-2 reflects the host immunologic function to a certain degree^[25]. In this experiment, the serum level of IL-2 in the Star-99 group was 6.63 ± 1.39 ng/ml, markedly higher than those of ethanol and saline groups ($P<0.05$). In another experiment of this study, the electron microscopy showed many lymphocytes in the tumor tissues of the Star-99 group^[26]. Figure 4 showed the microvilli on the surface of the lymphocytes attacked the cancer cells. The membrane of tumor cell in contact with the sensitized T lymphocyte became broken with the organelle and the nucleus dissolved and the vacuolation of the cytoplasm as well. This phenomenon further illustrate that the Star-99 could stimulate or induce the cellular immunity function of the organism. TNF- α is mainly produced by macrophage and activated T lymphocyte which can inhibit or destroy the cancer cells. It can also induce apoptosis by combining with TNF receptor and resulting in chain reactions^[27,28]. In the Star-99 group, the serum level of TNF- α was 3.98 ± 1.05 ng/ml, markedly higher than those of ethanol and saline groups. Significant correlation ($r=0.499$, $P<0.05$) was found between AI and serum levels of TNF- α . It indicated that the elevation of the serum TNF- α induced by Star-99 might be an important factor in the promotion of the HCC cells apoptosis.

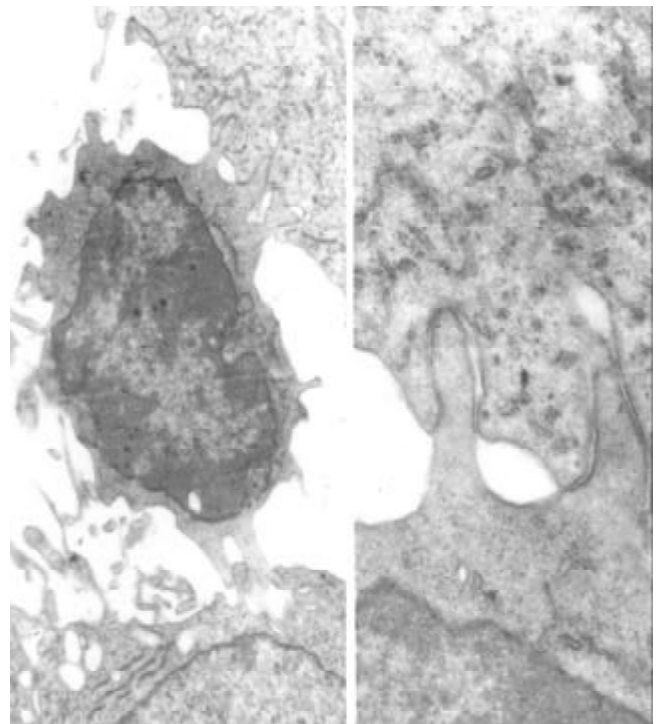


Figure 4 Many lymphocytes could be seen in the tumor tissues and the microvilli on the surface of the lymphocytes attacking the cancer cells in the Star-99 group (The right figure is a magnified image).

Cancer growth not only depends on proliferation^[29-35] but also on the reduced apoptosis^[36-39]. At present time, cancer therapy is now focusing on promoting apoptosis^[40,41]. The apoptotic cells could be identified by TUNEL assay^[5,42]. In this experiment, the apoptotic index in Star-99 group (48.98±5.09 %) was significantly higher than that in the ethanol group (11.95±2.24 %) and the saline group (10.48±3.85 %) ($P<0.01$), which was consistent with the result of FCM DNA analysis, the appearance rate of the apoptosis peak in Star-99 group was 92.9 %, markedly higher than that of the ethanol group (14.3 %) and the saline group (0.0 %) ($P<0.01$). These results showed that although the cancer cells in ethanol group were destroyed which was different from that by means of apoptosis. In the Star-99 group it was mainly by induction of apoptosis.

The results of this study illustrated that the compound Chinese medicine Star-99 has the strong effect on the growth restraint of the tumor. Apart from its direct destruction of cancer cells, the mechanism of the efficacy may be due to: (1) It can increase the serum levels of IL-2 and TNF- α and trigger the cellular immunity. (2) It can induce apoptosis of the cancer cells. The anti-cancer effect of Star-99 is more or less equivalent to the ethanol, but by different mechanisms. Based on the above findings, Star-99 may have great significance and good prospects in the future treatment of HCC.

REFERENCES

- Lin LW, Ye Z, Xue ES, Gao SD, He YM. A study of percutaneous hepatic quantified ethanol injection in treatment of hepatocarcinoma. *Zhongguo Chaosheng Yixue Zazhi* 2000; **16**: 514-516
- Arii S, Yamaoka Y, Futagawa S, Inoue K, Kobayashi K, Kojiro M, Makuuchi M, Nakamura Y, Okita K, Yamada R. Results of surgical and nonsurgical treatment for small-sized hepatocellular carcinomas: A retrospective and nationwide survey in Japan. *Hepatology* 2000; **32**: 1224-1229
- Livraghi T, Benedini V, Lazzaroni S, Meloni F, Torzilli G, Vettori C. Long term results of single session percutaneous ethanol injection in patients with large hepatocellular carcinoma. *Cancer* 1998; **83**: 48-57
- Tian G, Yu JP, Luo HS, Yu BP, Yue H, Li JY, Mei Q. Effect of Nimesulide on proliferation and apoptosis of human hepatoma SMMC-7721 cells. *World J Gastroenterol* 2002; **8**: 483-487
- Li J, Wang WL, Wang WY, Liu B, Wang BY. Apoptosis in human hepatocellular carcinoma by terminal deoxynucleotidyl transferase-mediate. *Huaren Xiaohua Zazhi* 1998; **6**: 491-494
- Wang LS, Pan LJ, Li MS, Sun Y, Shi L, Zhang YL, Zhou DY. Apoptosis of large bowel carcinoma induced by complete peptide polyose. *Shijie Huaren Xiaohua Zazhi* 1999; **7**: 710
- Zhang Z, Yuan Y, Gao H, Dong M, Wu HQ, Wang L, Wang MX. *In situ* observation of apoptosis and proliferation in gastric cancer and precanceration. *Shijie Huaren Xiaohua Zazhi* 1999; **7**: 802-803
- Pacella CM, Bizzarri G, Magnolfi F, Cecconi P, Caspani B, Anelli V, Bianchini A, Valle D, Pacella S, Manenti G, Rossi Z. Laser thermal ablation in the treatment of small hepatocellular carcinoma: results in 74 patients. *Radiology* 2001; **221**: 712-720
- Pacella CM, Bizzarri G, Magnolfi F, Cecconi P, Caspani B, Anelli V, Bianchini A, Valle D, Pacella S, Manenti G, Rossi Z. Hepatocellular carcinoma: long-term results of combined treatment with laser thermal ablation and transcatheter arterial chemoembolization. *Radiology* 2001; **219**: 669-678
- Lu MD, Chen JW, Xie XY, Liu L, Huang XQ, Liang LJ, Huang JF. Hepatocellular carcinoma: us-guided percutaneous microwave coagulation therapy. *Radiology* 2001; **221**: 167-172
- Ishida T, Murakami T, Shibata T, Inoue Y, Takamura M, Niinobu T, Sato T, Nakamura H. Percutaneous microwave tumor coagulation for hepatocellular carcinomas with interruption of segmental hepatic blood flow. *J Vasc Interv Radiol* 2002; **13**: 185-191
- Dick EA, Taylor-Robinson SD, Thomas HC, Gedroyc WMW. Ablative therapy for liver tumours. *Gut* 2002; **50**: 733-739
- Matsuda M, Fujii H, Kono H, Matsumoto Y. Surgical treatment of recurrent hepatocellular carcinoma based on the mode of recurrence: repeat hepatic resection or ablation are good choices for patients with recurrent multicentric cancer. *J Hepatobiliary Pancreat Surg* 2001; **8**: 353-359
- Gazelle GS, Goldberg SN, Solbiati L, Livraghi T. Tumor ablation with radio-frequency energy. *Radiology* 2000; **217**: 633-646
- Ahmed M, Lobo SM, Weinstein J, Kruskal JB, Gazelle GS, Halpern EF, Afzal SK, Lenkinski RE, Goldberg SN. Improved coagulation with saline solution pretreatment during radiofrequency tumor ablation in a canine model. *J Vasc Interv Radiol* 2002; **13**: 717-724
- Choi D, Lim HK, Kim SH, Lee WJ, Jang HJ, Kim H, Lee SJ, Lim JH. Assessment of therapeutic response in hepatocellular carcinoma treated with percutaneous radio frequency ablation: comparison of multiphase helical computed tomography and power doppler ultrasonography with a microbubble contrast agent. *J Ultrasound Med* 2002; **21**: 391-401
- Giorgio A, Francica G, Tarantino L, de Stefano G. Radio-frequency ablation of hepatocellular carcinoma lesions. *Radiology* 2001; **218**: 918-919
- Dupuy DE, Goldberg SN. Image-guided radiofrequency tumor ablation: challenges and opportunities-part II. *J Vasc Interv Radiol* 2001; **12**: 1135-1148
- Livraghi T, Goldberg SN, Lazzaroni S, Meloni F, Ierace T, Solbiati L, Gazelle GS. Hepatocellular carcinoma: radio-frequency ablation of medium and large lesions. *Radiology* 2000; **214**: 761-768
- Mc Dannold NJ, Jolesz FA, Hynynen KH. Determination of the optimal delay between sonications during focused ultrasound surgery in rabbits by using MR imaging to monitor thermal buildup *in vivo*. *Radiology* 1999; **211**: 419-426
- Wu F, Chen WZ, Bai J. Effect of high-intensity focused ultrasound on the patients with hepatocellular carcinoma: preliminary report. *Zhonghua Chaosheng Yingxiangxue Zazhi* 1999; **8**: 213-216
- Yamamoto J, Okada S, Shimada K, Okusaka T, Yamasaki S, Ueno H, Kosuge T. Treatment strategy for small hepatocellular carcinoma: Comparison of long-term results after percutaneous ethanol injection therapy and surgical resection. *Hepatology* 2001; **34**: 707-713
- Bruix J, Llovet JM. Prognostic prediction and treatment strategy in hepatocellular carcinoma. *Hepatology* 2002; **35**: 519-524
- Morimoto M, Sugimori K, Shirato K, Kokawa A, Tomita N, Saito T, Tanaka N, Nozawa A, Hara M, Sekihara H, Shimada H, Imada T, Tanaka K. Treatment of hepatocellular carcinoma with radiofrequency ablation: Radiologic-histologic correlation during follow-up periods. *Hepatology* 2002; **35**: 1467-1475
- Parslow TG, Stites DP, Terr AI, Imboden JB. Medical Immunology. *Beijing science Press* 2002: 154-156
- Lin LW, He YM, Gao SD, Yan FD. Percutaneous intratumoral injection of chinese traditional medicine "Star-99" in treatment of hepatic carcinoma: an experimental study. *Zhonghua Chaosheng Yingxiangxue Zazhi* 2002; **11**: 45-48
- Kimura K, Bowen C, Spiegel S, Gelmann EP. Tumor necrosis factor-alpha sensitizes prostate cancer cells to gamma-irradiation-induced apoptosis. *Cancer Res* 1999; **59**: 1606-1614
- Liang WJ, Huang ZY, Ding YQ, Zhang WD. Lovo cell line apoptosis induced by cycloheximide combined with TNF α . *Shijie Huaren Xiaohua Zazhi* 1999; **7**: 326-328
- Shen YF, Zhuang H, Shen JW, Chen SB. Cell apoptosis and neoplasms. *Shijie Huaren Xiaohua Zazhi* 1999; **7**: 267-268
- He SW, Shen KQ, He YJ, Xie B, Zhao YM. Regulatory effect and mechanism of gastrin and its antagonists on colorectal carcinoma. *World J Gastroenterol* 1999; **5**: 408-416
- Huang PL, Zhu SN, Lu SL, Dai SZ, Jin YL. Inhibitor of fatty acid synthase induced apoptosis in human colonic cancer cells. *World J Gastroenterol* 2000; **6**: 295-297
- Li J, Wang WL, Liu B. Angiogenesis and apoptosis in human hepatocellular carcinoma. *Huaren Xiaohua Zazhi* 1998; **6**: 1057-1060
- Liu HF, Liu WW, Fang DC, Yang SM, Wang RQ. Bax gene expression and its relationship with apoptosis in human gastric carcinoma and precancerous lesions. *Shijie Huaren Xiaohua Zazhi* 2000; **8**: 665-668
- Tu SP, Jiang SH, Tan JH, Jiang XH, Qiao MM, Zhang YP, Wu YL, Wu YX. Proliferation inhibition and apoptosis induction by ar-

- senic trioxide on gastric cancer cell SGC-7901. *Shijie Huaren Xiaohua Zazhi* 1999; **7**: 18-21
- 35 **Chen HY**, Liu WH, Qin SK. Induction of arsenic trioxide on apoptosis of hepatocarcinoma cell lines. *Shijie Huaren Xiaohua Zazhi* 2000; **8**: 532-535
- 36 **Liu HF**, Liu WW, Fang DC. Effect of combined anti-Fas mAb and IFN- γ on the induction of apoptosis in human gastric carcinoma cell line SGC-7901. *Shijie Huaren Xiaohua Zazhi* 2000; **8**: 1316-1364
- 37 **Sun BH**, Zhao XP, Wang BJ, Yang DL, Hao LJ. FADD and TRADD expression and apoptosis in primary human hepatocellular carcinoma. *World J Gastroenterol* 2000; **6**: 223-227
- 38 **Sun ZX**, Ma QW, Zhao TD, Wei YL, Wang GS, Li JS. Apoptosis induced by norcantharidin in human tumor cells. *World J Gastroenterol* 2000; **6**: 263-265
- 39 **Xue XC**, Fang GE, Hua JD. Gastric cancer and apoptosis. *Shijie Huaren Xiaohua Zazhi* 1999; **7**: 359-361
- 40 **Cheng J**, Huang HC. Programmed cell death and disease. *Peking Union Medical College Press* 1997: 1-8
- 41 **Brown JM**, Wouters BG. Apoptosis, p53, and tumor cell sensitivity to anticancer agents. *Cancer Res* 1999; **59**: 1391-1399
- 42 **Ikeda M**, Shomori K, Endo K, Makino T, Matsuura T, Ito H. Frequent occurrence of apoptosis is an early event in the oncogenesis of human gastric carcinoma. *Virchows Arch* 1998; **432**: 43-47

Edited by Wu XN

Right trisectionectomy for primary liver cancer

Jing-An Rui, Shao-Bin Wang, Shu-Guang Chen, Li Zhou

Jing-An Rui, Shao-Bin Wang, Shu-Guang Chen, Li Zhou,
Department of General Surgery, Peking Union Medical College
Hospital, Beijing 100032, China

Correspondence to: Prof. Jing-An Rui, Department of General
Surgery, Peking Union Medical College Hospital, Beijing 100032,
China. rlzhou@mail.bjmu.edu.cn

Telephone: +86-10-62091034 **Fax:** +86-10-62358270

Received: 2002-11-19 **Accepted:** 2003-01-02

Abstract

AIM: To evaluate the value of right trisectionectomy, previously named right trisegmentectomy, in the treatment of primary liver cancer by summarizing our 13-year experience for this procedure.

METHODS: Thirty three primary liver cancer patients undergoing right trisectionectomy from Apr. 1987 to Dec. 1999 were investigated retrospectively. The impacts in survival of patients by cancerous biological behavior, such as tumor thrombi and satellite nodules, were discussed respectively. All right trisectionectomies were performed under normothermic interruption of porta hepatis at single time. Ultrasonic dissector (CUSA system 200) was used in dissection of hepatic parenchyma from Nov. 1992, instead of finger fracture.

RESULTS: 1-, 3- and 5-year survival rates were 71.9 %, 40.6 % and 34.4 %, respectively. The longest survival term with free cancer was 150 months (alive). There were no significant differences in survival curves between cases with and without tumor thrombi (right branch of portal vein) and satellite nodules. Operative mortality was 3.0 % (1/33). Main surgical complications occurred in 5 cases.

CONCLUSION: Right trisectionectomy should be regarded as an effective and safe procedure for huge primary liver cancers and is worth using more widely.

Rui JA, Wang SB, Chen SG, Zhou L. Right trisectionectomy for primary liver cancer. *World J Gastroenterol* 2003; 9(4): 706-709
<http://www.wjgnet.com/1007-9327/9/706.htm>

INTRODUCTION

It has been documented that primary liver cancer has been the more common cancer killer worldwide, especially in the areas with high incidence, such as China^[1]. Several methods has been developed for the therapy of the malignancy^[2-11]. The outcomes have taken marked progress, but recurrence and metastasis rates remain high^[12,13]. Up to now, the difficult point is still existing in treatment of large liver cancers, due to worse results and higher risk^[14,15]. Since the middle of last century^[16], right trisectionectomy (previous trisegmentectomy) has been used for huge hepatic neoplasms covering right and left medial section. In 1975, Starzl described and clearly defined in detail a safe technique of right trisectionectomy^[17]. Then he reported on 30 cases of the operation in 1980, including malignant and benign hepatic lesion^[18]. In the past two decades, some papers described the

procedure in treatment of hepatic malignant neoplasm, such as liver infiltration of gallbladder cancer and metastatic and primary liver cancer^[19-23]. Most reports demonstrated that right trisectionectomy was effective in extensive hepatic malignancy, based on some individuals with long-term survival^[19,20]. But the risk (morbidity and mortality) of liver resection remains high according to some authors^[20,22,23], especially for primary liver cancer with cirrhosis. It is related to the fact that most primary liver cancer patients have a history of hepatitis and suffer a higher incidence of hepatic failure after major resection. Another reason perhaps, is occurrence of bleeding during the operation. Currently, we lack data about comprehensive evaluation of right trisectionectomy in treatment of primary liver cancer. In this study, we investigate 33 cases of right trisectionectomies retrospectively to explore the value of the procedure to deal with primary liver cancer patients.

MATERIALS AND METHODS

Patients

From April 1987 to December 1999, total of 459 primary liver cancer patients were hepatomized. Of them, 33 cases of right trisectionectomies were performed. There were 24 (72.7 %) males and 9 (27.3 %) females. Ages ranged from 15 to 69 years (mean \pm SD, 45.9 \pm 16.7 years). Hepatitis B surface antigen (HBsAg): 28 (84.8 %) were positive and 5 (15.2 %) were negative. There were 8 (24.2 %) with slight cirrhosis and 25 (75.8 %) without. Child-Pugh's classification: 22 (66.7 %) were A grade and 11 (33.3 %) were B grade when the patients were hospitalized, but they were all A grade before surgical procedures through positive hepatic protective therapy. α -fetoprotein (AFP): 27 (81.8 %) were elevated and 6 (18.2 %) were normal. And the highest value of AFP was 20 000 ng/ml. Sizes of tumor ranged from 8 to 20 cm (mean \pm SD, 13.9 \pm 3.4 cm). Staging (TNM^[24]) of Cancer: All tumors were stage IV_A (T₄N₀M₀). Pathology: 27 (81.8 %) were hepatocellular carcinoma, 2 (6.1 %) were cholangiocarcinoma and 4 (12.1 %) were mixed hepatocellular-cholangiocarcinoma. There were 17 cases (51.5 %) with tumor thrombi in the right branch of the portal vein. 19 macroscopic satellite nodules were found in 15 cases (45.5 %), and they didn't presented in left lateral section of the liver.

Evaluation for feasibility of surgery

The feasibility of right trisectionectomy for each patient was considered carefully according to the following standards: (1) Tumors (including satellite nodules no more than 2) were limited in right and left medial section of the liver. There weren't any evidence about cancer invasion in left lateral section. (2) Tumor masses had clear borders or pseudocapsule, and without tumor thrombus in trunk of portal vein and hepatic vein. (3) No evidence for distant metastasis. (4) Compensative enlargement of left lateral section. (5) Child-Pugh's classification of liver function was A and indocyanine green retention rate at 15 minutes (ICGR15)^[25] was lower than 15 % before surgery. (6) Serum bilirubin smaller than 34 mmol·L⁻¹, serum albumin higher than 30 g·L⁻¹ and serum prothrombin time larger than 60 % before surgery.

The situations of tumor were detected chiefly by image examinations, including B-type ultrasonography, computed tomography (CT), magnetic resonance imaging (MRI) and

angiography. To assess liver function reserve of these patients before operation, we adopted classical Child-Pugh's classification, ICGR test and some concrete parameters, as described in standards. 146 cases of huge primary liver cancer were eliminated from the indication according to above standards. Of them, 69 cases were due to advanced tumor and the rest 77 due to bad liver function reserve.

Surgical procedures

All of the right trisectionectomies were on standard style, i.e. the resection edges were along the falciform ligaments of the liver and removed blocks were Couinaud segments 4 to 8. From November 1992, the ultrasonic dissector (CUSA system 200) was adopted for dissecting hepatic parenchyma, instead of previous finger fracture technique, introduced by Lin *et al.*^[26]. The procedures were all performed under normothermic interruption of porta hepatis at single time. Interruption lasted 15 to 40 minutes (mean \pm SD, 25.3 \pm 6.8 minutes). The total surgical time ranged from 165 to 312 minutes (mean \pm SD, 236 \pm 63 minutes). The amount of bleeding ranged from 300 to 3 000 ml (mean \pm SD, 1 240 \pm 560 ml). The quantities of transfused blood ranged from 0 to 2 200 ml (mean \pm SD, 1 020 \pm 550 ml). There were 2 cases that did not require blood transfusion during right trisectionectomy. For dissection of the liver parenchyma, we used finger fracture in 9 cases (27.3 %) before November 1992 and ultrasonic dissector (CUSA System 200) in 24 cases (72.7 %) after the time. Net weight of specimens ranged from 1 500 to 3 100 g (mean \pm SD, 2 330 \pm 520 g).

Adjuvant therapy and follow-up

All patients were covered in our strict follow-up after the procedure. AFP, B-type ultrasonography, computed tomography (CT) magnetic resonance imaging (MRI) and angiography were used as monitors of recurrence and metastasis. Moreover, follow-ups by mail, E-mail and telephone were taken for patients without reexaminations every year. Follow-up terms were 3 to 150 months. The latest follow-up was in November 2000 and survival terms of patients alive were calculated to October 2000. When the recurrences were

found, they were treated by transcatheter arterial chemoembolization (TACE), percutaneous ethanol injection (PEI) etc. 11 patients underwent TACE, 5 patients underwent PEI and 7 patients underwent both.

Statistical analysis

Survival curves were analyzed by Kaplan-Meier and Log rank test. The χ^2 and Student *t* test were used to determine comparability of groups. Statistically significant *P* value was defined as <0.05.

RESULTS

Survival rates, recurrence and metastasis after right trisectionectomy

The postoperative survival rates at 1-, 2-, 3-, 4- and 5-years were 71.9 %, 50 %, 40.6 %, 37.5 % and 34.4 %, respectively (Kaplan-Meier method). Ten cases have survived from 13 to 150 months according to the November 2000 follow-up. Survival curve of all patients is shown in Figure 1. The longest tumor-free survival term was 150 months (alive). The clinicopathological features in cases with and without satellite nodules and tumor thrombi in the right branch of the portal vein are shown in Table 1, and their survival curves were presented in Figure 2 and 3, there were no significant differences (*P*>0.05, Log rank test). During follow-up term, recurrence and metastasis of cancer was found in 27 patients (81.8 %).

Operative mortality after right trisectionectomy

There was one patient who died of hepatic failure within one month after the operation. The operative mortality was 3.0 % (1/33).

Surgical complications after right trisectionectomy

There were 5 cases (15.2%) that developed main surgical complications after right trisectionectomies, including 2 cases of hepatic failure, 2 cases of bile leakage and 1 case of secondary bleeding. Four patients recovered by positive reoperation excluding 1 case of hepatic failure.

Table 1 Clinicopathological features of patients

Variables	TT present (17)	TT absent (16)	<i>P</i>	SN present (15)	SN absent (18)	<i>P</i>
Age	43.4(18.2)	47.6(16.5)	>0.05 ^b	46.8(17.6)	45.1(15.7)	>0.05 ^b
Sex			>0.05 ^a			>0.05 ^a
Male	14(82.4)	10(62.5)		13(86.7)	11(61.1)	
Female	3(17.6)	6(37.5)		2(13.3)	7(38.9)	
LC			>0.05 ^a			>0.05 ^a
Present	4(23.5)	4(25.0)		5(33.3)	3(16.7)	
Absent	13(76.5)	12(75.0)		10(66.7)	15(83.3)	
AFP			>0.05 ^a			>0.05 ^a
Elevated	15(88.2)	12(75.0)		13(86.7)	14(77.8)	
Normal	2(11.8)	4(25.0)		2(13.3)	4(22.2)	
TS (cm)	12.5(2.6)	16.7(5.8)	>0.05 ^b	14.4(3.8)	13.2(3.1)	>0.05 ^b
BL (ml)	1290(640)	1210(450)	>0.05 ^b	1300(680)	1220(390)	>0.05 ^b
BT (ml)	1100(720)	980(370)	>0.05 ^b	1050(510)	990(570)	>0.05 ^b
WS (g)	2280(490)	2350(530)	>0.05 ^b	2380(570)	2300(460)	>0.05 ^b
Pathology			>0.05 ^a			>0.05 ^a
HCC	13(76.5)	14(87.6)		12(80.0)	15(83.3)	
CC	1(5.9)	1(6.2)		1(6.7)	1(5.6)	
MHCC	3(17.6)	1(6.2)		2(13.3)	2(11.1)	

Values in parentheses are percentages or standard errors. TT, tumor thrombus; SN, satellite nodule; LC, liver cirrhosis; AFP, α -fetoprotein; TS, tumor size; BL, blood loss; BT, blood transfusion; WS, weight of specimen; HCC, hepatocellular carcinoma; CC, cholangiocarcinoma; MHCC, mixed hepatocellular-cholangiocarcinoma. ^a: χ^2 test, ^b: Student *t* test.

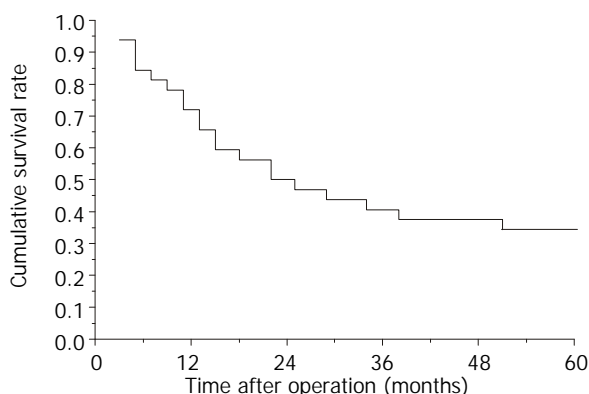


Figure 1 Survival curve of 32 patients underwent right trisectionectomy except 1 hospital death.

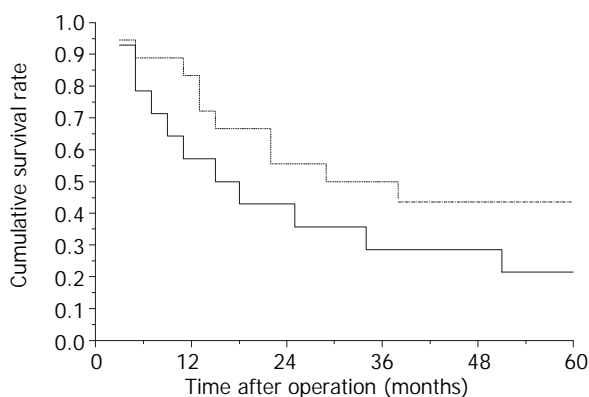


Figure 2 Survival curves of patients. —, with satellite nodules (SN); ---, without satellite nodules. $P > 0.05$, Log rank test.

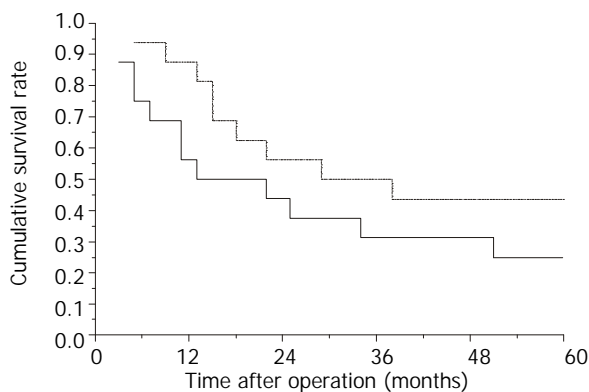


Figure 3 Survival curves of patients. —, with tumor thrombus (TT); ---, without tumor thrombus. $P > 0.05$, Log rank test.

DISCUSSION

In the therapy of primary liver malignancy, curative hepatic resection has been regarded as a primary method for radical treatment. But for hepatoma mainly in the right lobe and which invades the medial section of the left lobe, resection has always been difficult. Despite the fact that there has been research about right trisectionectomy, previous trisegmentectomy, mortality and morbidity remains high. There are few studies with large sample groups of primary liver cancer patients treated with right trisectionectomy. Starzl^[18] reported on 19 cases of primary hepatic malignant tumors (14 primary liver cancers and 5 other types of tumors) treated by the procedure. The 1-year survival rate was more than 50%. Holbrook *et al*^[27] reported on 13-years of experience in resection of malignant primary liver tumors, including 9 right trisectionectomies. Overall 1-, 2-, 3-, and 5-year survival rates were 57%, 52%, 40% and 33%, respectively. Mortality was 7% and

complication incidence was 26%. Kumada *et al*^[28] reported on 11 cases of tri- and bi-sectionectomy for HCC, mean survival time was 16 months, mortality was 15.4%. We had reported 4 right trisectionectomies to treat extensive primary liver cancers in 1991^[29]. Three cases survived more than 1 year. From April 1987 to December 1999, we performed 33 right trisectionectomies for primary liver cancer patients, 1-, 2-, 3-, 4- and 5-year survival rates were 71.9%, 50%, 40.6%, 37.5% and 34.4%, respectively. The longest term of survival with free cancer was 150 months. Mortality was 3.0% and the surgical complication rate was 15.2%. These results are related to new advances in liver surgery. To control severe intraoperative bleeding, we used normothermic interruption of the porta hepatis at single time. Previously, we reported on 20 cases of hemihepatectomy using this interruption method. Manipulation appeared simple and convenient. Mortality was 0%^[30]. These data suggested that normothermic interruption of the porta hepatis at single time should be regarded as an effective and safe method to limit bleeding in liver surgery. There were two patients in this study that were trisectionectomized without blood transfusion. Besides, the use of ultrasonic dissector in later period made the operative fields more clear. Thus, manipulations became more convenient and accurate. Meanwhile, the low incidence of complications and mortality were related to the accurate estimation of liver functional reserve prior to operation. We adopted the Child-Pugh's classification, some detailed parameters and ICGR test. Child-Pugh's classification was a classical method for estimating liver function. It could become more accurate if helped by other concrete markers, such as serum bilirubin, prothrombin time and albumin. Besides, ICGR test, a proven sensitive indicator of liver function reserve^[25], also provided important information. Our experience is that the combination of these parameters could accurately predict liver function reserve.

In the present study, we analyzed the influence of some pathological features on outcome of right trisectionectomy for huge primary liver cancers. The clinicopathological features showed in Table 1 suggested the comparability between patients with and without tumor thrombi or satellite nodules (all $P > 0.05$). And no significant differences could be found in their survival curves ($P > 0.05$), in spite of some differences in these curves. These findings suggest that surgeons should use curative resection in therapy of huge tumors, even in those with a few satellite nodules and tumor thrombi, if the tumor thrombi are only in the right branch of the portal vein, a satisfactory effect could be expected.

In conclusion, right trisectionectomy is an effective and safe procedure and should become one of strategies, and surgical arts in the treatment of huge tumor of primary liver cancers.

REFERENCES

- 1 **Pisani P**, Parkin DM, Bray F, Ferlay J. Estimates of the worldwide mortality from 25 cancers in 1990. *Int J Cancer* 1999; **83**: 18-29
- 2 **Makuuchi M**, Takayama T, Kubota K, Kimura W, Midorikawa Y, Miyagawa S, Kawasaki S. Hepatic resection for hepatocellular carcinoma-Japanese experience. *Hepatogastroenterology* 1998; **45** (Suppl 3): 1267-1274
- 3 **Yamamoto J**, Iwatsuki S, Kosuge T, Dvorchik I, Shimada K, Marsh JW, Yamasaki S, Starzl TE. Should hepatomas be treated with hepatic resection or transplantation? *Cancer* 1999; **86**: 1151-1158
- 4 **Shen P**, Hoffman A, Howerton R, Loggie BW. Cryosurgery of close or positive margins after hepatic resection for primary and metastatic hepatobiliary malignancies. *Am Surg* 2002; **68**: 695-703
- 5 **Pelletier G**, Ducreux M, Gay F, Lubinski M, Hagege H, Dao T, Van Steenberg W, Buffet C, Rougier P, Adler M, Pignon JP, Roche A. Treatment of unresectable hepatocellular carcinoma with lipiodol chemoembolization: a multicenter randomized trial. *Groupe CHC. J Hepatol* 1998; **29**: 129-134

- 6 **Livraghi T**, Benedini V, Lazzaroni S, Meloni F, Torzilli G, Vettori C. Long term results of single session percutaneous ethanol injection in patients with large hepatocellular carcinoma. *Cancer* 1998; **83**: 48-57
- 7 **Ohmoto K**, Tsuduki M, Shibata N, Takesue M, Kunieda T, Yamamoto S. Percutaneous microwave coagulation therapy for hepatocellular carcinoma located on the surface of the liver. *Am J Roentgenol* 1999; **173**: 1231-1233
- 8 **Livraghi T**, Goldberg SN, Lazzaroni S, Meloni F, Solbiati L, Gazelle GS. Small hepatocellular carcinoma: treatment with radio-frequency ablation versus ethanol injection. *Radiology* 1999; **210**: 655-661
- 9 **Cheng SH**, Lin YM, Chuang VP, Yang PS, Cheng JC, Huang AT, Sung JL. A pilot study of three-dimensional conformal radiotherapy in unresectable hepatocellular carcinoma. *J Gastroenterol Hepatol* 1999; **14**: 1025-1033
- 10 **Liu CL**, Fan ST, Ng IO, Lo CM, Poon RT, Wong J. Treatment of advanced hepato-cellular carcinoma with tamoxifen and the correlation with expression of hormone receptors: a prospective randomized study. *Am J Gastroenterol* 2000; **95**: 218-222
- 11 **Llovet JM**, Sala M, Castells L, Suarez Y, Vilana R, Bianchi L, Ayuso C, Vargas V, Rodes J, Bruix J. Randomized controlled trial of interferon treatment for advanced hepatocellular carcinoma. *Hepatology* 2000; **31**: 54-58
- 12 **Tang ZY**. Hepatocellular carcinoma-cause, treatment and metastasis. *World J Gastroenterol* 2001; **7**: 445-454
- 13 **Shuto T**, Hirohashi K, Kubo S, Tanaka H, Yamamoto T, Ikebe T, Kinoshita H. Efficacy of major hepatic resection for large hepatocellular carcinoma. *Hepatogastroenterology* 1999; **46**: 413-416
- 14 **Hanazaki K**, Kajikawa S, Shimozawa N, Shimada K, Hiraguri M, Koide N, Adachi W, Amano J. Hepatic resection for large hepatocellular carcinoma. *Am J Surg* 2001; **181**: 347-353
- 15 **Regimbeau JM**, Farges O, Shen BY, Sauvanet A, Belghiti J. Is surgery for large hepatocellular carcinoma justified? *J Hepatol* 1999; **31**: 1062-1068
- 16 **Quattlebaum JK**. Massive resection of the liver. *Ann Surg* 1953; **137**: 787-796
- 17 **Starzl TE**, Bell RH, Beart RW, Putnam CW. Hepatic trisegmentectomy and other liver resections. *Surg Gynecol Obstet* 1975; **141**: 429-437
- 18 **Starzl TE**, Koep LJ, Weil R 3rd, Lilly JR, Putnam CW, Aldrete JA. Right trisegmentectomy for hepatic neoplasms. *Surg Gynecol Obstet* 1980; **150**: 208-214
- 19 **Yamamoto M**, Miura K, Yoshioka M, Matsumoto Y. Disease-free survival for 9 years after liver resection for stage IV gallbladder cancer: report of a case. *Surg Today* 1995; **25**: 750-753
- 20 **Sugiura Y**, Nakamura S, Iida S, Hosoda Y, Ikeuchi S, Mori S, Sugioka A, Tsuzuki T. Extensive resection of the bile ducts combined with liver resection for cancer of the main hepatic duct junction: a cooperative study of the Keio Bile Duct Cancer Study Group. *Surgery* 1994; **115**: 445-451
- 21 **Chi DS**, Fong Y, Venkatraman ES, Barakat RR. Hepatic resection for metastatic gynecologic carcinomas. *Gynecol Oncol* 1997; **66**: 45-51
- 22 **Iwatsuki S**, Starzl TE. Experience with resection of primary hepatic malignancy. *Surg Clin North Am* 1989; **69**: 315-322
- 23 **Wakabayashi H**, Okada S, Maeba T, Maeta H. Effect of preoperative portal vein embolization on major hepatectomy for advanced-stage hepatocellular carcinomas in injured livers: a preliminary report. *Surg Today* 1997; **27**: 403-410
- 24 **Skeel RT**. Carcinomas of the pancreas, liver, gallbladder. In: Skeel RT, eds. Handbook of cancer chemotherapy (Fifth edition). Philadelphia: Lippincott Williams & Wilkins 1997: 249
- 25 **Lau H**, Man K, Fan ST, Yu WC, Lo CM, Wong J. Evaluation of preoperative hepatic function in patients with hepatocellular carcinoma undergoing hepatectomy. *Br J Surg* 1997; **84**: 1255-1259
- 26 **Lin TY**, Lee CS, Chen KM, Chen CC. Role of surgery in the treatment of primary carcinoma of the liver: a 31-year experience. *Br J Surg* 1987; **74**: 839-842
- 27 **Holbrook RF**, Koo K, Ryan JA. Resection of malignant primary liver tumors. *Am J Surg* 1996; **171**: 453-455
- 28 **Kumada K**, Ozawa K, Okamoto R, Takayasu T, Yamaguchi M, Yamamoto Y, Higashiyama H, Morikawa S, Sasaki H, Shimahara Y, Shimahara Y, Yamaoka Y, Takeuchi E. Hepatic resection for advanced hepatocellular carcinoma with removal of portal vein tumor thrombi. *Surgery* 1990; **108**: 821-827
- 29 **Rui JA**, Wang K, Su Y, Li ZW, Wang CF, Wu JX, Zhao P. Right trisegmentectomy for primary liver cancer-a report of 4 cases with review of literature. *Zhonghua Zhongliu Zazhi* 1991; **13**: 37-39
- 30 **Rui JA**, Qu JY, Su Y, Li ZW, Wang K, Zhu GJ, Wu JX, Chen GJ, Wang CF, Mao XW. Hemihepatectomy under hepato-portal interruption at normal temperature for liver malignancies: a report of 20 patients. *Zhonghua Zhongliu Zazhi* 1987; **9**: 221-223

Edited by Yuan HT

Glycylproline dipeptidyl aminopeptidase isoenzyme in diagnosis of primary hepatocellular carcinoma

Run-Zhou Ni, Jie-Fei Huang, Ming-Bing Xiao, Mei Li, Xian-Yong Meng

Run-Zhou Ni, Jie-Fei Huang, Ming-Bing Xiao, Mei Li, Xian-Yong Meng, Department of Gastroenterology, Affiliated Hospital of Nantong Medical College, Nantong 226001, Jiangsu Province, China
Correspondence to: Dr. Run-Zhou Ni, Department of Gastroenterology, Affiliated Hospital of Nantong Medical College, Nantong 226001, Jiangsu Province, China. nirz@public.nt.js.cn
Telephone: +86-513-5119461
Received: 2002-09-14 **Accepted:** 2002-10-17

Abstract

AIM: To investigate the role of glycylproline dipeptidyl aminopeptidase (GPDA) isoenzyme in the diagnosis of primary hepatocellular carcinoma (PHC), especially in patients with negative alpha-fetoprotein (AFP).

METHODS: A stage gradient polyacrylamide gel discontinuous electrophoresis system was developed to separate serum GPDA isoenzymes, which were determined in 102 patients with PHC, 45 cases with liver cirrhosis, 24 cases with chronic hepatitis, 35 cases with benign liver space-occupying lesions, 20 cases with metastatic liver cancer and 50 cases with extra-hepatic cancer, as well as 80 healthy subjects. The relationships between GPDA isoenzymes and AFP, the sizes of tumors, as well as alanine aminotransferase (ALT) were also analyzed.

RESULTS: Serum GPDA was separated into two isoenzymes, GPDA-S and GPDA-F. The former was positive in all subjects, while the latter was found mainly in majority of PHC (85.3 %) and a few cases with liver cirrhosis (11.1 %), chronic hepatitis (33.3 %), metastatic liver cancer (15.0 %) and non-hepatic cancer (16.0 %). GPDA-F was negative in all healthy subjects and patients with benign liver space-occupying lesions, including abscess, cysts and angioma. There was no correlation between GPDA-F and AFP concentration or tumor size. GPDA-F was consistently positive and not correlated with ALT in PHC, but GPDA-F often converted to negative as decline of ALT in benign liver diseases. The electrophoretic migration of GPDA-F became sluggish after the treatment of neuraminidase.

CONCLUSION: GPDA-F is a new useful serum marker for PHC. Measurement of serum GPDA-F is helpful in diagnosis of PHC, especially in patients with negative AFP. GPDA-F is one kind of glycoproteins rich in sialic acid.

Ni RZ, Huang JF, Xiao MB, Li M, Meng XY. Glycylproline dipeptidyl aminopeptidase isoenzyme in diagnosis of primary hepatocellular carcinoma. *World J Gastroenterol* 2003; 9(4): 710-713
<http://www.wjgnet.com/1007-9327/9/710.htm>

INTRODUCTION

Glycylproline dipeptidyl aminopeptidase (GPDA) was discovered by Hapsu-Hava and Glenner in 1966^[1]. It is widely distributed in human and animal tissues and catalyzes the

hydrolysis of N-terminal glycylproline from glycylprolyl- β -naphthylamide and glycylproline- β -nitroanilide. It was reported that serum GPDA activity increased in the patients with hepatobiliary diseases and in experimental hepatic cancer^[2,3]. Further studies demonstrated that GPDA activity was significantly higher in human hepatic cancer and embryonal tissues than in healthy adult liver tissues^[4]. However, serum GPDA cannot be used as a marker for PHC due to its low sensitivity and specificity in diagnosis.

In order to improve the diagnostic value of GPDA for PHC, a stage gradient polyacrylamide gel discontinuous electrophoresis system was established to separate serum GPDA into two isoenzymes, and clinical significances of serum GPDA isoenzymes in diagnosis of PHC were studied.

MATERIALS AND METHODS

Patients and healthy subjects

The resources of all patients in this study were from Affiliated Hospital of Nantong Medical College. The diagnosis of PHC met the diagnostic criterion of Liver Cancer Branch Committee of Chinese Anti-cancer Association. The diagnosis in 35 patients was confirmed pathologically. The origins of 20 metastatic liver cancers were gastrointestinal tract cancer (16 cases), lung cancer (2 cases) and breast cancer (2 cases). The origins in 50 cases with extra-hepatic cancer were gastrointestinal tract (22 cases), pancreas (5 cases), bile duct (6 cases), ovary (8 cases), bladder (4 cases), lung (4 cases) and kidney (1 case). Thirty-five benign liver space-occupying lesions were composed of 8 liver abscess, 2 liver cysts and 25 liver angioma. The diagnoses of 45 cases with hepatic cirrhosis and 24 chronic hepatitis were based on clinical manifestations and liver biopsy. The control samples came from healthy blood donor.

Detection of GPDA isoenzymes

Separation of GPDA isoenzymes was performed on stage gradient polyacrylamide gel with a vertical slab electrophoresis apparatus. The gel consists of one layer of stack gel and two layers of separating gels. The following solutions were used for the preparation of gels: (1) Solution A: 30 % acrylamide containing 0.8 % bisacrylamide; (2) Solution B: 4.95 % Tris base containing 0.05 % TEMED, pH6.9; (3) Solution C: 0.14 % ammonium persulfate. A gel of dimensions of 12.0 cm \times 10.0 cm \times 0.15 cm was prepared and loaded with 20 μ l of serum. The gel run at a constant voltage of 60 V for the first three hours and then at the voltage of 100 V for another 16 hours. After the electrophoresis, the gel was incubated at 37 $^{\circ}$ C for 30 min with a piece of acetate cellulose membrane of the gel size pre-soaked with a substrate solution, which consists of 15 mg of glycylproline- β -nitroanilide, 4.8 ml of 100 mmol \cdot L⁻¹ Tris-glycylglycine (pH 8.4), 0.1 ml of 100 ml \cdot L⁻¹ sodium nitrite and 0.1 ml of 50 g \cdot L⁻¹ N-(naphthyl)-ethylenediamine dihydrochloride. Finally red GPDA isoenzyme bands were visualized soon by immersing the acetate cellulose membrane into a solution composed of 100 ml \cdot L⁻¹ trichloroacetic acid and 250 ml \cdot L⁻¹ glycerol.

Measurement of AFP and ALT

ALT was measured with the method recommended by International Federation of Clinical Chemistry^[5] and AFP was determined with routine radioimmunoassay.

Treatment of serum with neuraminidase

Serum was incubated with 10 u/ml neuraminidase at 37 °C for 15 hr before electrophoresis.

Statistical analysis

Chi-square test and student *t* tests were used. $P < 0.05$ was considered as statistically significant.

RESULTS

Serum GPDA isoenzyme in patients with PHC and other diseases

Serum GPDA was separated into two isoenzyme bands with the electrophoresis system (Figure 1). The band in the anode was called as GPDA-F (fast band) and the band in cathode as GPDA-S (slow band). GPDA-S was positive in all subjects, including healthy persons and patients, while positive rates of GPDA-F varied in different diseases. GPDA-F was found in most patients with PHC and a few patients with benign liver diseases and extra-hepatic cancer, but no GPDA-F was found in all healthy persons and the patients with benign liver space-occupying lesions (Table 1). In patients with PHC, positive GPDA-F was considered as true positive and negative GPDA-F as false negative, while in patients with other diseases positive GPDA-F was considered as false positive and negative GPDA-F as true negative. Therefore, the sensitivity, specificity and accuracy of GPDA-F in diagnosis of PHC were 85.3 %, 86.2 % and 85.9 % respectively (Table 1).

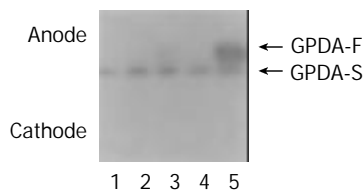


Figure 1 Serum GPDA isoenzymes separated with polyacrylamide electrophoresis. (Lane 1: healthy subject; lane 2: liver angioma; lane 3: chronic hepatitis; lane 4: liver cirrhosis; lane 5: PHC).

Table 1 Results of serum GPDA-F in patients and healthy subjects

	GPDA-F (+)		GPDA-F (-)	
	<i>n</i>	%	<i>n</i>	%
Healthy subjects	0	0	80	100.0
PHC	87 ^a	85.3	15	14.7
Liver cirrhosis	5	11.1	40	88.9
Chronic hepatitis	8	33.3	16	66.7
Benign liver space-occupying lesions	0	0	35	100.0
Metastatic hepatic cancer	3	15.0	17	85.0
Extra-hepatic cancer	8	16.0	42	84.0

^a $P < 0.05$ vs other groups. True positive (TP)=87; False positive (FP)=24(5+8+0+3+8); False negative (FN)=15; True negative (TN)=150(40+16+35+17+42); Sensitivity=TP/(TP+FN)×100 %; Specificity=TN/(TN+FP)×100 %; Diagnostic accuracy=(TP+TN)/(TP+TN+FP+FN)×100 %.

The complementary value of GPDA-F and AFP for PHC

There was no correlation between positive rates of GPDA-F and AFP concentration (Table 2). GPDA-F was positive in 75.0 % PHC cases with negative AFP (<50 ng/ml). If positive GPDA-F and AFP≥50 ng/ml were set as diagnostic criterion of PHC, the

sensitivity of AFP was 72.5 % and that of AFP with GPDA-F would reach up to 91.2 %. The diagnostic accuracy was also increased with the combination of AFP and GPDA-F (Table 3).

Table 2 Relationship between AFP and GPDA-F in sera of cases with PHC

AFP(ng/ml)	<i>n</i>	GPDA-F(+)
<50	28	21(75.0%)
-400	12	11(91.6%)
>400	62	55(88.7%)

Table 3 Diagnostic value of both AFP and GPDA-F in PHC

	Sensitivity (%)	Specificity (%)	Accuracy (%)
AFP alone	72.5	95.2	85.0
GPDA-F alone	85.3	87.1	86.3
AFP and GPDA-F	91.2	84.7	88.5

The relationship between GPDA-F and tumor size

One hundred and two cases with PHC were divided into two groups based on size of tumor, 23 cases were small liver cancer with tumor diameter ≤5 cm and 79 cases were advanced liver cancer with tumor diameter >5 cm. Positive rate of GPDA-F was 78.3 % (18/23) in small liver cancer, and 87.3 % (69/79) in advanced liver cancer. However, there was no statistical difference between the two groups ($P > 0.05$).

Characteristics of GPDA-F in PHC and benign liver diseases

In order to know whether GPDA-F is associated with inflammation of hepatocytes, GPDA-F and ALT were measured simultaneously. There was no significant difference of ALT activities between positive and negative GPDA-F groups in PHC, but ALT activities in positive GPDA-F group were significantly higher than that in negative group in liver cirrhosis and chronic hepatitis (Table 4), suggesting that GPDA-F was associated with elevated ALT in benign liver diseases, but not in PHC. It was also found that GPDA-F often converted to negative with the decrease of ALT in benign liver diseases but no in PHC (data not shown).

Table 4 Relationship between GPDA-F and ALT in different liver diseases

	ALT ($\bar{x} \pm s$, u/L)		
	PHC	Hepatic cirrhosis	Chronic hepatitis
Negative GPDA-F	31.0±9.6	31.6±3.6 ^a	67.3±13.2 ^a
Positive GPDA-F	50.1±10.2	67.6±31.6	159.8±46.6

^a $P < 0.05$ vs positive GPDA-F group.

Effects of neuraminidase on GPDA-F

Serum was treated with neuraminidase before electrophoresis as mentioned in materials and methods. The migration rate of GPDA-F became slower than that of GPDA-S following treatment of neuraminidase, while GPDA-S was not obviously affected (Figure 2).

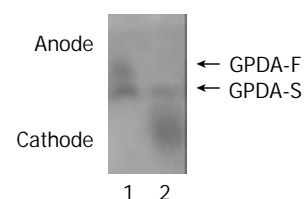


Figure 2 The effect of neuraminidase on migration of serum GPDA isoenzymes. (Lane 1: before treatment of neuraminidase; lane 2: after treatment of neuraminidase).

DISCUSSION

PHC is one of the most severe malignancies and ranks second mortality in malignant tumors in China^[6,7]. The prognosis is poor due to its delayed diagnosis and low resectable rate. Thus early diagnosis is important to improve the prognosis. Tumor markers are very useful in diagnosis. AFP is the most widely used tumor marker for PHC with a positive rate from 60 % to 70 %^[8-11]. AFP-L-3, one of the glycoforms of AFP, has higher specificity for PHC. However, it cannot increase the diagnostic sensitivity^[12-16]. Many studies have focused on other tumor markers to improve the diagnostic sensitivity for PHC. It has been found that there are some tumor markers, which are complementary to AFP in diagnosis of PHC, such as des-gamma-carboxy prothrombin (PIVKA-II)^[17-23], γ -glutamyltransferase isoenzyme^[24-26], transforming growth factor- β 1^[27-29] and α -L-fucosidase^[30-34].

In present study, we have investigated the value of GPDA isoenzymes in diagnosis of PHC. With a stage gradient polyacrylamide gel electrophoresis system, serum GPDA has been separated into two isoenzymes, GPDA-F and GPDA-S. GPDA-F was often detected in sera of patients with PHC, with a much higher positive rate than in other liver diseases, including liver cirrhosis, chronic hepatitis, metastatic liver cancer and extra-hepatic tumors; while GPDA-F was negative in healthy subjects and patients with benign liver space-occupying lesions. The sensitivity and specificity of GPDA-F in diagnosis of PHC were 85.3 % and 86.2 %, respectively. These results indicate that GPDA-F may be a valuable serum marker for PHC.

Serum GPDA-F in patients with benign liver diseases possibly originates from the inflammatory hepatocytes because in such cases positive GPDA-F was often accompanied by elevated ALT and changed to negative with the decline of ALT. On the contrary, GPDA-F in PHC is persistently positive and not correlated with ALT. Therefore, simultaneous determination and follow-up of ALT may help to rule out the false positive GPDA-F in benign liver diseases. It is known that some serum hepatoma markers are of predictive and early diagnostic value for PHC, such as AFP, des-gamma-carboxy prothrombin and gamma-glutamyltransferase isoenzyme II^[21-23, 26]. Whether persistent positive of GPDA-F in a few cases of liver cirrhosis is the precursor of hepatocarcinogenesis needs further investigation.

Although the diagnostic efficiency for PHC has been greatly improved in recent years with the use of many advanced image techniques, it is still difficult to make the diagnosis in some cases, especially for those at early stage or with negative AFP. Present study showed that GPDA-F and AFP were complementary for diagnosis of PHC. In these data, GPDA-F was positive in 75 % PHC cases of negative AFP but negative in all benign liver space-occupying lesions. Therefore, GPDA-F is of special value for the differential diagnosis of liver space-occupying lesions of unknown nature. Our data also showed that there was no correlation between tumor size and GPDA-F. In 23 cases of small liver cancer, the positive rate of GPDA-F was 78.3 %, suggesting that GPDA-F may be a good marker of PHC at early stage.

The exact mechanism by which GPDA-F appears in the sera of PHC cases is not clarified. It is possible that GPDA-F is produced by hepatoma tissues and then released into blood, since GPDA-F was only found in sera of those PHC cases in whose hepatoma tissues GPDA-F was positive (unpublished data). The electrophoretic migration of GPDA-F became slower than its isoenzyme GPDA-S after treatment with neuraminidase, indicating that GPDA-F is a kind of glycoprotein rich in sialic acids in its sugar chain. Therefore, the modification of the sugar chain after GPDA protein synthesis may be the main process of the production of GPDA-F. It has been known that several

kinds of glycoproteins synthesized by hepatoma cells are different from those produced by hepatocytes. For example, AFP and alpha-1-antitrypsin have higher percentage of lens culinaris agglutinin-reactive species in hepatocellular carcinoma than in benign liver diseases. It is also clear that the fucosylation of the sugar chain at the innermost N-acetylglucosamine is the molecular basis of this variation^[35, 36]. Whether there is the difference of fucosylation of GPDA isoenzymes between hepatocellular carcinoma and benign liver diseases needs to be studied further.

REFERENCES

- 1 **Hopsu-Havu VK**, Glenner GG. A new dipeptide naphthylamidase hydrolyzing glycyl-prolyl-beta-naphthylamide. *Histochemie* 1966; **7**: 197-201
- 2 **Hutchinson DR**, Halliwell RP, Lockhart JD, Parke DV. Glycylprolyl-p-nitroanilidase in hepatobiliary disease. *Clin Chem Acta* 1981; **109**: 83-89
- 3 **Kojima J**, Kanatani M, Nakamura N, Kashiwagi T, Tohjo F, Akiyama M. Serum and liver glycylproline dipeptidyl aminopeptidase activity in rats with experimental hepatic cancer. *Clin Chem Acta* 1980; **107**: 105-110
- 4 **Kojima J**, Ueno Y, Kasugai H, Okuda S, Akedo H. Glycylproline dipeptidyl aminopeptidase and gamma-glutamyl transpeptidase in human hepatic cancer and embryonal tissues. *Clin Chem Acta* 1987; **167**: 285-291
- 5 **Bergmeyer HU**, Horder M, Rej R. International federation of clinical chemistry (IFCC) scientific committee, analytical section: approved recommendation (1985) on IFCC methods for the measurement of catalytic concentration of enzymes. Part 3. IFCC method for alanine aminotransferase (L-alanine: 2-oxoglutarate aminotransferase, EC 2.6.1.2). *J Clin Chem Clin Biochem* 1986; **24**: 481-495
- 6 **Tang ZY**. Hepatocellular carcinoma-cause, treatment and metastasis. *World J Gastroenterol* 2001; **7**: 445-454
- 7 **Tang ZY**. Hepatocellular carcinoma. *J Gastroenterol Hepatol* 2000; **15** (Suppl): G1-7
- 8 **Rabe C**, Pilz T, Klostermann C, Berna M, Schild HH, Sauerbruch T, Caselmann WH. Clinical characteristics and outcome of a cohort of 101 patients with hepatocellular carcinoma. *World J Gastroenterol* 2001; **7**: 208-215
- 9 **Tangkijvanich P**, Anukulkarnkusol N, Suwangool P, Lertmaharit S, Hanvivatvong O, Kullavanijaya P, Poovorawa Y. Clinical characteristics and prognosis of hepatocellular carcinoma: analysis based on serum alpha-fetoprotein levels. *J Clin Gastroenterol* 2000; **31**: 302-308
- 10 **Yoshida S**, Kurokohchi K, Arima K, Masaki T, Hosomi N, Funaki T, Murota M, Kita Y, Watanabe S, Kuriyama S. Clinical significance of lens culinaris agglutini-reactive fraction of serum alpha-fetoprotein in patients with hepatocellular carcinoma. *Int J Oncol* 2002; **20**: 305-309
- 11 **Qin LX**, Tang ZY. The prognostic significance of clinical and pathological features in hepatocellular carcinoma. *World J Gastroenterol* 2002; **8**: 193-199
- 12 **Tamura A**, Oita T, Sakizono K, Nakajima T, Kasakura S. Clinical usefulness of lectin-reactive fraction of alpha-fetoprotein in hepatocellular carcinoma. *Rinsho Byori* 1998; **46**: 158-162
- 13 **Zaninotto M**, Ujka F, Lachin M, Bernardi D, Marafi C, Farinati F, Plebani M. Lectini-affinity electrophoresis for the detection of AFP microheterogeneities in patients with hepatocellular carcinoma. *Anticancer Res* 1996; **16**: 305-309
- 14 **Kumada T**, Nakano S, Takeda I, Kiriya S, Sone Y, Hayashi K, Katoh H, Endoh T, Sassa T, Satomura S. Clinical utility of Lens culinaris agglutinin-reactive alpha-fetoprotein in small hepatocellular carcinoma: special reference to imaging diagnosis. *J Hepatol* 1999; **30**: 125-130
- 15 **Hayashi K**, Kumada T, Nakano S, Takeda I, Sugiyama K, Kiriya S, Sone Y, Miyata A, Shimizu H, Satomura S. Usefulness of measurement of Lens culinaris agglutinin-reactive fraction of alpha-fetoprotein as a marker of prognosis and recurrence of small hepatocellular carcinoma. *Am J Gastroenterol* 1999; **94**: 3028-3033

- 16 **Li D**, Mallory T, Satomura S. AFP-L3: a new generation of tumor marker for hepatocellular carcinoma. *Clin Chim Acta* 2001; **313**: 15-19
- 17 **Sakon M**, Monden M, Gotoh M, Kanai T, Umeshita K, Nakano Y, Mori T, Sakurai M, Wakasa K. Relationship between pathologic prognostic factors and abnormal levels of des-gamma-carboxy prothrombin and alpha-fetoprotein in hepatocellular carcinoma. *Am J Surg* 1992; **163**: 251-256
- 18 **Lamerz R**, Runge M, Stieber P, Meissner E. Use of serum PIVKA-II (DCP) determination for differentiation between benign and malignant liver diseases. *Anticancer Res* 1999; **19**: 2489-2493
- 19 **Tanaka Y**, Kashiwagi T, Tsutsumi H, Nagasawa M, Toyama T, Ozaki S, Naito M, Ishibashi K, Azuma M. Sensitive measurement of serum abnormal prothrombin (PIVKA-II) as a marker of hepatocellular carcinoma. *Hepatogastroenterology* 1999; **46**: 2464-2468
- 20 **Sassa T**, Kumada T, Nakano S, Uematsu T. Clinical utility of simultaneous measurement of serum high-sensitivity des-gamma-carboxy prothrombin and lens culinaris agglutinin A-reactive alpha-fetoprotein in patients with small hepatocellular carcinoma. *Eur J Gastroenterol Hepatol* 1999; **11**: 1387-1392
- 21 **Ishii M**, Gama H, Chida N, Ueno Y, Shinzawa H, Takagi T, Toyota T, Takahashi T, Kasukawa R. Simultaneous measurements of serum alpha-fetoprotein and protein induced by vitamin K absence for detecting hepatocellular carcinoma. South tohoku district study group. *Am J Gastroenterol* 2000; **95**: 1036-1040
- 22 **Ikoma J**, Kaito M, Ishihara T, Nakagawa N, Kamei A, Fujita N, Iwasa M, Tamaki S, Watanabe S, Adachi Y. Early diagnosis of hepatocellular carcinoma using sensitive assay for serum des-gamma-carboxy prothrombin: a prospective study. *Hepatogastroenterology* 2002; **49**: 235-238
- 23 **Fujiyama S**, Tanaka M, Maeda S, Ashihara H, Hirata R, Tomita K. Tumor markers in early diagnosis, follow-up and management of patients with hepatocellular carcinoma. *Oncology* 2002; **62**(Suppl 1): 57-63
- 24 **Okuyama K**. Separation and identification of serum gamma-glutamyl transpeptidase isoenzymes by wheat germ agglutinin affinity electrophoresis: a basic analysis and its clinical application to various liver diseases. *Keio J Med* 1993; **42**: 149-156
- 25 **Sacchetti L**, Castaldo G, Cimino L, Budillon G, Salvatore F. Diagnostic efficiency in discriminating liver malignancies from cirrhosis by serum gamma-glutamyl transferase isoforms. *Clin Chim Acta* 1988; **177**: 167-172
- 26 **Xu K**, Meng XY, Wu JW, Shen B, Shi YC, Wei Q. Diagnostic value of serum gamma-glutamyl transferase isoenzyme for hepatocellular carcinoma: a 10-year study. *Am J Gastroenterol* 1992; **87**: 991-995
- 27 **Tsai JF**, Chuang LY, Jeng JE, Yang ML, Chang WY, Hsieh MY, Lin ZY, Tsai JH. Clinical relevance of transforming growth factor-beta 1 in the urine of patients with hepatocellular carcinoma. *Medicine* 1997; **76**: 213-226
- 28 **Sacco R**, Leuci D, Tortorella C, Fiore G, Marinosci F, Schiraldi O, Antonaci S. Transforming growth factor beta1 and soluble Fas serum levels in hepatocellular carcinoma. *Cytokine* 2000; **12**: 811-814
- 29 **Song BC**, Chung YH, Kim JA, Choi WB, Suh DD, Pyo SI, Shin JW, Lee HC, Lee YS, Suh DJ. Transforming growth factor-beta 1 as a useful serological marker of small hepatocellular carcinoma. *Cancer* 2002; **94**: 175-180
- 30 **Giardina MG**, Matarazzo M, Varriale A, Morante R, Napoli A, Martino R. Serum alpha-L-fucosidase. A useful marker in the diagnosis of hepatocellular carcinoma. *Cancer* 1992; **70**: 1044-1048
- 31 **Takahashi H**, Saibara T, Iwamura S, Tomita A, Maeda T, Onishi S, Yamamoto Y, Enzan H. Serum alpha-L-fucosidase activity and tumor size in hepatocellular carcinoma. *Hepatology* 1994; **19**: 1414-1417
- 32 **Giardina MG**, Matarazzo M, Morante R, Lucariello A, Varriale A, Guardasole V, De Marco G. Serum alpha-L-fucosidase activity and early detection of hepatocellular carcinoma: a prospective study of patients with cirrhosis. *Cancer* 1998; **83**: 2468-2474
- 33 **Ishizuka H**, Nakayama T, Matsuoka S, Gotoh I, Ogawa M, Suzuki K, Tanaka N, Tsubaki K, Ohkubo H, Arakawa Y, Okano T. Prediction of the development of hepato-cellular-carcinoma in patients with liver cirrhosis by the serial determinations of serum alpha-L-fucosidase activity. *Intern Med* 1999; **38**: 927-931
- 34 **Tangkijvanich P**, Tosukhowong P, Bunyongyod P, Lertmaharit S, Hanvivatvong O, Kullavanijaya P, Poovorawan Y. Alpha-L-fucosidase as a serum marker of hepatocellular carcinoma in Thailand. *Southeast Asian J Trop Med Public Health* 1999; **30**: 110-114
- 35 **Naitoh A**, Aoyagi Y, Asakura H. Highly enhanced fucosylation of serum glycoprotein in patients with hepatocellular carcinoma. *J Gastroenterol Hepatol* 1999; **14**: 436-445
- 36 **Mita Y**, Aoyagi Y, Suda T, Asakura H. Plasma fucosyltransferase activity in patients with hepatocellular carcinoma, with special reference to correlation with fucosylated species of alpha-fetoprotein. *J Hepatol* 2000; **32**: 946-954

Cloning and expression of ornithine decarboxylase gene from human colorectal carcinoma

Hai-Yan Hu, Xian-Xi Liu, Chun-Ying Jiang, Yan Zhang, Ji-Feng Bian, Yi Lu, Zhao Geng, Shi-Lian Liu, Chuan-Hua Liu, Xiao-Ming Wang, Wei Wang

Hai-Yan Hu, Xian-Xi Liu, Ji-Feng Bian, Yi Lu, Geng Zhao, Shi-Lian Liu, Chuan-Hua Liu, Xiao-Ming Wang, Yan Zhang, Wei Wang, Experimental Centre of Medical Molecular Biology, School of Medicine, Shandong University, Jinan 250012, Shandong Province, China

Chun-Ying Jiang, Department of colo-proctology, The affiliated Hospital of Shandong University of Tradition Chinese Medicine, Jinan 250012, Shandong Province, China

Supported by Scientific Research Fund of national Ministry of Health, No.98-1-173

Correspondence to: Xian-Xi Liu, Experimental Centre of Medical Molecular Biology, School of Medicine, Shandong University, Jinan 250012, Shandong Province, China. xianxi@sdu.edu.cn

Telephone: +86-531-8382346

Received: 2002-07-04 **Accepted:** 2002-10-31

Abstract

AIM: To construct and express ODC recombinant gene for further exploring its potential use in early diagnosis of colorectal carcinoma.

METHODS: Total RNA was extracted from colon cancer tissues and amplified by reverse-transcription PCR with two primers, which span the whole coding region of ODC. The synthesized ODC cDNA was cloned into vector pQE-30 at restriction sites BamH I and Sal I which constituted recombinant expression plasmid pQE30-ODC. The sequence of inserted fragment was confirmed by DNA sequencing, the fusion protein including 6His-tag was facilitated for purification by Ni-NTA chromatographic column.

RESULTS: ODC expression vector was constructed and confirmed with restriction enzyme digestion and subsequent DNA sequencing. The DNA sequence matching on NCBI Blast showed 99 % affinity. The vector was transformed into *E. coli* M15 and expressed. The expressed ODC protein was verified with Western blotting.

CONCLUSION: The ODC prokaryote expression vector is constructed and thus greatly facilitates to study the role of ODC in colorectal carcinoma.

Hu HY, Liu XX, Jiang CY, Zhang Y, Bian JF, Lu Y, Geng Z, Liu SL, Liu CH, Wang XM, Wang W. Cloning and expression of ornithine decarboxylase gene from human colorectal carcinoma. *World J Gastroenterol* 2003; 9(4): 714-716
<http://www.wjgnet.com/1007-9327/9/714.htm>

INTRODUCTION

Ornithine decarboxylase (ODC) is the first key enzyme of the biosynthesis of polyamine which catalyzes the decarboxylation of the amino acid ornithine to the diamine putrescine. Its activation regulates the metabolism of spermidine, spermine and their precursor putrescine. Activity of polyamine biosynthesis is closely associated with the proceeding of

physiological cell growth, proliferation and regeneration^[1] and pathological proliferation^[2]. It is necessary for cell to progress into S phase, or polyamine depletion arrest cells in G1^[3]. ODC activity and polyamine concentration in colorectal cancers are significantly elevated compared with that in normal adjacent and healthy control tissues on rodents^[4-7] and human beings. ODC repressor (eg. Difluoromethylornithine) has been considered to be one of the molecular targeted interventions of colon cancer^[8]. The changing of ODC activity is an early event during the expression of malignancy. In this study, an ODC expression vector expressing a 6His-tag fusion protein was successfully constructed. The 6His-tag enabled us to purify the fusion protein with high purity.

MATERIALS AND METHODS

Materials

Trizol, RNA extract reagent, were purchased from Life Technologies Inc. RT-PCR kit, T-A clone kit, DNA marker and all restrictive enzymes were purchased from TaKaRa Shuzo Co.Ltd. Primers were synthesized by Sangon. The QIAquick Gel Extraction Kit, and expression system were got from QIAGEN. Protein marker was purchased from Shanghai Lizhudongfeng biotechnologies Co.Ltd. Standard ODC was purchased from Sigma.

Tissues

Colorectal carcinoma and respective adjacent normal colorectal mucus were obtained during surgery. Once the specimens were removed during operation, the necrotic and ulcerated tumors were removed and the normal mucosa was dissociated from the muscle and connective tissue. All specimens were then kept in liquid nitrogen until further use.

Extraction of total RNA

The total cellular RNA was extracted from normal and cancer tissues, respectively. The method of RNA extraction was similar to the Trizol RNA extraction protocol (Life Technologies Inc.). The concentration of RNA extracted was determined at wavelength of 260nm using U-2000 spectrophotometer (HITACH Ltd, Tokyo, Japan).

Reverse transcription polymerase chain reaction (RT-PCR)

The sequence of ODC primers was as follows, up-stream primer: 5' - gca ggatcc acc atg aac aac ttt ggt aa; down-stream primer: 5' -gaa gtcgac cta cac att aat act agc cg. The 5' primer recognized the start codon of ODC in exon 3, and the 3' primer recognized the end-codon in exon 12. Restriction sites were BamH I and Sal I. The first strand of cDNA was synthesized at 55 °C for 30 min in the presence of AMV reverse transcriptase (0.5 unit/μl), RNase inhibitor 1 unit/ml, dNTP 1.0 mM, Mg²⁺ 2.5 mM. The PCR was processed through 35 cycles of denature (1 min at 95 °C), annealing (1.5 min at 58 °C), and extension (1 min at 72 °C) (Perkin-Elmer2400 PCR apparatus).

Purification of PCR product and T-A cloning

The PCR products were separated in 1 % agarose gel, and the

band containing ODC cDNA was cut off and placed into the QIAquick spin column, the ODC cDNA was purified and linked to plasmid pMD-18 with a polyA linker. The recombinant was transformed into *E. coli* DH5 α and selected by selective culture medium containing ampicillin.

Construction of pQE30-ODC

The pMD-ODC and pQE30 were digested by restrictive enzymes BamH I and SalI. The inserted fragment of pMD-ODC was collected from electrophoretic gel, then it was ligated with the linearized pQE30 by T4 Ligase at 18 °C overnight. The recombinant was transformed into *E. coli* DH5 α by CaCl₂ method and selected by agar plate containing ampicillin and confirmed by restriction enzyme mapping. The positive recombinant was transformed into *E. coli* M15. The sequence of inserted fragment was confirmed by DNA sequencing (Shanghai Sangon Bioengineering Co.Ltd.).

The expression of ODC fusion protein

The ampicillin-resistant colony of *E. coli* cells transformed with plasmid were cultured in LB cultural medium containing 100 mg/L ampicillin and 25 mg/L Kanamycin, and induced by 1 mM IPTG. The cultured cells were harvested at 1, 2, 3, 4hr after culture, respectively. The optimum time of maximum expression of proteins was analyzed through SDS-PAGE. The expressed ODC protein was tested through Western blot with specific antiserum.

RESULTS

RT-PCR amplification of ODC encoding sequence

RT-PCR was done with total RNA template extracted from human colon cancer. The designed primers include encoding sequence of ODC. Electrophoresis of RT-PCR products confirmed the length of RT-PCR fragment (1 480 bp) (Figure 1).

The purified ODC cDNA was ligated to pMD-18 by T-A complimentary pairing. ODC cDNA was inserted into pQE30 at BamH I and Sal I sites (Figure 2).

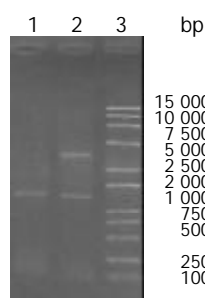


Figure 1 RT-PCR product on 1 % agarose gel. Lane 1: ODC RT-PCR product, 1 480 bp in length; Lane 2: pQE30-ODC plasmid digested by restriction enzyme BamHI and SalI.

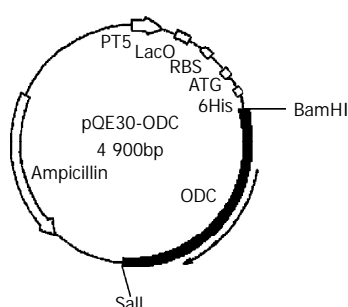


Figure 2 The pQE30-ODC expression vector including early promoter T5, Lac operator and 6His-Tag.

Sequence analysis

Sequence of inserted DNA was analyzed with automatic sequence analyzer and found to be about 1 500 bp in size and showed 99 % affinity in comparison with DNA sequence published on line [gi: 4505488].

SDS-PAGE and western blotting

Inserted ODC gene was expressed significantly in the prokaryotic expression system, and specific strip at 50kDa was demonstrated in Western blot. The optimum induction period is 4hr after administration of IPTG (Figure 3, 4).

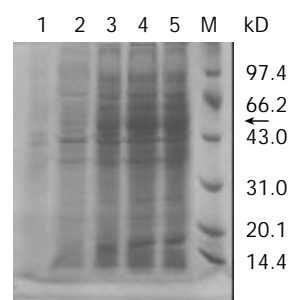


Figure 3 Expressed ODC protein on SDS-PAGE. Lane 1: M15 negative control; Lane 2-5: Expressed ODC proteins in M15 1 to 4 hour(s) after induction of IPTG; M: Protein marker; The arrow showed the expressed ODC protein.

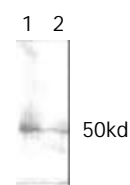


Figure 4 Western blot shows a strip of 50kD indicating the expression of ODC protein.

DISCUSSION

The polyamines are naturally occurring aliphatic polycations found in almost all living cells^[9]. They are positively charged at neutral pH and the charge is distributed along the length of the molecule. This facilitates their interaction with anionic molecules such as DNA and RNA^[9,10]. Polyamines have been shown to be essential for optimal rates of cell growth and differentiation, with high concentrations being found in rapidly growing cells and tissues^[11].

Cancer cells always have a higher intracellular polyamine content than the equivalent normal tissue^[12-15]. In addition to changes in polyamine content, ODC activity has also been found to be increased significantly in colon adenocarcinoma tissue compared to microscopically normal tissue from the same patients^[13,16]. Similar findings were observed in human colonic surgical specimens with both ODC activity and polyamine content of the malignant tissue being increased^[16,17]. Intratumour content of spermidine and spermine was increased in line with the increase in ODC activity.

Ornithine decarboxylase (ODC) is a rate-limiting enzyme in the biosynthesis of polyamines, and is induced in response to many growth stimuli such as hormones, growth factors, and tumor promoters, it has a rapid turnover rate with half-life at 15 minutes^[18]. Numerous studies have demonstrated that regulation of ODC can occur at multiple levels, including the transcription of protooncogene c-myc^[19-22], mRNA translation^[10,23,24], protein turnover^[10,25,26], and post-transcriptional interactions and modifications^[27-30]. Recent studies focus intensely on ODC and

polyamine regulation as therapeutic targets. Inhibitors of ODC were found to suppress tumor formation in experimental models of bladder, breast, colon, and skin carcinogenesis^[31-35].

Colorectal cancer is a major health problem in the western world and is associated with significant morbidity and mortality. First-line therapy is radical surgery with adjuvant chemotherapy commonly being treatment with antimetabolites such as 5-fluorouracil^[30]. Although great clinical efforts have been made for the therapy of colorectal cancer with new technologies, such as CT or MRI colography^[4,14], there is still much to be done on the early diagnosis and treatment. It is suggested that ODC activity and polyamine content may have interest in the diagnosis of malignancy and prognosis^[15]. As the change of ODC activity is an early event in the development of the disease, it may be helpful for early screening and diagnosis of colon cancer.

We designed two primers from human ODC gene including the start codon (ATG) in exon 3 and the termination codon (TAG) so as to amplify the whole encoding sequence about 1 480 bp of ODC. The exons encode a protein is identical to the 461-amino acid sequence derived from human ODC.

The restriction fragment mapping of the recombinant, pQE 30-ODC, indicated that the inserted fragment was about 1.5kb, which was consistent with the encoding sequence of ODC. ODC activity in the lysate of transformed M15 was demonstrated through Western blot. The expressed fusion protein is about 50kDa, which is similar to the known ODC protein. The construction and expression of recombinant ODC provide a tool for ODC related further study.

REFERENCES

- Jeevanandam M**, Petersen SR. Clinical role of polyamine analysis: problem and promise. *Curr Opin Clin Nutr Metab Care* 2001; **4**: 385-390
- Auvinen M**. Cell transformation, invasion, and angiogenesis: a regulatory role for ornithine decarboxylase. *J Natl Cancer Inst* 1997; **85**: 533-537
- Bowlin TL**, McKown BJ, Davis GF, Sunkara PS. Effect of polyamine depletion *in vivo* by DL-alpha-difluoromethylornithine on functionally distinct populations of tumoricidal effector cells in normal and tumor-bearing mice. *Cancer Res* 1986; **46**: 5494-5498
- Umar A**, Viner JL, Hawk ET. The future of colon cancer prevention. *Ann N Y Acad Sci* 2001; **952**: 88-108
- Rozhin J**, Wilson PS, Bull AW, Nigro ND. Ornithine decarboxylase activity in the rat and human colon. *Cancer Res* 1984; **44**: 3226-3230
- Hixson LJ**, Garewal HS, McGee DL, Sloan D, Fennerty MB, Sampliner RE, Gerner EW. Ornithine decarboxylase and polyamines in colorectal neoplasia and mucosa. *Cancer Epidemiol Biomarkers Prev* 1993; **2**: 369-374
- Giardiello FM**, Hamilton SR, Hylind LM, Yang VW, Tamez P, Casero RA Jr. Ornithine decarboxylase and polyamines in familial adenomatous polyposis. *Cancer Res* 1997; **57**: 199-201
- Pegg AE**, Shantz LM, Coleman CS. Ornithine decarboxylase as a target for chemoprevention. *J Cell Biochem (Suppl.)* 1995; **22**: 132-138
- Thomas T**, Thomas TJ. Polyamines in cell growth and cell death: molecular mechanisms and therapeutic applications. *Cell Mol Life Sci* 2001; **58**: 244-258
- Wallon UM**, Persson L, Heby O. Regulation of ornithine decarboxylase during cell growth. Changes in the stability and translatability of the mRNA, and in the turnover of the protein. *Mol Cell Biochem* 1995; **146**: 39-44
- Seiler N**, Atanassov CL, Raul F. Polyamine metabolism as target for cancer chemoprevention (review). *Raul F Int J Oncol* 1998; **13**: 993-1006
- Kingsnorth AN**, Wallace HM. Elevation of monoacetylated polyamines in human breast cancers. *Eur J Cancer Clin Oncol* 1985; **21**: 1057-1062
- Wallace HM**, Caslake R. Polyamines and colon cancer. *Eur J Gastroenterol Hepatol* 2001; **13**: 1033-1039
- Faaland CA**, Thomas TJ, Balabhadrapathruni S, Langer T, Mian S, Shirahata A, Gallo MA, Thomas T. Molecular correlates of the action of bis(ethyl)polyamines in breast cancer cell growth inhibition and apoptosis. *Biochem Cell Biol* 2000; **78**: 415-426
- Canizares F**, Salinas J, de las Heras M, Diaz J, Tovar I, Martinez P, Penafiel R. Prognostic value of ornithine decarboxylase and polyamines in human breast cancer: correlation with clinicopathologic parameters. *Clin Cancer Res* 1999; **5**: 2035-2041
- Linsalata M**, Caruso MG, Leo S, Guerra V, D' Attoma B, Di Leo A. Prognostic value of tissue polyamine levels in human colorectal carcinoma. *Anticancer Res* 2002; **22**: 2465-2469
- Takami H**, Koudaira H, Kodaira S. Relationship of ornithine decarboxylase activity and human colon tumorigenesis. *Jpn J Clin Oncol* 1994; **24**: 141-143
- Pegg AE**. Recent advances in the biochemistry of polyamines in eukaryotes. *Biochem J* 1986; **234**: 249-262
- Evan GI**, Wyllie AH, Gilbert CS, Littlewood TD, Land H, Brooks M, Waters CM, Penn LZ, Hancock DC. Induction of apoptosis in fibroblasts by c-myc protein. *Cell* 1992; **69**: 119-128
- Bello-Fernandez C**, Packham G, Cleveland JL. The ornithine decarboxylase gene is a transcriptional target of c-Myc. *Proc Natl Acad Sci U S A* 1993; **90**: 7804-7808
- Packham G**, Cleveland JL. Ornithine decarboxylase is a mediator of c-Myc-induced apoptosis. *Mol Cell Biol* 1994; **14**: 5741-5747
- Iyengar RV**, Pawlik CA, Krull EJ, Phelps DA, Burger RA, Harris LC, Potter PM, Danks MK. Use of a modified ornithine decarboxylase promoter to achieve efficient c-MYC- or N-MYC-regulated protein expression. *Cancer Res* 2001; **61**: 3045-3052
- Kahana C**, Nathans D. Translational regulation of mammalian ornithine decarboxylase by polyamines. *J Biol Chem* 1985; **260**: 15390-15393
- Shantz LM**, Pegg AE. Translational regulation of ornithine decarboxylase and other enzymes of the polyamine pathway. *Int J Biochem Cell Biol* 1999; **31**: 107-122
- Lu L**, Stanley BA, Pegg AE. Identification of residues in ornithine decarboxylase essential for enzymic activity and for rapid protein turnover. *Biochem J* 1991; **277**: 671-675
- Dircks L**, Grens A, Slezynger TC, Scheffler IE. Post-transcriptional regulation of ornithine decarboxylase activity. *J Cell Physiol* 1986; **126**: 371-378
- Heller JS**, Fong WF, Canellakis ES. Induction of a protein inhibitor to ornithine decarboxylase by the end products of its reaction. *Proc Nat Acad Sci USA* 1976; **73**: 1858-1862
- Fogel-Petrovic M**, Vujcic S, Miller J, Porter CW. Differential post-transcriptional control of ornithine decarboxylase and spermidine-spermine N1-acetyltransferase by polyamines. *FEBS Lett* 1996; **391**: 89-94
- Ruhl KK**, Pomidor MM, Rhim JS, Tuan RS, Hickok NJ. Post-transcriptional suppression of human ornithine decarboxylase gene expression by phorbol esters in human keratinocytes. *J Invest Dermatol* 1994; **103**: 687-692
- Flamigni F**, Campana G, Carboni L, Rossoni C, Spampinato S. Post-transcriptional inhibition of ornithine decarboxylase induction by zinc in a difluoromethylornithine resistant cell line. *Biochim Biophys Acta* 1994; **1201**: 101-105
- Thompson HJ**, Ronan AM. Effect of D,L-2-difluoromethylornithine and endocrine manipulation on the induction of mammary carcinogenesis by 1-methyl-1-nitrosourea. *Carcinogenesis* 1986; **7**: 2003-2006
- Nigro ND**, Bull AW, Boyd ME. Inhibition of intestinal carcinogenesis in rats: effect of difluoromethylornithine with piroxicam or fish oil. *J Natl Cancer Inst* 1986; **77**: 1309-1313
- Loprinzi CL**, Messing EM, O' Fallon JR, Poon MA, Love RR, Quella SK, Trump DL, Morton RF, Novotny P. Toxicity evaluation of difluoromethylornithine: doses for chemoprevention trials. *Cancer Epidemiol Biomarkers Prev* 1996; **5**: 371-374
- Carbone PP**, Douglas JA, Larson PO, Verma AK, Blair IA, Pomplun M, Tutsch KD. Phase I chemoprevention study of piroxicam and alpha-difluoromethylornithine. *Cancer Epidemiol Biomarkers Prev* 1998; **7**: 907-912
- Love RR**, Carbone PP, Verma AK, Gilmore D, Carey P, Tutsch KD, Pomplun M, Wilding G. Randomized phase I chemoprevention dose-seeking study of alpha-difluoromethylornithine. *J Natl Cancer Inst* 1993; **85**: 732-737

Pre-operative radiochemotherapy of locally advanced rectal cancer

Xiao-Nan Sun, Qi-Chu Yang, Jian-Bin Hu

Xiao-Nan Sun, Qi-Chu Yang, Jian-Bin Hu, Department of Radiation Oncology, Sir Run Run Shaw Hospital, College of Medicine, Zhejiang University, Hangzhou 310016, Zhejiang Province, China

Correspondence to: Dr. Xiao-Nan Sun, Department of Radiation Oncology, Sir Run Run Shaw Hospital, College of Medicine, Zhejiang University, Hangzhou 310016, Zhejiang Province, China. sunxiaonan@hotmail.com

Telephone: +86-571-86090073 **Fax:** +86-571-86044817

Received: 2002-08-01 **Accepted:** 2002-11-19

Abstract

AIM: To evaluate results of pre-operative radiochemotherapy followed by surgery for 15 patients with locally advanced un-resectable rectal cancer.

METHODS: 15 patients with advanced non-resectable rectal cancer were treated with pre-operative irradiation of 40-46 Gy plus concomitant chemotherapy (5-FU+LV and 5'-DFuR) (RCS group). For comparison, 27 similar patients, treated by preoperative radiotherapy (40-50 Gy) plus surgery were served as control (RS group).

RESULTS: No radiochemotherapy or radiotherapy was interrupted and then was delayed because of toxicities in both groups. The radical resectability rate was 73.3 % in the RCS group and 37.0 % ($P=0.024$) in RS group. Sphincter preservation rates were 26.6 % and 3.7 % respectively ($P=0.028$). Sphincter preservation rates of lower rectal cancer were 27.3 % and 0.0 % respectively ($P=0.014$). Response rates of RCS and RS groups were 46.7 % and 18.5 % ($P=0.053$). The tumor downstage rates were 8 (53.3 %) and 9 (33.3 %) in these groups ($P=0.206$). The 3-year overall survival rates were 66.7 % and 55.6 % ($P=0.485$), and the disease free survival rates were 40.1 % and 33.2 % ($P=0.663$). The 3-year local recurrent rates were 26.7 % and 48.1 % ($P=0.174$). No obvious late effects were found in either groups.

CONCLUSION: High resectability is possible following pre-operative radiochemotherapy and can have more sphincters preserved. It is important to improve the quality of the patients' life even without increasing the survival or local control rates. Preoperative radiotherapy with concomitant full course chemotherapy (5-Fu+LV and 5'-DFuR) is effective and safe.

Sun XN, Yang QC, Hu JB. Pre-operative radiochemotherapy of locally advanced rectal cancer. *World J Gastroenterol* 2003; 9 (4): 717-720

<http://www.wjgnet.com/1007-9327/9/717.htm>

INTRODUCTION

Neoadjuvant treatment is delivered as radiotherapy (RT) or radiochemotherapy (RCT) prior to surgery with the aim to devitalize primary and metastatic tumor cells and to shrink the tumor so that resection is facilitated even in case of primarily

nonresectable cases^[1-6]. The trials of several "neoadjuvant" radiochemotherapy have generated clear evidence downstaging is possible, resectability rates are increased, local relapse rates decreased, and survival rates possibly improved. Preoperative radiochemotherapy has been regarded as 'standard' therapy^[1,7].

The infusional chemotherapy protocol of 5-FU demonstrated a higher response rate and a marginal survival benefit in advanced colorectal cancer^[8]. The toxicity was lower in the infusion protocol than that in bolus protocol^[9]. In chemoradiotherapy with the infusion protocol, this advantage can still work and have a theoretically better chance of drug-radiation interaction as well^[10]. However, i.v. chemotherapy, either by infusion or bolus, is still a major source of discomfort to the patients.

Oral administration enables sustained exposure to 5-FU, avoids the technical barrier of intravenous (IV) administration and allows significant flexibility in choice of the dosage regimens, provided that efficacy is not compromised^[11,12]. Doxifluridine (5'-deoxy-5-fluorouridine, 5'-DFuR) is synthetic 5-deoxy-nucleoside derivative. In experimental murine tumor systems, doxifluridine has achieved a therapeutic index of 10-15 times greater than that of 5-FU or other fluoropyrimidines^[13]. This drug has been shown to be an effective agent when administered orally^[14]. The use of oral doxifluridine and leucovorin in chemoradiotherapy provides several advantages. Administration of the drug during the entire radiotherapy course offers more chances of interaction between the drug and radiation, similar to infusion chemoradiotherapy; i.v. infusion-associated complications can be avoided. The use of oral chemotherapy also provides convenience and a comfortable environment of drug administration to patients.

In our study, 15 patients received mean dose of 41.5 Gy of pelvic irradiation with concurrent chemotherapy of 5-FU+leucovorin (LV) was administered by bolus injection during d1-3 and d26-28 of RT. 5'-DFuR were given during d4-25 of RT (RCS group). 27 similar patients treated by preoperative radiotherapy (mean dose of 42.6 Gy) were served as control (RS group). The points of the study were to evaluate the toxicity, resectability rates and relative response rates of the treatment, 3-year survival rates and 3-year recurrent rates in the two groups.

MATERIALS AND METHODS

Patients

Patients with advanced non-resectable rectal cancer were considered eligible for radiochemotherapy plus surgery study (RCS group) if they fulfilled the following criteria: Below 72 years old, KPS of 60 or over, histologically confirmed adenocarcinoma of the rectum, advanced tethered and fixed primary tumor that were considered unresectable by surgeon. From December 1995 to January 1997, 15 patients were entered in the study. They were 12 men and 3 women and age ranging from 33 to 72 years (mean 50.6). For comparison, 27 similar patients, treated by preoperative radiotherapy (40-50 Gy) plus surgery served as control (RS group). They were 21 men and 6 women and age ranging from 18 to 71 (mean 58).

Table 1 summarized the main demography and baseline characteristics of all eligible patients. The two groups were well matched for all evaluated characteristics. All tumors of

two groups were middle and lower rectal cancers (5-11cm from anus). 11 and 20 lower rectal cancers in RCS group and RS group respectively. Before starting treatment all patients underwent a general examination and got CBC done. These examinations were repeated every week during the treatment period and before operation ultrasound and/or CT or MRI and digital examination were mandatory. Digital examination was done every week.

Table 1 Patient demography and disease characteristics at baseline

Parameter	RCS group	RS group
Male/female	12/3	21/6
Age(years):median(range)	56(33-72)	58(18-71)
Karnofsky performance status	70-90	70-90
Primary site		
Middle	4	7
lower	11	20
Degree of differentiation		
Well	1	2
Moderate	7	15
Poor	3	4
Not specified	4	6
TNM staging		
T3N0M0	5	14
T3N1M0	0	3
T4N0M0	6	3
T4N1M0	4	5
T4N2M0	0	2

Treatment

Radiation was delivered by linear accelerator (10 MV X-ray). Similar fields were used for treatment in both groups. The initial pelvic radiation therapy volume of AP/PA ports and two lateral fields treated to 4 000 cGy. The use of a boost field to the primary tumor bed and immediately adjacent lymph nodes were given in some patients. Total doses of 4 000cGy to 4 600 cGy (mean 4 150 cGy) were delivered in 4 to 5 weeks in RCS group. Total doses of 4 000cGy to 5 000cGy (mean 4 260 cGy) were delivered in 4 to 5 weeks in RS group. In RCS group, chemotherapy was given concomitantly and consisted of two courses of 5-FU at a dose of 500 mg/m²/day plus leucovorin at a dose of 300 mg by intravenous injection for 3 days in week 1 and week 4, 5'-DFuR was administered orally at a dose of 200 mg three times daily concomitantly during radiotherapy between interval of the two courses of intravenous chemotherapy. All patients in two groups underwent subsequent surgery 4 to 5 weeks after the preoperative treatment. 4 to 6 courses adjuvant chemotherapy (5-FU based) were given after surgery in two groups.

Evaluation of patients

Assessments of tumor dimensions and involved sites were performed before the start of treatment and were scheduled after week 4. Tumor dimensions were assessed by use of computed tomography scans, x-rays, magnetic resonance imaging. Tumor response classification was based on standard World Health Organization criteria. Disappearance of all known disease at all involved sites was considered a complete response (CR). Partial response (PR) was defined as residual disease with a decrease=50 % in sum of the products greatest perpendicular diameters (SPD) of all indicator lesions. Progressive disease (PD) was defined as the appearance of a

new lesion or an increase of 25 % in the SPD. Stable disease (SD) was defined as no change in SPD or a change not reaching to PR or PD. Total response rate was defined as CR plus PR. Surgical treatment results were summarized (the radical resectability rate, sphincter preservation rate and complication).

Patients were followed up every 3 months after the end of treatment with progression and survival of the disease recorded. The duration of follow-up ranged from 36-61 months (mean 43). Disease progression and survival time were analyzed according to Kaplan-Meier estimates and compared using the log-rank test. A one-sided chi-square test was used at an alpha level of 2.5 % to compare response data in two patient groups. The data of toxicity were scored retrospectively according to the World Health Organization (WHO) toxicity evaluation.

RESULTS

Tumor response

No radiochemotherapy or radiotherapy was interrupted and was then delayed because of toxicities in both groups. Obvious pain relief has been achieved in all patients of two groups presenting with buttock/sciatic/perineal pain, usually within days of commencing radiochemotherapy/radiotherapy. The median time of obvious pain relief was 7 days (range 5-10) in RCS group, 10 days (range 7-18) in RS group.

11 radical resection, 3 palliative surgery and 1 cytoreductive surgery were undertaken in RCS group. 10 radical resection, 15 palliative surgery and 2 cytoreductive surgery were undertaken in RS group. Table 2 summarizes the radical resectability, sphincter preservation, lower rectal cancer sphincter preservation, response and tumor downstage rates of the two groups. Pathologic complete response (pCR) of the primary tumor was observed in two patients of RCS group.

Table 2 The radical resectability, sphincter preservation, lower rectal cancer sphincter preservation, response and tumor downstage rates in the two groups

Parameter	RCS group	RS group	P
Radical resectability rate	73.3%	37.0%	0.024
Sphincter preservation rate	26.6%	3.7%	0.028
Lower rectal cancer sphincter preservation rate	27.3%	0.0%	0.014
Response rate	46.7%	18.5%	0.053
Tumor downstage rate	53.3%	33.3%	0.206

Follow-up results

In Table 3 the 3-year overall survival rates, the disease free survival rates and the 3-year local recurrent rates are compared in the patients of two groups. Four patients of RCS group had good to excellent sphincter function.

Table 3 The 3-year overall survival, disease free survival and local recurrent rates of the patients of two groups

Parameter	RCS group	RS group	P
3-year overall survival rate	66.7%	55.6%	0.485
3-year disease free survival rate	40.1%	33.2%	0.663
3-year local recurrent rate	26.7%	48.1%	0.174

Toxicity

Patients were scored according to the WHO grading. A detailed description of acute toxicities was given in Table 4. The most relevant toxic reactions included rectal tenesmus, diarrhea and perianal area skin reaction. No toxic death was observed in

this study. No patient interrupted the radiochemotherapy and delayed the operation because of these acute toxicities. Total incidence of grade 3/4 toxicity were 73.3 % in RCS group, 44.4 % in RS group ($P=0.071$) respectively. No severe late toxicity was found in the two groups.

Table 4 WHO modified scale for acute toxicity

Site	Grading (RCS group)					Grading (RS group)				
	0	1	2	3	4	0	1	2	3	4
Hematologic:										
Neutropenia	8	2	4	1	0	19	3	5	0	0
Non-hematologic:										
Small bowel	4	3	7	3	0	6	9	10	2	0
Bladder	6	4	5	0	0	10	11	6	0	0
Skin	0	2	6	7	0	0	10	8	9	0

DISCUSSION

Preoperative radiotherapy (RT) (45 Gy) with continuous infusion of 5-FU for 5 days per week with or without CDDP were used by the M.D. Anderson group^[15] in locally advanced tethered and fixed primary rectal cancer to downstage the tumors. It was concluded that preoperative radiochemotherapy decreased the local recurrence rate as compared to preoperative radiotherapy only, with no increase of surgical morbidity and late morbidity after a follow-up of 3 years. In this study, the acute toxicities of grade 3 in RCS group were more pronounced than that in RS group but without statistical differences and no patient had interrupted the radiochemotherapy and delayed the operation because of these acute toxicities. University of Uppsala study^[16] proved that the volume of bowel under radiation, rather than the energy of the radiation influence postoperative mortality, and emphasize the importance of precise radiotherapy planning to minimize normal tissue toxic reactions.

Continuous infusion of 5-FU led to significantly higher response rates than bolus 5-FU, and a meta-analysis identified a statistically significant increase in overall survival^[17]. However, this improvement was the only report, and other trials had failed to repeat the significant survival benefit. Continuous infusion 5-FU is not routinely practised, partly because of its inconvenience and cost and partly due to central venous access that might cause significant complications in 15 % to 20 % of patients^[18], including infections, bleeding, thrombosis, and pneumothorax. Each of these complications has a negative impact on quality of life. Several of the new chemotherapy drugs used in colorectal cancer also appear to be radiosensitizers. Pilot and phase II trials incorporating irinotecan and oxaliplatin^[19] into 5-FU-plus-radiation program are currently used, with encouraging results. Similarly, the oral 5-FU prodrugs^[20,21] represent promising new agents to combine with radiation. The oral route not only makes these drugs convenient to the patient but also gives prolonged therapeutic serum levels, simulating continuous venous infusion, which may be the preferable fluoropyrimidine schedule for radiosensitization.

5-FU as a radiosensitizer was given by continuous infusion. 5'-DFuR kills cancer cell through PyNPase transformation. The study by Watanabe *et al*^[22] found that fifty three patients with advanced colorectal cancer when given single oral doses of 5'-DFuR, high 5-FU concentration and PyNPase activity were noted in tumor tissue and lymph nodes. Effective 5-FU concentration in tumor tissue was maintained even 24 hours after treatment. Effective lymph node concentration of 5-FU was maintained even 8 hours after treatment. PyNPase activity in tumor tissue was significantly higher than that in the normal

intestinal mucosa ($P<0.05$). In this study, pre-operative radiochemotherapy was well tolerated. The relatively high rate of curative resections indicates that 5-FU and Oral 5'-DFuR treatment as radiosensitizers, maintaining higher concentrations of 5-FU during RT, are safe and effective. The aim of giving two courses of 5-FU intravenous injection was to relieve the local symptoms of the patients with local advanced rectal cancer and to improve systemic treatment efficacy. The appropriate dosage of oral 5'-DFuR as radiosensitizer during RT should be further studied.

Sphincter preservation rate and sphincter preservation rate of lower rectal cancer in RCS group were significantly higher than that of RS group. Therefore, this study at least demonstrates that sphincter preservation operation did not decrease local control and survival rates, although when local control and survival rates were analyzed, the RCS group had no significant advantage compared with RS group. But it is very important to meet the request of sphincter preservation by the rectal cancer patients and to improve their quality of life.

Local failure rates are high for locally irresectable primary or recurrent colorectal cancer, even when chemoradiation therapy is employed. A tumor-free surgical resection margins are paramount to achieve cure^[23-25]. In this study, the radical resectability rate in the RCS group was significantly higher than that in RS group, but without significant decrease local relapse rate, and no significant improvement of survival rate. Therefore, further study of this modality of treatment should be continued^[26-32].

REFERENCES

- 1 **Landry JC**, Koretz MJ, Wood WC, Bahri S, Smith RG, Costa M, Daneker GW, York MR, Sarma PR, Lynn M. Preoperative irradiation and fluorouracil chemotherapy for locally advanced rectosigmoid carcinoma: Phase I-II study. *Radiology* 1993; **188**: 423-426
- 2 **Chan A**, Wong A, Langevin J, Khoo R. Preoperative concurrent 5-fluorouracil infusion, mitomycin-c and pelvic radiation therapy in tethered and fixed rectal carcinoma. *Int J Radiat Oncol Biol Phys* 1993; **25**: 791-799
- 3 **Rich TA**, Skibber JM, Ajani JA, Buchholz DJ, Gleary KR, Dubrow RA, Levin B, Lynch PM, Meterissian SH, Roubein LD. Preoperative infusional chemoradiation therapy for stage T₃ rectal cancer. *Int J Radiat Oncol Biol Phys* 1995; **32**: 1025-1029
- 4 **Chen ET**, Mohiuddin M, Brodovsky H, Fishbein G, Marks G. Downstaging of advanced rectal cancer following combined preoperative chemotherapy and high dose radiation. *Int J Radiat Oncol Biol Phys* 1994; **30**: 169-175
- 5 **Minsky B**, Cohen A, Enker W, Kelsen D, Kemeng N, Ilson D, Guillem J, Saltz L, Frankel, Conti J. Preoperative 5-FU, low dose leucovorin and concurrent radiation therapy for rectal cancer. *Cancer* 1994; **73**: 273-280
- 6 **Yuan HY**, Li Y, Yang GL, Bei DJ, Wang K. Study on the causes of local recurrence of rectal cancer after curative resection: analysis of 213 cases. *World J Gastroenterol* 1998; **4**: 527-529
- 7 **Gunderson LL**. Indications for and results of combined modality treatment of colorectal cancer. *Acta Oncol* 1999; **38**: 7-21
- 8 **Rougier P**, Paillet B, La Planche A, Morvan F, Seits JF, Rekaewicz C, Laplaige P, Jacob J, Grandjouan S, Tigaud JW, Fabri MC, Luboinski M, Ducreux M. 5-Fluorouracil (5-FU) continuous intravenous infusion compared with bolus administration. Final results of a randomized trial in metastatic colorectal cancer. *Eur J Cancer* 1997; **33**: 1789-1793
- 9 **Rodel C**. Efficacy and toxicity spectrum of continuous infusion of 5-fluorouracil compared with bolus administration in advanced colorectal tumors. *Strahlenther Onkol* 1999; **175**: 294-295
- 10 **Byfield JE**, Frankel SS, Hombeck CL, Sharp TR, Callipari FB. Phase I and pharmacologic study of 72-hour infused 5-fluorouracil and hyperfractionated cyclical radiation. *Int J Radiat Oncol Biol Phys* 1985; **11**: 791-800
- 11 **Payne SA**. A study of quality of life in cancer patients receiving palliative chemotherapy. *Soc Sci Med* 1992; **35**: 1505-1509
- 12 **Liu G**, Franssen E, Fitch MI, Warner E. Patient preferences for

- oral versus intravenous palliative chemotherapy. *J Clin Oncol* 1997; **15**: 110-115
- 13 **Bollag W**, Hartmann HR. Tumor inhibitory effects of a new fluorouracil derivative: 5'-Deoxy-5-fluorouracil. *Eur J Cancer* 1980; **16**: 427-432
- 14 **Heintz RC**, Guentert TW, Ssutter C. Pharmacokinetic profile of doxifluridine (5' dFUR, furtulon), 5-fluorouracil (5-FU) prodrug. *Proc Am Assoc Cancer Res* 1986; **27**: 207
- 15 **Weinstein GD**, Rich TA, Shumate CR, Skibber JM, Cleary KR, Ajani JA, Ota DM. Preoperative infusional chemoradiation and surgery with or without an electron beam introoperative boost for advanced primary rectal cancer. *Int J Radiat Oncol Biol Phys* 1995; **32**: 197-204
- 16 **Frykholm GJ**, Isacson U, Nygard K, Montelius A, Jung B, Pahlman L, Glimelius B. Preoperative radiotherapy in rectal carcinoma: aspects of acute adverse effects and radiation technique. *Int J Radiat Oncol Biol Phys* 1996; **35**: 1039-1048
- 17 **Tsuji A**, Morita S, Horimi T, Takasaki M, Takahashi I, Shirasaka T. Combination chemotherapy of continuous 5-FU infusion and low-dose cisplatin infusion for the treatment of advanced and recurrent gastric and colorectal adenocarcinomas. *Gan To Kagaku Ryoho* 2000; **27**(Suppl 2): 528-534
- 18 **Grem JL**. Systemic treatment options in advanced colorectal cancer: Perspectives on combination 5-fluorouracil plus leucovorin. *Semin Oncol* 1997; **24**(Suppl 18): S8-S18
- 19 **Uzudun AE**, Battle JF, Velasco JC, Sanchez Santos ME, Carpeno Jde C, Grande AG, Juberias AM, Pineiro EH, Olivar LM, Garcia AG. Efficacy of preoperative radiation therapy for resectable rectal adenocarcinoma when combined with oral tegafur-uracil modulated with leucovorin: results from a phase II study. *Dis colon rectum* 2002; **45**: 1349-1358
- 20 **Janjan NA**, Crane C, Feig BW, Cleary K, Dubrow R, Curley S, Vauthey JN, Lynch P, Ellis LM, Wolff R, Lenzi R, Abbruzzese J, Pazdur R, Hoff PM, Allen P, Brown T, Skibber J. Improved overall survival among responders to preoperative chemoradiation for locally advanced rectal cancer. *Am J Clin Oncol* 2001; **24**: 107-112
- 21 **Van Cutsem E**, Peeters M, Verslype C, Filez L, Haustermans K, Janssens J. The medical treatment of colorectal cancer: actual status and new developments. *Hepatogastroenterology* 1999; **46**: 709-716
- 22 **Mori K**, Hasegawa M, Nishida M, Toma H, Fukuda M, Kobota T, Nagasue N, Yamana H, Hirakawa-YS Chung K, Ikeda T, Takasaki K, Oka M, Kameyama M, Toi M, Fujii H, Kitamura M, Murai M, Sasaki H, Ozono S, Makuuchi H, Shimada Y, Onishi Y, Aoyagi S, Mizutani K, Ogawa M, Nakao A, Kinoshita H, Tono T, Imamoto H, Nakashima Y, Manabe T. Expression levels of thymidine phosphorylase and dihydropyrimidine dehydrogenase in various human tumor tissues. *Int J Oncol* 2000; **17**: 33-38
- 23 **Farouk R**, Nelson H, Gunderson LL. Aggressive multimodality treatment for locally advanced irresectable rectal cancer. *Br J Surg* 1997; **84**: 741-749
- 24 **Farouk R**, Nelson H, Radice E, Mercill S, Gunderson L. Accuracy of computed tomography in determining respectability for locally advanced primary or recurrent colorectal cancers. *Am J Surg* 1998; **175**: 283-287
- 25 **Holm T**, Cedermark B, Rutqvist LE. Local recurrence of rectal adenocarcinoma after "curative" surgery with and without preoperative radiotherapy. *Br J Surg* 1994; **81**: 452-455
- 26 **Makin GB**, Breen DJ, Monson JR. The impact of new technology on surgery for colorectal cancer. *World J Gastroenterol* 2001; **7**: 612-621
- 27 **Shen LZ**, Wu WX, Xu DH, Zheng ZC, Liu XY, Ding Q, Hua YB, Yao K. Specific CEA-producing colorectal carcinoma cell killing with recombination adenoviral vect or containing cytosine deaminase gene. *World J Gastroenterol* 2002; **8**: 270-275
- 28 **Xiong B**, Gong LL, Zhang F, Hu MB, Yuan HY. TGF beta₁ expression and angiogenesis in colorectal cancer tissue. *World J Gastroenterol* 2002; **8**: 496-498
- 29 **Jiang Q**, Ge K, Xu DH, Sun LY, Zheng ZC, Liu XY. Expression of cytosine deaminase gene in human colon carcinoma cells by recombinant retroviral vector. *Shengwu Huaxue Yu Shengwu Wuli Xuebao(Shanghai)* 1997; **29**: 135-141
- 30 **Jiang Q**, Ge K, Xu DH, Sun LY, Zheng ZC, Liu XY. Use of carcinoembryonic antigen gene promoter in colorectal carcinoma-specific suicidal gene therapy. *Shengwu Huaxue Yu Shengwu Wuli Xuebao(Shanghai)* 1998; **30**: 1-8
- 31 **Pederson LC**, Buchsbaum DJ, Vickers SM, Kancharla SR, Mayo MS, Curiel DT, Stackhouse MA. Molecular chemotherapy combined with radiation therapy enhances killing of cholangiocarcinoma cells *in vitro* and *in vivo*. *Cancer Res* 1997; **57**: 4325-4332
- 32 **Chen G**, Li S, Yu B, An P, Cai H, Guo W. X-ray combined with cytosine deaminase suicide gene therapy enhances killing of colorectal carcinoma cells *in vitro*. *Zhonghua Waikexue* 2002; **40**: 136-138

Edited by Xu JY

Racial differences in the anatomical distribution of colorectal cancer: a study of differences between American and Chinese patients

San-Hua Qing, Kai-Yun Rao, Hui-Yong Jiang, Steven D. Wexner

San-Hua Qing, Kai-Yun Rao, Hui-Yong Jiang, Nan Fang Hospital, First Military Medical University, Guangzhou, 510515, Guangdong Province, China

Steven D. Wexner, Department of Colorectal Surgery, Cleveland Clinic Florida, Weston, Florida 33308, USA

Correspondence to: Dr. San-Hua Qing, Nan Fang Hospital, First Military Medical University, Guangzhou, 510515, Guangdong Province, China. sanhuaq@yahoo.com

Telephone: +86-20-61641696 **Fax:** +86-20-87280340

Received: 2002-07-08 **Accepted:** 2002-08-02

Abstract

AIM: To compare the racial differences of anatomical distribution of colorectal cancer (CRC) and determine the association of age, gender and time with anatomical distribution between patients from America (white) and China (oriental).

METHODS: Data was collected from 690 consecutive patients in Cleveland Clinic Florida, U.S.A. and 870 consecutive patients in Nan Fang Hospital affiliated to the First Military Medical University, China over the past 11 years from 1990 to 2000. All patients had colorectal adenocarcinoma diagnosed by histology and underwent surgery.

RESULTS: The anatomical subsite distribution of tumor, age and gender were significantly different between white and oriental patients. Lesions in the proximal colon ($P < 0.001$) were found in 36.3 % of white vs 26.0 % of oriental patients and cancers located in the distal colon and rectum in 63.7 % of white and 74 % of oriental patients ($P < 0.001$). There was a trend towards the redistribution from distal colon and rectum to proximal colon in white males over time, especially in older patients (> 80 years). No significant change of anatomical distribution occurred in white women and Oriental patients. The mean age at diagnosis was 69.0 years in white patients and 48.3 years in Oriental patients ($P < 0.001$).

CONCLUSION: This is the first study comparing the anatomical distribution of colorectal cancers in whites and Chinese patients. White Americans have a higher risk of proximal CRC and this risk increased with time. The proportion of white males with CRC also increased with time. Chinese patients were more likely to have distal CRC and developed the disease at a significantly earlier age than white patients. These findings have enhanced our understanding of the disease process of colorectal cancer in these two races.

Qing SH, Rao KY, Jiang HY, Wexner SD. Racial differences in the anatomical distribution of colorectal cancer: a study of differences between American and Chinese patients. *World J Gastroenterol* 2003; 9(4): 721-725
<http://www.wjgnet.com/1007-9327/9/721.htm>

INTRODUCTION

Colorectal cancer (CRC) is one of the most common cancers in the world and the second leading cause of cancer death in the United States^[1, 2]. It is estimated that 552 000 Americans died of cancer in the year 2000; about 55 000 of these cancer deaths were attributed to CRC. In recent years, the incidence of CRC has increased rapidly in China making it the fourth leading cause of cancer mortality in China^[3]. In general, majority of these cancers are distally located. During the last two decades many investigators have noted that the incidence rate of CRC vary widely by race and gender and the location also has changed with time^[4-15], with a trend towards redistribution of primary CRC from left to right^[16, 17]. Proximal cancers have a tendency to present at a more advanced stage and are associated with a poor prognosis. Increasing age, female gender, black, non-Hispanic race and the presence of comorbid illnesses were factors associated with a greater likelihood of developing colorectal cancer in a proximal location. Black patients with colon cancer are more likely to have a poorer survival than white patients^[13, 18-21]. However, it is not clear whether there are any differences in anatomical distribution of primary colorectal cancer between American (white) and Chinese (oriental) patients.

We hypothesized that there are significant differences of anatomical distribution of primary colorectal cancers between the white (American) and oriental (Chinese) patients. The purpose of this study is to compare the differences in anatomical distribution of colorectal cancers and to describe any association of age, gender and time with primary CRC in white and oriental patients.

MATERIALS AND METHODS

A retrospective study was undertaken. Data was collected from 690 consecutive white patients in Cleveland Clinic Florida U.S.A. and 870 consecutive Chinese patients in Nan Fang Hospital affiliated to the First Military Medical University in southern China over the past 11 years from 1990 to 2000. All the patients with CRC were diagnosed by histology and underwent surgery. Anatomical location of primary colorectal adenocarcinoma, race, age at diagnosis, gender and year of diagnosis were noted. Descriptive data on the type of treatment, patterns of recurrence and metastasis, survival, and the coexistence of disease were not the focus of our analysis. The Z-test and Fisher's Exact Test were performed to detect statistically significant differences in anatomical site distribution, age and gender over time between the white and oriental groups. In this study "proximal colon" includes the cecum, ascending colon, hepatic flexure, transverse colon and splenic flexure; "distal colon" includes the descending colon, sigmoid colon and rectum^[22]

RESULTS

664 Consecutive white patients in Cleveland Clinic Florida and 816 consecutive oriental patients in Nan Fang Hospital in China had documented histological diagnosis of colorectal

adenocarcinomas (Table 1). Patients with a diagnosis of adenocarcinoma only were included in this study.

Table 1 Histological diagnosis of patients with colorectal cancer

	No of patients (%)	
	White	Oriental
Adenocarcinoma	664 (96.2)	816 (93.8)
Nonadenocarcinoma	26 (3.8)	54 (6.2)
Total	690 (100.0)	870 (100.0)

Anatomical subsite distribution

Data on the anatomical distribution, race and gender in the two groups are shown in Table 2. The anatomical distribution of the lesions was markedly different between the two races. Comparison showed that 36.3 % of whites vs 26.0 % of oriental patients ($P<0.001$) had lesions in the proximal colon and 63.7 % of whites vs 74 % of orientals ($P<0.001$) had cancers located in the distal colon. The proportions of cancers located in the cecum, ascending and descending colon in white patients were higher than those in the orientals ($P<0.01$). Rectal and hepatic flexure tumors were less frequent in whites than in the orientals ($P<0.001$). There was no significant difference between cancers located in the transverse colon, splenic flexure and sigmoid colon.

Gender

Analysis by gender conforms to the overall racial differences. The proportions of cecal tumors was higher in the white men ($P<0.001$) and women ($P<0.001$) compared with their Oriental

counterparts. Ascending and descending colon cancers were also significantly more common in white men ($P<0.05$) but not in women ($P>0.05$). Rectal cancers were significantly more common in oriental men ($P<0.001$) and women ($P<0.001$). Oriental patients also had significantly more hepatic flexure cancers among men ($P<0.001$) and women ($P<0.001$). There was no significant difference in the rates of transverse colon, splenic flexure or sigmoid colon cancers.

There was a significant gender difference between the races (Table 3). The male: female ratio was slightly higher in whites (1.49:1) as compared with oriental patients (1.22:1). The gender ratio (m:f) in whites was 1.43:1 for proximal tumors and 1.52:1 for distal tumors; in oriental patients the ratio was 1.06:1 for proximal tumors and 1.29:1 for distal tumors.

Age

The mean age at diagnosis was 69.8 years (range 20-91) in white patients vs 48.3 years (range 13-84) years in oriental patients; oriental patients were therefore younger by twenty-one years ($P<0.001$). Incidence of CRC generally increased with age; it peaked between 70-79 years in white patients, whereas the highest incidence in oriental patients was observed between 50-59 years ($P<0.001$) (Figure 1).

We have further analyzed the age related distribution of proximal and distal tumors in the two racial groups (Figure 2). In white patients, the incidence of proximal tumors had an early peak by the age of 29 years; the incidence then declined significantly so that the lowest rates of proximal lesions were found in the 30-59 years; the incidence of proximal tumors then gradually rose to a peak at 70-79 years. There was a significant difference in the proportions of proximal tumors

Table 2 Anatomic subsite distribution of colorectal cancer by race

	Men				Women				Total			
	White		Oriental		White		Oriental		White		Oriental	
	n	%	n	%	n	%	n	%	n	%	n	%
Cecum	57	8.6	14	1.7 ^c	50	7.5	16	2.0 ^c	107	16.1	30	3.7 ^c
Ascending	45	6.8	31	3.8 ^a	32	4.8	29	3.6	77	11.6	60	7.4 ^b
Hepatic flexure	5	0.8	27	3.3 ^c	2	0.3	26	3.2 ^c	7	1.1	53	6.5 ^c
Transverse	27	4.1	20	2.5	13	1.9	25	3.0	40	6.0	45	5.5
Splenic flexure	8	1.2	17	2.1	2	0.3	7	0.8	10	1.5	24	2.9
Descending	20	3.0	9	1.1 ^a	11	1.7	7	0.9	31	4.7	16	2.0 ^b
Sigmoid	63	9.5	82	10.0	54	8.1	64	7.9	117	17.6	146	17.9
Rectum	172	25.9	249	30.5 ^c	103	15.5	193	23.7 ^c	275	41.4	442	54.2 ^c
Proximal	142	21.4	109	13.6 ^c	99	14.9	103	12.6 ^a	241	36.3	212	26.0 ^c
Distal	255	38.4	340	41.7 ^c	168	25.3	264	32.3 ^a	423	63.7	604	74.0 ^c
Total	397	59.8	449	55.0	267	44.2	367	45.0	664	100.0	816	100.0

^a $P<0.05$, ^b $P<0.01$, ^c $P<0.001$.

Table 3 Anatomic subsite distribution of colorectal cancer by race and time

Time		Proximal			Distal			Total		
		Man	Woman	Ratio	Man	Woman	Ratio	Man	Woman	Ratio
1990-1995	White	51	43	1.19	106	72	1.47	157	115	1.37
	Yellow	55	49	1.12	163 ^b	128 ^a	1.27	218 ^b	177	1.23
1996-2000	White	91	56	1.63	149	96	1.55	240	152	1.58
	Yellow	54 ^c	54 ^a	1.00	177	136	1.30	231 ^b	190	1.22
Total	White	142	99	1.43	255	168	1.52	397	267	1.49
	Yellow	109 ^c	103 ^a	1.06	340 ^c	264 ^a	1.29	449	367	1.22

^a $P<0.05$, ^b $P<0.01$, ^c $P<0.001$.

between various age groups: 0-29 years vs 30-59 years as well as 30-59 years vs. 60 years and older ($P < 0.001$). In oriental patients, the curve for incidence of proximal lesions was relatively flat. Young patients between 0-29 years had the lowest rate which was significantly lower than patients above 30 years ($P < 0.001$). The curves for proximal cancers in White and Oriental patients diverge at the extremes of age and there were significant differences between the two races at 0-29 years as well as above 70 years ($P < 0.01$). In White patients, there was a marked increase in the rates of proximal tumors whereas the frequency of distal tumors decreased with age. This trend was not observed in Oriental patients (Figure 2).

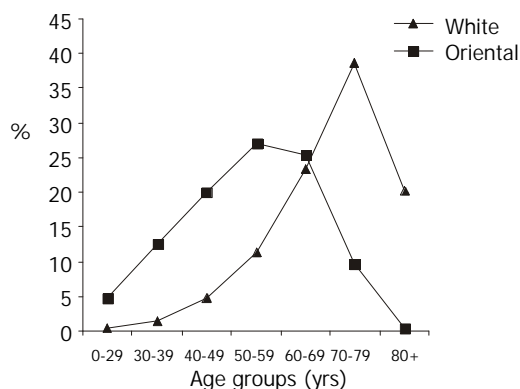


Figure 1 Age related incidence of colorectal cancers in two races.

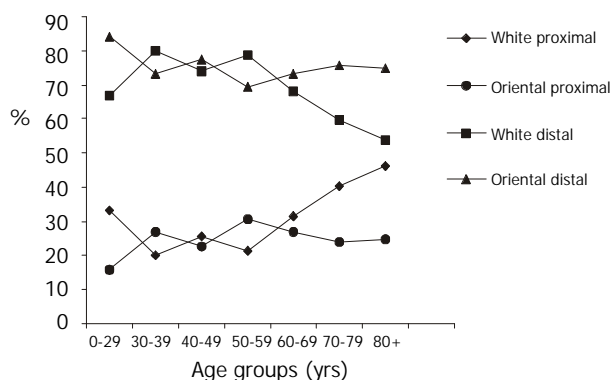


Figure 2 Age-related distribution of cancers.

Time

Generally, there was an increase in the proportion of white men with colorectal cancer from 1.37:1 during 90-95 to 1.58:1 during 96-2000 ($P < 0.05$) (Table 3). This increase was especially seen in proximal cancers of whites which increased from 1.19:1 in 90-95 to 1.63:1 in 96-2000 ($P < 0.01$); the gender ratio among whites for distal cancers changed from 1.47:1 in 90-95 to 1.55:1 in 96-2000 ($P > 0.05$). There was no significant change in the gender distribution of oriental patients ($P > 0.05$) between these two time periods.

Table 3 shows that in whites the proportion of proximal cancers increased from 34.6 % in 1990-1995 to 37.5 % between 1996-2000 and distal cancers decreased from 65.4 % to 62.5 % of all cancers between the same periods of time. There was a trend towards a redistribution of primary colorectal cancers from distal to proximal colon, but the difference was not significant. When we further compared the relationship between anatomical distribution and gender, a marked trend was found towards the redistribution of primary colorectal cancers from distal colorectum to proximal colon in white men with time, especially in the 80-99 years group, but this change was not significant ($P > 0.05$) (Figure 3). No significant change of anatomical distribution of tumor occurred in Oriental patients

over time ($P > 0.05$); in whom the proportion of cancers on the proximal side remained significantly higher. In addition, the proportion of proximal tumors remained significantly lower in white than in oriental patients.

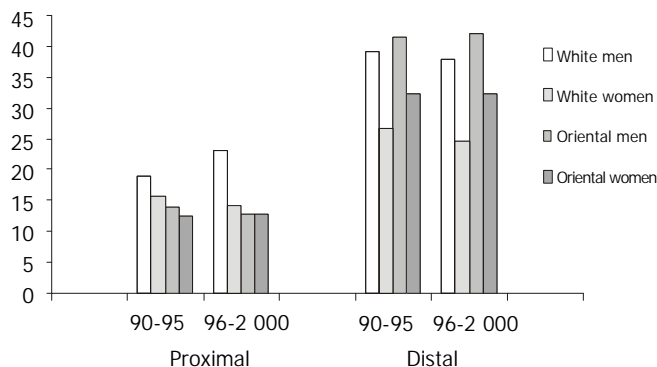


Figure 3 Gender and time based distribution of colorectal adenocarcinomas. The Y-axis shows percentage of tumors.

DISCUSSION

An important aspect of colorectal cancer is its anatomical site of origin, the majority of these cancers being diagnosed in the distal colon and rectum. Epidemiological characteristics of colorectal cancer differ by anatomical subsite, which suggests that other underlying subsite-specific differences may be present. There is evidence of a steady migration of colorectal cancer from distal to more proximal sites^[17], although a decrease in proximal cancers was reported^[22]. This is the first study comparing the anatomical distribution of colorectal cancers in these two large racial groups - American and Chinese. The study demonstrates that the most frequent anatomical subsite of origin of primary colorectal adenocarcinomas is the same - the rectum and sigmoid colon, in American and Chinese patients. The proportion of cancers located in the cecum and ascending colon in whites are significantly higher than those in the oriental patients; the latter did have significantly more tumors in the rectum. The proportion of cancers located in the transverse and sigmoid colon was similar in the two groups. Overall, the frequency of lesions in the proximal colon of white patients (36.3 %) was markedly higher than that of oriental patients (26.0 %). Likewise, the proportion of tumors located in the distal colon of oriental patients (74 %) was significantly higher than that of whites (63.7 %). CRC is considered a disease of western developed countries, which has an approximately 10 times greater incidence than developing countries of Africa^[23]. In general, the developed countries have a predominance of left-sided cancers, whereas low-risk communities have a higher proportion of right-sided cancers^[24]. Compared with America, China is a low risk community. The reasons for the significantly higher incidence of right-sided CRC in white patients are still not clear.

Many hypotheses have been developed based on histological differences between the left and right colon, differences in their functions, sex hormones, diet, and genetics. Proximal and distal sections of the colon also have different embryologic origins and morphology. The proximal colon is primarily involved with water absorption and solidification of fecal contents for storage. It is likely that there are differences in sensitivity and exposure to carcinogens for the proximal and distal sections of colon. There might even be differences in the etiologic agent between right-sided and left sided colorectal cancers; a study showed that different carcinogens produced cancers in different parts of the large bowel in experimental animals^[20].

No specific carcinogen has been found to cause CRC in humans, but the differences in the epidemiological patterns of CRC among various populations suggest the role of an environmental or dietary etiologic agent^[25]. The higher consumption of refined carbohydrates and fat and less dietary fiber may contribute to the increased incidence of colorectal cancers in the western countries^[16, 26]. Increased dietary fat resulted in increased bile acids in the intestine, a possible mechanism for carcinogenesis^[27]. High concentrations of fecal bile acids have been observed in people who eat a high fat diet. Bile acids in turn caused colonic bacteria to produce increased amounts of secondary bile acids and other metabolic by products, compounds that may be associated with the high risk of large bowel cancer^[19, 28-30].

Dietary fiber may play an important protective role against colorectal cancer by diluting the fecal concentration of mutagens and bile acids, and by altering the colonic luminal environment^[31]. Even the type of dietary fiber may be important in reducing the fecal mutagenic activity^[31]. It is said that, it is imperative to point out that the evidence linking fiber and colorectal cancer is not conclusive. Dietary fiber probably protects against carcinogenesis, if it is present in the diet from an early age^[32].

Another possible factor increasing the risk of rectal cancer is consumption of large amounts of alcoholic beverages, particularly beer. For example, alcohol has been shown to increase the relative risk for colon cancer by 1.71 when prospective study is made in black and white patients. In contrast, increased amount of vitamin C intake may be protective against rectal cancer^[22, 24, 33-34].

We have observed a trend toward a redistribution of CRC from distal to proximal in white men, especially in the older men, a finding that is similar to others in the literature which showed a trend towards the redistribution of primary CRC from left to right with increasing time^[35]. We found no significant change in the anatomical distribution of colorectal cancer in white women and oriental patients, the distribution remaining fairly stable in these two groups.

In recent years, the male: female ratio for CRC rose in many published reports^[4, 36]. This study showed that overall rates of colorectal cancers were higher among men than women in both races, but the proportion of white men was greater than that of oriental men, especially for proximal cancers. Between the periods 1990-95 and 1996-2000, we found the male-female ratio in whites rose from 1.19:1 to 1.68:1 for proximal colon cancers and 1.47:1 to 1.55:1 for distal colon cancers; over the same periods, in Oriental patients, the male-female ratio declined from 1.12:1 to 1:1 for proximal and rose from 1.27:1 to 1.30:1 for distal cancers (Table 3). There was no significant change in the oriental race, a finding in agreement with others^[9].

This gender-based disparity is largely unexplained. Recently it has been suggested that hormone replacement therapy may decrease the incidence of colorectal cancer in females. Female sex hormones are known to affect cholesterol metabolism which in turn affects bile acid production, a pathway linked to the development of colorectal cancer. Differences in bile acid metabolism between the proximal and distal colon may contribute to the gender-based disparity in colorectal cancer risk^[24].

Age at diagnosis was significantly different between the races. The mean age was 69.8 years in whites and 48.3 years in oriental patients; oriental patients being diagnosed about twenty-one years earlier. The whites presented most commonly between 70-79 years, but the oriental patients had the highest rate of presentation between 50-59 years. The greater proportion of proximal tumors with increasing age in older white patients has also been noted by others^[15, 37-40]. This trend was not observed in oriental patients. There was a higher

incidence of CRC in younger oriental patients of both sexes, the reasons for which are unknown.

The explanation for differences among racial or ethnic groups may lie in host, environmental, or behavioral factors that act alone or in combination. Heredity plays only a small role. As for colorectal adenocarcinoma, patients in China share the epidemiological characteristics of developing countries. It seems that behavioral factors, such as the dietary habits of Americans and Chinese are more likely to contribute to the difference.

We found that white Americans have a higher risk of proximal CRC and this risk increased with time. The proportion of white males with CRC also increased with time. Chinese patients were more likely to have distal CRC and developed the disease at a significantly earlier age than white patients. As colorectal cancer is one of the most common cancers in the world, it is important to conduct further study to explain subsite differences between the races and sexes. Evaluation of such differences will improve our understanding of colorectal carcinogenesis and may help formulate preventive strategies and perhaps guide research on therapy.

REFERENCES

- Ries LA**, Wingo PA, Miller DS, Howe HL, Weir HK, Rosenberg HM, Vernon SW, Cronin K, Edwards BK. The annual report to the nation on the status of cancer, 1973-1997, with a special section on colorectal cancer. *Cancer* 2000; **88**: 2398-2424
- Greenlee RT**, Murray T, Bolden S, Wingo PA. Cancer statistics, 2000. *CA Cancer J Clin* 2000; **50**: 7-33
- Shu Z**. Colorectal Cancer. *Gastrointestinal Surgery*. Ed Jiefu Wang, Beijing, Peoples Medical Publishing House, 2000: 920-923
- Coates RJ**, Greenberg RS, Liu MT, Correa P, Harlan LC, Reynolds P, Fenoglio-Preiser CM, Haynes MA, Hankey BF, Hunter CP. Anatomic site distribution of colon cancer by race and other colon cancer risk factors. *Dis Colon Rectum* 1995; **38**: 42-50
- Thomas CR Jr**, Jarosz R, Evans N. Racial differences in the anatomical distribution of colon cancer. *Arch Surg* 1992; **127**: 1241-1245
- Chattar-Cora D**, Onime GD, Coppa GF, Valentine IS, Rivera L. Anatomic, age, and sex distribution of colorectal cancer in a new york city hispanic population. *J Natl Med Assoc* 1998; **90**: 19-24
- Devesa SS**, Chow WH. Variation in colorectal cancer incidence in the United States by subsite of origin. *Cancer* 1993; **71**: 3819-3826
- Griffin PM**, Liff JM, Greenberg RS, Clark WS. Adenocarcinomas of the colon and rectum in persons under 40 years old. A population-based study. *Gastroenterology* 1991; **100**: 1033-1040
- Ji BT**, Devesa SS, Chow WH, Jin F, Gao YT. Colorectal cancer incidence trends by subsite in urban Shanghai, 1972- 1994. *Cancer Epidemiol Biomarkers Prev* 1998; **7**: 661-666
- Yoichi I**, Nobuhiro K, Masaki M, Minagawa S, Toyomasu T, Ezaki T, Tateishi H, Sugimachi K. Tumor stage in the proximal colon under conditions of a proximal shift of colorectal cancer with age. *Hepato-Gastroenterology* 1998; **45**: 1535-1538
- Chattar-Cora D**, Onime GD, Valentine IS, Rivera-Cora L. The anatomic distribution of colorectal cancer in a new york city puerto rican group. *Bol Asoc Med PR* 1998; **90**: 126-129
- Loffeld R**, Putten A, Balk A. Changes in the localization of colorectal cancer: implications for clinical practice. *J Gastroenterol Hepatol* 1996; **11**: 47-50
- Mayberry RM**, Coates RJ, Hill HA, Click LA, Chen VW, Austin DF, Redmond CK, Fenoglio-Preiser CM, Hunter CP, Haynes MA. Determinants of black/white differences in colon cancer survival. *J Natl Cancer Inst* 1995; **87**: 1686-1693
- Nelson RL**, Dollear T, Freels S, Persky V. The relation of age, race, and gender to the subsite location of colorectal carcinoma. *Cancer* 1997; **80**: 193-197
- Sharma VK**, Vasudeva R, Howden CW. Changes in colorectal cancer over a 15-year period in a single united states city. *Am J Gastroenterol* 2000; **95**: 3615-3619
- Wan J**, Zhang ZQ, Zhu C, Wang MW, Zhao DH, Fu YH, Zhang

- JP, Wang YH, Wu BY. Colonoscopic screening and follow-up for colorectal cancer in the elderly. *World J Gastroenterol* 2002; **8**: 267-269
- 17 **Gonzalez EC**, Roetzheim RG, Ferrante JM, Campbell R. Predictors of proximal vs distal colorectal cancers. *Dis Colon Rectum* 2001; **44**: 251-258
- 18 **Fireman Z**, Sandler E, Kopelman Y, Segal A, Sternberg A. Ethnic difference in colorectal cancer among arab and jewish neighbor isral. *Am J Gastroenterol* 2001; **96**: 204-207
- 19 **Chattar-Cora D**, Onime GD, Valentine IS, Cudjoe E, Rivera L. Colorectal cancer in a multi-ethnic urban group: its anatomical and age profile. *Int Surg* 2000; **85**: 137-142
- 20 **Nelson RL**, Dollear T, Freels S, Persky V. The relation of age, race, and gender to the subsites location of colonrectal carcinoma. *Cancer* 1997; **80**: 193-197
- 21 **Reddy BS**, Simi B, Engle A. Biochemical epidemiology of colon cancer: effect of types of dietary fiber on colonic diacylglycerols in women. *Gastroenterology* 1994; **106**: 883-889
- 22 **Holt PR**. Dairy foods and prevention of colon cancer: human studies. *J Am Coll Nutr* 1999; **18**(Suppl 5): 379S-391S
- 23 **Kim D**, Wong WD, Bleday R. Rectal Carcinoma: Etiology and evaluation. Beck DE, Wexner SD, eds. In fundamentals of. *Anorectal Surgery* 1998: 278-300
- 24 **Rudy DR**, Zdon MJ. Update on colorectal cancer. *Am Fam Physician* 2000; **61**: 1759-1770
- 25 **Chattar-Cora D**, Onime GD, Valentine IS, Cudjoe E, Rivera L. Colorectal cancer in a multi-ethnic urban group: its anatomical and age profile. *Int Surg* 2000; **85**: 137-142
- 26 **Marchand LL**. Combined influence of genetic and dietary factors on colorectal cancer incidence in Japanese Americans. *J Natl Cancer Inst Monogr* 1999; **26**: 101-105
- 27 **Cooper GS**, Yuan Z, Rimm AA. Radical disparity in the incidence and case-fatality of colorectal cancer: analysis of 329 United States countries. *Cancer Epidemiol Biomarkers Pre* 1997; **6**: 283-285
- 28 **Baquet CR**, Commiskey P. Colorectal cancer epidemiology in minorities: a review. *J Assoc Acad Minor Phys* 1999; **10**: 51-58
- 29 **Flood DM**, Weiss NS, Cook LS, Emerson JC, Schwartz SM, Potter JD. Colorectal cancer incidence in Asian migrants to the United States and their descendants. *Cancer Causes Control* 2000; **11**: 403-411
- 30 **Chattar-Cora D**, Onime GD, Coppa GF, Valentine IS, Rivera L. Anatomic, age, and sex distribution of colorectal cancer in a New York City Hispanic population. *J Natl Med Assoc* 1998; **90**: 19-24
- 31 **Jass JR**, Young J, Leggett BA. Evolution of colorectal cancer: change of pace and change of direction. *J Gastroenterol Hepatol* 2002; **17**: 17-26
- 32 **Sengupta S**, Tjandra JJ, Gibson PR. Dietary fiber and colorectal neoplasia. *Dis Colon Rectum* 2001; **44**: 1016-1033
- 33 **Taylor RH**, Moffet FJ. Profile of colorectal cancer at a community hospital with a multiethnic population. *Am J Surg* 1994; **167**: 509-512
- 34 **Zhang X**, Zhang B, Li X, Wang X, Nakama H. Relative risk of dietary components and colorectal cancer. *Eur J Med Res* 2000; **5**: 451-454
- 35 **Miller A**, Gorska M, Bassett M. Proximal shift of colorectal cancer in the australian capital territory over 20 years. *Aust N Z J Med* 2000; **30**: 221-225
- 36 **Ikeda Y**, Akagi K, Kinoshita J, Abe T, Miyazaki M, Mori M, Sugimachi K. Different distribution of Dukes' stage between proximal and distal colorectal cancer. *Hepatogastroenterology* 2002; **49**: 1535-1537
- 37 **Rodriguez-Bigas MA**, Mahoney MC, Weber TK, Petrelli NJ. Colorectal cancer in patients aged 30 years or younger. *Surg Oncol* 1996; **5**: 189-194
- 38 **Paraf F**, Jothy S. Colorectal cancer before the age of 40: a case-control study. *Dis Colon Rectum* 2000; **43**: 1222-1226
- 39 **Sahraoui S**, Acharki A, Tawfiq N, Jouhadi H, Bouras N, Benider A, Kahlain A. Colorectal cancer in patients younger than 40 years of age. *Cancer Radiother* 2000; **4**: 428-432
- 40 **Parramore JB**, Wei JP, Yeh KA. Colorectal cancer in patients under forty: presentation and outcome. *Am Surg* 1998; **64**: 563-567

Edited by Ma JY

Construction, expression and tumor targeting of a single-chain Fv against human colorectal carcinoma

Jin Fang, Hong-Bin Jin, Jin-Dan Song

Jin Fang, Hong-Bin Jin, Jin-Dan Song, Key Lab of Cell Biology, Ministry of Public Health of China, China Medical University, Shenyang 110001, Liaoning Province, China

Supported by the Natural Science Foundation of China, No.85-722-18-02

Correspondence to: Prof. Jin-Dan Song, Key Lab of Cell Biology, Ministry of Public Health of China, China Medical University, 92 Beier Road, Heping District, Shenyang 110001, Liaoning Province, China. jdsong@mail.cmu.edu.cn

Telephone: +86-24-23256666-5349

Received: 2002-11-26 **Accepted:** 2003-01-02

Abstract

AIM: A single-chain antibody fragment, ND-1scFv, against human colorectal carcinoma was constructed and expressed in *E. coli*, and its biodistribution and pharmacokinetic properties were studied in mice bearing tumor.

METHODS: V_H and V_L genes were amplified from hybridoma cell IC-2, secreting monoclonal antibody ND-1, by RT-PCR, and connected by linker $(Gly_4Ser)_3$ to form scFv gene, which was cloned into expression vector pET 28a(+) and finally expressed in *E. coli*. The expressed product ND-1scFv was purified by metal affinity chromatography using Ni-NTA, its purity and biological activity were determined using SDS-PAGE and ELISA. ND-1scFv was labeled with ^{99m}Tc , and then injected into mice bearing colorectal carcinoma xenograft for pharmacokinetic study *in vivo*.

RESULTS: SDS-PAGE analysis showed that the relative molecular weight of recombinant protein was 30kDa with purity of 94 %. ELIAS assay revealed that ND-1scFv retained the immunoactivity of parent mAb, being capable of binding specifically to human colorectal carcinoma cell line expressing associated antigen. Radiolabeled ND-1scFv exhibited rapid tumor targeting, with specific distribution in mice bearing colorectal carcinoma xenograft observed as early as 1 h following injection. *In vivo* pharmacokinetic studies also demonstrated that ND-1scFv had very rapid plasma clearance ($T_{1/2\alpha}$ of 5.7 min, $T_{1/2\beta}$ of 2.6 h).

CONCLUSION: ND-1scFv shows significant immunoactivity, and better pharmacokinetic and biodistribution characteristics compared with intact mAbs, demonstrating the possibility as a carrier for tumor-imaging.

Fang J, Jin HB, Song JD. Construction, expression and tumor targeting of a single-chain Fv against human colorectal carcinoma. *World J Gastroenterol* 2003; 9(4): 726-730

<http://www.wjgnet.com/1007-9327/9/726.htm>

INTRODUCTION

Colorectal carcinoma is one of the common malignant tumors with relatively high incidence, occupying the fourth rate of mortality in China. Therefore, efficient diagnosis and

therapeutic approaches are important for colorectal carcinoma research. Although in recent years some progress has been made in respect to application of monoclonal antibodies for the therapy and diagnosis of colorectal carcinoma, most mAbs are of murine origin, so that repeated administration can induce human anti-mouse antibodies (HAMA), moreover, intact mAbs are generally too large (M_r 150 000) to penetrate tumor masses, which can severely limit the efficacy of antibody in clinical utilization^[1]. To overcome such deficiencies, gene engineering antibody, including human origin antibodies, single chain Fv (scFv), human-murine chimed antibodies are developed to improve murine origin mAbs^[2-9]. ScFv, which is comprised of immunoglobulin heavy- and light-chain variable regions that are connected by a short peptide linker, is the gene engineered antibody employed most widely at present. The main advantages of scFv over intact mAbs and Fab fragment are their small size (M_r 30 000, amounting to one sixth of intact mAbs), making them penetrate a solid tumor mass rapidly and evenly. In addition, the lack of Fc domains makes them less immunogenic responsive and less capable of binding to Fc receptors distributed on normal cells. These characteristics make scFv potentially useful in tumor diagnosis and therapy as a carrier^[10,11].

ND-1 is a murine monoclonal antibody against tumor-associated antigen LEA, mainly expressed in human colorectal carcinoma, developed by Jindan Song in 1986, which was obtained by immunizing Balb/c mouse with CCL-187 human colorectal carcinoma cell line. The histochemical determination of one thousand pathologic samples showed that ND-1 binded specifically to well differentiated and moderately differentiated colorectal carcinoma tissues and its specificity is superior to mAbs against CEA. ^{131}I labeled ND-1 also exhibited excellent imaging of tumor tissue in mice bearing colorectal carcinoma xenograft. We constructed a scFv by gene engineering technology from the V_L and V_H of ND-1, a monoclonal antibody against human colorectal carcinoma, and determined the biological properties of ND-1 scFv *in vivo* and *in vitro*.

MATERIALS AND METHODS

Materials

IC-2 is murine hybridoma cell that secretes monoclonal antibody ND-1 against human colorectal carcinoma. Both IC-2 and HeLa human cervical carcinoma cell line were from our group. pET28a(+) expression vector and *E. coli* BL21 were kindly provided by Dr. YH. Chen. CCL-187 human colorectal carcinoma cell line was kindly provided by Tumor Research Institution of Medical College of Harvard University. pMD18-T vector, *E. coli* JM109 component cell, DNA polymerase, restriction enzyme, and DNA recovery kit were purchased from TarkaRa Biotechnology (Dalian, China). mRNA purification kit and T4 DNA ligase were bought from Pharmacia Biotech. Anti-His6 tag antibody was from Invitrogen. Ni-NTA resin was provided by Qaigen company. MDP and ^{99m}Tc were kindly provided by Department of Nuclear Medicine at China Medical University. Heavy chain primer 1 and 2, light chain primer mix, linker primer mix, and RS primer mix was purchased from Pharmacia Biotech.

Genetic construction of ND-1scFv

ND-1scFv gene was constructed as previously described. Briefly, mRNA was extracted from 5×10^6 hybridoma cells IC-2 and cDNA was synthesized by reverse transcription using random primer. V_H and V_L gene were separately amplified from the cDNA by PCR using heavy chain primer and light primer mix. The V_H and V_L gene fragments were recovered and mixed in equimolar ratios for two PCR reactions, the first one using linker primer mix for 7 cycles, followed by the second one using RS primer mix for 30 cycles. As a result, V_H and V_L gene fragments were connected to form scFv gene by extension overlap splicing PCR, and then, obtained ND-1 scFv gene was cloned into pMD18-T, and transformed into *E. coli* JM109, positive clones were identified by colony PCR and DNA sequencing.

Oligonucleotide primers S1 and S2 were designed to add *EcoRI* site at the 5' end of ND-1scFv, and *Hind III* site, *SalI* site at the 3' end. S1: 5' ACTGAATTCATGGCCAGGTGCAGCTGCAGC 3', S2: 5' CGCAAGCTTCTAGTCGAC TTTCCAGCTTGGTC 3'. pMD18-T-ND-1scFv was used as template for a PCR by primer S1 and S2, and the product was cloned into the vector pET28a(+) after digestion with *EcoRI* and *HindIII*, and then transformed into competent *E. coli* BL21 cells for protein expression.

DNA sequencing

ND-1scFv genes cloned into pMD18T and pET28a(+) were sequenced by the dideoxy chain termination method with M13 primer, T7 promoter primer and T7 terminator primer.

Expression and purification of ND-1scFv

E. coli BL21 cells containing pET28a(+)-ND-1scFv plasmid were grown in 100 ml LB broth with 50 µg/ml kanamycin at 37 °C, when O.D₆₀₀ of the culture attained about 0.6, IPTG was added in a final concentration of 1 mmol, and cells were shaken at 37 °C, after 3.5 h, the culture was centrifuged at 5 000 rpm for 10 min, the cell pellet was treated with lyses solution. After sonication and centrifugation, inclusion body containing scFv protein was solubilized and denatured in the presence of 6 mol/L Guanidine hydrochloride. Affinity chromatography on Ni-NTA resin was performed to purify scFv, the column was eluted with 8 mol/L urea at pH8.0, pH6.5 and pH4.2, and the component of pH4.2, containing scFv, was collected, following renaturing by dialysis. Purity and concentration of protein were determined with Bradford assay.

ELISA assay for activity of ND-1scFv

CCL-187 cells and HeLa cells (5×10^4) were grown in 96-well microtiter plates at 37 °C for 24 h, then fixed with 2.5 % glutaraldehyde and blocked with 1 % BSA, followed by incubation with ND-1IgG or ND-1scFv at 37 °C for 2 h; after washing 3 times with PBS, anti-His6 antibody was added into wells with ND-1scFv and incubated as above, the plate was washed and HRP-labeled goat anti-mouse IgG was added into both ND-1IgG and ND-1scFv wells, incubating at 37 °C for 2 h, substrate TMB was added, incubated in darkness for 30 min, the reaction was terminated with 1N H₂SO₄; PBS was used as a negative control.

Tumor model

Human colorectal carcinoma cells (1×10^6) were injected s.c. into the back of athymic mice (nu/nu)(4-6 weeks old). When a tumor developed at 0.5-1.5 cm in diameter, biodistribution and pharmacokinetics were studied.

Biodistribution and pharmacokinetics studies

ND-1scFv and ND-1IgG were labeled with ^{99m}Tc using MDP.

Excess β-mercaptoethanol was added to the solution containing ND-1scFv and ND-1IgG, reduced product (1 mg) was mixed with 40 µl MDP (2.5 mg/ml) and 370MBq ^{99m}Tc. Biodistribution study was performed using tumor-bearing mice injected i.p. with 0.2 ml ^{99m}Tc-ND-1scFv, the mice were killed at different periods. Blood, tumor and all the main organs were collected and weighed. The radioactivity was counted in a gamma scintillation counter. The T/NT value for each organ was calculated.

Pharmacokinetic study was performed by the tumor-bearing mice injected via the tail vein with 0.1 ml ^{99m}Tc-ND-1scFv and ^{99m}Tc-ND-1 IgG. Blood samples were obtained via tail bleeds at 0, 5, 10, 15, 30, 60, 120, 180 min and 24 h after injection, the radioactivity was counted in a gamma scintillation counter, and pharmacokinetic parameters were calculated.

RESULTS

Clone of ND-1scFv gene

V_H and V_L gene were amplified from hybridoma cell IC-2 that secreted monoclonal antibody against human colorectal carcinoma, and then were connected by a linker (Gly₃Ser)₄ using extension overlap splicing PCR to construct scFv gene, which had *EcoRI* site at 5' end and *HindIII* site at 3' end. scFv gene was cloned into the vector pET28a(+) and expressed in *E. coli* BL21. Restriction enzyme digestion analysis showed scFv gene had been accurately inserted into vector pET28a(+). Sequence analysis revealed that scFv gene consisted of 732bp, encoding 243 amino acids. Of which, 354bp for heavy chain gene, was located upstream of scFv gene, and 330bp for the light chain gene, was located downstream. They were connected by a 45bp linker sequence. The deduced protein sequence of ND-1scFv was showed in Figure 1.

```

MAQVQLQSGPGLVAPSSQL
SITCTVSGFSLTTDVHWVRQP
PRKGLEWLGGLVWANGRTNCT
SALMSRISITRDTSKNQVFLT
MNSLQTDDTAMYCYCARGSY
GAVDFWGGGTTVTVSSGGGG
SGGGSGGGGSDIELTQSPA
linker
SLAVSLGQRATISYRASKSVS
TSGYSYMHWNQKPKGQPPRL
LIYLVSNLESGVPAFSGSGS
GTDFTLNIIHPVEEEDATYYC
QHIRELTRSEGGPSWK

```

Figure 1 Amino acid sequences of ND-1scFv deduced from nucleotide sequences.

Expression and purification of ND-1scFv

Plasmid ND-1scFv-pET28a(+) was transformed into *E. coli* BL21, the protein was expressed with induction of IPTG. SDS-PAGE analysis showed that the lysates of BL21 cell expressing scFv protein exhibited a new protein band with molecular weight at 30kDa (Figure 2). Because a sequence encoding a short peptide His-tag exists at the upstream of multi-clone site (MCS) of vector pET28a(+), ND-1scFv was expressed as a recombinant fusion protein with His tag, consisting of 26kDa for scFv and 4kDa for His-tag and its upstream sequence, which was consistent with the theoretically predicted value. SDS-PAGE analysis also showed that no new protein component was found in the supernatant of cell lysate of *E. coli* BL21 induced by IPTG, which indicated scFv protein was expressed in the form of inclusion body. Inclusion body protein was purified by metal affinity chromatography using Ni-NTA resin which could bind to the His-tag protein marker located on the N terminal end of scFv specifically, purity of purified scFv was 94 % purity.

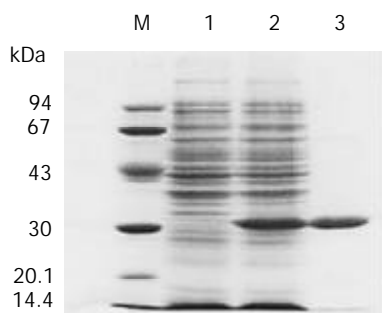


Figure 2 Expressed ND-1scFv. M: Protein marker; 1: Expression of pET28a(+)-ND-1scFv without induction; 2: Expression of pET28a(+)-ND-1scFv with induction of IPTG; 3: purified ND-1scFv protein.

Determination of immunoactivity of ND-1scFv

The immunoreactivity of purified ND-1scFv was determined by ELISA, the result revealed that scFv exhibited an immunoreactivity similar to the parent ND-1 antibody, and showed strong binding to CCL-187 cells expressing colorectal carcinoma associated antigen LEA, and weak binding to LEA-negative HeLa cells. This suggested that scFv had excellent specificity and still retained higher activity after undergoing refolding and purifying procedures.

Table 1 Immune activity of ND-1scFv determined by ELISA

Sample	OD _{450nm} ($\bar{x} \pm s$)	
	CCL-187	HeLa
ND-1IgG	1.92±0.28	0.20±0.06
ND-1scFv	0.87±0.17	0.19±0.03
PBS	0.14±0.03	0.13±0.01

In vivo distribution studies

ND-1scFv was labeled with ^{99m}Tc. ^{99m}Tc-ND-1scFv was injected into mice bearing the CCL-187 xenograft for biodistribution studies. Radioactivity in blood, tumor and normal tissue was determined at 1 and 3 h following injection, and the ratios of radioactivity between tumor tissue and normal tissue (T/NT) were evaluated. The result showed that labeled scFv displayed rapid localization in tumors, accumulation was found in tumors in high concentrations 1 hour after injection, and scFv uptake in tumor was significantly higher than that in other normal tissues (Table 2).

Table 2 Distribution of ^{99m}Tc- labeled ND-1scFv in mice-bearing tumor ($\bar{x} \pm s$)

Tissue	T/NT value	
	1 h	3 h
Blood	2.61±0.97	2.16±1.05
Liver	1.20±0.40	1.75±1.10
Spleen	2.72±0.10	1.23±0.65
Kidney	0.07±0.05	0.26±0.01
Heart	1.75±0.51	1.90±0.60
Lung	0.83±0.31	0.62±0.16

Pharmacokinetic studies

Studies were conducted to define the pharmacokinetic properties of plasma clearance of ^{99m}Tc labeled ND-1scFv in mice bearing tumor (Table 3). Compared with intact ND-1 IgG, ^{99m}Tc-ND-1scFv exhibited an extremely rapid clearance

from the plasma, 80 % of the scFv was cleared out of the plasma pool at 15 min following injection, T_{1/2}α phase for the scFv was 5.7 min, T_{1/2}β phase was 2.6 h, while T_{1/2}α and T_{1/2}β for the ND-1 were 60 min and 18 h, respectively.

Table 3 Pharmacokinetic parameter of ^{99m}Tc-labeled ND-1scFv in mice-bearing tumor

	ND-1IgG	ND-1scFv
Alpha half-life (min)	5.7	60
Beta half-life (h)	2.6	18

DISCUSSION

The critical issue in application of mAbs is its high specificity and good *in vivo* biological features. In this study, single chain Fv ND-1scFv against human colorectal carcinoma was constructed by fusing gene of variable region of heavy chain with gene of variable region of light chain, and the ND-1scFv protein was functionally expressed in *E.coli*. ELISA analysis showed that ND-1scFv had an immunoactivity similar to the parent ND-1 mAbs, and binded specifically to the CCL-187 human colorectal carcinoma cell that expressed associated antigen LEA. This suggests that ND-1 mAb with only a Fv segment still retained its immunoactivity of binding to corresponding antigens, which is consistent to the previous reports. In addition, ND-1scFv also exhibited excellent specific distribution and pharmacokinetic characteristic in tumor-bearing mice.

A linker sequence was required to connect V_H and V_L for the construction of scFv, the linker widely used at present was a 15-amino acid sequence consisting of repetition of four Gly and one Ser (GGGGS)^[12-15]. In this study, the (Gly₄Ser)₃ sequence was used, and the fusion molecule was constructed in V_H-linker-V_L order, the expressed ND-1scFv protein retained favorable stability during the renaturing and dialyzing, and retained biological activity similar to the parent antibody. In addition, a *SalI* site was provided at scFv 3' end except for adding a *HindIII* site for ligasing the vector. In another experiment, we have already constructed a fusion protein of ND-1scFv and yeast cytosine deaminase using the same restriction site.

E.coli gene expression system is known as the earliest developed and most widely applied system for gene engineering. Although expressed proteins are usually lack of the effective modification such as glycosylation, there are some evidences suggesting that a variety of antibody fragments expressed in *E.coli* were able to fold and assemble correctly into bioactive products without the processing^[16-20], which was also confirmed in own studies. pET vector which belongs to the T7 expression system propagating in *E.coli* was used to express of ND-1scFv. This vector contains T7 promoter, which can achieve high level controlled gene transcription in the presence of T7 RNA polymerase^[19,21-24]. ND-1scFv protein was intensively expressed to 17 % of the total bacterial protein. In addition, a 6×His tag sequence exists at the upstream of clone site in the pET vector, which was expressed in the form of fusion protein with the downstream scFv. Since it did not influence the bioactivity of expressed products, no enzyme hydrolysis process was required to remove it from the final products. This simplified the whole expression procedure. It was even more worth noticing that this sequence could be used as a protein marker for the determination and purification of expressed proteins^[25-27]. ND-1scFv protein was purified by metal affinity chromatography using Ni-NTA resin which can bind to His tag specifically located on -NH₃ of scFv. SDS-PAGE analysis showed that the purity of ND-1scFv was as

high as 94 %, and the concentration was 1.5 mg/ml, demonstrating its potential usefulness in clinical application.

After being reconstructed into small molecules, the molecular weight of mAbs usually reduced to as 1/3 or 1/6 of intact mAbs, which significantly increased their penetrability to tumor tissue. Related experimental observation revealed that intact mAbs mainly concentrated nearby the blood vessel, while scFv seemed to be distributed uniformly within the tumor tissue and performing targeting function with high efficiency^[28,29]. Furthermore, scFv exhibited two-phase pharmacokinetic characteristic *in vivo*, its $T_{1/2\alpha}$ (equilibrium phase) is much shorter than that of intact mAbs, implying that the *in vivo* equilibrated distribution of scFv may be reached rapidly, and its penetration into the interior of solid tumor could be achieved in a short time. In our experiment, ^{99m}Tc labeled ND-1scFv accumulated in tumor tissue in high concentration rapidly only 1 h after being injected into mice bearing xenograft. The radioactivity was significantly higher than that in most of normal tissues, while intact ND-1 required 20-24 h to obtain similar accumulation. Plasma pharmacokinetic studies in mice bearing tumor also showed a rapid plasma clearance of ND-1scFv superior to intact ND-1. Strong penetrability, rapid localization and elimination are the main biological behavior of scFv *in vivo*, making it an ideal localizing diagnostic agent for clinical applications. These were further validated by the immun imaging experiments in mice bearing tumor using a various of scFvs against different tumor antigen^[30-32]. Hitherto, the superiority of ND-1 developed by our group over the commercial product, mAb vs CEA, both in specificity and affinity, has been demonstrated in a number *in vivo* and *in vitro* experiments. Thus ND-1scFv, constructed from V_H and V_L of ND-1, may provide a new approach for clinical diagnosis and treatment of human colorectal carcinoma.

In this study, we observed that labeled scFv simultaneously accumulated intensively in kidney and in tumors of mice bearing xenograft, which also has been reported by other researchers^[30]. On one hand, relative small size of scFv promotes its rapid uptake by kidney, so that the accumulation in kidney occurs shortly after injection, on the other hand, the half life of ^{99m}Tc is shorter, which, although beneficial for *in vivo* fast imaging, also increases the uptake of labeled scFv by kidney^[28]. Recently, Goel *et al*^[33,34] constructed divalent [sc(Fv)₂] and tetravalent {[sc(Fv)₂]₂} by covalent interaction, which increased the valence of scFvs and improved their affinity. Compared to the monovalent scFv, the divalent scFvs showed approximately 20-fold higher affinities. Furthermore, the molecular weight of multivalent scFvs was larger than scFv, but still smaller than intact IgG, so the *in vivo* pharmacokinetic behavior would be more promising^[35-40]. Some researchers suggested that this uptake also may be related to the IP of the scFv, thus, there exists the possibility of directly modifying the isoelectric point of the scFv by introducing mutation in framework regions. A lower IP may reduce non-specific uptake into tissues such as the kidney^[31]. The ND-1scFv constructed in this study retained the immunoactivity of parent mAbs and the clinical application are demonstrated preliminarily in radiolabelling experiment with mice bearing tumor. With further development, it may become a promising targeting carrier for clinical diagnosis.

REFERENCES

- Borsi L**, Balza E, Bestagno M, Castellani P, Carnemolla B, Biro A, Leprini A, Sepulveda J, Burrone O, Neri D, Zardi L. Selective targeting of tumoral vasculature: Comparison of different formats of an antibody (L19) to the ED-B domain of fibronectin. *Int J Cancer* 2002; **102**: 75-85
- He FT**, Nie YZ, Chen BJ, Qiao TD, Fan DM, Li RF, Kang YS, Zhang Y. Expression and identification of recombinant soluble single-chain variable fragment of monoclonal antibody MC3. *World J Gastroenterol* 2002; **8**: 258-262
- Yu ZC**, Ding J, Nie YZ, Fan DM, Zhang XY. Preparation of single chain variable fragment of MG(7) mAb by phage display technology. *World J Gastroenterol* 2001; **7**: 510-514
- Kim SH**, Chun JH, Park SY. Characterization of monoclonal antibodies against carcinoembryonic antigen (CEA) and expression in *E. coli*. *Hybridoma* 2001; **20**: 265-272
- Pavlinkova G**, Colcher D, Booth BJ, Goel A, Batra SK. Pharmacokinetics and biodistribution of a light-chain-shuffled CC49 single-chain Fv antibody construct. *Cancer Immunol Immunother* 2000; **49**: 267-275
- Arakawa F**, Yamamoto T, Kanda H, Watanabe T, Kuroki M. cDNA sequence analysis of monoclonal antibody FU-MK-1 specific for a transmembrane carcinoma-associated antigen, and construction of a mouse/human chimeric antibody. *Hybridoma* 1999; **18**: 131-138
- De Kleijn EM**, Punt CJ. Biological therapy of colorectal cancer. *Eur J Cancer* 2002; **38**: 1016-1022
- Allison DE**, Gourlay SG, Koren E, Miller RM, Fox JA. Pharmacokinetics of rhuMAb CD18, a recombinant humanised monoclonal antibody fragment to CD18, in normal healthy human volunteers. *Bio Drugs* 2002; **16**: 63-70
- Al-Yasi AR**, Carroll MJ, Ellison D, Granowska M, Mather SJ, Wells CA, Carpenter R, Britton KE. Axillary node status in breast cancer patients prior to surgery by imaging with Tc-99m humanised anti-PEM monoclonal antibody, hHMFg1. *Br J Cancer* 2002; **86**: 870-878
- Pavlinkova G**, Beresford GW, Booth BJ, Batra SK, Colcher D. Pharmacokinetics and biodistribution of engineered single-chain antibody constructs of MAb CC49 in colon carcinoma xenografts. *J Nucl Med* 1999; **40**: 1536-1546
- Kim DJ**, Chung JH, Ryu YS, Rhim JH, Kim CW, Suh Y, Chung HK. Production and characterisation of a recombinant scFv reactive with human gastrointestinal carcinomas. *Br J Cancer* 2002; **87**: 405-413
- Kobayashi N**, Shibahara K, Ikegashira K, Shibusawa K, Goto J. Single-chain Fv fragments derived from an anti-11-deoxycortisol antibody. Affinity, specificity, and idiotype analysis. *Steroids* 2002; **67**: 733-742
- Ren X**, Gao H, Su K, Chen W, Yang A, Yu Z. Construction and nucleotide sequence assay of human anti-HBs variable region single-chain antibody gene. *Shengwu Yixue Gongchengxue Zazhi* 2000; **17**: 484-486
- Nakayashiki N**, Yoshikawa K, Nakamura K, Hanai N, Okamoto K, Okamoto S, Mizuno M, Wakabayashi T, Saga S, Yoshida J, Takahashi T. Production of a single-chain variable fragment antibody recognizing type III mutant epidermal growth factor receptor. *Jpn J Cancer Res* 2000; **91**: 1035-1043
- Hashimoto Y**, Ikenaga T, Tanigawa K, Ueda T, Ezaki I, Imoto T. Expression and characterization of human rheumatoid factor single-chain Fv. *Biol Pharm Bull* 2000; **23**: 941-945
- Luo YM**, Mu Y, Wei JY, Yan GL, Luo GM. Studies on the optimal expression condition, purification and its characterization of ScFv-2F3. *Shengwu Gongcheng Xuebao* 2002; **18**: 74-78
- Norton EJ**, Diekman AB, Westbrook VA, Flickinger CJ, Herr JC. RASA, a recombinant single-chain variable fragment (scFv) antibody directed against the human sperm surface: implications for novel contraceptives. *Hum Reprod* 2001; **16**: 1854-1860
- Zeng JZ**, Zhou ZY, Wu YQ, Liu ZP, Wang WX, Huang HL, Cai ZN, Yu JL. Expression of single-chain Fv antibody for anti-beet necrotic yellow vein virus in *Escherichia coli*. *Yichuan Xuebao* 2000; **27**: 1006-1011
- He HJ**, Yang WD, Chang YN, Shi HJ, Yang GZ, Wu XF, Yuan QS. Fusion and expression of the gene encoding human Mn-SOD to anti-CEA single-chain antibody in *Escherichia coli*. *Shengwu Gongcheng Xuebao* 2000; **16**: 566-569
- Fernandez LA**, Sola I, Enjuanes L, de Lorenzo V. Specific secretion of active single-chain Fv antibodies into the supernatants of *Escherichia coli* cultures by use of the hemolysin system. *Appl Environ Microbiol* 2000; **66**: 5024-5029
- Lee MH**, Park TI, Park YB, Kwak JW. Bacterial expression and *in vitro* refolding of a single-chain Fv antibody specific for human plasma apolipoprotein B-100. *Protein Expr Purif* 2002; **25**: 166-173

- 22 **Song LX**, Yu WY. Construction and expression of anticlonic cancer scFv fragment. *Shengwu Gongcheng Xuebao* 2000; **16**: 82-85
- 23 **Cho WK**, Sohn U, Kwak JW. Production and *in vitro* refolding of a single-chain antibody specific for human plasma apolipoprotein A-I. *J Biotechnol* 2000; **77**: 169-178
- 24 **Guo L**, Yan X, Qian S, Meng G. Selecting and expressing protective single-chain Fv fragment to stabilize L-asparaginase against inactivation by trypsin. *Biotechnol Appl Biochem* 2000; **31**: 21-27
- 25 **Sandee D**, Tungpradabkul S, Tsukio M, Imanaka T, Takagi M. Construction and high cytoplasmic expression of a tumoricidal single-chain antibody against hepatocellular carcinoma. *BMC Biotechnol* 2002; **2**: 16
- 26 **Goel A**, Beresford GW, Colcher D, Pavlinkova G, Booth BJ, Baranowska-Kortylewicz J, Batra SK. Divalent forms of CC49 single-chain antibody constructs in *Pichia pastoris*: expression, purification, and characterization. *J Biochem (Tokyo)* 2000; **127**: 829-836
- 27 **Hashimoto Y**, Tanigawa K, Nakashima M, Sonoda K, Ueda T, Watanabe T, Imoto T. Construction of the single-chain Fv from 196-14 antibody toward ovarian cancer-associated antigen CA125. *Biol Pharm Bull* 1999; **22**: 1068-1072
- 28 **Kang N**, Hamilton S, Odili J, Wilson G, Kupsch J. *In vivo* targeting of malignant melanoma by ¹²⁵Iodine- and ^{99m}Technetium-labeled single-chain Fv fragments against high molecular weight melanoma-associated antigen. *Clin Cancer Res* 2000; **6**: 4921-4931
- 29 **Kang NV**, Hamilton S, Sanders R, Wilson GD, Kupsch JM. Efficient *in vivo* targeting of malignant melanoma by single-chain Fv antibody fragments. *Melanoma Res* 1999; **9**: 545-556
- 30 **Reilly RM**, Maiti PK, Kiarash R, Prashar AK, Fast DG, Entwistle J, Dan T, Narang SA, Foote S, Kaplan HA. Rapid imaging of human melanoma xenografts using an scFv fragment of the human monoclonal antibody H11 labelled with ¹¹¹In. *Nucl Med Commun* 2001; **22**: 587-595
- 31 **Turatti F**, Mezzanzanica D, Nardini E, Luison E, Maffioli L, Bamberdieri E, de Lalla C, Canevari S, Figini M. Production and validation of the pharmacokinetics of a single-chain Fv fragment of the MGR6 antibody for targeting of tumors expressing HER-2. *Cancer Immunol Immunother* 2001; **49**: 679-686
- 32 **Mayer A**, Tsiompanou E, O' Malley D, Boxer GM, Bhatia J, Flynn AA, Chester KA, Davidson BR, Lewis AA, Winslet MC, Dhillon AP, Hilson AJ, Begent RH. Radioimmunoguided surgery in colorectal cancer using a genetically engineered anti-CEA single-chain Fv antibody. *Clin Cancer Res* 2000; **6**: 1711-1719
- 33 **Goel A**, Augustine S, Baranowska-Kortylewicz J, Colcher D, Booth BJ, Pavlinkova G, Tempero M, Batra SK. Single-Dose versus fractionated radioimmunotherapy of human colon carcinoma xenografts using ¹³¹I-labeled multivalent CC49 single-chain fvs. *Clin Cancer Res* 2001; **7**: 175-184
- 34 **Goel A**, Colcher D, Baranowska-Kortylewicz J, Augustine S, Booth BJ, Pavlinkova G, Batra SK. Genetically engineered tetra-valent single-chain Fv of the pancarcinoma monoclonal antibody CC49: improved biodistribution and potential for therapeutic application. *Cancer Res* 2000; **60**: 6964-6971
- 35 **Power BE**, Caine JM, Burns JE, Shapira DR, Hattarki MK, Tahtis K, Lee FT, Smyth FE, Scott AM, Kortt AA, Hudson PJ. Construction, expression and characterisation of a single-chain diabody derived from a humanised anti-Lewis Y cancer targeting antibody using a heat-inducible bacterial secretion vector. *Cancer Immunol Immunother* 2001; **50**: 241-250
- 36 **Wang F**, Ma QJ. Cloning and expressing of an anti-CD5 single chain antibody. *Shengwu Gongcheng Xuebao* 2001; **17**: 131-134
- 37 **Yazaki PJ**, Shively L, Clark C, Cheung CW, Le W, Szpikowska B, Shively JE, Raubitschek AA, Wu AM. Mammalian expression and hollow fiber bioreactor production of recombinant anti-CEA diabody and minibody for clinical applications. *J Immunol Methods* 2001; **253**: 195-208
- 38 **Yazaki PJ**, Wu AM, Tsai SW, Williams LE, Ikler DN, Wong JY, Shively JE, Raubitschek AA. Tumor targeting of radiometal labeled anti-CEA recombinant T84.66 diabody and t84.66 minibody: comparison to radioiodinated fragments. *Bioconjug Chem* 2001; **12**: 220-228
- 39 **Wu AM**, Yazaki PJ. Designer genes: recombinant antibody fragments for biological imaging. *Q J Nucl Med* 2000; **44**: 268-283
- 40 **Power BE**, Hudson PJ. Synthesis of high avidity antibody fragments (scFv multimers) for cancer imaging. *J Immunol Methods* 2000; **242**: 193-204

Edited by Ren SY

Follow up of infection of chacma baboons with inoculum containing a and non-a genotypes of hepatitis B virus

Marina Baptista, Anna Kramvis, Saffie Jammeh, Jocelyn Naicker, Jacqueline S. Galpin, Michael C. Kew

Marina Baptista, Anna Kramvis, Saffie Jammeh, Jocelyn Naicker, Michael C. Kew, University Molecular Hepatology Research Unit, Department of Medicine, University of the Witwatersrand, Johannesburg, South Africa

Jacqueline S. Galpin, School of Statistics and Actuarial Sciences, University of the Witwatersrand, Johannesburg, South Africa

Correspondence to: Professor Michael C. Kew, Department of Medicine, Witwatersrand University Medical School, 7 York Road, Parktown, 2193, Johannesburg, South Africa. kewmc@medicine.wits.ac.za

Telephone: +27-11-4883628 **Fax:** +27-11-6434318

Received: 2002-12-05 **Accepted:** 2002-12-22

Abstract

AIM: To determine whether one genotype (A or non-A genotypes of HBV) predominated over the other during the course of HBV infection.

METHODS: Four baboons were inoculated with HBV. DNA was extracted from serum obtained at monthly intervals post-inoculation for 52 weeks and HBV DNA was amplified using primers specific for the core region containing an insert characteristic of genotype A (nt 2 354-2 359, numbering from the *EcoRI* site). The amplicons were cloned into PCR-Script™ and a minimum of 15 clones per time point were sequenced in both directions.

RESULTS: Both genotypes persisted for the entire follow-up period of 52 weeks. Genotype non-A predominated in two baboons and genotype A in one baboon. Neither genotype predominated in the fourth baboon, as shown at a 5 % level of testing.

CONCLUSION: No conclusions concerning the dominance of either genotype or the natural progression or replication rates of HBV could be drawn because the pattern of the genotypes found may have been caused by sampling fluctuations at the time of DNA extraction and cloning as a result of the very low viral loads in the baboon sera.

Baptista M, Kramvis A, Jammeh S, Naicker J, Galpin JS, Kew MC. Follow up of infection of chacma baboons with inoculum containing a and non-a genotypes of hepatitis B virus. *World J Gastroenterol* 2003; 9(4): 731-735

<http://www.wjgnet.com/1007-9327/9/731.htm>

INTRODUCTION

Xenografts from closely related non-human primates or pigs have been suggested as one way to alleviate the chronic shortage of donor organs for human liver transplantation. Baboons (*Papio* species) which are phylogenetically close to humans, have reasonably large livers, and are not endangered. They have already been the source of xenografts for two humans undergoing liver transplantation^[1-3] (as well as for a few patients receiving kidney or heart transplants^[2,4-6]). The use of liver xenografts would, however, be precluded if they

were infected by zoonotic pathogens. In addition, because chronic hepatitis C and B virus infections are now the most frequent causes of end-stage liver disease requiring transplantation in humans^[7], the donor livers should be resistant to infection with these viruses. Our study has previously shown that Chacma baboons (*Papio ursinus orientalis*) are resistant to infection of hepatitis C virus^[8] but are susceptible to infection of hepatitis B virus (HBV)^[9].

In the latter study^[9], pooled serum from three patients with acute hepatitis B (the serum of all three was HBV surface (HBsAg)- and e antigen (HBeAg)-positive and had high titers of HBV DNA) had been injected into the baboons. Direct sequencing of HBV DNA amplified at various times post-inoculation indicated that the baboons had been inoculated with a mixed population of HBV. Cloning of the HBV DNA amplified from the inoculum revealed that it fortuitously contained approximately equal proportions of A and non-A genotypes of HBV. HBV has been classified into genotypes A-H, with an intergenotypic diversity of at least 8 %^[10-13]. Genotype A accounts for 80 % and genotype D for 10 % of the genotypes found in southern Africa, with the other genotypes being either absent or present in very few isolates^[14]. HBV genotypes have a characteristic geographical distribution^[15], which help in tracing the route of HBV infection^[16], and may influence the severity and outcome of infection with this virus^[17]. However, little is known about the natural progression and severity of the infection when more than one genotype is present^[18].

Co-infection with two or more genotypes may be the consequence of multiple exposures to infection at an early age when immune responses are immature or in older individuals with immune disorders^[19], or the result from genotype changes during seroconversion from e antigen positivity to negativity^[20]. Documented cases of co-infection with more than one genotype of HBV were rare^[18,19,21,22], and the natural progression of HBV infection in this circumstance has not been thoroughly evaluated. In one patient studied recently, infection with genotypes D and A (with D predominant) was serologically "silent" (HBsAg-negative but HBV DNA-positive), although with pathological consequences because the patient was cirrhotic and died of liver failure^[18]. This patient may be of particular interest in view of our failure to detect HBsAg in the serum of our HBV DNA-positive inoculated baboons^[9]. Therefore, the opportunity was taken in the present study to monitor the changes over time in the relative proportions of genotypes A and non-A in the inoculated baboons and to ascertain if the two genotypes differed in their rate of replication or in their ability to persist in the inoculated baboons.

MATERIALS AND METHODS

Samples

For this study, serum samples which were collected at 4-weekly intervals from 4 baboons infected by inoculated HBV^[9] were analyzed which was started at week 8. Because the initial phases of the study included the housing and inoculation of the baboons, the collection of serum samples were carried out at the Medical University of Southern Africa, this study was

undertook with the permission given by the Animal Ethics Committee of that institution. The Committee approved the procedures, and the care of the baboons according to its guidelines and those of the South African Medical Research Council. Each of the baboons had received intravenous injection of 1 ml pooled serum obtained from 3 HBV surface antigen (HBsAg) and HBV e antigen (HBeAg)-positive patients with clinically-overt acute hepatitis B. The concentration of HBV DNA in the pooled sera was 2 133 pg/ml (which was 2 982 pg/ml in another laboratory) using the Digene Hybrid Capture System (Digene Diagnosis Inc., Beltsville, MD, USA); the values in the individual isolates were 2 870 pg/ml, 6 660 pg/ml and 692 pg/ml, respectively. Using methods of amplification and cloning (see below), the HBV DNA amplified from the pooled inoculum was shown to contain equal proportions of genotype A and non-A of HBV. All of the baboon sera were tested for HBsAg, anti-HBc, and anti-HBs using commercially available assays (Abbott Laboratories, Chicago, IL, USA). All serum samples were stored at -20 °C.

PCR assay of HBV

HBV DNA levels were assessed with a quantitative PCR assay (Amplicor™ HBV monitor test, Roche Diagnostics). Briefly, 50 µl of serum were prepared with pre-treatment with polyethylene glycol, alkaline lysis of the pelleted viral particles, and neutralization of the lysate. After adding a fixed amount of internal standard and a PCR mix, 30 cycles of PCR amplification were performed according to the manufacturer's instructions. Biotinylated amplicons were captured on streptavidin-coated microwells and hybridized with specific dinitrophenyl-labelled oligonucleotide probes. It was incubated with alkaline phosphatase conjugated anti-DNP antibodies and a colorimetric substrate, then a kinetic of O.D. determination of HBV DNA levels was performed. The limit of detection of this PCR assay was 400 copies of viral genome per ml, and quantitation was linear up to 4×10^7 copies per ml^[23,24].

DNA extraction

DNA was extracted from serum using the QIAamp blood kit (Qiagen Inc., Hilden Germany), according to the manufacturer's instructions and as previously described^[25]. Known positive and negative sera, as well as best quality water were used as controls for the extraction procedure.

PCR of HBV DNA

HBV DNA in the core region was amplified using primers designed to amplify all the HBV genotypes (Table 1A and 1B). PCR was performed in 25 µL and 50 µL final reaction volumes for the first and second rounds, respectively. The reaction for the first round of the PCR consisted of 0.02 U/µL Dynazyme™ Taq DNA polymerase (version 2.0, Finnzymes OY, Espoo, Finland), 200 µmol/L of each of the nucleotide triphosphates, 1 µmol/L of each of the primers, 4 mmol/L MgCl₂ and 10 mmol/L Tris-HCl (pH 8.8 at 25 °C), 50 mmol/L KCl, and 0.1 % Triton® X-100. The reaction mixture for the second round of the PCR was the same as for the first round except that 1.5 mmol/L MgCl₂ was used. A third round of PCR was used on the serum from those time points that were negative after 2 rounds of PCR. The reaction mixture was the same as for the second round of PCR except that concentrations of MgCl₂ of 1.0 mmol/L, 1.5 mmol/L, and 1.5 mmol/L, were used for the first, second, and third rounds of PCR, respectively. All PCR assays were performed in a programmable thermal cycler (Perkin Elmer, Norwalk, CT, USA) with the 3-step cycling profile shown in Table 1B. Sera positive for HBsAg, HBeAg, and HBV DNA detected by slot-blot hybridization were used as positive controls and best quality water instead

of DNA as negative controls. To avoid cross-contamination and false-positive results, the precautions and procedures recommended by Kwok and Higuchi^[26] were strictly adhered to DNA extraction, the various stages of PCR amplification, and gel electrophoresis were performed in physically separate venues.

Table 1A Oligonucleotide primers

	Primer	Position ^a	Sequence
Double-round PCR	1687(+)	1687-1706	5' CGA CCG ACC TTG AGG CAT AC 3'
	2498(-)	2498-2477	5' AAG CCC AGT AAA GTT TCC CACC 3'
	2267(+)	2267-2284	5' GGA GTG TGG ATT CGC ACT 3'
Triple-round PCR	1687(+)	1687-1706	5' CGA CCG ACC TTG AGG CAT AC 3'
	2498(-)	2498-2477	5' AAG CCC AGT AAA GTT TCC CACC 3'
	1795(+)	1795-1812	5' TGG TCT GTC GAC CAG CAC 3'
PCR3	2436(-)	2436-2419	5' TGA GAT CTT CTG CGA CGC 3'
	2267(+)	2267-2284	5' GGA GTG TGG ATT CGC ACT 3'
	2400(-)	2400-2382	5' CTG CGA GGC GAG GGA GTT 3'

Table 1B Polymerase chain reaction cycling profiles

		Amplification conditions			Size ^b
		Denaturation	Annealing	Extension	
Double-round PCR	PCR1	94°C 30 sec	62°C 40 sec	72°C 80 sec	812bp
	PCR2	94°C 30 sec	57°C 50 sec	72°C 50 sec	170bp
Triple-round PCR	PCR1	94°C 30 sec	62°C 40 sec	72°C 80 sec	812bp
	PCR2	94°C 30 sec	48°C 60 sec	72°C 50 sec	642bp
	PCR3	94°C 30 sec	50°C 60 sec	72°C 50 sec	134bp

Notes: PCR1: the first round polymerase chain reaction; PCR2: the second round polymerase chain reaction; PCR3: the triple round polymerase chain reaction. (+) sense; (-) anti-sense. ^aDenotes the nucleotide position of hepatitis B virus *adv* genome (GenBank accession #V00866) where the *EcoRI* cleavage site is position 1. ^bSize of the amplicons in base pairs.

Detection of amplified products

A 5 µl aliquot of the amplified PCR product was electrophoresed in a 2 % agarose gel. Bands of the appropriate size (Table 1A and 1B) were visualised under ultraviolet light after ethidium bromide staining.

Cloning and nucleotide sequencing

Following the double or triple round PCR, amplicons were cloned using PCR-Script (Stratagene, La Jolla, CA, USA). Plasmid DNA was extracted using the QIAprep spin miniprep kit (Qiagen Inc., Hilden, Germany) and restricted with *Pvu II* to confirm the presence of the correct insert (Table 1A and 1B). Sequencing of positive clones was performed using the T7 Sequenase Version 2.0 DNA sequencing kit (Amersham Life Science Inc., Cleveland, OH, USA). Sequences were analyzed in both forward and reverse directions with primers T3 and T7 on 8 % glycerol-tolerant acrylamide gels and autoradiographed. The number of clones of A and non-A genotypes obtained at each time point was used as a measure of the relative proportions of the two genotypes in the serum at that time.

Statistical analysis

Fisher's Exact test and the Chi-squared tests were used for statistical analysis, where appropriate.

RESULTS

HBV DNA was detected in the serum using either double or triple round PCR in the four inoculated baboons at various time points during the 52-week follow up period. For baboons 1 and 13 HBV DNA concentration was determined at various time of post-inoculation using the Amplicor HBV Monitor™ Test (Table 2). When serum was available for further analysis and HBV DNA was successfully amplified, the amplicons were cloned and sequenced. Genotype A was distinguished from the other genotypes by the sequence 5' CGGGAC3' (nt 2 354-nt 2 359, numbering from the Eco R1 site) that is specific to this genotype (Figure 1). Depletion of inoculum serum prevented us from amplifying the S region and carrying out restriction fragment length polymorphisms in order to assign the non-A genotype to one of genotypes B to H. Although we could not preclude the possibility that the non-A isolates were comprised of more than one genotype, the most likely genotype would be genotype D, the genotype besides A commonly found in South Africa^[14].

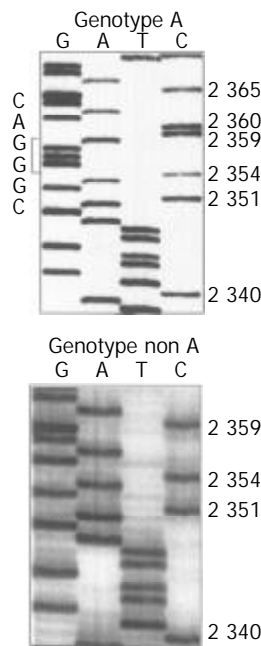


Figure 1 Sequence profiles of the core region (nucleotides 2 340-2 368 numbering from the *EcoRI* site) showing the insertion of 5' CGGGAC3' (nucleotide 2 354-2 359) found in genotype A and its absence in genotypes non-A. Tracks G, A, T and C are labelled.

Table 2 HBV DNA levels measured by the amplicor HBV monitor test

Time of post-inoculation (months)	HBV DNA Levels (genomes/ml)									
	2	3	4	5	6	7	8	9	10	10
Baboon 1	<400	<400	4 338	3 711	ns	ns	<400	ns	<400	<400
Baboon 13	<400	ns	ns	ns	ns	ns	2 6216	1 003	ns	ns

Notes: ns: no serum available.

Figure 2 showed the relative concentration of genotypes A and non-A at the various time points represented as a percentage of the total number of clones obtained and sequenced at that time point. The hypothesis of equal proportions of the genotypes over time was rejected for all four baboons ($P < 0.002$ in each instance). For each specific time/baboon combination, the hypothesis that the proportions of genotype A and non-A were equal was rejected in all but 4 cases, namely, at 10 months for baboons 2 and 12, and at 11 months for baboons 1 and 13.

Genotype non-A predominated in two baboons (baboon 2 and 13) and genotype A in one baboon (baboon 1); neither genotype predominated in the fourth baboon (baboon 12), as shown at a 5 % level of testing. In the three baboons in which one or other genotype predominated, there was at least one time-point at which the non-dominant genotype was present in the highest concentration at a proportion significantly different from zero.

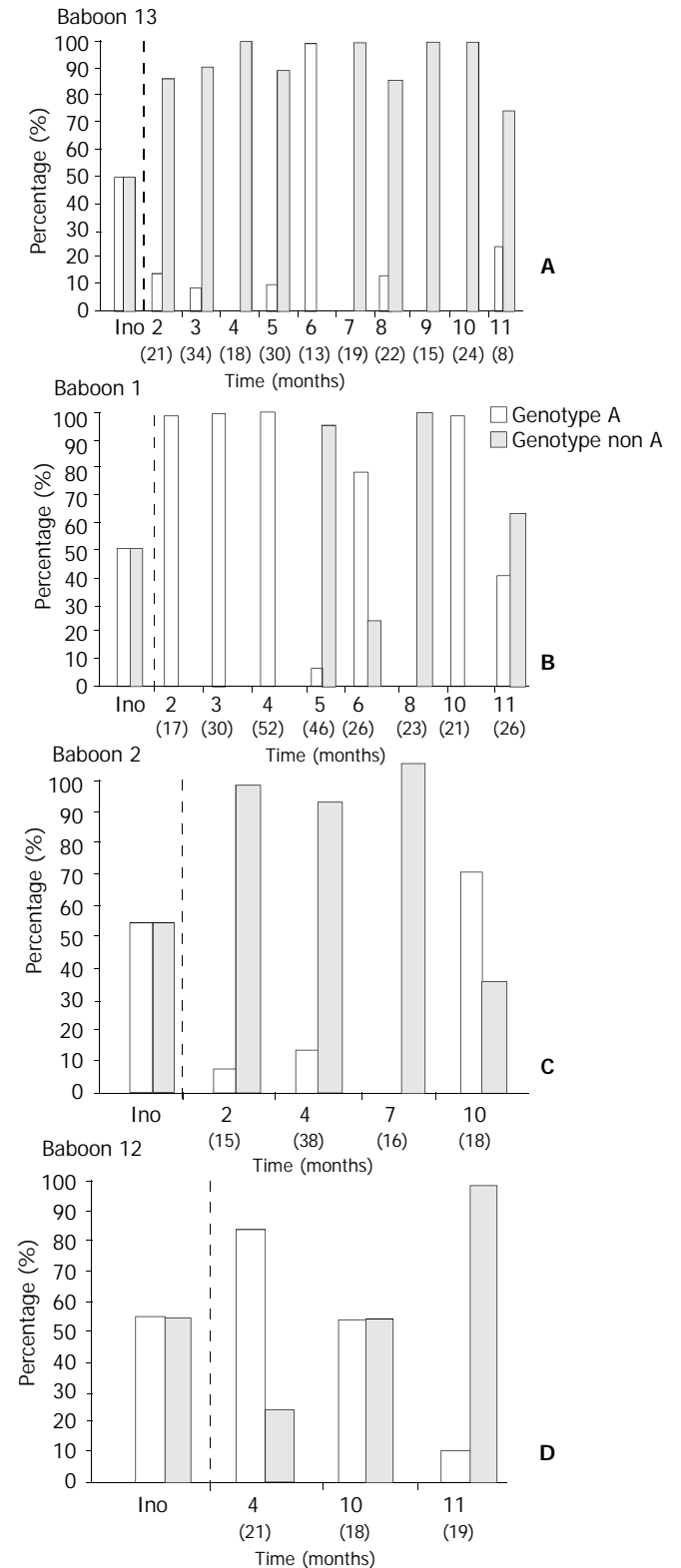


Figure 2 The change of genotype of hepatitis B virus at various time of post-infection which was represented as a percentage. The number of clones sequenced at each time point was showed in brackets. *ino: inoculum.

DISCUSSION

Neither HBsAg nor antibody to HBsAg (anti-HBs) was detected by conventional tests in the serum of the four inoculated baboons at any time during the 52 weeks they were monitored^[9]. HBV DNA identical to either the A or non-A HBV genotypes inoculated was, however, detected in each baboon throughout the follow-up period, and the presence of anti-HBc and Dane particles, small spherical particles and tubular particles was demonstrated in the serum at 16 weeks^[9]. The viral titers in the baboons were low (Table 2), as shown by the need to use nested PCR amplification to detect HBV DNA at all time points and three rounds of amplification at some time-points. No biochemical evidence of liver injury was evident at any stage and liver histology was normal at 52 weeks. These findings together suggested that the animals had become chronic asymptomatic carriers of the virus.

We had hoped that a clear pattern of different rates of replication of the two genotypes would be evident. However, no uniform pattern could be discerned in the relative concentration of genotypes A and non-A during the 52 weeks (Figure 2). Other explanations of a technical nature for the varying concentrations of the genotypes were needed therefore to be considered. One possibility was that the number of clones sampled at each time-point was too small to accurately assess the relative proportions of the genotypes in the serum at that time. This explanation was not supported by statistical analysis of the numbers of clones involved at each time point. A more likely explanation was that the low copy number of the genotypes resulted in sampling error at the time of HBV DNA extraction and cloning. This explanation was particularly apposite for the genotype pattern in baboon 13, in which genotype A alone was found in a single sample, whereas at all other time-points on either side of this sample, genotype non-A either predominated or was the sole genotype cloned (Figure 2A). It was also relevant that the conditions created in the study were artificial on two counts: the approximately equal concentrations of the two genotypes inoculated into the baboons resulted from the pooling of three serum samples from different patients, and we were assessing the effects of a human virus injected into a non-human primate.

Jeantet and co-workers were able to clone and sequence entire HBV genomes and found a number of mutations in the surface, precore and other regions affecting expression of the surface gene in both genotypes^[18]. The A genotype was fully replication competent, although, surprisingly, this was not true of the predominant D genotype. Sequencing of the subgenomic amplicons of HBV from our infected baboons did not reveal any mutations in the core region of the HBV isolates. Full genome analysis was impossible in our study because the study was carried out retrospectively. Either the serum samples were depleted or when serum was available full genome amplification did not work, possibly because of the low viral load.

The very low concentrations of HBV in the serum of the infected baboons (Table 2) and the resulting likelihood of sampling error during viral DNA extraction and cloning prevented us from drawing firm conclusions about the natural progression over time of genotypes A and non-A replication in baboons. The study did however show that both genotypes persisted for the entire period of 52-week of follow-up.

ACKNOWLEDGEMENTS

The authors thank Professor F. Chisari, The Scripps Research Institute for his helpful comments. The H.E. Griffin Cancer Trust supported this work.

REFERENCES

- 1 Lanford RE, Michaels MG, Chavez D, Brasky K, Fung J, Starzl TE. Persistence of extrahepatic hepatitis B virus DNA in the absence of detectable hepatic replication in patients with baboon liver transplants. *J Med Virol* 1995; **46**: 207-212
- 2 Starzl TE, Machioto TL, Peter GNH. Renal heterotransplantation from baboons to man: experience with 6 cases. *Transplantation* 1964; **2**: 752-756
- 3 Starzl TE, Fung J, Tzakis A, Todo S, Demetris AJ, Marino IR, Doyle H, Zeevi A, Warty V, Michaels M, Kusne S, Rudert WA, Trucco M. Baboon-to-human liver transplantation. *Lancet* 1993; **341**: 65-71
- 4 Bailey LL, Nehlsen-Cannarella SL, Concepcion W, Jolley WB. Baboon-to-human cardiac xenotransplantation in a neonate. *JAMA* 1985; **254**: 3321-3329
- 5 Barnard CN, Wolpowitz A, Losman JG. Heterotopic cardiac transplantation with a xenograft for assistance of the left heart in cardiogenic shock after cardiopulmonary bypass. *S Afr Med J* 1977; **52**: 1035-1038
- 6 Hitchcock CR, Kiser JC, Telander RL, Seljeskog EL. Baboon renal grafts. *J Am Med Assoc* 1964; **189**: 934-937
- 7 Sheiner PA. Hepatitis C after liver transplantation. *Semin Liver Dis* 2000; **20**: 201-209
- 8 Sithebe NP, Kew MC, Mphahlele MJ, Paterson AC, Lecatsas G, Kramvis A, de Klerk W. Lack of susceptibility of Chacma baboons (*Papio ursinus orientalis*) to hepatitis C virus infection. *J Med Virol* 2002; **66**: 468-471
- 9 Kedda MA, Kramvis A, Kew MC, Lecatsas G, Paterson AC, Aspinall S, Stark JH, De Klerk WA, Gridelli B. Susceptibility of chacma baboons (*Papio ursinus orientalis*) to infection by hepatitis B virus. *Transplantation* 2000; **69**: 1429-1434
- 10 Norder H, Courouce AM, Magnius LO. Complete genomes, phylogenetic relatedness, and structural proteins of six strains of the hepatitis B virus, four of which represent two new genotypes. *Virology* 1994; **198**: 489-503
- 11 Okamoto H, Tsuda F, Sakugawa H, Sastrosoewignjo RI, Imai M, Miyakawa Y, Mayumi M. Typing hepatitis B virus by homology in nucleotide sequence: comparison of surface antigen subtypes. *J Gen Virol* 1988; **69** (Pt 10): 2575-2583
- 12 Stuyver L, De Gendt S, Van Geyt C, Zoulim F, Fried M, Schinazi RF, Rossau R. A new genotype of hepatitis B virus: complete genome and phylogenetic relatedness. *J Gen Virol* 2000; **81**: 67-74
- 13 Arauz-Ruiz P, Norder H, Robertson BH, Magnius LO. Genotype H: a new Amerindian genotype of hepatitis B virus revealed in Central America. *J Gen Virol* 2002; **83**: 2059-2073
- 14 Bowyer SM, van Staden L, Kew MC, Sim JG. A unique segment of the hepatitis B virus group A genotype identified in isolates from South Africa. *J Gen Virol* 1997; **78** (Pt 7): 1719-1729
- 15 Courouce-Pauty AM, Plancon A, Soulier JP. Distribution of HBsAg subtypes in the world. *Vox Sang* 1983; **44**: 197-211
- 16 Yamishita Y, Kurashina S, Miyakawa Y, Mayumi M. South-to-north gradient in distribution of the r determinant of hepatitis B surface antigen in Japan. *J Infect Dis* 1975; **131**: 567-569
- 17 Mayerat C, Mantegani A, Frei PC. Does hepatitis B virus (HBV) genotype influence the clinical outcome of HBV infection? *J Viral Hepat* 1999; **6**: 299-304
- 18 Jeantet D, Chemin I, Mandrand B, Zoulim F, Trepo C, Kay A. Characterization of two hepatitis B virus populations isolated from a hepatitis B surface antigen-negative patient. *Hepatology* 2002; **35**: 1215-1224
- 19 Yamanaka T, Akahane Y, Suzuki H, Okamoto H, Tsuda F, Miyakawa Y, Mayumi M. Hepatitis B surface antigen particles with all four subtypic determinants: point mutations of hepatitis B virus DNA inducing phenotypic changes or double infection with viruses of different subtypes. *Mol Immunol* 1990; **27**: 443-449
- 20 Gerner PR, Friedt M, Oettinger R, Lausch E, Wirth S. The hepatitis B virus seroconversion to anti-HBe is frequently associated with HBV genotype changes and selection of preS2-defective particles in chronically infected children. *Virology* 1998; **245**: 163-172
- 21 Okamoto H, Imai M, Tsuda F, Tanaka T, Miyakawa Y, Mayumi M. Point mutation in the S gene of hepatitis B virus for a d/y or w/r subtypic change in two blood donors carrying a surface antigen of compound subtype adyr or adwr. *J Virol* 1987; **61**: 3030-3034
- 22 Paul DA, Purcell RH, Peterson DL. Use of monoclonal antibody

- ies to determine if HBsAg of mixed subtype is one particle or two. *J Virol Methods* 1986; **13**: 43-53
- 23 **Gerken G**, Gomes J, Lampertico P, Colombo M, Rothaar T, Trippler M, Colucci G. Clinical evaluation and applications of the Amplicor HBV Monitor test, a quantitative HBV DNA PCR assay. *J Virol Methods* 1998; **74**: 155-165
- 24 **Kessler HH**, Pierer K, Dragon E, Lackner H, Santner B, Stunzner D, Stelzl E, Waitzl B, Marth E. Evaluation of a new assay for HBV DNA quantitation in patients with chronic hepatitis B. *Clin Diagn Virol* 1998; **9**: 37-43
- 25 **Kramvis A**, Bukofzer S, Kew MC, Song E. Nucleic acid sequence analysis of the precore region of hepatitis B virus from sera of southern African black adult carriers of the virus. *Hepatology* 1997; **25**: 235-240
- 26 **Kwok S**, Higuchi R. Avoiding false positives with PCR. *Nature* 1989; **339**: 237-238

Edited by Xu XQ

Effects of hepatitis B virus infection on human sperm chromosomes

Jian-Min Huang, Tian-Hua Huang, Huan-Ying Qiu, Xiao-Wu Fang, Tian-Gang Zhuang, Hong-Xi Liu, Yong-Hua Wang, Li-Zhi Deng, Jie-Wen Qiu

Jian-Min Huang, Tian-Hua Huang, Xiao-Wu Fang, Tian-Gang Zhuang, Hong-Xi Liu, Department of Cell Biology and Medical Genetics, Shantou University Medical College, Shantou 515031, Guangdong Province, China

Huan-Ying Qiu, Yong-Hua Wang, Shantou University Hospital, Shantou 515063, Guangdong Province, China

Li-Zhi Deng, Jie-Wen Qiu, Department of Internal Medicine, Second Affiliated Hospital, Shantou University Medical College, Shantou 515041, Guangdong Province, China

Jian-Min Huang, Allergy and Inflammation Institute, Shantou University Medical College, Shantou 515031, Guangdong Province, China

Supported by the Natural Science Foundation of Guangdong Province, No. 940567; and by the National Natural Science Foundation of China, No. 39970374

Correspondence to: Dr. Tian-Hua Huang, Department of Cell Biology and Medical Genetics, Shantou University Medical College, Shantou 515031, Guangdong Province, China. thhuang@stu.edu.cn
Telephone: +86-754-8900497 **Fax:** +86-754-8557562

Received: 2002-08-06 **Accepted:** 2002-08-29

Abstract

AIM: To evaluate the level of sperm chromosome aberrations in male patients with hepatitis B, and to directly detect whether there are HBV DNA integrations in sperm chromosomes of hepatitis B patients.

METHODS: Sperm chromosomes of 14 tested subjects (5 healthy controls, 9 patients with HBV infection, including 1 with acute hepatitis B, 2 with chronic active hepatitis B, 4 with chronic persistent hepatitis B, 2 chronic HBsAg carriers with no clinical symptoms) were prepared using interspecific *in vitro* fertilization between zona-free golden hamster ova and human spermatozoa, and the frequencies of aberration spermatozoa were compared between subjects of HBV infection and controls. Fluorescence *in situ* hybridization (FISH) to sperm chromosome spreads was carried out with biotin-labeled full length HBV DNA probe to detect the specific HBV DNA sequences in the sperm chromosomes.

RESULTS: The total frequency of sperm chromosome aberrations in HBV infection group (14.8 %, 33/223) was significantly higher than that in the control group (4.3 %, 5/116). Moreover, the sperm chromosomes in HBV infection patients commonly presented stickiness, clumping, failure to staining, etc, which would affect the analysis of sperm chromosomes. Specific fluorescent signal spots for HBV DNA were seen in sperm chromosomes of one patient with chronic persistent hepatitis. In 9 (9/42) sperm chromosome complements containing fluorescent signal spots, one presented 5 obvious FISH spots, others presented 2 to 4 signals. There was significant difference of fluorescence intensity among the signal spots. The distribution of signal sites among chromosomes was random.

CONCLUSION: HBV infection can bring about mutagenic effects on sperm chromosomes. Integrations of viral DNA into sperm chromosomes which are multisites and

nonspecific, can further increase the instability of sperm chromosomes. This study suggested that HBV infection can create extensively hereditary effects by alteration genetic constituent and/or induction chromosome aberrations, as well as the possibility of vertical transmission of HBV via the germ line to the next generation.

Huang JM, Huang TH, Qiu HY, Fang XW, Zhuang TG, Liu HX, Wang YH, Deng LZ, Qiu JW. Effects of hepatitis B virus infection on human sperm chromosomes. *World J Gastroenterol* 2003; 9(4): 736-740

<http://www.wjgnet.com/1007-9327/9/736.htm>

INTRODUCTION

Hepatitis B virus (HBV) infection is a serious public health problem worldwide^[1-3], especially in Far-East Asia such as China. During HBV infection, HBV can be found in saliva, vaginal secretions, semen and other tissues beyond the liver and blood^[4-6]. It is well established that HBV DNA could integrate not only into the host hepatocytes but also into sperm cells^[7-19]. Extensive studies have confirmed that HBV DNA integrated into the hepatocytes will increase chromosome instability and cause genetic recombination and hepatocarcinogenesis^[7-17]. In this study, in order to clarify the inheritable influence of HBV on sperm chromosomes, we used interspecific *in vitro* fertilization with zona-free hamster eggs to prepare sperm chromosomes and compared the aberration frequencies of sperm chromosomes between patients with hepatitis B and the controls. In addition, FISH technique with HBV DNA as a probe was used to detect HBV sequences in sperm chromosomes and to analyze features of sperm chromosomes integrated HBV DNA. The genetic significance of the results from this investigation was discussed.

MATERIALS AND METHODS

Subjects

Nine men with HBV infection, including 1 subject with acute hepatitis, 6 with chronic hepatitis (2 with chronic active hepatitis, 4 with chronic persistent hepatitis), 2 chronic HBsAg carriers with no clinical symptoms, and 5 healthy men as controls were studied. The age range was from 22 to 38 years old (mean 27), without the history of exposure of radiation and use of mutagenic agent. The status of the markers of HBV infection of the subjects tested was listed in Table 1.

Preparation of sperm chromosomes

The technique of interspecific *in vitro* fertilization of zona-free golden hamster was used to prepare the sperm chromosomes. Those procedures included the treatment of semen samples from the tested subjects, superovulation of golden hamsters and egg processing, insemination and postinsemination culture and preparation of chromosome slides^[20,21].

Analysis of aberrations of sperm chromosome

Sperm chromosome slides were stained with 10-fold diluted

Giemsa in 50 ml Sorensen's buffer, pH6.8, for 20-30 min and observed under the light microscope. After the observation, the slides were stored at -70 °C for FISH test. Frequency distributions of spermatozoa with chromosome aberrations were evaluated by using Chi-square test.

Fluorescence *in situ* hybridization of sperm chromosomes

Labeling HBV DNA probe with biotin Recombinant plasmid, pHBV-1 containing 3.2kb HBV genomic DNA, was taken to amplify according to the routine method^[22]. The 3.2kb HBV DNA probe with its vector (altogether 6.2kb) was labeled with biotin-14-dATP by nick translation (GIBCOBRL No. 18247-015). Unincorporated nucleotides were separated by cold ethanol precipitation method.

***In situ* hybridization** Sperm chromosome slides were orderly treated with RNase (Sigma) at 100 mg/L for 60 min at 37 °C, then at 50 mg/L pepsin (Sigma) in 0.01N HCl for 10 min at 37 °C, at last at 1 % polyformaldehyde in PBS for 10 min at room temperature. Chromosomes were denatured at 75 °C for 4 min in 70 % formamide in 2×SSC. *In situ* hybridization with denatured DNA probe mentioned above was performed with a modification of the procedure described by our previous paper^[23]. Briefly, 10 µl hybridization buffer (50 % deionized formamide, 10 % dextran sulfate, and 2×SSC) containing 40 ng/µl biotin-labeled HBV DNA probe, 500 ng/µl sheared salmon sperm DNA was placed on each slide. A coverslip (18×18 mm) was then applied and sealed with rubber cement, followed by overnight incubation in a humidified chamber at 37 °C.

Detection of hybridization signals Post-hybridization washing was carried out, referring to Korenberg's methods for mapping small DNA probes^[24], once in 40 % formamide, 2×SSC for 10 min at 40 °C, then twice, each for 5 min, in 2×SSC at room temperature. Hybridization signals were detected with FITC-conjugated avidin and amplified with goat biotinylated anti-avidin antibody followed by another layer of FITC-avidin (avidin and anti-avidin, Vector Laboratories). To increase the intensity of the hybridization signal, a second round of amplification was applied by sandwich method as above. In order to reduce the nonspecific binding, the slides were preincubated in 4×SSC with 15 % nonfat dry milk for 10 min at 37 °C prior to each step of immunological reactions. The chromosomes were counterstained with propidium iodide (PI, Sigma) and 4, 6-diamidino-2-phenylindole (DAPI, Sigma), 2 µg/ml each in PBS/glycerol (1:9, v/v) containing 0.2 % (1,4)-diazobicyclo-(2, 2, 2) octane (DABCO, Sigma) as an anti-fade

agent. Photography was taken under a fluorescence microscope (BH-2, Olympus) with the G excitation filter, EY-455 help excitation filter and Y-475 barrier filter, using Fuji ASA 400 color film.

RESULTS

Analysis of chromosomal quality

Under the same conditions of the experiment, sperm of the subjects with HBV infection as well as healthy controls appeared to be able to penetrate into zona-free hamster oocytes and to develop to the first-cleavage metaphase. However, the quality of metaphase spreads of sperm chromosomes had significant difference between the above two groups ($P < 0.005$, χ^2 -test). The quality of a number of sperm chromosome plates of the subjects with HBV infection was low, showing generally hard to be stained, stickiness of chromosome, clumping, tortuosity and so on, making the analyzable metaphase spreads greatly decreased. Whereas, few of these phenomena occurred in the controls although a small proportion of sperm chromosome plates of the controls could not be analyzed because of poor separation of chromosomes (Table 2).

Incidence of chromosome aberrations

Among the analyzable metaphase spreads, chromosome aberrations observed included numerical anomaly (aneuploidy), gap, ring chromosome, triradial, dicentric chromosome, pulverization, acentric fragment and deletion, orderly. Of the 233 analyzable sperm metaphase spreads in the hepatitis group, 33 (14.8 %) complements contained chromosome aberrations, being significantly higher than 5 (4.3 %) chromosome aberrations in the control group ($P < 0.005$, χ^2 -test).

Signals of *in situ* hybridization

Using specific whole length HBV DNA as probe to perform *in situ* hybridization on sperm chromosome slides, the sperm metaphases of one patient with chronic persistent hepatitis (subject 6) presented positive signals, all other tested subjects' spermatozoa (50 per subject), as well as all hamster oocytes (more than 200) did not have FISH signal (Table 1). Of 42 chromosome complements of subject 6 with chronic persistent hepatitis, 9 complements showed clearly twin yellow spots on some chromosomes. In 9 sperm metaphase spreads with positive signals, one had 5 signals on different chromosomes, the rest ranged from 2 to 4 spots involving unrelated

Table 1 Markers of HBV infection of the tested subjects

Subjects	Age	Serum						Seminal fluid	
		HBsAg	Anti-HBc	HBeAg	Anti-HBs	Anti-HBe	HBV-DNA	HBsAg	HBV-DNA
Hepatitis^a									
1	38	+	+	-	-	-	+	+	-
2	32	+	+	+	-	-	+	-	+
3	25	+	+	-	-	+	+	-	-
4	22	+	+	+	-	-	-	+	+
5	26	+	+	-	-	+	-	+	+
6	23	+	+	-	-	+	-	-	+
7	27	+	+	+	-	-	+	+	-
8	22	+	+	-	-	+	-	-	-
9	25	+	+	-	-	-	+	-	+
Controls									
1	32	-	-	-	-	-	-	-	-
2	29	-	-	-	-	-	-	-	-
3	23	-	-	-	-	-	-	-	-
4	25	-	-	-	-	-	-	-	-
5	26	-	-	-	-	-	-	-	-

^a1: acute hepatitis; 2, 3: chronic active hepatitis; 4, 5, 6, 7: chronic persistent hepatitis; 8, 9: chronic HBsAg carriers.

Table 2 Analytical results of sperm chromosomes of the tested subjects

Sub-jects	Number of metaphase spreads observed	Number (%) of analyzable metaphase spreads	Number(%) of normal sperm karyotypes	Number of abnormal sperm							Rates (%) of abnormal sperm	FISH Re-sults	
				With aneu-ploidy	With structural aberrations								
					g	r	tr	dic	pul	ace			del
Hepatitis													
1	73	23(31.5)	20(87.0)	1	0	0	0	1	0	1	0	13.0	-
2	69	20(29.0)	15(75.0)	1	1	0	2	0	0	0	1	25.0	-
3	72	24(33.3)	22(91.7)	0	1	0	0	0	1	0	0	8.3	-
4	68	29(42.6)	25(86.2)	0	0	1	0	2	0	1	0	13.8	-
5	86	30(34.9)	28(93.3)	1(1) ^a	0	1	1 ^a	0	0	0	0	6.7	-
6	113	43(38.1)	30(69.8)	5(2) ^a	4(1) ^b	2(1) ^a	2(1) ^a	0	2	1 ^b	0	30.2	+
7	82	19(23.2)	19(100)	0	0	0	0	0	0	0	0	0.0	-
8	61	23(37.7)	20(87.0)	0	0	1	0	1	1	0	0	13.0	-
9	48	12(25.0)	11(91.7)	1	0	0	0	0	0	0	0	8.3	-
Total	672	223(33.2)	190(85.2)	9(3) ^a	6(1) ^b	5	5	4	4	3	1	14.8	-
Controls													
1	57	31(54.3)	29(93.5)	0	0	1	0	0	0	1	0	6.5	-
2	61	21(34.4)	21(100)	0	0	0	0	0	0	0	0	0.0	-
3	50	19(38.0)	19(100)	0	0	0	0	0	0	0	0	0.0	-
4	36	17(47.2)	16(94.1)	1	0	0	0	0	0	0	0	5.9	-
5	42	28(66.7)	26(92.9)	0	1	0	0	1	0	0	0	7.1	-
Total	246	116(47.2)	111(95.7)	1	1	1	0	1	0	1	0	4.3	-

g=Gap; r=Ring; tr=Triradial; dic=Dicentric chromosome; pul=Pulverization; ace=Acentric fragment; del=Deletion

^aFor containing both numerically and structurally chromosomal aberrations simultaneously

^bFor containing gap and acentric fragment chromosome aberrations simultaneously

chromosomes. The intensity of signal presented distinct difference among the spots. Positive signals detected were not identical in the chromosomes and in distribution (Figure1).

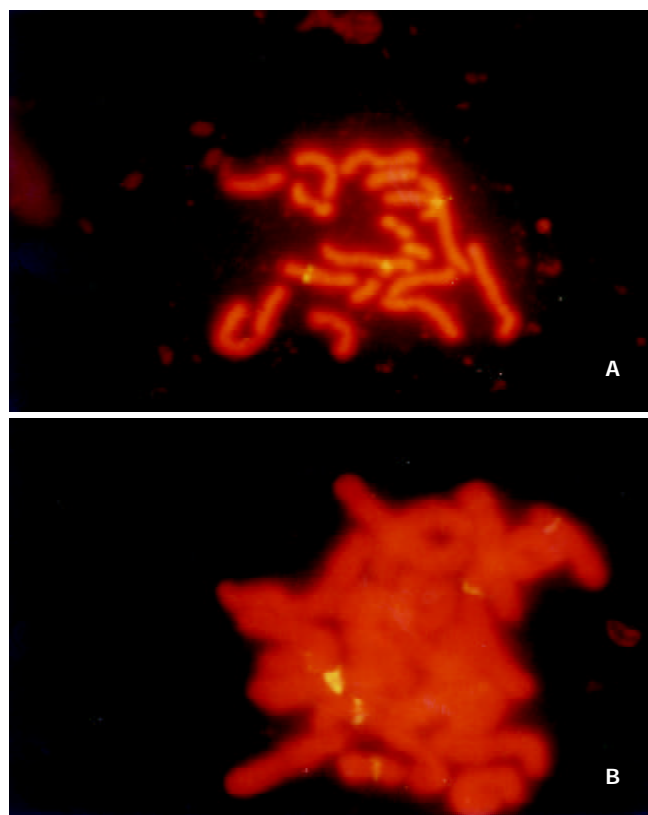


Figure 1 Detection of HBV DNA sequences in sperm chromosomes by FISH with biotinylated whole length HBV DNA probe: (A) a well separated chromosome plate from one patient (subject 6) with chronic persistent hepatitis, with three fluorescent signals on different chromosomes; (B) a poorly separated chromosome plate from the same patient with five fluorescent signals.

DISCUSSION

Our studies showed that the frequency of sperm chromosomal aberrations was greatly elevated after the infection of hepatitis B virus, and FISH could directly visualize the integration of HBV DNA sequences into sperm chromosomes. These results suggested that HBV infection could produce inheritable biological effects by carrying genetic materials damaged by virus or carrying altered genetic constituent due to the insertions of virus DNA in germ cells. As we know, this is the first report about the influence of biological factors on human sperm chromosomes.

In our study, we unexpectedly found that the sperm chromosomes frequently presented stickiness, faint stain and extreme tortuosity in the tested subjects with HBV infection and analyzable metaphases were low. Nevertheless, these changes were not found in the healthy controls under the strictly identical conditions. A previous report demonstrated that this manifestation had occurred in the chromosomes of somatic cells of HB patients with positive HBsAg^[25]. The reasons of causing chromosomal stickiness in the HBV infection patients were unclear. The possibilities we considered might include the following events: First, antigen components of HBV such as core protein might interfere with the assembly of chromosome from chromatin due to its interaction with histones, it was confirmed that the core protein of HBV had participated in the organization of nucleosomes with histones in the hepatitis B virus minichromosome^[26,27], so the condensation degree of chromosome was decreased and staining of chromosome became more difficult. Second, local despiralizations in the chromosomes occurred due to virus or its components. Third, premature chromosome condensation (PCC) might be induced by HBV, because virus-induced PCC was a common phenomenon^[28]. Chromosome stickiness itself may be a manifestation of chromosomal pulverizations.

Previous reports have indicated that HBV infection can induce genetic alterations in somatic cells including hepatocytes and blood cells etc, showing increase of the rate of chromosomal aberrations or SCEs^[29-35]. It was reported that influenza in spermatocytes of mice could greatly induce the

increase of chromosomal anomalies^[36]. Our studies revealed that the incidence of chromosomal aberrations in the HBV infection group was significantly higher than that in the controls. Although in the present study the individual sample sizes and analyzable chromosome numbers were not large enough and it was difficult to compare the differences of rates and types of aberrations among the different clinical and serological states of HBV infection, there were some features worthy to be considered: First, the incidence of chromosome aberrations did not appear to be closely correlated with the seminal fluid status of HBV infection; Second, the chromosome pulverizations were not observed in the controls but were present in 4 sperm cells in the HBV infection group; Third, subject 6 with proven HBV integrations in the sperm chromosomes had prominently higher level of chromosomal aberration than the other HBV infection subjects; Fourth, the chromosome breakages were more frequent in the HBV infection group than that in the controls.

FISH onto sperm chromosomes by specific HBV DNA as a probe had showed positive signals in an HBV patient. The results directly indicated that HBV could penetrate blood-testis barrier and enter male germ line and integrate into their genome. So the possibility of vertical transmission of HBV via the germ cells was further confirmed^[18,19]. Our preliminary observations showed that HBV integrations into sperm chromosomes had the feature of multi-site integrations and that the predilection site of HBV insertion into chromosomes seemed to be unlikely present. These results were similar with other previous reports about HBV-related hepatocellular carcinoma either in HCC-derived cell lines or in liver tumor samples^[7-17,32,33]. During spermatogenesis, the stem cells sequentially undergo proliferation by mitosis and differentiation into spermatocytes and formation into spermatozoa by meiosis. The occurred important events of meiosis were the pairing and recombination of chromosomes during the prophase of meiosis I^[37]. Thus it was possible that relocation of viral sequences and multi-site integrations could occur via genetic recombination when HBV was inserted into male reproductive cells, but the genetic effect of initial HBV insertion into various spermatogenic stages must have been greatly various. If the insertion occurred in stem cells, their all daughter cells would carry the integrated form of viral DNA and the effects would be long-term. In our studies, we were surprised by the fact that FISH showed strong signals in a patient using single small DNA probe. The reasonable explanations for this result included that the copies of HBV strand-invasion may be multiple, HBV sequence generated duplications *in situ* after the invasion into host genome, during the processes of making spermatozoa, unequal cross-over or DNA rearrangements occurred repeatedly due to HBV insertion into DNA of stem cells. According to the sperm chromosome aberration analysis (Table 2), such a subject with HBV integrations had relatively higher incidence of sperm chromosome aberration than that in other subjects without HBV integration. This correlation implied that viral DNA integrations into germ line significantly increased the instability of gametic genome. Thus, HBV integration into sperm cells would create extensively inheritable effects including offspring from such sperm fusion with ovum presenting HBV infection status in newborn infant and producing congenital or hereditary disease (for example, embryonal tumor) by altering genetic constituent and/or inducing mutations^[38-40].

We conclude that HBV infection can bring about mutagenic effects on sperm chromosomes which show that the incidence of sperm chromosome aberrations is significantly elevated after the infection of HBV. Integrations of viral DNA into sperm chromosomes with feature of multisites and nonspecific can further increase the instability of sperm chromosomes. Our

study suggests that HBV infection can create extensively inheritable effects not only by altering genetic constituent and/or inducing mutations but also possibly by vertical transmission of HBV via the germ line to the next generation.

REFERENCES

- 1 **Fang JN**, Jin CJ, Cui LH, Quan ZY, Choi BY, Ki M, Park HB. A comparative study on serologic profiles of virus hepatitis B. *World J Gastroenterol* 2001; **7**: 107-110
- 2 **Yan JC**, Ma JY, Pan BR, Ma LS. Studies on viral hepatitis B in China. *Shijie Huaren Xiaohua Zazhi* 2001; **9**: 611-616
- 3 **Rabe C**, Pilz T, Klostermann C, Berna M, Schild HH, Sauerbruch T, Caselmann WH. Clinical characteristics and outcome of a cohort of 101 patients with hepatocellular carcinoma. *World J Gastroenterol* 2001; **7**: 208-215
- 4 **Heathcote J**, Cameron CH, Dane DS. Hepatitis B antigen in saliva and semen. *Lancet* 1974; **1**: 71-73
- 5 **Darani M**, Gerber M. Letter: Hepatitis B antigen in vaginal secretions. *Lancet* 1974; **2**: 1008
- 6 **Dejean A**, Lugassy C, Zafrani S, Tiollais P, Brechot C. Detection of hepatitis B virus DNA in pancreas, kidney and skin of two human carriers of the virus. *J Gen Virol* 1984; **65**: 651-655
- 7 **Rogler CE**, Sherman M, Su CY, Shafritz DA, Summers J, Shows TB, Henderson A, Kew M. Deletion in chromosome 11p associated with a hepatitis B integration site in hepatocellular carcinoma. *Science* 1985; **230**: 319-322
- 8 **Hino O**, Shows TB, Rogler CE. Hepatitis B virus integration site in hepatocellular carcinoma at chromosome 17;18 translocation. *Proc Natl Acad Sci USA* 1986; **83**: 8338-8342
- 9 **Tokino T**, Fukushige S, Nakamura T, Nagaya T, Murotsu T, Shiga K, Aoki N, Matsubara K. Chromosomal translocation and inverted duplication associated with integrated hepatitis B virus in hepatocellular carcinoma. *J Virol* 1987; **61**: 3848-3854
- 10 **Zhou YZ**, Slagle BL, Donehower LA, vanTuinen P, Ledbetter DH, Butel JS. Structural analysis of a hepatitis B virus genome integrated into chromosome 17p of a human hepatocellular carcinoma. *J Virol* 1988; **62**: 4224-4231
- 11 **Urashima T**, Saigo K, Kobayashi S, Imaseki H, Matsubara H, Koide Y, Asano T, Kondo Y, Koike K, Isono K. Identification of hepatitis B virus integration in hepatitis C virus-infected hepatocellular carcinoma tissues. *J Hepatol* 1997; **26**: 771-778
- 12 **Pineau P**, Marchio A, Terris B, Mattei MG, Tu ZX, Tiollais P, Dejean A. At(3;8) chromosomal translocation associated with hepatitis B virus integration involves the carboxypeptidase N locus. *J Virol* 1996; **70**: 7280-7284
- 13 **Hino O**, Tabata S, Hotta Y. Evidence for increased *in vitro* recombination with insertion of human hepatitis B virus DNA. *Proc Natl Acad Sci USA* 1991; **88**: 9248-9252
- 14 **Hino O**, Ohtake K, Rogler CE. Features of two hepatitis B virus (HBV) DNA integrations suggest mechanisms of HBV integration. *J Virol* 1989; **63**: 2638-2643
- 15 **Tokino T**, Matsubara K. Chromosomal sites for hepatitis B virus integration in human hepatocellular carcinoma. *J Virol* 1991; **65**: 6761-6764
- 16 **Su TS**, Hwang WL, Yauk YK. Characterization of hepatitis B virus integrant that results in chromosomal rearrangement. *DNA Cell Biol* 1998; **17**: 415-425
- 17 **Shamay M**, Agami R, Shaul Y. HBV integrants of hepatocellular carcinoma cell lines contain an active enhancer. *Oncogene* 2001; **20**: 6811-6819
- 18 **Hadchouel M**, Scotto J, Huret JL, Molinier C, Villa E, Degos F, Brechot C. Presence of HBV DNA in spermatozoa: a possible vertical transmission of HBV via the germ line. *J Med Virol* 1985; **16**: 61-66
- 19 **Peng HW**, Su TS, Han SH, Ho CK, Ho CH, Ching KN, Chiang BN. Assessment of HBV persistent infection in an adult population in Taiwan. *J Med Virol* 1988; **24**: 405-412
- 20 **Huang TH**, Liu HX, Cai M, Huang JM. Chromosomal aberrations induced in human spermatozoa by mitomycin C. *Yichuan Xuebao* 1997; **24**: 291-295
- 21 **Kamiguchi Y**, Mikamo K. An improved, efficient method for analyzing human sperm chromosomes using zona-free hamster ova. *Am J Hum Genet* 1986; **38**: 724-740

- 22 **Sambrook J**, Fritsch EF, Maniatis. Molecular cloning-a laboratory manual. 3rd edition, New york: Clod Spring Harbor Laboratory Press 2001: 1.21-1.83
- 23 **Huang JM**, Huang TH, Fang XW, Zhuang TG, Liu HX. Detection of aneuploidy in human sperm by FISH. *Zhonghua Yixue Yichuanxue Zazhi* 1997; **14**: 248-249
- 24 **Korenberg JR**, Chen XN. Human cDNA mapping using a high-resolution R-banding technique and fluorescence *in situ* hybridization. *Cytogenet Cell Genet* 1995; **69**: 196-200
- 25 **Vianello MG**, Fasce LC, Mura MS, Andreoni G, Scalise G. Cytogenic analysis in HBsAg positive subjects, healthy carriers and patients with acute-phase hepatitis. *Boll Ist Sieroter Milan* 1979; **58**: 266-272
- 26 **Bock CT**, Schranz P, Schroder CH, Zentgraf H. Hepatitis B virus genome is organized into nucleosomes in the nucleus of the infected cell. *Virus Genes* 1994; **8**: 215-229
- 27 **Bock CT**, Schwinn S, Locarnini S, Fyfe J, Manns MP, Trautwein C, Zentgraf H. Structural organization of the hepatitis B virus minichromosome. *J Mol Biol* 2001; **307**: 183-196
- 28 **Aula P**. Virus-induced premature chromosome condensation (PCC) in single cells and G-bands of PCC-chromatin. *Hereditas* 1973; **74**: 81-87
- 29 **Chen HL**, Chiu TS, Chen PJ, Chen DS. Cytogenetic studies on human liver cancer cell lines. *Cancer Genet Cytogenet* 1993; **65**: 161-166
- 30 **Marchio A**, Meddeb M, Pineau P, Danglot G, Tiollais P, Bernheim A, Dejean A. Recurrent chromosomal abnormalities in hepatocellular carcinoma detected by comparative genomic hybridization. *Genes Chromosomes Cancer* 1997; **18**: 59-65
- 31 **Pang E**, Wong N, Lai PB, To KF, Lau JW, Johnson PJ. A comprehensive karyotypic analysis on a newly developed hepatocellular carcinoma cell line, HKCI-1, by spectral karyotyping and comparative genomic hybridization. *Cancer Genet cytogenet* 2000; **121**: 9-16
- 32 **Livezey KW**, Negorev D, Simon D. Hepatitis B virus-transfected Hep G2 cells demonstrate genetic alterations and de novo viral integration in cells replicating HBV. *Mutat Res* 2000; **452**: 163-178
- 33 **Livezey KW**, Negorev D, Simon D. Increased chromosomal alterations and micronuclei formation in human hepatoma HepG2 cells transfected with the hepatitis B virus HBX gene. *Mutat Res* 2002; **505**: 63-74
- 34 **Wang PL**, Liu SF, Shen SL, Dong XY. A study of sister-chromatid exchange in peripheral lymphocytes of hepatitis B patients with HBsAg positive and their children. *Mutat Res* 1986; **175**: 249-254
- 35 **Chatterjee B**, Ghosh PK. Constitutive heterochromatin polymorphism and chromosome damage in viral hepatitis. *Mutat Res* 1989; **210**: 49-57
- 36 **Sharma G**, Polasa H. Cytogenetic effects of influenza virus infection on male germ cells of mice. *Hum Genet* 1978; **45**: 179-187
- 37 **Hecht NB**. The making of a spermatozoon: a molecular perspective. *Dev Gen* 1995; **16**: 95-103
- 38 **Naumova AK**, Kisselev LL. Biological consequences of interactions between hepatitis B virus and human nonhepatic cellular genomes. *Biomed Sci* 1990; **1**: 233-238
- 39 **Kim H**, Lee MJ, Kim MR, Chung IP, Kim YM, Lee JY, Jang JJ. Expression of cyclin D1, cyclin E, cdk4 and loss of heterozygosity of 8p, 13q, 17p in hepatocellular carcinoma: comparison study of childhood and adult hepatocellular carcinoma. *Liver* 2000; **20**: 173-178
- 40 **Tanaka T**, Miyamoto H, Hino O, Kitagawa T, Koike M, Iizuka T, Sakamoto H. Primary hepatocellular carcinoma with hepatitis B virus-DNA integration in a 4-year-old boy. *Hum Pathol* 1986; **17**: 202-204

Edited by Xu XQ and Wu XN

TT virus and hepatitis G virus infections in Korean blood donors and patients with chronic liver disease

Mee Juhng Jeon, Jong Hee Shin, Soon Pal Suh, Young Chai Lim, Dong Wook Ryang

Mee Juhng Jeon, Division of Medical Research, Kwangju-Chonnam Red Cross Blood Center, Chonnam National University, Kwangju, Republic of Korea

Jong Hee Shin, Soon Pal Suh, Dong Wook Ryang, Department of Clinical Pathology, Chonnam National University, Kwangju, Republic of Korea

Young Chai Lim, Department of Pharmacology, Medical School, Chonnam National University, Kwangju, Republic of Korea

Jong Hee Shin, Soon Pal Suh, Young Chai Lim, Dong Wook Ryang, Research Institute of Medical Sciences, Chonnam National University, Kwangju, Republic of Korea

Correspondence to: Dong Wook Ryang M.D., Ph.D., Department of Clinical Pathology, Chonnam National University Medical School 8 Hak 1 dong, Dong-Ku, Kwangju, Korea. ryang@hitel.net

Telephone: +82-62-220-5353 **Fax:** +82-62-224-2518

Received: 2002-07-02 **Accepted:** 2002-07-27

Jeon MJ, Shin JH, Suh SP, Lim YC, Ryang DW. TT virus and hepatitis G virus infections in Korean blood donors and patients with chronic liver disease. *World J Gastroenterol* 2003; 9(4): 741-744

<http://www.wjgnet.com/1007-9327/9/741.htm>

INTRODUCTION

A novel human DNA virus, TT virus (TTV), was first discovered in the sera of three Japanese patients with post-transfusion hepatitis in 1997^[1]. TTV is a non-enveloped, single-stranded virus related to the Circoviridae family^[2,3]. Hepatitis G virus (HGV) is an enveloped RNA virus member of the Flaviviridae family^[4]. TTV and HGV infections in healthy blood donors as well as in patients with liver disease have been recently reported in many areas of the world^[3-22]. However, the role of these viruses in disease remains uncertain. Information regarding TTV and HGV infections in the Korean population is limited. Hepatitis B virus (HBV) and hepatitis C virus (HCV) are the viral agents most readily implicated in causing a liver disease in Korea^[23,24]. The aims of this study were to determine the prevalence of TTV and HGV in Korean blood donors and patients with type B or C chronic liver disease, to investigate the association between blood transfusion and TTV and HGV infections, and to assess the correlation between TTV and HGV viremia and hepatic damage.

MATERIALS AND METHODS

Materials

A total of 291 blood samples, derived from 110 healthy donors, 112 hepatitis B surface antigen (HBsAg)-positive donors, and 69 anti-hepatitis C virus antibody (anti-HCV Ab)-positive donors, were collected at the Kwangju-Chonnam Red Cross Blood Center. A total of 100 blood samples were obtained from 81 patients with type B chronic liver disease (46 chronic hepatitis, 15 liver cirrhosis, and 20 hepatocellular carcinoma) and 19 patients with type C chronic liver disease (10 chronic hepatitis and 9 hepatocellular carcinoma) at the Chonnam National University Hospital.

Serological and chemical studies

Blood samples were centrifuged and stored at -70 °C within hours of collection. HBsAg and anti-HCV Ab were tested with enzyme immunoassay (AxSYM, Abbott Laboratories, USA). Immunoblot assay (ProfiBlot IIN, SLT Lab Instruments, Austria) was used to confirm anti-HCV. Serum levels of alanine aminotransferase (ALT) and aspartate aminotransferase (AST) were also measured using an autoanalyzer (Hitachi 747, Hitachi, Japan).

DNA extraction and TTV PCR

DNA was extracted from 250 µL of sera using a kit (DNAzol, Molecular Research Center, USA) according to the manufacturer's guidelines. Nucleic acids were dissolved in 50 µL of NaOH (8 mM). A 7 µL volume was then removed and used for amplification of TTV DNA. The PCR reaction was performed in a volume of 50 µL containing 10 mM Tris-HCl

Abstract

AIM: To determine the prevalences of TTV and HGV infections among blood donors and patients with chronic liver disease in Korea, to investigate the association of TTV and HGV infections with blood transfusion, and to assess the correlation between TTV and HGV viremia and hepatic damage.

METHODS: A total of 391 serum samples were examined in this study. Samples were obtained from healthy blood donors ($n=110$), hepatitis B surface antigen (HBsAg)-positive donors ($n=112$), anti-hepatitis C virus (anti-HCV)-positive donors ($n=69$), patients with type B chronic liver disease ($n=81$), and patients with type C chronic liver disease ($n=19$). TTV DNA was detected using the hemi-nested PCR. HGV RNA was tested using RT-PCR. A history of blood transfusion and serum levels of alanine aminotransferase (ALT) and aspartate aminotransferase (AST) were also determined.

RESULTS: TTV DNA was detected in 8.2 % of healthy blood donors, 16.1 % of HBsAg-positive donors, 20.3 % of anti-HCV-positive donors, 21.0 % of patients with type B chronic liver disease, and 21.1 % of patients with type C chronic liver disease. HGV RNA was detected in 1.8 % of healthy blood donors, 1.8 % of HBsAg-positive donors, 17.4 % of anti-HCV-positive donors, 13.6 % of patients with type B chronic liver disease, and 10.5 % of patients with type C chronic liver disease. The prevalence of TTV and HGV infections in HBV- or HCV-positive donors and patients was significantly higher than in healthy blood donors ($P<0.05$), except for the detection rate of HGV in HBsAg-positive donors which was the same as for healthy donors. There was a history of transfusion in 66.7 % of TTV DNA-positive patients and 76.9 % of HGV RNA-positive patients ($P<0.05$). No significant increase in serum ALT and AST was detected in the TTV- or HGV-positive donors and patients.

CONCLUSION: TTV and HGV infections are more frequently found in donors and patients infected with HBV or HCV than in healthy blood donors. However, there is no significant association between TTV or HGV infections and liver injury.

(pH 8.3), 50 mM KCl, 1.5 mM MgCl₂, 200 μM dNTPs, 0.5 μM of NG059 (5' -ACAGACAGAGGAGAAGGCAACATG-3') as the sense primer, 0.5 μM of NG063 (5' -CTGGCATTTCACATTTCCAAAGTT-3') as the antisense primer, and 2 U of Taq polymerase to amplify a 286-bp product. The second-round PCR was done under identical conditions, except that the template was 5 μL product from the first-round PCR, and the sense primer was 0.5 μM of NG061 (5' -GGCAACATGTTATG GATAGACTGG-3'). The size of the second-round PCR product was 271 bp. Each PCR was performed in a programmable thermal cycler (GeneAmp PCR System 9 600, Perkin-Elmer Cetus, USA). The PCR program consisted of 35 cycles of denaturation for 15 seconds at 95 °C, annealing for 30 seconds at 58 °C, and extension for 30 seconds at 72 °C, followed by a final extension for 10 minutes at 72 °C. The amplification products were separated by 2 % agarose gel electrophoresis, stained with ethidium bromide, and photographed under UV light.

Nucleotide sequencing

To ascertain the specificity of the PCR products, DNA sequences of the amplified product were determined. The PCR product was purified with a PCR purification kit (Boehringer Mannheim, Mannheim, Germany). Nucleotide sequences of the amplicon were directly determined using an AccuPower DNA sequencing kit (Bioneer, Korea). The sequence homology between the PCR products and published TTV DNA was examined. Two randomly selected PCR products were sequenced, both of which were positive for TTV DNA. Sequence comparison with databases confirmed the specific amplification of TTV genomic DNA.

RNA extraction and HGV RT-PCR

To detect HGV RNA in a sample, nucleic acids were isolated from 250 μL of serum using Trizol LS Reagent (GIBCO, USA) and a reverse-transcription PCR (RT-PCR) was performed. A total of 35 cycles of PCR (94 °C for 30 seconds, 50 °C for 30 seconds, and 72 °C for 60 seconds for each cycle) were completed in a programmable thermal cycler (GeneAmp PCR System 9 600, Perkin-Elmer Cetus, USA). The size of the PCR product was 234 bp. The amplification products were separated by 2 % agarose gel electrophoresis, stained with ethidium bromide, and photographed under UV light.

Transfusion history

To examine the association of TTV and HGV infections with blood transfusion, previous transfusion history was investigated in both patients with chronic liver disease and blood donors, by examining their medical records or via telephone interviews.

Statistical analysis

Statistical analysis was conducted using the Chi-square test and analysis of variance (ANOVA). Statistical significance was set when $P < 0.05$.

RESULTS

Prevalences of TTV DNA and HGV RNA

The prevalences of TTV and HGV infections in blood donors and patients with chronic liver disease were shown in Table 1. TTV DNA was detected in 8.2 % (9/110) of healthy blood donors, 16.1 % (18/112) of HBsAg-positive donors, 20.3 % (14/69) of anti-HCV-positive donors, 21.0 % (17/81) of patients with type B chronic liver disease, and 21.1 % (4/19) of patients with type C chronic liver disease. The TTV prevalence was significantly higher both in HBsAg-positive or anti-HCV-positive donors and in patients with chronic liver disease than

in healthy blood donors ($P < 0.05$). HGV RNA was detected in 1.8 % (2/110) of healthy blood donors, 1.8 % (2/112) of HBsAg-positive donors, 17.4 % (12/69) of anti-HCV-positive donors, 13.6 % (11/81) of patients with type B chronic liver disease, and 10.5 % (2/19) of patients with type C chronic liver disease. The HGV prevalence was significantly lower in healthy blood donors or HBsAg-positive donors than in patients with chronic liver disease and anti-HCV-positive donors ($P < 0.05$). The detection rates for TTV or HGV were not significantly different between the three types of chronic liver disease. The TTV prevalence was about 4.6 times higher than the HGV prevalence in healthy blood donors. Co-infection of TTV and HGV was also observed in ten cases of HBV- or HCV-infected patients and donors.

Table 1 The prevalence of TTV and HGV infections in blood donors and patients with chronic liver disease from Korea

Subject	n	TTV (%)	HGV (%)	TTV & HGV (%)
Healthy blood donors	110	9 (8.2)	2 (1.8)	0 (0.0)
HBsAg(+) donors	112	18 (16.1) ^a	2 (1.8)	0 (0.0)
Anti-HCV(+) donors	69	14 (20.3) ^a	12 (17.4) ^b	3 (4.3)
Patients with type B chronic liver disease	81	17 (21.0) ^a	11 (13.6) ^b	6 (7.4)
Chronic hepatitis	6	10(21.7)	5 (10.9)	3 (6.5)
Liver cirrhosis	15	3 (20.0)	3 (20.0)	2 (13.3)
Hepatocellular carcinoma	20	4(20.0)	3 (20.0)	1 (5.0)
Patients with type C chronic liver disease	19	4 (21.1) ^a	2 (10.5) ^b	1 (5.3)
Chronic hepatitis	10	2 (20.0)	1 (10.0)	0 (0.0)
Hepatocellular carcinoma	9	2 (22.2)	1 (11.1)	1 (11.1)
Total	391	62 (15.9)	29 (7.4)	10 (2.6)

^a $P < 0.05$ vs healthy blood donors, ^b $P < 0.05$ vs healthy blood donors or HBsAg-positive donors.

Association of TTV and HGV infections with blood transfusion

To investigate the association of TTV and HGV infections with blood transfusion, the medical records for the previous transfusion history were reviewed in patients with chronic liver disease. The rate of transfusion history was higher in TTV- or HGV-positive patients than in TTV- or HGV-negative patients ($P < 0.05$) (Table 2).

Table 2 Transfusion history according to the detection of TTV and HGV in patients with chronic liver disease

Group	n	Transfusion history	
		Yes (%)	No (%)
TTV Positive	21	14 (66.7) ^a	7 (33.3)
Negative	77	33 (42.9)	44 (57.1)
HGV Positive	13	10 (76.9)	3 (23.1)
Negative	85	37 (43.5)	48 (56.5)
Total	98	47 (48.0)	51 (52.0)

^a $P < 0.05$ vs TTV- or HGV-negative patients.

Correlation between TTV or HGV viremia and hepatic damage

To evaluate the correlation between TTV or HGV infections and hepatic damage, the serum levels of ALT and AST were measured in all subjects (data not shown). No significant increase in serum ALT and AST was observed in TTV- or HGV-positive blood donors, compared with TTV- or HGV-negative donors. In addition, TTV or HGV co-infection did

not elicit any further significant increase in ALT and AST levels in patients with chronic liver disease. Furthermore, no increase in ALT and AST was observed in HBV- or HCV-positive patients or donors infected with both TTV and HGV. These observations suggested that there is no significant association between TTV or HGV infections and hepatic injury.

DISCUSSION

TTV was detected in 8.2 % of healthy blood donors from Korea. The prevalence of TTV infection among blood donors in other countries is 1.9 % in the United Kingdom^[5], 3.2 % in Germany^[6], 7.5-10 % in the United States^[7, 8], 12 % in Japan^[3], 29.4 % in Egypt^[9], 36 % in Thailand^[10], and 62 % in Brazil^[11]. These differences in prevalence between countries could be due to the different geographical distribution of TTV infections, and the heterogeneity and variability of TTV isolates^[3, 5]. Variation could also arise due to different experimental methods to determine TTV infection, such as the primers used, and the sensitivity of the PCR methods employed^[8, 25]. The primer used in our study was identical to that used in the aforementioned countries, suggesting that the discrepancies of TTV prevalence between countries were not due to variation in the primer used. The detection rate of HGV RNA in blood donors from many other countries ranged from 0.5 to 7.4 %^[19-22]. In healthy Korean blood donors, the detection rate of HGV was 1.8 %, and the prevalence of TTV was higher (about 4.6 times) than that of HGV.

We observed TTV and HGV co-infection in subjects with HBV or HCV findings that had also been reported elsewhere^[12-18]. The co-infection rate of TTV in HBV- and HCV-infected subjects was similar, a finding also reported by others^[10, 12]. However, there was some difference in the co-infection rate of HGV between HBV and HCV. The prevalence of HGV in HBsAg-positive donors was lower than in patients with chronic liver disease and also anti-HCV-positive donors. Giulivi *et al.* have reported similar findings^[26]. The discrepancy in the co-infection rate of HGV between HBV- and HCV-positive donors may have clinical significance. With the exception of HGV co-infection in HBV-positive donors, both HBV- and HCV-infected subjects had a higher detection rate of TTV or HGV than healthy donors. This suggested that HBV- or HCV-infected subjects had a greater exposure to a risk factor for viral infections. These viruses may also share a common route of transmission.

A total of 66.7 % of TTV DNA-positive patients and 76.9 % of HGV RNA-positive patients had a history of blood transfusion. This suggests the possibility of viral transmission via blood transfusion. TTV and HGV are prevalent in the sera of persons with hemophilia, intravenous drug users, and hemodialysis patients^[3, 8, 21, 27]. However, our results indicate that TTV and HGV were observed in donors and patients without a transfusion history, which suggests a non-parenteral route of transmission. TTV and HGV have reportedly been detected in urine, feces, and breast milk^[6, 28, 29]. Thus, TTV and HGV might be transmitted via several parenteral and non-parenteral routes.

No significant increase in ALT or AST was observed in healthy donors or liver disease patients infected with either TTV or HGV, compared to subjects without these viral infections. Kao *et al.* reported that TTV infection does not affect the disease process of type B or C hepatitis, or the response to interferon treatment^[15]. Oguchi *et al.* demonstrated that a TTV carrier state was maintained without hepatitis in hemodialysis patients over a 5-year follow-up period^[30]. Alter *et al.* showed that HGV infection was not associated with hepatitis and did not worsen the course of concurrent HCV infection^[31]. Considering all these results, TTV or HGV

infection seems not to be related to the initiation or potentiation of hepatic damage, which therefore suggests that the routine screening test for TTV and HGV on donated blood is not necessary. At present there also is no country that conducts the screening test for these viral infections.

REFERENCES

- Nishizawa T**, Okamoto H, Konishi K, Yoshizawa H, Miyakawa Y, Mayumi M. A novel DNA virus (TTV) associated with elevated transaminase levels in posttransfusion hepatitis of unknown etiology. *Biochem Biophys Res Comm* 1997; **241**: 92-97
- Mushahwar IS**, Erker JC, Muerhoff AS, Leary TP, Simons JN, Birkenmeyer LG, Chalmers ML, Pilot-Matias TJ, Dexai SM. Molecular and biophysical characterization of TT virus: evidence for a new virus family infecting humans. *Proc Natl Acad Sci USA* 1999; **96**: 3177-3182
- Okamoto H**, Nishizawa T, Kato N, Ukita M, Ikeda H, Iizuka H, Miyakawa Y, Mayumi M. Molecular cloning and characterisation of a novel DNA virus (TTV) associated with posttransfusion hepatitis of unknown etiology. *Hepatology* 1998; **10**: 1-16
- Simons JN**, Pilot-Matias TJ, Leary TP. Identification of two flavivirus-like genomes in the GB hepatitis agent. *Proc Natl Acad Sci* 1995; **92**: 3401-3405
- Simmonds P**, Davidson F, Lycett C, Prescott LE, MacDonald DM, Ellender J, Yap PL, Ludlam CA, Haydon GH, Gillon J, Jarvis LM. Detection of a novel DNA virus (TTV) in blood donors and blood products. *Lancet* 1998; **352**: 191-194
- Wolff C**, Diekmann A, Boomgaarden M, Korner MM, Kleesiek K. Viremia and excretion of TT virus in immunosuppressed heart transplant recipients and in immunocompetent individuals. *Transplantation* 2000; **69**: 351-356
- Charlton M**, Adjei P, Poterucha J, Zein N, Moore B, Therneau T, Krom R, Wiesner R. TT-virus infection in north American blood donors, patients with fulminant hepatic failure, and cryptogenic cirrhosis. *Hepatology* 1998; **28**: 839-842
- Desai SM**, Muerhoff AS, Leary TP, Erker JC, Simons JN, Chalmers ML, Birkenmeyer LG, Pilot-Matias TJ, Mushahwar IK. Prevalence of TT virus infection in US blood donors and populations at risk for acquiring parenterally transmitted viruses. *J Infect Disease* 1999; **179**: 1242-1244
- Gad A**, Tanaka E, Orii K, Kafumi T, Serwah AE, El-Sherif A, Nooman Z, Kiyosawa K. Clinical significance of TT virus infection in patients with chronic liver disease and volunteer blood donors in Egypt. *J Med Virol* 2000; **60**: 177-181
- Tanaka H**, Okamoto H, Luengrojanakul P, Chainuvata T, Tsuda F, Tanaka T, Miyakawa Y, Mayumi M. Infection with an unenveloped DNA virus (TTV) associated with posttransfusion non-A-G hepatitis in hepatitis patients and healthy blood donors in Thailand. *J Med Virol* 1998; **56**: 234-238
- Niel C**, de Oliveira JM, Ross RS, Gomes SA, Roggendorf M, Viazov S. High prevalence of TT virus infection in Brazilian blood donors. *J Med Virol* 1999; **57**: 259-263
- Naoumov NV**, Petrova EP, Thomas MG, Villians R. Presence of a newly described human DNA virus (TTV) in patients with liver disease. *Lancet* 1998; **352**: 195-197
- Orii K**, Tanaka E, Umemura T, Rokuhara A, Iijima A, Yoshisawa K, Imai H, Kiyosawa K. Prevalence and disease association of TT virus infection in Japanese patients with viral hepatitis. *Hepatology* 1999; **14**: 161-170
- Berg T**, Schreier E, Heuft HG, Hohne M, Bechstein WO, Leder K, Hopf U, Neuhaus P, Wiedenmann B. Occurrence of a novel DNA virus (TTV) infection in patients with liver diseases and its frequency in blood donors. *J Med Virol* 1999; **59**: 117-121
- Kao JH**, Chen W, Chen PJ, Lai MY, Chen DS. TT virus infection in patients with chronic hepatitis B or C: influence on clinical, histological and virological features. *J Med Virol* 2000; **60**: 387-392
- Schleicher S**, Chaves RL, Dehmer T, Gregor M, Hess G, Flehmig B. Identification of GBV-C hepatitis G RNA in chronic hepatitis C patients. *J Med Virol* 1996; **50**: 71-74
- Bralet MP**, Thorabla FR, Pawlowsky JM, Bastie A, Nhieu JTV, Duval J. Histopathologic impact of GB virus C infection on chronic hepatitis C. *Gastroenterology* 1997; **112**: 188-192

- 18 **Alter MJ**, Gallagher M, Morris T, Moyer LA, Meeks EL, Krawczynski K. Acute non-A-E hepatitis in the United States and the role of hepatitis G virus infection. *N Engl J Med* 1997; **336**: 741-746
- 19 **Simons JN**, Leary TP, Dawson GJ, Piolot-Matias TJ, Muerhoff AS, Schlauder GG, Desai SM, Mushahwar IK. Isolation of novel virus-like sequences associated with human hepatitis. *Nat Med* 1995; **1**: 564-569
- 20 **Buorkman P**, Sundstrom G, Widell A. Hepatitis C virus and GB virus C/hepatitis G virus viremia in Swedish blood donors with different alanine aminotransferase levels. *Transfusion* 1998; **38**: 378-384
- 21 **Hadlock KG**, Joung KH. GBV-C/HGV: a new virus within the Flaviviridae and its clinical implication. *Transfus Med Rev* 1998; **12**: 94-108
- 22 **Cheung RC**, Keeffe EB, Greenberg HB. Hepatitis G virus: Is it a hepatitis virus? *West J Med* 1997; **167**: 23-33
- 23 **Lee HS**, Han CJ, Kim CY. Predominant etiologic association of hepatitis C virus with hepatocellular carcinoma compared with hepatitis B virus in elderly patients in a hepatitis B-endemic area. *Cancer* 1993; **72**: 2564-2567
- 24 **Park BC**, Han BH, Ahn SY, Lee SW, Lee DH, Lee YN, Seo JH, Kim KW. Prevalence of hepatitis C antibody in patients with chronic liver disease and hepatocellular carcinoma in Korea. *J Viral Hepat* 1995; **2**: 195-202
- 25 **Mizokami M**, Albrecht JK, Kato T, Orito E, Lai VC, Goodman Z, Hong Z, Lau JY. TT virus infection in patients with chronic hepatitis C virus infection - effect of primers, prevalence, and clinical significance. Hepatitis Interventional Therapy Group. *J Hepatol* 2000; **32**: 339-343
- 26 **Giulivi A**, Slinger R, Tepper M, Sher G, Scalia V, Kessler G, Gill P. Prevalence of GBV-C/hepatitis G virus viremia and anti-E2 in Canadian blood donors. *Vox Sang* 2000; **79**: 201-205
- 27 **Aikawa T**, Sugai Y, Okamoto H. Hepatitis G infection in drug abusers with chronic hepatitis C. *N Engl J Med* 1996; **334**: 195-196
- 28 **Schröter M**, Polywka S, Zöllner B, Schäfer P, Laufs R, Feucht HH. Detection of TT virus DNA and GB virus type C/Hepatitis G virus RNA in serum and breast milk: Determination of mother-to-child transmission. *J Clin Microbiol* 2000; **38**: 745-747
- 29 **Okamoto H**, Akahane Y, Ukita M, Fukuda M, Tsuda F, Miyakawa Y, Mayumi M. Fecal excretion of a nonenveloped DNA virus (TTV) associated with posttransfusion non-A-G hepatitis. *J Med Virol* 1998; **56**: 128-132
- 30 **Oguchi T**, Tanaka E, Orii K, Kobayashi M, Hora K, Kiyosawa K. Transmission of and liver injury by TT virus in patients on maintenance hemodialysis. *J Gastroenterol* 1999; **34**: 234-240
- 31 **Alter HJ**, Nakatsuji Y, Melpolder J, Wages J, Wesley R, Shih WK, Kim JP. The incidence of transfusion-associated hepatitis G virus infection and its relation to liver disease. *N Engl J Med* 1997; **336**: 747-754

Edited by Ma JY and Xu XQ

Is laparoscopy an advantage in the diagnosis of cirrhosis in chronic hepatitis C virus infection?

Perdita Wietzke-Braun, Felix Braun, Peter Schott, Giuliano Ramadori

Perdita Wietzke-Braun, Felix Braun, Peter Schott, Giuliano Ramadori,
Department of Internal Medicine, Division of Gastroenterology and
Endocrinology, University of Goettingen, Germany

Correspondence to: Prof. Giuliano Ramadori, Medizinische
Universitätsklinik, Abteilung Gastroenterologie, Robert-Koch-Strasse
40, 37075 Goettingen, Germany. gramado@med.uni-goettingen.de
Telephone: +49-551-396301 **Fax:** +49-551-398596

Received: 2002-10-08 **Accepted:** 2002-11-04

Abstract

AIM: To evaluate the potential of laparoscopy in the diagnosis of cirrhosis and outcome of interferon treatment in HCV-infected patients.

METHODS: In this retrospective study, diagnostic laparoscopy with laparoscopic liver biopsy was performed in 72 consecutive patients with chronic HCV infection. The presence or absence of cirrhosis was analyzed macroscopically by laparoscopy and microscopically by liver biopsy specimens. Clinical and laboratory data and outcome of interferon-alfa treatment were compared between cirrhotic and noncirrhotic patients.

RESULTS: Laparoscopically, cirrhosis was seen in 29.2 % (21/72) and non-cirrhosis in 70.8 % (51/72) of patients. Cirrhotic patients were significantly older with a significant longer duration of HCV infection than noncirrhotic patients. Laboratory parameters (AST, γ -GT, γ -globulin fraction) were measured significantly higher as well as significantly lower (prothrombin index, platelet count) in cirrhotic patients than in non-cirrhotic patients. Histologically, cirrhosis was confirmed in 11.1 % (8/72) and non cirrhosis in 88.9 % (64/72). Patients with macroscopically confirmed cirrhosis ($n=21$) showed histologically cirrhosis in 38.1 % (8/21) and histologically non-cirrhosis in 61.9 % (13/21). In contrast, patients with macroscopically non-cirrhosis ($n=51$) showed histologically non cirrhosis in all cases (51/51). Thirty-nine of 72 patients were treated with interferon-alfa, resulting in 35.9 % (14/39) patients with sustained response and 64.1 % (25/39) with non response. Non-responders showed significantly more macroscopically cirrhosis than sustained responders. In contrast, there were no significant histological differences between non-responders and sustained responders.

CONCLUSION: Diagnostic laparoscopy is more accurate than liver biopsy in recognizing cirrhosis in patients with chronic HCV infection. Liver biopsy is the best way to assess inflammatory grade and fibrotic stage. The invasive marker for staging, prognosis and management, and treatment outcome of chronic HCV-infected patients need further research and clinical trials. Laparoscopy should be performed for recognition of cirrhosis if this parameter is found to be of prognostic and therapeutic relevance in patients with chronic HCV infection.

Wietzke-Braun P, Braun F, Schott P, Ramadori G. Is laparoscopy an advantage in the diagnosis of cirrhosis in chronic hepatitis C virus infection? *World J Gastroenterol* 2003; 9(4): 745-750
<http://www.wjgnet.com/1007-9327/9/745.htm>

INTRODUCTION

Hepatitis C virus (HCV) infection is the leading cause of chronic liver disease. Up to 85 % of HCV-infected patients develop chronic liver disease without elimination of the virus^[1-3]. Chronic HCV infected patients develop cirrhosis in 7 % and 20 % after 20 and 40 years of infection^[4], while symptoms and alarming biochemical markers appear late^[5,6]. Patients with cirrhosis secondary to chronic HCV infection also have an increased risks for development of hepatocellular carcinoma (HCC), estimated to be between 1-4 % per year^[7].

The diagnostic spectrum for chronic hepatitis C includes biochemical parameters, antibodies against HCV, qualitative and quantitative HCV RNA with genotyping, abdominal ultrasound and liver histology. Random core biopsy analysis can reveal information about the inflammatory grade and fibrotic stage of chronic HCV infection^[8]. Diagnosis of compensated liver cirrhosis can be made with a high accuracy neither by percutaneous liver biopsy nor by ultrasound^[9]. In comparison with percutaneous liver biopsy, laparoscopy allows macroscopic inspection of both liver lobes that might variate during progression of liver disease^[10]. Percutaneous liver biopsy only allows the interpretation of a small biopsy. It has been reported that histological analysis fail with error ranges above 25 % in the diagnosis of cirrhosis in chronic liver disease^[11,12], especially during the early phase of cirrhosis (Child A) and macronodular cirrhosis^[13]. In a retrospective study, Poniachik *et al.* compared the presence of cirrhosis in 434 patients by liver biopsy and laparoscopy. Cirrhosis was seen laparoscopically in 169 patients and was confirmed in 115 patients histologically. In contrast, only 2 of 265 histologically confirmed cirrhotic livers were macroscopically without cirrhosis^[14]. Ultrasound guided liver biopsy can result in a false negative histology due to the puncture of a regenerative nodule^[15]. Cardi *et al.* showed superiority of laparoscopy over ultrasonography in diagnosis of widespread liver diseases^[16]. Oberti *et al.* reported that only prothrombin index and serum hyaluronate were sensitive parameters for screening cirrhosis^[17]. Early cirrhosis may often be missed due to clinical inappearance especially in patients with chronic HCV infection and accurate noninvasive markers of disease activity and fibrosis are not available^[18]. The absence of early cirrhosis in chronic HCV infected patients might be a potential field for diagnostic laparoscopy that is not performed routinely and patients with early cirrhosis can be enrolled in the screening programs for HCC, too.

In the treatment of chronic HCV infection has proved beneficial interferon-alfa in the last two decades^[19-23]. Old age, high level of viraemia, HCV genotype II (1b), long duration of disease, high levels of hepatic iron store, especially the advanced liver damage represented by dimension of fibrosis were considered to be negative predictive factors in the outcome of interferon treatment^[22,24-34]. Two studies focused exclusively on interferon treatment in patients with HCV related cirrhosis^[35,36]. After introduction of pegylated interferon given only once a week, HCV-infected patients with cirrhosis or bridging fibrosis were treated in a clinical trial^[37]. These data implicated that HCV infected patients with liver cirrhosis need different therapeutic schedules with longer duration and higher dose of interferon.

Since cirrhosis is a negative predictor for antiviral therapy in chronic HCV-infected patients and liver histology might underestimate the frequency of cirrhosis, the aim of this retrospective study was to evaluate the potential of laparoscopy in the diagnosis of cirrhosis and outcome of interferon treatment in this particular group of patients.

MATERIALS AND METHODS

Patients

Laparoscopy and laparoscopic liver biopsy were performed in 72 chronic HCV-infected patients. Diagnosis of chronic HCV infection was based on elevated liver enzymes for at least 6 months, detection of anti-HCV antibodies in ELISA (2nd generation) and HCV RNA by RT/PCR. Patients with active viral coinfections (HBV, HIV, CMV, EBV), evidence for autoimmune hepatitis with positive serologic constellation of specific autoantibodies (ANA, AMA, anti-SLA, SMA, anti-LKM), alcohol and/or i.v. drug abusers and patients with signs of liver cirrhosis and/or hepatic decompensation (e.g. ascites, gastrointestinal bleeding, etc.) were excluded. Each patient was asked to sign a written informing consent for diagnostic laparoscopy and liver biopsy.

Biochemical and serological analysis

Serum levels of ALT, AST, γ -GT, AP and CHE, as well as concentrations of serum bilirubin, prothrombin index, γ -globuline fraction and platelet count were measured by established routine methods before laparoscopy, during and after interferon treatment. Anti-HCV antibodies were analyzed using an ELISA (2nd generation, Ortho Diagnostic Systems, Raritan, NJ, USA) according to the instructions of the manufacturer.

Detection of HCV RNA and determination of HCV genotypes

According to Okamoto *et al.* and Simmonds *et al.*^[38,39] determination of serum HCV RNA by a nested RT/PCR technique and determination of genotypes by a restriction enzyme analysis were carried out as described previously^[40].

Laparoscopy

Abdominal ultrasound, electrocardiogram and, in patients older than 60 years, a chest X-ray were performed before laparoscopy. The evening before laparoscopy, each patient received 75 mg promethazin orally. Two hours before examination, 50 mg promethazin and 30 minutes before exploration 50 mg pethidin and 0.5 mg atropine were injected intramuscularly. If necessary, patients received sedativa or analgetics during the laparoscopic intervention. During laparoscopy, each patient was given continuously an isotonic electrolyte solution intravenously. Patients were monitored by pulsoxymetry. After local anesthesia, the pneumoperitoneum was installed by puncturing at Monros' point with the Verres needle followed by insufflation of 2-3 L nitrous oxide. After insertion of the laparoscope in a trocar with a safety shield at Kalks' point, macroscopic exploration of liver, spleen and peritoneum followed. Liver biopsies were taken generally from an area on the anterior surface of the left lobe of the liver or of macroscopic suspect areas using a Menghini needle, at least 2 cm from the liver edge, containing at least five portal areas. Macroscopic diagnosis of cirrhosis was made based on the following criteria: (1) diffuse nodules on the liver surface, or (2) shallow nodules (i.e., nodules usually of large diameter, slightly protruding from the liver surface) if the liver was hard on palpation and rigid on lifting with a blunt probe and if clearcut features of portal hypertension were observed^[41,42].

Histopathological evaluation

Formalin-fixed and paraffin-embedded liver biopsies were

stained with hematoxylin-eosin, trichrome and by applying the Prussian blue reaction as described previously^[43]. One pathologist examined samples unblindedly. A modified "Histology Activity Index" (HAI) on the basis of reported staging scores served to assess the stage of fibrosis^[44-46]. Absent portal fibrosis was staged as fibrosis score I (HAI^b=0, no fibrosis), mild to moderate fibrosis as stage II (HAI^b=1, fibrotic portal expansion), marked fibrosis as stage III (HAI^b=3, bridging fibrosis) and complete fibrosis as cirrhosis (HAI^b=4).

Interferon treatment

Patients received recombinant interferon-alfa 2a (Roferon A, Hoffmann-La Roche, Basel, Switzerland) for initial treatment of chronic HCV infection. In our retrospective study, a dose of 6 MU three times a week was administered for 12 months according to Chemello *et al.*^[47]. Patients were classified as sustained responders if serum transaminases normalized (biochemical response) and serum HCV RNA became undetectable (virological response) during the treatment and at 6 months after the end of treatment (follow-up). During the follow-up, the re-emergence of both parameters after the end of treatment was defined as relapse. Patients with no improvement of biochemical or virological parameters within the first 3 months of treatment were classified as non-responders and treatment was stopped. For statistical analysis patients with relapse and non-response were classified as non-responders and compared with sustained responders. Patients who finished their course of treatment and 6 months of follow-up after the end of treatment were analysed.

Statistical analysis

Significant levels of differences between values were analyzed using the Chi-square test, Mann-Whitney test and student's *t*-test as indicated.

RESULTS

Mean ($M \pm SD$) age of the 72 patients (49 % female, 51 % male) with chronic HCV infection was 46.8 ± 12.1 years with a range of 27-72 years. Route and date of HCV infection were identified in 44 patients. The duration of HCV infection was 15.4 ± 9.7 years and route of viral transmission was blood transfusion in 23 %, intravenous drug abuse in 18 % and anti-D prophylaxis in 3 %.

Laparoscopy found no severe complications. Liver biopsy caused mild bleeding in 6 (8 %) patients which was controlled during laparoscopy by local compression. None of the patients required blood transfusion. One patient developed a mesenteric emphysema after insufflation of nitrous oxide.

Cirrhosis was found by laparoscopy in 21/72 (29.2 %) patients and by histology in 8/72 (11.1 %) patients. According to HAI, patients with macroscopic cirrhosis by laparoscopy ($n=21$) showed histologically fibrosis stage I in 14.3 % (3/21), fibrosis stage II in 19 % (4/21), fibrosis stage III in 28.6 % (6/21) and cirrhosis in 38.1 % (8/21) (Table 1). Therefore 13/21 (61.9 %) macroscopic cirrhosis was not identified histologically. No cirrhosis was detected by laparoscopy in 51/72 (70.8 %) patients. According to HAI, patients without macroscopic cirrhosis ($n=51$) showed histologically fibrosis stage I in 58.8 % (30/51), fibrosis stage II in 31.4 % (16/51), fibrosis stage III in 9.8 % (5/51) and cirrhosis in 0 (0/51).

For statistical analysis, patients were divided into two groups. Group A represented patients with macroscopic cirrhosis ($n=21$) and group B patients without macroscopic cirrhosis ($n=51$) diagnosed by laparoscopic criteria. The mean ($M \pm SD$) age of patients in group A was 56.4 ± 9.4 years, being significantly higher than in group B aged 41.7 ± 11.2 years ($P < 0.02$). There were 10 men and 11 women in group A and 27 men and 24 women in group B (n.s.). Mean ($M \pm SD$)

duration of chronic HCV infection in 44 patients of group A was 23.2 ± 8.3 years, being significantly longer than in patients without macroscopic cirrhosis (group B) aged 10.4 ± 5.7 years ($P < 0.02$) (Table 2). In blood chemistry, patients of group A had significantly higher AST, γ -GT and γ -globulin fraction in serum electrophoresis as well as significant lower prothrombin index and platelet count than patients of group B. No significant differences were found for ALT, AP, bilirubin and cholinesterase in both groups (Table 3). According to the Child-Pugh-Turcotte classification, 18 of the 21 patients with macroscopic cirrhosis were classified as Child A, 3 Child B and none Child C. In comparison of histological cirrhosis (8/21) and histologic non cirrhosis (13/21) of group A with macroscopic cirrhosis ($n=21$), significant differences were only found in AST and γ -GT (Table 4). Differences were not significant in prothrombin index, γ -globuline fraction and platelet count between cirrhosis (8/21) and histologic non-cirrhosis (13/21) of group A with macroscopic cirrhosis ($n=21$) (Table 4).

Table 1 Outcome of macroscopic laparoscopic exploration and histological analysis in 72 patients with chronic HCV infection

Histology (fibrosis stage score)	Laparoscopy	
	Patients without signs of cirrhosis ($n=51$)	Patients with signs of cirrhosis ($n=21$)
Fibrosis I	30	3
Fibrosis II	16	4
Fibrosis III	5	6
Cirrhosis	0	8

Absent portal fibrosis was judged as fibrosis score I ($HAI^b=0$, no fibrosis), mild to moderate fibrosis as stage II ($HAI^b=1$, fibros portal expansion), marked fibrosis as stage III ($HAI^b=3$, bridging fibrosis), and complete fibrosis as cirrhosis ($HAI^b=4$).

Table 2 Demographic and clinical data of patients with and without laparoscopically diagnosed cirrhosis

	Laparoscopy		<i>P</i>
	Patients with signs of Cirrhosis ($n=21$)	Patients without signs of Cirrhosis ($n=51$)	
Age (years)	56.36 ± 9.42	41.7 ± 11.2	$< 0.02^a$
Duration of disease (years) ($n=44$)	23.2 ± 8.3	10.4 ± 5.68	$< 0.02^a$
Sex ratio (m/f)	10/11	27/24	ns

^aStudent's *t*-test (unpaired); ns=not significant, years were showed as mean \pm standard deviation. Duration of disease could be evaluated in 44 cases by patients' history.

Table 3 Laboratory data of patients with and without laparoscopic macroscopic evidence of cirrhosis

Laboratory data	Laparoscopy		<i>P</i>
	Patients with evidence of cirrhosis ($n=21$)	Patients without evidence of cirrhosis ($n=51$)	
AST (U/l)	59.7 ± 54.2	29.3 ± 19.6	< 0.02
ALT (U/l)	82.5 ± 70.3	72.6 ± 47.2	ns
γ -GT (U/l)	72.6 ± 78.4	34.1 ± 38.2	< 0.02
AP (U/l)	129.8 ± 48.9	137.5 ± 49.6	ns
Bilirubin (mg/dl)	1.1 ± 0.93	1.86 ± 6.23	ns
CHE (U/l)	5114 ± 1331	5910 ± 1001	ns
Prothrombin index (%)	93.8 ± 12.6	102.2 ± 6.3	< 0.02
γ -globuline fraction (%)	19.9 ± 6.5	13.7 ± 2.9	< 0.02
Platelet count (cell/ μ l)	$172\ 940 \pm 65068$	$253\ 230 \pm 57096$	< 0.02

All data were showed as mean \pm standard deviation. Statistical analysis was performed by applying Mann-Whitney test. ns=not significant.

Table 4 Comparing laboratory data of patients with macroscopic laparoscopic signs of cirrhosis

Laboratory data	Histological analysis		<i>P</i>
	No cirrhosis ($n=13$)	Cirrhosis ($n=8$)	
AST (U/l)	35.9 ± 24.9	87.7 ± 67.8	< 0.02
ALT (U/l)	64.9 ± 72.2	97.0 ± 66.34	ns
γ -GT (U/l)	51.64 ± 39.78	103.0 ± 104.6	< 0.02
AP (U/l)	126.3 ± 54.6	144.6 ± 39.6	ns
Bilirubin (mg/dl)	0.36 ± 0.5	1.4 ± 3.438	ns
CHE (U/l)	5129 ± 1861	4685 ± 1773	ns
Prothrombin index (%)	95.8 ± 10.6	90.7 ± 14.3	ns
γ -globuline fraction (%)	16.3 ± 3.2	19.6 ± 10.6	ns
Platelet count (cells/ μ l)	$180\ 700 \pm 56\ 240$	$167\ 000 \pm 77\ 110$	ns

All data were showed as mean \pm standard deviation, statistical analysis were performed by Mann-Whitney test. ns=not significant.

Thirty-nine patients were treated with interferon-alfa 2a and followed up for 6 months after the end of treatment. HCV genotyping was performed in all 39 patients before start of therapy. HCV genotype II (1b) was the predominant genotype. The HCV genotypes of the 39 patients were 23 II (1b), 5 I (1a), 3 IV (2b), 5 V (3a) and 3 I (1a) combined with II (1b). Patients with macroscopic cirrhosis showed no significant difference of genotype distribution as compared with patients without cirrhosis. Interferon treatment resulted in 14/39 (35.9 %) sustained responders and 25/39 (64.1 %) non-responders including 2 relapsers. According to HCV genotype distribution, a significant higher rate of genotype II (1b) was observed in non-responders than sustained responders ($P < 0.02$). Non-responders had a higher rate of macroscopic cirrhosis than sustained responders ($P < 0.02$) (Table 5).

Table 5 Comparisons in pretreatment parameters between patients with sustained response and patients with non-response to interferon treatment ($n=39$)

	Sustained-responders	Non-responders	<i>P</i>
Number (%)	14 (35.9 %)	25 (64.1 %)	
Age (years)	50.6 ± 13.9	47.2 ± 10.6	ns
Genotype 1b (%)	5 (35.7 %)	18 (72 %)	$< 0.02^a$
Fibrosis staging score (%)			
I	7 (50.0 %)	9 (36.0 %)	
II	3 (21.4 %)	8 (32.0 %)	
III	3 (21.4 %)	3 (12.0 %)	
Cirrhosis	1 (7.0 %)	5 (20.0 %)	ns
Laparoscopic evidence of cirrhosis (%)	2 (14.2 %)	9 (36.0 %)	$< 0.02^a$

Data of age were showed as mean \pm standard deviation; ^aChi-square test, ns=not significant.

DISCUSSION

Diagnostic laparoscopy is recommended in the diagnosis of peritoneal diseases, evaluation of ascites of unknown origin, staging of abdominal cancer and chronic and focal liver disease^[48]. Laparoscopy is commonly not performed for the diagnosis of cirrhosis in patients with chronic HCV. The availability of percutaneous liver biopsy guided by ultrasound, CT- or MRI-scan offers selected biopsy of a suspicious area in the liver. The rate of laparoscopic liver biopsies in gastroenterology declined and also the number of training programs for this procedure^[49]. However, all imaging procedures do not allow a direct viewing of the liver. The direct

visual inspection of the liver and the abdomen is the privilege of laparoscopy.

In this study, more chronic HCV infected patients had been diagnosed of cirrhosis macroscopically by laparoscopic inspection of the liver than histologically by using the Menghini needle for laparoscopic liver biopsy. All patients with histological cirrhosis also had cirrhosis macroscopically, but 13/21 patients with macroscopic cirrhosis had no cirrhosis histologically. This discrepancy implicates an underestimation of cirrhosis in chronic HCV-infected patients, if diagnosis of cirrhosis is based only on liver biopsy using the Menghini needle. Poniachik *et al.* investigated the role of laparoscopy and laparoscopic liver biopsy in the diagnosis of cirrhosis in 434 patients with chronic liver disease including 169 patients with laparoscopic evidence of cirrhosis. The histological sampling error was 32 % among patients documented to have cirrhosis by laparoscopy^[14]. The selection of a suction or cutting needle for liver biopsy has a major impact at the stage of cirrhosis. The use of a cutting needle like Vim-Silverman or Tru-Cut is reported to give a more representative histology than suction needles like Menghini, Klatskin or Jamshidi, because fibrotic tissue tends to fragment with the use of suction needle^[49,50]. In a randomized study on 1192 patients with diffuse liver disease, Colombo *et al* investigated percutaneous liver biopsies comparing the Tru-Cut and the Menghini needle. For diagnosing cirrhosis accuracy of the Tru-Cut needle is significantly better (89.5 %) than the Menghini needle (65.5 %). Complication rates were very low with both needles^[51].

Comparing laparoscopy and laparoscopic biopsy for diagnosis of cirrhosis, laparoscopic diagnosis of macroscopic cirrhosis was of higher value than histological diagnosis of microscopic cirrhosis regarding blood chemistry and the response to interferon therapy. The rate of non-response to interferon therapy was 64.1 % in our study. Significant parameters for non-response were genotype II (1b) and laparoscopic evidence of cirrhosis, but not histological diagnosis of cirrhosis. Nowadays, new therapeutic regimes have replaced interferon monotherapy. The combination of interferon-alfa with ribavirin improved sustained response rate for chronic HCV-infected patients^[52] and for relapsers and non-responders after initially interferon monotherapy^[53-55]. Increased efficacy was shown with pegylated interferon as compared with standard interferons in cirrhotic and noncirrhotic patients with chronic hepatitis C^[37,56,57] and currently standard therapy is pegylated interferon in combination with ribavirin^[8]. In this treatment situation, the role of liver biopsy has increasingly been discussed^[58]. If patients with positive predictors of virological response, such as low viral load and infection with genotype 2 or 3, can be treated and have very high chances of response, a biopsy that reveals mild histologic changes may do little to dissuade the clinician and patients from immediate treatment^[8]. Liver biopsy may become recommended only in those patients whose pretreatment characteristics predict the lowest success rate^[8]. Paired liver biopsy specimens enable staging of inflammation and fibrosis before and after treatment to define histological response in those patients. Compared with our data, the rate of cirrhosis before treatment will be underestimated without performing laparoscopy in those patients. Both procedures, liver biopsy and laparoscopy, are invasive, but accurate noninvasive markers for staging disease activity, fibrosis and cirrhosis are not available^[18]. Our rate of complications related to laparoscopy and laparoscopic liver biopsy was 10 % and no severe complication was observed. These data are in accordance with other reports^[11,42,59-62]. The rate of severe complications using blind percutaneous liver biopsy is reported to be 0.3-1.5 % and is almost comparable with laparoscopic liver biopsy^[41,63-67]. Diagnostic laparoscopy and laparoscopic

liver biopsy are a safe and invasive procedure in patients with compensated liver disease. Minilaparoscopy has increasingly emerged as a less invasive diagnostic method in this field^[68].

Based on our data, diagnostic laparoscopy is indicated for recognition of early cirrhosis in patients with chronic HCV infection. In fact, as early diagnosis of cirrhosis affects management of chronic HCV infected patients, it should be the key factor in the decision-making process.

REFERENCES

- 1 **Alter MJ**, Margolis HS, Krawczynski K, Judson FN, Mares A, Alexander WJ, Hu PY, Miller JK, Gerber MA, Sampliner RE. The natural history of community-acquired hepatitis C in the united states. the sentinel counties chronic non-A, non-B hepatitis study team. *N Engl J Med* 1992; **327**: 1899-1905
- 2 **Hoofnagle JH**. Hepatitis C: the clinical spectrum of disease. *Hepatology* 1997; **26**: 15S-20S
- 3 **Ramadori G**, Meier V. Hepatitis C virus infection: 10 years after the discovery of the virus. *Eur J Gastroenterol Hepatol* 2001; **13**: 465-471
- 4 **Dore GJ**, Freeman AJ, Law M, Kaldor JM. Is severe liver disease a common outcome for people with chronic hepatitis C? *J Gastroenterol Hepatol* 2002; **17**: 423-430
- 5 **Di Bisceglie AM**, Goodman ZD, Ishak KG, Hoofnagle JH, Melpolder JJ, Alter HJ. Long-term clinical and histopathological follow-up of chronic posttransfusion hepatitis. *Hepatology* 1991; **14**: 969-974
- 6 **Zeuzem S**, Roth WK, Herrmann G. Viral hepatitis C. *Z Gastroenterol* 1995; **33**: 117-132
- 7 **Di Bisceglie AM**. Hepatitis C and hepatocellular carcinoma. *Hepatology* 1997; **26**: 34S-38S
- 8 **Herrine SK**. Approach to the patient with chronic hepatitis C virus infection. *Ann Intern Med* 2002; **136**: 747-757
- 9 **Gaiani S**, Gramantieri L, Venturoli N, Piscaglia F, Siringo S, D'Errico A, Zironi G, Grigioni W, Bolondi L. What is the criterion for differentiating chronic hepatitis from compensated cirrhosis? A prospective study comparing ultrasonography and percutaneous liver biopsy. *J Hepatol* 1997; **27**: 979-985
- 10 **Regev A**, Berho M, Jeffers LJ, Milikowski C, Molina EG, Pylsopoulos NT, Feng ZZ, Reddy KR, Schiff ER. Sampling error and intraobserver variation in liver biopsy in patients with chronic HCV infection. *Am J Gastroenterol* 2002; **97**: 2614-2618
- 11 **Jalan R**, Harrison DJ, Dillon JF, Elton RA, Finlayson ND, Hayes PC. Laparoscopy and histology in the diagnosis of chronic liver disease. *QJ Med* 1995; **88**: 559-564
- 12 **Nord HJ**. Biopsy diagnosis of cirrhosis: blind percutaneous versus guided direct vision techniques-a review. *Gastrointest Endosc* 1982; **28**: 102-104
- 13 **Vido I**, Wildhirt E. Correlation of the laparoscopic and histological findings in chronic hepatitis and liver cirrhosis. *Dtsch Med Wochenschr* 1969; **94**: 1633-1637
- 14 **Poniachik J**, Bernstein DE, Reddy KR, Jeffers LJ, Coelho-Little ME, Civantos F, Schiff ER. The role of laparoscopy in the diagnosis of cirrhosis. *Gastrointest Endosc* 1996; **43**: 568-571
- 15 **Mossner J**. Laparoscopy in differential internal medicine diagnosis. *Z Gastroenterol* 2001; **39**: 1-6
- 16 **Cardi M**, Muttillio IA, Amadori L, Petroni R, Mingazzini P, Barillari P, Lisi D, Bolognese A. Superiority of laparoscopy compared to ultrasonography in diagnosis of widespread liver diseases. *Dig Dis Sci* 1997; **42**: 546-548
- 17 **Oberti F**, Valsesia E, Pilette C, Rousselet MC, Bedossa P, Aube C, Gallois Y, Rifflet H, Maiga MY, Penneau-Fontbonne D, Cales P. Noninvasive diagnosis of hepatic fibrosis or cirrhosis. *Gastroenterology* 1997; **113**: 1609-1616
- 18 **Saadeh S**, Cammell G, Carey WD, Younossi Z, Barnes D, Easley K. The role of liver biopsy in chronic hepatitis C. *Hepatology* 2001; **33**: 196-200
- 19 **Davis GL**, Balart LA, Schiff ER, Lindsay K, Bodenheimer HC Jr, Perrillo RP, Carey W, Jacobson IM, Payne J, Dienstag JL. Treatment of chronic hepatitis C with recombinant interferon alfa. A multicenter randomized, controlled trial. Hepatitis Interventional Therapy Group. *N Engl J Med* 1989; **321**: 1501-1506

- 20 **Di Bisceglie AM**, Martin P, Kassianides C, Lisker-Melman M, Murray L, Waggoner J, Goodman Z, Banks SM, Hoofnagle JH. Recombinant interferon alfa therapy for chronic hepatitis C. A randomized, double-blind, placebo-controlled trial. *N Engl J Med* 1989; **321**: 1506-1510
- 21 **Poynard T**, Leroy V, Cohard M, Thevenot T, Mathurin P, Opolon P, Zarski JP. Meta-analysis of interferon randomized trials in the treatment of viral hepatitis C: effects of dose and duration. *Hepatology* 1996; **24**: 778-789
- 22 **Hoofnagle JH**, di Bisceglie AM. The treatment of chronic viral hepatitis. *N Engl J Med* 1997; **336**: 347-356
- 23 **Saracco G**, Borghesio E, Mesina P, Solinas A, Spezia C, Macor F, Gallo V, Chiandussi L, Donada C, Donadon V, Spirito F, Mangia A, Andriulli A, Verme G, Rizzetto M. Prolonged treatment (2 years) with different doses (3 versus 6 MU) of interferon alpha-2b for chronic hepatitis type C. Results of a multicenter randomized trial. *J Hepatol* 1997; **27**: 56-62
- 24 **Mizokami M**, Orito E, Gibo Y, Suzuki K, Ohba K, Ohno T, Lau JY. Genotype, serum level of hepatitis C virus RNA and liver histology as predictors of response to interferon-alpha 2a therapy in Japanese patients with chronic hepatitis C. *Liver* 1996; **16**: 23-27
- 25 **Rumi M**, Del Ninno E, Parravicini ML, Romeo R, Soffredini R, Donato MF, Wilber J, Russo A, Colombo M. A prospective, randomized trial comparing lymphoblastoid to recombinant interferon alfa 2a as therapy for chronic hepatitis C. *Hepatology* 1996; **24**: 1366-1370
- 26 **Jouet P**, Roudot-Thoraval F, Dhumeaux D, Metreau JM. Comparative efficacy of interferon alfa in cirrhotic and noncirrhotic patients with non-A, non-B, C hepatitis. Le Groupe Francais pour l' Etude du Traitement des Hepatites Chroniques NANB/C. *Gastroenterology* 1994; **106**: 686-690
- 27 **Pagliari L**, Craxi A, Cammaa C, Tine F, Di Marco V, Lo Iacono O, Almasio P. Interferon-alpha for chronic hepatitis C: an analysis of pretreatment clinical predictors of response. *Hepatology* 1994; **19**: 820-828
- 28 **Tsubota A**, Chayama K, Ikeda K, Yasuji A, Koida I, Saitoh S, Hashimoto M, Iwasaki S, Kobayashi M, Hiromitsu K. Factors predictive of response to interferon-alpha therapy in hepatitis C virus infection. *Hepatology* 1994; **19**: 1088-1094
- 29 **Martinot-Peignoux M**, Marcellin P, Pouteau M, Castelnau C, Boyer N, Poliquin M, Degott C, Descombes I, Le Breton V, Milotova V. Pretreatment serum hepatitis C virus RNA levels and hepatitis C virus genotype are the main and independent prognostic factors of sustained response to interferon alfa therapy in chronic hepatitis C. *Hepatology* 1995; **22** (4 Pt 1): 1050-1056
- 30 **Nousbaum JB**, Pol S, Nalpas B, Landais P, Berthelot P, Brechot C. Hepatitis C virus type 1b (II) infection in France and Italy. Collaborative Study Group. *Ann Intern Med* 1995; **122**: 161-168
- 31 **Kanazawa Y**, Hayashi N, Mita E, Li T, Hagiwara H, Kasahara A, Fusamoto H, Kamada T. Influence of viral quasispecies on effectiveness of interferon therapy in chronic hepatitis C patients. *Hepatology* 1994; **20**: 1121-1130
- 32 **Enomoto N**, Sakuma I, Asahina Y, Kurosaki M, Murakami T, Yamamoto C, Izumi N, Marumo F, Sato C. Comparison of full-length sequences of interferon-sensitive and resistant hepatitis C virus 1b. Sensitivity to interferon is conferred by amino acid substitutions in the NS5A region. *J Clin Invest* 1995; **96**: 224-230
- 33 **Van Thiel DH**, Friedlander L, Fagioli S, Wright HI, Irish W, Gavalier JS. Response to interferon alpha therapy is influenced by the iron content of the liver. *J Hepatol* 1994; **20**: 410-415
- 34 **Shindo M**, Arai K, Okuno T. The clinical value of grading and staging scores for predicting a long-term response and evaluating the efficacy of interferon therapy in chronic hepatitis C. *J Hepatol* 1997; **26**: 492-497
- 35 **Valla DC**, Chevallerie M, Marcellin P, Payen JL, Trepo C, Fonck M, Bourliere M, Boucher E, Miguet JP, Parlier D, Lemonnier C, Opolon P. Treatment of hepatitis C virus-related cirrhosis: a randomized, controlled trial of interferon alfa-2b versus no treatment. *Hepatology* 1999; **29**: 1870-1875
- 36 **Shiratori Y**, Yokosuka O, Nakata R, Ihori M, Hirota K, Katamoto T, Unuma T, Okano K, Ikeda Y, Hirano M, Kawase T, Takano S, Matsumoto K, Ohashi Y, Omata M. Prospective study of interferon therapy for compensated cirrhotic patients with chronic hepatitis C by monitoring serum hepatitis C RNA. *Hepatology* 1999; **29**: 1573-1580
- 37 **Heathcote EJ**, Shiffman ML, Cooksley WG, Dusheiko GM, Lee SS, Balart L, Reindollar R, Reddy RK, Wright TL, Lin A, Hoffman J, De Pamphilis J. Peginterferon alfa-2a in patients with chronic hepatitis C and cirrhosis. *N Engl J Med* 2000; **343**: 1673-1680
- 38 **Okamoto H**, Sugiyama Y, Okada S, Kurai K, Akahane Y, Sugai Y, Tanaka T, Sato K, Tsuda F, Miyakawa Y. Typing hepatitis C virus by polymerase chain reaction with type-specific primers: application to clinical surveys and tracing infectious sources. *J Gen Virol* 1992; **73**: 673-679
- 39 **Simmonds P**, McOmish F, Yap PL, Chan SW, Lin CK, Dusheiko G, Saeed AA, Holmes EC. Sequence variability in the 5' non-coding region of hepatitis C virus: identification of a new virus type and restrictions on sequence diversity. *J Gen Virol* 1993; **74** (Pt 4): 661-668
- 40 **Polzien F**, Schott P, Mihm S, Ramadori G, Hartmann H. Interferon-alpha treatment of hepatitis C virus-associated mixed cryoglobulinemia. *J Hepatol* 1997; **27**: 63-71
- 41 **Pagliari L**, Rinaldi F, Craxi A, Di Piazza S, Filippazzo G, Gatto G, Genova G, Magrin S, Maringhini A, Orsini S, Palazzo U, Spinello M, Vinci M. Percutaneous blind biopsy versus laparoscopy with guided biopsy in diagnosis of cirrhosis. A prospective, randomized trial. *Dig Dis Sci* 1983; **28**: 39-43
- 42 **Henning H**, Look D. Laparoskopie: Atlas und Lehrbuch. *Stuttgart Thieme* 1985: 32-46
- 43 **Mihm S**, Fayyazi A, Hartmann H, Ramadori G. Analysis of histopathological manifestations of chronic hepatitis C virus infection with respect to virus genotype. *Hepatology* 1997; **25**: 735-759
- 44 **Knodell RG**, Ishak KG, Black WC, Chen TS, Craig R, Kaplowitz N, Kiernan TW, Wollman J. Formulation and application of a numerical scoring system for assessing histological activity in asymptomatic chronic active hepatitis. *Hepatology* 1981; **1**: 431-435
- 45 **Desmet VJ**, Gerber M, Hoofnagle JH, Manns M, Scheuer PJ. Classification of chronic hepatitis: diagnosis, grading and staging. *Hepatology* 1994; **19**: 1513-1520
- 46 **Ishak K**, Baptista A, Bianchi L, Callea F, De Groote J, Gudat F, Denk H, Desmet V, Korb G, MacSween RN. Histological grading and staging of chronic hepatitis. *J Hepatol* 1995; **22**: 696-699
- 47 **Chemello L**, Bonetti P, Cavalletto L, Talato F, Donadon V, Casarin P, Belussi F, Frezza M, Noventa F, Pontisso P. Randomized trial comparing three different regimens of alpha-2a-interferon in chronic hepatitis C. The TriVeneto Viral Hepatitis Group. *Hepatology* 1995; **22**: 700-706
- 48 **Nord HJ**. What is the future of laparoscopy and can we do without it? *Z Gastroenterol* 2001; **39**: 41-44
- 49 **Bravo AA**, Sheth SG, Chopra S. Liver biopsy. *N Engl J Med* 2001; **344**: 495-500
- 50 **Goldner F**. Comparison of the Menghini, Klatskin and Tru-Cut needles in diagnosing cirrhosis. *J Clin Gastroenterol* 1979; **1**: 229-231
- 51 **Colombo M**, Del Ninno E, de Franchis R, De Fazio C, Festorazzi S, Ronchi G, Tommasini MA. Ultrasound-assisted percutaneous liver biopsy: superiority of the Tru-Cut over the Menghini needle for diagnosis of cirrhosis. *Gastroenterology* 1988; **95**: 487-489
- 52 **McHutchison JG**, Gordon SC, Schiff ER, Shiffman ML, Lee WM, Rustgi VK, Goodman ZD, Ling MH, Cort S, Albrecht JK. Interferon alfa-2b alone or in combination with ribavirin as initial treatment for chronic hepatitis C. hepatitis interventional therapy group. *N Engl J Med* 1998; **339**: 1485-1492
- 53 **Davis GL**, Esteban-Mur R, Rustgi V, Hoefs J, Gordon SC, Trepo C, Shiffman ML, Zeuzem S, Craxi A, Ling MH, Albrecht J. Interferon alfa-2b alone or in combination with ribavirin for the treatment of relapse of chronic hepatitis C. International Hepatitis Interventional Therapy Group. *N Engl J Med* 1998; **339**: 1493-1499
- 54 **Cheng SJ**, Bonis PA, Lau J, Pham NQ, Wong JB. Interferon and ribavirin for patients with chronic hepatitis C who did not respond to previous interferon therapy: a meta-analysis of controlled and uncontrolled trials. *Hepatology* 2001; **33**: 231-240
- 55 **Wietzke-Braun P**, Meier V, Braun F, Ramadori G. Combination of "low-dose" ribavirin and interferon alfa-2a therapy followed by interferon alfa-2a monotherapy in chronic HCV-infected non-responders and relapsers after interferon alfa-2a monotherapy.

- World J Gastroenterol* 2001; **7**: 222-227
- 56 **Zeuzem S**, Feinman SV, Rasenack J, Heathcote EJ, Lai MY, Gane E, O' Grady J, Reichen J, Diago M, Lin A, Hoffman J, Brunda MJ. Peginterferon alfa-2a in patients with chronic hepatitis C. *N Engl J Med* 2000; **343**: 1666-1672
- 57 **Reddy KR**, Wright TL, Pockros PJ, Shiffman M, Everson G, Reindollar R, Fried MW, Purdum PP 3rd, Jensen D, Smith C, Lee WM, Boyer TD, Lin A, Pedder S, DePamphilis J. Efficacy and safety of pegylated (40-kd) interferon alpha-2a compared with interferon alpha-2a in noncirrhotic patients with chronic hepatitis C. *Hepatology* 2001; **33**: 433-438
- 58 **Griffiths A**, Viiala CH, Olynyk JK. Liver biopsy in the 21st century: where and why? *Med J Aust* 2002; **176**: 52-53
- 59 **Phillips RS**, Reddy KR, Jeffers LJ, Schiff ER. Experience with diagnostic laparoscopy in a hepatology training program. *Gastrointest Endosc* 1987; **33**: 417-420
- 60 **Adamek HE**, Maier M, Benz C, Huber T, Schilling D, Riemann JF. Severe complications in diagnostic laparoscopy. 9 years experience in 747 examinations. *Med Klin* 1996; **91**: 694-697
- 61 **Bruhl W**. Incidents and complications in laparoscopy and directed liver puncture. Result of a survey. *Dtsch Med Wochenschr* 1966; **91**: 2297-2299
- 62 **Leinweber B**, Korte M, Kratz F, Gerhardt H, Matthes KJ. Laparoscopy. Results and experiences. *Med Welt* 1975; **26**: 1762-1765
- 63 **Terry R**. Risk of needle biopsy of the liver. *Br Med J* 1952; **1**: 1102-1105
- 64 **Sherlock S**, Dick R, Van Leeuwen DJ. Liver biopsy today. the royal free hospital experience. *J Hepatol* 1985; **1**: 75-85
- 65 **Piccinino F**, Sagnelli E, Pasquale G, Giusti G. Complications following percutaneous liver biopsy. A multicentre retrospective study on 68,276 biopsies. *J Hepatol* 1986; **2**: 165-173
- 66 **Perrault J**, McGill DB, Ott BJ, Taylor WF. Liver biopsy: complications in 1000 inpatients and outpatients. *Gastroenterology* 1978; **74**: 103-106
- 67 **Knauer CM**. Percutaneous biopsy of the liver as a procedure for outpatients. *Gastroenterology* 1978; **74**: 101-102
- 68 **Helmreich-Becker I**, Meyer zum Buschenfelde KH, Lohse AW. Safety and feasibility of a new minimally invasive diagnostic laparoscopy technique. *Endoscopy* 1998; **30**: 756-762

Edited by Ma JY and Xu XQ

Effect of alpha 2b interferon on inducement of mIL-2R and treatment of HCV in PBMC from patients with chronic viral hepatitis C

Jian Wang, Gui-Ju Xiang, Bing-Xiang Liu

Jian Wang, Department of Aetiology and Immunology, Anhui University of Science and Technology, Huainan 232001, Anhui Province, China

Gui-Ju Xiang, Department of Infectious Diseases, the Second Miner Hospital of Huainan, Huainan 232001, Anhui Province, China

Bing-Xiang Liu, Department of Infectious Diseases, Shibe Hospital of Shanghai, Shanghai 200435, China

Supported by the grants from Science Foundation of the Ministry of Coal Industry of China, No. 96-072

Correspondence to: Jian Wang, Department of Aetiology and Immunology, Anhui University of Science and Technology, Huainan 232001, Anhui Province, China. wangjian8237@sina.com

Telephone: +86-0554-6659942

Received: 2002-07-31 **Accepted:** 2002-08-23

Abstract

AIM: To study the level of membrane interleukin-2 receptor (mIL-2R) on surface of peripheral blood mononuclear cells (PBMC) and the therapeutic efficacy of alpha 2b interferon on the treatment of HCV-RNA in PBMC of patients with chronic hepatitis C and to compare the negative rates of HCV-RNA in PBMC, HCV-RNA and anti-HCV in serum.

METHODS: Before and after treatment of alpha 2b interferon, the level of mIL-2R of patients with chronic hepatitis C was detected by biotin-streptavidin (BSA). The therapeutic group (26 cases) was treated with alpha 2b interferon (3 MU/d) and control therapeutic group (22 cases) was treated with routine drugs (VitC, aspartic acid). The total course of treatment with alpha 2b interferon and routine drug was six months and per course of the treatment was three months. The levels of HCV-RNA in PBMC, HCV-RNA and anti-HCV in serum were detected before and after a course of the treatment.

RESULTS: Before and after treatment of alpha 2b interferon and routine drugs, the levels of mIL-2R in silence stage were (3.44±0.77) % and (2.95±0.72) %, the levels of mIL-2R in inducement stage were (33.62±3.95) % and (30.04±3.73) %. There was a significant difference between two groups ($P<0.01$ - $P<0.05$). After treatment of alpha 2b interferon with 3 MU/d for two courses of the treatment, the total negative rates of HCV-RNA in the PBMC and HCV-RNA, anti-HCV in serum were 42.31 % (11/26), 57.69 % (15/26), 65.38 % (17/26) respectively. After the treatment of routine drug, the negative rates of HCV-RNA in PBMC and HCV-RNA, anti-HCV in serum were 13.64 % (3/22), 22.73 % (5/22), 27.27 % (6/22) respectively. There was high significant difference in the group treated with alpha 2b interferon and the group treated with routine drugs ($P<0.01$ - $P<0.05$).

CONCLUSION: The mIL-2R can be induced by alpha 2b interferon during the treatment. The alpha 2b interferon has a definite effect on the treatment of HCV-RNA in PBMC.

The curative effect of alpha 2b interferon is better than that of the routine drugs.

Wang J, Xiang GJ, Liu BX. Effect of alpha 2b interferon on inducement of mIL-2R and treatment of HCV in PBMC from patients with chronic viral hepatitis C. *World J Gastroenterol* 2003; 9(4): 751-754

<http://www.wjgnet.com/1007-9327/9/751.htm>

INTRODUCTION

Treatment of interferon on the chronic viral hepatitis C has been shown to have a good curative effect on inhibition of HCV replication, reduction in transmission level in serum and liver cells^[1-8], but the improvement in clinical condition was not obvious and its effective rate was only 50 %^[9-17]. The curative effect of interferon was based on virostatic replication of HCV in serum and some improvement of liver function. The literatures show that the peripheral blood mononuclear cells (PBMC) have large different active immune cells and membrane interleukin-2 receptor (mIL-2R) is an important symbol of active T cells, and the immune function of PBMC will be inhibited after being infected by HCV and the scavenging effect limited^[18,19]. In order to study the effect of interferon on treatment of HCV in PBMC and the effect of interferon on inducement to mIL-2R, forty-eight patients with typical chronic hepatitis C were observed.

MATERIALS AND METHODS

Clinical data

Forty-eight patients with chronic viral hepatitis C were selected from the Second Miner Hospital of Huainan and our teaching hospital during 1997/03-2000/05. The total number of patients was 48 (male 27, female 21) and range of age was from 18 to 57 years old (average 37.3). The clinical diagnosis was based on the modified diagnosis criterion being affirmed on the Chinese viral hepatitis conference in Xian (2000). The patients all needed the following qualifications: (1) The positivity of anti-HCV in serum for more than six months. (2) The HCV-RNA in peripheral blood mononuclear cells and serum were positive. (3) The patients had been eliminated the infection of hepatitis A, B, D, E and G viruses. (4) There were no any systemic treatment of antiviral medicine, immunomodulator, cortical hormone for the patients. The normal control was 20 healthy students (male 12, female 8) with range age from 20 to 23 years old (average 22.5).

Treatment medicine

The alpha 2b interferon was produced by High Science and Technology of Anke Biology in Anhui Province.

Treatment methods

The patients with chronic hepatitis C were divided into two groups with treatment of alpha 2b interferon 3MU (26 cases)

and routine medicine (22 cases) respectively. The total course of treatment lasted sixty months, and per course was three months. Alpha 2b interferon was given intramuscularly injection (im) qd for two weeks and then alt dieb for two courses of treatment. The routine treatment group (22 cases) was given with Vit C, Aspartic acid, etc for six months.

Reagents

The diagnostic reagent of anti-HCV was purchased from Huamei Bioengineering Company of Shanghai, No:980811. The diagnostic reagent of HCV-RNA with RT-PCR was purchased from Shanghai Zhongya Gene Institute, No: 980805. The diagnostic reagent of mIL-2R was purchased from Immunology Institute of Shanghai. The lymphocytes separation medium was purchased from the Second Reagent Factory of Shanghai, No:970505. The reagent of RPMI 1640 culture was produced by Sigma (USA).

Instruments

The analysis instrument of Spector-I was made in USA; MDF-135 CO₂ incubator was made in Japan; The instrument for gene amplification (Hema-8000) was made in Hema Company of China.

Methods

The total volume of 5 ml peripheral venous blood from patients with hepatitis C before breakfast was taken before and after treatment, and distributed a sterile Eppendorf tube and an anticoagulant tube (heparin) respectively. For detection of anti-HCV, the process was performed strictly according to the direction, and with two blank, two negative and two positive pores as controls in each test. The average titer was examined by the analyser Spector-I. The average OD titer of test sample ≥ 2.1 times of average OD titer in negative control was considered to be positive. Detection of HCV-RNA in PBMC with RT-nested-PCR: After the heparin anticoagulant blood mixed with the equal volume Hank's liquid without Ca²⁺ and Mg²⁺, lymphocytes separation medium was used to separate the PBMC. The cells were washed twice with Hank's liquid without Ca²⁺, Mg²⁺ and diluted to (1-3) $\times 10^6$ /ml before detection of HCV-RNA. A positive and a negative control were set up at the same time for comparison in each test. The RT-nested-PCR was made by reverse transcription and primer selected from non-coded region and part of C region of HCV. The specific amplified fragment length was 248 bp. The synthesis parameters for cDNA were 94 °C 40 s, 55 °C 40 s, 72 °C 1 min, for 30 circles. The amplification parameters for cDNA were 94 °C 50 s, 55 °C 40 s and 72 °C 90 s, 35 circles, including initial denaturation for 4 min at 94 °C and last extension for 5 min at 72 °C. The amplification product was run for electrophoresis on gel with 2 % EB. The result that was uniform to the positive control was considered to be positive. The detection of mIL-2R in silence and inducement stages: 10 μ l suspension of the PBMC was smeared on the slide and left dry naturally and fixed with acetone for fifteen minutes or twenty minutes. The 10 μ l anti-Tac antibody was mixed with the membrane of smears. The cells were grown in continuous culture (37 °C, 50 ml·L⁻¹ CO₂ in atmosphere) for thirty minutes. The immune sheet glass pores were measured after staining with the color-developing agent and several washings with Tris Buffer Solution (TBS). Of the PBMC suspension, 0.5 ml was mixed with RPMI 1640 culture liquid, which had PHA 200 mg·L⁻¹. The cells were grown in continuous culture (37 °C, 50 ml·L⁻¹ CO₂ in atmosphere) 72 h and its mIL-2R induced by PHA could be measured by the antibodies against membrane of T cells. The Tac with biotin and SA-HRP were smeared on different sheet glasses. The immune

sheet glass pores were measured after staining with the color-developing agent and several washings with TBS. The total number of 200 PBMC was counted and its positive cells were statistically analyzed with the help of high power lens. The positive criterion was that the color of cytoplasm or cell membrane was brown.

Statistical analysis

Statistical analysis included analysis of Chi-square (χ^2) and *t* test.

RESULTS

The forty-eight patients with chronic hepatitis C were divided into two groups and treated with alpha 2b interferon (26 cases) and routine drugs (22 cases) respectively. The results had been shown that the high negative rates of anti-HCV and HCV-RNA in serum were in the group with treatment of alpha 2b interferon. There was very significant difference before and after treatment of alpha 2b interferon ($P < 0.01$ - $P < 0.05$, Table 1). The negative rate of HCV-RNA between in PBMC and in serum was similar ($P > 0.05$, Table 2). The level of mIL-2R in situation of silence and inducement stages after treatment with alpha 2b interferon was higher than that after treatment with routine drugs ($P < 0.05$, Table 3).

Table 1 The detective results of HCV-RNA in serum and PBMC after treatment with alpha 2b interferon (n, %)

Group	n	HCV-RNA in PBMC		HCV-RNA in serum		Anti-HCV	
		Negative	Negative rate	Negative	Negative rate	Negative	Negative rate
Interferon treatment	26	11	42.31 ^a	15	57.69 ^a	17	65.38 ^b
Routin treatment	22	3	13.64	5	22.73	6	27.27

^a $P < 0.05$, ^b $P < 0.01$ vs interferon treatment.

Table 2 The results of negative rate of HCV-RNA in serum and PBMC

HCV-RNA in serum	HCV-RNA in PBMC		Total	χ^2	P
	+	-			
+	7	4	11	0.75	>0.05
-	8	7	15		
Total	15	11	26		

Table 3 The level of mIL-2R before and after treatment of interferon (n, $\bar{x} \pm s$, %)

Group	n	mIL-2R (in silence)		mIL-2R (inducement)	
		Before treatment	After treatment	Before treatment	After treatment
Interferon treatment	26	2.63 \pm 0.70	3.44 \pm 0.77 ^{bcd}	30.34 \pm 3.55	33.62 \pm 3.95 ^{cd}
Routin treatment	22	2.43 \pm 0.78	2.95 \pm 0.72 ^{cd}	30.07 \pm 3.87	30.04 \pm 3.73 ^d
Normal control	20		4.54 \pm 1.48		37.42 \pm 4.10

^a $P < 0.05$, ^b $P < 0.01$ vs before and after treatment, ^c $P < 0.05$, ^d $P < 0.01$ vs interferon treatment.

DISCUSSION

There are three kinds of interferon, α , β , γ . Interferon alpha is the most active one. Alpha 2b interferon can not enter into the host cells and kill the virus directly, but can induce the production of protein kinase (2', 5' AS) in the infected cells.

The protein kinase and 2', 5' AS can be produced after being infected by virus in cells. The degradation of virus-RNA can be made by endogenous endonuclease induced with activated 2', 5' AS so that the necessary enzyme activity for synthesis of ribose is killed, the synthetic protein of virus can be decreased, the growth of hepatitis virus C is inhibited^[20-30].

The reports have been shown that interferon has definite curative effect of the treatment of chronic hepatitis C and elimination of HCV-RNA, anti-HCV in serum. Therefore, HCV-RNA is an important index to evaluate condition of the patient's^[4]. HCV-RNA in PBMC is a direct evidence of the existence of extrahepatic or latent infection, and is one of important reasons causing the chronicity of viral hepatitis C^[28-31]. The results of Table 1 had shown that the rate of change HCV-RNA into negative in PBMC and serum after treatment of alpha 2b interferon was similar between two groups ($P>0.05$). The curative effect was higher in the treatment group with alpha 2b interferon than that with routine treatment ($P<0.05$ - $P<0.01$). This result had showed that the inducing capability of alpha 2b interferon in lymphocytes of the patients was strong, and the high effect against HCV would be taken by activated lymphocytes obviously. Although the negative rate of HCV-RNA in PBMC was lower than that in serum, there was no significant difference ($P>0.05$). The results had shown that alpha 2b interferon had high effect on HCV-RNA both in PBMC and in serum. There were four cases of chronic hepatitis C with negative in serum and positive in PBMC. It indicated that with the T lymphocytes activation, multiple cell factors were released, that inhibited the replication of free HCV-RNA in serum, but not the HCV-RNA in PBMC. The cellular immune function was disorder in different extent in patients with chronic hepatitis C and so was their response to interferon and anti-HCV^[32-37]. Otherwise, the low level of membrane interleukin-2 receptor (mIL-2R) on the surface of PBMC decreased the activity in chronic hepatitis C, which limited the inducement of protein kinase and the activity of 2', 5' AS to eliminate HCV-RNA^[38].

Anti-HCV is an important index for the diagnosis of HCV and is one of the evidences for evaluating the curative effect on the treatment of hepatitis C. The anti-HCV diagnostic kits of the second generation were used in our laboratory testing for core antigen, NS₃, NS₄ and had high specificity and sensitivity^[39,40]. The rate of negative change of HCV-RNA was higher in alpha 2b interferon treatment group than that in routine treatment group ($P<0.01$). Among the twenty-six cases, there were six cases with anti-HCV(-) in serum and HCV-RNA(+) in PBMC, two cases with anti-HCV(-) in serum and HCV-RNA(+) in serum. This result showed that even the anti-HCV in serum became negative, HCV-RNA not stopping replication completely, some HCV-RNA could still be detected in some patients^[6]. The probable reasons were: (1) After being treatment of alpha 2b interferon, the level of anti-HCV in serum decreased obviously and could not be detected by routine test. (2) The degree of variation of HCV is high, the hydrophilic peptid chain on core protein is subjective to escape the attack of CTL and keep the infection persist in chronic state. (3) The variant antigen of HCV can not match the antibody produced.

mIL-2R is an important symbol of active T cells and plays key role on biologic effect of IL-2 and its level can reflect the course of activity of T cells and immune state^[38-41]. The levels of mIL-2R in silence stage detected by BSA were lower in patients with hepatitis C than those in normal controls ($P<0.01$). The probable reasons are: (1) The mIL-2R on surface of some T cells can be restrained by HCV. (2) The degree of variation of HCV is high, the hydrophilic peptid chain on core protein is subjective to escape the attack of CTL and keep the infection persist in chronic state. (3) The variant antigen of HCV can not match the antibody produced. A lot of soluble interleukin-

2 receptor (sIL-2R) can be released after replication of HCV-RNA in PBMC so that the expression of mIL-2R was restrained. It is not only a kind of manifestation of disorder and low cellular immune to HCV but also one of reasons of chronic hepatitis C. Some T cells receptor (TCR) on surface of some Tc cells can combine with the complement (HCV-MHC-I) and some perforation proteins can be released so that many liver cells will be injured. The sIL-2R, a kind of restrained factor, as well as mIL-2R all can combine with IL-2 competitively and induce infection of HCV from activity to chronicity. With the inducement of PHA, the level of mIL-2R in silence and inducement stages was obviously increased. This result showed that the mIL-2R could be induced by PHA and had strong compete ability against sIL-2R in serum.

After inducement of PHA, the level of mIL-2R of patients in inducement stage was higher than that in silence stage, and lower than that in normal controls ($P<0.01$). The results of our study showed that the effect of PHA was infirm for patients with hepatitis C and was similar to the reports published. The level of mIL-2R in silence and inducement stages were higher after treatment of alpha 2b interferon than that before treatment of alpha 2b interferon ($P<0.01$). The active T cells and high level of mIL-2R can be induced by alpha 2b interferon during the treatment. The results showed that alpha 2b interferon not only can induce the protein kinase and 2', 5' AS but also stimulate T cells and induce the effect of Tc cells against infected cells.

In conclusion, some active T cells and mIL-2R can be induced during the treatment of alpha 2b interferon. The patients with viremia are sensitive to treatment of alpha 2b interferon that have good effect on negative change of HCV-RNA in PBMC and serum and anti-HCV in serum. If the treatment time of alpha 2b interferon prolongs, the negative rate of anti-HCV and HCV-RNA will increase simultaneously. In treatment of HCV with alpha 2b interferon, the value of negative change of HCV-RNA in serum alone is limited. In well equipped hospital both HCV-RNA in serum and PBMC can be examined at the same time.

REFERENCES

- 1 **Piekarska A**, Sidorkiewicz M, Lewandowska U, Kuydowicz J. Evaluation of persistence of IFN-alpha treatment response in chronic hepatitis C patients according with HCV-RNA presence in PBMC. *Pol Arch Med Wewn* 2001; **106**: 939-944
- 2 **Piekarska A**, Kuydowicz J, Omulecka A. Interferon alpha-treatment predictive response factors in group of adults patients with chronic hepatitis C. *Pol Arch Med Wewn* 2001; **106**: 927-937
- 3 **Patel K**, McHutchison J. Peginterferon alpha-2b: a new approach to improving response in hepatitis C patients. *Expert Opin Pharmacother* 2001; **2**: 1307-1315
- 4 **Iwabuchi S**, Takatsuka K. Dynamics of serum HCV RNA levels during IFN therapy in patients with chronic hepatitis C for prediction of outcome of IFN therapy and beneficial dosing. *Nippon Rinsho* 2001; **59**: 1363-1368
- 5 **Fornai C**, Maggi F, Favilli F, Vatteroni ML, Pistello M, Marchi S, Cicciorossi P, Antonelli G, Bendinelli M. Rapid changes in hepatitis C virus quasispecies produced by a single dose of IFN-alpha in chronically infected patients. *J Interferon Cytokine Res* 2001; **21**: 417-422
- 6 **Malaguamera M**, Di Fazio I, Trovato BA, Pistone G, Mazzoleni G. Alpha-interferon (IFN-alpha) treatment of chronic hepatitis C: analysis of some predictive factors for the response. *Int J Clin Pharmacol Ther* 2001; **39**: 239-245
- 7 **Malaguamera M**, Laurino A, Di Fazio I, Pistone G, Castorina M, Guccione N, Rampello L. Neuropsychiatric effects and type of IFN-alpha in chronic hepatitis C. *J Interferon Cytokine Res* 2001; **21**: 273-278
- 8 **Reddy KR**, Wright TL, Pockros PJ, Shiffman M, Everson G, Reindollar R, Fried MW, Purdum PP, Jensen D, Smith C, Lee WM, Boyer TD, Lin A, Pedder S, DePamphilis J. Efficacy and safety of pegylated (40-kd) interferon alpha-2a compared with

- interferon alpha-2a in noncirrhotic patients with chronic hepatitis C. *Hepatology* 2001; **33**: 433-438
- 9 **Kraus MR**, Schafer A, Csef H, Faller H, Mork H, Scheurlen M. Compliance with therapy in patients with chronic hepatitis C: associations with psychiatric symptoms, interpersonal problems, and mode of acquisition. *Dig Dis Sci* 2001; **46**: 2060-2065
 - 10 **Suzuki T**, Yonemura K, Miyaji T, Suzuki H, Takahira R, Fujigaki Y, Fujimoto T, Hishida A. Progressive renal failure and blindness due to retinal hemorrhage after interferon therapy for hepatitis C virus-associated membranoproliferative glomerulonephritis. *Intern Med* 2001; **40**: 708-712
 - 11 **Nishiguchi S**, Shiomi S, Enomoto M, Lee C, Jomura H, Tamori A, Habu D, Takeda T, Yanagihara N, Shiraki K. Does ascorbic acid prevent retinopathy during interferon therapy in patients with chronic hepatitis C? *J Gastroenterol* 2001; **36**: 486-491
 - 12 **Ho SB**, Nguyen H, Tetrick LL, Opitz GA, Basara ML, Dieperink E. Influence of psychiatric diagnoses on interferon-alpha treatment for chronic hepatitis C in a veteran population. *Am J Gastroenterol* 2001; **96**: 157-164
 - 13 **Garcia-Suarez J**, Burgaleta C, Hernanz N, Albarran F, Tobaruela P, Alvarez-Mon M. HCV-associated thrombocytopenia: clinical characteristics and platelet response after recombinant alpha2b-interferon therapy. *Br J Haematol* 2000; **110**: 98-103
 - 14 **Hsieh MC**, Yu ML, Chuang WL, Shin SJ, Dai CY, Chen SC, Lin ZY, Hsieh MY, Liu JF, Wang LY, Chang WY. Virologic factors related to interferon-alpha-induced thyroid dysfunction in patients with chronic hepatitis C. *Eur J Endocrinol* 2000; **142**: 431-437
 - 15 **Hino K**, Yamaguchi Y, Fujiwara D, Katoh Y, Korenaga M, Okazaki M, Okuda M, Okita K. Hepatitis C virus quasispecies and response to interferon therapy in patients with chronic hepatitis C: a prospective study. *J Viral Hepat* 2000; **7**: 36-42
 - 16 **Sandres K**, Dubois M, Pasquier C, Payen JL, Alric L, Duffaut M, Vinel JP, Pascal JP, Puel J, Izopet J. Genetic heterogeneity of hypervariable region 1 of the hepatitis C virus (HCV) genome and sensitivity of HCV to alpha interferon therapy. *J Virol* 2000; **74**: 661-668
 - 17 **Poynard T**, Daurat V, Chevret S, Moussalli J, Degos F, Bailly F, Borotto E, Buffet C, Bartolomei-Portal I, Richardet JP, Riachi G, Calmus Y, Brechot C, Vidaud M, Olivi M, Bedossa P, Riffaud PC, Chastang C. A short induction regimen of interferon-alpha is not effective for treatment of relapse in chronic hepatitis C: a randomized trial. For the multicentre GER-CYT-01 group. *J Viral Hepat* 1999; **6**: 381-386
 - 18 **Weiss G**, Umlauf F, Urbanek M, Herold M, Lovevsky M, Offner F, Gordeuk VR. Associations between cellular immune effector function, iron metabolism, and disease activity in patients with chronic hepatitis C virus infection. *J Infect Dis* 1999; **180**: 1452-1458
 - 19 **Vertuani S**, Bazzaro M, Gualandi G, Micheletti F, Marastoni M, Fortini C, Canella A, Marino M, Tomatis R, Traniello S, Gavioli R. Effect of interferon-alpha therapy on epitope-specific cytotoxic T lymphocyte responses in hepatitis C virus-infected individuals. *Eur J Immunol* 2002; **32**: 144-154
 - 20 **Fujiwara T**, Kiura K, Ochi K, Matsubara H, Yamanari H, Shimomura H, Harada M. Giant negative T waves during interferon therapy in a patient with chronic hepatitis C. *Intern Med* 2001; **40**: 105-109
 - 21 **Fukuda A**, Kobayashi H, Teramura K, Yoshimoto S, Ohsawa N. Effects of interferon-alpha on peripheral neutrophil counts and serum granulocyte colony-stimulating factor levels in chronic hepatitis C patients. *Cytokines Cell Mol Ther* 2000; **6**: 149-154
 - 22 **Kakizaki S**, Takagi H, Yamada T, Ichikawa T, Abe T, Sohara N, Kosone T, Kaneko M, Takezawa J, Takayama H, Nagamine T, Mori M. Evaluation of twice-daily administration of interferon-beta for chronic hepatitis C. *J Viral Hepat* 1999; **6**: 315-319
 - 23 **Jensen DM**, Krawitt EL, Keeffe EB, Hollinger FB, James SP, Mullen K, Everson GT, Hoefs JC, Fromm H, Black M, Foust RT, Pimstone NR, Heathcote EJ, Albert D. Biochemical and viral response to consensus interferon (CIFN) therapy in chronic hepatitis C patients: effect of baseline viral concentration. Consensus Interferon Study Group. *Am J Gastroenterol* 1999; **94**: 3583-3588
 - 24 **Willson RA**, Fischer SH, Ochs HD. Long-term interferon alpha maintenance therapy for chronic hepatitis C infection in a patient with common variable immune deficiency. *J Clin Gastroenterol* 1999; **29**: 203-206
 - 25 **Fabris C**, Del Forno M, Falletti E, Toniutto P, Pirisi M. Kinetics of serum soluble tumour necrosis factor receptor (TNF-R) type-I and type-II after a single interferon-alpha (IFN-alpha) injection in chronic hepatitis C. *Clin Exp Immunol* 1999; **117**: 556-560
 - 26 **Begemann F**, Jablonowski H. Enhancing the response to interferon-alpha. *J Clin Virol* 1999; **13**: 1-7
 - 27 **Huraib S**, Tanimu D, Romeh SA, Quadri K, Al Ghamdi G, Iqbal A, Abdulla A. Interferon-alpha in chronic hepatitis C infection in dialysis patients. *Am J Kidney Dis* 1999; **34**: 55-60
 - 28 **Yagura M**, Murai S, Kojima H, Tokita H, Kamitsukasa H, Harada H. Interferon treatment in patients with chronic hepatitis C with normal alanine-aminotransferase activity. *Hepatogastroenterology* 1999; **46**: 1094-1099
 - 29 **Seifarth C**, Benninger J, Bohm BO, Wiest-Ladenburger U, Hahn EG, Hensen J. Augmentation of the immune response to islet cell antigens with development of diabetes mellitus caused by interferon-alpha therapy in chronic hepatitis C. *Z Gastroenterol* 1999; **37**: 2235-2239
 - 30 **Boran M**, Cetin S. The role of alpha-glutathione S-transferase in the monitoring of hemodialysis patients with hepatitis C virus infection undergoing high-dose interferon-alpha-2b therapy. *Nephron* 1999; **82**: 22-26
 - 31 **Woitars RP**, Petersen U, Moshage D, Brackmann HH, Matz B, Sauerbruch T, Spengler U. HCV-specific cytokine induction in monocytes of patients with different outcomes of hepatitis C. *World J Gastroenterol* 2002; **8**: 562-566
 - 32 **Zeuzem S**. The kinetics of hepatitis C virus infection. *Clin Liver Dis* 2001; **5**: 917-930
 - 33 **Cramp ME**, Rossol S, Chokshi S, Carucci P, Williams R, Naoumov NV. Hepatitis C virus-specific T-cell reactivity during interferon and ribavirin treatment in chronic hepatitis C. *Gastroenterology* 2000; **118**: 346-355
 - 34 **Kawamura C**, Nakajima S, Kuroki T, Monna T. Two-dimensional analysis of production of IL-6 and TNF-alpha can predict the efficacy of IFN-alpha therapy. *Hepatogastroenterology* 1999; **46**: 2941-2945
 - 35 **Song ZQ**, Hao F, Min F, Ma QY, Liu GD. Hepatitis C virus infection of human hepatoma cell line 7721 *in vitro*. *World J Gastroenterol* 2001; **7**: 685-689
 - 36 **Fukutomi T**, Fukutomi M, Iwao M, Watanabe H, Tanabe Y, Hiroshige K, Kinukawa N, Nakamura M, Nawata H. Predictors of the efficacy of intravenous natural interferon-beta treatment in chronic hepatitis C. *Med Sci Monit* 2000; **6**: 692-698
 - 37 **Xu JZ**, Yang ZG, Le MZ, Wang MR, He CL, Sui YH. A study on pathogenicity of hepatitis G virus. *World J Gastroenterol* 2001; **7**: 547-550
 - 38 **Li CP**, Wang KX, Wang J, Pan BR. mL-2R, T cell subsets and hepatitis C. *World J Gastroenterol* 2002; **8**: 298-300
 - 39 **Jimenez-Saenz M**, Rojas M, Pinar A, Salas E, Rebollo J, Carmona I, Herrerias-Esteban JM, Herrerias-Gutierrez JM. Sustained response to combination therapy in a patient with chronic hepatitis C and thrombocytopenia secondary to alpha-interferon. *J Gastroenterol Hepatol* 2000; **15**: 567-569
 - 40 **Yan FM**, Chen AS, Hao F, Zhao XP, Gu CH, Zhao LB, Yang DL, Hao LJ. Hepatitis C virus may infect extrahepatic tissues in patients with hepatitis C. *World J Gastroenterol* 2000; **6**: 805-811
 - 41 **Oketani M**, Higashi T, Yamasaki N, Shinmyozu K, Osame M, Arima T. Complete response to twice-a-day interferon-beta with standard interferon-alpha therapy in acute hepatitis C after a needle-stick. *J Clin Gastroenterol* 1999; **28**: 49-51

Anti-*Helicobacter pylori* immunoglobulin G (IgG) and IgA antibody responses and the value of clinical presentations in diagnosis of *H. pylori* infection in patients with precancerous lesions

Shao Li, Ai-Ping Lu, Lian Zhang, Yan-Da Li

Shao Li, Yan-Da Li, The Key Laboratory of Bioinformatics of Ministry of Education, Institute of Bioinformatics, Tsinghua University, Beijing 100084, China

Ai-Ping Lu, Institute of Basic Theory, China Academy of Traditional Chinese Medicine, Beijing 100700, China

Lian Zhang, Beijing Institute for Cancer Research, Beijing 100034, China

Supported by National Natural Science Foundation of China, No. 30200365

Correspondence to: Dr. Ai-Ping Lu, Institute of Basic Theory, China Academy of Traditional Chinese Medicine, Dongzhimen, Beijing 100700, China. catcm@public.bta.net.cn

Telephone: +86-10-64014411-2564 **Fax:** +86-10-64013896

Received: 2002-11-19 **Accepted:** 2002-12-18

Abstract

AIM: To determine the prevalence of *Helicobacter pylori* (*H. pylori*) infection, the serum anti-*H. pylori* immunoglobulin G (IgG) and IgA antibody responses, and the value of clinical presentations in diagnosis of *H. pylori* infection in patients with gastric atrophy, intestinal metaplasia and dysplasia.

METHODS: *H. pylori* infection was detected by histology in 209 patients with mild chronic atrophic gastritis (CAG, $n=76$), severe CAG ($n=22$), mild intestinal metaplasia (IM, $n=22$), severe IM ($n=58$), or dysplasia (DYS, $n=31$). Serum anti-*H. pylori* IgG and IgA were double sampled and evaluated by enzyme-linked immunosorbent assays. 35 clinical presentations were observed and their relationship with *H. pylori* infection was analyzed by the *k*-means cluster method.

RESULTS: Both IgG and IgA levels in *H. pylori* positive patients were significantly higher than those negative for *H. pylori* ($P<0.001-0.01$). The prevalence of *H. pylori* was highest in severe IM (84.5 %), and lowest in mild CAG (51.3 %) ($P<0.01$). They were similar in severe CAG (68.2 %), mild IM (72.7 %), and DYS (67.7 %). In *H. pylori* positive patients, the IgG levels in severe CAG were significantly higher than those in mild CAG ($P<0.01$). In *H. pylori* negative patients, both IgG and IgA levels increased remarkably in severe IM, compared to those in mild IM ($P<0.01-0.05$). *H. pylori* infection exhibited no association with patient's gender (62.1 % in males; 71.7 % in females) and age ($r=0.0814$, $P=0.241$). The diagnostic accuracy based on 35 clinical presentations was 65.7 %. It could be improved by 5.7 % when only the assemblage of digestive symptoms were engaged, or by 8.6 % when the pathogenic factors, general status and grossoscopy were combined. The diagnostic accuracy could be decreased when only the general symptoms were engaged, or when the pathogenic factors were accompanied with some common digestive symptoms.

CONCLUSION: *H. pylori* infection is a major risk factor for the process from atrophy, IM to DYS of gastric mucosa. Serum IgG and IgA are good indicators to evaluate this

progress with a certain rearrange. Investigation on the effective assemblages of clinical presentations may provide a better understanding in the pathogenesis, diagnosis and treatment for *H. pylori* infection.

Li S, Lu AP, Zhang L, Li YD. Anti-*Helicobacter pylori* immunoglobulin G (IgG) and IgA antibody responses and the value of clinical presentations in diagnosis of *H. pylori* infection in patients with precancerous lesions. *World J Gastroenterol* 2003; 9(4): 755-758

<http://www.wjgnet.com/1007-9327/9/755.htm>

INTRODUCTION

The persistence or repeated infection of pathogenic factors in the stomach may result in the chronic process of gastritis with glandular atrophy (AT), intestinal metaplasia (IM), dysplasia (DYS) and so on at different stages, which indicates diversiform prognosis. The roles of immune reactions in *Helicobacter pylori* (*H. pylori*) pathogenesis and chronic gastritis (CG) are research areas of rapid progress^[1-4]. It is now recognized that the clinical detection of serum antibody is effective in monitoring the *H. pylori* infection^[5,6]. However, *H. pylori* infection and the levels of serum anti-*H. pylori* immunoglobulin antibodies at different stages of CG are not fully investigated. Moreover, the complex clinical manifestations of *H. pylori* infection and associated CG leads to a diagnostic and therapeutic dilemma for CG^[7].

To determine the prevalence of *H. pylori* infection, the serum anti-*H. pylori* immunoglobulin G (IgG) and IgA antibody responses, and the value of clinical presentations in diagnosis of *H. pylori* infection in patients with gastric atrophy, intestinal metaplasia and dysplasia a population-based investigation was designed and a novel analytic method was proposed in this work. The study also took a different perspective in assessing the association between *H. pylori* infection and clinical presentations.

MATERIALS AND METHODS

Patients

A total of two hundred and nine patients with chronic gastritis, who were diagnosed through gastroscopy and mucosal biopsy, were included in the present study. All patients, who resided in Shandong province, were investigated by the Institute of Basic Theory, Chinese Academy of Traditional Chinese Medicine from 1999 to 2001. Among them 103 were males and 106 were females, aged from 45 to 72 with a mean age of 55 years old. Gastric biopsies were histologically evaluated for activity and chronicity of gastritis, and the presence of AT and/or IM according to the criterion of the visual analogue scale in Sydney classification and grading of gastritis^[8]. The patients consisted of 76 with mild chronic atrophic gastritis (CAG), 22 with severe (CAG), 22 with mild IM, 58 with severe IM and 31 with DYS accompanied with mild IM. All patients had not received any anti-*H. pylori* treatment.

Diagnosis of *H. pylori* infection

Two hundred and nine specimens of gastric mucosa were obtained from each patient via endoscopy. Gastric mucosa was sampled from the area of greater curvature at gastric antrum, and *H. pylori* was determined by pathological staining with hematoxylin and eosin (HE) followed by Giemsa staining. Under microscope, *Helicobacter-like organisms* can be identified as a typical curve like S or C. They look like a short bacilli or globular body with a slight curve.

Detection of anti-*H. pylori* IgG and IgA antibodies

Blood was sampled twice from patients. Enzyme-linked immunoadsorbent assays (ELISA) were used to detect the levels of serum anti-*H. pylori* IgG and IgA antibodies. The test kits for the detection of anti-*H. pylori* -IgG and anti-*H. pylori* -IgA were purchased from Bioseed Co., USA. The value of the optical density (OD) was read by a microtiter plate reader at 450 nm.

Clinical presentations observation

35 clinical presentations were observed as follows: (1) Symptoms of the digestive system including appetite, distending fullness in the stomach, stomachache, distending fullness in the abdomen, pain in the hypochondrium, pain in the abdomen, singultus, nausea, vomit, acid regurgitation and epigastric upset, and heartburn; (2) General status including ear, eye, physique, complexion, stool, urine, oropharynx, taste, swollen, head, limbs, chest, hand and foot; (3) Spirit and psychological status including spirit, sleep, and emotion; (4) Glossoscopy including quality of tongue, body of tongue, and fur of tongue and (5) Pathogenic factors including smoking, alcohol, dietary bias, and dietary regularity. Each investigated symptom consisted of two to four subordinate items.

Statistical analysis

A SPSS 10.0 statistical package program was used for data analysis. The variables were processed by chi-square test, student's *t* test, ANOVA analysis, and bivariate correlate analysis, where appropriate.

k-means cluster analysis

The *k*-means cluster analysis method has been applied in many areas including data mining, statistics, biology, and machine learning, and so on^[9]. In this study, the relationship between the *H. pylori* infection and the 35 clinical presentations of patients was analyzed by this method. The diagnostic accuracy was obtained by the *k*-means algorithms. The distance between clusters was further verified by an ANOVA test.

RESULTS

As shown in Table 1, the detected positive rates of *H. pylori* varied were 72.7 % (16/22) in mild IM, 84.5 % (49/58) in severe IM, 67.7 % (21/31) in DYS, 51.3 % (39/76) in mild CAG, and 68.2 % (15/22) in severe CAG, respectively. Analyses of chi-square test showed that the detected positive rates of *H. pylori* were similar in mild IM, mild CAG, DYS, and severe CAG groups. The *H. pylori* positive rate in severe IM group was statistically higher than those in other groups (all $P < 0.01$).

Table 2 shows the detective positive rates of *H. pylori* for the CG patients in relation to gender and age. There was no significant difference between the male (62.1 %, 64/103) and the female patients (71.7 %, 76/106) ($P > 0.05$). The *H. pylori* infection rate was highest in the ages from 42 to 49 (59/80, 73.8 %). However, the ANOVA analysis showed that there was no significant difference among four groups with different ages ($P > 0.05$). Bivariate correlation analysis also indicated that the detected positive rate of *H. pylori* was not remarkably associated with the age of patients ($r = 0.0814$, $P = 0.241$).

Table 3 lists the levels of serum anti-*H. pylori* IgG and IgA at different stage of CG. Both serum anti-*H. pylori* IgG and IgA levels were remarkably higher in *H. pylori* positive patients than those negative for *H. pylori* ($P < 0.001-0.01$). In *H. pylori* positive patients the IgG level was significantly greater in severe CAG than in mild CAG ($P < 0.01$). In *H. pylori* negative patients both the serum IgG and IgA levels increased significantly in severe IM, compared to those in mild IM ($P < 0.01-0.05$). There was no significant difference in IgG and IgA levels between mild and severe IM in the presence of *H. pylori* infection ($P > 0.05$).

Table 1 The detected positive rates of *H. pylori* at different stages of CG

<i>H. pylori</i>	Mild CAG	Severe CAG	Mild IM	Severe IM	DYS	Total
Number	76	22	22	58	31	209
Positive %	39 (51.3%)	15 (68.2%) ^a	16 (72.7%)	49 (84.5%) ^b	21 (67.7%)	140
Negative %	37 (48.7%)	7 (31.8%)	6 (27.3%)	9 (15.5%)	10 (32.3%)	69

CAG, chronic atrophic gastritis; IM, intestinal metaplasia; DYS, dysplasia. ^a $P < 0.05$, ^b $P < 0.01$, mild IM vs severe IM; mild CAG vs. severe CAG.

Table 2 The detected positive rates of *H. pylori* for CG patients in relation to gender and age

<i>H. pylori</i>	Males	Females	70-77 years old	60-69 years old	50-59 years old	42-49 years old
Number	103	106	16	47	66	80
Positive (%)	64 (62.1%)	76 (71.7%)	10 (62.5%)	32 (68.1%)	39 (59.1%)	59 (73.8%)
Negative (%)	39 (37.9%)	30 (28.3%)	6 (37.5%)	15 (31.9%)	27 (40.9%)	21 (26.2%)

Table 3 Comparison of serum anti-*H. pylori* IgG and IgA levels (the optical density value) at different stages of CG

	Mild CAG		Severe CAG		Mild IM		Severe IM		DYS	
	<i>H. pylori</i> (+)	<i>H. pylori</i> (-)	<i>H. pylori</i> (+)	<i>H. pylori</i> (-)	<i>H. pylori</i> (+)	<i>H. pylori</i> (-)	<i>H. pylori</i> (+)	<i>H. pylori</i> (-)	<i>H. pylori</i> (+)	<i>H. pylori</i> (-)
IgG(1)	2.86±1.8 ^b	0.38±0.27	4.48±2.14 ^{bc}	0.53±0.27	3.86±1.87 ^b	0.14±0.07	3.1±2.34 ^a	0.55±0.29 ^d	2.74±1.67 ^b	0.23±0.17
IgG(2)	3.26±2.16 ^b	0.46±0.24	4.52±3.27 ^a	0.54±0.29	4.44±2.56 ^b	0.3±0.18	3.5±1.98 ^b	0.54±0.29	3.33±1.87 ^b	0.72±0.97
IgA(1)	0.85±0.7 ^b	0.24±0.22	0.99±0.49 ^b	0.21±0.16	0.83±0.39 ^b	0.1±0.06	0.93±0.79	0.33±0.16 ^d	0.94±0.89 ^b	0.13±0.13
IgA(2)	0.96±0.83 ^b	0.25±0.21	1.08±0.59 ^a	0.27±0.16	0.99±0.72 ^a	0.12±0.07	0.89±0.63 ^a	0.32±0.19 ^d	0.78±0.6 ^b	0.15±0.13

CAG, chronic atrophic gastritis; IM, intestinal metaplasia; DYS, dysplasia. (1) The first detection. (2) The second detection. ^a $P < 0.01$, ^b $P < 0.001$, *H. pylori* (+) vs. *H. pylori* (-). ^c $P < 0.05$, *H. pylori* (+) mild CAG vs. *H. pylori* (+) severe CAG; ^d $P < 0.05$, *H. pylori* (-) mild IM vs. *H. pylori* (-) severe IM.

Table 4 Diagnostic accuracy of *H. pylori* infection determined by different assemblages of symptoms

Attributes	Assemblages of symptoms	Accuracy (%)	
		<i>H. pylori</i> (+)	<i>H. pylori</i> (-)
Pathogenic factors and general status	Smoking, alcohol, limbs, hand and foot (all ^a)	70.7%	42.3%
Pathogenic factors, general status and tongue	Smoking, alcohol, dietary regularity, limbs, and tongue quality (all ^a)	74.3%	39.1%
Pathogenic factors and digestive symptoms	Smoking, alcohol, limbs, hand and foot, distending fullness in the stomach, stomachache, distending fullness in the abdomen, and nausea (all ^a)	51.4%	52.2%
Digestive symptoms	Appetite, distending fullness in the stomach, stomachache, distending fullness in the abdomen, pain in the hypochondrium, pain in the abdomen, singultus, nausea, vomit, acid regurgitation and epigastric upset, heartburn, and stool (all ^a)	71.4%	26.1%
Digestive symptoms and tongue	Distending fullness in the stomach, stomachache, pain in the abdomen, nausea, and fur of tongue (all ^a)	72.1%	26.1%
General status	Taste, swollen, head, limbs, chest, hand and foot, spirit and sleep, emotion, complexion (all ^a)	50.7%	40.6%
Total symptoms	35 items ^b	65.7 %	40.6 %

^a $P < 0.05-0.001$, the difference between two classes tested by the ANOVA analysis. ^b $P < 0.05-0.001$, except dietary bias, dietary regularity, urine, oropharynx, eye, ear, physique, tongue quality, and tongue body.

Table 4 shows the diagnostic accuracy of *H. pylori* infection determined by different assemblages of clinical presentations. The overall diagnostic accuracy based on 35 presentations was 65.7 %. It could be improved by 5.7 % when the only digestive symptoms were engaged, or by 8.6 % when further information were referred such as the assemblage of pathogenic factors (smoking, alcohol), general status (tired limbs), and tongue observation according to the traditional Chinese medicine (TCM) method. However, the diagnostic accuracy could be decreased by the improper assemblages such as the general symptoms only, the pathogenic factors accompanied with some common digestive symptoms (distending fullness in the stomach, stomachache, distending fullness in the abdomen, and nausea) which had no special significance for the positive or negative *H. pylori*.

DISCUSSION

An increasing number of studies support a close relationship between *H. pylori* infection and CG, as previous described. However, the correlation between *H. pylori* infection, serum antibody and clinical symptoms at different stages of CG has not been well investigated so far. The chi-square test results in Table 1 show that the detected positive rates of *H. pylori* increase significantly in patients with mild CAG (51.3 %, 39/76), DYS and mild IM (67.7 %, 21/31), severe CAG (68.2 %, 15/22), and mild IM (72.7 %, 16/22). They reach the highest value in patients with severe IM (84.5 %, 49/58) ($P < 0.01$). However, *H. pylori* infection exhibited no remarkable association with patient's gender (62.1 % in males; 71.7 % in females) and age ($r = 0.08$, $P = 0.241$).

It has been reported that the adherence of *H. pylori* may play an important role in the pathogenesis of severe histological changes in CAG^[10], IM^[11] and DYS^[12]. Our investigation further explored the statistic probability of *H. pylori* infection at different stages of CG. Based on these, we suggest that *H. pylori* infection may be the key factor in accelerating the occurrence and development of CG, since *H. pylori* is a pathogenic bacterium that can adhere to gastric mucosa until the atrophy and intestinal metaplasia occurring in the course of CG.

A mostly pathological mechanism of *H. pylori* infection is the immunopathological response of host. When CG occurs, a detectable specific humoral immunological response will be established. The appearance of serum antibodies such as IgG and IgA may indicate an extensive immunoreaction causing by *H. pylori* infection. The serum anti-*H. pylori* -IgG antibody,

therefore, acts as a highly accurate, simple and noninvasive method in monitoring the status of *H. pylori* infection^[5, 13]. In our study, both serum anti-*H. pylori* IgG and IgA are remarkably higher in *H. pylori* positive patients than those negative for *H. pylori* ($P < 0.001-0.01$). On the one hand, in the presence of *H. pylori* infection the IgG level in severe CAG increased significantly, compared to those in mild CAG ($P < 0.01$). These imply that the serum anti-*H. pylori* IgG and IgA are appropriate indicators to evaluate the status of *H. pylori* infection in the process of CG. On the other hand, in absence of *H. pylori* infection both serum IgG and IgA are significantly greater in severe IM than those in mild IM ($P < 0.01-0.05$), whereas no significant difference ($P > 0.05$) was observed between mild and severe IM in the presence of *H. pylori* infection. The increase of antibody may be due to the reminiscence of *H. pylori* infection, resulting in a certain arrearage between serum antibody and *H. pylori*. It is reported that the IgA response of gastric mucoa in CG patients can be detected even in the quiescent period of negative *H. pylori* infection due to the recent exposure to the bacterial antigens^[6].

The clinical situations of CG patients are intricate. They are divergent by the pathological changes of gastric mucosa, and are affected by environmental factors^[14, 15]. By means of the cluster analysis method, we found that the proper assemblages such as digestive symptoms, pathogenic factors (smoking, alcohol), general status (tired limbs), and the tongue could improve the diagnostic accuracy of *H. pylori* infection. However, the improper assemblages, such as the general symptoms only, or the pathogenic factors accompanied with some common digestive symptoms decreased the diagnostic accuracy. A preferable symptomatic assemblage has been proposed in the present study. Based on this, the diagnostic accuracies of up to 74.3 % and 40.5 %, respectively, for positivity and negativity of *H. pylori* infection have been obtained. It has been demonstrated clinically that smoking, alcohol^[16] and the tongue change^[17] are pathogenic factors for the *H. pylori* infection. Our study indicates that the symptomatic assemblages rather than an individual factor are closely related to the clinic significance of *H. pylori* infection. Furthermore, it has been known that the validity of CG treatment in traditional Chinese medicine (TCM) is based on the differentiation of symptom-complexes^[18, 19]. Our investigation suggests that *H. pylori*-related symptomatic assemblages can be taken into consideration in practicality and methodology during the diagnoses and treatment of CG. More effective symptomatic assemblages and their effects

on *H. pylori* infection are still required.

In conclusion, the early genesis and further progression of CG are associated with *H. pylori* infection, which can be characterized by the increase of serum anti-*H. pylori* IgG and IgA with a certain arrangement. Due to the intricate clinical situation of CG, effective symptomatic assemblages are required in diagnosing *H. pylori* infection.

REFERENCES

- Aguilar GR**, Ayala G, Fierros-Zarate G. *Helicobacter pylori*: Recent advances in the study of its pathogenicity and prevention. *Salud Publica Mex* 2001; **43**: 237-247
- Gao HJ**, Yu LZ, Bai JF, Peng YS, Sun G, Zhao HL, Miu K, Lu XZ, Zhang XY, Zhao ZQ. Multiple genetic alterations and behavior of cellular biology in gastric cancer and other gastric mucosal lesions: *H. pylori* infection, histological types and staging. *World J Gastroenterol* 2000; **6**: 848-854
- Zhuang XQ**, Lin SR. Research of *Helicobacter pylori* infection in precancerous gastric lesions. *World J Gastroenterol* 2000; **6**: 428-429
- Prinz C**, Schoniger M, Rad R, Becker I, Keiditsch E, Wagenpfeil S, Classen M, Rosch T, Schepp W, Gerhard M. Key importance of the *Helicobacter pylori* adherence factor blood group antigen binding adhesin during chronic gastric inflammation. *Cancer Res* 2001; **61**: 1903-1909
- Zhu Y**, Lin J, Li D, Du Q, Qian K, Wu Q, Zheng S. *Helicobacter pylori* antigen and its IgG, IgA-type specific immunocomplexes in sera from patients with *Helicobacter pylori* infection. *Chin Med J (Engl)* 2002; **115**: 381-383
- Futagami S**, Takahashi H, Norose Y, Kobayashi M. Systemic and local immune responses against *Helicobacter pylori* urease in patients with chronic gastritis: distinct IgA and IgG productive sites. *Gut* 1998; **43**: 168-175
- Stankiewicz JA**, Chow JM. A diagnostic dilemma for chronic rhinosinusitis: definition accuracy and validity. *Am J Rhinol* 2002; **16**: 199-202
- Dixon MF**, Genta RM, Yardley JH, Correa P. Classification and grading of gastritis: the updated sydney system. International workshop on the histopathology of gastritis houston 1994. *Am J Surg Pathol* 1996; **20**: 1161-1181
- Han JW**, Kamber M. Data mining: concepts and techniques. *Morgan Kaufmann Publishers, USA* 2001: 16
- Domellof L**. Reversal of gastric atrophy after *Helicobacter pylori* eradication: is it possible or not? *Am J Gastroenterol* 1998; **93**: 1407-1408
- Meining A**, Stolte M. Close correlation of intestinal metaplasia and corpus gastritis in patients infected with *Helicobacter pylori*. *Z Gastroenterol* 2002; **40**: 557-560
- Gao H**, Wang JY, Shen XZ, Liu JJ. Effect of *Helicobacter pylori* infection on gastric epithelial cell proliferation. *World J Gastroenterol* 2000; **6**: 442-444
- Figueroa G**, Faundez G, Troncoso M, Navarrete P, Toledo MS. Immunoglobulin G antibody response to infection with coccoid forms of *Helicobacter pylori*. *Clin Diagn Lab Immunol* 2002; **9**: 1067-1071
- Kippen HM**, Fiedler N. The role of environmental factors in medically unexplained symptoms and related syndromes: conference summary and recommendations. *Environ Health Perspect* 2002; **110**(Suppl 4): 591-595
- Brown LM**, Thomas TL, Ma JL, Chang YS, You WC, Liu WD, Zhang L, Pee D, Gail MH. *Helicobacter pylori* infection in rural China: demographic, lifestyle and environmental factors. *Int J Epidemiol* 2002; **31**: 638-645
- Kamada T**, Haruma K, Komoto K, Mihara M, Chen X, Yoshihara M, Sumii K, Kajiyama G, Tahara K, Kawamura Y. Effect of smoking and histological gastritis severity on the rate of *H. pylori* eradication with omeprazole, amoxicillin, and clarithromycin. *Helicobacter* 1999; **4**: 204-210
- Ozdemir A**, Mas MR, Sahin S, Saglamkaya U, Ateskan U. Detection of *Helicobacter pylori* colonization in dental plaques and tongue scrapings of patients with chronic gastritis. *Quintessence Int* 2001; **32**: 131-134
- Chen ZQ**, Chen GL, Li XW, Zhao YQ, Shi LJ. Plasma L-ENK, AVP, ANP and serum gastrin in patients with syndrome of Liver-Qi-stagnation. *World J Gastroenterol* 1999; **5**: 61-63
- Zhang XC**, Gao RF, Li BQ, Ma LS, Mei LX, Wu YZ, Liu FQ, Liao ZL. Clinical and experimental study of therapeutic effect of Weixibaonizhuan pills on gastric precancerous lesions. *World J Gastroenterol* 1998; **4**: 24-27

Edited by Xia HHX

Immunotolerance of liver allotransplantation induced by intrathymic inoculation of donor soluble liver specific antigen

Chang-Ku Jia, Shu-Sen Zheng, Qi-Yong Li, Ai-Bin Zhang

Chang-Ku Jia, Shu-Sen Zheng, Qi-Yong Li, Ai-Bin Zhang, Department of Hepatobiliary Pancreatic Surgery, Key Lab of combined Multi-Organ Transplantation, Ministry of Public Health, The First Affiliated Hospital of College of Medicine, Zhejiang University, Hangzhou 310003, China

Supported by Science and Technology Department of Zhejiang Province Foundation, No.011106206

Correspondence to: Dr. Chang-Ku Jia, Department of Hepatobiliary Pancreatic Surgery, The First Affiliated Hospital of College of Medicine, Zhejiang University, Hangzhou 310003, China. jiachk@sohu.com

Telephone: +86-571-87236570 **Fax:** +86-571-87236570

Received: 2002-10-08 **Accepted:** 2002-11-14

Abstract

AIM: To study the effects of liver specific antigen (LSA) on the immunoreaction of liver allotransplantation and its significance.

METHODS: Orthotopic liver transplantation was used in this study. Group I: syngeneic control (Wistar-to-Wistar); Group II: acute rejection (SD-to-Wistar). Group III: acute rejection treated by intramuscular injection of cyclosporine A (CsA) (SD-to-Wistar+CsA). Group IV: Intrathymic inoculation of SD rat LSA one week before transplantation (LSA+SD-to-Wistar). The common situation and survival time, rejection grades, NF- κ B activity of splenocytes and intragraft cytokine gene expression were observed to analyze the acute rejection severity and immune state of animals.

RESULTS: The common situation of Wistar-to-Wistar group was very good after the transplantation and no signs of rejection were found. Recipients of SD-to-Wistar group lost body weight progressively. All died within 9 to 13 days after transplantation with the median survival time of 10.7 ± 0.51 days. It was an optimal control for acute rejection. The common situation of SD-to-Wistar+CsA group was bad during CsA medication but only with mild rejection. As for LSA+SD-to-Wistar group, 5 of 6 recipients survived for a long time and common situation was remarkably better than that of SD-to-Wistar group and SD-to-Wistar+CsA group. Its rejection grades were significantly lower than that of SD-to-Wistar group ($P=0.026$). Furthermore, no significant discrepancies of rejection were found between SD-to-Wistar group and LSA+SD-to-Wistar group at day7 and day12 ($P=0.067$). NF- κ B activity, IFN- γ and IL-2mRNA expression were significantly inhibited in LSA+SD-to-Wistar group compared with that of SD-to-Wistar group ($P<0.05$).

CONCLUSION: LSA is an important transplantation antigen which involves in the immunorejection of liver transplantation directly. We reported for the first time that intrathymic inoculation of LSA can induce immunotolerance of liver allotransplantation and grafts can survive for a long time thereby, thus leading to a novel way to liver transplantation immunotolerance.

Jia CK, Zheng SS, Li QY, Zhang AB. Immunotolerance of liver allotransplantation induced by intrathymic inoculation of donor soluble liver specific antigen. *World J Gastroenterol* 2003; 9 (4): 759-764

<http://www.wjgnet.com/1007-9327/9/759.htm>

INTRODUCTION

Although MHC-antigens have been extensively studied, the problem of rejection in liver transplantation was not resolved completely. Liver transplantation are not strict for HLA matching and both grafts and recipients can survive for a long time after immunotherapy^[1]. On the other hand, given HLA multiple loci matching in some cases, the likelihood of grafts dysfunction and rejection increased, which suggested that matching for HLA type may exert a dualistic effect on liver transplantation^[1,2]. No satisfactory explanations have been made about it up to date; and most studies were limited to HLA antigens themselves with the results still remaining controversial.

The specific antigens expressed only in liver cell membrane or liver cytoplasm and encoded by loci not linked to the MHC gene were called liver specific antigen (LSA). It was reported that this antigen could be detected in sera of almost all liver allotransplantation recipients but its effects remained unknown yet^[3]. Thus in this experiment, we aimed to find whether LSA was an transplantation antigen and its possible mechanism of inducing the tolerance of liver allotransplantation using intrathymic LSA inoculation pathway. And the roles of LSA in thymus tolerance were discussed in this research too.

MATERIALS AND METHODS

Materials

Inbred male Wistar and male SD rats weighing 200 to 250 g were purchased from Shanghai Experimental Animal Center; there were also materials used in this study as following: [γ -³²P]ATP (Furui bioengineering Corp, Beijing); EMSA assay kit (Promega); NF- κ B double stranded oligonucleotide, 5' - A G T T G A G G G A C T T T C C C A G G C - 3' , 3' - T C A A C T C C C C T G A A G G G T C C G - 5' (Santa Cruz), NF- κ B double stranded mutant oligonucleotide, 5' - A G T T G A G G - C G A C T T T C C C A G G C - 3' , 3' - T C A A C T C C G C T G A A G G G T C C G - 5' (Santa Cruz); TRIzol Reagent (Gibco, BRL); MuLV (MBI, Fermentas); Ultracentrifugator (Beckman); CHRIST lyophilizer (B.Braun Biotech).

Methods

Isolation of LSA Preparation of liver specific protein S100 was carried out by the method previously described^[4]. The protein contents was measured according to the method of Bradford. Then the protein was lyophilized by CHRIST lyophilizer and stored at -80 °C.

Surgical procedure, experimental groups and sample harvesting Rats were anesthetized with ether inhalation. Orthotopic rat liver transplantation was performed by Kamada's two-cuff technique^[5]. The animals surviving less

then 3 days after the transplantation were attributed to technical errors and were excluded from this study. Wistar rats serving as recipients were randomly divided into four groups, Group I: syngeneic control (Wistar-to-Wistar); Group II: acute rejection (SD-to-Wistar); Group III: acute rejection treated with intramuscular injection of CsA 3.0 mg/kg/d (SD-to-Wistar+CsA); Group IV: Intrathymic inoculation of 10 mg SD rat LSA one week before transplantation (LSA+SD-to-Wistar). All groups were subdivided into day 1, 3, 5, 7, 12 subgroup ($n=3$ each) after the transplantation respectively for sample harvesting and another subgroups ($n=6$) for observation of common situation and survival time. For observation of common situation and survival time in Group III, after the therapy of CsA for 12 days, animals received no additional immunosuppression. Graft specimens were harvested to determine morphological changes and cytokine gene expression. Recipient splenocytes were isolated and the NF- κ B activity were determined.

Histopathological examination Grafted liver samples were fixed in 10 % buffered formalin and embed in paraffin. Five micrometers thick sections were affixed to slides, deparaffinized, and stained with hematoxylin and eosin to assess morphologic changes and severity of acute rejection by the Kemnitz' s standard^[6].

Cytokine reverse transcription-polymerase chain reaction Primer sequences and reaction conditions: Primers sequences used were as follow: IL-2 sense primer, 5' - GACGCTTGCTCCTTGT CA-3', IL-2 antisense primer, 5' - ACCACAGTTGCTGGCTCATC-3' (size3 72bp); IFN- γ sense primer, 5' - ACTGCCAAGGCACATCATT-3', IFN- γ antisense primer, 5' - AGGTGCGAT TCGATGACACT-3' (size 235bp); β -actin sense primer, 5' - TCGTACCA CTGGCATTGTGA-3', β -actin antisense primer, 5' - TCCTGCTTGCTGATCCACAT-3' (size 645bp). Amplifications were performed under the following conditions: 95 °C for 2 minutes, 94 °C for 45 seconds, 56 °C for 45 seconds, 72 °C for 45 seconds, totally 32 cycles. The final extension step was performed by one cycle at 72 °C for 10 minutes. Reaction buffer: 10×Buffer 2.5 μ l, 10 mM dNTP 1 μ l, MgCl 2 μ l, cDNA 2 μ l and 1 μ l of each primer, ddH₂O was added to get the final volume of 25 μ l. RT-PCR: Total RNA was prepared from grafted liver with TRIzol Reagent according to the manufacturer' s recommendations. For cDNA synthesis, 4 μ g total RNA was reverse transcribed with MuLV reverse transcriptase according to the manufacturer' s recommendations. Two microliters from the resulting cDNA solution were then amplified using specific oligonucleotides under the reaction conditions using β -actin as a "housekeeping gene" in a volume of 25 μ l PCR buffer. Reaction products were run by electrophoresis on a 1.5 % agarose gel for 30-40 min at 100 V in 0.5×Tris/borate/EDTA buffer, and visualized with ethidium bromide under UV light. Relative expression of cytokines were defined as optical density ratio (cytokine/ β -actin) analyzed by Kodak digital science scanning system.

NF- κ B activity of splenocytes and EMSA competitive inhibition NF- κ B activity was detected by gel electrophoretic mobility shift assay (EMSA): Splenocytes of recipients were isolated and nuclear extracts were prepared according to the method described by Kravchenko^[7]. The contents of protein were determined by the method of Bradford. NF- κ B oligonucleotide was end-labeled with [γ -³²P]ATP according to the manufacturer' s recommendations. For EMSA, 10 μ g of each nuclear extract was mixed with 5×binding buffer at room temperature for 10 min. Then 1 μ l [γ -³²P] ATP-labeled double strand NF- κ B oligonucleotide probe was added in and incubated at room temperature for 20 min. The DNA/protein complex was electrophoresed on 4 % nondenaturing polyacrylamide gels in 0.5×Tris/borate/EDTA buffer to

separate probe binding to NF- κ B and free probe. Radioactive bands were detected by autoradiography at -70 °C followed by radiography to detect the level of retardation. The results were expressed as relative optical density (ROD)^[8]. To study whether the method of EMSA was specific, standard nuclear extract of Hela cells was used to bind with NF- κ B protein. The specificity of binding was confirmed by 100 fold excess unlabeled NF- κ B oligonucleotide as a specific competitor, 100 fold excess unlabeled non-related oligonucleotide as a nonspecific competitor and 100 fold excess unlabeled mutant NF- κ B oligonucleotide as a mutant competitor. All unlabeled oligonucleotides were preincubated with Hela nuclear extract at room temperature for 10 min then labeled NF- κ B oligonucleotide was added. The left steps were the same as mentioned above.

Statistics analysis

All data were expressed as mean \pm SD and analyzed by one-way repeated measures analysis of variance (ANOVA) using SPSS software (version 11.0 for windows). Pearson correlation analysis was used between parameters. $P<0.05$ was considered as statistically significant.

RESULTS

Postoperative common situation and survival time

The common situation of rats in the Wistar-to-Wistar group was very good after the transplantation. Recipients drank normally after 3rd day of posttransplantation. Normal coat recovered at day 7 with increase of body weight and all recipients survived for a long time. Recipients of rats in the SD-to-Wistar group ate badly with tarnished coat and progressive loss of body weight; all died within 9 to 13 days after the transplantation; median survival time was 10.7 \pm 0.51 days. Although 5 of 6 recipients of rats in the SD-to-Wistar+CsA group survived for a long time (one dead from abdominal inflammation and liver abscess day on 14 after the transplantation), they also drank badly with tarnished coat and ceased increase of body weight during CsA medication, which recovered after the cease of drug treatment. As for the LSA+SD-to-Wistar group, 5 of 6 recipients survived for a long time (one dead of bile duct obstruction on day 15 after the transplantation) and their common situation were remarkably better than that of rats in the SD-to-Wistar group and SD-to-Wistar+CsA group.

Histopathologic examination

No signs of rejection were found at any time point in the Wistar-to-Wistar group with minimal portal inflammatory infiltrates. In the SD-to-Wistar group, a few portal lymphocyte infiltrations combined with minimal vein endothelialitis on day 1 was found but there was no evidence of rejection. Significant portal lymphocyte infiltration with degeneration of hepatic parenchyma in some cases can be found on day 3 and day 5 with average rejection grade of 1.83 and 2.67, respectively. Severe inflammatory cells infiltration, severe vein subendothelialitis with bridging hepatocellular necrosis could be found on both day 7 and day 12 with rejection grade of 2.87 and 3, respectively. Owing to the immunosuppressive effect of CsA, rejection was greatly inhibited in the SD-to-Wistar+CsA group. No evidence of rejection was found at the first three time points. But mixed inflammatory infiltration and endothelialitis could be found on day 7 and day 12, in which grade 1 rejection was diagnosed. As for the LSA+SD-to-Wistar group, rejection grades was 0 and 1 on day 1 and 3, respectively. Mixed but mainly lymphocytic infiltration was found in both portal tract and parenchyma without focal necrosis of the hepatic parenchyma on day 5, 7 and 12. Thus their rejection grades were all defined as 1.25 which were significantly lower

than that in the SD-to-Wistar group ($P=0.026$). Furthermore, no significant discrepancies of rejection grades on day7 and day 12 were found between the the SD-to-Wistar+CsA group and LSA+SD-to-Wistar group ($P=0.067$) (Figure 1).

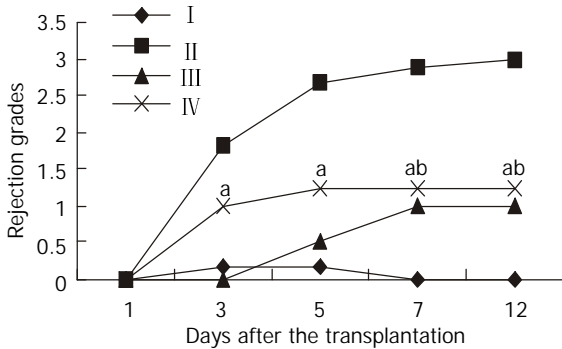


Figure 1 Rejection grades of grafted liver in different groups. Data were expressed as mean±SD. I, Wistar-Wistar group; II, SD-Wistar group; III, SD-Wistar+CsA group; IV, LSA+SD-Wistar group; Rejection grades of group IV were significantly lower than that in group II at all but day 1 time point. No significant discrepancies were found between group IV and group III on day 7 and day 12 time points. ^a $P<0.05$ vs group II, ^b $P>0.05$ vs group III.

Expression of cytokine gene

The kinetic changes of intragraft IL-2 mRNA expression in different groups were shown in Figure 2: no expression was detected at any time point in the Wistar-to-Wistar and the SD-to-Wistar+CsA group, whereas high level expression was detected at all time points in the SD-to-Wistar group and reached to the peak on day 7 and 12 after the transplantation ($P<0.001$, vs the Wistar -to-Wistar group). Low level expression was only detected on day 5 in the LSA+SD-to-Wistar group which was significantly lower than that in the SD-to-Wistar group ($P<0.001$). Intragraft IFN- γ mRNA expression in different groups was shown in Figure 3. Very weak IFN- γ mRNA expression was detected at any time point in the Wistar-to-Wistar group after the liver transplantation, whereas there was very strong expression in the SD-to-Wistar group at all time points ($P=0.006$, vs the Wistar -to-Wistar group). The expression of IFN- γ mRNA was significantly inhibited in the SD-to-Wistar+CsA group which was significantly lower than that in the SD-to-Wistar group ($P<0.001$). As for group IV, its kinetic change was similar to that in the SD-to-Wistar group but was significantly lower than that in the SD-to-Wistar group at any time points ($P=0.046$). Expression of IL-2 and IFN- γ mRNA was correlated to the histopathological damage.

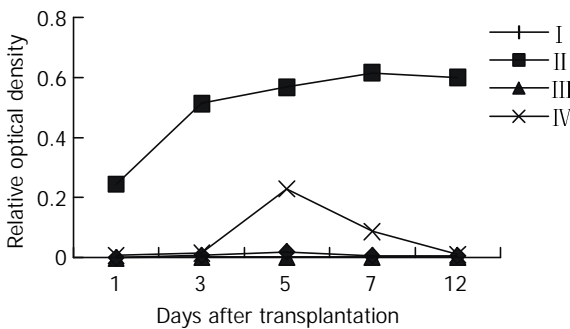


Figure 2 The kinetic change of intragraft IL-2mRNA expression in different groups. I, Wistar-Wistar group; II, SD-Wistar group; III, SD-Wistar+CsA group; IV, LSA+SD-Wistar group; IL-2mRNA expression of group IV were significantly lower than that in group II at all time point ($P<0.05$).

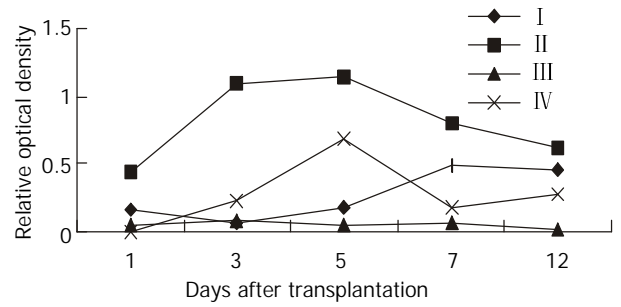


Figure 3 The kinetic change of Intragraft IFN- γ mRNA expression in different groups. I, Wistar-Wistar group; II, SD-Wistar group; III, SD-Wistar+CsA group; IV, LSA+SD-Wistar group; IL-2mRNA expression of group IV were significantly lower than that in group II at all time point ($P<0.05$).

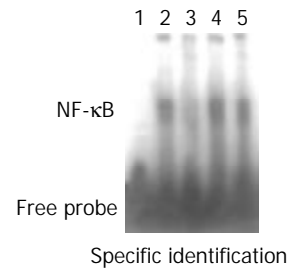


Figure 4 EMSA specific competitive inhibition. Lane 1, negative control; Lane 2, positive control; Lane 3, specific competition; Lane 4, non-specific competition; Lane 5, mutant competition.

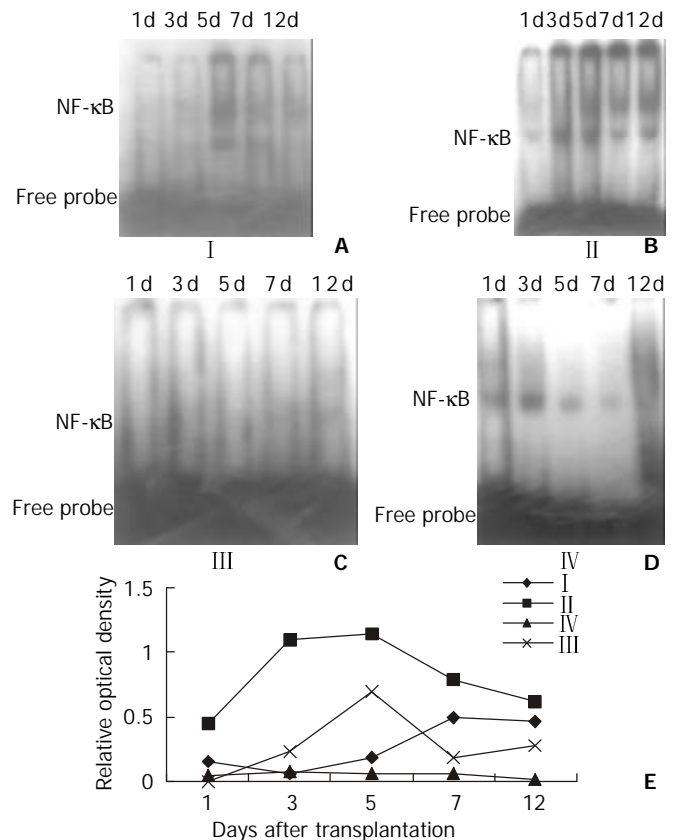


Figure 5 NF- κ B activity of splenocytes at different time points after the transplantation. A, Wistar-Wistar group; B, SD-Wistar group; C, SD-Wistar+CsA group; D, LSA+SD-Wistar group; E, the kinetic change of NF- κ B activity. NF- κ B activity of group IV were significantly lower than that in group II at all time point ($P<0.05$).

EMSA specific competitive inhibition and NF- κ B activity of splenocytes

The results of EMSA competitive inhibition showed that no NF- κ B activity was found after the specific competition, whereas NF- κ B activity was the same as the positive control after the nonspecific competition and mutant competition (Figure 4). This results showed that this method was specific. NF- κ B activity of splenocytes in Figure 5 showed the autoradiographic results of splenocyte NF- κ B DNA binding activity in different groups (A, B, C, D). Low NF- κ B activity was only detected on day 5 and day 7 in the Wistar-to-Wistar syngeneic group after the transplantation. In contrast, NF- κ B activity increased from day 3 after the transplantation in the SD-to-Wistar group and was significantly higher than that in the syngeneic group at all time points ($P=0.001$). Only very weak DNA binding activity was found on day 12 in the SD-to-Wistar+CsA group and NF- κ B activity was also inhibited in the LSA+SD-to-Wistar group which was significantly lower than that in the SD-to-Wistar group ($P=0.003$). NF- κ B activity was significantly inhibited in the SD-to-Wistar+CsA and LSA+SD-to-Wistar group (Figure 5E).

Correlation analysis

A good correlation was found between the activity of NF- κ B and intragraft IL-2 as well as IFN- γ mRNA expression in this study (pearson correlation analysis, $r=0.737$ and $r=0.742$ respectively, $P<0.01$, $n=20$). While intragraft IL-2 and IFN- γ mRNA expression were correlated to histopathological damage (pearson correlation analysis, $r=0.856$ and $r=0.680$ respectively, $P<0.01$, $n=20$).

DISCUSSION

Allotransplantation tolerance can be induced by intrathymic inoculation of donor cellular antigen^[9-12], and also by intrathymic inoculation of donor soluble MHC antigen^[13-15]. However, intrathymic inoculation of donor soluble non-MHC antigen have not been reported heretofore. In this study, we inoculated donor LSA into recipient thymus before the liver transplantation so that rejection was greatly inhibited. Only mild rejection was found in grafts and was significantly lower than that in the non-LSA inoculated group and similar to that in the CsA treated group. Recipients survived for a long time due to the induction of immunotolerance.

Although the rejection grades in the LSA+SD-to-Wistar group was increased obviously from day 3 and peaked at day 5 after transplantation, there was no significant difference between time points except for day 1 ($P>0.05$). This rejection kinetic change in the LSA+SD-to-Wistar group was similar to that in the Wistar -Wistar group and was significantly lower than that in the SD-to-Wistar group ($P=0.026$). Furthermore, the rejection grades in the LSA+SD-to-Wistar group did not significantly differ from that in the SD-to-Wistar+CsA group on day 7 and day 12 time point after the transplantation ($P=0.067$), which showed that intrathymic inoculation of LSA could greatly alleviate rejection. However, rejection in the SD-to-Wistar group was increased continuously and the rejection grade on day 3 after the transplantation was significantly different from its peak one ($P<0.05$). It was an optimal acute rejection control. As for the SD-to-Wistar+CsA group, rejection was greatly suppressed due to the effect of CsA and recipients survived for a long time, which was consistent with previous reports^[16]. The rejection grades in all but SD-to-Wistar+CsA group was increased rapidly within groups when compared with that on day 1 after the transplantation (Figure 1) showed that the high immunoresponses starting from day 3 to day 5 after the transplantation was the "rejection crisis" phase^[17].

Rejection crisis phase in the SD-to-Wistar+CsA group was postponed to start from day 5 to day 7 after the transplantation due to the strong immunosuppressive effect of CsA. Meanwhile, that rejection grades was not increase on day 7 after the transplantation both in the SD-to-Wistar+CsA group and LSA+SD-to-Wistar group and recipients survived for a long time suggested that the pathological damage in these two groups may be "self-limited". Given longer harvesting time point, more could probably be found.

For the expression of IL-2mRNA, the most related cytokine to rejection, detected using RT-PCR in grafts, low level expression was only detected on day 5 in the LSA+SD-to-Wistar group and it was significantly lower than that in the SD-to-Wistar group ($P<0.001$) (Figure 2). Although the expression of IFN- γ mRNA, another important cytokine to rejection, was slightly higher than that in the Wistar-to-Wistar group ($P=0.427$), it was also significantly inhibited in the LSA+SD-to-Wistar group ($P<0.046$, vs SD-to-Wistar group) (Figure3). IL-2 and IFN- γ are the representative cytokines secreted by Th1 cells which play important roles in transplant rejection^[18-20]. Both intragraft IFN- γ mRNA and protein were increased when grafts were rejected^[21,22]. IFN- γ not only increases expression of MHC class I and class II antigens of intragraft, but stimulates cells without expression of MHC class II antigens at quiescent state to express MHC class II antigens^[23]. Thus inhibiting the synthesis and secretion of IL-2 and IFN- γ is one of the mainly target for preventing transplantation rejection all the while.

As an important nuclear transcription factor, NF- κ B is a specific sequence binding protein which can bind to promoters or enhancers of multiple genes including closely related cytokines and adhesion molecules to organ transplantation rejection^[24], thus extensively regulating the expression of these genes. Apart from that the change of NF- κ B activity exerts crucial effects on the proliferation and activation of immune cells, NF- κ B is also an important antiapoptotic nuclear factor^[25,26]. So the change of NF- κ B activity may play a crucial role in the immunoresponses and directly influence the immunoreaction after the transplantation. In its quiescent state, NF- κ B is localized in cytoplasm in a complex with its inhibitory proteins (I κ Bs)^[27,28], which mask its nuclear localization signal and prevent its from translocation to the nucleus. NF- κ B is activated through phosphorylation and I κ Bs is subsequently degraded and then translocated into nucleus to bind with specific DNA sequences to regulate the expression of related genes^[26]. NF- κ B regulates the transcription of IL-2 mRNA through binding to its binding sites in down-stream of IL-2 gene promoter. It has been demonstrated *in vitro* that activated NF- κ B can directly result in high level expression of IL-2 mRNA and promote the proliferation and activation of T lymphocyte^[29]. IFN- γ gene belongs to lymphokine gene family and is related to transplantation rejection. Its transcription parallels that of other lymphokine genes such as IL-2 whose promoter activity can be enhanced by NF- κ B protein^[30,31]. In this regard, the ubiquitous factor NF- κ B controlling a number of cytokines may have roles in the transcription of IFN- γ gene. It has also been demonstrated that NF- κ B interacts with NF-AT to coregulate the gene expression of IFN- γ *in vitro*^[32] but not *in vivo* especially in the organ transplantation rejection. We used rat orthotopic liver transplantation model to study the relationship between the activity of NF- κ B and the expression of IL-2 and IFN- γ mRNA and its mechanisms with or without CsA and LAS treatment. A good correlation was found between the activity of NF- κ B and the expression of intragraft IL-2 as well as IFN- γ mRNA in this study (pearson correlation analysis, $r=0.737$ and $r=0.742$ respectively, $P<0.01$, $n=20$). While the expression of intragraft IL-2 and IFN- γ mRNA were correlated

to the histopathological damage (pearson correlation analysis, $r=0.856$ and $r=0.680$ respectively, $P<0.01$, $n=20$). Thus it is believable that allotransplantation rejection is partly due to the activation of NF- κ B at least. Both CsA and intrathymic inoculation of donor LSA can inhibit the activity of NF- κ B and further inhibit the expression of IL-2 and IFN- γ mRNA and rejection after the transplantation.

We preliminarily discuss the specific tolerance mechanisms induced by LSA: T lymphocytes recognition process of tissue specific antigens is MHC-restricted which includes direct and indirect recognition and the latter is the main one. In this experiment, before the transplantation, protein antigen was used to inoculate recipient thymus. No APC and MHC molecules of donor existed, so the recognition of LSA should be indirect. Modern immunology believes that TCR recognizes neither MHC molecules nor antigen peptides alone. What it recognizes is surface information of MHC-antigen peptides complex. So it is believed that although LSA is organ specific, space conformation, electric charge qualities and distributions of MHC-antigen peptides complex are not the same due to its polymorphism, thus activating allolymphocytes^[33]. But large numbers of activated lymphocytes may be clonally deleted due to high dose antigen immunization, which coincides with the "high-dose/activation-associated tolerance" mechanism^[34]; In addition, thymus reeducation may also be one of the mechanisms of this tolerance. T lymphocytes of recipient recognize donor LSA as self by reeducation mechanism.

Therefore it was postulated that given multiple MHC loci matching, the processing ability of tissue specific antigens by recipient MHC molecules will be enhanced or be equal to that of by donor's, thus bring about indirect recognition of T lymphocytes changing into direct recognition and increasing the occurrence of hepatopathy and rejection after the transplantation. This may be one of the reasons why multiple MHC loci matching, especially DR matching, can increase the rates of grafted liver dysfunction and rejection^[1,2]. This may be just as what Desquenue postulated that it should make it easier to induce tolerance of skin antigen as well as other tissue specific antigen when MHC incompatibilities prevail^[35]. Besides, special attention must be paid to the LSA+SD-to-Wistar group. The common situation of recipients without any transient immunosuppression were much better than that in the non-LSA or CsA-treated group and no such complications as inflammations happened. It showed that the tolerance did not result from down-regulation of body's immunofunction, in contrast recipients' immunofunction was normal. This is perhaps the optimal condition to induce donor specific tolerance and do not affect body's immunofunction. Reasonable explanation is that strong immunoreaction towards to liver parenchymal cells happened when transplanted liver was rejected. Thus the tolerance induced by LSA is towards to hepatocytes and is in real sense a donor and organ specific one.

The results of this experiment not only demonstrated that thymus had unusual effects on the tolerance induction, but also that allotolerance to non-MHC antigen can be induced after contacting of thymus microenvironment to non-MHC antigen. It may suggest that if immunodominant character or immunodominant non-MHC antigens were identified, differences of other MHC and non-MHC antigen may be neglected, thus leading to long-term allografts survival across complete MHC barrier. It also suggested that MHC antigens may be not the only obstacles to successful transplantation. It is reported here for the first time that intrathymic inoculation of LSA can induce permanent and specific immunotolerance of liver allotransplantation, which show that hepatocytes are directly involved in the immunoreaction of liver transplantation. It's an important supplement to the traditional theory of liver

transplantation rejection which considers that rejection is mainly involved in liver vascular bed, bile ducts and nonparenchymal cells, thus leading to a novel way to liver transplantation immunotolerance.

REFERENCES

- 1 **Donaldson P**, Underhill J, Doherty D, Hayllar K, Calne R, Tan KC, O'Grady J, Wight D, Portmann B, Williams R. Influence of human leukocyte antigen matching on liver allograft survival and rejection: "the dualistic effect". *Hepatology* 1993; **17**: 1008-1015
- 2 **Doran TJ**, Derley L, Chapman J, McCaughan G, Painter D, Dorney S, Sheil AG. Severity of liver transplantation rejection is associated with recipient HLA type. *Transplant Proc* 1992; **24**: 192-193
- 3 **Yan YH**, Liu GZ. Transplantation antigens. In: YiZhi MianYi Xue. Wuhan: Hubei Science and Technology Press 1998: 45-47
- 4 **Lohse AW**, Dienes HP, Meyer zum Buschenfelde KH. Suppression of murine experimental autoimmune hepatitis by T-cell vaccination or immunosuppression. *Hepatology* 1998; **27**: 1536-1543
- 5 **Kamada N**, Calne RY. A surgical experience with five hundred thirty liver transplants in the rat. *Surgery* 1983; **93**: 64-69
- 6 **Kemnitz J**, Ringe B, Cohnert TR, Gubernatis G, Choritz H, Georgii A. Bile duct injury as a part of diagnostic criteria for liver allograft rejection. *Hum Pathol* 1989; **20**: 132-143
- 7 **Kravchenko VV**, Pan Z, Han J, Herbert JM, Ulevitch RJ, Ye RD. Platelet-activating factor induces NF-kappa B activation through a G protein-coupled pathway. *J Biol Chem* 1995; **270**: 14928-14934
- 8 **Gong JP**, Liu CA, Wu CX, Li SW, Shi YJ, Li XH. Nuclear factor kB activity in patients with acute severe cholangitis. *World J Gastroenterol* 2002; **8**: 346-349
- 9 **Fujii Y**, Sugawara E, Hayashi K, Sano S. Neonatal intrathymic splenocyte injection yields prolonged cardiac xenograft survival. *Acta Med Okayama* 1998; **52**: 83-88
- 10 **Oluwole OO**, Depaz HA, Gopinathan R, Ali A, Garroville M, Jin MX, Hardy MA, Oluwole SF. Indirect allorecognition in acquired thymic tolerance: induction of donor-specific permanent acceptance of rat islets by adoptive transfer of allopeptide-pulsed host myeloid and thymic dendritic cells. *Diabetes* 2001; **50**: 1546-1552
- 11 **Torchia MG**, Aitken RM, Thliveris A. The effect of thymic inoculation to induce tolerance of allogeneic thyroid grafts in the outbred rabbit. *Histol Histopathol* 1998; **13**: 1061-1068
- 12 **Blom D**, Morrissey N, Mesonero C, Zuo XJ, Jordan S, Fisher T, Bronsther O, Orloff MS. Tolerance induction by intrathymic inoculation prevents chronic renal allograft rejection. *Transplantation* 1998; **65**: 272-275
- 13 **Chowdhury NC**, Saborio DV, Garroville M, Chandraker A, Magee CC, Waaga AM, Sayegh MH, Jin MX, Oluwole SF. Comparative studies of specific acquired systemic tolerance induced by intrathymic inoculation of a single synthetic Wistar-Furth (RT1U) allo-MHC class I (RT1.AU) peptide or WAG (RT1U)-derived class I peptide. *Transplantation* 1998; **66**: 1059-1066
- 14 **Fandrich F**, Zhu X, Schroder J, Dresske B, Henne-Bruns D, Oswald H, Zavazava N. Different in vivo tolerogenicity of MHC class I peptides. *J Leukoc Biol* 1999; **65**: 16-27
- 15 **Stadlbauer TH**, Schaub M, Magee CC, Kupiec Weglinski JW, Sayegh MH. Intrathymic immunomodulation in sensitized rat recipients of cardiac allografts: requirements for allorecognition pathways. *J Heart Lung Transplant* 2000; **19**: 566-575
- 16 **Gassel HJ**, Otto C, Gassel AM, Meyer D, Steger U, Timmermann W, Ulrichs K, Thiede A. Tolerance of rat liver allografts induced by short-term selective immunosuppression combining monoclonal antibodies directed against CD25 and CD54 with subtherapeutic cyclosporine. *Transplantation* 2000; **69**: 1058-1067
- 17 **Sharland A**, Shastry S, Wang C, Rokahr K, Sun J, Sheil AG, McCaughan GW, Bishop GA. Kinetics of intragraft cytokine expression, cellular infiltration, and cell death in rejection of renal allografts compared with acceptance of liver allografts in a rat model: early activation and apoptosis is associated with liver graft acceptance. *Transplantation* 1998; **65**: 1370-1377
- 18 **Coito AJ**, Shaw GD, Li J, Ke B, Ma J, Busuttill RW, Kupiec-Weglinski JW. Selectin-mediated interactions regulate cytokine networks and macrophage heme oxygenase-1 induction in cardiac allograft recipients. *Lab Invest* 2002; **82**: 61-70

- 19 **Ring GH**, Saleem S, Dai Z, Hassan AT, Konieczny BT, Baddoura FK, Lakkis FG. Interferon-gamma is necessary for initiating the acute rejection of major histocompatibility complex class II-disparate skin allografts. *Transplantation* 1999; **67**: 1362-1365
- 20 **Boehler A**, Bai XH, Liu M, Cassivi S, Chamberlain D, Slutsky AS, Keshavjee S. Upregulation of T-helper 1 cytokines and chemokine expression in post-transplant airway obliteration. *Am J Respir Crit Care Med* 1999; **159**: 1910-1917
- 21 **Moudgil A**, Bagga A, Toyoda M, Nicolaidou E, Jordan SC, Ross D. Expression of gamma-IFN mRNA in bronchoalveolar lavage fluid correlates with early acute allograft rejection in lung transplant recipients. *Clin Transplant* 1999; **13**: 201-207
- 22 **Affleck DG**, Bull DA, Albanil A, Shao Y, Brady J, Karwande SV, Eichwald EJ, Shelby J. Interleukin-18 production following murine cardiac transplantation: correlation with histologic rejection and the induction of INF-gamma. *J Interferon Cytokine Res* 2001; **21**: 1-9
- 23 **Gill RG**, Coulombe M, Lafferty KJ. Pancreatic islet allograft immunity and tolerance: the two-signal hypothesis revisited. *Immunol Rev* 1996; **149**: 75-96
- 24 **Bauerle PA, Baltimore D**. NF- κ B: ten years after. *Cell* 1996; **87**: 13-20
- 25 **Fonteh AN**, Marion CR, Barham BJ, Edens MB, Atsumi G, Samet JM, High KP, Chilton FH. Enhancement of mast cell survival: a novel function of some secretory phospholipase A(2) isotypes. *J Immunol* 2001; **167**: 4161-4171
- 26 **Akari H**, Bour S, Kao S, Adachi A, Strebel K. The human immunodeficiency virus type 1 accessory protein Vpu induces apoptosis by suppressing the nuclear factor kappaB-dependent expression of antiapoptotic factors. *J Exp Med* 2001; **194**: 1299-1311
- 27 **Granville DJ**, Carthy CM, Jiang H, Levy JG, McManus BM, Matroule JY, Piette J, Hunt DW. Nuclear factor-kappaB activation by the photochemotherapeutic agent verteporfin. *Blood* 2000; **95**: 256-262
- 28 **Tenjinbaru K**, Furuno T, Hirashima N, Nakanishi M. Nuclear translocation of green fluorescent protein-nuclear factor kappaB with a distinct lag time in living cells. *FEBS Lett* 1999; **444**: 1-4
- 29 **Kalli K**, Huntoon C, Bell M, McKean DJ. Mechanism responsible for T-cell antigen receptor- and CD28- or interleukin 1 (IL-1) receptor-initiated regulation of IL-2 gene expression by NF-kappaB. *Mol Cell Biol* 1998; **18**: 3140-3148
- 30 **Hemdon TM**, Juang YT, Solomou EE, Rothwell SW, Gourley MF, Tsokos GC. Direct transfer of p65 into T lymphocytes from systemic lupus erythematosus patients leads to increased levels of interleukin-2 promoter activity. *Clin Immunol* 2002; **103**: 145-153
- 31 **Zhou XY**, Yashiro-Ohtani Y, Nakahira M, Park WR, Abe R, Hamaoka T, Naramura M, Gu H, Fujiwara H. Molecular mechanisms underlying differential contribution of CD28 versus non-CD28 costimulatory molecules to IL-2 promoter activation. *J Immunol* 2002; **168**: 3847-3854
- 32 **Sica A**, Dorman L, Viggiano V, Cippitelli M, Ghosh P, Rice N, Young HA. Interaction of NF-kappaB and NFAT with the interferon-gamma promoter. *J Biol Chem* 1997; **272**: 30412-30420
- 33 **Liblau RS**, Tisch R, Shokat K, Yang X, Dumont N, Goodnow CC, McDevitt HO. Intravenous injection of soluble antigen induces thymic and peripheral T-cells apoptosis. *Proc Natl Acad Sci USA* 1996; **93**: 3031-3036
- 34 **Bishop GA**, Sun J, Sheil AG, McCaughan GW. High-dose/activation-associated tolerance: a mechanism for allograft tolerance. *Transplantation* 1997; **64**: 1377-1382
- 35 **Desquenne-Clark L**, Kimura H, Naji L, Silvers WK. Comparison of the abilities of MHC-compatible bone marrow cells and lymph node cells to induce tolerance of skin allografts in rats. *Transplantation* 1993; **56**: 1230-1233

Edited by Xu XQ

Expression of growth hormone receptor and its mRNA in hepatic cirrhosis

Hong-Tao Wang, Shuang Chen, Jie Wang, Qing-Jia Ou, Chao Liu, Shu-Sen Zheng, Mei-Hai Deng, Xiao-Ping Liu

Hong-Tao Wang, Jie Wang, Qing-Jia Ou, Chao Liu, Department of Hepato-biliary Surgery, Sun Yat-Sen Memorial Hospital, the Second Affiliated Hospital, Sun Yat-Sen University, Guangzhou 510120, Guangdong Province, China

Shuang Chen, Department of Gastroenteral Surgery, Sun Yat-Sen Memorial Hospital, the Second Affiliated Hospital, Sun Yat-Sen University, Guangzhou 510120, Guangdong Province, China

Shu-Sen Zheng, Molecular Medical Laboratory Center, Sun Yat-Sen Medical College, Sun Yat-Sen University, Guangzhou 510089, Guangdong Province, China

Mei-Hai Deng, Department of General Surgery, the Third Affiliated Hospital, Sun Yat-Sen University, Guangzhou 510630, Guangdong Province, China

Xiao-Ping Liu, Department of General Surgery, Shenzhen Central Hospital, Peking University, Shenzhen 518036, China

Supported by the Natural Science Foundation of Guangdong Province, No.984213 and Academic Foundation of Sun Yat-Sen University of Medical Sciences and Ministry of Health for Project 211, No.F000099075

Correspondence to: Dr. Hong-Tao Wang, M.D., Ph.D., Department of Hepato-biliary Surgery, Sun Yat-Sen Memorial Hospital, the Second Affiliated Hospital, Sun Yat-Sen University, Guangzhou 510120, Guangdong Province, China. sumswht@hotmail.com

Telephone: +86-20-81332020 **Fax:** +86-20-81332853

Received: 2002-10-05 **Accepted:** 2002-11-06

Abstract

AIM: To investigate the expression of growth hormone receptor (GHR) and mRNA of GHR in cirrhotic livers of rats with the intension to find the basis for application of recombinant human growth hormone (rhGH) to patients with liver cirrhosis.

METHODS: Hepatic cirrhosis was induced in Sprague-Dawley rats by administration of thioacetamide intraperitoneally for 9-12 weeks. Collagenase IV was perfused in situ for isolation of hepatocytes. The expression of GHR and its mRNA in cirrhotic livers was studied with radio-ligand binding assay, RT-PCR and digital image analysis.

RESULTS: One class of specific growth hormone-binding site, GHR, was detected in hepatocytes and hepatic tissue of cirrhotic livers. The binding capacity of GHR (R_T , fmol/mg protein) in rat cirrhotic liver tissue (30.8 ± 1.9) was significantly lower than that in normal control (74.9 ± 3.9) at the time point of the ninth week after initiation of induction of cirrhosis ($n=10$, $P<0.05$), and it decreased gradually along with the accumulation of collagen in the process of formation and development of liver cirrhosis ($P<0.05$). The number of binding sites ($\times 10^4/\text{cell}$) of GHR on rat cirrhotic hepatocytes (0.86 ± 0.16) was significantly lower than that (1.28 ± 0.24) in control ($n=10$, $P<0.05$). The binding affinity of GHR among liver tissue, hepatocytes of various groups had no significant difference ($P>0.05$). The expression of GHR mRNA (riOD, pixel) in rat cirrhotic hepatic tissues (23.3 ± 3.1) was also significantly lower than that (29.3 ± 3.4) in normal control ($n=10$, $P<0.05$).

CONCLUSION: The growth hormone receptor was expressed in a reduced level in liver tissue of cirrhotic rats, and lesser expression of growth hormone receptors was found in a later stage of cirrhosis. The reduced expression of growth hormone receptor was partly due to its decreased expression on cirrhotic hepatocytes and the reduced expression of its mRNA in cirrhotic liver tissue.

Wang HT, Chen S, Wang J, Ou QJ, Liu C, Zheng SS, Deng MH, Liu XP. Expression of growth hormone receptor and its mRNA in hepatic cirrhosis. *World J Gastroenterol* 2003; 9 (4): 765-770

<http://www.wjgnet.com/1007-9327/9/765.htm>

INTRODUCTION

Liver cirrhosis is a common pathway of a variety of chronic liver diseases^[1] and is associated with high protein catabolism, low anabolism and negative nitrogen balance^[2] resulting in hypoproteinemia which contributes to ascites, dysfunction of coagulation and suppressed immune responses^[3] as pathophysiological outcomes. In fact, progressive nutrition deficiencies and muscle wasting are universal problems and critical predictors of morbidity, mortality and survival^[4,5] after surgical intervention. Early reports showed that cirrhotic patients requiring emergency abdominal surgery exhibited a higher mortality^[6]. In retrospective studies of liver transplant recipients, protein-calorie malnutrition had been associated with adverse outcomes in patients with end-stage liver diseases^[7,8]. A prospective study showed that cirrhotic patients with hypermetabolism and body mass loss had a much higher mortality rate after liver transplantation than those with normometabolism^[9]. Nutritional support is critical for patients with hepatic cirrhosis. Yet, studies have shown that aggressive nutritional support is essential but not effective enough to prevent protein loss and optimize the care of these patients in severe catabolic illness, including cirrhosis^[10,11].

Recent research has investigated the role of exogenous growth factor therapy in catabolic illness. Recombinant human growth hormone (rhGH) has been used in catabolic states such as after abdominal operation^[12], organ transplantation^[13], major trauma^[14] and severe burns^[15] to enable them to survive an aggressive surgery and gain access to a new life^[16]. After treatment of rhGH, donor site healing rate in children with severe burns enhanced and thus decreased a 14-day hospitalization time^[17-19], Mortality rates in severely burned adults dropped 26 %^[20]. Cell-mediated immunity significantly enhanced, wound infection rates and length of hospitalization in a large group of post surgical patients decreased^[21]. Some clinical trial reported that growth hormone enhanced nitrogen retention in patients with chronic obstructive lung diseases^[22], severe sepsis^[23,24] and wasting status of AIDS^[25,26] and in fasted adult volunteers. Although there are many controversies^[27-31], it has been confirmed that rhGH is an effective drug to accelerate protein anabolism^[32] and plays a central role in metabolic intervention with a significant cost-effect benefit^[33].

The action of growth hormone depends on its binding with growth hormone receptor on cell membrane^[34]. Whether the cirrhotic hepatocytes express growth hormone receptors (GHR), and the relationship between the GHR expression and the staging of liver cirrhosis are not clear. So, we adopted multiple techniques such as radioligand binding assay and RT-PCR to measure the changes of GHR and its mRNA in an experimental liver cirrhosis model at cellular and histological levels for understanding of biological feature of expression of GHR in cirrhotic hepatocytes.

MATERIALS AND METHODS

Induction of liver cirrhosis

Liver cirrhosis in rats was induced by daily intraperitoneal injection of 3 % thioacetamide (TAA, Shanghai, China) 50 mg/kg for 9 to 12 weeks^[35,36]. Two hundreds male Sprague-Dawley rats (200-300 g, Medical Animal Center, Sun Yat-Sen University) were randomized and allotted to two groups, normal group ($n=82$) received saline intraperitoneally everyday; and cirrhotic group ($n=118$) received drugs for induction of hepatic cirrhosis. From each group, 80 rats were available for analysis. Rats were fed with regular chow and water *ad libitum* in cages placed in a room with 12-hour light-dark cycle and constant humidity and temperature (25 °C).

At the 3rd, 6th, 9th, 12th week and the 15th week (3 weeks after withdrawal of TAA) after induction of liver cirrhosis 10 rats from each group were fasted overnight and sacrificed. Liver tissue samples were obtained after hepatic sinusoids were flushed by perfusion of liver with normal saline through the portal vein. Tissue samples from the right major liver lobe were obtained and frozen in liquid nitrogen immediately and then stored at -80 °C until use, or fixed in 10 % neutral buffered formaldehyde solution and dehydrated and embedded in paraffin for regular pathological examination.

Digital image analysis

Liver collagen content was calculated by histomorphometric measurement in 4- μ m sections with Masson's trichrome stain. Under photographic analytic microscope (Carl Zeiss Axiotron, OPTON, Germany), three random areas in each section of liver slide were chosen and captured in RGB format with 24-bit true colors at a resolution of 768 \times 512 in real time by the JVC ky-F30B 3-CCD color video camera with digital conversion connected with a computer system of Kontron IBAS2.5 (OPTON, Germany) for digital image analysis. The total area and the area of fibrosis with positive staining were automatically selected, outlined and evaluated by planimetry. The relative content of collagen (RCC %) was expressed as a percentage of positive staining area in the total area^[37,38].

Hepatocyte isolation

At 9-12 weeks of the study, livers in 10 rats from each group were perfused *in situ* through portal vein with collagenase (type IV, 90 or 120 U/ml)^[39,40]. Hepatocytes were isolated at 4 °C by centrifugation (50 \times g, 5 min or 1 \times g, 10 min). Cells were re-suspended for radio-ligand binding assay in RPMI 1640 medium without serum to a final concentration of 1.0 \times 10⁶ cell/ml with a purity of more than 98 % and a viability of more than 90 % determined by trypan-blue exclusion.

Total RNA isolation

Total RNA of liver tissue was prepared from 10 rats in each group at the 9th week during the induction of cirrhosis by a single-step method^[41]. Integrity and quality of RNA were tested by electrophoresis in 1 % agarose-formaldehyde gels stained with ethidium bromide. The RNA concentration was evaluated

at spectrophotometric absorbance at 260 nm.

Primers for RT-PCR

Primers for the PCR amplification of GHR transcripts were purchased from Sangon Co. (Shanghai, China). The primers used for detection of GHR mRNA by RT-PCR were specific for the intracellular domain of the rat GHR, thus excluding detection of the smaller transcripts encoding GH-binding protein (GHRP)^[42]. The forward primer (GHR4548) was 5' - *ATGTGAGATCCAGACAACG-3' with the first base *A at the 5' end as an unmatched base of the original G and spanned from 876 to 894 located in exon 7 and the reverse one 5' - ATGTCAGGGTCATAACAGC-3' spanned from 1 356 to 1 374 located in exon 10. The PCR product was supposed to be 499 bp in length.

RT-PCR

RT-PCR was performed using the MasterAmp™ RT-PCR kit (Epicentre, Madison, USA) for detection of GHR mRNA^[43]. The procedure of RT-PCR was similar to that of literature^[44]. Negative controls in RT-PCR included reactions in the absence of RNA sample or primers or RT reaction to detect possible contamination of genomic DNA in RNA samples. The experiment was considered ineffective if there was any incidental band in lane of negative control. 10 μ l of each PCR products was subjected to electrophoresis for about 1 hour on 1 % agarose gel using electrophoresis apparatus (Bio-Rad, UK) and visualized by staining with ethidium bromide. The bands were observed using a ultraviolet gel device (UVI, UK) and captured into its computer system for digital image analysis. The level of GHR mRNA in each sample was expressed as: iOD (pixel)=the average optical density of each band \times its area (pixel).

Membrane microsome preparation

The microsomal liver membrane fraction was prepared by differential centrifugation of liver homogenate according to Papotti^[45]. About 1 g tissue from rat livers was chopped and homogenized with an electric homogenizer (Vorsicht, Malaysia) in ice-cold (4 °C) phosphate buffer (PBS) containing 0.25 M sucrose. The mixture was centrifuged at 1 500 \times g for 15 minutes. The supernatant was collected and centrifuged at 30 000 \times g for 30 minutes. The pellet was re-suspended in 3M MgCl₂ for 5 minutes to remove endogenous GH binding^[46] and centrifuged, the pellet was suspended in PBS. Protein concentration of the solution was determined by Lowry method.

GH binding assay

In radioreceptor assay, 100 μ l (approximately 20 000 cpm) of ¹²⁵I-hGH (NEN Inc, Boston, USA) with a specific activity of about 108 μ Ci/ μ g, 100 μ l of unlabeled hGH in PBS and 100 μ l of liver membrane microsomes or liver cells were mixed and incubated at 4 °C over night. Parallel incubations were performed with various amounts of hGH (0-3nM divided into 7-9 concentration gradients) in duplicate. An excess of hGH was used to determine nonspecific binding. At the end of the incubation, bound and free hormones were separated by filtration (0.18 μ m mesh filters, Shanghai, China)^[47]. The pellets on membrane were subjected to a gamma counter (SN γ 682, Rihuan, Shanghai, China). GH binding affinity constant (K_d, nM) and binding capacity (R_t, fmol/mg protein) or numbers of ¹²⁵I-GH binding sites of hepatocytes (\times 10⁴/cell) were calculated by Scatchard analysis using the LIGAND program^[48,49].

Statistical analysis

Results were expressed as the mean \pm SEM ($\bar{x}\pm s$) and analyzed by ANOVA and least significant difference (LSD) method with an acceptance of significance as $P<0.05$.

RESULTS

Changes of lobular structure and RCC in the development of liver cirrhosis

In control group, no evident pathological change of lobular structure was found in liver tissue over 15 weeks. In cirrhotic model group, 4 stages of pathological changes were manifested during the development of liver cirrhosis: (1) scattered necrosis and cellular degeneration at the 3rd week; (2) fibrous proliferation at the 6th week; (3) pseudo-lobule formation at the 9th week; (4) massive nodule formation at the 12th week and (5) partial reversion of cirrhosis at the 15th week.

In control group, there was no significant change of RCC ($P>0.05$) among the different time points during the period of 15 weeks (Table 1). While compared with that of the control group at the same time point, RCC kept no significant change at the 3rd week ($P>0.05$) and increased significantly at the 6th, 9th, 12th and 15th week respectively ($P<0.05$) in the cirrhotic model group. When compared among the different time points in the cirrhotic model group, RCC increased gradually at the 3rd, 6th, 9th week and reached to its turning point at the 12th week ($P<0.05$), then went down, but still above normal level at the 15th week.

Table 1 Dynamic alteration of RCC, R_T and K_d in cirrhotic liver tissues

Time	RCC (%)		R_T (fmol/mg protein)		K_d (nM)	
	Control Group	Model Group	Control Group	Model Group	Control Group	Model Group
3 rd week	1.29±0.23	1.56±0.35	75.8±5.1	55.2±4.5 ^b	0.62±0.03	0.61±0.07
6 th week	1.19±0.21	10.8±2.5 ^{ab}	77.3±4.3	42.6±2.1 ^{ab}	0.64±0.05	0.58±0.06
9 th week	1.16±0.18	20.2±3.6 ^{ab}	74.9±3.9	30.8±1.9 ^{ab}	0.61±0.09	0.60±0.04
12 th week	1.27±0.25	28.0±4.3 ^{ab}	73.2±5.4	17.5±2.5 ^{ab}	0.60±0.08	0.59±0.07
15 th week	1.13±0.24	15.2±2.6 ^{ab}	71.5±4.9	20.8±1.6 ^b	0.58±0.06	0.61±0.09

^a $P<0.05$ vs a previous time point, ^b $P<0.05$ vs control group. RCC: relative content of collagen (%) indicating severity of liver fibrosis; R_T : total binding capacity of receptors (fmol/mg protein) corresponding to the quantity of receptors; K_d : dissociation constant in equilibrium (nM) which is equal to the affinity of receptors.

GH binding in the development of liver cirrhosis

GH binding assay was carried out using liver membrane microsomes from rats at different time points in various groups and specific binding for ¹²⁵I-hGH was detected in all samples. The Scatchard analysis of GH binding capacity (R_T) and affinity (K_d) on each sample was performed and a single class of specific GH-binding sites on liver cell membranes, that is GHR, was revealed in both normal and cirrhotic liver tissue samples by linear Scatchard plots (Figure 1).

No significant change of R_T and K_d was found in liver tissue samples during the period of 15 weeks in control group ($P>0.05$) (Table 1 and Figure 1). While compared with that of the control group at the same time point, R_T decreased significantly ($P<0.05$) at the 3rd, 6th, 9th, 12th and 15th week although no change of K_d was observed in cirrhotic model group. When compared among the different time points in the cirrhotic model group, R_T decreased gradually at the 3rd, 6th, 9th week and reached to its lowest point ($P<0.05$) at the 12th week, then increased but still under normal level at the 15th week.

The correlation analysis manifested a significant negative linear correlation between R_T and RCC in rat liver cirrhotic tissue ($r=-0.82$, $n=50$, $P<0.05$) (Figure 2).

Quantitative analysis of GH binding sites on rats hepatocytes

There were linear Scatchard plots of normal and cirrhotic hepatocytes, which indicated the presence of a single class of

specific GH-binding sites, GHR, on hepatocyte membranes. The quantity of GH-binding sites ($\times 10^4$ /cell) on hepatocytes of cirrhotic model group (0.86 ± 0.16) was significantly less than that (1.28 ± 0.24) in normal control group ($n=10$, $P<0.05$) while the affinity (K_d , nM) of hepatocytes from model group (0.56 ± 0.08) and control group (0.61 ± 0.11) was similar ($n=10$, $P>0.05$).

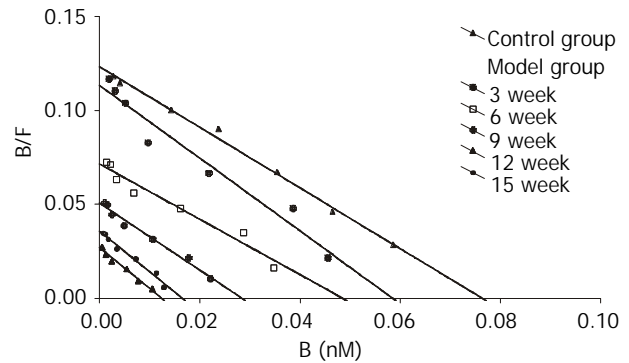


Figure 1 Scatchard analysis of GH-binding in rat liver tissue. Microsomes of liver tissues were incubated with ¹²⁵I-labeled hGH and increased concentrations of unlabeled hGH. The bound/free radioactivity ratio (Y axis) was plotted as a rectilinear function of bound hormone (X axis). GH binding capacities (B_{max} =intercept on X axis, $R_T=B_{max}$ /protein concentration) and affinities (K_d =negative reciprocal of slope) were calculated from the competition assays by Scatchard analysis.

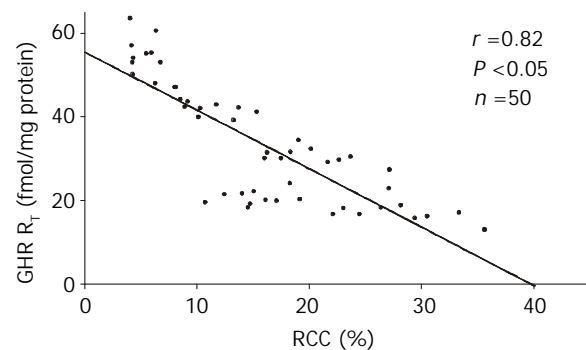


Figure 2 Correlation between R_T (quantity of GHR) and RCC (degree of cirrhosis) in rat cirrhotic liver samples.

GHR mRNA detected by RT-PCR

A specific band of RT-PCR products (499 bp in length) was detected in liver tissue samples from both control group and cirrhotic model group, indicating that GHR mRNA was expressed in both groups. The level of GHR mRNA (IOD, pixel) in cirrhotic liver (23.3 ± 3.1) was lower than that (29.3 ± 3.4) in normal liver ($n=10$, $P<0.05$) (Figure 3).

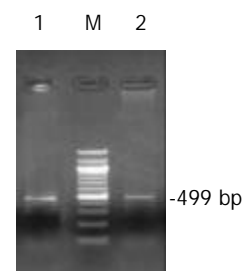


Figure 3 Comparison of GHR mRNA expression in liver tissue in normal control group and cirrhotic model group (the result of RT-PCR). Lane M: 100 bp DNA ladder; Lane 1: Normal control group; Lane 2: Cirrhotic model group.

DISCUSSION

Much has been done regarding the expression of GHR and signal transduction^[34, 47, 50, 51], but the expression of GHR in some pathological states such as cirrhotic hepatocytes, malignant cells is not clear. Chang^[52] reported that ¹²⁵I-rhGH binding activity in 6 cases of hepatocellular carcinoma and adjacent cirrhotic liver tissue could not be detected and believed that the GHR in cirrhotic hepatic tissue disappeared although the study only examined one aspect of the GHR, GH binding. Another study^[53] showed that specific binding of ¹²⁵I-hGH in liver tissue from liver transplant of 17 cases with end-stage liver diseases was lower than that in normal control, but only in 3 cirrhotic livers Scatchard analysis was performed for calculation of GH binding capacity and affinity. In this setting of tissue-based GH binding assay, it was not convincing enough to clear up the controversy about the expression of GHR on cirrhotic liver cells. So, GH binding assay at cellular level was used to analyze the expression of GHR on hepatocytes or in liver tissue of rats with cirrhosis. We have demonstrated that the growth hormone receptor was expressed on cirrhotic hepatocytes and lesser expression of GHR was found in a later stage of cirrhosis.

In present study, ¹²⁵I-hGH binding activity of cirrhotic hepatic tissue was studied with radioligand binding assay, and a single class of growth hormone specific binding sites with normal affinity was detected in the cirrhotic hepatic tissue, which indicated the expression of GHR in cirrhotic hepatic tissue. These results were compatible with those of clinical specimens from liver transplants^[53].

The relationship between the GHR expression in cirrhotic tissue and the stage of liver cirrhosis has not been reported. In our study, ¹²⁵I-hGH binding capacity (*i.e.* the quantity of GHR) decreased significantly even in the early stage of cirrhosis, and gradually decreased during the development of liver fibrosis and dropped to the lowest level in late stage of cirrhosis on week 12 after induction of hepatic cirrhosis, then increased but still below the normal level after withdrawal of TAA. This implicated that the quantity of GHR in liver tissue altered dynamically without any significant change of GH binding affinity over the development or recovery of liver cirrhosis. In other words, GHR expression was suppressed in the process of formation of liver cirrhosis. The more severe the cirrhosis was, the more significant the down regulation of GHR expression would be.

GH binding varied among liver samples^[47, 53]. Our results indicated that GH binding capacity in rat cirrhotic liver tissue differed in various stages of liver cirrhosis, and only slight variation (data not listed) of such binding was found in liver tissue with the same time point during the development of cirrhosis. Therefore, histological staging of liver cirrhosis was one of the important factors predisposing the down-regulation of GHR expression^[54].

Fibrotic tissue accumulated in the portal area during the reconstruction of lobule of cirrhotic liver while hepatocytes regenerated continuously after repeated necrosis in the development of liver cirrhosis. The fibrous structure, hepatocytes and interstitial cells with heterogeneous distribution and various combination in cirrhotic tissue should be considered respectively as we analyzed the expression of growth hormone receptor. In the present study, the result of GH-binding capacity (R_T) in cirrhotic liver tissue indicated the GHR expression on membrane microsomes in hepatocytes and interstitial cells and could be affected by non-parenchymal cells rather than fibrotic tissue^[53]. The quantitative measurement of GH binding sites on parenchymal cells from cirrhotic livers had not been reported previously. Therefore Scatchard analysis was resorted to again and a single class of growth hormone

specific binding sites with normal affinity was detected in isolated cirrhotic hepatocytes, suggesting the expression of GHR on cirrhotic hepatocytes disassociated *in vitro*. It was found that the binding sites on cirrhotic hepatocytes was significantly decreased as compared with that on normal hepatocytes, which implied that cirrhotic hepatocytes expressed GHR in a reduced level without any significant difference of binding affinity. So, the decreased expression of GHR in cirrhotic liver tissue should be attributed not only to accumulation of interstitial cells but to the reduced expression of GHR on cirrhotic hepatocytes themselves also.

It is possible that the reduced level of GH binding is partly owing to the reduced population of hepatocytes and increased numbers of interstitial cells in cirrhotic livers. But the mechanisms of the reduced GHR expression on cirrhotic hepatocytes has not been defined yet. The reduced GH binding level was unlikely due to changes in the receptor itself. Occupancy of the receptors by endogenous GH and ligand-induced internalization of GHR may affect the measurement of the binding, since dissociation of GH from its receptor and recycling of GHR is incomplete in several hours^[55]. Therefore, GH binding was determined on microsomes that had been desaturated by exposure to 3M MgCl₂ for 5 minutes^[46]. It was reported that the specific binding of ¹²⁵I-labelled bovine GH to a GHR-enriched low density membrane fraction from regenerating rat liver was reduced to 10-35 % between 12 and 24 h and remained low until 48 h after partial hepatectomy^[46], which indicated the amount of functional GHR on hepatocytes was decreased with repeated degeneration, necrosis and regeneration in the microenvironment of cirrhosis. In this situation several cytokines such as IL-1 β , TNF- α and glucocorticoids seemed to be involved in the likely mechanism of the reduced GHR expression^[40, 56, 57].

It is necessary to investigate the changes of GHR and its mRNA simultaneously in order to understand the biological events at different levels. Shen^[53] reported that the reduced expression of GHR mRNA identified by ribonuclease protection assay in human cirrhotic livers was in the similar order of magnitude as reduction in GH binding. Relative quantity of GHR mRNA in liver tissue of cirrhotic rats was tested with RT-PCR assay and a similar result of our study indicated that the expression of GHR mRNA in cirrhotic liver tissue was lower than that in normal controls. Accordingly, it was suggested that the reduced GH binding may be secondary to reduced GHR gene expression and decreased GHR synthesis.

In summary, GH binding assay with staging analysis of liver cirrhosis was applied and our study showed that the growth hormone receptor was expressed with normal binding affinity on cirrhotic hepatocytes and expression of growth hormone receptors in a later stage of cirrhosis reduced significantly. These results implicated that there was a physiological basis of GHR for GH action in cirrhotic livers, but the sensitivity of cirrhotic hepatocytes to growth hormone might be decreased. Further investigations should be concentrated on the signal transduction of GHR in cirrhotic hepatocytes^[58].

REFERENCES

- 1 **Strong RW.** Liver transplantation: current status and future prospects. *J R Coll Surg Edinb* 2001; **46**: 1-8
- 2 **Dichi JB,** Dichi I, Maio R, Correa CR, Angeleli AY, Bicudo MH, Rezende TA, Burini RC. Whole-body protein turnover in malnourished patients with child class B and C cirrhosis on diets low to high in protein energy. *Nutrition* 2001; **17**: 239-242
- 3 **Sobhonslidsuk A,** Roongpisuthipong C, Nantiruj K, Kulapongse S, Songchitsomboon S, Sumalnop K, Bussagorn N. Impact of liver cirrhosis on nutritional and immunological status. *J Med Assoc Thai* 2001; **84**: 982-988
- 4 **Alberino F,** Gatta A, Amodio P, Merkel C, Di Pascoli L, Boffo G,

- Caregaro L. Nutrition and survival in patients with liver cirrhosis. *Nutrition* 2001; **17**: 445-450
- 5 **Mendenhall CL**, Tosch T, Weesner RE, Garcia-Pont P, Goldberg SJ, Kiernan T, Seeff LB, Sorell M, Tamburro C, Zetterman R. VA cooperative study on alcoholic hepatitis. II. Prognostic significance of protein-calorie malnutrition. *Am J Clin Nutr* 1986; **43**: 213-218
 - 6 **Maull KI**, Turnage B. Trauma in the cirrhotic patient. *South Med J* 2001; **94**: 205-207
 - 7 **Moukarzel AA**, Najm I, Vargas J, McDiarmid SV, Busuttill RW, Ament ME. Effect of nutritional status on outcome of orthotopic liver transplantation in paediatric patients. *Transplant Proc* 1990; **22**: 1560-1563
 - 8 **Harrison J**, McKiernan J, Neuberger JM. A prospective study on the effect of recipient nutritional status on outcome in liver transplantation. *Transpl Int* 1997; **10**: 369-374
 - 9 **Muller MJ**, Lautz HU, Plogmann B, Burger M, Korber J, Schmidt FW. Energy expenditure and substrate oxidation in patients with cirrhosis: the impact of cause, clinical staging and nutritional state. *Hepatology* 1992; **15**: 782-794
 - 10 **Streat S**, Beddoe A, Hill GL. Aggressive nutritional support does not prevent protein loss despite fat gain in septic intensive care patients. *J Trauma* 1987; **27**: 262-266
 - 11 **Le Cornu KA**, McKiernan FJ, Kapadia SA, Neuberger JM. A prospective randomized study of preoperative nutritional supplementation in patients awaiting elective orthotopic liver transplantation. *Transplantation* 2000; **69**: 1364-1369
 - 12 **Wong WK**, Soo KC, Nambiar R, Tan YS, Yo SL. The effect of recombinant growth hormone on nitrogen balance in malnourished patients after major abdominal surgery. *Aust N Z J Surg* 1995; **65**: 109-113
 - 13 **Rodeck B**, Kardorff R, Melter M, Ehrlich JH. Improvement of growth after growth hormone treatment in children who undergo liver transplantation. *J Pediatr Gastroenterol Nutr* 2000; **31**: 286-290
 - 14 **Petersen SR**, Holaday NJ, Jeevanandam M. Enhancement of protein synthesis efficiency in parenterally fed trauma victims by adjuvant recombinant human growth hormone. *J Trauma* 1994; **36**: 726-733
 - 15 **Singh KP**, Prasad R, Chari PS, Dash RJ. Effect of growth hormone therapy in burn patients on conservative treatment. *Burns* 1998; **24**: 733-738
 - 16 **Iglesias P**, Diez JJ. Clinical applications of recombinant human growth hormone in adults. *Expert Opin Pharmacother* 1999; **1**: 97-107
 - 17 **Herndon DN**, Hawkins HK, Nguyen TT, Pierre E, Cox R, Barrow RE. Characterization of growth hormone enhanced donor site healing in patients with large cutaneous burns. *Ann Surg* 1995; **221**: 649-656
 - 18 **Aili Low JF**, Barrow RE, Mittendorfer B, Jeschke MG, Chinkes DL, Herndon DN. The effect of short-term growth hormone treatment on growth and energy expenditure in burned children. *Burns* 2001; **27**: 447-452
 - 19 **Hart DW**, Herndon DN, Klein G, Lee SB, Celis M, Mohan S, Chinkes DL, Wolf SE. Attenuation of posttraumatic muscle catabolism and osteopenia by long-term growth hormone therapy. *Ann Surg* 2001; **233**: 827-834
 - 20 **Knox J**, Demling R, Wilmore D, Sarraf P, Santos A. Increased survival after major thermal injury: the effect of growth hormone therapy in adults. *J Trauma* 1995; **39**: 526-530
 - 21 **Vara-Thorbeck R**, Guerrero JA, Rosell J, Ruiz-Requena E, Capitan JM. Exogenous growth hormone: effects on the catabolic response to surgically produced acute stress and on postoperative immune function. *World J Surg* 1993; **17**: 530-537
 - 22 **Pape GS**, Friedman M, Underwood LE, Clemmons DR. The effect of growth hormone on weight gain and pulmonary function in patients with chronic obstructive lung disease. *Chest* 1991; **99**: 1495-1500
 - 23 **Koea JB**, Breier BH, Douglas RG, Gluckman PD, Shaw JH. Anabolic and cardiovascular effects of rhGH in surgical patients with sepsis. *Br J Surg* 1996; **83**: 196-202
 - 24 **Li W**, Li J, Xu B, Yin L, Wang L, Gu J, Ren JA, Quan ZF. Effect of recombinant human growth hormone with total parenteral nutrition on albumin synthesis in patients with peritoneal sepsis. *Zhonghua Waikexue* 1998; **36**: 643-645
 - 25 **Schambelan M**, Mulligan K, Grunfeld C, Daar ES, LaMarca A, Kotler DP, Wang J, Bozzette SA, Breitmeyer JB. Recombinant human growth hormone in patients with HIV-associated wasting. A randomized, placebo-controlled trial. Serostim Study Group. *Ann Intern Med* 1996; **125**: 873-882
 - 26 **Waters D**, Danska J, Hardy K, Koster F, Qualls C, Nickell D, Nightingale S, Gesundheit N, Watson D, Schade D. Recombinant human growth hormone, insulin-like growth factor 1, and combination therapy in AIDS-associated wasting. A randomized, double-blind, placebo-controlled trial. *Ann Intern Med* 1996; **125**: 865-872
 - 27 **O'Leary MJ**, Ferguson CN, Rennie M, Hinds CJ, Coakley JH, Preedy VR. Effect of growth hormone on muscle and liver protein synthesis in septic rats receiving glutamine-enriched parenteral nutrition. *Crit Care Med* 2002; **30**: 1099-1105
 - 28 **Losada F**, Garcia-Luna PP, Gomez-Cia T, Garrido R N M, Pereira JL, Marin F, Astorga R. Effects of Human Recombinant Growth hormone on Donor-site Healing in Burned Adults. *World J Surg* 2002; **26**: 2-8
 - 29 **Carroll PV**, Van den Berghe G. Safety aspects of pharmacological GH therapy in adults. *Growth Horm IGF Res* 2001; **11**: 166-172
 - 30 **Takala J**, Ruokonen E, Webster NR, Nielsen MS, Zandstra DF, Vundelinckx G, Hinds CJ. Increased mortality associated with growth hormone treatment in critically ill adults. *N Engl J Med* 1999; **341**: 785-792
 - 31 **Jeschke MG**, Barrow RE, Herndon DN. Recombinant human growth hormone treatment in pediatric burn patients and its role during the hepatic acute phase response. *Crit Care Med* 2000; **28**: 1578-1584
 - 32 **Raguso CA**, Genton L, Kyle U, Pichard C. Management of catabolism in metabolically stressed patients: a literature survey about growth hormone application. *Curr Opin Clin Nutr Metab Care* 2001; **4**: 313-320
 - 33 **Wilmore DW**. Postoperative protein sparing. *World J Surg* 1999; **23**: 545-552
 - 34 **Carter-Su C**, Schwartz J, Smit LS. Molecular mechanism of growth hormone action. *Annu Rev Physiol* 1996; **58**: 187-207
 - 35 **Dashti H**, Jeppsson B, Hagerstrand I, Hultberg B, Srinivas U, Abdulla M, Bengmark S. Thioacetamide and carbon tetrachloride-induced liver cirrhosis. *Eur Surg Res* 1989; **21**: 83-91
 - 36 **Jeong DH**, Jang JJ, Lee SJ, Lee JH, Lim IK, Lee MJ, Lee YS. Expression patterns of cell cycle-related proteins in a rat cirrhotic model induced by CCl4 or thioacetamide. *J Gastroenterol* 2001; **36**: 24-32
 - 37 **Huang J**, Cai MY, Wei DP. HLA class I expression in primary hepatocellular carcinoma. *World J Gastroenterol* 2002; **8**: 654-657
 - 38 **Noutsias M**, Pauschinger M, Ostermann K, Escher F, Blohm JH, Schultheiss H, Kuhl U. Digital image analysis system for the quantification of infiltrates and cell adhesion molecules in inflammatory cardiomyopathy. *Med Sci Monit* 2002; **8**: MT59-71
 - 39 **Imanishi H**, Kothary PC, Bhora FY, Eckhauser FE, Raper SE. Impaired phorbol ester-induced hepatocyte proliferation in cirrhosis. *J Surg Res* 1995; **58**: 435-440
 - 40 **Thissen JP**, Verniers J. Inhibition by interleukin-1 beta and tumor necrosis factor-alpha of the insulin-like growth factor I messenger ribonucleic acid response to growth hormone in rat hepatocyte primary culture. *Endocrinology* 1997; **138**: 1078-1084
 - 41 **Chomczynski P**, Sacchi N. Single-step method of RNA isolation by acid guanidinium thiocyanate-phenol-chloroform extraction. *Anal Biochem* 1987; **162**: 156-159
 - 42 **Wolf M**, Bohm S, Brand M, Kreymann G. Proinflammatory cytokines interleukin 1 beta and tumor necrosis factor alpha inhibit growth hormone stimulation of insulin-like growth factor I synthesis and growth hormone receptor mRNA levels in cultured rat liver cells. *Eur J Endocrinol* 1996; **135**: 729-737
 - 43 **Rzucidlo SJ**, Bounous DI, Jones DP, Brackett BG. Acute acetaminophen toxicity in transgenic mice with elevated hepatic glutathione. *Vet Hum Toxicol* 2000; **42**: 146-150
 - 44 **Zhao J**, van Tol HT, Taverne MA, van der Weijden GC, Bevers MM, van den Hurk R. The effect of growth hormone on rat pre-antral follicles *in vitro*. *Zygote* 2000; **8**: 275-283
 - 45 **Papotti M**, Ghe C, Cassoni P, Catapano F, Deghenghi R, Ghigo E, Muccioli G. Growth hormone secretagogue binding sites in peripheral human tissues. *J Clin Endocrinol Metab* 2000; **85**: 3803-3807

- 46 **Husman B**, Andersson G. Regulation of the growth hormone receptor during liver regeneration in the rat. *J Mol Endocrinol* 1993; **10**: 289-296
- 47 **Hocquette JF**, Postel-Vinay MC, Kayser C, de Hemptinne B, Amar-Costesec A. The human liver growth hormone receptor. *Endocrinology* 1989; **125**: 2167-2174
- 48 **Golda V**, Fickova M, Pinterova L, Jurcovicova J, Macho L, Zorad S. Terguride attenuates prolactin levels and ameliorates insulin sensitivity and insulin binding in obese spontaneously hypertensive rats. *Physiol Res* 2001; **50**: 175-182
- 49 **Reynaud D**, Demin P, Pace-Asciak CR. Hepoxilin A3-specific binding in human neutrophils. *Biochem J* 1996; **313**: 537-541
- 50 **Husman B**, Andersson G, Norstedt G, Gustafsson JA. Characterization and subcellular distribution of somatogenic receptor in rat liver. *Endocrinology* 1985; **116**: 2605-2611
- 51 **van Neste L**, Husman B, Moller C, Andersson G, Norstedt G. Cellular distribution of somatogenic receptors and insulin-like growth factor-I mRNA in the rat liver. *J Endocrinol* 1988; **119**: 69-74
- 52 **Chang TC**, Lin JJ, Yu SC, Chang TJ. Absence of growth-hormone receptor in hepatocellular carcinoma and cirrhotic liver. *Hepatology* 1990; **11**: 123-126
- 53 **Shen XY**, Holt RI, Miell JP, Justice S, Portmann B, Postel-Vinay MC, Ross RJ. Cirrhotic liver expresses low levels of the full-length and truncated growth hormone receptors. *J Clin Endocrinol Metab* 1998; **83**: 2532-2538
- 54 **Wang H**, Chen S, Ou Q, Deng M, Liu X. Expression of growth hormone receptor and its mRNA in cirrhotic livers. *Zhonghua Yixue Zazhi* 2002; **82**: 168-171
- 55 **Allevato G**, Billestrup N, Goujon L, Galsgaard ED, Norstedt G, Postel-Vinay MC, Kelly PA, Nielsen JH. Identification of phenylalanine 346 in the rat growth hormone receptor as being critical for ligand-mediated internalization and down-regulation. *J Biol Chem* 1995; **270**: 17210-17214
- 56 **Tonshoff B**, Mehls O. Interactions between glucocorticoids and the growth hormone-insulin-like growth factor axis. *Pediatr Transplant* 1997; **1**: 183-189
- 57 **Wang P**, Li N, Li JS, Li WQ. The role of endotoxin, TNF- α , and IL-6 in inducing the state of growth hormone insensitivity. *World J Gastroenterol* 2002; **8**: 531-536
- 58 **Wang H**, Deng M, Ou Q, Wei J, Liu X, Chen S. Effects of rhGH on the expression of growth hormone receptor of liver cells in a murine experimental cirrhosis model. *Zhonghua Putong Waike Zazhi* 2002; **17**: 93-95

Edited by Ren SY

Influence of methionine/valine-depleted enteral nutrition on nucleic acid and protein metabolism in tumor-bearing rats

Yin-Cheng He, Jun Cao, Ji-Wei Chen, Ding-Yu Pan, Ya-Kui Zhou

Yin-Cheng He, Jun Cao, Ji-Wei Chen, Ding-Yu Pan, Ya-Kui Zhou, Department of general surgery, Zhongnan Hospital, Wuhan University, Wuhan 430071, China

Supported by Hubei Provincial Health Department, No.W98016 and The Education Department of Hubei Province, China, No. 2001A14005

Correspondence to: Dr. Yin-Cheng He, Department of general surgery, Zhongnan Hospital, Wuhan University, Wuhan 430071, China. w030508h@public.wh.hb.cn

Telephone: +86-27-67812963

Received: 2002-10-17 **Accepted:** 2002-11-16

Abstract

AIM: To investigate the effects of methionine/valine-depleted enteral nutrition (EN) on RNA, DNA and protein metabolism in tumor-bearing (TB) rats.

METHODS: Sprague-Dawley (SD) rats underwent jejunostomy for nutritional support. A suspension of Walker-256 carcinosarcoma cells was subcutaneously inoculated. 48 TB rats were randomly divided in 4 groups: A, B, C and D. The TB rats had respectively received jejunal feedings supplemented with balanced amino acids, methionine-depleted, balanced amino acids and valine-depleted for 6 days before injection of 740 KBq ³H- methionine/valine via jejunum. The ³H incorporation rate of the radioactivity into RNA, DNA and proteins in tumor tissues at 0.5, 1, 2, 4 h postinjection of tracers was assessed with liquid scintillation counter.

RESULTS: Incorporation of ³H into proteins in groups B and D was (0.500±0.020) % to (3.670±0.110) % and (0.708±0.019) % to (3.813±0.076) % respectively, lower than in groups A [(0.659±0.055) % to (4.492±0.108) %] and C [(0.805±0.098) % to (4.180±0.018) %]. Incorporation of ³H into RNA, DNA in group B was (0.237±0.075) % and (0.231±0.052) % respectively, lower than in group A (*P*<0.01). There was no significant difference in uptake of ³H by RNA and DNA between group C and D (*P*>0.05).

CONCLUSION: Protein synthesis was inhibited by methionine/valine starvation in TB rats and nucleic acid synthesis was reduced after methionine depletion, thus resulting in suppression of tumor growth.

He YC, Cao J, Chen JW, Pan DY, Zhou YK. Influence of methionine/valine-depleted enteral nutrition on nucleic acid and protein metabolism in tumor-bearing rats. *World J Gastroenterol* 2003; 9(4): 771-774

<http://www.wjgnet.com/1007-9327/9/771.htm>

INTRODUCTION

Parenteral nutrition (PN) is now a supportive therapy commonly used for cancer patients. However, some studies have suggested that PN with amino acid balanced solutions may prompt tumor

growth^[1-3]. Previous studies have shown that tumor growth was inhibited by a diet or PN lacking in methionine/valine. However, the mechanism is not yet known^[4-15]. In this study, we prepared methionine/valine-free amino acid imbalance solutions to investigate the effects of methionine/valine depleted EN on RNA, DNA and protein metabolism in TB rats.

MATERIALS AND METHODS

Radiopharmaceuticals

³H-methionine (³H-Met, specific activity of 148 MBq·mg⁻¹) and ³H-valine (³H-Val, specific activity of 240 MBq·mg⁻¹) was purchased from Chinese institute of atomic energy. The radiochemical purity was over 95 %.

Catheterization of jejunostomy

SD rats weighing (160±20) g were purchased from the animal center of Wuhan University, China. They were allowed to acclimate for one week. After fasting for 12 hours, rats were anesthetized with i.p. sodium pentobarbital (40 mg·kg⁻¹). The animals were undergone catheterization of jejunostomy (day 0). A silicone rubber catheter (2 mm ID, 3 mm OD) was inserted into the proximal jejunum. The catheter passed through a subcutaneous tunnel and emerged between the scapulae. The catheter was sutured to the animal's back to protect the lines and was connected to a swivel so that animals can move without any restrictions in individual metabolic cages. The cannulation system consists of an microinfusion pump, a swivel, rat-harness and a silicone-tube-jejunostomy. Coprophagy was prevented by an own model of faecal collection cup. Animals were fasted for 48 hours after operation but they were provided with water ad libitum, and then given normal rat diets.

Preparation of TB rats

Walker-256 carcinosarcoma cells were obtained from Chinese Center of Culture Preservation. On day 0, the rats were inoculated subcutaneously in the right flank with 10⁷ tumor cells of approximately 0.1 ml of cell suspension. Tumors were palpable in 7 days after transplantation.

Jejunal feeding

Enteral feedings were found to be a safe and cost-effective method for providing nutrition to cancer-bearing patients. On day 8, 48 TB rats were randomly divided into four groups (12 rats per group) and received enteral nutrition (jejunal feeding): Group A: TB rats were fed enteral nutrition solutions composed of balanced amino acids for 6 days before injection of 740 KBq ³H-MET.

Group B: TB rats were fed methionine-depleted enteral nutrition solutions for 6 days before injection of 740 KBq ³H-Met.

Group C: TB rats were fed enteral nutrition solutions composed of balanced amino acids for 6 days before injection of 740 KBq ³H-Val.

Group D: TB rats were fed valine-depleted enteral nutrition solutions for 6 days before injection of 740 KBq ³H-Val.

TB rats received continuous jejunal tube infusion with pump

for nutritional support at a daily dose of 330 ml·kg⁻¹, non-protein calorie was approximately 1160K J·kg⁻¹. A microinfusion pump was used for constant administration of EN solutions. TB rats were not fed during the entire infusion experiment, however they had free access to water.

Composition of amino acid solutions

Table 1 lists the components of amino acid solutions.

Table 1 Composition of amino acid solutions (g·L⁻¹)

Amino acids	Balanced amino acids (Group A, C)	Methionine-depleted (Group B)	Valine-depleted (Group D)
Isoleucine	5.5	5.5	5.5
Leucine	7.5	7.5	7.5
Lysine	7.0	7.0	7.0
Methionine	6.0	-	6.0
Phenylalanine	4.0	4.0	4.0
Threonine	5.0	5.0	5.0
Tryptophan	1.5	1.5	1.5
Valine	6.0	6.0	-
Arginine	6.0	6.0	6.0
Histidine	3.0	3.0	3.0
Proline	4.0	4.0	4.0
Tyrosine	1.0	1.0	1.0
Alanine	20.0	20.0	20.0
Glycine	7.5	7.5	7.5
Aspartic acid	4.0	4.0	4.0
Total amino acid	88.0	82.0	82.0
Total N	14.1	13.1	13.1

Composition of EN solutions

Table 2 summarizes the daily EN compositions infused into various groups.

Table 2 Compositions of EN solutions (ml·L⁻¹)

Amino acids	Balanced amino acids (group A, C)	Methionine-depleted (group B)	Valine-depleted (group D)
Amino acid solutions	350	350	350
50 % Glucose	300	300	300
20 % Intralipid	100	100	100
Electrolytes, vitamins	250	250	250
Total calorie (KJ·L ⁻¹)	3 513.3	3 507.9	3 507.9
Total N (g·L ⁻¹)	4.9	4.6	4.6
Non-protein calorie/N	122	131	131

Specimen sampling

After the infusions were completed, three rats per group were respectively killed by cervical dislocation at 0.5, 1, 2 and 4 hours postinjection of tracers. The whole tumor was dissected and used for the tissue uptake of radioactivity.

Nucleic acid and protein analysis

To assess the incorporation of the radioactivity into macromolecular materials, portions of the tumor tissues (70-120 mg) were divided into the acid-soluble fraction (ASF) and the acid-precipitate fraction (APF). Radiolabeled APF was divided into four fractions: lipids, RNA, DNA and proteins. To analyze ³H-Met and ³H-Val metabolites, the tumor tissues were homogenated in 1 ml of ice-cold 0.4 M HClO₄. The homogenate was centrifuged at 3 000 rpm for 5 min. The precipitate was resuspended in 1 ml of 0.4 M HClO₄. This wash was repeated twice. The precipitate was resuspended in 5 ml of CHCl₃:CH₃OH (2:1, V/V). After centrifugation at 3 000

rpm for 10 min, the CHCl₃:CH₃OH phase was separated. This extraction was repeated twice. The combined CHCl₃:CH₃OH fraction contains radiolabeled lipids. The precipitate was dissolved in 1 ml of 0.3 M KOH. After incubation of the solution at 37 °C for 1 hour to hydrolyze RNA, 0.32 ml of 3 N HClO₄ was added. The mixture was kept on ice for 5 min. The precipitate was then separated and washed with 1 ml 0.5 M HClO₄ as described above. The combined supernatant was designated as the alkaline-labile fraction containing the RNA hydrolysate. The precipitate was resuspended in 1 ml of 0.5 M HClO₄ and heated at 90 °C for 15 min to hydrolyze DNA. The solution was kept on ice for 5 min, and precipitate was separated and washed with 0.4 M HClO₄ twice. The combined supernatant and the final precipitate were assessed as the acid-labile fraction containing hydrolysates of DNA and protein fraction, respectively.

The radioactivities of fractions were counted by liquid scintillation counter. The tissue radioactivity was expressed as differential uptake ratio (DUR).

$$\text{DUR} = \frac{\text{Counts of tumor tissue (cpm)/sample weight (g)}}{\text{Injection dose counts (cpm)/body weight (g)}}$$

Statistical analysis

Student *t* test was used to examine the data. The difference was considered significant when *P* value was less than 0.05.

RESULTS

Three TB rats died of intestinal fistula, diarrhea, infection of abdominal cavity. Table 3 represented incorporation of ³H into nucleic acids and proteins in TB rats after treatment.

Table 3 Incorporation (DUR,%) of ³H into nucleic acids and proteins in TB rats after treatment

Group		0.5 h	1 h	2 h	4 h
RNA	A	0.208±0.002	0.300±0.002	0.349±0.007	0.405±0.007 ^c
	B	0.149±0.012	0.249±0.009	0.260±0.010	0.389±0.010
	C	0.200±0.007	0.250±0.036 ^b	0.283±0.029 ^{ac}	0.326±0.014 ^c
	D	0.180±0.013	0.210±0.024	0.300±0.034	0.320±0.030 ^b
DNA	A	0.210±0.013	0.300±0.020	0.339±0.039	0.400±0.002 ^c
	B	0.179±0.010 ^a	0.204±0.039 ^a	0.240±0.028 ^a	0.300±0.015 ^b
	C	0.200±0.011	0.250±0.040	0.283±0.031 ^c	0.340±0.057 ^c
	D	0.180±0.015	0.220±0.024	0.308±0.007	0.320±0.035
Proteins	A	0.659±0.055	2.410±0.149	3.450±0.125	4.492±0.108 ^c
	B	0.500±0.020 ^b	2.000±0.203 ^b	2.890±0.090 ^{bc}	3.670±0.110 ^b
	C	0.805±0.098	2.510±0.010	3.540±0.101 ^c	4.180±0.018 ^c
	D	0.708±0.019	1.887±0.020 ^b	2.916±0.085 ^b	3.813±0.076 ^b

^a*P*<0.05, ^b*P*<0.01, vs group A or C. ^cNumber of rats=2.

DISCUSSION

Influence of Methionine/Valine-depleted enteral nutrition on protein metabolism in TB rats

Patients with malignant tumors often show severe protein-amino acid metabolism disorder and uncorrectable negative nitrogen balance. Researchers have begun to reconsider the prescription of amino acid imbalance solution for cancer patients. Total parenteral nutrition deprived of methionine or valine cause tumor growth inhibition, but also have no significantly negative influences on the host animals^[16-18].

Table 3 shows the ³H incorporation rate in tumor tissues at

various times after ^3H -Met/Val injections. Regardless of Methionine/Valine-depleted enteral nutrition, the radioactivity into nucleic acids and proteins increased with time. In proteins we found an accumulation of the label which was up to 3-10-fold higher than in DNA and RNA. It represents the principle pathway for methionine and valine anabolism. Accumulation of ^3H -Met/Val into malignant tissue is thought to be due to amino acid metabolism of cancer cells such as increased active transport and incorporation of amino acid into protein fractions. In the complete absence of Methionine or Valine, the ^3H incorporation rate of the radioactivity into proteins in tumor tissues was from 75.8 % to 87.9 % of the control value. That is to say, in agreement with Xiao's study^[5], protein synthesis was inhibited by methionine/valine depletion, in this case suppressing tumor growth^[19-26].

Although essential amino acids are indispensable for physical well-being, the body lacks the ability to synthesize these compounds. Amino acids are an important materials of protein synthesis, amino acid imbalance are considered to principally involving alterations in intracellular protein synthesis, the deprivation of essential amino acids (Met, Val) leads to inhibit activity of tumor growth^[27,28].

Influence of Methionine/Valine-depleted enteral nutrition on RNA and DNA in TB rats

Methionine adenosyltransferase is the enzyme which is responsible for the synthesis of S-adenosyl-L-methionine (SAM) using methionine and adenosine triphosphate (ATP). Most of SAM are used in transmethylation reaction in which methyl groups are added to compounds and SAM is converted to S-adenosylhomocysteine. SAM is the principal biological methyl donor. SAM can easily transfer its methyl group to a large variety of acceptor substrates including rRNA, tRNA, mRNA, DNA, proteins, phospholipides, biological amines, and a long list of small molecules^[29-33]. So ^3H -Met is also incorporated into nucleic acids by transmethylation via S-adenosyl-L-methionine. Methionine depleted enteral nutrition can decrease methylation of tumor tissues and lead to further reduction in nucleic acid synthesis and inhibition of cancer growth at molecular levels.

Table 3 showed that the RNA and DNA incorporation rate in group B was lower than in control group (group A). Based on these findings, cancer cells were known to have lower levels of DNA and RNA synthesis on methionine-depleted enteral nutrition.

Theoretically, it is considered that ^3H -Val is incorporated into proteins but not into other high-molecular materials such as nucleic acids. The incorporation of ^3H -Val was detected in nucleic acids at negligible amounts, which possibly reflects contamination by labeled proteins during the experimental processes. However, because no metabolic pathway for the DNA incorporation of ^3H -Val is considered, the radioactivity in the acid-labile fraction is probably derived from basic proteins such as chromosomal histones.

REFERENCES

- 1 **Bozzetti F**, Gavazzi C, Cozzaglio L, Costa A, Spinelli P, Viola G. Total parenteral nutrition and tumor growth in malnourished patients with gastric cancer. *Tumori* 1999; **85**: 163-166
- 2 **Sasamura T**, Matsuda A, Kokuba Y. Tumor growth inhibition and nutritional effect of d-amino acid solution in AH109A hepatoma-bearing rats. *J Nutr Sci Vitaminol* 1998; **44**: 79-87
- 3 **Forchielli ML**, Paolucci G, Lo CW. Total parenteral nutrition and home parenteral nutrition: an effective combination to sustain malnourished children with cancer. *Nutr Rev* 1999; **57**: 15-20
- 4 **Sasamura T**, Matsuda A, Kokuba Y. Nutritional effects of a D-methionine-containing solution on AH109A hepatoma-bearing rats. *Biosci Biotechnol Biochem* 1998; **62**: 2418-2420
- 5 **Xiao HB**, Cao WX, Yin HR, Lin YZ, Ye SH. Influence of L-methionine-deprived total parenteral nutrition with 5-fluorouracil on gastric cancer and host metabolism. *World J Gastroenterol* 2001; **7**: 698-701
- 6 **Nagahama T**, Goseki N, Endo M. Doxorubicin and vincristine with methionine depletion contributed to survival in the Yoshida sarcoma bearing rats. *Anticancer Res* 1998; **18**: 25-31
- 7 **Cao WX**, Cheng QM, Fei XF, Li SF, Yin HR, Lin YZ. A study of preoperative methionine-depleting parenteral nutrition plus chemotherapy in gastric cancer patients. *World J Gastroenterol* 2000; **6**: 255-258
- 8 **Tang B**, Li YN, Kruger WD. Defects in methylthioadenosine phosphorylase are associated with but not responsible for methionine-dependent tumor cell growth. *Cancer Res* 2000; **60**: 5543-5547
- 9 **Komatsu H**, Nishihira T, Chin M, Doi H, Shineha R, Mori S, Satomi S. Effects of caloric intake on anticancer therapy in rats with valine-depleted amino acid imbalance. *Nutr Cancer* 1997; **28**: 107-112
- 10 **Yoshida S**, Ohta J, Shirouzu Y, Ishibashi N, Harada Y, Yamana H, Shirouzu K. Effect of methionine-free total parenteral nutrition and insulin-like growth factor I on tumor growth in rats. *Am J Physiol* 1997; **273**: E10-16
- 11 **Komatsu H**, Nishihira T, Chin M, Doi H, Shineha R, Mori S, Satomi S. Effect of valine depleted total parenteral nutrition on fatty liver development in tumor-bearing rats. *Nutrition* 1998; **14**: 276-281
- 12 **Tan Y**, Xu M, Guo H, Sun X, Kubota T, Hoffman RM. Anticancer efficacy of methioninase *in vivo*. *Anticancer Res* 1996; **16**: 3931-3936
- 13 **Guo H**, Tan Y, Kubota T, Moossa AR, Hoffman RM. Methionine depletion modulates the antitumor and antimetastatic efficacy of ethionine. *Anticancer Res* 1996; **16**: 2719-2723
- 14 **Sasamura T**, Matsuda A, Kokuba Y. Effects of D-methionine-containing solution on tumor cell growth *in vitro*. *Arzneimittelforschung* 1999; **49**: 541-543
- 15 **Bozzetti F**, Gavazzi C, Miceli R, Rossi N, Mariani L, Cozzaglio L, Bonfanti G, Piacenza S. Perioperative total parenteral nutrition in malnourished, gastrointestinal cancer patients: a randomized, clinical trial. *JPEN* 2000; **24**: 7-14
- 16 **Yoshioka T**, Wada T, Uchida N, Maki H, Yoshida H, Ide N, Kasai H, Hojo K, Shono K, Maekawa R, Yagi S, Hoffman RM, Sugita K. Anticancer efficacy *in vivo* and *in vitro*, synergy with 5-fluorouracil, and safety of recombinant methioninase. *Cancer Res* 1998; **58**: 2583-2587
- 17 **Jin D**, Phillips M, Byles JE. Effects of parenteral nutrition support and chemotherapy on the phasic composition of tumor cells in gastrointestinal cancer. *JPEN* 1999; **23**: 237-241
- 18 **Machover D**, Zittoun J, Broet P, Metzger G, Orrico M, Goldschmidt E, Schilf A, Tonetti C, Tan Y, Delmas-Marsalet B, Luccioni C, Falissard B, Hoffman RM. Cytotoxic synergism of methioninase in combination with 5-fluorouracil and folinic acid. *Biochem Pharmacol* 2001; **61**: 867-876
- 19 **Nishihira T**, Takagi T, Mori S. Leucine and manifestation of antitumor activity by valine-depleted amino acid imbalance. *Nutrition* 1993; **9**: 146-152
- 20 **Nishihira T**, Takagi T, Kawarabayashi Y, Izumi U, Ohkuma S, Koike N, Toyoda T, Mori S. Anti-cancer therapy with valine-depleted amino acid imbalance solution. *Tohoku J Exp Med* 1988; **156**: 259-270
- 21 **Nishihira T**, Komatsu H, Sagawa J, Shineha R, Mori S. Prevention of fatty liver and maintenance of systemic valine depletion using a newly developed dual infusion system. *JPEN* 1995; **19**: 199-203
- 22 **Machover D**, Zittoun J, Saffroy R, Broet P, Giraudier S, Magnaldo T, Goldschmidt E, Debuire B, Orrico M, Tan Y, Mishal Z, Chevallier O, Tonetti C, Jouault H, Ulusakarya A, Tanguy ML, Metzger G, Hoffman RM. Treatment of cancer cells with methioninase produces DNA hypomethylation and increases DNA synthesis. *Cancer Res* 2002; **62**: 4685-4689
- 23 **Hoshiya Y**, Kubota T, Inada T, Kitajima M, Hoffman RM. Methionine-depletion modulates the efficacy of 5-fluorouracil in human gastric cancer in nude mice. *Anticancer Res* 1997; **17**: 4371-4375
- 24 **Poirson-Bichat F**, Goncalves RA, Miccoli L, Dutrillaux B, Poupon

- MF. Methionine depletion enhances the antitumoral efficacy of cytotoxic agents in drug-resistant human tumor xenografts. *Clin Cancer Res* 2000; **6**: 643-653
- 25 **Poirson-Bichat F**, Lopez R, Bras Goncalves RA, Miccoli L, Bourgeois Y, Demerseman P, Poisson M, Dutrillaux B, Poupon MF. Methionine deprivation and methionine analogs inhibit cell proliferation and growth of human xenografted gliomas. *Life Sci* 1997; **60**: 919-931
- 26 **Hoshiya Y**, Kubota T, Matsuzaki SW, Kitajima M, Hoffman RM. Methionine starvation modulates the efficacy of cisplatin on human breast cancer in nude mice. *Anticancer Res* 1996; **16**: 3515-3517
- 27 **Samuels SE**, Knowles AL, Tilignac T, Debiton E, Madelmont JC, Attaix D. Protein metabolism in the small intestine during cancer cachexia and chemotherapy in mice. *Cancer Res* 2000; **60**: 4968-4974
- 28 **Poirson-Bichat F**, Gonfalone G, Bras-Goncalves RA, Dutrillaux B, Poupon MF. Growth of methionine-dependent human prostate cancer (PC-3) is inhibited by ethionine combined with methionine starvation. *Br J Cancer* 1997; **75**: 1605-1612
- 29 **Lu SC**. Methionine adenosyltransferase and liver disease: it's all about SMA. *Gastroenterology* 1998; **114**: 403-407
- 30 **Zhu SS**, Xiao SD, Chen ZP, Shi Y, Fang JY, Li RR, Mason JB. DNA methylation and folate metabolism in gastric cancer. *World J Gastroenterol*, 2000; **6**(Suppl 3): 18
- 31 **Avila MA**, Carretero MV, Rodriguez EN, Mato JM. Regulation by hypoxia of methionine adenosyltransferase activity and gene expression in rat hepatocytes. *Gastroenterology* 1998; **114**: 364-371
- 32 **Cao WX**, Ou JM, Fei XF, Zhu ZG, Yin HR, Yan M, Lin YZ. Methionine-dependence and combination chemotherapy on human gastric cancer cells *in vitro*. *World J Gastroenterol* 2002; **8**: 230-232
- 33 **Cui J**, Yang DH, Bi XJ, Fan ZR. Methylation status of *c-fms* oncogene in HCC and its relationship with clinical pathology. *World J Gastroenterol* 2001; **7**: 136-139

Edited by Xu JY

Action of progesterone on contractile activity of isolated gastric strips in rats

Fang Wang, Tian-Zhen Zheng, Wei Li, Song-Yi Qu, Di-Ying He

Fang Wang, Institute of Infectious Diseases, the Third Military Medical University Affiliated Southwest Hospital, Chongqing 400038, China

Tian-Zhen Zheng, Wei Li, Song-Yi Qu, Department of Physiology, Lanzhou Medical College, Lanzhou 730000, China

Di-Ying He, Department of Physical Culture, Gansu College of Education, Lanzhou 730000, China

Supported by Natural Science Foundation of Province of Gansu Province, No: ZR-96-085

Correspondence to: Fang Wang, Institute of Infectious Diseases, the Third Military Medical University Affiliated Southwest Hospital, Chongqing 400038, China. kaixin919@163.com

Telephone: +86-23-68754475-8020 **Fax:** +86-23-65334998

Received: 2002-07-23 **Accepted:** 2002-08-23

Abstract

AIM: To study the effect of progesterone on contractile activity of isolated gastric strips in rats.

METHODS: Wistar rats were sacrificed to remove whole stomach. Then, the stomach was opened and the mucosal layer was removed. Parallel to either the circular or the longitudinal fibers, muscle strips were cut from fundus, body, antrum and pylorus. Each muscle strip was suspended in a tissue chamber containing 5 mL Krebs solution. Then the motility of gastric strips in tissue chambers was simultaneously recorded. The preparations were subjected to 1 g load tension and washed with 5 ml Krebs solution every 20 min. After 1 h equilibration, progesterone or antagonists were added in the tissue chamber separately. The antagonists were added 3 min before using progesterone ($50 \mu\text{mol} \cdot \text{L}^{-1}$).

RESULTS: Progesterone decreased the resting tension of fundus and body longitudinal muscle (LM) ($P < 0.05$). It inhibited the mean contractile amplitude of body and antrum LM and circular muscle (CM), and the motility index of pyloric CM ($P < 0.05$). The inhibition of progesterone on the mean contractile amplitude could be partially blocked by phentolamine in LM of the stomach body (the mean contractile amplitude of body LM decreased from -7.5 ± 5.5 to -5.2 ± 4.5 $P < 0.01$), and by phentolamine or indomethacin in CM of body (The inhibition of progesterone on the mean contractile amplitude of body CM decreased from -5.6 ± 3.0 to -3.6 ± 2.7 by phentolamine and from -5.6 ± 3.0 to -3.5 ± 2.5 by indomethacin, $P < 0.01$). Hexamethonium, propranolol and L-NNA (inhibitor of NO synthetase) didn't affect the action of progesterone ($P > 0.05$).

CONCLUSION: The study suggested that progesterone can inhibit the contractile activity of isolated gastric strips in rats and the mechanism seems to be a direct one except that the action on gastric body is mediated through prostaglandin and adrenergic α receptor partly.

Wang F, Zheng TZ, Li W, Qu SY, He DY. Action of progesterone on contractile activity of isolated gastric strips in rats. *World J Gastroenterol* 2003; 9(4): 775-778
<http://www.wjgnet.com/1007-9327/9/775.htm>

INTRODUCTION

Nausea and vomiting are extremely common complaints of pregnancy and may precede even the patients are aware that she is pregnant^[1-4]. However, it's mechanism is poorly understood. The questions of whether gastric emptying of solids and liquids differs in men and women and whether emptying is influenced by the action of sex hormones on gastric smooth muscle remain unresolved^[5-8]. Whether gastric emptying of solids and liquids differs in women during the menstrual cycle is controversial^[9-12]. The results of several clinical and physiological studies have suggested that the aforementioned complaints of pregnancy may be related, at least in part, to decrease of resting tension within the lower esophageal sphincter and changes in gastric motility^[3,13-15]. The fact that a high serum sex hormone concentration is the characteristic of pregnancy tempts researchers to investigate the hormonal factor associated with gastrointestinal dysmotility. However, so far, the effect of pregnancy and sex hormone on gastric motility remains controversial. We studied the action of progesterone on the gastric strips in rats and explored the possible mechanism concerned.

MATERIALS AND METHODS

Materials

Progesterone, purchased from sigma, was dissolved and diluted in 1, 2-propanecol; hexamethonium and N^w-Nitro-L-Arginine (L-NNA), Sigma; indomethacin, Jiangsu Taicang Pharmaceutical Factory; propranolol, Beijing Second Pharmaceutical Factory; Phentolamine, Beijing Thirteen Pharmaceutical Factory; 1, 2-propanecol, Tianjing Chemical Factory; Krebs buffer solution [(mmol·L⁻¹: NaCl 120.6, KCl 5.9, NaH₂PO₄ 1.2, MgCl₂ 1.2, NaHCO₃ 15.4, CaCl₂ 2.5, C₆H₁₂O₆ 11.5, pH=7.4)].

JZ-BK external isometric force transducer, BK company; LMS-ZB two channel recorder, Chengdu Equipment Factory.

Wistar rats, 200-250 g, were provided by the Animal Center of Lanzhou Medical College.

Methods

Wistar rats were fasted with free access to water for 24 h, and sacrificed to remove whole stomach. Then, the stomach was opened along the great curvature, and rinsed with Krebs solution. The stomach was pinned on a wax block with mucosa side up, and the mucosal layer was gently rubbed with a tweezers. Parallel to either the circular or the longitudinal fibers, muscle strips (8×2 mm) were cut and named longitudinal muscle (LM) of fundus, circular muscle (CM) and LM of body and antrum and CM of pylorus^[16,17].

Each muscle strip with the mucosa removed was suspended in a tissue chamber containing 5 mL Krebs solution, constantly warmed by circulating water jacket at 37 °C and supplied with 95 % O₂ and 5 % CO₂. One end of the strip was fixed to a hook on the bottom of the chamber while the other end was connected by a thread to an external isometric force transducer at the top. Motility of gastric strips in tissue chambers were simultaneously recorded on recorders. Preparations were subjected to 1 g load tension and washed with 5 ml Krebs

solution every 20 min. After 1 h equilibration, progesterone (5, 10, 50 $\mu\text{mol}\cdot\text{L}^{-1}$) or antagonist was added in the tissue chamber (all were the final concentration) separately 3 min before using progesterone (50 $\mu\text{mol}\cdot\text{L}^{-1}$)^[16-20].

Analysis of data

We measured the resting tension of all strips, the mean contractile amplitude of body and antrum strips, and the motility index (MI = Σ [amplitude \times duration]) of pyloric strip. Frequencies of contraction were determined by counting the contraction waves. Values of the results was presented as $\bar{x}\pm s$. Statistical significances were measured by *t* test^[16,17].

RESULTS

Effect of progesterone on spontaneous contraction of gastric strips

Progesterone significantly decreased the resting tension of fundus and body LM (Table 1). It decreased the mean contractile amplitude of body and antrum, and the motility index of pylorus (Table 2). However it didn't influence the gastric contractile frequency ($P>0.05$).

Effect of antagonists added progesterone on spontaneous contraction of gastric strips

Hexamethonium (10 $\mu\text{mol}\cdot\text{L}^{-1}$), L-NNA (100 $\mu\text{mol}\cdot\text{L}^{-1}$) or propranolol (1 $\mu\text{mol}\cdot\text{L}^{-1}$) added 3 min before admistrated progesterone didn't influence the decreasing effect of progesterone on the gastric strips in rats ($P>0.05$), but phentolamine (1 $\mu\text{mol}\cdot\text{L}^{-1}$) partly blocked its effect on the mean contractile amplitude of body LM and CM, and indomethacin (10 $\mu\text{mol}\cdot\text{L}^{-1}$) also decreased the effect on the mean contractile amplitude of body CM (Table 3).

DISCUSSION

It has been shown from humans and animals that pregnancy is associated with alternations in the motor activity of the gastrointestinal tract, such as decreased gallbladder contractivity and lower esophageal sphincter pressure, reduced gastric emptying, small intestine and colonic transit^[13-15,21-29]. Although the factors responsible for the impaired gastric motility are obscure, there is evidence to suggest that pregnancy is associated with disturbances in the myoelectric and mechanical properties of gastrointestinal smooth muscle.

Table 1 Effect of progesterone on the resting tension of gastric smooth muscle in rats

Progesterone $\mu\text{mol}\cdot\text{L}^{-1}$	Resting tension/g					
	Fundus	Body		Antrum		Pylorus
	LM	LM	CM	LM	CM	CM
5	-0.08 \pm 0.12 ^a	-0.008 \pm 0.08	0	0.01 \pm 0.05	0	0
10	-0.08 \pm 0.08 ^b	-0.05 \pm 0.11	-0.03 \pm 0.06	0.04 \pm 0.09	0	0
50	-0.09 \pm 0.06 ^d	-0.12 \pm 2.0 ^a	0.01 \pm 0.15	0.02 \pm 0.04	0	-0.03 \pm 0.10

The values were expressed as differences in resting tension between 3 min before and after the addition of progesterone (5, 10 and 50 $\mu\text{mol}\cdot\text{L}^{-1}$) (The same in Tab 2). The resting tension of each strip in control (progesterone 0 $\mu\text{mol}\cdot\text{L}^{-1}$) was 1. LM: longitudinal muscle; CM: circular muscle. $\bar{x}\pm s$, $n=12$, ^a $P<0.05$, ^b $P<0.01$, ^d $P<0.001$, vs control by paired *t* test.

Table 2 Effect of progesterone on the mean contractile amplitude of body and antrum, and the motility index of pylorus in rats

Progesterone $\mu\text{mol}\cdot\text{L}^{-1}$		Contractile amplitude/mm				Motility index/cm.s ⁻¹
		Body		Antrum		Pylorus
		LM	CM	LM	CM	CM
5	B	13.4 \pm 17.0	12.0 \pm 13.2	13.6 \pm 8.6	14.1 \pm 15.0	92.4 \pm 16.2
	C	0.2 \pm 0.4	-0.9 \pm 3.0	-0.5 \pm 0.8 ^a	-0.8 \pm 1.7	1.7 \pm 4.8
10	B	12.8 \pm 17.6	11.2 \pm 14.0	14.0 \pm 7.1	13.6 \pm 12.9	98.5 \pm 20.0
	C	-2.1 \pm 3.8 ^a	-1.5 \pm 1.6 ^b	-1.8 \pm 2.0 ^b	-3.1 \pm 1.8 ^d	-22.5 \pm 16.6 ^d
50	B	12.0 \pm 16.9	11.8 \pm 12.9	12.6 \pm 8.0	12.6 \pm 14.8	110.2 \pm 22.8
	C	-7.5 \pm 5.5 ^a	-5.6 \pm 3.0 ^d	-5.4 \pm 3.8 ^d	-5.8 \pm 3.8 ^d	-47.4 \pm 31.2 ^d

B: basic values in 3 min before addition of progesterone; C: changes in 3 min after addition of progesterone (The same in Tab 3). $\bar{x}\pm s$, $n=12$. ^a $P<0.05$, ^b $P<0.01$, ^d $P<0.001$, vs corresponding B by paired *t* test.

Table 3 Effect of progesterone on the mean contractile amplitude of body after indomethacin or phentolamine pretreatment in rats

Gastric body muscle	Contractile amplitude/mm									
	Pr		I + Pr				Ph + Pr			
	B	C	B	C	B	C	B	C	B	C
LM	12.0 \pm 16.9	-7.5 \pm 5.5 ^b	12.9 \pm 17.1	-0.1 \pm 6.0	12.5 \pm 18.4	-8.2 \pm 6.9 ^b	12.1 \pm 19.2	1.4 \pm 3.8	15.4 \pm 16.5	-5.2 \pm 4.5 ^d
CM	11.8 \pm 12.9	-5.6 \pm 3.0 ^b	12.2 \pm 14.0	1.2 \pm 5.2	12.6 \pm 13.2	-3.5 \pm 2.5 ^d	11.7 \pm 12.6	0.2 \pm 0.5	11.4 \pm 13.0	-3.6 \pm 2.7 ^d

Phentolamine (1 $\mu\text{mol}\cdot\text{L}^{-1}$) or indomethacin (10 $\mu\text{mol}\cdot\text{L}^{-1}$) was added 3 min before the addition of progesterone (50 $\mu\text{mol}\cdot\text{L}^{-1}$). $\bar{x}\pm s$, $n=12$. Pr: progesterone, I: indomethacin, Ph: phentolamine. ^b $P<0.001$ vs corresponding B by paired *t* test; ^d $P<0.01$ vs Pr alone by two samples mean *t* test.

In our study, progesterone decreased the resting tension of fundus, which might be a cause of changed gastric motility during pregnancy. It had been agreed that decreased fundic resting tension mainly influenced the gastric emptying of liquids. Ryan also reported^[30] that pregnancy was associated with decreased gastric emptying of liquids in the guinea pig. The observation in our study that hexamethonium, L-NNA and propranolol didn't influence the effect of progesterone suggesting that the action of progesterone was not mediated via NO, β or N_1 receptors. Since phentolamine blocked partly the effect of body LM and CM, and indomethacin decreased that of body CM showed that the effect of the hormone on body LM partly via a receptor, and on body CM via prostaglandin and a receptor. In addition, the effect of progesterone might act on gastric smooth muscle cells directly. Progesterone receptor had been found in normal human gastric tissues. Another evidence was addition of progesterone to isolated denervated gallbladder muscle strips inhibited contraction in response to both acetylcholine or cholecystokinin^[31].

Parkman reported^[14] that spontaneous and bethanechol induced phasic antrum contraction of pregnant guinea pigs were significantly reduced in force compared with control virgin animals, and intracellular electrical recordings were obtained from antral smooth muscle cells to investigate the mechanism of the decreased contractivity of antral smooth muscle during pregnancy. The results showed that there were similar resting membrane potentials, slow wave frequency and slow wave duration vs those of the control, but the upstroke amplitude, plateau amplitude and number of spike per slow wave decreased significantly. Further study suggested that the decreased force of spontaneous antral contractions was associated with a reduction in the underlying electrical slow wave depolarization. Electrogastrogram recordings also suggested that gastric dysrhythmias were objective pathophysiologic event associated with symptoms of nausea and vomiting during pregnancy^[14,32,33].

Exogenous progesterone also inhibited the myoelectric and mechanical activity of gastrointestinal smooth muscle. Electrical spike potentials recorded from chronically implanted electrodes in the antrum and jejunum of ovariectomized dogs by Milenory decreased after 4 d of progesterone addition ($2 \text{ mg} \cdot \text{kg}^{-1} \cdot \text{d}^{-1}$) and the propagation velocity of the basic electrical rhythm from the antral region of the progesterone-treated animals also decreased^[34]. In another example, progesterone had been shown to reduce the propagation velocity of gastrointestinal slow waves possibly by decreasing the degree of electrical coupling between smooth muscle cells^[35]. Dysrhythmias were also induced in healthy, nonpregnant women by administration of progesterone in the dose that reproduces plasma level seen in pregnancy. The above results suggested that the inhibitory effect of progesterone on the gastric smooth muscle may contribute to the gastric dysmotility during pregnancy.

REFERENCES

- 1 **Chandra K**, Magee L, Koren G. Discordance between physical symptoms versus perception of severity by women with nausea and vomiting in pregnancy (NVP). *BMC Pregnancy Childbirth* 2002; **2**: 5-8
- 2 **Chandra K**, Einarson A, Koren G. Taking ginger for nausea and vomiting during pregnancy. *Can Fam Physician* 2002; **48**: 1441-1442
- 3 **Singer AJ**, Brandt LJ. Pathophysiology of the gastrointestinal tract during pregnancy. *Am J Gastrointestinal* 1991; **86**: 1695-1712
- 4 **DiIorio C**, van Lier D, Manteuffel B. Patterns of nausea during first trimester of pregnancy. *Clin Nurs Res* 1992; **1**: 127-140
- 5 **Hutson WR**, Roehrkasse RL, Wald A. Influence of gender and menopause on gastric emptying and motility. *Gastroenterology* 1989; **96**: 11-17
- 6 **Degen LP**, Phillips SF. Variability of gastrointestinal transit in healthy women and men. *Gut* 1996; **39**: 299-305
- 7 **Bennink R**, Peeters M, Van den Maegdenbergh V, Geypens B, Rutgeerts P, DeRoo M, Mortelmans L. Comparison of total and compartmental gastric emptying and antral motility between healthy men and women. *Eur J Nucl Med* 1998; **25**: 1293-1299
- 8 **Datz FL**, Christian PE, Moore J. Gender-related differences in gastric emptying. *J Nucl Med* 1987; **28**: 1204-1207
- 9 **Horowitz M**, Maddern GJ, Chatterton BE, Collins PJ, Petrucco OM, Seamark R, Shearman DJ. The normal menstrual cycle has no effect on gastric emptying. *Br J Obstet Gynaecol* 1985; **92**: 743-746
- 10 **Gill RC**, Murphy PD, Hooper HR, Bowes KL, Kingma YJ. Effect of the menstrual cycle on gastric emptying. *Digestion* 1987; **36**: 168-174
- 11 **Caballero-Plasencia AM**, Valenzuela-Barranco M, Martin-Ruiz JL, Herreras-Gutierrez JM, Esteban-Carretero JM. Are there changes in gastric emptying during the menstrual cycle? *Scand J Gastroenterol* 1999; **34**: 772-776
- 12 **Bovo P**, Paola Brunori M, di Francesco V, Frulloni L, Montesi G, Cavallini G. The menstrual cycle has no effect on gastrointestinal transit time. Evaluation by means of the lactulose H2 breath test. *Ital J Gastroenterol* 1992; **24**: 449-451
- 13 **Koch KL**. Gastrointestinal factors in nausea and vomiting of pregnancy. *Am J Obstet Gynecol* 2002; **185**: S198-203
- 14 **Parkman HP**, Wang MB, Ryan JP. Decreased electromechanical activity of guinea pig circular muscle during pregnancy. *Gastroenterology* 1993; **105**: 1306-1312
- 15 **Jones MJ**, Mitchell RW, Hindocha N, James RH. The lower oesophageal sphincter in the first trimester of pregnancy: comparison of supine with lithotomy positions. *Br J Anaesth* 1988; **61**: 475-476
- 16 **Qu SY**, Zheng TZ, Li W. Comparative study of ranitidine and cimetidine on contractile activity of isolated gastric muscle strips in rats. *Xin Xiaohuabingxue Zazhi* 1997; **5**: 75-76
- 17 **Wang F**, Luo JQ, Zhen TZ, Qu SY, Li W, He DY. Effect of oxytocin on the contractile activity of gastric strips of rats *in vitro*. *Zhongguo Yaolixueyudulixue Zazhi* 1999; **13**: 285-287
- 18 **Qu SY**, Zhen TZ, Li W. Effect of cholecystokinin and secretin on contractile activity of isolated gastric muscle strips in guinea pigs. *Shenlixuebao* 1995; **47**: 305-309
- 19 **Xie DP**, Li W, Qu SY, Zhen TZ, Yang YL, Ding YH, Wei YL, Chen LB. Effect of areca on contraction of colonic muscle strips in rats. *World J Gastroenterol* 2002; **8**: 350-352
- 20 **Li W**, He DY, Zhen TZ, Wang F, Qu SY. Effect of estradiol on the contractile activity of bladder strips of rats *in vitro*. *Jichuyixue Yu Lingchuang* 2001; **21**: 186-187
- 21 **Ryan JP**. Effect of pregnancy on intestinal transit: comparison of results using radioactive and non-radioactive test meals. *Life Sci* 1982; **31**: 2635-2640
- 22 **Scott LD**, Lester R, Van Thiel DH, Wald A. Pregnancy-related changes in small intestinal myoelectric activity in the rat. *Gastroenterology* 1983; **84**: 301-305
- 23 **Baron TH**, Ramirez B, Richter JE. Gastrointestinal motility disorders during pregnancy. *Ann Intern Med* 1993; **118**: 366-375
- 24 **Shah S**, Hobbs A, Singh R, Cuevas J, Ignarro LJ, Chaudhuri G. Gastrointestinal motility during pregnancy: role of nitergic component of NANC nerves. *Am J Physiol Regul Integr Comp Physiol* 2000; **279**: R1478-R1485
- 25 **Bainbridge ET**, Nicholas SD, Newton JR, Temple JG. Gastro-oesophageal reflux in pregnancy. Altered function of the barrier to reflux in asymptomatic women during early pregnancy. *Scand J Gastroenterol* 1984; **19**: 85-89
- 26 **Ryan JP**, Bhojwani A. Colonic transit in rats: effect of ovariectomy, sex steroid hormones, and pregnancy. *Am J Physiol* 1986; **251** (1Pt1): G46-50
- 27 **Brock-Utne JG**, Dow TG, Dimopoulos GE, Welman S, Downing JW, Moshal MG. Gastric and lower oesophageal sphincter (LOS) pressures in early pregnancy. *Br J Anaesth* 1981; **53**: 381-384
- 28 **Everson GT**, McKinley C, Lawson M, Johnson M, Kern F Jr. Gallbladder function in the human female: effect of the ovulatory cycle, pregnancy, and contraceptive steroids. *Gastroenterology* 1982; **82**: 711-719

- 29 **Braverman DZ**, Johnson ML, Kern F Jr. Effects of pregnancy and contraceptive steroids on gallbladder function. *N Engl J Med* 1980; **302**: 362-364
- 30 **Ryan JP**, Bhojwani A, Wang MB. Effect of pregnancy on gastric motility *in vivo* and *in vitro* in the guinea pig. *Gastroenterology* 1987; **93**: 29-34
- 31 **Everson GT**. Gastrointestinal motility in pregnancy. *Gastroenterol Clin North Am* 1992; **21**: 751-776
- 32 **Chen JD**, Mittal RK. Nausea and vomiting in pregnancy and cutaneous electrogastrogram. *Gastroenterology* 1993; **104**: 1569-1571
- 33 **Abell TL**. Nausea and vomiting of pregnancy and the electrogastrogram: old disease, newtechnology. *Am J Gastroenterol* 1992; **87**: 689-691
- 34 **Milenory K**. Effect of estradiol, progesterone and oxytocin on smooth muscle activity. In: *Physiology of Smooth Muscle*, edited by Bulbring E, Shuba MF. New York: Raven 1976: 395-402
- 35 **Bortoff A**. Progesterone reduces slow wave propagation velocity and decrease electrical coupling between intestinal muscle cells. In: Weinbeck M. *Motility of Digestive Tract*. New York: Raven 1982: 445-450

Edited by Wu XN

Relative efficacy of some prokinetic drugs in morphine-induced gastrointestinal transit delay in mice

AD Suchitra, SA Dkhar, DG Shewade, CH Shashindran

AD Suchitra, SA Dkhar, DG Shewade, CH Shashindran, Department of Pharmacology, JIPMER, Pondicherry 605006, INDIA
Correspondence to: DG Shewade, Department of Pharmacology, JIPMER, Pondicherry 605006, INDIA. shewade@eth.net
Telephone: +91-413-2278693 **Fax:** +91-413-2272067
Received: 2002-10-05 **Accepted:** 2002-11-04

Abstract

AIM: To study the relative efficacy of cisapride, metoclopramide, domperidone, erythromycin and mosapride on gastric emptying (GE) and small intestinal transit (SIT) in morphine treated mice.

METHODS: Phenol red marker meal was employed to estimate GE and SIT in Swiss albino mice of either sex. The groups included were control, morphine 1 mg/kg (s.c. 15 min before test meal) alone or with (45 min before test meal p.o.) cisapride 10 mg/kg, metoclopramide 20 mg/kg, domperidone 20 mg/kg, erythromycin 6 mg/kg and mosapride 20 mg/kg.

RESULTS: Cisapride, metoclopramide and mosapride were effective in enhancing gastric emptying significantly ($P < 0.001$) whereas other prokinetic agents failed to do so in normal mice. Metoclopramide completely reversed morphine induced delay in gastric emptying followed by mosapride. Metoclopramide alone was effective when given to normal mice in increasing the SIT. Cisapride, though it did not show any significant effect on SIT in normal mice, was able to reverse morphine induced delay in SIT significantly ($P < 0.001$) followed by metoclopramide and mosapride.

CONCLUSION: Metoclopramide and cisapride are most effective in reversing morphine-induced delay in gastric emptying and small intestinal transit in mice respectively.

Suchitra AD, Dkhar SA, Shewade DG, Shashindran CH. Relative efficacy of some prokinetic drugs in morphine-induced gastrointestinal transit delay in mice. *World J Gastroenterol* 2003; 9(4): 779-783

<http://www.wjgnet.com/1007-9327/9/779.htm>

INTRODUCTION

Opioids are effective analgesics for moderate to severe pain^[1]. Morphine is the most commonly prescribed opioid agonist for the treatment of chronic pain^[2,3]. However, when opioids are given to alleviate pain they cause undesirable gastrointestinal (GI) side effects namely nausea, vomiting and reduced gastrointestinal transit^[4]. Reduced GI transit can cause gastroesophageal reflux disease, bloating and idiopathic constipation^[5].

The pathophysiology of GI delay due to opioids has been well described. Possible etiologies include increased stationary segmentation, reduced peristalsis and depression of secretory activity^[6]. Due to the paucity of the data to guide practitioners

in the management of GI side effects of opioids much of the information is extrapolated from different patient populations experiencing the same symptoms due to different etiologies.

Use of opioid antagonists such as naloxone, nalmefene, for opioid-induced GI delay^[7-10], is limited by their cost and tendency to cause withdrawal symptoms in the doses used^[10,11]. Peripherally acting methyl naltrexone and ADL-2698 (Alvimopan) are in the stage of investigational^[11].

Mosapride, cisapride, metoclopramide, erythromycin and domperidone are commonly used prokinetic agents. At present, the data supporting their relative efficacy in opioid induced GI delay are lacking. Further their distinct mechanism of action leaves a scope for variation in their efficacy. The present work attempts to study the relative efficacy of various prokinetic drugs such as cisapride, metoclopramide, domperidone, erythromycin and mosapride on small intestinal transit (SIT) and gastric emptying (GE) in morphine treated mice.

MATERIALS AND METHODS

Animals

Randomly bred healthy adult Swiss albino mice of either sex weighing between 20-25 g were obtained from JIPMER animal house, Pondicherry. One week prior to the experimentation, six mice were housed in separate cages and had free access to food and water. The experiments were conducted between 09:00 AM and 1:00 PM. The animals were fed with the pellets obtained from Prestige Agro-industries, Aurangabad. The study was approved by the institutional animal ethics committee.

Drugs and chemicals

Morphine sulphate (Govt. opium and alkaloid works, Ghazipur), cisapride (Torrent Pharmaceuticals, Ahmedabad), metoclopramide hydrochloride (Ipca laboratories Ltd., Mumbai), domperidone (Torrent Pharmaceuticals, Ahmedabad), erythromycin ethylsuccinate (Emil pharmaceutical industries Pvt Ltd, Thane), mosapride citrate (Alembic chemical works Co. Ltd. Vadodara) and Thiopentone sodium (Abbot laboratories, Mumbai) were used. Other chemicals used were of analytical grade. Carboxymethyl cellulose (1 %, 0.2 ml) was used as vehicle to administer prokinetic drugs.

Phenol red meal

Phenol red indicator weighing 25 mg was dissolved in 50 ml of distilled water and filtered. The filtrate was heated to 70 °C and methylcellulose (0.75 g) was added to it with continuous stirring. The mixture was then cooled to 37 °C.

Gastric emptying (GE) and small intestinal transit (SIT)

The standard method of phenol red marker meal as performed by earlier workers was employed^[12,13]. Mice were deprived of food for 24 h prior to experimentation but had free access to water, and 0.5 ml of phenol red meal was administered with the aid of the oral feeding syringe. Animals were killed by cervical dislocation under i.v. thiopentone sodium anesthesia 15 min after the administration of the meal. Abdomen was

opened and stomach was dissected out after careful ligation at the cardiac and pyloric ends, and was washed with normal saline. The stomach was cut into pieces and homogenized with 25 ml of 0.1 N NaOH. To this 5 ml homogenate 0.5 ml of trichloroacetic acid (20 % w/v) was added and centrifuged at 3 000 rpm for 20 minutes. To one ml of supernatant 4 ml of 0.5 N NaOH was added. The absorbance of this pink colored liquid was measured using spectrophotometer at 560nm (Model: HITACHI 150-20). This correlates with the concentration of phenol red in the stomach, which in turn depends upon the gastric emptying. The percentage gastric emptying is derived as $(1-X/Y) \times 100$ where, X is absorbance of phenol red recovered from the stomach of animals sacrificed 15 minutes after test meal. Y is mean ($n=5$) absorbance of phenol red recovered from the stomachs of control animals (killed at 0 min following test meal).

The small intestine was dissected out from the pylorus and ileocaecal junction and the point to which meal had traversed was secured with thread to avoid change in the length of the transit due to handling. The total length of the small intestine and distance traveled by phenol red meal was measured. The small intestinal transit (SIT) was calculated considering the distance traveled by phenol red meal divided by total length of the small intestine multiplied by 100. Small intestinal transit was expressed as mean \pm sem. The observer was blinded for the drugs administered to the mice.

Drug treatment

Control groups received the equal volumes of vehicle through corresponding routes. The groups included were control, morphine 1 mg/kg (s.c.), cisapride 10 mg/kg (p.o.), metoclopramide 20 mg/kg (p.o.), domperidone 20 mg/kg (p.o.), erythromycin 6 mg/kg (p.o.) and mosapride 20 mg/kg (p.o.). The doses were selected based on the earlier reports^[14,17], recommended clinical doses^[18,20] and prior pilot experiments. Cisapride, metoclopramide, domperidone, erythromycin and mosapride in the dose mentioned above were given alone 45 minutes before the administration of phenol red meal. Morphine (s.c.) was injected 15 minutes before the administration of the meal.

Statistical analysis

Statistical analysis was carried out using Graph pad (Prism) software. One way analysis of variance (ANOVA) for small intestinal transit and gastric emptying was applied separately followed by bonferroni post-test for multiple comparisons. Values were expressed as mean \pm sem. $P < 0.05$ was considered significant.

RESULTS

Since significant difference was not noticed among inter-day and animals receiving saline or 1 % carboxymethyl cellulose, data from these groups were pooled to serve as control group. Similar results obtained from morphine (1 mg/kg s.c.) treated groups were pooled. Morphine in the dose of 1 mg/kg (s.c.) caused significant decrease (61 %) in SIT ($P < 0.001$) and (43 %) in gastric emptying ($P < 0.05$).

Gastric emptying

Cisapride, metoclopramide and mosapride in the doses employed increased gastric emptying significantly ($P < 0.001$) by 126 %, 102 %, 89 % respectively compared with control animals, while domperidone and erythromycin failed to show any significant effect (Table 1, Figure 1). When combined with morphine (1 mg/kg s.c.) only metoclopramide and mosapride reversed morphine induced delay significantly ($P < 0.05$) (Table 2, Figure 2).

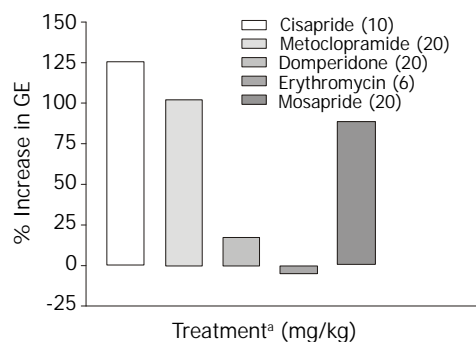


Figure 1 Percentage increase in gastric emptying by various prokinetic agents in mice. (Prokinetic agents were administered 45 minutes orally prior to the test meal).

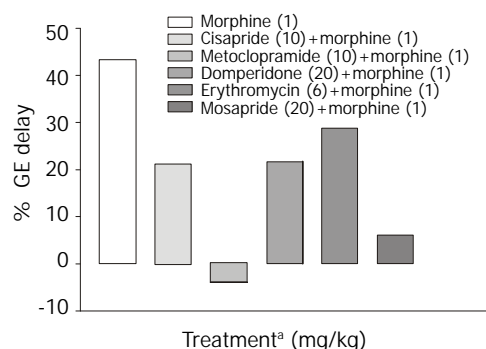


Figure 2 Effect of prokinetic agents on morphine induced delay of gastric emptying in mice. (Prokinetic agents were administered 45 minutes orally and morphine (s.c.) 15 minutes prior to test meal).

Table 1 Effect of prokinetic agents on gastric emptying and small intestinal transit in mice

Treatment* (mg/kg)	GE (%)	SIT(%)
Control	41.15 \pm 3.76	51.11 \pm 1.59
Cisapride (10) p.o.	92.98 \pm 1.76 ^a	61.46 \pm 3.01
Metoclopramide (20) p.o.	83.14 \pm 5.59 ^a	76.63 \pm 2.13 ^a
Domperidone (20) p.o.	48.15 \pm 2.31	58.94 \pm 1.25
Erythromycin (6) p.o.	39.08 \pm 5.10	52.91 \pm 1.50
Mosapride (20) p.o.	77.88 \pm 0.54 ^a	57.53 \pm 1.19

Each value represents mean \pm sem, $n=10$ in control group and $n=5$ in prokinetic drug treated group. *prokinetic agents were given 45 minutes prior to test meal. ^a $P < 0.001$ vs the control group.

Table 2 Effect of prokinetic agents on morphine induced delay in gastric emptying and small intestinal transit in mice

Treatment* (mg/kg)	GE (%)	SIT(%)
Control	41.15 \pm 3.76	51.11 \pm 1.59
Morphine(1) s.c.	23.30 \pm 2.83 ^a	19.73 \pm 1.25 ^b
Morphine (1) s.c. +		
Cisapride (10) p.o.	32.34 \pm 2.52	46.28 \pm 2.00 ^d
Metoclopramide (20) p.o.	42.77 \pm 2.04 ^c	34.01 \pm 1.75 ^d
Domperidone (20) p.o.	32.16 \pm 3.48	28.63 \pm 2.47
Erythromycin (6) p.o.	29.39 \pm 2.53	31.19 \pm 1.08
Mosapride (20) p.o.	38.59 \pm 1.98 ^c	38.01 \pm 1.61 ^d

Each value represents mean \pm sem, $n=5$ in treatment group and $n=10$ in control and morphine treated group. *prokinetic agents were given 45 minutes and morphine 15 minutes prior to the test meal. ^a $P < 0.05$ and ^b $P < 0.001$ vs control group. ^c $P < 0.05$ and ^d $P < 0.001$ vs morphine treated group.

Small intestinal transit

Only metoclopramide *per se*, significantly ($P < 0.001$) increased SIT by 50 % (Figure 3). However, when combined with morphine (1 mg/kg, s.c.) cisapride showed maximum efficacy followed by mosapride and metoclopramide (Figure 4). Domperidone and erythromycin did not exhibit any significant effect (Table 2).

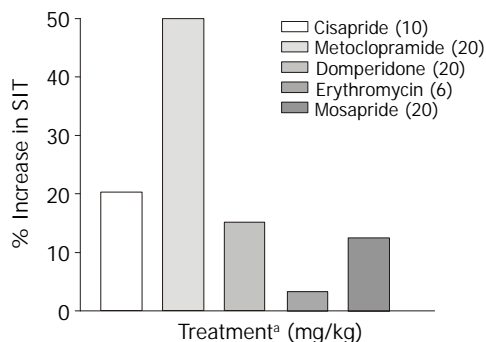


Figure 3 Effect of various prokinetic agents on small intestinal transit in mice. (^aProkinetic agents were administered orally 45 minutes prior to test meal).

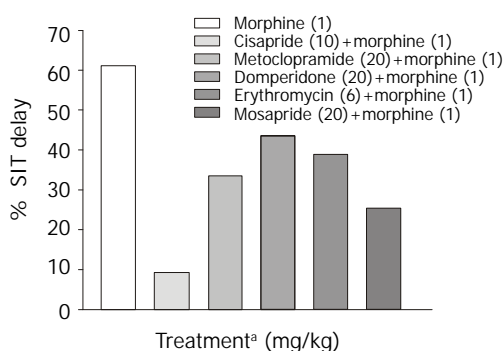


Figure 4 Effect of Prokinetic agents on morphine induced delay of small intestinal transit in mice. (^aProkinetic agents were administered orally 45 minutes and morphine s.c.15 minutes prior to test meal).

DISCUSSION

Opioids cause decrease in gastric emptying and intestinal motility, which leads to nausea, abdominal bloating and constipation^[21]. Both exogenous and endogenous opioids inhibit propulsive movements of the intestine by interfering with the enteric regulation of propulsive motility^[22]. They interact with μ and δ opioid receptors and cause decrease in cyclic AMP. Opioids increase the calcium dependent potassium conductance and thus, hyperpolarize myentric neurons, which reduce the entry of calcium during the action potential leading to decrease in intracellular calcium and thereby decreasing peristalsis^[23].

In mice μ agonists administered subcutaneously produced dose-related inhibitions of gastrointestinal transit^[24]. In our study there was significant decrease (61 %) in SIT with morphine (1 mg/kg s.c.) compared with control animals ($P < 0.001$). Decrease in SIT seen with 1 mg/kg (s.c) of morphine is in agreement with earlier reports^[14,16,17].

Prokinetic agents used to reverse morphine induced delay in GI transit showed variation in their efficacy. Cisapride (10 mg/kg, p.o.) though, did not show significant increase in SIT compared with control, it was most effective in reversing morphine induced delay in SIT (Figure 4). This finding is consistent with a clinical study where the effect of cisapride

was significantly greater than that of metoclopramide^[16]. Cisapride in the dose of 10 mg/kg (p.o.) showed significant increase in gastric emptying when compared with control animals but in morphine induced delay in gastric emptying it fails to show significant effect in overcoming the inhibition (Table 2).

Rectal administration of cisapride 30 mg 8th hourly had modest benefit in reversing small intestinal transit following intravenous meperidine in patients undergoing major abdominal surgery^[25]. This may reflect an inability of cisapride to attain effective plasma concentrations when given rectally and this is supported by another report where rectal cisapride was not able to overcome gastric stasis produced by morphine^[26]. Above observations indicate that in morphine treated mice, cisapride is more effective in reversing morphine induced delay in SIT rather than delay in gastric emptying.

Similar differential effect of metoclopramide and cisapride on the abdominal surgery induced decrease in transit was seen in which metoclopramide further inhibited whereas cisapride ameliorated the inhibition of transit^[27].

In our study metoclopramide (20 mg/kg p.o.) was found to be the most effective prokinetic agent when compared to control animals (Figure 3). Metoclopramide is a 5-HT₄ agonist, 5-HT₃ antagonist and antagonises the inhibitory effect of dopamine in the gastrointestinal tract. Despite above actions, it was only marginally effective in reversing morphine induced delay in SIT (Figure 2).

Metoclopramide in the dose of 20 mg/kg p.o. significantly increased gastric emptying when compared with controls (Table 1). In morphine induced gastric emptying delay, it reversed the morphine effect completely (Figure 2). In a clinical study conducted by McNeill *et al.*, it was shown that i.v. metoclopramide antagonised the opioid premedication induced delay in gastric emptying but not i.m. metoclopramide^[28]. There is also evidence that the effectiveness of metoclopramide may depend on the route of administration^[29,30].

Domperidone is a peripherally acting dopamine antagonist. Domperidone (20 mg/kg, p.o.) alone did not show any significant prokinetic effect as against control animals (Table 2). In our study, it was seen that in reversing morphine induced delay, though it could not significantly increase SIT, its efficacy was similar to that of metoclopramide (Figure 4). Since there is a risk of extrapyramidal effects with metoclopramide, domperidone may be useful in opioid induced delay in gastrointestinal transit where metoclopramide is contraindicated. Domperidone in the dose of 20 mg/kg p.o. did not show any significant increase in gastric emptying in normal and morphine treated animals (Table 1 and Table 2).

Erythromycin, a motilinomimetic in the dose of 6 mg/kg (p.o.) did not show any significant prokinetic effect (Table 1) and had the least efficacy in reversing morphine induced delay in gastrointestinal transit (Table 2). Erythromycin in the dose of 1 mg/kg did not show any effect in postoperative ileus^[27]. Erythromycin even at 40 mg/kg did not show any prokinetic effect in rats though motilin immunoreactivity has been demonstrated in the rat intestine^[31]. The motilin receptor status of mouse upper GI tract is not documented. De Winter *et al.* suggested by their experiments that rat might not be the ideal species to test erythromycin^[27]. The fact that erythromycin was not effective in our study indicates that mice too may not be the ideal species for these type of studies.

Mosapride, a derivative of cisapride so far was not tested in morphine-induced delay in small intestinal transit. In our study though it did not show significant prokinetic effect in the dose (20 mg/kg p.o.) used, however it was less effective than 10 mg cisapride in reversing morphine induced delay in SIT. Efficacy of mosapride and metoclopramide in reversing morphine effect on GE cannot be differentiated from the available data.

A look at the SIT values (Table 1) indicates that metoclopramide has maximum efficacy in normal mice while cisapride is most efficacious in reversing morphine induced delay in SIT followed by metoclopramide and mosapride (Table 2). The above differences may be due to interactions taking place at various levels viz. the central and the peripheral nervous system. It is known that morphine suppresses the cholinergic outflow^[32], while metoclopramide enhance cholinergic outflow^[20] via 5-HT₄ and D₂ receptor interaction. It is also known that cisapride is non-selective 5-HT₄ receptor agonist with affinity for D₂, 5-HT₂, α_1 adrenergic and muscarinic receptors^[33]. Further, mosapride a 5-HT₄ agonist shows efficacy less than cisapride in reversing morphine effects on SIT and less than metoclopramide in GE. The intrinsic activity of mosapride was less than that observed for cisapride which indicates that it may act as a partial agonist^[34]. Role of heterogeneity in 5-HT₄ receptors in the differential effect of 5-HT₄ agonists cannot be ruled out^[35].

Mechanism underlying the stimulation of gastric and small intestinal motility by prokinetic agents is 5-HT₄ receptor activation that involve cholinergic nerves. However the mechanism underlying the different profile of the effect of 5-HT₄ agonists on gastric emptying and small intestinal transit remains unexplained.

Gastric emptying in normal mice was enhanced by cisapride, metoclopramide and mosapride (Figure 1) but in morphine treated mice metoclopramide was most effective followed by mosapride (Figure 2). This suggests that in morphine treated mice, 5-HT₄ pathways may not play a major role. Effect of cisapride and metoclopramide on other receptors contributes predominantly in reversing the effect of morphine on SIT and gastric emptying respectively.

Results of this study and earlier reports indicate that efficacy of prokinetic agents is dependent on factors such as pathophysiology, species, site of gastrointestinal tract and pharmacological profile of the drug.

CONCLUSIONS

Morphine in the dose of 1 mg/kg (s.c.) inhibited the small intestinal transit by 61 % and to a lesser extent, gastric emptying (43 %) under the experimental conditions. Metoclopramide has significant prokinetic effect when compared with cisapride, domperidone, mosapride and erythromycin in normal mice. Metoclopramide, cisapride and mosapride enhance gastric emptying significantly compared to domperidone and erythromycin in normal mice. All the prokinetic agents used in our study differ in their prokinetic effects in counteracting the effect of morphine induced GI inertia. Cisapride is most effective in reversing morphine induced SIT delay followed by metoclopramide and mosapride. In morphine-induced GE delay metoclopramide is most effective followed by mosapride.

REFERENCES

- Barnett M.** Alternative opioids to morphine in palliative care: a review of current practice and evidence. *Postgrad Med J* 2001; **77**: 371-378
- Moulin DE, Iezz A, Amireh R, Sharpe WK, Boyd D, Merskey H.** Randomised trial of oral morphine for chronic non-cancer pain. *Lancet* 1996; **347**: 143-147
- McQuay H.** Opioids in pain management. *Lancet* 1999; **353**: 2229-2232
- Murphy DB, Sutton JA, Prescott LF, Murphy MB.** Opioid-induced delay in gastric emptying: a peripheral mechanism in humans. *Anesthesiology* 1997; **87**: 765-770
- McCallum RW.** Review of the current status of prokinetic agents in gastroenterology. *Am J Gastroenterol* 1985; **80**: 1008-1016
- De Luca A, Coupar IM.** Insights into opioid action in the intes-

- nal tract. Pharmacol Ther 1996; **69**: 103-115**
- Meissner W, Schmidt U, Hartmann M, Kath R, Reinhart K.** Oral naloxone reverses opioid-associated constipation. *Pain* 2000; **84**: 105-109
- Cheskin LJ, Chami TN, Johnson RE, Jaffe JH.** Assessment of nalmefene glucuronide as a selective gut opioid antagonist. *Drug Alcohol Depend* 1995; **39**: 151-154
- Culpepper-Morgan JA, Inturrisi CE, Portenoy RK, Foley K, Houde RW, Marsh F, Kreek MJ.** Treatment of opioid-induced constipation with oral naloxone: a pilot study. *Clin Pharmacol Ther* 1992; **52**: 90-95
- Yuan CS, Foss JF, O' Connor M, Toledano A, Roizen MF, Moss J.** Methylnaltrexone prevents morphine-induced delay in oral-cecal transit time without affecting analgesia: a double-blind randomized placebo-controlled trial. *Clin Pharmacol Ther* 1996; **59**: 469-475
- Schmidt WK.** Alvimopan* (ADL 8-2698) is a novel peripheral opioid antagonist. *Am J Surg* 2001; **182**(5A Suppl): 27S-38S
- Barquist E, Bonaz B, Martinez V, Rivier J, Zinner MJ, Tache Y.** Neuronal pathways involved in abdominal surgery-induced gastric ileus in rats. *Am J Physiol* 1996; **270**(4 Pt 2): R888-R894
- Matsuda H, Li Y, Yamahara J, Yoshikawa M.** Inhibition of gastric emptying by triterpene saponin, momordin, in mice: roles of blood glucose, capsaicin-sensitive sensory nerves, and central nervous system. *J Pharmacol Exp Ther* 1999; **289**: 729-734
- Fickel J, Bagnol D, Watson SJ, Akil H.** Opioid receptor expression in the rat gastrointestinal tract: a quantitative study with comparison to the brain. *Brain Res Mol Brain Res* 1997; **46**: 1-8
- Rowbotham DJ, Nimmo WS.** Effect of cisapride on morphine-induced delay in gastric emptying. *Br J Anaesth* 1987; **59**: 536-539
- Bianchi G, Ferretti P, Recchia M, Rocchetti M, Tavani A, Manara L.** Morphine tissue levels and reduction of gastrointestinal transit in rats. Correlation supports primary action site in the gut. *Gastroenterology* 1983; **85**: 852-858
- Patil CK, Kulkarni SK.** Effect of physostigmine and cisapride on morphine-induced delayed gastric transit in mice. *Ind J Pharmacol* 2000; **32**: 321-323
- Brogden RN, Carmine AA, Heel RC, Speight TM, Avery GS.** Domperidone. A review of its pharmacological activity, pharmacokinetics and therapeutic efficacy in the symptomatic treatment of chronic dyspepsia and as an antiemetic. *Drugs* 1982; **24**: 360-400
- Pandolfino JE, Howden CW, Kahrilas PJ.** Motility-modifying agents and management of disorders of gastrointestinal motility. *Gastroenterology* 2000; **118**: S32-S47
- Harrington RA, Hamilton CW, Brogden RN, Linkewich JA, Romankiewicz JA, Heel RC.** Metoclopramide. An updated review of its pharmacological properties and clinical use. *Drugs* 1983; **25**: 451-494
- Murphy DB, Sutton JA, Prescott LF, Murphy MB.** Opioid-induced delay in gastric emptying: a peripheral mechanism in humans. *Anesthesiology* 1997; **87**: 765-770
- Wong CL.** Central and peripheral inhibitory effects of morphine on intestinal transit in mice. *Exp Clin Pharmacol* 1986; **8**: 479-483
- Pasricha PJ.** Prokinetic agents, antiemetics and agents used in irritable bowel syndrome. In Hardman JG, Limbard LE, eds *The pharmacological basis of therapeutics*. McGraw-Hill, New York, 2001: 1021-1036
- Pol O, Ferrer I, Puig MM.** Diarrhea associated with intestinal inflammation increases the potency of mu and delta opioids on the inhibition of gastrointestinal transit in mice. *J Pharmacol Exp Ther* 1994; **270**: 386-391
- Benson MJ, Roberts JP, Wingate DL, Rogers J, Deeks JJ, Castillo FD, Williams NS.** Small bowel motility following major intra-abdominal surgery: the effects of opiates and rectal cisapride. *Gastroenterology* 1994; **106**: 924-936
- Kluger MT, Plummer JL, Owen H.** The influence of rectal cisapride on morphine-induced gastric stasis. *Anaesth Intensive Care* 1991; **19**: 346-350
- De Winter BY, Boeckxstaens GE, De Man JG, Moreels TG, Schuurkes JA, Peeters TL, Herman AG, Pelckmans PA.** Effect of different prokinetic agents and a novel enterokinetic agent on postoperative ileus in rats. *Gut* 1999; **45**: 713-718

- 28 **McNeill MJ**, Ho ET, Kenny GN. Effect of i.v. metoclopramide on gastric emptying after opioid premedication. *Br J Anaesth* 1990; **64**: 450-452
- 29 **Bateman DN**, Kahn C, Davies DS. Concentration effect studies with oral metoclopramide. *Br J Clin Pharmacol* 1979; **8**: 179-182
- 30 **Bateman DN**, Kahn C, Mashiter K, Davies DS. Pharmacokinetic and concentration-effect studies with intravenous metoclopramide. *Br J Clin Pharmacol* 1978; **6**: 401-407
- 31 **Trudel L**, Tomasetto C, Rio MC, Bouin M, Plourde V, Eberling P, Poitras P. Ghrelin/motilin-related peptide is a potent prokinetic to reverse gastric postoperative ileus in rat. *Am J Physiol Gastrointest Liver Physiol* 2002; **282**: G948-G952
- 32 **Cherubini E**, Morita K, North RA. Opioid inhibition of synaptic transmission in the guinea-pig myenteric plexus. *Br J Pharmacol* 1985; **85**: 805-817
- 33 **Briejer MR**, Akkermans LM, Schuurkes JA. Gastrointestinal prokinetic benzamides: the pharmacology underlying stimulation of motility. *Pharmacol Rev* 1995; **47**: 631-651
- 34 **Yoshida N**. Pharmacological effects of the gastroprokinetic agent mosapride citrate. *Nippon Yakurigaku Zasshi* 1999; **113**: 299-307
- 35 **Mine Y**, Yoshikawa T, Oku S, Nagai R, Yoshida N, Hosoki K. Comparison of effect of mosapride citrate and existing 5-HT₄ receptor agonists on gastrointestinal motility *in vivo* and *in vitro*. *J Pharmacol Exp Ther* 1997; **283**: 1000-1008

Edited by Ma JY and Xu XQ

Effect of transforming growth factor beta and bone morphogenetic proteins on rat hepatic stellate cell proliferation and trans-differentiation

Hong Shen, Guo-Jiang Huang, Yue-Wen Gong

Hong Shen, Guo-Jiang Huang, Yue-Wen Gong, Departments of Internal Medicine, Biochemistry and Medical Genetics, Faculty of Medicine, University of Manitoba, Winnipeg, Manitoba, Canada

Correspondence to: Dr. Yue-Wen Gong, John Buhler Research Centre, 803G - 715 McDermot Avenue, Winnipeg, Manitoba, Canada, R3E 3P4. ygong@ms.umanitoba.ca

Telephone: +1-204-7893567 **Fax:** +1-204-7893987

Received: 2002-10-04 **Accepted:** 2002-11-04

Abstract

AIM: To explore different roles of transforming growth factor beta (TGF- β) and bone morphogenetic proteins (BMPs) in hepatic stellate cell proliferation and trans-differentiation.

METHODS: Hepatic stellate cells were isolated from male Sprague-Dawley rats. Sub-cultured hepatic stellate cells were employed for cell proliferation assay with WST-1 reagent and Western blot analysis with antibody against smooth muscle alpha actin (SMA).

RESULTS: The results indicated that TGF- β 1 significantly inhibited cell proliferation at concentration as low as 0.1 ng/ml, but both BMP-2 and BMP-4 did not affect cell proliferation at concentration as high as 10 ng/ml. The effect on hepatic stellate cell trans-differentiation was similar between TGF- β 1 and BMPs. However, BMPs was more potent at trans-differentiation of hepatic stellate cells than TGF- β 1. In addition, we observed that TGF- β 1 transiently reduced the abundance of SMA in hepatic stellate cells.

CONCLUSION: TGF- β may be more important in regulation of hepatic stellate cell proliferation while BMPs may be the major cytokines regulating hepatic stellate cell trans-differentiation.

Shen H, Huang GJ, Gong YW. Effect of transforming growth factor beta and bone morphogenetic proteins on rat hepatic stellate cell proliferation and trans-differentiation. *World J Gastroenterol* 2003; 9(4): 784-787

<http://www.wjgnet.com/1007-9327/9/784.htm>

INTRODUCTION

Transforming growth factor beta (TGF- β) and bone morphogenetic proteins (BMPs) are the members of TGF- β superfamily^[7, 23]. Their biological effects are mediated through the receptors that have serine-threonine kinase activity^[1, 24]. However, they bind to their respective receptors. Moreover, the molecules involved in their signal transduction are different. It is generally considered that signal transduction pathway of BMPs is mediated by Smads 1, 5, and 8, while the signaling molecules of TGF- β are Smads 2 and Smads 3^[17, 29, 33]. The role of TGF- β in hepatic fibrogenesis has been investigated

because of the effect of TGF- β on extracellular matrix (ECM) production and degradation^[3, 27, 32]. But the effects of BMP on hepatic fibrogenesis have not been studied extensively. With recent understanding of hepatic fibrogenesis, hepatic stellate cells play an important role in the development of hepatic fibrosis^[8, 14]. It is documented that hepatic stellate cells are the main cell type that synthesize and secrete ECM in the liver. In addition, hepatic stellate cells migrate, proliferate and contract in response to liver injury, which contribute to the development of scar formation and portal hypertension. The effects of TGF- β 1 on hepatic stellate cell proliferation and activation have been documented with some studies showing the inhibitory effect of TGF- β 1^[2, 6, 25, 26] while others exhibited no effect on hepatic stellate cell proliferation^[20, 28]. However, there are no reports about the effects of BMPs on hepatic stellate cell proliferation and trans-differentiation. Therefore, the objective of this study is to examine the effects of TGF- β 1 and BMPs on rat hepatic stellate cell proliferation and expression of smooth muscle alpha actin (SMA) - a marker of hepatic stellate cell trans-differentiation.

MATERIALS AND METHODS

Materials

Collagenase D, pronase, DNase 1, cell proliferation reagent WST-1, and monoclonal antibody against smooth muscle alpha actin were purchased from Roche Diagnostics (Laval Quebec). Rabbit antibody against mouse IgG conjugated to horseradish peroxidase, and Enhanced Chemiluminescence Detection Kit were from Amersham Pharmacia Biotech, Inc. (Baie d'Urfe, Quebec). Dulbecco's Modified Eagle Medium (DMEM), fetal bovine serum (FBS) and Nycodenz were obtained from GIBCO/BRL (Burlington, Ontario). TGF- β 1, BMP-2 and BMP-4 were purchased from R&D systems (Minneapolis, MN).

Isolation of rat hepatic stellate cells

Male Sprague-Dawley rats (450-550 gram body weight) were purchased from Central Animal Care of the University of Manitoba and maintained under 12-hour light/dark cycles with food and water ad libitum. In conducting the research described in this report, all animals received humane care in compliance with the Institution's guidelines (Animal Protocol No. 98-053), which is in accordance with the Canadian Council on Animal Care's criteria. Hepatic stellate cells were isolated from rat liver by two steps of collagenase and pronase methods as previously described^[10]. The liver was perfused via the portal vein first with Ca²⁺ free Hanks' balanced salt solution (HBSS), pH 7.4, for 10 minutes at 37 °C and then with Ca²⁺ HBSS containing 0.125 mg/ml collagenase D, 0.5 mg/ml pronase and 15 μ g/ml DNase 1 for 20 minutes. After being dispersed gently, the cells were incubated with 0.125 mg/ml collagenase D, 0.5 mg/ml pronase and 15 μ g/ml DNase 1 for another 12 minutes with constant low speed stirring at 37 °C. Cell suspension was filtered through a 100 μ m mesh. After removing hepatocytes

by centrifugation at 500 rpm on a bench-top centrifuge, Hepatic stellate cells were separated from other non-parenchymal cells by density gradient centrifugation on 11.3 % Nycodenz with sodium chloride at 1 400 g for 17 minutes at 8 °C. Hepatic stellate cells were harvested from the interface between suspension buffer on the top and 11.3 % Nycodenz solution, washed and plated on uncoated plastic tissue culture dishes (Costar) at a density of 25 000 cells/cm². Hepatic stellate cells were identified by the typical star-like configuration under light microscopic appearance. The purity was always higher than 95 %. Hepatic stellate cells were incubated in DMEM supplemented with 10 % FBS, antibiotics (100 IU/ml penicillin and 100 mg/ml streptomycin) and 2 mM L-glutamine at 37 °C in a humidified atmosphere of 5 % CO₂. The first change of culture medium was made 24 hours after seeding and then change the medium every 48 hours. Sub-cultured Hepatic stellate cells were obtained from 9-day-old primary culture hepatic stellate cells by detaching from the dishes with trypsin-EDTA.

Cell proliferation assay

Cell proliferation was measured by cell proliferation reagents WST-1^[12]. Sub-cultured hepatic stellate cells (2×10³) in 200 μ l culture medium were seeded into 96 well plates. After incubation for 24 hours, the medium was changed with 100 μ l of fresh culture medium containing different concentrations of recombinant TGF- β 1, BMP-2 and BMP-4. The media and reagents were changed every other day. Cell proliferation was documented after 3, 6, 9 days of treatment. At the end of treatment, 10 μ l of WST-1 reagent were added into wells and incubated for 2 hours. The absorbance of the treated samples against a blank control was measured using a THERMOMax microplate reader (ELISA) (molecular Devices Co., Menlo Park, CA) with 420nm as detection wavelength and 650nm as reference wavelength for WST-1 assay.

Western blot analyses of SMA

Sub-cultured hepatic stellate cells were lysed in 100 μ l protein extract solution (1 mM Tris-HCl pH7.5, 1 mM EDTA pH 8.0, 10 mM NaCl, 1 % sodium dodecyl sulfate (SDS), 1 mM PMSF and 0.25 M sucrose)^[11]. Cell membrane was broken by sonicating the cells for 1 minutes with Sonicator (Vibra Cell, Sonics and Material Inc. Danbury, CT) and cell debris was pelleted by centrifugation at 14 000 rpm at 4 °C for 5 minutes. Protein concentration was determined by Lowry method^[9]. 20 g of protein from each sample was mixed with gel loading buffer (2×: 125 mM Tris-HCl, pH6.8, 4 % SDS, 20 % glycerol, 0.1 % bromophenol blue and 2.5 % β -mercaptoethanol), boiled for 5 minutes, separated on 12 % SDS-polyacrylamide gel under reducing conditions, and transferred to Nitroplus-2000 membrane (Micron Separations Inc. Westborough, MA). Nonspecific antibody binding was blocked by pre-incubation of the membranes in 1×Tris-buffered-saline (TBS) containing 5 % skim milk for 1 hour at room temperature. Membranes were then incubated overnight at 4 °C with primary antibody against SMA at dilution of 1:1 000 in 1×TBS containing 2 % skim milk. After washing, they were incubated for 1 hour at room temperature with sheep anti-mouse IgG at 1:1 000 dilutions. Bands were visualized by employing the enhanced chemiluminescence kit per the manufacturer's instruction.

Statistical analyses

Statistical significance of differences was performed by employing the ANOVA and Fisher's PLSD test as Post hoc test with StatView software (version 5.0, SAS Institute Inc. Cary, NC). Differences were considered to be significant when *P* was less than 0.05.

RESULTS

Effect of TGF- β 1, BMP2 and BMP4 on rat hepatic stellate cell proliferation

Effect of TGF- β 1, BMP2 and BMP4 on rat hepatic stellate cell proliferation was shown in Figure 1. TGF- β 1 significantly inhibited hepatic stellate cell proliferation after 6 days of incubation at the concentrations of 0.1, 0.5 and 1 ng/ml, respectively, *P*<0.05 (Figure 1A). The inhibition was more dramatic at 9-days treatment of TGF- β 1, *P*<0.01. However, both BMP2 and BMP4 did not affect hepatic stellate cell proliferation at the concentration as high as 10 ng/ml (Figure 1B and 1C).

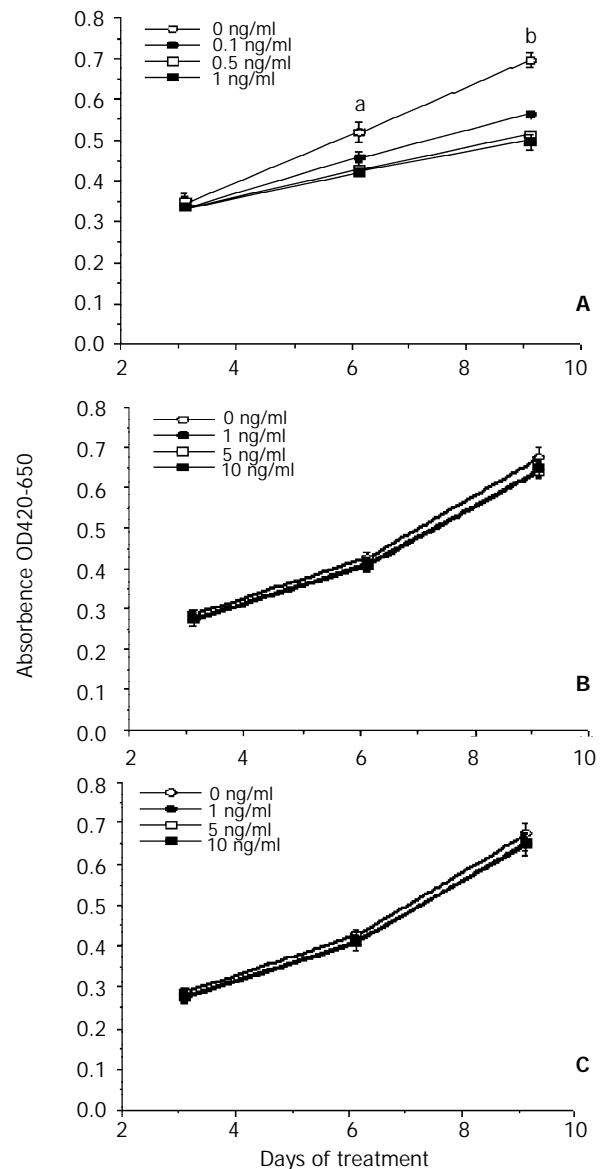


Figure 1 Regulating effect of TGF- β 1, BMP-2 and BMP-4 on the proliferation of rat hepatic stellate cells. Hepatic stellate cells were incubated with TGF- β 1 (A), BMP-2 (B) and BMP-4 (C) as described in Materials and methods. The data represent mean \pm SE from ten wells. The experiments were repeated two times. Denotes: a represents ^a*P*<0.05 vs the concentrations of 0.1, 0.5 and 1 ng/ml, b means ^b*P*<0.01 vs the concentrations of 0.1, 0.5 and 1 ng/ml.

Effect of TGF- β 1, BMP-2 and BMP-4 on SMA expression

TGF- β 1, BMP-2 and BMP-4 increased the expression of SMA, which is well recognized by the antibody as a 42-kDa protein. BMP-2 and BMP-4 seemed to have more potent effect on the expression of SMA than TGF- β 1. After incubation with TGF-

$\beta 1$ (concentrations from 0.1 to 1 ng/ml) for 3 days, SMA level was only elevated about 50 % as compared with control group (Figure 2). While after BMP-2 or BMP-4 treatment, SMA level was two to four times higher than that of the untreated group (Figure 3). Moreover, we observed that the abundance of SMA in hepatic stellate cells was reduced after 3 hours of TGF- $\beta 1$ treatment. The abundance of SMA was reduced to about 20 % of original level and the level of SMA was elevated (about 60 % higher than original level) after 18 hours' treatment (Figure 4).

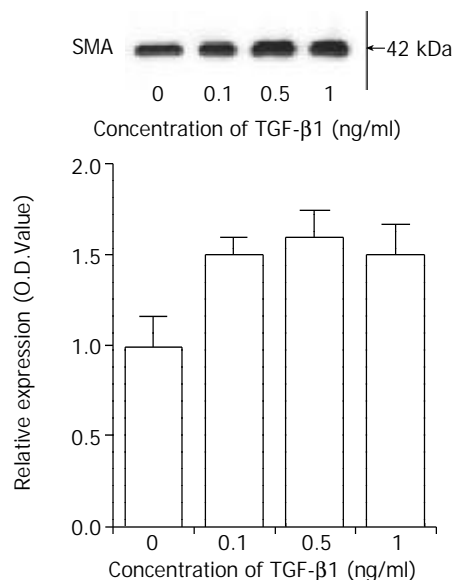


Figure 2 Regulating effect of TGF- $\beta 1$ on rat hepatic stellate cell trans-differentiation. Hepatic stellate cells were incubated with different concentrations of TGF- $\beta 1$ for three days. The media and TGF- $\beta 1$ were changed every other day. Western blot was performed as described in Materials and methods. The top panel represents typical Western blot of SMA. The lower panel represents histogram of densitometric data from four-separated Western blot (mean \pm SE).

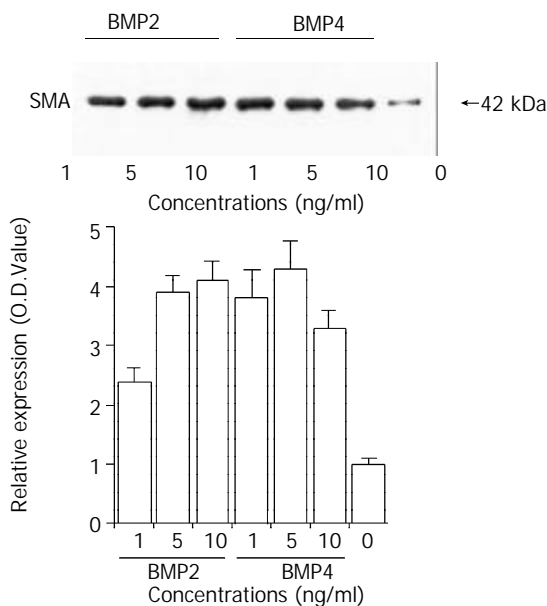


Figure 3 Regulating effect of BMP-2 and BMP-4 on hepatic stellate cell trans-differentiation. Hepatic stellate cells were incubated with different concentrations of BMP-2 or BMP-4 for three days. The media and BMPs were changed every other day. Western blot was performed as described in Materials and methods. The top panel represents typical Western blot of SMA. The lower panel represents histogram of densitometric data from four-separated Western blot (mean \pm SE).

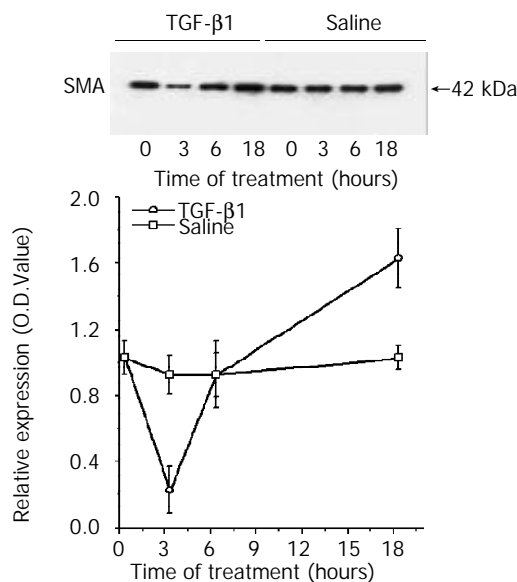


Figure 4 Regulating effect of TGF- $\beta 1$ on SMA protein expression. Hepatic stellate cells were cultured for three days and the media were removed. Media with 1 ng/ml TGF- $\beta 1$ or saline were added into culture dishes and cells were collected at different times as indicated. The data represent mean \pm SE from four experiments.

DISCUSSION

Hepatic stellate cells are non-parenchymal liver cells located at the perisinusoidal space. Recent studies have demonstrated that these cells proliferate and activate in response to liver injury. It is now established that hepatic stellate cells are the cell type involved in hepatic fibrogenesis^[4,5]. It is known that the proliferation of these cells is one response during hepatic fibrogenetic process. The other feature of these cells is their trans-differentiation, which is indicated by increased expression of SMA^[19]. During the trans-differentiation process of hepatic stellate cells, these cells are trans-differentiated into myofibroblast-like phenotype. To understand hepatic fibrogenesis, it is important to know the mechanism of proliferation and trans-differentiation of hepatic stellate cells. In this report, we employed TGF- $\beta 1$ and BMPs to examine their effects on hepatic stellate cell proliferation and trans-differentiation. Our study indicated that both TGF- $\beta 1$ and BMPs were important in the trans-differentiation of hepatic stellate cells. However, BMP-2 and BMP-4 had more potent effect on trans-differentiation of these cells than TGF- $\beta 1$ did. The difference can be due to the different signaling proteins involved in TGF- $\beta 1$ and BMPs signal transduction. It is known that Smads are the intracellular molecules for both TGF- β and BMP signal transduction pathways^[17, 29, 33]. However, Smad-2 and Smad-3 are believed to mediate TGF- β signal transduction while Smad-1, Smad-5 and Smad-8 mediate BMP signaling^[13, 16, 18, 21]. It has been demonstrated that Smad-3 is not necessary to the trans-differentiation of hepatic stellate cells but is required for TGF- $\beta 1$ mediated cell proliferation^[31]. Although TGF- $\beta 1$ had some effect on the trans-differentiation of hepatic stellate cells in this study, it might not be related to Smad-2 and Smad-3. It has been documented that TGF- $\beta 1$ can phosphorylate Smad-1 in human breast cancer cells^[22]. However, it still remained to be tested what is the mechanism mediating the transient reduction of SMA by TGF- $\beta 1$ in hepatic stellate cells. The direct TGF- $\beta 1$ regulation of SMA gene expression could not be excluded.

The inhibitory effect of TGF- $\beta 1$ on hepatic stellate cell proliferation was consistent with effect of TGF- $\beta 1$ on most mammalian cells. It inhibited the proliferation of hepatic stellate

cells. Studies relating the effect of TGF- β 1 on hepatic stellate cell proliferation from other groups have revealed some conflicting results. Most of the studies indicated that TGF- β 1 inhibited the proliferation of hepatic stellate cells^[2, 6, 25, 26, 28] while few studies had found no significant effect on these cell proliferation^[14, 20]. The difference of TGF- β 1 regulation of hepatic stellate cells may be related to stage of cell differentiation or the period of TGF- β 1 treatment. One of the interesting findings in this study is that both BMP-2 and BMP-4 did not affect the proliferation of hepatic stellate cells. It is well known that the main role of BMPs is bone morphogenesis, which is a sequential cascade with three key phases: chemotaxis and mitosis of mesenchymal cells, differentiation of the mesenchymal cells initially into cartilage, and replacement of the cartilage by bone. Its function is more related to differentiation than proliferation^[15, 30]. Therefore, no effect of BMPs on hepatic stellate cell proliferation is well consistent with their functions.

CONCLUSION

Our study documented that both TGF- β and BMPs play important roles in hepatic stellate cell proliferation and trans-differentiation. TGF- β is more important in the regulation of hepatic stellate cell proliferation while BMPs is more potent in the regulation of trans-differentiation of hepatic stellate cells. However, the *in vitro* observations of TGF- β and/or BMPs on hepatic stellate cell proliferation and trans-differentiation may represent one aspect of the complex interaction among varieties of factors in human body.

ACKNOWLEDGEMENTS

This work was supported by grants from Canadian Institute of Health Research and Manitoba Medical Service Foundation.

REFERENCES

- 1 **Atfi A**, Lepage K, Allard P, Chapdelaine A, Chevalier S. Activation of a serine/threonine kinase signaling pathway by transforming growth factor type beta. *Proc Natl Acad Sci USA* 1995; **92**: 12110-12114
- 2 **Bachem MG**, Riess U, Gressner AM. Liver fat storing cell proliferation is stimulated by epidermal growth factor/transforming growth factor alpha and inhibited by transforming growth factor beta. *Biochem Biophys Res Commun* 1989; **162**: 708-714
- 3 **Baricos WH**, Cortez SL, Deboisblanc M, Xin S. Transforming growth factor-beta is a potent inhibitor of extracellular matrix degradation by cultured human mesangial cells. *J Am Soc Nephrol* 1999; **10**: 790-795
- 4 **Brenner DA**, Waterboer T, Choi SK, Lindquist JN, Stefanovic B, Burchardt E, Yamauchi M, Gillan A, Rippe RA. New aspects of hepatic fibrosis. *J Hepatol* 2000; **32**: 32-38
- 5 **Davis BH**, Kresina TF. Hepatic fibrogenesis. *Clin Lab Med* 1996; **16**: 361-375
- 6 **Davis BH**, Rapp UR, Davidson NO. Retinoic acid and transforming growth factor beta differentially inhibits platelet-derived-growth-factor-induced Ito-cell activation. *Biochem J* 1991; **278**: 43-47
- 7 **Derynck R**, Chen RH, Ebner R, Filvaroff EH, Lawler S. An emerging complexity of receptors for transforming growth factor-beta. *Princess Takamatsu Symp* 1994; **24**: 264-275
- 8 **Friedman SL**. Hepatic stellate cells. *Prog Liver Dis* 1996; **14**: 101-130
- 9 **Fryer HJ**, Davis GE, Manthorpe M, Varon S. Lowry protein assay using an automatic microtiter plate spectrophotometer. *Anal Biochem* 1986; **153**: 262-266
- 10 **Gong W**, Roth S, Michel K, Gressner AM. Isoforms and splice variant of transforming growth factor beta-binding protein in rat hepatic stellate cells. *Gastroenterology* 1998; **114**: 352-363
- 11 **Gong Y**, Blok LJ, Perry JE, Lindzey JK, Tindall DJ. Calcium regulation of androgen receptor expression in the human prostate cancer cell line LNCaP. *Endocrinology* 1995; **136**: 2172-2178
- 12 **Gong Y**, Zhang M, Minuk GY. Regulation of transforming growth factor-beta1 gene expression and cell proliferation in human hepatocellular carcinoma cells (PLC/PRF/5) by tamoxifen. *J Lab Clin Med* 1999; **134**: 90-95
- 13 **Goumans MJ**, Mummery C. Functional analysis of the TGFbeta receptor/Smad pathway through gene ablation in mice. *Int J Dev Biol* 2000; **44**: 253-265
- 14 **Gressner AM**. Transdifferentiation of hepatic stellate cells (Ito cells) to myofibroblasts: a key event in hepatic fibrogenesis. *Kidney Int Suppl* 1996; **54**: S39-S45
- 15 **Hogan BL**. Bone morphogenetic proteins in development. *Curr Opin Genet Dev* 1996; **6**: 432-438
- 16 **Hullinger TG**, Pan Q, Viswanathan HL, Somerman MJ. TGFbeta and BMP-2 activation of the OPN promoter: roles of smad- and hox-binding elements. *Exp Cell Res* 2001; **262**: 69-74
- 17 **Itoh S**, Itoh F, Goumans MJ, Ten Dijke P. Signaling of transforming growth factor-beta family members through Smad proteins. *Eur J Biochem* 2000; **267**: 6954-6967
- 18 **Kawabata M**, Imamura T, Miyazono K. Signal transduction by bone morphogenetic proteins. *Cytokine Growth Factor Rev* 1998; **9**: 49-61
- 19 **Khan MA**, Poulos JE, Brunt EM, Li L, Solomon H, Britton RS, Bacon BR, Di Bisceglie AM. Hepatic alpha-smooth muscle actin expression in hepatitis C patients before and after interferon therapy. *Hepatology* 2001; **48**: 212-215
- 20 **Knittel T**, Janneck T, Muller L, Fellmer P, Ramadori G. Transforming growth factor beta 1-regulated gene expression of Ito cells. *Hepatology* 1996; **24**: 352-360
- 21 **Lagna G**, Hemmati-Brivanlou A. A molecular basis for Smad specificity. *Dev Dyn* 1999; **214**: 269-277
- 22 **Liu X**, Yue J, Frey RS, Zhu Q, Mulder KM. Transforming growth factor beta signaling through Smad1 in human breast cancer cells. *Cancer Res* 1998; **58**: 4752-4757
- 23 **Massague J**. The transforming growth factor-beta family. *Annu Rev Cell Biol* 1990; **6**: 597-641
- 24 **Massague J**, Weis-Garcia F. Serine/threonine kinase receptors: mediators of transforming growth factor beta family signals. *Cancer Surv* 1996; **27**: 41-64
- 25 **Matsuoka M**, Pham NT, Tsukamoto H. Differential effects of interleukin-1 alpha, tumor necrosis factor alpha, and transforming growth factor beta 1 on cell proliferation and collagen formation by cultured fat-storing cells. *Liver* 1989; **9**: 71-78
- 26 **Meyer DH**, Bachem MG, Gressner AM. Modulation of hepatic lipocyte proteoglycan synthesis and proliferation by Kupffer cell-derived transforming growth factors type beta 1 and type alpha. *Biochem Biophys Res Commun* 1990; **171**: 1122-1129
- 27 **Paulus W**, Baur I, Huettner C, Schmausser B, Roggendorf W, Schlingensiepen KH, Brysch W. Effects of transforming growth factor-beta 1 on collagen synthesis, integrin expression, adhesion and invasion of glioma cells. *J Neuropathol Exp Neurol* 1995; **54**: 236-244
- 28 **Pinzani M**, Gesualdo L, Sabbah GM, Abboud HE. Effects of platelet-derived growth factor and other polypeptide mitogens on DNA synthesis and growth of cultured rat liver fat-storing cells. *J Clin Invest* 1989; **84**: 1786-1793
- 29 **Schiffer M**, von Gersdorff G, Bitzer M, Susztak K, Bottinger EP. Smad proteins and transforming growth factor-beta signaling. *Kidney Int Suppl* 2000; **77**: S45-S52
- 30 **Schmitt JM**, Hwang K, Winn SR, Hollinger JO. Bone morphogenetic proteins: an update on basic biology and clinical relevance. *J Orthop Res* 1999; **17**: 269-278
- 31 **Schnabl B**, Kweon YO, Frederick JP, Wang XF, Rippe RA, Brenner DA. The role of Smad3 in mediating mouse hepatic stellate cell activation. *Hepatology* 2001; **34**: 89-100
- 32 **Tipton DA**, Dabbous MK. Autocrine transforming growth factor beta stimulation of extracellular matrix production by fibroblasts from fibrotic human gingiva. *J Periodontol* 1998; **69**: 609-619
- 33 **Visser JA**, Themmen AP. Downstream factors in transforming growth factor-beta family signaling. *Mol Cell Endocrinol* 1998; **146**: 7-17

IL-11 up-regulates Tie-2 expression during the healing of gastric ulcers in rats

Chun-Yang Wen, Masahiro Ito, Hui Wang, Long-Dian Chen, Zhao-Min Xu, Mutsumi Matsuu, Kazuko Shichijo, Toshiyuki Nakayama, Masahiro Nakashima, Ichiro Sekine

Chun-Yang Wen, Mutsumi Matsuu, Kazuko Shichijo, Toshiyuki Nakayama, Ichiro Sekine, Department of Molecular Pathology, Atomic Bomb Disease Institute, Nagasaki University School of Medicine, Japan

Chun Yang Wen, Long-Dian Chen, Zhao-Min Xu, Department of Digestive Disease, Nanjing Gu-Lou Hospital, Medical School of Nanjing University, Nanjing 210008, Jiangsu Province, China

Masahiro Ito, Department of Pathology, National Nagasaki Medical Center, Japan

Hui Wang, Department of Infectious Disease, Rui Jin Hospital, Shanghai Second Medical University, Shanghai 200025, China

Masahiro Nakashima, Tissue and Histopathology Section Division of Scientific Data Registry, Atomic Bomb Disease Institute, Nagasaki University School of Medicine, Japan

Correspondence to: Chun-Yang Wen, M.D., Ph.D., Department of Molecular Pathology, Atomic Bomb Disease Institute, Nagasaki University School of Medicine, 1-12-4 Sakamoto, Nagasaki 852-8523, Japan. cywen518@net.nagasaki-u.ac.jp

Telephone: +81-95-849-7107 **Fax:** +81-95-849-7108

Received: 2002-11-29 **Accepted:** 2003-01-13

Abstract

AIM: To investigate Tie-2 expression during the repair of acetic acid-induced gastric ulcers in rats treated with recombinant human IL-11 (rhIL-11) and in untreated control animals.

METHODS: Gastric ulcers were induced in male Wistar rats by applying acetic acid to the fundus of the stomach. RhIL-11 (100 µg/kg twice daily, subcutaneously) was administered from two days before ulcer induction and continued for five days after the induction. Control rats received bovine serum albumin. Gastric specimens were collected at 3 and 5 days after the induction of ulcer for immunohistochemical observation, Western blotting, and reverse transcription polymerase chain reaction (RT-PCR).

RESULTS: Immunohistochemical and Western blot analysis demonstrated that Tie-2 expression was enhanced in the rhIL-11-treated rats compared with the control animals at both intervals.

CONCLUSION: These findings suggested that IL-11 could accelerate ulcer healing, in part, by up-regulating Tie-2 expression and promoting angiogenesis.

Wen CY, Ito M, Wang H, Chen LD, Xu ZM, Matsuu M, Shichijo K, Nakayama T, Nakashima M, Sekine I. IL-11 up-regulates Tie-2 expression during the healing of gastric ulcers in rats. *World J Gastroenterol* 2003; 9(4): 788-790
<http://www.wjgnet.com/1007-9327/9/788.htm>

INTRODUCTION

IL-11 is a kind of pleiotropic cytokine that stimulates stem cell proliferation and affects multiple types of cells^[1]. RhIL-

11 may be useful in accelerating the recovery of both hematopoietic cells and gastrointestinal mucosal cells after cytoablative therapies^[2]. RhIL-11 is in Phase II clinical trials for the treatment of thrombocytopenia that occurs secondary to chemotherapy^[3]. Gross and microscopic evidence suggested that rhIL-11 treatment could improve acute colitis caused by both chemically-induced damage and chronic inflammatory bowel disease^[4]. Bruce *et al*^[5] recently reported that short-term treatment with rhIL-11 was well tolerated in patients with active Crohn's disease. Our previous study demonstrated that rhIL-11 facilitates gastric ulcer healing in rats^[6].

Angiogenesis is critical to ulcer healing since it regulates nutrient and oxygen delivery to the injured site and, thus, controls the healing rate. Tie-2 (tek) is a member of the endothelial cell-specific receptor tyrosine kinase family^[7, 8], and is essential for the formation of the embryonic vasculature^[9]. Our recent study suggests that Tie-2 plays an important role in the angiogenesis associated with the healing of gastric ulcers^[10]. The present study examined the effect of IL-11 on Tie-2 expression in acetic acid-induced gastric ulcers by comparing with in the rhIL-11-treated and control rats.

MATERIALS AND METHODS

Materials

This study was approved by the Animal Care Committee of Nagasaki University. Male Wistar rats, purchased from Charles River Japan (Atsugi, Japan) at 7 weeks of age, were housed 3 or 4 per cage in an air-conditioned room (24 °C, 12 hr light cycle) at the Laboratory Animal Center of Nagasaki University. The animals were fed with laboratory chow (F2, Japan CLEA, Tokyo, Japan) and tap water ad libitum.

Induction of gastric ulcer

Gastric ulcers were induced by luminal application of a 40 % acetic acid solution as reported previously^[11]. Under ether anesthesia, the stomach was exposed via a midline incision and the anterior and posterior walls of the gastric fundus were clamped together with ring forceps (ID, 6 mm). The acetic acid solution was injected into the clamped portion through the forestomach using 21 gauge needles. After forty-five seconds, the acid solution was removed, the abdomen closed and the animals fed and housed as above.

Treatment

RhIL-11 (Genetics Institute, Andover, MA, USA), courtesy of Yamanouchi Pharmaceutical Co., Ltd. (Tokyo, Japan), was diluted in 0.1 % bovine serum albumin (BSA) and administered subcutaneously (100 µg/kg/twice daily) for seven consecutive days beginning two days before ulcer induction as described previously ($n=16$)^[12]. Control animals ($n=16$) received the same volume of 0.1 % BSA twice daily. Eight rhIL-11-treated and eight untreated rats were sacrificed 3 and 5 days after the induction of gastric ulcers. Gastric tissues were collected for Western blot analysis, and reverse transcription polymerase chain reaction (RT-PCR). Tissues were fixed in 4 % paraformaldehyde solution for immunohistochemical examination of Tie-2 expression.

Immunohistochemistry analysis

Paraformaldehyde-fixed and paraffin-embedded tissues were cut into 4 μm sections, deparaffinized in xylene and rehydrated in phosphate-buffered saline. The tissues were subsequently preincubated in 3 % H_2O_2 for 30 minutes, followed by incubation in bovine serum to prevent nonspecific binding, and then incubated overnight at 4 $^\circ\text{C}$ (2 $\mu\text{g}/\text{ml}$) with rabbit anti-mouse Tie-2 (C-20, Santa Cruz Biotechnology, Inc., Santa Cruz, CA). The slides were subsequently incubated in biotinylated anti-rabbit immunoglobulin G followed by avidin-horseradish peroxidase and the reaction product was resolved using DAB (Vectastain ABC kit; Vector Laboratories, Burlingame, CA).

Western blot analysis

Fresh gastric tissues obtained from ulcerated areas were immediately frozen, suspended in RIPA buffer (50 mM Tris, 150 mM NaCl, 1 % NP-40, 1 % sodium deoxycholate and 0.05 % SDS, pH 7.4), broken into pieces on ice and subjected to three freeze-thaw cycles. Insoluble cell debris was removed by centrifugation at 14 000 $\times g$ at 0 $^\circ\text{C}$ for 10 minutes. The protein concentrations in the resultant supernates were quantified using a protein assay reagent (Bio-Rad Laboratories, Hercules, CA). Data from four rats were recorded at each time point and the assays were performed in duplicate. The proteins (30 μg) were separated by polyacrylamide gel electrophoresis (PAGE) under denaturing and reducing conditions, and transferred to a Hybond ECL Nitrocellulose Membrane (Amersham Life Science, Buckinghamshire, U.K.). The membranes were rinsed in TBS, blocked with 5 % low-fat dried milk in TBS containing 0.1 % Tween 20 (TTBS), and incubated for 2 hours at room temperature in a 1:500 dilution of mouse anti-rat Tie-2 antibodies. After extensive washing with TTBS, the membranes were incubated for 1 hour in TTBS with 1:2 000 dilution of horseradish-peroxidase-conjugated goat anti-mouse immunoglobulin G containing 3 % low-fat dried milk. The membranes were washed, developed with a horseradish peroxidase chemiluminescence detection reagent (ECL Plus System, Amersham, N.D.), and exposed to Hyperfilm ECL (Amersham).

RT-PCR analysis

Total RNA was prepared from gastric tissue using the acid guanidine phenol method. RNA (1 μg) was incubated at 37 $^\circ\text{C}$ for 1 hour in 50 μl reverse transcriptase buffer containing 20 units RNasin (Promega Corp., Madison, WI), 100 pmol of random hexamer primers (Boehringer Mannheim, Germany), and 400 units Moloney murine leukemic virus reverse transcriptase (GIBCO/BRL). Reverse transcription was terminated by heating to 95 $^\circ\text{C}$ for 10 minutes, and 20 % of the resulting cDNA was used for PCR. PCR samples were incubated with 50 pmol of each primer and 2.5 units of Taq DNA polymerase. The rat Tie-2 PCR primers were as followings: 5' -TGTTCTGTGCCACAGGCTG-3' (sense) and 5' -CACTGTCCCATCCGGCTTCA-3' (antisense). The human β -actin PCR primers were as followings: 5' -TCCTCCCTGGAGAAGAGCTA-3' (sense) and 5' -AGTACTTGCGCTCAGGAGGA-3' (antisense). The Tie-2 and β -actin primers were predicted to amplify 317 and 313 bp DNA products, respectively. Primer pairs were chosen to span introns of their respective rat genes. Samples were subjected to 40 cycles of PCR amplification, each cycle consisting of denaturation at 95 $^\circ\text{C}$ for 3 minutes, annealing at 50 $^\circ\text{C}$ for 1 minute, and primer extension at 72 $^\circ\text{C}$ for 1 minute. An aliquot of each amplification mixture was subjected to electrophoresis on 2 % agarose gel, and DNA was visualized by ethidium bromide staining.

RESULTS

Immunohistochemistry results

Immunohistochemical staining of Tie-2 was weakly positive in the endothelial cells of pre-existing vessels in the gastric wall. Tie-2 expression in the endothelial cells of new capillaries was enhanced in the rhIL-11-treated rats (Figure 1A) compared with the control rats (Figure 1B) after 3 and 5 days of the induction of ulcers.

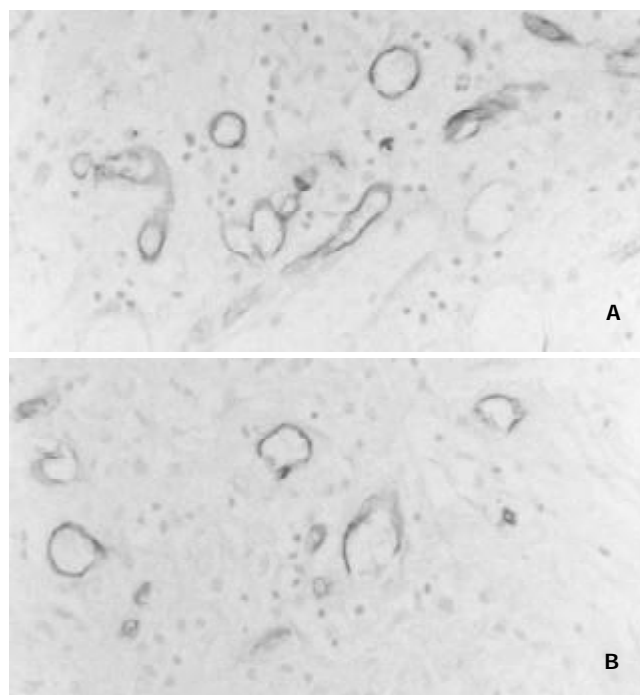


Figure 1 Three days after the induction of gastric ulcers, Tie-2 expression in the endothelial cells of new capillaries was enhanced in the rhIL-11-treated rats (A) in comparison to the untreated control animals (B).

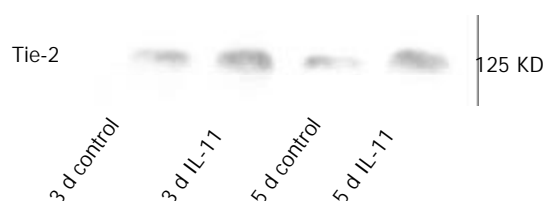


Figure 2 Western blots demonstrating Tie-2 expression. RhIL-11 treatment increased Tie-2 expression significantly 3 and 5 days after the induction of gastric ulcers compared with untreated control rats.

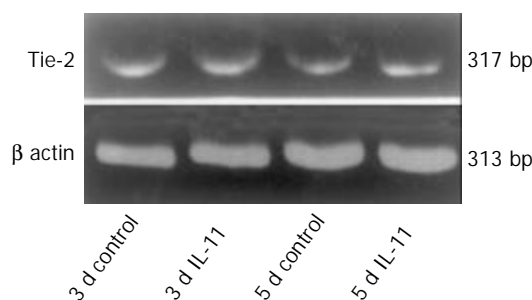


Figure 3 RT-PCR analysis of Tie-2 mRNA expression in ulcerative gastric tissues, using the specific primer pairs predicted to amplify Tie-2 (317 bp) and β -actin (313 bp). Lanes 1-4: rhIL-11-treated rats on days 3 (lane 2) and 5 (lane 4) and the untreated control rats on day 3 (lane 1) and 5 (lane 3).

Western blotting results

A major band of 125 KD representing Tie-2 protein was detected in the Western blots. Tie-2 expression was increased significantly after the appearance of ulcers in the rhIL-11-treated rats compared with the untreated control animals on day 3 and day5 (Figure2).

RT-PCR results

Tie-2 mRNA was detected between rhIL-11-treated rats and the control animals after 3 and 5 days of the induction of gastric ulceration. β -actin mRNA, a constitutively expressed transcript, was detected in all of the samples from both the rhIL-11 and untreated rats (Figure3).

DISCUSSION

Angiogenesis occurs in many physiological and pathological processes, including embryonic development, wound healing, and tumor growth^[13,14]. Ulcer healing consists of two processes, epithelial regeneration and mesenchymal reconstruction. The process of mesenchymal reconstruction consists of angiogenesis, fibrosis and smooth muscle regeneration. Therefore, angiogenesis is central to the formation of granulation tissue since newly formed vessels are required to supply oxygen and nutrients to the regenerating tissue. Tie-2 is a receptor tyrosine kinase expressed by endothelial cells^[15,16] and it has been reported to play an important role in embryonic angiogenesis^[17]. Furthermore, our own recent study revealed that Tie-2 was important in the angiogenesis that occurs during the healing of gastric ulcers^[10].

Our previous study was the first to demonstrate that IL-11 could promote gastric ulcer healing in rat model^[6]. This effect of IL-11 on the repair of mucosal injury most likely reflects its trophic action on mucosal epithelial and smooth muscle cells. RhIL-11 also exhibits an anti-apoptotic effect on the gastric mucosa. RhIL-11 most likely acts on epithelial cells via the regeneration of epithelial cell facilitated by IL-11 receptor. Concomitant smooth muscle hyperplasia may induce tissue contraction, thus promoting healing. The importance of smooth muscle contraction at the base of the ulcer has been previously demonstrated^[18]. Interestingly, IL-11 inhibits the production of nitric oxide, an agent that can relax smooth muscle cells^[19].

Our immunohistochemical and Western blot data showing that rhIL-11 enhanced Tie-2 expression suggest that IL-11 accelerates healing by promoting angiogenesis. The results of this study demonstrate that rhIL-11 up-regulates Tie-2 expression during the healing of gastric ulcer in rats and suggest that rhIL-11 may have clinical benefits in the treatment of gastric ulcers.

REFERENCES

- 1 **Du XX**, Williams DA. Interleukin-11: a multifunction growth factor derived from the hematopoietic microenvironment. *Blood* 1994; **83**: 2023-2030
- 2 **Gordon MS**, McCaskill-Stevens WJ, Battiatto LA, Loewy J, Loesch D, Breeden E, Hoffman R, Beach KJ, Kuca B, Kaye J, Sledge GW Jr. A phase I trial of recombinant human interleukin-11 (neumega rhIL-11 growth factor) in women with breast cancer receiving chemotherapy. *Blood* 1996; **87**: 3615-3624
- 3 **Gordon MS**. Thrombopoietic activity of recombinant human interleukin-11 in cancer patients receiving chemotherapy. *Cancer Chemother Pharmacol* 1996; **38**: S96-S98
- 4 **Keith JC Jr**, Albert L, Sonis ST, Pfeiffer CJ, Schaub RG. IL-11, a pleiotropic cytokine: Exciting new effects of IL-11 on gastrointestinal mucosal biology. *Stem Cells* 1994; **12**: 79-90
- 5 **Bruce ES**, Simmy B, Charles AS, Malcolm R, Seymour K, John WS, Philip BM Jr, Michael AS, Susan G, Stephen BH, Gary WV, Alan LB, Vance DR, Bruce S, Bin C, John L, Michael FD, Holly R, Mark S, Ullrich SS. Preliminary evaluation of safety and activity of recombinant human interleukin 11 in patients with active Crohn's disease. *Gastroenterology* 1999; **117**: 58-64
- 6 **Wen CY**, Ito M, Matsuo M, Fukuda E, Shichijo K, Nakashima M, Nakayama T, Sekine I. Mechanism of the antiulcerogenic effect of IL-11 on acetic acid-induced gastric ulcer in rats. *Life Sci* 2002; **70**: 2997-3005
- 7 **Schnurch H**, Risau W. Expression of tie-2, a member of a novel family of receptor tyrosine kinases, in the endothelial lineage. *Development* 1993; **119**: 957-968
- 8 **Maisonpierre PC**, Goldforb M, Yancopoulos GD, Gao G. Distinct rat genes with related profiles of expression define a TIE receptor tyrosine kinase family. *Oncogene* 1993; **8**: 1631-1637
- 9 **Sato TN**, Tozawa Y, Deutsch U, Wolburg-Buchholz K, Fujiwara Y, Gendron-Maguire M. Distinct roles of the receptor tyrosine kinases Tie-1 and Tie-2 in blood vessel formation. *Nature* 1995; **376**: 70-74
- 10 **Wen CY**, Ito M, Chen LD, Matsuo M, Shichijo K, Nakayama T, Nakashima M, Xu ZM, Ohtsuru A, Hsu CT, Sekine I. Expression of Tie-2 and Angiopoietin-1 and -2 in early phase of ulcer healing. *J Gastroenterol* 2003 (in press)
- 11 **Tsukimi Y**, Okabe S. Changes in gastric function and healing of chronic gastric ulcers in aged rats. *Jpn J Pharmacol* 1995; **68**: 103-110
- 12 **Potten CS**. Interleukin-11 protects the clonogenic stem cells in murine small-intestinal crypts from impairment of their reproductive capacity by radiation. *Int J Cancer* 1995; **62**: 356-361
- 13 **Millauer B**, Longhi MP, Plate KH, Shawver LK, Risau W, Ullrich A. Dominant-negative inhibition of Flk-1 suppresses the growth of many tumor types *in vivo*. *Cancer Res* 1996; **56**: 1615-1620
- 14 **Nakayama T**, Ito M, Ohtsuru A, Naito S, Nakashima M, Fagin JA, Yamashita S, Sekine I. Expression of the Ets-1 proto-oncogene in human gastric carcinoma. *Am J Pathol* 1996; **149**: 1931-1939
- 15 **Sato TN**, Qin Y, Kozak CA, Audus KL. Tie-1 and Tie-2 define another class of putative receptor tyrosine kinase genes expressed in early embryonic vascular system. *Proc Natl Acad Sci USA* 1993; **90**: 9355-9358
- 16 **Maisonpierre PC**, Goldfarb M, Yancopoulos GD, Gao G. Distinct rat genes with related profiles of expression define a TIE receptor tyrosine kinase family. *Oncogene* 1993; **8**: 1631-1637
- 17 **Korhonen J**, Polvi A, Partanen J, Alitalo K. The mouse tie receptor tyrosine kinase gene: expression during embryonic angiogenesis. *Oncogene* 1994; **12**: 395-403
- 18 **Tsukimi Y**, Okabe S. Acceleration of healing of gastric ulcers induced in rats by liquid diet: importance of tissue contraction. *Jpn J Pharmacol* 1994; **66**: 405-412
- 19 **Trepicchio WL**, Bozza M, Pedneault, Dorner AJ. Recombinant human IL-11 attenuates the inflammatory response through down-regulation of proinflammatory cytokine release and nitric oxide production. *J Immunol* 1996; **157**: 3627-3634

Changes of microvascular architecture, ultrastructure and permeability of rat jejunal villi at different ages

Yan-Min Chen, Jin-Sheng Zhang, Xiang-Lin Duan

Yan-Min Chen, Xiang-Lin Duan, Life Science College, Hebei Normal University, Shijiazhuang 050016, Hebei Province, China

Jin-Sheng Zhang, Department of Otolaryngology, Wayne State University School of Medicine, Detroit, Michigan 48201, USA

Supported by Natural Science Foundation of Hebei Province Educational Committee, No.2002136 and Natural Science Foundation of Hebei Province, No.303158

Correspondence to: Xiang-Lin Duan, Life Science College, Hebei Normal University, Shijiazhuang 050016, Hebei Province China. chyanmin@163.com

Telephone: +86-311-6049941 Ext 86480 **Fax:** +86-311-5828784
Received: 2002-11-26 **Accepted:** 2002-12-20

Abstract

AIM: To investigate the changes of microvascular architecture, ultrastructure and permeability of rat jejunal villi at different ages.

METHODS: Microvascular corrosion casting, scanning electron microscopy, transmission electron microscopy and Evans blue infiltration technique were used in this study.

RESULTS: The intestinal villous plexus of adult rats consisted of arterioles, capillary network and venules. The marginal capillary extended to the base part of the villi and connected to the capillary networks of adjacent villi. In newborn rats, the villous plexus was rather simple, and capillary network was not formed. The villous plexus became cone-shaped and was closely arrayed in ablation rats. In adult rats, the villous plexus became tongue-shaped and was enlarged both in height and width. In aged rats, the villous plexus shrank in volume and became shorter and narrower. The diametral ratio of villous arteriole to villous venule increased as animals became older. The number of endothelial holes, the thickness of basal membrane and the permeability of microvasculature were increased over the entire course of development from newborn period to aged period.

CONCLUSION: The digestive and absorptive functions of the rat jejunum at different ages are highly dependent upon the state of villous microvascular architecture and permeability, and blood circulation is enhanced by collateral branches such as marginal capillary, through which blood is drained to the capillary networks of adjacent villi.

Chen YM, Zhang JS, Duan XL. Changes of microvascular architecture, ultrastructure and permeability of rat jejunal villi at different ages. *World J Gastroenterol* 2003; 9(4): 795-799
<http://www.wjgnet.com/1007-9327/9/795.htm>

INTRODUCTION

The microvasculature of intestinal villi play an important role in the process of digestion, absorption and mucosal barrier protection^[1,2]. Intestinal diseases, such as diarrhea and enteritis, are reported to be related to the change of microvasculature^[3,4].

More recent studies on the intestinal microvasculature demonstrated that the damage to surface microvasculature is an early event inducing mucosal injury in the intestine^[5-7]. However, these studies were only limited in collecting pathological or clinical data, and tissue materials were obtained from adult subjects^[8-10]. In addition, little information is available regarding the changes of microvasculature throughout different age periods. Therefore, the current work was meant to elucidate the morphological and permeability changes of jejunal microvasculature at different ages. Microvascular corrosion casting technique, scanning electron microscopy (SEM), transmission electron microscopy (TEM), Evans blue infiltration methods were used and morphometry was conducted in this study.

MATERIALS AND METHODS

Animals

Fifty-four male Sprague-Dawley rats were used. They were divided into 4 groups according to their ages after birth: (1) newborn rats (1 day, $n=9$); (2) ablation rats (3 weeks, $n=15$); (3) adult rats (3 months, $n=15$) and (4) aged rats (24 months, $n=15$). For the groups with 15 animals, six were used for corrosion casting, three were observed under TEM, the other six were used to determine the permeability with Evans blue infiltration technique. The newborn rats were too small to be used in determining the permeability. All rats were fasting for 12 hours prior to each experiment.

Microvascular corrosion casting and SEM

Methyl-methacrylate and methacrylate were mixed at a ratio of 9:1. Polymerization was allowed by adding benzoyl-methacrylate at 80 °C. The viscosity of this solution was maintained to a level corresponding to that of 30 % glycerine. The solution was cooled for later use. The microvascular architecture was then performed in the following procedure. Animals were deeply anesthetized with ether and a catheter was inserted into the thoracic aorta. One percent of saline solution (500 ml/kg i.m.) was perfused to flush the blood out of cardiovascular system, and this step was immediately followed by a perfusion of 5 ml methyl-methacrylate. Meanwhile, the same volume of the pre-prepared solution mixed with N, N-dimethylaniline (1 % of the total volume) was added, serving as a polymerization accelerator. twelve hours later when polymerization was completed, the small intestine was sampled and stored in a 10 % NaOH solution for 1-2 weeks. The tissue was rinsed with tap water until the corroded tissue was washed out, and then trimmed under the dissection microscope and dried at 40 °C for 48 hours. The dried tissue was then coated using an IB-3 ionic splashing and shooting device. Photomicrographs were taken under a Hitachi S-570 scanning electron microscope.

TEM

Small pieces of the jejunum were immersed in phosphate-buffered 3 % glutaraldehyde for 2 hours, and then postfixed in phosphate-buffered 1 % OsO₄ for 2 hours. After postfixation, the tissue was dehydrated with ethanol and embedded in Epon

812. Ultra-thin sections stained with uranyl acetate and lead citrate were observed and photomicrographs were taken under a Hitachi TEM S-600.

Quantification of microvascular permeability of the jejunal tissue

Evans blue was used to measure the permeability of microvasculature. Rats were anesthetized with ether, and Evans blue (75 mg/kg i.m.) in 0.9 % saline solution was injected into a femoral vein. Two hours later, rats were perfused transcardially with 0.9 % saline solution (500 ml/kg i.m.). Evans blue was extracted from the jejunum by incubation in 5 ml of formamide at 54 °C for 24 hours. Evans blue was then quantified by measuring its absorption at wavelength of 620 nm using spectrometer. Results were expressed as μg Evans blue/gram fresh tissue.

Data processing

According to the methods of stereology^[11], the measurement and calculation of the thickness of basal membrane (nm), the number of endothelial hole (per mm capillary perimeter) and plasmalemmal vesicles (per mm² endothelium) were conducted on the photographs of TEM. Results were expressed as mean \pm SEM, and statistics was performed using Student's *t* test.

RESULTS

Microvascular architecture of adult rats villi

The villous plexi stood on the surface of the ileum. Between the adjacent villous plexi there were numerous different cryptal plexi. The villous plexus consisted of villous arteriole, villous capillary network and the villous venule. The villous capillaries connected to each other in a form of "net-basket" (Figure 1). The villous arteriole coming from the arterial plexus in the submucosa reached the base of the villi through the cryptal plexus gap, extending to the tip along the axis of the villi. The villous arterioles did not bifurcate within the villi, but formed the villous capillary network at the tips of the villi in the pattern of a "netted bag". This villous capillary wrapped the villous arteriole. The villous venules were formed in the middle and upper part of the villi, through which the blood from capillary venules converged into the venous plexus in the submucosa (Figure 1).

In addition, there was a straight capillary along the margin of the villous capillary network, and it is called marginal capillary. Its diameter was twice that of its adjacent capillaries (Figures 1 and 2). This capillary ran along the villous margin and did not merge into the villous venules of itself. It reached the base of the villi and connected to the basal part of its adjacent villous capillary networks (Figure 2).

Changes of microvascular architecture of jejunal villi at different ages

In newborn rats, the villous plexus was rather simple and was composed of only one or two loops of capillary vessels. A capillary network was not formed at this age and villous arteriole and venule could not be differentiated (Figure 3). For the ablation rats, the villous plexus became cone-shaped and was closely arrayed. The marginal capillary was as wide as villous arteriole. Each villous plexus had only one villous venule and was formed in the basal part of the villi. However, the diametral ratio of villous arteriole to it was very small (Figure 4). In adult rats, the villous plexus became tongue-shaped and was enlarged both in height and width. Each villous plexus usually had one villous venule which was formed in the middle and upper part of the villi, but the wide villi had two venules that were zygomorphous (Figure 1). In the aged rats, the villous plexus shrank in volume and became shorter and narrower. The capillaries were irregularly arrayed (Figure 5). The villous arteriole became wider and lower than villous venule (Figure 6). The diametral ratio of villous arteriole to venule was increased as animals became older (Table 1).

Changes of endothelial ultrastructure of villous capillary at different ages

Under TEM, the endothelium of capillary in the vicinity of epithelium of villi was so polarized that the nucleus was far away from epithelium and the side near the epithelium was thin. In the endothelium of newborn rats, bigger nucleus, more cytoplasm as well as several plasmalemmal vesicles were seen, but no endothelial hole and basal membrane were observed. However, endothelial hole and basal membrane were found in ablation animals (Figure 7). For the adult rats, a plenty of plasmalemmal vesicles were noticed in the endothelium (Figure 8). The endothelium in the aged rats, however, became thinner whereas its basal membrane became thicker. Endothelial holes were found to be increased whereas plasmalemmal vesicles were decreased (Figure 9). The number of endothelial holes, the thickness of basal membrane and the permeability of microvasculature were increased over the entire course of development from newborn period to aged period (Table 2).

Changes of microvascular permeability of villi at different ages

The microvascular permeability at different ages was determined with Evans Blue infiltration technique. The amount of Evans blue that penetrated into intestinal tissue was 28.1 $\mu\text{g/g}$ tissue in ablation rats and 64.4 $\mu\text{g/g}$ tissue in adult rats. The microvascular permeability of the aged rats was twice as high as that of the adult rats (Table 2).

Table 1 Comparison of the microvascular architecture of villi at different ages (mean \pm SEM)

	Ablactation rats	Adult rats	Aged rats
Diameter of arteriole (μm)	6.17 \pm 1.51	10.47 \pm 2.25 ^a	16.73 \pm 3.28 ^c
Diameter of venule (μm)	20.43 \pm 3.17	25.45 \pm 3.07 ^b	25.50 \pm 3.34
Ratio: arteriole/venule	0.30 \pm 0.04	0.41 \pm 0.04 ^a	0.65 \pm 0.06 ^c

^a*P*<0.01, ^b*P*<0.05 vs ablation rats; ^c*P*<0.01 vs adult rats.

Table 2 Comparison of the endothelial ultrastructure of villi at different ages (mean \pm SEM)

	Newborn	Ablactation	Adult	Aged rats
Endothelial holes (number/ μm)		3.01 \pm 0.38	3.51 \pm 0.35 ^b	5.19 \pm 0.48 ^d
Plasmalemmal vesicles (number/0.1 μm^2)	17.7 \pm 4.25	39.1 \pm 10.36 ^a	75.3 \pm 12.13 ^c	38.0 \pm 11.14 ^d
Basal membrane (nm)		25.2 \pm 5.26	43.5 \pm 5.86 ^c	60.5 \pm 6.89 ^d
Vascular permeability ($\mu\text{g/g}$)		28.1 \pm 4.64	64.4 \pm 9.34 ^c	116.4 \pm 15.63 ^d

^a*P*<0.01 vs newborn rats; ^b*P*<0.05, ^c*P*<0.01 vs ablation rats; ^d*P*<0.01 vs adult rats.

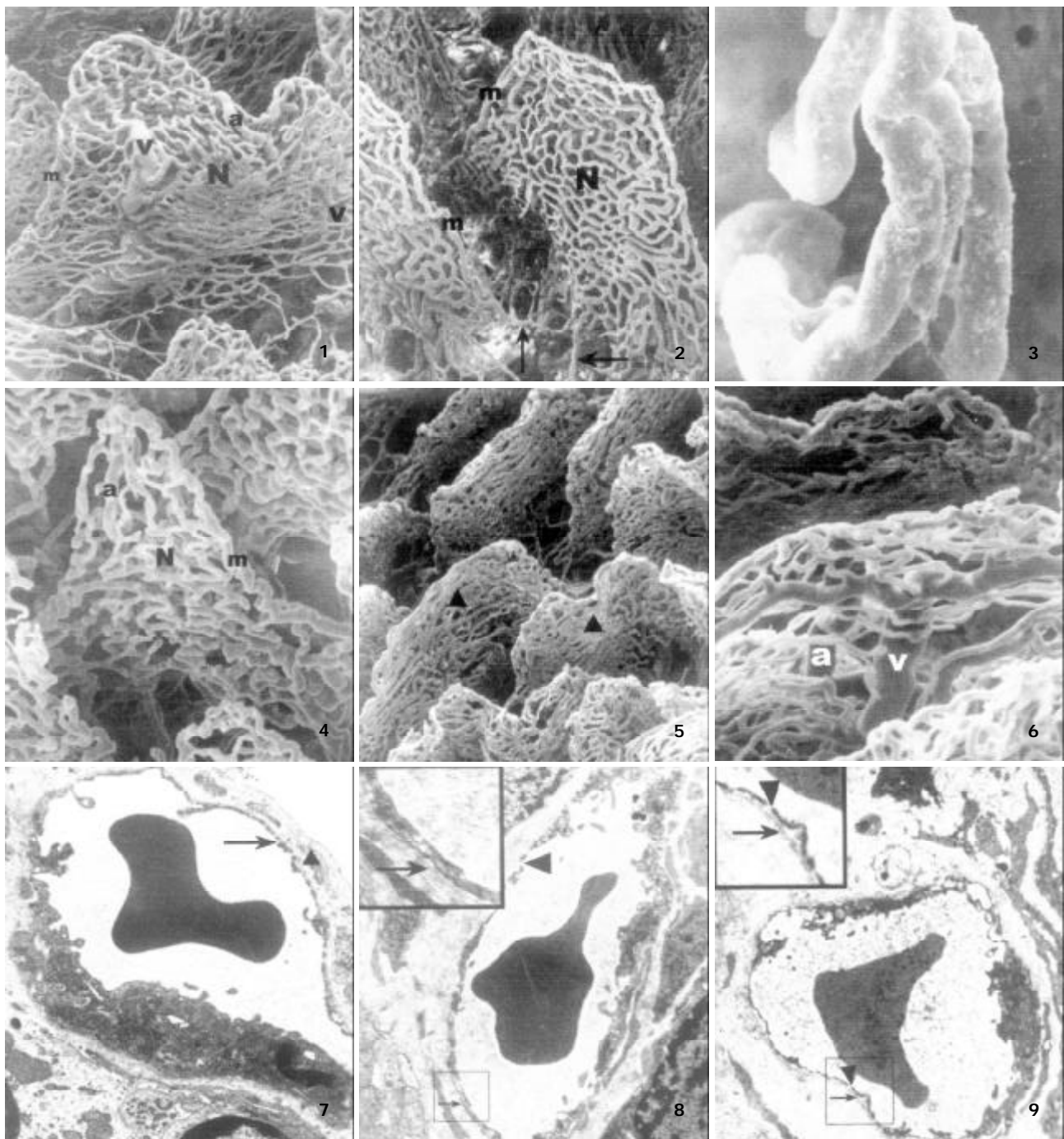


Figure 1 The microvascular architecture of adult rat jejunal villi, showing the villous arteriole (a), the villous capillary network (N), the villous venule(v), the marginal capillary(m) $\times 150$.

Figure 2 The microvascular architecture of adult rat jejunal villi, showing the marginal capillary(m) connecting to the basal part of its adjacent villous plexus (\uparrow) $\times 130$.

Figure 3 The microvascular architecture of newborn rat jejunal villi, $\times 400$.

Figure 4 The microvascular architecture of ablation rat jejunal villi, showing the villous arteriole (a), The villous capillary network(N),the marginal capillary(m) $\times 300$.

Figure 5 The microvascular architecture of aged rat jejunal villi $\times 100$.

Figure 6 The microvascular architecture of aged rat jejunal villi, showing the villous arteriole(a), the villous venule(v) $\times 250$.

Figure 7 The capillary endothelium of ablation rats, showing the endothelial hole (\uparrow) and the basal membrane (\blacktriangle) $\times 8\ 000$.

Figure 8 The capillary endothelium of adult rats, showing the basal membrane (\uparrow) and the endothelial hole (\blacktriangle) $\times 8\ 000$.

Figure 9 The capillary endothelium of aged rats, showing the basal membrane (\uparrow) and the endothelial hole (\blacktriangle) $\times 8\ 000$.

DISCUSSION

Injection of certain materials into blood vessels enables three dimensional visualization of vascular architecture and has provided abundant information which is not available by reconstruction of serial sections^[12-14]. A line of evidence demonstrated in rats, horses and human embryos, that the "fountain type" microvascular architecture of mammalian small

intestine is common^[15-17]. Among these studies, Ohashi *et al*^[16] found that two or more villous venules originating in the base of villi. The results of our study appear to suggest that the villous venules of the rat small intestine are formed in the middle and upper part of the villi, not in the base and at the tip. The villous venules are shorter than villous arterioles, and do not form arterio-venous anastomoses. There is big difference

in diameter between villous venules and villous arteries. The former is about one third of that of the latter. All of these properties are important in creating a low blood pressure and speedy circulatory system in the villous capillary network, which is important to the process of nutritional absorption and transportation^[18].

We found that branching did not take place when the villous arterioles climbed towards the tip of the villous and the capillary networks were not formed until the villous arteria reached the tip of the villous. After entering the villi, blood was supplied to the tip portion of villi and partially to its surrounding area. The cryptal plexus mainly supplied the blood to the basal part of the villi, which lacked artery terminals and branches. Therefore, this collateral circulation can provide blood supplies to the villi. Although there was supplementary blood supply in the base of the villi, blood supply was inefficient due to a long distance of transportation from the branching point at the tips of villi which were full of arterial blood^[19]. Therefore, the villi at the tip received much more arterial blood supply than in the base. From the base to the tip of the villi, the absorption rate of epithelium increased proportionately with the volume of its blood supply. However, there were still aging cells at the tip of villous that were less dynamic physiologically than the younger cells at the basal part. The cells of villi at the tip might not be able to adapt themselves very well to any abnormal blood circulation, and therefore would easily lose their normal physiology under certain harsh conditions^[20]. Injuries due to hypoxia usually emerged later in both intestinal crypts and basal part of villi than in the apical area of villi^[21]. This may indicate that the crypts, as compared with villi, are relatively more resistant to hypoxic injuries. Such resistance is important in maintaining the optimal endocrine function and the regenerative capability of mucosa even after shock resulting from excessive blood loss.

Our results also showed that there were marginal capillaries on both sides of the small intestinal villi. These capillaries descended from the apical part of the villi to the basal part along its margin. It crossed the cryptal plexus and connected to the capillary network. So far, there have been no report regarding this connection. Before this study, it had been considered that there was only one venous return path from the small intestinal capillary. In other words, blood from capillary venules converged into the venous plexus in the submucosa^[16,17,22]. Studies on marginal capillary have been developed since Mohiuddin^[19] described the marginal capillary. It was reported recently that marginal capillary was more manifest in jejunum than in ileum^[23,24], but its relationship with its adjacent villous plexus was not found in both jejunum and ileum. It is thus considered that the marginal capillary transports blood to the villous margin. Therefore, the findings from the this study regarding the marginal capillary and its relation with its adjacent villi suggest that the collateral circulation may exist before the venous return from the villi. That is, the marginal capillary delivers blood partially into the adjacent villous capillary networks. This architecture of the villous plexus may have been adapted to the movement of intestines as well as to the digestive and absorptive activities. After eating, the small intestine speeds up its motility. Villi not only have tight contacts with the chyme but also are subjected to mechanical pressure from the passing chyme. If the villous venules are depressed, blood return to the villi will be blocked. Therefore, blood can be collected into the adjacent villous plexi through the marginal capillary. This helps maintain a normal blood circulation in the villi, and their digestive and absorptive functions are carried out normally.

In the newborn rat villi, capillary network was not formed although only simple microvascular architecture was formed. The later developed capillary network is probably due to the

formation of slender transcapillary tissue pillars, which give rise to new vascular meshes^[25,26]. During villous formation, the developing vascular nets played an important role and the apical capillary loop in a villous was anchored to epithelial basal membrane or to the adjoining matrixes^[27]. After 3 weeks, the villous microvascular architecture tended to grow in full scale. During ablation period, the villous capillary network was formed, and the diametral ratio of villous arteriole to villous venule was one-third, which consolidated the normal digestion and absorption. The villous plexus in adult rats became higher and wider, providing more nutrition for the body. In aged rats, the tip of the villous plexus caved in, the position of villous venule was relatively high. The increases in diametral ratio of villous arteriole to villous venule caused high blood pressure, which degraded the transportation and absorption of nutrition. All of these demonstrate the important role of the vascular architecture in maintaining an efficient absorption of nutrition for the malfunctioned intestines in the aged animals.

The primary penetrating vessels in the submucosa formed an extensive submucosal plexus that supplied the tunica serosa, tunica muscularis, and tunica mucosa^[28]. Fewer branches of this plexus supply the muscle layers, and most of branches run towards the mucosa and to supply blood to the villous and the cryptal plexus^[29]. Therefore the vascular permeability mainly depends on the villous plexus, namely vascular architecture and endothelial structure. Under normal physiological condition, small molecules can easily enter or come out of blood vessels, but the large size substances must be transported through endothelial hole or plasmalemmal vesicle^[30]. Since there were no endothelial holes and very few plasmalemmal vesicles in newborn rats, these large size substances must be selected to pass through the endothelium, which may be a protection for the immature immune system. The emergence of a few of endothelial holes and plasmalemmal vesicles during ablation period indicate that the big molecular substances can be transported. The endothelium of adult rats have a plenty of plasmalemmal vesicles, and microvascular permeability was twice as high as that of the ablation rats. In the aged rats, the endothelium became thinner, and the number of plasmalemmal vesicles became smaller while the number of endothelial holes became bigger. The diametral ratio of villous arteriole to villous venule increased as animals become older. The blood pressure was higher in old rat villi. The larger number of endothelial holes and higher blood pressure resulted in double increase in the microvascular permeability of the aged rats as compared with the adult rats. The thickened basal membrane may be due to a compensatory response, which may prevent any injurants from entering the blood vessels in the aged rats. Based upon the above information, one can say that aging or degradation of blood vessels may underlie the mechanisms of systematic aging.

In summary, the microvascular architectures of rat intestinal villi are complex. Each villi has its own blood supply and venous return paths. Furthermore, one villi can supply blood to its adjacent villi through the marginal capillary. These complex connections in the villi help avoid a shortage of blood supply or blockade of venous blood return. Normal digestive and absorptive functions are thus protected. With regard to the small intestine of other species, whether there is a marginal capillary and venous return collateral circulation is a matter of future study.

REFERENCES

- 1 **Matheson PJ**, Wilson MA, Garrison RN. Regulation of intestinal blood flow. *J Surg Res* 2000; **93**: 182-196
- 2 **Mailman D**. Blood flow an intestinal absorption. *Fed Proc* 1982; **41**: 2096-2100

- 3 **Lun H.** Investigative survey of the intestinal blood vessels. *Jiepouxue Zazhi* 1997; **20**: 197-199
- 4 **Laroux FS,** Grisham MB. Immunological basis of inflammatory bowel disease: role of the microcirculation. *Microcirculation* 2001; **8**: 283-301
- 5 **Abbas B,** Boyle FC, Wilson DJ, Nelson AC, Carr KE. Radiation induced changes in the blood capillaries of rat duodenal villi: a corrosion cast, light and transmission electron microscopical study. *J Submicrosc Cytol Pathol* 1990; **22**: 63-70
- 6 **Kelly DA,** Piasecki C, Anthony A, Dhillon AP, Pounder RE, Wakefield AJ. Focal reduction of villous blood flow in early indomethacin enteropathy: a dynamic vascular study in the rat. *Gut* 1998; **42**: 366-373
- 7 **Ruh J,** Vogel F, Schmidt E, Werner M, Klar E, Secchi A, Gebhard MM, Glaser F, Herfarth C. Effects of hydrogen peroxide scavenger Catalase on villous microcirculation in the rat small intestine in a model of inflammatory bowel disease. *Microvasc Res* 2000; **59**: 329-337
- 8 **Hu S,** Sheng ZY. The effects of anisodamine and dobutamine on gut mucosal blood flow during gut ischemia/ reperfusion. *World J Gastroenterol* 2002; **8**: 555-557
- 9 **Nakajima Y,** Baudry N, Duranteau J, Vicaut E. Microcirculation in intestinal villi: a comparison between hemorrhagic and endotoxin shock. *Am J Respir Crit Care Med* 2001; **164**: 1526-1530
- 10 **Dabareiner RM,** Snyder JR, Sullins KE, White NA 2nd, Gardner IA. Evaluation of the microcirculation of the equine jejunum and ascending colon after ischemia and reperfusion. *Am J Vet Res* 1993; **54**: 1683-1692
- 11 **Zheng FS.** Steric metrology of cell morphology. *Beijing: The Former Beijing Medical University and PUMC Press* 1990
- 12 **Kondo S.** Microinjection methods for visualization of the vascular architecture of the mouse embryo for light and scanning electron microscopy. *J Electron Microsc* 1998; **47**: 101-113
- 13 **Poonkhum R,** Pongmayteegul S, Meeratana W, Pradidarcheep W, Thongpila S, Mingsakul T, Somana R. Cerebral microvascular architecture in the common tree shrew (*Tupaia glis*) revealed by plastic corrosion casts. *Microsc Res Tech* 2000; **50**: 411-418
- 14 **Zahner M,** Wille KH. Vascular system in the large intestine of the dog. *Anat Histol Embryol* 1996; **25**: 101-108
- 15 **Bellamy JE,** Latshaw WK, Nielsen NO. The vascular architecture of the porcine small intestine. *Can J Comp Med* 1973; **37**: 56-62
- 16 **Ohashi Y,** Kita S, Murakami T. Microcirculation of the rat small intestine as studied the injection replica scanning electron microscope method. *Arch Histol Jpn* 1976; **39**: 271-282
- 17 **Dart AJ,** Snyder JR, Julian D, Hinds DM. Microvascular circulation of the small intestine in horse. *Am J Vet Res* 1992; **53**: 995-1000
- 18 **Hummel R,** Schnorr B. The system of blood vessels of the small intestine of ruminants. *Anat Anz* 1982; **151**: 260-280
- 19 **Mohiuddin A.** Blood and lymph vessels in the jejunal villi of the white rat. *Anat Rec* 1966; **156**: 83-89
- 20 **Jiang L,** Zhao XM, Tian N, Liu YY, Li XH, Jiang CG. Simulation study of hemodynamic of small intestinal villosity microvessels in vitro. *Zhongguo Bingli Shengli Zazhi* 1999; **15**: 60-62
- 21 **Morini S,** Yacoub W, Rastellini C, Gaudio E, Watkins SC, Cicalese L. Intestinal microvascular patterns during hemorrhagic shock. *Dig Dis Sci* 2000; **45**: 710-722
- 22 **Metry JM,** Neff M, Knoblauch M. The microcirculatory system of the intestinal mucosa of the rat. An injection cast and scanning electron microscopy study. *Scand J Gastroenterol Suppl* 1982; **71**: 159-162
- 23 **Tahara T,** Yamamoto T. Morphological changes of the villous microvascular architecture and intestinal growth in rats with streptozotocin-induced diabetes. *Virchows Arch A Pathol Anat Histopathol* 1988; **413**: 151-158
- 24 **Kamyshova VV,** Karelina NR, Mironov AA, Mironov VA. Morphofunctional features of different divisions of the microcirculatory bed of jejunal villi in the white rat. *Arkh Anat Gistol Embriol* 1985; **88**: 44-50
- 25 **Patan S,** Alvarez MJ, Schittny JC, Burri PH. Intussusceptive microvascular growth: a common alternative to capillary sprouting. *Arch Histol Cytol* 1992; **55**(Suppl): 65-75
- 26 **Karelina NR.** Circulatory bed of the small intestinal villi of newborn infants. *Arkh Anat Gistol Embriol* 1978; **75**: 64-71
- 27 **Hashimoto H,** Ishikawa H, Kusakabe M. Development of vascular networks during the morphogenesis of intestinal villi in the fetal mouse. *Kaibogaku Zasshi* 1999; **74**: 567-576
- 28 **Yarbrough TB,** Snyder JR, Harmon FA. Jejunal microvascular architecture of the llama and alpaca. *Am J Vet Res* 1995; **56**: 1133-1137
- 29 **Chen YM,** Li J, Zhang J, Duan XL. The intestinal microvascular architecture of rat. *Shijie Huaren Xiaohua Zazhi* 2000; **8**: 1291-1293
- 30 **Komuro T,** Hashimoto Y. Three-dimensional structure of the rat intestinal wall (mucosa and submucosa). *Arch Histol Cytol* 1990; **53**: 1-21

Edited by Ma JY

Pleckstrin homology domain of G protein-coupled receptor kinase-2 binds to PKC and affects the activity of PKC kinase

Xing-Long Yang, Ya-Li Zhang, Zhuo-Sheng Lai, Fei-Yue Xing, Yu-Hu Liu

Xing-Long Yang, Ya-Li Zhang, Zhuo-Sheng Lai, Yu-Hu Liu, Institute of Gastroenterology, NanFang Hospital, First Military Medical University 510515, Guangzhou, Guangdong Province, China
Fei-Yue Xing, Key lab. for shock and microcirculation of PLA, Department of Preclinical Medicine, First Military Medical University 510515, Guangzhou, Guangdong Province, China

Correspondence to: Xing-Long Yang, Institute of Gastroenterology, NanFang Hospital, First Military Medical University 510515, Guangzhou, Guangdong Province, China. foru3000@hotmail.com
Telephone: +86-20-61364633 **Fax:** +86-20-61641544

Received: 2002-10-04 **Accepted:** 2002-11-28

Abstract

AIM: To study the detail mechanism of interaction between PKC and GRK₂ and the effect of GRK₂ on activity of PKC.

METHODS: The cDNA of pleckstrin homology (PH) domain located in GRK₂ residue 548 to 660 was amplified by PCR with the mRNA of human GRK₂ (β 1-adrenergic receptor kinase) as template isolated from human fresh placenta, the expression vector pGEX-PH inserted with the above cDNA sequence for GRK₂ PH domain protein and the expression vectors for GST (glutathion-s-transferase)-GRK₂ PH domain fusion protein, BTK (Bruton's tyrosine kinase) PH domain and GST protein were constructed. The expression of GRK₂ in culture mammalian cells (6 cell lines: PC-3, MDCK, SGC7901, Jurkat cell etc.) was determined by SDS-PAGE and Co-immunoprecipitation. The binding of GRK₂ PH domain, GST-GRK₂ PH domain fusion protein and BTK PH domain to PKC *in Vitro* were detected by SDS-PAGE and Western blot, upon prolonged stimulation of epinephrine, the binding of GRK₂ to PKC was also detected by western blot and Co-immunoprecipitation.

RESULTS: The binding of GRK₂ PH domain to PKC *in Vitro* was confirmed by western blot, as were the binding upon prolonged stimulation of epinephrine and the binding of BTK PH domain to PKC. In the present study, GRK₂ PH domain was associated with PKC and down-regulated PKC activity, but Btk PH domain up-regulated PKC activity as compared with GRK₂ PH domain.

CONCLUSION: GRK₂ can bind with PKC and down-regulated PKC activity.

Yang XL, Zhang YL, Lai ZS, Xing FY, Liu YH. Pleckstrin homology domain of G protein-coupled receptor kinase-2 binds to PKC and affects the activity of PKC kinase. *World J Gastroenterol* 2003; 9(4): 800-803

<http://www.wjgnet.com/1007-9327/9/800.htm>

INTRODUCTION

G protein-coupled receptor kinase-2 (GRK), also known as β 1-adrenergic receptor kinase (β -ARK1), plays an important role in agonist-induced desensitization of the β -adrenergic

receptors. Activation of protein kinase C (PKC) is able to stimulate phosphorylation and activation of GRKs and induce desensitization of G protein-coupled receptor. However, the detail mechanism of interaction between PKC and GRK₂ and the effect of GRK₂ on activity of PKC remain unknown. Pleckstrin homology (PH) domain is a kind of functional domain containing 120 amino acids, which exist on many protein molecules that involved in cellular signal transduction. A PH domain located in GRK₂ residue 548 to 660 may play a significant role in mediating interaction between PKC and GRK₂. In the present study, we showed that PKC could associate with PH domain of GRK₂ in pull-down assay *in vitro*. Co-immunoprecipitation displayed binding of PKC to GRK₂ in intact Jurkat cells after prolonged stimulation of epinephrine. Assay of PKC β 1 kinase activity indicated that the binding of the PH domain of GRK₂ to PKC β 1 could down-regulate the activity of PKC β 1 kinase. Thus, GRK₂ may play a negative feedback regulatory role on PKC β 1 activity in interaction between GRK₂ and PKC β 1.

G protein-coupled receptor kinase-2 is a member of the GRK family existing of at least 6 GRKs^[1]. GRKs are implicated in agonist-induced phosphorylation and homologous desensitization of G protein-coupled receptor (GPR). Phosphorylation sites of the GPR by GRK are located in the carboxyl tail of the receptor and involved amino acid residues at positions serine 404, 408, and 410^[2]. These phosphorylation sites are thought to initiate desensitization of GPR.

It has been recently reported that protein kinase C (PKC) could phosphorylate and activate GRK which sequentially mediated desensitization of GPR^[3]. In addition, PKC could directly phosphorylate GPR and initiate desensitization of the receptors^[4]. Thus, PKC likely participates in phosphorylation and homologous desensitization of adrenergic receptor at multiple levels. Furthermore, both activated GRK and PKC are recruited to the specific membrane and GRK may localize on the membrane via its PH domain binding to phosphatidylinositol phosphates. Both recruitment to membrane will facilitate the association of PKC with GRK. Deletion or mutation of the PH domain will abolish GRK faculty of phosphorylating and activating GPR^[5]. PH domain of GRK plays a pivotal role in mediating the phosphorylation and desensitization of the receptors. However, as to detail mechanism of PKC, how to interact with and activate GRK remains unclear.

PH domain has been distinguished from more than 100 molecules that are implicated in signaling and other biological function. The main function of PH domains is to mediate protein-phospholipid and protein-protein interaction. Up to now, several molecules such as phosphatidylinositol phosphates, G β γ , RACK1, PKC, G α subunit-12 and F-actin have been identified as ligands of PH domains. It was reported by Yao *et al* (1994)^[6] that the PH domain of Btk and Itk interacted with protein kinase C. Afterwards, the interactions between PKC and other PH domains of the molecules were also confirmed by different groups. Those PH domains that bind to PKC share a high homology in 1st-4th β strands^[7] which formats a relatively reserved face binding to PKC. But other PH domains that can interact with PKC remain to be identified.

PKC is a family of serine/threonine protein kinase, which plays significant roles in numerous cellular responses (including cell proliferation, differentiation, growth control, tumor progression, apoptosis etc.)^[8]. Besides the event of PKC phosphorylating GRK₂ discussed above, PKC can phosphorylate GRK₅ and modulate the activity of GRK₅^[9]; PKC can also lead to olfactory signal termination and desensitization^[17] via other GRK₂; Agonist stimulation results in oxytocin receptor interaction with GRK and PKC^[10]. Moreover, PKC presents a manner of phosphorylating directly to muscarinic receptor and leading to the desensitization receptor^[11].

Like most interaction between signaling molecules, PKC is likely associated with GRK₂ before phosphorylating and activating GRK₂. To elucidate detail mechanism of interaction between GRK₂ and PKC, we reported the study on interaction between PKC and GRK₂. It is expected that present study will provide new insights into understanding of the modulation mechanism of PKC in GRK₂ mediating signaling pathway. It is also expected that the present investigation can illustrate the importance of the GRK₂ PH domain in interaction with PKC.

MATERIALS AND METHODS

Materials

Anti-GRK₂, anti-PKCβ1 and secondary antibodies conjugated with horseradish peroxidase were purchased from Santa Cruz Biotechnology. **PKC assay kit (Sigma TECT™ PKC assay system) and reverse transcription kit** were from Promega. **Glutathione-agarose beads** was from Sigma. **Expression vector pGEX-4T-1 and ECL detection kit** (for western blotting) were from Amersham Pharmacia Biotech. **PVDF membrane** was from Millipore. **Rabbit IgG** was from Sino-American company (China). **Protein A-agarose** was from Pierce Inc.

Methods

Construction of expression vector pGEX-PH The mRNA of human GRK₂ (β1-adrenergic receptor kinase) was isolated from fresh human placenta^[12], and reverse transcription was performed according to the kit protocol. cDNA of PH domain (residue 548 to 660)^[13] was amplified by PCR with oligonucleotides containing BamHI sites (forward, CGGGATCCGGCCACGAGGAAGACTAC) and EcoRI sites (reverse, GGAATTCTCACCGCTGCACCAGCTGCTG). The products were purified from agarose gel and the resulting fragments were digested with Bam HI and EcoRI, respectively. The resulting fragments were ligated in frame between Bam HI and EcoRI sites of plasmid pUC-19. The resulting plasmid (termed pUC-PH) was resolved by sequencing. The fragments were excised from pUC-PH and ligated in frame into expression vector pGEX-4T-1, named pGEX-PH.

Expression and purification of GST fusion protein GST-GRK₂ PH domain, Btk PH domain and GST were expressed in *Escherichia coli* strain DH5α. Here was Btk PH domain positive control^[6]. The expression was induced with 0.2 mM of IPTG at 26 °C for 1 hour in LB medium containing 1 % glucose. Briefly, the bacteria were resuspended in ice-cold STE buffer (10 mM Tris-HCl, 150 mM NaCl, 1.0 mM EDTA, 1.0 mM phenylmethylsulfonyl fluoride and 0.1 mg/ml lysozyme, pH 8.0) on ice for 20 min. The treated bacteria were added dithiothreitol to 5.0 mM and sarkosyl to 1.5 % on ice until the solution became viscous, and then lysed by sonicate (30-40 output, 1 min×2, at 4 °C). Cell lysate was centrifuged at 10 000×g for 20 min at 4 °C. Component of both supernatant and the pellet was separated by SDS-PAGE to determine the distribution of the fusion protein. The supernatant was added Triton X-100 to 2 %, and then filtered with 0.45 mm membrane. The solution was saved as the fraction containing interested

proteins, and then the treated glutathione-agarose beads were added to solution at 4 °C for 2 hours with occasional gentle mixing. The beads were washed with PBS and centrifuged at 800×g, 4 °C for 3 min×5 times. The pellet was subjected to SDS-PAGE in 12 % gels. In order to utilize 1 equivalent amount of GST and fusion proteins for the following assay, the protein concentration was modulated according to band sizes in SDS-GAGE gel.

Determination of GRK2 expression in mammalian cell lines MDCK, SGC7901, DU145, PC-3, U937 and Jurkat cells were maintained in Dulbecco's modified eagle's medium or 1640 medium with 10 % (v/v) new born bovine serum and a 5 % CO₂ humidified atmosphere at 37 °C. In brief, the 10⁷ cells were harvested by centrifuging or scraping off, respectively, washed by PBS at 4 °C and then incubated with 1 ml of lysis buffer (20 mM Tris-HCl, pH 7.5, 10 mM KCl, 1 mM EDTA, 0.5 mM phenylmethylsulfonyl fluoride, 10 μg/ml leupeptin and 1 μg/ml aprotinin) on ice for 20 min with casually and vigorously vortexing. The mixtures were centrifuged at 12 000×g for 10 min at 4 °C. The supernatants were saved as GRK₂-contained or PKC-contained preparations for western blot.

Cell culture and lysis Jurkat T lymphocytes were maintained as above with RPMI 1640 medium. The 2×10⁷ cells were divided into 2 parts and were serum-freed for 8 h. followed by 0.5 h treatment without (Control) or with epinephrine. The stimulation was stopped by removal of the medium and adding 3 ml of ice-cold phosphate-buffered saline, which was also used for two similar washing steps with centrifugation at 500×g for 5 min.

Protein-protein interaction assay Approximately 20 μg of the GST and GST fusion proteins immobilized on glutathione-agarose beads was incubated with the 0.3 ml of Jurkat T lymphocyte supernatant at room temperature for 2 hours with gentle mixing. The beads were then washed five times with 1 ml of ice-cold PBST (PBS with 0.05 % tween-20). The eventual bead pellet was resolved by SDS-PAGE. Equivalent amount of the fusion protein or GST alone was used for the following assay.

Western blot-the resolved proteins were electrotransferred onto PVDF membrane. The membrane was blocked by incubating with 5 % gelatin in PBST at 37 °C for 1 h with gentle vibration, and then incubated with 1 μg of anti-PKCβ1 antibody at 4 °C overnight. The membrane was then washed 5 times with PBST and incubated with horseradish peroxidase-conjugated anti-rabbit secondary antibody at room temperature for 1 h with gentle vibration. The membrane was finally washed 6 times with PBST to remove unbound secondary antibody and visualized by using ECL (Amersham Pharmacia Biotech).

Co-immunoprecipitation assays 10⁷ Jurkat cells were lysed in 1 ml of lysis buffer (20 mM sodium phosphate, pH 7.5, 500 mM NaCl, 0.1 % SDS, 1 % NP-40, 0.5 % sodium deoxycholate, 0.02 % sodium azide, 0.5 mM phenylmethylsulfonyl fluoride, 2 μg/ml leupeptin and 2 μg/ml aprotinin). Briefly, 10 μg of anti-PKCβ1, or anti-GRK₂ antibodies and rabbit IgG were added to 200 μl of the lysate, respectively, then the samples were incubated overnight at 4 °C. The products were added 40 ml of immobilized protein A (Pierce Inc) and incubated at room temperature for 2 h with gentle mixing. The products were added 0.5 ml lysis buffer (without protease inhibitor) and centrifuged at 500×g, 4 °C for 3 min. The supernatant was discarded and this procedure was repeated for 6 times. In brief, the pellets were subjected to SDS-PAGE. The proteins were electrotransferred onto PVDF membranes. The membranes were blocked with gelatin and incubated with anti-PKCβ1 or anti-GRK₂ antibodies, respectively. The membranes were probed and visualized as described above.

PKC kinase assay The fusion proteins and GST were purified as described above, and washed extensively with PBST. After washing, the GST-fusion proteins and GST were eluted with

20 mM of reduced glutathione in 50 mM Tris·HCl (pH 8.0). The eluted proteins were concentrated using a Centricon (Millipore). Protein concentrations were determined with Bradford reagent (Bio-Rad). Equivalent amounts of the protein were added to the 100 μ l lysate of Jurkat cells. According to manufacturer's instruction (Sigma TECT™ PKC assay system), the activity of PKC in the lysate was determined by subtracting the radioactivity of the reaction with control buffer and 100 μ M PKC peptide inhibitor from that of the reaction without activated buffer nor the PKC inhibitor. The experiment was performed in triplicate samples for each groups. The data were presented as percentage of PKC activity and the control was used as 100 %.

RESULTS

Binding of GRK₂ PH domain to PKC *in vitro*

To search for potential binding between the expressed proteins (GST-GRK₂ PH domain, GST-Btk PH domain and GST) and PKC β 1, the proteins immobilized on glutathione-agarose beads were added to lysate of Jurkat cells, and then the products were subjected to SDS-PAGE and Western blot. The potential PKC β 1 was probed with anti-PKC β 1 antibody. As shown in Figure 1, the GST fusion proteins encompassing GRK₂ PH domain and GST-Btk PH domain associated specifically with PKC β 1 because the GST did not pull out PKC β 1 under the same experimental conditions. Binding of Btk PH domain to PKC β 1 was formerly approved. We confirmed the binding of GRK₂ PH domain to PKC β 1 which was specific *in vitro*.

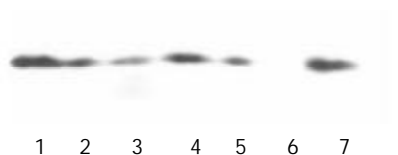


Figure 1 The binding of PH domain to PKC by Western blot with the antibody to PKC. Lane 1, 2, 3, 4 and 5 were the GST-PH domains of IRS-1, GRF/c, β -ARK1, PLC γ /n and Btk, respectively; lane 6 was the GST; lane 7 was lysate of Jurkat cells.

Determination of expression of GRK₂ in cultured mammalian cells

In order to detect the association of GRK₂ with PKC *in vivo*, GRK₂ expression of 6 cell lines were confirmed by western blot in advance. The same amount of the protein was utilized in SDS-PAGE. The results indicated GRK₂ were expressed in PC-3, MDCK, 7901 and Jurkat cell lines. The GRK₂-antibody could react with GRK₁ in MDCK and 7901 cell lines, and the antibody could specifically recognize GRK₂ in Jurkat cells. Thus, the following Co-immunoprecipitation assays was performed in Jurkat cells.

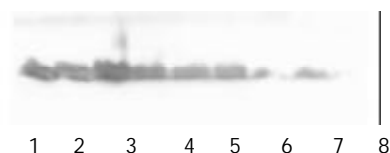


Figure 2 The expressing of GRK₂ by Western blot with the antibody to GRK₂. Lane 1, 2, 3, 4 were the results of Western blot in PC-3, MDCK, 7901 and Jurkat cell line respectively. Lane 5,6 was GST.

Binding of GRK₂ to PKC upon prolonged stimulation of epinephrine

Phosphorylation and activation of GRK by PKC enhance desensitization of G protein-coupled receptor. In the pull-down assay, our result indicated that the PH domain of GRK₂ was associated specifically with PKC *in vitro*. To determine the

association of PKC with GRK₂ *in vivo* after stimulation of the agonist of β -ARK, 100 μ M epinephrine was added to the cells in 1640 medium for 30 min. Co-immunoprecipitation was performed with specific anti-GRK₂ and anti-PKC antibodies in co-precipitation and detection of PKC and GRK. After stimulation of 100 μ M epinephrine for 30 min, PKC was detected out in the precipitate of GRK antibody and GRK was detected out in precipitate of PKC antibody, respectively. In contrast, the PKC did not bind to GRK₂ in the intact cells without stimulation of epinephrine. Thus, the results indicated that the association of PKC with GRK₂ was involved in GRK₂ activation and desensitization of G protein-coupled receptor.

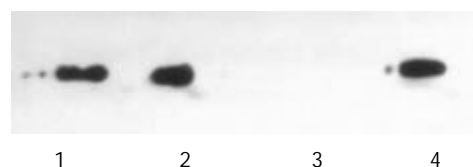


Figure 3 After stimulation of epinephrine, Co-immunoprecipitation was performed with anti-GRK₂ and anti-PKC in co-precipitation and detection of PKC and GRK₂. Lane 1 was PKC detected in precipitate of GRK antibody, lane 2 was GRK₂ detected in precipitate of PKC antibody. Lane 3 indicated the PKC did not bind to GRK₂ in the intact cells without stimulation of epinephrine, lane 4 was the lysate of Jurkat cell.

Effects of GRK₂ and Btk PH domains on PKC activity

Effects of proteins on PKC activity were determined as described under the experimental Procedures. After purification as described above, the expressed proteins were eluted and dialysed in PBS. Equivalent amounts (20 μ g) of GST-GRK₂ PH domain, GST-Btk PH domain and GST were added to the lysate of Jurkat cell lysate (100 μ l) in determining PKC activity. When Btk associated with PKC, Btk activity was down-regulated by PKC and PKC activity was up-regulated by Btk PH domain. In the present study, GRK₂ PH domain was associated with PKC and down-regulated PKC activity but Btk PH domain up-regulated PKC activity as compared with GST and untreated cells.

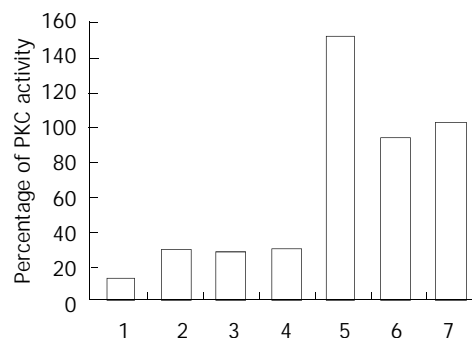


Figure 4 Effects of the PH domain on PKC activity measured by protein kinase C Assay System. The volume was percentage of PKC activity. The data were representation of two experiments. Lanes 1, 2, 3, 4 and 5 were GST-PH domain of IRS-1, GRF/c, β -ARK1, PLC γ /n and Btk, respectively; lane 6 was the GST; lane 7 was lysate of Jurkat cells.

DISCUSSION

The GRK family is composed of six members, namely GRK 1-6. Of these, GRK₂ phosphorylates G protein-coupled receptors (GPCRs) and plays an important role in mediating homologous desensitization of GPCRs. Chuang's work showed the activity of GRK₂ was increased^[14] in a protein kinase C (PKC)-dependent manner. Further study demonstrated that PKC could directly phosphorylate GRK. This study suggested that GRK could be

activated via phosphorylation of PKC. Recent work had led to the identification of phosphorylation site at GRK₂, the study of Krasel and co-worker showed that PKC phosphorylated GRK₂ at serine 29^[15], but the detail mechanism of PKC β 1 recognizing and binding to GRK₂ remains unknown. In present study, we reported that GRK₂ could bind to PKC via its carboxyl-terminal PH domain *in vitro*, which was a fundamental event in mediating interaction between PKC and GRK₂. The present result suggested the GRK ph domain had an analogous fashion to PH domain of Btk and Itk, which could interact with protein kinase C^[6] in our previous study. The PH domain of GRK₂ is probably involved in directly binding of GRK₂ to PKC and facilitates phosphorylation and activation of GRK₂ by PKC.

Stimulation of agonist (epinephrine) on adrenergic receptor results in association of PKC β 1 with GRK₂ in Jurkat cells. GRK₂ could through its PH domain can directly bind to PKC and then be phosphorylated by PKC. But in intact cells (without stimulation of epinephrine), PKC and GRK₂ are in dissociated state. The epinephrine stimulation on adrenergic receptor may activate phospholipase C (PLC), and initiates a cascade of events. The stimulation causes PLC-mediated hydrolysis of inositol phospholipids, and results in calcium mobilization and production of second messenger diacylglycerol (DAG). The DAG and Ca⁺⁺ are activators of PKC, and cause activation of PKC^[16]. In the present study, activated PKC is likely to bind to and phosphorylate GRK₂ directly, which phosphorylates G-protein coupled receptor and results in receptor desensitization. In this signaling pathway, activation of PKC appears to be prior to receptor desensitization and is of fundamental importance in regulating the receptor desensitization.

Those PH domains from Btk, β -spectrin, dynamin and amino-terminal of AFAP-110 known directly binding to PKC share a high homology at first three β -sheets^[7]. These β -sheets form conserved structure elements and may specifically bind to PKC. Table 1 showed the residue comparison of PH domains from GRK₂ and GRK₃ with these PH domains. The PH domain of GRK₂ and GRK₃ matches that consensus well. This may form a structured base of PH domains binding to PKC.

Table 1 First three β sheets of PH domains of GRK₂ and GRK₃ are compared with other PH domain known or predicted to bind to PKC

PH domain (source)	β 1	β 2	β 3
Btk	ESIFLKT--SQQKKKTSPLS--NFKKRLFLLT-VH-KLSYYEYDF		
β -spectrin	MEGFLNRKH-EWEAHNKKASSR-SWHNVYCVIN-NQ-EMGFYKDAK		
Dynamin	RKGWLTI---NNIGIMKGGG---KEYWVFLT--AE--NLSWYKDDDE		
AFAP, Nt PH domain	ICAFLLRKK-RFGQ-----WTKLLCVIK-EN-KLLCYKSSK		
Consensus	1* +*	++*****	+L 1p
GRK ₂	MHGYSKM--GNPFLTQ-----WQRRYFYLF--PN--RLEWRGEGEA		
GRK ₃	MHGMLKL--GNPFLTQ-----WQRRYFYLF--PN--RLEWRGEGES		

Consensus sequence is shown and symbols used are as in the paper of Baisden *et al.* 1 indicates aromatic residues, + indicates positively charged residues, * indicates hydrophobic residues, indicates polar residues. The sequences of GRK₂ and GRK₃ from Zheng *et al.*^[18].

The previous study revealed PKC inhibited the activity of Btk kinase via binding to Btk PH domain^[6], but the binding effect on PKC activity remains unclear. In the present study, the effects on PKC activity of Btk and GRK₂ PH domains were determined with GST. Compared with GST or control, Btk PH domain could increase PKC kinase activity, but GRK₂ PH domain inhibited PKC kinase activity. The mechanism of activation or inhibition of PKC activity might lie in the PH

domains binding to PKC regulatory domain and regulating activity of PKC kinase. Biological function of Btk PH domain inhibiting PKC activity will be laid in future investigation. The present study indicated that PKC through its binding to the PH domain of GRK and facilitates phosphorylation and activation of GRK by PKC when stimulated by epinephrine. On the other hand, GRK₂ PH domain appeared to play a negative feedback regulatory role on PKC activity. GRK₂ immediately turns off PKC kinase activity on GRK after PKC completed phosphorylation and activation of GRK.

REFERENCES

- 1 **Sallese M**, Iacovelli L, Cumashi A, Capobianco L, Cuomo L, De Blasi A. Regulation of G protein-coupled receptor kinase subtypes by calcium sensor proteins. *Biochim Biophys Acta* 2000; **1498**:112-121
- 2 **Diviani D**, Lattion AL, Cotecchia S. Characterization of the phosphorylation sites involved in G protein-coupled receptor kinase- and protein kinase C-mediated desensitization of the alpha1B-adrenergic receptor. *J Biol Chem* 1997; **272**: 28712-28719
- 3 **Winstel R**, Freund S, Krasel C, Hoppe E, Lohse MJ. Protein kinase cross-talk: Membrane targeting of the beta-adrenergic receptor kinase by protein kinase C. *Proc Natl Acad Sci USA* 1996; **93**: 2105-2109
- 4 **Garcia-Sainz JA**, Vazquez-Prado J, Del Carmen Medina L. Alpha 1-adrenoceptors: function and phosphorylation. *Eur J Pharmacol* 2000; **389**: 1-12
- 5 **Touhara K**. Effects of mutations in pleckstrin homology domain on beta-adrenergic receptor kinase activity in intact cells. *Biochem Biophys Res Commun* 1998; **252**: 669-674
- 6 **Yao L**, Kawakami Y, Kawakami T. The pleckstrin homology domain of Bruton tyrosine kinase interacts with protein kinase C. *Proc Natl Acad Sci USA* 1994; **91**: 9175-9179
- 7 **Baisden JM**, Qian Y, Zot HM, Flynn DC. The actin filament-associated protein AFAP-110 is an adaptor protein that modulates changed in actin filament integrity. *Oncogene* 2001; **20**: 6435-6447
- 8 **Nishizuka Y**. The protein kinase C family and lipid mediators for transmembrane signaling and cell regulation. *Alcohol Clin Exp Res* 2001; **25**: 3S-7S
- 9 **Pronin AN**, Benovic JL. Regulation of the G protein-coupled receptor kinase GRK5 by protein kinase C. *J Biol Chem* 1997; **272**: 3806-3812
- 10 **Berrada K**, Plesnicher CL, Luo X, Thibonnier M. Dynamic interaction of human vasopressin/oxytocin receptor subtypes with G protein-coupled receptor kinases and protein kinase C after agonist stimulation. *J Biol Chem* 2000; **275**: 27229-27237
- 11 **Hosey MM**, Benovic JL, DeBurman SK, Richardson RM. Multiple mechanisms involving protein phosphorylation are linked to desensitization of muscarinic receptors. *Life Sci* 1995; **56**: 951-955
- 12 **Chomczynski P**, Sacchi N. Single-step method of RNA isolation by acid guanidinium thiocyanate-phenol-chloroform extraction. *Anal Biochem*. 1987; **162**: 156-159
- 13 **Chuang TT**, LeVine H 3rd, De Blasi A. Phosphorylation and activation of beta-adrenergic receptor kinase by protein kinase C. *J Biol Chem* 1995; **270**: 18660-18665
- 14 **Chuang TT**, Sallese M, Ambrosini G, Parruti G, De Blasi A. High expression of beta-adrenergic receptor kinase in human peripheral blood leukocytes. Isoproterenol and platelet activating factor can induce kinase translocation. *J Biol Chem* 1992; **267**: 6886-6892
- 15 **Krasel C**, Dammeier S, Winstel R, Brockmann J, Mischak H, Lohse MJ. Phosphorylation of GRK₂ by protein kinase C abolishes its inhibition by calmodulin. *J Biol Chem* 2001; **276**: 1911-1915
- 16 **Rasmussen H**, Isales CM, Calle R, Throckmorton D, Anderson M, Gasalla-Herraiz J, McCarthy R. Diacylglycerol production, Ca²⁺ influx, and protein kinase C activation in sustained cellular responses. *Endocr Rev* 1995; **16**: 649-681
- 17 **Bruch RC**, Kang J, Moore ML Jr, Medler KF. Protein kinase C and receptor kinase gene expression in olfactory receptor neurons. *J Neurobiol* 1997; **33**: 387-394
- 18 **Zheng J**, Cahill SM, Lemmon MA, Fushman D, Schlessinger J, Cowburn D. Identification of the binding site for acidic phospholipids on the PH domain of dynamin: implications for stimulation of GTPase activity. *J Mol Biol* 1996; **255**: 14-21

Collagen fiber angle in the submucosa of small intestine and its application in gastroenterology

Yan-Jun Zeng, Ai-Ke Qiao, Ji-Dong Yu, Jing-Bo Zhao, Dong-Hua Liao, Xiao-Hu Xu, Gregersen Hans

Yan-Jun Zeng, Ai-Ke Qiao, Shantou University, Guangdong, 515031, China; Beijing University of Technology, Beijing, 100022, China
Ji-Dong Yu, Beijing Polytechnic University, Beijing, 100022, China
Jing-Bo Zhao, Department Gastrointestinal Surgery, Aalborg University, Denmark; China-Japan Friendship Hospital, Beijing, 100029, China
Dong-Hua Liao, Beijing University of Technology, Beijing, 100022, China; Department Gastrointestinal Surgery, Aalborg University, Denmark
Xiao-Hu Xu, Shantou University, Guangdong, 515031, China
Gregersen Hans, Department Gastrointestinal Surgery, Aalborg University, Denmark

Correspondence to: Yan-Jun Zeng, Professor and Director of Biomechanics & Medical Information Institute, Beijing University of Technology, No.100 Pingleyuan, Chaoyang District, Beijing 100022, China. yjzeng@bjpu.edu.cn

Telephone: +86-10-67392172 **Fax:** +86-10-67392297

Received: 2002-07-10 **Accepted:** 2002-07-25

Abstract

AIM: To propose a simple and effective method suitable for analyzing the angle and distribution of 2-dimensional collagen fiber in larger sample of small intestine and to investigate the relationship between the angles of collagen fiber and the pressure it undergoes.

METHODS: A kind of 2-dimensional visible quantitative analyzing technique was described. Digital image-processing method was utilized to determine the angle of collagen fiber in parenchyma according to the changes of area analyzed and further to investigate quantitatively the distribution of collagen fiber. A series of intestinal slice's images preprocessed by polarized light were obtained with electron microscope, and they were processed to unify each pixel. The approximate angles between collagen fibers were obtained via analyzing the images and their corresponding polarized light. The relationship between the angles of collagen fiber and the pressure it undergoes were statistically summarized.

RESULTS: The angle of collagen fiber in intestinal tissue was obtained with the quantitative analyzing method of calculating the ratio of different pixels. For the same slice, with polarized light angle's variation, the corresponding ratio of different pixels was also changed; for slices under different pressures, the biggest ratio of collagen fiber area was changed either.

CONCLUSION: This study suggests that the application of stress on the intestinal tissue will change the angle and content of collagen fiber. The method of calculating ratios of different pixel values to estimate collagen fiber angle was practical and reliable. The quantitative analysis used in the present study allows a larger area of soft tissue to be analyzed with relatively low cost and simple equipment.

Zeng YJ, Qiao AK, Yu JD, Zhao JB, Liao DH, Xu XH, Hans G. Collagen fiber angle in the submucosa of small intestine and its application in gastroenterology. *World J Gastroenterol* 2003; 9(4): 804-807 <http://www.wjgnet.com/1007-9327/9/804.htm>

INTRODUCTION

Several G.I. diseases can change the collagen fiber structure in the G.I. tract^[1-4]. The collagen fiber content and its distribution outside the cell are closely related to some diseases. For example, systemic sclerosis (scleroderma) will replace smooth muscle and deposit large amounts of collagen instead. Gastrointestinal scleroderma is a common clinical disorder; however, due to its complicated etiology, most of them are not easily diagnosed and all the patients with such disease manifested distinct collagen fiber transformations. Early collagen fiber transformations are swelling and homogenization and then become thickened, sclerosed and arranged in a close order^[5-9]. Collagen synthesis is increased especially the ratio of fine collagen fibers; at the same time, the smooth muscle fiber bundles become homogeneous, sclerosed and atrophic. There are changes occurred in the orientation of collagen fibers^[10-13]. Obstructive diseases could also change the collagen structure and content^[14-16]. In normal tissue the submucosal layer consist almost entirely of collagen, which is called the skeleton of the small intestine, and it is well known that the fibers run in a cross-cross pattern with 30 degrees angle in longitudinal direction^[17-20]. The directional distribution of collagen fibers has a very important role in studying the function and self-repair of soft tissue^[21].

The application of digital image-processing technology in medicine field has offered an accurate, simple, convenient and rapid method for the measurement and analysis of large amounts of medical images, especially for the quantitative analysis of smaller pictures, such as microscopic images. At the present time, the techniques for the quantitatively analyzing the distribution of collagen fibers consist mainly of several kinds as follows: that is, the method of quantitatively polarized light microscopy, small angle beam dispersion, image analysis and X-ray diffraction. These methods will sometimes be constrained by the image size, time cost or image connecting, and 90° orientation of template etc^[23].

The purpose of this paper is to propose a method suitable for analyzing the angle and distribution of 2-dimensional collagen fiber in larger sample and to investigate the relationship between the angles of collagen fiber and the pressure it undergoes. At the same time, this paper also offers an effective method for research of the large area collagen fiber distribution.

MATERIALS AND METHODS

Isolation of small intestine

Seven Sprague-Dawley (250-300 g body wt) rats were used in this study. They were fasted but free access to water for 24 hours before experiment. Approval of the protocol was obtained from the Danish Animal Experiment Committee. After animal was euthanized by cervical dislocation, its abdomen was opened and the small intestine was separated from the adjacent organs. An 18-cm-long segment from the middle part of small intestine was cut and excised within 2 min, then transferred to an organ bath containing oxygenated Krebs-Ringer-bicarbonate solution at pH 7.4 with 6 % Dextran and 2 mL EGTA.

Procedures

The specimen was further cut into six 3-cm-long segments. One of the six segments served as control and was fixed in 4 % formalin in no-load condition. The 5 segments left had one end ligated while the other end was connected via a tube to a fluid container for application of different pressures, which were 2, 5, 10, 15 and 20 cm H₂O respectively. Before we pressurized the intestinal segments, we placed some microbeads on surface of the middle part of the segments. Then the outlet was clamped to maintain the volume. After applying pressure for 3 minutes, a record of the whole intestine segment and the part with dots was obtained using video-camera (SONY CCD/RGB, JAPAN) to monitor the whole process (refer to Figure 1) performed under room temperature.

After the specimen was fixed in 4 % formalin for 24 hours, 1.0 cm long and 0.5 cm long transverse sections were taken from the middle part of specimen and dehydrated in a series of graded ethanol (70 %, 90 %, 95 % and 100 %) and embedded in paraffin respectively. 5 μ m serial slices were cut and stained with picosirius red for collagen analysis and HE (hemotoxylin and eosin) for general histological observation^[22-26].

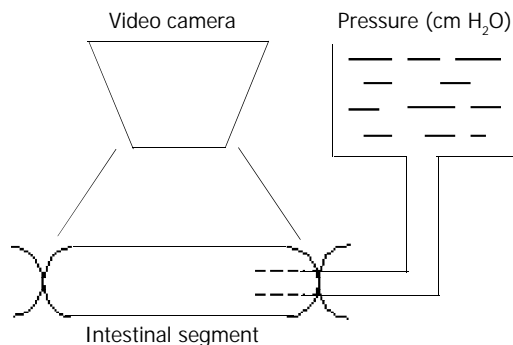


Figure 1 Slice record.

Image acquire

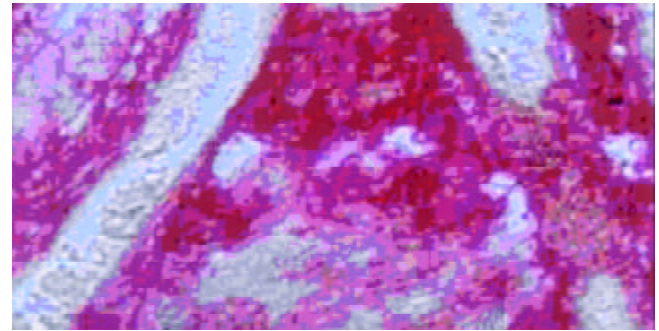
A series of polarized images of intestine slice was acquired by the recorder through microscope at every δ degree angle, and then stored in computer through image collecting card with TIFF format (RGB system type). The TIFF format, a very popular in use currently to reflect the details of the slice images distinctly, and the pixel values in the polarized images are suitable for the principles presented previously very well^[27-29]. Therefore we took the TIFF form to verify the method's feasibility and practicality.

In polarized light microscope, polarized light is delivered onto the sample to be analyzed and handled after being passed through two filter glasses. When the angle between optical axis of the two polarizing lens is 0 degree (that is, both of the two optical axis are parallel to the muscle direction), the blackest image area will be the part where the collagen fiber angle is 90 or 0 degree to the optical axis. Such an image area is also the part where the pixel values are minimum. Therefore, through image analysis we can find out all the area where the collagen fibers are parallel to muscle direction and thereby figure out the area ratio between the study area and the entire analysis Area (abcd). In the slice image analysis, the collagen fiber manifested as some pink striation (f) and the muscle fiber (e) some buff^[4] (refer to Figure 2).

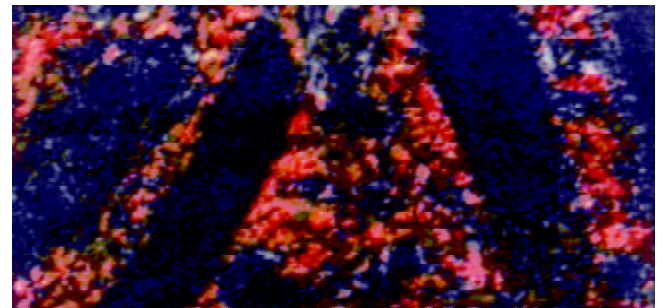
Rotating the polarizing eyepiece while maintaining the objective lens and the experiment sample stable can make muscle fiber direction coincide with the optical axis of polarizing objective. When the polarizing eyepiece is rotated δ degree, all the areas where the collagen fiber are δ degree or $90 + \delta$ degree with the muscle fiber will present in the blackest

part^[21], in this way, their ratio to the entire analyzing area can be figured out as well.

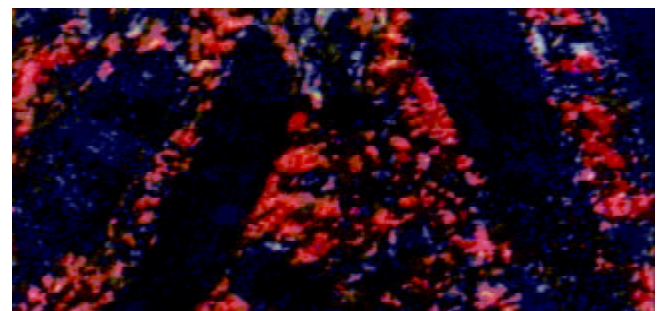
Accordingly, we can obtain the relationship between the angle and its area ratio to the entire area. Since the collagen fiber distribution is uniform, that is, reticular in shape, its longitude and latitude lines are +30 degree and -30 degree to the muscle fiber direction. The area ratio for which is therefore the biggest, we can utilize the area ratio to reckon the collagen fiber angle.



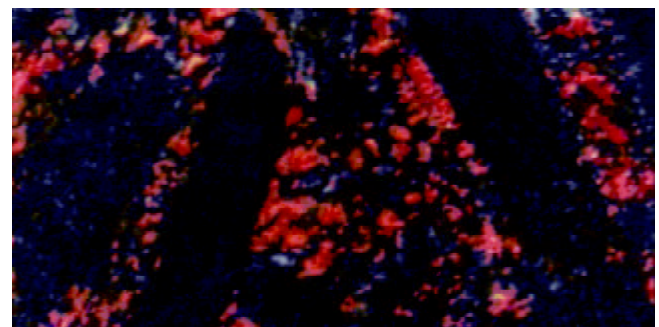
(a) Original image



(b) Polarized image ($\delta=0$ degree)



(c) Polarized image ($\delta=5$ degree)



(d) Polarized image ($\delta=10$ degree)

Figure 2 Image processing.

Image processing

The image processing is the key part of the research, which is eventually based on the analysis of every image's pixels, namely, first to normalize the pixel value and then to use proper algorithms to obtain results. When all the data are summed up, the distribution relationship of collagen fibers can be obtained reversely through the regression curve.

Since the scope of the images recorded is so large that there can include a great deal of muscle tissue and other unrelated background (Figure 2), which should be removed by the image filter before the analysis. The area selected for analysis should be done on the original image before it was polarized.

In this study, the background noises were excluded directly with a frequency domain strengthening method because both of the edge and noise in the image correspond to the high frequency section of the image's Fourier transformation, we could weaken this part of the frequency to lessen its influence in the frequency domain^[30-33].

Data processing

For the purpose of saving much more information of each pixel, the matrix was unified. Take matrix F (m,n) as the basis for further processing, the data less than the chosen threshold value were considered as the collagen fiber area in the polarized image. Figure out the pixel's number that was less than the chosen threshold value s (j)^[34,35]. And made:

$$b(j) = \frac{s(j)}{m \times n};$$

b(j) was equal to the area ratio of collagen fiber and the chosen observed area in polarized image j. From this we got series of the ratio sequence, which were stored into array Y(j).

RESULTS

According to the steps mentioned above, the calculation results were shown in Table 1, where the first column listed the pressures the tissue were received and the first row was the polarized light angles being rotated. We found that for the same slice, with polarized light angle's variation, its corresponding area ratio is not identical; for each tissue under different pressures, its biggest area ratio is not identical either. To obtain the smooth curve showing the relationship between the angle and the corresponding ratio, we made a nonlinear normality on the sample data^[36], the abscissa of the curve was δ's integer multiple and the ordinate the series value in array Y(i) (Figure 3).

The relationship between pressures tissue received and their corresponding fiber angle was shown in Figure 4.

The relationship between pressures tissue received and their corresponding biggest ratio was shown in Figure 5.

We tested other intestinal slice's images (of the same animal) and found that their properties above were similar by and large.

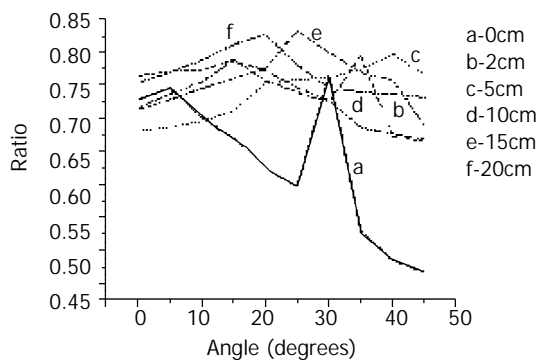


Figure 3 Relationship between angles of polarized light and their corresponding pixel ratio in series of slice images.

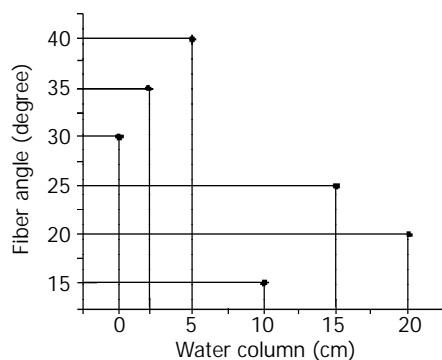


Figure 4 Relationship between pressures tissue received and their corresponding fiber angle.

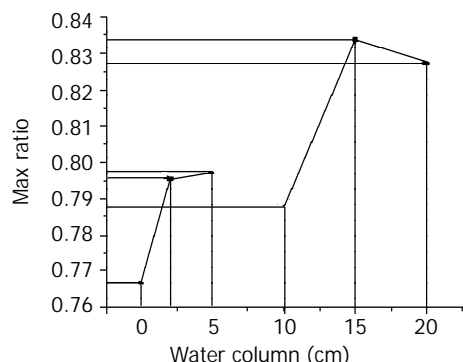


Figure 5 Relationship between pressures tissue received and their corresponding biggest ratio.

DISCUSSION

From the data in Table 1, we found that in the same tissue sample there exist obvious alterations in the collagen area ratio

Table 1 Area ratio of slice image at different angles within various distension pressures (δ=5°, *is the biggest area ratio of this slice image)

δ	0°	5°	10°	15°	20°	25°	30°	35°	40°	45°
H ₂ O										
0 cm	.7288	.7465	.7016	.6694	.6238	.5978	.7666*	.5290	.4852	.4669
2 cm	.7649	.7713	.7732	.7890	.7576	.7399	.7245	.7956*	.6730	.6654
5 cm	.6817	.6874	.6959	.7118	.7535	.7591	.7632	.7744	.7976*	.7664
10 cm	.7162	.7375	.7563	.7877*	.7730	.7469	.7272	.6866	.6764	.6684
15 cm	.7139	.7285	.7455	.7611	.7760	.8337*	.8000	.7693	.7580	.6873
20 cm	.7548	.7700	.7885	.8125	.8270*	.7807	.7457	.7400	.7372	.7320

as the angles of polarized light changed; In different slice's images with different pressures, its biggest ratio was also not identical (Figure 4), and the biggest value was fairly obvious. However, it can not be determined whether the magnitude of collagen fiber angle and the fiber content are all in direct proportion with the pressure that the intestines received (Figure 4, Figure 5), because this depends some degree on the way how it receives the pressure. Using other methods to change its stress still needs to be tested in future experiments. The method of calculating ratios of different pixel values to estimate collagen fiber angle has its feasibility and reliability, which allows a larger area of soft tissue being analyzed with relatively low cost and simple equipment. The disadvantage of this method is the difficulty in determining an appropriate threshold value as well as a definite scope suitable for analyzing which have very important influence on the study results. At the same time, the less δ is to be selected, the more accurate the angle will be.

This paper has tried to acquire the collagen fiber angle of soft tissue in intestine slice through introducing a quantitative analysis method for calculating different pixel values whose validity is verified with computer program, and suggested a practical and effective method for basic research on G.I. disease.

REFERENCES

- Sacks MS**, Gloeckner DC. Quantification of the fiber architecture and biaxial mechanical behaviour of porcine intestinal submucosa. *J Biomed Mater Res* 1999; **46**: 1-10
- Clarke KM**, Lantz GC, Salisbury SK, Badylak SF, Hiles MC, Voytik SL. Intestine submucosa and polypropylene mesh for abdominal wall repair in dogs. *J Surg Res* 1996; **60**: 107-114
- Badylak SF**, Lantz GC, Coffoy A, Geddes LA. Small intestinal submucosa as a large diameter vascular graft in the dog. *J Surg Res* 1989; **47**: 74-80
- Fackler K**, Klein L, Hiltner A, Microsc J. Polarizing light microscopy of intestine and its relationship to mechanical behaviour. *J Microsc* 1981; **124**: 305-311
- Klein L**, Eichelberger H, Mirian M, Hiltner A. Ultrastructural properties of collagen fibrils in rat intestine. *Connective Tissue Res* 1983; **12**: 71-78
- Gabella G**. The cross-ply arrangement of collagen fibers in the submucosa of the mammalian small intestine. *Cell Tissue Res* 1987; **248**: 491-497
- Doering CW**, Jalil JE, Janicki JS, Pick R, Aghili S, Abrahams C, Weber KT. Collagen network remodeling and diastolic stiffness of the rat left ventricle with pressure overload hypertrophy. *Cardiovasc Res* 1988; **22**: 686-695
- Whittaker P**, Boughner DR, Kloner RA. Role of collagen in acute myocardial infarct expansion. *Circulation* 1991; **84**: 2123-2134
- Yao YL**, Xu B, Zhang WD, Song YG. Gastrin, somatostatin, and experimental disturbance of the gastrointestinal tract in rats. *World J Gastroenterol* 2001; **7**: 399-402
- Jalil JE**, Janicki JS, Pick R, Abrahams C, Weber KT. Fibrosis-induced reduction of endomyocardium in the rat after isoproterenol treatment. *Circ Res* 1989; **65**: 258-264
- Jorgensen CS**, Assentoft JE, Knauss D, Gregersen H, Briggs GA, Jorgensen Claus S. Small intestine wall distribution of elastic stiffness measured with 500 MHz scanning acoustic microscopy. *Ann Biomed Eng* 2001; **29**: 1059-1063
- Eghbali M**, Robinson TF, Seifter S, Blumenfeld OO. Collagen accumulation in heart ventricles as a function of growth and aging. *Cardiovasc Res* 1989; **23**: 723-729
- Zou XP**, Liu F, Lei YX, Li ZS. Change and role of β -endorphine in plasma and gastric mucosa during the development of rat gastric stress ulceration. *Shanghai Shengwu Yixue Gongcheng* 2001; **22**: 3-5
- Jiang ZL**, Li HH, Liu B, Teng ZZ, Qing KR. Biomechanical properties of arteries in experimental hypotensive rats. *Shengwu Yixue Gongchengxue Zazhi* 2001; **18**: 381-384
- Wang ZS**, Chen JDZ. Blind separation of slow waves and spikes from gastrointestinal myoelectrical recordings. *IEEE Transactions on Information Technology in Biomedicine* 2001; **5**: 133-137
- Cui JH**, Krueger U, Henne-Bruns D, Kremer B, Kalthoff H. Orthotopic transplantation model of human gastrointestinal cancer and detection of micrometastases. *World J Gastroenterol* 2001; **7**: 381-386
- James X**, Horace HS, Nabil S, Helena TF, Gateno J, Wang DF, Tideman H. Three-dimensional virtual-reality surgical planning and soft-tissue prediction for orthognathic surgery. *IEEE Transaction on Information Technology in Biomedicine* 2001; **5**: 97-107
- Zhao J**, Sha H, Zhou S, Tong X, Zhuang FY, Gregersen H. Remodelling of zero-stress state of small intestine in streptozotocin-induced diabetic rats. Effect of gliclazide. *Dig Liver Dis* 2002; **34**: 707-716
- Orberg JM**, Klein L, Hiltner A. Scanning electron microscopy of collagen fibers in intestine. *Connective Tissue Research* 1982; **9**: 187-193
- Orberg J**, Baer E, Hiltner A. Organization of collagen fibers in the intestine. *Connective Tissue Research* 1983; **11**: 285-297
- Komuro T**. The lattice arrangement of the collagen fibers in the submucosa of the rat small intestine: scanning electron microscopy. *Cell Tissue Res* 1988; **251**: 117-121
- Gabella G**. The collagen fibrils in the collapsed and the chronically stretched intestinal wall. *J Ultrastruct Res* 1983; **85**: 127-138
- Dickey JP**, Hewlett BR, Dumas GA, Bednar DA. Measuring collagen fiber orientation: A two-dimensional quantitative macroscopic technique. *J Biomech Eng August* 1998; **120**: 537-540
- Pu YP**, Li YH, Han YS, Yuan CW, Wu L. Rat keratinocyte primary cultures based on conductive polypyrrole primary cell culture technique. *J Biomed Eng* 2001; **18**: 416-418
- Liu XP**, Li YM, Qiu XC, Li J, Yang YL. Effect and mechanism of melatonin on hemorrhheology in morphine withdrawal rats. *Beijing Shengwu Yixue Gongcheng* 2001; **20**: 143-145
- Jiang ZL**, Yang XQ, Ji KH, Chen EY. Effect of endothelin on zero-stress state of arteries in spontaneously hypertensive rats (SHR). *Zhongguo Shengwu Yixue Gongcheng Xuebao* 2001; **20**: 289-292
- Whittaker P**, Kloner RA, Boughner DR, Pickering JG. Quantitative assessment of myocardial collagen with picrosirius red staining and circularly polarized light. *Basic Res Cardiol* 1994; **89**: 397-410
- Slyater EM**. Optical methods in biology. *New York Wiley* 1970: 268-338
- Chandraratna PA**, Whittaker P, Chandraratna PM, Gallet J, Kloner RA, Hla A. Characterization of collagen by high-frequency ultrasound: evidence for different acoustic properties based on collagen fiber morphologic characteristics. *Am Heart J* 1997; **133**: 364-368
- Pickering JG**, Boughner DR. Quantitative assessment of the age of fibrotic lesions using polarized light microscopy and digital image analysis. *Am J Pathol* 1991; **138**: 1225-1231
- Zhang YJ**. Objective image quality measures and their applications in segmentation evaluation. *Journal of Electronics* 1997; **14**: 97-103
- Liu ZW**, Zhang YJ. Image retrieval using both color and texture features. *Tongxun Xuebao* 1999; **20**: 36-40
- Dong YN**. A New method for efficiently implementing parallel image rotations. *Dianzi Xuebao* 2001; **29**: 1671-1675
- Xue JH**, Zhang YJ, Lin XG. MAP pixel clustering method based on SEM estimation of scatter-plot for low quality image. *Dianzi Xuebao* 1999; **27**: 95-98
- Zhang YJ**, Xu Y, Liu ZW, Yao YR, Li Q. A test-bed for retrieving images with extracted features. *Zhongguo Tuxiang Tuxing Xuebao* 2001; **6**: 439-443
- Crowe JA**, Gibson NM, Woolfson MS, Somekh MG. Wavelet transform as a potential tool for ECG analysis and compression. *J Biomed Eng* 1992; **14**: 268-272

Hormonal regulation of dipeptide transporter (PepT1) in Caco-2 cells with normal and anoxia/reoxygenation management

Bing-Wei Sun, Xiao-Chen Zhao, Guang-Ji Wang, Ning Li, Jie-Shou Li

Bing-Wei Sun, Ning Li, Jie-Shou Li, Department of General Surgery, School of Medicine, Nanjing University, Nanjing 210093, Jiangsu Province, China
Research Institute of General Hospital, Chinese PLA General Hospital of Nanjing Military Area, Nanjing 210002, Jiangsu Province, China
Xiao-Chen Zhao, Guang-Ji Wang, Center of Drug Metabolism and Pharmacokinetics, China Pharmaceutical University, Nanjing 210009, Jiangsu Province, China

Supported by National Natural Science Foundation of China, No. 39970862

Correspondence to: Dr. Bing-Wei Sun, Research Institute of General Surgery, Chinese PLA General Hospital of Nanjing Military Area, 305 East Zhongshan Road, Nanjing 210002, Jiangsu Province, China. sunbinwe@hotmail.com

Telephone: +86-25-3387871 Ext 58088 **Fax:** +86-25-4803956

Received: 2002-10-04 **Accepted:** 2002-11-12

Abstract

AIM: To determine the regulation effects of recombinant human growth hormone (rhGH) on dipeptide transporter (PepT1) in Caco-2 cells with normal culture and anoxia/reoxygenation injury.

METHODS: A human intestinal cell monolayer (Caco-2) was used as the in vitro model of human small intestine and cephalixin as the model substrate for dipeptide transporter (PepT1). Caco-2 cells grown on Transwell membrane filters were preincubated in the presence of rhGH in the culture medium for 4 d, serum was withdrawn from monolayers for 24 h before each experiment. The transport experiments of cephalixin across apical membranes were then conducted; Caco-2 cells grown on multiple well dishes (24 pore) with normal culture or anoxia/reoxygenation injury were preincubated with rhGH as above and uptake of cephalixin was then measured.

RESULTS: The transport and uptake of cephalixin across apical membranes of Caco-2 cells after preincubation with rhGH were significantly increased compared with controls ($P=0.045$, 0.0223). Also, addition of rhGH at physiological concentration (34 nM) to incubation medium greatly stimulates cephalixin uptake by anoxia/reoxygenation injured Caco-2 cells ($P=0.0116$), while the biological functions of PepT1 in injured Caco-2 cells without rhGH were markedly downregulated. Northern blot analysis showed that the level of PepT1 mRNA of rhGH-treated injured Caco-2 cells was greatly increased compared to controls.

CONCLUSION: The present results of rhGH stimulating the uptake and transport of cephalixin indicated that rhGH greatly upregulates the physiological effects of dipeptide transporters of Caco-2 cells. The alteration in the gene expression may be a mechanism of regulation of PepT1. In addition, Caco-2 cells take up cephalixin by the Proton-dependent dipeptide transporters that closely resembles the transporters present in the intestine. Caco-2 cells represent an ideal cellular model for future studies of the dipeptide transporter.

Sun BW, Zhao XC, Wang GJ, Li N, Li JS. Hormonal regulation of dipeptide transporter (PepT1) in Caco-2 cells with normal and anoxia/reoxygenation management. *World J Gastroenterol* 2003; 9(4): 808-812

<http://www.wjgnet.com/1007-9327/9/808.htm>

INTRODUCTION

Transport of protein in the form of small peptides (di/tripeptides) across the small intestinal wall is a major route of dietary protein absorption. The H⁺-coupled dipeptide transporter, PepT1, is known to be located in the intestine and the kidney, and plays an important role in the absorption of di/tripeptide; in addition, it mediates the intestinal absorption of β -lactam antibiotics, angiotensin-converting enzyme inhibitors, and other peptide-like drugs^[1].

To investigate the properties of the human dipeptide transporter, the human intestinal cell line Caco-2 as an in vitro model was employed. The dipeptide transporters normally found in the small intestine are present in Caco-2 cells^[2-4]. Also, Caco-2 cells spontaneously differentiate in culture to polar cells possessing microvilli and enterocytic properties^[5]. Confluent monolayers form tight junctions between cells^[5], and exhibit dome formation^[6] and electrical properties of an epithelium^[7]. These cells have been evaluated in detail as a model to study both transcellular and paracellular transport of nutrients and drugs in the gut^[8-12].

Previous studies have shown that some hormones metabolically regulate the expression of the intestinal dipeptide transporter^[13,14]. For example, as the key hormone, insulin increases the membrane population of PepT1 by increasing its translocation from a preformed cytoplasmic pool^[14]. However, little is known whether another important hormone, growth hormone (GH), also metabolically regulate the functions of PepT1. The present study was undertaken to evaluate the potential effects of recombinant human growth hormone (rhGH) for the study of the properties of the human PepT1. Especially, we observed the regulation effects of rhGH to PepT1 in Caco-2 cells which were normally cultured or anoxia/reoxygenation injured. Because dipeptide and some β -lactam antibiotics (cephalexin, cefaclor etc.) share certain structural features such as a peptide bond with an α -amino group and a terminal carboxylic acid group (as illustrated in Figure 1 for cephalixin), it is not surprising that these compounds share a common transport mechanism. Unlike dipeptides, these orally absorbed antibiotics are not hydrolyzed by intestinal peptidases. Consequently, these kinds of drugs are ideal substrates to characterize the PepT1^[15-17]. In this study, the uptake and transport of cephalixin were examined.

MATERIALS AND METHODS

Materials

Cephalixin (Figure 1) was obtained from Nanjing No.2 Pharma.Co. Ltd. rhGH was purchased from Laboratoires Serono S.A. (Switzerland). All other chemicals were purchased from Sigma (St. Louis, MO), unless specified. Cell culture

reagents were obtained from Gibco (Grand Island, NY) and culture supplies from Corning (Corning, NY) and Falcon (Lincoln Park, NJ).

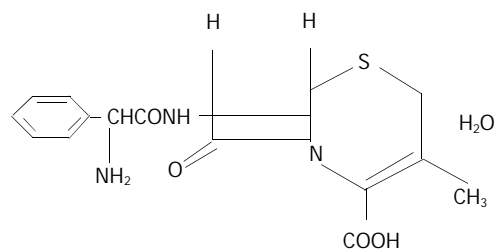


Figure 1 Structure of cephalexin used in this study.

Cell culture

The human adenocarcinoma cell line Caco-2 was obtained from American Tissue Culture Collection (ATCC, Rockville, MD, U.S.A). The cells were passaged as previously described^[18]. Caco-2 cells were grown in Dulbecco's Modified Eagle's Medium supplemented with 1 % nonessential amino acids, 10 % fetal calf serum (FCS), 1 000 U^L⁻¹ penicillin, and 1 mg·L⁻¹ streptomycin (Complete DMEM). For transport studies, Caco-2 cells were seeded on the polycarbonate filter (0.4- μ m pores, 4.71-cm² growth area) in the Transwell Cell Culture Chamber System (Costar, Cambridge, MA) at a density of 600 000 cells/filter. The cell monolayers were cultured with 1.5 and 2.6 ml of complete DMEM at the apical and the basolateral chamber, respectively. To assess the integrity of the monolayer, transepithelial electrical resistance (TEER) was monitored by measuring the transmembrane resistance. After subtracting intrinsic resistance (filter alone without cell monolayers) from the total resistance, TEER was corrected for surface area and expressed as Ω cm². Transport studies were carried out with cell monolayers that were 21-25 days old. For uptake studies, cells were seeded in the collagen-coated multiwell dishes (24 pore) with the same cell density. All the medium were replaced every day when each experiment began. Monolayers were kept at 37 °C, 5 % CO₂, and 90 % relative humidity.

Transport studies

Before the transport experiments, the culture medium was replaced every day from both sides of the monolayers, 1.5 ml pH 7.0 culture medium with 34nM rhGH were added to apical chamber of Transwell, while 2.6 ml pH 7.0 culture medium without rhGH were added to basolateral chamber. Then Caco-2 cells were cultured for 4 days. The controls were incubated with pH 7.0 culture medium both in apical side and basolateral side. All the monolayers were washed during each experiment. The apical chamber were then filled with 1.5 ml solution containing 1 mM cephalexin. Transport was examined within the time range of 0, 5, 10, 30, 60, 90, and 120 min. At the end of the incubation period, the inserts of Transwell were removed and the transport samples were obtained from the basolateral chambers. The concentrations of cephalexin of the transport samples were determined by High Performance Liquid Chromatography (HPLC, LC-10AT SHIMADU, Japan) using an isocratic solvent system described previously^[19] and the OD value was monitored at 254 nm.

Uptake studies

Using the same way as the transport experiments, the Caco-2 cells cultured in the multiwell dishes (24 pore) were cultured for 4 d with 34 nM rhGH. After washing the monolayers, the transport medium with 1 mM cephalexin was added to the pores and uptake was measured at 0, 5, 10, 30, 60, 90, and

120 min. At the end of the incubation period, cell monolayers were washed with pH 7.4 PBS to remove any extracellular cephalexin. Accumulated concentrations of cephalexin were determined by HPLC after the cells were lysed.

Anoxia-reoxygenation cells model

After Caco-2 cells were plated, media within the wells was reduced to a uniformly thin layer to reduce the diffusion distances for atmospheric gases, while maintaining cell ability. During culture, the monolayers were normally exposed to an atmosphere consisting of 95 % air and 5 % CO₂. Anoxia was produced with an atmosphere of 95 % N₂ and 5 % CO₂ for 90 min, reoxygenation was produced by restoration of the 95 % air, 5 % CO₂ for 30 min. After the period of reoxygenation, the volume of media was restored to the initial volume of 1.0 ml^[20] (Figure 2).

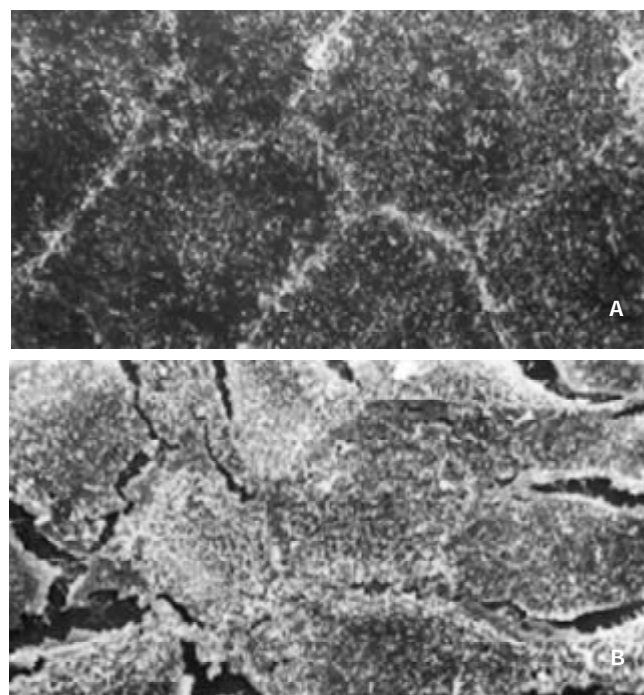


Figure 2 Appearance of scan electronic microscopy of Caco-2 cells. (A) Tight junction formation of normal Caco-2 cells. $\times 1\ 000$; (B) Tight junction of A/R Caco-2 cells was destroyed partially. $\times 1\ 000$.

Protein determination

Cells were lysed for 20 min or ice in 2 % Nonidet P-40, 0.2 % SDS, 1 mM dithiothreitol (DTT) in PBS, and total cellular protein was determined using Dc Protein Assay Reagent (BioRad).

Concentration dependence of cephalexin transport

To examine the kinetics of cephalexin transport by rhGH-treated Caco-2 cells, the different concentrations of cephalexin range of 20 to 80 μ g·ml⁻¹ were used.

Northern blotting

Total RNAs were isolated from the Caco-2 cell fractions by extraction with acid guanidine thiocyanate-phenol-chloroform. Total RNAs were denatured by heating at 70 °C in 10 mmol·L⁻¹ 3-(N-morpholino) propanesulfonic acid (pH 7.0) containing 5 mmol·L⁻¹ sodium acetate, 1 mmol·L⁻¹ ethylenediaminetetraacetic acid (EDTA), 2.2 mol·L⁻¹ formaldehyde, and 50 % (vol/vol) formamide for 5 minutes and subjected to electrophoresis in 1.2 % agarose gel containing 2.2 mol·L⁻¹ formaldehyde. Resolved RNA was transferred to hybridization

and was performed in a solution that contains 50 % formamide, 5x sodium chloride-sodium phosphate-EDTA, 2x Denhardt's solution, and 1 % sodium dodecyl sulfate (SDS). The membranes were exposed and analyzed by Fuji BAS-2000 system. The cDNA probe was prepared from human cDNA libraries.

Sense 5' TTTGGATCCCGGAGTAAGGCATTTCCCAAG 3',
Antisense 5' CCGAAGCTTTCAGGAAGGAGCCTGAGAATATGAG 3'.

Statistical analysis

Data were expressed as mean \pm SE. Differences between experimental groups were assessed by analysis of Variance. *P* values of <0.05 were considered statistically significant.

RESULTS

Transepithelial cephalixin transport in Caco-2 cell with normal culture

Caco-2 cells were seeded at a high density of 600 000 cells/filter, the transport of 1 mM cephalixin across rhGH-treated Caco-2 monolayers, apical-to-basolateral, was examined at PH 6.0 in the donor and pH 7.4 in the receiver compartment. Integrity of the monolayers was monitored by TEER. The apical-to-basolateral transport of cephalixin was significantly increased compared with the controls (*P*=0.0045) (Figure 3).

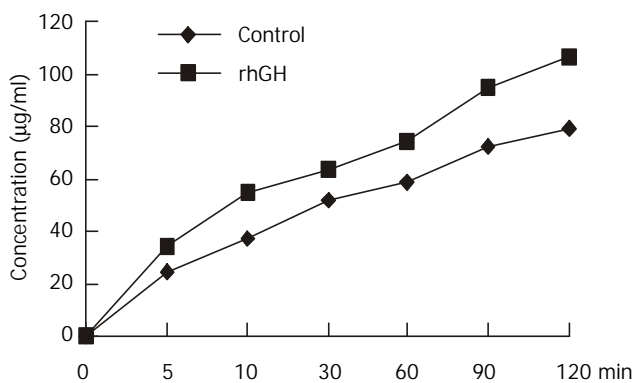


Figure 3 Transport of 1 mM cephalixin in Caco-2 cells. Caco-2 cells were cultured with rhGH in apical side for 4 days. The controls were incubated with PH 7.0 culture medium without rhGH both in apical side and basolateral side. All the monolayers were washed in each experiment. The apical chambers were then filled with 1.5 ml solution containing 1 mM cephalixin. Transport was examined within the time range of 0, 5, 10, 30, 60, 90, and 120 min. At the end of the incubation period, the inserts of Transwell were removed and the transport samples were obtained from the basolateral chambers. The concentrations of cephalixin of the transport samples were determined by HPLC. The apical-to-basolateral transport of cephalixin was significantly increased compared with the controls (*P*=0.0045).

Uptake of cephalixin in Caco-2 cells with normal culture

Uptake experiments with cephalixin were performed 6-8 days after seeding and 18 h after media replacement. Cephalixin uptake was measured in the presence and absence of 34nM of rhGH. The differences were significant (*P*=0.0223), and the results were summarized in Figure 4.

Uptake of cephalixin in anoxia/reoxygenation Caco-2 cells model

Caco-2 monolayers were initially subjected to a 90-minute period of anoxia followed by a 30-minute period of reoxygenation. This was selected as optimal for the main body of the experiment on the basis of the results of our initial experiments. Consequently, the effect of the presence of rhGH on cephalixin uptake via the PepT1 of anoxia/reoxygenation

Caco-2 cells were examined (Figure 5). The present studies indicated that uptake and transport of cephalixin by the normal and anoxia/reoxygenation Caco-2 cells were significantly increased under the influence of rhGH.

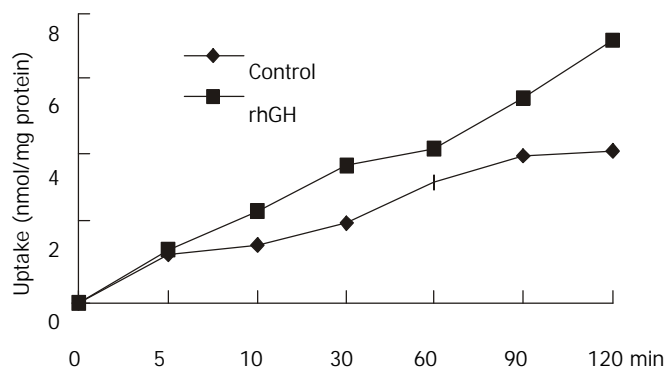


Figure 4 Uptake of 1 mM cephalixin in Caco-2 cells. Caco-2 cells cultured in the multiwell dishes (24 pore) were cultured for 4 d with 34 nM rhGH. After washing the monolayers, the transport medium with 1 mM cephalixin was added to the pores and uptake was measured at 0, 5, 10, 30, 60, 90, and 120 min. At the end of the incubation period, cell monolayers were washed with PH 7.4 PBS to remove any extracellular cephalixin. Accumulated concentrations of cephalixin were determined by HPLC after the cells were lysed. The differences were significant (*P*=0.0223).

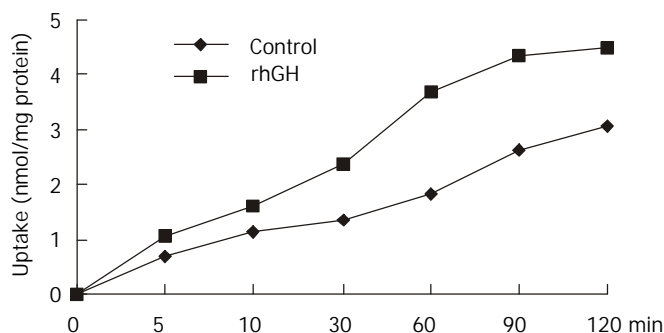


Figure 5 Uptake of 1 mM cephalixin in Caco-2 cells with anoxia/reoxygenation injury. Caco-2 monolayers were initially subjected to a 90-minute period of anoxia followed by a 30-minute period of reoxygenation. The effect of the presence of rhGH on cephalixin uptake via the PepT1 of anoxia/reoxygenation Caco-2 cells was examined. The differences were significant (*P*=0.0116).

Northern blot analysis

Northern blots of Poly (A)⁺ RNA, prepared from anoxia/reoxygenation Caco-2 cells grown either under control conditions or in medium supplemented with 34nM rhGH, were probed separately with ³²P-labelled hPepT1 and β -actin cDNAs. The studies showed that the level of mRNA in rhGH-treated Caco-2 Cells was increased 1.3-fold compared with the controls.

Concentration dependence of cephalixin transport

Transport experiments were performed across the rhGH-treated Caco-2 cells using the different concentrations of cephalixin range of 20 to 80 μ g \cdot ml⁻¹. The results (Figure 6) indicated that the transport of cephalixin was increased both in rhGH-treated Caco-2 cells and Controls. However, the extent of upregulation of rhGH on the transport was greater than the controls followed the increase of the concentration of cephalixin.

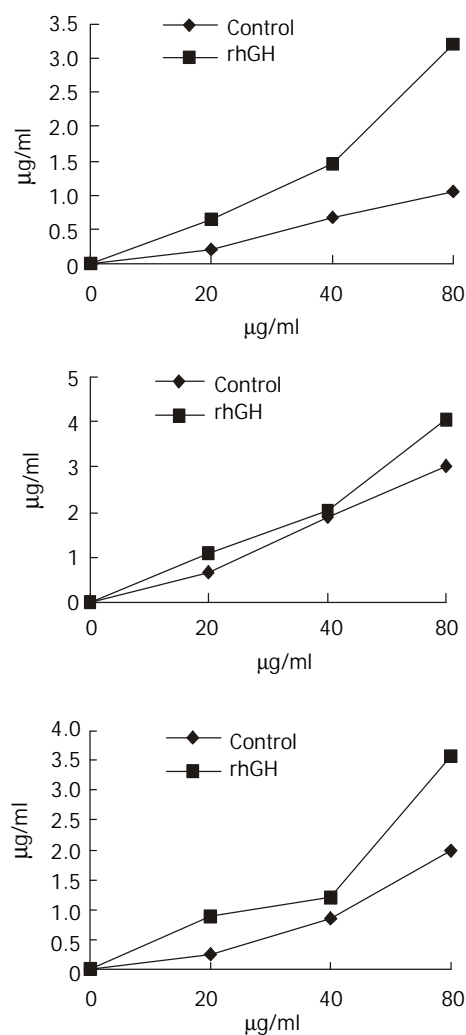


Figure 6 Concentration-dependent transport of cephalixin. The kinetics of cephalixin transport by rhGH-treated Caco-2 cells showed that the transport level of Caco-2 cells was in accordance with the concentration of cephalixin. The concentrations of cephalixin range of 20 to 80 $\mu\text{g}\cdot\text{ml}^{-1}$ were used. Transport was determined at the different time-point (a, 15 min; b, 30 min; c, 45 min). The extent of upregulation of rhGH on the transport was greater than the controls followed the increase of the concentration of cephalixin.

DISCUSSION

The nutritional importance of amino acid uptake in the form of short-chain peptides (di/tripeptides) is well known^[21]. The intraluminal products of protein digestion are predominantly small peptides^[22]. A significant fraction of the dietary amino nitrogen is absorbed as intact dipeptide rather than free amino acids. Absorption of these small peptides from the gastrointestinal (GI) tract of mammals occurs via the dipeptide transporter (PepT1). Previous studies have shown that the functions of intestine (including PepT1) were changed under the influence of many factors^[23,24]. PepT1 seems to play important roles in nutritional and pharmacological therapies; for example, it has allowed the use of small peptide as a source of nitrogen for enteral feeding and the use of oral route for delivery of peptidomimetic drugs such as β -lactam antibiotics. PepT1 was located at the brush-border membranes of the absorptive epithelial cells along the small intestine but absent in crypt and goblet cells^[25,26].

To examine the functions of PepT1, we used Caco-2 cells (the human adenocarcinoma cell line) as a unique *in vitro* intestinal model^[27]. One clear advantage of the Caco-2 cells is

that the cells stay viable throughout the transport studies. Also, a monolayer of cells may be grown on a porous support to represent an intact epithelium. Some β -lactam antibiotics (cephalexin) and dipeptides share certain structural features, and they are generally in the D-form, which allows them to escape hydrolysis by cytoplasmic peptidases. So these compounds share a common transport mechanism^[28]. In this study, we employed cephalixin as an ideal substrate.

The previous studies have shown that the insulin stimulates dipeptide transport by increasing membrane insertion of PepT1 from a preformed cytoplasmic Pool^[14], and cholera toxin decreases dipeptide transport by inhibiting the activity of PepT1 through an increase in the intracellular concentration of adenosine 3', 5'-cyclic monophosphate^[21]. It remains unclear, however, whether another key hormone, human growth hormone (hGH), also shows some significant importance. Strong evidence has demonstrated that growth hormone (GH) is an important growth factor for intestine^[28]. Complete GH depletion due to hypophysectomy caused pronounced hypoplasia of small intestinal mucosa with decreased villus height and reduced crypt cell proliferation^[29]. Simple replacement of GH can restore mucosal proliferative activity^[30]. rhGH promotes normal growth and development in the body by changing chemical activity in cells. It activates protein production in muscle cells and the release of energy from fats. rhGH significantly improves the anabolism in parenterally fed^[31]. It is typically used to stimulate growth in children with hormone deficiency, or to treat people with severe illness, burns or sepsis where destruction of human tissue and muscle occurs^[32-34]. Many of the effects of human growth hormone are brought about by the insulin-like growth factor 1 (IGF-1), which the growth hormone stimulates. IGF-1 plays an important part in growth-promoting effects of rhGH^[32]. The present studies showed that the uptake and transport of cephalixin in Caco-2 cells were greatly increased by using of rhGH. In addition, a specific injured cell model, anoxia/reoxygenation Caco-2 cells model, was established in our present experiment. The uptake of cephalixin in the injured Caco-2 cells was markedly decreased while the cephalixin uptake was significantly increased in the injured Caco-2 cells with treatment of rhGH. These results indicate that the functions of PepT1 in Caco-2 cells were upregulated by rhGH. The investigation of concentration-dependent transport of cephalixin in Caco-2 cells showed that the transport was increased both in rhGH-treated Caco-2 cells and controls. However, the upregulating extent of rhGH on the transport of cephalixin was greater than controls following the increase of the concentration of cephalixin. Northern blot analysis showed that the level of PepT1 mRNA of injured Caco-2 cells with rhGH treatment were increased. This result also provides novel information about the mechanism of regulation action of rhGH. It has suggested that the alteration in the gene expression may be a mechanism of regulation of PepT1.

Use of this experimental design leads to the following three questions. What is the detail mechanism of upregulating the functions of PepT1 by rhGH? How does the rhGH receptor distribute in Caco-2 cells? How does the rhGH receptor change in anoxia/reoxygenation Caco-2 cells? Clearly, the present study needs to be followed by further studies on physiology and biology of hormonal regulation of PepT1.

REFERENCES

- 1 **Hsu CP**, Walter E, Merkle HP, Rothen-Rutishauser B, Wunderli-Allenspach H, Hilfinger JM, Amidon GL. Function and immunolocalization of over expressed human intestinal H^+ /peptide cotransporter in adenovirus-transduced Caco-2 cells. *AAPS PharmSci* 1999; **1**: E12

- 2 **Vincent ML**, Russell RM, Sasak V. Folic acid uptake characteristics of a human colon carcinoma cell line, Caco-2. A newly-described cellular model for small intestinal epithelium. *Hum Nutr Clin Nutr* 1985; **39**: 355-360
- 3 **Mohrmann I**, Mohrmann M, Biber J, Murer H. Sodium-dependent transport of Pi by an established intestinal epithelial cell line(Caco-2). *Am J Physiol* 1986; **250**(3 Pt 1): G323-330
- 4 **Blais A**, Bissonnette P, Berteloot A. Common characteristics for Na⁺-dependent sugar transport in Caco-2 cells and human fetal colon. *J Member Biol* 1987; **99**: 113-125
- 5 **Rousset M**, Laburthe M, Pinto M, Chevalier G, Rouyer-Fessard C, Dussaulx E, Trugnan G, Boige N, Brun JL, Zweibaum A. Enterocytic differentiation and glucose utilization in the human colon tumor cell line Caco-2: modulation by forskolin. *J Cell Physiol* 1985; **123**: 377-385
- 6 **Romond MJ**, Martinot-Peignoux M, Erlinger S. Dome formation in the human colon carcinoma cell line Caco-2 in culture. Influence of ouabain and permeable supports. *Biol Cell* 1985; **54**: 89-92
- 7 **Grasset E**, Pinto M, Dussaulx E, Zweibaum A, Desjeux JF. Epithelial properties of human colonic carcinoma cell line Caco-2: electrical parameters. *Am J Physiol* 1984; **247**(3 Pt 1): C260-267
- 8 **Milovic V**, Turchanowa L, Stein J, Caspary WF. Transepithelial transport of putrescine across monolayers of the human intestinal epithelial cell line, Caco-2. *World J Gastroenterol* 2001; **7**: 193-197
- 9 **Hidalgo JJ**, Raub TJ, Borchardt RT. Characterization of the human colon carcinoma cell line (Caco-2) as a model system for intestinal epithelial permeability. *Gastroenterology* 1989; **96**: 736-749
- 10 **Artursson P**. Epithelial transport of drugs in cell culture. I: A model for studying the passive diffusion of drugs over intestinal absorptive (Caco-2) cells. *J Pharm Sci* 1990; **79**: 476-482
- 11 **Artursson P**, Karlsson J. Correlation between oral drug absorption in humans and apparent drug permeability coefficients in human intestinal epithelial (Caco-2) cells. *Biochem Biophys Res Commun* 1991; **175**: 880-885
- 12 **Artursson P**. Cell cultures as models for drugs absorption across the intestinal mucosa. *Crit Rev Ther Drug Carrier Syst* 1991; **8**: 305-330
- 13 **Thamotharan M**, Bawani SZ, Zhou X, Adibi SA. Hormonal regulation of oligopeptide transporter PepT1 in a human intestinal cell line. *Am J Physiol* 1999; **276**(4 Pt 1): C821-826
- 14 **Nielsen CU**, Amstrup J, Steffansen B, Frokjaer S, Brodin B. Epidermal growth factor inhibits glycy sarcosine transport and hPepT1 expression in a human intestinal cell line. *Am J Physiol Gastrointest Liver Physiol* 2001; **281**: G191-199
- 15 **Ganapathy V**, Mendicino JF, Leibach FH. Transport of glycyl-L-proline into intestinal and renal brush border vesicles from rabbit. *J Biol Chem* 1981; **256**: 118-124
- 16 **Rajendran VM**, Ansari SA, Harig JM, Adams MB, Khan AH, Ramaswamy K. Transport of glycyl-L-proline by human intestinal brush border membrane vesicles. *Gastroenterology* 1985; **89**: 1298-1304
- 17 **Berteloot A**. Membrane potential dependence of glutamic acid transport in rabbit jejunal brush-border membrane vesicles: K⁺ and H⁺ effects. *Biochim Biophys Acta* 1986; **861**: 447-456
- 18 **Dantzig AH**, Bergin L. Uptake of the cephalosporin, cephalixin, by a dipeptide transport carrier in the human intestinal cell line, Caco-2. *Biochim Biophys Acta* 1990; **1027**: 211-217
- 19 **Dantzig AH**, Bergin L. Carrier-mediated uptake of cephalixin in human intestinal cells. *Biochim Biophys Res Commun* 1988; **155**: 1082-1087
- 20 **Ratych RE**, Chuknyiska RS, Bulkley GB. The primary localization of free radical generation after anoxia/reoxygenation in isolated endothelial cells. *Surgery* 1987; **102**: 122-131
- 21 **Ferraris RP**, Diamond J, Kwan WW. Dietary regulation of intestinal transport of the dipeptide carnosine. *Am J Physiol* 1988; **255**(2 Pt 1): G143-150
- 22 **Ganapath V**, Brandsch M, Leibach FH. Intestinal transport of amino acids and peptides. In: Johnson LR, ed. Physiology of the gastrointestinal tract. Volum 2. 3rd ed. *New York: Raven* 1994: 1773-1794
- 23 **Li YS**, Li JS, Li N, Jiang ZW, Zhao YZ, Li NY, Liu FN. Evaluation of various solutions for small bowel graft preservation. *World J Gastroenterol* 1998; **4**: 140-143
- 24 **Liang LJ**, Yin XY, Luo SM, Zheng JF, Lu MD, Huang JF. A study of the ameliorating effects of carnitine on hepatic steatosis induced by total parenteral nutrition in rats. *World J Gastroenterol* 1999; **5**: 312-315
- 25 **Ogihara H**, Saito H, Shin BC, Terada T, Takenoshita S, Nagamachi Y, Inui K, Takata K. Immuno-localization of H⁺/peptide cotransporter in rat digestive tract. *Biochem Biophys Res Commun* 1996; **220**: 848-852
- 26 **Adibi SA**. The oligopeptide transporter (PepT1) in human intestine: Biology and Function. *Gastroenterology* 1997; **113**: 332-340
- 27 **Dantzig AH**, Bergin L. Uptake of the cephalosporin, cephalixin, by a dipeptide transport carrier in the human intestinal cell line, Caco-2. *Biochim Biophys Acta* 1990; **1027**: 211-217
- 28 **Zhou X**, Li YX, Li N, Li JS. Effect of bowel rehabilitative therapy on structural adaptation of remnant small intestine: animal experiment. *World J Gastroenterol* 2001; **7**: 66-73
- 29 **Bastie MJ**, Balas D, Laval J, Senegas-Balas F, Bertrand C, Frexinos J, Ribet A. Histological variations of jejunal and ileal mucosa on days 8 and 15 after hypophysectomy in rat: morphometrical analysis on light and electron microscopy. *Acta Anat (Basel)* 1982; **112**: 321-337
- 30 **Scow RO**, Hagan SN. Effect of testosterone Propionate and growth hormone on growth and chemical composition of muscle and other tissues in hypophysectomized male rats. *Endocrinology* 1965; **77**: 852-858
- 31 **Gu Y**, Wu ZH. The anabolic effects of recombinant human growth hormone and glutamine on parenterally fed, short bowel rats. *World J Gastroenterol* 2002; **8**: 752-757
- 32 **Jeschke MG**, Herndon DN, Wolf SE, Debroy MA, Rai J, Lichtenbelt BJ, Barrow RE. Recombinant human growth hormone alters acute phase reactant proteins, cytokine expression, and liver morphology in burned rats. *J Surg Res* 1999; **83**: 122-129
- 33 **Roth E**, Valentini L, Semsroth M, Holzenbein T, Winkler S, Blum WF, Ranke MB, Schemper M, Hammerle A, Karner J. Resistance of nitrogen metabolism to growth hormone treatment in the early phase after injury of patient with multiple injuries. *J Trauma* 1995; **38**: 136-141
- 34 **Postel-Vinay MC**, Finidori J, Sotiropoulos A, Dinerstein H, Martini JF, Kelly PA. Growth hormone receptor: structure and signal transduction. *Ann Endocrinol* 1995; **56**: 209-212

Experimental study on the feasibility and safety of radiofrequency ablation for secondary splenomegaly and hypersplenism

Quan-Da Liu, Kuan-Sheng Ma, Zhen-Ping He, Jun Ding, Xue-Quan Huang, Jia-Hong Dong

Quan-Da Liu, Kuan-Sheng Ma, Zhen-Ping He, Jun Ding, Jia-Hong Dong, Institute of Hepatobiliary Surgery, Southwest Hepatobiliary Surgery Hospital, Southwest Hospital, Third Military Medical University, Chongqing, 400038, China

Xue-Quan Huang, Department of Radiology, Southwest Hospital, Third Military Medical University, Chongqing, 400038, China

Supported by the "Tenth-Five" Fundamental Medical Scientific Research Projects of PLA, China, No. 02Z005

Correspondence to: Dr. Quan-Da Liu, Institute of Hepatobiliary Surgery, Southwest Hepatobiliary Surgery Hospital, Southwest Hospital, Third Military Medical University, Chongqing, 400038, China. liuquanda@sina.com

Telephone: +86-23-65398541

Received: 2002-10-08 **Accepted:** 2002-11-09

Abstract

AIM: To assess the feasibility and safety of radiofrequency ablation (RFA) in treatment of secondary splenomegaly and hypersplenism.

METHODS: Sixteen healthy mongrel dogs were randomly divided into two groups, group I ($n=4$) and group II ($n=12$). Congestive splenomegaly was induced by ligation of splenic vein and its collateral branches in both groups. At the end of 3rd week postoperation, RFA in spleen was performed in group II *via* laparotomy, complications of RFA were observed, CT scan was performed and the spleens were obtained. The radiofrequency (RF) thermal lesions and histopathology of spleen were examined regularly.

RESULTS: No complication or death was observed in both groups; CT revealed that the splenomegaly lasted over 2 months after ligation of splenic vein; the segmental RF lesions included hyperintense zone of coagulative necrosis and more extensive peripheral hypointense infarcted zone, the latter was called "bystander effect". The infarcted zone would be absorbed and subsequently disappeared in 4-6 weeks after RFA accompanied with shrinkage of the remnant spleen. The fundamental histopathological changes of splenic lesions caused by RF thermal energy included local coagulative necrosis, peripheral thrombotic infarction zone, subsequent tissue absorption and fibrosis in the zone of thrombotic infarction, the occlusion of vessels in remnant viable spleen, deposition of extensive fibrous protein, and disappearance of congestive splenic sinusoid - "splenic carnification". Those pathologic changes were underline of shrinkage of spleen.

CONCLUSION: It is feasible and safe to perform RFA in spleen to treat experimental splenomegaly and hypersplenism. The RFA could be safely performed clinically *via* laparotomy or laparoscopic procedure while spleen was strictly separated from surrounding organs.

Liu QD, Ma KS, He ZP, Ding J, Huang XQ, Dong JH. Experimental study on the feasibility and safety of radiofrequency ablation for secondary splenomegaly and hypersplenism. *World J Gastroenterol* 2003; 9(4): 813-817

<http://www.wjgnet.com/1007-9327/9/813.htm>

INTRODUCTION

Radiofrequency ablation (RFA) was developed in 1990s and thereafter evolved rapidly as a minimally invasive technique for the treatment of primary and secondary malignant tumors in solid organs^[1-25]. The fundamental principle is that alternating electric current operated in the range of radiofrequency (460-500 kHz) can produce a focal thermal injury in living tissue, the tip of the electrode conducts the current, causing local ionic agitation and subsequent frictional heat (90-110 °C). Temperatures over 60 °C produce uniform tissue coagulative necrosis, a 2-5 cm spherical thermal injury can be produced with each ablation. The potential benefits of these techniques over conventional surgical options include tumor ablation in nonsurgical candidates with low morbidity, and being used on an outpatient basis^[1-15].

One of the most manifestations of liver cirrhosis with portal hypertension was hypersplenism secondary to splenic congestion with intrasplenic sequestration and destruction of erythrocytes, leucocytes and platelets resulting in anemia, leucopenia and thrombocytopenia^[26]. Splenectomy is a routine therapy for hypersplenism and can correct the abnormal hematologic parameters^[26,27]. However, with the awareness of the role and importance of the spleen in the immune system, splenic conservative methods have gained prominence in the treatment of benign conditions of the spleen^[27-29]. Several minimally invasive treatment modalities such as transcatheter selective splenic arterial embolization^[30], absolute alcohol or ethanolamine oleate intrasplenic injection^[31,32] have been investigated clinically, but the clinical applications were restricted due to associated complications.

In order to establish an effective therapy for hypersplenism with splenomegaly, animal model with splenomegaly was induced by ligation of splenic vein (LSV), the computerized tomographic (CT) and pathologic changes of the thermal lesions in spleen after RFA were observed, and the feasibility and safety of RFA for secondary splenomegaly and hypersplenism and its potential clinical prospective were investigated.

MATERIALS AND METHODS

Animals and experimental design

Sixteen healthy adult mongrel dogs (12 to 17 kg) were randomly divided into two groups. LSV *plus* Laparotomy were performed in Group I ($n=4$), and LSV *plus* RFA were done in Group II ($n=12$).

After fasting overnight, the animals were anesthetized generally with sodium pentobarbital (25 mg/kg) and maintained with supplemental doses of sodium pentobarbital. The great saphenous vein was cannulated for transfusion with 500 ml of acetate Ringer's solution. Midline incision was used to access the spleen, splenic veins in both groups were ligated at the confluent to portal vein, and then the main branches of splenic vein were further ligated separately at the splenic hilus in order to minimize collateral formation. The animals were cared in cages at 24±2 °C and fed with standard diet and water *ad libitum* after operation. At the end of the third week, under general anesthesia again, the animals in group I were performed laparotomy only; and both laparotomy and RFA of spleen were done in group II.

Ablation procedures

RFA was performed with the RF 2000 generator system (Radio Therapeutics Corp., CA, USA), which consists of a generator generating [up to 90 W in power, a leVein monopolar array needle electrode (3.5 cm maximum array diameter), and two electrode pads (grounding pads) placed on the animal's shaved thighs. The leVein needle electrode is a 15-gauge, 15-20 cm in length insulated cannula containing 10 individual hook-shaped retractable electrode arms that deployed in situ after placement of the needle electrode in splenic parenchyma. The probe was inserted perpendicularly into the splenic parenchyma in lateral region of superior or inferior pole of spleen, and the spleen was elevated to avoid to contact with adjacent organs and skin. A 90 W monopolar radiofrequency generator (RF 2000, Radiotherapeutics) was used as the energy source. Power output was initially set at 30 W and manually titrated 10 W per 60 sec until the maximum power. Thereafter, impedance could rise with automatic power adjustment until power output was terminated. The electrode 0.5 cm retrograded in situ and above session repeated. The needle track was cauterized on needle removal.

During RFA procedure, the temperatures on the sites of thermal lesions, hilum of spleen and the tail of pancreas were measured frequently by thermosensors, and cold saline was used to lower the temperature on the hilum of spleen, and tail of pancreas. Five-hundred ml of acetate Ringer's solution and 0.8M IU of penicillin were given intravenously.

Observation of animals

The complications during RFA, such as hemorrhage, thermal injury of other organs, the appetites, eating and activities of animals, morbidity and mortality after RFA were carefully documented.

CT imaging and histopathology on splenic lesions

Splenic sizes in group I after LSV were documented with CT scans (Siemens Medical System, Germany) at 3, 6, 9 weeks after laparotomy. CT imaging (plain scan plus enhancement) performed for the dogs in group II after RFA on day 1, and at 1, 2, 4, 6 and 9 weeks after RFA to study the thermal injured lesions in spleens. Two dogs in group II were killed immediately after CT scan, and all dogs were sacrificed at the end of the 9th week. Before sacrificing the dogs, spleens were removed, specimen of liver and pancreas were harvested and fixed in 10 % formaldehyde, and routine histopathological studies were processed and examined under light microscopy.

RESULTS

Animals

The RFA procedure took 30 to 58 minutes, the temperatures on 0.5 cm in depth of thermal lesion in spleens were over 100 °C as reaching to the maximum impedance. The temperatures on the hilum of spleen were 45-50 °C, the temperatures were kept below 42 °C with iced cold saline. There was a temperature gradient rising from lateral to center of splenic hilum due to blood inflow. Thus, choosing puncture site on lateral region of superior or inferior pole of spleen could enlarge the size of thermal lesions, and approximately 40-50 % of spleen could be damaged on each episode of RFA. Minor or mild bleeding from the puncture site of spleen immediately after inserting the electrode may occur and would be stopped automatically in 5 minutes due to thermal coagulation if the electrode was kept still. The animals could well tolerate the RFA, distressing in 5 dogs due to high tension of spleen capsule caused by thermal injury was resolved after administration of tranquilizer. The dogs fasted on the day of RFA were lethargic or anorexic. All dogs were fed normally after RFA. Restlessness, vomiting

and anorexia, significant body weights change and complications of surgery such as gastrointestinal perforation, peritonitis, intra-abdominal hemorrhage, rupture of spleen or hydrothorax and death were not observed at all.

CT imaging of spleens

Splenomegaly in group I could persist over 2 months. The enhanced CT revealed that each RF thermal lesion could destroy one lobe or multiple splenic segments, and the splenic capsule was intact except small part of hilum. The ablated lesion included two zones: (a) hyperintense zone of coagulative necrosis; (b) more extensive peripheral hypointense infarcted zone - the latter was called "bystander effect". No perisplenic or splenic abscess was formed (Figure 1). The infarcted zone would be absorbed in 4 to 6 weeks after RFA, and subsequently disappeared in two months, and the size of remnant spleen shrunk significantly (Figure 2, 3).

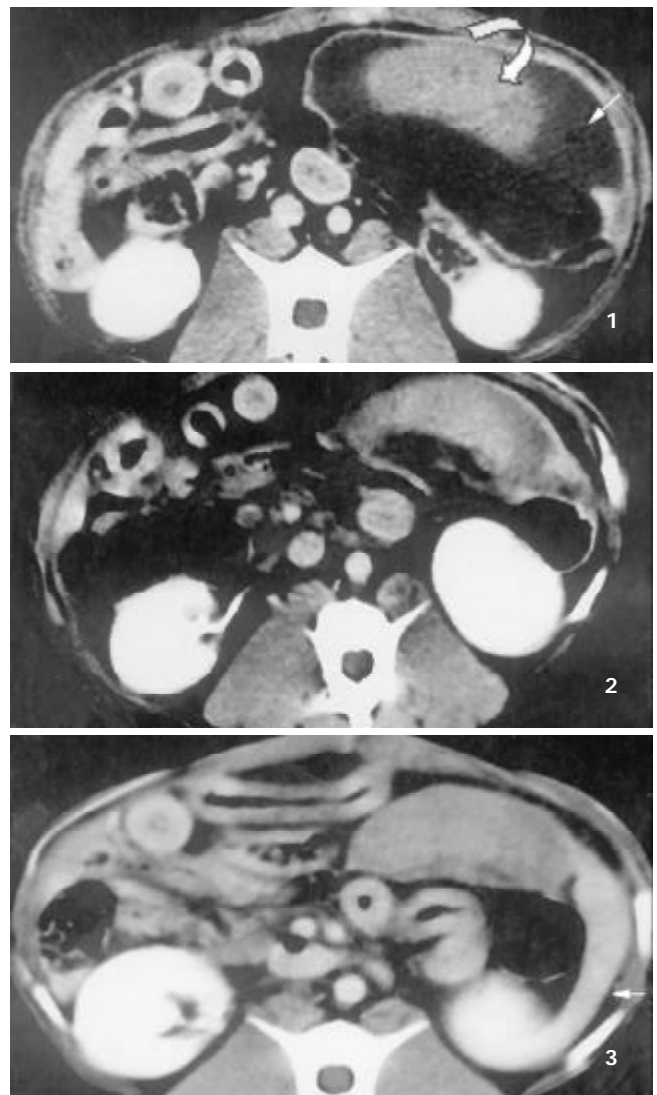


Figure 1 Enhanced CT demonstrated multiple segmental ablated lesion at the end of 2nd week after RFA, the splenic capsule was continuous, the thermal lesion included 2 zones, namely hyperintense zone of coagulative necrosis and peripheral hypointense infarcted zone; no perisplenic or splenic abscess was seen.

Figure 2 The lesion of infarcted zone was mostly absorbed at the end of 6th week after RFA.

Figure 3 The lesion of infarcted zone was absorbed absolutely at the end of 9th week after RFA, however, the lesion of coagulative necrosis hardly altered, the remnant spleen shrank significantly (arrow).

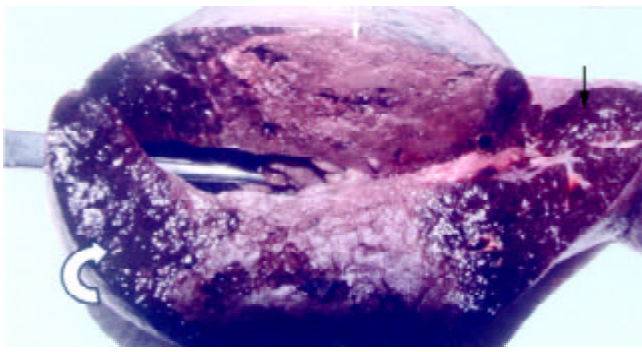


Figure 4 The appearance of the spleen the day after RFA, showed the lesion included the zone of soild-yellow dry necrosis (white arrow) and dark-red zone of thrombotic infarction (curve arrow), and the bright red normal spleen (black arrow); each ablation created a lesion with maximum diameter of 9 cm.

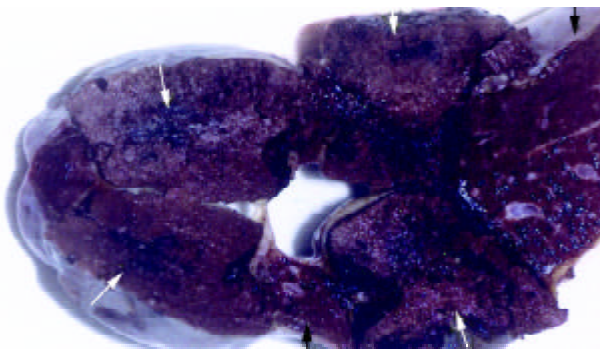


Figure 5 The lesion of infarcted zone was absorbed absolutely at the end of 9th week after RFA, however, the lesion of coagulative necrosis hardly altered (arrow).

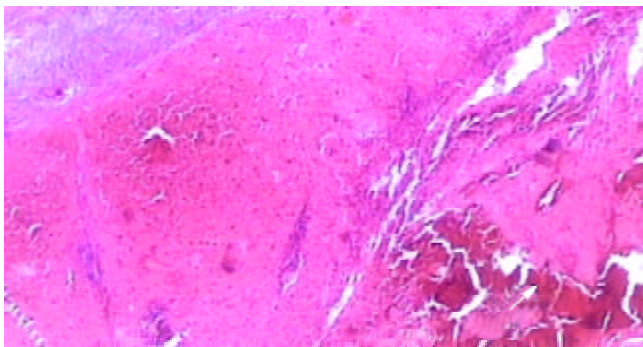


Figure 6 Light microscopic appearance of the coagulative necrosis at the end of 2nd week after RFA, the intrasplenic hemorrhage at the probe insertion site could see (arrow), the splenic capsule thickened (HE. $\times 40$).

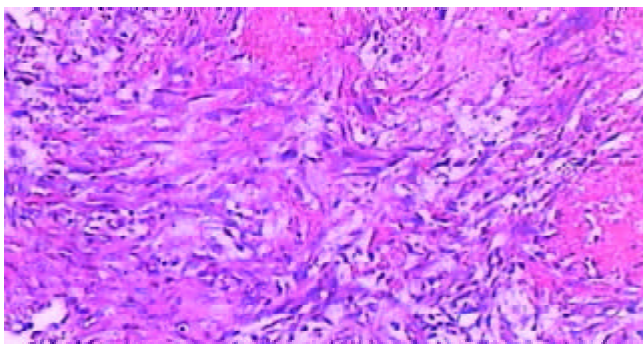


Figure 7 Microscopic examination at the junction of the necrotic region and infarcted region at the end of 2nd week after

RFA, massive fibroblasts and inflammatory cells aggregated, the microthrombus dissolved (HE. $\times 200$).

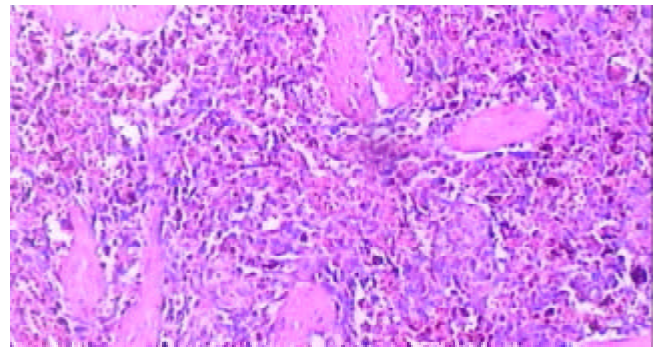


Figure 8 Microscopic examination of the thrombotic infarction at the end of 4th week after RFA, the microthrombus dissolved, and extensive macrophages with hemosiderin deposition presented (HE. $\times 100$).

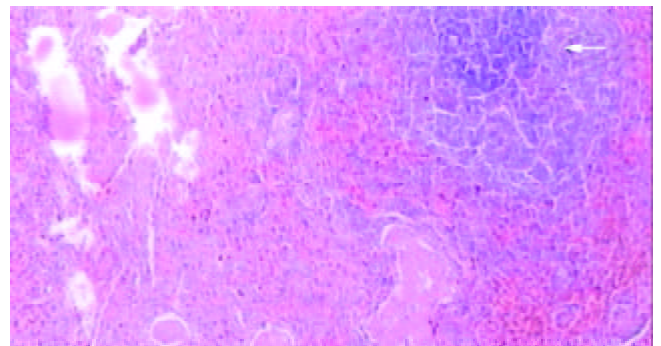


Figure 9 Microscopic appearance of "splenic carnification" of the normal viable splenic tissue distant from ablative lesion at the end of 9th week after RFA, the tissue structure consolidated, larger vessels occluded, extensive fibrous protein deposited, and the congestive splenic sinusoid disappeared; however, the structure of splenic lymphoid nodule was intact (arrow) (HE. $\times 40$).

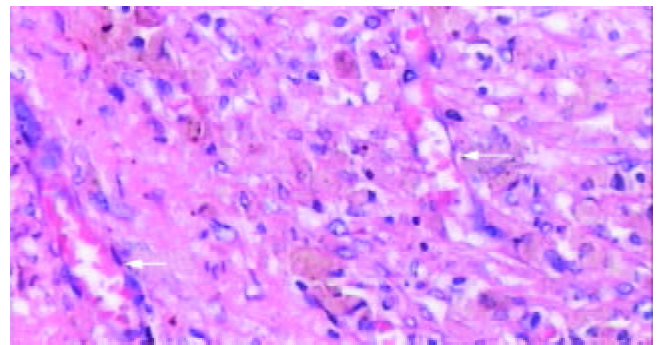


Figure 10 The typical appearance of poorly vascularized splenic tissue due to "splenic carnification" after RFA. The splenic sinusoid disappeared, tissue structure consolidated, granular hemosiderin deposition and sparsely neovascularized vessels (arrow) presented clearly (HE. $\times 200$).

Histopathology

Splenomegaly in gross appearance was existed in 2 months after ligation of splenic veins. The areas of ablated lesions had dot swollen dark red appearance, the spleens shrunk significantly and approached to the normal size at the end of ninth week after RFA. The macroscopic and microscopic of liver and pancreas were normal. The omentum was adherent to the ablated surface of the spleen in most cases. The appearances of cut surface of the ablated lesions matched

with the CT imaging, including the zone of soil-yellow dry necrosis and zone of thrombotic infarction (Figure 4), and the lesions became dry necrosis after the thrombotic infarction was absorbed (Figure 5). No obvious intrasplenic hemorrhage except the puncture tract was seen with microscopic examination (Figure 6). The RF energy caused focal tissue coagulative necrosis, massive vessels in the spleen were damaged thermally and occluded, consequently broad microthrombus led to the peripheral thrombotic infarction, which is called as bystander effect corresponding to the CT finding. Thrombotic infarction zone had absorbed by macrophages gradually in 4-6 weeks, where fibroblasts proliferation and local fibrosis were demonstrated. Even though some part of spleen appeared normal and viable, there had obvious thickened intima, occluded vessels, extensive fibrous protein deposition, and the absence of congestive splenic sinusoid, which we called as splenic carnification, the most important pathological basis of the shrunken spleen (Figure 7-10).

DISCUSSION

Hypersplenism is one of the common manifestations, 70-80 % patients with cirrhotic hypertension present with various degrees of splenomegaly and hypersplenism. The immune function in patients with hypersplenism would be reduced due to leucopenia, thrombocytopenia and erythropenia. Splenectomy is the traditional treatment for hypersplenism. However, patients with cirrhotic splenomegaly and hypersplenism often have many complications, which are the contraindication of splenectomy. Furthermore, endoscopic ligation or sclerosing of varices for esophageal varices bleeding due to cirrhotic portal hypertension was advocated as first line treatment in western countries, splenectomy plus devascularization are commonly abandoned^[33-38]. With the awareness of the role and importance of the spleen in the immune system, it is recommended to reserve the splenic tissue and function as much as in the treatment of benign conditions of the spleen. Thereby, new safe, effective and minimal invasive modalities should be established.

Radiofrequency ablation (RFA) technique is a safe and effective minimally invasive modality and has been clinically used in treatment of many malignant tumors and some benign tumors in solid organs^[1-25]. Until now, only two cases in treatment of colorectal and renal splenic metastasis using RFA were reported^[39, 40], no data of experimental or clinical study regarding the safety and efficacy of RFA for hypersplenism is available. The safety and effectiveness may be the cardinal considerations that impede the attempts. The limited necrotic volume identical to the lesion in liver for hepatocellular carcinoma with 3-5 cm maximal diameter could scarcely reduce the size of splenomegaly, consequently could be futile to ameliorate cytopenia for hypersplenism. However, theoretically, RFA could be used for hypersplenism due to portal hypertension: (a) spleen is a solid organ, thermal energy can cause focal tissue coagulative necrosis, and the RF heat energy has the role of electric coagulation^[39,40]; (b) certain time of RF thermal energy can lead to endothelial cells degeneration of vessels and sinus, thrombosis, and occlusion of vessels and splenic sinusoid, therefore produces effect of ablating larger lesion^[17]; (c) puncture of spleen with needle is relative safe, the morbidity rate of biopsy reported using 18-22 gauge needles for splenic lesions including splenomegaly is 0-5.2 %, without mortality^[41-43]; (d) the inflammatory reaction and neo-vascularization at the site of RFA lesion could create extensive collateral circulation between portal-cava vein systems, and reduce blood inflow to portal vein due to smaller spleen, sequentially depress the portal hypertension^[28]. Clinically, we

performed RFA for splenomegaly intraoperatively before splenectomy, only minor or mild bleeding occurred but stopped within few minutes (data not shown), and we found this procedure was practicable.

For these reasons, we carried out the study on RFA for splenomegaly and hypersplenism in canine models (the blood counts of peripheral samples in splenomegaly models also showed thrombocytopenia, erythropenia without leucopenia, which is similar to the result of Sahin *et al*^[44], and the hematologic abnormalities could be corrected by RFA; data not shown), results of preliminary study confirmed part of above presumptions.

First, RFA procedure for spleen is relative safe. Although bleeding occurred immediately following inserting of electrodes into the spleen, it ceased soon due to thermal coagulation. In order to avoid the potential risks, several important steps should be followed, the puncture site must be kept away from large vessels at hilum of spleen, the electrode should be fixed to reduce bleeding; the spleen should be elevated to avoid to contact with adjacent organs and skin; cool saline should be used on the surface of the hilum of spleen, tail of pancreas to reduce energy deposition and avoid thermal damage of pancreas. In our preliminary experiment, dog's thighs were burned due to insufficient shave of thigh and thus incomplete attachment of electrode pads; and another dog died from severe burning of internal organs, because spleen was not isolated from skin and intra-abdominal viscera. However, no morbidity and mortality occurred after procedures above in experiment were followed strictly. In addition, puncture of needle at lower pole of spleen is preferable to reduce the pulmonary complications and referred pain. If this procedure were used clinically, exposure and protection of spleen would be helpful in avoiding complications.

Second, the area of RF thermal ablated lesion is so large that compasses one lobe or multiple segments of spleen. The area of coagulative necrosis zone in spleen is similar to that of RF lesion in liver^[12,25], but the RFA in spleen also has "bystander effect" - the RF energy causes multiple segmental thrombotic infarction, enables for the management of hypersplenism effectively. The RF energy triggers occlusion of broad intrasplenic microthrombi and vessels, and absorption of area with thrombotic infarction. Even in the remaining normal splenic tissue, obvious occluded vessels, extensive fibrous protein deposition with no congestion of splenic sinusoid are still existed. The changes of "splenic carnification" are responsible for the shrinking of the remnant spleen, which could explain precisely why splenic RFA ameliorated the cytopenia.

In summary, it is feasible and safe to perform RFA in spleen to treat secondary splenomegaly and hypersplenism in a canine model, and yet its clinical application is worthy of further study. The peculiar radiological and pathological splenic changes after RFA could be used as clinical indicators for therapeutic effect and the follow-up in the therapy of hypersplenism. With the development of technique, such as RFA with the minimally invasive procedures, it would provide promising effect on selected patients with hypersplenism^[17].

REFERENCES

- 1 **Ma K**, Min C, Ian HX, Jiahong D. Prevention and cure of complications from multiple-electrode radiofrequency treatment of liver tumors. *Dig Dis* 2001; **19**: 364-366
- 2 **Liu LX**, Jiang HC, Piao DX. Radiofrequency ablation of liver cancers. *World J Gastroenterol* 2002; **8**: 393-399
- 3 **Tang ZY**. Hepatocellular carcinoma-Cause, treatment and metastasis. *World J Gastroenterol* 2001; **7**: 445-454
- 4 **Qin LX**, Tang ZY. The prognostic significance of clinical and pathological I features in hepatocellular carcinoma. *World J Gastroenterol* 2002; **8**: 193-199

Analysis of gene expression profile of pancreatic carcinoma using cDNA microarray

Zhi-Jun Tan, Xian-Gui Hu, Gui-Song Cao, Yan Tang

Zhi-Jun Tan, Xian-Gui Hu, Gui-Song Cao, Yan Tang, Department of General Surgery, Changhai Hospital, Second Military Medical University, Shanghai 200433, China

Correspondence to: Xian-Gui Hu, Department of General Surgery, Changhai Hospital, Second Military Medical University, Shanghai 200433, China. hxgchw@sh163.net

Telephone: +86-21-25070571 **Fax:** +86-21-25070571

Received: 2002-11-06 **Accepted:** 2002-12-07

Abstract

AIM: To identify new diagnostic markers and drug targets, the gene expression profiles of pancreatic cancer were compared with that of adjacent normal tissues utilizing cDNA microarray analysis.

METHODS: cDNA probes were prepared by labeling mRNA from samples of six pancreatic carcinoma tissues with Cy5-dUTP and mRNA from adjacent normal tissues with Cy3-dUTP respectively through reverse transcription. The mixed probes of each sample were then hybridized with 12 800 cDNA arrays (12 648 unique human cDNA sequences), and the fluorescent signals were scanned by ScanArray 3 000 scanner (General Scanning, Inc.). The values of Cy5-dUTP and Cy3-dUTP on each spot were analyzed and calculated by ImaGene 3.0 software (BioDiscovery, Inc.). Differentially expressed genes were screened according to the criterion that the absolute value of natural logarithm of the ratio of Cy5-dUTP to Cy3-dUTP was greater-than 0.69.

RESULTS: Among 6 samples investigated, 301 genes, which accounted for 2.38 % of genes on the microarray slides, exhibited differentially expression at least in 5. There were 166 over-expressed genes including 136 having been registered in Genbank, and 135 under-expressed genes including 79 in Genbank in cancerous tissues.

CONCLUSION: Microarray analysis may provide invaluable information on disease pathology, progression, resistance to treatment, and response to cellular microenvironments of pancreatic carcinoma and ultimately may lead to improving early diagnosis and discovering innovative therapeutic approaches for cancer.

Tan ZJ, Hu XG, Cao GS, Tang Y. Analysis of gene expression profile of pancreatic carcinoma using cDNA microarray. *World J Gastroenterol* 2003; 9(4): 818-823

<http://www.wjgnet.com/1007-9327/9/818.htm>

INTRODUCTION

The morbidity of pancreatic carcinoma has taken an upward trend all over the world. In occidental countries, the morbidity of pancreatic carcinoma has increased by 3 to 7 times in nearly thirty years, and pancreatic carcinoma has become one of the ten commonest malignant tumors. In China, the morbidity was 1.16/100 000 in Shanghai in 1963, and reached on 3.80/100 000

in 1974. Then, it took the 14th place of the morbidity of the malignant tumors, and jumped to fifth in 1984. The statistical results showed that it was 5.1/100 000, which was four times higher than that of twenty years before. In some medical centers, curative resections were given to minority of patients in early stage who were highly selected, and their five-year survival of these patients might even rise to 15 to 25 percent. But generally speaking, treatment of pancreatic cancer is still a serious challenge to us. The key problem to improve the current situation of treatment is to seek novel diagnostic markers, effective adjunctive therapy and mechanism of genesis and evolution of pancreatic cancer. Hence, more and more attention has been paid to the research on molecular pathology and related genes of pancreatic cancer.

Over the past decade, many studies involving pancreatic cancer have searched for cancer-causing gene. As a result, several cancer-related genes have been identified. DPC4, p53, and p16 are the three most frequently inactivated tumor suppressor genes. Other tumor suppressor genes that are altered in pancreatic cancer include BRCA2, ALK-5, MKK4, and STK11. Mutations of K-ras oncogene are commonly seen in pancreatic cancer, with its incidence as high as 90 %. Some other cancer-related genes, such as Her-2/neu, COX-2, VEGF have also been reported to be overexpressed in pancreatic cancer. Development and progression of pancreatic cancer is a very complicated process, so it is reasonable to predict that many other genes, as yet undiscovered, might be potential tumor markers or drug targets.

Microarray is the technique that a large number of cDNAs are arranged orderly on the carrier, such as glass chip or else in high density. Data are obtained by examining the signals of fluorescence, analyzed and compared by computer software. A large number of genes can be examined simultaneously, accurately, and effectively in one experiment. In this study, we have used a high-density cDNA microarray technique to assess the gene expression profile of pancreatic carcinoma versus adjacent normal tissue. Several genes, we identified, may be involved in pancreatic tumorigenesis as well as its potential clinical biomarkers that may be used to improve early diagnosis, and to constitute potential novel therapeutic targets.

MATERIALS AND METHODS

Materials

cDNA microarray slides used in this study were fabricated in United Gene Technique, Ltd. Briefly, each slide has 12 800 spots, containing 112 genes as negative control, such as ripe U2 RNA gene (8 spots), HCV coat protein gene (8 spots), spotting solution (96 spots); and 40 housekeeping genes as positive control. Each slide has 12 648 unique human cDNA sequences. Six samples of pancreatic carcinoma were obtained from patients undergoing pancreaticoduodenectomy in department of general surgery, Changhai Hospital, the Second Military Medical University. All cases were proved pathologically as carcinoma of pancreatic head. Normal tissues as control were taken from tissue adjacent to the cutting margin of the carcinoma and proved pathologically to be free from tumor invasion. Samples were snap-frozen in liquid nitrogen within 15 to 20 minutes after resection and then stored at -80 °C.

Cy3-dUTP and Cy5-dUTP were purchased from Amersham Pharmacia Biotech, Inc. and Oligotex mRNA Midi Kit from Quagen, Inc. ScanArray 3 000 scanner was manufactured by General Scanning, Inc. ImaGene3.0 software came from BioDiscovery, Inc.

Methods

Probe preparation Total RNA isolated from pancreas tissues and normal adjacent tissues by using modified single step extraction. Briefly, frozen tissues were crushed down and homogenized in solution D and 1 % mercaptoethanol. The supernatant was then extracted by phenol: chloroform (1:1) two times, and phenol: chloroform (5:1) and NaAc (PH=4.5) once. Afterward, the supernatant was precipitated in equal volume of isopropanol at -20 °C for 1.5 hours and was precipitated in LiCl for purification. Both kinds of mRNAs were purified using Oligotex mRNA Midi Kit. The fluorescent cDNA probes were prepared by reverse transcription and then purified, according to the protocol of Schena (Schena *et al.*, 1995). The mRNA from normal tissue was labeled with Cy3- dUTP, and that from cancerous tissue with Cy5- dUTP. Then the two probes were mixed with equivalence, precipitated by ethanol, and resolved in 20 µl hybridization buffer (5×SSC + 0.4 % SDS, 50 % Formamide, 5×denhardt' s solution).

Hybridization Microarray slides were pre-hybridized in hybridization buffer, which contained 0.5 mg/ml denatured clupeine DNA, at 42 °C for 6 hours. After denatured at 95 °C for 5 minutes, the probes mixture were added on the pre-hybridized slides and sealed with cover glass. After hybridizing

in HybChamber at 60 °C for 15 to 17 hours, the slides were subsequently washed in solutions of 2×SSC + 0.2 % SDS, 0.1×SSC+0.2 % SDS and 0.1×SSC respectively for 10 minutes, then dried at room temperature.

Scanning and analysis The slides were scanned by ScanArray 3 000 laser scanner at two wavelengths to obtain fluorescence intensities for both dyes (Cy3 and Cy5). The original value of each spot was normalized by the values of 40 housekeeping genes selected on the slides. The fluorescence intensities of Cy3 and Cy5 were analyzed and the ratios of Cy5 to Cy3 were calculated by ImaGene 3.0 software. The intensities of two fluorescent signals represented the quantities of two tagged probes. The ratio of Cy5 to Cy3 of certain spot on the slides demonstrated that mRNA abundance of this gene expressed in cancerous tissues versus normal.

RESULTS

Verification of microarray technique system

There were 12 800 spots on each slide, including 6 170 known genes and 6 478 unknown ones. In order to monitor entire process of microarray technique system, negative and positive control genes were set on the slides. They were ripe U2 RNA gene (8 spots), HCV coat protein gene (8 spots), spotting solution (96 spots), which served as negative control; and 40 housekeeping genes as positive control. In present study, the individual result of six hybridization showed that all of positive control signals are distinct, and all of negative control signals were very low. These prove the reliability of the data.

Table 1 Over-expressed genes in pancreatic carcinoma

Accession number	Gene name	Gene function	Ratio value
U06863	Alpha 1 (III) collagen	Extracellular matrix	33.89
X91148	Microsomal triglyceride transfer protein	Microsomal triglyceride transfer	21.89
AF017986	Secreted apoptosis related protein 1 (SARP1)	Repress apoptosis	20.32
Y00755	Extracellular matrix protein BM-40	Extracellular matrix	20.23
Z74616	Alpha2 (I) collagen	Extracellular matrix	12.52
D32039	Proteoglycan PG-M(V3)	Extracellular matrix	11.90
J03607	40-kDa keratin intermediate filament precursor	Extracellular matrix	11.62
AF144103	Novel chemokine family member with altered expression in human head and neck squamous cell carcinoma	Cytokine	9.93
AF141201	Ubiquitin fusion-degradation 1 protein (UFD1)	Protease	8.29
X02761	Fibronectin (FN)	Extracellular matrix	8.01
U06863	Follistatin-related protein precursor	Nucleoprotein	6.92
M14219	Chondroitin/dermatan sulfate proteoglycan (PG40) core protein	Extracellular matrix	6.65
M17783	Glia-derived nexin (GDN)	Protease inhibitor	6.49
U59877	Low-Mr GTP-binding protein (RAB31)	Signal transduction	5.97
AF000989	Thymosin beta 4 Y isoform (TB4Y)	Thymosin isoform	5.71
L20688	GDP-dissociation inhibitor protein (Ly-GDI)	Signal transduction	5.62
X57351	1-8D gene from interferon-inducible gene	Signal transduction	5.51
U18728	Lumican	Extracellular matrix	5.15
L02326	Lambda-like gene	Immunity correlation	4.77
M14144	Vimentin	Extracellular matrix	4.64
J05633	Integrin beta-5 subunit	Cell adhesion molecule	4.42
AF070523	JWA protein	-	4.32
M27749	Immunoglobulin-related 14.1 protein	Immunity correlation	4.28
S83308	Sry-related HMG box gene (SOX5)	Transcription factor	4.16
U05875	Interferon gamma receptor accessory factor-1 (AF-1)	Immunity correlation	3.92
M17733	Thymosin beta-4	Thymosin isoform	3.89
M20259	Thymosin beta-10	Thymosin isoform	3.75
M36501	Alpha-2-macroglobulin	Protease inhibitor	3.72
AF026977	Microsomal glutathione S-transferase 3 (MGST3)	Oxidation-reduction	3.62
M14630	Prothymosin-α	Nucleoprotein	3.45

Table 2 Under-expressed genes in pancreatic carcinoma

Accession number	Gene name	Gene function	Ratio value
U96628	Nuclear antigen H731-like protein	Tumor suppressor	0.16
U72649	B-cell translocation gene 2 (BTG2)	Tumor suppressor	0.18
Y15409	Putative glucose 6-phosphate translocase	Gluconeogenesis	0.18
Z21507	Elongation factor-1-delta	Translation factor	0.20
L13463	Helix-loop-helix basic phosphoprotein (G0S8)	Cell cycle correlation	0.21
S68805	L-arginine:glycine amidinotransferase	Amino transferase	0.22
AF041474	BAF53a (BAF53a)	Chromatin reformation	0.22
X05130	Prolyl 4-hydroxylase beta subunit	Hydroxylase	0.22
AF067855	Geminin	Cell cycle correlation	0.25
D87810	Phosphomannomutase	Glycometabolism	0.25
D28540	CDC10 homologue	Cell cycle correlation	0.27
L37368	RNA-binding protein	RNA metabolism	0.27
Y00711	Lactate dehydrogenase B (LDH-B)	Dehydrogenase	0.27
M24103	Trans-golgi network glycoprotein 51 (TGN)	-	0.29
M64930	Protein phosphatase 2A beta subunit	Signal transduction	0.29
X81197	Archain	Membranin	0.31
U75686	Polyadenylate binding protein	Signal transduction	0.32
AF133659	ATP-binding cassette 7 iron transporter (ABC7)	Iron transfer	0.32
M61832	S-adenosylhomocysteine hydrolase (AHCY)	Hydrolase	0.33
Z23064	HnRNP G protein	RNA-binding protein	0.34
X85960	TRK-T3 oncogene	Oncogene	0.35
L18887	Calnexin	Calcium binding protein	0.35
J02966	Mitochondrial ADP/ADT translocator	ATP/ADP transport	0.35
X78678	Ketohexokinase	Glycometabolism	0.35
M58460	75-kD autoantigen (PM-Sc1)	Autoantigen	0.35
L12711	Transketolase (tk)	Ribose metabolism	0.35
S75311	Glycosyl phosphatidylinositol (GPI)-linked glycoprotein CD24	Signal transduction	0.35
U46838	MCM105 protein	Cell cycle correlation	0.36
Y11312	Phosphoinositide 3-kinase	Signal transduction	0.36
U83908	PDCD4 (programmed cell death 4)	Tumor suppressor	0.36

Judgement of differentially expressed genes

Hybridization of each couple of probes repeated two times. The standard of determination for differentially expressed genes was that, the absolute value of natural logarithm of the ratio of Cy5 to Cy3 was greater than 0.69, that was to say change of gene expression was above 2 times, and the signal value of either Cy3 or Cy5 needed to be greater than 600.

Genes expressed differentially

Among 6 samples investigated, 301 genes, which accounted for 2.38 % of genes on the microarray slides, exhibited differentially expression at least in 5. There were 166 over-expressed genes including 136 having been registered in Genebank, and 135 under-expressed genes including 79 in Genebank. Some of these genes, which took superior places of differentially expression, were listed in Table 1 and Table 2.

DISCUSSION

There are altogether 215 previously reported genes differently expressed in cancer tissues in our research, including urokinase plasminogen activator surface receptor (uPAR)^[1], glyceraldehyde-3-phosphate dehydrogenase (GAPDH), lumican^[2], phospholipase A2^[3], vascular cell adhesion molecule 1^[4], which have been reported to play certain role in evolution of pancreatic carcinoma. However, the relationship between the majority of these genes and development of pancreatic carcinoma has not been covered in any study up to the present. These genes are involved in various cytobiological functions, such as signal transduction, transcription and translation,

cytoskeleton, cell adhesion, extracellular matrix and matrix degradation, cell cycle and apoptosis, chromosome instability, tumor suppressor genes, enzyme, and "others". Moreover, some genes exhibit differently expression in pancreatic cancer in our study, as well as in other cancers. They are fibronectin^[5], caltractin^[6], glyceraldehyde-3-phosphate dehydrogenase (GAPDH)^[7], lipocortin II, uPAR^[8] in hepatic cancer; FN^[9], glutathione peroxidase^[10], phospholipase A2^[11], thymosin beta-10^[12], uPAR^[13], uracil DNA glycosylase^[14] in colorectal cancer; N-cadherin^[15], uPAR^[16], alpha-2-macroglobulin^[17], caltractin^[6], syntenin^[18] in gastric cancer; phospholipase A2^[19] in cholangiocarcinoma; fibronectin^[20], glutathione peroxidase^[21,22], prothymosin alpha^[23,24], thymosin beta-10^[25], uPAR^[26], caltractin^[6], GAPDH^[27], proteoglycan PG-M(V3), syntenin^[18], lumican^[28] in mammary cancer and glutathione peroxidase^[29], SPARC/osteonectin^[29], thymosin beta-10^[30], uPAR^[31] in thyroid carcinoma. These data indicated that we have obtained the same results by using cDNA microarray as by other methods. Meanwhile, these confirmed the feasibility, accuracy and effectiveness of microarray as a method to investigate the expression profiles of pancreatic cancer. On the other hand, we might get the conclusion that genesis and progression of various neoplasms have some common mechanisms. Further study on these common mechanisms might lead us go into depth the knowledge of molecular biology of cancer, and find the key to the improvement of diagnosis and treatment of cancer.

Pancreatic carcinoma is one of the most malignant tumors, and is characterized by aggressive growth behavior and high incidence rate of recurrence. During proliferation of a primary tumor or the establishment of metastatic foci, there is

continuous remodeling of the extracellular matrix including various degrees of biosynthesis, reformation and degradation. Among over-expressed genes, several genes, such as alpha1 (III) collagen, extracellular matrix protein BM-40, alpha2 (I) collagen, proteoglycan PG-M (V3), fibronectin, chondroitin/dermatan sulfate proteoglycan (PG40) core protein, lumican, vimentin, chondroitin sulfate proteoglycan versican V0 splice-variant, and versican V2 splice-variant core protein, component analysis related to extracellular matrix (ECM), take the superior places. Versican belongs to the family of large aggregating proteoglycans (PGs). In mammals, versican appears as four possible spliced variants, V₀, V₁, V₂, and V₃. It has been described that the versican-rich extracellular matrices exert an anti-adhesive effect on the cells, thus facilitating tumor cell migration and invasion. Besides decreasing cell adhesion, versican is also able to increase the cell proliferation. The study on melanoma has shown that this PG could serve as a good marker for primary malignant as well as metastatic lesion^[32]. Lumican is the member of the small leucine-rich proteoglycan (SLRP) family, whose members are known as keratocan, mimecan, decorin, biglycan, fibromodulin, epiphygan, osteoadherin, and lumican. SLRP proteins can modulate cellular behaviour, including cell migration and proliferation during embryonic development, tissue repair, and tumor growth. In breast cancer tissues, lumican mRNA is reported to be overexpressed. Furthermore, its high expression level was associated with high tumor grade, low estrogen receptor levels, and young age of patients^[28]. It is also found that lumican is not synthesized by the exocrine components of the normal pancreas, but that these cells ectopically synthesize and secrete the lumican in cancer tissues, which may play a role in pancreatic cancer cell growth^[2]. Extracellular matrix protein BM-40, an anti-adhesive protein, is proposed to modulate cell migration and vascular morphogenesis either by directly interacting with ECM proteins or by initiating a receptor-mediated signaling event. It may directly affect cell motility by inducing intracellular changes of cytoplasmic components; or indirectly promote cell migration by modulating the expression of proteolytic enzymes that degrade the ECM, such as collagenase, stromelysin and MMP-9. It may promote infiltration of tumor cells, serve as a cellular marker of invasion, and correlate to angiogenesis^[33]. Fibronectin connects with the cancer cell via its receptors, including integrins $\alpha_5\beta_1$ and $\alpha_v\beta_3$. The abilities in adhesion to fibronectin and migration increased markedly, after hepatocellular carcinoma cells were transfected with H-ras oncogene^[34]. In addition, fibronectin is the primary protein involved in the displacement of MMP-2 produced by adjacent normal cells to cancer tissues^[35]. MMP-2 can associate with the cell surface through its COOH-terminal and hemopexin-like domain via a number of mechanisms, including binding to cell-associated collagen I and IV. In our present study, we also find that collagen I and IV overexpress in cancerous tissues. This may enhance the fibronectin-induced displacement of MMP-2, and facilitates invasion of cancerous cells. Vimentin is also a component of ECM. Enhanced expression of the vimentin is associated with high degree of motility, poor differentiation and metastasis of prostate carcinoma^[36]. It has been shown that vimentin was immunohistochemically positive in basaloid squamous carcinoma of esophagus^[37]. Moreover, uPAR and cathepsin O2 are also found to be over-expressed in our study. All of these changes endow pancreatic cancer with the trait of aggressive growth, and may be potential markers of invasion.

On the other hand, recurrence to chemotherapy after resection remains a major obstacle to the cure of pancreatic cancer. It is well known that cancerous cells are surrounded by an extensive stroma of ECM at both primary and metastatic sites, which contains, among other proteins, fibronectin,

laminin and collagen IV. Adhesion of pancreatic cancer cells to these proteins confers resistance to apoptosis induced by standard chemotherapeutic agents. The study on small-cell lung cancer showed that β_1 -integrin-mediated cell adhesion to ECM proteins results in tyrosine phosphorylation, which, weaken persistent chemotherapy-induced DNA damage, prevents caspase activation and apoptosis^[38]. Alpha-tubulin^[39], lipocortin II and uracil DNA glycosylase^[14] were also found to be contributed to resistance to chemotherapy. These genes over-express in pancreatic cancer in our study, and may play the same role. It is indicated that the regulation routes of these genes may be potential targets for treatment of pancreatic carcinoma.

There are still some genes that should be mentioned. Prothymosin alpha (PTA) is a nuclear protein that is present throughout the cell cycle. It has been shown that it binds histones *in vitro* and has been proposed to affect the chromatin state. PTA is expressed in various human tumor tissues of different origins, supporting the idea that PTA expression is required for tumor growth. Recent study has shown that in breast cancer, whose tumor with low or moderate PTA level demonstrated a statistically significant decreased rate of tumor recurrence and a statistically significant increased overall survival in comparison with those whose tumor had high PTA levels. It is proposed that PTA could be used as a predictor of the potential malignancy of breast tumors that might help to identify patients at high risk of fatality^[23,24]. Fas-binding protein and secreted apoptosis related protein-1 (SARP-1) are proposed to repress apoptosis. SARP-1 may inhibit phosphorylation of liberated β -catenin and degradation by ubiquitin-protease system via Wnt signaling way. Subsequently, β -catenin accumulates in cytoplasm, and cell apoptosis is suppressed. SARP-1 thus promotes excessive proliferation and transformation. Fas-binding protein can arrest Fas-induced apoptosis. Thymosin beta-4 and Thymosin beta-10 are also up-regulated. These genes may serve as markers for measuring proliferation of pancreatic cancer cells.

There are two tumor suppressors, B-cell translocation gene 2 (BTG2) and programmed cell death 4 (PDCD4), which are down-regulated in cancer tissues. PDCD4 gene is homologous to the mouse gene (MA-3/Pdcd4/A7-1), which is associated with apoptosis and is shown to suppress tumor promoter-induced neoplastic transformation. The ORF of human PDCD4 encodes a protein of 458 aa with a predicted molecular size of 50.6 kDa. It has been demonstrated that PDCD4 protein inhibits neoplastic transformation and must be down-regulated for progression to occur^[40]. BTG2, which is induced by p53, displays an antiproliferative activity in different cell types, such as fibroblasts and PC12 cells. It is well known that the control of the cell cycle plays an essential role in cell growth and in the activation of important cellular processes, such as differentiation and apoptosis. pRb and p53 are two molecules identified as key regulators of the cell cycle. Some suggestions came from a recent report, which showed that BTG2 interacted with a protein-arginine N-methyltransferase (Prmt1) by positively modulating its activity. Prmt1, in turn, has been found to bind the interferon receptors and to be required for interferon-mediated growth inhibition. A further investigation on BTG2 demonstrated that this gene inhibited G₁/S progression in an Rb-dependent manner and that this effect was correlated with its ability to inhibit cyclin D₁ expression. Furthermore, the impairment in the ability of BTG2 to lower cyclin D₁ levels, seen in consequence of mutations of the BTG2 molecule, correlated with the extent of impairment in growth arrest^[41].

DNA replication is initiated at discrete sites on chromosomes through the coordinate action of a number of replication initiation factors. It is believed that a complex of proteins called

the origin recognition complex (ORC) associates with specific DNA sequences near origins of replication to recruit other replication initiation factors during the G₁ phase of the cell cycle. The other replication initiation factors, Cdc6p, Cdt1p, and the Mcm2-7p complex, associate with the origin sequence in an ORC-dependent reaction to form a pre-replicative complex (pre-RC). At the G₁-S transition, the activation of cyclin-dependent kinases leads to the recruitment of elongation factors, CDC45, DNA polymerases, and RPA to the pre-RCs at origins. The action of these replication elongation proteins leads to the initiation of DNA synthesis, the hallmark of S phase. Geminin interacts with Cdt1p and prevents the recruitment of the Mcm2-7p complex to origins during S, G₂, and early M phases of the cell cycle and thereby inhibits replication initiation, leading to the expectation that the protein acts as an inhibitor of cell proliferation^[42]. The research on these under-expressed genes may render invaluable information to find novel targets for the treatment of pancreatic cancer.

In summary, though some genes have been missed in present study, the genes we have identified may be important to the tumorigenesis of pancreatic cancer, and potential to serve as tumor markers or drug targets.

REFERENCES

- Han H**, Bearss DJ, Browne LW, Calaluce R, Nagle RB, Von Hoff DD. Identification of differentially expressed genes in pancreatic cancer cells using cDNA microarray. *Cancer Res* 2002; **62**: 2890-2896
- Ping Lu Y**, Ishiwata T, Asano G. Lumican expression in alpha cells of islets in pancreas and pancreatic cancer cells. *J Pathol* 2002; **196**: 324-330
- Kashiwagi M**, Friess H, Uhl W, Berberat P, Abou-Shady M, Martignoni M, Anghelacopoulos SE, Zimmermann A, Buchler MW. Group II and IV phospholipase A(2) are produced in human pancreatic cancer cells and influence prognosis. *Gut* 1999; **45**: 605-612
- Tempia-Caliera AA**, Horvath LZ, Zimmermann A, Tihanyi TT, Korc M, Friess H, Buchler MW. Adhesion molecules in human pancreatic cancer. *J Surg Oncol* 2002; **79**: 93-100
- Nejjari M**, Hafdi Z, Gouysse G, Fiorentino M, Beatrix O, Dumortier J, Pourreyron C, Barozzi C, D'errico A, Grigioni WF, Scoazec JY. Expression, regulation, and function of alpha V integrins in hepatocellular carcinoma: an *in vivo* and *in vitro* study. *Hepatology* 2002; **36**: 418-426
- Tian DY**, Hayashi M, Yoshida T, Sakakura T, Kawarada Y, Tanaka T. Overexpression of caltractin gene in tumor-infiltrating lymphocytes. *Int J Oncol* 1998; **13**: 1135-1140
- Yamagata M**, Mori M, Begum NA, Shibuta K, Shimoda K, Barnard GF. Glycerolaldehyde-3-phosphate dehydrogenase mRNA expression in hepatocellular carcinoma. *Int J Oncol* 1998; **12**: 677-683
- Zhou L**, Hayashi Y, Itoh T, Wang W, Rui J, Itoh H. Expression of urokinase-type plasminogen activator, urokinase-type plasminogen activator receptor, and plasminogen activator inhibitor-1 and -2 in hepatocellular carcinoma. *Pathol Int* 2000; **50**: 392-397
- Lopez-Conejo MT**, Olmo N, Turnay J, Lopez De Silanes I, Lizarbe MA. Interaction of fibronectin with human colon adenocarcinoma cells: effect on the *in vivo* tumorigenic capacity. *Oncology* 2002; **62**: 371-380
- Skrzydawska E**, Stankiewicz A, Sulkowska M, Sulkowski S, Kasacka I. Antioxidant status and lipid peroxidation in colorectal cancer. *J Toxicol Environ Health A* 2001; **64**: 213-222
- Osterstrom A**, Dimberg J, Fransén K, Soderkvist P. Expression of cytosolic and group X secretory phospholipase A (2) genes in human colorectal adenocarcinomas. *Cancer Lett* 2002; **182**: 175-182
- Nimmrich I**, Erdmann S, Melchers U, Finke U, Hentsch S, Moyer MP, Hoffmann I, Müller O. Seven genes that are differentially transcribed in colorectal tumor cell lines. *Cancer Lett* 2000; **160**: 37-43
- Baker EA**, Bergin FG, Leaper DJ. Plasminogen activator system, vascular endothelial growth factor, and colorectal cancer progression. *Mol Pathol* 2000; **53**: 307-312
- Dusseau C**, Murray GI, Keenan RA, O' Kelly T, Krokan HE, McLeod HL. Analysis of uracil DNA glycosylase in human colorectal cancer. *Int J Oncol* 2001; **18**: 393-399
- Yanagimoto K**, Sato Y, Shimoyama Y, Tsuchiya B, Kuwano S, Kameya T. Co-expression of N-cadherin and alpha-fetoprotein in stomach cancer. *Pathol Int* 2001; **51**: 612-618
- Choi YK**, Yoon BI, Kook YH, Won YS, Kim JH, Lee CH, Hyun BH, Oh GT, Siple J, Kim DY. Overexpression of urokinase-type plasminogen activator in human gastric cancer cell line (AGS) induces tumorigenicity in severe combined immunodeficient mice. *Jpn J Cancer Res* 2002; **93**: 151-156
- Allgayer H**, Babic R, Grutzner KU, Beyer BC, Tarabichi A, Schildberg FW, Heiss MM. Tumor-associated proteases and inhibitors in gastric cancer: analysis of prognostic impact and individual risk protease patterns. *Clin Exp Metastasis* 1998; **16**: 62-73
- Koo TH**, Lee JJ, Kim EM, Kim KW, Kim HD, Lee JH. Syntenin is overexpressed and promotes cell migration in metastatic human breast and gastric cancer cell lines. *Oncogene* 2002; **21**: 4080-4088
- Wu T**, Han C, Lunz JG 3rd, Michalopoulos G, Shelhamer JH, Demetris AJ. Involvement of 85-kd cytosolic phospholipase A (2) and cyclooxygenase-2 in the proliferation of human cholangiocarcinoma cells. *Hepatology* 2002; **36**: 363-373
- Jiang Y**, Harlocker SL, Molesh DA, Dillon DC, Stolk JA, Houghton RL, Repasky EA, Badaro R, Reed SG, Xu J. Discovery of differentially expressed genes in human breast cancer using subtracted cDNA libraries and cDNA microarrays. *Oncogene* 2002; **21**: 2270-2282
- Perquin M**, Oster T, Maul A, Froment N, Untereiner M, Bagrel D. The glutathione-related detoxification system is increased in human breast cancer in correlation with clinical and histopathological features. *J Cancer Res Clin Oncol* 2001; **127**: 368-374
- Gorodzanskaya EG**, Larionova VB, Zubrikhina GN, Kormosh NG, Davydova TV, Laktionov KP. Role of glutathione-dependent peroxidase in regulation of lipoperoxide utilization in malignant tumors. *Biochemistry* 2001; **66**: 221-224
- Bianco NR**, Montano MM. Regulation of prothymosin alpha by estrogen receptor alpha: molecular mechanisms and relevance in estrogen-mediated breast cell growth. *Oncogene* 2002; **21**: 5233-5244
- Magdalena C**, Dominguez F, Loidi L, Puente JL. Tumour prothymosin alpha content, a potential prognostic marker for primary breast cancer. *Br J Cancer* 2000; **82**: 584-590
- Santelli G**, Califano D, Chiappetta G, Maria Teresa Vento, Bartoli PC, Zullo F, Trapasso F, Viglietto G, Fusco A. Thymosin beta-10 gene overexpression is a general event in human carcinogenesis. *Am J Pathol* 1999; **155**: 799-804
- Gong SJ**, Rha SY, Chung HC, Yoo NC, Roh JK, Yang WI, Lee KS, Min JS, Kim BS, Chung HC. Tissue urokinase-type plasminogen activator receptor levels in breast cancer. *Int J Mol Med* 2000; **6**: 301-305
- Revellion F**, Pawlowski V, Hornez L, Peyrat JP. Glycerolaldehyde-3-phosphate dehydrogenase gene expression in human breast cancer. *Eur J Cancer* 2000; **36**: 1038-1042
- Leygue E**, Snell L, Dotzlaw H, Troup S, Hiller-Hitchcock T, Murphy LC, Roughley PJ, Watson PH. Lumican and decorin are differentially expressed in human breast carcinoma. *J Pathol* 2000; **192**: 313-320
- Takano T**, Hasegawa Y, Matsuzuka F, Miyauchi A, Yoshida H, Higashiyama T, Kuma K, Amino N. Gene expression profiles in thyroid carcinomas. *Br J Cancer* 2000; **83**: 1495-1502
- Takano T**, Hasegawa Y, Miyauchi A, Matsuzuka F, Yoshida H, Kuma K, Amino N. Quantitative analysis of thymosin Beta-10 messenger RNA in thyroid carcinomas. *Jpn J Clin Oncol* 2002; **32**: 229-232
- Kim SJ**, Shiba E, Taguchi T, Tsukamoto F, Miyoshi Y, Tanji Y, Takai S, Noguchi S. uPA receptor expression in benign and malignant thyroid tumors. *Anticancer Res* 2002; **22**: 387-393
- Touab M**, Villena J, Barranco C, Arumi-Uria M, Bassols A. Versican is differentially expressed in human melanoma and may play a role in tumor development. *Am J Pathol* 2002; **160**: 549-557
- Vajkoczy P**, Menger MD, Goldbrunner R, Ge S, Fong TAT, Vollmar B, Schilling L, Ullrich A, Hirth KP, Tonn JC, Schmiedek P, Rempel SA. Targeting angiogenesis inhibits tumor infiltration

- and expression of the pro-invasive protein SPARC. *Int J Cancer* 2000; **87**: 261-268
- 34 **Wang Q**, Lin ZY, Feng XL. Alterations in metastatic properties of hepatocellular carcinoma cell following H-ras oncogene transfection. *World J Gastroenterol* 2001; **7**: 335-339
- 35 **Saad S**, Gottlieb DJ, Bradstock KF, Overall CM, Bendall LJ. Cancer cell-associated fibronectin induces release of matrix metalloproteinase-2 from normal fibroblasts. *Cancer Res* 2002; **62**: 283-289
- 36 **Lang SH**, Hyde C, Reid IN, Hitchcock IS, Hart CA, Bryden AA, Villette JM, Stower MJ, Maitland NJ. Enhanced expression of vimentin in motile prostate cell lines and in poorly differentiated and metastatic prostate carcinoma. *Prostate* 2002; **52**: 253-263
- 37 **Zhang XH**, Sun GQ, Zhou XJ, Guo HF, Zhang TH. Basaloid squamous carcinoma of esophagus: a clinicopathological, immunohistochemical and electron microscopic study of sixteen cases. *World J Gastroenterol* 1998; **4**: 397-403
- 38 **Rintoul RC**, Sethi T. Extracellular matrix regulation of drug resistance in small-cell lung cancer. *Clin Sci* 2002; **102**: 417-424
- 39 **Kyu-Ho Han E**, Gehrke L, Tahir SK, Credo RB, Cherian SP, Sham H, Rosenberg SH, Ng S. Modulation of drug resistance by alpha-tubulin in paclitaxel-resistant humanlung cancer cell lines. *Eur J Cancer* 2000; **36**: 1565-1571
- 40 **Cmarik JL**, Min H, Hegamyer G, Zhan S, Kulesz-Martin M, Yoshinaga H, Matsuhashi S, Colburn NH. Differentially expressed protein Pdc4 inhibits tumor promoter-induced neoplastic transformation. *Proc Natl Acad Sci U S A* 1999; **96**: 14037-14042
- 41 **Guardavaccaro D**, Corrente G, Covone F, Micheli L, Dagnano I, Starace G, Caruso M, Tirone F. Arrest of G₁ S progression by the p53-inducible gene PC3 is Rb dependent and relies on the inhibition of cyclin D1 transcription. *Mol Cell Biol* 2000; **20**: 1797-1815
- 42 **Wohlschlegel JA**, Dwyer BT, Dhar SK, Cvetic C, Walter JC, Dutta A. Inhibition of eukaryotic DNA replication by geminin binding to Cdt1. *Science* 2000; **290**: 2309-2312

Edited by Xu JY

Association of two polymorphisms of tumor necrosis factor gene with acute biliary pancreatitis

Dian-Liang Zhang, Jie-Shou Li, Zhi-Wei Jiang, Bao-Jun Yu, Xing-Ming Tang, Hong-Mei Zheng

Dian-Liang Zhang, Jie-Shou Li, Zhi-Wei Jiang, Bao-Jun Yu, Xing-Ming Tang, Research Institute of General Surgery, Jinling Hospital, School of Medicine, Nanjing University, Nanjing 210093, Jiangsu Province, China

Hong-Mei Zheng, Department of Nephrology, the Hospital affiliated with Binzhou Medical College, Binzhou 256603, Shandong Province, China

Supported by the 10th five-year plan for medicine and health, PLA, No.013012 and is also supported by the General Hospital of Nanjing Command, No.2002059

Correspondence to: Dian-Liang Zhang and Jie-Shou Li, Research Institute of General Surgery, Jinling Hospital, Nanjing 210093, China. phdzdl@yahoo.com

Telephone: +86-25-4825061 **Fax:** +86-25-4803956

Received: 2002-10-08 **Accepted:** 2003-01-02

Abstract

AIM: To investigate TNF- α -308 and TNFB polymorphisms in acute biliary pancreatitis (ABP) and to related them to the plasma TNF- α levels.

METHODS: Genomic DNA was prepared from peripheral blood leukocytes. Genotypes and allele frequencies were determined in patients ($n=127$) and healthy controls ($n=102$) using restriction fragment length polymorphism analysis of polymerase chain reaction (PCR) products. Reading the size of digested bands from polyacrylamide gel demonstrated the two alleles TNF1 and TNF2, or the two alleles TNFB1 and TNFB2.

RESULTS: The frequencies of TNF2 polymorphism and TNFB2 polymorphism were both similar in patients with mild or severe pancreatitis, so were in pancreatitis patients and in controls. Patients with septic shock showed a significantly higher prevalence of the TNF2 than those without. No significant differences were found in the genotype distribution of TNF- α -308 and TNFB among different groups. Plasma TNF- α levels did not differ significantly in ASBP patients displaying different alleles of the TNF gene studied.

CONCLUSION: Results indicate that TNF gene polymorphisms studied play no part in determination of disease severity or susceptibility to acute biliary pancreatitis; however, TNF2 polymorphism is associated with septic shock from ASBP. Genetic factors are not important in determining plasma TNF- α levels in ASBP.

Zhang DL, Li JS, Jiang ZW, Yu BJ, Tang XM, Zheng HM. Association of two polymorphisms of tumor necrosis factor gene with acute biliary pancreatitis. *World J Gastroenterol* 2003; 9(4): 824-828 <http://www.wjgnet.com/1007-9327/9/824.htm>

INTRODUCTION

In China and most other countries, gallstones are the most common cause of acute pancreatitis. There are reports that

gallstones account for between one third and two thirds of cases, with an average of 40 to 50 %^[1]. Acute severe pancreatitis (ASP) is a serious disease, with highly persistent morbidity and mortality. Generally speaking, the natural course of severe acute pancreatitis progresses in two phases. The first 14 days are characterized by the systemic inflammatory response syndrome resulting from the release of inflammatory mediators. The second stage, beginning approximately 2 weeks after the onset of the disease, is dominated by septic-related complications resulting from infection of pancreatic necrosis or bacteria translocation. Today, with improvements in the care of the critically ill, many patients with ASP survive over early systemic inflammatory response and enter a second phase of illness dominated by sepsis and the consequences of organ failure. More than two thirds of deaths in ASP are due to late septic organ complications^[2]. However, the susceptibility and mechanism of septic shock related to ASP are still unclear.

Tumor necrosis factor- α (TNF- α), the early cytokine to be released, is a principal mediator of immune responses to endotoxin. It can be produced in large amounts in several organs during ASP and is also believed to mediate pathophysiological changes^[3,4]. Systemic release of TNF- α is associated with septic shock and fatal outcome. TNF- α levels are increased in patients with ASP and septic shock and appear to correlate with clinical outcome.

Because of its short half-life, the value of TNF- α as a marker of susceptibility or severity for ASP is limited. The production and response of TNF- α are partly regulated at the transcription level, the role of polymorphisms of TNF promoter in determination inflammatory disease susceptibility or as a marker of severity has been the subject of intense research^[5]. There are many single nuclear polymorphisms within the TNF- α gene promoter. The TNF- α gene shows a polymorphism at position -308 in the promoter region. This polymorphism results in two allele forms, 1 in which a guanine defines the common allele TNF1 and 1 in which an adenosine defines the uncommon allele TNF2^[6]. The TNF2 allele has been associated with a variety of inflammatory disorders, including systemic lupus erythematosus, dermatitis herpetiformis, and celiac disease^[7]. Furthermore, TNF2 allele has been found to be a stronger transcription activator than the TNF1 allele^[8-12], resulting in higher TNF- α levels. Moreover, TNF2 polymorphism has been associated with morbidity and mortality of severe forms of cerebral malaria^[13], mucocutaneous leishmaniasis^[14], meningococcal disease^[15] and septic shock^[16].

A polymorphism is also found at position +252 located in the first intron of the TNF β gene, with a G in the TNFB1 allele and an A in the TNFB2 allele^[17]. In contrast to TNF- α , which is expressed mainly by macrophages, TNF β is expressed and released by lymphocytes. Genes encoding either cytokine are positioned next to each other within the cluster of human leukocyte antigen class III genes on chromosome 6. With respect to high homology and location in the genome, evolutionary studies suggest a common ancestor for both genes that duplicated during evolution. The TNFB1 allele has been associated with a higher TNF β response at both the mRNA and the protein levels^[17]. Furthermore, some studies have found

that the TNFB2 allele results in a higher TNF- α secretory capacity than the TNFB1 allele^[8], and higher plasma TNF- α levels^[18], whereas others could not confirm this observation.

The present study was focused on ABP. The aim was to investigate TNF- α -308 and TNFB polymorphisms in ABP patients, and to related the polymorphisms studied to plasma TNF- α levels.

MATERIALS AND METHODS

Subjects

127 consecutive patients with a first attack of unequivocal acute biliary pancreatitis (ABP) were prospectively considered from January 2001 to August 2002. The diagnosis of acute pancreatitis was based on clinical criteria, an increased -amylase activity (enzymatic colorimetric test) in serum and CT verification of pancreatitis. Etiology of acute pancreatitis was gallstones, in the presence of appropriate radiological of endoscopic retrograde cholangiopancreatography (ERCP) findings. Pancreatitis is classified as severe when APACHE II score is ≥ 8 ^[19] and CT severity index ≥ 4 ^[20]. Septic shock was defined according to ACCP/SCCM consensus conference criteria^[21]. The control Group came from 102 healthy volunteers. In order to be eligible for the enrollment, all of the subjects from the two groups had to be yellow Chinese Han. The exclusion criteria were defined as follows: (1) age > 75 years; (2) cardiac failure(class>III); (3) liver insufficiency (Child C); (4) White blood cell counts $< 0.4 \times 10^9/L$; (5) immunosuppression; (6) there was a delay of more than 36 hours from onset of abdominal pain and hospitalization; (7) patients who had clinical, radiological, or ERCP evidence suggestive of a diagnosis of chronic pancreatitis. The study was approved by the local Ethics Committee and informed consent had been obtained from the patient or a close relative.

Measurement of plasma TNF- α concentrations

Peripheral venous plasma samples were collected (EDTA anticoagulation) from only ASBP patients at admission, centrifuged and stored at $-70^\circ C$ before analysis. Plasma TNF- α concentrations were measured by enzyme immunoassay kit (Quantikine HS Human TNF- α immunoassay kit, R & D Systems, Inc, Minneapolis, MN). The limit of sensitivity was 2.5 pg/mL.

TNF- α -308 G to A substitution

Each patient's DNA was extracted from whole blood using Wizard Genomic DNA Purification kit (Promega) according to the manufacture's instruction. PCR was used to amplify a 107 basepairs fragment of the TNF- α genomic sequence using primers. Upstream: 5' -AGGCAATAGGTTTTGAGGGCCAT 3', downstream: 5' -TCCTCCCTGCTCCGATTCCG 3' (Nanjing Bio Eng Co.Ltd.). The following PCR protocol was used: $94^\circ C$ for 3 minutes; 35 cycles of $94^\circ C$ for 45 seconds, $60^\circ C$ for 45 seconds, $72^\circ C$ for 45 seconds; $72^\circ C$ for 5 minutes using reagents purchased from Promega on a Gene Cyclor™ (BIO-RAD, Japan). The PCR product was digested directly with 2 U NcoI restriction enzyme (Promega) at $37^\circ C$ for 6 hours. Digested DNA was analyzed on 5 % polyacrylamide gels. Ethidium bromide staining of the gel demonstrated the original 107 basepairs fragment (homozygous patients for allele TNF2, lacking NcoI site), three fragments of 102, 87 and 20 basepairs (heterozygous patients), or two fragments of 87 and 20 basepairs of size (homozygous patients for the allele TNF1), (Figure 1).

TNF- β NcoI polymorphism

A 782 basepairs fragment of the TNF- β genomic sequence, including the polymorphic NcoI site, was amplified using PCR.

The following nucleotide sequences were used for PCR amplification^[18]: 5' -CCGTGCTTCGTGCTTTGGACTA 3' and 5' -AGAGGGGTGGATGCTTGGGTTTC3' (Nanjing Bio Eng Co.). The following PCR protocol was used: $95^\circ C$ for 3 minutes; 37 cycles of $95^\circ C$ for 1 minute, $50^\circ C$ for 1 minute, $72^\circ C$ for 1 minute; $72^\circ C$ for 5 minutes using reagents purchased from Promega on a Gene Cyclor™ (BIO-RAD, Japan). The PCR product was digested directly with 2 U NcoI restriction enzyme (Promega) at $37^\circ C$ for 6 hours. Digested DNA was analyzed on 5 % polyacrylamide gels. Ethidium bromide staining of the gel demonstrated the original 782 basepairs fragment (homozygous patients for allele TNFB2), three fragments of 782, 586 and 196 basepairs (heterozygous patients), or two fragments of 586 and 196 basepairs of size (homozygous patients for the allele TNFB1), (Figure 2).

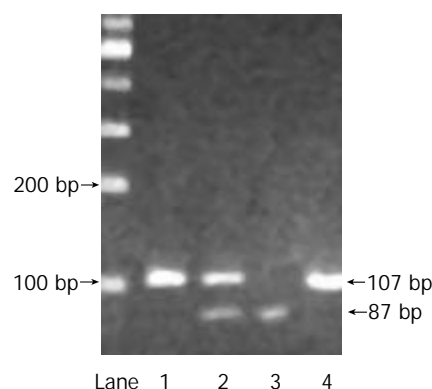


Figure 1 Lane 1 and 4, TNF2 homozygote; Lane 2, TNF1/TNF2 heterozygote; Lane 3, TNF1 homozygote.

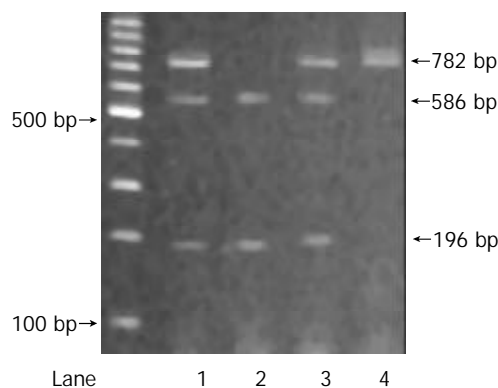


Figure 2 Lane 1 and 3, TNFB1/TNFB2 heterozygote; Lane 2, TNFB1 homozygote; Lane 4, TNFB2 homozygote.

Statistical analysis

Comparison of allelic and genotype frequencies was examined for statistical significance with chi-square test. Descriptive data of continuous variables were tested by Student's *t*-test. Plasma TNF- α levels were reported as median \pm SD. Analysis was completed by SPSS 10.0, and a 2-tailed $P < 0.05$ was considered statistically significant.

RESULTS

Characteristics of the patients

According to the selected criteria, 61 patients (36 females, males 25) with acute severe pancreatitis were studied. The mean age (\pm SD) was 54.6 ± 19 years. APACHE II, 11.5 ± 1 ; CT, 6 ± 1 . Of these, 18 had developed septic shock. The APACHE II score and CT score at the time of admission was similar in both septic shock and no septic shock patients. This study was

undertaken in selected patients with acute mild biliary pancreatitis (AMBP, $n=66$) as defined by APOCHE II score^[19] and CT severity index^[20], and matched with ASBP for age, sex, and cause of pancreatitis. Patients with AMBP had an uneventful recovery. The control group included 102 healthy volunteers, the mean age (\pm SD) was 44.5 ± 10 years. The distribution of gender was 59 females and 43 males.

Two polymorphisms of tumor necrosis factor gene

The frequency distribution of genotypes for TNF polymorphisms studied is shown in Table 1. There was no significant difference in the TNF-308 or TNFB genotype frequency distributions between patients with mild or severe disease. For the TNF-308 polymorphism, TNF2 was found in 18 (29.5 %) of patients with ASBP compared with 17 (25.8 %) of patients with AMBP ($\chi^2=0.223$, $P=0.636$). Likewise TNFB2 occurred in 42 (68.9 %) of patients with ASBP compared with 44 (66.7 %) of patients with AMBP ($\chi^2=0.147$, $P=0.702$).

Further there were no significant differences in the TNF-308 or TNFB genotype frequency distributions between patients with ASBP and controls (Table 1). As to TNF2 frequency, it was found in 35 (27.6 %) of patients with ASBP compared with 26 (25.5 %) of controls ($\chi^2=0.124$, $P=0.725$). Likewise TNFB2 occurred in 86 (67.7 %) of patients with ASBP compared with 63 (61.8 %) of controls ($\chi^2=0.882$, $P=0.348$ respectively).

TNF2 was found in 9 (50 %) of ASBP patients who developed septic shock compared with 9 (20.1 %) of ASBP patients with no septic shock ($\chi^2=5.155$, $P=0.023$). However, TNFB2 occurred in 13 (72.2 %) of ASBP patients with septic shock compared with 29 (67.4 %) of ASBP patients with no septic shock ($\chi^2=0.135$, $P=0.713$), (Table 2).

Table 1 Comparison of TNF Genotype among different groups

	TNF-308			TNFB		
	G/G	G/A	A/A	1/1	1/2	2/2
ASBP	43 (70.5)	15 (24.6)	3 (4.9)	19 (31.1)	25 (41.0)	17 (27.9)
AMBP	49 (74.2)	14 (21.2)	3 (4.5)	22 (33.3)	26 (39.4)	18 (27.3)
	$\chi^2=0.040$, $P=0.980$			$\chi^2=0.197$, $P=0.906$		
ABP	92 (72.4)	29 (22.8)	6 (4.7)	41 (32.3)	51 (40.1)	35 (27.6)
Control	76 (74.5)	21 (20.6)	5 (4.9)	39 (38.2)	35 (34.3)	28 (27.5)
	$\chi^2=2.545$, $P=0.280$			$\chi^2=3.594$, $P=0.166$		

Note. Comparison by chi-square test. No significant differences were found in the distribution of each genotype frequency [no. (%)] between any of the two groups.

Table 2 Comparison of TNF2 frequency and TNFB2 frequency between septic shock group and no septic shock group

	Septic shock ($n=18$)	No septic shock ($n=43$)	P
TNF2	9 (44.4%)	9 (20.9%)	0.023
TNFB2	13 (72.2%)	29 (67.4%)	0.713

Patients with septic shock showed a significantly higher prevalence of the TNF2 than those without. No such association was seen in TNFB2.

Baseline concentrations of TNF- α at inclusion in ASBP

Plasma TNF- α levels at inclusion were detectable in all of the patients with ASBP and shown in Figure 3. At inclusion, among the 61 patients who were admitted for ASBP, 31 (50.8 %) had an increased concentration of TNF- α (normal value <20 pg/mL). There was no significant difference in baseline

concentrations of TNF- α , between ASBP patients who developed septic shock and ASBP patients who didn't.

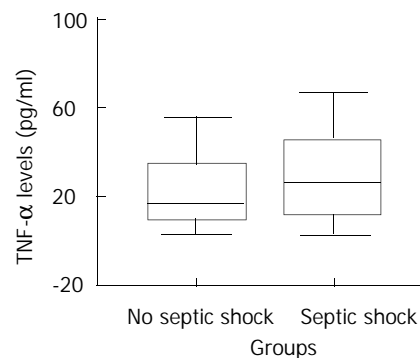


Figure 3 Baseline concentrations of TNF- α at inclusion in ASBP complicated by septic shock or not. $P=0.643$. No significant differences were found in baseline TNF- α levels between septic shock group and no septic shock group.

Association of two polymorphisms of TNF gene with TNF- α levels

In ASBP patients, no association was found in baseline TNF- α levels between TNF2 carrier and TNF1 carrier (30.73 ± 23.05 vs 25.65 ± 22.63 , $P=0.430$), neither was found between TNFB2 carrier and TNFB1 carrier (25.53 ± 23.71 vs 30.73 ± 20.38 , $P=0.412$), (Figure 4 and Figure 5).

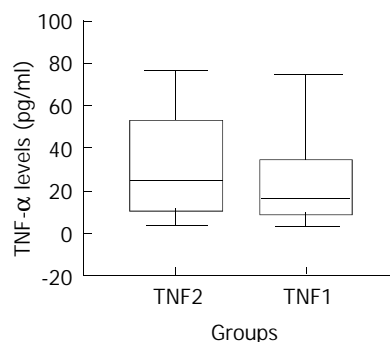


Figure 4 Comparison of TNF- α levels (pg/mL) in ASBP patients based on TNF2 allele. No significant difference was found in TNF- α levels between TNF2 carrier and TNF1 carrier.

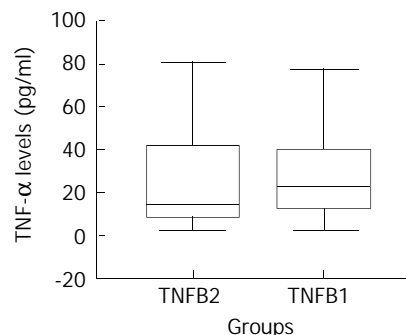


Figure 5 Comparison of TNF- α levels (pg/mL) in ASBP patients based on TNFB2 allele. No significant difference was found in TNF- α levels between TNFB2 carrier and TNFB1 carrier.

DISCUSSION

In the study we have found no association between either TNF- α -308 or TNFB biallelic polymorphism and ASBP or ABP, and thus no evidence that these loci contribute to ASBP susceptibility

or severity. This was in line with previous study^[22, 23]. However, the distribution of TNF- α -308 polymorphisms within the ASBP patients varied, and TNF2 allele was found significantly more frequently in the septic shock patients than in no septic shock ones ($P < 0.05$). The association between the septic shock patients and TNF polymorphism was restricted to the TNF- α -308 polymorphism (TNF2 allele), no such association being seen with TNFB2. The finding of an apparent association between the TNF- α -308 polymorphism and the septic shock raises the possibility that genetic factors may play a role in controlling the onset of septic shock related to ASBP.

In our study an increased TNF- α value was documented in 50.8 % of ASBP patients at inclusion. This finding confirms two previous clinical studies in which TNF- α was documented in 29 % to 78 % of patients studied^[24, 25]. However, there was no significant difference in baseline TNF- α levels between patients who developed septic shock and patients who didn't. The result suggested that plasma baseline TNF- α level was of little value predicting whether septic shock would occur in ASP.

In sepsis and other diseases TNF polymorphisms have been associated with morbidity and mortality of severe forms^[13-16, 26]. The present study did not find an association in the distribution of either TNF2 allele frequency or TNFB2 allele frequency between ASBP patients and AMBP patients ($\chi^2 = 0.223$, $P = 0.636$ and $\chi^2 = 0.147$, $P = 0.702$ respectively). The results showed no correlation between the gene polymorphisms studied and disease severity. Comparison of TNF2 allele frequency or TNFB2 allele frequency in patients with ABP and in healthy controls suggested that these polymorphisms studied did not influence disease susceptibility ($\chi^2 = 0.124$, $P = 0.725$ and $\chi^2 = 0.882$, $P = 0.348$ respectively). However, significant difference was found in TNF2 allele frequencies between septic shock patients and non-septic shock patients ($\chi^2 = 5.155$, $P = 0.023$). Indeed, only in severe forms of cerebral malaria^[13], mucocutaneous leishmaniasis^[14], meningococcal disease^[15] and septic shock^[16], were morbidity and mortality linked with TNF2 allele or TNFB2 allele. In mild conditions, no such relationship was found between sepsis and the TNF2 allele^[27]. As to TNF- α -308 and TNFB genotype, there were no significant difference in the distribution of either type between ASBP patients and AMBP patients, neither was found between ABP patients and controls. It suggested that TNF- α -308 genotype and TNFB genotype were both not related to the susceptibility or severity of ABP.

Although polymorphisms may only be markers of other functionally significant gene polymorphism, at least one of the TNF gene polymorphisms studied is known to have functional significance. It seems that environmental factors trigger cytokine secretion, genetic factors may be important in determining levels of secretion^[28]. In vitro studies have identified that individuals may demonstrate consistent differences in leukocyte cytokine secretion^[29] and that these difference are probably genetically predetermined^[28]. In our study, plasma TNF- α concentrations of ASBP patients with TNF2 allele or TNFB2 allele were not significantly higher than that of patients without TNF2 allele or TNFB2 allele respectively. It suggested that there was no significant correlation between TNF- α concentration and TNF2 or TNFB2 allele carriage. However, many factors could influence plasma TNF- α concentrations. Of these, an important one is its relatively short half-life^[30], so we were at great risk of missing the intravascular secretion of this cytokine. Another reason for low plasma TNF- α concentrations may be the breakdown of TNF- α by enzyme released from pancreas into circulation^[31, 32]. Furthermore, this detectable level does not take into account the membrane-bound form of TNF- α . In addition, in complex biologic systems, the effect of a single gene polymorphism in determining cytokine production may be minimized through

the interaction of other factors^[33]. Maybe circulating TNF- α levels do not correspond with the TNF2 and TNFB2 polymorphisms, however, circulating TNF- α levels might be under a multifactoral regulatory process. Local TNF- α levels might be of greater importance and under more control by specific polymorphisms.

To the best of our knowledge, there have two different studies on the association of two polymorphisms of tumor necrosis factor gene with acute severe pancreatitis^[23, 35], and our results are in line with theirs. However, they both failed to study the association of two polymorphisms with septic shock due to ASBP. The finding of our study for the first time, to our knowledge, raise the possibility that TNF2 allele may play some role in the susceptibility of septic shock related to ASBP. However, the role, if any, of genetic factors in influencing the occurrence of septic shock awaits confirmation in further prospective studies. If the association between TNF2 allele and septic shock is confirmed, it would have implications not only for understanding of mechanisms of septic shock from ASBP, but also in the clinical management of patients, with the possibility that TNF2 carriers at high risk of septic shock may be identifiable early in the disease course, allowing early and aggressive therapy to be instituted. In addition, the study offers new opportunities for studying intervention with anti-TNF therapies. Determining a patient's TNF2 genotype before starting the treatment may permit the selection of a TNF2 group of high-risk patients who could benefit from treatment with anti-TNF. Such a possibility deserves further study, since an effective therapy for ASBP patients with septic shock would have important clinical and economic consequences.

In conclusion, our study demonstrated that there was no association between acute biliary pancreatitis and the two polymorphisms of tumor necrosis factor gene studied; however, TNF2 allele were associated with the susceptibility to septic shock related to acute severe biliary pancreatitis. Genetic factors are not important in determining plasma TNF- α levels in ASBP.

REFERENCES

- 1 **Forsmark CE.** The clinical problem of biliary acute necrotizing pancreatitis: epidemiology, pathophysiology, and diagnosis of biliary necrotizing pancreatitis. *J Gastrointest Surg* 2001; **5**: 235
- 2 **Schmid SW,** Buchler MW. The role of infection in acute pancreatitis. *Gut* 1999; **45**: 311-316
- 3 **Xia Q,** Jiang JM, Gong X, Chen GY, Li L, Huang ZW. Experimental study of Tong Xia purgative method in ameliorating lung injury in acute necrotizing pancreatitis. *World J Gastroenterol* 2000; **6**: 115-118
- 4 **Grewal HP,** Kotb M, el Din AM, Ohman M, Salem A, Gaber L, Gaber AO. Induction of tumor necrosis factor in severe acute pancreatitis and its subsequent reduction after hepatic passage. *Surgery* 1994; **115**: 213-221
- 5 **Chiche JD,** Siami S, Dhainaut JF, Mira JP. Cytokine polymorphisms and susceptibility to severe infectious disease. *Sepsis* 2001; **4**: 209-215
- 6 **Wilson AG,** de Vries N, Pociot F, di Giovine FS, van der Putte LB, Duff GW. An allelic polymorphism within the human tumor necrosis factor α promoter region is strongly associated with HLA A1, B8, and DR3 alleles. *J Exp Med* 1993; **177**: 557-560
- 7 **McManus R,** Wilson AG, Mansfield J, Weir DG, Duff GW, Kelleher D. TNF2, a polymorphism of the tumor necrosis- α gene promoter, is a component of the celiac disease major histocompatibility complex haplotype. *Eur J Immunol* 1996; **26**: 2113-2118
- 8 **Pociot F,** Briant L, Jongeneel CV, Molvig J, Worsaae H, Abbal M, Thomsen M, Nerup J, Cambon-Thomsen A. Association of tumor necrosis factor (TNF) and class II major histocompatibility complex alleles with the secretion of TNF- α and TNF- β by human mononuclear cells: a possible link to insulin-dependent diabetes mellitus. *Eur J Immunol* 1993; **23**: 224-231

- 9 **Kroeger KM**, Carville KS, Abraham LJ. The -308 tumor necrosis factor α promoter polymorphism effects transcription. *Mol Immunol* 1997; **34**: 391-399
- 10 **Wilson AG**, Symons JA, McDowell TL, McDevitt HO, Duff GW. Effects of a polymorphism in the human tumor necrosis factor α promoter on transcriptional activation. *Proc Natl Acad Sci USA* 1997; **94**: 3195-3199
- 11 **Braun N**, Michel U, Ernst BP, Metzner R, Bitsch A, Weber F, Rieckmann P. Gene polymorphism at position -308 of the tumor-necrosis-factor-alpha (TNF-alpha) in multiple sclerosis and its influence on the regulation of TNF-alpha production. *Neurosci Lett* 1996; **215**: 75-78
- 12 **Brinkman BM**, Zuijdeest D, Kaijzel EL, Breedveld FC, Verweij CL. Relevance of the tumor necrosis factor alpha (TNF- α)-308 promoter polymorphism in TNF alpha gene regulation. *J Inflamm* 1996; **46**: 32-41
- 13 **McGuire W**, Hill AV, Allsopp CE, Greenwood BM, Kwiatkowski D. Variation in the TNF-alpha promoter region associated with susceptibility to cerebral malaria. *Nature* 1994; **371**: 508-510
- 14 **Cabrera M**, Shaw MA, Sharples C, Williams H, Castes M, Convit J, Blackwell JM. Polymorphism in tumor necrosis factor genes associated with mucocutaneous leishmaniasis. *J Exp Med* 1995; **182**: 1259-1264
- 15 **Nadel S**, Newport MJ, Booy R, Levin M. Variation in the tumor necrosis factor-alpha gene promoter region may be associated with death from meningococcal disease. *J Infect Dis* 1996; **174**: 878-880
- 16 **Mira JP**, Cariou A, Grall F, Delclaux C, Losser MR, Heshmati F, Cheval C, Monchi M, Teboul JL, Riche F, Leleu G, Arbibe L, Mignon A, Delpech M, Dhainaut JF. Association of TNF2, a TNF-alpha promoter polymorphism, with septic shock susceptibility and mortality: a multicenter study. *JAMA* 1999; **282**: 561-568
- 17 **Messer G**, Spengler U, Jung MC, Honold G, Blomer K, Pape GR, Riethmuller G, Weiss EH. Polymorphic structure of the tumor necrosis factor (TNF) locus: an NcoI polymorphism in the first intron of the human TNF- β gene correlates with a variant amino acid in position 26 and a reduced level of TNF- β production. *J Exp Med* 1991; **173**: 209-219
- 18 **Stuber F**, Petersen M, Bokelmann F, Schade U. A genomic polymorphism within the tumor necrosis factor locus influences plasma tumor necrosis factor- α concentrations and outcome of patients with severe sepsis. *Crit Care Med* 1996; **24**: 381-384
- 19 **Dominguez-Munoz JE**, Carballo F, Garcia MJ, de Diego JM, Campos R, Yanguela J, de la Morena J. Evaluation of the clinical usefulness of APACHEII and SAPS systems in the initial prognostic classification of acute pancreatitis: a multicenter study. *Pancreas* 1993; **8**: 682-686
- 20 **Balthazar EJ**, Robinson DL, Megibow AJ, Ranson JH. Acute pancreatitis: value of CT in establishing prognosis. *Radiology* 1990; **174**: 331-336
- 21 **Muckart DJ**, Bhagwanjee S. American college of chest physicians/society of critical care medicine consensus conference definitions of the systemic inflammatory response syndrome and allied disorders in relation to critically injured patients. *Crit Care Med* 1997; **25**: 1789-1795
- 22 **Zhang D**, Li J, Jiang Z, Yu B, Tang X. Significance of tumor necrosis factor-alpha gene polymorphism in patients with acute severe pancreatitis. *Zhonghua Yixue Zazhi* 2002; **82**: 1529-1531
- 23 **Sargen K**, Demaine AG, Kingsnorth AN. Cytokine gene polymorphisms in acute pancreatitis. *JOP* 2000; **1**: 24-35
- 24 **de Beaux AC**, Goldie AS, Ross JA, Carter DC, Fearon KC. Serum concentrations of inflammatory mediators related to organ failure in patients with acute pancreatitis. *Br J Surg* 1996; **83**: 349-353
- 25 **Brivet FG**, Emilie D, Galanaud P. Pro- and anti-inflammatory cytokines during acute severe pancreatitis: an early and sustained response, although unpredictable of death. Parisian Study Group on Acute Pancreatitis. *Crit Care Med* 1999; **27**: 749-755
- 26 **Majetschak M**, Flohe S, Obertacke U, Schroder J, Staubach K, Nast-Kolb D, Schade FU, Stuber F. Relation of a TNF Gene Polymorphism to Severe Sepsis in Trauma Patients. *Ann Surg* 1999; **230**: 207-214
- 27 **Stuber F**, Udalova IA, Book M, Drutskaya LN, Kuprash DV, Turetskaya RL, Schade FU, Nedospasov SA. -308 tumor necrosis factor (TNF) polymorphism is not associated with survival in severe sepsis and is unrelated to lipopolysaccharide inducibility of the human TNF promoter. *J Inflamm* 1996; **46**: 42-50
- 28 **Westendorp RG**, Langermans JA, Huizinga TW, Elouali AH, Verweij CL, Boomsma DI, Vandenbroucke JP, Vandenbroucke JP. Genetic influence on cytokine production and fatal meningococcal disease. *Lancet* 1997; **349**: 170-173
- 29 **van der Linden MW**, Huizinga TW, Stoeken DJ, Sturk A, Westendorp RG. Determination of tumor necrosis factor-alpha and interleukin-10 production in a whole blood stimulation system: assessment of laboratory error and individual variation. *J Immunol Methods* 1998; **218**: 63-71
- 30 **Kaufmann P**, Tilz GP, Lueger A, Demel U. Elevated plasma levels of soluble tumor necrosis factor receptor (sTNFp60) reflect severity of acute pancreatitis. *Intensive Care Med* 1997; **23**: 841-848
- 31 **Steer ML**. How and where does acute pancreatitis begin? *Arch Surg* 1992; **127**: 1350-1353
- 32 **Dominguez-Munoz JE**, Carballo F, Garcia MJ, de Diego JM, Rabago L, Simon MA, de la Morena J. Clinical usefulness of polymorphonuclear elastase in predicting the severity of acute pancreatitis: results of a multicentre study. *Br J Surg* 1991; **78**: 1230-1234
- 33 **Powell JJ**, Fearon KC, Siriwardena AK, Ross JA. Evidence against a role for polymorphisms at tumor necrosis factor interleukin-1 and interleukin-1 receptor antagonist gene loci in the regulation of disease severity in acute pancreatitis. *Surgery* 2001; **129**: 633-640

The development of a new bioartificial liver and its application in 12 acute liver failure patients

Yi-Tao Ding, Yu-Dong Qiu, Zhong Chen, Qing-Xiang Xu, He-Yuan Zhang, Qing Tang, De-Cai Yu

Yi-Tao Ding, Yu-Dong Qiu, Zhong Chen, Qing-Xiang Xu, Qing Tang, De-Cai Yu, Hepatobiliary Surgery Department, affiliated Drum Tower Hospital of Medical College of Nanjing University, Hepatobiliary Institute of Nanjing University; Hepatobiliary Surgery Institute of Nanjing, Jiangsu Province, 210008, China
He-Yuan Zhang, Biochemistry Department in Nanjing University, Jiangsu Province, China

Supported by the Public Health Bureau of Jiangsu Province, China, BQ200020 and Social Development Plan of Scientific and Technological Council of Nanjing Municipal, China. SS200002

Correspondence to: Dr. Yi-Tao Ding, Hepatobiliary Surgical Department, Affiliated Drum Tower Hospital of Medical College in Nanjing University, Zhongshan road, 321, Nanjing, 210008, Jiangsu Province, China. xqx008@hotmail.com

Telephone: +86-25-3304616-11601 **Fax:** +86-25-3317016

Received: 2002-07-31 **Accepted:** 2002-09-12

Abstract

AIM: Bioartificial liver is a hope of supporting liver functions in acute liver failure patients. Using polysulfon fibers, a new bioartificial liver was developed. The aim of this study was to show whether this bioartificial liver could support liver functions or not.

METHODS: Hepatocytes were procured from swine using Seglen's methods. The bioartificial liver was constructed by polysulfon bioreactor and more than 10^{10} hepatocytes. It was applied 14 times in 12 patients, who were divided into 7 cases of simultaneous HBAL and 5 cases of non-simultaneous HBAL. Each BAL treatment lasted 6 hours. The general condition of the patients and the biochemical indexes were studied.

RESULTS: After treatment with bioartificial liver, blood ammonia, prothrombin time and total bilirubin showed significant decrease. 2 days later, blood ammonia still showed improvement. within one month period, 1 case (1/7) in simultaneous group died while in non-simultaneous group 2 cases (2/5) died. The difference was significant. Mortality rate was 25 %.

CONCLUSION: The constructed bioartificial liver can support liver functions in acute liver failure. The simultaneous HBAL is better than non-simultaneous HBAL.

Ding YT, Qiu YD, Chen Z, Xu QX, Zhang HY, Tang Q, Yu DC. The development of a new bioartificial liver and its application in 12 acute liver failure patients. *World J Gastroenterol* 2003; 9 (4): 829-832

<http://www.wjgnet.com/1007-9327/9/829.htm>

INTRODUCTION

Acute liver failure (ALF) is commonly seen in the mainland of China. The patients are always characterized by infection of hepatitis B. Liver cell damage is the main reason of ALF.

When the amount of normal cells decrease below its limit, liver function will deteriorate and a vicious cycle will be formed.

Liver transplantation (LT) has already been a wise choice for these patients^[1-3]. The 1 year survival rate could be improved to more than 70 % when LT is applied^[4,5]. But the donor is scarce, so it limits the wide practice of LT. Many patients exacerbated and died during the period of waiting donor liver.

Bioartificial liver (BAL) is designed to take the responsibility of supporting liver functions temporarily in acute liver failure^[6-9]. It consists of a semi-permeable membrane and living allogeneic or syngeneic liver cells. The flow of blood or plasma from the patient can exchange the substances with those cells through this membrane. The ammonia and other toxins in blood then are detoxified, as well as some useful factors are secreted into blood. Many scholars reported that BAL was effective and could be used as a bridge to LT^[8-10]. Also this technique gave the chance of spontaneous recovery of the native function because of liver cell regeneration in some cases^[8,11].

It is estimated that 1×10^9 hepatocytes are the lowest limit that are needed in BAL^[10]. Such large number of hepatocytes are very difficult to be cultured in a small bioreactor. Enlarging the volume of the bioreactor and adding a hepatocytes cell pool are both good methods to solve such problems.

Using a bioreactor made of polysulfon, we developed a bioartificial liver recently and applied it in 12 patients. The results were exciting.

MATERIALS AND METHODS

Animals

Healthy Chinese experimental miniature swine were purchased from the Animal Center of Beijing Agriculture University. On receipt, swine were kept in a temperature and humidity controlled environment (20-25 °C, humidity 50-70 %) in a 12/12 hour light/dark cycle and fed with a cereal based diet with free access to water. More than a week later, they were used to get the hepatocytes. 12 hours before procedure only free water *ad libitum* was allowed. The animals were treated in accordance with the guidelines established by Affiliated Drum Tower Hospital of Medical College of Nanjing University.

Hepatocytes preparation

Hepatocytes were isolated from the swine by in situ liver perfusion and enzymatic collagenase digestion according to the process described by Seglen^[12]. Briefly, under katamine (50 mg/kg) anesthesia, a median laparotomy and cannulation of the portal vein were performed. The inferior vena cava was ligated just above the renal vein and then was cannulated close to the heart. The liver was perfused at 4 °C and pH 7.6 with 3 000 ml Hanks solution through the portal vein. Then the liver was circularly perfused with 500 ml 0.5 % collagenase IV solution (Gibco, New York, USA) at a constant flow of 20 ml/minute. The softened liver was then excised and hepatocytes were separated from the connective liver tissue by gentle

agitation. The resulting cell suspension was filtered through 50 μm sterile metal mesh. The cells were washed three times, suspended in non serum RPMI 1640 culture medium (Sigma, Louis, USA) with 200 $\mu\text{g/L}$ hydrocortisone, 1 mg/L HGF, 10 $\mu\text{g/L}$ EGF, 20 $\mu\text{g/L}$ NGF, 100 $\mu\text{g/L}$ insulin, 4 $\mu\text{g/L}$ glucagon, 6.25 mg/L transferrin, 10 mg/L linoleic acid, 2 mmol glutamine, 0.5 g/L bovine serum albumin, 3nmol sodium selenate, 0.1 $\mu\text{g/L}$ $\text{CuSO}_4 \cdot 5\text{H}_2\text{O}$, 50pM $\text{ZnSO}_4 \cdot 7\text{H}_2\text{O}$, 15 mmol HEPES, 200 $\mu\text{g/L}$ cefaperazone, $1 \times 10^3 \text{U/L}$ penicillin and 100 mg/L streptomycin. Cell viability was determined by the trypanum exclusion test. Only suspensions with cell viability of $\geq 95\%$ were used. Cells suspension was then stirring incubated overnight in that non serum RPMI 1640 culture medium at 37 $^\circ\text{C}$.

Configuration of bioartificial liver

Polysulfon bioreactor was purchased from TECA Corp. (Hongkong, China). The molecular cutoff of the membrane was 100 kD. Total fiber internal surface area was 1 620 cm^2 , external surface area was 2 060 cm^2 . Before use, the bioreactor was sterilized and rinsed by 3 000 ml normal saline. A hepatocytes reservoir, a rolling pump and a circulation cycle were designed to connect to the extra-fiber compartment of bioreactor. The aim was to ensure more than 10^{10} hepatocytes being used and enough nutrition could be provided. Then the cultured suspended cells were filled into the extra-fiber compartment of bioreactor. The rolling rate of the pump was 80 ml/minute.

Blood was removed from the patient through a double lumen catheter in superficial femoral vein at a rate of 100 ml/minute and run through a plasma separator. The separated plasma passed through a charcoal column or bilirubin absorption column and then run into the intra-fiber compartment of bioreactor in simultaneous HBAL, while in non-simultaneous HBAL the plasma run directly into the intra-fiber compartment of bioreactor. The reacted plasma were then reconstituted with red blood cells and returned to the patient via the venous cannula. (Figure 1).

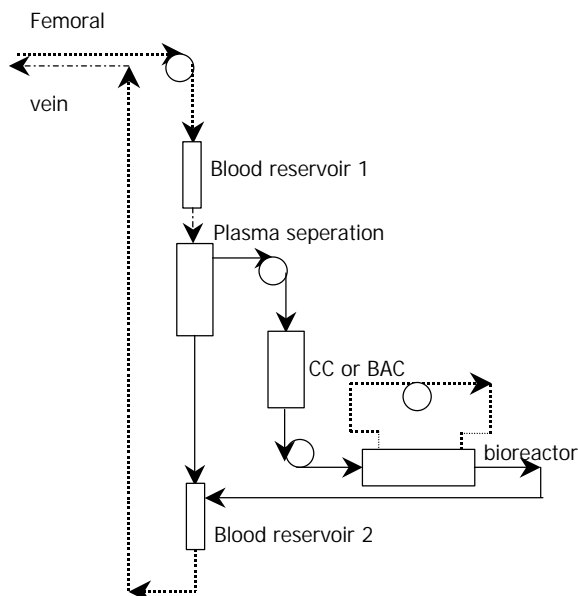


Figure 1 The constructed bioartificial liver. CC: charcoal column. BAC: bilirubin absorption column.

Clinical use

12 patients, which include 9 male and 3 female, suffering from acute liver failure were adopted to this study. The age ranged

from 13 to 56. All the patients were found having hepatitis B infection (Table 1). Before the BAL supporting treatment, an evaluation of the patient's psychic state was conducted by a psychologist, and an agreement of BAL application was signed by the patient and/or his direct relatives.

The treatment regimen included simultaneous HBAL and non-simultaneous HBAL. The only difference was bilirubin absorption treatment or plasma exchange treatment being used 1 day before the bioreactor was applied in non-simultaneous HBAL while in simultaneous HBAL they were applied simultaneously. Other traditional treatments were all the same. Some liver function indexes and the one month mortality rate were used to evaluate the function of BAL.

Table 1 Clinical data of the patients

Patient No.	Sex	Age	Hepatitis B infection	Regimen of treatment	Number of treatment	Result
1	M	13	+	HBAL(CC)	1	Improved
2	M	38	+	1. HBAL(BAC) 2. BAL	1	Improved
3	F	34	+	HBAL(BAC)	1	Improved
4	M	55	+	HBAL(BAC)	1	Death
5	M	52	+	HBAL(BAC)	1	Improved
6	M	46	+	HBAL(BAC)	1	Improved
7	M	58	+	HBAL(BAC)	1	Improved
8	M	33	+	PE and BAL	1	Improved
9	F	50	+	PE and BAL	2	Death
10	F	52	+	HF and BAL	1	Death
11	M	40	+	HF and BAL	1	Improved
12	M	30	+	BAC and BAL	1	Improved

M: male, F: female, +: positive, HBAL: hybrid bioartificial liver, BAL: bioartificial liver, (CC): with charcoal column, (BAC): with bilirubin absorption column, PE and BAL: plasma exchange and 24 hours later BAL only, HF and BAL: hemofiltration and 24 hours later BAL only, BAC and BAL: bilirubin absorption and 24 hours later BAL only.

Statistical analysis

Mortality rate was expressed as percentage. Others were expressed as mean \pm SD. Paired T test was used (SPSS software, SPSS Inc. USA). Probability of less than 0.05 was accepted as significant.

RESULTS

In 12 patients, 14 times BAL treatments were conducted. The period of one BAL treatment lasted 6 hours. All patients experienced the procedure successfully.

3 patients died soon after the procedure and 9 were improved. The mortality rate was 25%. The criteria of improvement included improvement of general condition of the patient, persistent hepatic function improvement, improved psychic state, and recovery.

In biochemical test, ALT showed slight decrease in post-treatment period and restored to pre-treatment level 2 days later. No change in blood albumin. Blood ammonia, prothrombin time and total bilirubin indexes showed significant decrease after treatment. 2 days later, only blood ammonia still maintained significant low level (Figure 2).

In non-simultaneous HBAL, the mortality rate was 40%. While in simultaneous HBAL, the mortality rate was 14.3%. Significant difference was found comparing them (Figure 3).

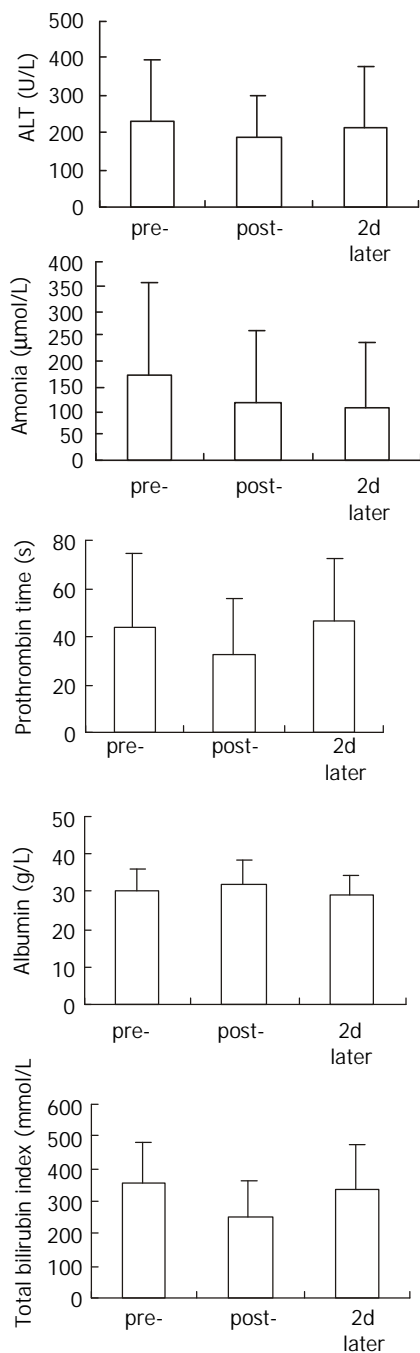


Figure 2 Change of ALT, ammonia, prothrombin time, albumin and total bilirubin index in 12 patients. Compared with pre-, ammonia, prothrombin time and total bilirubin index showed significant decrease in post-. 2 days later, only ammonia showed significant lowering. pre-: pre-treatment, post-: post-treatment, 2d later: 2 days after the treatment. Paired T test was used to test the difference.

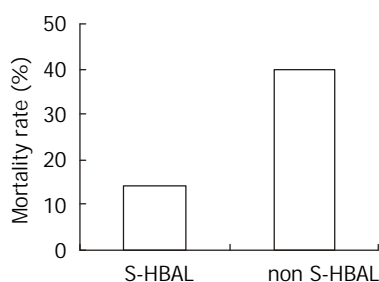


Figure 3 The mortality rate of simultaneous HBAL and non-simultaneous HBAL. Significant difference was found between this two groups ($P < 0.05$).

Typical case report: A male, aged 38 years old, was admitted for “fatigue and yellow urine for a week”. Physical examination showed yellowish face, moderate jaundice in skin and sclera, palpable liver that was 2 cm below the costal arch in right mid-clavicular line, and tenderness in right upper abdomen. Laboratory examination showed positive HBs antibody, Hbe antibody and HBc antibody, abnormal liver function. B type ultrasound examination showed image of liver injury. The diagnosis was severe acute hepatitis with hepatitis B virus infection. After admission, the patient was given conventional treatment without any improvement and ran downhill. One week later, He received a simultaneous HBAL (bilirubin absorption) treatment. Total bilirubin and prothrombin time decreased immediately. 6 days later he received another HBAL treatment because of worsening some biochemical indexes. 2 weeks after that the patient was recovered and was waiting for liver transplantation. (Table 2).

Table 2 Change of some biochemical index after the HBAL treatment

Time	ALT (U/L)	GOT (U/L)	TBI (μmol/L)	DBI (μmol/L)	TP (g/L)	ALB (g/L)	PT (s)
Admission	77.5	58.8	341.8	265.4	60.1	32.8	68.8
2 hours later	58.7	52.5	343.0	255.2	52.4	31.9	32.2
HBAL 4 hours later	66.3	69.5	345.7	280.4	52.9	31.4	40.9
(BA) 6 hours later	68.7	79.9	260.8	291.6	54.5	31.4	26.7
2 days later	80.6	68.0	423.2	336.0	70.4	37.1	20.2
Before HBAL	421.2	371.9	375.4	109.0	44.6	27.4	21.9
2 hours later	427.9	412.0	389.0	102.1	42.7	26.5	28.5
HBAL 4 hours later	431.8	411.4	373.9	99.5	43.0	26.7	28.7
6 hours later	371.0	218.0	339.8	122.1	45.6	28.8	17.4
2 days later	301.2	159.6	444.6	125.7	43.6	26.5	28.7

HBAL: hybrid bioartificial liver; BA: bilirubin absorption.

DISCUSSION

ALF is a severe disease in clinical practice with a mortality rate of 30-80 %^[1-5]. OLT is thought to be the most effective method to improve the prognosis. But it is greatly limited due to shortage of donor liver^[3,4]. HBAL is designed to take responsibility of improving the poor physical state of the patients and supporting liver function for a short time which may serve as a bridge to OLT^[6-11].

The ideal HBAL should support the patients to pass through the worst period of the course by its metabolic, synthetic, toxin and drug degradational functions. When it works, immune reactions to the living cells may be avoided^[13,14], while toxins and some useful factors might be capable to pass the membrane freely.

Construction of HBAL

The external BAL is being studied in many medical centers. Living hepatocytes are first needed in this apparatus. Human hepatocytes are the ideal choice. But the only available human livers are all used for liver transplantation. Human cell strains from some liver neoplasmas were also reported. But the danger of this application is unknown. Porcine hepatocytes are the commonest choice of many centers, because pigs are cheap and easy to get, without any ethical contradictions of killing them.

When the liver cells are procured, the membranes might be damaged by the enzymes or the mechanical factors^[15]. The damaged membrane needs 1 to 3 days for recovery^[16]. Our experience shows 1 day stirring culture of the procured hepatocytes is enough.

Enough viable hepatocytes are also important in BAL. It was estimated that 1×10^9 hepatocytes are the lowest limit^[10]. Such a large number of hepatocytes are very difficult to live and maintain its function in a small bioreactor, through which hepatocytes may exchange substance with blood. If the volume of bioreactor is enlarged greatly, hemodynamics of the patient may be disturbed. We designed a two cycles bioreactor. The first cycle was to supply the nutrition and the other one was to connect to a cell reservoir which ensured 10^{10} cells were used in this system.

The toxins in blood are sometimes harmful to living hepatocytes. To decrease this effect, mechanical filtration or absorption is used in this system. Due to long period of time to construct the system and urgent situation of the patient requiring this treatment, we designed a non-simultaneous HBAL, that used mechanical filtration or carbon absorption or bilirubin absorption or plasma exchange first, then BAL was applied the next day. The results were not satisfactory. The mortality rate was higher than the simultaneous HBAL.

Effects of HBAL

The material of the bioreactor and the characters of it are most important. Polysulfon was chosen because of its good histocompatibility with body and little toxicity. In dialysis medicine the polysulfon is already widely used as dialyzer. The molecular cut-off is another important index for the bioartificial liver. If it is large enough, cells in it may not be protected completely. Otherwise the toxins cannot be detoxified and useful factors secreted by hepatocytes cannot enter the body. The molecular cut-off we choosed was 100 kD because IgG is about 150 kD and albumin or hepatic growth factor is about 70-80 kD.

Our experiments showed that BAL could function well when applied to the patients. The ammonia, prothrombin time and total bilirubin showed significant decrease in post-treatment examination. ALT also showed a slight decrease in post-treatment study, although no significant difference was found.

Also HBAL showed a delayed reaction, 2 days after application as ammonia still showed significant decrease. We considered that this function might be due to the synthetic function of HBAL.

REFERENCES

- 1 Emond JC, Whittington PF, Thistlethwaite JR, Cherqui D, Alonso

- EA, Woodle IS, Vogelbach P, Busse-Henry SM, Zucker AR, Broelsch CE. Transplantation of two patients with one liver. *Ann Surg* 1990; **212**: 14-22
- 2 Shaw BW. More questions than answers. *Liver Transplant Surg* 1995; **1**: 404-407
- 3 Everhart JE, Lombardero M, Detre KM, Zetterman RK, Wiesner RH, Lake JR, Hoofnagle JH. Increased waiting time for liver transplantation results in higher mortality. *Transplantation* 1997; **64**: 1300-1306
- 4 Bilsuttill W, Klintmalm B. Transplantation of the liver Philadelphia. W. B. Saunders Company 1996: 861
- 5 Emond JC, Whittington PF, Thistlethwaite JR, Alonso EM, Broelsch CE. Reduced-size orthotopic liver transplantation: use in the management of children with chronic liver disease. *Hepatology* 1989; **10**: 867-872
- 6 Friedman AL. Why bioartificial liver support remains the holy grail. *ASAIO* 1998; **44**: 241-243
- 7 Kamihira M, Yamada K, Hamamoto R, Iijima S. Spheroid formation of hepatocytes using synthetic polymer. *Ann NY Acad Sci* 1997; **831**: 398-407
- 8 Sussman NL, Gislason GT, Conlin CA, Kelly JH. The Hepatix extracorporeal liver assist device: Initial clinical experience. *Artif Organs* 1994; **18**: 390-396
- 9 Dixit V. Development of a bioartificial liver using isolated hepatocytes. *Artif Organs* 1994; **18**: 371-384
- 10 Hui T, Rozga J, Demetriou AA. Bioartificial liver support. *J Hepatobiliary Surg* 2001; **8**: 1-15
- 11 Suh KS, Lilja H, Kamohara Y, Eguchi S, Arkadopoulos N, Neuman T, Demetriou AA, Rozga J. Bioartificial liver treatment in rats with fulminant hepatic failure: effect on DNA-binding activity of liver-enriched and growth-associated transcription factors. *J Surg Res* 1999; **85**: 243-250
- 12 Seglen PO. Preparation of isolated rat liver cells. *Methods Cell Biol* 1976; **13**: 23-28
- 13 Rozga J, Williams F, Ro MS, Neuzil DF, Giorgio TD, Backfisch G, Moscioni AD, Hakim R, Demetriou AA. Development of a bioartificial liver: properties and function of a hollow fiber module inoculated with liver cells. *Hepatology* 1993; **17**: 258-265
- 14 Cuervas-Mons V, Colas A, Rivera JA, Prados E. In vivo efficacy of a bioartificial liver in improving spontaneous recovery from fulminant hepatic failure: a controlled study in pigs. *Transplantation* 2000; **69**: 337-344
- 15 Flendrig LM, La-Soe JW, Jorning GGA, Steenbeek A, Karlsen OT, Bovee WMM, Ladiges NC, te Velde AA, Chamuleau RA. In vitro evaluation of a novel bioreactor based on an integral oxygenator and spirally wound nonwoven polyester matrix for hepatocyte culture as small aggregates. *J Hepatol* 1997; **26**: 1379-1392
- 16 Chen Z, Ding Y, Zhang H. Cryopreservation of suckling pig hepatocytes. *Ann Clin Lab Sci* 2001; **31**: 391-398

Edited by Xu JY

Serum positive cagA in patients with non-ulcer dyspepsia and peptic ulcer disease from two centers in different regions of Turkey

Ender Serin, Uður Yılmaz, Ganiye Künefecı, Birol Özer, Yüksel Gümürdülü, Mustafa Güçlü, Fazilet Kayaselçuk, Sedat Boyacıođlu

Ender Serin, Ganiye Künefecı, Birol Özer, Yüksel Gümürdülü, Mustafa Güçlü, Ba kent University Faculty of Medicine, Department of Gastroenterology, Adana Teaching and Medical Research Center, Dadalođlu Mahallesi, 39 Sokak, No: 6, 01250 Adana, Turkey
Uður Yılmaz, Sedat Boyacıođlu, Ba°kent University Faculty of Medicine, Department of Gastroenterology, Ankara Hospital, Dadalođlu Mahallesi, 39 Sokak, No: 6, 01250 Adana, Turkey
Fazilet Kayaselçuk, Ba°kent University Faculty of Medicine, Department of Pathology, Adana Teaching and Medical Research Center Dadalođlu Mahallesi, 39 Sokak, No: 6, 01250 Adana, Turkey
Correspondence to: Ender Serin, Ba°kent Üniversitesi Týp Fakóltesi, Adana Uygulama ve Arařtırma Merkezi, Dadalođlu Mahallesi, 39 Sokak, No: 6, 01250 Adana, Turkey. eserin@baskent-adn.edu.tr
Telephone: +90-322-3272727 **Fax:** +90-322-3271273
Received: 2002-12-07 **Accepted:** 2003-01-03

Abstract

AIM: To investigate and compare frequencies of serum positive cagA in patients from two separate regions of Turkey who were grouped according to the presence of peptic ulcer disease or non-ulcer dyspepsia.

METHODS: One hundred and eighty *Helicobacter pylori*-positive patients with peptic ulcer disease or non-ulcer dyspepsia were included in the study. One hundred and fourteen patients had non-ulcer dyspepsia and 66 had peptic ulcer disease (32 with gastric ulcers and/or erosions and 34 with duodenal ulcers). Each patient was tested for serum antibody to *H. pylori* cagA protein by enzyme immunoassay.

RESULTS: The total frequency of serum positive cagA in the study group was 97.2 %. The rates in the patients with peptic ulcers and in those with non-ulcer dyspepsia were 100 % and 95.6 %, respectively. These results were similar to those reported in Asian studies, but higher than those that have been noted in other studies from Turkey and Western countries.

CONCLUSION: The high rates of serum positive cagA in these patients with peptic ulcer disease and non-ulcer dyspepsia were similar to results reported in Asia. The fact that there was high seroum prevalence regardless of ulcer status suggests that factors other than cagA might be responsible for ulceration or other types of severe pathology in *H. pylori*-positive individuals.

Serin E, Yılmaz U, Künefecı G, Özer B, Gümürdülü Y, Güçlü M, Kayaselçuk F, Boyacıođlu S. Serum positive cagA in patients with non-ulcer dyspepsia and peptic ulcer disease from two centers in different regions of Turkey. *World J Gastroenterol* 2003; 9(4): 833-835
<http://www.wjgnet.com/1007-9327/9/833.htm>

INTRODUCTION

Helicobacter pylori (*H. pylori*) infection is very common, especially in developing countries; however, patients with this

infection rarely develop clinically significant conditions, such as peptic ulcer disease. This situation has prompted researchers to investigate the possible roles of host and environmental factors, and factors related to the bacterium itself in cases that show severe pathologies^[1-3]. Earlier works identified associations between *H. pylori* strains that harbor cytotoxin-associated gene A (cagA) and significant gastroduodenal pathology; however, the results of more recent studies are conflicting. In Europe, investigators have reported a significantly higher seroprevalence of cagA antigen in gastroduodenal ulcer cases than that in non-ulcer dyspepsia cases^[4,5]. In contrast, most studies from Asian countries have noted that there was no significant difference between these patient groups with respect to anti-cagA antibody positivity^[5-7]. Interpretation of these findings has been further complicated by reports from Japan and China. Some of these results differ from those of other Asian studies, and are in line with findings in Western countries^[8,9].

Turkey is geographically situated between two continents that are reported to have different cagA seroprevalence rates. Our aim in this study was to compare the frequencies of serum positive cagA in Turkish patients with peptic ulcer disease and those with non-ulcer dyspepsia.

MATERIALS AND METHODS

General data of patients

The study included 180 patients (79 males and 101 females; mean age 43.4±11.2 years old) with dyspepsia who were confirmed *H. pylori*-positive by rapid urease testing. The patients came from two Baskent University medical centers in two different Turkish cities. Ninety-nine were from the southern city of Adana, and 81 were from Ankara in central Turkey. Individuals who met at least one of the following criterias were excluded from the study: history of *H. pylori* eradication treatment; anti-secretory and/or non-steroidal anti-inflammatory drug therapy in the 4 weeks prior to the study; chronic organ failure (chronic renal, pulmonary, or liver disease); chronic alcohol intake and cigarette smoking.

Methods

Gastric specimens from the antrum and corpus of each patient from the Adana Hospital were examined with hematoxylin/eosin and Giemsa stains. For each specimen, chronic inflammation, neutrophil activity, and *H. pylori* density were scored separately, according to the updated Sydney system: 0=normal, 1=mild, 2=moderate, and 3=severe^[10]. We modified the four-point scale for histological scoring slightly in order to facilitate statistical analysis. Scores of 0-1 were categorized together as "low score" and scores of 2-3 were categorized together as "high score." The same pathologist examined all the histological sections.

Three groups were divided according to the patients' endoscopic findings: a non-ulcer dyspepsia (NUD) group ($n=114$); a duodenal ulcer (DU) group ($n=34$); and a gastric ulcer and/or erosion (GU/E) group ($n=32$).

Enzyme immunoassay (Equipar Diagnostici, Rome, Italy) was used to test for the presence of serum IgG and IgA

antibodies to *H. pylori* cagA protein. Since there is no international standard for IgG levels, this was quantitated by means of a standard curve calibrated in arbitrary units per milliliter (Uarb/mL). Serum levels above 5 Uarb/mL were considered to indicate positivity.

Statistical analysis

The unpaired Student's *T*-test and the χ^2 test were used to analyze the data, as appropriate. It was considered to be statistical significant when $P < 0.05$.

RESULTS

Of the 180 patients, 175 (97.2 %) were cagA (+). The rate serum positive cagA in the NUD group was 95.6 %, and they were 100 % in both DU and GU/E groups. The overall rate in each hospital and the group rates in each center were shown in Table 1. The NUD, DU, and GU/E groups had similar mean serum levels of IgG-type cagA antibodies (45.2±40.3 Uarb/mL, 54.3±42.4 Uarb/mL, and 51.2±41.3 Uarb/mL, respectively; $P > 0.05$).

Table 1 The rates of serum positive cagA overall and according to endoscopic diagnosis in the patients from the two different centers

	cagA+		<i>P</i>
	Adana hospital n (%)	Ankara hospital n (%)	
Total patients	98/99 (98.9)	77/81 (95.1)	NS
NUD patients	73/74 (98.6)	36/40 (90.0)	NS
GU/E patients	12/12 (100)	20/20 (100)	NS
DU patients	13/13 (100)	21/21 (100)	NS

Denotes: NUD: Non-ulcer dyspepsia; DU: Duodenal ulcer; GU/erosion: Gastric ulcer and/or erosions.

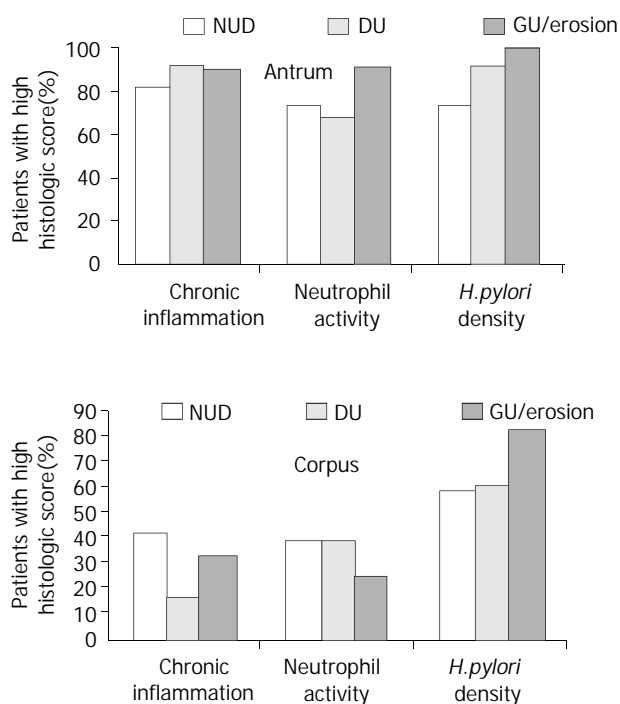


Figure 1 The percentages of patients with high scores (moderate or severe findings) for inflammation, neutrophil activity, and *H. pylori* density in the antrum and corpus. (NUD: Non-ulcer dyspepsia; DU: Duodenal ulcer; GU/erosion: Gastric ulcer and/or erosions).

In each group, the percentages of patients with high scores for each histologic parameter were calculated. Separate calculations were made for the antrum and the corpus specimens. The results were then compared to demonstrate whether there was any difference among gastroduodenal pathologies (NUD, DU, and GU/E) with respect to severity of gastritis and *H. pylori* density in each stomach region (Figure 1). In the antrum, there were no significant differences in the group rates for chronic inflammation, neutrophil activity, and *H. pylori* density ($P > 0.05$), and all three groups had very high frequencies of high scores for chronic inflammation and *H. pylori* density. Analysis of the corpus findings showed that the DU group had a lower percentage of patients with high inflammation scores than those in the other two groups ($P < 0.05$). Also, the GU/E group had a higher percentage of patients with high *H. pylori* density scores than those in the other two groups ($P < 0.05$).

DISCUSSION

Many studies have suggested that cagA+ strains of *H. pylori* are associated with severe gastrointestinal lesions, such as severe gastritis, peptic ulcer disease, and gastric cancer^[11-13]. In infected patients, the cagA protein is translocated into epithelial cells and induces structural changes in these cells^[14,15]. A number of investigations have shown that infection with these strains leads to increased secretion of interleukin-8, which plays a pivotal role in the inflammatory response^[16,17]. Despite these findings and observations, recent studies of the frequency of cagA+ *H. pylori* strains in patients with NUD have suggested that factors other than cagA may contribute to severe gastrointestinal pathologies^[5-7].

Studies of patients with and without peptic ulcer disease in different countries, and in different regions within countries, have revealed wide variations in cagA serum prevalence in these two groups. This variation is evident if we compared the data from our study group overall (180 *H. pylori*-positive patients from health centers in central and southern Turkey) and a previously published study of patients from western Turkey^[18]. The latter report showed that the rate of serum positive cagA was significantly higher in peptic ulcer patients than that in NUD patients, whereas our results showed higher but similar rates when our patients were categorized in these two groups. When we analyzed our data of patients categorized according to hospital/city origin (Table 1), the overall rates of serum positive cagA were similar, and the corresponding rates were similar when the patients were divided into NUD, GU/E, and DU groups. These observations supported the suggestion that cagA should not be considered a universal marker for the prediction of severe gastrointestinal pathology. The reasons for, and the clinical aspects associated with this variation in serum positive cagA are not clear. Two possible reasons for the discrepancy among studies even from same country are the possible differences between commercial kits in the detection of cagA antibody in the sera of patients and variation in the prevalence of serum positive cagA strains even in areas showing geographical proximity.

In our study, we were unable to compare the severity of gastritis and *H. pylori* density in patients with cagA(+) and cagA(-) strains because almost all of the 180 patients tested positive for cagA antibodies, regardless of the endoscopic diagnosis. We performed an indirect analysis in attempt to determine whether cagA+ *H. pylori* strains were associated with severe gastritis. For this, we focused only on individuals with high histological scores, and determined the percentage of patients in each group that had high scores for chronic inflammation, neutrophil activity, and *H. pylori* density, respectively. The NUD, GU/E, and DU groups all had very high frequencies of high inflammation scores in the antrum.

However, in the corpus, the DU group had a significantly lower frequency of high inflammation scores than the other two groups. These findings suggested that cagA may have some impact on the severity of gastritis, but not on duodenal ulcer development. Previous work has shown a negative correlation between severe corpus gastritis and the presence of DU, most likely due to changes in the pattern of gastric acid secretion^[19,20]. Our findings were in line with this reported relationship.

Figura *et al* reported that most patients with NUD have both cagA(+) and cagA(-) strains of *H. pylori* simultaneously, and suggested that a particular pathological finding may be determined by the dominant strain that colonizes a particular gastric area^[21]. This may explain the conflicting results of different studies concerning the serum prevalence of cagA in NUD patients. According to this concept, a patient with anti-cagA antibody in his or her serum may clinically show NUD if the majority of the *H. pylori* organisms in the gastric mucosa are cagA(-).

There is also another possible explanation for why some patients with cagA(+) strains develop milder upper gastrointestinal pathology than those who show more severe pathology but have the same bacterial strain. The reason may be variations in genetic make-up, as a number of different cagPaI genes are required for the cagA protein to be able to enter epithelial cells. Investigation has shown that inactivation of some of these genes abolishes cagA delivery and phosphorylation^[14,22].

In conclusion, our findings reveal that the rates of cagA serum prevalence are high and similar in *H. pylori*-positive patients from two Turkish cities that are approximately half thousand of kilometers apart. These rates indicate that cagA serum prevalence in the Turkish population is close to the rates reported in Asian countries. The fact that we observed similar frequencies of cagA(+) *H. pylori* strains in all our dyspeptic patients, regardless of ulcer status, suggests that factors other than cagA may contribute to severe gastrointestinal pathology in patients with *H. pylori*.

REFERENCES

- 1 **Go MF**. What are the host factors that place an individual at risk for *Helicobacter pylori*-associated disease? *Gastroenterology* 1997; **113**(Suppl 6): S15-S20
- 2 **Kurata JH**, Nogawa AN. Meta-analysis of risk factors for peptic ulcer. Nonsteroidal anti-inflammatory drugs, *Helicobacter pylori* and smoking. *J Clin Gastroenterol* 1997; **24**: 2-17
- 3 **Atherton JC**. The clinical relevance of strain types of *Helicobacter pylori*. *Gut* 1997; **40**: 701-703
- 4 **Warburton VJ**, Everett S, Mapstone NP, Axon AT, Hawkey P, Dixon MF. Clinical and histological associations of cagA and vacA genotypes in *Helicobacter pylori* gastritis. *J Clin Pathol* 1998; **51**: 55-61
- 5 **Jenks PJ**, Megraud F, Labigne A. Clinical outcome after infection with *Helicobacter pylori* does not appear to be reliably predicted by the presence of any of the genes of the cag pathogenicity island. *Gut* 1998; **43**: 752-758
- 6 **Hua J**, Zheng PY, Yeoh KG, Ho B. The status of the cagA gene does not predict *Helicobacter pylori*-associated peptic ulcer disease in Singapore. *Microbios* 2000; **102**: 113-120
- 7 **Yang JC**, Wang TH, Wang HJ, Kuo CH, Wang JT, Wang WC. Genetic analysis of the cytotoxin-associated gene and the vacuolating toxin gene in *Helicobacter pylori* strains isolated from Taiwanese patients. *Am J Gastroenterol* 1997; **92**: 1316-1321
- 8 **Takata T**, Fujimoto S, Anzai K, Shirohani T, Okada M, Sawae Y, Ono J. Analysis of the expression of CagA and VacA and the vacuolating activity in 167 isolates from patients with either peptic ulcers or non-ulcer dyspepsia. *Am J Gastroenterol* 1998; **93**: 30-34
- 9 **Ching CK**, Wong BC, Kwok E, Ong L, Covacci A, Lam SK. Prevalence of CagA-bearing *Helicobacter pylori* strains detected by the anti-CagA assay in patients with peptic ulcer disease and in controls. *Am J Gastroenterol* 1996; **91**: 949-953
- 10 **Dixon MF**, Genta RM, Yardley JH, Correa P. Classification and grading of gastritis The updated Sydney System. International Workshop on the Histopathology of Gastritis, Houston 1994. *Am J Surg Pathol* 1996; **20**: 1161-1181
- 11 **Crabtree JE**, Taylor JD, Wyatt JJ, Heatley RV, Shallcross TM, Tompkins DS, Rathbone BJ. Mucosal IgA recognition of *Helicobacter pylori* 120 kDa protein, peptic ulceration, and gastric pathology. *Lancet* 1991; **338**: 332-335
- 12 **Kuipers EJ**, Perez-Perez GI, Meuwissen SG, Blaser MJ. *Helicobacter pylori* and atrophic gastritis: importance of the cagA status. *J Natl Cancer Inst* 1995; **33**: 28-32
- 13 **Rudi J**, Kolb C, Maiwald M, Zuna I, von Herbay A, Galle PR, Stremmel W. Serum antibodies against *Helicobacter pylori* proteins VacA and CagA are associated with increased risk for gastric adenocarcinoma. *Dig Dis Sci* 1997; **42**: 1652-1659
- 14 **Asahi M**, Azuma T, Ito S, Ito Y, Suto H, Nagai Y, Tsubokawa M, Tohyama Y, Maeda S, Omata M, Suzuki T, Sasakawa C. *Helicobacter pylori* cagA protein can be tyrosine phosphorylated in gastric epithelial cells. *J Exp Med* 2000; **191**: 593-602
- 15 **Segal ED**, Cha J, Lo J, Falkow S, Tompkins LS. Altered states: involvement of phosphorylated CagA in the induction of host cellular growth changes by *Helicobacter pylori*. *Proc Natl Acad Sci USA* 1999; **96**: 14559-14564
- 16 **Crabtree JE**, Covacci A, Farmery SM, Xiang Z, Tompkins DS, Perry S, Lindley IJ, Rappuoli R. *H. pylori*-induced interleukin-8 expression in gastric epithelial cells associated with cagA-positive phenotype. *J Clin Pathol* 1995; **48**: 41-45
- 17 **Sharma SA**, Tummuru M, Miller G, Blaser MJ. Interleukin-8 response of gastric epithelial cell lines to *Helicobacter pylori* stimulation *in vitro*. *Infect Immun* 1995; **63**: 1681-1687
- 18 **Demirturk L**, Ozel AM, Yazgan Y, Solmazgul E, Yildirim S, Gultepe M, Gurbuz AK. CagA status in dyspeptic patients with and without peptic ulcer disease in Turkey: association with histopathological findings. *Helicobacter* 2001; **6**: 163-168
- 19 **Kim HY**, Kim YB, Park CK, Yoo JY, Graham DY. Co-existing gastric cancer and duodenal ulcer disease: Role of *Helicobacter pylori* infection. *Helicobacter* 1997; **2**: 205-209
- 20 **El-Zimaity HMT**, Gutierrez O, Kim JG, Akamatsu T, Gurer IE, Simjee AE, Graham DY. Geographic differences in the distribution of intestinal metaplasia in duodenal ulcer patients. *Am J Gastroenterol* 2001; **96**: 666-672
- 21 **Figura N**, Vindigni C, Covacci A, Presenti L, Burrioni D, Vernillo R, Banducci T, Roviello F, Marrelli D, Biscontri M, Kristodhullu S, Gennari C, Vaira D. CagA-positive and -negative *H. pylori* strains are simultaneously present in the stomach of most patients with non-ulcer dyspepsia: relevance to histological damage. *Gut* 1998; **42**: 772-778
- 22 **Odenbreit S**, Puls J, Sedlmaier B, Gerland E, Fischer W, Haas R. Translocation of *Helicobacter pylori* CagA into gastric epithelial cells by type IV secretion. *Science* 2000; **287**: 1497-1500

Study on the classification of chronic gastritis at molecular biological level

Goang-Yao Yin, Wu-Ning Zhang, Xue-Fen He, Yi Chen, Xiao-Jing Shen

Goang-Yao Yin, Xue-Fen He, Xiao-Jing Shen, Wuxi No.3 Peoples Hospital, Wuxi 214041, Jiangsu Province, China

Wu-Ning Zhang, Yi Chen, Department of National Microanalysis Center, Fudan University, Shanghai 200433, Shanghai, China

Correspondence to: Dr. Goang-Yao Yin, Wuxi No.3 Peoples Hospital, 230 Eastern Tonghuhui Road Wuxi 214041, Jiangsu Province, China. yinyao@pub.wx.jsinfo.net

Received: 2002-10-04 **Accepted:** 2002-12-03

Abstract

AIM: To explore the pathophysiological basis for the fact that patients with digestive tract symptoms do not necessarily have gastric mucosal pathology and those without clinical symptoms do not necessarily have no gastric mucosal pathology.

METHODS: The ultrastructure, trace elements, cAMP, DNA, SOD and LPO in the gastric mucosa and its epithelial cells of 188 patients without organic lesions of heart, lung, liver, gallbladder, pancreas, kidney or intestine and basically histopathological normal persons (F) were detected synchronously by SEM, TEM, EDAX, Image analysis system RIA and ³H-TdR Lymphocyte Transfer Test.

RESULTS: The content of Zn, Cu, cAMP and ³H-TdR LCT in gastric mucosa and the content of Zn, Cu, DNA and LPO in gastric mucosa epithelial nuclei of each group were shown as follows: Normal control (4.1±1.0, 5.2±0.8, 15.9±1.5, 1079.7±227.4, 7.6±0.4, 58.4±0.3, 12.6±2.7, 2.6±0.6); CSG without symptoms group (3.7±1.2, 5.1±1.8, 15.6±0.9, 924.5±234.9, 7.8±0.3, 58.6±0.4, 13.0±3.1, 2.9±0.4); CAG without symptoms group (3.3±1.0, 4.8±0.9, 14.9±0.7, 887.7±243.6, 7.8±0.3, 58.7±0.3, 14.3±2.8, 3.1±0.4); F type with symptoms group (3.5±1.4, 4.5±1.0, 15.7±1.4, 932.1±2449.3, 7.9±0.4, 58.7±0.5, 13.5±4.6, 2.9±0.7); CSG with symptoms group (2.8±1.9, 4.0±1.5, 14.2±1.8, 867.3±240.5, 8.1±0.5, 58.9±0.5, 15.2±3.2, 4.2±0.7); CAG with symptoms group (2.0±1.8, 3.4±1.5, 13.4±1.8, 800.9±221.8, 8.6±0.4, 59.3±0.5, 16.5±3.1, 4.5±0.6). The contents of Zn, Cu in mitochondria and SOD in gastric mucosa of each group were shown as follows: Normal control group (9.2±0.5, 58.3±0.3, 170.5±6.1), CSG without symptoms group (8.9±0.5, 58.2±0.3, 167.2±5.3), CAG without symptoms group (8.8±0.4, 57.5±0.2, 166.1±4.2); F type with symptoms group (8.9±0.5, 58.0±0.3, 167.9±5.7), CSG with symptoms group (8.6±0.5, 57.8±0.3, 163.3±5.6); CAG with symptoms group (8.3±0.4, 57.5±0.3, 161.2±4.3). There were significant differences in these cases, $P < 0.05-0.001$. There were synchronous changes of gastric mucosa epithelial cellular ultrastructure. The "background lesions" (focal atrophic gastritis, focal intestinal metaplasia, micro-ulcer) in nonfocal gastric mucosa of all groups had significant differences ($P < 0.05-0.001$).

CONCLUSION: Disease with symptoms, disease without symptoms, nondisease with symptoms occur on the basis

of the quantitative changes of gastric mucosa epithelial cellular ultrastructure and related bioactive substances.

Yin GY, Zhang WN, He XF, Chen Y, Shen XJ. Study on the classification of chronic gastritis at molecular biological level. *World J Gastroenterol* 2003; 9(4): 836-842

<http://www.wjgnet.com/1007-9327/9/836.htm>

INTRODUCTION

After undergoing gastroscopy with mucosal biopsy, patients with digestive tract symptoms and volunteer blood donors without any clinical symptoms were found to be of two types: those with gastric mucosa pathological changes, and others without evident pathology. In order to explore the pathophysiological basis, we detected synchronously the epithelial cell ultrastructure, trace element, cAMP, DNA, gastric mucosa SOD, serum LPO and ³H-TdRLCT by means of histopathology, SEM, TEM with EDAX, image analysis technique, RIA and chemiluminescence method. The results were reported as follows.

MATERIALS AND METHODS

Materials

188 patients with digestive tract symptoms, had been ruled out from organic lesions of heart, lung, liver, gallbladder, pancreas, kidney or intestine by physical examination, fluoroscopy of chest, GI x-ray examination, type ultrasonography, blood biochemistry, gastroscopy with histopathological examination. According to diagnostic criteria of "the standards for the classification of chronic gastritis, gastroscopy atrophic gastritis", 68 cases were diagnosed as CSG (43 males, 25 females, average age 43, average course of disease 4a); 64 cases as CAG (37 males, 27 females, average age 47, average course of disease 6a.); 56 cases as having basically normal gastric mucosa (F group) (22 males, 34 females, average age 39, average course of disease 2a). Among 42 volunteer blood donors without any clinical symptoms, through gastroscopy and histopathological biopsy, 18 cases were diagnosed as CSG (13 males, 5 females, average age 39), 9 cases as CAG (7 males, 2 females, average age 41); 15 cases as having basically normal gastric mucosa (6 males, 9 females, average age 37) thus also referred to as normal control group (NC group).

Methods

During gastroscopy, three pieces of gastric mucosa were taken from the focal, nonfocal areas of antral region of stomach and body of stomach for histopathological examination, SEM, TEM, the determination of cAMP and SOD. Blood specimens were taken to determine LPO and ³H-TdRLCT. For the study of gastric mucosa ultrastructure and determination of its trace elements, 501B SEM with 9100/60 EDAX were used taking three pieces of specimens from each patient and determine the weight percentage (WT%)^[1-4] of each element between the elements of gastric mucosa. Radioimmuno-assay was adopted

to detect gastric mucosa cAMP content (pmol/g)^[5], blood ³H-TdRLCT (Bq/L)^[5]. For the observation of gastric mucosa epithelial cellular ultrastructure and the determination of its trace elements, EM 430 TEM with 9100/60 EDAX^[1-4] were used. The three pieces of mucosa specimens of every patient were magnified in unison by five magnifying powers (3 600, 7 200, 14 000, 19 000, 29 000) to randomly take pictures of the panoragram, local area and organelle and to determine the atomic number percentage (AT %) of each nuclear and mitochondrial element between the trace elements. 50 nuclei and 50 mitochondria of each patient were determined, with average WT% of each element taken as its actual WT%. For the determination of DNA in gastric mucosa epithelial nuclei, IBAS 2000 image analysis technique was used to determine IOD with gastric mucosa cell smear after Feulgen staining, taken as the relative content of nuclear DNA^[4]. Chemiluminescence method was adopted to determine the activity of SOD (u/g) in gastric mucosa^[5]. Thiobarbituric acid development process was adopted to determine serum LPO (umol/L)^[5].

Statistical method

χ^2 and *t* test.

RESULTS

Histopathological changes of gastric mucosa

In NC group and F group, there were extremely small number of mononuclear cells and lymphocytes in lamina propria of gastric mucosa, there was no abnormality in gastric gland. Therefore their gastric mucosa were defined as relatively normal. In CG gastric mucosa, in there were various degrees of infiltration of lymphocyte, plasmocyte, eosinophil and neutrophil in lamina propria, there were various degrees of degeneration necrosis, erosion and atrophy in mucosa epithelial cells. Glands decreased due to destruction and some glands had cystic dilatation. As for the inflammatory cell infiltration degree in gastric mucosa and the decrease degree of original glands (<1/3 low-grade, >1/3 <2/3 middle-degree, >2/3 heavy-grade). There was greater significant difference in CSG without symptom (CSG-woS) group, CAG without symptom (CAG-woS) group, CSG with symptom (CSG-wS) group, CAG with symptom (CAG-wS) group than in HC group and F group ($P<0.05-0.001$). There was significant difference between the first four groups ($P<0.05-0.001$, Table 1).

Ultrastructure of gastric mucosa

The relatively normal gastric mucosa had clear surface, which was divided by crisscross small groves into many lesser gastric areas, assuming convolution shape, in which there were many gastric pits (the mouths of gastric glands). The gastric pits were shaped like craters and their concave walls had round or oval epithelial cells of almost the same size (Figure 1). When magnified, the surfaces of cells were found to be rough and uneven, with short and thin microvilli as well as many semicircular cumuli, several micro processus and small fossae. The fossae were marks left by cumuli after rupture and excretion of mucus. The crater periphery projections were shaped like dykes. The gastric antrum mucosa were rough, apparently folded, the small craters were mostly groves of different lengths with deep bottoms. In low power observation, as far as gastric mucosa of chronic gastritis was concerned, the crisscross groves of the focal mucosa are shallow, the convolution structures were smooth and even, craters were deformed and of different sizes at different heights and ill-distributed; the dykes form projections that are undulating, of different width (Figure 2).

In high power observation, the focal gastric mucosa had scattering denatured, diabrotic and necrotic exfoliated epithelial cells, on it's surfaces S-shape helicobacter pylori were found (Figure 3). Massive epithelial cells were diabrotic, anabrotic and exfoliated forming micro ulcers. The ulcers spread from their centers, with adjacent cells crushed and destructed, in irregular shapes and arrangement. The epithelial cells of the crater walls were atrophic and denatured of different sizes and derangement (Figure 5), and the cells became diabrotic and necrotic and had inflammatory cell infiltration (Figure 6). The glands propria of the serious cases were shaped like grid framework structure (Figure 7). The surfaces of the epithelial cells of IM gastric mucosa were covered with a thick coating, villi were invisible, and the intercellular boundaries were not clear (Figure 8). The hollowed crateriform cells were round or polygon cavities, with ejected mucus at mouths scattering like tiny white dots. In nonfocal gastric mucosa, focal atrophic inflammatory changes, IM cell population, micro ulcers and helicobacter pylori (can be found also), they were generally referred to as "background lesion".

Comparing CSG-woS group, CAG-woS group, CSG-wS group and CAG-wS group, there were significant differences in background lesion of nonfocal gastric antrum mucosa ($P<0.05-0.001$). The incidence rate of background lesion of nonfocal gastric mucosa is especially high in CAG-wS group (Table 2).

The ultrastructure of gastric mucosa epithelial cells

The mucous cells on epithelial cell surface of relatively normal gastric mucosa were columnar epithelial cells covering endogastric surfaces and inside wall of gastric pits. Their free surfaces had short microvilli and nuclei were relatively big, at the bottoms of the cells. In cytoplasm were mucous granules of various sizes, a great deal of RERs and scattered mitochondria. The mucous neck cells were distributed over the necks of gastric glands, round or crescent shape. In the upper part of cytoplasmic nuclei, there were a great deal of secretory granules, developed Golgi's bodies, a few RERs and scattered mitochondria. On the tops of cells were a few short thick micro villi. Chief cells were distributed over the bodies and bottoms of gastric glands and their nuclei were round. In cytoplasm there are many parallel RERs, a great deal of secretory granules, well-developed Golgi's bodies and scattered mitochondria (Figure 9). The parietal cells were big and conic in shape and their conical tops turned towards gland cavities. The nuclei were in the centers of the cells. The cytosols are filled with vesicular smooth RERs (secreting hydrochloric acid), intracellular canaliculi (conveying hydrochloric acid) and many mitochondria. The endocrine cells lay between chief cells and parietal cells. They were small and their nuclei are round, at the bottoms of cellular matrixes. In cytoplasm, there are great deal of spherical endocrine granules, RERs, and a few mitochondria, Golgi's bodies lie nearby nuclei (Figure 10). The normal gastric mucosa epithelial cell nuclei were round or oval; the nuclei envelopes are slightly bending; lobulated nuclei were few; the nucleocytoplasmic ratio was less than 1; the nuclei chromatins were scattered, associated with nucleoli or distributed around the nuclei. The light bright zones between heterochromatins in the nucleoli were euchromatins; the nucleoli had high electron density without capsules (Figure 11). The normal epithelial cell mitochondria of gastric mucosa were round or oval, scattered around nuclei. The mitochondria consist of outer membrane, inner membrane, outer ventricle, inner ventricle and cristae. Crista, the inward folded inner membrane, was a hollow canal leading to outer ventricle. Some mitochondrial cristae lead directly to

cytoplasm. Cristas were generally in tabular arrangement, parallel to each other and vertical to mitochondrial long axes (Figure 12). The free surfaces of epithelial cells of CG gastric mucosa have dropped off micro villi. The intercellular space expands and cell junctions decrease; mitochondria decrease, become swollen or cristae break and had vacuolar degeneration (Figure 13). RERs dilate and were in circular arrangement. The Golgi's bodies became atrophic and had lost their typical structures; the cytoplasmic secretory granules decreased; nuclei expand or shrink; parietal cell intracytoplasmic canaliculi dilate and micro villi become short and thin or even disappear. The karyoplasmic ratio of the cells with undifferentiated nuclei and IM cells of CG gastric mucosa epithelial cells were greater than 1 and there is increase in nuclear lobulation (Figure 14), interchromatic granules, perichromatic granular density and euchromatins. The nucleoli were hypertrophic and lie close to nuclear margins (referred to as nucleolar margination). The obsolescent epithelial nuclei shrink and the nucleocyto-plasmic ratio was still less. The heterochromatins lie densely around nuclei; the electron density was low in the center of nuclei and nuclei were loop in shape (referred to as chromatic margination) (Figure 15). The shrunk nuclei were denticular, in which the electron density was moderately homogeneous and chromatin were not found (referred to as chromatic homogenization). As for the above changes, there was significant difference between NC group, CSG-woS group, CAG-woS group, F-wS group, CSG-wS group and CAG-wS group ($P<0.05-0.001$, Table 3). There were mitochondrial swelling, hypertrophy, pyknosis, hyaline degeneration as well as vacuolar degeneration in epithelial cells of CG gastric mucosa.

Deformed mitochondria were in C-shape or U-shape. There were zigzag, longitudinal, sparse, pyknosis and deranged cristae (Figure 16). There was an decrease in the number of mitochondria and their cristae. In the above changes, there is significant difference between NC group, CSG-woS group, CAG-woS group, F-wS group, CSG-wS group and CAG-wS group ($P<0.05-0.001$, Table 4).

Gastric mucosa trace elements, cAMP, SOD and blood $^3\text{H-TdRLCT}$

Under the direct vision of SEM with EDAX probe that automatically detected the samples within 0.1-0.01 mm² range all the elements under 12 in atomic number and automatically calculates the weight percentage (WT%) of each element in the element series. 15 points were fixed in the three pieces of mucosa from every patient to carry out 15 detections and in every detection, 21 elements were detected to get their respective average WT% as its actual WT%. Zn and Cu were taken as index. The gastric mucosa Zn, Cu, cAMP, SOD and $^3\text{H-TdRLCT}$ decrease progressively in the sequence of NC group, CSG-woS group, CAG-woS group, F-wS group, CSG-wS group and CAG-wS group ($P<0.05-0.001$, Table 5).

Biochemical changes in gastric mucosa and blood serum

The quantity of nuclei DNA, Zn, Cu and serum LPO increased progressively in the sequence of NC group, CSG-woS group, CAG-woS group, F-wS group, CSG-wS group, CAG-wS group. While mitochondrial Zn, Cu, decreased progressively in the same sequence and there were significant differences between these groups ($P<0.05-0.001$, Table 6).

Table 1 Degree of inflammatory cell infiltration compared with the degree of decrease of original glands in gastric mucosa $n(\%)$

Group	n	Degree of inflammatory cell infiltration			Degree decrease of glands propria		
		<1/3	>1/3<2/3	>2/3	<1/3	1/3<2/3	>2/3
NC	15						
CSG-woS	18	11(61.1)	6(33.3)	1(5.6)	1(5.6)		
CAG-woS	9	5(55.6)	3(33.3)	1(11.1)	5(55.6) ^d	3(33.3)	
F-TwS	56						
CSG-wS	68	26(38.2) ^c	32(47.1)	10(14.7)			
CAG-Ws	64	19(29.7) ^{df}	21(32.8)	24(37.5) ^{df}	23(35.9) ^d	23(35.9)	18(28.1)

Compared with NC group. ^a $P<0.05$, ^b $P<0.01$; compared with CSG-woS group. ^c $P<0.05$, ^d $P<0.01$; compared with CAG-woS group. ^e $P<0.05$, ^f $P<0.01$, Compared with F-wS group, ^g $P<0.05$, ^h $P<0.01$, Compared with CSG-wS group, ⁱ $P<0.05$, ^j $P<0.01$, In table 2-6, the marks are the same as here.

Table 2 Focal background lesions in non-focal site of gastric mucosa $n(\%)$

Focal lesions	CSG-woS ($n=18$)		CAG-woS ($n=9$)		CSG-wS ($n=68$)		CAG-Ws ($n=64$)	
	Gastric antrum	Gastric body	Gastric antrum	Gastric body	Gastric antrum	Gastric body	Gastric antrum	Gastric body
Atrophic	1 (5.6)	0 (0.0)	1 (11.1) ^a	0 (0.0)	21 (30.9) ^{bd}	11 (16.2)	47 (73.4) ^{bdj}	27 (42.2) ^j
inflammatory lesion								
IM	4 (22.2)	1 (5.6)	5 (55.6) ^b	2 (22.2) ^b	27 (39.7) ^{bc}	5 (7.4) ^d	59 (92.2) ^{bdj}	13 (20.3) ^b
Micro ulcer	1 (5.6)	1 (5.6)	3 (33.3) ^b	1 (11.1) ^a	11 (16.2)	2 (2.9) ^c	28 (43.8) ^{bdj}	9 (14.1) ^{aj}

Table 3 Ultrastructures of gastric mucosa epithelial cell nuclei *n* (%)

Group	<i>n</i>	Appearance		Chromatin		Nucleoli	
		nucleoplasmic ratio >1	nuclear lobulation	margination or homogeneity	perinuclear concentration	hypertrophy or margination	looping
NC	15			1 (6.7)	1 (6.7)		
CSG-woS	18	1 (5.6)		4 (22.2) ^b	1 (5.6)	1 (5.6)	1 (5.6)
CAG-woS	9	2(22.2) ^d	2(22.2)	7 (77.8) ^{bd}	3 (33.3) ^{bd}	2 (22.2) ^d	4 (44.4) ^d
F-TwS	56			3 (5.4) ^{df}	3 (5.4) ^f	1 (1.8) ^f	
CSG-wS	68	5 (5.7) ^f	2(2.9) ^f	7 (10.3) ^{cf}	5 (7.4) ^f	2 (2.9) ^f	2 (2.9) ^f
CAG-Ws	64	20(31.3) ^{dj}	9(29.7) ^j	33 (51.6) ^{bdhj}	29 (45.3) ^{dffhj}	27 (42.2) ^{dffhj}	14 (21.9) ^{dgi}

Table 4 Mitochondria ultrastructures of gastric mucosa epithelial cells. ($\bar{x}\pm s$)

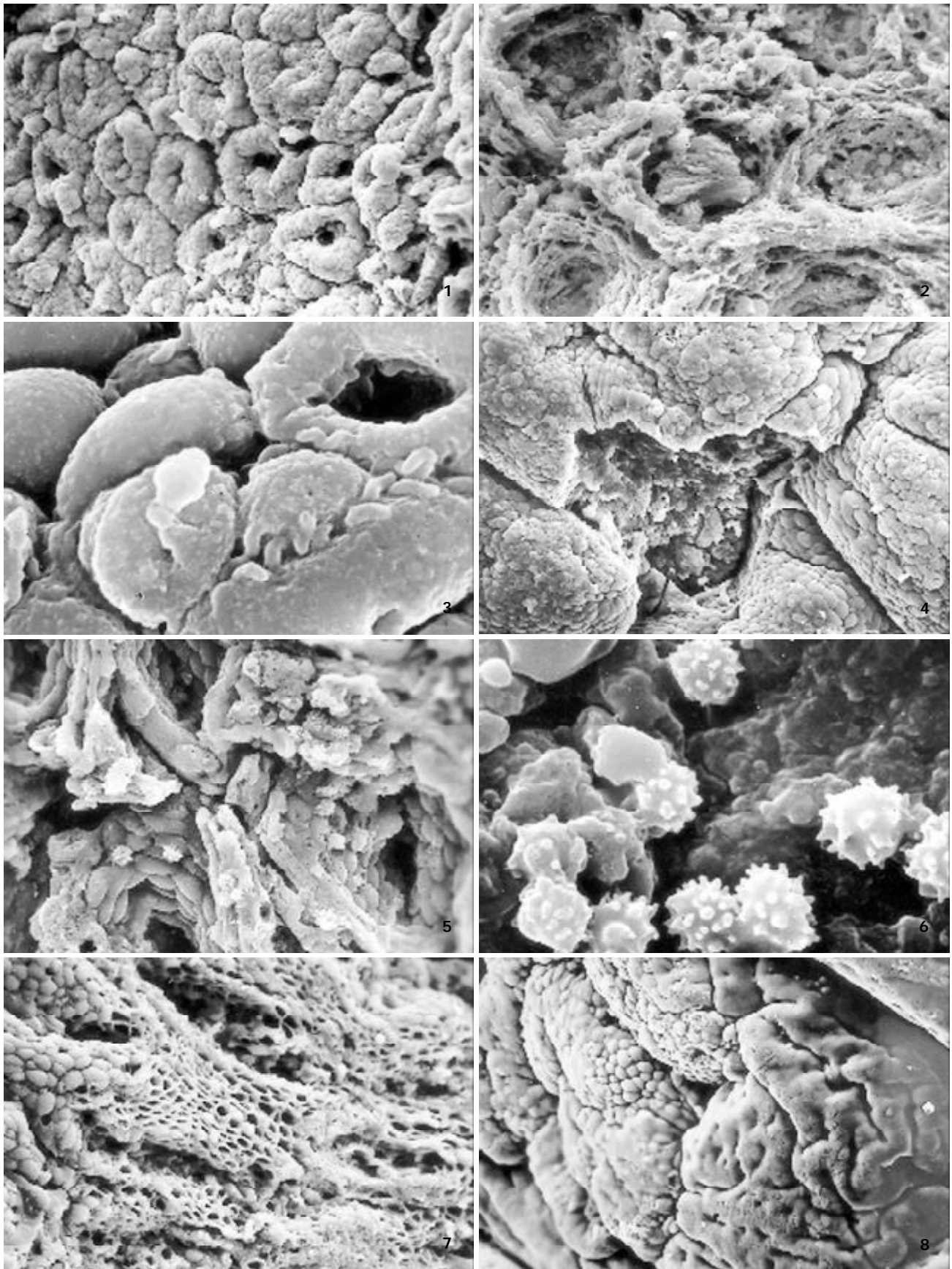
Group	<i>n</i>	Number	Swelling & overgrowth (%)	Matrix-discoloration (%)	Vacuolar degeneration (%)	Pyknosis (%)	Crista number	Crista fragmentation & derangement (%)
NC	15	86.5±27.3	3.4±1.6	3.0±1.1	2.9±1.9	1.1±0.8	12.8±3.2	2.2±1.1
CSG-woS	18	85.3±22.2	3.9±1.1	3.9±2.2	3.2±1.2	1.4±0.9	11.4±2.4	3.1±1.3
CAG-woS	9	83.8±17.3	4.4±2.4	4.3±2.9	3.3±1.1	1.7±0.8	11.4±2.1	3.2±1.2
F-TwS	56	83.1±22.8	5.4±2.9 ^{bd}	4.4±2.4	2.9±1.8	1.2±0.7	11.2±2.3	3.9±1.2 ^{bc}
CSG-wS	68	65.4±21.1 ^{bdfh}	7.2±3.8 ^{bdfig}	7.9±5.0 ^{bdfh}	6.4±4.5 ^{bdfh}	1.9±0.9 ^{bch}	8.2±3.2 ^{bdfh}	5.8±3.1 ^{bdfh}
CAG-wS	64	52.2±20.8 ^{bdfhj}	10.9±4.5 ^{bdfhj}	11.7±8.6 ^{bdfhj}	11.6±7.7 ^{bdfhj}	3.7±1.1 ^{bdfhj}	6.9±3.5 ^{bdfhji}	8.9±3.7 ^{bdfhj}

Table 5 Gastric mucosa trace elements, cAMP and ³H-TdRLCT ($\bar{x}\pm s$)

Group	<i>n</i>	Gastric mucosa				Blood
		Zn (WT%)	Cu (WT%)	cAMP (Pmol/g)	SOD (u/g)	³ H-TdRLCT (Bq/L)
NC	15	4.1±1.0	5.2±0.8	15.9±1.5	170.5±6.1	1079.7±227.4
CSG-woS	18	3.7±1.2	5.1±1.8	15.6±0.9	167.2±5.3	924.5±234.9
CAG-woS	9	3.3±1.0	4.8±0.9	14.9±0.7 ^a	166.1±4.2 ^a	887.7±243.6
F-TwS	56	3.5±1.4 ^a	4.5±1.0 ^a	15.7±1.4 ^e	167.9±5.7	932.1±2449.3 ^a
CSG-wS	68	2.8±1.9 ^{bcg}	4.0±1.5 ^{aceg}	14.2±1.8 ^{bdeh}	163.3±5.6 ^{bdh}	867.3±240.5 ^{bc}
CAG-wS	64	2.0±1.8 ^{bdfhi}	3.4±1.5 ^{bdfhj}	13.4±1.8 ^{bdfhi}	161.2±4.3 ^{bdfhi}	800.9±221.8 ^{bdi}

Table 6 Epithelial nuclei and mitochondria Zn, Cu in gastric mucosa ($\bar{x}\pm s$)

Group	<i>n</i>	Nuclei			Mitochondria		Serum
		Zn (AT%)	Cu(AT%)	DNA(IOD)	Zn (AT%)	Cu(AT%)	LPO(umol/L)
NC	15	7.6±0.4	58.4±0.3	12.6±2.7	9.2±0.5	58.3±0.3	2.6±0.6
CSG-woS	18	7.8±0.3	58.6±0.4	13.0±3.1	8.9±0.5	58.2±0.3	2.9±0.4
CAG-woS	9	7.8±0.3 ^a	58.7±0.3 ^a	14.3±2.8	8.8±0.4 ^a	57.5±0.2 ^{bd}	3.1±0.4
F-TwS	56	7.9±0.4 ^a	58.7±0.5 ^a	13.5±4.6	8.9±0.5 ^a	58.0±0.3 ^{af}	2.9±0.7
CSG-wS	68	8.1±0.5 ^{bdfh}	58.9±0.5 ^{bdh}	15.2±3.2 ^{bcg}	8.6±0.5 ^{bh}	57.8±0.3 ^{bdfh}	4.2±0.7 ^{bdfh}
CAG-Ws	64	8.6±0.4 ^{bdfhj}	59.3±0.5 ^{bdfhj}	16.5±3.1 ^{bdehi}	8.3±0.4 ^{bdfhj}	57.5±0.3 ^{bdfhj}	4.5±0.6 ^{bdfhi}



- Figure 1** Mouth of gastric glands, like craters, The concave walls have round or oval epithelial cells, of almost same size. $\times 160$.
- Figure 2** Craters are deformed, the crater periphery projections are of different heights and width. $\times 320$.
- Figure 3** On cell surfaces, S-shape *Helicobacter pylori* are found. $\times 2\ 500$.
- Figure 4** Micro ulcers. $\times 320$.
- Figure 5** Epithelial cells of crater concave walls are atrophic, denatured, of different sizes and deranged. $\times 640$.
- Figure 6** Inflammatory cell infiltration. $\times 2\ 500$.
- Figure 7** Glands propria of grid framework structure. $\times 320$.
- Figure 8** Surface of IM gastric mucosa epithelial is thickly coated, villi are invisible, intercellular boundaries are not clear. $\times 320$.

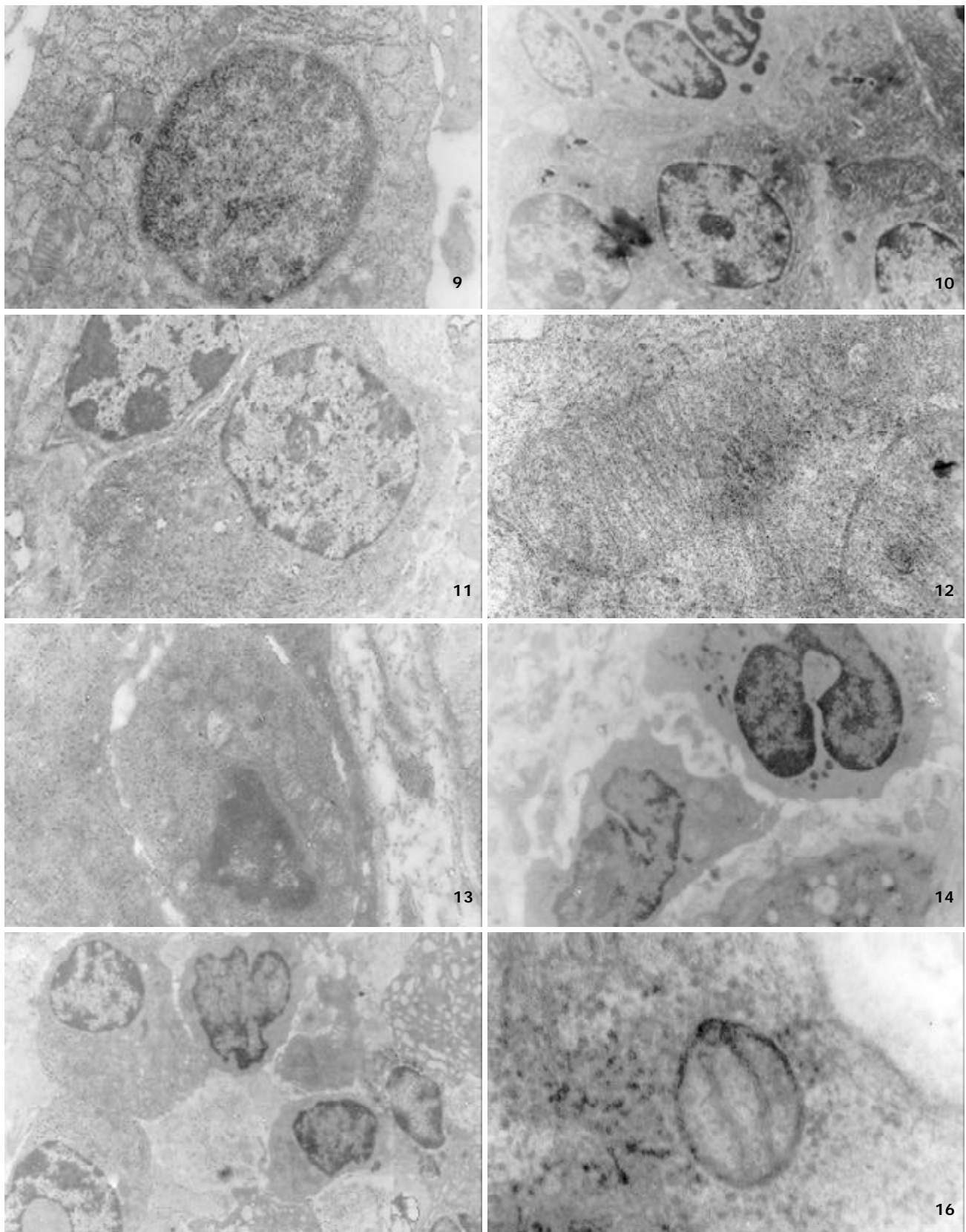


Figure 9 Normal epithelial nuclei are round, there are RERS, secretory granules, Golgi's bodies and mitochondrias in cytoplasm. $\times 7\ 200$.

Figure 10 The normal epithelial secretory cells are relatively small, nuclei are round, a great deal of spherical incretory granules in cytoplasm. $\times 14\ 000$.

Figure 11 Normal gastric mucosa epithelial nuclei are round. or oval, nucleocytoplasmic ratio < 1 ; the nucleoli have no capsules. $\times 14\ 000$.

Figure 12 Normal cristas are hollow canals leading to outer ventricles. cristas are vertical to mitochondrial long axles. $\times 14\ 000$.

Figure 13 Intercellular space expands, decrease of cellular conjuctions; mitochondria decrease, swollen or cristae break, have vacuolar degeneration. $\times 29\ 000$.

Figure 14 Nucleocytoplasmic ratio > 1 , lobulated nuclei. $\times 7\ 200$.

Figure 15 Heterochromatins lie densely around nuclei, the electron density is low in the centers of nuclei. the nuclei are loop in shape (referred to as chromatic homogenization). $\times 14\ 000$.

Figure 16 Longitudinal cristas, sparse cristae, deranged cristae. $\times 14\ 000$.

DISCUSSION

Compared with NC group, 188 patients with digestive tract symptoms without other organic disease and 27 patients without any clinical symptoms have a tendency of decreasing of quality in the submicrostructure of gastric mucosa epithelial cells -mitochondria. The incidence rate of karyoplasmic ratio > 1, nuclear lobulation, chromatin peripheral granule densification, hypertrophy of nucleoli, mitochondrial degeneration, and quantitative changes of nucleolar DNA, Zn, Cu and LPO increase progressively in the sequence of NC group, CSG-woS group, CAG-woS group, F-wS group, CSG-wS group and CAG-wS group. While gastric mucosa Zn, Cu, cAMP, SOD and mitochondrial Zn, Cu and the number of mitochondria and crista decrease progressively in the same sequence.

When gastric mucosa is damaged by noxious substances or ischemia, the metabolism of Zn, Cu becomes disordered with the body and thus enzyme system is disturbed. In human body, Zn is the important component and activator of over a hundred varieties of enzymes such as carbonic anhydrase, DNA polymerase, peptase, phosphatase, peroxide dismutase etc. By regulating the activity of these enzymes, it participates and regulates the metabolism of sugars, lipids, proteins, nuclei acid and vitamins, contends for mercaptan to inhibit free radical reaction. Cu participates the composition of over 30 kinds of proteins and enzymes in the body, regulates the protein metabolism and influences cellular respiration and division. When the level of Zn and Cu in the body declines, the synthesis and activity of SOD will be inhibited. Because of NADPH oxidation reduction circulation and the catalytic function of xanthine oxidase, a great deal of oxygen free radicals will be produced, far beyond the clearing ability of SOD. The excessive accumulated oxygen free radicals react in peroxidation with unsaturated fatty acid of inner and outer mitochondrial membranes and produce LPO, therefore serum LPO level will rise. The inner and outer mitochondrial membranes will accordingly be damaged, resulting in the decrease and derangement of mitochondrial cristae, the change of the ratio of mitochondrial ventricle diameter to cavity diameter and eventually the retrograde affection, the decrease of ATP production, inadequate energy supply, which in turn cause debility, structural atrophy, decrease of gastric acid secretion and even cytonecrosis. The participation of Zn and Cu dependence enzymes is essential in nuclear protein synthetic metabolism (including DNA duplication) and mitochondrial energy metabolism. When nuclear took in more Zn and Cu, the protein synthesis was brisk, nuclei division and hyperplasia were accelerated, which increased the chance of gene mutation. As the second messenger substance, cAMP regulate some vital activities in the body. Once the quantity of cyclic nucleoside phosphate in nuclei changes abnormally, pathological state will occur. The quantitative changes of cAMP result in the changes of cellular metabolism, immunity and vegetative functions. The decrease of cyclic nucleoside phosphate, especially cAMP in the body results in the inhibition of sympathetic nerve (including purinergic nerve) function, and relative hyperfunction of parasympathetic nerve function. As a result, digestive tract symptoms occur such as abdominal distention, loose stool, involuntary drooling, poor appetite, pale enlarged tongue with tooth marks. Through influencing lymphocyte metabolism, the quantitative changes of Zn and cAMP in turn influence cell respiration, differentiation and inhibit lymphocyte transformation^[4,6-13] and cause decline of ³H-TdRLCT level. As a result: (1) When gastric mucosa Zn, Cu and blood ³H-TdRLCT are nearly equal to that of NC group and gastric mucosa cAMP was markedly lower than that of

HC group, clinical phenomena as CSG-woS and CAG-woS will occur; (2) When gastric mucosa Zn, Cu and ³H-TdRLCT were markedly lower than that of NC group and gastric mucosa cAMP is nearly equal to that of NC group, the phenomenon of F type with symptoms (non-disease with symptoms) will occur; (3) When the levels of gastric mucosa Zn, Cu, cAMP and ³H-TdRLCT were all markedly lower than those of NC group, the clinical phenomena such as CSG-wS and CAG-wS will occur. The occurrences of these clinical phenomena were consistent with the change of gastric mucosa ultrastructure and histopathology, forming the pathophysiological basis in the classification of chronic gastritis. Thus it can be seen that changes of gastric mucosa epithelial cell ultrastructures and the quantitative changes of their bioactive substances are the pathophysiological bases that determines the classification of chronic gastritis with different classification has respective clinical symptoms.

REFERENCES

- 1 **Yin GY**, Zhang WN, He XF, Chen Y, Shen XJ. Detection of ultrastructural changes and contents DNA, Zn, Cu and LPO in subgroups of chronic gastritis. *Shijie Huaren Xiaohua Zazhi* 2002; **10**: 663-667
- 2 **Yin GY**, Zhang WN, Shen XJ, Chen Y, He XF. Ultrastructural and molecular biological changes of chronic gastritis and gastric cancer: a comparative study. *Shijie Huaren Xiaohua Zazhi* 2002; **10**: 668-672
- 3 **Yin GY**, Zhang WN, He XF, Chen Y, Shen XJ. Alterations of ultrastructures, trace elements, cAMP and cytoimmunity in subgroups of chronic gastritis. *Shijie Huaren Xiaohua Zazhi* 2002; **10**: 673-676
- 4 **Yin GY**, Zhang WN, He XF, Chen Y, Yin YF, Shen XJ. Histocytological study on gastric mucosa of spleen deficiency syndromes. *Zhongguo Zhongxiyi Jiehe Zazhi* 1999; **19**: 660-663
- 5 **Yin GY**, Xu FC, Zhang WN, Li GC, He XF, Chen Y, Shen XJ. The effect of weikangfu on cytopathology of gastric mucosa tissue when treating gastric precancerous lesion of patients with spleen deficiency syndromes. *Zhongguo Zhongxiyi Jiehe Zazhi* 2000; **6**: 241-243
- 6 **Yin GY**, Zhang WN, Xu FC, He XF, Chen Y, Shen XJ. Effect of Weikangfu chongji on ultrastructure of precancerous gastric mucosa of patients with spleen deficiency Syndromes. *Zhongguo Zhongxiyi Jiehe Zazhi* 2000; **20**: 667-670
- 7 **Yin GY**, Zhang WN, Xu FC, Chen Y, He XF, Li GC, Shen XJ. Study on the modern pathophysiologic basis of the syndrome classification of spleen deficiency with chronic gastritis and of (treatment) verification of clinical syndromes and prescriptions. *Jiangsu Yiyao Zazhi* 2001; **27**: 46-47
- 8 **Yin GY**, He XF, Yin YF, Du YQ, Jiao JH. Study on mitochondrial ultrastructure, trace elements and correlative factors of gastric mucosa in patients with spleen deficiency syndrome. *Zhongguo Zhongxiyi Jiehe Zazhi* 1996; **15**: 719-723
- 9 **Yin GY**, Zhang WN, Xu FC, He XF, Chen Y, Shen XJ. Effect of weikangfu chongji on epithelial cellular ultrastructure of precancerous gastric mucosa of patients with spleen deficiency syndrome. *Jiangsu Yiyao Zazhi* 2000; **26**: 514-517
- 10 **Yin GY**, Zhang WN, Xu FC, He XF, Chen Y, Li GC, Shen XJ. Effect of weikangfu on Zn, Cu and DNA in precancerous gastric mucosa epithelial nuclei and mitochondria of patients with spleen deficiency syndromes. *Zhongguo Zhongxiyi Jiehe Zazhi* 2000; **8**: 221-224
- 11 **Yin GY**, Zhang WN, Shen XJ, Chen Y, He XF. A comparative study on ultrastructure of chronic gastritis gastric mucosa IM, ATP and their molecular biology. *Jiangsu Yiyao Zazhi* 2002; **28**: 4-7
- 12 **Yin GY**, He XF, Zhang WN, Chen Y. Relationship between the classification of spleen deficiency and the quantitative changes of bio-active substances in mitochondria of gastric mucosa epithelial cell nuclei. *Zhongguo Zhongxiyi Jiehe Zazhi* 1999; **7**: 145-148
- 13 **Yin GY**, Zhang WN, Li GC, Huang JR, Chen Y, He XF, Shen XJ. Therapeutic effect of weikangfu on gastric precancerous disorder with spleen deficiency syndrome and its effect of gastric mucosal zinc, copper, cyclic adenosine monophosphate, superoxide dismutase, lipid peroxide and ³H-TdR lymphocyte conversion test. *Zhongguo Zhongxiyi Jiehe Zazhi* 2000; **20**: 176-179

The influence of Enteral Nutrition in postoperative patients with poor liver function

Qing-Gang Hu, Qi-Chang Zheng

Qing-Gang Hu, Qi-Chang Zheng, Department of Surgery, Xiehe hospital, Tongji Medical College, Huazhong University of Science and Technology, Wuhan 430022, Hubei Province, China

Supported by the Scientific Foundation of Wuhan city, No.92251106

Correspondence to: Dr. Qing-Gang Hu, Department of Surgery, Xiehe hospital, Tongji Medical College, Huazhong University of Science and Technology, Wuhan 430022, Hubei Province China. mailbox_1@163.net

Telephone: +86-27-85726201 **Fax:** +86-10-85726942

Received: 2002-08-09 **Accepted:** 2002-09-03

Abstract

AIM: To investigate the safety, rationality and the practicality of enteral nutritional (EN) support in the postoperative patients with damaged liver function and the protective effect of EN on the gut barrier.

METHODS: 135 patients with liver function of Child B or C grade were randomly allocated to enteral nutrition group (EN, 65 cases), total parenteral nutrition group (TPN, 40 cases) and control group (CON, 30 cases). Nutritional parameters, hepatic and kidney function indexes were measured at the day before operation, 5th and 10th day after the operation respectively. Comparison was made to evaluate the efficacy of different nutritional support. Urinary concentrations of lactulose(L) and mannitol(M) were measured by pulsed electrochemical detection(HPLC-PED) and the L/M ratio calculated to evaluate their effectiveness on protection of gut barrier.

RESULTS: No significant damages in hepatic and kidney function were observed in both EN and TPN groups between pre- and postoperatively. EN group was the earliest one reaching the positive nitrogen balance after operation and with the lowest loss of body weight and there was no change in L/M ratio after the operation (0.026 ± 0.004) at the day 1 before operation, 0.030 ± 0.004 at the day 5 postoperative and 0.027 ± 0.005 at the day 10 postoperative), but the change in TPN group was significant at the day 5 postoperative (0.027 ± 0.003 vs 0.038 ± 0.009 , $P<0.01$).

CONCLUSION: EN is a rational and effective method in patients with hepatic dysfunction after operation and has significant protection effect on the gut barrier.

Hu QG, Zheng QC. The influence of Enteral Nutrition in postoperative patients with poor liver function. *World J Gastroenterol* 2003; 9(4): 843-846
<http://www.wjgnet.com/1007-9327/9/843.htm>

INTRODUCTION

Liver is the central organ for production and utilization of nutrients and plays a key role in metabolism. In chronic liver disease severe protein-calorie malnutrition can seriously damaging the capacity of liver regeneration, however

nutritional support can improve the postoperative outcome^[1]. Parenteral nutrition (PN) has been used clinically^[2], but its limitations of the incomplete nutritional constituent^[3], catheter-related or endogenous complication^[4], metabolic complications and liver dysfunction restrict its use in hepatic damaged patients^[5]. In the mid 1980s, along with the recognition of the relevance of the gut barrier and endogenous infection^[6,7], enteral nutrition (EN) has been widely used^[8], but how does it effect on poor liver function remaining unclarified.

It is the aim of this study: (1) To investigate the safety, rationality and feasibility in performing EN in postoperative patients with poor liver function. (2) To study the influence of EN on gut barrier.

MATERIALS AND METHODS

Patients and groups

According to the later Enrolled criterion, 135 patients were enrolled and randomly divided into 3 groups: EN ($n=65$), TPN ($n=40$) and CON ($n=30$) (Table 1).

Enrolled criterion is: (1) Hospitalized adult patients from July 1998 to October 2001 with chronic liver damage requiring operative treatment; (2) The hepatic function was graded as Child B or C; (3) A patient of at least 7 days' nutritional support after the operation; (4) Except the primary disease, no other factors affecting the metabolism (5) With the agreement of the patients to join the program.

Table 1 Grouping of patients

	CON ($n=30$)			TPN($n=40$)			EN($n=65$)		
	Cases	Grade		Cases	Grade		Cases	Grade	
		B	C		B	C		B	C
PVH	13	10	3	14	8	6	21	10	11
HCC	4	2	2	11	7	4	10	5	5
CLA	1	-	1	3	1	2	8	-	8
ROBD	7	3	4	7	3	4	15	5	10
CLT	3	1	2	3	2	1	10	3	7
Others	2	1	1	2	-	2	1	-	1

PVH: Portal venous hypertension; HCC: hepatocellular carcinomar; CLA: Cholangiocarcinoma; ROBD: Reoperation of bile duct; CLT: cholelithiasis.

Reagents used

(1) 20 % and 30 % Intralipid (Beijing, Fresenius); (2) 8.5 % Novamin (Sino-swed Pharmaceutical Corp. LTD); (3) Nutrison Fibre (Nutrisia); (4) manitol (Sigma); (5) lactulose (Sigma).

Procedures

Deferent Nutrition supports were used: In TPN group, 30 cal·kg⁻¹·d⁻¹ energy and 0.16 g·kg⁻¹·d⁻¹ nitrogen were given. 1/4-1/3 nonprotein calories were provided by fat and carbohydrate. The ratio of N: nonprotein calorie=1:168. The source of nitrogen was Novamin (8.5 %) and the source of fat was from Intralipid (20 % or 30 %). Essential trace elements

and vitamins were given and the solution was given via peripheral infusion from the day 1 after the operation and lasted at least 7 days. In EN group, Nutrison Fibre was given. After 2 days of TPN, EN begun on the day 3 after the operation via the jejunostomy tube placed during the operation. On the first day, 500 ml Nutrison Fibre was given, which was increased progressively each day till 1 500 ml/d while TPN was decreased progressively till totally substituted. This was used given at least for 7 days. The temperature of Nutrison Fibre were kept at 25-30 °C and infused in 12-24 h. The rate was adjusted according to the need. In CON group, nutritional support was not performed or performed not regularly.

The sample preparation including: (1) urine sample: The patient drank the test solution, containing 2 g lactulose, 1 g mannitol in fasted condition or injected on 1 day before operation, 5th and 10th day after the operation respectively. Urine was collected for a total of 6 h and being added 0.1 ml of 10 g/L thimerosal as preservative. The total volume was recorded and 20 ml sample was stored at -20 °C until analysis by the HPLC-PED; (2) blood sample: Venous blood samples were achieved during fasting on 1 day before operation, 5th and 10th day after operation respectively for analysis.

Such Monitoring markers were measured: (1) Nutritional status marker: Transferrin (TRF), Prealbumin (PAB), Total protein (TP), Albumin (ALB), the alteration of weight (w) and circumference of upper arm (COUA) postoperatively, and accumulative nitrogen balances in the first 7 days after operation (ANE); (2) Liver and kidney function, electrolytes: Total bilirubin (TB), Direct bilirubin (DB), Albumin (ALB), Total protein (TP), Alanine aminotransferase (ALT), Aspartate aminotransferase

(AST), Creatinine (Cr), Blood urea nitrogen(BUN), Potassium (k+), Sodium (Na+), Calcium (Ca2+); (3) Gut barrier marker: Urinary ratio of lactulose and Mannitol (L/M)^[9,10].

Statistical analysis

The data was expressed as mean ± standard error. Experimental results were analyzed by analysis of variance and *t* tests for multiple comparisons. *P*<0.05 was considered statistically significant.

RESULTS

All 135 patients, except one cirrhotic patient (CON) with portal hypertension died due to MSOF at the 26th day after operation, all completed the treatment and were discharged. In EN group, there were 32 patients complained for abdominal distention and diarrhea but disappeared by adjusting the temperature and infusion rate, given domperidone or antidiarrheal agent.

Nutritional status marker (Table 2)

In all three groups, on the 5th day postoperatively, the level of TRF, TP, and ALB declined significantly (*P*<0.05), but in EN and TPN groups, they recovered on the 10th day. Comparing with TPN, the level of TP in EN group on the 10th day was higher with significant difference (*P*<0.05). In CON group, on the 10th day PO, the level of TRF, PAB, TP and ALB were all significantly lower than these in EN and TPN groups (*P*<0.05). The W and COUA loss in CON group were significantly more than those in EN and TPN groups (*P*<0.05), and in EN group were lower than that in TPN group. Among these, EN group reached positive nitrogen balance the earliest (*P*<0.05).

Table 2 Changes of nutritional status

Parameters	Control(n=30)			TPN(n=40)			EN(n=65)		
	1st BO*	5th PO**	10th PO	1st BO	5th PO	10th PO	1st BO	5th PO	10th PO
TRF(g/L)	1.1±0.6	0.9±0.3	0.8±0.6	1.2±0.4	1.0±0.6	1.2±0.3	1.3±0.6	1.2±0.5	1.2±0.6
PAB(mg/L)	657±232	591±220	595±213	690±214	669±228	667±239	681±228	719±177	690±221
TP(g/L)	63.6±12.9	46.3±9.7	48.1±9.7	66.6±12.2	48.3±10.1	50.4±9.6	70.1±7.9	55.7±7.8	63.5±8.9
ALB(g/L)	30.8±4.9	29.2±5.9	29.1±4.8	31.4±4.9	30.8±7.1	31.8±5.0	36.5±6.1	30.7±4.0	32.9±3.9
ANE	32.4±10.8 mg·kg ⁻¹ ·7 d ⁻¹			105.3±9.4 mg·kg ⁻¹ ·7 d ⁻¹			185.3±8.4 mg·kg ⁻¹ ·7 d ⁻¹		
W(kg)	-3.3±1.7			-2.4±1.1			-2.1±0.9		
COUA	23.5±1.2	-	22.2±1.3	23.6±1.1	-	23.2±1.3	24.4±2.6	-	23.7±2.2

BO: Before operation; PO: After operation; ANE: accumulated nitrogen balance; W: weight change; COUA: circumference of upper arm.

Table 3 Changes of liver and kidney function, electrolytes

Parameters	Control(n=20)			TPN(n=26)			EN(n=30)		
	1st BO	5th PO	10th PO	1st BO	5th PO	10th PO	1st BO	5th PO	10th PO
TB (μmol/L)*	92.3±37.8	71.7±34.5	41.8±35.8	86.3±46.8	68.7±33.8	45.7±33.2	119.8±73.0	96.3±54.4	64.3±47.3
DB(μmol/L)*	53.3±28.6	39.2±23.3	16.5±11.7	50.4±33.7	38.4±22.6	17.7±12.3	60.8±50.2	42.8±32.7	31.9±29.2
TP(g/L)*	63.6±12.9	46.3±9.7	48.1±9.7	66.6±12.2	48.3±10.1	50.4±9.6	70.1±7.9	55.7±7.8	63.5±8.9
ALB(g/L)	30.8±4.9	29.2±5.9	29.1±4.8	31.4±4.9	30.8±7.1	31.8±5.0	36.5±6.1	30.7±4.0	32.9±3.9
AST(U/L)#	71.7±28.9	91.3±33.5	78.7±28.1	73.4±30.6	89.9±35.7	67.7±39.1	94.8±47.8	104.4±80.7	69.6±23.8
ALT(U/L)#	54.7±31.1	101.4±44.9	85.3±33.7	58.7±32.3	99.3±56.2	78.7±35.5	109.1±82.7	148.4±180	67.1±50.1
Cr(μmol/L)	72.9±28.8	82.1±23.3	69.5±37.9	73.9±35.3	80.1±22.9	67.5±33.7	77.4±16.5	80.6±24.7	77.1±19.6
BUN(mmol/L)	6.9±3.3	8.4±3.5	5.9±3.4	7.1±4.1	8.2±3.7	5.6±3.2	5.5±1.8	6.9±4.9	6.0±3.2
K(mmol/L)	3.9±0.5	5.3±1.1	3.8±0.7	3.8±0.6	4.4±0.9	4.3±1.1	4.1±0.5	4.3±0.8	4.4±0.2
Na(mmol/L)	136.5±14.7	139.3±18.3	145.8±15.4	132.7±15.9	140.3±13.7	138.8±7.3	138.3±7.1	135.3±5.7	137.0±7.4
Ca(mmol/L)	2.35±0.39	1.99±0.18	2.17±0.31	2.32±0.43	2.67±0.27	2.27±0.34	2.21±0.22	2.07±0.14	2.24±0.17

*among all 3 groups, between day 1 preoperatively and day 10 postoperatively, *P*<0.01; # at day 10 postoperatively, the levels were lower in EN and TPN group than in CON group, *P*<0.05.

Liver and kidney function, electrolytes (Table 3)

After operation, the levels of TB, DB declined significantly in all three groups ($P < 0.01$). Same increase could be found in patients with hepatic lobectomy, radical operation of Cholangiocarcinoma, severe portal hypertension and emergency operation, but with no statistical significance. On the 10th PO, the levels of AST and ALT were lower in EN and TPN group than those in CON group ($P < 0.05$), but no difference was seen between EN and TPN group. The levels of Cr and BUN increased in EN and TPN group on the 5th day, but recovered on the 10th day. No electrolyte imbalance occurred in EN and TPN group.

Gut barrier marker (Table 4)

In EN group, the L/M ratio did not change after operation. In TPN and CON groups, they increased on the 5th day ($P < 0.01$) and declined at 10th day. In both TPN and CON groups, the difference of L/M ratio between preoperation and postoperation was significant.

Table 4 Changes of L/M ratio

	1st BO	5th PO	10th PO
CON($n=30$)	0.028±0.004	0.037±0.017	0.031±0.010
TPN($n=40$)	0.027±0.003	0.038±0.009	0.030±0.006
EN($n=65$)	0.026±0.004	0.030±0.004	0.027±0.005

DISCUSSION**Present status of clinical nutritional support in patients with poor hepatic function**

The liver plays a central role in nutritional homeostasis and any liver disease can lead to abnormal nutrient metabolism with the subsequent malnutrition. Severe protein-calorie malnutrition in patients with advanced liver disease can seriously undermine the capacity for liver regeneration and functional restoration. Appropriate nutritional support is helpful to these patients.

PN and EN are two major nutritional supports clinically. What has been proved is that long-term TPN may aggravate the liver damage^[11]. In recent years, there have been some advance in studies on various formulas including the branched chain amino acid (BCAA)^[13] and MCT/LCT^[14] in patients with poor hepatic function^[12], but there are still some problems: (1) How does lipid affect the nutrient metabolism; (2) What is the rational and safe dose and the suitable percentage of lipid supplied as the energy source^[15,16]; (3) The expensive cost. These problems impede the extensive use of PN which on long-term use may cause atrophy of intestinal mucosa and lead to the gut barrier dysfunction^[17]. The consequent enteric bacterial translocation would also cause endogenous infection even multiple organ failure (MOF) and death. EN is a more physiological, cheaper and has protection function on gut barrier. But when using EN^[18,19], the later three facts are inevitable: (1) The gastrointestinal tract should be intact; (2) Patient should be able to tolerate the indwelling nasogastric tube; (3) In case of hypertonic, patient may have abdominal distention, diarrhea, and sometimes nausea and vomiting and enhancement of the liver burden. There had been reported on using EN in patients with alcoholic cirrhosis and obstructive jaundice^[20,21], but in patients with worse liver function or sustain the hepatic lobectomy, radical operation of cholangiocarcinoma, severe portal hypertension with upper gastrointestinal hemorrhage, the selection of nutritional support is troublesome.

Evaluation of EN and its influence on liver function

En has been proven to be an efficient nutritional support^[22,23],

which is prefer to TPN. In this study, in both EN and PN groups, the patients' nutritional status was much better than CON group. Compare with PN groups, in weight loss and circumference of upper arm, EN group were much less and the positive nitrogen balance was reached much earlier.

Liver is the key organ in maintaining the carbohydrate, lipid and protein metabolism and the stabilization of internal environment. Also it is the site of biochemical pathways responsible for production and utilization of nutrients and other chemicals. It plays a central role in carbohydrate, lipid and nitrogen metabolism. Therefore it is not surprising that chronic liver disease has great metabolic impact. On the base of this, the impact and irritated responsiveness of the operation may aggravate the burden of liver and ultimately affect the outcome of the patients^[24-26]. On the other hand, we can suspect that if the nutrients were absorbed via liver, the liver could utilize the nutrient as the substrate to repair and rebuilt hepatic cell so as to promote its recover^[27]. Whether it is beneficial or harmful, our study have performed some useful study in finding this method for support sufficient nutriment at the same time to avoid further liver damage in such patients.

In 42/65 patients of Child C grade EN group, after EN, had their levels of ALT, AST, TB and DB declined, and their Cr and BUN did not increased. There were no signs of aggravating damage of liver and kidney. The successful use of Nutrison Fibre indicates that whether the BCAA is absolutely necessary in EN needs further study.

EN can protect the gut barrier

In patients with poor liver function, infection is a familiar complication and threat^[28]. Except for the depression of cellular immunity^[29], the bacteria translocation is the most probable reason of infection after the operation^[30]. Because of the translocation of the germ and endotoxin, the consequent systemic inflammatory reaction and sepsis and the dysfunction of renal, lung and cardiac system would even threaten the patient's life. The gut barrier plays a the major role in preventing bacteria translocation and block the subsequent malign reaction, which is the "trigger" of MSOF^[31,32]. Keeping the integrity of gut barrier is important to decrease the morbidity and mortality after operation.

In our study, the L/M probe was selected to monitor the status of gut barrier. The result showed: the L/M ratio of EN group was 0.026±0.004 in day 1 before the operation, 0.030±0.004 in day 5 postoperatively and 0.027±0.005 in day 10 postoperatively, the change was not significant, but it was markedly elevated in TPN and CON group after operation as follow. It indicated: EN could protect the gut barrier remarkably, the rational mechanisms were (1) The stimulation on the bowl wall may increase the blood perfusion^[33,34]; (2) The stimulation on the bowl wall may accelerate the secretion of pancreas and biliary duct to prevent shrinking of gut mucosa; (3) EN supplies the substrate of intestinal mucosal cell metabolism directly; (4) The fiber^[35-38] ingredient of Nutrison may also protect the gut barrier.

Clinical observation

In our study, we found through the upper jejunostomy tube placed during the operation, good nutrition support and good tolerance and good controllability are approached. The tube can be hold for at least 4 weeks. With good nursery, it can be kept fairly long, the longest one in our study is 94 days and no complications occurred.

In our study, the rate of ascites was 83.6 %, 93.3 % and 90.0 % in EN group, PN group and CON group, respectively, till discharge, the subsidence of them were 86.6 %, 61.3 % and 75 %. In EN group the ascites subsided earliest and liver function recovered faster.

The lowest rate of fever and the shortest fever time indicated that the risk of infection is low in EN. It is owed to the protection of the gut barrier.

REFERENCES

- 1 **Zhang LH**, Li JS. Perioperative nutrition in hepatic surgery. *Gandan Waiké Zazhi* 1994; **2**: 121-123
- 2 **Yeatman TJ**. Nutritional support for the surgical oncology Patient. *JMCC* 2000; **7**: 563-565
- 3 **Jeejeebhoy KN**. Enteral and parenteral nutrition: evidence-based approach. *Proc Nutr Soc* 2001; **60**: 399-402
- 4 **Waitzberg DL**, Plopper C, Terra RM. Access routes for nutritional therapy. *World J Surg* 2000; **24**: 1468-1476
- 5 **Nompleggi DJ**, Bonkovsky HL. Nutritional supplement in chronic liver disease: an analytical review. *Hepatology* 1994; **19**: 518-533
- 6 **Wu CT**, Huang QC, Li ZL. The increase of intestinal mucosal permeability and bacterial translocation. *Shijie Huaren Xiaohua Zazhi* 1999; **7**: 605-606
- 7 **Wilmore DW**, Smith RJ, O' D-wyer ST, Jacobs DO, Ziegler TR, Wang XD. The gut: a central organ after surgical stress. *Surgery* 1988; **104**: 917-923
- 8 **Zhu WM**, Li L. Enteral nutritional support. *Zhongguo Shiyong Waiké Zazhi* 2001; **21**: 506-510
- 9 **Sun M**, Liu YW, Liu W, Deng GY, Tang WS, Jiang ZM. Lactulose mannitol ratio in patients after operation. *Zhonghua Waiké Zazhi* 1999; **37**: 298-300
- 10 **Hu QG**, Zheng QC. The effect of enteral nutrition on gut barrier in patients with hepatic dysfunction. *Parenteral&Enteral Nutrition* 2002; **9**: 1-3
- 11 **Bavdekar A**, Bhave S, Pandit A. Nutrition management in chronic liver disease. *Indian J Pediatr* 2002; **69**: 427-431
- 12 **Fang CH**, Yang JZ. Arginine regulation of cellular immunity in patients with obstructive jaundice. *Huaren Xiaohua Zazhi* 1998; **6**: 902-904
- 13 **Abou-Assi S**, Vlahcevic ZR. Hepatic encephalopathy. Metabolic consequence of cirrhosis often is reversible. *Postgrad Med* 2001; **109**: 52-54, 57-60, 63-65 passim
- 14 **Qin HL**, Wu ZH. Influence of lipofundin vs intralipid on surgical patients with liver diseases. *Zhongguo Linchuang Yingyang Zazhi* 1999; **7**: 129-132
- 15 **Ling PR**, Ollero M, Khaodhiar L, McCowen K, Keane-Ellison M, Thibault A, Tawa N, Bistrrian BR. Disturbances in essential fatty acid metabolism in patients receiving long-term home parenteral nutrition. *Dig Dis Sci* 2002; **47**: 1679-1685
- 16 **Jia QB**, Wu YT, Mao HX, Wang BY, Tang Y. The influence of fat emulsion on liver function and fatty metabolism in patients after surgery of obstructive jaundice. *Zhongguo Linchuang Yingyang Zazhi* 1999; **7**: 112-114
- 17 **Takagi K**, Yamamori H, Toyoda Y, Nakajima N, Tashiro T. Modulating effects of the feeding route on stress response and endotoxin translocation in severely stressed patients receiving thoracic esophagectomy. *Nutrition* 2000; **16**: 355-360
- 18 **Zhou X**, Chen QP. Prevention and cure of complications of enteral nutrition. *Shijie Huaren Xiaohua Zazhi* 2000; **8**: 1393-1394
- 19 **Zhi XT**, Shou NH. Accommodation and contraindication of enteral nutrition. *Shijie Huaren Xiaohua Zazhi* 2000; **8**: 1389-1390
- 20 **Teran JC**. Nutrition and liver diseases. *Curr Gastroenterol Rep* 1999; **1**: 335-340
- 21 **Wu XT**, Yan LN. Enteral nutrition in liver disease and pancreatic disease. *Shijie Huaren Xiaohua Zazhi* 2000; **8**: 1397-1398
- 22 **Li JS**. The experience of nutritional support in gastric surgery. *Zhonghua Putong Waiké Zazhi* 2000; **15**: 172-173
- 23 **Zhu L**, Yang ZC, Li A, Cheng DC. Protective effect of early enteral feeding on postburn impairment of liver function and its mechanism in rats. *World J Gastroenterol* 2000; **6**: 79-83
- 24 **Li N**, Li JS. Improve and prospect of surgical nutrition in current 20 years. *Zhongguo Shiyong Waiké Zazhi* 2002; **22**: 6-8
- 25 **Wu GH**, Wu ZH. Selection of perioperative nutrition. *Zhonghua Putong Waiké Zazhi* 2000; **15**: 766-767
- 26 **Heubi JE**, Wiechmann DA, Creutzinger V, Setchell KD, Squires R Jr, Couser R, Rhodes P. Tauroursodeoxycholic acid (TUDCA) in the prevention of total parenteral nutrition-associated liver disease. *J Pediatr* 2002; **141**: 237-242
- 27 **Mochizuki H**, Togo S, Tanaka K, Endo I, Shimada H. Early enteral nutrition after hepatectomy to prevent postoperative infection. *Hepatogastroenterology* 2000; **47**: 1407-1410
- 28 **Xu BH**, Wang X, Wang XX, Wang BT, Li JG. 52 cases of decompensated in liver cirrhosis with multiple organ failure. *Huaren Xiaohua Zazhi* 1998; **6**: 918
- 29 **Zhang J**, Liu YH, Jiang XH, Xu KS. Relationship between endotoxemia and cellular immunity in obstructive jaundice. *Huaren Xiaohua Zazhi* 1998; **6**: 305-306
- 30 **Xu DZ**, Lu Q, Deitch EA. Elemental diet-induced bacterial translocation associated with systemic and intestinal immune suppression. *Journal of Parenteral and Enteral Nutrition* 1998; **22**: 37-41
- 31 **Yue MX**. Research method in therapy of multiple organ failure. *Huaren Xiaohua Zazhi* 1998; **6**: 729-730
- 32 **Sugiura T**, Tashiro T, Yamamori H, Takagi K, Hayashi N, Itabashi T, Toyoda Y, Sano W, Nitta H, Hirano J, Nakajima N. Effects of total parenteral nutrition on endotoxin translocation and extent of the stress response in burned rats. *Nutrition* 1999; **15**: 570-575
- 33 **Fu TL**, Chen QP. The protection of enteral nutrition on gut barrier. *Shijie Huaren Xiaohua Zazhi* 2000; **8**: 1395-1396
- 34 **Zhu WM**, Li L. Enteral nutritional support in gastric surgery. *Shijie Huaren Xiaohua Zazhi* 2000; **8**: 1396-1397
- 35 **Zheng QC**, Wang JJ, Li JS, Zhang SX. Elemental diet supplemented with intestinal nutrient ingredients protects stressed rat's gut barrier. *Zhonghua Linchuang Yingyang Zazhi* 1997; **5**: 145-148
- 36 **Gong SJ**, Luo MD, Chen DW, Quan SW, Shen J, Chu BF, Zhang YC, Cai W, Tang QY, Xia ZM, Feng Y. Elementary diet supplemented with fiber in alimentary tract operative patients. *Shijie Huaren Xiaohua Zazhi* 2001; **9**: 483-484
- 37 **Yu Y**, Tian HM, Shi ZG, Yao YM, Wang YP, Lu LR, Yu Y, Chang GY, Ma NS, Sheng ZY. Relationship between endotoxemia and dysfunction of intestinal immuno-barrier after scald in rats. *Huaren Xiaohua Zazhi* 1998; **6**: 703-704
- 38 **Wu WX**, Xu Q, Hua YB, Shen LZ. Early enteral nutrition after colorectal resections: a prospective clinical trial. *Shijie Huaren Xiaohua Zazhi* 1999; **7**: 1024-1029

Edited by Wu XN

Operative stress response and energy metabolism after laparoscopic cholecystectomy compared to open surgery

Kai Luo, Jie-Shou Li, Ling-Tang Li, Kei-Hui Wang, Jing-Mei Shun

Kai Luo, Jie-Shou Li, Ling-Tang Li, Kei-Hui Wang, Jing-Mei Shun, Research Institute of General Surgery, Nanjing General Hospital, Nanjing Command of People's Liberation Army, and Clinical School of Medical College, Nanjing University, Nanjing Jiangsu Province 210002, China

Supported by grants from the Health Department of General Logistics Department of People's Liberation Army, China, No 01Z011

Correspondence to: Dr. Kai Luo, Research Institute of General Surgery, Nanjing General Hospital, Nanjing Command of People's Liberation Army, and Clinical School of Medical College, Nanjing University, Nanjing 210002, Jiangsu Province, China. lokai@jlonline.com

Telephone: +86-25-4491878

Received: 2002-03-14 **Accepted:** 2002-08-13

Abstract

AIM: To determine the least invasive surgical procedure by comparing the levels of operative stress hormones, response-reactive protein (CRP) and rest energy expenditure (REE) after laparoscopic (LC) and open cholecystectomy (OC).

METHODS: Twenty-six consecutive patients with noncomplicated gallstones were randomized for LC (14) and OC (12). Plasma concentrations of somatotropin, insulin, cortisol and CRP were measured. The levels of REE were determined.

RESULTS: In the third postoperative day, the insulin levels were lower compared to that before operation ($P < 0.05$). In the first postoperative day, the levels of somatotropin and cortisol were higher in OC than those in LC. After operation the parameters of somatotropin, CRP and cortisol increased, compared to those in the preoperative period in the all patients ($P < 0.05$). In the all-postoperative days, the CRP level was higher in OC than that in LC (7.46 ± 0.02 ; 7.38 ± 0.01 , $P < 0.05$). After operation the REE level all increased in OC and LC ($P < 0.05$). In the all-postoperative days, the REE level was higher in OC than that in LC (1438.5 ± 418.5 ; 1222.3 ± 180.8 , $P < 0.05$).

CONCLUSION: LC results in less prominent stress response and smaller metabolic interference compared to open surgery. These advantages are beneficial to the restoration of stress hormones, the nitrogen balance, and the energy metabolism. However, LC can also induce acidemia and pulmonary hypoperfusion because of the pneumoperitoneum it uses during surgery.

Luo K, Li JS, Li LT, Wang KH, Shun JM. Operative stress response and energy metabolism after laparoscopic cholecystectomy compared to open surgery. *World J Gastroenterol* 2003; 9(4): 847-850

<http://www.wjgnet.com/1007-9327/9/847.htm>

INTRODUCTION

The superiority of laparoscopic cholecystectomy (LC) has justified its universal usage in recent years. It induces less

surgical response compared to open cholecystectomy (OC). A great many literatures had proved such an advantage^[1-4]. However, there were few studies concerning the difference between LC and OC in operative stress response and energy metabolism. In this prospective, randomized study, we compared the effects of LC and OC on body oxygen supply, metabolic hormones and response-reactive protein (CRP) levels, body energy metabolism, and acid-base balance.

MATERIALS AND METHODS

Clinical data

Twenty-six patients with uncomplicated gallstones were recruited for the study from April 2001 to Oct. 2001. They were randomized to undergo LC ($n=14$) or OC ($n=12$). The two groups of patients had comparable demographic data (Table 1). All enrolled patients were asymptomatic for at least 6 weeks prior to admission without any history of abdominal surgery. Ultrasonography was routinely performed to exclude the common bile duct stone. The patients with jaundice, severe infection, or metabolic abnormalities were also excluded in this study. Anesthesia was induced and maintained using a standard intravenous protocol in both groups. LC was undertaken by a standard 4-trochar approach with electrocautery dissection; pneumoperitoneum was established with carbon dioxide (CO₂) insufflation, and OC was performed via a sub-costal incision.

Table 1 Comparison of general conditions between the two groups

Group	Number	M/F	Median age (yrs)	Height (cm)	BW (Kg)
OC	12	3/9	45.5±12.6	161.3±7.1	61.0±3.6
LC	14	6/8	46.6±15.8	163.9±6.1	65.8±9.4

Blood samples and evaluation method

Fast venous blood was taken at 6 AM on the day prior to surgery, and days 1 and 3 postoperatively. Samples should be analyzed within 2 hours after stored *in vitro*. All hormones were quantitatively assayed. In CRP assay, rate immunonephometry with specific protein analyzer (BN 100 Analyzer) was adopted. Growth hormones (GH) levels were determined by double-antibody RIA with reagents from Jiuding Bio-medical Co. Ltd, Tianjing. Serum cortisol and insulin analysis were both carried out by competitive RIA, using reagents from 3V Diagnostic Technique Co. Ltd. and Chinese Institute of Atomic Energy, respectively.

Energy metabolism was assessed by indirect calorimeter on the day prior to operation, and days 1 and 3 postoperatively. During analysis, patients should be reposed, with ambient temperature 18-26 °C and humidity 50-60 %. Oxygen consumption (VO₂) and CO₂ production (VCO₂) per unit time were determined at first. Then, based on the indirect calorimetry theory, REE and RQ were figured out according to the value of VO₂ and VCO₂. All energy consumption measurements were carried out using Medical Graphics Critical Care Monitor Desktop Analysis System (Medical Graphics Co.,

Minneapolis, MN). Artery and acid-base balance were assayed by automatic gas analyzer.

Statistical analysis

Data were given as means and standard error of the mean. The intergroup comparison was made using the Student's *t* test. All the statistical procedures were accomplished with SPSS 8.0. A two-tailed $P < 0.05$ was taken as significant.

RESULTS

Median surgical duration was not different between the LC (50.9±8.9 min) and OC (58.5±6.3 min) group ($P > 0.05$), while the length of hospital stay and the time to first passage of flatus were significantly shorter in LC than those in OC group (Table 2).

Table 2 Postoperative intestinal transit recovery

	OC (n=12)	LC (n=14)
Time to first passage of flatus (days)	2.8±0.4	1.5±0.3 ^a
Postoperative length of stay (days)	6.7±0.2	3.2±0.3 ^a

^a $P < 0.05$ vs OC.

Insulin levels rose significantly on the 3rd postoperative day above baseline measurements in OC group, with no intergroup difference throughout the postoperative period. GH levels elevated in both groups at all phases postoperatively. However, there was a more prominent response in patients undergoing OC. A significant intergroup difference was detected on day 1 following operation with higher values for OC than that for LC. Cortisol levels increased from baseline on both of the postoperative days in the two groups, but more remarkably in OC group. Intergroup comparison indicated that concentrations were significantly higher in patients undergoing OC on day 1, postoperatively. But on the 3rd postoperative day, cortisol concentrations were comparable in the two groups (Table 3).

Table 3 GH, Insulin, and cortisol levels before and after surgery

	Prior to surgery	1st postoperative day	3rd postoperative day
Insulin			
LC (n=14)	14.4±2.1	16.1±2.8	14.6±2.5
OC (n=12)	17.9±2.1	17.2±3.4	12.3±0.9 ^b
GH			
LC	1.0±0.2	2.7±1.0 ^{ab}	1.5±0.5 ^b
OC	1.8±0.4	5.4±2.5 ^b	2.2±0.9
Cortisol			
LC	0.46±0.01	0.56±0.11 ^{ab}	0.74±0.05 ^b
OC	0.71±0.15	1.12±0.25 ^b	0.89±0.02 ^b

^a $P < 0.05$, vs OC ^b $P < 0.05$, vs the preoperative period.

In OC groups, REE levels raised 165.3Kcal from baseline on day 1 postoperatively. The difference was significant. But on the 3rd postoperative day, it was 57.3Kcal higher than baseline only (not significant). A similar pattern was seen in the patients undergoing LC, and there was a marked increase (60.1Kcal) on day 1 but not on day 3. On both of the postoperative days, REE levels were significantly higher in OC than those in LC group. RQ fell significantly from baseline on the 1st postoperative day in both groups. There was a significant elevation of CRP concentrations from baseline

levels in both groups. However, in patients undergoing OC, the increase was more remarkable. CRP levels were significantly higher in OC than those in LC group on both of the postoperative days (Table 4).

Table 4 REE, RQ, and CRP levels before and after surgery

	Prior to surgery	1st postoperative day	3rd postoperative day
REE			
LC (n=14)	1162.2±159.6	1222.3±180.8 ^{ab}	1152.8±150.2 ^a
OC (n=12)	1273.2±304.8	1438.5±418.5 ^b	1330.5±353.8
RQ			
LC	0.87±0.10	0.78±0.06 ^b	0.85±0.09
OC	0.88±0.12	0.78±0.04 ^b	0.84±0.08
CRP			
LC	8.00±0.01	15.10±2.47 ^{ab}	34.44±7.88 ^{ab}
OC	12.37±3.55	64.50±15.20 ^b	94.25±13.43 ^b

^a $P < 0.05$, vs OC ^b $P < 0.05$, vs the preoperative period.

Artery oxygen pressure did not change remarkably after surgery in OC group, while it declined significantly on the 1st postoperative day in the LC group and returned to preoperative levels on the 3rd day. Oxygen saturation (SO₂) in blood fell significantly on the 1st postoperative day in both groups. On the 3rd day, it was much higher in LC than that in OC group. There was no significant change of PCO₂ in both groups after surgery. (Table 5) On the 3rd postoperative day, HCO₃⁻ level and BE rose significantly in LC group, and BE was significantly higher in LC than that in OC group. PH was significantly lower in LC than that in OC group on the 1st postoperative day (Table 6).

Table 5 Artery PO₂, PCO₂ and SO₂ before and after surgery

	Prior to surgery	1st postoperative day	3rd postoperative day
PO₂			
LC (n=14)	87.7±4.0	75.9±3.2 ^b	80.94±4.3
OC (n=12)	80.2±2.2	86.5±9.2	79.81±0.6
PCO₂			
LC	36.79±1.19	37.09±1.64	34.48±1.75
OC	35.01±1.76	31.83±2.63	37.96±1.88
SO₂			
LC	96.4±0.40	94.6±0.86 ^b	95.4±0.40 ^a
OC	95.4±0.40	92.73±1.70 ^b	94.0±0.67

^a $P < 0.05$, vs OC ^b $P < 0.05$, vs the preoperative period.

Table 6 REE, RQ, and CRP levels before and after surgery

	Prior to surgery	1st postoperative day	3rd postoperative day
REE			
LC (n=14)	22.5±0.61	21.7±0.61	22.15±0.83
OC (n=12)	21.02±0.58	20.32±2.1	24.8±0.72 ^b
RQ			
LC	-1.77±0.48	-2.85±0.46	-1.77±0.78 ^a
OC	-1.66±0.54	-2.17±1.38	1.23±0.65 ^b
CRP			
LC	7.40±0.006	7.387±0.008 ^a	7.43±0.008 ^b
OC	7.42±0.013	7.46±0.022	7.44±0.018

^a $P < 0.05$, vs OC ^b $P < 0.05$, vs the preoperative period.

DISCUSSION

Laparoscopic cholecystectomy is becoming the choice of surgery for uncomplicated cholelithiasis because it had induced less tissue trauma response throughout the course of wound healing compared to open cholecystectomy. Surgery stimulates a series of hormonal and metabolic changes that constitute the stress response. Surgery also induces neurohormonal events that include activation of sympathetic nervous system and stimulation of hypothalamic-pituitary-adrenal axis initially. Then the adrenal cortex is activated, promoting the release of neurohormonal transmitters that would influence the intensity of postoperative pain and duration of postoperative ileus^[5-7]. ACTH, catecholamine, cortisol, and glucagon all played crucial roles in the mediation of stress response. In response to sepsis and trauma, massive catecholamine, cortisol, and glucagons are released, while serum insulin concentrations decrease relatively, and decrease of insulin levels is in correlation with the severity of the sepsis and trauma^[8-12]. In the present study, we found a marked decrease of insulin levels from baseline in OC group on the 3rd postoperative day, while the intergroup difference was not significant on either 1st or 3rd postoperative day. GH and cortisol levels increased from baseline in both groups on the 1st and 3rd postoperative day, and there was a more marked increase in OC group. On the 1st postoperative day GH and cortisol concentrations were both higher in OC than those in LC group.

The cytokines and CRP were objective markers of operative stress response as well as the mediators of host immunologic reaction. Derived from immune system or other tissues, TNF, IL-1 and IL-6 were the major mediators of the acute-phase response^[13-15]. In a recent study, Bruce and coworkers^[16] examined the changes of CRP, IL-1 Ra, IL-6, and TNF- α in LC and OC patients after surgery. A marked and persistent raise of IL-6 levels was detected from 8 hours to 7 days postoperatively in OC group, while the concentrations of CRP and albumin were comparable in the two groups. IL-1ra levels were significantly raised as early as 4 hours following incision in OC group, compared to LC group. IL-6 levels rose significantly and early (1 hour) in both groups, but there was a more prominent and prolonged response in patients undergoing OC. Significant intergroup difference of IL-6 levels was present as early as 8 hours following incision^[17-21]. In our study, we found that CRP levels rose significantly from baseline on both day 1 and day 3 after surgery in the two groups, but more prominently in OC group.

In response to the surgical trauma, the body usually presents with a hyper-metabolic state. Such a state is directly linked to the activation of sympathetic nervous system, the increase of oxygen and energy consumption, the negative nitrogen balance, and the synthesis of CRP. All surgical traumas will induce neuroendocrine activation and protein catabolism, and the nitrogen excretion is therefore increased (mainly as BUN, sometimes as SCr)^[22,23]. The amount of the increased nitrogen excretion was determined by the extent of stress, which is proportional to the intensity of injury response. Thus, the degree of metabolic restoration could be acquired using systemic nitrogen balance measurements^[8]. To our knowledge, this study is the first to assess the effect of mini-invasive surgery on body REE consumption. In the study, we observed the perioperative changes of REE levels of LC and OC groups using indirect calorimeter. As the result, REE increased significantly (165.3 Kcal) from baseline in the 1st postoperative day in OC group, while on the 3rd day the elevation was not significant (57.3 Kcal). The LC group also revealed marked increase (60.1 Kcal) in the 1st postoperative day, but not in the 3rd day. The intergroup difference of REE levels was significant (with higher levels in OC group) at all phases postoperatively. RQ decreased significantly on the 1st

postoperative day in both groups. Thus, our study revealed that LC was less invasive and induced less host stress response and metabolic disturbance compared with traditional OC and it therefore might be more beneficial to the restoration of nitrogen balance and metabolism.

During LC, pneumoperitoneum is induced by insufflation of carbon dioxide, which may be accompanied with disturbance of acid-base balance and pulmonary perfusion^[24-27]. Open surgery, on the other hand, usually results in pulmonary dysfunction. Previous studies have shown that on the 1st postoperative day, FVC and FEV1 decreased 40-70 % in patients undergoing OC, compared to 20-40 % in patients undergoing LC. There are possibly two explanations for this. One is that postoperative wound pain often causes shallow respiration, which may lead to small bronchiole closure, the pulmonary blood shunt, and hence the hyponoxia. Increased oxygen consumption after surgery may be another explanation^[28-31]. In this study, we observed that artery oxygen consumption fell significantly from baseline on day 1 and restored to preoperative levels on the day 3 postoperatively in LC patients, with no significant reduction in OC patients. SO₂ decreased significantly on the 1st postoperative day on both groups, and on the 3rd postoperative day it was higher in LC group than in OC group. Penumoperitonium could explain the reduced oxygen supply at early postoperative phases in LC patients. However, the influence of wound pain on respiration is more pronounced and permanent OC than in LC patients, this may be the reason why the intergroup difference is significant on the 3rd postoperative day. HCO₃ and BE raised significantly from baseline in OC group on the 3rd postoperative day, and BE was significantly higher in LC group than that in OC group on the day. PH levels were much lower in LC group than those in OC group on the 1st postoperative day. This is possibly because of the postoperative acidemia elicited by the retention of CO₂ during pneumoperitonium. Much attention should be paid to this change during LC.

In conclusion, LC results in less prominent stress response and metabolic interference compared to open surgery. These advantages are beneficial to the restoration of stress hormones, the nitrogen balance, and the energy metabolism. However, LC can also induce acidemia and pulmonary hypoperfusion because of the pneumoperitonium it uses during surgery.

REFERENCES

- 1 **Chen L**, Dai N, Shi X, Tao S, Zhang W. Life quality of patients after cholecystectomy. *Zhonghua Waike Zazhi* 2002; **40**: 762-765
- 2 **Champault A**, Vons C, Dagher I, Amerlinck S, Franco D. Low-cost laparoscopic cholecystectomy. *Br J Surg* 2002; **89**: 1602-1607
- 3 **Bosch F**, Wehrman U, Saeger HD, Kirch W. Laparoscopic or open conventional cholecystectomy: clinical and economic considerations. *Eur J Surg* 2002; **168**: 270-277
- 4 **Topcu O**, Ka rakayali F, Kuzu MA, Ozdemir S, Erverdi N, Elhan A, Aras N. Comparison of long-term quality of life after laparoscopic and open cholecystectomy. *Surg Endosc* 2003; **17**: 291-295
- 5 **Dubois M**, Pickar D, Cohen MR, Roth YF, Macnamara T, Bunney WE Jr. Surgical stress in humans is accompanied by an increase in plasma beta-endorphin immunoreactivity. *Life Sci* 1981; **29**: 1249-1254
- 6 **Hearing SD**, Thomas LA, Heaton KW, Hunt L. Effect of cholecystectomy on bowel function: a prospective, controlled study. *Gut* 1999; **45**: 889-894
- 7 **Fox JE**, Daniel EE. Exogenous opiates: their local mechanisms of action in the canine small intestine and stomach. *Am J Physiol* 1987; **253**(2 Pt 1): G179-188
- 8 **Byrne J**, Hallett JW Jr, Ilstrup DM. Physiologic responses to laparoscopic aortofemoral bypass grafting in an animal model. *Ann Surg* 2000; **231**: 512-518
- 9 **Blanc-louvy IL**, Coquerel A, Koning E. Operative stress response

- is reduced after laparoscopic compared to pen cholecystectomy. *Dig Dis Sic* 2000; **45**: 1703-1713
- 10 **Emirer S**, Karadayi K, Simsek S, Erverdi N, Bumin C. Comparison of postoperative acute-phase reactants in patients who underwent laparoscopic v open cholecystectomy: a randomized study. *J Laparoendosc Adv Surg Tech A* 2000; **10**: 249-252
- 11 **Schauer PR**, Sirinek KR. The laparoscopic approach reduces the endocrine response to elective cholecystectomy. *Am Surg* 1995; **61**: 106-111
- 12 **Yoshida S**, Ohta J, Yamasaki K, Kamei H, Harada Y, Yahara T, Kaibara A, Ozaki K, Tajiri T, Shirouzu K. Effect of surgical stress on endogenous morphine and cytokine levels in the plasma after laparoscopic or open cholecystectomy. *Surg-Endosc* 2000; **14**: 137-140
- 13 **Mendoza-Sagaon M**, Hanly EJ, Talamini MA, Kutka MF, Gitzelmann CA, Herreman-Suquet K, Poulouse BF, Paidas CN, De Maio A. Comparison of the stress response after laparoscopic and open cholecystectomy. *Surg Endosc* 2000; **14**: 1136-1141
- 14 **Leung KL**, Lai PB, Ho RL, Meng WC, Yiu RY, Lee JF, Lau WY. Systemic cytokine response after laparoscopic-assisted resection of rectosigmoid carcinoma: A prospective randomized trial. *Ann Surg* 2000; **231**: 506-511
- 15 **Sendt W**, Amberg R, Schoffel U, Hassan A, von-Specht BU, Farthmann EH. Local inflammatory peritoneal response to operative trauma: studies on cell activity, cytokine expression, and adhesion molecules. *Eur J Surg* 1999; **165**: 1024-1030
- 16 **Bruce DM**, FRCS And smith M. Minimal Access Surgery for cholelithiasis induces an attenuated acute phase response. *Am J Surg* 1999; **178**: 232-234
- 17 **Jess P**, Schultz K, Bendtzen K, Nielsen OH. Systemic inflammatory responses during laparoscopic and open inguinal hernia repair: a randomised prospective study. *Eur J Surg* 2000; **166**: 540-544
- 18 **Chaudhary D**, Verma GR, Gupta R, Bose SM, Ganguly NK. Comparative evaluation of the inflammatory mediators in patients undergoing laparoscopic versus conventional cholecystectomy. *Aust N Z J Surg* 1999; **69**: 369-372
- 19 **Mansour MA**, Stiegmann GV, Yamamoto M, Berguer R. Neuroendocrine stress response after minimally invasive surgery in pigs. *Surg Endosc* 1992; **6**: 294-297
- 20 **Kristiansson M**, Saraste L, Soop M, Sundqvist KG, Thorne A. Diminished interleukin-6 and C-reactive protein responses to laparoscopic versus open cholecystectomy. *Acta Anaesthesiol Scand* 1999; **43**: 146-152
- 21 **Janicki K**, Bicki J, Radzikowska E, Pietura R, Madej B, Burdan F. C-reactive protein (CRP) as a response to postoperative stress in laparoscopic cholecystectomy using the abdominal wall lift, with performed pneumoperitoneum (CO₂), and in open cholecystectomy. *Ann Univ Mariae Curie Sklodowska* 2001; **56**: 397-402
- 22 **Bistran BR**. A simple technique to estimate severity of stress. *Surg Gynecol Obstet* 1979; **148**: 675-678
- 23 **Cerra FB**, Siegal JH, Border JR. Correlations between metabolic and cardiopulmonary measurement in patients after trauma, general surgery and sepsis. *J trauma* 1979; **19**: 621-629
- 24 **Coskun I**, Hatipoglu AR, Topaloglu A, Yoruk Y, Yalcinkaya S, Caglar T. Laparoscopic versus open cholecystectomy: effect on pulmonary function tests. *Hepatogastroenterology* 2000; **47**: 341-342
- 25 **Mimica Z**, Biocic M, Bacic A, Banovic I, Tocilj J, Radonic V, Ilic N, Petricevic A. Laparoscopic and laparotomic cholecystectomy: a randomized trial comparing postoperative respiratory function. *Respiration* 2000; **67**: 153-158
- 26 **Singh-Ranger D**. Pulmonary function after laparoscopic and open cholecystectomy. *Surg Endosc* 2002; **16**: 1496-1497
- 27 **Koivusalo AM**, Kellokumpu I, Scheinin M, Tikkanen I, Makisalo H. A comparison of gasless mechanical and conventional carbon dioxide pneumoperitoneum methods for laparoscopic cholecystectomy. *Anesth Analg* 1998; **86**: 153-158
- 28 **Ali J**, Gana TJ. Lung volumes 24 h after laparoscopic cholecystectomy - justification for early discharge. *Can Respir J* 1998; **5**: 109-113
- 29 **Chumillas MS**, Ponce JL, Delgado F, Viciano V. Pulmonary function and complications after laparoscopic cholecystectomy. *Eur J Surg* 1998; **164**: 433-437
- 30 **Larsen JF**, Ejstrud P, Svendsen F, Pedersen V, Redke F. Systemic response in patients undergoing laparoscopic cholecystectomy using gasless or carbon dioxide pneumoperitoneum: a randomized study. *J Gastrointest Surg* 2002; **6**: 582-586
- 31 **Hendolin HI**, Paakonen ME, Alhava EM, Tarvainen R, Kempainen T, Lahtinen P. Laparoscopic or open cholecystectomy: a prospective randomised trial to compare postoperative pain, pulmonary function, and stress response. *Eur J Surg* 2000; **166**: 394-399

Edited by Zhang JZ

Ultrastructure and molecular biological changes of chronic gastritis, gastric cancer and gastric precancerous lesions: a comparative study

Goang-Yao Yin, Wu-Ning Zhang, Xiao-Jing Shen, Yi Chen, Xue-Fen He

Goang-Yao Yin, Xiao-Jing Shen, Xue-Fen He, Wuxi No.3 Peoples Hospital, Wuxi 214041, Jiangsu Province, China

Wu-Ning Zhang, Yi Chen, Department of National Microanalysis Center, Fudan University, Shanghai 200433, Shanghai, China

Correspondence to: Dr. Goang-Yao Yin, Wuxi No.3 Peoples Hospital, 230 Eastern Tonghuhui Road Wuxi 214041, Jiangsu Province, China. yinyao@pub.wx.jsinfo.net

Received: 2002-10-04 **Accepted:** 2002-12-03

Abstract

AIM: To carry out a comparative study on ultrastructure and molecular biological changes of chronic gastritis (CG), gastric cancer (GC) and gastric precancerous lesions.

METHODS: By the use of histochemical staining, SEM with EDAX, TEM with EDAX, image analysis technique, RIA and chemiluminescence method, gastric mucosa of 168 patients were synchronously analyzed in morphology, trace elements, DNA, cAMP, SOD, ³H-TdR LCT and serum LPO were also done.

RESULTS: The incidence of epithelial nucleoplasmic ratio >1, lobulated nuclei, inter-chromatin aggregation of granules, nucleolar hypertrophy, and the content of DNA, Zn, Cu in nuclei and serum LPO of each group were showed as follows: normal control group (0.0, 0.0, 6.7, 0.0, 12.6±2.7, 7.6±0.4, 58.4±0.3, 2.6±0.6), CSG group (5.7, 2.9, 7.4, 2.9, 15.2±3.1, 8.1±0.5, 58.9±0.5, 4.2±0.7), CAG group (31.3, 29.7, 45.3, 42.2, 16.5±3.1, 8.6±0.4, 59.3±0.5, 4.5±0.6), CA group (100.0, 100.0, 72.2, 50.0, 30.7±8.2, 8.8±0.3, 59.5±0.4, 6.8±1.6), ATP⁺⁺ group (61.5, 38.5, 23.1, 38.5, 23.5±8.9, 8.3±0.4, 59.1±0.4, 5.1±1.2), IM⁺⁺⁺ ATP⁺⁺ group (77.8, 55.5, 33.3, 44.4, 25.1±7.2, 8.4±0.5, 59.5±0.4, 6.5±1.1), IM⁺⁺⁺ ATP⁺⁺ group (100.0, 100.0, 75.0, 62.5, 28.5±9.1, 8.9±0.5, 59.7±0.4, 7.6±0.7), IMII_b group (100.0, 62.5, 75.0, 50.0, 27.3±10.3, 8.6±0.3, 59.5±0.4, 6.1±0.9); whereas the content of Zn, Cu in mitochondria and cAMP, SOD in gastric mucosa, and ³H-TdR LCT of each group were shown as follows: normal control group (9.2±0.5, 58.3±0.3, 15.9±1.5, 170.5±6.1, 1079.7±227.4), CSG group (8.6±0.5, 57.8±0.3, 14.6±1.8, 163.3±5.6, 867.3±240.5), CAG group (8.3±0.4, 57.5±0.3, 13.4±1.8, 161.2±4.3, 800.9±221.8), CA group (8.9±0.4, 57.1±0.3, 10.2±3.9, 152.2±3.8, 325.7±186.8), ATP⁺⁺ group (9.1±0.4, 57.0±0.3, 12.4±1.8, 161.5±3.8, 642.9±174.3), IM⁺⁺⁺ ATP⁺⁺ group (8.6±0.4, 56.9±0.3, 12.0±2.3, 152.2±2.5, 326.3±160.3), IM⁺⁺⁺ ATP⁺⁺ group (8.5±0.3, 56.8±0.2, 10.4±0.9, 147.4±2.6, 316.1±170.7), IMII_b group (8.6±0.3, 56.9±0.3, 11.9±1.9, 150.0±2.8, 318.9±145.8), there were significant differences between groups ($P < 0.05-0.01$).

CONCLUSION: There was a significant difference between CG and GC in their ultrastructure and molecular biology. Only on the condition of changes of internal environment in combination with the harmful effect of external

environment, chronic atrophic gastritis can then develop into gastric cancer. Hence it might have similar epithelial cell ultrastructure and molecular biological changes in ATP⁺⁺, IMII_b and cancer, hence there were similar patterns of occurrence, development and transformation. Recognition of this trend might help to explore problems of prevention and cure.

Yin GY, Zhang WN, Shen XJ, Chen Y, He XF. Ultrastructure and molecular biological changes of chronic gastritis, gastric cancer and gastric precancerous lesions: a comparative study. *World J Gastroenterol* 2003; 9(4): 851-857

<http://www.wjgnet.com/1007-9327/9/851.htm>

INTRODUCTION

We conducted histochemical staining, detection of cAMP, SOD and DNA of gastric mucosa of 168 patients with chronic gastritis (CG) or gastric cancer (GC); SEM and TEM with EDAX were used to synchronously determine ultrastructures and trace elements and image analysis technique was used to determine nuclear DNA. ³H-TdR LCT and serum LPO were also carried out. Following was the comparative study.

MATERIALS AND METHODS

Materials

168 patients definitely diagnosed as suffering from CSG, CAG and GC were our subjects of study. According to "The standards for the classification of chronic gastritis, for gastrofiberscopic diagnosis and for histopathological diagnosis of atrophic gastritis", gastric mucosa tissue slices underwent HE staining and AB_{PH2.5}/PAS, Hid/AB_{PH2.5} and HiD/AB_{PH2.5} histochemical staining. ATP was classified into low-grade, middle-grade and heavy-grade and IM into IM I_a, IM I_b, IM II_a, IM II_b. 68 cases were definitely diagnosed as CSG, including 43 males, 25 females, average age 43 years, average course of disease 4a, 26 cases without IM or ATP; 31 cases with concomitant or solitary IM-19 cases low-grade, 10 cases middle-grade and 2 cases heavy-grade; 9 cases with solitary ATP-8 cases low-grade, 1 case middle-grade; 2 cases with IM and concomitant ATP, IM and ATP were both middle-grade. 64 cases were definitely diagnosed as CAG, including 37 males, 27 females, average age 47 years average course of disease 6a, 3 cases without IM or ATP; 39 cases with concomitant solitary IM (17 cases low-grade, 4 cases middle-grade and 18 cases heavy-grade); 8 cases with solitary ATP (2 cases low-grade, 6 cases middle-grade.) 14 cases with IM concomitant ATP (12 cases middle-grade IM, 2 cases heavy-grade IM, 8 cases low-grade ATP, 6 cases middle-grade ATP). 36 cases were definitely diagnosed as GC, including 22 males, 14 females, average age 52 years, average course of disease, 2a, all with IM or ATP. 12 cases with solitary IM (6 cases low-grade, 3 cases middle-grade, 3 cases heavy-grade); 7 cases with solitary ATP (1 case low-grade, 6 cases middle-grade);

17 cases with IM concomitant ATP (5 cases middle-grade IM, 12 cases heavy-grade IM; 7 cases low-grade ATP, 9 cases middle-grade ATP, 1 case heavy-grade ATP). Of the 45 healthy volunteers who underwent gastroscopy and biopsy, 15 cases had basically normal gastric mucosa tissues, including 6 males 9 females, average age 37, and they were referred to as normal control (NC) group.

Methods

Under gastroscopy, three pieces of gastric mucosa were taken from the focal and nonfocal areas in antral region and body of stomach as specimens for section preparation, SEM, TEM, detection of DNA, cAMP and SOD. Blood was taken for ^3H -TdRLCT and LPO. For the observation of gastric mucosa ultrastructure and determination of its trace elements^[1-4], 501B SEM with 9100/60 EDAX was used to observe the three pieces of specimens of each patient, under the direct vision of SEM, the EDAX probe automatically detected the samples within 0.1-0.01 mm² range all the elements under 12 in atomic number and automatically calculated the weight percentage (WT%) of each element in element series. 15 points were fixed in the three pieces of mucosa of every patient to carry out 15 detections, and the average WT% of each element was taken as its actual WT%. In every detection, 21 elements such as Na, Mg, Al, Si, P, S, K, Ca, Fe, Cu, Zn, Ti, Cr etc were detected, and weight percentage (WT%) of each element between elements of gastric mucosa was calculated.

By using EM430 TEM with 9100/60 EDAX, three pieces of mucosa specimens of every patient were magnified in unison by five magnifying powers (3 600, 7 200, 14 000, 19 000, 29 000) to randomly take the pictures of the panoramagram, local area and organelle and to detect the atomic number percentage (AT%) of each nuclear and mitochondrial element between trace elements^[5-10]. After gastric mucosa cell smear was stained by Feulgen staining, IBAS 2000 image analysis technique was adopted to detect IOD, which is taken as the relative content of nuclear DNA^[7,8]. RIA was adopted to detect the content of gastric mucosa cAMP (Pmol/g); chemiluminescence method was adopted to detect the activity of SOD (u/g)^[4]. ^3H -TdRLCT. (Bq/L whole blood) was carried out; thiobarbituric acid development process was adopted to detect serum LPO (u mol/L)^[4].

Statistical method

χ^2 and t test.

RESULTS

Histopathology of gastric mucosa

Between NC group. CSG group. CAG group and CA group, there were significant differences in the incidence rate and degree of different types of IM and ATP in glands propria of gastric mucosa ($P < 0.05-0.001$, Table 1). The surface of normal gastric mucosa was isolated by crisscross small groves into many lesser gastric areas, assuming convolution shape (Figure 1). In these areas, there were many gastric pits (the mouths of gastric glands), which were shaped like craters. The concave walls had round or oval epithelial cells of almost the same size. In CSG gastric mucosa there were scattered denatured, diabrotic and necrotic exfoliated epithelial cells, on whose surface S-shape *Helicobacter pylori* (HP) were found (Figure 2). Massive epithelial cells became diabrotic, anabrotic and exfoliated forming micro ulcers. The ulcers spread out from their centers, with adjacent cells crushed, destructed in irregular shapes and arrangement. In CSG gastric mucosa, cyst was found accidentally (Figure 3), the epithelial cells of crater walls were atrophic and denatured,

of different sizes and deranged; the cells became diabrotic and necrotic and had inflammatory cell infiltration and the glands propria of the serious cases were shaped like grid framework structure (Figure 4). The surfaces of the epithelial calls of IM gastric mucosa were thickly coated, villi were invisible and the intercellular boundaries were not clear (Figure 5). SEM was not able to definitely indentify gastric mucosa ATP, but only able to distinguish whether cells were hyperplastic or not. Degeneration, hyperplasia or cellular regeneration occurred in gastric mucosa. The hyperplastic cells are of different sizes and states and the active memberanes were shaped like lesser tubercles (Figure 6, 7). The cells of gastric cancer were different sizes and shapes, deranged, characterized by obvious heteromorphic nature, conglobated and shaped like grapes or cauliflower. There were nearby or basal infiltration, destruction and ulceration of cancer cells, which have developed into ulcers.

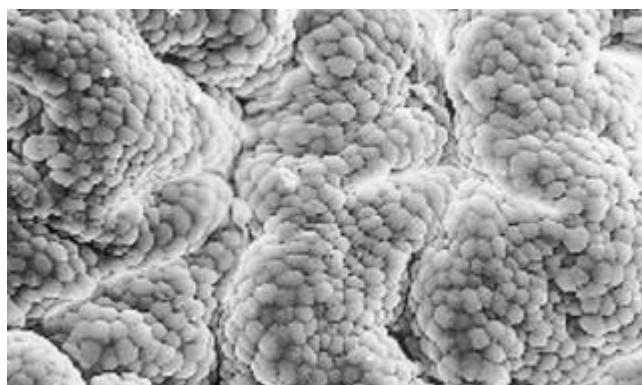


Figure 1 Convolution shape of mucosa surface. $\times 320$.

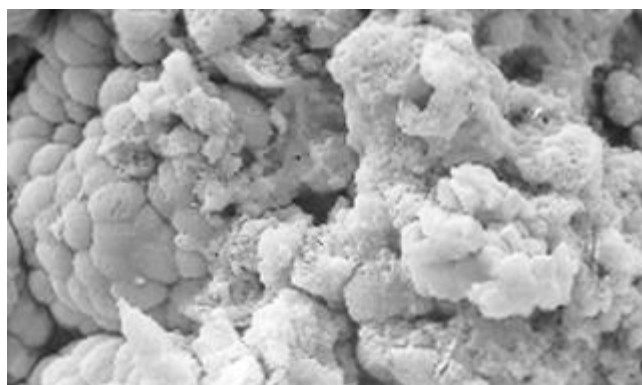


Figure 2 Degeneration, diabrosis, necrosis and exfoliation of gastric mucosa epithelial cells. $\times 640$.

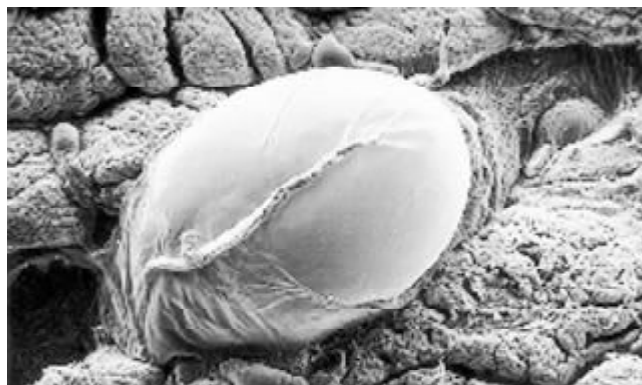


Figure 3 Cysts of gastric mucosa. $\times 64$.

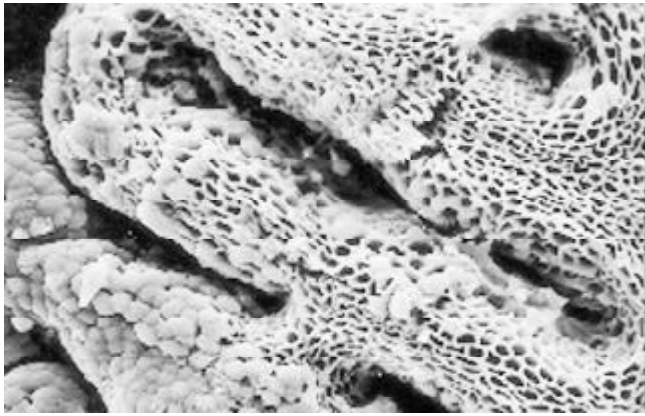


Figure 4 Atrophic and denatured glands propria in grid framework structure. $\times 320$.

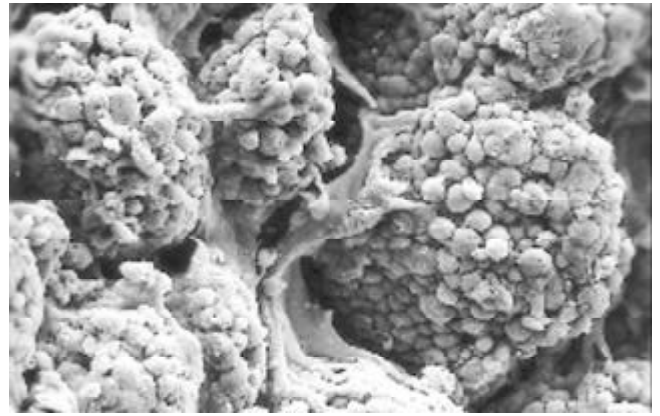


Figure 8 The cells of gastric cancer are conglobated and shaped like grapes. $\times 320$.

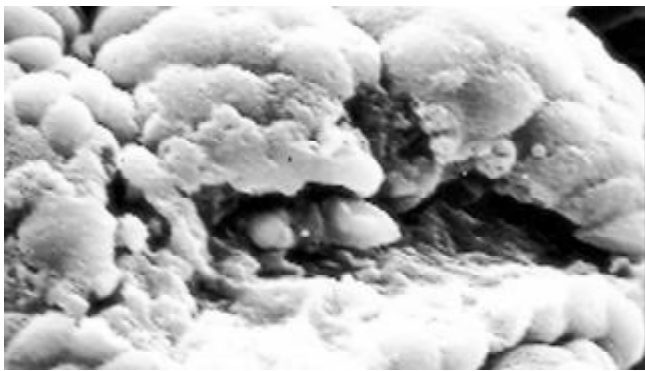


Figure 5 The surface of IM cells is thickly coated, intercellular boundaries are not clear. $\times 1\ 250$.

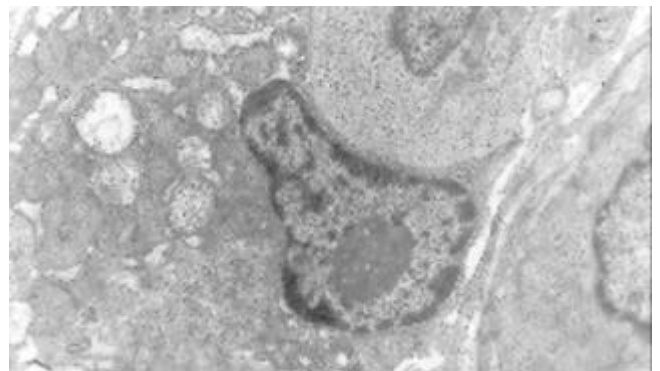


Figure 9 There is an increase in inter chromatinic granules densification, nucleolar granules become thick nucleoli expand with irregular margins. $\times 14\ 000$.

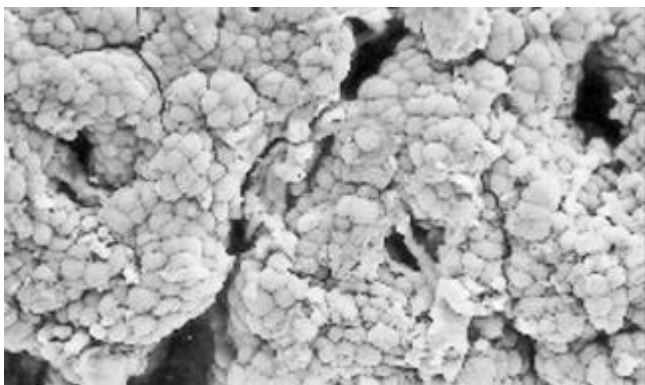


Figure 6 The hyperplastic cells are of different sizes and states, the active membranes are shaped like lesser tubercles. $\times 320$.

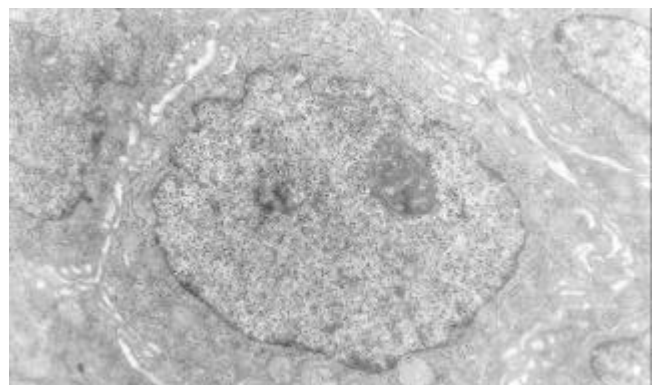


Figure 10 Nucleolar margination. $\times 7\ 200$.

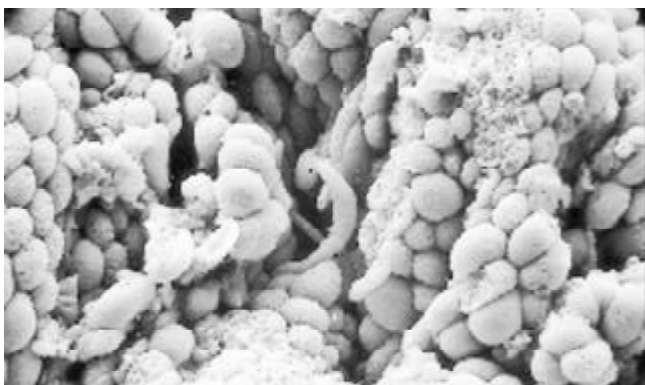


Figure 7 The hyperplastic cells are of different sizes and states, the active membranes are shaped like lesser tubercles. $\times 640$.

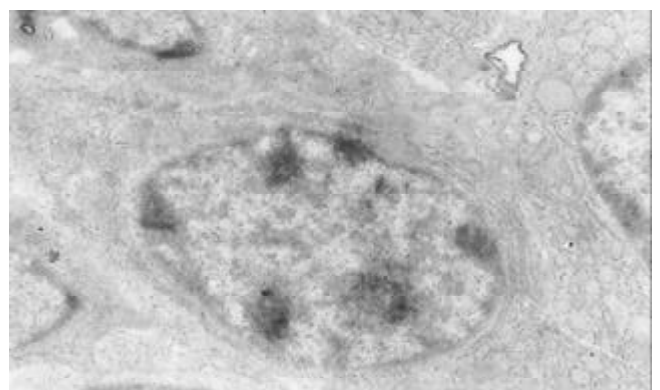


Figure 11 Multi nucleoli. $\times 14\ 000$.

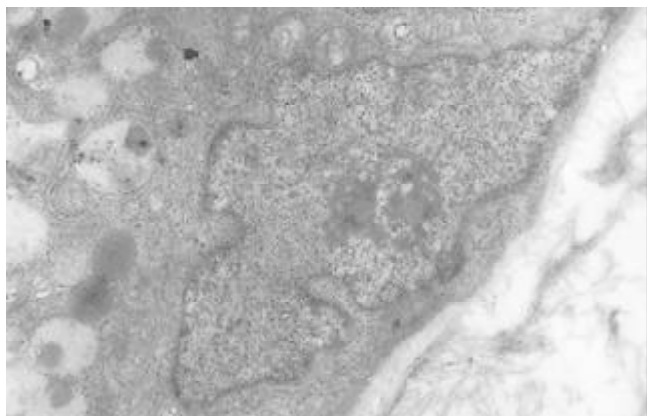


Figure 12 Nucleolar division. $\times 14\ 000$.

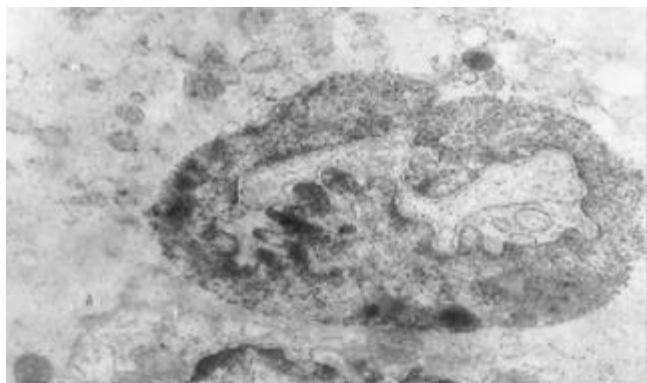


Figure 13 Intranuclear inclusion. $\times 14\ 000$.

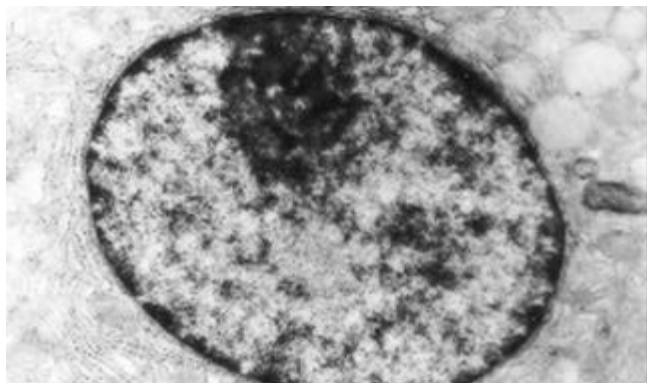


Figure 14 The densification of inter chromatinic grandules. $\times 14\ 000$.

The ultrastructure of gastric mucosa epithelial cells

The mucous cells on epithelial cell surface of relatively normal gastric mucosa were columnar epithelial cells covering endogastric surfaces and inside wall of gastric pit. Their free surfaces had short micro villi; the mucous neck cells were distributed over the necks of gastric glands, and on the tops of these cells were a few short thick micro villi. Chief cells were distributed over the bodies and bottoms of gastric glands; parietal cells were big and conic and their conical tops turned towards gland cavities; the endocrine cells lied between chief cells and parietal cells and they were small, and their nuclei are round or oval, the nuclei envelopes are slightly bent, lobulated nuclei were few, the nucleocytoplasmic ratio was less than 1.

The nuclear chromatins were scattered, or associated with nucleoli or along nuclear perimeters. The light bright zones between heterochromatins in the nucleoli are euchromatins; the nucleoli had high electron density without capsule.

Mitochondria were round or oval, scattering around nuclei. The mitochondria consisted of outer membrane, inner membrane, outer ventricle, inner ventricle and cristae. Crista, the inward folded inner membrane, was a hollow canal leading to outer ventricle. Some mitochondrial cristae directly led to cytoplasm. Cristae were generally in tabular arrangement, parallel to each other and vertical to mitochondrial long axes. In cytoplasm were many parallel rough surfaced endoplasmic reticulus (RERs), secretory granules, well-developed Golgi's bodies and scattered mitochondria. The free surfaces of epithelial cells of CG gastric mucosa had dropped micro villi; the intercellular space expanded and cell conjunctions decreased; the karyoplasmic ratio of both ill-differentiated epithelial cells and IM cells was greater than 1, and lobulated nuclei increased; nucleolar granules became thick and nucleoli expanded with irregular margins (Figure 9).

There occurred nucleolar margination (Figure 10), multinucleoli (Figure 11) and nucleolar division (Figure 12). The obsolescent epithelial nuclei shrank and the karyoplasmic ratio was still less; the heterochromatins lied densely around nuclei; the electron density was low in the center of nuclei and nuclei were loop in shape. (referred to as chromatin margination); the shrunk nuclei were denticular, in which the electron density was moderately homogeneous and chromatins were not found (referred to as chromatin homogenization). There were mitochondrial swelling, hypertrophy, pyknosis, hyaline degeneration as well as vacuolar degeneration. The deformed mitochondrias were in C-shape or U-shape. There were zigzag, longitudinal, sparse and pyknosis cristae, and deranged cristas. There was an decrease in the number of mitochondrias and their cristae. There were mitochondrial decreases in number, mitochondrial swelling, or crista fragmentation, vacuolar degeneration, and RERs in circular arrangement; the Golgi's bodies become atrophic and had lost their typical structures; the cytoplasmic incretory granules decreased. There were still greater epithelial cell changes in cancer cells of gastric cancer than in cells of gastric mucosa of chronic gastritis, intranuclear inclusion appeared (Figure 13). There was an increase in peri-chromatinic and interchromatinic granular densification (Figure 14). In euchromatins; there was a significant difference between CSG group and CAG group in nucleolar margination and nucleolar looping ($P < 0.05-0.001$, Table 2, 3); between IM II_b group, ATP⁺⁺ group, IM⁺⁺+ATP⁺⁺ group and IM⁺⁺⁺+ATP⁺⁺ group, compared with NC group, CSG group and CAG group, the difference was also significant ($P < 0.05-0.001$, Table 2, 3). There is no significant difference between IM⁺⁺⁺+ATP⁺⁺ group, IM II_b group and CA group ($P > 0.05$, Table 2, 3).

The biochemical assay in gastric mucosa and serum

The content of nuclear Zn and Cu increased progressively in the sequence of NC group, CSG group, CAG group and CA group; the content of mitochondrial Zn and Cu decreased progressively in the same sequence. There was significant differences between these groups ($P < 0.05-0.001$, Table 4). The content of Zn, Cu, cAMP and SOD in gastric mucosa decreased progressively in the same sequence; the content of DNA increased progressively in the above sequence. There were significant differences between these groups ($P < 0.05-0.001$, Table 5). The content of ³H-TdRLCT decreased in the sequence of NC group, CSG group, CAG group and CA group; content of serum LPO increased in the same sequence; there was significant difference between these groups ($P < 0.05-0.001$, Table 6). Between IMII_b group, ATP⁺⁺ group, IM⁺⁺+ATP⁺⁺ group and IM⁺⁺⁺+ATP⁺⁺ group, NC group, CSG group and CAG group, there was also significant difference ($P < 0.05-0.001$, Table 4, 5, 6). Between IM⁺⁺⁺+ATP⁺⁺ group, IM II_b group and CA group, There was no significant difference ($P > 0.05$, Table 4, 5, 6).

Table 1 Comparison between classification of IM and grading of ATP in CG and GC gastric mucosa *n* (%)

Groups	<i>n</i>	IM classification				Grading of ATP						
		I _a	I _b	II _a	II _b	ATP ⁺	ATP ⁺⁺	IM ⁺⁺⁺ +ATP ⁺	IM ⁺⁺⁺ +ATP ⁺⁺	IM ⁺⁺⁺ +ATP ⁺	IM ⁺⁺⁺ +ATP ⁺⁺	IM ⁺⁺⁺ +ATP ⁺⁺⁺
NC	15	2(13.3)	1(6.7)									
CSG	68	16(23.5)	8(11.8)	6(8.8)	3(4.4)	8(11.8)	1(1.5)		2(2.9)			
CAG	64	16(25.0) ^b	11(17.2) ^b	13(20.3) ^d	13(20.3) ^d	2(3.1) ^d	6(9.4) ^d	7(10.9)	5(7.8) ^c	1(1.5)	1(1.6)	
CA	36		4(11.1)	9(25.0) ^c	16(44.4) ^{df}	1(2.8) ^d	6(16.7) ^d	3(8.3)	2(5.6) ^c	4(11.1) ^f	7(19.4) ^f	1(2.8)

Either Solitary IM or IM with concomitant ATP in CSG, CAG or CA is included in IM classification statistically, compared with NC group. ^a*P*<0.05, ^b*P*<0.01; compared with CSG group. ^c*P*<0.05, ^d*P*<0.01; compared with CAG group. ^e*P*<0.05, ^f*P*<0.01. In table 2-6, the marks are the same as here.

Table 2 The ultrastructures of epithelial nuclei of gastric mucosa in CG and GC *n* (%)

Group	<i>n</i>	Appearance		Chromatin		Nucleons	
		Nucleoplasmic ratio >1	Nucleus lobulated	Margination or homogeneity	Perinuclear concentrated	Hypertrophy or margination	looping
NC	15			1(6.7)	1(6.7)		
CSG	68	5(5.7)	2(2.9)	7(10.3)	5(7.4)	2(2.9)	2(2.9)
CAG	64	20(1.3) ^d	19(9.7) ^d	33(51.6) ^{bd}	29(45.3) ^{bd}	27(42.2) ^d	14(21.9)
CA	36	36(100.0) ^{bf}	36(100.0) ^{bf}	17(47.2) ^d	26(72.2) ^{bdf}	18(50.0) ^d	17(47.2) ^{df}
IMII _b	8	8(100.0) ^b	5(62.5) ^h	5(62.5) ^b	6(75.0) ^b	4(50.0)	3(37.5)
ATP ⁺⁺	13	8(61.5) ^{hi}	5(38.5) ^{hj}	4(30.8) ^{bgi}	3(23.1) ^{bhj}	5(38.5)	1(7.7) ^{hj}
IM ⁺⁺⁺ +ATP ⁺⁺	9	7(77.8) ^{hhik}	5(55.5) ^{hk}	3(33.3) ^{bgi}	3(33.3) ^{bhj}	4(44.4)	3(33.3) ^l
IM ⁺⁺⁺ +ATP ⁺⁺	8	8(100.0) ⁱⁿ	8(100.0) ^{ikm}	5(62.5) ^{bkm}	6(75.0) ^{blm}	5(62.5) ^{lm}	3(37.5) ^l

Compared with CA group, ^g*P*<0.05, ^h*P*<0.01, Compared with IMII_b group, ⁱ*P*<0.05, ^j*P*<0.01, Compared with ATP⁺⁺ group, ^k*P*<0.05, ^l*P*<0.01. Compared with IM⁺⁺⁺+ATP⁺⁺ group, ^m*P*<0.05, ⁿ*P*<0.01. In table 3-6, the marks are the same as here.

Table 3 Mitochondria ultrastructures of gastric mucosa epithelial cells in CG and GC ($\bar{x}\pm s$)

Group	<i>n</i>	Number	Swelling or Ovegrowth (%)	Matrix fading (%)	Vacuolar degeneration (%)	Pyknosis (%)	Crista number	Fragmentation and derangement of cristas(%)
NC	15	86.5±27.3	3.4±1.6	3.0±1.1	2.9±1.9	1.1±0.8	12.8±3.2	2.2±1.1
CSG	68	65.4±21.1 ^b	7.2±3.8 ^b	7.8±5.0 ^b	6.4±4.5 ^b	1.9±0.9 ^b	8.2±3.2 ^b	5.8±3.1 ^b
CAG	64	52.2±20.8 ^{bd}	10.9±4.5 ^{bd}	11.7±8.6 ^{bd}	11.6±7.7 ^{bd}	3.7±1.1 ^{bd}	6.9±3.5 ^{bc}	8.9±3.7 ^{bd}
CA	36	38.8±31.5 ^{bde}	12.9±4.2 ^{bde}	15.6±5.4 ^{bdf}	14.6±5.8 ^{bde}	3.9±0.6 ^{bd}	8.1±1.9 ^{bde}	10.5±2.7 ^{bde}
IMII _b	8	36.8±30.8 ^b	13.8±3.2 ^b	14.1±4.3 ^b	12.5±3.9 ^b	3.3±0.8 ^{bg}	9.3±2.1 ^b	7.6±1.1 ^{bh}
ATP ⁺⁺	13	49.1±27.9 ^b	11.3±2.9 ^b	8.3±3.5 ^{bh}	9.3±4.7 ^b	1.9±0.5 ^{bhj}	11.3±1.8 ^{hi}	5.2±1.2 ^{bhj}
IM ⁺⁺⁺ +ATP ⁺⁺	9	41.3±30.8 ^b	12.8±2.1 ^b	12.1±2.8 ^{bg}	11.2±3.7 ^b	2.3±0.3 ^{bhjk}	11.0±1.5 ^{ahi}	6.2±1.3 ^{bhi}
IM ⁺⁺⁺ +ATP ⁺⁺	8	35.4±31.5 ^b	13.3±4.3 ^b	15.2±5.3 ^{bi}	12.8±4.3 ^b	3.9±0.5 ^{bbin}	8.4±2.1 ^{bin}	8.6±1.0 ^{bhin}

Table 5 Gastric mucosa Zn, Cu, DNA, cAMP and SOD in CG and GC ($\bar{x}\pm s$)

Group	<i>n</i>	Zn (WT%)	Cu(WT%)	DNA(IOD)	cAMP(pmol/g)	SOD(u/g)
NC	15	4.1±1.0	5.2±0.8	12.6±2.7	15.9±1.5	170.5±6.1
CSG	68	2.8±1.9 ^b	4.0±1.5 ^a	15.2±3.1 ^b	14.6±1.8 ^b	163.3±5.6 ^b
CAG	64	2.0±1.8 ^{bc}	3.4±1.5 ^{bd}	16.5±3.1 ^{bc}	13.4±1.8 ^{bc}	161.2±4.3 ^{bc}
CA	36	1.5±1.2 ^{bde}	2.8±0.9 ^{bde}	30.7±8.2 ^{bdf}	10.2±3.9 ^{bdf}	152.2±3.8 ^{bdf}
IMII _b	8	1.7±0.9 ^b	3.5±0.9 ^b	27.3±10.3 ^b	11.9±1.9 ^b	150.0±2.8 ^b
TP ⁺⁺	13	2.7±1.3 ^{bhi}	4.4±0.9 ^{ahi}	23.5±8.9 ^{bg}	12.4±1.8 ^{bg}	161.5±3.8 ^{aj}
IM ⁺⁺⁺ +ATP ⁺⁺	9	2.3±1.5 ^b	4.1±0.9 ^{bh}	25.1±7.2 ^b	12.0±2.3 ^b	152.2±2.5 ^{bl}
IM ⁺⁺⁺ +ATP ⁺⁺	8	1.5±0.8 ^{bkm}	2.9±0.8 ^{bhin}	28.5±9.1 ^b	10.4±0.8 ^{bil}	147.4±2.6 ^{bhin}

Table 4 Nuclear and mitochondrial Zn, Cu of gastric mucosa in CG and GC ($\bar{x}\pm s$)

Group	n	Nuclear		Mitochondria	
		Zn (AT%)	Cu(AT%)	Zn (AT%)	Cu(AT%)
NC	15	7.6±0.4	58.4±0.3	9.2±0.5	58.3±0.3
CSG	68	8.1±0.5 ^b	58.9±0.5 ^b	8.6±0.5 ^b	57.8±0.3 ^b
CAG	64	8.6±0.4 ^{bd}	59.3±0.5 ^{bd}	8.3±0.4 ^{bd}	57.5±0.3 ^{bd}
CA	36	8.8±0.3 ^{bde}	59.5±0.4 ^{bde}	8.9±0.4 ^{bde}	57.1±0.3 ^{bde}
IMII _b	8	8.6±0.3 ^b	59.5±0.4 ^b	8.6±0.3 ^b	56.9±0.3 ^b
ATP ⁺⁺	13	8.3±0.4 ^{bhi}	59.1±0.4 ^{bhi}	9.1±0.4 ⁱ	57.0±0.3 ^b
IM ⁺⁺ +ATP ⁺⁺	9	8.4±0.5 ^{bg}	59.5±0.4 ^{bk}	8.6±0.4 ^{bi}	56.9±0.3 ^b
IM ⁺⁺⁺ +ATP ⁺⁺	8	8.9±0.5 ^{bl}	59.7±0.4 ^b	8.5±0.3 ^{agl}	56.8±0.2 ^{bh}

Table 6 LPO and ³H-TdRLCT of CG and GC ($\bar{x}\pm s$)

Group	n	LPO(umol/L)	³ H-TdRLCT(Bq/L)
NC	15	2.6±0.6	1079.7±227.4
CSG	68	4.2±0.7 ^b	867.3±240.5 ^b
CAG	64	4.5±0.6 ^{bc}	800.9±221.8 ^{bc}
CA	36	6.8±1.6 ^{bdf}	325.7±186.8 ^{bdf}
IMII _b	8	6.1±0.9 ^b	318.9±145.8 ^b
ATP ⁺⁺	13	5.1±1.2 ^{bhi}	642.9±174.3 ^{bhj}
IM ⁺⁺ +ATP ⁺⁺	9	6.5±1.1 ^b	326.3±160.6 ^{bk}
IM ⁺⁺⁺ +ATP ⁺⁺	8	7.6±0.7 ^{bgilm}	316.1±170.7 ^{bl}

DISCUSSION

Chronic gastritis, CAG in particular, is generally acknowledged as precancerous state. However, not all CAGs are likely to develop into gastric cancer because there is significant difference between chronic gastritis and gastric cancer in the ultrastructure and molecular biology of gastric mucosa. In the grading and classification of IM, grading of ATP of gastric mucosa, incidence rate of epithelial karyoplasmic ratio >1, incidence rate of perichromatinic granular densification and of nucleolar hypertrophy, the number of mitochondria and cristae as well as the incidence rate of mitochondrial degeneration; as well as in the quantitative changes of nuclear DNA, Zn, Cu, cAMP, SOD and serum LPO and ³H-TdRLCT, there were significant differences between NC group, CSG group, CAG group, CA group, IM II_b group, ATP⁺⁺ group, IM⁺⁺+ATP⁺⁺ group and IM⁺⁺⁺+ATP⁺⁺ group ($P<0.05-0.0001$); There was no significant difference between IM⁺⁺⁺+ATP⁺⁺ group, IM II_b group and CA group ($P>0.05$). There are similar epithelial ultrastructures and molecular biochemical changes in ATP⁺⁺, IM II_b and CA. Consequently they should have similar law of occurrence, development and transformation, which might contribute to the exploration of prevention and treatment of the disease.

Clinically, only a few chronic gastritis patients' gastric mucosa epithelial cells are likely to develop into cancer cells, but it is essential that there should be a process which causes genetic variation of cells, the key of which is the quantitative changes of epithelial nuclear DNA. The DNA molecular is coded with nucleotide sequence fragments of special genetic codes, every fragment is a functional group, referred to as gene. The gene order has great stability. Only when intracellular cAMP declines, cytodifferentiation is disturbed. The metabolism of Zn, Cu in the body is disturbed, which in turn disturbs the enzyme system and inhibits the synthesis and activity of SOD; because of the NADPH oxidation reduction circulation and the catalytic function of xanthine oxidase, a great deal of oxygen free radicals are produced far beyond the

cleaning ability of SOD. The excessive accumulated oxygen free radicals react in lipid peroxidation with unsaturated fatty acid of inner and outer membranes of mitochondria, producing LPO. Thus level of serum LPO rises. The inner and outer membranes of mitochondria are destructed, causing decrease and derangement of mitochondrial cristae, mitochondrial degeneration decrease of adenosine triphosphate production, and inadequate energy supply of gastric mucosa epithelial cells. When nuclei take up more Zn and Cu, the protein synthesis is enhanced nuclear division and hyperplasia are accelerated; through influencing lymphocyte metabolism, the quantitative changes of Zn and cAMP in turn inhibit lymphocyte transformation and result in the decline of ³H-TdRLCT level and immunity of the organism. The above changes of intraorganism environment, only if stimulated by certain external causes such as ionizing radiation, chemical injuries, infection S-shape HP and virus, are likely to cause the change of sequences in gene group, which is referred to as gene mutation; and genetic codes change accordingly, the changed codes are transferred to heterogenous cell descendants, causing cellular differentiation disturbance and even cancerous change. Human body is an integrity organism, in which the components of tissue and cell, and the bioactive substances including trace elements, enzymes, hormones, immunity and messenger substances exist with a definite content and a definite quantitative ratio. It's important to measure the "absolute" content of each bioactive substance, but it's more important to measure quantitative ratio of each bioactive substance because it can explain the trends and laws of variation of the whole body and inner circumstance^[9,10]. These ratios in normal body keep in a state of dynamic balance within a definite range. If this balance is broken, pathological phenomena and functional disturbance will arise. The ratio fluctuation of bioactive substances higher or lower than normal value, can lead to a series of ratio variation, and then cause both a definite disease diagnosed by modern medicine and clinical expression of Chinese medical syndrome (a synthesis of symptoms without peculiarity). The composite nature of Chinese medicine treats disease through adjusting the above mentioned pathological ratio is one of it's therapeutic mechanisms. This is why Chinese medicines have multilevel, multitarget, two-way adjusting effects on human body, and how the medicines regulate pathological ratio. It's a slow process for Chinese medicines to regulate pathological ratio, so It's therapeutic effect is slow too. Measuring the "quantitative ratio" of a series of bioactive substances not only will be the research direction of medical science and biological science, but also the research kernel of the basic theory of traditional Chinese medicine^[11-13].

REFERENCES

- 1 Yin GY, Zhang WN, He XF, Chen Y, Shen XJ. Detection of ultrastructural changes and contents DNA, Zn, Cu and LPO in subgroups of chronic gastritis. *Shijie Huaren Xiaohua Zazhi* 2002; **10**: 663-667
- 2 Yin GY, Zhang WN, Shen XJ, Chen Y, He XF. Ultrastructural and molecular biological changes of chronic gastritis and gastric cancer: a comparative study. *Shijie Huaren Xiaohua Zazhi* 2002; **10**: 668-672
- 3 Yin GY, Zhang WN, He XF, Chen Y, Shen XJ. Alterations of ultrastructures, trace elements, cAMP and cytoimmunity in subgroups of chronic gastritis. *Shijie Huaren Xiaohua Zazhi* 2002; **10**: 673-676
- 4 Yin GY, Zhang WN, He XF, Chen Y, Yin YF, Shen XJ. Histocytological study on gastric mucosa of spleen deficiency syndromes. *Zhongguo Zhongxiyi Jiehe Zazhi* 1999; **19**: 660-663
- 5 Yin GY, Xu FC, Zhang WN, Li GC, He XF, Chen Y, Shen XJ. The effect of weikangfu on cytopathology of gastric mucosa tissue

- when treating gastric precancerosis lesion of patients with spleen deficiency syndromes. *Zhongguo Zhongxiyi Jiehe Zazhi* 2000; **6**: 241-243
- 6 **Yin GY**, Zhang WN, Xu FC, He XF, Chen Y, Shen XJ. Effect of Weikangfu chongji on ultrastructure of precancerosis gastric mucosa of patients with spleen deficiency Syndromes. *Zhongguo Zhongxiyi Jiehe Zazhi* 2000; **20**: 667-670
- 7 **Yin GY**, Zhang WN, Xu FC, Chen Y, He XF, Li GC, Shen XJ. Study on the modern pathophysiologic basis of the syndrome classification of spleen deficiency with chronic gastritis and of (treatment) verification of clinical syndromes and prescriptions. *Jiangsu Yiyao Zazhi* 2001; **27**: 46-47
- 8 **Yin GY**, He XF, Yin YF, Du YQ, Jiao JH. Study on mitochondrial ultrastructure, trace elements and correlative factors of gastric mucosa in patients with spleen deficiency syndrome. *Zhongguo Zhongxiyi Jiehe Zazhi* 1996; **15**: 719-723
- 9 **Yin GY**, Zhang WN, Xu FC, He XF, Chen Y, Shen XJ. Effect of weikangfu chongji on epithelial cellular ultrastructure of precancerotic gastric mucosa of patients with spleen deficiency syndrome. *Jiangsu Yiyao Zazhi* 2000; **26**: 514-517
- 10 **Yin GY**, Zhang WN, Xu FC, He XF, Chen Y, Li GC, Shen XJ. Effect of weikangfu on Zn, Cu and DNA in precancerosis gastric mucosa epithelial nuclei and mitochondria of patients with spleen deficiency syndromes. *Zhongguo Zhongxiyi Jiehe Zazhi* 2000; **8**: 221-224
- 11 **Yin GY**, Zhang WN, Shen XJ, Chen Y, He XF. A comparative study on ultrastructure of chronic gastritis gastric mucosa IM, ATP and their molecular biology. *Jiangsu Yiyao Zazhi* 2002; **28**: 4-7
- 12 **Yin GY**, He XF, Zhang WN, Chen Y. Relationship between the classification of spleen deficiency and the quantitative changes of bio-active substances in mitochondria of gastric mucosa epithelial cell nuclei. *Zhongguo Zhongxiyi Jiehe Zazhi* 1999; **7**: 145-148
- 13 **Yin GY**, Zhang WN, Li GC, Huang JR, Chen Y, He XF, Shen XJ. Therapeutic effect of weikangfu on gastric precancerosis disordddeer with spleen deficiency syndrome and its effect of gastric mucosal zinc, copper, cyclic adenosine monophosphate, superoxide dismutase, lipid peroxide and ³H-TdR lymphocyte conversion test. *Zhongguo Zhongxiyi Jiehe Zazhi* 2000; **20**: 176-179

Edited by Xu JY

Neuroendocrine markers in adenocarcinomas: an investigation of 356 cases

Gen-You Yao, Ji-Lin Zhou, Mao-De Lai, Xiao-Qing Chen, Pei-Hui Chen

Gen-You Yao, Ji-Lin Zhou, Mao-De Lai, Xiao-Qing Chen, Pei-Hui Chen, Department of Pathology, Zhejiang University Medical School, Hangzhou 310031, China

Supported by Foundation of Health Bureau of Zhejiang Province

Correspondence to: Gen-You Yao, Research fellow of Pathology, Department of Pathology, Zhejiang University Medical School, Hangzhou, 310031 China. yaogy@zjuem.zju.edu.cn

Telephone: +86-0571-87217167

Received: 2002-10-25 **Accepted:** 2002-11-18

Abstract

AIM: To investigate the incidence of neuroendocrine (NE) cells and their hormone products in adenocarcinomas and evaluate their significance in clinical pathology and prognosis.

METHODS: By using tissue sectioning and immunocytochemistry, 356 cases of adenocarcinomas were studied to examine the presence of chromogranin and polypeptide hormones in adenocarcinoma samples from our hospital.

RESULTS: The positive rate of NE cells and hormone products was 41.5 % (54/130) and 59.3 % (32/54), respectively in large intestinal adenocarcinoma cases; 39.6 % (38/96) and 36.8 % (14/38), respectively in gastric cancer cases; 38.1 % (8/21) and 50.0 % (4/8), respectively in prostatic cancer cases; 21.0 % (17/81) and 17.6 % (3/17), respectively in breast cancer cases; 17.9 % (5/28) and 60.0 % (3/5), respectively in pancreatic cancer cases. Among carcinomas of large intestine, pancreas and breast, the highly differentiated NE cell numbers were higher than the poorly differentiated NE cell numbers; while the gastric carcinoma cases had more poorly differentiated NE cells than highly differentiated NE cells. The higher detection rate of NE cells and their hormone products, the higher 5-year survival rate among the large intestine cancer cases.

CONCLUSION: Close correlation was observed between NE cells and their hormone products with the cancer differentiations. For colorectal carcinomas, there is a close correlation of the presence of NE cells and their hormone products with the tumor staging and prognosis.

Yao GY, Zhou JL, Lai MD, Chen XQ, Chen PH. Neuroendocrine markers in adenocarcinomas: an investigation of 356 cases. *World J Gastroenterol* 2003; 9(4): 858-861
<http://www.wjgnet.com/1007-9327/9/858.htm>

INTRODUCTION

Compared with neuroendocrine cancers, little investigation is carried out on the relationship of neuroendocrine cells and their hormone products in non- neuroendocrine cancers, especially in the common adenocarcinoma cases. By using nine different antibodies and immunocytochemistry, NE cells and their hormone products in 356 adenocarcinomas was observed with the aim of revealing the incidence and distribution of NE cells

and the correlation between the cancer differentiation with the biological behaviors was evaluated.

MATERIALS AND METHODS

Materials

All the 365 adenocarcinoma samples were got from the first affiliated hospital of Zhejiang University Medical College from 1975 to 1994. There were 96 cases of gastric cancer samples (31 samples were got from the clinical biopsy; 65 samples were got from radical operation and 22 samples had lymph nodes metastasis); there were 130 cases of large intestine cancer samples got from radical operations (110 cases had the follow-up data); there were 81 and 28 cases of breast and pancreatic cancer, respectively. The remaining 21 samples were got from prostatic cancer biopsy.

Methods

All the samples were fixed with 10 % formaldehyde with paraffin embedding and continuous sectioning at 4 μ m in thickness. Gross pathological observation was made on the HE stain slides followed by immunocytochemistry. All the samples were treated with anti-chromogranin serum for the primary screening positive cases. Further immunocytochemistry was carried out for those positive NE samples by using peptide hormone antibodies such as ST (diluted at 1:10 000, provided by the 4th Military Medical Academy) and other Dako's antibodies (somatostatin diluted at 1:300; glucagon diluted at 1:800; pancreatic polypeptide diluted at 1:800; gastrin diluted at 1:350; insulin diluted at 1:150; ACTH diluted at 1:800 and calcitonin diluted at 1:150). The immunostains were done by ABC method and coloured with AEC. The antiserum of serotonin and gastrin was used in the gastric mucosa; the pancreas tissue was used to detect the chromogranin, somatostatin, glucagon, insulin and pancreatic polypeptide; calcitonin antiserum was used in the medullary carcinoma of the thyroid gland while ACTH in the pituitary was used as the positive control. The negative control was carried out by using normal sheep serum to replace the 1st antibody. Based on the chromogranin positive NE cell numbers, all the samples were divided into three grades as the following. Negative: there was no NE cells; Positive(+): the number of NE cells was fewer than 5/mm²; Super positive(++): the number of NE cells was over 5/mm².

Statistical analysis

The data were analysed by χ^2 test.

RESULTS

Morphology of NE cells and their incidence

Among the five common adenocarcinomas from different tissue sources, the incidence rate was 41.5 % (54/130) for the large intestinal carcinomas; 39.6 % (38/96) for the gastric carcinoma; 38.1 % (8/21) for the prostatic carcinoma; 21.0 % (17/81) for the breast cancer and 17.9 % (5/28) for the pancreatic cancers, respectively. The highest incidence was

seen in large intestinal carcinomas while the lowest in the pancreatic carcinomas. When observing the chromogranin stained slides, clear edges of NE cells and brownish granules could be seen in the cytoplasm under the microscopy. In the low differentiated carcinomas, the NE cells presented as an oval, round or irregular shape without polarizations. Abnormal structural characteristics were observed among these low differentiated NE cells, which was similar to the adjacent tumor cells; while for those highly differentiated carcinomas, the NE cells were pyramid or bar shaped with the apex pointing to the cavity of the gland. A few NE cell processes could be observed reaching the gland cavity surfaces. The distribution of NE cells were scattered or localized infiltrating all the layers with the cancer cells. NE cells could be seen in both of the primary carcinoma and the metastasis sites.

Relationship between NE cells and carcinoma differentiation

No exact correlation between NE cells and carcinoma differentiation was observed among different carcinomas. The highly differentiated NE cell incidences were 41.7 % (5/12) for the large intestinal carcinomas, 42.9 % (3/7) for the pancreas carcinomas and 32.5 % (14/43) for the breast cancers, which was much higher than that of the low differentiated carcinomas. Prostatic carcinomas had the same tendency but there was no statistical significance due to fewer case numbers. In the low differentiated gastric carcinomas, 50 % (27/54) had the positive NE cells, which was significantly higher than that of the highly differentiated carcinomas.

Distribution of hormone products of NE cells in tumors

From Table 1, the number of hormone products types was more in large intestinal and gastric carcinomas (5 types of hormone products); hormone products detected in breast cancers were the fewest (only three in 17 cases). Most of them were the tumor origin tissue hormones, but few of them were ecotopic hormones.

Relationship between positive cell of hormone products and tumor differentiation

In the large intestinal carcinomas, 9 cases were low differentiated carcinomas whose positive cell percentage of hormone products against the total NE cells was 27.0 %, which was obviously lower than that in high differentiated carcinomas (15 cases with the percentage of 43.9 %) ($\chi^2=115.9$, $P<0.01$); It was also the same in the highly differentiated large intestinal carcinomas whose percentage was lower than that in the normal mucus membrane (10 cases with the percentage of 83.1 %) ($\chi^2=212.3$, $P<0.01$) and the mucus membranes adjacent to the tumors (25 cases with the percentage of 88.7 %) ($\chi^2=168.8$, $P<0.01$). The gastric carcinoma had the similar results: the positive cell percentage of hormone products against the total

NE cells was 17.5 %. But in the positive cells of hormone products from 5 gastric sinus mucus membranes, the positive cell percentage of hormone products against the total NE cells was 78.6 % ($\chi^2=1611.8$, $P<0.01$); the samples adjacent to the gastric sinus areas had the obviously higher percentage (46.6 %, $\chi^2=266.4$, $P<0.01$). Significant difference was also observed between the percentage of the adjacent mucus membrane tissues of the tumors and the normal mucus membranes ($\chi^2=242.0$, $P<0.01$).

Ecotopic hormones and tumor differentiation

Except for the pancreatic carcinomas, ecotopic hormones were revealed in other four types of the adenocarcinomas. One of the large intestinal carcinomas cases showed gastrin positive; Six gastric carcinoma cases showed ACTH positive; Two prostatic cancer cases were glucagons positive; One breast cancer case was somatostatin positive while another breast cancer case was calcitonin positive. Except for the large intestinal and gastric carcinomas, all the other nine cases were low differentiated carcinomas among the ecotopic hormone carcinomas.

NE cells and tumor differentiation

Observed in large intestinal carcinomas, Dukes A stage accounted for 41.7 % of the NE cell (++) cases (12 cases), which was much higher than that in NE(-) group (19.7 %, 76 cases). ($\chi^2=4.668$, $P<0.05$). Among the 110 cases with following-up, the 5-year survival rate was 81.8 % in NE cell (++) group, which was obviously higher than that in the NE (+) group (45.7 %, 35 cases) ($\chi^2=4.000$, $P<0.05$) and in NE cell (-) group (42.2 %, 64 cases) ($\chi^2=4.397$, $P<0.05$).

Among the 32 hormone products positive cases with polypeptide hormones (PH), Dukes A stage cases accounted for 44.1 %, which was higher than that of NE cell positive cases with hormone products negative (36.1 %), yet no statistical difference was found between the two groups ($\chi^2=0.351$, $P>0.05$). In hormone products (+) group (17 cases), the 5-year survival rate was 70.6 %, which was higher than that of hormone products (-) group (37.9 %, 29 cases) ($\chi^2=4.148$, $P<0.05$).

DISCUSSION

The commonly used staining methods for revealing NE cells include silver staining, neuron-specific enolase (NSE), synaptophysin (SY) and chromogranin (CG) immunocytochemistry. Silver staining is the traditional staining method with less specificity and sensitivity. Although NSE, CG and SY are all the common markers, NSE has poor specificity with distributions in different tissues but is localized in the cytoplasm. CG is distributed in neuroendocrine granules. Both CG and SY are good markers and corresponding to

Table 1 Distribution of hormone productions of NE cells in tumors

Type	NE Positive Case	Serotonin Case (%)	Somatostatin Case (%)	Glucagon Case (%)	P P Case (%)	Gastrin Case (%)	Calcitonin Case (%)	ACTH Case (%)
Colorectal carcinomas	54	30(55.6)	14(25.9)	11(20.4)	5(9.3)	1(1.9)	0	0
Gastric carcinomas	38	5(13.2)	5(13.2)	5(13.2)	0	3(7.9)	0	6(15.8)
Pancreatic Carcinomas	5	1(20.0)	0	1(20.0)	2(40.0)	0	0	0
Breast Carcinomas	17	1(5.9)	1(5.9)	0	0	0	1(5.9)	0
Prostatic Carcinomas	8	4(50.0)	0	2(25.0)	0	0	0	0

respective subcellular structures. CG is a specific matrix component of endocrine granules^[1-3]. While SY is localized within small capsule membranes related to the secretion granules, whose specificity and sensitivity are less than those of CG. That's why CG is considered as a realistic marker for NE cells^[4-8]. Studies have confirmed that CG could be served as a new way of revealing NE cells and for the diagnosis of NE tumors^[9].

Our study demonstrated that NE cell numbers were closely correlated to the tumor differentiation in large intestinal, pancreatic, breast and prostatic carcinomas^[10]. The higher differentiated tumors had the higher incidence of the NE cells^[8]. That was contradicted to our gastric carcinoma observations, but corresponding to the publication reports^[11]. Further studies are needed to be conducted to reveal these differences to see if they are related to the embryology, etiology and tissue development of the tumors.

No serial report were seen about the hormone products of NE cells from the common adenocarcinomas. We observed 5 types of adenocarcinomas and found out that large intestinal and gastric carcinomas had the higher hormone products in their NE cells; but in the gastric and highly differentiated carcinomas, they had lower hormone products in NE cell than those of poor differentiated carcinomas. The hormone products were more in the large intestinal and gastric carcinomas than those in normal mucus membranes and tissues adjacent to the carcinomas. Neoplastic NE cells had lower hormone products and they were decreased with anaplasia which may be due to the fact that these cells were in immature state with lower hormone synthesis. Thus, the amount of hormone products in NE cells of the carcinomas can serve as an index for the determination of tumor differentiation and the diagnosis of benign and malignant tumors^[12-15].

Based on the study of the large intestinal carcinomas, we found that hormone products and distribution of NE cells were closely correlated to the tumor grade, clinical pathological stage of the tumor and prognosis of the patients^[16-23]. Carcinomas with NE (++) releasing PH were the early stage carcinomas. The higher 5-year survival rate may be due to the somatostatin's inhibition of the tumors^[24-29]. Zollinger-Ellison syndrome was reported in some gastric carcinoid cases^[30-32], but our study only revealed there were only different hormone products but without sign and symptoms of Zollinger-Ellison syndrome as well as other hormone signs and symptoms, which may be the fact that the hormone products produced by NE cells were not enough in the inactivated form or inactivated by the liver enzymes. Further study is required to examine whether these hormone products participate in the immune regulations of the tumor or the hormone products exert the direct effects on the tumor development and growth.

REFERENCES

- 1 **Papotti M**, Macri L, Finzi G, Capella C, Eusebi V, Bussolati G. Neuroendocrine differentiation in carcinomas of the breast: a study of 51 cases. *Semin Diagn Pathol* 1989; **6**: 174-188
- 2 **Van Laarhoven HA**, Gratama S, Wereldsma JC. Neuroendocrine carcinoid tumours of the breast: a variant of carcinoma with neuroendocrine differentiation. *J Surg Oncol* 1991; **46**: 125-132
- 3 **Giovanella L**, Marelli M, Ceriani L, Giardina G, Garancini S, Colombo L. Evaluation of chromogranin A expression in serum and tissues of breast cancer patients. *Int J Biol Markers* 2001; **16**: 268-272
- 4 **Kimura N**, Sasano N, Yamada R, Satoh J. Immunohistochemical study of chromogranin in 100 cases of pheochromocytoma, carotid body tumour, medullary thyroid carcinoma and carcinoid tumour. *Virchows Arch A Pathol Anat Histopathol* 1988; **413**: 33-38
- 5 **Kimura N**, Hoshi S, Takahashi M, Takeha S, Shizawa S, Nagura H. Plasma chromogranin A in prostatic carcinoma and neuroendocrine tumors. *J Urol* 1997; **157**: 565-568
- 6 **Portel-Gomes GM**, Grimelius L, Johansson H, Wilander E, Stridsberg M. Chromogranin A in human neuroendocrine tumors: an immunohistochemical study with region-specific antibodies. *Am J Surg Pathol* 2001; **25**: 1261-1267
- 7 **Bernini GP**, Moretti A, Ferdeghini M, Ricci S, Letizia C, D' Erasmio E, Argenio GF, Salvetti A. A new human chromogranin 'A' immunoradiometric assay for the diagnosis of neuroendocrine tumours. *Br J Cancer* 2001; **84**: 636-642
- 8 **Yao GY**, Chen PH, Lai MD, Hong LY. Study of 9 neuroendocrine markers in pancreatic tumors. *Zhenjiang Yike Daxue Xuebao* 1995; **24**: 56-58
- 9 **Chen FX**, Corti A, Siccardi AG. DIBIT; San Raffaele H. Characterization of antigenic sites of Human Chromogranin A. *Shanghai Mian Yixue Zazhi* 1998; **18**: 215-219
- 10 **di Sant' Agnese PA**. Neuroendocrine differentiation in prostatic carcinoma: an update. *Prostate Suppl* 1998; **8**: 74-79
- 11 **Chen BF**, Yin H. Neuro-endocrine type of gastric carcinoma. Immunohistochemical and electron microscopic studies of 100 cases. *Chin Med J* 1990; **103**: 561-564
- 12 **Yu JY**, Wang LP, Meng YH, Hu M, Wang JL, Bordi C. Classification of gastric neuroendocrine tumors and its clinicopathologic significance. *World J Gastroenterol* 1998; **4**: 158-161
- 13 **Chabot V**, de Keyzer Y, Gebhard S, Uske A, Bischof-Delaloye A, Rey F, Dusmet M, Gomez F. Ectopic ACTH Cushing's syndrome: V3 vasopressin receptor but not CRH receptor gene Expression in a pulmonary carcinoid tumor. *Horm Res* 1998; **50**: 226-231
- 14 **Mao C**, el Attar A, Domenico DR, Kim K, Howard JM. Carcinoid tumors of the pancreas. Status report based on two cases and review of the world's literature. *Int J Pancreatol* 1998; **23**: 153-164
- 15 **Duchesne G**, Cassoni A, Pera M. Radiosensitivity related to neuroendocrine and endodermmal differentiation in lung carcinoma lines. *Radiother Oncol* 1988; **13**: 153-161
- 16 **Tezel E**, Nagasaka T, Nomoto S, Sugimoto H, Nakao A. Neuroendocrine-like differentiation in patients with pancreatic carcinoma. *Cancer* 2000; **89**: 2230-2236
- 17 **Yao G**, Zhou J, Zhao Z. Studies on the DNA content of breast carcinoma cells with neuroendocrine differentiation. *Chin Med J* 2002; **115**: 296-298
- 18 **Maluf HM**, Zukerberg LR, Dickersin GR, Koerner FC. Spindle-cell argyrophilic mucin-producing carcinoma of the breast. Histological, ultrastructural, and immunohistochemical studies of two cases. *Am J Surg Pathol* 1991; **15**: 677-686
- 19 **Scopsi L**, Andreola S, Pilotti S, Testori A, Baldini MT, Leoni F, Lombardi L, Hutton JC, Shimizu F, Rosa P. Argyrophilia and granin (chromogranin/secretogranin) expression in Female breast carcinomas. Their relationship to survival and other disease parameters. *Am J Surg Pathol* 1992; **16**: 561-576
- 20 **Grabowski P**, Schindler I, Anagnostopoulos I, Foss HD, Riecken EO, Mansmann U, Stein H, Berger G, Buhr HJ, Scherubl H. Neuroendocrine differentiation is a relevant prognostic factor in stage III-IV colorectal cancer. *Eur J Gastroenterol Hepatol* 2001; **13**: 405-411
- 21 **Sapino A**, Papotti M, Righi L, Cassoni P, Chiusa L, Bussolati G. Clinical significance of neuroendocrine carcinoma of the breast. *Ann Oncol* 2001; **12**(Suppl 2): S115-117
- 22 **Matsui T**, Kataoka M, Sugita Y, Itoh T, Ichihara T, Horisawa M, Koide A, Ichihara S, Nakao A. A case of small cell carcinoma of the stomach. *Hepatogastroenterology* 1997; **44**: 156-160
- 23 **Yang GC**, Rotterdam H. Mixed (composite) glandular-endocrine cell carcinoma of the stomach. Report of a case and review of literature. *Am J Surg Pathol* 1991; **15**: 592-598
- 24 **Upp JR Jr**, Olson D, Poston GJ, Alexander RW, Townsend CM Jr, Thompson JC. Inhibition of growth of two human pancreatic adenocarcinomas in vivo by somatostatin analog SMS 201-995. *Am J Surg* 1988; **155**: 29-35
- 25 **Anderson JV**, Bloom SR. Neuroendocrine tumours of the gut: long-term therapy with the somatostatin analogue SMS 201-995. *Scand J Gastroenterol Suppl* 1986; **119**: 115-128
- 26 **Oda Y**, Tanaka Y, Naruse T, Sasanabe R, Tsubamoto M, Funahashi H. Expression of somatostatin receptor and effects of somatostatin analog on pancreatic endocrine tumors. *Surg Today* 2002; **32**: 690-694
- 27 **O' Byrne KJ**, Carney DN. Somatostatin and the lung. *Lung Can-*

- cer* 1993; **10**: 151-172
- 28 **Taylor JE**, Moreau JP, Baptiste L, Moody TW. Octapeptide analogues of somatostatin inhibit the clonal growth and vasoactive intestinal peptide-stimulated cyclic AMP formation in human small cell lung cancer cells. *Peptides* 1991; **12**: 839-843
- 29 **Taylor JE**, Bogden AE, Moreau JP, Coy DH. *In vitro* and *in vivo* inhibition of human small cell lung carcinoma (NCI-H69) growth by a somatostatin analogue. *Biochem Biophys Res Commun* 1988; **153**: 81-86
- 30 **Diaz-Sanchez CL**, Molano Romero RA, Martinez Gonzalez M, Marquez Rivera ML, Halabe-Cherem J. Gastric neuroendocrine tumor. *Rev Gastroenterol Mex* 1998; **63**: 97-100
- 31 **Tomassetti P**, Migliori M, Lalli S, Campana D, Tomassetti V, Corinaldesi R. Epidemiology, clinical features and diagnosis of gastroenteropancreatic endocrine tumours. *Ann Oncol* 2001; **12** (Suppl 2): S95-99
- 32 **Eriksson B**, Oberg K, Stridsberg M. Tumor markers in neuroendocrine tumors. *Digestion* 2000; **62**: 33-38

Edited by Xu XQ

Primary jejunoileal neoplasmas: a review of 60 cases

Yun-Sheng Yang, Qi-Yang Huang, Wei-Feng Wang, Gang Sun, Li-Hua Peng

Yun-Sheng Yang, Qi-Yang Huang, Wei-Feng Wang, Gang Sun, Li-Hua Peng, Department of Gastroenterology, China PLA General Hospital, Beijing 100853, China

Correspondence to: Yun-Sheng Yang M.D.&Ph.D, Department of Gastroenterology, China PLA General Hospital, Beijing 100853, China. yangys@163bj.com

Telephone: +86-10-66939747 **Fax:** +86-10-68154357

Received: 2002-07-12 **Accepted:** 2002-08-13

Abstract

AIM: Primary neoplasmas of the jejunum and ileum are infrequent and lack specific manifestations and inaccessibility of conventional endoscopy, so the diagnosis of these tumors are usually delayed. So far the data of primary jejunoileal neoplasmas is still scarce, especially in Chinese medical literature in English. There may be some differences among the Chinese and the westerners in jejunoileal neoplasmas.

METHODS: A retrospective analysis was made on clinical findings and pathological types.

RESULTS: Of the 60 patients with jejunal or ileal neoplasmas, the most frequent symptom was abdominal pain (57 %), followed by tarry stool (43 %) and hematochezia (10 %). Abdominal mass (40 %) was the most common finding on physical examination, followed by anemia and weight loss (35 %). 67 % of the jejunoileal neoplasms were located in the jejunum. Among the malignant neoplasmas (68 %), malignant stroma (47 %) was most common, while the benign stromoma (20 %) was the most common benign neoplasmas. Preoperatively, 40 patients (67 %) were diagnosed as small bowel neoplasmas, of which 34 were found by enteroclysis. Abdominal mass was shown by CT in 18 cases and by ultrasonography in 13. The mean duration of symptoms before diagnosis was 7 months. In 41 patients with malignant tumors, the duration of symptoms before diagnosis exceeded 12 months in 21 cases, lymphatic or distant metastases were found in 26 (63 %)cases during operation. An emergency laparotomy was performed in 4 patients (7 %) owing to intestinal obstruction or perforation.

CONCLUSION: Primary jejunoileal neoplasmas in Chinese present some difference from Westerners on clinical features and histopathologic types. Enteroclysis remains the major relevant diagnostic procedure in this study, the misdiagnostic rate is high preoperatively due to failure of detection by conventional imaging procedures such as CT and inaccessibility of routine endoscopy. For the suspected patients, combined application of aforementioned procedures may facilitate early diagnosis. The wireless capsule endoscopy may improve the diagnostic rate of jejunoileal neoplasmas in the future.

Yang YS, Huang QY, Wang WF, Sun G, Peng LH. Primary jejunoileal neoplasmas: a review of 60 cases. *World J Gastroenterol* 2003; 9(4): 862-864
<http://www.wjgnet.com/1007-9327/9/862.htm>

INTRODUCTION

Primary neoplasmas of jejunum and ileum, benign or malignant, are infrequent. Clinical manifestations of jejunoileal neoplasmas are nonspecific and the neoplasma-related symptoms occur late, moreover, such neoplasms are beyond the scope of conventional gastroscopy or colonoscopy. The rarity, nonspecific and inaccessibility make them liable to be overlooked, with delayed or erroneous diagnosis^[1], and are responsible for high mortality rates. So far the data on small bowel cancers are scarce^[2]. To our knowledge, there may be some differences between the Chinese and the Westerner in jejunoileal neoplasmas. Herein we reported a series of consecutive cases of primary jejunal and ileal neoplasmas in our hospital over the past 8 years, and analyzed their clinical manifestations, pathologic types and diagnostic process.

MATERIALS AND METHODS

Cases of primary jejunal and ileal neoplasmas from January 1993 to August 2001 were retrieved through the inpatient computer registry system of PLA General Hospital, Beijing. The medical records were reviewed by the authors. Cases of duodenal and metastatic small bowel tumors were excluded. A total of 60 cases of primary jejunal and ileal neoplasmas were collected. All cases underwent surgery and were confirmed by histopathology.

RESULTS

Demographic features

There were 42 males (70 %) and 18 females (30 %) with an average age of 48 years (16-77 years). The majority (51 %) of patients were over 50 years of age.

Clinical manifestations

Symptoms, signs and complications were listed in the following Table 1. Abdominal pain and tarry stool were the most common symptoms in both benign and malignant jejunoileal tumors. Abdominal mass and anemia were common findings on physical examination in both benign and malignant neoplasmas, while the weight loss was frequent in malignant ones. Complications at presentation such as intestinal obstruction and perforation were more common in malignant tumors.

Table 1 Clinical manifestations of 60 cases of jejunoileal tumors

	Benign (n)	Malignant (n)	Total
Symptoms			
Abdominal pain	8	26	34 (57%)
Tarry stool	9	17	26 (43%)
Hematochezia	2	4	6 (10%)
Signs			
Abdominal mass	9	15	24 (40%)
Anemia	6	15	21 (35%)
Weight loss	1	20	21 (35%)
Complications			
Intestinal obstruction	2	5	7 (12%)
Intestinal perforation	0	1	1

Histopathology and sites of distribution

Histopathology and sites of distribution of jejunoileal neoplasmas were summarized in Table 2. Of the 60 cases, 40 (67 %) were located in the jejunum, and 20 (33 %) in the ileum. Malignant tumors ($n=41$, 68 %) was nearly twice that of the benign ones ($n=19$, 32 %). Benign and malignant stromoma were predominant histological entities.

Table 2 Histopathology and distribution sites of 60 cases of jejunal and ileal tumors

Tumor types	Jejunum	Ileum	Total
Benign	14 (23.3%)	5 (8.3%)	19 (\approx 32%)
Stromoma	8	4	12 (20%)
Adenoma	2	0	2 (3.3%)
Angioleiomyoma	2	0	2 (3.3%)
Lipoma	0	1	1 (1.7%)
Lymphangioma	1	0	1 (1.7%)
Neurofibroma	1	0	1 (1.7%)
Malignant	26 (43%)	15 (25%)	41 (\approx 68%)
Malignant stromoma	17	11	28 (46.7%)
Adenocarcinoma	7	1	8 (13.3%)
Non-Hodgkin's lymphoma	0	2	2 (3.3%)
Carcinoid	0	1	1 (1.7%)
Neuroendocrine carcinoma	1		1 (1.7%)
Malignant histiocytosis	1	0	1 (1.7%)
Total	40(67%)	20(33%)	60 (100%)

Diagnostic procedures

Before operation, small intestinal diseases were suspected in 73 % (44/60) on admission. There were 40/60 patients (67 %) correctly diagnosed preoperatively. Among the 40 patients, 34 jejunoileal neoplasmas were correctly diagnosed by enteroclysis. Other preoperative diagnoses were made by angiography, colonoscopy, CT and Ultrasonography. Angiography was performed in 5 cases, of which 4 (80 %) of them were discovered preoperatively. One case of lymphoma of terminal ileum was detected by colonoscopy, and one jejunal tumor was diagnosed by CT scan only.

Of the 60 patients, 56 underwent CT scan, abdominal masses or intestinal wall thickening were visualized in 18 (32 %) cases, but two of them were misinterpreted as ovarian cancer, one as renal lipoma and one as intestinal tuberculosis. Ultrasonography was carried out in all 60 patients, and solid abdominal masses were demonstrated in 13 (22 %).

20 patients remained obscure diagnosis preoperatively, final diagnoses were disclosed during laparotomy. The mean duration of symptoms before diagnosis was 7 months. In 41 patients with malignant neoplasms, the duration of symptoms exceeded 12 months in 21 (52 %) cases.

Surgical findings

Of the 60 patients, three cases of intestinal obstruction and one case of intestinal perforation underwent emergency laparotomy (7 %). The rest underwent selective laparotomy (93%).

Of the 41 of malignant tumors, the masses within the intestinal walls were found in 15 without metastases; local lymph node metastasis in 12, distant and mesenteric lymph node metastasis in 9, liver metastases in 4 and urinary bladder metastasis in 1, the total rate of metastases was 63 % among the malignant tumors. lymph node metastasis was commonest in 51 % of malignant tumors.

DISCUSSION

Primary neoplasmas of jejunum and ileum are only <2 % of

the gastrointestinal malignant tumors, the incidence was 1.4 per 100 000 compared to 35.7/100 000 for colorectal and 92.9/100 000 for breast cancer^[2,3]. The jejunoileal neoplasmas are preponderant in male with a ratio of 2:1 between male and female^[3,4]. Our result showed 70 % in male and 30 % in female, similar to that reported in the literature. The patients with jejunoileal tumors were usually old people with an average age of over 50 years^[1-5], in this article, 51 % were over 50 years.

The small bowel neoplasmas located in the jejunum usually more frequent than that in ileal. In our results, the jejunal neoplasmas were twice as many as the ileal ones, higher than that reported in the literature^[4]; but the ratio of malignant and benign in small bowel tumors was concordant with those in the literature^[7]. As to the histopathologic types, the commonest pathologies of jejunoileal tumors were lymphoma, adenocarcinoma and carcinoids, followed by leiomyosarcomas, neuroendocrine tumors and other entities in Western countries^[1-7], which were significantly different from those in our study, in which the benign and malignant stromoma was predominant. In addition, some very rare tumors were seen in our investigation including angioleiomyoma, lymphangioma and malignant histiocytosis etc. The above results indicated that there were some differences between the Chinese and the Westerners in the pathologic types of jejunoileal tumors.

The clinical manifestations of jejunoileal neoplasmas were nonspecific and symptoms usually occurred late. The abdominal pain, gastrointestinal bleeding and weight loss were most frequent complaints in our patients and as well as in the other reports^[4-6], followed by nausea and/or vomiting^[4,6]. Abdominal mass and anemia were the most common physical findings in our study and related literatures^[4,6], followed by abdominal distension, muscle guarding and rigidity^[4]. The diagnosis of small bowel neoplasmas was often made when symptoms presented several months late, the median duration of symptoms before diagnosis was 7 months in our study, 3.6 and 6 months in others^[4,6]. The metastasises of jejunoileal neoplasms were common as they were usually identified late, the metastatic rate of leiomyosarcoma ranged from 24 % to 50 %, with the liver being most frequently involved^[5], distant metastasis occurred in 27 %^[2]. In our study, metastasis was found in 63 % of the malignant tumors, lymph node metastasis was the commonest (51 %) similar to that reported in the literature^[4], followed by liver metastases in 10 % of cases.

The preoperative diagnosis of primary jejunoileal neoplasmas remains difficult for clinicians owing to the nonspecific symptomatic presentation. The enteroclysis, enteroscopy and imaging methods have been used generally for small bowel diseases. Radiographic study of small bowel malignant tumors showed abnormality in 87 %^[4]. In our study, 34 cases of jejunoileal neoplasmas were diagnosed by enteroclysis. Both ultrasonography (US) and CT are also useful for detection of small bowel tumours. CT was found to detect leiomyoma and leiomyosarcoma most successfully and had the additional advantage of locating metastatic lesions^[5]. Moreover, CT offered the possibility of a preoperative staging by evaluating tumour extension through the bowel wall, involvement of lymph node and possible metastases^[8]. Other preoperative diagnoses were made through angiography, colonoscopy, CT and Ultrasonography. Angiography was performed in 5 cases, of which 4 (80 %) of small intestinal neoplasmas were discovered preoperatively. A case of lymphoma of terminal ileum was detected by colonoscopy, and one case of jejunum tumor was diagnosed by CT scan only.

Of the 60 patients, 56 underwent CT scan, abdominal masses or intestinal wall thickening were visualized in 18 (32 %), but two cases were misinterpreted as ovarian cancer, one as renal lipoma and one as intestinal tuberculosis. Ultrasonography was

carried out in all 60 patients, and the solid abdominal masses were demonstrated in 13 cases (22 %).

Final diagnoses were disclosed during laparotomy for those 20 patients whose diagnoses remained obscure preoperatively. The mean duration of symptoms before diagnosis was 7 months. In 41 patients with malignant neoplasms, the duration of symptoms exceeded 12 months in 21 cases (52 %).

Jejunum and ileum are difficult to visualize directly. Colonoscopy with retrograde ileoscopy is useful in the diagnosis of neoplasm of the terminal ileum^[4]. Enteroscopy is capable of observing most of the small intestine^[5], but it is hard for the patients to endure. Small bowel enteroclysis is still a good choice for the detection of jejunoileal neoplasms^[6], albeit a third of cases of this series may be missed in the examination. Angiography is carried out in only a small proportion of patients, though it is relatively sensitive, especially for those lesions with abundant vascularity, the expense and invasive property limit its application^[7]. Spiral CT is thought to be comparatively accurate in detecting small bowel tumors^[8], however its diagnostic accuracy is poor in this series with possible misinterpretations, probably due to lack of experience of some radiologists in this field. Despite the interference by intestinal gas, ultrasonography proves to be helpful in a fifth of cases to demonstrate thickened intestinal wall or unsuspected mass. Wireless capsule endoscopy is optimal for those patients without intestinal obstruction when it is available. Laparotomy is justified in those suspected cases as a last resort.

Thanks to a variety of investigations, the correct diagnosis is reached in the majority of patients before operation, though the delay between the onset of symptoms and the final diagnosis

is often significant. As a result, more than 60 % of patients with malignant tumors has advanced beyond the early stage of neoplasm. Recognition of this entity, with high index of suspicion, rational application of aforementioned investigation procedures, the advent of capsule endoscopy and justified early laparotomy, may facilitate the diagnosis and improve the outcome.

REFERENCES

- 1 **Baillie CT**, Williams A. Small bowel tumors: a diagnostic challenge. *J R Coll Surg Edinb* 1994; **39**: 8-12
- 2 **DiSario JA**, Burt RW, Vargas H, McWhorter WP. Small bowel cancer: epidemiological and clinical characteristics from a population-based registry. *Am J Gastroenterol* 1994; **89**: 699-701
- 3 **North JH**, Pack MS. Malignant tumors of the small intestine: a review of 144 cases. *Am Surg* 2000; **66**: 46-51
- 4 **Garcia Marcilla JA**, Sanchez Bueno F, Aguilar J, Parrilla Paricio P. Primary small bowel malignant tumors. *Eur J Surg Oncol* 1994; **20**: 630-634
- 5 **Blanchard DK**, Budde JM, Hatch GF 3rd, Wertheimer-Hatch L, Hatch KF, Davis GB, Foster RS Jr, Skandalakis JE. Tumors of the small intestine. *World J Surg* 2000; **24**: 421-429
- 6 **O'Boyle CJ**, Kerin MJ, Feeley K, Given HF. Primary small intestinal tumours: increased incidence of lymphoma and improved survival. *Ann R Coll Surg Engl* 1998; **80**: 332-334
- 7 **Brucher BL**, Roder JD, Fink U, Stein HJ, Busch R, Siewert JR. Prognostic factors in resected primary small bowel tumors. *Dig Surg* 1998; **15**: 42-51
- 8 **Maccioni F**, Rossi P, Gourtsoyiannis N, Bezzi M, Di Nardo R, Broglia L. US and CT findings of small bowel neoplasms. *Eur Radiol* 1997; **7**: 1398-1409

Edited by Wu XN

Prospective study of scoring system in selective intraoperative cholangiography during laparoscopic cholecystectomy

Xiao-Dong Sun, Xiao-Yan Cai, Jun-Da Li, Xiu-Jun Cai, Yi-Ping Mu, Jin-Min Wu

Xiao-Dong Sun, Xiao-Yan Cai, Jun-Da Li, Xiu-Jun Cai, Yi-Ping Mu, Jin-Min Wu, Department of General Surgery, The Affiliated Sir Run Run Shaw Hospital, Zhejiang University Medical College, Hangzhou 310016, Zhejiang Province, China

Correspondence to: Dr Xiao-Dong Sun, Department of General Surgery, The Affiliated Sir Run Run Shaw Hospital, Zhejiang University Medical College, Hangzhou 310016, Zhejiang Province, China. s.xiaodong@sohu.com

Telephone: +86-571-86090073 **Fax:** +86-571-86044817

Received: 2002-07-26 **Accepted:** 2002-08-23

Abstract

AIM: To evaluate of scoring system in predicting choledocholithiasis in selective intraoperative cholangiography (IOC) during laparoscopic cholecystectomy (LC).

METHODS: The scoring system of predicting choledocholithiasis was developed during the retrospective study in 264 cases, and was tested in 184 to evaluate its predictive value in choledocholithiasis.

RESULTS: The scoring system was developed in a retrospective study of 264 cases, the statistical analyses showed the predictive factors included sex, transaminase levels, alkaline phosphatase level, bilirubin level, and common bile duct diameter on ultrasonography. The scoring system was used in 184 cases prospectively, of which, 3 of 162 (1.9 %) cases scoring <3 had choledocholithiasis, 17 of 22 (77.3 %) cases scores ≥ 3 had choledocholithiasis. A case of scores ≥ 3 or more prospectively should be considered highly intraoperative cholangiography during laparoscopic cholecystectomy.

CONCLUSION: The scoring system can predict choledocholithiasis and is helpful in selection patients for intraoperative cholangiography.

Sun XD, Cai XY, Li JD, Cai XJ, Mu YP, Wu JM. Prospective study of scoring system in selective intraoperative cholangiography during laparoscopic cholecystectomy. *World J Gastroenterol* 2003; 9(4): 865-867

<http://www.wjgnet.com/1007-9327/9/865.htm>

INTRODUCTION

Laparoscopic cholecystectomy (LC) has been extensively accepted since Mouret first successfully finished the procedure in 1987^[1]. Whether intraoperative cholangiogram (IOC) during LC should be applied routinely is still controversial. Thus, we develop a scoring system to predict choledocholithiasis and recommend selection of IOC during LC.

MATERIALS AND METHODS

Retrospective study

Two hundred sixty-four cases of LC from January 1996 to June

1999 were analyzed. Before operation, choledocholithiasis in cases with cholecystolithiasis was not discovered by ultrasonography (US). During operation, 54 cases of cholecystolithiasis with choledocholithiasis and 210 cases of cholecystolithiasis without choledocholithiasis were confirmed by IOC. Sex, age, history of pancreatitis, jaundice, transaminase levels, alkaline phosphatase level, bilirubin level and diameter of common bile duct (CBD) on ultrasonography were evaluated as predictors of choledocholithiasis, and scoring system of selective IOC was designed.

Prospective study

From January 2000 to June 2001, the scoring system was carried out prospectively in 184 patients undergoing LC. Following evaluation, LC and IOC were performed, then the correlation of scoring results with choledocholithiasis was studied.

RESULTS

No choledocholithiasis in 264 patients undergoing LC was discovered by ultrasonography prior to operation. During LC, IOC found choledocholithiasis in 54 patients (Table 1).

Table 1 Factors predicting choledocholithiasis in 264 patients

Factor	No of cases with choledocholithiasis (54 cases)	No of cases without choledocholithiasis (210 cases)	Percentage (%)	P
Sex				
Male	27	40	40	<0.05
Female	27	170	14	
Age				
<55ys	34	112	23	
≥ 55 ys	20	98	17	<0.05
Pancreatitis				
Present	15	30	33	>0.05
Absent	39	180	18	
Jaundice				
Present	10	22	31	>0.05
Absent	44	188	19	
Transaminase				
Normal	31	201	13	
Elevated	23	9	72	<0.05
Alkaline phosphatase				
Normal	36	189	16	
Elevated	18	21	46	<0.05
Bilirubin				
Normal	31	205	13	
Elevated	23	5	82	<0.05
CBD diameter on US				
≤ 8 mm	33	204	14	
>8 mm	21	6	78	<0.05

Multivariate analysis found that independent predictors of choledocholithiasis included sex, serum level of transaminase, alkaline phosphatase, and bilirubin, and CBD diameter on US. Therefore, the scoring system in regression analysis was established (Table 2).

Table 2 Scoring system of predicting choledocholithiasis

Factor	Criteria	Score
Sex	Female	0
	Male	1
Transaminase	Normal	0
	Elevated	2
Alkaline phosphatase	Normal	0
	Elevated	2
Bilirubin	Normal	0
	Elevated	3
CBD diameter on US	≤8 mm	0
	>8 mm	3
Total		11

The scoring system was used in 184 patients undergoing LC before operation. During LC, all of the patients were performed IOC (Table 3).

Table 3 Results of scores in 184 patients before LC

	Score											
	0	1	2	3	4	5	6	7	8	9	10	11
No of patients	107	49	6	3	1	2	1	3	2	2	2	6

During LC, choledocholithiasis was found in 20 patients by IOC, the relationship between scores and choledocholithiasis was showed in Table 4.

Table 4 Relationship between scoring results and choledocholithiasis in 184 patients undergoing LC

Score	No of patients with choledocholithiasis	No of patients without choledocholithiasis	Percentage
<3	3	159	1.9
≥3 ^a	17	5	77.3

^a*P*<0.05 vs score of less than 3.

A significant difference in predicting value scoring 3 or more and that of less than 3 was found according to the χ^2 test. Thus, evaluation of LC patient with scoring system preoperatively would be helpful in predicting choledocholithiasis. If patient were scored more than 3, IOC should be performed during LC.

DISCUSSION

With the popularization of laparoscope, the age of micro-traumatic surgery has come and great changes have occurred in surgical operation and surgical ideology^[2]. Gallstone is one of the common primary diseases of biliary tract. LC has become a conventional method to treat patient with symptomatic gallstones. IOC is one of the accurate and safe procedure used in LC, is helpful in finding abnormality of pancreaticobiliary tract^[3], avoiding common bile duct injury^[4-8], and detecting choledocholithiasis^[9-11], thus, some recommended a routine IOC during LC^[4,5,12]. Because majority of gallstones patients do not have choledocholithiasis, IOC will increase the patient's cost

and exposure to X-ray, however, some researches found that the value of IOC were limited^[13-15], it is unnecessary to perform a routine IOC during LC. However, there are still 10-15 % of choledocholithiasis patients who have choledocholithiasis^[16]. Preoperative ERCP and IOC may be helpful to find choledocholithiasis^[17-20].

Mahmud suggested that, some gallstones might slip into the cystic duct or the common bile duct during LC, and IOC is valuable of determining the choledocholithiasis, ERCP and EST were regarded as effective methods detecting choledocholithiasis^[21]. Edey retrospectively analyzed 31 patients with choledocholithiasis treated by EST, and ERCP showed completely cleared common bile duct, but IOC during subsequent LC revealed common duct residual stones in 8 of these 31 patients. The author suggested that even after presumed endoscopic clearance of the bile duct stone, many patients (26 %) still harbored stones in common bile duct at the time of cholecystectomy. Therefore IOC during LC was recommended even after successful ERCP^[22]. Some studies revealed that preoperative ultrasound is neither sensitive nor specific for detecting common bile duct dilatation or the presence of residual stones^[23]. Some studies assessed the use of endoscopic retrograde cholangiopancreatography (ERCP), IOC, intraoperative laparoscopic ultrasonography (IOUS)^[24-27]. Bege manifested that combined endoscopic and laparoscopic management of cholecystolithiasis and choledocholithiasis were a viable option and were optimized by endoscopic ultra-sonography^[28]. The combined procedures of endoscopic sphincterotomy and LC included one-stage treatment of cholelithiasis and choledocholithiasis, elimination of potential return to the operating room when postoperative ERCP were unsuccessful^[29,30]. Ichihara concluded that intraoperative real time cholangiograms were helpful in detecting bile duct injuries or anomalies, and unsuspected bile duct stones^[31].

We recommend that IOC during LC should be performed selectively. Digital C-arm can provide real-time imaging and obtain a clear cholangiogram easily. The protocol of selective IOC is still debatable. Snow analyzed the results of 2034 LC, and found that there were no false negative, bile duct injuries, or other complications attributable to routine IOC or selective IOC, and suggested that selective IOC were an effective method of verifying suspected choledocholithiasis and were safer and less expensive than routine IOC^[32]. Abboud performed a meta-analysis of published data to evaluate preoperative indicators of choledocholithiasis, which included cholangitis, jaundice, dilated CBD on ultrasound, hyperbilirubinemia, elevated levels of alkaline phosphatase, pancreatitis, cholecystitis, and hyperamylasemia. The results showed that these predictors could be applied as guidelines for whether to investigate for duct stones before cholecystectomy^[33]. Kim also suggested selective IOC, and the risk levels of the presence of choledocholithiasis were determined by the independent predictor including preoperative clinical, biochemical and sonographic variables^[34]. However, Koo reviewed 420 cases of elective LC, IOC was routinely performed and acted as the reference standard for the presence of choledocholithiasis, and found that there were no predictive tests that could sufficiently increase an observer's probability estimate of the presence or absence of choledocholithiasis to allow for "selective" IOC decisions^[35].

By logistic regression analysis, our studies showed that sex, transaminase levels, alkaline phosphatase level, bilirubin level and common bile duct diameter on ultrasonography were independent predictors of choledocholithiasis. A scoring system was therefore designed with a total score of 11. Our prospective studies also showed that patients scoring more than 3 were at significant risk to have choledocholithiasis, and IOC should be performed during LC.

REFERENCES

- 1 **Huang ZQ**. Present status of biliary surgery in china. *World J Gastroenterol* 1998; **4** (Suppl 2): 8-9
- 2 **Shi JS**, Ma JY, Zhu LH, Pan BR, Wang ZR, Ma LS. Studies on gallstone in China. *World J Gastroenterol* 2001; **7**: 593-596
- 3 **Fujisaki S**, Tomita R, Koshinaga T, Fukuzawa M. Analysis of pancreaticobiliary ductal union based on intraoperative cholangiography in patients undergoing laparoscopic cholecystectomy. *Scand J Gastroenterol* 2002; **37**: 956-959
- 4 **Ludwig K**, Bernhardt J, Steffen H, Lorenz D. Contribution of intraoperative cholangiography to incidence and outcome of common bile duct injuries during laparoscopic cholecystectomy. *Surg Endosc* 2002; **16**: 1098-1104
- 5 **Ludwig K**, Bernhardt J, Lorenz D. Value and consequences of routine intraoperative cholangiography during cholecystectomy. *Surg Laparosc Endosc Percutan Tech* 2002; **12**: 154-159
- 6 **Podnos YD**, Gelfand DV, Dulkanchainun TS, Wilson SE, Cao S, Ji P, Ortiz JA, Imagawa DK. Is intraoperative cholangiography during laparoscopic cholecystectomy cost effective? *Am J Surg* 2001; **182**: 663-669
- 7 **Cai XJ**, Wang XF, Hong DF, Li LB, Li JD, Bryan F. The application of intraoperative cholangiography in laparoscopic cholecystectomy. *Zhonghua Waike Zazhi* 1999; **37**: 427-428
- 8 **Flum DR**, Koepsell T, Heagerty P, Sinanan M, Dellinger EP. Common bile duct injury during laparoscopic cholecystectomy and the use of intraoperative cholangiography: adverse outcome or preventable error? *Arch Surg* 2001; **136**: 1287-1292
- 9 **Cemachovic I**, Letard JC, Begin GF, Rousseau D, Nivet JM. Intraoperative endoscopic sphincterotomy is a reasonable option for complete single-stage minimally invasive biliary stones treatment: short-term experience with 57 patients. *Endoscopy* 2000; **32**: 956-962
- 10 **Mitchell SA**, Jacyna MR, Chadwick S. Choledocholithiasis: a controversy revisited. *Br J Surg* 1993; **80**: 759-760
- 11 **Kama NA**, Atli M, Doganay M, Kologlu M, Reis E, Dolapci M. Practical recommendations for the prediction and management of choledocholithiasis in patients with gallstones. *Surg Endosc* 2001; **15**: 942-945
- 12 **Waldhausen JH**, Graham DD, Tapper D. Routine intraoperative cholangiography during laparoscopic cholecystectomy minimizes unnecessary endoscopic retrograde cholangiopancreatography in children. *J Pediatr Surg* 2001; **36**: 881-884
- 13 **Li LB**, Cai XJ, Li JD, Mu YP, Wang YD, Yuan XM, Wang XF, Bryner B, Finley RK Jr. Will intraoperative cholangiography prevent biliary duct injury in laparoscopic cholecystectomy? *World J Gastroenterol* 2000; **6**(Suppl 3): 21
- 14 **Falcone RA Jr**, Fegelman EJ, Nussbaum MS, Brown DL, Bebbe TM, Merhar GL, Johannigman JA, Luchette FA, Davis K Jr, Hurst JM. A prospective comparison of laparoscopic ultrasound vs intraoperative cholangiogram during laparoscopic cholecystectomy. *Surg Endosc* 1999; **13**: 784-788
- 15 **Arul GS**, Rooney PS, Gregson R, Steele RJ. The standard of laparoscopic intraoperative cholangiography: a quality control study. *Endoscopy* 1999; **31**: 248-252
- 16 **Hong DF**, Gao M, Bryner U, Cai XJ, Mou YP. Intraoperative endoscopic sphincterotomy for choledocholithiasis during laparoscopic cholecystectomy. *World J Gastroenterol* 2000; **6**: 448-450
- 17 **Silverstein JC**, Wavak E, Millikan KW. A prospective experience with selective cholangiography. *Am Surg* 1998; **64**: 654-658
- 18 **Stuart SA**, Simpson TI, Alvord LA, Williams MD. Routine intraoperative laparoscopic cholangiography. *Am J Surg* 1998; **176**: 632-637
- 19 **Meyer C**, Le JV, Rohr S, Duclos B, Reimund JM, Baumann R. Management of choledocholithiasis in a single operation combining laparoscopic cholecystectomy and peroperative endoscopic sphincterotomy. *J Hepatobiliary Pancreat Surg* 2002; **9**: 196-200
- 20 **Halpin VJ**, Dunnegan D, Soper NJ. Laparoscopic intracorporeal ultrasound versus fluoroscopic intraoperative cholangiography: after the learning curve. *Surg Endosc* 2002; **16**: 336-341
- 21 **Mahmud S**, Hamza Y, Nassar AH. The significance of cystic duct stones encountered during laparoscopic cholecystectomy. *Surg Endosc* 2001; **15**: 460-462
- 22 **Edye M**, Dalvi A, Canin-Endres J, Baskin-Bey E, Salky B. Intraoperative cholangiography is still indicated after preoperative endoscopic cholangiography for gallstone disease. *Surg Endosc* 2002; **16**: 799-802
- 23 **Lichtenbaum RA**, McMullen HF, Newman RM. Preoperative abdominal ultrasound may be misleading in risk stratification for presence of common bile duct abnormalities. *Surg Endosc* 2000; **14**: 254-257
- 24 **Barwood NT**, Valinsky LJ, Hobbs MS, Fletcher DR, Knuiman MW, Ridout SC. Changing methods of imaging the common bile duct in the laparoscopic cholecystectomy era in Western Australia: implications for surgical practice. *Ann Surg* 2002; **235**: 41-50
- 25 **Biffl WL**, Moore EE, Offner PJ, Franciose RJ, Burch JM. Routine intraoperative laparoscopic ultrasonography with selective cholangiography reduces bile duct complications during laparoscopic cholecystectomy. *J Am Coll Surg* 2001; **193**: 272-280
- 26 **Liu TH**, Consorti ET, Kawashima A, Tamm EP, Kwong KL, Gill BS, Sellin JH, Peden EK, Mercer DW. Patient evaluation and management with selective use of magnetic resonance cholangiography and endoscopic retrograde cholangiopancreatography before laparoscopic cholecystectomy. *Ann Surg* 2001; **234**: 33-40
- 27 **Luo XZ**, Wang LS, Lin SZ. An analysis of the relationship between ultrasonography and laparoscopic cholecystectomy. *World J Gastroenterol* 1998; **4**(Suppl 2): 83
- 28 **Berdah SV**, Orsoni P, Bege T, Barthet M, Grimaud JC, Picaud R. Follow-up of selective endoscopic ultrasonography and/or endoscopic retrograde cholangiography prior to laparoscopic cholecystectomy: a prospective study of 300 patients. *Endoscopy* 2001; **33**: 216-220
- 29 **Kalimi R**, Cosgrove JM, Marini C, Stark B, Gecelter GR. Combined intraoperative laparoscopic cholecystectomy and endoscopic retrograde cholangiopancreatography: lessons from 29 cases. *Surg Endosc* 2000; **14**: 232-234
- 30 **Park AE**, Mastrangelo MJ Jr. Endoscopic retrograde cholangiopancreatography in the management of choledocholithiasis. *Surg Endosc* 2000; **14**: 219-226
- 31 **Ichihara T**, Suzuki N, Horisawa M, Kataoka M, Uchida Y, Sekiya M, Matsui T, Chen H, Sakamoto J, Nakao A, Koide A. The importance of the real-time fluoroscopic intraoperative direct cholangiogram in the laparoscopic cholecystectomy using a new strumet. *Hepatogastroenterology* 1996; **43**: 1296-1304
- 32 **Snow LL**, Weinstein LS, Hannon JK, Lane DR. Evaluation of operative cholangiography in 2043 patients undergoing laparoscopic cholecystectomy: a case for the selective operative cholangiogram. *Surg Endosc* 2001; **15**: 14-20
- 33 **Abboud PA**, Malet PF, Berlin JA, Staroscik R, Cabana MD, Clarke JR, Shea JA, Schwartz JS, Williams SV. Predictors of choledocholithiasis prior to cholecystectomy: a meta-analysis. *Gastrointest Endosc* 1996; **44**: 450-455
- 34 **Kim KH**, Kim W, Lee HI, Sung CK. Prediction of choledocholithiasis: its validation in laparoscopic cholecystectomy. *Hepatogastroenterology* 1997; **44**: 1574-1579
- 35 **Koo KP**, Traverso LW. Do preoperative indicators predict the presence of choledocholithiasis during laparoscopic cholecystectomy? *Am J Surg* 1996; **171**: 495-499

Use of endoscopic naso-pancreatic drainage in the treatment of severe acute pancreatitis

Zhu-Fu Quan, Zhi-Ming Wang, Wei-Qin Li, Jie-Shou Li

Zhu-Fu Quan, Zhi-Ming Wang, Wei-Qin Li, Jie-Shou Li, Research Institute of General Surgery, Jinling Hospital, Medical College of Nanjing University, Nanjing 210002, Jiangsu Province, China

Correspondence to: Dr. Zhu-Fu Quan, Institute of General Surgery, Jinling Hospital, Medical College of Nanjing University, Nanjing 210002, Jiangsu Province, China. quanzf@x263.net

Telephone: +86-25-4810649 **Fax:** +86-25-4803956

Received: 2002-10-05 **Accepted:** 2002-11-06

Abstract

AIM: To review the experience on the use of endoscopic nasopancreatic drainage (ENPD) in the treatment of severe acute pancreatitis (SAP).

METHODS: Since March 1998, under the regular management of SAP with non-operative method, ENPD has been randomly used in 14 patients. The average age of the patients was 41.3 ± 15.9 (years), with 8 males and 6 females. The time from onset to admission was 32.9 ± 22.8 (hours). 8 cases were found to have gallbladder stone. The daily output of pancreatic fluid was measured. The body temperature, heart rate, WBC count, blood glucose, blood calcium, PaO_2 , blood and urine levels of amylase were detected on the fifth day and compared with their respective data on the first day. Therapeutic results and hospitalization times were recorded.

RESULTS: The time of drainage was 7.3 ± 4.0 days. The daily drainage outputs of the first five days were 236.4 ± 176.6 , 287.1 ± 164.7 , 284.6 ± 216.4 , 435.0 ± 357.8 and 377.8 ± 223.8 ml, respectively. The decreases in body temperature, heart rate, WBC counts, blood and urine levels of amylase and the increase in PaO_2 were significant on the fifth day when compared with those on the first day. Infection of pancreatic necrosis was found in one patient and controlled by anti-infectives. 6 out of 8 patients with gallbladder stone were operated during hospital stay. All patients were cured and discharged and the average hospital stay was 28.1 ± 11.6 days.

CONCLUSION: ENPD is an effective method for the drainage of pancreatic fluid and might have an important role in the treatment of SAP. Further observation, comparison and summary by this method are worthy to be considered.

Quan ZF, Wang ZM, Li WQ, Li JS. Use of endoscopic nasopancreatic drainage in the treatment of severe acute pancreatitis. *World J Gastroenterol* 2003; 9(4): 868-870

<http://www.wjgnet.com/1007-9327/9/868.htm>

INTRODUCTION

Acute pancreatitis (AP) is a common clinical emergency. For the reason of urgency of episode, severity of patient's condition, frequent complications and high mortality, extensive attention has been paid to severe acute pancreatitis (SAP) in clinical practice^[1-10]. Since August 1995, we have adopted the principle of combination therapy mainly by non-operative methods, the

therapeutic efficacy of SAP has been increased significantly and hospital stay has been shortened. Therein, the method of endoscopic naso-pancreatic drainage (ENPD) was used in 14 cases since March 1998, with significant results.

MATERIALS AND METHODS

General clinical data

A total of 14 patients were treated, with average age of 41.3 ± 15.9 (27-77) years, 8 males and 6 females. From onset of the disease to admission was 32.9 ± 22.8 (6-72) hours. In 8 cases (8/14, 57.1%), gallbladder stone was detected by B ultrasonography or computerized tomography (CT). All patients were diagnosed as SAP in accord with the diagnostic criteria set by Surgical Pancreatic Group of the Surgical Society of Chinese Medical Association^[11,12]. Within 24 hours after hospitalization, their APACHE-II scores were ≥ 8 , Balthazar CT grades $\geq \text{II}$, and all accompanied by one or more organ dysfunction.

Routine non-operative monitoring therapy

All patients in fasting were installed with gastric tube to decompress and drain gastrointestinal fluid, and were given oxygen therapy (nasal catheter oxygen inhalation, 5 L/min), prophylactic application of antibiotics and somatostatin (14 peptide or 8 peptide). At the same time, internal homeostasis including water-electrolyte balance, acid-base balance, and the change of organ functions such as heart, lung, liver and kidney were monitored. Proper supportive therapy was given on time if necessary.

Endoscopic nasopancreatic drainage (ENPD)

After hospitalization, with the use of fiberoptic duodenoscope spectacle (Olympus TJF-30 model), nasopancreatic drainage-tube was inserted through the scope in the ward instantly after admission. The procedure was as follows: after intramuscular injection of 50 mg meperidine and 10 mg 654-2 with topical anaesthesia of throat, the endoscope was advanced to duodenum, searching for the papilla. Once found, it was observed about its shape, size, and position of the orifice. A tube was inserted into pancreatic duct for 5-10 cm through the orifice. The catheter was 1.95 m in length, 1.95 mm in outside diameter and 1.70 mm in inside diameter with 3 to 5 side holes near the distal end. If pancreatic juice could be drawn out, it indicated that insertion of the catheter was successful. The endoscope was then withdrawn and the drainage tube was guided from oral cavity to nasal cavity by a guiding catheter and fixed. Thereafter, the patency of the nasopancreatic tube was closely observed daily and was washed with gentamycin saline solution if necessary. When the abdominal symptoms and signs subsided, the tube was pulled out.

Observation index

Volume of the drainage from nasopancreatic tube was observed and recorded everyday. The body temperature, heart rate, WBC counts, blood glucose, blood calcium, PaO_2 , and blood and urine levels of amylase were surveyed on the fifth day and compared with that on the first day. The therapeutic results and the time of hospital stay were recorded.

Data processing

All data were expressed as mean ± standard deviation, and *t*-test was used for statistical analysis.

RESULTS

Information of drainage by nasopancreatic tube

The pancreatic fluid of all patients drained out was feculent achromatic or white fluid in the first 1 to 3 days, and then turned to clear transparent pancreatic fluid. The time of nasopancreatic drainage was 7.3±4.0 days. The drainage output of pancreatic fluid during the first five days was shown in Figure 1. The radiogram of naso-pancreatic catheter in a patient was shown in Figure 2.

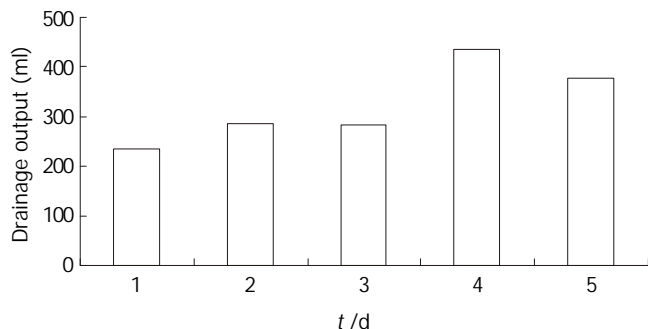


Figure 1 The drainage output of pancreatic fluid during the first five days.



Figure 2 The radiogram of naso-pancreatic catheter in a patient.

Changes of the relevant monitoring indices

The decrease of body temperature, heart rate, WBC count, blood and urine levels of amylase and the increase of PaO₂ were significant on the fifth day when compared with that on the first day. The change of blood glucose or blood calcium had no significant difference. The details were shown in Table 1.

Table 1 Changes in several related indexes

	The first day	The fifth day
Body temperature (°C)	38.2±0.6	37.2±0.8 ^b
Heart rate (bpm)	102.3±17.0	82.9±14.5 ^b
WBC count (×10 ⁹ /L)	14.6±4.2	10.1±5.4 ^a
Blood amylase (U/L)	695.7±445.2	82.6±47.1 ^b
Urine amylase (U/L)	3174.1±2542.5	286.8±260.9 ^b
PaO ₂ (mmHg)	78.0±16.3	113.0±41.6 ^b
Blood glucose (mmol/L)	10.0±4.9	8.6±3.3
Blood calcium (mmol/L)	2.1±0.2	2.2±0.2

^a*P*<0.05, ^b*P*<0.01, vs the first day.

Therapeutic result of treatment and time of hospital stay

Bacterial infection of pancreatic necrosis was found in one patient and controlled after changing the anti-infectives. Cholecystectomy was performed in 6 patients with cholecystolithiasis before discharge. All patients were cured and the time of hospital stay was 28.1±11.6 days.

DISCUSSION

There has been a steady increase in the incidence or the admission rate of AP^[13-15]. Generally, it is recognized that the pathogenesis of AP is correlated with the common channel of biliary and pancreatic ducts which is also called the common biliary pancreatic duct. The most common cause (60-80 %) is gallbladder stone and alcoholism^[16]. The former cause was more extensively studied than the latter. Incarceration by the calculus which enters the common channel and/or the inflammatory reaction and tissue edema caused by the passage of the calculus have often been proposed as the mechanism of AP and we name this type of AP the gallbladder stone-originated AP.

The obstruction of common biliary pancreatic duct results in the bile flowing into the pancreatic duct, activating the pancreatic enzymes and then causing the occurrence of AP. This is the classical bile reflux-common channel theory. This theory does not explain why AP happens in patients who have no calculus incarceration in or obstruction of common biliary pancreatic duct. In our group, 8 out of 14 cases, which amounted to 57.1 %, were diagnosed as having with cholecystolithiasis. But no one showed incarceration of the calculus or obstruction of common biliary pancreatic duct. We found that there was no bile mixed in the pancreatic fluid in our SAP patients with or without cholecystolithiasis, although the initial drain was feculent.

Nevertheless, the experiment of Lerch, *et al*^[17] made it clear that both pancreatic duct ligation alone and common biliary pancreatic duct ligation could cause the occurrence of AP, with pathological changes of similar severity. This result suggested that pancreatic duct obstruction, especially increase of pancreatic intraductal pressure was the main factor of the occurrence of AP. It may be the main mechanism in patients suffering from AP with or without cholecystolithiasis. Pancreatic ischaemia has an important role in the pathophysiology of AP^[18,19]. Shi and his colleagues^[20] reported that pancreatic duct obstruction was the first step causing ischaemia in AP and early decompression of the pancreatic duct prevented the early pancreatic ischaemia. The study of Choudari, *et al*^[21] proved that improving drainage of the pancreatic ductal system by endoscopic means effectively relieved the pain and reduced the number of attacks of pancreatitis in the majority of patients with hereditary pancreatitis. Aiming directly on this mechanism, we used the method of ENPD in treating SAP patients. All the patients accepted the routine non-operative therapy. Amelioration of abdominal symptoms and signs was very rapid with the drainage. Comparing with that on the first day, the decrease in body temperature, heart rate, WBC counts, blood and urine levels of amylase and the increase in PaO₂ were significant on the fifth day. Although blood glucose decreased and blood calcium increased, but they had no statistic significance. Bacterial infection of pancreatic necrosis was found only in one patient and was controlled after changing the anti-infectives. All 14 patients of this group were cured.

Studies have shown that duration of the obstruction of common biliary pancreatic duct was related directly with the severity of pancreatic necrosis and prognosis of the patient. Removal of the obstruction or decreasing the pressure on time can prevent the appearance of pancreatic necrosis or its further

development. The earlier the time of removal of the obstruction or decreasing the pressure, the better the prognosis^[16,22-24]. Beger, *et al*^[25] found that if the course of AP was longer than 3-4 days, the pancreas would necrotize irreversibly. It is important in the therapy of SAP to remove the obstruction or lower the high pressure of the pancreatic duct as early as possible. The time from onset to admission was 32.9±22.8 (6-72) hours in this group and the application of ENPD was carried out in the ward immediately after the admission. This is another important factor to get the curative effect.

This is our preliminary experience of the clinical application of ENPD in the treatment of SAP. The real value of this therapeutic modality should be further studied by strict randomised control study.

REFERENCES

- Howard TJ, Temple MB. Prophylactic antibiotics alter the bacteriology of infected necrosis in severe acute pancreatitis. *J Am Coll Surg* 2002; **195**: 759-767
- De La Mano A, Sevillano S, De Dios I, Vicente S, Manso MA. Low enzyme content in the pancreas does not reduce the severity of acute pancreatitis induced by bile-pancreatic duct obstruction. *Mol Cell Biochem* 2002; **240**: 75-81
- Srikanth G, Sikora SS, Baijal SS, Ayyagiri A, Kumar A, Saxena R, Kapoor VK. Pancreatic abscess: 10 years experience. *ANZ J Surg* 2002; **72**: 881-886
- Ammori BJ, Cairns A, Dixon MF, Larvin M, McMahon MJ. Altered intestinal morphology and immunity in patients with acute necrotizing pancreatitis. *J Hepatobiliary Pancreat Surg* 2002; **9**: 490-496
- Hartwig W, Werner J, Muller CA, Uhl W, Buchler MW. Surgical management of severe pancreatitis including sterile necrosis. *J Hepatobiliary Pancreat Surg* 2002; **9**: 429-435
- Hartwig W, Werner J, Uhl W, Buchler MW. Management of infection in acute pancreatitis. *J Hepatobiliary Pancreat Surg* 2002; **9**: 423-428
- Mayumi T, Ura H, Arata S, Kitamura N, Kiriyama I, Shibuya K, Sekimoto M, Nago N, Hirota M, Yoshida M, Ito Y, Hirata K, Takada T. Evidence-based clinical practice guidelines for acute pancreatitis: proposals. *J Hepatobiliary Pancreat Surg* 2002; **9**: 413-422
- Balthazar EJ. Complications of acute pancreatitis: clinical and CT evaluation. *Radiol Clin North Am* 2002; **40**: 1211-1227
- Balthazar EJ. Staging of acute pancreatitis. *Radiol Clin North Am* 2002; **40**: 1199-1209
- Uhl W, Warshaw A, Imrie C, Bassi C, McKay CJ, Lankisch PG, Carter R, Di Maggio E, Banks PA, Whitcomb DC, Dervenis C, Ulrich CD, Satake K, Ghaneh P, Hartwig W, Werner J, McEntee G, Neoptolemos JP, Buchler MW. IAP Guidelines for the Surgical Management of Acute Pancreatitis. *Pancreatology* 2002; **2**: 565-573
- Surgical Pancreatic Group of the Surgical Society of Chinese Medical Association. The clinical diagnosis and grading criteria of acute pancreatitis. *Zhonghua Waikē Zazhi* 1997; **35**: 773-775
- Surgical Pancreatic Group of the Surgical Society of Chinese Medical Association. The treatment guideline of severe acute pancreatitis. *Zhongguo Shiyong Waikē Zazhi* 2001; **21**: 513-514
- Tinto A, Lloyd DA, Kang JY, Majeed A, Ellis C, Williamson RC, Maxwell JD. Acute and chronic pancreatitis-diseases on the rise: a study of hospital admissions in England 1989/90-1999/2000. *Aliment Pharmacol Ther* 2002; **16**: 2097-2105
- Birgisson H, Moller PH, Birgisson S, Thoroddsen A, Asgeirsson KS, Sigurjonsson SV, Magnusson J. Acute pancreatitis: a prospective study of its incidence, aetiology, severity, and mortality in Iceland. *Eur J Surg* 2002; **168**: 278-282
- Lopez MJ. The changing incidence of acute pancreatitis in children: a single-institution perspective. *J Pediatr* 2002; **140**: 622-624
- Steer ML. Pathogenesis of acute pancreatitis. *Digestion* 1997; **58** (Suppl 1): 46-49
- Lerch MM, Saluja AK, Runzi M, Dawra R, Saluja M, Steer ML. Pancreatic duct obstruction triggers acute necrotizing pancreatitis in the opossum. *Gastroenterology* 1993; **104**: 853-861
- Zhou ZG, Chen YD. Influencing factors of pancreatic microcirculatory impairment in acute pancreatitis. *World J Gastroenterol* 2002; **8**: 406-412
- Zhou ZG, Chen YD, Sun W, Chen Z. Pancreatic microcirculatory impairment in experimental acute pancreatitis in rats. *World J Gastroenterol* 2002; **8**: 933-936
- Shi CX, Chen JW, Carati CJ, Schlothe AC, Toouli J, Saccone GT. Effects of acute pancreatic duct obstruction on pancreatic perfusion: implication of acute pancreatic duct decompression. *Scand J Gastroenterol* 2002; **37**: 1328-1333
- Choudari CP, Nickl NJ, Fogel E, Lehman GA, Sherman S. Hereditary pancreatitis: clinical presentation, ERCP findings, and outcome of endoscopic therapy. *Gastrointest Endosc* 2002; **56**: 66-71
- Runzi M, Saluja AK, Lerch MM, Dawra R, Nishino H, Steer ML. Early ductal decompression prevents the progression of biliary pancreatitis: an experimental study in the opossum. *Gastroenterology* 1993; **105**: 157-164
- Feng BX, Huang B, Zhai CB, Li DW, Yang LQ, Lin HJ. Role of pancreatic duct cannulation in the treatment of experimental acute haemorrhagic necrotizing pancreatitis of dogs. *Zhonghua Putong Waikē Zazhi* 1998; **13**: 295-297
- Kueppers PM, Russell DH, Moody FG. Reversibility of pancreatitis after temporary pancreaticobiliary duct obstruction in rats. *Pancreas* 1993; **8**: 632-637
- Beger HG, Rau B, Mayer J, Pralle U. Natural course of acute pancreatitis. *World J Surg* 1997; **21**: 130-135

Edited by Xu JY

Local excision carcinoma in early stage

Ji-Dong Gao, Yong-Fu Shao, Jian-Jun Bi, Su-Sheng Shi, Jun Liang, Yu-Hua Hu

Ji-Dong Gao, Yong-Fu Shao, Jian-Jun Bi, Department of General Surgical Oncology, Cancer Hospital, Chinese Academy of Medical Sciences, Peking Union Medical College, Beijing 100021, China

Su-Sheng Shi, Department of Pathology, Cancer Hospital, Chinese Academy of Medical Sciences, Peking Union Medical College, Beijing 100021, China

Jun Liang, Yu-Hua Hu, Department of Radiotherapy Oncology, Chinese Academy of Medical Sciences, Peking Union Medical College, Beijing 100021, China

Correspondence to: Ji-Dong Gao, Department of General Surgical Oncology, Cancer Hospital, Chinese Academy of Medical Sciences, Peking Union Medical College, Beijing 100021, China. ab168@vip.sina.com

Telephone: +86-10-87708308

Received: 2002-12-22 **Accepted:** 2003-01-16

Abstract

AIM: To assess the validity of local excision for the early stage low rectal cancer as an effective treatment alternative to radical resection.

METHODS: A retrospective medical chart review was done in 47 patients with early stage low rectal carcinoma who underwent local excision from November 1980 through November 1999 at Cancer Hospital of Chinese Academy of Medical Sciences (CAMS). The patients were treated by either transanal (40 cases), trans-sacral (5 cases), or trans-vaginal (2 cases) excision of tumors and no death was related to surgery. Sixteen patients received postoperative radiotherapy.

RESULTS: T1 and T2 lesion was found in 36 (76.6 %) and 11 patients (23.4 %) respectively. The overall local tumor recurrence rate was 14.9 % (7/47), with an average recurrence time of 21 months. Among these 7 recurrent patients, there were 4 T1 and 3 T2 lesions. Microscopically, the surgical incisional margin was negative in 45 (95.7 %) and positive in 2 patients (4.3 %); Both of the later had developed local recurrence. The overall 5-year survival rate was 91.7 %, in which there were 94.4 % for T1 and 83.3 % for T2 tumors. T stage, intravessel tumor thrombosis, lymphocytic infiltration and histological grade were not found to be significant by related to the local recurrence and survival ($P>0.05$).

CONCLUSION: Local tumor excision was a safe procedure for the treatment of early stage low rectal carcinoma with minimal morbidity and mortality, which might serves as one of the primary surgical treatment methods for the disease of this kind.

Gao JD, Shao YF, Bi JJ, Shi SS, Liang J, Hu YH. Local excision carcinoma in early stage. *World J Gastroenterol* 2003; 9(4): 871-873

<http://www.wjgnet.com/1007-9327/9/871.htm>

INTRODUCTION

Abdominoperineal resection (APR) has traditionally been used to treat the Adenocarcinoma of the low rectum^[1-2]. In which a

permanent colostomy has to be performed, leading to the risk of complications, inconvenience of patients and even death^[3,4]. More recently, local excision has been performed with the curative intent to remove the well-differentiated lesions that are less than 3 cm in diameter and limited to the mucosa or submucosa^[5-7], which offers these patients fewer operative complications and long-term survival outcome^[8-13]. The increasing evidence based on the local tumor recurrence and survival rates supports the use of local excision as a primary treatment modality in the selected patients^[14-18].

The aim of the present study was to review our experience in the local excision of the early rectal cancers and to assess the validity of this therapeutic strategy as an effective treatment alternative to radical resection.

MATERIALS AND METHODS

Materials

Forty-seven 47 patients with early stage low rectal carcinomas were treated by local excision from November 1980 to November 1999 at the Department of General Surgical Oncology, Cancer Hospital of Chinese Academy of Medical Sciences (CAMS). They were 23 male and 24 female and with an average age 57 years (ranging from 31 to 80 years). The rectal carcinomas were located 3 to 8 cm from the anal verge (Table 1).

Table 1 Patient and treatment characteristics (n=47)

Characteristic	No. patients
Sex	
Male	23
Female	24
Surgical margin	
Negative	45
Positive	2
Radiotherapy	
No	31
Yes	16
T stage	
T1	36
T2	11
Grade	
Well differentiated	22
Moderately differentiated	23
Poorly differentiated	2
Surgical Procedure	
Transanal excision	40
Trans-sacral excision	5
Trans-vaginal excision	2

Treatment

Patients were treated by either transanal (40 cases), trans-sacral (5 cases), or trans-vaginal (2 cases) excision of tumors, in which 16 patients received postoperative radiotherapy.

Pathological diagnosis

All available pathohistological sections were reviewed by a single pathologist to assess the depth and extent of tumor invasion, the lymphocytic infiltration, mucinous status, and the degree of tumor differentiation. The tumor was staged according to the American Joint Committee on Cancer Staging System (AJCC1996).

Statistical analysis

The end points of this study were local and distant tumor recurrence and patient survival. Obtained data were analyzed using the Statistical Package for the Social Sciences (Release 11.0, SPSS, Inc). Survival curves were estimated using the Kaplan-Meier method and were compared using the log-rank test. Significance was defined as $P < 0.05$.

RESULTS

There was no death related to surgery. The most severe complication was the fistula formation, which was necessitated to perform a temporary diverting colostomy in two patients treated with trans-sacral excision. Other complications included bleeding in 2 patients and anal stricture in one patient (Table 1).

The median tumor diameter was 2.0 cm (ranging from 0.4 to 3 cm). Thirty-six patients (76.6 %) had T1 and 11 patients (23.4 %) had T2 lesion. The resected tumors in most cases were well or moderately differentiated, poorly differentiated were only seen in two patients. For those pathological sections were available, intravessel tumor thrombosis was identified in 10 patients (21.3 %) and lymphocytic infiltration in 8 patients (17.0 %). Tumor cells appeared on the surgical incisional margin were negative in 45 patients (95.7 %) and positive in 2 cases (4.3 %).

The average time for follow-up survey was 53 months. The overall local tumor recurrence rate was 14.9 % (7 patients) with the median recurrence time of 21 months (ranging from 12 to 48 months) postoperation. Among those with local recurrence, T1 and T2 tumors were found in 4 and 3 cases respectively. Five patients had immediate reoperation (APR or anterior resection). Both of the two patients with tumor cell positive incisional margin developed local recurrence. The overall 5-year survival rate was 91.7 %, in which there were 94.4 % for T1 and 83.3 % for T2 tumors.

T stage, intravessel tumor thrombosis, lymphocytic infiltration, histological grade and mucinous differentiation were not found to be significant predictors for local tumor recurrence and survival ($P > 0.05$).

DISCUSSION

Abdominoperineal resection, the mainstay of treatment for rectal cancer nowadays, has been reported bearing a death rate of 2.3 % to 3.2 % and 30 % to 46 % postoperative complications in the patient. permanent colostomy, urinary and sexual dysfunction are common sequelae of radical proctectomy that impair seriously affecting the patient's quality of life^[14]. In the past, local excision was performed only if the patient was in poor medical condition or refused to have a colostomy. Recent data suggest that the combination of local excision and postoperative chemo-radiation therapy may be an option for some patients with early stage rectal cancer. Encouraging results of local treatment of early rectal cancer and the development of new diagnostic technology providing accurate preoperative staging have greatly increased the interest of surgical oncology in this therapeutic strategy^[14-19].

However, broad acceptance of local excision as the primary treatment rectal cancer has been limited by the high local tumor recurrence that was difficult to be interpreted because the

literature was dominated by retrospective analyses of heterogeneous groups of patients. Included the patients with the tumors undifferentiated and penetrating the perirectal fat, with questionable or even positive tumor cell incisional margins, or with different surgical approaches, even palliative surgery^[20,21]. Besides specific reference was not always made to the lymphatic and blood vessel invasion, and the role of salvage surgery after failed local excision has also not been clearly stated^[22-26]. Therefore, There is an almost uniform agreement at present that only the well- or moderately differentiated T1 and T2 tumors, without blood vessel or lymphatic invasion or mucinous components could be treated by local excision with curative intent.

The present study there was no death related to the surgery, postoperative mortality. Complications occurring more and with a minimal in patients treated with trans-sacral excision was the fistula that was necessitated to perform a temporary diverting colostomy in two patients. Transanal excision was associated with less morbidity than any other local excision procedures.

Our data suggested that longer follow-up was necessary to identify those who would have a relapse, as shown by the fact that the median time for the local tumor recurrence in our study was about 21 months, with a range of 12 to 48 months postoperation. Recurrence rates were 11.1 % and 27.3 % in T1 and T2 tumors, respectively, which suggested that T stage was an important factor affecting recurrence.

The fact that both of the 2 patients with tumor cell positive incisional margin developed local recurrence suggested that tumor-free incisional margin and completely tumor excision was crucial for the prevention of local tumor recurrence, which was difficult to achieve for T3 lesion because the tumor had invaded the perirectal fat or anal sphincter. Therefore, if a tumor cell negative incisional margin could not be achieved in the operation, the patient was not considered as a good candidate for the local excision^[27,28]. Statistical analysis showed that intravessel tumor thrombosis, lymphocytic infiltration, histologic grade and mucinous differentiation were not found to be the significant predictors for the local tumor recurrence and survival ($P > 0.05$).

In summary, on the basis of our retrospective data, the sphincter-preserving local excision can be used as one of the primary surgical treatment methods for the early-stage low rectal cancer with minimal morbidity and mortality.

REFERENCES

- 1 **Nissan A**, Guillem JG, Paty PB, Douglas Wong W, Minsky B, Saltz L, Cohen AM. Abdominoperineal resection for rectal cancer at a specialty center. *Dis Colon Rectum* 2001; **44**: 27-35
- 2 **Zheng S**, Liu XY, Ding KF, Wang LB, Qiu PL, Ding XF, Shen YZ, Shen GF, Sun QR, Li WD, Dong Q, Zhang SZ. Reduction of the incidence and mortality of rectal cancer by polypectomy: a prospective cohort study in Haining County. *World J Gastroenterol* 2002; **8**: 488-492
- 3 **Luna-Perez P**, Rodriguez-Ramirez S, Vega J, Sandoval E, Labastida S. Morbidity and mortality following abdominoperineal resection for low rectal adenocarcinoma. *Rev Invest Clin* 2001; **53**: 388-389
- 4 **McLeod RS**. Comparison of quality of life in patients undergoing abdominoperineal extirpation or anterior resection for rectal cancer. *Ann Surg* 2001; **233**: 157-158
- 5 **Sengupta S, Tjandra JJ**. Local excision of rectal cancer: what is the evidence? *Dis Colon Rectum* 2001; **44**: 1345-1361
- 6 **Masaki T**, Sugiyama M, Atomi Y, Matsuoka H, Abe N, Watanabe T, Nagawa H, Muto T. The indication of local excision for T2 rectal carcinomas. *Am J Surg* 2001; **181**: 133-137
- 7 **Taylor RH**, Hay JH, Larsson SN. Transanal local excision of selected low rectal cancers. *Am J Surg* 1998; **175**: 360-363
- 8 **Bleday R**, Steele G Jr. Current protocols and outcomes of local

- therapy for rectal cancer. *Surg Oncol Clin N Am* 2000; **9**: 751-758
- 9 **Rothenberger DA**, Garcia-Aguilar J. Role of local excision in the treatment of rectal cancer. *Semin Surg Oncol* 2000; **19**: 367-375
- 10 **Chorost MI**, Petrelli NJ, McKenna M, Kraybill WG, Rodriguez-Bigas MA. Local excision of rectal carcinoma. *Am Surg* 2001; **67**: 774-779
- 11 **Blair S**, Ellenhorn JD. Transanal excision for low rectal cancers is curative in early-stage disease with favorable histology. *Am Surg* 2000; **66**: 817-820
- 12 **Hall NR**, Finan PJ, al-Jaberi T, Tsang CS, Brown SR, Dixon MF, Quirke P. Circumferential margin involvement after mesorectal excision of rectal cancer with curative intent. Predictor of survival but not local recurrence? *Dis Colon Rectum* 1998; **41**: 979-983
- 13 **Chakravarti A**, Compton CC, Shellito PC, Wood WC, Landry J, Machuta SR, Kaufman D, Ancukiewicz M, Willett CG. Long-term follow-up of patients with rectal cancer managed by local excision with and without adjuvant irradiation. *Ann Surg* 1999; **230**: 49-54
- 14 **Wagman RT**, Minsky BD. Conservative management of rectal cancer with local excision and adjuvant therapy. *Oncology (Huntingt)* 2001; **15**: 513-519
- 15 **Daniels IR**, Simson JN. Local excision and chemoradiation for low rectal T1 and T2 cancers is an effective treatment. *Am Surg* 2000; **66**: 512
- 16 **Medich D**, McGinty J, Parda D, Karlovits S, Davis C, Caushaj P, Lembersky B. Preoperative chemoradiotherapy and radical surgery for locally advanced distal rectal adenocarcinoma: pathologic findings and clinical implications. *Dis Colon Rectum* 2001; **44**: 1123-1128
- 17 **Benson R**, Wong CS, Cummings BJ, Brierley J, Catton P, Ringash J, Abdolell M. Local excision and postoperative radiotherapy for distal rectal cancer. *Int J Radiat Oncol Biol Phys* 2001; **50**: 1309-1316
- 18 **Varma MG**, Rogers SJ, Schrock TR, Welton ML. Local excision of rectal carcinoma. *Arch Surg* 1999; **134**: 863-867
- 19 **Akasu T**, Kondo H, Moriya Y, Sugihara K, Gotoda T, Fujita S, Muto T, Kakizoe T. Endorectal ultrasonography and treatment of early stage rectal cancer. *World J Surg* 2000; **24**: 1061-1068
- 20 **Weber TK**, Petrelli NJ. Local excision for rectal cancer: an uncertain future. *Oncology (Huntingt)* 1998; **12**: 933-943
- 21 **Bouvet M**, Milas M, Giacco GG, Cleary KR, Janjan NA, Skibber JM. Predictors of recurrence after local excision and postoperative chemoradiation therapy of adenocarcinoma of the rectum. *Ann Surg Oncol* 1999; **6**: 26-32
- 22 **Graham RA**, Hackford AW, Wazer DE. Local excision of rectal carcinoma: a safe alternative for more advanced tumors? *J Surg Oncol* 1999; **70**: 235-238
- 23 **Benoist S**, Panis Y, Martella L, Nemeth J, Hautefeuille P, Valleur P. Local excision of rectal cancer for cure: should we always regard rigid pathologic criteria? *Hepatogastroenterology* 1998; **45**:1546-1551
- 24 **Mellgren A**, Sirivongs P, Rothenberger DA, Madoff RD, Garcia-Aguilar J. Is local excision adequate therapy for early rectal cancer? *Dis Colon Rectum* 2000; **43**: 1064-1071
- 25 **Wexner SD**, Rotholtz NA. Surgeon influenced variables in resectional rectal cancer surgery. *Dis Colon Rectum* 2000; **43**: 1606-1627
- 26 **Lopez-Kostner F**, Fazio VW, Vignali A, Rybicki LA, Lavery IC. Locally recurrent rectal cancer: predictors and success of salvage surgery. *Dis Colon Rectum* 2001; **44**: 173-178
- 27 **Kim CJ**, Yeatman TJ, Coppola D, Trotti A, Williams B, Barthel JS, Dinwoodie W, Karl RC, Marcet J. Local excision of T2 and T3 rectal cancers after downstaging chemoradiation. *Ann Surg* 2001; **234**: 352-358
- 28 **Beart RW Jr**. Predictors of recurrence after local excision. *Ann Surg Oncol* 1999; **6**: 26-32

Edited by Zhu L

Acaroid mite, intestinal and urinary acariasis

Chao-Pin Li, Yu-Bao Cui, Jian Wang, Qing-Gui Yang, Ye Tian

Chao-Pin Li, Yu-Bao Cui, Jian Wang, Qing-Gui Yang, Ye Tian, Department of Etiology and Immunology, School of Medicine, Anhui University of Science & Technology, Huainan 232001, Anhui Province, China

Correspondence to: Dr. Chao-Pin Li, Department of Etiology and Immunology, School of Medicine, Anhui University of Science & Technology, Huainan 232001, Anhui Province, China. yxfy@aust.edu.cn
Telephone: +86-554-6658770 **Fax:** +86-554-6662469

Received: 2002-11-11 **Accepted:** 2002-12-20

Abstract

AIM: To investigate epidemiology and pathogenic mite species of intestinal and urinary acariasis in individuals with different occupations.

METHODS: A total of 1994 individuals were tested in this study. History collection, skin prick test and pathogen identification were conducted. The mites were isolated from stool and urine samples by saturated saline flotation methods and sieving following centrifugation, respectively.

RESULTS: Among the 1994 individuals examined, responses to the skin prick test of "+++", "++", "+", "±" and "-" were observed at frequencies of 3.96 % (79), 3.21 % (64), 2.31 % (46), 1.25 % (25) and 89.27 % (1780), respectively. A total number of 161 (8.07 %) individuals were shown to carry mites, with 92 (4.61 %) positive only for stool samples, 37 (1.86 %) positive only for urine samples and 32 (1.60 %) for both. The positive rate of mites in stool samples was 6.22 % (124/1994), being 6.84 % (78/1140) for males and 5.39 % (46/854) for females. No gender difference was observed in this study ($\chi^2=1.77$, $P>0.05$). The mites from stool samples included *Acarus siro*, *Tyrophagus putrescentiae*, *Dermatophagoides farinae*, *D. pteronyssinus*, *Glycyphagus domesticus*, *G. ornatus*, *Carpoglyphus lactis* and *Tarsonemus granaries*. The positive rate of mites in urine samples was 3.46 % (69/1994). The positive rates for male and female subjects were found to be 3.95 % (45/1140) and 2.81 % (24/854) respectively, with no gender difference observed ($\chi^2=1.89$, $P>0.05$). Mites species in urine samples included *Acarus siro*, *Tyrophagus putrescentiae*, *T. longior*, *Aleuroglyphus ovatus*, *Caloglyphus berlesei*, *C. mycophagus*, *Suidasia nesbitti*, *Lardoglyphus konoii*, *Glycyphagus domesticus*, *Carpoglyphus lactis*, *Lepidoglyphus destructor*, *Dermatophagoides farinae*, *D. pteronyssinus*, *Euroglyphus magnei*, *Caloglyphus hughesi*, *Tarsonemus granarus* and *T. hominis*. The species of mites in stool and urine samples were consistent with those separated from working environment. A significant difference was found among the frequencies of mite infection in individuals with different occupations ($\chi^2=82.55$, $P<0.001$), with its frequencies in those working in medicinal herb storehouses, those in rice storehouse or mills, miners, railway workers, pupils and teachers being 15.89 % (68/428), 12.96 % (53/409), 3.28 % (18/549), 2.54 % (6/236), 5.10 % (13/255) and 2.56 % (3/117), respectively.

CONCLUSION: The prevalence of human intestinal and urinary acariasis was not associated with gender, and these

diseases are more frequently found in individuals working in medicinal herb, rice storehouses or mills and other sites with high density of mites. More attention should be paid to the mite prevention and labor protection for these high-risk groups.

Li CP, Cui YB, Wang J, Yang QG, Tian Y. Acaroid mite, intestinal and urinary acariasis. *World J Gastroenterol* 2003; 9(4): 874-877
<http://www.wjgnet.com/1007-9327/9/874.htm>

INTRODUCTION

Various species of mites often infest stored foodstuffs and various drugs, and cause losses in food and drug products, especially in humid and warm area^[1-9]. They are small creatures of about half a millimeter in body size and creamy white in color, proving difficult to be detected from drugs and food products. Therefore, the incidence of various forms of human acariasis presumably caused by the ingestion of mite-infested food is unusually high in China^[10]. In this study we investigate the epidemiological characteristics and pathogenic mite species of intestinal and urinary acariasis in individuals with different occupations in Anhui Province.

MATERIALS AND METHODS

Population

A total of 1994 subjects with the average age of 35 years (6-63 years), 1 140 males and 854 females, were examined in this study, including medicinal herb storehouse workers ($n=428$), rice storehouse or mill workers ($n=409$), miners ($n=549$), railway workers ($n=236$), pupils ($n=255$) and teachers ($n=117$). Special attention was paid to individuals with intestinal or/and urinary symptoms.

Methods

History collection, skin prick test and etiological examination were carried out on the 1994 subjects.

History collection A questionnaire, administered by a nurse, was used to collect information from each subject investigated. Information was collected by means of in-person, telephone, interview, including age, gender, history of present illness, anamnesis, symptomatology (i.e. abdominal pain, diarrhea, abdominal cramps, urethrorrhage, urodynia, cloudy urine, frequency of micturition), onset date and duration of symptoms, personal habits, living environmental hygiene and the date of stool and urine sample collection.

Skin prick test Skin prick test were performed with the concentrations of 1:100 (W/V) of the test extract. After skin disinfection, a little of extract (about 0.01 ml) was dripped on skin surface of right forearm flexor, then a special disinfectant needle was used to prick into the skin through the drop of the extract. The depth of needle in skin was limited about 0.5-1 mm and there was no bloodshed. About 5 cm apart from the extract drop, normal saline in proximal and histamine in distalis were used for negative and positive control solution. The mean diameter of the wheals or areolae was measured 15-20 min after the test. The reactions with the mean diameter up to 1.5

mm, 2 mm, 3 mm, 5 mm and 10 mm were regarded as \pm , +, ++, +++ and ++++, respectively.

The test extract was made according to NIBSC82/518 approved by World Health Organization (WHO) in 1984. The purified fraction was prepared as follows: the mites were then frozen and thawed several times after having been cultured in the initial medium for several months. A 48-hr maceration in a borate buffer (pH 8.5) was followed by centrifugation. The supernatant was neutralized and submitted to precipitation with a series of acetone. The fraction precipitated at 80 % acetone was isolated, washed and dried. This purified extract was lyophilized or stored as a solution in the presence of 50 % glycerol and 5 % pheno^[11-14].

Etiological examination All individuals were asked to provide stool and urine samples for etiological examination. Mites in stool samples were separated by saturated saline flotation methods, and the mites were identified under microscope. Each stool sample was examined for three times. Specimens containing adult or larval mites, eggs, or hypopus were considered positive.

Samples of the first urine in the morning and 24 hours' urine of all individuals were collected for separation of mites. After centrifugation and filtration with a copper sieve, they were examined under a microscope for adult or larval mites, eggs or hypopus.

Blood examination Leukocytes were also counted and sorted in 30 patients with mites detected.

Detection of mites from working environment Directcopy, waterenacopy and tullgren were used to identify mites from mill floor dust, stores of medicinal herbs including wolfberry fruit, ophiopogon root liquorice, boat-fruited sterculia seed and safflower.

Colonoscopy After defecation, the patients with mites found in their stools were examined by routine colonoscopy.

Cystoscopy After emiction, the patients with mites detected in their urine were examined by routine cystoscopy.

Statistical analysis

The positivity rates were expressed as percentages, and the statistical analysis was carried out by using χ^2 test. A probability value of less than 0.05 was considered statistically significant.

RESULTS

Skin prick test

The skin prick test was definitely positive in 189 subjects, with the results “+++”, “++”, “+”, “ \pm ” and “-” observed in 79 (3.96 %), 64 (3.21 %), 46 (2.31 %), 25 (1.25 %) and 1 780 (89.27 %), respectively among the 1994 individuals examined.

Etiological examination

Of 1994 individuals investigated, mites were detected from stool or/and urine samples in 161 (8.07 %) subjects, with the positive rates in stool, urine and in both being 4.61 % (92), 1.86 % (37) and 1.60 % (32), respectively.

The positive rate of mites in stool samples was 6.22 % (124/1 994), with that for male and female subjects being 6.84 % (78/1 140) and 5.39 % (46/854), respectively. No gender difference was found in this series ($\chi^2=1.77$, $P>0.05$). The mites from stool samples included *Acarus siro*, *Tyrophagus putrescentiae*, *Dermatophagoides farinae*, *D. pteronyssinus*, *Glycyphagus domesticus*, *G. ornatus*, *Carpoglyphus lactis* and *Tarsonemus granaries*. Among 124 cases with mites in stool samples, 54 (43.55 %) were positive for adult mites, 13 (10.48 %) for larval mites, 43 (34.68 %) for both adult and larval mites, 3 (2.42 %) for both adult mites and eggs, 6 (4.84 %) for adult and larval mites and eggs, 3 (2.42 %) for both larval mites and

eggs and 2 (1.61 %) for both hypopus and eggs. Mite concentration was also estimated, being 1-2 /cm³, 2-4 /cm³ and >5 /cm³ in 6, 30 and 88 cases, respectively.

Totally, mites were detected from urine samples at a frequency of 3.46 % (69/1 994). The positive rate for male and female subjects were 3.95 % (45/1140) and 2.81 % (24/854), respectively, with no gender difference found in this series ($\chi^2=1.89$, $P>0.05$). The mites in urine samples were separated and identified, including *Acarus siro*, *Tyrophagus putrescentiae*, *T. longior*, *Aleuroglyphus ovatus*, *Caloglyphus berlessei*, *C. mycophagus*, *Suidasia nesbitti*, *Lardoglyphus konoi*, *Glycyphagus domesticus*, *Carpoglyphus lactis*, *Lepidoglyphus destructor*, *Dermatophagoides farinae*, *D. pteronyssinus*, *Euroglyphus magnei*, *Caloglyphus hughesi*, *Tarsonemus granarius* and *T. hominis*. Among the 69 positive cases, 19 cases (27.54 %) were found to be positive for adult mites, 18 (26.09 %) for larval mites, 11 (15.94 %) both adult and larval mites, 3 (4.35 %) for adult mites and eggs, 11 (15.94 %) adult and larval mites and eggs, 6 (8.70 %) for larval mites and eggs, and 1 (1.44 %) for both hypopus and eggs. The mite concentrations were shown to be <0.5 /ml, 0.6-1 /ml, 1.1-1.5 /ml and >1.5 /ml, respectively, in 32, 25, 10 and 2 cases, reflecting the verity infectiosity of mites among different individuals.

Relationship between skin prick test and etiological examination

The results of etiological examination are correlative to skin prick test. One hundred and sixty-one of the 189 cases (85.19 %) positive skin-prick reaction were found to be positive for mites in their stool or / and urine samples. The intensities of the skin prick reaction were also found to be associated to mite concentrations in stool or / and urine samples, with the reactions “+++”, “++” and “+” corrective to 100 % (79/79), 90.63 % (58/64) and 37.50 % (24/46), respectively.

Blood examination

Leukocytes were counted and sorted in 30 cases, most of them being in the range of (5.55-10.4)×10⁹/L with the exception of 4 cases [(11.0-12.9)×10⁹/L]. The eosinophilic granulocyte count was high [(0.32-0.78)×10⁹/L]. The average value of constituent ratio of eosinophilic granulocyte was 0.09 (0.04-0.11) and was higher than the normal range ($P<0.01$).

Mites separated from working environment

The samples of mill floor dust (30 shares), stores of medicinal herbs (146 species) including wolfberry fruit, ophiopogon root liquorice, boat-fruited sterculia seed, safflower and other working environmental foodstuffs were collected and used for mites isolation. Numbers of mites per gram were shown to be 91-1862, 21-186, 0-483, 10-348, 51-712, and 311-1193, in mill floor dust, traditional Chinese medicine stores, traditional Chinese herbs including candied fruit, dry fruit, brown sugar, and expired cake. Twenty-two species, from 9 families of mites were separated and identified out of them, including *Acaridae*, *Lardoglyphidae*, *Glycyphagidae*, *Chortoglyphidae*, *Carpoglyphidae*, *Histiostomidae*, *Pyroglyphidae*, *Tarsonemus*, *Cheyletus*. The mite species isolates from working environment were shown to be similar to those from stored food staffs.

Relationship between acariasis and occupation

Of the 1994 subjects investigated, mites were detected in 68 individuals (15.89 %) working in traditional Chinese medical storehouses, and 53 rice storehouse or mill workers 53 (12.96 %), being higher than those with other occupations (Table 1).

Table 1 Prevalence of intestinal and urinary tract mite infection in individuals with different occupations

Occupations	n	Only in stool		Only in urine		Both in stool and urine		Total	
		n	%	n	%	n	%	n	%
Traditional medical storehouse workers	428	32	7.48	24	5.61	12	2.80	68	15.89 ^a
Rice storehouse or mill workers	409	28	6.85	12	2.93	13	3.18	53	12.96 ^a
Miners	549	16	2.91	0	0	2	0.36	18	3.28 ^a
Railway workers	236	5	2.12	0	0	1	0.42	6	2.54 ^a
Pupils	255	9	3.53	1	0.39	3	1.18	13	5.10 ^a
Teachers	117	2	1.71	0	0	1	0.85	3	2.56 ^a
Total	1994	92	4.61	37	1.90	32	1.65	161	8.07

^a $\chi^2=82.55$, $P<0.001$.

Colonoscopy

Colonoscopy performs in 16 patients with mites found only in stool, showing pale intestinal wall, punctate ulcer, and exfoliated cell from intestinal wall. In addition, live mites and eggs were observed in tissues, especially in marginal zone of ulcer.

Cystoscopy

Cystoscopy was performed in the 11 patients with mites only found in urine samples, showing Pachymucosa, uroepithelial hyperplasia, lymphocyte and plasmaocyte infiltration in membrana propria and a lot of dense pink abscess in the trigone. In addition, trabecularism of inner wall of urinary bladder changed slightly, local of lateral wall was congestive, and blood capillary was also congestive and dilated. By cystoscopy, 4 adult mites were found in 3 of 11 subjects, which were identified to be *Lardoglyphus konoii*, *Euroglyphus magnei*, *Tarsonemus granarus*, and neither larval mite nor egg was found.

DISCUSSION

The acaroid mite is a kind of arthropod and its geographic distribution appears to be global^[15,16]. Acaroid mites infestation is a well-known problem for stored grain, often influencing quality and hygienic condition of the grain^[1-9]. However, little is known about acariasis. Acaroid mite can survive in many environments including the storehouse, human and animal bodies. Its infestation in human can cause acariasis in several organs including the lung, intestine and urinary tract^[17-26].

In this study, mites were identified in 124 of the 1994 stool samples. The mite species observed in stool samples included *Acaridae*, *Glycyphagidae*, *Carpoglyphidae*, *Pyroglyphidae* and *Tarsonemus*, being in accordance with those found in the working places of the patients. This confirmed that mites being able to live in intestinal tract and causing intestinal acariasis were transmitted through living environment and stored foods. The respiratory infection through the polluted air may also be an alternative pathway. Eight sampling sites had been set up in a traditional Chinese medicine plant, and 13 mites had been isolated from the dust samples collected from the 640 L volume of air in the working environment of the plant. When dust with mites ingested, some of mites might go into intestine through mouth, nasal cavity or gorge. The mites living in intestinal tract may stimulate mechanically and damage intestinal tissues with its gnathosoma, chelicera, feet, and other structures^[27,28]. In addition, they may also intrude into mucous layer and deep tissues, and cause necroinflammation and ulcers^[29-33]. This has been approved in this study by colonoscopy, with spotty necrosis, petechial hemorrhage and ulcer observed. The most frequent symptoms of the intestinal acariasis were abdominal pain, diarrhea and pyohemofecia^[10, 34,45].

Urinary acariasis was caused by mites parasitizing in human urinary tract. Mite isolation from urine is essential for its

diagnosis. In the present study, 1994 individuals with different occupation were surveyed 69 patients found from their urine samples, 17 mite species were identified, with most of them being *Acaridida*. Apparently the pathogenic mites come from environment. Regarding the transmission path, the following possibilities have been proposed. First, the insects may enter the urinary tract by crawling from vulva. Second, they may enter the body through skin and reach urinary tract in some way. Third, mites in respiratory or alimentary system may enter the blood circulation, and reach kidney and urinary tract^[46-50]. Acarid in human urinary system may damage urethral epithelia, for the mites are good at digging. Furthermore, they can also invade loose connective tissue and small blood vessel in urinary tract, and caused an ulcer. Under cystoscopy, a lot of dense pink abscess were found in trigone of urinary bladder in this study.

The incidence of intestinal and urinary acariasis was shown in this study to vary greatly and was linked to occupations, being higher in individuals working in traditional Chinese medicine (16 %) and rice storehouses or mills (13 %) than in those with other occupations (2.5-8.1 %). The densities of mites in traditional Chinese medicine and rice storehouses were shown to be high. When peoples exposed to these environment for a long time, the possibility to be infected may be greater than those in environments with low densities of mites. It is important to note that some patients with acariasis have habits of having teas immersed by traditional Chinese herbs, such as *Liriope longipedicellata*, *Radix glycyrrhizae*, boat-fruited *sterculia* seed, and eating dried kern like dateplum persimmon, candied jujube and *Crataegus cuneata*. Therefore, the prevalence of acariasis was related to personal habits and densities of mites in working environment and stored foodstuffs.

REFERENCES

- 1 Sun HL, Lue KH. Household distribution of house dust mite in central Taiwan. *J Microbiol Immunol Infect* 2000; **33**: 233-236
- 2 Croce M, Costa-Manso E, Baggio D, Croce J. House dust mites in the city of Lima, Peru. *Investig Allergol Clin Immunol* 2000; **10**: 286-288
- 3 Arlian LG, Neal JS, Vyszenski-Moher DL. Reducing relative humidity to control the house dust mite *Dermatophagoides farinae*. *J Allergy Clin Immunol* 1999; **104**: 852-856
- 4 Mumcuoglu KY, Gat Z, Horowitz T, Miller J, Bar-Tana R, Ben-Zvi A, Naparstek Y. Abundance of house dust mites in relation to climate in contrasting agricultural settlements in Israel. *Med Vet Entomol* 1999; **13**: 252-258
- 5 Arlian LG, Neal JS, Vyszenski-Moher DL. Fluctuating hydrating and dehydrating relative humidities effects on the life cycle of *Dermatophagoides farinae* (Acari: Pyroglyphidae). *J Med Entomol* 1999; **36**: 457-461
- 6 Racewicz M. House dust mites (Acari: Pyroglyphidae) in the cities of Gdansk and Gdynia (northern Poland). *Ann Agric Environ Med* 2001; **8**: 33-38
- 7 Solarz K. Risk of exposure to house dust pyroglyphid mites in Poland. *Ann Agric Environ Med* 2001; **8**: 11-24

- 8 **Sadaka HA**, Allam SR, Rezk HA, Abo-el-Nazar SY, Shola AY. Isolation of dust mites from houses of Egyptian allergic patients and induction of experimental sensitivity by *Dermatophagoides pteronyssinus*. *J Egypt Soc Parasitol* 2000; **30**: 263-276
- 9 **Boquete M**, Carballada F, Armisen M, Nieto A, Martin S, Polo F, Carreira J. Factors influencing the clinical picture and the differential sensitization to house dust mites and storage mites. *J Investig Allergol Clin Immunol* 2000; **10**: 229-234
- 10 **Li CP**, Wang J. Intestinal acariasis in Anhui Province. *World J Gastroenterol* 2000; **6**: 597-600
- 11 **Nuttall TJ**, Lamb JR, Hill PB. Characterisation of major and minor *Dermatophagoides* allergens in canine atopic dermatitis. *Res Vet Sci* 2001; **71**: 51-57
- 12 **Basomba A**, Tabar AI, de Rojas DH, Garcia BE, Alamar R, Olaguibel JM, del Prado JM, Martin S, Rico P. Allergen vaccination with a liposome-encapsulated extract of *Dermatophagoides pteronyssinus*: a randomized, double-blind, placebo-controlled trial in asthmatic patients. *J Allergy Clin Immunol* 2002; **109**: 943-948
- 13 **Akcakaya N**, Hassanzadeh A, Camcioglu Y, Cokugras H. Local and systemic reactions during immunotherapy with adsorbed extracts of house dust mite in children. *Ann Allergy Asthma Immunol* 2000; **85**: 317-321
- 14 **Hillier A**, Kwochka KW, Pinchbeck LR. Reactivity to intradermal injection of extracts of *Dermatophagoides farinae*, *Dermatophagoides pteronyssinus*, house dust mite mix, and house dust in dogs suspected to have atopic dermatitis: 115 cases (1996-1998). *J Am Vet Med Assoc* 2000; **217**: 536-540
- 15 **Musken H**, Franz JT, Wahl R, Paap A, Cromwell O, Masuch G, Bergmann KC. Sensitization to different mite species in German farmers: clinical aspects. *J Investig Allergol Clin Immunol* 2000; **10**: 346-351
- 16 **van Hage-Hamsten M**, Johansson E. Clinical and immunologic aspects of storage mite allergy. *Allergy* 1998; **53**(Suppl 48): 49-53
- 17 **Beco L**, Petite A, Olivry T. Comparison of subcutaneous ivermectin and oral moxidectin for the treatment of notoedric acariasis in hamsters. *Vet Rec* 2001; **149**: 324-327
- 18 **Hiraoka E**, Sato T, Shirai W, Kimura J, Nogami S, Itou M, Shimizu K. A case of pulmonary acariasis in lung of Japanese macaque. *J Vet Med Sci* 2001; **63**: 87-89
- 19 **van der Geest LP**, Elliot SL, Breeuwer JA, Beerling EA. Diseases of mites. *Exp Appl Acarol* 2000; **24**: 497-560
- 20 **Hammerberg B**, Bevier D, DeBoer DJ, Olivry T, Orton SM, Gebhard D, Vaden SL. Auto IgG anti-IgE and IgG x IgE immune complex presence and effects on ELISA-based quantitation of IgE in canine atopic dermatitis, demodectic acariasis and helminthiasis. *Vet Immunol Immunopathol* 1997; **60**: 33-46
- 21 **Morris DO**, Dunstan RW. A histomorphological study of sarcoptic acariasis in the dog: 19 cases. *J Am Anim Hosp Assoc* 1996; **32**: 119-124
- 22 **Jungmann P**, Guenet JL, Cazenave PA, Coutinho A, Huerre M. Murine acariasis: I. Pathological and clinical evidence suggesting cutaneous allergy and wasting syndrome in BALB/c mouse. *Res Immunol* 1996; **147**: 27-38
- 23 **Jungmann P**, Freitas A, Bandeira A, Nobrega A, Coutinho A, Marcos MA, Minoprio P. Murine acariasis. II. Immunological dysfunction and evidence for chronic activation of Th-2 lymphocytes. *Scand J Immunol* 1996; **43**: 604-612
- 24 **Ponsonby AL**, Kemp A, Dwyer T, Carmichael A, Couper D, Cochran J. Feather bedding and house dust mite sensitization and airway disease in childhood. *J Clin Epidemiol* 2002; **55**: 556-562
- 25 **Pauffler P**, Gebel T, Dunkelberg H. Quantification of house dust mite allergens in ambient air. *Rev Environ Health* 2001; **16**: 65-80
- 26 **Zhou X**, Li N, Li JS. Growth hormone stimulates remnant small bowel epithelial cell proliferation. *World J Gastroenterol* 2000; **6**: 909-913
- 27 **Fryauff DJ**, Prodjodipuro P, Basri H, Jones TR, Mouzin E, Widjaja H, Subianto B. Intestinal parasite infections after extended use of chloroquine or primaquine for malaria prevention. *J Parasitol* 1998; **84**: 626-629
- 28 **Barrett KE**. New insights into the pathogenesis of intestinal dysfunction: secretory diarrhea and cystic fibrosis. *World J Gastroenterol* 2000; **6**: 470-474
- 29 **He ST**, He FZ, Wu CR, Li SX, Liu WX, Yang YF, Jiang SS, He G. Treatment of rotaviral gastroenteritis with Qiwei Baizhu powder. *World J Gastroenterol* 2001; **7**: 735-740
- 30 **Zhou JL**, Xu CH. The method of treatment on protozoon diarrhea. *Shijie Huaren Xiaohua Zazhi* 2000; **8**: 93-95
- 31 **Lee JD**, Wang JJ, Chung LY, Chang EE, Lai LC, Chen ER, Yen CM. A survey on the intestinal parasites of the school children in Kaohsiung county. *Kaohsiung J Med Sci* 2000; **16**: 452-458
- 32 **Herwaldt BL**, de Arroyave KR, Wahlquist SP, de Merida AM, Lopez AS, Juranek DD. Multiyear prospective study of intestinal parasitism in a cohort of Peace Corps volunteers in Guatemala. *J Clin Microbiol* 2001; **39**: 34-42
- 33 **Komatsu S**, Nimura Y, Granger DN. Intestinal stasis associated bowel inflammation. *World J Gastroenterol* 1999; **5**: 518-521
- 34 **Davis MD**, Richardson DM, Ahmed DD. Rate of patch test reactions to a *Dermatophagoides* mix currently on the market: a mite too sensitive? *Am J Contact Dermat* 2002; **13**: 71-73
- 35 **Lebbad M**, Norrgren H, Naucler A, Dias F, Andersson S, Linder E. Intestinal parasites in HIV-2 associated AIDS cases with chronic diarrhoea in Guinea-Bissau. *Acta Trop* 2001; **80**: 45-49
- 36 **Menon BS**, Abdullah MS, Mahamud F, Singh B. Intestinal parasites in Malaysian children with cancer. *J Trop Pediatr* 1999; **45**: 241-242
- 37 **Vandenplas Y**. Diagnosis and treatment of gastroesophageal reflux disease in infants and children. *World J Gastroenterol* 1999; **5**: 375-382
- 38 **Germani Y**, Minnsart P, Vohito M, Yassibanda S, Glaziou P, Hocquet D, Berthelemy P, Morvan J. Etiologies of acute, persistent, and dysenteric diarrheas in adults in Bangui, Central African Republic, in relation to human immunodeficiency virus serostatus. *Am J Trop Med Hyg* 1998; **59**: 1008-1014
- 39 **Spiewak R**, Gora A, Horoch A, Dutkiewicz J. Atopy, allergic diseases and work-related symptoms among students of agricultural schools: first results of the Lublin study. *Ann Agric Environ Med* 2001; **8**: 261-267
- 40 **Fan WG**, Long YH. Diarrhea in travelers. *Shijie Huaren Xiaohua Zazhi* 2000; **8**: 937-938
- 41 **Feng ZH**. Application of gene vaccine and vegetable gene in infective diarrhea. *Shijie Huaren Xiaohua Zazhi* 2000; **8**: 934-936
- 42 **Xiao YH**. Treatment of infective Diarrhea with antibiotic. *Shijie Huaren Xiaohua Zazhi* 2000; **8**: 930-932
- 43 **Walusiak J**, Palczynski C, Wyszynska-Puzanska C, Mierzwa L, Pawlukiewicz M, Ruta U, Krakowiak A, Gorski P. Problems in diagnosing occupational allergy to flour: results of allergologic screening in apprentice bakers. *Int J Occup Med Environ Health* 2000; **13**: 15-22
- 44 **Barret JP**, Dardano AN, Hegggers JP, McCauley RL. Infestations and chronic infections in foreign pediatric patients with burns: is there a role for specific protocols? *J Burn Care Rehabil* 1999; **20**: 482-486
- 45 **Xia B**, Shivananda S, Zhang GS, Yi JY, Crusius JBA, Peka AS. Inflammatory bowel disease in Hubei Province of China. *China Natl J New Gastroenterol* 1997; **3**: 119-120
- 46 **Bertot GM**, Corral RS, Fresno M, Rodriguez C, Katzin AM, Grinstein S. *Trypanosoma cruzi* tubulin eliminated in the urine of the infected host. *J Parasitol* 1998; **84**: 608-614
- 47 **Snowden KF**, Didier ES, Orenstein JM, Shaddock JA. Animal models of human microsporidial infections. *Lab Anim Sci* 1998; **48**: 589-592
- 48 **Mqoqi NP**, Appleton CC, Dye AH. Prevalence and intensity of *Schistosoma haematobium* urinary schistosomiasis in the Port St Johns district. *S Afr Med J* 1996; **86**: 76-80
- 49 **Greiff L**, Andersson M, Svensson J, Wollmer P, Lundin S, Persson CG. Absorption across the nasal airway mucosa in house dust mite perennial allergic rhinitis. *Clin Physiol Funct Imaging* 2002; **22**: 55-57
- 50 **Obase Y**, Shimoda T, Tomari SY, Mitsuta K, Kawano T, Matsuse H, Kohno S. Effects of pranlukast on chemical mediators in induced sputum on provocation tests in atopic and aspirin-intolerant asthmatic patients. *Chest* 2002; **121**: 143-150

Primary biliary cirrhosis and ulcerative colitis: A case report and review of literature

Wen-Bin Xiao, Yu-Lan Liu

Wen-Bin Xiao, Yu-Lan Liu, Department of Gastroenterology, People's Hospital, Peking University, Beijing 100044, China
Correspondence to: Dr. Wen-Bin Xiao, Department of Gastroenterology, People's Hospital, Peking University, Beijing 100044, China. hhxwb@263.net
Telephone: +86-10-68314422 Ext 5726 **Fax:** +86-10-68318386
Received: 2002-11-26 **Accepted:** 2002-12-25

Abstract

AIM: To summarize the characteristics of patients suffered from primary biliary cirrhosis associated with ulcerative colitis.

METHODS: To report a new case and review the literature.

RESULTS: There were 18 cases (including our case) of primary biliary cirrhosis complicated with ulcerative colitis reported in the literature. Compared with classical primary biliary cirrhosis, the patients were more often males and younger similar. The bowel lesions were usually mild with proctitis predominated. While ulcerative colitis was diagnosed before primary biliary cirrhosis in 13 cases, the presentation of primary biliary cirrhosis was earlier than that of ulcerative colitis in our new case reported here. The prevalence of primary biliary cirrhosis among patients of ulcerative colitis was almost 30 times higher than in general population.

CONCLUSION: Association of primary biliary cirrhosis with ulcerative colitis is rare. It should be considered in the differential diagnosis of hepatobiliary disease in patients with ulcerative colitis, and vice versa.

Xiao WB, Liu YL. Primary biliary cirrhosis and ulcerative colitis: A case report and review of literature. *World J Gastroenterol* 2003; 9(4): 878-880
<http://www.wjgnet.com/1007-9327/9/878.htm>

INTRODUCTION

A variety of hepatobiliary diseases have been described in patients with ulcerative colitis (UC). The incidence is 3-15 % with persistent abnormal liver function tests, and up to 90 % with abnormal liver histology at surgery or autopsy^[1]. These include primary sclerosing cholangitis, pericholangitis of the small bile ducts, chronic active hepatitis, cholangiocarcinoma and cirrhosis. The association of primary biliary cirrhosis (PBC) and UC has occasionally been reported^[2-4]. We hereby presented an additional case.

CASE REPORT

A 50-year-old woman was admitted to our hospital because of skin pruritus for two years. One year ago she was found to have jaundice and examined in another hospital. The results of all hepatitis virus test were negative, and she was diagnosed as cryptogenic hepatitis. Six months ago she had diarrhea 2-3

times per day. Upon physical examination icterus was evident on the skin and sclera. Hepatomegaly and splenomegaly were found. Blood routine test revealed hemoglobin 106 g/L, WBC and platelet counts normal. ESR 78 mm/h. IgM elevated to 7.73 g/L, IgA and IgG normal. Liver function tests showed ALT 81 U/L, AST 139 U/L, serum total bilirubin 223.2 umol/L, direct bilirubin 138.3 umol/L and GGT 1042 U/L. Cholesterol was 12.2 mmol/L. Immunological tests, by indirect immunofluorescence were as follows: ANA, 1:10 positive, anti-mitochondria antibody (AMA), negative, anti-LK (anti-liver and anti-kidney) microsome antibody and anti-smooth muscle antibody negative. Hepatomegaly, splenomegaly and portal hypertension were seen in abdominal computed tomography (Figure 1). No intra- and extrahepatic bile duct abnormalities were found by ERCP. Liver biopsy disclosed an increased portal infiltration consisting of lymphocytes, plasmacytes, and scattered eosinophils with fibrosis and pseudolobulation. Two portal areas had hyperplastic ductule. The findings were compatible with PBC stage 3-4 (Figure 2). Colonoscopy showed up to 20 cm continuous lesions of the mucosa with numerous ulcers and adherent mucopurulent exudate (Figure 3). Histological examination demonstrated loss of goblet cells, neutrophilic microabscesses in the crypts, and infiltration with mononuclear cells and plasma cells in the lamina propria (Figure 4). Ulcerative colitis limited to rectosigmoid was diagnosed. Ursodeoxycholic acid (UDCA) was prescribed. One month later serum bilirubin and liver function tests returned to normal. But diarrhea persisted and sulfasalazine was given. The bowel symptoms were then relieved.

Table 1 Review of patients of PBC associated with UC^a

Refer-ences	Patient	Sex	Age (yr)	Comorbidity	AMA (titer)
3	1	F	65	Pancolitis, chronic pancreatitis	1/64
4	2	F	20	Proctitis	Strongly
4	3	M	22	Proctitis	1/160
4	4	M	44	Proctitis	1/320
4	5	F	28	Left-side colitis	1/200
5	6	F	49	Proctitis, chronic myelocytic leukemia	Positive
6	7	F	45	Proctitis, chronic pancreatitis	Positive
7	8	M	40	Left-side colitis	1/160
8	9	F	48	Pancolitis, renal cell carcinoma	1/160
9	10	M	58	Proctitis	1/160
9	11	F	68	Proctitis	1/160
10	12	F	43	Pancolitis	>1/160
11	13	M	61	Proctitis	Positive
Present	14	F	50	Proctitis	Negative

^aFour cases with incomplete data were not shown here.

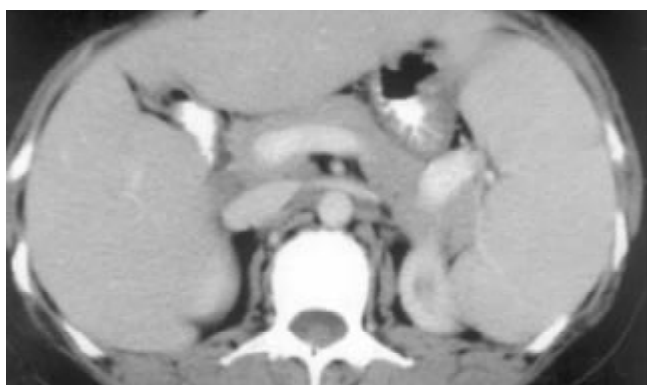


Figure 1 Abdominal CT disclosed hepatomegaly, splenomegaly and portal hypertension.

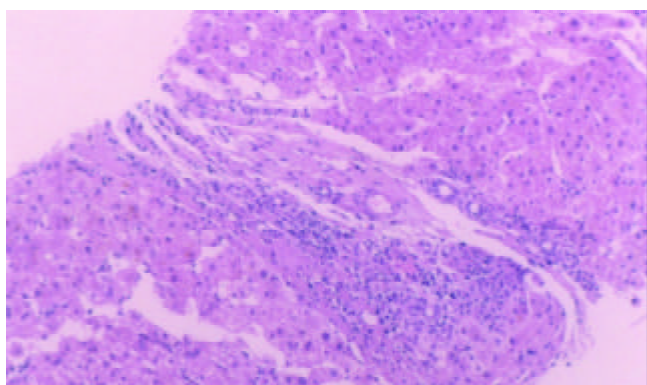


Figure 2 Liver biopsy revealed portal infiltration of lymphocytes, plasmacytes, and scattered eosinophils with fibrosis and pseudolobule (H&E, 10×10).



Figure 3 Colonoscopy showed continuous mucosal ulceration.

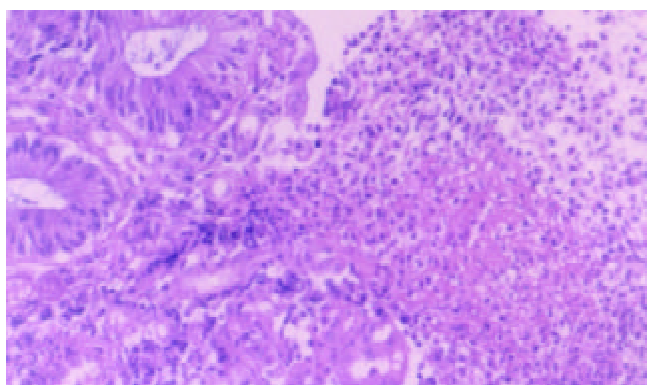


Figure 4 Histological examination demonstrated neutrophilic microabscesses in the crypts (H&E, 10×20).

DISCUSSION

Hepatobiliary diseases are commonly found in association with UC. Primary sclerosing cholangitis (PSC) involving the large bile ducts is the most common associated hepatopathy, affecting 2.4-7.5 % of UC patients. PBC is another autoimmune hepatobiliary disease similar to PSC. The typical features include skin pruritus, with hyperbilirubinemia, increased IgM levels and hypercholesterolemia. AMA is present in about 95 % of patients, that is in about 5 % AMA is negative. Cholangiogram is normal. Granulomatous inflammation of the periportal areas is a typical finding. The clinical manifestation and histologic features of our patient were compatible with PBC, although AMA was negative.

PBC associated with UC is rare. There were 18 cases (including our case) reported in the literature. In 4 cases from Sweden and Taiwan data were incomplete. In the remaining 14 patients, their presentations were different from that of typical PBC without UC (Table 1). It is well known that PBC usually affects middle-aged women. The sex ratio is 10:1 (women to men), and the mean age at diagnosis was 57.5 years. It is quite obvious that these figures differ in the patients of table 1. The sex ratio was low (2:1) and the mean age was younger similar to that of UC. In addition, UC was mild and limited with proctitis predominating. Only 3 of 12 patients had pancolitis. Similarly, UC associated with PSC tends to be mild, but usually involving the whole bowel.

The prevalence of PBC in Europe is about 15/100 000. In a cohort of 412 cases of UC, 2 cases of PBC were diagnosed estimating the prevalence of PBC among these patients 485/100 1 000, almost 30 times higher as compared with the general population^[2]. It is believed that both PBC and UC are autoimmune disease, and have similar pathogenesis. Associated autoimmune conditions are frequent in both PBC and UC. PBC and UC may be an additional example of a true association between syndromes of autoimmune etiology. But the detail remains to be clarified. In 13 out of the 14 patients UC were diagnosed many years before the diagnosis of PBC. Symptoms of PBC usually presented during the active stage of UC. In other words, PBC runs a course depending the activity of UC. So most authors considered PBC as the extraintestinal (hepatobiliary) manifestation of UC. But in our case it is clear that the presentation of PBC is earlier than that of UC. We believe that UC also could be regarded as extrahepatic manifestation of PBC.

Treatment of these patients presents some difficulties. Prednisolone, which is indicated for the treatment of the active stage of UC, might lead to extensive osteoporosis in PBC. But as mentioned above, UC associated with PBC is usually mild, so sulfasalazine is the first choice. If the presentation of PBC is evident, UDCA could be added.

In conclusion the reported association between UC and PBC is rare, and it has not yet been established whether it occurs coincidentally or is due to a common immunogenetic basis. PBC should be considered in the differential diagnosis of hepatobiliary disease in patients with UC, and vice versa. Liver biopsy and serum AMA are two diagnostic criteria that clearly distinguish PBC from PSC.

REFERENCES

- 1 **Monsen U**, Sorstad J, Hellers G, Johansson C. Extracolonic diagnoses in ulcerative colitis: an epidemiological study. *Am J Gastroenterol* 1990; **85**: 711-716
- 2 **Chien RN**, Sheen IS, Chen TJ, Liaw YF. A clinicopathological study in primary biliary cirrhosis. *J Formos Med Assoc* 1992; **91** (Suppl 2): S117-121
- 3 **Kato Y**, Morimoto H, Unoura M, Kobayashi K, Hattori N, Nakanuma Y. Primary biliary cirrhosis and chronic pancreatitis

- in a patient with ulcerative colitis. *J Clin Gastroenterol* 1985; **7**: 425-427
- 4 **Bush A**, Mitchison H, Walt R, Baron JH, Boylston AW, Summerfield JA. Primary biliary cirrhosis and ulcerative colitis. *Gastroenterology* 1987; **92**: 2009-2013
- 5 **Akahoshi K**, Miyata Y, Hashimoto M, Koga S, Chijiwa Y, Misawa T, Suematsu E, Nishimura J, Nawata H. A case of combined primary biliary cirrhosis, ulcerative colitis and chronic myelocytic leukemia. *Gastroenterol Jpn* 1992; **27**: 252-257
- 6 **Veloso FT**, Dias LM, Carvalho J, Fraga J, Saleiro J. Ulcerative colitis, primary biliary cirrhosis, and chronic pancreatitis: coincident or coexistent? *J Clin Gastroenterol* 1993; **16**: 55-57
- 7 **Lever E**, Balasubramanian K, Condon S, Wat BY. Primary biliary cirrhosis associated with ulcerative colitis. *Am J Gastroenterol* 1993; **88**: 945-947
- 8 **Satsangi J**, Marshall J, Roskell D, Jewell D. Ulcerative colitis complicated by renal cell carcinoma: a series of three patients. *Gut* 1996; **38**: 148-150
- 9 **Kourentaki M**, Koutroubakis IE, Petinaki E, Tzardi M, Oekonomaki H, Mouzas I, Kouroumalis EA. Ulcerative colitis associated with primary biliary cirrhosis. *Dig Dis Sci* 1999; **44**: 1953-1956
- 10 **Ohge H**, Takesue Y, Yokoyama T, Hiyama E, Murakami Y, Imamura Y, Shimamoto F, Matsuura Y. Progression of primary biliary cirrhosis after proctocolectomy for ulcerative colitis. *J Gastroenterol* 2000; **35**: 870-872
- 11 **Nakayama M**, Tsuji H, Shimono J, Azuma K, Ogata H, Matsumoto T, Aoyagi K, Fujishima M, Iida M. Primary biliary cirrhosis associated with ulcerative colitis. *Fukuoka Igaku Zasshi* 2001; **92**: 354-359

Edited by Xu JY

Congenital H-type anovestibular fistula

Mesut Yazlcl, Barlas Etensel, Harun Gürsoy, Sezen Özklsack

Mesut Yazlcl, Barlas Etensel, Harun Gürsoy, Sezen Özklsack,
Department of Pediatric Surgery, Faculty of Medicine, Adnan
Menderes University, Aydlın, Turkey

Correspondence to: Mesut Yazlcl, Department of Pediatric Surgery,
Faculty of Medicine, Adnan Menderes University, 09100 Aydlın,
Turkey. myazici@adu.edu.tr

Telephone: +90-256-2120020 **Fax:** +90-256-2120146

Received: 2002-12-22 **Accepted:** 2003-01-13

Abstract

The congenital H-type fistula between the anorectum and genital tract besides a normal anus is a rare entity in the spectrum of anorectal anomalies. We described a girl with an anovestibular H-type fistula and left vulvar abscess. A 40-day-old girl presented symptoms after her parents noted the presence of stool at the vestibulum. On the physical examination, anus was in normal location and size, and had normal sphincter tone. A vestibular opening was seen in the midline just below of the hymen. A fistulous communication was found between the vestibular opening and the anus, just above the dentate line. There was a vulvar abscess which had a left lateral vulvar drainage opening 15 mm left lateral to the perineum. After the management of local inflammation and abscess, the patient was operated for primary repair of the fistula. A protective colostomy wasn't performed prior the operation. A profuse diarrhea started after 5 hours of postoperation. After the diarrhea, a recurrent fistula was occurred on the second postoperative day. A divided sigmoid colostomy was performed. 2 months later, and anterior sagittal anorectoplasty was reconstructed and colostomy was closed 1 month later. Various surgical techniques with or without protective colostomy have been described for double termination repair. But there is no consensus regarding surgical management of double termination.

Yazlcl M, Etensel B, Gürsoy H, Özklsack S. Congenital H-type anovestibular fistula. *World J Gastroenterol* 2003; 9(4): 881-882
<http://www.wjgnet.com/1007-9327/9/881.htm>

INTRODUCTION

The congenital H-type fistula between the anorectum and genital tract without anal atresia is a rare entity in the spectrum of anorectal anomalies. This type of anomaly has been termed as "double termination" of the alimentary tract in girls^[1-3]. Most of the fistulas localized between the anorectum and vestibule of the vagina, and this type anomaly was described as Perineal Canal^[1,2,4-6]. We described a 40-day-old girl with a congenital anovestibular H-type fistula complicated with a vulvar abscess.

CASE REPORT

A 40-day-old girl referred to our university medical center with a passage of stool through vestibulum as well as through the normal anal passage from birth. She had been swelling and tenderness on her left vulvar region for one week. On the physical examination, anus was at the normal location and size,

and it had normal sphincter tone. A vestibular opening was found in the midline just below of the hymen. With insertion of an 8 Fr catheter through the vestibular opening, a fistulous communication was detected between the vestibule of the vagina and the anus at the dentate line. Nearly 3 mm to the left side of this opening, there was a second opening about 3 mm in diameter. A metal sound was inserted through this opening and it was found that it had a subcutaneous continuity with a vulvar abscess. This abscess was detected to drain through a cutaneous opening 15 mm lateral to the perineum (Figure 1). No associated anomaly was detected.



Figure 1 8 Fr catheter was placed in the perineal canal and metal sound was passed through vestibular and cutaneous openings of the abscess.

After the management of local inflammation and abscess, the patient was operated for primary repair of the fistula. The bowel preparation was performed with saline enemas. A protective colostomy was not performed either prior or during the definitive operation. We used the technique of anterior sagittal anorectoplasty described by Kulshrestha *et al.* in 1998^[1]. At the operation, a metal sound was passed through the fistula from the vestibule of the vagina into the anal canal in the lithotomy position. Then the perineal body that remained over the sound vertically was incised. This incision included skin, subcutaneous tissue, a few fibers of external sphincter muscle, wall of the fistulous tract and anal canal mucosa. The mucosa of the opened fistulous tract was dissected off the underlying muscle. Then, perineal reconstruction was performed by stitching the vestibule, perineal body, sphincter muscle and the anorectum with interrupted 4/0 PDS sutures. Perineal skin was closed with 4/0 Prolene. Five hours following the transfer of the patient to the ward, a profuse diarrhea started resulting in 16 defecations on the first postoperative day. Unfortunately, this caused a partial breakdown of the wound on the second postoperative day, which caused the recurrence of the fistula. And the divided sigmoid colostomy was performed.

Two months later, we operated with the same technique and this attempt was successful. One month following the repair of the fistula, we closed her colostomy and started a rectal dilatation program. Her first year postoperative follow-up was uneventful.

DISCUSSION

The incidence of double termination among female anorectal malformations ranged between 4-14 % in different Asian series^[1,5-8]. On the basis of Wingspread classification, these H-type fistulas were divided into three groups according to their level. Low type double termination included cases in which the fistula was lying between the anal canal and the vestibule and this was named as "perineal canal". In the intermediate type, communication was found between the rectum and the vestibule. High type of double termination consisted of a fistula between the rectum and the vagina^[1]. Our case had a low type double termination and an abscess which was detected in her vulvar region complicated her anomaly. When we reviewed the cases reported in the literature, we found out that Rintala *et al.* reported vulvar abscess formation in three girls with double termination^[2]. In another report by Brem *et al.* abscess formation was claimed to be secondary to the infection in either a congenital blind-ending sinus or an existing fistula leading to additional openings^[9].

On the other hand, high type of vestibular fistula demands a more specific operation and it may be named as vestibulorectal pull-through procedure. Without protective colostomy, this type of repair is reported to have a fairly high recurrence rate^[7]. Various surgical techniques have been described for low-type double termination repair. These techniques were utilized either with or without protective colostomy in different series. Chatterjee described a simple perineal procedure without colostomy and with good results^[3]. Tsuchida *et al* did not use diversion during definitive procedure they named as "pull-through of the anterior wall of the rectum" in 3 of his 7 cases with perineal canal. Their results were satisfactory for both diverted and non-diverted cases. However, they were not as successful as above with their cases managed with another different simple repair technique and without diversion^[5]. Kulshrestha *et al.* described anterior sagittal anorectoplasty in 1998 as a surgical technique for all types of double termination without colostomy and without no complications^[1]. This series which were the most recent and had a successful outcome for the repair of perineal canal directed us to prefer this technique in our series. Furthermore,

avoiding a colostomy in using this technique was another major factor for our selection.

Unfortunately, our case's fistula recurred. This may have resulted not from insufficiency of the technique, but from some factors that did not take place in Kulshrestha's series. A major reason for breakdown of the repair may be due to the unexpected and unwanted profuse diarrhea of the patient that started after 5 hours of the post-operation. The sufficiency of the technique may be thought of when one thinks that in the redo operation, it was proved to be a good result.

In conclusion, it is believed that definitive repair can be performed without protective colostomy when no abscess formation is present in the vulvar region. If an abscess is detected, it should be well managed before the operation.

REFERENCES

- 1 **Kulshrestha S**, Kulshrestha M, Prakash G, Gangopadhyay AN, Sarkar B. Management of congenital and acquired H-type anorectal fistulae in girls by anterior sagittal Anorectovaginoplasty. *J Pediatr Surg* 1998; **33**: 1224-1228
- 2 **Rintala RJ**, Mildh L, Lindahl H. H-type anorectal malformations: incidence and clinical characteristics. *J Pediatr Surg* 1996; **31**: 559-562
- 3 **Chatterjee SK**, Talukder BC. Double termination of the alimentary tract in female infants. *J Pediatr Surg* 1969; **4**: 237-243
- 4 **Rao KL**, Choudhury SR, Samujh R, Narasimhan KL. Perineal canal-repair by a new surgical technique. *Pediatr Surg Int* 1993; **8**: 449-450
- 5 **Tsuchida Y**, Saito S, Honna T, Makino S, Kaneko M, Hazama H. Double termination of the alimentary tract in females: a report of 12 cases and a literature review. *J Pediatr Surg* 1984; **19**: 292-296
- 6 **Wakhlu A**, Pandey A, Prasad A, Kureel SN, Tandon RK, Wakhlu AK. Anterior Sagittal anorectoplasty for anorectal malformations and perineal trauma in the female child. *J Pediatr Surg* 1996; **31**: 1236-1240
- 7 **Chatterjee SK**. Double termination of the alimentary tract-a second look. *J Pediatr Surg* 1980; **15**: 623-627
- 8 **Bagga D**, Chadha R, Malhotra CJ, Dhar A. Congenital H-type vestibuloanorectal fistula. *Pediatr Surg Int* 1995; **10**: 481-484
- 9 **Brem H**, Guttman FM, Laberge JM, Doody D. Congenital anal fistula with normal anus. *J Pediatr Surg* 1989; **24**: 183-185

Edited by Xu XQ

A case of enterolith small bowel obstruction and jejunal diverticulosis

Buhussan Hayee, Hamed Noor Khan, Talib Al-Mishlab, John F McPartlin

Buhussan Hayee, Hamed Noor Khan, Talib Al-Mishlab, John F McPartlin, Department of Surgery, William Harvey Hospital, Ashford, Kent TN24, U.K.

Correspondence to: Dr. Hamed Khan, Flat 11, the Point, 6 Bellargate, Nottingham, NG1 1JN, U.K. hamed4Khan@aol.com

Telephone: +44 -115-9242809

Received: 2002-11-19 **Accepted:** 2003-01-13

Abstract

We reported a case of 79-year old woman with known large bowel diverticulosis presenting with small bowel obstruction due to stone impaction - found on plain abdominal X-ray. Contrast studies demonstrated small bowel diverticulosis. At laparotomy, the gall bladder was normal with no stones and no abnormal communication with small bowel - excluding the possibility of a gallstone ileus. Analysis of the stone revealed a composition of bile pigments and calcium oxalate. This was a rare case of small bowel obstruction due to enterolith formation - made distinctive by calcification (previously unreported in the proximal small bowel).

Hayee B, Khan HN, Al-Mishlab T, McPartlin JF. A case of enterolith small bowel obstruction and jejunal diverticulosis. *World J Gastroenterol* 2003; 9(4): 883-884
<http://www.wjgnet.com/1007-9327/9/883.htm>

INTRODUCTION

Diverticulosis of the small bowel (excluding Meckel's) is uncommon - being found in less than 5 % of post-mortem examinations, although the prevalence increases with age^[1]. The condition can be complicated by diverticulitis, haemorrhage or perforation^[2,3]. Small bowel obstruction due to an enterolith formed and extruded from a diverticulum is a rare complication^[4-6].

Enteroliths form in small bowel diverticula either *de novo* or around a central nidus such as a fruit stone or undigested vegetable matter (the latter is termed a bezoar). The usual composition of true enteroliths is choleic acid^[7] - an end product of bile salt metabolism - postulated to form as a result of acidic pH shift within a small bowel diverticulum. Radiological diagnosis of such stones is rare, unless calcified (which usually occurs only in the more alkaline ileum)^[7]. Diagnosis is therefore made at laparotomy with the presence of the stone, diverticula and the finding of a normal gall bladder (excluding a gallstone ileus). It is unclear how stones are extruded from small bowel diverticula lacking a muscular coat, but larger stones will be extruded and pass distally to cause obstruction - an enterolith ileus.

CASE REPORT

A 79-year-old lady presented with a two-day history of vomiting and central, colicky abdominal pain. She had been constipated prior to this episode and had taken senna with only a little effect on the previous day. She had a known history of

sigmoid diverticular disease and had been admitted only once previously for suspected diverticulitis. She appeared dehydrated with fever of 37.6 degrees. Her abdomen was distended but soft with some central and left-sided tenderness. Bowel sounds were heard and digital rectal examination was unremarkable. Blood tests revealed a white cell count of $21.6 \times 10^9/L$ without other abnormality. A plain abdominal film demonstrated opacity on the left side (Figure 1) and a gastrograffin study revealed numerous small bowel diverticula of varying sizes. The opacity now was presumed to be a stone, was noted within the small bowel (Figure 2).



Figure 1 Radio-opaque stone was clearly seen in the plain abdominal radiograph (arrow).



Figure 2 Contrast study (105 mins) demonstrated multiple jejunal diverticula and minimal passage of barium beyond the mid-jejunum. Stone was still visible (arrow).

At laparotomy, the presence of large jejunal diverticula was confirmed and the stone was found impacted in the mid-

jejunum. The gall bladder appeared normal without stones. The stone approximately 3×4 cm and weighing 10.60 g appeared greyish and hard which was removed via a small enterotomy close to it. The patient made a good recovery from operation, delayed only by post-operative nausea. Analysis of the stone revealed a composition of bile pigments and calcium oxalate.

DISCUSSION

We reported the first case of proximal small bowel obstruction due to a calcified enterolith. It is postulated that diverticulas provide the more acidic environment necessary for choleic acid precipitation and stone formation^[7]. However calcification cannot occur without an alkaline pH shift, which normally occurs in the ileum. Our case confirmed calcification occurring in the proximal small bowel which made this theory less definitive but facilitated the diagnosis.

The consensus management of enterolith ileus at laparotomy is to first attempt manual lysis of the stone without enterotomy and to milk the smaller parts into the colon where they are passed through rectum^[8]. If this is proved to be impossible or inappropriate, the stone is removed through an enterotomy which is made in a less edematous segment of proximal small bowel.

The rarity of enterolith small bowel obstruction is well recognised with the condition occurring in conjunction with

cases of diverticulosis. However the diagnosis should be considered in patients presenting with clinical features of small bowel obstruction without evidence of previous abdominal surgery or incarcerated hernia.

REFERENCES

- 1 **Noer T**. Non-Meckelian diverticula of the small bowel. *Acta Chir Scand* 1960; **120**: 175-179
- 2 **Longo WE**, Vernava AM 3rd. Clinical implications of jejunal diverticular disease. *Dis Colon & Rectum* 1992; **35**: 381-388
- 3 **Sibille A**, Wilcox R. Jejunal diverticulitis. *Am J Gastroenterol* 1992; **87**: 655-658
- 4 **Yang HK**, Fondacaro PF. Enterolith ileus: a rare complication of duodenal diverticula. *Am J Gastroenterol* 1992; **77**: 621-624
- 5 **Ishizuka D**, Shirai Y, Hatakeyama K. Duodenal obstruction caused by gallstone obstruction into an intraluminal duodenal diverticulum. *Am J Gastroenterol* 1997; **92**: 182-183
- 6 **Klingler PJ**, Seelig MH, Floch NR, Branton SA, Metzger PP. Small intestinal enteroliths: unusual cause of small intestinal obstruction: report of three cases. *Dis Colon & Rectum* 1999; **42**: 676-679
- 7 **Shocket E**, Simon SA. Small bowel obstruction due to enterolith (bezoar) formed in a duodenal diverticulum: a case report and review of the literature. *Am J Gastroenterol* 1982; **77**: 621-624
- 8 **Yang HK**, Fondacaro PF. Enterolith ileus: a rare complication of duodenal diverticula. *Am J Gastroenterol* 1992; **87**: 1846-1848

Edited by Xu XQ

Expression of hepatitis C virus hypervariable region 1 and its clinical significance

Xin-Xin Zhang, Shen-Ying Zhang, Jing Liu, Zhi-Meng Lu, Yuan Wang

Xin-Xin Zhang, Jing Liu, Yuan Wang, State Key Laboratory of Molecular Biology, Institute of Biochemistry and Cell Biology, Shanghai Institutes for Biological Sciences, Chinese Academy of Sciences, Shanghai, 200031, China

Xin-Xin Zhang, Shen-Ying Zhang, Zhi-Meng Lu, Department of Infectious Diseases, Rui Jin Hospital, Shanghai Second Medical University, Shanghai, 200025, China

Correspondence to: Dr. Yuan Wang, Institute of Biochemistry and Cell Biology, 320 Yue Yang Road, Shanghai, 200031, China. wangyuan@server.shnc.ac.cn

Telephone: +86-21-54921103 **Fax:** +86-21-64675170

Received: 2002-12-22 **Accepted:** 2003-01-16

Abstract

AIM: To explore the properties of hypervariable region 1 (HVR1) in the envelope 2 gene of hepatitis C virus by analyzing the reactivity of HVR1 fusion proteins from different Chinese HCV strains with sera of patients with chronic hepatitis C and by comparing their reactivity between interferon therapy responders and non-responders.

METHODS: Gene fragments of HVR1 of four HCV strains (three genotype 1b and one genotype 2a) were amplified from pGEMT-E2 plasmids and sub-cloned into pQE40 vectors respectively to construct recombinant expression plasmids which expressed HVR1 fused downstream to DHFR in *Escherichia coli* strain TG1. The purified DHFR-HVR1 proteins were then used to detect the anti-HVR1 antibodies in 70 serum samples of patients with chronic hepatitis C.

RESULTS: Four DHFR- HVR1 fusion proteins were successfully expressed in *E. coli* (320-800 µg fusion proteins per 100 ml culture). Each fusion protein (SH1b, BJ1b, SD1b and SD2a) reacted with 72.8 % (51/70), 60 % (42/70), 48.6 % (34/70), and 58.6 % (41/70) of the anti-HCV positive patients' sera respectively by ELISA. 57.1 % (4/7) of non responders reacted with all four HVR1 fusion proteins, while only 15.3 % (2/13) of responders reacted with all of them. The O.D. values of sera from IFN therapy responders were significantly higher than those of non responders ($P < 0.05$).

CONCLUSION: The selected HVR1 fusion proteins expressed in *E. coli* can broadly react with HCV-infected patients' sera. The intensity and/or quality of the immune response against HCV may be a critical factor determining the response to interferon treatment. With the evolution of virus strains, anti-HVR1 antibodies can not neutralize all the quasispecies. A polyvalent and high immunogenic vaccine comprising a mixture of several HVR1 sequences that cover the reactivity of most HCV isolates may be useful.

Zhang XX, Zhang SY, Liu J, Lu ZM, Wang Y. Expression of hepatitis C virus hypervariable region 1 and its clinical significance. *World J Gastroenterol* 2003; 9(5): 1003-1007
<http://www.wjgnet.com/1007-9327/9/1003.htm>

INTRODUCTION

Hepatitis C virus (HCV) is the major etiologic agent of blood transfusion-associated and sporadic non-A non-B hepatitis worldwide. About 70 % of the infections become chronic, among which a significant proportion eventually develops cirrhosis and hepatocellular carcinoma. Despite recent success after the combination therapy with Interferon- α and ribavirin^[1-3], about 60 % of patients still fail to respond. Thus, the development of HCV vaccine is especially important, but it remains an urgent challenge due to the high mutation rate of HCV.

Multiple lines of evidence indicate that one of the principal neutralization determinants corresponds to the hypervariable region 1 (HVR1), which is located in the amino-terminus of E2 of HCV (nt1150-1230). Zibert *et al*^[4] found that an early appearance of antibodies directed to HVR1 is associated with acute self-limiting infection of HCV, while the persistence of HVR1 antibodies is associated with chronic HCV infection. Antibodies against HVR1 have been shown to block adsorption to susceptible cells *in vitro*^[5,6]. Animal antibodies raised against this region have provided effective prophylaxis in chimpanzee challenge experiments^[7-9], but attempts to develop a HVR1 vaccine against HCV were hampered by the frequent mutations of HVR1. Although anti-HVR1 antibodies react with HVR1 proteins specifically, a single fraction of antibodies has potentiality to react with more than one HVR1 protein sharing a similar amino acid sequence^[10]. These findings suggest that HVR1 may play an important role in the prevention of HCV infection.

Our previous study^[11] analyzed the variability of HCV envelope region in 12 dominant strains from different cities of China and predicted the immunogenicity with computer programs, demonstrating that genotypes and epidemic areas should be considered when identifying the cross-reactive epitopes for vaccine design. In this study, we selected four HCV strains of two genotypes from three regions (Shanghai, Beijing and Shandong) of China according to the results of the variant analysis and immunogenicity prediction of the envelope region in Chinese HCV strains. The gene fragments of HVR1 were amplified from four corresponding pGEMT-E2 plasmids and sub-cloned into pQE 40 vectors respectively to construct four recombinant prokaryotic expression plasmids that can express HVR1 as fusion proteins with DHFR. The purified DHFR- HVR1 proteins were then used to detect the anti-HVR1 antibodies in sera of patients with chronic hepatitis C to further explore their antigenicity and analyze the different reactivity between IFN therapy responders and non-responders.

MATERIALS AND METHODS

Patients

Fifty HCV-infected patients were studied, who were all anti-HCV positive by commercial anti-HCV assays (third generation of enzyme-linked immunosorbent assay [ELISA], Abbott, North Chicago, IL). Of these, 20 patients received interferon (IFN) therapy, Roferon (Roche, Switzerland), 3 million units three times a week for 6 months. 13 patients who showed negativity of serum HCV RNA and normalization of

alanine aminotransferase (ALT) level after cessation of IFN were considered as responders, while the other 7 patients who remained HCV RNA positive and/or presented fluctuation of ALT were designed non responders (Table 1). Quantitation of serum HCV RNA was performed using commercial kit from Fu Hua Gene Company, Shanghai. Informed consent was obtained from all the patients, and study protocol was approved by the committee on human ethics. 20 healthy blood donors who were anti-HCV negative were also analyzed as negative control.

Table 1 Characteristics of chronic hepatitis C patients treated with IFN- α

	Responders	Non responders
Number	13	7
Age (Yr)	41	40
Sex (F/M)	5/8	2/5
Known duration of infection (Yr)	10.6	9.9
Baseline ALT (IU/ml)	185	126 (P=0.1660)
Baseline viral load (copies/ml)	4.37 $\times 10^6$	2.92 $\times 10^6$ (P=0.6908)

Methods

Construction of recombinant expression plasmids Part of E2/NS1 regions was cloned from sera of the patients and sequenced as described before^[11]. From these plasmids pGEMT-E2, DNA fragments containing HVR1 (nt1150-1233, aa384-411) were amplified by PCR. The primers for HCV strain Shanghai 1b (SH1b), sense: nt1150-1161, 5' TTAGATCTGCAACCTACACG3', anti-sense: nt1225-1233, 5' CCCAAGCTTAGATTTTCTG3'; the primers for strain Beijing 1b (BJ1b), sense: nt1150-1161, 5' TTAGATCTGGCACCTATACG3', anti-sense: same as SH1b; the primers for strain Shandong 1b (SD1b), sense: nt1150-1159, 5' TTAGATCTGAGACCCGTG3', anti-sense: same as SH1b, and the primers for Shandong 2a (SD2a), sense: nt1150-1159, 5' TTAGATCTAGCACCCACG 3', anti-sense: nt1225-1233, 5' CCCAAGCTTAGATGTTCTG3'. The PCR products were purified and ligated into the Hind III, Bgl II sites of the expression vector pQE40 which allows fusion of HVR1 encoding sequences downstream to the murine dihydrofolate reductase (DHFR) with a N-terminal 6 \times His tag.

The recombinant plasmids were identified by digestion with Hind III and Bgl II. The inserts were then sequenced to ensure that the DNA encoded the authentic HCV sequence. The identified plasmids were named as pQE40-HVR1-SH1b, BJ1b, SD1b and SD2a respectively.

Expression and purification of the fusion proteins The recombinant plasmids and pQE40 vector were transformed to E.coli strain TG1.DHFR-HVR1 fusion proteins were expressed by induction with 1 mmol/l isopropyl- β -D-thiogalactotyranside (IPTG) in 100 ml of LB/ampicillin media cultured at 37 $^{\circ}$ C with vigorous shaking. After 6 h of induction, cells were harvested by centrifugation at 4 $^{\circ}$ C and 5 000 g for 30 min.

Harvested cells were re-suspended in 10 ml of 8M urea/20mM β -ME/PBS pH8.0, and cell disruption was performed using an ultrasound sonication method. After centrifugation at 20 000 g and 4 $^{\circ}$ C for 30 min, the supernatant was saved for purification on Ni²⁺-nitrilotriacetate (NTA)-agarose (Qiagen) according to manufacture's instructions at room temperatures. Denatured crude extract was allowed to bind to Ni²⁺-NTA-agarose pre-equilibrated in 8M urea/20mM β -ME/PBS pH8.0 for 2 h. The gel matrice were then washed with the same solution pH6.3 and gel-bound proteins were eluted with that of pH4.3.

The purified fusion proteins were run on 12 % sodium

dodecyl sulfate -polyacrylamide gel electrophoresis (SDS-PAGE) for identification. For protein visualization and quantification, gels were stained with Coomassie brilliant blue (Sigma). The purity and yield of recombinant proteins were calculated from densitometric scanning results by comparing with known quantity of BSA (Bio-Rad) run on the same gel.

ELISA The plates were coated with four purified fusion proteins respectively or combined at of 0.2 μ g/well for 1 hour at 37 $^{\circ}$ C and then overnight at 4 $^{\circ}$ C in carbonate buffer pH 9.5. After blocking with 1 % BSA for 1 hour at 37 $^{\circ}$ C, sera were dispended in wells at a dilution of 1:20 and incubated for 45 min at 37 $^{\circ}$ C, followed by washing. HRP conjugated goat anti-human IgG (Sino-American Biological Company) diluted 1:8 000 was then added and plates were incubated for 45 min at 37 $^{\circ}$ C. After washing, the color was developed using TMB according to standard procedures, and the optical density values were measured at 450nm (OD₄₅₀) in automatic photometer (Wellsan K3, Labssystem Company).

Statistical analysis

The results were analyzed by the *t* test. In all analyses, a *P* value less than 0.05 was considered statistically significant.

RESULTS

Construction of the recombinant plasmids

Four recombinant plasmids expressing HVR1 fused with DHFR were constructed as described in methods. Obtained clones were digested with Hind III and Bgl II, 95bp fragments of HVR1 coding sequences could be detected from each of them (Figure 1). Automatic sequencing confirmed that the inserted HVR1 fragments corresponded to reported data (Figure 2). The reading frames of the recombinant plasmids were correct.

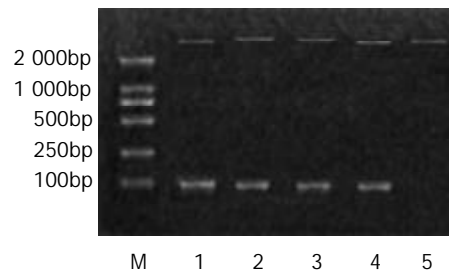


Figure 1 Digestion of the recombinant plasmids with HindIII and Bgl II. M is DNA marker (DL 2000). Lane 1-lane 4 show four recombinant plasmid digestion results, SH1b, BJ1b, SD1b and SD2a respectively. Lane 5 is the control (pQE40).

```
HVR1-SH1b  GCAACCTACA  CGACGGGGGG  GCGCGCTTCC
          CACAACACCC
HVR1-BJ1b  -GC----T-  -----  ---CAGGG-  -GTGC----
HVR1-SD1b  -AG---CGTG  T-----  --T-CAAAG-  T-T-C-CT--
HVR1-SD2a  AGC--C-G  TC--T-T--  CATT--G-G  -G-GC-G--A
```

```
HVR1-SH1b  GGGGGTTTAC  GTCCCTCTTT  AGTTCTGGGT  CGCAGCAGAA
HVR1-BJ1b  A---CC-C-  -----  TCACG-----  --GCT----
HVR1-SD1b  ----CC-C-  -----  -CG-----C  -AGCT----
HVR1-SD2a  -CA-T-CGT  CAG-T-GC-C  -CCC---ACG  -TA-A-----
```

```
HVR1-SH1b  A
HVR1-BJ1b  -
HVR1-SD1b  -
HVR1-SD2a  C
```

Figure 2A The nucleotide sequences of the four HVR1 frag-

ments in recombinant pQE40-HVR1 plasmids. Dashes represent nucleotides identical to those of HVR1-SH1b.

```

384                               410
CONSENSUS ETHVTGGVAG HTTSGFTSLF TSGPSQK
HVR1-SH1b A-YT---A-S -N-R-----S--SQ--
HVR1-BJ1b G-YT---AQ- RA-Q-L----R-SA--
HVR1-SD1b --R-----QS Y-LA-L-----A--
HVR1-SD2a G-----I-A RAA-S-V--L -PDAK--

```

Figure 2B Deduced amino acid sequence of the HVR1 fragments in pQE40-HVR1. Sequences are shown with a single-letter amino acid code where residue is different from the consensus sequence of genotype 1b defined by Hattori *et al.*, and with a dash where residue is identical.

Expression and purification of the fusion proteins

The proteins expressed in transformed *E. coli* were analyzed by SDS-PAGE. The fusion proteins migrated as an approximately 28 kDa band, approximately 3 kDa larger than DHFR (Figure 3A), in accordance with the fusion of 28 aa HVR1. Figure 3B shows the SDS-PAGE result of four purified fusion proteins and DHFR. The concentrations estimated by BSA grades are 0.4–1.0 $\mu\text{g}/\mu\text{l}$, so about 320–800 μg of purified protein can be obtained from every 100 ml of bacteria culture.

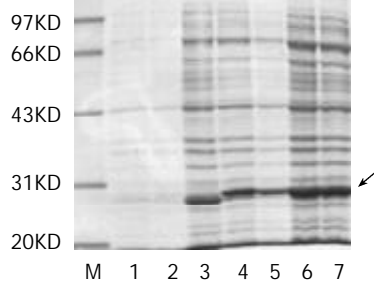


Figure 3A SDS-PAGE of the fusion proteins expressed in *E. coli* strain TG1. M: protein molecular marker. Lane 1 is vector pQE40 before induction, Lane 2 is one of the recombinant plasmids before induction. Lane 3–7, are recombinant plasmids pQE40-SH1b, BJ1b, SD1b, and SD2a after 4 hours of induction with 1 mmol/l IPTG respectively.

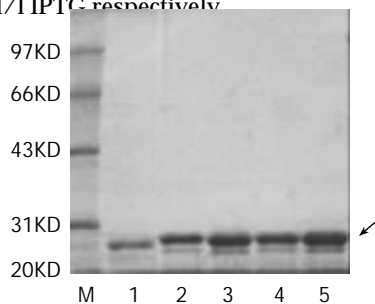


Figure 3B Results of the purified proteins. M is protein marker. Lane 1 is plain DHFR. Lane 2–5 are the fusion proteins SH1b, BJ1b, SD1b and SD2a serially.

Detection of anti-HVR1 Ab in HCV infected patients' sera

Anti-HVR1 antibodies were detected in 70 serum samples from 50 patients with chronic hepatitis C (sera were tested before and after IFN therapy for 20 patients) using the four DHFR-HVR1 fusion proteins respectively. None of the healthy blood donors, who were anti-HCV negative, was anti-HVR1 positive. Anti-HCV seronegative healthy donors had mean OD₄₅₀ value of 0.06. Sera were scored positive showing OD value >0.2 (cut off = 3 time mean neg + 10%) in at least two experiments.

Each fusion protein (SH1b, BJ1b, SD1b and SD2a) reacted with 72.8% (51/70), 60% (42/70), 48.6% (34/70), and 58.6% (41/70) of the anti-HCV positive patients respectively. SH1b was the most broadly reactive fusion protein. 91.4% (64/70) of the tested sera reacted positively with one or more fusion proteins, and among these, 89.1% (57/64) can react with more than one fusion proteins, 20.3% (13/64) samples of these sera were shown to react with all four fusion proteins.

The reactivity of sera was compared between responders and non-responders in 20 patients who received interferon therapy (Table 2). The reactive rates of sera with the four fusion proteins were higher in non-responders than in responders before interferon therapy, but there was no statistical significance. 57.1% (4/7) of non-responders reacted with all four DHFR-HVR1 fusion proteins, while only 15.3% (2/13) of responders react with all of them (Figure 4). With the three fusion proteins (SH1b, BJ1b and SD2a), the ODs of the serum reactivity of the non-responders were higher than those of responders, and the difference had statistical significances for the four mixed proteins between the two groups of patients ($P < 0.05$) (Figure 5).

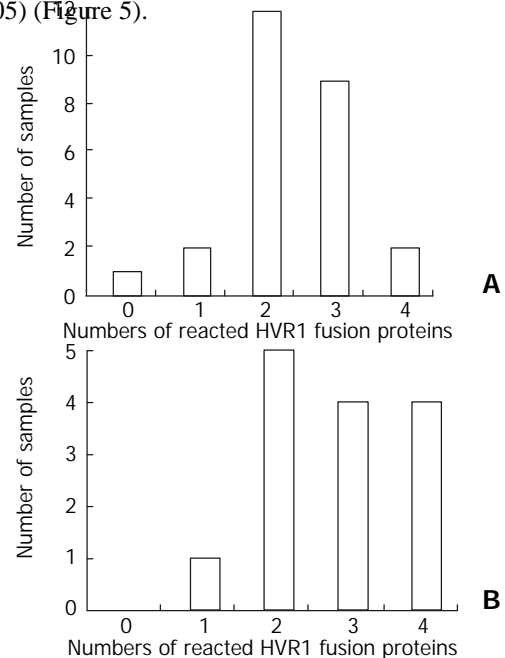


Figure 4 The serum of hepatitis C patients reacted with different numbers of HVR1 fusion proteins. A shows that the sera of IFN responders reacted with 0–4 kinds of HVR1 sequence; B shows that the sera of IFN non-responders reacted with 1–4 kinds of HVR1 sequence.

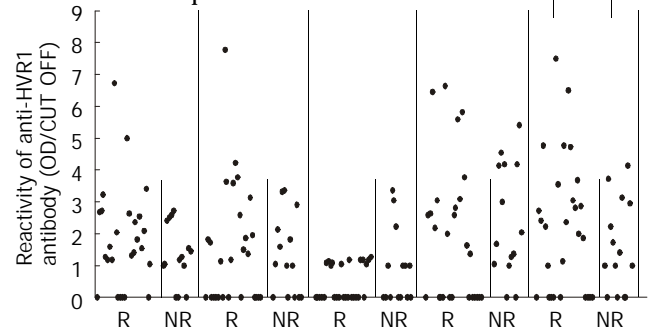


Figure 5 The OD values of 40 HCV-infected patients' sera reacted with the four HVR1 fusion proteins respectively or totally, which were compared between R (IFN-responders) and NR

(IFN-non responders). For the mixed fusion proteins, the values (OD/CUT OFF) of the responders' sera were significantly higher than those of non-responders ($P=0.0358$).

Table 2 The serum reactive rates of chronic hepatitis C patients with the four HVR1 fusion proteins before IFN therapy

Proteins	Responders(13)	Non responders(7)	Total(20)
SH1b	69.2 % (9/13)	85.7 % (6/7)	75 % (15/20)
BJ1b	53.8 % (7/13)	57.1 % (4/7)	55 % (11/20)
SD1b	30.8 % (4/13)	71.4 % (5/7)	45 % (9/20)
SD2a	69.2 % (9/13)	71.4 % (5/7)	70 % (14/20)
MIX	69.2 % (9/13)	71.4 % (5/7)	70 % (14/20)

DISCUSSION

Antibodies against HVR1 of the main envelope protein of HCV are hypothesized to be neutralizing, but frequent mutation in HVR1 is driven by the host's humoral immune response^[12] and is a major mechanism of viral persistence by escaping host immune recognition^[13,14]. The relationship between the severity of liver diseases and the molecular evolution of HCV during chronic infection remains unclear and controversial^[15]. HVR1 has the potential to provide a viral antigen for vaccine development, and the cross-reactivity of HVR1 sequences is an essential consideration in the development of a broadly protective vaccine to prevent HCV infection. Cerino *et al*^[16] reported that the appearance of anti-HVR1 is earlier than anti-E2, and the early appearance of anti-HVR1 antibodies may be predictive of the later clearance of HCV. It has also been found that HVR1 sequences could induce anti-HVR1 antibodies capable of reacting with many HVR1 sequences *in vitro* other than the original immunogen sequence^[17]. It might be the conserved sub-regions in HVR1 sequences that determined the observed immunological cross-reactivity, by which it may eventually be possible to develop a polyvalent vaccine using a mixture of several HVR1 sequences that cover the reactivity of most HCV isolates.

Synthetic HVR1 peptides have been used in many studies, but this method is too expensive to be used widely. Hattori *et al*^[10] successfully expressed HVR1 (aa383-410) as fusion proteins with GST (about 32kDa) in *E.coli* DH5 α , and each fusion protein reacted with 36.1 % to 59.3 % of HCV infected patients' sera. Others reported different reactivity of chronic hepatitis C patients' sera with HVR1 proteins from 15 % to 67 %^[18,19]. In this study, we selected four HCV strains of two genotypes from our previous reported clones (SH1b, BJ1b, SD1b and SD2a), because the HVR1 fragments in these four strains was predicted to have higher hydrophilicity and possess 2-3 immunogenic epitopes in each of them^[11]. We used pQE40 vector to express HVR1 fused with DHFR in *E.coli*. pQE40 is constructed for expression of N-terminally 6 \times his-tagged DHFR-fusion proteins and is recommended for expression of poorly expressed proteins or short peptides. DHFR could enhance both stability and antigenicity of the fusion protein, while DHFR itself displays little immunogenicity^[20].

The reactivity of the fusion proteins with HCV-infected patients' sera, especially SH1b was higher than most reports. We selected the HVR1 sequences according to computer prediction. The reason that the selected HVR1 sequence reacted with a considerable proportion of HCV-infected patients' sera may be that cross-reactive antibodies react with the different HVR1 proteins through common epitopes, as suggested by Scarselli *et al*^[21]. It might also be the consequence of exposure to multiple strains of HCV.

HCV genotype and the baseline level of viremia have been pointed out as the most important predictive factors of responsiveness to IFN therapy^[22]. However, several studies

suggested that other factors, such as the heterogeneity of virus population^[23] and replication in PBMC^[24], might also influence the effectiveness of therapy. Like most RNA viruses, HCV circulates in the human host as a complex population of different but closely related viral variants, commonly referred to as quasispecies^[25]. It has been suggested that a reduction in genetic diversity leading to an increasingly homogeneous viral population in the envelope genes, and especially in the HVR1 of the E2 gene, is likely to be the result of a more successful and balanced cellular and humoral immune response^[26], which can be observed in IFN therapy responders with viral clearance^[27,28]. It was also reported that the broad reactivity of serum anti-HVR1 antibodies correlated with viral loads and response to IFN in genotype-1b-infected patients^[10]. But Del porto *et al*^[29] found that the frequency of anti-HVR1 T cell response was significantly higher in patients who recovered after IFN therapy than that in those who did not, while no difference in the anti-HVR1 antibody reactivities were detected. In our study, the reactive rates of the four HVR1 fusion proteins with patients' sera were higher in non-responders than those in responders, although there was no statistical difference, which might be due to insufficient number of patients. Meanwhile, 57.1 % (4/7) of non responders reacted with all four HVR1 fusion proteins, while only 15.3 % (2/13) of responders reacted with all of them. These facts suggested that the genetic diversity of HCV was greater in non responders than that in responders. The broad cross-reactivity of anti-HVR1 anti-bodies causes the inefficiency of neutralizing activity as proposed by the theory of "viral antigenic sin"^[21,30]. According to this theory, after the exposure to the first immunodominant and cross-reactive virus strain, patients produce not a new antibody to the second related virus strain, but an antibody to the original antigen, which is inefficient to neutralize the new variant. The findings that the serum reactive rates with the four HVR1 fusion proteins were higher in non responders than in responders may be interpreted by this theory. On the other hand, the O.D. values of anti-HVR1 antibodies were higher in responders than those in non responders. This reflected the immune status of these patients and implied that the pre-therapy immune response is a major factor determining eventual virus elimination as suggested by others^[31,32].

In conclusion, the selected HVR1 fusion proteins expressed in *E. coli* can broadly react with HCV-infected patients' sera. The intensity and/or quality of the immune response against HCV could be a critical factor determining the response to treatment. With the evolution of virus strains, anti-HVR1 antibodies could not neutralize all the quasispecies. A polyvalent and high immunogenic vaccine combining a mixture of several HVR1 sequences that cover the reactivity of most HCV isolates might be useful.

REFERENCES

- 1 **Poynard T**, Marcellin P, Lee SS, Niederau C, Minuk GS, Ideo G, Bain V, Heathcote J, Zeuzem S, Trepo C, Albrecht J. Randomized trial of interferon alpha 2b plus ribavirin for 48 weeks or for 24 weeks versus interferon alpha 2b plus placebo for 48 weeks for treatment of chronic infection with hepatitis C virus. International Hepatitis Interventional Therapy Group (IHIT). *Lancet* 1998; **352**: 1426-1432
- 2 **Wietzkebetaun P**, Meier V, Braun F, Ramadori G. Combination of "low-dose" ribavirin and interferon alfa-2a therapy followed by interferon alfa-2a monotherapy in chronic HCV-infected non-responders and relapsers after interferon alfa-2a monotherapy. *World J Gastroenterol* 2001; **7**: 222-227
- 3 **Arase Y**, Ikeda K, Tsubota A, Suzuki Y, Saitoh S, Kobayashi M, Kobayashi M, Suzuki F, Akuta N, Someya T, Kumada H. Efficacy of prolonged interferon therapy for patients with chronic hepatitis C with HCV-genotype 1b and high virus load. *J*

- Gastroenterol* 2003; **38**: 158-163
- 4 **Zibert A**, Meisel H, Kraas W, Schulz A, Jung G, Roggendorf M. Early antibody response against hypervariable region 1 is associated with acute self-limiting infections of hepatitis C virus. *Hepatology* 1997; **25**: 1245-1249
 - 5 **Shimizu YK**, Igarashi H, Kiyohara T, Cabezon T, Farci P, Purcell RH. A hyperimmune serum against a synthetic peptide corresponding to the hypervariable region 1 of hepatitis C virus can prevent viral infection in cell cultures. *Virology* 1996; **223**: 409-412
 - 6 **Zhou YH**, Takekoshi M, Maeda F, Ihara S, Esumi M. Recombinant antibody Fab against the hypervariable region 1 of hepatitis C virus blocks the virus adsorption to susceptible cells in vitro. *Antiviral Res* 2002; **56**: 51-59
 - 7 **Choo QL**, Kuo G, Ralston R, Weiner A, Chien D, Nest GV, Han J, Berger K, Thudium K, Kuo C, Kansopon J, McFarlad J, Tabrizi A, Ching K, Moos B, Cummins LB, Houghton M, Muchmore E. Vaccination of chimpanzees against infection by the hepatitis C virus. *Proc Natl Acad Sci USA* 1994; **91**: 1294-1298
 - 8 **Esumi M**, Rikihisa T, Nishimura S, Goto J, Mizuno K, Zhou YH, Shikata T. Experimental vaccine activities of recombinant E1 and E2 glycoproteins and hypervariable region 1 peptides of hepatitis C virus in chimpanzees. *Arch Virol* 1999; **144**: 973-980
 - 9 **Goto J**, Nishimura S, Esumi M, Makizumi K, Rikihisa T, Nishihara T, Mizuno K, Zhou Y, Shikata T, Fujiyama S, Tomita K. Prevention of hepatitis C virus infection in a chimpanzee by vaccination and epitope mapping of antiserum directed against hypervariable region 1. *Hepatitis Res* 2001; **19**: 270-283
 - 10 **Hattori M**, Yoshioka K, Aiyama T, Iwata K, Terazawa Y, Ishigami M, Yano M, Kakumu S. Broadly reactive antibodies to hypervariable region 1 in hepatitis C virus-infected patient sera: relation to viral loads and response to interferon. *Hepatology* 1998; **27**: 1703-1710
 - 11 **Cai Q**, Zhang XX, Tian LF, Yuan M, Jin GD, Lu ZM. Variant analysis and immunogenicity prediction of envelope gene of HCV strains from China. *J Med Virol* 2002; **67**: 490-500
 - 12 **Gaud U**, Langer B, Petropoulou T, Thomas HC, Karayiannis P. Changes in hypervariable region 1 of the envelope 2 glycoprotein of hepatitis C virus in children and adults with humoral immune defects. *J Med Virol* 2003; **69**: 350-356
 - 13 **Weiner AJ**, Geysen HM, Christopherson C, Hall JE, Mason TJ, Saracco G, Bonino F, Crawford K, Marion CD, Crawford KA, Brunetto M, Barr PJ, Miyamura T, McHutchinson J, Houghton M. Evidence for immune selection of hepatitis C virus (HCV) putative envelope glycoprotein variants: potential role in chronic HCV infection. *Proc Natl Acad Sci USA* 1992; **89**: 3468-3472
 - 14 **Mondelli MU**, Cerino A, Lisa A, Brambilla S, Segagni L, Cividini A, Bissolati M, Missale G, Bellati G, Meola A, Bruniercole B, Nicosia A, Galfre G, Silini E. Antibody responses to hepatitis C virus hypervariable region 1: evidence for cross-reactivity and immune-mediated sequence variation. *Hepatology* 1999; **30**: 537-545
 - 15 **Curran R**, Jameson CL, Craggs JK, Grabowska AM, Thomson BJ, Robins A, Irving WL, Ball JK. Evolutionary trends of the first hypervariable region of the hepatitis C virus E2 protein in individuals with differing liver disease severity. *J Gen Virol* 2002; **83**: 11-23
 - 16 **Cerino A**, Bissolati M, Cividini A, Nicosia A, Esumi M, Hayashi N, Mizuno K, Slobbe R, Oudshoorn P, Silini E, Asti M, Mondelli MU. Antibody responses to the hepatitis C virus E2 protein: relationship to viremia and prevalence in Anti-HCV seronegative subjects. *J Med Virol* 1997; **51**: 1-5
 - 17 **Zhou YH**, Moriyama M, Esumi M. Multiple sequence-reactive antibodies induced by a single peptide immunization with hypervariable region 1 of hepatitis C virus. *Virology* 1999; **256**: 360-370
 - 18 **Zibert A**, Schreier E, Roggendorf M. Antibodies in human sera specific to hypervariable region 1 of hepatitis C virus can block viral attachment. *Virology* 1995; **208**: 653-661
 - 19 **Lechner S**, Rispeter K, Meisel H, Kraas W, Jung G, Roggendorf M, Zibert A. Antibodies directed to envelope proteins of hepatitis C virus outside of hypervariable region 1. *Virology* 1998; **243**: 313-321
 - 20 **Gu J**, Stephenson CG, Iadarola MJ. Recombinant proteins attached to a nicked-NTA column: use in affinity purification of antibodies. *BioTechniques* 1994; **17**: 257
 - 21 **Scarselli E**, Cerino A, Esposito G, Silini E, Mondelli MU, Traboni C. Occurrence of antibodies reactive with more than one variant of the putative envelope glycoprotein (gp70) hypervariable region 1 in viremic hepatitis C virus-infected patients. *J Virol* 1995; **69**: 4407-4412
 - 22 **Davis GL**, Lau JY. Factors predictive of a beneficial response to therapy of hepatitis C. *Hepatology* 1997; **26**(Suppl 3): 122S-127S
 - 23 **Sandres K**, Dubois M, Pasquier C, Payen JL, Alric L, Duffaut M, Vinel JP, Pascal JP, Puel J, Izopet J. Genetic heterogeneity of hypervariable region 1 of the hepatitis C virus (HCV) genome and sensitivity of HCV to alpha interferon therapy. *J Virol* 2000; **74**: 661-668
 - 24 **Gong GZ**, Lai LY, Jiang YF, He Y, Su XS. HCV replication in PBMC and its influence on interferon therapy. *World J Gastroenterol* 2003; **9**: 291-294
 - 25 **Martell M**, Esteban JL, Quer J, Genesca J, Weiner A, Esteban R, Guardia J, Gomez J. Hepatitis C virus (HCV) circulates as a population of different but closely related genomes: quasispecies nature of HCV genome distribution. *J Virol* 1992; **66**: 3225-3229
 - 26 **Klenerman P**, Lechner F, Kantzanou M, Ciurea A, Hengartner H, Zinkernagel R. Viral escape and the failure of cellular immune responses. *Science* 2000; **289**: 2003
 - 27 **Farci P**, Strazzeria R, Alter HJ, Farci S, Degioannis D, Coiana A, Peddis G, Usai F, Serra G, Chessa L, Diaz G, Balestrieri A, Purcell RH. Early changes in hepatitis C viral quasispecies during interferon therapy predict the therapeutic outcome. *Proc Natl Acad Sci USA* 2002; **99**: 3081-3086
 - 28 **Grahovac B**, Bingulac-Popovic J, Vucelic B, Hratic I, Ostojic R, Drazic V, Balija M, Grgicevic D. Hypervariable region 1 of hepatitis C virus genome and response to interferon therapy. *Clin Chem Lab Med* 2000; **38**: 905-910
 - 29 **Del Porto P**, Puntoriero G, Scotta C, Nicosia A, Piccolella E. High prevalence of hypervariable region 1-specific and cross-reactive CD4+ T cells in HCV-infected individuals responsive to IFN- α treatment. *Virology* 2000; **269**: 313-324
 - 30 **Dimmock NJ**. Neutralization of animal viruses. *Curr Top Microbiol Immunol* 1993; **183**: 1-149
 - 31 **Hadlock KG**, Gish R, Rowe J, Rajyaguru SS, Newsom M, Warford A, Fong SK. Cross-reactivity and clinical impact of the antibody response to hepatitis C virus second envelope glycoprotein (E2). *J Med Virol* 2001; **65**: 23-29
 - 32 **Boulestin A**, Sandres-Sauné K, Payen JL, Alric L, Dubois M, Pasquier C, Vinel JP, Pascal JP, Puel J, Izopet J. Genetic heterogeneity of the envelope 2 gene and eradication of hepatitis C virus after a second course of interferon- α . *J Med Virol*, 2002; **68**: 221-228

A small yeast RNA inhibits HCV IRES mediated translation and inhibits replication of poliovirus *in vivo*

Xue-Song Liang, Jian-Qi Lian, Yong-Xing Zhou, Qing-He Nie, Chun-Qiu Hao

Xue-Song Liang, Jian-Qi Lian, Yong-Xing Zhou, Qing-He Nie, Chun-Qiu Hao, The center of diagnosis and treatment for infectious diseases of Tangdu Hospital of Military Medical University of PLA, Xi'an 710038, Shaanxi Province, China

Supported by the Youth Natural Scientific Foundation of China, No. 30000147

Correspondence to: Dr Jian-Qi Lian, The center of diagnosis and treatment for infectious diseases of Tangdu Hospital of Military Medical University of PLA, Xi'an 710038, Shaanxi Province, China. lianjq@sohu.com

Telephone: +86-29-3377595

Received: 2002-11-19 **Accepted:** 2002-12-20

Abstract

AIM: To investigate the anti-virus infection activity of internal ribosome entry site (IRES) specific inhibitor RNA (IRNA).

METHODS: IRNA eukaryotic vector pcRz-IRNA or miRNA eukaryotic vector pcRz-miRNA was transfected into human hepatocarcinoma cells (HHCC), then selected with neomycin G418 for 4 to 8 weeks, and then infected with polio virus vaccinas line. The cytopathogenesis effect was investigated and the cell extract was collected. At last the polio virus titer of different cells was determined by plaque assay.

RESULTS: Constitutive expression of IRNA was not detrimental to cell growth. HCV IRES-mediated cap-independent translation was markedly inhibited in cells constitutively expressing IRNA compared to control hepatoma cells. However, cap-dependent translation was not significantly affected in these cell line. Additionally, HHCC cells constitutively expressing IRNA became refractory to infection of polio virus.

CONCLUSION: IRES specific IRNA can inhibit HCV IRES mediated translation and poliovirus replication.

Liang XS, Lian JQ, Zhou YX, Nie QH, Hao CQ. A small yeast RNA inhibits HCV IRES mediated translation and inhibits replication of poliovirus *in vivo*. *World J Gastroenterol* 2003; 9 (5): 1008-1013

<http://www.wjgnet.com/1007-9327/9/1008.htm>

INTRODUCTION

IRES is one of the key structures of some virus such as poliovirus and hepatitis C virus. The structure stability and integrality of IRES are crucial for the virus life cycle^[1-8]. IRNA is one IRES specific yeast small RNA. We constructed the human hepatoma cells constitutively expressing the IRNA. Using polio vaccine virus infected the cells, we demonstrated that the cells expressing IRNA became refractory to infection of poliovirus.

MATERIALS AND METHODS

Materials

Human hepatocarcinoma cell (HHCC) was grown in

RPMI1640 medium supplemented with 100 mL/L newborn calf serum. PV I tenuate vaccinas line (Third Department of vaccinia, Chinese Drug and Bioproduct Identified Agent) was amplified in Hep2 cells, and the virus titer was calculated by plaque assay.

Methods

Plasmid construction By using subcloning methods, the IRNA and miRNA sequence were cloned into the pcDNA3 vector, yielding pcRz-IRNA and pcRz-miRNA which introduced the ribozyme sequence over the both sites of IRNA and miRNA to generate the correct site of IRNA and miRNA. In summary, by using PCR methods the sequences of target RNA were generated from pGRz-IRNA or pGRz-miRNA which were constructed by our laboratory. Then the PCR product was cloning into the *BamHI-ApaI* sites of the pcDNA3 vector.

Construction of HHCCs expressing IRNA or miRNA Plasmids pcRz-IRNA and pcRz-miRNA were transfected into HHCC cells respectively by using Lipofectamine 2000 reagent (Gibco) and screened for neomycin resistance with 300 µg of G418 (Invitrogen) per milliliter for 4 weeks. The antibiotic-resistant cell clones were harvested and further screened by dilution titer. The control cells were also prepared by using similar method using plasmid pcDNA3.

Detection of IRNA/miRNA in the cells IRNA or miRNA expression in the cells was measured by isolating total RNA from these cells and the IRNA or miRNA were detected by reverse transcriptase (RT)-mediated PCR (RT-PCR) by using IRNA or miRNA specific oligonucleotide primers. 1 to 2 µg of total RNA isolated from the IRNA or miRNA expressing cells, and 2 µg total RNA from HHCC control cells were reversely transcribed by murine leukemia virus RT using random hexamer primers in a 20 µl reaction mixture according to the TaKaRa RNA PCR kit protocol. 20pmol of each primer (corresponding to 5' nt 1 to 20 and 3' nt 1 to 20 of the IRNA or miRNA sequence) was used to amplify the 60-nt fragment in a 100 µl PCR reaction. The cycling parameters were as follows: denaturation, 95 °C for 1 min; annealing, 65 °C for 1 min; extension, 72 °C for 1 min, total extension, 72 °C for 10 mins; a total of 50 cycles. Twenty microliters of each reaction product were loaded onto 20 g/L gel and visualized by ethidium bromide staining.

Detection of cell protein levels by laser confocal microscopy Monolayers of HHCCs were plated on cover glass and fixed with pure ethanol for 10 mins. Monoclonal antibody of β-actin was properly diluted and covered on the glass with HHCC cells for 1h at 37 °C, and then the glass was washed with PBS 3 times (10 mins each). Then FITC labeled second antibody was covered on the glass at 37 °C for 1 h and the glass was washed with PBS 3 times again. At last the cells were examined by using the laser confocal microscopy.

Plaque assay Plaque assay were performed as described below. HHCCs (10⁶ cells) were infected with PV I tenuate line, and after 72 h, cytopathic effect was observed and cell extracts were prepared. Two hundred microliters of cell extracts was used to further infect Hep2 cells (5×10⁶ cells in 60

millimeter diameter plates). After 3 days of inoculation at 37 °C, the plaques were developed by staining with 10 g/L crystal violet.

Mobility shift electrophoresis assay Fifty micrograms of rabbit reticulocyte lysate (RRL) was preincubated at 30 °C for 10 mins with 4 µg of poly (dI-dC) (Pharmacia) in a 15 µl reaction mixture containing 5 mmol/L HEPES (N-2-hydroxyethylpiperazine-N'-2-ethanesulfonic acid) (pH 7.5), 25 mmol/L KCl₂, 2 mmol/L MgCl₂, 38g/L glycerol, and 2 mmol/L dithiothreitol. For competition experiments, 25 to 50-fold excess of unlabeled competitor RNAs were added to the reaction mixture and incubated for 10 min at 30 °C. Finally, 5 to 10 fmol of labeled RNA probes were added to respective reaction mixture and incubation was continued for another 30 min at 30 °C. The nonspecific RNA used in competition assay was the sequence of the polylinker region of the pGEM 3Z vector (Promega). Three microliters of gel loading dye was added to the reaction mixture to a final concentration of 100 g/L glyceol and 2 g/L each of bromophenol blue and xylene cyanol. RNA-protein complexes were then analyzed on a 40 g/L polyacrylamide gel (39:1 ratio of acrylamide: bis) in a 0.5×TBE.

RESULTS

Construction of hepatoma cells expressing IRNA or miRNA constitutionally

To determine the long-term effect of expression of IRNA in HHCC cells, the cells constitutionally expressing IRNA were generated by using a pcDNA-based vector as described in Material and Methods. In order to obtain the correct and stable both sides of the expressed IRNA, the ribozyme sequences were introduced into the both sides of the IRNA and miRNA. The IRNA or miRNA was examined by RT-PCR using appropriate primers. As can be seen in Figure 1, IRNA and miRNA was expressed stably in the cloning cells.

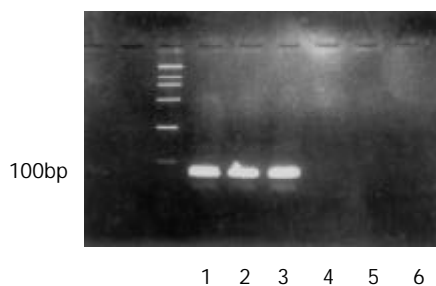


Figure 1 Detection IRNA or miRNA in the total RNA of HHCCs which constitutionally expressing IRNA or miRNA. 1: DNA Marker DL2000; 2 and 3: RT-PCR of cell lines expressing IRNA; 4: RT-PCR of cell lines expressing miRNA; 5 and 6: PCR of cell lines expressing IRNA or miRNA.

Effect of long-term IRNA expression on cellular protein expression

To determine whether constitutionally expressing of IRNA interfered with cellular protein translation, levels of cellular protein β-actin was determined by laser confocal microscopy. As can be seen in Figure 2A and 2B, no differences were detected in the overall expression of the cellular protein between HHCC (control) and IRNA-expressing cells (11.74 ± 6.52 vs 10.06 ± 5.75 , $P > 0.05$).

Inhibition of long-term expressing IRNA on HCV IRES mediated translation

To test the inhibitor activity of long-term expressing IRNA on

HCV IRES mediated translation, the control cells (HHCC) and cells expressing IRNA or miRNA were transiently cotransfected with pCMVNCRLuc and pSV40/β-Gal. Additionally, in order to exclude the nonspecific effect of nonspecific small RNA on the protein translation, the cells expressing pcDNA3 were cotransfected with pCMVNCRLuc and pSV40/β-Gal as well. Cell extracts were used to measure both luciferase and β-Gal activities. The results were plotted as percent of control after normalizing for β-Gal activity and protein concentration. Maximum inhibition of luciferase expression was 80 % in the cells expressing IRNA compared to the control, but no differences were observed in the cells expressing miRNA and pcDNA3.

To determine the effect of long-term expressing IRNA on cap-dependent translation, the cells were transfected with pcDNA-luc. As seen in Figure 3, no significant inhibition of cap-dependent translation from the pcDNA-luc construct was observed in cells expressing IRNA compared to the control cells.

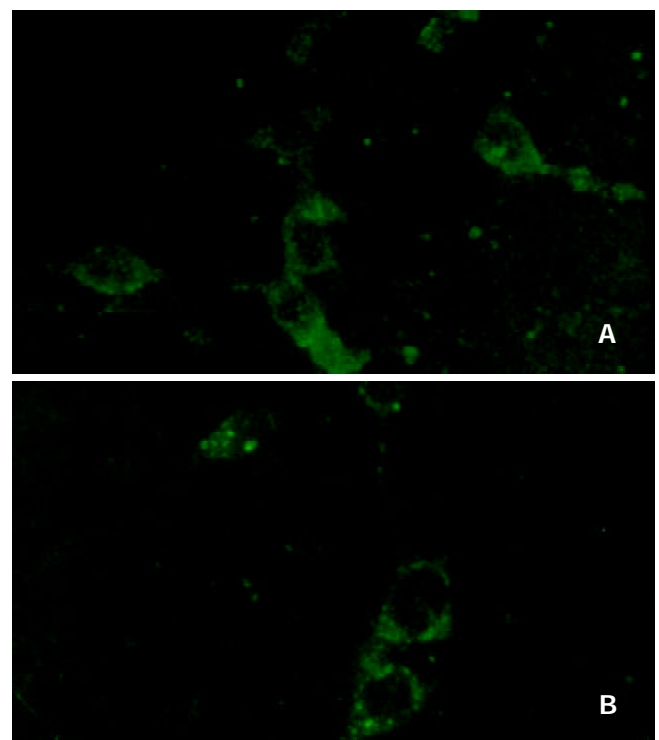


Figure 2 The translation level of β-actin in HHCC and IRNA-expressing lines. (Laser confocal, 400×1.00). A: IRNA-expressing cell lines, B: Control cell lines.

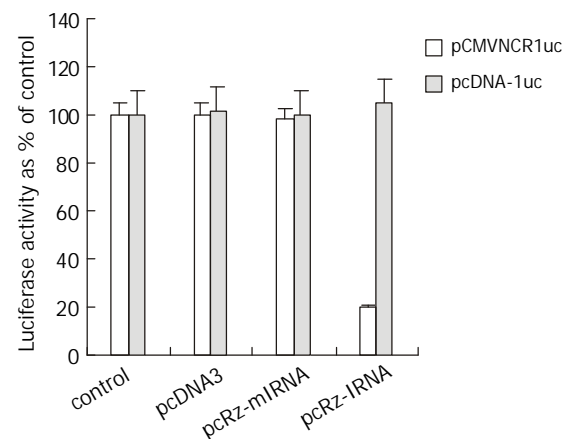


Figure 3 The effect of long-term expressing IRNA on cap-independent and cap-dependent protein translation.

Hepatoma cells constitutionally expressing IRNA are refractory to infection by a PV tenuate virus

To determine the inhibit effect of IRNA on IRES mediated protein translation during virus infection, the pcRz-IRNA and pcRz-mIRNA cells were infected with a vaccinia PV. After infection with PV, the cells were stained and the cytopathic effects were observed and we found that the pcRz-mIRNA cells and control cells were appeared marked cytopathic effect compared to the cells prior to the infection, but the cells expressing IRNA were almost totally protected from the cytopathic effect of PV (Figure 4). Following the infection,

cell extracts were prepared from infected cells which were then used to further infect Hep2 monolayer cells. Plaques characteristic of PV were apparent in Hep2 cells infected with cell extract from control hepatoma cells and pcRz-mIRNA cells (Figure 5A, B). Evidently viral replication was drastically affected in the cels expressing IRNA (Figure 5D).

To rule out the possibility that the nonspecific small RNA expressing cells affected the viral replication, the pcDNA3 cells were infected under the same condition. As can be seen in the Figure 4C and Figure 5C, the PV replication was not affected in the pcDNA3 cells.

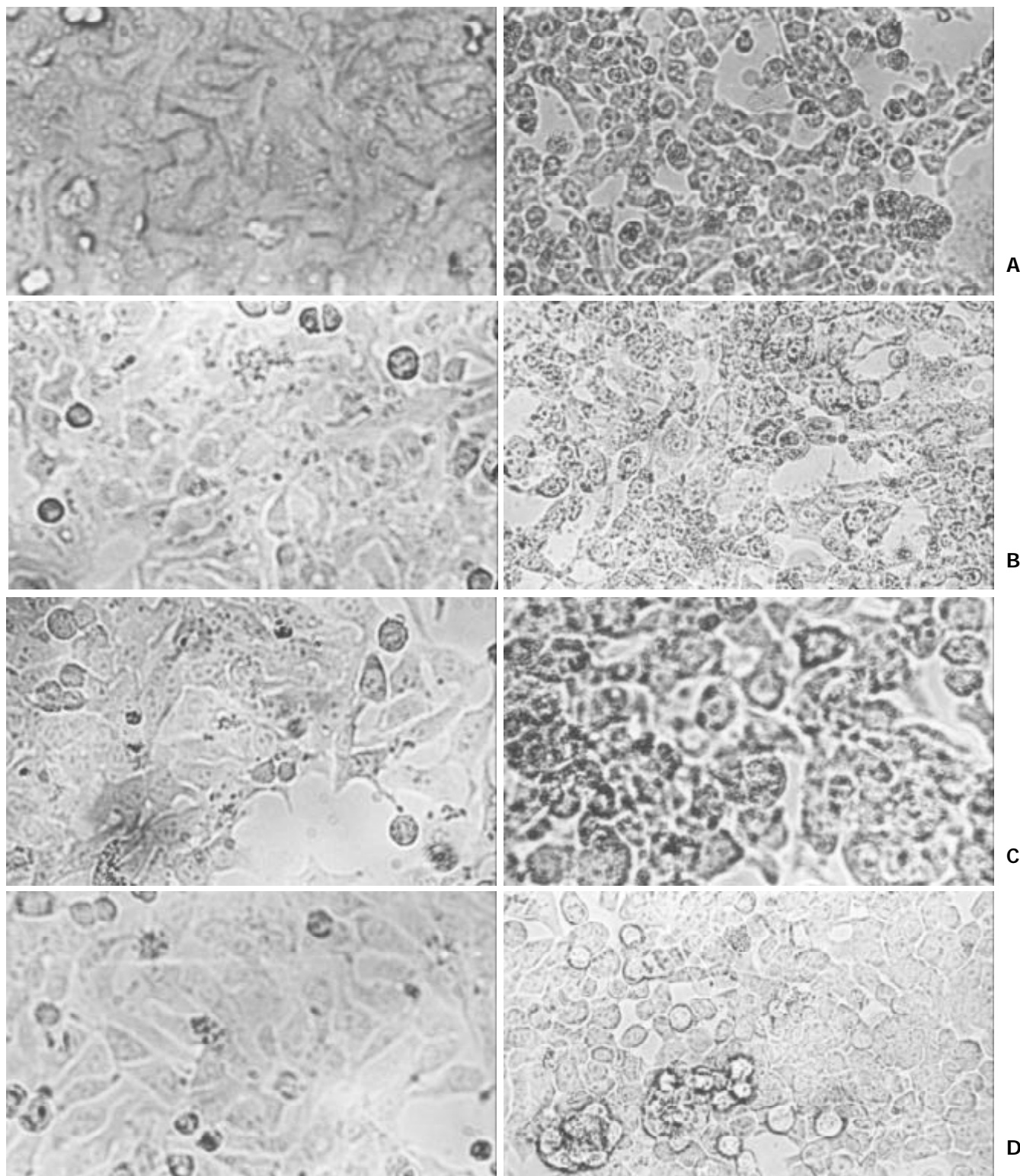


Figure 4 The cytopathic effect of different HHCC cells infected with PV. A: control HHCC cells; B: mIRNA cells ; C: pcDNA3 cells; D: IRNA cells.

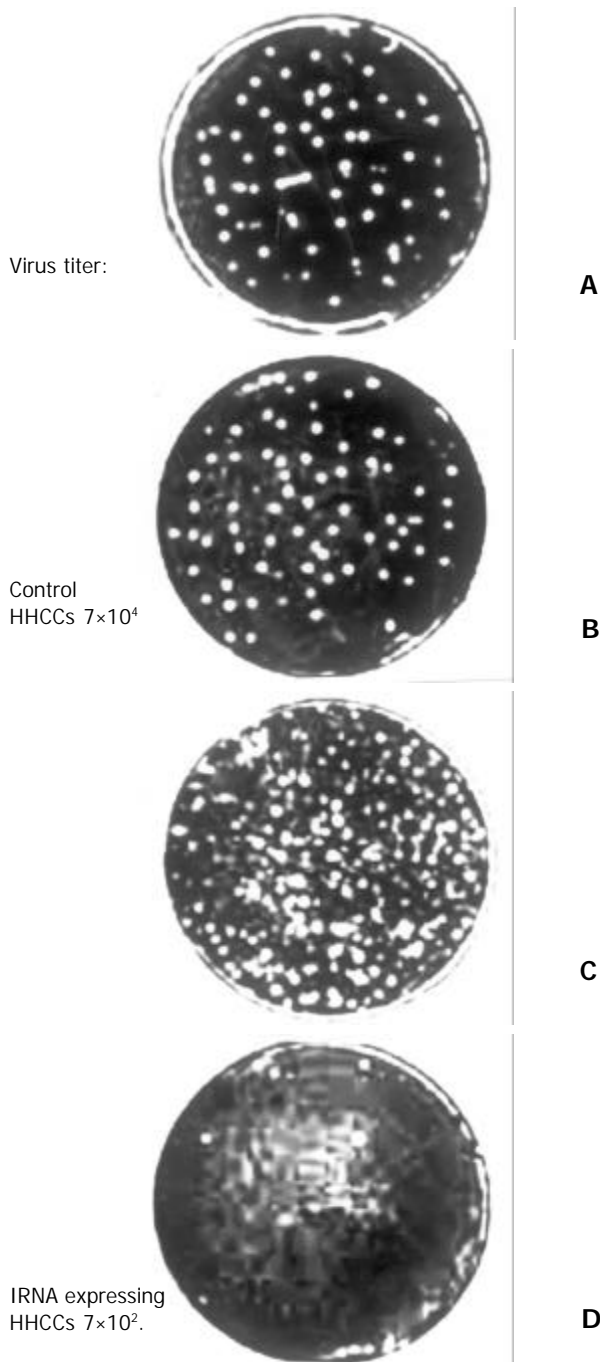


Figure 5 Plaque characteristic of different HHCC infected of PV. A: control HHCC; B: mIRNA cells; C: pcDNA3 cells; D: IRNA cells.

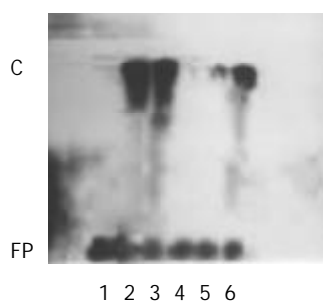


Figure 6 IRNA forms a gel-retarded complex which is inhibited by 5' UTR of HCV RNA. ^{32}P -labeled IRNA was incubated with RRL extract in the absence (lane 2) or presence of an unlabeled 25- or 50-fold molar excess of IRNA (lane 3 and lane 4, respectively) or 5' UTR (lane 5) or of a 50-fold molar excess of

nonspecific RNA (lane 6). Protein-RNA complexes were analyzed on a nondenaturing gel. In lane 1, RRL extract was not added. FP: free probe; C: complexes.

IRNA forms a gel-retarded complex that is inhibited by UTR

In order to study the mechanism of IRNA inhibitor activity on IRES mediated protein translation, ^{32}P -body-labeled IRNA probe was prepared and mixed with RRL extract, and the resulting RNA-protein complexes were analyzed by nondenaturing polyacrylamide gel electrophoresis. As shown in Figure 6, lane 2, a single complexes (denoted C).

DISCUSSION

IRES-dependent protein translation mechanism was first discovered in picornavirus, including PV, rhinovirus and hepatitis A virus, as well as certain flavivirus, such as hepatitis C virus^[9-12]. Although there is very little sequence homology between these different IRES elements, structural similarity do appear to exist. In fact for keeping the activity of IRES, it is more important to maintain the secondary structure than to maintain the integrality of certain genome sequences^[1-3,7,8]. IRES is the key structure for some virus RNA replication, so it has been the target for antiviral infection^[13-20]. We have constructed the self-cleavage plasmid of IRNA, and affirmed that IRNA can inhibit IRES-dependent protein translation both *in vivo* and *in vitro*^[21]. In order to further confirm the long-term expressing IRNA effect on cellular protein and virus protein translation, we cloned the HHCCs expressing IRNA, and confirmed that long-term expressing IRNA could inhibit IRES mediated protein translation significantly compared to the control cells and mIRNA expressing cells. Das and his collaborates prepared the a number of human hepatoma (Huh-7) cell lines expressing IRNA by using the similar methods. They found that HCV IRES-mediated cap-independent translation was markedly inhibited in cells constitutively expressing IRNA compared to control hepatoma cells^[22].

Additionally, We have shown here that the long-term expression of IRNA did not affect the overall translation of cellular protein as shown by laser confocal microscopy. This was surprising since some cellular mRNAs such as the immunoglobulin heavy-chain-binding protein, mouse androgen receptor, and *Drosophila antennapedia* mRNAs has been shown to use IRES-mediated translation. It is possible that cellular mRNAs having IRES elements are also translated in a cap-dependent manner, as almost all mRNAs synthesized *in vivo* are capped. Das and his collaborates also confirmed that the constitutive expression of IRNA was not detrimental to cell growth^[22].

Recent studies on picornavirus-IRES-mediated translation have demonstrated that cellular *trans*-acting proteins distinct from canonical translation initiation factors play an important role in IRES-mediated translation. These proteins bind to the IRES and presumably help to facilitate the binding of ribosomes to the IRES. Some of the *trans*-acting proteins have been identified as the La autoantigen, polypyrimidine tract-binding (PTB) protein, glyceraldehydes 3-phosphate dehydrogenase (GAPDH). The La polypeptide binds to both PV and HCV IRES elements and stimulates IRES-mediated translation. Similarly, the PTB protein interacts with HCV and other picornavirus IRES sequences and stimulated viral 5' UTR mediated translation^[23-25]. Because HCV IRES and PV IRES bind the similar cellular protein, and we lack effective HCV culture system *in vitro*, we studied the long-term expressing IRNA blocking viral replication ability by using PV infection *in vitro*. Our results demonstrated that long-term expressing IRNA blocks the PV replication effectively. Das and his collaborates constructed PV-HCV chimera in which PV IRES

was replaced by the HCV IRES. They demonstrated that Huh-7 cells constitutively expressing IRNA became refractory to infection by the PV-HCV chimera, but the replication of a PV-encephalomyocarditis virus (ECMV) chimera containing the ECMV IRES element was not affected significantly in the IRNA-producing cell line^[22].

At low multiplicities of infection of the virus, cells expressing IRNA showed significant resistance to virus infection compared to control cells. This could be due to inhibition of primary translation of the input viral RNA in cells expressing IRNA. Multiple rounds of replication and reinfection of control cells, but not of IRNA-expressing cells, resulting in an amplified effect seen in the plaque assay was shown in Figure 5. At higher multiplicities of infections, the virus titer was approximately 10-fold lower in IRNA cells compared to control cells. This could be due to one or more of the following reasons: (1) the level of IRNA expression was relatively low in the cell line; (2) the viral 5' UTR, which competed with IRNA for binding of relevant protein factors, has significantly higher affinity for these proteins than IRNA; (3) the amount of IRNA in the cytoplasm was low compared to the total amount of expressed IRNA; and finally (4) all of the IRNA molecules in the cell line might not have been properly folded to assume the right secondary structure required for its translation-inhibitory activity.

Theoretically, IRNA could inhibit IRES-mediated translation by two possible mechanisms. It could bind to some sequences in the UTR as antisense RNA or it could bind protein factors necessary for the internal entry of ribosome, thus inhibiting IRES-dependent translation. The possibility that the IRNA acted by binding protein factors required for IRES-mediated translation was plausible for the following reasons. First, purified RNA was not complementary to 5' UTR sequences nor did it hybridize with virus 5' UTR. Secondly, inhibition of the translation of PV RNA could be overcome by the addition of increasing concentrations of HeLa extract but not of PV RNA or 5' UTR sequence. In fact, in order to identify the mechanism of IRNA inhibitor activity, several laboratories by using the UV-crossing linking methods and Gel retardation methods studied the mechanism respectively. They found that IRNA specifically binds proteins which interact with RNA secondary structures within the virus 5' UTR presumably involved in internal initiation. Furthermore, they demonstrated that purified IRNA specifically competed with virus RNA structures within the 5' UTR which bind a cellular protein with an approximate molecular mass of 52 KD, 57KD. Then they determined that p52 protein appears to be identical to human La autoantigen and the binding of the La autoantigen to the HCV IRES element was specifically and efficiently competed by IRNA. The data present here (Figure 6) also suggested that the IRNA inhibit viral IRES mediated protein translation through binding specific cellular factors^[22, 26-31]. Additionally, Das and his collaborator determined the secondary structure of IRNA and founded that both a stem and a loop formed by intramolecular folding of IRNA were important for inhibition of viral IRES mediated translation. Venkatesan had also predicted the secondary structure of the IRNA and its complementary RNA (cIRNA) using biosoftware MFOLD by energy minimal principle and further determined the structure using enzyme methods and chemical modification methods. They found that IRNA and cIRNA have not only same secondary structure but also similar inhibitor activity on PV IRES mediated protein translation^[31]. Our laboratory have also modeled the secondary structure of IRNA and cIRNA and got the similar results to the Venkatesan (data reported in other file).

In summary, we could get the conclusion that (1) IRNA expressing cells could significantly anti polio virus infection; (2) IRNA long-term expression has no significant affect on

cellular protein translation; (3) IRNA expressing cells significantly inhibit the HCV IRES mediated protein translation.

REFERENCES

- 1 **Malnou CE**, Poyry TA, Jackson RJ, Kean KM. Poliovirus internal ribosome entry segment structure alterations that specifically affect function in neuronal cells: molecular genetic analysis. *J Virol* 2002; **76**: 10617-10626
- 2 **Schwantes A**, Ortlepp I, Lochelt M. Construction and functional characterization of feline foamy virus-based retroviral vectors. *Virology* 2002; **301**: 53
- 3 **Ki Kim Y**, Key Jang S. Continuous heat shock enhances translational initiation directed by internal ribosomal entry site. *Biochem Biophys Res Commun* 2002; **297**: 224
- 4 **Mason PW**, Bezborodova SV, Henry TM. Identification and characterization of a cis-acting replication element (cre) adjacent to the internal ribosome entry site of foot-and-mouth disease virus. *J Virol* 2002; **76**: 9686-9694
- 5 **Ray PS**, Das S. La autoantigen is required for the internal ribosome entry site-mediated translation of Coxsackievirus B3 RNA. *Nucleic Acids Res* 2002; **30**: 4500-4508
- 6 **Kaku Y**, Chard LS, Inoue T, Belsham GJ. Unique characteristics of a picornavirus internal ribosome entry site from the porcine teschovirus-1 talfan. *J Virol* 2002; **76**: 11721-11728
- 7 **Kim I**, Lukavsky PJ, Puglisi JD. NMR study of 100 kDa HCV IRES RNA using segmental isotope labeling. *J Am Chem Soc* 2002; **124**: 9338-9339
- 8 **Royal RE**, Kershaw MH, Reeves ME, Wang G, Daly T, Treisman J, Lam J, Hwu P. Increased functional expression of transgene in primary human lymphocytes using retroviral vectors modified with IRES and splicing motifs. *Gene Ther* 2002; **9**: 1085-1092
- 9 **Dai YM**, Shou ZP, Ni CR, Wang NJ, Zhang SP. Localization of HCV RNA and capsid protein in human hepatocellular carcinoma. *World J Gastroenterol* 2000; **6**: 136-137
- 10 **Wietzke-Betaraun P**, Meier V, Braun F, Ramadori G. Combination of "low-dose" ribavirin and interferon alpha-2a therapy followed by interferon alpha-2a monotherapy in chronic HCV-infected non-responders and relapsers after interferon alpha-2a monotherapy. *World J Gastroenterol* 2001; **7**: 222-227
- 11 **Meier V**, Mihm S, Braun-Wietzke P, Ramadori G. HCV-RNA positivity in peripheral blood mononuclear cells of patients with chronic HCV-infection: does it really mean viral replication? *World J Gastroenterol* 2001; **7**: 228-234
- 12 **Zhou HC**, Xu DZ, Wang XP, Zhang JX, Huang Y, Yan YP, Zhu Y, Jin BQ. Identification of the epitopes on HCV core protein recognized by HLA-A2 restricted cytotoxic T lymphocytes. *World J Gastroenterol* 2001; **7**: 583-586
- 13 **Jin J**, Yang JY, Liu J, Kong YY, Wang Y, Li GD. DNA immunization with fusion genes encoding different regions of hepatitis C virus E2 fused to the gene for hepatitis B surface antigen elicits immune responses to both HCV and HBV. *World J Gastroenterol* 2002; **8**: 505-510
- 14 **Woitars RP**, Petersen U, Moshage D, Brackmann HH, Matz B, Sauerbruch T, Spengler U. HCV-specific cytokine induction in monocytes of patients with different outcomes of hepatitis C. *World J Gastroenterol* 2002; **8**: 562-566
- 15 **Yu YC**, Mao Q, Gu CH, Li QF, Wang YM. Activity of HDV ribozymes to trans-cleave HCV RNA. *World J Gastroenterol* 2002; **8**: 694-698
- 16 **You J**, Tang BZ, Zhuang L, Zhang HB, Zhang L. Seven-years follow-up on trial of Interferon alpha in patients with HCV RNA positive chronic hepatitis C. *World J Gastroenterol* 2000; **6**: 68
- 17 **Li LF**, Zhou Y, Xia S, Zhao LL, Wang ZX, Wang CQ. The epidemiologic feature of HCV prevalence in Fujian. *World J Gastroenterol* 2000; **6**: 80
- 18 **Kang JA**, Funkhouser AW. A proposed vestigial translation initiation motif in VP1 of hepatitis A virus. *Virus Res* 2002; **87**: 11-19
- 19 **Kato J**, Kato N, Moriyama M, Goto T, Taniguchi H, Shiratori Y, Omata M. Interferons specifically suppress the translation from the internal ribosome entry site of hepatitis C virus through a double-stranded RNA-activated protein kinase-independent pathway. *J Infect Dis* 2002; **186**: 155-163

- 20 **Soler M**, Pellerin M, Malnou CE, Dhumeaux D, Kean KM, Pawlotsky JM. Quasispecies heterogeneity and constraints on the evolution of the 5' noncoding region of hepatitis C virus (HCV): relationship with HCV resistance to interferon-alpha therapy. *Virology* 2002; **298**: 160-173
- 21 **Liang XS**, Zhou YX. Effect of inhibitor RNA on intracellular inhibition of viral gene expression in 5' noncoding region of hepatitis C virus. *Zhonghua Neike Zazhi* 2002; **10**: 661-662
- 22 **Das S**, Kenan DJ, Bocskai D, Keene JD, Dasgupta A. Sequences within a small yeast RNA required for inhibition of initiation of translation: interaction with La and other cellular proteins influences its inhibitory activity. *J Virol* 1996; **70**: 1624-1632
- 23 **Padilla-Noriega L**, Paniagua O, Guzman-Leon S. Rotavirus protein NSP3 shuts off host cell protein synthesis. *Virology* 2002; **298**: 1-7
- 24 **Laporte J**, Bain C, Maurel P, Inchauspe G, Agut H, Cahour A. Differential distribution and internal translation efficiency of hepatitis C virus quasispecies present in dendritic and liver cells. *Blood* 2002; **28**: 122-126
- 25 **Lopez De Quinto S**, Saiz M, De La Morena D, Sobrino F, Martinez-Salas E. IRES-driven translation is stimulated separately by the FMDV 3' NCR and poly(A) sequences. *Nucleic Acids Res* 2002; **30**: 4398-4405
- 26 **Shiroki K**, Ohsawa C, Sugi N, Wakiyama M, Miura K, Watanabe M, Suzuki Y, Sugano S. Internal ribosome entry site-mediated translation of Smad5 in vivo: requirement for a nuclear event. *Nucleic Acids Res* 2002; **30**: 2851-2861
- 27 **Han B**, Zhang JT. Regulation of gene expression by internal ribosome entry sites or cryptic promoters: the eIF4G Story. *Mol Cell Biol* 2002; **22**: 7372-7384
- 28 **Otto GA**, Lukavsky PJ, Lancaster AM, Sarnow P, Puglisi JD. Ribosomal proteins mediate the hepatitis C virus IRES-HeLa 40S interaction. *RNA* 2002; **8**: 913-923
- 29 **Lytle JR**, Wu L, Robertson HD. Domains on the hepatitis C virus internal ribosome entry site for 40s subunit binding. *RNA* 2002; **8**: 1045-1055
- 30 **Isoyama T**, Kamoshita N, Yasui K, Iwai A, Shiroki K, Toyoda H, Yamada A, Takasaki Y, Nomoto A. Lower concentration of La protein required for internal ribosome entry on hepatitis C virus RNA than on poliovirus RNA. *J Gen Virol* 1999; **80**: 2319-2327
- 31 **Venkatesan A**, Das S, Dasgupta A. Structure and function of a small RNA that selectively inhibits internal ribosome entry site-mediated translation. *Nucleic Acids Res* 1999; **27**: 562-572

Edited by Wu XN

The study between the dynamics and the X-ray anatomy and regularizing effect of gallbladder on bile duct sphincter of the dog

Jing-Guo Wei, Yao-Cheng Wang, Guo-Min Liang, Wei Wang, Bao-Ying Chen, Jia-Kuan Xu, Li-Jun Song

Jing-Guo Wei, Yao-Cheng Wang, Guo-Min Liang, Wei Wang, Bao-Ying Chen, Jia-Kuan Xu, Li-Jun Song, Radiology Department of Tangdu Hospital, Fourth Military Medical University, Xi'an 710038, Shaanxi Province, China

Correspondence to: Dr Jing-Guo Wei, Department of Radiology, Tangdu Hospital, Fourth Military Medical University, Xi'an 710038, Shaanxi Province, China. tdradio1@fmmu.edu.cn

Telephone: +86-29-3377163 **Fax:** +86-29-3377163

Received: 2002-10-17 **Accepted:** 2002-11-13

Abstract

AIM: To study the relationship between the radiological anatomy and the dynamics on bile duct sphincter in bile draining and regulatory effect of gallbladder.

METHODS: Sixteen healthy dogs weighing 18 kg to 25 kg were divided randomly into control group and experimental group (cholecystectomy group). Cineradiography, manometry with perfusion, to effect of endogenous cholecystokinin and change of ultrastructure were employed.

RESULTS: According to finding of the choledochography and manometry, in control group the intraluminal basal pressure of cephalic cyclic smooth muscle of choledochal sphincter cCS was 9.0 ± 2.0 mmHg and that of middle oblique smooth muscle of choledochal sphincter (mOS) was 16.8 ± 0.5 mmHg, the intraluminal basal pressure of cCS segment was obviously lower than that of mOS ($P < 0.01$) in the interval period of bile draining, but significant difference of intraluminal basal pressure of the mOS segment was not found between the interval period of bile draining (16.8 ± 0.5 mmHg) and the bile flowing period (15.9 ± 0.9 mmHg) ($P > 0.05$). The motility of cCS was mainly characterized by rhythmically concentric contraction, just as motility of cCS bile juice was pumped into the mOS segment in control group. And motility of mOS segment showed mainly diastolic and systolic activity of autonomically longitudinal peristalsis. There was spasmodic state in cCS and mOS segment and reaction to endogenous cholecystokinin was debased after cholecystectomy. The change of ultrastructure of cCS portion showed mainly that the myofilaments of cell line in derangement and mitochondria is swelling.

CONCLUSION: During fasting, the cCS portion has a function as similar cardiac "pump" and it is main primary power source in bile draining, and mOS segment serves mainly as secondary power in bile draining. The existence of the intact gallbladder is one of the important factors in guaranteeing the functional coordination between the cCS and mOS of bile duct sphincter. There is dysfunction in the cCS and mOS with cholecystectomy.

Wei JG, Wang YC, Liang GM, Wang W, Chen BY, Xu JK, Song LJ. The study between the dynamics and the X-ray anatomy and regularizing effect of gallbladder on bile duct sphincter of the dog. *World J Gastroenterol* 2003; 9(5): 1014-1019
<http://www.wjgnet.com/1007-9327/9/1014.htm>

INTRODUCTION

The sphincter of Oddi regulates both bile and pancreatic juice flowing into the duodenum, and one of important feature is that the time of bile draining was delayed when the sphincter of Oddi dysfunction in postcholecystectomy. Obviously, this is relative to the abnormal dynamic change of choledochal sphincter in bile draining^[1-7]. But the mechanism of sphincter of Oddi dysfunction remains speculative^[8-19]. Up to now there was no report the relationship between the abnormal changes of bile draining and the functional anatomy of choledochal sphincter.

At the opening site of terminal bile duct there was a bundle of cyclic smooth muscles. Afterwards Ruger Oddi reported his results that this sphincter played a "valve"-like role in bile and pancreatic juice output. This bundle of muscles encysted the ampulla of Vater at the confluence of bile duct and pancreatic duct, thus was called ampulla sphincter or sphincter of Oddi. Boyden EA and Eichhorn EP, however, had also confirmed that, situated at the cephalic side of ampulla of Vater, in bile duct and in pancreatic duct there were two bundles of sphincter respectively which were independent to each other. The independent bile duct sphincter showed its own remarkable structural features that there was cyclic smooth muscle at the cephalic side portion, it was called cephalic cyclic segment of choledochal sphincter (cCS), and there was oblique and longitudinal smooth muscle following the cCS portion, it was called middle oblique smooth muscle segment of choledochal sphincter (mOS) because it was between in the cCS and classical SO. According to the above mentioned anatomical data, it seems that up to now the anatomical structures of sphincters involved in the studies of the function of sphincter of Oddi should include cCS, mOS and SO, which are referred to as the sphincter of Oddi. Obviously it is significantly different in concept and range from the classical sphincter of Oddi suggested by Ruger Oddi earlier. Based on the analysis of the anatomical characteristics, cCS and mOS are considered as the chief constitutive part of bile duct sphincter, thus it is suggested that the physiological role of cCS and mOS in regulating the bile flow is different from that of the classical sphincter of Oddi in this semi-enclosed hydrostatic system. In order to this objective, the methods of cholangiography, pressure measurement by perfusion, and microscopic observation were employed in this research primarily to observe the radiological anatomy of cCS and mOS, before and or after cholecystectomy, the morphologic features during bile draining, and the histological changes of cCS and mOS. The functional features of Ccs, mOS and its role in bile draining were investigated to find out the regulatory factors that affected the function of cCS and mOS.

MATERIALS AND METHODS

Experimental instruments and animal model

Unicameral manometry Teflon catheter with an 0.8 mm internal diameter and 1.7 mm outer diameter (Cook Co, USA), PT-16M pressure sensor (external pressure transducer, Shanghai, China), RM-6200C polygraph recorder (Chengdu, China), WZ-50 trace perfusion apparatus (Zhejiang, China) were used to

record pressures. Sixteen healthy hybrid dogs (Weighing 18-25 kg) raised in Shaanxi were randomly classified as control group and experimental group. The cholecystectomy were undertaken under they had received intraperitoneal injection with amobarbital, then they were fed for 4-6 weeks in experimental dogs.

Manometry and cholangiography

Anaesthesia was introduced with ketamine (100 mg/h). The operation was performed through thorax-abdomen-combined incision while autonomous respirator was being used to control animals' respiration. The cystic ducts of the experimental dogs were ligated. A vertical incision was then made on the proximal choledochus in order to insert the manometry catheter. Cholangiography was performed with 30 % meglumine diatrizoate injected through the manometry catheter (based on the calibration of developing in secondary branch of intrahepatic bile duct), and the bile excretion at portion of bile duct sphincter was recorded by cineradiography at the rate of 25 width/Sec. The intraluminal pressures at the portion of cCS and mOS were measured after the completion of contrast radiography.

The catheter that had been inserted into bile duct was introduced into duodenum again and measured the pressures in duodenal lumen. The manometric catheter system (the compliance of this system was low) was infused with 0.85 % NaCl solution at a flow rate of 25 ml/h, while the velocity of recording paper was 60 mm/min. The curves of changes in intraluminal pressures in the duodenum, the mOS and cCS portion of the bile duct sphincter were recorded respectively for 5 min. The intraluminal pressure in the duodenum was calibrated as zero basal level of pressure. In addition, a Teflon catheter was inserted into the stoma opening of stomach wall, with its top being placed in duodenal lumen for next experiment.

Observational parameters

Manometric parameters The numbers of the mOS segment contraction per min were regarded as the mOS contractile frequency (mOSCF). The difference between the diastolic pressure at the mOS portion and the duodenal intraluminal pressure was considered as the mOS basal pressure (mOSBP), and the difference between the contractile wave peak and its diastolic period intraluminal pressure as the mOS contractile amplitude (mOSCA). The difference between the cCS and the duodenal intraluminal pressure was classified as the cCS basal pressure (cCSBP).

Maximal inner diameter of bile duct and contrast draining time The maximal inner diameter of bile duct during cholangiography period was referred as the maximal inner diameter of choledochus, which was corrected by the magnification of contrast duct diameter. The biliary draining time (BDT) was referred as the time between the period when contrast medium completely filled the extrahepatic bile duct and the period when it completely disappeared. And the time in which biliary flows in choledochus was between the period when the bile duct sphincter began to drain bile and the period when it stopped draining bile. The time interval between the two biliary draining times was regarded as the interval of biliary draining.

Pathological examination

The intact choledochal sphincter segment of bile duct was fixed with 2.5 % glutaral, then with 1 % osmium acid, and finally embedded with epoxy resin after dehydration with 95 % alcohol. The ultra-thin section of the sample was sliced and stained with plumbum acid citrate. Then the observation was

done under JEM-2000EX electromicroscope. Two dogs were involved in both the control and experimental groups.

Statistical analysis

The "t" test was used to evaluate the results. A *P* value less than or equal to 0.05 was regarded as significant.

RESULTS

The diameter of bile duct

The maximal diameter of bile duct was 3.5-4.5 mm in controls, and that of experimental group was 4.7-7.5 mm, the average diameter of bile duct was 6.1 ± 1.3 mm in experimental group in 46 days and 58 days. There was significant difference between the control and the experimental group ($P < 0.01$). There were no stones and obstruction in the dilatants bile duct.

The contrast results in the control group

During interval period of bile draining, the mOS was in a state of shutting up, thus the terminal end of cCS portion shaped like "pestle", while the distal end of bile duct showed a cyclic notch which was the radiological marker of the initial part of cCS. With the concentric contraction of cCS segment, the bile was pumped into the mOS segment. The mOS segment appeared to be a narrow, slender lumen. An uneven caliber could be seen in peristalsis contraction, and at the same time the bile was squeezed into the duodenum (Figure 1). 10 min after 20 ml of 33.3 % MgSO₄ was injected through the catheter placed in duodenum, there was no significant change in the shape of cCS segment, but while the mOS lumen was significantly dilated in 3 fold, compared with that before the injection, there was no significant contraction and peristalsis in the mOS segment.



Figure 1 During bile draining in control group. It was showed that the mOS portion was in a peristaltic movement (↑→▲), and the narrow distal segment (▲→▲) was portion of the mOS and SO segment of bile duct. Between the end of choledochus and the cCS portion was demarcated by in notch (↑).

Image in the experimental group

During the bile draining period, between the distal end of bile duct, and cCS portion, there was a remarkable notch which appeared to be in a "infundibulum" shape at the cCS portion in connection with mOS segment. There was no significant contraction in the form of the spastic cCS segment and no significant peristaltic movement of the mOS segment, and lumen of the mOS segment appeared to be a narrow lumen as a "thin line", to last until the bile draining period ended (Figure 2). 10 min after the bile duct was injected with 20 ml of 33.3 % MgSO₄ through the intestinal tract, and significant change did not demonstrated in the diameter of cCS part and the diameter of mOS segment.

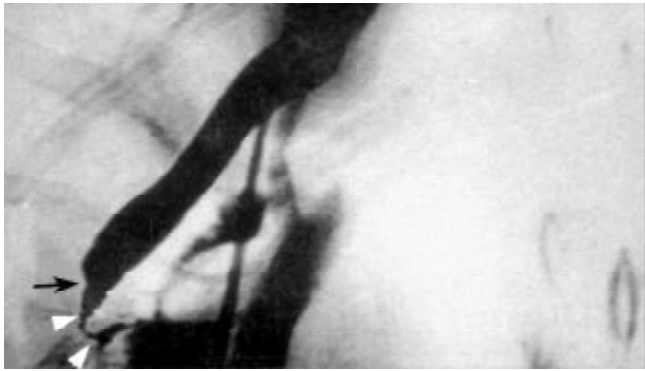


Figure 2 In experimental group of bile drainage. During bile draining the remarkable notch to keep up still in between the choledochus and the cCS portion, and it appeared to be in an “infundibulum” shape at the cCS portion and there was no significant contraction in the form of spastic cCS portion of bile duct and no significant peristelsis movement and there appeared to be a narrow lumen as a “thin line”, to last until the bile draining period ended at the mOS segment. Infusion of 33.3% MgSO₄ after, no significant change was seen in the diameter of cCS partion (↑→▲) and mOS segment (▲→▲) of bile duct.

Manometric results

The pressure of cCS and mOS segments in the control and experimental groups (Table 1).

Table 1 The pressures of cCS and mOS segments before MgSO₄ infusion in interval period of bile draining (mmHg)

Group	cCSBP	mOSBP
Control (n=7)	9.0±2.0 ^a	16.8±0.5 ^b
Study (n=7)	14.0±2.0	14.7±0.7

^aP<0.01, t=6.195; ^bP<0.05, t=2.717. vs the study group.

It is indicated that the cCSBP of control and experimental groups were lower than the mOSBP, which suggested that there was a retrograde pressure gradient between cCS and mOS segments in interval period of the bile draining. Although mOSBP in the study group was lower than that in the controls before infused MgSO₄, but the pressures of cCS segment in the study group were significantly higher than those in the controls (P<0.05), suggesting that the cCS and the mOS segment was in state of spastic contraction in the study group. **The pressure of mOS in the control** Manometric results and reaction of mOS to 33.3 % MgSO₄ infusion in the control group (Table 2) and pressure curve of mOS (Figure 3,4).

Table 2 The manometric results of mOS segment before and after MgSO₄ infusion in the controls (x±s)

	mOSBP (mmHg)	mOSCA (mmHg)	mOSCF (No/min)	BDT (min)
Before Infusion (n=7)	16.8±0.5	21.9±0.9	15.2±0.7	17.1±0.9
After Infusion (n=7)	15.7±0.9 ^a	15.1±2.1 ^b	11.4±0.3 ^c	10.8±1.1 ^d

^aP<0.05, t=2.651; ^bP<0.01, t=7.344; ^cP<0.01, t=35.155; ^dP<0.01, t=33.375. vs before MgSO₄ infusion.

It is showed that the high-pressure zone of the sphincters of bile duct was mainly located at mOS segment, and the resistance and contractile frequencies of mOS were significantly reduced by endogenous cholecystokinin (CCK) while the intact gallbladder remained. (Table 2 and Figures 3,4).

In addition, it was founded, that there was no significantly different between the mOSBP in interval period of bile draining (16.8±0.07 mmHg), and the mOSBP in bile draining period (15.9±0.7 mmHg) in control group (P>0.05).

Manometric results and reaction of mOS segment to MgSO₄ infusion in the experimental group The pressure curves and the changes in pressures of mOS segment before and after MgSO₄ infusion are shown in Table 3 and Figures 5,6.

Table 3 The manometric results of mOS segment before and after MgSO₄ infusion in the study group (x±s)

	mOSBP (mmHg)	mOSCA (mmHg)	mOSCF (No/min)	BDT (min)
Before Infusion (n=7)	14.7±0.7	14.2±1.3	15.9±0.7	27.0±3.4
After Infusion (n=7)	14.3±1.3	14.0±1.4	15.1±0.7	26.3±2.3

There were no significant differences in each parameter before and after infusion in the experimental group (P>0.05). This indicated that the sensitivity of mOS segment to endogenous CCK decreased after cholecystectomy, and that the diastolic and systolic movements of mOS segment were damaged, resulting in the elevation of resistance in bile draining. (Figures 5,6).

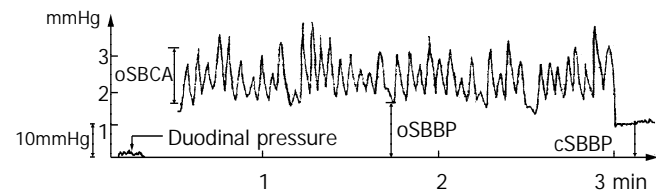


Figure 3 Pressure curves of the cCS and mOS portion and duodenum in control group. There is high pressure zone and rythmical contractile movement was appeared in the mOS portion of bile duct and pressure of the cCS portion of bile duct is lower than pressure of the mOS and the SO portion of bile duct.

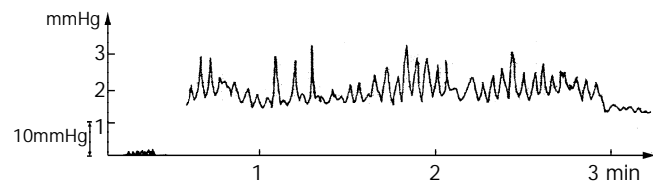


Figure 4 Reaction to the injection of 33.3 % MgSO₄ in control group. 10 min after 20 ml of 33.3 % MgSO₄ was injected through the catheter placed in duodenum, the pressure of mOS segment of bile duct is decreased, compared that before the injection, and unregular pressure curves was appeared in the mOS segment of bile duct.

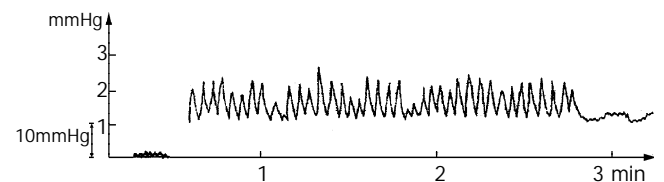


Figure 5 A pressure curves before MgSO₄ solution infusion in

the study group. Signs of the pressure curves is similar to the control group in the mOS segment of bile duct.

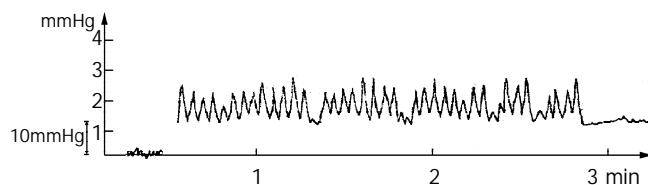


Figure 6 A pressure curves after $MgSO_4$ solution infusion in the study group. Signs of the pressure curves is similar to the pressure curves before $MgSO_4$ solution infusion.

Microscopic results of histopathology of the cCS portion

The results of the transection of cCS portion in the controls are showed in Figure 7.

The results of the transection of cCS portion in the study group: The light microscope results showed no the degeneration of muscular fibers of cCS, mOS portion and infiltration of inflammatory cells. Under the electromicroscope, the changes of smooth muscular cells are showed in Figure 8.



Figure 7 The figure is a transection of cCS portion of bile duct in the control group. It is showed that the smooth muscular cell membrane (\uparrow) was flat, the myofilament and dense body appeared to be longitudinal arrangement in parallel to the long axis of smooth muscular cell and the dense body like spindles (\blacktriangle). The structure of the mitochondrion was normal, which evenly distributed itself among the cytoplasm.

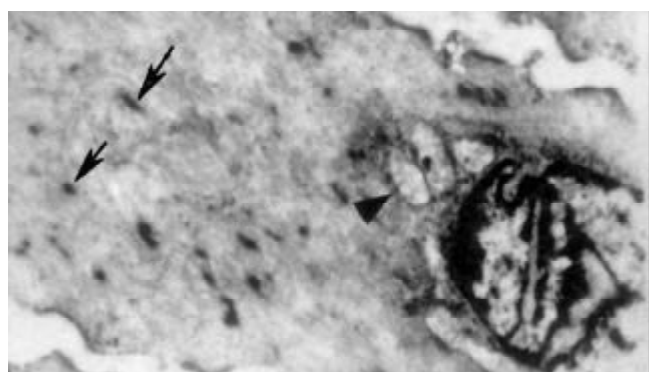


Figure 8 The figures is a transection of cCS portion of bile duct in experimental group. Under the electromicroscope the cell membrane twisted like billows, and the myofilament density was not even, shaping like “whirl”. The dense body showed derangement and various shapes (\uparrow). The mitochondrions clustered at the end of the nucleus, and vacuolation (\blacktriangle) was seen.

DISCUSSION

Evaluation of infused catheter manometry as a method of functional analysis of bile duct sphincter

The manometry with ERCP, which began in 1970s, has been widely used in functional evaluation and experimental studies of bile duct sphincter^[20,21]. Based on the manifestation of manometry, Venu and Sherman suggested that the lesions of bile duct sphincter could be classified as functional and structural lesions. It is reported that the functional disturbances of bile duct sphincter are further classified in four types^[22-26]: sphincter spasm, high-frequency contraction, abnormally directory contraction and abnormal response to CCK based on the results of manometry. Combined with the observations of clinically therapeutic effect, it is now generally accepted that the directory manometry with infused catheter is a golden criterion in evaluating the function of bile duct sphincter.

Dodds firstly reported the manometry of inner pressure of esophagus. He believed that the accuracy of infused manometry with catheter was negatively correlated with the compliance of catheter, but positively with the speed of infused fluid. In order to increase the accuracy of manometry, the catheter used must be characterized with less elasticity and thick wall. As far as the speed of infused fluid is concerned, Some people believed that it was suitable to have a speed of 0.25-0.6 ml/min^[27-29]. The physical character of catheter and the speed of infused fluid employed in this study meet the above criteria, and manometric results obtained can objectively reflect the characteristic changes in pressures of CS segment in dogs.

The anatomical and functional study of CS

Eichhorn and Barraya confirmed in their study on the bile duct sphincter in dogs that there were successively from cephalic to distal ends of bile duct sphincter the cyclic sphincter (cCS), oblique and longitudinal sphincter (mOS) and classic SO (a strong cyclic sphincter encysting the terminal opening of bile duct). There is no anatomical definite boundary between the classic SO and mOS, but their arrangements show the remarkable differences. Because the anatomical structure and distributive position of the cCS and mOS segments are different from classical SO, there would be differences in their functions. Up to now, however, there has been no report on the functional features of the cCS and mOS segments.

The bile is a kind of important digestive fluid in the digestion of fatty substances. Dodds reported that 75 % bile secreted by liver is stored in the gallbladder, then being drained into the duodenum after alternating with the bile which already remains in the gallbladder, and the rest of it (25 %) directly flows into the duodenum through the bile duct sphincter. Eating causes the gallbladder contracting and results a large quantity of bile draining into duodenum to digest food within a short time. Only a small quantity of bile from the duct is directly drained into duodenum through the bile duct sphincter during the fasting period. Obviously, they are two different processes in bile draining. Only when the function of bile duct sphincter remains intact and coordinative, two different processes of bile draining can be successfully completed.

Nowadays there are arguments about the mechanism of bile duct sphincter in bile draining^[30-37]. Toouli believed that the intramural type of choledochal sphincter, only plays a role of a “valve” in bile draining. Some people reported that the SO takes an active part in bile draining, and the power in bile draining comes from the spontaneous peristalsis contraction of bile duct sphincter. Scott, however, explained that the SO acts as a power source in bile draining while SO contracts moderately, and as a “valve” while contracting strongly. But our research results have confirmed that during fasting the lumen of mOS segment is not uniform in caliber. It can be

determined based on the study on the physiological function of smooth muscle that peristalsis-like diastolic and systolic motions are apparently not the patterns of characteristic manifestation of motions of cCS segment. Compared and analyzed with the manometric results, the peristaltic motility can only originate from the high-pressure area of bile duct sphincter, where the mOS segment of bile duct locates. It is further demonstrated by the manometric results in this study that cCS segment is a low-pressure lumen (9.0 ± 2.0 mmHg), than that the pressure are of the mOS segment (16.8 ± 0.5 mmHg), during the interval period of bile draining, and there is apparently a retrograde pressure gradient between cCS portion and mOS segment. It is apparent that the existing of high-pressure area in mOS segment is beneficial for preventing from the reflux of duodenal fluid, and even at the bile draining period the pressure in mOS segment does not decrease significantly, obviously, it is that the retrograde pressure gradient between the cCS segment and the mOS segment form the resistance in bile draining. But it is showed by cholangiography that cCS segment reveals concentric contraction in bile draining in the controls when fasting period, and its luminal volume reduces, resulting in the bile being "pressed" into mOS segment. With the peristaltic contraction of mOS segment, the bile filled in mOS segment ejects like "squeezed milk" into the duodenum. Obviously in order to overcome the resistance in bile draining cCS segment should play a role of similar cardiac "pump" in the process of changing the retrograde pressure gradient, that prevented reflux of duodenal juice, into a positive pressure gradient during bile draining. It is just because of the different roles of cCS and mOS segments play in bile draining, that the bile duct sphincter takes not only a part in inhibiting the reflux of duodenal fluid as a "valve", but also a part in regulating the stability of pressure in bile duct.

Effect of gallbladder to the movement of cCS and mOS segments

It is suggested that the functional coordination of cCS portion and mOS segment is closely related to whether the gallbladder is intact or not. It is showed by cholangiography that cCS segment has apparently dilative and contractile functions, while the peristaltic motion exists in the mOS segment that appears to be in a functional high pressure zone during the process of bile draining in the controls. But in the experimental group, cCS and mOS segments are constantly, and the notch remains still at the inferior extremity of bile duct and the lumen of mOS segment appears narrow like a "line". After infusion with $MgSO_4$, the notch at the inferior extremity of bile duct doesn't disappear, and the "line"-shaped narrow lumen of the mOS segment shows neither significant dilation nor apparent peristaltic motion, and it showed that the cCS and the mOS segment are in the state of spasm. Grace has also confirmed that there was a decline of the sensitivity of the bile duct sphincter to the endogenous CCK after cholecystectomy. Tokunaga and his men has discovered that, with a concentration of $1 \mu\text{mol} \cdot \text{L}^{-1}$, 0.11 ± 0.03 gm of CCK-8 is needed to relax the cyclic muscle stripe of bile duct sphincter, but with the same concentration, only 0.02 ± 0.01 gm of CCK-8 can relax the mOS segment. It seems to suggest from the above results that mOS segment is very sensitive to CCK-8 than that of the cCS, and its functional regulation is closely related to the content of endogenous cholecystokinin. In this study the results obtained from the choledochography confirm that Tokunaga Y's viewpoint is right. Our results indicate that the functional regulation between the cCS and mOS segment is manifested in intact gallbladder. Further, our results showed that there is a significant change in spatial structure of smooth muscle cells

of bile duct sphincter: the morphological manifestation of which is that the cell membrane is like billows, and myofilaments line in derangement and twist like "whirlpool". The form and size of the attachment points of corresponding myofilaments-dense bodies, are different and lose their behaviors of normal fusiform arrangement in parallel to the long axis of cells. There have been no reports about its pathological significance. If the changes are considered, this change in spatial structure of cytoskeleton may be related to the strong contraction and dragging of the myofilaments. The spastic state of cCS segment and the reduced range of concentric contraction, furthermore, will unavoidably result in decreasing in its bile draining volume. Although the basal pressure in mOS segment during bile draining somewhat decreases, the resistance produced by mOS segment in bile draining cannot be completely overcome by the motility obtained from contraction of cCS segment in bile draining, this may mostly be the important cause that the bile cannot drain smoothly from the bile duct and the time for emptying the contrast medium is elongated in the experimental group. The direct result is that the bile flow slows down and the relative stasis exists, and the bile duct is dilated.

REFERENCES

- 1 **Wang XJ**, Wei JG, Wang CM, Wang YC, Wu QZ, Xu JK, Yang XX. Effect of cholesterol liposomes on calcium mobilization in muscle cells from the rabbit sphincter of Oddi. *World J Gastroenterol* 2002; **8**: 144-149
- 2 **Wang XJ**, Wei JG, Wang YC, Xu JK, Wu QZ, Wu DC, Yang XX. Effect of cholesterol liposome on contractility of rabbit Oddi's sphincter smooth muscle cells. *Shijie Huaren Xiaohua Zazhi* 2000; **8**: 633-637
- 3 **Chen BY**, Wei JG, Wang YC, Yang XX, Qian JX, Yu J, Chen ZN, Wu DC. Effect of cholesterol on proliferation of cultured fibroblasts of bile duct in rabbit. *Shijie Huaren Xiaohua Zazhi* 2002; **10**: 566-570
- 4 **Ishibashi Y**, Murakami G, Honma T, Sato TJ, Takahashi M. Morphometric study of the sphincter of oddi (hepatopancreatic) and configuration of the submucosal portion of the sphincteric muscle mass. *Clin Anat* 2000; **13**: 159-167
- 5 **Liashchenko SN**. The microsurgical anatomy of the major duodenal papilla and of the sphincter of the hepatopancreatic ampulla. *Morfologiya* 1999; **116**: 50-53
- 6 **Avisse C**, Flament JB, Delattre JF. Ampulla of Vater. Anatomic, embryologic, and surgical aspects. *Surg Clin North Am* 2000; **80**: 201-212
- 7 **Aymerich RR**, Prakash C, Aliperti G. Sphincter of oddi manometry: is it necessary to measure both biliary and pancreatic sphincter pressures? *Gastrointest Endosc* 2000; **52**: 183-186
- 8 **Linder JD**, Geels W, Wilcox CM. Prevalence of sphincter of Oddi dysfunction: can results from specialized centers be generalized? *Dig Dis Sci* 2002; **47**: 2411-2415
- 9 **Toouli J**. Biliary Dyskinesia. *Curr Treat Options Gastroenterol* 2002; **5**: 285-291
- 10 **Craig AG**, Toouli J. Sphincterotomy for biliary sphincter of Oddi dysfunction. *Cochrane Database Syst Rev* 2001; **3**: CD001509
- 11 **Cicala M**, Habib FI, Fiocca F, Pallotta N, Corazziari E. Increased sphincter of Oddi basal pressure in patients affected by gall stone disease: a role for biliary stasis and colicky pain? *Gut* 2001; **48**: 414-417
- 12 **Blaut U**, Sherman S, Fogel E, Lehman GA. Influence of cholangiography on biliary sphincter of Oddi manometric parameters. *Gastrointest Endosc* 2000; **52**: 624-629
- 13 **Kuo KK**, Utsunomiya N, Nabae T, Takahata S, Yokohata K, Chijiwa K, Sheen PC, Tanaka M. Sphincter of Oddi motility in patients with hepatolithiasis and common bile duct stones. *Dig Dis Sci* 2000; **45**: 1714-1718
- 14 **Toouli J**, Craig A. Clinical aspects of sphincter of Oddi function and dysfunction. *Curr Gastroenterol Rep* 1999; **1**: 116-122
- 15 **Toouli J**, Craig A. Sphincter of Oddi function and dysfunction. *Can J Gastroenterol* 2000; **14**: 411-419

- 16 **Deng ZL**, Nabae T, Konomi H, Takahata S, Yokohata K, Ogawa Y, Chijiwa K, Tanaka M. Effects of proximal duodenal transection and anastomosis on interdigestive sphincter of Oddi cyclic motility in conscious dogs. *World J Surg* 2000; **24**: 863-869
- 17 **Wehrmann T**, Lembcke B, Caspary WF, Seifert H. Sphincter of Oddi dysfunction after successful gallstone lithotripsy (postlithotripsy syndrome): manometric data and results of endoscopic sphincterotomy. *Dig Dis Sci* 1999; **44**: 2244-2250
- 18 **Eversman D**, Fogel EL, Rusche M, Sherman S, Lehman GA. Frequency of abnormal pancreatic and biliary sphincter manometry compared with clinical suspicion of sphincter of Oddi dysfunction. *Gastrointest Endosc* 1999; **50**: 637-641
- 19 **Wei JG**, Wang YC, Du F, Yu HJ. Dynamic and ultrastructural study of sphincter of Oddi in early-stage cholelithiasis in rabbits with hypercholesterolemia. *World J Gastroenterol* 2000; **6**: 102-106
- 20 **Madacsy L**, Middelfart HV, Matzen P, Hojgaard L, Funch-Jensen P. Quantitative hepatobiliary scintigraphy and endoscopic sphincter of Oddi manometry in patients with suspected sphincter of Oddi dysfunction: assessment of flow-pressure relationship in the biliary tract. *Eur J Gastroenterol Hepatol* 2000; **12**: 777-786
- 21 **Wehrmann T**, Schmitt T, Schonfeld A, Caspary WF, Seifert H. Endoscopic sphincter of Oddi manometry with a portable electronic microtransducer system: comparison with the perfusion manometry method and routine clinical application. *Endoscopy* 2000; **32**: 444-451
- 22 **Manning BP**, Mawe GM. Tachykinins mediate slow excitatory postsynaptic transmission in guinea pig sphincter of Oddi ganglia. *Am J Physiol Gastrointest Liver Physiol* 2001; **281**: G357-364
- 23 **Lee SK**, Kim MH, Kim HJ, Seo DS, Yoo KS, Joo YH, Min YI, Kim JH, Min BI. Electroacupuncture may relax the sphincter of Oddi in humans. *Gastrointest Endosc* 2001; **53**: 211-216
- 24 **Shima Y**, Mori M, Takakura N, Tanaka N, Yokoi I, Kabuto H, Yamazato T. Continuous monitoring of nitric oxide release induced by cholecystokinin from the choledochal sphincter in guinea pigs. *Digestion* 2000; **61**: 135-139
- 25 **Chiu JH**, Kuo YL, Lui WY, Wu CW, Hong CY. Somatic electrical nerve stimulation regulates the motility of sphincter of Oddi in rabbits and cats: evidence for a somatovisceral reflex mediated by cholecystokinin. *Dig Dis Sci* 1999; **44**: 1759-1767
- 26 **Sand J**, Arvola P, Porsti I, Jantti V, Oja OS, Baer G, Nordback I. Histamine in the control of porcine and human sphincter of Oddi activity. *Neurogastroenterol Motil* 2000; **12**: 573-579
- 27 **Di Francesco V**, Brunori MP, Rigo L, Toouli J, Angelini G, Frulloni L, Bovo P, Filippini M, Vaona B, Talamini G, Cavallini G. Comparison of ultrasound-secretin test and sphincter of Oddi manometry in patients with recurrent acute pancreatitis. *Dig Dis Sci* 1999; **44**: 336-340
- 28 **Chen SZ**, Sha JP, Chen XC, Hou CC, Fu WH, Liu W. Dysrelaxation of Sphincter of Oddi in patients with bile reflux gastritis: study on effect of nifedipine on gallbladder emptying. *Shijie Huaren Xiaohua Zazhi* 1999; **7**: 1020-1023
- 29 **Li XP**, Ouyang KQ, Cai SX. The regulation of bile secretion and education. *Shijie Huaren Xiaohua Zazhi* 2001; **9**: 1066-1070
- 30 **Yang CM**, Mao GP, Zhang XR, Zhang YH, Jian YP. The effects of ethanol on rabbit Oddi's sphincter. *Shijie Huaren Xiaohua Zazhi* 2000; **8**: 87
- 31 **Wu PJ**. The motility and dysfunction of bile duct system. *Shijie Huaren Xiaohua Zazhi* 1999; **7**: 603-604
- 32 **Zapata R**, Severin C, Manriquez M, Valdivieso V. Gallbladder motility and lithogenesis in obese patients during diet-induced weight loss. *Dig Dis Sci* 2000; **45**: 421-428
- 33 **Greaves RR**, O'Donnell LJ, Farthing MJ. Differential effect of prostaglandins on gallstone-free and gallstone-containing human gallbladder. *Dig Dis Sci* 2000; **45**: 2376-2381
- 34 **Craig A**, Toouli J. Sphincter of Oddi dysfunction: is there a role for medical therapy? *Curr Gastroenterol Rep* 2002; **4**: 172-176
- 35 **Kawiorski W**, Herman RM, Legutko J. Pathogenesis and significance of gastroduodenal reflux. *Przegl Lek* 2001; **58**: 38-44
- 36 **Chen BY**, Wei JG, Wang YC, Wang CM, Yu J, Yang XX. Effects of cholesterol on the phenotype of rabbit bile duct fibroblasts. *World J Gastroenterol* 2003; **9**: 351-355
- 37 **Craig AG**, Chen LD, Saccone GT, Chen J, Padbury RT, Toouli J. Sphincter of Oddi dysfunction associated with choledochal cyst. *J Gastroenterol Hepatol* 2001; **16**: 230-234
- 38 **Nabae T**, Yokohata K, Otsuka T, Inoue K, Yamaguchi K, Chijiwa K, Tanaka M. Effect of truncal vagotomy on sphincter of oddi cyclic motility in conscious dogs. *Ann Surg* 2002; **236**: 98-104

Edited by Ren SY

Effect of vanadium on colonic aberrant crypt foci induced in rats by 1,2 Dimethyl hydrazine

P Suresh Kanna, CB Mahendrakumar, T Chakraborty, P Hemalatha, Pratik Banerjee, M Chatterjee

P Suresh Kanna, CB Mahendrakumar, T Chakraborty, P Hemalatha, Pratik Banerjee, M Chatterjee, Division of Biochemistry, Department of Pharmaceutical Technology, Jadavpur University, Kolkata -700032 (Calcutta), India

Supported by financial assistance of Department of Science & Technology, Government of India for during execution of the study (Ref No. SP/SO/B36/2000 dated 4/7/2002)

Correspondence to: M Chatterjee, P.O.17028, Division of Biochemistry, Department of Pharmaceutical Technology, Jadavpur University, Kolkata-700032 (Calcutta), India. m_chatterjee@lycos.com

Telephone: +91-33-24146393 **Fax:** +91-33-24146393

Received: 2003-01-14 **Accepted:** 2003-02-19

Abstract

AIM: To investigate the chemo preventive effects of vanadium on rat colorectal carcinogenesis induced by 1,2-dimethylhydrazine (DMH).

METHODS: Male Sprague-Dawley Rats were randomly divided into four groups. Rats in Group A received saline vehicle alone for 16 weeks. Rats in Group B were given DMH injection once a week intraperitoneally for 16 weeks; rats in Group C, with the same DMH treatment as in the Group B, but received 0.5-ppm vanadium in the form ammonium monovanadate *ad libitum* in drinking water. Rats in the Group D received vanadium alone as in the Group C without DMH injection.

RESULTS: Aberrant crypt foci (ACF) were formed in animals in DMH-treated groups at the end of week 16. Compared to DMH group, vanadium treated group had less ACF ($P < 0.001$). At the end of week 32, all rats in DMH group developed large intestinal tumors. Rats treated with vanadium contained significantly few colonic adenomas and carcinomas ($P < 0.05$) compared to rats administered DMH only. In addition, a significant reduction ($P < 0.05$) in colon tumor burden (sum of tumor sizes per animal) was also evident in animals of Group C when compared to those in rats of carcinogen control Group B. The results also showed that vanadium significantly lowered PCNA index in ACF ($P < 0.005$). Furthermore, vanadium supplementation also elevated liver GST and Cyt P-450 activities ($P < 0.001$ and $P < 0.02$, respectively).

CONCLUSION: Vanadium in the form of ammonium monovanadate supplemented in drinking water *ad libitum* has been found to be highly effective in reducing tumor incidence and preneoplastic foci on DMH-induced colorectal carcinogenesis. These findings suggest that vanadium administration can suppress colon carcinogenesis in rats.

Kanna PS, Mahendrakumar CB, Chakraborty T, Hemalatha P, Banerjee P, Chatterjee M. Effect of vanadium on colonic aberrant crypt foci induced in rats by 1,2 Dimethyl hydrazine. *World J Gastroenterol* 2003; 9(5): 1020-1027

<http://www.wjgnet.com/1007-9327/9/1020.htm>

INTRODUCTION

Colon cancer is one of the most common malignancies in many regions of the world^[1]. The idea that this cancer might be a root cause for chemoprevention stems from epidemiological evidence that some factors in the diet may play important roles in its development, where others may reduce the risk^[2,3]. Experimental Colon carcinogenesis is a multistep process involving three distinct stages, initiation, that alters the molecular message of a normal cell, followed by promotion and progression that ultimately ends up with a phenotypically altered "transformed cell"^[4]. In animal studies, treated with a carcinogen, such as, 1,2 dimethylhydrazine (DMH), methylnitrosurea, N-methyl-N'-nitro-N-nitrosoguanidine will induce colon tumors in experimental animals particularly in rodents^[5,6]. Colon carcinogenesis models using DMH or the related azoxymethane, with putative preneoplastic aberrant crypt foci (ACF) as end-point marker lesions have been used to assess the influence of modulatory factors^[7,8].

ACF are readily discernible 'preadenomatous' morphological putative lesions within the colonic mucosa of rodents and even in cancer patients that may contribute to the stepwise progression to colon cancer^[9-11]. The formation and growth of ACF are associated with the induction of colon tumors in rats and are influenced by exposure to chemopreventive agents^[12,13]. Natural compounds that inhibit ACF induced colon carcinogenesis have proved to be protective against colon cancer in rodents^[14].

Besides the DMH-target tissue colon, the liver was preferentially selected for assaying the biotransformation and detoxification pattern^[15,16]. Many chemical changes of the liver are detectable prior to the onset of secondary pathological and nutritional changes associated with conditions such as neoplasia. The pathological alterations in the liver often act as an indicator of overall damage caused by a carcinogen since liver enzymes provide more sensitive indicators of pathogenesis than blood^[17]. Efficient inactivation of both xenobiotics and endogenous toxins result in the preservation of cellular integrity and inhibition of cytotoxic events, which lead to several diseases including cancer^[18]. Glutathione S-transferases (GST) are a family of multifunctional proteins, which act as binding proteins and also as enzymes in various detoxification processes^[19-21]. GSTs have been acknowledged as preneoplastic and neoplastic markers^[22]. Cytochrome P-450s, also known as mixed function oxidases having a very broad range of substrate specificity in both exogenous and endogenous including drugs, chemical carcinogens and xenobiotics^[23,24] carry out biotransformation and reduction. Aberration in epithelial colonic crypt cell proliferation leads to hyperplasia with higher risk of colon cancers both in humans and experimental animal models^[25]. Assessment of PCNA expression as an indicator of colonic crypt cell proliferation is suggested as a putative intermediate marker of colon cancer risk^[26].

Vanadium, an element of complex chemistry is of considerable scientific and biological interest nowadays, because of its diverse physiological properties with narrow thresholds between essential and toxic doses^[27]. Various studies from our laboratory have established vanadium for the very first time to be a novel biological regulator in assessing the

physiological and biochemical state of animals in a dose related manner in the detoxification of a number of xenobiotics, including electrophilic chemical carcinogens. Vanadium is observed to be capable of exhibiting some unique beneficial effects particularly, its anticarcinogenic potential under a very low dose^[28-30] without any adverse toxicity. Our laboratory has documented a number of works involving vanadium as a potential antineoplastic agent in rat liver carcinogenesis. Furthermore, this element has shown to be able to inhibit chromosomal and molecular damages by abating the generation of DNA single stranded-breaks and thereby maintaining the genomic integrity^[31]. Thus, there are good reasons to suspect that this micronutrient vanadium may be considered as a potential cancer chemopreventive agent.

In the present study, we had focused on the inhibitory effect of vanadium against the early stages of neoplastic transformation in a defined DMH-induced rat colon carcinogenesis model, since no reports from any other laboratories have documented the same, by morphometric evaluation of the ACF in colonic mucosa and colonic tumors in terms of tumor incidence, colon tumor multiplicity and tumor burden along with histological typings. Furthermore, the chemopreventive efficacy of the trace element was also investigated on certain hepatic drug metabolizing and phase II detoxifying enzyme activity patterns e.g. on liver glutathione S-transferase [GST] and Cytochrome P-450 [Cyt P-450] activities. Finally, PCNA expression as an indicator of cellular proliferation was carried out to correlate the morphometric and enzymological parameters with the protein expression to establish the possible antineoplastic potential of the said element at the cellular level.

MATERIALS AND METHODS

Animals

40 Male Sprague Dawley rats (3-4 weeks old) weighing 80-100 grams were purchased from Indian Institute of Chemical Biology (CSIR), Kolkata (Calcutta), India and quarantined for a week. They were housed 10 per cage under controlled conditions of a 12:12 hour light and dark cycle at 28±3 °C. All rats were maintained on a semi purified basal diet (Lipton, Calcutta, India) and water *ad libitum*. All rats received human care according to the criteria outlined in the "Guide for the Care and Use of Laboratory Animals" prepared by the National Academy of Sciences and published by the National Institutes of Health (NIH publication 86-23, revised 1985). Body weights were recorded every 2 weeks.

Chemicals

1, 2 Dimethylhydrazine (DMH) and Vanadium as Ammonium monovanadate was purchased from E. Merck Ltd, Bombay, India.

Experimental protocols

Rats were randomly assigned into experimental and control groups. Group A: animals constituted the normal untreated controls and received saline vehicle intraperitoneally, once a week, throughout the entire course of experimental study, till 32 weeks. Group B: comprised of carcinogen control animals. 1,2 DMH was administered intraperitoneally at a dose of 20-mg/kg-body weight, once a week in 0.9 % NaCl solution (pH 7.2) for a total period of 16 weeks. Group C: included the experimental animals, which received both DMH and Vanadium treatment. Vanadium as ammonium monovanadate at a dose of 0.5-ppm was administered *ad libitum* through drinking water while DMH was injected in the same dose mentioned earlier for Group A animals. Vanadium treatment

was initiated simultaneously with the DMH injection (termed day 0). Group D: animals were vanadium controls and received vanadium alone as ammonium monovanadate at a dose of 0.5 ppm *ad libitum* through drinking water. They were not subjected to any DMH injection.

Interim sacrifice was performed at 16 weeks from the day of initiation in order to evaluate the preventive efficacy of vanadium in the initial stages of carcinogenesis in terms of histology and ACF studies. The terminal sacrifice was carried out at end of 32nd week as shown in Figure 1. All animals were fasted overnight before termination and sacrifice under light ether anesthesia. The length of the colon was recorded.

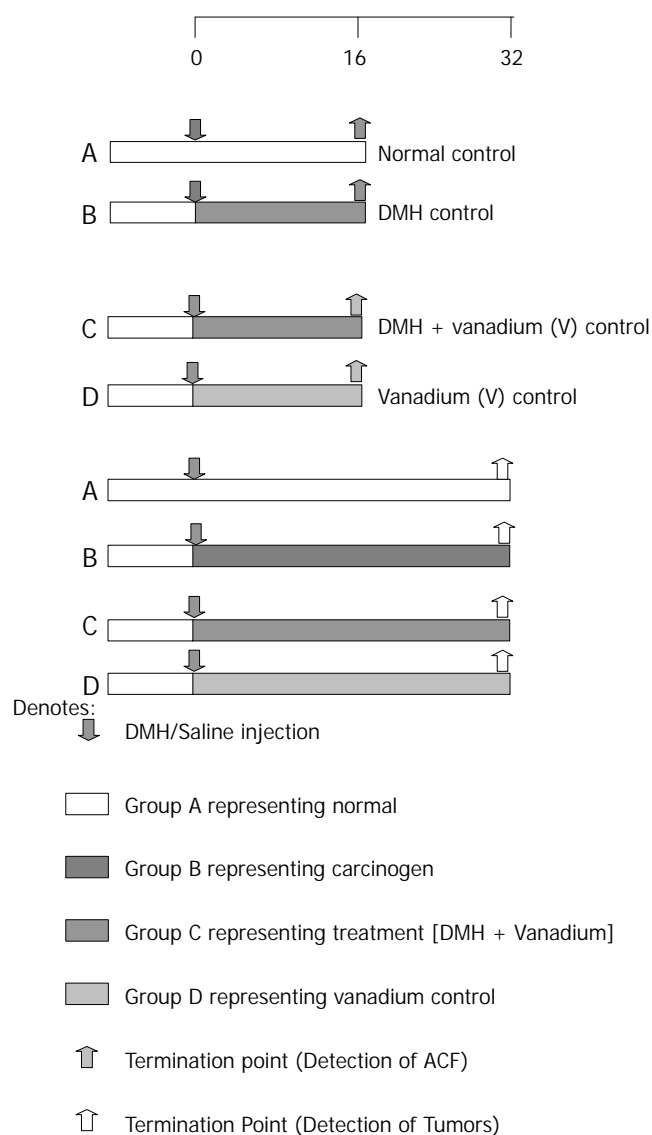


Figure 1 Grouping and different time point of the experiment.

Histological evaluation and ACF assay

The method of Bird^[32] was used to stain and highlight ACF. The number of ACF was evaluated in the 0.3 % methylene blue stained colon. ACF was scored under a light microscope with 40 times magnification to transilluminate the colon. Only ACF meeting the criteria given by McLellan and Bird were chosen. These included crypts of increased size with a thicker and deeply stained epithelial lining and increased pericryptal zone compared with normal crypts.

Morphometric evaluation

After the terminal sacrifice at 32 weeks, colons were excised from the rats, blotted dry, cut open longitudinally and the inner

surface was examined whether there were visible macroscopic lesions (neoplastic tumors). Tumors were easily discernable in the inflamed sections of the colon. The number and size of the tumors were noted for tumor incidence, multiplicity and burden studies. Tumors were classified as adenomas/carcinomas based on the evidence of invasion through the muscularis mucosa. Those with clear-cut invasion were considered to be carcinomas while the rest were classified as adenomas^[33]. The three main axes of each macroscopic tumor from rats were measured using a vernier caliper with 0.1 mm graduation. Preneoplastic lesions were not included in tumor counts.

Assay of GST and Cyt P-450 activities

To determine whether vanadium could modify liver GST and Cyt P-450 activities, livers were excised immediately from all rats necropsy. The livers were perfused with saline to remove blood and minced into small pieces. Aliquots from minced livers were processed to obtain the cytosolic fraction as described^[34]. The activities of GST with 1,2-dichloro-4-nitrobenzene (DCNB) as substrates, and Cyt P-450 assay was determined as described^[35-37]. All assays were performed with UV-Visible Spectrophotometer (Jasco V-530). One unit of enzyme activity was the amount of enzyme catalyzing the conversion of 1 μ mol of substrate to produce per min at 25 °C. Cytosolic protein concentrations were determined by the method of Lowry *et al*^[38] using bovine serum albumin as the standard.

Immunohistochemistry of proliferating cell nuclear antigen (PCNA)

Immunohistochemical staining for PCNA was performed by the avidin-biotin complex method (Sigma). Tissue sections were deparaffinized with xylene, hydrated through a graded ethanol series, immersed in 0.3 % hydrogen peroxide in absolute methanol for 30 minutes at room temperature to block endogenous peroxidase activity and then washed in phosphate-buffered saline (pH 7.2). Following incubation with normal rabbit serum at room temperature for 10 minutes to block background staining, the sections were incubated with an anti-PCNA antibody (mouse monoclonal PC 10; Sigma, USA; a 1:100 dilution) for 12 hours in a humidified chamber at room temperature. They were then reacted with 3,3'-diaminobenzidine and counterstained with Harris' hematoxylin. For determination of PCNA-positive index, 10 full-length crypts (aberrant crypts, normal-appearing crypts or normal crypts) of each colon were examined. The number of PCNA positively stained nuclei in each crypt column was recorded. The PCNA positive index (number of positive stained nuclei X 100/total number of nuclei counted) was then calculated.

Statistical analysis

The statistical analysis for morphometric studies between different groups was performed by Fischer's exact probability test for tumor incidence. Student's *t* test was used to analyzed the tumor multiplicity and tumor burden.

RESULTS

Food and water intake

No appreciable change in food consumption was observed among different groups of rats. The daily food and water intakes were measured with a measuring cylinder and it was found that rats took on an average of 8-10 ml of water/day per rat.

Mortality

All animals survived during the entire course of the experiment.

Body weight of rats

Figure 2 showed the body weight of the rats in different groups sacrificed on the 32nd weeks following the first DMH injection. DMH treatment did not appreciably decrease rat body weight when compared with saline treatment, for first few weeks but by the end of the experimental study at 32nd weeks, differences between normal and carcinogen control Group A were statistically significant ($P < 0.05$). In Group C, animals undergoing treatment with vanadium, maintained near normal body weights. Animals in vanadium control Group D displayed body weights close to those in normal Group B.

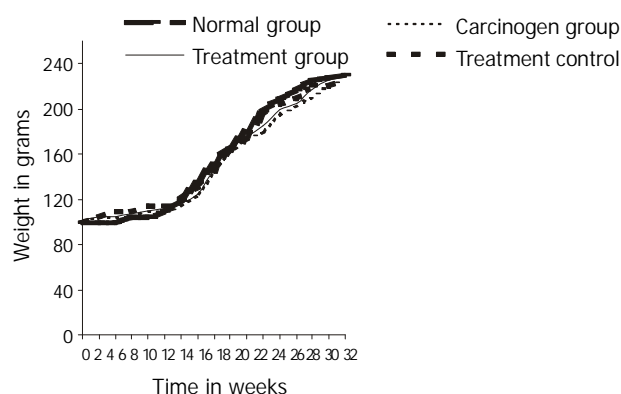


Figure 2 Depicts the body weights of different group of animals.

Aberrant crypt assay

The effect of vanadium on the growth and development of ACF, induced by DMH, in rats was given in Table 1. There was a remarkable decrease in the incidence of aberrant crypts, expressed in terms of percentage, from 100 % in carcinogen group B to 66.07 % in vanadium treatment Group C in early stages of colon carcinogenesis. The average yield of aberrant crypts for the carcinogen group was 112 ± 3.2 ACF/Colon and the range was 90-115 ACF/Colon. For the vanadium treatment Group C, this was significantly reduced ($P < 0.001$ when compared with Group B) to a mean value of 38 ± 3.1 and ranged between 15-40 ACF/Colon. There were no observable foci witnessed in rats of Group D which had administration of vanadium alone *ad libitum* throughout the experiment.

Table 1 Chemopreventive efficacy of vanadium on DMH-induced ACF in Sprague Dawley rats

Group	Number of rats/Group	Number of ACF per rat colon (mean \pm SE)	Inhibition (%)
Normal Control A	10	-	-
DMH Control B	10	112 \pm 3.2	-
DMH + V C	10	38 \pm 3.1 ^a	66.07
V Control D	10	-	-

^a $P < 0.001$ vs DMH-only group B by Student's *t* test.

Histology

Tissue sections of Group A displayed normal colonic architecture with no signs of apparent abnormality (Figure 3.1 a,b). In the Carcinogen group B, well-differentiated signs of neoplasia were evident. Nuclei were enlarged and hyperchromatic with mitosis. Simultaneously, there was a loss in nuclear polarity. Connective tissues showed edema and swelling of endothelial cells (Figure 3.2 a,b). In the vanadium treatment Group C, histology revealed no loss of nuclear polarity. Tubules were well formed while crypts lie parallel

to each other. The size and shape of the cells were uniform. Occasionally, hyper chromatic nucleus was evident. However, connective tissue invasion was not seen. No oedema or infiltration of polymorph nuclear leucocytes was sighted (Figure 3.3 a,b). There were no signs of neoplasia or toxicity observed in Group D rats administered with vanadium supplementation (Figure 4.3 a,b).

Colonic tumor analysis

Administration of ammonium monovanadate at the dose of 0.5 ppm, *ad libitum* through drinking water for each animal, brought about a significant reduction of tumor incidence in DMH-induced colon carcinogenesis (Table 2). In the carcinogen Group B, tumor incidence was 100 % (Figure 4.

1 a,b). It dropped to a significant 60 % in the vanadium treated Group C ($P < 0.01$ when compared to DMH control group B by Fischer's exact probability test) (Figure 4.2 a,b). The average number of tumor (classified as adenomas, carcinomas) per tumor bearing rat was also considered in the study. Rats treated with vanadium in Group C contained significantly few colonic adenomas and carcinomas ($P < 0.05$ by Student's *t* test) compared to rats administered with DMH only (Table 2). In addition, a significant reduction ($P < 0.05$) in colon tumor burden (sum of tumor sizes per animal) was also evident in Group C when compared to those in carcinogen control Group B. The results were statistically significant (Table 3). There were no marked changes observed in Group D (Figure 4.3 a,b).

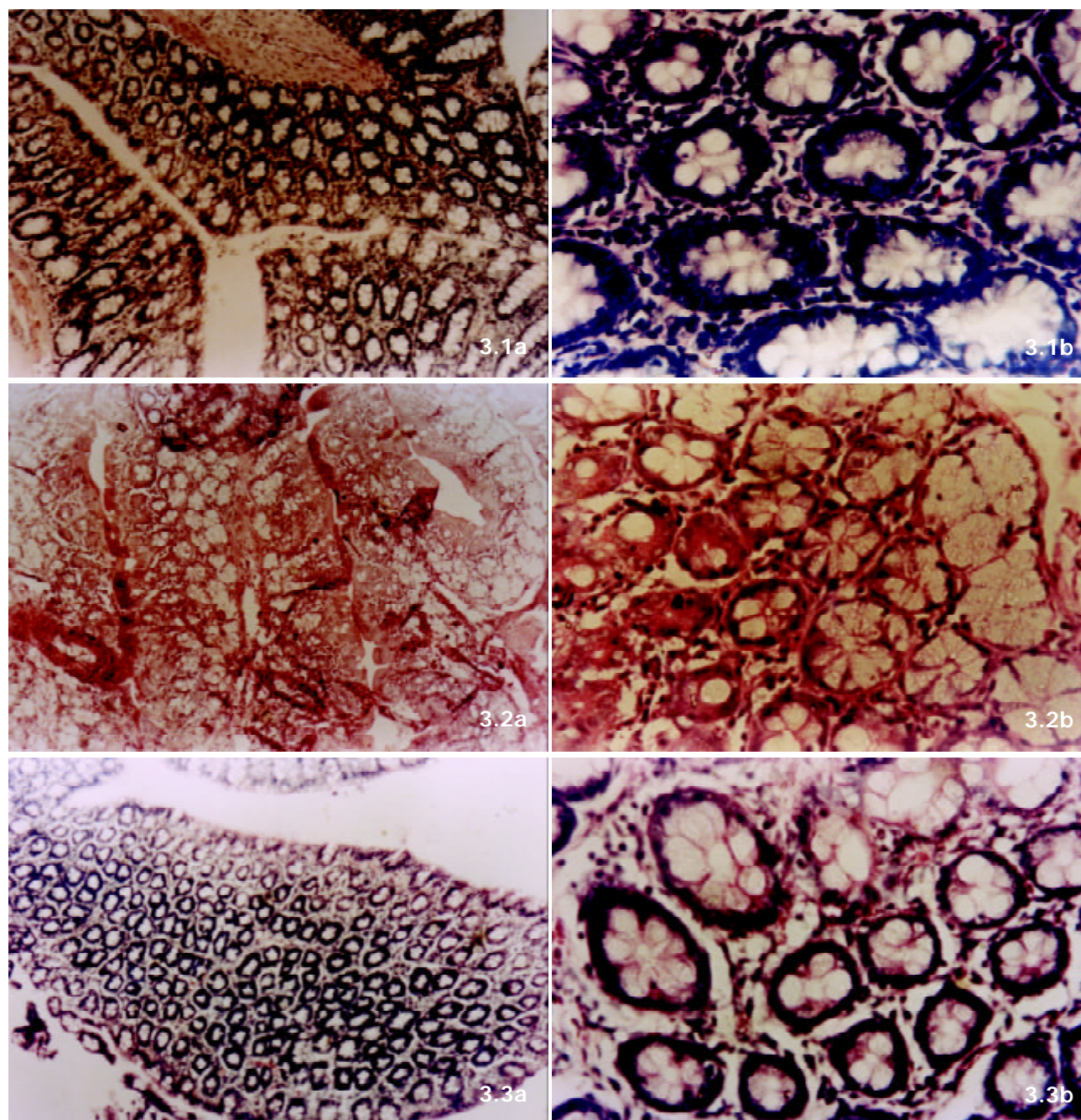


Figure 3 3.1 (a): showing the normal colonic architecture view of rats sacrificed at end of week 16 (Low power).
 3.1 (b): showing the normal colonic architecture view of rats sacrificed at end of week 16 (High power).
 3.2 (a): representing the carcinogen-induced group B rats sacrificed at end of week 16 (Low power).
 3.2 (b): representing the carcinogen-induced group B rats sacrificed at end of week 16 (High power).
 3.3 (a): showing the treatment with vanadium group C rats sacrificed at the end of week 16 (Low power).
 3.3 (b): showing the treatment with vanadium group C rats sacrificed at the end of week 16 (High power).

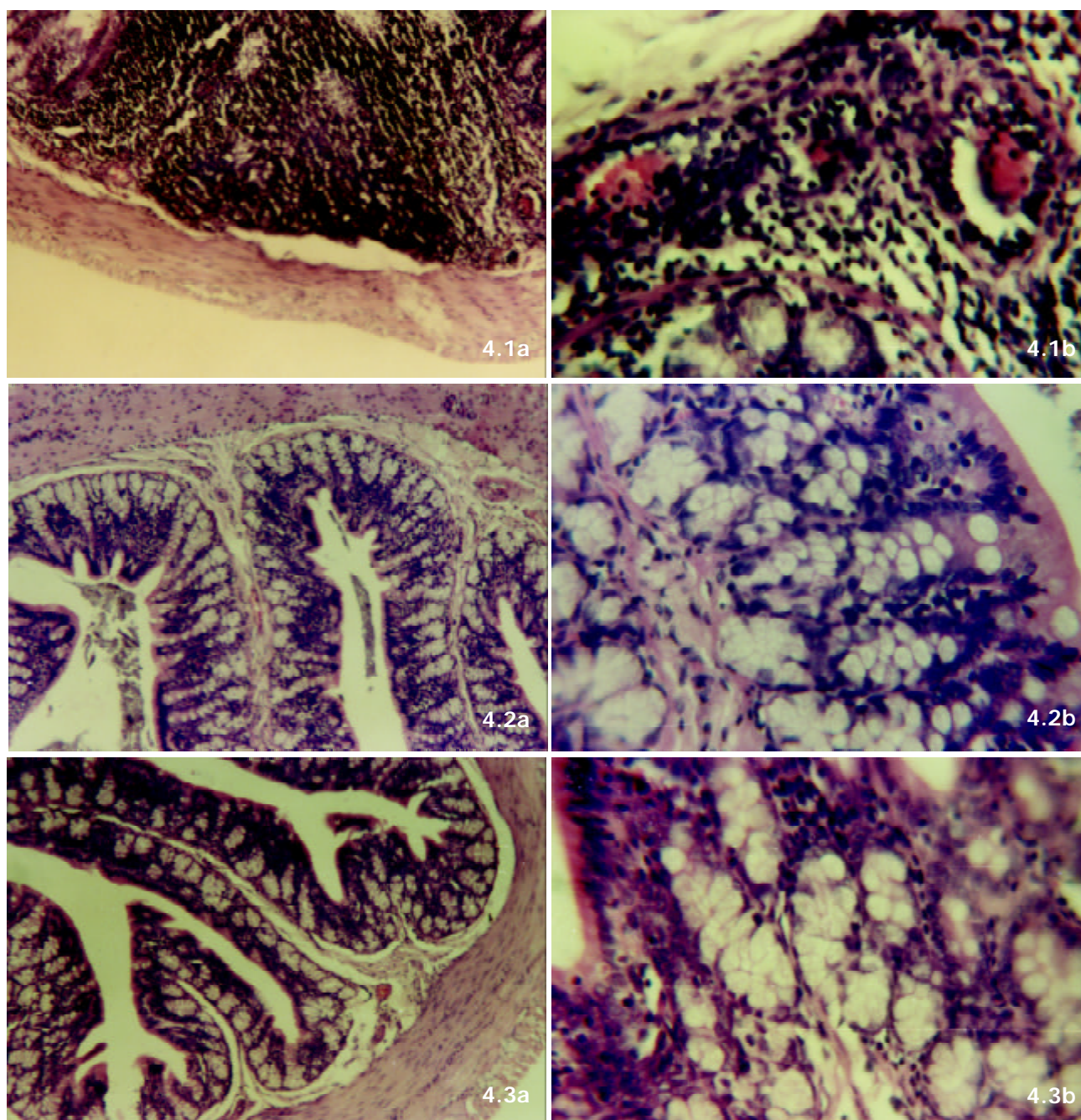


Figure 4 4.1 (a): showing the carcinogen-induced group B rats sacrificed at end of week 32 (Low power).
 4.1 (b): showing the carcinogen-induced group B rats sacrificed at end of week 32 (High power).
 4.2 (a): showing the treatment with vanadium group C rats sacrificed at the end of week 32 (Low power).
 4.2 (b): showing the treatment with vanadium group C rats sacrificed at the end of week 32 (High power).
 4.3 (a): showing the vanadium control group D rats with no signs of toxicity sacrificed at the end of week 32 (Low power).
 4.3 (b): showing the vanadium control group D rats with no signs of toxicity sacrificed at the end of week 32 (High power).

Table 2 Chemopreventive efficacy of 0.5-ppm vanadium (supplemented ad libitum through drinking water) on the incidence and multiplicity of DMH induced rat colonic tumors

Group	Number of rats		Colon tumor incidence (percentage of tumor-bearing rats)	Total number of tumors			Colon tumor multiplicity (mean tumor/animal, Mean±SD)		
	Total	Tumor counts		Adenoma	Carcinoma	All neoplasia	Adenoma	Carcinoma	All neoplasia
A	10	-	-	-	-	-	-	-	-
B	10	10	100	97	64	120	9.7±0.3	6.4±0.1	12±0.1
C	10	06	60 ^a	23	16	31	2.3±0.2	1.6±0.2	3.1±0.1 ^b
D	10	-	-	-	-	-	-	-	-

^a $P < 0.01$ vs DMH-only group B by Fischer's exact probability test; ^b $P < 0.05$ vs Group B by Student's *t*-test.

Table 3 DMH-induced colon tumor burden in Male Sprague Dawley rats fed Vanadium (0.5 ppm) *ad libitum* through drinking water

Group	Number of rats/group	Mean colonic length (cm)(Y)	Mean colon tumor burden (sum of the tumor size, mean±SD) (cm)			X/Y
			Adenoma	Carcinoma	All Neoplasia (X)	
A	10	24	-	-	-	-
B	10	24	3.67±3.2 ^b	5.96±9.7	9.56±12.05	0.39
C	10	22	0.87±1.6	1.19±2.9	1.92±2.93 ^a	0.08
D	10	20	-	-	-	-

^a $P < 0.05$ vs Group B by Student's *t*-test.

Liver GST and CYT P-450 activities

Liver GST and Cyt P-450 activities at the end of the study were shown in Table 4. DMH treatment in Group B significantly elevated liver GST ($P < 0.05$) and Cyt P-450 ($P < 0.001$) activities using CDNB as a substrate when compared with those of Group A. GST activities in Group C was significantly greater than those in Group B ($P < 0.02$) and Cyt P-450 activities in Group C was also significantly greater than those in Group B ($P < 0.001$).

Table 4 Liver GST and Cyt P-450 activities (mean ± SE, $n=10$)

Group	Cyt P-450 activity (mU/mg protein)	GST-CDNB (mU/mg protein)
A Normal Control	0.62±0.06	0.83±0.10
B DMH-Control	0.20±0.03 ^d	0.45±0.03 ^a
C DMH + V	0.41±0.01 ^e	1.98±0.09 ^f
D V-Control	0.47±0.05	0.90±0.19

^a $P < 0.001$ vs Group A, ^b $P < 0.05$ vs Group A, ^c $P < 0.001$ vs Group B, ^d $P < 0.02$ vs Group B.

PCNA-labeling index in ACF

The PCNA-labeling indices in ACF were shown in Table 5. The mean PCNA-labeling indices in ACF of Group C were significantly lower than that of Group B ($P < 0.005$ and $P < 0.005$, respectively).

Table 5 PCNA-labeling index of colonic mucosa of rats treated with DMH, supplemented with vanadium (V) 0.5-ppm *ad libitum* in drinking water (means ± SD)

Group	No of rats	ACF(Numbers of ACF or crypts)
A Normal control	10	-
B DMH control	10	35±5 (10)
C DMH + V	10	23.6±2 ^a (10)
D V Control	10	-

^a $P < 0.005$ vs Group B by Student's *t*-test.

DISCUSSION

Variable inhibitory effects of vanadium on the incidence of preneoplastic lesions (ACF) were observed during different phases of colorectal carcinogenesis. The finding of the histological and morphometric study clearly supports that trace element vanadium holds a promising anticancer potential with respect to colon carcinogenesis^[39]. The results suggest that chemically induced carcinogenesis in the rat colon follows a distinct pathway where histogenesis obeys the ACF-adenoma-carcinoma sequence in the mid and distal colon and the ACF are an intermediate stage only existed in better-differentiated tumors. A linear relationship between AC formation and colon tumor induction for the same group of laboratory animals could also be established.

As there is strong correlation between ACF formation and colon carcinogenesis, the observation amply imply that supplementation by 0.5-ppm vanadium under the conditions of the experiment, can greatly affect the post initiation stages of colon carcinogenesis by altering the efficacy at which DMH can initiate foci appearance. Increased mitotic activity, which have been proposed as a biomarker of the early stages of colon cancer^[40] was observed in most of the ACF induced by DMH administration alone. Treatment with vanadium greatly restored normalcy in the colonic epithelial cells. The ability of vanadium to reduce the number of ACF per colon also indicates that the anti-carcinogenic potential of vanadium could be mediated through an enhanced repair or remodeling of preneoplastic lesions^[41].

In our observation, we have studied vanadium mediated inhibition of the tumor multiplicity coupled with tumor burden as a percentage of the colonic length. This observation is of interest if one considers that there was no major difference in body weights among the normal rats and rats in Group C. This is particularly important because nutritional deprivation causing body weight loss may parallel a decrease in tumor burden^[42]. The variation in weight gain among the different groups under experiment, thus, do not seem to be significant when evaluating possible causes for the observed differences in the induction of AC or tumors.

Treatment of rats with drinking water supplemented with vanadium for 16 and 32 weeks not only decreased the number of preneoplastic foci but also caused a decrement in the tumor incidence/tumor multiplicity with a concomitant reduction in tumor burden as a percentage of colonic length. This strongly suggests the potentiality of vanadium in inhibiting/slowing tumorigenesis in the rat colon.

Phase II enzymes help to inhibit the formation of electrophiles and catalyze their conversion to inactivate conjugates making them more water soluble and readily excretable from the cell. It is the cellular balance between the Phase I activating enzymes and Phase II detoxifying enzymes that contribute to one's risk of developing cancer^[43]. GSTs catalyze the reaction of the compounds with thiol group of GSH, thus neutralize their electrophilic sites and render the product more water soluble^[44]. 1, 2-DMH is a colon specific procarcinogen that is metabolically activated to the active carcinogen in the liver through a sequential radical generating mechanism^[45] implying a need for detoxification through antioxidant as well as biotransformation mechanism. Cellular GSH by itself or together with GST can function as a non-critical nucleophile for conjugation reactions and play an important role in the inactivation of electrophilic compounds^[46]. Therefore, an elevation of GSH level indicates an increase in the systemic ability to detoxify electrophilic compounds including carcinogens. Data from several laboratories continue to suggest a relationship between decreased GST expression and an increased risk for cancer^[47-49]. The decrease may be associated further with interference of protein synthesis and accumulation of electrophilic metabolites. Increased GST level towards normal value clearly indicates that the tumor genesis burden

is not high, at the same time shows that vanadium is a good protective agent against DMH induced colon carcinogenesis.

Preliminary studies from our laboratory^[50,51] have shown that under a certain optimum dose of 0.5 ppm, the trace element could lead to stable induction of GST activity without any apparent signs of toxicity. A probable mechanistic explanation could be increased transcription of GST gene and/or allosteric modification of the enzyme. Alternatively, this increase in GST activity by vanadium can be viewed as the host cellular response in boosting up the GSH-related conjugation system against the possible free radical mediated stress.

In the present study, we also report that vanadium functions as an anticarcinogen by altering the activity of Cyt P-450 related enzyme. Vanadium might have induced the Cyt P-450 level due to its property as a heavy metal. Since the dose used is non-toxic^[52], it is having a positive action on inhibiting tumor promotion. The induction of Cyt P-450 may also be due to alteration of the ATP/ADP ratio by the inhibition of oxidative phosphorylation thereby increasing the NADPH content rapidly for the mixed function oxidase system to act. Alternatively, vanadium may elevate the Cyt P-450 level by regulating the transcriptional activation of the P-450 gene^[53]. Considering the relative persistence of oxidative damage, antioxidant defense and biotransformation alterations, we could predict that the biochemical markers measured in the liver may well be a prognostic marker of the distant neoplasm of the colon, even at the early stages of preneoplasia at 16 weeks.

Finally, PCNA-labeling index, an intermediate biomarker of carcinogenesis, was decreased in DMH-treated ACF by supplementation of vanadium in the drinking water. Cell proliferation plays an important role in multistage carcinogenesis with multiple genetic changes^[54]. PCNA is an auxiliary protein of the DNA polymerase delta, reaching an expression peak during the S-phase of the cell cycle and playing an important role in cellular proliferation^[55]. PCNA has been used as an intermediate biomarker in chemoprevention of colorectal cancer^[56]. Zheng *et al*^[57] observed that Vitamin A significantly decreased PCNA in the AOM-induced colorectal cancer animal model. Thus, the inhibitory effect of vanadium may be due, in part, to modification of cell proliferation through the above mechanisms.

One of the predominating factors which often limit the therapeutic efficacy of many antineoplastic elements and their complexes is their considerable toxic side effects associated with hepato and nephrotoxicity. However in the present study, supplementing vanadium at 0.5 ppm have shown no clinical signs of toxicity such as decrease in food and water intake, retarded growth or eventual death.

In conclusion, the results of this study suggest that daily supplementation of 0.5 ppm vanadium in the form of ammonium monovanadate in the drinking water has a positive beneficial effect against chemically induced colonic preneoplastic progression in rats induced by DMH, which provides an effective dietary chemopreventive approach to disease management. However, other definitive bioassay including protein expression and documentation of specific molecular markers is now being planned in our laboratory to establish the surrogate end-point biomarker in vanadium-mediated cancer chemoprevention.

REFERENCES

- 1 **Shike M**, Winawer SJ, Greenwald PH, Bloch A, Hill MJ, Swaroop SV. Primary prevention of colorectal cancer: The WHO collaborating centre for prevention of colorectal cancer. *Bull World Health Org* 1990; **68**: 377-385
- 2 **Potter JD**, McMichael AJ. Diet and cancer of the colon and rectum: a case-control study. *J Natl Cancer Inst* 1986; **76**: 557-569
- 3 **Mukhtar H**, Athar M. Dietary anticarcinogens and cancer prevention. *Cleaveland Clin J Med* 1988; **55**: 507-508
- 4 **Pitot HC**. Fundamentals of Oncology. New York: *Marcel Dekker, Inc* 1986
- 5 **Pozharisski KM**, Likhachev AJ, Klimashevski VF, Shaposhnikov JD. Experimental intestinal cancer research with special reference to human pathology. *Adv Cancer Research* 1979; **30**: 165-237
- 6 **Druckrey E**. Organ-specific carcinogenesis in the digestive tract. In: Nakahara W, Takayama S, Sugimura T, Odashima S, eds. Topics in Chemical Carcinogenesis. Baltimore Maryland: *University Park* 1972:73-101
- 7 **Bird RP**. Role of ACF in understanding the pathogenesis of colon cancer. *Cancer Letters* 1995; **93**: 55-71
- 8 **McLellan EA**, Bird RP. Aberrant crypts: Potential preneoplastic lesions in the murine colon. *Cancer Research* 1988; **48**: 6187-6192
- 9 **McLellan EA**, Medline A, Bird RP. Dose response and proliferate characteristics of aberrant crypt foci: putative preneoplastic lesions in rat colon. *Carcinogenesis* 1991; **12**: 2093-2098
- 10 **McLellan EA**, Bird RP. Aberrant crypts: Potential preneoplastic lesions in the murine colon. *Cancer Research* 1988; **48**: 6187-6192
- 11 **McLellan EA**, Medline A, Bird RP. Sequential analyses of the growth and morphological characteristics of aberrant crypt foci: putative preneoplastic lesions. *Cancer Research* 1991; **51**: 5270-5274
- 12 **Pereira MA**, Barnes LH, Rassman VL, Kolloff GV, Steele VE. Use of azoxymethane-induced foci of aberrant crypts in rat colon to identify potential cancer chemopreventive agents. *Carcinogenesis* 1994; **15**: 1049-1054
- 13 **Pretlow TP**, O' Riordan MA, Somich GA, Amini SB, Pretlow TG. Aberrant crypts correlate with tumor incidence in F344 rats treated with azoxymethane and phytate. *Carcinogenesis* 1992; **13**: 1509-1512
- 14 **Tanaka T**, Mori H. Inhibition of colon carcinogenesis by nonnutritive constituents in foods. *J Toxicol Pathol* 1996; **9**: 139-149
- 15 **Albano E**, Tomasi A, Gorla-Gatti L, Iannone A. Free radicals activation of monomethyl and dimethylhydrazines in isolated hepatocytes and liver microsomes. *Free Radical Biol Med* 1989; **6**: 3-8
- 16 **Pence CB**. Dietary selenium and antioxidant status: toxic effects of 1,2-dimethyl hydrazine in rats. *J Nutr* 1991; **121**: 138-144
- 17 **Herzfeld A**, Greengard O. The effect of lymphoma and other neoplasms on hepatic and plasma enzymes of the host rat. *Cancer Research* 1977; **37**: 231-238
- 18 **Jakoby WB**, Ziegler DM. The enzymes of detoxification. *J Biol Chem* 1990; **265**: 20715-20718
- 19 **Jakoby WB**, Habig WH. Enzymatic basis of detoxification. *Vol II Acad Press* 1980; **12**: 63-94
- 20 **Manavick B**, Alin P, Gluthenbeg C, Jensson H, Tahir MK, Warholm M, Jornvall H. Identification of three classes of cytosolic glutathione transferase common to several mammalian species. *Proc Natl Acad Sci USA* 1985; **82**: 7202-7206
- 21 **Ketterer B**, Meyer DJ, Coles B, Taylor JB, Pemble S. Glutathione transferases and carcinogenesis. *Basic Life Sci* 1986; **39**: 103-126
- 22 **Sato K**. Glutathione S-transferases as markers of preneoplasia and neoplasia. *Adv Cancer Res* 1990; **52**: 205-255
- 23 **Jakoby WB**. Enzymatic basis of detoxification. New York: *Acad Press* 1983: 135-182
- 24 **Guengerich FP**. Roles of Cytochrome P-450 enzymes in chemical carcinogenesis and cancer chemotherapy. *Cancer Res* 1988; **48**: 2946-2954
- 25 **Chapkin RS**, Lupton JR. Colonic cell proliferation and apoptosis in rodent species. Modulation by diet. *Adv Exp Med Biol* 1999; **470**: 105-118
- 26 **Yamada K**, Yoshitke K, Sato M, Ahnen DJ. Proliferating cell nuclear antigen expression in normal, preneoplastic colonic epithelium of the rat. *Gastroenterology* 1992; **103**: 160-167
- 27 **Nriagu JO**. Advances in environmental science and technology. *Wiley J and Sons USA*; 31
- 28 **Bishayee A**, Chatterjee M. Increased lipid peroxidation in tissues of the cat fish *Clarias batrachus* following vanadium treatment: in vivo and in vitro evaluation. *Journal Inorganic Biochemistry* 1994; **54**: 277-284
- 29 **Chakraborty A**, Bhattacharjee S, Chatterjee M. Alterations in enzymes in an Indian Cat fish *Clarias batrachus* (L) exposed to vanadium. *Bulletin of Environmental Contamination Toxicology* 1995; **54**: 281-288

- 30 **Chakraborty A**, Ghosh R, Roy K, Ghosh S, Choudhury PK, Chatterjee M. Vanadium-a modifier of drug metabolizing enzyme patterns and its critical role in cellular proliferation in transplantable murine lymphoma. *Oncology* 1995; **52**: 310-314
- 31 **Chatterjee M**, Bishayee A. Vanadium-A new tool for cancer prevention. Vanadium in Environment Part 2 1998; John Wiley & Sons, Inc
- 32 **Bird RP**. Role of aberrant crypt foci in understanding the pathogenesis of colon cancer. *Cancer Letters* 1995; **93**: 55-71
- 33 **Jacobs LR**. Enhancement of rat colon carcinogenesis by wheat bran consumption during the stage of 1,2 Dimethylhydrazine administration. *Cancer Research* 1983; **43**: 4057-4061
- 34 **Benson AM**, Batzinger RP, Ou SY, Bueding E, Cha YN, Talalay P. Elevation of hepatic glutathione S-transferase activities and protection against metabolites of benzo [a] pyrene by dietary antioxidants. *Cancer Research* 1978; **38**: 4486-4495
- 35 **Benson AM**, Hunkeler MJ, Talalay P. Increase of NAD (P) H: quinone reductase by dietary antioxidants: possible role in protection against carcinogenesis and toxicity. *Pro Natl Acad Sci USA* 1980; **77**: 5216-5220
- 36 **Habig WH**, Pabst MJ, Jakoby WB. Glutathione S-transferase: The first enzymatic step in mercapturic acid formation. *Biol Chem* 1974; **249**: 7130-7139
- 37 **Omura T**, Sato R. The carbon monoxide binding pigment of liver microsomes I and II. *J Biol Chem* 1964; **239**: 2370-2378
- 38 **Lowry OH**, Rosebrough NJ, Farr AL, Randall RJ. Protein measurement with the folin phenol reagent. *J Biol Chem* 1951; **193**: 265-275
- 39 **Bishayee A**, Chatterjee M. Inhibitory effect of vanadium on rat liver carcinogenesis initiated with diethylnitrosamine and promoted by Phenobarbital. *British J Cancer* 1995; **71**: 1214-1220
- 40 **Lipkin M**. Biomarkers of increased susceptibility to gastrointestinal cancer: new application to studies of cancer prevention in human subjects. *Cancer Research* 1988; **48**: 235-245
- 41 **Farber E**, Parker S, Gruenstein M. The resistance of putative pre-malignant liver cell populations, hyperplastic nodules to the acute cytotoxic effects of some hepatocarcinogenesis. *Cancer Research* 1976; **36**: 3879-3887
- 42 **Waitzberg DL**, Goncalves EL, Faintuch J, Bevilacqua LR, Rocha CL, Cologni AM. Effects of diets with different protein levels on the growth of Walker 256 carcinosarcoma in rats. *Brazil J Med Biol Res* 1989; **22**: 447-455
- 43 **Wilkinson J**, Clapper ML. Detoxification enzymes and chemoprevention. *Pro Soc Exp Biol Med* 1997; **216**: 192-200
- 44 **Habig WH**, Pabst MJ, Jakoby WB. Glutathione S-transferase: The first enzymatic step in mercapturic acid formation. *Biol Chem* 1974; **249**: 7130-7139
- 45 **Albano E**, Tomasi A, Goria-Gatti L, Iannone A. Free radicals activation of monomethyl and dimethylhydrazines in isolated hepatocytes and liver microsomes. *Free Radical Biol Med* 1989; **6**: 3-8
- 46 **Uhlig S**, Wendel A. The physiological consequences of glutathione variations. *Life Sci* 1992; **51**: 1083-1094
- 47 **Zhou T**, Evans AA, London WT, Xia X, Zou H, Shen F, Clapper ML. Glutathione- S-transferase expression in hepatitis B virus associated and human hepatocellular carcinogenesis. *Cancer Research* 1997; **57**: 2749-2753
- 48 **Szarka CE**, Pfeiffer GR, Hum ST, Everley LC, Balshem AM, Moore DF, Litwin S, Goosenberg EB, Frucet H, Engstrom PF. Glutathione S-transferase activity and glutathione S-transferase mu expression in subjects with risk for colorectal cancer. *Cancer Research* 1995; **55**: 2789-2793
- 49 **Clapper ML**, Adrian RH, Murthy S. Proceedings Am. Gastroenterol Assoc 1997; 3122, Washington D.C.97
- 50 **Bishayee A**, Chatterjee M. Selective enhancement of glutathione S-transferase activity in liver and extra hepatic tissues of rats following oral administration of vanadate. *Acta Physiol Pharmacol* 1993; **19**: 83-89
- 51 **Bishayee A**, Chatterjee M. Time-course effects of vanadium supplement on cytosolic reduced glutathione level and glutathione S-transferase activity. *Biological Trace Element Research* 1995; **48**: 275-285
- 52 **Bishayee A**, Chatterjee M. Inhibitory effect of vanadium on rat liver carcinogenesis initiated with diethylnitrosamine and promoted by Phenobarbital. *British J Cancer* 1995; **71**: 1214-1220
- 53 **Dahl AR**, Hadley WM, Hahn FH, Benson JM, Mc Clellan RO. Cytochrome P-450 dependent monooxygenase in olfactory epithelium of dogs: Possible role in tumorigenicity. *Science* 1982; **216**: 57-59
- 54 **Cohen SM**. Cell proliferation and carcinogenesis. *Drug Metab Rev* 1998; **30**: 339-357
- 55 **Hall PA**, Levinson DA, Woods AL, Yu CC, Kellock DB, Watkins JA, Barnes DM, Gillett CE, Camplejohn R, Dover R. Proliferating cell nuclear antigen (PCNA) immunolocalization in paraffin sections: an index of cell proliferation with evidence of deregulated expression in some neoplasm. *J Pathol* 1990; **162**: 285-294
- 56 **Zang XQ**. Progress of study on suppressor, EGFR and PCNA in colorectal cancer. *Xin Xiaohuabingxue Zazhi* 1996; **4**: 327-328
- 57 **Zheng Y**, Kramer PM, Lubet RA, Steele VE, Kelloff GJ, Pereira MA. Effect of retinoids on AOM-induced colon cancer in rats: modulation of cell proliferation, apoptosis and aberrant crypt foci. *Carcinogenesis* 1999; **20**: 255-260

Edited by Xu XQ

Downregulation of electroacupuncture at ST36 on TNF- α in rats with ulcerative colitis

Li Tian, Yu-Xin Huang, Min Tian, Wei Gao, Qing Chang

Li Tian, Yu-Xin Huang, Wei Gao, Qing Chang, Department of Gastroenterology, Tangdu Hospital, Fourth Military Medical University, Xi'an 710038, Shaanxi Province, China

Min Tian, Department of Ultrasound, Heping Hospital of Changzhi Medical College, Changzhi 046000, Shanxi Province, China

Supported by the National Nature Science Foundation of China, No.39970888

Correspondence to: Dr Yu-Xin Huang, Department of Gastroenterology, Tangdu Hospital, 4th Military Medical University, Xi'an 710038, Shaanxi Province, China. tianli72@263.net

Telephone: +86-29-3577597

Received: 2002-11-12 **Accepted:** 2002-12-30

Abstract

AIM: To investigate the regulatory effect of electroacupuncture (EA) at Zusanli (ST36) on tumor necrosis factor- α (TNF- α) in rats with ulcerative colitis (UC), and further elucidate the therapeutic mechanism of EA on UC.

METHODS: Thirty-two male Sprague-Dawley (SD) rats were randomly divided into four groups ($n=8$): normal control group, UC control group, UC+ST36 group and UC+non-acupoint group. A solution containing ethanol and 2,4,6-trinitrobenzenesulfonic acid (TNBS) was instilled into the distal colon in the rat (at a dose of 100 mg/kg) to set up UC rat model. Rats in wakefulness state of UC+ST36 group were stimulated at ST36 by EA once a day, while those of UC+non-acupoint group were done at 0.5 cm beside ST36. After 10 d treatment, all rats were sacrificed simultaneously. Colon mucosal inflammation and damage were assessed by measuring colon mass, morphologic damage score, colonic myeloperoxidase enzyme (MPO) activity, serum TNF- α and colonic TNF- α mRNA level. Morphologic damage score was examined under stereomicroscope. Colonic MPO activity was measured by spectrophotometer method. Serum TNF- α concentration was determined by radioimmunoassay (RIA). Colonic TNF- α mRNA expression level was analyzed by semiquantitative reverse transcription polymerase chain reaction (RT-PCR).

RESULTS: Ratio of colonic mass/body mass (m_c/m_b) and activity of colonic MPO ($\mu\text{kat/g}$ tissue) markedly increased (8.5 ± 2.6 vs 2.5 ± 0.4 ; 145 ± 25 vs 24 ± 8 , $P<0.01$ vs normal control group). Compared with normal control rats, serum TNF- α and colonic TNF- α mRNA level in UC control group were increased 2.5 fold ($2\ 278\pm 170$ vs 894 ± 248 , $P<0.01$) and 4.3 fold (0.98 ± 0.11 vs 0.23 ± 0.11 , $P<0.01$) respectively. After EA at ST36, m_c/m_b and MPO activity were reduced significantly (5.3 ± 2.0 vs 8.5 ± 2.6 ; 104 ± 36 vs 145 ± 25 , $P<0.01$, 0.05) compared with those of UC control group. Serum TNF- α and colonic TNF- α mRNA level were inhibited by EA stimulation at ST36 ($P<0.01$). The inhibitory rate was 16 % and 44 % respectively. Morphologic damage score was also increased markedly in rat with UC ($P<0.01$), whereas it was decreased by EA at ST36 ($P<0.05$). There was no significant difference between UC control group and UC+EA at non-acupoint

($P>0.05$). Furthermore, these parameters were highly correlated with each other ($P<0.01$).

CONCLUSION: Serum TNF- α concentration and colonic TNF- α mRNA expression level are increased significantly in UC rats in correlation with the severity of disease. It indicates that TNF- α is closely involved in the immune abnormalities and inflammatory responses in UC. EA at ST36 has therapeutic effect on UC by downregulating serum TNF- α and colonic TNF- α mRNA expression. High levels of TNF- α and its corresponding mRNA expression seem to be implicated in the pathogenesis of UC.

Tian L, Huang YX, Tian M, Gao W, Chang Q. Downregulation of electroacupuncture at ST36 on TNF- α in rats with ulcerative colitis. *World J Gastroenterol* 2003; 9(5): 1028-1033
<http://www.wjgnet.com/1007-9327/9/1028.htm>

INTRODUCTION

The incidence of ulcerative colitis (UC) has become higher in China^[1]. It is characterized by intestinal inflammation and ulceration^[22-26]. Its pathogenesis has not been elucidated yet. A number of clinical and experimental studies, however, have suggested that imbalance between proinflammatory cytokines and anti-inflammatory cytokines is involved in the pathogenesis of UC^[5,6]. High levels of proinflammatory cytokines (interleukin-1 β , interleukin-6, interleukin-8 and TNF- α) in the intestinal mucosa are thought to be the pivotal factors in the pathogenesis of intestinal inflammation and ulceration in UC. These proinflammatory cytokines concentrations and their corresponding mRNA expression levels elevated significantly in colonic mucosa, perfusion fluids, spleen and serum of UC patients. It has been suggested that TNF- α may be an important mediator involved in the initiation and perpetuation of intestinal inflammation in UC. TNF- α can cause inflammation directly, and indirectly by inducing the production of other proinflammatory cytokines.

Nearly all drug treatments for UC have many side effects, which limit patients' acceptance. Acupuncture is characteristic technique of traditional oriental medicine. It has been accepted by patients for its better clinical therapeutic effects and fewer side effects on many diseases including UC. Recent studies have demonstrated that acupuncture has immunoregulatory role. It can modulate the production and expression of many cytokines. But the therapeutic mechanism of acupuncture on UC is still uncertain. As an important acupoint, ST36 is not only for disorders of the lower limbs, but also for the whole digestive system, even with certain effect on immunity. The effect of EA at ST36 on UC has rarely been reported yet.

In this study, we induced UC in rats and stimulated them with EA at ST36 (Zusanli). The aim of this study was to assess the effect of EA stimulation at ST36 on UC, further investigate its role of regulating TNF- α , explain the therapeutic mechanism of EA on UC and provide new thought to acupuncture and moxibustion.

MATERIALS AND METHODS

Materials

Male SD rats weighed 220 ± 20 g were purchased from Experimental Animal Research Center, Fourth Military Medical University. The rats were housed in an air-conditioned animal room at 25 ± 2 °C and 60 % humidity with food and water available ad libitum, and drinking water was changed every day. Hadecyltrimethylammonium bromide (HATB) was purchased from Xizhong Chemical Co (Beijing, China). TNBS was purchased from Sigma Chemical Co (St.Louis, MO). TNF- α RIA kit was purchased from Dongya Biotechnology (Beijing, China). Access RT-PCR System Kit was obtained from Promega (Madison, WI). TRIzol Reagents were purchased from Gibco BRL (Gercy-Pontoise, France).

Induction of ulcerative colitis

The rats were randomized into 4 groups (8 rats for each group): normal control group, UC control group, UC+ EA at ST36 group and UC+ non-acupoint group. Rats were fast for 24 hours. Being gently anesthetized by ether, a rubber catheter (OD, 2 mm) was inserted through anus into its colon whose length in the lumen was 8 cm proximally. TNBS dissolved in 300 mL ethanol was instilled into the lumen of the colon through the rubber catheter at the dose of 100 mg/kg^[28,29]. Rats of normal control group were treated by 90 mL/L NaCl solution at the same dose.

EA stimulation

Rats in wakefulness state of UC+ST36 group were stimulated at ST36 (bilateral) which lies just 0.5 cm below fibular head of hinder leg in rat, while those of UC+non-acupoint group were done at 0.5 cm beside ST36^[33,35,40]. These rats were immobilized in special cages, and then were stimulated by the intermittent pulse with 2Hz frequency, 4mA intensity for 30 minutes once a day and 10 times in all. Rats in other two groups were immobilized in the same way with sham acupuncture stimulation.

Preparation of the samples

All rats were weighed after 10 d treatment. Serum was separated from blood drawn from carotid and then stored at -20 °C until analysis. All rats were sacrificed simultaneously. The colon was taken from the region, which was 8 cm proximal to the anus. Along its mesenteric border, the colon was opened and gently rinsed out of its contents with an iced NaCl solution 90 mL/L. The colon was then placed flat, with mucosal surface upwards, on a plate chilled at 4 °C. The colon was immediately examined under a stereomicroscope and any visible damage was scored on a 0-5 scale by two independent observers blinded to the treatment^[28]. There was a highly significant linear correlation between the scores assigned by the two observers ($r=0.98$, $P<0.001$). The colon tissue was weighed after being dried on a filter paper. Three tissue samples (1 mm³) were excised from affected region of each colon and then were fixed in 40 g/L glutaraldehyde for electro microscopic examination. The remaining colon was stored at -70 °C.

Colonic MPO activity assay

The distal 6 cm segment of the colon was homogenized in 5 mL/L HTAB in 20 mmol/L phosphate buffer (pH=6.0, 50 mg of tissue/ml). Homogenates were sonicated and centrifuged for 15 min (15 000 r/min). The supernatant was assayed for MPO activity by using a spectrophotometer, and 0.1 ml of supernatant was mixed with 2.9 ml of 20 mmol/L phosphate buffer (pH=6.0) containing 20 mmol/L guaiacol and 5 mL/L hydrogen peroxide. The changes in absorbance at 460 nm were measured with an Uvikon 860 spectrophotometer (Kontron

Instrument, St. Quentin, France). MPO activity was expressed as $\mu\text{kat/g}$. One $\mu\text{kat/g}$ was defined as that degrading 1 μmol of peroxides per second at 25 °C for 1 g of tissue.

Measurement of serum TNF- α concentration by TNF- α RIA kit Measurement of TNF- α mRNA expression in colonic tissue

Total RNA of 100 mg colonic tissue was purified by TRIzol Reagents. Reverse transcription (RT) was performed in a final volume of 50 μl containing nuclease-free water, AMV/tfl 5 \times reaction buffer, dNTP mix (10 mM each dNTP), 50 pmol specific primers, 25 mmol/L MgSO₄, 5Mu/L AMV Reverse Transcriptase, 5Mu/L tfl DNA Polymerase and 1 μg RNA. cDNA was synthesized by incubating the solution for 50 minutes at 48 °C and heating them for 2 minutes at 94 °C. Then 45 cycles of PCR were performed in a thermal cycler, using the following conditions: denaturation, 30 seconds at 94 °C; annealing, 1 minute at 55 °C for TNF- α and 57 °C for β -actin; and extension, 2 minutes at 68 °C. At the end of the 45 cycles, further extension was continued for 7 minutes at 68 °C. The primers were TNF- α sense, 5' -AGAACTCCAGGCGGTGTCT-3'; TNF- α antisense, 5' -TCCCTCAGGGGTGCCTTAG-3' (484bp); β -actin sense, 5' -AACCTAAGGCCAACCGTGAAAAG-3'; β -actin antisense, 5' -GCTCGAAGTCTAGGGCAACATA-3' (343bp). Amplification of β -actin was used for the determination of TNF- α mRNA expression level. 10 μl aliquots of the synthesized PCR products were separated by electrophoresis on a 22 g/L agarose gel and analyzed by Gel-Pro version 3.1 software (Media Cybernetics). The ratio of arbitrary unit (AU, $D_{\text{area}} \cdot D_{\text{density}}$) of TNF- α over β -actin was used for expressing the relative level of mRNA expression.

Statistical analysis

The results are expressed as mean \pm SEM. All data were analyzed by using ANOVA. P values <0.05 were considered significant. All statistical calculations were performed using the SPSS for windows version 10.0 software package.

RESULTS

Effect of EA on colonic morphology of UC rats

The levels of colonic tissue damage score and m_c/m_B of rats in UC control group were increased significantly compared with those of normal control group ($P<0.01$). In comparison with those of UC control group, EA at ST36 made them decreased markedly ($P<0.01$). EA stimulation at non-acupoint had few effects on these two parameters ($P>0.05$, Table 1, Figure 1).

Table 1 Effect of EA on colonic tissue damage score

Group	n_A	n_B	P
1 2	8	8	0.000
1 3	8	8	0.000
1 4	8	8	0.000
2 3	8	8	0.006
2 4	8	8	1.000
3 4	8	8	0.040

1: Normal control; 2: UC Control; 3: UC+EA at ST36; 4: UC+EA at non-acupoint. These classifications are qualified for all figures.

Histological ultrastructure of colonic tissue was assessed by electron microscopy. Colonic ultrastructure manifestations of rats in UC control group and those in UC+non-acupoint group were similar: exiguous goblet cells, scanty microvilli, dilatations of endoplasmic reticula, mitochondria swelling

and rounding, with loss of cristae and many inflammatory cells infiltration. While in UC+EA at ST36 group, the results of colonic electron microscopy were more microvilli with well organized appearance, more goblet cells filled with numerous mucous drop in colonic mucosa and only slight mitochondria swelling compared with those of UC control group (Figure 2-4).

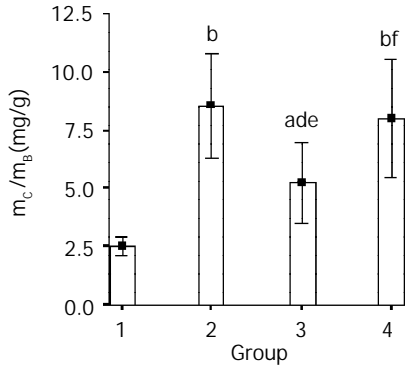


Figure 1 Effect of EA on m_c/m_g . ^a $P < 0.05$, ^b $P < 0.01$ vs normal control; ^d $P < 0.01$, ^f $P > 0.05$ vs UC control; ^e $P < 0.05$ vs UC+EA at non-acupoint.

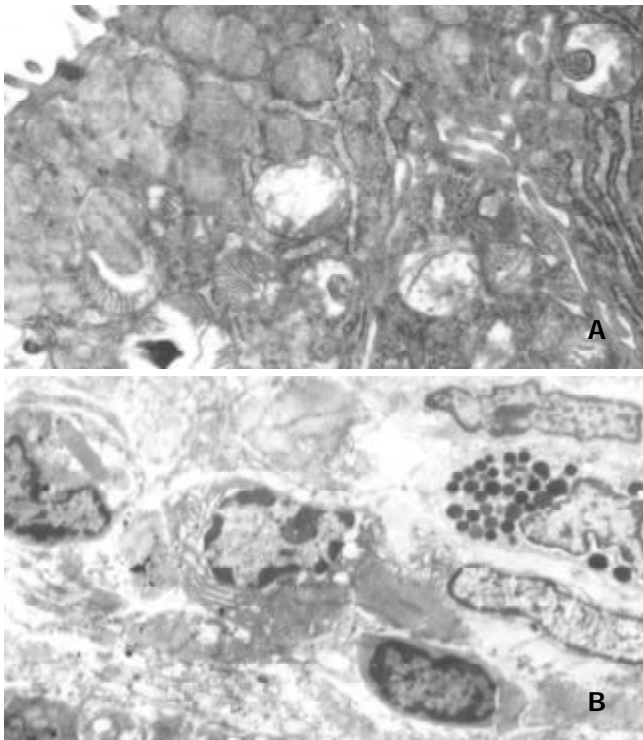


Figure 2 Colonic ultrastructure of UC control group: A, goblet cells, microvilli, endoplasmic reticula and mitochondria (TEM x10 000); B, inflammatory cells (TEM x2 500).

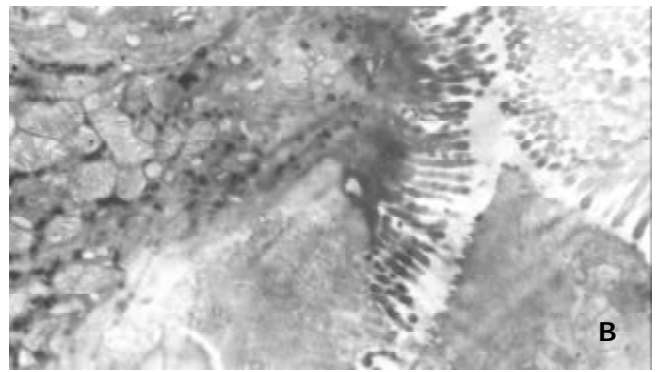
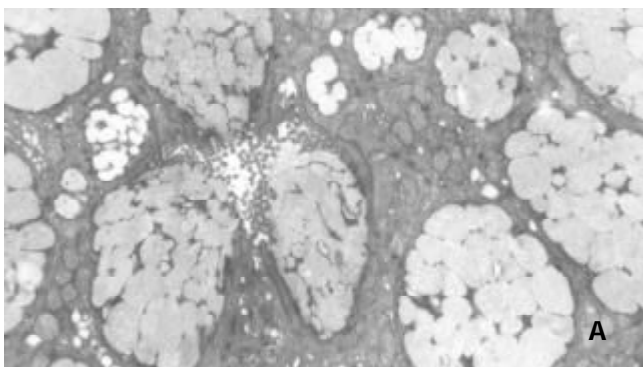


Figure 3 Colonic ultrastructure of UC+EA at ST36 group: A, goblet cells (TEM x4 000); B microvilli and mitochondria (TEM x8 000).

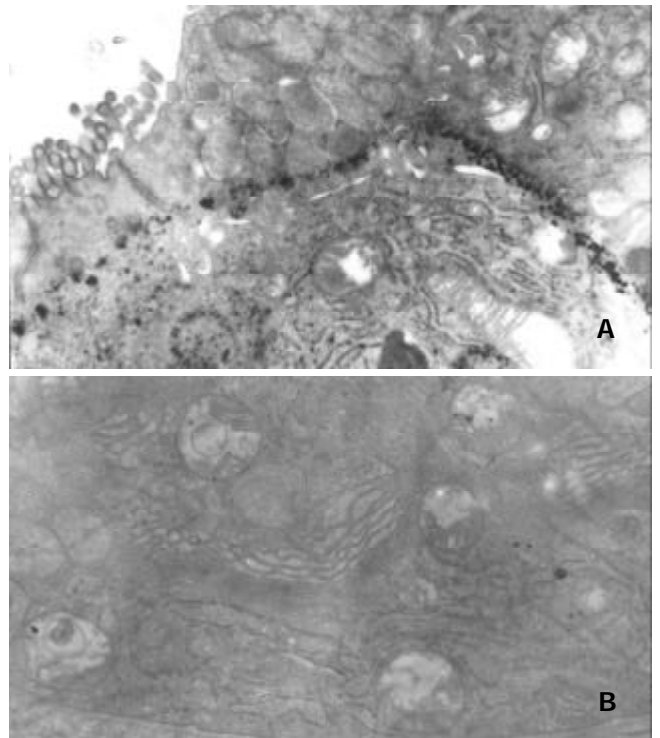


Figure 4 Colonic ultrastructure of EA+non-acupoint group: A, goblet cells, microvilli and mitochondria (TEM x8 000); B, endoplasmic reticula and mitochondria (TEM x10 000).

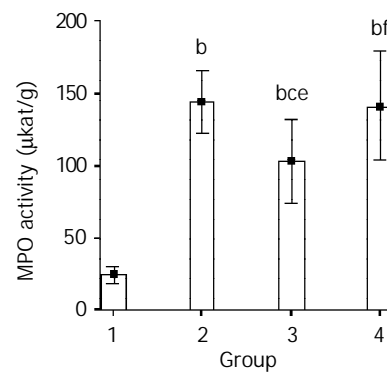


Figure 5 Effect of EA on colonic MPO activity. ^b $P < 0.01$ vs normal control; ^c $P < 0.05$, ^f $P > 0.05$ vs UC control; ^e $P < 0.05$ vs UC+EA at non-acupoint.

Effect of EA on colonic MPO activity

Colonic MPO activity of rats in UC control group was significant higher than that in normal control group (145 ± 25

vs 24 ± 8 , $P < 0.01$). After EA stimulation at ST36, colonic MPO activity became lower than that in UC control group (104 ± 36 vs 145 ± 25 , $P < 0.05$). There was no significant difference between UC control group and UC+non-acupoint group (142 ± 45 vs 145 ± 25 , $P > 0.05$, Figure 5).

Effect of EA on the production and expression of TNF- α

Compared with normal control rats, serum TNF- α concentration and colonic TNF- α mRNA expression level increased 2.5 fold ($2\ 278 \pm 170$ vs 894 ± 248 , $P < 0.01$) and 4.3 fold (0.98 ± 0.11 vs 0.23 ± 0.11 , $P < 0.01$). Serum TNF- α and colonic TNF- α mRNA expression were inhibited by EA stimulation at ST36. The inhibitory rate was 16 % ($1\ 913 \pm 232$ vs $2\ 278 \pm 170$, $P < 0.01$) and 44 % (0.55 ± 0.13 vs 0.98 ± 0.11 , $P < 0.01$), respectively. While the production of serum TNF- α and the level of TNF- α mRNA expression were not affected by EA stimulation at non-acupoint ($2\ 183 \pm 209$ vs $2\ 278 \pm 170$, 0.92 ± 0.17 vs 0.98 ± 0.11 , $P > 0.05$, Figure 6, 7).

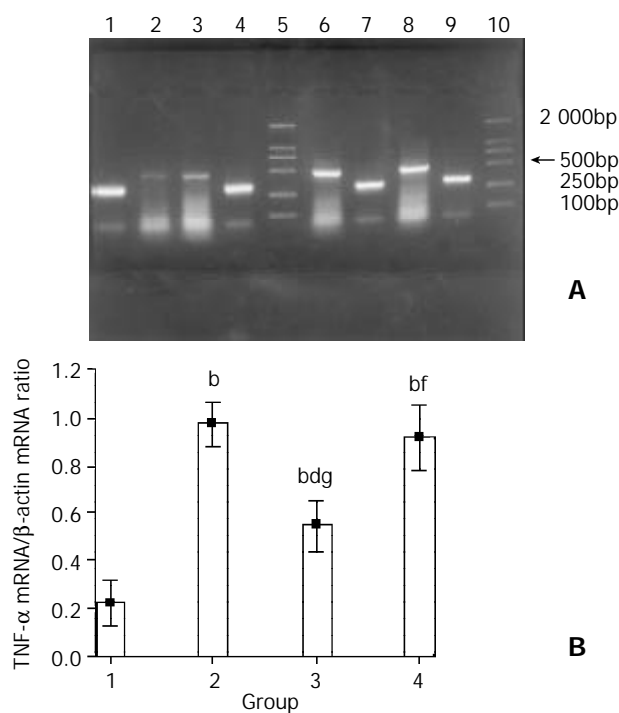


Figure 6 Effect of EA on TNF- α mRNA expression. A: Representative pictures of RT-PCR. Lane 1, 4, 7, 9: β -actin. Lane 2, 3, 6, 8: TNF- α . Lane 5, 10: DNA Marker (DL2000). B: Relative level of TNF- α mRNA expression. ^b $P < 0.01$ vs normal control; ^d $P < 0.01$, ^f $P > 0.05$ vs UC control; ^g $P < 0.01$ vs UC+EA at non-acupoint.

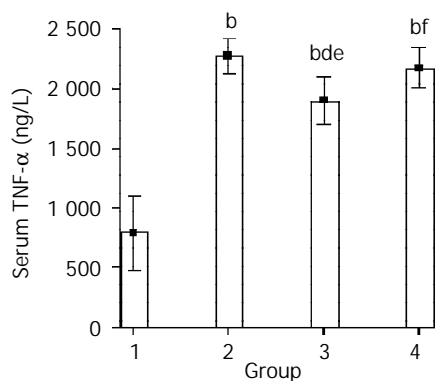


Figure 7 Effect of EA on serum TNF- α concentration. ^b $P < 0.01$ vs normal control; ^d $P < 0.01$, ^f $P > 0.05$ vs UC control; ^e $P < 0.05$ vs UC+EA at non-acupoint.

Correlation among parameters quantified above

There were significant correlations between serum TNF- α concentration and colonic MPO activity ($r = 0.815$, $P < 0.01$), serum TNF- α and damage scores ($r = 0.877$, $P < 0.01$), serum TNF- α and m_c/m_b ($r = 0.691$, $P < 0.01$). colonic TNF- α mRNA expression level was highly correlated with colonic MPO activity ($r = 0.791$, $P < 0.01$), damage scores ($r = 0.827$, $P < 0.01$), and m_c/m_b ($r = 0.686$, $P < 0.01$). The correlation matrix is shown in Table 2.

Table 2 Correlations among the parameters (r)

Parameters	TNF- α	TNF- α mRNA	m_c/m_b	MPO	Damage scores
TNF- α	1	0.814	0.691	0.815	0.877
TNF- α mRNA		1	0.686	0.791	0.827
m_c/m_b			1	0.759	0.770
MPO				1	0.902
Damage scores					1

DISCUSSION

UC is a non-specific inflammatory bowel disease. Many factors including infection, environment and immune abnormality may involve in the pathogenesis of UC, in which abnormal immunoregulation plays an important role^[2-4]. There is strong evidence that inflammatory immunoregulation in the intestinal mucosa is characterized by increased concentrations of proinflammatory cytokines with apparent inability to adequately downregulate immune activation. UC showed significantly increased mRNA expression of interleukin-1beta (IL-1 β), interleukin-6 (IL-6), interleukin-8 (IL-8) and TNF- α in large numbers of cells throughout the inflamed intestine but also in some macroscopically unaffected tissue specimens. Elevated concentrations of proinflammatory cytokines were also found in serum, colonic mucosa, spleen and colorectal perfusion fluids in UC^[7-12]. There is significant correlation between the production of these cytokines and the activity of UC. The increased production of proinflammatory cytokines is thought to be a pivotal factor in the pathogenesis of UC. It is accepted that TNF- α may be particularly important for inducing and sustaining intestinal inflammation in UC. It is known from many studies that TNF- α is expressed in human gastrointestinal mucosa, and that the expression is strongly enhanced in the inflammatory course of UC. TNF- α production in the gut has been attributed to monocytes, macrophages, natural killer cells, T lymphocytes and mast cells. TNF- α is known to induce the synthesis of IL-6 and IL-8. TNF- α and IL-1 β induce each other. The effects of IL-1 β and TNF- α appear synergistic. These cytokines regulate many nuclear factor kappaB inducible genes that control expression of other cytokines, cell adhesion molecules, immunoregulatory molecules, and proinflammatory mediators^[13]. Enhanced production of TNF- α and IL-1 β may induce some key enzymes of the inflammation cascade and neutrophils chemotaxis. TNF- α can also induce more production of nitric oxide (NO) and inducible nitric oxide synthase (iNOS), which further promotes inflammation than IL-1 β ^[14-20]. High levels of proinflammatory cytokines in the mucosa lead to the excessive production of matrix degrading enzymes by gut fibroblasts, loss of mucosa integrity and ulceration^[21].

MPO is an enzyme found predominantly in the azurophilic granules of polymorphonuclear neutrophils (PMN) and has been used as a quantitative index of inflammation in several tissues, including intestine. PMN are the most abundant cell type in intestinal lesions in UC. PMN carry the capacity to secrete increased amounts of TNF- α and IL-1 β in active UC

and infectious colitis. Neutrophils may be important contributors to the initiation and perpetuation of mucosa inflammation^[27].

Quantitative indexes of inflammation (damage scores, colon mass and MPO activity) were elevated significantly in UC^[22-26]. This study showed that in UC control group, erosion and ulceration induced by TNBS were so particularly severe in rectum and even extended to the proximal colon that damage scores and colon mass were increased markedly, neutrophil infiltration was characteristically present in the lesions and surrounding mucosa, MPO activity at lesions sites was increased, serum TNF- α concentration and colonic TNF- α mRNA expression level elevated significantly compared with those of normal control rats. All these parameters correlated significantly with each other. So TNF- α is a key inflammatory mediator in the pathogenesis of UC.

Based on recent studies, several new therapeutic strategies are currently tested in clinical practice including inhibitors of proinflammatory cytokines (TNF- α , IL-12) and their receptors (TNF- α , IL-6R), in which anti-TNF- α has been impressive. These new therapeutic strategies have demonstrated efficacy in refractory UC patients. But there are still many problems to solve including the best way of therapy and side effects before they are formally applied to UC patients. Other potent medications with side effects limit patients' acceptance. While the advantages of acupuncture treatment for UC have been obvious^[39].

Acupuncture is one of the most important part of traditional Chinese medicine (TCM) which possesses a unique theoretical systems, rich clinical experience and excellent clinical effects. TCM theory says: inharmony between Qi and blood, and imbalance between Yin and Yang can lead to disease. EA at acupoint is able to stimulate meridians to transport Qi and blood, regulate Yin and Yang keeping the functions and activities of all parts of the body in harmony and balance relatively.

As an important acupoint in TCM, ST36 is the lower He-(Sea) point. This point has a tonifying function. It is an important point for health maintenance and disorder of stomach and abdomen. Recent studies have shown that EA stimulation at ST36 may regulate nerve-endocrine-immune network by influencing the production and expression of neurotransmitters, hormones and cytokines^[30-37]. EA stimulation at ST36 significantly restores brain-derived neurotrophic factor (BDNF) mRNA expression declined by emergency^[38]. EA stimulation at ST36 improves the immune function by inducing interleukin-2 (IL-2) and interferon-gamma (IFN- γ) production of spleen lymphocytes in traumatized rats. ST36 stimulated by EA can also inhibit abnormal IL-1 increment induced by trauma and even disease. Li *et al*^[40] found that high levels of serum IL-1 β , IL-6, TNF- α and NO induced by lipopolysaccharide in rats were decreased significantly by EA stimulation at ST36.

Acupuncture at acupoints such as Tianshu(ST25), Guanyuan (Ren4) has a marked curative effects with few side ones on UC, and therefore was readily acceptable to the patients^[39]. But its therapeutic mechanism is still unclear. There are only a few studies on its corresponding theory. Some studies showed that EA stimulation at Qihai(RN6) and Tianshu(ST25) may downregulate the expression of proinflammatory cytokines mRNA (IL-1 β mRNA, IL-6 mRNA) and iNOS mRNA of spleen and colon in UC rats, whereas it could upregulate IL-1 α mRNA expression. It is reported that acupuncture stimulation at acupoint reduces the excessive production of TNF- α positive cells of colonic mucosa in rats with UC. The study of effect of EA stimulation at ST36 on UC has rarely been reported yet.

This study showed that in UC+EA at ST36 group, lesion formation was inhibited grossly and microscopically,

neutrophil infiltration and MPO activity in and around lesions were lessened, serum TNF- α concentration and colonic TNF- α mRNA expression level were decreased significantly. These results suggest that EA stimulation at ST36 can inhibit effectively inflammation cascade in UC. But these parameters were not restored to normal levels by EA stimulation at ST36 without being accompanied by other acupoint.

In summary, this study showed EA stimulation at ST36 has therapeutic effect on UC by reducing serum TNF- α concentration and colonic TNF- α mRNA expression level, decreasing colonic MPO activity and alleviating colonic inflammation damage. Its therapeutic mechanism is attributed to its downregulation effect on TNF- α , which is a key proinflammatory cytokine. It is still unknown whether EA can keep the balance between proinflammatory cytokines and anti-inflammatory cytokines by upregulating the key anti-inflammatory cytokines (IL-4, IL-10, IL-13) when it downregulates proinflammatory cytokines. Its mechanism of regulating cytokines needs further study.

REFERENCES

- 1 **Kirsner JB**. Historical origins of current IBD concepts. *World J Gastroenterol* 2001; **7**: 175-184
- 2 **Bing X**. The pathogenesis and etiology of inflammatory bowel disease. *Shijie Huaren Xiaohua Zazhi* 2001; **9**: 246-250
- 3 **Jiang XL**, Cui HF. An analysis of 10218 ulcerative colitis cases in China. *World J Gastroenterol* 2002; **8**: 158-161
- 4 **Blumberg RS**, Strober W. Prospects for research in inflammatory bowel disease. *JAMA* 2001; **285**: 643-647
- 5 **Ishizuka K**, Sugimura K, Homma T, Matsuzawa J, Mochizuki T, Kobayashi M, Suzuki K, Otsuka K, Tashiro K, Yamaguchi O, Asakura H. Influence of interleukin-10 on the interleukin-1 receptor antagonist/interleukin-1 beta ratio in the colonic mucosa of ulcerative colitis. *Digestion* 2001; **63**: 22-27
- 6 **Bulois P**, Tremaine WJ, Maunoury V, Gambiez L, Hafraoui S, Leteurtre L, Cortot A, Sandborn W J, Colombel JF, Desreumaux P. Pouchitis is associated with mucosal imbalance between interleukin-8 and interleukin-10. *Inflamm Bowel Dis* 2000; **6**: 157-164
- 7 **Akazawa A**, Sakaida I, Higaki S, Kubo Y, Uchida K, Okita K. Increased expression of tumor necrosis factor-alpha messenger RNA in the intestinal mucosa of inflammatory bowel disease, particularly in patients with disease in the inactive phase. *J Gastroenterol* 2002; **37**: 345-353
- 8 **Van Heel DA**, Udalova IA, De Silva AP, McGovern DP, Kinouchi Y, Hull J, Lench NJ, Cardon LR, Carey AH, Jewell DP, Kwiatkowski D. Inflammatory bowel disease is associated with a TNF polymorphism that affects an interaction between the OCT1 and NF-(kappa)B transcription factors. *Hum Mol Genet* 2002; **11**: 1281-1289
- 9 **Indaram AV**, Visvalingam V, Locke M, Bank S. Mucosal cytokine production in radiation-induced proctosigmoiditis compared with inflammatory bowel disease. *Am J Gastroenterol* 2000; **95**: 1221-1225
- 10 **Komatsu M**, Kobayashi D, Saito K, Furuya D, Yagihashi A, Araake H, Tsuji N, Sakamaki S, Niitsu Y, Watanabe N. Tumor necrosis factor-alpha in serum of patients with inflammatory bowel disease as measured by a highly sensitive immuno-PCR. *Clin Chem* 2001; **47**: 1297-1301
- 11 **Wang Q**, Xu L. Experimental examination and active assessment of ulcerative colitis. *Shijie Huaren Xiaohua Zazhi* 2000; **8**: 336-337
- 12 **Guo J**, Sheng ZX, Tan SY. Active index of inflammatory bowel disease. *Shijie Huaren Xiaohua Zazhi* 2001; **9**: 1431-1434
- 13 **Bingham CO 3rd**. The pathogenesis of rheumatoid arthritis: pivotal cytokines involved in bone degradation and inflammation. *J Rheumatol* 2002; **29**: 3-9
- 14 **Ljung T**, Herulf M, Beijer E, Jacobsson H, Lundberg J, Finkel Y, Hellstrom PM. Rectal nitric oxide assessment in children with Crohn disease and ulcerative colitis. Indicator of ileocaecal and colorectal affection. *Scand J Gastroenterol* 2001; **36**: 1073-1076
- 15 **Guihot G**, Guimbaud R, Bertrand V, Narcy-Lambare B, Coutu-

- rier D, Duee PH, Chaussade S, Blachier F. Inducible nitric oxide synthase activity in colon biopsies from inflammatory areas: correlation with inflammation intensity in patients with ulcerative colitis but not with Crohn's disease. *Amino Acids* 2000; **18**: 229-237
- 16 **Perner A**, Andresen L, Normark M, Fischer-Hansen B, Sorensen S, Eugen-Olsen J, Rask-Madsen J. Expression of nitric oxide synthases and effects of L-arginine and L-NMMA on nitric oxide production and fluid transport in collagenous colitis. *Gut* 2001; **49**: 387-394
- 17 **Dijkstra G**, Zandvoort AJ, Kobold AC, de Jager-Krikken A, Heeringa P, van Goor H, van Dullemen HM, Tervaert JW, van de Loosdrecht A, Moshage H, Jansen PL. Increased expression of inducible nitric oxide synthase in circulating monocytes from patients with active inflammatory bowel disease. *Scand J Gastroenterol* 2002; **37**: 546-554
- 18 **Colon AL**, Menchen LA, Hurtado O, De Cristobal J, Lizasoain I, Leza JC, Lorenzo P, Moro MA. Implication of TNF-alpha convertase (TACE/ADAM17) in inducible nitric oxide synthase expression and inflammation in an experimental model of colitis. *Cytokine* 2001; **16**: 220-226
- 19 **Zhang K**, Deng CS, Zhu YQ, Yang YP, Zhang YM. Significance of nuclear factor- κ B, cyclooxygenase 2 and inducible nitric oxide synthase expression in human ulcerative colitis tissues. *Shijie Huaren Xiaohua Zazhi* 2002; **10**: 575-578
- 20 **Goodstone NJ**, Hardingham TE. Tumour necrosis factor alpha stimulates nitric oxide production more potently than interleukin-1beta in porcine articular chondrocytes. *Rheumatology (Oxford)* 2002; **41**: 883-891
- 21 MacDonald TT, Monteleone G, Pender SL. Recent developments in the immunology of inflammatory bowel disease. *Scand J Immunol* 2000; **51**: 2-9
- 22 **Padol I**, Huang JQ, Hogaboam CM, Hunt RH. Therapeutic effects of the endothelin receptor antagonist Ro 48-5695 in the TNBS/DNBS rat model of colitis. *Eur J Gastroenterol Hepatol* 2000; **12**: 257-265
- 23 **Tjandra K**, Le T, Swain MG. Experimental colitis attenuates development of toxin-induced cholangitis in rats. *Dig Dis Sci* 2002; **47**: 1216-1223
- 24 **Ogawa Y**, Kanatsu K, Iino T, Kato S, Jeong Y, Shibata N, Takada K, Takeuchi K. Protection against dextran sulfate sodium-induced colitis by microspheres of ellagic acid in rats. *Life Sci* 2002; **71**: 827-839
- 25 **Nosal' ova V**, Bobek P, Cerna S, Galbavy S, Stvrtina S. Effects of pleuran (beta-glucan isolated from *Pleurotus ostreatus*) on experimental colitis in rats. *Physiol Res* 2001; **50**: 575-581
- 26 **Peng ZS**, Hu PJ, Lin HL, Cui Y, Chen W. Evaluation of biopsy pathology in diagnosis of ulcerative colitis. *Shijie Huaren Xiaohua Zazhi* 2001; **9**: 1169-1173
- 27 **Carlson M**, Raab Y, Seveus L, Xu S, Hallgren R, Venge P. Human neutrophil lipocalin is a unique marker of neutrophil inflammation in ulcerative colitis and proctitis. *Gut* 2002; **50**: 501-506
- 28 **Zheng L**, Gao ZQ, Wang SX. A chronic ulcerative colitis model in rats. *World J Gastroenterol* 2000; **6**: 150-152
- 29 **Zhou SY**, Mei QB, Liu L, Guo X, Qiu BS, Zhao DH, Cho CH. Delivery of glucocorticoid in rat gastrointestinal tract and its treatment for ulcerative colitis. *Acta Pharmacol Sin* 2001; **22**: 761-764
- 30 **Gao W**, Huang YX, Chen H, Zhao NX, Sun DY, Zhang HX, Wang QL. Regulatory mechanism of electroacupuncture on the stomach channel-brain gut peptide-immune network. *Shijie Huaren Xiaohua Zazhi* 2001; **9**: 279-283
- 31 **Li YM**, Huang YX. The effects of brain gut peptides and cytokines on the acupuncture's modulatory mechanism in the gastrointestinal immunity. *Shijie Huaren Xiaohua Zazhi* 2001; **9**: 329-332
- 32 **Xu GS**, Yang YX, Liu Y, Zhu QF, Zhang FB. The mechanism of acupuncture and moxibustion effect on gastrointestinal. *Shijie Huaren Xiaohua Zazhi* 2000; **8**: 27
- 33 **Zhang J**, Huang YX, Gao W, Pan BR, Wang JJ, Li YM, Wang QL. Effects of acupuncture on gastrointestinal mucosa immunologic function in rats. *Shijie Huaren Xiaohua Zazhi* 2001; **9**: 1116-1119
- 34 **Tian L**, Huang YX. The modulatory significance of electroacupuncture on cytokines in ulcerative colitis. *Shijie Huaren Xiaohua Zazhi* 2001; **9**: 1435-1438
- 35 **Gao W**, Huang YX, Chen H, Song DY, Wang QL. Regulatory effects of electro-acupuncture at Zusanli on ir-SP content in rat pituitary gland and peripheral blood and their immunity. *World J Gastroenterol* 2000; **6**: 581-584
- 36 **Zhao BM**, Huang YX, Wang QL, Chu ZH, Zhao NX. Effect of electroacupuncture on gastric acid secretion and its relationship with gastrin and epidermal growth factor in rats. *Shijie Huaren Xiaohua Zazhi* 2000; **8**: 276-278
- 37 **Ou YW**, Han L, Da CD, Huang YL, Cheng JS. Influence of acupuncture upon expressing levels of basic fibroblast growth factor in rat brain following focal cerebral ischemia-evaluated by time-resolved fluorescence immunoassay. *Neurol Res* 2001; **23**: 47-50
- 38 **Yun SJ**, Park HJ, Yeom MJ, Hahm DH, Lee HJ, Lee EH. Effect of electroacupuncture on the stress-induced changes in brain-derived neurotrophic factor expression in rat hippocampus. *Neurosci Lett* 2002; **318**: 85-88
- 39 **Moum B**. Medical treatment: does it influence the natural course of inflammatory bowel disease? *Eur J Intern Med* 2000; **11**: 197-203
- 40 **Li YM**, Huang YX, Zhang J, Wang QL. Effect of electroacupuncture on gastric emptying of rats treated with lipopolysaccharide and its relationship with serum cytokines. *Shijie Huaren Xiaohua Zazhi* 2001; **9**: 1110-1115

Leptin receptor expression in the basolateral nucleus of amygdala of conditioned taste aversion rats

Zhen Han, Jian-Qun Yan, Guo-Gang Luo, Yong Liu, Yi-Li Wang

Zhen Han, Jian-Qun Yan, Department of Physiology, Xi'an Jiaotong University School of Medicine, Xi'an 710061, Shaanxi Province, China

Guo-Gang Luo, Department of Neurology, First Hospital of Xi'an Jiaotong University, Xi'an 710061, Shaanxi Province, China

Yong Liu, Institute for Neurobiology, Xi'an Jiaotong University School of Medicine, Xi'an 710061, Shaanxi Province, China

Yi-Li Wang, Institute for Cancer Research, Xi'an Jiaotong University School of Life Science & Technology, Xi'an 710061, Shaanxi Province, China

Supported by China Natural Science Foundation, No.30270454 and Natural Science Foundation of Xi'an JiaoTong University, No. 1600.573004

Correspondence to: Professor Jian-Qun Yan, Department of Physiology, Xi'an Jiaotong University School of Medicine, Xi'an 710061, Shaanxi Province, China. jqyan@mail.xjtu.edu.cn

Received: 2002-12-07 **Accepted:** 2003-01-08

Abstract

AIM: To determine whether serum leptin level and the leptin receptor (OB-R) expression in the basolateral amygdala (BLA) change following conditioned taste aversion (CTA) formation.

METHODS: The serum leptin concentration was measured by rat leptin RIA kit, long and short forms of leptin receptor (OB-Rb and OB-Ra) mRNA in the brain sections were examined by in situ hybridization (ISH) and the expression of OB-R was assessed by immunohistochemistry ABC method with a highly specific goat anti-OB-R antibody.

RESULTS: The level of serum leptin didn't show significant difference between CTA and control group. Comparing with the control group, the CTA group had an increase on count of OB-R immunohistochemistry positive-stained cells in the BLA (127 ± 12 vs 48 ± 9 per 1 mm^2). The OB-Rb mRNA expression level enhanced by 11.9% in the BLA, while OB-Ra mRNA level increased by 7.4% on the choroid plexus in CTA group. So BLA was supposed to be a region where interactions between gustatory and vagal signals take place.

CONCLUSION: BLA is one of the sites, which are responsible for CTA formation in the brain. Leptin and OB-R maybe involved in neuronal communication for CTA. So leptin and its receptors probably take part in CTA and integration of autonomic and exteroceptive information.

Han Z, Yan JQ, Luo GG, Liu Y, Wang YL. Leptin receptor expression in the basolateral nucleus of amygdala of conditioned taste aversion rats. *World J Gastroenterol* 2003; 9(5): 1034-1037
<http://www.wjgnet.com/1007-9327/9/1034.htm>

INTRODUCTION

Conditioned taste aversion (CTA) is a protective reflex by which an animal learns to discriminate and to reject potentially harmful substances by their flavor. When the consumption of novel flavored food is followed by internal malaise, animals

avoid ingesting the food on subsequent presentations^[1,2]. The anatomical substrates responsible for CTA learning have been well established^[3]. But the neurotransmitters involved in neuronal communication for CTA are not yet well known.

Leptin has been discovered since 1994 by Zhang *et al* (*Nature* 1994; 372:425-431) as the product of the *ob* gene. Leptin (OB protein) is produced primarily by adipose tissue and secreted into the bloodstream, then delivered to the brain. In the brain some specific receptors of leptin have been characterized, especially in hypothalamic nuclei where express neuropeptides and neurotransmitters that were involved in the long-term regulation of food intake and metabolism rate^[4-7], therefore, leptin serves as a unique feedback signal system to submit information regarding to adipose tissue energy store into the central nervous system^[8]. As leptin level growth coincidence with adiposity increment in rodents and mankind, it is proposed to act as a negative feedback 'adipostatic signal' to brain centers and control energy homeostasis, prevent from obesity in time of nutritional abundance^[9].

In recent years leptin receptor has been found to be expressed in the amygdala^[10], especially in the basolateral amygdala (BLA)^[11]. The interest in amygdala which acts as a regulator of weight and intake behavior has also been warming up. Amygdala is one of critical centers to regulate weight and ingestive behavior. Robust increases in body weight and food intake has been observed in rats with lesions of the BLA and postrodorsal amygdala (PDA) (*Brain Res* 1996;740:193-200). In addition to food intake alteration, lesions (electrolytic and excitotoxic) in the amygdala have also been known to disrupt the formation of conditioned taste aversion (CTA), particularly lesions placed in the BLA^[12-15]. The sense of taste lies in the interface between the external and internal of milieu and participates in control of motivational processes which guide dietary selection. The amygdala plays an important role in the initiation and guidance of autonomic and exteroceptive information^[16].

The present study was undertaken to further investigate possible changes of the leptin receptor expression accompanied with learning and maintaining of CTA.

MATERIALS AND METHODS

Animals

Twenty healthy adult male Sprague-Dawley rats, weighing 200-250 g, were used in all experiments. Every rat was housed at one cage in a temperature-controlled room (18-24 °C) on a 12 h light/dark cycle and allowed food (rodent chow) and water ad libitum for 3 days. All rats were randomly grouped into 2 groups. Each group consisted of 10 rats.

Behavior experiment

Rats were water-deprived for 24 h prior to test day. At 08:30 to 09:00 from day 1 to 5, the rats were trained to drink distilled water for 30 min in the home cages. At the same time on day 6, each rat in test group received an ip injection of 0.15 mol/L LiCl (2% body weight) as an unconditioned stimulus (US) soon after 30 min of free access to 1 g/L (0.005 mol/L) sodium

saccharin instead of water as a conditioned stimulus (CS). Rats in control group received an ip injection of an equivalent volume of 0.15 mol/L NaCl. From day 7 to 9, all rats have accessed to distilled water for 30 min. On day 10, the rats were presented with 1 g/L saccharin for 30 min. The volumes of intake of the CS were recorded on day 6 and 10.

Sample collection

Rats were anaesthetized with urethane (1.2 g/kg, ip). Then the tail was cut, the whole blood glucose level was measured by One Touch Brand blood glucose meter (Lifescan inc, USA). Then opened thorax and 2 mL blood was drawn from the aorta and put into dry tube allowing to clot for 1 h. Serum was separated by centrifugation (2 000 r/min) for 20 min. Then the rats were perfused via the ascending aorta with 300 ml of 8.5 g/L saline (room temperature) followed by 300 mL of paraformaldehyde (PFA, 4 g/L, pH 7.4). Brains were dissected out and then post-fixed in the same fixative for 3 hours at 4 °C. After being paraffin embedded, three series of sections were cut coronally at a thickness of 5 µm, thaw-mounted on poly-L-lysine-coated glass slides and stored at -70 °C. One of the series was used for immunohistochemical staining, another for ISH. The remaining series of sections were stained with hematoxylin-eosin.

The assay of serum leptin

Serum leptin and insulin were measured by radioimmunoassay (RIA) (rat leptin RIA kit, rat insulin RIA kit, Linco Research, St, Louis, MO). The lower limits of sensitivity of the assay are 0.5 µg/L and 0.1 µg/L.

Immunohistochemistry

Endogenous peroxidase activity was blocked with 0.01 mol/L PB containing 0.3 mL/L hydrogen peroxide. Then the sections were heated to 92 °C in citric acid (pH 6.0). After that the sections were rinsed with 0.01 mol/L phosphate-buffered saline (PBS), incubated with 15 mL/L blocking serum in PBS for 1 h. The sections were incubated at 4 °C for 40 h with goat polyclonal antiserum against leptin receptor (antiserum Sc-1834 with dilution at 1:100, Santa-Cruz Biotechnology, CA, USA). After incubation, the sections were immunostained by the avidin-biotin complex method (goat ABC staining system, Sc-2023, Santa-Cruz Biotechnology, CA, USA). The sections were mounted on slide glasses, dried and dehydrated in a graded ethanol series, and covered with balata.

To verify the specificity of staining, some sections were incubated with non-immune serum instead of the primary antiserum, or with the primary antiserum without the second antiserum to serve as a negative control. No LR-IR was observed in the negative control tissue.

In situ hybridization

Prior to hybridization, the sections were deparaffinized, incubated at 37 °C in 2 mg/L of proteinase K for 25 min. Post fixation was performed in a PFA solution and the sections were treated with 2 mol/L HCl. The specific oligonucleotide probes are 5' -GGC TCC AGA AGA AGA CCA AAT ATC (Nucleotide number 2 712-2 738 of Genebank sequence D84500) for OB-Rb and 5' -CAA GCA TGG GCT GCA GTG ACA TTA GAG (Nucleotide number 671-697 of Genebank sequence D84550) for OB-Ra. The probe was terminally labeled with digoxigenin-dUTP (Dig Oligonucleotide Tailing Kit, Cat No.1417231, Roche, Germany) and tested by Dig nucleic acid detection kit (1175041, Roche, Germany). Its concentration was 100 nmol/L. Probe was prepared in a solution containing 500 g/L formamide, 0.3 mol/L NaCl, 10 mmol/L Tris, 1 g/L ssDNA, 1× Denhardt's solution, and 100 g/L dextran

sulfate, then they were hybridized to sections at 50 °C for 16-18 h. After hybridization, the slides were washed sequentially in 2× saline-sodium citrate (SSC) for 30 min followed by rinses in 1×SSC, 0.5×SSC. Then they were incubated with phosphatase-labeled anti-digoxigenin antibody (1:400) at 37 °C for 2 h. Staining was performed with a freshly prepared substrate solution of Nitro Blue Tetrazolium and 5-bromo-4-chloro-3-indolyl phosphate. Then the sections were restained by methyl green.

To assess the specificity of labelling, control sections were co-incubated with a 100-fold excess of unlabelled probe in addition to the corresponding DIG-labelled probe. No labelling above background was detected in those sections.

Quantification and data analysis

On the basis of volumes of following two test days, we calculated a CTA index as an indicator of the strength of CTA formation. The larger this index, the stronger the acquisition of CTA: CTA index=1-(total saccharin intake on day 10/total saccharin intake on day 6).

Some sections were photographed. Then expression of leptin receptor immunoreactivity was quantified by counting positive-stained cells in BLA of five adjacent brain sections. All films of ISH were analyzed by using a computer-assisted image analysis system, multi-analyst, connected to a GS 690 Imaging Densitometer (Bio-Rad, USA). Quantification of mRNA expression levels was obtained by measuring the average density of each region in five adjacent brain sections. All data are shown as the $\bar{x} \pm s_x$ for groups based on eight rats in each group. Analysis was performed by SPSS software. Unpaired, two tailed *t*-test and Anova comparison test were used with $P < 0.05$ be considered as sufficient to reject no difference hypothesis.

RESULTS

There were no significant differences of weight, glucose level, serum leptin and serum insulin level (Compared with control rats, $P > 0.05$) between test and control groups (Table 1).

Table 1 Comparison of weight, glucose level, serum leptin and insulin between test and control groups ($\bar{x} \pm s$)

Group	<i>n</i>	Weight (g)	Glucose	Leptin (µg/L)	Insulin(µg/L)
CTA	8	227.2±11.7	6.2±0.8	2.2±0.4	1.2±0.4
Control	9	226.3±10.2	6.4±1.2	2.1±0.4	1.4±0.5

Many neuronal cell bodies and dendritic processes in the amygdala expressed leptin receptor immunoreactivity (LR-IR). The expressed immunoreactivity was quantified by counting positive-stained cells. Compared with the control group, the expression of leptin receptor was increased by 166.7 % in BLA. The average number of LR-IR positive cell was 127±12 vs 48±9 per 1 mm² ($t=12.67$, $P=0.000$). LR-IR was mainly found in the membrane of cells in the control group. In CTA rats, it was shown that LR-IR mostly deposited in cytoplasm and membrane. That is to say, LR-IR immigrated into cells after CTA leaning (Figure 1).

By means of CTA learning, rats displayed a significant difference at the level of OB-Rb mRNA expression in the BLA. Compared with the control group, the levels of OB-Rb mRNA increased by + 11.9 % (116.5±10.8 vs 104.3±10.9). The level of OB-Ra mRNA on the choroid plexus also rose up by 7.4 % (114.2±12.0 vs 106.1±13.8 (Figure 2, 3)). After CTA learning, the expression of both OB-Rb mRNA in the BLA and Ob-Ra mRNA on the choroid plexus have significantly enhanced.

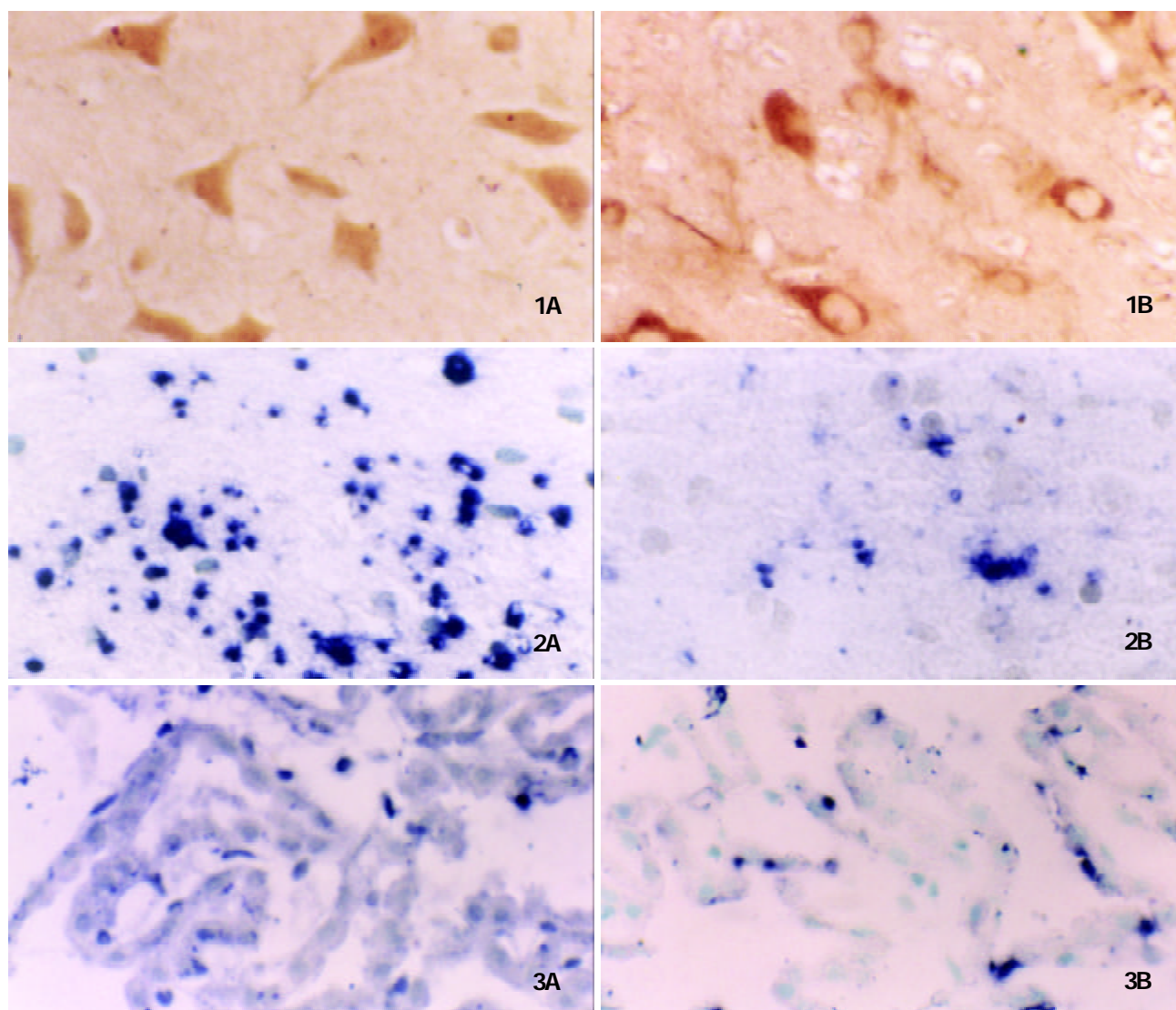


Figure 1 LR-IR positive cells in BLA of rats. A: CTA group; B: control group.

Figure 2 OB-Rb mRNA expression in BLA of rats. A: CTA group; B: control group.

Figure 3 OB-Ra mRNA expression on choriod plexus of rats. A: CTA group; B: control group.

DISCUSSION

BLA and CTA

Many researches have observed deficits in the CTA paradigm after functional disruption of the BLA, which included electrolytic lesions, ibotenic acid lesions^[17-20]. The amygdala has long been believed to be associated with the control of emotions, motivation, and hedonic tone^[21,22]. The amygdala receives information from various sensory modalities via the neocortex and directly from the thalamus, brain stem and plays an important role in ingestive behaviors. In rodents, the amygdala is one of the major recipients of gustatory projections to forebrain. The nucleus tractus solitarius (NTS) in the medulla receives taste information from peripheral taste nerves and sends gustatory information to the pontine parabrachial nucleus (PBN). Gustatory neurons in the PBN pass through two parallel ascending paths, one path goes to thalamocortical axis and the other directly goes to the amygdala^[23]. Gustatory and visceral information from the PBN may travel through the insular cortex or the thalamus, ultimately reaching the BLA. All these appear to be the routes relevant to CTA^[2]. On the basis of the typical CTA paradigm in which ingestion of a taste solution is paired with an ip injection of LiCl as an illness-inducing agent, CTA can be thought in a simple framework of association learning between taste information via the taste nerves and general

visceral information via the vagus nerve.

So BLA has been characterized as a region where presents of the internal and external worlds overlap, and it permits the animal to assess physiological needs in relation to the external resources, which are available to fulfill. As a result, the amygdala plays a critical role in the initiation and guidance of feeding, on which relies an integration of autonomic and exteroceptive information. Nishijo's study suggested that the activity of the amygdaloid neurons was altered when animals must modulate ingestive behavior by learning a new stimulus associated with food and being exposed to stress. The amygdala may not contribute to gustatory processing by precise discrimination, but by imparting hedonic appreciation and emotional significance to the taste experience, and by mediating the effects of conditional and of physiological needs on taste perception^[24].

Leptin and CTA

Leptin is a hormone believed to control appetite and regulate body weight via receptors^[25]. The leptin receptor is widely distributed in the brain, including hypothalamus^[26], pituitary^[27] and amygdala^[10]. These observations suggest that leptin may be involved not only in the control of energy expenditure, but also in other neuroendocrine functions^[28,29]. The expression of OB-

Rb and OB-Ra mRNA increased following by CTA formation indicate that leptin and its receptors may take part in CTA learning and interactions between gustatory and vagal signals.

To date, six different alternatively spliced isoforms have been identified, referred to as OB-Ra-f (*Nature* 1996;379:632-635). They are classified by the length of intracellular domains of the receptors. The long form of the receptor, OB-Rb is taken as the main functional receptor, which is capable of signaling, and is thus able to mediate the biological effects of leptin^[30]. Short forms, especially OB-Ra may play a role not only in transport but also in clearance or as a source of soluble receptor (*J Biol Chem* 1997; 272:6093-6096). The leptin receptor on the choroid plexus plays an important role in transporting plasma leptin into the brain^[31].

In the present study, although the level of serum leptin has not changed, strong expression of OB-R protein and OB-Rb mRNA has been found in the BLA and OB-Ra mRNA level increasing on the choroid plexus after CTA formation. All these results suggest that leptin receptor may participate in the formation of CTA. After CTA formation, LR-IR was expressed in the cytoplasm and the membrane of cells. It can be predicted that the function or activity of leptin receptor maybe change in the formation and maintenance of CTA.

Leptin is well known for its regulation of food intake and body weight. It also acts as a sweet-sensing suppressor. After i.p. injection of recombinant leptin, the sucrose and saccharin responses decreased parallely along with the serum leptin level increased^[4]. So leptin and its receptors possibly act as a mediate factor between feeding and taste. It maybe a sweet-sensing modulator that takes part in regulation of food intake. But in the present immunohistochemistry staining, the primary antibody reacts with all isoforms, including the long and short forms of receptors. Thus the antiserum could not discriminate the isoforms. Further studies are necessary to clarify the functional significance of OB-R isoforms of different aspects in taste aversion learning.

In summary, we have discovered (1) Expression of OB-Rb mRNA and OB-R protein were increased by means of CTA learning in the BLA; (2) OB-Ra mRNA levels enhanced followed by CTA formation on the choroid plexus; (3) LR-IR immigrated into cells after CTA formation.

ACKNOWLEDGEMENT

Mrs. Song and Mr. Lai for their technical assistance.

REFERENCES

- 1 **Yasoshima Y**, Morimoto T, Yamamoto T. Different disruptive effects on the acquisition and expression of conditioned taste aversion by blockades of amygdalar ionotropic and metabotropic glutamatergic receptor subtypes in rats. *Brain Res* 2000; **869**: 15-24
- 2 **Welzl H**, D' Adamo P, Lipp HP. Conditioned taste aversion as a learning and memory paradigm. *Behav Brain Res* 2001; **125**: 205-213
- 3 **Sakai N**, Yamamoto T. Possible routes of visceral information in the rat brain in formation of conditioned taste aversion. *Neurosis Res* 1999; **35**: 53-61
- 4 **Kawai K**, Sugimoto K, Nakashima K, Mirhito M, Ninomiya Y. Leptin as a modulator of sweet taste sensitivities in mice. *Proc Natl Acad Sci* 2000; **97**: 11044-11049
- 5 **Scott TR**, Verhagen JV. Taste as a factor in the management of nutrition. *Ingest Behav and Obes* 2000; **16**: 874-885
- 6 **Hofbauer KG**. Molecular pathways to onesity. *Int J Obes Relat Metab Disord* 2002; **26**: s18-27
- 7 **Strubbe J**, van Dijk G. The temporal organization of ingestive behavior and its interaction with regulation of energy balance. *Neurosci Biobehav Rev* 2002; **26**: 485
- 8 **Tschop M**, Morrison KM. Weight loss at high altitude. *Adv Exp Med Biol* 2002; **502**: 237-247
- 9 **Blundell JE**, Goodson S, Halford JC. Regulation of appetite: role of leptin in signaling systems for drive and satiety. *Int J Obes Relat Metab Disord* 2001; **25**: s20-34
- 10 **Burguera B**, Couce ME, Long J, Lamsam J, Laakso K, Jensen MD, Parisi JE, Lloyd RV. The long form of the leptin receptor (OB-Rb) is widely expressed in the human brain. *Neuroendocrinology* 2000; **71**: 187-195
- 11 **Lundy RF Jr**, Norgren R. Pontine gustatory activity is altered by electrical stimulation in the central nucleus of the amygdala. *J Neurophysiol* 2001; **85**: 770-783
- 12 **Miranda MI**, Ferreria G, Ramirez-Lugo L, Bermudez-Rattoni F. Glutamatergic activity in the amygdala signals visceral input during taste memory formation. *Proc Natl Acad Sci* 2002; **99**: 11417-11422
- 13 **Gutierrez H**, Gutierrez R, Ramirez-Trejo L, Silva-Gandarias R, Ormsby CE, Miranada MI, Bermudez-Rattoni F. Redundant basal forebrain modulation in taste aversion memory formation. *J Neurosci* 1999; **19**: 7661-7669
- 14 **Wig GS**, Barnes SJ, Pinel JP. Conditioning of a flavor aversion in rats by amygdala kindling. *Behav neurosci* 2002; **116**: 347-350
- 15 **Ganaraja B**, Jeganathan PS. Increased sweet taste preference following the lesion of basolateral nucleus of amygdala(BLA) in rat. *Indian J Physiol Pharmacol* 1999; **43**: 443-448
- 16 **Ganaraja B**, Jeganathan PS. Effect of basolateral amygdala & ventromedial hypothalamic lesions on ingestion & taste preference in rat. *Indian J Med Res* 2000; **112**: 65-70
- 17 **Ferry B**, Di Scala G. Basolateral amygdala NMDA receptors are selectively involved in the acquisition of taste potentiated odor aversion in the rat. *Behav Neurosci* 2000; **114**: 1005-1010
- 18 **Rollins BL**, King BM. Amygdala-lesion obesity: What is the role of the basolateral and central nuclei? *Am J Physiol* 2000; **279**: R1348-1376
- 19 **Rollins BL**, Stimas SG, McGuire HR, King BM. Effects of amygdala lesions on body weight, conditioned taste aversion and neophobia. *Physiol & Behav* 2001; **72**: 735-742
- 20 **Morris R**, Frey S, Kasambira T, Petrides M. Ibotenic acid lesions of the basolateral, but not the central amygdala interfere with conditioned taste aversion: evidence from a combined behavioral and anatomical tract-tracing investigation. *Behav neurosci* 1999; **113**: 291-302
- 21 **Daenen EW**, Wolterink G, Gerrits MA, Van Ree JM. The effects of neonatal lesions in the amygdala or ventral hippocampus on social behavior later in life. *Behav Brain Res* 2002; **136**: 571-582
- 22 **Nishijo H**, Uwano T, Tamura R, One T. Gustatory and multimodal neuronal responses in the amygdala during licking and discrimination of sensory stimuli in awake rats. *J Neurophysiol* 1998; **79**: 21-36
- 23 **Pritchard TC**, Hamilton RB, Norgren R. Projections of the parabrachial nucleus in the old world monkey. *Exp Neurol* 2000; **165**: 101-117
- 24 **Nishijo H**, One T, Uwano T, Torii K. Hypothalamic and amygdalar neurons responses to various testant solutions during ingestive behavior in rats. *J Nutr* 2000; **130**: 954s-959s
- 25 **Vernon RG**, Denis RG, Sorensen A. Signals of adiposity. *Domest Anim Endocrinol* 2001; **21**: 197-214
- 26 **Sahu A**, Nguyen L, O' Doherty RM. Nutritional regulation of hypothalamic leptin receptor gene expression is defective in diet-induced obesity. *J Neuroendocrinol* 2002; **14**: 887-893
- 27 **Jin L**, Zhang S, Burguera BG, Couce ME, Osamura RY, Kulig E, Lloyd R. Leptin and leptin receptor expression in rat and mouse pituitary cells. *Endocrinology* 2000; **141**: 333-339
- 28 **Pralong FP**, Gaillard RC. Neuroendocrine effects of leptin. *Pituitary* 2001; **41**: 25-32
- 29 **Fruhbeck G**. Peripheral actions of leptin and its involvement in disease. *Nutr Rev* 2002; **60**: s47-55
- 30 **Heshka JT**, Jones PJ. A role of dietary fat in leptin receptor, OB-Rb, function. *Life Sci* 2001; **69**: 987-1003
- 31 **Kastin AJ**, Pan W, Maness LM, Koletsky RJ, Rnsberger P. Decreased transport of leptin across the blood-brain barrier in rats lacking the short form of the leptin receptor. *Peptides* 1999; **20**: 1449-1453

The mRNA expression patterns of tumor necrosis factor- α and TNFR-I in some vital organs after thermal injury

Wen-Hui Fang, Yong-Ming Yao, Zhi-Guo Shi, Yan Yu, Ye Wu, Lian-Rong Lu, Zhi-Yong Sheng

Wen-Hui Fang, Yong-Ming Yao, Zhi-Guo Shi, Yan Yu, Ye Wu, Lian-Rong Lu, Zhi-Yong Sheng, Department of Microbiology and Immunology, Burns Institute, 304th Hospital of PLA, Beijing 100037, China

Supported by the National Key Program for Fundamental Research and Development, No.G1999054203, the National Natural Science Outstanding Youth Foundation of China, No.30125020, and the National Natural Science Foundation of China, No.30200293

Correspondence to: Yong-Ming Yao, M.D., Department of Microbiology and Immunology, Burns Institute, 304th Hospital of PLA, 51 Fu-Cheng Road, Beijing 100037, China. c_fanf@sina.com

Telephone: +86-10- 66867394 **Fax:** +86-10-68429998

Received: 2002-10-30 **Accepted:** 2002-11-25

I in some vital organs after thermal injury. *World J Gastroenterol* 2003; 9(5): 1038-1044

<http://www.wjgnet.com/1007-9327/9/1038.htm>

Abstract

AIM: To investigate changes of tumor necrosis factor- α (TNF- α) and TNFR-I expression in vital organs and their significance in the pathogenesis of multiple organ damage associated with endogenous endotoxin following major burns.

METHODS: Wistar rats subjected to a 35 % full-thickness scald injury were sacrificed at 12 h, 24 h, 48 h, and 72 h postburn, respectively. Meanwhile, eight rats were taken as normal controls. Tissue samples from liver, spleen, kidney, lung and intestine were collected to assay tissue endotoxin levels and measure TNF- α and TNFR-I expression. In addition, blood samples were obtained for the determination of organ function parameters.

RESULTS: Endotoxin levels in liver, spleen and lung increased markedly after thermal injury, with the highest level in liver. The gene expression of TNF- α in liver, lung and kidney was up-regulated after thermal injury, while the TNFR-I mRNA expression in liver, lung, kidney and intestine was shown decreased throughout the observation period. Thus, the mRNA expression ratio of TNF- α to TNFR-I was significantly increased postburn, particularly in pulmonary tissue (67-fold). In addition, the significant correlations between the expression of TNFR-I or the expression ratio of TNF- α /TNFR mRNA in liver tissue and serum aspartate aminotransferase levels were noted ($P < 0.05-0.01$). Similar results were also obtained between pulmonary TNF- α mRNA expression and myeloperoxidase activities ($P < 0.01$), whereas there was a highly negative correlation between levels of renal TNFR-I mRNA expression and serum creatinine.

CONCLUSION: Burn injury could result in the translocation of gut-derived endotoxin that was mainly distributed in the liver, spleen and lung. The translocated endotoxin then made the expression of TNF- α and TNFR-I mRNA up-regulated and down-regulated respectively in various organs, which might be involved in the pathogenesis of multiple organ damage following burns.

Fang WH, Yao MY, Shi ZG, Yu Y, Wu Y, Lu LR, Sheng ZY. The mRNA expression patterns of tumor necrosis factor- α and TNFR-

INTRODUCTION

Gram-negative bacterial sepsis with resulting multiple organ dysfunction syndrome (MODS) and death continues to be a major problem in critical surgical patients. Lipopolysaccharide (LPS), an integral component of the gram-negative bacterial cell membrane, is responsible for many, if not all, of the toxic effects that occur during gram-negative sepsis. Both experimental and clinical data recently implicated that gut-derived bacteria or endotoxin translocation might play a role in the development of sepsis and multiple organ damage in critically ill patients, especially after trauma, thermal injury, hemorrhagic shock and major elective surgical procedure^[1-3]. It has also become clear that endotoxin initiates an inflammatory cytokine and mediator cascade, and these mediators, in turn, act on additional target cells to produce an array of pro-inflammatory cytokines leading to cardiovascular shock, MODS, or even death^[4-7]. Among these inflammatory mediators, tumor necrosis factor- α (TNF- α) in particular occupies a pivotal role in the pathogenesis of inflammation, cachexia, septic shock and tissue injury.

TNF- α exerts its pleiotropic effect by interacting with two high affinity receptors termed TNFR-I (55 kilodaltons) and TNFR-II (75 kilodaltons) on a variety of cells^[8]. Both TNFRs also exist in soluble forms^[9]. The soluble TNFRs (sTNFRs) are produced by proteolytic cleavage of the extracellular domain of TNFRs. The biological role of sTNFR appears to be dose-dependent. For instance, at low concentrations, sTNFRs stabilize the trimeric structure of TNF- α , thereby slowing its spontaneous decay of bioactivity, and augmenting the long-term effects of TNF- α by providing a reservoir of bioactive TNF- α that is slowly released. When more quantities of sTNFRs are present, however, they reduce the bioactivity of TNF- α by competing for TNF- α binding with cell-associated receptors. These above regulatory processes may modulate TNF- α activity in response to inflammation. In this regard, to obtain a complete view of the *in vivo* pathophysiologic roles of TNF- α , one should further study the regulation of TNF- α /TNFR and the balance between them. Since most of the known cellular TNF- α responses occur through TNFR-I, we investigated the expression changes of TNF- α and TNFR-I in vital organs, and their significance in the pathogenesis of multiple organ damage associated with endogenous endotoxin following major burns.

MATERIALS AND METHODS

Animals and thermal injury

Male Wistar rats (weight range 250-300 g), purchased from the Laboratory Animal Center, Beijing, China, were used for the study. The animals were housed in separate cages in a temperature-controlled room with alternating 12-h light-dark cycles, and were allowed to acclimatize for at least 7 days

before being used. All animals had free access to water, but were fasted overnight prior to the experiment. After the rats were anesthetized by the intraperitoneal (i.p.) injection of pentobarbital sodium (40 mg/kg), their dorsal hair was shaved and a 35 % of total body surface area with full-thickness burn was inflicted by immersion of the dorsal skin in a 100 °C water bath for 12 s. All animals received Ringer's solution (50 ml/kg) administered i.p. after burn injury for resuscitation, and the burn wounds were treated with an antibacterial agent everyday as a prophylactic measure against wound infection. All experimental manipulations were undertaken in accordance with the National Institute of Health Guide for the Care and Use of Laboratory Animals, and with the approval of the Scientific Investigation Board of the Burns Institute, Postgraduate Medical College, Beijing.

Experimental design

A total of 46 animals were sacrificed at each of following time points: 12 h, 24 h, 48 h and 72 h postburn. Meanwhile, eight rats were taken as normal controls. Under anesthesia, systemic blood samples were obtained. Then tissue specimens were taken from mesenteric lymph nodes (MLNs), liver, spleen, kidneys, lungs, and intestine.

Bacterial translocation

The MLNs, spleen, liver, kidney, lung and subeschar tissues were removed aseptically in this order. Each organ sample was weighed, homogenized in 2 ml of sterile saline under aseptic conditions, and 100 μ l of the homogenate were plated on Chinese blue agar and 5 % sheep blood agar. After 48 h of aerobic incubation at 37 °C, all agar plates were examined for growth. The number of viable microorganisms per gram of organ tissue was calculated, and the obtained organisms were identified by standard bacteriological techniques.

Tissue endotoxin measurement

Tissue specimens from liver, spleen, kidneys and lungs were aseptically removed, and were homogenized in 3-fold volume pyrogen-free saline on ice. The homogenate was stored at -20 °C until analyzed. The tissue endotoxin levels were measured by the chromogenic Limulus Amebocyte Lysate (LAL) assay with the procedure based on the LS-1 kit (Seikagaku Corp., Tokyo, Japan) protocol modified by perchloric acid (PCA) treatment of samples to remove nonspecific activators or inhibitors of the lysate^[10]. Briefly, 150 μ l of 0.32 M PCA were added to 75 μ l of homogenate in an ice bath, and the mixture was incubated at 37 °C for 20 min. After centrifuged (Kubota Corp., Japan) at 3 000 rpm for 15 min, the supernatant was neutralized with an equal volume of 0.18 N NaOH. Then, 100 μ l of the supernatant was incubated for 18 min at 37 °C with 50 μ l of amebocyte lysate. Chromogenic substrate then was added, and after 3 min of further incubation, the reaction was stopped. The amount of *p*-nitroaniline (pNA) released from the substrate was determined, after diazo-coupling, by the absorbance of the solution at 545 nm (Beckman Corp. U.S.). The endotoxin concentration expressed as endotoxin units per gram of organ tissue was calculated from a standard curve derived from the assay of a standard endotoxin (Lot EC-5, endotoxin unit (EU) =100 pg of U.S. standard endotoxin). The detection limit with this method was 0.01 EU/ml.

RNA extraction and reverse-transcription-polymerase chain reaction

Tissue samples from liver, lungs, kidneys and intestine were stored in liquid nitrogen until analysis. Extraction of total tissue RNA was performed with guanidine isothiocyanate according to the method by Chomczynski and Sacchi^[11]. First-strand

cDNA was synthesized using oligo-dT primer and the AMV reverse transcriptase (Promega Corp., Madison, WI). In brief, 2 μ g of total RNA was reversely transcribed by adding 20 μ l of a master mixed with 1 U/ μ l RNase inhibitor, 0.025 μ g of random hexamers, 5 mmol/L MgCl₂, 1 \times reverse transcriptase buffer, 1 mmol/L of dNTP mixture, and 0.7 U/ml AMV reverse transcriptase (final concentrations indicated). Samples were incubated at 42 °C for 60 min.

For the cDNA amplification, the PCR with hot start technique was used, in which *Taq* polymerase was added to each tube at 88 °C with Thermal Cycler (Perkin-Elmer Corp., U.S.). The PCR mixture contained a final concentration of 0.2 μ mol/L specific primers for TNF- α and TNFR-I (from Beijing Medical University), 1 \times PCR buffer, 1.5 mmol/L MgCl₂, 0.2 mmol/L of each dNTP and 0.5 U/25 μ l *Taq* polymerase (Promega Corp., Madison, WI). After a 5-min initial melting step at 97 °C, the PCR with 28 to 32 cycles was carried out [94 °C 1 min for denaturation; 58 °C (TNF- α) or 63 °C (TNFR-I) 1 min for annealing; and 72 °C 1 min for extension]. The final cycle was followed by a 10-min soak at 72 °C. The sequences of primer pairs, and predicted sizes of the amplified PCR fragments were shown in Table 1. The house keeping gene β -actin was used as internal controls for standardization of PCR product^[14].

Table 1 Primer sequences used for polymerase chain reaction (PCR)

Target gene	Oligonucleotide primers	Size of PCR production, bp	Ref.
TNF- α	5'-AGA ACT CCA GGC GGT GTC TCT G-3'	415	8
	5'-GT GGC AAA TCG GCT GAC GGT GT-3'		
TNFR	5'-CC ATC TGC TGC ACC AAG TGC CA-3'	347	9
	5'-AA TCC TCG GTG GCA GTT ACA CA-3'		

PCR products and molecular weight markers were subjected to electrophoresis and visualized by means of ethidium bromide staining. The cycle number of each study was chosen in a linear range to avoid the plateau effect. The gel then was photographed, and the negative scanned with a densitometer (Pharmacia Corp., Sweden). Final data were expressed as a ratio of the band of interest to the unregulated control (β -actin).

Tumor necrosis factor- α protein analysis

Liver, lung, kidney and intestine tissues were respectively homogenized in 9-fold volume 0.01 mmol/L sodium phosphate buffer, pH 7.2 in an ice bath, and centrifuged (Haerus Corp., Germany) for 20 min at 1 400 rpm, 4 °C. The supernatant was stored at -20 °C until analysis. TNF- α concentration was determined by a commercially available protocol (rat tumor necrosis factor ELISA test kit; Endogen Corp., U.S.). In brief, aliquots of freshly diluted standard concentrations of recombinant rat TNF- α or samples were incubated in duplicate on ELISA plates. ELISA wells were then sequentially exposed to biotinylated antibody, streptavidin-HRP, and finally TMB substrate. The reaction was terminated using stop solution. The sample absorbance was detected at 450 nm with a plate reader (Denley Corp., England) and the TNF- α concentrations were determined by the reading of the standard curve. The sample protein was measured by the method of Bradford^[15], and the detected tissue TNF- α was finally expressed as pg/mg protein.

Myeloperoxidase assay

Lung tissue was homogenized in a 9-fold volume of 20 mmol/L potassium phosphate buffer, pH 7.4, and centrifuged (Hitachi Corp., Japan) for 30 min at 35 000 rpm, 4 °C^[16]. The pellet was

resuspended in 1 ml of 50 mmol/L potassium phosphate buffer, pH 6.0, containing 0.5 mg/dl hexadecyltrimethylammonium bromide and frozen overnight at -70°C . Then, the samples were thawed, sonicated for 90 s at full power, incubated in a 60°C water bath for 2 h, and centrifuged for 10 min at 35 000 rpm, 4°C . 0.1 ml of supernatant, was added to 2.9 ml of 50 mmol/L potassium phosphate buffer, pH 6.0, containing 0.167 mg/ml o-dianisidine and 0.0005 hydrogen peroxide. The sample absorbance was measured at 460 nm visible light (A_{460}) for 2 min (Beckman Corp., U.S.). Myeloperoxidase (MPO) activity per gram wet lung (gwl) was calculated by the following formula: Myeloperoxidase activity (units/gwl) = $(\Delta A_{460}) \times (13.5) / \text{lung weight (g)}$, where ΔA_{460} was the changes in absorbance at 460 nm from 30 to 90 s after the initiation of the reaction. The coefficient 13.5 was empirically determined such that 1 unit MPO activity was the amount of enzyme that would reduce 1mmole peroxide/min.

Diamine oxidase activity measurement

The small intestines were removed and stored in liquid nitrogen before analysis. For measurement of intestinal diamine oxidase (DAO) activity, the small intestine was homogenized in a threefold volume of ice-cold phosphate buffer (0.1M, pH 7.2) and centrifuged (Haerus Corp., Germany) for 30 min at 10 000 rpm, 4°C . After the resulting upper layer was discarded, the supernatant left was used as the source of the enzyme. DAO activity was assayed according to the modified method^[17]. The assay mixture contained 3 ml of phosphate buffer (0.2 M, pH 7.2); 0.1 ml (4 μg) of horseradish peroxidase solution (Shanghai Biochemistry Institute, China), 0.1 ml of o-dianisidine (Sigma Chemical, St. Louis, MO) methanol solution (500 μg), 0.5 ml of intestinal homogenate or freshly diluted DAO standard, and 0.1 ml of substrate (cadaverine dihydrochloride from Sigma Chemical, St. Louis, MO) solution (175 μg), which was incubated for 30 min at 37°C . Then, the absorbance was measured at 436 nm (Beckman Corp. Germany), and the DAO activity was read on the standard curve. Sample protein was measured as described previously^[15]. The intestinal DAO activity was calculated by the following formula: DAO activity (units/mg protein) = DAO activity \times (60)/protein concentration.

Organ function parameters measurement

Systemic blood samples were collected and serum was prepared by centrifugation for 10 min at 2 000 rpm. Then, the samples were stored at -20°C until analysis. Serum aminoleucine transferase (ALT), aspartate aminotransferase (AST), MB isoenzyme of creatine kinase (CK-MB) and creatinine (Cr) levels were determined with a biochemical autoanalyzer (Model 7170; Hitachi Ltd., Japan).

Statistical analysis

Statistical analyses were done by using the statistical package SAS 6.04, and the data were expressed as the mean \pm SEM. Statistical evaluation of the continuous data were performed by one-way analysis of variance (ANOVA), following by either Dunnett's *t* test or Kruskal-Wallis test for inter-group comparisons. Correlations between variables were tested by Spearman's correlation coefficients. The level of significance was considered to be $P < 0.05$.

RESULTS

Bacterial translocation and endotoxin levels in tissues

Microbiologic cultures from subschar tissues were all negative throughout the observation period, while the bacterial translocation was significantly increased at various

time points after severe burns ($P < 0.05$), which was predominantly detected in MLNs (the incidence was 30.0 %) with the higher cultured bacterial number than that in other organs (control: negative, postburn: $4.748 \pm 0.313 \log_{10}\text{CFU/g}$). The translocating organisms were predominantly *E. coli*, but *Klebsiella spp.* and *Enterococcus* species were also identified. Meanwhile, the endotoxin levels in liver, spleen and lungs were significantly elevated at 12 h postburn, with the liver highest (control: $1.388 \pm 0.312 \text{ EU/g}$, 12 h postburn: $17.337 \pm 3.687 \text{ EU/g}$, $P < 0.01$). Endotoxin levels in liver and spleen then fell quickly, and elevated again at 48 h ($2.805 \pm 0.306 \text{ EU/g}$ in liver, $2.623 \pm 0.321 \text{ EU/g}$ in spleen, $P < 0.01$ compared with the controls). On the other hand, endotoxin levels in lungs maintained a high level till 72 h (control: $4.510 \pm 1.139 \text{ EU/g}$, 72 h postburn: $6.938 \pm 1.715 \text{ EU/g}$). There was no significant difference in endotoxin levels in kidneys at any time point postburn.

Expression of TNF- α and TNFR-I in Tissues

The expressions of TNF- α mRNA in tissues (liver, lungs, kidneys and intestine) were examined by RT-PCR as shown in Figure 1, which revealed a constitutively lower level in the control animals and a marked increase in burned subjects. The expression of TNF- α mRNA in liver was increased to a maximum at 12 h postburn (control: 0.020 ± 0.013 , 12 h postburn: 0.140 ± 0.032 , $P < 0.05$) and decreased thereafter (Figure 1A), whereas that in the kidneys and lungs peaked at 48 h postburn with the increased expression by 10-fold and 8-fold respectively (Figure 1B), among which the pulmonary mRNA expression maintained at a higher level up to 72 h postburn ($P < 0.05$ compared with the controls). However, there was a trend of lower expression of TNF- α mRNA in intestine (Figure 1B).

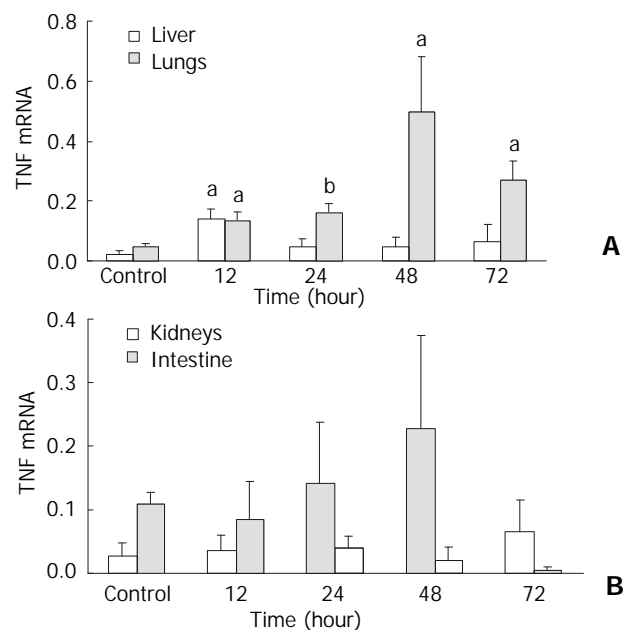


Figure 1 Semiquantitative analysis of tumor necrosis factor- α (TNF- α) mRNA in various organs after thermal injury. Values are reported as the ratio of TNF- α to β -actin signals. ^a $P < 0.05$ and ^b $P < 0.01$ as compared to the control values.

Tissue TNF- α protein assayed by ELISA exhibited higher levels in both liver and intestine (Figure 2, A and B), with the former that was increased by 25 % at 72 h postburn compared with control values, and the latter that peaked at 48 h postburn (control: $45.723 \pm 1.133 \text{ pg/mg protein}$, 48 h postburn: $80.448 \pm 14.018 \text{ pg/mg protein}$, $P < 0.05$) and maintained at a higher levels until 72 h postburn ($61.357 \pm 4.902 \text{ pg/mg protein}$).

However, there was no significant difference in TNF- α levels in lungs at each time point postburn compared with the controls. So was TNF- α levels in kidneys.

TNFR-I mRNA expression in vital organs by RT-PCR was shown in Figure 3, in which abundant expression was observed in the control animals, with the highest level in the liver (1.029 \pm 0.215). After burn injury, however, TNFR mRNA expression in liver, kidneys and lungs was shown to reduce dramatically, with the lowest levels at 24-48 h postburn (26.1-46.7 % of the control values). Though increased gradually thereafter, TNFR mRNA levels in these organs were shown lower than the control values at 72 h after thermal injury. A remarkable decrease in intestinal TNFR mRNA expression was also noted (17.3 % of the control values, $P<0.05$) and maintained throughout the observation period.

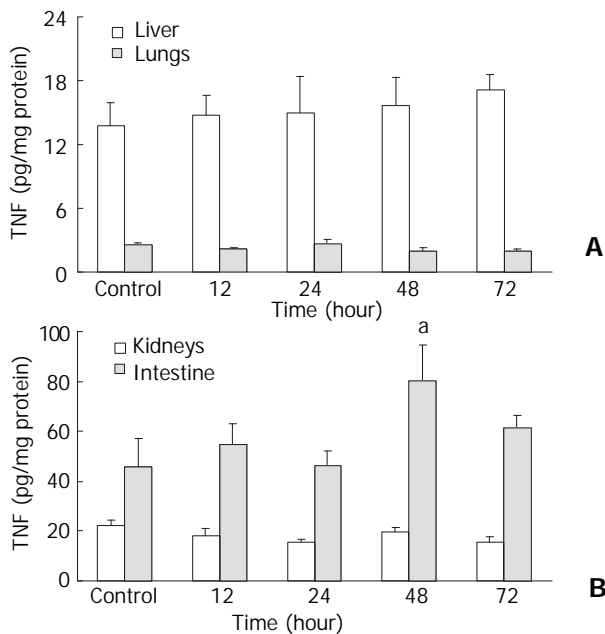


Figure 2 TNF- α protein levels in various organs after thermal injury. Values are reported as pg/mg protein. ^a $P<0.05$ as compared to the control values.

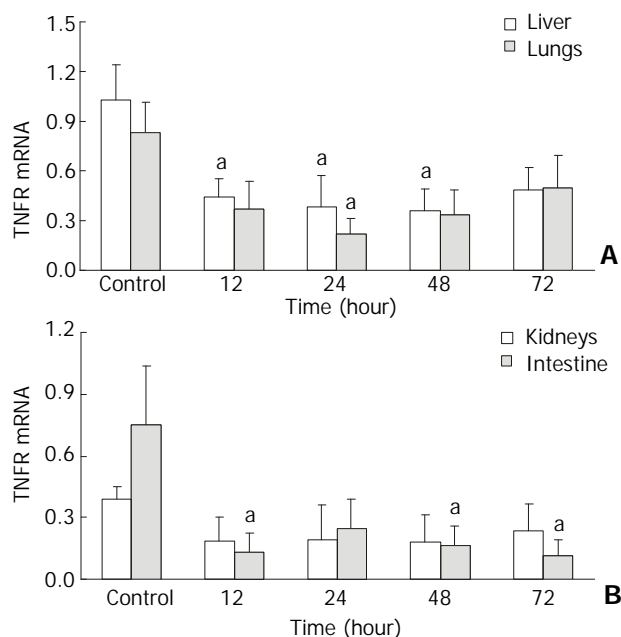


Figure 3 Semiquantitative analysis of tumor necrosis factor- α receptor-I (TNFR-I) mRNA in observed organs after thermal injury. Values are reported as the ratio of TNFR-I to β -actin signals. ^a $P<0.05$ as compared to the control values.

The ratio of TNF- α to TNFR-I mRNA (T/R ratio) in various organs was investigated in the present study as shown in Figure 4, which revealed that T/R ratio in these organs was significantly increased postburn, particularly in pulmonary tissue that was 67-fold of control values at 48 h after burn injury. T/R ratios in liver and kidneys reached at their maximums between 24 and 48 h ($P<0.05-0.01$), whereas the elevated ratio in lungs and intestine existed till 72 h postburn.

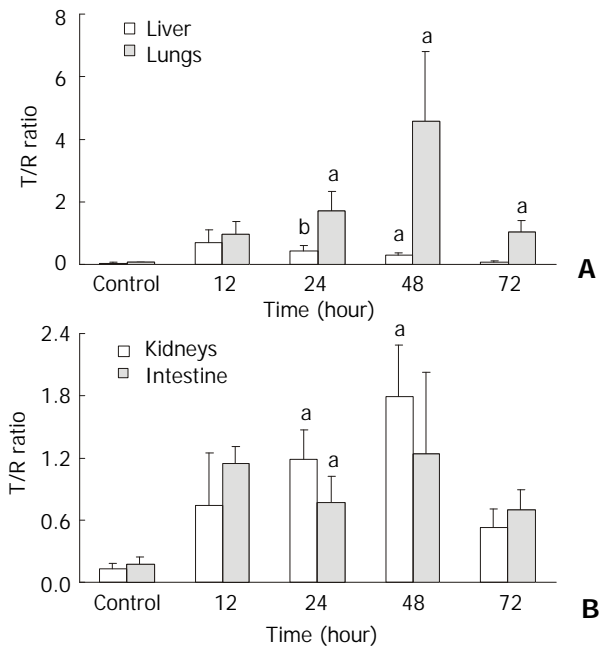


Figure 4 mRNA expression ratio of tumor necrosis factor- α to TNFR-I (T/R ratio) in observed organs after thermal injury. ^a $P<0.05$ and ^b $P<0.01$ as compared to the control values.

Organ function parameters

Serum ALT and AST levels markedly increased after scald injury, reaching a maximum between 12 and 24 h (4-5 folds of control values, $P<0.01$ compared with the controls), and remaining higher than control levels at 72 h postburn ($P<0.05-0.01$). Similarly, levels of serum CK-MB increased rapidly postburn, peaking at 12 h (control: 1 193.875 \pm 195.427 U/L, 12 h postburn: 3 626.100 \pm 410.073 U/L, $P<0.01$), and then decreasing gradually to baseline. However, serum Cr levels were not significantly different between normal and burned animals. There was a negative correlation between hepatic TNFR mRNA and serum AST levels ($r=-0.3930$, $P=0.0121$). Similar results were also obtained between renal TNFR mRNA and serum Cr levels ($r=-0.9295$, $P=0.0001$). In addition, it was noted significant correlation between T/R ratio in liver tissues and serum AST levels ($r=0.4409$, $P=0.0056$).

MPO and DAO activities

The pulmonary MPO activity that stood for the neutrophil sequestration was markedly increased after burns with the peaking at 12 h and elevating till 72 h postburn. The mucosal DAO activity, which might serve as a useful marker of intestinal injury, tended to be decreased at each time point postburn. It was noted that there was a significant correlation between pulmonary TNF- α mRNA levels and MPO activities ($r=0.4289$, $P=0.0091$), but there wasn't between intestinal TNF- α mRNA levels and DAO activities, as well as between MPO or DAO activities and TNFR mRNA in lungs and intestine ($P>0.05$).

DISCUSSION

The role of endotoxin in the pathogenesis of septic shock and

organ failure has been well established. It is almost an opinion in unison that LPS initiates a cytokine cascade, and among these cytokines TNF- α is recognized as the pivotal one to evoke systemic responses to sepsis and injury^[18]. Most of our current knowledge on the *in vivo* induction and regulation of TNF- α has been attained by measurement of serum cytokine levels. To date, only a few studies have addressed the gene regulation of the tissue-specific cytokines *in vivo*. In the current study, we investigated mRNA of TNF- α as well as its receptor and TNF- α protein expression in vital organs following severe burns. It was found that thermal injury induced a marked increase in mRNA of TNF- α . Hepatic TNF- α mRNA expression increased early and transiently with a peak at 12 h, whereas sustained elevation of TNF- α gene expression was observed in kidneys and lungs. Especially in the latter, the highest induced levels of TNF- α mRNA were found, suggesting a possible role for TNF- α in mediating pulmonary damage, which is commonly encountered in sepsis.

The investigations of Furse *et al.* have shown that TNF- α mRNA levels were increased in monocytes of trauma patients, and an increased amount of TNF- α protein was produced^[19]. In the present study, we attempt to determine the association between TNF- α mRNA expression and TNF- α protein production by comparing their respective time course of exhibition. Recent studies document that cytokines exert their primary effects in a paracrine fashion at the local tissue level^[20]. Andrejko *et al.* reported that the changes in TNF- α -dependent hepatic gene expression accompanied an animal model of the systemic inflammatory response syndrome correlated with intrahepatic, and not plasma concentrations of TNF- α ^[21]. Since circulating levels of cytokines may not appreciably reflect their true biological activity in the affected tissues^[22], we determined tissue TNF- α protein expression in various organs instead of plasma levels of TNF- α . To our surprise, the results revealed that the changes in TNF- α protein did not correlate temporally with increased expression of TNF- α mRNA in vital organs. To explain the discrepancy, we offer the following possibilities. Firstly, TNF- α is short-lived in plasma^[23]. There was a transient rise in TNF- α after the injection of *E. coli* or endotoxin, and TNF- α became undetectable by 4-6 h^[24]. Therefore it is likely that the TNF- α response is too transient to be detected. Secondly, shed soluble TNF- α receptors may interfere with TNF- α activity in immunoassay^[25]. Finally, despite of transcriptional control, TNF- α production is also regulated posttranscriptionally^[26]. Thus, TNF- α protein concentration is a cesspool of complex interactions regarding binding and release from cell membranes, magnitude and kinetics of the soluble receptors and natural cytokine antagonists, and rates of catabolisms. Account of the aforementioned interfering factors, we suggest that determination of TNF- α mRNA expression may be more reliable to reflect the kinetics of cytokine at the local tissue level.

A large body of clinical and experimental evidence suggests that gut-derived endotoxemia following trauma, burns and circulatory shock could result in TNF- α production, which may play a key role in mediating subsequent septic response and systemic tissue injury^[27-29]. In burn injury, however, the causative effect of locally accumulated endotoxin on TNF- α mRNA expression in various organs is still not completely understood. In the present study, it was found that endotoxin levels in the liver, spleen and lung rose markedly after thermal injury, peaking at 12 h. Endotoxin levels in liver and spleen then lowered gradually, while pulmonary endotoxin levels maintained a high level till 72 h. The temporal relationship between the kinetic changes of TNF- α mRNA and that of endotoxin levels in the visceral organs, as observed in the present study, suggests that endotoxin originated from the gastrointestinal tract appears to be one of the most potential

triggers for TNF- α gene expression. Hadjimines *et al.* demonstrated that TNF- α mRNA in peritoneal exudated macrophages of mice rose fourfold after intraperitoneal administration of endotoxin^[30]. Similarly, cecal ligation and puncture was shown to induce a rapid increase in hepatic and pulmonary TNF- α mRNA by 3 h, remaining high for 18 h^[31]. These findings are consistent with our data suggesting that endotoxin can induce TNF- α gene expression in various tissues.

Monocytes have been demonstrated to be major producers of the elevated TNF- α seen post-trauma. In the model used here, hepatic macrophages appear to be the principal cellular source of TNF- α , as the Kupffer cell population within the liver is the largest fixed tissue macrophage population in the body. Recent study had shown that Kupffer cells were the major source of TNF- α in culture supernatants of hepatic perfusate mononuclear cells from ethanol-consuming rats injected LPS^[32,33]. Additionally, blood monocytes, pulmonary macrophages and peritoneal macrophages were also possibly involved in TNF- α formation^[30, 34-36], since endotoxin distributing to lung and spleen was evident after burns in the present study. Unexpectedly, correlation analysis between tissue endotoxin concentrations and TNF- α mRNA levels did not reveal any significant correlation. From that, endotoxin translocation originated from the gut may serve purely as an initial trigger. Moreover, although endotoxin translocation occur following severe burns, endotoxin may not be the sole agent responsible for the subsequent induction of cytokine, whereas a variety of factors, such as hypoxemia, shock, and necrosis tissues, may be also involved in cytokine production^[37].

The majority of human cells express high-affinity receptors that mediated the biological activities of TNF- α . The potent regulatory abilities of TNF- α are transduced by two distinct cell surface receptors, namely 55 kd (TNFR-I) and 75 kd (TNFR-II) relative molecule mass^[38]. In inflammation, the receptors activate both unique and synergistic responses. Studies of TNFR knockout mice have established that TNFR-I plays a predominant role in LPS-induced inflammatory diseases and mediate the lethal effects of endotoxin^[39-41]. Furthermore, mice lacking TNFR-I showed resistance to endotoxin challenge^[42]. Therefore, we attempted to observe the mRNA expression of this receptor in vital organs. It was found that although normal tissue expressed TNFR mRNA abundantly, with the highest level in liver, TNFR mRNA expression in various organs plummeted after burn injury. Previous study has shown that loss of monocyte surface TNFRs is an early event in the response to endotoxemia^[43]. The nadir of this response occurred 2 h after endotoxin administration, and the monocyte surface TNFR levels then returned to baseline within 6 h after endotoxin challenge. These results indicate that monocyte surface TNFR levels rapidly decrease in response to an inflammatory stimulus *in vivo* and also rapidly normalize when the stimulus is no longer present. Thus, the significant and sustained decrease in TNFR mRNA levels observed in present study may represent an ongoing condition of systemic inflammation. Our findings are consistent with the recent observations of Calvano *et al.*, who reported a significant and sustained (up to 4 days) decrease in monocyte surface TNFR levels in non-surviving patients with sepsis^[44]. On the other hand, the extracellular domains of the TNFR apparently are shed from the cell surface in response to many of the same inflammatory stimuli that are known to induce TNF- α production^[25]. Our data may thus imply that a dual deregulation in TNFR reflects decreased expression of TNFR on the cell surface concomitant to decreased cell shedding of TNFR.

The shedding of TNFR and resultant acute decrease in the number of TNFR on the cell surface may serve to transiently desensitize cells, thereby providing a mechanism for inhibition of TNF- α activity. This process may have additional

significance, as released soluble receptors (sTNFR) may inhibit TNF- α bioactivity by binding to the molecule and preventing ligand binding to the cellular TNFR. *In vitro* studies demonstrated that sTNFR in critical ill patients and in experimental endotoxemia are sufficient to neutralize the bioactivity associated with TNF- α concentrations observed in mild inflammation, whereas such levels are inadequate to neutralize the cytotoxicity associated with TNF- α levels seen in overwhelming or lethal sepsis^[45]. Thus, imbalance of TNF- α to TNFR may reflect more than one dysfunction in monocyte TNF- α production and regulation, which may contribute to overwhelming activation of the inflammation cascade.

Pellegrini *et al.* reported that monocyte membrane associated TNF- α (mTNF- α) elevated and TNFR shedding decreased in trauma patients^[46]. There was a correlation between increased mTNF- α and decreased TNFR shedding to increased MODS score, but this lacked specificity. However, when mTNF- α and TNFR are assessed as the mTNF- α /TNFR ratio, an increased ratio correlated with higher specificity to development of organ failure. In this paper, we investigated for the first time the ratio of TNF- α to TNFR mRNA (T/R ratio) in various tissues. Our results revealed that tissue T/R ratio was significantly increased postburn. It is impressive that the magnitude of T/R ratio elevation was much higher than TNF- α (10-60 folds in T/R ratios *vs.* 8-10 folds in TNF- α). Combined with the persistently elevated levels found in tissues, this suggests that T/R ratio would better reflect the inflammatory status than TNF- α or TNFR alone. Moreover, it was noted that T/R ratio in liver tissue and serum AST level were significantly correlated, suggesting that this kind of cytokine regulation appears to be in sufficient in counteracting overwhelming sepsis, and the imbalance of TNF- α to TNFR might be involved in liver dysfunction. Hence, assessment of T/R ratio might provide a more sensitive indicator of organ damage or even outcome.

In this study, it was found that significant correlation between T/R ratio in liver tissues and serum AST levels. Similar results were also obtained between pulmonary TNF- α mRNA and MPO activities, whereas there were highly negative correlations between hepatic TNFR mRNA and serum AST levels, and between renal TNFR mRNA and serum Cr levels, suggesting imbalance of TNF- α to TNFR might be involved in the development of multiple organ damage following burns. Since TNF- α has been shown to be a pivotal cytokine of sepsis and MODS induced by endotoxin translocation post-trauma, we have evaluated the protective effect of anti-TNF- α monoclonal antibody (MoAb) for vital organs following intestinal ischemia-reperfusion or thermal injury. In rat intestinal ischemia-reperfusion model, prophylactic treatment with anti-TNF- α MoAb resulted in striking decreases in systemic TNF- α levels, and associated with such a neutralization effect were amelioration of hypotension and distant organ injury, including liver, kidneys, and lungs, as well as significant improvement in survival^[47-49]. Similarly, early treatment with anti-TNF- α MoAb could attenuate endotoxemia-mediated multiple organ damage resulting from severe burns, which might be associated with the down-regulation effects of tissue lipopolysaccharide binding protein (LBP) gene expression by use of MoAb^[50]. Moreover, a recent series of investigations have shown that recombinant sTNFR protected animals from death caused by endotoxin and gram-negative bacteria, and these promising experimental results prompted large scale randomized clinical trials^[51]. Additionally, TNFR-deficient mice were resistant to endotoxin shock and sepsis induced by cecal ligation and puncture^[42, 52]. Thus, appropriate use of agents to interrupt the chains of cytokine cascade might provide more balanced cytokine response, which may be beneficial to the host.

In summary, the present study demonstrated that burn injury *per se* could result in gut-derived endotoxin translocation that was mainly to the liver, spleen and lungs. The translocated endotoxin might be responsible at least in part, for the up-regulating of TNF- α and down-regulating of TNFR-I mRNA expression in these organs. The expression imbalance between TNF- α and TNFR might play a part in the development of multiple organ damage following burns.

REFERENCES

- 1 **Yao YM**, Redl H, Bahrami S, Schlag G. The inflammatory basis of trauma/shock associated multiple organ failure. *Inflamm Res* 1998; **47**: 201-210
- 2 **Swank GM**, Deitch EA. Role of the gut in multiple organ failure: bacterial translocation and permeability changes. *World J Surg* 1996; **20**: 411-417
- 3 **Fang WH**, Yao YM, Shi ZG, Yu Yan, Wu Ye, Lu LR, Sheng ZY. The effect of recombinant bactericidal/permeability-increasing protein on endotoxin translocation and lipopolysaccharide-binding protein/CD14 expression in rats following thermal injury. *Crit Care Med* 2001; **29**: 1452-1459
- 4 **Deitch EA**. Multiple organ failure: Pathophysiology and potential future therapy. *Ann Surg* 1992; **216**: 117-134
- 5 **Fang CW**, Yao YM, Shi ZG, Yu Yan, Wu Ye, Lu LR, Sheng ZY. The effect of endotoxin translocation on lipopolysaccharide-binding protein and lipopolysaccharide receptor CD14 gene expression after thermal injury and its potential mechanism(s). *J Trauma* 2002; **53**: 957-967
- 6 **Wu RQ**, Xu YX, Song XH, Chen LJ, Meng XJ. Relationship between cytokine mRNA expression and organ damage following cecal ligation and puncture. *World J Gastroenterol* 2002; **8**: 131-134
- 7 **Yu YY**, Si CW, Tian XL, He Q, Xue HP. Effect of cytokines on liver necrosis. *World J Gastroenterol* 1998; **4**: 311-313
- 8 **Remick DG**. Applied molecular biology of sepsis. *J Crit Care* 1995; **10**: 198-212
- 9 **Tracey KJ**, Cerami A. Tumor necrosis factor: An updated review of its biology. *Crit Care Med* 1993; **21**: S415-S422
- 10 **Yao YM**, Yu Y, Sheng ZY, Tian HM, Wang YP, Lu LR, Yu Y. Role of gut-derived endotoxaemia and bacterial translocation in rats after thermal injury: effects of selective decontamination of the digestive tract. *Burns* 1995; **21**: 580-585
- 11 **Chomczynski P**, Sacchi N. Single-step method of RNA isolation by acid guanidinium thiocyanate-chloroform extraction. *Anal Biochem* 1987; **162**: 156-159
- 12 **Estler HC**, Grewe M, Gaussling R, Pavlovic M, Decker K. Rat tumor necrosis factor- α : transcription in rat kupffer cells and *in vitro* posttranslational processing based on a PCR-derived cDNA. *Biol Chem Hoppe Seyle* 1992; **373**: 271-281
- 13 **Himmler A**, Maurer-Fogy I, Kronke M, Scheurich P, Pfizenmaier K, Lantz M, Olsson I, Hauptmann R, Stratowa C, Adolf GR. Molecular cloning and expression of human and rat tumor necrosis factor receptor chain (p60) and its soluble derivative, tumor necrosis factor-binding protein. *DNA Cell Biol* 1990; **9**: 705-715
- 14 **Nanji AA**, Zhao S, Sadrzadeh SM, Waxman DJ. Use of reverse transcription-polymerase chain reaction to evaluate *in vivo* cytokine gene expression in rats fed ethanol for long periods. *Hepatology* 1994; **19**: 1483-1487
- 15 **Bradford MM**. A rapid and sensitive method for the quantitation of microgram quantities of protein utilizing the principle of protein-dye binding. *Anal Biochem* 1976; **72**: 248-254
- 16 **Koike K**, Moore FA, Moore EE, Poggetti RS, Tuder RM, Banerjee A. Endotoxin after gut ischemia/reperfusion causes irreversible lung injury. *J Surg Res* 1992; **52**: 656-662
- 17 **Suzuki T**, Okuyama T. Estimation of diamine oxidase activity by o-dianisidine peroxidase coupling. *Seikagaku* 1967; **39**: 399-404
- 18 **Dellinger RP**. Tumor necrosis factor in septic shock and multiple system trauma. *Crit Care Med* 1997; **25**: 1771-1773
- 19 **Furse RK**, Kodys K, Zhu D, Miller Graziano CL. Increased monocyte TNF- α message stability contributes to trauma patients' increased TNF production. *J Leukoc Biol* 1997; **62**: 524-534

- 20 **Marie C**, Losser MR, Fitting C, Kermarrec N, Payen D, Cavaillon JM. Cytokines and soluble cytokine receptors in pleural effusions from septic and nonseptic patients. *Am J Respir Crit Care Med* 1997; **156**: 1515-1522
- 21 **Andrejko KM**, Deutschman CS. Acute-phase gene expression correlates with intrahepatic tumor necrosis factor-alpha abundance but not with plasma tumor necrosis factor concentrations during sepsis/systemic inflammatory syndrome in the rat. *Crit Care Med* 1996; **24**: 1947-1952
- 22 **Kox WJ**, Volk T, Kox SN, Volk HD. Immunomodulatory therapies in sepsis. *Intensive Care Med* 2000; **26**: S124-S128
- 23 **Schroder J**, Stuber F, Gallati H, Schade FU, Kremer B. Pattern of soluble TNF receptors I and II in sepsis. *Infection* 1995; **23**: 143-148
- 24 **Murphey ED**, Traber DL. Pretreatment with tumor necrosis factor-alpha attenuates arterial hypotension and mortality by endotoxin in pig. *Crit Care Med* 2000; **28**: 2015-2021
- 25 **Kasai T**, Inada K, Takakuwa T, Yamada Y, Inoue Y, Shimamura T, Taniguchi S, Sato S, Wakabayashi G, Endo S. Anti-inflammatory cytokine levels in patients with septic shock. *Res Commun Mol Pathol Pharmacol* 1997; **98**: 34-42
- 26 **Minei JP**, Williams JG, Hill SJ, McIntyre K, Bankey PE. Augmented tumor necrosis factor response to lipopolysaccharide after thermal injury is regulated posttranscriptionally. *Arch Surg* 1994; **129**: 1198-1203
- 27 **Li JY**, Lu Y, Hu S, Sun D, Yao YM. Preventive effect of glutamine on intestinal barrier dysfunction induced by severe trauma. *World J Gastroenterol* 2002; **8**: 168-171
- 28 **Sheng ZY**, Yao YM, Yu Y. The relationship between gut-derived endotoxemia and tumor necrosis factor, neopterin: experimental and clinical studies. *Chin Med J* 1997; **110**: 30-35
- 29 **Yao YM**, Sheng ZY, Yu Y, Tian HM, Wang YP, Lu LR, Xu SH. The potential etiologic role of tumor necrosis factor in mediating multiple organ dysfunction in rats following intestinal ischemia-reperfusion injury. *Resuscitation* 1995; **29**: 157-168
- 30 **Hadjiminas DJ**, McMasters KM, Peyton JC, Cheadle WG. Tissue tumor necrosis factor mRNA expression following cecal ligation and puncture or intraperitoneal injection of endotoxin. *J Surg Res* 1994; **56**: 549-555
- 31 **Salkowski CA**, Detore G, Franks A, Falk MC, Vogel SN. Pulmonary and hepatic gene expression following cecal ligation and puncture: monophosphoryl lipid A prophylaxis attenuates sepsis-induced cytokine and chemokine expression and neutrophil infiltration. *Infect Immun* 1998; **66**: 3569-3578
- 32 **Batey R**, Cao Q, Madsen G, Pang G, Russell A, Clancy R. Decreased tumor necrosis factor-alpha and interleukin-1 alpha production from intrahepatic mononuclear cells in chronic ethanol consumption and upregulation by endotoxin. *Alcohol Clin Exp Res* 1998; **22**: 150-156
- 33 **Gong JP**, Wu CX, Liu CA, Li SW, Shi YJ, Yang K, Li Y, Li XH. Intestinal damage mediated by Kupffer cells in rats with endotoxemia. *World J Gastroenterol* 2002; **8**: 923-927
- 34 **Wang JE**, Solberg R, Okkenhang C, Jorgensen PF, Krohn CD, Aasen AO. Cytokine modulation in experimental endotoxemia: characterization of an ex vivo whole blood model. *Eur Surg Res* 2000; **32**: 65-73
- 35 **Hirakata Y**, Kirikae T, Kirikae F, Yamaguchi T, Izumikawa K, Takemura H, Maesaki S, Tomono K, Yamada Y, Kamihira S, Nakano M, Kitamura S, Kohno S. Effect of *Pseudomonas aeruginosa* exotoxin A on endotoxin-induced tumor necrosis factor production in murine lung. *J Med Microbiol* 1999; **48**: 471-477
- 36 **Cong B**, Li SJ, Yao YX, Zhu GJ, Ling YL. Effect of cholecystokinin octapeptide on tumor necrosis factor alpha transcription and nuclear factor-kappaB activity induced by lipopolysaccharide in rat pulmonary interstitial macrophages. *World J Gastroenterol* 2002; **8**: 718-723
- 37 **Qin RY**, Zou SQ, Wu ZD, Qiu FZ. Experimental research on production and uptake sites of TNFalpha in rats with acute hemorrhagic necrotic pancreatitis. *World J Gastroenterol* 1998; **4**: 144-146
- 38 **Peschon JJ**, Torrance DS, Stocking KL, Glaccum MB, Otten C, Willis CR, Charrier K, Morrissey PJ, Ware CB, Mohler KM. TNF receptor-deficient mice reveal divergent roles for p55 and p75 in several models of inflammation. *J Immunol* 1998; **160**: 943-952
- 39 **Leist M**, Gantner F, Jilg S, Wendel A. Activation of the 55 kDa TNF receptor is necessary and sufficient for TNF-induced liver failure, hepatocyte apoptosis and nitrite release. *J Immunol* 1995; **154**: 1307-1316
- 40 **Yin M**, Wheeler MD, Kono H, Bradford BU, Gallucci RM, Luster MI, Thurman RG. Essential role of tumor necrosis factor alpha in alcohol-induced liver injury in mice. *Gastroenterology* 1999; **117**: 942-952
- 41 **Pryhuber GS**, O'Brien DP, Baggs R, Huyck H, Sanz I, Nahm MH. Ablation of tumor necrosis factor receptor type I (p55) alters oxygen-induced lung injury. *Am J Physiol Lung Cell Mol Physiol* 2000; **278**: L1082-L1090
- 42 **Acton RD**, Dahlberg PS, Uknis ME, Klaerner HG, Fink GS, Norman JG, Dunn DL. Differential sensitivity to *Escherichia coli* infection in mice lacking tumor necrosis factor p55 or interleukin-1 p80 receptors. *Arch Surg* 1996; **131**: 1216-1221
- 43 **van der Poll T**, Calvano SE, Kumar A, Braxton CC, Coyle SM, Barbosa K, Moldawer LL, Lowry SF. Endotoxin induces downregulation of tumor necrosis factor receptors and circulating monocytes and granulocytes in humans. *Blood* 1995; **86**: 2754-2759
- 44 **Calvano SE**, van der Poll T, Coyle SM, Moldawer LL, Lowry SF. Monocyte tumor necrosis factor receptor levels as a predictor of risk in human sepsis. *Arch Surg* 1996; **131**: 434-437
- 45 **Van Zee KJ**, Kohno T, Fischer E, Rock CS, Moldawer LL, Lowry SF. Tumor necrosis factor soluble receptors circulate during experimental and clinical inflammation and can protect against excessive tumor necrosis factor *in vitro* and *in vivo*. *Proc Natl Acad Sci USA* 1992; **89**: 4845-4849
- 46 **Pellegrini JD**, Puyana JC, Lapchak PH, Kodys K, Miller Graziano CL. A membrane TNF-alpha/TNFR ratio correlates to MODS score and mortality. *Shock* 1996; **6**: 389-396
- 47 **Yao YM**, Yu Y, Wu Y, Shi ZG, Sheng ZY. The role of the gut as a cytokine-generating organ in remote organ dysfunction after intestinal ischemia and reperfusion. *Chin Med J* 1998; **111**: 514-518
- 48 **Yao YM**, Bahrami S, Redl H, Schlag G. Monoclonal antibody to tumor necrosis factor-alpha attenuates hemodynamic dysfunction secondary to intestinal ischemia/reperfusion in rats. *Crit Care Med* 1996; **24**: 1547-1553
- 49 **Yao YM**, Bahrami S, Redl H, Fuerst S, Schlag G. IL-6 release after intestinal ischemia/reperfusion in rats is under partial control of TNF. *J Surg Res* 1997; **70**: 21-26
- 50 **Zhai H**, Yao Y, Lu L, Fang W, Yu Y, Shi Z, Zhou B, Tian H, Sheng Z. Effect of TNF-alpha monoclonal antibody on tissue lipopolysaccharide-binding protein mRNA expression in rats after thermal injury. *Zhonghua Waikae Zazhi* 1998; **36**: 633-635
- 51 **Baumgartner JD**, Calandre T. Treatment of sepsis: past and future avenues. *Drugs* 1999; **57**: 127-132
- 52 **Leon LR**, White AA, Kluger MJ. Role of IL-6 and TNF in thermoregulation and survival during sepsis in mice. *Am J Physiol* 1998; **275**: R269-277

Fos expression in tyrosine hydroxylase-containing neurons in rat brainstem after visceral noxious stimulation: an immunohistochemical study

Feng Han, Yu-Fei Zhang, Yun-Qing Li

Feng Han, Yu-Fei Zhang, Yun-Qing Li, Department of Anatomy and K.K. Leung Brain Research Centre, the Fourth Military Medical University, Xi'an 710032, Shaanxi Province, China

Supported by Grants-in-Aid from the National Natural Science Foundation of China (Nos. 39970239, 30070389, 3000052), the Foundation for University Key Teacher by the Ministry of Education of China and the National Program of Basic Research of China (G1999054004)

Correspondence to: Dr. Yun-Qing Li, Department of Anatomy and K. K. Leung Brain Research Centre, the Fourth Military Medical University, Xi'an 710032, Shaanxi Province, China. deptanat@fmmu.edu.cn

Fax: +86-29-3283229

Received: 2002-10-09 **Accepted:** 2002-11-04

Abstract

AIM: To prove that neurons in the different structures of the brainstem that express tyrosine hydroxylase (TH) are involved in the transmission and modulation of visceral or somatic nociceptive information in rat.

METHODS: Immunohistochemical double-staining method was used to co-localize TH and Fos expression in neurons of the rat brainstem in visceral or subcutaneous noxious stimulation models.

RESULTS: Neurons co-expressing TH/Fos were observed in lateral reticular nucleus (LRT), rostroventrolateral reticular nucleus (RVL), solitary tract nucleus (SOL), locus coeruleus (LC), A5, A7 neuronal groups and ventrolateral subdivision of the periaqueductal gray (vlPAG) in both models. But the proportion and number of the double-labeled neurons responding to the two noxious stimuli were significantly different in the LRT, RVL and LC nuclei. The proportion and number of the TH/Fos double-labeled neurons in the visceral pain model were smaller than that in the subcutaneous pain model. However, in the case of SOL, they were similar in the two models.

CONCLUSION: Differences of Fos expression in TH immunoreactive neurons in animals after visceral and somatic noxious stimulation indicate that the mechanisms of the transmission and modulation of visceral nociceptive information in the brainstem may be different from that of somatic nociceptive information.

Han F, Zhang YF, Li YQ. Fos expression in tyrosine hydroxylase-containing neurons in rat brainstem after visceral noxious stimulation: an immunohistochemical study. *World J Gastroenterol* 2003; 9(5): 1045-1050

<http://www.wjgnet.com/1007-9327/9/1045.htm>

INTRODUCTION

Tyrosine hydroxylase (TH) is a catecholamine (including

noradrenaline, adrenaline and dopamine) synthesis enzyme. In the brainstem, except that substantia nigra (SN) TH is mainly involved in the locomotive modulation, TH immunoreactive (TH-ir) neurons are mainly located in the lateral reticular nucleus (LRT), rostroventrolateral reticular nucleus (RVL), solitary tract nucleus (SOL), locus coeruleus (LC), A5, A7 neuronal groups and ventrolateral subdivision of the midbrain periaqueductal gray (vlPAG). All these regions, except for RVL and SOL, are regarded as the origins of the descending inhibitory system, which uses predominantly noradrenaline (NA) and 5-hydroxytryptamine (5-HT) as neurotransmitters^[1,2]. Morphological evidence has shown that these nuclei directly or indirectly project to the superficial laminae of the spinal and medullary dorsal horns and SOL, forming intrinsic circuits that modulate the visceral and peripheral nociceptive message transmission^[1]. Electrophysiological results proved that NTS, VLM, PBL, and vlPAG were involved in visceral message transmission and modulation and electrical stimulation of vlPAG depressed visceral message transmission^[3-6]. RVL is mainly associated with cardiovascular regulation^[7] and projects to spinal autonomic nuclei^[8], while SOL is mainly involved in the visceral nociceptive message transmission, convergence and cardiovascular reflection^[9,10].

c-fos proto-oncogene is expressed within the neurons following voltage-gated calcium entry into the cell^[11,12]. Fos protein, which is encoded by *c-fos*, has been regarded as a third messenger molecule which coupled the short term extracellular signals with the long term alteration in cell function after neurons were excited^[13,14]. Mapping studies have shown that noxious stimulation could induce Fos expression in the central neuronal system and visceral organs^[15-21]. Thus, Fos is usually used as a marker to indicate the activation of neurons^[22].

It is well known that the brainstem noradrenergic (NAergic) system plays an important role in the process of antinociception and that the mechanism of visceral noxious message modulation is different from those of somatic noxious message modulation^[23]. It is reasonable for us to propose that the location of Fos expression, under the effects of different noxious stimuli in the structures of brainstem, which express TH, could be diverse. In order to prove this hypothesis, we studied the expression pattern of Fos induced by visceral or subcutaneous noxious stimuli as well as the co-localization of Fos and TH protein expression using an immunohistochemical double-staining method.

MATERIALS AND METHODS

Materials

Experiments were carried out using 40 Sprague-Dawley male rats (weighing 200-250 g). The rats were kept in a dark facility for 24 hours before the experiment, and then randomly divided into two experimental groups and two control groups (for each group, $n=10$). All procedures described below were approved by the Committee for Animal Care and Usage for Research

and Education from the Fourth Military Medical University (Xi'an, P. R. China).

Methods

All rats were anesthetized by being placed into a transparent glass container with methoxyflurane gas. After anesthesia, 2 mL of 100 mL/L formalin or 2 mL distilled water was perfused into the oesophagus and stomach through a fine plastic tube, or 0.1 mL of 100 mL/L formalin or 0.1 mL distilled water was injected subcutaneously into the left forepaw in the rats of experimental or control groups respectively. Then the animals were put back into the cages and 2 hours later, all rats were anesthetized with sodium pentobarbital intraperitoneally (60 mg/kg) were intracardially perfused with 100 mL of saline followed by 500 mL of 4% paraformaldehyde in 0.1 mol/L phosphate buffer (PB, pH 7.4). The brainstems were immediately removed, placed into the same fresh fixative for 4 hours (4 °C), and saturated with a solution of 300 g/L sucrose in 0.1 mol/L PB (pH 7.4) overnight at 4 °C. Thirty- μ m thick serial frontal sections were cut on a cryostat and serially collected into 5 dishes separately. Then all sections were washed with 0.01 mol/L phosphate-buffered saline (PBS, pH 7.4).

The first section was initially incubated overnight at room temperature with rabbit antisera against Fos (1:1 000 dilution; Santa Cruz, USA) in 0.01 mol/L PBS containing 50 mL/L normal horse serum, 3 g/L Triton X-100, 0.05 g/L NaN₃ and 5 g/L carrageenan (PBS-NHS). Secondly, the sections were incubated with goat anti-rabbit IgG (1:100 dilution; Cappel, USA) in PBS-NHS for 3 hours, and followed by rabbit peroxidase anti-peroxidase (PAP) complex (1:200 dilution; Polysciences, USA) in PBS for 1 hour. Finally, Fos-immunoreactive (Fos-ir) neurons were visualized by incubated the sections with 0.05 mol/L Tris-HCl buffer (pH 7.6) containing 0.4 g/L diaminobenzidine tetrahydrochloride (DAB) (Dojin, Japan), 0.03 mL/L H₂O₂ and 0.4 g/L Ni(NH₄)₂SO₄ for 30-40 minutes.

The second section was incubated at room temperature with mouse antisera against TH (1:3 000 dilution; Chemicon, USA) overnight, followed by biotinylated horse anti-mouse IgG (1:100 dilution; Vector, USA) for 3 hours, and then with ABC (avidin-biotin peroxidase complex) Elite kit (1:50 dilution; Vector) for 1 hour. Finally, TH-immunoreactive (TH-ir) neurons were visualized by incubated the sections with 0.05 mol/L Tris-HCl buffer (pH 7.6) containing 0.4 g/L DAB, 0.03 mL/L H₂O₂ and 0.4 g/L Ni(NH₄)₂SO₄ for 30-40 minutes.

The third section was incubated overnight at room temperature with a mixture of rabbit anti-Fos and mouse anti-TH, followed by goat anti-rabbit IgG or biotinylated horse anti-mouse IgG for 3 hours, and then with rabbit PAP for 1 hour. The sections were firstly reacted with 0.05 mol/L Tris-HCl buffer (pH 7.6) containing 0.4 g/L DAB, 0.03 mL/L H₂O₂ and 0.4 g/L Ni(NH₄)₂SO₄ for 30-40 minutes to intensify DAB-based reaction to Fos-ir neurons. Then the reacted sections were washed three times in PBS for 30 minutes and incubated with ABC Elite kit for 1 hour, and finally reacted in the same reaction solution without Ni(NH₄)₂SO₄ for 30-40 minutes to detect TH-ir neurons and TH/Fos double-labeled neurons. The number of TH-ir neurons, Fos-ir neurons, and TH/Fos double-labeled neurons was counted from the sections from the third section of each rat. The distribution of the immunohistochemically stained neurons in two animals in each model was charted with the aid of a camera and one rat was used to represent each experimental group.

A mixture of normal rabbit serum and normal mouse serum was used to replace rabbit anti-Fos and mouse anti-TH antisera to incubate the fourth section. The subsequent staining procedures were the same as those used for the third section.

All the sections were washed and mounted onto gelatin-coated glass slides and examined with light microscope (BH-2; Olympus, Japan).

The fifth section was mounted onto gelatin-coated slides and processed for Nissl staining.

Statistical analysis

Values were expressed as $\bar{x}\pm s$. Statistical differences between means of TH/Fos double-labeled neurons were determined by Student's *t* test. The difference in proportion of TH/Fos double-labeled neurons to Fos-ir neurons was analyzed by Crosstab's test. A *P*<0.05 is considered to be significant.

RESULTS

On the first, second, and third sections from the experimental groups, three kinds of immunocytochemically positive neurons were identified in the nuclei of the brainstem: Fos-ir neurons, TH-ir neurons and TH/Fos double-labeled neurons. The cellular nuclei of the Fos-ir neurons were dark with oval or round shape, leaving their cytoplasm unstained. In contrast to Fos-ir neurons, TH-ir neurons showed brownish cytoplasm and dendrites with unstained nuclei. Scattered among those Fos- and TH-ir neurons, some neurons with dark nuclei and brownish cytoplasm exhibiting the co-localization of Fos and TH in the neurons were also observed.

On the first sections of experimental groups, Fos-ir neurons were mainly located in the caudal subnucleus of the spinal trigeminal nucleus (Sp5C), lateral reticular nucleus (LRT), rostroventrolateral reticular nucleus (RVL), nucleus solitary tract (SOL), nucleus raphe obscurus (ROb), nucleus raphe pallidus (RPa), paramedian raphe nucleus (PMN), lateral paragigantocellular nucleus (LPGi), alpha part of gigantocellular reticular nucleus (G_{ia}), nucleus raphe magnus (NRM), locus coeruleus (LC), parabrachial nuclear complex (PBNC), nucleus raphe pontis (RPn), dorsal raphe nucleus (DR), ventrolateral subregion of the midbrain periaqueductal gray (vlPAG), and median raphe nucleus (MnR) (Figure 1, 2). Fos-ir neurons in these nuclei of the subcutaneous noxious stimulation group was somewhat more than that in the visceral noxious stimulation group, but in the SOL, the number of the Fos-ir neurons in both visceral and subcutaneous noxious stimulations was similar between the experiment groups (Table 1). On the sections of the control groups, only a few Fos-ir neuronal cell bodies were observed in the superficial part of the Sp5C or SOL.

Table 1 The number and distribution of the immunopositive neurons in the brainstem

Nuclei	TH		Fos		TH/Fos	
	Visc	Sub	Visc	Sub	Visc	Sub
SOL	203±13	214±17	254±31	99±7	60±5	54±5
LRT and RVL	42±15	252±24	57±7	151±13 ^a	31±4	90±10 ^a
LC	328±26	330±25	42±6	103±12 ^a	26±3	72±9 ^a

Data are shown as ($\bar{x}\pm s$) ^a*P*<0.05 Sub vs Visc. Visc: visceral noxious stimulation; Sub: subcutaneous noxious stimulation; TH: TH-ir neurons; Fos: Fos-ir neurons; TH/Fos: TH/Fos double-labeled neurons.

On the second sections of both experimental and control groups, the distribution of TH-ir neuronal cell bodies were mainly in LRT, RVL, SOL, A4, A5, LC, A7, vlPAG and substantia nigra (SN) (Figures 1 and 2). There was no remarkable difference in the number and distribution of TH-ir neurons between the experimental and control groups.

Immunohistochemical staining of the third sections from experimental groups showed, except that TH-ir and Fos-ir neurons were the same as that seen on the first and second sections of the experimental groups, TH/Fos double-labeled

neurons were mainly distributed in the LRT, RVL, SOL, A5, LC, A7 and vlPAG in both visceral (Figures 1, 3a, 3a', 3c, 3c', 3e and 3e') and subcutaneous (Figures 2, 3b, 3b', 3d, 3d', 3f and 3f') pain models. In LRT, RVL, A5, A7, LC, and vlPAG, the proportion and number of TH/Fos double-labeled neurons in visceral pain model were less than those in subcutaneous pain model (Table 1). It is interesting to note that in the SOL,

TH/Fos double-labeled neurons in both visceral and subcutaneous pain models were similar (Table 1). TH/Fos double-labeled neurons, with medium to large (20-35 μm) fusiform, oval, multipolar shaped neuronal cellular bodies, were observed.

In the brainstem, there was no expression of Fos and/or TH in the neurons from the fourth dish of both the groups.

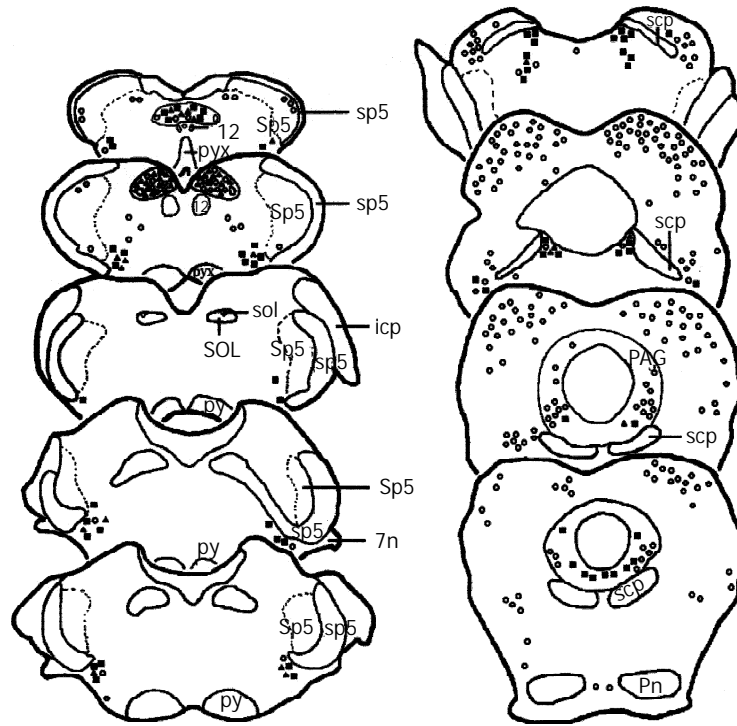


Figure 1 Drawing of the brainstem areas showing the distribution of TH, Fos and TH/Fos immunoreactive neurons after visceral noxious stimulation. Each ■ represents three TH-ir neurons. Each ○ represents five Fos-ir neurons. Each ▲ represents one TH/Fos double-labeled neuron. Abbreviations: 12: hypoglossal nuclei; 7n: facial nerve or its root; icp: inferior cerebellar peduncle; PAG: the midbrain periaqueductal gray; Pn: pontine nuclei; py: pyramidal tract; pyx: pyramidal decussation; scp: superior cerebellar peduncle; sol: solitary trace; SOL: solitary trace nuclei; sp5: spinal trigeminal tract; Sp5: spinal trigeminal nuclei.

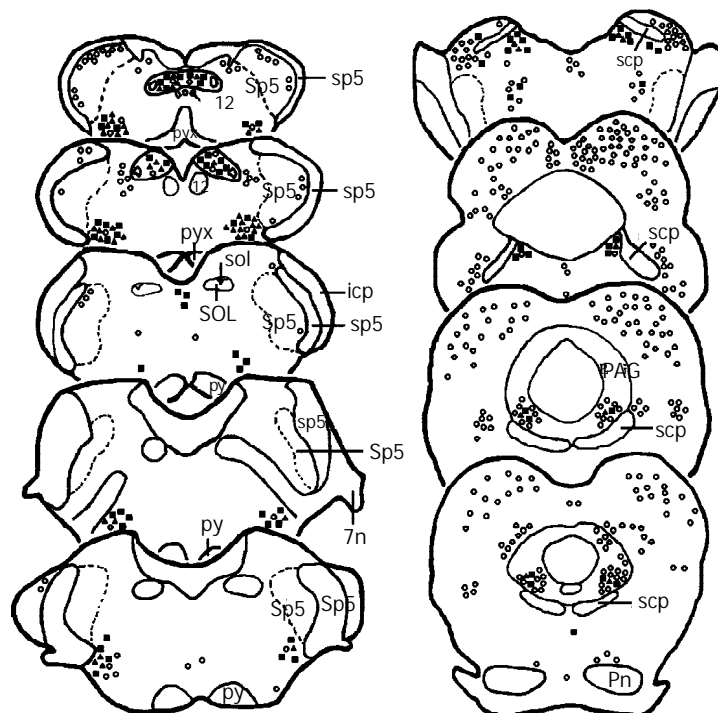


Figure 2 Drawing of the brainstem areas showing the distribution of TH (■), Fos (○) and TH/Fos (▲) immunoreactive neurons after subcutaneous noxious stimulation on the left forepaw. The ratios for each marker to present the number of TH, Fos and TH/Fos immunoreactive neurons and the abbreviations are the same as Figure 1.

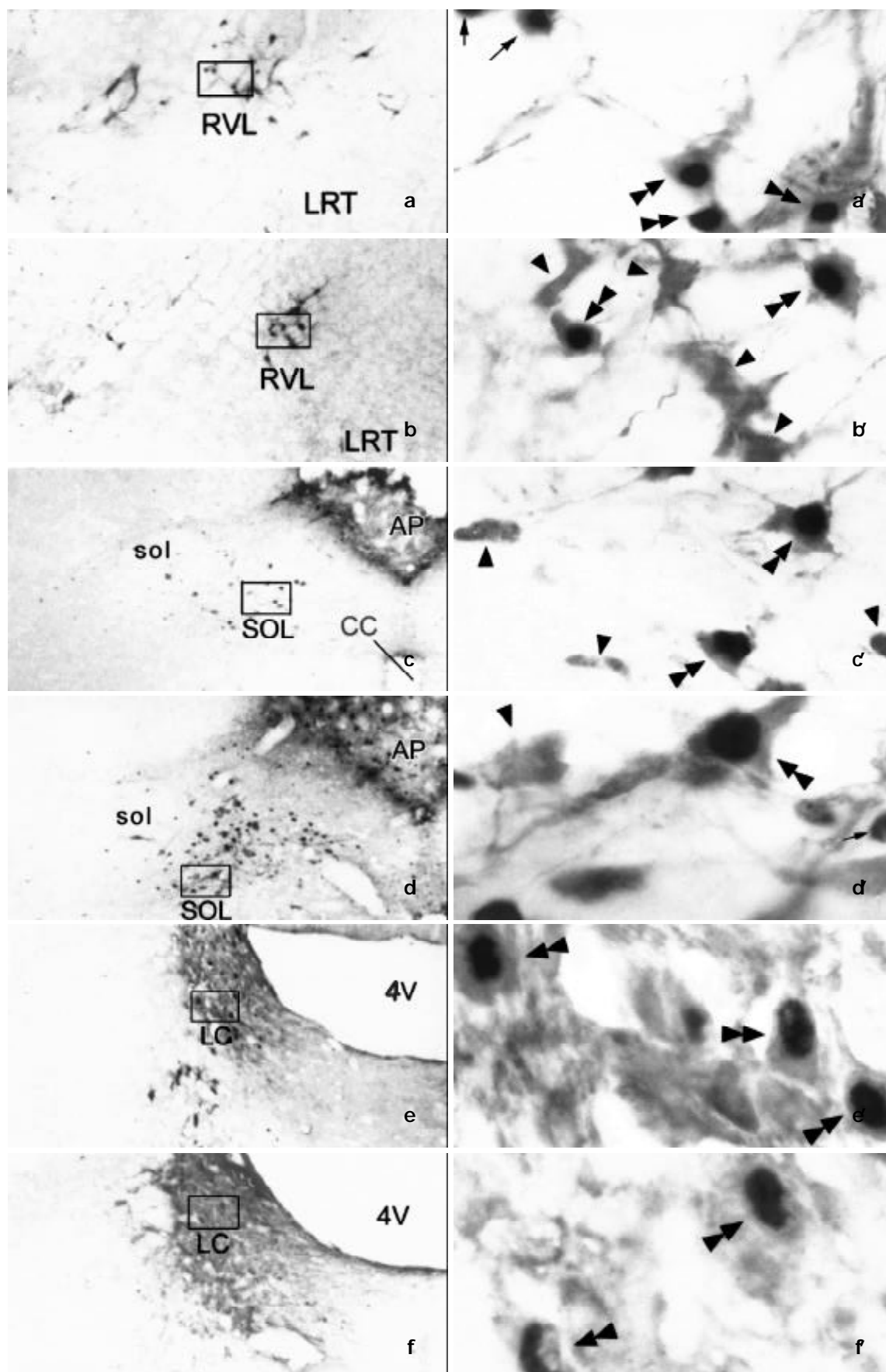


Figure 3 Photomicrographs showing the distribution and morphological characteristics of TH-ir neurons (arrowheads), Fos-ir neurons (arrows) and TH/Fos double-labeled neurons (double arrowheads) in SOL (a, a' and b, b'), RVL (c, c' and d, d') and LC (e, e' and f, f'). a, a', c, c' and e, e' were taken from visceral noxious stimulating rats, while b, b', d, d' and f, f' were taken from subcutaneous noxious stimulating rats, respectively. a, b, c, d, e and f are lower magnification photomicrograph (original magnification $\times 100$). a', b', c', d', e' and f' are higher magnification photomicrograph (original magnification $\times 1000$) of the rectangle in a, b, c, d, e and f, respectively. Abbreviations: 4V: the fourth ventricle. cc: central canal. LC: locus coeruleus. LRT: lateral reticular nucleus. RVL: rostroventrolateral reticular nucleus. sol: solitary tract. SOL: solitary tract nucleus.

DISCUSSION

TH is a critical enzyme for the synthesis of catecholamine. NA is thought to be one of the two neurotransmitters in descending inhibitory system, which can exert potent superspinal control of nociceptive information *via* various pathways^[24, 25]. In the brainstem, the descending inhibitory system is mainly composed of LRT, LC, vPAG, rostral ventral ventromedial medulla and its surrounding reticular nuclei and other brainstem raphe nuclei^[1]. NA can inhibit either excitatory transmitters (glutamate, substance P, *etc.*) released from primary afferent terminals or the EPSCs produced by primary afferent fibers *via* postsynaptic G-protein^[23, 26]. Intrathecal injection of naloxone could reverse the NA-produced antinociception at the spinal level^[27], indicating the involvement of endogenous opiate peptides in the antinociceptive effects of the NA. LRT and LC including NAergic neurons project to SOL and are thought to be involved in visceral nociceptive message modulation and antinociception, which is proved by the electrophysiological experiments^[28, 29]. These results suggest that NA is an important neurotransmitter for the control of the nociceptive transmission in the central nervous system. In RVL and SOL, the neurons containing TH receive nociceptive message and produce somatic-visceral or viscera-somatic reflection^[7, 10], which do not belong to the descending inhibitory system. There exist many diseases with pain in visceral organs, and therapeutic methods for visceral pain are similar to those for somatic pain^[30-34]. But it is not clear whether the neurons containing NA play different roles in different pain models. In order to clarify the functional roles of the NAergic neurons in the visceral and somatic pain models, we observed the expression pattern of both Fos and TH in which Fos protein was used as a marker to indicate TH-ir neurons activation using a immunohistochemical double-staining method.

In the present study, we observed TH/Fos double-labeled neurons in the LRT, RVL, SOL, A5, LC, A7 and vPAG and then compared the distribution, number and proportion of TH-ir neurons related to visceral and somatic noxious stimuli. Our results suggested that visceral and subcutaneous nociceptive inputs triggered similar TH immunoreactive in neurons in the brainstem, and indicated that these nuclei in the brainstem were involved in both visceral and subcutaneous nociceptive message convergence and modulation. Our results also indicated that the mechanisms involved could be different. As we know neither the factors resulting in *c-fos* expression nor the consequences of Fos protein expression, caution must be taken in interpreting these data. It might not be the case that all labeled neurons are nociceptive; on the other hand, the absence of Fos in these neurons does not exclude that these neurons are nociceptive since some nociceptive neurons might not be activated by the experimental conditions used. Nevertheless, this method allows us to monitor the response of a large number of neurons to noxious stimulation in awaken animals, which complements to the electrophysiological tests on anesthetized animals.

It is accepted that anesthesia is effective in triggering Fos expression in many brain regions, such as descending inhibitory system, RVL and SOL. More Fos-ir neurons were found in the experiment groups than those in the control groups. Based on these phenomena, we suggest that in addition to anesthetic effect, the noxious stimuli might be one of the inducing factors of Fos expression.

In LRT and RVL, there were fewer TH/Fos double-labeled neurons in visceral pain model than those in subcutaneous pain model. Both visceral and subcutaneous noxious stimuli can induce Fos expression in TH-ir neurons of LRT and RVL, indicating the occurrence of nociceptive neurons in this area. As this area is known to be crucial for vasomotor functions^[28, 35],

and connected with SOL^[36], NAergic neurons in this region are probably involved in eliciting the neurovegetative reaction induced by pain and producing somatic-visceral reflection.

Several evidences have suggested that the LC played a significant role in the descending inhibitory system^[1, 4]. TH/Fos double-labeled neurons were observed in the LC in both visceral and subcutaneous noxious stimuli models. This indicates the induction of NAergic neuronal activation in the LC in both models. The localization of these neurons is correspondent with the functional data implicating a role of LC in antinociception^[29]. Therefore, we suggest that NAergic neurons in the LC probably receive the visceral nociceptive convergence and probably mediate the behavioral and physiological characteristics of visceral pain as well. The difference in the proportion and number of TH/Fos double-labeled neurons in visceral and subcutaneous pain models shows that NAergic neurons in LRT, RVL and LC may be mainly involved in somatic nociceptive message transmission and modulation.

SOL, which receives most of the visceral primary terminations from the majority of organs in the neck, chest and abdomen, is closely related to visceral nociceptive message transmission and convergence and pain-induced sensory-cardiovascular reflection^[2, 4, 37]. Neurons in the SOL also projected to lateral parabrachial nucleus (LPB)^[36]. These results provide anatomical evidence for physiological data, confirms the involvement of this nucleus in nociceptive transmission. In addition, our data proved that TH/Fos double-labeled neurons were mainly located in the middle portion of SOL in both models, but TH/Fos double-labeled neurons in the subcutaneous nociceptive model were more rostral than those in the visceral nociceptive model. These results indicate that TH/Fos double-labeled neurons are distributed topographically in two pain models and the mechanism that the NAergic neurons in SOL are involved in transmission and modulation of nociceptive information in visceral pain models is different from that in subcutaneous pain models.

ACKNOWLEDGMENTS

The authors are grateful to Ms. Yue-Ping Yuan and Ms. Miao-Li Zhang for their photographic assistance.

REFERENCES

- 1 **Jones SL.** Descending noradrenergic influences on pain. *Prog Brain Res* 1991; **88**: 381-394
- 2 **Mason P.** Central mechanisms of pain modulation. *Curr Opin Neurobiol* 1999; **9**: 436-441
- 3 **Hudson PM, Semenenko FM, Lumb BM.** Inhibition effects evoked from the rostral ventrolateral medulla are selective for the nociceptive responses of spinal dorsal horn neurons. *Neuroscience* 2000; **99**: 541-547
- 4 **Benarroch EE.** Pain-autonomic interactions: a selective review. *Clin Auton Res* 2001; **11**: 331-333
- 5 **Krout KE, Jansen AS, Loewy AD.** Periaqueductal gray matter projection to the parabrachial nucleus in rat. *J Comp Neurol* 1998; **401**: 437-454
- 6 **Okada K, Murase K, Kawakita K.** Effects of electrical stimulation of thalamic nucleus submedius and periaqueductal gray on the visceral nociceptive responses of spinal dorsal horn neurons in the rat. *Brain Res* 1999; **834**: 112-121
- 7 **Dampney RA.** Functional organization of central pathways regulating the cardiovascular system. *Physiol Rev* 1994; **74**: 323-364
- 8 **Romagnano MA, Harshbarger RJ, Hamill RW.** Brainstem enkephalinergic projections to spinal autonomic nuclei. *J Neurosci* 1991; **11**: 3539-3555
- 9 **Boscan P, Paton JF.** Nociceptive afferents selectively modulate the cardiac component of the peripheral chemoreceptor reflex *via* actions within the solitary tract nucleus. *Neuroscience* 2002;

- 110:** 319-328
- 10 **Boscan P**, Paton JF. Role of the solitary tract nucleus in mediating nociceptive evoked cardiorespiratory responses. *Auton Neurosci* 2001; **86**: 170-182
- 11 **Morgan JI**, Curran T. Role of ion flux in the control of *c-fos* expression. *Nature* 1986; **322**: 552-555
- 12 **Premkumar DR**, Adhikary G, Overholt JL, Simonson MS, Cherniack NS, Prabhakar NR. Intracellular pathways linking hypoxia to activation of *c-fos* and AP-1. *Adv Exp Med Biol* 2000; **475**: 101-109
- 13 **Gurran T**, Morgan JT. Superinduction of Fos by nerve growth factor in the presence of peripherally active benzodiazepines. *Science* 1985; **229**: 1265-1268
- 14 **Saria A**, Fischer HS, Humpel C, Pfaffner A, Schatz DS, Schuligoi R. Margatoxin and iberiotoxin, two selective potassium channel inhibitors, induce *c-fos* like protein and mRNA in rat organotypic dorsal striatal slices. *Amino Acids* 2000; **19**: 23-31
- 15 **Yuan SL**, Huang RM, Wang XJ, Song Y, Huang GQ. Reversing effect of Tanshinone on malignant phenotypes of human hepatocarcinoma cell line. *World J Gastroenterol* 1998; **4**: 317-319
- 16 **He SW**, Shen KQ, He YJ, Xie B, Zhao YM. Regulatory effect and mechanism of gastrin and its antagonists on colorectal carcinoma. *World J Gastroenterol* 1999; **5**: 408-416
- 17 **Feng DY**, Zheng H, Tan Y, Cheng RX. Effect of phosphorylation of MAPK and Stat3 and expression of *c-fos* and *c-jun* proteins on hepatocarcinogenesis and their clinical significance. *World J Gastroenterol* 2001; **7**: 33-36
- 18 **Wang X**, Wang BR, Zhang XJ, Xu Z, Ding YQ, Ju G. Evidences for vagus nerve in maintenance of immune balance and transmission of immune information from gut to brain in STM-infected rats. *World J Gastroenterol* 2002; **8**: 540-545
- 19 **Omote K**, Kawamata T, Kawamata M, Namiki A. Formalin-induced nociception activates a monoaminergic descending inhibitory system. *Brain Res* 1998; **814**: 194-198
- 20 **Traub RJ**, Murphy A. Colonic inflammation induces *fos* expression in the thoracolumbar spinal cord increasing activity in the spinoparabrachial pathway. *Pain* 2002; **95**: 93-102
- 21 **Liu XJ**, Yang L, Mao YQ, Wang Q, Huang MH, Wang YP, Wu HB. Effects of the tyrosine protein kinase inhibitor genistein on the proliferation, activation of cultured rat hepatic stellate cells. *World J Gastroenterol* 2002; **8**: 739-745
- 22 **Harris JA**. Using *c-fos* as a neural marker of pain. *Brain Res Bull* 1998; **45**: 1-8
- 23 **Leao RM**, Von Gersdorff H. Noradrenaline increases high-frequency firing at the calyx of held synapse during development by inhibiting glutamate release. *J Neurophysiol* 2002; **87**: 2297-2306
- 24 **Al-Adawi S**, Dawe GS, Bonner A, Stephenson JD, Zarei M. Central noradrenergic blockade prevents autotomy in rat: implication for pharmacological prevention of postdenervation pain syndrome. *Brain Res Bull* 2002; **57**: 581-586
- 25 **Li P**, Zhuo M. Cholinergic, noradrenergic, and serotonergic inhibition of fast synaptic transmission in spinal lumbar dorsal horn of rat. *Brain Res Bull* 2001; **54**: 639-647
- 26 **Devilbiss DM**, Waterhouse BD. Norepinephrine exhibits two distinct profiles of action on sensory cortical neuron responses to excitatory synaptic stimuli. *Synapse* 2000; **37**: 273-282
- 27 **Ma J**, Qiao JT, Dafny N. Opiate-like substances mediate norepinephrine-induced but not serotonin-induced antinociception at spinal level: reevaluation by an electrophysiological model of formalin test in rats. *Life Sci* 2001; **69**: 969-976
- 28 **Potts JT**, Lee SM, Anguelov PI. Tracing of projection neurons from the cervical dorsal horn to the medulla with the anterograde tracer biotinylated dextran amine. *Auton Neurosci* 2002; **98**: 64-69
- 29 **Perez H**, Ruiz S, Laurido C, Hernandez A. Locus coeruleus-mediated inhibition of chemosensory responses in the rat nucleus tractus solitarius is mediated by alpha2-adrenoreceptors. *Neurosci Lett* 1998; **249**: 37-40
- 30 **Xia PY**, Zheng J, Zhou H, Pan WD, Qin XJ, Xiao GX. Relationship between lymphocyte apoptosis and endotoxin translocation after thermal injury in rats. *World J Gastroenterol* 2002; **8**: 546-550
- 31 **Meng AH**, Ling YL, Zhang XP, Zhang JL. Anti-inflammatory effect of cholecystokinin and its signal transduction mechanism in endotoxic shock rat. *World J Gastroenterol* 2002; **8**: 712-717
- 32 **Diao TJ**, Yuan TY, Li YL. Immunologic role of nitric oxide in acute rejection of golden hamster to rat liver xenotransplantation. *World J Gastroenterol* 2002; **8**: 746-751
- 33 **Rabe C**, Pilz T, Klostermann C, Berna M, Schild HH, Sauerbruch T, Caselmann WH. Clinical characteristics and outcome of a cohort of 101 patients with hepatocellular carcinoma. *World J Gastroenterol* 2001; **7**: 208-215
- 34 **He XS**, Su Q, Chen ZC, He XT, Long ZF, Ling H, Zhang LR. Expression, deletion and mutation of p16 gene in human gastric cancer. *World J Gastroenterol* 2001; **7**: 515-521
- 35 **Lima D**, Albino-Teixeira A, Tavares I. The caudal medullary ventrolateral reticular formation in nociceptive-cardiovascular integration. An experimental study in the rat. *Exp Physiol* 2002; **87**: 267-274
- 36 **Acuna-Goycolea C**, Fuentealba P, Torrealba F. Anatomical substrate for separate processing of ascending and descending visceral information in the nucleus of the solitary tract of the rat. *Brain Res* 2000; **883**: 229-232
- 37 **Kwon YB**, Kang MS, Han HJ, Beitz AJ, Lee JH. Visceral antinociception produced by bee venom stimulation of the Zhongwan acupuncture point in mice: role of alpha (2) adrenoreceptors. *Neurosci Lett* 2001; **308**: 133-137

Edited by Yuan HT and Zhang JZ

Effects of two methods of reconstruction of digestive tract after total gastrectomy on gastrointestinal motility in rats

Xin-Yu Qin, Yong Lei, Feng-Lin Liu

Xin-Yu Qin, Yong Lei, Feng-Lin Liu, Department of General Surgery, ZhongShan Hospital, Fudan University, Shanghai 200032, China

Supported by the National Natural Science Foundation of China, No. 30070738

Correspondence to: Professor Xin-Yu Qin, Department of General Surgery, ZhongShan Hospital, 180 Fenglin Road, Shanghai 200032, China. xyqin@zshospital.net

Telephone: +86-21-64037287 **Fax:** +86-21-64038472

Received: 2002-10-09 **Accepted:** 2002-11-04

Abstract

AIM: To compare the effects of Roux-en-Y and jejunum interposition reconstruction procedures after total gastrectomy on intestinal motility.

METHODS: Fifty male Sprague-Dawley rats were randomly divided into 5 groups: the control group (C), the laparotomy group (L), the jejunal transection group (JT) where the jejunum was transected 10 cm distal from the Treitz ligament and anastomosed, the Roux-en-Y group (RY) and the jejunal interposition group (JI) after total gastrectomy. To evaluate intestinal transit, the animals were given 0.1 ml Evans Blue solution through an orogastric tube. The rats were executed by CO₂ inhalation 30 minutes later and the intestinal transit was determined as the distance between the site of esophageojejunal anastomosis and the most distal site of small intestine colored with blue.

RESULTS: One month after operation, the body weight of rats among JI and RY were almost identical (274.6 ± 9.5 vs 270.4 ± 10.6 , $P > 0.05$), but were significantly lighter than those of JT and L group. Four months after the operation, the body weight in the JI group increased compared to the preoperative level (345.2 ± 15.7 g vs 299.5 ± 8.3 g, $P < 0.01$). However, the body weight of RY group decreased compared to preoperative (255.1 ± 11.3 g vs 295.0 ± 12.0 g, $P < 0.01$). The difference was more significant at six months postoperative. Small bowel transit time in RY was slower than that in JI group and C group ($P < 0.01$).

CONCLUSION: Changes of body weight and intestinal motility in JI group are less influenced than in RY group.

Qin XY, Lei Y, Liu FL. Effects of two methods of reconstruction of digestive tract after total gastrectomy on gastrointestinal motility in rats. *World J Gastroenterol* 2003; 9(5): 1051-1053 <http://www.wjgnet.com/1007-9327/9/1051.htm>

INTRODUCTION

Total gastrectomy is one of the popular operative procedures for gastric malignancy, but there still are debates on the recommended method of gastrointestinal reconstruction after total gastrectomy. The choice of suitable method is crucial to

the patients' quality of life. To a great extent, surgeons choose the reconstruction methods according to personal experiences. We compared the prognosis of the different reconstruction methods and explored their effects on gastrointestinal motility in rats.

MATERIALS AND METHODS

Animal and grouping

Fifty male Sprague-Dawley rats (weight 280-310 g) were randomly divided into 5 groups, each of which contained 10 subjects. Five groups included controlled group (C), laparotomy group (L), jejunal transection group (JT) receiving transection of jejunum at 10 cm distal to the Treitz ligament and anastomosis in situ in each rat, jejunal interposition group (JI) receiving jejunal interposition with the segment of 5 cm length after total gastrectomy, and esophageojejunal Roux-en-Y anastomosis group (RY). All rats in RY underwent anastomosis of esophagus and jejunum after total gastrectomy with the R-Y loop of 10 cm. Rats resumed to normal diet on day 3 post-surgery.

Methods

Body weight of each rat was measured before operation and 1, 4, 6 months after operation, respectively. After fasting for 12 hours (free access to water), rat underwent corresponding operation. After six months, weight and the time of intestinal transition were recorded. Each rat was given 0.1 ml Evans Blue solution (50 mg/ml, Sigma, St Louis, USA) through orogastric tube to stomach directly or esophageojejunal junction in the JI and RY groups.

Statistic analysis

Statistical analysis was performed with statistical software SPSS 10.0. The results were expressed as mean \pm SD and comparisons among groups were performed by Student's *t* Test, ANOVA test and *q* test. All tests were two sided. *P* values < 0.01 were considered significant.

RESULTS

Body weight

No significant difference in body weight of rats before operation was detected among L, JT, JI and RY group, though the weight of C group was significantly lower than other groups ($P < 0.01$) (Table 1); One month after operation ($F > F_{(0.01, 49)}$, $P < 0.01$), body weight in L and JT was significantly higher than that in JI and RY, while no significant differences between L and JT group, as well as between RY and JI ($P > 0.01$) were not observed; At fourth month postoperatively, weight in C, L and JT group were similar, while these of JI and RY were significantly lower than those in other groups. Furthermore, the weight of RY was much lower than that of JI ($P < 0.01$); At 6 months after operation, rats in group C, L and JT gained weight significantly ($P < 0.01$). Although the weight of rats in group JI was not as much as that of group C, L and JT ($P < 0.01$), it still increased significantly compared to preoperative weight

(385.0±21.2 g vs 299.5±8.3, $P<0.01$). Nevertheless, the rats in group RY lost weight compared to preoperative weight (247.7±13.4 g vs 295.0±12.0 g, $P<0.01$), and they were significantly lighter than those of other groups at 6 months after operation, including JI group ($P<0.01$).

Transit time of intestine

Transit time of intestine (TTI) was 24.8±10.3 cm/30 min in group RY, which was significantly longer than that of group C (54.7±6.7 cm/30 min) ($P<0.01$). No significant differences in TTI were found among group JI, JT, L and C (Table 2).

Table 1 Weight of rats pre-and postoperative (g)

	C	L	JT	JI	RY
Preoperative	249.5±10.4	297.5±11.1	294.7±11.9	299.5±8.3	295.0±12.0
Postoperative 1 month	287.4±12.3	320.4±9.3	322.3±10.6	274.6±9.5	270.4±10.6
Postoperative 4 month	368.3±13.5	381.7±15.5	384.0±19.3	345.2±15.7	255.1±11.3
Postoperative 6 month	430.0±30.9	453.0±32.2	457.0±29.8	385.0±21.3	247.7±13.4

Table 2 Postoperative TTI of rats

Group	Postoperative TTI
C	54.6±6.7
L	55.8±6.4
JT	58.2±7.1
JI	48.6±7.8
RY	24.8±10.3*

∗: $P<0.01$, RY vs TTI of other groups.

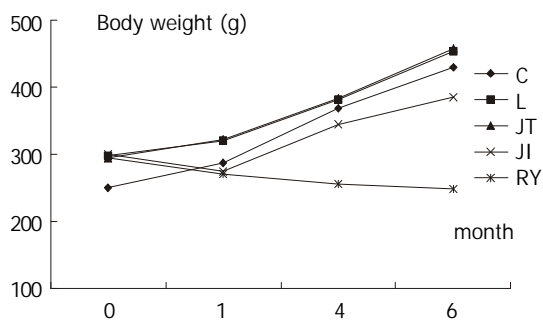


Figure 1 Body weight of rats before and after operation.

DISCUSSION

Since Karl Schlatter first successfully performed total gastrectomy in 1897, it has been mainly indicated for Zollinger-Ellison syndrome and for potentially curable gastric carcinoma^[1]. Formerly, it was quite common to apply esophagus-jejunum anastomosis after total gastrectomy. Although this procedure has merit of simple, the operative complication of reflux esophagitis restricts its application^[2]. To avoid the complication, many surgeons adopt Roux-en-Y anastomosis of esophagus and jejunum to reconstruct digestive tract. At first, the results were quite promising; later, many patients complained about fullness, abdominal pain, nausea, even food vomiting. Many studies indicated that the gastrointestinal motility of patients underwent Roux-en-Y anastomosis of esophagus and jejunum was obviously weakened. Such symptoms were nominated as "Roux stasis syndrome"^[3-5]. Nowadays, many researches advocate jejunal pouch with Roux-en-Y reconstruction as a modified method^[6].

Recently, some researchers advocate gastric substitution by interposition of jejunum. As the procedure is more accordant with physiology, it can eliminate the shortcomings of Roux-en-Y esophagojejunostomy induced by chyme bypass of duodenum^[7, 8]. Moreover, interposition of jejunum makes preparatory assimilation possible by mixing of chyme with bile and pancreatic fluid in duodenum. Also, such procedure has fewer disturbances on gastrointestinal motility. Our results indicated that the rats in group JI gained weight six months after operation and had similar gastrointestinal motility as control group, which means the nutrition and growth of rats were not impaired. But Miholic J measured the emptying of gastric substitute after total gastrectomy and compared the differences between jejunal interposition and Roux-y esophagojejunostomy and contended that the concept of a gastric substitute pouch was not supported^[9].

Our study illuminated that the rats lost weight in group RY and group JI at one month after total gastrectomy, but rats in group C, L and JT steadily gained weight during the same time. At four months after operation, the growth curves of group RY and group JI were markedly different. After initial fall in weight of 8% in the gastrectomized rats (274.6±9.5 vs 299.5±8.3), a sizable rise was observed in the rats of group JI. As for RY group, the rats constantly lost weight till 6 months after gastrectomy. Our results revealed that procedure of jejunal interposition may affect the nutrition status of rats and the effect may last less than four months, which was consistent with results of other researches^[10, 11]. But rats among RY group still lost weight at six months after operation, and it indicated the Roux-en-Y esophagojejunostomy might influence the nutrition status of rats for at least 6 months, much longer than jejunal interposition. So it seems that the jejunal interposition is superior to Roux-en-Y esophagojejunostomy after total gastrectomy.

Rats in RY group revealed delayed transit time of intestine at six months after the operation, just as Pellegrini reported^[12], which also supports that gastrointestinal motility was impaired after Roux-en-Y esophagojejunostomy. Meanwhile, rats in group C, L, JT and JI revealed similar intestinal transit time, which was significantly different from that in group RY. The result was consistent with the growth curve of body weight of rats (Figure 1). Thus slowed intestinal transit may be one main etiological factor in postgastrectomy malnutrition. But some studies did not find abnormal intestinal transit after total gastrectomy^[13], more conclusive research is required.

Although no significant differences in TTI in other 4 groups were observed at six months after operation, previous study has revealed that different operative procedure and anesthesia do affect the gastrointestinal motility^[14]. Although we did not measure the TTI soon after operation, our results showed that TTI could resume to preoperative level after several months for some surgical procedures. In addition to abdominal operation, prior study indicated that gastric emptying was markedly delayed after cardiac surgery^[15]. Some researchers advocate that motilin may be one of possible reason for such changes^[16], which is a widely distributed neuropeptide and has been located in digestive tract and brain^[17]. Specific receptor of motilin has been isolated and located on chromosome^[18], and is proved at mucosa^[19]. And new neuropeptide has been identified and proved to be related with gastrointestinal activity^[20].

In conclusion, the procedure of jejunal interposition has fewer disturbances on intestinal transit than Roux-en-Y, and the gastrointestinal motility and nutrition status of rats of group JI are much better than those of rats of group RY.

REFERENCES

- Schrock TR, Way LW. Total gastrectomy. *Am J Surg* 1978; **135**: 348-355

- 2 **Morrow D**, Passaro ER Jr. Alkaline reflux esophagitis after total gastrectomy. *Am J Surg* 1976; **132**: 287-291
- 3 **Gustavsson S**, Ilstrup DM, Morrison P, Kelly KA. Roux-Y stasis syndrome after gastrectomy. *Am J Surg* 1988; **155**: 490-494
- 4 **Schimmer BD**. Gastric atony and the Roux syndrome. *Gastroenterol Clin North Am* 1994; **23**: 327-343
- 5 **Eagon JC**, Medema BW, Kelly KA. Postgastrectomy syndrome. *Surg Clin North Am* 1992; **72**: 445-465
- 6 **Iivonen MK**, Mattila JJ, Nordback IH, Matikainen MJ. Long-term follow-up of patients with jejunal pouch reconstruction after total gastrectomy. A randomized prospective study. *Scand J Gastroenterol* 2000; **35**: 679-685
- 7 **Ambrecht U**, Lundell L, Stockbrugger RW. Nutrient malassimilation after total gastrectomy and possible intervention. *Digestion* 1987; **37**: 56-60
- 8 **Olbe L**, Lundell L. Intestinal function of total gastrectomy and possible consequences of gastric replacement. *World J Surg* 1987; **11**: 713-719
- 9 **Miholic J**, Meyer HJ, Kotzerke J, Balks J, Aebert H, Jahne J, Weimann A, Pichlmayr R. Emptying of the gastric substitute after total gastrectomy. Jejunal interposition versus Roux-y esophagojejunostomy. *Ann Surg* 1989; **210**: 165-172
- 10 **Morsiani E**, Tassinati E, Rescazzi R, Benea G. Rapid intestinal transit and postgastrectomy malnutrition. An experimental study in growing rats. *Ital J Surg Sci* 1985; **15**: 139-144
- 11 **Miholic J**, Meyer HJ, Muller MJ, Weimann A, Pichlmayr R. Nutritional consequences of total gastrectomy: the relationship between mode of reconstruction, postprandial symptoms, and body composition. *Surgery* 1990; **108**: 488-494
- 12 **Pellegrini CA**, Deveney CW, Patti MG, Lewin M, Way LW. Intestinal transit of food after total gastrectomy and Roux-Y esophagojejunostomy. *Am J Surg* 1986; **151**: 117-125
- 13 **Sategna-Guidetti C**, Bianco L. Malnutrition and malabsorption after total gastrectomy. A pathophysiologic approach. *J Clin Gastroenterol* 1989; **11**: 518-524
- 14 **Le Blanc-Louvry I**, Coquerel A, Koning E, Maillot C, Ducrotte P. Operative stress response is reduced after laparoscopic compared to open cholecystectomy: the relationship with postoperative pain and ileus. *Dig Dis Sci* 2000; **45**: 1703-1713
- 15 **Goldhill DR**, Whelpton R, Winyard JA, Wilkinson KA. Gastric emptying in patients the day after cardiac surgery. *Anaesthesia* 1995; **50**: 122-125
- 16 **Schwarz A**, Buchler M, Usinger K, Rieger H, Glasbrenner B, Friess H, Kunz R, Beger HG. Importance of the duodenal passage and pouch volume after total gastrectomy and reconstruction with the Ulm pouch: prospective randomized clinical study. *World J Surg* 1996; **20**: 60-66
- 17 **Huang YX**, Xu CF, Liao H, Wang QL. Genesis and distribution of motilin in human fetus. *China Natl J New Gastroenterol* 1995; **1**: 37-40
- 18 **McKee KK**, Tan CP, Palyha OC, Liu J, Feighner SD, Hreniuk DL, Smith RG, Howard AD, Van der Ploeg LH. Cloning and characterization of two human G protein-coupled receptor genes (GPR38 and GPR39) related to the growth hormone secretagogue and neurotensin receptors. *Genomics* 1997; **46**: 426-434
- 19 **Alcalde AI**, Plaza MA, Marco R. Study of the binding of motilin to the membranes of enterocytes from rabbit jejunum. *Peptides* 1996; **17**: 1237-1241
- 20 **Wang H**, Zhang YQ, Ding YQ, Zhang JS. Localization of neurokinin B receptor in mouse gastrointestinal tract. *World J Gastroenterol* 2002; **8**: 172-175

Edited by Ren SY

Expression of a novel immunoglobulin gene SNC73 in human cancer and non-cancerous tissues

Jian-Bin Hu, Shu Zheng, Yong-Chuan Deng

Jian-Bin Hu, Department of Radiation Oncology, Sir Run Run Shaw Hospital, Zhejiang University Medical College, Hangzhou 310016, Zhejiang Province, China

Shu Zheng, Cancer Institute, Zhejiang University, Hangzhou 310009, Zhejiang Province, China

Yong-Chuan Deng, Department of Surgical Oncology, The Second Affiliated Hospital of Zhejiang University Medical College, Hangzhou 310009, Zhejiang Province, China

Supported by the National Nature Scientific Foundation of China, No. 30070832

Correspondence to: Shu Zheng, Cancer Institute, Zhejiang University, Hangzhou 310009, Zhejiang Province, China. zhengshu@mail.hz.zj.cn

Telephone: +86-571-87783868 **Fax:** +86-571-87214404

Received: 2002-06-11 **Accepted:** 2002-07-12

Abstract

AIM: To investigate the expression of immunoglobulin gene SNC73 in malignant tumors and non-cancerous normal tissues.

METHODS: Expression level of SNC73 in tumors and non-cancerous tissues from the same patient was determined by reverse transcription polymerase chain reaction and enzyme-linked immunosorbent assay (RT-PCR-ELISA) in 90 cases of malignant tumors, including colorectal cancer, gastric cancer, breast cancer, lung cancer and liver cancer. Analysis on the correlation of SNC73 expression with sex, age, site, grade of differentiation, depth of invasion, and metastases in colorectal cancer patients was made.

RESULTS: Expression level of SNC73 in non-cancerous colorectal mucosa and colorectal cancerous tissues was 1.234 ± 0.842 and 0.737 ± 0.731 , respectively ($P < 0.01$), with the mean ratio of 7.134 ± 14.092 (range, 0.36-59.54). Expression of SNC73 showed no significant difference among gastric cancer, breast cancer, lung cancer and liver cancer when compared with non-cancerous tissues ($P > 0.05$). No correlation was found between SNC73 expression level and various clinicopathological factors, including sex, age, site, grade of differentiation, depth of invasion and metastases of CRC patients.

CONCLUSION: Down-regulation of SNC73 expression may be a relatively specific phenomenon in colorectal cancer. SNC73 is a potential genetic marker for the carcinogenesis of colorectal cancer. The relationship of SNC73 expression and carcinogenesis of colorectal cancer merits further study.

Hu JB, Zheng S, Deng YC. Expression of a novel immunoglobulin gene SNC73 in human cancer and non-cancerous tissues. *World J Gastroenterol* 2003; 9(5): 1054-1057

<http://www.wjgnet.com/1007-9327/9/1054.htm>

INTRODUCTION

Colorectal cancer (CRC) is the second leading cause of cancer-related deaths in developed western countries^[1]. A series of

molecular changes are involved in colorectal carcinogenesis, including activation of oncogenes, inactivation and/or mutational changes of tumor suppressor genes, microsatellite instability, and so on^[2-10]. Fearon *et al* proposed a genetic model of colorectal tumorigenesis^[11]. However, despite the tremendous efforts that have been made, there are still many problems unsolved for the model of CRC due to the complexity of carcinogenesis. The early detection and new therapeutic target of CRC have yet to be found. Modern medicine proves that almost all diseases arise from gene function change, which is mainly reflected by the differential gene expression^[12]. Hopefully the identification and characterization of genes expressed differently in tumor tissues and normal mucosa will shed light on the mechanisms of CRC and provide useful molecular markers for screening, diagnosis, prognosis and therapeutic monitoring.

To explore new molecular events that are related to carcinogenesis of CRC, Cancer Institute of Zhejiang University constructed CRC negative-associated cDNA libraries by subtractive hybridization^[13-17]. Subtractive hybridization between cDNA of normal mucosal tissues and mRNA of CRC tissues was performed and a total of 46 cDNA clones that were expressed in normal mucosal tissues but were either expressed at a significantly reduced level or not expressed at all in cancerous tissues were isolated. SNC73 is one of the 46 CRC negative-associated complement DNA (cDNA) clones. Northern blot, reverse transcription-polymerase chain reaction (RT-PCR), in situ hybridization, and in situ PCR confirmed expression of SNC73 in normal epithelial cells and several non-hematopoietic cancer cell strains^[17]. The aim of this study was to confirm the negative association between CRC and SNC73 expression and to examine whether such association also exists in other tumors. In the present study, expression level of SNC73 in 90 cases of malignant tumors (31 cases colorectal cancer, 24 cases gastric cancer, 15 cases breast cancer, 11 cases lung cancer and 9 cases liver cancer) and non-cancerous tissues from the same patient was determined by RT-PCR-ELISA.

MATERIALS AND METHODS

Tissue sample preparation

Fresh samples of surgically resected cancer and its non-cancerous tissues were obtained from the same patient at the Second Affiliated Hospital of Zhejiang University Medical College, and were immediately frozen in liquid nitrogen until used. Several paired specimens were collected for replication. The total RNA was extracted with Trizol reagent (Gibco BRL, USA). RNA integrity was checked on 1 % formaldehyde agarose gel. RNA samples were accepted only when the ratio between absorbance optical density values at 260 nm and at 280 nm was higher than 1.65.

RT-PCR (DIG Labeling)

RNA samples were reverse transcribed with AMV reverse transcriptase (Promega Co.). The primers were labeled with biotin for following immobilization by streptavidin coated microtiter plate modules. The primer for SNC73 was designed

based on its cDNA sequence according to previous study. The sequence is 5' biotin-AAA CAC ATT CCG GCC CGA G 3' and 5' biotin-AGC GGT CGA TGG TCT TCT G 3'. The sequence of primer for β -actin is 5' biotin-TCG ACA ACG GCT CCG GCA 3' and 5' biotin-CGT ACA TGG CTG GGG TGT 3'. RT-PCR was carried out to amplify the mRNA of SNC73 and β -actin. The PCR products were labeled with digoxigenin (dig) by using mixture of dATP, dCTP, dGTP, dTTP and DIG-dUTP in reaction mixture during the amplification process. PCR reaction mixture contained 15.7 μ l sterile water, 2.5 μ l PCR buffer (10 \times conc., with MgCl₂), 2.5 μ l 2 mM PCR DIG labeling mix, 2 μ l 10 mM primers mixture, 0.3 μ l Taq DNA polymerase and 2 μ l template cDNA. The cycling program was denaturation of the template 94 °C for 3 min, 22 cycles of amplification: 94 °C for 10 s (denaturation), 58 °C for 20 s (hybridization), 72 °C for 30 s (elongation) and elongation (72 °C) for 5 min was added after last cycle to ensure the completion of the reaction. PCR products quality was confirmed by electrophoresis in 1 % agarose gel stained with ethidium bromide.

PCR ELISA (DIG Detection)

DIG detection of PCR ELISA was carried out using a modification of the assay protocol according to reagent kit (Boehringer Mannheim Co., German). DIG labelled PCR products were immobilized by incubating appropriate dilutions of amplification reaction at 55 °C for 3 h. The solution was discarded and each well was washed 5 times with washing solution. The strips were incubated with anti-digoxigenin peroxidase conjugate at 37 °C for 30 min. The solution was discarded and each well was washed 5 times again with washing solution. The colorimetric substrate ABTS was added and

incubated at 37 °C for 30 min. Absorbance was read in an ELISA-reader at 405 nm. The absorbance optical density values at 405 nm (A_{405}) represented the relative concentrations of PCR products. The results were normalized by the absorbance optical density values of β -actin, which was used as an endogenous standard because of its equal expression in various tissues. This would correct the variation in product abundance due to differences in the efficiencies of individual RT-PCR reaction.

Statistical analysis

The expression level of SNC73 in both cancerous tissues and non-cancerous tissues was interpreted as the ratio of its OD value relative to that of β -actin. SNC73 expression level in various cancerous tissues and non-cancerous tissues and the ratio of non-cancerous tissues to cancerous tissues were calculated. All results were expressed as means \pm SD. Statistical differences between means of various cancerous tissues and non-cancerous tissues were determined by Wilcoxon nonparametric test (2-related samples). The differences were considered significant at $P < 0.05$.

To get more information about the down-regulation of SNC73, which may be helpful to determine its characteristics, we investigated the relationship between SNC73 expression level and various clinicopathological factors of CRC patients. All CRC patients were grouped according to sex, age, site, grade of differentiation, depth of invasion and metastases (including lymph node metastases and distant metastases). The same functions as those used between various cancerous tissues and non-cancerous tissues were applied among different groups. Statistical differences of means among different groups were determined by analysis of variance. The differences were considered significant at $P < 0.05$.

Table 1 SNC73 expression level in human cancerous tissues and non-cancerous tissues (Mean \pm SD). The expression level of SNC73 in both cancerous tissues and non-cancerous tissues was expressed as the ratio of its OD value relative to that of β -actin. ($\bar{x} \pm s$)

Tumor	n	SNC73 expression level		Non-cancerous tissues / Cancerous tissues
		Non-cancerous tissues	Cancerous tissues	
CRC	31	1.234 \pm 0.842	0.737 \pm 0.731 ^a	7.134 \pm 14.092
Gastric cancer	24	1.098 \pm 0.413	1.069 \pm 0.606	1.438 \pm 1.392
Breast cancer	15	1.279 \pm 1.705	0.900 \pm 0.690	1.836 \pm 2.541
Lung cancer	11	0.834 \pm 0.533	1.428 \pm 1.904	0.877 \pm 0.469
Liver cancer	9	0.793 \pm 0.285	0.799 \pm 0.322	1.140 \pm 0.467

^a $P < 0.01$ vs non-cancerous tissues.

Table 2 The relationship between SNC73 expression level and various clinicopathological factors of CRC patients. The expression level of SNC73 was interpreted as the ratio of its OD value relative to that of β -actin. ($\bar{x} \pm s$)

Factor	Group	n	SNC73 expression level		Non-cancerous tissues / Cancerous tissues
			Non-cancerous tissues	Cancerous tissues	
Sex	Male	15	1.360 \pm 1.011	0.748 \pm 0.438	8.822 \pm 18.358
	Female	16	1.116 \pm 0.657	0.726 \pm 0.943	5.551 \pm 8.782
Age	<60	14	1.524 \pm 0.979	0.737 \pm 0.458	9.444 \pm 18.843
	\geq 60	17	0.995 \pm 0.644	0.736 \pm 0.911	5.231 \pm 8.681
Site	Rectal	17	1.209 \pm 0.715	0.616 \pm 0.497	10.890 \pm 18.260
	Colon	14	1.264 \pm 1.002	0.883 \pm 0.942	2.572 \pm 2.652
Grade of differentiation	Well	14	1.284 \pm 1.034	0.756 \pm 0.430	2.378 \pm 2.488
	Moderately	12	1.188 \pm 0.746	0.776 \pm 1.086	14.030 \pm 21.033
	Poorly	5	1.203 \pm 0.536	0.587 \pm 0.358	3.898 \pm 4.226
Depth of invasion	Mucosa or muscle	8	1.258 \pm 0.847	0.973 \pm 1.233	9.066 \pm 20.511
	Serosa or beyond	23	1.226 \pm 0.859	0.654 \pm 0.467	6.462 \pm 11.624
Metastases	Positive	22	1.225 \pm 0.914	0.638 \pm 0.479	6.672 \pm 11.854
	Negative	9	1.257 \pm 0.682	0.977 \pm 1.144	8.263 \pm 19.334

RESULTS

Expression of SNC73 was significantly down-regulated in CRC compared with non-cancerous colorectal mucosa from the same patient. Expression level of SNC73 in normal colorectal mucosa and colorectal cancerous tissues was 1.234 ± 0.842 and 0.737 ± 0.731 , respectively ($P < 0.01$), with the mean ratio between them of 7.134 ± 14.092 (range, 0.36-59.54). Among 31 cases of CRC, cancerous tissues of 24 cases (77.4 %) expressed lower level SNC73 as compared with non-cancerous colorectal mucosa from the same patient. Study on the expression of SNC73 in other kinds of carcinomas revealed that no differential expression of SNC73 was found in gastric cancer, breast cancer, lung cancer and liver cancer as compared with non-cancerous tissues from the same patient ($P > 0.05$, Table 1).

Further analysis on the relationship between SNC73 expression level and various clinicopathological factors of CRC patients revealed that no correlation was found between SNC73 expression level and various clinicopathological factors, including sex, age, site, grade of differentiation, depth of invasion and metastases of CRC patients ($P > 0.05$, Table 2).

DISCUSSION

RT-PCR-ELISA allows convenient and sensitive detection of PCR products. The sensitivity of the PCR ELISA is in general about one hundredfold higher than conventional analysis of the PCR products in ethidium bromide stained agarose gels^[18-20]. The high sensitivity makes detection of low or unknown expression level of genes closer to the real status. The whole process of RT-PCR-ELISA takes no more than ten hours, and a group of samples can be detected at the same time. These are the reasons why this method was used to get a relative estimates about expression levels of SNC73 in different human carcinomas in this study.

SNC73 is one of the 46 cDNA clones of CRC negative-associated cDNA libraries constructed by Cancer Institute of Zhejiang University by subtractive hybridization technique. Sequence analysis revealed that full-length cDNA of SNC73 is 1651bp. Open reading frame analysis showed SNC73 encodes one immunoglobulin (Ig) heavy chain molecule with 384 amino acids, with its constant region identical to that of IgA1. The predicted structure of SNC73 had no apparent difference from other matured IgA molecules that serve in the immune system. Northern Blot, RT-PCR, in situ hybridization and in situ PCR confirmed expression of SNC73 in normal epithelial cells of colorectal mucosa and several non-hematopoietic cancer cell strains^[17]. There are several reports about Ig and Ig-like genes expressed in non-hematopoietic cell lines^[21-30], and Ig gene rearrangement was confirmed in the epithelial malignant cells^[24]. These findings raise the possibility that immunoglobulin genes, whose expression is generally considered to be restricted to lymphocytes-origin cells, can be expressed by non-lymphoid cells. Maybe some factors during de-differentiation of cells activated the rearrangement of Ig genes in malignant cells, but it remains to be explored how Ig genes undergo rearrangement in epithelial cells.

Expression level of SNC73 in CRC and non-cancerous mucosa had been determined by the method of RT-PCR-imaging, Northern-blot and in situ hybridization. The present study confirmed the initial findings that CRC expresses lower level SNC73 than non-cancerous mucosa^[17,30]. Expression level of SNC73 in other human cancerous tissues and non-cancerous tissues was also determined. No significantly different expression was found in gastric cancer, lung cancer, breast cancer and liver cancer compared with non-cancerous tissues from the same patient. This is the first semi-quantitative analysis about SNC73 expression in different human cancers. In this study the number of cases of breast cancer, lung cancer

and liver cancer was small, and more cases are needed to draw a conclusion. Interestingly, beyond our expectation, gastric cancer, which also originates from gastrointestinal tract, expressed no significantly different level of SNC73 compared with normal gastric mucosa. Conclusion drawn from the results of this study suggests that down-regulation of SNC73 expression may be a relatively specific phenomenon in CRC, and SNC73 may serve as a potential genetic marker for carcinogenesis of CRC. Further study on expression of SNC73 in tissues of different pathological status, such as adenoma, dysplastic mucosa and para-cancerous tissues, may provide clearer conclusion^[31].

The relation between SNC73 and carcinogenesis of CRC remains to be explored. Carcinogenesis of tumor is closely related to immunological surveillance of host. Previous study proved the significance of immune responses to mucosal carcinogens in carcinogenesis^[32]. Recently, Ig molecules or Ig-like proteins have been reported to influence the development of tumor directly or through interaction with oncogenes or tumor suppressor genes^[24,33,34]. So the relationship between Ig and carcinogenesis of tumor should be further explored besides the conventional hormonal immunity. These clues implicate some role of SNC73 in carcinogenesis of CRC. SNC73 encoded protein can be assumed to be an immune molecule secreted by normal epithelial cells, together with Ig secreted by plasma cells, participating in local anti-tumor activity. The protein affects carcinogenesis of CRC through the similar influence on adhesion or signal transduction to other Ig superfamily components or interaction with some oncogenes or tumor suppressor genes is also possible. Further study on the mechanisms of down-regulation of SNC73 in CRC and the biological function of SNC73 will provide important clues for determining its role in screening, diagnosis, prognosis and therapy of CRC. The relationship of SNC73 expression and carcinogenesis of colorectal cancer merits further study.

REFERENCES

- 1 **Schulmann K**, Reiser M, Schmiegel W. Colonic cancer and polyps. *Best Pract Res Clin Gastroenterol* 2002; **16**: 91-114
- 2 **Gan YB**, Zheng S, Cai XH. Detection of a gene mutation in familial adenomatous polyposis families by PCR-RFLP method. *Zhonghua Yixue Zazhi* 1994; **74**: 352-354, 390-391
- 3 **Cao J**, Teng L, Cai X. Inhibition effect of p53 antisense RNA on malignant phenotype of colorectal cancer cells. *Zhonghua Zhongliu Zazhi* 1997; **19**: 123-126
- 4 **Kruse R**, Rutten A, Lamberti C, Hosseiny-Malayeri HR, Wang Y, Ruelfs C, Jungck M, Mathiak M, Ruzicka T, Hartschuh W, Bisceglia M, Friedl W, Propping P. Muir-Torre phenotype has a frequency of DNA mismatch-repair-gene mutations similar to that in hereditary nonpolyposis colorectal cancer families defined by the Amsterdam criteria. *Am J Hum Genet* 1998; **63**: 63-70
- 5 **Yuan Y**, Zheng S. Mutations of hMLH1 and hMSH2 genes in suspected hereditary nonpolyposis colorectal cancer. *Zhonghua Yixue Zazhi* 1999; **79**: 346-348
- 6 **Xiong B**, Zheng S, Cai X. Study of microsatellite instability of colotectal cancer and its clinical significance. *Zhonghua Zhongliu Zazhi* 1999; **21**: 199-201
- 7 **Yuan Y**, Huang J, Zheng S. Mutation of human mismatch repair genes in hereditary nonpolyposis colorectal cancer (HNPCC) families. *Zhonghua Zhongliu Zazhi* 1999; **21**: 105-107
- 8 **Ozawa A**, Konishi F, Fukayama M, Kanazawa K. Apoptosis and its regulation in flat-type early colorectal carcinoma: comparison with that in polypoid-type early colorectal carcinoma. *Dis Colon Rectum* 2000; **43**: S23-28
- 9 **Borchers R**, Heinzlmann M, Zahn R, Witter K, Martin K, Loeschke K, Folwaczny C. K-ras mutations in sera of patients with colorectal neoplasias and long-standing inflammatory bowel disease. *Scand J Gastroenterol* 2002; **37**: 715-718
- 10 **Grady WM**, Markowitz SD. Genetic and epigenetic alterations in colon cancer. *Annu Rev Genomics Hum Genet* 2002; epub ahead of print

- 11 **Fearon ER**, Volgelstein B. A genetic model for colorectal tumorigenesis. *Cell* 1990; **61**: 759-767
- 12 **Chester KA**, Robson L, Begent RH, Pringle H, Primrose L, Talbot IC, Macpherson AJ, Owen SL, Boxer G, Malcolm AD. In situ and slot hybridization analysis of RNA in colorectal tumors and normal colon shows distinct distributions of mitochondrial sequences. *J Pathol* 1990; **162**: 309-315
- 13 **Cao J**, Cai XH, Zheng L, Geng LY, Shi ZZ, Pao CC, Zheng S. Characterization of colorectal-cancer-related cDNA clones obtained by subtractive hybridization screening. *J Cancer Res Clin Oncol* 1997; **123**: 447-451
- 14 **Zheng S**, Cai X, Cao J, Geng L, Zhang Y, Gu J, Shi Z. Screening and identification of down-regulated genes in colorectal carcinoma by subtractive hybridization: a method to identify putative tumor suppressor genes. *Chin Med J* 1997; **110**: 543-547
- 15 **Zheng S**, Cai X, Cao J. Application of subtractive hybridization in screening for colorectal cancer negatively related genes. *Zhonghua Yixue Zazhi* 1997; **77**: 256-259
- 16 **Cao J**, Zheng S, Zheng L, Cai X, Zhang Y, Geng L, Fang Y. A novel serine protease SNC19 associated with human colorectal cancer. *Chin Med J (Engl)* 2001; **114**: 726-730
- 17 **Zheng S**, Cao J, Geng LY, Peng JP, Fang YM, Dong Q, Zhang SZ. Structure and expression of colorectal related immunoglobulin novel gene SNC73. *Zhonghua Yixue Zazhi* 2001; **81**: 485-488
- 18 **Whitby JE**, Heaton PR, Whitby HE, O' Sullivan E, Johnstone P. Rapid detection of rabies and rabies-related viruses by RT-PCR and enzyme-linked immunosorbent assay. *J Virol Methods* 1997; **69**: 63-72
- 19 **Shamloul AM**, Hadidi A. Sensitive detection of potato spindle tuber and temperate fruit tree viroids by reverse transcription-polymerase chain reaction-probe capture hybridization. *J Virol Methods* 1999; **80**: 145-155
- 20 **Hall LL**, Bicknell GR, Primrose L, Pringle JH, Shaw JA, Furness PN. Reproducibility in the quantification of mRNA levels by RT-PCR-ELISA and RT competitive-PCR-ELISA. *Biotechniques* 1998; **24**: 652-658
- 21 **Cao Y**, Sun Y, Poirier S, Winterstein D, Hegamyer G, Seed J, Malin S, Colburn NH. Isolation and partial characterization of a transformation-associated sequence from human nasopharyngeal carcinoma. *Mol Carcinog* 1991; **4**: 297-307
- 22 **Borova TS**, Chuev YuV. An immunoglobulin-like antigen in human cell lines and sera of cancer patients. *Neoplasma* 1992; **39**: 101-105
- 23 **Hu WX**, Cao Y, Li XY, Lee LM, Yao KT. Comparison of homology of Tx gene with Ig kappa gene and its expression in different cell lines. *Shengwu Huaxue Yu Shengwu Wuli Xuebao* 1995; **27**: 215-221
- 24 **Qiu XY**, Yang GZ. Structural analysis of Ig gene existed in the epithelial malignant cells. *Zhongguo Zhongliu Shengwu Zhiliao Zazhi* 1997; **4**: 157-158
- 25 **Deng X**, Cao Y, Hu W, Gu H, Yao K. No point mutation of the 2.8 kb EcORI fragment of the nasopharyngeal carcinoma transforming gene TX in nasopharyngeal carcinoma. *Hunan Yike Daxue Xuebao* 1997; **22**: 102-104
- 26 **Kimoto Y**. Expression of heavy-chain constant region of immunoglobulin and T-cell receptor gene transcripts in human non-hematopoietic tumor cell lines. *Genes Chromosomes Cancer* 1998; **22**: 83-86
- 27 **Luo MJ**, Lai MD. Identification of differentially expressed genes in normal mucosa, adenoma and adenocarcinoma of colon by SSH. *World J Gastroenterol* 2001; **7**: 726-731
- 28 **Li M**, Tang M, Deng X. Positive immunoglobulin A expression in human epithelial carcinoma cell lines. *Zhonghua Zhongliu Zazhi* 2001; **23**: 451-453
- 29 **Li M**, Ren W, Weng XX, Liao W, Xia LQ, Deng X, Cao Y. Nucleotide sequence analysis of a transforming gene isolated from nasopharyngeal carcinoma cell line CNE2: an aberrant human immunoglobulin kappa light chain which lacks variable region. *DNA Seq* 2001; **12**: 331-335
- 30 **Ye F**, Zheng S, Fang SC, Peng JP, Dong Q, Geng LY, Cao J. Expression of novel immunoglobulin gene SNC73 in colorectal cancer by In Situ Hybridization. *Ai Zheng* 2001; **20**: 460-463
- 31 **Jubb AM**, Bell SM, Quirke P. Methylation and colorectal cancer. *J Pathol* 2001; **195**: 111-134
- 32 **Keren DF**, Silbart LK, Lincoln PM, Annesely TM. Significance of immune responses to mucosal carcinogens: a hypothesis and a workable model system. *Pathol Immunopathol Res* 1986; **5**: 265-277
- 33 **Nussenzweig MC**, Schmidt EV, Shaw AC, Sinn E, Campos - Torres J, Mathey-Prevot B, Pattengale PK, Leder P. A human immunoglobulin gene reduces the incidence of lymphomas in c-myc-bearing transgenic mice. *Nature* 1988; **66**: 446-450
- 34 **Brummer J**, Neumaier M, Gopfert C, Wagener C. Association of pp60-src with biliaryglycoprotein (CD66a), an adhesion molecule of the carcinoembryonic antigen family downregulated in colorectal carcinomas. *Oncogene* 1995; **11**: 1649-1655

Edited by Bo XN

Developmental patterns of GHr and SS mRNA expression in porcine gastric tissue

Dong Xia, Ru-Qian Zhao, Xi-Hui Wei, Qing-Fu Xu, Jie Chen

Dong Xia, Ru-Qian Zhao, Qing-Fu Xu, Xi-Hui Wei, Jie Chen, Key Laboratory of Animal Physiology and Biochemistry, Ministry of Agriculture, Nanjing Agricultural University, Nanjing 210095, Jiangsu Province, China

Supported by National Natural Science Foundation of China, No. 39830290

Correspondence to: Professor Ru-Qian Zhao, Key Laboratory of Animal Physiology and Biochemistry, Ministry of Agriculture, Nanjing Agricultural University, Nanjing 210095, Jiangsu Province, China. lapb@njau.edu.cn

Telephone: +86-25-4395047

Received: 2002-11-26 **Accepted:** 2002-12-20

Abstract

AIM: The present study was aimed to investigate the developmental patterns of growth hormone receptor (GHr) and somatostatin (SS) mRNA expression in porcine gastric tissue and its relationship with gastric growth and gastric functional development.

METHODS: Erhualian and Large White boars were selected randomly and sampled at birth (D0), 3, 20, 30, 90, 120 and 180 days of age respectively, meanwhile the bodyweight and gastric weight were recorded. The single tube semi-quantitative RT-PCR was applied in this experiment to investigate the developmental patterns of gastric GHr and SS mRNA expression, the correlations between the patterns of mRNA expression and the relative gastric weight (ratio of gastric weight to bodyweight) and the pepsin contents in gastric mucous membrane were analyzed. In order to further elucidate the effect of GH on gastric function, the primary cultures of gastric fundic mucosal cells were treated with 2 ng/ml, 20 ng/ml and 200 ng/ml of rpGH for 18 hrs respectively, and the pepsin contents in culture medium were measured.

RESULTS: The expression of GHr mRNA was high at birth, followed by a significant decrease at 3 days of age (D3) in both breeds. In Large White boars, the expression of GHr mRNA reached a peak at D90 and remained a plateau afterward. In Erhualian pigs, however, a slight yet significant increase occurred at D30 reaching a level that was kept constant thereafter. From birth to D30, the expression of GHr mRNA in gastric tissue was higher in Erhualian boars than that in Large White boars, but from D90 to D180, the higher expression of GHr mRNA was found in Large White boars. The gastric GHr mRNA expression was significantly correlated with the relative gastric weight ($r=0.541$, $P<0.05$) and pepsin content in gastric mucosa ($r=0.625$, $P<0.05$) respectively.

The gastric SS mRNA expression was high at birth (Erhualian 1.59, Large White 0.80), but dropped significantly at D3 (Erhualian 0.95, Large White 0.19, $P<0.05$), a stepwise increase was followed thereafter until a peak at D30 (Erhualian 1.71, Large White 0.95). In general, Erhualian pigs expressed higher levels of SS mRNA in gastric tissue as compared with Large White pigs at the same age ($P<0.05$). No significant correlations between SS mRNA and relative gastric weight or pepsin content were found.

In vitro, 2 ng/ml of rpGH elicited significant increase in pepsin secretion from primary cultures of gastric mucosal cells ($P<0.05$), and no responses were observed at 20 ng/ml and 200 ng/ml.

CONCLUSION: The results suggested that: 1, GHr and SS mRNA in porcine stomach are expressed according to strain specific developmental patterns; 2, GH acts directly at the gastric tissue and regulates the structural and functional growth of stomach.

Xia D, Zhao RQ, Wei XH, Xu QF, Chen J. Developmental patterns of GHr and SS mRNA expression in porcine gastric tissue. *World J Gastroenterol* 2003; 9(5): 1058-1062

<http://www.wjgnet.com/1007-9327/9/1058.htm>

INTRODUCTION

The growth hormone (GH) regulates numerous cellular functions by direct binding to its receptors (growth hormone receptor, GHr) in many different tissues, such as liver, muscle, lymph and adipose tissue, etc. It has been reported that GHr was expressed in the stomach of rat^[1,2], rabbit^[3] and human^[4], respectively, suggesting that stomach is the target organ of GH.

Somatostatin (SS) is a typical brain-gut-peptide, and it is expressed both in the brain and gastrointestinal system. Hypothalamic SS serves as an inhibitory factor to regulate GH secretion from anterior pituitary^[5], while gastric SS works to inhibit the secretion of pepsin, gastric acid, as well as gastrin, hence plays an important role in the regulation of gastric function^[6].

The retardation of gastric functional development, such as insufficient gastric acid and pepsin secretion, results in dyspepsia, diarrhea, poor growth and even death in newborn piglets. It is postulated that GH and gastric SS might be involved in the regulation of porcine stomach development, but no much data available to date. Therefore, the present study employed two breeds of pig with different genetic backgrounds, Large White and Erhualian pigs, as animal model to investigate the developmental patterns of growth hormone receptor (GHr) and somatostatin (SS) mRNA expression in porcine gastric tissue. The correlation between the patterns of GHr and SS mRNA expression and the gastric growth as well as the gastric functional development were analyzed. In addition, an *in vitro* cell culture trial was conducted to study the effect of GH on gastric pepsin secretion.

MATERIALS AND METHODS

Animals and Sampling

Eight litters newborn purebred piglets respectively from 2nd or 3rd farrowing Large White and Erhualian sows were kept for experiment, and water and feed were available ad libitum. The diet was formulated according to the requirement of each breed. Large White piglets weaned at D30 of age, while Erhualian piglets at D45. Erhualian boars ($n=4$) and Large White boars ($n=4$) were selected randomly and sacrificed at birth, 3, 20, 30, 90, 120 and 180 days of age respectively, meanwhile the bodyweight and gastric weight were recorded.

The fundic tissue were sampled and frozen in liquid nitrogen immediately, then stored at -70°C . The fundic mucosa were taken and stored at -20°C .

Pepsin detection

One gram fundic mucosa was homogenized with 3 ml 0.85 % NaCl, then the homogenate was centrifuged at 4°C for 30 min at 5 000 rpm. The supernatant was collected for pepsin activity analysis according to the procedure modified by Robinson (1972), using hemoglobin as the substrate. Since hemoglobin was diluted with hydrochloric acid ($\text{pH}=1.6$), at such acidic condition, all pepsinogen were activated, so the gastric pepsin activity measured accounted for the total pepsin content of gastric mucosa. The protein content in the same supernatant of the homogenate was measured for normalizing the pepsin content as follows:

$$\text{Gastric mucosa pepsin activity (U/g)} = \frac{\text{Pepsin (U)/homogenate liquid (ml)}}{\text{Protein (g)/homogenate liquid (ml)}}$$

Semi-quantitative RT-PCR

Total RNA was isolated from porcine gastric tissue using guanidinium thiocyanate-phenol-chloroform one-step method. RNA was reverse transcribed into cDNA with random hexamer primers. An RT control tube containing all RT reagents except reverse transcriptase was included to monitor genomic DNA contamination.

The primers for GHR were designed according to the cDNA sequence published on Gene Bank (X54429): sense, 5' -ctcgatattgatgacctga-3', and anti-sense, 5' -gatgagtgtagtcagttcca-3', and the predicted PCR product was 341bp. SS primers were achieved according to the code region of porcine genomic DNA (Gene Bank, U36385): sense, 5' -AGCTGCTGTCTGAACCCAAC-3', and anti-sense, 5' -GAAATTCTTGCAGCCAGCTT-3'. Classic 18S rRNA internal standards (Ambion Inc. USA) was used to adjust the variation in pipetting and amplification.

PCR conditions were optimized for both GHR and SS. The reaction volume for GHR was 50 μl , including 5 μl 10 \times PCR buffer, 1.3 mmol/L MgCl_2 , 10 mmol/L dNTP, 0.66 mmol/L GHR sense and anti-sense primer, 2 μl 18S primer pair, 2 μl 18S competitor, 2 μl RT product, 1.0 U Tag DNA polymerase (Promega, Shanghai). Amplification conditions included: denaturation at 94°C for 5 min, denaturation at 94°C for 30 sec, annealing at 52°C for 1 min, extension at 72°C for 1 min, total in 32 cycles, finally an additional extension step at 72°C for 5 min was done. The SS PCR reaction mix contained 5 μl 10 \times PCR buffer, 1.5 mmol/L MgCl_2 , 10 mmol/L dNTP, 1 mmol/L SS sense and anti-sense primer, 2 μl 18S primer pair, 2 μl 18S competitor, 2 μl RT product, and 1.0 U Tag DNA polymerase (Promega, Shanghai). Total volume was 50 μl . Amplification conditions included: denaturation at 94°C for 5 min; denaturation at 94°C for 30 sec, annealing at 55°C for 30 sec, extension at 72°C for 1 min, total in 32 cycles, finally it was finished by an extension step at 72°C for 5 min. All samples were amplified in the same PCR run together with quality and contamination controls on GeneAmp PCR system 9600 (Perkin Elmer, U.S.A.).

Twenty μl PCR products were separated through 2 % agarose gel electrophoresis. The band intensities were analyzed by Kodak ID Electrophoresis Documentation and Analysis System 120 (Kodak Photo Film Co., Ltd., U.S.). The ratio of target gene intensity to 18S intensity was used to represent the abundance of GHR and SS mRNA expression.

Cell culture

Animal and reagent Four Landrace X Large White crossbred gilts at the age of D35 were used in this trial. HEPES and DMEM/F-12 were products of Hyclone, collagenase type I

was bought from Sigma and the fetal bovine serum was purchased from Hangzhou Sijiqing Company, China.

Sample and culture Piglets were sacrificed and the fundic mucosa was isolated. The tissue was washed in Hank's solution thoroughly and dipped in Hank's solution containing 500 U/ml of antibiotics for 30 min. Then the fundic mucosa were dispersed by 600 U/ml of collagenase I at 37°C for 2 hrs, filtrated and centrifuged (1 000 r/min, 5 min). Thereafter cells at the density of 1×10^5 per cm^2 were cultured (37°C , 5 % CO_2) in DEME/F-12 supplemented with 10 % fetal bovine serum, 5 mM HEPES buffer, and 100 U/ml antibiotics. After 24 hrs, the culture medium was refreshed by new medium containing 2 ng/ml, 20 ng/ml and 200 ng/ml GH respectively. The GH challenge lasted for 18 hrs before the medium were collected for pepsin analysis.

Statistical analysis

All data were analyzed by SPSS10. Significant difference analysis were conducted by *t*-test, one-way ANOVA and LSD. The correlation between the GHR, SS mRNA expression and the relative gastric weight, as well as the gastric mucosa pepsin content were determined.

RESULTS

Gastric growth

As shown in Figure 2, the gastric growth rate is low before weaning both in Large White and Erhualian pigs, especially during the period from D3 to D20. Highest growth rate is seen between D30 and D90. From D90 onwards, the gastric weight of Large White Boars keeps increase while that of Erhualian boars maintains a plateau, which results in a higher gastric growth rate in Large White boars than that of Erhualian boars. Compared to the body weight changes shown in Figure 1, the stomach weight changes display different patterns, which is more obvious in Erhualian pigs. Figure 3 shows the developmental pattern of relative gastric weight, it seems that the gastric growth lags behind the body growth during the period from D20 to D30.

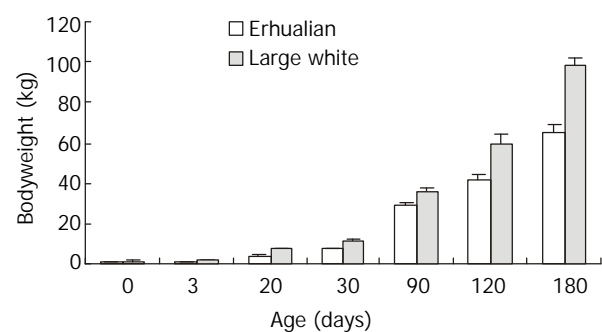


Figure 1 The developmental patterns of body weight in Erhualian and Large White boars.

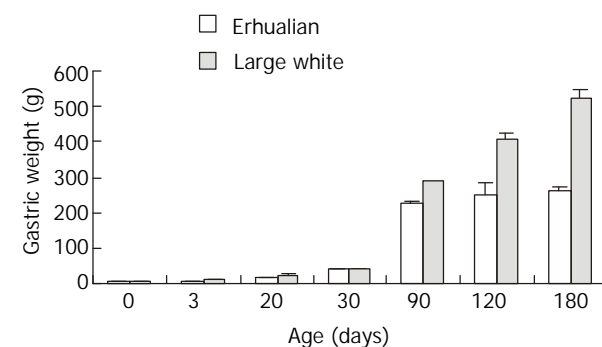


Figure 2 The developmental patterns of gastric weight in Erhualian and Large White boars.

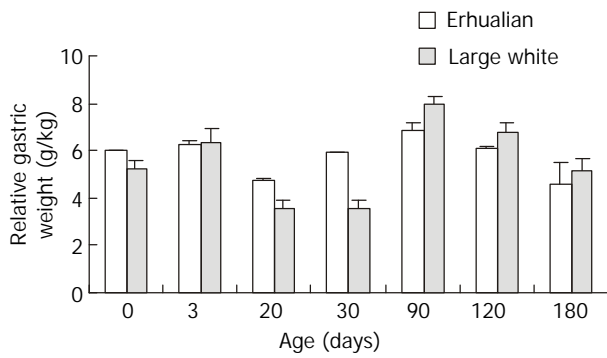


Figure 3 The developmental patterns of the relative gastric weight in Erhualian and Large White boars.

Developmental changes of pepsin contents in gastric mucosa

From birth to D30, no notable variation was found in gastric pepsin content in Large White boars, but after D30, the gastric pepsin content increased significantly ($P<0.05$) and kept constant thereafter (Figure 4). However in Erhualian pigs, the gastric pepsin content was high at birth, but dropped significantly at D3 and D20 ($P<0.05$). A significant up-regulation occurred at D30 for gastric pepsin content until a peak level was reached at D120.

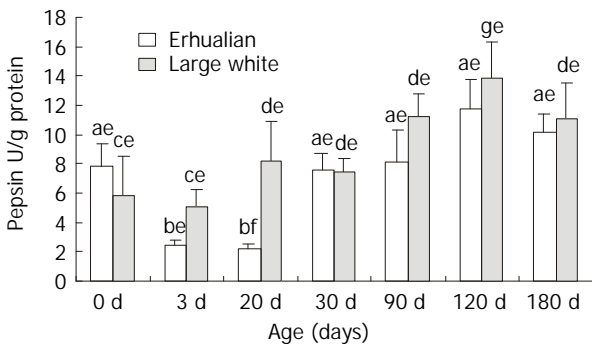


Figure 4 The developmental patterns of the pepsin activity (U/g protein) of fundic mucosa in Letters a and b for Erhualian boars, letters c and d and g for Large White boars, letter e and f for the different breeds at same ages, different letters differ significantly $P<0.05$.

Developmental changes of gastric GHr mRNA expression

Figure 6 shows the the expression patterns of GHr mRNA in gastric tissue. The GHr mRNA was high at birth, but dropped dramatically at D3 in both breeds. In both breeds of pigs, the expression of GHr mRNA increased from D30 but followed different patterns thereafter. In Large White pigs, the GHr mRNA expression continue increased till D90 when a plateau was reached. While in Erhualian pigs, the gastric GHr mRNA expression went up in a much lesser extent and reached a much lower plateau earlier at D30. As the result, the expression of GHr mRNA in gastric tissue was higher in Erhualian boars than that in Large White boars in earlier stages from birth to D30, whereas the opposite was true in later stages from D90 to D180. The statistic analysis revealed that the gastric GHr mRNA expression was positively correlated with the relative gastric weight ($r=0.541$, $P<0.05$) and the pepsin content in gastric mucosa ($r=0.625$, $P<0.05$), respectively.

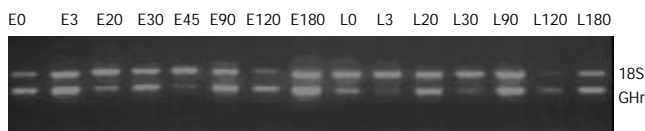


Figure 5 Representative agarose gel electrophoreses photo of

RT-PCR product for gastric GHr mRNA in Erhualian and Large White boars. (M is marker pUC19, E0-E180 represents Erhualian boars at day 0-180 respectively, and L0-L180 represents Large White boars at day 0-180 respectively).

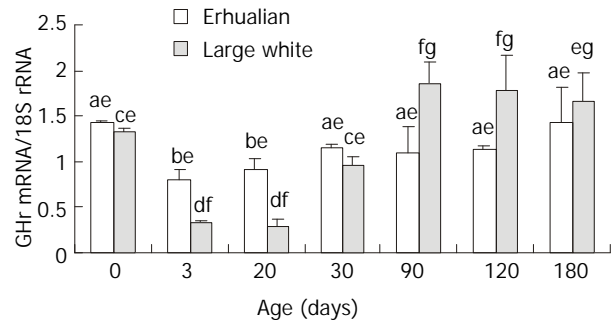


Figure 6 The developmental pattern of GHr mRNA expression in stomach of Erhualian and Large Letters a and b for Erhualian boars, letters c and d and g for Large White boars, letter e and f for the different breeds at same ages, different letters differ significantly $P<0.05$.

The developmental changes of porcine gastric SS mRNA expression

The gastric SS mRNA expression followed a similar pattern in two breeds of pigs (Figure 8). The SS mRNA expression was high at birth, but significantly decreased at D3 ($P<0.05$), soon after a stepwise increase was found reaching a peak at D30 in both breeds of pigs. In general, Erhualian pigs expressed higher levels of SS mRNA in gastric tissue as compared with Large White pigs at the same age in early stages ($P<0.05$) but this difference diminished in later stages at D120 and D180. No clear correlation was found between gastric SS mRNA expression and relative gastric weight or pepsin content in gastric mucosa.

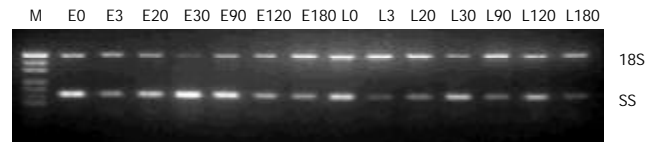


Figure 7 Representative agarose gel electrophoreses photo of RT-PCR product for gastric SS mRNA in Erhualian and Large White boars. (M is marker pUC19, E0-E180 represents Erhualian boars at day 0-180 respectively, and L0-L180 represents Large White boars at day 0-180 respectively).

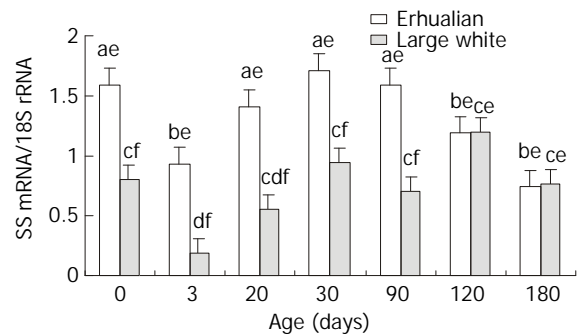


Figure 8 The developmental pattern of SS mRNA expression in stomach of Erhualian and Large Letters a and b for Erhualian boars, letters c and d for Large White boars, letter e and f for the different breeds at same ages, different letters differ significantly $P<0.05$.

The effect of GH on pepsin secretion in vitro

As shown in Figure 9, 2 ng/ml of rpGH significantly stimulated

pepsin secretion ($P < 0.05$), but 20 and 200 ng/ml of GH failed to show any influence in terms of pepsin secretion *in vitro*.

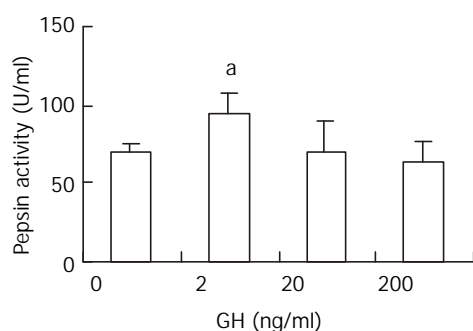


Figure 9 Effects of rpGH on the pepsin secretion from gastric mucous cells *in vitro* (a indicating significant difference between different treatment, $P < 0.05$).

DISCUSSION

The effects of GH on growth can be mediated via: (1) binding to the hepatic GHr to stimulate the IGF-1 secretion from liver into circulation, in which IGF-1 then works in an endocrine manner to promote the growth of target organs, (2) directly binding to GHr in extra-hepatic tissues to induce IGF-1 expression, in which IGF-1 works in both endocrine and paracrine manner to stimulate target tissue development, (3) directly binding to the GHr of extra-hepatic tissues to regulate the development of target organs⁷. It was reported by Lobie *et al.* (1992) that bGH (bovine GH) administration significantly increased rat gastric weight, relative gastric weight, as well as the height of mucosa². There are evidences for the localization of GHr mRNA expression in the gastric mucous membrane of rat, rabbit, human¹⁻⁴. Using semi-quantitative RT-PCR, the present experiment proved the expression of GHr mRNA in stomach of both Large White and Erhualian pigs. Furthermore, the gastric GHr mRNA expressed in an age-dependent manner which is positively correlated to relative gastric weight. This positive correlation implies that GH may directly act on stomach to regulate its growth. However, from birth to D3, the expression of gastric GHr significantly decreased, but the stomach was in a rapid growth period, it may be contributed by maternal influences through colostrum. Xu (1996) reviewed that there are high concentrations of hormones and growth-promoting peptides, such as insulin, cortisol, epidermal growth factor (EGF) and insulin-like growth factor I (IGF-I) in the maternal colostrums and there are evidences that colostrum-borne EGF and IGF-I play a role in postnatal stomach development¹⁸. Many researches have proved that IGF-1 can stimulate gastric mucosal cell proliferation¹⁹⁻¹². Coerper *et al.* (2001) reported that IGF-1 at low dose of 0.4 mg/kg BW and 4 mg/kg BW significantly stimulated gastric cell proliferation and ulcer healing¹³. However, it is not clear whether the maternal growth factors in colostrum contribute to the down regulation of gastric GHr mRNA expression at 3 days of age.

The GH actions are tissue-specific, which depends on the sensitivities of target tissues to GH stimulation. The tissue sensitivity depends upon the abundance of GHr¹⁴. Studies of Ikbahar. (1995)¹⁵, Klempt *et al.* (1993)¹⁶, Schnoebelen-Combes *et al.* (1996)¹⁷ and Peng *et al.* (1998)¹⁸ on mice, sheep and pigs, proved that the developmental patterns of GHr mRNA expression varied among different tissues, species and breeds. Our results also showed that the developmental patterns of GHr expression in stomach differ from that in liver, spleen and muscle. This tissue-specific GHr expression may account for the different functions and regulatory mechanisms of GH in different tissues or organs.

Our results also showed that the expression of GHr mRNA in gastric tissues was higher in Erhualian boars in early stages from birth to D30, but from D90 to D180, the higher expression of GHr mRNA was found in Large White boars. This result was in accordance with the differences in stomach growth between the two breeds of pigs. The present results suggest that GH play an important role in the regulation of gastric growth through the GHr expressed in stomach.

The significant correlation between gastric GHr mRNA expression and the pepsin content in mucous membrane provided an important hint that GH may be involved in the regulation of gastric function apart from its role in gastric growth. To date, however, controversy results have been published in this regard. Drago *et al.* (1997) proved that GH stimulated the gastric acid secretion in rats but failed to restore the decreased peptic activity in hypophysectomized rats¹⁹. On the contrary, however, GH did restore peptic activity in hypophysectomized dog^{11,2}. In order to clarify the effect of GH on pepsin secretion from gastric mucosa membrane, we performed an *in vitro* trial in primary cell culture and found that 2 ng/ml of GH significant elevated pepsin secretion ($P < 0.05$), but 20 ng/ml and 200 ng/ml of GH did not show significant effect on pepsin secretion compared with the control. The results suggest that GH is indeed involved in the regulation of pepsin secretion in a dose-related manner.

It is well known that gastric SS located in D-cell of autrum and fundus is a key player in the gastric function regulation. SS inhibits gastric acid, pepsin, and gastrin secretion via both paracrine and endocrine pathways²¹. It was reported that SS inhibits gastrin secretion by down-regulating the gastrin mRNA expression. Sheep immunized against SS boosted gastric acid and gastrin secretion⁶. *In vitro* studies proved that SS antisera significantly increased gastric acid release from perfused stomach of rat, mouse and pig²².

There have been some publications on the ontogeny of gastric SS. Yee *et al.* (1996) concluded that, in the fetal rabbit stomach, the expression of gastrin and somatostatin may regulate the onset of acid secretion from parietal cells²³. Read *et al.* (1992) found that in ovine, the developmental pattern of gastric SS mRNA was on the contrary to that patterns of gastrin mRNA and H⁺/K⁺-ATPase mRNA. It was proposed that the gastrin, H⁺/K⁺-ATPase and SS work in synergy to initiate gastric acid secretion²⁴. In present experiment, the developmental changes of gastric SS expression negatively correlated with the changes in gastric acid secretion in general. The gastric SS mRNA decreased significantly from birth to D3, which coincided with the increase in gastric acid secretion in the same period²⁰. Before weaning, the inhibition of gastric acid secretion agreed with the up-regulation of gastric SS expression. Our results confirmed that SS is the inhibiting factor for gastric acid secretion. Gastric SS inhibits both gastric acid and gastrin secretion, and it has negative effect on pepsin secretion as well²⁵. We found in present experiment significant differences in the expression of gastric SS mRNA between two breeds of pigs, which was negatively correlated with the pepsin content in fundic mucosa during the sucking period. However, the correlation between gastric SS mRNA expression and pepsin content was low, suggesting that the gastric SS is not the major regulator of pepsin secretion.

In conclusion, GH and gastric SS play important roles in the regulation of porcine stomach development and gastric functions, but the interaction between GH and gastric SS is still unclear. Drago *et al.* (1997) reported that the stimulation of GH on gastric acid secretion may be related to GH down-regulating gastric SS secretion¹⁹. Our unpublished data indicated that GH mRNA expression in the pituitary of Large White pigs was higher than that of Erhualian pigs. It might be presumed that the lower expression of gastric SS mRNA in

Large White pigs was resulted from, to some extent, the higher expression of GH in pituitary. However, the positive correlation between gastric SS and GHr mRNA expression over the period of investigation did not support this presumption. The complex interactions between GH and gastric SS are still to be illuminated.

REFERENCES

- 1 **Lobie PE**, Breipohl W, Waters MJ. Growth hormone receptor expression in the rat gastrointestinal tract. *Endocrinology* 1990; **126**: 299-306
- 2 **Lobie PE**, Garcia-Aragon J, Waters MJ. Growth hormone (GH) regulation of gastric structure and function in the GH-deficient rat: up-regulation of intrinsic factor. *Endocrinology* 1992; **130**: 3015-3024
- 3 **Delehay-Zervas MC**, Mertani H, Martini JF, Nihoul-Fekete C, Morel G, Postel-Vinay MC. Expression of the growth hormone receptor gene in human digestive tissue. *J Clin Endocrinol Metab* 1994; **78**: 1473-1480
- 4 **Nagano M**, Chastre E, Choquet A, Bara J, Gespach C, Kelly P. Expression of prolactin and growth hormone receptor genes and their isoforms in the gastrointestinal tract. *Am J Physiol* 1995; **268**: G431-G442
- 5 **Muller EE**, Vittorio L, Daniela C. Neuroendocrine control of growth hormone secretion. *Physiological Reviews* 1999; **70**: 511-579
- 6 **Yana Z**, Fleming WR, Shulkes A. 1999. Concurrent elevation of fundic somatostatin prevents gastrin stimulation by GRP. *Gastrointestinal and Liver Physiology* 1999; **276**: 21-27
- 7 **Lupu F**, Terwilliger JD, Lee K, Segre GV, Efstratiadis A. Roles of growth hormone and insulin-like growth factor 1 in mouse post-natal growth. *Dev Biol* 2001; **229**: 141-162
- 8 **Xu RJ**. Development of the newborn GI tract and its relation to colostrum /milk intake: a review. *Reprod Fertil Dev* 1996; **8**: 35-48
- 9 **Kato S**, Tanaka A, Ogawa Y, Kanatsu K, Seto K, Yoneda T, Takeuchi K. Effect of polaprezinc on impaired healing of chronic gastric ulcers in adjuvant-induced arthritic rats-role of insulin-like growth factors (IGF)-1. *Med Sci Monit* 2001; **7**: 20-25
- 10 **Shen WH**, Xu RJ. Stability of insulin-like growth factor I in the gastrointestinal lumen in neonatal pigs. *J Pediatr Gastroenterol Nutr* 2000; **30**: 299-304
- 11 **Korolkiewicz RP**, Tashima K, Fujita A, Kato S, Takeuchi K. Exogenous insulin-like growth factor (IGF)-1 improves the impaired healing of gastric mucosal lesions in diabetic rats. *Pharmacol Res* 2000; **41**: 221-229
- 12 **Tremblay E**, Chailier P, Menard D. Coordinated control of fetal gastric epithelial functions by insulin-like growth factors and their binding proteins. *Endocrinology* 2001; **142**: 1795-1803
- 13 **Coerper S**, Wolf S, von Kiparski S, Thomas S, Zittel TT, Ranke MB, Hunt TK, Becker HD. Insulin-like growth factor I accelerates gastric ulcer healing by stimulating cell proliferation and by inhibiting gastric acid secretion. *Scand J Gastroenterol* 2001; **36**: 921-927
- 14 **Hull KL**, Harvey S. Autoregulation of central and peripheral growth hormone receptor mRNA in domestic fowl. *Journal of Endocrinology* 1998; **156**: 323-329
- 15 **Ilkbahar YN**, Wu K, Thordarson G, Talamantes F. Expression and distribution of messenger ribonucleic acids for growth hormone (GH) receptor and GH-binding protein in mice during pregnancy. *Endocrinology* 1995; **136**: 386-392
- 16 **Klempt M**, Bingham B, Breier BH, Baumbach WR, Gluckman PD. Tissue distribution and ontogeny of growth hormone receptor messenger ribonucleic acid and ligand binding to hepatic tissue in the midgestation sheep fetus. *Endocrinology* 1993; **132**: 1071-1077
- 17 **Schnoebelen-Combes S**, Louveau I, Postel-Vinay MC, Bonneau M. Ontogeny of GH receptor and GH-binding protein in the pig. *J Endocrinol* 1996; **148**: 249-255
- 18 **Peng M**, Abribat T, Calvo E, LeBel D, Palin MF, Bernatchez G, Morisset J, Pelletier G. Ontogeny of insulin-like growth factors (IGF), IGF binding proteins, IGF receptors, and growth hormone receptor mRNA levels in porcine pancreas. *J Anim Sci* 1998; **76**: 1178-1188
- 19 **Drago F**, Montoneri C. Growth hormone and somatostatin interaction in the ulcerogenic effect of cysteamine in female rats. *J Physiol Paris* 1997; **91**: 127-130
- 20 **Xu RJ**, Cranwell PD. Development of gastric acid secretion in pigs from birth to thirty six days of ages: the response to pentagastrin. *J Dev Physiol* 1990; **13**: 315-326
- 21 **Shulkes A**, Read M. Regulation of somatostatin secretion by gastrin-and acid-dependent mechanisms. *Endocrinology* 1991; **129**: 2329-2334
- 22 **Simon LW**, Graham HM, Keneth JH, Arthur S. Active immunization against somatostatin alters regulation of gastrin in response to gastric acid secretagogues. *Gastrointestinal and Liver Physiology* 1998; **274**: 751-756
- 23 **Yee LF**, Wong HC, Calaastro EQ, Mulvhill SJ. Roles of gastrin and somatostatin in the regulation of gastric acid secretion in the fetal rabbit. *J Surg Res* 1996; **63**: 364-368
- 24 **Read MA**, Patricia C, Knenneth JH, Shulkes A. Ontogeny of gastrin, somatostatin, and the H⁺/K⁺-ATPase in the ovine fetus. *Endocrinology* 1992; **130**: 1688-1697
- 25 **Felley CP**, O' Doris TM, Howe B, Coy DH, Mantey SA, Pradhan TK, Sutliff VE, Jensen RT. Chief cells possess somatostatin receptors regulated by secretagogues acting through the calcium or cAMP pathway. *Am J Physiol* 1994; **266**: G780-G798

Edited by Zhang JZ

Contents of chemical elements in stomach during prenatal development: different age-dependent dynamical changes and their significance

Shao-Fan Hou, Hai-Rong Li, Li-Zhen Wang, De-Zhu Li, Lin-Sheng Yang, Chong-Zheng Li

Shao-Fan Hou, Hai-Rong Li, Li-Zhen Wang, De-Zhu Li, Lin-Sheng Yang, Institute of Geographical Sciences and Natural Resources Research, CAS, Beijing 100101, China

Chong-Zheng Li, Beijing University of Chinese Medicine Pharmacy Huguosi Hospital, Beijing 100035, China

Supported by the National Natural Science Foundation of China, No. 49971003

Correspondence to: Professor Shao-Fan Hou, Institute of Geographical Sciences and Natural Resources Research, CAS, Beijing 100101, China. lihr@igsnr.ac.cn

Telephone: +86-10-64889796 **Fax:** +86-10-64851844

Received: 2002-10-30 **Accepted:** 2002-12-18

Abstract

AIM: To observe dynamic of different chemical elements in stomach tissue during fetal development.

METHODS: To determine contents of the 21 chemical elements in each stomach samples from fetus aging four to ten months. The content values were compared to those from adult tissue samples, and the values for each month group were also analyzed for dynamic changes.

RESULTS: Three representations were found regarding the relationship between contents of the elements and ages of the fetus, including the positive correlative (K), reversely correlative (Na, Ca, P, Al, Cu, Zn, Fe, Mn, Cr, Sr, Li, Cd, Ba, Se) and irrelevant groups (Mg, Co, Ni, V, Pb, Ti).

CONCLUSION: The chemical elements' contents in stomach tissues were found to change dynamically with the stomach weights. The age-dependent representations for different chemical elements during the prenatal development may be of some significance for assessing development of fetal stomach and some chemical elements. The data may be helpful for the nutritional balance of fetus and mothers during prenatal development and even the perinatal stages.

Hou SF, Li HR, Wang LZ, Li DZ, Yang LS, Li CZ. Contents of chemical elements in stomach during prenatal development: different age-dependent dynamical changes and their significance. *World J Gastroenterol* 2003; 9(5): 1063-1066
<http://www.wjgnet.com/1007-9327/9/1063.htm>

INTRODUCTION

Embryonic stomach develops from the caudal side of foregut, and then the primitive stomach expands towards abdomen. With its enlargement, a 90 degrees clockwise rotation occurs around its major axis, giving the rise to the shape similar to the adult stomach. During the prenatal development, stomach is one of the fast growing organs, and all nutritious elements for the growth are supplied by mother through the placenta. The stomach is mainly for digestion of food and absorption of

nutrients, so its development and functional maturation after birth is important for its adaptability to the changing nutrient intaking way. In this article, we reported the dynamics contents of 21 chemical elements in gastric tissues during the development of fetal stomach.

MATERIALS AND METHODS

Materials

The fetuses were 4-10 months old (every 4 weeks are one month), all begin from countryside of Henan Province. Those gland 10 months old were obtained through unexpected abortion and those with shorter pregnancies were collected after the induced abortion. No case of the abortion could be attributed to environmental pollution, or their maternal health or nutrition problems. The stomach was taken from the fetus, using redistilled water, and then dried in an oven at 70-80 °C. The samples were crushed into powder and kept in the desiccator for use. Stainless steel scalpel and Teflon scissors were used during the sample processing, and contamination was avoided in the whole course.

Methods

Se was measured using the method of 2,3 - di-aminonaphthalene fluorescence, with a fluorescence spectrometer (Model MPF-4, Hitachi). The other elements were detected using the method of ICP-AES^[1], with a sequential plasma emission spectrometer (ICP-2070 Barid Company's Model). All reagents employed were of commercial reagent-grade quality. Quality control was carried out by national first grade references including ox liver powder (ESA-1) and the pork (GBW08552). Statistical computations were conducted using the soft package SPSS 10.0.

Analysis data of adult

All data of adults were taken from the literature^[2], covering reference parameters from the 100 persons (68 men, 32 women, 31.3 ± 1.0 years old) 4 provinces in South and Northern China. The original values, presumed to contain 71.6 % of water, were converts into those by dry weight.

RESULTS

Contents of constant elements in fetal stomach

Table 1 showed the contents of six constant elements of stomach of fetus aging 4-10 month, with that of K increasing with age, the values of Na, Ca, P, and Al were found to decrease with the fetus age, but the change for Mg was not significant. Contents of K, Na, Ca, P, Al and Mg in stomach tissues from fetus 10 month-old were 112.4 %, 60.6 %, 53.3 %, 78.0 %, 44.3 %, 86.1 % respectively of those from fetus 4 month-old. This indicates that the gastric tissues at embryo stages, contain more K than those at later pregnancy, and that Na, Ca, P, Al and Mg are higher in the embryonic stomach. In addition, K, Na, Ca and Mg contents were higher in the fetal stomach than in the adult samples.

Contents of essential elements in fetal stomach

Table 2 showed the contents of ten essential elements of stomach of fetus at the ages of 4-10 months. A tendency of age-dependent reduction was observed for all of 10 trace

elements, with the changes of Cu, Zn, Fe, Mn, Cr, Se and being more pronounced, and Cu, Zn, Fe, Mn, Cr, Sr, Se, Co, Ni, V contents in fetal stomach age of 10 month were 67.5 %, 38.8 %, 69.8 %, 78.0 %, 54.6 %, 95.8 %, 72.7 %, 99.0 %,

Table 1 Contents of constant elements in fetal stomachs, with comparison to those in adult^[2] (μg/g dry weight)

Age (mon)	4	5	6	7	8	9	10	Adult
K	7995.7	8148.9	8712.2	8583.1	8838.4	9091.5	8987.2	5193.7
	2309.1(6)	2783.7(19)	1969.6(14)	1405.1(9)	1731.5(7)	2308.9(6)	894.2(5)	1457.7
Na	13237.5	11255.8	10708.8	9368.1	7859.1	9673.3	8023.6	4894.4
	1540.3(6)	2096.0(19)	2718.0(14)	2112.5(9)	2433.1(7)	1855.6(6)	1853.8(5)	1626.8
Ca	972.7	676.1	704.5	662.6	699.4	575.5	518.8	89.7
	60.3(6)	191.9(19)	147.3(14)	110.4(9)	243.8(7)	103.7(6)	159.0(5)	47.5
Mg	591.8	589.5	627.4	622.7	648.1	519.7	509.8	494.0
	203.3(6)	155.6(19)	99.6(14)	91.9(9)	71.5(7)	96.5(6)	84.6(5)	159.7
P	7850.8	7668.5	7029.8	6213.7	6117.3	6216.3	6122.4	
	2113.8(6)	1092.0(19)	969.1(14)	946.3(9)	752.4(7)	722.9(6)	312.9(5)	
Al	12.922	14.486	14.152	14.792	10.786	10.096	5.722	
	8.947(6)	5.794(19)	8.620(14)	8.608(9)	4.513(7)	7.342(6)	5.208(5)	

Data in the upper row for each element is average mean, those in the lower is standard deviation with the case numbers in bracket. Case number of adult is 100.

Table 2 Contents of essential elements in fetal stomachs, with comparison to those in adult^[2] (μg/g dry weight)

Month-age	4	5	6	7	8	9	10	Adult
Cu	47.33	37.26	38.98	37.67	38.28	27.65	32.20	4.95
	13.95(6)	14.74(19)	9.02(14)	16.44(9)	17.42(7)	8.53(6)	8.43(5)	1.52
Zn	310.7	311.1	279.6	215.2	150.6	136.0	120.5	71.87
	38.8(6)	124.6(19)	50.3(14)	44.7(9)	81.2(7)	34.9(6)	12.6(5)	15.42
Fe	765.1	677.0	550.9	503.1	559.8	530.1	534.3	138.6
	188.5(6)	257.3(19)	158.1(14)	147.4(9)	98.9(7)	260.0(6)	131.3(5)	61.4
Mn	3.266	2.849	2.833	2.918	3.068	2.370	2.547	2.440
	0.797(6)	0.881(19)	1.015(14)	0.934(9)	0.859(7)	0.387(6)	0.512(5)	1.116
Se	-	0.565	0.553	0.539	0.471	0.468	0.411	
	0.042(2)	0.186(10)	0.161(9)	0.240(7)	0.089(6)	0.137(5)		
Co	0.575	0.613	0.711	0.709	0.648	0.595	0.569	0.060
	0.380(6)	0.292(19)	0.320(14)	0.547(9)	0.259(7)	0.229(6)	0.188(5)	0.377
Cr	0.595	0.565	0.513	0.510	0.359	0.302	0.325	3.958
	0.291(6)	0.309(19)	0.396(14)	0.397(9)	0.241(7)	0.154(6)	0.181(5)	6.511
Ni	0.511	0.898	0.517	0.483	0.780	0.530	0.211	0.662
	0.254(6)	1.551(19)	0.584(14)	0.302(9)	0.293(7)	0.426(6)	0.096(5)	0.556
Sr	1.231	0.785	0.922	0.735	0.651	0.374	0.564	
	0.554(6)	0.394(19)	0.502(14)	0.238(9)	0.236(7)	0.170(6)	0.178(5)	
V	0.707	0.500	0.702	0.581	0.640	0.556	0.327	
	0.521(6)	0.386(19)	0.524(14)	0.170(9)	0.261(7)	0.413(6)	0.173(5)	

Table 3 Contents of harmful elements in fetal stomachs, with comparison to those in adult^[2] (μg/g dry weight)

Month-age	4	5	6	7	8	9	10	Adult
Li	0.707	0.720	0.699	0.653	0.567	0.479	0.383	
	0.903(6)	0.328(19)	0.374(14)	0.318(9)	0.189(7)	0.258(6)	0.165(5)	
Cd	0.266	0.197	0.129	0.128	0.103	0.108	0.081	0.835
	0.357(6)	0.189(19)	0.080(14)	0.070(9)	0.065(7)	0.053(6)	0.039(5)	0.553
Pb	1.091	0.882	0.881	0.851	0.879	0.884	0.835	0.426
	0.607(6)	0.565(19)	1.245(14)	0.578(9)	0.948(7)	0.461(6)	0.370(5)	0.356
Ba	2.542	1.361	1.055	0.911	1.053	0.415	0.705	
	1.214(6)	0.789(19)	0.447(14)	0.770(9)	1.445(7)	0.183(6)	0.228(5)	
Ti	0.347	0.567	0.474	0.497	0.543	0.533	0.419	
	0.154(6)	0.298(19)	0.275(14)	0.286(9)	0.353(7)	0.385(6)	0.290(5)	

41.3 % and 46.3 % respectively of that of 4 month. This indicates that the embryonic stomachs contain more essential elements than the fetal stomach. In comparison to the adult tissues, the gastric samples from fetuses aging 10 months contain more Cu, Zn, Fe and Co, less Cr and Ni, but the Mn content was similar. There were no analytical datum of Se, Sr, V in stomach of China Reference Person.

Contents of harmful elements in fetal stomach and comparison with those in adult

Table 3 showed the contents of five harmful elements of stomach of fetus ageing 4-10 months. Except Ti, other elements reduced with the fetal development. Li, Cd, Ba, Pb and Ti contents in fetal stomach at the age of 10 month were 54.2 %, 30.5 %, 27.8 %, 78.2 % and 120.7 % respectively of those at the age of 4 month. In comparison to the published data for the adult group^[2], the stomach tissue in fetuses at the age of 10 month contained less Cd and more Pb.

Change regulation of contents of chemical elements in Fetus' stomach and its significance

Table 4 showed the stomach weights of fetuses from 4 to 10 months. The data in agreement with those reported elsewhere^[3]. The stomach weight was positively correlative the age ($r=0.961$, $P=0.001$). Table 5 showed the relation between contents of 21 elements and the age of fetus, with both parameters positively correlative for K, negatively correlative for 14 elements and statistically independent for the remaining elements.

Table 4 Stomach weights of fetus aging from 4 to 10 months

Month-age	4	5	6	7	8	9	10
Weight (gram)	0.35 0.12(6)	0.94 0.45(19)	1.73 0.64(14)	3.17 0.74(9)	4.20 1.19(7)	5.41 0.76(6)	8.93 2.10(5)
Fixed ratio (%)	100	268.6	494.3	905.7	1200.0	1545.7	2551.4
Circular ratio (%)	-	268.6	184.0	183.2	132.5	128.8	165.1

The data in the upper row was average mean, that in the lower row was standard deviation, with the case number in bracket.

$$\text{Fixed ratio} = \frac{\text{stomach weight of fetus age of } i \text{ month}}{\text{stomach weight of fetus age of } j \text{ month}} \times 100 \%$$

$$\text{Circular ratio} = \frac{\text{stomach weight of fetus age of } j \text{ month}}{\text{stomach weight of fetus age of } i \text{ month}} \times 100 \%$$

$$(i=4,5,\dots,10; j=i+1, j_{\max}=10)$$

Table 5 Relation between elements' contents and age of fetus

Remarkable positive relativity (Pearson r)	Remarkable negative relativity (Pearson r)	Unobvious relativity (Pearson r)
K(0.9301) ^b	Na(-0.8815) ^b	Mn(-0.7364) ^a
	Ca(-0.9222) ^b	Cr(-0.9515) ^b
	P(-0.7221) ^a	Sr(-0.8734) ^b
	Al(-0.7983) ^a	Li(-0.9419) ^b
	Cu(-0.8259) ^a	Cd(-0.9051) ^b
	Zn(-0.9700) ^a	Ba(-0.8369) ^b
	Fe(-0.7883) ^a	Se(-0.9648) ^b
		Co(-0.1858)
		Ni(-0.4872)
		V(-0.6348)
		Pb(-0.0002)
		Ti(0.2161)

^a $P<0.05$, ^b $P<0.01$.

DISCUSSION

Embryo's development is a special stage in human life. It can be divided into the embryo, fetus and neonate stage. There are respective characteristics during each stage. Main character of fetus is that embryo differentiates into different organs for

fetal development and storage for material and energy. Neonate characteristic is the adaptation of outer-environment of womb, and fetal metabolism changes from anabolism to catabolism. These characters are extremely easy to be interfered by environment, different dangers happen in different stages, and this is one of reasons that changes happen in the later stage of fetus appear after birth^[4]. At present, there is very deficient knowledge to the variety of the chemical elements and understanding of their physiological function in the special changes that happen in the stage of fetus, it is helpful to solve these problems through dynamic observation of chemical elements of fetal tissues.

In this article, the correlation analysis between chemical elements in stomach and fetal age indicates that elements that are positively correlative with age in per gram stomach tissue increases with the development of the stomach, and elements' contents in fetus are lower than neonate; 14 elements that are reversely correlative with age in per gram stomach tissue reduce notably with the development of the stomach, and the elements contents in fetus are higher than neonate; 6 elements that are statistically independent with age in stomach of fetus may be basically unanimous of those of neonate. These results may be of some significance for studying the relation between elements and stomach development and physiological function.

In eleven essential elements that have datum of "China reference person", there are eight elements' contents of stomach of fetus higher than those of adult. For example, Ca of fetus stomach is 5.8 times of the adult's, Cu is 6.5 times, Fe is 3.8 times, and Zn is 1.7 times. It is well known that Ca, Cu, Fe, Zn are the elements that are easy to be lack and affect on the organs' development, cause a lot of physiology biochemical pathological changes and health problems in neonate, infant and children^[5-9], the character that there are higher contents in the stage of fetus not only reflects the material' storage function of fetus, but also reveals the regulation of "adaptation to outer-environment of womb" after birth. The contaminative trace elements' contents are remarkably lower than adult (Cr, Ni), such as Cr content in stomach of adult is 12.2 times of that of fetus, this indicates that the increase of this kind of elements' contents in adult is closely related with environment^[2]. Harmful elements like Cd and Pb, their contents decrease with the increase of age, for example, the contents of Cd of stomach of fetus 10 month age is 30.45 % of that of fetus 4 month age, and the content of Pb of children over 7 is 37.5 % that of the neonate, which indicates that the content of Cd, Pb doesn't bring harm to fetus, and the accumulations of Cd, Pb in body of children result from environmental pollution, bad living and sanitary custom *et al*^[8, 10-20], this can consult for environmental monitoring.

Our series study of 21 elements contents' dynamics in other tissues of fetus (liver, kidney, brain, heart, lung, spleen), the same to stomach, majority of 21 elements' contents in per gram tissue remarkably reduce with the fetal age, the decreasing rate is especially large before birth. This common character of elements' change in different tissues indicates the sensitivities to these elements deficiency in the stage of neonate and infant, if the supply of this kind of elements from mother-environmental system is insufficient, it may bring nutritional lack of this kind of elements. Intervene experiment shows that it will take good effects on fetus and infant development with this kind of elements supplement singly to pregnant women^[21-25], however, supplement with Ca, Fe, Zn jointly to pregnant women, the mean values of the weight and height of their baby at birth are largest than other groups, this indicates that Ca, Fe, Zn supplement to pregnant woman is benefit for fetus and infant development^[26-28]. Our study not only provides basis for adjusting and controlling nutrition of neonate, infant and pregnant and breast-feeding

woman, at the same time, furthermore can offer physiological foundation for focus viewpoint that some diseases of adult originate from fetus^[29-32].

REFERENCES

- 1 **Wang LZ.** Determination of elements in viscera by method of ICP-AES. *Guangpu Shiyanshi* 1997; **14**: 61-64
- 2 **Wang JX,** Chen RS, Zhu HD, Zhou YZ, Ma RW. Anatomical physiology and metabolizing datum of china reference person. Beijing: *Atomic Energy Press* 1998: 177-195
- 3 **Gu HY.** Chinese embryo developing sequence and prevention of abnormality. Shanghai: *Shanghai Medical University Press* 1993: 88-117
- 4 **Zhang X,** Liu YG. Toxicology. Beijing: Beijing Medical University and China. *Beijing Union Medical College United Press* 1997: 364-376
- 5 **Keen CL,** Uriu-Hare JY, Hawk SN, Jankowski MA, Daston GP, Kwik-Urbe CL, Rucker RB. Effect of copper deficiency on prenatal development and pregnancy outcome. *Am J Clin Nutr* 1998; **67**(Suppl 5): 1003S-1011S
- 6 **Nishiyama S,** Kiwaki K, Miyazaki Y, Hasuda T. Zinc and IGF-I concentrations in pregnant women with anemia before and after supplementation with iron and/or zinc. *J Am Coll Nutr* 1999; **18**: 261-267
- 7 **Rathi SS,** Srinivas M, Grover JK, Mitra D, Vats V, Sharma JD. Zinc levels in women and newborns. *Indian J Pediatr* 1999; **66**: 681-684
- 8 **Srivastava S,** Mehrotra PK, Srivastava SP, Tandon I, Siddiqui MK. Blood lead and zinc in pregnant women and their offspring in intrauterine growth retardation cases. *J Anal Toxicol* 2001; **25**: 461-465
- 9 **Black RE.** Micronutrients in pregnancy. *Br J Nutr* 2001; **85**(Suppl 2): S193-197
- 10 **Salpietro CD,** Gangemi S, Minciullo PL, Briuglia S, Merlino MV, Stelitano A, Cristani M, Trombetta D, Saija A. Cadmium concentration in maternal and cord blood and infant birth weight: a study on healthy non-smoking women. *J Perinat Med* 2002; **30**: 395-399
- 11 **Bjerregaard P,** Hansen JC. Organochlorines and heavy metals in pregnant women from the Disko Bay area in Greenland. *Sci Total Environ* 2000; **245**: 195-202
- 12 **Qi Q,** Yang Y, Yao X, Ding L, Wang W, Liu Y, Chen Y, Yang Z, Sun Y, Yuan B, Yu C, Han L, Liu X, Hu X, Liu Y, Du Z, Qu L, Sun F. Blood lead level of children in the urban areas in China. *Zhonghua Liuxingbingxue Zazhi* 2002; **23**: 162-166
- 13 **Sallmen M,** Lindbohm ML, Nurminen M. Paternal exposure to lead and infertility. *Epidemiology* 2000; **11**: 148-152
- 14 **Yan C,** Wu S, Shen X, Zhang Y, Jiang F, Yin J, Zhou J, He J, Ao L, Zhang Y, Li R. The trends of changes in children's blood lead levels since the introduction of lead free gasoline in Shanghai. *Zhonghua Liuxingbingxue Zazhi* 2002; **23**: 172-174
- 15 **Rothenberg SJ,** Khan F, Manalo M, Jiang J, Cuellar R, Reyes S, Acosta S, Jauregui M, Diaz M, Sanchez M, Todd AC, Johnson C. Maternal bone lead contribution to blood lead during and after pregnancy. *Environ Res* 2000; **82**: 81-90
- 16 **Moura M,** Goncalves Valente J. Blood lead levels during pregnancy in women living in Rio de Janeiro, Brazil. *Sci Total Environ* 2002; **299**: 123-129
- 17 **Black AP,** Knight R, Batty J, Haswell SJ, Lindow SW. An analysis of maternal and fetal hair lead levels. *BJOG* 2002; **109**: 1295-1297
- 18 **Kaul PP,** Srivastava R, Srivastava SP, Kamboj M, Chand S. Relationships of maternal blood lead and disorders of pregnancy to neonatal birthweight. *Vet Hum Toxicol* 2002; **44**: 321-323
- 19 **Klitzman S,** Sharma A, Nicaj L, Vitkevich R, Leighton J. Lead poisoning among pregnant women in New York City: risk factors and screening practices. *J Urban Health* 2002; **79**: 225-237
- 20 **Tao Y,** Bai X, Zhang H, Liu J. Effect of lead exposure in prenatal and postnatal duration on infant growth. *Weisheng Yanjiu* 2001; **30**: 102-104
- 21 **Koo WW,** Walters JC, Esterlitz J, Levine RJ, Bush AJ, Sibai B. Maternal calcium supplementation and fetal bone mineralization. *Obstet Gynecol* 1999; **94**: 577-582
- 22 **Beard JL.** Effectiveness and strategies of iron supplementation during pregnancy. *Am J Clin Nutr* 2000; **71**(5 Suppl): 1288S-1294S
- 23 **Ashworth A,** Morris SS, Lira PI, Grantham-McGregor SM. Zinc supplementation, mental development and behaviour in low birth weight term infants in northeast Brazil. *Eur J Clin Nutr* 1998; **52**: 223-227
- 24 **Hamadani JD,** Fuchs GJ, Osendarp SJ, Huda SN, Grantham-McGregor SM. Zinc supplementation during pregnancy and effects on mental development and behaviour of infants: a follow-up study. *Lancet* 2002; **360**: 290-294
- 25 **O'Brien KO.** Regulation of mineral metabolism from fetus to infant: metabolic studies. *Acta Paediatr Suppl* 1999; **88**: 88-91
- 26 **An HB,** Yin SA, Xu QM, Hu SM, Zhao XF, Meng J. Effects of supplementing calcium, iron and zinc on the fetus development and growth during pregnancy. *Zhonghua Yufang Yixue Zazhi* 2001; **35**: 370-373
- 27 **Leung PL,** Huang HM, Sun DZ, Zhu MG. Hair concentrations of calcium, iron, and zinc in pregnant women and effects of supplementation. *Biol Trace Elem Res* 1999; **69**: 269-282
- 28 **Huang HM,** Leung PL, Sun DZ, Zhu MG. Hair and serum calcium, iron, copper, and zinc levels during normal pregnancy at three trimesters. *Biol Trace Elem Res* 1999; **69**: 111-120
- 29 **Barker DJ.** Early growth and cardiovascular disease. *Arch Dis Child* 1999; **80**: 305-307
- 30 **Cheung YB,** Low L, Osmond C, Barker D, Karlberg J. Fetal growth and early postnatal growth are related to blood pressure in adults. *Hypertension* 2000; **36**: 795-800
- 31 **Godfrey KM,** Barker DJ. Fetal nutrition and adult disease. *Am J Clin Nutr* 2000; **71**: 1344-1452
- 32 **Mi J,** Law C, Zhang KL, Osmond C, Stein C, Barker D. Effects of infant birth weight and maternal body mass index in pregnancy on components of the insulin resistance syndrome in China. *Ann Intern Med* 2000; **132**: 253-260

Edited by Su Q

Effect of 1,25-dihydroxyvitamin D₃ on preventing allograft from acute rejection following rat orthotopic liver transplantation

Ai-Bin Zhang, Shu-Sen Zheng, Chang-Ku Jia, Yan Wang

Ai-Bin Zhang, Shu-Sen Zheng, Chang-Ku Jia, Yan Wang, Department of Hepatobiliary Pancreatic Surgery, The First Affiliated Hospital of Medicine School, Zhejiang University, Key Lab of Combined Multi-Organ Transplantation, Ministry of Public Health, Hangzhou 310003, Zhejiang Province, China

Correspondence to: Ai-Bin Zhang, Department of Hepatobiliary Pancreatic Surgery, The First Affiliated Hospital of Medicine School, Zhejiang University, Hangzhou 310003, Zhejiang Province, China. cheung163@163.com

Telephone: +86-571-87236570

Received: 2002-11-06 **Accepted:** 2002-12-16

Abstract

AIM: To study the mechanism and the preventive role of 1, 25-dihydroxyvitamin D₃ in acute rejection following orthotopic liver transplantation.

METHODS: Rats were randomly divided as donors or recipients for orthotopic liver allotransplantation model. Four groups were designed in the study, Group I: syngenic control (Wistar to Wistar); Group II: acute rejection (SD to Wistar); Group III: acute rejection treated with cyclosporine A, and Group IV: acute rejection treated with 1,25-(OH)₂D₃. Liver function, rejection activity index and mRNA of IFN- γ , IL-10 intragraft in recipients were measured on day 1, 5, 7, 15, 30 posttransplant for assessing graft function, severity of acute rejection and immune state of recipients.

RESULTS: Survival time of recipients in Group IV was significantly prolonged (4/6 recipients survived for over 100 days. vs Group II, $P < 0.001$; vs Group III, $P > 0.05$). After treatment with 1,25-(OH)₂D₃, mean value of all the assay tested on each experimental time was compared, liver function in group IV was significantly improved (AST 127 ± 41 U/L- 360 ± 104 U/L, BIL 13 ± 5 mmol/l- 38 ± 11 mmol/l; vs Group II, $P < 0.05$; vs Group III, $P > 0.05$). Rejection activity index was significantly decreased ($0.3.3 \pm 1.6$; vs Group II, $P < 0.05$; vs Group III, $P > 0.05$). Level of hepatic IFN- γ mRNA in group IV was decreased, while level of hepatic IL-10 mRNA was increased (vs Group II, $P < 0.05$; vs Group III, $P > 0.05$).

CONCLUSION: Our results indicated that 1,25-(OH)₂D₃ induced the secretion of cytokine toward to Th2 type, which would alleviate acute rejection, protect liver function and prolong survival of recipient after orthotopic liver transplantation.

Zhang AB, Zheng SS, Jia CK, Wang Y. Effect of 1,25-dihydroxyvitamin D₃ on preventing allograft from acute rejection following rat orthotopic liver transplantation. *World J Gastroenterol* 2003; 9(5): 1067-1071

<http://www.wjgnet.com/1007-9327/9/1067.htm>

INTRODUCTION

1,25-dihydroxyvitamin D₃ (1,25-(OH)₂D₃), the functional metabolite of vitamin D, is a key regulator of calcium and

phosphorus^[1], has important immunomodulatory action^[2,3], and was demonstrated to be able to prevent graft from acute rejection after transplantation of heart and renal, and prolong the survival of graft significantly^[4-7]. In previous study, we demonstrated that 1,25-(OH)₂D₃ played important role in preventing the rejection of allograft after liver transplantation. The kinetic characteristic of 1,25-dihydroxyvitamin D₃ on liver allograft viability and rejection after liver transplantation was explored in present study with orthotopic rat liver transplantation model. Furthermore, expression of IFN and IL-10 was determined to examine the immunomodulatory effect of 1,25-dihydroxyvitamin D₃.

MATERIALS AND METHODS

Animals, surgical procedure and experimental groups

Male Sprague-Dawley (SD) and Wistar rats (200-250 g, purchased from Shanghai Animal Center, Academy of Science, Shanghai) were selected randomly as transplant donors or recipients. Under ether inhalation, orthotopic rat liver transplantation was performed according to Kamada's two-cuff technique^[8]. Four experimental groups were designed in this study, Group I: syngenic control (Wistar-to-Wistar); Group II: acute rejection (SD-to-Wistar); Group III: acute rejection treated with cyclosporine A 3.0 mg·kg⁻¹·d⁻¹ intramuscularly, from day 0 to 13 posttransplant (SD-to-Wistar+CsA); Group IV: acute rejection treated with 1,25-(OH)₂D₃ 1.0 μ g·kg⁻¹·d⁻¹ intraperitoneally, from day 0 to day 13 posttransplant (SD-to-Wistar+1,25-(OH)₂D₃). Recipient animals had an experimental diet containing 0.47 % calcium 7 days before transplantation; only recipients in Group IV received experimental diet for 15 days following transplantation.

Sample harvesting

On day 1, 5, 7, 15, and 30 posttransplant, three rats were selected from each group for sample harvesting. Serum calcium levels were measured to study the effect of 1,25-(OH)₂D₃ on calcium metabolism. Serum aspartate aminotransferase (AST) and total bilirubin (BIL) were measured to study the effect of 1,25-(OH)₂D₃ on liver functions. Liver allografts were taken for histology and cytokine determination. Another 6 rats in each group were bred for observing survival time. Rocaltrol[®], 1,25-dihydroxyvitamin D₃ product of Roche Pharma, and Sandimmune[®], Cyclosporine A product of Novartis Pharma were used in this study.

Histopathologic examination

Grafted liver samples were fixed in 10 % buffered formalin and embed in paraffin. Five-micrometer-thick sections were affixed on slides, deparaffinized, and stained with hematoxylin and eosin. Morphologic change of graft was observed and severity of acute rejection was assessed with Rejection Activity Index according to Banff 97 working classification of hepatic allograft pathology^[9].

Cytokine reverse transcription-polymerase chain reaction

Primer sequences and reaction conditions The sequences of primers, synthesized by Bioengine-ering Corp at Shanghai

are as follow, IFN- γ sense primer 5' -ACT GCC AAG GCA CAC TCA TT-3', antisense primer 5' -AGG TGC GAT TCG ATG ACA CT-3' (size 235bp); IL-10 sense primer 5' -TGC TCT TAC TGG CTG GAG TG-3', IL-10 antisense primer 5' -GTC GCA GCT GTA TCC AGA GG-3' (size 345bp). β -actin sense primer, 5' -TCG TAC CAC TGG CAT TGT GA-3', β -actin antisense primer, 5' -TCC TGC TTG CTG ATC CAC AT-3' (size 645bp). Amplification was performed using an initial denaturation step of 95 °C for 2 minutes, followed by 32 cycles consisting of 94 °C for 45 seconds, 56 °C for 45 seconds and 72 °C for 45 seconds. The final extension step was one cycle at 72 °C for 10 minutes.

RT-PCR Total RNA was prepared from grafted liver with TRIzol Reagent (Gibco, BRL) according to the manufacturer's recommendations. For cDNA synthesis, 4 μ g total RNA was reverse transcribed with MuLV (MBI, Fermentas) reverse transcriptase according to the manufacturer's recommendations. Two microliters from the resulting cDNA solution were then amplified in a volume of 25 μ l PCR buffer using specific oligonucleotides under the conditions aforementioned. Reaction products were run on a 1.5 % agarose gel for 20-30 min at 100 V, and visualized with ethidium bromide under UV light. Relative expression of cytokines was defined as optical density ratio (cytokine/ β -actin) analyzed by Kodak science scanning system.

Statistics

All data were expressed as mean values and standard deviations and analyzed using SPSS software (version 10.0 for windows). Difference in mean value between the groups was tested by Independent-Samples *t* test. Differences in pathological Rejection Activity Index score between the groups were tested with the Mann-Whitney U nonparametric test. Recipient's survival was estimated with the Kaplan-Mier product limit estimator. Statistically significance was defined at $P < 0.05$.

RESULTS

Survival of recipient posttransplantation

All the recipients in Group I survived for over 100 days; all the recipients in Group II died at day 7 to day 19 posttransplantation and median survival time was 12.3 \pm 4.0 days. Five out of 6 recipients in Group III, and 4 out of 6 recipients in Group IV survived for long term. Difference between Group IV and II was statistically significant, but not for that between group IV and III. Kaplan-Mier Survival Curve was showed in Figure 1.

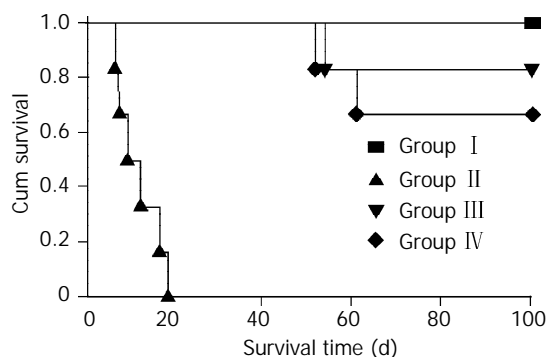


Figure 1 Effect of 1,25-(OH) $_2$ D $_3$ on survival of rat recipients of an orthopic liver allograft (Kaplan-Meier Survival Curve). When Group III was compared with Group II: $P=0.0005$. When Group IV was compared with Group II: $P=0.0005$. When Group IV was compared with Group III: $P=0.70$.

Effect of 1,25-(OH) $_2$ D $_3$ on serum calcium and liver function

An obvious limitation to the use of vitamin D $_3$ derivatives in transplantation was hypercalcemia. Serum calcium in Group I

on day 7 posttransplant was defined as basal value. If value was not significant in comparison with basal value, no significant effect of 1,25-(OH) $_2$ D $_3$ or CsA on calcium metabolism was considered (Table 1). Level of AST and BIL in Group I increased slightly within 7 days posttransplant and then gradually restored to normal after 7 days posttransplant. In Group II, liver function deteriorated dramatically on day 5 posttransplant, and levels of bilirubin and AST increased steadily until the death of recipients. In contrast, administration of either CsA or 1,25-(OH) $_2$ D $_3$ prevented deterioration of the graft function during the first 30 days after transplantation. The average values of AST were 146 \pm 33 U/L-241 \pm 107 U/L, and BIL 17 \pm 6 mmol/l-25 \pm 9 mmol/l in Group III, while mean level of AST, BIL in Group IV posttransplant was 127 \pm 41 U/L-360 \pm 104 U/L and 13 \pm 5 mmol/l-38 \pm 11 mmol/l, respectively. Difference of these values between Group II and IV was statistically significant while difference between group III and IV was not (Figure 2).

Table 1 Serum calcium assessment (mmol/l, $\bar{x}\pm s$)^a

Group	Time posttransplant (d)		
	7	15	30
I	2.29 \pm 0.13	2.16 \pm 0.05	2.22 \pm 0.16
II	2.34 \pm 0.04		
III	2.25 \pm 0.11	2.32 \pm 0.07	2.12 \pm 0.09
IV	2.60 \pm 0.31	2.47 \pm 0.27	2.33 \pm 0.31

a: Serum calcium of Group I on 7 d posttransplant was supposed as basal values, each value was not significant in comparison with basal values ($P > 0.05$).

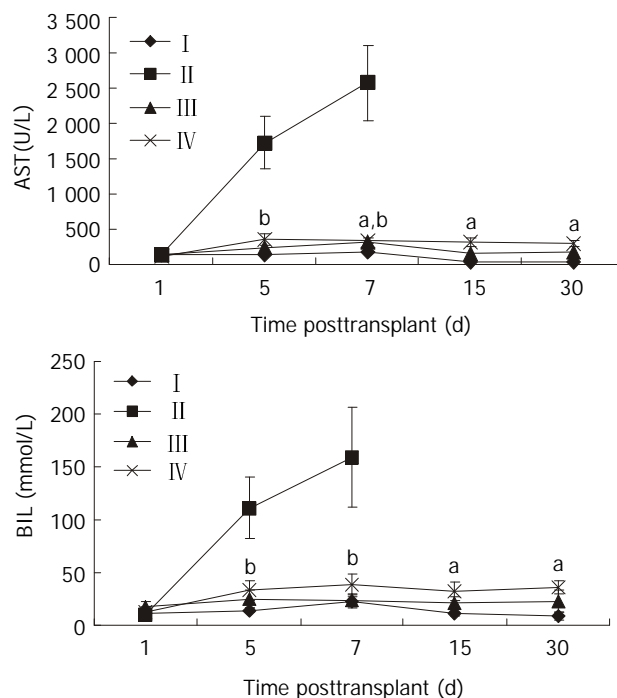


Figure 2 Effect of 1,25-(OH) $_2$ D $_3$ on graft function ($\bar{x}\pm s$). ^a $P < 0.05$, vs Group I; ^b $P < 0.05$, vs Group II.

Histological assessment of graft rejection

In Group I no signs of rejection were found all the time, on day 5 posttransplant, minimal inflammation on portal area was found, average RAI score was 0.3 \pm 0.6. On all other experimental times, RAI score was 0; In group II, a few lymphocytes infiltrated in portal area with minimal vein endothelialitis on day 1 posttransplant. Lymphocytes infiltrated

in portal area obviously with degeneration of hepatic parenchyma in all cases on day 5 posttransplant with average RAI 8.3 ± 1.1 . Marked mononuclear infiltration, severe vein subendothelialitis with bridging hepatocellular necrosis can be found on day 7 posttransplant with average RAI 8.7 ± 0.6 . Rejection reaction was greatly inhibited in Group III due to the immunosuppressive effect of CsA. No evidence of rejection was found on day 1 and day 5 posttransplant. But both inflammatory infiltration and endothelialitis can be found on day 7 with RAI at 2.3 ± 0.6 was evaluated. Infiltration in portal area and bile duct hyperplasia in some cases were detected on day 15 and day 30 posttransplant. As for Group IV, RAI was 0 on day 1 posttransplant. On day 5 posttransplant, RAI was 2.3 ± 0.6 . Inflammatory was mild. Vein subendothelial tissue and bile duct were cuffed by lymphocytic infiltrate occasionally. Necrosis of hepatocytes was not detected. On day 7 and 15, mild to moderate portal inflammatory was continuously mild to moderate. Various degree endothelialitis or hepatocyte necrosis existed in some cases. On day 30 posttransplant, mild to moderate portal infiltrate was still existed. Mild bile duct hyperplasia was found in 2/3 cases. RAI in Group IV was lower than in Group II significantly ($P < 0.05$) on each time point. In comparison with Group III, RAI in group IV was slightly higher without any significance ($P > 0.05$) on each time point (Figure 3).

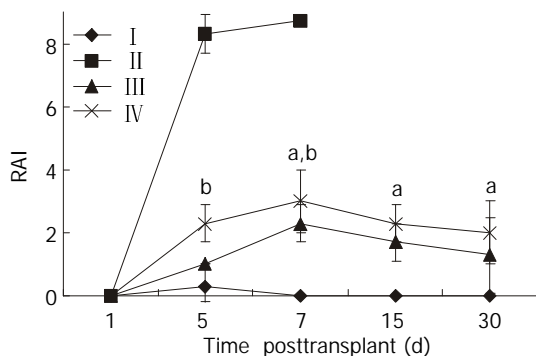


Figure 3 Effect of $1,25\text{-(OH)}_2\text{D}_3$ on Rejection Activity Index (RAI). ($\bar{x} \pm s$). ^a $P < 0.05$, vs Group I; ^b $P < 0.05$ vs Group II.

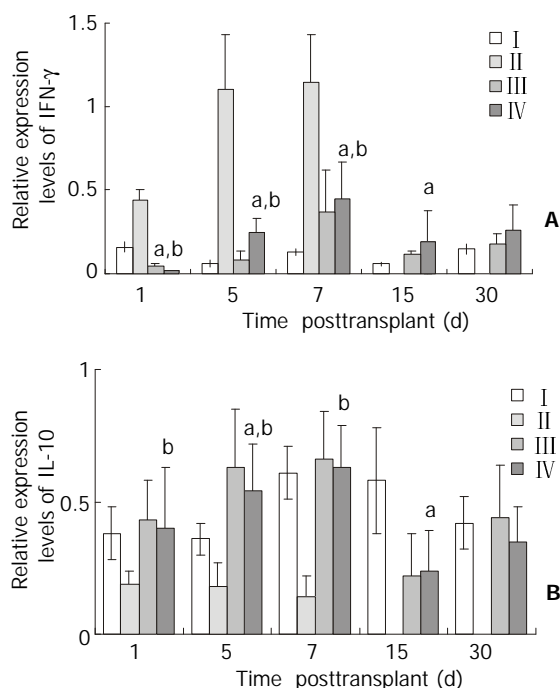


Figure 4 Effect of $1,25\text{-(OH)}_2\text{D}_3$ on IFN- γ and IL-10 gene transcription ($\bar{x} \pm s$, analyzed by RT-PCR). ^a $P < 0.05$, vs Group I; ^b $P < 0.05$ vs Group II.

Effect of $1,25\text{-(OH)}_2\text{D}_3$ on IFN- γ mRNA and IL-10 mRNA

On each defined time posttransplant, the expression of IFN- γ mRNA intra-graft was little in Group I and strong in Group II. After administration of CsA, the expressed level of IFN- γ mRNA decreased significantly ($P < 0.05$, vs Group II). After treatment with $1,25\text{-(OH)}_2\text{D}_3$ $1.0 \mu\text{g} \cdot \text{kg}^{-1} \cdot \text{d}^{-1}$, the expressed level of IFN- γ mRNA decreased significantly ($P < 0.05$, vs Group I; $P > 0.05$, vs Group III).

In contrast, expression of IL-10 mRNA intra-graft was strong and obvious in Group, but very weak in Group II. The expression level increased significantly ($P < 0.05$, vs Group II) after treatment with CsA. As for Group IV, the expression level increased markedly ($P < 0.05$, vs Group II; $P > 0.05$, vs Group III) (Figure 4).

DISCUSSION

As a newly recognized hormone, $1,25\text{-(OH)}_2\text{D}_3$ has immune activity *in vitro* and its role in organ transplantation has been highlighted last decade. For instance, MC1288, a analogue of $1,25\text{-(OH)}_2\text{D}_3$, could prolong survival of cardiac and small-bowel allografts in rats^[4]. $1,25\text{-(OH)}_2\text{D}_3$ was demonstrated to inhibit neonatal as well as vascularized heart transplantation rejection much effectively than a high-dose CsA regimen^[5]. However, no effect was observed in graft survival in a neonatal nonvascularized murine heart transplantation model in another report^[10]; Jordan *et al.*^[11] reported a marginal effect of vitamin D on rat cardiac allograft survival. In all cases, significant toxicity of hypercalcemia was observed. In our study, we showed that $1,25\text{-(OH)}_2\text{D}_3$ can effectively inhibit acute rejection following liver transplantation, and prolong recipients' survival markedly. Our study also showed that hypercalcemic effect of $1,25\text{-(OH)}_2\text{D}_3$ can be mitigated by a low-calcium diet. The major differences between these studies were the administrative route of $1,25\text{-(OH)}_2\text{D}_3$. It was given every other day intraperitoneally in previous study. Since the half-life of $1,25\text{-(OH)}_2\text{D}_3$ is few hours^[1], the administration of this compound every other day would not be sufficient. Furthermore, several studies used various analogues of vitamin D such as KH1060, MC1288. These analogues had varied side effect of hypercalcemia by changing its stereochemistry at C-20^[12-14], and allowed to take higher dosage of this agents and thus increased its immune effect in therapy.

In present study, it has been confirmed that the beneficial of $1,25\text{-(OH)}_2\text{D}_3$ on survival was due to a marked inhibition of rejection and amelioration of graft function. At the cellular level, $1,25\text{-(OH)}_2\text{D}_3$ interferes with function of antigen-presenting cells by decreasing MHC class II expression, and blocks mitogen stimulated T-cell proliferation^[15-17]. As a result, $1,25\text{-(OH)}_2\text{D}_3$ reduces the immunogenicity of allograft and the cytotoxicity of CTL, prevents the allograft from immune attack. In present study, the allografts of rats that did not receive $1,25\text{-(OH)}_2\text{D}_3$ demonstrated moderate to severe acute rejection. Marked lymphocytic infiltration, severe bile duct injury, subendothelialitis and hepatic necrosis were observed. The RAI score and bilirubin concentration, AST activity increased continuously until the death of recipients. In contrast, allografts of rats receiving $1,25\text{-(OH)}_2\text{D}_3$ showed significant improvement. Lymphocytic infiltration intra-graft and hepatocellular necrosis were mild, and the rejection activity was inhibited. On each time point observed, the differences in values of RAI, BIL and AST between Group III and IV were not significant statistically. It suggested that the effect of $1,25\text{-(OH)}_2\text{D}_3$ and CsA in protecting graft function was equal.

Some studies^[18-21] showed that in allografting Th1 cells delayed rejection by priming the cytotoxicity of CTL and delayed-type hypersensitivity reaction through cytokine, and Th2 cells induced allografts tolerance by receding the activity

of Th1 cells through cytokine. 1,25-(OH)₂D₃ interacted with a nuclear receptor (VDR). In nuclear, VDR combined with RXR to form a heterodimer, then bound to the target gene. Once 1, 25-(OH)₂D₃ combined with the VDR, DNA bending occurs. Ultimately it affected the RNA polymerase activity for either stimulation or suppression of transcription^[22-24]. The present study has demonstrated that 1,25-(OH)₂D₃ can inhibit transcription of IFN- γ , and stimulate transcription of IL-10. Thus, our results provide further evidence that a high IL-10 and low IFN- γ expression state may protect allografts^[25,26]. It was manifested *in vitro* that 1,25-(OH)₂D₃ could inhibit interleukin 12^[27] which was produced by myelomonocytic cells and played a pivotal role in the development of Th1 cells, as well as inhibition the excretion of cytokine such as IFN- γ ^[28,29] and IL-2^[30,31]. In the other hand, 1,25-(OH)₂D₃ can directly stimulate Th2 cells to excrete cytokine such as IL-4, IL-5 and IL-10^[32-34]. The effect of vitamin D3 on cytokine may shift the immune response from the Th1 pathway, which leads to allograft rejection to the Th2 pathway, which can induce allograft tolerance.

In kinetic surveillance, some common characteristic can be found in all groups. In isograft, variation of each index was relatively gentle. The allografts of rats that did not take 1,25-(OH)₂D₃ demonstrated a obvious tidemark of rejection on day 5 posttransplant. In Group III and IV, the rejection reaction was inhibited markedly due to the immunosuppressive effect of 1,25-(OH)₂D₃ and CsA. The kinetic in the two groups and IFN- γ mRNA and RAI were similar, that is, the severe rejection reaction appeared on day 7 posttransplant, meanwhile expression of IL-10 mRNA and liver function were very low. Previous studies^[35,36] showed that high immunoresponses occurred day 3 to day 5 posttransplantation and thus called a transient "rejection crisis". It may be due to the strong immunosuppressive effect of 1,25-(OH)₂D₃ and CSA that rejection crisis phase in Group III and IV was postponed. Interesting, although majority of recipients in group III and IV survived for long-term, all of grafts in these two groups were demonstrated various degree of rejection activity. Further studies^[37,38] have confirmed that majority of this rejection was self-limited, and it could resolve spontaneously by day 50 posttransplant without immunosuppressive agents.

In conclusion, our study proved that 1,25-(OH)₂D₃ could effectively modulate the cytokine net, induce TH1/TH2 shifting, and thus postpone the "rejection crisis", inhibit the acute rejection and protect the graft function.

REFERENCES

- Brown AJ**, Dusso A, Slatopolsky E. Vitamin D. *Am J Physiol* 1999; **277**: 157-175
- Lemire J**. 1,25-Dihydroxyvitamin D₃-a hormone with immunomodulatory properties. *Z Rheumatol* 2000; **59**: 24-27
- van Etten E**, Branisteanu DD, Verstuyf A, Waer M, Bouillon R, Mathieu C. Analogs of 1,25-dihydroxyvitamin D₃ as dose-reducing agents for classical immunosuppressants. *Transplantation* 2000; **69**: 1932-1942
- Johnsson C**, Tufveson G. MC 1288-a vitamin D analogue with immunosuppressive effects on heart and small bowel grafts. *Transpl Int* 1994; **7**: 392-397
- Hullett DA**, Cantorna MT, Redaelli C, Humpal-Winter J, Hayes CE, Sollinger HW, Deluca HF. Prolongation of allograft survival by 1,25-dihydroxyvitamin D₃. *Transplantation* 1998; **66**: 824-828
- Redaelli CA**, Wagner M, Gunter-Duwe D, Tian YH, Stahel PF, Mazzucchelli L, Schmid RA, Schilling MK. 1 α ,25-dihydroxyvitamin D₃ shows strong and additive immunomodulatory effects with cyclosporine A in rat renal allotransplants. *Kidney Int* 2002; **61**: 288-296
- Griffin MD**, Lutz W, Phan VA, Bachman LA, McKean DJ, Kumar R. Dendritic cell modulation by 1 α ,25-dihydroxyvitamin D₃ and its analogs: a vitamin D receptor-dependent pathway that promotes a persistent state of immaturity *in vitro* and *in vivo*. *Proc Natl Acad Sci U S A* 2001; **98**: 6800-6805
- Kamada N**, Calne RY. A surgical experience with five hundred thirty liver transplants in the rat. *Surgery* 1983; **93**: 64-69
- An international panel**. Banff schema for grading liver allograft rejection: an international consensus document. *Hepatology* 1997; **25**: 658-663
- Lemire JM**, Archer DC, Khulkarni A, Ince A, Uskokovic MR, Stepkowski S. Prolongation of the survival of murine cardiac allografts by the vitamin D₃ analogue 1,25-dihydroxy-delta 16-cholecalciferol. *Transplantation* 1992; **54**: 762-763
- Jordan SC**. 1,25-dihydroxyvitamin D₃ prolongs allograft rat cardiac allograft survival, in molecular, cellular and clinical endocrinology. In: Norman AW, Schaefer K, Grigoleit HG, eds. Berlin: *Walter de Gruyter* 1988: 334-339
- Tocchini-Valentini G**, Rochel N, Wurtz JM, Mitschler A, Moras D. Crystal structures of the vitamin D receptor complexed to superagonist 20-epi ligands. *Proc Natl Acad Sci U S A* 2001; **98**: 5491-5496
- Vaisanen S**, Ryhanen S, Saarela JT, Maenpaa PH. Structure-function studies of new C-20 epimer pairs of vitamin D₃ analogs. *Eur J Biochem* 1999; **261**: 706-713
- Nishii Y**, Okano T. History of the development of new vitamin D analogs: studies on 22-oxacalcitriol (OCT) and 2 β -(3-hydroxypropoxy)calcitriol (ED-71). *Steroids* 2001; **66**: 137-146
- Penna G**, Adorini L. 1 α ,25-dihydroxyvitamin D₃ inhibits differentiation, maturation, activation, and survival of dendritic cells leading to impaired alloreactive T cell activation. *J Immunol* 2000; **164**: 2405-2411
- Canning MO**, Grotenhuis K, de Wit H, Ruwhof C, Drexhage HA. 1- α , 25-Dihydroxyvitamin D₃ (1,25(OH)₂D₃) hampers the maturation of fully active immature dendritic cells from monocytes. *Eur J Endocrinol* 2001; **145**: 351-357
- Piemonti L**, Monti P, Sironi M, Fraticelli P, Leone BE, Dal Cin E, Allavena P, Di Carlo V. Vitamin D₃ affects differentiation, maturation, and function of human monocyte-derived dendritic cells. *J Immunol* 2000; **164**: 4443-4451
- Ke B**, Ritter T, Kato H, Zhai Y, Li J, Lehmann M, Busuttill RW, Volk HD, Kupiec-Weglinski JW. Regulatory cells potentiate the efficacy of IL-4 gene transfer by up-regulating Th2-dependent expression of protective molecules in the infectious tolerance pathway in transplant recipients. *J Immunol* 2000; **164**: 5739-5745
- Affleck DG**, Bull DA, Albanil A, Shao Y, Brady J, Karwande SV, Eichwald EJ, Shelby J. Interleukin-18 production following murine cardiac transplantation: correlation with histologic rejection and the induction of INF-gamma. *J Interferon Cytokine Res* 2001; **21**: 1-9
- Mukai M**, Bohgaki T, Kondo M, Notoya A, Kohno M. Changes in the T-helper cell 1/T-helper cell 2 balance of peripheral T-helper cells after autologous peripheral blood stem cell transplantation for non-Hodgkin's lymphoma. *Ann Hematol* 2001; **80**: 715-721
- Tan L**, Howell WM, Smith JL, Sadek SA. Sequential monitoring of peripheral T-lymphocyte cytokine gene expression in the early post renal allograft period. *Transplantation* 2001; **71**: 751-759
- DeLuca HF**, Zierold C. Mechanisms and functions of vitamin D. *Nutr Rev* 1998; **56**: S4-10
- Nagpal S**, Lu J, Boehm MF. Vitamin D analogs: mechanism of action and therapeutic applications. *Curr Med Chem* 2001; **8**: 1661-1679
- Towers TL**, Staeva TP, Freedman LP. A two-hit mechanism for vitamin D₃-mediated transcriptional repression of the granulocyte-macrophage colony-stimulating factor gene: vitamin D receptor competes for DNA binding with NFAT1 and stabilizes c-Jun. *Mol Cell Biol* 1999; **19**: 4191-4199
- Zuo Z**, Wang C, Carpenter D, Okada Y, Nicolaidou E, Toyoda M, Trento A, Jordan SC. Prolongation of allograft survival with viral IL-10 transfection in a highly histoincompatible model of rat heart allograft rejection. *Transplantation* 2001; **71**: 686-691
- Halloran PF**, Miller LW, Urmson J, Ramassar V, Zhu LF, Kneteman NM, Solez K, Afrouzian M. IFN-gamma alters the pathology of graft rejection: protection from early necrosis. *J Immunol* 2001; **166**: 7072-7081
- D' Ambrosio D**, Cippitelli M, Cocciolo MG, Mazzeo D, Di Lucia P, Lang R, Sinigaglia F, Panina-Bordignon P. Inhibition of IL-12 production by 1,25-dihydroxyvitamin D₃. Involvement of NF-kappaB downregulation in transcriptional repression of the p40

- gene. *J Clin Invest* 1998; **101**: 252-262
- 28 **Mattner F**, Smirolto S, Galbiati F, Muller M, Di Lucia P, Poliani PL, Martino G, Panina-Bordignon P, Adorini L. Inhibition of Th1 development and treatment of chronic-relapsing experimental allergic encephalomyelitis by a non-hypercalcemic analogue of 1,25-dihydroxyvitamin D(3). *Eur J Immunol* 2000; **30**: 498-508
- 29 **Takeuchi A**, Reddy GS, Kobayashi T, Okano T, Park J, Sharma S. Nuclear factor of activated T cells (NFAT) as a molecular target for 1alpha, 25-dihydroxyvitamin D3-mediated effects. *J Immunol* 1998; **160**: 209-218
- 30 **Staeva-Vieira TP**, Freedman LP. 1,25-dihydroxyvitamin D3 inhibits IFN-gamma and IL-4 levels during in vitro polarization of primary murine CD4+ T cells. *J Immunol* 2002; **168**: 1181-1189
- 31 **Gregori S**, Casorati M, Amuchastegui S, Smirolto S, Davalli AM, Adorini L. Regulatory T cells induced by 1 alpha,25-dihydroxyvitamin D3 and mycophenolate mofetil treatment mediate transplantation tolerance. *J Immunol* 2001; **167**: 1945-1953
- 32 **Boonstra A**, Barrat FJ, Crain C, Heath VL, Savelkoul HF, O'Garra A. 1alpha,25-Dihydroxyvitamin d3 has a direct effect on naive CD4(+) T cells to enhance the development of Th2 cells. *J Immunol* 2001; **167**: 4974-4980
- 33 **Cantorna MT**, Woodward WD, Hayes CE, DeLuca HF. 1,25-dihydroxyvitamin D3 is a positive regulator for the two anti-encephalitogenic cytokines TGF-beta 1 and IL-4. *J Immunol* 1998; **160**: 5314-5319
- 34 **Overbergh L**, Decallonne B, Waer M, Rutgeerts O, Valckx D, Casteels KM, Laureys J, Bouillon R, Mathieu C. 1alpha,25-dihydroxyvitamin D3 induces an autoantigen-specific T-helper 1/T-helper 2 immune shift in NOD mice immunized with GAD65 (p524-543). *Diabetes* 2000; **49**: 1301-1307
- 35 **Sharland A**, Shastry S, Wang C, Rokahr K, Sun J, Sheil AG, McCaughan GW, Bishop GA. Kinetics of intragraft cytokine expression, cellular infiltration, and cell death in rejection of renal allografts compared with acceptance of liver allografts in a rat model: early activation and apoptosis is associated with liver graft acceptance. *Transplantation* 1998; **65**: 1370-1377
- 36 **Rokahr KL**, Sharland AF, Sun J, Wang C, Sheil AG, Yan Y, McCaughan GW, Bishop GA. Paradoxical early immune activation during acceptance of liver allografts compared with rejection of skin grafts in a rat model of transplantation. *Immunology* 1998; **95**: 257-263
- 37 **Gassel HJ**, Otto C, Gassel AM, Meyer D, Steger U, Timmermann W, Ulrichs K, Thiede A. Tolerance of rat liver allografts induced by short-term selective immunosuppression combining monoclonal antibodies directed against CD25 and CD54 with subtherapeutic cyclosporine. *Transplantation* 2000; **69**: 1058-1067
- 38 **Lord R**, Goto S, Pan T, Chiang K, Chen C, Sunagawa M. Peak protein expression of IL-2 and IFN-gamma correlate with the peak rejection episode in a spontaneously tolerant model of rat liver transplantation. *Cytokine* 2001; **13**: 155-161

Edited by Ren SY

Modulation of GdCl₃ and Angelica Sinensis polysaccharides on differentially expressed genes in liver of hepatic immunological injury mice by cDNA microarray

Hong Ding, Gang-Gang Shi, Xin Yu, Jie-Ping Yu, Jie-An Huang

Hong Ding, Gang-Gang Shi, Medical College, Shantou University, Shantou, 515031, Guangdong Province, China

Xin Yu, College of Pharmacy, Wuhan University, Wuhan, 430072, Hubei Province, China

Jie-Ping Yu, Jie-An Huang, Department of Gastroenterology, The First Affiliated Hospital, Clinical Medical College, Wuhan University, Wuhan, 430064, Hubei Province, China

Correspondence to: Dr. Hong Ding, College of Pharmacy, Wuhan University, Wuhan 430072, Hubei Province, China. dinghong2000@263.net

Telephone: +86-27-87682339 **Fax:** +86-27-87682339

Received: 2002-09-13 **Accepted:** 2002-11-28

Abstract

AIM: To study the modulating effect of GdCl₃ and Angelica Sinensis polysaccharides (ASP) on differentially expressed genes in liver of hepatic immunological mice by cDNA microarray.

METHODS: Hepatic immunological injury was induced by lipopolysaccharide (LPS ip, 0.2 mg·kg⁻¹) in bacillus calmetteguerin (BCG ip, 1 mg·kg⁻¹) primed mice; A single dose of 20 mg·kg⁻¹ GdCl₃ was simultaneously pretreated and 30 mg·kg⁻¹ ASP (ig, qd×7 d) was administrated when the BCG+LPS was primed. The mice were sacrificed at the end of the 7th day after ip LPS for 6 h and the liver was removed quickly. The PCR products of 512 genes were spotted onto a chemical material-coated glass plate in array. The DNAs were fixed to the glass plate after series of treatments. The total RNAs were isolated from the liver tissue, and were purified to mRNAs by Oligotex. Both mRNAs from the normal liver tissue and the liver tissue from the mice with hepatic immunological injury or that pretreated with GdCl₃ or ASP were reversely transcribed to cDNAs with the incorporation of fluorescent dUTP to prepare the hybridization probes. The mixed probes were hybridized to the cDNA microarray. After high-stringent washing, the cDNA microarray was scanned for fluorescent signals and showed differences between the two tissues.

RESULTS: Among the 512 target genes, 18 differed in liver tissue of hepatic immunological injury mice, and 6 differed in those pretreated by ASP, 7 differed in those pretreated by GdCl₃.

CONCLUSION: cDNA microarray technique is effective in screening the differentially expressed genes between two different kinds of tissue. Further analysis of those obtained genes will be helpful to understand the molecular mechanism of hepatic immunological injury and to study the intervention of drug. Both ASP and GdCl₃ can decrease the number of the differentially expressed genes in liver tissue of mice with hepatic immunological injury.

Ding H, Shi GG, Yu X, Yu JP, Huang JA. Modulation of GdCl₃ and Angelica Sinensis polysaccharides on differentially expressed genes in liver of hepatic immunological injury mice by cDNA microarray. *World J Gastroenterol* 2003; 9(5): 1072-1076

<http://www.wjgnet.com/1007-9327/9/1072.htm>

INTRODUCTION

The advanced technique of DNA microarray makes it possible to monitor the expression of ten out of thousand genes simultaneously in one hybridization experiment^[1,2]. The past year has demonstrated the versatility of microarrays for the analysis of whole model-organism genomes and has seen the development of chips to measure the expression of 40 000 human genes. Microarray technology has also become considerably more robust and sensitive^[3]. The technology of microarrays has advanced from reverse Northern blots on filters detected using radioactive probes to a highly technical field involving miniaturized synthesis, multi-color fluorescent labeling, and database management. Recently, whole genome has been analyzed^[4,5]. Microarray analyses typically follow the steps of gene selection, microarray synthesis, sample preparation, array hybridization, detection, and data analysis with appropriate controls required for each. Functional genomics is the study of gene function through the parallel expression measurements of genomes, most commonly using the technologies of microarrays and serial analysis of gene expression. Microarray could use in some other field also, such as, basic research of drug and target discovery, biomarker determination, pharmacology, toxicogenomics, target selectivity, development of prognostic tests and disease-subclass determination^[6]. In this experiment, the DNA segments were spotted on a slide with high density. Then cDNA retro-transcribed from mRNA derived from normal or pathological tissues, which were labeled with Cy3 and Cy5 fluorescence, hybridized with the microarray slide^[7]. Through this technique, detection of differentially expressed genes and the construction of differential gene expression profiles are greatly facilitated. The BioDoor 512DNA microarray was used for investigating the changes of gene expression in liver tissue of hepatic immunological mice and studying the effective mechanisms of ASP and GdCl₃, which might give important health benefits to understanding, diagnosing and treating the liver injury.

MATERIALS AND METHODS

Animals and treatments

Hepatic immunological injury was induced by lipopolysaccharide (LPS ip, 0.2 mg·kg⁻¹) in bacillus calmetteguerin (BCG ip, 1 mg·kg⁻¹) primed mice (Model); A single dose of 20 mg·kg⁻¹ GdCl₃ was pretreated simultaneously (Model+GdCl₃) and 30 mg·kg⁻¹ ASP (Model+ASP, ig, qd×7 d) was administrated when the BCG+LPS was primed. The mice were sacrificed at the end of the 7th day after ip LPS for 6 h and the liver was collected for analysis of cDNA microarray.

Construction of microarrays^[4]

The BioDoor 512 microarray consisted of a total of 512 novel or known genes (provided by United Gene Holdings, Ltd). These genes were amplified through PCR using universal primers and then purified; the purity of PCR production was dissolved in 3×SSC solution, and these target genes were spotted on silylated slides (Tele Chem, Inc.) by Cartesian 7 500 Spotting Robotics (Cartesian, Inc.). After spotting, the slides were hydrated (2 h), dried (0.5 h) at room temperature, UV cross-linked (65 mJ/cm), and then treated with 0.2 % SDS (10 min). The slides were dried again and ready for use.

Probe preparation^[4]

The method of total RNA extraction was modified from the original single step extraction with Trizol agent. The liver tissue stored in liquid nitrogen were ground completely into tiny granules in 100 mm ceramic mortar (RNase free) and homogenized in Trizol. The pellet of total RNA was dissolved with Milli-Q H₂O. The mRNAs were purified using Oligotex mRNA Midi Kit (Qiagen, Inc.). The fluorescent cDNA probes were prepared through reverse transcription and then purified (referring to the protocol of Mark. Schena.). The probes from normal tissues were labeled with Cy3-dUTP, those from the pathological tissues were with Cy5-dUTP.

Hybridization and washing^[4]

The probes were mixed and precipitated by ethanol, and resolved in 20 μl hybridization solution (5×SSC + 0.4 % SDS +50 % formamide + 5×denhardt's solution). Chip was prehybridized with Hyb sol +3 μl denatured salmon sperm DNA at 42 °C for 6 h. After denaturing at 95 °C for 5 min, the probe mixture was added on the prehybridized chip and covered with glass. The chips were incubated at 42 °C for 15-17 h. The slide was then washed in solutions of 2×SSC + 0.2 % SDS,

0.1×SSC+ 0.2 % SDS and 0.1×SSC at 60 °C, respectively for 10 min each, then dried at room temperature.

Detection and analysis^[4]

The chip was scanned by ScanArray 5000 laser scanner (General Scanning, Inc) at 2 wavelengths. The acquired image was analyzed by ImaGene 3.0 software (BioDiscovery, Inc.). The intensity of each spot at the 2 wavelengths represented the quantity of Cy3-dUTP and Cy5-dUTP, respectively. The ratio of Cy3 to Cy5 was calculated. The two overall intensity was normalized by a coefficient according to the ratios of the located 40 housekeeping genes.

RESULTS***Differentially expressed gene in liver tissues between mice with or without hepatic immunological injury***

Total 18 differentially expressed genes that might be associated with hepatic immunological injury were selected from microarray. 4 genes showed up-regulation and 14 genes showed down-regulation (Table1, Figures 1 and 2).

Differentially expressed gene in liver tissues between mice with hepatic immunological injury and those pretreated by GdCl₃

6 differentially expressed genes associated with the effect of GdCl₃ on hepatic immunological injury were selected from the microarray. 1 gene showed up-regulation and 5 genes showed down-regulation (Table 2, Figures 1 and 2).

Differentially expressed gene in liver tissues between mice with hepatic immunological injury and those pretreated by ASP

7 differentially expressed genes associated with the effect of ASP on hepatic immunological injury were selected from the microarray. 1 gene showed up-regulation and 6 genes showed down-regulation (Table3, Figures 1 and 2).

Table 1 Differentially expressed gene in liver tissues between hepatic immunological injury mice and normal mice

Genbank-ID	Ratio(Cy5/Cy3)	Classification	Definition
Humipasa	0.253	Metabolism	Human mRNA for ATP synthase alpha subunit, complete cds.
Hsngmrna	0.285		H. sapiens hng mRNA for uracil DNA glycosylase.
Humoat	0.290	Modulators/Effectors/ intracellular transduction	Human ornithine aminotransferase mRNA, complete cds.
Hsncadhe	0.294	Cell Surface Antigens & Adhesion	Human mRNA for N-cadherin
Humpparp	0.307	0	Human acidic ribosomal phosphoprotein P0 mRNA, complete cds.
Humorf06	0.319	Other	Human mRNA for KIAA0106 gene, complete cds.
Hsgcsab	0.373	Modulators/Effectors/ intracellular transduction	H. sapiens soluble guanylate cyclase small subunit mRNA.
Humhspa2	0.379	Stress Response Proteins	Human heat shock protein HSPA2 gene, complete cds.
Hspbx3	0.439	Other	Human PBX3 mRNA
Hsef1gmr	0.452		H.sapiens mRNA for elongation factor-1-gamma
Hsgagmr	0.460	Other	Human mRNA for GARS-AIRS-GART
Humhhr23	0.467	DNA Synthesis, Repair & Recombination F	Human mRNA for XP-C repair com;lamenting protein(p58/HHR23B), complete cds.
Hscatr	0.470	Metabolism	Human kidney mRNA for catalase.
Humscp2a	0.5	Ion Channel & Transport Proteins	Human sterol carrier protein X.sterol carrier protein 2 mRNA, complete cds.
Humnpm	2.062	Other	Human nucleophosmin mRNA, complete cds.
Hsrpl32	2.074	DNA Binding/Transcription/ transcription F	Human mRNA for ribosomal protein L32.
Hsu32944	2.244	Apoptosis-Related proteins	Human cytoplasmic dynein light chain1(hdlc1) mRNA, complete cds.
Hsu32944	3.239	Oncogenes & Tumor Suppressors mRNA, com;oete cds.	Human cytoplasmic dynein light chain 1 (hdlc1)

Ratio is Cy5/Cy3: high expression (ratio >2.0), low expression (ratio<0.5).

Table 2 Differentially expressed gene in liver tissues between mice with hepatic immunological injury and those pretreated by GdCl₃

Genbank-ID	Ratio(Cy5/Cy3)	Classification	Definition
Hsung	0.313	DNA Binding/Transcription/Transcription Factors	Human cDNA for uracil-DNA glycosylase.
Hsu09564	0.343	Modulators/Effectors/intracellular Transduction	Human serine kinase mRNA, complete cds.
Hsu83843	0.374	Cell Surface Antigens & Adhesion	Human HIV-1 Nef interacting protein (Nip7-1)mRNA, Partial cds.
Hsmyc1	0.441	Oncogenes & Tumor Suppressors	Human mRNA encoding the c-myc oncogene.
Humoat	0.454	Modulators/Effectors/intracellular transduction	Human ornithine aminotransferase mRNA, complete cds.
Hsu70323	2.200	Extracellular Cell signaling & Communication proteins	Human ataxin-2(SCA2) mRNA, complete cds.

Ratio is Cy5/ Cy3: high expression (ratio >2.0), low expression (ratio<0.5).

Table 3 Differentially expressed gene in liver tissues between mice with hepatic immunological injury and those pretreated by ASP

Genbank-ID	Ratio(Cy5/Cy3)	Classification	Definition
Humscp2a	0.283	Ion channel & transport proteins	Human sterol carrier protein X.sterol carrier protein 2 mRNA, complete cds.
Humoat	0.421	Modulators/Effectors/intracellular transduction	Human ornithine aminotransferase mRNA, complete cds.
Hsngmrna	0.431		H. sapiens hng mRNA for uracil DNA glycosylase.
humpafaa	0.461	Modulators/Effectors/intracellular transduction	Human mRNA for platelet activating factor acetylhydrolase IB gamma-subunit, complete cds.
humhbgfb	0.481	Extracellular cell signaling & communication proteins	Human heparin-binding growth factor receptor (HBGF-R-alpha-a2) mRNA, complete cds.
Hsu83843	0.493	Cell surface antigens and adhesion	Human HIV-1 Nef interacting protein(Nip7-1)mRNA, Partial cds.
Humnlk	2.353	Modulators/Effectors/intracellular transduction	Human neroleukin mRNA, complete cds.

Ratio is Cy5/ Cy3: high expression (ratio >2.0), low expression (ratio<0.5).

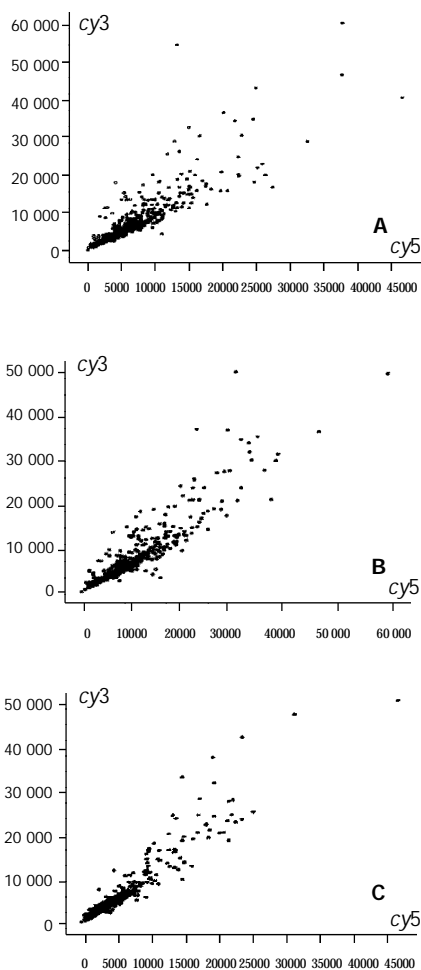


Figure 1 The scatter plots of gene expression pattern by cDNA microarray. A: Model liver(Cy5)/normal liver(Cy3); B: Model+GdCl₃ liver (Cy5)/normal liver; C: Model+ASP liver (Cy5)/normal liver (Cy3). Ratio is Cy5/Cy3: high expression (ratio >2.0), low expression (ratio<0.5), no change in expression (0.5<ratio<2.0).

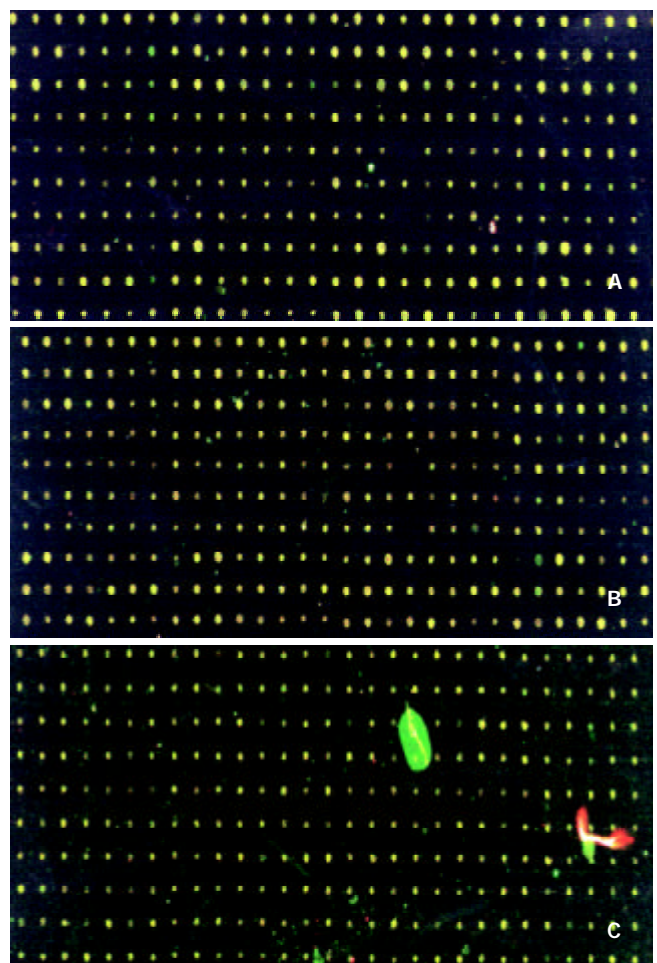


Figure 2 Scanning results of hybridizing signals by cDNA microarray. A: Model liver(Cy5)/normal liver(Cy3); B: Model+GdCl₃ liver (Cy5)/normal liver; C: Model+ASP liver (Cy5)/normal liver (Cy3). Color of spots in the merged image of Cy3 image and Cy5 image: high expression (red), low expression (green), no change in expression (yellow).

DISCUSSION

Hepatic immunological injury is a result of altering multiple genes expression. cDNA microarray method can simultaneously determine a number of genes altered in the different pathological and physiological status, so gene chip is a useful tool for studying the target cause of disease and the effect of drug^[10]. The DNA microarray hybridization applications reviewed include the important areas of gene expression analysis and genotyping for point mutations, single nucleotide polymorphisms (SNPs), and short tandem repeats (STRs)^[11,12]. In addition to the many molecular biological and genomic research uses, systems for pharmacogenomic research and drug discovery^[13,14], infectious and genetic disease and cancer diagnostics, and forensic and genetic identification purposes^[15-17]. Additionally, microarray technology being developed and applied to new areas of proteomic and cellular analysis are reviewed^[18,19]. Now, microarray has been developed many kinds, such as, protein microarray, GEM microarray, tissue microarray, they also have different kinds uses^[20-22].

The present study showed that 18 differentially expressed genes that might be associated with hepatic immunological injury were found, 4 genes showed up-regulation and 14 genes showed down-regulation. These genes expression could recover to normal level by GdCl₃ except the HIV-1 Nef interacting protein (Nip7-1) mRNA (Hsu83843). And by ASP except the HIV-1 Nef interacting protein (Nip7-1) mRNA (Hsu83843), sterol carrier protein X/sterol carrier protein 2 Mrna (Humsnp2a), and H.sapiens hug mRNA for uracil DNA glycosylase (Hsngmna).

Furthermore, cDNA or uracil-DNA glycosylase, serine kinase mRNA, encoding the c-myc oncogene expression (Hsmycl) showed down-regulation in the mice pretreated with GdCl₃. In this study we find that using GdCl₃ and ASP to pretreat mice with hepatic immunological liver both would cause down-regulation of Hsung and Hsngmna. Hsung and Hsngmna both related to encoding uracil-DNA glycosylase. In humans, uracil appears in DNA at the rate of several hundred bases per cell each day as a result of misincorporation of deoxyuridine (dU) or deamination of cytosine. The human UNG-gene at position 12q24.1 encodes nuclear (UNG2) and mitochondrial (UNG1) two forms of uracil-DNA glycosylase^[23]. Repair of uracil-DNA is a base-excision pathway initiated by a uracil-DNA glycosylase (UDG) enzyme of which have four families^[24]. The most efficient and well characterized of these uracil-DNA glycosylases is UDG which releases uracil from DNA, restores the correct DNA sequence, excises U from single- or double-stranded DNA and is associated with DNA replication forks^[25,26]. Uracil DNA glycosylase (UDG) and DNA polymerase beta (beta pol) are the two enzymes of base excision repair (BER)^[10]. Krokan *et al* propose that BER is important both in the prevention of cancer and for preserving the integrity of germ cell DNA during evolution^[23]. But Kvaløy *et al* find mutations affecting the function of human UNG gene are seemingly infrequent in human tumor cell lines^[26,27]. So we infer down-regulation of these genes may affect cell proliferation, and GdCl₃ and ASP protect liver depend on this mechanism in some degree. Although ornithine aminotransferase mRNA (Humoat) also showed down-regulation, its expression showed a little improvement (Cy5/Cy3 increased from 0.290 to 0.454). Ataxin-2 Mrna (Hsu70323) expression showed up-regulation in the mice pretreated with GdCl₃. As for the mice pretreated with ASP, Humoat expression also showed some improvement (Cy5/Cy3 increased from 0.290 to 0.421). TNF alpha can cause liver cell apoptosis through the TNF-alpha receptor or Fas/CD95, which is expressed by liver cells. The TNF-alpha induced expression of the nuclear oncogene c-myc in intact hepatocytes has been

studied^[28]. The expression of Hsmycl is down-regulation, which may be the reason of preventing hepatic cell from apoptosis. The liver plays a central role in nitrogen metabolism. Nitrogen enters the liver as free ammonia and as amino acids of which glutamine and alanine are the most important precursors. Detoxification of ammonia to urea involves deamination and transamination. Half of the extra NH₃ removed by the liver was, apparently, utilized by periportal glutamate dehydrogenase and aspartate aminotransferase for sequential glutamate and aspartate synthesis and converted to urea as the 2-amino moiety of aspartate^[29]. Ornithine aminotransferase is the most important enzyme to metabolize free ammonia and amino acids. The gene exists as a single copy in the malarial genome and is located on chromosomes 6/7/8^[30]. Ornithine-delta-aminotransferase (OAT) (EC 2.6.1.13) is a pyridoxal-5' phosphate dependent mitochondrial matrix enzyme. It controls the L-ornithine (Orn) level in tissues by catalysing the transfer of the delta-amino group of Orn to 2-oxoglutarate. The products of this reaction are L-glutamate-gamma-semialdehyde and L-glutamate^[31]. Boon L proves that high protein diet would cause ornithine aminotransferase increased^[32]. NOX significantly reduced serum levels of ornithine carbamoyltransferase and aspartate aminotransferase as hepatic injury^[33]. The present study showed ornithine aminotransferase mRNA (Humoat) showed down-regulation, but its expression showed a little improvement (Cy5/Cy3 increased from 0.290 to 0.454) and (Cy5/Cy3 increased from 0.290 to 0.421) with GdCl₃ and ASP. So we think ornithine aminotransferase is important aspect in hepatic injury. Protective effect of GdCl₃ and ASP on the hepatic immunological injury depends on regulating the expression of ornithine aminotransferase. While the heparin-binding growth factor receptor (HBGF-R-alpha-a2) mRNA (humhbgfb) expression showed down-regulation and neuroleukin mRNA (Humnlk) expression showed up-regulation in the mice. Neuroleukin (NLK) is a multifunctional protein, involved in neuronal growth, glucose metabolism, cell motility, and differentiation. Neuroleukin (NLK), autocrine motility factor (AMF) and phosphohexose isomerase (PHI) have been identified same structure, so they have many kinds on functions and expressed in many tissues and organs, such as, brain, bone, liver, etc. NLK could mediate leukemia cell^[34]. Romagnoli *et al* show that the block of NLK commits PC12 cells to caspase-dependent apoptosis, and suggest a general protective role of NLK in the control of cell death in neuronal cells^[35]. NLK may be modulating inflammation and is probably involved in protecting CN and the cerebellums against apoptosis^[36]. When ASP pretreat mice with hepatic immunological injury, the expression of Humnlk up-regulation may show ASP prevent cell apoptosis. It remains to be demonstrated whether the altered genes are target of protective effect of GdCl₃ or ASP on the immunological liver injury, and further analysis the function of these genes is needed.

REFERENCES

- 1 **Aharoni A**, Keizer LC, Bouwmeester HJ, Sun Z, Alvarez-Huerta M, Verhoeven HA, Blaas J, van Houwelingen AM, De Vos RC, van der Voet H, Jansen RC, Guis M, Mol J, Davis RW, Schena M, van Tunen AJ, O'Connell AP. Identification of the SAAT gene involved in strawberry flavor biogenesis by use of DNA microarrays. *Plant Cell* 2000; **12**: 647-662
- 2 **Schena M**, Mulatero P, Schiavone D, Mengozzi G, Tesio L, Chiandussi L, Veglio F. Vasoactive hormones induce nitric oxide synthase mRNA expression and nitric oxide production in human endothelial cells and monocytes. *Am J Hypertens* 1999; **12**: 388-397
- 3 **Leethanakul C**, Knezevic V, Patel V, Amornphimoltham P, Gillespie J, Shillitoe EJ, Emko P, Park MH, Emmert-Buck MR, Strausberg RL, Krizman DB, Gutkind JS. Gene discovery in oral

- squamous cell carcinoma through the Head and Neck Cancer Genome Anatomy Project: confirmation by microarray analysis. *Oral Oncol* 2003; **39**: 248-258
- 4 **Jiang Y**, Harlocker SL, Molesh DA, Dillon DC, Stolk JA, Houghton RL, Repasky EA, Badaro R, Reed SG, Xu J. Discovery of differentially expressed genes in human breast cancer using subtracted cDNA libraries and cDNA microarrays. *Oncogene* 2002; **21**: 2270-2282
- 5 **DeRisi JL**, Lyer VR, Brown PO. Exploring the metabolic and genetic control of gene expression on a genomic scale. *Science* 1997; **278**: 680-686
- 6 **Butte A**. The use and analysis of microarray data. *Nat Rev Drug Discov (Nature reviews Drug discovery)* 2002; **1**: 951-960
- 7 **Shalon D**, Smith SJ, Brown PO. A DNA microarray system for analyzing complex DNA samples using two-color fluorescent probe hybridization. *Genome Res* 1996; **6**: 639-645
- 8 **Welford SM**, Gregg J, Chen E. Detection of differentially expressed genes in primary tumor tissues using representational differences analysis coupled to microarray hybridization. *Nucleic Acids Res* 1998; **26**: 3059-3065
- 9 **Heller MJ**. DNA microarray technology: devices, systems, and applications. *Annu Rev Biomed Eng (Annual review of biomedical engineering)* 2002; **4**: 129-153
- 10 **Armour JA**, Barton DE, Cockburn DJ, Taylor GR. The detection of large deletions or duplications in genomic DNA. *Hum Mutat* 2002; **20**: 325-337
- 11 **Stickney HL**, Schmutz J, Woods IG, Holtzer CC, Dickson MC, Kelly PD, Myers RM, Talbot WS. Rapid mapping of zebrafish mutations with SNPs and oligonucleotide microarrays. *Genome Res* 2002; **12**: 1929-1934
- 12 **Santacroce R**, Ratti A, Caroli F, Foglieni B, Ferraris A, Cremonesi L, Margaglione M, Seri M, Ravazzolo R, Restagno G, Dallapiccola B, Rappaport E, Pollak ES, Surrey S, Ferrari M, Fortina P. Analysis of clinically relevant single-nucleotide polymorphisms by use of microelectronic array technology. *Clin Chem* 2002; **48**: 2124-2130
- 13 **Butte A**. The use and analysis of microarray data. *Nat Rev Drug Discov* 2002; **1**: 951-960
- 14 **Petricoin EF**, Zoon KC, Kohn EC, Barrett JC, Liotta LA. Clinical proteomics: translating benchside promise into bedside reality. *Nat Rev Drug Discov* 2002; **1**: 683-695
- 15 **Hoffman EP**, Rao D, Pachman LM. Clarifying the boundaries between the inflammatory and dystrophic myopathies: insights from molecular diagnostics and microarrays. *Rheum Dis Clin North Am* 2002; **28**: 743-757
- 16 **Maier S**, Olek A. Diabetes: a candidate disease for efficient DNA methylation profiling. *J Nutr* 2002; **132**: 2440S-2443S
- 17 **Macgregor PF**, Squire JA. Application of microarrays to the analysis of gene expression in cancer. *Clin Chem* 2002; **48**: 1170-1177
- 18 **Martinez MJ**, Aragon AD, Rodriguez AL, Weber JM, Timlin JA, Sinclair MB, Haaland DM, Werner-Washburne M. Identification and removal of contaminating fluorescence from commercial and in-house printed DNA microarrays. *Nucleic Acids Res* 2003; **31**: e18
- 19 **Nam JH**, Yu CH, Hwang KA, Kim S, Ahn SH, Shin JY, Choi WY, Joo YR, Park KY. Application of cDNA microarray technique to detection of gene expression in host cells infected with viruses. *Acta Virol* 2002; **46**: 141-146
- 20 **Reynolds MA**. Microarray technology GEM microarrays and drug discovery. *J Ind Microbiol Biotechnol (Journal of industrial microbiology & biotechnology)* 2002; **28**: 180-185
- 21 **Templin MF**, Stoll D, Schrenk M, Traub PC, Vöhringer CF, Joos TO. Protein microarray technology. *Drug Discov Today (Drug discovery today)* 2002; **7**: 815-822
- 22 **Rimm DL**, Camp RL, Charette LA, Costa J, Olsen DA, Reiss M. Tissue microarray: a new technology for amplification of tissue resources. *Cancer J (Cancer journal (Sudbury, Mass.))* 2001; **7**: 24-31
- 23 **Krokan HE**, Otterlei M, Nilsen H, Kavli B, Skorpen F, Andersen S, Skjelbred C, Akbari M, Aas PA, Slupphaug G. Properties and functions of human uracil-DNA glycosylase from the UNG gene. *Prog Nucleic Acid Res Mol Biol (Progress in nucleic acid research and molecular biology.)* 2001; **68**: 365-386
- 24 **Pearl LH**. Structure and function in the uracil-DNA glycosylase superfamily. *Mutat Res (Mutation research.)* 2000; **3-4**: 165-181
- 25 **Dinner AR**, Blackburn GM, Karplus M. Uracil-DNA glycosylase acts by substrate autocatalysis. *Nature (Nature.)* 2001; **413**: 725-752
- 26 **Kvaløy K**, Nilsen H, Steinsbekk KS, Nedal A, Monterotti B, Akbari M, Krokan HE. Sequence variation in the human uracil-DNA glycosylase (UNG) gene. *Mutat Res (Mutation research.)* 2001; **4**: 325-338
- 27 **Mendez F**, Sandigursky M, Franklin WA, Kenny MK, Kureekattil R, Bases R. Heat-shock proteins associated with base excision repair enzymes in HeLa cells. *Radiat Res (Radiation research.)* 2000; **2**: 186-195
- 28 **Globa AG**, Solovyev AS, Terentyev AA, Demidova VS, Shulgina MF, Alesenko AV, Karelin AA. TNF alpha-induced aerobic synthesis of ATP on plasma membranes of target cells. The relation to the expression of the nuclear oncogene c-myc. *Biochem Mol Biol Int (Biochemistry and molecular biology international.)* 1998; **6**: 1169-1178
- 29 **Milano GD**, Hotston-Moore A, Lobley GE. Influence of hepatic ammonia removal on ureagenesis, amino acid utilization and energy metabolism in the ovine liver. *Br J Nutr (The British journal of nutrition.)* 2000; **3**: 307-315
- 30 **Gafan C**, Wilson J, Berger LC, Berger BJ. Characterization of the ornithine aminotransferase from *Plasmodium falciparum*. *Mol Biochem Parasitol (Molecular and biochemical parasitology.)* 2001; **1**: 1-10
- 31 **Seiler N**. Ornithine aminotransferase, a potential target for the treatment of hyperammonemias. *Curr Drug Targets (Current drug targets.)* 2000; **2**: 119-153
- 32 **Boon L**, Geerts WJ, Jonker A, Lamers WH, Van Noorden CJ. High protein diet induces pericentral glutamate dehydrogenase and ornithine aminotransferase to provide sufficient glutamate for pericentral detoxification of ammonia in rat liver lobules. *Histochem Cell Biol (Histochemistry and cell biology.)* 1999; **6**: 445-452
- 33 **Nadler EP**, Dickinson EC, Beer-Stolz D, Alber SM, Watkins SC, Pratt DW, Ford HR. Scavenging nitric oxide reduces hepatocellular injury after endotoxin challenge. *Am J Physiol Gastrointest Liver Physiol (American journal of physiology. Gastrointestinal and liver physiology.)* 2001; **1**: G173-181
- 34 **Chiao JW**, Xu W, Seiter K, Feldman E, Ahmed T. Neuroleukin mediated differentiation induction of myelogenous leukemia cells. *Leuk Res (Leukemia research.)* 1999; **1**: 13-18
- 35 **Romagnoli A**, Oliverio S, Evangelisti C, Iannicola C, Ippolito G, Piacentini M. Neuroleukin inhibition sensitises neuronal cells to caspase-dependent apoptosis. *Biochem Biophys Res Commun (Biochemical and biophysical research communications.)* 2003; **3**: 448-453
- 36 **Stiles JK**, Meade JC, Kucerova Z, Lyn D, Thompson W, Zakeri Z, Whittaker J. Trypanosoma brucei infection induces apoptosis and up-regulates neuroleukin expression in the cerebellum. *Ann Trop Med Parasitol (Annals of tropical medicine and parasitology.)* 2001; **8**: 797-810

Repression of allo-cell transplant rejection through CIITA ribonuclease P⁺ hepatocyte

Rong Guo, Ping Zou, Hua-Hua Fan, Feng Gao, Qing-Xin Shang, Yi-Lin Cao, Hua-Zhong Lu

Rong Guo, Ping Zou, Institute of Hematology, the Union Hospital, Affiliated to Tongji Medical College, Huazhong University of Science and Technology, Wuhan 430022, Hubei Province, China

Hua-Hua Fan, Feng Gao, Hua-Zhong Lu, The Department of Blood Engineering, Shanghai Municipal Blood Center, Shanghai 200051, China

Qing-Xin Shang, Yi-Lin Cao, Shanghai Municipal Tissue Engineering Research and Developing Center, Shanghai 200011, China

Supported by the Science and Technology Development Foundation of Shanghai municipality, No. 0143nm068 and the Great Branch Project of the Science and Technology Development Foundation of Shanghai Municipality, No. 00DJ14001-8

Correspondence to: Dr. Rong Guo, Institute of Hematology, the Union Hospital, 1127 Jiefang Dadao, Wuhan 430022, Hubei Province China. gh7311@yahoo.com.cn

Telephone: +86-27-85730575

Received: 2002-11-06 **Accepted:** 2002-12-16

Abstract

AIM: Allo-cell transplant rejection and autoimmune responses were associated with the presence of class II major histocompatibility complex (MHC II) molecules on cells. This paper studied the effect of Ribonuclease P (RNase P) against CIITA, which was a major regulator of MHCII molecules, on repressing the expression of MHCII molecules on hepatocyte.

METHODS: M1-RNA is the catalytic RNA subunit of RNase P from *Escherichia coli*. It were constructed that M1-RNA with guide sequences (GS) recognizing the 452, 3408 site of CIITA by PCR from *pTK117* plasmid, then were cloned into the *EcoRI/BglII* or *EcoRI/SalI* site of vector *psNAV* (*psNAV-M1-452-GS*, *psNAV-M1-3408-GS*) respectively. The target mould plate (3176-3560) of CIITA was obtained from Raji cell by RT-PCR, and then inserted into the *XhoI/EcoRI* of *pGEM-7zf(+)* plasmid (*pGEM-3176*). These recombinant plasmids were screened out by sequence analysis. *psNAV-M1-452-GS*, *psNAV-M1-3408-GS* and its target RNA *pGEM-3176* were transcribed and then mixed up and incubated *in vitro*. It showed that M1-3408-GS could exclusively cleave target RNA that formed a base pair with the GS. Stable transfectants of hepatocyte cell line with *psNAV-M1-3408-GS* were tested for expression of class II MHC through FCM, for mRNA abundance of MHCII, Ii and CIITA by RT-PCR, for the level of IL-2 mRNA on T cell by mixed lymphocyte reaction.

RESULTS: When induced with recombinant human interferon-gamma (*IFN-γ*), the expression of HLA-DR, -DP, -DQ on *psNAV-M1-3408-GS*⁺ hepatocyte was reduced 83.27 %, 88.93 %, 58.82 % respectively, the mRNA contents of CIITA, HLA-DR, -DP, -DQ and Ii decreased significantly. While T cell expressed less IL-2 mRNA in the case of *psNAV-M1-3408-GS*⁺ hepatocyte.

CONCLUSION: The Ribonuclease P against CIITA-M1-

3408-GS could effectively induce antigen-specific tolerance through cleaving CIITA. These results provided insight into the future application of M1-3408-GS as a new nucleic acid drug against allo-transplantation rejection and autoimmune diseases.

Guo R, Zou P, Fan HH, Gao F, Shang QX, Cao YL, Lu HZ. Repression of allo-cell transplant rejection through CIITA ribonuclease P⁺ hepatocyte. *World J Gastroenterol* 2003; 9 (5): 1077-1081

<http://www.wjgnet.com/1007-9327/9/1077.htm>

INTRODUCTION

The donor shortage has become the major restriction on liver transplantation with the increasing demands for it^[1]. Now people are trying to produce artificial liver with hepatocytes and various biological materials^[2,3], but are faced with the challenge of rejection in allo-hepatocyte transplantation^[4]. Allo-transplant rejection, was associated with the presence of class II major histocompatibility complex (MHCII) on the tissues and organs^[5,6]. MHCII played a critical role in the induction of immune responses by presenting fragments of alloantigenic peptides to CD4⁺ T lymphocytes, then resulting in the activation of CD8⁺ T lymphocytes. So it was more important for compatibility of MHCII in allo-transplantation. Moreover, the abnormal expression of MHCII molecules was associated with autoimmune disease too^[7-9]. There are codominance and multiple allele for MHCII molecules which lead to their complicated polymorphism, so it is difficult to repress every MHCII molecules expression directly. MHC class II transactivator (CIITA) was the major rate-limiting factor for both constitutive and inducible MHCII expression., and with rare exceptions, its expression parallels to that of MHCII transcripts^[10-12]. There was no rejection in allo-skin graft^[5] or prolonged survival time in allo-cardiac graft^[13] of CIITA(-/-) according to the latest investigation.

Ribozymes included hammerhead-, hairpin-, Ribonuclease P (RNase P), *et al.* M1-RNA was the catalytic RNA subunit of RNase P from *Escherichia coli*. RNase P was a ribonucleoprotein complex that catalyzed the hydrolysis reaction by removing a 5' leader sequence from tRNA precursors^[14]. Hammerhead ribozymes required presence of specific nucleotide sequences in the target RNA to be cut^[15,16], and these requirements could not always be fulfilled. M1-RNA could be used as a tool to cleave any specific mRNA sequence simply by the 3' terminal addition to the ribozyme sequence of a so-called guide sequence (GS) complementary to the target mRNA, that formed a base-pair with it and left a 5' -ACCAC-3' unpaired stretch needed for the M1-GS RNA to recognize and cleave this artificially created substrate (Figure 1B). Thus, M1-GS RNA, apart from some requirements to improve its cleavage efficiency, could be specifically directed to cut any mRNA sequences. This study represents, to our knowledge, the first gene therapy approach that makes use of the catalytic activity of M1-RNA for allo-cell transplant rejection in hepatic tissue engineering and the autoimmune diseases.

MATERIALS AND METHODS

Plasmids

PTK117, a *pUC19* derivative in which the DNA sequence coding for *E.coli* M1RNA is under the control of the T7 RNA polymerase promoter, was provided by Dr Chen BB^[14]. *pGEM-7zf(+)* vector was purchased from Shanghai BioEngineering Company, adeno-associated virus vector (*psNAV*) was provided by Dr Lu HZ.

Enzymes and chemicals

T4 DNA ligase and restriction endonucleases *EcoRI*, *Sall*, *BglII*, *XhoI* were purchased from MBI; mouse anti-human isotype control (IgG2a)-FITC, HLA-DR (IgG2a, *k*), -DQ (IgG2a, *k*) monoclonal antibody and recombinant human IFN- γ were obtained from PharMingen, mouse anti-HLA-DP (IgG2b, BRA-FB6) from CYMBUS, GENETICIN (G418) from GIBCO. TRIZOL^R from GIBCOBRL, TITANIUM^R one-step RT-PCR kit from Clontech.

Cell culture

Cell line used included L-02 cell line (from human fetal liver) and Raji cell line (human B lymphoma), all purchased from Cell Bank of Shanghai Academy of Science. Cells were maintained in RPMI1640 (GIBCOBRL) medium supplemented with 15 % fetal calf serum (HyClone).

In vitro cleavage of anti-CIITA RNaseP

RNaseP construction The M1-RNA with the anti-CIITA-directed GS (M1-452-GS or M1-3408-GS) were constructed by the polymerase chain reaction (PCR) with the gene for M1-RNA as found in plasmid *pTK117* as a template. The 5' primer, OliT7: 5' -gcggaattcTAATACGACTCACTATAG-3', annealing with the T7 promoter and providing a 5' *EcoRI* site for cloning. The 3' primers contained the appropriate GS and were OliP3408: 5' -acgcgtcgacGTGGTGCAGCTCGCTGATTACGCCAAGC-3' and OliP452: 5' -gaagatctGTGGTTCTTCCAGGACTGCCAAGCTTGC-3'. The 3' proximal sequences of 15 nucleotides in OliP3408 and 11 nucleotides in OliP452 served as primers for the PCR with the *pTK117* sequence. The lowercase sequences, the underlined sequences, and the black ones corresponded, respectively, to the *Sall* in OliP3408 or *BglII* in OliP452, the ACCAC-3' sequence, and the GS. The two different PCR products were obtained according to the instructions of 2 \times HiFi Master PCR kit (Shanghai Bioengineering Company), and cloned into *psNAV* (*psNAV*-M1-3408-GS, *psNAV*-M1-452-GS), then completely sequenced to exclude any mutation during the PCR reaction.

Construction of artificial substrate The CIITA (3176-3560) mould mRNA was obtained from Raji cell line by RT-PCR, according to instructions of TRIZOL^R and TITANIUM^R one-step RT-PCR kit. The 5' primer: 5' -ccgctcgagAGCTGAAGTCCTTGAA-3', The 3' primers: 5' -gcggaattcGAACATGCCTGTCCAGAGC-3'. The RT-PCR product, containing 384 nucleotides spanning at the point of 3408, was cloned into the *XhoI/EcoRI* site of *pGEM-7zf(+)* (*pGM-3176*).

Assays for cleavage by M1-GS RNA^[16] Plasmid *pGM-3176* was linearized with *EcoRI*, *psNAV*-M1-3408-GS and *psNAV*-M1-452-GS were linearized with *BglII*, then purified by EndoFree^R Plasmid Maxi kit (QIAGEN), and transcribed in vitro from the *pGEM-7zf* or M1-RNA T7 promoter in the presence of [³²P]-GTP, with Ribomax large scale RNA production system-T7 (Promega), then transcribed ribozyme and substrate RNA were phenol chloroform extracted and precipitated with ethanol, and their integrity was checked by either acrylamide/urea or agarose electrophoresis. RNaseP

RNA and uniformly labeled substrates were incubated for 4 h at 50 °C in 25 mM Tris HCl(pH7.5), 50 mM MgCl₂, 50 mM NH₄Cl buffer in a final reaction volume of 20 μ l. Reactions were stopped by the addition of 6 μ l of a solution containing 95 % formamide, 20 mM EDTA, 0.05 % bromophenol blue, and 0.05 % xylene cyanol FF boiled for 5 min and chilled on ice. The reaction products were analyzed on 10 % polyacrylamide/8 mol/L urea gels (Figure 1C).

A

M1-3408-GS specific mRNA (*pGM-3176*)

5' GCAGCUCGCUGCCAGCCUUCGGAGGUGUCCUCAUGUGGA3'

M1-452-GS specific mRNA

5' UCUUCCAGGACUCCAGCUGGAGGGCCUGAGCAAGGACA3'

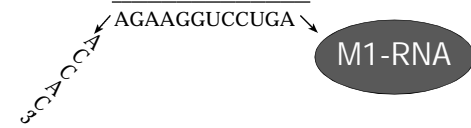
B

In vitro transcribed mould plate RNA of unrelated CIITA

Cleavage point (452)



5' UCUUCCAGGACUCCAGCUGGAGGGCCUGA 3'

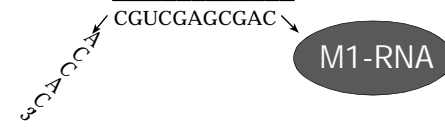


In vitro transcribed mould plate RNA of *pGM-3176* in CIITA

Cleavage point (3408)



5' GCAGCUCGCUGCCAGCCUUCGGAGGUGUCCU 3'



C

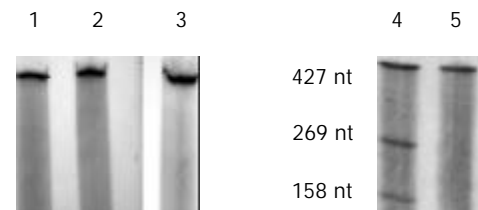


Figure 1 Cleavage of CIITA substrate by M1-GS RNA *in vitro* (A): The mould plate RNA of CIITA *pGM-3176* (3176-3560) include the cutting point of only M1-3408-GS, not M1-452-GS. (B): Schematic representation of targeting the CIITA mRNA by M1-RNA: GS encoding 12 or 11 nucleotides complementary to CIITA was covalently linked to the 3' end of M1-452-GS or M1-3408-GS. So M1-452-GS and M1-3408-GS specifically cut CIITA on the site of 452 and 3408 respectively. (C): Sequence-specific cleavage of *pGM-3176* substrate by M1-3408-GS: autoradiograph of transcripts of M1-452-GS (lane 1), M1-3408-GS (lane 2) and *pGM-3176* (lane 3), and *pGM-3176* substrate was incubated either with M1-3408-GS (lane 4), or with M1-452-GS (lane 5). So only M1-3408-GS (not M1-452-GS) could cleave *pGM-3176*.

Cell transfection through nanometer vector

Hepatocytes were transfected with 0.4 μ g *psNAV*-M1-3408-GS by nanometer vector. According to Effectene (QIAGEN) kit's instructions, seeded 2.5 \times 10⁵ cells/well the day before transfection. The cell number seeded should produce 40-80 % confluence on the day of transfection. *psNAV*-M1-3408-GS were diluted in 100 μ l EC buffer, mixed with Enhancer 3.2 μ l, incubating 2-4 min at RT, then adding Effectene 10 μ l, at RT 7-8 min, mixed with 600 μ l medium containing serum and antibiotics, and immediately transferred the total volume to the above cells in the 6-well plate.

The expression of MHCII antigens on hepatocyte by FCM

Hepatocytes were collected and washed with 1.5 g/L MPBS buffer (10 g/L BSA and 1 g/L NaN₃) once at the density of 1×10^6 /ml, adding IgG2a, HLA-DR, DP, DQ 10 μ l respectively, incubating at 4 °C for 30 min, detecting the expression of MHCII molecules by Flow cytometry (COULTER, EPICSXL).

RNA analysis

RT-PCR was done according to the instructions of TRIZOL^R and TITANIUM^R one-step RT-PCR kit. In a total 50 μ l volume, 50 °C 1 h, 94 °C 5 min, 94 °C 30 s, 65 °C 30 s, 68 °C 1 min, 30 cycles, 72 °C extending 7 min. Primers sequences (synthesized by Shanghai Bioengineering Company) referred to Table 1.

Table 1 The primers of CIITA, MHCII and RNaseP

Primer	Sequence	Length
CIITA mould	L 5'-CCGCTCGAGAGCTGAAGTCTTGGAA-3'	384bp
	R 5'-GCGGAATTCGAACATGCCTGTCCAGAGC-3'	
CIITA	L 5'-CCG CTC GAG GCT GCC TGG CTG GGA TT -3'	410bp
	R 5'-GCG GAA TTC CGA TCA CTT CAT CTG GTC CTAT-3'	
M1-452-GS	L 5'-GCGGAATTCTAATACGACTCACTATAG-3'	446bp
	R 5'-GAAGATCTGTGGTTCTCCAGGACTGCCAAGCTTGC-3'	
M1-3408-GS	L 5'-GCGGAATTCTAATACGACTCACTATAG-3'	454bp
	R 5'-ACGCGTCGACGTGGTGCAGCTCGTGATTACGCCAAGC-3'	
HLA-DR	5'-AAT GGC CAT AAG TGG AGT CC-3'	335bp
	5'-GGA GGT ACA TTG GTG ATC GG-3'	
HLA-DP	5'-CAG AGC TGT GAT CTT GAG AG-3'	197bp
	5'-AGA TGC CAG ACG GTC TCC TT-3'	
HLA-DQ	5'-CTC TGA CCA CCG TGA TGA GC-3'	153bp
	5'-CTC TCC AGG TCC ACG TAG AA-3'	
Ii	5'-CCA GAT GCA CAG GAG GAG AA-3'	714bp
	5'-CCT CTG CTG CTC TCA CAT GG-3'	
Neo gene	L 5'-ACA ATC GGC TGC TCT GAT -3'	349bp
	R 5'-CTC GCT CGA TGC GAT GIT -3'	
β -actin	L 5'-ATC ATG TTT GAG ACC TTC AA -3'	310bp
	R 5'-CAT CTC TTG CTC GAA GTC CA -3'	

Mixed lymphocyte reaction (MLR)

It were incubated at 37 °C, 5 % CO₂ (keeping away light) after adding mitocin-C (25 μ g/ml, Sigma) into IFN- γ induced psNAV-M1-3408-GS⁺ hepatocyte (1×10^7 /ml), and washed with RPMI1640 twice, plated at a density of 1×10^6 /well as stimulating cells. Then added peripheral blood mono-nucleated cells (PBMNC, 1×10^6) from healthy donors into above stimulating cells. The level of IL-2 mRNA from PBMNC after 48 h incubation was Detected through RT-PCR^[17].

RESULTS

The expression of MHCII molecules on hepatocyte

Hepatocyte without IFN- γ induction The expression of HLA-DR, DP, DQ on hepatocyte was low, (0.14 \pm 0.04) %, (26.76 \pm 5.26) %, (2.12 \pm 0.56) % respectively.

Hepatocyte after IFN- γ induction The expression of HLA-DR, DP, DQ on hepatocyte with IFN- γ (40 ng/ml) induction for 3 d increased significantly, (18.68 \pm 2.94) %, (41.78 \pm 4.90) %, (4.78 \pm 1.26) % respectively.

Rnase P down-modulating MHCII expression on hepatocyte

The expression of MHCII on psNAV-M1-3408-GS⁺ hepatocyte after the induction of IFN- γ (40 ng/ml) for 3 d was repressed. Compared with void-vector⁺ hepatocyte, the expression of HLA-DR, DP, and DQ on psNAV-M1-3408-GS⁺ hepatocyte was inhibited 83.27 %, 88.93 %, and 58.82 % respectively.

The expression of MHCII, Ii and CIITA mRNA through RT-PCR detection

The induction of MHCII, Ii and CIITA mRNA on psNAV-M1-3408-GS⁺ hepatocyte was detected through RT-PCR (Figure 2). Compared with void vector, the amount of MHCII and Ii mRNA of psNAV-M1-3408-GS⁺ hepatocyte was significantly down-modulated, the CIITA mRNA was down-modulated 71 %.

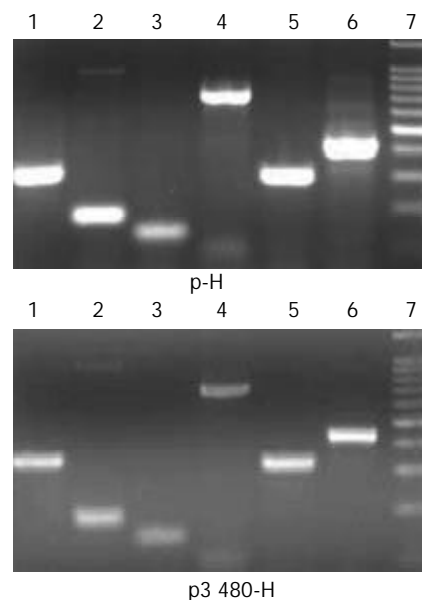


Figure 2 Comparison of CIITA, MHCII mRNA abundance of psNAV-M1-3408-GS⁺ hepatocyte with void vector⁺ following IFN- γ induction. The total RNA of psNAV-M1-3408-GS⁺ (p3408-H) or void vector⁺ (p-H) hepatocyte after IFN- γ (30 ng/ml, 3 d) induction was both extracted, then RT-PCR. 1: HLA-DR (335bp); 2: HLA-DP (197bp); 3: HLA-DQ (153bp); 4: Ii (714bp); 5: β -actin (310bp); 6: CIITA (410bp); 7: 100bp DNA Ladder.

Hepatocyte inducing mixed lymphocyte reaction

The excretion of IL-2 from PBMNC stimulated by psNAV-M1-3408-GS⁺ hepatocyte after the induction of IFN- γ for 3 d referred to Figure 3. Void-vector⁺ hepatocyte could induce PBMNC high amount of IL-2 mRNA, but negative control and psNAV-M1-3408-GS⁺ hepatocyte could hardly induce the excretion of IL-2 mRNA from PBMNC.

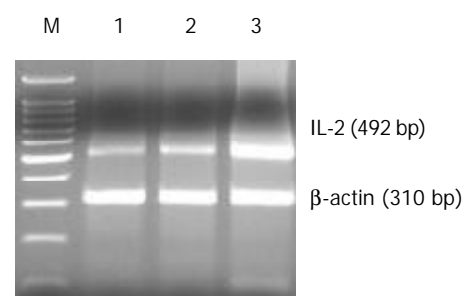


Figure 3 The secretion of IL-2 mRNA from PBMNC through RT-PCR. M: 100bp DNA ladder; 1: Negative control; 2: The IL-2 from PBMNC stimulated by psNAV-M1-3408-GS⁺ hepatocyte after IFN- γ induction; 3: The IL-2 from PBMNC stimulated by void vector control after IFN- γ induction.

DISCUSSION

In allo-cell transplantation or autoimmune diseases, some cytokines such as IFN- γ , induced some low/non MHCII antigen expressing cells to express these molecules highly^[18,19]. We selected IFN- γ to induce hepatocyte for 3 days, the expression

of HLA-DR, DP, DQ antigens increased exactly, while the expression of HLA-DP was most apparent.

CIITA regulated the transcription of MHCII gene by interacting with the trans-acting factors such as RFX, X2BP and NFY. The expression of CIITA paralleled to that of MHCII molecules and appeared only in the MHCII-positive cells^[10,11]. In the hepatocyte detected by us, the expression of CIITA was consistent with that of MHCII molecules: without IFN- γ induction, all hepatocytes didn't express MHCII molecules and CIITA gene; following IFN- γ induction, these cells expressed MHCII molecules and CIITA gene simultaneously; in the case of anti-CIITA psNAV-M1-3408-GS positive hepatocytes, the induced MHCII expression on their surface was nearly completely lost, and their CIITA mRNA detected by RT-PCR was also defect, perhaps the latter was the direct reason that MHCII expression didn't react to IFN- γ induction. This view was coincidence with that of Luder *et al*^[18,20]: TOXO plasma gondi parasite lowered the MHCII expression by inhibiting its induced CIITA expression. Moreover, HMG-CoA reductase inhibitors, cyclosporine and phosphatidylethanolamine-linked hyaluronic acid (HYPE) could completely repress MHCII expression of human microvascular endothelial cells by reducing its induced CIITA mRNA contents *ex vitro*^[19,21-23].

Gene blocking techniques were mainly made up of anti-sense oligonucleotide, anti-sense RNA, ribozyme and RNA interference (RNAi), and so on. Anti-sense oligonucleotide referred to a small fragment of single-strand deoxyribonucleic acid (14-23 bases) synthesized artificially, which could hybridize with target DNA or mRNA. However, there were still some problems of stability and efficiency of entering cell *in vivo* about it. Anti-sense RNA, ribozyme and RNAi all took action on target mRNA, namely anti-sense complementation, cutting and interference respectively. The novel RNAi technique was the double-strand RNA connected by anti-sense RNA and sense RNA in essence, and was more efficient than single anti-sense RNA^[24,25]. The mechanism of which was still not clear and might be related to activating ribonuclease to degrade target mRNA. But when it is larger than 30bp, the action of it was not specific^[24]. Compared with above-mentioned gene blocking techniques, ribozyme not only sealed mRNA, but also cut mRNA with specificity. Moreover, ribozyme could be used repeatedly, so it had higher efficiency. Both hammerhead ribozyme and hairpin ribozyme require GUC sequence to identify in target sequence. However, RnaseP was not limited to this and could aim at any site in the target sequence, so it had wider selective range^[14]. There was no report on RnaseP yet at home. According to human RNA sequences published in the NCBI Gene Bank, our experiment selected 452, 3408 site in the CIITA gene as target sites of M1-RNA after eliminating the possibility of their homology. PST and LRR regions initiated by 452, 3408 site were very essential to the transcription activation of CIITA. Moreover, the secondary structure around them was relatively simple and accessible. The GS of M1-3408-GS and M1-452-GS were programmed as 11 and 12 nucleotides respectively, to fit for the combination with their own substrate, the disconnection of cutting products with the ribozyme, and the specificity of the ribozyme. The 5' -terminal of M1-RNA had a TAATA box (T7 promoter), and M1-RNA was cloned into the psNAV vector (without T7 promoter), then the transcription was gone on owing to T7 promoter in the ribozyme itself. This could avoid supplementary sequence of the psNAV vector and objectively reflect the cutting activity of the Rnase P. The result of our experiment revealed the expected cutting stripes in the electrophoresis of cutting products of M1-3408-GS and CIITA mould plate *ex vitro*.

The reason why our experiment used nanometer-vector to mediate the transfection of M1-RNA into hepatocyte was that

nanometer had the advantages of both virus vector and non-virus vector^[26,27]. For instance, adenovirus vector^[28,29] or retroviral vectors^[30] could cause too strong immunological reaction of body to fit for the study of inhibiting the immunological rejection in our experiment; Especially, nanometer-vector could mediate exogenous gene to integrate into the chromosome DNA of host cell so that the long-term and stable expression of transgene could be obtained. In our experiment using the novel nanometer vector Effectene to transfect human hepatocyte, the rate was about 11 %, and it could rise to 60-80 % after the screening with G418 for 1 wk. Nanometer vector, however, has just begun to be used in the field of gene therapy. So far, internationally, there has no report on it used in the gene therapy of clinical or pre-clinical study.

Moreover, hepatocytes induced by IFN- γ could stimulate the secretion of IL-2 mRNA from exogenous T cell, while psNAV-M1-3408-GS⁺ hepatocyte after IFN- γ induction lost this ability. Therefore, M1-3408-GS inhibited CIITA mRNA and thus the family of MHCII molecules regulated by CIITA, then down-regulated the ability of stimulating mixed lymphocyte reaction. In conclusion, our research will have important theoretical and practical meaning on the study of transplantation immune in the whole hepatocyte tissue engineering and the therapy of autoimmune diseases.

REFERENCES

- Zhu XF**, Chen GH, He XS, Lu MQ, Wang GD, Cai CJ, Yang Y, Huang JF. Liver transplantation and artificial liver support in fulminant hepatic failure. *World J Gastroenterol* 2001; **7**: 566-568
- Wang YJ**, Li MD, Wang YM, Nie QH, Chen GZ. Experimental study of bioartificial liver with cultured human liver cells. *World J Gastroenterol* 1999; **5**: 135-137
- Wang YJ**, Wang XH, Li MD, Wang YM. Effect of cultured human hepatocytes on D-Gal induced acute hepatic failure in mice. *Shijie Huaren Xiaohua Zazhi* 1998; **6**: 383-385
- Bumgardner GL**, Li J, Prologo JD, Heining M, Orosz CG. Patterns of immune responses evoked by allogeneic hepatocytes: evidence for independent co-dominant roles for CD4+ and CD8+ T-cell responses in acute rejection. *Transplantation* 1999; **68**: 555-562
- Felix NJ**, de Serres S, Meyer AA, Ting JP. Comparison of Abeta (b-/-), H2-DM(-), and CIITA(-/-) in second-set skin allograft rejection. *J Surg Res* 2002; **102**: 185-192
- Lei H**, Madsen JC, Sachs DH. Strain variation of constitutive expression of MHC class II on coronary vascular endothelium. *Zhongguo Miyanixue Zazhi* 1996; **12**: 350-352
- Tsark EC**, Wang W, Teng YC, Arkfeld D, Dodge GR, Kovats S. Differential MHC class II-mediated presentation of rheumatoid arthritis autoantigens by human dendritic cells and macrophages. *J Immunol* 2002; **169**: 6625-6633
- Czaja AJ**. Understanding the pathogenesis of autoimmune hepatitis. *Am J Gastroenterol* 2001; **96**: 1224-1231
- Stuve O**, Youssef S, Slavin AJ, King CL, Patarroyo JC, Hirschberg DL, Brickey WJ, Soos JM, Piskurich JF, Chapman HA, Zamvil SS. The role of the MHC class II transactivator in class II expression and antigen presentation by astrocytes and in susceptibility to central nervous system autoimmune disease. *J Immunol* 2002; **169**: 6720-6732
- Holling TM**, van der Stoep N, Quinten E, van den Elsen PJ. Activated Human T Cells Accomplish MHC Class II Expression Through T Cell-Specific Occupation of Class II Transactivator Promoter III. *J Immunol* 2002; **168**: 763-770
- Waldburger JM**, Suter T, Fontana A, Acha-Orbea H, Reith W. Selective abrogation of major histocompatibility complex class II expression on extrahematopoietic cells in mice lacking promoter IV of the class II transactivator gene. *J Exp Med* 2001; **194**: 393-406
- Nagarajan UM**, Bushey A, Boss JM. Modulation of gene expression by the MHC class II transactivator. *J Immunol* 2002; **169**: 5078-5088
- June Brickey W**, Felix NJ, Griffiths R, Zhang J, Wang B, Piskurich JF, Itoh-Lindstrom Y, Coffman TM, Ting JP. Prolonged survival

- of class II transactivator-deficient cardiac allografts. *Transplantation* 2002; **74**: 1341-1348
- 14 **Cobaleda C**, Sanchez-Garcia I. *In vivo* inhibition by a site-specific catalytic RNA subunit of RNase P designed against the BCR-ABL oncogenic products: a novel approach for cancer treatment. *Blood* 2000; **95**: 731-737
- 15 **Hao ZM**, Luo JY, Cheng J, Wang QY, Yang GX. Design of a ribozyme targeting human telomerase reverse transcriptase and cloning of its gene. *World J Gastroenterol* 2003; **9**: 104-107
- 16 **Sullivan JM**, Pietras KM, Shin BJ, Misasi JN. Hammerhead ribozymes designed to cleave all human rod opsin mRNAs which cause autosomal dominant retinitis pigmentosa. *Mol Vis* 2002; **8**: 102-113
- 17 **Okimoto T**, Yahata H, Fukuda Y, Dohi K. The mechanism of donor specific unresponsiveness in renal transplant recipients. *Nihon Rinsho Meneki Gakkai Kaishi* 1998; **21**: 118-128
- 18 **Luder CG**, Lang C, Giraldo-Velasquez M, Algnier M, Gerdes J, Gross U. Toxoplasma gondii inhibits MHC class II expression in neural antigen-presenting cells by down-regulating the class II transactivator CIITA. *J Neuroimmunol* 2003; **134**: 12-24
- 19 **Yard BA**, Yedgar S, Scheele M, van der Woude D, Beck G, Heidrich B, Krimsky M, van der Woude FJ, Post S. Modulation of IFN-gamma-induced immunogenicity by phosphatidylethanolamine-linked hyaluronic acid. *Transplantation* 2002; **73**: 984-992
- 20 **Luder CG**, Walter W, Beuerle B, Maeurer MJ, Gross U. Toxoplasma gondii down-regulates MHC class II gene expression and antigen presentation by murine macrophages via interference with nuclear translocation of STAT1alpha. *Eur J Immunol* 2001; **31**: 1475-1484
- 21 **Youssef S**, Stuve O, Patarroyo JC, Ruiz PJ, Radosevich JL, Hur EM, Bravo M, Mitchell DJ, Sobel RA, Steinman L, Zamvil SS. The HMG-CoA reductase inhibitor, atorvastatin, promotes a Th2 bias and reverses paralysis in central nervous system autoimmune disease. *Nature* 2002; **420**: 78-84
- 22 **Charreau B**, Coupel S, Boulday G, Soulillou JP. Cyclosporine inhibits class II major histocompatibility antigen presentation by xenogeneic endothelial cells to human T lymphocytes by altering expression of the class II transcriptional activator gene. *Transplantation* 2000; **70**: 354-361
- 23 **Sadeghi MM**, Tiglio A, Sadigh K, O'Donnell L, Collinge M, Pardi R, Bender JR. Inhibition of interferon-gamma-mediated microvascular endothelial cell major histocompatibility complex class II gene activation by HMG-CoA reductase inhibitors. *Transplantation* 2001; **71**: 1262-1268
- 24 **Elbashir SM**, Harborth J, Lendeckel W, Yalcin A, Weber K, Tuschl T. Duplexes of 21-nucleotide RNAs mediate RNA interference in cultured mammalian cells. *Nature* 2001; **411**: 494-498
- 25 **Yamamoto T**, Omoto S, Mizuguchi M, Mizukami H, Okuyama H, Okada N, Saksena NK, Brisibe EA, Otake K, Fuji YR. Double-stranded nef RNA interferes with human immunodeficiency virus type 1 replication. *Microbiol Immunol* 2002; **46**: 809-817
- 26 **Esfand R**, Tomalia DA. Poly (amidoamine) (PAMAM) dendrimers: from biomimicry to drug delivery and biomedical applications. *Drug Discov Today* 2001; **6**: 427-436
- 27 **Dennig J**, Duncan E. Gene transfer into eukaryotic cells using activated polyamidoamine dendrimers. *J Biotechnol* 2002; **90**: 339-347
- 28 **Yang ZY**, Wyatt LS, Kong WP, Moodie Z, Moss B, Nabel GJ. Overcoming immunity to a viral vaccine by DNA priming before vector boosting. *J Virol* 2003; **77**: 799-803
- 29 **Sailaja G**, HogenEsch H, North A, Hays J, Mittal SK. Encapsulation of recombinant adenovirus into alginate microspheres circumvents vector-specific immune response. *Gene Ther* 2002; **9**: 1722-1729
- 30 **Podevin G**, Pichard V, Durand S, Aubert D, Heloury Y, Ferry N. *In vivo* retroviral gene transfer to the liver is cancelled by an immune response against the corrected cells. Can it be avoided? *Pediatr Surg Int* 2002; **18**: 595-599

Edited by Yuan HT

Radio frequency "sutureless" fistulotomy- a new way of treating fistula in anus

Pravin J. Gupta

Pravin J. Gupta, Gupta Nursing Home, D/9, Laxminagar, NAGPUR-440022, India

Correspondence to: Dr Pravin J. Gupta, Gupta Nursing Home, D/9, Laxminagar, NAGPUR- 440022, India. drpjpg@yahoo.co.in

Received: 2002-08-06 **Accepted:** 2002-11-04

Abstract

AIM: To explore the effect of the classical lay open technique or fistulotomy with the radio frequency surgical device in the treatment of fistula in anus.

METHODS: In our study, the conventional 'lay open' technique, or 'fistulotomy' was performed by employing the radio frequency surgical device as an alternative to the traditional knife and scissors. In a span of 18 months starting from July 1999 to December 2000, 210 cases with fistula in anus of varied types were operated in our nursing home exclusively applying the radio frequency device.

RESULTS: The results of the study were not only encouraging but also were satisfactory. A follow up of the operated patients with radio frequency surgery over a period of 15 months, i.e. from December 2000 to March 2002 was summarized as below: (a) average time taken by the patient to resume routine - 7 days; (b) none of the patient had any interference with the continence; (c) the wounds were found healed within an average time of 47 days; (d) delayed wound healing was noticed only in 7 patients; (e) recurrence/ failure rate was reduced to as low as 1.5 percent.

CONCLUSION: This technique has been found superior to the conventional fistulotomy in the sense that the time taken for the whole procedure is reduced to almost half, chances of bleeding are reduced to a minimum and the use of suture material is dispensed with. The procedure can safely be called a "Sutureless fistulotomy".

Gupta PJ. Radio frequency "sutureless" fistulotomy- a new way of treating fistula in anus. *World J Gastroenterol* 2003; 9(5): 1082-1085

<http://www.wjgnet.com/1007-9327/9/1082.htm>

INTRODUCTION

Fistula in anus is defined as an abnormal communication lined by granulation tissue between the anal canal and the exterior i. e. the skin, which causes a chronic inflammatory response.

Etiology

The most common cause is secondary to an anorectal abscess. These abscesses either have been treated inadequately, or have bursts spontaneously. Abscess is commonly formed secondary to infection of an anal gland (cryptoglandular hypothesis of Eisenhammer)^[1]. Other causes are as follows: (a) Secondary to inflammatory bowel disease- Crohn's or Ulcerative

proctocolitis; (b) Secondary to introduction of a foreign body e.g. probing of an abscess or a low fistula; (c) Associated with anal fissure, i.e. post fissure fistula; (d) Rectum cancer especially the colloid carcinoma.

Causes of multiple fistulae include T.B, Crohn's disease, ulcerative proctocolitis, lymphogranuloma inguinale, bilharziasis, hidradenitis suppurativa, etc.

Clinical features

History Patients had the history of seropurulent discharge, persistent pruritus and discomfort in the surrounding skin^[2]. Patients feel pain if the fistula tract is blocked for accumulation of secretions under pressure.

Inspection The external opening can usually be seen as an elevation of granulation tissue often active with purulent discharge. The number and location of external openings and the relationships to the anal canal provide a clue as to the internal origin. According to Goodsall's rule, if the opening is anterior to a transverse anal line (coronal plane), the internal opening will be in a direct radial line to the nearest crypt. If the opening is posterior to the coronal line, the internal opening will usually be in a posterior midline crypt, and the tract will be curved^[3]. Exceptions to Goodsall's rule include anterior openings that are more than 3 cm far from the anal margin and multiple openings. In these situations, the internal opening is more likely to be located in one of the posterior crypts. Other clinical conditions can simulate the appearance of a fistula, including hidradenitis suppurativa, pilonidal sinus, and Bartholin's gland abscess or sinus^[4].

Palpation Palpation may reveal an indurated cord beneath the skin in the direction of the internal opening^[5]. Digital anal palpation may reveal a suspicious scarred or retracted crypt. Further internal palpation may reveal posterior or lateral induration, indicating fistulas deep in the postanal space or horseshoe fistulas. Digital rectal examination also provides assessment of sphincter tone and voluntary squeeze pressure, which may indicate the need for preoperative manometry.

Anoscopy It may aid in identifying the internal opening in the anal canal. Massaging the tract may produce a bead of pus at the dentate line. Proctosigmoidoscopy may exclude a proximal internal opening, inflammatory bowel disease, or neoplasia. Colonoscopy is appropriate if the diagnosis of Crohn's disease is suspected based on a history of recurrent or multiple fistulas or if examination is suggestive of inflammatory bowel disease. A small-bowel series also may be appropriate for patients with recurrent or multiple fistulas.

Fistulography This may have a role in evaluation of recurrent fistula, particularly when the prior surgical procedure has failed to identify the internal opening. The external opening is cannulated with a small caliber feeding tube, and contrast material is gently injected into the tract. X-ray images are then taken in the anteroposterior, oblique, and lateral positions. Complications are rare, and limiting the volume and pressure of contrast injection can minimize patient discomfort. Accuracy rates have been reported to range from 16 to 48 percent, with a false-positivity rate of 10 %^[6].

Classification There are four main types described: (1)

Transphincteric low; (2) Transphincteric high; (3) Supralevator; and (4) Intersphincteric. However, numerous variations of each can occur^[7].

Treatment The classical lay open technique is still the most favoured procedure^[8]. Slitting the complete tract from the external to internal opening is the basis of the traditional fistulotomy. Tissues around the external openings and internal opening are excised along with a small margin of tissue lining the tract and the wound is kept open for healing by secondary intention.

The traditional approach is as follows^[9]. Preoperative cleansing enema is given. The patient is kept in lithotomic position. Anesthesia: general or regional block is OK. The procedures were as follows: Digital palpation- the tract is felt as nodule or cord. Proctoscopy- a hypertrophied anal papilla may be the point of internal opening. Probing- It is done with delicate hand either retrograde (preferred) or antegrade. Methylene blue dye or milk with hydrogen peroxide is injected from the external opening to locate the direction and path of the tract^[10].

A director probe is inserted inside the fistula. Tract is cut along probe. Edges of wounds were trimmed and 1-3 mm of tissue margins was removed. The excised tract is sent for histopathological examination.

This conventional procedure encounters a lot of bleeding from the cut surfaces needing multiple ligatures to tie the bleeding vessels. At times, certain raw areas, which cannot be tied individually, may need under-running also. Due to all these hindrances, the whole procedure becomes somewhat messy and time consuming.

MATERIALS AND METHODS

In our study, the radio frequency surgical device was used instead of the surgical knife and scissors. The device is called as the *Ellman Dual Frequency 4MHz* unit from Ellman International, Hewlett, N.Y.

In a span of 18 months starting from July 1999 to December 2000, 210 cases with fistula in anus of varied types have been operated in our nursing home exclusively employing the aforesaid radio frequency surgery device. There were 187 males and 23 females. The mean age was 37 years old (age range: from 22 to 63 years old). The mean duration of the disease was 19 months (ranging from 4 months to 11 years). Seventeen patients had an operation for fistula once before and they had a recurrence.

Radio frequency surgery is a technique for cutting and coagulating the tissues using a high frequency alternate current. It is a method of coagulating the tissues, which occurs because of heat produced by the tissue resistance to the passage of high frequency wave. The heat makes the intracellular water boil, increasing the cell inner pressure to the point of breaking it from inside to outside explosion^[11]. This phenomenon is called as cellular volatilization. The principle of radio frequency wave surgery is using high frequency radio waves at 4.0 MHz, which delivers low temperature through RF micro-fiber electrodes and is similar to the frequency of marine band radio frequencies. The tissue serves as the resistance instead of the electrode; hence, there is no heating of the RF micro-fiber electrode. Instead, the intracellular tissue water provides the resistance and vaporizes without causing the heat and damage seen in electro surgery. This tissue vaporization also results in significant hemostasis without actually burning the tissue. In addition, there is no danger of shocking or burning the patient. Most important is the fact that there is controlled and minimal lateral tissue damage with the 4.0 MHz high frequency, low temperature radio frequency wave surgery^[12].

The unit is provided with a handle to which different

electrodes can be attached as per the requirement of the procedure. A ball electrode meant for coagulation, a needle electrode to incise the fistula tract and round loop electrode to shave the surrounding infected tissue has been used in our procedure.

All the patients under study were given to understand the use of the new technique to be employed in the procedure and were clearly explained the potential drawbacks like relapses and need for repetition that may follow. The patients were allowed an option to choose between the conventional method and the radio frequency technique. An informed consent was obtained from them before subjecting them to this new technique.

Exclusion criteria of the study

Only low fistulas having opening below the anus rectal ring were included for study. High trans sphincteric fistulas with or without high blind tract, suprasphincteric, extrasphincteric, and horseshoe fistulas as well as fistulas associated with inflammatory bowel disease were excluded from the study.

Radio frequency surgical fistulotomy procedures

The steps in the fistulotomy^[13] were the same as described above with the following modifications. (1) Injection of methylene blue dye with hydrogen peroxide. (2) Director probe inserted in the fistula. (3) To begin with, the skin overlying the probe, which is in the fistula tract, was coagulated by moving the ball electrode over its complete length. This reduced the amount of bleeding when the tract is slit opened. (4) The track was cut open along the probe with the help of the needle electrode that was kept in cutting and coagulation mode. This reduced the bleeding while cutting and the dissection became smooth without a drag on the tissues. (5) The bleeding edges were caught in the hemostat and were coagulated with the ball electrode kept in coagulation mode. This avoided need of suturing or under running of the bleeding points and raw areas. (6) The edges along with the surrounding infected, fibrotic tissues were shaved with the loop electrode on cut and coagulation mode. As cutting and coagulation worked simultaneously, the brisk bleeding often encountered in the conventional knife and scissor dissection was avoided. (7) At this stage, we used an accessory called the suction coagulator. This was an accessory supplied with the radio frequency surgical device. This helped in removing the ooze of blood from the raw area while the bleeding points are being coagulated. The use of this additional tool eliminated frequent mopping of the operative field while coagulating the bleeding point, as both could be done simultaneously.

Apart from the main procedure of fistulotomy, this radio frequency surgical device could also be used in coagulating associated skin tags, and internal pile masses if present.

Postoperative care

This consisted of dressing the wound twice a day after warm sitz bath. The wound could be covered with sanitary napkin, which helped in mopping up the discharge and kept the wound dry. The patient was required to stay in the hospital for a day or two. Time off work was between 5-7 days after which patient could resume his routine.

Comparative study

Encouraged by the outcome of the radio frequency fistulotomy, we carried out a separate study. This study was to compare the efficacy of radio frequency surgical fistulotomy over the conventional one. One hundred patients of low anal fistula treated by the classical 'lay open' technique were examined. Fifty patients were operated by conventional method, while

fifty were operated by radio frequency fistulotomy.

RESULTS

Failure occur mainly due to premature union of the skin edges, failure to excise the internal opening, failure to locate an extra tract, failure to detect a cavity leading upwards from the main tract, presence of foreign bodies and poor post fistulotomy wound care^[14]. In our study, the failure rate was as low as 1.5 %.

Follow up findings

A follow up of the operated patients of fistulotomy with radio frequency surgery over a period of 15 months, i.e. from December 2000 to March 2002 was as follows. None of patients lost during the follow up of 9 days. Average time taken for complete wound healing was 47 days. Average time taken by the patient to resume routine was 7 days. Delayed wound healing happened in 7 patients (took about 80-90 days for complete healing). It was observed that the fistula wounds which were close to the midline, i.e., near 12 or 6' O clock positions when the patient was in lithotomic position took longer time to heal than wounds at other places. The reason possibly could be an excess of stress on the wounds in that situation due to proximity with joints.

Four patients had a premature closure of the proximal wound while the distal remained unhealed. In case of these patients, the healed edges of the proximal wound were slit opened with needle electrode under local anaesthesia. One of them thereafter had an uneventful healing, while the wound remained unhealed in the remaining three.

The remaining three patients continued to have discharge from a small wound left behind, which despite repeated attempts of refreshing the edges remained unresolved. So, they were labeled as cases of ' failure of wound healing' , rather than of recurrence. Out of these three patients, one patient was from the series of those seventeen patients who came with a recurrence after conventional procedure in the past.

None of these patients had any interference with the continence, anal stenosis, or mucosal prolapse^[15].

The data of follow up findings was shown in Figure 1.

Follow up findings after radio surgical fistulotomy



Figure 1 Follow up findings after radio frequency fistulotomy.

Complications

No major complications were encountered. Few minor ones were discussed as follows. Deep dissection may cause more scarring and longer time for healing. Excessive power of the unit can cause more smoke and charring. Either accidental burns on the part of the patient or operator due to unintended activation of hand piece has been noted. Development of edema in the surrounding tissue would occur, if power was too high. Excessive discharge from the open wound was found in few patients. This usually happened when the tissues at the base were coagulated in excess.

Results of Comparative study

The comparative data of events observed after conventional and radio frequency surgical fistulotomy were shown in Table 1 and Figure 2.

Table 1 Comparative data of events after conventional and RF fistulotomy

Events observed	Conventional fistulotomy (n=50)	Radio frequency surgical fistulotomy (n=50)
Average time of procedure	37 minutes	22 minutes
Average bleeding during procedure	134 ml	47 ml
Need of Suture material	100 %	8 %
Post operative pain	9 days	5 days
Hospital Stay [Mean]	56 hrs	37 hrs
Recurrence/Failure of Treatment	6 %	2 %
Time off work	11 days	7 days
Mean healing time	64 days	47 days
Impairment of continence	12 % for flatus	4 % for flatus

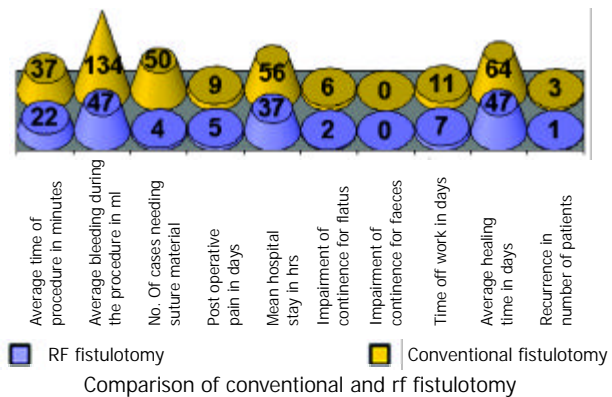


Figure 2 Comparative findings of the results of radio frequency and conventional fistulotomy.

DISCUSSION

Radio frequency surgery, not to be confused with electro surgery, diathermy, spark-gap circuitry, or electrocautry, uses a very high frequency radio frequency wave. Unlike electrocautry or diathermy, the electrode remains cold^[16]. This is possible because of use of very high frequency current of 4 MHz, as compared to 0.5 to 1.5 MHz used in the electrocautry. As contrast to true cautry, which causes damage similar to 3rd degree burns, the tissue damage that does occur is very superficial and is comparable to that which occurs with Lasers. Histologically, it has been shown that tissue damage with radio frequency surgery is actually less than with a conventional scalpel and equals cold scalpel^[17]. Radio frequency surgery creates minimal collateral heat damage in the tissue resulting in rapid healing and leaves no ugly scar. Biopsies performed of the skin tissue indicate a maximum thickness of heat-denatured collagen to be 75 micrometer. This is equal to or even better than carbon dioxide laser used for cutting^[18].

Rapidity of treatment, a nearly bloodless field, minimal postoperative pain, and rapid healing are but few advantages of radio frequency surgery. Once proper technique is established, a scar by this method of treatment is often less pronounced than those produced by other surgical techniques. Excising too deeply increases the likelihood of scars^[19].

Precautions to be taken

Removing a lesion on someone who is on aspirin or anticoagulant therapy may be accompanied by increased bleeding.

The unit should not be used in presence of flammable or

explosive liquids or gases. The surgeon must also remember to deactivate the hand piece whenever the electrodes are changed^[20].

As with all radio frequency surgery machines, smoke is produced, this needs to be attended to avoid the unpleasant smell of burning. This could be achieved by employing a vacuum extractor with the help of the assistant^[21].

The various techniques used for treating fistula^[22] are fistulectomy, fistulotomy, fistulotomy with marsupialisation^[23] of fistula, curettage of fistula and placement of flaps of mucosa or skin, placement of medicated Setons, insertion of antibiotic beads, and injection of commercial or autologous fibrin glue^[24]. Out of these options available to the surgeon, majorities of them still rely on the classical lay open technique (fistulotomy) as the gold standard of treatment in over 90 % of anal fistula cases^[25].

Patients' satisfaction after the surgical treatment for fistula-in-anus is associated with recurrence of the fistula, the development of anal incontinence, and the effects of anal incontinence on patient lifestyle^[26]. The radio frequency surgical technique of fistulotomy has been found more acceptable than the conventional fistulotomy in the sense that the time taken for the whole procedure is reduced to half, bleeding is reduced to a minimum and the use of suture material is dispensed with. None of the patients in our study had any interference with the continence and the recurrence rate was as low as 1.5 %.

If compared to electrocautery or laser, the active electrode does not heat up, so there is minimal or no heat generated to the surgical site. This allows the surgeon to work in direct proximity of the functional tissues that needs to be preserved^[27].

CONCLUSION

This technique has been found superior to the conventional and can safely be called a "sutureless fistulotomy".

REFERENCES

- 1 **Adams D**, Kovalcik PJ. Fistula in ano. *Surg Gynecol Obstet* 1981; **153**: 731-732
- 2 **Vasilevsky CA**. Fistula-in-ano and abscess. In: Beck DE, Wexner SD, eds. Fundamentals of anorectal surgery. *New York: McGraw-Hill* 1992: 131-144
- 3 **Seow-Choen F**, Nicholls RJ. Anal fistula. *Br J Surg* 1992; **79**: 197-205
- 4 **Isbister WH**. Fistula in ano: a surgical audit. *Int J Colorectal Dis* 1995; **10**: 94-96
- 5 **Kuypers JH**. Diagnosis and treatment of fistula-in-ano. *Neth J Surg* 1982; **34**: 147-152
- 6 **Kuipers HC**, Schulpen T. Fistulography for fistula in ano: is it useful? *Dis Colon Rectum* 1985; **28**: 103-104
- 7 **Parks AG**, Gordon PH, Hardcastle JD. A classification of fistula-in-ano. *Br J Surg* 1976; **63**: 1-12
- 8 **Kronborg O**. To lay open or excise a fistula-in-ano: a randomized trial. *Br J Surg* 1985; **72**: 970
- 9 **McLeod RS**. Management of fistula-in-ano. Roussel Lecture. *Can J Surg* 1991; **34**: 581-585
- 10 **Gingold BS**. Reducing the recurrence risk of fistula in ano. *Surg Gynecol Obstet* 1983; **156**: 661-662
- 11 **Pfenninger JL**, Zainea GG. Common anorectal conditions: Part II. *Am Fam Physician* 2001; **64**: 77-88
- 12 **Plant RL**. Radiofrequency treatment of tonsillar hypertrophy. *Laryngoscope* 2002; **112**: 20-22
- 13 **Golighar J**, Duthie H, Nixon H. Surgery of the anus rectum and colon. 5th ed. *London: Bailliere Tindal* 1992: 196-197
- 14 **Vasilevsky CA**, Gordon PH. Results of treatment of fistula-in-ano. *Dis Colon Rectum* 1985; **28**: 225-231
- 15 **Gustafsson UM**, Graf W. Excision of anal fistula with closure of the internal opening: functional and manometric results. *Dis Colon Rectum* 2002; **45**: 1672-1678
- 16 **Olivar AC**, Rorouhar FA, Gillies CG, Servanski DR. Transmission of Electron Microscopy: Evaluation of Damage in human oviducts caused by different surgical instruments. *Ann Clin Laboratory Sci* 1999; **29**: 135-139
- 17 **Saidi MH**, Setzler FD Jr, Sadler RK, Farhart SA, Akright BD. Comparison of office loop electrosurgical conization and cold knife conization. *J Am Assoc Gynecol Laparosc* 1994; **1**: 135-139
- 18 **Bridenstine JB**. Use of ultra-high frequency electrosurgery [Radio surgery] for cosmetic surgical procedures. *Dermatol Surg* 1998; **24**: 397-400
- 19 **Pfenninger JL**, DeWitt DE. Radio frequency frequency surgery. Procedures for primary care physicians. *St Louis: Mosby* 1994: 91-101
- 20 **Valinsky MS**, Hettinger DF, Gennett PM. Treatment of Verrucae via Radio frequency wave Surgery. *J Am Podiatr Med Assoc* 1990; **80**: 482-488
- 21 **Inoue Y**, Yozu R, Cho Y, Kawada S. Video-Assisted thoracoscopy system guidance in linear radiofrequency ablation. *Surgery Today* 2000; **30**: 811-815
- 22 **Belliveau P**. Anal fistula. In: Fazio VW, eds. Current therapy in colon and rectal surgery. *Toronto: BC Decker* 1990: 22-27
- 23 **Eu KW**. Fistulotomy and marsupialisation for simple fistula-in-ano. *Singapore Med J* 1992; **33**: 532
- 24 **Abel ME**, Chiu YS, Russell TR, Volpe PA. Autologous fibrin glue in the treatment of rectovaginal and complex fistulas. *Dis Colon Rectum* 1993; **36**: 136-138
- 25 **Ewerth S**, Ahlberg J, Collste G, Holmstrom B. Fistula-in-ano. A six-year follow up study of 143 operated patients. *Acta Chir Scand Suppl* 1978; **482**: 53-55
- 26 **Garcia-Aguilar J**, Davey CS, Le CT, Lowry AC, Rothenberger DA. Patient satisfaction after surgical treatment for fistula-in-ano. *Dis Colon Rectum* 2000; **43**: 1206-1212
- 27 **Pfenninger JL**. Modern treatments for internal hemorrhoids. *BMJ* 1997; **314**: 1211-1212

Edited by Xu XQ

Laparoscopic splenectomy: the latest technical evaluation

Min Tan, Chao-Xu Zheng, Zhi-Mian Wu, Guo-Tai Chen, Liu-Hua Chen, Zhen-Xian Zhao

Min Tan, Chao-Xu Zheng, Zhi-Mian Wu, Guo-Tai Chen, Liu-Hua Chen, Zhen-Xian Zhao, Department of General Surgery, the First Affiliated Hospital of Sun Yat-sen University, Guangzhou 510080, Guangdong Province, China

Correspondence to: Professor Min Tan, Department of General Surgery, The First Affiliated Hospital of Sun Yat-sen University, 58 Zhongshan 2 Road Guangzhou 510080, Guangdong Province, China. tommyt@vip.163.com

Telephone: +86-20-87766335 **Fax:** +86-20-87750632

Received: 2002-10-21 **Accepted:** 2002-11-25

Abstract

AIM: To introduce our latest innovation on technical manipulation of laparoscopic splenectomy.

METHODS: Under general anesthesia and carbon dioxide (CO₂) pneumoperitoneum, 86 cases of laparoscopic splenectomy (LS) were performed. The patients were placed in three different operative positions: 7 cases in the lithotomic position, 31 cases in the right recumbent position and 48 cases in the right lateral position. An ultrasonic scissors was used to dissect the pancreaticosplenic ligament, the splenocolic ligament, lienorenal ligament and the lienophrenic ligament, respectively. Lastly, the gastrosplenic ligament and short gastric vessels were dissected. The splenic artery and vein were resected at splenic hilum with Endo-GIA. The impact of different operative positions, spleen size and other events during the operation were studied.

RESULTS: The laparoscopic splenectomy was successfully performed on all 86 patients from August 1997 to August 2002. No operative complications, such as peritoneal cavity infection, massive bleeding after operation and adjacent organs injured were observed. There was no death related to the operation. The study showed that different operative positions could significantly influence the manipulation of LS. The right lateral position had more advantages than the lithotomic position and the right recumbent position in LS.

CONCLUSION: Most cases of LS could be accomplished successfully when patients are placed in the right lateral position. The right lateral position has more advantages than the conventional supine approach by providing a more direct view of the splenic hilum as well as other important anatomies. Regardless of operation positions, the major axis of spleen exceeding 15 cm by B-ultrasound in vitro will surely increase the difficulties of LS and therefore prolong the duration of operation. LS is a safe and feasible modality for splenectomy.

Tan M, Zheng CX, Wu ZM, Chen GT, Chen LH, Zhao ZX. Laparoscopic splenectomy: the latest technical evaluation. *World J Gastroenterol* 2003; 9(5): 1086-1089
<http://www.wjgnet.com/1007-9327/9/1086.htm>

INTRODUCTION

Endoscopic surgery has continued to gain popularity in almost

all fields of general surgery. Since the first case of LS described by Delaitre and his colleagues^[1] in 1991, more and more LS have been reported in the world^[2-13]. LS has been proven to be a safe modality and become now the first choice of treatment for most patients requiring a splenectomy^[14-20]. LS will be the best choice in laparoscopic surgery followed by the laparoscopic cholecystectomy^[21,22]. However, we noticed that some anatomical and technical factors could significantly influence the outcome of LS. We herein report our latest results of 86 cases with LS.

MATERIALS AND METHODS

Patients

From August 1997 to August 2002, there were 86 patients with various splenic disorders shown in Table 1 received LS. There were thirty-five males and fifty-one females, with the mean age of 41 years (range 16-71). The platelet count (PLT) of 47 patients, in this study, with immune thrombocytopenic purpura (ITP) ranged 12-77×10⁹/L. The major axis of spleen by B-ultrasound in vitro preoperatively were less than 12 cm in fifty-four cases, 12-15 cm in twenty-one cases, 15-20 cm in eight cases and more than 20 cm in three cases. The patient with the largest spleen (23 cm) in this study was a case who suffered from portal hypertension, hypersplenism disease. Accessory spleen was detected in 6 cases with the size of 8 mm to 20 mm. The same surgeon performed all LSs.

Table 1 Diagnosis of 86 Patients in this study

Diagnosis	Cases (percentage %)
Hematologic disorders	
ITP	47 (54.7 %)
Hereditary spherocytosis (HS)	7 (8.1 %)
Autoimmune hemolytic anemia	4 (4.7 %)
Aplastic anemia (AA)	3 (3.5 %)
Hodgkin's lymphoma	3 (3.5 %)
Systemic lupus erythematosus (SLE)	2 (2.3 %)
Other disorders	
Hypersplenism	12 (13.9 %)
Multiple splenic cysts	3 (3.5 %)
Splenic tuberculosis	3 (3.5 %)
Splenic hemangioma	2 (2.3 %)
Total	86 (100 %)

Preoperative managements

Patients with non-hematologic disorders were similar to those receiving traditional open splenectomy in preoperative management. Patients with ITP received an oral administration of prednisone 30-40 mg twice a day and high doses of immunoglobulin G (400 mg/kg per day) 3-5 days for at least one week prior to the operation to raise the platelet count to a mean value of 80 (range 14-110)×10⁹/L. Intravenous administration of prophylactic antibiotics and hydrocortisone 200-300 mg were needed immediately before operation. Prednisone should be given continuously after the operation and reduced in dose gradually according to clinical situations.

Operative technique

All patients received the general anesthesia and were placed in three different operative positions: 7 cases in the lithotomic position, 31 cases in the right recumbent position and 48 cases in the right lateral position. In the right recumbent position and the lateral position, three trocars were usually used to perform the LS (Figure 1). Once all ports were placed, a 30° telescope was introduced through the 10 mm trocar into the peritoneal cavity. Ultrasonic scissors were used to dissect the pancreaticosplenic ligament, splenocolic ligament, lienorenal ligament and lienophrenic ligament, respectively. Lastly, the gastrosplenic ligament and short gastric vessels were dissected. The splenic artery and vein were resected at splenic hilum with Endo-GIA staplers (Autosuture CO; USA), which enabled safe vascular operation for larger vessels. Finally, the spleen was extracted in a plastic or nylon bag through a port wound which enlarged to about 3 cm.

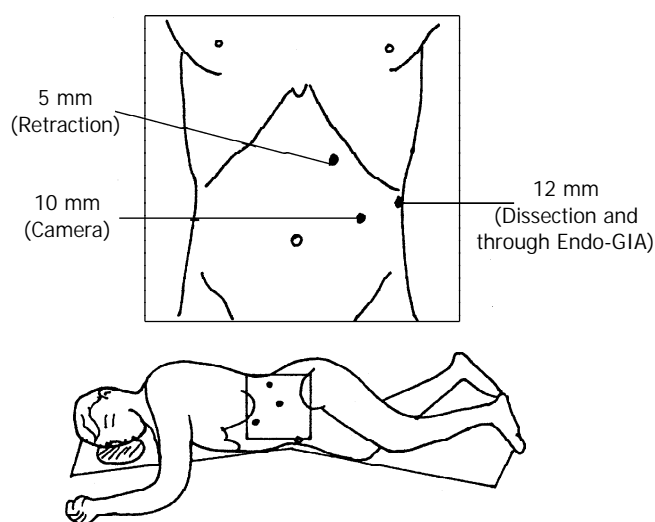


Figure 1 Trocar placement for laparoscopic splenectomy in the lateral position. Three trocars are required.

RESULTS

No postoperative complications or mortality occurred in any patients with LS. All patients were hemodynamically stable during the perioperative period.

Eighty-six cases underwent a successful LS with a mean operating time of 110 minutes (range 50-270 minutes) except one case with extensive dense adhesion around the spleen due to severe perisplenitis, for whom it took nearly six hours to accomplish the operation. The situations of patients with operating time over 120 minutes were: the initial five cases of our patients being conducted LS and eleven cases with spleen major axis exceeding 15 cm. The case with 23 cm in major axis of spleen took 270 minutes to finish the LS. Blood loss was estimated between 50-800 ml during operation in all patients. Three cases received intraoperative transfusion of 400 ml red blood cell. Fifty-two of eighty-six cases (60.5 %) needed to place the drainage tube in lienalis recess postoperatively, which was removed within three days (1 to 3 days). The total amount of draining fluids was less than 100 ml (range 15-100 ml). Recovery of bowel movement occurred within an average of twenty-two (range 18-50) hours after LS. Patients were discharged from hospital in three to six days postoperatively. For patients with ITP, a positive immediate response to splenectomy was defined as a PLT more than $100 \times 10^9/L$ after surgery, which maintained without therapy. In 39 of the 47 patients with ITP, the effective rate of LS was 82.9 % (39/47).

DISCUSSION

Splenectomy for those patients with hereditary spherocytosis (HS) was initially described by Sutherland and Burghard in 1910. With the advancement of laparoscopic instruments and surgeon's experience, minimally invasive approach has been used extensively in many surgical procedures including splenectomy. Now LS has been recognized as a safe and effective treatment for hematologic disorders and other splenic diseases^[23-26]. However, the spleen is fragile and is located deeply in the left upper quadrant, and the abdominal organs like stomach, omentum, and pancreas tail obscure the splenic hilum. Operators are faced with a great deal of difficulty and risk when dealing with LS.

Since the initial reports, early experience has been gained in patients with immune thrombocytopenic purpura and other splenic disorders in a number of centers. In all these early reports, patients received LS either in the supine or the lithotomic position, and laparoscope was placed through a port near the umbilicus. In our seven early LS cases, the patients were placed in the lithotomic position too. This position, however, may take exposure and dissection suboptimal, or even cumbersome. In the lithotomic position, the laparoscope is usually inserted through the trocar near the umbilicus, when peri-splenic adhesion or splenomegaly, causes trouble to expose and dissect the peri-splenic ligaments, such as lienorenal ligament and lienophrenic ligament. Also, this position is very difficult for surgeons to expose posterior-dorsal vessels of spleen clearly and retract spleen to the medial abdomen against its gravity, when attempted to dissect the superior splenic ligaments. For these reasons, we made the rest LS patients lie in the right recumbent position or the right lateral position. We found that the abdominal organs like stomach, omentum and colon all went to the right by their gravity, dorsal side of spleen was exposed satisfactorily, and the peri-splenic ligaments are dissected easily in these two positions. In our experience, it is easy to dissect ligaments, to mobilize spleen and to place the stapler without any tension when using the right lateral approach. The procedure we used can also reduce operating time and avoid spleen or capsule fractures. In this study, there was no massive intraoperative bleeding, and no injury to great splenic vessels was observed.

Splenomegaly was initially considered as a contraindication of laparoscopic splenectomy^[27-32]. With the advancement of laparoscopic technology, LS of enlarged spleen has been performed successfully with laparoscopy^[33-38]. However, the difficulty in conducting LS on splenomegaly is certainly greater than that on the spleen with normal size. As operative area is stuffed with enlarged spleen, the peri-splenic ligaments is relative shorter, and the splenic hilum is deeply hidden in the enlarged spleen, the manipulation of LS becomes very difficult. It is hard to dissect the dorsal and upper pole ligaments of spleen in this situation. A tear of splenic capsule and splenic pedicle hemorrhage can often occur. It is a common cause to alter LS to open splenectomy in splenomegaly. In our study, we found that the right lateral approach is particularly suitable for patients with splenomegaly. Surgeons easily manipulate in right lateral position by taking advantage of gravity of spleen to expose the retroperitoneal attachments and to dissection even in the presence of dense diaphragmatic adhesions. The right lateral position offers a better laparoscopic view and space for manipulation than other positions. Moreover, only three trocars are typically required, and splenic pedicle exposition can be performed easily with less risk of capsular disruption. In fact, we have used this position in all LS cases regardless of the size of spleen since 2000^[39,40]. However, The disadvantage of the right lateral position is lack of wide visual field, which presents the possibility of missing the accessory spleen not

located in the neighborhood of splenic hilum. In addition, the distance between costal margin and iliac crest is rather short in some patients with obesity being placed in the right lateral position, which may cause difficulty for laparoscopic manipulation.

After exploring the abdominal cavity, the lower pole ligament of spleen and splenocolic ligament should be dissected firstly. Then, lienorenal ligament and lienophrenic ligament were dissected in order. The gastrosplenic ligament should be dissected after dealing with all peri-splenic ligaments, because these ligaments, especially lienophrenic ligament, create a narrow area between stomach and spleen. When the peri-splenic ligaments are dissected, the spleen will be turned down easily, the space between stomach and spleen will be enlarged, and the gastrosplenic ligament as well as short gastric vessels can be transected by ultrasonic scissors^[41,42] or titanium clips. Following this procedure, the injury to stomach or the tear of upper pole of spleen can be avoided when dissecting the upper part of gastrosplenic ligament. At last, the splenic artery and vein are isolated and divided by endoscopic vascular staplers. Individual ligation of splenic vessels requires dissecting the artery and vein of splenic hilum, which may increase the risk of damage to the tail of pancreas and hilum vessels. The high success rate in our group may be related to the operative position we adopted which provides a nice exposure of hilum of the spleen, so that it is certain for endoscopic vascular stapler to cross the entire splenic hilar vessels completely. By the way, the application of stapling instrument is safer than other manners when dealing with the splenic hilum vessels.

Perisplenitis may lead to contraction of ligaments and adhesion of the spleen to the adjacent organs, which increases the difficulty of manipulation and the risk of operation. The adhesion and peri-splenic ligaments should be dissected with ultrasonic scissors carefully in order to avoid possible capsular being torn or great vessels broken, which will result in uncontrollable bleeding. Once the splenic hilum is exposed clearly, transection procedure should be taken before handling the upper pole of spleen. This procedure is very important for the enlarged spleen, which usually has autoinfection leading to inflammatory adhesions to the diaphragm and omentum. To mobilize all the peri-splenic ligaments before transecting the splenic hilum for patients with splenomegaly, it will take the branch for the root and easily lead to uncontrollable bleeding. In one of our cases, the operation took nearly six hours on the patient who suffered from severe perisplenitis and extensive dense adhesion around the spleen. Another two cases received intraoperative transfusion of 400 ml red blood cell, in which the possible causes of bleeding were considered as massively enlarged spleen (more than 20 cm), severe extensive dense adhesion and in the lithotomic position. Although more and more reports defined LS as a safe and easy operation in massive splenomegaly^[43-47], we thought the major axis of spleen exceeding 15 cm will surely raise the difficulty and risk in LS.

For patient with hematology disorders, accessory spleen often results in unfavorable therapeutic outcome or recurrence of primary disease^[48]. It is reported that the incidence of accessory spleens are 10 % to 30 % in patients with hematologic diseases^[49-55]. In this series, we found six patients (12.8 %) with accessory spleen. The "cure" rates of the patients with ITP in our group are approximately 83 %, showing a good response to LS. However, it is considered that the period of follow-up was short in our study. So far there has been no data available of long-term cure rates of ITP by means of LS. The long-term follow-up is needed to answer this question. Notably, in a comparative study, the rate of discovery of accessory spleens was 3 times higher in open splenectomy than that in laparoscopic splenectomy^[56]. The observation showed the need

for a systematic search, in various sites such as splenic hilum, tail of pancreas, splenocolic and gastrosplenic ligaments, and the greater omentum, for accessory spleens during laparoscopic splenectomy.

Laparoscopic surgery has more advantages for improving postoperative course. The majority of our patients started to drink water eight hours after the operation. And the hospitalization ranged from three to six days.

In conclusion, laparoscopic splenectomy for patients with hematologic disorders and some other splenic diseases is technically safe and feasible. It is believe that it is easy to conduct laparoscopic splenectomy in the right lateral position. While in case of splenomegaly, the right lateral position provides better visualization than the lithotomic position and the right recumbent position. The lateral position offers many advantages than the conventional supine approach as it provides a more direct view of the splenic hilum by using the gravity of spleen to expose important anatomy. Regardless of the operative position, the major axis of spleen exceeding 15 cm by B-ultrasound in vitro surely increases the difficulty of LS and therefore prolongs the duration of operation.

REFERENCES

- 1 **Delaitre B**, Maignien B. Splenectomy by the laparoscopic approach. Report of a case. *Presse Med* 1991; **20**: 2263
- 2 **Hamamci EO**, Besim H, Bostanoglu S, Sonisik M, Korkmaz A. Use of laparoscopic splenectomy in developing countries: analysis of cost and strategies for reducing cost. *J Laparoendosc Adv Surg Tech A* 2002; **12**: 253-258
- 3 **Mostafa G**, Matthews BD, Sing RF, Prickett D, Heniford BT. Elective laparoscopic splenectomy for grade III splenic injury in an athlete. *Surg Laparosc Endosc Percutan Tech* 2002; **12**: 283-286
- 4 **Tagaya N**, Oda N, Furihata M, Nemoto T, Suzuki N, Kubota K. Experience with laparoscopic management of solitary symptomatic splenic cysts. *Surg Laparosc Endosc Percutan Tech* 2002; **12**: 279-282
- 5 **Tagaya N**, Rokkaku K, Kubota K. Splenectomy using a completely needlescopic procedure: report of three cases. *J Laparoendosc Adv Surg Tech A* 2002; **12**: 213-216
- 6 **Chapman WH 3rd**, Albrecht RJ, Kim VB, Young JA, Chitwood WR Jr. Computer-assisted laparoscopic splenectomy with the da Vinci surgical robot. *J Laparoendosc Adv Surg Tech A* 2002; **12**: 155-159
- 7 **Corcione F**, Esposito C, Cuccurullo D, Settembre A, Miranda L, Capasso P, Piccolboni D. Technical standardization of laparoscopic splenectomy: experience with 105 cases. *Surg Endosc* 2002; **16**: 972-974
- 8 **Torelli P**, Cavaliere D, Casaccia M, Panaro F, Grondona P, Rossi E, Santini G, Truini M, Gobbi M, Bacigalupo A, Valente U. Laparoscopic splenectomy for hematological diseases. *Surg Endosc* 2002; **16**: 965-971
- 9 **Pace DE**, Chiasson PM, Schlachta CM, Mamazza J, Poulin EC. Laparoscopic splenectomy does the training of minimally invasive surgical fellows affect outcomes? *Surg Endosc* 2002; **16**: 954-956
- 10 **Fielding GA**. Technical developments and a team approach leads to an improved outcome: Lessons learnt implementing laparoscopic splenectomy. *ANZ J Surg* 2002; **72**: 459
- 11 **Rosen M**, Ponsky J. Minimally invasive surgery. *Endoscopy* 2001; **33**: 358-366
- 12 **Brodsky JA**, Brody FJ, Walsh RM, Malm JA, Ponsky JL. Laparoscopic splenectomy. *Surg Endosc* 2002; **16**: 851-854
- 13 **Anthony ML**, Hardee EM. Laparoscopic splenectomy in children with sickle cell disease. *AORN J* 1999; **69**: 567-577
- 14 **Rescorla FJ**, Engum SA, West KW, Tres Scherer LR 3rd, Rouse TM, Grosfeld JL. Laparoscopic splenectomy has become the gold standard in children. *Am Surg* 2002; **68**: 297-301
- 15 **Ho CM**. Splenic cysts: a new approach to partial splenectomy. *Surg Endosc* 2002; **16**: 717
- 16 **Rosen M**, Brody F, Walsh RM, Tarnoff M, Malm J, Ponsky J. Outcome of laparoscopic splenectomy based on hematologic

- indication. *Surg Endosc* 2002; **16**: 272-279
- 17 **Szold A**, Kais H, Keidar A, Nadav L, Eldor A, Klausner JM. Chronic idiopathic thrombocytopenic purpura (ITP) is a surgical disease. *Surg Endosc* 2002; **16**: 155-158
- 18 **Katkhouda N**, Mavor E. Laparoscopic splenectomy. *Surg Clin North Am* 2000; **80**: 1285-1297
- 19 **Brodsky JA**, Brody FJ, Walsh RM, Malm JA, Ponsky JL. Laparoscopic splenectomy. *Surg Endosc* 2002; **16**: 851-854
- 20 **Walsh RM**, Heniford BT, Brody F, Ponsky J. The ascendance of laparoscopic splenectomy. *Am Surg* 2001; **67**: 48-53
- 21 **Fass SM**, Hui TT, Lefor A, Maestroni U, Phillips EH. Safety of laparoscopic splenectomy in elderly patients with idiopathic thrombocytopenic purpura. *Am Surg* 2000; **66**: 844-847
- 22 **Katkhouda N**, Manhas S, Umbach TW, Kaiser AM. Laparoscopic splenectomy. *J Laparoendosc Adv Surg Tech A* 2001; **11**: 383-390
- 23 **Park AE**, Birgisson G, Mastrangelo MJ, Marcaccio MJ, Witzke DB. Laparoscopic splenectomy: outcomes and lessons learned from over 200 cases. *Surgery* 2000; **128**: 660-667
- 24 **Delaitre B**, Champault G, Barrat C, Gossot D, Bresler L, Meyer C, Collet D, Samama G. Laparoscopic splenectomy for hematologic diseases. Study of 275 cases. French Society of Laparoscopic Surgery. *Ann Chir* 2000; **125**: 522-529
- 25 **Jaroszewski DE**, Schlinkert RT, Gray RJ. Laparoscopic splenectomy for the treatment of gastric varices secondary to sinistral portal hypertension. *Surg Endosc* 2000; **14**: 87
- 26 **Budzynski A**, Bobrzynski A, Krzywon J. Laparoscopic surgery of the spleen. *Przegl Lek* 2001; **58**: 158-161
- 27 **Targarona EM**, Espert JJ, Cerdan G, Balague C, Piulachs J, Sugranes G, Artigas V, Trias M. Effect of spleen size on splenectomy outcome. A comparison of open and laparoscopic surgery. *Surg Endosc* 1999; **13**: 559-562
- 28 **Kobayashi S**, Sekimoto M, Tomita N, Monden M. Laparoscopic splenectomy for a massive splenomegaly using a transcatheter technique. *Nippon Geka Gakkai Zasshi* 1998; **99**: 733-736
- 29 **Terrosu G**, Donini A, Baccarani U, Vianello V, Anania G, Zala F, Pasqualucci A, Bresadola F, Pasqualucci A. Laparoscopic versus open splenectomy in the management of splenomegaly: our preliminary experience. *Surgery* 1998; **124**: 839-843
- 30 **Yuan RH**, Chen SB, Lee WJ, Yu S C. Advantages of laparoscopic splenectomy for splenomegaly due to hematologic diseases. *J Formos Med Assoc* 1998; **97**: 485-489
- 31 **Targarona EM**, Espert JJ, Balague C, Piulachs J, Artigas V, Trias M. Splenomegaly should not be considered a contraindication for laparoscopic splenectomy. *Ann Surg* 1998; **228**: 35-39
- 32 **Nicholson IA**, Falk GL, Mulligan SC. Laparoscopically assisted massive splenectomy. A preliminary report of the technique of early hilar devascularization. *Surg Endosc* 1998; **12**: 73-75
- 33 **Glasgow RE**, Mulvihill SJ. Laparoscopic splenectomy. *World J Surg* 1999; **23**: 384-388
- 34 **Hebra A**, Walker JD, Tagge EP, Johnson JT, Hardee E, Othersen HB Jr. A new technique for laparoscopic splenectomy with massively enlarged spleens. *Am Surg* 1998; **64**: 1161-1164
- 35 **Rosin D**, Brasesco O, Rosenthal RJ. Laparoscopic splenectomy: new techniques and indications. *Chirurg* 2001; **72**: 368-377
- 36 **Stanek A**, Gruca Z, Hellmann A, Makarewicz W, Ciepluch H, Kaska L, Oseka T. Laparoscopic splenectomy with a postero-lateral approach in patients with idiopathic thrombocytopenic purpura. *Pol Merkurizus Lek* 2000; **9**: 764-766
- 37 **Park A**, Targarona EM, Trias M. Laparoscopic surgery of the spleen: state of the art. *Langenbecks Arch Surg* 2001; **386**: 230-239
- 38 **Esposito C**, Schaarschmidt K, Settimi A, Montupet P. Experience with laparoscopic splenectomy. *J Pediatr Surg* 2001; **36**: 309-311
- 39 **de Csepel J**, Quinn T, Gagner M. Laparoscopic exclusion of a splenic artery aneurysm using a lateral approach permits preservation of the spleen. *Surg Laparosc Endosc Percutan Tech* 2001; **11**: 221-224
- 40 **Tan M**, Okada M, Wu Z. Application of laparoscopic technique in splenectomy. *Zhonghua Waike Zazhi* 2001; **39**: 599-601
- 41 **Pampaloni F**, Valeri A, Mattei R, Presenti L, Noccioli B, Tozzini S, Di Lollo S, Pampaloni A. Laparoscopic decapsulation of a large epidemoid splenic cyst in a child using the UltraCision LaparoSonic Coagulating Shears. *Pediatr Med Chir* 2002; **24**: 59-62
- 42 **Schaarschmidt K**, Kolberg-Schwerdt A, Lempe M, Saxena A. Ultrasonic shear coagulation of main hilar vessels: A 4-year experience of 23 pediatric laparoscopic splenectomies without staples. *J Pediatr Surg* 2002; **37**: 614-616
- 43 **Terrosu G**, Baccarani U, Bresadola V, Sistu MA, Uzzau A, Bresadola F. The impact of splenic weight on laparoscopic splenectomy for splenomegaly. *Surg Endosc* 2002; **16**: 103-107
- 44 **Kercher KW**, Matthews BD, Walsh RM, Sing RF, Backus CL, Heniford BT. Laparoscopic splenectomy for massive splenomegaly. *Am J Surg* 2002; **183**: 192-196
- 45 **Heniford BT**, Park A, Walsh RM, Kercher KW, Matthews BD, Frenette G, Sing RF. Laparoscopic splenectomy in patients with normal-sized spleens versus splenomegaly: does size matter? *Am Surg* 2001; **67**: 854-857
- 46 **Hashizume M**, Tomikawa M, Akahoshi T, Tanoue K, Gotoh N, Konishi K, Okita K, Tsutsumi N, Shimabukuro R, Yamaguchi S, Sugimachi K. Laparoscopic splenectomy for portal hypertension. *Hepatogastroenterology* 2002; **49**: 847-852
- 47 **Greene AK**, Hodin RA. Laparoscopic splenectomy for massive splenomegaly using a Lahey bag. *Am J Surg* 2001; **181**: 543-546
- 48 **Ribo JM**, Garcia Aparicio L, Morales I. Laparoscopic splenectomy in the treatment of hematologic diseases. *Cir Pediatr* 2001; **14**: 69-72
- 49 **Anglin BV**, Rutherford C, Ramus R, Lieser M, Jones DB. Immune thrombocytopenic purpura during pregnancy: laparoscopic treatment. *JSL* 2001; **5**: 63-67
- 50 **Reddy VS**, Phan HH, O' Neill JA, Neblett WW, Pietsch JB, Morgan WM, Cywes R. Laparoscopic versus open splenectomy in the pediatric population: a contemporary single-center experience. *Am Surg* 2001; **67**: 859-863
- 51 **Cogliandolo A**, Berland-Dai B, Pidoto RR, Marc OS. Results of laparoscopic and open splenectomy for nontraumatic diseases. *Surg Laparosc Endosc Percutan Tech* 2001; **11**: 256-261
- 52 **Marcaccio MJ**. Laparoscopic splenectomy in chronic idiopathic thrombocytopenic purpura. *Semin Hematol* 2000; **37**: 267-274
- 53 **Torelli P**, Cavaliere D, Casaccia M, Panaro F, Grondona P, Rossi E, Santini G, Truini M, Gobbi M, Bacigalupo A, Valente U. Laparoscopic splenectomy for hematological diseases. *Surg Endosc* 2002; **16**: 965-971
- 54 **Bresler L**, Guerci A, Brunaud L, Ayav A, Sebbag H, Tortuyaux JM, Lederlin P, Boissel P. Laparoscopic splenectomy for idiopathic thrombocytopenic purpura: outcome and long-term results. *World J Surg* 2002; **26**: 111-114
- 55 **Tanoue K**, Okita K, Akahoshi T, Konishi K, Gotoh N, Tsutsumi N, Tomikawa M, Hashizume M. Laparoscopic splenectomy for hematologic diseases. *Surgery* 2002; **131**: S318-S323
- 56 **Tsiotos G**, Schlinkert RT. Laparoscopic splenectomy for immune thrombocytopenic purpura. *Arch Surg* 1997; **132**: 642-646

A new technique of combined endoscopic sclerotherapy and ligation for variceal bleeding

Radha K. Dhiman, Yogesh K. Chawla

Radha K. Dhiman, Yogesh K. Chawla, Department of Hepatology, Postgraduate Institute of Medical Education & Research, Chandigarh 160012, India

Correspondence to: Dr Radha K. Dhiman, M.D., D.M., F.A.C.G., Consultant gastroenterologist, Department of Internal Medicine, Salmaniya Medical complex, PO Box 12, Manama, Bahrain, India. rkpsdhiman@hotmail.com

Telephone: +91-172-747585

Received: 2002-09-13 **Accepted:** 2002-11-04

Abstract

AIM: To develop a technique of combined endoscopic sclerotherapy and ligation (ESL) in which both techniques of endoscopic sclerotherapy (ES) and endoscopic variceal ligation (EVL) can be optimally used.

METHODS: ESL was performed in 10 patients (age 46.4 ± 7.9 ; 9 males, 1 female) with cirrhosis of liver using sclerotherapy needle and Speedband, Superview multiple band ligater (Boston Scientific, Microvasive, Watertown, MA). A single band was placed 5-10 cm proximal to the gastro-esophageal junction over each varix from proximal to distal margin, followed by intravariceal injection of 1.5 % ethoxysclerol (4 ml each) 2 to 3 cm proximal to the gastroesophageal junction on the ligated varices distal to deployed band. EVL was then performed at the injection site. Similarly other varices were also injected and ligated from distal to proximally. In the subsequent sessions, ES alone was performed to sclerose small varices at the gastroesophageal junction.

RESULTS: ESL was successfully performed in all patients. A median of 3 (ESL 1, ES 2) sessions (ranged 1-4) were required to eradicate the varices in 9 (90 %) of 10 patients. Recurrence of varices without bleed was seen in 1 patient during a mean follow-up of 10.3 months (ranged 6-15). Two patients died of liver failure. None died of variceal bleeding. None of the patients had procedure related complications.

CONCLUSION: ESL may be useful in the fast eradication of esophageal varices. However, randomised controlled trials are required to find out its relative efficacy and impact on variceal recurrence in comparison to ES or EVL.

Dhiman RK, Chawla YK. A new technique of combined endoscopic sclerotherapy and ligation for variceal bleeding. *World J Gastroenterol* 2003; 9(5): 1090-1093

<http://www.wjgnet.com/1007-9327/9/1090.htm>

INTRODUCTION

Endoscopic sclerotherapy (ES) and endoscopic variceal ligation (EVL) are well-established nonsurgical procedures for the secondary prevention of bleeding from esophageal varices. EVL, developed by Stiegmann *et al*^[1], has been

shown to have lesser complications and also require fewer endoscopy sessions to obliterate esophageal varices^[2]. However, EVL is associated with higher variceal recurrence rate in the long term^[3-7]. High recurrence rates following EVL could be related to inability to further ligate varices once they became small and had no effect on perforating veins and paraesophageal collaterals^[8-10]. The presence of paraesophageal varices predicts the recurrence of esophageal varices and recurrent bleeding^[8-10]. The mechanisms of ES and EVL in achieving variceal sclerosis are quite different. The effect induced by EVL is localized to the submucosa, whereas the chemical effect of ES is deeper, i.e. on perforating veins and paraesophageal collaterals^[8-10]. We have proposed a new technique of combined endoscopic sclerotherapy and ligation (ESL) in which both techniques of ES and EVL can be optimally utilized to achieve rapid eradication and decreased recurrence of esophageal varices^[11]. In this pilot study, we reported our initial experience with this new technique of ESL.

MATERIALS AND METHODS

Patients

Ten patients (mean age 46.4 ± 7.9 years, ranged 38-60; 9 males, 1 female) with cirrhosis of liver and upper gastrointestinal bleeding underwent ESL for variceal eradication. None of the patients was actively bleeding. The diagnosis of cirrhosis was based on clinical, biochemical and ultrasound findings. All patients had a patent splenoportovenous axis on Doppler ultrasound. The etiology of cirrhosis was related to alcohol in 6 patients, hepatitis B virus in 2, autoimmune hepatitis in 1 and cryptogenic in 1. One patient was in Child's grade A, 3 in Child's grade B and 6 patients were in Child's grade C. All patients received first session of ESL followed by ES alone with 1.5 % ethoxysclerol every 2 to 3 weeks.

Methods

ESL was performed with the Olympus EVIS GIF-Type 100 or OES GIF-XQ20 forward-viewing fiberoptic endoscope and Superview, a multiple band ligator device (Boston Scientific Co., Watertown, MA, USA) and a locally fabricated sclerotherapy needle with an outer diameter of 1.8 mm^[12]. The scope was loaded with multiple band ligator devices according to manufacturer's instructions. A small nick with a sharp, pointed blade was made in the plastic covering near the trip wire of the handle unit for the introduction of the sclerotherapy needle (Figure 1). The sclerotherapy needle was thus passed through the working channel of the scope and could be brought out distally through the cylinder of the ligating unit for ES (Figure 2). The scope was loaded with multiple band ligator device containing 5 or 8 bands, then it was introduced into the esophagus and a single band was applied 5-10 cm proximal to the gastroesophageal junction over the varix starting from proximal to distal margin (Figure 3). This was followed by intravariceal injection of 1.5 % ethoxysclerol (4 ml each) 2 to 3 cm proximal to gastroesophageal junction on the ligated varices distal to the deployed bands. The sclerotherapy needle

was removed and EVL was then performed at the injection site. Similarly, other varices were also injected and ligated from distal to proximal margin. The scope was then removed after ensuring complete hemostasis.

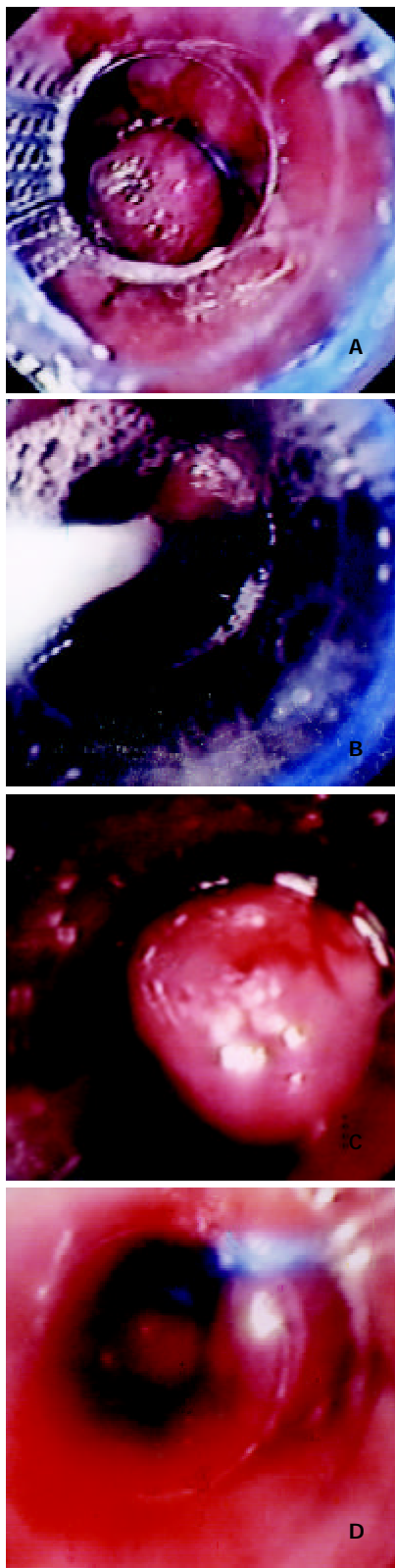


Figure 3 ESL using Speedband, Superview multiple band ligator (Boston Scientific Co., Watertown, MA) and sclerotherapy needle. (a) EVL at least 5 cm or more proximal to gastroesophageal junction, (b) sclerotherapy 2 to 3 cm proximal to gastroesophageal junction on the same varix, (c) EVL on the injection site (arrow) and (d) proximal (large arrow) and distal (small arrow) EVL on the same varix.



Figure 1 Handle unit with trip wire and scope fastener. Injector was passed along the trip wire after making a small nick in the plastic covering (arrow) with a sharp blade.



Figure 2 Endoscope loaded with the ligating unit at its distal end. An injector was coming out from the cylinder of the ligating device through the working channel of the scope.

There was marked reduction in the size of esophageal varices after the ESL; therefore in the subsequent treatment sessions, ES alone was performed with 1.5 % ethoxysclerol to eradicate the remaining varices by intravariceal injection method every 2 to 3 weeks. The patients were then followed-up every 3 to 4 months.

RESULTS

All results were shown in Table 1. Eight patients had large esophageal varices (grade 3 or 4) and 2 patients had small (grade 2) varices. Each patient received 1 session of ESL as described. Esophageal varices were eradicated in 9 (90 %) patients. Marked reduction in variceal size was found following ESL in all patients on the first follow-up of ES session after 2 to 3 weeks. One patient need not require ES as the varices were completely eradicated after the first session of ESL. Three patients each required 1 and 2 sessions of ES with 1.5 % ethoxysclerol, respectively and two patients required 3 ES sessions for complete eradication of esophageal varices. Thus, eradication of varices was achieved in a median of 3 (ESL 1, ESL 2) sessions (range 1-4). None of the patient had procedure-related complications. None of them underwent a "second look" endoscopy after the therapy for evaluation of any symptoms. Large liner superficial ulcers were seen in 3 patients on the first follow-up endoscopy after 2 weeks, which healed uneventfully with marked reduction in variceal size. None of the patient received β -blockers.

Nine patients, in whom variceal eradication was achieved, were followed-up for a mean of 10.3 months (range 6-15). Small (grade 2) esophageal varices recurred in 1 (11.1 %) patient without variceal bleeding. ES was carried out to eradicate the varices again. Two patients died of liver failure. While 1 patient died before the varices could be eradicated,

another died during follow-up for 9 months after the eradication of varices. None of the patient died of variceal bleeding.

One patient had large fundal varices with cherry red spots. This patient received undiluted 2.5 ml of intravariceal injection of n-butyl-2-cyanoacrylate into the fundal varices in 2 sessions. Fundal varices disappeared following extrusions of cyanoacrylate cast 3 months later. Mild portal hypertensive gastropathy was present in 1 patient before the eradication of esophageal varices and in 3 patients after the eradication of varices.

Table 1 Endoscopic parameters

Grade of esophageal varices	Number of patients
Grade 3 or 4	8
Grade 2	2
ESL sessions	1
Follow-up ES sessions (median, range)	2(0-3)
Total ESL + ES sessions (median, range)	3(1-4)
Gastric varices	
Before eradication of esophageal varices ^a	1
After eradication of esophageal varices	0
Portal hypertensive gastropathy	
Before	1
After	3
Death ^b	2

^aThe patient received n-butyl-2-cyanoacrylate for large gastric (fundal) varices, ^bLiver failure.

DISCUSSION

We successfully performed this new technique in all patients with cirrhosis of liver, thus showing its efficacy in a clinical setting. Large paraesophageal collaterals on endosonography predict recurrence of esophageal varices^[10,13]. We have earlier shown that the ES has an effect on the perforating veins and paraesophageal collaterals as evidenced by reduction in their number and size, while no effect could be demonstrated on these venous structures with EVL^[7,8]. In order to reduce the early recurrence of the varices, the present technique aimed at augmenting the effect of sclerosant on perforating veins and on paraesophageal collaterals, while at the same time maintaining the efficacy of EVL to quickly obliterate the esophageal varices.

In this technique, proximal ligation of varices with a band not only interrupts the cephalic variceal blood flow but also divert it into the paraesophageal collaterals via perforating veins, thereby, augmenting the effect of sclerosant on the perforating veins and paraesophageal collaterals or feeders. The effect of this technique may be similar to the technique of ESL used by Umehara *et al*^[4], or the technique of ES used by Takase *et al*^[14] where the effect of sclerosant on feeder vessels of the varices could be increased by interrupting variceal blood flow by inflating the proximal balloon affixed to endoscope. In both the techniques, fluoroscopy was used to confirm the opacification of feeders with sclerosant and contrast mixture. However, our technique was simple and did not require fluoroscopy thereby reducing the radiation exposure to the patient. This method had another advantage. The effectiveness of ES also depended on the time that sclerosant remained in contact with endothelial cells in blood vessels^[15]. Proximal ligation of varices in this technique thus increased the effectiveness of sclerosant by increasing the contact time with endothelial cells. After the ES, a band was placed either on the injection site or distal to it, to achieve complete hemostasis

and the optimal effect of EVL. The endoscopist however must be careful while negotiating the scope beyond the proximally ligated varices. We did not experience the displacement of proximally deployed band.

If the effect of EVL and ES in this technique is additive then the variceal eradication rate should be higher, the varices should be eradicated in fewer sessions and the recurrence of the varices should be low. In this pilot study, complete eradication of esophageal varices was achieved in 9 (90 %) patients in a median of 3 (ESL1, ES2) sessions (range 1-4), while our previous experience with ES alone showed that 6.8±4.9 (mean ± SD) sessions were required to obliterate varices in 45 % of patients with cirrhosis of liver^[16]. Recurrence of esophageal varices in our previous experience was 25.9 %^[16]. These results comparing with historical control, indicate that the present technique of ESL is not only effective in reducing the number of sessions for eradication of esophageal varices but also in achieving eradication of varices in a higher proportion of patients. However, prospective, multi-center randomised trials are required to substantiate these results as well as to observe the impact on variceal recurrence with this technique.

ES was done easily without any complication as the injector could be passed though the working channel of the scope. We, however, observed large linear superficial ulcers over the varices on follow-up endoscopy. This finding is not unexpected as the effect of sclerosant is increased by the interruption of the variceal blood flow proximally by a band. These ulcers were superficial and healed without any complication, and were associated with eradication or marked reduction in the variceal size.

In conclusion, our new technique of ESL may be useful in the fast eradication and in achieving lower recurrence of esophageal varices. It, however, requires further randomised controlled trials with EVL or ES to find out its efficacy and impact on the variceal recurrence.

REFERENCES

- 1 **Van Stiegmann GV**, Cambre T, Sun TH. A new endoscopic elastic band ligating device. *Gastrointest Endosc* 1986; **32**: 230-233
- 2 **Laine L**, Cook D. Endoscopic ligation compared with sclerotherapy for treatment of esophageal varices and bleeding: a meta-analysis. *Ann Intern Med* 1995; **123**: 280-287
- 3 **Hou MC**, Lin HC, Kuo BIT, Chan CH, Lee FY, Lee SD. Comparison of endoscopic variceal injection sclerotherapy and ligation for the treatment of esophageal variceal hemorrhage: a prospective randomized trial. *Hepatology* 1995; **21**: 1517-1522
- 4 **Umehara M**, Onda M, Tajiri T, Toba M, Yoshida H, Yamashita K. Sclerotherapy plus ligation versus ligation for the treatment of esophageal varices: a prospective randomized study. *Gastrointest Endosc* 1999; **50**: 7-12
- 5 **Baroncini D**, Milandri GL, Borioni D. A prospective randomized trial of sclerotherapy versus ligation in the elective treatment of bleeding esophageal varices. *Endoscopy* 1997; **29**: 235-240
- 6 **Sarin SK**, Govil A, Jain AK, Guptan RC, Issar SK, Jain M. Prospective randomized trial of endoscopic sclerotherapy versus variceal band ligation for esophageal varices: influence on gastropathy, gastric varices and variceal recurrence. *J Hepatol* 1997; **26**: 826-832
- 7 **Bohnacker S**, Sriram PV, Soehendra N. The role of endoscopic therapy in the treatment of bleeding varices. *Baillieres Best Pract Res Clin Gastroenterol* 2000; **14**: 477-499
- 8 **Dhiman RK**, Choudhuri G, Saraswat VA, Agarwal DK, Naik SR. Role of paraesophageal collaterals and perforating vein on outcome of endoscopic sclerotherapy for esophageal varices: an endosonographic study. *Gut* 1996; **38**: 759-764
- 9 **Choudhuri G**, Srivastava A, Agarwal DK, Dhiman RK. Endosonographic evaluation of venous changes around the gastroesophageal junction during sclerotherapy and band ligation

- of varices. *Gastroenterology* 1996; **110**: A1170
- 10 **Lo GH**, Lai KH, Chang JS, Huang RL, Wang SJ, Chiang HT. Prevalence of paraesophageal varices and gastric varices in patients achieving variceal obliteration by banding ligation and by injection sclerotherapy. *Gastrointest Endosc* 1999; **49**: 428-436
- 11 **Dhiman RK**, Chawla YK. Is the technique of endoscopic sclerotherapy and ligation (ESL) optimum? *Gastrointest Endosc* 2000; **51**: 639-640
- 12 **Dilawari JB**, Chawla Y, Locham HS, Prakash S. A low cost endoscopic sclerotherapy needle. *Trop Gastroenterol* 1985; **6**: 104-106
- 13 **Leung VK**, Sung JJ, Ahuja AT, Tumala IE, Lee YT, Lau JYW. Large para-oesophageal varices on endosonography predict recurrence of esophageal varices and rebleeding. *Gastroenterology* 1997; **112**: 1811-1816
- 14 **Takase Y**, Shibuya S, Chikamori F, Oril K, Iwasaki Y. Recurrence factors studied by percutaneous transhepatic portography before and after endoscopic sclerotherapy for esophageal varices. *Hepatology* 1990; **11**: 348-352
- 15 **Masaki M**, Obara K, Suzuki S, Orikasa K, Mitsunashi H, Iwasaki K. The destructive effect of sclerosant elanalamine oleate on mammalian vessel endothelium. *Gastroenterol Japonica* 1990; **25**: 230-235
- 16 **Chawla YK**, Dilawari JB, Kaur U. Variceal sclerotherapy in cirrhosis. *Indian J Gastroenterol* 1998; **7**: 215-217

Edited by Xu XQ

Bile from a patient with anomalous pancreaticobiliary ductal union promotes the proliferation of human cholangiocarcinoma cells via COX-2 pathway

Gao-Song Wu, Sheng-Quan Zou, Zheng-Ren Liu, Da-Yu Wang

Gao-Song Wu, Sheng-Quan Zou, Zheng-Ren Liu, Da-Yu Wang, Department of General Surgery, Tongji Hospital, Tongji Medical College, Huazhong University of Science and Technology, Wuhan, 430030, Hubei Province, China

Correspondence to: Dr Gao-Song Wu, Department of General Surgery of Tongji Hospital, 1095 Jiefang Road, Wuhan, 430030, Hubei Province, China. wugaosong9172@sina.com

Telephone: +86-27-83662851 **Fax:** +86-27-83662851

Received: 2002-08-24 **Accepted:** 2002-10-12

Abstract

AIM: To explore the effects of COX-2 gene in the proliferative activity induced by bile from anomalous pancreaticobiliary ductal union (APBDU) on human cholangiocarcinoma cell line.

METHODS: Bile sample from APBDU and normal bile sample were used for this study. The proliferative effect of bile was measured by methabenzthiazuron (MTT) assay; COX-2 mRNA was examined by semi-quantitative reverse transcription polymerase chain reaction (RT-PCR). Cell cycle was analyzed by flow cytometry (FCM), and the PGE₂ levels in the supernatant of cultured cholangiocarcinoma cells were quantitated by enzyme-linked immunoabsorbent assay (ELISA).

RESULTS: Bile from APBDU can significantly promote the proliferation of human cholangiocarcinoma QBC939 cells compared with normal bile ($P=0.005$) and up-regulated remarkably their COX-2 mRNA expression ($P=0.004$). The proliferative activity of APBDU bile can be abolished by addition of cyclooxygenase-2 specific inhibitor celecoxib.

CONCLUSION: Bile from APBDU can promote the proliferation of human cholangiocarcinoma QBC939 cells via COX-2 pathway.

Wu GS, Zou SQ, Liu ZR, Wang DY. Bile from a patient with anomalous pancreaticobiliary ductal union promotes the proliferation of human cholangiocarcinoma cells via COX-2 pathway. *World J Gastroenterol* 2003; 9(5): 1094-1097
<http://www.wjgnet.com/1007-9327/9/1094.htm>

INTRODUCTION

It is well known that APBDU is associated with choledochal cyst^[1-9]. Recently, a frequent association of biliary tract carcinoma and APBDU without choledochal cyst is well recognized, but its underlying mechanism is unclarified. For the purpose of resolving these mechanism we used the APBDU bile to act directly on the QBC939 cells to determine the effects of bile from APBDU on the cholangiocarcinoma cells growth.

MATERIALS AND METHODS

Materials

Bile samples collection and treatment: APBDU bile was obtained from the common bile duct of a patient (male, 39) with polypoid lesion of the gallbladder who underwent cholecystectomy in the Department of Surgery, Tongji hospital, Wuhan, China. Preoperative MRCP revealed the length of the pancreaticobiliary common channel was 19 mm with absence of dilation of the common bile duct, the pancreatic duct merged with the bile duct (P-B type) and the pancreaticobiliary ductal union was located proximal to the narrow distal segment, which represented the sphincter of Oddi, APBDU was diagnosed by intraoperative cholangiography concordant with the MRCP diagnosis. Normal control bile was obtained from the common bile duct of another patient (male, 41) with gastric cancer and a normal hepatobiliary tract. Both patients had not taken any nonsteroidal anti-inflammatory drugs, antibiotics or anti-tumor drugs before the operation. Bile samples were sterile and filtered (0.22 μm, Millipore) twice immediately and stored at -80 °C. PBS (pH7.2) was used as negative control. Human extrahepatic cholangiocarcinoma cell line QBC939 was gifted by professor Wang (Third Military Medical University, China)^[10], the cells were maintained as monolayers in Dulbecco's modified Eagle's medium (DMEM) supplemented with 10 % fetal bovine serum (FBS, Gibco. USA.), 100 units/ml penicillin and 100 mg/ml streptomycin in a humidified atmosphere of 95 % air and 5 % CO₂ at 37 °C. PGE₂ ELISA detection kit was purchased from Jingmei Biotech Co., Wuhan, China. Celecoxib was provided by Dr. Mei (Wuhan University, China)^[11]. Stock solution was prepared in dimethylsulfoxide (DMSO) and stored at -20 °C. In all experiments the final concentration of DMSO in the medium was ≤0.1 %.

Methods

Cytotoxicity pretesting Cytotoxicity pretesting was taken with each of the gradient in diluted bile sample to determine the concentration of experimental bile samples. Our results showed that 1 % bile (10 μL bile/mL medium) was not cytotoxic to QBC939 cells.

MTT assay The proliferating status of human cholangiocarcinoma cells QBC939 was determined by MTT assay. Cholangiocarcinoma cells were seeded at a density of 1×10⁴ cells per well in flat-bottomed 96-well microplates. 12 h after incubation, the cells were treated with 1 % bile with or without 20 μmol/L celecoxib. After 72 h incubation, 20 μL MTT (5 g/L) was added to each well and cultured for 4 h. Upon removal of the supernatant, added DMSO 150 μL and shook for 5 min until the crystals were dissolved. OD490nm value was measured by enzyme-linked immunoabsorbent assay. The negative control well was used as zero point of absorbance. Each assay was performed three times in triplicate. **ELISA** The PGE₂ levels in the supernatant of the cultured human cholangiocarcinoma cells QBC939 were quantitated

by ELISA. Cells were seeded into 24-well microplates (4.0×10^5 /well) and allowed to adhere overnight. The cells were then incubated in presence 1 % bile with or without 20 $\mu\text{mol/L}$ celecoxib for 48 h. The supernatants were aspirated and centrifuged to prepare for the detection of PGE_2 . 0.5 mL supernatant was added into 1 N HCl 0.1 mL and centrifuged for 10 min at room temperature; then 1.2 N NaOH 0.1 mL was used to neutralize the acidified samples. Standard solution (200 μL /well) or activated samples were added into the microplates. Then the steps were proceeded as instructed. The value of OD of each well was determined at 450nm. The supernatants were harvested in triplicate and the experiment was performed three times.

Flow cytometric analysis Human cholangiocarcinoma cells QBC939 were trypsinized and plated in 6-well culture dishes in presence of 1 % APBDU bile or 1 % normal bile. After 24 h, the cells were harvested, centrifuged at low speed and fixed in 70 % ethanol. After overnight incubation at 4 °C, the cells were stained with 50 $\mu\text{g/ml}$ propidium iodide in presence of RNasin A (10 $\mu\text{g/ml}$) and 0.1 % Triton X-100 and determined by flow cytometer.

RT-PCR QBC939 cells were cultured in presence of 1 % APBDU bile, 1 % normal bile or 1 % PBS for 3 d. The total RNA was prepared from subconfluent cultures with RNA-SOLV reagent (Omega) according to the manufacture' instruction. The primers were designed to amplify a fragment of COX-2 cDNA based on the reported sequence for human COX-2. To normalize the amount of input RNA, RT-PCR was performed with primers for the constitutively expressed β -actin gene. The COX-2 primers were 5' - ACAATGCTGACTATGGCTAC-3' (sense) and 5' - AACTGATGCGTGAAGTGCTG-3' (antisense), giving rise to a 238 base pair polymerase chain reaction production. The β -actin primers were 5' -GTGCGTGACATTAAGGAG-3' (sense) and 5' -CTAAGTCATAGTCCGCCT-3' (antisense), giving rise to a 520 base pair polymerase chain reaction production. The first strand cDNA synthesis and the subsequent PCR were performed with RNA PCR kit (AMV) using a programmed temperature control system set for 30 cycles of denaturation at 94 °C for 45 s, annealing at 58 °C for 30 s, and extension at 72 °C for 60 s. 10 μL reaction mixture was electrophoresed on a 1.5 % agarose gel, and the PCR products were visualized by ethidium bromide staining and quantified by an ImageQuant software. COX-2 mRNA expression level was determined by COX-2/ β -actin protein.

Statistical analysis

The data were expressed as $\bar{x} \pm s$. Student's *t*-test was used for statistical analysis. $P < 0.05$ indicated significant difference.

RESULTS

Assay of COX-2 activity

PGE_2 levels in the supernatant released by the cultured human cholangiocarcinoma cells QBC939 determined the COX-2 activity. The concentrations of PGE_2 in culture medium of QBC939 cells treated with 1 % APBDU bile or 1 % normal bile with or without 20 $\mu\text{mol/L}$ celecoxib for 48 h were quantitated by ELISA. APBDU bile could induce the release of PGE_2 in QBC939 cells: the PGE_2 level was higher significantly ($P=0.004$) in APBDU bile group (187.1 ± 14.0 ng/well) as compared with that in normal bile group (139.4 ± 15.3 ng/well). Celecoxib could suppress PGE_2 production of the QBC939 cells, the PGE_2 concentration was (65.2 ± 10.6) ng/well and (57.0 ± 9.8) ng/well in APBDU bile group and normal bile group respectively when pre-treated with 20 $\mu\text{mol/L}$ celecoxib, there was no statistical difference between the two group ($P=0.09$).

Effects of bile on the proliferation activity of QBC939

QBC939 cells were incubated in 1 % bile with or without 20 $\mu\text{mol/L}$ celecoxib, and the cells density was measured by MTT assay. APBDU bile could significantly promote the proliferation of QBC939 cells as compared with normal bile ($P=0.005$), and the proliferative effect of APBDU bile could be abolished by addition of 20 $\mu\text{mol/L}$ celecoxib ($P=0.103$, Table 1).

Table 1 Effects of bile on the growth of QBC939 with or without celecoxib

Group	OD ₄₉₀	P	+CE OD ₄₉₀	P
A	0.82±0.19	^b $P=0.008$, ^d $P=0.005$	0.33±0.14	^b $P=0.297$, ^d $P=0.103$
B	0.47±0.14	^b $P=0.398$	0.26±0.07	^b $P=0.052$
C	0.43±0.10		0.24±0.09	

QBC939 cells were incubated in 1 % APBDU bile (A), 1 % normal bile (B) or 1 % PBS (C) with or without 20 $\mu\text{mol/L}$ celecoxib (+CE), and the cells density (OD_{490nm}) was measured by using MTT assay. Data were expressed as $\bar{x} \pm s$, b vs C, d vs B.

Flow cytometric analysis of proliferative index of QBC939 cells

The QBC939 cells proliferative index (PI) increased significantly ($P=0.003$) after treatment with 1 % APBDU bile (60.59 ± 4.06) as compared with that of the normal bile (28.69 ± 1.79 , Figure 2), $\text{PI} = \text{S} + \text{G2/M} \times 100\%$.

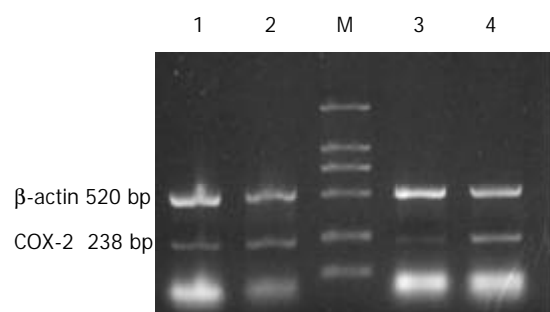


Figure 1 Expression of COX-2 mRNA, β -actin served as control. M: DL2,000 marker; 1: normal bile; 2 and 4: APBDU; 3: PBS.

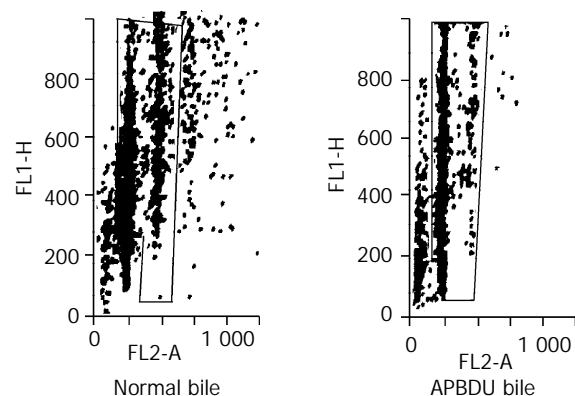


Figure 2 Representative data of cell cycle from QBC939 cells in the presence of 1 % APBDU bile ($\text{S} + \text{G2/M} = 65.12\%$) or 1 % normal bile ($\text{S} + \text{G2/M} = 30.47\%$) for 24 h was analyzed by flow cytometry.

Expression level of COX-2 mRNA

APBDU bile could markedly ($P=0.004$) up-regulate the COX-2 mRNA expression of QBC939 cells (Figure 1, Table 2).

Table 2 Expression level of COX-2 mRNA

Group	n	COX-2/ β -actin	t	P
A	6	0.4322 \pm 0.0448	^b t=11.556, ^d t=5.010	^b P<0.001, ^d P=0.004
B	6	0.2267 \pm 0.0638	^b t=1.820	^b P=0.128
C	6	0.1367 \pm 0.0653		

COX-2 mRNA expression level was determined by COX-2/ β -actin protein. Data were expressed as $\bar{x}\pm s$, b vs C (PBS), d vs B (normal bile), A: APBDU.

DISCUSSION

A frequent association of biliary tract carcinoma and APBDU is well recognized^[12-19], especially in the undilated type APBDU^[20, 21]. Mori^[7] had reported that among 698 patients subjected to endoscopic retrograde cholangiopancreatography, APBDU was found in 6 patients (0.9 %). 4 of these 6 patients had no associated congenital choledochal cyst, and two patients had advanced gallbladder cancer. The remaining 2 patients had no associated carcinoma of the biliary tract. They further studied 28 such APBDU without choledochal cyst cases. The clinicopathological data showed that the thickness of the gallbladder wall was visualized in 26/28 (92.9 %) patients. Some researchers^[20-22] had reported that patients with adenomyomatosis (a presumed premalignant lesion of the gallbladder) were frequently associated with the undilated type APBDU. Tanno^[23] reported 15/24 (63 %) of APBDU patients had epithelial hyperplasia of the gallbladder, the incidence of which was significantly higher in the gallbladders of undilated type APBDU patients (91 %) than that in dilated type patients (38 %). Ki-67 labeling index was significantly higher in hyperplastic mucosa than that in the control gallbladder mucosa. 2/9 (22 %) high grade hyperplasia cases had K-ras mutations. Their results suggested that hyperplasia of the gallbladder mucosa in APBDU patients was an early change. Cell kinetic studies of gallbladder epithelial cells by Yang^[24] had shown the Ki-67 labeling index, PCNA labeling index and BrdU labeling index of the noncancerous mucosa in patients with APBDU and/or gallbladder carcinoma were significantly higher than those in patients without APBDU and gallbladder carcinoma.

Increase of the secondary and free bile acid concentrations is considered a risk factor for biliary carcinogenesis in APBDU patients. Sugiyama^[25] had suggested that elevation of the lysolecithin (LL) in the bile was one of the factors for development of biliary tract carcinoma in patients with APBDU: the LL in the phospholipid produced from lecithin by activated phospholipase A₂ in the refluxed pancreatic juice, was significantly elevated in the APBDU group. Yoon^[26] also indicated that bile acids induced both EGFR phosphorylation and enhanced COX-2 protein expression. EGFR was activated by bile acids to induce COX-2 expression by a MAPK cascade. The induction of COX-2 might participate in the genesis and progression of cholangiocarcinoma.

In an effort to delineate the underlying mechanism of the carcinogenesis in APBDU and the effects of COX-2 gene in the proliferative activity induced by APBDU bile, we used the bile from APBDU to see the direct effect on the human cholangiocarcinoma QBC939 cells *in vitro* to determine the effect of APBDU bile on the growth of human cholangiocarcinoma cells. Our data show that APBDU bile could significantly promote the proliferation of human cholangiocarcinoma QBC939 cells and up-regulated remarkably their COX-2 mRNA expression, and the proliferative activity of APBDU bile could be abolished by adding cyclooxygenase-2 specific inhibitor celecoxib. Our

study indicated that APBDU bile promoted the proliferation of human cholangiocarcinoma QBC939 cells via COX-2 pathway.

Substantial evidences have shown that COX-2 is important in carcinogenesis^[27-33]. Celecoxib as a new COX-2 selective inhibitor has shown its safety and efficiency in human and animals. Several studies have demonstrated that celecoxib has significant efficacy in animal models: Celecoxib inhibited intestinal tumor multiplicity up to 71 % as compared with controls in the Min mouse model, and inhibited colorectal tumor burden in the rat azoxymethane (AOM) model^[34-36]. Recently celecoxib has been approved by the FDA to reduce the number of adenomatous colorectal polyps in patients with familial adenomatous polyposis (FAP). Our data suggested that celecoxib as a chemopreventive and chemotherapeutic agent might be effective in cholangiocarcinoma and could be used as a chemopreventive strategy in the people of high-risk conditions for the development of cholangiocarcinoma such as APBDU. Our study demonstrated that the QBC939 cells proliferative index increased significantly after treated with APBDU bile for 24 h. These data suggested that APBDU bile could affect the QBC939 cell proliferation cycle.

In conclusion, APBDU bile can promote the proliferative activity of human cholangiocarcinoma QBC939 cells and the effect is via COX-2 pathway.

REFERENCES

- 1 **Han SJ**, Hwang EH, Chung KS, Kim MJ, Kim H. Acquired choledochal cyst from anomalous pancreatobiliary duct union. *J Pediatr Surg* 1997; **32**: 1735-1738
- 2 **Komuro H**, Makino S, Tahara K. Choledochal cyst associated with duodenal obstruction. *J Pediatr Surg* 2000; **35**: 1259-1262
- 3 **Qiao Q**, Sun Z, Huang Y. Diagnosis and treatment of congenital choledochal cysts in adults. *Zhonghua Waikē Zazhi* 1997; **35**: 610-612
- 4 **Chijiwa K**, Tanaka M. Carcinoma of the gallbladder in anomalous pancreatobiliary ductal junction. *Nippon Geka Gakkai Zasshi* 1996; **97**: 599-605
- 5 **Chijiwa K**, Tanaka M. Surgical strategy for patients with anomalous pancreatobiliary ductal junction without choledochal cyst. *Int Surg* 1995; **80**: 215-217
- 6 **Song HK**, Kim MH, Myung SJ, Lee SK, Kim HJ, Yoo KS, Seo DW, Lee HJ, Lim BC, Min YI. Choledochal cyst associated the with anomalous union of pancreaticobiliary duct (AUPBD) has a more grave clinical course than choledochal cyst alone. *Korean J Intern Med* 1999; **14**: 1-8
- 7 **Mori K**, Akimoto R, Kanno M, Kamata T, Hirono Y, Matsumura A. Anomalous union of the pancreaticobiliary ductal system without dilation of the common bile duct or tumor: case reports and literature review. *Hepatogastroenterology* 1999; **46**: 142-147
- 8 **Ohtsuka T**, Inoue K, Ohuchida J, Nabae T, Takahata S, Niiyama H, Yokohata K, Ogawa Y, Yamaguchi K, Chijiwa K, Tanaka M. Carcinoma arising in choledochocoele. *Endoscopy* 2001; **33**: 614-619
- 9 **Okamura K**, Hayakawa H, Kuze M, Takahashi H, Kosaka A, Mizumoto R, Katsuta K. Triple carcinomas of the biliary tract associated with congenital choledochal dilatation and pancreatobiliary maljunction. *J Gastroenterol* 2000; **35**: 465-471
- 10 **Wang SG**, Han BL, Duan HC, Chen YS, Peng ZM. Establishment of the extrahepatic cholangiocarcinoma cell line. *Zhonghua Shiyān Waikē Zazhi* 1997; **14**: 67-68
- 11 **Mei ZY**, Shi Z, Wang XH, Luo XD. Synthesis of COX-2 Inhibitor Celecoxib. *Zhongguo Yiyao Gongye Zazhi* 2000; **31**: 433-434
- 12 **Kobayashi S**, Asano T, Yamasaki M, Kenmochi T, Nakagohri T, Ochiai T. Risk of bile duct carcinogenesis after excision of extrahepatic bile ducts in pancreatobiliary maljunction. *Surgery* 1999; **126**: 939-944
- 13 **Funabiki T**, Matsubara T, Ochiai M, Marugami Y, Sakurai Y, Hasegawa S, Imazu H. Surgical strategy for patients with pancreatobiliary maljunction without choledochal dilatation. *Keio J Med* 1997; **46**: 169-172

- 14 **Miyano T**, Ando K, Yamataka A, Lane G, Segawa O, Kohno S, Fujiwara T. Pancreaticobiliary maljunction associated with nondilatation or minimal dilatation of the common bile duct in children: diagnosis and treatment. *Eur J Pediatr Surg* 1996; **6**: 334-337
- 15 **Okada A**. Pancreatico-biliary maljunction and congenital dilatation of bile duct. *Nippon Geka Gakkai Zasshi* 1996; **97**: 589-593
- 16 **Funabiki T**, Matsubara T, Ochiai M. Symptoms, diagnosis and treatment of pancreaticobiliary maljunction associated with congenital cystic dilatation of bile duct. *Nippon Geka Gakkai Zasshi* 1996; **97**: 582-588
- 17 **Nakamura T**, Okada A, Higaki J, Tojo H, Okamoto M. Pancreaticobiliary maljunction-associated pancreatitis: an experimental study on the activation of pancreatic phospholipase A2. *World J Surg* 1996; **20**: 543-550
- 18 **Shi LB**, Peng SY, Meng XK, Peng CH, Liu YB, Chen XP, Ji ZL, Yang DT, Chen HR. Diagnosis and treatment of congenital choledochal cyst: 20 years' experience in China. *World J Gastroenterol* 2001; **7**: 732-734
- 19 **Wu GS**, Zou SQ, Luo XW, Wu JH, Liu ZR. Proliferative activity of bile from congenital choledochal cyst patients. *World J Gastroenterol* 2003; **9**: 184-187
- 20 **Tanno S**, Obara T, Maguchi H, Mizukami Y, Shudo R, Fujii T, Takahashi K, Nishino N, Arisato S, Saitoh Y, Ura H, Kohgo Y. Thickened inner hypoechoic layer of the gallbladder wall in the diagnosis of anomalous pancreaticobiliary ductal union with endosonography. *Gastrointest Endosc* 1997; **46**: 520-526
- 21 **Tanno S**, Obara T, Fujii T, Mizukami Y, Yanagawa N, Izawa T, Ura H, Kohgo Y. Epithelial hyperplasia of the gallbladder in children with anomalous pancreaticobiliary ductal union. *Hepatogastroenterology* 1999; **46**: 3068-3073
- 22 **Tanno S**, Obara T, Maguchi H, Fujii T, Mizukami Y, Shudo R, Takahashi K, Nishino N, Arisato S, Ura H, Kohgo Y. Association between anomalous pancreaticobiliary ductal union and adenomyomatosis of the gall-bladder. *J Gastroenterol Hepatol* 1998; **13**: 175-180
- 23 **Tanno S**, Obara T, Fujii T, Mizukami Y, Shudo R, Nishino N, Ura H, Klein-Szanto AJ, Kohgo Y. Proliferative potential and K-ras mutation in epithelial hyperplasia of the gallbladder in patients with anomalous pancreaticobiliary ductal union. *Cancer* 1998; **83**: 267-275
- 24 **Yang Y**, Fujii H, Matsumoto Y, Suzuki K, Kawaoi A, Suda K. Carcinoma of the gallbladder and anomalous arrangement of the pancreaticobiliary ductal system: cell kinetic studies of gallbladder epithelial cells. *J Gastroenterol* 1997; **32**: 801-807
- 25 **Sugiyama Y**, Kobori H, Hakamada K, Seito D, Sasaki M. Altered bile composition in the gallbladder and common bile duct of patients with anomalous pancreaticobiliary ductal junction. *World J Surg* 2000; **24**: 17-21
- 26 **Yoon JH**, Higuchi H, Werneburg NW, Kaufmann SH, Gores GJ. Bile acids induce cyclooxygenase-2 expression via the epidermal growth factor receptor in a human cholangiocarcinoma cell line. *Gastroenterology* 2002; **122**: 985-993
- 27 **Tian G**, Yu JP, Luo HS, Yu BP, Yue H, Li JY, Mei Q. Effect of Nimesulide on proliferation and apoptosis of human hepatoma SMMC-7721 cells. *World J Gastroenterol* 2002; **8**: 483-487
- 28 **Gao HJ**, Yu LZ, Sun G, Miao K, Bai JF, Zhang XY, Lu XZ, Zhao ZQ. The expression of Cox-2 Proteins in gastric cancer tissue and accompanying tissue. *Shijie Huaren Xiaohua Zazhi* 2000; **8**: 578-579
- 29 **Zhuang ZH**, Wang LD. Non-steroid anti-inflammatory drug and digestive tract tumors. *Shijie Huaren Xiaohua Zazhi* 2001; **9**: 1050-1053
- 30 **Wu YL**, Sun B, Zhan XI, Wang SN, He HY, Qiao MM, Zhong J, Xu JY. Growth inhibition and apoptosis induction of sulindac on human gastric cancer cells. *World J Gastroenterol* 2001; **7**: 796-800
- 31 **Sun B**, Wu YL, Zhang XJ, Wang SN, He HY, Qiao MM, Zhang YP, Zhong J. Effects of Sulindac on growth inhibition and apoptosis induction in human gastric cancer cells. *Shijie Huaren Xiaohua Zazhi* 2001; **9**: 997-1002
- 32 **Tian G**, Yu TP, Luo HS, Yu BP, Li JY. The expression and effect of cyclooxygenase-2 in acute hepatic injury. *Shijie Huaren Xiaohua Zazhi* 2002; **10**: 24-27
- 33 **Gao HJ**, Yu LZ, Bai JF, Peng YS, Sun G, Zhao HL, Miu K, Lü XZ, Zhang XY, Zhao ZQ. Multiple genetic alterations and behavior of cellular biology in gastric cancer and other gastric mucosal lesions: *H. pylori* infection, histological types and staging. *World J Gastroenterol* 2000; **6**: 848-854
- 34 **Hosomi Y**, Yokose T, Hirose Y, Nakajima R, Nagai K, Nishiwaki Y, Ochiai A. Increased cyclooxygenase 2 (COX-2) expression occurs frequently in precursor lesions of human adenocarcinoma of the lung. *Lung Cancer* 2000; **30**: 73-81
- 35 **Tsubouchi Y**, Mukai S, Kawahito Y, Yamada R, Kohno M, Inoue K, Sano H. Meloxicam inhibits the growth of non-small cell lung cancer. *Anticancer Res* 2000; **20**: 2867-2872
- 36 **Souza RF**, Shewmake K, Beer DG, Cryer B, Spechler SJ. Selective inhibition of cyclooxygenase-2 suppresses growth and induces apoptosis in human esophageal adenocarcinoma cells. *Cancer Res* 2000; **60**: 5767-5772

A clinical dilemma: abdominal tuberculosis

Oya Uygur-Bayramiçli, Gül Dabak, Resat Dabak

Oya Uygur-Bayramiçli, Resat Dabak, Head of Endoscopy Unit, Kartal State Hospital, Istanbul, Turkey

Gül Dabak, Heybeliada Chest Diseases Hospital, Istanbul, Turkey
Correspondence to: Oya Uygur-Bayramiçli, Altunizade mah. Atıf bey sok Çamlık sit II.Kıyım A Blok No53/10, Üsküdar 81020 - Istanbul, Turkey. bayramicli@hotmail.com

Telephone: +90-216-4184063 **Fax:** +90-216-3511994

Received: 2003-01-18 **Accepted:** 2003-02-19

Abstract

AIM: To evaluate the clinical, radiological and microbiological properties of abdominal tuberculosis (TB) and to discuss methods needed to get the diagnosis.

METHODS: Thirty-one patients diagnosed as abdominal TB between March 1998 and December 2001 at the Gastroenterology Department of Kartal State Hospital, Istanbul, Turkey were evaluated prospectively. Complete physical examination, medical and family history, blood count erythrocyte sedimentation rate, routine biochemical tests, Mantoux skin test, chest X-ray and abdominal ultrasonography (USG) were performed in all cases, whereas microbiological examination of ascites, upper gastrointestinal endoscopy, colonoscopy or barium enema, abdominal tomography, mediastinoscopy, laparoscopy or laparotomy were done when needed.

RESULTS: The median age of patients (14 females, 17 males) was 34.2 years (range 15-65 years). The most frequent symptoms were abdominal pain and weight loss. Eleven patients had active pulmonary TB. The most common abdominal USG findings were ascites and hepatomegaly. Ascitic fluid analysis performed in 13 patients was found to be exudative and acid resistant bacilli were present in smear and cultured only in one patient with BacTec (3.2 %). Upper gastrointestinal endoscopy yielded nonspecific findings in 16 patients. Colonoscopy performed in 20 patients showed ulcers in 9 (45 %), nodules in 2 (10 %) and, stricture, polypoid lesions, granulomatous findings in terminal ileum and rectal fistula each in one patient (5 %). Laparoscopy on 4 patients showed dilated bowel loops, thickening in the mesentery, multiple ulcers and tubercles on the peritoneum. Patients with abdominal TB were divided into three groups according to the type of involvement. Fifteen patients (48 %) had intestinal TB, 11 patients (35.2 %) had tuberculous peritonitis and 5 (16.8 %) tuberculous lymphadenitis. The diagnosis of abdominal TB was confirmed microbiologically in 5 (16 %) and histopathologically in 19 patients (60.8 %). The remaining nine patients (28.8 %) had been diagnosed by a positive response to antituberculous treatment.

CONCLUSION: Neither clinical signs, laboratory, radiological and endoscopic methods nor bacteriological and histopathological findings provide a gold standard by themselves in the diagnosis of abdominal TB. However, an algorithm of these diagnostic methods leads to considerably higher precision in the diagnosis of this insidious disease

which primarily necessitate a clinical awareness of this serious health problem.

Uygur-Bayramiçli O, Dabak G, Dabak R. A clinical dilemma: abdominal tuberculosis. *World J Gastroenterol* 2003; 9(5): 1098-1101

<http://www.wjgnet.com/1007-9327/9/1098.htm>

INTRODUCTION

Tuberculosis (TB) was a prevalent infection even in Ancient Greek and Egypt. The disease could be taken under control only after the advent of antimicrobial therapy in 1946. However, it has started to resurge worldwide in the last 10 years, due to HIV epidemic and to primary resistance to first-line drugs. One-third of the world population is under the risk of acquiring TB according to WHO and more than 30 million deaths had been expected due to TB in the nineties especially in Africa and Asia^[1]. Not surprisingly, there is also an increase in the percentage of patients with atypical presentations and atypical extra-pulmonary forms of TB. Extra-pulmonary organ involvement of TB is estimated as 10-15 % of patients not infected with HIV whereas the frequency is about 50-70 % in patients infected with HIV^[2].

Abdominal TB is one of the most prevalent forms of extra-pulmonary disease. Gastrointestinal involvement had been reported to be 55-90 % in patients with active pulmonary TB before the advent of specific anti-TB treatment. But it was regressed to 25 % after the development of specific drugs^[3]. The abdominal form of TB has an insidious course like any other chronic infectious disease without any specific laboratory, radiological or clinical findings. Due to this non-specificity there are great difficulties in its diagnosis. Various methods of investigation had been reported as the gold standard of diagnosis in earlier studies; however there are great difficulties in clinical practice. As a result, the diagnosis of abdominal TB is still a challenge to the physician. In the present prospective study, we analyzed the clinical, laboratory, radiologic, endoscopic and microbiological features of abdominal TB patients in order to evaluate the diagnostic value of various methods and to define the correct tool of diagnosis.

MATERIALS AND METHODS

Thirty-one patients were diagnosed as abdominal TB in Gastroenterology Department of Kartal State Hospital-Istanbul, between March 1998 and December 2001. On admission, every patient had a complete physical examination, medical and family history, blood count and erythrocyte sedimentation rate (ESR), routine biochemical tests, Mantoux skin test, chest X-ray and abdominal ultrasonography (USG). After these basic investigations, an algorithm of diagnostic evaluation was applied according to the presence of certain symptoms, namely, ascites, upper gastrointestinal symptoms, chronic or bloody diarrhea, change in bowel habits, malabsorption, and additional suspicious lesions in other body parts. If present, ascites was taken for direct examination and culture for *Mycobacterium tuberculosis*. Patients complaining of dyspepsia, abdominal pain, vomiting, upper gastrointestinal bleeding or gastric

distention had an upper gastrointestinal endoscopy. 3 to 4 gastric biopsies were routinely taken from corpus and antrum during the endoscopy and the specimens were investigated for mycobacterium tuberculosis or the presence of granulomas. If the patient had symptoms suggestive of intestinal TB like chronic diarrhea, bloody stools or change in bowel habit, stool was examined for bacilli and culture for mycobacterium tuberculosis was done. Then, colonoscopy, or in patients with problems of performing colonoscopy, barium enema was performed. Eight to ten biopsies were taken for histopathologic and microbiological examinations if any lesions were found present during colonoscopy. Signs of small bowel involvement like malabsorption were evaluated with small bowel series. Any abnormality of abdominal organs, lymph nodes, mesentery and peritoneum seen on abdominal USG examination was evaluated by abdominal CT. Otherwise routine abdominal CT was not done. If necessary for any additional suspected lesions, mediastinoscopy, laparoscopy or laparotomy was also performed. In the presence of any pathological findings, multiple biopsies were taken and sent for bacteriological and histopathological investigations. A microbiological diagnosis was attempted in all cases. However, in some of the patients where no microbiological diagnosis could be met despite every effort, the histopathological finding of typical caseating granulomas was accepted as a definite evidence of TB. In patients where none of the diagnosis was available and clinical suspicion of abdominal TB was high, a therapeutic trial of anti-TB treatment with four agents (Rifampicin, Ethambutol, Isoniazid and Morphozinamide) was started, and response to treatment was evaluated after three months.

We treated all patients with the standard four-drug regimens (streptomycin or ethambutol, rifampin, pyrazinamide, isoniazid) for 9 months and the patients were reevaluated again at the end of this time. If there was no resolution of symptoms and Mycobacterium tuberculosis was still present in any specimen, an additional 9-months of treatment was given.

RESULTS

Thirty-one patients with abdominal TB (14 females, 17 males) with a median age of 34.2 years (range 15-65 years) were diagnosed in 5 years. A past medical history of pulmonary TB was obtained in 6 patients (19.2 %) and of bone TB in 2 patients (6.4 %). There was a family history of TB (in the first-degree relatives of index patient) in 8 (25.6 %). The mean duration of symptoms showed great variation among the patients (range 1 month-11 years).

The presenting symptoms and signs were summarized in Table 1. Abdominal pain and weight loss appeared to be the most frequent symptoms among these.

Laboratory investigations revealed anemia in 22 (70.4 %), elevated ESR in 20 (64 %), and hypoalbuminaemia in 15 (48 %) patients as the most prominent features. Other findings were leucocytosis in 2 (6.4 %), positive CRP in 5 (16 %), elevated transaminases in 7 patients (22.4 %). Of these 7 patients, 2 were chronic HBV carriers, 1 was immune to HBV and 1 was anti-HCV positive. In 4 patients (12.8 %), all laboratory examinations were within normal limits.

Mantoux skin test was found positive in 6 (19.2 %) of the patients. There was ascites in 13 (41.6 %). Ascitic fluid analysis performed in those patients was found to be exudative in character and only in one patient acid-fast bacilli (ARB) were present in smear and cultured only in one patient with BacTec (3.2 %).

In 11 patients (35.2 %), chest X-ray showed lesions compatible with active pulmonary TB, like fibrocavitary lesions, effusions, or lymphadenopathies. Thorax CT was carried out on these patients and lung lesions such as pleural

involvement, lymphadenopathy or nodular infiltration were present in all of them. Thorax CT did not provide additional data in comparison to chest X-ray.

Abdominal USG was performed on all patients except in five because of technical problems due to recent operations. USG findings of 26 patients were summarized in Table 2. Abdominal CT was performed on 22 of these patients who presented with abnormal findings in USG. Ascites in 8 (36.3 %), thickening of mesentery in 5 (22.7 %), abdominal lymphadenopathy in 3 (13.6 %), omental pathology in 3 (13.6 %) and lymphadenopathy in liver hilum, cholelithiasis, destruction in sacral bone, ovary cyst and splenomegaly each for one (4.5 %) occasions had been observed as the most important CT findings among these patients. Only 3 patients (13.6 %) presented with completely normal CT examination.

Table 1 Presenting symptoms (*may be more than one in each patient*) and signs and their frequency in patients (*n=32*)

Symptoms and signs	Number of patients	Percentage (%)
Abdominal pain	16	51.2
Weight loss	16	51.2
Ascites	12	38.4
Diarrhea	10	32
Cough and sputum	6	19.2
Vomiting and nausea	5	16
Fever	4	12.8
Perforation	3	9.6
Bone pain	2	6.4
Night sweats	2	6.4
Urinary symptoms	1	3.2
Mass in the lower quadrant	1	3.2
Cervical pain	1	3.2
Evisceration following laparotomy	1	3.2
Incidental	1	3.2
Operation because of brid ileus	1	3.2

Table 2 Abdominal ultrasonographic findings (*may be more than one in each patient*) and their frequency in the patients (*n=26*)

Abdominal USG findings	Number of patients	Percentage (%)
Normal	4	17.2
Ascites	14	53.2
Hepatomegaly	4	17.2
Thickening	3	11.4
Atrophic	2	7.6
Abdominal	2	7.6
Hepatosteatosis	2	7.6
Splenomegaly	1	3.8
Pericardial	1	3.8
LAP	1	3.8
Calcifications	1	3.8

Small bowel follow-up was done on seven patients and the bowel was significantly shortened due to extensive resection because of perforation in one of them. Barium enema was performed on two, and there was irregularity and ulcers in the bowel wall of one patient's.

Upper gastrointestinal endoscopy was performed in 17 patients and showed nonspecific findings in 16. In every case, gastric biopsies were taken but no acid-resistant bacilli (ARB) or granulomas were identified in tissue sections.

Colonoscopy was performed in 20 patients. There was no abnormality in 8 patients (40 %). Ulcers in 9 (45 %), nodules in 2 (10 %) and, stricture, polypoid lesions, granulomatous

findings in terminal ileum and rectal fistula each in one (5 %), occasions were found in these patients.

Laparoscopy was performed on 4 patients and there were positive findings in all of them. Dilated bowel loops, thickening in the mesentery, multiple ulcers and tubercles on the peritoneum, each for once, were observed in these patients. Peritoneal biopsies confirmed the diagnosis of tuberculosis in three of these patients. In the fourth patient, a peritoneal biopsy could not be taken because of high bleeding risk due to a very long prothrombin time.

Mediastinoscopy in one patient, and fine needle aspiration biopsy of the lymphadenopathy in liver hilum in another one were performed to confirm the diagnosis. In only 2 patients of the whole series, the diagnosis was clarified by biopsies taken in an operation under general anesthesia (one was operated because of bulging cervical disc and the other because of intestinal obstruction).

Patients with abdominal TB were divided into three groups according to the type of involvement. 15 patients (48 %) had intestinal TB, 11 patients (35.2 %) tuberculous peritonitis and 5 (16.8 %) tuberculous lymphadenitis.

It was able to confirm the diagnosis of abdominal tuberculosis microbiologically in 5 patients (16 %). Two of these patients were diagnosed by positive ARB smears of sputum, 1 with ARB in enterocutaneous fistula discharge, 1 with ARB in ascitic fluid, and 1 with ARB in biopsy material. Two patients were found positive in BacTec, but none of these patients had positive culture on Löwenstein medium. Nineteen patients (60.8 %) were diagnosed histopathologically and the diagnosis in the remaining nine patients (28.8 %) have been reached by a positive response to antituberculous treatment. In 2 patients, there were both, histopathologic and microbiologic diagnosis of tuberculosis.

Twenty-eight patients were symptom-free after 9 months of treatment. Furthermore, no pathological findings were observed in the next follow-up visits after six months. In the remaining 3 patients, the disease had a complicated course and although antituberculous treatment with four agents (streptomycin or ethambutol, rifampin, pyrazinamide, isoniazid) was begun, mammarian abscess developed in one of them, osteomyelitis and enterocutaneous fistula in the second patient, and incisional enterocutaneous fistula in the last patient.

DISCUSSION

Abdominal TB is again on the rise all over the world with the resurgence of multidrug resistant TB and with AIDS pandemic. It is also an increasing health problem because of the immigrants from underdeveloped countries where it is more common. However, this topic is still restricted within a few paragraphs in the textbooks and the current knowledge of abdominal TB has to be updated. Sensitivity of various methods have already been speculated in previous studies without any serious conclusion. In the present study we aimed to investigate the relative reliability of these tools in the diagnosis of abdominal TB which has an exceptionally insidious course. As shown in the present study, the clinical and laboratory features of abdominal TB are nonspecific and lead to the suspicion of only a chronic infectious disease.

Three diagnostic stages have been evaluated in the diagnosis of abdominal TB. The first two stages, clinical evaluation of the patient and the radiologic examination, give indirect evidence of the disease. The third stage includes the invasive techniques to achieve direct evidence. However, the diagnosis of TB has its own difficulties that these evidences generally come out to be relatively direct in practice.

The vague character of symptoms has been previously defined in many studies^[4,5] and the radiographic presentation of this disease which frequently mimics many other conditions

has already been described^[6,7]. The combination of mesenteric thickening of 15 mm with associated mesenteric lymphadenopathy has been stated as a prominent sonographic finding in abdominal TB^[8,9] which could not be confirmed in our study. We found rather nonspecific findings in abdominal ultrasonography such as ascites and hepatomegaly. However, CT features of abdominal TB have been reported to be of value in the diagnosis^[10] and the ability to differentiate TB peritonitis from malignant diseases of the peritoneum could be increased by combining some CT findings^[11]. The same is true for this study; we had a positive finding in 88 % of the patients in abdominal CT. The results obtained on CT scans are comparable to USG findings in the literature^[4]. Thus abdominal CT findings appear to provide more objective data about the disease than other radiological methods.

The invasive diagnostic tools have the very real advantage of examining the lesion itself either macroscopically or microscopically. However, even these direct methods have their own drawbacks in clinical practice.

Colonoscopic findings of abdominal TB are problematic because of segmentary involvement of the disease^[12] and because of low yield of granulomas as a result of submucosal disease. In a study of Singh and associates^[13], granulomas were seen in 44 % of the patients, and 19 % of them had caseation. We could find colonoscopic abnormalities in 60 % of the patients and confirm TB histopathologically. However, colonoscopy is still mandatory to obtain tissue for culturing the agent which is very important for the diagnosis of intestinal TB.

The sensitivity of endoscopic biopsy ranges between 30 and 80 % and Bhargawa *et al*^[14] suggested obtaining 8 to 10 biopsies for histology and 3 to 4 specimens for culture.

In patients with palpable abdominal masses, direct fine needle aspiration cytology can also be applied^[5]. This method is not feasible in any of our patients because we could not palpate these masses in any of them.

Laparoscopic pattern and biopsies obtained from the peritoneum have been reported to be more helpful and that this finding could be used even for treating patients with abdominal TB without any histopathologic or bacteriologic confirmation^[15]. In the present study, laparoscopy was performed in 4 patients and confirmed the diagnosis histopathologically in 3 and macroscopically in one patient. Thus, it appeared to be a highly sensitive diagnostic tool in all selected patients. In a study of Lisehora *et al*^[16], even mini laparotomy was reported as the most sensitive and specific diagnostic procedure in abdominal TB.

The diagnosis of abdominal TB classically requires microbiological and culture confirmation of mycobacterium tuberculosis, whereas, the diagnosis can be established histopathologically in many studies^[4,15]. Also in the current study, the diagnosis could be reached histopathologically in 60.8 % of the patients. If the isolation of Mycobacterium tuberculosis is accepted as "sine qua non" for this infectious disease according to the postulates of Koch, histopathological diagnosis can not be regarded as standard. However, microbiological isolation of the agent is very rare for patients with abdominal TB. It has remained under 50 % in all the reported series. Isolation of bacilli in endoscopic biopsy materials has been postulated as even to be zero^[12,13]. It is known that Mycobacterium tuberculosis can be occasionally isolated in stool of persons with healthy conditions. Therefore special decontamination techniques and BacTec technology must be used for culture of this agent^[17]. Interestingly, we could not be able to confirm the existence of Mycobacterium tuberculosis in any of our patients using Löwenstein medium that was said to be the ideal culture medium for this bacterium. Even in patients who were ARB positive in direct smear, culture in Löwenstein was not positive; but we had culture positivity in

two patients with BacTec technique. In a case report of Anand and associates^[17], PCR was used on endoscopic biopsy specimens obtained from a patient with chronic diarrhea and the result was found positive.

The isolation of Mycobacterium tuberculosis with BacTec or PCR are promising methods for the future but even these methods appear to be far from ideal since it is not enough for the treatment of the disease because of the lack of culture. We think that we have to refine our isolation procedures for the bacterium and in every case of extrapulmonary TB, not only histopathological but also microbiological confirmation should still be sought in order to break the vicious circle of multidrug resistancy.

A past history of pulmonary TB or a family history of TB is quite frequent in patients with abdominal TB^[19] which is also the case in our study. It is known that patients with multidrug resistant organisms acquire the organisms through multiple ineffective courses of treatment with various drugs^[20]. Thus, it can be concluded that most of the cases with abdominal TB have a primary resistance to conventional chemotherapy.

The isolation of mycobacterium tuberculosis is also essential for susceptibility tests which are now performed on every patient with pulmonary TB because of the high incidence of multidrug resistance (it has increased from 2 % to 9 % in the past three decades)^[20].

Based upon our clinical observation with abdominal TB, we can stress on these patient with high resistance because of the long course of the disease and because of frequency of complications. If a better way of isolating the organism cannot be found and if the resistance cannot be detected before starting with the antituberculous treatment, the increase of new TB cases will be inevitable. The problem of mutant strains could also be expected in the future. It is known that two different mutant strains can coexist in the same patient which further complicates the resistance problem. Although the molecular fingerprinting of mycobacterium tuberculosis may help to solve these problems in some extent^[21], these facts should be taken into consideration for future directions in the diagnosis and treatment of abdominal TB.

CONCLUSION

Neither clinical signs, laboratory, radiological and endoscopic methods nor bacteriological and histopathological findings provide a gold standard by themselves in the diagnosis of abdominal TB. However, an algorithm of these diagnostic methods leads to considerably higher precision in the diagnosis of this insidious disease which primarily necessitate a clinical awareness of this serious health problem.

ACKNOWLEDGMENT

We are grateful to Mehmet Bayramiçli, M.D. for his assistance in preparation of the manuscript.

REFERENCES

- 1 **WHO.** Tuberculosis control and research strategies for the 1990' s. Memorandum from a WHO-meeting. *Bull WHO* 1992; **70**: 17
- 2 **Runyon BA.** *Textbook of Gastroenterology*. 2nded. Philadelphia: Lippincott 1995: 928
- 3 **Haddad FS,** Ghossain A, Sawaya E, Nelson AR. Abdominal tuberculosis. *Dis Colon Rectum* 1987; **30**: 724-735
- 4 **Al-Quorain AA,** Satti MB, Al-Freih HM, Al-Gindan YM, Al-Awad N. Abdominal tuberculosis in Saudi Arabia: A clinicopathological study of 65 cases. *Am J Gastroenterol* 1993; **88**: 75-79
- 5 **Lewis S,** Field S. Intestinal and peritoneal tuberculosis. In: Rom WN, Garay S, eds. *Tuberculosis*. Boston: *Little Brown and Company* 1996: 585-597
- 6 **Nyman RS,** Brismar J, Hugosson C, Larsson SG, Lundstedt C. Imaging of tuberculosis-experience from 503 patients I. Tuberculosis of the chest. *Acta Radiologica* 1996; **37**: 482-488
- 7 **Lundstedt C,** Nyman RS, Brismar J, Hugosson C, Kagevi I. Imaging of tuberculosis II. Abdominal manifestations in 112 patients. *Acta Radiologica* 1996; **37**: 489-495
- 8 **Jain R,** Sawhney S, Bhargava DK, Berry M. Diagnosis of abdominal tuberculosis: Sonographic findings in patients with early disease. *AJR* 1995; **165**: 1391-1395
- 9 **Kedar RP,** Shah PP, Shivde RS, Malde HM. Sonographic findings in gastrointestinal and peritoneal tuberculosis. *Clin Radiol* 1994; **49**: 24-29
- 10 **Epstein BM,** Mann JH. CT of abdominal tuberculosis. *AJR Am J Roentgenol* 1982; **139**: 861-866
- 11 **Ha HK,** Jung JI, Lee MS, Choi BG, Lee M, Kim YH, Kim PN, Auh YH. CT differentiation of tuberculous peritonitis and peritoneal carcinomatosis. *AJR Am J Roentgenol* 1996; **167**: 743-748
- 12 **Shah S,** Thomas V, Mathan M, Chacko A. Colonoscopic study of 50 patients with colonic tuberculosis. *Gut* 1992; **33**: 347-351
- 13 **Singh V,** Kumar P, Kamal J, Prakash V, Vaiphei K, Singh K. Clinicocolonoscopy profile of colonic tuberculosis. *Am J Gastroenterol* 1996; **91**: 565-568
- 14 **Bhargava DK,** Tandon HD, Chawla TC, Shrinivas S, Tandon BN, Kapur BML. Diagnosis of ileocecal and colonic tuberculosis by colonoscopy. *Gastrointest Endosc* 1985; **31**: 68-70
- 15 **Bhargava DK,** Shrinivas S, Chopra P, Nijhawan S, Dasarathy S, Kushwaha AKS. Peritoneal tuberculosis: Laparoscopic patterns and its diagnostic accuracy. *Am J Gastroenterol* 1992; **87**: 109-112
- 16 **Lisehora GB,** Peters CC, Lee YT, Barcia PJ. Tuberculous peritonitis-do not miss it. *Dis Colon Rectum* 1996; **39**: 394-399
- 17 **Pfaller MA.** Application of new technology to the detection, identification and antimicrobial susceptibility testing of mycobacteria. *Am J Clin Pat* 1994; **101**: 329-337
- 18 **Anand BS,** Schneider FE, El-Zaatari FAK, Shawar RM, Clarridge JE, Graham DY. Diagnosis of intestinal tuberculosis by polymerase chain reaction on endoscopic biopsy specimens. *Am J Gastroenterol* 1994; **89**: 2248-2249
- 19 **Gorbach SL.** Infectious diarrhea and bacterial food poisoning. In: Sleisenger MH, Fordtran JS, eds. *Gastrointestinal disease*. Philadelphia: *Saunders* 1993: 1128-1161
- 20 **Iseman MD.** Treatment of multidrug resistant tuberculosis. *N Engl J Med* 1993; 784-791
- 21 **Behr MA,** Small PM. Molecular fingerprinting of Mycobacterium tuberculosis: how can it help the clinician? *Clin Infect Dis* 1997; **25**: 806-810

Edited by Xu XQ

Factors predisposing to severe acute pancreatitis: evaluation and prevention

Bei Sun, Ha-Li Li, Yue Gao, Jun Xu, Hong-Chi Jiang

Bei Sun, Ha-Li Li, Yue Gao, Jun Xu, Hong-Chi Jiang, Department of General Surgery, First Clinical Hospital, Harbin Medical University, Harbin 150001, China

Correspondence to: Bei Sun, Department of General Surgery, First Clinical Hospital, Harbin Medical University, Harbin 150001, China. sunbei70@163.net

Telephone: +86-451-3600281 **Fax:** +86-451-3600286

Received: 2002-10-30 **Accepted:** 2002-12-24

Abstract

AIM: To analyze factors predisposing to the infections associated with severe acute pancreatitis (SAP) and to work out ways for its prevention.

METHODS: Total 208 cases of SAP treated in this hospital from Jan. 1980 to Dec. 2001 were retrospectively analyzed.

RESULTS: Statistical difference in the incidence of the aforementioned infections was found between the following pairs: between the groups of bloody or non-bloody ascites, paralytic ileus lasting shorter or longer than 5 days, Ranson scores lower or higher than 5, hematocrit lower or higher than 45 %, CT Balthazar scores lower or higher than 7 and between 1980.1-1992.6 or 1992.7-2001.12 admissions ($\chi^2 > 3.84$, $P < 0.05$), while no statistical difference was established between the groups of biliogenic and non-biliogenic pancreatitis, serum amylase < 200 U/L and ≥ 200 U/L, serum calcium < 2 mmol/L and ≥ 2 mmol/L or groups of total parenteral nutrition shorter or longer than 7 days ($\chi^2 < 3.84$, $P > 0.05$).

CONCLUSION: Occurrence of infection in patients with SAP is closely related with bloody ascites, paralytic ileus ≥ 5 days, Ranson scores ≥ 5 , hematocrit ≥ 45 % and CT Balthazar Scores ≥ 7 , but not with pathogens, serum calcium and total parenteral nutrition (TPN). Comprehensive prevention of pancreatic infection and practice of individualized therapy contribute to reducing the incidence of infection.

Sun B, Li HL, Gao Y, Xu J, Jiang HC. Factors predisposing to severe acute pancreatitis: evaluation and prevention. *World J Gastroenterol* 2003; 9(5): 1102-1105

<http://www.wjgnet.com/1007-9327/9/1102.htm>

INTRODUCTION

Severe acute pancreatitis (SAP) characterized by atrocious progression, multi-complications and unquenchable mortality rate is a very dangerous acute abdomen^[1-3]. SAP progresses in two consecutive stages: the earlier stage marked by serious physiological disorder and the later stage presenting with necrosis and infection. The earlier-stage mortality mainly caused by hypovolaemia, shock, adult respiratory distress syndromes (ARDS) and cardiac or renal insufficiency has been

remarkably lowered as a result of the improvement on intensive care for severe diseases in recent years, however the later-stage mortality as a consequence of pancreatic or peri-pancreatic infections and their complications is still above 50 %^[4-6]. Though the primary choice for pancreatic infection was surgery, surgical intervention can not obviously bring down the formidable mortality, thus rendering it extremely valuable to study the predisposing factors and to work out ways for effective prevention.

MATERIALS AND METHODS

Clinical data

Total 208 SAP cases treated in this hospital since Jan. 1980 to Dec. 2001 were selected, which consisted of 112 males and 96 females with an average age of 49 ranging from 18 to 82 years old. All the patients were diagnosed by clinical presentations, biochemical findings and CT scanning on pancreas according to the universal standard for SAP diagnosis in China. Among these 208 cases, 68 were diagnosed as secondary pancreatic infection and the other 114 non-infections. 94 cases admitted between Jan. 1980 and June. 1992 underwent operations in the earlier stage, while the other 114 cases between July 1992 and Dec. 2001 were treated by the principle of "Individualized therapy", which, with emphasis on conservative management in the earlier stage, exploited comprehensive individualized treatments to prevent secondary pancreatic infection. Preventive measures include: (1) volume supplementation, shock correction and protection against multiple organ dysfunction syndrome (MODS); (2) improving pancreatic micro-circulation; (3) decontamination of intestinal tract to facilitate the recovery of gastrointestinal function; (4) preventive prescription of antibiotics; (5) nutritional support; (6) peritoneal lavage or drainage in case of retention with a great amount of exudates in the abdominal cavity. The criteria for diagnosis of pancreatic infection are: (1) body temperature continuously ≥ 38.5 °C, white blood cell count (WBC) $\geq 20 \times 10^9/L$ and signs of peritoneal irritation in more than 2 quadrants; (2) air bubbles in necrotic tissue of the pancreas by enhanced CT scanning; (3) bacteria found by culture or smear examination on fine needle aspirate.

Statistical analysis

All the data was analyzed by chi-square test.

RESULTS

Analysis of factors inducing pancreatic infection

Table 1 shows that statistical difference existed between the groups of bloody and non-bloody ascites, paralytic ileus lasting shorter or longer than 5 days, Ranson scores lower or higher than 5, hematocrit lower or higher than 45 %, CT Balthazar scores lower or higher than 7 and between 1980.1-1992.6 or 1992.7-2001.12 admissions ($\chi^2 > 3.84$, $P < 0.05$), while no statistical difference was found between the groups of biliogenic and non-biliogenic pancreatitis, serum amylase < 200 U/L and ≥ 200 U/L, serum calcium < 2 mmol/L and

≥ 2 mmol/L or groups of total parenteral nutrition shorter or longer than 7 days ($\chi^2 < 3.84$, $P > 0.05$).

Table 1 Factors predisposing to infections associated with SAP

Factors	Total cases	Incidence of infections			P values
		cases	%	χ^2	
Admission					
1980.1-1992.6	94	40	42.6	7.58	<0.01
1992.7-2001.12	114	28	24.6		
Ascites					
Non-bloody	156	40	25.6	14.1	<0.01
Bloody	52	28	53.8		
Paralytic ileus					
<5 days	150	43	28.7	3.96	<0.05
≥ 5 days	58	25	43.1		
Ranson Scores					
<5	144	40	27.8	5.14	<0.05
≥ 5	64	28	43.8		
Hematocrit					
<45 %	128	35	27.3	4.33	<0.05
≥ 45 %	80	33	41.2		
CT Balthazar Scores					
<7	138	38	27.5	4.95	<0.05
≥ 7	70	30	42.9		
Etiology					
Biliogenic SAP	90	35	38.9	2.77	>0.05
Non-biliogenic SAP	118	33	28.0		
Serum amylase					
<200 U/L	83	25	30.1	0.41	>0.05
≥ 200 U/L	125	43	34.4		
Serum calcium					
<2 mmol/L	88	34	38.6	2.45	>0.05
≥ 2 mmol/L	120	34	28.3		
TPN					
<7 days	126	37	29.4	1.61	>0.05
≥ 7 days	82	31	37.8		

DISCUSSION

More than 80 % of mortality in SAP is related with infection, mainly the secondary infection in the tissues^[7-9]. Secondary pancreatic infections including infective pancreatic necrosis, pancreatic abscess and infective pancreatic pseudocyst are responsible for more than 90 % of systematic infections and predispose to acute injury of gastric mucosa, hemorrhage in the abdominal cavity, fistula of digestive tract and multiple organ failure. Baron *et al* deemed that the morbidity of secondary infection was 30-70 %^[10], while a morbidity of 32.7 % was demonstrated in this study. The mechanisms of secondary infection have not been fully elucidated yet. Gastrointestinal paralysis and edema of the intestinal mucosa caused by pancreatic enzymes and many other bioactive and toxic substances released in the acute stage give rise to disorder and translocation of bacterial clusters as well as atrophy of the intestinal mucosa lack of stimulus from food as a result of long-term (more than 1 week) gastric decompression. TPN impairs the mononuclear phagocytic system and thus weakens the intestinal immunity, which in turn promotes intestinal bacteria translocation making secondary infection inevitable^[11-13]. In our experience the main cause of mortality in the later stage of SAP (after 2 weeks) was pancreatic infection or multiple organ

system failure (MOSF). To prevent secondary pancreatic infection is essential to reducing the mortality of SAP. Therefore it is of chief importance to understand the factors related to pancreatic infection before any prevention is undertaken against it^[14,15].

Our data did not indicate obvious relationship between the incidence of secondary infection and etiology of pancreatitis, serum amylase, serum calcium and TPN. Biliogenic pancreatitis is generally considered as a high risk factor to pancreatic infection, since it is always accompanied by biliary tract infection. However such consequence is not confirmed by our data, which may be that the secondary infection of SAP is mainly entero-genic. Whether TPN increases the incidence of secondary infection is still controversial^[16-18], but there is an evidence that long-term central venous catheter deposit, tedious intubating manipulation and improper nursing of catheter lead to certain catheter-related infections, which are proved to give priority to G⁻ bacteria, whereas in our study, to G⁺ bacteria instead. Accordingly, it may be concluded that TPN has no marked relationship with infections caused by intestinal bacteria translocation.

According to our data, bloody ascites, paralytic ileus ≥ 5 days, Ranson scores ≥ 5 , hematocrit ≥ 45 % and CT Balthazar scores ≥ 7 predispose to secondary pancreatic infection. Great amount of bloody ascites indicating severe hemorrhage and necrosis of the pancreas and dissemination of inflammatory mediators throughout the abdominal cavity can not be absorbed in most cases if not timely eliminated, and it acts as an important initiator giving rise to or worsening the ongoing intra-peritoneal infection. The relationship between pancreatic infection and the extent of pancreatic or peri-pancreatic necrosis graded by CT Balthazar scoring has been confirmed by many investigations^[19,20], but intestinal malfunction as an initiative to bacteria translocation and pancreatic infection has been ignored although the latter two are being investigated more deeply, producing the concept of preventive prescription of intra-intestinal antibiotics in view of pancreatic infection. Recently, some traditional Chinese medical doctors, who have achieved prominent efficacy using prescriptions emphasized on Tungli (an acupoint) and purgation, found the earlier the intestinal malfunction corrected, the lower the incidence of secondary pancreatic infection in the later stage was, otherwise the high incidence of both MOSF in the earlier stage and secondary pancreatic infection in the later stage persists. Ranson's grading system as a standard to evaluate the severity of acute pancreatitis and to determine its prognosis went into practice in 1974 and has been proved efficient ever since by both domestic and foreign researchers. In our study, the coincidence of secondary infection with the Ranson's score of SAP was established.

Recently, some scholars pointed out that pachyhememia poses threat in the earlier stage of SAP, as Hayakawa demonstrated that apparent reduction of circulation volume and pachyhememia existed in patients with SAP and suggested hemoglobin >150 g/L as a preliminary indicator to pachyhememia^[21]. Baillargeon's study demonstrated that pachyhememia with hematocrit ≥ 47 % at admission or HCT staying high in 24 hours after admission points to SAP and helps evaluate the extent of pancreatic necrosis and predict the onset of MOSF^[22,23]. In this study, hematocrit was obtained in the earlier stage of SAP before any intervention, which precisely reflected the extent of pachyhememia. Our data further demonstrated that pachyhememia is closely related with secondary infection of SAP, but the mechanism was unknown. We deem it may be that the exudation of large amount of plasma from circulation into the third space through the capillary bed with enhanced permeability by activated pancreatic enzymes and other vaso-active substances produced by SAP results in systemic

pachyhemias, elevated HCT count and deteriorated pancreatic micro-circulation and eventually leads to pancreatic infection. We also found that the incidence of pancreatic infection in the group admitted in 1992-07/2001-12 was significantly lower than that in the group of 1980-01/1992-06 admission. The reasons were: (1) application of "individualized therapy" on SAP; (2) adoption of comprehensive prevention against secondary pancreatic infection. The patients admitted during 1980-01/1992-06 underwent operations in the earlier stage, which as a matter of fact, not only aggravated the instability of circulation in the earlier stage or even caused shock rather than reduced the incidence of MOSF, but also destroyed the integrity of the pancreas, hampered its self-healing process, gave rise to further ischemia and necrosis after the operation and rendered it a site vulnerable to bacteria translocation increasing the incidence of pancreatic infection.

While in recent years, as to the patients admitted in 1992-07/2001-12 "Individualized therapy" was adopted, which with emphasis on conservative management in the earlier stage employs comprehensive individualized treatments to prevent secondary pancreatic infection and alternates to surgical operations if failed. Comprehensive preventions include: (1) blood volume supplementation, shock correction and especially preventions against multi-organ low perfusion injury and MOSF in the earlier stage of SAP. Ischemia and anoxia are responsible for pancreatic necrosis, damage to gastrointestinal mucosal barrier, bacteria translocation and even malfunction of the heart, the kidneys or the lungs; (2) to improve the microcirculation: by decreasing the fragility of RBC and lowering blood viscosity, the combined administration of Dextran, Saliva miltorrhiza, Ca²⁺-blocker and large dosages of dexamethason maintains hyperdynamic circulation, which is efficient in oxygen transportation. Therefore, pancreatic and systemic micro-circulation is protected and intracellular Ca²⁺ overload prevented, resulting in alleviated necrosis of the pancreatic acinar, suppression of various inflammatory mediators and lowered incidence of micro-thrombocytosis; (3) intestinal decontamination to facilitate the recovery of gastrointestinal function: traditional Chinese cathartic herbs including castor oil and magnesium sulfate were early administered to achieve decontamination, which not only decrease the population of intestinal bacteria but also promote gastrointestinal peristalsis eliminating "dead cavities". Translocation of intestinal bacteria as the principal cause of secondary infection is thus constrained. Moreover, physical therapy targeted at the gastrointestinal tract is helpful for the recovery of its function; (4) preventive administration of antibiotics: the antibiotics against G⁻ bacilli especially those capable of passing through the blood-pancreas barrier such as third generation cephalosporin, imipenem, tinidazole, etc are effective, while other antibiotics such as first generation cephalosporin, ampicillin, amikacin, etc have been proved ineffective thus improper for prescription^[24,25]. (5) nutritional support: enough energy should be supplemented by means of EN (enteral nutrition) or TPN (total parenteral nutrition) to stop self burning, potentiate resistance against infection and accelerate tissue healing^[26]. Recent study shows that pure TPN reduces the production of saliva, gastric juice, intestinal juice and bile, which are essential to the integrity of gastrointestinal barrier and function. Though a necessary part of the therapeutic planning, single application of TPN can not reverse hypercatabolism in the earlier stage but together with fasting, enhances the permeability of the intestinal mucosa. It is suggested that TPN should give way to EN when the digestive tract restore the ability to bear food load; (6) peritoneal lavage and drainage of effusion^[27]: Beger argued that severe intraperitoneal hyperbaric status might lead to the death of patients with SAP^[28,29]. When large amount of ascites develops in SAP

patients, active peritoneal lavage or ultrasonic B or CT guided drainage through a small abdominal incision should be employed to eliminate activated inflammatory mediators and toxic peritoneal exudates, so that toxin intake and intraperitoneal hyperbaric status can be alleviated. By these measures certain cases, on which conservative treatment is ineffective, avoid the operations aimed at establishing peripancreatic drainage in the earlier stage and the incidence of secondary pancreatic infection is thus reduced.

REFERENCES

- 1 **Ammori BJ**, Fitzgerald P, Hawkey P, McMahon MJ. The early increase in intestinal permeability and systemic endotoxin exposure in patients with severe acute pancreatitis is not associated with systemic bacterial translocation: molecular investigation of microbial DNA in the blood. *Pancreas* 2003; **26**: 18-22
- 2 **Hartwig W**, Werner J, Muller CA, Uhl W, Buchler MW. Surgical management of severe pancreatitis including sterile necrosis. *J Hepatobiliary Pancreat Surg* 2002; **9**: 429-435
- 3 **Hartwig W**, Werner J, Uhl W, Buchler MW. Management of infection in acute pancreatitis. *J Hepatobiliary Pancreat Surg* 2002; **9**: 423-428
- 4 **Howard TJ**, Temple MB. Prophylactic antibiotics alter the bacteriology of infected necrosis in severe acute pancreatitis. *J Am Coll Surg* 2002; **195**: 759-767
- 5 **Balthazar EJ**. Complications of acute pancreatitis: clinical and CT evaluation. *Radiol Clin North Am* 2002; **40**: 1211-1227
- 6 **Gecelter G**, Fahoum B, Gardezi S, Schein M. Abdominal compartment syndrome in severe acute pancreatitis: an indication for a decompressing laparotomy? *Dig Surg* 2002; **19**: 402-405
- 7 **Uhl W**, Warshaw A, Imrie C, Bassi C, McKay CJ, Lankisch PG, Carter R, Di Magno E, Banks PA, Whitcomb DC, Dervenis C, Ulrich CD, Satake K, Ghaneh P, Hartwig W, Werner J, McEntee G, Neoptolemos JP, Buchler MW. IAP guidelines for the surgical management of acute pancreatitis. *Pancreatology* 2002; **2**: 565-573
- 8 **Samel S**, Lanig S, Lux A, Keese M, Gretz N, Nichterlein T, Sturm J, Lohr M, Post S. The gut origin of bacterial pancreatic infection during acute experimental pancreatitis in rats. *Pancreatology* 2002; **2**: 449-455
- 9 **Olah A**, Belagyi T, Issekutz A, Gamal ME, Bengmark S. Randomized clinical trial of specific lactobacillus and fibre supplement to early enteral nutrition in patients with acute pancreatitis. *Br J Surg* 2002; **89**: 1103-1107
- 10 **Baron TH**, Morgan DE. Acute necrotizing pancreatitis. *N Engl J Med* 1999; **340**: 1412-1417
- 11 **Karsenti D**, Bourlier P, Dorval E, Scotto B, Giraudeau B, Lanotte R, de Calan L, Mesny J, Lagarrigue F, Metman E. Morbidity and mortality of acute pancreatitis: prospective study in a French university hospital. *Presse Med* 2002; **31**: 727-734
- 12 **Bose SM**, Verma GR, Mazumdar A, Giridhar M, Ganguly NK. Significance of serum endotoxin and antiendotoxin antibody levels in predicting the severity of acute pancreatitis. *Surg Today* 2002; **32**: 602-607
- 13 **Moriguchi T**, Hirasawa H, Oda S, Shiga H, Nakanishi K, Matsuda K, Nakamura M, Yokohari K, Hirano T, Hirayama Y, Watanabe E. A patient with severe acute pancreatitis successfully treated with a new critical care procedure. *Ther Apher* 2002; **6**: 221-224
- 14 **Oda S**, Hirasawa H, Shiga H, Nakanishi K, Matsuda K, Nakamura M. Continuous hemofiltration/ hemodiafiltration in critical care. *Ther Apher* 2002; **6**: 193-198
- 15 **Bank S**, Singh P, Pooran N, Stark B. Evaluation of factors that have reduced mortality from acute pancreatitis over the past 20 years. *J Clin Gastroenterol* 2002; **35**: 50-60
- 16 **Norton ID**, Clain JE. Optimising outcomes in acute pancreatitis. *Drugs* 2001; **61**: 1581-1591
- 17 **Beger HG**, Rau B, Isenmann R. Prevention of severe change in acute pancreatitis: prediction and prevention. *J Hepatobiliary Pancreat Surg* 2001; **8**: 140-147
- 18 **Gloor B**, Muller CA, Worni M, Martignoni ME, Uhl W, Buchler MW. Late mortality in patients with severe acute pancreatitis. *Br J Surg* 2001; **88**: 975-979
- 19 **Al-Omran M**, Groof A, Wilke D. Enteral versus parenteral nutri-

- tion for acute pancreatitis. *Cochrane Database Syst Rev* 2001; **2**: CD002837
- 20 **Gurlich R**, Peskova M, Lukas M, Maruna P. Pathophysiology of development of acute pancreatitis. *Sb Lek* 1999; **100**: 269-277
- 21 **Hayakawa T**. Physiopathology and treatment of severe acute pancreatitis. *Nippon Naika Gakkai Zasshi* 2001; **90**: 434-439
- 22 **Baillargeon JD**, Orav J, Ramagopal V, Tenner SM, Banks PA. Hemoconcentration as an early risk factor for necrotizing pancreatitis. *Am J Gastroenterol* 1998; **93**: 2130-2135
- 23 **Wyncoll DL**. The management of severe acute necrotizing pancreatitis: an evidence-based review of the literature. *Intensive Care Med* 1999; **25**: 146-156
- 24 **Kramer KM**, Levy H. Prophylactic antibiotics for severe acute pancreatitis: the beginning of an era. *Pharmacotherapy* 1999; **19**: 592-602
- 25 **Lehocky P**, Sarr MG. Early enteral feeding in severe acute pancreatitis: can it prevent secondary pancreatic infection? *Dig Sur* 2000; **17**: 571-577
- 26 **Okabe A**, Hirota M, Nozawa F, Shibata M, Nakano S, Ogawa M. Altered cytokine response in rat acute pancreatitis complicated with endotoxemia. *Pancreas* 2001; **22**: 32-39
- 27 **Gloor B**, Uhl W, Muller CA. The role of surgery in the management of acute pancreatitis. *Can J Gastroenterol* 2000; **14**: 136D-140D
- 28 **Beger HG**, Isenmann R. Surgical management of necrotizing pancreatitis. *Surg Clin North Am* 1999; **79**: 783-800
- 29 **Bradley EL III**, Allen K. A prospective longitudinal study of observation versus surgical intervention in the management of necrotizing pancreatitis. *Am J Surg* 1991; **161**: 19-24

Edited by Zhang JZ

Prevalence of nonalcoholic fatty liver among administrative officers in Shanghai: an epidemiological survey

Lei Shen, Jian-Gao Fan, Yan Shao, Min-De Zeng, Jun-Rong Wang, Guo-Hao Luo, Ji-Qiang Li, Si-Yao Chen

Lei Shen, Min-De Zeng, Guo-Hao Luo, Ji-Qiang Li, Department of Gastroenterology, Renji Hospital, Second Medical University, Shanghai 200001, China

Jian-Gao Fan, Yan Shao, Department of Gastroenterology, First People's Hospital, Shanghai, China

Jun-Rong Wang, Central Hospital of Putou District, Shanghai, China
Si-Yao Chen, Zhongshan Hospital, Fudan University, Shanghai, China

Correspondence to: Dr Jian-Gao Fan, Department of Gastroenterology, First People's Hospital, Shanghai 200080, China. fanjg@citiz.net

Telephone: +86-21-63240090-3141 **Fax:** +86-21-63240825

Received: 2002-06-28 **Accepted:** 2002-07-25

Abstract

AIM: To determine the prevalence of nonalcoholic fatty liver in a specific population in Shanghai by an epidemiological survey, and to analyze risk factors of fatty liver.

METHODS: Total 4009 administrative officers who denied regular alcohol drinking participated in the survey, and underwent physical examination and laboratory tests. The important parameters were body mass index (BMI), waist hip circumferences ratio (WHR) and levels of serum lipids. Diagnosis of fatty liver was based on established real-time ultrasonographic criteria, the presence of an ultrasonographic pattern consistent with "bright liver", with evident ultrasonographic contrast between hepatic and renal parenchyma, vessel blurring, and narrowing of the lumen of the hepatic veins. Analysis of data was performed through SPSS for Windows statistical package.

RESULTS: The overall prevalence of fatty liver was 12.9 %, 15.8 % in males and 7.5 % in females, and the prevalence of fatty liver in males younger than 50 years old, was significantly higher (13.3 %) than that of in females (2.7 %). But the difference between the sexes became less significant in people older than 50 years (19.1 % vs 18.1 %). The prevalence of fatty liver was increased with age; this was markedly presented in females younger than 50 years. Multiple variant regression analysis demonstrated that the prevalence of fatty liver was positively correlated to several risk factors, including male, aging (>50yr), hyperlipidemia, impaired glucose tolerance/diabetes mellitus, hypertension and overweight/obesity.

CONCLUSION: There is a high prevalence of nonalcoholic fatty liver among certain population in Shanghai, to which overweight and hyperlipidemia are closely relevant.

Shen L, Fan JG, Shao Y, Zeng MD, Wang JR, Luo GH, Li JQ, Chen SY. Prevalence of nonalcoholic fatty liver among administrative officers in Shanghai: an epidemiological survey. *World J Gastroenterol* 2003; 9(5): 1106-1110

<http://www.wjgnet.com/1007-9327/9/1106.htm>

INTRODUCTION

Fatty liver has increasingly been recognized as an important

and common form of chronic liver disease over the past 20 years^[1]. Fatty liver consists the intrahepatic accumulation of lipids. It is the commonest liver disease, accounting for abnormal liver function tests in the majority of asymptomatic subjects^[2]. Although generally unprogressive, fatty liver is an important precursor to the development of fibrosis in aetiologically diverse conditions such as hepatitis C, and alcoholic and nonalcoholic liver disease^[3]. Furthermore, it has the potential to lead to end-stage liver failure^[4] via steatohepatitis from lipid peroxidation, even in the nonalcohol drinker, an entity that is being studied with growing interest in the affluent society^[5]. Fatty liver is an increasingly common problem worldwide and has been reported in Japan^[6,7], Australia^[8], America^[4,9], Europe^[10,11], and the Middle East^[12], although geographic variations in prevalence are evident. Along with the steady improvement of living level and wide use of ultrasonography, the number of patients with diagnosis of fatty liver is increasing in China recently. The objective of this study was to determine the prevalence of fatty liver in a specific population in Shanghai by epidemiological survey, and analysis of its risk factors.

MATERIALS AND METHODS

Study participants (demographics)

A total of 4375 administrative officers, who took part in annual regular physical examination from September 1 to November 30 in 1999 (in Renji Hospital and Central Hospital of Putuo District in Shanghai) were recruited. Complete laboratory data were obtained from 4009 participants, who denied regular alcohol drinking and included in this study. 2583 were males and 1426 females. The mean age of participants was 46±14 years with ranged was 20-81 years.

Methods of examination

For each participant, an extensive medical history was obtained that included alcohol intake, history of chronic liver disease in first-degree relatives; a detailed history of viral hepatitis, gallstone disease and drug abuse; previous diagnosis of diabetes, hypertension and coronary heart disease.

Each participant also underwent a detailed physical examination, including of measurement of body weight, height, waist and hip circumferences. The body mass index (BMI) was calculated as: body weight in kg/(height in meter)². The waist hip circumferences ratio (WHR) was calculated by dividing waist girth (halfway between the lower costal margin and the iliac crest in the mid expiratory phase of breathing while the subject was standing) by hip girth (maximum circumference around the buttocks) previously measured while the subject was wearing light underwear.

Laboratory tests included routine blood and urine analysis, serum alanine aminotransferase (ALT), total cholesterol (Tch), triglycerine (TG), low-density lipoprotein cholesterol (LDL-Ch), high-density-lipoprotein cholesterol (HDL-Ch), plasma glucose levels, hepatitis B surface antigen (HB_sAg), routine chest fluorography, electrocardiography and optic fundus examination.

Ultrasonographic examination of liver and gallbladder was performed by two experienced ultrasonographers, using the Simens Sonoline-SI450 unit with 3.5MHz probe. Fatty liver was defined as the presence of an ultrasonographic pattern consistent with "bright liver," with evident ultrasonographic contrast between hepatic and renal parenchyma, vessel blurring, and narrowing of the lumen of the hepatic veins in the absence of findings suggestive of chronic liver disease^[13,14].

Statistical analysis

All statistical analysis was processed by Clinical Epidemiological Network in Zhongshan Hospital, Fudan University with Software SPSS. Statistical analysis was performed by using the SPSS statistical package, version 7.1(SPSS, Inc.). The following tests were applied, unpaired Student's *t*-test, chi-squared test with Fisher's exact test, analysis of variance, and logistic regression analysis (LRA). Rejection of the null hypothesis was set at $P < 0.05$. Analysis of data was performed through SPSS for Windows statistical package.

RESULTS

Body-mass index (BMI)

The mean BMI was 22.93 ± 2.82 . Among them 31.6 % had BMI > 24, which were considered as overweight, 53.3 % had BMI between 20-24; and 15.1 % had BMI < 20.

Waist-hip-circumference ratio (WHR)

The mean value of WHR was 0.83 ± 0.06 . Among them 2.78 % had WHR > 0.94, 21.1 % had WHR between 0.88-0.94 and 76.2 % had WHR < 0.88.

Blood lipids

The mean TG was 115.9 ± 84.6 mg/dl (1.31 ± 0.95 mmol/L), TCh 189.0 ± 56.7 mg/dl (4.89 ± 1.47 mmol/L). Among them 627 had hypertriglycerinemia only; 282 participants had hypercholesterolemia only and 256 participants had mixed hyperlipidemia. Thus, the prevalence of hyperlipidemia among participants was 28.9 %. Each patient was classified into the following four previously defined hyperlipidemia phenotypes according to 12-hr fasting plasma lipid levels: hypertriglycerinemia (≥ 150 mg/dl, 1.7 mmol/L), hypercholesterinemia (≥ 220 mg/dl, 5.7 mmol/L), mixed hyperlipidemia and normal blood lipids.

Blood glucose, liver function and HB_sAg

Among participants 86 (2.2 %) suffered from impaired glucose tolerance, 93 (2.3 %) had diabetes mellitus (DM); 59 (1.5 %) suffered from increased ALT, and 257 (6.4 %) were HB_sAg positive.

Fatty liver and cholelithiasis

Fatty liver was detected with ultrasound examination in 516 participants (12.9 %); cholesterol crystal in gallbladder was detected in 54 persons (1.3 %), Gallstone or cholecystoectomy was noted in 358 participants (8.9 %).

Influence of sex and aging on parameters

In this study, the mean age of male participants (47.3 ± 14.7 years) was older than the female participants (43.4 ± 23.5 years, $P < 0.01$). BMI, WHR, serum level of TG and glucose in male group was significantly higher than those in female group. Levels of serum TCh and LDL -Ch were similar in both groups (Table 1).

As presented in Table 2, there are more participants with increased ALT, positive HB_sAg and arteriosclerosis of optic fundus in male group. Prevalence of DM, coronary artery disease, hypertension and fatty liver are significantly higher

in male group than those in female group; but the prevalence of cholelithiasis is similar in both groups.

Table 3 shows sex and age related change of hyperlipidemia. In participants younger than 50 years old, more cases of hypertriglycerinemia are detected, whereas participants older than 50 years old, prevalence of hypercholesterolemia increase significantly, especially in females. In whole group the prevalence of three hyperlipidemia types increase significantly with aging.

Among females younger than 50 years old, the prevalence of hyperlipidemia is lower than that among males. After 50 years of age this prevalence was significantly higher than in males.

As in showed the Table 4, the prevalence of fatty liver increased with aging, which is markedly presented in females younger than 50 years. The prevalence of fatty liver in males younger than 50 years is significantly higher (13.3 %) than that in females (2.7 %). In participants older than 50 years, no significant difference of prevalence of fatty liver is noted between males and females (19.1 % vs 18.1 %).

Table 1 Obesity indices and lipid parameters in males and females

Parameters	Male	Female	P value
BMI	23.5 ± 2.7	21.5 ± 2.6	<0.001
WHR	0.86 ± 0.05	0.79 ± 0.06	<0.001
TG(mg/dl)	126.3 ± 87.7	97.2 ± 75.2	<0.001
TCh(mg/dl)	188.8 ± 56.7	189.3 ± 56.6	>0.05
HDL-Ch(mg/dl)	81.4 ± 75.4	84.4 ± 57.0	>0.05
LDL-Ch(mg/dl)	143.1 ± 166.0	133.5 ± 153.7	>0.05

Table 2 Difference of prevalences of several diseases in males and females

Diseases	Male%	Female%	P value
Abnormal ALT	2.1	0.35	<0.001
Positive HB _s Ag	7.3	4.8	<0.001
Arteriosclerosis of optic fundus	13.4	6.3	<0.001
Diabetes mellitus	5.1	3.3	<0.001
Coronary artery disease	3.5	2.3	<0.001
Hypertension	15.3	8.2	<0.001
Gallstone	8.9	8.9	>0.05
Fatty liver	15.8	7.5	<0.001

Table 3 Relation between hyperlipidemia and age in males and females

Age (yr)	Sex	n	Hypertriglycerinemia %	Hypercholesterolemia %	Mixed hyperlipidemia %	Sum%
<30	Male	314	11.6	1.5	1.2	14.3
	Female	257	1.1	2.7	0.7	4.5
	Total	571	6.9	2.1	1.0	9.0
30-50	Male	1202	17.3	3.9	4.9	26.1
	Female	726	4.5	4.9	1.3	10.7
	Total	1928	12.5	4.3	3.6	20.3
51-64	Male	702	22.6	6.9	9.2	38.7
	Female	324	16.9	18.5	17.5	52.9
	Total	1026	20.8	10.6	11.8	43.2
≥ 65	Male	365	28.5	12.9	11.3	52.7
	Female	119	24.2	25.0	14.3	63.5
	Total	484	27.4	27.4	12.0	55.4

Table 4 Prevalence of fatty liver in groups of different sex and ages

Age(years)	Sex	Number	Fatty liver n%
<30	Males	314	11 (6.4)
	Females	257	2 (1.6)
	Total	571	13 (2.3)
30-50	Males	1202	190 (20.7)
	Females	726	25 (5.4)
	Total	1928	215 (11.2)
51-64	Males	702	125 (17.9)
	Females	324	57 (19.7)
	Total	1026	182 (17.7)
≥65	Males	365	83 (22.7)
	Females	119	23 (19.3)
	Total	484	106 (21.9)

In this survey 516 patients (12.9 %) with fatty liver were detected by ultrasonography. The age, BMI, WHR, levels of serum TG and TCh of patients with fatty liver were significantly higher than participants without fatty liver (3493 persons). The details were presented in Table 5. The results of monovariant regression analysis of relation between prevalence of fatty liver and other factors was presented in Table 6. Prevalence of fatty liver was associated with several parameters, including sex, BMI, and WHR.

Stepwise logistic multivariant regression analysis of relationship between prevalence of fatty liver and other parameters demonstrated that 9 parameters were closely related with prevalence of fatty liver. As presented in order of importance, these were WHR, increased ALT, BMI, and hypertension, DM and impaired glucose tolerance, hyperlipidemia, male sex and arteriosclerosis of optic fundus.

Table 5 Obesity indices and lipid parameters in groups with and without fatty liver

	Age (years)	BMI (kg/m ²)	WHR	TG (mg/dl)	TCh (mg/dl)
Group without fatty liver	44.6±14.3	22.2±2.4	0.8±0.1	105.0±78.4	186.2±59.5
Group with fatty liver	52.3±13.0	26.0±2.4	0.9±0.1	168.6±93.4	202.2±37.7

Table 6 Results of monovariant regression analysis of fatty liver and various parameters

Parameters	B value	βvalue	T value	P value
Sex	0.038	0.063	2.59	0.0000
Age	0.53	0.062	2.79	0.0018
BMI	0.073	0.522	23.89	0.0000
Waist circumference	0.010	0.216	5.87	0.0000
WHR	0.782	0.129	4.96	0.0000
TG	0.000	0.084	3.08	0.0021
TCh	-0.0000	-0.079	-3.12	0.0016
HDL-Ch	-0.000	-0.047	-2.17	0.0300
LDL-Ch	-0.000	0.332	2.61	0.0092
Hyperlipidemia	0.094	0.160	7.27	0.0000
Arteriosclerosis	0.062	0.087	3.59	0.0000
Hypertension	0.068	0.099	4.45	0.0000
Diabetes mellitus	0.149	0.130	3.42	0.0000
Coronary heart disease	0.142	0.067	3.14	0.0018
Abnormal ALT	0.156	0.069	3.24	0.0012
Positive HB _s Ag	-0.09	0.063	-3.02	0.0026

Table 7 Results of Logistic multivariant regression analysis

	B	SE	Wald	df	Sig	R	Exp(B)
WHR	2.2	0.19	139.2	1	0.00	0.30	9.1
Abnormal ALT	1.3	0.26	27.0	1	0.00	0.08	3.8
BMI 0.90.15	35.3	1	0.00	0.15	2.4		
Positive HB _s Ag	-0.7	0.24	9.3	1	0.00	-0.04	0.05
Hyperlipidemia	0.6	0.06	99.9	1	0.00	0.16	1.8
Diabetes mellitus	0.5	0.11	21.5	1	0.00	0.07	1.7
Hyperlipidemia	0.4	0.05	81.0	1	0.00	0.15	1.5
Sex	0.4	0.05	55.1	1	0.00	0.12	1.5
Arteriosclerosis	0.2	0.09	6.8	1	0.01	0.04	1.3

DISCUSSION

The natural history of fatty liver ranges from asymptomatic indolent to end stage liver disease. Diagnosis of nonalcoholic fatty liver (NAFL) and nonalcoholic steatohepatitis (NASH) may involve ultrasonography, liver biopsy and recognition of related condition^[1]. Fatty liver is a common disease of liver without specific clinical features and lack of confirmatory laboratory tests^[15-17]. In patients undergoing liver biopsy, the prevalence of NAFL ranges between 15 % and 39 %^[18]. This wide range in the prevalence of NAFL is probably related to differences in the study design. Because patients undergoing liver biopsy were highly selected, these data might not reflect the true prevalence of NAFL in the general population. Therefore, current best estimates make the prevalence of NAFL approximately 20 % and of NASH 2-3 % in the general population^[18].

While it could be argued that in the absence of histology this figure may not reflect the true prevalence of fatty infiltration, previous studies in which ultrasound findings were compared to histologic results indicate that the overall sensitivity and specificity of ultrasound examinations for the diagnosis of fatty liver are approximately 80-95 % and 90-95 % respectively^[13,19-21]. In the present study, the prevalence of NAFL was 15.8 % in males and 7.5 % in females according to ultrasonic criteria of diagnosis for fatty liver.

This study was limited in survey of the administrative officers in two districts of Shanghai. Nevertheless, these participants were representatives of the health status of administrative officers. In comparison with general population, participants of this study had better living condition and less physical exercises. The results of this study showed higher prevalence of hyperlipidemia and fatty liver in participants than those in general population in Shanghai.

Several authors suggested that fatty liver should be included in "metabolic syndrome"^[2,14,22]. Evidence for this hypothesis derives, in our opinion, from epidemiology, metabolism, and experimental pathology. The results of this survey showed that overweight was detected in 31.6 % of participants and hyperlipidemia in 28.8 %, and the prevalence of fatty liver was 12.9 %. The prevalence of DM, hypertension and coronary heart disease was 4.5 %, 12.8 % and 3.1 % respectively, suggesting that overweight and associated diseases are becoming common diseases among administrative officers in Shanghai.

Hyperlipidemia is considered as a risk factor for fatty infiltration of the liver^[23,24]. The pathogenesis of nonalcoholic steatohepatitis is poorly understood, but lipid peroxidation and oxidative stress are the leading culprits^[16, 25]. Diabetes and hypertriglyceridemia were the two states predictive of fatty liver that is consistent with the presence of insulin resistance^[23]. NAFL correlates significantly with both anthropometrical data BMI, WHR and with abdominal fat^[26]. In clinical practice BMI over

24 used as diagnostic criteria for overweight in China.

In this study, both monovariant and multivariant regression analysis demonstrated a close correlation between BMI and fatty liver. High WHR suggests increased abdominal fatty tissue, which is a strong predictive factor for DM and other metabolism abnormalities^[27-30]. Increased WHR is considered as the most important risk factor for fatty liver. The development of fatty liver may be a result of transportation of the abnormal fatty tissue into the liver^[23,31,32]. BMI was found to be an independent predictor of fatty liver in either sex^[33]. Both monovariant and multi variant regression analysis revealed that hypertension is correlated with fatty liver. The relation between fatty liver and impaired glucose tolerance, DM and hyperlipidemia has been well established^[34-43], and was confirmed again in this study. Fatty liver could be gender-related^[33]. The results of this study showed that in male participants younger than 50 years old, the prevalence of three types of hyperlipidemia and fatty liver were markedly higher than those in females. In participants older than 50 years old the prevalence were similar in males and females. This result suggested that female hormones might have favorable effects on lipid metabolism in liver. Monovariant analysis showed that many factors were correlated with prevalence of fatty liver. However, logistic multivariant regression analysis demonstrated that only nine parameters were closely correlated with fatty liver.

In majority of patients with fatty liver, the hepatic function is normal, therefore determination of ALT can not reflect the content of fat retention in liver^[7,44]. Results of this study showed negative correlation between positive HB_sAg and fatty liver, which might explain that chronic hepatitis B infection would not induce the development of fatty liver. The sensibility by liver function tests to detect fatty liver was inferior to that of BMI^[7]. But hepatitis C may be linked to hepatic steatosis^[45-47].

This epidemiological survey demonstrated that fatty liver is a common disease among administrative officers in Shanghai. Overweight, hyperlipidemia, and DM are high risk factors for fatty liver. It is clear that NAFL is a chronic liver disease with the potential for progression to cirrhosis and to cause liver-related death^[48,50]. Although ultrasonography provides the prevalence of NAFL, it can not delineate the different histologic form of NAFL^[18]. If it is clinically indicated, a liver biopsy to assess the degree of inflammation and fibrosis should be performed during follow-up^[10]. To reduce the incidence of fatty liver, comprehensive measures are necessary^[32,51-53].

REFERENCES

- 1 **Brunt EM.** Nonalcoholic steatohepatitis: definition and pathology. *Semin Liver Dis* 2001; **21**: 3-16
- 2 **Lonardo A.** Fatty liver and nonalcoholic steatohepatitis. Where do we stand and where are we going? *Dig Dis Sci* 1999; **17**: 80-89
- 3 **McCullough AJ, Falck-Ytter Y.** Body composition and hepatic steatosis as precursors for fibrotic liver disease. *Hepatology* 1999; **29**: 1328-1330
- 4 **Matteoni CA, Younossi ZM, Gramlich T, Boparai N, Liu YC, McCullough AJ.** Nonalcoholic fatty liver disease: a spectrum of clinical and pathological severity. *Gastroenterology* 1999; **116**: 1413-1419
- 5 **James O, Day C.** Non-alcoholic steatohepatitis: another disease of affluence. *Lancet* 1999; **353**: 1634-1636
- 6 **Tominaga K, Kurata JH, Chen YK, Fujimoto E, Miyagawa S, Abe I, Kusano Y.** Prevalence of fatty liver in Japanese children and relationship to obesity. An epidemiological ultrasonographic survey. *Dig Dis Sci* 1995; **40**: 2002-2009
- 7 **Yano E, Tagawa K, Yamaoka K, Mori M.** Test validity of periodic liver function tests in a population of Japanese male bank employees. *J Clin Epidemiol* 2001; **54**: 945-951
- 8 **Powell EE, Cooksley WG, Hanson R, Searle J, Halliday JW, Powell LW.** The natural history of nonalcoholic steatohepatitis: a follow-up study of forty-two patients for up to 21 years. *Hepatology* 1990; **11**: 74-80
- 9 **Araujo LM, De Oliveira DA, Nunes DS.** Liver and biliary ultrasonography in diabetic and non-diabetic obese women. *Diabetes Metab* 1998; **24**: 458-462
- 10 **Bellentani S, Saccoccio G, Masutti F, Croce LS, Brandi G, Sasso F, Cristanini G, Tiribelli C.** Prevalence of and risk factors for hepatic steatosis in Northern Italy. *Ann Intern Med* 2000; **132**: 112-117
- 11 **Mathiesen UL, Franzen LE, Fryden A, Foberg U, Bodemar G.** The clinical significance of slightly to moderately increased liver transaminase values in asymptomatic patients. *Scand J Gastroenterol* 1999; **34**: 85-91
- 12 **el-Hassan AY, Ibrahim EM, al-Mulhim FA, Nabhan AA, Chammas MY.** Fatty infiltration of the liver: analysis of prevalence, radiological and clinical features and influence on patient management. *Br J Radiol* 1992; **65**: 774-778
- 13 **Joseph AE, Saverymuttu SH, al-Sam S, Cook MG, Maxwell JD.** Comparison of liver histology with ultrasonography in assessing diffuse parenchymal liver disease. *Clin Radiol* 1991; **43**: 26-31
- 14 **Lonardo A, Bellini M, Tartoni P, Tondelli E.** The bright liver syndrome. Prevalence and determinants of a "bright" liver echopattern. *Ital J Gastroenterol Hepatol* 1997; **29**: 351-356
- 15 **Skelly MM, James PD, Ryder SD.** Findings on liver biopsy to investigate abnormal liver function tests in the absence of diagnostic serology. *J Hepatol* 2001; **35**: 195-199
- 16 **Reid AE.** Nonalcoholic steatohepatitis. *Gastroenterology* 2001; **121**: 710-723
- 17 **Angulo P, Keach JC, Batts KP, Lindor KD.** Independent predictors of liver fibrosis in patients with nonalcoholic steatohepatitis. *Hepatology* 1999; **30**: 1356-1362
- 18 **Falck-Ytter Y, Younossi ZM, Marchesini G, McCullough AJ.** Clinical features and natural history of nonalcoholic steatosis syndromes. *Semin Liver Dis* 2001; **21**: 17-26
- 19 **Hultcrantz R, Gabrielsson N.** Patients with persistent elevation of aminotransferases: Investigation with ultrasonography, radio-nuclide imaging and liver biopsy. *J Intern Med* 1993; **233**: 7-12
- 20 **Layer G, Zuna I, Lorenz A, Zerban H, Haberkorn U, Bannasch P, van Kaick G, Rath U.** Computerized ultrasound B-scan texture analysis of experimental diffuse parenchymal liver disease: Correlation with histopathology and tissue composition. *J Clin Ultrasound* 1999; **19**: 193-201
- 21 **Mendler MH, Bouillet P, LeSidaner A, Lavoine E, Labrousse F, Sautereau D, Pillegand B.** Dual-energy CT in the diagnosis and quantification of fatty liver: Limited clinical value in comparison to ultrasound scan and single-energy CT, with special reference to iron overload. *J Hepatol* 1998; **28**: 785-794
- 22 **Marceau P, Biron S, Hould FS, Marceau S, Simard S, Thung SN, Kral JG.** Liver pathology and the metabolic syndrome X in severe obesity. *J Clin Endocrinol Metab* 1999; **84**: 1513-1517
- 23 **Assy N, Kaita K, Mymin D, Levy C, Rosser B, Minuk G.** Fatty infiltration of liver in hyperlipidemic patients. *Dig Dis Sci* 2000; **45**: 1929-1934
- 24 **Ludwig J, Viggiano TR, McGill DB, Oh BJ.** Nonalcoholic steatohepatitis: Mayo Clinic experiences with a hitherto unnamed disease. *Mayo Clin Proc* 1980; **55**: 434-438
- 25 **Fan JG, Zeng MD, Wang GL.** Pathogenesis of fatty liver. *Shijie Huaren Xiaohua Zazhi* 1999; **7**: 75-76
- 26 **Sabir N, Sermez Y, Kazil S, Zencir M.** Correlation of abdominal fat accumulation and liver steatosis: importance of ultrasonographic and anthropometric measurements. *Eur J Ultrasound* 2001; **14**: 121-128
- 27 **Mensenkamp AR, Havekes LM, Romijn JA, Kuipers F.** Hepatic steatosis and very low density lipoprotein secretion: the involvement of apolipoprotein E. *J Hepatol* 2001; **35**: 816-822
- 28 **Nehra V, Angulo P, Buchman AL, Lindor KD.** Nutritional and metabolic considerations in the etiology of nonalcoholic steatohepatitis. *Dig Dis Sci* 2001; **46**: 2347-2352
- 29 **Sharabi Y, Eldad A.** Nonalcoholic fatty liver disease is associated with hyperlipidemia and obesity. *Am J Med* 2000; **109**: 171
- 30 **Fong DG, Nehra V, Lindor KD, Buchman AL.** Metabolic and nutritional considerations in nonalcoholic fatty liver. *Hepatology* 2000; **32**: 3-10
- 31 **Loguercio C, De Girolamo V, de Sio I, Tuccillo C, Ascione A, Baldi F, Budillon G, Cimino L, Di Carlo A, Di Marino MP, Morisco**

- F, Picciotto F, Terracciano L, Vecchione R, Verde V, Del Vecchio Blanco C. Non-alcoholic fatty liver disease in an area of southern Italy: main clinical, histological, and pathophysiological aspects. *J Hepatol* 2001; **35**: 568-574
- 32 **Fan JG**. Steatohepatitis studies in China. *Shijie Huaren Xiaohua Zazhi* 2001; **9**: 6-10
- 33 **Lonardo A**, Trande P. Are there any sex differences in fatty liver? A study of glucose metabolism and body fat distribution. *J Gastroenterol Hepatol* 2000; **15**: 775-782
- 34 **Sonsuz A**, Basaranoglu M, Bilir M, Senturk H, Akin P. Hyperinsulinemia in nondiabetic, both obese and nonobese patients with nonalcoholic steatohepatitis. *Am J Gastroenterol* 2002; **97**: 495
- 35 **Urso R**, Visco-Comandini U. Metformin in non-alcoholic steatohepatitis. *Lancet* 2002; **359**: 355-356
- 36 **Chitturi S**, Abeygunasekera S, Farrell GC, Holmes-Walker J, Hui JM, Fung C, Karim R, Lin R, Samarasinghe D, Liddle C, Weltman M, George J. NASH and insulin resistance: Insulin hypersecretion and specific association with the insulin resistance syndrome. *Hepatology* 2002; **35**: 373-379
- 37 **Pagano G**, Pacini G, Musso G, Gambino R, Mecca F, Depetris N, Cassader M, David E, Cavallo-Perin P, Rizzetto M. Nonalcoholic steatohepatitis, insulin resistance, and metabolic syndrome: further evidence for an etiologic association. *Hepatology* 2002; **35**: 367-372
- 38 **Willner IR**, Waters B, Patil SR, Reuben A, Morelli J, Riely CA. Ninety patients with nonalcoholic steatohepatitis: insulin resistance, familial tendency, and severity of disease. *Am J Gastroenterol* 2001; **96**: 2957-2961
- 39 **Paradis V**, Perlemuter G, Bonvoust F, Dargere D, Parfait B, Vidaud M, Conti M, Huet S, Ba N, Buffet C, Bedossa P. High glucose and hyperinsulinemia stimulate connective tissue growth factor expression: a potential mechanism involved in progression to fibrosis in nonalcoholic steatohepatitis. *Hepatology* 2001; **34**: 738-744
- 40 **Marchesini G**, Brizi M, Bianchi G, Tomassetti S, Bugianesi E, Lenzi M, McCullough AJ, Natale S, Forlani G, Melchionda N. Nonalcoholic fatty liver disease: a feature of the metabolic syndrome. *Diabetes* 2001; **50**: 1844-1850
- 41 **Sanyal AJ**. Insulin resistance and nonalcoholic steatohepatitis: fat or fiction? *Am J Gastroenterol* 2001; **96**: 274-276
- 42 **Luyckx FH**, Lefebvre PJ, Scheen AJ. Non-alcoholic steatohepatitis: association with obesity and insulin resistance, and influence of weight loss. *Diabetes Metab* 2000; **26**: 98-106
- 43 **Marchesini G**, Brizi M, Morselli-Labate AM, Bianchi G, Bugianesi E, McCullough AJ, Forlani G, Melchionda N. Association of non-alcoholic fatty liver disease with insulin resistance. *Am J Med* 1999; **107**: 450-455
- 44 **Sonsuz A**, Basaranoglu M, Ozbay G. Relationship between aminotransferase levels and histopathological findings in patients with nonalcoholic steatohepatitis. *Am J Gastroenterol* 2000; **95**: 1370-1371
- 45 **Lai MM**. Hepatitis C virus proteins: direct link to hepatic oxidative stress, steatosis, carcinogenesis and more. *Gastroenterology* 2002; **122**: 568-571
- 46 **Giannini E**, Ceppa P, Testa R. Steatosis in chronic hepatitis C: can weight reduction improve therapeutic efficacy? *J Hepatol* 2001; **35**: 432-433
- 47 **Ong JP**, Younossi ZM, Speer C, Olano A, Gramlich T, Boparai N. Chronic hepatitis C and superimposed nonalcoholic fatty liver disease. *Liver* 2001; **21**: 266-271
- 48 **Bacon BR**, Farahvash MJ, Janney CG, Neuschwander-Tetri BA. Nonalcoholic steatohepatitis: an expanded clinical entity. *Gastroenterology* 1994; **107**: 1103-1109
- 49 **Kumar KS**, Malet PF. Nonalcoholic steatohepatitis. *Mayo Clin Proc* 2000; **75**: 733-739
- 50 **Xu ZJ**, Fan JG, Wang GL, Ding XD, Tian LY, Zheng XY. Rat model of nonalcoholic steatohepatitis with fibrosis by a fat-rich diet. *Shijie Huaren Xiaohua Zazhi* 2002; **10**: 392-396
- 51 **Angulo P**, Lindor KD. Treatment of nonalcoholic fatty liver: present and emerging therapies. *Semin Liver Dis* 2001; **21**: 81-88
- 52 **Chitturi S**, Farrell GC. Etiopathogenesis of nonalcoholic steatohepatitis. *Semin Liver Dis* 2001; **21**: 27-41
- 53 **Cortez-Pinto H**, Chatham J, Chacko VP, Arnold C, Rashid A, Diehl AM. Alterations in liver ATP homeostasis in human non-alcoholic steatohepatitis: a pilot study. *JAMA* 1999; **282**: 1659-1664

Edited by Zhang JZ

Cloning of HBsAg-encoded genes in different vectors and their expression in eukaryotic cells

Shan Qin, Hong Tang, Lian-San Zhao, Fang He, Yong Lin, Li Liu, Xiao-Mei He

Shan Qin, Hong Tang, Lian-San Zhao, Fang He, Yong Lin, Li Liu, Key Laboratory for Molecular Biology of Infectious Diseases of Sichuan Province, West China Hospital, Sichuan University, Chengdu 610041, Sichuan, China

Xiao-Mei He, Analytical and Testing Center, Sichuan University, Chengdu 610064, Sichuan, China

Shan Qin, Center for Discovery of Drugs and Diagnostics, Biomolecular Science Center, University of Central Florida, 12722 Research Parkway, Orlando, Florida 32826, USA

Supported by the National Science Foundation of China, No. 39670670

Correspondence to: Dr Shan Qin, Key Laboratory for Molecular Biology of Infectious Diseases of Sichuan Province, West China Hospital, Sichuan University, Chengdu 610041, Sichuan, China. shanqin@hotmail.com

Telephone: +86-28-5422650

Received: 2001-09-14 **Accepted:** 2001-10-26

Abstract

AIM: To compare the efficiency of different plasmids as DNA vectors by cloning three HBsAg-encoded genes into two eukaryotic expression vectors, pRc/CMV and pSG5UTPL/Flag, and to express HBsAg S, MS, and LS proteins in SP2/0 cells, and to establish monoclonal SP2/0 cell strains that are capable of expressing S or S₂S proteins stably.

METHODS: Segments of S, preS₂-S, preS₁-preS₂-S genes of Hepatitis B virus were amplified by routine PCR and preS₁-S fragment was amplified by Over-Lap Extension PCR. The amplified segments were cleaved with restricted endonuclease Hind III/Not I followed by ligation with pRc/CMV, or BamHI/EcoR I followed by ligation with pSG5UTPL/Flag. After the plasmid vectors were cleaved with the correspond enzymes, the amplified segments were inserted into pRc/CMV or pSG5UTPL/Flag plasmid vectors with T4 DNA ligase. KOZAK sequence was added before the initial ATG code of each fragment using specific primer. The inserted segments in the recombinant plasmids were sequenced after subcloning. BALB/c mice myeloma cells (SP2/0 cell line) were transfected with the recombinant plasmids. The expressions of the different recombinants were compared by Western-blot, using a monoclonal anti-HBs antibody as the primary antibody and peroxidase-labeled multi-linker as the secondary. Stable SP2/0-pRc/CMV-S or SP2/0-pRc/CMV-MS clones were established through clone screening with G418.

RESULTS: Fragments with anticipated size were harvested after PCR. After recombination and screening, the sequences of the inserted segments in the recombinants were confirmed to be S, preS₂S, preS₁-preS₂S and preS₁S encoding genes, determined by sequencing. The results of Western-blot hybridization were positive for the anticipated proteins. Among them, pRc/CMV-S or pRc/CMV-MS demonstrated the highest expressing their respective antigen.

CONCLUSION: Eight recombinant plasmids expressing S,

M, L or preS₁S proteins are obtained. For hepatitis surface antigen expression in eukaryotic cells, the vector pRc/CMV is superior to pSG5UTPL/Flag, and pRc/CMV-S and pRc/CMV-MS are the most efficient in the pRc/CMV clones. SP2/0 cells stably expressing HBsAg are established, and may be used as target cells for evaluating the CTL activity of a DNA vaccine in vitro.

Qin S, Tang H, Zhao LS, Lin Y, Liu L, He XM. Cloning of HBsAg-encoded genes in different vectors and their expression in eukaryotic cells. *World J Gastroenterol* 2003; 9(5): 1111-1113

<http://www.wjgnet.com/1007-9327/9/1111.htm>

INTRODUCTION

Hepatitis B virus (HBV) infection is epidemic worldwide^[1-3]. Unfortunately, there are no satisfactory drugs to cure HBV-related diseases, and the only way to control the epidemic is through vaccination^[4-6]. Great efforts have been made to develop more successful vaccines than those currently available to prevent or to treat HBV infection. The newest approach is genetic immunization. This involves the transfer of a viral gene into host somatic cells by a plasmid vector, with subsequent endogenous production and intracellular processing of the virus' structural proteins into small peptides. The processed peptides eventually induce a broad-based immune response^[7-11]. Hepatitis B virus surface antigen consists of S (S, small surface), MS (medium surface, S+preS₂), and LS (large surface, S+preS₁+preS₂) HBsAg molecules. We have reported that DNA vaccine expressing HBsAg S molecule induced humoral and cellular immune responses against HBsAg^[12,13]. Because the preS antigen is necessary for HBV to penetrate the cell membrane of the host, vaccines containing the preS antigen are more effective. Hence, we constructed a series of plasmids encoding small (S), medium (M), or large (L) envelope proteins of HBsAg utilizing different promoters. In addition, the expression levels of these recombinant plasmids were evaluated, in order to choose a better vector for designing future DNA vaccines.

MATERIALS AND METHODS

Gene fragments expressing S, MS, LS, and preS₁S proteins

Plasmid pBHB₄ (containing the *adr* subtype of HBV genome DNA) was used as a template to amplify S, preS₂ and preS₁ fragments. The following primers were used: the forward primers: SF (nt 28-41), 5' - GCG AAT TCT AGC TTA TCG ATC ACC ATG GAG AAC ACA AC, complementary to the S gene; S₂F (nt 3077-3090), 5' - GCG AAT TCA AGC TTA TCG ATC ACC ATG CAG TGG AAC ACA TC, complementary to the preS₂ gene; and S₁F (nt 2179-2733), 5' - GCG AAT TCA AGC TTA TCG ATC ACC ATG GGA GGT TGG TC, complementary to the preS₁ gene. The same reverse primer was used for all reactions: SR (nt 705-693): GCG CGG CCG CTT AGG ATC CAA TCG ATA CCC AA. The primers contain a flanking sequence having endonuclease enzyme sequence

bands when detected by Western-Blot. Cytosolic HBsAg was detected by immunocytochemistry. The 7 cell strains above were also positive for pRc/CMV-S or pRc/CMV-S₂S when detected by *in situ* hybridization.

DISCUSSION

DNA immunization involves the recombination of the genes of interest with the selected eukaryotic expression plasmid/vector and the transfer of the recombinant plasmid into muscle or skin cells of the host, with a subsequent induction of specific immune responses^[16-20]. DNA immunization is attractive for its advantages over traditional vaccines, and is discussed in elsewhere^[21-24]. We have reported that HBV DNA vaccine NV-HB/s could express HBsAg in muscle cells after injecting into mouse muscle, followed by the induction of an immune response, including the switchover of anti-HBs production in peripheral blood^[12,13].

HBsAg-encoded genes include S, preS₁, and preS₂. All the proteins expressed by these genes are antigenic. The elicited response is strongest with preS₁ and preS₂. The titer of preS antibody in rabbits immunized with preS protein is 400 times greater than that of S antibody in rabbits immunized with S protein. In addition, some mice are non-responsive to S protein of HBV, which is determined by an allele of H₂ gene. Vaccines containing HBV preS₁ and/or preS₂ antigen may alter this inherited non-responsive state, inducing anti-HBs in mice which were previously immunized with vaccines only containing S. Moreover, preS proteins are necessary in order for HBV to infect hepatocytes. preS₁ protein can bind hepatocytes specifically while preS₂ can bind hepatocytes through PHS (polymerase human serum albumin). Because of the importance of HBV preS proteins, we constructed plasmids, which can be used for DNA vaccines containing the preS₁ and/or preS₂ genes. Several plasmids were constructed by different promoters in order to compare their expression proficiency. All these recombinant plasmids demonstrated expression in SP2/0 cells, while the vector pRc/CMV was the most effective, with the highest expression demonstrated as pRc/CMV-S and pRc/CMV-S₂S. pRc/CMV-S and pRc/CMV-S₂S may be used as good candidates for DNA immunization. Their efficacy in inducing immune responses is still in experimental process.

Long-term expression cell strains transfected with pRc/CMV-S or pRc/CMV-S₂S were established in our experiment through selection with G418 more than 30 generations. The cell lines SP2/0-pRc/CMV-S and SP2/0-pRc/CMV-S₂S can express HBsAg S protein or S₂S protein effectively and may be used as target cells for CTL test in the study of DNA immunization for HBV in the near future.

ACKNOWLEDGEMENTS

We are grateful to Prof. Senshi Murukami, Kanazawa University in Japan, for generous gift of plasmid pBHB4 and plasmid vector pSG5UTPL. The authors thank Kathleen N from Biomolecular Science Center of University of Central Florida for her reviewing of the manuscript.

REFERENCES

1 **Christensen PB**, Krarup HB, Niesters HG, Norder H, Schaffalitzky de Muckadell OB, Jeune B, Georgsen J. Outbreak

- of Hepatitis B among injecting drug users in Denmark. *J Clin Virol* 2001; **1**: 133-141
- 2 **Yerly S**, Quadri R, Negro F, Barbe KP, Cheseaux JJ, Burgisser P, Siegrist CA, Perrin L. Nosocomial outbreak of multiple bloodborne viral infections. *J Infect Dis* 2001; **3**: 369-372
- 3 **Whalley SA**, Murray JM, Brown D, Webster GJ, Emery VC, Dusheiko GM, Perelson AS. Kinetics of acute hepatitis B virus infection in humans. *J Exp Med* 2001; **7**: 847-854
- 4 **Lin OS**, Keefe EB. Current treatment strategies for chronic hepatitis B and C. *Annu Rev Med* 2001; **52**: 29-49
- 5 **Vryheid RE**, Yu ES, Mehta KM, McGhee J. The declining prevalence of hepatitis B virus infection among Asian and Pacific Islander children. *Asian Am Pac Isl J Health* 2001; **2**: 162-178
- 6 **Merle P**, Trepo C, Zoulim F. Current management strategies for hepatitis B in the elderly. *Drugs Aging* 2001; **10**: 725-735
- 7 **von Reyn CF**, Vuola JM. New vaccines for the prevention of tuberculosis. *Clin Infect Dis* 2002; **4**: 465-474
- 8 **Riedl P**, El-Kholy S, Reimann J, Schirmbeck R. Priming biologically active antibody responses against an isolated, conformational viral epitope by DNA vaccination. *J Immunol* 2002; **3**: 1251-1260
- 9 **Heinen PP**, Rijsewijk FA, De Boer-Luijze EA, Bianchi AT. Vaccination of pigs with a DNA construct expressing an influenza virus M2-nucleoprotein fusion protein exacerbates disease after challenge with influenza A virus. *J Gen Virol* 2002; **8**: 1851-1859
- 10 **Coban C**, Ishii KJ, Sullivan DJ, Kumar N. Purified malaria pigment (hemozoin) enhances dendritic cell maturation and modulates the isotype of antibodies induced by a DNA vaccine. *Infect Immun* 2002; **7**: 3939-3943
- 11 **Kraehenbuhl JP**. Mucosa-targeted DNA vaccination. *Trends Immunol* 2001; **12**: 646-648
- 12 **Zhao LS**, Qin S, Zhou TY, Tang H, Liu Li, Lei BJ. DNA-based vaccination induces humoral and cellular immune responses against hepatitis B virus surface antigen in mice without activation of C-myc. *World J Gastroenterol* 2000; **6**: 239-243
- 13 **Qin S**, Zhao LS, Tang H. Detection of NV-HB/s DNA and C-myc mRNA in mice inoculated with hepatitis B nucleic acid vaccine-NV-HB/s. *Zhonghua Ganzangbing Zazhi* 1999; **1**: 6-7
- 14 **Sambrook J**, Russell DW. Calcium-phosphate-mediated transfection of Adherent Cells. In: Sambrook J, Russell DW, eds. *Molecular Cloning*. 3rd Edition, New York, Cold Spring Harbor Laboratory Press 2001; **16**: 25-26
- 15 **Qin S**, Huang CY, He F, Zhao LS, Liu L. Eukaryotic cell SP2/0 transfection by calcium phosphate method and detection of their expressions. *Lett Biotechnol* 2000; **2**: 115
- 16 **Fearon DT**. Innate immunity-beginning to fulfill it's promise? *Nat Immunol* 2000; **2**: 102-103
- 17 **Monzavi-Karbassi B**, Kieber-Emmons T. Current concepts in cancer vaccine strategies. *Biotechniques* 2001; **1**: 170-176
- 18 **Qin S**, Zhao LS. Applications of DNA-immunization in prevention and treatment of infectious diseases. *Zhonghua Chuanranbing Zazhi* 1999; **1**: 65-66
- 19 **Shedlock DJ**, Weiner DB. DNA vaccination: antigen presentation and the induction of immunity. *J Leukoc Biol* 2000; **6**: 793-806
- 20 **Robinson HL**, Pertmer TM. DNA vaccines for viral infections: basic studies and applications. *Adv Virus Res* 2000; **55**: 1-74
- 21 **Vecino WH**, Morin PM, Agha R, Jacobs WR, Fennelly GJ. Mucosal DNA vaccination with highly attenuated Shigella is superior to attenuated Salmonella and comparable to intramuscular DNA vaccination for T cells against HIV. *Immunol Lett* 2002; **3**: 197-204
- 22 **Robinson HL**. New hope for an AIDS vaccine. *Nat Rev Immunol* 2002; **4**: 239-250
- 23 **Rodriguez F**, Harkins S, Slifka MK, Whitton JL. Immunodominance in virus-induced CD8(+) T-cell responses is dramatically modified by DNA immunization and is regulated by gamma interferon. *J Virol* 2002; **9**: 4251-4259
- 24 **Haupt K**, Roggendorf M, Mann K. The potential of DNA vaccination against tumor-associated antigens for antitumor therapy. *Exp Biol Med (Maywood)* 2002; **4**: 227-237

Three-dimensional contrast-enhanced MR angiography in diagnosis of portal vein involvement by hepatic tumors

Jiang Lin, Kang-Rong Zhou, Zu-Wang Chen, Jian-Hua Wang, Zhi-Quan Wu, Jia Fan

Jiang Lin, Kang-Rong Zhou, Zu-Wang Chen, Jian-Hua Wang, Department of Radiology, Affiliated Zhongshan Hospital, Fudan University, Shanghai 200032, China

Zhi-Quan Wu, Jia Fan, Institute of Liver Cancer, Affiliated Zhongshan Hospital, Fudan University, Shanghai 200032, China

Supported by National Natural Science Foundation of China, No. 39670230

Correspondence to: Dr Jiang Lin, Department of Radiology, Affiliated Zhongshan Hospital, Fudan University, Shanghai 200032, China. linjiang@zshospital.net

Telephone: +86-21-64041990 Ext 2463 **Fax:** +86-21-64038472

Received: 2003-01-04 **Accepted:** 2003-02-13

Abstract

AIM: To assess the accuracy of three-dimensional contrast-enhanced magnetic resonance angiography (3D CE MRA) in evaluation of the portal vein involvement in patients with hepatic tumors.

METHODS: 3D CE MRA was performed in 62 patients with hepatic tumors to assess the patency of the main, right and left portal veins before hepatic surgery. A total of 186 veins were examined for encasement, occlusion and tumor thrombosis. The results of 3D CE MRA diagnosis were then correlated with the surgical-pathological and intra-operative sonographic findings.

RESULTS: 3D CE MRA correctly detected 48 of 49 involved and 135 of 137 noninvolved portal veins with the sensitivity of 98 %, specificity of 99 %, positive predictive value of 96 % and negative predictive value of 99 %.

CONCLUSION: 3D CE MRA is accurate in evaluation of the portal vein involvement in patients with hepatic tumors.

Lin J, Zhou KR, Chen ZW, Wang JH, Wu ZQ, Fan J. Three-dimensional contrast-enhanced MR angiography in diagnosis of portal vein involvement by hepatic tumors. *World J Gastroenterol* 2003; 9(5): 1114-1118

<http://www.wjgnet.com/1007-9327/9/1114.htm>

INTRODUCTION

Evaluation of the patency of the portal vein (PV) is essential before surgical resection of hepatic tumors. There are advantages and limitations to the conventional methods for PV imaging. Ultrasound (US) is noninvasive and relatively inexpensive, but it is operator dependent and may not be successful when the acoustic window is restricted^[1,2]. Contrast-enhanced computed tomography (CT) is readily available and can demonstrate the PV, but it uses ionizing radiation and requires intravenous administration of a large amount of iodinated contrast medium with the risk of nephrotoxicity and possible allergic reaction^[2-5]. X-ray portography is the standard technique for evaluation of the PV due to its superb spatial resolution^[2], but it is invasive, uncomfortable and, like CT,

involves radiation and use of iodinated contrast medium. Occasionally, opacity of the PV is poor by intra-arterial portography in patients with portal hypertension^[2,6,7]. The disadvantages of x-ray portography also include high cost, requirement for operator expertise and associated complications such as hemorrhage and aortic dissection^[8]. Non-enhanced magnetic resonance angiography (MRA) with time-of-flight (TOF) and phase-contrast (PC) techniques is another means for non-invasive demonstration of the PV. However, it is limited by long acquisition time, motion and flow artifacts and saturation effects^[1,9-13].

Three-dimensional contrast-enhanced MRA (3D CE MRA) is a recently developed, non-invasive and fast and easy to perform technique which is suited for evaluation of the portal venous system^[14-21]. With this technique, the imaging of the PV is accomplished in a single breath hold. It requires only a peripheral venous injection of a small amount of gadolinium, which is much safer than iodine-based contrast media. Using gadolinium to shorten the T1 value of the blood, it overcomes flow artifacts and saturation effects in TOF and PC. Moreover, it involves no radiation. 3D CE MRA has been frequently used in our hospital in patients with liver tumors for the preoperative diagnosis of the patency of the portal venous system. The goal of this study was to evaluate the accuracy of this technique for the assessment of the PV involvement in hepatic tumors.

MATERIALS AND METHODS

Patients

Sixty-two consecutive patients who required evaluation of their portal venous system before surgical resection of hepatic tumors were recruited. They consisted of 56 men and 6 women ranging in age from 26 to 78 years (mean age 54 years) and were diagnosed clinically as hepatocellular carcinoma (55 patients), hepatic metastasis (4 patients), hemangioma (1 patient), hepatic adenoma (1 patient) and right adrenal carcinoma with liver involvement (1 patient).

MR examinations

MR scans were performed using a 1.5T MR imager (Signa, General Electric Medical Systems, Milwaukee, WI, USA) and a body coil. After images located were acquired, a breath-hold T1-weighted fast multiplanar spoiled gradient-echo (FMPSGR) sequence (repetition time/echo time, 150/4.2 ms; flip angle, 90°; field of view, 360 mm; matrix, 128×256; 18 slices of 7.0 mm thickness each; gap, 3.0 mm; one signal acquired) and a respiratory-triggered T2-weighted fast spin-echo sequence (repetition time/echo time, 2800-4200/80 ms; echo train length 8-12, field of view, 360 mm; matrix, 128×256; 18 slices of 7.0 mm thickness each; gap, 3.0 mm; 2 signals acquired) were performed in the liver. For 3D CE MRA, a breath-hold 3D fast spoiled gradient-echo sequence (repetition time/echo time, 5.2-10.2/1.2-1.9 ms; flip angle, 30° or 45°; field of view, 360-480 mm; matrix, 128×256; imaging volume, 75-168 mm; number of partitions, 24-30; one signal acquired; and acquisition time, 19-28 s) was used.

With T1-weighted and T2-weighted images as references the imaging volume of 3D CE MRA was acquired in a coronal plane to cover the main PV and its left and right intrahepatic branches. The imaging volume was determined by a radiologist depending on each patient's liver size and ability of breathholding. A gadolinium chelate called gadopentetate-dimeglumine (Magnevist; Schering AG, Berlin, Germany) was used as a contrast medium for all examinations, with a concentration of 0.15 mmol per kg body weight. The contrast medium was injected by an experienced MR technician through an antecubital vein at an injection rate of approximately 3 ml/s. Acquisition was commenced immediately after the injection and repeated three times with a 6-second delay between each acquisition to allow patient breathing. The second acquisition coincided with portal venous phase, while the first acquisition was the arterial phase and the third acquisition was the equilibrium phase. Source images of portal venous phase were reviewed first. These images were then reconstructed on a workstation (Advantage Windows Workstation, General Electric Medical Systems, Milwaukee, WI) to produce projectional images like x-ray portography. Both maximum intensity projection and multiplanar reconstruction techniques were performed and reviewed.

Image analysis

The patency of the main PV and intrahepatic left and right PV including their anterior and posterior branches on 3D CE MRA were assessed by two radiologists who were unaware of the patient's clinical status. A consensus reading between them was reached in every case. The PV involvement was considered to be present if the veins were encased, occluded and thrombosed. Encasement was diagnosed when the PV was surrounded by a tumor and showed mural irregularity or had an indistinct wall or irregular lumen narrowing. The PV was considered to be occluded if the lumen was obstructed, interrupted or not visualized due to tumor invasion. Tumor thrombosis was diagnosed when the PV was widened with linear, nodular or irregular filling defect.

Surgery was performed 1-20 days (mean, 6 days) after the MR imaging. Tumor location and portal venous status were recorded by the surgeon in the surgical report for each case. In 12 of 49 patients who underwent hepatic resection, tumor

thrombi were removed from the stump and/or main trunk of the PV during the operation. In 13 patients whose tumors were found to be unresectable at surgery, intra-operative US was performed to demonstrate the PV. In these unresectable cases, small amount of tumor tissue was taken for pathological examination and 3 of them had tumor thrombi removed from the main PV. The results of 3D CE MRA for assessment of the PV involvement were compared with the surgeon's findings. Sensitivity, specificity, positive and negative predictive values of 3D CE MRA were calculated using surgical-pathologic and intra-operative US findings as the references. All cases with false positive and negative diagnosis were further analyzed to determine the cause of the error.

RESULTS

All 3D CE MRA examinations were performed successfully. The main PV and intrahepatic left PV and right PV including their anterior and posterior branches were shown well without diagnostic difficulty in each case.

Forty-nine of 186 PVs were found to be involved at surgery. Encasement was present in 7 veins, occlusion in 13 veins and tumor thrombosis in 29 veins (Figures 1-3). The site and type of the PV involvement were summarized in Table 1. The remaining 137 PVs were normal. 3D CE MRA correctly depicted 48 of 49 (98 %) involved PVs and 135 of 137 (99 %) noninvolved PVs with an overall sensitivity of 98 %, specificity of 99 %, positive predictive value of 96 %, and negative predictive value of 99 % for the evaluation of all PVs including the main, left and right PVs. The accuracy in examination of the patency of the main PV reached 100 %. The relationship between 3D CE MRA for each of the PVs and the surgical findings is shown in Table 2. Use of 3D CE MRA resulted in two false positive interpretations involving the left PV (Figure 4) and one false negative interpretation involving the right PV (Figure 5). The two false positive diagnoses were made in which the left PVs were interpreted as occluded at 3D CE MRA, whereas at surgery they were found to be compressed but not invaded by tumors in left lobes. For the false negative diagnosis, the right PV was diagnosed as normal by 3D CE MRA, but surgical-pathologic examination revealed that the right posterior PV was thrombosed with tumor.

Table 1 Surgical-pathologic findings of portal vein involvement

	Type of involvement				
	Total involved	Encasement	Occlusion	Tumor thrombosis	Normal
Main PV	12	0	0	12	50
Left PV	18	3	8	7	44
Right PV	19	4	5	10	43
Total	49	7	13	29	137

Note: Data are number of cases. PV is portal vein.

Table 2 Relationship between 3-dimensional contrast-enhanced MR angiography diagnosis of portal vein involvement and surgical-pathologic findings

	True positive	True negative	False negative	False positive	Sensitivity (%)	Specificity (%)	Positive predictive (%)	Negative predictive (%)
Main PV	12	50	0	0	100	100	100	100
Left PV	18	42	0	2	100	95	90	100
Right PV	18	43	1	0	95	100	100	98
Total	48	135	1	2	98	99	96	99

Note: Data are number of cases except otherwise indicated. PV is portal vein.

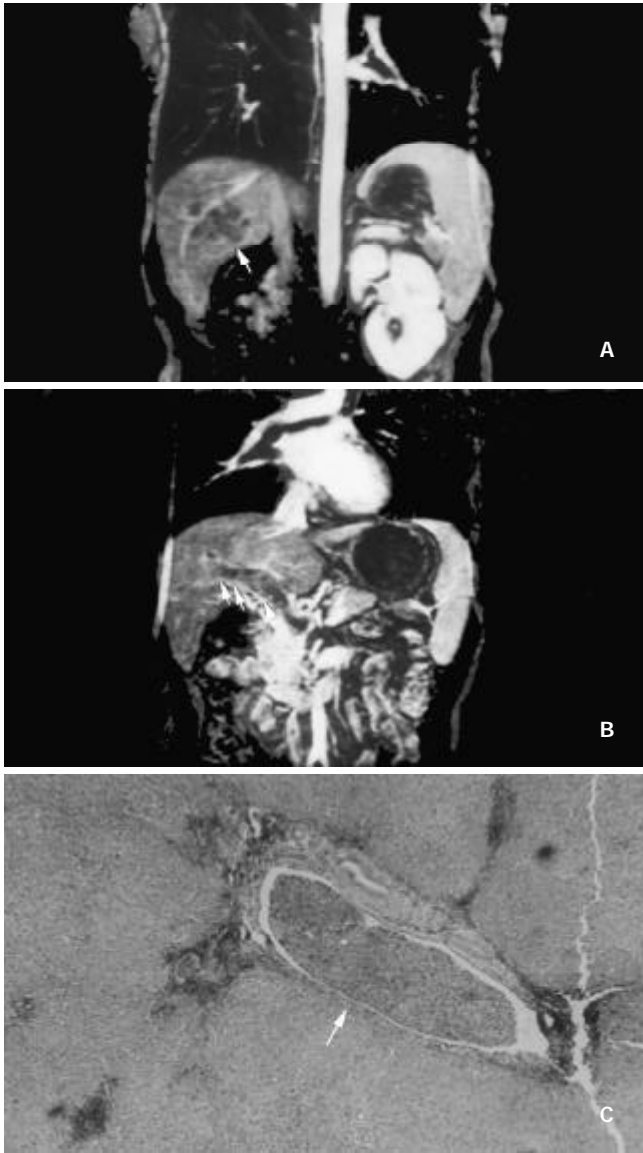


Figure 1 A patient with hepatocellular carcinoma in the right lobe. (A) Source image of 3-dimensional contrast-enhanced MR angiography demonstrates a hypointense tumor in the right lobe (arrow). (B) Multiplanar reconstruction of 3-dimensional contrast-enhanced MR angiography shows widened main and right portal vein with filling defects (arrow). (C) The patient underwent tumor resection and removal of tumor thrombi in the portal vein. Histopathology (HE ×40) reveals tumor thrombus in the portal vein (arrow).

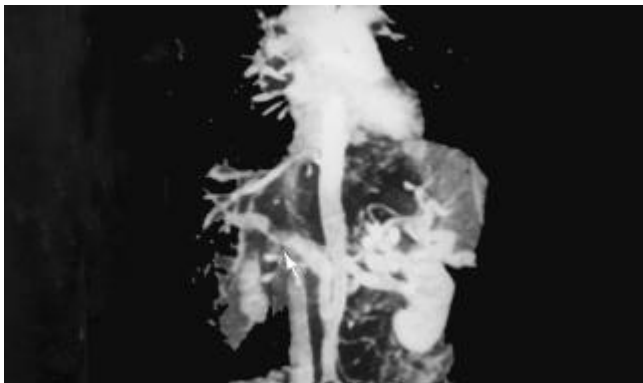


Figure 3 A patient with hepatocellular carcinoma in the left lobe. 3-dimensional contrast-enhanced MR angiography demonstrates occluded left portal vein and irregular filling defects in the main portal vein (arrow). The right portal vein is normal.

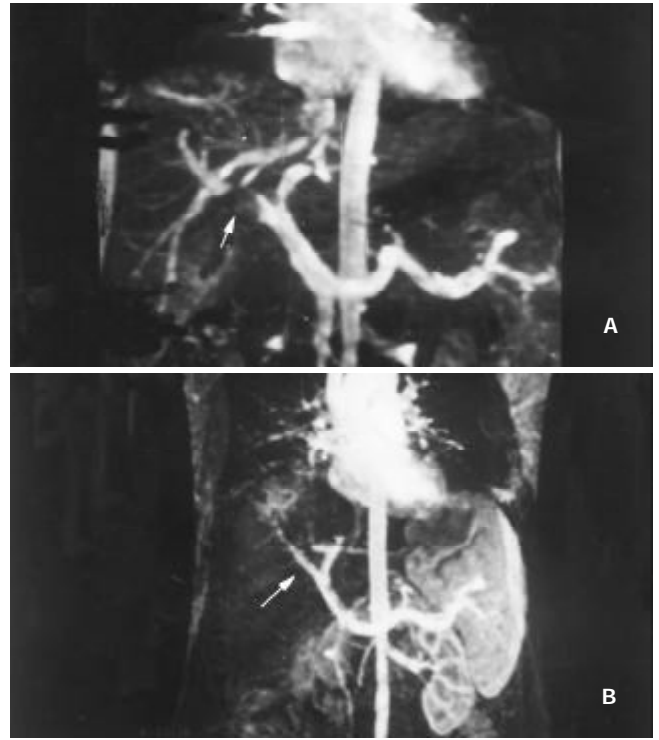


Figure 2 A patient with hepatocellular carcinoma in the right lobe. (A) 3-dimensional contrast-enhanced MR angiography depicts a nodular filling defect in the right portal vein (arrow). (B) After partial right hepatic resection and removal of the tumor thrombi, the right portal vein is shown patent (arrow).

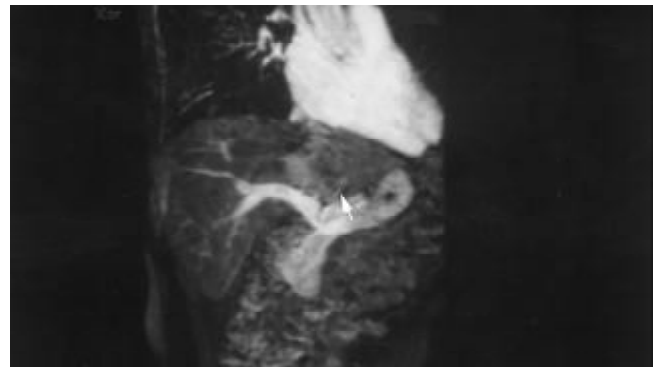


Figure 4 A patient with hepatocellular carcinoma in the left lobe (arrow). The left portal vein is not visualized and interpreted as occlusion. But at surgery, however, it was only compressed by the tumor.

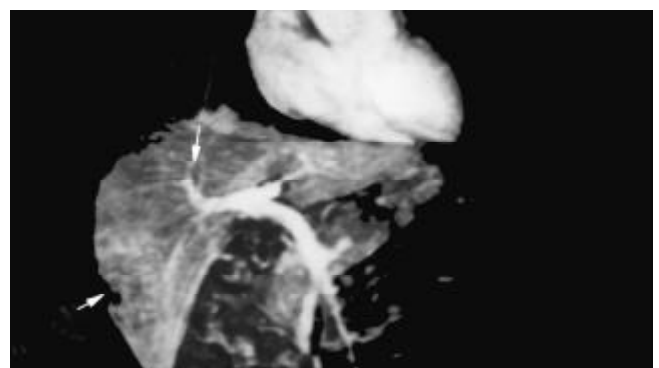


Figure 5 A patient with hepatocellular carcinoma in the right lobe (thick arrow). The normal right anterior portal vein (thin arrow) is misinterpreted as the right portal vein. But at surgery, the right posterior portal vein was involved by the tumor.

DISCUSSION

Hepatocellular carcinoma often invades the portal venous system^[22]. Once this system is involved, the prognosis and quality of life of the patients become extremely poor as a result of increased portal pressure, intrahepatic spread of the tumor, and deteriorated liver function^[22-24]. Traditionally, involvement of the main PV or the bifurcation of the PV is the indications of the unresectability. However, with the advances in surgical technique for hepatic resection, the survival of these patients can be prolonged by combination of hepatic resection, removal of tumor thrombi in the PV and post-operative transarterial embolization^[23]. The removal of tumor thrombi in the main PV can relieve portal hypertension, lower the risk of variceal bleeding and partially restore the liver function. Accordingly, prior to the appropriate surgical or interventional planning to be made, it is crucial to determine whether the portal venous system is patent or invaded and the site and the extent of the invasion.

In our results, 3D CE MRA was 98 % sensitive and 99 % specific in the diagnosis of the involvement of the main PV and its intrahepatic branches. The accuracy in depicting main PV involvement was 100 %. A minor compromise of positive predictive value (96 %) of 3D CE MRA was due to the false positive diagnosis for evaluation of the left PV. However, for the main and right PV, the positive predictive value reached 100 %. Using a technique similar to ours, Kreft *et al.*^[25] reported a sensitivity and specificity of 100 % and 98 % for identifying PV thrombosis in 36 patients.

US is currently the screening technique for the PV. Tessler *et al.*^[26] evaluated the main PV with color Doppler US in 215 patients and showed 9 of them with PV thrombosis. The sensitivity was 89 %, specificity was 92 %, negative predictive value was 98 %, and positive predictive value was 62 %. Bach *et al.*^[27] found that color Doppler US had a sensitivity of 93 %, specificity of 99 %, positive predictive value of 97 % and negative predictive value of 98 % for evaluation of the main, left and right PV in 63 patients with hepatic tumors. In a recent study by Marshall *et al.*^[28], microbubble contrast-enhanced color Doppler US was used to improve the visualization of the PV, but the accuracy was only 87 % for diagnosis of PV thrombosis in 15 patients. CT during arterial portography (CTAP) is also frequently employed to assess the portal venous system. According to Bach's study^[27], it gave a sensitivity of 90 %, specificity of 99 %, positive predictive value of 95 % and negative predictive value of 97 % for evaluation of the PV involvement. Compared with the findings using US or CTAP, our study showed that 3D CE MRA was more accurate in demonstration of the PV involvement by hepatic tumors, especially regarding its higher sensitivity. Although US is the first-choice imaging modality, it is observer dependent and sometimes hampered by patient's habitus and presence of bowel gas, ascites and heterogenous cirrhotic liver. When venous flow in patent PV was slow or stagnant, a PV thrombosis might be misdiagnosed. Similarly, false negative results might occur when flow was detected in a collateral vein and it was erroneously thought to be a patent main PV, which was actually thrombosed^[2,26-28]. Thus, 3D CE MRA should be a useful noninvasive alternative when the visualization of the PV on US was inadequate or when the involvement was suspected clinically but the US diagnosis was indeterminate. In comparison to CTAP, 3D CE MRA is readily acceptable by patients owing to its noninvasive nature, the lack of allergic reaction to iodine and the lack of radiation. With a higher sensitivity and equal specificity, 3D CE MRA can replace CTAP for evaluation of the PV.

Nevertheless, the two false positive results of 3D CE MRA in demonstration of the patency of the left PV indicate that the assessment of the left PV could be compromised by the

presence of large masses in left lobes. These masses caused substantial compression of the left PV. When collapsed, the left PV was underfilled with contrast medium injected from a peripheral vein and hardly distinguishable from the surrounding enhanced tumor. Therefore, 3D CE MRA had limitation in distinguishing compression of the small-caliber left PV from occlusion by tumor, which might adversely affect the surgical or interventional treatment options.

As for one false negative diagnosis occurred on the right PV, an anatomic variation of the PV found at surgery was thought to be the reason. In that case, the main PV trifurcated directly into the left and right anterior and right posterior PV at the porta hepatis. Although the right posterior PV was invaded by tumor, the right anterior PV was normal. On 3D CE MRA, we erroneously interpreted the normal right anterior PV as the right PV. In studies by Atri and Akgul *et al.*^[29,30], variation of the intrahepatic PV branching was common and trifurcation of the main PV could occur in 10.8 % and 12.3 % of patients respectively. As a result, the images of 3D CE MRA must be interpreted meticulously, with an understanding of the vascular anatomy and variation, and also with attention to the other potential sources of error noted above.

In summary, 3D CE MRA is an excellent noninvasive alternative to US for imaging the portal venous system. It is highly accurate in the evaluation of the PV involvement by hepatic tumors and is able to provide valuable information before surgery and interventional treatment for liver tumors.

REFERENCES

- 1 **Finn JP**, Kane RA, Edelman RR, Jenkins RL, Lewis WD, Muller M, Longmaid HE. Imaging of the portal venous system in patients with cirrhosis: MR angiography vs duplex Doppler sonography. *Am J Roentgenol* 1993; **161**: 989-994
- 2 **Pieters PC**, Miller PC, Demeo JH. Evaluation of the portal venous system: complementary roles of invasive and noninvasive imaging strategies. *Radiographics* 1997; **17**: 879-895
- 3 **Sahani D**, Saini S, Pena C, Nichols S, Prasad SR, Hahn PF, Halpern EF, Tanabe KK, Mueller PR. Using multidetector CT for preoperative vascular evaluation of liver neoplasms: technique and results. *Am J Roentgenol* 2002; **179**: 53-59
- 4 **Bradbury MS**, Kavanagh PV, Chen MY, Therese MW, Bechtold RE. Noninvasive assessment of portomesenteric venous thrombosis: current concepts and imaging strategies. *J Comput Assist Tomogr* 2002; **26**: 392-404
- 5 **Matsumoto A**, Kitamoto M, Lmamura M, Nakanishi T, Ono C, Ito K, Kajiyama G. Three-dimensional portography using multislice helical CT is clinically useful for management of gastric fundic varices. *Am J Roentgenol* 2001; **176**: 899-905
- 6 **Rodgers PM**, Ward J, Baudouin CJ, Ridgway JP, Robinson PJ. Dynamic contrast-enhanced MR imaging of the portal venous system: comparison with x-ray angiography. *Radiology* 1994; **191**: 741-745
- 7 **Parvey HR**, Raval B, Sandler CM. Portal vein thrombosis: Imaging findings. *Am J Roentgenol* 1994; **162**: 77-81
- 8 **Sakamoto I**, Hayashi K, Matsunaga N, Matsuoka Y, Uetani M, Fukuda T, Fujisawa H. Aortic dissection caused by angiographic procedures. *Radiology* 1994; **191**: 467-467
- 9 **Nghiem HV**, Freeny PC, Winter III, Mack LA, Yuan C. Phase-contrast MR angiography of the portal venous system: preoperative findings in liver transplant recipients. *Am J Roentgenol* 1994; **163**: 445-450
- 10 **Hughes LA**, Hartnell GG, Fin JP, Longmaid H, Volpe J, Wheeler H, Clouse M. Time-of-flight MR angiography of the portal venous system: value compared with other imaging procedures. *Am J Roentgenol* 1996; **166**: 375-378
- 11 **Burkart DJ**, Johnson CD, Morton MJ, Ehman RL. Phase-contrast MR angiography in chronic liver disease. *Radiology* 1993; **187**: 407-412
- 12 **Lomas DJ**, Britton PD, Alexander GJM, Calne RY. A comparison of MR and duplex doppler ultrasound for vascular assessment prior to orthotopic liver transplantation. *Clin radiol* 1994; **49**: 307-310

- 13 **Silverman JM**, Podesta L, Villamil F, Sher L, Vierling J, Rojter S, Lopez R, Rosenthal P, Woolf G, Memsic L, Herfkens R, Petrovich LM, Makowka L. Portal vein patency in candidates for liver transplantation: MR angiographic analysis. *Radiology* 1995; **197**: 147-152
- 14 **Laissy JP**, Trillaud H, Douek P. MR angiography: noninvasive vascular imaging of the abdomen. *Abdom imaging* 2002; **27**: 488-506
- 15 **Saddik D**, Frazer C, Robins P, Reed W, Stephen D. Gadolinium-enhanced three-dimensional MR portal venography. *Am J Roentgenol* 1999; **172**: 413-417
- 16 **Okumura A**, Watanabe Y, Dohke M, Ishimori T, Amoh Y, Oda K, Dodo Y. Contrast-enhanced three-dimensional MR portography. *Radiographics* 1999; **19**: 973-987
- 17 **Hawighorst H**, Schoenberg SO, Knopp MV, Essig M, Miltner P, van Kaick G. Hepatic lesions: morphological and functional characterization with multiphase breath-hold 3D gadolinium-enhanced MR angiography-initial results. *Radiology* 1999; **210**: 89-96
- 18 **Kopka L**, Rodenwaldt J, Vosshenrich R, Fischer U, Renner B, Lorf T, Graessner J, Ringe B, Grabbe E. Hepatic blood supply: comparison of optimized dual phase contrast-enhanced three-dimensional MR angiography and digital subtraction angiography. *Radiology* 1999; **211**: 51-58
- 19 **Leung DA**, Mckinnon GC, Davis CP, Pfammater T, Krestin GP, Debatin JF. Breath-hold, contrast-enhanced, three-dimensional MR angiography. *Radiology* 1996; **200**: 569-571
- 20 **Zeh H**, Choyke PL, Alexander HR, Bartlett D, Libutti SK, Chang R, Summers RM. Gadolinium-enhanced 3D MRA prior to isolated hepatic perfusion for metastases. *J Comput Assist Tomogr* 1999; **23**: 664-669
- 21 **Glockner JF**, Forauer AR, Solomon H, Varma CR, Perman WH. Three-dimensional gadolinium-enhanced MR angiography of vascular complication after liver transplantation. *Am J Roentgenol* 2000; **174**: 1447-1453
- 22 **Cedrone A**, Rapaccini GL, Pompili M, Aliotta A, Trombino C, DeLuca F, Caputo S, Gasbarrini G. Portal vein thrombosis complicating hepatocellular carcinoma. Value of ultrasound-guided fine-needle biopsy of the thrombus in the therapeutic management. *Liver* 1996; **16**: 94-98
- 23 **Tanaka A**, Morimoto T, Yamaoka Y. Implications of surgical treatment for advanced hepatocellular carcinoma with tumor thrombi in the portal vein. *Hepato-gastroenterology* 1996; **43**: 637-643
- 24 **Tang ZY**. Hepatocellular carcinoma-cause, treatment and metastasis. *World J Gastroenterol* 2001; **7**: 445-454
- 25 **Kreft B**, Strunk H, Flacke S, Wolff M, Conrad R, Gieseke J, Pauleit D, Bachmann R, Hirner A, Schild HH. Detection of thrombosis in the portal venous system: comparison of contrast-enhanced MR angiography with intraarterial digital subtraction angiography. *Radiology* 2000; **216**: 86-92
- 26 **Tessler FN**, Gehring BJ, Gomes AS, Perrella RR, Ragavendra N, Busuttill RW, Grant EG. Diagnosis of portal vein thrombosis: value of color Doppler imaging. *Am J Roentgenol* 1991; **157**: 293-296
- 27 **Bach AM**, Hann LE, Brown KT, Getrajdman GI, Herman SK, Fong Y, Blumgart LH. Portal vein evaluation with US: Comparison to angiography combined with CT arterial portography. *Radiology* 1996; **201**: 149-154
- 28 **Marshall MM**, Beese RC, Muiesan P, Sarma DI, O'Grady J, Sidhu PS. Assessment of portal venous system patency in the liver transplant candidate: a prospective study comparing ultrasound, microbubble-enhanced color Doppler ultrasound, with arteriography and surgery. *Clin Radiol* 2002; **57**: 377-383
- 29 **Atri M**, Bret PM, Fraser-Hill MA. Intrahepatic portal venous variations: prevalence with US. *Radiology* 1992; **184**: 157-158
- 30 **Akgul E**, Inal M, Soyupak S, Binokay F, Aksungur E, Oguz M. Portal venous variations. Prevalence with contrast-enhanced helical CT. *Acta Radiol* 2002; **43**: 315-319

Edited by Liu HX

Recombinant *Helicobacter pylori* catalase

Yang Bai, Ya-Li Zhang, Jian-Feng Jin, Ji-De Wang, Zhao-Shan Zhang, Dian-Yuan Zhou

Yang Bai, Ya-Li Zhang, Ji-De Wang, Dian-Yuan Zhou, PLA Institute for Digestive Medicine, Nanfang Hospital, the First Military Medical University, Guangzhou 510515, Guangdong Province, China
Jian-Feng Jin, Chemistry university of Beijing, Beijing 100071, China
Zhao-Shan Zhang, Institute of Biotechnology, Chinese Academy of Military Medical Sciences, Beijing 100071, China
Supported by the National Natural Science Foundation of China, No.30270078

Correspondence to: Dr Yang Bai, PLA Institute for Digestive Medicine, Nanfang Hospital, the First Military Medical University, Guangzhou 510515, Guangdong Province, China. baiyang1030@hotmail.com
Telephone: +86-20-61641532

Received: 2002-11-06 **Accepted:** 2002-12-07

Abstract

AIM: To construct a recombinant strain which highly expresses catalase of *Helicobacter pylori* (*H. pylori*) and assay the activity of *H. pylori* catalase.

METHODS: The catalase DNA was amplified from *H. pylori* chromosomal DNA with PCR techniques and inserted into the prokaryotic expression vector pET-22b (+), and then was transformed into the BL21 (DE3) *E. coli* strain which expressed catalase recombinant protein. The activity of *H. pylori* catalase was assayed by the Beers&Sizers.

RESULTS: DNA sequence analysis showed that the sequence of catalase DNA was the same as GenBank's research. The catalase recombinant protein amounted to 24.4 % of the total bacterial protein after induced with IPTG for 3 hours at 37 °C and the activity of *H. pylori* catalase was high in the BL21 (DE3) *E. coli* strain.

CONCLUSION: A clone expressing high activity *H. pylori* catalase is obtained, laying a good foundation for further studies.

Bai Y, Zhang YL, Jin JF, Wang JD, Zhang ZS, Zhou DY. Recombinant *Helicobacter pylori* catalase. *World J Gastroenterol* 2003; 9(5): 1119-1122

<http://www.wjgnet.com/1007-9327/9/1119.htm>

INTRODUCTION

Helicobacter pylori (*H. pylori*) is a bacillus first isolated from human gastric antral epithelium in 1982. It is recognized as a human-specific gastric pathogen that colonizes the stomachs of at least half of the world population^[1,2]. *H. pylori* infection is the major cause of chronic gastritis and peptic ulcer^[3-13], and is also closely related to adenocarcinoma of stomach and mucosa-associated lymphoid tissue (MALT) lymphoma and primary gastric non-Hodgkin's lymphoma^[14-32]. This organism was recently categorized as a class I carcinoma by the World Health Organization^[33], and direct evidence of carcinogenesis was recently demonstrated in an animal model^[34-36]. In addition, seroepidemiologic studies indicate that *H. pylori* infection is also associated with the occurrence of circulatory, respiratory and alimentary (except stomach and duodenum) system diseases and autoimmune diseases^[37-41]. With discoveries that

H. pylori may play an important role in many diseases, *H. pylori* is being studied thoroughly, especially the mechanism of escaping from host killing and clearing. Because of only escaping from host killing and clearing, *H. pylori* can locate in body steadily and cause diseases. The effect of catalase is emphasized increasingly in escaping from killing of host's free radical and sustaining the balance of self-oxygen metabolism. No study in expressing high activity *H. pylori* catalase had been reported in China and abroad. In this study, PCR technology was performed to obtain catalase gene, and construct expressing vectors. The sequence analysis and activity detection were performed in order to obtain the clone, effective expression and activity evaluation of catalase gene, thus laying a good foundation for further studying the associated functions.

MATERIALS AND METHODS

Plasmids and strains and growth conditions

Plasmid pET-22b (+) was obtained from Novagen. *Escherichia coli* (*E. coli*) DH5 α (Biodev) was used as a host for recombinant DNA manipulation, *E. coli* BL21 (DE3) was used for expression of the catalase gene. *H. pylori* was stored in this lab. *E. coli* was grown in Luria-Bertani medium containing 100 mg of ampicillin liter⁻¹.

Recombinant DNA techniques

All restriction enzyme digestions, ligations and other common DNA manipulations, unless otherwise stated, were performed by standard procedures. The genome of *H. pylori* was prepared from the cells collected from the colonies on the agar plate. The gene of *H. pylori* catalase was amplified from the genome of *H. pylori* by PCR (Techne PROGENE) using the primers cat1 (5' -TG GCC ATG GAT GTT AAT AAA GAT GTG AAA C-3') as upstream primer and cat2 (5' -AG TGC GGC CGC CTT TTT CTT TTT TGT GTG-3') as downstream primer as described in the literature^[42]. Cat1 and cat2 contained *Nco* I and *Not* I sites, respectively. The PCR product was recovered from agarose gel, digested with *Nco* I and *Not* I, and inserted into the *Nco* I and *Not* I restriction fragment of the expression vector pET-22b(+) using T4 DNA ligase. The resulting plasmid pET-CAT was transformed into competent *E. coli* BL21 (DE3) cells using ampicillin resistance for selection. The insert was confirmed using *Xho* I digestion to check for a 1.5-kb increase in size and *Nco* I and *Not* I digestion to show a 1.5-kb fragment.

Microbiological manipulations

Strain BL21 (DE3) BL21 (DE3) containing pET-22b(+)-CAT, was incubated overnight at 37 °C while shaking in 5 ml LB with 100 μ g/mL ampicilline. Fifty mL LB was inoculated and the cells grew until the optical density at 600nm reached 0.4-0.6. Isopropyl- β -D-thiogalactopyranoside (IPTG) was added to a final concentration of 1mM.

Enzyme assay

Catalase activity was assayed according to the modified method of Aebi. The assay was performed in a reaction mixture (1 ml) containing 10mM H₂O₂ in 50mM potassium phosphate buffer (pH 7.0, buffer B) at 30 °C. The rate of disappearance of H₂O₂ was measured spectrophotometrically at 240nm using a

Shimadzu UV-3000 spectrophotometer (Kyoto). One unit of catalase activity was defined as the amount of enzyme that decomposed 1 $\mu\text{mol H}_2\text{O}_2$ per minute under the assay conditions.

Preparation of cell fractionation

E. coli cells from a 50 mL growth 5 h after induction were harvested by centrifugation at $12\,000\times g$ for 10 min and the pellet was resuspended in 1 mL 30mM Tris buffer (pH8.0) containing 1 mmol/L EDTA (pH8.0), 20 % sucrose. The suspension was put on ice for 10 min, then centrifuged for 10 min at $12\,000\times g$, and the resulting supernatant contained proteins from the periplasm. The resulting pellet was resuspended in 5 mL 50mM Tris buffer (pH8.0) containing 2mM EDTA, 0.1 mg/mL lysozyme and 1 % Triton X-100. The suspension was incubated at 30 °C for 20 min and then sonicated on ice until it became clarified. The lysate was centrifuged at $12\,000\times g$ for 15 min at 4 °C, and the resulting supernatant contained proteins from the cytoplasm, while pelleted proteins were derived from inclusion bodies.

Optimization of expression

Induction of glycolate oxidase expression as a function of the concentration of IPTG: Seven flasks each with 50 mL medium containing 100 $\mu\text{g/mL}$ ampicillin were inoculated with BL21 (DE3) carrying plasmid pET-CAT. At OD_{600} of 0.6, expression of CAT was induced with IPTG, of which the concentrations were 0, 0.1, 0.2, 0.4, 0.6, 0.8, 1.0mM, respectively. After 5 hours the cells were harvested, crude extracts were compared by SDS-gel electrophoresis. CAT activity of the cells was determined as described above.

Induction of glycolate oxidase expression as a function of cell density: Three flasks each with 50 mL medium containing 100 $\mu\text{g/mL}$ ampicillin were inoculated with BL21 (DE3) carrying plasmid pET-CAT. At OD_{600} of 0.4, 0.6 and 1.0, respectively, expression of CAT was induced with IPTG (final concentration 0.2mM). After 5 hours cells were harvested, crude extracts were compared and CAT activity was determined as described above.

RESULTS

Cloning of *H. pylori* catalase gene

The *H. pylori* catalase gene was amplified by PCR using the *H. pylori* genome as the template and cloned into plasmid pET-22b(+). The recombinant plasmids pET-CAT were all digested by Xho I, and by Nco I and Not I simultaneously, then digestive products were visualized on $10\text{ g}\cdot\text{L}^{-1}$ agarose gel electrophoreses (Figure 1). It demonstrated that recombinant plasmid contained the objective gene. The DNA sequencing proved that the entire sequence of the gene was consistent with the results reported before^[42].

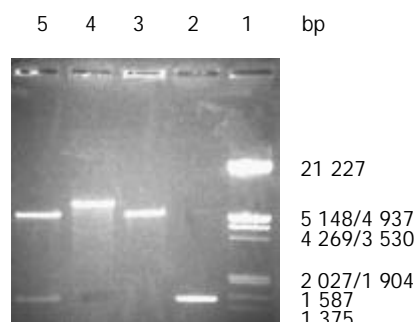


Figure 1 Agarose gel electrophoresis of PCR products and plasmid pET-CAT digested with restriction enzymes. Lane 1: DNA marker; Lane 2: PCR product; Lane 3: pET-22b (+) / Xho I; Lane 4: pET-CAT / Xho I; Lane 5: pET-CAT / NcoI + NotI.

Expression of *H. pylori* catalase in *E. coli*

Following recombinant vector transformed into BL21 *E. coli* strains, recombinant *E. coli* strains expressing catalase were obtained. The expressed protein amounted to 24.4 % of the total bacterial protein after induced with IPTG for 3 h at 37 °C. Its molecular mass was M_r 58 000 by 100 g/L SDS-PAGE gel analysis. After preparation of cell fractionation, the expressed protein amounted to 11.5 % of the bacterial periplasm protein, 14.9 % of the bacterial sonicate supernatant and 58.1 % of the bacterial inclusion body (Figure 2).

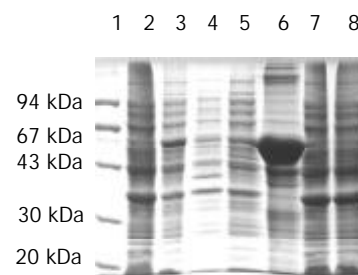


Figure 2 SDS-PAGE analysis of catalase recombinant protein expressed in BL21 (DE3). Lane 1: Molecular weight marker ($20, 30, 43, 67, 94$) $\times 10^3$; Lane 2: BL21 (pET-CAT) cells before induction; Lane 3: BL21 (pET-CAT) cells after 3 h induction with IPTG; Lane 4: BL21 (pET-CAT) cells periplasm protein after 3 h induction with IPTG; Lane 5: sonicate supernatant of BL21 (pET-CAT) cells after 3 h induction with IPTG; Lane 6: inclusion body of BL21 (pET-CAT) cells after 3 h induction with IPTG; Lane 7: control strain BL21 (pET) before induction; Lane 8: control strain BL21 (pET) after 3 h induction with IPTG.

Optimization of expression

An important factor that might affect the expression is the concentration of the inducer. Since IPTG is a rather costly component we decided to investigate the dependency of the expression system on the IPTG concentration. We found that in the range of 0.1-1 mM final concentration of IPTG, the expression level was independent of the inducer concentration, and the catalase activity of the whole cells was from 633.6 U/mg cells (dry weight) to 660.1 U/mg cells (dry weight). The data are shown in Table 1.

Table 1 Induction of glycolate oxidase expression at different IPTG concentrations

IPTG concentration (mM)	0.1	0.2	0.4	0.6	0.8	1.0
Activity (U/mg cells (dry weight))	638.5	653.6	660.1	642.3	646.7	631.2

In order to further optimize the conditions for expression we induced the bacterial cultures at various cell densities. The expression was the highest at $\text{OD}_{600}=0.6$, and at the same time the activity was also optimal at $\text{OD}_{600}=0.6$, (Table 2).

Table 2 Induction of *H. pylori* catalase expression at different cell densities

Induction at OD_{600}	Activity (U/mg cells (dry weight))
0.4	603.2
0.6	661.2
1.0	584.1

DISCUSSION

For a long time, people had presumed that transferring poisonous oxygen metabolite into nonpoisonous water,

sustaining self-metabolite equilibrium and protecting *H. pylori* from the killing of neutrophilic leukocyte were the main functions of *H. pylori* catalase^[43]. However, Bauerfeind *et al.* found that *H. pylori* catalase accounts only for 1.5 %, while urease accounts for 10 % of thallus' s gross protein at pH 6 or 7. The activity of urease could not be detected at pH 5. On the other hand, the activity of catalase is still sustained at pH 3. This finding indicated that catalase may play a more important role than urease when *H. pylori* survives in an acid environment^[44]. In addition, recent studies found that catalase may play an important role in preventing *H. pylori* from bacillus to coccus^[45-47].

Most interestingly, Radcliff *et al.* have suggested that the protective rate of natural catalase can reach 80 %, while that of recombinant catalase can reach 90 %, based on their animal experiments, which indicated that catalase is a new antigen for the preparation of *H. pylori* vaccine^[42].

Overall, further studies on catalase are essential, in order to understand the effect of catalase on *H. pylori* mechanism of causing disease, as well as immune prevention and treatment. In this study, *H. pylori* catalase gene was cloned and inserted into fused cloning strain, which was demonstrated by catalase activity. An important experimental basis for further studies on mechanism of catalase causing disease, and immune protective effects has been laid.

Plasmid pET-22b(+) was a secretion vector and the foreign protein was transported into periplasm directed by the signal peptide Pel B. Soluble and functional expression of catalase was achieved by secreting the recombinant protein to periplasm, which provided an environment favorable for the folding of this protein. These may explain why the cloning strain has the high activity. The high activity of the cloning strain may provide better measures to treat diseases caused by free radicals, such as sequela radiotherapy on neoplasm, all kinds of phlogosis, several kinds of dermatosis, second perfusion in open cardiac operation and so on.

REFERENCES

- 1 **Michetti P**, Kreiss C, Kotloff K, Porta N, Blanco JL, Bachmann D, Herranz M, Saldinger P, Cortesy-Theulaz I, Losonsky G, Nichols R, Simon J, Stolte M, Ackerman S, Monath TP, Blum AL. Oral immunization with urease and Escherichia coli heat-labile enterotoxin is safe and immunogenic in *Helicobacter pylori*-infected adults. *Gastroenterology* 1999; **116**: 804-812
- 2 **Xu CD**, Chen SN, Jiang SH, Xu JY. Seroepidemiology of *Helicobacter pylori* infection among asymptomatic Chinese children. *World J Gastroenterol* 2000; **6**: 759-761
- 3 **Xiao SD**, Liu WZ. Current status in treatment of *Hp* infection. *Shijie Huaren Xiaohua Zazhi* 1999; **7**: 3-4
- 4 **Jiang Z**, Tao XH, Huang AL, Wang PL. A study of recombinant protective *H. pylori* antigens. *World J Gastroenterol* 2002; **8**: 308-311
- 5 **Meyer JM**, Silliman NP, Dixon CA, Siepmann NY, Sugg JE, Hopkins RJ. *Helicobacter pylori* and early duodenal ulcer status post-treatment: a review. *Helicobacter* 2001; **6**: 84-92
- 6 **Xia HX**, Fan XG, Talley Nicholas J. Clarithromycin resistance in *Helicobacter pylori* and its clinical relevance. *World J Gastroenterol* 1999; **5**: 263-265
- 7 **Peng ZS**, Liang ZC, Liu MC, Ouang NT. Studies on gastric epithelial cell proliferation and apoptosis in *Hp* associated gastric ulcer. *Shijie Huaren Xiaohua Zazhi* 1999; **7**: 218-219
- 8 **Vandenplas Y**. *Helicobacter pylori* infection. *World J Gastroenterol* 2000; **6**: 20-31
- 9 **Casella G**, Buda CA, Maisano R, Schiavo M, Perego D, Baldini V. Complete regression of primary gastric MALT-lymphoma after double eradication *Helicobacter pylori* therapy: role and importance of endoscopic ultrasonography. *Anticancer Res* 2001; **21**: 1499-1502
- 10 **Kate V**, Ananthakrishnan N, Badrinath S. Effect of *Helicobacter pylori* eradication on the ulcer recurrence rate after simple closure of perforated duodenal ulcer: retrospective and prospective randomized controlled studies. *Br J Surg* 2001; **88**: 1054-1058
- 11 **Hobsley M**, Tovey FI. *Helicobacter pylori*: the primary cause of duodenal ulceration or a secondary infection? *World J Gastroenterol* 2001; **7**: 149-151
- 12 **Hou P**, Tu ZX, Xu GM, Gong YF, Ji XH, Li ZS. *Helicobacter pylori* vacA genotypes and cagA status and their relationship to associated diseases. *World J Gastroenterol* 2000; **6**: 605-607
- 13 **Zhang H**, Jiang SL, Yao XX. Study of T-lymphocyte subsets, nitric oxide, hexosamine and *Helicobacter pylori* infection in patients with chronic gastric diseases. *World J Gastroenterol* 2000; **6**: 601-604
- 14 **Guo CQ**, Wang YP, Ma SW, Ding GY, Li LC. Study on *Helicobacter pylori* infection and P53, c-erbB-2 gene expression in carcinogenesis of gastric mucosa. *Shijie Huaren Xiaohua Zazhi* 1999; **7**: 313-315
- 15 **Hiyama T**, Haruma K, Kitadai Y, Masuda H, Miyamoto M, Ito M, Kamada T, Tanaka S, Uemura N, Yoshihara M, Sumii K, Shimamoto F, Chayama K. Clinicopathological features of gastric mucosa-associated lymphoid tissue lymphoma: a comparison with diffuse large B-cell lymphoma without a mucosa-associated lymphoid tissue lymphoma component. *J Gastroenterol Hepatol* 2001; **16**: 734-739
- 16 **Quan J**, Fan XG. Progress in experimental research of *Helicobacter pylori* infection and gastric carcinoma. *Shijie Huaren Xiaohua Zazhi* 1999; **7**: 1068-1069
- 17 **Delchier JC**, Lamarque D, Levy M, Tkoub EM, Copie-Bergman C, Deforges L, Chaumette MT, Haioun C. *Helicobacter pylori* and gastric lymphoma: high seroprevalence of CagA in diffuse large B-cell lymphoma but not in low-grade lymphoma of mucosa-associated lymphoid tissue type. *Am J Gastroenterol* 2001; **96**: 2324-2328
- 18 **Hua JS**. Effect of *Hp*: cell proliferation and apoptosis on stomach cancer. *Shijie Huaren Xiaohua Zazhi* 1999; **9**: 647-648
- 19 **Hu PJ**. *Hp* and gastric cancer: challenge in the research. *Shijie Huaren Xiaohua Zazhi* 1999; **7**: 1-2
- 20 **Gao HJ**, Yu LZ, Bai JF, Peng YS, Sun G, Zhao HL, Miu K, Lü XZ, Zhang XY, Zhao ZQ. Multiple genetic alterations and behavior of cellular biology in gastric cancer and other gastric mucosal lesions: *H. pylori* infection, histological types and staging. *World J Gastroenterol* 2000; **6**: 848-854
- 21 **Yao YL**, Zhang WD. Relation between *Helicobacter* and gastric cancer. *Shijie Huaren Xiaohua Zazhi* 2001; **9**: 1045-1049
- 22 **Nakamura S**, Matsumoto T, Suekane H, Takeshita M, Hizawa K, Kawasaki M, Yao T, Tsuneyoshi M, Iida M, Fujishima M. Predictive value of endoscopic ultrasonography for regression of gastric low grade and high grade MALT lymphomas after eradication of *Helicobacter pylori*. *Gut* 2001; **48**: 454-460
- 23 **Uemura N**, Okamoto S, Yamamoto S, Matsumura N, Yamaguchi S, Yamakido M, Taniyama K, Sasaki N, Schlemper RJ. *Helicobacter pylori* infection and the development of gastric cancer. *N Engl J Med* 2001; **345**: 784-789
- 24 **Morgner A**, Miehle S, Fischbach W, Schmitt W, Muller-Hermelink H, Greiner A, Thiede C, Schetelig J, Neubauer A, Stolte M, Ehninger G, Bayerdorffer E. Complete remission of primary high-grade B-cell gastric lymphoma after cure of *Helicobacter pylori* infection. *J Clin Oncol* 2001; **19**: 2041-2048
- 25 **Zhuang XQ**, Lin SR. Progress in research on the relationship between *Hp* and stomach cancer. *Shijie Huaren Xiaohua Zazhi* 2000; **8**: 206-207
- 26 **Wang RT**, Wang T, Chen K, Wang JY, Zhang JP, Lin SR, Zhu YM, Zhang WM, Cao YX, Zhu CW, Yu H, Cong YJ, Zheng S, Wu BQ. *Helicobacter pylori* infection and gastric cancer: evidence from a retrospective cohort study and nested case-control study in China. *World J Gastroenterol* 2002; **8**: 1103-1107
- 27 **Yao YL**, Xu B, Song YG, Zhang WD. Overexpression of cyclin E in Mongolian gerbil with *Helicobacter pylori*-induced gastric precancerosis. *World J Gastroenterol* 2002; **8**: 60-63
- 28 **Morgner A**, Miehle S, Stolte M, Neubauer A, Alpen B, Thiede C, Klann H, Hierlmeier FX, Ell C, Ehninger G, Bayerdorffer E. Development of early gastric cancer 4 and 5 years after complete remission of *Helicobacter pylori* associated gastric low grade marginal zone B cell lymphoma of MALT type. *World J Gastroenterol* 2001; **7**: 248-253
- 29 **Miehle S**, Kirsch C, Dragosics B, Gschwantler M, Oberhuber G, Antos D, Dite P, Lauter J, Labenz J, Leodolter A, Malfertheiner P, Neubauer A, Ehninger G, Stolte M, Bayerdorffer E. *Helicobacter pylori* and gastric cancer: current status of the Austrain Czech

- German gastric cancer prevention trial (PRISMA Study). *World J Gastroenterol* 2001; **7**: 243-247
- 30 **Zhuang XQ**, Lin SR. Research of *Helicobacter pylori* infection in precancerous gastric lesions. *World J Gastroenterol* 2000; **6**: 428-429
- 31 **Cai L**, Yu SZ, Zhang ZF. *Helicobacter pylori* infection and risk of gastric cancer in Changle County, Fujian Province, China. *World J Gastroenterol* 2000; **6**: 374-376
- 32 **Liu WZ**, Zheng X, Shi Y, Dong QJ, Xiao SD. Effect of *Helicobacter pylori* infection on gastric epithelial proliferation in progression from normal mucosa to gastric carcinoma. *World J Gastroenterol* 1998; **4**: 246-248
- 33 **Suganuma M**, Kurusu M, Okabe S, Sueoka N, Yoshida M, Wakatsuki Y, Fujiki H. *Helicobacter pylori* membrane protein 1: a new carcinogenic factor of *Helicobacter pylori*. *Cancer Res* 2001; **61**: 6356-6359
- 34 **Goto T**, Nishizono A, Fujioka T, Ikewaki J, Mifune K, Nasu M. Local secretory immunoglobulin A and postimmunization gastritis correlated with protection against *Helicobacter pylori* infection after oral vaccination of mice. *Infect Immun* 1999; **67**: 2531-2539
- 35 **Watanabe T**, Tada M, Nagai H, Sasaki S, Nakao M. *Helicobacter pylori* infection induces gastric cancer in Mongolian Gerbils. *Gastroenterology* 1998; **115**: 642-648
- 36 **Honda S**, Fujioka T, Tokieda M, Satoh R, Nishizono A, Nasu M. Development of *Helicobacter pylori*-induced gastric carcinoma in Mongolian Gerbils. *Cancer Res* 1998; **58**: 4255-4259
- 37 **Bulajic M**, Stimec B, Milicevic M, Loehr M, Mueller P, Boricic I, Kovacevic N, Bulajic M. Modalities of testing *Helicobacter pylori* in patients with nonmalignant bile duct diseases. *World J Gastroenterol* 2002; **8**: 301-304
- 38 **Pena A**. Genetic factors determining the host response to *Helicobacter pylori*. *World J Gastroenterol* 2000; **6**: 624-625
- 39 **Gocyk W**, Niklinski T, Olechnowicz H. *Helicobacter pylori*, gastrin and cyclooxygenase-2 in lung cancer. *Med Sci Monit* 2000; **6**: 1085-1092
- 40 **Tsai CJ**, Huang TY. Relation of *Helicobacter pylori* infection and angiographically demonstrated coronary artery disease. *Dig Dis Sci* 2000; **45**: 1227-1232
- 41 **Dauden E**, Jimenez A I, Garcia D A. *Helicobacter pylori* and idiopathic chronic urticaria. *Int J Dermatol* 2000; **39**: 446-452
- 42 **Radcliff FJ**, Hazell SL, Kolesnikow T. Catalase, a novel antigen for *Helicobacter pylori* vaccination. *Infect Immun* 1997; **65**: 4668-4674
- 43 **Nilius M**, Malfertheiner P. *Helicobacter pylori* enzymes. *Aliment Pharmacol Ther* 1996; **10**: 65-71
- 44 **Bauerfeind P**, Garner R, Dunn BE. Synthesis and activity of *Helicobacter pylori* urease and catalase at low Ph. *Gut* 1997; **40**: 25-30
- 45 **She FF**, Su DH, Lin JY, Zhou LY. Virulence and potential pathogenicity of coccoid *Helicobacter pylori* induced by antibiotics. *World J Gastroenterol* 2001; **7**: 254-258
- 46 **Khin MM**, Hua JS, Ng HC, Wadstrom T, Bow H. Agglutination of *Helicobacter pylori* coccoids by lectins. *World J Gastroenterol* 2000; **6**: 202-209
- 47 **Nakamura A**, Park A, Nagata K. Oxidative cellular damage associated with transformation of *Helicobacter pylori* from a bacillary to a coccoid form. *Free Radic Biol Med* 2000; **28**: 1611-1618

Edited by Ma JY

Effects of antireflux treatment on bronchial hyper-responsiveness and lung function in asthmatic patients with gastroesophageal reflux disease

Shan-Ping Jiang, Rui-Yun Liang, Zhi-Yong Zeng, Qi-Liang Liu, Yong-Kang Liang, Jian-Guo Li

Shan-Ping Jiang, Rui-Yun Liang, Qi-Liang Liu, Yong-Kang Liang, Jian-Guo Li, Department of Respiratory Medicine, The Second Affiliated Hospital, Sun Yat-Sen University, Guangzhou 510120, Guangdong Province, China

Zhi-Yong Zeng, Department of Gastroenterology, The Second Affiliated Hospital, Sun Yat-Sen University, Guangzhou 510120, Guangdong Province, China

Correspondence to: Professor Shan-Ping Jiang, Department of respiratory Medicine, The Second Affiliated Hospital, Sun Yat-sen University, 107 Yanjiang West Road, Guangzhou 510120, Guangdong Province China. zengzhiyong99@hotmail.com

Telephone: +86-20-81332441 **Fax:** +86-20-81332441

Received: 2002-12-22 **Accepted:** 2003-01-16

Abstract

AIM: To investigate the effects of antireflux treatment on bronchial hyper-responsiveness and lung function in asthmatic patients with gastroesophageal reflux disease (GERD).

METHODS: Thirty asthmatic patients with GERD were randomly divided into two groups (group A and group B). Patients in group A ($n=15$) only received asthma medication including inhaled salbutamol 200 μg four times a day and budesonide 400 μg twice a day for 6 weeks. Patients in Group B ($n=15$) received the same medication as group A, and also antireflux therapy including oral omeprazole 20 mg once a day and domperidone 10 mg three times a day for 6 weeks. Pulmonary function tests and histamine bronchoprovocation test were performed before and after the study.

RESULTS: There was no significant difference in the baseline values of pulmonary function and histamine $\text{PC}_{20\text{-FEV}_1}$ between the two groups. At the end of the study, the mean values for VC, VC%, FVC, FVC%, FEV₁, FEV₁%, PEF, PEF%, $\text{PC}_{20\text{-FEV}_1}$ were all significantly improved in group B, compared with group A.

CONCLUSION: Antireflux therapy may improve pulmonary function and inhibit bronchial hyper-responsiveness in asthmatic patients with GERD.

Jiang SP, Liang RY, Zeng ZY, Liu QL, Liang YK, Li JG. Effects of antireflux treatment on bronchial hyper-responsiveness and lung function in asthmatic patients with gastroesophageal reflux disease. *World J Gastroenterol* 2003; 9(5): 1123-1125
<http://www.wjgnet.com/1007-9327/9/1123.htm>

INTRODUCTION

Bronchial asthma is likely to be associated with gastroesophageal reflux disease (GERD). Bronchial hyper-responsiveness is one of the characteristics of asthma.

Numerous observations have suggested that GERD may be causally related to the reactive airways condition, and may at least be a trigger causing airways to react^[1-4]. Our study was carried out to determine the effects of antireflux treatment on bronchial hyper-responsiveness and lung function in asthmatic patients with GERD.

MATERIALS AND METHODS

Thirty asthmatic patients with GERD were included in our study. All patients were recruited in the Second Affiliated Hospital Sun Yat-Sen University from December 2000 to December 2001. The diagnosis of asthma was established according to the Global Initiative for Asthma issued by the National Heart, Lung, and Blood Institute. The presence of GERD was determined in accordance with below standards^[5]: typical clinical symptom of GERD such as postprandial chest pain and sour regurgitation, signs of erosive esophagitis shown by barium esophagogram and/or lower esophageal erosions shown by endoscopic examination and mucosal biopsy.

The patients were randomly divided into two groups. Group A included 15 patients (7 men, 8 women; range of age 23-60 years, mean 34.9 ± 19.2 years), with duration of asthma ranging from 1-19 years (mean 8.2 ± 6.3 years). Group B included 15 patients (6 men, 9 women; range of age 20-65 years, mean 35.6 ± 17.4 years), with duration of asthma ranging from 1-25 years (mean 7.8 ± 6.1 years). There was no significant difference in age, sex, and duration of asthma between these two groups.

Patients in group A only received asthma medication which included inhaled salbutamol 200 μg four times a day and budesonide 400 μg twice a day for 6 weeks. Patients in Group B received the same medication as group A, and also antireflux therapy which included oral omeprazole 20 mg once a day and domperidone 10 mg three times a day for 6 weeks. Pulmonary function tests and histamine bronchoprovocation test were performed before and at the end of the medications.

Pulmonary function tests included vital capacity (VC), forced vital capacity (FVC), forced expiratory volume at the first second (FEV₁), and the peak expiratory flow rate (PEF), and the percentage of the above parameters over the predicted values (i.e. VC%; FVC%; FEV₁% and PEF%). Bronchial hyper-responsiveness was detected by histamine bronchoprovocation test (HIT). Briefly, the patients were asked to orderly inhale a series of histamine solutions with increasing concentrations ranging from 0.03, 0.06, 0.12, 0.24, 0.48, 1, 2, 4 to 8 g/L for two minutes with an interval of 5 minutes. Every 30 seconds and 90 seconds after each inhalation, FEV₁ was detected. The test was stopped when FEV₁ fell by 20 % from baseline value. Histamine- $\text{PC}_{20\text{-FEV}_1}$, the concentration of histamine required to produce a 20 % fall from baseline in FEV₁, calculated from Cockcroft formula^[6], represented the degree of bronchial responsiveness. Pulmonary function tests and inhaled histamine bronchoprovocation test were performed with the Spiroanalyzer ST-300, Fukuda Sangyo, Japan.

Statistical analysis

The differences of mean values \pm SD were determined by *t* test. The distribution of frequency of histamine PC_{20-FEV1} was skewed distribution. When the values were expressed as geometric mean, it became a normal distribution. A *P* value of < 0.05 was considered statistically significant.

RESULTS

There was no significant difference in the baseline values of pulmonary function and histamine PC_{20-FEV1} between the two groups. At the end of the study, the mean values for VC, VC%, FVC, FVC%, FEV₁, FEV₁%, PEF, PEF%, PC_{20-FEV1} did not change significantly in group A, while in group B the mean values for VC, VC%, FVC, FVC%, FEV₁, FEV₁%, PEF, PEF%, PC_{20-FEV1} all significantly increased. Also, at the end of the study, the mean values for above indices were all significantly higher in group B than in group A. The changes in pulmonary function and bronchial responsiveness were showed in Table 1.

Table 1 Changes in pulmonary function and bronchial responsiveness in asthmatic patients with GERD (mean values \pm SD)

Index	Group A n=15		Group B n=15	
	Before therapy	After therapy	Before therapy	After therapy
VC(L)	2.9 \pm 0.4	2.7 \pm 0.9	2.8 \pm 0.7	3.7 \pm 0.7 ^{ab}
VC%	86.3 \pm 14.6	85.9 \pm 1.9	84.9 \pm 18.9	111.2 \pm 13.6 ^{ab}
FVC(L)	2.9 \pm 0.6	2.7 \pm 0.8	2.8 \pm 0.4	3.6 \pm 0.9 ^{ab}
FVC%	88.4 \pm 19.2	85.1 \pm 23.6	86.3 \pm 21.7	102.6 \pm 16.1 ^{ab}
FEV ₁ (L)	2.3 \pm 0.9	2.4 \pm 0.6	2.2 \pm 0.8	2.8 \pm 0.5 ^{ab}
FEV ₁ %	76.8 \pm 11.6	77.5 \pm 16.3	75.6 \pm 14.5	84.6 \pm 12.7 ^{ab}
PEF(L/S)	4.4 \pm 1.5	4.8 \pm 1.7	4.6 \pm 1.2	5.9 \pm 1.6 ^{ab}
PEF%	74.8 \pm 19.6	75.1 \pm 16.3	70.5 \pm 20.4	85.1 \pm 23.1 ^{ab}
PC _{20-FEV1} (g/L)	0.31 \pm 0.11	0.28 \pm 0.16	0.33 \pm 0.14	0.84 \pm 0.22 ^{ab}

^a*P* < 0.05 vs. group A after therapy, the *t* values were 2.34, 2.59, 2.31, 2.55, 2.49, 2.26, 2.63, 2.22, and 2.68, respectively. ^b*P* < 0.01 vs. group B before therapy, the *t* values were 3.93, 4.16, 3.87, 4.04, 3.95, 3.62, 4.46, 3.98, and 4.33, respectively.

DISCUSSION

It has been indicated that there is a causal relationship between asthma and GERD: asthma may cause or precipitate GERD and vice versa, and so much as a vicious cycle^[11-13]. On one hand, asthma may be the cause of GERD in some patients. Prolonged period of cough, wheezing and greater respiratory muscle effort in asthma increase abdominal pressure, and facilitate the movement of gastric secretions towards the lower esophageal sphincter (LES). Moreover, the diaphragm's contribution to sphincter tone is decreased in asthma. Furthermore, bronchodilator therapies (both beta-agonists and theophylline) appear to reduce LES pressure^[7]. It has become clear that the pressure gradient across the LES is increased in asthma, which promotes the development of GERD.

On the other hand, GERD may cause or facilitate asthma. Mechanisms of bronchospasm inspired by reflux include^[8,9]: (1) acid in the inflamed esophagus may stimulate exposed acid sensitive receptors which act through vagal afferents to the airways to cause an increase in bronchial hyper-responsiveness which leads to bronchoconstriction; (2) microaspiration, with stimulation of upper-airway vagal receptor, causes bronchoconstriction; and (3) microaspiration of gastric contents into the lung results into exudative mucosal reaction.

GERD has been found to occur in 30-80 % of asthmatic

patients. Kiljander *et al* found that the prevalence of GERD in asthmatic patients is 53 %^[11]. Dal Negro *et al* reported that GERD was found in 78.9 % of atopic asthmatic patients^[12]. Sontag *et al* demonstrated that more than 80 % of asthmatic patients had abnormal GERD^[13]. A number of authors have suggested that some factors may be associated with an increased risk for the development of GERD in asthmatic patients, and thus further diagnostic tests should be proposed to evaluate the presence of GERD in such patients. These factors include^[10]: (1) asthma of adult onset; (2) asthmatic symptoms that are largely or predominantly nocturnal; (3) large meals, which might cause or worsen cough and wheezing; (4) asthma of non-smokers; (5) sour dietary and drinks that can cause cough and wheezing; (6) non-allergic (it may be changed to no allergen identified); (7) responders to antacid therapy; and (8) steroid resistant asthma.

Many diagnostic tests have been used to prove the presence of GERD, including barium esophagogram, endoscopic examination and mucosal biopsy, measurement of the LES pressure, esophageal acid perfusion tests, gastroesophageal scintiscan, and twenty-four-hour esophageal PH monitoring.

In 1985, Barish *et al* established a series of procedures to determine the prevalence of GERD in asthmatic patients^[5] including barium esophagogram, endoscopic examination, mucosal biopsy and measurement of the LES pressure. It was suggested that GERD be definitely diagnosed if there are two positive results from above examinations. Otherwise, ambulatory 24-hour esophageal PH monitoring can be used as the gold standard to determine the prevalence of GERD^[14,15]. However, Barish *et al* emphasized that this test should only be used in cases with diagnostic difficulties because of long time of catheter inserting or shortage of equipment^[5]. David *et al* established that in patients with predominant reflux symptoms and supportive evidence from endoscopy, the diagnosis of GERD was straightforward^[10]. Allescher *et al* suggested that in patients with persistent reflux problems and erosive reflux esophagitis indicated by endoscopy, the diagnosis of GERD was certain^[17]. Hollenz *et al* also proposed that gastroesophageal reflux was diagnosed when endoscopy revealed typical esophageal lesions^[16]. In some uncertain cases, 24-hour pH monitoring can be used to verify and objectify an acid gastroesophageal reflux^[17].

All the thirty cases in our study had classic symptoms of GERD and positive signs by both barium esophagogram and endoscopic examination. Therefore, the presence of GERD is certain.

A variety of different treatments aiming at the improvement of reflux symptoms have been used in adult asthmatic patients with GERD. Most investigators^[10,18] have suggested the three-step procedures. The first step includes elevation of the head of the beds 15-20 cm, no eating or drinking for three hours before sleeping, avoidance of large meals, weight loss, restricted consumption of caffeine, alcohol, spicy foods and chocolate and no smoking. The second step consists of medical management including antacids, H₂-receptor antagonists, proton pump inhibitors, pro-kinetic agents and cytoprotective agents. The third step consists of surgical management. In asthmatic patients with GERD, many studies have indicated that medical antireflux therapy can improve the symptoms of asthma. Harding *et al* reported improvements in both symptoms and pulmonary function in asthmatic patients with GERD after antireflux therapy^[19]. Levin *et al* demonstrated that omeprazole improved PEF and quality of life in asthmatic patients with GERD^[20]. Teichtahl *et al* found that omeprazole therapy significantly increased evening PEF in asthmatic patients with GERD^[21]. Meier *et al* indicated that medical antireflux therapy by omeprazole might predispose to improve respiratory function in asthmatics with GERD^[22]. Our observation also

demonstrated that antireflux medications could make an obvious favor in the improvement of pulmonary function and inhibition of bronchial hyper-responsiveness in asthmatic patients with GERD. These results provide strong evidence that GERD can precipitate asthma. Therefore, in such subset of patients, elimination of GERD may be proven to be especially beneficial.

In patients with GERD, esophageal acid exposure is reduced by up to 80 % with H₂-receptor antagonists and up to 95 % with proton pump inhibitors^[10]. So, proton pump inhibitors are superior to H₂-receptor antagonists. In addition, pro-kinetic agents also decrease GERD by improving gastric emptying.

In conclusion, our observations indicate that antireflux therapy by proton pump inhibitors and pro-kinetic agents is beneficial to asthmatic patients with GERD.

REFERENCES

- 1 **Larrain A**, Carrasco E, Galleguillos F, Sepulveda R, Pope CE 2nd. Medical and surgical treatment of non-allergic asthma associated with gastroesophageal reflux. *Chest* 1991; **99**: 1330-1335
- 2 **Sontag S**, O'Connell S, Greenlee H, Schnell T, Chintam R, Nemchausky B, Chejfec G, Van Drunen M, Wanner J. Is gastroesophageal reflux a factor in some asthmatics? *Am J Gastroenterol* 1987; **82**: 119-126
- 3 **Tuchman DN**, Boyle JT, Pack AI, Schwartz J, Kokonos M, Spitzer AR, Cohen S. Comparison of airway response following tracheal or esophageal acidification in the cat. *Gastroenterology* 1984; **87**: 872-881
- 4 **Mansfield LE**, Hameister HH, Spaulding HS, Smith NJ, Glab N. The role of the vagus nerve in airway narrowing caused by intraesophageal hydrochloric acid provocation and esophageal distension. *Ann Allergy* 1981; **47**: 431-434
- 5 **Barish CF**, Wu Wc, Castell DO. Respiratory complications of gastroesophageal reflux. *Arch Intern Med* 1985; **145**: 1882-1888
- 6 **Cockcroft DW**, Murdock KY, Mink JT. Determination of histamine PC₂₀. Comparison of linear and logarithmic interpolation. *Chest* 1983; **84**: 505-506
- 7 **Field SK**, Underwood M, Brant R, Cowie RL. Prevalence of gastroesophageal reflux symptoms in asthma. *Chest* 1996; **109**: 316-322
- 8 **Harding SM**. Gastroesophageal reflux, asthma, and mechanisms of interaction. *Am J Med* 2001; **111**(Suppl 8A): 8S-12S
- 9 **Sontag SJ**. Gastroesophageal reflux and asthma. *Am J Med* 1997; **103**(5A): 84S-90S
- 10 **Bowrey DJ**, Peters JH, DeMeester TR. Gastroesophageal reflux disease in asthma: effects of medical and surgical antireflux therapy on asthma control. *Ann Surg* 2000; **231**: 161-172
- 11 **Kiljander TO**, Salomaa ER, Hietanen EK, Terho EO. Gastroesophageal reflux in asthmatics: A double-blind, placebo-controlled crossover study with omeprazole. *Chest* 1999; **116**: 1257-1264
- 12 **Dal-Negro R**, Pomari C, Micheletto C, Turco P, Tognella S. Prevalence of gastroesophageal reflux in asthmatic patients: an Italian study. *Ital J Gastroenterol Hepatol* 1999; **31**: 371-375
- 13 **Sontag SJ**, O'Connell S, Khandelwal S, Miller T, Nemchausky B, Schnell TG, Serlovsky R. Most asthmatic patients have reflux with or without bronchodilator therapy. *Gastroenterology* 1990; **99**: 613-620
- 14 **Richter JE**. Extraesophageal presentations of gastroesophageal reflux disease: the case for aggressive diagnosis and treatment. *Cleve Clin J Med* 1997; **64**: 37-45
- 15 **Vaezi MF**, Richter JE. Twenty-four-hour ambulatory esophageal pH monitoring in diagnosis of acid reflux-related chronic cough. *South Med J* 1997; **90**: 305-311
- 16 **Hollenz M**, Stolte M, Labenz J. Prevalence of gastro-oesophageal reflux disease in general practice. *Dtsch Med Wochenschr* 2002; **127**: 1007-1012
- 17 **Allescher HD**. Diagnosis of gastroesophageal reflux. *Schweiz Rundsch Med Prax* 2002; **91**: 779-790
- 18 **Harper PC**, Bergner A, Kaye MD. Antireflux treatment for asthma, Improvement in patients with associated gastroesophageal reflux. *Arch Intern Med* 1987; **147**: 56-60
- 19 **Harding SM**, Richter JE, Guzzo MR, Schan CA, Alexander RW, Bradley LA. Asthma and gastroesophageal reflux: acid suppressive therapy improves asthma outcome. *Am J Med* 1996; **100**: 395-405
- 20 **Levin TR**, Sperling RM, McQuaid KR. Omeprazole improves peak expiratory flow rate and quality of life in asthmatic patients with gastroesophageal reflux. *Am J Gastroenterol* 1998; **93**: 1060-1063
- 21 **Teichtahl H**, Kronborg IJ, Yeomans ND, Robinson P. Adult asthma and gastroesophageal reflux: the effects of omeprazole therapy on asthma. *Aust N Z J Med* 1996; **26**: 671-676
- 22 **Meier JH**, McNally PR, Punja M, Freeman SR, Sudduth RH, Stocker N, Perry M, Spaulding HS. Does omeprazole (Prilosec) improve respiratory function in asthmatic patients with gastroesophageal reflux? A double-blind, placebo-controlled crossover study. *Dig Dis Sci* 1994; **39**: 2127-2133

Edited by Xia HHX

Type 2 diabetes mellitus affects eradication rate of *Helicobacter pylori*

Mehmet Sargın, Oya Uygur-Bayramiçli, Haluk Sargın, Resat Dabak, Ekrem Orbay, Dilek Yavuzer, Ali Yayla

Mehmet Sargın, Oya Uygur-Bayramiçli, Haluk Sargın, Reşat Dabak, Ekrem Orbay, Dilek Yavuzer, Ali Yayla, Departments of Endocrinology and Diabetes, Gastroenterology, Family Medicine, Pathology and Internal Medicine; Kartal Education and Research Hospital, Istanbul, Turkey

Correspondence to: Oya Uygur-Bayramiçli, Altunizade mah. Atıf Bey sok. Çamlık sitesi II. Kısım A Blok No: 53/9, 81020 Uskudar/ISTANBUL, Turkey. bayramicli@hotmail.com

Telephone: +90-216-4184063 **Fax:** +90-216-4188637

Received: 2002-12-05 **Accepted:** 2003-01-03

Abstract

AIM: To study the eradication rate of *Helicobacter pylori* (*Hp*) in a group of type 2 diabetes and compared it with an age and sex matched *non-diabetic* group.

METHODS: 40 diabetic patients (21 females, 19 males; 56±7 years) and 40 *non-diabetic* dyspeptic patients (20 females, 20 males; 54±9 years) were evaluated. Diabetic patients with dyspeptic complaints were referred for upper gastrointestinal endoscopies; 2 corpus and 2 antral gastric biopsy specimens were performed on each patient. Patients with positive *Hp* results on histopathological examination comprised the study group. *Non-diabetic* dyspeptic patients seen at the Gastroenterology Outpatient Clinic and with the same biopsy and treatment protocol formed the control group. A triple therapy with amoxicillin (1 g b.i.d), clarithromycin (500 mg b.i.d) and omeprazole (20 mg b.i.d.) was given to both groups for 10 days. Cure was defined as the absence of *Hp* infection assessed by corpus and antrum biopsies in control upper gastrointestinal endoscopies performed 6 weeks after completing the antimicrobial therapy.

RESULTS: The eradication rate was 50 % in the diabetic group versus 85 % in the *non-diabetic* control group ($P<0.001$).

CONCLUSION: Type 2 diabetic patients showed a significantly lower eradication rate than controls which may be due to changes in microvasculature of the stomach and to frequent antibiotic usage because of recurrent bacterial infections with the development of resistant strains.

Sargın M, Uygur-Bayramiçli O, Sargın H, Orbay E, Yavuzer D, Yayla A. Type 2 diabetes mellitus affects eradication rate of *Helicobacter pylori*. *World J Gastroenterol* 2003; 9(5): 1126-1128 <http://www.wjgnet.com/1007-9327/9/1126.htm>

INTRODUCTION

Helicobacter pylori (*Hp*) is the most prevalent infection all over the world and has been considered as the causative agent of many gastrointestinal diseases^[1,2]. Type 2 diabetes mellitus can present with many protean gastrointestinal symptoms and *Hp* can play a role in this context^[3,4].

Although a number of studies has been performed on the association of *Hp* and diabetes mellitus, the results have been

controversial. In a large study performed by Xia *et al.*, the seroprevalance of *Hp* infection was not statistically different in patients with diabetes mellitus and *non-diabetic* controls^[5]. In earlier studies, the prevalence of *Hp* was reported to be 62 % versus 21%, but according to Xia *et al.*, the prevalence of *Hp* should be corrected for age and gender and there are no differences if an adjustment has been done for these variables^[6].

The literature is even scarce about treatment regimens of *Hp* infection in diabetes mellitus. We also know that the eradication of *Hp* shows great differences between different ethnic groups and in patients with some chronic conditions^[1,7]. Therefore we proposed that the eradication rate of *Hp* may be also different in type 2 diabetics in comparison to *non-diabetic* controls and we planned a prospective study to elucidate the eradication rate of *Hp* infection in type 2 diabetic subjects.

MATERIALS AND METHODS

Patients

Diabetic patients with dyspeptic complaints from Diabetes Outpatient Clinic were referred for upper gastrointestinal endoscopies in the Gastroenterology Department. Upper gastrointestinal endoscopies were performed in a standard fashion with a videoendoscope (Pentax G-2940, Japan) by the same endoscopist. Endoscopic findings were noted and *Hp* infection was assessed using 2 gastric antrum and 2 gastric corpus biopsy specimens, which were evaluated with the rapid urease test and the pathological examination (Haematoxylin-Eosin staining and Giemsa if the first stain was negative). Only patients with positive results for *Hp* in pathological specimens were included in the study. The study population consisted of 40 patients with type 2 diabetic (21 females and 19 males; mean age 56±7 years) and 40 *non-diabetic* dyspeptic patients as a control group from Gastroenterology Outpatient Clinic (20 females and 20 males; mean age 54±9 years) matched for sex and age (Table 1). All patients had detailed information about the study and written informed consent.

Table 1 Characteristics of the patients in diabetic and control groups

	Diabetics	Control	P
n (F/M)	40 (21/19)	63 (25/40)	>0.05
Age (y)	56±7	54±9	>0.05
Diabetes duration (y)	7.2±5	-	
HbA1c (%)	7.4±1.3	-	

Methods

At enrolment and at the end of the treatment, each patient completed a dyspepsia questionnaire proposed by Buckley *et al.*, which had been slightly modified^[8]. A triple therapy with amoxicillin (1 g b.i.d), clarithromycin (500 mg b.i.d) and omeprazole (20 mg b.i.d) was given for 10 days. After 10 days, the patients received 20 mg omeprazole for 5 weeks if a gastric or duodenal ulcer was identified in the initial endoscopy or 40 mg of famotidin if there was gastritis. Cure was defined as the

absence of *Hp* infection assessed by corpus and antrum biopsies in control upper gastrointestinal endoscopies performed 6 weeks after completing the antimicrobial therapy. Endoscopic findings were evaluated again in control endoscopy and compared with initial endoscopic findings. Any side effects due to the treatment were reported.

During the same study period, dyspeptic patients seen at the Gastroenterology Outpatient Clinic were taken as the control group if there was no history of type 2 diabetes, and their fasting plasma glucose levels were in normal limits (between 80-110 mg/dl) and pathological *Hp* positivity was found in gastric antrum and corpus specimens. The same triple therapy and a control upper gastrointestinal endoscopy after 6 weeks were also applied to the control group.

Statistical analysis

Results were expressed as means \pm SEM. Statistically significant differences between groups were assessed using either Student *t* test, Fischer's exact test or ANOVA test, as appropriate. $P < 0.05$ was considered to be significant.

RESULTS

All enrolled patients completed the study. *Hp* was eradicated in 50 % (20/40) type 2 diabetic patients and in 85 % (34/40) *non-diabetic* dyspeptic patients. The eradication rate was significantly lower in diabetics in comparison to the controls ($P < 0.05$).

There were no side effects in both groups, which led to discontinuation of the treatment.

At baseline, type 2 diabetic patients infected with *Hp* showed a high prevalence of gastrointestinal symptoms. There was a statistically significant decrease in epigastric pain, nausea and belching after *Hp* eradication treatment (Table 2).

Table 2 Prevalence of gastrointestinal symptoms in type 2 diabetic patients before and after the treatment

	Before (%)	After (%)	<i>P</i>
Epigastric pain	75 (30/40)	30 (12/40)	<0.05
Bloating	68 (27/40)	43 (17/40)	NS
Pyrosis	63 (25/40)	38 (15/40)	NS
Nausea	55 (22/40)	23 (9/40)	<0.05
Belching	63 (25/40)	30 (12/40)	<0.05
Early satiety	30 (12/40)	20 (8/40)	NS

Denotes: NS=not significant

Age, duration of the diabetes and Haemoglobin A1c levels were not significantly different between the diabetics in whose *Hp* was eradicated and whose *Hp* was not eradicated (Table 3).

Table 3 Comparison of demographic data of diabetic patients in whom *Hp* was eradicated and *Hp* was not eradicated

	<i>Hp</i> (+) at control endoscopy	<i>Hp</i> (-) at control endoscopy	<i>P</i>
Female sex (%)	53	47	>0.05
Age (y)	56.2 \pm 8	55.8 \pm 8	>0.05
Diabetes duration (y)	7.3 \pm 5	7.2 \pm 5	>0.05
HbA1c (%)	7.2 \pm 1.2	7.2 \pm 1.2	>0.05

DISCUSSION

Hp infection is responsible for up to 90 % of upper gastrointestinal diseases and is linked to the development of

gastric carcinoma, MALT associated lymphoma and has to be eradicated whenever it's possible^[9,10].

Standard triple therapy (Omeprazole, Clarithromycin and Amoxicillin) has been shown to be highly effective in the eradication of *Hp* in *non-diabetic* subjects in many previous studies (91 %)^[11,12]. In our control group, we found an eradication rate of 85 %, which was compatible with the results in the literature.

Many authors have extensively explored the relationship between *Hp* and diabetes mellitus. There has been controversial results in previous studies but in a larger, well-designed study of Xia *et al.*, there was no difference of the seroprevalence of *Hp* infection between patients with diabetes mellitus and *non-diabetic* controls^[5]. But there were no studies which explored the efficacy of anti *Hp* protocols in type 2 diabetics, whereas in a study of Gasbarrini *et al.* in type 1 diabetics, the *Hp* eradication rate was 65 % in comparison to 92 % in controls^[13]. In another study performed on type 1 diabetics, the eradication rate was 62 % with different triple antibiotic regimens and this could be increased by quadruple regimen to 88 %^[14]. In the present study performed on type 2 diabetics, a much lower eradication rate of *Hp* (50 %) was found. Histopathological examination was used in this study for the detection of pre and post treatment *Hp* and as the gold standard, it was more reliable and reproducible than the ¹³C urea breath test, which has been used in the studies by Gasbarrini *et al.*^[13,14].

Immunosuppression in diabetes might predispose to the low eradication rate of *Hp* infection but other mechanisms may also explain the low eradication rate of *Hp* in type 2 diabetics. Type 2 diabetics are more susceptible to many bacterial and mycotic infections, which may lead to frequent use of antibiotics, and to the development of resistance^[15-18].

Due to absorption problems in gastric mucosa, the extent of antibiotic absorption may be less^[19]. This study showed a high rate of pathological endoscopic findings in type 2 diabetics, which may lead to disorders in gastrointestinal motility and to insufficient absorption of the drugs. Autonomic neuropathy has also been accused as a culprit. But studies in the literature suggested that there was no correlation between *Hp* positivity and delay in gastric emptying.

A standard 10 days triple therapy with conventional antibiotics seems not to be warranted in diabetics. Due to problems of absorption and motility, alternative regimens with longer duration seem to be necessary for a higher eradication rate. In particular, if we take into consideration that gastrointestinal symptoms, which are quite frequent in diabetics, are significantly improving when it is possible to eradicate *Hp*, we should try to eradicate *Hp* in diabetic subjects. But this is a new area of research and the larger prospective studies with different anti *Hp* regimens for type 2 diabetics are needed.

ACKNOWLEDGEMENT

The authors thank endoscopy assistants Aygün İbýk, RN and Elvan Ýmþir, RN for their assistance .

REFERENCES

- 1 **Dunn BE**, Cohen H, Blaser MJ. Epidemiology of *H. Pylori* Infection. *Clinical Microbiology Reviews* 1997; **10**: 720-741
- 2 **D' Elios MM**, Andersen LP, Prete GD. Inflammation and host response. *Current Opinion in Gastroenterology: The year in Helicobacter pylori* 1998; **14** (Suppl 1): 15-19
- 3 **Güvener N**, Akcan Y, Paksoy I, Soylu AR, Aydın M, Arslan O. *Helicobacter pylori* associated gastric pathology in patients with type 2 diabetes mellitus and its relationship with gastric emptying: The Ankara study. *Exp Clin Endocrinol Diab* 1999; **107**: 172-176
- 4 **Gentile S**, Turco S, Olivero B, Torella R. The role of autonomic

- neuropathy as a risk factor of *Helicobacter pylori* infection in dyspeptic patients with type 2 diabetes mellitus. *Diab Res Clin Pract* 1998; **42**: 41-48
- 5 **Xia HHX**, Talley JN, Kam EPY, Young LJ, Hammer J, Horowitz M. *Helicobacter pylori* infection is not associated with diabetes mellitus, nor with upper gastrointestinal symptoms in diabetes mellitus. *Am J Gastroenterol* 2001; **96**: 1039-1046
- 6 **Simon L**, Tornoczky J, Toth M, Jambor M, Sudar Z. The significance of *Campylobacter pylori* infection in gastroenterologic and diabetic practice. *Orvosi Hetilap* 1989; **130**: 1325-1329
- 7 **Uygur-Bayramiçli O**, Kılıç D, Yavuzer D, Telatar B, Kavaklı B. *Helicobacter pylori* colonization and immunological disease. *Eur J Gastroenterol Hepatol* 2001; **13**: 301-302
- 8 **Buckley MJ**, Scanion C, McGurgan P, O' Morian CA. A validated dyspepsia symptom score. *Ital J Gastroenterol Hepatol* 1997; **29**: 495-500
- 9 **Delchier JC**, Ebert M, Maltfertheiner P. *Helicobacter pylori* in gastric lymphoma and carcinoma. *Current Opinion in Gastroenterology: The year in Helicobacter pylori* 1998; **14** (Suppl 1): 41-45
- 10 **Eslick GD**, Lim LL-Y, Byles JE, Xia HH, Talley NJ. Association of *Helicobacter pylori* infection with gastric carcinoma: A meta analysis. *Am J Gastroenterol* 1999; **94**: 2373-2379
- 11 **Wurzer H**, Rodrigo L, Stamler D, Archambult A, Rokkas T, Skandalis N, Fedorak R, Bazzoli F, Hentschel E, Mora P, Archmandritis A, Megraud F. For the ACT-10 Study Group. Short course therapy with amoxicillin-clarithromycin triple therapy for 10 days (ACT-10) eradicates *Helicobacter pylori* and heals duodenal ulcer. *Aliment Pharmacol Ther* 1997; **11**: 81-87
- 12 **Viara D**, Ali A, Gatta L, O' Morain C. Treatment of *Helicobacter pylori*. *Current Opinion in Gastroenterology: The year in Helicobacter pylori* 1998; **14** (Suppl 1): 71-78
- 13 **Gasbarrini A**, Ojetti V, Pitocco D, Franceschi F, Candelli M, Torre EL, Gabrielli M, Cammarota G, Armuzzi A, Pola P, Ghirlanda G, Gasbarrini G. Insulin-dependent diabetes mellitus affects eradication rate of *Helicobacter pylori* infection. *Eur J Gastroenterol Hepatol* 1999; **11**: 713-716
- 14 **Gasbarrini A**, Ojetti V, Pitocco D, Armuzzi A, Silveri NG, Pola P, Ghirlanda G, Gasbarrini G. Efficacy of different *Helicobacter pylori* eradication regimens in patients affected by insulin-dependent diabetes mellitus. *Scand J Gastroenterol* 2000; **35**: 260-263
- 15 **Zwet VAA**, Megraud F. Diagnosis. *Current Opinion in Gastroenterology: The year in Helicobacter pylori* 1998; **14** (Suppl 1): 27-33
- 16 **Gwilt PR**, Nahas RR, Tracewell WG. The effects of diabetes mellitus on pharmacokinetics and pharmacodynamics in humans. *Clin Pharmacokinet* 1991; **20**: 477-490
- 17 **Megraud F**. Resistance of *Helicobacter pylori* to antibiotics. *Aliment Pharmacol Ther* 1997; **11** (Suppl 1): 43-53
- 18 **Bessman AN**, Sapico FL. Infections in the diabetic patient: the role of immune dysfunction and pathogen virulence factors. *J Diabetic Complications* 1992; **6**: 258-262
- 19 **Jaap AJ**, Shore AC, Tooke JE. Relationship of insulin resistance to microvascular dysfunction of subjects with fasting hyperglycaemia. *Diabetologia* 1997; **40**: 238-243

Edited by Xu XQ

Postmyotomy dysphagia after laparoscopic surgery for achalasia

Yutaka Shiino, Ziad T. Awad, Gleb R. Haynatzki, Richard E. Davis, Ronald A. Hinder, Charles J. Filipi

Yutaka Shiino, Ziad T. Awad, Richard E. Davis, Charles J. Filipi, Department of Surgery, Creighton University, 601 N. 30th Street, Omaha, NE 68131, USA

Gleb R. Haynatzki, Department of Medicine, Creighton University, 601 N. 30th Street, Omaha, NE 68131, USA

Ronald A. Hinder, Department of Surgery, Mayo Clinic Jacksonville, 4500 San Pablo Road, Jacksonville, FL 32224, USA

Correspondence to: Charles J. Filipi, Professor of Surgery, Department of Surgery, Suite 3740, Creighton University School of Medicine, 601 No. 30th Street, Omaha, NE 68131, USA. cjfilipi@Creighton.edu

Telephone: +1-402-2804213 **Fax:** +402-2804593

Received: 2002-12-22 **Accepted:** 2003-01-20

Abstract

AIM: To determine predictive factors for postoperative dysphagia after laparoscopic myotomy for achalasia.

METHODS: Logistic regression was used to investigate the possible association between the response (postoperative dysphagia, with two levels: none/mild and moderate/severe) and several plausible predictive factors.

RESULTS: Eight patients experienced severe or moderate postoperative dysphagia. The logistic regression revealed that only the severity of preoperative dysphagia (with four levels: mild, moderate, severe, and liquid) was a marginally significant ($P=0.0575$) predictive factor for postoperative dysphagia.

CONCLUSION: The severity of postoperative dysphagia is strongly associated with preoperative dysphagia. Preoperative symptomatology can significantly impact patient outcome.

Shiino Y, Awad ZT, Haynatzki GR, Davis RE, Hinder RA, Filipi CJ. Postmyotomy dysphagia after laparoscopic surgery for achalasia. *World J Gastroenterol* 2003; 9(5): 1129-1131
<http://www.wjgnet.com/1007-9327/9/1129.htm>

INTRODUCTION

Results of laparoscopic Heller myotomy are as effective as traditional surgery and have the additional advantages of a shorter hospital stay and less discomfort^[1,2]. Although the early results of mini-invasive surgery for achalasia appear satisfactory in general, postmyotomy dysphagia remains a problem^[3,4]. Most reports do not describe the cause of postoperative dysphagia although its incidence is quantified.

Aperistalsis, incomplete relaxation of the lower esophageal sphincter, exposure of the esophageal mucosa to reflux material, incomplete myotomy and a too tight or a distorted Dor fundoplication can result in dysphagia. In addition, operation-related trauma such as perforation, edema, vagal nerve injury and fibrosis may cause dysphagia. For further improvement of laparoscopic Heller myotomy, additional factors affecting results should be determined for postmyotomy dysphagia is not rare. This study was conducted to investigate the causes of persistent symptomatology and to assist in predicting poor results of laparoscopic surgery for achalasia.

MATERIALS AND METHODS

Patients

36 patients (18 females and 18 males) who underwent laparoscopic Heller myotomy and fundoplication were investigated retrospectively. All patients underwent a preoperative barium swallow, esophagogastroscopy and manometry to establish the diagnosis of achalasia.

Manometry

Lower esophageal sphincter (LES) manometry was performed utilizing the station pull-through method and the esophageal body study was completed using 10 wet swallows with the distal tip of the manometry catheter located 3 cm above the upper border of the LES.

Surgical procedures

Two surgeons performed these procedures at the same institution. Myotomy was performed in all cases from approximately 4 cm above the esophagogastric junction to 2 cm distal to the gastroesophageal junction. Methods used to establish the location of the esophagogastric junction included identifying an outward tapering of the stomach, a change in the thickness of muscularis, the angle of the circular muscles and observation with intraoperative esophagoscopy in selected cases. Either an anterior or posterior fundoplication was performed in conjunction with the Heller myotomy, according to the surgeon's preference.

Grouping

The response variable, postoperative dysphagia, was classified into 2 categories according to the severity: severe or moderate dysphagia (Group A), and mild or no dysphagia (Group B). A category of "severe dysphagia" represented debilitating dysphagia requiring therapeutic intervention; "moderate dysphagia" represented frequent but not requiring intervention, "mild dysphagia" represented occasional symptoms not requiring therapy and "no dysphagia" represented absence of symptoms.

Parameters

Fourteen predictive factors for postoperative dysphagia as the response / dependent variables were evaluated. These included age, weight, preoperative symptom duration, LES pressure, abdominal and overall length of the LES, relaxation of the LES, contraction pressure of the esophageal body, percentage of simultaneous contractions, preoperative pneumatic dilation, the type of fundoplication, severity of preoperative dysphagia (*D*), heartburn (*HB*) and regurgitation (*R*). Factors *D*, *HB* and *R* were numerically ranked by an independent observer according to their severity, as 1-4 for mild through liquid dysphagia, 0-3 and 0-3, respectively. Preoperative forceful dilation and the type of fundoplication were categorized as binary (0-1) variables.

Statistical analysis

Since our response variable was binary, we had chosen the logistic regression approach and expressed the logarithm of the odds ratio for the response as a linear function of the

explanatory variables, i.e. we had fitted a model of the form:

$$\text{Log} \left(\frac{P}{1-P} \right) = \beta_0 + \beta_1 \times \text{Age} + \dots + \beta_{12} \times D + \beta_{13} \times \text{HB} + \beta_{14} \times R \quad \{\text{I}\}$$

Where P was the probability of poor outcome (moderate/severe postoperative dysphagia) and $1-p$ is the probability of favorable outcome (none/mild postoperative dysphagia). We used the statistical package SAS® 8.0 to implement the maximum likelihood estimation of the coefficients of the above equation. As a result, the final model included only one predictive factor.

RESULTS

Six patients experienced severe dysphagia after the operation and required interventional treatment. A 43 year-old female complaining of severe postoperative dysphagia and weight loss underwent repeat laparoscopic myotomy which was completed uneventfully 16 months after the primary myotomy. Only dense adhesions of the anterior esophagus were found.

Five patients underwent endoscopic dilatation 1 to 18 months after the primary operation. Two patients required two balloon dilatations while the remaining 3 patients underwent Hurst Maloney bouginage.

Two additional patients complained of moderate postoperative dysphagia. Their dysphagia lasted several months but improved without further intervention. Seven of the 8 patients with postoperative severe or moderate dysphagia experienced no complications. One patient had gastric stasis requiring 9 days of hospitalization.

As a result of the logistic regression analysis (equation {I}), only preoperative dysphagia, D , was marginally significant ($P=0.0575$); all the rest had P -values larger than 0.20 and were not significant. Thus, the final model involves only one predictive factor, D :

$$\text{Log} \left(\frac{P}{1-P} \right) = \beta_0 + \beta_{11} \times D \quad \{\text{II}\}$$

where $\beta_0 = -2.7953$, $\beta_{11} = 0.9366$. Therefore, the odds ratio increased as D increased, and as a result of {II} the odds in favor of having moderate/severe postoperative dysphagia for somebody with mild preoperative dysphagia were approximately 39.2 % of that for somebody with moderate preoperative dysphagia. Similarly, the chance of somebody with moderate preoperative dysphagia to have moderate/severe postoperative dysphagia was 39.2 % of that for somebody with severe preoperative dysphagia and, finally, somebody with severe preoperative dysphagia had only 39.2% of that chance for somebody with moderate preoperative dysphagia. The last number was derived by first exponentiating 0.9366 which gave 2.551, and then finding its reciprocal, 0.392.

What we could derive from {II} was the fact that there existed a positive association between the probability of poor outcome (severe or moderate postoperative dysphagia) and the explanatory variable, the severity of preoperative dysphagia, D . The fact that we obtained only marginal significance ($P=0.0575$) was apparently due to the small sample size. Should the sample size be increased, the result would have been statistically significant at a level 0.05.

DISCUSSION

The objective of this study was to clarify causes for postoperative dysphagia after laparoscopic Heller myotomy for achalasia.

The severity of preoperative dysphagia is marginally significant with a P value of 0.0575 and was positively

associated with postoperative dysphagia. Numerous articles on laparoscopic Heller myotomy have been published since the first case report^[5]. However, none have specifically addressed the cause of failed myotomy. Some studies were instructive in surgical technique and others are simply case reports^[6,7].

The type of fundoplication and the extent of myotomy onto the gastric wall are extremely important for this operation^[8,9]. A previous report has shown that patients undergoing anterior fundoplication in conjunction with myotomy were more likely to experience postmyotomy dysphagia or heartburn than those undergoing posterior fundoplication^[9]. Posterior fundoplication is considered effective because it is capable of keeping the edges of myotomy apart^[10].

We demonstrated a positive association between the probability of poor outcome and the severity of preoperative dysphagia. Why does the severity of preoperative dysphagia make the outcome poor? Preoperative manometry showed that patients with the more severe preoperative dysphagia did not always have higher LES pressure or poor relaxation of the LES. There also was no evidence of poorer esophageal peristalsis (all patients were 100 % dysfunctional).

Patients with short-term dysphagia (5 to 6 months) were included in the analysis because they presented a significant problem for the clinician. Early postoperative dysphagia (< 2 months) was well tolerated by the patient. More prolonged difficulty required explanation. The degree of preoperative dysphagia could be explained preoperatively as a postoperative risk factor and would assist in reducing patient anxiety and expectations.

The length of myotomy is believed to be a critical technical feature of the operation. The extent of the gastric myotomy appears to play a key role in prevention of dysphagia. Some surgeons prefer to extend the myotomy 1 cm beyond gastroesophageal junction^[11,12], while others recommend 2 cm or longer^[9,13]. Generally, a shorter gastric myotomy is performed in conjunction with the transthoracic or thoracoscopic approach. On the other hand, longer myotomy is usually performed with concomitant fundoplication with open transabdominal or laparoscopic approach^[14,15]. The former operation is prone to gastroesophageal reflux disease as documented by pH monitoring^[10,16]. Several authors have demonstrated the necessity of fundoplication. They have shown that patients undergoing myotomy without fundoplication have a higher chance of experiencing postoperative gastroesophageal reflux^[17,18]. Mattioli *et al.* has clearly shown in a prospective study that a significantly better long-term outcome results from a transabdominal long cardiomyotomy plus anterior fundoplication as compared to transabdominal long myotomy alone or a transthoracic short cardiomyotomy^[8].

REFERENCES

- 1 **Decanini TC**, Varela GG, Galicia JA. Laparoscopic esophagomyotomy and antireflux procedure with intraoperative manometry. *Surg Laparosc Endosc* 1996; **6**: 398-402
- 2 **Esposito PS**, Sosa JL, Sleeman D, Santelices. Laparoscopic management of achalasia. *Am Surg* 1997; **63**: 221-223
- 3 **Morino M**, Rebecchi F, Festa V, Garrone C. Preoperative pneumatic dilatation represents a risk factor for laparoscopic Heller myotomy. *Surg Endosc* 1997; **11**: 359-361
- 4 **Peracchia A**, Rosati R, Bona S, Fumagalli U, Bonavina L, Chella B. Laparoscopic treatment of functional diseases of the esophagus. *Int Surg* 1995; **80**: 336-340
- 5 **Shimi S**, Nathanson LK, Cuschieri A. Laparoscopic cardiomyotomy for achalasia. *J R Coll Surg Edinb* 1991; **36**: 152-154
- 6 **Holzman MD**, Sharp KW, Ladipo JK, Eller RF, Holcomb GW III, Richards WO. Laparoscopic surgical treatment of achalasia. *Am J Surg* 1997; **173**: 308-311

- 7 **Xynos E**, Tzouvaras G, Petrakis I, Chrysos E, Vassilakis JS. Laparoscopic Heller's cardiomyotomy and Dor's fundoplication for esophageal achalasia. *J Laparoendosc Surg* 1996; **6**: 253-258
- 8 **Mattioli S**, Di Simone MP, Bassi F, Pilotti V, Felice V, Pastina M, Lazzari A, Gozzetti G. Surgery for esophageal achalasia. Long-term results with three different techniques. *Hepatogastroenterology* 1996; **43**: 492-500
- 9 **Raiser F**, Perdakis G, Hinder RA, Swanstrom LL, Filipi CJ, McBride PJ, Katada N, Neary PJ. Heller myotomy via minimal-access surgery. An evaluation of antireflux procedures. *Arch Surg* 1996; **131**: 593-597
- 10 **Swanstrom LL**, Pennings J. Laparoscopic esophagomyotomy for achalasia. *Surg Endosc* 1995; **9**: 286-290
- 11 **Hunter JG**, Trus TL, Branum GD, Waring JP. Laparoscopic Heller myotomy and fundoplication for achalasia. *Ann Surg* 1997; **225**: 655-664
- 12 **Pellegrini CA**, Leichter R, Patti M, Somberg K, Ostroff JW, Way L. Thoracoscopic esophageal myotomy in the treatment of achalasia. *Ann Thorac Surg* 1993; **56**: 680-682
- 13 **Bonavina L**, Nosadini A, Bardini R, Baesatto M, Peracchia A. Primary treatment of esophageal achalasia. Long-term results of myotomy and Dor fundoplication. *Arch Surg* 1992; **127**: 222-226
- 14 **Donahue PE**, Schlesinger PK, Sluss KF, Richter HM, Liu KJM, Rypins EB, Nyhus LM. Esophagocardiomyotomy - Floppy Nissen fundoplication effectively treats achalasia without causing esophageal obstruction. *Surgery* 1994; **116**: 719-725
- 15 **Jamieson WR**, Miyagishima RT, Carr DM, Stordy SN, Sharp FR. Surgical management of primary motor disorders of the esophagus. *Am J Surg* 1984; **148**: 36-42
- 16 **Gerzic Z**, Knezevic J, Milicevic M, Rakic S, Dunjic M, Randjelovic T. Results of 8 transabdominal cardiomyotomy with Dor partial fundoplication in the management of achalasia. In: Siewert JR, Holscher AH, eds. *Diseases of the Esophagus*. Berlin:Springer-Verlag 1988: 970-974
- 17 **Björck S**, Dernevik L, Gatzinsky P, Sandberg N. Oesophagocardiomyotomy and antireflux procedures. *Acta Chir Scand* 1982; **148**: 525-529
- 18 **Tomlinson P**, Grant A. A review of 74 patients with oesophageal achalasia: the results of Heller's cardiomyotomy, with and without Nissen fundoplication. *Aust N Z J Surg* 1981; **51**: 48-51

Edited by Xu XQ

Immunogenicity and reactogenicity of a recombinant hepatitis B vaccine in subjects over age of forty years and response of a booster dose among nonresponders

Kunal Das, R. K. Gupta, V. Kumar, P. Kar

Kunal Das, R. K. Gupta, V. Kumar, P. Kar, Department of Medicine, Maulana Azad Medical College & L. N. Hospital, New Delhi. Medical Advisor, Panacea Biotec Co., New Delhi

Correspondence to: Dr P. Kar, MD. DM. Professor of Medicine Maulana Azad Medical College, New Delhi-110002, India. pkar@vsnl.com

Telephone: +91-11-26889271 **Fax:** +91-11-23230132

Received: 2002-03-19 **Accepted:** 2002-05-10

Abstract

AIM: The study was initiated to evaluate the reactogenicity and immunogenicity of a recombinant hepatitis B vaccine in age group >40 years and to study the response of a single booster dose in primary non-responders to the hepatitis B vaccination.

METHODS: A total of 102 volunteers without markers of hepatitis B infection (negative for HBsAg, anti-HBc antibody, HBeAg and anti-HBs antibody) received 20 µg of recombinant HB vaccine intramuscularly at 0, 1, and 6 months. Anti HBs titers were evaluated by a quantitative Elisa kit at 90 and 210 days. A booster dose of 20 µg HB vaccine was given after 6 months of the 3rd vaccine dose to the 15 non-responders and anti-HBs titers were measured after 1 month.

RESULTS: Seroprotection (anti-HBs GMT³ 10 IU/L) was achieved in 85.3 % (87/102) volunteers. The mean GMT titers of the vaccine responders was 136.1 IU/L. Of the seroprotected individuals, there were 32.4 % (33/102) hyporesponders (anti-HBs titers <10-99 mIU/ml) and 52.9 % (54/102) were responders (anti-HBs titers >100 IU/L). All the non-responders (15/15) responded to a single dose of the booster dose of recombinant HB vaccine and their mean anti-HBs antibody titers were more than 100.5 mIU/ml after the booster dose.

CONCLUSION: Recombinant hepatitis B vaccine offers good seroprotection in the age group >40 years and has a good safety profile. A single booster dose after 6 months in primary non-responders leads to good seroprotective anti-HBs antibody titers. However, larger population based studies are needed to evaluate the role of a booster dose in selected group of non-responders and whether such an approach will be cost effective.

Das K, Gupta RK, Kumar V, Kar P. Immunogenicity and reactogenicity of a recombinant hepatitis B vaccine in subjects over age of forty years and response of a booster dose among nonresponders. *World J Gastroenterol* 2003; 9(5): 1132-1134 <http://www.wjgnet.com/1007-9327/9/1132.htm>

INTRODUCTION

Hepatitis B infection is a major public health problem worldwide due to its long-term sequelae which include chronic

hepatitis, cirrhosis and hepatocellular carcinoma. The situation is grim in developing countries like India, where blood bank infrastructure is non-existent outside the major metropolitan cities and safe blood handling practice standards are low. India comes under intermediate zone of HBV prevalence, and with a carrier rate of 4.7 %^[1,2] has a estimated 42 million carriers, next only to China. Hepatitis B vaccination has been one of the success stories of the 20th century and has been extensively used in a wide range of groups throughout the world. Hepatitis B vaccination programmes have successfully reduced the prevalence of hepatitis B, e.g. in Taiwan, where universal HB vaccination^[3] has led to a significant reduction of hepatitis B prevalence and incidence of hepatocellular carcinoma in children. The immunogenicity, efficiency and safety profile of hepatitis B vaccine has been well established. More than 90 % seroconversion has been achieved in adult populations consistently^[4-7]. The safety profile of the recombinant vaccine has been very good^[8]. No response to hepatitis B vaccination is increased among certain risk groups like smokers, diabetes, chronic renal failure patients, elderly obese individuals. It is important to predict vaccine non-responders as they are susceptible to break through hepatitis B infection^[9]. The study was designed to evaluate the immunogenicity and reactogenicity and safety profile of a recombinant hepatitis B vaccine in subjects above the age of 40 yr and to study the response of a single booster dose in primary non-responders to hepatitis B vaccination.

MATERIALS AND METHODS

Volunteer selection

The study was conducted in L. N. Hospital, New Delhi over the period of one year (1996-1997). A total of 147 healthy volunteers (volunteers were attendants of the patients attending the medical OPD services) in the age group more than 40 yrs out of 387 healthy persons who were none obese and non-smokers attending the medical outpatient services consented to be included in the study. All of these volunteers were tested for markers of HBV infection. All the subjects were screened by the serological tests including HBsAg (Ranbaxy Diagnostics, India) and anti-HBc (Melotec, Spain) using commercially available ELISA kits. 102 volunteers who were negative for all the serological markers of hepatitis B infection, completed the hepatitis B vaccination programme.

HBV vaccination and sample collection

In a total of 102 volunteers after their informed consent, 20 mg of recombinant DNA hepatitis B vaccine (EnivachHB, Panacea Biotec) was administered intramuscularly at a dosing schedule of 0, 1 and 6 months. Five dropped out after the first vaccine dose themselves, hence 102 volunteers received all the three doses of HBV vaccination. Serum samples for anti-HBs antibody titres were determined at 90 and 210 days. Anti-HBs antibodies were done using a commercially available quantitative ELISA kit (AUSAB-EIA, Abbot Labs, USA).

Protection with hepatitis B vaccination is considered to be achieved when concentration of anti-HBs antibody titers is more than 10 IU/L. A non-response was defined as mean anti-HBs antibody titers below 10 IU/L, low responders were those with titers between 10-99 IU/L, and those with anti-HBs titers more than 100 IU/L^[13-26] were responders. A high response was on with titers more than 1 000 IU/L.

Booster schedule

All the non-responders (15/15) received an additional booster dose (20 µg) at 6 months after the third vaccination dose (12 months from the first vaccine dose) and the anti-HBs titers were measured after one month of booster dose.

Statistical analysis

Statistical analysis was done using Chi-square test and Student's test.

RESULTS

A total of 102 subjects were enrolled in the study. The mean age of the study group was 44.6±5.6 yr. with male: female ratio of 1.9:1. At day 90, after administration of two doses of recombinant vaccine 87.3 % (89/102) subjects achieved seroprotective levels of anti-HBs. At day 210 after administration of the third dose of recombinant vaccine 87/102 (85.3 %) subjects achieved seroprotective levels of anti-HBs. The mean anti-HBs titres achieved after the third dose of vaccine in the responders was 136.1 IU/L. The age distribution of mean anti-HBs levels achieved after the third dose of vaccine are given in Table 1. The peak anti-HBs levels achieved are lower in patients with increasing age. Further more, 13.3 % (11/83) subjects in the age group 40-49 years did not achieve seroprotective levels. Whereas ¼(25 %) subjects in the age group >60 years did not respond but the difference was not statistically significant. Also the number of high responders (anti-HBs levels >1 000 IU/L) was not significantly higher in the age group 40-49 years as compared to the age group 50-59 years [85.7 % (18/21) in the age group 40-49 years and 14.3 % (3/21) in the age group 50-59 years]. The mean age of 15 non-responders was 46.4±6.9 yr which was, however, not statistically different from the mean age of responders. 11.9 % (8.67) males were non-responders whereas 20 % (7/35) females were non-responders but the difference was not statistically significant.

All the non-responders, who were given an additional booster dose of 20 µg recombinant vaccine, responded and this achieved seroprotective levels.

Table 1 Age distribution of (GMT) anti-HBs titers

	Age (years)			Total
	40 - 49	50 - 59	> 60	
Male	52 (76.5%)	13 (19.1%)	3 (4.4%)	68
Mean GMT	136.0	105.9	107.5	
Female	30 (91.1%)	2 (5.8%)	1 (2.9%)	33
Mean GMT	145.4	177.6	41.56	

DISCUSSION

Risk factors that have been associated with non-response to hepatitis B vaccine include increasing age, male gender, obesity, history of smoking, administration of vaccine in buttock rather than deltoid^[4,8,10-13], diabetes and chronic renal failure^[14,15]. In many of the non-responders not explained by the above risk factors, certain HLA types have been found to

be associated with non response^[16-19]. The relationship of hepatitis B vaccination response with age is controversial. Our study suggests that seroconversion in age group >40 years is 85.7 %, which is considered high compared to most other studies^[20,21] where a seroconversion rate of around 60 % has been reported. However, as all the above studies, we too found a decreasing seroconversion rate with increasing age (Table 1). Our study suggests that 85.7 % of the high responders (mean titers >1 000 IU/L) occurred in the relatively younger age groups. These findings favor the hypothesis that increasing age decreases seroprotective antibody formation after vaccination. This finding is of clinical importance as non-responders who do not develop protective antibody level remain susceptible to break-through hepatitis B infection. Although no comparative Indian study of HBV vaccine in elderly is available, reports in adults show a 90-100 % seroconversion rate for 20 µg recombinant HBV vaccine administered intramuscularly^[22] not different from Western rates. For management of non-responders, there are no exact guidelines. Most unresponsive subjects are not absolute non-responders, since it has been shown that most of them can develop protective anti-HBsAg titers after a fourth or fifth dose of vaccination^[23-25]. Most studies in literature have found a variable response rate of 40-60 %^[28-30] to booster dose vaccination among nonresponders. Our study suggests a 100 % seroprotection rate after a single booster dose that is higher than most reports in the literature. One of the reasons for higher rate of seroprotection in our study compared to other reports in literature could be: (i) volunteers had received the booster dose after 6 months from the last vaccine dose and (ii) The selection of non-obese and non-smoking volunteers. If further such reports of 100 % seroprotection are available from other centers as well, an additional vaccine dose among the older populations could be recommended routinely after evaluation of cost effectiveness of such a strategy. There were no major side effects and relatively few minor side effects viz pain at injection site, fever etc. in 36/102 (35.3 %) of the cases. To conclude, the study suggests that the recombinant HBV vaccine is highly immunogenic with good safel profile among the age group >40 yr and a single booster dose is effective in non-responders. Further larger population based studies need to be undertaken to confirm our findings.

ACKNOWLEDGEMENT

We wish to thank Sanjay Singh and Abhijit Kumar of Panacea Biotec for extending co-operation and providing us the vaccine for the clinical trial.

REFERENCES

- 1 **Thyagarajan SP**, Jayaram S, Mohanavalli B. Prevalance of HBV in the general population of India. In: Sarin SK, Singal AK (eds). Hepatitis B in India: Problems and prevention. CBS publishers, New Delhi, India 1996: 5-15
- 2 **John TJ**, Abraham P. Hepatitis B in India: A review of disease epidemiology. *Indian Pediatr* 2001; **38**: 1318-1325
- 3 **Chen CJ**, You SL, Lin LH, Hsu WL, Yang YW. Cancer Epidemiology and control in Taiwan: a brief review. *Jpn J Clin Oncol* 2002; **32** (Suppl): S66-81
- 4 **Arslanoglu I**, Cetin B, Isguven P, Karavus M. Anti-HBs response to Standard Hepatitis B vaccination in children and adolescents with diabetes mellitus. *J Pediatr Endocrinol Metab* 2002; **15**: 389-395
- 5 **Cook IF**, Murtagh J. Comparative immunogenicity of hepatitis B vaccine administered into the ventrogluteal area and anterolateral thigh in infants. *J Paediatr Child Health* 2002; **38**: 393-396
- 6 **Abraham B**, Baine Y, De-Clercq N, Tordeur E, Gerard PP, Manovriez PL, Parenti DL. Magnitude and quality of antibody response to a combination hepatitis A and hepatitis B vaccine. *Antiviral Res* 2002; **53**: 63-73

- 7 **Cassidy WM.** Adolescent hepatitis B vaccination. A review. *Minerva Pediatr* 2001; **53**: 559-566
- 8 **Elkayam O,** Yaron M, Caspi D. Safety and efficacy of vaccination against hepatitis B in patients with rheumatoid arthritis. *Ann Rheum Dis* 2002; **61**: 623-625
- 9 **Leroux-Roels G,** Cao T, De Knibber A, Meuleman P, Roobrouck A, Farhoudi A, Vanlandschoot P, Desombere I. Prevention of hepatitis B infections: vaccination and its limitations. *Acta Clin Belg* 2001; **56**: 209-219
- 10 **National Health and Medical Research Council.** The Australian Immunization Handbook. Australian Government publication Service (AGPS). *Canberra* 2000
- 11 **Leroy V,** Bourliere M, Durand M, Abergel A, Tran A, Baud M, Botta-Fridlund D, Gerolami A, Ouzan D, Halfon P, Zarski JP. The antibody response to hepatitis B vaccination is negatively influenced by the hepatitis C virus viral load in patients with chronic hepatitis C: a case control study. *Eur J Gastroenterol & Hepatol* 2002; **14**: 485-489
- 12 **Frciologlu C,** Mikla S, Midilli K, Aydin A, Cam H, Ergin S. Reduced immune response to hepatitis B vaccine in children with insulin dependent diabetes. *Acta Paediatr Jpn* 1995; **37**: 687-690
- 13 **Bouter KP,** Diepersloot RJ, Wismans PJ, Gmelig Meyling FH, Hoekstra JB, Heijtkink RA, van Hattum J. Humoral response to a Yeast-derived hepatitis B vaccine in patients with type 1 diabetes mellitus. *Diabet Med* 1992; **9**: 66-69
- 14 **Oguz Y,** Doganci L, Vural A. Seroconversion rates of two different doses of Hepatitis B vaccine in Turkish haemodialysis patients. *Cent Eur J Public Health* 2001; **9**: 44-45
- 15 **Tele SA,** Martins RM, Lopes CL, dos Santos Carneiro MA, Souza KP, Yoshida CF. Immunogenicity of a recombinant hepatitis B vaccine (Eurax B) in haemodialysis patients and staff. *Eur J Epidemiol* 2001; **17**: 145-149
- 16 **Desombere I,** Willems A, Zeroux-Roels G. Respaue to hepatitis B vaccine: multiple HLA genes are involved. *Tissue Antigens* 1998; **51**: 593-604
- 17 **Lango-Warensjo A,** Cardell K, Lindblom B. Haptotypes comprising subtypes of the DQBI* 06 allele direct the antibody response after immunization with hepatitis B surface antigen. *Tissue Antigens* 1998; **52**: 374-380
- 18 **Caillat-Zucman S,** Gimenez JJ, Wambergue R, Albouze G, Lebkiri B, Naret C, Moynot A, Jungers P, Bach JF. Distinct HLA class II alleles determine antibody response to vaccination with hepatitis B surface antigen. *Kidney Int* 1998; **53**: 1626-1630
- 19 **Durupinar B,** Okten G. HLA Tissue types in non-responders to hepatitis B vaccine. *Indian J Pediatr* 1996; **63**: 369-373
- 20 **Looney RJ,** Hasan MS, Coffin D, Campbell D, Falsey AR, Kolassa J, Agosti JM, Abraham GN, Evans TG. Hepatitis B Immunization of healthy elderly adults: relationship between naïve CD4+ T Cells and primary immune response and evaluation of GM-CSF as an adjuvant. *J Clin Immunol* 2001; **21**: 30-36
- 21 **Bennett RG,** Powers DC, Remsburg RE, Scheve A, Clements ML. Hepatitis B virus vaccination for older adults. *J Am Geriatr Soc* 1996; **44**: 699-703
- 22 **Murhekar MV,** Murhekar KM, Arankalle VA, Sehgal SC. Immune response to an indigenously developed hepatitis-B (Shanvac-B) vaccine in a tribal community of India. *Vaccine* 2002; **20**: 3431-3435
- 23 **Zannolli R,** Morgese G. Hepatitis B vaccine: current issues. *Ann Pharmacother* 1997; **31**: 1059-1067
- 24 **Wismans P,** van Huttum J, Stelling T, Poel J, de Gast GC. Effect of Supplementary vaccination in healthy non-responders to hepatitis B vaccination. *Hepatogastroenterology* 1998; **35**: 78-79
- 25 **Clemens R,** Sanger R, Kruppenbacher J, Hobel W, Stanbury W, Bock HL, Jilg W. Booster immunization of low- and non-responders after a standard three dose hepatitis B vaccine schedule-results of a post marketing surveillance. *Vaccine* 1997; **15**: 349-352

Edited by Zhang JZ

The treatment of the “untreatable” patient-revisited

Joseph B. Kirsner

Joseph B. Kirsner, The Louis Block Distinguished Service Professor of Medicine, Section of Gastroenterology, Department of Medicine, university of Chicago, USA

Based upon a paper published in the Illinois Medical Journal (117 - June 1960 - with permission of the Illinois State Medical Society)

Correspondence to: Joseph B. Kirsner, M.D., Ph.D., The Louis Block Distinguished Service Professor of Medicine, Section of Gastroenterology, Department of Medicine, university of Chicago, USA. gponce@medicine.bsd.uchicago.edu

Telephone: +1-773-7026101 **Fax:** +1-773-7024028

Received: 2003-01-11 **Accepted:** 2003-02-19

Abstract

The limits of medicine have not yet been reached. Numerous human illnesses initially thought to be incurable are reversible under unique and unpredictable individual circumstances. This paper, and the preceding companion publication, describes instances of the successful treatment of patients previously labeled as untreatable, including instances of severe ulcerative colitis and Crohn's disease.

Kirsner JB. The treatment of the “untreatable” patient-revisited. *World J Gastroenterol* 2003; 9(5): 885-887

<http://www.wjgnet.com/1007-9327/9/885.htm>

“We simply cannot predict what will happen to every given patient.”

—James S. Goodwin and Jean M. Goodwin - 1987

The recent (2002) social visit with a former, now healthy patient, first seen 54 years earlier, prompted the review of my 1960 paper entitled “The Treatment of the Untreatable Patient”^[1]. In that publication, I described the improvement and recovery of a group of patients, some with organic disease (cancer, inflammatory bowel disease, and septicemia) and some with emotionally-related disorders who responded to sustained nutritional aid and emotionally supportive therapy after having been evaluated elsewhere as “medically untreatable.”

My former patient, R.K., had immigrated with his parents to the USA from Germany in 1938. Now age 66, and in good health, he was first seen by me in 1948 when he was 12 years old. He had been diagnosed at two major medical centers as having severe ulcerative colitis, “untreatable medically”, and “requiring a total colectomy and ileostomy”. His parents then had brought him to the University of Chicago for admission to my hospital service. Physical examination revealed a pale, undernourished boy, obviously sick. Diagnostic studies confirmed the presence of severe idiopathic ulcerative colitis involving the entire colon. Laboratory tests documented the presence of a severe iron-deficiency anemia and a lowered serum albumin of 2.8 grams (normal 4.0 grams).

In the 1940s and 1950s, it was possible at the University of Chicago Medical Center, and very helpful, to keep seriously ill patients in the hospital for extended periods of time, and R. K. remained for approximately three months. Therapy initially included blood transfusions, nutritional support, and sulfonamides. Supportive psychotherapy, emphasizing

personal improvement and ultimate recovery, was provided for the patient. The patient's parents were informed daily as to progress and provided daily encouragement. In an ambience of optimism, expectations of success, and the involvement of an enthusiastic and caring hospital staff, the patient began to improve. Steroids, immunosuppressive compounds, and biological agents, of course, were not yet available. After the anemia had been corrected with several blood transfusions and the serum albumin had been restored to normal, with infusions of human albumin, the diarrhea, rectal bleeding and the abdominal discomfort gradually diminished. His appetite improved and he began to gain weight. When he returned home after three months in the hospital, he also had increased in height. At home, the improvement continued without interruption. After six months, and in the absence of any symptoms, all medications and dietary limitations were discontinued. At age 21, he was 6' 2" tall and weighed 190 lbs. He has remained well ever since. He married and raised a family of three children and 8 grandchildren, all healthy. Today, he continues in excellent health and is a successful businessman. In retrospect, R.K. and his colon were not “medically untreatable” initially, but rather difficult to treat. What was the therapeutic difference? It was probably the sustained therapy, the optimistic approach, and the strong nutritional and psychosocial personal support. The patient himself includes the interest, skill and unwavering optimism of his physician.

While less common than hoped for, such instances of recovery from ulcerative colitis are not rare, as described in earlier papers^[2,3]. In a second recent experience, A. T., first seen by me in 1952, with severe ulcerative colitis, had developed the disease in 1951; the treatment included nutritional and emotional support supplemented with injections of ACTH. The colitis recurred intermittently until 1959, when the patient “changed his life style” and “totally eliminated stress from his life”. The diagnosis of “multiple polypoid defects” on barium examination performed elsewhere, in 1991 had led to a recommendation of colectomy; but follow-up examinations found no evidence of colonic polyps. Expert colonoscopy was performed in April 2000 at the University of Chicago, and except for a mild “vascular distortion”, was unremarkable; colonic biopsies were negative for dysplasia. The patient has remained free of symptoms since 1960, now continuing for more than 40 years. Living in Hawaii, he organized and became president of a successful chemical company. In this patient also, the explanation for the apparent recovery from ulcerative colitis remains unclear: although “the avoidance of stress,” may be a contributing factor. Noteworthy in both patients with ulcerative colitis, therapy had emphasized nutritional and psychological support. In each instance, IBD improvement had coincided with personal achievement; issues rarely emphasized in today's world of molecules and genes. Biologic therapy, cytokine inhibition and gene transfer are exciting treatment possibilities for the future; but until these complex measures are realized, and perhaps irregardless of their availability, treatment of inflammatory bowel disease should continue to emphasize detailed attention to the nutritional and personal needs of the patient.

The word “untreatable” does not appear in Webster's dictionary; the Random House Dictionary of the English language, the American Heritage dictionary, nor in Roget's

Thesaurus. Webster's Medical Desk dictionary blandly defines untreatable as "not susceptible to medical treatment". Medicine has never fully accepted Hippocrates' observation^[4], "... for it is impossible to make all the sick well . . .", and has made remarkable progress in reducing the ranks of the "untreatable". Indeed, as the Goodwins^[5] have indicated: "Twentieth Century Medicine can be seen as a systematic denial of the impossible." Nevertheless, uncertainty in the course of human disease, and in its prognosis has characterized Medicine, throughout history as reviewed by J. Baroness^[6] and by R. Fox^[7].

The designation "untreatability" in medicine is both arbitrary and absolute. It may be a relative term, reflecting non-cooperation of the patient or an inadequate therapeutic approach, rather than the illness itself. Occasionally, "untreatability" is the inappropriate label for an initially erroneous diagnosis, as illustrated in the following patient, first described in 1960. A.J., a 62-year old photo-engraver, in 1940, had developed severe pain in the epigastrium and in the back with nausea, vomiting, and weight loss. Surgery at another hospital demonstrated an "inoperable carcinoma of the pancreas," and the abdomen was closed. The patient then was referred to the University of Chicago for possible chordotomy to relieve the intractable pain. Here, the pain and vomiting continued. The alert hospital resident noted the vomitus as clear, watery-appearing, fluid; and having learned earlier that gastric acid secretion is a watery appearing fluid; he tested the vomitus with Töpfer's reagent, and indeed identified the fluid as gastric secretion containing hydrochloric acid. The intragastric instillation of hydrochloric acid reproduced the pain and vomiting, and gastric aspiration, removing the acid secretion, relieved the pain. X-rays demonstrated a huge duodenal ulcer crater. Large amounts of calcium carbonate hourly, day and night, atropine sulphate, and frequent gastric aspirations were required to diminish the pain and heal the ulcer, events consistent with duodenal ulcer, penetrating into the pancreas, causing pancreatitis. The surgeon presumably had misinterpreted the inflammatory thickening of the pancreas as neoplasm. In August 1941, an appendectomy was performed for acute appendicitis; and confirmed the absence of carcinoma. Ulcer recurrences necessitated a supradiaphragmatic vagotomy; and gastroenterostomy in June 1944, with complete recovery. He later succumbed to a heart attack 35 years after the initial erroneous diagnosis of pancreatic carcinoma.

At times, the determined patient provides the vital spark, transforming an apparently hopeless situation into one of renewed hope and improved health. A striking example, cited in the 1960 paper, is that of a man, then 53 years old, with a history of alcoholism, cirrhosis of the liver and malnutrition, who was hospitalized with ascites and thrombophlebitis of superficial veins in the abdominal wall. X-rays revealed not only esophageal varices, but also a linitis plastica-type carcinoma of the stomach. When he became confused, the situation appeared hopeless indeed. It seemed only humane to grant the patient's plea for simply orange juice and coffee. Astonishingly, instead of deteriorating, he improved. The thrombophlebitis subsided; the ascites gradually diminished, and in several weeks the patient returned home. Additional history revealed that he had swallowed lye during childhood, causing the gastric deformity simulating neoplasm. The patient survived for many years thereafter; and occasionally revisited us to demonstrate his continuing viability. The hepatic disease eventually became "untreatable", and he died following a massive hemorrhage from esophageal varices; but had he been untreatable initially?

Patients with emotional difficulties and associated gastrointestinal symptoms may be especially challenging, because of the difficulty in fully understanding emotionally generated symptoms^[8,9] prematurely prompting the label of

"untreatability". This important problem has been reviewed recently^[10]. Useful therapy includes the exclusion of structural disease and evaluation of the life situation of the patient, a reassuring explanation of the physiologic basis of the symptoms, avoiding criticism, and sustained supportive therapy^[11]. Medication alone often does not suffice in these circumstances, and the art of medicine is as necessary as its science. Indeed, hope, faith and trust, together with sustained therapeutic effort salvage more sick people than many physicians realize^[12,13]. H.G. Wolff^[14] has pointed out that "hope, like faith and purpose in life, is medicinal".

The significant beneficial impact of religious beliefs in some patients with chronic illness also has been documented^[15]. The treatment of such patients, often is prolonged, and demanding; but the satisfaction following successful therapy is one of the rewarding personal experiences in the practice of medicine. An example of this type of "medical untreatability", noted in the 1960 paper, is that of M.V., then a 50 year-old man, who repeatedly sought treatment for digestive symptoms, including a bitter taste, belching, flatulence, constipation and diarrhea, abdominal pain, and fatigue; diagnosed as an irritable bowel. Many laboratory and diagnostic studies were normal; and many consultations with physicians in other areas of medicine did not reveal additional problems. Psychiatric evaluation of the patient included the following: ". . . a passive, inhibited male. . . his hypochondriacal expressions are at once expressions of his primary concern with himself and defenses against object relationships (which are threatening because of their homosexual character . . .) . . . Psychotherapy could be of little value and is not indicated in the present circumstances". However, the patient was regularly employed. In time he became involved in the affairs of his community and was recognized for this activity. The many medical visits undoubtedly provided him with a measure of support, though the continuing need for reassurance reflected limited acquired understanding of his situation. The patient was perhaps "untreatable" in that his basic emotional difficulty was not fully resolved. However, he was relatively treatable in that, with support, reassurance, and personal attention, he was able to function as a useful citizen. Since then, modern research has documented significant biological and physiologic relationships between mind and body^[3,16,17] and has provided a scientific basis for the understanding and management of emotionally associated gastrointestinal symptomatology.

The limits of medicine, as these clinical experiences illustrate, are by no means rigid or irreversible. While much has been learned about human illness and its molecular nature, there is much more knowledge yet to be acquired about individual human illness^[18], its neurological, immunological and genetic dimensions. Hopefully, as expressed by Baroness^[6], ". . . through continued research and technologic innovation, fueled by curiosity and personal drive, by institutional agendas and by the insightful and compassionate physician in the service of human needs", additional progress can be anticipated in the successful management of the "untreatable patient."

REFERENCES

- 1 **Kirsner JB**. The treatment of the untreatable patient. *Illinois Medical J* 1960; **117**: 385-400
- 2 **Kirsner JB**, Palmer WL, Klotz AP. Reversibility in ulcerative colitis. *Radiology* 1951; **57**: 1-14
- 3 **Kirsner JB**, VanWoert M. Reversibility and irreversibility in ulcerative colitis. *Med Clin North Am* 1964; **48**: 143-157
- 4 **Adams F**. The Genuine Works of Hippocrates. Baltimore: *Williams Wilkins Co* 1939
- 5 **Goodwin JS**, Goodwin JM. Impossibility in medicine. In: Davis PJ, Park D, eds. No Way - the Nature of the Impossible. *New York:WH Freeman and Company* 1987

- 6 **Barondess JA.** The impossible in medicine. *Perspectives in Biology and Medicine* 1986; **29**: 521-529
- 7 **Fox RC.** The evolution of medical uncertainty. *Milbank Quarterly Health and Society* 1980; **58**: 1-49
- 8 **Brosin HW.** The doctor and his patients. *Post Med* 1956; **20**:528-531
- 9 **Smith CA,** Chapman EM, Chase PP, Beck IA, Clark SL. Help for the hopeless. *Rhode Island MJ* 1956; **39**: 491
- 10 **Dewar MJ,** Pies RV. The difficult to treat psychiatric patient. Washington DC: *Am Psych Publi* 2001
- 11 **Kirsner JB,** Palmer WL. The irritable colon. *Gastroenterology* 1958; **34**: 491-501
- 12 **Cabot RC,** Dicks RL. The art of ministering to the sick. New York: *Mac Mill Comp* 1936
- 13 **Cousins N.** Anatomy of an illness (as perceived by the patient). *Saturd Review Literat* 1977; **28**: 1458-1463
- 14 **Wolff HG.** What hope does for man. *Saturday Review (Science and Humanity)* 1957
- 15 **Koenig HG.** An 83-year old woman with chronic illness and strong religious beliefs. *JAMA* 2002; **288**: 487-492
- 16 **Steinberg EM.** Emotions and disease - from balance of humors to balance of molecules. *Nature Med* 1993; **3**: 264-267
- 17 **Steinberg EM.** Neural-immune interactions in health and disease. *J Clin Investigation* 1997; **100**: 2641-2647
- 18 **Fessel WJ.** The nature of illness and diagnosis. *Am J Med* 1983; **75**: 555-560

Edited by Xu XQ

Response of human *REV3* gene to gastric cancer inducing carcinogen *N*-methyl-*N'*-nitro-*N*-nitrosoguanidine and its role in mutagenesis

Feng Zhu, Cai-Xia Jin, Tao Song, Jun Yang, Lei Guo, Ying-Nian Yu

Feng Zhu, Tao Song, Jun Yang, Lei Guo, Ying-Nian Yu, Department of Pathophysiology, Zhejiang University School of Medicine, Hangzhou 310031, Zhejiang Province, China

Cai-Xia Jin, Department of Biology, Ningxia Medical College, Yingchuan 750004, Ningxia Self-governing Region, China

Supported by a grant from the National Natural Science Foundation of China for Key Program, No.39830210, and a grant from the National Natural Science Foundation of China, No. 39960067, and a grant from National Key Basic Research and Development Program, No. 2002CB512904

Correspondence to: Professor Ying-Nian Yu, Department of Pathophysiology, Zhejiang University School of Medicine, Hangzhou 310031, Zhejiang Province, China. ynyu@mail.hz.zj.cn

Telephone: +86-571-87217149 **Fax:** +86-571-87217149

Received: 2002-12-07 **Accepted:** 2003-01-13

Abstract

AIM: To understand the response of human *REV3* gene to gastric cancer inducing carcinogen *N*-methyl-*N'*-nitro-*N*-nitrosoguanidine (MNNG) and its role in human mutagenesis.

METHODS: The response of the human *REV3* gene to MNNG was measured in human 293 cells and FL cells by RT-PCR. By using antisense technology, mutation analysis at *HPRT* locus (on which lesion-targeted mutation usually occurs) was conducted in human transgenic cell line FL-*REV3*⁻ by 8-azaguanine screening, and mutation occurred on undamaged DNA template was detected by using a shuttle plasmid pZ189 as the probe in human transgenic cell lines 293-*REV3*⁻ and FL-*REV3*⁻. The blockage effect of *REV3* was measured by combination of reverse transcription-polymerase chain reaction to detect the expression of antisense *REV3* RNA and Western blotting to detect the *REV3* protein level.

RESULTS: The human *REV3* gene was significantly activated by MNNG treatment, as indicated by the upregulation of *REV3* gene expression at the transcriptional level in MNNG-treated human cells, with significant increase of *REV3* expression level by 0.38 fold, 0.33 fold and 0.27 fold respectively at 6 h, 12 h and 24 h in MNNG-treated 293 cells ($P < 0.05$); and to 0.77 fold and 0.65 fold at 12 h and 24 h respectively in MNNG-treated FL cells ($P < 0.05$). In transgenic cell line (in which *REV3* was blocked by antisense *REV3* RNA), high level of antisense *REV3* RNA was detected, with a decreased level of *REV3* protein. MNNG treatment significantly increased the mutation frequencies on undamaged DNA template (untargeted mutation), and also at *HPRT* locus (lesion-targeted mutation). However, when *REV3* gene was blocked by antisense *REV3* RNA, the MNNG-induced mutation frequency on undamaged DNA templates was significantly decreased by 3.8 fold ($P < 0.05$) and 5.8 fold ($P < 0.01$) respectively both in MNNG-pretreated transgenic 293 cells and FL cells in which *REV3* was blocked by antisense RNA, and almost recovered to their spontaneous mutation levels.

The spontaneous *HPRT* mutation was disappeared in *REV3*-disrupted cells, and induced mutation frequency at *HPRT* locus significantly decreased from 8.66×10^{-6} in FL cells to 0.14×10^{-6} in transgenic cells as well ($P < 0.01$).

CONCLUSION: The expression of the human *REV3* can be upregulated at the transcriptional level in response to MNNG. The human *REV3* gene plays a role not only in lesion-targeted DNA mutagenesis, but also in mutagenesis on undamaged DNA templates that is called untargeted mutation.

Zhu F, Jin CX, Song T, Yang J, Guo L, Yu YN. Response of human *REV3* gene to gastric cancer inducing carcinogen *N*-methyl-*N'*-nitro-*N*-nitrosoguanidine and its role in mutagenesis. *World J Gastroenterol* 2003; 9(5): 888-893

<http://www.wjgnet.com/1007-9327/9/888.htm>

INTRODUCTION

It has long been known that exposure to certain chemicals is associated with the development of specific human cancers, which is largely the outcome of interaction between environmental agents and genetic susceptibility. Examples include the associations between amine dyes and bladder cancer, benzene and leukemia, aflatoxin and hepatocellular carcinoma, and tobacco smoke and lung cancer^[1-5]. Recent studies have also revealed that tobacco smoke significantly increases the risks for oral^[6, 7], esophageal^[3-5, 8], bladder^[9-12], pancreas^[11], gastric^[13] and colorectal cancers^[14]. In addition, men who have a history of chronic indigestion or gastroduodenal ulcer have substantially higher mortality rates associated with concurrent cigarette smoking^[13].

Tobacco smoke consists of many chemicals. One important substance found in tobacco smoke is chemical carcinogen *N*-methyl-*N'*-nitro-*N*-nitrosoguanidine (MNNG), a direct acting carcinogen, that targets the cellular DNA and induces severe genotoxic stress to the cell that can result in various DNA damages^[15]. Epidemiologic studies have suggested an etiological role for *N*-nitroso compounds from dietary sources in the development of gastric and colorectal cancer in humans^[16, 17], and animal experiments have shown that MNNG induces gastric cancer^[18-21] and colorectal cancer^[22, 23]. Obviously, the link between DNA damages and MNNG induced cancers is closely related to mutagenesis. To ensure normal growth control and accuracy in DNA replication, cells have developed a variety of responses to stress, such as DNA repair, cell cycle checkpoints, DNA damage avoidance, or in extreme cases, apoptosis^[24]. In addition, cells have also evolved a sophisticated lesion bypass system (also called translation synthesis, or TLS) to repair the damaged DNA, resulting in DNA damage lesion-targeted mutation. However, mutation can also occur on undamaged DNA template, which is designated untargeted mutation (UTM), which has been described in SOS-induced mutagenesis in *E. coli*^[25]. It has been known that untargeted and targeted mutations caused by SOS response in *E. coli* both are resulted from the inhibition of DNA polymerase functions

that normally maintain fidelity and the involvement of DNA polymerases with low fidelity, which include DNA pol IV (dinB), pol V (UmuD' 2C) and other factors^[26-30]. In eukaryote, it has been found that up to 40 % of cycl-91 revertants induced by ultraviolet (UV) is untargeted using mating experiments with excision deficient strains of *Saccharomyces cerevisiae*^[31], and that stress response induced by DNA damaging agents (8-methoxy-psoralen or UV) leads to specific and delayed UTM in mouse T-lymphoma cells^[32]. Previous studies in our laboratory also shown that low concentration MNNG induces UTM in mammalian cells^[33]. Currently, it has been known that specialized DNA polymerases are responsible for DNA damage lesion-targeted mutation in eukaryote. However, it is not clear which factor can be activated and involved in UTM on undamaged DNA templates.

The human *REV3* gene, encoding the catalytic subunit REV3 of human pol ζ , has been received intensive attention in recent years^[34]. *REV3* gene is thought to be the major component of error-prone TLS pathway^[34, 35], although a number of other polymerases might also be involved in this process^[36]. It is responsible for most of spontaneous and UV-induced mutation in yeast and humans, as well as somatic hypermutation in humans^[34, 35, 37-43, 44-47]. The expression of *REV3* appears to be elevated at the transcriptional level in some tumor cell lines^[48]. However, the response of *REV3* gene to gastric cancer inducing carcinogen MNNG and its role in MNNG-induced mutagenesis are still not clear. In order to understand the relationship between the human *REV3* gene and the etiology of gastric cancer and colorectal cancer in humans, the response of *REV3* to MNNG and its role in MNNG-induced mutagenesis, including both lesion-targeted and untargeted mutation, were explored.

MATERIALS AND METHODS

Cell culture and treatment

Human 293 cells were grown in DMEM (Dulbecco's Modified Eagle Medium, Gibco) containing 10 % fetal bovine serum (Gibco), 200 units/ml penicillin, 100 μ g/ml streptomycin and 200 μ g/ml kanamycin. Human FL cells were grown in MEM (Minimum Essential Medium, Gibco), containing 10 % newborn calf serum (Gibco), 200 units/ml penicillin, 100 μ g/ml streptomycin and 200 μ g/ml kanamycin. Transgenic cell line 293-*REV3*^[49] and FL-*REV3*⁻ (unpublished data) were established in this laboratory by transfecting 293 cells and FL cells with pM-RS⁻ plasmid^[50] that can express anti *REV3* RNA when induced by dexamethasone (dex). 293-M and FL-M cell line were established by transfecting 293 cells and FL cells with the control vector pMAM neo-amp⁻ alone. These transgenic cell lines were grown in MEM containing 200 mg/ml of G418 (geneticin, Gibco). For MNNG treatment, cells were exposed to 0.2 μ M of MNNG (Sigma, dimethyl sulfoxide (DMSO) as solvent) in serum-free DMEM (for 293 cells) or MEM (for FL cells) for 2.5 h, and then MNNG was removed and replaced with fresh medium. DMSO treated cells were used as control.

Response of human *REV3* to MNNG

The response of the human *REV3* gene to MNNG was measured at the transcriptional level by using reverse transcription-polymerase chain reaction (RT-PCR) with *ARF1* (encoding ADP-ribosylation factor 1) as the internal control. RNA from 2×10^6 293 or FL cells was extracted at different time point using TRIzol agent (Gibco) after 0.2 μ M MNNG treatment, followed by the first-strand cDNAs synthesis with 3 μ g of RNA using M-MuLV reverse transcriptase (MBI fermentas) and random hexamer primer. After exponential

phase selection, PCR was performed with the appropriate cycles: 5 min pre-denaturation at 95 $^{\circ}$ C, 30 sec denaturation at 94 $^{\circ}$ C, 30 sec annealing at 59 $^{\circ}$ C, 1 min extension at 72 $^{\circ}$ C, and an additional 10 min extension at 72 $^{\circ}$ C. PCR primers: *REV3*, 5' -TGT CCA AGG CAC CAT ATC TC-3' (sense), 5' -TGC TAC ACG TGG TAC TAC TG-3' (antisense); *ARF1*, 5' -GAA CAT CTT CGC CAA CCT CTT C-3' (sense), 5' -ACA GCC AGT CCA GTC CTT CAT A-3' (antisense). The sizes of the expected products are 635bp for *REV3* and 515bp for *ARF1*. Ratios of OD_{*REV3*}/OD_{*ARF1*} representing *REV3* transcript level were calculated.

Identification of the antisense blocking effect on *REV3* function in transgenic cells

The antisense blocking effect on *REV3* function was analyzed by detecting the expression of antisense *REV3* fragment with RT-PCR and the *REV3* protein level with Western blotting. RNA was extracted from transgenic cells, which could express antisense *REV3* fragment after 10 μ M dex treatment for 3 days. 0.1 μ g RNA from 1 μ g RNA sample digested by 1 unit DNaseI (Gibco) was reverse transcribed using the *REV3* specific sense primer (5' -AAG GCC AGC ATA CAA GAC-3'). For the positive control (with no dex treatment), a random hexamer primer was used as the reverse transcription. Each cDNA sample was amplified with the specific primers: 5' -GCC AAG GAA TAC AGA GGA AGT-3' (sense), 5' -CCA GCT GAA GAC ATC AAT ACC-3' (antisense). The PCR cycling parameter is as following: 5 min pre-denaturation at 94 $^{\circ}$ C, 30 cycles of 30 sec denaturation at 94 $^{\circ}$ C, 30 sec annealing at 59 $^{\circ}$ C, and 1 min extension at 72 $^{\circ}$ C. Amplifications were completed by an additional 8 min extension at 72 $^{\circ}$ C. For Western blotting, the nuclear protein were extracted from the cell strains as described before^[24]. Each nuclear extract (30 μ g) was used for Western blotting, and the Ku70 protein was used as the loading control.

Detection of mutation at *HPRT* locus^[51]

2×10^5 cells of the FL, FL-M or FL-*REV3*⁻ were seeded in 100 ml culture flasks, respectively. After 1 day incubation, the media were replaced with HAT medium (Gibco) for 24 h and HT medium (Gibco) for the next 48 h to remove the pre-existed *HPRT*⁻ cells in the population, then the cells were induced with 10 μ M dex for another 48 h. After treatment with 0.2 μ M MNNG or DMSO for 2.5 h, the medium was removed and replaced with a fresh medium containing 10 μ M dex for an additional 24 h incubation. Cells reaching approximately 80 % confluent were subcultured three or four times, with a consistent density at 10^6 cells/flask. Then 200 cells were transferred to a 9-cm plate (5 plates total) for 15 days to count the relative cloning efficiency. In the meantime, 2×10^5 cells were seeded in 100 ml culture flask (5 flasks total). After 24 h, the medium was replaced with fresh one containing 5 μ g/ml 8-azaguanine (Gibco). Cells were then maintained for 30 days, with the medium changed every 3 days. After washing with 0.9 % NaCl, the clones were fixed with ethanol: acetic acid (3:1), stained with 1 % methylene blue, and the number counted. The mutation frequency was calculated as following:

Mutation frequency = (number of mutant clones/ 10^6 cells) \times (1/relative cloning efficiency).

Statistical analysis was performed according to the method described by Kastenbaum and Bowman^[52].

Detection of untargeted mutation on shuttle plasmid pZ189

The detection of untargeted mutation was performed as described (Figure 1)^[33].

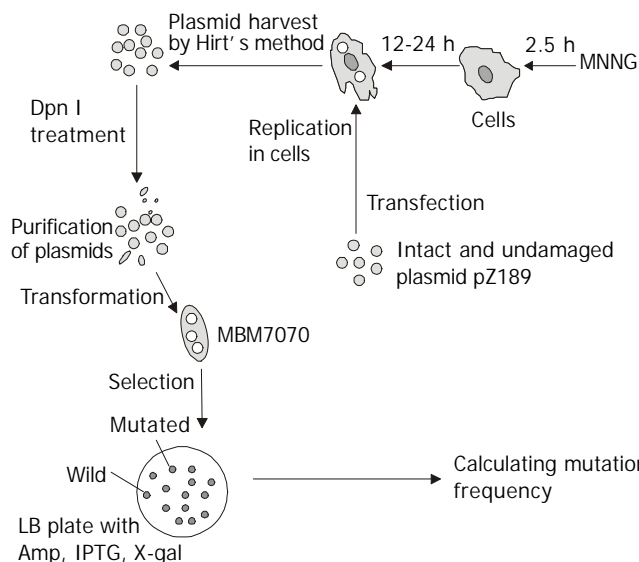


Figure 1 The detection system of untargeted mutation occurring on undamaged DNA template. Cells were pretreated by MNNG, and then intact and undamaged shuttle plasmid pZ189 was transfected into cells after removing MNNG. After replication for 48 h in cells, replicated pZ189 plasmid was rescued and then transformed to host bacterial MBM7070 to screen pZ189 mutants.

RESULTS

Response of human mutator *REV3* to MNNG

It was found that PCR with 31 cycles for 293 cells and 28 cycles for FL cells ensured the exponential amplification of *REV3* and *ARF1* within the same tube (data not shown). The expression of *REV3* was upregulated at the transcriptional level in both 293 cells and FL cells after MNNG treatment. In MNNG-treated 293 cells, the level of *REV3* expression was significantly increased by 0.38 fold at 6 h, 0.33 fold at 12 h and 0.27 fold at 24 h, when compared with the control ($P < 0.05$, Figure 2). Similarly, the transcriptional level of *REV3* was also significantly increased by 0.77 fold at 12 h and 0.65 fold at 24 h in MNNG-treated FL cells, when compared with the control (all $P < 0.05$, Figure 2). The data suggest that the human mutator *REV3* gene was activated by low concentration MNNG treatment and could be regulated at the transcriptional level.

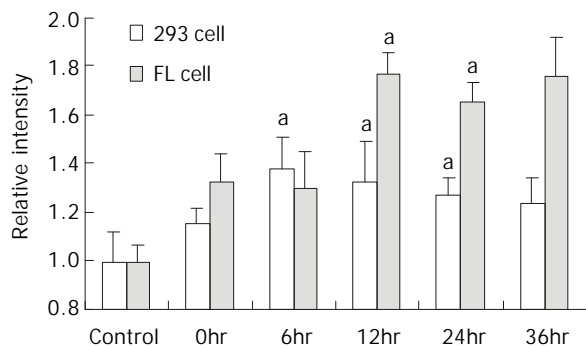


Figure 2 The response of the human *REV3* to MNNG at different time points. The response of *REV3* to MNNG was measured in human 293 cells and FL cells at the transcriptional level by using RT-PCR. ^a $P < 0.05$, compared with the control.

Identification of the antisense blocking effect on *REV3* function in transgenic cells

An expected high level of 297bp antisense RNA to C-terminal of *REV3* was detected in transgenic cells by RT-PCR (Figure

3). In addition, the results of Western blotting showed that the *REV3* protein level was obviously reduced in transgenic cells (Figure 4). Therefore, it was indicated that the function of *REV3* protein was partially blocked by antisense *REV3* fragment in transgenic cells.

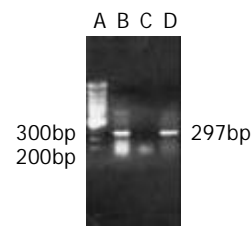


Figure 3 Detection of antisense *REV3* RNA fragment expressed in 293-*REV3* cells using RT-PCR. A, 100bp DNA ladder; B, RT-PCR result in Dex-treated 293-*REV3* cells; C, RT-PCR result in 293-*REV3* cells (Dex-free); D, a positive control.

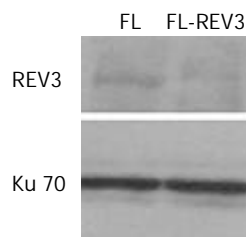


Figure 4 Western blotting showing the loss of *REV3* protein in transgenic FL-*REV3* cells. Western analysis showing the level of expression of *REV3* protein in nuclear extracts from *REV3* antisense-expressing transfectant FL-*REV3*⁻ and its parental strain FL. Ku-70 was used as the loading control.

Decreased formation of MNNG induced *HPRT* mutants in transgenic cells

HPRT locus is traditionally used as a genetic marker for genome instability. Normally the spontaneous mutation frequency at *HPRT* locus was quite low. In the present study, we observed that the spontaneous mutation frequency was 2.87×10^{-6} in FL cells, and 4×10^{-6} in FL-M cells. Interestingly, in FL-*REV3*⁻ cells, no spontaneous mutants were observed. This observation led to the speculation that *REV3* may be involved in the process of spontaneous mutagenesis.

Previous studies found that MNNG could induce *HPRT* mutation in human cells^[53]. It would be of interest to know if MNNG had the same effect on FL and the derived FL-M and FL-*REV3*⁻ cells. As shown in Table 1, we observed that MNNG treatment significantly elevated the mutation frequency from 2.87×10^{-6} to 8.66×10^{-6} at *HPRT* locus in FL cells. Similarly, the mutation frequency was also increased in FL-M cells by MNNG treatment from 4×10^{-6} to 18.75×10^{-6} . On the other hand, the induced mutation frequency was only 0.14×10^{-6} cells in FL-*REV3*⁻ cells, which was significantly lower than that of the spontaneous mutation frequency in FL cells (Table 1).

Decreased untargeted mutation frequency on undamaged plasmid transfected into MNNG pretreated transgenic cells

Intact and undamaged shuttle plasmid pZ189 DNA was introduced into MNNG pretreated human cells. Progeny plasmids were harvested 48 h after transfection, and used to transform MBM7070. White and light blue colonies were picked and the frequency of *supF* *tRNA* mutants was scored. As shown in Table 2, the spontaneous mutation frequencies were at comparable level between each cell lines. Untargeted mutation on undamaged DNA templates was increasingly

Table 1 Detection of the spontaneous and induced mutation frequency at *HPRT* locus in FL, FL-M and FL-REV3⁻ cells

Cell line	MNNG (0.3 μ M)	Antisense block of <i>REV3</i>	No. of mutants per 10 ⁶ cells selected	Mutation frequency (10 ⁻⁶)
FL	0	None	2.87	2.87
	0.3		19.25 ^{bc}	8.66
FL-M	0	None	4.00	4
	0.3		18.75 ^{bc}	18.75
FL-REV3 ⁻	0	Yes	0 ^a	0
	0.3		7 ^a	0.14

^a: mutants screened from 5 \times 10⁷ cells; ^b P <0.01 compared with spontaneous mutants in FL cell and FL-M cell; ^c P <0.01 compared with FL-REV3⁻ cells.

Table 2 Mutation frequency of *supF* *tRNA* gene in intact plasmid pZ189 after replicated in cultured human cells

Cell line	DMSO			MNNG		
	Number of transformant	Number of mutant	Mutation frequency(10 ⁻⁴)	Number of transformant	Number of mutant	Mutation frequency(10 ⁻⁴)
293	7954	1	1.26	12205	9	7.37 ^{ab}
293-M	15358	2	1.30	12040	7	5.81 ^{ab}
293-REV3 ⁻	39236	9	2.29	19758	3	1.52
FL	13495	7	5.2	13854	38	27.4 ^{cd}
FL-M	13272	7	5.3	10310	28	27.2 ^{cd}
FL-REV3 ⁻	10967	3	2.7	12609	5	4.0

a, c χ test P <0.05 and 0.01 respectively as compared with spontaneous mutation frequency; b, d χ test P <0.05 and 0.01 as compared with induced mutation frequency in 293-REV3⁻ and FL-REV3⁻ cells respectively.

induced in MNNG-pretreated 293, 293-M, FL and FL-M cells, with the mutation frequencies occurred in these cells being 4.5-5.8-fold higher than those in control groups. However, the untargeted mutation frequencies significantly decreased by 3.8 fold (from 7.37 \times 10⁻⁴ to 1.52 \times 10⁻⁴, P <0.05) and 5.8 fold (from 27.4 \times 10⁻⁴ to 4.0 \times 10⁻⁴, P <0.01) respectively in MNNG-pretreated transgenic 293 cells and FL cells in which *REV3* was blocked by antisense RNA, and the mutation frequencies were almost similar to their spontaneous mutation levels.

DISCUSSION

The interconnections between environment and human health have been increasingly recognized. With the increasing cases of environmental cancer in the world range, especially in developing countries, investigation on the potential biomarkers for environmental risk assay or new targets for gene therapy is an emergent task to prevent and control the carcinogenesis. In China, the incidence of gastric cardia cancer has greatly increased in the past 2-3 decades, and dietary habits might be one of the risk factors for the cardia carcinogenesis among Chinese population^[54]. Recently, it was found that COX-2 may contribute to progression of tumor in human gastric adenocarcinoma^[55]. However, it has become clear that the induction of carcinogenesis is a complex multi-step process involving a series of genetic and epigenetic changes. For example, the induction of colon cancer requires alterations in at least three tumor-suppressor genes (*MCC*, *DCC*, and *p53*) and activation of the oncogene *K-ras*^[56-58]. The genetic changes mainly occur in initiation, malignant conversion and progression stages in the development of malignant tumors^[59]. DNA damaging agents can induce lesions in DNA template, causing the block on DNA replication fork. However, it also leads to the activation of several TLS DNA polymerases, especially the activation of pol ζ , to restart the replication process by replacing the normal replication polymerases and finally result in lesion-targeted mutation^[40, 42, 60]. On the other hand, UV-light or chemical carcinogen can induce the UTM on undamaged DNA templates^[31-33].

It was interesting to find that human *REV3* gene, which

encodes the catalytic subunit of TLS polymerase ζ , was activated by the carcinogen MNNG that can induce gastric and colorectal cancer. Our computational analysis indicated that transcriptional factor binding sites for CREB, AP-1 and NF- κ B were found in the promoter region of *REV3* (data not shown). Previous studies in our laboratory have shown that MNNG treatment activates CREB^[61], AP-1 and NF- κ B (unpublished data) in mammalian cells as early epigenetic events, which indicates that *REV3* could be activated by MNNG via the activation of specific transcriptional factors in advance.

Mutation at *HPRT* locus can be used as an indicator to reflect the degree of genome instability^[62]. It has been recognized that *HPRT* mutants are generated directly by DNA damage^[62, 63], i. e., the mutation spectrum belongs to lesion-targeted mutation. In human fibroblasts, the number of UV-induced *HPRT* mutants is significantly increased, whereas, the mutation is remarkably depressed in the human cells that express high levels of *REV3* antisense RNA^[47]. In this study, our data showed that the spontaneous mutation of *HPRT* locus in human cells was dependent on the function of *REV3*, since mutation at *HPRT* locus was eliminated in cells expressing antisense *REV3* (Table 1). On the other hand, *REV3* gene was also involved in MNNG-induced *HPRT* mutation, like in UV-induced mutation^[47], as the antisense block of *REV3* function significantly decreased the MNNG-induced mutation frequency. It is also possible that other factors might be involved in MNNG-induced *HPRT* mutagenesis, for example, the function of human *REV1* gene is required for mutagenesis at *HPRT* locus induced by UV light^[64].

Interestingly, our data further indicated that human *REV3* gene also played a role in mutation genesis occurred on undamaged DNA templates. Unlike the role of *REV3* in lesion-targeted mutation, the spontaneous mutagenesis in *SupF* *tRNA* gene in pZ189 replicated in human cells was *REV3*-independent, i. e., the antisense block of *REV3* has no effect on the spontaneous mutations (Table 2). It was suggested that most of the spontaneous mutation occurring in such an experimental system are due to the deletion damage induced by the shear force during transfection. Different mechanisms are involved in repairing the base damage and deletion damage,

in the later case no evidence was presented of *REV3* dependent. In this study, however, we proved that MNNG-induced mutation on undamaged DNA templates was *REV3*-dependent (Table 2). To date, we still do not know whether there are other factors involved in untargeted mutation in addition to the human *REV3* gene. Taken together, these data strongly suggest that human *REV3* gene is capable of inducing mammalian genome instability, and this mutator gene could be a potential target for gastric and colorectal cancer prevention and gene therapy.

REFERENCES

- 1 **Yang J**, Duerksen-Hughes P. A new approach to identifying genotoxic carcinogens: p53 induction as an indicator of genotoxic damage. *Carcinogenesis* 1998; **19**: 1117-1125
- 2 **Li Y**, Su JJ, Qin LL, Yang C, Luo D, Ban KC, Kensler T, Roebuck B. Chemopreventive effect of oltipraz on AFB(1)-induced hepatocarcinogenesis in tree shrew model. *World J Gastroenterol* 2000; **6**: 647-650
- 3 **Boring CC**, Squires TS, Tong T, Heath CW. Mortality trends for selected smoking-related cancers and breast cancer-United States, 1950-1990. *Morb Mortal Wkly Rep* 1993; **42**: 857, 863-866
- 4 **Bollschweiler E**, Holscher AH. Carcinoma of the esophagus-actual epidemiology in Germany. *Onkologie* 2001; **24**: 180-184
- 5 **Bonnin-Scaon S**, Lafon P, Chasseigne G, Mullet E, Sorum PC. Learning the relationship between smoking, drinking alcohol and the risk of esophageal cancer. *Health Educ Res* 2002; **17**: 415-424
- 6 **Balaram P**, Sridhar H, Rajkumar T, Vaccarella S, Herrero R, Nandakumar A, Ravichandran K, Ramdas K, Sankaranarayanan R, Gajalakshmi V, Munoz N, Franceschi S. Oral cancer in southern India: the influence of smoking, drinking, paan-chewing and oral hygiene. *Int J Cancer* 2002; **98**: 440-445
- 7 **Bartal M**. Health effects of tobacco use and exposure. *Monaldi Arch Chest Dis* 2001; **56**: 545-554
- 8 **Wang AH**, Sun CS, Li LS, Huang JY, Chen QS. Relationship of tobacco smoking CYP1A1 GSTM1 gene polymorphism and esophageal cancer in Xi'an. *World J Gastroenterol* 2002; **8**: 49-53
- 9 **Badawi AF**, Habib SL, Mohammed MA, Abadi AA, Michael MS. Influence of cigarette smoking on prostaglandin synthesis and cyclooxygenase-2 gene expression in human urinary bladder cancer. *Cancer Invest* 2002; **20**: 651-656
- 10 **Bernardini S**, Adessi GL, Chezy E, Billerey C, Carbillet JP, Bittard H. Influence of cigarette smoking on P53 gene mutations in bladder carcinomas. *Anticancer Res* 2001; **21**: 3001-3004
- 11 **Borras J**, Borras JM, Galceran J, Sanchez V, Moreno V, Gonzalez JR. Trends in smoking-related cancer incidence in Tarragona, Spain, 1980-1996. *Cancer Causes Control* 2001; **12**: 903-908
- 12 **Castelao JE**, Yuan JM, Skipper PL, Tannenbaum SR, Gago-Dominguez M, Crowder JS, Ross RK, Yu MC. Gender- and smoking-related bladder cancer risk. *J Natl Cancer Inst* 2001; **93**: 538-545
- 13 **Chao A**, Thun MJ, Henley SJ, Jacobs EJ, McCullough ML, Calle EE. Cigarette smoking, use of other tobacco products and stomach cancer mortality in US adults: The Cancer Prevention Study II. *Int J Cancer* 2002; **101**: 380-389
- 14 **Casimiro C**. Etiopathogenic factors in colorectal cancer. Nutritional and life-style aspects. 2. *Nutr Hosp* 2002; **17**: 128-138
- 15 **Yang J**, Duerksen-Hughes PJ. Activation of a p53-independent, sphingolipid-mediated cytolytic pathway in p53-negative mouse fibroblast cells treated with N-methyl-N-nitro-N-nitrosoguanidine. *J Biol Chem* 2001; **276**: 27129-27135
- 16 **Palli D**, Saieva C, Coppi C, Del Giudice G, Magagnotti C, Nesi G, Orsi F, Airolidi L. O6-alkylguanines, dietary N-nitroso compounds, and their precursors in gastric cancer. *Nutr Cancer* 2001; **39**: 42-49
- 17 **Knekt P**, Jarvinen R, Dich J, Hakulinen T. Risk of colorectal and other gastro-intestinal cancers after exposure to nitrate, nitrite and N-nitroso compounds: a follow-up study. *Int J Cancer* 1999; **80**: 852-856
- 18 **Sherenesheva NI**, Mashkovtsev Iu V. Electron microscopy study of experimental stomach cancer. *Eksp Onkol* 1985; **7**: 29-35
- 19 **Sasako M**. The effect of Nd: YAG laser irradiation on gastric cancer in rats induced by N-methyl-N'-nitro-N-nitrosoguanidine as a model of endoscopic laser treatment for early gastric cancers. *Nippon Geka Gakkai Zasshi* 1985; **86**: 443-454
- 20 **Newberne PM**, Charnley G, Adams K, Cantor M, Suphakarn V, Roth D, Schragger TF. Gastric carcinogenesis: a model for the identification of risk factors. *Cancer Lett* 1987; **38**: 149-163
- 21 **Yamashita S**, Wakazono K, Sugimura T, Ushijima T. Profiling and selection of genes differentially expressed in the pylorus of rat strains with different proliferative responses and stomach cancer susceptibility. *Carcinogenesis* 2002; **23**: 923-928
- 22 **Amberger H**. Different autochthonous models of colorectal cancer in the rat. *J Cancer Res Clin Oncol* 1986; **111**: 157-159
- 23 **Narayan S**, Jaiswal AS. Activation of adenomatous polyposis coli (APC) gene expression by the DNA-alkylating agent N-methyl-N'-nitro-N-nitrosoguanidine requires p53. *J Biol Chem* 1997; **272**: 30619-30622
- 24 **Li Z**, Xiao W, McCormick JJ, Maher VM. Identification of a protein essential for a major pathway used by human cells to avoid UV-induced DNA damage. *Proc Natl Acad Sci USA* 2002; **99**: 4459-4464
- 25 **Maenhaut-Michel G**. Mechanism of SOS-induced targeted and untargeted mutagenesis in *E. coli*. *Biochimie* 1985; **67**: 365-369
- 26 **Pham P**, Bertram JG, O'Donnell M, Woodgate R, Goodman MF. A model for SOS-lesion-targeted mutations in *Escherichia coli*. *Nature* 2001; **409**: 366-370
- 27 **Otterlei M**, Kavli B, Standal R, Skjelbred C, Bharati S, Krokan HE. Repair of chromosomal abasic sites *in vivo* involves at least three different repair pathways. *EMBO J* 2000; **19**: 5542-5551
- 28 **Kim SR**, Maenhaut-Michel G, Yamada M, Yamamoto Y, Matsui K, Sofuni T, Nohmi T, Ohmori H. Multiple pathways for SOS-induced mutagenesis in *Escherichia coli*: an overexpression of dinB/dinP results in strongly enhancing mutagenesis in the absence of any exogenous treatment to damage DNA. *Proc Natl Acad Sci USA* 1997; **94**: 13792-13797
- 29 **Tang M**, Bruck I, Eritja R, Turner J, Frank EG, Woodgate R, O'Donnell M, Goodman MF. Biochemical basis of SOS-induced mutagenesis in *Escherichia coli*: reconstitution of *in vitro* lesion bypass dependent on the UmuD'2C mutagenic complex and RecA protein. *Proc Natl Acad Sci U S A* 1998; **95**: 9755-9760
- 30 **Tang M**, Pham P, Shen X, Taylor JS, O'Donnell M, Woodgate R, Goodman MF. Roles of *E. coli* DNA polymerases IV and V in lesion-targeted and untargeted SOS mutagenesis. *Nature* 2000; **404**: 1014-1018
- 31 **Lawrence CW**, Christensen RB. The mechanism of untargeted mutagenesis in UV-irradiated yeast. *Mol Gen Genet* 1982; **186**: 1-9
- 32 **Boesen JJ**, Stuijvenberg S, Thyssens CH, Panneman H, Darroudi F, Lohman PH, Simons JW. Stress response induced by DNA damage leads to specific, delayed and untargeted mutations. *Mol Gen Genet* 1992; **234**: 217-227
- 33 **Zhang X**, Yu Y, Chen X. Evidence for nontargeted mutagenesis in a monkey kidney cell line and analysis of its sequence specificity using a shuttle-vector plasmid. *Mutat Res* 1994; **323**: 105-112
- 34 **Lawrence CW**, Maher VM. Mutagenesis in eukaryotes dependent on DNA polymerase zeta and Rev1p. *Philos Trans R Soc Lond B Biol Sci* 2001; **356**: 41-46
- 35 **Quah SK**, von Borstel RC, Hastings PJ. The origin of spontaneous mutation in *Saccharomyces cerevisiae*. *Genetics* 1980; **96**: 819-839
- 36 **Rechkoblit O**, Zhang Y, Guo D, Wang Z, Amin S, Krzeminsky J, Louneva N, Geacintov NE. Trans-lesion synthesis past bulky benzo[a]pyrene diol epoxide N2-dG and N6-dA lesions catalyzed by DNA bypass polymerases. *J Biol Chem* 2002; **277**: 30488-30494
- 37 **Morrison A**, Christensen RB, Alley J, Beck AK, Bernstine EG, Lemontt JF, Lawrence CW. *REV3*, a *Saccharomyces cerevisiae* gene whose function is required for induced mutagenesis, is pre-

- dicted to encode a nonessential DNA polymerase. *J Bacteriol* 1989; **171**: 5659-5667
- 38 **Roche H**, Gietz RD, Kunz BA. Specificity of the yeast rev3 delta antimutator and REV3 dependency of the mutator resulting from a defect (rad1 delta) in nucleotide excision repair. *Genetics* 1994; **137**: 637-646
- 39 **Lawrence CW**, Hinkle DC. DNA polymerase zeta and the control of DNA damage induced mutagenesis in eukaryotes. *Cancer Surv* 1996; **28**: 21-31
- 40 **Nelson JR**, Lawrence CW, Hinkle DC. Thymine-thymine dimer bypass by yeast DNA polymerase zeta. *Science* 1996; **272**: 1646-1649
- 41 **Holbeck SL**, Strathern JN. A role for REV3 in mutagenesis during double-strand break repair in *Saccharomyces cerevisiae*. *Genetics* 1997; **147**: 1017-1024
- 42 **Baynton K**, Bresson-Roy A, Fuchs RP. Analysis of damage tolerance pathways in *Saccharomyces cerevisiae*: a requirement for Rev3 DNA polymerase in translesion synthesis. *Mol Cell Biol* 1998; **18**: 960-966
- 43 **Xiao W**, Fontanie T, Bawa S, Kohalmi L. REV3 is required for spontaneous but not methylation damage-induced mutagenesis of *Saccharomyces cerevisiae* cells lacking O6-methylguanine DNA methyltransferase. *Mutat Res* 1999; **431**: 155-165
- 44 **Diaz M**, Velez J, Singh M, Cerny J, Flajnik MF. Mutational pattern of the nurse shark antigen receptor gene (NAR) is similar to that of mammalian Ig genes and to spontaneous mutations in evolution: the translesion synthesis model of somatic hypermutation. *Int Immunol* 1999; **11**: 825-833
- 45 **Diaz M**, Verkoczy LK, Flajnik MF, Klinman NR. Decreased frequency of somatic hypermutation and impaired affinity maturation but intact germinal center formation in mice expressing antisense RNA to DNA polymerase zeta. *J Immunol* 2001; **167**: 327-335
- 46 **Zan H**, Komori A, Li Z, Cerutti A, Schaffer A, Flajnik MF, Diaz M, Casali P. The translesion DNA polymerase zeta plays a major role in Ig and bcl-6 somatic hypermutation. *Immunity* 2001; **14**: 643-653
- 47 **Gibbs PE**, McGregor WG, Maher VM, Nisson P, Lawrence CW. A human homolog of the *Saccharomyces cerevisiae* REV3 gene, which encodes the catalytic subunit of DNA polymerase zeta. *Proc Natl Acad Sci U S A* 1998; **95**: 6876-6880
- 48 **Xiao W**, Lechler T, Chow BL, Fontanie T, Agustus M, Carter KC, Wei YF. Identification, chromosomal mapping and tissue-specific expression of hREV3 encoding a putative human DNA polymerase zeta. *Carcinogenesis* 1998; **19**: 945-949
- 49 **Xu F**, Yu Y, Song TN. Establishment of cell lines whose hREV3 gene expression was inhibited by transfection of antisense RNA expression plasmids and their biological characteristics. *Zhongguo Bingli Shengli Zazhi* 2000; **16**: 293-297
- 50 **Xu F**, Yu YN, Wu WW. Construction of eukaryotic expression plasmid expressing antisense fragment of hREV3. *Zhongguo Bingli Shengli Zazhi* 1999; 703-706
- 51 **Qian Y**, Yu Y, Cheng X, Luo J, Xie H, Shen B. Molecular events after antisense inhibition of hMSH2 in a HeLa cell line. *Mutat Res* 1998; **418**: 61-71
- 52 **Kastenbaum MA**, Bowman KO. Tables for determining the statistical significance of mutation frequencies. *Mutat Res* 1970; **9**: 527-549
- 53 **Wang R**. Studies on human cervical carcinoma cell line. II. Establishment of HGPRT- cell line CC-80IAR2 and its biological characteristics. *Zhongguo Yixue Kexueyuan Xuebao* 1992; **14**: 461-464
- 54 **Cai L**, Zheng ZL, Zhang ZF. Risk factors for the gastric cardia cancer: a case-control study in Fujian Province. *World J Gastroenterol* 2003; **9**: 214-218
- 55 **Xue YW**, Zhang QF, Zhu ZB, Wang Q, Fu SB. Expression of cyclooxygenase-2 and clinicopathologic features in human gastric adenocarcinoma. *World J Gastroenterol* 2003; **9**: 250-253
- 56 **Vogelstein B**, Fearon ER, Kern SE, Hamilton SR, Preisinger AC, Nakamura Y, White R. Allelotype of colorectal carcinomas. *Science* 1989; **244**: 207-211
- 57 **Fearon ER**, Cho KR, Nigro JM, Kern SE, Simons JW, Ruppert JM, Hamilton SR, Preisinger AC, Thomas G, Kinzler KW. Identification of a chromosome 18q gene that is altered in colorectal cancers. *Science* 1990; **247**: 49-56
- 58 **Vogelstein B**, Kinzler KW. The multistep nature of cancer. *Trends Genet* 1993; **9**: 138-141
- 59 **Best Robert C**, Kufe Donald W, Pollock Raphael E, Weichselbaum Ralph R, Holland James F, Frei E, editors. Chemical carcinogenesis: Multi-stage carcinogenesis. *Cancer Medicine 5th ed.* Canada: BC Decker Inc 2000
- 60 **Kunz BA**, Straffon AF, Vonarx EJ. DNA damage-induced mutation: tolerance via translesion synthesis. *Mutat Res* 2000; **451**: 169-185
- 61 **Wang G**, Yu Y, Chen X, Xie H. Low concentration *N*-methyl-*N*-nitro-*N*-nitrosoguanidine activates DNA polymerase- β expression via cyclic-AMP-protein kinaseA-cAMP response element binding protein pathway. *Mutat Res* 2001; **478**: 177-184
- 62 **Wilson VL**, Wade KR, Yin X, Albertini RJ. Temporal delineation of sequential HPRT mutations arising *in vivo* in a T-cell clone with a mutator phenotype. *Mutat Res* 2001; **473**: 181-199
- 63 **Leonhardt EA**, Trinh M, Chu K, Dewey WC. Evidence that most radiation-induced HPRT mutants are generated directly by the initial radiation exposure. *Mutat Res* 1999; **426**: 23-30
- 64 **Gibbs PE**, Wang XD, Li Z, McManus TP, McGregor WG, Lawrence CW, Maher VM. The function of the human homolog of *Saccharomyces cerevisiae* REV1 is required for mutagenesis induced by UV light. *Proc Natl Acad Sci U S A* 2000; **97**: 4186-4191

Edited by Xia HHX

Effect of ZNRD1 gene antisense RNA on drug resistant gastric cancer cells

Yu-Mei Zhang, Yan-Qiu Zhao, Yang-Lin Pan, Yong-Quan Shi, Xiao-Hang Jin, Hui Yi, Dai-Ming Fan

Yu-Mei Zhang, Yan-Qiu Zhao, Yang-Lin Pan, Yong-Quan Shi, Xiao-Hang Jin, Hui Yi, Dai-Ming Fan, Department of Gastroenterology, Xijing Hospital, the Fourth Military Medical University, Xi'an 710033, Shaanxi Province, China
Supported by National Natural Science Foundation of China, No. 30030140

Correspondence to: Dai-Ming Fan, Institute of Gastroenterology, Xijing Hospital, Fourth Military Medical University, Xi'an 710033, Shaanxi Province, China. fandaim@fmmu.edu.cn
Telephone: +86-29-3375221 **Fax:** +86-29-2539041
Received: 2002-07-08 **Accepted:** 2002-08-02

Abstract

AIM: To investigate the expression level of ZNRD1 gene in gastric cancer cells SGC7901 and gastric cancer MDR (multidrug resistant) cells SGC7901/VCR, and to observe the drug sensitizing and proliferation effect of ZNRD1 antisense nucleic acid transduction on SGC7901/VCR cells.

METHODS: Amplification of sequences encoding ZNRD1 from SGC7901/VCR cDNA by PCR. The levels of ZNRD1 mRNA expression were demonstrated using semiquantitative reverse transcription polymerase chain reaction (RT-PCR). Eukaryotic expression vector pcDNA3.1-anti ZNRD1 was constructed and transfected into SGC7901/VCR cells by lipofectamine. Immunohistochemical method was used to detect the expression of protein in SGC7901/VCR cells and transfectants. The cell cycle alteration and the intracellular adriamycin (ADM) accumulation were observed by FACS. Growth curve and drug sensitization of cells for vincristine (VCR) were analyzed with MTT assay.

RESULTS: We cloned the open reading frame of full-length ZNRD1. The expression of ZNRD1 showed higher in SGC7901/VCR than in SGC7901 cells. The antisense ZNRD1 drug-resistant clones were selected after gene transfection. Immunohistochemical results showed that the expression level of ZNRD1 protein was lower in anti ZNRD1-SGC7901/VCR cells than that in non-transfectants. Comparing to SGC7901/VCR and pcDNA3.1-SGC7901/VCR, anti ZNRD1-SGC7901/VCR showed gradually accumulated in G₁ phase, with a concomitant decrease of cell population in S phase. FACS also suggested intracellular ADM accumulation increased 2fold in SGC7901/VCR cells after transfected with antisense ZNRD1. MTT assay showed that transfectants cells proliferation was lagged and more sensitive to VCR than non-transfectants.

CONCLUSION: ZNRD1 gene displayed highly expression in VCR resistant gastric cancer cells. Expression of ZNRD1 protein was effectively blocked in anti ZNRD1-SGC7901/VCR cells by gene transfection. ZNRD1 antisense nucleic acid transfection sensitized drug resistant gastric cancer cells to VCR, increased ADM accumulation and inhibited the cells proliferation. ZNRD1 antisense RNA transduction could reverse the MDR of human drug-resistant gastric cancer cell SGC7901/VCR to a degree.

Zhang YM, Zhao YQ, Pan YL, Shi YQ, Jin XH, Yi H, Fan DM. Effect of ZNRD1 gene antisense RNA on drug resistant gastric cancer cells. *World J Gastroenterol* 2003; 9(5): 894-898
<http://www.wjgnet.com/1007-9327/9/894.htm>

INTRODUCTION

Chemotherapy is one of the major methods in tumor treatment, but it often does not work due to MDR. In previous studies, we examined the expression of ZNRD1 is higher in VCR-resistant (SGC7901/VCR) cells than in parental cells SGC7901 by Subtractive Hybridization. The purpose of this study was to investigate the expression and effect of ZNRD1. We transfected ZNRD1 antisense nucleic acid, which is a Homo sapiens transcription-associated zinc ribbon protein, into VCR-resistant gastric cancer cells, and observed the expression of target protein in transfectants and the sensitivity of transfectants to chemotherapeutic agents in order to find the ground for reversing gastric cancer MDR.

MATERIALS AND METHODS

Material

Gastric cancer cell line SGC7901, VCR-resistant gastric cancer SGC7901/VCR cells, DH5 α bacterial strain and rat anti human ZNRD1 polyclonal antibody were kept in our department. The expression vector pcDNA3.1⁺ was from our department. EcoRV, Xba I, BamHI, cloning vector pUCm-T and T4 DNA ligase were purchased from Takara; MTT, DEPC from Sigma. TRIZOL, M-MuLV RT enzyme, Taq DNA polymerase, DMEM, Lipofectamine and G418 were products of Gibco BRL, and Primer from Sangon, Shanghai. Avidin biotin peroxidase complex (ABC) kit was obtained from Vector. VCR from Shanghai Hualian Pharmaceutical Co. Ltd, and ADM from Meiji Pharmaceutical Co. Ltd.

Methods

Cell culture The MDR subline SGC7901/VCR was developed by exposing the parental SGC7901 cells to stepwise increasing concentrations of anticancer drugs VCR. All cells were cultivated in DMEM supplemented with 10 % heat-inactivated fetal bovine serum at 37 °C in 5 % CO₂ atmosphere. Medium for SGC7901/VCR cells was further supplemented with VCR (1.0 μ g/ml). Before use in experiments, SGC7901/VCR cells were cultured in drug-free medium for 2 weeks. Cell stocks were cultivated in these conditions until nearly confluent and subcultured at 1:20 dilution or plated for experiments.

RT-PCR of ZNRD1 Total cellular RNA was extracted from SGC7901 and SGC7901/VCR cells using TRIZOL reagent, cDNA was transcribed from mRNA by RT-PCR. Total RNA (5 μ g) and random primer (2 μ g) in DEPC water were denatured at 65 °C for 15 min, then 4 μ L 5 \times reverse transcriptase buffer, 3 μ L 10 mmol \cdot L⁻¹ dNTP, 1 μ L M-MuLV reverse transcriptase (200 U) and DEPC water were added to have the total volume of 20 μ L. The reaction was performed at 25 °C for 10 min, then 42 °C for 1 hour, and 70 °C for 10 min to inactivate the reverse transcriptase. PCR was performed in a 50 μ L reaction mixture

containing 2 μ L reactant, 2.5 U *Taq* DNA polymerase, deoxynucleoside triphosphates (0.2 mM each), and 1.5 mM $MgCl_2$. The sense primer (5' -ccaactcctcctcagaccgg-3') and antisense primer (5' -cctgggcaaatatacagtc-3') designed according to the DNA sequence of ZNRD1 (GenBank accession no. AF024617). The PCR consisted of initial denaturation at 94 °C for 5 min, followed by 30 reaction cycles (50 s at 94 °C and 60 °C, and 30 s at 70 °C) and a final cycle at 72 °C for 10 min. The β_2 -microglobulin was used to internal standard. The amplified fragments were detected by agarose gel electrophoresis.

Construction of recombinant pUCm-T-ZNRD1 and sequencing of ZNRD1 The PCR product of about 434 bp was isolated and ligated with pUCm-T vector by T4 DNA ligase. *E. Coli* DH5 α was transformed with the resulted recombinants pUCm-T-ZNRD1 and the positive bacteria colonies were screened by ampicillin resistant and blue-white screening with X-gal and IPTG. The cDNA of ZNRD1 cloned in pUCm-T was sequenced by the dideoxynucleotide termination procedure of Sanger.

Construction and identification of antisense nucleic acid The ZNRD1 cDNA was generated by digestion of pUCm-T-ZNRD1 plasmid with EcoR V and BamHI restriction enzyme site. Under T4 DNA ligase, cDNA fragment was inserted in the reverse orientation into the pcDNA3.1⁺ expression vector that was linearized with the same enzymes. The recombinant plasmid was identified through enzyme digestion and agarose gel electrophoresis.

Gene transfection and selection The pcDNA3.1-anti ZNRD1 (1 μ g) diluted in 100 μ L DMEM was mixed with 2 μ L lipofectamine, and placed at room temperature for 10 min. The mixture was then transfected into 1×10^5 SGC7901/VCR cells. After 24 h incubation at 37 °C, the culture was rinsed and re-fed with fresh growth medium. After transfection 48 h, the culture was split and then selected in the culture medium containing the neomycin analogue G418 (400 mg/L). At the same time, pcDNA3.1⁺ vector that lacked target genes transfected cells and non-transfectants served as negative controls.

Immunocytochemistry The expression of ZNRD1 was detected by immunocytochemical staining with the ABC kit. Cells were seeded in glass slides in DMEM at 37 °C for further 24 h, slides were washed with phosphate-buffered saline (PBS) for 3-5 min, then fixed in cold acetone for 5 min; 50 mL L^{-1} H_2O_2 was added and incubated at room temperature for 10-15 min then added 3 g L^{-1} TritonX-100 for another 15 min. The rabbit-anti-human polyclonal antibody ZNRD1 and normal rabbit serum were used at dilution of 1:100, and incubated at 4 °C overnight; Biotinylated goat anti-rabbit IgG was added and incubated at 37 °C for 1 h, then incubated with avidin DH-Biotinylated peroxidase for 45 min. Finally, color was developed by immersion of the sections in a peroxidase substrate solution DAB.

Cell cycle Cells were harvested, washed with PBS twice and fixed with ethanol at 4 °C overnight. Fixed cells were washed twice with PBS and stained with propidium iodide. The fluorescence intensity of propidium iodide-stained nuclei was determined by flow cytometric analysis.

Adriamycin accumulation According to described previously^[1], cells were cultured in 6-well culture plates at 37 °C for 48 h, ADM was added to the final concentration of 5 mg L^{-1} . After further culture for 1 h, PBS was used as negative controls. Cells were harvested and suspended in cold PBS; intracellular adriamycin fluorescence intensity was determined by flow cytometric analysis with the stimulative and acceptant wave length at 488 nm and 575 nm, respectively.

Growth curve Exponentially growing cells (10^3) were trypsinized and inoculated in 96-well plates. The cells were allowed to attach overnight and then incubated for eight days. Cell number and viability were determined by MTT cytotoxic assay. The cells in three wells were supplemented with 20 μ L MTT solution (5 g/L) every day. After 4 h, culture media were discarded followed by

addition of 150 μ L DMSO to melt crystal. The absorbance (A) was measured at 490nm using a microplate reader.

Drug sensitivity assay Dose-survival curves defining the sensitivity of SGC7901/VCR, pcDNA3.1-SGC7901/VCR and anti ZNRD1-SGC7901/VCR transfectants to VCR was obtained using MTT cytotoxic assay. Cells (10^3 - 10^4) diluted with 200 μ L 10 % DMEM were seeded into 96 well plates, after culturing for 12 h, added VCR (0.05, 0.5, 5 and 50 μ g/mL) according to the clinically established plasma peak concentration. Three days later, the absorbance (A) was measured as previously described above. The percentage of viable cells was calculated as follow: (A of experimental group / A of control group) \times 100 %. The IC₅₀ was obtained by Nosa soft.

Statistical analysis

Student's *t* test was used to assess statistical significance of differences. If $P < 0.05$, the difference was considered significant.

RESULTS

Semiquantitative RT-PCR

To examine ZNRD1 gene expression in MDR subline SGC7901/VCR and SGC7901 cell line with Semiquantitative RT-PCR. Two fragments were amplified, ZNRD1 cDNA (434bp) and endogenous control gene β_2 -microglobulin (118bp). It is revealed significantly higher ZNRD1 expression in SGC7901/VCR than in SGC7901 cell line (Figure 1).

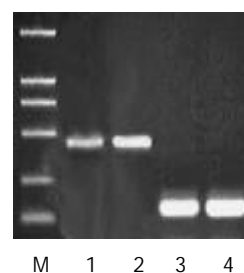


Figure 1 Semiquantitative RT-PCR for ZNRD1 and β_2 -microglobulin. M: Marker (DL2000); Lane 1,3: SGC7901 cells; 2,4: SGC7901/VCR cells.

Construction of recombinants

The recombinant of pUCm-T-ZNRD1 was constructed with the human ZNRD1 inserted into the cloning site of vector pUCm-T. Selection and identification of the recombinant was carried out by EcoRV/XbaI endonuclease digestion and agarose electrophoresis (Figure 2). The cloned DNA segments in selected recombinants were sequenced completely. According to the results of DNA sequencing, the cDNA in a selected recombinant was identical to the DNA sequence of ZNRD1 (GenBank accession no. AF024617) in the reading frame.

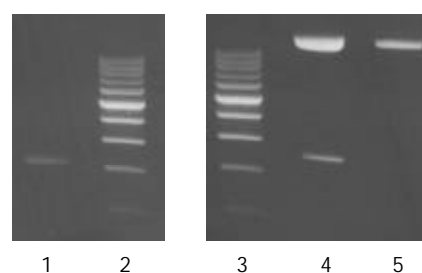


Figure 2 Electrophoresis of PCR product and pUCm-T-ZNRD1 digested with enzymes. Lane 1: PCR product; Lane 2,3: Marker (200bp); Lane 4: recombinant of pUCm-T-ZNRD1 cleaved by EcoRV and XbaI; Lane 5: recombinant of pUCm-T-ZNRD1.

Construction of eukaryotic expression vector

The EcoRV/BamHI fragment containing the complete ZNRD1 cDNA was subcloned into the pcDNA3.1⁺ expression vector. Selection and identification of the recombinants were carried out by EcoRV/BamHI endonuclease digestion and agarose electrophoresis (Figure 3). The pcDNA3.1⁺ vector carrying the neomycin-resistance gene for the selection of transfected cells.

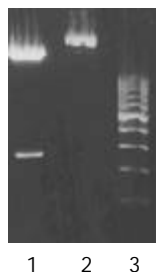


Figure 3 Electrophoresis identification of pcDNA3.1-anti ZNRD1. Lane 1: pcDNA3.1-anti ZNRD1/EcoRV+BamHI; Lane 2: pcDNA3.1-anti ZNRD1; Lane 3: Marker (200bp).

Establishment of transfectants

When transfected cells were cultured selectively by G418 for 4-5 weeks, resistant clones formed gradually. In contrast, all nontransfectants died two weeks after G418 selection. Resistant clones were further incubated in the presence of low dose G418 for 40-50 days. We got resistant clones, anti ZNRD1-SGC7901/VCR cells.

Expression of ZNRD1

We detected ZNRD1 protein expression in transfectants by immunocytochemistry. All cells had positive staining, staining on anti ZNRD1-SGC7901/VCR cells was weaker than that on SGC7901/VCR, ZNRD1 protein was expressed mostly in the nucleus (Figure 4).

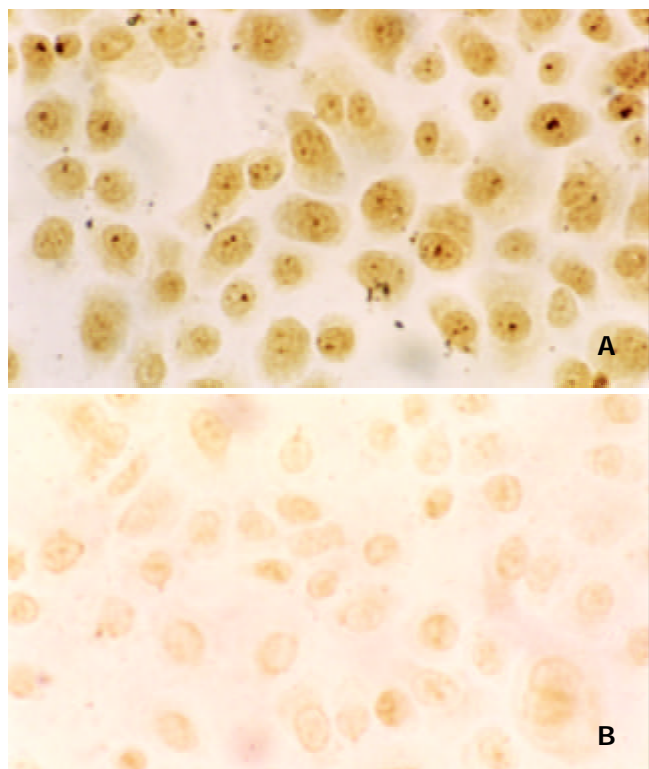


Figure 4 Detection of ZNRD1 expression in cells by immunocytochemical staining. $\times 200$. A: SGC7901/VCR; B: anti ZNRD1-SGC7901/VCR.

Adriamycin accumulation

The effects of ZNRD1 antisense nucleic acid on ADM accumulation in SGC7901/VCR cells were determined by flow cytometric analysis. When cells were cultured in drug-DMEM, intracellular drug concentration would increase and finally stabilized at the highest plateau value, which was called adriamycin accumulation. The fluorescence intensity of SGC7901/VCR, pcDNA3.1-SGC7901/VCR and anti ZNRD1-SGC7901/VCR cells, mean fluorescence of 10^4 cells, is 3.68, 5.70, and 7.24 respectively. The intracellular ADR accumulation marked increase 2fold.

Inhibition of cell proliferation by ZNRD1 antisense nucleic acid

Cell cycle When transfected SGC7901/VCR cells with ZNRD1 antisense nucleic acid, the cell cycle obtained by FCM was as shown in Table 1. The anti ZNRD1-SGC7901/VCR cells gradually accumulated in G₁ phase, with a concomitant decrease of cell population in S phase.

Table 1 Cell cycle distribution of three kinds of cell lines (Number fraction)

Cell line	G1	G2	S	G1/G2
SGC7901/VCR	0.572	0.111	0.317	1.900
pcDNA3.1-SGC7901/VCR	0.652	0.091	0.256	1.887
Anti ZNRD1-SGC7901/VCR	0.744	0.118	0.138	1.881

Growth curves The cells viability were daily measured by MTT proliferation analysis. The growth curve showed that cell growth was suppressed after transfected with ZNRD1 antisense nucleic acid (Figure 5).

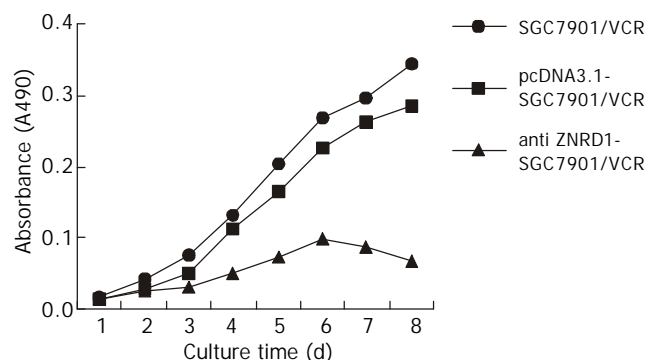


Figure 5 Growth curve of cells.

Drug sensitivity assay

The IC₅₀ of SGC7901/VCR, pcDNA3.1-SGC7901/VCR and anti ZNRD1-SGC7901/VCR cells treated with VCR is 50.51 ± 0.3 , 42.68 ± 0.79 , 10.87 ± 0.25 ($\mu\text{g/mL}$), respectively. The anti ZNRD1-SGC7901/VCR cells were more sensitive to VCR ($P < 0.01$).

DISCUSSION

Multidrug resistance (MDR), the principal mechanism by which many cancers develop resistance to chemotherapeutic drugs, is a major factor in the failure of many forms of chemotherapy. There are several ways for cancer cells to develop resistance or defense mechanisms against cytotoxic drugs^[2-4]. Several molecules have been found to confer MDR phenotype of tumor cells, such as P-gp, MRP, LRP, BCRP, GSH/GSH, TopoII, apoptosis associated proteins and anti-apoptosis proteins. We found the MDR markers are differently over-expressed and no coexpression exists in gastric cancer, MGr1-Ag was a novel MDR protein^[5-7]. However, these

molecules could not interpret completely how tumor cells develop MDR. The key to the clinical use of reversal agents therefore lies in searching for agents with low toxicity and high reversal activity. For gene therapy has very low toxicity, it might therefore be suitable for clinical use.

SGC7901/VCR is a vincristine-resistant SGC7901 cell line, and it overexpresses P-gp and is cross-resistant to several anti-cancer drugs. In previous studies, we have identified that 54 cDNA fragments were preferentially expressed in SGC 7901/VCR cells by DD-PCR^[8]. We isolated differentially expressed genes from drug-resistant human gastric adenocarcinoma cell lines using a polymerase chain reaction-based subtractive hybridization technique, and the expression of ZNRD1 is higher in SGC7901/VCR cells than in parental cells SGC7901^[9]. ZNRD1 is a new zinc ribbon gene that cloned from the human MHC class I region, named the gene ZNRD1 for zinc ribbon domain-containing 1 protein^[10]. Alignment with genomic DNA demonstrates that this gene spans 3.6 kb and consists of four exons and three introns. The full-length cDNA contains an open reading frame of 378 bp. Within the putative polypeptide of 126 amino acids, two zinc-ribbon domains were identified: Cx2Cx15Cx2C at the N-terminal and Cx2Cx24Cx2C at the C-terminal. The C-terminal domain is actually folded as three β -sheets stabilized by a zinc ion instead of finger like helices, compared to TFIIS zinc ribbon folds, they fit each other very well. The conserved amino acid sequence, CxRCx6Yx3QxRSADEx2TxFxCx2C is highly homologous to the yeast RNA polymerase A subunit 9 and transcription-associated proteins.

Transcriptional initiation and elongation provide control points in gene expression. The highly conserved eukaryotic transcriptional elongation factor TFIIS helps overcome elongation barriers and enhances proofreading by RNA polymerase II (RNAPII). The nucleic acid binding domain of TFIIS contains a Cys4 Zn⁽²⁺⁾-binding site with no homology to previously characterized Cys4, Cys6, or Cys2-His2 Zn fingers. Its solution structure exhibits a novel three-stranded antiparallel beta-sheet (designated the Zn ribbon), extends the repertoire of Zn-mediated peptide architectures and highlights the growing recognition of the beta-sheet as a motif of nucleic-acid recognition. The TFIIS functions may be modulated by the Zn ribbon domain through interactions with nucleic acids in the elongation complex. The RNAPII contain a Zn ribbon, in as much as the polymerase's 15-kDa subunit contains a sequence that aligns well with the TFIIS Zn ribbon sequence, including a similarly placed pair of acidic residues. It has demonstrated that TFIIS Zn ribbon is critical for stimulation of both elongation and RNA cleavage activities of RNAPII. Eukaryotic RNA polymerase II subunit 9 (Rpb9) contains Zn ribbon motifs homologous to TFIIS; it regulates start-site selection and elongational arrest. RNAPII lacking the Rpb9 subunit uses alternate transcription initiation sites *in vitro* and *in vivo* and is unable to respond to the transcription elongation factor TFIIS *in vitro*. Alanine substitutions in the C-terminal zinc ribbon domain of Rpb9, like amino acid substitutions in the homologous part of TFIIS, completely eliminated elongation activity. It has show that RPB9 has a synthetic phenotype with the TFIIS gene^[11].

DNA primases are enzymes whose continual activity is required at the DNA replication fork. They catalyze the synthesis of short RNA molecules used as primers for DNA polymerases. All DNA primases contain a metal binding site, which is composed of four conserved Cys or His residues that could potentially coordinate zinc^[12]. Motif IV in the small subunit contains four cysteines that could form a zinc ribbon motif as a member of the zinc ribbon subfamily of zinc binding motifs.

The ability to selectively regulate the expression of genes

implicated in cancer could have important ramifications for both basic research and for therapy. Using peptide combinatorial libraries expressed in yeast, Bartsevich^[13] has screened for a novel zinc finger proteins that selectively bind to an overlapping EGR1/SP1/WT1 regulatory site in the promoter of the MDR1 multidrug resistance gene. The novel proteins were only moderately effective in blocking transcription by simple masking of the target site. However, when coupled to mammalian transactivator or repressor domains, they could selectively modulate the expression of reporter genes having promoters containing the MDR1 target site. Moreover, they could also regulate transcription of the chromosomal MDR1 gene. These studies potentially provide a novel alternative approach to the control of multidrug resistance. They also provide important insights into strategies for developing selective regulators of gene expression.

Thus, zinc ribbon is related to transcription and DNA replication, and the construction is same to zinc finger. It may regulate the expression of genes to control MDR.

Semiquantitative RT-PCR analysis is a sensitive and specific method; it is revealed that the RNA expression levels of ZNRD1 were significantly higher in SGC7901/VCR cells than that in SGC7901 cells. We transfected ZNRD1 antisense RNA into SGC7901/VCR cells, then found that intrinsic ZNRD1 protein was decreased, and transfected cells were more sensitive to VCR and cell growth was suppressed, the cell cycle was notably changed, the G1 phase cells were gradually increased, with a concomitant decrease of cell population in S phase, these observations suggest that ZNRD1 antisense RNA may be involved in the action of the G1 checkpoint and inhibition of DNA replication. ADR can emit fluorescence; its intensity represents its accumulation, which was markedly enhanced in transfectants. The results suggested that the formation of MDR in SGC7901/VCR cells was associated with over expression of ZNRD1. Because gastric cancer is common in China and some areas in the world^[14-33], these results may be important for further study.

REFERENCES

- Han Y**, Han ZY, Zhou XM, Shi R, Zheng Y, Shi YQ, Miao JY, Pan BR, Fan DM. Expression and function of classical protein kinase C isoenzymes in gastric cancer cell line and its drug-resistant sublines. *World J Gastroenterol* 2002; **8**: 441-445
- Monden N**, Abe S, Hishikawa Y, Yoshimura H, Kinugasa S, Dhar DK, Tachibana M, Nagasue N. The role of P-glycoprotein in human gastric cancer xenografts in response to chemotherapy. *Int J Surg Investig* 1999; **1**: 3-10
- Liu B**, Staren E, Iwamura T, Appert H, Howard J. Effects of Taxotere on invasive potential and multidrug resistance phenotype in pancreatic carcinoma cell line SUI-2. *World J Gastroenterol* 2001; **7**: 143-148
- Yin F**, Shi YQ, Zhao WP, Xiao B, Miao JY, Fan DM. Suppression of P-gp induced multiple drug resistance in a drug resistant gastric cancer cell line by overexpression of Fas. *World J Gastroenterol* 2000; **6**: 664-670
- Fan K**, Fan D, Cheng LF, Li C. Expression of multidrug resistance-related markers in gastric cancer. *Anticancer Res* 2000; **20**: 4809-4814
- Shi Y**, Han Y, Wang X, Zhao Y, Ning X, Xiao B, Fan D. MGr1-Ag is associated with multidrug-resistant phenotype of gastric cancer cells. *Gastric Cancer* 2002; **5**: 154-159
- Shi Y**, Zhai H, Wang X, Wu H, Ning X, Han Y, Zhang D, Xiao B, Wu K, Fan D. Multidrug-resistance-associated protein MGr1-Ag is identical to the human 37-kDa laminin receptor precursor. *Cell Mol Life Sci* 2002; **59**: 1577-1583
- Wang X**, Lan M, Shi YQ, Lu J, Zhong YX, Wu HP, Zai HH, Ding J, Wu KC, Pan BR, Jin JP, Fan DM. Differential display of vincristine-resistance-related genes in gastric cancer SGC7901 cell. *World J Gastroenterol* 2002; **8**: 54-59

- 9 **Zhao Y**, You H, Liu F, An H, Shi Y, Yu Q, Fan D. Differentially expressed gene profiles between multidrug resistant gastric adenocarcinoma cells and their parental cells. *Cancer Lett* 2002; **185**: 211-218
- 10 **Fan W**, Wang Z, Kyzysztof F, Prange C, Lennon G. A new zinc ribbon gene (ZNRD1) is cloned from the human MHC class I region. *Genomics* 2000; **63**: 139-141
- 11 **Hemming SA**, Jansma DB, Macgregor PF, Goryachev A, Friesen JD, Edwards AM. RNA polymerase II subunit Rpb9 regulates transcription elongation *in vivo*. *J Biol Chem* 2000; **275**: 35506-35511
- 12 **Frick DN**, Richardson CC. DNA primases. *Annu Rev Biochem* 2001; **70**: 39-80
- 13 **Bartsevich VV**, Juliano RL. Regulation of the MDR1 gene by transcriptional repressors selected using peptide combinatorial libraries. *Mol Pharmacol* 2000; **58**: 1-10
- 14 **Xu L**, Zhang SM, Wang YP, Zhao FK, Wu DY, Yan X. Relationship between DNA ploidy, expression of ki-67 antigen and gastric cancer metastasis. *World J Gastroenterol* 1999; **5**: 10-11
- 15 **Wu YA**, Lu B, Liu J, Li J, Chen JR, Hu SX. Consequence alimentary reconstruction in nutritional status after total gastrectomy for gastric cancer. *World J Gastroenterol* 1999; **5**: 34-37
- 16 **Ji F**, Peng QB, Zhan JB, Li YM. Study of differential polymerase chain reaction of C-erbB 2 oncogene amplification in gastric cancer. *World J Gastroenterol* 1999; **5**: 152-155
- 17 **Zhan WH**, Ma JP, Peng JS, Gao JS, Cai SR, Wang JP, Zheng ZQ, Wang L. Telomerase activity in gastric cancer and its clinical implications. *World J Gastroenterol* 1999; **5**: 316-319
- 18 **Ji F**, Wang WL, Yang ZL, Li YM, Huang HD, Chen WD. Study on the expression of matrix metallo proteinase-2MRNA in human gastric cancer. *World J Gastroenterol* 1999; **5**: 455-457
- 19 **Wang H**, Zheng MH, Zhang HB, Zhu J, He JR, Lu AG, Ji YB, Zhang MJ, Jiang Y, Yu BM, Li HW. Study on incisional implantation of tumor cells by carbon dioxide pneumo peritoneum in gastric cancer of a murine model. *World J Gastroenterol* 1999; **5**: 544-546
- 20 **Zou SC**, Qiu HS, Zhang CW, Tao HQ. A clinical and long-term follow-up study of peri operative sequential triple therapy for gastric cancer. *World J Gastroenterol* 2000; **6**: 284-286
- 21 **Cai L**, Yu SZ, Zhang ZF. *Helicobacter pylori* infection and risk of gastric cancer in Changle County, Fujian Province, China. *World J Gastroenterol* 2000; **6**: 374-376
- 22 **Zhang FX**, Zhang XY, Fan DM, Deng ZY, Yan Y, Wu HP, Fan JJ. Antisense telomerase RNA induced human gastric cancer cell apoptosis. *World J Gastroenterol* 2000; **6**: 430-432
- 23 **Gu QL**, Li NL, Zhu ZG, Yin HR, Lin YZ. A study on arsenic trioxide inducing *in vitro* apoptosis of gastric cancer cell lines. *World J Gastroenterol* 2000; **6**: 435-437
- 24 **Wang ZN**, Xu HM. Relationship between collagen IV expression and biological behavior of gastric cancer. *World J Gastroenterol* 2000; **6**: 438-439
- 25 **Tu SP**, Zhong J, Tan JH, Jiang XH, Qiao MM, Wu YX, Jiang SH. Induction of apoptosis by arsenic trioxide and hydroxy camptothecin in gastric cancer cells *in vitro*. *World J Gastroenterol* 2000; **6**: 532-539
- 26 **Jiang BJ**, Sun RX, Lin H, Gao YF. Study on the risk factors of lymphatic metastasis and the indications of less invasive operations in early gastric cancer. *World J Gastroenterol* 2000; **6**: 553-556
- 27 **Deng DJ**. Progress of gastric cancer etiology: N-nitrosamides 1990s. *World J Gastroenterol* 2000; **6**: 613-618
- 28 **Gao HJ**, Yu LZ, Bai JF, Peng YS, Sun G, Zhao HL, Miu K, Lü XZ, Zhang XY, Zhao ZQ. Multiple genetic alterations and behavior of cellular biology in gastric cancer and other gastric mucosal lesions: *H. pylori* infection, histological types and staging. *World J Gastroenterol* 2000; **6**: 848-854
- 29 **Miehlke S**, Kirsch C, Dragosics B, Gschwantler M, Oberhuber G, Antos D, Dite P, Lauter J, Labenz J, Leodolter A, Malfertheiner P, Neubauer A, Ehninger G, Stolte M, Bayerdorffer E. *Helicobacter pylori* and gastric cancer: current status of the Austrian-Czech-German gastric cancer prevention trial (PRISMA Study). *World J Gastroenterol* 2001; **7**: 243-247
- 30 **Xu AG**, Li SG, Liu JH, Gan AH. Function of apoptosis and expression of the proteins Bcl-2, p53 and C-myc in the development of gastric cancer. *World J Gastroenterol* 2001; **7**: 403-406
- 31 **Cai L**, Yu SZ, Zhang ZF. Glutathione S-transferases M1, T1 genotypes and the risk of gastric cancer: A case control study. *World J Gastroenterol* 2001; **7**: 506-509
- 32 **He XS**, Su Q, Chen ZC, He XT, Long ZF, Ling H, Zhang LR. Expression, deletion and mutation of p16 gene in human gastric cancer. *World J Gastroenterol* 2001; **7**: 515-521
- 33 **Fang DC**, Yang SM, Zhou XD, Wang DX, Luo YH. Telomere erosion is independent of microsatellite instability but related to loss of heterozygosity in gastric cancer. *World J Gastroenterol* 2001; **7**: 522-526

Edited by Bo XN

Imbalance between expression of matrix metalloproteinase-9 and tissue inhibitor of metalloproteinase-1 in invasiveness and metastasis of human gastric carcinoma

Sheng Zhang, Li Li, Jian-Yin Lin, Hua Lin

Sheng Zhang, Hua Lin, Department of Pathology, The First Affiliated Hospital, Fujian Medical University, Fuzhou 350005, Fujian Province, China

Li Li, Jian-Yin Lin, Department of Molecular Medicine, Fujian Medical University, Fuzhou, 350004, Fujian Province, China

Supported by Fujian Province Educational Bureau Science Foundation, No JA98103 and Fujian Province Health Bureau Science Foundation, No 96048

Correspondence to: Professor Jian-Yin Lin, Department of Molecular Medicine, Fujian Medical University, Fuzhou 350004, China. jylin@fjmu.edu.cn

Telephone: +86-591-3574445 **Fax:** +86-591-3351345

Received: 2002-11-06 **Accepted:** 2002-12-22

Abstract

AIM: The expressive balance between matrix metalloproteinase-9 (MMP-9) and its tissue inhibitor of metalloproteinase-1 (TIMP-1) plays a critical role in maintaining the degradation and synthesis of extracellular matrix. Loss of such balance is associated with invasion and metastasis of tumors. This study aimed to determine the expression of MMP-9 and TIMP-1 in gastric carcinoma, and the association of the expressive imbalance between MMP-9 and TIMP-1 with the invasion and metastasis and prognosis of gastric carcinoma.

METHODS: We used immunohistochemistry to determine the expressions of MMP-9, TIMP-1 and proliferating cell nuclear antigen Ki-67 in the gastric specimens taken from 256 patients with primary gastric carcinoma. The patients were followed-up for up to 96 months.

RESULTS: No association between the expression of MMP-9 and TIMP-1 and patients' sex and age, tumor size and location of gastric carcinoma was observed. The incidence of the positive expression of MMP-9 in cases with tumors invasion to muscularis propria and visceral peritoneum (70.13 % and 69.09 %, respectively) was significantly higher than that in cases with tumor invasion only to lamina propria or submucosa (42.50 %, $P=0.0162$). The positive correlation between MMP-9 expression and the depth of tumor invasion was observed (Pearson correlation coefficient=0.2129, $P=0.016$). Along with the increase of the metastatic station of lymph nodes, the incidence of the MMP-9 expression was increased by degrees; a positive correlation between them was observed (Pearson correlation coefficient=0.2910, $P=0.0001$). There was also a significant correlation between MMP-9 expression and the TNM stage in gastric carcinoma (Pearson correlation coefficient=0.3027, $P<0.0001$). The incidence of MMP-9 expression in stage II and III/IV (75.00 % and 76.15 %, respectively) was significantly higher than those in stage I (46.15 %, $P<0.0001$). A negative correlation between TIMP-1 immunoreactivity and the depth of invasion, status of lymph node metastasis and TNM stage was observed (Pearson correlation coefficient = -0.1688, -0.3556

and -0.3004, $P=0.023$, <0.0001 and <0.0001 , respectively). Four types of co-expression of MMP-9 and TIMP-1 were observed; i.e. MMP-9 positive but TIMP-1 negative ($n=115$), both positive ($n=52$), both negative ($n=62$) and MMP-9 negative but TIMP-1 positive ($n=27$). The frequency of serosal invasiveness was significant higher in patients with MMP-9 but without TIMP-1 expression than those with other types of the co-expression ($P=0.0303$). The incidence of lymph node metastasis was highest in patients with MMP-9 but without TIMP-1 expression, and lowest in those with TIMP-1 but without MMP-9 expression ($P<0.0001$). The survival rate in patients with MMP-9 but without TIMP-1 expression was lower than that in those with TIMP-1 but without MMP-9 expression ($P=0.0014$).

CONCLUSION: Our results in gastric carcinoma demonstrated a significant positive association of MMP-9 over-expression with proliferation of tumor cells, the depth of invasiveness, lymph node metastasis and TNM stage, suggesting MMP-9 can serve as a molecular marker of tumor invasion and metastasis. We also demonstrate a significant negative relationship of TIMP-1 expression with the depth of invasiveness and lymph node metastasis, which provide a new idea in the tumor biological and genetic treatment. The interaction between MMP-9 and TIMP-1 in the processes of tumor invasion and metastasis is that MMP-9 mainly promotes tumor invasion and metastasis and TIMP-1 inhibits functions of MMP-9. The imbalance between MMP-9 and TIMP-1 expression may suggest the occurrence of tumor invasion and metastasis, predict poor prognosis. For patients with imbalanced MMP-9 and TIMP-1 expression, the optimal treatment scheme needs to be selected.

Zhang S, Li L, Lin JY, Lin H. Imbalance between expression of matrix metalloproteinase-9 and tissue inhibitor of metalloproteinase-1 in invasiveness and metastasis of human gastric carcinoma. *World J Gastroenterol* 2003; 9(5): 899-904
<http://www.wjgnet.com/1007-9327/9/899.htm>

INTRODUCTION

The malignant behavior of tumor cells mainly depends on the capability of invasion and metastasis of cancer cells. After the components of the extracellular matrix (ECM) are degraded, tumor cells invade the surrounding tissue and the vascular or lymphatic vessels to form metastatic colonies at distant sites. Matrix metalloproteinase-9 (MMP-9) can degrade the main components of the ECM, type IV and V collagen and gelatin^[1-6], thus, its activities are closely related to the ability of the invasiveness and metastasis of tumor cells^[7,8]. Increased expression of matrix metalloproteinases (MMPs) renders the tumor cells capable of digesting essential tissue barriers especially basement membranes lining the blood vessels, thereby promoting the cells' motility. By forming a 1:1 complex with MMP-9 and inhibiting its enzymatic activity^[2,9,10], tissue

inhibitor of metalloproteinase-1 (TIMP-1) plays negative role in the invasion and metastasis of tumor cells^[11]. Therefore, attentions have been paid to the role of MMP-9 and TIMP-1 in the progress of tumor, and it has been reported that the expression of MMP-9 and TIMP-1 was correlated^[12], but the relationship of their expressive imbalance to the invasion and metastasis in gastric carcinoma was rarely reported. In the present study, we study the expressive pattern of MMP-9 and TIMP-1 in 256 patients with primary gastric carcinoma by immunohistochemistry, as well as the relationship of their expressive imbalance to invasion and lymph node metastasis and prognosis of gastric carcinoma. We demonstrated that the expressive imbalance of MMP-9 and TIMP-1 was significantly associated with the invasion and metastasis of gastric carcinoma.

MATERIALS AND METHODS

Materials

Two hundred fifty-six patients who underwent a surgery for the primary gastric carcinoma at the First Affiliated Hospital of Fujian Medical University, between 1991 and 1999, and had sufficient clinical materials were selected for this study. These patients comprised 186 males and 70 females. The median age was 60 with a range from 23 to 84 years. All studied patients had not been accepted for radiation therapy and chemotherapy before the operation. The histological findings, lymph node metastasis and TNM stage were evaluated based on World Health Organization Classification of Tumors^[13,14]. Follow-up information was available for 167 patients.

Methods

The specimens were fixed in formalin and embedded in paraffin wax, sliced serial step sections of 4 μ m thickness and stained by hematoxylin-eosin.

Immunohistochemistry

Paraffin sections (4 μ m thick) were immunostained with anti-mouse monoclonal antibodies for MMP-9 (GE-213, 1:10, NeoMarkers), TIMP-1 (102D1, 1:10, NeoMarkers) and Ki-67 (MB67, Ready, NeoMarkers) by the peroxidase-conjugated streptavidin complex method. Sections were deparaffinized and heated in a microwave oven for 10 min to retrieve the antigens. They were immersed in 3 % hydrogen peroxide in 100 % methanol for 10 min to block the endogenous peroxidase activity. After incubated in normal horse serum for 20 min, the tissue sections were incubated with the primary antibodies for 120 min at room temperature. The sections were incubated with biotinylated rabbit anti-mouse immunoglobulins G for 20 min and then treated with peroxidase-conjugated streptavidin for 20 min. The sections were immersed into DAB solution. The slides were counterstained with haematoxylin solution, dehydrated and mounted. Between steps, the slides were washed three times with phosphate buffered saline (PBS). As a negative control, PBS was used instead of the primary antibody.

Two independent observers without knowledge of the clinical outcomes evaluated the degree of immunohistochemical staining. All sections for which the two observers disagreed were re-evaluated until there was a complete agreement on the classification.

Immunohistochemical analyses of MMP-9, TIMP-1 and Ki-67 labeling index

Figures 1 and 2 show a positive expression of MMP-9 and TIMP-1, respectively. They were expressed within the cell membrane and/or cytoplasm. The intensity of staining in cell membrane and cytoplasm and the percentage of immunoreactive cells to total tumor cells were evaluated. The intensity of staining was graded as 0, when staining not greater

than negative control, 1, for light staining, and 2, for heavy staining. Immunoreactivity was scored according to the percentage of immunoreactive cells over total tumor cells counted as 0, if <5 % cells were stained; 1 if 5-25 % cells were immunoreactive, 2 if 26-50 % cells were immunoreactive and 3 if >50 % cells were immunoreactive. The expression of MMP-9 and TIMP-1 was finally defined according to the score obtained from the grade of intensity multiplied by the score of cell immunoreactivity, i.e. negative (-, score 0-1), positive (+, score 2-3), and strong positive (++, score 4 or above).

The positive expression of Ki-67 staining was in the nuclei of the carcinoma cells. Ki-67 labeling index was defined as the ratio of immunoreactive cells over 1 000 tumor cells counted labeling.

Statistical analysis

The χ^2 analysis was used for univariable categorical analysis. The relationship of the expressive imbalance between MMP-9 and TIMP-1 to the postoperative survival was tested for prognostic significance in gastric carcinoma specific survival using Kaplan-Meier survival curves and the log-rank test. All statistical analysis was performed using the SPSS 6.0 statistical software program. A value of $P < 0.05$ was considered statistically significant.

RESULTS

Relationship between MMP-9 expression and the clinical pathological parameters of gastric carcinoma

MMP-9 was mainly expressed within the cytoplasm and cytoplasmic membranes of the gastric carcinoma cells (Figure 1). Among 256 primary gastric carcinomas, the incidence of a positive expression of MMP-9 in carcinoma cells was 65.23 % (167/256), with the incidence of strong immunoreactivity of 13.67 % (35/256). No significant correlations between the expression of MMP-9 and sex, age, location and size of tumors were observed. As shown in Table 1, the incidence of the positive expression of MMP-9 in cases whose tumors invaded to muscularis propria and visceral peritoneum (70.13 % and 69.09 %, respectively) were significantly higher than those whose tumors only invaded to lamina propria or submucosa (42.50 %, $P = 0.0162$). A significant correlation between MMP-9 expression and the depth of tumor invasion was observed (Pearson correlation coefficient = 0.2129, $P = 0.016$). Along with the increase of the metastatic station of lymph nodes, the incidence of the MMP-9 expression was increased by degrees; a positive correlation between them was observed (Pearson correlation coefficient = 0.2910, $P = 0.0001$). We also demonstrated a significant correlation between MMP-9 expression and the TNM stage of gastric carcinoma (Pearson correlation coefficient = 0.3027, $P < 0.0001$), the incidence of MMP-9 expression was significantly higher in stage II and III/IV (75.00 % and 76.15 %, respectively) than in stage I (46.15 %, $P < 0.0001$, Table 1).

Relationship between TIMP-1 expression and the clinical pathological parameter in gastric carcinoma

A total of 79 (30.89 %) patients had positive immunohistochemical staining for TIMP-1 in the cytoplasm and cytoplasmic membrane of the gastric carcinoma cells, with the strong positive staining only five (1.95 %) cases (Figure 2). No statistical correlation between TIMP-1 immunoreactivity and sex, age, location and tumor size was observed. There were significant negative correlations between TIMP-1 immunoreactivity and the depth of invasion, status of lymph node metastasis and TNM stage (Pearson correlation coefficient = -0.1688, -0.3556 and -0.3004, $P = 0.023$, < 0.0001 and < 0.0001 , respectively, Table 1).

Table 1 MMP-9 (matrix metalloproteinase-9) and TIMP-1 (tissue inhibitor of metalloproteinase-1) expression and clinicopathological characteristics of gastric carcinoma

	<i>n</i>	Expressing levels of MMP-9				<i>P</i> value	Expressing levels of TIMP-1			<i>P</i> value
		-	+	++	Positive rate (%)		-	+	Positive rate (%)	
(1) Sex										
Male	186	61	100	25	67.20	>0.05	127	59	31.72	>0.05
Female	70	28	32	10	60.00		50	20	28.57	
(2) Age										
Mean		55.00	58.33	61.36			57.28	58.64		
±		±	±	±		>0.05	±	±		>0.05
SD		12.19	11.31	8.48			12.19	10.22		
(3) Location										
Cardia	63	14	36	13	77.78	>0.05	39	24	38.10	>0.05
Corpus	33	10	18	5	69.70		23	10	30.30	
Antrum	140	55	71	14	60.71		101	39	27.86	
Others	20	10	7	3	50.00		14	6	30.00	
(4) Tumor size(cm)										
<5	124	52	59	13	58.06	>0.05	80	44	34.38	>0.05
≥5	132	37	73	22	71.69		97	35	26.51	
(5) Histological type										
Well-moderately differentiated	109	24	61	24	77.98	>0.05	63	46	42.20	>0.05
Poorly differentiated	98	38	53	7	61.22		77	21	21.43	
Undifferentiated	18	13	4	1	27.78		14	4	22.22	
Mucinous	31	14	14	3	54.84		23	8	25.81	
(6) Depth of invasion										
Lamina propria or submucosa	40	23	15	2	42.50	<0.05	23	17	42.50	<0.05
Muscularis propria	77	23	54	10	70.13		48	29	37.66	
Visceral peritoneum	139	43	73	23	69.06		106	33	23.74	
(7) Lymph node metastasis										
Negative	98	51	40	7	47.96	<0.01	47	51	52.04	<0.01
N1	130	34	73	23	73.85		103	27	20.77	
N2	28	4	19	5	85.71		27	1	3.57	
(8) TNM stage										
I	91	49	36	6	46.15	<0.01	46	45	49.45	<0.01
II	56	14	35	7	75.00		40	16	28.57	
III-IV	109	26	61	22	76.15		91	18	16.51	
(9) Ki-67 labeling index										
Mean		669.83	720.09	751.77			716.95	684.53		
±		±	±	±		<0.01	±	±		>0.05
SD		129.48	126.64	120.81			119.67	122.34		

SD: Standard deviation.

Table 2 Association between the expression of MMP-9 (matrix metalloproteinase-9) and TIMP-1 (tissue inhibitor of metalloproteinase-1) and invasion and metastasis of gastric carcinoma

MMP-9 expression	TIMP-1 expression	<i>n</i>	Penetrating visceral peritoneum		Lymph node metastasis	
			<i>n</i>	Ratio(%)	<i>n</i>	Ratio(%)
+	-	115	74	64.35	97	84.35
	+	52	22	42.31 ^a	23	44.23 ^{ab}
-	-	62	32	51.61 ^a	33	53.32 ^{ab}
	+	27	12	44.44 ^a	5	15.52 ^a

^a*P*<0.05 vs MMP-9(+)TIMP-1(-); ^b*P*<0.05 vs MMP-9(-)TIMP-1(+).

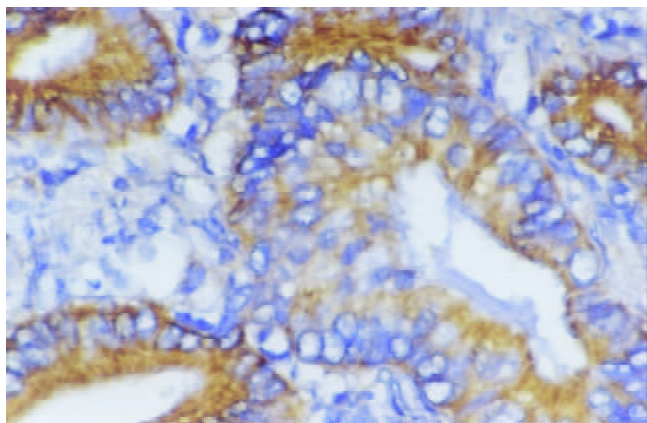


Figure 1 MMP-9 (matrix metalloproteinase-9) strongly positive staining. Membrane or cytoplasm of gastric cancer cells was stained brown. (SP method $\times 400$).

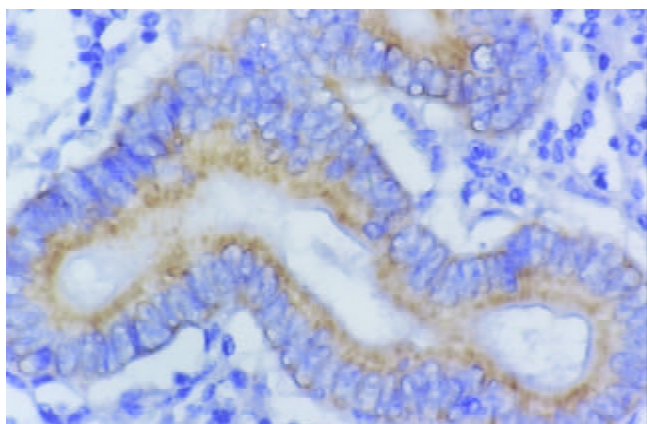


Figure 2 TIMP-1 (tissue inhibitor of metalloproteinase-1) strongly positive staining. Membrane or cytoplasm of gastric cancer cells was stained brown. (SP method. $\times 400$).

Relationship between MMP-9 and TIMP-1 expression and Ki-67 labeling index

As shown in Table 1, the higher the expression of MMP-9 in gastric carcinoma, the higher the Ki-67 labeling indexes in tumor cells ($F=6.7013$, $P=0.0015$). There was no significant difference in Ki-67 labeling index between the positive group and negative group of TIMP-1 expression in gastric carcinoma ($F=3.4474$, $P>0.05$).

Relationship of the expressive imbalance between MMP-9 and TIMP-1 to the invasiveness and metastasis of gastric carcinoma

According to the expression of MMP-9 and TIMP-1 in gastric carcinoma tissues, four patterns of co-expression were observed: 1, MMP-9 positive but TIMP-1 negative, or MMP-9 expression greater than TIMP-1 expression, $n=115$ (44.92 %); 2, MMP-9 and TIMP-1 both positive, $n=52$ (20.13 %); 3, MMP-9 and TIMP-1 both negative, $n=62$ (24.22 %); 4, MMP-9 negative but TIMP-1 positive, or TIMP-1 expression greater than MMP-9 expression, $n=27$ (10.55 %). Whereas patterns 2 and 3 of the co-expression of MMP-9 and TIMP-1 were defined as balanced, the co-expression patterns in 1 and 4 were defined as imbalanced. The frequency of the serosa invasiveness in patients with the co-expression pattern 1 was significant higher than those with other patterns ($P=0.0303$). Similarly, the incidence of lymph node metastasis was highest in patients with the co-expression pattern 1 and lowest in those with the pattern 4 ($P<0.0001$, Table 2).

Relationship of the expression of MMP-9 and TIMP-1 to the postoperative survival of patients with gastric carcinoma

Follow-up (6-97 months) information was available for 167 patients with gastric carcinoma. The postoperative survival rate appeared to decrease in patients with MMP-9 expression compared with those without MMP-9 expression, and in patients without TIMP-1 expression compared with those with TIMP-1 expression, although their difference was not statistically significant ($P>0.05$). However, the correlation between the expressive imbalance of MMP-9 and TIMP-1 and the postoperative survival was demonstrated. The survival rate was significantly decreased in patients with the co-expression pattern 1 compared with those with the co-expression pattern 4 ($P=0.0014$, Table 3, Figure 3).

Table 3 Association between the expression of MMP-9 (matrix metalloproteinase-9) and TIMP-1 (tissue inhibitor of metalloproteinase-1) and the prognosis of patients with gastric carcinoma

	n	Survival (%)			P value
		1 yr	2 yr	5 yr	
MMP-9 expression					
-	50	80.42	70.33	60.92	>0.05
+	117	68.09	55.77	44.15	
TIMP-1 expression					
-	121	67.48	56.62	41.23	>0.05
+	46	82.93	68.81	68.81	
Co-expression of MMP-9 and TIMP-1					
A	83	64.87	53.62	36.75	<0.05
B	34	76.08	60.90	60.90	
C	38	73.48	63.74	49.42	
D	12	100.00	88.89	88.89 ^a	

Note: A: MMP-9(+)/TIMP-1(-); B: MMP-9(+)/TIMP-1(+); C: MMP-9(-)/TIMP-1(-); D: MMP-9(-)/TIMP-1(+), ^a $P<0.05$ vs A.

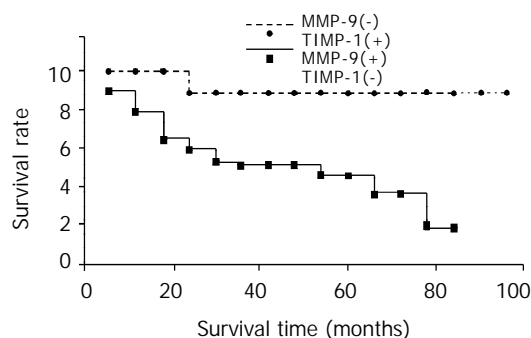


Figure 3 The association between expressive imbalance of MMP-9 (matrix metalloproteinase-9) and TIMP-1 (tissue inhibitor of metalloproteinase-1) and postoperative survival in gastric carcinoma.

DISCUSSION

Expression of MMP-9 and invasiveness, metastasis and prognosis of gastric carcinoma

Degradation of extracellular matrix (ECM) and basement membranes by the tumor cells is a critical step in the processes of tumor invasion and metastasis. MMP-9 is one member of the matrix metalloproteinase families, and characterized by substrate high-specificity and capable of degrading several components of ECM, including type IV collagen molecules which form the major component of the basement membrane.

Increased levels of MMP-9 have been implicated in the invasive potential of tumors^[11-4]. There was a trend towards a higher proportion of active MMP-9 with an increasing grade of breast carcinoma, endometrial carcinoma, colorectal carcinoma, papillary thyroid carcinoma and squamous cell carcinoma of the head and neck^[15-19]. In this study, we observed positive expression of MMP-9 in 65.23 % of patients with gastric carcinoma, but no association of the expression of MMP-9 with sex, age, tumor size and location. These results were similar to the results reported by Murray *et al*^[12] and Hou *et al*^[20]. In contrast to the Murray's and Hou's study, we also demonstrated there was a significant correlation between MMP-9 expression and proliferation of tumor cells, the depth of invasiveness, lymph node metastasis and TNM stage of gastric carcinoma. Pereda *et al* also found that high levels of matrix metalloproteinases promoted the proliferation of pituitary adenomas cells^[21]. Kabashima *et al* reported that MMP-9 expression correlated with lymph node metastasis in intramucosal gastric carcinoma^[22]. Torri *et al* reported that preoperative plasma MMP-9 concentration correlated closely with severity of T, N and M classification, and stage^[23]. These results suggest that over-expression of MMP-9 plays an important role in the progress of gastric carcinoma, and MMP-9 protein may be served as a marker for invasiveness and metastasis of gastric carcinoma. We also noticed that MMP-9 expression increased dramatically in advanced tumors compared with early tumors, whereas there was no such difference between different stages of the advanced tumors. These results suggested that MMP-9 expression might play an important role in the early progress of gastric carcinoma. Sier *et al* reported that the expression and activation of MMP-9 in tumor tissues were of prognostic significance for poor overall survival of the patients with gastric carcinoma, independent of the major clinicopathological parameters^[8,24]. Although there was a decreasing trend of survival in the patients with MMP-9 expression compared with those without the expression, the difference was no significant. Maatta *et al* reported the similarly results in hepatocellular carcinoma and pancreatic adenocarcinoma^[25]. The relation of MMP-9 to the prognosis of gastric carcinoma still needs to be further investigated.

Expression of TIMP-1 and invasiveness, metastasis and prognosis of gastric carcinoma

During the process of invasiveness and metastasis of tumors, the secretion and activation of metalloproteinases (MMPs) is not sufficient to degrade ECM components, as its enzymatic activity can be inhibited by a family of endogenous inhibitors, the tissue inhibitors of metalloproteinase (TIMPs). TIMP-1, a 28.5 kDa glycoprotein, is the first member of the TIMP family, and known to form a complex of 1:1 stoichiometry with activated collagenase, stromelysin and MMP-9 to inhibit their activities. Watanabe *et al* found that the transfection of the complete human TIMP-1 cDNA into highly metastatic human gastric carcinoma cell line KKLS notably decreased the formation of liver metastases when transplanted into nude mice^[11]. It is suggested that TIMP-1 is a negative regulators in the process of tumor metastasis. The expression of TIMP-1 in gastric carcinoma has not been widely examined so far. In our study, a negative association between TIMP-1 expression and invasiveness and metastasis and TNM stage was observed, but there was no association between TIMP-1 expression and sex, age, tumor size and location in gastric carcinoma. These results were opposite to the results reported by Mimori *et al* that the expression of TIMP-1 mRNA in the biopsy samples from human gastric carcinoma tissues (T) was higher than in the biopsy samples from the corresponding normal tissues (N), and a higher T/N ratio of TIMP-1 mRNA correlated with lately advanced stage and poor prognosis of human gastric

carcinoma^[26]. Other studies also showed that the increased TIMP-1 expression correlated with poor prognosis variables, including shortened survival, in patients with renal cell carcinoma and lung cancer^[8,27]. Several studies have shown that TIMP-1 possesses two activities, i.e. inhibitory activity of metalloproteinases, and growth promoting function^[2,28]. Our findings suggest that, TIMP-1 in the progress of human gastric carcinoma functions mainly as an inhibitor of metalloproteinases, subsequently blocking the invasiveness and metastasis of tumor cells. Our findings may offer a new idea in the biological and genetic treatment for gastric carcinoma^[29-34]. In our study, the survival rate of patients with TIMP-1 expression was higher than those without TIMP-1 expression, although difference was not significant. Further studies are needed to determine whether or not TIMP-1 expression alone can serve as a marker predicting the prognosis of patients with gastric cancer.

Imbalance between expression of MMP-9 and TIMP-1 in the invasiveness, metastasis and prognosis of gastric carcinoma

Under physiological conditions the expression of MMPs and TIMPs is highly coordinated at the level of gene expression, and this balanced expression guarantees normal tissue structure and organ function, and prevents both excessive ECM deposition and increased ECM degradation. As some factors in malignant tumors contributes to the over-expression of MMPs without matched TIMP expression, and thus, this balance was broken, thereby, the ECM was degraded and the cancer metastasis was occurred. By contraries, over-expression of TIMPs can prevent the degradation of ECM and inhibit the cancer invasion and metastasis. TIMP-1 can bind to the catalytic domain of MMP-9 in a 1:1 stoichiometry to form complex, so inhibiting the enzymatic activity of MMP-9^[2,9,10]. Murray *et al* revealed the correlation between the expression of MMP-9 and the expression of TIMP-1 in gastric carcinoma^[12,27,35]. However, observation concerning the association of imbalance between the expression of MMP-9 and TIMP-1 with invasion and metastasis in gastric carcinoma has rarely been published. We found that the tumor invasion and metastasis was more frequent in the cases with positive expression of MMP-9. However, the extents of invasion and metastasis in gastric carcinoma significantly decreased if the TIMP-1 was also expressed in these cases at the same time. This suggests that MMP-9 mainly exert functions of promoting cancer invasion and metastasis, while TIMP-1 independently exerts the inhibiting function for cancer invasion and metastasis during the processes of the invasion and metastasis of gastric carcinoma. We also found that the incidence of visceral peritoneum invasion and lymph node metastasis was the highest in the cases with MMP-9 expression but without TIMP-1 expression, whereas, the incidence of lymph node metastasis in the cases with the TIMP-1 expression but without MMP-9 expression was the lowest, with the modest incidence in cases with balanced expression of MMP-9 and TIMP-1. These findings strongly support the hypothesis the expressive imbalance between MMP-9 and TIMP-1 is an important factor in tumor invasion and metastasis. In brief, altered balance of expression between MMP-9 and TIMP-1 plays a central role in progression of gastric carcinoma. According to our follow-up information, we found, for the first time, that although MMP-9 or TIMP-1 alone may not serve as an indicator for patient prognosis, there is a significant association of the expressive imbalance between MMP-9 and TIMP-1 with the postoperative survival of patients with gastric carcinoma. Our data suggest that patients with over-expression of MMP-9 and no expression of TIMP-1 have more aggressive tumor progression and a lower survival rate.

In conclusion, our results indicate a significant positive association between MMP-9 expression and proliferation of tumor cells, the depth of invasiveness, lymph node metastasis

and TNM stage of gastric carcinoma, suggesting MMP-9 can serve as a molecular marker of tumor invasion and metastasis. Our results also demonstrate a significant negative association of TIMP-1 expression with the depth of invasiveness and lymph node metastasis, which provides a new idea in tumor biological and genetic treatment. The interaction between MMP-9 and TIMP-1 in the processes of tumor invasion and metastasis is that MMP-9 mainly promotes tumor invasion and metastasis whereas TIMP-1 inhibits the functions of MMP-9. Imbalance between MMP-9 and TIMP-1 expression may predict the occurrence of tumor invasion and metastasis and poor prognosis. For these patients with imbalanced MMP-9 and TIMP-1 expression, the optimal treatment scheme needs to be selected.

REFERENCES

- Aznavoorian S**, Murphy AN, Stetler-Stevenson WG, Liotta LA. Molecular aspects of tumor cell invasion and metastasis. *Cancer* 1993; **71**: 1368-1383
- Nagase H**, Woessner JF Jr. Matrix metalloproteinases. *J Biol Chem* 1999; **274**: 21491-21494
- Westenmarck J**, Kahari VM. Regulation of matrix metalloproteinase expression in tumor invasion. *FASEB J* 1999; **13**: 781-792
- Ellenrieder V**, Adler G, Gress TM. Invasion and metastasis in pancreatic cancer. *Ann Oncol* 1999; **10**(S): 41-45
- Yoshizaki T**, Sato H, Furukawa M. Recent advances in the regulation of matrix metalloproteinase 2 activation: from basic research to clinical implication. *Oncol Rep* 2002; **9**: 607-611
- Hofmann UB**, Westphal JR, Van Muijen GN, Ruiter DJ. Matrix metalloproteinases in human melanoma. *J Invest Dermatol* 2000; **115**: 337-344
- Ramos-DeSimone N**, Hahn-Dantona E, Siple J, Nagase H, French DL, Quigley JP. Activation of matrix metalloproteinase-9 (MMP-9) via a converging plasmin/stromelysin-1 cascade enhances tumor cell invasion. *J Biol Chem* 1999; **274**: 13066-13076
- Kallakury BV**, Karikehalli S, Haholu A, Sheehan CE, Azumi N, Ross JS. Increased expression of matrix metalloproteinases 2 and 9 and tissue inhibitors of metalloproteinases 1 and 2 correlate with poor prognostic variables in renal cell carcinoma. *Clin Cancer Res* 2001; **7**: 3113-3119
- Goldberg GI**, Strongin A, Collier IE, Genrich LT, Marmer BL. Interaction of 92-kDa type IV collagenase with the tissue inhibitor of metalloproteinases prevents dimerization, complex formation with interstitial collagenase, and activation of the proenzyme with stromelysin. *J Biol Chem* 1992; **267**: 4583-4591
- Olson MW**, Gervasi DC, Mobashery S, Fridman R. Kinetic analysis of the binding of human matrix metalloproteinase-2 and -9 to tissue inhibitor of metalloproteinase (TIMP)-1 and TIMP-2. *J Biol Chem* 1997; **272**: 29975-29983
- Watanabe M**, Takahashi Y, Ohta T, Mai M, Sasaki T, Seiki M. Inhibition of metastasis in human gastric cancer cells transfected with tissue inhibitor of metalloproteinase 1 gene in nude mice. *Cancer* 1996; **77**: 1676-1680
- Murray GI**, Duncan ME, Arbuckle E, Melvin WT, Fothergill JE. Matrix metalloproteinases and their inhibitors in gastric cancer. *Gut* 1998; **43**: 791-797
- Fenoglio-Preiser C**, Munoz N, Carneiro F, Powell SM, Correa P, Rugge M, Guilford P, Sasako M, Lambert R, Stolte M, Megraud F, Watanabe H. Tumours of the stomach. In: Hamilton SR, Aaltonen LA eds. World health organization classification of tumours: Pathology and genetics of tumours of the digestive system. 1st ed. Lyon: IARC Press 2000: 37-67
- Owen DA**. The stomach In: Sternberg SS eds. Diagnostic surgical pathology. 3rd ed. Philadelphia: Lippincott Williams And Wilkins 1999: 1330-1334
- Davies B**, Miles DW, Happerfield LC, Naylor MS, Bobrow LG, Rubens RD, Balkwill FR. Activity of type IV collagenases in benign and malignant breast disease. *Br J Cancer* 1993; **67**: 1126-1131
- Di Nezza LA**, Misajon A, Zhang J, Jobling T, Quinn MA, Ostor AG, Nie G, Lopata A, Salamonsen LA. Presence of active gelatinases in endometrial carcinoma and correlation of matrix metalloproteinase expression with increasing tumor grade and invasion. *Cancer* 2002; **94**: 1466-1475
- Baker EA**, Bergin FG, Leaper DJ. Matrix metalloproteinases, their tissue inhibitors and colorectal cancer staging. *Br J Surg* 2000; **87**: 1215-1221
- Maeta H**, Ohgi S, Terada T. Protein expression of matrix metalloproteinases 2 and 9 and tissue inhibitors of metalloproteinase 1 and 2 in papillary thyroid carcinomas. *Virchows Arch* 2001; **438**: 121-128
- O-Charoenrat P**, Rhys-Evans PH, Eccles SA. Expression of matrix metalloproteinases and their inhibitors correlates with invasion and metastasis in squamous cell carcinoma of the head and neck. *Arch Otolaryngol Head Neck Surg* 2001; **127**: 813-820
- Hou L**, Li Y, Jia YH, Wang B, Xin Y, Ling MY, L ü S. Molecular mechanism about lymphogenous metastasis of hepatocarcinoma cells in mice. *World J Gastroenterol* 2001; **7**: 532-536
- Paez Pereda M**, Ledda MF, Goldberg V, Chervin A, Carrizo G, Molina H, Muller A, Renner U, Podhajcer O, Arzt E, Stalla GK. High levels of matrix metalloproteinases regulate proliferation and hormone secretion in pituitary cells. *J Clin Endocrinol Metab* 2000; **85**: 263-269
- Kabashima A**, Maehara Y, Kakeji Y, Baba H, Koga T, Sugimachi K. Clinicopathological features and overexpression of matrix metalloproteinases in intramucosal gastric carcinoma with lymph node metastasis. *Clin Cancer Res* 2000; **6**: 3581-3584
- Torii A**, Kodera Y, Uesaka K, Hirai T, Yasui K, Morimoto T, Yamamura Y, Kato T, Hayakawa T, Fujimoto N, Kito T. Plasma concentration of matrix metalloproteinase 9 in gastric cancer. *Br J Surg* 1997; **84**: 133-136
- Sier CF**, Kubben FJ, Ganesh S, Heerding MM, Griffioen G, Hanemaaijer R, van Krieken JH, Lamers CB, Verspaget HW. Tissue levels of matrix metalloproteinases MMP-2 and MMP-9 are related to the overall survival of patients with gastric carcinoma. *Br J Cancer* 1996; **74**: 413-417
- Maatta M**, Soini Y, Liakka A, Autio-Harmanen H. Differential expression of matrix metalloproteinase (MMP)-2, MMP-9, and membrane type 1-MMP in hepatocellular and pancreatic adenocarcinoma: implications for tumor progression and clinical prognosis. *Clin Cancer Res* 2000; **6**: 2726-2734
- Mimori K**, Mori M, Shiraishi T, Fujie T, Baba K, Haraguchi M, Abe R, Ueo H, Akiyoshi T. Clinical signification of tissue inhibitor of metalloproteinase expression in gastric carcinoma. *Br J Cancer* 1997; **76**: 531-536
- Ylisirnio S**, Hoyhtya M, Makitaro R, Paakko P, Risteli J, Kinnula VL, Turpeenniemi-Hujanen T, Jukkola A. Elevated serum levels of type I collagen degradation marker ICTP and tissue inhibitor of metalloproteinase (TIMP) 1 are associated with poor prognosis in lung cancer. *Clin Cancer Res* 2001; **7**: 1633-1637
- Chesler L**, Golde DW, Bersch N, Johnson MD. Metalloproteinase inhibition and erythroid potentiation are independent activities of tissue inhibitor of metalloproteinase-1. *Blood* 1995; **86**: 4506-4515
- Coussens LM**, Fingleton B, Matrisian LM. Matrix metalloproteinase inhibitors and cancer: trials and tribulations. *Science* 2002; **295**: 2387-2392
- Tosetti F**, Ferrari N, De Flora S, Albini A. 'Angioprevention': angiogenesis is a common and key target for cancer chemopreventive agents. *FASEB J* 2002; **16**: 2-14
- Yoshizaki T**, Sato H, Furukawa M. Recent advances in the regulation of matrix metalloproteinase 2 activation: from basic research to clinical implication. *Oncol Rep* 2002; **9**: 607-611
- Hoekstra R**, Eskens FA, Verweij J. Matrix metalloproteinase inhibitors: current developments and future perspectives. *Oncologist* 2001; **6**: 415-427
- Verhagen AM**, Lock P. Revealing the intricacies of cancer. *Genome Biol* 2002; **3**: reports4015.1-4015.5
- Brown PD**. Matrix metalloproteinases in gastrointestinal cancer. *Gut* 1998; **43**: 161-163
- Arnold SM**, Young AB, Munn RK, Patchell RA, Nanayakkara N, Markesbery WR. Expression of p53, bcl-2, E-cadherin, matrix metalloproteinase-9, and tissue inhibitor of metalloproteinases-1 in paired primary tumors and brain metastasis. *Clin Cancer Res* 1999; **5**: 4028-4033

Relationship between inactivation of p16 gene and gastric carcinoma

Guo-Hai Zhao, Tie-Chen Li, Liang-Hui Shi, Ya-Bin Xia, Lin-Ming Lu, Wen-Bin Huang, Hui-Lan Sun, Yi-Sheng Zhang

Guo-Hai Zhao, Liang-Hui Shi, Ya-Bin Xia, Yi-Sheng Zhang, Department of Surgery, the Affiliated Yijishan Hospital, Wannan Medical College, Wuhu 241001, Anhui Province, China

Tie-Chen Li, Hui-Lan Sun, Department of Biology, Wannan Medical College, Wuhu 241001, Anhui Province, China

Lin-Ming Lu, Wen-Bin Huang, Department of pathology, Wannan Medical College, Wuhu 241001, Anhui Province, China

Supported by the Department of Education Natural Science Foundation of Anhui Province, China, No.99j10216

Correspondence to: Guo-Hai Zhao, Department of Surgery, the Affiliated Yijishan Hospital, Wannan Medical College, Wuhu 241001, Anhui Province, China. zhaoguohai@163.net

Telephone: +86-553-5738856-2107 **Fax:** +86-553-5738279

Received: 2002-10-09 **Accepted:** 2003-01-03

Abstract

AIM: To investigate the relationship between inactivation of p16 gene and gastric carcinoma, and the mechanism of inactivation of p16 gene in gastric carcinogenesis.

METHODS: 40 fresh tumor tissue specimens were taken from primary gastric cancer patients. Expression of P16 protein was detected by immunohistochemical method. Deletion and point mutation of p16 gene were analyzed by polymerase chain reaction (PCR) and DNA sequencing, respectively.

RESULTS: The frequency of loss of P16 protein expression in the gastric cancer tissue, adjacent nontumor tissue, and distal normal tissue was 77.5 % (31/40), 55.0 % (22/40), and 17.5 % (7/40), respectively ($P < 0.005$). Homozygous deletion of exon 1 and exon 3 was observed in two and three cases, respectively, giving an overall frequency of homozygous deletion of 12.5 %. All five cases had diffuse type gastric carcinoma. No p16 gene point mutation was detected.

CONCLUSION: These findings suggest a close correlation between inactivation of p16 gene and gastric carcinoma. Further investigations are needed to testify the mechanism of inactivation of p16 gene in gastric carcinogenesis.

Zhao GH, Li TC, Shi LH, Xia YB, Lu LM, Huang WB, Sun HL, Zhang YS. Relationship between inactivation of p16 gene and gastric carcinoma. *World J Gastroenterol* 2003; 9(5): 905-909 <http://www.wjgnet.com/1007-9327/9/905.htm>

INTRODUCTION

Gastric carcinoma (GC) is common in China^[1-19]. From 1991 to 2000, 18,029 inpatients with malignant tumor had been treated in the Affiliated Yijishan Hospital of Wannan Medical College. 2,859 cases were GC sufferers, which accounted for 16 % of the total inpatients and ranked the first in malignant tumor. The statistical data showed that GC was one of the commonest tumors in South Anhui province. Therefore, it

would have clinical significance to explore the pathogenesis of gastric carcinogenesis.

Early in 1994, Kamb *et al*^[20] and Norobi *et al*^[21] reported their studies on p16 gene simultaneously but independently. p16 gene is located in chromosome 9p21, consisting of 2 introns and 3 exons. Exon 1 contains a region of 126 bp, while exon 2 contains a region of 307 bp, and exon 3 contains a region of 11 bp. In recent years, studies have revealed homozygous deletion and mutation of p16 gene, predominantly in exon 2, in various malignant tumor, suggesting that p16 gene is a multiple tumor suppressor 1 (MTS1)^[20-33].

The mechanism of p16 gene in gastric carcinogenesis remains unidentified. Some studies have suggested that p16 gene alteration in GC presents itself in different mechanism from other tumors. The alteration is infrequent in exon 2, but exists predominantly in exon 1 and 3^[34-36]. In this study, using polymerase chain reaction (PCR), DNA sequencing analysis and an immunohistochemical method, the fresh tumor specimens of 40 GC patients were examined for homozygous deletion, point mutation of p16 gene and expression of P16 protein to verify the relationship between p16 gene alteration and GC.

MATERIALS AND METHODS

Gastric carcinoma specimens

Under sterile conditions, fresh tumor specimens and their adjacent non-tumor (≤ 3 cm away from the tumor) and distal (≥ 5 cm away from the tumor) normal appearing tissues were obtained in the course of surgery from 40 patients with primary GC at the Affiliated Yijishan Hospital of Wannan Medical College. None of the patients had received either chemotherapy or radiotherapy prior to surgery. All of the primary tumors were pathologically confirmed to be GC cases, among which there were 26 males and 14 females. The age ranged from 31 to 68 (mean 55.4) years old. 14 cases had intestinal type and 26 cases diffuse type by histopathological typing. 12 cases had well-differentiated and 28 cases poorly differentiated.

DNA extraction

Approximately 50 mg tissue of GC was abraded with routine methods and digested with proteinase K. DNA was extracted by means of the routine phenol-chloroform method. The purity and concentration of extracted DNA were detected with ultraviolet spectrophotometer (Daojin Company, UV-2201 type). The extracted DNA was stored at 4 °C until use.

Polymerase chain reaction

The three exons of p16 gene were amplified by employing 3 pairs of primers. The primers 1 and 3 were synthesized by Shanghai Boya Company, and the primer 2 by Saer Biotechnology Company of Shanghai Cell Biology Institution. The sequence of primers and the length of PCR products were listed in Table 1.

PCR was performed in 50 μ L reaction volume containing 0.2 μ g DNA template, 2 U Taq DNA polymerase (Shanghai Sangon

Company), 10 pmol/L each pair of primers, 0.2 mmol/L dNTP, 1.5 mmol/L MgCl₂, 5 μL 10×buffer. PCR reaction was carried out in a thermal cycle machine (Perkin-Elmer, 480 type) for an initial 5 min denaturation step at 98 °C. After Taq DNA polymerase was added, the thermal cycle followed. The reaction conditions consisted of denaturation at 94 °C for 45 s, annealing at 58 °C for 50 s for exon 1, 56 °C for 60 s for exon 2, 52 °C for 50 s for exon 3, extension at 72 °C for 60 s, on completion of 35 cycles, at last extension at 72 °C for 5 min. 10 μL of PCR product was loaded into the gel, and a 100 bp DNA ladder was used as a marker. The PCR products were electrophoresed at voltage of 100 V on 2 % agarose gel for 30 min and visualized under UV illumination using an ethidium bromide stain. The results were photographed by a digital camera.

Table 1 The primer sequence of the p16 gene

Exon	Sequence of the primer	Product of PCR (bp)	Temperature for annealing (°C)
1S	5' TCTGCGGAGAGGGGAGAGCAG 3'	280	58
1A	5' GCGCTACCTGATTCCAATTC 3'		
2S	5' TTCCTTCCGTCATGCCGG 3'	394	56
2A	5' GTACAAATCTCAGATCATCAGTCCTC 3'		
3S	5' GGATGTTCCACACATCTTTG 3'	189	52
3A	5' ATGAAAACACTACGAAAGCGGG 3'		

S: sense; A: antisense.

DNA sequencing analysis

The GC specimens that produced amplified product were reamplified by PCR. PCR was performed in 100 μL reaction volume. The products were purified using Spin PCRapid Purification kit (Promage Company), and then together with PCR primers were sequenced (dideoxy chain termination) by an ABI Prism 377 DNA sequencer (Perkin-Elmer Company) in Shanghai Sangon Company.

Immunohistochemistry

The sections were deparaffined, boiled and retrieved in citric acid buffer for 10 min. Then, the immunohistochemical streptavidin-in-peroxidase (SP) method was used according to the specification of SP kit. The known positive sections were used as a positive control. Phosphatic buffer solution (PBS) replacing the primary antibody was used as a negative control in every experiment. Mouse-anti-human P16 (ZJ11) and SP kit were products of Fuzhou Maixin Biotechnology Company.

RESULTS

Deletion and mutation of p16 gene

Of 40 GC specimens in PCR products, exon 1 and exon 3 were not detected in 2 cases and 3 cases, respectively. But all of specimens were detected the PCR product of exon 2. These findings indicate that homozygous deletion of p16 gene exon 1 and exon 3 exist in GC (Figure 1, 2, 3). The frequency of deletion of p16 gene was 12.5 % (5/40). All five cases with p16 gene deletion had poorly differentiated were all diffuse type GC, with staging of PT₃N₂M₀, as assessed by pathological section analysis.

Amongst the 35 GC cases in whom p16 deletion was not detected, 10 cases were randomly selected for DNA sequencing. No point mutation was detected in these GC specimens when compared with the normal p16 gene cDNA sequence^[37].

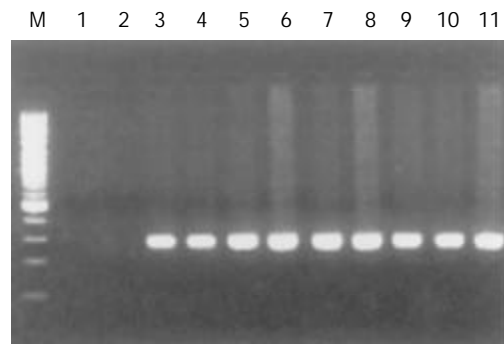


Figure 1 The PCR products of p16 gene exon 1. M: marker 100 bp ladder; Line 1-11: gastric carcinoma; Line 1-2: homozygous deletion.

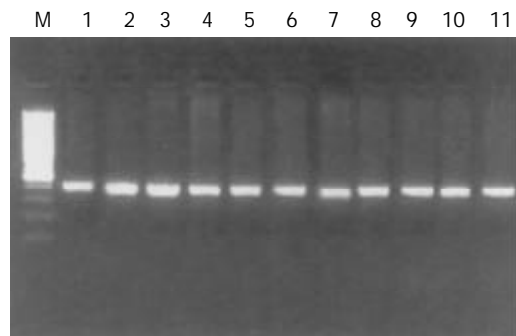


Figure 2 The PCR products of p16 gene exon 2. M: marker 100 bp ladder; Line 1-11: gastric carcinoma.

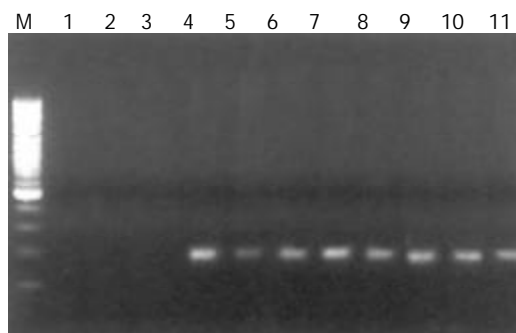


Figure 3 The PCR products of p16 gene exon 3. M: marker 100 bp ladder; Line 1-11: gastric carcinoma; Line 1-3: homozygous deletion.

Expression of P16 protein

Expression of P16 protein in GC tissues, adjacent nontumor tissue (≤3 cm) and distal normal tissue (≥5 cm) were summarized in Table 2 and Figure 4, 5, 6. Using χ^2 test, the value of χ^2 was 29.40, $P < 0.005$, which has significant difference. These data revealed a strong correlation between inactivation of p16 gene and gastric carcinogenesis.

Table 2 P16 protein expression at GC

Histological types	n	The frequency of P16 protein expression loss (%)	
		Positive	Negative
Gastric carcinoma	40	9	31
Adjacent nontumor tissue (≤3 cm)	40	18	22
Distal normal tissue (≥5 cm)	40	33	7

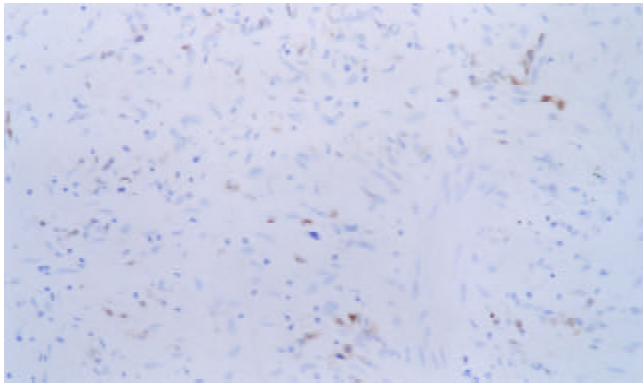


Figure 4 p16 protein expression in gastric carcinoma $\times 200$.

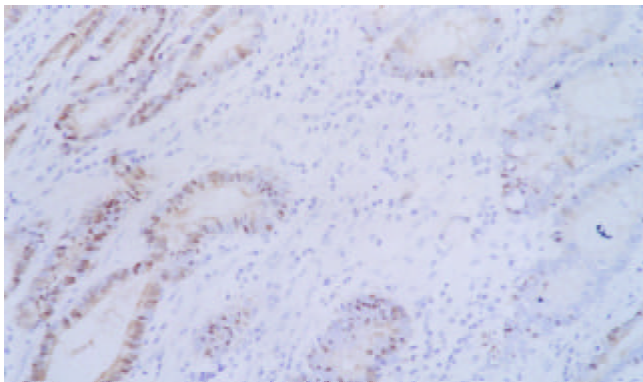


Figure 5 p16 protein expression in adjacent nontumor tissue $\times 200$.

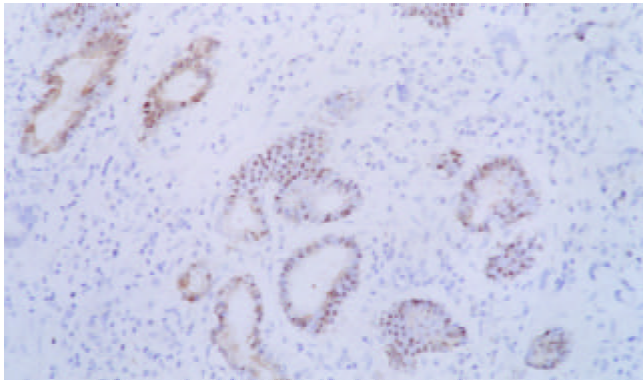


Figure 6 p16 protein expression in distal normal tissue $\times 200$.

DISCUSSION

Fission of tumor cells undergoes a regular cell cycle as normal cells do, which is commonly divided into G1, S, G2, and M phase. When a cell goes into the cell cycle, the cell depends on activation of cyclin dependent kinase (CDK). Only combined with a cyclin, can CDK be activated, and inhibited when it combines with a series of proteins. These proteins known as cyclin dependent kinase inhibitors are a group of small molecular proteins that are involved in the negative regulation of the cell cycle. Alteration of these proteins results in uncontrollable cell proliferation and thus carcinogenesis. P16 protein is one of these proteins so that mutation and deletion of p16 gene lead to uncontrollable cell proliferation, and then carcinogenesis^[1, 20, 21, 37-40]. The relationship between alteration of p16 gene and carcinogenesis of various tumors has been verified^[1, 20-36, 41].

In this study, homozygous deletion of exon 1 and exon 3 was observed, respectively, in 2 cases and 3 cases with poorly

differentiated diffuse type GC amongst 40 samples. The frequency of deletion was 12.5 %. Our results showed that alteration in p16 gene was highly associated with poorly differentiated GC, which is almost identical to the observations by Lu *et al.*^[34] and Lee *et al.*^[35]. Therefore, it is suggested that alteration of p16 gene is associated with the differentiation degree and metastasis of GC. In contrast, Wu *et al.*^[36] reported that deletion of p16 gene was frequently encountered in the intestinal type, with a lower frequency in the diffuse type. Furthermore, He *et al.*^[41] reported that there was homozygous deletion of p16 gene exon 2 in GC, with a frequency of 20.0 %. Our finding does not tally with above observation^[34-36]. We randomly selected 10 of the 35 GC cases without p16 gene deletion for DNA sequencing, no point mutation was detected. The results reveal that point mutation of p16 gene is rare in gastric carcinogenesis. It coincides with previous findings^[34-36, 41].

In human primary GC, deletion and point mutation of p16 gene are infrequent, but loss of expression of P16 protein is common. Some studies have found^[1, 35, 40-42] that the frequency of loss of P16 protein expression ranges from 52 % to 90 %. Our results agree with these studies. We found that the frequency of loss of expression of P16 protein was 77.5 %. It had statistically significant difference with adjacent non-tumor tissue (55.0 %) and distal normal appearing tissue (17.5 %) ($P < 0.005$). These results suggest that inactivation of p16 gene is strongly associated with gastric carcinogenesis, however, deletion and point mutation of p16 gene are not the major mechanism of p16 inactivation in GC.

The methylation-specific PCR (MSP) method established by Herman *et al.*^[43] in 1996 has significantly promoted the research on the interrelationship between hypermethylation and gene silencing. Subsequent studies have revealed high frequency of hypermethylation in p16 gene 5' promotor regions in various tumors, with frequency ranging from 60 % to 89 %^[44-48]. Inactivation of p16 gene correlates with hypermethylation of 5' promotor regions CpG island in GC. Some studies have found that hypermethylation in the promotor regions CpG island is an important mechanism for p16 gene inactivation in GC, whereas deletion and point mutation of the gene are rarely seen^[49-56]. The CpG island hypermethylation occurred early in multistep gastric carcinogenesis tends to accumulate along the process^[55]. P16 gene with methylated promotor regions would reexpress P16 protein when it is treated with 5-aza-2'-deoxycytidine which demethylates^[35] or when the inducers of hypermethylation are eliminated^[57, 58]. The effect mechanism of p16 gene is to inhibit cell cycle directly, and it is easy to perform gene targeting or protein modification because p16 gene is small. Therefore, it is needed to further investigate the relationship between p16 gene inactivation and gastric carcinogenesis, and the mechanism of p16 gene inactivation, since it is of significant clinical implications in early diagnosis, therapy and prognosis.

REFERENCES

- 1 **Zhao Y**, Zhang XY, Shi XJ, Hu PZ, Zhang CS, Ma FC. Clinical significance of expressions of P16, P53 proteins and PCNA in gastric cancer. *Shijie Huaren Xiaohua Zazhi* 1999; 7: 246-248
- 2 **Tu SP**, Jiang SH, Tan JH, Jiang XH, Qiao MM, Zhang YP, Wu YL, Wu YX. Proliferation inhibition and apoptosis induction by arsenic trioxide on gastric cancer cell SGC-7901. *Shijie Huaren Xiaohua Zazhi* 1999; 7: 18-21
- 3 **Gao P**, Jiang XW, Yuan WJ. Effects of gastrin and gastrin receptor antagonist proglumide on gastric cancer line. *Shijie Huaren Xiaohua Zazhi* 1999; 7: 22-24
- 4 **Li JQ**, Wan YL, Cai WY. Biological significance of cyclin E expression in early gastric cancer. *Shijie Huaren Xiaohua Zazhi* 1999; 7: 31-33
- 5 **Dong WG**, Yu JP, Luo HS, Yu BP, Xu Y. Relationship between

- human papillomavirus infection and the development of gastric carcinoma. *Shijie Huaren Xiaohua Zazhi* 1999; **7**: 46-48
- 6 **Liu ZM**, Shou NH. Significance of mdr1 gene expression in gastric carcinoma tissue. *Shijie Huaren Xiaohua Zazhi* 1999; **7**: 145-146
- 7 **Shi YQ**, Xiao B, Miao JY, Zhao YQ, You H, Fan DM. Construction of eukaryotic expression vector pBK fas and MDR reversal test of drug-resistant gastric cancer cells. *Shijie Huaren Xiaohua Zazhi* 1999; **7**: 309-312
- 8 **Fang DC**, Zhou XD, Luo YH, Wang DX, Lu R, Yang SM, Liu WW. Microsatellite instability and loss of heterozygosity of suppressor gene in gastric cancer. *Shijie Huaren Xiaohua Zazhi* 1999; **7**: 479-481
- 9 **Qin LJ**. *In situ* hybridization of P53 tumor suppressor gene in human gastric precancerous lesions and gastric cancer. *Shijie Huaren Xiaohua Zazhi* 1999; **7**: 494-497
- 10 **Liu HF**, Liu WW, Fang DC. Study of the relationship between apoptosis and proliferation in gastric carcinoma and its precancerous lesion. *Shijie Huaren Xiaohua Zazhi* 1999; **7**: 649-651
- 11 **Mi JQ**, Zhang ZH, Shen MC. Significance of CD_{44v6} protein expression in gastric carcinoma and precancerous lesions. *Shijie Huaren Xiaohua Zazhi* 2000; **8**: 156-158
- 12 **Gao GL**, Yang Y, Yang S, Ren CW. Relationship between proliferation of vascular endothelial cells and gastric cancer. *Shijie Huaren Xiaohua Zazhi* 2000; **8**: 282-284
- 13 **Wang RQ**, Fang DC, Liu WW. MUC2 gene expression in gastric cancer and preneoplastic lesion tissues. *Shijie Huaren Xiaohua Zazhi* 2000; **8**: 285-288
- 14 **Liu HF**, Liu WW, Fang DC, Yang SM, Wang RQ. Bax gene expression and its relationship with apoptosis in human gastric carcinoma and precancerous lesions. *Shijie Huaren Xiaohua Zazhi* 2000; **8**: 665-668
- 15 **Gu HP**, Ni CR, Zhan RZ. Relationship between CD₁₅ mRNA and its protein expression and gastric carcinoma invasion. *Shijie Huaren Xiaohua Zazhi* 2000; **8**: 851-854
- 16 **Wang DX**, Fang DC, Liu WW. Study on alteration of multiple genes in intestinal metaplasia, atypical hyperplasia and gastric cancer. *Shijie Huaren Xiaohua Zazhi* 2000; **8**: 855-859
- 17 **Guo SY**, Gu QL, Liu BY, Zhu ZG, Yin HR, Lin YZ. Experimental study on the treatment of gastric cancer by TK gene combined with mIL-2 gene. *Shijie Huaren Xiaohua Zazhi* 2000; **8**: 974-978
- 18 **Guo YQ**, Zhu ZH, Li JF. Flow cytometric analysis of apoptosis and proliferation in gastric cancer and precancerous lesion. *Shijie Huaren Xiaohua Zazhi* 2000; **8**: 983-987
- 19 **Xia JZ**, Zhu ZG, Liu BY, Yan M, Yin HR. Significance of immunohistochemically demonstrated micrometastases to lymph nodes in gastric carcinomas. *Shijie Huaren Xiaohua Zazhi* 2000; **8**: 1113-1116
- 20 **Kamb A**, Gruis NA, Weaver-Feldhaus J, Liu QY, Harshman K, Tavtigian SV, Stockert E, Day III RS, Johnson BE, Skolnick MK. A cell cycle regulator potentially involved in genesis of many tumor types. *Science* 1994; **264**: 436-440
- 21 **Nobori T**, Miura K, Wu DJ, Lois A, Takabayashi K, Carson DA. Deletions of the cyclin-dependent kinase-4 inhibitor gene in multiple human cancers. *Nature* 1994; **368**: 753-756
- 22 **Lu JG**, Huang ZQ, Wu JS, Wang Q, Ma QJ, Yao X. Significance of tumor suppressor gene p16 expression in primary biliary cancer. *Shijie Huaren Xiaohua Zazhi* 2000; **8**: 638-640
- 23 **Zhou YA**, Gu ZP, Wang XX, Ma QF, Huang LJ. Reexpression of p16^{INK4a} gene suppresses growth of human esophageal carcinoma cells. *Shijie Huaren Xiaohua Zazhi* 2001; **9**: 877-881
- 24 **Jin S**, Peng Q, Lu S, Chen R, Zhou C, Su T. Deletion of MTS1/p16 gene in human esophageal carcinoma. *Zhonghua Zhongliu Zazhi* 1998; **20**: 9-11
- 25 **Peng Q**, Jin S, Lu S, Chen R. p16 gene suppresses growth of human esophageal carcinoma cells. *Zhonghua Zhongliu Zazhi* 1999; **21**: 175-177
- 26 **Lu G**, Chen X, Cao W, Zhang G, Dai H, Jiang Y, Sun W. Multiple tumor suppressor 1/p16 gene alterations in human esophageal squamous-cell carcinoma: clinical significance and regional difference. *Zhonghua Zhongliu Zazhi* 1999; **21**: 359-362
- 27 **Cheng J**, Lin C, Xing R, Zhang X, Kui Y, Mou J, Wang X, Wu M. Apoptosis of human melanoma cell line WM-983A by p16 gene transduction. *Zhonghua Zhongliu Zazhi* 1999; **21**: 89-92
- 28 **Hashemi J**, Platz A, Ueno T, Stierner U, Ringborg U, Hansson J. CDKN2A germ-line mutation in individuals with multiple cutaneous melanomas. *Cancer Res* 2000; **60**: 6864-6867
- 29 **Wang X**, Sun Y, Li W, Wang X, Zhang H, Chen J, Ding F, Wu M. Alterations of FHIT gene and p16 gene in lung cancer and metastatic hilar lymph nodes. *Zhonghua Zhongliu Zazhi* 1999; **21**: 108-111
- 30 **Fu X**, Zhang S, Ran R, Shen Z, Gu J, Cao S. Effect of exogenous p16 gene on the growth of wild-type p53 human lung adenocarcinoma cells. *Zhonghua Zhongliu Zazhi* 1999; **21**: 102-104
- 31 **Zhou J**, Yang D, Zhang L, Wang J, Yao Q, Su Z, Fan Y. Study on the relationship of alteration and expression of p16 gene to pancreatic carcinoma. *Zhonghua Yixue Yi Chuanxue Zazhi* 2000; **17**: 399-403
- 32 **Wang GL**, Lo KW, Tsang KS, Chung NYF, Tsang YS, Cheung ST, Lee JCK, Huang DP. Inhibiting tumorigenic potential by restoration of p16 in nasopharyngeal carcinoma. *Br J Cancer* 1999; **81**: 1122-1126
- 33 **Huang Q**, Tao Y, Yandell DW. Mutations of several tumor suppressor genes in primary retinoblastoma. *Zhonghua Zhongliu Zazhi* 1999; **21**: 10-12
- 34 **Lu Y**, Gao C, Cui J, Sun M, Cheng J. Deletion and down-regulation of MTS1/p16 gene in human gastric cancer. *Zhonghua Zhongliu Zazhi* 1996; **18**: 189-191
- 35 **Lee YY**, Kang SH, Seo JY, Jung CW, Lee KU, Choe KJ, Kim BK, Kim NK, Koeffler HP, Bang YJ. Alterations of p16^{INK4A} and p15^{INK4B} genes in gastric carcinomas. *Cancer* 1997; **80**: 1889-1896
- 36 **Wu MS**, Shun CT, Sheu JC, Wang HP, Wang JT, Lee WJ, Chen CJ, Wang TH, Lin JT. Overexpression of mutant p53 and c-erbB-2 proteins and mutations of the p15 and p16 genes in human gastric carcinoma: with respect to histological subtypes and stages. *J Gastroenterol Hepatol* 1998; **13**: 305-310
- 37 **Serrano M**, Hannon GJ, Beach D. A new regulatory motif in cell-cycle control causing specific inhibition of cyclin D/CDK4. *Nature* 1993; **366**: 704-707
- 38 **Shapiro GI**, Edwards CD, Ewen ME, Rollins BJ. p16^{INK4A} participates in a G1 arrest checkpoint in response to DNA damage. *Mol Cell Biol* 1998; **18**: 378-387
- 39 **Quan J**, Fan XG. Progress in experimental research of *Helicobacter pylori* infection and gastric carcinoma. *Shijie Huaren Xiaohua Zazhi* 1999; **7**: 1068-1069
- 40 **Wu SH**, Ma LP, Jin W, Sui YF. The relation between suppressor gene p16, p21, PRB and gastric cancer. *Shijie Huaren Xiaohua Zazhi* 1999; **7**: 551
- 41 **He XS**, Su Q, Chen ZC, He XT, Long ZF, Ling H, Zhang LR. Expression, deletion and mutation of p16 gene in human gastric cancer. *World J Gastroenterol* 2001; **7**: 515-521
- 42 **Zhou Y**, Gao SS, Li YX, Fan ZM, Zhao X, Qi YJ, Wei JP, Zou JX, Liu G, Jiao LH, Bai YM, Wang LD. Tumor suppressor gene p16 and Rb expression in gastric cardia precancerous lesions from subjects at a high incidence area in northern China. *World J Gastroenterol* 2002; **8**: 423-425
- 43 **Herman JG**, Graff JR, Myohanen S, Nelkin BD, Baylin SB. Methylation-specific PCR: A novel PCR assay for methylation status of CpG islands. *Proc Natl Acad Sci USA* 1996; **93**: 9821-9826
- 44 **Lehmann U**, Hasemeier B, Lilischkis R, Kreipe H. Quantitative analysis of promoter hypermethylation in laser-microdissected archival specimens. *Lab Invest* 2001; **81**: 635-638
- 45 **Matsuda Y**, Ichida T, Matsuzawa J, Sugimura K, Asakura H. p16^{INK4} is inactivated by extensive CpG methylation in human hepatocellular carcinoma. *Gastroenterology* 1999; **116**: 394-400
- 46 **Liew CT**, Li HM, Lo KW, Leow CK, Chan JY, Hin LY, Lau WY, Lai PBS, Lim BK, Huang J, Leung WT, Wu S, Lee JCK. High frequency of p16^{INK4A} gene alterations in hepatocellular carcinoma. *Oncogene* 1999; **18**: 789-795
- 47 **Foster SA**, Wong DJ, Barrett MT, Galloway DA. Inactivation of p16 in human mammary epithelial cells by CpG island methylation. *Mol Cell Biol* 1998; **18**: 1793-1801
- 48 **Salem C**, Liang G, Tsai YC, Coulter J, Knowles MA, Feng AC, Groshen S, Nichols PW, Jones PA. Progressive increases in *de novo* methylation of CpG islands in bladder cancer. *Cancer Res* 2000; **60**: 2473-2476
- 49 **Suzuki H**, Itoh F, Toyota M, Kikuchi T, Kakiuchi H, Hinoda Y, Imai K. Distinct methylation pattern and microsatellite instability in sporadic gastric cancer. *Int J Cancer* 1999; **83**: 309-313

- 50 **Toyota M**, Ahuja N, Suzuki H, Itoh F, Toyota MO, Imai K, Baylin SB, Issa JPI. Aberrant methylation in gastric cancer associated with the CpG island methylator phenotype. *Cancer Res* 1999; **59**: 5438-5442
- 51 **Tsujie M**, Yamamoto H, Tomita N, Sugita Y, Ohue M, Sakita I, Tamaki Y, Sekimoto M, Doki Y, Inoue M, Matsuura N, Monden T, Shiozaki H, Monden M. Expression of tumor suppressor gene p16^{INK4} products in primary gastric cancer. *Oncology* 2000; **58**: 126-136
- 52 **Shim YH**, Kang GH, Ro JY. Correlation of p16 hypermethylation with p16 protein loss in sporadic gastric carcinomas. *Lab Invest* 2000; **80**: 689-695
- 53 **Song SH**, Jong HS, Choi HH, Kang SH, Ryu MH, Kim NK, Kim WH, Bang YJ. Methylation of specific CpG sites in the promoter region could significantly down-regulate p16^{INK4a} expression in gastric adenocarcinoma. *Int J Cancer* 2000; **87**: 236-240
- 54 **Leung WK**, Yu J, Ng EKW, To KF, Ma PK, Lee TL, Go MYY, Chung SCS, Sung JY. Concurrent hypermethylation of multiple tumor-related genes in gastric carcinoma and adjacent normal tissues. *Cancer* 2001; **91**: 2294-2301
- 55 **Kang GH**, Shim YH, Jung HY, Kim WH, Ro JY, Rhyu MG. CpG island methylation in premalignant stages of gastric carcinoma. *Cancer Res* 2001; **61**: 2847-2851
- 56 **Bae SI**, Lee HS, Kim SH, Kim WH. Inactivation of O⁶-methylguanine-DNA methyltransferase by promoter CpG island hypermethylation in gastric cancers. *Br J Cancer* 2002; **86**: 1888-1892
- 57 **Toyota M**, Itoh F, Imai K. Can DNA methylation be a molecular marker for eradication of *Helicobacter pylori* in MALT lymphoma? *J Gastroenterol* 2002; **37**: 73-74
- 58 **Kim YS**, Kim JS, Jung HC, Lee CH, Kim CW, Song IS, Kim CY. Regression of low-grade gastric mucosa-associated lymphoid tissue lymphoma after eradication of *Helicobacter pylori*: possible association with p16 hypermethylation. *J Gastroenterol* 2002; **37**: 17-22

Edited by Xia HHX

Expression of TFF2 and *Helicobacter pylori* infection in carcinogenesis of gastric mucosa

Guo-Yong Hu, Bao-Ping Yu, Wei-Guo Dong, Mu-Qi Li, Jie-Ping Yu, He-Sheng Luo, Zong-Xue Rang

Guo-Yong Hu, Bao-Ping Yu, Wei-Guo Dong, Mu-Qi Li, Jie-Ping Yu, He-Sheng Luo, Zong-Xue Rang, Gastroenterology Department, Renmin Hospital of Wuhan University, Wuhan 430060, Hubei Province, China

Correspondence to: Bao-Ping Yu, Gastroenterology Department, Renmin Hospital of Wuhan University, 238 Jie-Fang Road, Wuhan 430060, Hubei Province, China. yubaoping62@yahoo.com.cn

Telephone: +86-27-88041911-8469

Received: 2002-07-23 **Accepted:** 2002-10-29

Abstract

AIM: To investigate the expression of TFF2 and *Helicobacter pylori* infection in carcinogenesis of gastric mucosa.

METHODS: The expression of TFF2 was immunohistochemically analyzed in paraffin-embedded samples from 119 patients with endoscopic biopsy and subtotal gastrectomy specimens of gastric mucosal lesions, including 16 cases of chronic superficial gastritis (CSG), 20 chronic atrophic gastritis (CAG), 35 intestinal metaplasia (IM), 23 gastric epithelial dysplasia (GED) and 25 gastric carcinoma (CA), and *Helicobacter pylori* infection was detected by Warthin-Starry staining.

RESULTS: 1: TFF2 was located in the cytoplasm of gastric mucous neck cell. The expression of TFF2 was 100 %, 100 %, 0, 56.5 % and 0 in CSGs, CAGs, IMs, GEDs and CAs, respectively. 2: The value of TFF2 positive cell density in CSG with *Helicobacter pylori* infection was higher than that without *Helicobacter pylori* infection. (52.89 ± 7.27 vs 46.49 ± 13.04 , $P > 0.05$); But the value of TFF2 positive cell density in CAG and GED with *Helicobacter pylori* infection was significantly lower than that without *Helicobacter pylori* infection (18.17 ± 4.09 vs 37.93 ± 13.80 , $P < 0.01$ and 14.44 ± 9.32 vs 24.84 ± 10.22 , $P < 0.05$).

CONCLUSION: Increase of TFF2 expression in CSG is perhaps associated with the protective mechanism after gastric mucosal injury. Decrease of TFF2 expression in CAG possibly attributes to the decrease in the number of gastric gland cell expressing TFF2. Re-expression of TFF2 in gastric epithelial dysplasia implies that TFF2 possibly contributes to the initiation of gastric carcinoma. The effect of *Helicobacter pylori* on the expression of TFF2 depends on the status of gastric mucosa.

Hu GY, Yu BP, Dong WG, Li MQ, Yu JP, Luo HS, Rang ZX. Expression of TFF2 and *Helicobacter pylori* infection in carcinogenesis of gastric mucosa. *World J Gastroenterol* 2003; 9(5): 910-914

<http://www.wjgnet.com/1007-9327/9/910.htm>

INTRODUCTION

Trefoil factor family 2 (TFF2), also known as spasmodic polypeptide (SP), is one of three known mammalian trefoil peptides. Trefoil peptides are small (7-12 kDa) protease-

resistant proteins secreted by the gastrointestinal mucosa in a lineage-specific manner. While expressed and secreted preferentially by gastric mucous neck cell^[1,2], TFF2 is upregulated in diverse pathological conditions of gastrointestinal tract, which involves regeneration and restitution of epithelial lineage during the epithelial cell injury, mucosal protection and healing of ulcer^[3-5]. However, the relationship between TFF2 expression and gastric carcinoma is still not fully elucidated. In the present study, we evaluated the expression of TFF2 and *Helicobacter pylori* infection in a series of gastric mucosal lesions. The aim of this study was in two aspect: to characterize the expression pattern of TFF2 on carcinogenesis of gastric mucosa; and to study the relationship between the expression of TFF2 and *Helicobacter pylori* infection.

MATERIALS AND METHODS

Tissue material

The gastric mucosal lesions of all 119 patients who had undergone surgical resection or endoscopic biopsy in the Renmin Hospital of Wuhan University from March 2001 to March 2002 were studied. There were 16 cases of chronic superficial gastritis (CSG), 20 chronic atrophic gastritis (CAG), 35 intestinal metaplasia (IM), 23 gastric epithelial dysplasia (GED) and 25 gastric carcinoma (CA). Tissue fragments were fixed in 10 % formaldehyde and embedded in paraffin. Serial sections of 4 μ m were stained with haematoxylin and eosin (HE), Warthin-Starry and by immunohistochemistry.

Immunohistochemistry of TFF2 protein

A modification of the streptavidin-peroxidase method was applied to immunohistochemistry and with 3, 3'-diaminobenzidine (DAB) as the chromogen (Ultrasensitive SP Kit, DAB, FuZhou Maixin Biotechnology Co). Sections was incubated for one hour at 37 °C with monoclonal antibody against human TFF2 (hSP, diluted 1:35, Novocastra Laboratories Ltd). All batches of staining included positive control. Negative control was performed by replacing the primary mAbs with Tris buffer solution (TBS). The value of positive cell density was determined by image analysis system of HPIAS2000.

Warthin-Starry staining

Histological examination with Warthin-Starry staining technique was used for *Helicobacter pylori* infection diagnosis in all cases, and was identified as positive brown-black or black staining of *Helicobacter pylori*.

Scoring of immunoreactivity

Immunoreactivity was scored according to the presence of immunoreactive cells: -, none or rate positive cells (<5 %); +, 5-25 %; ++, 25-75 %; +++, >75 %.

Statistical analysis

All results are expressed as means plus or minus SD unless otherwise stated, and analyzed by software of SPSS 10.00.

The statistical significance of difference was evaluated with the Student's *t* test. A *P* value of less than 0.05 was considered statistically significant.

RESULTS

Expression pattern of TFF2 protein in carcinogenesis of gastric mucosa

TFF2 protein was located in the cytoplasm of gastric epithelial cells and gastric gland mucous neck cells by immunohistochemistry, and positive cells were stained brown-yellow. TFF2 protein was expressed in all the chronic superficial gastritis and chronic atrophic gastritis (Figure 1-2), but the scoring of TFF2 staining was higher in chronic superficial gastritis than in that chronic atrophic gastritis. The expression of TFF2 was partly detected (56.5 %) in the gastric epithelial dysplasia (Figure 3). There was no expression of TFF2 in the intestinal metaplasia and gastric carcinoma. (Figure 4-5) (Table 1).

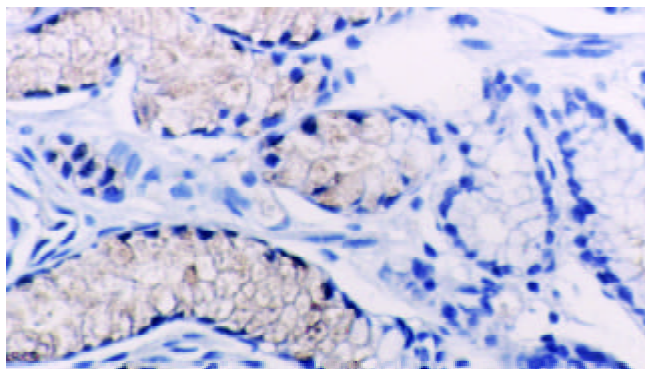


Figure 1 The expression of TFF2 protein in chronic superficial gastritis by immunohistochemistry (SP×200).

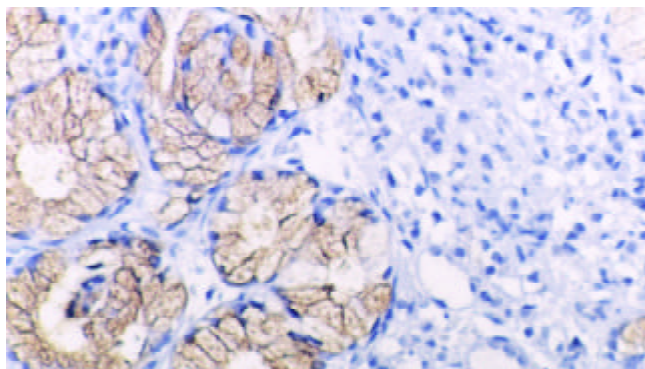


Figure 2 The expression of TFF2 protein in chronic atrophic gastritis by immunohistochemistry (SP×200).

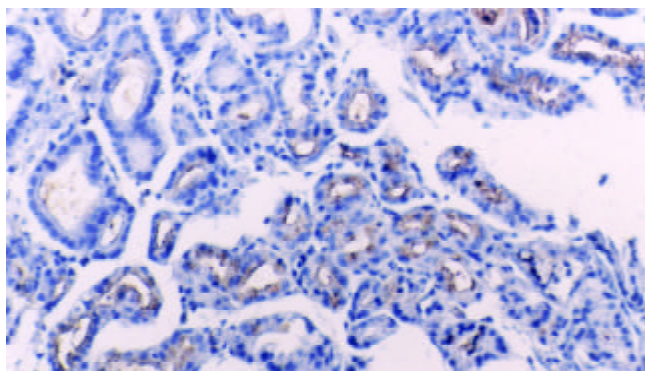


Figure 3 The expression of TFF2 protein in gastric epithelial dysplasia by immunohistochemistry (SP×100).

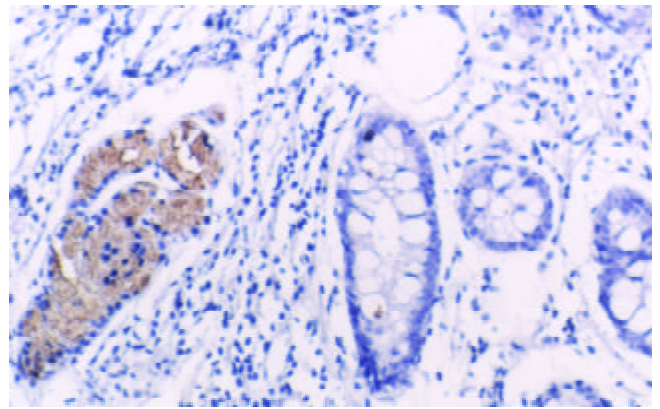


Figure 4 No expression of TFF2 protein in intestinal metaplasia, but the expression observed in its surrounding tissues (SP×100).

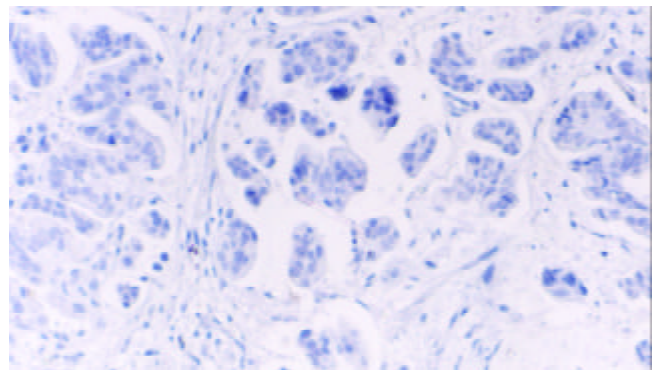


Figure 5 No expression of TFF2 protein in gastric carcinoma (SP×100).

Table 1 The expression pattern of TFF2 protein in carcinogenesis of gastric mucosa

Classification	Cases	TFF2				Rates of positivity
		-	+	++	+++	
CSG	16	0	1	5	10	100 %
CAG	20	0	5	11	4	100 %
IM	35	35	0	0	0	0
GED	23	10	9	2	2	56.5 %
CA	25	25	0	0	0	0

Table 2 The relationship between the expression of TFF2 and *H.pylori* infection

Classification	Cases	TFF2	<i>t</i> test
CSG			
<i>H.pylori</i> (+)	8	52.89±7.27	<i>P</i> >0.05
<i>H.pylori</i> (-)	8	46.49±13.04	
CAG			
<i>H.pylori</i> (+)	12	18.17±4.09	<i>P</i> <0.01
<i>H.pylori</i> (-)	8	37.93±13.80	
IM			
<i>H.pylori</i> (+)	16	0	
<i>H.pylori</i> (-)	19		
GED			
<i>H.pylori</i> (+)	12	14.44±9.32	<i>P</i> <0.05
<i>H.pylori</i> (-)	11	24.84±10.22	
CA			
<i>H.pylori</i> (+)	15	0	
<i>H.pylori</i> (-)	9		

The relationship between the expression of TFF2 and *Helicobacter pylori* infection

The positive rate of *Helicobacter pylori* was 53.8 % (64/119) in our cases. The value of TFF2 positive cell density in chronic superficial gastritis with *Helicobacter pylori* infection was higher than that without *Helicobacter pylori* infection (52.89 ± 7.27 vs 46.49 ± 13.04 , $P > 0.05$), but the difference was not statistically significant; While the value of that in chronic atrophic gastritis and dysplasia with *Helicobacter pylori* infection was significantly lower than that without *Helicobacter pylori* infection (18.17 ± 4.09 vs 37.93 ± 13.80 , $P < 0.01$ and 14.44 ± 9.32 vs 24.84 ± 10.22 , $P < 0.05$), and the difference was statistically significant (Table 2).

DISCUSSION

We undertook the present study in order to characterize the pattern of TFF2 protein expression in carcinogenesis of gastric mucosa. In conformity with data in the literature^[2], immunohistochemical expression of TFF2 was not observed at the surface epithelium, although expression of the corresponding mRNA was previously detected by *in situ* hybridization^[2]. We observed, as did others, the expression of TFF2^[2,6] in the mucous cells of the antrum, the chief cells of the body and neck zone cells.

In this study, we have clarified the expression pattern of TFF2 protein in carcinogenesis of gastric mucosa. In chronic superficial gastritis and atrophic gastritis, the high expression of TFF2 was observed in all cases. As a cytoprotective factor, TFF2 protein was induced as a result of gastric mucosal injury. Our results confirmed an important cytoprotective and restitutive role for TFF2. The mechanism of protective and healing effect of TFF2 on the gastric mucosa is still not fully elucidated. *In vitro*, TFF2 stimulated cell migration^[7]. It has recently been shown that hTFF decreased proton permeation through interacting with mucus *in vivo* and *in vitro*^[8], and oral TFF2 binds to the mucus layer of the stomach^[9], which accelerates the gastric ulcer healing in rat. Further, we also discovered that the scores of TFF2 staining were higher in chronic superficial gastritis than that in chronic atrophic gastritis, which might attribute to the decrease in the number of mucous neck cell expressing TFF2 in chronic atrophic gastritis. There was no expression of TFF2 protein in intestinal metaplasia and gastric carcinoma, but TFF2 protein was observed in surrounding tissues of intestinal metaplasia and gastric carcinoma, which suggested the expression of TFF2 could be associated with the phenotype of gastric epithelial cell differentiation. Although it had been reported by Machado *et al*^[10], the expression of TFF2 was observed in 10 (10.4 %) of 96 cases of gastric carcinomas.

Furthermore, we also found that there were 13 out of 20 cases with re-expression of TFF2 in gastric epithelial dysplasia. It was well known that dysplasia is a precancerous lesion of stomach, and TFF2 could contribute to the initiation of gastric carcinoma. In 1999, Schemidt *et al*^[11] found the SPEM (SP-expressing metaplasia) lineage was detected in 91 % of gastric carcinoma, typically located in mucosa adjacent to the carcinoma or areas of dysplasia. And others studies^[12] also discovered that SPEM was identified in 88 % of the surrounding mucosa in the remnant cancers, as well as 61 % of the follow-up biopsies. In the malignant resections, 67 % of the surface dysplasia displayed SP positive cells. All findings implicated a strong association of the SPEM lineage with gastric carcinoma. At present, no confirmed relationship could be found between TFF2 and carcinoma^[11-19]. However, Farrell *et al*^[20] generated a model of TFF2-deficient mice, and suggested a physiologic role of TFF2 in promoting mucosal healing through the stimulation of proliferation and downregulation of gastric

acid secretion. In other words, increased TFF2 expression and secretion could contribute directly to gastric cancer risk not only through stimulation of proliferation, but also through inhibition of acid secretion. Meanwhile, our results and others^[11] showed there was loss of TFF2 in all gastric carcinoma cases. Therefore, it is impossible that TFF2 expression plays an important role in the progression of gastric carcinoma. Whether TFF2 can directly or indirectly contribute to carcinogenesis of gastric mucosa will be required for further studies.

Gastric carcinoma is the most common tumor in gastrointestinal tract^[21-32], more and more studies suggested that *Helicobacter pylori* infection was significantly associated with gastric carcinoma and was a high risk factor for gastric carcinoma^[33-52]. It has been reported that an increase in the number of mucous neck cells expressing TFF2 has been observed in both *Helicobacter* infected human patients^[12] and *Helicobacter*-infected mice with both preneoplastic^[53] and neoplastic^[54] changes of the gastric mucosa. In all of these findings, it was likely that *Helicobacter pylori* infection would contribute to the expression of TFF2 by promoting the proliferation of gastric mucosal cell, which would be a mechanism of *Helicobacter pylori* contributing to carcinogenesis of gastric mucosa. Then, we examined retrospectively the *Helicobacter pylori* infection of all cases by Warthin-Starry staining, and found that the value of TFF2 positive cell density was higher in chronic superficial gastritis with *Helicobacter pylori* infection than that without, which suggested that TFF2 was induced in the early stage of *Helicobacter pylori* infection. Nevertheless, its value was significantly lower in chronic atrophic gastritis and dysplasia with *Helicobacter pylori* infection than that without. We inferred that low expression of TFF2 was associated with a decrease in the number of gastric mucosal cell as result of *Helicobacter pylori* infection. As a result, the effect of *Helicobacter pylori* on the expression of TFF2 could depend on the status of gastric mucosa.

In conclusion, early-stage or short-term upregulation of TFF2 appears to be helpful in healing of gastric mucosa, but prolonged upregulation may in fact contribute to carcinogenesis. Further studies will be needed to define the role of TFF2 in *Helicobacter pylori*-associated chronic gastritis and gastric carcinoma.

REFERENCES

- 1 Tomasetto C, Rio MC, Gautier C, Wolf C, Hareuveni M, Chambon P, Lathe R. HSP, the domain-duplicated homolog of pS2 protein, is co-expressed with pS2 in stomach but not in breast carcinoma. *EMBO J* 1990; **9**: 407-414
- 2 Hanby AM, Poulosom R, Singh S, Elia G, Jeffery RE, Wright NA. Spasmolytic polypeptide is a major antral peptide: distribution of the trefoil peptides human spasmolytic polypeptide and pS2 in the stomach. *Gastroenterology* 1993; **105**: 1110-1116
- 3 McKenzie C, Thim L, Parsons ME. Topical and intravenous administration of trefoil factors protect the gastric mucosa from ethanol-induced injury in the rat. *Aliment Pharmacol Ther* 2000; **14**: 1033-1040
- 4 Tran CP, Cook GA, Yeomans ND, Thim L, Giraud AS. Trefoil peptide TFF2 (spasmolytic polypeptide) potentially accelerates healing and reduces inflammation in a rat model of colitis. *Gut* 1999; **44**: 636-642
- 5 Cook GA, Familiari M, Thim L, Giraud AS. The trefoil peptides TFF2 and TFF3 are expressed in rat lymphoid tissues and participate in the immune response. *FEBS Lett* 1999; **456**: 155-159
- 6 Playford RJ, Marchbank T, Chinery R, Evison R, Pignatelli M, Boulton RA, Thim L, Hanby AM. Human spasmolytic polypeptide is a cytoprotective agent that stimulates cell migration. *Gastroenterology* 1995; **108**: 108-116
- 7 Dignass A, Lynch-Devaney K, Kindon H, Thim L, Podolsky DK. Trefoil peptides promote epithelial migration through a trans-

- forming growth factor beta-independent pathway. *J Clin Invest* 1994; **94**: 376-383
- 8 **Tanaka S**, Podolsky DK, Engel E, Guth PH, Kaunitz JD. Human spasmodic polypeptide decreases proton permeation through gastric mucus *in vivo* and *in vitro*. *Am J Physiol* 1997; **272**(6 Pt 1): G1473-1480
 - 9 **Poulsen SS**, Thulesen J, Christensen L, Nexø E, Thim L. Metabolism of oral trefoil factor 2 (TFF2) and the effect of oral and parenteral TFF2 on gastric and duodenal ulcer healing in the rat. *Gut* 1999; **45**: 516-522
 - 10 **Machado JC**, Nogueira AM, Carneiro F, Reis CA, Sobrinho-Simoes M. Gastric carcinoma exhibits distinct types of cell differentiation: an immunohistochemical study of trefoil peptides (TFF1 and TFF2) and mucins (MUC1, MUC2, MUC5AC, and MUC6). *J Pathol* 2000; **190**: 437-443
 - 11 **Schmidt PH**, Lee JR, Joshi V, Playford RJ, Poulosom R, Wright NA, Goldenring JR. Identification of a metaplastic cell lineage associated with human gastric adenocarcinoma. *Lab Invest* 1999; **79**: 639-646
 - 12 **Yamaguchi H**, Goldenring JR, Kaminishi M, Lee JR. Identification of spasmodic polypeptide expressing metaplasia (SPEM) in remnant gastric cancer and surveillance postgastroectomy biopsies. *Dig Dis Sci* 2002; **47**: 573-578
 - 13 **Terris B**, Blaveri E, Crnogorac-Jurcovic T, Jones M, Missiaglia E, Ruzsniowski P, Sauvanet A, Lemoine NR. Characterization of gene expression profiles in intraductal papillary-mucinous tumors of the pancreas. *Am J Pathol* 2002; **160**: 1745-1754
 - 14 **Azarschab P**, Al-Azzeh E, Kornberger W, Gott P. Aspirin promotes TFF2 gene activation in human gastric cancer cell lines. *FEBS Lett* 2001; **488**: 206-210
 - 15 **Ohshio G**, Suwa H, Kawaguchi Y, Imamura M, Yamaoka Y, Yamabe H, Matsumoto M, Yoshioka H, Hashimoto Y, Takeda H. Differential expression of human spasmodic polypeptide (trefoil factor family-2) in pancreatic carcinomas, ampullary carcinomas, and mucin-producing tumors of the pancreas. *Dig Dis Sci* 2000; **45**: 659-664
 - 16 **Nogueira AM**, Machado JC, Carneiro F, Reis CA, Gott P, Sobrinho-Simoes M. Patterns of expression of trefoil peptides and mucins in gastric polyps with and without malignant transformation. *J Pathol* 1999; **187**: 541-548
 - 17 **Labouvie C**, Machado JC, Carneiro F, Sarbia M, Vieth M, Porschen R, Seitz G, Blin N. Differential expression of mucins and trefoil peptides in native epithelium, Barrett's metaplasia and squamous cell carcinoma of the oesophagus. *J Cancer Res Clin Oncol* 1999; **125**: 71-76
 - 18 **Efstathiou JA**, Liu D, Wheeler JM, Kim HC, Beck NE, Ilyas M, Karayiannakis AJ, Mortensen NJ, Kmiot W, Playford RJ, Pignatelli M, Bodmer WF. Mutated epithelial cadherin is associated with increased tumorigenicity and loss of adhesion and of responsiveness to the motogenic trefoil factor 2 in colon carcinoma cells. *Proc Natl Acad Sci USA* 1999; **96**: 2316-2321
 - 19 **dos Santos Silva E**, Kayadmir T, Regateiro F, Machado JC, Savas S, Dobosz T, Blin N, Gott P. Variable distribution of TFF2 (Spasmodic) alleles in Europeans does not indicate predisposition to gastric cancer. *Hum Hered* 1999; **49**: 45-47
 - 20 **Farrell JJ**, Taupin D, Koh TJ, Chen D, Zhao CM, Podolsky DK, Wang TC. TFF2/SP-deficient mice show decreased gastric proliferation, increased acid secretion, and increased susceptibility to NSAID injury. *J Clin Invest* 2002; **109**: 193-204
 - 21 **Cai L**, Yu SZ, Zhan ZF. Cytochrome P450 2E1 genetic polymorphism and gastric cancer in Changle, Fujian province. *World J Gastroenterol* 2001; **7**: 792-795
 - 22 **Xiao HB**, Cao WX, Yin HR, Lin YZ, Ye SH. Influence of L-methionine-deprived total parenteral nutrition with S-fluorouracil on gastric cancer and host metabolism. *World J Gastroenterol* 2001; **7**: 698-701
 - 23 **He XS**, Su Q, Chen ZC, He XT, Long ZF, Ling H, Zhang LR. Expression, deletion [was deletion] and mutation of p16 gene in human gastric cancer. *World J Gastroenterol* 2001; **7**: 515-521
 - 24 **Cai L**, Yu SZ, Zhang ZF. Glutathione S-transferases M1, T1 genotypes and the risk of gastric cancer: a case-control study. *World J Gastroenterol* 2001; **7**: 506-509
 - 25 **Liu DH**, Zhang XY, Fan DM, Huang YX, Zhang JS, Huang WQ, Zhang YQ, Huang QS, Ma WY, Chai YB, Jin M. Expression of vascular endothelial growth factor and its role in oncogenesis of human gastric carcinoma. *World J Gastroenterol* 2001; **7**: 500-505
 - 26 **Niu WX**, Qin XY, Liu H, Wang CP. Clinicopathological analysis of patients with gastric cancer in 1200 cases. *World J Gastroenterol* 2001; **7**: 281-284
 - 27 **Xin Y**, Li XL, Wang YP, Zhang SM, Zheng HC, Wu DY, Zhang YC. Relationship between phenotypes of cell-function differentiation and pathobiological behavior of gastric carcinomas. *World J Gastroenterol* 2001; **7**: 53-59
 - 28 **Gao HJ**, Yu LZ, Bai JF, Peng YS, Sun G, Zhao HL, Miu K, L XZ, Zhang XY, Zhao ZQ. Multiple genetic alterations and behavior of cellular biology in gastric cancer and other gastric mucosal lesions: *H. pylori* infection, histological types and staging. *World J Gastroenterol* 2000; **6**: 848-854
 - 29 **Cai L**, Yu SZ, Ye WM, Yi YN. Fish sauce and gastric cancer: an ecological study in Fujian Province, China. *World J Gastroenterol* 2000; **6**: 671-675
 - 30 **Deng DJ**. Progress of gastric cancer etiology: N-nitrosamides 1999s. *World J Gastroenterol* 2000; **6**: 613-618
 - 31 **Jiang BJ**, Sun RX, Lin H, Gao YF. Study on the risk factors of lymphatic metastasis and the indications of less in vasive operations in early gastric cancer. *World J Gastroenterol* 2000; **6**: 553-556
 - 32 **Wang ZN**, Xu HM. Relationship between collagen IV expression and biological behavior of gastric cancer. *World J Gastroenterol* 2000; **6**: 438-439
 - 33 **Lu SY**, Pan XZ, Peng XW, Shi ZL, Lin L, Chen MH. Effect of *Hp* infection on gastric epithelial cell kinetics in stomach diseases. *Shijie Huaren Xiaohua Zazhi* 2000; **8**: 386-388
 - 34 **Wang DX**, Fang DC, Li W, Du QX, Liu WW. A study on relationship between infection of *Helicobacter pylori* and inactivation of antioncogenes in cancer and pre-cancerous lesion. *Shijie Huaren Xiaohua Zazhi* 2001; **9**: 984-987
 - 35 **Guo CQ**, Wang YP, Liu GY, Ma SW, Ding GY, Li JC. Study on *Helicobacter pylori* infection and -p53, c-erbB-2 gene expression in carcinogenesis of gastric mucosa. *Shijie Huaren Xiaohua Zazhi* 1999; **7**: 313-315
 - 36 **He XX**, Wang JML, Wu JL, Yuan SY, Ai L. Telomerase expression, *Hp* infection and gastric mucosal carcinogenesis. *Shijie Huaren Xiaohua Zazhi* 2000; **8**: 505-508
 - 37 **Lu W**, Chen LY, Gong HS. PCNA and c-erbB-2 expression in gastric mucosal intestinal metaplasia with *Helicobacter pylori* infection. *Shijie Huaren Xiaohua Zazhi* 1999; **7**: 111-113
 - 38 **Yang Y**, Deng CS, Yao XJ, Liu HY, Chen M. Effect of *Helicobacter pylori* on morphology and growth of gastric epithelial cells. *Shijie Huaren Xiaohua Zazhi* 2000; **8**: 500-504
 - 39 **Lu SY**, Pan XZ, Peng XW, Shi ZL. Effect of *Hp* infection on gastric epithelial cell kinetics in stomach diseases. *Shijie Huaren Xiaohua Zazhi* 1999; **7**: 760-762
 - 40 **Liang HJ**, Gao JH, Liu WW, Fang DC, Men RP. Longterm effects of concentrated *Helicobacter pylori* culture supernatant on gastric mucosa of rats. *Shijie Huaren Xiaohua Zazhi* 1999; **7**: 861-863
 - 41 **Gao JH**, Liang HJ, Liu WW, Fang DC, Wang ZH. Expression of C-myc gene protein and epidermal growth factor receptor in gastric mucosa pre and post *Helicobacter pylori* clearance. *Shijie Huaren Xiaohua Zazhi* 1999; **7**: 1018-1019
 - 42 **Peng ZS**, Liang ZC, Liu MC, Ouyang NT. Studies on gastric epithelial cell proliferation and apoptosis in *Hp* associated gastric ulcer. *Shijie Huaren Xiaohua Zazhi* 1999; **7**: 218-219
 - 43 **Liu HF**, Liu WW, Fang DC, Gao JH, Wang ZH. Apoptosis and proliferation induced by *Helicobacter pylori* and its association with p53 protein expression in gastric epithelial cells. *Shijie Huaren Xiaohua Zazhi* 2001; **9**: 1265-1268
 - 44 **Liu HF**, Liu WW, Fang DC, Yang SM, Zhao L. Gastric epithelial apoptosis induced by *Helicobacter pylori* and its relationship with Bax protein expression. *Shijie Huaren Xiaohua Zazhi* 2000; **8**: 860-862
 - 45 **Maeda S**, Yoshida H, Ogura K, Mitsuno Y, Hirata Y, Yamaji Y, Akanuma M, Shiratori Y, Omata M. *H. pylori* activates NF-kappaB through a signaling pathway involving IkappaB kinases, NF-kappaB-inducing kinase, TRAF2, and TRAF6 in gastric cancer cells. *Gastroenterology* 2000; **119**: 97-108
 - 46 **Ekstrom AM**, Held M, Hansson LE, Engstrand L, Nyren O. *Helicobacter pylori* in gastric cancer established by CagA immunoblot as a marker of past infection. *Gastroenterology* 2001;

- 121:** 784-791
- 47 **Xue FB**, Xu YY, Wan Y, Pan BR, Ren J, Fan DM. Association of *H. pylori* infection with gastric carcinoma: a Meta analysis. *World J Gastroenterol* 2001; **7**: 801-804
- 48 **Zhang Z**, Yuan Y, Gao H, Dong M, Wang L, Gong YH. Apoptosis, proliferation and p53 gene expression of *H. pylori* associated gastric epithelial lesions. *World J Gastroenterol* 2001; **7**: 779-782
- 49 **Yao YL**, Xu B, Song YG, Zhang WD. Overexpression of cyclin E in Mongolian gerbil with *Helicobacter pylori*-induced gastric precancerosis. *World J Gastroenterol* 2002; **8**: 60-63
- 50 **Morgner A**, Miehlike S, Stolte M, Neubauer A, Alpen B, Thiede C, Klann H, Hierlmeier FX, Ell C, Ehninger G, Bayerdorffer E. Development of early gastric cancer 4 and 5 years after complete remission of *Helicobacter pylori* associated gastric low grade marginal zone B cell lymphoma of MALT type. *World J Gastroenterol* 2001; **7**: 248-253
- 51 **Miehlike S**, Kirsch C, Dragosics B, Gschwantler M, Oberhuber G, Antos D, Dite P, Lauter J, Labenz J, Leodolter A, Malfertheiner P, Neubauer A, Ehninger G, Stolte M, Bayerdorffer E. *Helicobacter pylori* and gastric cancer: current status of the Austrain Czech German gastric cancer prevention trial (PRISMA Study). *World J Gastroenterol* 2001; **7**: 243-247
- 52 **Cai L**, Yu SZ, Zhang ZF. *Helicobacter pylori* infection and risk of gastric cancer in Changle County, Fujian Province, China. *World J Gastroenterol* 2000; **6**: 374-376
- 53 **Wang TC**, Goldenring JR, Dangler C, Ito S, Mueller A, Jeon WK, Koh TJ, Fox JG. Mice lacking secretory phospholipase A2 show altered apoptosis and differentiation with *Helicobacter felis* infection. *Gastroenterology* 1998; **114**: 675-689
- 54 **Wang TC**, Dangler CA, Chen D, Goldenring JR, Koh T, Raychowdhury R, Coffey RJ, Ito S, Varro A, Dockray GJ, Fox JG. Synergistic interaction between hypergastrinemia and *Helicobacter* infection in a mouse model of gastric cancer. *Gastroenterology* 2000; **118**: 36-47

Edited by Zhang JZ

Nimesulide inhibits proliferation via induction of apoptosis and cell cycle arrest in human gastric adenocarcinoma cell line

Jian-Ying Li, Xiao-Zhong Wang, Feng-Lin Chen, Jie-Ping Yu, He-Sheng Luo

Jian-Ying Li, Xiao-Zhong Wang, Feng-Lin Chen, Department of Gastroenterology, Affiliated Union Hospital, Fujian Medical University, Fuzhou 350001, Fujian Province, China
Jie-Ping Yu, He-Sheng Luo, Department of Gastroenterology, Renmin Hospital of Wuhan University, Wuhan 430060, Hubei Province, China

Correspondence to: Dr. Jian-Ying Li, Department of Gastroenterology, Affiliated Union Hospital, Fujian Medical University, Fuzhou 350001, Fujian Province, China. jyli99@hotmail.com

Telephone: +86-3357896-8450

Received: 2002-11-11 **Accepted:** 2002-12-20

Abstract

AIM: To evaluate the potential role of Nimesulide, a selective COX-2 inhibitor, in proliferation and apoptosis of gastric adenocarcinoma cells SGC7901.

METHODS: Cell counts and MTT assay were used to quantify the influence of Nimesulide in the proliferation of SGC7901 cells. Transmission electron microscopy and flow cytometry were used to observe the induction of Nimesulide the apoptosis of SGC7901 cells and influence in the distribution of cell cycle. The expression of P27^{kip1} protein was observed by immunocytochemical staining.

RESULTS: SGC-7901 Cells treated with Nimesulide at various concentrations exhibited a profound dose- and time-dependent reduction in the proliferation rate over the 72 h test period. The highest survival rate of the cells was 78.7 %, but the lowest being 22.7 %. Nimesulide induced apoptosis of the cells in a dose-dependent and non-linear manner and increased the proportion of cells in the G₀/G₁ phase and decreased the proportion in the S and G₂/M phase of the cell cycle. Meanwhile, Nimesulide could up-regulate the expression of P27^{kip1} protein.

CONCLUSION: The induction of apoptosis and cell cycle arrest are both anti-proliferative responses that likely contribute to the antineoplastic action of nimesulide on SGC-7901 cells. The up-regulation of P27^{kip1} gene may contribute to the accumulation of these cells in the G₀/G₁ phase following treatment with Nimesulide. Selective COX-2 inhibitor may be a new channel of the chemoprevention and chemotherapy for gastric carcinoma.

Li JY, Wang XZ, Chen FL, Yu JP, Luo HS. Nimesulide inhibits proliferation via induction of apoptosis and cell cycle arrest in human gastric adenocarcinoma cell line. *World J Gastroenterol* 2003; 9(5): 915-920

<http://www.wjgnet.com/1007-9327/9/915.htm>

INTRODUCTION

Nonsteroidal anti-inflammatory drugs (NSAIDs) are among the most commonly used medications. Recently, numerous studies have shown that NSAIDs can reduce the risk of

colorectal cancer. The mechanism of action of NSAIDs is principally due to the inhibition of cyclooxygenase (COX). COX exists in two isozyme forms: COX-1 is a constitutive form of the enzyme, and COX-2, a cytokine-inducible form of the enzyme. Enhanced COX-2 expression was observed in esophageal, gastric, colorectal, liver, lung, prostate, the head and neck cancers^[1-10]. These findings suggest that COX-2 may play an important role in carcinogenesis. It is thought that inhibition of COX-2 activity by NSAIDs as the antineoplastic mechanism of this class of drugs and gastrointestinal complications of using NSAIDs attribute to the inhibition of COX-1. For this reason, development of selective COX-2 inhibitors was promoted. Current, studies on the relationship between COX-2 and NSAIDs with neoplasm focused on the studies of colorectal carcinomas^[11-15]. Gastric carcinoma is the most common malignancy and the first leading cause of cancer deaths in our country, its pathogenesis is not completely understood and treatment for advanced tumors are relatively poor^[16-21]. Therefore, an increased understanding of pathogenesis of gastric carcinoma and developing effective treatment approaches are very important. Prophylaxis and treatment of NSAIDs for gastric carcinoma are emphasized. Epidemiological studies show that NSAIDs can also reduce the incidence rate and mortality from gastric carcinoma. Nimesulide, a selective COX-2 inhibitor, was found to be between 5 and 16 fold selective that for COX-2^[22]. However, effects of Nimesulide on the growth of gastric carcinoma cells have not been studied.

In this study, we have tested the effects of Nimesulide in proliferation, apoptosis and distribution of cell cycle of SGC-7901 gastric adenocarcinoma cells, In order to seek theoretical evidences for chemoprevention action of selective COX-2 inhibitor on gastric carcinoma.

MATERIALS AND METHODS

Cell culture

Human gastric adenocarcinoma cell line SGC-7901, purchased from Shanghai Institute of Cell Biology, Chinese Academy of Sciences, was routinely maintained in RPMI 1640 containing 10 % fetal bovine serum (FBS), 100 U· ml⁻¹ penicillin, 100 U· ml⁻¹ streptomycin at 37 °C in a humidified atmosphere containing 5 % CO₂.

Cell viability assay

SGC-7901 cells were plated at 3×10⁴ cells/well in 24 well plates for 24 h. At day 0, the medium was changed, incubations were continued without or with increasing concentrations of Nimesulide (50, 100, 200, 400 μmol· L⁻¹) for 72 h. For the time course experiments, cells were incubated with or without Nimesulide and harvested at various intervals. Dead cells were removed by gentle washing with PBS, and the number of living cells after treatment was counted by a hemocytometer.

MTT assay

Cells were seeded at a density of 4×10³ per well in 96-well plates in RPMI-1640 containing 10 % FBS. After 24 h, fresh

medium was added, containing Nimesulide at concentrations of 0 to 400 $\mu\text{mol}\cdot\text{L}^{-1}$. During 72 h incubation, MTT assay was performed every 24 h. Twenty μl of stock MTT (5 $\text{mg}\cdot\text{ml}^{-1}$) was added to each well, and the cells were further incubated at 37 $^{\circ}\text{C}$ for 4 h. The supernatant was removed and 150 μl DMSO was added to each well. A ELISA reader measured the absorbance at a wavelength of 570nm.

Transmission electron microscopy

SGC-7901 cells were treated with Nimesulide at various concentrations for 72 h. Then the cells were centrifugated and fixed in glutaraldehyde for observation of transmission electron microscopy.

Flow cytometry

SGC-7901 cells were treated with Nimesulide at a concentration of 0 to 400 $\mu\text{mol}\cdot\text{L}^{-1}$ for 72 h. Cells were digested by 2.5 $\text{g}\cdot\text{L}^{-1}$ trypsin, washed by 0.01M PBS, fixed by cold alcohol at 4 $^{\circ}\text{C}$ and dyed with PI (propidium iodide), and then were analyzed by flow cytometry.

Immunocytochemistry

SGC-7901 cells were added to 24-well plates with cover glass-slides at 3×10^4 cells/well, after being incubated with Nimesulide at the different concentrations of 0 to 400 $\mu\text{mol}\cdot\text{L}^{-1}$ for 72 h and fixed in 95 % alcohol. After washing in 0.01M PBS, the cells were incubated in 0.5 % H_2O_2 solution to inactive endogenous peroxidase, nonspecific binding was blocked with normal goat serum at room temperature for ten minutes. The cells were incubated with anti-P27kip1 protein monoclonal antibody (impromptu type, Zhong Shan Co) 2 h at 37 $^{\circ}\text{C}$. Immunocytochemical staining for P27kip1 was performed using SP technique according to SP immunostain kit instructions (Zhong Shan Co). PBS was used as substitutes of protein antibody for negative controls. The positive signal of immunocytochemical staining showed brown particles, and distributed in the cytoplasm or nuclei. The absorbance value (A value) of positive cells was detected by image analysis software. The mean value under five random fields was regarded as the relative quantity of P27^{kip1} protein expression.

Statistical analysis

Data were presented as $\bar{x}\pm s$. Statistical analysis of the data was performed using the Student's *t* test, $P<0.05$ was considered statistically significant.

RESULTS

Effect of Nimesulide on cell growth

Cell counts The number of viable cells following incubation with either Nimesulide or control medium, is shown in Figure 1. This figure demonstrates that control SGC-7901 cells entered a line growth and increased by approximately 7-fold within 72 h. Compared with control cultures, cultures treated with Nimesulide displayed a dose-dependent reduction of viable cell number in their proliferation rate over the 72 h test period. At 200 $\mu\text{mol}\cdot\text{L}^{-1}$ and 400 $\mu\text{mol}\cdot\text{L}^{-1}$, Nimesulide strongly inhibited the proliferation of these cells. At 400 $\mu\text{mol}\cdot\text{L}^{-1}$, the proliferation curve was flat over the entire 72 h.

MTT assay In order to further investigate the growth inhibition of Nimesulide on SGC-7901 cells, cell growth was determined by MTT assay. The result was similar to cell counts. The survival rate of the control groups is regarded as 100 %, and the survival rate of Nimesulide group is expressed as the % absorbance for treated wells/controls. As shown in Figure 2, the highest survival rate of the cells was 78.7 %, but the lowest was 22.7 %.

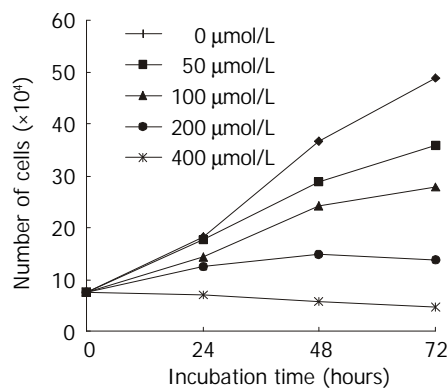


Figure 1 Effects of various concentration of nimesulide on the proliferation of SGC7901 cells for different time periods analysing by cell counts ($n=3$).

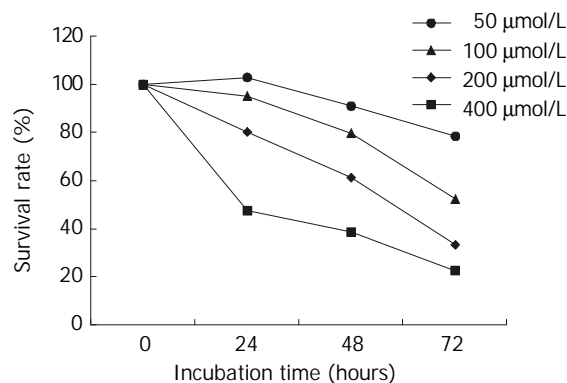


Figure 2 Effects of nimesulide on SGC-7901 cells analyzing the cell survival using the MTT assay.

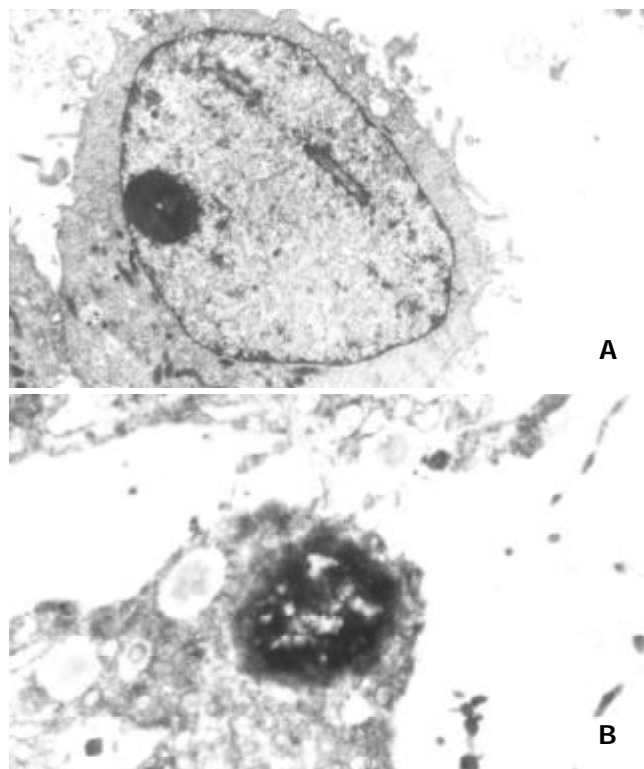


Figure 3 (A) control group: Microvilli of SGC7901 cells were enrichment, nucleus was large and round, chromatin was disperse, nucleolus was distinct. TEM $\times 6000$. (B) Treated with nimesulide at the concentration of 400 $\mu\text{mol/L}$ for 72 h: Disappearance of microvilli, margination of nuclear chromatin, the organelle swelled up and physallization. TEM $\times 8000$.

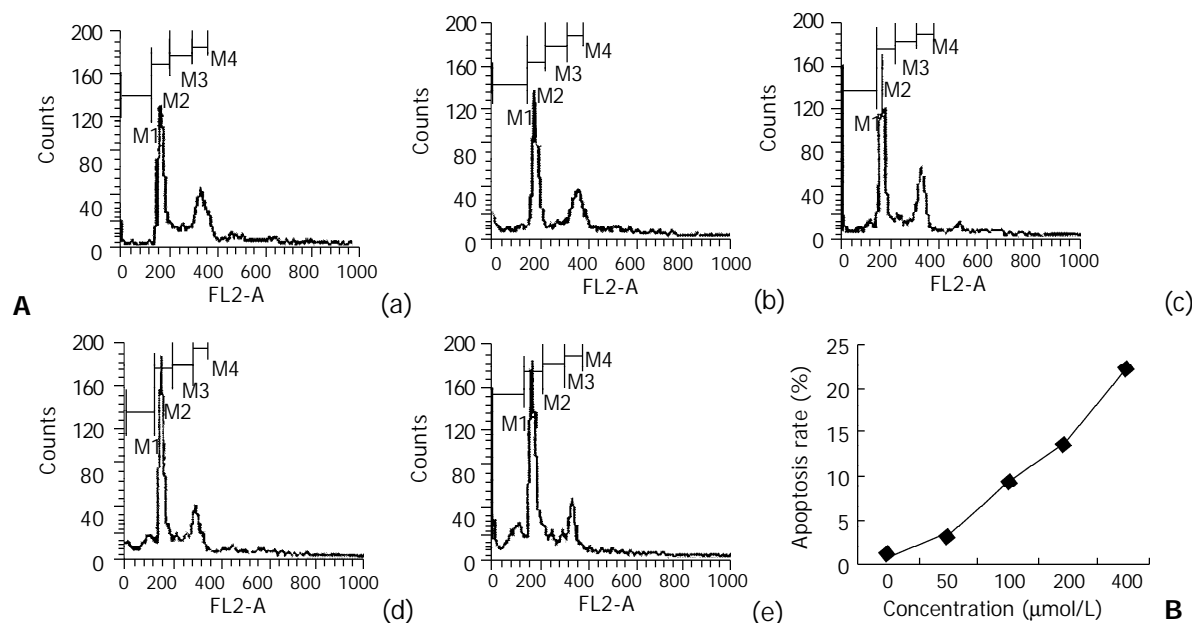


Figure 4 The results of flow cytometry analysis of SGC7901 cells treated with nimesulide for 72 h and their DNA content was determined by flow cytometry. A: DNA histogram: (a) control, (b) 50 μmol/L nimesulide, (c) 100 μmol/L nimesulide, (d) 200 μmol/L nimesulide, (e) 400 μmol/L nimesulide. B: The apoptosis percentage of nimesulide-treated SGC7901 cells.

Apoptosis of SGC-7901 cells induced by nimesulide

The TEM images of the normal SGC-7901 cells: Microvilli of SGC7901 cells were abundant, nucleus was large and round, chromatin was disperse, and nucleolus was distinct. After treated with various concentrations of nimesulide for 72 h, disappearance of microvilli, margination and condensation of nuclear chromatin, nuclear shrinkage, the swollen organelle and cytoplasmic blebbing with maintenance of the integrity of the cell membrane (Figure 3). SGC-7901 cells were treated with various concentrations of nimesulide for 72 h, DNA content of cells was measured by PI staining and flow cytometry analysis was made to detect apoptotic cells. The apoptotic cells can be observed on a DNA histogram as subdiploid or pre-G₁ peak, which was especially remarkable at the 400 μmol·L⁻¹ concentration, and the percentage of apoptotic cells increased to 22.02±1.27 % of the total cell population. Nimesulide induced apoptosis of the cells in a dose-dependent and non-linear manner (Figure 4).

Effect of Nimesulide on cell cycle phase distribution

We assessed the effect of Nimesulide in cell cycle phase distribution of SGC-7901 cells using flow cytometry analysis. The SGC-7901 cells incubated for 72 h in control or nimesulide medium is shown in Table 1. After 72 h treatment, Nimesulide caused a dose-dependent alteration in the cell cycle distribution of SGC-7901 cells, it increased the proportion of cells in the G₀/G₁ phase and decreased the proportion in the S and G₂/M phases of the cell cycle.

Table 1 Effect of Nimesulide in cell cycle progression of gastric cancer cells ($\bar{x}\pm s$)

Concentration (μmol/L)	Percentage of cell cycle (%)		
	G ₀ /G ₁	S	G ₂ /M
0	48.24±2.12	23.51±1.75	28.10±2.17
50	51.14±2.28	22.67±2.30	26.15±1.56
100	57.71±1.51 ^b	20.76±1.45	21.52±2.07 ^a
200	64.82±2.16 ^b	17.06±1.72 ^b	18.12±1.71 ^b
400	75.89±2.61 ^b	10.16±0.79 ^b	13.45±1.20 ^b

^aP<0.05, ^bP<0.01, vs the control.

Expression of P27^{kip1} protein

Before treatment with Nimesulide, the expression of P27^{kip1} protein was mainly located in the cytoplasm of SGC-7901 cells. After Incubated with different concentrations of Nimesulide for 72 h, P27^{kip1} immunoreactivity in cytoplasm was significantly increased, meanwhile nucleus exhibited positive staining. Compared with controls, absorbance value of P27^{kip1} positive cells was increased after Nimesulide treatment (Figures 5-6).

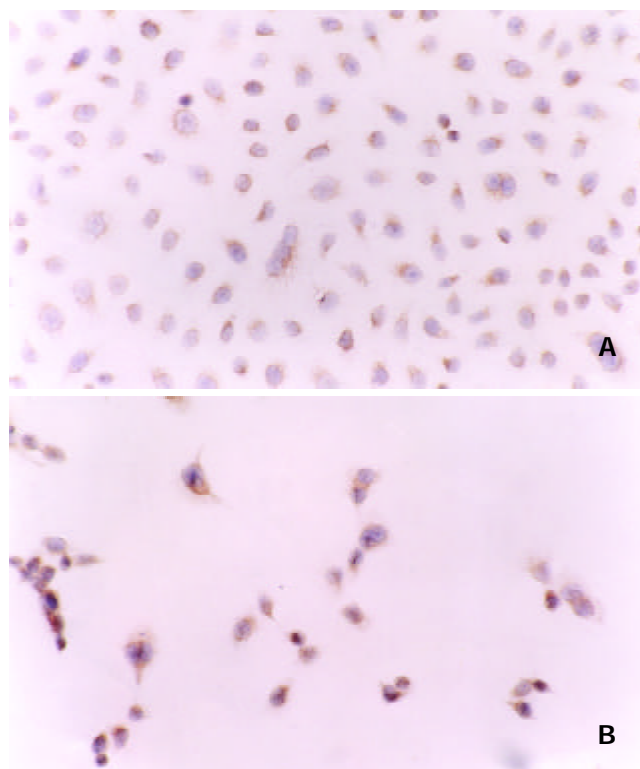


Figure 5 (A) Positive staining of P27^{kip1} protein was mainly in cytoplasm of SGC-7901 cells before treated with nimesulide. (B) Strong positive staining of P27^{kip1} protein was in cytoplasm and in nuclei of SGC-7901 cells after treated with nimesulide at the concentration of 400 μmol/L. SP×200.

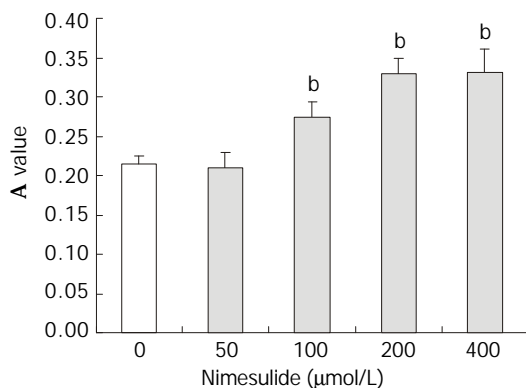


Figure 6 Effects of nimesulide on P27^{kip1} proteins expression in SGC-7901 cells. The data present $\bar{x} \pm s$, $n=3$. ^b $P < 0.01$ vs control.

DISCUSSION

Accumulating evidence indicates that NSAIDs can lower the incidence of colorectal carcinomas. The anti-neoplastic property of NSAIDs has been shown in epidemiological studies with human, clinical studies of the human disease familial adenomatous polyposis (FAP) and in experimental carcinogenesis studies with animals^[23-26]. NSAIDs may be active on epithelial cancer other than colon cancer, such as esophageal^[27], pancreas^[28], lung^[29] and breast cancer^[30]. However, long-term uses of non-selective NSAIDs can lead to gastrointestinal toxicity from sustained inhibition COX-1. With the recent development of highly selective COX-2 inhibitors, an evaluation of the effectiveness of these agents in chemoprevention of cancer would be very important. Several selective COX-2 inhibitors have been tested for their possible utility as chemopreventive agents in colon cancer^[31,32]. However, studies on the role of selective COX-2 inhibitor in human gastric cancer are limited.

There are a lot of sensitive tests of anti-tumor medicine *in vitro*. However, each test method has its merits and weak points. So we detected growth inhibitive effect of Nimesulide on SGC-7901 gastric cancer cells by two methods of cell counts and MTT assay. We found that Nimesulide has anti-proliferative effect on cultured SGC-7901 gastric cancer cells *in vitro* in a dose- and time-dependent manner. Our findings that Nimesulide have profound anti-proliferative effects on SGC-7901 gastric adenocarcinoma cells are in agreement with previous studies demonstrating that many of the selective COX-2 inhibitors inhibit the proliferation of tumor cell line^[33-35].

A number of studies have shown that NSAIDs have an effect of growth inhibition of cancer cells, but the mechanism of the antineoplastic effect of NSAIDs is unknown. These theoretically could be related to the changes of the dynamics of cell proliferation. This hypothesis is supported by the work of Bayer *et al*, who demonstrated that indomethacin reversibly inhibits the proliferation of human fibroblasts and rat hepatoma cells and arrests them in the G₁ phase of cell cycle^[36]. An explanation for the antineoplastic properties of NSAIDs was first suggested by Adolphie, who reported that certain NSAIDs were capable of inhibiting the proliferation of cultured HeLa cells by causing cell cycle arrest^[37]. Since NSAIDs may inhibit proliferation of non-gastric cancer cells and change the distribution of cell cycle, we guess that it may have the similar effects on gastric cancer cells. We further studied the effects of Nimesulide on cell cycle of SGC-7901 gastric cancer cells *in vitro*.

We found that Nimesulide can result in changes in cell cycle distribution of SGC-7901 cells. There is an increase in the proportion of cells in G₀/G₁ and a relative decrease in the percentage of cells in S phase and G₂/M. Shiff found^[38] that NSAIDs caused colon cancer cells to accumulate in the G₀/G₁

phase of cell cycle. This effect was produced by influencing signaling pathways in these cells that control the levels and activity of certain cdk proteins. Goldberg *et al*^[39] found that the G₀/G₁ block induced by sulindac and sulindac sulfide in HT-29 cells was associated with an initial rise, followed by an abrupt decrease in P34^{cdk2}, an increase in P21^{WAF/cip1}, and a reduction in mutant p53. We can speculate reasonably that Nimesulide may increase the fraction of cells with G₀/G₁ DNA content by arresting them in the G₁ or G₀ phase of the cell cycle through an effect on the molecular components that regulate cell cycle transitions.

The cell cycle is a complex process, regulated by many factors, which can be divided into three groups: cyclins; cyclin-dependent kinases(CDK); and CDK inhibitors(CDKI). p27^{kip1} is a member of the Cip1/Kip1 family of CDKI and is a potential tumor suppressor gene. It possessed the ability to inhibit several cyclin-Cdk complexes *in vitro* but seem to target preferentially those containing Cdk2, which control progression through G₁, and inhibit the G₁/S transition^[40,41]. Before treatment with Nimesulide, the expression of P27^{kip1} protein mainly was located in the cytoplasm of SGC-7901 cells. After treated with Nimesulide, P27^{kip1} immunoreactivity in cytoplasm was significantly increased, meanwhile nucleus exhibited positive staining. Interestingly, there was a change in subcellular localization of P27^{kip1} protein expression. Singh's studies suggested that the nuclear location of p27 was essential for its growth-inhibiting function^[42]. So, the result of nuclear localization of P27^{kip1} protein after Nimesulide treatment indicates the anti-proliferation of Nimesulide. We found that Nimesulide could increase the proportion of SGC-7901 cells at G₀/G₁ phase and reduce the cells at S and G₂/M phase. P27^{kip1} is generally associated with the G₁ checkpoint. In our study, overexpression of P27^{kip1} may be associated with the accumulation of cells at G₀/G₁ phase after Nimesulide treatment.

It is also possible that mechanisms responsible for the anti-proliferative effects of the NSAIDs on cultured cells are multifactorial. Apoptotic cell death is another mechanism that could contribute to reduced cell growth. Additional recent reports have demonstrated that NSAIDs induced apoptosis in different tumor cells^[43-48]. It is also conceivable that apoptosis might occur in the human gastric cancer cells in response to Nimesulide. To evaluate the antiproliferative mechanisms of Nimesulide, we tested the apoptosis of SGC-7901 cells induced by Nimesulide. Evidence that apoptosis was induced by Nimesulide was based on the detection of morphological changes of apoptosis and a sub-diploid peak of DNA content on flow cytometry analysis. The results showed Nimesulide also induced apoptosis in SGC-7901 cells at concentrations that affected their proliferation. Thus, apoptosis may be one of the mechanisms responsible for the inhibition of cell growth in Nimesulide-treated SGC-7901 cells. The intracellular molecular events involved in the role of COX-2 inhibitors in the induction of apoptosis are still by far unknown. It might be associated with the changes of expression of bcl-2^[49] and c-myc^[50].

In summary, we conclude that selective COX-2 inhibitor Nimesulide, has anti-proliferative effects in cultured SGC-7901 gastric cancer cells *in vitro*. The up-regulation of P27^{kip1} gene may contribute to the accumulation of these cells in the G₀/G₁ phase following treatment with Nimesulide. The induction of apoptosis and cell cycle arrest are both anti-proliferative responses that likely contribute to the inhibition of SGC-7901 cell proliferation treated with Nimesulide. The selective COX-2 inhibitor Nimesulide, may be useful as a novel approach to the treatment of gastric carcinoma without undesirable side effects.

REFERENCES

- 1 Wu QM, Li SB, Wang Q, Wang DH, Li XB, Liu CZ. The expres-

- sion of COX-2 in esophageal carcinoma and its relation to clinicopathologic characteristics. *Shijie Huaren Xiaohua Zazhi* 2001; **9**: 11-14
- 2 **Zimmermann KC**, Sarbia M, Weber AA, Borchard F, Gabbert HE, Schror K. Cyclooxygenase 2 expression in human esophageal carcinoma. *Cancer Res* 1999; **59**: 198-204
 - 3 **Murata H**, Kawano S, Tsuji S, Tsuji M, Sawaoka H, Kimura Y, Shiozaki H, Hori M. Cyclooxygenase-2 overexpression enhances lymphatic invasion and metastasis in human gastric carcinoma. *Am J Gastroenterol* 1999; **94**: 451-455
 - 4 **Ohno R**, Yoshinaga K, Fujita T, Hasegawa K, Iseki H, Tsunozaki H, Ichikawa W, Nihei Z, Sugihara K. Depth of invasion parallels increased cyclooxygenase-2 levels in patients with gastric carcinoma. *Cancer* 2001; **91**: 1876-1881
 - 5 **Shen ZX**, Cao G, Sun J. Expression of COX-2 mRNA in colorectal carcinoma and their relation with clinical pathological characters. *Shijie Huaren Xiaohua Zazhi* 2001; **9**: 1082-1084
 - 6 **Dimberg J**, Samuelsson A, Hugander A, Soderkvist P. Differential expression of cyclooxygenase 2 in human colorectal cancer. *Gut* 1999; **45**: 730-732
 - 7 **Koga H**, Sakisaka S, Ohishi M, Kawaguchi T, Taniguchi E, Sasatomi K, Harada M, Kusaba T, Tanaka M, Kimura R, Nakashima Y, Nakashima O, Kojiro M, Kurohiji T, Sata M. Expression of cyclooxygenase-2 in human hepatocellular carcinoma: relevance to tumor dedifferentiation. *Hepatology* 1999; **29**: 688-696
 - 8 **Ochiai M**, Oguri T, Isobe T, Ishioka S, Yamakido M. Cyclooxygenase-2 (COX-2) mRNA expression levels in normal lung tissues and non-small cell lung cancers. *Jpn J Cancer Res* 1999; **90**: 1338-1343
 - 9 **Chan G**, Boyle JO, Yang EK, Zhang F, Sacks PG, Shah JP, Edelstein D, Soslow RA, Koki AT, Woerner BM, Masferrer JL, Dannenberg AJ. Cyclooxygenase-2 expression is up-regulated in squamous cell carcinoma of the head and neck. *Cancer Res* 1999; **59**: 991-994
 - 10 **Yoshimura R**, Sano H, Masuda C, Kawamura M, Tsubouchi Y, Chargui J, Yoshimura N, Hca T, Wada S. Expression of cyclooxygenase-2 in prostate carcinoma. *Cancer* 2000; **89**: 589-596
 - 11 **Fournier DB**, Gordon GB. COX-2 and colon cancer: potential targets for chemoprevention. *J Cell Biochem* 2000; **34**(Suppl): 97-102
 - 12 **Zhang Z**, DuBois RN. Par-4, a proapoptotic gene, is regulated by NSAIDs in human colon carcinoma cells. *Gastroenterology* 2000; **118**: 1012-1017
 - 13 **Elder DJ**, Halton DE, Playle LC, Paraskeva C. The MEK/ERK pathway mediates COX-2-selective NSAID-induced apoptosis and induced COX-2 protein expression in colorectal carcinoma cells. *Int J Cancer* 2002; **99**: 323-327
 - 14 **Konturek PC**, Bielanski W, Konturek SJ, Hartwich A, Pierzchalski P, Gonciarz M, Marlicz K, Starzngska T, Zuchowicz M, Darasz Z, Gotze JP, Rehfeld JF, Hahn EG. Progastrin and cyclooxygenase-2 in colorectal cancer. *Dig Dis Sci* 2002; **47**: 1984-1991
 - 15 **Tang X**, Sun YJ, Half E, Kuo MT, Sinicrope F. Cyclooxygenase-2 overexpression inhibits death receptor 5 expression and confers resistance to tumor necrosis factor-related apoptosis-inducing ligand-induced apoptosis in human colon cancer cells. *Cancer Res* 2002; **62**: 4903-4908
 - 16 **Lu YY**. The review and the outlook of the related gene research of Chinese stomach cancer. *Shijie Huaren Xiaohua Zazhi* 1998; **6**(Suppl 7): 10-11
 - 17 **Xue XC**, Fang GE, Hua JD. Gastric cancer and apoptosis. *Shijie Huaren Xiaohua Zazhi* 1999; **7**: 359-361
 - 18 **Zou SC**, Qiu HS, Zhang CW, Tao HQ. A clinical and long term follow up study of peri operative sequential triple therapy for gastric cancer. *World J Gastroenterol* 2000; **6**: 284-286
 - 19 **He XX**, Wang JL, Wu JL, Yuan SY, Ai L. Telomerase expression, Hp infection and gastric mucosal carcinogenesis. *Shijie Huaren Xiaohua Zazhi* 2000; **8**: 505-508
 - 20 **Wang GT**, Zhu JS, Xu WY, Wang Y, Zhou AG. Clinical and experimental studies on fuzheng anti-cancer granula combined with chemotherapy in advanced gastric cancer. *Huaren Xiaohua Zazhi* 1998; **6**: 214-218
 - 21 **Deng DJ**, E Z. Overview on recent studies of gastric carcinogenesis: human exposure of N nitrosamides. *Shijie Huaren Xiaohua Zazhi* 2000; **8**: 250-252
 - 22 **Hawkey CJ**. COX-2 inhibitors. *Lancet* 1999; **353**: 307-314
 - 23 **Thun MJ**, Namboodiri MM, Calle EE, Flanders WD, Heath CW Jr. Aspirin use and risk of fatal cancer. *Cancer Res* 1993; **53**: 1322-1327
 - 24 **Giovannucci E**, Egan KM, Hunter DJ, Stampfer MJ, Colditz GA, Willett WC, Speizer FE. Aspirin and the risk of colorectal cancer in women. *N Engl J Med* 1995; **333**: 609-614
 - 25 **Schmid K**, Nair J, Winde G, Velic I, Bartsch H. Increased levels of promutagenic etheno-DNA adducts in colonic polyps of FAP patients. *Int J Cancer* 2000; **87**: 1-4
 - 26 **Oshima M**, Murai N, Kargman S, Arguello M, Luk P, Kwong E, Taketo MM, Evans JF. Chemoprevention of intestinal polyposis in the Apcdelta716 mouse by rofecoxib a specific cyclooxygenase-2 inhibitor. *Cancer Res* 2001; **61**: 1733-1740
 - 27 **Shureiqi I**, Xu X, Chen D, Lotan R, Morris JS, Fischer SM, Lippman SM. Nonsteroidal anti-inflammatory drugs induce apoptosis in esophageal cancer cells by restoring 15-lipoxygenase-1 expression. *Cancer Res* 2001; **61**: 4879-4884
 - 28 **Molina MA**, Sitja-Arnau M, Lemoine MG, Frazier ML, Sinicrope FA. Increased cyclooxygenase-2 expression in human pancreatic carcinomas and cell lines: Growth inhibition by nonsteroidal anti-inflammatory drugs. *Cancer Res* 1999; **59**: 4356-4362
 - 29 **Hida T**, Leyton J, Makheja AN, Ben-Av P, Hla T, Martinez A, Mulshine J, Malkani S, Chung P, Moody TW. Non-small cell lung cancer cyclooxygenase activity and proliferation are inhibited by non-steroidal anti-inflammatory drugs. *Anticancer Res* 1998; **18**: 775-782
 - 30 **Planchon P**, Veber N, Magnien V, Prevost G, Starzec AB, Israel L. Evidence for separate mechanisms of antiproliferative action of indomethacin and prostaglandin on MCF-7 breast cancer cells. *Life Sci* 1995; **57**: 1233-1240
 - 31 **Sheng H**, Shao J, Kirkland SC, Isakson P, Coffey RJ, Morrow J, Beauchamp RD, DuBois RN. Inhibition of human colon cancer cell growth by selective inhibition of cyclooxygenase-2. *J Clin Invest* 1997; **99**: 2254-2259
 - 32 **Kawamori T**, Rao CV, Seibert K, Reddy BS. Chemopreventive activity of celecoxib, a specific cyclooxygenase-2 inhibitor against colon carcinogenesis. *Cancer Res* 1998; **58**: 409-412
 - 33 **Souza RF**, Shewmake K, Beer DG, Cryer B, Spechler SJ. Selective inhibition of cyclooxygenase-2 suppresses growth and induces apoptosis in human esophageal adenocarcinoma cells. *Cancer Res* 2000; **60**: 5767-5772
 - 34 **Tsubouchi Y**, Mukai S, Kawahito Y, Yamada R, Kohno M, Inoue K, Sano H. Meloxicam inhibits the growth of non-small cell lung cancer. *Anticancer Res* 2000; **20**: 2867-2872
 - 35 **Tian G**, Yu JP, Luo HS, Yu BP, Yue H, Li JY, Mei Q. Effect of Nimesulide on proliferation and apoptosis of human hepatoma SMMC-7721 cells. *World J Gastroenterol* 2002; **8**: 483-487
 - 36 **Bayer BM**, Beaven MA. Evidence that indomethacin reversibly inhibits cell growth in the G₁ phase of the cell cycle. *Biochem Pharmacol* 1979; **28**: 441-443
 - 37 **Adolphe M**, Deysson G, Lechat P. Action of some steroid and non-steroid anti-inflammatory agents on the cell cycle: cytophotometric study of the DNA content. *Rev Eur Etud Clin Biol* 1972; **17**: 320-323
 - 38 **Shiff SJ**, Qiao L, Tsai LL, Rigas B. Sulindac sulfide, an aspirin-like compound, inhibits proliferation, causes cell cycle quiescence, and induces apoptosis in HT-29 colon adenocarcinoma cells. *J Clin Invest* 1995; **96**: 491-503
 - 39 **Goldberg Y**, Nassif I I, Pittas A, Tsai LL, Dynlacht BD, Rigas B, Shiff SJ. The anti-proliferative effect of sulindac and sulindac sulfide on HT-29 colon cancer cells: alterations in tumor suppressor and cell cycle-regulatory proteins. *Oncogene* 1996; **12**: 893-901
 - 40 **Nourse J**, Firpo E, Flanagan WM, Coats S, Polyak K, Lee MH, Massague J, Crabtree GR, Roberts JM. Interleukin-2-mediated elimination of the p27kip1 cyclin-dependent kinase inhibitor prevented by rapamycin. *Nature* 1994; **372**: 570-573
 - 41 **Peng D**, Fan Z, Lu Y, DeBlasio T, Scher H, Mendelsohn J. Anti-epidermal growth factor receptor monoclonal antibody 225 up-regulates p27kip1 and induces G₁ arrest in prostatic cancer cell line DU145. *Cancer Res* 1996; **56**: 3666-3669
 - 42 **Singh SP**, Lipman J, Goldman H, Ellis FH Jr, Aizenman L, Cangi MG, Signoretti S, Chiaur DS, Pagano M, Loda M. Loss or

- altered subcellular localization of P27 in Barrett's associated adenocarcinoma. *Cancer Res* 1998; **58**: 1730-1735
- 43 **Piazza GA**, Rahm AL, Krutzsch M, Sperl G, Paranka NS, Gross PH, Brendel K, Burt RW, Alberts DS, Ppamukcu R, Ahnen DJ. Antineoplastic drugs sulindac sulfide and sulfone inhibit cell growth by inducing apoptosis. *Cancer Res* 1995; **55**: 3110-3116
- 44 **Lu X**, Xie W, Reed D, Bradshaw WS, Simmons DL. Nonsteroidal anti-inflammatory drugs cause apoptosis and induce cyclooxygenases in chicken embryo fibroblasts. *Proc Natl Acad Sci USA* 1995; **92**: 7961-7965
- 45 **Arber N**, DuBois RN. Nonsteroidal anti-inflammatory drugs and prevention of colorectal cancer. *Curr Gastroenterol Rep* 1999; **1**: 441-448
- 46 **Wu YL**, Sun B, Zhang Xj, Wang SN, He HY, Qiao MM, Zhong J, Xu JY. Growth inhibition and apoptosis induction of Sulindac on Human gastric cancer cells. *World J Gastroenterol* 2001; **7**: 796-800
- 47 **Piazza GA**, Rahm A K, Finn TS, Fryer BH, Li H, Stoumen AL, Pamukcu R, Ahnen DJ. Apoptosis primarily accounts for the growth-inhibitory properties of sulindac metabolites and involves a mechanism that is independent of cyclooxygenase inhibition, cell cycle arrest, and P53 induction. *Cancer Res* 1997; **57**: 2452-2459
- 48 **Qiao L**, Hanif R, Sphicas E, Shiff SJ, Rigas B. Effect of aspirin of induction of apoptosis in HT-29 human colon adenocarcinoma cells. *Biochemical pharmacology* 1998; **55**: 53-64
- 49 **Zhu GH**, Wong BC, Eggo MC, Ching CK, Yuen ST, Chan EY, Lai KC, Lam SK. Non-steroidal anti-inflammatory drug-induced apoptosis in gastric cancer cells is blocked by protein kinase C activation through inhibition of c-myc. *Br J Cancer* 1999; **79**: 393-400
- 50 **Liu XH**, Yao S, Kirschenbaum A, Levine AC. NS398, a selective cyclooxygenase-2 inhibitor, induces apoptosis and down-regulates bcl-2 expression in LNCaP Cells. *Cancer Res* 1998; **58**: 4245-4249

Edited by Ma JY

Laminin induces the expression of cytokeratin 19 in hepatocellular carcinoma cells growing in culture

Qin Su, Yong Fu, Yan-Fang Liu, Wei Zhang, Jie Liu, Chun-Mei Wang

Qin Su, Yong Fu, Wei Zhang, Jie Liu, Department of Pathology, Tangdu Hospital, The Fourth Military Medical University, Xi'an 710038, Shaanxi Province, China

Yan-Fang Liu, Department of Pathology, Faculty of Basic Medicine, The Fourth Military Medical University, Xi'an 710032, Shaanxi Province, China

Chun-Mei Wang, Departments of Electron Microscopy, Faculty of Basic Medicine, The Fourth Military Medical University, Xi'an 710032, Shaanxi Province, China

Supported by the Natural Science Foundation of China (NSFC), Grants No. 39470778 and No. 30171052

Correspondence to: Prof. Dr. Qin Su, Department of Pathology, Tangdu Hospital, The Fourth Military Medical University, Xi'an 710038, Shaanxi Province, China. qinsu@fmmu.edu.cn

Telephone: +86-29-3377467 **Fax:** +86-29-3552079

Received: 2002-12-05 **Accepted:** 2003-01-08

Abstract

AIM: To study the abnormal cytokeratin (CK) expression, emergence of CK19 with or without CK7, in liver parenchymal cells and the role of laminin (LN), a basement membrane protein, in this process.

METHODS: Six hepatocellular carcinoma (HCC) cell lines were examined for different CKs, LN and its receptor by immunocytochemistry and Western blotting. Double immunofluorescent reaction, laser-scanning confocal microscopy and an *in vitro* induction procedure were used to demonstrate the role of LN in regulating CK19 expression in these cells.

RESULTS: Immunoreactivities for CK8, CK18, CK7 and the receptor for LN were observed in all the six HCC cell lines examined. However, CK19 was merely found in four of the six cell lines, and was in any case associated with LN expression. Laser-scanning confocal microscopy demonstrated the concomitant presence of these two molecules in most of the positive cells. In the two HCC cell lines, originally negative for CK19, addition of LN to the culture medium resulted in an induction of CK19 in a dose-dependent manner. Both the artificially induced and the intrinsic production of CK19 were completely blocked by an antibody to LN.

CONCLUSION: LN can induce expression of CK19 in HCC cells *in vitro*, providing direct evidence for our hypothesis that the abnormal hepatocytic CK19 expression *in situ* is due to pathologic LN deposition.

Su Q, Fu Y, Liu YF, Zhang W, Liu J, Wang CM. Laminin induces the expression of cytokeratin 19 in hepatocellular carcinoma cells growing in culture. *World J Gastroenterol* 2003; 9(5): 921-929 <http://www.wjgnet.com/1007-9327/9/921.htm>

INTRODUCTION

Cytokeratins (CKs) constitute the cytoskeleton of intermediate

filament type in most epithelial cells. They consist of at least 20 members, designated CK1 to CK20 according to their molecular weights and isoelectric points^[1,2]. Each type of epithelial cell has a rather stable CK composition, termed CK pattern, which has been used in identification of different epithelial tissues and their neoplasms^[1-3]. In normal adult liver, hepatocytes contain only CK18 and CK8 ("hepatocytic" CKs), while the epithelial cells lining the human biliary tree additionally express CK19 and CK7 ("bile duct type" CKs). This difference has been traced back to the early stage of morphogenesis of intrahepatic bile ducts both in rat^[4-6] and in man^[7]. It was believed that the characteristic adult CK pattern of each cell type is maintained in various liver diseases including neoplasia (reviewed by Moll *et al*^[1] and Cooper *et al*^[3]). However, CK19 expression, with or without appearance of CK7, has been observed under many pathologic conditions including human hepatocellular carcinoma (HCC)^[8,9], chronic hepatitis and cirrhosis caused by alcoholism^[10-12], cholestasis^[10,12], hepatitis B virus (HBV) infection^[13] and exposure of rats to carbon tetrachloride^[14,15], butter yellow, and local frostbite injury caused by liquid nitrogen^[16] (for more literatures see Van Eyken *et al*^[17] and Fu *et al*^[18]).

The additional expression of CK19 in liver parenchymal cells has been considered a phenotypic change involved in three common pathologic processes, namely 1) remodeling of the liver parenchyma or cirrhotic nodules (destruction of the limiting plate), 2) the capillarization of hepatic sinusoids, and 3) ductular (oval) cell proliferation^[16]. However, little is known about the molecular mechanism resulting in CK19 expression under these conditions.

The hepatocytes in normal liver are characterized by the absence of a basement membrane (BM)^[5,15,16,19-23] and simplicity of their CK composition^[1,17,18]. All the three pathologic processes mentioned above are associated with an increase in production of laminin (LN), a BM glycoprotein, and its deposition within the involved sinusoids to form an LN-positive BM^[15,16,24-27]. The abnormal deposition of LN was postulated to be a common cause for CK19 expression in liver parenchymal cells^[15,16]. In the present study, we provide direct evidence for this hypothesis in human HCC cell lines using laser-scanning confocal microscopy (LSCM), Western blotting, and an *in vitro* assay for the induction of CK19.

MATERIALS AND METHODS

Cell lines and cell culture

Six well characterized and intensively used human HCC cell lines, including HepG2^[28], Hep3B^[29], HCC-9724^[30,31], HHCC (kindly supplied by Dr. Xian-Hui Wang), HCC-9204^[32,33], and SMMC7721^[9,34-38], were examined in this study. The cells were cultured in RPMI1640 medium (Gibco BRL, Life Technologies Inc, Gaithersburg, MD, USA) containing 100 mL/L newborn calf serum (Biotech Shaanxi, Xi'an, China), 10⁵ u/L penicillin, 10⁵ u/L streptomycin and 2 g/L glutamine at 37 °C in the air containing 50 mL/L CO₂. After two to three days, the cell monolayers growing on coverslips were taken out from the 12-well plastic flasks, rinsed in 10 mmol/L, pH 7.4 phosphate-buffered saline (PBS) for 2 min and fixed for 10 min in the

methanol/acetone (1:1 in volume) solution precooled at 4 °C. After being washed with PBS for three times, 5 min each, the cell monolayers were ready for the immunostaining as detailed below.

Immunocytochemical reactions

The cell monolayers fixed on coverslips were treated in 800 mL/L methanol solution containing 3 mL/L H₂O₂ to block the endogenous peroxidase, washed with PBS for three times. After pretreatment with 100 mL/L bovine serum in PBS, separate incubation with monoclonal antibodies to the following proteins was conducted overnight at 4 °C: CK8 (M0631, Dako A/S, Copenhagen, Denmark; 1:40), CK18 (M7010, Dako; 1:40), CK7 (M7018, Dako; 1:40), CK19 (M0772, Dako; 1:75), LN (M0638, Dako; 1:25) and LN receptor (MAB0273, Clone MLUC5, Maxim Biol Fuzhou, China; 1:30). The antigen-antibody conjugation *in situ* was demonstrated by consecutive incubation with biotinylated anti-mouse/rabbit IgG and streptavidin-labeled peroxidase (S-P) using an Ultrasensitive™ S-P kit (KIT-9730, Maxim Bio Fuzhou). Finally, the immunoreactions were visualized by incubation in a 3,3'-diaminobenzidine-H₂O₂ solution for 10 min, and the monolayers were slightly counterstained with hematoxylin. Normal mouse and rabbit IgG of the same concentrations were used to substitute for the mouse monoclonal and rabbit polyclonal antibodies, respectively, as negative controls.

Double immunofluorescence reactions for LN and CK19 and LSCM

After blocking with 30 mL/L bovine serum in PBS, the cell monolayers were incubated with an antibody mixture (1:1) of mouse monoclonal anti-CK19 (1:75) and rabbit polyclonal anti-LN (Z0097, Dako; 1:38). The reactions were demonstrated by incubation with an antibody mixture (1:1) of the fluorescein isothiocyanate (FITC)-labeled goat anti-mouse IgG (Dako; 1:15) and tetramethylrhodamine isothiocyanate (TRITC)-labeled swine anti-rabbit IgG (Dako; 1:30), and observed under a laser-scanning confocal microscope (Zeiss 100) equipped with the Biorad MRC-1024 system. The FITC- and TRITC-labeled signals were visualized at 488 nm and 568 nm, respectively, as their emission wavelength.

Western blotting analysis

Sodium dodecyl sulfate (SDS)-polyacrylamide gel electrophoresis (PAGE) and Western blotting were carried out as described previously^[39]. Briefly, five cell lines, including HHCC, HCC-9204, HepG2, HCC-9724 and SMMC7721, were cultured in the RPMI1640 medium supplemented with newborn calf serum (100 mL/L). Cells were harvested by digestion with trypsin. For all cell lines examined, 10⁷ cells were used for each protein extraction. The cells were washed in precooled PBS for two times, 5 min each, and then extracted with 1 mL of a Tris-HCl solution (50 mmol/L, pH 8.0) containing 150 mmol/L NaCl, 100 mg/L Nonidet P-40, 50 mg/L Sodium deoxycholate, 10 mg/L SDS, 2 mg/L pepstadin, 2 mg/L leupeptins and 100 mg/L phenylmethylsulfonyl fluoride. After centrifugation at 2 000 r/min for 2 min, the supernatant was collected. Lysates of the cell lines, 10 µL for each, were loaded on to a 100-g/L SDS-polyacrylamide gel. Proteins were resolved through electrophoresis at 150 V using a miniVE vertical unit (Hoefer Pharmacia Biotech Inc, San Francisco, CA) and transferred onto a nitrocellulose membrane (Biotech Shaanxi) by using the same unit according to the instructions of the manufacturer. After the blocking with 1 mL/L bovine serum albumin in PBS for 2 h, the blots were incubated overnight at 4 °C separately with monoclonal antibodies to CK18 (1:600), CK7 (1:600) and CK19 (1:750). The reactions were demonstrated by incubation with alkaline phosphatase (AP)-labeled anti-mouse IgG (Dako; 1:2 000) and visualized

by incubating the filters in 5-bromo-4-chloro-3-indolyl phosphate (BCIP)/nitro blue tetrazolium (NBT) solution for 10 min.

Induction of CK19 expression by exogenous LN and its blocking test

Two HCC cell lines, HHCC and HCC-9724, did not produce LN and were negative for CK19 when growing in the ordinary complete medium (see below). They were transferred into the medium containing LN at concentrations ranging from 2.5 mg/L to 60 mg/L. The LN preparation, isolated and purified from mouse Engelbreth-Holm-Swarm tumor, was supplied by Department of Cell Biology, Health Science Center, Peking University. Sterilized PBS of the same volume was used to substitute for LN as a negative control for the assay. After growing for 60 h, the coverslips with cell monolayers within each well were taken out and immunostained for CK19 using the S-P kit as described above.

In order to show specificity of the induction role of exogenous LN, a blocking test was carried out using the cell line, HHCC. The cells were transferred into the complete RPMI1640 medium supplemented with LN (20 mg/L), and then divided into three groups. In one group, the rabbit polyclonal anti-LN IgG, with its concentrations ranging from 20 mg/L to 0.002 mg/L, was added into the LN-containing medium. The two remaining groups, in which normal rabbit IgG at corresponding concentrations or sterilized PBS of the same volume, respectively, were added to the medium, served as negative controls.

Inhibition test of the CK19 expression associated with intrinsic LN

In order to elucidate the mechanism of CK19 expression in HCC cells with intrinsic production of LN (see below), SMMC7721 cells were cultured in the ordinary medium without addition of LN, and divided into three groups. As for the blocking test in HHCC, the rabbit anti-LN IgG was added to the culture medium at corresponding concentrations, and normal rabbit IgG or sterilized PBS, respectively, were used for negative controls.

Statistical analyses

Intensities of the immunoreaction in single cells were graded into negative (-), weakly positive (+), moderately positive (2+) and strongly positive (3+) as described previously^[15,40]. For assessment of expression levels of the antigens tested, ten high-power microscopical fields were determined randomly in different samples, all cells within these areas were counted, and their immunoreactions were evaluated.

In each cell lines immunoreactivities for the antigens detected were graded into negative (-, reaction being absent or too weak to be identified from background), weak (+, definite reaction visible but weak in its intensity or smaller in number of immunoreactive cells) and strong (2+, brown or darker brown reaction in up to half of cells). Statistical computations were conducted using the software package SLPM^[41]. The semiquantitative data obtained were analyzed by Karl-Pearson and Krushal-Wallis tests. The *P* value below 0.05 was regarded as statistical significance.

RESULTS

Expression of CKs, LN and its receptor in different HCC cell lines

Immunoreactivities for CK18 and CK8 were observed by the immunoperoxidase reaction in cytoplasm of all the six HCC cell lines examined (Table 1). CK7-immunoreactivity was also found in all of these cell lines (Figure 1 A, B), but its intensity varied markedly, being stronger in SMMC7721 and HCC-

9204, and weaker in the others. CK19 and LN expression correlated well, both being present in the cell lines SMMC7721, HepG2 (Figure 1 C, E), Hep3B and HCC-9204, but undetectable in the cell lines HHCC and HCC-9724 (Figure 1 D, F). All of these cell lines were positive for the LN receptor, its immunoreactivity being localized at and beneath the cytoplasmic membrane (Figure 1 G, H).

Expression of CK18 and CK7 was also demonstrated by Western blotting in cell lines SMMC7721, HepG2, HCC-9204, HCC-9724 and HHCC, as shown in Figure 2 A to E, respectively. However, CK19 was only identified in the former three cell lines (Figure 2 A-C), and not in the latter two (Figure 2 D, E).

Table 1 Expression of CKs, LN and its receptor in six HCC cell lines in culture

Antigens	SMMC7721	Hep3B	HCC-9204	HepG2	HHCC	HCC-9724
CK8	++	++	++	++	++	++
CK18	++	++	++	++	++	++
CK7	++	+	++	+	+	+
CK19	+	+	+	+	-	-
LN	+	+	+	+	-	-
LN receptor	+	+	+	+	+	+

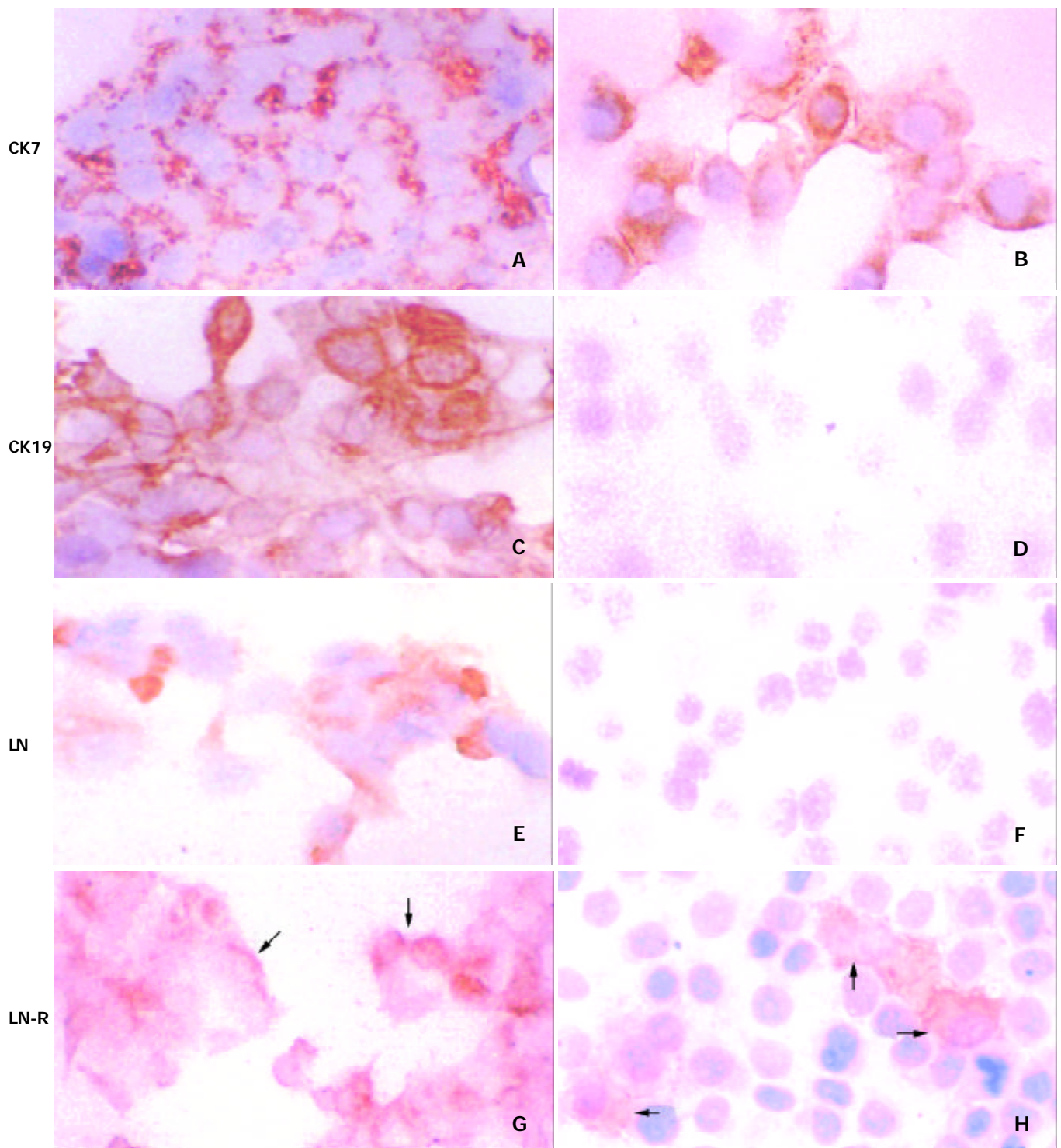


Figure 1 Expression of CK7 (A, B), CK19 (C, D), LN (E, F) and its receptor (*LN-R*, the reactivity denoted by *arrows*; G, H) in the representative HCC cell lines, HepG2 (A, C, E, G) and HCC-9724 (B, D, F, H). Both CK19 and LN present in HepG2 (C and E) and absent in HCC-9724 (D and F). S-P reaction, slightly counterstained with hematoxylin. $\times 250$.

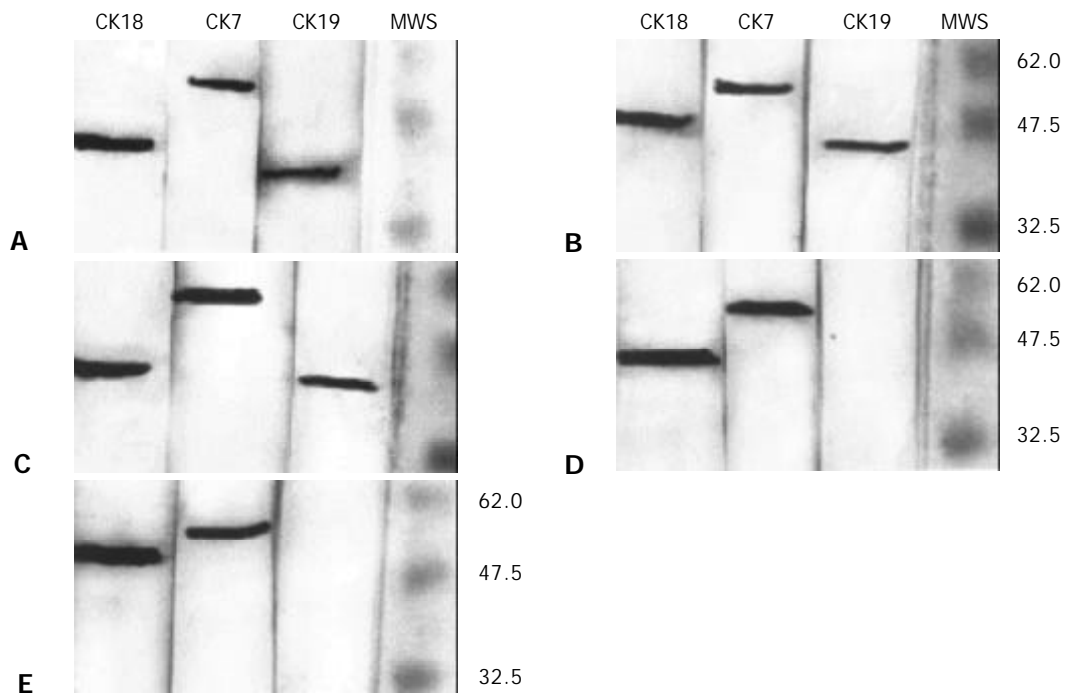


Figure 2 Western blotting for CK18, CK7 and CK19 using the intermediate filament cytoskeleton extracts from HCC cell lines SMMC7721 (A), HCC-9204 (B), HepG2 (C), HHCC (D) and HCC-9724 (E). Immunoreactions were demonstrated by AP-labeled anti-mouse IgG and visualized in a BCIP/NBT solution. The right lanes show molecular weight standards (MWS) visualized by staining with Coomassie R250, with three indicated by the short bars (from top to bottom, M_r 62 000, M_r 47 500 and M_r 32 500, respectively).

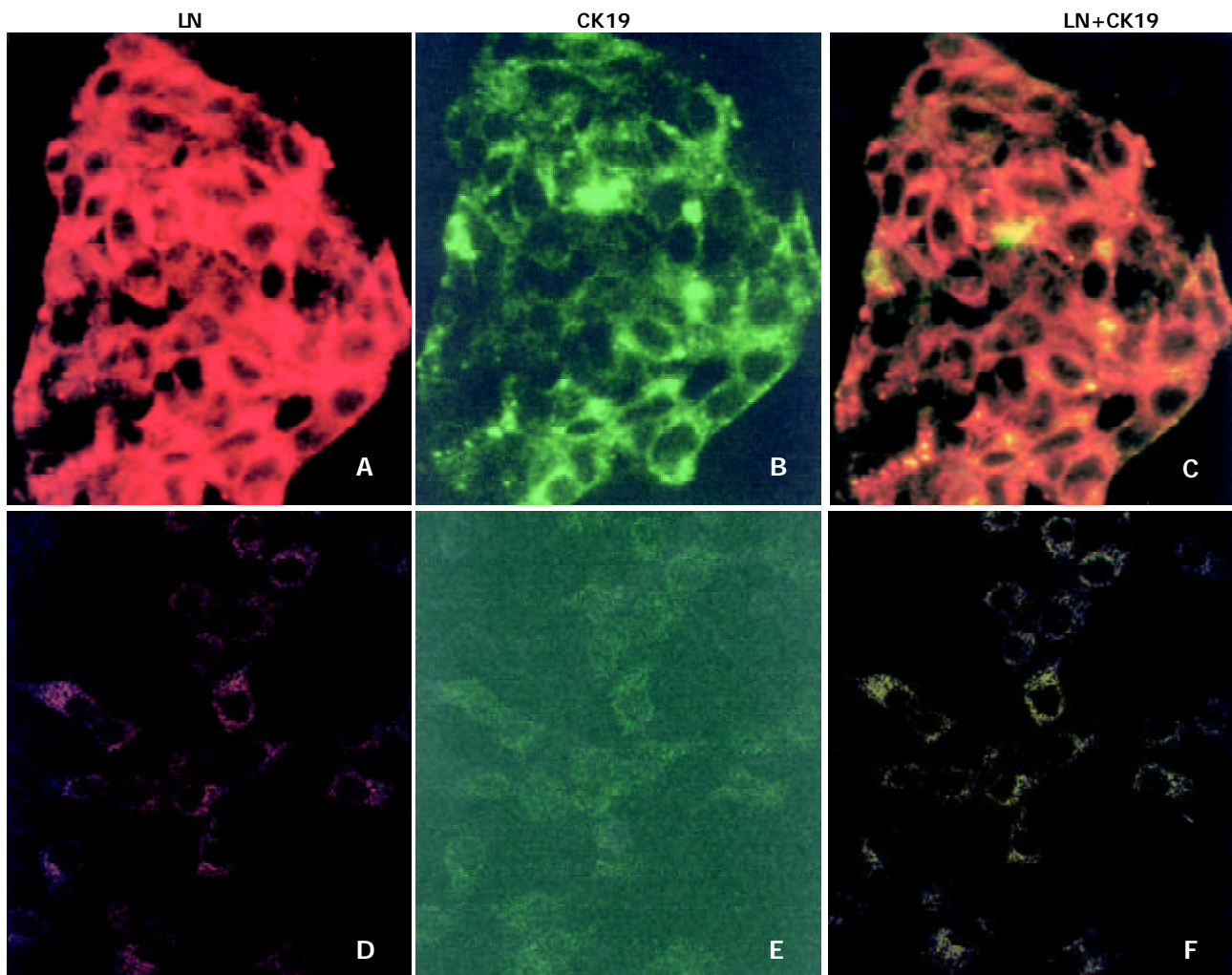


Figure 3 Double immunofluorescence reaction for LN (TRITC-labeled, red) and CK19 (FITC-labeled, green) in HCC cell lines HepG2 (A-C) and HCC-9724 (D-F) under a laser-scanning confocal microscope. Definite signals for LN and CK19, frequently coexisting within cytoplasmic compartment (orange), were found only in the cell line HepG2. $\times 400$.

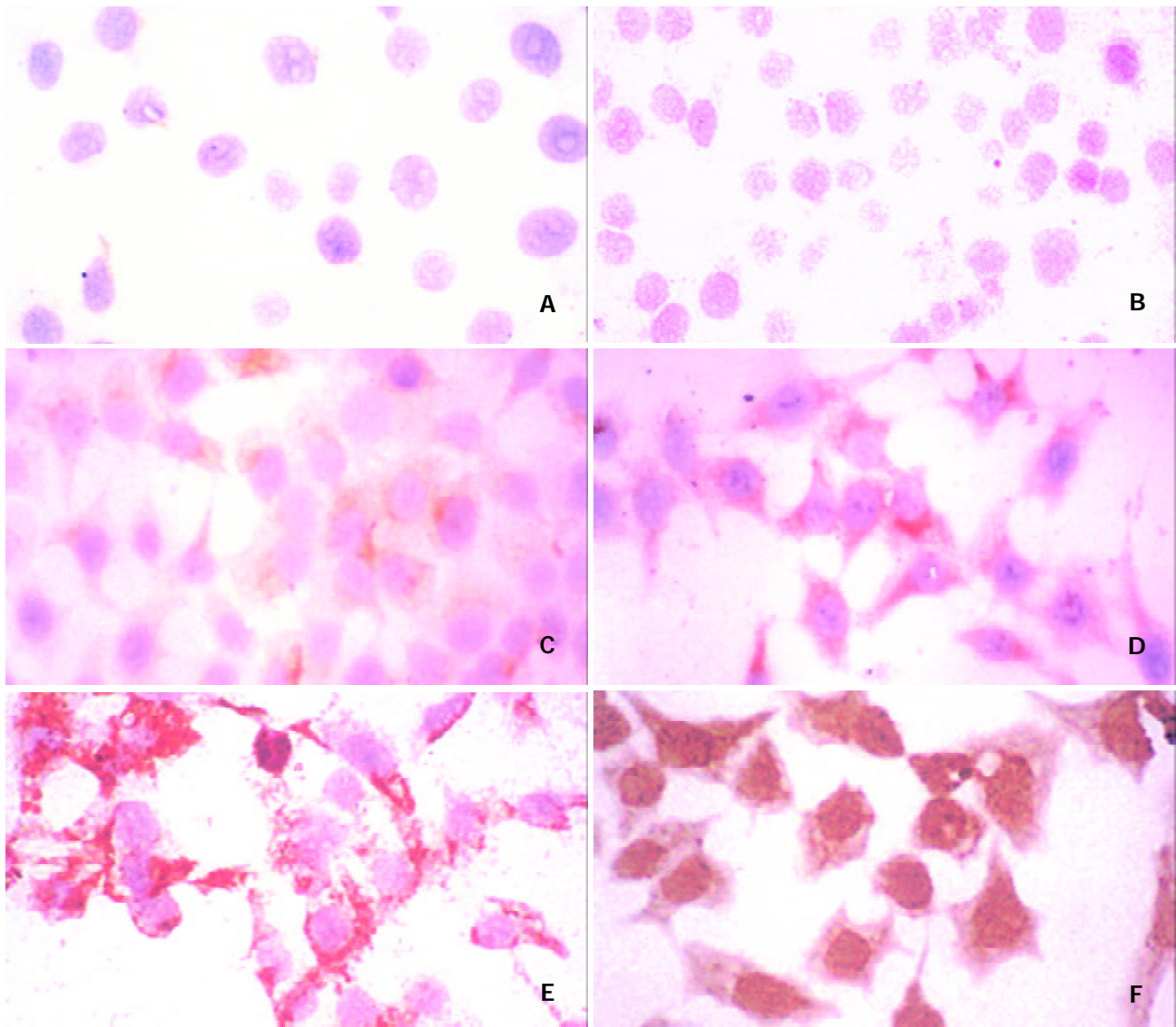


Figure 4 Induction test using the HCC cell line HCC-9724. Cells were inoculated in RPMI1640 medium containing LN at concentrations of 2.5 (A), 5 (B), 10 (C), 20 (D), 40 (E) and 60 mg/L (F), respectively. CK19 expression was found in cells incubated with LN starting at a concentration of 10 mg/L (C), and increasing with LN concentrations (D-F). S-P reaction, slightly counterstained with hematoxylin. $\times 250$.

Concomitant emergence of CK19 and LN as demonstrated by LSCM

CK19 and LN were labeled by double immunofluorescence staining in the same five cell lines showing these proteins on Western blots. The reactions were examined by LSCM, the results being similar to those obtained by the S-P procedure (Table 1). The concomitant occurrence of CK19 and LN was observed in the positive cell lines SMMC7721, HepG2 and HCC-9204, the majority of the positive cells expressing both elements with close correlation of the intensities of the immunoreactivities (Figure 3 A-C). In the cell lines HHCC and HCC-9724, both reactions were negative, showing only some faint background staining (Figure 3 D-F).

Induction of CK 19 expression by addition of LN to the medium

The data described above verified the link between the aberrant expression of CK19 in liver parenchymal cells and abnormal LN deposition. However, more direct evidence is needed to unequivocally establish the role of LN for the induction of abnormal CK19 expression. For this reason, an induction test was carried out in two HCC cell lines, HHCC and HCC-9724. Growing of both cell lines in the medium containing LN resulted in the appearance of CK19 when the concentration of

LN reached 10 mg/L (Figure 4). The expression level of CK19 was found to increase along with concentration of LN in the medium (Figure 5). In the control group, addition of the same volume of sterilized PBS to the medium did not give rise to any CK19-positive cell.

Blocking of LN-induced CK19 expression by LN antibody

If LN added to culture medium is indeed responsible for the emergence of CK19 expression in the LN-negative cell lines as described above, the effect should be blocked, or at least be partially inhibited, by the addition of LN antibody. This assay was performed using the cell line HHCC. The cells, being negative for both LN and CK19 when growing in ordinary medium, were found to express CK19 with the presence of exogenous LN in the medium (20 mg/L). Its levels in HHCC cells growing in the medium containing different amounts of rabbit anti-LN IgG were assessed. CK19 became undetectable in the cells when the final concentration of LN antibody reached 0.2 mg/L in the LN-containing medium (Figure 6A), while addition of the same amount of normal rabbit IgG or sterilized PBS did not inhibit the expression of CK19 (Figure 6B). These data prove that exogenous LN can induce CK19 expression in HCC cells growing *in vitro*.

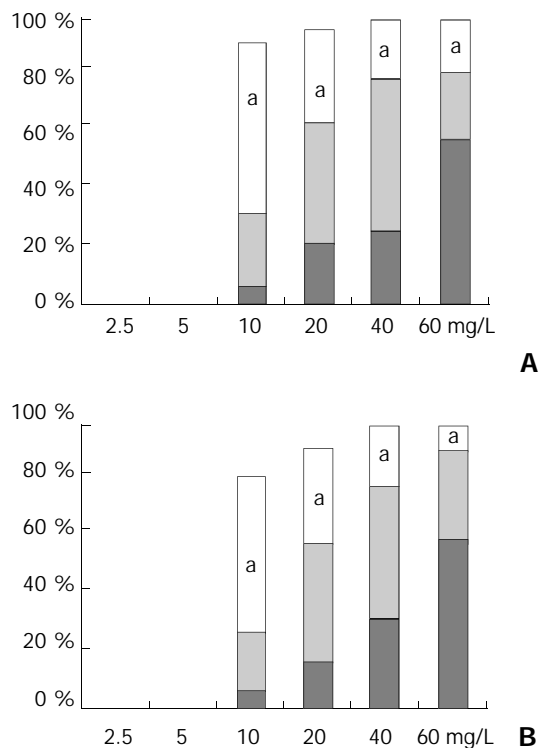


Figure 5 Induction of CK19 expression in HCC cell lines, HHCC (A) and HCC-9724 (B), by LN. Concentrations of LN in culture medium ranging from 2.5 mg/L to 60 mg/L. Numbers of cells expressing CK19 were presented in percentages, and the expression levels indicated by column colors (white, +; gray, 2+; black, 3+). ^a $P < 0.05$ (compared to group on the left).

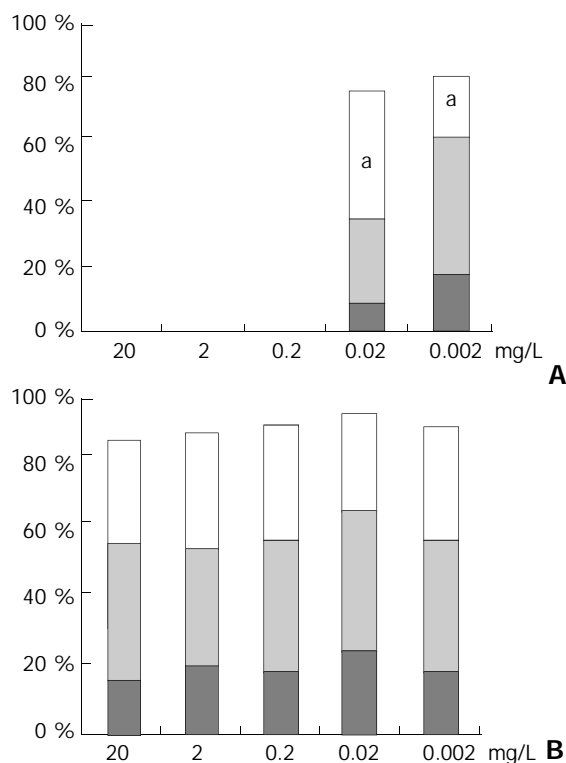


Figure 6 Blocking test of the CK19 expression in HHCC cells induced by exogenous LN. A. CK19 expression completely blocked with concentration of the polyclonal anti-LN up to 0.2 mg/L in the LN-conditioned medium (20 mg/L). B. Addition of the same amount of normal rabbit IgG having no effect on the CK19 expression. Numbers of cells expressing CK19 presented in percentages, and CK19 expression levels indicated by column colors (white, +; gray, 2+; black, 3+). ^a $P < 0.05$ (compared to group on the left).

For the HHCC cells whose CK19 expression was completely inhibited by LN antibody, CK19 reappeared when cells were transferred back to the medium containing LN (20 mg/L) and cultured for 14 d. This demonstrates that the inhibition effect by LN antibody is reversible.

The antibody inhibition test was also conducted in the HCC cell line SMMC7721, whose endogenous production of LN has been described above and whose expression of CK19 has been observed when growing in the ordinary medium. Levels of CK19 expression in the cells growing in the medium containing different amounts of rabbit anti-LN IgG were assessed. CK19 became undetectable in the cells when the final concentration of rabbit anti-LN IgG reached 0.02 mg/L in the medium (Figure 7A), while addition of the same amount of normal rabbit IgG or sterilized PBS did not exert this effect (Figure 7B). Similarly, CK19-immunoreactivity reappeared when the cells were transferred to the medium without LN antibody and cultured for 14 d. These data demonstrate that endogenous LN is also responsible for maintaining CK19 expression in HCC cells growing *in vitro*.

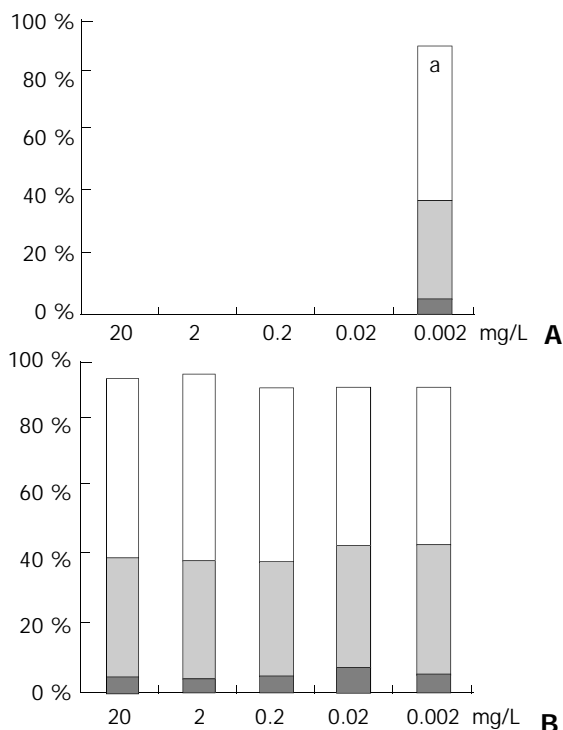


Figure 7 Blocking test of the CK19 expression in SMMC7721 cells associated with endogenous LN. A. CK19 expression completely blocked with concentration of the polyclonal anti-LN up to 0.02 mg/L in the ordinary medium. B. Addition of the same amount of normal rabbit IgG having no effect on the CK19 expression. Numbers of cells expressing CK19 were presented in percentages, and CK19 expression levels indicated by column colors (white, +; gray, 2+; black, 3+). ^a $P < 0.05$ (compared to group on the left).

DISCUSSION

The data obtained in this and other groups during last decade have demonstrated that the CK expression in hepatocytes^[10-16,40] and hepatocytic neoplasms^[8,9] is not so stable as considered before^[17,18]. The expression of CK18 and CK8, the "hepatocytic" CKs, may change greatly in some phenotypically altered hepatocytes^[42]. Moreover, expression of CK19, with or without CK7, has been observed in parenchymal cells in some liver diseases, indicating that hepatocytes can also express the so-called "bile duct type" CKs under certain pathological conditions^[17,18]. The abnormal CK19 expression is found in

chronic hepatitis, cholestasis and cirrhosis^[10-15], as well as in some HCCs^[8,9] and HCC cell lines^[9,35,43], and has been considered an adaptive reaction to some alterations of the local microenvironment^[15,16,18]. This change has been linked to three common pathologic processes including remodeling of the parenchyma in livers with chronic hepatitis or cirrhosis, capillarization of hepatic sinusoids and ductular (oval) cell proliferation^[16]. The ductular (oval) cells are frequently seen in rodent liver under some pathological conditions which suppress regeneration of the parenchymal cells^[16,44,45] (for more references see a review by Vessey and de la Hall^[46]). Cells with similar morphologic and immunohistochemical phenotypes have also been described in human livers with chronic hepatitis^[13,47-50]. In addition, some of the small epithelial liver cells, identified in human livers with chronic hepatitis or cirrhosis and possibly involved in reparative regeneration of liver parenchyma^[40] and progression of the preneoplastic foci of altered hepatocytes^[42,51], were also shown to express CK19^[40,52]. It seems to be true that these CK19-positive cells correspond to a subpopulation of small hepatocytes, being phenotypically intermediate between ductular (oval) cells and typical hepatocytes^[40,52]. Considering the frequent abnormal CK19 expression in extrafocal parenchyma in livers with progressive diseases and in HCC cells^[8-15,35,43], occurrence of CK19-immunoreactivity in some small-cell preneoplastic foci, as recently observed by Libbrecht *et al.*^[52], fails to provide any unequivocal evidence for their speculation that ductular (oval) cells give rise to the small-cell foci, and does not argue against the hepatocytic origin of hepatic preneoplastic foci as demonstrated in both rodents^[53-55] and man^[42,51,56].

Apparently, the frequent occurrence of CK19 expression reflects the complexity in the differentiation of hepatic epithelial cells, and implies great difficulties in using these "bile duct type" CKs for the differential diagnosis between hepatocellular and cholangiocellular neoplasms^[9]. Moreover, its mode of origin has not been fully established. Several lines of indirect evidence have related the aberrant CK19 expression, at least partially, to ductular metaplasia of hepatocytes and glandular differentiation of HCC cells, and indicated its association with abnormal deposition of LN. It has been shown that the morphogenesis of intrahepatic bile ducts in fetal liver, which is characterized by the occurrence of CK19 expression^[4,7], is linked to the deposition of LN around portal vein branches^[5]. Secondly, all of the three pathologic processes related to the CK19 expression as discussed above were associated with an abnormal deposition of LN within the hepatic sinusoids involved^[15,16,18-27], the patterns of histological distribution of these two immunohistochemical reactions being largely correlated with each other^[15,16,27]. Thirdly, both CK19 expression and LN production were also found in some hepatocytes in primary culture and in some HCC cell lines growing *in vitro*^[9,18,35,43,57], and a coexpression of these two molecules has been noted under these conditions^[35,43,58]. The recent data from Blaheta *et al.*^[59] and Nishikawa *et al.*^[60] proved that fetal hepatocytes growing in culture differentiated in response to some extracellular extracts, containing collagen types I and IV, fibronectin, LN and many other extracellular matrix components. The differentiation was reflected by changes in their CK composition^[59-62]. However, these data failed to demonstrate which of the extracellular elements was responsible for the effect.

In this study, the immunocytochemical and Western blotting data proved the concomitant occurrence of LN and CK19 in four of the six HCC cell lines examined, both elements were colocalized in most of the positive cells as demonstrated by LSCM. The data strongly, though still indirectly, suggest a role of LN for the induction of CK19 expression in liver parenchymal cells.

Our induction assay was conducted in two HCC cell lines, HHCC and HCC-9724, which did not produce LN and were negative for CK19 when growing in ordinary medium. CK19 expression emerged with a certain amount of LN added to the culture medium. The effect was found to be dose-dependent, and was completely blocked by a polyclonal antibody against LN. The blocking test was also done with the HCC cell line SMMC7721, which was found to produce LN itself and was positive for CK19 as observed previously^[35,43]. LN antibody added to the medium completely inhibited the CK19 expression. These data clearly demonstrate that LN, either of exogenous origin or produced intrinsically, can induce the expression of CK19 in HCC cells *in vitro*.

Based on results from this and previous studies, we believe that LN, being frequently deposited in hepatic sinusoids as a common response to various kinds of liver injury, is one of the key molecules causing the abnormal CK19 expression. It has been noted that LN is able to induce the hepatocytes to express its receptor, a type of integrin molecules. The receptor takes part in the regulation of cellular differentiation and replication^[61-64]. Immunoreactivity for LN receptor was also observed in all the six HCC cell lines examined in this study. In addition, the successful blocking of the induction effect of intrinsically produced LN by anti-LN IgG molecules added to the medium, as well as the reversibility of this reaction, indicate that a receptor-mediated pathway is needed for LN to exert its effect. Therefore, we suggest that LN induce CK19 expression in hepatocytes and HCC cells through its receptors located on the surface of their cytoplasmic membrane.

In summary, this study provided direct evidence for an essential role of LN in the induction of CK19 expression in liver parenchymal cells, and established abnormal LN deposition as a key causative factor for the development of aberrant expression of CK19. This will be helpful for the further understanding of differentiation and transformation of liver cells, as well as for evaluating CK19 immunohistochemistry in differential diagnosis of hepatocellular and cholangiocellular carcinomas.

ACKNOWLEDGEMENTS

Technical assistance of Ling-Zhi Hu, Dan Chen and Shu-Jie Yang; statistical advice by Dr. Yu-Hai Zhang; helpful discussions with Dr. Lui-Sheng Si, Yi-Li Wang and Xiao-Feng Huang; Dr. Xin-You Shi, Xian-Hui Zhang and Ji-Suai Zhang for providing cell lines; Prof. Peter Bannasch and Bo-Rong Pan for their critical reading of the manuscript.

REFERENCES

- 1 **Moll R**, Franke WW, Schiller DL, Genger B, Krepler R. The catalog of human cytokeratins: pattern of expression in normal epithelia tumors and cultured cells. *Cell* 1982; **31**: 11-24
- 2 **Moll R**, Löwe A, Laufer J, Franke WW. Cytokeratin 20 in human carcinomas, a new histodiagnostic marker detected by monoclonal antibodies. *Am J Pathol* 1992; **140**: 427-447
- 3 **Cooper D**, Schermer A, Sun TT. Classification of human epithelia and their neoplasms using monoclonal antibodies to keratins: strategies, applications, and limitations. *Lab Invest* 1985; **52**: 243-256
- 4 **Su Q**, Gong MZ, Liu YF. Immunocytochemical localization of epidermal keratin in the livers of rat and its embryos. *Dongwu Xuebao* 1988; **34**: 344-347
- 5 **Su Q**, Liu YF, Gong MZ. Mechanism of the morphogenesis of intrahepatic bile ducts in rat embryos, a cytokeratin and laminin-immunohistochemical study. *Di-Si Junyi Daxue Xuebao* 1994; **15**: 168-172
- 6 **Van Eyken P**, Sciort R, Desmet VJ. Intrahepatic bile development in the rat: a cytokeratin-immunohistochemical study. *Lab Invest* 1988; **59**: 52-59

- 7 **Van Eyken P**, Sciort R, Callea F, Van der Steen K, Moerman P, Desmet VJ. The development of intrahepatic bile ducts in man: a keratin-immunohistochemical study. *Hepatology* 1988; **8**: 1586-1595
- 8 **Van Eyken P**, Sciort R, Paterson A, Callea F, Kew MC, Desmet VJ. Cytokeratin expression in hepatocellular carcinoma: an immunohistochemical study. *Hum Pathol* 1988; **19**: 562-568
- 9 **Liu YF**, Su Q, Gong MZ. Expression of cytokeratins in hepatocellular and cholangiocellular carcinomas and their cell lines of human and rat. *Cell Vision* 1996; **3**: 119-125
- 10 **Ray MB**. Distribution of patterns of cytokeratin antigen determinants in alcoholic and nonalcoholic liver diseases. *Hum Pathol* 1987; **18**: 61-66
- 11 **Ray MB**, Mendenhall CL, French SW, Gartside PS. Bile duct changes in alcoholic liver disease. *Liver* 1993; **13**: 36-45
- 12 **Van Eyken P**, Sciort R, Desmet VJ. A Cytokeratin immunohistochemical study of cholestatic liver disease: evidence that hepatocytes can express 'bile-duct type' cytokeratins. *Histopathol* 1989; **15**: 125-135
- 13 **Su Q**, Liu YF, Zhang YG. The abnormal cytokeratin expression in HBV-caused hepatitis, early-cirrhotic and cirrhotic livers, its mechanism and significance. *Zhonghua Binglixue Zazhi* 1992; **21**: 287-289
- 14 **Su Q**, Liu YF, Shen WH, Wei ZQ. The changes in the intermediate filament cytoskeleton and its antigenic determinants in hepatocytes in CCl₄-injured liver. *Dianzi Xianwei Xuebao* 1993; **12**: 469-475
- 15 **Su Q**, Liu YF, Wei ZQ. Abnormal cytokeratin expression in experimental liver injury caused by carbon tetrachloride administration in rats. *Cell Vision* 1996; **3**: 297-305
- 16 **Su Q**, Liu YF. The abnormal cytokeratin expression in hepatocytes and its mechanism in three models of experimental liver injury in rat. *Di-Si Junyi Daxue Xuebao* 1993; **14**: 257-262
- 17 **Van Eyken P**, Desmet VJ. Cytokeratins and the liver. *Liver* 1993; **13**: 113-122
- 18 **Fu Y**, Su Q, Liu YF. Expression of cytokeratins in hepatocytes and hepatic extracellular matrix. *Xibao Yu Fenzi Mianyixue Zazhi* 2001; **17**(Suppl): 80-82
- 19 **Hahn E**, Wick G, Pencev D, Templ R. Distribution of basement membrane proteins in normal and fibrotic liver: collagen type IV, laminin, and fibronectin. *Gut* 1980; **21**: 63-71
- 20 **Bianchi FB**, Biagini G, Ballardini G, Cenacchi G, Fancani A, Pisi E, Laschi R, Liotta L, Garbisa S. Basement membrane production by hepatocytes in chronic liver disease. *Hepatology* 1984; **4**: 1167-1172
- 21 **Clement B**, Rescan PY, Baffet G, Loreal O, Lehry D, Champion JP, Guillouzo A. Hepatocytes may produce laminin in fibrotic liver and in primary culture. *Hepatology* 1988; **8**: 794-803
- 22 **Martinez-Hernandez A**, Delgado FM, Amenta PS. The extracellular matrix in hepatic regeneration: localization of collagen types I, III, IV, laminin, and fibronectin. *Lab Invest* 1991; **64**: 157-166
- 23 **Reid LM**, Fiorino AS, Sigal SH, Brill S, Holst PA. Extracellular matrix gradients in the space of Disse: relevance to liver biology. *Hepatology* 1992; **15**: 1198-1203
- 24 **Martinez-Hernandez A**. The hepatic extracellular matrix. II. Electron immunohistochemical studies in rats with CCl₄-induced cirrhosis. *Lab Invest* 1985; **53**: 166-186
- 25 **Bloula SP**, Lafon M, Leball B, Dennis JA, Martin AB. Ultrastructure of sinusoids in liver diseases. In: Arias IM, Balabaud C, eds. *Sinusoids in human liver: health and disease*. The Netherlands, Rijswijk: The Kupffer Cell Foundation 1988:223-228
- 26 **Slott PA**, Liu MH, Tavoloni N. Origin, pattern, and mechanism of bile duct proliferation following biliary obstruction in the rat. *Gastroenterology* 1990; **99**: 466-477
- 27 **Matsumoto S**, Yamamoto K, Nagano T, Okamoto R, Ibuki N, Tagashira M, Tsuji T. Immunohistochemical study on phenotypical changes of hepatocytes in liver disease with reference to extracellular matrix composition. *Liver* 1999; **19**: 32-38
- 28 **Morris KM**, Aden DP, Knowles BB, Colten HR. Complement biosynthesis by the human hepatoma-derived cell line HepG2. *J Clin Invest* 1982; **70**: 906-913
- 29 **Ting LP**, Jeng KS, Chou CK, Su TS, Hu CP, Wong FH, Chang HK, Chang CM. Expression of oncogenes in human hepatoma cell lines. *Chung Hua Min Kuo Wei Sheng Wu Chi Mien I Hsueh Tsa Chih* 1988; **21**: 141-150
- 30 **Shi CH**, Shi Y, Shi XY, Zhu DS. Establishment and characterization of a human hepatocellular carcinoma cell line, HCC-9724. *Di-Si Junyi Daxue Xuebao* 2000; **21**: 709-712
- 31 **Yang LJ**, Wang WL. Preparation of monoclonal antibody against apoptosis-associated antigens of hepatoma cells by subtractive immunization. *World J Gastroenterol* 2002; **8**: 808-814
- 32 **Hu CM**, Liu YF, Shui YF, Xu LQ, Liu CG. Establishment and characterization of a human hepatocellular carcinoma cell line, HCC-9204. *Di-Si Junyi Daxue Xuebao* 1995; **16**: 92-95
- 33 **Li J**, Yang XK, Yu XX, Ge ML, Wang WL, Zhang J, Hou YD. Overexpression of p27KIP1 induced cell cycle arrest in G1 phase and subsequent apoptosis in HCC-9204 cell line. *World J Gastroenterol* 2000; **6**: 513-521
- 34 **Dung YC**, Zhou RH, Lui FD, Tao YC. Establishment of a human hepatocellular cell line, SMMC7721, and its biologic characteristics. *Di-Er Junyi Daxue Xuebao* 1980; **1**: 5-10
- 35 **Han YP**, Su Q, Liu YF. Expression of insulin-like growth factor II in hepatocellular carcinoma cells growing in culture. *Di-Si Junyi Daxue Xuebao* 1992; **13**: 84-87
- 36 **Song ZQ**, Hao F, Min F, Ma QY, Liu GD. Hepatitis C virus infection of human hepatoma cell line 7721 *in vitro*. *World J Gastroenterol* 2001; **7**: 685-689
- 37 **Wang X**, Liu FK, Li X, Li JS, Xu GX. Inhibitory effect of endostatin expressed by human liver carcinoma SMMC7721 on endothelial cell proliferation *in vitro*. *World J Gastroenterol* 2002; **8**: 253-257
- 38 **Tian G**, Yu JP, Luo HS, Yu BP, Yue H, Li JY, Mei Q. Effect of Nimesulide on proliferation and apoptosis of human hepatoma SMMC-7721 cells. *World J Gastroenterol* 2002; **8**: 483-487
- 39 **Su Q**, Schröder CH, Hofmann WJ, Otto G, Pichlmayr R, Bannasch P. Expression of hepatitis B virus (HBV) X protein in HBV-infected human livers and hepatocellular carcinomas. *Hepatology* 1998; **27**: 1109-1120
- 40 **Su Q**, Liu YF, Zhang JF, Zhang SX, Li DF, Yang JJ. Expression of insulin-like growth factor II in hepatitis B, cirrhosis and hepatocellular carcinoma: its relationship with hepatitis B virus antigen expression. *Hepatology* 1994; **20**: 788-799
- 41 **Cao XT**. An introduction to the statistic software package, SPLM of the Windows version. In: Guo Z-C, ed. *Medical statistics*. Beijing: Renmin Junyi Press 1999: 259-270
- 42 **Su Q**, Zerbán H, Otto G, Bannasch P. Cytokeratin expression is reduced in glycogenotic clear hepatocyte but increased in ground glass cells in chronic human and woodchuck hepadnaviral infection. *Hepatology* 1998; **28**: 347-359
- 43 **Fu Y**, Zhang W, Liu YF, Wang CM, Chen D, Liu J, Su Q. Abnormal expression of cytokeratins in hepatocellular carcinoma cell lines and its mechanism. *Di-Si Junyi Daxue Xuebao* 2001; **22**: 598-603
- 44 **Paku S**, Schnur J, Nagy P, Thorgeirsson SS. Origin and structural evolution of the early proliferating oval cells in rat liver. *Am J Pathol* 2001; **158**: 1313-1323
- 45 **Goumay J**, Auvigne I, Pichard V, Ligeza C, Bralet MP, Ferry N. *In vivo* cell lineage analysis during chemical hepatocarcinogenesis in rats using retroviral-mediated gene transfer: evidence for dedifferentiation of mature hepatocytes. *Lab Invest* 2002; **82**: 781-788
- 46 **Vessey CJ**, de la Hall PM. Hepatic stem cells: a review. *Pathology* 2001; **33**: 130-141
- 47 **Hsia CC**, Thorgeirsson SS, Tabor E. Expression of hepatitis B surface and core antigens and transforming growth factor-alpha in "oval cells" of the liver in patients with hepatocellular carcinoma. *J Med Virol* 1994; **43**: 216-221
- 48 **Libbrecht L**, Desmet V, Van Damme B, Roskams T. Deep intralobular extension of human hepatic 'progenitor cells' correlates with parenchymal inflammation in chronic viral hepatitis: can 'progenitor cells' migrate? *J Pathol* 2000; **192**: 373-378
- 49 **Kiss A**, Schnur J, Szabo Z, Nagy P. Immunohistochemical analysis of atypical ductular reaction in the human liver, with special emphasis on the presence of growth factors and their receptors. *Liver* 2001; **21**: 237-246
- 50 **Ma X**, Qiu DK, Peng YS. Immunohistochemical study of hepatic oval cells in human chronic viral hepatitis. *World J Gastroenterol* 2001; **7**: 238-242

- 51 **Su Q**, Benner A, Hofmann WJ, Otto G, Pichlmayr R, Bannasch P. Human hepatic preneoplasia: phenotypes and proliferation kinetics of foci and nodules of altered hepatocytes and their relationship to liver cell dysplasia. *Virchows Arch* 1997; **431**: 391-406
- 52 **Libbrecht L**, Desmet V, Van Damme B, Roskams T. The immunohistochemical phenotype of dysplastic foci in human liver: correlation with putative progenitor cells. *J Hepatol* 2000; **33**: 76-84
- 53 **Steinberg P**, Hacker HJ, Dienes HP, Oesch F, Bannasch P. Enzyme histochemical and immunohistochemical characterization of oval and parenchymal cells proliferating in livers of rats fed a choline-deficient/DL-ethionine-supplemented diet. *Carcinogenesis* 1991; **12**: 225-231
- 54 **Gindi T**, Ghazarian DM, Deitch D, Farber E. An origin of presumptive preneoplastic foci and nodules from hepatocytes in chemical carcinogenesis in rat liver. *Cancer Lett* 1994; **83**: 75-80
- 55 **Anilkumar TV**, Golding M, Edwards RJ, Lalani EN, Sarraf CE, Alison MR. The resistant hepatocyte model of carcinogenesis in the rat: the apparent independent development of oval cell proliferation and early nodules. *Carcinogenesis* 1995; **16**: 845-853
- 56 **Su Q**, Bannasch P. Relevance of hepatic preneoplasia for human hepatocarcinogenesis. *Toxicol Pathol* 2003; **31**: 126-133
- 57 **Albrechtsen R**, Wewer UM, Thorgeirsson SS. *De novo* deposition of laminin-positive basement membrane *in vitro* by normal hepatocytes and during hepatocarcinogenesis. *Hepatology* 1988; **8**: 538-546
- 58 **Cable EE**, Isom HC. Exposure of primary rat hepatocytes in long-term DMSO culture to selected transition metals induces hepatocyte proliferation and formation of duct-like structures. *Hepatology* 1997; **26**: 1444-1457
- 59 **Blaheta RA**, Kronenberger B, Woitaschek D, Auth MK, Scholz M, Weber S, Schuldes H, Encke A, Markus BH. Dedifferentiation of human hepatocyte by extracellular matrix proteins *in vitro*: quantitative and qualitative investigation of cytokeratin 7, 8, 18, 19 and vimentin filaments. *J Hepatol* 1998; **28**: 677-690
- 60 **Nishikawa Y**, Tukasashi Y, Kadohama T, Nishimori H, Ogawa K. Hepatocytic cells form bile duct-like structure with a three-dimensional collagen gel matrix. *Exp Cell Res* 1996; **223**: 357-371
- 61 **Kono Y**, Yang S, Letarte M, Roberts EA. Establishment of a human hepatocyte line derived from primary culture in a collagen gel sandwich culture system. *Exp Cell Res* 1995; **221**: 478-485
- 62 **Le Bail B**, Faouzi S, Boussarie L, Balabaud C, Bioulac-Sage P, Rosenbaum J. Extracellular matrix composition and integrin expression in early hepatocarcinogenesis in human cirrhotic liver. *J Pathol* 1997; **181**: 330-337
- 63 **Yuan ST**, Hu XQ, Lu JP, Kei KH, Zhai WR, Zhang YE. Changes of integrin expression in rat hepatocarcinogenesis induced by 3'-Me-DAB. *World J Gastroenterol* 2000; **6**: 231-233
- 64 **Liu LX**, Jiang HC, Liu ZH, Zhou J, Zhang WH, Zhu AL, Wang XQ, Wu M. Integrin gene expression profiles of human hepatocellular carcinoma. *World J Gastroenterol* 2002; **8**: 631-637

Edited by Pang LH

Effect of arsenic trioxide on rat hepatocarcinoma and its renal cytotoxicity

Shao-Shan Wang, Ti Zhang, Xi-Lu Wang, Li Hong, Qing-Hui Qi

Shao-Shan Wang, Ti Zhang, Xi-Lu Wang, Li Hong, Department of Surgery of Dagang Hospital 300270, Tianjin, China
Qing-Hui Qi, Department of Chinese and Western Integral Surgery of Master Hospital of Tianjin Medical University 300052, Tianjin, China
Supported by Natural Scientific Foundation of Tianjin, No. 993703211

Correspondence to: Dr. Shao-Shan Wang, Department of Surgery of Dagang Hospital 300270, Tianjin, China. wsss@public.tpt.tj.cn
Telephone: +86-22-25997553 **Fax:** +86-22-25991440

Received: 2002-08-13 **Accepted:** 2002-10-22

Abstract

AIM: To study the effect of arsenic trioxide (As_2O_3) on rat experimental hepatocarcinoma and its renal cytotoxicity.

METHODS: The hepatocarcinoma model was established by diethylnitrosamine perfusion in stomach of 120 Wistar rats, and the treatment began at the end of 20 weeks. Before the treatment, the rat models were randomly divided into 5 groups. In the treatment groups, three doses of As_2O_3 were injected into rat abdominal cavity, the total time of drug administration was 4 weeks. Cisplatin control or the blank group was injected into abdominal cavity with equal amount of cisplatin or saline at the same time, respectively. On the 7th, 14th and 28th day after the treatment, the hepatocarcinoma nodules were obtained and the morphologic changes of hepatocarcinoma cells were observed under light and electron microscopes; Immunohistochemistry (S-P methods) was employed to detect the expression of bcl-2, bax and PCNA in hepatocarcinoma tissues; flow cytometry (TUNEL assay) was used to detect the apoptosis of liver cancer cells and the change of cytokinetics. On the 28th day, the kidneys were obtained and their histologic changes were observed under light microscope, and immunohistochemistry (SP stain) was also employed to detect the expression of bcl-2 and PCNA. Cisplatin and saline solution were used as the control.

RESULTS: As_2O_3 could induce the apoptosis of rat liver cancer cells and exhibited typical morphologic changes. The incidence of apoptosis of hepatocarcinoma cells was elevated ($P=0.001$). The elevation was the most higher in the group of middle-dose of As_2O_3 ($1\text{ mg}\cdot\text{kg}^{-1}$), significantly higher than that of the other arsenic groups and the controls ($P=0.001$). Large dose of As_2O_3 ($5\text{ mg}\cdot\text{kg}^{-1}$) was able to arise the incidence of apoptosis, but also produced a large amount of necrosis and inflammatory reaction. Middle dose of As_2O_3 dramatically increased the cell number in G2/M phase ($P=0.0001$), and apoptosis happened apparently. The expression of bcl-2 and bax was related to the dose of As_2O_3 . With the up-regulation of apoptotic incidence, the ratio of bcl-2/bax decreased. But the incidence of apoptosis was not the highest status and the ratio of bcl-2/bax was at the lowest when the highest-dose of As_2O_3 was used. There was significant difference among the PCNA indexes (PCNA L1) of the five groups. Of them, three arsenic groups all showed decrease of different degrees, and this down-

regulation was most obvious in group A. There was significant difference among the three groups ($P=0.016$). Under the light microscope, the rat kidney in the cisplatin group exhibited tubular epithelium swelling and degeneration, protein casts in collecting tubules; While all arsenic groups didn't show the significant changes ($P=0.013$). In the arsenic groups, the expression of bcl-2 in the renal tubular epithelium was increased ($P=0.005$), no obvious changes happened to PCNA L1. But in the group of cisplatin, the PCNA L1 increased significantly ($P=0.001$).

CONCLUSION: As_2O_3 can induce apoptosis of rat hepatocellular carcinoma cells. And there is optimum dose; too high dose will induce the cytotoxic effect, while certain dose of As_2O_3 is able to block the cell cycle at G2/M phase. As_2O_3 had the most remarkable influence on G2/M cells, and it can also induce apoptosis to cells at other phases. As_2O_3 can restrain the proliferation of rat hepatocellular carcinoma cells, in a dose-time dependent manner. Compared with cisplatin, As_2O_3 didn't show obvious renal toxicity, which was related to the increasing expression of bcl-2 in renal tubular epithelium, the inhibition of apoptosis and the anti-oxidation effects.

Wang SS, Zhang T, Wang XL, Hong L, Qi QH. Effect of arsenic trioxide on rat hepatocarcinoma and its renal cytotoxicity. *World J Gastroenterol* 2003; 9(5): 930-935
<http://www.wjgnet.com/1007-9327/9/930.htm>

INTRODUCTION

Primary hepatocellular carcinoma has been found to be one of the most common malignancies worldwide. In the recent years, the diagnosis rate of early hepatocellular carcinoma has increased and the curative effect of surgery resection also improved. However, most of the early hepatocellular carcinoma is subclinical, once it is symptomatic, it is mainly in its middle or later stage. As the update statistic indicates, hepatocellular carcinoma ranked the second cause of cancer mortality since 1990s in China^[1]. Presently, what challenges us most is the mid-or-late stage hepatocarcinoma, unresectable hepatocarcinoma, high postoperative reoccurrence and high metastasis. Thus efficient nonsurgical methods are urgent^[2,31-36].

Recently, it has been reported that arsenic (mainly arsenic trioxide, As_2O_3) in the treatment of leukemia has obvious curative effect through inducing tumor cell apoptosis^[3,4]. But whether arsenic chemist can be used in the treatment of other malignancy such as hepatocellular carcinoma is still under the exploration. The blockage of apoptosis plays a more important role not only in the cause of malignancy but also in the out of control of proliferation. Thus in the two strategies of tumor treatment: inhabiting tumor cells' proliferation and inducing their apoptosis, the later seems to be more preferable^[5-7]. Our study is to establish a rat hepatocellular carcinoma model with the treatment of As_2O_3 , then observe the apoptosis and proliferation of hepatocellular carcinoma cells and influence of it on the cell cycle, as well as the possibly noxious side effect on kidney of As_2O_3 .

MATERIALS AND METHODS

Materials

Arsenic trioxide (As₂O₃ Sigma) was dissolved by PBS and diluted to 0.2 % (m/m), kept under 4 °C. Diethylnitrosamine (DEN Sigma) was diluted to 1 % (v/v) by water solution. Cisplatin (QiLu Pharmaceutical Department) was diluted to 0.08 % (m/m) by injection solution. There were also key reagents as follows: murine monoclonal antibody against human Bcl-2 (1:50, SANTA CRUZ) and murine monoclonal antibody Bax (1:70, SANTA CRUZ) and murine monoclonal antibody against rat proliferation cell nuclear antigen (PCNA) (1:100, Zhongshan Biotech Ltd, Beijing); Histostain™-Plus Immunohistochemical reagent box (Zymed), DAB stain kit (Zhongshan Biotech Ltd, Beijing) APO-BRDU™ apoptosis quantitative test reagent box (Becton Dickinson).

FACS Vantage flow cytometry (Becton Dickinson), H600-4 transmission electron microscope (HITACHI) were used in this study.

Animal model, grouping and treatment

120 Wistar rats (60 males and 60 females, 6 weeks old) were supplied by the Fourth Institute of Military Medical Academy of Science. According to the method in the reference^[8], the hepatocarcinoma model was established by DEN perfusion in stomach, and the treatment began at the end of 20 weeks. Before the treatment, the rat models were randomly divided into 5 groups. There were no difference in the number, sex and weight among the 5 groups. Group A: high-dose of As₂O₃ (5 mg·kg⁻¹), group B: middle-dose of As₂O₃ (1 mg·kg⁻¹), group C: low-dose of As₂O₃ (0.2 mg·kg⁻¹), group D: cisplatin control (2 mg·kg⁻¹), group E: blank control (saline solution).

In the treatment groups, three doses of As₂O₃ were injected into rat abdominal cavity, once a day, after two weeks, it is changed to twice a week, and the total time of drug administration was 4 weeks. Cisplatin control or the blank group was injected into abdominal cavity with equal amount of cisplatin or saline at the same time, respectively.

The choice of the dose of As₂O₃ was based on the curative dose on human leukemia (10 mg·d⁻¹)^[4], obtained by calculating the ratio of equal effective dose of body surface area between the human and rat. The dose of cisplatin was chosen according to the reference^[9].

Methods

Sample preparation After the treatment, all rats were operated to obtain the liver nodules through 3 operations under anesthesia of sodium pentobarbital (abdominal cavity injection, 40-50 mg·kg⁻¹) on the 7th, 14th and 28th day, respectively. The specimens with the formation of carcinoma proved by pathologic examination were chosen as experimental objects. At the last operation, the rats' kidneys were obtained at the same time and the rats were killed.

The hepatocellular carcinoma nodules were divided into three parts along the center, one part (about 0.2 mg, fresh tissue) was made into monocyte suspending solution, used in the detection of flow cytometry; one part was fixed in 10 % formaldehyde, embedded in paraffin with 4 μm successive section and HE staining. The pathologic changes of cancer nodules were observed under light microscope or by immunohistochemistry (IHC). The third part was processed into thin slice (<1 mm) and immediately immersed into 2.5 % glutaraldehyde phosphoric buffer. The embedded sections were made using the common electron microscope specimens. The ultrastructure of the hepatocellular carcinoma cells was observed under the transmission electron microscope^[37].

Flow cytometry analysis The FACS Vantage flow cytometry was employed with the 5w argon laser as emission resource, and the wavelength of emission light was 488 nm. The variation

coefficient (CV) of the machine was regulated as < 4 % using chicken blood erythrocytes fixed by glutaraldehyde. 1×10⁴ cells were analyzed and the data was analyzed using MODifit LT software. Referring to the kit protocol, PI stain was used to label the cellular DNA to analyze cell cycle TdT to catalyze dUTP combined with external bromides (Br-dUTP) ligated to the 3' -OH terminal end of DNA fragments, then it was combined with anti- Br-dUTP mono-antibody labeled by FITC, and then the intensity of fluorescence of FITC was detected through the flow cytometry to estimate the number of DNA breakage points to qualitatively examine the cell apoptosis. The occurrence of apoptosis in different phases was analyzed combining with the staining result of PI.

Histology analysis The paraffin-embedded rat hepatocellular carcinoma tissues after 7 days of treatment were successively cut into 4 μm sections and the HIC (SP stain) was employed to detect the expression of bcl-2, bax and PCNA. The successive 4 μm sections were obtained from the paraffin-embedded rat hepatocellular carcinoma tissues after 28 days of treatment and stained with HE. And the histomorphologic change was observed under light microscope. IHC (SP stain) was used to detect the expression of bcl-2 and PCNA. PCNA labeling index (LI) = PCNA positive cells number / 500 (using % to denote).

Statistical analysis

All the data were processed by statistical software SPSS10.0. The total VAR difference of each group was analyzed by Bartlett test. If it was the same, then analyzed by the one way ANOVA or student *t* test, otherwise by Kruskal-Wallis *H* test, or Mann Whitney *U* test which as for the multi-sample comparison; to the quantity material analysis, χ² test was used (test standard: two-side α=0.05).

RESULTS

On 7th, 14th, 28th day after the treatment, the hepatocarcinoma nodules of the rats (No. 65, 43, 34) were collected respectively (proved by pathology). The other rats were repelled out of the experiment due to the absence of carcinoma nodules. The kidneys of hepatocarcinoma rats were obtained on the 28th day after the treatment.

Morphologic change

Macroscopic observation The liver was yellow or pale with dramatically increase of the volume and weight. The liver grew as multi-nodular mass. The nodules were of variable size ranging from 3 mm to 3.5 cm. Some nodules were hemorrhagic. The liver was firm in texture, pale on section and with necrosis. Some nodules were dark red on section accompanied by the hemorrhagic necrosis (more obviously seen in Group A and D than in the others).

Light microscopic observation Hepatocarcinoma cells were arrayed in column or gland-like, most commonly presented middle- or highly- differentiated status, few were poorly differentiated status. In some specimens, the hepatocarcinoma cells showed patched or focal necrosis with red-stained non-structural materials. The nucleic chromatin disappeared, prominently seen in group A and D. The necrosis region and portal tracts were infiltrated by inflammatory cells with vascular dilation and hyperemia. Group B, C and E mainly exhibited point necrosis, slight inflammatory reaction in portal tracts, and vascular dilation was less obvious than the former groups. In the treated groups, some hepatocarcinoma cells presented apoptotic features, cell membrane was shrunken but intact, chromatin was condensed and accumulated at side or broken up forming nucleic bodies in different sizes within cells, without inflammatory cells invasion, seen more commonly in group A, B and D. Under microscope, group D (4/7) exhibited relatively extensive renal tubular epithelium cloudy swelling

and degeneration. Protein casts was formed in the collecting tubules (4/7), there were no casts formed in group A, B, C and E (0/6, 0/6, 0/8, 0/7) without or occasionally tubular epithelium swelling and denaturalization. There was significant difference among the five groups ($\chi^2=12.69, P=0.013$).

Electron microscope observation The chromatin was accumulated at the side of the nucleic membranes which was condensed. The nucleic shape was irregular and the surface of nucleic membrane was rough. The nucleus was broken but encapsulated by intact membrane, containing intact organelles and apoptotic bodies.

Flow cytometry analysis of hepatocarcinoma cells

Tumor cell apoptotic rate in each group and influence of treatment time On the 7th, 14th, 28th day of treatment, there was significant difference of tumor cell apoptotic rate presents among each group ($P=0.001$). Compared with group E, apoptotic rate of group A, B, C, D all increased evidently, especially that of group B ($P=0.000$). The apoptotic rate of Group B depended on time, firstly it was increased then decreased ($P=0.004$), but there was no significant difference between them on the 14th day and 28th day ($P=0.224$). The relationship of apoptosis and treatment time between group A and group C was almost the same (Table 1).

Table 1 Relationship between tumor cells apoptotic rate in each group and treatment time ($\bar{x}\pm s$)

Specimen	7days	14days	28days
Group A	18.30±3.43 ^a	20.16±5.31 ^a	16.92±4.03 ^a
Group B	40.99±5.89 ^b	51.59±7.67 ^b	47.49±3.23 ^b
Group C	11.80±7.02	12.24±4.41 ^a	10.77±3.45 ^a
Group D	22.41±7.09 ^a	17.31±6.16 ^a	13.88±3.83 ^a
Group E	7.66±2.23	6.72±2.31	6.30±1.15

^a $P<0.05$, vs group E; ^b $P<0.001$, vs group E.

Compared with group E, apoptotic rate of G_0/G_1 , G_2/M phase cell in group B was significantly increased ($P<0.05$), especial that of G_2/M phase cell ($P=0.001$). Cell apoptosis presented during the whole cell cycle in group A, C, D, without distinct specificity (Table 2). In group B, apoptotic rate of G_0/G_1 phase cell is lower than that of G_2/M phase cell, but the number

of apoptotic cells at G_0/G_1 phase still accounted for a rather large proportion of the whole apoptotic cells.

Tumor cell cycle changes in each group (Table 3)

The tumor cells apoptotic distribution at G_0/G_1 , G_2/M phase in each group Compared with group E, on the 7th, 14th, 28th day after the treatment, the percentage of G_0/G_1 phase cells in group A was increased significantly ($P=0.001$), while that in group D was significantly decreased ($P=0.001$), and no statistical difference in group B, C ($P>0.05$); the percentage of S phase cell in group A, B, C was reduced ($P=0.001$); while that of G_2/M phase cell in group B, C, D was increased ($P=0.001$).

Immunohistochemical analysis

Immunohistochemical result of hepatocarcinoma tissue Among the 65-rat hepatocarcinoma tissue obtained after the treatment for 7 days, bc1-2 expressed positively in 57 of them. The intensity of bc1-2 positive expression was evidently differed among the 5 groups (chi-square test, $P=0.034$), it was lower expressed in group A, B, C, especial group B, which was significantly lower than that in the controls. Among the 65 specimens, 54 of them presented positive expression of bax. The intensity and rate of positive expression had significant difference among the 5 groups (chi-square test, $P=0.022$ and $P=0.006$). It was significantly higher in group A, B, C than that in the controls, whereas there was no statistical difference among the former. PCNA was expressed positively in 63 specimen, with significant difference among the 5 groups (Kruskal-Wallis test, $P=0.001$). Compared with group E, PCNA LI expression was down regulated in group A, B, C, and D, especially in group A.

Immunohistochemical analyzing of renal tissue There was no significant difference in the expression of bcl-2 among the 5 groups, but among different positions. In group D and E, bc1-2 was positively expressed commonly in stroma cells without significant difference among the 5 groups. But in the renal tubular epithelium its positive expression was obviously enhanced ($\chi^2=14.93, P=0.005$) (Figure 1, 2). PCNA LI was significantly different (Kruskal-Wallis test, $P=0.001$). Compared to group E, PCNA LI expression was increased evidently (Mann-Whitney, $P=0.001$), without significant difference between Group A, B, C. Expression of PCNA LI renal tubular epithelium and stroma cells had significant difference among the 5 groups; while that of stroma cells, cortex-

Table 2 Apoptosis distribution of tumor cells at G_0/G_1 , G_2/M phase in each group (%)

Specimen	7days		14days		28days	
	G_0/G_1	G_2/M	G_0/G_1	G_2/M	G_0/G_1	G_2/M
Group A	21.79 ^a	10.67	24.93 ^b	8.65	15.84	36.21 ^a
Group B	23.43 ^a	78.64 ^b	42.53 ^b	80.68 ^b	27.90 ^a	78.95 ^b
Group C	5.97	25.50 ^a	13.24	15.99	10.42	14.21
Group D	21.91 ^a	40.33 ^b	20.94 ^a	25.71 ^a	10.95	20.66
Group E	10.19	12.80	8.56	8.07	7.07	8.87

^a $P<0.05$, vs group E; ^b $P<0.001$, vs group E.

Table 3 Variety of tumor cells in each group (%)

Specimen	7days			14days			28days		
	G_0/G_1	S	G_2/M	G_0/G_1	S	G_2/M	G_0/G_1	S	G_2/M
Group A	74.81 ^a	5.65 ^a	19.54 ^a	80.17 ^a	7.71 ^a	12.12	85.16 ^a	5.58 ^a	9.25
Group B	54.04	12.63 ^a	33.79 ^a	69.50	8.50 ^a	22.01 ^a	67.83	11.14 ^a	21.04 ^a
Group C	60.34	6.45 ^a	33.21 ^a	66.92	11.18 ^a	21.90 ^a	62.63	12.21 ^a	25.17 ^a
Group D	44.71 ^a	23.42 ^a	31.94 ^a	37.97 ^a	30.64 ^a	31.39 ^a	32.84 ^a	23.25	43.91 ^a
Group E	58.89	29.93	11.18	63.47	26.21	10.33	66.54	22.07	11.4

^a $P<0.05$, vs group E.

medulla cells and renal tubular epithelium all rose obviously without significant changes in Group A, B, C (Figure 3, 4).

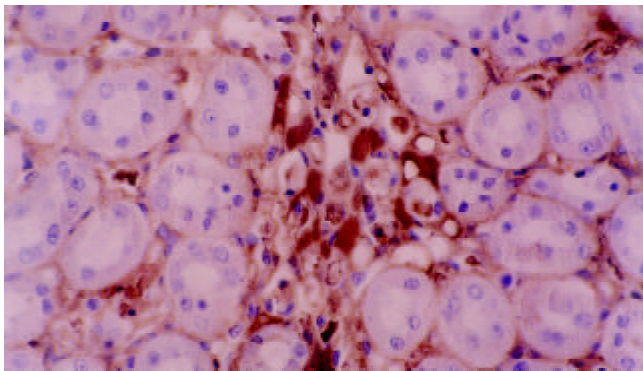


Figure 1 Positive expression of bcl-2 in the renal stroma cell, while negative in tubular epithelium in the cisplatin group (SP, ×400).

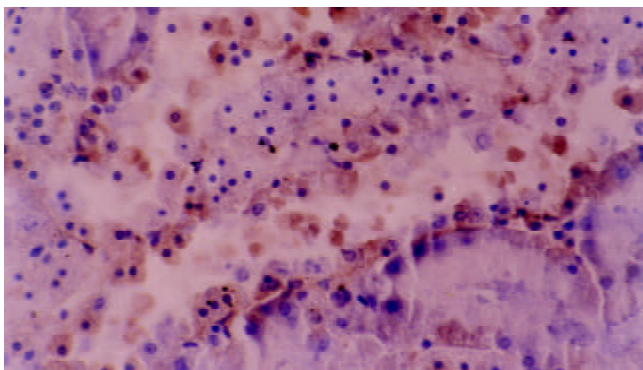


Figure 2 Positive expression of bc1-2 in renal tubular epithelium in medium dose arsenic group (SP, ×400).

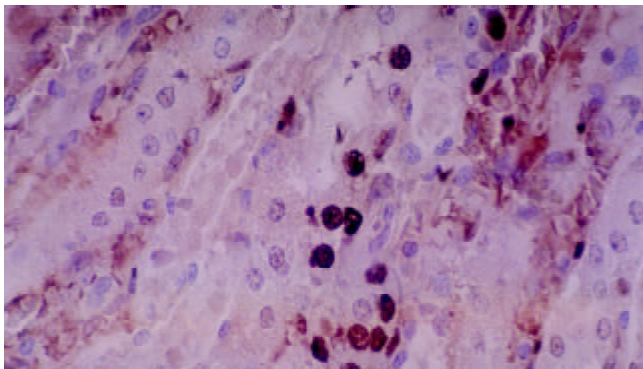


Figure 3 PCNA expression in renal collecting tubular epithelium and stroma cells in the cisplatin group (SP, ×400).

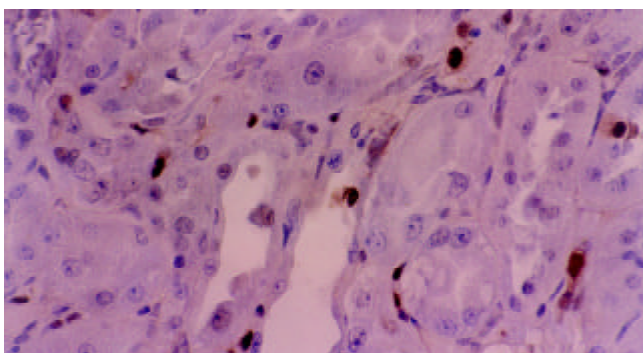


Figure 4 PCNA expression in renal cortex tubular cells in medium dose in arsenic group epithelium (SP, ×400).

DISCUSSION

At present, the pathogenesis and progression of tumor are thought to relate to cellular abnormal proliferation^[16, 37, 39], and as well as the abnormal apoptosis^[19, 41]. Exploring the origination and development of tumor from the viewpoint of apoptosis may elucidate the pathogenesis of tumor and helpfully open a new way to the therapy of tumor.

Studies indicated that As_2O_3 was able to induce hepatocarcinoma cells apoptosis^[41-44], and to inhibit the growth of transplanted hepatocarcinoma of nude mice^[11-14]. However, there is no report on the effect of chemocarcinogen on hepatocarcinoma *in vitro*. The result in this study revealed that As_2O_3 could induce the apoptosis of hepatic carcinoma cells and inhibited the proliferation of carcinoma cells after treatment of hepatocarcinoma induced by DEN in rat. There was no apparent damage to the renal, especially to the tubular epithelial cells. Different dosages of arsenic had different effects on the apoptosis, showing a problem of an optimum dose. As for the morphologic changes, it was assumed that two death mechanisms worked at the same time when the arsenic dose was too high. Though it could induce the apoptosis in certain degree, it could also produce cellular toxic phenomena^[17-23], leading to necrosis and inflammation of carcinoma cells, and kill the normal cells. While too low dose had weak cytotoxicity, it couldn't take effect in spite of the ability to induce apoptosis of carcinoma cells. Moderate dose could induce the apoptosis of amount of cancer cells, but produce obvious cytotoxic effect^[41-45].

Apoptosis has a close relationship with cell cycle. Among the current anti-cancer drugs, whether the cellular cycle-specific drugs or the non-specific ones, both of them have the first-class kinetics, which is that they cannot kill all of the tumor cells but some proportion of them. Studies showed that some carcinoma cell lines, such as human hepatocarcinoma^[14, 22], stomach cancer and pancreatic cancer and so on^[36], may show blockage of G₂/M phase after treated with As_2O_3 *in vitro*. While in human mammary carcinoma cell line, cell cycle was blocked at different phases with different dose of As_2O_3 . The results in this study indicated that As_2O_3 could induce the change of cell cycle in rat. The prominent feature was that middle-dose of As_2O_3 would lead to G₂/M blockage and large-dose of As_2O_3 would lead to G₀/G₁ blockage. It was thought that different dose of As_2O_3 held different influence on cell cycle of rat carcinoma cells and they correspondingly maybe had different end of cell cycle blockage. This study showed that with middle-dose of As_2O_3 , the cells at G₂/M phase had very high incidence of apoptosis, while the rate of apoptosis was low at G₁ and S phase, presenting very strong cell cycle-specific manner. However, at the same time, in spite of the low incidence of apoptosis at G₁ and S phase, at both of them, especially at G₁ phase, the proportion of apoptotic cells to total apoptotic cells couldn't be ignored. In the high- or low- dose of arsenic group, apoptosis didn't present the highest sensitivity at some phase. The above results suggested that arsenic may belong to a kind of non-typical cell cycle-specific drugs, and would get better therapy effect after combination with other cell cycle-specific drugs.

PCNA is an assistant protein of DNA polymerase, directly participating in the DNA replication during the cell proliferation. PCNA is lowly expressed in rest cells, and gets its peak at G₁ late phase and S phase, and then significantly descends at G₂/M phase. The content and expression degree of PCNA reflect the activity of cellular proliferation, which is a main biologic index of cellular proliferation. The present study showed that PCNA LI of the rat hepatocarcinoma cells was decreased to different level after the treatment of As_2O_3 . Different dosages of As_2O_3 resulted in different degree of

reduction of PCNA LI. The higher dose resulted in more significant reduction, proving that there did exist certain dose effect relationship in the inhibition of proliferation of As₂O₃ on hepatocarcinoma cells.

Cisplatin is one of the most effective chemotherapy drugs on hepatocarcinoma at present, but the serious renal-toxicity limits its use. Under microscope the renal toxicity of cisplatin manifests acute denaturalization tubular epithelium, necrosis, interstitial edema and tubular dilation. Our study showed these changes were showed in the cisplatin group (4/7) while no significant changes happened in the As₂O₃ group.

Studies showed that the renal toxicity had close relation with its oxidized damage to tubules. Bcl-2 is an apoptosis inhibitor and a strong anti-oxidant^[18-21]. With the action of cisplatin, the expression of bcl-2 was strikingly decreased in the renal tubular epithelium. Preliminary treatment with some medicines (Midkine, uranyl acetate) can increase the expression of bcl-2 and decrease the apoptosis resulting from cisplatin, and subsequently on low its damage on tubules^[9,19]. In this study, after administration of As₂O₃, the expression of bcl-2 in renal tubular epithelium was increased, while PCNA LI was not significantly changed. It was supposed that with the effect of As₂O₃, expression of apoptosis repression gene bcl-2 was increased, resulting in the inhibition of apoptosis, meanwhile, the anti-oxidated effect of bcl-2 was able to counteract possible oxidated damage, therefore it didn't have obvious toxic side effect on renal tubular epithelium.

In conclusion, this study indicated that As₂O₃ could induce apoptosis of rat hepatocarcinoma cells. And there exists optimization dose, too high dose will cause the cytotoxic effect, while proper dose of As₂O₃ is able to block the cell cycle at G₂/M phase. As₂O₃ had the most remarkable influence on cells at G₂/M phase, and it can also induce apoptosis to the cells at other phases. As₂O₃ can restrain the proliferation of rat hepatocarcinoma cells, presenting a dose-time relationship. Compared with cisplatin, As₂O₃ didn't show obvious renal toxicity which maybe was related to the increase of expression of bcl-2 in renal tubular epithelium, the inhibition of apoptosis and its anti-oxidation effects^[45].

REFERENCES

- Tang ZY.** Hepatocellular carcinoma-Cause, treatment and metastasis. *World J Gastroenterol* 2001; **7**: 445-454
- Vucenik I, Tantivejkul K, Zhang ZS, Cole KE, Saied I, Shamsuddin AM.** IP6 in treatment of liver cancer I. IP6 inhibits growth and reverses transformed phenotype in HepG2 human liver cancer cell line. *Anticancer Res* 1998; **18**: 4083-4090
- Chen GQ, Zhu J, Shi XG, Ni JH, Zhong HJ, Si GY, Jin XL, Tang W, Li XS, Xiong SM, Shen ZX, Sun GL, Ma J, Zhang P, Zhang TD, Gazin C, Naoe T, Chen SJ, Wang ZY, Chen Z.** *In vitro* studies on cellular and molecular mechanisms of arsenic trioxide (As₂O₃) in the treatment of acute promyelocytic leukemia: As₂O₃ induces NB4 cell apoptosis with downregulation of Bcl-2 expression and modulation of PML-RAR alpha/PML proteins. *Blood* 1996; **88**: 1052-1061
- Shen ZX, Chen GQ, Ni JH, Li XS, Xiong SM, Qiu QY, Zhu J, Tang W, Sun GL, Yang KQ, Chen Y, Zhou L, Fang ZW, Wang YT, Ma J, Zhang P, Zhang TD, Chen SJ, Chen Z, Wang ZY.** Use of arsenic trioxide (As₂O₃) in the treatment of acute promyelocytic leukemia (APL): II. Clinical efficacy and pharmacokinetics in relapsed patients. *Blood* 1997; **89**: 3354-3360
- Kerr JFR, Winterford CM, Harmon V.** Apoptosis: Its significance in cancer and cancer therapy. *Cancer* 1994; **73**: 2013-2026
- Jiang MC, Yang-Yen HF, Lin JK, Yen JJ.** Differential regulation of p53, c-Myc, Bcl-2 and Bax protein expression during apoptosis induced by widely divergent stimuli in human hepatoblastoma cells. *Oncogene* 1996; **13**: 609-616
- Fisher DE.** Apoptosis in cancer therapy: Crossing the threshold. *Cell* 1994; **78**: 539-542
- Zhou H, Miyaji T, Kato A, Fujigaki YK, Hishida A.** Attenuation of cisplatin-induced, acute renal failure is associated with less apoptotic cell death. *J Lab Clin Med* 1999; **134**: 649-658
- Chen Z, Chen GQ, Shen ZX, Sun GL, Tong JH, Wang ZY, Chen SJ.** Expanding the use of arsenic trioxide: leukemias and beyond. *Semin Hematol* 2002; **39**: 22-26
- Liao C, Zhao MJ, Zhao J, Jia D, Song H, Li ZP.** Over-expression of LPTS-L in hepatocellular carcinoma cell line SMMC-7721 induces crisis. *World J Gastroenterol* 2002; **8**: 1050-1052
- Oketani M, Kohara K, Tuvdendorj D, Ishitsuka K, Komorizono Y, Ishibashi K, Arima T.** Inhibition by arsenic trioxide of human hepatocarcinoma cell growth. *Cancer Lett* 2002; **183**: 147-153
- Siu KP, Chan JY, Fung KP.** Effect of arsenic trioxide on human hepatocellular carcinoma HepG2 cells: inhibition of proliferation and induction of apoptosis. *Life Sci* 2002; **71**: 275-285
- Xu HY, Yang YL, Gao YY, Wu QL, Gao GQ.** Effect of arsenic trioxide on human hepatocarcinoma cell line BEL-7402 cultured *in vitro*. *World J Gastroenterol* 2000; **6**: 681-687
- Zeng WJ, Liu GY, Xu J, Zhou XD, Zhang YE, Zhang N.** Pathological characteristics, PCNA labeling index and DNA index in prognostic evaluation of patients with moderately differentiated hepatocellular carcinoma. *World J Gastroenterol* 2002; **8**: 1040-1044
- Niu ZS, Li BK, Wang M.** Expression of p53 and C-myc genes and its clinical relevance in the hepatocellular carcinomatous and pericarcinomatous tissues. *World J Gastroenterol* 2002; **8**: 822-826
- Chen XP, Zhao H, Zhao XP.** Alternation of AFP-mRNA level detected in blood circulation during liver resection for hepatocarcinoma and its significance. *World J Gastroenterol* 2002; **8**: 818-821
- Qiu DK, Ma X, Peng YS, Chen XY.** Significance of cyclooxygenase-2 expression in human primary hepatocellular carcinoma. *World J Gastroenterol* 2002; **8**: 815-817
- Jiang Y, Zhou XD, Liu YK, Wu X, Huang XW.** Association of hTcf-4 gene expression and mutation with clinicopathological characteristics of hepatocellular carcinoma. *World J Gastroenterol* 2002; **8**: 804-807
- Yang LJ, Wang WL.** Preparation of monoclonal antibody against apoptosis-associated antigens of hepatocarcinoma cells by sub-tractive immunization. *World J Gastroenterol* 2002; **8**: 808-814
- Huang J, Cai MY, Wei DP.** HLA class I expression in primary hepatocellular carcinoma. *World J Gastroenterol* 2002; **8**: 654-657
- Huang GW, Yang LY.** Metallothionein expression in hepatocellular carcinoma. *World J Gastroenterol* 2002; **8**: 650-653
- Liu L, Qin S, Chen H, Wang J, Chen H, Ma J, Liu W.** An experimental study on arsenic trioxide-selectively induced human hepatocarcinoma cell lines apoptosis and its related genes *Zhonghua Ganzhangbing Zazhi* 2000; **8**: 367-369
- Yang JY, Luo HY, Lin QY, Liu ZM, Yan LN, Lin P, Zhang J, Lei S.** Subcellular daunorubicin distribution and its relation to multidrug resistance phenotype in drug-resistant cell line SMMC-7721/R. *World J Gastroenterol* 2002; **8**: 644-649
- Liu LX, Jiang HC, Liu ZH, Zhou J, Zhang WH, Zhu AL, Wang XQ, Wu M.** Integrin gene expression profiles of human hepatocellular carcinoma. *World J Gastroenterol* 2002; **8**: 631-637
- Jiang HC, Liu LX, Piao DX, Xu J, Zheng M, Zhu AL, Qi SY, Zhang WH, Wu LF.** Clinical short-term results of radiofrequency ablation in liver cancers. *World J Gastroenterol* 2002; **8**: 624-630
- Su JM, Gui L, Zhou YP, Zha XL.** Expression of focal adhesion kinase and alpha5 and beta1 integrins in carcinomas and its clinical significance. *World J Gastroenterol* 2002; **8**: 613-618
- Liu H, Wang Y, Zhou Q, Gui SY, Li X.** The point mutation of p53 gene exon7 in hepatocellular carcinoma from Anhui Province, a non hepatocarcinoma prevalent area in China. *World J Gastroenterol* 2002; **8**: 480-482
- Li MS, Li PF, He SP, Du GG, Li G.** The promoting molecular mechanism of alpha-fetoprotein on the growth of human hepatocarcinoma Bel7402 cell line. *World J Gastroenterol* 2002; **8**: 469-475
- Wang FS, Liu MX, Zhang B, Shi M, Lei ZY, Sun WB, Du QY,**

- Chen JM. Antitumor activities of human autologous cytokine-induced killer (CIK) cells against hepatocellular carcinoma cells *in vitro* and *in vivo*. *World J Gastroenterol* 2002; **8**: 464-468
- 30 **Qin LX**, Tang ZY, Ma ZC, Wu ZQ, Zhou XD, Ye QH, Ji Y, Huang LW, Jia HL, Sun HC, Wang L. P53 immunohistochemical scoring: an independent prognostic marker for patients after hepatocellular carcinoma resection. *World J Gastroenterol* 2002; **8**: 459-463
- 31 **Liu LX**, Jiang HC, Piao DX. Radiofrequency ablation of liver cancers. *World J Gastroenterol* 2002; **8**: 393-399
- 32 **Qin LX**, Tang ZY. The prognostic molecular markers in hepatocellular carcinoma. *World J Gastroenterol* 2002; **8**: 385-392
- 33 **Zhang G**, Long M, Wu ZZ, Yu WQ. Mechanical properties of hepatocellular carcinoma cells. *World J Gastroenterol* 2002; **8**: 243-246
- 34 **Zhao WH**, Ma ZM, Zhou XR, Feng YZ, Fang BS. Prediction of recurrence and prognosis in patients with hepatocellular carcinoma after resection by use of CLIP score. *World J Gastroenterol* 2002; **8**: 237-242
- 35 **Zheng N**, Ye SL, Sun RX, Zhao Y, Tang ZY. Effects of cryopreservation and phenylacetate on biological characters of adherent LAK cells from patients with hepatocellular carcinoma. *World J Gastroenterol* 2002; **8**: 233-236
- 36 **Hao MW**, Liang YR, Liu YF, Liu L, Wu MY, Yang HX. Transcription factor EGR-1 inhibits growth of hepatocellular carcinoma and esophageal carcinoma cell lines. *World J Gastroenterol* 2002; **8**: 203-207
- 37 **Qin LX**, Tang ZY. The prognostic significance of clinical and pathological features in hepatocellular carcinoma. *World J Gastroenterol* 2002; **8**: 193-199
- 38 **Wang ZX**, Hu GF, Wang HY, Wu MC. Expression of liver cancer associated gene hepatocarcinomaA3. *World J Gastroenterol* 2001; **7**: 821-825
- 39 **Tang ZY**. Hepatocellular carcinoma-cause, treatment and metastasis. *World J Gastroenterol* 2001; **7**: 445-454
- 40 **Rabe C**, Pilz T, Klostermann C, Berna M, Schild HH, Sauerbruch T, Caselmann WH. Clinical characteristics and outcome of a cohort of 101 patients with hepatocellular carcinoma. *World J Gastroenterol* 2001; **7**: 208-215
- 41 **Sun BH**, Zhang J, Wang BJ, Zhao XP, Wang YK, Yu ZQ, Yang DL, Hao LJ. Analysis of *in vivo* patterns of caspase 3 gene expression in primary hepatocellular carcinoma and its relationship to p21(WAF1) expression and hepatic apoptosis. *World J Gastroenterol* 2000; **6**: 356-360
- 42 **Yang SM**, Zhou H, Chen RC, Wang YF, Chen F, Zhang CG, Zhen Y, Yan JH, Su JH. Sequencing of p53 mutation in established human hepatocellular carcinoma cell line of HHC4 and HHC15 in nude mice. *World J Gastroenterol* 1998; **4**: 506-510
- 43 **Oketani M**, Kohara K, Tuvdendorj D, Ishitsuka K, Komorizono Y, Ishibashi K, Arima T. Inhibition by arsenic trioxide of human hepatocarcinoma cell growth. *Cancer Lett* 2002; **183**: 147-153
- 44 **Siu KP**, Chan JY, Fung KP. Effect of arsenic trioxide on human hepatocellular carcinoma HepG2 cells: inhibition of proliferation and induction of apoptosis. *Life Sci* 2002; **71**: 275-285
- 45 **Guo XZ**, Shao XD, Liu MP, Xu JH, Ren LN, Zhao JJ, Li HY, Wang D. Effect of bax, bcl-2 and bcl-xL on regulating apoptosis in tissues of normal liver and hepatocellular carcinoma. *World J Gastroenterol* 2002; **8**: 1059-1062

Edited by Xu XQ

Synergistic effects of nimesulide and 5-fluorouracil on tumor growth and apoptosis in the implanted hepatoma in mice

Xiao-Hong Li, Xiao-Kun Li, Shao-Hui Cai, Fu-Xing Tang, Xue-Yun Zhong, Xian-Da Ren

Xiao-Hong Li, Shao-Hui Cai, Xian-Da Ren, Department of Pharmacokinetics, Pharmacy College, Jinan University, Guangzhou 510632, Guangdong Province, China

Xiao-Kun Li, Biopharmaceutical R&D Center of Jinan University, Guangzhou 510632, Guangdong Province, China

Fu-Xing Tang, Electron microscopy Center of Jinan University, Guangzhou 510632, Guangdong Province, China

Xue-Yun Zhong, Department of Pathology, Medical College, Jinan University, Guangzhou 510632, Guangdong Province, China

Supported by National Natural Science Foundation of China, No. 39770300, and the Overseas Chinese Affairs Office of the State Council Foundation, No. 98-33

Correspondence to: Professor Xian-Da Ren, Department of Pharmacokinetics, Pharmacy College, Jinan University, Guangzhou 510632, Guangdong, China. tsam@jnu.edu.cn

Telephone: +86-20-8522-0261

Received: 2002-11-26 **Accepted:** 2002-12-25

Abstract

AIM: To compare the effect of nimesulide or/and 5-fluorouracil (5-FU) on tumor growth inhibition and apoptosis in mice with the implanted hepatoma and to observe their possible interactions.

METHODS: The inhibitory effects on tumor growth was evaluated by inhibition rate. Apoptosis was assessed by the ultrastructural, flow cytometry features and the DNA ladder demonstrated by agarose gel electrophoresis. PGE₂ level was determined by radioimmunoassay. Expression levels of c-jun, c-fos and p53 were evaluated by western blotting.

RESULTS: Nimesulide or 5-FU alone inhibited the growth of hepatoma, while a synergistic effect was observed for a combined use of both. More pronounced morphologic changes for tumor cell apoptosis and the DNA ladder were found for the latter treatment. Expression levels of c-jun and p53 were found to be elevated for the tumors from mice treated with nimesulide and 5-FU comparing to those with either of them, but a reduced PGE₂ level was observed only for the treatment with nimesulide. No change was detected on c-fos expression.

CONCLUSION: Nimesulide and 5-FU appear to have synergistic effects for the growth inhibition and apoptosis induction. Both were found to be overexpressed in p53 and c-jun proteins, rather than that of c-fos, associations with the resulted apoptosis.

Li XH, Li XK, Cai SH, Tang FX, Zhong XY, Ren XD. Synergistic effects of nimesulide and 5-fluorouracil on tumor growth and apoptosis in the implanted hepatoma in mice. *World J Gastroenterol* 2003; 9(5): 936-940

<http://www.wjgnet.com/1007-9327/9/936.htm>

INTRODUCTION

5-Fluorouracil (5-FU) is widely used in the chemotherapies

for many malignancies including gastrointestinal, breast and head and neck cancers. Its intravenous or intra-arterial delivery was often used as a monotherapy or in combination with other chemotherapeutic agents. It can cause DNA damage and induces apoptosis in some cancers^[1-3]. Further works are being done to potentiate 5-FU cytotoxicity by improving the dosing schedule and biochemical modulation of 5-FU. However, one of the major hindrances for its clinical application is the development of resistance by neoplastic cells, being innate or acquired for 5-FU^[4]. 5-FU, therefore is often used in combination with other anti-cancer therapies in the treatment of solid tumors. Experimental have indicated that pre-exposure of MCF-7 breast cancer cells to paclitaxel followed by 5-FU was preferable^[5].

During the last 20 years, accumulating data have shown an anti-proliferative effect of non-steroidal anti-inflammatory drugs (NSAIDs) in a variety of malignant cell lines^[6-12]. PGs and their synthesizing enzyme COX-2 was suggested to be involved in carcinogenesis^[13]. Reducing the COX-2 and PGE₂ expression proved to be an alteration approach to inhibit tumor growth. Some selective COX-2 inhibitors may be of the therapeutic significance. Nimesulide, a sulfonanilide class COX-2 inhibitor, can bind specifically to the large catalytic moiety of COX-2, with much less adverse effects on the gastrointestinal tract compared to the non-specific NSAIDs^[14]. In our previous studies, nimesulide was found to reduce the COX-2 and PGE₂ levels in association with the resulted apoptosis in mice implanted Hepatoma. In the present study a synergistic effect was observed for nimesulide and 5-FU on the growth and apoptosis of mouse hepatoma, and its possible molecular mechanism(s) was also investigated.

MATERIALS AND METHODS

Drugs and reagents

5-FU was purchased from Dongrui Pharmaceutical Co (Jiangsu, China). Nimesulide and other chemicals were purchased from Sigma Chemical Co (St. Louis, MO, USA) and suspended in PBS (pH 7.2). Monoclonal anti-mouse antibodies were supplied from Santa Cruz.

Animals and tumor model

Kunming breed mice, with their body weights ranging from 18 g to 22 g, were used. Subcutaneous inoculation was conducted in the flank with 1×10⁷/ml mouse hepatoma cell line HepA^[15]. The mice were bred on standard mouse chow and tap water under standard conditions. Nimesulide was given ig daily in a volume of 0.2 ml. 5-FU was injected ip every three days. Mice were randomly separated into five groups, 10 mice each: vehicle control, nimesulide 20 mg/kg, 5-FU 10 mg/kg, 5-FU 20 mg/kg, and nimesulide 20 mg/kg plus 5-FU 10 mg/kg. Throughout the experimentation period, food and water was available to animals *ad libitum*. After 21d test period animals were killed by cervical dislocation. Tumor was weighed, and fixed or minced using a mortar and pestle.

Tumor inhibition rate

Tumor growth was evaluated by the inhibition rate as assessed

by the formula: $IR=(1-T/C)\times 100\%$. IR represents inhibition rate, T and C indicate the mean tumor weights in the treatment and control groups, respectively.

Morphological analysis of apoptosis

Morphological changes indicative of apoptosis were detected by electron microscopy (EM). Briefly, dissected tumor samples were fixed with 20 ml/L glutaraldehyde in PBS for 1 h. After being washed with buffer for 3 times, the samples were post-fixed in OsO_4 in cacodylate buffer for 1 h. Subsequently, the samples were dehydrated in ethanol and embedded in epoxy resin (Agar 100). Thin sections (70nm) were stained in uranyl acetate and Reynolds lead citrate and viewed at 75 kV in an electron microscope (JEM-100CX 11/T).

Flow cytometry

Cell suspension was fixed in ice-cold 70 % ethanol in PBS, and stored at $-20\text{ }^\circ\text{C}$. Prior to analysis, the cells were washed and resuspended in PBS and incubated with RNase I 1 g/L and propidium iodide 20 mg/mL at $37\text{ }^\circ\text{C}$ for 30 min. The analysis of samples was performed using a flow cytometer.

DNA ladder visualization

Pulverized tumors were lysed with 150 μl hypotonic lysis buffer (10 mmol/L EDTA, 0.5 % Triton X-100 in 1 mmol/L Tris-HCl, pH7.4) for 15 min on ice and were precipitated with 2.5 % polyethyleneglycol and 1 mol/L NaCl for 15 min at 4 %. After centrifugation at 16 000 g for 10 min at room temperature, the supernatant was incubated in the presence of proteinase K (0.3 g/L) at $37\text{ }^\circ\text{C}$ for one hour and precipitated with isopropanol at $-20\text{ }^\circ\text{C}$. After centrifugation, each pellet was dissolved in 10 μl of Tris-EDTA (pH7.6) and electrophoresed on a 1.5 % agarose gel containing ethidium bromide 2 mg/mL. DNA fragments were visualized by ultraviolet transillumination.

Detection of prostaglandin E2 (PGE₂) by radioimmunoassay (RIA)

The amounts of immunoreactive PGE₂ in samples of solid tumor from mice were determined by RIA using a kit (Institute of Blood, Suzhou Medical university, China) following to the manufacturer's instructions. Briefly, to each polypropylene RIA tube, 100 μl of anti-PGE₂, ¹²⁵I-PGE₂, and PGE₂ or a sample were added. Immune complexes were precipitated 24 h later with 1 ml of polyethylene glycol solution, and the radioactivity in the precipitate was determined by a gamma counter. There was no nonspecific interference of the assay by the components of the sample. Assays were carried out in triplicate and the mean and standard deviations were obtained.

Western blotting for c-jun, c-fos, and p53

Samples were extracted with a lysis buffer (1 % Triton-100, 50 mM NaCl, 50 mM NaF, 20 mM Tris pH 7.4, 1 mM EDTA, 1 mM EGTA, 1 mM sodium vanadate, 0.2 mM phenylmethylsulfonyl fluoride, and 0.5 % Nonidet P-40). The cell lysates, 60 mg each, were solubilized in sample buffer by boiling for 5 min, and then subjected to 10 % SDS-PAGE. The resolved proteins were electrotransferred onto a nitrocellulose filter. The filter was incubated consecutively with a primary antibody and with peroxidase-conjugated anti-mouse immunoglobulin G (IgG). The reactions were visualized using the ECL detection system.

Statistical analysis

Results are expressed as $\bar{x}\pm s$. Statistical analysis of the results was performed using the student's *t*-test. $P<0.05$ was considered statistically significant.

RESULTS

Tumor inhibition rate

Administrated nimesulide and 5-FU suppressed tumor growth of the implanted hepatoma. The growth inhibitory rate was about 30 % after treatment with nimesulide (20 mg/kg). Application of 5-FU (20 mg/kg) also resulted in a marked inhibitory effect on the growth of the implanted tumors, while no significant effect was observed with the lower dose (10 mg/kg). It showed a greater inhibitory effect with a combined use of nimesulide and 5-FU than with either of them (Table 1).

Table 1 Effect of nimesulide and 5-FU on tumor inhibition in mouse implanted hepatomas ($n=10$, $\bar{x}\pm s$)

Group	X1	R1	X2	R2
Control	3.67 \pm 1.7	-	3.69 \pm 1.6	-
Nimesulide 20mg/kg	2.59 \pm 0.9 ^c	30%	2.56 \pm 0.9 ^c	31%
5-FU 10mg/kg	2.63 \pm 0.9 ^c	28%	2.61 \pm 1.0 ^c	29%
5-FU 20mg/kg	1.11 \pm 0.6 ^{ab}	70%	1.01 \pm 0.6 ^{ab}	73%
Nimesulide 20mg/kg +5-FU 10mg/kg	0.43 \pm 0.2 ^a	88%	0.49 \pm 0.2 ^a	87%

^a $P<0.01$ vs control, ^b $P<0.05$, ^c $P<0.01$ vs nimesulide+5-FU. X1: the first mean tumor weights; R1: the first mean inhibition rates; X2: the second mean tumor weights; R2: the second mean inhibition rates.

Effect of nimesulide and 5-FU on apoptosis in HepA cells

The tumor growth-inhibiting effect was found to be associated with apoptosis as demonstrated by EM, and characterized by cell shrinkage and blebbing, condensation of unclear chromatin and nuclear fragment (Figure 1). Administration of 20 mg/kg of nimesulide or 20 mg/kg of 5-FU alone resulted in slight increases in apoptotic cell numbers, whereas the combined use of 20 mg/kg of nimesulide and 10 mg/kg of 5-FU caused markedly increased number of apoptotic cells.

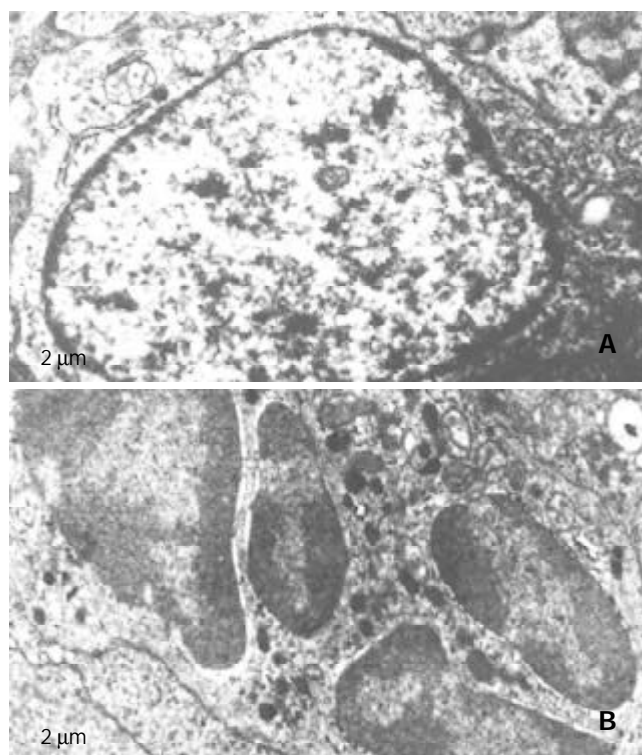


Figure 1 Electro micrographs of nimesulide plus 5-FU treated mice hepatoma. A, control; B, nimesulide plus 5-FU.

Agarose gel electrophoresis showed DNA ladder in the hepatoma tissue 21 d after the treatment. Compared to those caused by nimesulide or 5-FU alone, the DNA ladder appeared more pronounced for the combined treatment with 5-FU (10 mg/kg) and nimesulide. (Figure 2).

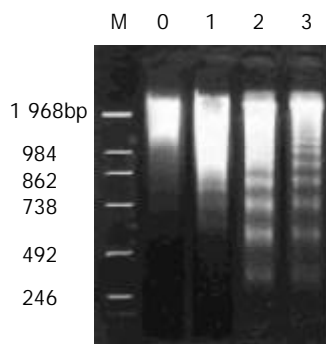


Figure 2 DNA ladder pattern of hepatoma tissues as demonstrated by agarose gel 1.5 % electrophoresis. M, DNA markers; lanes 0-3, control, nimesulide 20 mg/kg, 5-FU 20 mg/kg, nimesulide 20 mg/kg +5-FU 10 mg/kg.

The pro-apoptotic effect of nimesulide was further confirmed by flow cytometry. After treatment with nimesulide and/or 5-FU for 21 d, the profiles of the DNA histograms were different from control (Figure 3). With 5-FU and nimesulide administered, a striking SubG₁ peak was found and the apoptotic index increased from (4.3±1.5) % to (72±2.5) % (Table 2).

Table 2 Apoptotic indices of nimesulide and 5-FU in mouse hepatoma tissues after the treatment with determined by FCM. *n*=3, $\bar{x}\pm s$

	Control	Nimesulide (20 mg/kg)	5-FU (20 mg/kg)	Nimesulide (20 mg/kg)+ 5-FU (10 mg/kg)
Apoptotic Index	4.3±1.5	29.0±2.6 ^{ac}	49.0±2.0 ^{ac}	72.0±2.5 ^a

^a*P*<0.01 vs control; ^c*P*<0.01 vs nimesulide +5-FU.

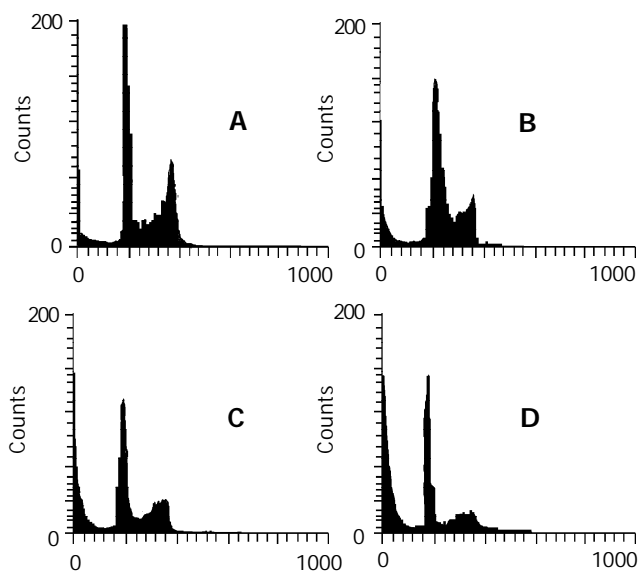


Figure 3 Data of flow cytometry of mouse hepatoma without any treatment as a control (A), or following 21 d treatment with nimesulide 20 mg/kg (B), 5-FU 20 mg/kg (C) and nimesulide 20 mg/kg+5-FU 10 mg/kg (D). The sub-G₁ peak to the left of the G₁ peak represents apoptotic cells.

Expression of PGE₂

The PGE₂ contents of the implanted hepatoma tissue was 636.67±17.9 ng/ml after treatment with 20 mg/kg of 5-FU, being at the same level as in the control group. However, it was significantly reduced with nimesulide administered, alone or combined with 5-FU (10 mg/kg) (Figure 4). Apparently, the mechanisms for the growth inhibition by nimesulide and 5-FU may be different, the former being associated with, and the latter independent of, PGE₂ content in tumor tissue.

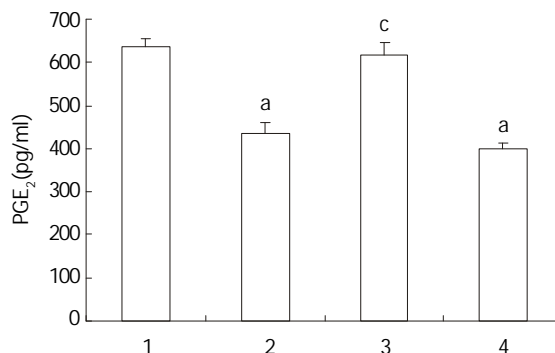


Figure 4 Effect of Nimesulide and 5-FU on PGE₂ content in mouse hepatoma. Each column is the mean ± SD of the sample. 1-4, control, nimesulide 20 mg/kg, 5-FU 20 mg/kg, and nimesulide 20 mg/kg+5-FU 10 mg/kg. *n*=3. $\bar{x}\pm s$. ^a*P*<0.01 vs control, ^c*P*<0.01 vs nimesulide+5-FU.

Effect on c-jun, c-fos, and p53 expressions

Western blotting showed that nimesulide or 5-FU induced expression of c-jun and p53 in mouse hepatoma. Treatment with nimesulide plus 5-FU resulted in up regulation of the expression of these genes, while it was not for the c-fos expression. Treatment with of 5-FU, 20 mg/kg in dose, also gave rise to expression of c-jun and p53. However, the effect of the combined application of nimesulide and a low dose of 5-FU (10 mg/kg) was more pronounced compared to those of 5-FU or nimesulide alone (Figure 5).

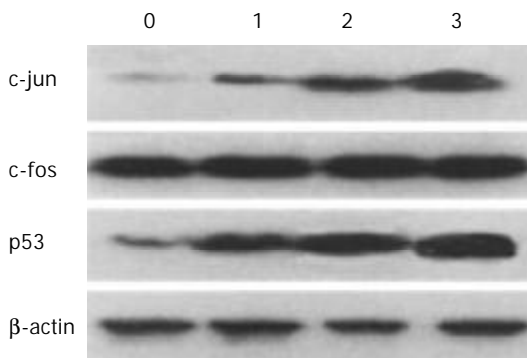


Figure 5 Effect of nimesulide and 5-FU on expression of c-fos, c-jun, and p53 in mouse hepatoma. 0-3, control, nimesulide 20 mg/kg, 5-FU 20 mg/kg, nimesulide 10 mg/kg+5-fu 10 mg/kg. The β -actin was used as an intrinsic reference molecule.

DISCUSSION

Previous observations showed that indomethacin, a non-selective COX inhibitor, improved hematopoietic recovery following 5-FU. 5-FU toxicity, increased with its dose, and indomethacin caused a generalized alleviation of 5-FU toxicity, but only if given concurrently with 5-FU^[16]. By the subsequent treatment with interferon γ , indomethacin, and phenylbutyrate in human

colon carcinoma cells, the recurrence of colon carcinomas, occurring frequently between cycles of 5-FU treatment, can be prevented or at least effectively retarded^[17].

The present study demonstrated that both nimesulide and 5-FU can inhibit the tumor growth and induce apoptosis, the combination of nimesulide and 5-FU being more effective compared to that of 5-FU or nimesulide alone. Apparently, apoptosis may be associated with the growth-inhibiting effect of 5-FU combined with nimesulide, and a synergistic effect was observed for these two agents. As demonstrated in this report, 5-FU (20 mg/kg) or nimesulide alone stimulated c-jun and p53 expression in hepatoma at a low level, this effect being greatly enhanced its combination with nimesulide.

The mechanism involved in growth inhibition and cell apoptosis by combination nimesulide with 5-FU treatment remains obscure. The ultimate outcome of tumor treatment with anti-cancer agents is the effect of many intrinsic and extrinsic factors, functioning independently or cooperatively^[18-20]. In the present study the possible role of c-fos and c-jun protein on tumor growth and apoptosis was evaluated^[21]. The well-characterized substrate of JNK is c-Jun, a component of the AP-1 transcription factor^[22,23]. Expression of c-jun was repeatedly shown to be involved in apoptosis induction and growth inhibition of many anti-cancer agents. In the present study, the level of c-jun was up-regulated by the treatment with nimesulide or 5-FU alone, and that with nimesulide plus 5-FU were even more effective. No significant change was observed in the c-fos levels in tumors after treatment with nimesulide or 5-FU alone, or their combined use, indicating that the anti-cancer effects on mouse hepatoma were associated with c-jun rather than c-fos.

The tumor suppressor gene, p53, is a key component in regulating cell cycle progression^[24]. Strikingly, many apoptotic stimuli are known to be p53-dependent^[25-30]. For example, p53 is required for the bleomycin-induced cerebellar granule cell death, following c-jun protein overexpression^[31]. MIF, a local proinflammatory cytokine, is capable of functionally inactivating p53. The observation provides a mechanistic link between inflammation and cancer^[32]. Moreover it is well known that selective COX-2 inhibitors have anti-inflammation and anti-cancer effects through inhibition COX-2. The elevated p53 level in mouse hepatoma treated with nimesulide alone or plus 5-FU may be due to inhibit COX-2 and PGE₂ level. Furthermore 5-FU induces cell apoptosis in a p53-dependent way^[33]. Our results raise the possibility that p53 is required for c-jun-dependent apoptosis induced by nimesulide or/and 5-FU treatment. It is possible that these two drugs increase p53 expression though different intracellular pathway for activating cell death processes.

In conclusion, a synergistic effect was observed between nimesulide and 5-FU on apoptosis in murine hepatoma, indicating its potential application in the management of human hepatocellular carcinomas.

REFERENCES

- 1 **Yoneda K**, Yamamoto T, Osaki T. p53- and p21-independent apoptosis of squamous cell carcinoma cells induced by 5-fluorouracil and radiation. *Oral Oncol* 1998; **34**: 529-537
- 2 **Warr JR**, Bamford A, Quinn DM. The preferential induction of apoptosis in multidrug-resistant KB cells by 5-fluorouracil. *Cancer Lett* 2002; **175**: 39-44
- 3 **Mizutania Y**, Nakanishia H, Yoshidab O, Fukushima M, Bonavidad B, Mikia T. Potentiation of the sensitivity of renal cell carcinoma cells to TRAIL-mediated apoptosis by subtoxic concentrations of 5-fluorouracil. *Eur J Cancer* 2002; **38**: 167-176
- 4 **Fukushima M**, Fujioka A, Uchida J, Nakagawa F, Takechi T. Thymidylate synthase (TS) and ribonucleotide reductase (RNR) may be involved in acquired resistance to 5-fluorouracil (5-FU) in human cancer xenografts *in vivo*. *Eur J Cancer* 2001; **37**: 1681-1687
- 5 **Jean LG**, Diana N, Brian PM, Vivian K, Francois JG. Sequence-dependent antagonism between fluorouracil and paclitaxel in human breast cancer cells. *Biochem Pharmacol* 1999; **58**: 477-486
- 6 **Smith ML**, Hawcroft G, Hull MA. The effect of non-steroidal anti-inflammatory drugs on human colorectal cancer cells: evidence of different mechanisms of action. *Eur J Cancer* 2000; **36**: 664-674
- 7 **Wu YL**, Sun B, Zhang XJ, Wang SN, He HY, Qiao MM, Zhong J, Xu JY. Growth inhibition and apoptosis induction of Sulindac on human gastric cancer cells. *World J Gastroenterol* 2001; **7**: 796-800
- 8 **Li HL**, Chen DD, Li XH, Zhang HW, Lü JH, Ren XD, Wang CC. JTE-522-induced apoptosis in human gastric adenocarcinoma cell line AGS cells by caspase activation accompanying cytochrome C release, membranane translocation of Bax and loss of mitochondrial membrane potential. *World J Gastroenterol* 2002; **8**: 217-223
- 9 **Li HL**, Zhang HW, Chen DD, Zhong L, Ren XD, Si-Tu R. JTE-522, a selective COX-2 inhibitor, inhibits cell proliferation and induces apoptosis in RL95-2 cells. *Acta Pharmacol Sin* 2002; **23**: 631-637
- 10 **Geng HZ**, Benjamin CYW, Chi KC, Kam CL, Lam SK. Differential apoptosis by indomethacin in gastric epithelial cells through the constitutive expression of Wild-Type p53 and/or Up-regulation of c-myc. *Biochem Pharmacol* 1999; **58**: 193-200
- 11 **Yaniv E**, Fiorenza P, Galit L, Na' am K, Amiram R. Comparative effects of indomethacin on cell proliferation and cell cycle progression in tumor cells grown *in vitro* and *in vivo*. *Biochem Pharmacol* 2001; **61**: 565-571
- 12 **Maria P**, Montserrat B, Mireia D, Beatriz B, Gabriel P. Aspirin induces apoptosis through mitochondrial cytochrome c release. *FEBS Lett* 2000; **480**: 193-196
- 13 **Munkarah AR**, Morris R, Baumann P. Effects of prostaglandin E2 on proliferation and apoptosis of epithelial ovarian cancer cells. *J Soc Gynecol Investig* 2002; **9**: 168-173
- 14 **Ayumi D**, Wakashi K, Akiko M, Hideki K, Yasutaka S, Osamu K, Toshifumi T, Masahiro T, Dai N, Hidetoshi T, Yoichi K. Increased expression of cyclooxygenase-2 protein during rat hepatocarcinogenesis caused by a choline-deficient, L-amino acid-defined diet and chemopreventive efficacy of a specific inhibitor, nimesulide. *Carcinogenesis* 2002; **23**: 245-256
- 15 **Wang W**, Qin SK, Chen BA, Chen HY. Experimental study on antitumor effect of arsenic trioxide in combination with cisplatin or doxorubicin on hepatocellular carcinoma. *World J Gastroenterol* 2001; **7**: 702-705
- 16 **Djordjevic B**, Lange CS, Schwartz MA, Rotman M. Clonogenic inactivation of colon cancer-derived cells treated with 5-Fluorouracil and indomethacin in Hybrid Spheroids. *Acta Oncol* 1998; **37**: 735-739
- 17 **Yicong H**, Curt MH, Samuel W. Regrowth of 5-Fluorouracil-treated human colon cancer cells is prevented by the combination of interferon γ , indomethacin, and phenylbutyrate. *Cancer Res* 2000; **60**: 3200-3206
- 18 **Xu CT**, Huang LT, Pan BK. Current gene therapy for stomach carcinoma. *World J Gastroenterol* 2001; **7**: 752-759
- 19 **Shen ZY**, Shen J, Li QS, Chen CY, Chen JY, Zeng Y. Morphological and functional changes of mitochondria in apoptosis esophageal carcinoma cells induced by arsenic trioxide. *World J Gastroenterol* 2002; **8**: 31-35
- 20 **Huang S**, Li JY, Wu J, Meng L, Shou CC. Mycoplasma infections and different human carcinomas. *World J Gastroenterol* 2001; **7**: 266-269
- 21 **Huang X**, Martindale JL, Liu Y, Holbrook NJ. The cellular response to oxidative stress: influences of mitogen-activated protein kinase signalling pathways in cell survival. *Biochem J* 1998; **333**: 291-300
- 22 **Behens A**, Sibilina M, Wagner EF. Amino-terminal phosphorylation of c-Jun regulates stress-induced apoptosis and cellular proliferation. *Nat Genet* 1999; **21**: 326-329
- 23 **Hengartner MO**. The biochemistry of apoptosis. *Nature* 2000; **407**: 770-776
- 24 **Fuchs SY**, Adler V, Pincus MR, Ronai Z. MEKK1/JNK signaling stabilizes and activates p53. *Proc Natl Acad Sci USA* 1998; **95**:

- 10541-10546
- 25 **Andrea R**, Shabbir M, Peter MY, Gohc SSN. Expression of nitric oxide synthase, cyclooxygenase, and p53 in different stages of human gastric cancer. *Cancer Lett* 2001; **172**: 177-185
- 26 **Li HL**, Ren XD, Zhang HW, Ye CL, Lü JH, Zheng PE. Synergism between heparin and adriamycin on cell proliferation and apoptosis in human nasopharyngeal carcinoma CNE2 cells. *Acta Pharmacol Sin* 2002; **23**: 167-172
- 27 **Zhao AG**, Zhao HL, Jin XJ, Yang JK, Tang LD. Effects of Chinese Jianpi herbs on cell apoptosis and related gene expression in human gastric cancer grafted onto nude mice. *World J Gastroenterol* 2002; **8**: 792-796
- 28 **Qin LX**, Tang ZY. The prognostic molecular markers in hepatocellular carcinoma. *World J Gastroenterol* 2002; **8**: 385-392
- 29 **Zhang Z**, Yuan Y, Gao H, Dong M, Wang L, Gong YH. Apoptosis, proliferation and p53 gene expression of *H. pylori* associated gastric epithelial lesions. *World J Gastroenterol* 2001; **7**: 779-782
- 30 **Xu AG**, Li SG, Liu JH, Gan AH. Function of apoptosis and expression of the proteins Bcl-2, p53 and C-myc in the development of gastric cancer. *World J Gastroenterol* 2001; **7**: 403-406
- 31 **Toshiyuki A**, Yasushi E, Naoko I, Shinichi A, John CR, Hiroshi H. Changes in c-Jun but not Bcl-2 family proteins in p53-dependent apoptosis of mouse cerebellar granule neurons induced by DNA damaging agent bleomycin. *Brain Res* 1998; **794**: 239-247
- 32 **James DH**, Mahmood AS, Roberta M, Amancio C, Gregory JH, David HB. A proinflammatory cytokine inhibits p53 tumor suppressor activity. *J Exp Med* 1999; **190**: 1375-1382
- 33 **Pritchard MD**, Jackmanb A, Christopher SP, John AH. Chemically-induced apoptosis: p21 and p53 as determinants of enterotoxin activity. *Toxicol Lett* 1998; **102-103**: 19-27

Edited by Su Q

Biological characteristics of HCC by ultrasound-guided aspiration biopsy and its clinical application

Li-Wu Lin, Xue-Ying Lin, Yi-Mi He, Shang-Da Gao, Xiao-Dong Lin

Li-Wu Lin, Xue-Ying Lin, Yi-Mi He, Shang-Da Gao, Xiao-Dong Lin, Fujian Provincial Ultrasonic Medicine Institute, Ultrasound Department, Union Hospital of Fujian Medical University, Fuzhou 350001, Fujian Province, China

Correspondence to: Li-Wu Lin, Ultrasound Department, Union Hospital of Fujian Medical University, Fuzhou 350001, Fujian Province, China. lxdghl@163.net

Telephone: +86-591-3357896-8352 **Fax:** +86-591-3357896-8352

Received: 2002-11-19 **Accepted:** 2003-01-02

Abstract

AIM: To probe the pathological biological characteristics of hepatocellular carcinoma (HCC) by the ultrasound-guided aspiration biopsy and assess the clinical application value of this method.

METHODS: The biopsy and DNA analysis by flow cytometry (FCM) were taken in 46 cases with HCC nodules, including 26 cases and 20 cases with nodules ≤ 3 cm and > 3 cm in diameters respectively, and 12 cases with intrahepatic benign hyperplastic nodules. They were taken in 22 cases of 46 cases with HCC before and after the therapy. Fine-needles and automatic histological incised biopsy needles were used. The fresh biopsy tissue was produced into the single cell suspension, which was sent for DNA detection and ratio analysis of cell period. The ratio of each DNA period of cell proliferation of each group was calculated and compared with each other. The DNA aneuploid (AN) and apoptosis cell peak were observed and their percentages were calculated.

RESULTS: The ratios of S and G_2/M periods of DNA, which reflect cell hyperproliferation, in the group with HCC tumors > 3 cm in diameter were markedly higher than those of the group with HCC nodules ≤ 3 cm in diameter and the group with the benign hyperplastic nodules ($P < 0.01$ except A:B of S period, $P < 0.05$). The ratios of the middle group were also apparently higher than those of the latter group ($P < 0.01$). The ratio of DNA AN of 46 cases with HCC nodules was 34.8 % (16/46). None of the cases with the intrahepatic hyperplastic nodules appeared AN. The DNA AN appeared more apparently with the growth of the tumors. The AN ratio of the group with tumors > 3 cm in diameter was 55 % (11/20), markedly higher than that of the group with tumors ≤ 3 cm in diameter which was 19.2 % (5/26) ($P < 0.01$). The FCM DNA analysis of 22 specimens of hepatic carcinoma tissue before therapy showed that the aneuploid peaks appeared in 5 cases (22.7 %). The ratio of G_1 period rose after therapy while the S period and G_2/M ratios fell ($P < 0.01$). The aneuploid peak disappeared in the 5 cases after the therapy, while the apoptosis peaks in 12 cases (54.5 %) appeared.

CONCLUSION: Addition to supply the information of the pathological morphology of the tumor, the ultrasound-guided fine-needle aspiration tissue could be sent for FCM DNA

analysis to comprehend its pathological biological characteristics. This can not only provide the clinic the reliable information about the occurrence, development, diagnosis, curative effect and prognosis of tumors but also supply biological information for clinic to choose therapeutic schemes.

Lin LW, Lin XY, He YM, Gao SD, Lin XD. Biological characteristics of HCC by ultrasound-guided aspiration biopsy and its clinical application. *World J Gastroenterol* 2003; 9 (5): 941-945

<http://www.wjgnet.com/1007-9327/9/941.htm>

INTRODUCTION

Recently, with the wide use of flow cytometry (FCM) in clinic, it becomes possible to make pathological diagnosis develop from qualitative analysis of the morphology to quantitative analysis^[1-5]. The study of DNA analysis of the biological characteristics of hepatocellular carcinoma (HCC) model and hepatectomy specimens of man HCC has greatly developed^[6-18]. But the study of DNA analysis of the pathological biological characteristics of HCC specimens acquired from the ultrasound-guided aspiration biopsy has been rarely reported^[15,19]. In our study, the ultrasound-guided aspiration biopsy and the FCM DNA analysis were taken in 46 cases with HCC, including 22 cases with HCC before and after the therapy and 12 cases with intrahepatic benign hyperplastic nodules (IBHN) in order to probe the biological characteristics of HCC and assessed the clinical application value of this research.

MATERIALS AND METHODS

Subjects

Forty-six cases with HCC, including 26 cases and 20 cases with nodules 3 cm and > 3 cm in diameters respectively, consisted of 39 males and 7 females. The mean age was 53.7 years (range, 29-72). Twenty-two of 46 cases taking ultrasound-guided interventional therapy included 16 males and 6 females. Twelve cases with IBHN comprised 7 males and 5 females and the average age was 47.5 years (range, 27-58). The diagnosis was established by cytopathological and / or histological examinations.

Instruments and methods

The apparatuses were Aloka-650 and 1700 with 3.5-MHz probe. All cases took aspiration biopsy with 22G PTC needles. Twenty-two cases with HCC took percutaneous ethanol or other anti-tumor drug injection therapy for 5-8 times after biopsy, then took aspiration biopsy once again. The 18G automatic histological incised biopsy needle (produced by C.R. Bard, Inc, American) was used if the specimen taken by the fine needle aspiration was unsatisfactory. The amount of platelet of the patient must be $> 60 \times 10^9/L$ and the mobility of thrombogen of the cases must be > 50 %. The process of fine-needle aspiration biopsy was as follows. The point of puncture

in the skin was determined by ultrasonography. Then sterilization, drape and local paralysis were done. The fine needle punctured through the point into the focus. The needle was twitched up and down in the focus. At the same time, the negative pressure was kept in the syringe. The needle was taken out when the tissue and / or tissue with blood were seen in the syringe. The aspirated material was divided into three parts. One part was smeared on glass slides for pathological examination. The second part was placed in 10 % formalin or electron microscope (EM) liquid for electron microscopy. The last part was placed in 10 ml physiological saline for cytometric DNA analysis. The process of puncture of automatic histological incised biopsy was similar to that of fine-needle aspiration biopsy. The needle punctured to the periphery of the mass, ejected and excised the tumor tissue, then was extracted quickly. The sample was 19.0 mm in length and 1.0 mm in diameter.

The examination method of FCM

The FACScan (B.D. company, America) was adopted. At first, the fresh biopsy tissue was produced into the single cell suspension^[1]. Then it was stained by PI for DNA analysis. DNA content was measured and the ratio of each DNA period of cell proliferation was analyzed. The ratio of each DNA period, the percentage of the DNA aneuploid (AN) and the percentage of apoptosis cell peak were observed.

Statistical analysis

The average value and standard deviation of the percentage of the ratio of cell proliferation and DNA AN stem-line of each group were calculated respectively. The student-*t* test or student-*t'* test was used to test whether the mean of each group was different from each other. A difference was regarded as significance if $P < 0.05$.

RESULTS

Table 1 showed the ratio of each DNA period of cell proliferation of each group. Statistical analysis showed that the ratio of S and G₂/M periods of DNA, which reflect cell hyperproliferation, in the group with HCC tumors >3 cm in diameter were markedly higher than those of the group with nodules ≤3 cm in diameter and the group with the benign hyperplastic nodules ($P < 0.01$ except A:B of S period, $P < 0.05$). The ratios of the middle group were also apparently higher than those of the latter group ($P < 0.01$). The apparent characteristics were that the DNA of IBHN was steadily in G₁ period, which means the nonproliferation diploid (2c) state (Figure 1). While the DNA of HCC cell stayed in unstable division stage and appeared the cell hyperproliferation state (Figure 2) with the development of foci.

Table 1 The ratios of cell proliferation of HCC in different diameter and benign hyperplastic nodules (% , $\bar{x} \pm s$)

Characteristics of foci	Number of cases	DNA analysis of each period		
		G ₁ period	S period	G ₂ /M period
The group with HCC >3 cm (A)	20	40.3±6.8	43.5±7.4	16.2±1.7
The group with HCC ≤3 cm (B)	26	57.7±5.8	30.4±5.2	11.9±1.1
The group with IBHN (C)	12	94.8±0.7	2.6±0.5	2.6±0.4

G₁ period A:B A:C B:C $P < 0.01$; S period A:B $P < 0.05$, S period B:C A:C $P < 0.01$; G₂/M period A:B B:C A:C $P < 0.01$.

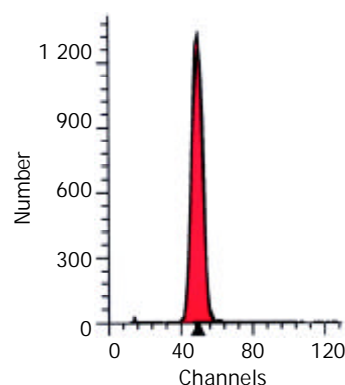


Figure 1 DNA analysis of aspiration biopsy tissues acquired from intrahepatic benign hyperplastic nodules showed steady diploid (2C) peak that stayed in G₁ period (single red peak).

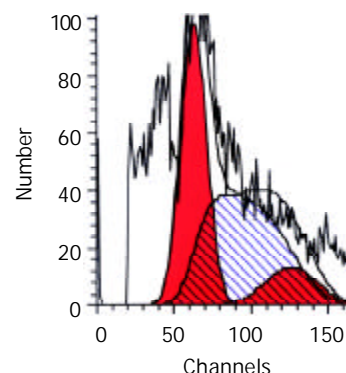


Figure 2 DNA analysis of aspiration biopsy tissues acquired from HCC nodules showed S period of hyperproliferation (the peak with oblique lines) and G₂/M period (the second red peak).

The statistical materials also showed that the ratio of DNA AN stem-line of 46 cases with HCC nodules was 34.8 % (16/46) (Figure 3). While none of cases with IBHN appeared AN stem-line. The DNA appeared AN more apparently with the growth of the tumors. The AN ratio of the group with tumors >3 cm in diameter was 55 % (11/20), markedly higher than that of the group with tumors ≤3 cm in diameter which was 19.20 % (5/26) ($P < 0.01$).

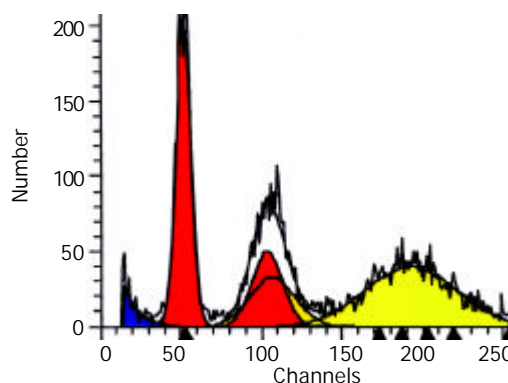


Figure 3 DNA analysis of HCC nodules showed aneuploid (AN) peak (the orange peak).

The pathological results of 22 cases among 46 cases with HCC after the ultrasound-guided percutaneous interventional therapy showed that the tumor cells appeared pyknosis and necrosis in various degrees. The Table 2 showed the results of FCM DNA analysis of the aspiration tissue. The ratio of G₁ period which reflects cell steady state rose apparently after therapy ($P < 0.01$). While the ratios of S period and G₂/M period

which reflect cell hyperproliferation fell ($P < 0.01$). After therapy the AN peaks disappeared in 5 cases which appeared before therapy and the apoptosis peaks appeared in 12 cases (54.5 %) (Figure 4) which was consistent with the cell pyknosis and dark nuclear staining showed by the histopathologic examination and the typical apoptosis cell or/and apoptosis body showed by the electron microscopy (Figure 5).

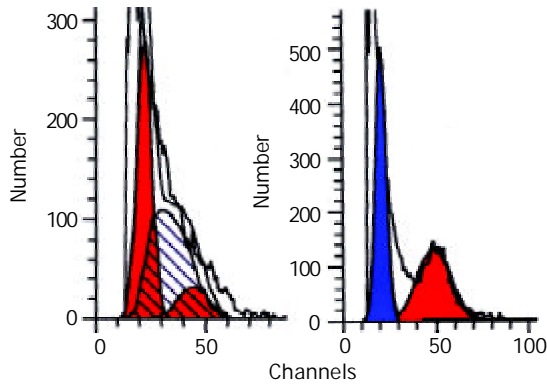


Figure 4 DNA analysis of HCC nodules showed hyperproliferation state before therapy (left) and apoptosis peak after therapy (the blue peak).

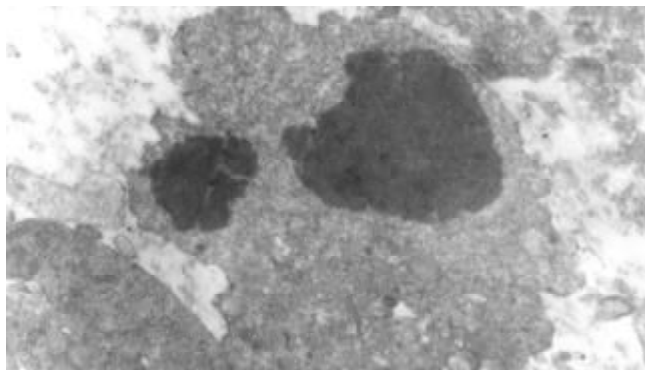


Figure 5 The same cases as those in figure.4 appeared typical apoptosis cells and apoptosis bodies after therapy.

Table 2 Cell proliferative ratios of 22 cases with HCC before and after ultrasound-guided interventional therapy (% , $\bar{x} \pm s$)

Time of detect	Each period of cell proliferation (%)		
	G ₁ period	S period	G ₂ /M period
Before therapy(a)	52.6±7.2	37.5±8.1	9.9±1.9
After therapy(b)	94.7±4.1	3.7±2.5	1.6±0.5

a:b of each period $P < 0.01$.

DISCUSSION

The application value of cytopathological and histological examinations using ultrasound-guided aspiration biopsy has been affirmed in clinic^[20-22]. There are also many scholars using many immunological methods to study the biological characteristics of hepatic tumors^[23-45]. But the study of DNA detection of intrahepatic tumor tissue by ultrasound-guided fine-needle aspiration or incising biopsy^[15,19] is rarely reported. On the basis of comparative study between ultrasound-guided fine-needle and heavy-needle biopsy, we made pathomorphological examination of HCC nodules that were different in diameter, HCC nodules before and after therapy as well as benign hyperplastic nodules by ultrasound-guided

puncturing biopsy. At the same time^[46-48], the fresh biopsy tissue was produced into the single cell suspension which was sent for FCM DNA detection and ratio analysis of cell period. The changing process of cell proliferation was observed. Through the study of biological characteristics of hepatic carcinoma and pathological comparison of hepatic carcinoma tissue before and after the therapy, we probed the application value of DNA analysis in assessment of the therapeutic efficacy and prognosis.

It is determined by the biological behavior of the cell itself that the normal tissue, reactive tissue and benign tumor all have normal diploid DNA. Like most other malignant tumors, HCC appears polyploid DNA, especially AN DNA. AN has become a reliable cytobiological signs of human malignant tumors^[49]. On the other side, like other malignant tumors, the occurrence and development pattern of HCC also relate to a biological behavior that changes from a relative steady benign state in the early period to a high proliferative malignant state^[3,4,7,50]. The study of HCC model of animal shows that, acted by the carcinogen the animal based on the hepatic cirrhosis appears the proliferation group of new born hepatocytes with diploid DNA stem-line which has highly proliferative activity and the potential ability of malignant tendency. That is the cytological basis of carcinogenesis later. The continuous changes of DNA stem-line in the process of occurrence and development of HCC form the characteristics of the various biological dynamic mechanism from early relative benign state to markedly malignant state of high proliferation. The course of DNA stem-line changing from 2C to AN is an important pathobiological sign. So the study of biological characteristics of HCC has the important clinical practical value for early diagnosis, selection of therapeutic schemes and judgment of prognosis of HCC. In our study, DNA analysis of HCC tissue by ultrasound-guided puncturing aspiration biopsy was made before and after therapy. The ratio of each period in cell period showed that the ratios of synthesis phase (S period) and mitosis phase (G₂/M period) which reflect high proliferation of HCC group were apparently higher than those of benign hyperplastic group ($P < 0.01$) and that the ratios of S and G₂/M period apparently rose with the growth of the tumors. As we all know, DNA, as the material basis of heredity of biotic bodies, is mainly located in chromosome of nucleus. The degree of maturation is closely relative to DNA content. The cell in non-proliferative state is characterized by 2C DNA stem-line. The DNA content increases multiply when cells enter division stage and DNA changes into AN stem-line. With the increasing of malignant degree of cell, the structure and amount of chromosome are more abnormal and the phenomena of changing into high proliferative state and AN is more remarkable. On the basis of the studies of animal HCC model and hepatectomic human HCC sample, Cong MW regards that the smaller HCC <3 cm in diameter is mainly characterized by diploid DNA stem-line which indicates relatively slow growth, lower malignant degree, tumors mostly having capsules, foci limiting, lower distant metastasis rate and lower occurring rates of thrombosis and satellite foci of tumor^[3,4]. All these are the pathological basis of conducting radical operation. Our material also shows that 34.8 % of 46 cases with HCC appeared AN. The ratio of AN of the group with tumor >3 cm in diameter reached 55.0 % (11/20), markedly higher than that of the group with tumor ≤3 cm in diameter which was 19.2 % (5/26) ($P < 0.01$). None of the cases with IBHN appeared AN. It is worth mentioning that, with the growth of tumor, the DNA gradually changes from low proliferation to AN stem-line at certain extent, which reflects that pathobiological characteristics is in relation to the size of tumor nodules. But it is not consistent thoroughly. In our study, the diameter of a small HCC nodule was only 1.1 cm, yet the DNA analysis characterized it by typical AN stem-

line (Figure 3).

Many scholars have made the researches in the relationship between the ploidy type and the prognosis of many tumors including HCC by FCM DNA analysis^[51-55]. But the study of DNA analysis by ultrasound-guided fine-needle biopsy to assess the therapeutic efficacy has been rarely reported^[56]. In our study, DNA analysis of tumor biopsy tissue shows that the AN stem-line which appeared before therapy disappeared after the ultrasound-guided interventional therapy with the cancer cell being killed. The ratios of S and G₂/M periods all fell obviously ($P < 0.01$) and 54.5 % cases appeared physiological death process which was different from common necrosis, in another word, appeared apoptosis peak before G₀-G₁ period. All these changes were consistent with what had been seen in pathological examination. DNA content rose multiply and the cell appeared polyploid when the cell entered division stage. In pathological state, especially for cancer cells, the structure and amount of chromosome became abnormal and the phenomenon of polyploid and/or AN became more remarkable. Summarily, the content and periods of DNA decreased and increased with dying and recurring of the cancer cell^[2,5,57]. The materials also show that DNA analysis could supply reliable biological information and objective quantification index.

This study shows that besides providing pathomorphological information of cytology and histology, the tissues acquired by ultrasound-guided puncturing biopsy could also be sent for FCM DNA analysis to comprehend the biological characteristics of tumors. So this method attains the objective of "one needle, three uses" and provides valuable clinical basis for diagnosis, therapeutic efficacy and prognosis assessment of tumors and is worth further studying.

REFERENCES

- 1 **Qi J**, Zhang YC. Using flow cytometry to process DNA analysis and several problems of this method. *Baiqiuen Yike Daxue Xuebao* 1993; **19**: 516-517
- 2 **Chen MF**, FACS, Hwang TL, Tsao KC, Sun CF, Chen TJ. Flow cytometric DNA analysis of hepatocellular carcinoma: preliminary report. *Surgery* 1991; **109**: 455-458
- 3 **Nagasue N**, Yamanoi A, Takemoto Y, Kimoto T, Uchida M, Chang YC, Taniura H, Kohno H, Nakamura T. Comparison between diploid and aneuploid hepatocellular carcinomas: a flow cytometric study. *Br J Surg* 1992; **79**: 667-670
- 4 **Yamanaka N**, Okamoto E, Toyosaka A, Mitunodu M, Fujihara S, Kato T. Prognostic factors after hepatectomy for hepatocellular carcinomas. *Cancer* 1990; **65**: 1104-1110
- 5 **Coon JS**, Landay AL, Weinstein RS. Flow cytometric analysis of paraffin-embedded tumors: implications for diagnostic pathology. *Hum Pathol* 1986; **17**: 435-437
- 6 **Cong WM**, Wu MC, Zhang XZ. Characteristic changes of DNA stemlines during hepatocarcinogenesis in rats. *Chinese Medical Journal* 1992; **105**: 535-538
- 7 **Cong WM**, Wu MC, Chen H. Development of diagnosis and therapy in hepatocellular carcinoma. *Zhongguo Shiyong Waike Zazhi* 1997; **17**: 3-4
- 8 **Lu DD**. The DNA analysis of hepatocarcinoma. *Yixue Tongxun Zazhi* 1999; **28**: 21-24
- 9 **Cheng HH**, Zheng ZY, Gao Z, Yang RY, Yu YH. The clinical value of the detect of DNA content and cell proliferative activity of primary hepatocellular carcinoma. *Zhongguo Zhongliu Linchuang Yu Kangfu* 1996; **3**: 25-26
- 10 **Cong WM**, Wu MC. The biopathologic characteristics of DNA content of hepatocellular carcinomas. *Cancer* 1990; **66**: 498-501
- 11 **Fujimoto J**, Okamoto E, Yamanaka N, Toyosaka A, Mitsunobu M. Flow cytometric DNA analysis of hepatocellular carcinoma. *Cancer* 1991; **67**: 939-944
- 12 **Rua S**, Comino A, Fruttero A, Torchio P, Bouzari H, Taraglio S. Flow cytometric DNA analysis of cirrhotic liver cells in patients with hepatocellular carcinoma can provide a new prognostic factor. *Cancer* 1996; **78**: 1195-1202
- 13 **Wen XF**, Ma ZC, Lin ZY, Ye QH, Tang ZQ. The clinical value of DNA content in the recurrence of hepatocellular carcinoma-Logistic model. *Zhongguo Puwai Jichu Yu Linchuang Zazhi* 2001; **8**: 236-238
- 14 **Shi GJ**, Hu YL, Zhao YR. The relationship of DNA content and morphometric data of nuclear feature in primary hepatocellular carcinoma and clinical value. *Gandan Waike Zazhi* 1997; **5**: 233-235
- 15 **Anti M**, Marra G, Rapaccini GL, Rumi C, Bussa S, Fadda G, Vecchio FM. DNA ploidy pattern in human chronic liver diseases and hepatic nodular lesions. *Cancer* 1994; **73**: 281-288
- 16 **Joensuu H**, Klemi PJ. Comparison of nuclear DNA content in primary and metastatic differentiated thyroid carcinoma. *Am J Clin Pathol* 1988; **89**: 35-40
- 17 **Wersto RP**, Liblit RL, Koss LG. Flow cytometric DNA analysis of human solid tumors: a review of the interpretation of DNA histo ams. *Hum Gr Pathol* 1991; **22**: 1085-1098
- 18 **Ezaki T**, Kanematsu T, Okamura T, Sonoda T, Sugimachi K. DNA analysis of hepatocellular carcinoma and clinicopathologic implications. *Cancer* 1988; **61**: 106-109
- 19 **Cottier M**, Jouffre C, Maubon I, Sabido O, Barthelemy C, Cuilleron M, Veyret C, Laurent JL, Audigier JC. Prospective flow cytometric DNA analysis of hepatocellular carcinoma specimens collected by ultrasound-guided fine needle aspiration. *Cancer* 1994; **74**: 599-605
- 20 **Chen YL**, Chen F, Hu ZQ, Wang HP. Study on technological improvement by ultrasound-guided percutaneous renal biopsy. *Zhonghua Chaosheng Yingxiangxue Zazhi* 2000; **9**: 234-236
- 21 **Tang J**, Li S, Xu JH, Yang YY, Li JL, Luo YK, Dong BW. Evaluation of biopsy guided by ultrasound in the diagnosis of prostatic intraepithelial neoplasia. *Zhonghua Chaosheng Yingxiangxue Zazhi* 2000; **9**: 465-468
- 22 **Dong BW**, Liang P, Yu XL, Su L, Yu DJ, Zhang J. The clinical usefulness of color Doppler ultrasonography-guided percutaneous biopsy for pancreatic masses. *Zhonghua Chaosheng Yingxiangxue Zazhi* 2001; **10**: 219-221
- 23 **Deng ZL**, Ma Y. Aflatoxin sufferer and p53 gene mutation in hepatocellular carcinoma. *World J Gastroenterol* 1998; **4**: 28-29
- 24 **Sun JJ**, Zhou XD, Liu YK, Zhou G. Phase tissue intercellular adhesion molecule-1 expression in nude mice human liver cancer metastasis model. *World J Gastroenterol* 1998; **4**: 314-316
- 25 **Yang SM**, Zhou H, Chen RC, Wang YF, Chen F, Zhang CG, Zhen Y, Yan JH, Su JH. Sequencing of p53 mutation in established human hepatocellular carcinoma cell line of HHC4 and HHC15 in nude mice. *World J Gastroenterol* 1998; **4**: 506-510
- 26 **Zhang LF**, Peng WW, Yao JL, Tang YH. Immunohistochemical detection of HCV infection in patients with hepatocellular carcinoma and other liver diseases. *World J Gastroenterol* 1998; **4**: 64-65
- 27 **Luo D**, Liu QF, Gove C, Naomov NV, Su JJ, Williams R. Analysis of N-ras gene mutation and p53 gene expression in human hepatocellular carcinomas. *World J Gastroenterol* 1998; **4**: 97-99
- 28 **Jiang SM**, Xu ZH. Serum deprivation enhances DNA synthesis of humanhepatoma SMMC-7721 cells. *World J Gastroenterol* 1998; **4**: 121-124
- 29 **Peng XM**, Peng WW, Yao JL. Codon 249 mutations of p53 gene in development of hepatocellular carcinoma. *World J Gastroenterol* 1998; **4**: 125-127
- 30 **Sun JJ**, Zhou XD, Zhou G, Liu YK. Expression of intercellular adhesive molecule-1 in liver cancer tissues and liver cancer metastasis. *World J Gastroenterol* 1998; **4**: 202-205
- 31 **Huang B**, Wu ZB, Ruan YB. Expression of nm23 gene in hepatocellular carcinoma tissue and its relation with metastasis. *World J Gastroenterol* 1998; **4**: 266-267
- 32 **Liu Y**, Zhang BH, Qian GX, Chen H, Wu MC. Detection of blood AFPmRNA in nude mice bearing human HCC using nested RT-PCR and its significance. *World J Gastroenterol* 1998; **4**: 268-270
- 33 **Zheng N**, Ye SL, Sun RX, Zhao Y, Tang ZY. Effects of cryopreservation and phenylacetate on biological characters of adherent LAK cells from patients with hepatocellular carcinoma. *World J Gastroenterol* 2002; **8**: 233-236
- 34 **Liu LX**, Jiang HC, Liu ZH, Zhou J, Zhang WH, Zhu AL, Wang XQ, Wu M. Intergrin gene expression profiles of human hepatocellular carcinoma. *World J Gastroenterol* 2002; **8**: 631-637

- 35 **Wang X**, Liu FK, Li X, Li JS, Xu GX. Inhibitory effect of endostatin expressed by human liver carcinoma SMMC7721 on endothelial cell proliferation *in vitro*. *World J Gastroenterol* 2002; **8**: 253-257
- 36 **Sun ZJ**, Pan CE, Liu HS, Wang GJ. Anti-hepatoma activity of resveratrol *in vitro*. *World J Gastroenterol* 2002; **8**: 79-81
- 37 **Tian G**, Yu JP, Luo HS, Yu BP, Yue H, Li JY, Mei Q. Effect of nimesulide on proliferation and apoptosis of human hepatoma SMMC-7721 cells. *World J Gastroenterol* 2002; **8**: 483-487
- 38 **Liu H**, Wang Y, Zhou Q, Gui SY, Li X. The point mutation of p53 gene exon7 in hepatocellular carcinoma from anhui province, a non HCC prevalent area in china. *World J Gastroenterol* 2002; **8**: 480-482
- 39 **Wang FS**, Liu MX, Zhang B, Shi M, Lei ZY, Sun WB, Du QY, Chen JM. Antitumor activities of human autologous cytokine induced killer (CIK) cells against hepatocellular carcinoma cells *in vitro* and *in vivo*. *World J Gastroenterol* 2002; **8**: 464-468
- 40 **Qin LX**, Tang ZY, Ma ZC, Wu ZQ, Zhou XD, Ye QH, Ji Y, Huang LW, Jia HL, Sun HC, Wang L. P53 immunohistochemical scoring: an independent prognostic marker for patients after hepatocellular carcinoma resection. *World J Gastroenterol* 2002; **8**: 459-463
- 41 **Huang GW**, Yang LY. Metallothionein expression in hepatocellular carcinoma. *World J Gastroenterol* 2002; **8**: 650-653
- 42 **Feng DY**, Chen RX, Peng Y, Zheng H, Yan YH. Effect of HCV NS-3 protein on p53 protein expression in esophageal carcinoma cells. *World J Gastroenterol* 1999; **5**: 45-46
- 43 **He P**, Tang ZY, Ye SL, Liu BB. Relationship between expression of α fetoprotein messenger RNA and some clinical parameters of human hepatocellular carcinoma. *World J Gastroenterol* 1999; **5**: 111-115
- 44 **Lee JH**, Ku JL, Park YJ, Lee KU, Kim WH, Park JG. Establishment and characterization of four human hepatocellular carcinoma cell lines containing hepatitis B virus DNA. *World J Gastroenterol* 1999; **5**: 289-295
- 45 **Martins C**, Kedda MA, Kew MC. Characterization of six tumor suppressor genes and microsatellite instability in hepatocellular carcinoma in southern African blacks. *World J Gastroenterol* 1999; **5**: 470-476
- 46 **Lin LW**, He YM, Gao SD, Yang FD, Ye Z, Xue ES, Yu LY, Lin XD. Value of ultrasound-guided fine-needle aspiration biopsy and ejection heavy needle biopsy in diagnosis and assessment of therapeutic effect for hepatic carcinoma. *Zhonghua Chaosheng Yingxiangxue Zazhi* 2001; **10**: 608-610
- 47 **Zhang W**, Lv GR, Jia JW, Ran WQ, Miao LY, Shi XD, Huang MW, Zhao R, Ding LH, Feng LZ, Li ZP. Clinical applications of automatic biopsy technique under the guidance of ultrasound. *Zhonghua Chaosheng Yingxiangxue Zazhi* 1993; **2**: 38-41
- 48 **Dong BW**, Liang P, Yu XL, Su L, Yu DJ, Zhang J. Comparison of clinical usefulness of US-guided core (18G) and fine (21G) needles biopsy analysis. *Zhonghua Chaosheng Yingxiangxue Zazhi* 2000; **9**: 71-73
- 49 **Zhang YH**. The use of flow cytometry in laboratory medical. *Zhonghua Yixue Jianyan Zazhi* 1997; **20**: 203-205
- 50 **Fujimoto J**, Okamoto E, Yamanaka N, Toyosaka A, Mitsunobu M. Flow cytometric DNA analysis of hepatocellular carcinoma. *Cancer* 1991; **67**: 939-944
- 51 **Liu LN**, Zhang CH. DNA ploidy analysis and Ki-67 examination on renal neoplasms: investigation of degree of malignancy and biological behavior of small renal tumors. *Zhonghua Binglixue Zazhi* 2001; **30**: 39-42
- 52 **Rugge M**, Sonogo F, Sessa F, Leandro G, Capella C, Sperti C, Pasquali C, Mario FD, Pedrazzoli S, Ninfo V. Nuclear DNA content and pathology in radically treated pancreatic carcinoma. *Cancer* 1996; **77**: 459-465
- 53 **Southern JF**, Warshaw AL, Lewandrowski KB. DNA ploidy analysis of mucinous cystic tumors of the pancreas. *Cancer* 1996; **77**: 58-63
- 54 **Huang T**, Yu EX, Cao SL. Relationship between DNA ploidy and prognosis in hepatocellular carcinoma after radiation therapy. *Zhongguo Aizheng Zazhi* 1999; **9**: 203-205
- 55 **Qin XL**, Jia HL, Tang ZQ. The characteristics and prognosis of hepatic carcinoma. *Zhongliu* 2001; **21**: 473-476
- 56 **Lin LW**, He YM, Gao SD, Yu LY, Ye Z, Xue ES, Lin XD. Value of DNA analysis of ultrasound-guided fine-needle aspiration biopsy in assessment of therapeutic efficacy for hepatic carcinoma. *Zhonghua Chaosheng Yingxiangxue Zazhi* 2001; **10**: 538-541
- 57 **Peng LM**. Development of the study of cytoapoptosis detect. *Zhonghua Yixue Jianyan Zazhi* 1996; **19**: 336-338

Edited by Ren SY

Signal transduction of gap junctional genes, connexin32, connexin43 in human hepatocarcinogenesis

Xiang-Dong Ma, Xing Ma, Yan-Fang Sui, Weng-Liang Wang, Chun-Mei Wang

Xiang-Dong Ma, Department of Obstetrics & Gynecology, Xijing Hospital, Fourth Military Medical University, 17 Changle Xilu, Xi'an 710033, Shaanxi Province, China

Xing Ma, Department of Orthopaedics, Xijing Hospital, Fourth Military Medical University, 17 Changle Xilu, Xi'an 710033, Shaanxi Province, China

Yan-Fang Sui, Weng-Liang Wang, Department of Pathology, Fourth Military Medical University, 17 Changle Xilu, Xi'an 710033, Shaanxi Province, China

Chun-Mei Wang, Department of Electronic Microscopy, Fourth Military Medical University, 17 Changle Xilu, Xi'an 710033, Shaanxi Province, China

Correspondence to: Dr. Xiang-Dong Ma, Department of Obstetrics & Gynecology, Xijing Hospital, Fourth Military Medical University, 17 Changle Xilu, Xi'an 710033, Shaanxi Province, China. mapping@fmmu.edu.cn

Telephone: +86-29-3373569

Received: 2002-06-01 **Accepted:** 2002-07-15

Abstract

AIM: To investigate gap junctional intercellular communication (GJIC) in hepatocellular carcinoma cell lines, and signal transduction mechanism of gap junction genes connexin32(cx32), connexin43(cx43) in human hepatocarcinogenesis.

METHODS: Scraped loading and dye transfer (SLDT) was employed with Lucifer Yellow (LY) to detect GJIC function in hepatocellular carcinoma cell lines HHCC, SMMC-7721 and normal control liver cell line QZG. After Fluo-3AM loading, laser scanning confocal microscope (LSCM) was used to measure concentrations of intracellular calcium $[Ca^{2+}]_i$ in the cells. The phosphorylation on tyrosine of connexin proteins was examined by immunoblot.

RESULTS: SLDT showed that ability of GJIC function was higher in QZG cell than that in HHCC and SMMC-7721 cell lines. By laser scanning confocal microscopy, concentrations of intracellular free calcium $[Ca^{2+}]_i$ was much higher in QZG cell line (108.37 nmol/L) than those in HHCC (35.13 nmol/L) and SMMC-7721 (47.08 nmol/L) cells. Western blot suggested that only QZG cells had unphosphorylated tyrosine in Cx32 protein of 32 ku and Cx43 protein of 43 ku; SMMC-7721 cells showed phosphorylated tyrosine Cx43 protein.

CONCLUSION: The results indicated that carcinogenesis and development of human hepatocellular carcinoma related with the abnormal expression of cx genes and disorder of its signal transduction pathway, such as decrease of $[Ca^{2+}]_i$, post-translation phosphorylation on tyrosine of Cx proteins which led to a dramatic disruption of GJIC.

Ma XD, Ma X, Sui YF, Wang WL, Wang CM. Signal transduction of gap junctional genes, connexin32, connexin43 in human hepatocarcinogenesis. *World J Gastroenterol* 2003; 9(5): 946-950

<http://www.wjgnet.com/1007-9327/9/946.htm>

INTRODUCTION

Hepatocellular carcinoma has been one of the most common malignant threatening human health^[1-9], and much higher incidences of human hepatocellular carcinoma (HCC) are observed recently^[10-18]. Gap junctional intercellular communication (GJIC) is performed by intercellular hemichannels^[19], which are formed by six basic protein subunits named connexin (Cx) expressed in neighboring cells^[20]. Six connexins form around a central pore^[21], through which adjacent cells can exchange low weight molecules of information and energy directly^[22]. At least 16 members of connexin super gene family have been identified, which are divided into two groups according to amino acid sequence. GJIC mediated via gap junctions plays important roles in tissue homeostasis, embryonic development as well as carcinogenesis^[23-25]. The mechanisms of carcinogenesis may be related with the block of GJIC of homologous and heterologous communication between tumor cells and surrounding normal cells^[26].

Connexin32 (Cx32) and connexin43 (Cx43) are the major kinds of gap junction proteins expressing in hepatocytes^[18]. Our works showed that expressions of Cx32, Cx43 proteins decreased in hepatocellular carcinoma tissues and cell lines whereas increased in normal tissues and cell lines^[19-21], but cx32 mRNA and cx43 mRNA kept a high level in both hepatocellular carcinoma and normal liver cells lines described previously^[22,23]. It suggested that the mechanism involved in abnormal processes in post-translation or signal transduction is worthy of discussing^[24].

MATERIALS AND METHODS

Cell culture

Hepatocellular carcinoma cell lines HHCC, SMMC-7721 and normal hepatocyte cell line QZG, were kindly provided by professor Chen in 863 Project Group in Fourth Military Medical University. The cells were cultured in RPMI 1640 medium (Gibco BRL, USA), supplemented with 10 mL/L fetal bovine serum (Gibco BRL, USA), incubated in a humidified atmosphere which contains 950 mL/L air and 5 mL/L CO₂ at 37 °C.

Scrape loading dye transfer (SLDT)

Functions of gap junctional intercellular communication (GJIC) in adjacent cells were assessed by scrape loading dye transfer (SLDT) with fluorescent dye Lucifer Yellow (LY, Sigma, USA). The cultures were rinsed three times with serum free RPMI 1640 medium, several scrapes were made on the monolayer using a surgical scalpel, cells were exposed to 100 g/L LY in 0.33 mol/L LiCl, incubated for 3 min, and rinsed by serum free RPMI 1640 medium for several times to remove any background fluorescence. The GJIC function in adjacent cells revealed by LY dye transfer could be detected under fluorescent microscope (Nikon UFX-II, Japan).

Concentration of intracellular calcium ($[Ca^{2+}]_i$) measured by laser scanning confocal microscopy (LSCM)

Digested by trypsin and collected, HHCC, SMMC-7721 and QZG cells were loaded by 100 nmol/L special fluorescent dye

indicator of calcium Fluo-3 AM (Sigma, USA) in serum free RPMI-1640 medium, 37 °C for 90 min, rinsed by Ca²⁺ free D-Hank's for three times. MRC-1024 laser scanning confocal microscope imaging system (Bio-Rad, USA) was used to obtain the images determining the location and intensity of intracellular Ca²⁺ in various cell lines.

MRC-1024 laser scanning confocal microscope imaging system consists of a laser scanning system intermediate optics and a detector controlled by lasership software (Bio-Rad, USA). Images were obtained by Zesis 100 microscope and images of interest were saved to a 512×512 pixel, Zoom was 4.0. Besides analysis of location of Ca²⁺, quantities of intracellular concentration [Ca²⁺]_i were counted with formation below: [Ca²⁺]_i=kd×(F-Fmin)/(Fmax-F), kd=400 nmol/L.

Immunoblot analysis of phosphorylation on tyrosine

Western blot was performed to analyses the phosphorylation on tyrosine. Cells were rinsed with cold 0.01 mol/L PBS containing 5 mmol/L EDTA, 10 mmol/L NaF and 1 mmol/L PMSF on ice for 20 min, harvested by scraping in the same solution, and centrifuged at 13 000 r/min at 4 °C for 30 min. Pellets were rinsed dissolved in 20 g/L SDS. Concentrations of proteins were measured by the Bio-Rad DC protein assay (Bio-Rad, USA).

20 ug protein of various cells in equal amounts of 2×SDS denatured at 100 °C for 4 min. 100 g/L SDS-PAGE vertical electrophoretically Min-PROTEAN II (Bio-Rad, USA) was used at 80V for 30 min and 120V for 60 min. Mini Trans-Blot transferred proteins form gel to NC membranes (Hybond, USA) by transferring electrophoretically (Bio-Rad, USA) at 100V 350 mA 4 °C for 2 h.

Normal serum blocked NC membranes at room temperature for 2 h. Cx32 and Cx43 protein bands were detected using a mouse monoclonal anti-Cx32 antibody (1:2 000, Zymed, USA), a mouse monoclonal anti-Cx43 antibody(1:2 000, Zymed, USA). Phosphorylations on tyrosine were detected by special anti- phosphorylation tyrosine mAb 4G10 (1:2 000, CA, USA) at room temperature for 2 h. NC membranes were washed by TBST for 10 min for several times, incubated with a biotin-streptavidin alkaline phosphatase conjugated secondary IgG (1:32, Johnson, USA) at room temperature for 2 h and washed by TBST for 10 min for several times again. The enhanced chemiluminescence (ECL) detection kit (Amersham, UK) was employed to detect immunoblot signal.

RESULTS

Gap junctional intercellular communication of various cells

After stained with special fluorescent dye Lucifer Yellow (LY), function of gap junctional intercellular communication were detected by scrape loading and dye transfer (SLDT). Molecular weight of LY is below 1 000 u that can pass via gap junction smoothly. Normal liver cell line QZG showed stronger intensity and amount yellow fluorescent among neighboring cells, whereas hepatocellular carcinoma cells HHCC and SMMC-7721 showed much slight fluorescent staining limited among adjacent cells.

Analysis of concentrations and location of intracellular Ca²⁺ ([Ca²⁺]_i) LSCM was used to determine intracellular Ca²⁺ in cultured cells after being loaded with special indicator of Ca²⁺ Fluo-3 AM. The results showed that intensity of Ca²⁺ was much higher with a very bright and higher peak signal of Ca²⁺ in QZG cells. Intracellular concentration of Ca²⁺ in QZG cells was 108.37 nmol/L. In HHCC and SMMC-7721 cells peak signals of Ca²⁺ were lower. [Ca²⁺]_i in HHCC cell decreased to 35.13 nmol/L, SMMC-7721 cells also had lower peak Ca²⁺ and its [Ca²⁺]_i decreased to 47.08 nmol/L as shown in Figure 1-3.

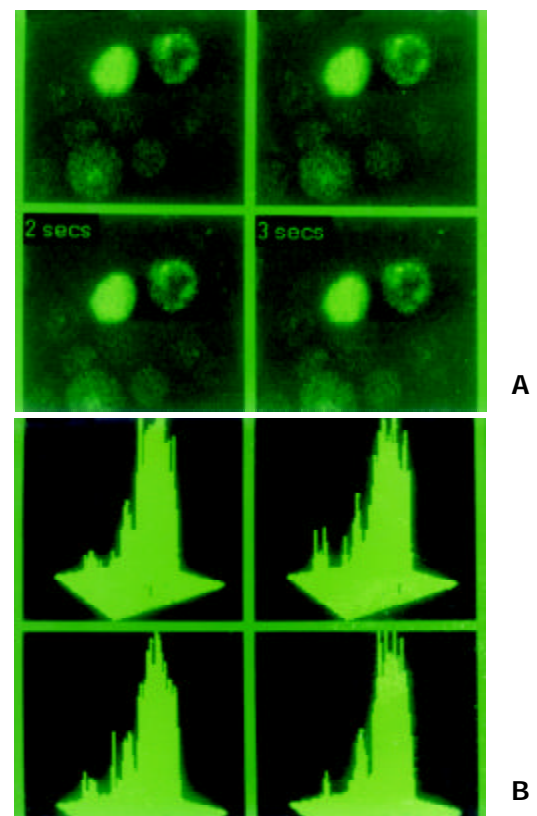


Figure 1 Special indicator Fluo-3 AM was loading at 37 °C for 90 min in hepatocarcinoma cell lines in order to examine localization and concentration of intracellular calcium in MRC-1024 laser scanning confocal microscope imaging system. (A). In normal hepatocyte cell line QZG, stronger signal of calcium with lower peak released. (B). Concentration of intracellular calcium in HHCC was 108.37 nmol/L.

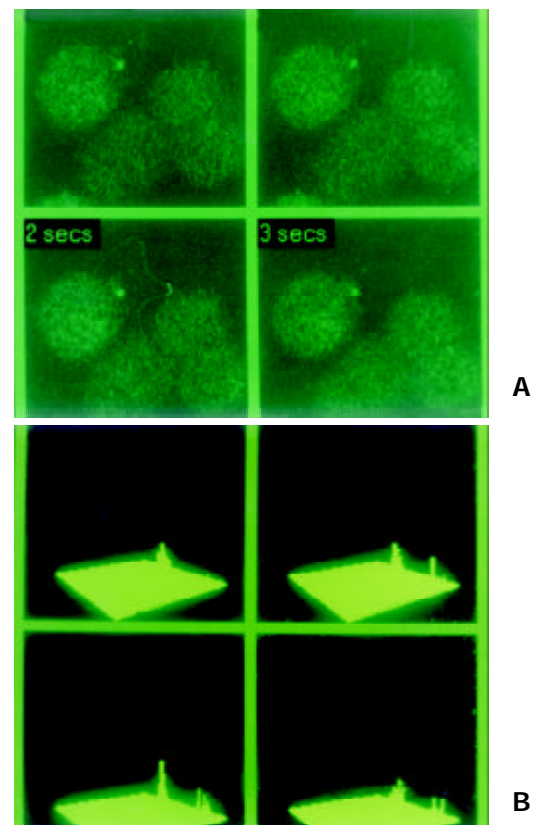


Figure 2 Special indicator Fluo-3 AM was loading at 37 °C for 90 min in hepatocarcinoma cell lines in order to examine local-

ization and concentration of intracellular calcium in MRC-1024 laser scanning confocal microscope imaging system. (A). In hepatocarcinoma cell line HHCC, slight signal of calcium with lower peak was observed. (B). Concentration of intracellular calcium in HHCC was 35.13 nmol/L.

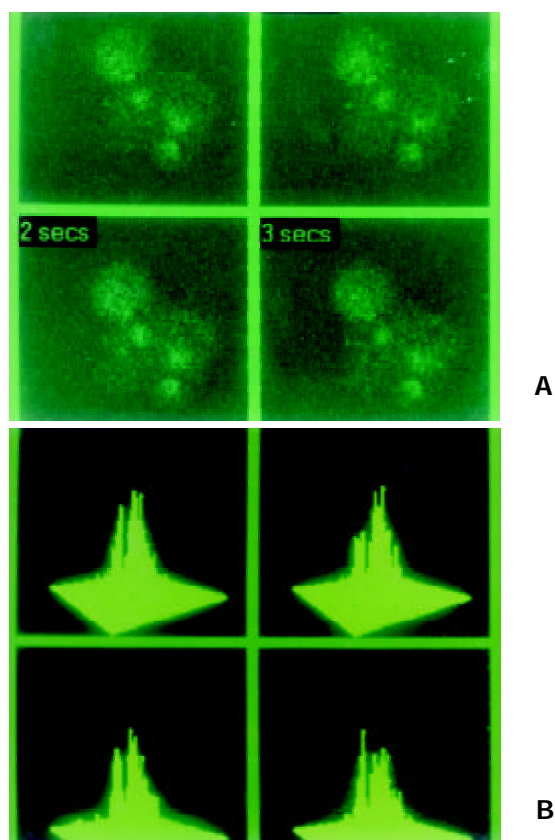


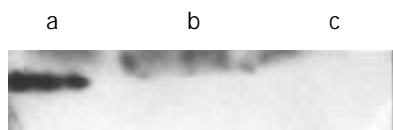
Figure 3 Special indicator Fluo-3 AM was loading at 37 °C for 90 min in hepatocarcinoma cell lines in order to examine localization and concentration of intracellular calcium in MRC-1024 laser scanning confocal microscope imaging system. (A). Loading by Fluo-3 AM, dark signal of calcium and lower peak was also absent in hepatocarcinoma cell line SMMC-7721. (B). Concentration of intracellular calcium was 47.08 nmol/L.

Phosphorylation on tyrosine of Cx32, Cx43 proteins

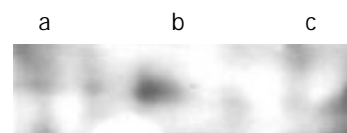
The expressions of Cx32, Cx43 proteins were assessed using western blot analysis with anti-Cx32 mAb, anti-Cx43 mAb. We also verified the phosphorylation on tyrosine using western blot analysis with anti-phosphorylated tyrosine mAb 4G10.

Western blot showed that major bands at 32 ku, 44 ku in a blot is unphosphorylated tyrosine in QZG cells. It recognized a band at 32 ku phosphorylated tyrosine Cx32 protein and phosphorylated tyrosine Cx43 protein of 43 ku in SMMC-7721 cells. No evidence of phosphorylated tyrosine at 32 ku of Cx32 and 44 ku of Cx43 proteins were detected in HHCC cells.

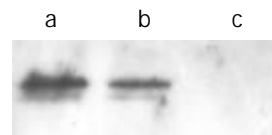
These results conform that the mouse monoclonal antibody selectively binds phosphorylated tyrosine Cx43 proteins was corresponding decrease of concentrations of calcium and block of gap junctional intercellular communication in same hepatocellular carcinoma cell lines as shown in Figure 4A-D.



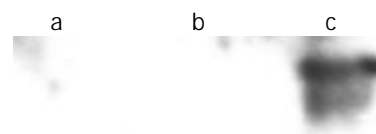
A. a. QZG, b. HHCC, c. SMMC-7721



B. a. QZG, b. HHCC, c. SMMC-7721



C. a. QZG, b. HHCC, c. SMMC-7721



D. a. QZG, b. HHCC, c. SMMC-7721

Figure 4 Western blot analysis of phosphorylation on tyrosine of Cx32, Cx43 proteins in various cell lines. Cells were harvested and lysed, equal amount of cell lysates were resolved of SDS-PAGE, transferred to NC membranes, and then probed with anti-phosphorylation tyrosine mAb 4G10. (A). Expressions of Cx32 proteins in cell lines with special anti-Cx32 mAb. Cx32 showed high immunoblot signal only in normal hepatocyte cell line QZG with very slight signal in hepatocarcinoma cell lines HHCC, SMMC-7721. (B). Expressions of Cx43 proteins in cell lines with special anti-Cx43 mAb. Cx43 appeared in both QZG and SMMC-7721 cells but no in HHCC. (C). Phosphorylation on tyrosine of Cx43 with special anti-phosphorylation tyrosine 4G10, unphosphorylation appeared in QZG cells even they showed high level expression of Cx32, Cx43. (D). Phosphorylated tyrosine of Cx43 protein was detected in SMMC-7721 cells.

DISCUSSION

Gap junctions are channels between neighboring cells, which allow small molecules, and ions (mass molecules are below 1 000 u) to pass through directly. Normal hepatocytes express high quantities of connexin32, connexin43 as the major gap junction forming proteins^[20,27]. As described previously, immunohistochemical analysis showed gap junctional proteins Cx32, Cx43 frequently decreased in hepatocellular carcinoma tissues and cell lines^[28-31]. But by in situ hybridization (ISH), cx32 mRNA, cx43 mRNA in hepatocellular carcinoma tissues and cell lines showed same strong positive rates and density without significant difference^[32,33]. The aberrant location of Cx32 and Cx43 proteins might be responsible for hepatocarcinogenesis^[34], the mechanism might be defect of cx genes in post-translational processing^[35].

In various neoplasm, including hepatocellular carcinoma cells often express less connexin, but the mechanisms are unknown. It suggested that decrease of expression and lacking of function of Cx32, Cx43 might keep close relationship with liver hepatocarcinogenesis. Disruption of GJIC activity could contribute to the multi-step, multi-mechanism process of carcinogenesis^[36]. Most tumors demonstrate a reduction between either homologous and heterologous gap junctional intercellular communication (GJIC). GJIC was assessed by transfer of the fluorescent dye Lucifer Yellow (LY) after scrape loading dye transfer (SLDT) in hepatocellular carcinoma cell lines HHCC, SMMC-7721 and normal liver cell line QZG. Molecular mass of LY is below 1 000 u, which can pass via gap

junction smoothly^[37]. Our results showed that QZG had high ability of GJIC function than that in HHCC and SMMC-7721 cell lines, which were almost blocked.

Presumably down-regulation of GJIC activity would lead to the removal of growth inhibitory signaling. It was hypothesized that an initiated cell would be growth suppressed by being coupled by gap junctions to surrounding normal cells. Disturbance of GJIC facilitate cells to escape from intercellular signals involved regulations on proliferation, differentiation and apoptosis. Many factors, tumor-promoting chemicals^[38] and oncogenes influence signal transduction in the initiated and surrounding normal cells, which would cause the down-regulation of GJIC. Many kinds of tumor promoting agents have been shown to decrease expressions of gap junction proteins or block GJIC associated with hepatocarcinogenesis^[39]. H-ras, v-myc also cooperate malignancy^[40]. Connexin genes might belong to the group of tumor suppressor genes.

Our results suggested that multiple mechanisms likely contributed to block of GJIC, including decrease of expressions of gap junction proteins and abnormal pathway of signal transduction including decreased level of intracellular Ca^{2+} , phosphorylation on tyrosine and other potential mechanisms. In different tissues molecules smaller than approximately 1 000 u may pass through gap junctions which implies that the most common second messengers cAMP, inositol-1,4,5-trisphosphate (IP₃) and intracellular free calcium ions Ca^{2+} can be transferred. The mechanisms of intracellular calcium signaling are currently being investigated. Mechanisms during hepatocarcinogenesis are related to multiple pathophysiological processes including decreased in intracellular Ca^{2+} . Calcium signals might be an important mechanism for controlling and synchronizing physiology. With intact gap junctional coupling, calcium in connected hepatocytes can communicate directly through gap junctions.

Whereas, gap junctional permeability and conductance affected by the calcium concentrations spikes in hepatocytes, a reduction of junctional conductance by calcium concentrations has been observed in hepatoma cells^[42,43]. In our study, after special indicator of calcium Fluo-3AM loading, LSCM was used to measure concentrations of intracellular calcium [Ca^{2+}]_i in hepatocellular carcinoma cell lines HHCC, SMMC-7721 and normal liver cell line QZG. Concentrations of intracellular calcium [Ca^{2+}]_i was much higher in QZG (108.37 nmol/L) cell line than that in HHCC (35.13 nmol/L) and SMMC-7721 (47.08 nmol/L) cell lines. QZG cells showed much higher calcium peaks than HHCC, SMMC-7721 cells which was associated with disruption of GJIC in these cell lines. Decreased level of intracellular Ca^{2+} contributed to conduction abnormalities of GJIC which immediate loss of calcium fluxes and influence the calcium dynamics in hepatocellular carcinoma cell lines.

Gap junctions are modulated by a multi-step molecular components and signaling pathway. Our observations also suggested that disruption of GJIC in hepatoma cells was associated with multiple distinct steps such as phosphorylation on tyrosine of Cx32, Cx43 proteins^[43]. Cx contains phosphorylations sites for several protein kinases including protein kinase C (PKC) and mitogen-activated protein kinase (MAPK) which are involved in Cx phosphorylation leading to the closure of GJIC^[44,45]. Disruption of GJIC requires Cx43 phosphorylation and interaction with other cellular factors. Phosphorylation of Cx proteins has been postulated to be a critical regulatory element for gap junctional communication^[46]. In our study, western blot suggested that only QZG cells had unphosphorylated tyrosine in Cx32 protein at 32ku and Cx43 protein at 43ku; SMMC-7721 cells had phosphorylated tyrosine Cx43 proteins. Change in the amount and distribution of phosphorylated and nonphosphorylated isoforms of Cx32 and

Cx43 were measured by immunoblot using isoform-specific antibodies anti-Cx32 mAb, anti-Cx43 mAb. Dramatic decreases in gap junctional communication and loss of phosphorylation on tyrosine^[47]. It indicated post-translation phosphorylation on tyrosine of Cx proteins, which associated with a dramatic disruption of GJIC^[48]. Functional recovery was associated with increased levels of unphosphorylated Cx43.

As above all, disruption of GJIC in hepatocellular carcinoma cells could also be achieved by multi-mechanisms. We could make conclusions that the establishment and permanent of functional gap junctions were regulated by transcriptions as well as post-translational controls including reduce of concentrations of intracellular calcium and phosphorylation on tyrosine of connexin proteins even the biological consequences of specific changes in Cx proteins phosphorylation are not understood in detail. The decrease of Cx proteins or the disorder of signal transduction of cx genes might keep close relationships with hepatocellular carcinoma.

REFERENCES

- 1 **Wang Y**, Liu H, Zhou Q, Li X. Analysis of point mutation in site 1896 of HBV procore and its detection in the tissues and serum of HCC patients. *World J Gastroenterol* 2000; **6**: 395-397
- 2 **Mei MH**, Xu J, Shi QF, Yang JH, Chen Q, Qin LL. Clinical significance of serum intercellular adhesion molecule detection in patients with hepatocellular carcinoma. *World J Gastroenterol* 2000; **6**: 408-410
- 3 **Qin Y**, Li B, Tan YS, Sun ZL, Zuo FQ, Sun ZF. Polymorphism of p16INK4a gene and rare mutation of p15INK4b gene exon2 in primary hepatocarcinoma. *World J Gastroenterol* 2000; **6**: 411-414
- 4 **Wang XZ**, Jiang XR, Chen XC, Chen ZX, Li D, Lin JY, Tao QM. Seek protein which can interact with hepatitis B virus X protein from human liver cDNA library by yeast two-hybrid system. *World J Gastroenterol* 2000; **8**: 95-98
- 5 **Yin ZZ**, Jin HL, Yin XZ, Li TZ, Quan JS, Jin ZN. Effect of boschniakia rossica on expression of GSTP, p53 and p21ras proteins in early stage of chemical hepatocarcinogenesis and its anti inflammatory activities in rats. *World J Gastroenterol* 2000; **6**: 812-818
- 6 **Lin GY**, Chen ZL, Lu CM, Li Y, Ping XJ, Huang R. Immunohistochemical study on p53, Hrasp21, cerbB2 protein and PCNA expression in HCC tissues of Han and minority ethnic patients. *World J Gastroenterol* 2000; **6**: 234-238
- 7 **Liu L**, Jiang Z, Teng GJ, Song JZ, Zhang DS, Guo QM, Fang W, He SC, Guo JH. Clinical and experimental study on regional administration of phosphorus 32 glass microspheres in treating hepatic carcinoma. *World J Gastroenterol* 1999; **5**: 492-505
- 8 **Liu LX**, Liu ZH, Jiang HC, Qu X, Zhang WH, Wu LF, Zhu AL, Wang XQ, Wu M. Profiling of differentially expressed genes in human gastric carcinoma by cDNA expression array. *World J Gastroenterol* 2002; **8**: 580-585
- 9 **Lin NF**, Tang J, Ismael HS. Study on environmental etiology of high incidence areas of liver cancer in China. *World J Gastroenterol* 2000; **6**: 572-576
- 10 **Tian DY**, Yang DF, Xia NS, Zhang ZG, Lei HB, Huang YC. The serological prevalence and risk factor analysis of hepatitis G virus infection in Hubei Province of China. *World J Gastroenterol* 2000; **6**: 585-587
- 11 **Zhong DR**, Ji XL. Hepatic angiomyolipoma misdiagnosis as hepatocellular carcinoma: A report of 14 cases. *World J Gastroenterol* 2000; **6**: 608-612
- 12 **Riordan SM**, Williams R. Transplantation of primary and reversibly immortalized human liver cells and other gene therapies in acute liver failure and decompensated chronic liver disease. *World J Gastroenterol* 2000; **6**: 636-642
- 13 **Li Y**, Su JJ, Qin LL, Yang C, Luo D, Ban KC, Kensler T, Roebuck B. Chemopreventive effect of oltipraz on AFB1 induced hepatocarcinogenesis in tree shrew model. *World J Gastroenterol* 2000; **6**: 647-650
- 14 **Xu HY**, Yang YL, Gao YY, Wu QL, Gao GQ. Effect of arsenic trioxide on human hepatoma cell line BEL7402 cultured *in vitro*. *World J Gastroenterol* 2000; **6**: 681-687

- 15 **Zang GQ**, Zhou XQ, Yu H, Xie Q, Zhao GM, Wang B, Guo Q, Xiang YQ, Liao D. Effect of hepatocyte apoptosis induced by TNF α on acute severe hepatitis in mouse models. *World J Gastroenterol* 2000; **6**: 688-692
- 16 **Huang XF**, Wang CM, Dai XW, Li ZJ, Pan BR, Yu LB, Qian B, Fang L. Expressions of chromogranin A and cathepsin D in human primary hepatocellular carcinoma. *World J Gastroenterol* 2000; **6**: 693-698
- 17 **Xu HY**, Yang YL, Guan XL, Song G, Jiang AM, Shi LJ. Expression of regulating apoptosis gene and apoptosis index in primary liver cancer. *World J Gastroenterol* 2000; **6**: 721-724
- 18 **Chen YP**, Liang WF, Zhang L, He HT, Luo KX. Transfusion transmitted virus infection in general populations and patients with various liver diseases in south China. *World J Gastroenterol* 2000; **6**: 738-741
- 19 **Falk MM**. Biosynthesis and structural composition of gap junction intercellular membrane channels. *Eur J Cell Biol* 2000; **79**: 564-574
- 20 **Kumar NM**, Gilula NB. The gap junction communication channel. *Cell* 1996; **84**: 381-389
- 21 **Windoffer R**, Beile B, Leibold A, Thomas S, Wilhelm U, Leube RE. Visualization of gap junction mobility in living cells. *Cell Tissue Res* 2000; **299**: 347-362
- 22 **Verselis VK**, Trexler EB, Bukauskas FF. Connexin hemichannels and cell-cell channels: comparison of properties. *Braz J Med Biol Res* 2000; **33**: 379-389
- 23 **Yamasaki H**, Naus CC. Role of connexin genes in growth control. *Carcinogenesis* 1996; **17**: 1199-1213
- 24 **Yamasaki H**, Krutovskikh V, Mesnil M, Tanaka T, Zaidan-Dagli ML, Omori Y. Role of connexin (gap junction) genes in cell growth control and carcinogenesis. *C R Acad Sci III* 1999; **322**: 151-159
- 25 **Krutovskikh V**, Yamasaki H. The role of gap junctional intercellular communication (GJIC) disorders in experimental and human carcinogenesis. *Histol Histopatol* 1997; **12**: 761-768
- 26 **Iwai M**, Harada Y, Muramatsu A, Tanaka S, Mori T, Okanou T, Katoh F, Ohkusa T, Kashima K. Development of gap junctional channels and intercellular communication in rat liver during ontogenesis. *J Hepatol* 2000; **32**: 11-18
- 27 **Steinberg TH**. Gap junction function: the messenger and the message. *Am J Pathol* 1998; **152**: 851-854
- 28 **Ma XD**, Sui YF, Wang WL. Expression of gap junction proteins Cx32, Cx43 in human hepatocarcinoma cell lines and normal liver cell line: Study with laser scanning confocal microscope. *Zhongguo Aizheng Zazhi* 2000; **10**: 1-2
- 29 **Ma XD**, Sui YF, Wang WL, Xiu LQ. A flow cytometric study of gap junction cx32, cx43 in human hepatocellular carcinoma cell lines. *Fenzi Yu Xibao Mianyixue Zazhi* 1999; **15**: 51-54
- 30 **Ma XD**, Sui YF, Wang WL. The expression of gap junction protein connexin32 in human hepatocellular carcinoma, cirrhotic and viral hepatitis liver tissues. *Zhongguo Aizheng Zazhi* 1999; **18**: 133-135
- 31 **Ma XD**, Sui YF, Wang WL. Expression of gap junction genes connexin32, connexin43 and their proteins in human hepatocellular carcinoma cell lines and normal liver cell line. *Shiyong Aizheng Zazhi* 1999; **14**: 161-163
- 32 **Ma XD**, Sui YF, Wang WL. Expression of gap junction genes connexin 32, connexin 43 and their proteins in hepatocellular carcinoma and normal liver tissues. *World J Gastroenterol* 2000; **6**: 66-69
- 33 **Ma XD**, Ma X, Sui YF, Wang WL. Expression of gap junction genes connexin 32 and connexin 43 mRNAs and proteins, and their role in hepatocarcinogenesis. *World J Gastroenterol* 2002; **8**: 64-68
- 34 **Neveu MJ**, Hully JR, Babcock KL, Hertzberg EL, Paul DL, Pitot HC. Multiple mechanisms are responsible for altered expression of gap junction genes during oncogenesis in rat liver. *J Cell Sci* 1994; **107**: 83-95
- 35 **Piechocki MP**, Burk RD, Ruch RJ. Regulation of connexin32 and connexin43 gene expression by DNA methylation in rat liver cells. *Carcinogenesis* 1999; **20**: 401-406
- 36 **Niessen H**, Willecke K. Strongly decreased gap junctional permeability to inositol 1,4,5-trisphosphate in connexin32 deficient hepatocytes. *FEBS Lett* 2000; **466**: 112-114
- 37 **Juul MH**, Rivedal E, Stokke T, Sanner T. Quantitative determination of gap junction intercellular communication using flow cytometric measurement of fluorescent dye transfer. *Cell Adhes Commun* 2000; **7**: 501-512
- 38 **Ren P**, Ruch RJ. Inhibition of gap junctional intercellular communication by barbiturates in long-term primary cultured rat hepatocytes is correlated with liver tumor promoting activity. *Carcinogenesis* 1996; **17**: 2119-2124
- 39 **Moennikes O**, Buchmann A, Romualdi A, Ott T, Werringloer J, Willecke K, Schwarz M. Lack of phenobarbital-mediated promotion of hepatocarcinogenesis in connexin 32-null mice. *Cancer Res* 2000; **60**: 5087-5091
- 40 **DeoCampo ND**, Wilson MR, Trosko JE. Cooperation of bcl-2 and myc in the neoplastic transformation of normal rat liver epithelial cells is related to the down-regulation of gap junction-mediated intercellular communication. *Carcinogenesis* 2000; **21**: 1501-1506
- 41 **Rottingen JA**, Camerer E, Methiesen I, Prydz H, Iversen JG. Synchronized Ca²⁺ oscillations induced in Madin Darby canine kidney cells by bradykinin and thrombin but not by ATP. *Cell Calcium* 1997; **21**: 195-211
- 42 **Peracchia C**, Wang XG, Peracchia LL. Slow gating of gap junctions channels and calmodulin. *J Membr Biol* 2000; **178**: 55-70
- 43 **Matesic DF**, Rupp HL, Bonney WJ, Ruch RJ, Trosko JE. Changes in gap-junction permeability, phosphorylation, and number mediated by phorbol-ester and nonphorbol-ester tumor promoters in rat liver epithelial cells. *Mol Carcinogenesis* 1994; **10**: 226-236
- 44 **Elcock FJ**, Deag E, Roberts RA, Chipman JK. Nafenopin cause protein kinase C mediated serine phosphorylation and loss of function of connexin32 protein in rat hepatocytes with aberrant expression or localization. *Toxicol Sci* 2000; **56**: 86-94
- 45 **Hossain MZ**, Jagdale AB, Ao P, Boynton AL. Mitogen-activated protein kinase and phosphorylation of connexin43 are not sufficient for the disruption of gap junctional communication by platelet-derived growth factor and tetradecanoylphorbol acetate. *J Cell Physiol* 1999; **179**: 87-96
- 46 **Kwak BR**, Hermans MM, De Jonge HR, Lchmann SM, Chanson M. Differential regulation of distinct types of gap junction channels by similar phosphorylating conditions. *Mol Biol Cell* 1995; **6**: 1707-1719
- 47 **Omori Y**, Krutovskikh V, Mironov N, Tsuda H, Yamasaki H. Cx32 gene mutation in a chemically induced rat liver tumor. *Carcinogenesis* 1996; **17**: 2077-2080
- 48 **Hossain MZ**, Ao P, Boynton AL. Rapid disruption of gap junctional communication and phosphorylation of connexin 43 by platelet-derived growth factor in T518B rat liver epithelial cells expressing platelet-derived growth factor receptor. *J Cell Physiol* 1998; **174**: 66-77

Continuous release of interleukin 12 from microencapsulated engineered cells for colon cancer therapy

Shu Zheng, Zuo-Xiang Xiao, Yue-Long Pan, Ming-Yong Han, Qi Dong

Shu Zheng, Zuo-Xiang Xiao, Yue-Long Pan, Ming-Yong Han, Qi Dong, Cancer Institute, Zhejiang University, Hangzhou 310009, Zhejiang Province, China

Supported by National Natural Science Foundation of China, No. 40621130

Correspondence to: Dr. Shu Zheng, Cancer Institute, Zhejiang University, 88 Jiefang Road, Hangzhou 310009, Zhejiang Province, China. zhengshu@zju.edu.cn

Telephone: +86-571-87784501 **Fax:** +86-571-87214404

Received: 2002-12-10 **Accepted:** 2003-01-16

Abstract

AIM: To explore the anti-tumor immunity against CT26 colon tumor of the microencapsulated cells modified with murine interleukine-12 (mIL-12) gene.

METHODS: Mouse fibroblasts (NIH3T3) were stably transfected to express mIL-12 using expression plasmids carrying mIL-12 gene (p35 and p40), and NIH3T3-mIL-12 cells were encapsulated in alginate microcapsules for long-term delivery of mIL-12. mIL-12 released from the microencapsulated NIH3T3-mIL-12 cells was confirmed using ELISA assay. Transplantation of the microencapsulated NIH3T3-mIL-12 cells was performed in the tumor-bearing mice with CT26 cells. The anti-tumor responses and the anti-tumor activities of the microencapsulated NIH3T3-mIL-12 cells were evaluated.

RESULTS: Microencapsulated NIH3T3-mIL-12 cells could release mIL-12 continuously and stably for a long time. After the microencapsulated NIH3T3-mIL-12 cells were transplanted subcutaneously into the tumor-bearing mice for 21 d, the serum concentrations of mIL-12, mIL-2 and mIFN- γ , the cytotoxicity of the CTL from the splenocytes and the NK activity in the treatment group were significantly higher than those in the controls. Moreover, mIL-12 released from the microencapsulated NIH3T3-mIL-12 cells resulted in a significant inhibition of tumor proliferation and a prolonged survival of tumor-bearing mice.

CONCLUSION: The microencapsulated NIH3T3-mIL-12 cells have a significant therapeutic effect on the experimental colon tumor by activating anti-tumor immune responses *in vivo*. Microencapsulated and genetically engineered cells may be an extremely versatile tool for tumor gene therapy.

Zheng S, Xiao ZX, Pan YL, Han MY, Dong Q. Continuous release of interleukin 12 from microencapsulated engineered cells for colon cancer therapy. *World J Gastroenterol* 2003; 9(5): 951-955
<http://www.wjgnet.com/1007-9327/9/951.htm>

INTRODUCTION

Alginate microcapsules have been used extensively for different applications, particularly for the encapsulation of pancreatic islet cells and insulin delivery^[1]. This method has

also been used for the encapsulation of cells that release growth hormone, β -endorphin, endostatin and other agents for gene therapy^[2-5]. The alginate membranes allow the free exchange of nutrients and oxygen between the implanted cells, and could prevent the escape and elimination of encapsulated cells. More important, this approach provides a prolonged sustained delivery of recombinant protein produced by the cells, thus maintaining high levels of the agent.

In recent years, interleukine-12 (IL-12) has received considerable interest in cancer biologic therapy. *In vivo* IL-12 was found to have a potent antitumor efficacy in a variety of murine tumor models^[6,7]. Local or systemic treatment with recombinant IL-12 protein (rIL-12) was shown to inhibit the growth of established subcutaneous tumor and tumor metastasis^[8-10]. However, systemic administration of rIL-12 caused severe dose-dependent toxicity and led to an interruption of the first human trial^[11]. In contrast, the local transfer of cytokine genes as a means for gene therapy could circumvent such systemic toxicity and provide effective and persistent local cytokine levels for immune cells activation^[12-15]. Some studies using an *ex vivo* IL-12 gene therapy yielded encouraging results, showing that murine fibroblasts or tumor cells transduced *in vitro* with IL-12 cDNA, using a retroviral vector, were able to induce antitumor immune responses in the absence of apparent toxicities^[16]. This strategy, however, has many obstacles precluding successful clinical application: e.g. autologous somatic cells or tumor cells are difficult to culture and transfect, and selection for transfected cells requires prolonged culture and the attendant costs of these process are expensive. To avoid these potential disadvantages, an alternative approach to obtain prolonged local cytokine secretion is adopted to use microencapsulated engineered cells to secrete IL-12.

In the present study, NIH3T3 cells engineered to continuously secrete high levels of mIL-12 were encapsulated with alginate. The ability of this system to secrete biologically active mIL-12 capable of inhibiting the tumor growth of a murine colon carcinoma xenograft in the mouse was investigated.

MATERIALS AND METHODS

Mice and cell lines

Male BALB/C mice aged between 6 and 8 weeks were purchased from Joint Ventures Sipper BK Experimental Animal Company (Shanghai, China) and housed in a specific pathogen-free condition for all experiments. Mouse fibroblasts (NIH3T3) and the murine colon adenocarcinoma cell line (CT26) were donated by the Institute of Immunology, Zhejiang University (Hangzhou, China). Cells were cultured in RPMI-1640 medium (GIBCO-BRL, Gaithersburg, MD, USA) supplemented with 10 % heat-inactivated fetal calf serum (FCS; HyClon, Logan, UT, USA), 2 mM glutamine, penicillin 100 U/ml, and streptomycin 100 μ g/ml.

Expression plasmids and transfection of NIH3T3 cells

Murine p35 and p40 subunits of mIL-12 were subcloned into pcDNA3.1 plasmids containing a cytomegalovirus (CMV) immediate-early enhancer promoter and a G418 selected gene.

NIH3T3 cells were stably transfected with these expression plasmids using LF2000™ (Ivotrogen, Life Technologies, USA). To obtain stably transfected clones (NIH3T3-mIL-12), transfected cells were grown in G418 containing medium (400 g/L, Ivotrogen, Life Technologies, USA) for 14 days, and resistant clones were propagated separately. With subsequent determination of mIL-12 expression by ELISA kit (R&D systems, Inc., USA).

Microencapsulation of NIH3T3-mIL-12

NIH3T3-mIL-12 cells were encapsulated within microspheres composed of Ba²⁺-alginate. Briefly, cells were resuspended in sodium alginate-saline (1.5 % wt/vol, purified by Syringe Driven Filter Unit) (Sigma, St Louis, MO, USA) to a final ratio of 0.5×10⁹ cells/L of alginate. The suspension was sprayed through an air jet-head droplet-forming apparatus, into a solution of 4.9 % Barium chloride (pH 7.4, Sigma), where they were allowed to gel for 10 min, washed three times with PBS, then cultured in the conditioned medium described above. The number of cells encapsulated and the viability of the cells in the microcapsules were evaluated weekly using a modified MTT assay.

In vitro release of mIL-12 from encapsulated NIH3T3-mIL-12 cells

Microencapsulated NIH3T3-mIL-12 cells were suspended in the conditioned medium described above at a density of 2×10⁵ cells/well. The medium was collected every 2 hrs. and assayed for mIL-12 using ELISA assay (Endogen, Woburn, MA, USA). Medium from NIH3T3-mIL-12 monolayer cells was used as a positive control.

Murine studies

The BALB/C mice were inoculated subcutaneously in the right-behind armpit with CT26 cells (2×10⁵ tumor cells/injection). Mice were randomly divided into four groups of twenty each. Group 1 received a single subcutaneous injection of microcapsules containing NIH3T3-mIL-12 cells within 0.5 cm apart from the area where CT26 cells were inoculated (1×10⁵ encapsulated cells/animal); Group 2 RPMI-1640 (control), Group 3 microcapsules containing NIH3T3 (1×10⁵ cells), and Group 4 RPMI injected at the same region of mice. The length and width of the tumor mass were measured with calipers every other day after tumor inoculation. Tumor size was expressed as 1/2 (length + width). Twenty-one days after tumor inoculation, ten mice taken randomly from each group were sacrificed, and spleen was resected, and blood was collected from the mice eyeballs. The rest ten mice in each group were observed for their survival period until 60 days after injection.

Cytotoxic assay of CTL and NK cells

Spleen cells derived from each group of experimental mice were unstimulated or were stimulated with irradiated CT26 cells (1×10⁵) for 7 days *in vitro* and processed for the NK or cytotoxic T lymphocyte (CTL) assay, respectively. The NK activity and CTL activity were determined by lactate dehydrogenase (LDH) release assay with Non-Radioactive Cytotoxicity Assay kit (Promega, Madison, WI, USA). The target cells (YAC-1 cells for the NK assay, and CT26 cells for the CTL assay) were washed three times with RPMI 1640 medium containing 50 ml·L⁻¹ FCS to remove adherent LDH derived from lysed cells. The cell suspension was diluted with RPMI 1640 medium containing 50 ml·L⁻¹ FCS to give a final concentration of 1×10⁸ cells/L; and 100 μl target cell suspension and 100 μl different ratios of effector cells were pipetted together into the wells of a round-bottomed microtiter plate. Suspensions containing exclusively effector cells, target cells,

or culture medium, respectively, served as controls to estimate the LDH background. The plates were incubated for 4 hrs in a humidified 50 ml·L⁻¹ CO₂ atmosphere at 37 °C. After incubation, they were centrifuged for 10 min. Then 100 μl of the supernatant from each well was transferred to the corresponding well of enzymatic assay plate. Fifty μl reconstituted substrate mix (containing lactate and NAD⁺) was added to each well. The plate was covered and incubated at room temperature (protected from light). Thirty minutes later, 50 μl stop solution was added to each well. The reaction was measured in an ELISA reader at a wavelength of 490 nm. Calculations were carried out according to the following formula: percent specific lysis=100×(mean experimental cpm - mean spontaneous cpm)/(mean maximum cpm - mean spontaneous cpm).

Determination of serum cytokine production

Blood samples were collected from the mice 21 days after tumor inoculation. Stored serum were separated from the whole blood and frozen at -70 °C until analyzed for cytokine production. mIL-2, mIL-12, mIL-4, mIL-10 and mIFN-γ were measured using a standard sandwich ELISA technique with corresponding kits purchased from Endogen (Woburn, MA, USA).

Statistical analysis

Data were expressed as mean ±SD. Statistical analysis was performed using the *t* test and log-rank test (for survival analysis). The difference was considered statistically significant when the *P* value was less than 0.05. The SPSS software package version 10.0 was used for statistical calculation.

RESULTS

In vitro expression and release of mIL-12 from encapsulated cells

NIH3T3 cells were transfected with a mIL-12 expression vector and clonal populations of stably transfected NIH3T3 cells were obtained (NIH3T3-mIL-12). The microcapsules have an average diameter of 0.45 mm±0.05 mm (Figure 1). Both encapsulated and nonencapsulated NIH3T3-mIL-12 cells were cultured *in vitro*, and the conditioned medium was collected every week for six weeks. The encapsulated cells were viable in culture as determined by MTT assay. ELISA method was used to determine mIL-12 in the medium collected at all time points. The average concentration of mIL-12 secreted by 2×10⁵ cultured encapsulated NIH3T3-mIL-12 cells or nonencapsulated NIH3T3-mIL-12 cells were 5.12 μg·L⁻¹ and 5.45 μg·L⁻¹ for every 24hrs, and the optimal expression up to 46.8 and 48.2 ng of mIL-12 per 24 hrs per 10⁵ cells, respectively. These results indicate that mIL-12 protein could release freely from the microencapsulated NIH3T3-mIL-12 cells.

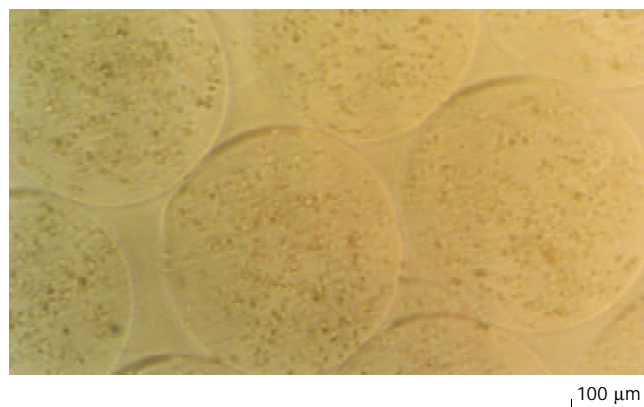


Figure 1 NIH3T3-mIL-12 cells-loaded microcapsules (average capsule diameter 450 μm).

Increased NK activity after delivery of microencapsulated NIH3T3-mIL-12 cells

Twenty-one days after treatment of tumor-bearing mice with various injections, the splenocytes were used in cytolytic assay against YAC-1 cells at effector:target (E:T) ratios at 20:1, 40:1, 80:1. As shown in Figure 2, NK activity in mice treated with NIH3T3-mIL-12 cells capsule increased significantly when compared with the mice treated with NIH3T3-mIL-12 cells, NIH3T3 cells capsule or RPMI-1640 ($P<0.01$). These data suggested that nonspecific immunity was enhanced significantly by the local delivery of IL-12 with NIH3T3-mIL-12 cells capsule.

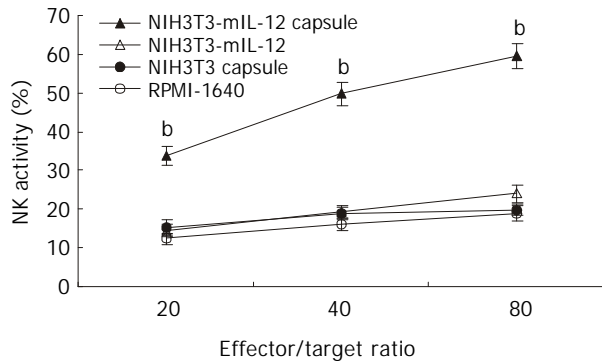


Figure 2 NK activity induced by various treatment. $\bar{x}\pm s$, $n=10$, ^b $P<0.01$ for the group treated with NIH3T3-mIL-12 cells capsule versus other three counterpart groups, respectively.

Potent CTL activity induced by delivery of microencapsulated NIH3T3-mIL-12 cells

The splenocytes collected from various groups were restimulated *in vitro* with inactivated CT26 tumor cells for CTL induction. As shown in Figure 3, the mice treated with NIH3T3-mIL-12 cells capsule exhibited a CT26 colon carcinoma-specific CTL response that was higher than that of mice treated with NIH3T3-mIL-12 cells, NIH3T3 cells capsule or RPMI-1640 ($P<0.01$). It suggested that CTL activity against tumor was induced significantly by the local delivery of IL-12 with NIH3T3-mIL-12 cells capsule.

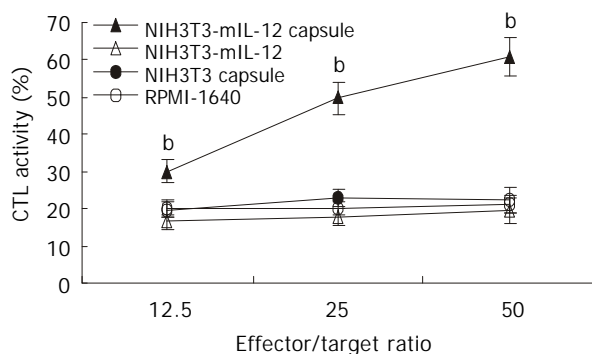


Figure 3 CTL activity against CT26 induced by various treatment. $\bar{x}\pm s$, $n=10$, ^b $P<0.01$ for the group treated with NIH3T3-mIL-12 cells capsule versus other three counterpart groups, respectively.

Serum cytokine production

Twenty-one days after the microencapsulated NIH3T3-mIL-12 cells were injected into the tumor-bearing mice, blood was collected for analysis of serum mIL-12, mIL-2, mIFN- γ and mIL-4, mIL-10. The serum average concentrations of mIL-12, mIL-2 and mIFN- γ in the group treated with

microencapsulated NIH3T3-mIL-12 cells were 542 ± 48 , 176 ± 25 and 982 ± 12 ng \cdot L⁻¹, respectively, which were significantly higher as compared with the counterpart control groups ($P<0.01$), but the serum concentrations of mIL-4 and mIL-10 were lowered significantly compared to the controls ($P<0.01$). The results of the studies are shown in Figure 4.

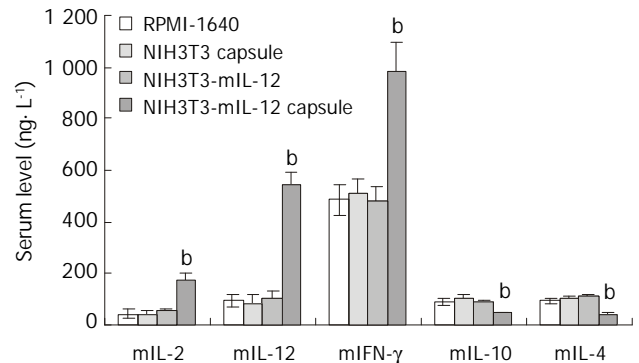


Figure 4 Cytokines levels in serum after various treatment in the tumor-bearing model. $\bar{x}\pm s$, $n=10$, ^b $P<0.01$ for the group treated with NIH3T3-mIL-12 cells capsule versus other three counterpart groups, respectively.

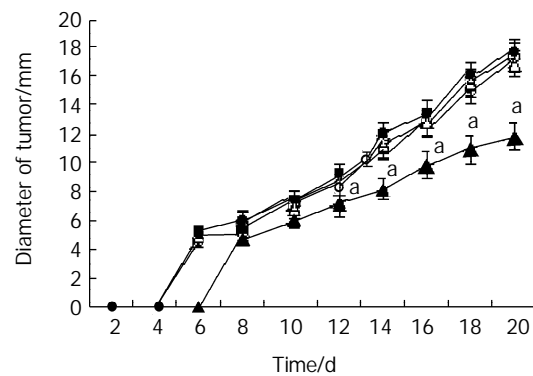


Figure 5 Inhibition of tumor growth by microencapsulated NIH3T3-mIL-12. Two days after tumor inoculation, mice were injected sc with NIH3T3-mIL-12 cells capsule (▲), NIH3T3-mIL-12 cells (△), NIH3T3 cells capsule (●) or RPMI-1640 (○). $\bar{x}\pm s$, $n=20$, ^a $P<0.05$ for the group treated with NIH3T3-mIL-12 cells capsule versus other three counterpart groups respectively.

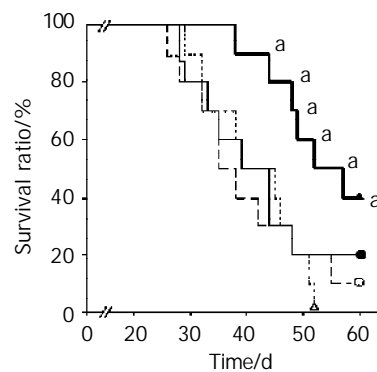


Figure 6 Survival time after various treatment in the tumor-bearing model. Two days after tumor inoculation, mice were injected sc with RPMI-1640 (○), NIH3T3 cells capsule (●), NIH3T3-mIL-12 cells (△) and NIH3T3-mIL-12 cells capsule (▲), respectively. Ten tumor-bearing mice ($n=10$) in each group were observed for their survival time. All surviving mice were monitored for at least 60 d. ^a $P<0.05$, compared with other three counterpart groups, respectively.

Effects of encapsulated NIH3T3-mIL-12 cells on subcutaneous tumor xenografts

The subcutaneous tumor size was calculated as follows: tumor size = (maximum diameter + vertical diameter)/2. The growth of tumor xenografts was significantly inhibited by a single dose of microcapsules containing NIH3T3-mIL-12 cells when compared with both control groups ($P < 0.05$) (Figure 5).

Survival time after delivery of microencapsulated NIH3T3-mIL-12 cells in the tumor-bearing model

When treated mice were observed up to 60 days after implantation of CT26 tumor, the mice survival time of the group treated with microencapsulated NIH3T3-mIL-12 cells was longer than other counterpart control groups ($P < 0.05$) (Figure 6).

DISCUSSION

Encapsulation of living cells in a protective, biocompatible, and semipermeable polymeric membrane has been proven to be an effective method for immunoprotection of desired cells, regardless of the type recipient involved (allograft, xenograft)^[17]. Alginate microcapsules have been applied for various purposes, and the molecular cutoff of alginate microcapsule membrane was 75 kDa^[18], so the IL-12 protein (a molecular weight of 70 kDa) could pass through the membrane. In the present study, we observed that mIL-12 protein could release freely from the microencapsulated NIH3T3-mIL-12 cells. Twenty-one days after the microencapsulated NIH3T3-mIL-12 cells were transplanted subcutaneously into the tumor-bearing mice, both the NK and CTL activities were significantly enhanced, and the mice serum average concentrations of mIL-12, mIL-2 and mIFN- γ were upregulated, but the mIL-4 and mIL-10 were downregulated in the treated group as compared with those of other control groups. In tumor bearing mice, Th1 cytokine production (IL-2, IFN- γ) is suppressed and Th2 cytokine production (IL-4, IL-10) was increased, as compared with those of normal mice. The administration of microencapsulated NIH3T3-mIL-12 cells to tumor bearing mice transferred the balance of Th1/Th2 cell responses from Th2 dominant state to the Th1 dominant state. These findings are consistent with the results of previous studies showing that production of IFN- γ , NK cell activation, CTL differentiation, and Th1 differentiation were the main mechanisms of antitumor activity of IL-12^[19].

The present study developed an alternative approach for local long-term delivery of mIL-12 by a single administration of alginate microcapsules containing cells secreting mIL-12. Using this system, the microencapsulated engineered cells could supply the appropriate doses of effective mIL-12 protein in a paracrine fashion to induce potent anti-tumor immune response and constituted an efficacious therapy in mouse colon models. This system differs from other cytokine gene therapy models, which utilize engineered autologous somatic cells^[20,21], tumor cells^[22-24] or intratumoral injection of adenovirus expressing cytokine^[25,26]. Considering the difficulties of prolonged culture and transduction of human autologous somatic cells or primary tumor cells for each patient, and in contrast, the ready availability of microencapsulated cells, the use of microencapsulated engineered cells for prolonged cytokine administration is an attractive alternate method for clinical application of gene therapy. With respect to the finding that local secretion of IL-12 at the site of tumor might induce an immune response against poorly immunogenic tumor without severe toxicities that were often observed with systemic administration, this system has significant advantages for initiating studies of the prolonged delivery effect of IL-12 with

microencapsulated engineered cells on tumor growth.

The transplantation of the microencapsulated NIH3T3-mIL-12 cells could lead to prolonged, homogeneous expression of mIL-12 and continuous stimulation of TILs, with tumor-specific immunity ultimately being established. Such immunity is advantageous because it could result in continued destruction of tumor cells even after expression of mIL-12 had declined^[27]. Moreover, no side effects of IL-12 were noticed in treated mice, which is in contrast to the results of trials using recombinant IL-12 protein, where severe toxicity (e.g. fur ruffling or lethargy) was often observed with systemic administration. This is probably because mIL-12 mainly restricted to the vicinity of tumors, a prolonged appropriate blood concentration of cytokines could stimulate an antitumor immune response without causing excessive systemic inflammatory and immunoreaction^[28]. Thus this approach should be a better-tolerated and safer strategy than systemic administration of recombinant IL-12 protein. In this study, by treatment of a single dose of microcapsules containing NIH3T3-mIL-12 cells, the growth of tumor xenografts was significantly inhibited and the mice survival time was significantly prolonged. This result also showed that the approach for local and sustained release of interleukin 12 could induce both innate and adaptive antitumor immune responses resulting in significant growth suppression and metastases of tumor^[29-31].

It should also be emphasized that controlling the amount of encapsulated cells makes an appropriate concentration of IL-12 obtainable. Preliminary *in vitro* test for IL-12 expression revealed that the microencapsulated NIH3T3-mIL-12 cells secreted up to 468 ng of mIL-12 per 24hrs per 10^6 cells. This result indicates that using an optimized amount of encapsulated cells may lead to more powerful antitumor effects and less side effects. Furthermore, using this approach, the antitumor effects of IL-12 may be augmented by combination with other therapeutic genes (e.g., genes encoding other cytokines and apoptotic genes), which is probably necessary in destruction and prevention of recurrence of not only primary tumors, but also metastases^[32].

Colorectal carcinomas are generally not very sensitive to the established chemotherapeutic agents and most patients with colorectal carcinoma will die from distant metastases that are not detectable at the initiation of treatment, the alternative antitumor therapy approaches, such as biotherapy, are necessary for the patients suffering from colorectal cancer^[33-35]. This study show that microencapsulated engineered cells could supply appropriate doses of effective mIL-12 protein locally to induce potent anti-tumor immune response and constitute an efficacious therapy in mouse colon models. Investigation of optimal combinations of genes used with encapsulated cells has the potential to contribute to a successful anticancer gene therapy for colon cancer.

ACKNOWLEDGEMENTS

We could like to thank Professor LH Zhang and Dr. HP Yao for their encouragement and Mr. M Zhu for technical assistance.

REFERENCES

- 1 **Soon-Shiong P**, Heintz RE, Merideth N, Yao QX, Zheng T, Murphy MK, Schmehl M. Insulin independence in a type 1 diabetic patient after encapsulated islets transplantation. *Lancet* 1994; **343**: 950-951
- 2 **Ross CJ**, Ralph M, Chang PL. Delivery of recombinant gene products to the central nervous system with nonautologous cells in alginate microcapsules. *Hum Gene Ther* 1999; **10**: 49-59
- 3 **Stockley TL**, Robinson KE, Delaney K, Ofosu FA, Chang PL. Delivery of recombinant product from subcutaneous implants of encapsulated recombinant cells in canines. *J Lab Clin Med* 2000;

- 135: 484-492
- 4 **Machluf M**, Orsola A, Atala A. Controlled release of therapeutic agents: slow delivery and cell encapsulation. *World J Urol* 2000; **18**: 80-83
 - 5 **Joki T**, Machluf M, Atala A, Zhu J, Seyfried NT, Dunn IF, Abe T, Carroll RS, Black PM. Continuous release of endostatin from microencapsulated engineered cells for tumor therapy. *Nat Biotechnol* 2001; **19**: 35-39
 - 6 **Rakhmievich AL**, Turner J, Ford MJ, McCabe D, Sun WH, Sondel PM, Grota K, Yang NS. Gene gun-mediated skin transfection with interleukin 12 gene results in regression of established primary and metastatic murine tumors. *Proc Natl Acad Sci USA* 1996; **93**: 6291-6296
 - 7 **Kodama T**, Takeda K, Shimozato O, Hayakawa Y, Atsuta M, Kobayashi K, Ito M, Yagita H, Okumura K. Perforin-dependent NK cell cytotoxicity is sufficient for anti-metastatic effect of IL-12. *Eur J Immunol* 1999; **29**: 1390-1396
 - 8 **Mu J**, Zou JP, Yamamoto N, Tsutsui T, Tai XG, Kobayashi M, Herrmann S, Fujiwara H, Hamaoka T. Administration of recombinant interleukin 12 prevents outgrowth of tumor cells metastasizing spontaneously to lung and lymph nodes. *Cancer Res* 1995; **55**: 4404-4408
 - 9 **Takeda K**, Seki S, Ogasawara K, Anzai R, Hashimoto W, Sugiura K, Takahashi M, Satoh M, Kumagai K. Liver NK1.1+CD4+ alpha beta T cells activated by IL-12 as a major effector in inhibition of experimental tumor metastasis. *J Immunol* 1996; **156**: 3366-3373
 - 10 **Cavallo F**, Di Carlo E, Butera M, Verrua R, Colombo MP, Musiani P, Forni G. Immune events associated with the cure of established tumors and spontaneous metastases by local and systemic interleukin 12. *Cancer Res* 1999; **59**: 414-421
 - 11 **Atkins MB**, Robertson MJ, Gordon M, Lotze MT, DeCoste M, DuBois JS, Ritz J, Sandler AB, Edington HD, Garzone PD, Mier JW, Canning CM, Battiatto L, Tahara H, Sherman ML. Phase I evaluation of intravenous recombinant human interleukin 12 in patients with advanced malignancies. *Clin Cancer Res* 1997; **3**: 409-417
 - 12 **Xu CT**, Huang LT, Pan BR. Current gene therapy for stomach carcinoma. *World J Gastroenterol* 2001; **7**: 752-759
 - 13 **Weber SM**, Shi F, Heise C, Warner T, Mahvi DM. Interleukin 12 gene transfer results in CD8-dependent regression of murine CT26 liver tumors. *Ann Surg Oncol* 1999; **6**: 186-194
 - 14 **Shi FS**, Weber S, Gan J, Rakhmievich AL, Mahvi DM. Granulocyte-macrophage colony-stimulating factor (GM-CSF) secreted by cDNA-transfected tumor cells induces a more potent antitumor response than exogenous GM-CSF. *Cancer Gene Ther* 1999; **6**: 81-88
 - 15 **Oshikawa K**, Rakhmievich AL, Shi F, Sondel PM, Yang N, Mahvi DM. Interleukin 12 gene transfer into skin distant from the tumor site elicits antimetastatic effects equivalent to local gene transfer. *Hum Gene Ther* 2001; **12**: 149-160
 - 16 **Tahara H**, Zeh HJ 3rd, Storkus WJ, Pappo I, Watkins SC, Gubler U, Wolf SF, Robbins PD, Lotze MT. Fibroblasts genetically engineered to secrete interleukin 12 can suppress tumor growth and induce antitumor immunity to a murine melanoma *in vivo*. *Cancer Res* 1994; **54**: 182-189
 - 17 **Chang TM**. Artificial cells with emphasis on bioencapsulation in biotechnology. *Biotechnol Annu Rev* 1995; **1**: 267-295
 - 18 **Chang TM**. Pharmaceutical and therapeutic applications of artificial cells including microencapsulation. *Eur J Pharm Biopharm* 1998; **45**: 3-8
 - 19 **Shurin MR**, Esche C, Peron JM, Lotze MT. Antitumor activities of IL-12 and mechanisms of action. *Chem Immunol* 1997; **68**: 153-174
 - 20 **Kang WK**, Park C, Yoon HL, Kim WS, Yoon SS, Lee MH, Park K, Kim K, Jeong HS, Kim JA, Nam SJ, Yang JH, Son YI, Baek CH, Han J, Ree HJ, Lee ES, Kim SH, Kim DW, Ahn YC, Huh SJ, Choe YH, Lee JH, Park MH, Kong GS, Park EY, Kang YK, Bang YJ, Paik NS, Lee SN, Kim SH, Kim S, Robbins PD, Tahara H, Lotze MT, Park CH. Interleukin-12 gene therapy of cancer by peritumoral injection of transduced autologous fibroblasts: Outcome of a phase I study. *Hum Gene Ther* 2001; **12**: 671-684
 - 21 **Tang ZH**, Qiu WH, Wu GS, Yang XP, Zou SQ, Qiu FZ. The immunotherapeutic effect of dendritic cells vaccine modified with interleukin-18 gene and tumor cell lysate on mice with pancreatic carcinoma. *World J Gastroenterol* 2002; **8**: 908-912
 - 22 **Hara S**, Nagai H, Miyake H, Yamanaka K, Arakawa S, Ichihashi M, Kamidono S, Hara I. Secreted type of modified interleukin-18 gene transduced into mouse renal cell carcinoma cells induces systemic tumor immunity. *J Urol* 2001; **165**: 2039-2043
 - 23 **Coze C**, Leimig T, Jimeno MT, Mannoni P. Retrovirus-mediated gene transfer of the cytokine genes interleukin-1beta and tumor necrosis factor-alpha into human neuroblastoma cells: consequences for cell line behavior and immunomodulatory properties. *Eur Cytokine Netw* 2001; **12**: 78-86
 - 24 **Hu JY**, Li GC, Wang WM, Zhu JG, Li YF, Zhou GH, Sun QB. Transfection of colorectal cancer cells with chemokine MCP-3 (monocyte chemoattractant protein-3) gene retards tumor growth and inhibits tumor metastasis. *World J Gastroenterol* 2002; **8**: 1067-1072
 - 25 **Chen JP**, Lin C, Xu CP, Zhang XY, Wu M. The therapeutic effects of recombinant adenovirus RA538 on human gastric carcinoma cells *in vitro* and *in vivo*. *World J Gastroenterol* 2000; **6**: 855-860
 - 26 **Mazzolini G**, Qian C, Xie X, Sun Y, Lasarte JJ, Drozdziak M, Prieto J. Regression of colon cancer and induction of antitumor immunity by intratumoral injection of adenovirus expressing interleukin-12. *Cancer Gene Ther* 1999; **6**: 514-522
 - 27 **Gambotto A**, Tuting T, McVey DL, Kovessi I, Tahara H, Lotze MT, Robbins PD. Induction of antitumor immunity by direct intratumoral injection of a recombinant adenovirus vector expressing interleukin-12. *Cancer Gene Ther* 1999; **6**: 45-53
 - 28 **Xu YX**, Gao X, Janakiraman N, Chapman RA, Gautam SC. IL-12 gene therapy of leukemia with hematopoietic progenitor cells without the toxicity of systemic IL-12 treatment. *Clin Immunol* 2001; **98**: 180-189
 - 29 **Egilmez NK**, Jong YS, Sabel MS, Jacob JS, Mathiowitz E, Bankert RB. *In situ* tumor vaccination with interleukin-12-encapsulated biodegradable microspheres: induction of tumor regression and potent antitumor immunity. *Cancer Res* 2000; **60**: 3832-3837
 - 30 **Hill HC**, Conway TF Jr, Sabel MS, Jong YS, Mathiowitz E, Bankert RB, Egilmez NK. Cancer immunotherapy with interleukin 12 and granulocyte-macrophage colony-stimulating factor-encapsulated microspheres: coinduction of innate and adaptive antitumor immunity and cure of disseminated disease. *Cancer Res* 2002; **62**: 7254-7263
 - 31 **Sabel MS**, Hill H, Jong YS, Mathiowitz E, Bankert RB, Egilmez NK. Neoadjuvant therapy with interleukin-12-loaded polylactic acid microspheres reduces local recurrence and distant metastases. *Surgery* 2001; **130**: 470-478
 - 32 **Tamura T**, Nishi T, Goto T, Takeshima H, Dev SB, Ushio Y, Sakata T. Intratumoral delivery of interleukin 12 expression plasmids with *in vivo* electroporation is effective for colon and renal cancer. *Hum Gene Ther* 2001; **12**: 1265-1276
 - 33 **Deng YC**, Zhen YS, Zheng S, Xue YC. Activity of boanmycin against colorectal cancer. Activity of boanmycin against colorectal cancer. *World J Gastroenterol* 2001; **7**: 93-97
 - 34 **Zheng S**, Liu XY, Ding KF, Wang LB, Qiu PL, Ding XF, Shen YZ, Shen GF, Sun QR, Li WD, Dong Q, Zhang SZ. Reduction of the incidence and mortality of rectal cancer by polypectomy: a prospective cohort study in Haining County. *World J Gastroenterol* 2002; **8**: 488-492
 - 35 **Chau I**, Cunningham D. Adjuvant therapy in colon cancer: current status and future directions. *Cancer Treat Rev* 2002; **28**: 223-236

hOGG1 Ser326Cys polymorphism modifies the significance of the environmental risk factor for colon cancer

Jae-II Kim, Young-Jin Park, Ki-Hong Kim, Ji-II Kim, Byung-Joo Song, Meung-Soo Lee, Chul-Num Kim, Seok-Hyo Chang

Jae-II Kim, Young-Jin Park, Ki-Hong Kim, Ji-II Kim, Byung-Joo Song, Meung-Soo Lee, Chul-Num Kim, Seok-Hyo Chang, Department of Surgery, Ilsan Paik Hospital, Inje University College of Medicine, 2240, Daehwa-dong, Ilsan-gu, Koyang shi, Kyunggi-do 412-270, Korea

Supported by the grants from the Korea Research Foundation, No. 2001-003-F00117

Correspondence to: Dr. Young-Jin Park, Department of Surgery, Ilsan Paik Hospital, Inje University College of Medicine, 2240, Daehwa-dong, Ilsan-gu, Koyang shi, Kyunggi-do 412-270, Korea. yjpark@ilsanpaik.ac.kr

Telephone: +82-31-9107307 **Fax:** +82-31-9107319

Received: 2002-12-07 **Accepted:** 2002-12-24

Abstract

AIM: To determine the association of *hOGG1* (8-oxoguanine glycosylase I, *OGG1*) polymorphism of Ser326Cys substitution with colon cancer risk and possible interaction with known environmental risk factors.

METHODS: A case-control study with 125 colon cancer cases and 247 controls was conducted.

RESULTS: There was no major difference in Ser326Cys genotype distribution between cases and controls. The meat intake tended to increase the odds ratio for colon cancer with an OR of 1.72 (95 % confidence interval; CI=1.12-2.76). Such tendency was more prominent in Cys/Cys carriers (OR=4.31, 95 % CI=1.64-11.48), but meat intake was not a significant risk factor for colon cancer in Ser/Ser or Ser/Cys carriers. The OR for colon cancer was elevated with marginal significance in smokers who were Cys/Cys carriers (OR=2.75, 95 % CI=1.07-7.53) but not in Ser/Ser or Ser/Cys carriers.

CONCLUSION: These results suggest that the *hOGG1* Ser326Cys polymorphism is probably not a major contributor to individual colon cancer susceptibility overall, but the Cys/Cys genotype may alter the impact of some environmental factors on colon cancer development.

Kim JI, Park YJ, Kim KH, Kim JI, Song BJ, Lee MS, Kim CN, Chang SH. *hOGG1* Ser326Cys polymorphism modifies the significance of the environmental risk factor for colon cancer. *World J Gastroenterol* 2003; 9(5): 956-960
<http://www.wjgnet.com/1007-9327/9/956.htm>

INTRODUCTION

Reactive oxygen species are formed continuously in living cells through both endogenous and exogenous processes. The reaction of reactive oxygen species results in various forms of both cellular and DNA damage^[1]. Oxidative damage to DNA is thought to cause mutations, which in turn can activate oncogenes or inactivate tumor suppressor genes and may finally lead to carcinogenesis^[2-4]. 7,8-Dihydro-8-oxoguanine

(8oxoG) is one of the most important lesions produced in DNA by oxygen radical forming agents. Due to its mispairing with deoxyadenosine, it causes mutagenic transversion of G:C to T:A *in vitro* and *in vivo*^[5,6]. The *hOGG1* gene encodes a DNA glycosylase/AP-lyase that catalyzes the removal of 8oxoG adducts as part of the base excision repair pathway. The *hOGG1* gene is expressed as multiple alternatively-spliced isoforms with only the 1 α -form containing a nuclear localization signal^[7,8]. Previous studies have revealed the presence of several polymorphisms at the *hOGG1* locus. A C/G polymorphism at position of 1245 in the 1 α -specific exon 7 of the *hOGG1* gene results in an amino acid substitution from serine to cysteine in codon 326^[9]. Although no difference in catalytic activity was observed between Ser326 and Cys326 variants in some studies^[10,11], the *hOGG1* protein encoded by the Ser326 allele exhibited substantially higher activities than the Cys326 variants in an *in vitro Escherichia coli* complementation activities assay^[9].

Several studies have suggested that Cys326 type allele is associated with increased risk for lung^[12], esophageal^[13] and a subset of stomach cancer^[14]. The possible causal relationship between oxygen free radicals and cancer development has been reported mainly in organs under a high burden of oxygen free radicals, including the lung and oro-laryngeal cancer associated with smoking history. Among the smokers, the Cys/Cys carriers who are supposed to have decreased capability in coping with the oxidative DNA damage tended to be more susceptible to lung cancer than the Ser/Ser or Ser/Cys carriers. The colon may be continuously exposed to the attack of oxygen free radicals. The relatively high concentrations of iron in feces, together with the ability of bile pigments to act as iron chelators that support Fenton chemistry, may very well permit efficient hydroxyl radical (-OH) generation from superoxide and hydrogen peroxide produced by bacterial metabolism^[15]. The abundant free radical generation in colon supports the free radical related colon carcinogenesis.

We previously demonstrated that the impact of genetic defect on carcinogenesis is modulated by an environmental risk factor in hereditary nonpolyposis colorectal cancer patients^[16]. In addition, we tried to delineate the relationship between *hOGG1* enzyme activity and the allele type harbored in Ser326Cys polymorphism *in vivo*^[17]. However, any clear conclusion was not made despite of possible relevance. The available information makes it plausible to hypothesize that the Ser326Cys polymorphism may alter colon cancer risk, particularly in association with the environmental risk factors. We will conduct a case control study to examine the hypothesis.

MATERIALS AND METHODS

Study populations and sample processing

Case subjects consisted of 125 patients operated with primary colorectal cancer. All the patients agreed to participate in this study and consented. Community-based controls consisted of subjects who were visited the health-screening center of Ilsan-Paik hospital. At this center, screenings of common cancers as

well as evaluation on the general status of health were performed. All control subjects were recruited after an initial verbal screening to determine whether they had no previous diagnosis of cancer, and none of the controls recruited into this study were diagnosed with any form of cancer after screening. The eligible pool of control subjects was restricted to those individuals of the same age (± 5 years) and sex as case subjects. The controls pair-matched into a 2 to 1 ratio in terms of those cases studied. Ninety-five percent of the control subjects ($n=247$) consented. A trained interviewer conducted in-person interviews. Information was collected on life-long smoking, alcohol consumption, diet habits, physical activity and family history of colorectal cancer.

Genotypic assays

The genotypes of *hOGG1* alleles were determined by a polymerase chain reaction - restriction endonuclease length polymorphism (PCR-RELP) analysis. Briefly, a 251 bp fragment was amplified by PCR in a 25 μ L reaction volume that contained 50 ng of genomic DNA, 10 mmol/L Tris-HCl, 50 mmol/L KCl, 1 mmol/L MgCl₂, 0.2 mmol/L of each dNTP, 10 pmol of the *hOGG1* sense (*hOGG1F*; 5' - AGTGGATTCTCATTGCCTTCG-3', corresponding to nucleotide 8 919 through 8 939 of *hOGG1* intron 6 DNA sequences; Genbank accession #HSA131341) and antisense (*hOGG1R*; 5' - GGTGCTTGGGGAATTTCTTT-3', corresponding to nucleotide 9 150 through 9 169 of *hOGG1* exon 7 sequences) primers and 2 units of Taq DNA polymerase. Cycling conditions were as follows: initial denaturation at 94 °C for 5 min following 30 cycles of denaturation at 94 °C for 30 sec, annealing at 57 °C for 30 and elongation at 72 °C for 40. Ten μ L of each PCR sample was digested with 2 units of Fsp4HI (Bioneer, Taejeon, Korea) at 37 °C for 12 h and resolved on 30 g/L agarose gels to detect differences in RFLP patterns.

Statistical analysis

The association between the *hOGG1* polymorphism and colorectal cancer risk was estimated by the odds ratio (OR), using the unconditional logistic regression model. We calculated not only crude ORs, but also values adjusted for age, sex, drinking habits, smoking and diet habits to control the effect of potential confounding environmental factors. Because the Ser/Ser genotype was thought to have the highest effective enzymatic activity, we used this genotype as reference for colorectal cancer risk. Thus, the ORs for the Ser/Cys and Cys/Cys types relative to the Ser/Ser were calculated. The ORs for the Cys/Cys type versus other types combined were also calculated because only the Cys/Cys type could potentially influence the individual repair activity. Statistical differences of the categorical comparison and the probability of the Hardy-Weinberg equilibrium were tested using χ^2 test.

RESULTS

The mean age of the case and control groups were 57.2 and 56.1 years, respectively, and the case and control groups consisted of 36.5 % and 37.2 % females, respectively. There were no significant statistical differences in age and gender between the case and control groups.

Three banding patterns were observed depending on the genotypes; a single 251 bp band corresponding to the Ser326/Ser326 genotype, a 251, 153 and 98 bp bands that corresponded to the Ser326/Cys326 genotype, and 153 and 98 bp bands corresponding to the 326Cys/Cys326 genotype (Figure 1A). The specificity of the amplification products was verified by sequencing (Figure 1B).

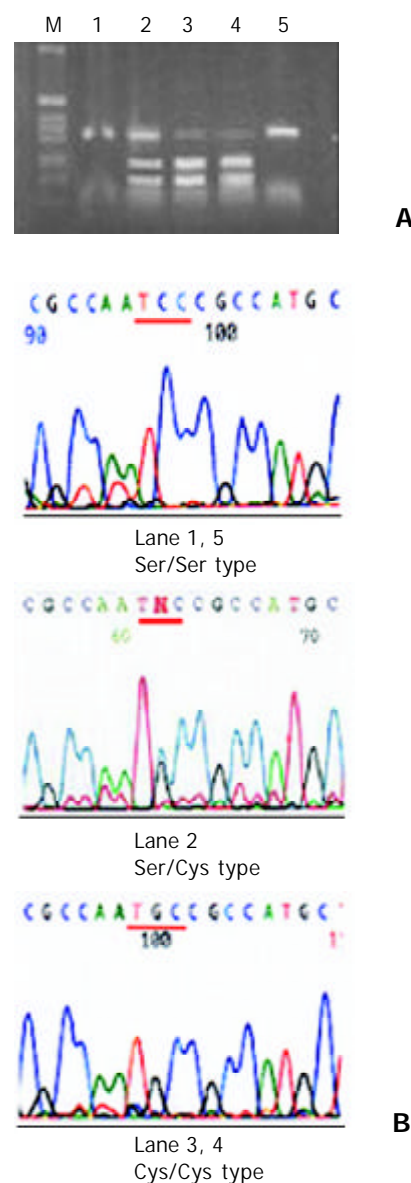


Figure 1 A: The representative PCR-RFLP analysis of *hOGG1* Ser326Cys polymorphism. Lane 1, 5, undigested PCR-amplified product observed in homozygous Ser326 carriers; Lane 2, Fsp4HI-digested PCR product from subject with heterozygous *hOGG1* genotype; Lane 3, 4, Fsp4HI-digested PCR product from subject with homozygous Cys326 genotype. B: DNA sequence histogram revealing the indicated sequence changes (underlined). In the 2nd histogram, both the cytosine (blue line) and guanine (black line) are observed in the codon 326 site (marked as N), indicating the heterozygous genotype.

The allelic frequency was not significantly different between cases and controls, slightly more homozygous Cys326 alleles were found in the case group than that in the controls (Table 1). The prevalence of the *hOGG1* Ser/Cys polymorphism followed the Hardy-Weinberg equilibrium.

Table 1 Odds ratios for colon cancer according to the genotypes of *hOGG1* Ser326Cys polymorphism

	Number (%)		OR (95% CI)	P for trend
	Controls	Cases		
Ser / Ser	52 (21.1)	24 (19.2)	1.00	
Ser / Cys	131 (53.0)	66 (52.8)	1.09 (0.60-2.00)	P=0.871
Cys / Cys	64 (25.9)	35 (28.0)	1.18 (0.60-2.35)	
Total	247 (100)	125 (100)		

To examine the relationship between the *hOGGI* genotype and colon cancer risk in the presence of selected environmental risk factors, study subjects were stratified by *hOGGI* genotype and several known colon cancer risk factors. Table 2 represented the frequency distribution of the *hOGGI* genotype stratified with the risk factors and ORs with

a 95 % confidence interval (95 % CI) for colon cancer cases compared with controls. None of the risk factors analyzed in the present study significantly elevated the ORs for colon cancer in the total number of subjects studied. Only frequent meat intake increased the OR with marginal statistical significance.

Table 2 ORs for colon cancer according to individual habits and familial history of colon cancer with reference to the *hOGGI* Ser326Cys polymorphism

	Total			<i>hOGGI</i> Ser326Cys polymorphism					
	Ca/Co	OR	95% CI	Ser/Ser + ser/Cys			Cys/Cys		
				Ca/Co	OR	95%CI	Ca/Co	OR	95%CI
Smoking									
No	44/106	1.00	-	35/75	1.00	-	9/31	1.00	-
Yes	81/141	1.53	0.94-2.52	55/108	1.08	0.62-1.84	26/33	2.75	1.07-7.53
Drinking									
< 2 times/wk	73/161	1.00	-	53/122	1.00	-	20/39	1.00	-
> 2 times/wk	52/86	1.37	0.87-2.32	37/61	1.49	0.87-2.77	15/25	1.21	0.49-3.02
Meat									
< 2 time/week	66/159	1.00	-	52/112	-	-	14/47	1.00	-
> 2 time/week	59/88	1.72	1.12-2.76	38/71	1.27	0.73-2.13	21/17	4.31	1.64-11.48
Vegetable intake									
Low	50/89	1.00	-	36/70	1.00	-	14/19	1.00	-
High	75/158	0.80	0.49-1.31	54/113	0.90	0.46-1.67	21/45	1.55	0.50-4.19
Soybean product									
< 3/wk	55/115	1.00	-	37/87	1.00	-	18/28	1.00	-
> 3/wk	70/132	1.11	0.70-1.75	53/96	1.30	0.76-2.23	17/36	0.73	0.30-1.82
Activity									
< 4 hs/wk	61/104	1.00	-	43/75	-	-	18/29	1.00	-
> 4hs/wk	64/143	0.76	0.48-1.20	47/108	0.76	0.44-1.30	17/35	0.78	0.32-1.94
Familial history of colon cancer									
No	84/185	1.00	-	62/138	-	-	22/47	1.00	-
Yes	41/62	1.46	0.80-2.40	28/45	1.38	0.76-2.51	13/17	1.63	0.62-4.32

Denotes: Ca/Co=Cases/Controls.

In the subgroup analysis with reference to the Ser326Cys polymorphism, the smoking habit did not increase the ORs for colon cancer in Ser/Ser or Ser/Cys carriers. In contrast, a near-significant increase in risk was observed for smokers with the Cys/Cys genotype (OR=2.75, 95 % CI=1.07-7.53). Meat intake was associated with increased colon cancer incidence with borderline significance among the total number of subjects (OR=1.72, 95 % CI=1.12-2.76). The OR for colon cancer with frequent meat intake was further increased in the Cys/Cys subgroup (OR=4.31, 95 % CI=1.64-11.48), while the OR was not increased in Ser/Ser or Ser/Cys carriers. Except for the meat intake factor, the intake of selected foods including alcohol, vegetable and soybean products did not alter the ORs for colon cancer neither in the entire group of subjects studied nor in the Cys/Cys subgroup. No significant alteration in the OR for colon cancer according to the extent of physical activity was observed in either genotype carriers.

Because the presence of colon cancer in relatives, particularly in 1st or 2nd degree relatives, has been known to be associated with colon cancer risk and because the genetic polymorphism could be one of the possible causes, changing patterns of OR for colon cancer according to the *hOGGI* Ser326Cys polymorphism when there was at least one colon cancer patient within a family were investigated. Although the risk was increased with the presence of colon cancer within a family among the total number of subjects studied, there was no apparent increase in the OR among subjects with Cys/Cys genotype.

DISCUSSION

It is theoretically possible that the incidence of cancer differs depending on the genotypes of *hOGGI* Ser326Cys polymorphism. This view is supported by the difference in DNA repairing capability depending on the allele type^[9] and increase of the incidence of cancer in certain organs in Cys326 allele carriers^[12,13,18].

Colon is the most susceptible organ for cancer development in hereditary non-polyposis colorectal cancer (HNPCC), where the DNA mismatch repair activity is defective^[19]. As the role of defects in DNA mismatches repair process in colon carcinogenesis is very clear, attention has also recently focused on the possible role of alternative DNA repair pathways such as base excision repair in colon cancer formation.

In the present investigation, however, the *hOGGI* Ser326Cys polymorphism did not alter the overall odds ratios for colon cancers despite of the theoretical relevancies. Subgroup analysis revealed an increased tendency of ORs with smoking habit or frequent meat intaking in Cys/Cys carriers although the statistical significance of the former factor is marginal.

The intake of meat and animal fat was almost consistently associated with the increased risk of large-bowel cancer in the previous studies^[20-22]. It was suggested that the abundant fecal iron after red meat intake, together with the ability of bile pigments to act as iron chelators, supports the superoxide-driven Fenton reaction^[15]. Meanwhile, excessive fat ingestion increases the concentrations of bile acids in the colon. The increased fatty acids and secondary bile acids in the colonic

lumen, which acts as cytotoxic surfactants, can damage colonic epithelial cells and thus induce a compensatory hyperproliferation of crypt cells^[23]. In addition, the high intake of polyunsaturated fatty acid induces peroxidative reaction with plasma low-density lipoproteins, which in turn generate free radicals. Meat is a major source of dietary animal fat. Thus, the question is still unresolved whether the association of meat with colorectal cancer seen in some epidemiologic investigations reflects the effect of fat, or meat in general, or just particular types of meat. One prospective study showed that red meat, but not the chicken or fish could be an independent risk factor for colon cancer^[24]. The result of the present investigation together with a literature review consists with the suggestion that oxidative damage after meat intake may play a role in colon carcinogenesis and that the role may be more pronounced in Cys/Cys carriers, who have a lower activity in terms of repair of DNA.

Some discussion is required on the credibility of the answer concerning the meat intake habit. The dietary environment has been rapidly changing in Korea in accordance with economic development. Meat consumption per capita has increased more than 3 times during the past 3 decades^[25]. A possible problem under this circumstance is that the answers on the questionnaire might be more influenced by recent dietary habits rather than lifelong ones, although we tried to reduce such problems to a minimum during the interview.

Among the various lifestyle factors, tobacco smoking might provide the strongest oxygen radical generating environment. An array of studies demonstrated the increased oxidative DNA damage in smokers compared to non-smokers^[26,27]. The carcinogenic role of tobacco in association with the oxygen free radical seems clear in airway tract tissues. Recent studies showed that an increased risk of squamous type lung cancer, orolaryngeal cancer in smokers, was particularly found in homozygous Cys 326 gene carriers. In general, the biologic role of tobacco smoke as an etiology of cancer in the gastrointestinal tract might be less prominent than that in the airway tract. Tobacco smoking history is often inconsistent with the incidence of colorectal cancers although it shows a near consistent positive relationship with the presence of colorectal adenomas^[28,29]. The previous studies, which investigated the effect of smoking in gastric cancer development in connection with the Ser326Cys polymorphism, showed only a weak association^[14]. In the present study, the OR for colon cancer among smokers tended to be higher in Cys/Cys carriers than that in Ser/Ser and Ser/Cys carriers, the interaction being of borderline statistical significance. The result of present findings suggested that the oxygen free radical generated from tobacco smoke might be involved in colon carcinogenesis although the role is probably limited.

The role of oxidative DNA damage in alcohol-related carcinogenesis is still controversial. Alcohol consumption was associated with increased DNA damage or induction of 8oxoG in some studies^[30,31] in contrast, but not in others^[32,33]. The present study showed that alcohol intake did not increase the risk of colon cancer even in Cys/Cys carriers. It suggested that the role of alcohol consumption in colon cancer formation, particularly in association with the 8oxoG adduct induction, was limited. The other factors including vegetable or soybean product intake, physical exercise and family history of colon cancer did not increase OR for colon cancer in the total number of subjects studied as well as in Cys/Cys carriers. Thus, it was difficult to interpret whether these factors play a role during colon carcinogenesis, particularly in interaction with the *hOGG1* Ser326Cys polymorphism.

In summary, the *hOGG1* Ser/Cys polymorphism does not significantly alter the overall risk of colon cancer. The Cys type allele, however, may exert an impact on colon

carcinogenesis through an interaction with certain environmental factors such as smoking or meat consumption. There are lines of complex biologic factors involved in colon carcinogenesis. The present study suggests the possibility that an inter-individual difference in DNA repair capacity can be one such factor, however, the influence of such a role is believed to be limited. Further studies with a large number of subjects are warranted to better assess the role of *hOGG1* polymorphism in colon carcinogenesis.

REFERENCES

- 1 **Poulsen HE**, Prieme H, Loft S. Role of oxidative damage in cancer initiation and promotion. *Eur J Cancer Prev* 1998; **7**: 9-16
- 2 **Fearon ER**. Human cancer syndrome: clues to the origin and nature of cancer. *Science* 1997; **278**: 1043-1050
- 3 **Loft S**, Deng XS, Tuo J, Wellejus A, Sorensen M, Poulsen HE. Experimental study of oxidative DNA damage. *Free Radic Res* 1998; **29**: 525-539
- 4 **Marnett LJ**. Oxyradicals and DNA damages. *Carcinogenesis* 2000; **21**: 361-370
- 5 **Shibutani S**, Takeshita N, Grollman AP. Insertion of specific bases during DNA synthesis past the oxidation-damaged base 8-oxodG. *Nature* 1991; **349**: 431-434
- 6 **Michaels ML**, Miller JH. The GO system protects organisms from the mutagenic effect of the spontaneous lesion 8-hydroxyguanine. *J Bacteriol* 1992; **174**: 6321-6325
- 7 **Nishioka K**, Ohtsubo T, Oda H, Fujiwara T, Kang D, Sugimachi K, Nakappu Y. Expression and differential intracellular localization of two major forms of human 8-oxoguanine DNA glycosylase encoded by alternatively spliced OGG1 mRNAs. *Mol Biol Cell* 1999; **10**: 1637-1652
- 8 **Shinmura K**, Kohno T, Tekeuchi-Sasaki M, Maeda M, Segawa T, Kamo T, Sugimura H, Yokota J. Expression of the OGG1 type 1a (nuclear form) protein in cancerous and non-cancerous human cells. *Int J Oncol* 2000; **16**: 701-707
- 9 **Kohno T**, Shinmura K, Tosaka M, Tani M, Kim SR, Sugimura H, Nohmi T, Kasai H, Yokota J. Genetic polymorphisms and alternative splicing on the *hOGG1* gene, that is involved in the repair of 8-hydroxyguanine in damaged DNA. *Oncogene* 1998; **16**: 3219-3225
- 10 **Dherin C**, Radicella JP, Dizdaroglu M, Boiteux S. Excision of oxidatively damaged DNA base by the human alpha-*hOGG1* protein and polymorphic alpha-*hOGG1*(Ser326Cys) which is frequently found in human populations. *Nucl Acids Res* 1999; **27**: 4001-4007
- 11 **Janssen K**, Schlink K, Gotte W, Hipper B, Kaina B, Oesch F. DNA repair activity of 8-oxoguanine DNA glycosylase 1 in human lymphocytes is not dependent on genetic polymorphism Ser³²⁶/Cys³²⁶. *Mutat Res* 2001; **486**: 207-216
- 12 **Sugimura H**, Kohno T, Wakai K, Nagura K, Genka K, Igarashi H, Morris BJ, Baba S, Ohno Y, Gao C, Li Z, Wang J, Takezaki T, Tajima K, Varga T, Sawaguchi T, Lum JK, Martinson JJ, Tsugane S, Iwamasa T, Shinmura K, Yokota J. *hOGG1* Ser326Cys polymorphism and lung cancer susceptibility. *Cancer Epidemiol Biomarkers Prev* 1999; **8**: 669-674
- 13 **Xing DY**, Tan W, Song N, Lin DY. Ser326Cys polymorphism in *hOGG1* gene and risk of esophageal cancer in a Chinese population. *Int J Cancer* 2001; **95**: 140-143
- 14 **Takezaki T**, Gao CM, Wo JZ, Li ZU, Wang JD, Ding JH, Liu YT, Hu X, Xu TL, Tajima K, Sugimura H. *hOGG1* Ser326Cys polymorphism and modification by environmental factors of stomach cancer risk in Chinese. *Int J Cancer* 2002; **99**: 624-627
- 15 **Babbs CF**. Free radicals and the etiology of colon cancer. *Free Radic Biol Med* 1990; **8**: 191-200
- 16 **Park JG**, Park YJ, Wijnen JT, Vasen HF. Gene-environment interaction in hereditary nonpolyposis colorectal cancer with implications for diagnosis and genetic testing. *Int J Cancer* 1999; **82**: 516-519
- 17 **Park YJ**, Choi EY, Choi JY, Park JG, You HJ, Chung MH. Genetic changes of *hOGG1* and the activity of oh8Gua glycosylase in colon cancer. *Eur J Cancer* 2001; **37**: 340-346
- 18 **Elahi A**, Zheng Z, Park J, Eyring K, McCaffrey T, Lazarus P. The

- human OGG1 DNA repair enzyme and its association with orolaryngeal cancer risk. *Carcinogenesis* 2002; **23**: 1229-1234
- 19 **Fisbel R**, Lescoe MK, Rao MR, Copeland NG, Jenkins NA, Garber J, Kane M, Kolodner R. The human mutator gene homolog MSH2 and its association with hereditary nonpolyposis colon cancer. *Cell* 1993; **75**: 1027-1038
- 20 **Drasar BS**, Irving D. Environmental factors and cancer of the colon and breast. *Br J Cancer* 1973; **27**: 167-172
- 21 **Giovannucci E**, Rimm EB, Stampfer MJ, Colditz GA, Ascherio A, Willett WC. Intake of fat, meat, and fiber in relation to risk of colon cancer in men. *Cancer Res* 1994; **54**: 2390-2397
- 22 **Neugut AI**, Garbowski GC, Lee WC, Murray T, Nieves JW, Forde KA, Treat MR, Wayne JD, Fenoglio-Preiser C. Dietary risk factors for the incidence and recurrence of colorectal adenomatous polyps. A case-control study. *Ann Intern Med* 1993; **118**: 91-95
- 23 **Van der Meer R**, Lapre JA, Govers MJ, Kleibeuker JH. Mechanisms of the intestinal effects of dietary fats and milk products on colon carcinogenesis. *Cancer Lett* 1997; **114**: 75-83
- 24 **Willett WC**, Stampfer MJ, Colditz GA, Rosner BA, Speizer FE. Relation of meat, fat, and fiber intake to the risk of colon cancer in a prospective study among women. *N Engl J Med* 1990; **323**: 1664-1672
- 25 **Korea National statistical office**. Available from: URL:<http://www.nso.go.kr>
- 26 **Nakayama T**, Kaneko M, Kodama M, Nagata C. Cigarette smoke induces DNA single-strand breaks in human cells. *Nature* 1985; **314**: 462-464
- 27 **Asami S**, Hirano T, Yamaguchi R, Tomioka Y, Itoh H, Kasai H. Increase of a type of oxidative DNA damage, 8-hydroxyguanine, and its repair activity in human leukocytes by cigarette smoking. *Cancer Res* 1996; **56**: 2546-2549
- 28 **Kune GA**, Kune S, Vitetta L, Watson LF. Smoking and colorectal cancer risk: data from the Melbourne colorectal cancer study and brief review of literature. *Int J Cancer* 1992; **50**: 369-372
- 29 **Heineman EF**, Zahm SH, McLaughlin JK, Vaught JB. Increased risk of colorectal cancer among smokers: results of a 26-year follow-up of US veterans and a review. *Int J Cancer* 1994; **59**: 728-738
- 30 **Nakajima M**, Takeuchi T, Takeshita T, Morimoto K. 8-Hydroxydeoxyguanosine in human leukocyte DNA and daily health practice factors: effects of individual alcohol sensitivity. *Environ Health Perspect* 1996; **104**: 1336-1338
- 31 **Ye XB**, Fu H, Zhu JL, Ni WM, Lu YW, Kuang XY, Yang SL, Shu BX. A study on oxidative stress in lead-exposed workers. *J Toxicol Environ Health* 1999; **57**: 161-172
- 32 **van Zeeland AA**, de Groot AJ, Hall J, Donato F. 8-Hydroxydeoxyguanosine in DNA from leukocytes of healthy adults: relationship with cigarette smoking, environmental tobacco smoke, alcohol and coffee consumption. *Mutat Res* 1999; **439**: 249-257
- 33 **Lodovici M**, Casalini C, Cariaggi R, Michelucci L, Dolara P. Levels of 8-hydroxydeoxyguanosine as a marker of DNA damage in human leukocytes. *Free Radic Biol Med* 2000; **28**: 13-17

Edited by Xu XQ

Dose surgical sub-specialization influence survival in patients with colorectal cancer?

Cameron Platell, Daniel Lim, Nazreen Tajudeen, Ji-Li Tan, Karen Wong

Cameron Platell, Daniel Lim, Nazreen Tajudeen, Ji-Li Tan, Karen Wong, Department of Surgery, University of Western Australia, Fremantle Hospital, Australia

Correspondence to: Cameron Platell, Associate Professor, University Department of Surgery, Fremantle Hospital, PO Box 480, Fremantle, 6160, Australia. cplatell@cyllene.uwa.edu.au

Telephone: +61-8-94312500 **Fax:** +61-8-94312623

Received: 2003-01-04 **Accepted:** 2003-01-17

Abstract

AIM: To perform a review of patients with colorectal cancer to a community hospital and to compare the risk-adjusted survival between patients managed in general surgical units versus a colorectal unit.

METHODS: The study evaluated all patients with colorectal cancer referred to either general surgical units or a colorectal unit from 1/1996 to 6/2001. These results were compared to a historical control group treated within general surgical units at the same hospital from 1/1989 to 12/1994. A Kaplan-Meier survival analysis compared the overall survivals (all-cause mortality) between the groups. A Cox proportional hazards model was used to determine the influence of a number of independent variables on survival. These variables included age, ASA score, disease stage, emergency surgery, adjuvant chemotherapy and/or radiotherapy, disease location, and surgical unit.

RESULTS: There were 974 patients involved in this study. There were no significant differences in the demographic details for the three groups. Patients in the colorectal group were more likely to have rectal cancer and Stage I cancers, and less likely to have Stage II cancers. Patients treated in the colorectal group had a significantly higher overall 5-year survival when compared with the general surgical group and the historical control group (56 % versus 45 % and 40 % respectively, $P < 0.01$). Survival regression analysis identified age, ASA score, disease stage, adjuvant chemotherapy, and treatment in a colorectal unit (Hazards ratio: 0.67; 95 % CI: 0.53 to 0.84, $P = 0.0005$), as significant independent predictors of survival.

CONCLUSION: The results suggest that there may be a survival advantage for patients with colon and rectal cancers being treated within a specialist colorectal surgical unit.

Platell C, Lim D, Tajudeen N, Tan JL, Wong K. Dose surgical sub-specialization influence survival in patients with colorectal cancer? *World J Gastroenterol* 2003; 9(5): 961-964
<http://www.wjgnet.com/1007-9327/9/961.htm>

INTRODUCTION

The question of who should be performing surgery on patients with colorectal cancer has important implications for both specialist colorectal surgeons and general surgeons. This is

because it impacts on not only patient management, but also surgical training and the provision of surgical services in regional areas.

A significant volume of literature has been devoted to try and define if sub-specialization benefits patients with colorectal cancer^[1-3]. However, there is currently little convincing evidence that specialist colorectal surgeons can achieve superior results when compared to general surgeons. The Australian NHMRC guidelines for the management of colorectal cancer^[4] address only the issue of who should perform elective rectal cancer surgery. It states rather enigmatically that “*such surgery should be performed by surgeons who have undergone a period of special exposure to this form of surgery and who have satisfactory experience in the surgical management of rectal cancer*”.

The aim of this study was to determine if there was a risk-adjusted survival advantage for patients with colorectal cancer being treated within a specialist colorectal surgical unit when compared to general surgical units.

MATERIALS AND METHODS

The colorectal service was established at Fremantle Hospital in 1996 with the appointment of a single surgeon who had received accredited training in colorectal surgery. The management of these patients was standardized through the use of treatment pathways, and protocols for the use of adjuvant chemo and/or radiotherapy. All patients referred to the service with a histologically proven colorectal cancer were prospectively entered into a designated colorectal computer database (Filemaker Pro 3.0 and 5.0, Claris) managed by the service. The three general surgical units at the hospital comprised of 10 different general surgeons who were employed by the hospital over the study period. All patients referred to these units with a histologically proven colorectal cancer were prospectively entered into the general surgical database managed through the Department of Surgery. A medical student group crosschecked these database entries with the patients' medical records and pathological records to accurately determine tumour stage, use of adjuvant therapy, and whether the operation was an emergency. These data were validated by the author. The study period was from 1/1/1996 to 1/6/2001. Patients presenting with recurrent colorectal cancers for management were included in the analysis.

The historical control group consisted of a cohort of patients with colorectal cancer who had been managed at Fremantle Hospital from 1/1989 to 12/1994 by a group of 8 general surgeons. This group of 475 patients had previously been part of a retrospective analysis performed in 1996 by the author, and the results published in 1997^[5]. In view of the retrospective nature of the data collection, some areas of information were not collected as accurately as in the present prospective trial. In particular, the information required to calculate cancer free survivals was not available. This control group was chosen because it predated the widespread acceptance and use of adjuvant chemotherapy and radiotherapy at Fremantle Hospital. All the endpoints were defined prior to the collection of data.

The surgical procedure was termed curative if there was macroscopic removal of all the tumour and histological assessment showed there to be clear margins. A palliative procedure was where the surgeon had left tumour remaining following surgery, or where no attempt had been made to remove the tumour. Histological assessment of the resected specimen was required to adequately determine this. A positive surgical margin was defined as the presence of tumour within 1 mm of the resection line.

Primary was defined as the first presentation with a colorectal neoplasia, or if a second presentation, where the tumour occurred in a metachronous location. The rectum was defined as commencing in the area where the taenia coli of the sigmoid colon coalesce into a uniform outer longitudinal muscular wall. At colonoscopy, it included the area up to 18 cm from the anal verge. An emergency procedure was where a patient underwent urgent surgery (i.e. within 24 hours of admission) without recourse to the normal pre-operative work up which includes colonoscopy and bowel preparation (including presentations with acute obstruction, perforation, and massive bleeding). The American Society of Anaesthesia score (ASA score) was used as a general measure of patient well-being. The TNM staging system was used in this study. For those patients who received pre-operative radiotherapy to their rectal cancers, and where there had been complete resolution of the primary tumour, the staging was based upon the pre-treatment endoanal ultrasound and CT scan.

In the colorectal group, adjuvant chemotherapy was offered to all patients with Stage III colon cancers and a selected group of Stage II colon cancers if there was evidence of poor prognostic markers (i.e. poorly differentiated, lymphovascular invasion) or if they were of young age (<50 years). Adjuvant preoperative radiotherapy was offered to patients with rectal cancers if the lesion was - (1) less than or equal to 12 cm from the anal verge, (2) fixed in position, (3) mobile lesions if found on endorectal ultrasound to be T3 or T4 in staging, (4) no associated metastatic disease found on abdominal CT scan. The general surgeons did not maintain guidelines for the use of adjuvant chemo/radio therapy. There was minimal use of adjuvant therapy in the historical control group.

The three data sets (a. colorectal group, b. general surgeon group, c. historical group) were then linked to the Mortality Registry of the Health Department of Western Australia. This enabled cross checking of the date of death of patients, and the survival curves were calculated from this information.

Statistical analysis

The mean, standard deviation, and range were used as descriptive statistics. Survival was calculated using the Kaplan-Meier product-limit estimate of survival. The survival time was calculated from the time of initial surgery (or if no surgery was performed, from initial consultation) to either death or 1-12-2002. The survival analysis was an overall analysis and included patients dying - (1) in the 30 day postoperative period, (2) from colorectal cancer, or (3) from unrelated causes (e.g. myocardial infarct). Patients presenting with recurrent cancer were included in the survival analysis. Comparisons of the overall (all-cause mortality) survival data were made between the study groups using the log rank test and the Breslow-Gehan-Wilcoxon test. The latter test was chosen because it could give greater weight to times with more observations in the risk set, and was therefore less sensitive than the log rank test to late events when few subjects remained in the study. The Chi-square test was used in comparisons of nominal data.

A Cox proportional hazards model (Statview 5.0, SAS Institute Inc.) was then applied to identify those factors associated with the improved survival of patients with

colorectal cancer. The variables which were evaluated were: (1) patients age, (2) stage of disease, (3) location - colon versus rectum, (4) surgical timing - elective versus emergency, (5) surgical management group - colorectal group and the general surgical group versus the historical control group, (6) use of adjuvant chemotherapy, (7) use of adjuvant radiotherapy (8) ASA score. Those factors identified on univariate analysis as significant predictors of survival were then included in a forward multiple linear regression analysis (Statview 5.0, SAS Institute Inc.). Significance was defined as the probability of a type I error of less than 5 %.

RESULTS

There were 974 patients involved in this study. The basic demographic data for the study groups was detailed in Table 1. The only significant differences noted were that patients in the colorectal group were more likely to have a rectal cancer, and those patients in the colorectal group and general surgical groups were more likely to have an ASA score of 3 or 4 when compared with the controls. The mean follow up time in the colorectal group was shorter than that in the general surgical group. This was because the rate of referrals was increasing in the former and declining in the latter. For example, the general surgical group managed only 11 colorectal cancers during 2000.

Table 1 Basic demographic data for the study groups of patients with colorectal cancer

	Colorectal group	General surgical group	Historical group
Number	362	137	475
Mean age-years	69 (±12)	70 (±11)	69 (±13)
Age range-years	29 to 93	38 to 93	32 to 95
Sex ration M:F	1.3:1	1.4:1	1.4:1
ASA score of 3 or 4	40 %	39 %	22 %
Elective vs emergency procedures	319 vs 43 (88% vs 12%)	112 vs 25 (78% vs 18%)	394 vs 81 (79% vs 17%)
Curative vs palliative pesections	264 vs 80 (73 % vs 22%)	101 vs 23 (74 % vs 17%)	366 vs 85 (77 % vs 18%)
No surgery	18 (5%)	13 (9%)	24 (5%)
Colon cancer	170 (47%) ^a	90 (66%)	314 (66%)
Rectal cancer	192 (53%) ^b	47 (34%)	161 (34%)
Adjuvant chemotherapy	116 (32%) ^c	19 (14%)	17 (4%)
Adjuvant radiotherapy	65 (18%) ^d	9 (7%)	14 (4%)
Mean follow-up-years	2.75 (±1.2) ^e	4.5 (±1.4)	5.1 (±4.5)
Max follow-up-years	6.8	6.9	13.9

^{a,b,c,d,e,f} $P < 0.05$ vs the other two group.

The information for staging for both colon and rectal cancers for the three groups was presented in Table 2. Patients in the colorectal group were significantly more likely to have a stage I cancer, and had significantly fewer stage II cancers, when compared with the other two groups. There was also a significant difference between the two groups in the use of adjuvant chemotherapy for patients who were less than 75 years of age and who had stage III colorectal cancers. For this group of patients, the percentage receiving adjuvant therapy was 89 % in the colorectal group, versus 41 % in the general surgery group, and 5.8 % in the historical group. For patients with stage II colorectal cancer, adjuvant chemotherapy was administered to 11 % of patients in the colorectal group, and no patients in the general surgery or historical groups. No patients with stage I cancer received adjuvant chemotherapy in either group.

Table 2 Staging information for colorectal cancers for the study groups

Stage	Colorectal group number (%)	General surgical group number (%)	Historical group number (%)
Stage I	81 (22 %) ^a	9 (7 %)	57 (12 %)
Stage II	95 (26 %) ^b	53 (39 %)	159 (33 %)
Stage III	91 (25 %)	41 (30 %)	146 (31 %)
Stage IV	91 (25 %)	29 (21 %)	106 (22 %)
Stage unknown	4 (1 %)	4 (3 %)	7 (2 %)

^{a,b} $P < 0.05$ vs the other two group with the Chi-square test.

A comparison of the survival between the study groups found that patients in the colorectal group had a significantly higher overall 5 year survival when compared with the general surgical group and historical groups (56 % versus 45 % and 40 % respectively, $P < 0.0001$). The survivals for the various study groups based on the tumour stage were presented in Table 3. Patients in the colorectal group who had either Stage I or Stage III cancers were noted to have significantly higher survivals when compared to the other two groups.

Table 3 A comparison of the overall 5 year survival based on stage for the study groups

Stage	Colorectal group	General surgical group	Historical group
I	90 % ^a	67 %	72 %
II	62 %	57 %	58 %
III	60 % ^b	46 %	34 %
IV (2 year survivals)	22 %	21 %	19 %

^{a,b} $P < 0.05$ vs the other two group.

In the uni-variate analysis, those factors that were found to be significant predictors of overall survival were: age, ASA score, emergency surgery, and stage of disease, adjuvant chemotherapy, adjuvant radiotherapy, and the surgical unit the patients were managed in. These independent variables were then entered into a multiple logistic regression analysis (Table 4) that identified: age, ASA score, stage of disease, the use of adjuvant chemotherapy, and management in the colorectal surgical group as significant independent predictors of survival. The comparisons for the surgical groups were made against the historical control group, with the general surgical group showing no improvement in survival when compared with the controls.

Table 4 Cox survival regression analysis of independent predictors of the overall survival in the 974 patients with colorectal cancer

Independent variables	<i>P</i>	Hazard ratio	95% Confidence interval
Age	0.15	1.011	1.002-1.020
ASA score	<0.0001	1.477	1.29-1.69
Adjuvant chemotherapy	0.047	0.634	0.405-0.993
Stage I	<0.0001	0.211	0.107-0.418
Stage II	0.003	0.397	0.214-0.738
Stage III	0.19	0.665	0.358-1.237
Stage IV	0.009	2.27	1.229-4.186
Colorectal surgical unit vs control	0.0005	0.667	0.531-0.837

DISCUSSION

The results of this study suggest that there was a survival advantage for patients with colorectal cancer being managed within a specialist colorectal surgical unit at a community based teaching hospital. These improvements in survival appear to be independent of other known predictors of survival that include stage of disease at presentation, emergency procedures, and the use of adjuvant chemotherapy. It remains to be determined as to why these differences exist. Do they simply reflect a higher surgical case load, or are they a result of improved surgical technique, better utilization of adjuvant therapy, or even standardized care through the use of treatment pathways?

There are a number of difficulties in designing a study to determine if there is a survival advantage in patients with colorectal cancer being managed by different groups of surgeons. A review of the surgical literature will show that rarely have clinical trials been conducted which compared the performance of different groups of surgeons. The logistics of trying to randomize patients into such a trial are very difficult. In this study, we have attempted to compare the risk adjusted survival of patients managed in general surgical units with those in a colorectal unit, and have compared these results with a well studied control group to see if there have been any improvements. Evaluating risk-adjusted survival in large cohorts of patients using historical controls is one recognized technique for addressing this issue. Clearly there were significant differences between the groups, with those patients in the colorectal group more likely to have Stage I disease and rectal cancers and with a trend towards fewer emergency procedures. However, the multivariate analysis is designed to account for these differences, and to include those factors that have been identified as independent predictors of survival. The individual surgeon was not included as an independent risk factor in this study because the majority of the general surgeons performed less than 20 cases during the study period. Such a small number makes it difficult to assess an individual surgeon's performance.

There have been a number of reports in the literature detailing wide variations in outcomes between surgeons managing patients with malignant disease^[1-3]. An important aspect to this variation appears to be case loads^[6-8]. In both patients with breast cancer^[6], oesophageal cancer^[7] and rectal cancer^[1], surgeons managing higher numbers of patients seem to gain improved results. A comprehensive review of the relationship between volume of surgical procedures and outcome has recently been published^[9,10]. This review assessed 88 studies and found that 77 % of the trials demonstrated a positive relationship between volume of work and reduced mortality, with the other 23 % of studies showing no relationship. None of the studies demonstrated a negative relationship.

The question of whether a surgeon who is sub-specialized in colorectal surgery can achieve improved results remains an unresolved issue. Porter *et al.*^[11], in their study on factors which influenced survival and local recurrence rates in patients treated for rectal cancer, found that surgeons who were trained in colorectal cancer had significantly improved survivals and reduced local recurrence rates when compared to general surgeons performing less than 21 procedures over the eight year study period. Nonetheless, their results were not significantly better than when compared to general surgeons performing greater than 21 procedures in the study period. Yet again this study focuses on rectal cancer and ignores colonic cancers. It remains to be determined whether these improvements relate to factors such as accuracy of tumour excision, minimizing tissue trauma, reduced incidence of septic

complications (which may influence cancer survival)^[11], and even possible to reduced blood loss and transfusion requirements.

In conclusion, there appears to be a survival advantage for patients with colorectal cancer being managed within a specialized colorectal unit. However, it remains to be determined which aspects of the management in such a unit are the most important determinates in this improvement in out-come.

ACKNOWLEDGEMENTS

I would like to thank Dr Di Rosman at the Health Department of Western Australia for her assistance in linking information with the Deaths Registry of Western Australia. I would also like to thank Dr James Semmens of the Department of Public Health at the University of Western Australia for acting as a consultant for the statistical analysis used in this paper.

REFERENCES

- 1 **Porter GA**, Soskolne CL, Yakimets WW, Newman SC. Surgeon related factors and outcome in rectal cancer. *Ann Surg* 1998; **227**: 157-167
- 2 **Khuri SF**, Daley J, Henderson W, Hur K, Hossain M, Saybel D, Kizer KW, Aust JB, Bell RH, Chang V, Demakis J, Faleri PJ, Gibbs JO, Graver F, Hammermeister K, McDonald G, Passaro E, Phillips L, Scamman F, Spencer J, Stremple JF. Relation of surgical volume to outcome in eight common operations. Results from the VA national surgical quality improvement program. *Ann Surg* 1999; **230**: 414-432
- 3 **Singh KK**, Barry MK, Ralston P, Henderson MA, McCormick JS, Walls AD, Auld CD. Audit of colorectal cancer surgery by non-specialist surgeons. *Br J Surg* 1997; **84**: 343-347
- 4 **NHMRC**. Guidelines for the prevention, early detection and management of colorectal cancer. 1999
- 5 **Platell C**. A community-based hospital experience with colorectal cancer. *Aust NZ J Surg* 1997; **67**: 420-423
- 6 **Sainsbury R**, Haward B, Rider L, Johnston C, Round C. Influence of clinician workload and patterns of treatment on survival from breast cancer. *Lancet* 1995; **345**: 1265-1270
- 7 **Matthews HR**, Powell DJ, McConkey CC. Effects of the result of surgical experience on the results of resection for oesophageal carcinoma. *Br J Surg* 1986; **73**: 621-623
- 8 **McArdle CS**, Hole D. Impact of variability among surgeons on postoperative morbidity and mortality and ultimate survival. *Br Med J* 1991; **302**: 1501-1505
- 9 **Committee on Quality of Health Care in America and the National Cancer Policy Board**. Interpreting the volume-outcome relationship in the context of health care quality. *Washington: Institute of Medicine* 2000
- 10 **Birkmeyer JD**, Finlayson EV, Birkmeyer BS. Volume standards for high-risk surgical procedures: Potential benefits of the Leapfrog initiative. *Surgery* 2001; **130**: 415-422
- 11 **Fujita S**, Teramoto T, Watanabe M, Kodaira S, Kitajima M. Anastomotic leakage after colorectal cancer surgery: a risk factor for recurrence and poor prognosis. *Jap J Clin Oncol* 1993; **23**: 299-302

Edited by Xu XQ

Tumor necrosis factor-related apoptosis-inducing ligand gene on human colorectal cancer cell line HT29

Xiang-Ming Xu, Chao He, Xiao-Tong Hu, Bing-Liang Fang

Xiang-Ming Xu, Department of Colorectal Surgery of the First Affiliated Hospital, College of Medicine, Zhejiang University, Hangzhou 310003, Zhejiang Province, China

Chao He, Xiao-Tong Hu, Clinical Research Institute of Sir Run Run Shaw Hospital, Zhejiang University, Hangzhou 310016, Zhejiang Province, China

Bing-Liang Fang, Department of Thoracic and Cardiovascular Surgery, the University of Texas M.D.Anderson Cancer Center, Box109, 1515 Holcombe Boulevard, Houston, TX77030, Texas, USA
Supported by the Scientific Committee Foundation of Zhejiang Province, No.001103163

Correspondence to: Chao He, Clinical Research Institute of Sir Run Run Shaw Hospital, Zhejiang University, Hangzhou 310016, Zhejiang Province, China. drhe@zju.edu.cn

Telephone: +86-571-86048962

Received: 2002-10-09 **Accepted:** 2002-11-06

Abstract

AIM: To evaluate the therapeutic efficiency of Tumor Necrosis Factor-related Apoptosis-inducing Ligand (TRAIL) gene on human colorectal cancer cell line HT29.

METHODS: Human embryonal kidney cells transformed by introducing sheared fragments of Ad5 DNA (293 cell) were used for amplification of adenoviral vectors: Ad/GT-TRAIL, Ad/GT-Bax, Ad/GT-LacZ and Ad/PGK-GV16. Human colorectal cancer cell line HT29 was transfected with binary adenovirus-mediated TRAIL gene. Bax gene was used as positive control, LacZ gene was used as the vector control, and cells treated with PBS only were used as a mock control. The morphological changes, cell growth and apoptosis were measured by reversmicroscope, MTT method and flow cytometry.

RESULTS: All adenoviral vectors titer determined by optical absorbency at A260nm were 1×10^{10} viral particle/ml(vp/ml). Obviously morphological changes of HT29 cells were observed when infected with Ad/GT-TRAIL, and these changes were much more obviously when Ad/PGK-GV16 was coinfecting. The cell suppression percentage and the percentage of apoptotic cells were 52.5 % and 16.5 % respectively when infected with Ad/GT-TRAIL alone, while combining with Ad/PGK-GV16, the growth of HT29 was suppressed by 85.2 % and the percentage of apoptotic cells was 35.9 %. It showed a significantly enhanced therapeutic efficiency with binary system ($P < 0.05$).

CONCLUSION: A binary adenoviral vector system provides an effective approach to amplify viral vectors that express potentially toxic gene, TRAIL. Ad/GT-TRAIL showed a significantly enhanced therapeutic efficiency for HT29 when coinfecting with Ad/PGK-GV16. Ad/GT-TRAIL could induce apoptosis of HT29 and inhibit its growth.

Xu XM, He C, Hu XT, Fang BL. Tumor necrosis factor-related apoptosis-inducing ligand gene on human colorectal cancer cell line HT29. *World J Gastroenterol* 2003; 9(5): 965-969
<http://www.wjgnet.com/1007-9327/9/965.htm>

INTRODUCTION

Tumor necrosis factor-related apoptosis-inducing ligand, is also called Apo-2L, a new member of TNF family. It was first identified through a search of an expressed sequence tag (EST) database using a conserved sequence contained in many TNF family members. TRAIL is a type II transmembrane protein whose extracellular region forms a soluble molecule on cleavage. Both membrane-bound TRAIL and soluble TRAIL rapidly induce apoptosis in a wide variety of tumorigenic cells via interaction with the death receptors DR4 and DR5. However, unlike its relatives, TNF and CD95L, TRAIL appears to induce apoptosis only in tumorigenic or transformed or virus infected cells and not in normal cells. Because of its selective cellular toxicity, TRAIL may act as a safe agent for tumor gene therapy^[1,2]. In our experiment, human colorectal cancer cell line HT29 was transfected with binary adenovirus-mediated TRAIL gene. Bax gene was used as positive control, LacZ gene was used as the vector control, and cells treated with PBS only were used as a mock control. To evaluate the therapeutic efficiency of TRAIL on human colorectal cancer cell line HT29, reversmicroscope, MTT method and flow cytometry were used.

MATERIALS AND METHODS

Materials

Adenoviral vectors and cell lines: Ad/GT-TRAIL, Ad/GT-Bax, Ad/GT-LacZ and Ad/PGK-GV16 were presented by Dr. Bingliang Fang (Department of Thoracic and Cardiovascular surgery, The University of Texas M.D.Anderson Cancer center). Human embryonal kidney cells transformed by introducing sheared fragments of Ad5 DNA (293 cell) was maintained in our laboratory (Clinical research institute of Sir Run Run Shaw Hospital, Zhejiang University). Human colorectal cancer cell line HT29, a kind gift from Dr. Junhui Cui (Medical School, Zhejiang University).

Methods

Construction, amplification and titration of adenoviruses^[3]
Adenoviral vectors Ad/GT-Bax, Ad/GT-LacZ and Ad/PGK-GV16 were constructed as described previously^[14]. Ad/GT-TRAIL, an adenoviral vector expressing TRAIL, was also constructed. Briefly, a cDNA containing the entire coding sequence of human TRAIL was inserted into an expression cassette driven by a GT promoter to generate shuttle plasmid pAd/GT-TRAIL. This shuttle plasmid was then cotransfected into 293 cells along with a 35-kb ClaI fragment from adenovirus type 5. Then, recombinant vector Ad/GT-TRAIL was generated by homologous recombination and plaque-purified. To produce large quantities of the virus, when 293 cells (transformed primary human embryonal kidney cells) are grown to 60-70 % confluency on 75 cm² bottle, the media were changed using RPMI1640 supplemented with 10 % FBS and antibiotics. Purified virus is added to the bottles at a multiplicity of infection (MOI) of 100:1. Every 15 min gently rock the bottles to redistribute the liquid over the entire bottle, and rotate the bottles to allow for even distribution of the viral

suspension. After one hour incubation, add 15 ml fresh media to each bottle. Incubate the bottles in a 37 °C, 5 % CO₂ incubator for 48-72 h, harvest the cells when a complete cytopathic effect (CPE) is evident (95-100 % cells rounded with 10-20 % floating). The cells should be lifted off the bottle by gently pipetting medium over them and collect cells into 50 ml centrifuge tubes. Centrifuge in a clinical centrifuge at room temperature for 3-4 min at 1 500 rpm. The supernatant may be placed directly at -70 °C for further infection. The cell pellet may also be placed directly at -70 °C until ready for purification. After three cycles of freeze-thaw the cell pellets, remove the cellular debris by centrifuging in a clinical centrifuge at 2 500 rpm for 5 min. The titer determined by the absorbency of the dissociated virus at A260 nm (one A260 nm unit=10¹² viral particles/ml) was used in this study. All of the viral preparations were found to be free of the E1+ adenovirus by PCR assay and endotoxin by testing with a Limulus amoebocyte lysate endotoxin detection kit.

MTT assay of cell growth

Cell growth was measured by MTT methods. Cells were seeded onto 96-well plates at a density of 10⁴ in 100 µl of medium per well. When HT29 cells were grown to 80 % confluency, PBS, Ad/GT-LacZ, Ad/GT-Bax, Ad/GT-TRAIL, Ad/GT-LacZ+Ad/PGK-GV16 (1:1), Ad/GT-Bax+Ad/PGK-GV16 (1:1), Ad/GT-TRAIL+Ad/PGK-GV16 (1:1) were added respectively. The optimal MOI was determined by infecting HT29 cell with Ad/GT-LacZ+Ad/PGK-GV16 (1:1) and assessing the expression of β-galactosidase via X-gal staining. The MOI that resulted in >85 % of cells being stained blue were used in this experiment. The MOI was 1 000 particles for HT29 cells. Unless otherwise specified, Bax was used as positive control, LacZ was used as the vector control, and cells treated with PBS only were used as a mock control. At 0, 1 d, 3 d and 5 d, cells were incubated with 0.5 % MTT for 4 hours. The medium was then removed and 150 µl DMSO solution was added, followed by incubation at 37 °C for another 4 hours. The absorbance of the reaction solution at 490 nm was measured. These data were used to make growth curves. The cell suppression percentage=(1-absorbance of experimental group/absorbance of control group)×100 %.

Assay of apoptosis (FCM)

HT29 cells were seeded onto 6-well plates at a density of 4×10⁶ in 2.5 ml of medium per well. The cells were given the same treatment as we did in the MTT assay. The MOI was 1 000, reverse microscope was used to watch the morphological changes. Cells were harvested by trypsinization at 5 d after treatment, then FCM analysis for cell surface molecules was performed using Annexin V Kit (Immunotech, Annexin-FITC), according to the following procedure: wash cells twice with cold PBS, resuspend cells in 1×Binding Buffer at a concentration of 1×10⁶cells/ml, transfer 100 µl to a 5 ml culture tube, add 5 µl Annexin V-FITC and 10 µlPI, gently vortex the tube and incubate for 15 min at room temperature in the dark, add 400 µl 1×Binding Buffer to each tube, analyze by flow cytometry as soon as possible (within one hour). PI/Annexin V-negative cells were regarded as living cells; PI-positive/Annexin-negative cells were regarded as injured ones; PI-negative/Annexin V-positive cells were regarded as early apoptotic cells; PI/Annexin V-positive cells were regarded as late apoptotic or secondary necrotic ones.

Statistical analysis

Differences among the treatment groups were assessed by paired *t*-test using SPSS10.0 statistical software. *P*<0.05 indicates significant difference.

RESULTS

Titers of recombinant adenovirus

All adenoviral vectors titer determined by optical absorbency at A260nm were 1×10¹⁰ viral particle/ml(vp/ml).

Morphological changes of recombinant adenovirus on HT29 cell

When HT29 were transfected with Ad/GT-TRAIL, Ad/GT-Bax, obviously morphological changes of HT29 were found. These changes were found to be much more early and obviously when Ad/PGK-GV16 was cultured together. Over 80 % of the cells showed signs of cytopathology, and became rounded and detached. However, when HT29 were transfected with Ad/GT-LacZ, Ad/GT-LacZ+Ad/PGK-GV16, no significant morphological changes were found, the cells remained in monolayers with normal morphology.

Cell growth inhibition of recombinant adenovirus on HT29 cell

Cell viability was measured by MTT assay as showed in Figure 1 and Figure 2. Cultured with Ad/GT-TRAIL, Ad/GT-Bax, Ad/GT-LacZ, the cell growth of HT29 was inhibited by 52.5 %, 30.3 % and 10.5 % respectively (Table 1). When Ad/PGK-GV16 was added, the cell growth inhibition rates were 85.2 %, 61.5 % and 12.1 % respectively (Table 2). There were significant difference between TRAIL, Bax and LacZ, and PBS treatment, Ad/GT-TRAIL and Ad/GT-TRAIL+ Ad/PGK-GV16, Ad/GT-Bax and Ad/GT-Bax+ Ad/PGK-GV16 (*P*<0.05). There were also shown significant difference between TRAIL and Bax treatment when combined with Ad/PGK-GV16. The result showed TRAIL was more efficient to inhibit cell growth than Bax on HT29.

Table 1 Cell growth inhibition of recombinant adenovirus on HT29 cell

Group	OD ($\bar{x}\pm s$)	Cell growth inhibition rates (%)
Ad/GT-TRAIL	0.57±0.12 ^{ac}	52.5
Ad/GT-Bax	0.84±0.08 ^a	30.3
Ad/GT-LacZ	1.07±0.13	10.5
PBS	1.20±0.17	0.0

^a*P*<0.05, vs LacZ, PBS groups; ^c*P*<0.05, vs Bax group.

Table 2 Cell growth inhibition of recombinant adenovirus on HT29 cell when combined with Ad/PGK-GV16

Group	OD ($\bar{x}\pm s$)	Cell growth inhibition rates (%)
Ad/GT-TRAIL+Ad/PGK-GV16	0.18±0.03 ^{ac}	85.2
Ad/GT-Bax +Ad/PGK-GV16	0.46±0.09 ^a	61.5
Ad/GT-LacZ +Ad/PGK-GV16	1.05±0.07	12.1
PBS	1.20±0.17	0.0

^a*P*<0.05, vs LacZ, PBS groups; ^c*P*<0.01, vs Bax group.

Apoptosis detected by flow cytometry

Apoptosis was detected by flow cytometry (Figure 3). The percentage of apoptotic cells treated with Ad/GT-TRAIL, Ad/GT-Bax, Ad/GT-LacZ and PBS (120 h after treatment) were 16.5 %, 14.7 %, 7.45 %, and 6.15 % respectively (Table 3). There were significant difference between Ad/GT-TRAIL, Ad/GT-Bax and Ad/GT-LacZ, PBS group (*P*<0.05). When combined with Ad/PGK-GV16, the percentage of apoptotic cells were significantly increased (*P*<0.05), 35.9 %, 29.0 % and 11.2 % respectively (Table 4). There were no significant difference between Ad/GT-TRAIL and Ad/GT-Bax treatment,

but there were significant difference between Ad/GT-TRAIL+Ad/PGK-GV16, Ad/GT-Bax+Ad/PGK-GV16 and Ad/GT-LacZ+Ad/PGK-GV16, PBS treatment ($P<0.01$).

Table 3 The percentage of apoptotic cells of recombinant adenovirus on HT29 cell after 5 d treatment

Group	The percentage of apoptotic cells (% , $\bar{x}\pm s$)
Ad/GT-TRAIL	16.50±1.13 ^a
Ad/GT-Bax	14.70±0.46 ^a
Ad/GT-LacZ	7.45±0.75
PBS	6.15±0.23

^a $P<0.05$, compared with LacZ, PBS groups.

Table 4 The percentage of apoptotic cells of recombinant adenovirus on HT29 cell when combined with Ad/PGK-GV16 after 5 d treatment

Group	The percentage of apoptotic cells (% , $\bar{x}\pm s$)
Ad/GT-TRAIL+Ad/PGK-GV16	35.90±1.32 ^a
Ad/GT-Bax+Ad/PGK-GV16	29.00±1.66 ^a
Ad/GT-LacZ+Ad/PGK-GV16	11.23±1.14
PBS	6.15±0.23

^a $P<0.01$, compared with LacZ, PBS groups.

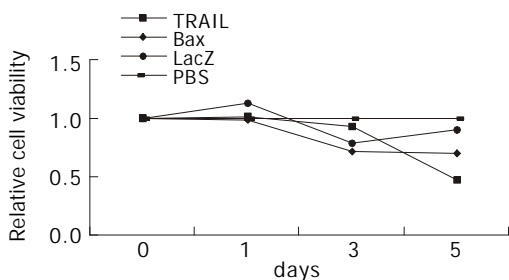


Figure 1 Cell viability determined by MTT assay.

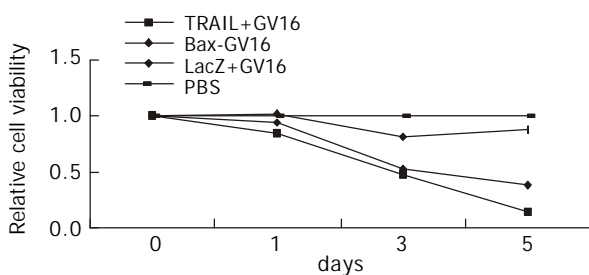


Figure 2 Cell viability determined by MTT assay.

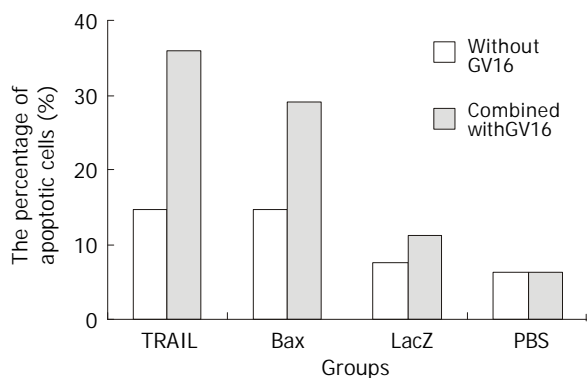


Figure 3 Apoptosis detected by flow cytometry.

DISCUSSION

Colorectal cancer is one of the malignant tumors that threaten human life severely. The main treatments of colorectal cancer are surgical resection, chemotherapy and radiotherapy. Because of local recurrence and metastasis, the 5-year survival rate after surgical resection is about 50 %. Gene therapy is a new method of introducing genetic material into cells developed in modern medicine and molecular biology. It is certain that occurrence of colorectal cancer is the result of interaction between hereditary and environmental factors, research on colorectal gene therapy has been undertaken in recent years, including suicide gene therapy (HSV-TK/GCV system, CD/5-FC system), tumor suppressor gene, immunogene therapy and anti-VEGF gene therapy. The idea of them is to induce apoptosis of tumor cells^[4-9].

Tumor necrosis factor-related apoptosis-inducing ligand (TRAIL), which is a new member of the TNF family, showed a promising result for tumor gene therapy because of its selective cytotoxic effect. TRAIL is present on many normal cell surfaces. It appears to induce apoptosis only in tumorigenic or transformed cells or virus infected cells but not in normal cells^[10,11]. It has five receptors: DR4^[12], DR5^[13], DcR1^[14], DcR2^[15], OPG^[16] (Osteoprotegerin). Both member-bound TRAIL and soluble TRAIL induce apoptosis rapidly via interaction with death receptors DR4, DR5. DcR1, with no death domain and DcR2, with a truncated death domain are not capable of inducing apoptosis, however by competing for TRAIL, they are capable of inhibiting TRAIL-induced apoptosis, thereby protecting normal cells from the cytotoxic effect^[17,18]. In addition, it is important for tumor gene therapy that TRAIL may elicit bystander effects either through interaction of surface TRAIL molecules with receptors on neighboring cells or through the action of soluble TRAIL from the TRAIL-expressing cells^[19].

Recent studies showed that TRAIL induced apoptosis in a wide variety of tumor cell lines, both *in vitro* and *in vivo*. Because of the TRAIL gene's high apoptotic activity and its toxic effect on packaging 293 cells, constructing an adenoviral vector that can express TRAIL remain to be a problem. In this study, we constructed adenoviral vectors expressing the human TRAIL gene using a binary vector system that allows expression of a highly apoptotic gene. Briefly, the TRAIL gene's promoter was replaced by GT, a synthetic promoter consisting of five GAL4-binding sites and a TATA box, which has very low transcriptional activity *in vitro* and *in vivo* when placed in an adenoviral backbone. Moreover, the transgene activity can be substantially induced *in vitro* and *in vivo* by administering this construct along with an adenoviral vector (Ad/PGK-GV16) expressing a GT transactivator, namely, the GAL4-VP16 fusion protein^[20]. This means TRAIL protein expression could be induced by coinfected target cells with Ad/GT-TRAIL and Ad/PGK-GV16. One potential problem that may arise in using this system is that not all the target cells may be transduced by both the transgene-expressing and transactivator-expressing vector. Our early study showed *in vitro* transduction of H1299 cells with Ad/CMV-LacZ or Ad/GT-LacZ+Ad/PGK-GV16(1:1) at the same MOI showed equivalent blue cells by X-gal staining, which suggested that transduction efficiency may not be hampered by using two vectors. The binary adenoviral vector system was effective for expressing high levels of the proapoptotic gene, it was also confirmed in Bax gene study^[21]. Here Bax gene was used as positive control. The results showed Ad/GT-TRAIL and Ad/GT-Bax were able to induce apoptosis of HT29 and inhibit its growth. When combined with Ad/PGK-GV16, the effects were enhanced significantly, it was testified again that the binary adenoviral vector system was simple and effective for

expressing high levels of the proapoptotic gene. This method may provide an alternative approach for colorectal cancer biotherapy. Our result also provides experimental evidences for preclinical research on colorectal cancer gene therapy. There are several advantages using adenoviral vector: high transduction efficiency; high expression of report gene; high viral titer; simpler to construct recombinant virus; insert size up to 8kb. Direct intratumoral injection of recombinant adenoviral vector can induce tumor cell apoptosis, suppress tumor progression and even ablate the tumor with TRAIL gene's antitumor and bystander effect. Recent studies showed that repeated i.v. injection of recombinant and biologically active TRAIL induced tumor cell apoptosis, suppressed tumor progression, and improved survival in mice bearing colorectal cancer model (DLD-1), with no detectable toxicity^[19]. Whereas toxic effects of TRAIL on human hepatocytes *in vitro* were observed, concern must be raised about the potential toxicity of TRAIL, especially when administered systemically. A non-tagged, soluble, native-sequence form of TRAIL (amino acids 114-281) failed to induce hepatotoxicity in cynomolgus monkeys^[10]. A recombinant, soluble version of the ligand fused to a trimerizing leucine zipper (amino acids 95-281) also lacked hepatotoxicity in mice^[11]. More recently, a polyhistidine-tagged recombinant soluble form of TRAIL (amino acids 114-281) was reported to induce apoptosis in cultured human hepatocytes^[22]. Although the recent report of hepatocyte death after treatment with TRAIL *in vitro* must be taken seriously, it is important that the limitations of the model system used in these experiments are also understood^[23]. Fortunately, further research showed that the proapoptotic activity of the TRAIL gene is mainly elicited via membrane-bound TRAIL, and soluble factors contribute little to antitumor and bystander effect. The possible explanation is that the effects of the soluble TRAIL may be dose-dependent, conformation-dependent. It has been reported that only the trimerized recombinant TRAIL is the most effective. With direct intratumoral injection of TRAIL, the release of soluble TRAIL from such TRAIL-expressing tumor cells is not substantial enough to cause liver damage, and toxicity may be reduced by vector-targeting strategies. TRAIL has a strong bystander effect, but our preliminary data showed the bystander effect was mediated by the membrane-bound TRAIL, and it was cell-contact dependent. Therefore, efficient delivery of the TRAIL gene into as many cancer cells as possible is still an important goal in treating cancer patients.

Although our data showed TRAIL and Bax gene can significantly inhibit the growth of HT29, the percentage of apoptotic cell are not very high. It has been shown that different kinds of tumors, even different cell lines of the same tumor have different sensitivity to TRAIL, which had relation to level of FLIP, low expression or mutation or loss of DR4 gene, activation or not of NF- κ B, overexpression of Bcl-2, etc. However with the addition of chemotherapeutic agent or immunoregulator^[24-26], TRAIL-resistant tumor cells recovered its sensitivity to TRAIL. For examples, addition of actinomycin D to TRAIL-resistant melanomas resulted in decreased intracellular concentrations of FLIP, which correlated with their acquisition of TRAIL sensitivity^[27]. The same results were found, when treated with Doxorubicin or 5-Fu to induce apoptosis of breast cancer, Doxorubicin or Camptothecin to human hepatocellular carcinoma dramatically augmented TRAIL-induced cytotoxicity^[28]. In experiment of the antitumor activity of recombinant TRAIL on mice bearing human colon carcinoma, Gliniak^[29] found that these tumors displayed a differential sensitivity to TRAIL *in vivo* that paralleled their susceptibility to TRAIL-induced apoptosis *in vitro*. It demonstrated that TRAIL alone was a potent antitumor agent *in vivo*, and its activity could be significantly enhanced in

combination with the chemotherapeutic agent CPT-11. However, one of these reports also mentioned that normal cells could be sensitized to TRAIL-induced apoptosis^[30]. This suggests that such a combination treatment may also increase toxicity. Nevertheless such an increase in toxicity in response to this combination therapy may be avoided if TRAIL expression can be limited locally to tumors. With the combination of TRAIL and chemotherapy, the dose of chemotherapeutic agent could be reduced, and thus decreased the side effects of chemotherapy. In order to explore a more effective approach to deliver TRAIL gene for colorectal treatment, or to evaluate the effect of TRAIL gene on liver metastasis (through liver metastasis models of human colorectal carcinoma established in nude mice)^[31], further research on it is necessary.

REFERENCES

- 1 **Wiley SR**, Schooley K, Smolak PJ, Din WS, Huang CP, Nicholl JK, Sutherland GR, Smith TD, Rauch C, Smith CA. Identification and characterization of a new member of the TNF family that induces apoptosis. *Immunity* 1995; **3**: 673-682
- 2 **Pitti RM**, Marsters SA, Ruppert S, Donahue CJ, Moore A, Ashkenazi A. Induction of apoptosis by Apo-2 ligand, a new member of the tumor necrosis factor cytokine family. *J Biol Chem* 1996; **271**: 12687-12690
- 3 **Graham FL**, Prevec L. Manipulation of adenovirus vectors frank L.Graham and ludvik prevec. *Vol7.Clifton, NJ:Humane Press Inc* 1991: 109-128
- 4 **Lechanteur C**, Princen F, Lo Bue S, Detroz B, Fillet G, Gielen J, Bours V, Merville MP. HSV-1 thymidine kinase gene therapy for colorectal adenocarcinoma-derived peritoneal carcinomatosis. *Gene Ther* 1997; **4**: 1189-1194
- 5 **Hirschowitz EA**, Ohwada A, Pascal WR, Russi TJ, Crystal RG. *In vivo* adenovirus-mediated gene transfer of the Escherichia coli cytosine deaminase gene to human colon carcinoma-derived tumors induces chemosensitivity to 5-Fluorocytosine. *Hum Gen Ther* 1995; **6**: 1055-1063
- 6 **Fujiwara T**, Tanaka N. Molecular surgery for human colorectal cancer with tumor suppressor P53 gene transfer. *Nippon Geka Gakkai Zasshi* 1998; **99**: 463-468
- 7 **Mazzolini G**, Qian C, Narvaiza I, Barajas M, Borrás-Cuesta F, Xie X, Duarte M, Melero I, Prieto J. Adenoviral gene transfer of interleukin 12 into tumors synergizes with adoptive T cell therapy both at the induction and effector level. *Hum Gen Ther* 2000; **11**: 113-125
- 8 **Shen LZ**, Wu WX, Xu DH, Zheng ZC, Liu XY, Ding Q, Hua YB, Yao K. Specific CEA-producing colorectal carcinoma cell killing with recombinant adenoviral vector containing cytosine deaminase gene. *World J Gastroenterol* 2002; **8**: 270-275
- 9 **Cao GW**, Qi ZT, Pan X, Zhang XQ, Miao XH, Feng Y, Lu XH, Kuriyama S, Du P. Gene therapy for human colorectal carcinoma using human CEA promoter controlled bacterial ADP-ribosylating toxin genes human CEA: PEA & DTA gene transfer. *World J Gastroenterol* 1998; **4**: 388-391
- 10 **Ashkenazi A**, Pai RC, Fong S, Leung S, Lawrence DA, Marsters SA, Blackie C, Chang L, McMurtrey AE, Hebert A, DeForge L, Koumenis IL, Lewis D, Harris L, Bussiere J, Koeppen H, Shahroksh Z, Schwall RH. Safety and antitumor activity of recombinant soluble Apo2 ligand. *J Clin Invest* 1999; **104**: 155-162
- 11 **Walczak H**, Miller RE, Ariail K, Gliniak B, Griffith TS, Kubin M, Chin W, Jones J, Woodward A, Le T, Smith C, Smolak P, Goodwin RG, Rauch CT, Schuh JC, Lynch DH. Tumor necrosis factor-related apoptosis-inducing ligand *in vivo*. *Nat Med* 1999; **5**: 157-163
- 12 **Pan G**, O'Rourke K, Chinnaiyan AM, Gentz R, Ebner R, Ni J, Dixit VM. The receptor for the cytotoxic ligand TRAIL. *Science* 1997; **276**: 111-113
- 13 **Walczak H**, Degli-Esposti MA, Johnson RS, Smolak PJ, Waugh JY, Boiani N, Timour MS, Gerhart MJ, Schooley KA, Smith CA, Goodwin RG, Rauch CT. TRAIL-R2: a novel apoptosis-mediating receptor for TRAIL. *EMBO J* 1997; **16**: 5386-5397
- 14 **Degli-Esposti MA**, Smolak PJ, Walczak H, Waugh J, Huang CP, DuBose RF, Goodwin RG, Smith CA. Cloning and character-

- ization of TRAIL-R3, a novel member of the emerging TRAIL receptor family. *J Exp Med* 1997; **186**: 1165-1170
- 15 **Marsters SA**, Sheridan JP, Pitti RM, Huang A, Skubatch M, Baldwin D, Yuan J, Gurney A, Goddard AD, Godowski P, Ashkenazi A. A novel receptor for Apo-2L/TRAIL contains a truncated death domain. *Curr Biol* 1997; **7**: 1003-1006
- 16 **Emery JG**, McDonnell P, Burke MB, Deen KC, Lyn S, Silverman C, Dul E, Appelbaum ER, Eichman C, DiPrinzio R, Dodds RA, James IE, Rosenberg M, Lee JC, Young PR. Osteoprotegerin is a receptor for the cytotoxic ligand TRAIL. *J Biol Chem* 1998; **273**: 14363-14367
- 17 **Ashkenazi A**, Dixit VM. Apoptosis control by death and decoy receptors. *Curr Opin Cell Biol* 1999; **11**: 255-260
- 18 **Griffith TS**, Lynch DH. TRAIL: a molecule with multiple receptors and control mechanisms. *Curr Opin Immunol* 1998; **10**: 559-563
- 19 **Kagawa S**, He C, Gu J, Koch P, Rha SJ, Roth JA, Curley SA, Stephens LC, Fang B. Antitumor activity and bystander effects of the tumor necrosis factor-related apoptosis-inducing ligand (TRAIL) gene. *Cancer Res* 2001; **61**: 3330-3338
- 20 **Fang B**, Ji L, Bouvet M, Roth JA. Evaluation of GAL4/TATA *in vivo*. Induction of transgene expression by adenovirally mediated gene codelivery. *J Biol Chem* 1998; **273**: 4972-4975
- 21 **Kagawa S**, Pearson SA, Ji L, Xu K, McDonnell TJ, Swisher SG, Roth JA, Fang B. A binary adenoviral vector system for expressing high levels of the proapoptotic gene bax. *Gene Ther* 2000; **7**: 75-79
- 22 **Jo M**, Kim TH, Seol DW, Esplen JE, Dorko K, Billiar TR, Strom SC. Apoptosis induced in normal human hepatocytes by tumor necrosis factor-related apoptosis-inducing ligand. *Nat Med* 2000; **6**: 564-567
- 23 **Gores GJ**, Kaufmann SH. Is TRAIL hepatotoxic? *Hepatology* 2001; **34**: 3-6
- 24 **Hu JY**, Wang S, Zhu JG, Zhou GH, Sun QB. Expression of B7 costimulation molecules by colorectal cancer cells reduce tumorigenicity and induces anti-tumor immunity. *World J Gastroenterol* 1999; **5**: 147-151
- 25 **Bonavida B**, Ng CP, Jazirehi A, Schiller G, Mizutani Y. Selectivity of TRAIL-mediated apoptosis of cancer cells and synergy with drugs: the trail to non-toxic cancer therapeutics. *Int J Oncol* 1999; **15**: 793-802
- 26 **Gibson SB**, Oyer R, Spalding AC, Anderson SM, Johnson GL. Increased expression of death receptors 4 and 5 synergizes the apoptosis response to combined treatment with etoposide and TRAIL. *Mol Cell Biol* 2000; **20**: 205-212
- 27 **Griffith TS**, Chin WA, Jackson GC, Lynch DH, Kubin MZ. Intracellular regulation of TRAIL-induced apoptosis in human melanoma cells. *J Immunol* 1998; **161**: 2833-2840
- 28 **Yamanaka T**, Shiraki K, Sugimoto K, Ito T, Fujikawa K, Ito M, Takase K, Moriyama M, Nakano T, Suzuki A. Chemotherapeutic agents augment TRAIL-induced apoptosis in human hepatocellular carcinoma cell lines. *Hepatology* 2000; **32**: 482-490
- 29 **Gliniak B**, Le T. Tumor necrosis factor-related apoptosis-inducing ligands antitumor activity *in vivo* is enhanced by the chemotherapeutic agent CPT-11. *Cancer Res* 1999; **59**: 6153-6158
- 30 **Keane MM**, Ettenberg SA, Nau MM, Russell EK, Lipkowitz S. Chemotherapy augments TRAIL-induced apoptosis in breast cell lines. *Cancer Res* 1999; **59**: 734-741
- 31 **Liu QZ**, Tuo CW, Wang B, Wu BQ, Zhang YH. Liver metastasis models of human colorectal carcinoma established in nude mice by orthotopic transplantation and their biologic characteristic. *World J Gastroenterol* 1998; **4**: 409-411

Edited by Xu JY

Effect of extended radical resection for rectal cancer

Xing-Shu Dong, Hai-Tao Xu, Zhi-Wei Yu, Ming Liu, Bin-Bin Cui, Peng Zhao, Xi-Shan Wang

Xing-Shu Dong, Hai-Tao Xu, Zhi-Wei Yu, Ming Liu, Bin-Bin Cui, Peng Zhao, Xi-Shan Wang, Department of Abdominal Surgery, the Third Affiliated Hospital, Harbin Medical University, Harbin 150040, Heilongjiang Province, China

Correspondence to: Xing-Shu Dong, Department of Abdominal Surgery, the Third Affiliated Hospital, Harbin Medical University, Harbin 150040, Heilongjiang Province, China. happy-satisfied@sina.com
Telephone: +86-451-6677580-2146 **Fax:** +86-451-6663760

Received: 2002-09-14 **Accepted:** 2002-10-18

Abstract

AIM: To discuss the rationality of extended radical resection (ERR) and to guide the surgical treatment of rectal cancer.

METHODS: Total 211 patients who underwent ERR from 1981 to 1987 (follow-up rate of 94.8 %) were selected to study the patterns of lymphatic metastasis and therapeutic effect. The control group was made of 293 patients with rectal cancer who underwent conventional radical resection (CRR) and its follow-up rate was 98.5 %. The lymph node specimens, obtained by the triple-approach lymph node resection during the radical resection of rectal cancer, were studied by conventional pathological method. The extended radical resection, guided by the patterns of lymphatic metastasis, was applied in the clinical practice.

RESULTS: The incidence of lymphatic metastasis in Chinese patients with advanced rectal cancer was 43.6 %, and that of the upper 2nd and 3rd groups and the lateral group was 14.2 %, 10.9 % and 11 % respectively. The 5, 10-year-survival rates of the ERR were 68.0 % and 47.0 %, respectively, which were much higher than those of the conventional radical resection (42.9 % and 25.3 %).

CONCLUSION: The ERR for rectal cancer removes all the lymph nodes, prevents possible metastasis and finally improves the survival rate.

Dong XS, Xu HT, Yu ZW, Liu M, Cui BB, Zhao P, Wang XS. Effect of extended radical resection for rectal cancer. *World J Gastroenterol* 2003; 9(5): 970-973
<http://www.wjgnet.com/1007-9327/9/970.htm>

INTRODUCTION

Early in 1970s, the opinion for extended radical resection (ERR) of rectal cancer, which was suggested by some Japanese scholars, caused great controversy among the scholars who majored in colorectal cancer all over the world. In 1980s, to study the rationality of surgical treatment for Chinese rectal cancer, our hospital first got the patterns of lymphatic metastasis in Chinese rectal cancer with studying rectal normal lymphatic drainage and lymphatic metastasis of rectal cancer. And the EER, guided by the patterns of lymphatic metastasis, has been applied in our hospital for about 20 years. These caused a lot of controversy as well. Here, the patterns of

lymphatic metastasis in rectal cancer and therapeutic effect of ERR are reviewed and analyzed, then the scholar's doubts are discussed.

MATERIALS AND METHODS

Materials

All cases of advanced rectal cancer were received and treated in our hospital. 211 cases used to study the patterns of lymphatic metastasis and therapeutic effect were chosen within the patients who underwent ERR (include all upper and lateral lymph nodes cleaning) from 1981 to 1987 (follow-up rate of 94.8 %). The control group was made of 293 cases that underwent conventional radical resection (CRR) and its follow-up rate was 98.5 %. Between two groups, there was no significant difference in the clinical data such as location, pathological type, degree of infiltration, lymphatic metastasis and so on.

Methods

During operation, the upper lymph nodes were resected from the root of inferior mesenteric artery. The periaorta lymph nodes were cleaned partially. Then the lymph nodes around common, internal and external iliac arteries were resected, as well as those of obturator foramen. The inferior mesenteric artery or superior rectal artery and middle rectal artery was ligated and cut off at the root. And the rectal lateral ligament was cut off along the pelvic wall. In the Miles operation, the levator muscle of anus was cut off along the pelvic wall as well. And the connective tissue in the ischioanal fossa should be cleaned.

These lymph nodes included those of perirectum, superior rectal artery, inferior mesenteric artery and its root, middle rectal artery, and external iliac artery, common iliac artery, obturator, aorta, inferior vena cava and deep inguinal.

The lymph nodes were collected by touch and modified transparent methods. Both the nodes and the primary locus were analyzed by conventional pathological method. The survival rate of both groups was compared by direct method.

RESULTS

The patterns of lymphatic metastasis

Total 6894 lymph nodes were collected among 211 patients who underwent the extended radical resection, 32.7 nodes per patient in average. There were 92 cases (43.6 %) and 616 nodes (8.9 %) with metastasis. The metastasis rate of upper 2nd and 3rd group was respectively 14.2 % and 10.9 %. 16 cases of rectal cancer below the peritoneum reflex had lateral metastasis (11 %). The metastasis rate of the cases with >1/2 rectal circumference involved was 53.7 %, and that with <1/2 circumference involved was 26.7 % ($P<0.01$). The metastasis rate of the cases with serosal invasion was 63.5 %, and that of muscular invasion was 26.0 % ($P<0.01$). The metastasis rate of the cases with invasive type was 58.9 %, local type 32.3 % ($P<0.01$). Poorly differentiated and mucinous adenocarcinoma had a metastasis rate of 68.6%, well and moderately differentiated ones 31.8 % ($P<0.01$), invasive type of growth 70.0 %, and expanding type of growth 22.9 % ($P<0.01$). (Tables 1-5).

Table 1 Relationship between lymphatic metastasis and invasive rate

Circumference	<i>n</i>	Lymphatic metastasis (-)	Lymphatic metastasis (+)	Positive rate (%)
≤1/2	90	66	24	26.7 %
<1/2	121	56	65	53.7 % ^a

^a*P*<0.01, vs ≤1/2 circumference.

Table 2 Relationship between lymphatic metastasis and invasive depth

Depth	<i>n</i>	Lymphatic metastasis (-)	Lymphatic metastasis (+)	Positive rate (%)
Muscular	96	71	25	26.0 %
Serosa	115	42	73	63.5 % ^b

^b*P*<0.01, vs. Muscular.

Table 3 Relationship between lymphatic metastasis and macrotype

Macrotype	<i>n</i>	Lymphatic metastasis (-)	Lymphatic metastasis (+)	Positive rate (%)
Local	99	67	32	32.3 % ^c
Invasive	112	46	66	58.9 %

^c*P*<0.01, vs. invasive type.

Table 4 Relationship between lymphatic metastasis and histological type

Histological type (adenocarcinoma)	<i>n</i>	Lymphatic metastasis (-)	Lymphatic metastasis (+)	Positive rate (%)
Well and moderately differentiated	160	109	51	31.8 %
Poorly differentiated and mucinous	51	16	35	68.6 % ^d

^d*P*<0.01, vs. well and moderately differentiated type.

Table 5 Relationship between lymphatic metastasis and growth type

Growth type	<i>n</i>	Lymphatic metastasis (-)	Lymphatic metastasis (+)	Positive rate (%)
Expanding	61	47	14	22.9 %
Invasive	150	46	105	70.0 % ^e

^e*P*<0.01, vs. expanding type.

Table 6 Survival rate of extend radical resection (ERR) and conventional radical resection (CRR)

	<i>n</i> ₁	5-year-survival rate	<i>n</i> ₂	10-year-survival rate
Dukes A				
CRR	54/103	52.4 %	16/55	29.1 %
ERR	63/73	86.3 %	5/9	55.69 %
Dukes B				
CRR	32/71	45.1 %	12/43	27.9 %
ERR	28/47	59.5 %	1/3	33.3 %
Dukes C				
CRR	38/115	33.0 %	12/60	20.0 %
ERR	52/91	57.1 %	2/12	40.0 %
Total				
CRR	124/289	42.9 %	40/158	25.3 %
ERR	136/200	68.0 %	8/17	47.0 %

The therapeutic effect of the ERR

Table 6 shows that the 5- and 10-year-survival rate of patients with advanced rectal cancer who underwent ERR (68.0 % and 47.0 %) is obvious higher than that of patients with CRR (42.9 % and 25.3 %), *P*<0.05.

DISCUSSION

The lymphatic drainage of rectum and the patterns of lymphatic metastasis of rectal cancer

The research on anatomy of rectum^[1,16,19,36] had played an important role in operation of rectal cancer. Numbers of researches have showed that there are three routes of lymphatic drainage. The upper way drains the lymph of the whole anorectum, the lateral one drains that of the anal canal and the rectum below the level of peritoneal reflection, and inferior one only drains that of the anal canal^[1]. Then this result of the anatomic research has been used to guide the operations in clinical practice^[2-6, 17, 20, 23, 28,37]. Early in 1980s, our hospital first began to study the principle of lymphatic metastasis in Chinese patients with rectal cancer and showed that lymphatic metastasis followed the normal lymphatic drainage^[6, 27].

The ERR

According to the patterns, we concluded that ERR could be used for advanced rectal cancer. During cleaning of lymphatic tissue, the upper level of the cleaning should reach the root of inferior mesenteric artery, or 10 % lymphatic metastasis would have been left. For the rectal cancer beneath the level of peritoneal reflection, the lateral cleaning with internal iliac artery and obturator nodes should be carried out, or else another 10 % would have been left.

The indications for EER should be fitful. The advanced rectal cancer with no transperitoneal and distant metastasis and the one with the local invasion but resectable would be preferred. The patients must have no serious disease and could endure the surgical operation and the anaesthesia. The ERR cleaned all the upper, lateral and partial lower lymphatic tissue with potential metastasis, and thus improve the survival rate^[7, 8, 26].

The influence of EER to the immune function

For the extended radical resection, the experts in the field of rectal cancer wondered whether the cleaning of the lymphatic tissue affected the immune function of the patients. So we carried out the comparative study of the immune function, which included the "E" wreath test and the IgA, IgG, IgE determination before operation and after operation. And the results showed that the ERR have no negative influence of the immune reaction.

The problem about how to clean all the nodes with metastasis and maintain the normal ones

It was not always correct to judge whether it metastasize or not with nude eyes. That is to say, we could not confirm the Dukes stage of the rectal cancer during the operation. The misdiagnosis rate is about 25 %. The lymphatic micrometastasis^[30-32] of rectal cancer, that was a new challenge for judging the lymphatic metastasis, was investigated by Silva^[25] and Sterk *et al*^[35] using lymphoscintigraphy and lymphangiography^[34], but there is still controversy^[34]. Still now, there is no effective method to judge whether lymphatic metastasis took place in one lymph node during the operation yet^[38].

Key points of studying the principle of lymphatic metastasis

In the European scholar's studies, the metastasis rate was not so high and that of lateral way was only 2 %. But the Japanese scholars showed that the metastasis rate was 10-20 %. There

was a significant difference between them. So we thought the following conditions should be important to study the patterns of lymphatic metastasis: 1. The quantity of lymphatic nodes resected during the operation must be enough to study. 2. All the nodes should be checked out by use of correct methods. 3. The careful pathological examination should be carried out.

Whether ERR would cause more bleeding and trauma

According to our statistics, the average quantity of blood transfusion in ERR was 760 ml, and that of conventional radical resection was 700 ml. There was no significant difference between them. The common damages in rectal operation included the injuries of ureter, sacral venous plexus and pelvis autonomic nerve. During the operation, the ureters were dissociated for about 20 cm, and then the resection of lymphatic nodes was carried out directly in sight. In our study, the ureter-injury rate in the extended resection was 1.4 % (3/211), and that in the conventional radical resection was 1.7 % (5/289). There was no significant difference between the both groups. The ischemia and necrosis caused by insufficient ureter dissociation never took place in our study. To avoid the injury of sacral venous plexus, we should get familiar with the anatomy of pelvis and operate directly in sight.

Early in 1980s, Japanese experts made lots of researches on preventing these complications^[9,10,18,33]. We also began to carry out the ERR with pelvis autonomic nerve reservation from 1988. And the rate of post-operative bladder and sex dysfunction was effectively reduced. The western scholars such as Mass *et al*^[24] and Di Matteo *et al*^[29] had drawn the similar conclusions. So we ensured that the functional ERR should be one of the most satisfactory operations for advanced rectal cancer.

The relationship between the functional ERR and the total mesenteric excision (TME)

TME^[11-13] was recently paid attention to by the scholars^[15,21,22,26] all over the world. Japanese experts^[14,26] divided the cleaning of perirectal connective tissue into three regions, A, B and C, and TME was similar to A region only^[14]. Our opinion is that TME should be one portion of the functional preserved EER. Early in 1980s, when ERR was established, we mentioned that total perirectal connective tissue should be resected along the lateral wall of pelvis, so did in Miles operation. In low anterior resection (LAR) operation, the perirectal connective tissue should be resected at least beneath the lower transect of the rectum. Therefore we believe that a throughout ERR should include TME.

REFERENCES

- 1 **Wang YX**. Anatomy of lymphatic system. 1st edition. Beijing: People's Medical Publishing House 1984: 237-243
- 2 **Enker WE**, Havenga K, Porgak T, Thaler H, Cranor M. Abdominoperineal resection via total mesorectal excision and automatic nerve preservation for low rectal cancer. *World J Surg* 1997; **21**: 715-720
- 3 **Scott N**, Jackson P, Al-Jaberi T, Dixon MF, Quirke P, Finan PJ. Total mesorectal excision and local recurrence: A study of tumour spread in the mesorectum distal to rectal cancer. *Br J Surg* 1995; **82**: 1031-1033
- 4 **Takahashi T**. The vicissitudes and new topic of the radical operation of rectal cancer. *Gastroenterological Surg* 1998; **21**: 271-277
- 5 **Takeo M**, Keiichi T, Masayuki O, Tatsuro Y. Advanced rectal cancer. *Gastroenterological Surg* 2001; **24**: 1897-1902
- 6 **Dong XS**, Yan FC, Zhao TZ, Ding L, Jia EM. The clinicopathological study of the lymphatic metastasis in rectal cancer. *Zhonghua Waike Zazhi* 1985; **23**: 463-466
- 7 **Moriya Y**, Sugihara K, Akasu T, Fujita S. Importance of extended lymphadenectomy with lateral node dissection for advanced lower rectal cancer. *World J Surg* 1997; **21**: 728-732
- 8 **Susumu K**. The vicissitudes and future of the operation in colorectal carcinoma. *Gastroenterological Surg* 1998; **21**: 2012-2016
- 9 **Takeo M**, Keiichi T, Masamichi Y. Saving pelvic autonomic nerve in the operation of lowrectal cancer. *Gastroenterological Surg* 1999; **22**: 1373-1379
- 10 **Takahashi T**. Function-save vs. anatomy of rectal. *Gastroenterological Surg* 2000; **23**: 1225-1232
- 11 **Heald RJ**, Husband EM, Ryall RDH. The mesorectum in rectal cancer surgery-the clue to pelvic recurrence. *Br J Surg* 1982; **69**: 613-616
- 12 **Heald RJ**, Ryall RDH. Recurrence and survival after total mesorectal excision for rectal cancer. *The Lancet* 1986; **1**: 1479-1482
- 13 **Heald RJ**, Chir M, Karanjia ND. Results of radical surgery for rectal cancer. *World J Surg* 1992; **16**: 848-857
- 14 **Maeda K**, Maruta M, Utsumi T, Togama K, Masumori K. The modern standard radical resection (D₂, D₃) advanced radical resection and decrease-size operation of rectal cancer. *Gastroenterological Surg* 1998; **21**: 279-287
- 15 **Maeda K**, Maruta M, Utsumi T, Sato H, Matsumoto M. Indications for and limitations of low anterior resection. *Nippon Geka Gakkai Zasshi* 2000; **101**: 449-453
- 16 **Takahashi T**, Ueno M, Azekura K, Ohta H. Lateral ligament: its anatomy and clinical importance. *Semin Surg Oncol* 2000; **19**: 386-395
- 17 **Jatzko GR**, Jagoditsch M, Lisborg PH, Denk H, Klimpfinger M, Stetner HM. Long-term results of radical surgery for rectal cancer: multivariate analysis of prognostic factors influencing survival and local recurrence. *Eur J Surg Oncol* 1999; **25**: 284-291
- 18 **Mori T**, Takahashi K, Yasuno M. Radical resection with autonomic nerve preservation and lymph node dissection techniques in lower rectal cancer surgery and its results: the impact of lateral lymph node dissection. *Langenbecks Arch Surg* 1998; **383**: 409-415
- 19 **Gu J**, Ma Z, Xia J. Anatomical basis of autonomic nerve-preserving radical resection for rectal cancer. *Zhonghua Waike Zazhi* 2000; **38**: 128-130
- 20 **Stipa S**, Stipa F, Lucandri G, Ziparo V. Surgery of rectal tumors. *Przegl Lek* 2000; **57**(Suppl 5): 66-68
- 21 **Aeberhard P**, Fasolini F. Total mesorectal excision for cancer of the rectum. *Recent Results Cancer Res* 1998; **146**: 66-70
- 22 **Law WL**, Chu KW. Strategies in the management of mid and distal rectal cancer with total mesorectal excision. *Asian J Surg* 2002; **25**: 255-264
- 23 **Maurer CA**, Renzulli P, Kasperek MS, Hager F, Tabrizi SA, Mazzucchelli L, Buchler MW. The role of lymph nodes in colon carcinoma. *Zentralbl Chir* 2000; **125**: 863-869
- 24 **Maas CP**, Moriya Y, Steup WH, Kiebert GM, Kranenbarg WM, van de Velde CJ. Radical and nerve-preserving surgery for rectal cancer in The Netherlands: a prospective study on morbidity and functional outcome. *Br J Surg* 1998; **85**: 92-97
- 25 **Silva JH**. Pelvic lymphoscintigraphy: contribution to the preoperative staging of rectal cancer. *Rev Hosp Clin Fac Med Sao Paulo* 2002; **57**: 55-62
- 26 **Hojo K**. Treatment strategy for cancer of the colorectum-difference with western approach. *Gan To Kagaku Ryoho* 1998; **25**: 1123-1130
- 27 **Dong X**, Wang X, Yu Z. Clinico-pathologic study on extended radical resection for rectal cancer. *Zhonghua Zhongliu Zazhi* 2001; **23**: 323-325
- 28 **Gao Y**, Jiang B, Sun R. Colorectal cancer: lymphatic metastasis and choice of operation. *Zhonghua Waike Zazhi* 1999; **37**: 721-723
- 29 **Di Matteo FM**, Peparini N, Maturo A, Zeri KP, Torretta A, Mascagni D, Redler A, Di Matteo G. Compatibility, indications, and limits of nerve sparing technique in lateral pelvic lymphadenectomy for advanced rectal carcinoma. *Chir Ital* 2000; **52**: 203-213
- 30 **Zhang ZS**, Zhang YL. Research of rectal cancer in China. *Shijie Huaren Xiaohua Zazhi* 2001; **9**: 489-494
- 31 **Yamamoto H**, Miyake Y, Noura S, Ohnishi T, Takayama O, Ikenaga M, Fujiwara Y, Nakamori S, Sekimoto M, Monden M. Clinical significance of micrometastasis to lymph nodes in gastrointestinal tract cancers. *Gan To Kagaku Ryoho* 2001; **28**: 776-783
- 32 **Rosenberg R**, Hoos A, Mueller J, Baier P, Stricker D, Werner M,

- Nekarda H, Siewert JR. Prognostic significance of cytokeratin-20 reverse transcriptase polymerase chain reaction in lymph nodes of node-negative colorectal cancer patients. *J Clin Oncol* 2002; **20**: 1049-1055
- 33 **Shirouzu K**, Ogata Y, Araki Y, Sasatomi T, Nozoe Y, Nakagawa M, Matono K. Total mesorectal excision, lateral lymphadenectomy and autonomic nerve preservation for lower rectal cancer: significance in the long-term follow-up study. *Kurume Med J* 2001; **48**: 307-319
- 34 **Feigen M**, Crocker EF, Read J, Crandon AJ. The value of lymphoscintigraphy, lymphangiography and computer tomography scanning in the preoperative assessment of lymph nodes involved by pelvic malignant conditions. *Surg Gynecol Obstet* 1987; **165**: 107-110
- 35 **Sterk P**, Keller L, Jochims H, Klein P, Stelzner F, Bruch HP, Markert U. Lymphoscintigraphy in patients with primary rectal cancer: the role of total mesorectal excision for primary rectal cancer—a lymphoscintigraphic study. *Int J Colorectal Dis* 2002; **17**: 137-142
- 36 **Su Q**, Zhao Y, Chen CS, Liu EQ, Feng Y, Wang W, Li GQ. The proliferating ability of transitional mucosa adjacent to rectal carcinoma and its clinical significance in sphincter preserving operations. *World J Gastroenterol* 2000; **6**(Suppl 3): 43
- 37 **Liu DW**, Xu L, Shen JW, Jia EM. How to prolong the survival time of postoperative rectal cancer and to prevent its recurrence. *World J Gastroenterol* 2000; **6** (Suppl 3): 39
- 38 **Makin GB**, Breen DJ, Monson JRT. The impact of new technology on surgery for colorectal cancer. *World J Gastroenterol* 2001; **7**: 612-621

Edited by Zhang JZ

Expression of survivin protein in human colorectal carcinogenesis

Lian-Jie Lin, Chang-Qing Zheng, Yu Jin, Ying Ma, Wei-Guo Jiang, Tie Ma

Lian-Jie Lin, Chang-Qing Zheng, Yu Jin, Department of Gastroenterology of the 2nd Hospital Affiliated to China Medical University, Shenyang 110004, Liaoning Province, China

Ying Ma, Wei-Guo Jiang, Tie Ma, Department of Pathology of the 2nd Hospital Affiliated to China Medical University, Shenyang 110004, Liaoning Province, China

Correspondence to: Lian-Jie Lin, Department of Gastroenterology of the 2nd Hospital Affiliated to China Medical University, 36 Sanhao Heping, Shenyang 110004, Liaoning Province, China. audreylin73@hotmail.com

Telephone: +86-24-83956416

Received: 2002-11-19 **Accepted:** 2002-12-22

Abstract

AIM: To identify the role of survivin in colorectal carcinogenesis and the relationship between Survivin and histological differentiation grade of colorectal carcinoma.

METHODS: Immunohistochemical staining of survivin by using the monoclonal antibody was performed by the standard streptavidin-peroxidase (SP) technique for the 188 paraffin sections which included 30 normal colorectal mucosas, 41 adenomas with low grade dysplasia, 30 adenomas with high grade dysplasia, and 87 colorectal carcinomas which were classified as high, middle and low differentiated subgroups which included 33, 28, 26 cases respectively.

RESULTS: Expression of survivin was observed in the cytoplasm of adenoma with dysplasia and colorectal carcinoma cells. No immunoreactivity of survivin was seen in normal mucosas. The positive rate of survivin increased in the transition from normal mucosas to adenomas with low grade dysplasia to high grade dysplasia/ carcinomas (0.0 %, 31.7 %, 56.7 % and 63.2% respectively). But the difference between high grade dysplasia and carcinomas had no statistical significance. Positive rate was not related to histological differentiation grade of colorectal carcinoma. Moreover, there was no correlation between histological differentiation grade of colorectal carcinoma and immunoreactive intensity of survivin.

CONCLUSION: The expression of survivin is the essential event in the early stage of colorectal carcinogenesis and plays an important role in the transition sequence and it is not related to histological differentiation grade of colorectal carcinoma. It thus may provide a new diagnostic and therapeutic target in colorectal cancer.

Lin LJ, Zheng CQ, Jin Y, Ma Y, Jiang WG, Ma T. Expression of survivin protein in human colorectal carcinogenesis. *World J Gastroenterol* 2003; 9(5): 974-977

<http://www.wjgnet.com/1007-9327/9/974.htm>

INTRODUCTION

Disturbance of apoptosis is thought to be very important in neoplastic transformation and progression. Several tumor

suppressor genes and oncogenes, such as p53 and the bcl-2 family, are involved in regulation of cell apoptosis, which were thoroughly studied^[1-12]. Moreover, a gene family of inhibitor of apoptosis (IAP) has been identified recently. Survivin, a novel member of IAP family, directly inhibits caspase-3 and -7 activity^[13] or conjugates caspase-9^[14], and regulates the cell cycle in the G2/M phase by interact with spindle microtubules^[15]. Survivin shows markedly different tissue expression compared with other IAPs. It is present during embryonic and fetal development, but is downregulated in normal adult tissues. However, it becomes re-expressed in a variety of cancers^[16-20]. The unique feature makes it attractive as a target for cancer therapy^[21]. In this study, we sought to investigate the expression of survivin in normal colorectal mucosas, adenomas with low grade dysplasia, adenomas with high grade dysplasia, and colorectal carcinomas by immunohistochemical staining method in order to identify the role of survivin in colorectal carcinogenesis and the relationship between survivin and histological differentiation grade of colorectal carcinoma.

MATERIALS AND METHODS

Tissue samples

Tissue specimens used for this study were obtained from 188 patients which were resected surgically or endoscopically at the 2nd Hospital Affiliated to China Medical University from 1998 to 2002. There were 105 males and 83 females, and the mean age of the patients was 56.2 years. Materials were composed of 30 cases of normal colorectal mucosas, 41 cases of adenomas with low grade dysplasia, 30 cases of adenomas with high grade dysplasia, and 87 cases of colorectal carcinomas, their mean ages were 52.3, 55.4, 57.9 and 57.4 respectively. According to histological differentiation grade, 87 cases of colorectal carcinoma were classified to high, middle and low differentiated subgroups which included 33, 28, 26 cases and the mean ages were 62.0, 57.9, and 51.1 respectively. The patients had received neither chemotherapy nor radiation therapy before tumor resection.

Methods

Routinely processed formalin fixed, paraffin embedded, serial sections of 5 µm were prepared from the cut surface of blocks at the maximum cross-section. For morphologic analysis, tissue sections were routinely stained with hematoxylin and eosin. At least 2 experienced pathologists studied the sections. The immunohisto-chemical staining for survivin antigen was carried out by the standard streptavidin /peroxidase (SP) technique. Briefly, before labeling with primary antibody, paraffin sections were dewaxed, and then incubated with 30 ml/L hydrogen peroxide for 10 minutes, and antigen retrieval was performed by boiling in EDTA (0.01M, pH7.4). The sections were cooled and washed in PBS. Nonspecific reactions were blocked by incubating the sections in a solution containing normal serum. The sections were incubated with a primary antibody overnight at 4 °C. The anti-survivin antibody was sc-8806 antibody (Sant Cruz Biotechnology, Inc) at a 1:50 dilution. Rinsed with PBS, then the sections were incubated for 30 minutes at 37 °C with biotinylated

secondary antibody and streptavidin conjugated to horseradish peroxidase, respectively. After three rinses with PBS, the sections were incubated with diaminobenzidine substrate, then rinsed with distilled water and counterstained with hematoxylin.

Scoring criteria

The mean percentage of positive cells for the expression of survivin was determined in at least 5 areas at 400-fold magnification, and cases with less than 10 % positively stained cells were defined as negative. Cases with 10 to 29 % positively stained cells were defined as “+”, 30 to 59 % as “++”, and 60 % or more than 60 % as “+++”. These scorings were performed in a blinded fashion.

Statistical analysis

The difference and correlation were analyzed by χ^2 test. A value of $P < 0.05$ was considered statistically significant.

RESULTS

By immunohistochemical staining, we examined the expression of survivin in adenoma-carcinoma sequence. Representative results were shown in Figure 1. The expression of survivin was observed in the cytoplasm of the benign and malignant tumor cells, whereas not in normal tissues. As shown in Table 1, the positive rate for survivin expression increased gradually from normal colorectal mucosas to adenomas with low grade dysplasia, adenomas with high grade dysplasia, and carcinomas. The expression rates were 0.0 %, 31.7 %, 56.7 %, and 63.2% respectively. Analyzed by χ^2 test, there were significant differences in the expressions of survivin between the normal mucosas group and any one of the other groups, between adenomas with low grade dysplasia and carcinomas, and between adenomas with low grade dysplasia and adenomas with high grade dysplasia ($P < 0.05$), while there were no significant differences between adenomas with high grade dysplasia and carcinomas ($\chi^2 = 0.40$, $0.5 < P < 0.75$).

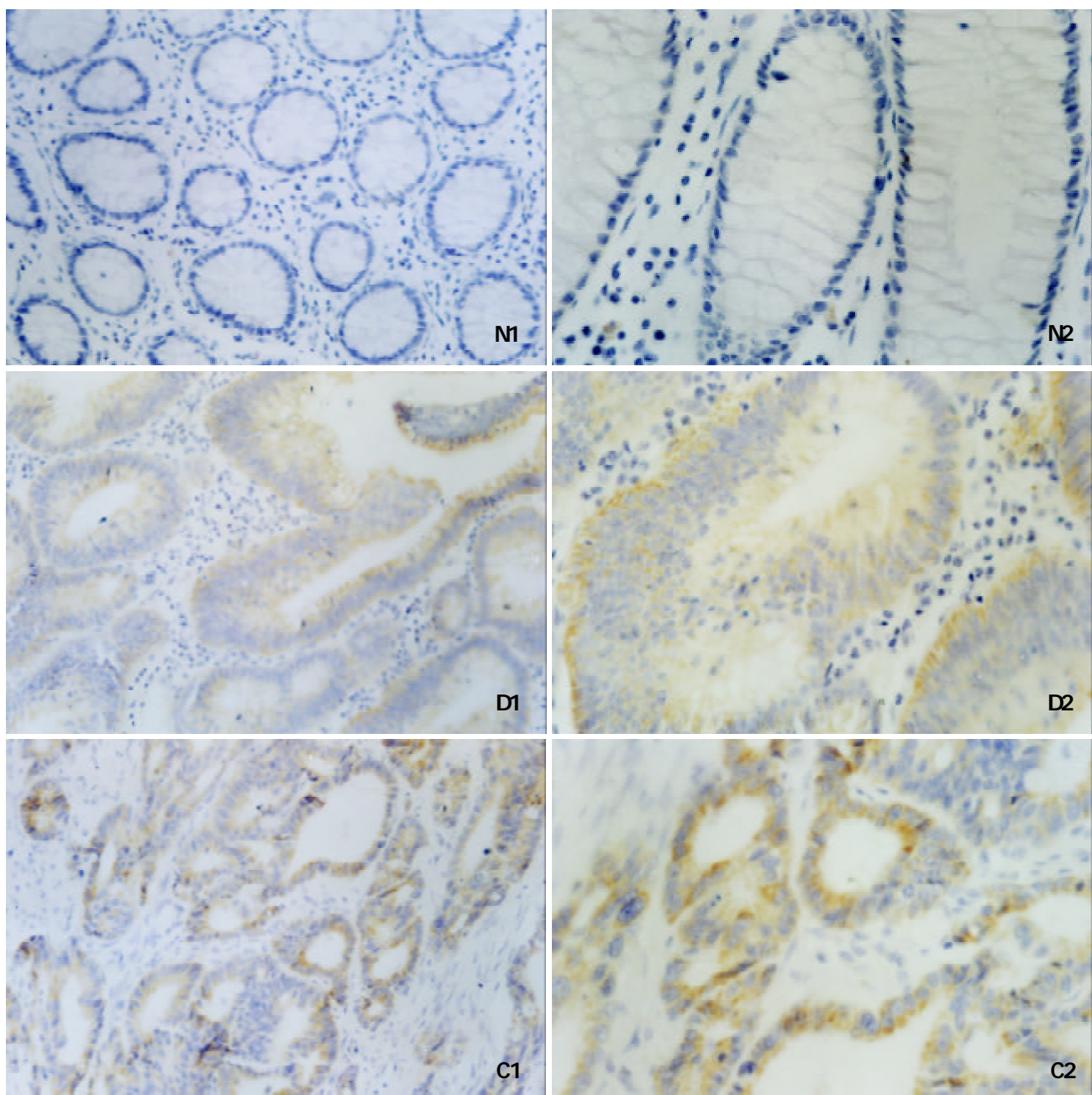


Figure 1 Immunohistochemical staining of survivin in adenoma-carcinoma sequence. The expression of survivin was observed in the cytoplasm of the benign and malignant tumor cells, whereas not in normal tissues. N: normal tissue. D: adenoma with dysplasia; C: carcinoma; 1: $\times 200$ fold; 2: $\times 400$ fold.

Table 1 Expression of survivin in the colorectal carcinogenesis

Lesion	n	Expression intensity				Expression rate %
		-	+	++	+++	
Normal mucosas	30	30	0	0	0	0.0
Adenomas with low grade dysplasia	41	28	7	5	0	31.7
Adenomas with high grade dysplasia	30	13	3	7	7	56.7
Carcinomas	87	32	8	20	27	63.2

To study the relationship between survivin and histological differentiation grade of colorectal carcinoma, 87 cases of colorectal carcinoma were classified to high, middle and low differentiated subgroups. The results were shown in Table 2. Analyzed by χ^2 test, there were no significant differences in the expressions of survivin among the subgroups ($P>0.90$). Moreover, there was no relationship between the differentiation grade of colorectal carcinoma and the expression intensity ($P>0.75$).

Table 2 Correlation between the differentiation grade of colorectal carcinoma and the expression intensity of survivin

Lesion	n	Expression intensity				Expression rate %
		-	+	++	+++	
High differentiation	33	12	3	10	8	63.6
Middle differentiation	28	11	2	4	11	60.7
Low differentiation	26	9	3	6	8	65.4
Total	87	32	8	20	27	63.2

DISCUSSION

The development of colorectal carcinoma proceeds through a series of genetic changes involving the activation of oncogenes and loss of tumor suppressor genes. During this process, a disturbance in the balance between cell proliferation and apoptosis may underlie neoplastic development. Previous investigations have well studied the role of p53 and bcl-2 family^[1-12]. The IAPs is a widely expressed gene family of apoptosis inhibitors. Survivin, a novel and structurally unique member of the IAP gene family, is the strongest apoptosis inhibitor. A characteristic finding of survivin is that it is expressed during embryonic and fetal development but not in normal adult differentiated tissues, and prominently reexpressed in the most common human carcinomas. The mechanism is unclear. In this study, we aimed to identify the role of survivin in colorectal carcinogenesis and the relationship between survivin and histological differentiation grade of colorectal carcinoma.

In our study, we demonstrated that survivin was not expressed in normal colorectal mucosas, which coincided with previous reports. The expression of survivin was localized in the cytoplasm of the adenoma and carcinoma cells, and the positive rate for survivin expression increased gradually from normal colorectal mucosas to adenomas with low grade dysplasia, adenomas with high grade dysplasia, and to carcinomas. The expression rates were 0.0 %, 31.7 %, 56.7 % and 63.2 % respectively. Analyzed by χ^2 test, there were significant differences in the expressions of survivin between the normal mucosa group and any one of the other groups ($P<0.05$), between adenomas with low grade dysplasia and carcinomas ($P<0.05$), and between adenomas with low grade dysplasia and adenomas with high grade dysplasia, while there were no significant differences between adenomas with high

grade dysplasia and carcinomas. We analyze the adenomas with high grade dysplasia and the carcinoma groups. The positive rates of them were 56.7 % and 63.2 % respectively, and the total number of cases were 30 and 87 respectively, then, the value of χ^2 was 0.40 and P was more than 0.5 but less than 0.75. Thus, we consider that there is no difference between them. This result has not been analyzed by other studies, but it coincides with the clinical practice that the treatment of adenomas with high grade dysplasia is similar to that of the carcinomas.

To study the relationship between survivin and histological differentiation grade of colorectal carcinoma, 87 cases of colorectal carcinoma were classified to high, middle and low differentiated subgroups. The number of cases were 33, 28, and 26 respectively, and the positive rates were 63.6 %, 60.7 % and 65.4 % respectively. Analyzed by χ^2 test, there was no significant difference in the expressions of survivin among the subgroups ($P>0.90$). Moreover, there was no relationship between the differentiation grade of colorectal carcinoma and the expression intensity ($P>0.75$). These results conflict with those of Wang Mei *et al*^[22], who thought the expression of survivin was related to the tumor histological grade in cervical carcinoma. These may be due to the different tissue origin. There was no significant difference in the expressions of survivin among the different grade of colorectal carcinoma, which makes it possible to use survivin as a tumor-specific target for therapy or diagnosis. That is, no matter what historical grade the colorectal carcinoma is, the cancer can be diagnosed by detecting survivin and be treated by targeting survivin. Meanwhile, the normal cells will not be killed because survivin is not expressed in normal cells. Survivin is an attractive candidate for cancer therapy. Therefore, our study gives some directions to diagnose and treat colorectal cancer. Whether the expression of survivin can predict prognosis in cancer or not is still under discussion^[23-36].

Survivin, a novel mammalian IAP molecule, has interested scholars for its unique developmentally regulated expression and mechanism. There are still many problems to be solved, such as the molecular mechanism for its selective expression, the details about its anti-apoptosis, and so on. The targeting therapy is just beginning. Therefore, it is worthy to be further studied to settle a firm basis of tumor diagnosis and therapy.

REFERENCES

- 1 **Lan J**, Xiong YY, Lin YX, Wang BC, Gong LL, Xu HS, Guo GS. *Helicobacter pylori* infection generated gastric cancer through p53-Rb tumor-suppressor system mutation and telomerase reactivation. *World J Gastroenterol* 2003; **9**: 54-58
- 2 **Jain D**, Srinivasan R, Patel FD, Kumari Gupta S. Evaluation of p53 and Bcl-2 Expression as Prognostic Markers in Invasive Cervical Carcinoma Stage IIb/III Patients Treated by Radiotherapy. *Gynecol Oncol* 2003; **88**: 22-28
- 3 **Kim KY**, Seol JY, Jeon GA, Nam MJ. The combined treatment of aspirin and radiation induces apoptosis by the regulation of bcl-2 and caspase-3 in human cervical cancer cell. *Cancer Lett* 2003; **189**: 157-166
- 4 **Pepper C**, Thomas A, Hoy T, Bentley P. Antisense oligonucleotides complementary to Bax transcripts reduce the susceptibility of B-cell chronic lymphocytic leukaemia cells to apoptosis in a bcl-2 independent manner. *Leuk Lymphoma* 2002; **43**: 2003-2009
- 5 **Iyer R**, Ding L, Batchu RB, Naugler S, Shammas MA, Munshi NC. Antisense p53 transduction leads to overexpression of bcl-2 and dexamethasone resistance in multiple myeloma. *Leuk Res* 2003; **27**: 73-78
- 6 **Selim AG**, El-Ayat G, Wells CA. Expression of c-erbB2, p53, Bcl-2, Bax, c-myc and Ki-67 in apocrine metaplasia and apocrine change within sclerosing adenosis of the breast. *Virchows Arch* 2002; **441**: 449-455
- 7 **Choi YH**, Kim MJ, Lee SY, Lee YN, Chi GY, Eom HS, Kim ND,

- Choi BT. Phosphorylation of p53, induction of Bax and activation of caspases during beta-lapachone-mediated apoptosis in human prostate epithelial cells. *Int J Oncol* 2002; **21**: 1293-1299
- 8 **Kasimir-Bauer S**, Beelen D, Flasshove M, Noppeney R, Seeber S, Scheulen ME. Impact of the expression of P glycoprotein, the multidrug resistance-related protein, bcl-2, mutant p53, and heat shock protein 27 on response to induction therapy and long-term survival in patients with de novo acute myeloid leukemia. *Exp Hematol* 2002; **30**: 1302-1308
 - 9 **Rincheval V**, Renaud F, Lemaire C, Godefroy N, Trotot P, Boulo V, Mignotte B, Vayssiere JL. Bcl-2 can promote p53-dependent senescence versus apoptosis without affecting the G1/S transition. *Biochem Biophys Res Commun* 2002; **298**: 282-288
 - 10 **Sakuragi N**, Salah-eldin AE, Watari H, Itoh T, Inoue S, Moriuchi T, Fujimoto S. Bax, Bcl-2, and p53 expression in endometrial cancer. *Gynecol Oncol* 2002; **86**: 288-296
 - 11 **Nagler R**, Kerner H, Laufer D, Ben-Eliezer S, Minkov I, Ben-Itzhak O. Squamous cell carcinoma of the tongue: the prevalence and prognostic roles of p53, Bcl-2, c-erbB-2 and apoptotic rate as related to clinical and pathological characteristics in a retrospective study. *Cancer Lett* 2002; **186**: 137
 - 12 **Li HL**, Chen DD, Li XH, Zhang HW, Lu YQ, Ye CL, Ren XD. Changes of NF-kB, p-53, Bcl-2 and caspase in apoptosis induced by JTE-522 in human gastric adenocarcinoma cell line AGS cells: role of reactive oxygen species. *World J Gastroenterol* 2002; **8**: 431-435
 - 13 **Shin S**, Sung BJ, Cho YS, Kim HJ, Ha NC, Hwang JI, Chung CW, Jung YK, Oh BH. An anti-apoptotic protein human survivin is a direct inhibitor of caspase-3 and -7. *Biochemistry* 2001; **40**: 1117-1123
 - 14 **O' Connor DS**, Grossman D, Plescia J, Li F, Zhang H, Villa A, Tognin S, Marchisio PC, Altieri DC. Regulation of apoptosis at cell division by p34cdc2 phosphorylation of survivin. *Proc Natl Acad Sci USA* 2000; **97**: 13103-13107
 - 15 **Giordini A**, Kallio MJ, Wall NR, Gorbisky GJ, Tognin S, Marchisio PC, Symons M, Altieri DC. Regulation of microtubule stability and mitotic progression by survivin. *Cancer Res* 2002; **62**: 2462-2467
 - 16 **Sarela AI**, Verbeke CS, Ramsdale J, Davies CL, Markham AF, Guillou PJ. Expression of survivin, a novel inhibitor of apoptosis and cell cycle regulatory protein, in pancreatic adenocarcinoma. *Br J Cancer* 2002; **86**: 886-892
 - 17 **Mori A**, Wada H, Nishimura Y, Okamoto T, Takemoto Y, Kakishita E. Expression of the antiapoptosis gene survivin in human leukemia. *Int J Hematol* 2002; **75**: 161-165
 - 18 **Das A**, Tan WL, Teo J, Smith DR. Expression of survivin in primary glioblastomas. *J Cancer Res Clin Oncol* 2002; **128**: 302-306
 - 19 **Lehner R**, Lucia MS, Jarboe EA, Orlicky D, Shroyer AL, McGregor JA, Shroyer KR. Immunohistochemical localization of the IAP protein survivin in bladder mucosa and transitional cell carcinoma. *Appl Immunohistochem Mol Morphol* 2002; **10**: 134-138
 - 20 **Sasaki T**, Lopes MB, Hankins GR, Helm GA. Expression of survivin, an inhibitor of apoptosis protein, in tumors of the nervous system. *Acta Neuropathol* 2002; **104**: 105-109
 - 21 **Yamamoto T**, Tanigawa N. The role of survivin as a new target of diagnosis and treatment in human cancer. *Med Electron Microsc* 2001; **34**: 207-212
 - 22 **Wang M**, Wang B, Wang X. A novel antiapoptosis gene, survivin, bcl-2, p53 expression in cervical carcinomas. *Zhonghua Fuchanke Zazhi* 2001; **36**: 546-548
 - 23 **Nakanishi K**, Tominaga S, Hiroi S, Kawai T, Aida S, Kasamatsu H, Aurues T, Hayashi T, Ikeda T. Expression of survivin does not predict survival in patients with transitional cell carcinoma of the upper urinary tract. *Virchows Arch* 2002; **441**: 559-563
 - 24 **Rodel F**, Hoffmann J, Grabenbauer GG, Papadopoulos T, Weiss C, Gunther K, Schick C, Sauer R, Rodel C. High survivin expression is associated with reduced apoptosis in rectal cancer and may predict disease-free survival after preoperative radiochemotherapy and surgical resection. *Strahlenther Onkol* 2002; **178**: 426-435
 - 25 **Dong Y**, Sui L, Watanabe Y, Sugimoto K, Tokuda M. Survivin expression in laryngeal squamous cell carcinomas and its prognostic implications. *Anticancer Res* 2002; **22**: 2377-2383
 - 26 **Sui L**, Dong Y, Ohno M, Watanabe Y, Sugimoto K, Tokuda M. Survivin expression and its correlation with cell proliferation and prognosis in epithelial ovarian tumors. *Int J Oncol* 2002; **21**: 315-320
 - 27 **Takai N**, Miyazaki T, Nishida M, Nasu K, Miyakawa I. Survivin expression correlates with clinical stage, histological grade, invasive behavior and survival rate in endometrial carcinoma. *Cancer Lett* 2002; **184**: 105-116
 - 28 **Ikehara M**, Oshita F, Kameda Y, Ito H, Ohgane N, Suzuki R, Saito H, Yamada K, Noda K, Mitsuda A. Expression of survivin correlated with vessel invasion is a marker of poor prognosis in small adenocarcinoma of the lung. *Oncol Rep* 2002; **9**: 835-838
 - 29 **Wurl P**, Kappler M, Meye A, Bartel F, Kohler T, Lautenschlager C, Bache M, Schmidt H, Taubert H. Co-expression of survivin and TERT and risk of tumour-related death in patients with soft-tissue sarcoma. *Lancet* 2002; **359**: 943-945
 - 30 **Sandler A**, Scott D, Azuhata T, Takamizawa S, O' Dorisio S. The survivin:Fas ratio is predictive of recurrent disease in neuroblastoma. *J Pediatr Surg* 2002; **37**: 507-511
 - 31 **Ikeguchi M**, Ueda T, Sakatani T, Hirooka Y, Kaibara N. Expression of survivin messenger RNA correlates with poor prognosis in patients with hepatocellular carcinoma. *Diagn Mol Pathol* 2002; **11**: 33-40
 - 32 **Chakravarti A**, Noll E, Black PM, Finkelstein DF, Finkelstein DM, Dyson NJ, Loeffler JS. Quantitatively determined survivin expression levels are of prognostic value in human gliomas. *J Clin Oncol* 2002; **20**: 1063-1068
 - 33 **Sarela AI**, Scott N, Ramsdale J, Markham AF, Guillou PJ. Immunohistochemical detection of the anti-apoptosis protein, survivin, predicts survival after curative resection of stage II colorectal carcinomas. *Ann Surg Oncol* 2001; **8**: 305-310
 - 34 **Tajiri T**, Tanaka S, Shono K, Kinoshita Y, Fujii Y, Suita S, Ihara K, Hara T. Quick quantitative analysis of gene dosages associated with prognosis in neuroblastoma. *Cancer Lett* 2001; **166**: 89-94
 - 35 **Kato J**, Kuwabara Y, Mitani M, Shinoda N, Sato A, Toyama T, Mitsui A, Nishiwaki T, Moriyama S, Kudo J, Fujii Y. Expression of survivin in esophageal cancer: correlation with the prognosis and response to chemotherapy. *Int J Cancer* 2001; **95**: 92-95
 - 36 **Okada E**, Murai Y, Matsui K, Isizawa S, Cheng C, Masuda M, Takano Y. Survivin expression in tumor cell nuclei is predictive of a favorable prognosis in gastric cancer patients. *Cancer Lett* 2001; **163**: 109-116

Hepatitis B virus infection of transplanted human hepatocytes causes a biochemical and histological hepatitis in immunocompetent rats

Catherine H. Wu, Edwin C. Ouyang, Cherie Walton, Kittichai Promrat, Faripour Forouhar, George Y. Wu

Catherine H. Wu, Edwin C. Ouyang, Cherie Walton, Kittichai Promrat, George Y. Wu, Department of Medicine, Division of Gastroenterology-Hepatology, University of Connecticut Health Center, Farmington, CT, USA

Faripour Forouhar, Department of Pathology, University of Connecticut Health Center, Farmington, CT, USA

Supported by the grants from the NIDDK: DK-42182 (GYW), Connecticut Innovations, Inc. (CHW), a Blowitz-Ridgeway grant of the American Liver Foundation (CHW), and the Herman Lopata Chair in Hepatitis Research (GYW)

Correspondence to: George Y. Wu, Ph.D., Department of Medicine, Division of Gastroenterology-Hepatology, University of Connecticut Health Center, Rm. AM-045263 Farmington Avenue, Farmington, CT 06030-1845, USA. wu@nso.uconn.edu

Telephone: +1-860-6793158 **Fax:** +1-860-6793159

Received: 2002-10-25 **Accepted:** 2002-11-07

Abstract

AIM: To characterize the host response to hepatitis B virus (HBV) infection in human hepatocytes transplanted into immunocompetent rodent rats tolerized by, and transplanted with primary human hepatocytes.

METHODS: One week after the transplantation, rats were inoculated with HBV, and viral gene expression, replication, and host response was monitored.

RESULTS: HBV DNA was detectable in serum for at least 60 days. HBsAg levels rose steadily for 3 weeks post-inoculation and then plateaued at a level of about 0.6 pg/ml. HBV RNA was also found in liver at levels that remained constant through the time course. Immunofluorescence revealed clusters of hepatocytes that stained positive for HBcAg. The presence of HBV covalently closed circular DNA (cccDNA) in liver was demonstrated using nuclease digestion of single-stranded DNA followed by PCR. Serum ALT levels rose and reached a peak level of 180 IU/L on day 18, but remained elevated for 60 days. Histology revealed a progressive predominantly mononuclear lobular hepatitis.

CONCLUSION: These data indicate that human hepatocytes transplanted into rats rendered tolerant to these cells, when infected by HBV, results in biochemical as well as histological evidence of hepatitis that accompanies viral gene expression, and DNA replication.

Wu CH, Ouyang EC, Walton C, Promrat K, Forouhar F, Wu GY. Hepatitis B virus infection of transplanted human hepatocytes causes a biochemical and histological hepatitis in immunocompetent rats. *World J Gastroenterol* 2003; 9 (5): 978-983

<http://www.wjgnet.com/1007-9327/9/978.htm>

INTRODUCTION

It has been shown recently that primary human hepatocytes can be transplanted into rats and infected with human hepatitis

B virus^[1]. This was accomplished by rendering normal rats tolerant to human hepatocytes by intrafetal injection of primary hepatocytes. The rats were then transplanted with the same batches of cells, and then infected by inoculation of those animals with purified HBV. This resulted in production of HBV antigens. The current studies were performed to evaluate the effects of this infection on the host liver.

MATERIALS AND METHODS

Animals

Pregnant Sprague-Dawley rats, 250 to 300 g of body weight (Charles River Co., Inc., Wilmington, MA) were maintained on 12 hour light-dark cycles, and fed *ad lib* with standard rat chow in the Center for Laboratory Animal Care at the University of Connecticut Health Center. All animal procedures were approved by Institutional Animal Care and Use Committee and conformed to USDA and NIH animal usage guidelines.

Cells

Human hepatocytes were obtained from Clonetics Corp (Walkersville, MD). HepG2 2.2.15^[2] cells, a transformed human liver cell line that constitutively produces infectious HBV, were grown in Dulbecco Modified Eagle's medium (DMEM) with 10 % fetal bovine serum (FBS) and antibiotics.

Intrafetal intraperitoneal injections of human hepatocytes

Rats were rendered tolerant to human hepatocytes by intrafetal injection of those cells as described previously^[1]. In brief, at 15 to 17 days of gestation, groups of pregnant rats were anesthetized by intramuscular injections of ketamine (40 mg/kg body weight) and xylazine (5 mg/kg body weight) as described previously^[3]. Laparotomies were performed under sterile conditions; gravid uteri were exposed, and transilluminated by a high intensity lamp (Fiber-lite MI-150, Dolan-Jenner Industries, Lawrence, MA). Human hepatocytes, 1×10⁵ cells in 10 µl PBS, were injected through the uterine wall into the peritoneal cavities of rat fetuses using a sterile 200 µl Hamilton syringe with a 28 gauge beveled point needle (Hamilton Inc., Reno, NV).

Cell transplantation

Within 24 hours of birth, newborn rats were placed on ice for 2-5 min, and 2×10⁶ human hepatocytes in 200 µl PBS were injected into the spleen by sterile Hamilton syringe.

Sample collection

Peripheral blood samples were drawn from tail veins, spun, and serum stored at -20 °C. Liver samples were collected either by sacrificing animals or by performing partial hepatectomies. Samples were fresh frozen in liquid nitrogen, and stored at -80 °C.

HBV inoculation of rats

One week following human hepatocyte transplantation, tolerized rats were inoculated with 10⁵ HBV particles in 100

μ l TEN (0.02 M Tris-HCl, pH 7.5, 1 mM EDTA, 0.15 M NaCl) buffer by intrasplenic injection. Controls consisted of tolerized neonatal rats from the same litter that did not receive human hepatocyte transplantation, but were also inoculated identically with HBV, as well as tolerized rats from the same litter that transplanted with human hepatocytes, but no HBV, and tolerized rats from the same litter with saline injection only.

Detection and quantitation of HBsAg in serum

Levels of HBsAg in rat serum were measured as a function of time after inoculation using an enzyme-linked immunoassay kit for HBV surface antigen (Abbott Labs) according to the manufacturer's protocol. Antigen was quantitated using a spectrophotometer at 492 nm. Assays were done in triplicate, and the results expressed as means \pm S.D. in units of pg/ml serum.

Detection and time course of HBV DNA in serum

To detect circulating virus, HBV DNA was extracted from 30 μ l of rat serum, incubated with 100 μ g/ml proteinase K in 0.05 M Tris-HCl, pH 8.0, 0.1 M EDTA and 0.5 % SDS, overnight at 55 °C. DNA was purified by phenol-chloroform extraction^[4]. An antisense primer 5' - ATCTTCTGCGACGCGGATGGAGATC-3' and a sense primer 5' - CTCTGCTGGGGGAATTGATGACTCTAGC-3' were used to generate an expected 355 bp fragment of adw HBV genome spanning nt 2079-2434. One third of total cDNA was mixed with 100 pmol of amplification primers, and 2.5 U Taq polymerase, and amplified by 1 cycle of 94 °C for 3 min; 38 cycles of 94 °C for 1 min, 55 °C for 1 min, 72 °C for 1 min; and the final elongation reaction at 72 °C for 5 min. The PCR products were analyzed on 1.0 % agarose gels in Tris-borate-acetate buffer and visualized by ethidium bromide staining.

Detection and time course of HBV RNA levels in rat liver

Total liver RNA was extracted from 100 mg liver samples from rats tolerized only, rats tolerized and transplanted with human hepatocytes, rats tolerized and transplanted with human hepatocytes followed by HBV inoculation. Samples obtained at 1, 6 and 14 weeks following HBV inoculation were homogenized in a guanidinium isothiocyanate solution^[5]. RNA concentrations were determined by spectrophotometric measurement, and samples either used immediately or stored at -80 °C. In some experiments, total RNA was passed through an oligo-dT cellulose column and poly A(+) RNA isolated^[6]. 10 μ g total RNA or 1 μ g poly A(+) RNA was reverse transcribed using reverse transcriptase (Gibco/BRL Life Technologies) with random primers. One third of the reverse transcriptase reaction sample was used for PCR generation of a 355 bp fragment using the same primers as mentioned above. One third of total RNA was mixed with 100 pmol of amplification primers, and 2.5 U Taq polymerase, and amplified for 1 cycle at 95 °C for 5 min; 38 cycles at 95 °C for 5 min, 55 °C for 1 min, 72 °C for 1 min; and the final elongation reaction at 72 °C for 5 min. The PCR products were analyzed on 1.0 % agarose gels in Tris-borate-acetate buffer and visualized by ethidium bromide staining.

Detection of HBcAg in rat liver

Immunohistochemical staining was performed as described previously^[1]. In brief, frozen rat liver tissue slides were immersed in acetone for 2 min at 25 °C and washed with PBS (pH 7.4). Endogenous peroxidase activity was blocked by incubation in a solution containing hydrogen peroxide (Sigma) and methanol for 20 min at 25 °C. Slides were washed with PBS (pH 7.4), and non-specific activity was blocked by incubation in PBS (pH 7.4) and 1 % BSA (Sigma) for 10 min

at 25 °C. Primary antibody, rabbit anti-HBV core (Sigma), was diluted 1:1 000 in PBS (pH 7.4) and 1 % BSA and slides were incubated with primary antibody for 3 hrs at 25 °C. Washes were performed using PBS (pH 7.4) and 1 % BSA with 1 % Tween-20 (Sigma). Secondary antibody, rhodamine conjugated anti-rabbit IgG (Jackson ImmunoResearch Lab., West Grove, Pa), was diluted 1:200 in PBS (pH 7.4) and 1 % BSA. Slides were incubated for 1 hour at 25 °C and washed with PBS and 1 % BSA with 1 % Tween-20, and finally washed in PBS (pH 7.4). Slides were sealed and immunofluorescence visualized using a Zeiss Scanning laser confocal microscope (Model LSM-410).

Detection of HBV cccDNA in rat liver

Low molecular weight DNA was isolated using fractionation as described by Yeh, *et al.*^[7] and originally by Hirt^[8]. 5 μ g of extracted DNA were subjected to the following conditions: (a) no treatment or (b) digestion with 0.1 unit of Mung Bean nuclease (New England Biolabs, Beverly, MA) in 50 mM sodium acetate (pH 5.0), 30 mM NaCl, 1 mM ZnCl₂ at 25 °C for 5 min and inactivation at 70 °C for 15 min. Samples were then mixed with 100 pmol primers in 1 \times PCR buffer (Invitrogen, Carlsbad, CA), 500 mM MgCl₂, 100 mM dNTPs, and 2.5 U Taq DNA polymerase (Invitrogen). The cycler was programmed for 5 min at 95 °C, 2 min at 55 °C, 38 cycles of 1 min at 95 °C, 1 min at 55 °C, 1 min at 72 °C with a final cycle of 5 min at 72 °C. Samples were analyzed on a 1 % agarose gel stained with ethidium bromide. The primers used were: a 21-mer sense strand (5' AGGCTGTAGGCACAAATTGGT 3') and a 20-mer antisense strand (5' GTATGGTGAGGTGAGCAATG 3') spanning 1 780 to 2 060 of the adwR2 HBV genome which generates a predicted 280 bp fragment after PCR.

Serum aminotransferase assays

To detect possible liver damage following inoculation of HBV, 10 μ l aliquots of rat serum were assayed for ALT spectrophotometrically using kits (Sigma) as instructed by the manufacturer. All assays were performed in triplicate and results expressed as means \pm S.D. in units of IU/L.

Liver histology

Liver specimens were fixed in formalin, and stained with hematoxylin and eosin to evaluate liver architecture, and cellular reaction, and examined in a blinded fashion.

RESULTS

Time course of HBV DNA and HBsAg in serum

Figure 1 showed the results of assays of serum for HBsAg and HBV DNA as a function of time after inoculation of HBV into rats tolerized and transplanted with human hepatocytes cells. Surface antigen levels were detectable at a level of 0.2 pg/ml on day 1, declined slightly by day 4, but increased to a maximum of 0.7 pg/ml by day 21. There was no significant change in levels thereafter as the levels plateaued through day 60. Serum HBV DNA was detected on day 7, and remained positive on up to day 70 of post-inoculation. These data confirmed the results from our previous study^[1], and were presented here to show the dynamics of the parameters in a single figure.

HBV mRNA is present in livers from transplanted and HBV inoculated rats

To be certain that the HBsAg detected in serum was actually produced in the liver, and not simply remnants of injected virus, the presence of viral messenger (poly A(+) RNA) was sought in liver by RT-PCR as a function of time after inoculation.

Figure 2 showed that, as expected, neither normal untreated rat liver, lane 2, nor Huh7, a transformed human liver cell line, lane 3, produced any signal corresponding to the expected 355 bp fragment from amplification of HBV RNA in the core-polymerase reading frames. As a positive control, RNA from HepG2 2.2.15 cells which constitutively produced infectious HBV particles, lane 4, did produce a band of the predicted size. Livers from rats after tolerization and transplantation with human hepatocytes and subsequently inoculated with HBV, also produced a band at 355 bp when assayed after one week, lane 5. This signal remained detectable at week 6, lane 6, and through week 14, lane 7.

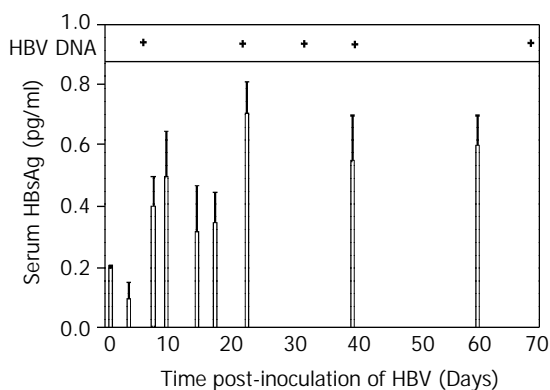


Figure 1 Composite time course of HBsAg, HBV DNA in serum. Levels of HBsAg in rat serum were measured as a function of time after inoculation using an enzyme-linked immunoassay kit as described in Materials and Methods. Assays were done in triplicate, and the results expressed as means \pm S.D. in units of pg/ml serum. HBV DNA was extracted from rat serum, and amplified with primers spanning nt 2 079-2 434 of the adw HBV genome. Upper panel, serum positive for HBV DNA. Lower panel, HBsAg levels.

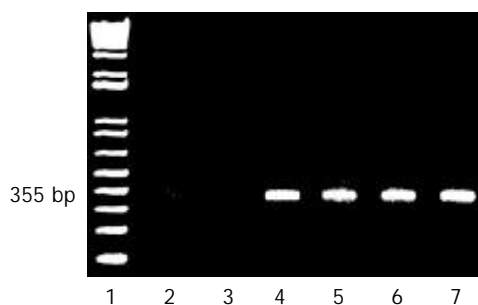


Figure 2 Detection and time course of HBV RNA in liver. Poly A(+) RNA from livers were isolated, reverse transcribed and amplified by PCR as described in Materials and Methods to generate a 355 bp fragment. Lane 1, molecular size markers; lane 2, normal untreated rat liver; lane 3, Huh7 human liver cell line; lane 4, HepG2 2.2.15 cells which constitutively produce infectious HBV particles. Livers from rats after tolerization and transplantation with human hepatocytes and subsequent inoculation with HBV after 1 week, lane 5; 6 weeks, lane 6, and 14 weeks, lane 7.

HBcAg was detectable in HBV infected rats

To obtain evidence of HBV replication, the presence of HBcAg was sought by immunofluorescence. Figure 3 showed a representative immunofluorescence pattern from the liver of a rat tolerized and transplanted with human hepatocytes, and subsequently inoculated with HBV. Clumps of cells can be seen with cytoplasmic staining for HbcAg, Figure 3A. In contrast, livers from rats without transplantation, but inoculated with the same amount of HBV as the rat in Figure 3A had no staining, Figure 3B, indicating that the observed staining in

Figure 3A could not have been due to uptake or artifact from the input injected virus. Similarly, control untreated rats in Figure 3C had no HBcAg staining confirming that the observed results in Figure 3A were not due to non-specific cross reactivity to a rat antigen.

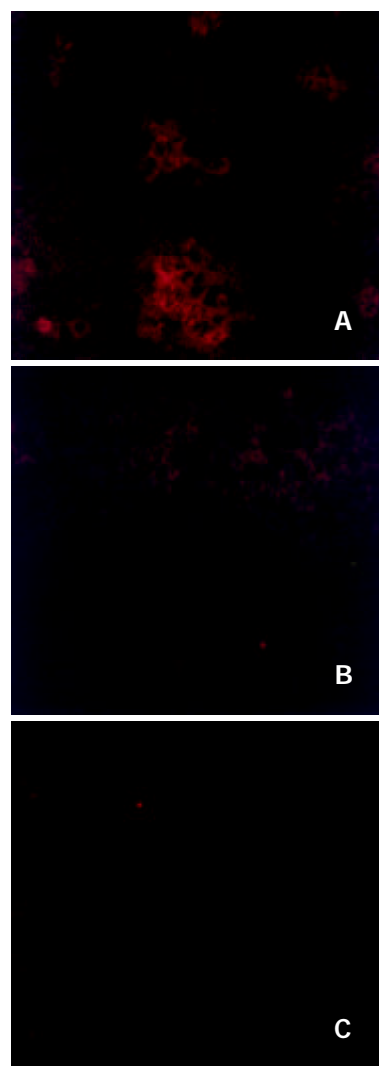


Figure 3 Detection of HBcAg in livers of rats transplanted and inoculated with HBV. Livers were removed 14 weeks after inoculation with HBV, incubated with anti-HbcAb and rhodamine-conjugated secondary antibody as described in Materials and Methods. Figure 3A, a rat tolerized, transplanted, and inoculated with HBV; Figure 3B a rat tolerized and inoculated, but not transplanted; Figure 3C, an untreated rat.

HBV cccDNA is detectable in HBV infected rat liver

Further evidence supporting HBV replication was obtained from assays for HBV covalently closed circular DNA (cccDNA). In these experiments, Mung Bean nuclease, a DNA nuclease with a cleavage preference for single-stranded DNA was used to distinguish partially double stranded viral DNA from completely double stranded cccDNA. At low concentrations of enzyme, the partially double-stranded region DNA of the virus should be digested, and only cccDNA should survive exposure to the nuclease. In Figure 4, lane 2 showed that media from HepG2 2.2.15 cells known to secrete intact virus into the medium, produced after amplification, a band corresponding to an expected size of 280 nt. However, lane 3 showed that when first digested with Mung nuclease, and then amplified, no signal could be produced even with 5 times the amount of DNA sample from media compared to lane 2. DNA

extracted from cell layers of HepG2 2.2.15 cells produced a smear when amplified as shown in lane 4. However, prior exposure to Mung nuclease yielded a surviving band at 280 nt indicating that Mung nuclease resistant DNA was present in the low molecular weight extracts of the cell layers. Lane 6 showed that DNA extracted from livers of rats tolerized, transplanted and inoculated with HBV also generated a smear in the absence of nuclease. However, lane 7 showed that even after prior exposure to Mung nuclease, a 280 nt band spanning the partially double stranded region in the virus was still evident, supporting the presence of cccDNA in that rat liver. In contrast, DNA from rats without transplantation, but inoculated with the same amount of HBV DNA failed to generate any signal with, lane 9, or without nuclease, lane 8, indicating the signal detected in lane 7 was not due to an artifact of input viral DNA. Similarly, liver from untreated rats failed to generate the 280 nt band either with or without nuclease digestion, lanes 11, and 10 respectively, indicating that the observed band in lane 7 was not due to nonspecific amplification of host rat sequences.

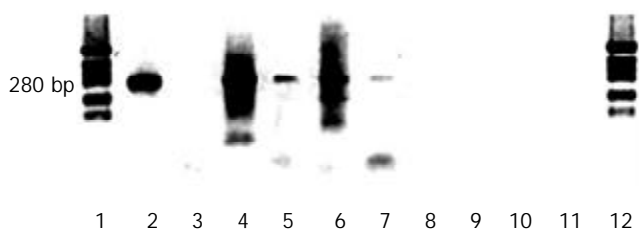


Figure 4 Detection of HBV cccDNA in liver. Low molecular weight DNA was extracted from liver, digested with Mung Bean nuclease or amplified by PCR without nuclease digestion as described in Materials and Methods. Lane 1, molecular weight markers; lane 2, 5 μ g DNA from HepG2 2.2.15 cell media (containing partially double stranded viral DNA); lane 3, 25 μ g DNA from HepG2 2.2.15 cell media plus 0.1 U Mung Bean nuclease pretreatment; lane 4, 5 μ g DNA from HepG2 2.2.15 cell layer; lane 5, 5 μ g DNA from HepG2 2.2.15 cell layer plus 0.1 U nuclease pretreatment; lane 6, 5 μ g liver DNA from a tolerized, transplanted and HBV inoculated rat; lane 7, 5 μ g liver DNA from a tolerized, transplanted and HBV inoculated rat; plus 0.1 U nuclease; lane 8, 5 μ g liver DNA from a non-transplanted rat inoculated with HBV; lane 9, 5 μ g liver DNA from a non-transplanted rat inoculated with HBV plus 0.1 U nuclease; lane 10, 5 μ g DNA from an untreated rat; lane 11, 5 μ g DNA from an untreated rat plus 0.1 U nuclease; lanes 1 and 12, molecular size markers.

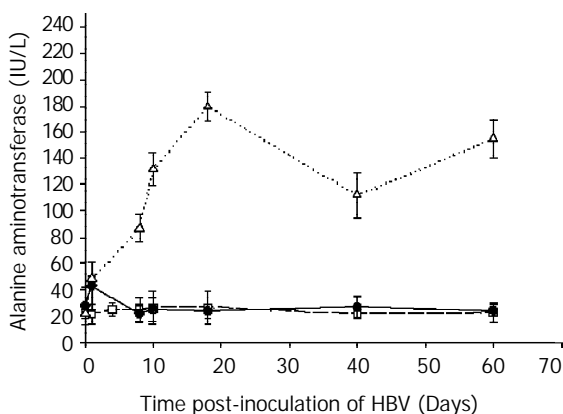


Figure 5 Time course of ALT. To detect possible liver damage following inoculation of HBV, aliquots of rat serum, 10 μ l, were assayed for ALT spectrophotometrically as described in Mate-

rials and methods. All assays were performed in triplicate and results expressed as means \pm S.D. in units of IU/L. Rats tolerized transplanted and inoculated with HBV, open triangles; rats inoculated with HBV, had a slight increase in ALT on the first day, solid squares; rats transplanted, but not inoculated with HBV, open squares.

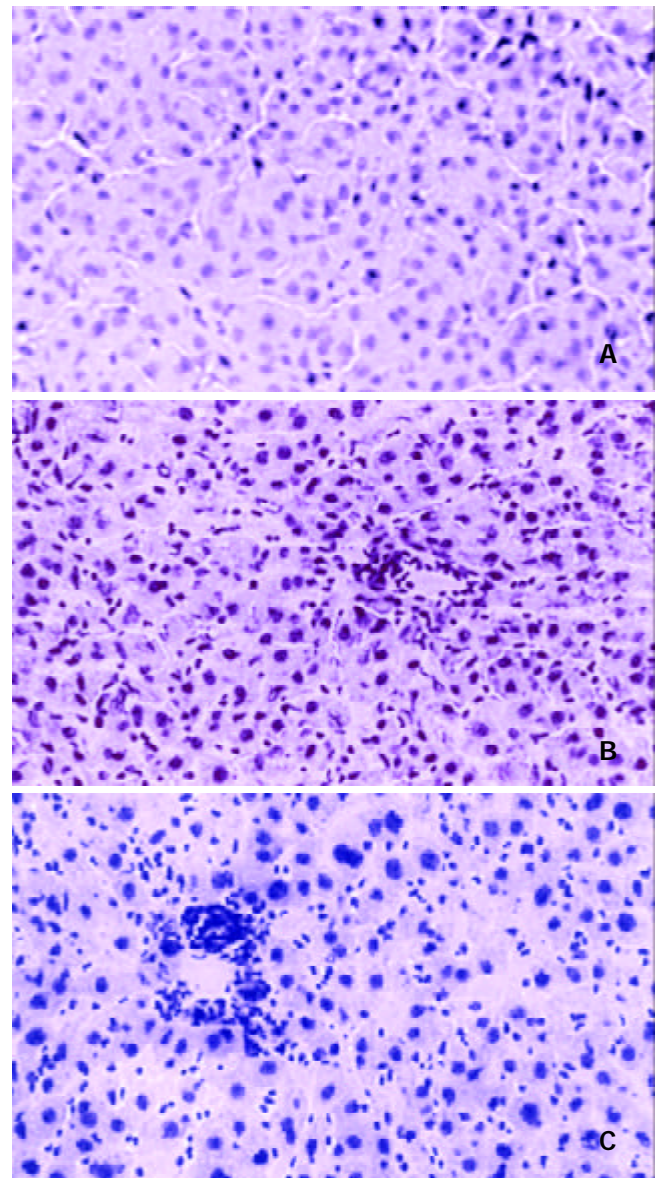


Figure 6 Histological examination. Liver specimens were obtained at various time points after inoculation with HBV, fixed in formalin and stained with hematoxylin and eosin as described in Materials and Methods. Figure 6A, 1 week; Figure 6B, 6 weeks, Figure 6C, 14 weeks.

HBV infection results in biochemical evidence of liver damage

To determine whether HBV inoculation was associated with liver damage, serum alanine aminotransferase (ALT) activities were measured as a function of time after inoculation. Figure 5 showed that in animals that were transplanted with human hepatocytes, and inoculated with HBV, ALT levels rose from normal levels of 20 IU/L on the first day to a peak of 180 IU/L on day 18, and remained significantly above normal throughout the study with a value of 160 IU/L on day 60. In contrast, rats which were not transplanted, but were inoculated with HBV, had a slight increase in ALT on the first day, but returned to normal levels throughout the course. Rats that were transplanted, but not inoculated with HBV, had no increases in ALT levels at any time.

Histology confirms an immune response following HBV inoculation

To determine whether the biochemical abnormalities were associated with any pathological evidence of liver damage, livers were examined histologically as a function of time after HBV inoculation. Figure 6A showed no significant abnormalities at one week after inoculation. However, by the sixth week, Figure 6B, there was moderate inflammation characterized by lymphocytic and neutrophilic infiltration of the lobules, Kupffer cell hyperplasia, and mild portal inflammation. Figure 6C showed that at 14 weeks of post-inoculation, the inflammation was maintained, with characteristics similar to that seen in Figure 6B: moderate lobular hepatitis with lymphocytic and neutrophilic infiltration in the lobules and portal inflammation. There were no significant differences in fibrosis among any of the samples. Control livers from rats transplanted, but not inoculated with HBV, or rats not transplanted, but were inoculated with HBV failed to show any inflammation (data not shown). These data taken together with the ALT measurements indicated that inoculation of HBV into rats transplanted with human hepatocytes was associated not only with viral replication, but also liver damage mediated at least in part by a host immune response.

DISCUSSION

The developing immune system in the fetus allows a unique opportunity for the induction of tolerance to specific cells without generalized suppression of the immune system. *In utero* injection of donor cells directly into the peritoneal cavities of fetuses during gestation has been shown previously to result in a donor-specific tolerance^[9-11].

Chimeric liver models have been described previously, but in immunocompromised hosts. For example, normal adult woodchuck hepatocytes were transplanted into uPA/RAG2 knock out mice via intrasplenic injection. These cells eventually reconstituted 90 % of those mouse livers^[12]. Similarly, immortalized primary human hepatocytes have been transplanted into RAG-2 knock out mice^[13]. Primary human hepatocytes transplanted under the kidney capsule of SCID/NOD mice were shown to be susceptible to HBV infection^[14, 15]. Recently, primary human hepatocytes were transplanted into SCID-Alb-uPA mice and shown to be susceptible to hepatitis C viral infection^[16]. The results demonstrate that when transplanted into immunocompromised hosts, human hepatocytes can not only survive, but also maintain susceptibility to human hepatitis viruses. Our current data on infection and HBV replication confirmed this observation, and further indicated that general immune deficiency or suppression was not required, and intrafetal tolerization was sufficient to prevent rejection. As the mouse models described above were immunodeficient, no inflammatory response was observed as expected, in contrast to our results.

The sustained elevated levels of serum HBsAg, liver HBV RNA and serum ALT levels through 60 days of observation were not characteristics of an acute infection. Given that the viral inoculations were performed shortly (two week) after birth, the situation may be analogous to perinatal HBV infections in man. In these cases, the frequency of progression to chronic infection is extremely high, unlike the situation in adults^[17]. Some data suggest that the viral load of the inoculum is predictive of the outcome of the infection in neonates^[18]. Therefore, the development of chronicity in our model may be dependent on, and possibly controlled by the amount of virus in the inoculations.

While susceptibility of transplanted human hepatocytes to

HBV was not totally unexpected, the development of liver damage was. It is generally accepted that the majority of the liver damage by human hepatitis B viral infection in man is due to the host immune response. However, in the case of our model, because of the mismatch between host rat immunocytes and human hepatocyte MHC, no significant recognition or interaction between HBV antigens and immune cells was anticipated. Thus, the finding of evidence of hepatitis was surprising. However, non-specific immune-mediated toxicity has been described in other systems^[19]. The mechanism of the response observed in the present study is unknown, and is presently under investigation.

Nevertheless, the model system in its present form may be useful in the evaluation of new antiviral agents for efficacy, including those with immunostimulatory properties that can only be assessed in the presence of a functional immune system. Eventually, models such as this might also permit evaluation of hepatocyte toxicity of agents as well.

ACKNOWLEDGEMENT

We thank Martha Schwartz for her secretarial assistance.

REFERENCES

- 1 **Sells MA**, Chen ML, Acs G. Production of hepatitis B virus particles in HepG2 cells transfected with cloned hepatitis B virus DNA. *Proc Natl Acad Sci USA* 1987; **84**: 1005-1009
- 2 **Hawk CT**, Leary SL. Formulary for laboratory animals. Ames, Iowa: *Iowa State University Press* 1987
- 3 **Gross-Bellard M**, Oudet P, Chambon P. Isolation of high-molecular DNA from mammalian cells. *Eur J Biochem* 1973; **36**: 32-38
- 4 **Chomczynski P**, Sacchi N. Single-step method of RNA isolation by acid guanidinium thiocyanate-phenol-chloroform extraction. *Anal Biochem* 1987; **162**: 156-159
- 5 **Aviv J**, Leder P. Preparation of biologically active globin messenger RNA by chromatography on oligothymidylic acid-cellose. *Proc Natl Acad Sci USA* 1972; **69**: 1408-1412
- 6 **Wu CH**, Ouyang EC, Walton CM, Wu GY. Human hepatocytes transplanted into genetically immunocompetent rats are susceptible to infection by hepatitis B virus *in situ*. *J Viral Hep* 2001; **8**: 111-119
- 7 **Yeh CT**, Wong SW, Fung YK, Ou JH. Cell cycle regulation of nuclear localization of hepatitis B core protein. *Proc Natl Acad Sci USA* 1993; **90**: 6459-6463
- 8 **Hirt BJ**. Selective extraction of polyoma DNA from infected mouse cell cultures. *J Mol Biol* 1967; **26**: 365-369
- 9 **Yuh DD**, Gandy KL, Hoyt G, Reitz BA, Robbins RC. Tolerance to cardiac allografts induced *in utero* with fetal liver cells. *Circulation* 1996; **94** (Suppl 9): II304- II 307
- 10 **Yuh DD**, Gandy KL, Hoyt G, Reitz BA, Robbins RC. A rodent model of *in utero* chimeric tolerance induction. *J Heart Lung Transplant* 1997; **16**: 222-230
- 11 **Kline GM**, Shen Z, Mohiuddin M, Ruggiero V, Rostami S, DiSesa VJ. Development of tolerance to experimental cardiac allografts *in utero*. *Ann Thor Surg* 1994; **57**: 72-74
- 12 **Petersen J**, Dandri M, Gupta S, Rogler CE. Liver repopulation with xenogenic hepatocytes in B and T cell-deficient mice leads to chronic hepadnavirus infection and clonal growth of hepatocellular carcinoma. *Proc Natl Acad Sci USA* 1998; **95**: 310-315
- 13 **Brown JJ**, Parashar B, Moshage H, Tanaka KE, Engelhardt D, Rabbani E, Roy-Chowdhury N, Roy-Chowdhury J. A long-term hepatitis B viremia model generated by transplanting nontumorigenic immortalized human hepatocytes in Rag-2-deficient mice. *Hepatology* 2000; **31**: 173-181
- 14 **Ohashi K**, Marion PL, Nakai H, Meuse L, Cullen JM, Bordier BB, Schwall R, Greenberg HB, Glenn JS, Kay MA. Sustained survival of human hepatocytes in mice: A model for *in vivo* infection with human hepatitis B and hepatitis delta viruses. *Nat Med* 2000; **6**: 327-331

- 15 **Mercer DF**, Schiller DE, Elliott JF, Douglas DN, Hao C, Rinfret A, Adison WR, Fischer KP, Churchill TA, Lakey JR, Tyrrell DL, Kneteman NM. Hepatitis C virus replication in mice with chimeric human livers. *Nat Med* 2001; **7**: 927-933
- 16 **Chang MH**, Hwang LY, Hsu HC, Lee CY, Beasley RP. Prospective study of asymptomatic HBsAg carrier children infected in the perinatal period: clinical and liver histologic studies. *Hepatology* 1988; **8**: 374-377
- 17 **Burk RD**, Hwang LY, Ho GY, Shafritz DA, Beasley RP. Outcome of perinatal hepatitis B virus exposure is dependent in maternal virus load. *J Infect Dis* 1994; **170**: 1418-1423
- 18 **Lafferty KJ**, Prowse SJ, Simeonovic CJ, Warren HS. Immunobiology of tissue transplantation: a return to the passenger leukocytes concepts. *Ann Rev Immunol* 1983; **1**: 143-173

Edited by Xu XQ

Mix-infections with different genotypes of HCV and with HCV plus other hepatitis viruses in patients with hepatitis C in China

Yuan-Ding Chen, Ming-Ying Liu, Wen-Lin Yu, Jia-Qi Li, Qin Dai, Zhen-Quan Zhou, Sergio G. Tisminetzky

Yuan-Ding Chen, Ming-Ying Liu, Jia-Qi Li, Qin Dai, Key Laboratory, Institute of Medical Biology, Chinese Academy of Medical Sciences & Peking Union Medical College, Kunming 650118, Yunnan Province, China

Wen-Lin Yu, Zhen-Quan Zhou, Kunming Hospital for Infectious Diseases, Kunming 650041, Yunnan Province, China

Sergio G. Tisminetzky, International Centre for Genetic Engineering and Biotechnology, Trieste 34012, Italy

Supported by the research grants from International Centre for Genetic Engineering and Biotechnology (ICGEB) Collaborative Research Program, CRP/CHN96-05 and from China Yunnan Provincial Science & Technology Commission International Collaborative Research Program, No. 97C009

Correspondence to: Dr. Yuan-Ding Chen, The Key laboratory, Institute of Medical Biology, Chinese Academy of Medical Sciences & Peking Union Medical College, 379 Jiaoling Road, Kunming 650118, Yunnan Province, China. chenyd@km169.net

Telephone: +86-871-8334689 **Fax:** +86-871-8334483

Received: 2002-01-14 **Accepted:** 2002-12-22

Abstract

AIM: Clinical therapy and prognosis in HCV infections are not good, and mix-infections with different HCV genotypes or quasiespecies and mix-infections with HCV plus other hepatitis viruses are important concerns worldwide. The present report describes the sequence diversity and genotyping of the 5' NCR of HCV isolates from hepatitis patients mix-infected with different HCV genotypes or variants, and the conditions of mix-infections with HCV plus other hepatitis viruses, providing important diagnostic and prognostic information for more effective treatment of HCV infections.

METHODS: The 5' non-coding region (5' NCR) of HCV was isolated from the patients sera and sequenced, and sequence variability and genotypes of HCV were defined by nucleotide sequence alignment and phylogenetic analysis, and the patients mix-infected with HCV plus other hepatitis viruses were analyzed. The conditions and clinical significance of mix-infections with HCV plus other hepatitis viruses were further studied.

RESULTS: Twenty-four out of 43 patients with chronic hepatitis C were defined as mix-infected with different genotypes of HCV. Among these 24 patients, 9 were mix-infected with genotype 1 and 3, 7 with different variants of genotype 1, 2 with different variants of genotype 2, 6 with different variants of genotype 3. No patients were found mix-infected with genotype 1 and 2 or with genotype 2 and 3. The clinical virological analysis of 60 patients mix-infected with HCV plus other hepatitis viruses showed that 45.0 % of the patients were mix-infected with HCV plus HAV, 61.7 % with HCV plus HBV, 6.7 % with HCV plus HDV/HBV, 8.4 % with HCV plus HEV, 3.3 % with HCV plus HGV. Infections with HCV plus other hepatitis viruses may exacerbate the pathological lesion of the liver.

CONCLUSION: The findings in the present study imply

that mix-infections with different HCV genotypes and mix-infections with HCV plus other hepatitis viruses were relatively high in Yunnan, China, providing important diagnostic and prognostic information for more effective treatment of HCV infections.

Chen YD, Liu MY, Yu WL, Li JQ, Dai Q, Zhou ZQ, Tisminetzky SG. Mix-infections with different genotypes of HCV and with HCV plus other hepatitis viruses in patients with hepatitis C in China. *World J Gastroenterol* 2003; 9(5): 984-992

<http://www.wjgnet.com/1007-9327/9/984.htm>

INTRODUCTION

Hepatitis C virus (HCV) is the major causative agent of non-A, non-B posttransfusional hepatitis, possessing a positive-stranded RNA genome of 9.4 kb^[1]. Since the discovery of HCV, investigations showed that HCV genome has great diversity, proposing that HCV isolates be classified into different groups (genotypes) or subtypes. HCV sequence diversity observed among isolates relevant to the process of viral evolution as it occurred during the history of human populations^[2]; therefore, it has been largely exploited to classify viral variants showing different epidemiological and pathogenic features^[3]. Conversely genetic diversity within individuals is more pertinent to the long-term adaptation of the virus to the host and reflect the dynamics of viral population and the selective mechanisms operating during the course of the infection^[4], formation of persistent and chronic infections^[5,6].

Clinic therapy and prognosis in HCV infections are not good. More than 50 % of individuals exposed to HCV develop chronic infection, and of those individuals chronically infected, approximately 20 % to 30 % will develop liver cirrhosis and/or hepatocellular carcinoma when followed a twenty to thirty years^[5,7]. For those results, in addition to HCV infection, mix-infection (co-infection or super-infection) with HCV plus other hepatitis viruses might have important significance in these situations. It was previously believed that some of the individuals with hepatitis C might in fact be mix-infected by HCV plus other hepatitis viruses. In such cases, HCV viremia clearance might be observed after clinical treatment directed to HCV infection, but the serum ALT level be not normalized or only transiently decreased. Mix-infection with HCV plus other hepatitis viruses is an important concern worthy further investigation.

The present report described the sequence diversity and genotyping of the 5' NCR of HCV isolates from hepatitis patients mix-infected with different HCV genotypes or variants, and the conditions of mix-infections with HCV plus other hepatitis viruses in Yunnan, China.

MATERIALS AND METHODS

Subjects

The cases described in this study are all Chinese patients in Yunnan province clinically diagnosed with liver diseases mix-infected with different HCV genotypes or variants, or with

HCV plus other hepatitis viruses. The serum specimens were collected from the patients for virological tests.

Sequencing and genotyping of HCV genome

HCV-RNA extraction HCV-RNA was extracted from the sera of patients with hepatitis C by the guanidinium lysis and phenol-chloroform method described previously^[8]. The HCV RNA extract from 450 µl of serum was finally dissolved in 45 µl of distilled water.

HCV PCR HCV-positive serum specimens were obtained from patients with hepatitis infected by HCV, and the details of RT-PCR method used to generate the double-stranded cDNA fragment have been described elsewhere^[8], with some modification. Briefly, 45 µl of RNA was extracted from 450 µl of serum as described previously, and the antisense primer AS-1 (5' -GTGCACGGTCTACGAGACCT-3') derived from the 5' NCR was used in a reverse transcriptase reaction to generate a cDNA copy of the antisense strand. Synthesis of HCV cDNA was performed from 2 µl of RNA extract, mixed with 13 µl of pre-RT buffer (50 mM Tris-HCl, 50 mM KCl, 10 mM MgCl₂, 0.5 mM spermidine, 10 mM DTT, 1.25 mM of the four dNTPs [Promega Biological Products Ltd., Shanghai, China] and 150 ng of the AS-1). After heat treated for 30 s at 92 °C and quick chilling, the above mix was added with 5 µl of RT buffer containing 20 u of RNasin and 10 u AMV reverse transcriptase (Promega, Shanghai, China) and then incubated for 1 hr at 42 °C.

Twenty microliters of cDNA from each reverse transcriptase reaction was used as a template for the first subsequent PCR in a DNA Thermal Cycler (Perkin-Elmer/Cetus, CA., USA). The first PCR was performed in a reaction volume of 100 µl containing 10 mM Tris-HCl (pH9.0), 50 mM KCl, 25 mM MgCl₂, 0.1 % Triton x-100, 5 mM of each dNTPs, 5 u Taq DNA polymerase [Promega], 150 ng of primers AS-1 and S-1 (5' -GCCATGGCGTTAGTATGAGT-3') and 20 µl of cDNA. The PCR was performed for 30 cycles at 94 °C for 45 s, 56 °C for 45 s and 72 °C for 45 s.

Cloning and sequencing One µl aliquot of the first PCR product (comprising nucleotides -240 to -22) was used as a template for the second of PCR amplification, using a new pair of primers AS-2 (5' -CGGGGAGCTCGCAAGCACCCCTAT-3'), S-2 (5' -GTCGTGGTACCTCCAGGACC-3'). The conditions of the second PCR reaction were the same as described above, except the primers AS-2 and S-2 which induced restriction endonuclease sites (underlined) Kpn I (GGTACC) and Sac I (GAGCTC) on the 5' - and 3' -end of the PCR product. The second PCR product (comprising nucleotides -220 to -47) was then cut with enzymes Kpn I/Sac I and inserted into pBluescript II K/S +/- (pBS) cloning vector by standard procedures. Clones were sequenced by the dideoxy chain termination method with phage T7 DNA polymerase (¹⁷SequencingTM, Pharmacia Biotech Inc. USA) (Figure 1). To minimize sequencing errors due to sequencing reaction and electrophoresis artifacts, all the clones were sequenced in both directions.

Sequence analysis To make a comparative analysis with reported sequences, sequences of the 5' NCR were compared with the consensus sequence of HCV-1^[9]. Genalign was used for sequence alignments and comparison (Intelligenetics). A phylogenetic tree for HCV was constructed by the previously described method^[10]. Briefly, evolutionary distance (i.e. those corrected for multiple substitution) between pairs of sequences were estimated using the DNADIST program in the PHYLIP package^[11]. Phylogenetic analysis was carried out using the programs DNADIST, NEIGHBOR and DRAWTREE in the PHYLIP package^[11].

Seral and virological tests

Anti-HAV detection Serum anti-HAV IgM was examined with an ELISA kit (Beijing Science & Health Clinic

Diagnostics Company, Beijing) as described in the manual.

HBV detection HBV infection markers including HBsAg, anti-HBs, anti-HBc, HBeAg were examined with ELISA kits (Beijing Biochemical & Immunological Reagent Company, Beijing). HBV-DNA was examined by PCR. The patients positive for at least two of the above markers were considered HBV-infected cases.

HCV detection Serum anti-HCV was examined with a second generation ELISA kit (AxSYM, Abbott Laboratories Diagnostics Division, USA) and the 5' NCR of HCV genome was examined by reverse transcription PCR (RT-PCR) as described previously^[8]. The patients positive for both anti-HCV and HCV-RNA were considered HCV-infected cases.

Anti-HDV detection Serum anti-HDV was examined with an ELISA kit (Beijing Science & Health Clinic Diagnostics Company, Beijing).

Anti-HEV detection Anti-HEV IgM was examined with an ELISA kit (Genelab Diagnostics PTE LTD, Singapore).

Anti-HGV detection HGV-RNA was examined by RT-PCR with HGV specific primers^[12].

Serum ALT detection Serum ALT was examined by Rate' s method.

Statistical analysis

Statistical analysis was performed using the Mann Witney test and Fisher' s exact test^[13].

Nucleotide sequence accession numbers

The nucleotide sequence data reported in this study have been deposited in the Genbank and EMBL Databases under the following accession numbers: AJ388314 to AJ388391. Genbank accession numbers of the previously reported sequences cited in this study are HCV1 (1a), M62321; HCVJ (1b), D90208; HC-J6 (2a), D00944; HC-J8(2b), D10988; NE92 (2d), X78862; Eb1 (3a), D10114; HCV-TR (3b), D11433; NE048 (3c), D16612; NE125 (3f), D16614; IND1751 (3g), X91421; T983 (2c), Ref. 14.

RESULTS

Mix-infections with different HCV genotypes or variants and sequence diversity

Forty-three serum samples from HCV antibody-positive patients with chronic hepatitis were analyzed by RT-PCR. The alignment of the DNA sequences (Figure 1 and 2) showed that 24 patients were mix-infected with different HCV genotypes or variants. Among these 24 patients, 9 were mix-infected with genotype 1 and 3 (Figure 1), 7 with different variants of genotype 1, 2 with variants of genotype 2, and 6 with variants of genotype 3 (Figure 2). There were no patients mix-infected with genotype 1 and 2 or mix-infected with genotype 2 and 3. Phylogenetic analysis with DNADIST (Figure 3 and 4) clearly demonstrated these results.

Nineteen isolates were cloned from the nine patients mix-infected with genotype 1 and 3 (Figure 1). Of them only 2 isolates (YS233-3 and YS245-3) were found possessing the sequence completely identical to the previously reported genotype 1b (HCVJ)^[15]. Two isolates (YS203-3 and YS232-2) possessed high sequence homology with genotype 1b. The remaining sequences were quite different from the existing (classified) genotypes reported previously.

Fourteen isolates were cloned from the seven individuals mix-infected with different variants of genotype 1, and only 2 isolates (YS246-2 and YS248-1) were found possessing the sequences completely identical to HCVJ (1b). Four isolates were cloned from the two patients mix-infected with different variants of genotype 2, and only one (R4-1) was found possessing sequence quite similar to T983 (genotype 2c)^[14].

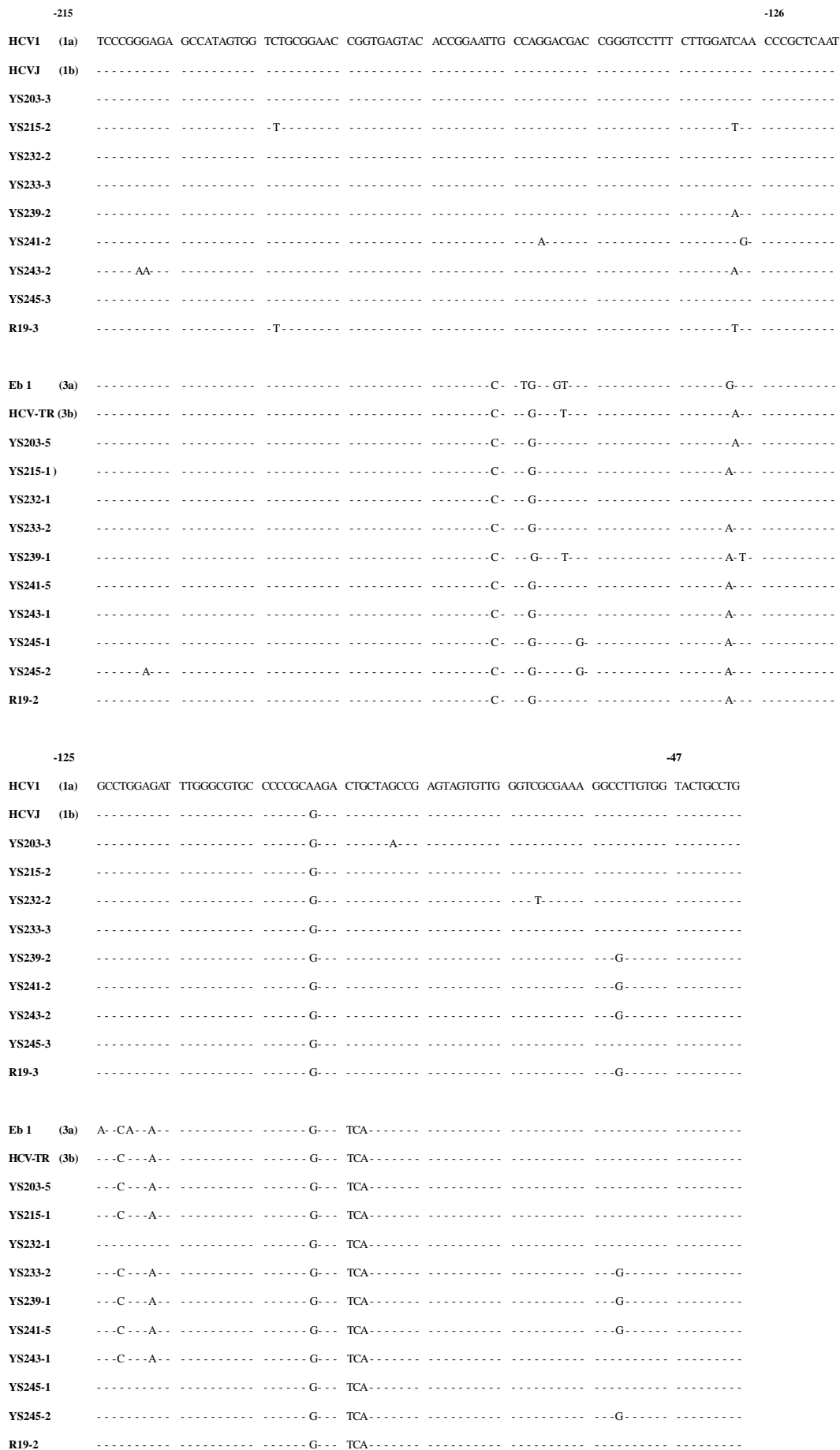


Figure 1 Alignment of DNA sequence of the 5' NCR of HCV isolated from the patients mix-infected with genotypes 1 and 3 mix-infected patients. Comparison of nucleotide sequences in the 5' NCR from Chinese patients (YS-, R-) with previously published HCV sequences. Nucleotide numbering corresponds to that described for the prototype HCV1^[9]. Dashes indicate identity with sequence of HCV1 (top line). Nucleotide substitutions are indicated. Numbers in parentheses indicates the genotype of that sequence. Source of published sequences referred to Materials and Methods.

-215	-126
HCV1 (1a)	TCCCCGGGAGA GCCATAGTGG TCTGCGGAAC CCGTGAGTAC ACCGGAATTG CCAGGACGAC CGGGTCCTTT CTTGGATCAA CCCGCTCAAT
HCVJ (1b)
YS204-5
YS204-9
YS205-3
YS205-2 A
YS219-2
YS219-1 A
YS224-3 T
YS224-1 T
YS226-3 C
YS226-2
YS246-2 T
YS246-3 T
YS248-1
YS248-2
HC-J6 (2a) G - A - T - A - A - T -
HC-J8 (2b) A - G - A - T - A - A - T -
T983 (2c) G - A - T - A - A - T -
NE92 (2d) A - T - A - A - T -
R4-1 G - A - T - A - A - T -
R4-2 G - A - T - A - A - T -
R3-1 A - G - A - T - A - A - T -
R3-2 G - A - T - A - A - T -
Eb 1 (3a) C - TG - GT - G -
HCV-TR (3b) C - G - T - A -
YS194-2 G - C - G - A -
YS194-3 G - G - C - G - A -
YS198-2 C - G - A -
YS198-3 A - G - C - G - A -
YS201-4 C - G - A -
YS201-2 C - G - A - G -
YS201-1 C - G - A -
YS225-6 C - TG - GT - AT -
YS225-10 C - TG - GT - AT -
YS225-7 C - G - GT - AT -
YS245-1 C - G - G - A -
YS245-2 A - C - G - G - A -
YS250-3 C - G - A -
YS250-1 C - G - A -
YS252-7 C - G - T - A - T -
YS252-1 C - G - T - A - T -

(continued)

	-125	-47
HCV1 (1a)	GCCTGGAGAT TTGGGCGTGC CCCCACAAGA CTGCTAGCCG AGTAGTGTG GGTCCGAAA GGCCTTGTGG TACTGCCTG	
HCVJ (1b)	-----G-----	
YS204-5	-----C-----G-----	
YS204-9	-----G-----G-----	
YS205-3	-----G-----G-----	
YS205-2	-----GG-----G-----	
YS219-2	-----G-----G-----	
YS219-1	-----G-----G-----	
YS224-3	-----G-----G-----	
YS224-1	-----G-----C-----G-----	
YS226-3	-----G-----G-----	
YS226-2	-----G-----G-----	
YS246-2	-----G-----G-----	
YS246-3	-----G-----G-----	
YS248-1	-----G-----G-----	
YS248-2	-----G-----G-----	
HC-J6 (2a)	--C--TC-- -----C-----T-----	
HC-J8 (2b)	-T-C--TC-- -----AC-- -----C-----T-----	
T983 (2e)	--C--CC-- -----C-----T	
NE92 (2d)	-----TC-- -----C-----T	
R4-1	--C--TC-- -----C-----T-----A-----	
R4-2	--C--TC-- -----G-----	
R3-1	--C--TC-- -----G-----	
R3-2	--C--TC-- -----G-----G-----	
Eb 1 (3a)	A--CA--A-- -----G-- TCA-----	
HCV-TR (3b)	--C--A-- -----G-- TCA-----	
YS194-2	--C--A-- -----G-- TCA-----G-----	
YS194-3	--C--A-- -----G-- TCA-----G-----	
YS198-2	--C--A-- -----G-- TCA-----G-----	
YS198-3	--CA--A-- -----G-- TCA-----C-----	
YS201-4	--C--A-- -----G-- TCA-----	
YS201-2	--C--A-- -----G-- TCA-----	
YS201-1	--C--A-- -----G-- TCA-----G-----	
YS225-6	A--CA--A-- -----G-- TCA-----	
YS225-10	A--CA--A-- -----G-- TCA-----G-----	
YS225-7	A--CA--A-- -----G-- TCA-----	
YS245-1	--C--A-- -----G-- TCA-----	
YS245-2	--C--A-- -----G-- TCA-----G-----	
YS250-3	--C--A-- -----G-- TCA-----	
YS250-1	--C--A-- -----G-- TCA-----G-----	
YS252-7	--C--A-- -----G-- TCA-----G-----	
YS252-1	--C--A-- -----G--G TCA-----G-----	

Figure 2 Alignment of DNA sequence of the 5' NCR of HCV isolated from the patients mix-infected with different variants of the same genotype. Comparison of nucleotide sequences in the 5' NCR from Chinese patients (YS-, R-) with previously published HCV sequences. Patients were presumably divided in three groups, as shown in the left column. Nucleotide numbering corresponds to that described for the prototype HCV1^[9]. Dashes indicate identity with sequence of HCV1 (top line). Nucleotide substitutions are indicated. Numbers in parentheses indicates the genotype of that sequence. Source of published sequences referred to Materials and Methods.

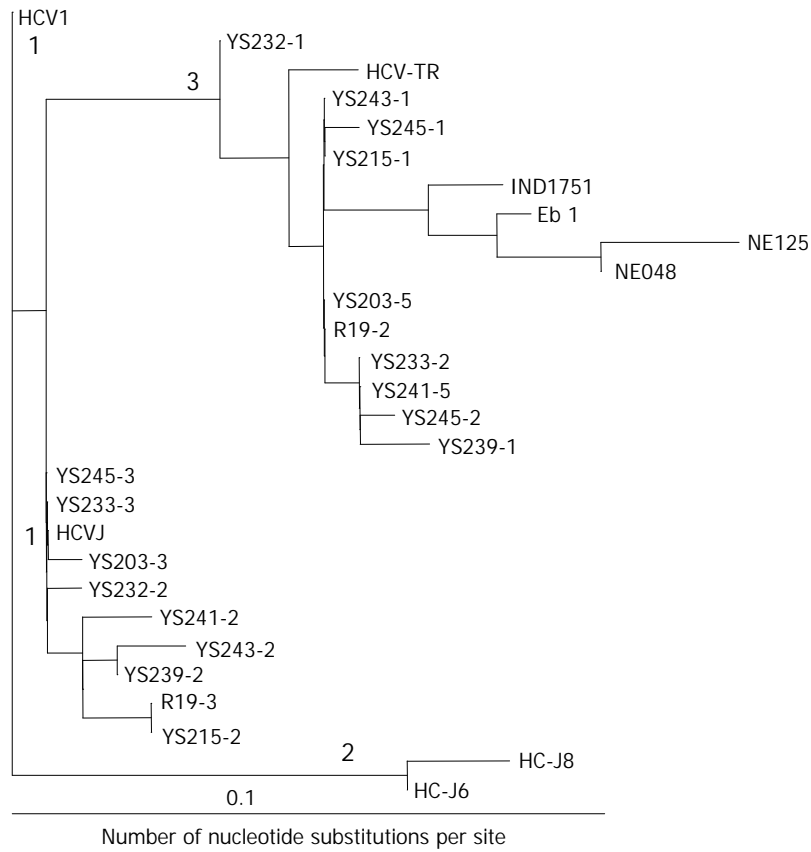


Figure 3 Phylogenetic tree constructed with Chinese (YS-, R-) and previously reported sequences, based on nucleotide (nt) identity of 5' NCR sequence (nt -220 to -47). Dendrogram shows 19 Chinese isolates distributed within 2 major genotypes (genotypes 1 and 3). Source of published sequences referred to Materials and Methods.

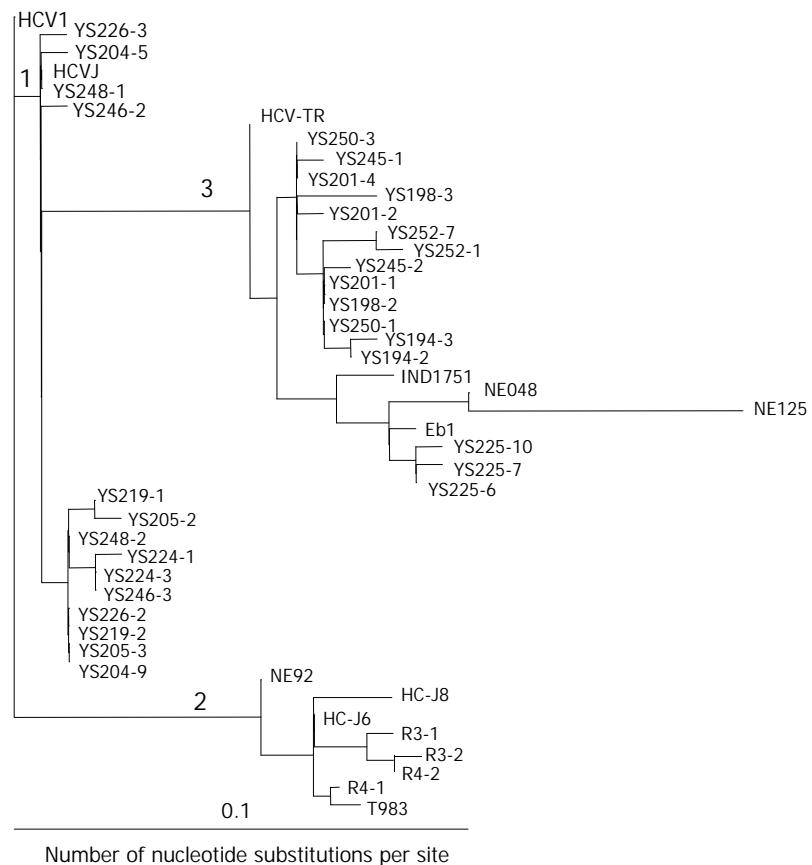


Figure 4 Phylogenetic tree constructed with Chinese (YS-, R-) and previously reported sequences, based on nucleotide (nt) identity of 5' NCR sequence (nt -220 to -47). Dendrogram shows 34 different Chinese isolates distributed within 3 major genotypes, 14 isolates in genotype 1, 4 in genotype 2, and 16 in genotype 3. Source of published sequences referred to materials and Methods.

Variation in the HCV 5' NCR sequences

Fifty one isolates were obtained from the 24 mix-infected patients, and only 5 isolates were found possessing the sequences completely identical to the known HCVJ (genotype 1b), the remaining possess high variability from the known genotypes. On the other side, isolates cloned from different individuals might possess the completely identical sequences, such as YS233-3 and YS245-3 (Figure 1); YS203-5, YS215-1, YS243-1, R19-2 (Figure 1), YS201-4 and YS250-3 (Figure 2); YS233-2 (Figure 1) and YS250-1 (Figure 2); YS239-1 (Figure 1) and YS252-7 (Figure 2).

The sequence analyzing found that out of 51 isolates, 29 (57 %) possessed a G at nucleotide position -61, in place of the

“T” that was present in all previously reported sequences. Of them, 14 were in genotype 1, 2 in genotype 2, 13 in genotype 3.

Clinic virus detection

In order to detect the conditions of mix-infection with HCV plus other hepatitis viruses, HAV, HBV, HDV, HEV and/or HGV infection markers were detected in 82 patients HCV chronically infected. The results showed that 60 patients were mix-infected with HCV plus other hepatitis viruses. The incidence was very high. Among these cases, 30.0 % (18/60) were mix-infected with HCV plus HAV, 46.7 % (28/60) with HCV plus HBV, 18.3 % (11/60) with HCV plus other two or three hepatitis viruses (Table 1). The individuals mix-infected

Table 1 Virological test in different groups

Cases	Positive cases (%)										
	HCV+ HAV+	HCV+ HBV+	HCV+ HEV+	HCV+ HGV+	HCV+ HAV+ HBV+	HCV+ HAV+ HEV+	HCV+ HAV+ HGV+	HCV+ HBV+ HDV+	HCV+ HBV+ HEV+	HCV+ HAV+ HBV+ HDV+	HCV+ HBV+ HEV+
60	18	28	2	1	3	1	1	1	1	3	1
(%)	(30.0)	(46.7)	(3.3)	(1.7)	(5.0)	(1.7)	(1.7)	(1.7)	(1.7)	(5.0)	(1.7)

Table 2 Virus detection in HCV-infected patients

Cases	Positive cases (%)				
	HAV	HBV	HDV	HEV	HGV
60	27	37	4	5	2
	(45.0 %)	(61.2 %)	(6.7 %)	(8.3 %)	(3.3 %)

Table 3 Mean age and ALT level of patients infected with HCV and mix-infected with HCV plus other hepatitis viruses

Group	Subtotal		Male		Female	
	Age (years)	ALT (U/L)	Age (years)	ALT (U/L)	Age (years)	ALT (U/L)
HCV ⁺	35.9 (20-57) [718/20]	577.7 (20-1890) [11553/20]	33.5 (20-57) [368/11]	580.8 (20-1890) [6970/12]	38.9 (20-48) [350/9]	572.9 (121-1000) [4583/8]
HCV ⁺ +HAV ⁺	18.9 (4-40) [302/16]	1253.4 (92-2350) [20055/16]	18.8 (6-40) [150/8]	1108.5 (92-2080) [8868/8]	19 (4-37) [152/8]	1398.4 (208-2350) [11187/8]
HCV ⁺ +HBV ⁺	34.6 (18-71) [970/28]	741 (30-2745) [20748/28]	35.7 (18-53) [678/19]	610.4 (30-1905) [11598/19]	32.4 (19-71) [292/9]	1016.7 (35-2745) [9150/9]
HCV ⁺ +other hepatitis viruses	29.3 (14-64) [439/15]	1266.5 (49-4160) [18998/15]	27.6 (14-54) [276/10]	1090.4 (49-3800) [10904/10]	32.6 (16-64) [163/5]	1618.8 (345-4160) [8094/5]
Total	30.7 (4-71) [2429/79]	803.2 (20-4160) [71354/79]	30.7 (6-57) [1472/48]	799.5 (21-3800) [38375/48]	30.9 (4-71) [95/31]	1100.5 (35-4160) [33014/30]

*Patients were divided into different groups: HCV-infected group (HCV⁺), HCV plus HAV mix-infected group (HCV⁺+HAV⁺), HCV plus HBV mix-infected group (HCV⁺+HBV⁺), and, HCV plus other hepatitis viruses mix-infected group (HCV⁺+other viruses). Refer to table 1.

Table 4 Mean ages and ALT levels of patients mix-infected with HCV plus HAV and other hepatitis viruses and with HCV plus HBV and other hepatitis viruses

Group	Total		Male		Female	
	Age (years)	ALT (U/L)	Age (years)	ALT (U/L)	Age (years)	ALT (U/L)
HCV ⁺ +HAV ⁺	26.9 (14-64) [242/9]	1521.9 (233-4160) [13697/9]	21.6 (14-41) [108/5]	1552.6 (233-3800) [7763/5]	33.5 (16-64) [134/4]	1483.5 (345-4160) [5934/4]
HCV ⁺ +HBV ⁺	34.3 (26-64) [309/9]	771.8 (49-2680) [6406/9]	31.8 (26-50) [191/6]	772 (49-2680) [4632/6]	39.3 (54-64) [118/3]	591.3 (234-1429) [1774/3]

with HCV plus HDV were all infected with HBV. Among these HCV infected patients, the positive rates of HAV, HBV, HDV, HEV and HGV were 45.0 %, 61.2 %, 6.7 %, 8.3 % and 3.3 %, respectively (Table 2).

Agas and serum ALT

The ages and serum ALT levels in different group patients were showed in Table 3.

The mean age of individuals infected singly with HCV was 35.9 years old, older than those mix-infected with HCV plus other hepatitis viruses. The mean age of the patients mix-infected with HCV plus HAV was 18.9 years old, which was significantly younger than that (35.9 years) singly infected with HCV ($P<0.001$), mix-infected with HCV plus HBV (34.6 %) ($P<0.001$) or mix-infected with HCV plus other one or more viruses (29.3 years) ($P<0.001$). The serum ALT level of the patients mix-infected with HCV plus HAV was 1 253.4 U/L, which was significantly higher than that (577.7 U/L) singly infected with HCV ($P<0.001$) or than that (741 U/L) mix-infected with HCV plus HBV ($P<0.05$) (Table 3). The mean age of the patients mix-infected with HCV plus HAV was significantly younger than that mix-infected with HCV plus HBV ($P<0.001$), no matter whether they were mix-infected with other hepatitis viruses or not (Table 3 and 4).

There were no significant differences in mean ages or in mean ALT levels between two sex individuals within different groups.

DISCUSSION

Conditions and features of different genotype HCV mix-infections

High variability of HCV genome appears not only in its highly variable region (HVR) of E2 protein, but also in the most highly conserved 5' NCR. The 5' NCR is the first generation of direct sequencing tests which provide complete sequence information to characterize HCV genotypes^[8,14]. However, the previously reported sequence comparisons between isolates were mainly cloned from the same individuals and focused on HVR of E2 or C protein region^[6,16-18], and largely within the same genotype. Isolates of HCV genome cloned from the same individual could belong to the same genotype^[16] or the different genotype^[19]. The previous report showed that HVR1 of HCV variation had an adaptive significance and was associated with favorable features of liver disease^[6] and the 5' NCR did so as showed in the present study. The findings in the present study showed that mix-infections within the same individual with different HCV genotypes or variants commonly existed, and mix-infection with genotype 1 plus genotype 3 were only found in the present study up to now in China. No genotype 1/2 or genotype 2/3 mix-infected cases were found in the present study. Different HCV genotypes or variants existed within the same individual. Most of the viral sequences found in the present study had high diversity from previously reported, implying that HCV genotypes in China had specific geographic distributions and epidemiological features.

Considerable sequence diversity exists both among isolates from unrelated individuals and within the same individual, implying that the virus is not a single molecular species, but as a variable population of closely related or unrelated genomes, according to the model of the viral genotypes or quasispecies. The pathogenetic mechanisms responsible for persistent HCV infection and progressive liver disease are largely unclear; nonetheless, variant genotypes or quasispecies presence was thought favorable to escaping from immune surveillance, leading to chronicity. In fact, the immune response failed to eradicate HCV infection and did not confer protection^[20],

despite the continuous presence of antibodies^[21-23] and cytotoxic T-cell^[24,25]. This phenomenon is likely to result in the continuous selection of new variants.

The previous reports showed that different HCV genotypes had different clinical pathological features and had different response to interferon therapy, while very few reports described clinical pathologic implications of mix-infection with different genotypes or variants. This is worthy to further study.

Clinical implications of mix-infections with HCV plus other hepatitis viruses

A considerable number of HCV/HAH or HCV/HBV mix-infections were observed in this study. Among the studied cases, only 26.8 % (22/82) of the patients were singly infected with HCV. The results showed that the mean age was lower and the mean ALT level was higher in the patients mix-infected with HCV plus other hepatitis virus than in the patients singly infected with HCV. These findings implied mix-infection with HCV plus other hepatitis virus might exacerbate pathological lesion of the liver, accelerating the progress of liver disease. Affections by HAV super-infection were most significant.

HCV infection has become an important public health problem worldwide including China^[26], and mix-infections among the patients with liver diseases with HCV plus other hepatitis viruses in China seems to be also a common problem. There were a lot of investigations about infections with only single HCV or other hepatitis viruses, but only few involved in mix-infections with HCV plus HAV^[27], HCV plus HBV^[28-31], HCV plus HDV^[28,32], or HCV plus HGV^[12,28,33-35], with high incidence rate has been reported in China. While there were no investigations involved the cases mix-infected with HCV plus so many hepatitis viruses with clinical features in China and even abroad. The findings in the present study showed that patients might get mix-infections with HCV plus one, two or three other hepatitis viruses. The positive rate in the patients mix-infected with HCV plus HBV was very high, implying that mix-infection with HCV plus HBV have great significance in diagnosis and treatment of HCV infected patients. Besides, mix-infection with HCV plus HIV would not be another ignorable public health problem in China today, especially in blood donors and drug abusers^[26,36,37]. The preliminary results obtained in the present study would provide important diagnostic and prognostic information for more effective treatment of HCV infections. In order to get better insight in the whole conditions of mix-infection of different hepatitis viruses more investigations are still necessary.

ACKNOWLEDGEMENT

We are indebted to Professor Francisco E. Baralle (International Centre for Genetic Engineering and Biotechnology, ICGEB) for his technical assistance in the present study, careful reading of the manuscript and for helpful discussions. This study was supported by research grants from ICGEB Collaborative Research Program (CRP/CHN96-05) and from China Yunnan Provincial Science & Technology Commission International Collaborative Research Program (97C009).

REFERENCES

- 1 **Choo QL**, Kuo G, Weiner AJ, Overby LR, Bradley DW, Houghton M. Isolation of a cDNA clone derived from a blood-borne non-A, non-B viral hepatitis genome. *Science* 1989; **244**: 359-362
- 2 **Bukh J**, Miller RH, Purcell RH. Genetic heterogeneity of hepatitis C virus: quasispecies and genotypes. *Semin Liver Dis* 1995; **15**: 41-63
- 3 **Mondelli MU**, Silini E. Clinical significance of hepatitis C virus genotypes. *J Hepatol* 1999; **31** (Suppl 1): 65-70

- 4 **Holland JJ**, De La Torre JC, Steinhauer DA. RNA virus populations as quasispecies. *Curr Top Microbiol Immunol* 1992; **176**: 1-20
- 5 **Heintges T**, Wands JR. Hepatitis C virus: Epidemiology and transmission. *Hepatology* 1997; **26**: 521-526
- 6 **Brambilla S**, Bellati G, Asti M, Lisa A, Candusso ME, D' Amico M, Grassi G, Giacca M, Franchini A, Bruno S, Ideo G, Mondelli MU, Silini EM. Dynamics of hypervariable region 1 variation in hepatitis C virus infection and correlation with clinical and virological features of liver diseases. *Hepatology* 1998; **27**: 1678-1686
- 7 **Cuthbert JA**. Hepatitis C: Progress and problems. *Clin Microbiol Rev* 1994; **7**: 505-532
- 8 **Chen YD**, Liu MY, Yu WL, Li JQ, Peng M, Dai Q, Wu J, Liu X, Zhou ZQ. Sequence variability of the 5' UTR in isolates of hepatitis C virus in China. *HBPDI INT* 2002; **1**: 541-552
- 9 **Choo QL**, Richman KH, Han JH, Berger K, Lee C, Dong C, Gallegos C, Coit D, Medina-Selby R, Barr PJ, Weiner AJ, Bradley DW, Kuo G, Houghton M. Genetic organization and diversity of the hepatitis C virus. *Proc Natl Acad Sci USA* 1991; **88**: 2451-2455
- 10 **Simmonds P**, Mellor J, Sakuldamrongpanich T, Nuchaprayoon C, Tanprasert S, Holmes EC, Smith DB. Evolutionary analysis of variants of hepatitis C virus found in Southeast Asia: comparison with classifications based upon sequence similarity. *J Gen Virol* 1996; **77**: 3013-3024
- 11 **Felsenstein J**. PHYLIP (Phylogeny Inference Package) version 3.5c. Distributed by the author. Department of Genetics, University of Washington, Seattle, USA 1993
- 12 **McHutchinson JG**, Nainan OV, Alter MJ, Sedghi-Vaziri A, Detmer J, Collins M, Kolberg J. Hepatitis C and G co-infection: Response to interferon therapy and quantitative changes in serum HGV-RNA. *Hepatology* 1997; **26**: 1322-1327
- 13 **Tsiminetzky SG**, Gerotto M, Pontisso P, Chemello L, Ruvoletto MG, Baralle F, Alberti A. Genotypes of hepatitis C virus in Italian patients with chronic hepatitis C. *Int Hepatol Commun* 1994; **2**: 105-112
- 14 **Halfon P**, Trimoulet P, Bourliere M, Khiri H, de Ledinghen V, Couzigou P, Feryn JM, Alcaraz P, Renou C, Fleury HJ, Ouzan D. Hepatitis virus genotyping based on 5' noncoding sequence analysis (trugene). *J Clin Microbiol* 2001; **39**: 1771-1773
- 15 **Bhattacharjee V**, Prescott LE, Pike I, Rodgers B, Bell H, El-Zayadi AR, Kew MC, Conradie J, Lin CK, Marsden H, Saeed AA, Parker D, Yap P-L, Simmonds P. Use of NS-4 peptides to identify type-specific antibody to hepatitis C virus genotype 1, 2, 3, 4, 5, and 6. *J Gen Virol* 1995; **76**: 1737-1748
- 16 **Pan W**, Wang H, Wang T. Comparison of hypervariable region gene of hepatitis C virus between an individual infected persistently and an individual recovered from infection. *Zhonghua Ganzangbing Zazhi* 1999; **7**: 26-28
- 17 **Fang F**, Pan W, Qi ZT, Song YB, Zhu SY. Sequence characterization of hypervariable region 1 of the putative envelope protein 2 in Chinese HCV isolates. *Zhongguo Bingduxue* 1998; **13**: 35-39
- 18 **Zhang WQ**, Yu H, Wang XF, Wang Q, Lu R, Wang HQ, Shao JJ. Analysis of the nucleotide sequence for C and NS5 regions and the genotype of HCV isolate in Shandong Province. *Zhonghua Shiyuan He Linchuangbing Duxue Zazhi* 2001; **15**: 219-221
- 19 **Song HS**, Wang HT, Tang SX, Ji BX, Wang TX, Zhang XT. HCV genotypes and distributions in patients coinfecting with different HCV genotypes. *Zhonghua Liuxingbingxue Zazhi* 1999; **20**: 227
- 20 **Farci P**, Alter HJ, Govindarajan S, Wong DC, Engle R, Lesniewski RR, Mushahwar IK, Desai SM, Miller RH, Ogata N, Purcell RH. Lack of protective immunity against reinfection with hepatitis C virus. *Science* 1992; **258**: 135-140
- 21 **Weiner AJ**, Geysen HM, Christopherson C, Hall JE, Mason TJ, Saracco G, Bonino F, Crawford K, Marion CD, Crawford KA, Brunetto M, Barr PJ, McHutchinson J, Houghton M. Evidence for immune selection of hepatitis C virus (HCV) putative envelope glycoprotein variants: potential role in chronic HCV infections. *Proc Natl Acad Sci USA* 1992; **89**: 3468-3472
- 22 **Taniguchi S**, Okamoto H, Sakamoto M, Kojima M, Tsuda F, Tanaka T, Munekata E, Muchmore EE, Peterson DA, Mishiro S. A structurally flexible and antigenically variable N-terminal domain of the hepatitis C virus E2/NS1 protein: implication for an escape from antibody. *Virology* 1993; **195**: 297-301
- 23 **Kato N**, Sekiya H, Ootsuyama Y, Nakazawa T, Hijikata M, Ohkoshi S, Shimotohno K. Humoral immune response to hypervariable region 1 of the putative envelope glycoprotein (gp70) of hepatitis C virus. *J Virol* 1993; **67**: 3923-3930
- 24 **Koziel MJ**, Dudley D, Afdhal N, Grakoui A, Rice CM, Choo Q-L, Houghton M, Walker BD. HLA class I-restricted cytotoxic T lymphocytes specific for hepatitis C virus. Identification of multiple epitopes and characterization of patterns of cytokine release. *J Clin Invest* 1995; **96**: 2311-2321
- 25 **Rehermann B**, Chang KM, McHutchinson J, Kokka R, Houghton M, Rice CM, Chisari FV. Differential cytotoxic T-lymphocyte responsiveness to the hepatitis B and C viruses in chronically infected patients. *J Virol* 1996; **70**: 7092-7102
- 26 **Chen YD**, Liu MY, Yu WL, Li JQ, Peng M, Dai Q, Liu X, Zhou ZQ. Hepatitis C virus infections and genotypes in China. *HBPDI INT* 2002; **2**: 194-201
- 27 **Tang BY**, Huang ZH, Li J, Min X. Investigation of anti-HCV in sera from patients with viral hepatitis in part areas in Jiangsu Province. *Nanjing Yikedaxue Xuebao* 1993; **13**: 252-255
- 28 **Fan XL**, Peng WW, Yao JL, Zhou YP, Lu L, Zheng XC, Chen Q. Infection of HBV, HCV and HDV in hepatocellular carcinoma. *Zhonghua Chuanranbing Zazhi* 1995; **13**: 129-132
- 29 **Du S**, Tao Q, Chang J. Studies on multiple infection with hepatitis B, C and G viruses. *Zhonghua Yufangyixue Zazhi* 1998; **32**: 13-15
- 30 **Wang J**, Zhao H, Zhao S. Prevalence of HCV and HBV infection in patients with primary hepatocellular carcinoma in Shanxi Province. *Zhonghua Liuxingbingxue Zazhi* 1999; **20**: 215-217
- 31 **Shimbo S**, Zhang ZW, Gao WP, Hu ZH, Qu JB, Watanabe T, Nakatsuka H, Matsuda-Inokuchi N, Higashikawa K, Ikeda M. Prevalence of hepatitis B and C infection markers among adult women in urban and rural areas in Shaanxi Province, China. *Southeast Asian J Trop Med Public Health* 1998; **29**: 263-268
- 32 **Wei JR**, Liu JL, Zhang YK, Zhang QS. Hepatitis B and Hepatitis C virus infection and hepatocellular carcinoma. *Zhonghua Chuanranbing Zazhi* 1997; **15**: 151-153
- 33 **Wang H**, Sun Y, Chang JH, Tao QM. The coinfection of hepatitis C virus with hepatitis G virus and its reaction to interferon treatment. *Zhonghua Shiyuan He Linchuangbing Duxue Zazhi* 1998; **12**: 377-379
- 34 **Wang Y**, Chen HS, Fan MH, Liu HL, An P, Sawada N, Tanaka T, Truda F, Okamoto H. Infection with GB virus C and hepatitis C virus in hemodialysis patients and blood donors in Beijing. *J Med Virol* 1997; **52**: 26-30
- 35 **Wu RR**, Mizokami M, Cao K, Nakano T, Ge XM, Wang SS, Orito E, Ohba K, Mukaide M, Hikiji K, Lao JY, Iino S. GB virus C/hepatitis G virus infection in southern China. *J Infect Dis* 1997; **175**: 168-171
- 36 **Zhu B**, Wu N, Qiang L, Shao Y. The serologic study on the blood transmission origin of HIV. *Zhonghua Liuxingbingxue Zazhi* 2000; **21**: 140-142
- 37 **Zhang C**, Yang R, Xia X, Qin S, Dai J, Zhang Z, Peng Z, Wei T, Liu H, Pu D, Luo J, Takebe Y, Ben K. High prevalence of HIV-1 and hepatitis C virus coinfection among injection drug users in the southeastern region of Yunnan, China. *J Acquir Immune Defic Syndr* 2002; **29**: 191-196

Prevalence of hepatitis B and C markers among refugees in Athens

Anastasios Roussos, Constantin Goritsas, Thomas Pappas, Maria Spanaki, Panagiota Papadaki, Angeliki Ferti

Anastasios Roussos, Constantin Goritsas, Thomas Pappas, Angeliki Ferti, Department of Internal Medicine, General Regional Hospital "Sotiria", Athens, Greece

Maria Spanaki, Panagiota Papadaki, Blood Bank, General Regional Hospital "Sotiria", Athens, Greece

Correspondence to: Dr Anastasios Roussos, 20 Ierosolinon Street, P.O. 11252, Athens, Greece. roumar26@yahoo.com

Telephone: +301-210-8646215 **Fax:** +301-210-8646215

Received: 2003-01-18 **Accepted:** 2003-02-19

Abstract

AIM: To assess the prevalence of hepatitis B and C serological markers in a population of refugees living in Athens.

METHODS: One hundred and thirty refugees (81 males and 49 females, mean age \pm SD: 31.7 \pm 8 years) were included in the study. The hepatitis B virus surface antigen (HBsAg), the hepatitis B virus core antibody (anti-HBc) and the hepatitis C virus antibody (anti-HCV) were detected using a third-generation immunoassay.

RESULTS: Twenty individuals (15.4 %) were HBsAg positive and 69 (53.1 %) were anti-HBc positive. The prevalence of HBsAg and anti-HBc was higher among refugees from Albania and Asia (statistical significant difference, $P < 0.008$ and $P < 0.001$ respectively). The prevalence of these markers was found irrelevant to age or sex. Anti-HCV was detected in the serum of 3 individuals (2.3 %). No differences among age, sex or ethnicity regarding anti-HCV prevalence were found.

CONCLUSION: It can be concluded that refugees living in Athens are an immigrant population characterized by a high incidence of HBV infection. The prevalence of HBV markers is higher among refugees from Albania and Asia. It is therefore believed that the adherence to general precautions and the initiation of HBV vaccination programs will be necessary in the future, especially in these communities. Although the prevalence of HCV infection seems to be relatively low, extended epidemiological surveys are needed to provide valid results.

Roussos A, Goritsas C, Pappas T, Spanaki M, Papadaki P, Ferti A. Prevalence of hepatitis B and C markers among refugees in Athens. *World J Gastroenterol* 2003; 9(5): 993-995

<http://www.wjgnet.com/1007-9327/9/993.htm>

INTRODUCTION

During the last decade, refugees from countries with an increased prevalence of infectious diseases, (i.e. viral hepatitis, AIDS and tuberculosis) have settled in Greece. The crowded living conditions and the avoidance of well-organized places of sheltering, due to the fear of deportation or expulsion, characterize immigrant populations and facilitate the spread of these diseases^[1].

Assessing the prevalence of viral hepatitis among refugees

is necessary in order to plan health control measures regarding primary and secondary prevention and prophylaxis for the entire population^[2,3]. Both prevention and prophylaxis are of great importance for public health, as chronic viral hepatitis remains the main etiology for the development of hepatocellular carcinoma, in our country^[4] and worldwide^[5-7]. In Greece, previous studies on Albanian refugees showed a high prevalence of hepatitis B^[8,9]. However, data regarding refugees of other nationalities is limited. Moreover, insufficient information is available on the prevalence of hepatitis C.

The aim of this study was to assess the prevalence of hepatitis B and C serological markers in a population of refugees of various nationalities, living in Athens.

MATERIALS AND METHODS

Materials

The study involved all refugees referred to the outpatient clinic of our Department for a health certificate, during a six-month period. A total of 130 refugees (81 men and 49 women), aged between 18 and 69 years (mean age \pm SD: 31.7 \pm 8 years old), were studied. The local ethics committee approved the study and signed informed consent was obtained from each participant.

Methods

All subjects were interviewed by means of a structured questionnaire for general demographic details (age, sex, ethnic origin) and risk factors for hepatitis B and C infections (blood transfusions, intravenous drug use, tattoos). Thereafter, 10 ml of blood was obtained by venesection and the serum was separated by centrifugation. Each serum sample was coded and stored at -20 °C. The hepatitis B virus surface antigen (HBsAg), the hepatitis B virus core antibody (anti-HBc) and the hepatitis C virus antibody (anti-HCV) were detected by a third-generation enzyme-linked immunosorbent assay (ELISA, ABBOTT, EIA-3). This immunoassay method was used according to the instructions of the manufacturer.

Statistical analysis

Results were expressed as mean \pm SD. A Chi - squared (χ^2) test with Yate's correction was used to detect differences between groups and predictive indices. χ^2 -analysis was performed using the SPSS program (version 9.0, SPSS Inc., IL, USA). $P < 0.05$ were considered statistically significant.

RESULTS

Albanian refugees represented the higher proportion (59 %) in our study population. Refugees from eastern European countries (the former USSR, Poland, Bulgaria and Romania), Asia and Africa, were also examined. The mean age did not differ among the various ethnic groups. Male sex was prominent in Albanian (67 %) and Asian (100 %) refugees. The demographic characteristics of the 130 subjects were shown analytically in Table 1.

Twenty individuals (15.4 %) were HBsAg positive and 69 (53.1 %) were anti-HBc positive. Table 2 showed the distribution of hepatitis B markers according to sex. The

prevalence of HBsAg and anti-HBc was higher in men than that in women but the difference was not statistically significant ($P=0.23$ and $P=0.14$ respectively). Finally, the mean age did not differ significantly between seropositive and seronegative for these markers groups [HBsAg (+): 31.8 ± 6 years, HBsAg (-): 32.7 ± 7 years, $P=0.66$; and anti-HBc (+): 30.9 ± 7 years, anti-HBc (-): 32.8 ± 6 years, $P=0.23$].

A total of 3 individuals (2.3%), two men (aged 32 and 34) and one woman aged 33 were anti-HCV positive. No differences in age ($P=0.71$) and sex ($P=0.87$) regarding anti-HCV prevalence were found.

Table 3 showed the distribution of hepatitis B and C serological markers according to ethnicity. The prevalence of HBsAg and anti-HBc was higher among refugees from Albania and Asia (statistically significant difference, $P<0.008$ and $P<0.001$, respectively). Although a high prevalence of hepatitis C infection (12.5%) characterized African refugees, no statistically significant difference among the various groups ($P=0.76$) was found.

Table 1 Demographic characteristics of refugees

Ethnicity	n (%)	Sex (M/F)	Age (mean±SD)
Albania	76 (59)	51/25	31.8±8.5
East europe	35 (27)	15/20	32.5±10.2
Asia	11 (8.5)	11/0	31.4±6.2
Africa	8 (6.2)	4/4	31.1±6.7
Total	130	81/49	31.7±8.5

Table 2 Distribution of hepatitis B serological markers according to sex

Sex	n	HBsAg(+)	Anti-HBc(+)	HBsAg, anti-HBc(-)
Males	81	15 (18.5%)	47 (58%)	19 (23.5%)
Females	49	5 (10.2%)	22 (45%)	22 (44.8%)
Total	130	20 (15.4%)	69 (53.1%)	41 (31.5%)

Table 3 Distribution of hepatitis B and C serological markers according to ethnicity

Ethnicity	n	HBsAg(+)	Anti-HBc(+)	Anti-HCV(+)
Albania	76	17 (22.4%) ^a	54 (71%) ^a	1 (1.3%)
E Europe	35	0 (0)	8 (23%)	1 (2.8%)
Asia	11	3 (27.3%) ^b	5 (45%) ^b	0 (0)
Africa	8	0 (0)	2 (25%)	1 (12.5%)
Total	130	20 (13.4%)	69 (53.1%)	3 (2.3%)

^a $P<0.008$, ^b $P<0.001$.

DISCUSSION

Hepatitis B and C are widespread infectious diseases representing major health problems. The worldwide seroprevalence of HBsAg and anti-HCV is estimated to be 5% and 1%, respectively. However, marked geographic variation exists. Local factors, such as the ethnic composition of the population, influence the prevalence of these infections in a particular community^[2,3]. It is well known that refugees constitute a special social group in a geographical area. They often live under conditions that facilitate the spread of infectious diseases. Moreover, the prevalence of chronic infections among them depends on the endemicity of these diseases in the country of origin. In the present study, the prevalence of hepatitis B and C serological markers among

refugees of various nationalities living in Athens was evaluated. Greece has been traditionally considered as a region of intermediate endemicity for HBV infection and estimated prevalence rates for HBsAg and anti-HBc were 3% and 30-40%, respectively^[10]. Recent information regarding the seroprevalence of these markers in the Greek population is not available. However, in recent studies, blood donors and recruits in the army had an HBsAg positivity below 1%, possibly indicating a shift towards lower endemicity in Greece^[11]. In the population of our study, the prevalence of HBsAg and anti-HBc was extremely high (15.4% and 53.1%, respectively), similar to that reported in countries of high endemicity for HBV infection. In Greece, the reported HBsAg prevalence even in high-risk groups for HBV infection, such as HIV-patients (13.3%)^[12] and drug addicts (6.9%)^[13,14], is lower than that observed in our population. Higher HBsAg prevalence (17.2%) has been reported only in Kurdish of a refugee camp in Athens, a social group characterized by particularly unhealthy living conditions^[15].

An increased prevalence of hepatitis B serological markers has been reported in previous studies concerning Albanian refugees in Greece and Italy^[8,9,16,17]. Our results confirm that Albanian refugees have a high seroprevalence of HBV markers, which possibly reflects the high endemicity of HBV infection in Albania. It is also suggested that Asian refugees should be considered as another group with high prevalence of chronic HBV infection. If a larger epidemiological research confirms our results, then future preventive intervention could be conducted for those communities of refugees that are at highest risk.

The prevalence of anti-HCV in the population of refugees was relatively low (2.3%) and no differences among various nationalities were found. A previous study among Albanian refugees in northwestern Greece showed anti-HCV seroprevalence of 1.75%^[8]. To our knowledge, the present study is the first concerning refugees living in Athens. In Greece, several reports have shown the important role of HCV in the development of cirrhosis and hepatocellular cancer^[18,19]. However, most of the epidemiological research for the prevalence of hepatitis C concerns specific population groups, such as blood donors, medical staff, and chronic alcoholics^[20-22]. Recently, a random community-based study of the general population in the Greek Island of Zakynthos showed lower prevalence of hepatitis C (1.25%) compared to our results^[23]. However, this difference is slight. Therefore, refugees living in Athens cannot be considered as a potential reservoir of HCV infection for the indigenous population.

It is concluded that refugees living in Athens are characterized by a high prevalence of HBV infection. The seroprevalence of HBV markers is higher among refugees from Albania and Asia. We, therefore, believe that the adherence to general precautions and an effort to improve living conditions will be necessary in the future, especially in these communities. The initiation of HBV vaccination programs is also needed. Although the prevalence of HCV infection seems to be relatively low among refugees living in Athens, extended epidemiological surveys are needed to provide valid results.

REFERENCES

- Ackerman LK. Health problems of refugees. *J Am Board Fam Pract* 1997; **10**: 337-348
- Terrault N, Wright T. Viral Hepatitis A through G. In: Sleisenger and Fortdran's, eds. *Gastrointestinal and Liver Disease. Pathophysiology, diagnosis and management*. 6th ed. Philadelphia: Saunders 1998: 1123-1170
- Sherlock S. Chronic Hepatitis. In: Sherlock S, Dooley J, eds. *Diseases of the liver and biliary system*. 10th ed. London: Blackwell Science Ltd 1997: 303-336

- 4 **Kuper HE**, Tzonou A, Kaklamani E, Hadziyannis S, Tasopoulos N, Lagiou P, Trichopoulos D, Stuver S. Hepatitis B and C viruses in the etiology of hepatocellular carcinoma; a study in Greece using third-generation assays. *Cancer Causes Control* 2000; **11**: 171-175
- 5 **Yang JM**, Wang RQ, Bu BG, Zhou ZC, Fang DC, Luo YH. Effects of HCV infection on expression of several cancer-associated gene products in hepatocellular carcinoma. *World J Gastroenterol* 1999; **5**: 25-27
- 6 **Rabe C**, Pilz T, Klostermann C, Berna M, Schild HH, Sauerbruch T, Caselmann WH. Clinical characteristics and outcome of a cohort of 101 patients with hepatocellular carcinoma. *World J Gastroenterol* 2001; **7**: 208-215
- 7 **Tang ZY**. Hepatocellular carcinoma-cause treatment and metastasis. *World J Gastroenterol* 2001; **7**: 445-454
- 8 **Dalekos GN**, Zervou E, Karabini F, Tsianos EV. Prevalence of viral markers among refugees from southern Albania: increased incidence of infection with hepatitis A, B, and D viruses. *Eur J Gastroenterol Hepatol* 1995; **7**: 553-558
- 9 **Malamitsi PA**, Papacharitonos S, Sotos D, Tzala E, Psychogios G, Hatzakis A. Prevalence study of different hepatitis markers among pregnant Albanian refugees in Greece. *Eur J Epidemiol* 1996; **12**: 297-301
- 10 **Kyriakis KP**, Foudoulaki LE, Papoulia EI, Sofroniadou KE. Seroprevalence of hepatitis B surface antigen (HBsAg) among first-time and sporadic blood donors in Greece: 1991-1996. *Transfus Med* 2000; **10**: 175-180
- 11 **Stamouli M**, Gizaris V, Totos G, Papaevangelou G. Decline of hepatitis B infection in Greece. *Eur J Epidemiol* 1999; **15**: 447-449
- 12 **Dimitrakopoulos A**, Takou A, Haida A, Molangeli S, Gialeraki A, Kordossis T. The prevalence of hepatitis B and C in HIV-positive Greek patients: relationship to survival of deceased AIDS patients. *J Infect* 2000; **40**: 127-131
- 13 **Roumeliotou-Karayannis A**, Tassopoulos N, Kotsianopoulou M, Karpodini E, Trichopoulou E, Papaevangelou G. Prevalence of HBV HDV and LAV/HTLV-III infections among Greek drug addicts. *Prog Clin Biol Res* 1987; **234**: 403-404
- 14 **Roumeliotou A**, Karayiannis A, Tassopoulos N, Karpodini E, Trichopoulou E, Kotsianopoulou M. Prevalence of HBV, HDV and HIV infections among intravenous drug addicts in Greece. *Eur J Epidemiol* 1987; **3**: 143-146
- 15 **Skliros E**, Lionis C, Foudoulaki L, Sotiropoulos A, Kouroumalis E, Spandidos D. Hepatitis B and C markers in a Kurdish refugee camp in Greece. *J Gastroenterol Hepatol* 2001; **16**: 839-840
- 16 **Santantonio T**, Lo Caputo S, Germinario C, Squarcione S, Greco D, Laddago V. Prevalence of hepatitis virus infections in Albanian refugees. *Eur J Epidemiol* 1993; **9**: 537-540
- 17 **Chironna M**, Germinario C, Lopalco PL, Quarto M, Barbuti S. HBV, HCV and HDV infections in Albanian refugees in Southern Italy (Apulia region). *Epidemiol Infect* 2000; **125**: 163-167
- 18 **Hadziyannis SJ**, Gianhoulis G, Hadziyannis E, Kaklamani E, Alexopoulou A, Dourakis S. Hepatitis C virus infection in Greece and its role in chronic liver disease and hepatocellular carcinoma. *J Hepatol* 1993; **17**(Suppl 3): 72-77
- 19 **Goritsas C**, Athanasiadou A, Arvaniti A, Lampropoulou-Karatza C. The leading role of Hepatitis B and C viruses as risk factors for the development of hepatocellular carcinoma. *J Clin Gastroenterol* 1995; **20**: 220-224
- 20 **Manesis E**. Hepatitis C in the general Greek population. In: S Hadziyannis, eds. *Hepatitis C*. Athens: *Paschalidis Editions* 1997; 25-33
- 21 **Koulentaki M**, Spanoudakis S, Kantidaki E, Drandakis P, Tzagarakis N, Biziagos. Prevalence of hepatitis B and C markers in volunteer blood donors in Crete. A 5-year study. *J viral Hepat* 1999; **6**: 243-248
- 22 **Dalekos GN**, Zervou E, Merkouropoulos MH, Tsianos EV. Prevalence of hepatitis B and C viruses infection in chronic alcoholics with or without liver disease in Ioannina, Greece: low incidence of HCV infection. *Eur J Epidemiol* 1996; **12**: 21-25
- 23 **Goritsas C**, Plerou I, Agaliotis S, Spinthaki R, Mimidis K, Velissaris D. HCV infection in the general population of a Greek island: Prevalence and risk factors. *Hepatogastroenterology* 2000; **47**: 782-785

Oral immunization of animals with transgenic cherry tomatillo expressing HBsAg

Yi Gao, Ying Ma, Mei Li, Tong Cheng, Shao-Wei Li, Jun Zhang, Ning-Shao Xia

Yi Gao, Ying Ma, Tong Cheng, Shao-Wei Li, Jun Zhang, Ning-Shao Xia, The Key Laboratory Ministry of Education for Cell Biology and Tumor Cell Engineering, Xiamen University, Xiamen 361005, Fujian Province, China

Mei Li, Xiamen Overseas Chinese Introduction Garden, Xiamen 361002, Fujian Province, China

Supported by the grant from Natural Scientific Fundation of Fujian Province, No. C9910004 and Xiamen Kaili Biologic Product Limited Company

Correspondence to: Professor Ning-Shao Xia, The Key Laboratory Ministry of Education for Cell Biology and Tumor Cell Engineering, Xiamen University, Xiamen 361005, Fujian Province, China. nsxia@jingxian.xmu.edu.cn

Telephone: +86-592-2184110 **Fax:** +86-592-2184110

Received: 2002-12-07 **Accepted:** 2003-01-02

Abstract

AIM: To investigate the expression of recombinant HBsAg (rHBsAg) in transgenic cherry tomatillo in order to explore the feasibility of producing HBV oral vaccine with cherry tomatillo by animal immune tests.

METHODS: The recombinant plant expression vector containing HBsAg gene was constructed. Mediated with *Agrobacterium tumefaciens*, HBsAg gene was transferred into cotyledons of cherry tomatillo. Transformed cherry tomatillos were obtained through hygromycin delay-selection. Integrated DNA in transgenic cherry tomatillo was confirmed by hygromycin resistance selection, Gus detection, polymerase chain reaction (PCR) and dot blotting analysis. Antigenicity of rHBsAg was examined by ELISA and the immunogenicity of rHBsAg derived from transgenic cherry tomatillo tissues was confirmed by oral feed of transformed tissues to BALB/c mice primed with commercial HBV vaccines. Specific antibody titers in mice's serum were examined by ELISA every week.

RESULTS: By far, 10 positive lines of transgenic cherry tomatillos containing HBsAg gene were obtained. Among different organs of the same transgenic cherry tomatillo, level of rHBsAg expressed in leaves was the highest with the yield up to 300ng/g fresh weight. And the rHBsAg expression level in fruits was about 10 ng/g fresh weight. In animal immune tests, oral delivery with transgenic tissues to mice primed with commercial vaccine instead of naive mice resulted in significant immune response.

CONCLUSION: The result of this animal immune test indicated the rHBsAg derived from transgenic cherry tomatillo possessed normal immunogenicity. This work demonstrated the feasibility to generate oral immunogenic rHBsAg in transgenic cherry tomatillo, and would provide some experimental approach for the production of low-cost oral vaccines using transgenic cherry tomatillo in large scale.

Gao Y, Ma Y, Li M, Cheng T, Li SW, Zhang J, Xia NS. Oral immunization of animals with transgenic cherry tomatillo expressing HBsAg. *World J Gastroenterol* 2003; 9(5): 996-1002 <http://www.wjgnet.com/1007-9327/9/996.htm>

INTRODUCTION

Hepatitis B virus infection is one of the most widespread viral infections of humans, especially in China. HBV DNA were found in most of newborns of HBsAg positive mothers^[1]. HBV vaccines have prevented numerous infections. However, administration of vaccine intramuscularly causes some pain, it is not accepted widely, especially in children. In recent years, a novel production system of vaccines- "edible vaccines" or "oral vaccines" is developed. Oral vaccines can serve multiple immunization priorities, including simplicity of use, increase in compliance (as a result of increased comfort of delivery), enhanced immune responses at mucosal sites, and stimulation of humoral immunity^[2-5].

The use of transgenic vegetables and fruits for the expression and delivery of recombinant protein antigens as edible vaccines has become an attractive topic for plant molecular biologists. Plants are potential source of antigen protein that is not dependent upon process technology to ensure protein folding and particle assembly. In addition, a plant-based antigen protein expression system makes possible the testing of an oral immunization strategy by simply feeding the plant tissues. So far, the production of oral vaccines in transgenic plant has focus on viral and bacterial subunit antigen, including *E.coli* heat-labile enterotoxin B subunit (LT-B)^[6-12], cholera toxin B subunit (CT-B)^[13,14], hepatitis B surface antigen (HBsAg)^[15-21], Norwalk virus capsid protein (NVCP)^[22,23], rabies virus glycoprotein^[24], etc. The results of oral immune tests in human bodies with transgenic potato and lettuce expressing rHBsAg have been reported, and the special antibody was detected in serum of the volunteers who were given edible tissues of transgenic plant^[25]. As we know, potato and lettuce could not be eaten in raw in certain population. But cooking process would destroy the target protein and affect its immunogenicity. So the plant acceptor should not only be easy to handle in genetic constructs, but also be able to be consumed in raw. In our study, we chose cherry tomatillo as the plant system for producing recombinant antigen.

Tomatillo, *Physalis ixocarpa* Brot. is grown in Mexico annually. It is a good source of vitamin C. The flesh of tomatillo is solid and seedy. And the pulp is glutinous, a little sweeter than tomato, and the flavor is somewhat similar to green apple. It is a key ingredient of many Mexican recipes, raw or cooked. Ripe fruits can be eaten raw, in sandwiches and salads. As an important commercial vegetable crop in the diets of Mexicans and Central Americans, tomatillo has been known by more and more researchers. The aim of this study that chose tomatillo as the plant acceptor was to investigate the feasibility of producing HBV oral vaccine with transgenic cherry tomatillo.

MATERIALS AND METHODS

Materials

Plant materials Cherry tomatillo (*Physalis ixocarpa* Brot.). The seeds were obtained from Xiamen ITG Seed IMP&EXP CO., LTD.

Bacterium and plasmids *Agrobacterium tumefaciens* strain EHA105, was kindly provided by Prof. Zhang Qi-fa, Huazhong Agricultural University. p1301HBs, recombinant mini Ti

plasmid of the binary expression vector (containing hygromycin-resistant gene, kanamycin-resistant gene, Gus gene and HBsAg-S gene), was constructed in our lab^[20,21].

Animals in immune tests BALB/c mice aged 4-6 weeks were purchased from the Center of Cancer Research, Xiamen University.

Methods

Construction of plant expression vector A 0.8 kb DNA fragment containing HBsAg-S gene was obtained by a PCR-based assembly from patient's serum and inserted into pBPF Ω 7 between the constitutively-expressed cauliflower mosaic virus (CaMV) 35S promoter and Nos terminator at the Xho I/EcoR I site by substituting the Ω gene to form pBHBS, then the 2.4 kb DNA fragment containing the HBsAg-S gene, the CaMV35S promoter and the nos terminator was cleaved with Pst I from pBHBS and ligated into the binary plant vector pCAMBIA1301 (containing hygromycin-resistant gene, kanamycin-resistant gene, Gus gene) digested by Pst I to give the resulting plasmid, p1301HBs (Figure 1).

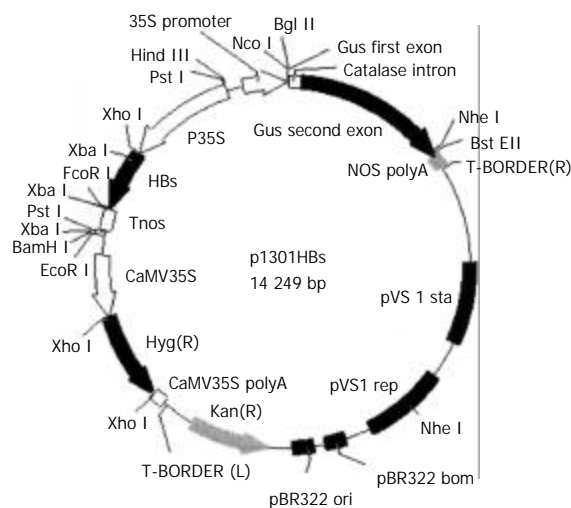


Figure 1 Plasmid p1301HBs.

Plant transformation and regeneration p1301HBs was introduced into *Agrobacterium tumefaciens* strain EHA105 directly by the freeze-thaw method with slight modifications. Subsequently, *Agrobacterium tumefaciens* carrying p1301HBs was used to transform cherry tomatillo cotyledons disks. Ten-days post germination cotyledons were excised from *in vitro*-germinated seedlings, and co-cultivated for 48-72 h with an overnight-grown culture of *Agrobacterium tumefaciens* carrying p1301HBs on a shooting medium containing 2 mg/l 6-benzyladenine (6-BA) and 0.2 mg/l indole-3-acetic acid (IAA). Cotyledons were then rinsed with sterilized water added 500 mg/l cefotaxime to kill the *A. tumefaciens* on the surface of explants, blotted dry on a sterilized paper towel, and placed onto a shooting medium added 500 mg/l cefotaxime for recovery. After seven days' recovery period, the explants were transferred to a shooting medium added 300 mg/l cefotaxime and 25 mg/l hygromycin to select transgenic progeny. About eight weeks later, hygromycin-resistant shoot regenerants were removed to a rooting medium containing 0.2 mg/l IAA and 25 mg/l hygromycin. Rooted plantlets were acclimatized and transferred to a greenhouse for fruiting.

Analysis of transgenic plants

Detection of expression activity of reporter gene-Gus gene Histochemical quantification of Gus activity was performed.

Different tissues were cut from transgenic plantlets and immersed into Gus reaction buffer (889 mg/l X-Gluc, 100 mg/l chloramphenicol, 50 mM NaH₂PO₄, 1 % Triton-X100, 20 % methanol, pH 7.0-8.0). After incubation at 37 °C for 24 h, the tissues were bleached with absolute alcohol, then observed and photographed under the dissecting microscope. Tissues from non-transformed cherry tomatillo were used as negative control.

PCR amplification of plant genomic DNA Transgenic plants were checked for the presence of target gene in leaf tissue using PCR and dot-blot analysis. Genomic DNA samples extracted from leaves of regenerated cherry tomatillo plants by the CTAB method^[26] were used as templates in PCR reactions using the following primers: forward primer 5' - ATGGAGAACAACATC-3'; reverse primer 5' - GGATCCTTTTGC GGAAGCCCA-3', such that amplification would yield a PCR product of 480 bps. The DNA was denatured at 94 °C for 10 min. Forty cycles of PCR were performed at: 94 °C for 50 sec, 45 °C for 45 sec, 72 °C for 50 sec; followed by a 72 °C incubation for 7 min. A positive control (p1301HBs) and a negative control (DNA from non-transformed tomatillo leaves) were included in this experiment. Analysis of PCR products was carried out by loading samples onto a 1.2 % agarose gel containing ethidium bromide (EB), followed by electrophoresis and visualization via ultraviolet transillumination. A molecular weight standard (DL-2000, Takara) was used.

Dot blotting The denatured genomic DNA samples were loaded onto a nitrocellulose membrane (Millipore). A positive control (p1301HBs) and a negative control (DNA from non-transformed tomatillo leaves) were included in this experiment. Pre-hybridization was followed by DNA hybridization using a DIG-labelled probe generated from the same 480 bps fragment that was amplified from p1301HBs. Pre-hybridization and hybridization conditions were both at 42 °C. After washing procedure, the membrane was incubated with alkaline phosphatase-conjugated anti-DIG antibody for 2 h at room temperature. The membrane was finally soaked in the color solution at room temperature for up to 4 h in the dark, and the reaction was stopped by rinsing the membrane in distilled water when satisfactory color was observed.

ELISA Different organs of Cherry tomatillo were harvested, frozen in liquid N₂, and ground to a fine power. The power was suspended in extraction buffer (50 mM Tris-HCl, 0.029 % NaN₃, pH9.5) at room temperature overnight. The slurry was then centrifuged at 12 000 rpm for 10 min at 4 °C, and supernatants were tested for HBsAg by ELISA (Double Antibody sandwich-ELISA Kit, provided by Beijing Wantai Biological Medicine Co.) following the corresponding protocol. Total soluble protein was quantified using Molecular Biology Assistant (MBA2000, Perkin-Elmer Co.).

Immunization of animals

Oral primary immunization Two four-week-old BALB/c mice were fed 20 g transgenic tomatillo tissues (containing the equivalent of approximate 1 μ g HBsAg) every day. Two control mice were fed wild-type tomatillo tissues. After four weeks, two groups of mice were all boosted parenterally with a subimmunogenic dose (containing 0.5 μ g HBsAg) of commercial vaccine (Chuangchun Institute of Biological Products).

Oral booster immunization Four four-week-old BALB/c mice were administered parenterally with commercial vaccine (containing 2 μ g HBsAg) as primary immunization. Once the serum antibody levels of the mice decreased apparently, three mice were fed transgenic cherry tomato tissues (20 g/day, containing the equivalent of approximately 1 μ g HBsAg) and negative control one was fed wild-type tomatillo tissues.

Antibody assays Mice sera were collected once every week and evaluated for anti-HBsAg-specific antibodies using a

commercially available enzyme immunoassay (EIA) diagnostic kit (Double Antigen sandwich-ELISA Kit, Beijing Wantai Biological Medicine Co.).

RESULTS

Transformation and regeneration of cherry tomatillo

The plasmid for expression of HBsAg in plants (p1301HBs, Figure 1) was introduced into *Agrobacterium tumefaciens* and used in transformation experiments. Hygromycin incorporated

into tissue culture media allowed for selection of transformed callus tissue from which shoots and thereafter mature cherry tomatillo plants were regenerated over a period of about 2-3 months. Ten independent hygromycin-resistant lines of transgenic plants were generated finally. Some lines grew poorly in tissue culture. Such effects could result from insertional mutagenesis. Four lines appearing similar in morphology to wild-type plants were transferred to a greenhouse for fruiting (Figure 2). And F1 progeny of one line was obtained.

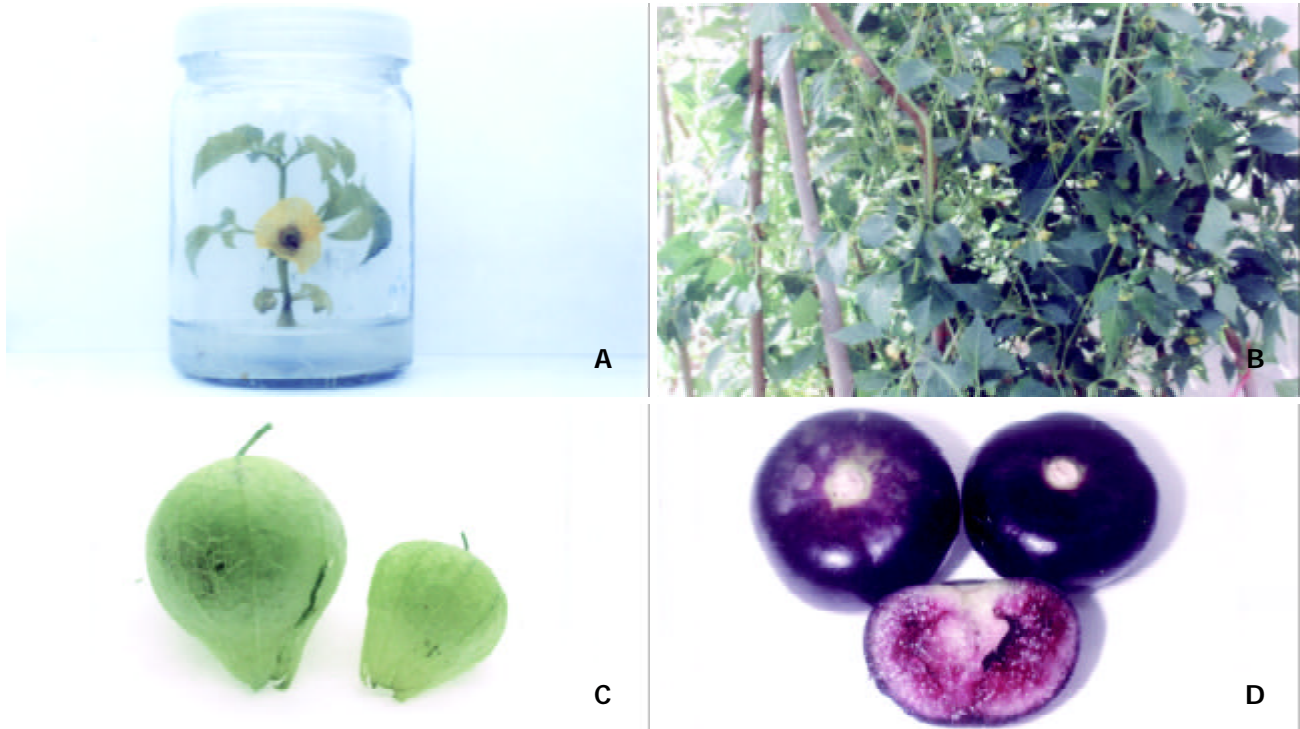


Figure 2 Transgenic cherry tomatillo. A, Transgenic plant in tissue culture; B, Transgenic plant in greenhouse; C, Green transgenic fruits; D, Ripe transgenic fruits.

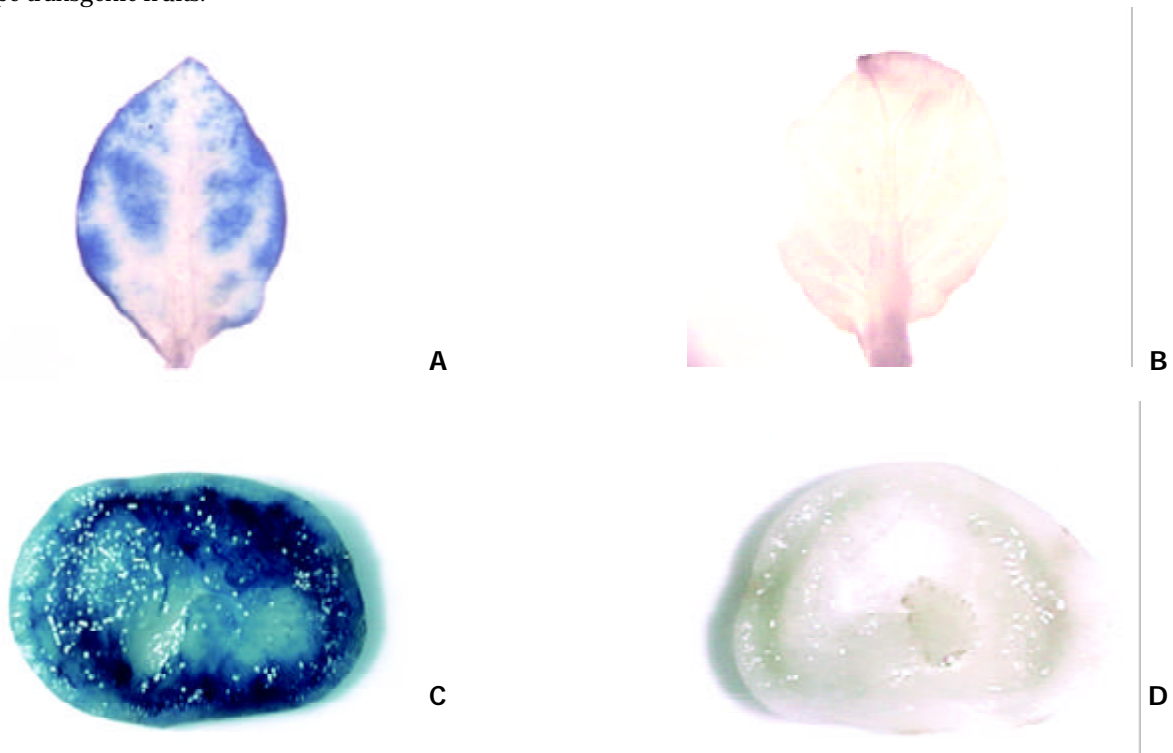


Figure 3 Analysis of Gus activity in transformed cherry tomatillo tissues. A, Leaf of transformed cherry tomatillo; B, Leaf of non-transformed cherry tomatillo; C, Fruit of transformed cherry tomatillo; D, Fruit of non-transformed cherry tomatillo.

Detection of expression activity of reporter gene (*Gus*)

The transformed plants, containing *Gus* gene as the report gene, were tested for the *Gus* activity (Figure 3). The results demonstrated that *Gus* gene was stably integrated into nuclear chromosomal DNA of tomatillo and different organs all presented a remarkably high *Gus* activity.

PCR screening for the presence of HBsAg gene

To verify that these plants contained the target gene, genomic DNA extracted from young leaves was subjected to PCR amplification and the PCR products were electrophoresed through agarose. Samples containing the target gene were identified by the presence of an amplified product of 480 bp, representing a fragment of the HBsAg-S coding sequence in p1301HBs. The results obtained demonstrated the presence of an amplified product of the expected size in all the hygromycin-resistant plants tested, which was absent in non-transformed plants (Figure 4 A).

Analysis of genomic DNA by dot blotting

To further confirm that HBsAg coding gene was stably integrated into nuclear chromosomal DNA of transgenic cherry tomatillo, genomic DNA was analyzed by dot blotting, which showed that all the transgenic samples had the same hybridization signals as the positive control (p1301HBs) (Figure 4 B).

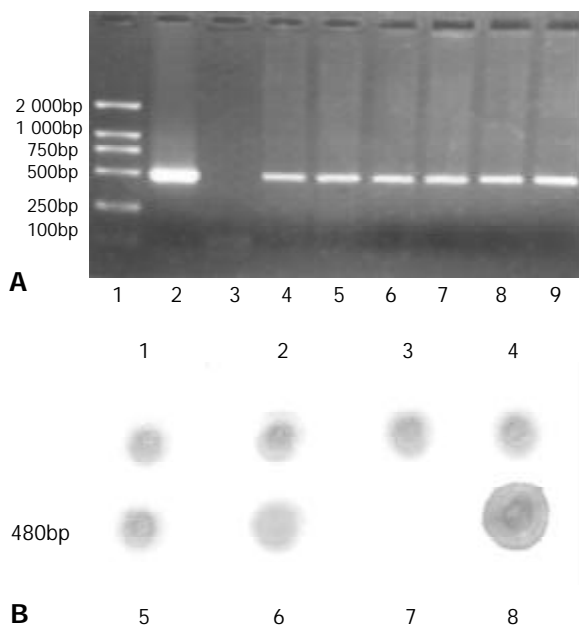


Figure 4 Identification of HBsAg gene in transgenic cherry tomatillo by PCR (A) and dot blot (B). A1, DNA marker; A2, Positive Control; A3, Non-transformed plants; A4-9, Transformed plants. B1-6, Transformed plants; B7, Non-transformed plants; B8, Positive control.

Immunological detection and quantification of rHBsAg in transgenic tomatillo

Plants positive in PCR and dot blotting were further tested by ELISA to detect and quantitatively analyze the target protein. The rHBsAg levels in different organs from a representative one of several tactile lines are presented in Table 1. The results indicated that the expression levels of rHBsAg varied among different organs of the same plant. Apparently, the amount of rHBsAg produced in leaf was much higher than any of the other organs. rHBsAg protein levels in fruit and stem were in a similar range. However, rHBsAg/TSP (total soluble protein) value of fruit was somewhat higher than that of leaf. No

significant variation was observed among the rHBsAg/TSP values of the same kind of organs in different individuals reproduced from the same line, but striking difference in the absolute expression levels of rHBsAg was observed and the level of TSP in leaves of the plantlets in tissue culture was significantly lower than that in leaves of the plants in greenhouse. The difference might be due to growth condition of these plants.

The rHBsAg levels in leaves of tissue-cultured plantlets of four different lines were shown in Table 2. ELISA analysis demonstrated that rHBsAg was expressed in these different lines ranging from 21 to 90 nag/g fresh weight.

Table 1 Expression of HBsAg in different organs and different plants of same line

Plant No.	Organ	Total soluble protein (mg/g fresh weight)	Content of HBsAg (nag/g fresh weight)	HBsAg/TSP (1/1000 000)
1#	Leaf	31.6	300	9
	Stem	5.8	15	3
	Fruit	0.7	7	10
2#	Leaf	30.0	240	8
	Stem	5.0	9	2
	Fruit	0.6	6	10
3#	Leaf	27.3	210	8
	Stem	3.6	7	2
	Fruit	0.6	6	10
4#	Leaf	11.3	90	8
	Stem	2.6	5	2
CK	Leaf	28.4	-	-
	Stem	4.7	-	-
	Fruit	0.6	-	-

Note: 1#, 2#, 3#, 4# were different plants of same transgenic cherry tomatillo line; 1#, 2#, 3# were transferred to soil in the greenhouse; 4# was still in tissue culture; CK was a non-transformed plant growing in the greenhouse.

Table 2 Expressed target protein

Line No.	Total soluble protein (mg/g fresh weight)	Content of HBsAg (ng/g fresh weight)	HBsAg/TSP (1/1000 000)
1#	16.0	45	3
2#	15.5	24	2
3#	12.6	21	2
4#	13.1	90	7
CK	13.7	-	-

Note: 1#, 2#, 3# and 4# were four different lines of transgenic cherry tomatillo with normal phenotype, and these materials were all leaves of transgenic plants in the condition of tissue culture; CK was leaf of a non-transformed tomatillo in tissue culture.

Oral immunogenicity of rHBsAg derived from transgenic tomatillo in mice

The immunogenicity of plant-derived rHBsAg was tested by oral immunizing BALB/c mice with transgenic tissues from plant line with highest production of rHBsAg. Then vaccinated mice were bled weekly, and the sera were assessed for the presence of specific antibodies by ELISA.

Oral primary immunization

Oral immunization of two naive mice by feeding transgenic tissues did not evoke primary antibody within four weeks. Then mice in two groups were both injected with a subimmunogenic dose (0.5 μ g HBsAg) of commercial HBV vaccine via an

intramuscularly route as booster. However, none of the mice developed measurable specific serum antibodies in the following examination. There was no significant difference between serum antibody titers of the mice primed with transgenic tissues and those of the control mice in this experiment (Figure 5).

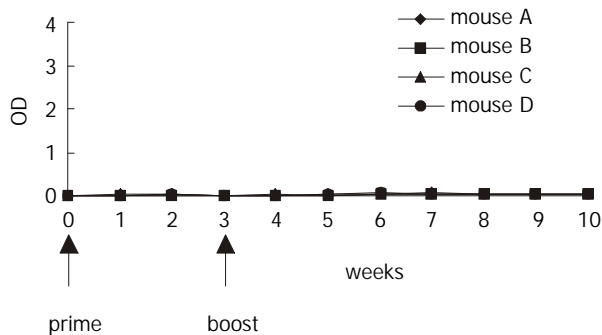


Figure 5 Serum antibody response elicited by oral prime with transgenic cherry tomatillo. A.B: Mice were fed non-transformed tissues until week 4, then boosted with a subimmunogenic dose of commercial vaccine; C.D: Mice were fed transformed tissues until week 4, then boosted parenterally with a subimmunogenic dose of commercial vaccine.

Oral booster immunization

After a single dose ($2 \mu\text{g}$ HBsAg) of commercial vaccine as priming, titers of serum antibody in mice rose sharply in response to antigen initially and then declined. Three mice primed were orally immunized with tissues of the transgenic tomatillo tissues as booster, and elicited an immediate high-level recall antibody response within the following 3-5 weeks. Antibody titers in serum were augmented significantly. In comparison, one negative control mouse fed with wild type tomatillo tissues did not show any booster response. Serum titers of antibody remained same (Figure 6).

We concluded that immune memory cells were established in mice following parenteral immunization of commercial vaccine and a recall response was elicited by oral delivery of HBsAg in transgenic tissues.

Our results showed that tomatillo-derived rHBsAg had same immunogenicity as commercial vaccine in stimulating production of HBsAg-specific antibodies in animal. The present experiment was limited by the total amount of plant tissues that mice ingested in 24 h and the amount of rHBsAg produced in the transgenic tissues. Absence of expected anti-HBsAg response in the oral priming study might be due to inadequate immunization schedule, such as low doses of antigen, or low sensitivity of the detection system and interference of plant material with development of an immune response. In contrast, active immune response to orally administered antigens in parenterally primed animals might be due to altered antigen processing in favoring of active antibody production rather than oral immunotolerance.

DISCUSSION

Oral vaccination using transgenic plants is a viable approach to the development of a novel HBV vaccine. Availability of the vaccine in an edible form as a fruit or vegetable would enhance vaccination coverage by providing an inexpensive, easy to deliver and relatively heat-stable package for distribution. Such a vaccine would have the potential to enable rates of vaccination to reach the targets required for global eradication.

In this study a new foreign breed of cherry tomatillo was used as the vector of producing transgenic plant vaccine. Through the research of transforming HBsAg gene into

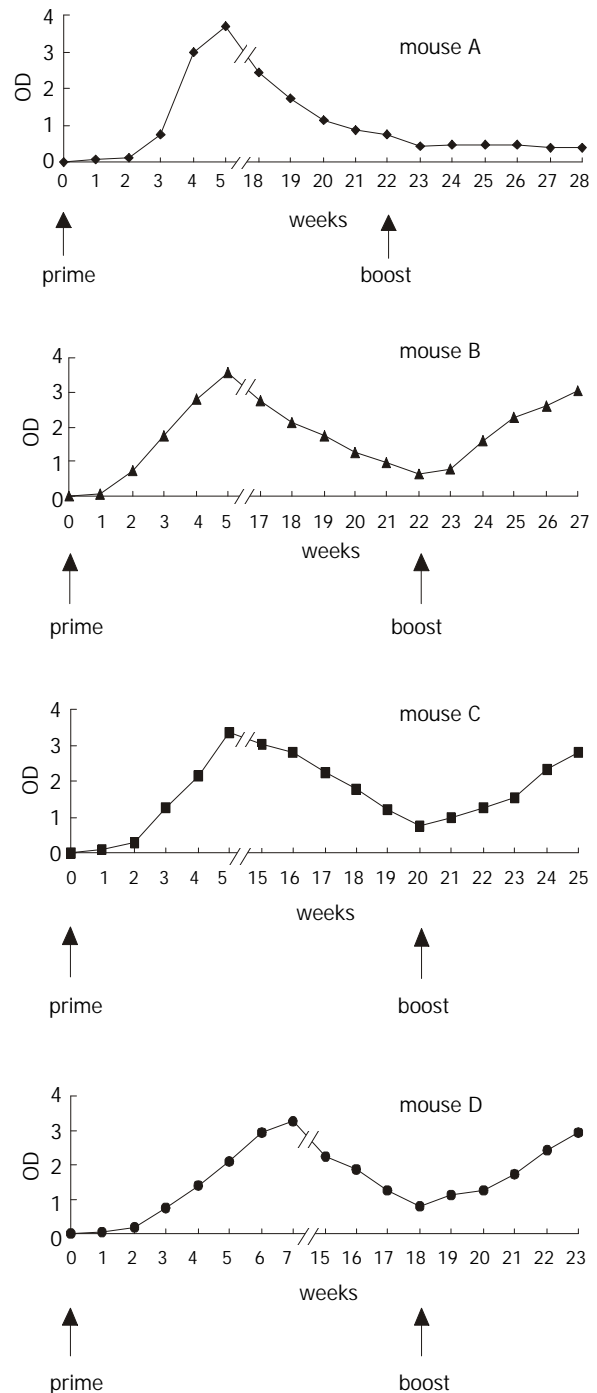


Figure 6 Serum antibody response elicited by oral boost with transgenic cherry tomatillo. A: Mouse was primed parenterally with $2 \mu\text{g}$ commercial rHBsAg, and when its serum antibody level descends to $\text{OD} < 1.0$, mouse was fed with untransformed tissues; B.C.D: Mice were primed parenterally with $2 \mu\text{g}$ yeast-derived rHBsAg, and when their serum antibody levels descend to $\text{OD} < 1.0$, mice were fed with transformed tissues as boost.

tomatillo, a high efficient transformation system of tomatillo was produced, and the recombinant protein from transgenic plants possessed good immunogenicity. The work demonstrated the feasibility of expressing the oral immunogenic rHBsAg in transgenic tomatillo, and provided some theoretic and experimental directions for the production oral vaccines using transgenic tomatillo in large scale.

Transgenic plants expressing recombinant antigens have been developed successfully since it was first described by Mason *et al.* A corollary of this research is the goal of developing subunit vaccines that are produced in edible plant

products, such that the plant-derived vaccine can be ingested directly without prior purification or processing. It appears to be a very promising alternative to other methods for expressing recombinant protein. Nevertheless, a number of questions and challenges still remain to be solved. And its main disadvantage is low yields of antigen expressed. To our knowledge, in most cases at present expression levels of vaccine proteins in transgenic plants are lower than 0.1 %. We encountered the same problem in the study. Although plant-derived rHBsAg had good immunogenicity, the maximal level of rHBsAg in transgenic tomatillos was inadequate for use practically.

Bioencapsulation of the recombinant antigen within plant cells may protect it from degradation by gastrointestinal proteinases and allow important epitopes to be recognized. It may result in greater stability of the antigen in the stomach, effectively increasing the amount of antigen available for uptake in the gut. However, foreign antigens expressed in edible plant tissues for use as oral vaccines also will consist of impure mixtures with numerous other plant proteins. The stability of such a protein in the gut is unknown yet, but high protein levels and localization in the cell wall should ensure that at least some of the antigen will be delivered to the intestine. To address these possibilities, we need edible plant tissues that produce higher levels of rHBsAg, and thus our further studies will focus on increasing the accumulation of rHBsAg in transgenic tomatillos.

Over the past decade increasing endeavors have been directed towards how to augment expression levels of foreign genes in transgenic plants. Some modifications of expression vectors have been successfully assayed to have the function to lead to increased levels of expression of the recombinant genes, including the use of stronger promoters^[15], plant-optimized synthetic genes^[8], plant-derived leader sequences, signal peptides which can target the protein for retention in intercellular compartments^[7,10,27], the fruit-specific expressed promoter^[28,29], and the chloroplast expression system^[30] etc.

Although this study was not yet complete, we could demonstrate that plant-derived rHBsAg was active as an oral immunogen and cherry tomatillo might be a potential source of vaccines for direct application. Transgenic tomatillos could induce specific immune response depending on the route of administration and immune status of the animal. In our hands, oral immunization solely by feeding transgenic tissues was not effective. Activation of the immune system by a primary immunization via a parenteral route followed by booster via the oral route resulted in significant antibody responses. The results showed that the administration of edible vaccines in primed instead of naive subjects revealed a more sensitive test system and higher probability of success. The mechanisms underlying the increased responsiveness of parenterally primed animals to orally delivered antigens are not clear yet. Further research is required to optimize this approach and to identify the underlying mechanisms. Combinations of parenteral and oral delivery may eventually prove to be most efficient, and in this regard, the present study provides a platform for ongoing and future investigations.

In conclusion, more and more attentions have been paid to the study on oral vaccine using transgenic plants in the recent years, and many great achievements have been attained in this field. However, there is a long way to go before practical use of oral vaccine. Many problems still need to be solved, such as how to improve the accumulation of target protein in edible tissues of transgenic plant, how to enlarge the production scale of plant oral vaccine, how to properly determine the suitable delivery method and dosage of plant oral vaccine.

REFERENCES

1 **Wang SP**, Xu DZ, Yan YP, Shi MY, Li RL, Zhang JX, Bai GZ, Ma

- JX. Hepatitis B virus infection status in the PBMC of newborns of HBsAg positive mothers. *World J Gastroenterol* 2000; **6**(Suppl 3): 58
- 2 **Daniell H**, Streatfield SJ, Wycoff K. Medical molecular farming: production of antibodies, biopharmaceuticals and edible vaccine in plants. *Trends Plant Sci* 2001; **6**: 219-226
- 3 **Walmsley AM**, Arntzen CJ. Plants for delivery of edible vaccines. *Curr Opin Biotechnol* 2000; **11**: 126-129
- 4 **Koprowski H**, Yusibov V. The green revolution: plants as heterologous expression vectors. *Vaccine* 2001; **19**: 2735-2741
- 5 **Liu DH**. Plant as a system for production of pharmaceutical proteins. *Shengwu Jishu Tongbao* 1999; **4**: 1-5
- 6 **Tacket CO**, Reid RH, Boedeker EC, Losonsky G, Nataro JP, Bhagat H, Edelman R. Enteral immunisation and challenge of volunteers given enterotoxigenic *E. coli* CFA/II encapsulated in biodegradable microspheres. *Vaccine* 1994; **12**: 1270-1274
- 7 **Haq TA**, Mason HS, Clements JD, Arntzen CJ. Oral immunization with a recombinant bacterial antigen produced in transgenic plants. *Science* 1995; **268**: 714-716
- 8 **Mason HS**, Haq TA, Clements JD, Arntzen CJ. Edible vaccine protects mice against *Escherichia coli* heat-labile enterotoxin (LT): potatoes expressing a synthetic LT-B gene. *Vaccine* 1998; **16**: 1336-1343
- 9 **Tacket CO**, Mason HS, Losonsky G, Clements JD, Levine MM, Arntzen CJ. Immunogenicity in humans of a recombinant bacterial antigen delivered in a transgenic potato. *Nat Med* 1998; **4**: 607-609
- 10 **Lauterslager TG**, Florack DE, Wal TJ, Molthoff JW, Langeveld JP, Bosch D, Boersma WJ, Hilgers LA. Oral immunization of naive and primed animals with transgenic potato tubers expressing LT-B. *Vaccine* 2001; **19**: 2749-2755
- 11 **Streatfield SJ**, Jilka JM, Hood EE, Turner DD, Bailey MR, Mayor JM, Woodard SL, Beifuss KK, Horn ME, Delaney DE, Tizard IR, Howard JA. Plant-based vaccines: unique advantages. *Vaccine* 2001; **19**: 2742-2748
- 12 **Chikwamba R**, Cunnick J, Hathaway D, McMurray J, Mason H, Wang K. A functional antigen in a practical crop: LT-B producing maize protects mice against *Escherichia coli* heat labile enterotoxin (LT) and cholera toxin (CT). *Transgenic Res* 2002; **11**: 479-493
- 13 **Arakawa T**, Chong DK, Langridge WH. Efficacy of a food plant-based oral cholera toxin B subunit vaccine. *Nat Biotechnol* 1998; **16**: 292-297
- 14 **Daniell H**, Lee SB, Panchal T, Wiebe PO. Expression of the native cholera toxin B subunit gene and assembly as functional oligomers in transgenic tobacco chloroplasts. *J Mol Biol* 2001; **311**: 1001-1009
- 15 **Mason HS**, Lam DMK, Arntzen CJ. Expression of hepatitis B surface antigen in transgenic plants. *Proc Natl Acad Sci USA* 1992; **89**: 11745-11749
- 16 **Richter LJ**, Thanavala Y, Arntzen CJ, Mason HS. Production of hepatitis B surface antigen in transgenic plants for oral immunization. *Nat Biotechnol* 2000; **18**: 1167-1171
- 17 **Kong QX**, Richter L, Yang YF, Arntzen CJ, Mason HS, Thanavala Y. Oral immunization with Hepatitis B surface antigen expressed in transgenic plants. *PNAS* 2001; **98**: 11539-11544
- 18 **Smith ML**, Mason HS, Shuler ML. Hepatitis B surface antigen (HBsAg) expression in plant cell culture: Kinetics of antigen accumulation in batch culture and its intracellular form. *Biotechnol Bioeng* 2002; **80**: 812-822
- 19 **Zhao CH**, Wang R, Zhao CS, Wang GL, Tian P. Expression of human hepatitis B virus surface antigen gene with and without preS in transgenic tomato. *Nongye Shengwu Jishu Xuebao* 2000; **8**: 85-88
- 20 **Chen HY**, Zhang J, Gao Y, Du HL, Ma Y, Zheng WZ, Xia NS. Transforming HBsAg into peanut and detection of its immunogenicity. *Shengwu Jishu Tongxun* 2002; **13**: 245-250
- 21 **Ma Y**, Lin SQ, Gao Y, Zhang J, Lu LX, Xia NS. Transformation of HBsAg (hepatitis B virus surface antigen) into tomato plants. *Fujian Nonglin Daxue Xuebao (Ziran Kexueban)* 2002; **31**: 223-227
- 22 **Mason HS**, Ball JM, Shi JJ, Jiang X, Estes MK, Arntzen CJ. Expression of Norwalk virus capsid protein in transgenic tobacco and potato and its oral immunogenicity in mice. *Proc Natl Acad Sci* 1996; **93**: 5335-5340

- 23 **Tacket CO**, Mason HS, Losonsky G, Estes MK, Levine MM, Arntzen CJ. Human immune responses to a novel Norwalk virus vaccine delivered in transgenic potatoes. *J Infect Dis* 2000; **182**: 302-305
- 24 **McGarvey PB**, Hammond J, Dienelt MM, Hooper DC, Fu ZF, Dietzschold B, Koprowski H, Michaels FH. Expression of the rabies virus glycoprotein in transgenic tomatoes. *Biotechnology* 1995; **13**: 1484-1487
- 25 **Kapusta J**, Modelska A, Figlerowicz M, Pniewski T, Letellier M, Lisowa O, Yusibov V, Koprowski H, Plucienniczak A, Legocki AB. A plant-derived edible vaccine against hepatitis B virus. *FASEB J* 1999; **13**: 1796-1799
- 26 **Wang GL**, Fang HJ. Principle and technology of plant genetic engineering, 1st ed, Beijing: *Science Press* 1998
- 27 **Tackaberry ES**, Dudani AK, Prior F, Tocchi M, Sardana R, Altosaar I, Ganz PR. Development of biopharmaceuticals in plant expression systems: cloning, expression and immunological reactivity of human cytomegalovirus glycoprotein B (UL55) in seeds of transgenic tobacco. *Vaccine* 1999; **17**: 3020-3029
- 28 **Clendennen SK**, López-Gómez R, Gómez-Lim M, May GD, Arntzen CJ. The abundant 31-kilodalton banana pulp protein is homologous to class-III acidic chitinases. *Phytochemistry* 1998; **47**: 613-619
- 29 **Sandhu JS**, Krasnyanski SF, Domier LL, Korban SS, Osadjan MD, Buetow DE. Oral immunization of mice with transgenic tomato fruit expressing respiratory syncytial virus-F protein induces a systemic immune response. *Transgenic Res* 2000; **9**: 127-135
- 30 **Cosa BD**, Moar W, Lee SB, Miller M, Daniell H. Over-expression of the Bt Cry2Aa2 operon in chloroplasts leads to formation of insecticidal crystals. *Nat Biotechnol* 2001; **19**: 71-74

Edited by Ren SY

Severe acute respiratory syndrome and its lesions in digestive system

Jian-Zhong Zhang

Jian-Zhong Zhang, Department of Pathology, 306 Hospital of PLA, Beijing 100101, China

Correspondence to: Professor Jian-Zhong Zhang, Director of Department of Pathology, Beijing 306 Hospital, 9 North Anxiang Road, P.O.Box 9720, Chaoyang District, Beijing 100101, China. zhangjz55@sina.com

Telephone: +86-10-66356237 **Fax:** +86-10-64871261

Received: 2003-05-20 **Accepted:** 2003-05-27

Abstract

Severe acute respiratory syndrome (SARS) is an infectious atypical pneumonia that has recently been recognized in the patients in 32 countries and regions. This brief review summarizes some of the initial etiologic findings, pathological description, and its lesions of digestive system caused by SARS virus. It is an attempt to draw gastroenterologists and hepatologists' attention to this fatal illness, especially when it manifests itself initially as digestive symptoms.

Zhang JZ. Severe acute respiratory syndrome and its lesions in digestive system. *World J Gastroenterol* 2003; 9(6): 1135-1138 <http://www.wjgnet.com/1007-9327/9/1135.asp>

INTRODUCTION

In November 2002, a so-called atypical pneumonia with unknown etiology appeared in Guangdong Province, China, followed by reports from Hong Kong, Vietnam, Singapore, Canada and Beijing of severe febrile respiratory illness that spread to household members and health care workers^[1-6,23-26]. This disease was designated "severe acute respiratory syndrome (SARS)" later by the World Health Organization (WHO) and global efforts to understand the cause of this illness and prevent its spread were instituted in March 2003. Many cases could be linked through chains of transmission to a health care worker from Guangdong Province, China, who visited Hong Kong, where he was hospitalized with SARS and died. Till May 19, 2003, a cumulative total of 7 864 SARS cases were reported to WHO from 29 countries; 643 deaths (case-fatality proportion: 8.2 %) have been reported, in which most cases occurred in China (7291 cases)^[7]. The incubation period for the disease is usually 2 to 7 days. Infection is characterized by fever, non-productive cough, and shortness of breath, and the presence of minimal auscultatory findings with consolidation on chest radiographs. Lymphopenia, leucopenia, thrombocytopenia, and elevated liver enzymes and creatinine kinase may also present in most cases.

In response to this outbreak, WHO coordinated an international collaboration that included clinical, epidemiologic, and laboratory investigation, and initiated efforts to control the spread of SARS. Rapid research progress has been made in last three months. This brief review is to focus on the etiologic and pathologic findings with an emphasis on the known lesions in the liver and intestine.

ETIOLOGICAL FINDINGS

The isolation of a novel coronavirus was obtained from the respiratory secretions of patients with SARS and subsequently demonstrating this virus or a serologic response to this virus, points to a possible etiologic association with SARS^[5,6,17,20,22,27]. The discovery of this new virus occurred through a broad-based and multidisciplinary effort by clinical, epidemiologic, and laboratory investigators.

Researchers around the world have sequenced the genetic codes of SARS virus, and are searching for clues to the virus' s origins, behavior, and future. Science is set to publish online a paper analyzing the genome from the BCCA Genome Sciences Center in Vancouver, as well as one from the Centers for Disease Control and Prevention (CDC) in Atlanta (www.sciencemag.org/feature/data/sars). Now that sequencing technology has become cheap and widely available, almost every country or area affected by SARS is sequencing its own version, including Hong Kong, Singapore and China^[8-10]. The viruses themselves are something of an oddity. With a genome of the complete -29 700 nucleotides, coronaviruses are relative giants, and they have a complex two-step replication mechanism. Many RNA virus genomes contain a single, large gene that is translated by the host' s cellular machinery to produce all viral proteins. Coronaviruses, instead, can have up to 10 separate genes. Most ribosomes translate the biggest one of these, called replicase, which by itself is twice the size of many other RNA viral genomes. The replicase gene produces a series of enzymes that use the rest of the genome as a template to produce a set of smaller, overlapping messenger RNA molecules, which are then translated into the so-called structural proteins - the building blocks of new viral particles. Most coronaviruses cause either a respiratory or an enteric disease, and some do both. But the differences among these types can be small. In 1999, for instance, a team led by Luí s Enjuanes of the Autonomous University of Madrid, Spain, showed that just two point mutations can change a mostly enteric virus that can kill piglets into a nondeadly one that excels at the respiratory route but replicates poorly in the gut^[11].

Researchers have grouped coronaviruses into three categories based on cross-reactivity of antibodies backed up by genetic data; the two previously known human viruses fell into different groups. Investigators have hoped that the genome sequence of the new virus would help pinpoint its origins. But a first glance at the data has yielded few clues. The new coronavirus does not fit into any of the clusters but is a new one by itself. Phylogenetic analysis of the predicted viral proteins indicates that the virus does not closely resemble any of the three previously known groups of coronaviruses. The genome sequence will aid in the diagnosis of SARS virus infection in humans and potential animal hosts (using PCR and immunological tests), in the development of antivirals (including neutralizing antibodies), and in the identification of putative epitopes for vaccine development.

PATHOLOGICAL CHANGES IN THE LUNG

Pathological studies of patients who died of SARS from Guangdong, Hongkong, Beijing and Singapore showed diffuse

alveolar damage (DAD) in the lung as the most notable feature^[5,6,12,15,21]. In those individuals with severe disease resulting in death, scattered type II pneumocytes showed marked cytologic changes including multinucleation, cytomegaly, nucleomegaly, clearing of nuclear chromatin, and prominent nucleoli. Although these changes were severe, they were within the spectrum of epithelial changes seen in other cases of DAD. Definite viral inclusions were not always found in the cytoplasm of epithelial cells. Nicholis *et al*^[12] found that DAD was common but not universal. Morphologic changes identified were bronchial epithelial denudation, loss of cilia, and squamous metaplasia. Other findings included focal intraalveolar hemorrhage, hemophagocytosis, necrotic inflammatory debris in small airways, organizing pneumonia or secondary bacterial pneumonia.

DAD is a pattern of acute lung injury characterized, in the acute phase, by hyaline membranes, interstitial and intraalveolar edema, patchy type II pneumocyte hyperplasia, microthrombi, and scant interstitial infiltrates of mononuclear cells. The acute phase forms a continuum with the proliferative or organizing phase in which proliferation of interstitial fibroblasts and prominent type II pneumocyte hyperplasia are the histologic hallmarks. In addition to DAD, the autopsy cases showed acute bronchopneumonia and variable intravascular thrombosis, all of which are common as terminal events. Biopsy material from milder cases or earlier in the course of illness may better define the initial lesion in SARS.

Multinucleated syncytial cells were identified in the alveolar spaces in a few patients. These cells contained abundant vacuolated cytoplasm with cleaved and convoluted nuclei, which show either CD68 or cytokeratin positive. No obvious intranuclear or intracytoplasmic viral inclusions were identified, and electron-microscopical examination of a limited number of these syncytial cells revealed no coronavirus particles. No definitive immunostaining was identified in tissues from a patient with SARS, with the use of a battery of immunohistochemical stains reactive with coronavirus from antigenic groups I, II, and III. In addition, no staining of patient tissues was identified with the use of immunohistochemical stains for influenza viruses A and B, adenoviruses, Hendra and Nipah viruses, metapneumoviruses, respiratory syncytial virus, measles virus, *Mycoplasma pneumoniae*, and *Chlamydia pneumoniae*^[14].

Evaluation of Vero E6 cells infected with coronavirus isolated from a patient with SARS revealed viral cytopathic effect that included occasional multinucleated syncytial cells but no obvious viral inclusions. Immunohistochemical assays with various antibodies reactive with coronavirus from antigenic group I, including human coronavirus 229E, feline infectious peritonitis virus 1, and porcine transmissible gastroenteritis virus, and with an immune serum specimen from a patient with SARS demonstrated strong cytoplasmic and membranous staining of infected cells. No staining was identified with any of several monoclonal or polyclonal antibodies reactive with coronavirus in antigenic group II (human coronavirus OC43, bovine coronavirus, and mouse coronavirus) or group III (turkey coronavirus and infectious bronchitis virus). Electron-microscopical examination of a bronchoalveolar-lavage specimen from one patient revealed many coronavirus-infected cells^[14].

Ksiazek and colleagues^[5] noticed that the primary histopathological lesions are consistent with a nonspecific acute response to lung injury that can be caused by infections, trauma, drugs, or toxic chemicals. The multinucleated syncytial cells without viral inclusions seen in the lungs of two patients, however, are suggestive of a number of viral infections including measles and parainfluenzavirus, respiratory syncytial virus, and Nipah virus infection. Multinucleated syncytial cells

associated with some human coronavirus infections have occasionally been observed in cell culture, but most often in cell cultures inoculated with animal coronaviruses. To detect this novel coronavirus antigen, the investigators used an extensive panel of antibodies against coronaviruses that are representative of the three antigenic groups, including several group 1 antiserum specimens that reacted against Urbani SARS-associated coronavirus infected tissue-culture material. A possible explanation for the failure of this antiserum to react with antigens in these patients on immunohistochemical analysis is that the host immune response has cleared the virus from these tissues. The tissues were available late in the course of the illness, 14 to 20 days after its onset. For many viral respiratory infections, viral antigens and nucleic acids are cleared within two weeks after the onset of disease.

Electron microscopic examination showed that virus-like particles with 100-150 nm in diameter were found in cytoplasm and dilated reticular endoplasm of the infected alveolar epithelial cells and endothelial cells^[5,15-17]. Other agents, such as paramyxovirus, metapneumovirus and chlamydia, were also identified in the pulmonary tissues^[16,22]. It could be that the coronavirus may by itself produce the disease but it may also open the door for other viruses, or nonviruses, to aggravate the disease.

The pathogenesis of this disorder remains to be determined. However, the mechanism of acute lung injury could involve direct damage by the virus to the alveolar wall by targeting either endothelial cells or epithelial cells. Alternatively, the virus could infect inflammatory cells with the injury mediated through cytokines, interleukins, or tumor necrosis factor-alpha. It is also possible that the tissue damage in SARS is not directly related to viral infection in tissues but is a secondary effect of cytokines or other factors induced by viral infection proximal to but not within the lung tissue. In influenza infections, viral antigens are seen predominantly in respiratory epithelium of large airways and are only rarely identified in pulmonary parenchyma, despite concomitant and occasionally severe interstitial pneumonitis.

LESIONS IN DIGESTIVE ORGANS

As previously described, most coronaviruses cause either a respiratory or an enteric disease, which is also transmitted by the faecal-oral route. During this outbreak of SARS, symptoms of gastrointestinal tract in the patients were noticed. Many investigators^[13,19,24] found that gastrointestinal symptoms are not uncommon at presentation, including diarrhea (19-50 percent), nausea and vomiting (19.6 percent), and abdominal pain (13 percent) manifested in SARS patients.

As many as 66 % of the patients in the Amoy Garden SARS outbreak in Hong Kong also had diarrhea, contributing to a significant virus load being discharged in the sewerage, which caused 361 cases of SARS^[3]. During hospitalization, some patients were present with mildly elevated aminotransferase levels (indicating liver damage), or developed dysfunction of the liver at the later stage of the disease. Some patients presented with severe acute abdominal pain requiring exploratory laparotomy. All these patients developed typical SARS. These clinical findings suggest that SARS virus does involve the digestive system, especially the epithelial cells of intestinal mucosa.

Pathologic evaluation of the fatal cases showed that, except the lung changes, hepatocytes underwent fatty degeneration, cloudy swelling, apoptosis and dot necrosis, with Kupffer cell proliferation and portal infiltrates of lymphocytes^[15,16]. There were regional hemorrhages, vascular congestion and lymphocytic infiltration in gastrointestinal walls of the patient. Suckling mice inoculated with SARS-infected samples also

demonstrated hepatocytic lesions, including swelling, vacuolar and hydropic degenerations, focal cellular condensation and necrosis. But no coronavirus-like particles were found in hepatocytes.

Epidemiologic investigation also showed that the virus could survive in stools for at least two days and in diarrhoeal stools, which has a higher pH, for up to four days. It can also survive on plastic surfaces for up to 48 hours, but it is not yet known how big a dose of the virus is required to cause infection^[18].

According to the experience of Prince of Wales Hospital in Hong Kong^[20], where SARS outbreak happened, the difficulty of making a firm diagnosis until chest radiographic changes appear has important implications for health-care personnel and for surveillance. Three major reasons for spread of infection to health-care workers are: failure to apply isolation precautions to cases not yet identified as SARS, breaches of procedure, and inadequate precautions. Every patient must now be assumed to have SARS, which has major long-term implications for the health-care system. Another reason for spread among health-care workers is infected workers continuing to work despite symptoms, such as mild fever. Such individuals must now cease working. However, staying at home can also have disastrous consequences for exposed family members. Potential cases therefore require early isolation from both workplace and household. Extreme measures are required to protect health-care workers, who account for about 20 % of cases. Therefore, gastroenterologists and hepatologists should pay more attention when contacting the patients.

SARS has been appropriately elicited because current knowledge regarding the transmission of this disease is rapidly evolving and clinicians must provide patient care while dealing with a degree of uncertainty. The Centers for Disease Control and Prevention have published and regularly update logical recommendations for preventing the spread of the causative agent. The causative organism appears to spread predominantly by contact and droplets and may spread by airborne routes as well. The use of N-95 masks, gowns, double gloves, hand hygiene, and eye protection seem well advised and appear to have substantially curtailed spread within hospitals.

Global efforts have described this new syndrome with dramatic speed, and identified and sequenced the apparent etiologic agents. With expedited efforts to develop a specific diagnostic test, effective infection-control techniques, and to develop effective therapies and vaccines for SARS-associated coronavirus, and to create a true global health network, there is much reason for optimism. To be prepared for that challenge, health care professionals must not forsake their patients, the research community must help provide answers to the unanswered questions, and health care leadership must take the knowledge from that research to rapidly implement whatever strategies necessary to better combat this newly emerging infectious disease^[28].

REFERENCES

- 1 **Centers for Disease Control and Prevention.** CDC update: outbreak of severe acute respiratory syndrome-worldwide, 2003. *MMWR* 2003; **52**: 241-248
- 2 **World health organization.** Situation Update-SARS. Available at <http://www.who.int/mediacentre/releases/2003/pr31/en/>
- 3 **Hong Kong Department of Health Report.** Main findings of an investigation into the outbreak of severe acute respiratory syndrome at Amoy Gardens. <http://www.info.gov.hk/dh/ap.htm> (accessed April 19, 2003)
- 4 **Booth CM,** Matukas LM, Tomlinson GA, Rachlis AR, Rose DB, Dwosh HA, Walmsley SL, Mazzulli T, Avendano M, Derkach P, Ephthimios LE, Kitai I, Mederski BD, Shadowitz SB, Gold WL, Hawrylurk LA, Rea E, Chenkin JS, Cescon DW, Poutanen SM, Detsky AS. Clinical features and short-term outcomes of 144 patients with SARS in the Greater Toronto Area. *JAMA* 2003; **289**: 1-9
- 5 **Ksiazek TG,** Erdman D, Goldsmith C, Zaki SR, Peret T, Emery S, Tong S, Urbani C, Comer JA, Lim W, Rolin PE, Dowell S, Ling AE, Humphrey C, Shieh WJ, Guarner J, Paddock CD, Rota P, Fields B, DeRisi J, Yang JY, Cox N, Hughes J, LeDuc JW, Bellini W, Anderson LJ, the SARS Working Group. A Novel Coronavirus Associated with Severe Acute Respiratory Syndrome. *New Eng J Med*, 2003. <http://www.nejm.org>, May 10, 2003
- 6 **Rota PA,** Oberste MS, Monroe SS, Nix A, Campagnoli R, Icenogle JP, Penaranda S, Bankamp B, Maher K, Chen MH, Tong S, Tamin A, Lowe L, Frace M, DeRisi JL, Chen Q, Wang D, Erdam D, Peret TC, Burns C, Ksiazek TG, Rollin PE, Sanchez A, Liffick S, Holloway B, Limor J, McCausland K, Olsen-Rasmussen M, Fouchier S, Gunther S, Osterhaus ADME, Drosten C, Paliash MA, Anderson LJ, Bellini WJ. Characterization of a novel coronavirus associated with severe acute respiratory syndrome. *Science*. Available at [Sciencexpress/www.sciencexpress.org/1](http://www.sciencexpress.org/1) May 2003/10.1126/science.1085952
- 7 **World Health Organization.** Cumulative probable cases of severe acute respiratory syndrome (SARS). <http://www.who.int/csr/sars/cases> (accessed May 19, 2003)
- 8 **Enserink M,** Vogel G. Hungry for details, scientists zoom in on SARS genomes. *Science* 2003; **300**: 715-716
- 9 **Marra MA,** Jones SJM, Astel CR, Holt RA, Brooks-Wilson A, Butterfield YS, Khattra J, Asano JK, Barber SA, Chan SY, Cloutier A, Coughlin SM, Freeman D, Girn N, Griffith OL, Leach SR, Mayo M, McDonald H, Montgomery SB, Pandoh PK, Petrescu AS, Robertson AG, Schein JE, Siddiqui A, Smailus DE, Stott JM, Yang GS, Plummer F, Andonov A, Artsob H, Bastien N, Bernard K, Booth TF, Bowness D, Drebot M, Fernando L, Flick R, Garbutt M, Gray M, Grolla A, Jones S, Feldmann H, Meyers A, Kabani A, Li Y, Normand S, Stroher U, Tipples GA, Tyler S, Vogri R, Ward D, Watson B, Brunham RC, Krajden M, Petric M, Skowronski DM, Upton C, Roper RL. The genome sequence of the SARS-associated coronavirus. *Scienceexpress/www.sciencexpress.org/1* May 2003/10.1126/science.1085953
- 10 **Center for Disease Control and Prevention.** SARS coronavirus sequencing. Available at: <http://www.cdc.gov/ncidod/sars/sequence.htm>
- 11 **Enserink M.** Calling all coronavirologists. *Science* 2003; **300**: 413-414
- 12 **Nicholls JM,** Poon LLM, Lee KC, Ng WF, Lai ST, Leung CY, Chu CM, Hui PK, Mak KL. Lung pathology of fatal severe acute respiratory syndrome. *Lancet*, Published online May 16, 2003/<http://image.thelancet.com/extras/03art4347web.pdf>
- 13 **Lee N,** Hui D, Wu A, Chan P, Cameron P, Joynt GM, Ahuja A, Yung MY, Leung CB, To KF, Lui SF, Szeto CC, Chung S, Sung JY. A Major Outbreak of Severe Acute Respiratory Syndrome in Hong Kong. *N Engl J Med* 2003; **348**: 1986-1994
- 14 **Zhao JM,** Zhou GD, Sun YL, Wang SS, Yang JF, Mao LY, Pan D, Mao PY, Cheng Y, Wang YD, Xin SJ, Zhou XZ, Lu JY, Li L, Chen JM. Pathological and etiological findings in a dead case of severe acute respiratory syndrome in China. *Jifangjun Yixue Zazhi* 2003; **28**: 379-382
- 15 **Wang CE,** Qin ED, Gan YH, Li YC, Wu XH, Cao JT, Yu M, Si BY, Yan G, Li JF, Zhu QY. Pathological observation on sucking mice and Vero E6 cells inoculated with SARS samples. *Jifangjun Yixue Zazhi* 2003; **28**: 383-384
- 16 **Hong T,** Wang JW, Sun YL, Duan SM, Chen LB, Qu JG, Ni AP, Liang GD, Ren LL, Yang RQ, Guo L, Zhou WM, Chen J, Li DX, Wen XB, Xu H, Guo YJ, Dai SL, Bi SL, Dong XP, Ruan L. Chlamydia-like and coronavirus-like agents found in dead cases of atypical pneumonia by electron microscopy. *Zhonghua Yixue Zazhi* 2003; **83**: 632-636
- 17 **Ksiazek TG,** Drosten C, Gunther S, Preiser W, Finkelstein S, Rose D, Green K, Tellier R, Draker R, Adachi D, Ayers M, Chan AK, Skowronski DM, Salit I, Simor AE, Slutsky AS, Doyle PW, Krajden M, Petric M, Brunham R, Geer AJ. Identification of a novel coronavirus in patients with severe acute respiratory syndrome. *N Eng J Med*, 2003 <http://www.nejm.org>, May 10, 2003
- 18 **Donnelly CA,** Ghani AC, Leung GM, Hedley AJ, Fraser C, Riley S, Abu-Raddad LJ, Ho ML, Thach TQ, Chau P, Chan KP, Lam TH, Tse LY, Tsang T, Liu SH, Kong JHB, Lau EMC, Ferguson

- NM, Roy M, Anderson RM. Epidemiological determinants of spread of causal agent of severe acute respiratory syndrome in Hong Kong. *Lancet*. Published online May 7, 2003/<http://image.thelancet.com/extras/03art4453web.pdf>, t
- 19 **Tomlinson B**, Cockram C. SARS: experience at Prince of Wales Hospital, Hong Kong. *Lancet* 2003; **361**: 1486-1487
- 20 **Poon LLM**, Wong OK, Luk W, Yuen KY, Peris JSM, Guan Y. Rapid diagnosis of a coronavirus associated severe acute respiratory syndrome (SARS). *Clin Chem* 2003; **49**: 1-3
- 21 **Chan WY**, Hui PK. Pathology of SARS 2003 Hong Kong. Available at <http://www.eelab.com>
- 22 **Peiris JSM**, Lai ST, Poon LLM, Guan Y, Yam LYC, Lim W, Nicholls J, Yee WKS, Yan WW, Cheung MT, Cheng VCC, Chan KH, Tsang DNC, Yung RWH, Ng TK, Yuen KY, and members of the SARS study group*. Coronavirus as a possible cause of severe acute respiratory syndrome. *Lancet* 2003; **361**: 1319-1325
- 23 **Poutanen SM**, Low DE, Henry B, Finkelstein S, Rose D, Green K, Tellier R, Draker R, Adachi D, Ayers M, Chan AK, Skowronski DM, Salit I, Simor AE, Slutsky AS, Doyle PW, Krajden M, Petric M, Brunham RC, McGeer AJ. National Microbiology Laboratory, Canada; Canadian Severe Acute Respiratory Syndrome Study Team. Identification of severe acute respiratory syndrome in Canada. *N Engl J Med* 2003; **348**: 1995-2005
- 24 **Tsang KW**, Ho PL, Ooi GC, Yee WK, Wang T, Chan-Yeung M, Lam WK, Seto WH, Yam LY, Cheung TM, Wong PC, Lam B, Ip MS, Chan J, Yuen KY, Lai KN. A cluster of cases of severe acute respiratory syndrome in Hong Kong. *N Engl J Med* 2003; **348**: 1977-1985
- 25 **Lee N**, Hui D, Wu A, Chan P, Cameron P, Joynt GM, Ahuja A, Yung MY, Leung CB, To KF, Lui SF, Szeto CC, Chung S, Sung JJ. A major outbreak of severe acute respiratory syndrome in Hong Kong. *N Engl J Med* 2003; **348**: 1986-1994
- 26 **Drosten C**, Gunther S, Preiser W, Van Der Werf S, Brodt HR, Becker S, Rabenau H, Panning M, Kolesnikova L, Fouchier RA, Berger A, Burguiere AM, Cinatl J, Eickmann M, Escriou N, Grywna K, Kramme S, Manuguerra JC, Muller S, Rickerts V, Sturmer M, Vieth S, Klenk HD, Osterhaus AD, Schmitz H, Doerr HW. Identification of a Novel Coronavirus in Patients with Severe Acute Respiratory Syndrome. *N Engl J Med* 2003; [epub ahead of print]
- 27 **Fouchier RA**, Kuiken T, Schutten M, Van Amerongen G, Van Doornum GJ, Van Den Hoogen BG, Peiris M, Lim W, Stohr K, Osterhaus AD. Aetiology: Koch's postulates fulfilled for SARS virus. *Nature* 2003; **423**: 240-241
- 28 **Masur H**, Emanuel E, Lane HC. Severe Acute Respiratory Syndrome: Providing Care in the Face of Uncertainty. *JAMA* 2003; **289**: (DOI 10.1001/jama.289.21.JED30036)

Edited by Zhu LH

Advances in clinical diagnosis and treatment of severe acute respiratory syndrome

Qing-He Nie, Xin-Dong Luo, Wu-Li Hui

Qing-He Nie, Xin-Dong Luo, The Chinese PLA Center of Diagnosis and Treatment for Infectious Diseases, Tangdu Hospital, Fourth Military Medical University, Xi'an 710038, Shaanxi Province, China
Wu-Li Hui, Department of Epidemiology, Chinese People's Armed Police Force Medical College, Tianjin 300162, China

Correspondence to: Dr. Qing-He Nie, The Chinese PLA Center of Diagnosis and Treatment for Infectious Diseases, Tangdu Hospital, Fourth Military Medical University, Xi'an 710038, Shaanxi Province, China. nieqinghe@hotmail.com

Currently, Dr. Qing-He Nie works at Xiao Tang Shan Hospital in Beijing as a member of SARS expert committee

Telephone: +86-29-3377452 **Fax:** +86-29-3537377

Received: 2003-05-31 **Accepted:** 2003-06-04

Abstract

It has been proved that severe acute respiratory syndrome (SARS) is caused by SARS-associated coronavirus, a novel coronavirus. SARS originated in Guangdong Province, the People's Republic of China at the end of 2002. At present, it has spread to more than 33 countries or regions all over the world and affected 8 360 people and killed 764 by May 31, 2003. Identification of the SARS causative agent and development of a diagnostic test are important. Detecting disease in its early stage, understanding its pathways of transmission and implementing specific prevention measures for the disease are dependent upon swift progress. Due to the efforts of the WHO-led network of laboratories testing for SARS, tests for the novel coronavirus have been developed with unprecedented speed. The genome sequence reveals that this coronavirus is only moderately related to other known coronaviruses. WHO established the definitions of suspected and confirmed and probable cases. But the laboratory tests and definitions are limited. Until now, the primary measures included isolation, ribavirin and corticosteroid therapy, mechanical ventilation, etc. Other therapies such as convalescent plasma are being explored. It is necessary to find more effective therapy. There still are many problems to be solved in the course of conquering SARS.

Nie QH, Luo XD, Hui WL. Advances in clinical diagnosis and treatment of severe acute respiratory syndrome. *World J Gastroenterol* 2003; 9(6): 1139-1143

<http://www.wjgnet.com/1007-9327/9/1139.asp>

INTRODUCTION

On 12 March 2003, the World Health Organization (WHO) issued a global alert on the atypical pneumonia, also called severe acute respiratory syndrome (SARS), after reports from the Department of Health of Hong Kong of an outbreak of pneumonia in one of its public hospitals. At about the same time, WHO received reports of the syndrome from China, Singapore, Vietnam, Thailand, Indonesia, Taiwan, and the Philippines, as well as from countries in other continents including Canada, the United States, and Germany. The disease

originated in Guangdong Province at the end of 2002 and has affected 8 360 people and killed 764 by May 31, 2003. Dr. Carlo Urbani reported the disease first in a Vietnam French Hospital of Hanoi^[1]. WHO took prompt measures to avoid wider spread of SARS according to his alarm. It has been proved that a novel coronavirus is associated with SARS (SARS-CoV), and that this virus plays an etiologic role in SARS^[2-9]. Because of the death of Dr. Carlo Urbani (46 years old, an expert of infectious diseases, Italian) from SARS, Ksiazek and his colleagues proposed that their first isolate be named the Urbani strain of SARS-associated coronavirus.

On 17 March 2003, WHO called upon 11 laboratories in 9 countries to join a collaborative multi-center research project on SARS diagnosis. This network took advantage of modern communication technologies to share outcomes of investigation of clinical samples from SARS cases in real time. Clinicians from China, Hong Kong and the USA introduced their own experience of treatment on SARS. Scientists have made great progress in the clinical diagnosis and treatment of SARS. However, there are still many difficulties and problems to be solved in the course of conquering SARS.

DIAGNOSIS

Identification of SARS causative agent and development of a diagnostic test are of paramount importance. Detecting disease in its early stage, understanding its pathways of transmission and implementing disease specific prevention measures are dependent upon swift progress and results in aetiological and diagnostic research.

Clinical presentations

Booth *et al*^[10] reported that features of the clinical examination most commonly found in the patients at admission were self-reported fever (99 %), documented elevated temperature (85 %), nonproductive cough (69 %), myalgia (49 %), and dyspnea (42 %). The reports from Zhong^[11] and Chan-Yeung *et al*^[12] were similar to this.

Laboratory tests

Due to the efforts of the WHO-led international multi-center collaborative network of laboratory testing for SARS, tests for the novel coronavirus have been developed with unprecedented speed^[13].

Early in the course of the disease, the absolute lymphocyte count is often decreased. Overall white blood cell counts are generally normal or decreased. At the peak of the respiratory illness, approximately 50 % of patients have leukopenia and thrombocytopenia or low platelet counts within normal range. Early in the respiratory phase, elevated creatine phosphokinase levels (as high as 3 000 IU/L) and hepatic transaminases (two to six times of the upper limits of normal) have been noted. In the majority of patients, renal function is normal. Common laboratory features include elevated lactate dehydrogenase (87 %), hypocalcemia (60 %), and lymphopenia (54 %). Only 2 % of patients have rhinorrhea^[10] (Tables 1 and 2).

Table 1 Earliest symptoms of SARS^a

Symptom	No. (%) of patients (n=144)
Fever (n=106)	
Alone	33(23)
With prodrome	33(23)
With prodrome and cough or dyspnea	16(11)
With cough or dyspnea	15(11)
With other combinations	9(6)
Prodrome alone	19(13)
Cough or dyspnea alone	13(9)
Symptom reported first	
Prodrome	74(52)
Fever	106(74)
Cough or dyspnea	51(35)
Diarrhea	9(6)

^aProdrome includes headache, malaise, or myalgia.

Table 2 Laboratory features of SARS at admission and during hospitalization

	At admission		During hospitalization ^a	
	Median (IQR)	No./Total(%) Abnormal ^b	Median (IQR)	No./Total(%) Abnormal ^b
Lymphocytes, / μ L	900 (700-1300)	104/122 (85)	500 (400-800)	106/120 (88)
Lactate dehydrogenase, U/L	396 (219-629)	86/99 (87)	630 (363-1156)	115/123 (94)
Creatine kinase, U/L	157 (70-310)	43/109 (39)	370 (208-959)	64/118 (54)
Potassium, mEq/L	3.7 (3.4-4.0)	36/137 (26)	3.2 (2.9-3.4)	60/140 (43)
Calcium, mg/dL ^c	8.52 (8.2-9.16)	53/89 (60)	8.1 (7.76)	71/101 (70)
Magnesium, mg/dL	1.94 (1.7-2.19)	12/68 (18)	1.43 (0.97-1.51)	55/96 (57)
Phosphorus, mg/dL	3.10 (2.76-3.69)	17/64 (27)	2.17 (1.83-2.48)	41/78 (53)

Abbreviations: IQR, interquartile range; SI conversions: To convert calcium to mmol/L, multiply by 0.25. To convert magnesium to mmol/L, multiply by 0.411. To convert phosphorus to mmol/L, multiply by 0.323. ^aThe most abnormal value recorded used. ^bDefined as lymphocytes <1 500/ μ L; lactate dehydrogenase >190 U/L; creatine kinase >240 U/L for men and >190 U/L for women; potassium <3.5 mEq/L; calcium <8.8 mg/dL; magnesium <1.70 mg/dL; phosphate <2.79 mg/dL. ^cCalcium values have been corrected for serum albumin.

Radiographic findings of SARS

Wong *et al*^[14] found that initial chest radiographs were abnormal in 108 of 138 (78.3 %) patients and showed air-space opacity. Lower lung zone (70 of 108, 64.8 %) and right lung (82 of 108, 75.9 %) were more preferably involved. In most patients, peripheral lung involvement was more common (81 of 108, 75.0 %). Unifocal involvement (59 of 108, 54.6 %) was more frequent than multifocal or bilateral involvement.

Molecular test (PCR)

Sequencing of the about 30000-base genome of the SARS-associated coronavirus has completed^[15-21]. The genome sequence revealed that this coronavirus was only moderately related to other known coronaviruses, including two human coronaviruses, HCoV-OC43 and HCoV-229E. A valid positive PCR result indicated that there was genetic material (RNA) from the SARS-CoV in the sample. However, it does not mean the virus present is infectious, or that it is present in a large

enough quantity to infect another person. Negative PCR results do not exclude SARS. Besides the possibility of obtaining false-negative test results, specimens may not have been collected at a time when the virus or its genetic material was present.

The SARS-CoV-specific RNA can be detected in various clinical specimens such as blood, stool, respiratory secretions or body tissues by PCR. A number of PCR protocols developed by members of the WHO laboratory network are available on a WHO website^[22].

Despite their high sensitivity, the existing PCR tests cannot rule out the presence of the SARS virus in patients on account of possible false negative results. On the other hand, contamination of samples in laboratories may lead to false positive results.

SARS-CoV isolation

The presence of the infectious virus can be detected by inoculating suitable cell cultures (e.g. Vero cells) with patient's specimens (such as respiratory secretions, blood or stool) and propagating the virus *in vitro*. Once isolated, the virus must be identified as SARS-CoV using further tests. Cell culture is a very demanding test, but is currently (with the exception of animal trials) the only means to show the existence of a live virus. Positive cell culture results indicate the presence of live SARS-CoV in the sample. Negative cell culture results do not exclude SARS.

Antibody detection

Various methods provide a means for the detection of antibodies produced in response to infection with SARS-CoV. Different types of antibodies (IgM or IgG) appear and change in level during the course of infection. They can be undetectable in the early stages of infection. IgG usually remains detectable after resolution of the illness. It was reported that IgG would reach peak value 60 days after obvious symptoms and then keep it, while IgM would reach peak value on day 14 after onset of apparent symptoms. Enzyme-linked immunosorbent assay (ELISA), immunofluorescence assay (IFA), neutralisation test are being developed, but are not yet commercially available.

WHO CASE DEFINITION^[23]

The definitions of suspected and confirmed and probable case according to the WHO Case Definition are as follows:

Suspect case

A person presenting after 1 November 2002, with history of: high fever (>38 °C) and cough or breathing difficulty, and one or more of the following exposures during the 10 days prior to onset of symptoms: (1) close contact, with a person who is a suspect or probable case of SARS; (2) history of travel, to an area with recent local transmission of SARS; (3) residing in an area with recent local transmission of SARS. Close contact means having cared for, lived with, or had direct contact with respiratory secretions or body fluids of a suspect or probable case of SARS.

A person with an unexplained acute respiratory illness resulting in death after 1 November 2002, but on whom no autopsy has been performed, and one or more of the following exposures during the 10 days prior to onset of symptoms: (1) close contact with a person who is a suspect or probable case of SARS; (2) history of travel to an area with recent local transmission of SARS, and (3) residing in an area with recent local transmission of SARS.

Probable case

(1) A suspect case with radiographic evidence of infiltrates

consistent with pneumonia or respiratory distress syndrome (RDS) on chest X-ray (CXR). (2) A suspect case of SARS that is positive for SARS coronavirus by one or more assays. See Use of laboratory methods for SARS diagnosis. (3) A suspect case with autopsy findings consistent with the pathology of RDS without an identifiable cause.

Exclusion criteria

A case should be excluded if an alternative diagnosis can fully explain their illness.

Reclassification of cases

As SARS is currently a diagnosis of exclusion, the status of a reported case may change over time. A patient should always be managed as clinically appropriate, regardless of their case status. (1) A case initially classified as suspect or probable, for whom an alternative diagnosis can fully explain the illness, should be discarded after carefully considering the possibility of co-infection. (2) A suspect case who, after investigation, fulfils the probable case definition should be reclassified as "probable". (3) A suspect case with a normal CXR should be treated, as deemed appropriate, and monitored for 7 days. Those cases in whom recovery is inadequate should be re-evaluated by CXR. (4) Those suspect cases in whom recovery is adequate but whose illness cannot be fully explained by an alternative diagnosis should remain as "suspect". (5) A suspect case who died, on whom no autopsy was conducted, should remain classified as "suspect". However, if this case is identified as being part of a chain transmission of SARS, the case should be reclassified as "probable". (6) If an autopsy was conducted and no pathological evidence of RDS was found, the case should be "discarded".

The surveillance period began on 1 November 2002 to capture cases of atypical pneumonia in China now recognized as SARS. International transmission of SARS was first reported in March 2003 for cases with onset in February 2003. The Centers for Disease Control and Prevention have added laboratory criteria for evidence of infection with SARS-CoV to the interim surveillance case definition^[24]. Using the new laboratory criteria, a SARS case is laboratorily confirmed if one of the following is met: detection of the SARS-CoV antibody by indirect fluorescent antibody (IFA) or enzyme-linked immunosorbent assay (ELISA), isolation of SARS-CoV in tissue culture, detection of SARS-CoV RNA by reverse transcriptase-polymerase chain reaction (RT-PCR), which must be confirmed by a second PCR test. Negative laboratory results for PCR, viral culture, or antibody tests obtained within 21 days of illness do not rule out SARS-CoV infection. In these cases, an antibody test of a specimen obtained more than 21 days after the onset of illness is needed to determine infection. Unless PCR confirms the initial suspicion of SARS infection, the diagnosis of SARS is based on the clinical findings of an atypical pneumonia not attributed to any other cause as well as a history of exposure to a suspect or probable case of SARS, or to their respiratory secretions or other body fluids. The initial diagnostic testing for suspected SARS patients should include chest radiography, pulse oximetry, blood cultures, sputum Gram stain and culture, and testing for viral respiratory pathogens, obviously influenza A and B and respiratory syncytial virus. A specimen for Legionella and pneumococcal urinary antigen testing should also be considered.

Clinicians should save any available clinical specimens (respiratory, blood, and serum) for additional testing until a specific diagnosis is made. Acute and convalescent (greater than 21 days after the onset of symptoms) serum samples should be collected from each patient who meets the definition criteria for SARS. Specific instructions for collecting specimens from suspected SARS patients are available on the Internet.

In the early stages, SARS may be hard to differentiate from other viral infections, and diagnostic delays may contribute to the spread of the epidemic. Nevertheless, until standardized reagents for virus and antibody detection become available and methods have been adequately tested, the diagnosis of SARS remains based on clinical and epidemiological findings. The revised case definition for the first time includes laboratory results: a suspected case of SARS, that is positive for SARS-CoV in one or more assays, should be reclassified as a probable case. At present there are no defined criteria for SARS-CoV test results to confirm or reject the diagnosis of SARS.

Positive laboratory test results for other known agents that are able to cause atypical pneumonia such as Legionella pneumophila, influenza and parainfluenza viruses, mycoplasma pneumoniae etc. may serve as exclusion criteria; according to the case definition, a case should be excluded if an alternative diagnosis can fully explain the illness. However, the possibility of dual infection must not be ruled out completely. According to our clinical experience and correlative papers, we think that exact diagnosis of a confirmed case must need a history of close contact and persistent symptoms (fever or influenza-like symptom). To observe the chest x-ray of patient continuously is also necessary.

TREATMENT

From initial clinical experience, SARS can develop in stages, including acute constitutional symptoms, acute viral pneumonitis, acute lung injury, and even acute respiratory distress syndrome, evolving over 1 to 2 weeks. Initial infection followed by a hyperactive immune response appears to underlie the severe manifestations of SARS. Therefore, corticosteroids can be used to dampen excessive lung damage due to an inflammatory response.

Ribavirin and glucocorticoid therapy

A series of 31 patients with probable SARS were treated according to a treatment protocol consisting of antibacterials and a combination of ribavirin and methylprednisolone in Hong Kong^[25]. One patient recovered by antibacterial treatment alone, 17 showed rapid and sustained responses, and 13 achieved improvements with step-up or pulsed methylprednisolone. Four patients required short periods of non-invasive ventilation. No patient required intubation or mechanical ventilation. There was no mortality or treatment morbidity in this series. The following is the standard protocol.

Antibacterial treatment

- (1) Levofloxacin 500 mg once daily intravenously or orally;
- (2) Or clarithromycin 500 mg twice daily orally plus coamoxiclav (amoxicillin and clavulanic acid), 375 mg three times daily orally if patient is <18 years old, pregnant, or suspected to have tuberculosis.

Ribavirin and methylprednisolone

Combination treatment with ribavirin and methylprednisolone when: (1) Extensive or bilateral chest radiographic involvement; (2) Or persistent chest radiographic involvement and persistent high fever for 2 days; (3) Or clinical, chest radiographic, or laboratory findings suggestive of worsening; (4) Or oxygen saturation <95 % in room air.

Standard corticosteroid regimen for 21 days

- (1) Methylprednisolone 1 mg/kg every 8 h (3 mg/kg daily) intravenously for 5 days; (2) Then methylprednisolone 1 mg/kg every 12 h (2 mg/kg daily) intravenously for 5 days; (3) Then prednisolone 0.5 mg/kg twice daily (1 mg/kg daily) orally

for 5 days; (4) Then prednisolone 0.5 mg/kg daily orally for 3 days; (5) Then prednisolone 0.25 mg/kg daily orally for 3 days; (6) Then off.

Ribavirin regimen for 10-14 days

(1) Ribavirin 400 mg every 8 h (1 200 mg daily) intravenously for at least 3 days (or until condition becomes stable); (2) Then ribavirin 1 200 mg twice daily (2 400 mg daily) orally.

Pulsed methylprednisolone

(1) Give pulsed methylprednisolone if clinical condition, chest radiograph, or oxygen saturation worsens (at least two of these), and lymphopenia persists; (2) Give methylprednisolone 500 mg twice daily intravenously for 2 days, then back to standard corticosteroid regimen.

Mechanical ventilation

Traditional approaches to mechanical ventilation use tidal volumes of 10 to 15 ml per kilogram of body weight and may cause stretch-induced lung injury in patients with acute lung injury and the acute respiratory distress syndrome. The Acute Respiratory Distress Syndrome Network therefore conducted a trial. The mean tidal volumes on days 1 to 3 were 6.2 ± 0.8 and 11.8 ± 0.8 ml per kilogram of predicted body weight. They found that in patients with acute lung injury and acute respiratory distress syndrome, mechanical ventilation with a lower tidal volume than traditionally used resulted in decreased mortality and increased number of days without ventilator use^[26-29].

Cordingley *et al*^[30] suggests that reduced mortality may be achieved by using a strategy that aims at preventing overdistension of the lungs. There is no clinical evidence to support the use of specific FiO_2 thresholds, but it is common clinical practice to decrease FiO_2 below 0.6 as quickly as possible. SaO_2 values of around 90 % are commonly accepted. PaCO_2 is allowed to rise during lung protective volume and pressure limited ventilation. PaCO_2 levels of 2-3 times 3 normal seem to be well tolerated for prolonged periods. Renal compensation for respiratory acidosis occurs over several days. Many clinicians infuse sodium bicarbonate slowly if arterial pH falls below 7.20, Set PEEP at a relatively high level such as 15 cm H_2O in patients with ARDS. It is common practice during pressure control ventilation to increase the I:E ratio to 1:1 or 2:1 (inverse ratio ventilation) with close monitoring of intrinsic PEEP and haemodynamics.

Other therapies being studied

At present, serum therapy is being studied for SARS patients. 40 patients were divided into two groups in the Medical College of Hong Kong Chinese University. One group was treated with convalescent plasma and another group not. The effect was obviously different among two groups after one month, the therapy group died no patients while another group 3 patients, but it needs more clinical trial to be proved. In their opinion, to use convalescent plasma within earlier two weeks will shorten the in-hospital period and fever time and reduce mortality. Serum therapy was used to dying patients and aged patients with other severe or chronic disease and pregnant women.

As to another trial in Hong Kong^[31], treatment of a SARS patient followed by 200 ml convalescent plasma donated by SARS patients in their convalescent phase. No adverse reaction occurred after administration of convalescent plasma. The fever subsided, chest X-ray showed further resolution of basal lung infiltrates, and she made an uneventful recovery. Although no probable SARS case has been ascribed to transmission by labile blood products or blood derivatives, there is a theoretical risk

of transmission of the SARS virus through transfusion of labile blood products, since low viraemia has been detected up to approximately 10 days after the onset of symptoms from probable SARS patients^[32].

Moller *et al*^[33] reported that bovine surfactant therapy in severe ARDS improved oxygenation immediately after administration. This improvement was sustained only in the subgroup of patients without pneumonia but with an initial $\text{PaO}_2/\text{FIO}_2$ ratio higher than 65. The SARS studies on antisense oligonucleotide drug, polypeptide, and vaccine will benefit the treatment of this disease.

It has been proved that a novel coronavirus is the cause of SARS with strong infectivity. Up to now, we have only understood the preliminary pathogenesis and epidemiology of SARS. After all SARS is a disease seen never before in human. To control and defend human being from this disease, further studies are needed, such as: (1) origin, mutation, life cycle, transmission pathways of SARS-CoV; (2) the mechanisms of SARS-CoV replicating and coming into the host cell; (3) pathogenesis of acute lung injury and abnormal immune response; (4) rapid diagnosis and vaccine, and (5) effective medicine such as inhibitory polypeptide. With rapid progress in the basic studies of the disease all over the world, more effective drugs and treatment measures will be discovered in the days to come and SARS will be put under complete control by mankind soon.

REFERENCES

- 1 **Reilley B**, Van Herp M, Sermand D, Dentico N. SARS, Carlo Urbani. *N Engl J Med* 2003; **348**: 1951-1952
- 2 **Ksiazek TG**, Erdman D, Goldsmith CS, Zaki SR, Peret T, Emery S, Tong S, Urbani C, Comer JA, Lim W, Rollin PE, Dowell SF, Ling AE, Humphrey CD, Shieh WJ, Guarner J, Paddock CD, Rota P, Fields B, DeRisi J, Yang JY, Cox N, Hughes JM, LeDuc JW, Bellini WJ, Anderson LJ. A novel coronavirus associated with severe acute respiratory syndrome. *N Engl J Med* 2003; **348**: 1953-1966
- 3 **Rota PA**, Oberste MS, Monroe SS, Nix WA, Campagnoli R, Icenogle JP, Penaranda S, Bankamp B, Maher K, Chen MH, Tong S, Tamin A, Lowe L, Frace M, DeRisi JL, Chen Q, Wang D, Erdman DD, Peret TC, Burns C, Ksiazek TG, Rollin PE, Sanchez A, Liffick S, Holloway B, Limor J, McCaustland K, Olsen-Rasmussen M, Fouchier R, Gunther S, Osterhaus AD, Drosten C, Pallansch MA, Anderson LJ, Bellini WJ. Characterization of a novel coronavirus associated with severe acute respiratory syndrome. *Science* 2003; **300**: 1394-1399
- 4 **Falsey AR**, Walsh EE. Novel coronavirus and severe acute respiratory syndrome. *Lancet* 2003; **361**: 1312-1313
- 5 **Drosten C**, Gunther S, Preiser W, van der Werf S, Brodt HR, Becker S, Rabenau H, Panning M, Kolesnikova L, Fouchier RA, Berger A, Burguiera AM, Cinatl J, Eickmann M, Escriou N, Grywna K, Kramme S, Manuguerra JC, Muller S, Rickerts V, Sturmer M, Vieth S, Klenk HD, Osterhaus AD, Schmitz H, Doerr HW. Identification of a novel coronavirus in patients with severe acute respiratory syndrome. *N Engl J Med* 2003; **348**: 1967-1976
- 6 **Peiris JS**, Lai ST, Poon LL, Guan Y, Yam LY, Lim W, Nicholls J, Yee WK, Yan WW, Cheung MT, Cheng VC, Chan KH, Tsang DN, Yung RW, Ng TK, Yuen KY. Coronavirus as a possible cause of severe acute respiratory syndrome. *Lancet* 2003; **361**: 1319-1325
- 7 **No authors listed**. Severe acute respiratory syndrome (SARS) and coronavirus testing-United States, 2003. *Mmwr Morb Mortal Wkly Rep* 2003; **52**: 297-302
- 8 **No authors listed**. From the centers for disease control and prevention. severe acute respiratory syndrome (SARS) and coronavirus testing-united states, 2003. *JAMA* 2003; **289**: 2203-2206
- 9 Update 31 - Coronavirus never before seen in humans is the cause of SARS. http://www.who.int/csr/sarsarchive/2003_04_16/en/
- 10 **Booth CM**, Matukas LM, Tomlinson GA, Rachlis AR, Rose DB, Dwosh HA, Walmsley SL, Mazzulli T, Avendano SB, Derkach P, Ephantymios IE, Kitai I, Mederski BD, Shadowitz SB, Gold WL, Hawryluck LA, Rea E, Chenkin JS, Cescon DW, Poutanen SM,

- Detsky AS. Clinical features and short-term outcomes of 144 patients with SARS in the greater toronto area. *JAMA* 2003; [epub ahead of print]
- 11 **Zhong NS.** The Clinical Diagnosis and Treatment of SARS at present. *Zhong Guoyi Xuelun Tanbao* 2003; **4**: 29
- 12 **Chan-Yeung M,** Yu WC. Outbreak of severe acute respiratory syndrome in hong kong special administrative region: case report. *BMJ* 2003; **326**: 850-852
- 13 SARS: Laboratory diagnostic tests. 29 April 2003. <http://www.who.int/csr/sars/diagnostictests/en>
- 14 **Wong KT,** Antonio GE, Hui DS, Lee N, Yuen EH, Wu A, Leung CB, Rainer TH, Cameron P, Chung SS, Sung JJ, Ahuja AT. Severe acute respiratory syndrome: radiographic appearances and pattern of progression in 138 patients. *Radiology* 2003; [epub ahead of print]
- 15 **Marra MA,** Jones SJ, Astell CR, Holt RA, Brooks-Wilson A, Butterfield YS, Khattri J, Asano JK, Barber SA, Chan SY, Cloutier A, Coughlin SM, Freeman D, Girn N, Griffith OL, Leach SR, Mayo M, McDonald H, Montgomery SB, Pandoh PK, Petrescu AS, Robertson AG, Schein JE, Siddiqui A, Smailus DE, Stott JM, Yang GS, Plummer F, Andonov A, Artsob H, Bastien N, Bernard K, Booth TF, Bowness D, Czub M, Drebot M, Fernando L, Flick R, Garbutt M, Gray M, Grolla A, Jones S, Feldmann H, Meyers A, Kabani A, Li Y, Normand S, Stroher U, Tipples GA, Tyler S, Vogrig R, Ward D, Watson B, Brunham RC, Krajden M, Petric M, Skowronski DM, Upton C, Roper RL. The Genome sequence of the SARS-associated coronavirus. *Science* 2003; **300**: 1399-1404
- 16 **Dye C,** Gay N. Modeling the SARS Epidemic. *Science* 2003; [epub ahead of print]
- 17 **Lipsitch M,** Cohen T, Cooper B, Robins JM, Ma S, James L, Gopalakrishna G, Chew SK, Tan CC, Samore MH, Fisman D, Murray M. Transmission dynamics and control of severe acute respiratory syndrome. *Science* 2003; [epub ahead of print]
- 18 **Riley S,** Fraser C, Donnelly CA, Ghani AC, Abu-Raddad LJ, Hedley AJ, Leung GM, Ho LM, Lam TH, Thach TQ, Chau P, Chan KP, Lo SV, Leung PY, Tsang T, Ho W, Lee KH, Lau EM, Ferguson NM, Anderson RM. Transmission dynamics of the etiological agent of SARS in hong kong: impact of public health interventions. *Science* 2003; [epub ahead of print]
- 19 **Lipsitch M,** Cohen T, Cooper B, Robins JM, Ma S, James L, Gopalakrishna G, Chew SK, Tan CC, Samore MH, Fisman D, Murray M. Transmission dynamics and control of severe acute respiratory syndrome. *Science* 2003; [epub ahead of print]
- 20 **Fisher DA,** Chew MH, Lim YT, Tambyah PA. Preventing local transmission of SARS: lessons from singapore. *Med J Aust* 2003; **178**: 555-558
- 21 **Stohr K.** A multicentre collaboration to investigate the cause of severe acute respiratory syndrome. *Lancet* 2003; **361**: 1730-1733
- 22 PCR primers for SARS developed by WHO Network Laboratories. 17 April 2003 <http://www.who.int/csr/sars/primers/en/>
- 23 Case Definitions for Surveillance of Severe Acute Respiratory Syndrome SARS. <http://www.who.int/csr/sars/casedefinition/en/>
- 24 Updated Interim U.S. Case Definition of Severe Acute Respiratory Syndrome (SARS). May 23, 2003, 10:00 PM. <http://www.cdc.gov/ncidod/sars/diagnosis.htm>
- 25 **So LK,** Lau AC, Yam LY, Cheung TM, Poon E, Yung RW, Yuen KY. Development of a standard treatment protocol for severe acute respiratory syndrome. *Lancet* 2003; **361**: 1615-1617
- 26 **The Acute Respiratory Distress Syndrome Network.** Ventilation with lower tidal volumes as compared with traditional tidal volumes for acute lung injury and the acute respiratory distress syndrome. *N Engl J Med* 2000; **342**: 1301-1308
- 27 **Allegra L,** Blasi F. Problems and perspectives in the treatment of respiratory infections caused by atypical pathogens. *Pulm Pharmacol Ther* 2001; **14**: 21-27
- 28 **Atabai K,** Matthay MA. The pulmonary physician in critical care. 5: Acute lung injury and the acute respiratory distress syndrome: definitions and epidemiology. *Thorax* 2002; **57**: 452-458
- 29 **The Acute Respiratory Distress Syndrome Network.** Ventilation with lower tidal volumes as compared with traditional tidal volumes for acute lung injury and the acute respiratory distress syndrome. *N Engl J Med* 2000; **342**: 1301-1308
- 30 **Cordingley JJ,** Keogh BF. The pulmonary physician in critical care. 8: Ventilatory management of ALI/ARDS. *Thorax* 2002; **57**: 729-734
- 31 **Wong VWS,** Dai D, Wu AKL, Sung JY. Treatment of severe acute respiratory syndrome with convalescent plasma. *H K MJ* <http://www.hkmj.org.hk/hkmj/update/SARS/cr1606.htm>
- 32 WHO Recommendations on SARS and Blood Safety. <http://www.who.int/csr/sars/guidelines/bloodsafety/en/>
- 33 **Moller JC,** Schaible T, Roll C, Schiffmann JH, Bindl L, Schrod L, Reiss I, Kohl M, Demirakca S, Hentschel R, Paul T, Vierzig A, Groneck P, Von Seefeld H, Schumacher H, Gortner L. Treatment with bovine surfactant in severe acute respiratory distress syndrome in children: a randomized multicenter study. *Intensive Care Med* 2003; **29**: 437-446

Edited by Zhu LH and Zhang JZ

Mechanism and its regulation of tumor-induced angiogenesis

Manoj Kumar Gupta, Ren-Yi Qin

Manoj Kumar Gupta, Ren-Yi Qin, Department of Surgery, Tongji Hospital, Tongji Medical College, Huazhong University of Science and Technology, Wuhan, 430030, Hubei Province, China

Supported by National Natural Science Foundation of China, No 30271473

Correspondence to: Professor Ren-Yi Qin, Department of Surgery, Tongji Hospital, Tongji Medical College, Huazhong University of Science and Technology, Wuhan, 430030, Hubei, China. ryqin@tjh.tjmu.edu.cn

Telephone: +86-27-83662389

Received: 2002-11-29 **Accepted:** 2003-01-13

Abstract

Tumor angiogenesis is the proliferation of a network of blood vessels that penetrates into cancerous growths, supplying nutrients and oxygen and removing waste products. The process of angiogenesis plays an important role in many physiological and pathological conditions. Solid tumors depend on angiogenesis for growth and metastasis in a hostile environment. In the prevascular phase, the tumor is rarely larger than 2 to 3 mm³ and may contain a million or more cells. Up to this size, tumor cells can obtain the necessary oxygen and nutrient supplies required for growth and survival by simple passive diffusion. The properties of tumors to release and induce several angiogenic and anti-angiogenic factors which play crucial roles in regulating endothelial cell (EC) proliferation, migration, apoptosis or survival, cell-cell and cell-matrix adhesion through different intracellular signaling are thought to be the essential mechanisms during tumor-induced angiogenesis. Tumor angiogenesis actually starts with tumor cells releasing molecules that send signals to surrounding normal host tissue. This signaling activates certain genes in the host tissue that, in turn, make proteins to encourage growth of new blood vessels. In this review, we focus the mechanisms of tumor-induced angiogenesis, with an emphasis on the regulatory role of several angiogenic and anti-angiogenic agents during the angiogenic process in tumors. Advances in understanding the mechanisms of tumor angiogenesis have led to the development of several most effective anti-angiogenic and anti-metastatic therapeutic agents and also have provided several techniques for the regulation of cancer's angiogenic switch. The suggestion is made that standard cytotoxic chemotherapy and angiogenesis inhibitors used in combination may produce complementary therapeutic benefits in the treatment of cancer.

Gupta MK, Qin RY. Mechanism and its regulation of tumor-induced angiogenesis. *World J Gastroenterol* 2003; 9(6): 1144-1155
<http://www.wjgnet.com/1007-9327/9/1144.asp>

MECHANISM OF ANGIOGENESIS

Angiogenesis is a complex multi-step process involving extensive interplay between cells, soluble factors, and extracellular matrix (ECM) components. Four distinct sequential steps in angiogenesis include: (1) degradation of basement membrane by proteases; (2) migration of endothelial cells (ECs) into the interstitial space and sprouting; (3) ECs

proliferation at the migrating tip; (4) lumen formation, generation of new basement membrane with the recruitment of pericyte, formation of anastomoses and finally blood flow^[1]. The angiogenic response in the microvasculature is associated with changes in cellular adhesive interactions between adjacent ECs, pericytes and surrounding ECM. In the process of active neovascularization, activated ECs reorganize their cytoskeleton, express cell surface adhesion molecules such as integrins and selectins, secrete proteolytic enzymes, and remodel their adjacent ECM. These events are followed by the formation of capillary buds. Autocrine and/or paracrine angiogenic factors must be present to induce EC migration, proliferation, elongation, orientation and differentiation leading to the re-establishment of the basement membrane, lumen formation and anastomosis with other new or pre-existing vessels, eventually leading to the formation of intact microvessels.

CANCER'S ANGIOGENIC SWITCH

Angiogenic phenotype serves the development of malignant tumor at multiple stages. Tumor cells may overexpress one or more of the positive regulators of angiogenesis, may mobilize an angiogenic protein from the ECM, may recruit host cells such as macrophages (which produce their own angiogenic proteins), or may engage in a combination of these processes. Tumor angiogenesis is mediated by tumor-secreted angiogenic growth factors that interact with their surface receptors expressed on ECs. The most commonly found angiogenic growth factors such as VEGF and bFGF, when encounter ECs, they bind to the tyrosine kinase receptors on ECs membrane. Binding leads to dimerization of the receptors and activation of autophosphorylation of tyrosines on the receptor surface and thereby initiates the several signaling proteins (including PI3-kinase, Src, Grb2/m-SOS-1 (a nucleotide exchange factor for Ras) and signal transducers and activators of transcriptions (STATs) each of which contains src-homology-2 (SH-2) domains^[2]. Binding of the SH-2 regions of these proteins to the phosphotyrosines on the receptor tyrosine kinases (RTKs) activates several pathways that are crucial for triggering the cell cycle machinery. The most well studied pathway passes through the GTP-binding protein Ras and activates the mitogen activated protein kinase (MAPK) cascade and subsequently transcription factors in the nucleus^[2]. Up-regulation of an angiogenic factor is not sufficient in itself for a tumor cell to become angiogenic, however, certain negative regulators or inhibitors of vessel growth may need to be down-regulated^[3]. If there is a preponderance of angiogenic factors in the local milieu, the neovasculature may persist as capillaries, or differentiate into mature venules or arterioles. If instead, the local milieu changes such that there is a preponderance of angiostatic factors, the neovessels can regress. The angiostatic factors that mediate regression can do so either by inducing apoptosis or cell cycle arrest of ECs. Thus, the switch to the angiogenic phenotype is regulated by a change in the local equilibrium between positive and negative regulators of the growth of microvessels^[1,3].

FACTORS INVOLVED IN TUMOR ANGIOGENESIS

Vascular endothelial growth factor and receptors

Vascular endothelial growth factor (VEGF), also known as

vascular permeability factor (VPF), is a heparin-binding angiogenic growth factor, and is highly expressed in various types of tumors. It may increase ECs permeability by enhancing the activity of vesicular-vacuolar organelles, clustered vesicles in ECs lining small vessels that facilitate transport of metabolites between luminal and abluminal plasma membranes^[4]. Alternatively, VEGF may enhance permeability through mitogen-activated protein (MAP) kinase signal transduction cascade by loosening adhering junctions between ECs in a monolayer via rearrangement of cadherin/catenin complexes^[5,6]. In addition, recent studies have shown that VEGF enhances ECs permeability by activating PKB/Akt, endothelial nitric oxide synthase (eNOS), and MAP kinase dependent pathways using human umbilical vein endothelial cell^[7] (Figure 1). Increased vascular permeability may allow the extravasation of plasma proteins and formation of ECM favorable to endothelial and stromal cell migration.

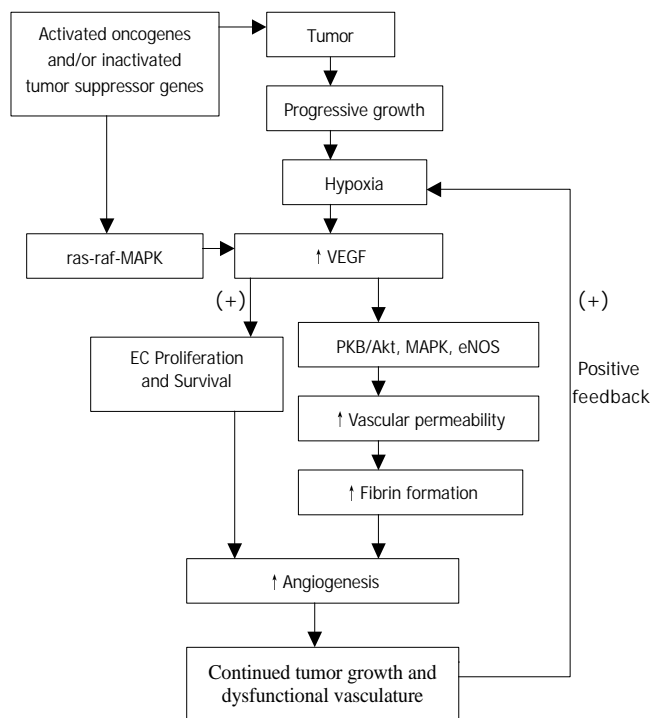


Figure 1 The triggering mechanism in tumor angiogenesis: inactivated tumor suppressor genes/activated oncogenes versus hypoxia.

VEGF is an EC specific mitogen. VEGF, after binding to its high affinity receptors (Flt-1/VEGFR-1, Flk-1/KDR/VEGFR-2), promotes the formation of the second messenger via hydrolysis of inositol, thus induces the autophosphorylation of the receptors in the presence of heparin-like molecules, and open phosphatidylinositol metabolic signal transduction pathways, activates MAP kinases in EC and thereby VEGF exerts its mitogenic effect by promoting EC proliferation^[8,9].

VEGF induces a balanced system of proteolysis that can remodel ECM components necessary for angiogenesis. VEGF stimulates EC production of urokinase-like plasminogen activator (uPA), tissue type plasminogen activator (tPA) and plasminogen activator inhibitor-1 (PAI-1)^[10,11], proteolytic enzymes, tissue factors, and interstitial collagenase^[12]. Plasminogen activators activate plasminogen to plasmin, which can break down ECM components. In addition to remodeling the basement membrane, uPA bound to uPAR also mediates intracellular signal transduction in ECs. Tang *et al.* have demonstrated that uPAR occupancy on ECs results in the phosphorylation of focal adhesion proteins and the activation

of MAP kinase^[13] through which uPA influences EC migration and proliferation (Figure 2).

Moreover, VEGF has been shown to exhibit its angiogenic effect by inducing expression of the $\alpha_1\beta_1$, $\alpha_2\beta_1$ and $\alpha_v\beta_3$ integrins, which promote cell migration, proliferation and matrix reorganization (Figure 2), and $\alpha_1\beta_1$, $\alpha_2\beta_1$ and $\alpha_v\beta_3$ antagonists may prove effective on inhibiting VEGF-driven angiogenesis associated with cancers and other pathologies through apoptosis^[14,15]. VEGF, in addition to a very specific mitogen for vascular EC, is a potent pro-survival factor for ECs in newly formed immature vessels. Several endothelial survival factors (VEGF, angiopoietin-1 and $\alpha_v\beta_3$) suppress p53, p21, p16 and p27, and proapoptotic protein Bax, whereas they variably activate the survival PI3K/Akt, p42/44 MAP kinases, bcl-2, A1 and survivin pathways^[16-20] (Figure 2). It was reported that p42/p44 MAP kinases promoted VEGF expression by activating its transcription via recruitment of the AP-2/Sp1 (activator protein-2) complex on the proximal region (-88/-66) of the VEGF promoter and by direct phosphorylation of hypoxia-inducible factor 1 alpha (HIF-1 alpha)^[21]. Pharmacological inhibition of PI3K or transfection with a dominant-negative Akt mutant abolished the antiapoptotic effect of VEGF on ECs. In addition to the PI3K/Akt pathway, ras-dependent signaling pathways might also play an important role at least for VEGF signaling. Thus, H-rasV12G down-regulation leads to profound tumor regression, which is initially characterized by massive apoptosis of tumor- and host-derived ECs^[22]. Therefore, apoptosis induction is resistant to enforced VEGF expression, suggesting that VEGF requires an intact Ras-dependent signaling pathway to mediate its apoptosis inhibitory effect^[22]. And also, VEGF via the KDR/Flt-1 receptor induces enhanced expression of the serine-threonine protein kinase Akt^[19], a downstream target of PI3-kinase, which potentially blocks apoptosis by interfering with various apoptosis signaling pathways^[23,24], promotes EC migration^[25], and enhances the expression of the hypoxia-inducible factor (HIF), which is known to stimulate VEGF expression^[26], suggesting a potent proangiogenic effect^[27,28]. These findings have identified the VEGFR2 and the PI3K/Akt signal transduction pathway as crucial elements in promoting EC survival induced by VEGF. The downstream effector pathways mediating the antiapoptotic VEGF effect include Akt-dependent activation of the endothelial nitric oxide synthase (NOS)^[29,30], resulting in an enhanced endothelial NO synthesis, which, in turn promotes EC survival (Figure 2). Gupta *et al.* demonstrated that the VEGF-induced activation of the MAPK/extracellular signal-regulated kinase (ERK) pathway and inhibition of the stress-activated protein kinase/c-Jun amino-terminal kinase pathway is also implicated in the antiapoptotic effect mediated by VEGF^[31] (Figure 2). Interestingly, the activation of the PI3K/Akt pathway mediates not only the antiapoptotic effect but also the migratory effect of VEGF on ECs via Akt-dependent phosphorylation and activation of eNOS^[32] (Figure 2).

The expression of VEGF mRNA is highest in hypoxic tumor cells adjacent to necrotic areas. Hypoxia-induced transcription of VEGF mRNA is apparently mediated, at least in part, by the binding of hypoxia-inducible factor 1 (HIF-1) to an HIF-1 binding site located in the VEGF promoter, and by the activation of a stress inducible PI3K/Akt pathway^[26,33]. In fact, progressive growth of tumor creates ongoing hypoxia, which up-regulates several pro-angiogenic compounds including VEGF, bFGF, IL-8, TNF- α , TGF- β etc. These compounds, via several mechanisms such as increase of vessel hyperpermeability, release of plasma proteins, induction of proteases, fibrin formation, EC proliferation, migration etc, promote angiogenesis and fibrinolysis resulting in continued tumor growth and dysfunctional vasculature, which further positively feedback to create continuing hypoxia inside tumors (Figure 1).

Fibroblast growth factors

Fibroblast growth factors (FGFs) and their receptors are overexpressed in various types of cancers, and are important tumor angiogenic and ECs survival factors. Pardo *et al.* reported that bFGF induced expression of the antiapoptotic proteins bcl-XL and bcl-2 via the MEK/ERK signaling pathway^[34] (Figure 2). Expression of VEGF mRNA in the tumor is increased by bFGF overexpression, and the bFGF-induced tumor development is significantly inhibited by treatment with KDR/Flk-1 neutralizing monoclonal antibody (mAb), which suggests that bFGF synergistically augments VEGF-mediated hepatocellular carcinoma development and angiogenesis, at least in part, by induction of VEGF through KDR/Flk-1^[35]. In addition, bFGF induces an increase of VEGF mRNA in vascular smooth muscle cells^[36] and an increase in VEGF receptors in microvascular ECs^[37]. aFGF and bFGF are mitogenic for ECs and stimulate ECs migration as well as ECs production of plasminogen activator (PA) and collagenase that are capable of degrading basement membrane^[38] (Figure 2). FGFs are responsible for production of ECM and release of matrix metalloproteinases (MMPs) for selective degradation and organization of ECM^[39] (Figure 2).

Binding of FGFs to their high affinity receptors causes the activation of the intrinsic tyrosine kinase and a cascade of events, leading eventually to the induction of immediate early gene transcription, and to cell proliferation. FGFs receptors dimerize upon ligand binding, and transphosphorylate at tyrosine residue. Angiogenic growth factors, like bFGF and VEGF165, require interaction with heparin sulfate (HS) in order to induce a proliferative signal through tyrosine kinase receptors. Binding of bFGF to high affinity cell surface receptor sites can be modulated by heparin-mimicking compounds (i. e. RG-13577) that can modulate abnormal bFGF signaling by disrupting bFGF mediated autocrine loop, compete with heparin sulfate (HS) on binding to bFGF, bind the growth factor, and prevent receptor binding and/or dimerization^[40], and by proteolytic enzymes (e.g. MMP-2) that cleave the ectodomain of the receptor. These effects are associated with profound inhibition of bFGF mediated signal transduction (tyrosine phosphorylation) and proliferation of vascular ECs^[40]. Spontaneous migration of ECs is inhibited by neutralizing antibodies to bFGF, suggesting an autocrine of bFGF synthesized and released by the ECs themselves^[38]. A dominant-negative receptor, which, when co-expressed with

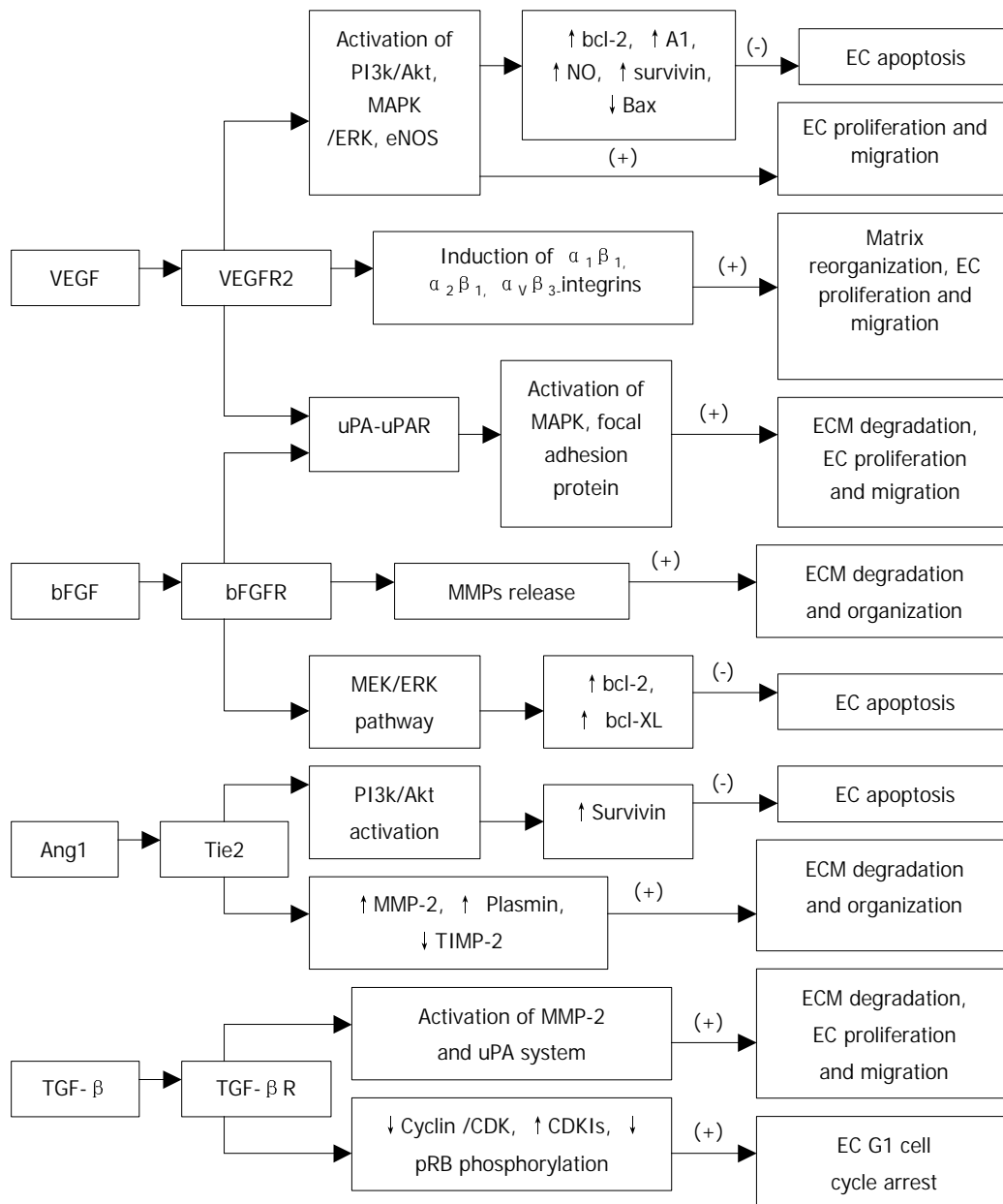


Figure 2 Mechanism of angiogenesis by angiogenic factors.

FGF receptors (FGFRs), can block the activation and signal transduction. In addition, the ligand-specific targeting of toxin to tumor cells expressing FGFRs and the compounds that bind and inactivate FGF ligands, can block ECs proliferation.

Angiopoietins and tie receptors

It has been proposed that angiopoietin-1 (Ang1) and angiopoietin-2 (Ang2) are pro-angiogenic and anti-angiogenic owing to their respective agonist and antagonist signaling action through the Tie2 receptor^[41]. Lobov *et al.* have demonstrated that *in vivo*, in the presence of endogenous VEGF-A, Ang2 promotes a rapid increase in capillary diameter, remodeling of the basal lamina, proliferation and migration of ECs, and stimulates sprouting of new blood vessels^[41]. By contrast, Ang2 promotes ECs death and vessel regression if the activity of endogenous VEGF is inhibited^[41]. It was reported that Ang1 induced phosphorylation of Tie2 and the p85 subunit of PI 3'-kinase and increased PI 3'-kinase activity in a dose-dependent manner, suggesting that the Tie2 receptor, PI 3'-kinase, and Akt are crucial elements in signal transduction pathway leading to EC survival induced by the paracrine activity of Ang1^[42] (Figure 2). Alternatively, Ang1 prevents EC apoptosis via Akt/survivin pathway by activating a critical survival messenger, Akt, and by up-regulating a broad spectrum apoptosis inhibitor, survivin^[43, 44] (Figure 2), but has no effect on the expression of bcl-2 and XIAP^[44]. Moreover, Ang1-induced migratory effect might be mediated through PI 3'-kinase activity dependent tyrosine phosphorylation of p125^{FAK}, which plays a key role in regulating dynamic changes in actin cytoskeleton organization during EC migration^[45]. Increased plasmin and MMP-2 secretion, and suppressed TIMP-2 secretion by Ang1 from ECs are also important determinants for inducing ECs sprouting^[45] (Figure 2). In contrast, the PI 3'-kinase inhibitors have been found to inhibit Ang1-stimulated tyrosine phosphorylation of p125^{FAK}, and secretion of MMP-2 and plasmin from ECs and migration^[45]. Ang2 blocks Ang1-mediated Tie2 autophosphorylation in ECs and acts as a check point on Ang1/Tie2-mediated angiogenesis to prevent excessive branching and sprouting of blood vessels by promoting destabilization of blood vessels.

Transforming growth factor- β

Transforming growth factor- β s (TGF- β s) are multifunctional polypeptides that regulate cell growth and differentiation, ECM deposition, cellular adhesion properties, angiogenesis and immune functions. TGF- β 1 acts through the TGF- β type I and type II receptors to activate intracellular mediators, such as Smad proteins, the p38 MAPK, and the ERK pathway^[46]. TGF- β 1 mRNA levels by activin receptor-like kinase 5 (ALK5) independent of p38 MAPK activation^[46]. In contrast, TGF- β 1 induction of fibronectin (FN) mRNA requires p38 MAPK activity^[46]. TGF- β 1 induction of PAI-1 and TSP-1 mRNA uses at least ALK5 and possibly the p38 MAPK pathway^[46]. TGF- β secreted by most cultured cells is in biologically inactive form, and cannot bind TGF- β receptors; the latent TGF- β is activated by proteases such as plasmin and cathepsin D, low pH, chaotropic agents such as urea, and heat^[47, 48]. Several studies suggested that VEGF increases plasminogen activator (PA) activity in vascular ECs^[11] and that plasmin is able to activate latent TGF- β ₁^[49, 50] which decreases Flk-1 expression and thereby negatively regulates the VEGF/Flk-1 signal transduction pathway in EC^[51], raise the possibility that a complex self-regulating mechanism of VEGF signal transduction may exist during angiogenesis^[50]. However, immunohistochemical study has shown that TGF- β 1 might be associated with tumor progression by indirectly stimulating angiogenesis through the up-regulation of VEGF expression in gastric carcinoma^[52]. In addition, TGF- β ₁ inhibits the

generation of the anti-angiogenic molecule angiostatin by human pancreatic cancer cells in a time- and dose-dependent manner, and this effect is mediated through modulation of the plasminogen/plasmin system^[53].

TGF- β not only inhibits the activity and expression of cyclins and CDKs but also induces the cyclin-dependent kinase inhibitors (CDKIs) p15, p27 and p16, which bind to the cyclin/CDKs, preventing phosphorylation of pRB and thereby arresting most epithelial cells (including ECs) at late G1 phase^[54] (Figure 2). The effects of TGF- β ₁ on endothelial tube formation may be mediated through a net antiproteolytic activity by modulating uPA and PAI levels^[55]. Ellenrieder *et al.* reported that TGF- β treatment of PANC-1 and IMIM-PC1 cells resulted in strong up-regulation of expression and activity of both matrix metalloproteinase-2 (MMP-2) and the uPA system, and treatment with MMP inhibitors or inhibitors of the uPA system caused significant reduction of TGF- β -induced invasiveness in both cell lines suggesting that TGF- β acts in an autocrine manner to induce tumor cell invasion, which is mediated by MMP-2 and the uPA system^[56] (Figure 2). Furthermore, TGF- β indirectly stimulates angiogenesis by the recruitment of inflammatory mediators that secrete angiogenic factors. Thus, TGF- β regulates vascular remodeling through its pleiotropic effects on different cell types.

Interleukin-8 and matrix metalloproteinase-2

Up-regulation of MMP activity, favoring proteolytic degradation of the basement membrane and ECM, has been linked to tumor growth and metastasis, as well as tumor-associated angiogenesis. IL-8 mRNA is up-regulated in neoplastic tissues, such as non-small cell lung cancer^[57] and that its expression correlates with the extent of neovascularization, tumor progression and survival. And also, MMP-2 mRNA level is increased in tumor cells transfected with IL-8, but VEGF and bFGF mRNA levels are unchanged^[58, 59] suggesting that IL-8-induced MMP-2 production is a major mechanism by which tumor cells induce angiogenesis. IL-8 can also be up-regulated by hypoxia, suggesting that the environment plays a major role in regulating IL-8 expression and metastasis^[58]. MMPs induce tumor angiogenesis by degrading ECM and thereby release angiogenic mitogens that have been shown to be stored within the matrix. In addition, MMP-2 and MMP-3 are able to release soluble FGF receptor 1 (FGFR1)^[60] and soluble 12-kDa immunoreactive and mitogenic heparin-binding epidermal growth factor (HB-EGF)^[61], respectively. MMP-2 has been shown to directly modulate melanoma cell adhesion, spreading on ECM and invasion^[62], and an inhibitor of MMP-2 significantly inhibits growth and neovascularization of tumors implanted into chick chorioallantoic membrane (CAM) by preventing MMP-2 binding to α v β ₃ and blocking cell surface collagenolytic activity^[63]. Furthermore, MMP-9, as well as MMP-2 proteolytically cleave and activate latent TGF- β , and promote tumor invasion and angiogenesis^[64].

Oncogene and tumor suppressor genes

Oncogenes are found to be activated and tumor suppressor genes are found to be inactivated in tumor, and hence promote tumor growth and angiogenesis through different mechanisms (Figure 1). It has been shown that VEGF is introduced by K- or H-ras mutant gene, v-src and v-raf in transformed fibroblast and ECs. Other angiogenic factors such as VEGF, TNF- α , TGF- β have been shown to be up-regulated by mutant ras^[65]. These effect may be mediated through a ras-raf-MAP kinase signal transduction pathway (Figure 1), which results in activation of promoter regions of genes of angiogenic growth factors^[66]. Moreover, expression of ras, either constitutive or transient, potentiated the induction of VEGF by hypoxia^[67].

p53 is an important suppressor gene, which inhibits the angiogenic process by inducing thrombospondin-1, down-regulating VEGF and NOS and, in addition, down-regulating hypoxia-induced angiogenesis, either inducing apoptosis or enhancing anti-angiogenic factors^[68]. A transient transfection of mutated p53 results in up-regulation of VEGF mRNA in NIH3T3 cells^[69]. In contrast, adenovirus-mediated wild-type p53 overexpression down-regulates CD40-induced VEGF expression and transmigration in human multiple myeloma cells expressing mutant p53^[70]. And, we have previously demonstrated that the expression of Flt-1 receptor is significantly correlated with p53 mutation gene, not obviously with ras mutation gene in pancreatic carcinoma cells, which suggest that wild type p53, after mutation, might lose the suppressive function to the expression of Flt-1 receptor, thus results in neovascularization of pancreatic neoplasm and promotes the growth of tumor cells, whereas ras mutation may take part in neovascularization through other approaches. Recombinant wild type p53 represses bFGF mRNA translation in rabbit reticulocyte lysate, in a dose- dependent manner via blocking translation initiation by preventing 80S ribosome formation on an mRNA bearing the bFGF mRNA leader sequence^[71]. Moreover, adenoviral vector-mediated wild type p53 transduction results in tumor regression, at least in part, via anti-angiogenesis mediated by the down-modulation of FGF binding protein, a secreted protein required for the activation of angiogenic factor bFGF^[72]. In addition, wild type p53 gene transfer significantly reduces cell invasiveness *in vitro* via a decrease in the secreted levels of MMP-2 in mutated p53 human melanoma cell lines^[73]. Biologically, p53 acts at a G1/S check point, postponing DNA replication after certain cell stress, such as DNA damage^[74], and also induces the apoptotic pathway of cell death^[75].

THE ANGIOGENIC INHIBITORS

Mechanism of angiogenesis inhibitors

Leading anti-angiogenic targets that have been identified are^[76, 77]: (1) inhibition of the growth factors that promote endothelial proliferation; (2) inhibition of the proteases required for ECs to penetrate basement membrane and form new blood vessels; (3) disruption of specific intracellular signal transduction pathway; (4) induction of EC apoptosis or inhibition of EC survival; (5) inhibition of endothelial bone marrow precursor cells; and (6) inhibition of $\alpha v \beta_3$ -integrin-vitronectin interaction that is pivotal in mediating ECs adhesion to ECM during neovascularization^[77].

Inhibitors of angiogenic growth-factors and their receptors

One broad class of angiogenesis inhibitors is made up of drugs that target growth factors such as bFGF and VEGF. The factors tend to bind to heparin, a property that may trap them within the ECM and may thereby govern their bioavailability. Hence, the early generation of drugs is heparin-like (e.g. Pentosan polysulfate), especially with regard to carrying multiple negative charges that promote growth factor binding. However, receptor targeting agents can impede tumor growth and metastasis by interfering, at specific growth-factor receptors, such as those for FGFs and VEGF, with the transduction of angiogenic stimuli into intracellular responses. In these pathways, the receptors are transmembrane tyrosine kinases, in which ligand binding to an extracellular domain induces autophosphorylation of an intracellular kinase domain. Each kinase then functions as an activator of downstream signals. To disrupt such a sequence, a drug may compete for receptor binding and prevent tyrosine kinase autophosphorylation. Inhibitors of VEGF family include: (1) anti-VEGF mAb^[78]: directly neutralizes VEGF proteins, and inhibits biological

activities of VEGF; (2) soluble VEGF receptors: specifically bind to VEGF, indirectly block the function of VEGF with receptors; (3) inhibitors of VEGF receptors^[79]: bind to VEGF receptors and block their functions with VEGF; (4) inhibitors of VEGF signal transduction: interfere a series of signal transduction pathways by blocking autophosphorylation of VEGF receptors; (5) VEGF antisense^[80]: is a specific nucleotide sequence, which binds to VEGF mRNA and thereby interferes VEGF mRNA translation and VEGF protein formation. A recent study has shown that the VEGFR2 DNzyme can cleave its substrate efficiently in a concentration- and time-dependent manner, inhibit the proliferation of EC with a concomitant reduction of VEGFR2 mRNA, and inhibit tumor growth *in vivo*^[81].

Endogenous angiogenesis inhibitors

More than 40 endogenous angiogenesis inhibitors have been characterized, and they are divided into 4 major groups: interferons (IFNs), proteolytic fragments, interleukins (ILs), and tissue inhibitors of metalloproteinases (TIMPs)^[82].

Interferons The interferons (INF- α , - β , and - γ) are members of a family of secreted glycoproteins, which have direct or indirect inhibitory effect on tumor angiogenesis and growth. IFN- α/β have been reported to down-regulate the expression of pro-angiogenic factor MMP-9 mRNA and protein in different cancers^[83-86]. Also, IFN- α/β down-regulate IL-8 expression in bladder cancer^[83-84]. Several studies demonstrated that the administration of optimal biological dose of IFN- α/β decreased the expression of bFGF mRNA and protein and microvessel density in the tumors and, in addition, induced EC apoptosis^[83-85, 87]. Sasamura *et al.* demonstrated that IFN- γ had mild inhibitory effects on VEGF mRNA and bFGF mRNA expression, whereas IFN- α did not significantly decrease the level of either VEGF mRNA or bFGF mRNA in renal cell carcinoma^[88]. However, some studies demonstrated that IFN- α/β treatment did not cause the reduction of bFGF and VEGF levels in serum from patients with carcinoid tumours^[89] and leukemia^[86]. Thus, anti-angiogenic effect of IFNs treatment might be mediated by the regulation of different angiogenic factors in different tumors in dose- and time-dependent manner. Moreover, IFN- γ is presumed to induce its anti-angiogenic effects through the secretion of IFN- γ inducible protein 10 (IP-10) and monokine induced by IFN- γ ^[90]. Finally, IFNs have antitumor properties, which may be mediated through a direct cytotoxic effect on tumor cells, augmentation of immunogenicity of tumor by up-regulation of major histocompatibility (MHC) classes *I and II* and tumor associated antigens, and/or activation of macrophages, T lymphocytes and natural killer cells^[89].

Interleukins It was reported that interleukins (ILs) having a Glu-Leu-Arg (ELR) motif at the NH₂ terminus, such as IL-8, enhance angiogenesis, and those that lack this sequence, such as IL-4, inhibit it^[91]. IL-4 inhibits *in vivo* neovascularization induced by bFGF in the rat cornea and blocks the migration of microvascular ECs toward bFGF *in vitro*^[92]. However, it has been shown that IL-1 α , a representative cytokine of activated macrophages, induces angiogenesis through the enhanced expression of various angiogenic factors such as VEGF, IL-8, and bFGF^[93]. And also, IL-6 was found to counteract the apoptotic effect mediated by wild type p53^[75]. Several studies have reported that IL-12 suppresses the expression of VEGF mRNA^[94, 95], bFGF^[94] and MMP-9 mRNA^[94]. Additionally, IL-12 was found to stimulate mRNA expression of IFN- γ and its inducible anti-angiogenic chemokine IFN- γ inducible protein (IP-10) in ECs cultured with IL-12^[95]. IL-12 significantly promotes apoptosis and inhibits proliferation rate of human tumors and extensive necrosis in the murine, and thereby reducing tumor vessel density^[95]. Furthermore, the *in vivo* inhibition of neovascularization in IL-10-secreting tumors

might be mediated by the ability of IL-10 to down-regulate the synthesis of VEGF, IL-1 β , TNF- α , IL-6, and MMP-9 in tumor-associated macrophages^[96]. And also, IL-10 inhibits tumor metastasis through a natural killer (NK) cell-dependent mechanism^[96].

Tissue inhibitors of metalloproteinases Remodeled ECM components comprise a scaffold upon which ECs can adhere, migrate, and form tubes, and deposition of these components forms the basal lamina that ensheathes endothelial and mural cells. *In vitro* migration of ECs through gelatin is significantly inhibited by overexpressed TIMP-1^[97]. Murphy *et al.* reported that TIMP-2, but not TIMP-1, inhibited bFGF-induced EC proliferation^[98]. TIMP-2 is able to inhibit soluble FGFR1 released by MMP-2^[60]. Transfection of the highly metastatic B6F10 murine melanoma cell line with TIMP-2 cDNA showed the reduced levels of blood vessel formation and diminished induction of EC migration and invasion^[99]. Studies have shown that the overexpression of TIMP-3 induces the apoptotic cell death of a number of cancer cell lines and rat vascular smooth muscle cells through the stabilization of TNF-alpha receptors on the cell surface, perhaps by inhibiting a receptor shedding metalloproteinase^[100, 101]. Furthermore, anti-angiogenic and antitumor effects of TIMP-3 appear to be mediated, in part, by decreased expression of vascular endothelial (VE)-cadherin by ECs in the presence of TIMP-3 in an *in vitro* assay and in TIMP-3-overexpressing tumors^[102]. Finally, TIMP-1, TIMP-2, TIMP-3 and TIMP-4 inhibit neovascularization by inhibiting MMP-1, MMP-2, and MMP-9 induced breakdown of surrounding matrix^[103]. Thus, the multiple effects of TIMPs on both endothelial and tumor cells migration render MMPs attractive targets for tumor therapy.

Proteolytic fragments Most of these fragments are derived from ECM components, such as collagen or fibronectin, or from enzymes such as plasminogen and MMP-2 that remodel ECM. Perhaps the most characterized inhibitors in this class are angiostatin and endostatin.

Angiostatin The anti-angiogenic effect of angiostatin, a 38-kDa internal fragment of plasminogen, may be mediated, at least in part, by their ability to down-regulate VEGF expression within the tumor^[104]. Angiostatin inhibits hepatocyte growth factor (HGF)-induced phosphorylation of c-met, Akt, and ERK1/2, and thereby exerts its anti-angiogenic effect via disruption of HGF/c-met signaling^[105]. Intraperitoneal administration of angiostatin potentially inhibits the neovascularization and metastasis formation in mice observed after a primary tumor has been removed^[106]. It has been shown that binding of angiostatin to the α/β -subunits of plasma membrane-localized ATP synthase may suppress endothelial-surface ATP metabolism and thereby mediates its anti-angiogenic effects and the down-regulation of EC proliferation and migration^[107, 108] (Figure 3). Further, adenoviral mediated angiostatin gene transfer selectively inhibits EC proliferation and disrupts the G₂/M transition induced by M-phase-promoting factors, and that ECs show a significant mitosis arrest that is correlated with the down-regulation of the M-phase phosphoproteins^[109]. Other studies have shown that angiostatin treatment significantly increases the apoptosis of EC and tumor cells, and decreases density of tumor blood vessels^[109-111]. Angiostatin was found to produce a transient increase in ceramide that correlates with actin stress fiber reorganization, detachment and death^[112] and, in addition, treatment with angiostatin or ceramide resulted in the activation of RhoA, an important effector of cytoskeletal structure^[112] (Figure 3). Angiostatin can selectively regulate the expression of E-selectin and thereby inhibits the proliferation of ECs.

Endostatin It is a 20-kDa fragment of type XVIII collagen that has been identified as a factor produced by hemangioendothelioma cells that inhibits ECs proliferation,

angiogenesis and tumor growth. The mechanisms by which endostatin inhibits VEGF-induced proliferation and migration of ECs are (Figure 3): First, endostatin blocks the VEGF-induced tyrosine phosphorylation of KDR/Flk-1 in ECs^[113]. Second, endostatin suppresses the VEGF-induced activation of ERK, p38 MAPK, and p125^{FAK}, which are downstream events of the KDR/Flk-1 signaling and are involved in the mitogenic and motogenic activities of VEGF in ECs^[113]. Third, endostatin inhibits the binding of VEGF to ECs and to its cell surface receptor, KDR/Flk-1^[113]. Finally, endostatin directly binds to KDR/Flk-1 but not to VEGF^[113]. Endostatin was found to exhibit its anti-migratory effect by reducing VEGF-induced phosphorylation of endothelial NOS (eNOS)^[114] (Figure 3). Rehn *et al.* demonstrated that soluble endostatin was capable of binding to α_v - and α_5 -integrins, thereby inhibiting the integrin functions, such as EC migration^[115] (Figure 3). In addition, endostatin may exert its antiproliferative and anti-angiogenic effects by competing with bFGF for binding to cell surface heparan sulphate proteoglycans, which could disrupt the mitogenic growth factor signaling^[116]. Endostatin induces a significant decrease in EC proliferation in the basal state and after stimulation by neuropeptide Y and bombesin^[117]. Endostatin potentially inhibits both the extracellular activation of proMMP-2 by inhibition of membrane-type 1 MMP (MT1-MMP) and the catalytic activity of MMP-2 and thereby can block the invasiveness of ECs and tumor cells^[118]. The proapoptotic activity of endostatin appears to be mediated via tyrosine kinase signaling^[119] and reduction of antiapoptotic proteins bcl-2 and bcl-XL without affecting the level of the proapoptotic Bax protein^[120] (Figure 3). Furthermore, the Shb adaptor protein has been suggested to be involved in the mediation of the apoptotic signaling of endostatin^[119] (Figure 3).

Somatostatin and its analogs

Somatostatin (SS) and its analogs inhibit the proliferation of somatostatin receptors (SSTRs) positive endocrine neoplasm. The antiproliferative action of SS is signaled via five specific G-protein coupled receptors (SSTR1-SSTR5), which initiate pertussis toxin sensitive-G protein dependent, and tyrosine phosphatase mediated cell growth arrest or apoptosis according to receptor subtypes and target cells. It has been shown that activation of SSTR1, 2, 4, and 5 induce G1 cell cycle arrest through the ability of SS to maintain high levels of CDKIs p27^(Kip1) and p21, and inactivate cyclin E-CDK2 complexes, thus leading to hypophosphorylation of pRb^[121, 122] (Figure 3). Moreover, somatostatin-mediated growth inhibition of normal and cancer pancreatic acinar cells is triggered via an inhibition of PI3-kinase signaling pathway^[123]. SS may directly stimulate tumor apoptosis via sstr3-dependent G protein signaling, causing the induction of suppressor gene p53 and proapoptotic protein Bax^[124] (Figure 3). Our recent investigation reported that the low expression or loss of SSTR2 gene was more negatively correlated with the over-expression of p53 and ras mutation genes, which might take part in the angiogenesis of pancreatic neoplasm, whereas there was no significant relationship between SSTR2 and DPC4 (deleted in pancreatic cancer, locus 4), which suggested that there was different regulatory pathway in neovascularization of pancreatic neoplasm. Albini *et al.* provided evidence that SS inhibits Kaposi sarcoma associated angiogenesis by inhibiting both EC proliferation and invasion, and also by inhibiting migration of monocytes, which are important mediators of the angiogenic cascade, and are able to produce survival factors that, in turn, activate ECs^[125]. In addition, SS induces a significant decrease in basal and stimulates EC proliferation in HUVEC, and also decreases number of capillaries^[117]. CAM model study showed that unlabeled SS analogs inhibited angiogenesis, which was

proportional to the ability of the analogs to inhibit growth hormone (GH) production^[126].

It is defined that SSTR subtypes are responsible for the specific post-receptor signal transduction mechanisms involved in octreotide's inhibition of angiogenesis^[126]. The intracellular signal transduction mechanisms involved in this angiogenic inhibition include the G^α_i-binding protein, cAMP, and calcium^[127]. Further, SS and its analogs induce their biologic effects by interacting with specific receptors that are coupled to a variety of signal transduction pathways involving adenylate cyclase, guanylate cyclase, ionic conductance channels, phospholipase C-β, phospholipase A₂, and tyrosine phosphatase and protein dephosphorylation and thereby regulate cell growth^[128, 129]. The best characterized pathway involves the inhibition of adenylate cyclase, leading to a reduction in intracellular cAMP levels. Antiproliferative effects that are mediated through SSTR1 and SSTR2, involve the stimulation of tyrosin phosphatases, however SSTR5 appears to be coupled to inositol phospholipid/calcium pathway^[130]. Mentlein *et al.* reported that cultivated cells from solid human gliomas of different stages and glioma cell lines secreted variable amounts of VEGF, which was reduced between 25 and 80 % of control levels depending on the glioma by co-incubation with SS or

SSTR2-selective agonists (octreotide and L-054 522) in dose-dependent manner^[131]. Growth factor-induced (EGF, bFGF) VEGF synthesis could also be suppressed to <50 % by co-incubation with SS or SSTR2-selective agonists, which was less pronounced in hypoxia-induced VEGF synthesis^[131]. And also, SS and octreotide diminished the proliferative activity of cultured murine ECs HECa10 *vs.* controls; however, SS and octreotide did not change the release of VEGF into supernatants of 24-h or 72-h EC cultures^[132]. A recent study has demonstrated that SS 14 can reduce bFGF-induced corneal angiogenesis^[133].

In summary, the mechanisms of action of tumor growth inhibition by SS and its analogs are^[134]: (1) inhibition of the secretion of hormones, such as GH, insulin and/or gastrointestinal hormones; (2) direct or indirect (via GH) inhibition of IGF-1 and/or other growth factors that exert a stimulatory effect on tumor growth. On the other hand, SS analogs can selectively stimulate the formation of IGF-binding protein 1, and thereby interfering with IGF-1 action at the receptor level; (3) inhibition of angiogenesis through different mechanisms; (4) direct antimitotic effects of growth factors, which act on tyrosine kinase receptors such as EGF and FGF, via SSTRs on the tumor cells; (5) modulation of immunological activity.

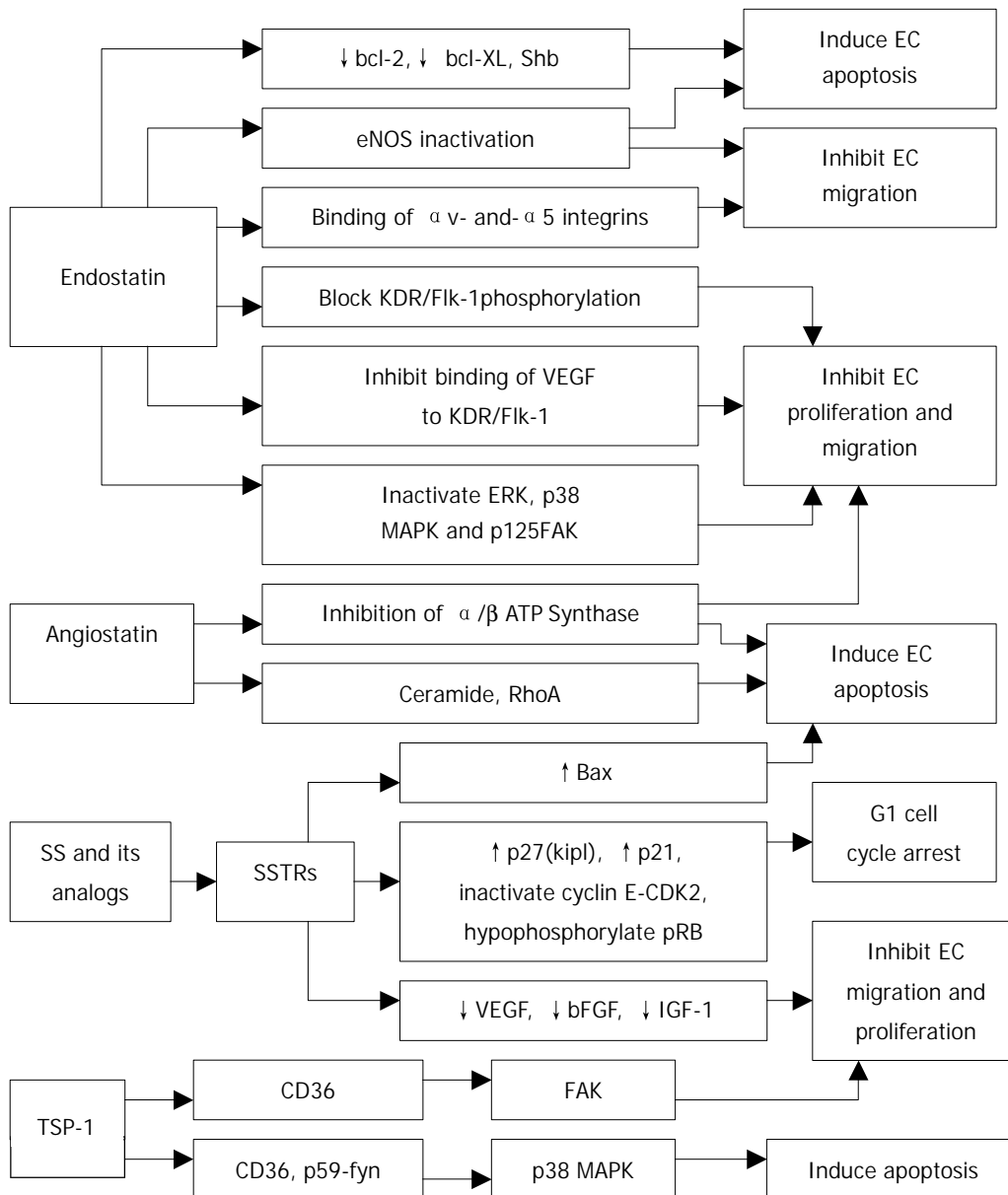


Figure 3 Proposed effector pathways of angiogenic inhibitors.

Thrombospondin-1

Thrombospondin-1 (TSP-1) is a naturally occurring inhibitor of angiogenesis that limits vessel density in normal tissues and curtails tumor growth. TSP-1 exerts its anti-angiogenic activity via binding to the CD36 receptor by triggering an apoptotic signaling pathway^[135]. Binding of TSP-1 to CD36 receptor leads to the recruitment of the Src-related kinase, p59-fyn, and to activation of p38 MAPK. The activation of the p38 MAPK has been shown to be p59-fyn-dependent and to require a caspase-3-like proteolytic activity^[135]. Furthermore, activated p38 MAPK leads to the activation of caspase-3 and to apoptosis^[135] (Figure 3). Interestingly, the apoptotic effect of TSP-1 is restricted to ECs activated to take part in the angiogenic process and not in quiescent vessels^[135]. TSP-1 acts through CD36 to modulate the activity of focal adhesion kinase (FAK) and thus inhibits EC migration and proliferation^[136] (Figure 3). TSP-1 can effectively inhibit chemotaxis *in vitro* and neovascularization *in vivo*, induced by several angiogenic stimuli. These include protein that acts via tyrosine kinase receptors (VEGF, bFGF, aFGF, PDGF), via G proteins (IL-8), via serine/threonine kinase receptors (TGF- β), and also lipids (PGE-1)^[137, 138].

SUMMARY AND CONCLUSION

Developmental status and evaluation of anti-angiogenic therapy in human clinical trials

Angiogenesis is a complex process that depends on the coordination of many different activities in several cell types. The angiogenic response in the microvasculature is associated with changes in cellular adhesive interactions between adjacent ECs, pericytes, fibroblasts, and immune mediators express many different cytokines and growth factors that react with other cells or ECM components to affect ECs migration, proliferation, tube formation, and vessel stabilization. As one or more of the positive regulators of angiogenesis are up-regulated, and simultaneously, certain negative regulators of angiogenesis are down-regulated, tumors become angiogenic. Interestingly, different angiogenic regulators, sometimes, function through the same mechanism and a single angiogenic regulator, sometimes, functions through different mechanisms. Hence, the anti-angiogenic therapy can be realized through the regulation of 'angiogenic switch' by interfering with different mechanisms.

Anti-angiogenic agents, if administered before a tumor develops or becomes vascular supply dependent, would therefore theoretically act similarly to a vaccine in preventing tumor development, not just tumor growth. However, it is notable that anti-angiogenic therapy represents a treatment, not a cure, for cancer. A cure for cancer can be realized only by targeting the agents and mechanisms that cause normal cells to become tumorigenic. The anti-angiogenic therapy of cancer, nonetheless, represents a highly effective strategy for destroying tumors because fundamental requirement of tumor growth is dependent on a blood supply. Unlike standard chemotherapy that targets tumor cells and other proliferating cells, angiogenesis inhibitors target dividing ECs that have been recruited into the tumor bed. For example, certain tubulin-binding agents such as combretastin A-4, exhibit a selective toxicity for proliferating ECs *in vitro* and causing a vascular collapse in tumor models *in vivo* via apoptosis and the subsequent death of much larger numbers of tumor cells^[139]. Thus, specific anti-angiogenic therapy has little or no toxicities such as gastrointestinal symptoms and myelosuppression that are characteristic of standard chemotherapeutic regimens, does not require that the therapeutic agent enter any tumor cells nor cross the blood brain barrier, controls tumor growth independently of growth fraction or tumor cell heterogeneity or even tumor cell type, and does not induce acquired drug resistance^[140]. Further, since normal vasculature in the adult is

quiescent, the appropriate use of selective angiogenic inhibitors may be expected to confer a degree of specificity that is not obtainable with the nonspecific modalities of chemotherapy and radiation therapy and to allow for relatively nontoxic, long-term treatment of tumors.

Because anti-angiogenic agents are expected to be cytostatic rather than cytotoxic, they may be particularly effective in combination with cytotoxic agents, even used in advanced cases of pancreatic, colon, and hormone-refractory prostate cancer, thereby targeting not only DNA synthesis and cell division but also the biologic behavior of tumor cells. The following guidelines are suggested to improve the therapeutic efficacy of endogenous angiogenesis inhibitors in clinical trials: (1) after surgery or radiotherapy to prevent recurrence of distant metastases; (2) combinatorial therapies, for example, in combination with conventional chemotherapy, radiotherapy and vaccine therapy or immunotherapy, and also, in combination with several angiogenesis inhibitors rather than a single inhibitor; (3) targeting therapy. Angiogenesis inhibitors may be specifically targeted to the disease locus at high concentrations rather than be widely distributed in the entire body; (4) gene therapy, several advantages including prolonged therapy, low doses of DNA molecules, and less frequent injections may be achieved by anti-angiogenic gene therapy with endogenous angiogenesis inhibitors; (5) more potent angiogenesis inhibitors should be discovered; (6) prolonged half-lives. Slow-release of angiogenesis inhibitors in the body reaches a steady-state level in the circulation.

Remarkably diverse groups of anti-angiogenic drugs are currently undergoing evaluation in phase I, II or III clinical trials. However, there are still some difficulties associated with the clinical evaluation of these drugs efficacy. In the experimental animal model, tumors can be removed and examined for therapeutic efficacy such as changes in the extent of vascularization, vascular structure, EC viability or apoptosis, as well as for markers of angiogenic activity, e.g. VEGF expression. But in the clinical situation, taking serial biopsies of metastatic tumors may not be a particularly practical or desirable approach. For this, reliable surrogate markers of tumor angiogenesis in serum or urine, and non-invasive strategy may be necessary. Several studies have successfully used various non-invasive medical imaging strategies (e.g. MRI, Doppler ultrasound) to monitor changes in tumor blood flow, vascular structure and permeability^[141-143]. Indeed, there are considerable research efforts underway in this field. In addition, there are obvious concerns about delayed toxicity associated with long-term anti-angiogenic therapy, and physiological angiogenesis affected by anti-angiogenic drugs such as wound healing in a cancer patient, reproductive angiogenesis (e.g. corpus luteum development in adult females, development of the vasculature in developing embryos), in neonates and children. In this concern, a potentially significant development in the near future could be the use of genomics based technologies to uncover a large number of highly (or even totally) specific molecular markers for the activated ECs of newly formed blood vessels.

In the near future, the outcome of ongoing clinical trials will give us more insights into the potential of anti-angiogenic approaches to treat cancer.

REFERENCES

- 1 **Bussolino F**, Mantovani A, Persico G. Molecular mechanisms of blood vessel formation. *Trends Biochem Sci* 1997; **22**: 251-256
- 2 **Sebti SM**, Hamilton AD. Design of growth factor antagonists with antiangiogenic and antitumor properties. *Oncogene* 2000; **19**: 6566-6573
- 3 **Dameron KM**, Volpert OV, Tainsky MA, Bouck N. Control of angiogenesis in fibroblasts by p53 regulation of thrombospondin-1. *Science* 1994; **265**: 1582-1584

- 4 **Kohn S**, Nagy JA, Dvorak HF, Dvorak AM. Pathways of macromolecular tracer transport across venules and small veins. Structural basis for the hyperpermeability of tumor blood vessels. *Lab Invest* 1992; **67**: 596-607
- 5 **Esser S**, Lampugnani MG, Corada M, Dejana E, Risau W. Vascular endothelial growth factor induces VE-cadherin tyrosine phosphorylation in endothelial cells. *J Cell Sci* 1998; **111**: 1853-1865
- 6 **Kevil CG**, Payne DK, Mire E, Alexander JS. Vascular permeability factor/vascular endothelial cell growth factor-mediated permeability occurs through disorganization of endothelial junctional proteins. *J Biol Chem* 1998; **273**: 15099-15103
- 7 **Lal BK**, Varma S, Pappas PJ, Hobson RW 2nd, Duran WN. VEGF increases permeability of the endothelial cell monolayer by activation of PKB/akt, endothelial nitric-oxide synthase, and MAP kinase pathways. *Microvasc Res* 2001; **62**: 252-262
- 8 **Ferrara N**. Role of vascular endothelial growth factor in regulation of physiological angiogenesis. *Am J Physiol Cell Physiol* 2001; **280**: C1358-C1366
- 9 **Doanes AM**, Hegland DD, Sethi R, Kovsesi I, Bruder JT, Finkel T. VEGF stimulates MAPK through a pathway that is unique for receptor tyrosine kinases. *Biochem Biophys Res Commun* 1999; **255**: 545-548
- 10 **Mandriota SJ**, Seghezzi G, Vassalli JD, Ferrara N, Wasi S, Mazzei R, Mignatti P, Pepper MS. Vascular endothelial growth factor increases urokinase receptor expression in vascular endothelial cells. *J Biol Chem* 1995; **270**: 9709-9716
- 11 **Pepper MS**, Ferrara N, Orci L, Montesano R. Vascular endothelial growth factor (VEGF) induces plasminogen activators and plasminogen activator inhibitor-1 in microvascular endothelial cells. *Biochem Biophys Res Commun* 1991; **181**: 902-906
- 12 **Unemori EN**, Ferrara N, Bauer EA, Amento EP. Vascular endothelial growth factor induces interstitial collagenase expression in human endothelial cells. *J Cell Physiol* 1992; **153**: 557-562
- 13 **Tang H**, Kerins DM, Hao Q, Inagami T, Vaughan DE. The urokinase-type plasminogen activator receptor mediates tyrosine phosphorylation of focal adhesion proteins and activation of mitogen-activated protein kinase in cultured endothelial cells. *J Biol Chem* 1998; **273**: 18268-18272
- 14 **Senger DR**, Claffey KP, Benes JE, Perruzzi CA, Sergiou AP, Detmar M. Angiogenesis promoted by vascular endothelial growth factor: regulation through alpha1beta1 and alpha2beta1 integrins. *Proc Natl Acad Sci U S A* 1997; **94**: 13612-13617
- 15 **Senger DR**, Ledbetter SR, Claffey KP, Papadopoulos-Sergiou A, Peruzzi CA, Detmar M. Stimulation of endothelial cell migration by vascular permeability factor/vascular endothelial growth factor through cooperative mechanisms involving the alpha5beta3 integrin, osteopontin, and thrombin. *Am J Pathol* 1996; **149**: 293-305
- 16 **Carmeliet P**. Mechanisms of angiogenesis and arteriogenesis. *Nat Med* 2000; **6**: 389-395
- 17 **Watanabe Y**, Lee SW, Detmar M, Ajioka I, Dvorak HF. Vascular permeability factor/vascular endothelial growth factor (VPF/VEGF) delays and induces escape from senescence in human dermal microvascular endothelial cells. *Oncogene* 1997; **14**: 2025-2032
- 18 **Gerber HP**, Dixit V, Ferrara N. Vascular endothelial growth factor induces expression of the antiapoptotic proteins Bcl-2 and A1 in vascular endothelial cells. *J Biol Chem* 1998; **273**: 13313-13316
- 19 **Gerber HP**, McMurtrey A, Kowalski J, Yan M, Keyt BA, Dixit V, Ferrara N. Vascular endothelial growth factor regulates endothelial cell survival through the phosphatidylinositol 3'-kinase/Akt signal transduction pathway. Requirement for Flk-1/KDR activation. *J Biol Chem* 1998; **273**: 30336-30343
- 20 **Wheeler-Jones C**, Abu-Ghazaleh R, Cospedal R, Houliston RA, Martin J, Zachary I. Vascular endothelial growth factor stimulates prostacyclin production and activation of cytosolic phospholipase A2 in endothelial cells via p42/p44 mitogen-activated protein kinase. *FEBS Lett* 1997; **420**: 28-32
- 21 **Berra E**, Milanini J, Richard DE, Le Gall M, Vinals F, Gothie E, Roux D, Pages G, Pouyssegur J. Signaling angiogenesis via p42/p44 MAP kinase and hypoxia. Signaling angiogenesis via p42/p44 MAP kinase and hypoxia. *Biochem Pharmacol* 2000; **60**: 1171-1178
- 22 **Chin L**, Tam A, Pomerantz J, Wong M, Holash J, Bardeesy N, Shen Q, O'Hagan R, Pantginis J, Zhou H, Horner JW 2nd, Cor-don-Cardo C, Yancopoulos GD, DePinho RA. Essential role for oncogenic Ras in tumour maintenance. *Nature* 1999; **400**: 468-472
- 23 **Khwaja A**. Akt is more than just a Bad kinase. *Nature* 1999; **401**: 33-34
- 24 **Fujio Y**, Walsh K. Akt mediates cytoprotection of endothelial cells by vascular endothelial growth factor in an anchorage-dependent manner. *J Biol Chem* 1999; **274**: 16349-16354
- 25 **Morales-Ruiz M**, Fulton D, Sowa G, Languino LR, Fujio Y, Walsh K, Sessa WC. Vascular endothelial growth factor-stimulated actin reorganization and migration of endothelial cells is regulated via the serine/threonine kinase Akt. *Circ Res* 2000; **86**: 892-896
- 26 **Mazure NM**, Chen EY, Laderoute KR, Giaccia AJ. Induction of vascular endothelial growth factor by hypoxia is modulated by a phosphatidylinositol 3-kinase/Akt signaling pathway in Haras-transformed cells through a hypoxia inducible factor-1 transcriptional element. *Blood* 1997; **90**: 3322-3331
- 27 **Dimmeler S**, Zeiher AM. Akt takes center stage in angiogenesis signaling. *Circ Res* 2000; **86**: 4-5
- 28 **Jiang BH**, Zheng JZ, Aoki M, Vogt PK. Phosphatidylinositol 3-kinase signaling mediates angiogenesis and expression of vascular endothelial growth factor in endothelial cells. *Proc Natl Acad Sci U S A* 2000; **97**: 1749-1753
- 29 **Dimmeler S**, Fleming I, Fisslthaler B, Hermann C, Busse R, Zeiher AM. Activation of nitric oxide synthase in endothelial cells by Akt-dependent phosphorylation. *Nature* 1999; **399**: 601-605
- 30 **Fulton D**, Gratton JP, McCabe TJ, Fontana J, Fujio Y, Walsh K, Franke TF, Papapetropoulos A, Sessa WC. Regulation of endothelium-derived nitric oxide production by the protein kinase Akt. *Nature* 1999; **399**: 597-601
- 31 **Gupta K**, Kshirsagar S, Li W, Gui L, Ramakrishnan S, Gupta P, Law PY, Hebbel RP. VEGF prevents apoptosis of human microvascular endothelial cells via opposing effects on MAPK/ERK and SAPK/JNK signaling. *Exp Cell Res* 1999; **247**: 495-504
- 32 **Dimmeler S**, Dernbach E, Zeiher AM. Phosphorylation of the endothelial nitric oxide synthase at ser-1177 is required for VEGF-induced endothelial cell migration. *FEBS Lett* 2000; **477**: 258-262
- 33 **Buchler P**, Reber HA, Buchler M, Shrinkante S, Buchler MW, Friess H, Semenza GL, Hines OJ. Hypoxia-inducible factor 1 regulates vascular endothelial growth factor expression in human pancreatic cancer. *Pancreas* 2003; **26**: 56-64
- 34 **Pardo OE**, Arcaro A, Salerno G, Raguz S, Downward J, Seckl MJ. Fibroblast growth factor-2 induces translational regulation of Bcl-XL and Bcl-2 via a MEK-dependent pathway: correlation with resistance to etoposide-induced apoptosis. *J Biol Chem* 2002; **277**: 12040-12046
- 35 **Yoshiji H**, Kuriyama S, Yoshiji H, Ikenaka Y, Noguchi R, Hicklin DJ, Huber J, Nakatani T, Tsujinoue H, Yanase K, Imazu H, Fukui H. Synergistic effect of basic fibroblast growth factor and vascular endothelial growth factor in murine hepatocellular carcinoma. *Hepatology* 2002; **35**: 834-842
- 36 **Stavri GT**, Zachary IC, Baskerville PA, Martin JF, Erusalimsky JD. Basic fibroblast growth factor upregulates the expression of vascular endothelial growth factor in vascular smooth muscle cells. Synergistic interaction with hypoxia. *Circulation* 1995; **92**: 11-14
- 37 **Mandriota SJ**, Pepper MS. Vascular endothelial growth factor-induced in vitro angiogenesis and plasminogen activator expression are dependent on endogenous basic fibroblast growth factor. *J Cell Sci* 1997; **110**: 2293-2302
- 38 **Sato Y**, Rifkin DB. Autocrine activities of basic fibroblast growth factor: regulation of endothelial cell movement, plasminogen activator synthesis, and DNA synthesis. *J Cell Biol* 1988; **107**: 1199-1205
- 39 **Ausprunk DH**, Folkman J. Migration and proliferation of endothelial cells in preformed and newly formed blood vessels during tumor angiogenesis. *Microvasc Res* 1977; **14**: 53-65
- 40 **Miao HQ**, Ornitz DM, Aingorn E, Ben-Sasson SA, Vlodavsky I. Modulation of fibroblast growth factor-2 receptor binding, dimerization, signaling, and angiogenic activity by a synthetic heparin-mimicking polyanionic compound. *J Clin Invest* 1997; **99**: 1565-1575
- 41 **Lobov IB**, Brooks PC, Lang RA. Angiopoietin-2 displays VEGF-dependent modulation of capillary structure and endothelial cell survival *in vivo*. *Proc Natl Acad Sci U S A* 2002; **99**: 11205-11210

- 42 **Kim I**, Kim HG, So JN, Kim JH, Kwak HJ, Koh GY. Angiopoietin-1 Regulates Endothelial Cell Survival Through the Phosphatidylinositol 3'-Kinase/Akt Signal Transduction Pathway. *Circulation Research* 2000; **86**: 24-29
- 43 **Papapetropoulos A**, Fulton D, Mahboubi K, Kalb RG, O'Connor DS, Li F, Altieri DC, Sessa WC. Angiopoietin-1 inhibits endothelial cell apoptosis via the Akt/survivin pathway. *J Biol Chem* 2000; **275**: 9102-9105
- 44 **Harfouche R**, Hassessian HM, Guo Y, Faivre V, Srikant CB, Yancopoulos GD, Hussain SN. Mechanisms which mediate the antiapoptotic effects of angiopoietin-1 on endothelial cells. *Microvasc Res* 2002; **64**: 135-147
- 45 **Kim I**, Kim HG, Moon SO, Chae SW, So JN, Koh KN, Ahn BC, Koh GY. Angiopoietin-1 induces endothelial cell sprouting through the activation of focal adhesion kinase and plasmin secretion. *Cir Res* 2000; **86**: 952-959
- 46 **Laping NJ**, Grygielko E, Mathur A, Butter S, Bomberger J, Tweed C, Martin W, Fornwald J, Lehr R, Harling J, Gaster L, Callahan JF, Olson BA. Inhibition of transforming growth factor (TGF)-beta1-induced extracellular matrix with a novel inhibitor of the TGF-beta type I receptor kinase activity: SB-431542. *Mol Pharmacol* 2002; **62**: 58-64
- 47 **Lawrence DA**, Pircher R, Jullien P. Conversion of a high molecular weight latent beta-TGF from chicken embryo fibroblasts into a low molecular weight active beta-TGF under acidic conditions. *Biochem Biophys Res Commu* 1985; **133**: 1026-1034
- 48 **Lyons RM**, Keski-Oja J, Moses HL. Proteolytic activation of latent transforming growth factor-beta from fibroblast-conditioned medium. *J Cell Biol* 1988; **106**: 1659-1665
- 49 **Lyons RM**, Gentry LE, Purchio AF, Moses HL. Mechanism of activation of latent recombinant transforming growth factor beta 1 by plasmin. *J Cell Biol* 1990; **110**: 1361-1367
- 50 **Sato Y**, Tsuboi R, Lyons RM, Moses HL, Rifkin DB. Characterization of the activation of latent TGF-beta by co-cultures of endothelial cells and pericytes or smooth muscle cells: a self-regulating system. *J Cell Bio* 1990; **111**: 757-763
- 51 **Mandriota SJ**, Menoud PA, Pepper MS. Transforming growth factor beta 1 down-regulates vascular endothelial growth factor receptor 2/flk-1 expression in vascular endothelial cells. *J Biol Chem* 1996; **271**: 11500-11505
- 52 **Saito H**, Tsujitani S, Oka S, Kondo A, Ikeguchi M, Maeta M, Kaibara N. The expression of transforming growth factor-beta1 is significantly correlated with the expression of vascular endothelial growth factor and poor prognosis of patients with advanced gastric carcinoma. *Cancer* 1999; **86**: 1455-1462
- 53 **O'Mahony CA**, Albo D, Tuszynski GP, Berger DH. Transforming growth factor-beta 1 inhibits generation of angiostatin by human pancreatic cancer cells. *Surgery* 1998; **124**: 388-393
- 54 **Sherr CJ**. Cancer cell cycle. *Science* 1996; **14**: 309-318
- 55 **Pepper MS**, Belin D, Montesano R, Orci L, Vassalli JD. Transforming growth factor-beta 1 modulates basic fibroblast growth factor-induced proteolytic and angiogenic properties of endothelial cells *in vitro*. *J Cell Biol* 1990; **111**: 743-755
- 56 **Ellenrieder V**, Hendlar SF, Ruhland C, Boeck W, Adler G, Gress TM. TGF-beta-induced invasiveness of pancreatic cancer cells is mediated by matrix metalloproteinase-2 and the urokinase plasminogen activator system. *Int J Cancer* 2001; **93**: 204-211
- 57 **Yuan A**, Yang PC, Yu CJ, Chen WJ, Lin FY, Kuo SH, Luh KT. Interleukin-8 messenger ribonucleic acid expression correlates with tumor progression, tumor angiogenesis, patient survival, and timing of relapse in non-small-cell lung cancer. *Am J Respir Crit Care Med* 2000; **162**: 1957-1963
- 58 **Bar-Eli M**. Role of interleukin-8 in tumor growth and metastasis of human melanoma. *Pathobiology* 1999; **67**: 12-18
- 59 **Kitadai Y**, Takahashi Y, Haruma K, Naka K, Sumii K, Yokozaki H, Yasui W, Mukaida N, Ohmoto Y, Kajiyama G, Fidler IJ, Tahara E. Transfection of interleukin-8 increases angiogenesis and tumorigenesis of human gastric carcinoma cells in nude mice. *Br J Cancer* 1999; **81**: 647-653
- 60 **Levi E**, Fridman R, Miao HQ, Ma YS, Yayon A, Vlodavsky I. Matrix metalloproteinase 2 releases active soluble ectodomain of fibroblast growth factor receptor 1. *Proc Natl Acad Sci U S A* 1996; **93**: 7069-7074
- 61 **Suzuki M**, Raab G, Moses MA, Fernandez CA, Klagsbrun M. Matrix metalloproteinase-3 releases active heparin-binding EGF-like growth factor by cleavage at a specific juxtamembrane site. *J Biol Chem* 1997; **272**: 31730-31737
- 62 **Ray JM**, Stetler-Stevenson WG. Gelatinase A activity directly modulates melanoma cell adhesion and spreading. *EMBO J* 1995; **14**: 908-917
- 63 **Brooks PC**, Silletti S, von Schalscha TL, Friedlander M, Cheresh DA. Disruption of angiogenesis by PEX, a noncatalytic metalloproteinase fragment with integrin binding activity. *Cell* 1998; **92**: 391-400
- 64 **Yu Q**, Stamenkovic I. Cell surface-localized matrix metalloproteinase-9 proteolytically activates TGF-beta and promotes tumor invasion and angiogenesis. *Genes Dev* 2000; **14**: 163-176
- 65 **Rak J**, Filmus J, Finkenzeller G, Grugel S, Marme D, Kerbel RS. Oncogenes as inducers of tumor angiogenesis. *Cancer Metastasis Rev* 1995; **14**: 263-277
- 66 **Relf M**, LeJeune S, Scott PA, Fox S, Smith K, Leek R, Moghaddam A, Whitehouse R, Bicknell R, Harris AL. Expression of the angiogenic factors vascular endothelial cell growth factor, acidic and basic fibroblast growth factor, tumor growth factor beta-1, platelet-derived endothelial cell growth factor, placenta growth factor, and pleiotrophin in human primary breast cancer and its relation to angiogenesis. *Cancer Res* 1997; **57**: 963-969
- 67 **Mazure NM**, Chen EY, Yeh P, Laderoute KR, Giaccia AJ. Oncogenic transformation and hypoxia synergistically act to modulate vascular endothelial growth factor expression. *Cancer Res* 1996; **56**: 3436-3440
- 68 **Chiarugi V**, Magnelli L, Gallo O, Cox-2, iNOS and p53 as play-makers of tumor angiogenesis. *Int J Mol Med* 1998; **2**: 715-719
- 69 **Kieser A**, Weich HA, Brandner G, Marme D, Kolch W. Mutant p53 potentiates protein kinase C induction of vascular endothelial growth factors expression. *Oncogene* 1994; **9**: 963-969
- 70 **Tai YT**, Podar K, Gupta D, Lin B, Young G, Akiyama M, Anderson KC. CD40 activation induces p53-dependent vascular endothelial growth factor secretion in human multiple myeloma cells. *Blood* 2002; **99**: 1419-1427
- 71 **Galy B**, Creancier L, Prado-Lourenco L, Prats AC, Prats H. p53 directs conformational change and translation initiation blockade of human fibroblast growth factor 2 mRNA. *Oncogene* 2001; **20**: 4613-4620
- 72 **Sherif ZA**, Nakai S, Pirolo KF, Rait A, Chang EH. Downmodulation of bFGF-binding protein expression following restoration of p53 function. *Cancer Gene Ther* 2001; **8**: 771-782
- 73 **Toschi E**, Rota R, Antonini A, Melillo G, Capogrossi MC. Wild-type p53 gene transfer inhibits invasion and reduces matrix metalloproteinase-2 levels in p53-mutated human melanoma cells. *J Invest Dermatol* 2000; **114**: 1188-1194
- 74 **Kastan MB**, Onyekwere O, Sidranski D, Kastan MB, Onyekwere O, Sidranski D. Participation of p53 protein in the cellular response to DNA damage. *Cancer Res* 1991; **51**: 6304-6311
- 75 **Yonish-Rouach E**, Resnitzky D, Lotem J, Sachs L, Kimchi A, Oren M. Wild-type p53 induces apoptosis of myeloid leukaemic cells that is inhibited by interleukin-6. *Nature* 1991; **352**: 345-347
- 76 **Eckhardt SG**. Angiogenesis inhibitors as cancer therapy. *Hosp Pract (Off Ed)* 1999; **34**: 63-68, 77-79, 83-84
- 77 **Oehler MK**, Bicknell R. The promise of anti-angiogenic cancer therapy. *Br J Cancer* 2000; **82**: 749-752
- 78 **Zhang W**, Ran S, Sambade M, Huang X, Thorpe PE. A monoclonal antibody that blocks VEGF binding to VEGFR2 (KDR/Flk-1) inhibits vascular expression of Flk-1 and tumor growth in an orthotopic human breast cancer model. *Angiogenesis* 2002; **5**: 35-44
- 79 **Witte L**, Hicklin DJ, Zhu Z, Pytowski B, Kotanides H, Rockwell P, Bohlen P. Monoclonal antibodies targeting the VEGF receptor-2 (Flk1/KDR) as an anti-angiogenic therapeutic strategy. *Cancer Metastasis Rev* 1998; **17**: 155-161
- 80 **Im SA**, Gomez-Manzano C, Fueyo J, Liu TJ, Ke LD, Kim JS, Lee HY, Steck PA, Kyritsis AP, Yung WK. Anti-angiogenesis treatment for gliomas: transfer of antisense-vascular endothelial growth factor inhibits tumor growth *in vivo*. *Cancer Res* 1999; **59**: 895-900
- 81 **Zhang L**, Gasper WJ, Stass SA, Ioffe OB, Davis MA, Mixson AJ. Angiogenic inhibition mediated by a DNzyme that targets vas-

- cular endothelial growth factor receptor 2. *Cancer Res* 2002; **62**: 5463-5469
- 82 **Feldman AL**, Libutti SK. Progress in antiangiogenic gene therapy of cancer. *Cancer* 2000; **89**: 1181-1194
- 83 **Slaton JW**, Perrotte P, Inoue K, Dinney CP, Fidler IJ. Interferon-alpha-mediated down-regulation of angiogenesis-related genes and therapy of bladder cancer are dependent on optimization of biological dose and schedule. *Clin Cancer Res* 1999; **5**: 2726-2734
- 84 **Izawa JI**, Sweeney P, Perrotte P, Kedar D, Dong Z, Slaton JW, Karashima T, Inoue K, Benedict WF, Dinney CP. Inhibition of tumorigenicity and metastasis of human bladder cancer growing in athymic mice by interferon-beta gene therapy results partially from various antiangiogenic effects including endothelial cell apoptosis. *Clin Cancer Res* 2002; **8**: 1258-1270
- 85 **Ozawa S**, Shinohara H, Kanayama HO, Bruns CJ, Bucana CD, Ellis LM, Davis DW, Fidler IJ. Suppression of angiogenesis and therapy of human colon cancer liver metastasis by systemic administration of interferon-alpha. *Neoplasia* 2001; **3**: 154-164
- 86 **Bauvois B**, Dumont J, Mathiot C, Kolb JP. Production of matrix metalloproteinase-9 in early stage B-CLL: suppression by interferons. *Leukemia* 2002; **16**: 791-798
- 87 **Marler JJ**, Rubin JB, Trede NS, Connors S, Grier H, Upton J, Mulliken JB, Folkman J. Successful antiangiogenic therapy of giant cell angioblastoma with interferon alfa 2b: report of 2 cases. *Pediatrics* 2002; **109**: E37
- 88 **Sasamura H**, Takahashi A, Miyao N, Yanase M, Masumori N, Kitamura H, Itoh N, Tsukamoto T. Inhibitory effect on expression of angiogenic factors by antiangiogenic agents in renal cell carcinoma. *Br J Cancer* 2002; **86**: 768-773
- 89 **Nilsson A**, Janson ET, Eriksson B, Larsson A. Levels of angiogenic peptides in sera from patients with carcinoid tumours during alpha-interferon treatment. *Anticancer Res* 2001; **21**: 4087-4090
- 90 **Jonasch E**, Haluska FG. Interferon in oncological practice: review of interferon biology, clinical applications, and toxicities. *Oncologist* 2001; **6**: 34-55
- 91 **Strieter RM**, Polverini PJ, Kunkel SL, Arenberg DA, Burdick MD, Kasper J, Dzau BA, Van Damme J, Walz A, Marriott D. The functional role of the ELR motif in CXC chemokine-mediated angiogenesis. *J Biol Chem* 1995; **270**: 27348-27357
- 92 **Volpert OV**, Fong T, Koch AE, Peterson JD, Waltenbaugh C, Tepper RI, Bouck NP. Inhibition of angiogenesis by interleukin 4. *J Exp Med* 1998; **188**: 1039-1046
- 93 **Toritsu H**, Ono M, Kiryu H, Furue M, Ohmoto Y, Nakayama J, Nishioka Y, Sone S, Kuwano M. Macrophage infiltration correlates with tumor stage and angiogenesis in human malignant melanoma. *Int J Cancer* 2000; **85**: 182-188
- 94 **Oshikawa K**, Rakhmievich AL, Shi F, Sondel PM, Yang N, Mahvi DM. Interleukin 12 gene transfer into skin distant from the tumor site elicits antimetastatic effects equivalent to local gene transfer. *Hum Gene Ther* 2001; **12**: 149-160
- 95 **Duda DG**, Sunamura M, Lozonschi L, Kodama T, Egawa S, Matsumoto G, Shimamura H, Shibuya K, Takeda K, Matsuno S. Direct *in vitro* evidence and *in vivo* analysis of the antiangiogenesis effects of interleukin-12. *Cancer Res* 2000; **60**: 1111-1116
- 96 **Huang S**, Ullrich SE, Bar-Eli M. Regulation of tumor growth and metastasis by interleukin-10: the melanoma experience. *J Interferon Cytokine Res* 1999; **19**: 697-703
- 97 **Fernandez HA**, Kallenbach K, Seghezzi G, Grossi E, Colvin S, Schneider R, Mignatti P, Galloway A. Inhibition of endothelial cell migration by gene transfer of tissue inhibitor of metalloproteinases-1. *J Surg Res* 1999; **82**: 156-162
- 98 **Murphy AN**, Unsworth EJ, Stetler-Stevenson WG. Tissue inhibitor of metalloproteinases-2 inhibits bFGF-induced human microvascular endothelial cell proliferation. *J Cell Physiol* 1993; **157**: 351-358
- 99 **Valente P**, Fassina G, Melchiori A, Masiello L, Cilli M, Vacca A, Onisto M, Santi L, Stetler-Stevenson WG, Albini A. TIMP-2 overexpression reduces invasion and angiogenesis and protects B16F10 melanoma cells from apoptosis. *Int J Cancer* 1998; **75**: 246-253
- 100 **Smith MR**, Kung H, Durum SK, Colburn NH, Sun Y. TIMP-3 induces cell death by stabilizing TNF-alpha receptors on the surface of human colon carcinoma cells. *Cytokine* 1997; **9**: 770-780
- 101 **Baker AH**, Zaltsman AB, George SJ, Newby AC. Divergent effects of tissue inhibitor of metalloproteinase-1, -2, or -3 overexpression on rat vascular smooth muscle cell invasion, proliferation, and death *in vitro*. TIMP-3 promotes apoptosis. *J Clin Invest* 1998; **101**: 1478-1487
- 102 **Spurbeck WW**, Ng CY, Strom TS, Vanin EF, Davidoff AM. Enforced expression of tissue inhibitor of matrix metalloproteinase-3 affects functional capillary morphogenesis and inhibits tumor growth in a murine tumor model. *Blood* 2002; **100**: 3361-3368
- 103 **Gomez DE**, Alonso DF, Yoshiji H, Thorgeirsson UP. Tissue inhibitors of metalloproteinases: structure, regulation and biological functions. *Eur J Cell Biol* 1997; **74**: 111-122
- 104 **Hajitou A**, Grignet C, Devy L, Berndt S, Blacher S, Deroanne CF, Bajou K, Fong T, Chiang Y, Foidart JM, Noel A. The antitumoral effect of endostatin and angiostatin is associated with a down-regulation of vascular endothelial growth factor expression in tumor cells. *FASEB J* 2002; **16**: 1802-1804
- 105 **Wajih N**, Sane DC. Angiostatin selectively inhibits signaling by hepatocyte growth factor in endothelial and smooth muscle cells. *Blood* 2002 oct 24; [epub ahead of print]
- 106 **Cao Y**, Ji RW, Davidson D, Schaller J, Marti D, Sohndel S, McCance SG, O'Reilly MS, Llinas M, Folkman J. Kringle domains of human angiostatin. Characterization of the anti-proliferative activity on endothelial cells. *J Biol Chem* 1996; **271**: 29461-29467
- 107 **Moser TL**, Stack MS, Asplin I, Enghild JJ, Hojrup P, Everitt L, Hubchak S, Schnaper HW, Pizzo SV. Angiogenesis binds ATP synthase on the surface of human endothelial cells. *Proc Natl Acad Sci U S A* 1999; **96**: 2811-2816
- 108 **Moser TL**, Kenan DJ, Ashley TA, Roy JA, Goodman MD, Misra UK, Cheek DJ, Pizzo SV. Endothelial cell surface F₁-F₀ ATP synthase is active in ATP synthesis and is inhibited by angiostatin. *Proc Natl Acad Sci U S A* 2001; **98**: 6656-6661
- 109 **GrisCELLI F**, Li H, Bennaceur-GrisCELLI A, Soria J, Opolon P, Soria C, Perricaudet M, Yeh P, Lu H. Angiostatin gene transfer: inhibition of tumor growth *in vivo* by blockage of endothelial cell proliferation associated with a mitosis arrest. *Proc Natl Acad Sci U S A* 1998; **95**: 6367-6372
- 110 **Sun X**, Kanwar JR, Leung E, Lehnert K, Wang D, Krissansen GW. Angiostatin enhances B7.1-mediated cancer immunotherapy independently of effects on vascular endothelial growth factor expression. *Cancer Gene Ther* 2001; **8**: 719-727
- 111 **Lucas R**, Holmgren L, Garcia I, Jimenez B, Mandriota SJ, Borlat F, Sim BK, Wu Z, Grau GE, Shing Y, Soff GA, Bouck N, Pepper MS. Multiple forms of angiostatin induce apoptosis in endothelial cells. *Blood* 1998; **92**: 4730-4741
- 112 **Gupta N**, Nodzinski E, Khodarev NN, Yu J, Khorasani L, Beckett MA, Kufe DW, Weichselbaum RR. Angiostatin effects on endothelial cells mediated by ceramide and RhoA. *EMBO Rep* 2001; **2**: 536-540
- 113 **Kim YM**, Hwang S, Kim YM, Pyun BJ, Kim TY, Lee ST, Gho YS, Kwon YG. Endostatin Blocks Vascular Endothelial Growth Factor-mediated Signaling via Direct Interaction with KDR/Flk-1. *J Biol Chem* 2002; **277**: 27872-27879
- 114 **Urbich C**, Reissner A, Chavakis E, Dernbach E, Haendeler J, Fleming I, Zeiher AM, Kaszkin M, Dimmeler S. Dephosphorylation of endothelial nitric oxide synthase contributes to the antiangiogenic effects of endostatin. *FASEB J* 2002; **16**: 706-708
- 115 **Rehn M**, Veikkola T, Kukk-Valdre E, Nakamura H, Ilmonen M, Lombardo C, Pihlajaniemi T, Alitalo K, Vuori K. Interaction of endostatin with integrins implicated in angiogenesis. *Proc Natl Acad Sci U S A* 2001; **98**: 1024-1029
- 116 **Hohenester E**, Sasaki T, Olsen BR, Timpl R. Crystal structure of the angiogenesis inhibitor endostatin at 1.5 angstrom resolution. *EMBO J* 1998; **17**: 1656-1664
- 117 **Marion-Audibert AM**, Nejari M, Pourroyon C, Anderson W, Gouysson G, Jacquier MF, Dumortier J, Scoazec JY. Effects of endocrine peptides on proliferation, migration and differentiation of human endothelial cells. *Gastroenterol Clin Biol* 2000; **24**: 644-648
- 118 **Kim YM**, Jang JW, Lee OH, Yeon J, Choi EY, Kim KW, Lee ST, Kwon YG. Endostatin inhibits endothelial and tumor cellular invasion by blocking the activation and catalytic activity of matrix metalloproteinase. *Cancer Res* 2000; **60**: 5410-5413
- 119 **Dixelius J**, Larsson H, Sasaki T, Holmqvist K, Lu L, Engstrom A, Timpl R, Welsh M, Claesson-Welsh L. Endostatin-induced tyrosine kinase signaling through the shb adaptor protein regulates endothelial cell apoptosis. *Blood* 2000; **95**: 3403-3411

- 120 **Dhanabal M**, Ramchandran R, Waterman MJ, Lu H, Knebelmann B, Segal M, Sukhatme VP. Endostatin induces endothelial cell apoptosis. *J Biol Chem* 1999; **274**: 11721-11726
- 121 **Pages P**, Benali N, Saint-Laurent N, Esteve JP, Schally AV, Tkaczuk J, Vaysse N, Susini C, Buscail L. sst2 somatostatin receptor mediates cell cycle arrest and induction of p27(Kip1). Evidence for the role of SHP-1. *J Biol Chem* 1999; **274**: 15186-15193
- 122 **Sharma K**, Patel YC, Srikant CB. C-terminal region of human somatostatin receptor 5 is required for induction of Rb and G1 cell cycle arrest. *Mol Endocrinol* 1999; **13**: 82-90
- 123 **Charland S**, Boucher MJ, Houde M, Rivard N. Somatostatin inhibits Akt phosphorylation and cell cycle entry, but not p42/p44 mitogen-activated protein (MAP) kinase activation in normal and tumoral pancreatic acinar cells. *Endocrinology* 2001; **142**: 121-128
- 124 **Sharma K**, Patel YC, Srikant CB. Subtype-selective induction of wild-type p53 and apoptosis, but not cell cycle arrest, by human somatostatin receptor 3. *Mol Endocrinol* 1996; **10**: 1688-1696
- 125 **Albini A**, Florio T, Giunciuglio D, Masiello L, Carlone S, Corsaro A, Thellung S, Cai T, Noonan DM, Schettini G. Somatostatin controls Kaposi's sarcoma tumor growth through inhibition of angiogenesis. *FASEB J* 1999; **13**: 647-655
- 126 **Woltering EA**, Watson JC, Alperin-Lea RC, Sharma C, Keenan E, Kurozawa D, Barrie R. Somatostatin analogs: angiogenesis inhibitors with novel mechanisms of action. *Invest New Drugs* 1997; **15**: 77-86
- 127 **Gulec SA**, Gaffga CM, Anthony CT, Su LJ, O'Leary JP, Woltering EA, Gulec SA, Gaffga CM, Anthony CT, Su LJ, O'Leary JP, Woltering EA. Antiangiogenic therapy with somatostatin receptor-mediated in situ radiation. *Am Surg* 2001; **67**: 1068-1071
- 128 **Patel YC**. Molecular pharmacology of somatostatin receptor subtypes. *J Endocrinol Invest* 1997; **20**: 348-367
- 129 **Lewin MJ**. The somatostatin receptor in the GI tract. *Annu Rev Physiol* 1992; **54**: 455-468
- 130 **Buscail L**, Esteve JP, Saint-Laurent N, Bertrand V, Reisine T, O'Carroll AM, Bell GI, Schally AV, Vaysse N, Susini C. Inhibition of cell proliferation by the somatostatin analogue RC-160 is mediated by somatostatin receptor subtypes SSTR2 and SSTR5 through different mechanisms. *Proc Natl Acad Sci U S A* 1995; **92**: 1580-1584
- 131 **Mentlein R**, Eichler O, Forstreuter F, Held-Feindt J. Somatostatin inhibits the production of vascular endothelial growth factor in human glioma cells. *Int J Cancer* 2001; **92**: 545-550
- 132 **Lawnicka H**, Stepien H, Wyczolkowska J, Kolago B, Kunert-Radek J, Komorowski J. Effect of somatostatin and octreotide on proliferation and vascular endothelial growth factor secretion from murine endothelial cell line (HECa10) culture. *Biochem Biophys Res Commun* 2000; **268**: 567-571
- 133 **Wu PC**, Liu CC, Chen CH, Kou HK, Shen SC, Lu CY, Chou WY, Sung MT, Yang LC. Inhibition of experimental angiogenesis of cornea by somatostatin. *Graefes Arch Clin Exp Ophthalmol* 2003; **241**: 63-69
- 134 **Lamberts SW**, Krenning EP, Reubi JC. The role of somatostatin and its analogs in the diagnosis and treatment of tumors. *Endocr Rev* 1991; **12**: 450-482
- 135 **Jimenez B**, Volpert OV, Crawford SE, Febbraio M, Silverstein RL, Bouck N. Signals leading to apoptosis-dependent inhibition of neovascularization by thrombospondin-1. *Nat Med* 2000; **6**: 41-48
- 136 **Gilmore AP**, Romer LH. Inhibition of focal kinase protein (FAK) signaling in focal adhesion decreases cell motility and proliferation. *Mol Biol Cell* 1996; **7**: 1209-1224
- 137 **Volpert OV**, Lawler J, Bouck NP. A human fibrosarcoma inhibits systemic angiogenesis and the growth of experimental metastases via thrombospondin-1. *Proc Natl Acad Sci U S A* 1997; **95**: 6343-6348
- 138 **Panetti TS**, Chen H, Misenheimer TM, Getzler SB, Mosher DF. Endothelial cell mitogenesis induced by LPA: inhibition by thrombospondin-1 and thrombospondin-2. *J Lab Clin Med* 1997; **129**: 208-216
- 139 **Iyer S**, Chaplin DJ, Rosenthal DS, Boulares AH, Li LY, Smulson ME. Induction of apoptosis in proliferating human endothelial cells by the tumor-specific antiangiogenesis agent combretastatin A-4. *Cancer Res* 1998; **58**: 4510-4514
- 140 **Boehm T**, Folkman J, Browder T, O'Reilly MS. Antiangiogenic therapy of experimental cancer does not induce acquired drug resistance. *Nature* 1997; **390**: 404-407
- 141 **Jayson GC**, Zweit J, Jackson A, Mulatero C, Julyan P, Ranson M, Broughton L, Wagstaff J, Hakansson L, Groenewegen G, Bailey J, Smith N, Hastings D, Lawrance J, Haroon H, Ward T, McGown AT, Tang M, Levitt D, Marreaud S, Lehmann FF, Herold M, Zwierzina H. Molecular imaging and biological evaluation of HuMV833 anti-VEGF antibody: implications for trial design of antiangiogenic antibodies. *J Natl Cancer Inst* 2002; **94**: 1484-1493
- 142 **Gossmann A**, Helbich TH, Kuriyama N, Ostrowitzki S, Roberts TP, Shames DM, van Bruggen N, Wendland MF, Israel MA, Brasch RC. Dynamic contrast-enhanced magnetic resonance imaging as a surrogate marker of tumor response to anti-angiogenic therapy in a xenograft model of glioblastoma multiforme. *J Magn Reson Imaging* 2002; **15**: 233-240
- 143 **Kim SW**, Park SS, Ahn SJ, Chung KW, Moon WK, Im JG, Yeo JS, Chung JK, Noh DY. Identification of angiogenesis in primary breast carcinoma according to the image analysis. *Breast Cancer Res Treat* 2002; **74**: 121-129

Primary adenocarcinomas of lower esophagus, esophagogastric junction and gastric cardia: in special reference to China

Li-Dong Wang, Shu Zheng, Zuo-Yu Zheng, Alan G. Casson

Li-Dong Wang, Cancer Institute, Zhejiang University, Hangzhou 310009, Jiangsu Province, China and Laboratory for Cancer Research, College of Medicine, Zhengzhou University, Zhengzhou 450052, Henan Province, China

Shu Zheng, Cancer Institute, Zhejiang University, Hangzhou 310009, Jiangsu Province, China

Zuo-Yu Zheng, Laboratory for Cancer Research, College of Medicine, Zhengzhou University, Zhengzhou 450052, Henan Province, China

Alan G. Casson, Department of Surgery, Dalhousie University, Halifax, Nova Scotia, Canada

Supported by National Distinguished Young Scientist Foundation of China, No. 30025016 and Foundation of Henan Education Committee, No. 1999125

Correspondence to: Li-Dong Wang, M.D., Professor of Pathology and Oncology, Invited Profesor of Henan Province, Director fo Laboratory for Cancer Research, College of Medicine, Zhengzhou University, Zhengzhou, 450052, Henan Province, China. lidong0823@sina.com
Telephone: +86-371-6970165 **Fax:** +86-371-6970165

Received: 2003-05-20 **Accepted:** 2003-06-02

Abstract

Gastric cardia adenocarcinoma (GCA) is an under-studied subject. The pathogenesis, molecular changes in the early stage of carcinogenesis and related risk factors have not been well characterized. There is evidence, however, that GCA differs from cancer of the rest of the stomach in terms of natural history and histopathogenesis. Adenocarcinomas of the lower esophagus, esophagogastric junction (EGJ) and gastric cardia have been given much attention because of their increasing incidences in the past decades, which is in striking contrast with the steady decrease in distal stomach adenocarcinoma. In China, epidemiologically, GCA shares very similar geographic distribution with esophageal squamous cell carcinoma (SCC), especially in Linzhou (formerly Linxian County), Henan Province, North China, the highest incidence area of esophageal SCC in the world. Historically, both GCA and SCC in these areas were referred to as esophageal cancer (EC) by the public because of the common syndrome of dysphagia. In Western countries, Barrett's esophagus is very common and has been considered as an important precancerous lesion of adenocarcinoma at EGJ. Because of the low incidence of Barrett's esophagus in China, it is unlikely to be an important factor in early stage of EGJ adenocarcinoma development. However, Z line up-growth into lower esophagus may be one of the characteristic changes in these areas in early stage of GCA development. Whether intestinal metaplasia (IM) is a premalignant lesion for GCA is still not clear. Higher frequency of IM observed at adjacent GCA tissues in Henan suggests the possibility of IM as a precancerous lesion for GCA in these areas. Molecular information on GCA, especially in early stage, is very limited. The accumulated data about the changes of tumor suppressor gene, such as p53 mutation, and ontogeny, such as C-erbB2, especially the similar alterations in GCA and SCC in the same patient, indicated that there might be some similar risk factors,

such as nitrosamine, involved in both GCA and SCC in Henan population. The present observations also suggest that GCA should be considered as a distinct entity.

Wang LD, Zheng S, Zheng ZY, Casson AG. Primary adenocarcinomas of lower esophagus, esophagogastric junction and gastric cardia: in special reference to China. *World J Gastroenterol* 2003; 9(6): 1156-1164

<http://www.wjgnet.com/1007-9327/9/1156.asp>

INTRODUCTION

Adenocarcinomas of the gastric cardia are currently classified as gastric cancers^[1, 2]. However, recent studies have suggested that these tumors have distinct epidemiological and biological characteristics^[3, 4]. In the last two decades, the incidence of primary adenocarcinomas of the lower esophagus, esophagogastric junction (EGJ) and adenocarcinomas of the gastric cardia has increased dramatically in North America and Western European countries^[3-6]. In contrast, the incidence of adenocarcinoma of the distal stomach has decreased steadily in recent years.

In China, adenocarcinomas of the gastric cardia have unique epidemiological features distinguishing these tumors from the adenocarcinomas of the distal stomach. Linzhou (formerly Linzhou County), the region with the highest incidence rate of esophageal cancer in the world, also has a high incidence of adenocarcinoma of the gastric cardia. However, the incidence of adenocarcinoma arising from the distal stomach is very low in this area. Therefore, previously, adenocarcinomas arising from the EGJ (gastric cardia) were referred to as esophageal cancers, because they shared similar clinical symptoms such as dysphagia. As most of the adenocarcinomas arising from the cardia are diagnosed at an advanced stage, it is very difficult to accurately define whether these tumors have a primary esophageal or gastric origin. Therefore, adenocarcinomas of the EGJ (gastric cardia) are now generally referred to as gastric cardia adenocarcinomas (GCA). With the exception of Barrett's esophagus (a well documented premalignant lesion of esophageal adenocarcinoma in Caucasians)^[7, 8], the role of other risk factors, such as *H. pylori* infection, diet, alcohol and tobacco exposure, still remains unclear.

Most studies of esophageal carcinoma in Linzhou have evaluated only esophageal squamous cell carcinoma (SCC). Few have studied adenocarcinoma (AC) of the gastric cardia, particularly as a separate pathological entity in China. In this review, recent epidemiological, histopathological and molecular biological advances were summarized to provide clues about the risk factors and the molecular carcinogenesis of adenocarcinomas of the lower esophagus, and EGJ (gastric cardia).

EPIDEMIOLOGY OF ADENOCARCINOMA OF THE GASTRIC CARDIA

GCA shares several common features with the adenocarcinoma arising from the distal esophagus: a lower mean age of

presentation, a higher incidence in the Caucasian population, a higher male to female ratio, and similar risk factors^[4, 9]. Epidemiological studies have demonstrated that smoking, alcohol consumption, increased body mass index (reflecting obesity), and lower socioeconomic status are risk factors for adenocarcinomas of both the distal esophagus and gastric cardia^[10-12]. In Linzhou, China, adenocarcinoma of the gastric cardia was previously classified as esophageal cancer by the local registry for the past several decades, primarily because of comparable clinical features and similarity in therapy. Reviewing hospital records of patients with dysphagia, our research group reported that while approximately 60 percent of patients were found to have a diagnosis of SCC, the remaining 40 percent were found to have adenocarcinomas of the lower esophagus or gastric cardia^[13]. A case-control study performed on the patients with presumed distal esophageal or gastric cardia cancer in Linzhou found that one third of all these tumors was adenocarcinomas of the gastric cardia^[14]. While there is considerable evidence implicating that dietary factors, including certain nutrient deficiencies and consumption of nitrosamine-contaminated food, and drinking water are associated with the development of SCC^[15-18], it is not clear whether adenocarcinomas of the gastric cardia share the same risk factors in this high-incidence area in China.

DIAGNOSTIC CRITERIA FOR ADENOCARCINOMA OF THE GASTRIC CARDIA

It is generally difficult to distinguish where cardia adenocarcinomas originate, as most tumors present in advanced stage at diagnosis, often involving both esophagus and stomach. Imprecise clinical and pathological definitions of adenocarcinomas of the lower esophagus, EGJ or gastric cardia may be the reason underlying inconsistencies between different studies. An adenocarcinoma is considered to be of cardia origin when the epicenter of the tumor is at the esophagogastric junction, or within 2 cm distally^[19]. Strict clinicopathologic criteria have been used also to define primary esophageal adenocarcinomas^[20]. A new classification for adenocarcinomas of the esophagogastric junction was proposed at a recent conference of the International Gastric Cancer Association (IGCA) and the International Society for Diseases of the Esophagus (ISDE). Adenocarcinomas of the cardia has been defined as tumors that have their centres within 5 cm of the anatomic esophagogastric junction. Three distinct tumor entities (Type I, II and III) have been proposed^[21].

RELEVANT PATHOLOGICAL CONDITIONS OF ADENOCARCINOMA OF THE GASTRIC CARDIA

Barrett's esophagus

Barrett's esophagus is the condition in which columnar epithelium replaces the squamous epithelium that normally lines the distal esophagus^[22]. The endoscopic appearance is characteristic, with a salmon-pink color and velvety texture. This upward extension may be circumferential, or limited to finger-like projections, or even islands of columnar epithelium that only involve part of the distal esophageal wall^[23]. In healthy individuals, the squamo-columnar junction (SCJ) does not always correspond with the anatomic EGJ. The juxtaposition of pale squamous epithelium and reddish columnar epithelium forms a visible line called the Z line, or the SCJ. The EGJ is the most proximate part of gastric folds. The Z line and gastroesophageal junction often coincide. When the Z line is located above the EGJ, there is a columnar lined segment of esophagus. Barrett's esophagus is diagnosed endoscopically if columnar mucosa extending greater than 3 cm above the EGJ, or by histologic finding of intestinal metaplasia

(specialized mucosa) existing at any level of the tubular esophagus^[22].

The pathogenesis of Barrett's esophagus is still unclear. Most Barrett's esophagus develops from approximately 10 % of persons who have chronic gastroesophageal reflux^[24]. In addition to gastroesophageal reflux diseases (GERD), Barrett's esophagus is associated with several other esophageal disorders, such as hiatal hernia^[25], and occasionally familial groupings are reported^[26-28].

The significance of Barrett's esophagus is its association with the development of esophageal malignancy^[29,30]. Patients with Barrett's esophagus have (by conservative estimates) a 30- to 40-fold higher risk of developing esophageal adenocarcinoma than those without^[23]. Since the diagnostic criteria for Barrett's esophagus now include the histological finding of intestinal metaplasia, a columnar-lined esophagus less than 3 cm in length is now recognized as short-segment Barrett's esophagus (SSBE), in contrast to the traditional long-segment Barrett's esophagus (LSBE)^[31]. The risk of malignancy in SSBE still needs to be determined^[32].

In China, Barrett's esophagus used to be regarded as a rare condition, and consequently has not been studied in detail. However, based on an endoscopic survey performed by our research group in the high-risk population in Linzhou, Barrett's esophagus was detected with a frequency of 0.7 % (3/402); not as rare as it was considered previously^[33]. It has been identified that there is an apparent change of Z line upgrowth among symptom free subjects in the high-incidence area for esophageal cancer in Henan Province. Z line upgrowth is related with epithelial cell hyperproliferation both in gastric cardia and lower segment of esophagus. These results suggest that Z line upgrowth may be one of the characteristic changes, or precancerous lesions related with EGJ carcinogenesis in the high-risk population for GCA in Henan^[11]. Further characterizing Barrett's Esophagus, Z line upgrowth, and esophageal and gastric reflux esophagitis in this population may provide new insights into understanding of cardia carcinogenesis^[34].

Intestinal metaplasia

Since the diagnostic criteria for Barrett's esophagus based on endoscopy are arbitrary, recent definitions of Barrett's esophagus have included the histologic finding of intestinal metaplasia, regardless of the length of the columnar-lined esophagus^[35]. Histologically, three types of columnar epithelium have been observed in Barrett's esophagus: gastric fundic type, junctional type and specialized intestinal metaplasia (IM). Based on the mucin content of the columnar and goblet cells, intestinal metaplasia is histopathologically divided into three types: the complete form (Type I), in which the columnar cells are absorptive and contain neutral mucins, and the two incomplete forms, in which the columnar cells are partly secretory and contain acidic sialomucins (Type II) or sulphomucins (Type III)^[36,37]. Type I is the predominant form of intestinal metaplasia found in the stomach, including both benign and malignant conditions. Type III is the least common form in the stomach, but the one most strongly associated with gastric cancer^[38]. The incomplete form of intestinal metaplasia also termed specialized columnar epithelium (SCE), is the histological mark of Barrett's esophagus^[39].

IM is also associated with GERD, and the frequency of IM is increased with the extension of columnar lining in the esophagus^[40]. However, gastritis rather than GERD seems to be a risk factor of cardiac intestinal metaplasia^[41]. While complete intestinal metaplasia is a manifestation of multifocal atrophic gastritis, the incomplete form may result from carditis and GERD^[42].

It has been hypothesized that Barrett's adenocarcinoma follows the metaplasia-dysplasia-adenocarcinoma sequence (MCS)^[43]. Whether intestinal metaplasia is a premalignant lesion for adenocarcinoma of the gastric cardia is still not clear^[44]. Several studies showed that dysplasia was infrequently observed in EGJ or gastric cardia with intestinal metaplasia^[42, 44, 45]. These suggest that intestinal metaplasia at the EGJ or gastric cardia is not a high-risk precursor lesion for adenocarcinoma. However, progression from intestinal metaplasia at the EGJ or gastric cardia to dysplasia still requires further characterization^[46].

Examination of the adjacent gastric cardia cancer tissue by our research group showed that IM was frequently observed in as high as 20 % of the specimens^[47]. In contrast, only 0.7 % symptom-free subjects in Linzhou were identified with IM in gastric cardia biopsies^[33]. Goblet cell was invariably identified on HE stained specimen. Half of the IM lesion was found to have dysplasia. These suggest that IM may be a precursor of gastric cardia adenocarcinoma in Henan, which is not consistent with that in Western countries. The reason is not clear. Standard histologic evaluation fails to reliably differentiate between IM in the esophagus and IM in native cardiac mucosa. Further characterization for subtypes of IM with biohistochemistry and immunohistochemistry will provide important evidence for elucidating the significance of IM in gastric cardia carcinogenesis.

Chronic carditis: *H. pylori* infection or gastroesophageal reflux disease

IM in the distal stomach is usually a consequence of chronic inflammation, mainly caused by *H. pylori* infection^[48], while the intestinal metaplasia of Barrett's esophagus has been demonstrated to be associated with GERD^[49]. Furthermore, recent studies suggested that gastric infection with *H. pylori* might protect the esophagus from developing of reflux esophagitis and Barrett's esophagus^[50-54]. It is reasonable to hypothesize that intestinal metaplasia at the gastric cardia may develop as a consequence of chronic inflammation due to either GERD or infection. Several recent studies have focused on the relative contribution of *H. pylori* infection and GERD to gastric carditis, however, results have been inconsistent, to date^[55-58]. One possible reason may be related to the use of different histopathologic criteria for identification of the gastric cardia. A study of 33 consecutive autopsies in children showed that the length of cardiac epithelium ranged from 1 to 4 mm, with a mean extent of 1.8 mm^[59]. Ormsby expanded the study to 223 adult autopsies, finding that the mean extent of cardiac epithelium in patients aged <18, 19-50, and >50 years was 1.7, 2.6, and 3.3 mm, respectively^[60]. Such a narrow range makes accurate sampling extremely difficult. Therefore, biopsies from the gastric cardia may have two origins: esophagus or stomach.

MOLECULAR BASIS FOR ADENOCARCINOMA OF GASTRIC CARDIA

The pathogenesis of carcinoma has been demonstrated to be a progressive, multi-step process, manifested as an uncontrolled cell cycle and abnormal proliferation. The molecular basis of human cancer has been investigated widely in the recent two decades, and has implicated deregulation of tumor suppressor genes, activation of oncogenes, and aberrant expression of growth factors. Different genetic alterations have been observed between the two different histologic sub-types of esophageal cancer. Meanwhile, molecular evidence is also accumulating to support the hypothesis that adenocarcinomas of the gastric cardia are distinct from adenocarcinomas of the esophagus and stomach.

Loss of heterozygosity (LOH)

LOH has been demonstrated to play an important role in tumorigenesis, and to be frequently associated with the loss of tumor suppressor gene function. LOH was initially observed at several tumor suppressor gene loci (17p, 13q, 5q, 18q and 9p for p53, Rb, APC, MSH2, DCC and p16, E-cadherin, 19p, respectively) in human esophageal and gastric cancer^[61-67]. At present, LOH has been used to localize putative tumor suppressor genes. LOH has also been reported at 1p, 3p, 4q, 9q, 11p and 17q in esophageal adenocarcinomas^[68, 69]. Allelic loss of the tumor suppressor gene p73 on 1p is frequently observed in neuroblastoma^[70, 71], and hMLH-1, a mismatch repair gene associated with hereditary non-polyposis colorectal cancer, is located on 3q21^[72]. The tylosis esophageal cancer (TOC) gene, initially reported in families with autosomal dominant tylosis families who developed esophageal cancer, has been located on chromosome 17q25. Allelic loss at this region has been implicated in both sporadic SCC and Barrett's adenocarcinoma^[73]. BCRA1, associated with susceptibility to breast and ovarian cancer, is located on 17q^[74]. Using comparative genomic hybridization (CGH), deletion of a specific region at 14q31-32.1 occurred significantly more frequently in Barrett's adenocarcinomas in the distal esophagus than in gastric cardia cancers, suggesting genetic divergence in this group of closely related cancers^[75]. Allelotype analysis performed on 38 gastric cardia adenocarcinomas even differentiated this allelic imbalance between the intestinal-type and diffuse-type adenocarcinomas, and a higher frequency of allelic imbalance on chromosome 16q was detected in the diffuse-type adenocarcinomas^[76].

Dysfunction of tumor suppressor genes

Tumor suppressor gene p53 P53 is located on chromosome 17p13, encoding a phosphoprotein with a molecular weight of 53kd. Abnormalities in p53 gene function cause uncontrolled cell cycles and abnormal cell proliferation. P53 mutations are the most frequent genetic alterations found in human cancers^[77]. Over 90 percent of p53 mutations are observed in exons 5-8, which is the highly conserved region for DNA binding. Comparison of p53 mutations in premalignant (basal cell hypertrophy, BCH; dysplasia, DYS; carcinoma *in situ*, CIS) esophageal tissues matched with corresponding invasive SCC tumor tissues, showed similar p53 mutations in DYS, CIS and tumors^[78]. Similar studies with Barrett's adenocarcinoma showed that p53 mutations in Barrett's epithelia (metaplasia, non-dysplastic) did not necessarily correspond to the matched adenocarcinoma^[20]. The high coincident alterations for P53 in SCC and GCA from the same patient indicate the possibility of similar molecular mechanisms, which provides important molecular basis and etiological clue for similar geographic distribution and risk factors in SCC and GCA^[79, 80]. These results suggest that some p53 mutations may have a selective tumorigenic advantage during tumor progression. And some findings suggest p53, bcl-2 and caspase-3 may play an important role in the induction of apoptosis in AGS cells^[81]. In the course of the formation of gastric carcinoma, proliferation of gastric mucosa can be greatly increased by *H. pylori* infection, which can strengthen the expression of mutated p53 gene^[82]. Less aggressive mutations may increase the genetic instability of Barrett's mucosa, promoting abnormal cellular proliferation, but as they are incapable of transformation independently, additional molecular or epigenetic events are required for tumorigenesis.

About 90 percent of p53 mutations are located within the DNA binding domain (exons 5 to 8). They may occur either at the binding surface or at the hydrophobic core, disrupting the structure for DNA binding. P53 mutations do not distribute in a random manner through the whole encoding region. Several

“hot spot” mutations have been located such as codon 175, 176, 245, 248, 249, 273 and 282 in all the human cancers^[83], implying that there may be a general pathway for the pathogenesis of tumors with a high percentage of p53 mutations. However, mutation sites also appear to be organ specific and cell-dependent. In esophageal adenocarcinomas, p53 mutations occur most frequently at codon 175 (9 %), 248 (16 %) and 273 (16 %), which are also hot spot mutations for all human cancers recorded, while mutations at codon 248 and 273 are much less frequently observed, even though the mutation at codon 175 accounts for 8 % in SCC. Relatively high frequencies of p53 mutations at codons 193, 194, 195 and 270 are unique in comparison to other human cancers^[77].

P53 mutations may result from endogenous processes or exogenous carcinogens^[84], and the spectrum of mutations may be indicative of specific carcinogenic mechanisms. Mutation profiles of p53 also help to identify the DNA damage arising from environmental carcinogens. Approximately 31 % of p53 mutations occur at the A:T base pairs in the SCC, which are usually caused by exogenous carcinogenic compounds. But in esophageal adenocarcinoma, p53 mutations have a very high frequency of transition at the CpG dinucleotides. This alteration is thought to result from spontaneous deamination of 5-methylcytosine, suggesting a defective DNA mismatch repair^[77, 85]. Differences in p53 mutation spectra between SCC and esophageal adenocarcinoma are consistent with the results of epidemiological studies, suggesting that SCC and esophageal adenocarcinoma have different etiology.

Adenocarcinomas of gastric cardia share similar epidemiological and histological features to esophageal adenocarcinomas in North America and some European countries. Gleeson *et al.*^[86] compared the p53 abnormalities in adenocarcinoma of the distal esophagus and gastric cardia, and reported that p53 mutations were detected in 70 % and 63 % of adenocarcinoma of esophagus and gastric cardia, respectively. 85 % of the p53 mutations in esophageal adenocarcinoma occurred as G:C→A:T transitions, with 69 % at the CpG dinucleotides. Similar p53 mutations were observed in adenocarcinoma of the gastric cardia, in which 82 % were base transitions with 55 % occurring at the CpG dinucleotides. One study from Linzhou based on the p53 gene mutation analysis identified 6 mutations among 14 adenocarcinomas of the gastric cardia, 3 of which were G to T transversions, a mutation that is rarely observed in Barrett's adenocarcinoma^[87]. Further investigation and comparison of mutation analysis of p53 gene between SCC and adenocarcinoma of the gastric cardia in this population are needed so to provide more insights into the etiology of both SCC and adenocarcinomas of esophagus and the gastric cardia.

p53 gene family Recently, discovery of p53 homologues such as p73 and p63 suggests a more complex pathway. p73 and p63, similar to p53, may result in transactivation, DNA binding and oligomerization domains^[88], capable of activating the transcription of p53-responsive genes and inducing apoptosis^[89-91]. p73 is located on chromosome 1p36, a region that is frequently deleted in neuroblastoma^[73, 74], but unlike p53, p73 mutations have been detected infrequently in other types of tumor, including esophageal and gastric carcinoma^[92-100]. Silencing of p73 gene due to hypermethylation at its promoter region was observed in a subset of lymphoblastic leukaemia and Burkett's lymphoma^[101, 102], but increased level of mRNA was more commonly observed in other tumors^[95, 103-105]. p73 is characterized by loss of imprinting (LOI), resulting in monoallelic expression in normal tissues. It has been observed that p73 is overexpressed in several tumors, which is thought to be due to the switching from monoallelic to biallelic expression^[93, 95]. Meanwhile, p73 isoforms, caused by alternative splicing, have been observed in rare types of brain

tumors, suggesting tissue-specificity in the regulation of p73 gene transcription^[106]. However, the precise function of p73 isoforms in tumor development is still unclear. Specific mutations of p73 or p63 causing amino acid substitutions are not identified. Neither p53, p73 nor p63 is related to prognosis. p73 and p63 have rarely been found to be mutated in gastric carcinomas, but both proteins are expressed in only a subset of tumors. The status of these p53 homologues is discordant among all patients with multiple simultaneous gastric carcinomas. The increased expression of p63 (TAp63 and black triangleNp63) in less well-differentiated gastric carcinomas may indicate that p63 can act to promote neoplastic growth in the gastric epithelium^[107]. In 15 SCC samples from Henan, no p73 mutations were found in exons 4-7, but a high frequency of LOI and LOH was observed in these samples. The SCC samples with p53 defects were significantly correlated with those, which had elevated expression of p73. These results suggest that increased expression of p73, including that by LOI, could be a partial compensatory mechanism for defective p53^[100].

The p63 gene also encodes multiple isoforms through alternative splicing with different abilities to transactivate p53-responsive genes. However, p63 is more closely related to p73 than to p53, and p63 mutations have been rarely observed in human tumors^[108, 109]. The predominant isoform of p63, lacking in an acidic N-terminus corresponding to the transactivation domain of p53, has been detected in many kinds of epithelial tissue. This truncated protein may act as a dominant-negative agents toward transactivation by p53^[110]. Up to date, p63 has not been studied in esophageal adenocarcinoma or adenocarcinomas of the cardia.

Rb gene One study compared LOH with the expression of Rb gene in SCC, finding that 90 % of the tumor samples containing LOH showed low or no Rb expression, while only 20 % of those without LOH had altered expression of Rb, suggesting LOH is the principal molecular alteration of Rb in SCC^[111]. Recent studies of SCC cell lines demonstrated that the hypophosphorylated Rb protein was also associated with G2 arrest^[112]. Besides inhibition of the cell cycle progression, Rb protein appears to have other distinct mechanisms to suppress cellular proliferation^[113]. In the gastric carcinogenesis, *H. pylori* might cause severe imbalance of proliferation and apoptosis in the precancerous lesions (IMIII and DysIII) first, leading to p53-Rb tumor-suppressor system mutation and telomerase reactivation, and finally causing gastric cancer^[114]. Wang *et al.*^[115] suggested the alteration of Rb protein might play a role in the early stages of gastric cardia carcinogenesis.

p16INK4a, p15INK4b and p14ARF LOH of p16INK4a has been detected with high frequencies in both SCC (65 %) and esophageal adenocarcinoma (69 %)^[116]. Several studies have demonstrated that hypermethylation of the promoter region of p16INK4a is the main mechanism causing gene silencing rather than point mutation, which rarely occurs in esophageal carcinomas^[116-119]. Distinct from p16INK4a, p15INK4b, which inhibits the cell growth in response to extracellular stimuli such as TGF- β ^[120], is more frequently deleted, at a frequency of 40 %^[118]. Though p16INK4a regulates cell cycle through inhibiting the phosphorylation of Rb protein, p14ARF is closely associated with p53 by attenuating mdm2-mediated degradation of p53^[121, 122]. Similar to p15INK4b, p14ARF is also deleted frequently in SCC, losing its function to protect p53 from ubiquitin-dependent degradation^[123].

Abnormalities of oncogenes Point mutation, amplification, rearrangement and overexpression are the most frequent mechanisms for oncogene activation. Amplification of cyclinD1, HER-2/neu(c-erbB2), c-myc, c-ras, Int-2/hst-1 and c-erbB (EGFR) has been observed in gastric and esophageal carcinomas^[124-130]. The amplification of c-erbB2 was followed

by overexpression in the same gastric adenocarcinoma tissue^[125,129]. No amplification of *c-erbB2* was detected in SCC. Amplification of oncogenes that encode growth factor receptors is more commonly found in adenocarcinomas. *Int-2* and *hst-1*, encoding FGF-3 and FGR-4 respectively, are located at chromosome 11q13 with the oncogene *cyclinD1*. Coamplification of *int-2* and *hst-1* was observed at a frequency of 28-47 % in primary esophageal carcinomas and much higher in metastatic tumors, suggesting an association with tumor progression and distal metastasis^[131,132]. *CyclinD1*, a cell cycle protein, facilitates cell cycle progression from G1 to S phase through combining with CDK4. Both the amplification and overexpression of *cyclinD1* were detected in esophageal carcinomas^[133,134]. Abnormal expression of *cyclin E* and *p27* may be one of the important molecular changes in the early stage of esophageal carcinogenesis, and the high-expression of *cyclin E* and low-expression of *p27* may be one of the mechanisms driving the mild lesion towards carcinogenesis^[135]. In contrast to other gastrointestinal tumors, the *ras* oncogene is rarely mutated in human esophageal adenocarcinoma^[127]. However, overexpression of *ras* and *ras*-regulated genes (*osteopontin*, *cathepsin L*) has been reported in 58 % of primary esophageal adenocarcinomas^[136].

DIFFERENCES BETWEEN ADENOCARCINOMAS OF LOWER ESOPHAGUS, GASTRIC CARDIA AND SUBCARDIAC STOMACH

Though adenocarcinomas of the lower esophagus and gastric cardia share similar epidemiological characteristics, new clinicopathologic classifications have established criteria to differentiate these two entities. *Taniere*^[137] compared molecular markers in esophageal adenocarcinomas with those in adenocarcinomas of the gastric cardia. The male to female ratio and *p53* mutation frequency were higher in esophageal adenocarcinomas, while *mdm2* amplification was more frequent in the adenocarcinomas of the gastric cardia. Patterns of cytokeratin immunostaining were also different between these two tumors. *Flejou*^[138] performed a study to compare *p53* protein expression immunohistochemically between esophageal and gastric carcinomas, and reported a higher prevalence of *p53* protein overexpression was found in esophageal and cardiac adenocarcinomas compared with gastric antral adenocarcinoma. This was confirmed by an additional study, which reported *p53* mutation rates in adenocarcinomas of distal stomach were significantly lower than those in adenocarcinomas of esophagus and gastric cardia^[139]. These results suggest that adenocarcinoma of the gastric cardia may be a distinct entity from adenocarcinoma of the distal stomach.

Comparison between gastric cardia adenocarcinoma and esophageal squamous cell carcinoma, with special reference to Linzhou

Because of the highly concurrent incidence of gastric cardia adenocarcinoma and esophageal squamous cell carcinoma in Linzhou^[140], it is highly desirable to characterize the molecular differences between these tumors of different histological types to explore the possible clues related with etiological risk factors. However, useful information concerning this topic is very limited. In Linzhou, it is not uncommon clinically to identify patients with both gastric cardia adenocarcinoma and esophageal squamous cell carcinoma^[141], which is the most common pattern of multiple primary malignant neoplasm (MPN) with an incidence of 0.4-2.5 %^[142]. Recent studies from Wang's laboratory showed that there was a highly consistent positive immunostaining rate for *p53* in SCC and GCA from the same patient (60 %, 12/25 vs 40 %, 10/25)^[79] similar results were observed for PCNA. *p53* mutation analysis in patients with either SCC or GCA from Linzhou indicated that G:C to

A:T transition was the most frequent mutation pattern both in SCC and GCA. The consistency of *P53* gene mutation was as high as 64 %^[143]. G to A mutation pattern may be resulted from DNA methylation induced by nitrosamine^[141]. These results are of important value in explaining the similar geographic distribution of SCC and GCA in this area. Protein file analysis also showed similar expression pattern in SCC and GCA, such as *PTEN*^[144], *c-erbB-2* and *c-myc*^[145], *MUC1*^[146], *CYP1A1* and *2E1*^[147], *MUC3*^[148], *mEH*^[149], *GSTM1*, *GSTT1* and *GSTP*^[150], *EGFR*^[151], etc from the samples in Linzhou.

CONCLUSION

In summary, the incidence of adenocarcinomas arising from the distal esophagus, EGJ and gastric cardia is increasing at a dramatic rate in North America and Europe. It is suggested that adenocarcinomas of the esophagus develop in a metaplasia-dysplasia-carcinoma sequence. Whether adenocarcinomas of the gastric cardia follow the same pattern needs further study. Although both esophageal squamous cell carcinomas and adenocarcinomas of the gastric cardia have a high incidence in the same high-risk population in Linzhou, little information is available on the molecular and etiological differences between these two tumor types. Metaplasia is a frequent finding in the gastric cardia, but its significance in the development of adenocarcinoma of the gastric cardia is not clear. *H.pylori* infection, a main factor causing atrophy of the mucosa of distal stomach, also leads to chronic inflammation of the gastric cardia. Though *H.pylori* has been classified as a Type I carcinogen, the role it plays in gastric cardia carcinogenesis remains unclear. To study adenocarcinoma of the gastric cardia in China, researchers are beginning to evaluate epidemiological, histopathologic and molecular characteristics of the tumor.

ACKNOWLEDGEMENTS

We acknowledge the help given by graduate students in Laboratory for Cancer Research, College of Medicine, Zhengzhou University (Drs. Dao-Cun Wang, Ning-Bo Wang, Hui-Xing Yi, Xin-Wei He, She-Gan Gao, Xin-Na Yi, Zhi-Wei Chang, Dong-Ling Xie, Ran Wang, Ya-Nan Jiang, Xiao-Dong Lü, Xiao-Li Liu) in preparation of the manuscript.

REFERENCES

- 1 **Hermanek P**, Sobin LH. TNM classification of malignant tumors. International Union Against Cancer (UICC). 4th ed. 2nd revision. Berlin: Springer 1992; page: 455-460
- 2 **Beahrs OH**, Henson DE, Hutter RVP, Kennedy BJ, eds. American Joint Committee on Cancer: Manual for Staging of Cancer. 4th ed. Philadelphia, Pennsylvania: JB Lippincott 1992; page: 175-200
- 3 **Powell J**, McConkey CC. Increasing incidence of adenocarcinoma of the gastric cardia and adjacent sites. *Br J Cancer* 1990; **62**: 440-443
- 4 **Blot WJ**, Devesa SS, Kneller RW, Fraumeni F. Rising incidence of adenocarcinoma of the esophagus and gastric cardia. *JAMA* 1991; **265**: 1287-1289
- 5 **Blot WJ**, Devesa SS, Fraumeni JF. Continuing climb in rates of esophageal adenocarcinoma: An update. *JAMA* 1993; **270**: 1320-1322
- 6 **Pera M**, Cameron AJ, Trastek VF, Carpenter HA, Zinsmeister AR. Increasing incidence of adenocarcinoma of the esophagus and esophogastriac junction. *Gastroenterology* 1993; **104**: 510-513
- 7 **Spechler SJ**, Robbins AH, Bloomfield RH, Vincent ME, Heeren T, Doos WG, Colton T, Shimmel EM. Adenocarcinoma and Barrett's esophagus: an overrated risk? *Gastroenterology* 1984; **87**: 927-933
- 8 **Cameron AJ**, Ott BJ, Payne WS. The incidence of adenocarcinoma in columnar-lined (Barrett's) esophagus. *N Engl J Med* 1985; **313**: 857-859

- 9 **Wang HH**, Antonioli DA, Goldman H. Comparative features of esophageal and gastric adenocarcinomas: recent changes in type and frequency. *Hum Pathol* 1986; **17**: 482-487
- 10 **Vaughan TL**, Davis S, Kristal A, Thomas DB. Obesity, alcohol, and tobacco as risk factors for cancers of the esophagus and gastric cardia: adenocarcinoma versus squamous cell carcinoma. *Cancer Epidemiol Biomarkers Prev* 1995; **2**: 85-92
- 11 **Zhang ZF**, Kurtz RC, Sun M, Karpeh MJ, Yu GP, Gargon N, Fein JS, Georgopoulos SK, Harlap S. Adenocarcinomas of the esophagus and gastric cardia: medical conditions, tobacco, alcohol, and socio-economic factors. *Cancer Epidemiol Biomarkers Prev* 1996; **1**: 761-768
- 12 **Gammon MD**, Schoenberg JB, Ahsan H, Risch HA, Vaughan TL, Chow WH, Rotterdam H, West AB, Dubrow R, Stanford JL, Mayne ST, Farrow DC, Niwa S, Blot WJ, Fraumeni JF Jr. Tobacco, alcohol, and socioeconomic status and adenocarcinomas of the esophagus and gastric cardia. *J Natl Cancer Inst* 1997; **89**: 1277-1284
- 13 **Wang LD**, Gao WJ, Yang WC, Li XF, Li J, Zou JX, Wang DC, Guo RX. Preliminary analysis of the statistics on 3,933 cases with esophageal cancer and gastric cardia cancer from the subjects in People's Hospital of Linzhou in 9 years. *Henan Yike Daxue Xuebao* 1997; **32**: 9-11
- 14 **Li JY**, Ershow AG, Chen ZJ, Wacholder S, Li GY, Guo W, Li B, Blot WJ. A case-control study of cancer of the esophagus and gastric cardia in Linzhou. *Int J Cancer* 1989; **43**: 755-761
- 15 **Yang CS**. Research on esophageal cancer in China: a review. *Cancer Res* 1980; **40**: 2633-2644
- 16 **Lu SH**, Chui SX, Yang WX, Hu XN, Guo LP, Li FM. Relevance of N-nitrosamines to esophageal cancer in China. *IARC Sci Pub* 1991; **105**: 11-17
- 17 **Yu Y**, Taylor PR, Li JY, Dawsey SM, Wang GQ, Guo WD, Wang W, Liu BQ, Blot WJ, Shen Q. Retrospective cohort study of risk-factors for esophageal cancer in Linzhou, People's Republic of China. *Cancer Causes Control* 1993; **4**: 195-202
- 18 **Guo W**, Blot WJ, Li JY, Taylor PR, Liu BQ, Wang W, Wu YP, Zheng W, Dawsey SM, Li B. A nested case-control study of oesophageal and stomach cancers in the Linzhou nutrition intervention trial. *Int J Epidemiol* 1994; **23**: 444-450
- 19 **Wijnhoven BP**, Siersema PD, Hop WC, van Dekken H, Tilanus HW. Adenocarcinomas of the distal oesophagus and gastric cardia are one clinical entity. Rotterdam Esophageal Tumour Study Group. *Br J Surg* 1999; **86**: 529-535
- 20 **Casson AG**, Mukhopadhyay T, Cleary KR, Ro JY, Levin B, Roth JA. P53 gene mutations in Barrett's epithelium and esophageal cancer. *Cancer Res* 1991; **51**: 4495-4499
- 21 **Siewert JR**, Stein HJ. Classification of adenocarcinoma of the oesophagogastric junction. *Br J Surg* 1998; **85**: 1457-1459
- 22 **Spechler SJ**. Barrett's esophagus and esophageal adenocarcinoma: pathogenesis, diagnosis, and therapy. *Med Clin North Am* 2002; **86**: 1423-1445
- 23 **Spechler SJ**, Goyal RK. Barrett's esophagus. *N Engl J Med* 1986; **315**: 362-371
- 24 **Vaughan TL**, Kristal AR, Blount PL, Levine DS, Galipeau PC, Prevo LJ, Sanchez CA, Rabinovitch PS, Reid BJ. Nonsteroidal anti-inflammatory drug use, body mass index, and anthropometry in relation to genetic and flow cytometric abnormalities in Barrett's esophagus. *Cancer Epidemiol Biomarkers Prev* 2002; **11**: 745-752
- 25 **Spechler SJ**. Clinical practice. Barrett's Esophagus. *N Engl J Med* 2002; **346**: 836-842
- 26 **Everhart CWJ**, Holzapple PG, Humphries TJ. Barrett's esophagus: inherited epithelium or inherited reflux? *J Clin Gastroenterol* 1983; **5**: 357-358
- 27 **Crabb DW**, Berk MA, Hall TR, Conneally PM, Biegel AA, Lehman GA. Familial gastroesophageal reflux and development of Barrett's esophagus. *Ann Intern Med* 1985; **103**: 52-54
- 28 **Smith RRL**, Hamilton SR, Boitnott JK, Rogers EL. The spectrum of carcinoma arising in Barrett's esophagus: a clinicopathologic study of 26 patients. *Am J Surg Pathol* 1984; **8**: 563-557
- 29 **Bonelli L**. Barrett's esophagus: results of a multicentric survey. *Endoscopy* 1993; **25**: 652-654
- 30 **Reid BJ**, Sanchez CA, Blount PL, Levine DS. Barrett's esophagus: cell cycle abnormalities in advancing stages of neoplastic progression. *Gastroenterology* 1993; **105**: 119-129
- 31 **Weston AP**, Krmpotich P, Makdisi WF, Cheriam R, Dixon A, McGregor DH, Banerjee SK. Short segment Barrett's esophagus: clinical and histological features, associated endoscopic findings, and association with gastric intestinal metaplasia. *Am J Gastroenterol* 1996; **91**: 981-986
- 32 **Hamilton SR**, Smith RR, Cameron JL. Prevalence and characteristics of Barrett's esophagus in patients with adenocarcinoma of the esophagus or esophagogastric junction. *Hum Pathol* 1988; **19**: 942-948
- 33 **Wang LD**, Feng CW, Zhou Q. Analysis of the screening result of esophageal disease in high risk urban and rural areas of esophageal carcinoma. *Henan Yike Daxue Xuebao* 1997; **32**: 6-8
- 34 **Wang LD**, Zheng S, Fan ZM, Liu B, Feng CW, Sun C, Gao SG, Zhang YR, Guo HQ, Li JL, Jiao XY. Changes of Z-line at the gastroesophageal junction in symptom-free subjects from high-incidence area for esophageal cancer in Henan. *Zhengzhou Daxue Xuebao Yixueban* 2002; **37**: 733-736
- 35 **Gottfried MR**, McClave SA, Boyce HW. Incomplete intestinal metaplasia in the diagnosis of columnar lined esophagus (Barrett's esophagus). *Am J Clin Pathol* 1989; **92**: 741-746
- 36 **Jass JR**. Role of intestinal metaplasia in the histogenesis of gastric carcinoma. *J Clin Pathol* 1980; **33**: 801-810
- 37 **Filipe MI**, Potet F, Bogomoletz WV, Dawson PA, Fabiani B, Chauveinc P, Fenzy A, Gazzard B, Goldfain D, Zeegen R. Incomplete sulphomucin-secreting intestinal metaplasia for gastric cancer. Preliminary data from a prospective study from three centers. *Gut* 1985; **26**: 1319-1326
- 38 **Spechler SJ**. The role of gastric carditis in metaplasia and neoplasia at the gastroesophageal junction. *Gastroenterology* 1999; **117**: 218-228
- 39 **Haggitt RC**. Barrett's esophagus, dysplasia, and adenocarcinoma. *Hum Pathol* 1994; **25**: 982-993
- 40 **Gulizia JM**, Wang H, Antonioli D, Spechler SJ, Zeroogian J, Goyal R, Shahsafaei A, Chen YY, Odze RD. Proliferative characteristics of intestinalized mucosa in the distal esophagus and gastroesophageal junction (short-segment Barrett's esophagus): a case control study. *Hum Pathol* 1999; **30**: 412-418
- 41 **El-Serag HB**, Sonnenberg A, Jamal MM, Kunkel D, Crooks L, Feddersen RM. Characteristics of intestinal metaplasia in the gastric cardia. *Am J Gastroenterol* 1999; **94**: 622-627
- 42 **Voutilainen M**, Farkkila M, Juhola M, Mecklin JP, Sipponen P. The Central Finland Endoscopy Study Group. Complete and incomplete intestinal metaplasia at the esophagogastric junction: prevalences and associations with endoscopic erosive esophagitis and gastritis. *Gut* 1999; **45**: 644-648
- 43 **Prach AT**, MacDonald TA, Hopwood DA, Johnston DA. Increasing incidence of Barrett's esophagus: education, enthusiasm or epidemiology? *Lancet* 1997; **350**: 933
- 44 **Morales TG**, Bhattacharyya A, Johnson C, Sampliner R. Is Barrett's esophagus associated with intestinal metaplasia of the gastric cardia? *Am J Gastroenterol* 1997; **92**: 1818-1822
- 45 **Morales TG**, Sampliner RE, Bhattacharyya A. Intestinal metaplasia of the gastric cardia. *Am J Gastroenterol* 1997; **92**: 414-418
- 46 **van Sandick JW**, van Lanschoot JB, van Felius L, Haringsma J, Tytgat GN, Dekker W, Driltenburg P, Offerhaus GJ, ten Kate FJ. Intestinal metaplasia of the esophagus or esophagogastric junction: Evidence of distinct clinical, pathologic, and histochemical staining features. *Am Soci Clin Pathol* 2002; **117**: 117-125
- 47 **Chen H**, Wang LD, Fan ZM, Gao SG, Guo HQ, Guo M. The comparison study of the three histochemical staining methods in gastric cardia intestinal metaplasia staining. *Henan Yixue Yanjiu* 2003; **12**: 10-13
- 48 **Asaka M**, Takeda H, Sugiyama T, Kato M. What role does *Helicobacter pylori* play in gastric cancer? *Gastroenterology* 1997; **113**: 556-560
- 49 **Spechler SJ**. Barrett's esophagus. *Semin Oncol* 1994; **21**: 431-437
- 50 **Oberg S**, Peters JH, DeMeester TR, Chandrasoma P, Hagen JA, Ireland AP, Ritter MP, Mason RJ, Crookes P, Bremner CG. Inflammation and specialized intestinal metaplasia of cardiac mucosa is a manifestation of gastroesophageal reflux disease. *Ann Surg* 1997; **226**: 522-532
- 51 **Csendes A**, Smok G, Burdiles P, Sagastume H, Rojas J, Puente G, Quezada F, Korn O. "Carditis": an objective histological marker for pathologic gastroesophageal reflux disease. *Dis Esophagus*

- 1998; **11**: 101-105
- 52 **Goldblum JR**, Vicari JJ, Falk GW, Rice TW, Peek RM, Easley K, Richter JE. Inflammation and intestinal metaplasia of the gastric cardia: the role of gastroesophageal reflux and *H.pylori* infection. *Gastroenterology* 1998; **114**: 633-639
- 53 **Chen YY**, Antoniolli DA, Spechler SJ, Zeroogian JM, Goyal RK, Wang HH. Gastroesophageal reflux disease versus *Helicobacter pylori* infection as the cause of gastric carditis. *Mod Pathol* 1998; **11**: 950-956
- 54 **Zhang YR**, Gao SS, Liu G, An JY, Li JL, Jiao XY, Wang LD. Comparison of *Helicobacter pylori* (HP) infection in the cardia and *pylori* parts of the stomach from symptom-free subjects at high-incidence area for esophageal and gastric cardia cancer in Henan. *Zhengzhou Daxue Xuebao Yixueban* 2002; **37**: 777-779
- 55 **Loffeld RJ**, van der Hulst RW. *Helicobacter pylori* and gastro-oesophageal reflux disease: association and clinical implications. To treat or not to treat with anti-*H. pylori* therapy? *Scand J Gastroenterol Suppl* 2002; **236**: 15-18
- 56 **Labenz J**, Blum AL, Bayerdorffer E, Meining A, Stolte M, Borsch G. Curing *Helicobacter pylori* infection in patients with duodenal ulcer may provoke reflux esophagitis. *Gastroenterology* 1997; **112**: 1442-1447
- 57 **Chow WH**, Blaser MJ, Blot WJ, Gammon MD, Vaughan TL, Risch HA, Perez-Perez GI, Schoenberg JB, Stanford JL, Rotterdam H, West AB, Fraumeni JFJ. An inverse relation between *cagA*+ strains of *Helicobacter pylori* infection and risk of esophageal and gastric cardia adenocarcinoma. *Cancer Res* 1998; **58**: 588-590
- 58 **Vicari JJ**, Peek RM, Falk GW, Goldblum JR, Easley KA, Schnell J, Perez-Perez GI, Halter SA, Rico TW, Blaser MJ, Richter JE. The seroprevalence of *CagA*-positive *Helicobacter pylori* strains in the spectrum of gastroesophageal reflux disease. *Gastroenterology* 1998; **115**: 50-57
- 59 **Ormsby AH**, Kilgore SP, Goldblum JR, Richter JE, Rice TW, Gramlich TL. The location and frequency of intestinal metaplasia at the esophagogastric junction in 223 consecutive autopsies: implications for patient treatment and preventive strategies in Barrett's esophagus. *Mod Pathol* 2000; **13**: 614-620
- 60 **Ormsby AH**, Goldblum JR, Rice TW, Richter JE, Falk GW, Vaezi MF, Gramlich TL. Cytokeratin subsets can reliably distinguish Barrett's esophagus from intestinal metaplasia of the stomach. *Hum Pathol* 1999; **30**: 288-294
- 61 **El-Rifai W**, Powell SM. Molecular biology of gastric cancer. *Semin Radiat Oncol* 2002; **12**: 128-140
- 62 **Zhang QX**, Ding Y, Le XP, Du P. Studies on microsatellite instability in p16 gene and expression of hMSH2 mRNA in human gastric cancer tissues. *World J Gastroenterol* 2003; **9**: 437-441
- 63 **Chae KS**, Ryu BK, Lee MG, Byun DS, Chi SG. Expression and mutation analyses of MKK4, a candidate tumor suppressor gene encoded by chromosome 17p, in human gastric adenocarcinoma. *Eur J Cancer* 2002; **38**: 2048-2057
- 64 **Rees BP**, Caspers E, Hausen A, den Brule A, Drillenburger P, Weterman MA, Offerhaus GJ. Different pattern of allelic loss in Epstein-Barr virus-positive gastric cancer with emphasis on the p53 tumor suppressor pathway. *Am J Pathol* 2002; **161**: 1207-1213
- 65 **Chang YT**, Wu MS, Chang CJ, Huang PH, Hsu SM, Lin JT. Preferential loss of Fhit expression in signet-ring cell and Krukenberg subtypes of gastric cancer. *Lab Invest* 2002; **82**: 1201-1208
- 66 **Becker KF**, Kremmer E, Eulitz M, Schulz S, Mages J, Handschuh G, Wheelock MJ, Cleton-Jansen AM, Hofler H, Becker I. Functional allelic loss detected at the protein level in archival human tumors using allele-specific E-cadherin monoclonal antibodies. *J Pathol* 2002; **197**: 567-574
- 67 **Wang Q**, Chen H, Bai J, Wang B, Wang K, Gao H, Wang Z, Wang S, Zhang Q, Fu S. Analysis of loss of heterozygosity on 19p in primary gastric cancer. *Zhonghua Yixue Yichuanxue Zazhi* 2001; **18**: 459-461
- 68 **Hammoud ZT**, Kaleem Z, Cooper JD, Sundaresan RS, Patterson GA, Goodfellow PJ. Allelotyping analysis of esophageal adenocarcinomas: evidence for the involvement of sequences on the long arm of chromosome 4. *Cancer Res* 1996; **56**: 4499-4502
- 69 **Dolan K**, Garde J, Gosney J, Sissons M, Wright T, Kingsnorth AN, Walker SJ, Sutton R, Meltzer SJ, Field JK. Allelotyping analysis of esophageal adenocarcinoma: loss of heterozygosity occurs at multiple sites. *Br J Cancer* 1998; **78**: 950-957
- 70 **Kaghad M**, Bonnet H, Yang A, Creancier L, Biscan JC, Valent A, Minty A, Chalon P, Lelias JM, Dumont X, Ferrara P, McKeon F, Caput D. Monoallelically expressed gene related to p53 at 1p36, a region frequently deleted in neuroblastoma and other human cancers. *Cell* 1997; **90**: 809-819
- 71 **White PS**, Maris JM, Beltinger C, Sulman E, Marshall HN, Fujimori M, Kaufman BA, Biegel JA, Allen C, Hilliard C, Valentine MB, Lod AT, Enomoto H, Skiyama S, Brodeur GM. A region consistent deletion in neuroblastoma maps within human chromosome 1p36.2-36.3. *Proc Natl Acad Sci USA* 1995; **92**: 5520-5524
- 72 **Papadopoulos N**, Nicolaides NC, Wei YF, Ruben SM, Carter KC, Rosen CA, Haseltine WA, Fleischmann RD, Fraser CM, Adams MD. Mutation of a mutL homolog in hereditary colon cancer. *Science* 1994; **262**: 1625-1629
- 73 **Risk JM**, Mills HS, Garde J, Dunn JR, Evans KE, Hollstein M, Field JK. The tylosis esophageal cancer (TOC) locus: more than just a familial cancer gene. *Dis Esophagus* 1999; **12**: 173-176
- 74 **Mori T**, Aoki T, Matsubara T, Iida F, Du X, Nishihira T, Mori S, Nakamura Y. Frequent loss of heterozygosity in the region including BRCA1 on chromosome 17q in squamous cell carcinomas of the esophagus. *Cancer Res* 1994; **54**: 1638-1640
- 75 **van Dekken H**, Geelen E, Dinjens WN, Wijnhoven BP, Tilanus HW, Tanke HJ, Rosenberg C. Comparative genomic hybridization of cancer of the gastroesophageal junction: deletion of 14Q31-32.1 discriminates between esophageal (Barrett's) and gastric cardia adenocarcinomas. *Cancer Res* 1999; **59**: 748-752
- 76 **Gleeson CM**, Sloan JM, McGuigan JA, Ritchie AJ, Weber JL, Russel SEH. Allelotyping analysis of adenocarcinoma of the gastric cardia. *Br J Cancer* 1997; **76**: 1455-1465
- 77 **Hollstein M**, Shormer B, Greenblatt M, Soussi T, Hovig E, Montesano R, Harris CC. Somatic point mutations in the p53 gene of human tumors and cell lines: update compilation. *Nucleic Acids Res* 1996; **24**: 141-146
- 78 **Shi ST**, Yang GY, Wang LD, Xue Z, Feng B, Ding W, Xing EP, Yang CS. Role of p53 gene mutations in human esophageal carcinogenesis: results from immunohistochemical and mutation analysis of carcinomas and nearby non-cancerous lesions. *Carcinogenesis* 1999; **20**: 591-597
- 79 **Chen H**, Wang LD, Guo M, Gao SG, Guo HQ, Fan ZM, Li JL. Alterations of p53 and PCNA in cancer and adjacent tissues from concurrent carcinomas of the esophagus and gastric cardia in the same patient in Linzhou, a high incidence area for esophageal cancer in northern China. *World J Gastroenterol* 2003; **9**: 16-21
- 80 **Feng CW**, Wang LD, Jiao LH, Liu B, Zheng S, Xie XJ. Expression of p53, inducible nitric oxide synthases and vascular endothelial growth factor in gastric precancerous and cancerous lesions: Correlation with clinical features. *BMC Cancer* 2002; **2**: 1-7
- 81 **Li HL**, Chen DD, Li XH, Zhang HW, Lu YQ, Ye CL, Ren XD. Changes of NF- κ B, p53, Bcl-2 and caspase in apoptosis induced by JTE-522 in human gastric adenocarcinoma cell line AGS cells: role of reactive oxygen species. *World J Gastroenterol* 2002; **8**: 431-435
- 82 **Zhang Z**, Yuan Y, Gao H, Dong M, Wang L, Gong YH. Apoptosis, proliferation and p53 gene expression of *H. pylori* associated gastric epithelial lesions. *World J Gastroenterol* 2001; **7**: 79-82
- 83 **Wang LD**, Liu B, Zheng S. Analysis of p53 mutational spectra of esophageal squamous cell carcinomas from Linzhou: comparison with esophageal and other cancers from other areas. *Zhonghua Liuxing Bingxue Zazhi* 2003; **24**: 202-205
- 84 **Greenblatt MS**, Bennett WP, Hollstein M, Harris CC. Mutations in the p53 tumor suppressor gene: clues to cancer etiology and molecular pathogenesis. *Cancer Res* 1994; **54**: 4855-4878
- 85 **Montesano R**, Hollstein M, Hainaut P. Genetic alterations in esophageal cancer and their relevance to etiology and pathogenesis: a review. *Int J Cancer* 1996; **69**: 225-235
- 86 **Gleeson CM**, Sloan JM, McManus DT, Maxwell P, Arthur K, McGuigan JA, Ritchie AJ, Russell SEH. Comparison of p53 and DNA content abnormalities in adenocarcinoma of the esophagus and gastric cardia. *Br J Cancer* 1998; **77**: 277-286
- 87 **Liang YY**, Esteve A, Martel-Planche G, Takahashi S, Lu SH, Montesano R, Hollstein M. p53 mutations in esophageal tumors from high-incidence areas of China. *Int J Cancer* 1995; **61**: 611-614
- 88 **Arrowsmith CH**. Structure and function in the p53 family. *Cell*

- Death Differ* 1999; **6**: 1169-1173
- 89 **Kaelin WJ**. The emerging p53 gene family. *J Natl Cancer Inst* 1999; **91**: 594-598
- 90 **Sheikh MS**, Fornace AJ Jr. Role of p53 family members in apoptosis. *J Cell Physiol* 2000; **182**: 171-181
- 91 **Benard J**, Douc-Rasy S, Ahomadegbe JC. TP53 family members and human cancers. *Hum Mut* 2003; **21**: 182-191
- 92 **Takahashi H**, Ichiniya S, Nimura Y, Watanabe M, Furusato M, Wakui S, Yatani R, Aizawa S, Nakagawara A. Mutation, allelotyping and transcription analyses of the p73 gene in prostatic carcinoma. *Cancer Res* 1998; **58**: 2076-2077
- 93 **Mai M**, Yokomizo A, Qian C, Yang P, Tindall DJ, Smith DI, Liu W. Activation of p73 silent allele in lung cancer. *Cancer Res* 1998; **58**: 2347-2349
- 94 **Tsao H**, Zhang X, Majewski P, Haluska FG. Mutational and expression analysis of the p73 gene in melanoma cell lines. *Cancer Res* 1999; **59**: 172-174
- 95 **Chi SG**, Chang SG, Lee SJ, Lee CH, Kim JI, Park JH. Elevated and biallelic expression of p73 is associated with progression of human bladder cancer. *Cancer Res* 1999; **59**: 2791-2793
- 96 **Yoshikawa H**, Nagashima M, Knan MA, Mcmenamin MG, Hagiwara K, Harris CC. Mutational analysis of p73 and p53 in human cancer cell lines. *Oncogene* 1999; **18**: 3415-3421
- 97 **Yokozaki H**, Shitara Y, Fujimoto J, Hiyama T, Yasui W, Tahara E. Alterations of p73 preferentially occur in gastric adenocarcinomas with foveolar epithelial phenotype. *Int J Cancer* 1999; **83**: 192-196
- 98 **Mihara M**, Nimura Y, Ichimiya S, Sakiyama S, Kajikawa S, Adachi W, Amano J, Nakagawara A. Absence of mutation of the p73 gene localized at chromosome 1p36.3 in hepatocellular carcinoma. *Br J Cancer* 1999; **79**: 164-167
- 99 **Nimura Y**, Mihara M, Ichimiya S, Sakiyama S, Seki N, Ohira M, Nomura N, Fujimori M, Adachi W, Amano J, He M, Ping YM, Nakagawara A. p73, a gene related to p53, is not mutated in esophageal carcinomas. *Int J Cancer* 1998; **78**: 437-440
- 100 **Cai YC**, Yang GY, Nie Y, Wang LD, Zhao X, Song Y, Seril D N, Liao J, Xing EP, Yang CS. Molecular alteration of p73 in human esophageal squamous cell carcinomas: loss of heterozygosity occurs frequently; loss of imprinting and elevation of p73 expression may be related to defective p53. *Carcinogenesis* 2000; **21**: 683-689
- 101 **Kawano S**, Miller CW, Gombart AF, Bartram CR, Matsuo Y, Asou H, Sakashita A, Said J, Tatsumi E, Koeffler HP. Loss of p73 gene expression in leukemias/lymphomas due to hypermethylation. *Blood* 1999; **94**: 1113-1120
- 102 **Corn PG**, Kuerbitz SJ, van Noesel MM, Esteller M, Compitello N, Baylin SB, Herman JG. Transcriptional silencing of the p73 gene in acute lymphoblastic leukemia and Burkett's lymphoma is associated with 5' CpG island methylation. *Cancer Res* 1999; **59**: 3352-3356
- 103 **Zaika AI**, Kovalev S, Marchenko ND, Moll UM. Overexpression of the wild type p73 gene in breast cancer tissues and cell lines. *Cancer Res* 1999; **59**: 3257-3263
- 104 **Tokuchi Y**, Hashimoto T, Kobayashi Y, Hayashi M, Nishida K, Hayashi S, Imai K, Nakachi K, Ishikawa Y, Nakagawa K, Kawakami Y, Tsuchiya E. The expression of p73 is increased in lung cancer, independent of p53 gene alteration. *Br J Cancer* 1999; **80**: 1623-1629
- 105 **Yokomizo A**, Mai M, Tindall DJ, Cheng L, Bostwick DG, Naito S, Smith DI, Liu W. Overexpression of the wild type p73 gene in human bladder cancer. *Oncogene* 1999; **18**: 1629-1633
- 106 **Loiseau H**, Arsaut J, Demotes-Mainard J. p73 gene transcripts in human brain tumors: overexpression and altered splicing in ependymomas. *Neurosci Lett* 1999; **263**: 173-176
- 107 **Tannapfel A**, Schmelzer S, Benicke M, Klimpfinger M, Kohlhaw K, Mossner J, Engeland K, Wittekind C. Expression of the p53 homologues p63 and p73 in multiple simultaneous gastric cancer. *J Pathol* 2001; **195**: 163-170
- 108 **Hagiwara K**, McMenamin MG, Miura K, Harris CC. Mutational analysis of the p63/p73L/p51/p40/CUSP/KET gene in human cancer cell lines using intronic primers. *Cancer Res* 1999; **59**: 4165-4169
- 109 **Kato S**, Shimada A, Osada M, Ikawa S, Obinata M, Nakagawara A, Kanamaru R, Ishioka C. Effects of p51/p63 missense mutations on transcriptional activities of p53 downstream gene promoters. *Cancer Res* 1999; **59**: 5908-5911
- 110 **Yang A**, Kaghad M, Wang Y, Gillett E, Fleming MD, Dotsch V, Andrews NC, Caput D, McKeon F. p63, a p53 homolog at 3q27-29, encodes multiple products with transactivating, death-inducing, and dominant-negative activities. *Mol Cell* 1998; **2**: 305-316
- 111 **Xing EP**, Yang GY, Wang LD, Shi ST, Yang CS. Loss of heterozygosity of the Rb gene correlates with pRb protein expression and associates with p53 alteration in human esophageal cancer. *Clin Cancer Res* 1999; **5**: 1231-1240
- 112 **Rigberg DA**, Kim FS, Sebastian JL, Kazanjian KK, McFadden DW. Hypophosphorylated retinoblastoma protein is associated with G2 arrest in esophageal squamous cell carcinoma. *J Surg Res* 1999; **84**: 101-105
- 113 **Knudsen KE**, Weber E, Arden KC, Cavenee WK, Feramisco JR, Knudsen ES. The retinoblastoma tumor suppressor inhibits cellular proliferation through two distinct mechanisms: inhibition of cell cycle progression and induction of cell death. *Oncogene* 1999; **18**: 5239-5245
- 114 **Lan J**, Xiong YY, Lin YX, Wang BC, Gong LL, Xu HS, Guo GS. *Helicobacter pylori* infection generated gastric cancer through p53-Rb tumor-suppressor system mutation and telomerase reactivation. *World J Gastroenterol* 2003; **9**: 54-58
- 115 **Zhou Y**, Gao SS, Li YX, Fan ZM, Zhao X, Qi YJ, Wei J P, Zou J X, Liu G, Jiao L, Bai YM, Wang LD. Tumor suppressor gene p16 and Rb expression in gastric cardia precancerous lesions from subjects at a high incidence area in northern China. *World J Gastroenterol* 2002; **8**: 423-425
- 116 **Muzeau F**, Flejou JF, Thomas G, Hamelin R. Loss of heterozygosity on chromosome 9 and p16 (MTS1, CDKN2) gene mutations in esophageal cancers. *Int J Cancer* 1997; **72**: 27-30
- 117 **Wong DJ**, Barrett MT, Stoger R, Emond MJ, Reid BJ. p16INK4a promoter is hypermethylated at a high frequency in esophageal adenocarcinomas. *Cancer Res* 1997; **57**: 2619-2622
- 118 **Xing EP**, Nie Y, Wang LD, Yang GY, Yang CS. Aberrant methylation of p16INK4a and deletion of p15INK4b are frequent events in human esophageal cancer in Linzhou, China. *Carcinogenesis* 1999; **20**: 77-84
- 119 **Tsujimoto H**, Hagiwara A, Sugihara H, Hattori T, Yamagishi H. Promoter methylations of p16INK4a and p14ARF genes in early and advanced gastric cancer. Correlations of the modes of their occurrence with histologic type. *Pathol Res Pract* 2002; **198**: 785-794
- 120 **Hannon GJ**, Beach D. p15INK4B is a potential effector of TGF-beta-induced cell cycle arrest. *Nature* 1994; **371**: 257-261
- 121 **Bates S**, Phillips AC, Clark PA, Stott F, Peters G, Ludwig RL, Vousden KH. p14ARF links the tumour suppressors RB and p53. *Nature* 1998; **395**: 124-125
- 122 **Stott FJ**, Bates S, James MC, McConnell BB, Starborg M, Brookes S, Palmero I, Ryan K, Vousden KH, Peters G. The alternative product from the human CDKN2A locus, p14(ARF), participates in a regulatory feedback loop with p53 and MDM2. *EMBO* 1998; **17**: 5001-5014
- 123 **Xing EP**, Nie Y, Song YL, Yang GY, Cai YC, Wang LD, Yang CS. Mechanisms of inactivation of p14ARF, p15INK4b and p16INK4a genes in human esophageal squamous cell carcinoma. *Clin Cancer Res* 1999; **5**: 2704-2713
- 124 **Yokota J**, Yamamoto T, Miyajima N, Toyoshima K, Nomura N, Sakamoto H, Yoshida T, Terada M, Sugimura T. Genetic alterations of the c-erbB-2 oncogene occur frequently in tubular adenocarcinoma of the stomach and are often accompanied by amplification of the v-erbA homologue. *Oncogene* 1988; **2**: 283-287
- 125 **Park JB**, Rhim JS, Park SC, Kimm SW, Kraus MH. Amplification, overexpression, and rearrangement of the erbB-2 protooncogene in primary human stomach carcinomas. *Cancer Res* 1989; **49**: 6605-6609
- 126 **Persons DL**, Croughan WS, Borilli KA, Cherian R. Interphase cytogenetics of esophageal adenocarcinoma and precursor lesions. *Cancer Genet Cytogenet* 1998; **106**: 11-17
- 127 **Hollstein MC**, Smith AM, Galiana C, Yamasaki H, Bos JL, Mandard A, Partensky C, Montesano R. Amplification of epidermal growth factor receptor gene but no evidence of ras mutation in primary human esophageal cancers. *Cancer Res* 1988; **48**: 5119-5123

- 128 **Tsuda T**, Tahara E, Kajiyama G, Sakamoto H, Terada M, Sugimura T. High incidence of coamplification of hst-1 and int-2 genes in human esophageal carcinoma. *Cancer Res* 1989; **49**: 5505-5508
- 129 **Houldsworth J**, Cordon-cardo C, Ladanyi M, Kelsen DP, Chaganti RSK. Gene amplification in gastric and esophageal adenocarcinomas. *Cancer Res* 1990; **50**: 6417-6422
- 130 **Chen H**, Wang LD, Gao SG, Fan ZM, Guo HQ. Alterations of MUC1, C-erbB2 in concurrent cancers of the esophagus and gastric cardia from the same patient in Linzhou, Henan province, a high incidence area for esophageal cancer. *Zhengzhou Daxue Xuebao (Yixueban)* 2002; **37**: 758-761
- 131 **Tsuda T**, Tahara E, Kajiyama G, Sakamoto H, Terada M, Sugimura T. High incidence of coamplification of hst-1 and int-2 genes in human esophageal carcinomas. *Cancer Res* 1989; **49**: 5505-5508
- 132 **Kitagawa Y**, Ueda M, Anda N, Shinozawa, Y, Shimizu N, Abe O. Significance of int-2/hst-1 coamplification as a prognostic fact or in patients with esophageal squamous carcinoma. *Cancer Res* 1991; **51**: 1504-1508
- 133 **Jiang W**, Kahn SM, Tomita N, Zhang YJ, Lu SH, Weinstein IB. Amplification and expression of the human cyclin D gene in esophageal cancer. *Cancer Res* 1992; **52**: 2980-2983
- 134 **Adelaide J**, Monges G, Derderian C, Seitz JF, Birnbaum D. Oesophageal cancer and amplification of the human cyclin D gene CCND1/PRAD1. *Br J Cancer* 1995; **71**: 64-68
- 135 **Qin YR**, Liu Z, Guo HQ, Gao SS, Fan ZM, Li JX. Expression of tumor suppressor gene p27 and cyclinE in esophageal precancerous lesions from the subjects at high-incidence area for esophageal cancer in Henan. *Zhengzhou Daxue Xuebao (Yixueban)* 2002; **37**: 733-736
- 136 **Casson AG**, Wilson SE, McCart JA, O' Malley FP, Ozcelik H, Tsao MS, Chambers AF. Ras mutation, and expression of the ras regulated genes osteopontin and cathepsin L, in human esophageal cancer. *Int J Cancer* 1997; **72**: 739-745
- 137 **Tniere P**, Martel-Planche G, Maurici D, Lombard-Bohas C, Scoazec JY, Montesano R, Berger F, Hainaut P. Molecular and clinical differences between adenocarcinomas of the esophagus and of the gastric cardia. *Am J Path* 2001; **158**: 33-40
- 138 **Flejou JF**, Muzeau F, Potet F, Lepelletier F, Fekete F, Henin D. Overexpression of the p53 tumor suppressor gene product in esophageal and gastric carcinoma. *Path Res Prac* 1994; **190**: 1141-1148
- 139 **Ireland AP**, Shibata DK, Para Chandrasoma P, Lord RVN, Peters JH, DeMeester TR. Clinical significance of p53 mutations in adenocarcinoma of the esophagus and cardia. *Ann Surg* 2000; **231**: 179-187
- 140 **Chen H**, Wang LD, Gao SG, Fan ZM, Guo HQ, Li JL, Guo M. Alterations of MUC1, C-erbB2 in concurrent cancers of the esophagus and gastric cardia from the same patient in Linzhou, Henan province, a high incidence area for esophageal cancer. *Zhengzhou Daxue Xuebao (Yixueban)* 2002; **37**: 758-760
- 141 **Wang LD**, Zheng S. Mechanisms of human esophageal and gastric cardia cancer on the subjects in Henan, the high incidence area for esophageal cancer. *Zhengzhou Daxue Xuebao (Yixueban)* 2002; **37**: 717-729
- 142 **Zhou Q**, Wang LD. Biological characteristics of gastric cardia adenocarcinoma. *ShiJie Xiaohua Zazhi* 1998; **6**: 636-637
- 143 **Zhou Q**, Zheng ZY, Wang LD, Liu B, Qin YR, Wang DC, Chang ZW, Yi HX, Fan ZM, Li JL. p53 protein accumulation and p53 gene mutation in esophageal and gastric cardia cancer from the patients at Linzhou, Henan. *Zhengzhou Daxue Xuebao (Yixueban)* 2003; **38**: 313-316
- 144 **An JY**, Wang LD, He XW, Wang QM, Fan ZM, Gao SS, Guo HQ. Changes of PTEN expression in esophageal squamous cell carcinomas and gastric cardia adenocarcinoma from the patients at high-incidence area for esophageal cancer in Henan. *Zhengzhou Daxue Xuebao (Yixueban)* 2002; **37**: 750-753
- 145 **Wang LD**, Liu B, Guo RF, Bai YM, Sun C, Yi XN, He XW, Xie DL, Fan ZM, Ding ZH. Changes of c-erbB-2 and c-myc expression in esophageal and gastric cardia carcinogenesis from the subjects at high-incidence area for esophageal cancer in Henan, China. *Zhengzhou Daxue Xuebao (Yixueban)* 2002; **37**: 739-742
- 146 **Zhuang ZH**, Wang LD, Gao SS, Fan ZM, Song ZB, Qi YJ, Li YJ, Li JX. Expression of MUC1 in esophageal and gastric cardia carcinoma: a study on the subjects at high-incidence area for esophageal cancer in Henan, China. *Zhengzhou Daxue Xuebao (Yixueban)* 2002; **37**: 774-777
- 147 **Zhou Q**, Zheng ZY, Wang LD, Liu B, Gao SHG, Guo RF, Fan ZM, Guo HQ, Li JL. Prevalence of genetic polymorphisms of CYP1A1 and 2E1 in subjects with gastric cardia adenocarcinoma at Linzhou, Henan. *Zhengzhou Daxue Xuebao (Yixueban)* 2003; **38**: 317-320
- 148 **Zhou Q**, Bai YM, Wang LD, Liu B, Gao SS, Fan ZM, Guo HQ, Wang QM, Qin YJ, Li JL, Jiao XY. Alterations of MUC3 in gastric-cardia precancerous and cancerous lesions: A comparative study between the high- and low-risk populations. *Zhengzhou Daxue Xuebao (Yixueban)* 2003; **38**: 324-326
- 149 **Zhou Q**, Zheng ZY, Wang LD, Fan ZM, Guo HQ, Gao SHG, Qin YR, An JY, He XW, Wang QM, Wang DC, Liu B, Li JL. Polymorphism of mEH in gastric cardia carcinogenesis from the subjects at Linzhou, Henan. *Zhengzhou Daxue Xuebao (Yixueban)* 2003; **38**: 321-323
- 150 **Zhou Q**, Zheng ZY, Wang LD, Yi XN, Wang DC, Chang ZW, Liu B, Li JL. Prevalence of genetic polymorphisms of GSTM1, GSTT1 and GSTP1 in subjects with gastric cardia adenocarcinoma at Linzhou, Henan. *Zhengzhou Daxue Xuebao (Yixueban)* 2003; **38**: 327-329
- 151 **Zhou Q**, Bai YM, Liu B, He XW, Fan ZM, Li JL, Gao SS, Guo HQ, Wang DC, He XW, Chang ZW, Yih X, Wang NB, Wang LD. Alterations of EGFR in gastric-cardia precancerous and cancerous lesions: A comparative study between the high and low risk populations. *Zhengzhou Daxue Xuebao (Yixueban)* 2003; **38**: 332-334

DNA polymerase ζ : new insight into eukaryotic mutagenesis and mammalian embryonic development

Feng Zhu, Ming Zhang

Feng Zhu, Department of Pathophysiology, Zhejiang University School of Medicine, Hangzhou 310031, Zhejiang Province, China
Ming Zhang, College of Life Science, Zhejiang University, Hangzhou 310012, Zhejiang Province, China

Correspondence to: Professor Ming Zhang, College of Life Science, Zhejiang University, Hangzhou 310012, Zhejiang Province, China. zhangming_ls@zju.edu.cn

Telephone: +86-571-88273423 **Fax:** +86-571-88273423

Received: 2003-01-04 **Accepted:** 2003-02-17

Abstract

Information about the mechanisms that generate mutations in eukaryotes is likely to be useful for understanding human health concerns, such as genotoxicity and cancer. Eukaryotic mutagenesis is largely the outcome of attacks by endogenous and environmental agents. Except for DNA repair, cell cycle checkpoints and DNA damage avoidance, cells have also evolved DNA damage tolerance mechanism, by which lesion-targeted mutation might occur in the genome during replication by specific DNA polymerases to bypass the lesions (translesion DNA synthesis, TLS), or mutation on undamaged DNA templates (untargeted mutation) might be induced. DNA polymerase ζ (pol ζ), which was found firstly in budding yeast *Saccharomyces cerevisiae* and consists of catalytic subunit scRev3 and stimulating subunit scRev7, has received more attention in recent years. Pol ζ is a member of DNA polymerase δ subfamily, which belongs to DNA polymerase B family, and exists in almost all eukaryotes. Human homolog of the scRev3 gene is located in chromosome region 6q21, and the mouse equivalent maps to chromosome 10, distal to the *c-myb* gene and close to the *Macs* gene. Alternative splicing, upstream out-of frame ATG can be found in yeast scRev3, mouse and human homologs. Furthermore, the sequence from 253-323 immediate upstream of the AUG initiator codon has the potential to form a stem-loop hairpin secondary structure in REV3 mRNA, suggesting that human REV3 protein may be expressed at low levels in human cells under normal growth conditions. The functional domain analysis showed that yeast Rev3-980 tyrosine in conserved region II is at the polymerase active site. Human REV3 amino acid residues 1 776-2 195 provide a REV7 binding domain, and REV7 amino acid residues 1-211 provide a bind domain for REV1, REV3 and REV7 itself. More interestingly, REV7 interacts with hMAD2 and therefore might function in the cell cycle control by affecting the activation of APC (anaphase promoting complex). Currently it has been known that pol ζ is involved in most spontaneous mutation, lesion-targeted mutation via TLS, chemical carcinogen induced untargeted mutation and somatic hypermutation of antibody genes in mammalian. In TLS pathway, pol ζ acts as a "mismatch extender" with combination of other DNA polymerases, such as pol ι . Unlike in yeast, it was found that pol ζ also functioned in mouse embryonic development more recently. It was hypothesized that the roles of pol ζ in TLS and cell cycle control might contribute to mouse embryonic lethality.

Zhu F, Zhang M. DNA polymerase ζ : new insight into eukaryotic mutagenesis and mammalian embryonic development. *World J Gastroenterol* 2003; 9(6): 1165-1169

<http://www.wjgnet.com/1007-9327/9/1165.asp>

INTRODUCTION

The increase of environmental cancer has been received intensive attention in recent years^[1-6]. An arresting example is that tobacco smoke significantly increases the risks for oral^[7,8], esophageal^[3,6,9,10], bladder^[11-14], pancreas^[13], gastric^[15] and colorectal cancers^[16]. To understand the relationship between environmental agents and cancer is a noteworthy hotspot, by which it is possible to establish a system to prevent and control environmental cancers.

Information about the mechanisms that generate mutations in eukaryotes is likely to be useful for understanding human health concerns, such as genotoxicity and cancer. Eukaryotic mutagenesis is largely the outcome of attacks by endogenous and environmental agents. However, the cells have evolved sophisticated systems in response to DNA damage, including DNA repair and cell cycle checkpoints. Even when DNA repair systems and cell cycle checkpoints are fully functional, some damage can still persist in the genome during replication under circumstances such as: (i) when cells sustain significant DNA damage; (ii) when a particular damage is poorly repaired; or (iii) when some genomic regions are inefficiently repaired. DNA damage frequently blocks replication. Such blockage can be overcome by error-free or error-prone translesion DNA synthesis (TLS) bypass, employing specialized DNA polymerases and proteins for promoting continuous nascent strand extension at forks blocked by the presence of unrepaired DNA damage at the cost of increasing mutation frequency^[17]. Alternatively, mutation can be avoided by DNA damage avoidance^[18], or occur on undamaged DNA template and lead to untargeted mutation via damage tolerance^[19].

DNA polymerase ζ (pol ζ), consisting of catalytic subunit scRev3 and stimulating scRev7 in budding yeast *Saccharomyces cerevisiae*, has received more attention in recent years. It is thought to be the major component of error-prone TLS pathway^[20-24], although a number of other polymerases might be involved in this process^[25]. In *Saccharomyces cerevisiae*, TLS pathway pasting many types of DNA damage in yeast depends on the activities of pol ζ and Rev1p, which is a major source of DNA-damage-induced substitutions and frameshifts and of spontaneous mutations^[21,22,26-30]. It has been speculated and demonstrated later that human pol ζ plays a major role in UV-induced mutagenesis and somatic hypermutation in antibody genes^[31-34]. More recently, it was found that human pol ζ was also involved in mammalian untargeted mutagenesis, and the expression of human mutator REV3 could be upregulated at transcriptional level in response to chemical carcinogen *N*-methyl-*N'*-nitro-*N*-nitrosoguanidine (MNNG)^[35], which could induce gastric cancer^[36-39] and colorectal cancer^[40,41]. Evidences also suggested that pol ζ was concerned with cell cycle control and early

embryonic development^[42-45]. The aim of this paper was to review the structural and functional features of pol ζ , and its roles in mutagenesis and embryonic development as well.

PROPERTIES OF STRUCTURE AND FUNCTION DOMAIN OF POL ζ

In the budding yeast *Saccharomyces cerevisiae*, the scRev3-scRev7 complex is the sixth eukaryotic DNA polymerase to be described, and is therefore called DNA polymerase ζ ^[22]. The catalytic subunit Rev3 is a member of family B DNA polymerases, which contains six conserved motifs^[46, 47]. Mutation analysis *in vivo* and the X-ray crystal structures of family B polymerases reveal that yeast scRev3-980 tyrosine in conserved region II is at the polymerase active site^[48]. Investigation suggests that homologues of the yeast scRev3 gene are found in almost all eukaryotes, including *Arabidopsis thaliana*, *Drosophila melanogaster*, *Schizosaccharomyces pombe*, mouse and specifically humans^[30, 31, 49-53].

Human homolog of the *Saccharomyces cerevisiae* scRev3 gene is located on chromosome region 6q21, and the mouse equivalent maps to chromosome 10, distal to the *c-myc* gene, and close to the *Mac3* gene^[50, 52]. The full-length cDNA of human REV3 consists of 10 919 nucleotides, with a putative open reading frame of 9 390 bp^[31, 50, 51]. Human REV3 gene contains 33 exons in about 200 kb of genomic DNA, in which an additional exon, alternative splicing event and an upstream out-of frame ATG have been demonstrated^[31, 50]. The same alternative splicing has also been observed in mouse, with a 128bp exon inserted between nt +139 and +140 in approximately 50 % of the transcripts^[52]. An upstream out-of-frame ATG with an ORF that terminates within the main ORF is also found in the yeast gene^[21], suggesting that it may be evolutionally conserved in all pol ζ genes. The sequence context of the upstream gene performs a similar function to that of its yeast counterpart. Interestingly, three stretches of sequences, GGCAGTGGCGGC, AGGGGAGGGGGC, and GCCGCCGCCGCTGC, are duplicated in the 5' untranslated region constituting 323 nucleotides. Furthermore, the sequence from 253-323 immediate upstream of the AUG initiator codon has the potential to form a stem-loop hairpin secondary structure in REV3 mRNA^[51]. Such primary structural features and the secondary structure in the 5' untranslated region are expected to reduce the translational efficiency of the message, suggesting that human REV3 protein may be expressed at low levels in human cells under normal growth conditions.

The predicted homologous proteins in human and mouse are a little over twice the length of the yeast scRev3 protein (1 504 residues), i.e., 3 130 amino acids with an expected mass of 353 kDa and a calculated *pI* of 8.7 in human, and 3 122 amino acids in mouse respectively. The homologous proteins of yeast scRev3 are highly conserved^[31, 51, 52]: (i) in the N-terminal part, the overall homology between yeast scRev3/*Drosophila* DmRev3, yeast scRev3/human REV3 and *Drosophila* DmRev3/human REV3 amounts to respectively 33.3 %, 35.0 % and 50.5 % identical amino acids. (ii) in a region of 850 residues at the carboxyl terminus, the overall homology between yeast scRev3/human REV3 amounts to 39 % identical amino acids, and (iii) in a 55-residue region in the middle of both scRev3 and REV3 proteins, with 29 % identity. But little similarity can be found in the intervening regions^[31].

The carboxyl terminus region of yeast Rev3 homologue proteins in human, mouse and *Drosophila* contains the six conserved sequence motifs characterized by DNA polymerases in the right order, including the canonical hexapeptide motifs within regions 1 and 2, YGDTDS and SLYPSI, which are found jointly only in type B DNA polymerases^[46, 47]. Further alignment shows that pol ζ is a member of DNA polymerase δ

family with two specifically conserved motifs ζ I and ζ II in pol ζ , and in the N-terminal part, a conserved glycine repeat motif (G-x4-G-x2-G-x8-G-x3-YFY) in pol δ is also present in the homologues which have been implicated in nucleotide binding^[51]. Outside the six DNA polymerase motifs in the C-terminal, both yeast scRev3 and human REV3 proteins contain a putative zinc finger DNA binding region, and the location of this putative zinc finger is also highly conserved from yeast to humans^[51]. Such structural features are consistent with the notion that the C-terminal region of scRev3 homologue serves as the catalytic domain during nucleotide polymerization, while its N-terminal region may provide sites for protein-protein interactions with other factors such as a putative yeast scRev7 homologue during translesional DNA synthesis.

However, the existence of a much larger nonhomologous or species-specific region in the expected human protein suggests that pol ζ may perform a wider range of functions in the higher eukaryotes. In *Saccharomyces cerevisiae*, it was found that LexA-scRev3 and Gal4-scRev7 fusions interacted with each other^[22]. More recently, studies showed that human REV3 amino acid residues 1 776-2 195 provided a REV7 binding domain, and REV7 amino acid residues 1-211 provided a bind domain for REV1, REV3 and REV7 itself^[54, 55]. REV7, the stimulating subunit of pol ζ which is located on chromosome 1p36, displays 23 % identity and 53 % similarity with scRev7, as well as 23 % identity and 54 % similarity with the human mitotic checkpoint protein hMAD2. And yeast two-hybrid assay suggests that REV7 may interact with hMAD2 but not with hMAD1^[54]. It is possible that REV3, REV7, and hMAD2 might be capable of forming a stable triprotein complex.

CHARACTERISTICS AND ROLES OF POL ζ INVOLVED IN EUKARYOTIC MUTAGENESIS

DNA damage induced elevation of mutations during the course of translesion replication is likely to be an important contributory cause in the development of many cancers^[27]. With *in vitro* and *in vivo* investigation, it has been clear that pol ζ plays a role in an error-prone way. Yeast pol ζ can bypass T-T cyclobutane dimer, but not (6-4) T-T photoproduct and abasic site, inserting an incorrect nucleotide with relatively low efficiency *in vitro* (f_{inc} values range from 4.1×10^{-3} to 1.9×10^{-5})^[22, 56]. When combined with REV1 (transfers a dCMP residue from dCTP to the 3' end of a DNA primer in a template-dependent reaction opposite abasic site), pol ι (inserts a deoxynucleotide opposite the (6-4) T-T photoproduct and abasic site) or pol η (bypasses T-T cyclobutane dimer with relative high accuracy and efficiency), pol ζ can bypass all three types of lesions with more efficiency (F_{ext} values range from 10^{-1} to 10^{-2}) at elongating from a mismatched terminus, which develops the TLS two-step model (Figure 1)^[56-58].

Mutation caused by TLS is usually designated targeted mutation. However, mutation can also occur on undamaged DNA template and therefore is called untargeted mutation (UTM), which has been described in SOS-induced mutagenesis in *E. coli*^[59]. It has been known that untargeted and targeted mutations caused by SOS response in *E. coli* both result from the inhibition of DNA polymerase functions that normally maintain fidelity and the involvement of DNA polymerases with low fidelity, which include DNA pol III, pol IV (dinB), pol V (UmuD' 2C) and other factors (RecA*, β -sliding clamp, γ -clamp loading complex and single-stranded binding protein)^[60-64]. Using mating experiments with excision deficient strains of *Saccharomyces cerevisiae*, Lawrence and Christensen found that up to 40 % of cycl-91 revertants induced by UV were untargeted, showing that a reduction in fidelity of DNA replication^[65]. In mouse T-lymphoma cells, stress response induced by DNA damage agents (8-methoxy-psoralen or UVA)

leads to specific, delayed and untargeted mutations^[66]. It has been found that low concentration *N*-methyl-*N'*-nitro-*N*-nitrosoguanidine (MNNG), a carcinogen which can induce gastric cancer, could induce mammalian UTM^[19]. However, it is not clear which factor capable of inhibiting fidelity can be induced or activated. More recently, it was found that pol ζ might be involved in the mammalian UTM induced by MNNG. The transcriptional level of *REV3* gene is upregulated when human cells are treated by low concentration MNNG. Furthermore, human cells, in which the function of pol ζ is inhibited by antisense *REV3* RNA, display characteristics of both anti UTM and targeted mutation^[35].

Pol ζ also functions in somatic hypermutation^[33,34]. Accumulation of somatic mutations in the V(H) genes of memory B cells from transgenic mice which express antisense RNA to a portion of mouse *REV3* is decreased, particularly among those that generate amino acid replacements enhancing the affinity of the B cell receptor to the hapten^[33]. In addition, inhibition of the mouse mRev3 by specific phosphorothioate-modified oligonucleotides impairs Ig and bcl-6 hypermutation and UV damage-induced DNA mutagenesis, without affecting cell cycle or viability^[34].

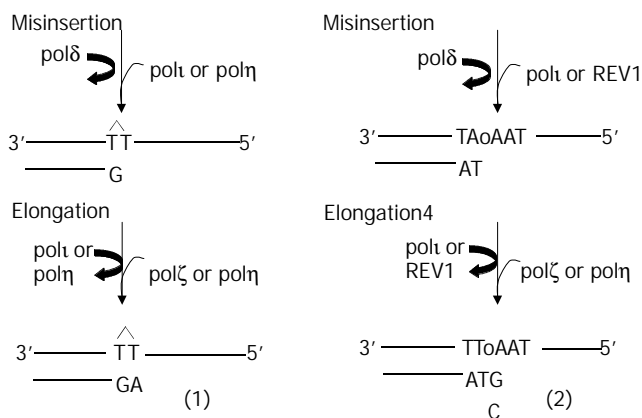


Figure 1 TLS two-step model in human cells. (1) The main replicase in humans, pol δ , has difficulty in replicating through *cis-syn* T-T cyclobutane dimer and (6-4) T-T photoproduct. This recruits specialized polymerases such as pol η , pol ι to insert or misinsert deoxynucleotides, and then pol ζ functions as a mismatch extender. (2) Opposite the abasic site, pol ι or REV1 inserts a deoxynucleotide, and bypass of this lesion occurs when combined with pol ζ .

ROLE OF POL ζ IN MAMMALIAN EMBRYONIC DEVELOPMENT

In *Saccharomyces cerevisiae*, pol ζ is not essential for cell viability, as indicated by the fact that haploids carrying a complete deletion of *Rev3* are viable^[21]. Besides, human fibroblast cells expressing high levels of an *REV3* antisense RNA fragment grow normally^[31]. However, recent evidences have shown that pol ζ is essential for cell viability during embryonic development in mammals (Table 1)^[43-45, 67].

Table 1 Characteristics of *mRev3*^{-/-} embryo

Size	Reduced at day 10.5
Viability	Usually aborted around day 12.5
Inner cell mass (ICM)	Diminished expansion
Haematopoietic cells	No haematopoietic cells developed other than erythrocytes
Morphogenesis of embryo	1. Abnormalities in the development and maintenance of embryonic mesoderm 2. Predominant disorder and lack of integrity mainly in mesenchymal tissues, including heart and large blood vessels

It has been realized that numerous DNA lesions caused by unavoidable oxidative and hydrolytic processes are constantly formed in genomes^[68]. Double-strand breaks can form when DNA replication forks encounter nicked templates, and these stalled replication forks must be reactivated by replication or repair. Unlike cells in adult tissues or in culture, which have mechanisms to cease division or DNA replication temporarily in order to allow accurate and specific DNA repair enzymes to act before proceeding through the cell cycle, embryonic development adheres to a strict temporal program that requires rapid cell division. Under such conditions, enzymes that can rapidly bypass DNA lesions may be expected to be particularly important, and an intolerable load of damaged DNA in critical embryonic or extra-embryonic cells would then lead to death. On the other hand, the proliferating cells in the embryo might gradually accumulate DNA damage and ES cells may be a special case of a cell type primed to undergo apoptosis after accumulated low levels of DNA damage^[69]. During the developmental stage of the *mRev3*-defective mouse embryos before embryonic death, the embryos are still able to propagate rapidly and differentiate through many cell divisions.

It is noteworthy that mouse *mRev3* is most highly expressed in mesodermal tissues and embryonic death coincides with the period of more widely distributed *mRev3l* expression. High-level expression of mouse *mRev3* is developmentally regulated during embryogenesis, occurring first in early somatogenesis and then in other mesodermal tissues up to at least 11.5 days *post coitum*^[45]. This differential expression seems likely to account for the predominant disorder and lack of integrity found mainly in mesenchymal tissues. Lack of proper development of the heart and large blood vessels might in itself be the immediate cause of death. Also, as mouse *mRev3* is normally expressed within extraembryonic membranes, the absence of functional mRev3 in mouse *mRev3*^{-/-} embryos could be the cause of the pericardial sac edema, yolk sac fragility and weak attachment to the decidual implantation site. Yolk-sac malfunction can induce osmotic imbalance, leading to edema, whereas delayed and/or suboptimal chorioallantoic fusion can result in an implantation defect. Defects of the chorioallantoic placenta or yolk sac are a common cause of murine lethality *in utero* and could contribute to the embryonic lethality of mouse *mRev3* disruption. Therefore, ES cells may have a special need for the activity of pol ζ if certain types of DNA damage accumulate within them, and bypass of specific types of DNA lesions by pol ζ is essential for cell viability during embryonic development in mammals.

However, it is also possible that mouse mRev3 has an additional unknown function. In view of the fact that yeast scRev7 shares a region of homology, termed the HORMA (Hop1p, Rev7p and Mad2) domain with Mad2, which associates with unattached kinetochores and functions in the spindle assembly mitotic checkpoint^[71]. Mad2, Rev3 and Rev7 proteins might therefore have the potential to interact *in vitro*. It has been demonstrated that human REV7 may interact with hMAD2^[54]. Interestingly, the tumor suppressor p33ING1, which has recently been demonstrated to have no synergistic effect with p53 in camptothecin-induced cell death in melanoma cells^[72], strongly associates with mRev3 protein in a two-hybrid assay^[30]. It was observed that mouse *mRev3*^{-/-} embryonic death occurred in a p53-independent pathway indicating mRev3 functions with no direct or indirect interaction with p53^[67]. Furthermore, it has been found that *Saccharomyces cerevisiae* lacking Snm1, scRev3 or Rad51 have a normal S-phase but arrest permanently in G₂ after cisplatin treatment^[42]. Therefore, pol ζ can play a central role in apoptosis, cell proliferation, and the control of cell cycle by protein-protein interaction, and thus affect the embryonic development.

REFERENCES

- 1 **Li Y**, Su JJ, Qin LL, Yang C, Luo D, Ban KC, Kensler T, Roebuck B. Chemopreventive effect of oltipraz on AFB(1)-induced hepatocarcinogenesis in tree shrew model. *World J Gastroenterol* 2000; **6**: 647-650
- 2 **Bollschweiler E**, Holscher AH. Carcinoma of the esophagus-actual epidemiology in Germany. *Onkologie* 2001; **24**: 180-184
- 3 **Bonnin-Scaon S**, Lafon P, Chasseigne G, Mullet E, Sorum PC. Learning the relationship between smoking, drinking alcohol and the risk of esophageal cancer. *Health Educ Res* 2002; **17**: 415-424
- 4 **Cai L**, Zheng ZL, Zhang ZF. Risk factors for the gastric cardia cancer: a case-control study in Fujian Province. *World J Gastroenterol* 2003; **9**: 214-218
- 5 **Xue YW**, Zhang QF, Zhu ZB, Wang Q, Fu SB. Expression of cyclooxygenase-2 and clinicopathologic features in human gastric adenocarcinoma. *World J Gastroenterol* 2003; **9**: 250-253
- 6 **Wang AH**, Sun CS, Li LS, Huang JY, Chen QS. Relationship of tobacco smoking CYP1A1 GSTM1 gene polymorphism and esophageal cancer in Xi' an. *World J Gastroenterol* 2002; **8**: 49-53
- 7 **Balaram P**, Sridhar H, Rajkumar T, Vaccarella S, Herrero R, Nandakumar A, Ravichandran K, Ramdas K, Sankaranarayanan R, Gajalakshmi V, Munoz N, Franceschi S. Oral cancer in southern India: the influence of smoking, drinking, paan-chewing and oral hygiene. *Int J Cancer* 2002; **98**: 440-445
- 8 **Bartal M**. Health effects of tobacco use and exposure. *Monaldi Arch Chest Dis* 2001; **56**: 545-554
- 9 **Boring CC**, Squires TS, Tong T, Heath CW. Mortality trends for selected smoking-related cancers and breast cancer—United States, 1950-1990. *Morb Mortal Wkly Rep* 1993; **42**: 857, 863-866
- 10 **Bollschweiler E**, Holscher AH. Carcinoma of the esophagus-actual epidemiology in Germany. *Onkologie* 2001; **24**: 180-184
- 11 **Badawi AF**, Habib SL, Mohammed MA, Abadi AA, Michael MS. Influence of cigarette smoking on prostaglandin synthesis and cyclooxygenase-2 gene expression in human urinary bladder cancer. *Cancer Invest* 2002; **20**: 651-656
- 12 **Bernardini S**, Adessi GL, Chezy E, Billerey C, Carbillet JP, Bittard H. Influence of cigarette smoking on P53 gene mutations in bladder carcinomas. *Anticancer Res* 2001; **21**: 3001-3004
- 13 **Borras J**, Borras JM, Galceran J, Sanchez V, Moreno V, Gonzalez JR. Trends in smoking-related cancer incidence in Tarragona, Spain, 1980-96. *Cancer Causes Control* 2001; **12**: 903-908
- 14 **Castelao JE**, Yuan JM, Skipper PL, Tannenbaum SR, Gago-Dominguez M, Crowder JS, Ross RK, Yu MC. Gender- and smoking-related bladder cancer risk. *J Natl Cancer Inst* 2001; **93**: 538-545
- 15 **Chao A**, Thun MJ, Henley SJ, Jacobs EJ, McCullough ML, Calle EE. Cigarette smoking, use of other tobacco products and stomach cancer mortality in US adults: The Cancer Prevention Study II. *Int J Cancer* 2002; **101**: 380-389
- 16 **Casimiro C**. Etiopathogenic factors in colorectal cancer. Nutritional and life-style aspects. 2. *Nutr Hosp* 2002; **17**: 128-138
- 17 **Kunz BA**, Straffon AF, Vonarx EJ. DNA damage-induced mutation: tolerance via translesion synthesis. *Mutat Res* 2000; **451**: 169-185
- 18 **Li Z**, Xiao W, McCormick JJ, Maher VM. Identification of a protein essential for a major pathway used by human cells to avoid UV-induced DNA damage. *Proc Natl Acad Sci USA* 2002; **99**: 4459-4464
- 19 **Zhang X**, Yu Y, Chen X. Evidence for nontargeted mutagenesis in a monkey kidney cell line and analysis of its sequence specificity using a shuttle-vector plasmid. *Mutat Res* 1994; **323**: 105-112
- 20 **Quah SK**, Von Borstel RC, Hastings PJ. The origin of spontaneous mutation in *Saccharomyces cerevisiae*. *Genetics* 1980; **96**: 819-839
- 21 **Morrison A**, Christensen RB, Alley J, Beck AK, Bernstine EG, Lemontt JF, Lawrence CW. REV3, a *Saccharomyces cerevisiae* gene whose function is required for induced mutagenesis, is predicted to encode a nonessential DNA polymerase. *J Bacteriol* 1989; **171**: 5659-5667
- 22 **Nelson JR**, Lawrence CW, Hinkle DC. Thymine-thymine dimer bypass by yeast DNA polymerase zeta. *Science* 1996; **272**: 1646-1649
- 23 **Baynton K**, Bresson-Roy A, Fuchs RP. Analysis of damage tolerance pathways in *Saccharomyces cerevisiae*: a requirement for Rev3 DNA polymerase in translesion synthesis. *Mol Cell Biol* 1998; **18**: 960-966
- 24 **Lawrence CW**, Maher VM. Eukaryotic mutagenesis and translesion replication dependent on DNA polymerase zeta and Rev1 protein. *Biochem Soc Trans* 2001; **29**: 187-191
- 25 **Rechkoblit O**, Zhang Y, Guo D, Wang Z, Amin S, Krzeminsky J, Louneva N, Geacintov NE. Trans-lesion synthesis past bulky benzo[a]pyrene diol epoxide N2-dG and N6-dA lesions catalyzed by DNA bypass polymerases. *J Biol Chem* 2002; **277**: 30488-30494
- 26 **Roche H**, Gietz RD, Kunz BA. Specificity of the yeast rev3 delta antimutator and REV3 dependency of the mutator resulting from a defect (rad1 delta) in nucleotide excision repair. *Genetics* 1994; **137**: 637-646
- 27 **Lawrence CW**, Hinkle DC. DNA polymerase zeta and the control of DNA damage induced mutagenesis in eukaryotes. *Cancer Surv* 1996; **28**: 21-31
- 28 **Holbeck SL**, Strathern JN. A role for REV3 in mutagenesis during double-strand break repair in *Saccharomyces cerevisiae*. *Genetics* 1997; **147**: 1017-1024
- 29 **Xiao W**, Fontanie T, Bawa S, Kohalmi L. REV3 is required for spontaneous but not methylation damage-induced mutagenesis of *Saccharomyces cerevisiae* cells lacking O6-methylguanine DNA methyltransferase. *Mutat Res* 1999; **431**: 155-165
- 30 **Lawrence CW**, Maher VM. Mutagenesis in eukaryotes dependent on DNA polymerase zeta and Rev1p. *Philos Trans R Soc Lond B Biol Sci* 2001; **356**: 41-46
- 31 **Gibbs PE**, McGregor WG, Maher VM, Nisson P, Lawrence CW. A human homolog of the *Saccharomyces cerevisiae* REV3 gene, which encodes the catalytic subunit of DNA polymerase zeta. *Proc Natl Acad Sci U S A* 1998; **95**: 6876-6880
- 32 **Diaz M**, Velez J, Singh M, Cerny J, Flajnik MF. Mutational pattern of the nurse shark antigen receptor gene (NAR) is similar to that of mammalian Ig genes and to spontaneous mutations in evolution: the translesion synthesis model of somatic hypermutation. *Int Immunol* 1999; **11**: 825-833
- 33 **Diaz M**, Verkoczy LK, Flajnik MF, Klinman NR. Decreased frequency of somatic hypermutation and impaired affinity maturation but intact germinal center formation in mice expressing antisense RNA to DNA polymerase zeta. *J Immunol* 2001; **167**: 327-335
- 34 **Zan H**, Komori A, Li Z, Cerutti A, Schaffer A, Flajnik MF, Diaz M, Casali P. The translesion DNA polymerase zeta plays a major role in Ig and bcl-6 somatic hypermutation. *Immunity* 2001; **14**: 643-653
- 35 **Zhu F**, Jin C, Song T, Yang J, Guo L, Yu Y. Response of human REV3 gene to gastric cancer inducing carcinogen N-methyl-N'-nitro-N-nitrosoguanidine and its role in mutagenesis. *World J Gastroenterol* 2003; **9**: 888-893 (in press)
- 36 **Sherenesheva NI**, Mashkovtsev IV. Electron microscopy study of experimental stomach cancer. *Eksp Onkol* 1985; **7**: 29-35
- 37 **Sasako M**. The effect of Nd:YAG laser irradiation on gastric cancer in rats induced by N-methyl-N'-nitro-N-nitrosoguanidine as a model of endoscopic laser treatment for early gastric cancers. *Nippon Geka Gakkai Zasshi* 1985; **86**: 443-454
- 38 **Newberne PM**, Charnley G, Adams K, Cantor M, Suphakarn V, Roth D, Schrager TF. Gastric carcinogenesis: a model for the identification of risk factors. *Cancer Lett* 1987; **38**: 149-163
- 39 **Yamashita S**, Wakazono K, Sugimura T, Ushijima T. Profiling and selection of genes differentially expressed in the pylorus of rat strains with different proliferative responses and stomach cancer susceptibility. *Carcinogenesis* 2002; **23**: 923-928
- 40 **Amberger H**. Different autochthonous models of colorectal cancer in the rat. *J Cancer Res Clin Oncol* 1986; **111**: 157-159
- 41 **Narayan S**, Jaiswal AS. Activation of adenomatous polyposis coli (APC) gene expression by the DNA-alkylating agent N-methyl-N'-nitro-N-nitrosoguanidine requires p53. *J Biol Chem* 1997; **272**: 30619-30622
- 42 **Grossmann KF**, Ward AM, Moses RE. *Saccharomyces cerevisiae* lacking Snn1, Rev3 or Rad51 have a normal S-phase but arrest permanently in G2 after cisplatin treatment. *Mutat Res* 2000; **461**: 1-13
- 43 **Bemark M**, Khamlichi AA, Davies SL, Neuberger MS. Disruption of mouse polymerase zeta (Rev3) leads to embryonic lethality and impairs blastocyst development in vitro. *Curr Biol* 2000; **10**: 1213-1216
- 44 **Esposito G**, Godindagger I, Klein U, Yaspo ML, Cumano A,

- Rajewsky K. Disruption of the Rev3l-encoded catalytic subunit of polymerase zeta in mice results in early embryonic lethality. *Curr Biol* 2000; **10**: 1221-1224
- 45 **Wittschieben J**, Shivji MK, Lalani E, Jacobs MA, Marini F, Gearhart PJ, Rosewell I, Stamp G, Wood RD. Disruption of the developmentally regulated Rev3l gene causes embryonic lethality. *Curr Biol* 2000; **10**: 1217-1220
- 46 **Braithwaite DK**, Ito J. Compilation, alignment, and phylogenetic relationships of DNA polymerases. *Nucleic Acids Res* 1993; **21**: 787-802
- 47 **Wong SW**, Wahl AF, Yuan PM, Arai N, Pearson BE, Arai K, Korn D, Hunkapiller MW, Wang TS. Human DNA polymerase alpha gene expression is cell proliferation dependent and its primary structure is similar to both prokaryotic and eukaryotic replicative DNA polymerases. *EMBO J* 1988; **7**: 37-47
- 48 **Pavlov YI**, Shcherbakova PV, Kunkel TA. *In vivo* consequences of putative active site mutations in yeast DNA polymerases alpha, epsilon, delta, and zeta. *Genetics* 2001; **159**: 47-64
- 49 **Kajiwara K**, Nagawawa H, Shimizu-Nishikawa S, Ookuri T, Kimura M, Sugaya E. Molecular characterization of seizure-related genes isolated by differential screening. *Biochem Biophys Res Commun* 1996; **219**: 795-799
- 50 **Morelli C**, Mungall AJ, Negrini M, Barbanti-Brodano G, Croce CM. Alternative splicing, genomic structure, and fine chromosome localization of REV3L. *Cytogenet Cell Genet* 1998; **83**: 18-20
- 51 **Lin W**, Wu X, Wang Z. A full-length cDNA of hREV3 is predicted to encode DNA polymerase zeta for damage-induced mutagenesis in humans. *Mutat Res* 1999; **433**: 89-98
- 52 **Van Sloun PP**, Romeijn RJ, Eeken JC. Molecular cloning, expression and chromosomal localisation of the mouse Rev3l gene, encoding the catalytic subunit of polymerase zeta. *Mutat Res* 1999; **433**: 109-116
- 53 **Eeken JC**, Romeijn RJ, de Jong AW, Pastink A, Lohman PH. Isolation and genetic characterisation of the Drosophila homologue of (SCE) REV3, encoding the catalytic subunit of DNA polymerase zeta. *Mutat Res* 2001; **485**: 237-253
- 54 **Murakumo Y**, Roth T, Ishii H, Rasio D, Numata S, Croce CM, Fishel R. A human REV7 homolog that interacts with the polymerase zeta catalytic subunit hREV3 and the spindle assembly checkpoint protein hMAD2. *J Biol Chem* 2000; **275**: 4391-4397
- 55 **Murakumo Y**, Ogura Y, Ishii H, Numata S, Ichihara M, Croce CM, Fishel R, Takahashi M. Interactions in the error-prone postreplication repair proteins hREV1, hREV3, and hREV7. *J Biol Chem* 2001; **276**: 35644-35651
- 56 **Johnson RE**, Washington MT, Haracska L, Prakash S, Prakash L. Eukaryotic polymerases iota and zeta act sequentially to bypass DNA lesions. *Nature* 2000; **406**: 1015-1019
- 57 **Nelson JR**, Lawrence CW, Hinkle DC. Deoxycytidyl transferase activity of yeast REV1 protein. *Nature* 1996; **382**: 729-731
- 58 **Woodgate R**. Evolution of the two-step model for UV-mutagenesis. *Mutat Res* 2001; **485**: 83-92
- 59 **Maenhaut-Michel G**. Mechanism of SOS-induced targeted and untargeted mutagenesis in *E. coli*. *Biochimie* 1985; **67**: 365-369
- 60 **Pham P**, Bertram JG, O'Donnell M, Woodgate R, Goodman MF. A model for SOS-lesion-targeted mutations in Escherichia coli. *Nature* 2001; **409**: 366-370
- 61 **Otterlei M**, Kavli B, Standal R, Skjelbred C, Bharati S, Krokan HE. Repair of chromosomal abasic sites *in vivo* involves at least three different repair pathways. *EMBO J* 2000; **19**: 5542-5551
- 62 **Kim SR**, Maenhaut-Michel G, Yamada M, Yamamoto Y, Matsui K, Sofuni T, Nohmi T, Ohmori H. Multiple pathways for SOS-induced mutagenesis in Escherichia coli: an overexpression of dinB/dinP results in strongly enhancing mutagenesis in the absence of any exogenous treatment to damage DNA. *Proc Natl Acad Sci USA* 1997; **94**: 13792-13797
- 63 **Tang M**, Bruck I, Eritja R, Turner J, Frank EG, Woodgate R, O'Donnell M, Goodman MF. Biochemical basis of SOS-induced mutagenesis in Escherichia coli: reconstitution of *in vitro* lesion bypass dependent on the UmuD'2C mutagenic complex and RecA protein. *Proc Natl Acad Sci USA* 1998; **95**: 9755-9760
- 64 **Tang M**, Pham P, Shen X, Taylor JS, O'Donnell M, Woodgate R, Goodman MF. Roles of *E. coli* DNA polymerases IV and V in lesion-targeted and untargeted SOS mutagenesis. *Nature* 2000; **404**: 1014-1018
- 65 **Lawrence CW**, Christensen RB. The mechanism of untargeted mutagenesis in UV-irradiated yeast. *Mol Gen Genet* 1982; **186**: 1-9
- 66 **Boesen JJ**, Stuijvenberg S, Thyssens CH, Panneman H, Darroudi F, Lohman PH, Simons JW. Stress response induced by DNA damage leads to specific, delayed and untargeted mutations. *Mol Gen Genet* 1992; **234**: 217-227
- 67 **O-Wang J**, Kajiwara K, Kawamura K, Kimura M, Miyagishima H, Koseki H, Tagawa M. An essential role for REV3 in mammalian cell survival: absence of REV3 induces p53-independent embryonic death. *Biochem Biophys Res Commun* 2002; **293**: 1132-1137
- 68 **Lindahl T**, Wood RD. Quality control by DNA repair. *Science* 1999; **286**: 1897-1905
- 69 **Van Sloun PP**, Jansen JG, Weeda G, Mullenders LH, Van Zeeland AA, Lohman PH, Vrieling H. The role of nucleotide excision repair in protecting embryonic stem cells from genotoxic effects of UV-induced DNA damage. *Nucl Acids Res* 1999; **27**: 3276-3282
- 70 **Copp AJ**. Death before birth: clues from gene knockouts and mutations. *Trends Genet* 1995; **11**: 87-93
- 71 **Aravind L**, Koonin EV. The HORMA domain: a common structural denominator in mitotic checkpoints, chromosome synapsis and DNA repair. *Trends Biochem Sci* 1998; **23**: 284-286
- 72 **Cheung KJr**, Li G. The tumour suppressor p33ING1 does not enhance camptothecin-induced cell death in melanoma cells. *Int J Oncol* 2002; **20**: 1319-1322

Detection of human papillomavirus in Chinese esophageal squamous cell carcinoma and its adjacent normal epithelium

Xiao-Bo Zhou, Mei Guo, Lan-Ping Quan, Wei Zhang, Zhe-Ming Lu, Quan-Hong Wang, Yang Ke, Ning-Zhi Xu

Xiao-Bo Zhou, Lan-Ping Quan, Wei Zhang, Ning-Zhi Xu, Laboratory of Cell and Molecular Biology, Cancer Institute & Cancer Hospital, Chinese Academy of Medical Sciences, Beijing 100021, China
Mei Guo, Zhe-Ming Lu, Yang Ke, Laboratory of Genetics, Beijing Institute for Cancer Research, School of Oncology, Peking University, No. 1 Da Hong Luo Chang St, Beijing 100034, China

Quan-Hong Wang, Department of Pathology, the Third People's Hospital of Shanxi Province, Taiyuan 030013, China

Supported in part by grants from the National Natural Science Foundation of China, No. 39925020 and from State Key Basic Research Program, No.G1998051204

Correspondence to: Dr Ning-Zhi Xu, Laboratory of Cell and Molecular Biology, Cancer Institute & Cancer Hospital, Chinese Academy of Medical Sciences, Beijing 100021, China. xningzhi@public.bta.net.cn
Telephone: +86-10-67738220 **Fax:** +86-10-67767548

Dr Yang Ke, Laboratory of Genetics, Beijing Institute for Cancer Research, School of Oncology, Peking University, No. 1 Da Hong Luo Chang St, Beijing 100034, China. keyang@bjmu.edu.cn

Telephone: +86-10-62091204 **Fax:** +86-10-62015681

Received: 2002-12-22 **Accepted:** 2003-03-05

Abstract

AIM: To investigate the putative role of human papillomavirus (HPV) infection in the carcinogenesis of esophageal squamous cell carcinoma in China.

METHODS: Twenty-three esophageal squamous cell carcinoma samples and the distal normal epithelium from Shanxi Province, and 25 more esophageal squamous cell carcinoma samples from Anyang city, two areas with a high incidence of esophageal cancer in China, were detected for the existence of HPV-16 DNA by PCR, mRNA *in situ* hybridization (ISH) and immunohistochemistry (IHC) targeting HPV-16 E6 gene.

RESULTS: There were approximately 64 % (31/48) patients having HPV-16 DNA in tumor samples, among them nearly two-thirds (19/31) samples were detected with mRNA expression of HPV-16 E6. However, in the normal esophageal epithelium from cancer patients, the DNA and mRNA of HPV-16 were found with much less rate: 34.7 % (8/23) and 26.1 % (6/23) respectively. In addition, at protein level detected by IHC assay, 27.1 % (13/48) tumor samples had virus oncoprotein E6 expression, while only one case of normal epithelium was found positive.

CONCLUSION: HPV infection, especially type 16, should be considered as a risk factor for esophageal malignancies in China.

Zhou XB, Guo M, Quan LP, Zhang W, Lu ZM, Wang QH, Ke Y, Xu NZ. Detection of human papillomavirus in Chinese esophageal squamous cell carcinoma and its adjacent normal epithelium. *World J Gastroenterol* 2003; 9(6): 1170-1173
<http://www.wjgnet.com/1007-9327/9/1170.asp>

INTRODUCTION

Esophageal squamous cell carcinoma (ESCC) is one of the leading causes among Chinese cancer mortality, and the

incidence is mainly aggregated in North China, from which Henan and Shanxi Provinces are two high-incidence areas. The distinct geographical distribution suggests a dominant role of environmental factors in the etiology of this disease. Furthermore, other risk factors have been speculated, such as nutrition imbalance (lack or absence of vitamins and minerals), improper life style (cigarette smoking and consumption of pickled food), exposure to nitrosamines, during the carcinogenesis of ESCC in China^[1-2]. Nevertheless, the real causes and the mechanism of ESCC have not been elucidated yet.

Human papillomavirus (HPV) as one kind of important tumor-related virus has been firmly recognized in cervical cancer. But its oncogenic role in other tumors is still disputed^[3-5]. As to its role in ESCC, it was firstly suggested by Syrjanen 20 years ago, when he found the HPV infection in ESCC by pathological observation^[6]. Since then, many reports regarding this topic have been published, but the HPV infection rate in ESCC varied from zero to 67 %^[7,8], depending on the specimens obtained from low- or high-risk area around the world and the methods used in each study^[9-12]. In our previous study, we found that the prevalence of HPV-16 E6 and E7 genes in high incidence area was higher than that in low incidence area, detected by means of PCR and ISH, from the samples of balloon cytologic examination in Anyang area of China^[13]. In order to confirm and further investigate the prevalence of HPV infection in ESCC, the tumor samples and the distal normal epithelia from Shanxi Province, another high incidence region in China, with the tumor samples from Anyang city together, were tested for the existence of HPV-16 DNA.

Based on our previous data^[13], in this study, we focused on the HPV-16 E6 gene, a major viral oncogene of high-risk HPV type. In addition to detecting its DNA and mRNA by using PCR and ISH, the E6 protein expression was simultaneously analyzed by IHC for all the samples. Furthermore the status of HPV-16 infection was compared between tumor samples and their adjacent "normal" esophageal epithelium.

MATERIALS AND METHODS

Clinical samples

A total of 48 primary esophageal carcinoma specimens and 23 normal samples were obtained. Among them, 25 cases were from Anyang City Cancer Hospital and 23 from Shanxi Province Cancer Hospital. Distal end of the 23 surgical samples was pathologically diagnosed as normal esophageal mucous in morphology. Both areas are high incidence region of ESCC in China. The group included 36 males and 12 females with an average age of 57.4 years.

All the samples were esophageal squamous cell carcinomas. None of the patients had radical therapy or chemotherapy before surgery. The paraffin-embedded, formaldehyde fixed samples were cut into 5 μ m slides continuously, one for H&E staining and others for DNA extraction, immunohistochemistry and ISH analysis.

DNA extraction and PCR

The methods were as described previously^[13]. Briefly, 5-10

slides were deparaffinized in xylene and graded alcohol, then the lysis buffer (300 mmol/l NaCl; 50 mmol/l Tris·HCl pH 8.0; 0.2 % SDS) was added into the tube with proteinase K (200 mg/l), and the solution was incubated at 55 °C overnight until it became clear. Then DNA was extracted using phenol/chloroform, precipitated with cold alcohol, and dissolved in ion-free water and the concentration was determined from its optical density. Quality of the extracted DNA was tested by PCR with β -actin primer: 5' GGC GGC ACC ACC ATG TAC CCT 3' and 5' AGG GGC CGG ACT CGT CAT ACT 3'. The usable DNA went through PCR amplification using primer: 5' -CAAGCAACAGTTACTGCGA-3' and 5' -CAACAAG-ACATACATCGACC-3' targeting HPV-16 E6 gene under conditions at 94 °C denaturing for 1 min, at 60 °C annealing for 1 min, and at 72 °C prolonging for 1 min with 30 cycles.

The PCR product was about 321 bp. The plasmid containing full of length of HPV-16 genome as template was the positive control, and the water as template was the negative control.

In situ hybridization assay

HPV-16 E6 gene by PCR from the plasmid containing full length of HPV-16 was obtained and cloned into PGEM-T easy vector (Promega). After Sal I digestion, a digoxin-labelled E6 probe was made via *in vitro* transcription with the kit (Roche, No, 1175025).

The slides were deparaffinized and hydrated in xylene and graded ethanol continuously, then were treated with 0.2 mol/L HCl for 10 min at room temperature, followed by digestion with proteinase K 100 mg/l at 37 °C for 15 min. Twenty-five to fifty ng probe was added into hybridization solution (50 % formamide, 4×SSC, 5 % dextran sulfate, 5×Denhardt's solution and 200 g/l denatured salmon sperm DNA), then the solution containing E6 probe was dropped on the slides. The hybridization reaction was completed overnight in wet-chamber at 42 °C. After this, the slides were washed by 2×SSC, 1×SSC orderly twice, 30 min each time. The anti-digoxin antibody conjugated with alkaline phosphatase was added to the samples for 30 min at 37 °C. The purple-blue ISH signals were developed by adding substrate NBT/BCIP (Roche, No, 1175041) on the slides. The slides were incubated with hybridizing solution without E6 probe as negative control, and the cervical cancer biopsies were used as positive control.

Immunohistochemical staining for HPV-16 E6

The sections were deparaffinized in xylene and hydrated in graded ethanol continuously. Then the sections were covered with 3 % hydrogen peroxide in PBS to block the endogenous peroxidase activity for 10 min. The sections were pre-treated in citrate buffer (0.01 M, pH=6.0) under microwave heating for 20 min to retrieve the antigen. Normal goat serum was added to the slides for 30 min at room temperature. After that, the sections were incubated overnight at 4 °C with mouse monoclonal primary antibody against HPV-16 E6 (Santa Cruz, sc-460#), while the negative control was incubated with PBS instead of primary antibody under the same conditions. After the slides were washed three times in PBS for 5 min each, the biotinylated goat anti-mouse secondary antibody was added for 30 min followed by the avidin-biotinylated peroxidase complex for another 30 min at room temperature. After being washed with PBS, the slides were stained with DAB, and then counterstained in haematoxylin. The cervical cancer biopsies were used as positive control.

Evaluation of ISH and IHC results

If more than 10 % of epithelial cells in one slide showed

the positive signals, the case was regarded as positive. And the data were calculated by χ^2 -test. $P < 0.05$ was regarded as significant.

RESULTS

PCR analysis

All the extracted DNA samples showed good quality of DNA after PCR with β -actin primer. After PCR amplification using HPV-16 E6 specific primer, HPV infection was found in tumor patients from both regions, with an infection rate of 80 % in Anyang, and 47.8 % in Shanxi Province (Figure 1 and Table 1).

Furthermore, we detected the positive rate of 34.7 % of HPV-16 DNA in the morphologically normal epithelium adjacent to tumor tissue. But comparing the positive rate of cancer and normal samples, the difference of HPV infection in DNA level was significant (Table 1).

ISH and IHC assays

To identify whether HPV-16 infection can definitely cause mRNA transcription and protein expression of E6 oncogene, we further detected these two levels by ISH and IHC.

Using digoxin-labelled HPV-16 E6 specific cRNA probe, a total of 19 samples showed positive ISH signals in the cytoplasm of cancer cells. Among them, only 2 had nuclear positive signals (Figure 1). And 6 samples from adjacent normal esophageal epithelium were positive for HPV-16.

Among 48 cancer samples from both regions, 13 had HPV-16 E6 protein expression, while only one normal epithelium sample showed IHC positive signals. The difference between cancer and normal epithelia was significant ($P < 0.05$, Table 1).

The immunohistochemistry dark-brown signals scattered in the infected cancer cells, was similar to those mentioned before^[14] (Figure 2).

Table 1 HPV-16 infection rate detected by PCR, ISH and IHC in normal and tumor esophageal epithelium from two high-incidence regions in China

Samples	Region	n	PCR	ISH	IHC
Normal	Shanxi	23	8(34.7%) ^a	6(26.1%)	1(4.3%) ^a
Tumor	Shanxi	23	11(47.8%)	6(26.1%)	5(21.7%)
	Anyang	25	20(80.0%)	13(52.0%)	8(32.0%)
Total		48	31(64.6%)	19(39.6%)	13(27.1%)

^a $P < 0.05$, from PCR and IHC data, HPV infection rate in normal esophageal epithelium was distinctly different from those in esophageal cancer samples.

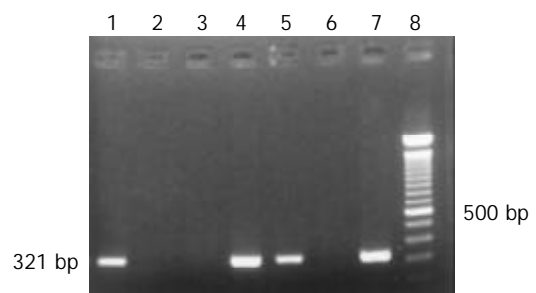


Figure 1 PCR results of Chinese esophageal cancer samples using HPV-16 E6 specific primer. Lane 1,2 were the positive and negative control; Lane 4,5,7 were the positive samples; Lane 3,6 were the negative samples; Lane 8 was 100 bp ladder.

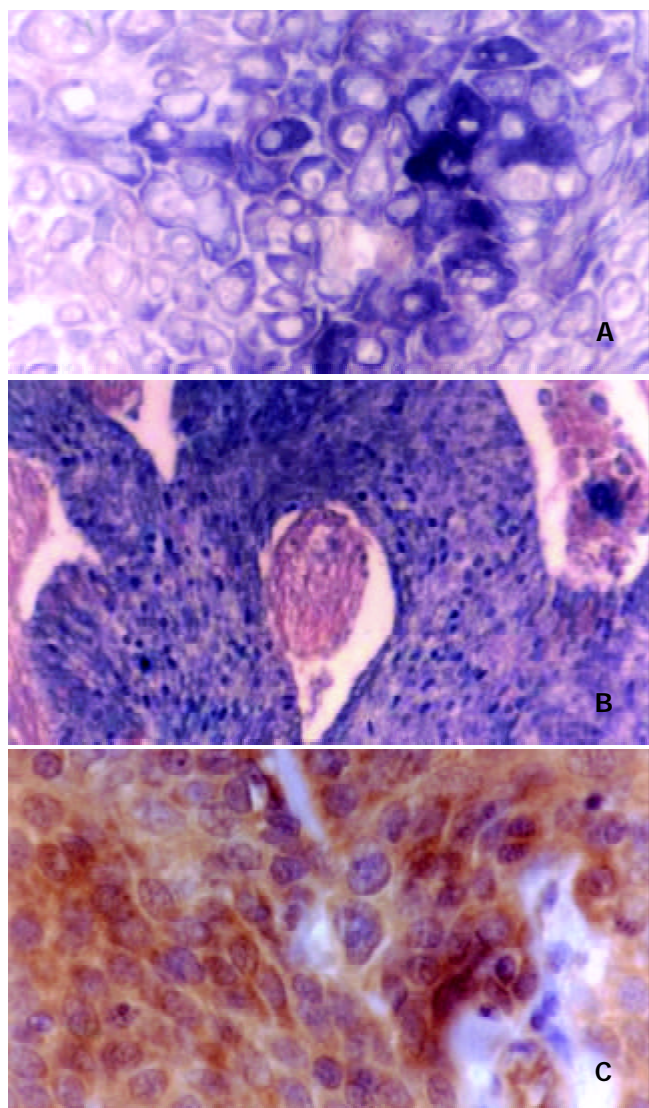


Figure 2 ISH and IHC results of tumor samples targeting HPV-16 E6 gene. A, the positive purple-blue ISH signal is mainly located in the cytoplasm of esophageal cancer cell. $\times 200$; B, the positive purple-blue ISH signal is mainly located in the nuclear of the carcinoma cell. $\times 100$; C, note the dark-brown IHC signals located mainly in the cytoplasm of cancer cell. SP methods, haematoxylin counterstained $\times 200$.

DISCUSSION

HPV infection of the esophagus was first suggested by Syrjanen in 1982, who found that 40 % of the esophageal specimens with squamous cell carcinoma presented histological changes identical to those of condylomatous lesions in or around these carcinomas, and demonstrated the presence of HPV antigen in one case of esophageal squamous cell papilloma using immunohistochemistry. This finding was subsequently confirmed by others who demonstrated HPV antigens as well as HPV DNA in benign and malignant esophageal lesions^[15-19]. But the infection rate reported in the literature varied largely, such as in India, one of Asian high ESCC regions, the detection rate could reach as high as 67 %^[8], while in some Western countries such as France^[20], Slovenia^[21], Sweden^[22], Belgium^[23] and Finland^[24], the HPV infection rate is close to zero. Based on our previous study^[13], and after carefully reviewing the literature, we share the opinion with others^[21,25] that HPV infection plays a much more significant role in ESCC in those regions of the world with a high prevalence of disease than in areas with a moderate or low risk^[26-28].

Besides the influence of geographic, environmental and

racial differences, the sensitivity of the detection techniques and the different methodologies should not be ignored for the variation around the world. For example, consensus L1 primers were frequently used as the proper PCR primers for its ability to detect a wide spectrum of HPV types^[12,26,29]. But during virus integration into the host genome, L1 and L2 were often lost. Therefore, the detection using consensus primers against the L1 gene would likely lead to a low rate. This has been demonstrated clearly by our previous and other studies^[13,25].

HPV type 16 has been most commonly implicated in ESCC, and in addition, it is known that the E6 amplification system is retained during viral integration into the host genome^[25]. In this study, we used specific primer targeting E6 gene of HPV-16 as before^[13]. The presence of HPV-16 DNA was found in 65 % tumor patients from Anyang city and Shanxi Province, two high-incidence regions in ESCC in China. Furthermore, E6 mRNA expression of HPV-16 was detected in nearly two-thirds samples among those viral DNA positive patients, while the positive rate of E6 protein expression not found as high as that of mRNA, but still in more than 40 % (13/31) tumor samples, the E6 protein could be detected by IHC when HPV-16 infection occurred among those patients. From this study, it is demonstrated that HPV-16 infection of esophageal epithelium is very common within ESCC patients from Anyang city, and this observation is truly the same as within those from Shanxi Province.

Comparing the status of HPV-16 infection between some adjacent "normal" esophageal epithelium and their tumor samples, the most significant difference was E6 expression at protein level, rather than DNA and mRNA level between them (Table 1). Therefore, it is confirmed that not only existence of the viral DNA, but also the expression of E6 gene may play an important role in the carcinogenesis of ESCC in those high incidence regions.

It is well known that HPV oncogenes expressed in cervical cancer cells are involved in their transformation and immortalization, and are required for the progression towards malignancy^[30-35]. In cervical cancer, the knowledge has been firmly established that HPV infection could interfere normal cell cycles by degrading tumor suppressor protein P53 and Rb and cause host genomic instability through its DNA integrating host genome randomly and increasing centrosome number. As for the exact function of HPV infection during the carcinogenesis of ESCC, it is still unclear. But in recent years, more evidences suggested the possible mechanism of high-risk HPV in transforming esophageal epithelial cells, such as induction of HPV on the activity of telomerase^[36], interaction of E6 with P53^[37] the association of HPV-16 E6 with nuclear matrix^[38] and others^[39-40].

In conclusion, from our previous study and this study, as well as others, HPV infection should be considered as a risk factor for ESCC, at least in high incidence area in China, and in order to further explore the role of viral DNA infection during the carcinogenesis of ESCC, more works are needed in the future.

REFERENCES

- 1 **Wang DX**, Li W. Advances in esophageal neoplasms etiology. *Shijie Huaren Xiaohua Zazhi* 2000; **8**: 1029-1031
- 2 **Chang F**, Syrjanen S, Wang L, Syrjanen K. Infectious agents in the etiology of esophageal cancer. *Gastroenterology* 1992; **103**: 1336-1348
- 3 **Heino P**, Eklund C, Fredriksson-Shanazarian V, Goldman S, Schiller JT, Dillner J. Association of serum immunoglobulin G antibodies against human papillomavirus type 16 capsids with anal epidermoid carcinoma. *J Natl Cancer Inst* 1995; **87**: 437-440
- 4 **Hemminki K**, Jiang Y, Dong C. Second primary cancers after anogenital, skin, oral, esophageal and rectal cancers: etiological links? *Int J Cancer* 2001; **93**: 294-298

- 5 **Zumbach K**, Hoffmann M, Kahn T, Bosch F, Gottschlich S, Gorogh T, Rudert H, Pawlita M. Antibodies against oncoproteins E6 and E7 of human papillomavirus types 16 and 18 in patients with head-and-neck squamous-cell carcinoma. *Int J Cancer* 2000; **85**: 815-818
- 6 **Syrjanen KJ**. Histological changes identical to those of condylo-matous lesions found in esophageal squamous cell carcinomas. *Arch Geschwustforsch* 1982; **52**: 283-292
- 7 **Talamini G**, Capelli P, Zamboni G, Mastromauro M, Pasetto M, Castagnini A, Angelini G, Bassi C, Scarpa A. Alcohol, smoking and papillomavirus infection as risk factors for esophageal squamous-cell papilloma and esophageal squamous-cell carcinoma in Italy. *Int J Cancer* 2000; **86**: 874-878
- 8 **Sobti RC**, Kochar J, Singh K, Bhasin D, Capalash N. Telomerase activation and incidence of HPV in human gastrointestinal tumors in North Indian population. *Mol Cell Biochem* 2001; **217**: 51-56
- 9 **Han C**, Qiao G, Hubbert NL, Li L, Sun C, Wang Y, Yan M, Xu D, Li Y, Lowy DR, Schiller JT. Serologic association between human papillomavirus type 16 infection and esophageal cancer in Shannxi province, China. *J Natl Cancer Inst* 1996; **88**: 1467-1471
- 10 **Bjorge T**, Hakulinen T, Engeland A, Jellum E, Koskela P, Lehtinen M, Luostarinen T, Paavonen J, Sapp M, Schiller J, Thoresen S, Wang Z, Youngman L, Dillner J. A prospective, seroepidemiological study of the role of human papillomavirus in esophageal cancer in Norway. *Cancer Res* 1997; **57**: 3989-3992
- 11 **Tripodi S**, Chang F, Syrjanen S, Shen Q, Cintorino M, Alia L, Santopietro R, Tosi P, Syrjanen K. Quantitative image analysis of oesophageal squamous cell carcinoma from the high-incidence area of China, with special reference to tumour progression and papillomavirus (HPV) involvement. *Anticancer Res* 2000; **20**: 3855-3862
- 12 **Kawaguchi H**, Ohno S, Araki K, Miyazaki M, Saeki H, Watanabe M, Tanaka S, Sugimachi K. p53 polymorphism in human papillomavirus-associated esophageal cancer. *Cancer Res* 2000; **60**: 2753-2755
- 13 **Li T**, Lu ZM, Chen KN, Guo M, Xing HP, Mei Q, Yang HH, Lechner JF, Ke Y. Human papillomavirus type 16 is an important infectious factor in the high incidence of esophageal cancer in Anyang area of China. *Carcinogenesis* 2001; **22**: 929-934
- 14 **Kim KH**, Yoon DJ, Moon YA, Kim YS. Expression and localization of human papillomavirus type 16 E6 and E7 open reading frame proteins in human epidermal keratinocyte. *Yonsei Med J* 1994; **35**: 1-9
- 15 **Chang F**, Syrjanen S, Shen Q, Cintorino M, Santopietro R, Tosi P, Syrjanen K. Human papillomavirus involvement in esophageal carcinogenesis in the high-incidence area of China. A study of 700 cases by screening and type-specific in situ hybridization. *Scand J Gastroenterol* 2000; **35**: 123-130
- 16 **Chang F**, Syrjanen S, Shen Q, Ji HX, Syrjanen K. Human papillomavirus(HPV) DNA in esophageal precancer lesions and squamous cell carcinomas from China. *Int J Cancer* 1990; **45**: 21-25
- 17 **Ravakhah K**, Midamba F, West BC. Esophageal papillomatosis from human papilloma virus proven by polymerase chain reaction. *Am J Med Sci* 1998; **316**: 285-288
- 18 **Agarwal SK**, Chatterji A, Bhambhani S, Sharma BK. Immunohistochemical co-expression of human papillomavirus type 16/18 transforming (E6) oncoprotein and p53 tumour suppressor gene proteins in oesophageal cancer. *Indian J Exp Biol* 1998; **36**: 559-563
- 19 **Syrjanen KJ**. HPV infections and oesophageal cancer. *J Clin Pathol* 2002; **55**: 721-728
- 20 **Benamouzig R**, Jullian E, Chang F, Robaskiewicz M, Flejou JF, Raoul JL, Coste T, Couturier D, Pompidou A, Rautureau J. Absence of human papillomavirus DNA detected by polymerase chain reaction in French patients with esophageal carcinoma. *Gastroenterology* 1995; **109**: 1876-1881
- 21 **Poljak M**, Cerar A, Seme K. Human papillomavirus infection in esophageal carcinomas: a study of 121 lesions using multiple broad-spectrum polymerase chain reactions and literature review. *Hum Pathol* 1998; **29**: 266-271
- 22 **Lagergren J**, Wang Z, Bergstrom R, Dillner J, Nyren O. Human papillomavirus infection and esophageal cancer: a nationwide seroepidemiologic case-control study in Sweden. *J Natl Cancer Inst* 1999; **91**: 156-162
- 23 **Lambot MA**, Haot J, Peny MO, Fayt I, Noel JC. Evaluation of the role of human papillomavirus in oesophageal squamous cell carcinoma in Belgium. *Acta Gastroenterol Belg* 2000; **63**: 154-156
- 24 **Chang F**, Janatuinen E, Pikkarainen P, Syrjanen S, Syrjanen K. Esophageal squamous cell papillomas. Failure to detect human papillomavirus DNA by in situ hybridization and polymerase chain reaction. *Scand J Gastroenterol* 1991; **26**: 535-543
- 25 **Sur M**, Cooper K. The role of the human papillomavirus in esophageal cancer. *Pathology* 1998; **30**: 348-354
- 26 **Lavergne D**, de Villiers EM. Papillomavirus in esophageal papillomas and carcinomas. *Int J Cancer* 1999; **80**: 681-684
- 27 **Ma QF**, Jiang H, Feng YQ, Wang XP, Zhou YA, Liu K, Jia ZL. Detection of human papillomavirus DNA in squamous cell carcinoma of the esophagus. *Shijie Huaren Xiaohua Zazhi* 2000; **8**: 1218-1224
- 28 **Liu J**, Su Qin, Zhang W. Relationship between HPV-E6, p53 protein and esophageal squamous cell carcinoma. *Shijie Huaren Xiaohua Zazhi* 2000; **8**: 494-496
- 29 **Peixoto Guimaraes D**, Hsin Lu S, Snijders P, Wilmotte R, Herrero R, Lenoir G, Montesano R, Meijer CJ, Walboomers J, Hainaut P. Absence of association between HPV DNA, TP53 codon 72 polymorphism, and risk of oesophageal cancer in a high-risk area of China. *Cancer Lett* 2001; **162**: 231-235
- 30 **Zur Hausen H**. Immortalization of human cells and their malignant conversion by high risk human papillomavirus genotypes. *Semin Cancer Biol* 1999; **9**: 405-411
- 31 **Zur Hausen H**. Papillomaviruses and cancer: from basic studies to clinical application. *Nat Rev Cancer* 2002; **2**: 342-350
- 32 **Duensing S**, Munger K. Human papillomaviruses and centrosome duplication errors: modeling the origins of genomic instability. *Oncogene* 2002; **21**: 6241-6248
- 33 **Munger K**. The role of human papillomaviruses in human cancers. *Front Biosc* 2002; **7**: d641-649
- 34 **Cottage A**, Dowen S, Roberts I, Pett M, Coleman N, Stanley M. Early genetic events in HPV immortalized keratinocytes. *Genes Chromosomes Cancer* 2001; **30**: 72-79
- 35 **Duensing S**, Munger K. Centrosome abnormalities, genomic instability and carcinogenic progression. *Biochim Biophys Acta* 2001; **1471**: M81-88
- 36 **Shen ZY**, Xu LY, Li C, Cai WJ, Shen J, Chen JY, Zeng Y. A comparative study of telomerase activity and malignant phenotype in multistage carcinogenesis of esophageal epithelial cells induced by human papillomavirus. *Int J Mol Med* 2001; **8**: 633-639
- 37 **Zou JX**, Wang LD, Shi ST, Yang GY, Xue ZH, Gao SS, Li YX, Yang CS. p53 gene mutations in multifocal esophageal precancerous and cancerous lesions in patients with esophageal cancer in high-risk northern China. *Shijie Huaren Xiaohua Zazhi* 1999; **7**: 280-284
- 38 **Chen HB**, Chen L, Zhang JK, Shen ZY, Su ZJ, Cheng SB, Chew EC. Human papillomavirus 16 E6 is associated with the nuclear matrix of esophageal carcinoma cells. *World J Gastroenterol* 2001; **7**: 788-791
- 39 **Shen Z**, Cen S, Shen J, Cai W, Xu J, Teng Z, Hu Z, Zeng Y. Study of immortalization and malignant transformation of human embryonic esophageal epithelial cells induced by HPV18 E6E7. *J Cancer Res Clin Oncol* 2000; **126**: 589-594
- 40 **Zou SY**, Liu XM, Tang XP, Wang P. Immunohistochemical and electron microscopic observation on positive HPV-16-E6 protein in esophageal cancer. *Huaren Xiaohua Zazhi* 1998; **6**: 47-48

Expression of ECRG4, a novel esophageal cancer-related gene, downregulated by CpG island hypermethylation in human esophageal squamous cell carcinoma

Chun-Mei Yue, Da-Jun Deng, Mei-Xia Bi, Li-Ping Guo, Shih-Hsin Lu

Chun-Mei Yue, Mei-Xia Bi, Li-Ping Guo, Shih-Hsin Lu, Department of Etiology and Carcinogenesis, Cancer Institute, Peking Union Medical College and Chinese Academy of Medical Sciences, Beijing, 100021, China

Da-Jun Deng, Beijing Institute for Cancer Research, School of Oncology, Peking University, Beijing, 100034, China

Supported by grant from State Key Basic Program (G1998051204) and from the Ministry of Education, China

Correspondence to: Shih-Hsin Lu, Department of Etiology and Carcinogenesis, Cancer Institute, Chinese Academy of Medical Sciences, Beijing 100021, China. shlu@public.bta.net.cn

Telephone: +86-10-67712368 **Fax:** +86-10-67712368

Received: 2003-03-02 **Accepted:** 2003-03-29

Abstract

AIM: To study the mechanisms responsible for inactivation of a novel esophageal cancer related gene 4 (ECRG4) in esophageal squamous cell carcinoma (ESCC).

METHODS: A pair of primers was designed to amplify a 220 bp fragment, which contains 16 CpG sites in the core promoter region of the *ECRG 4* gene. PCR products of bisulfite-modified CpG islands were analyzed by denaturing high-performance liquid chromatography (DHPLC), which were confirmed by DNA sequencing. The methylation status of *ECRG 4* promoter in 20 cases of esophageal cancer and the adjacent normal tissues, 5 human tumor cell lines (esophageal cancer cell line-NEC, EC109, EC9706; gastric cancer cell line-GLC; human embryo kidney cell line-Hek293) and 2 normal esophagus tissues were detected. The expression level of the *ECRG 4* gene in these samples was examined by RT-PCR.

RESULTS: The expression level of *ECRG 4* gene was varied. Of 20 esophageal cancer tissues, nine were unexpressed, six were lowly expressed and five were highly expressed compared with the adjacent tissues and the 2 normal esophageal epithelia. In addition, 4 out of the 5 human cell lines were also unexpressed. A high frequency of methylation was revealed in 12 (8 unexpressed and 4 lowly expressed) of the 15 (80 %) downregulated cancer tissues and 3 of the 4 unexpressed cell lines. No methylation peak was observed in the two highly expressed normal esophageal epithelia and the methylation frequency was low (3/20) among the 20 cases in the highly expressed adjacent tissues. The methylation status of the samples was consistent with the result of DNA sequencing.

CONCLUSION: These results indicate that the inactivation of *ECRG 4* gene by hypermethylation is a frequent molecular event in ESCC and may be involved in the carcinogenesis of this cancer.

Yue CM, Deng DJ, Bi MX, Guo LP, Lu SH. Expression of ECRG4, a novel esophageal cancer-related gene, downregulated by CpG

island hypermethylation in human esophageal squamous cell carcinoma. *World J Gastroenterol* 2003; 9(6): 1174-1178
<http://www.wjgnet.com/1007-9327/9/1174.asp>

INTRODUCTION

Esophageal cancer (EC) is one of the most common malignant tumors in the world. Previous studies have shown several genetic abnormalities including amplification of *c-myc*, *int-2* and *Hst*, mutation and/or deletion of *p53* and *Rb* in human EC and EC cell lines^[1,2]. However, the genetic events leading to the development of EC are not clear yet. In recent years, many studies of EC focused on the clone and identification of novel EC-related genes, which might play an important role in the carcinogenesis and development of esophageal cancer^[3-5].

Recently, we have cloned and identified a novel tumor candidate suppressor gene, *ECRG 4* (Genbank Accession NO. AF 325503), from human normal esophageal epithelium^[6,7]. The *ECRG 4* gene located in chromosome 2q14.1-14.3 contains 4 exons, spans about 13 kb and has a full-length cDNA of 772 bp. Analysis by bioinformatics has shown that the protein coded by *ECRG 4* shows a 31 % homology with mouse IgG V region. The results of SAGE and RT-PCR detection have demonstrated the *ECRG 4* gene is expressed in adult esophageal epithelium but is downregulated in esophageal squamous cell carcinoma (ESCC) and tumor cell lines. These findings suggest that the *ECRG 4* gene might be involved in the development of ESCC, but the mechanism inactivating it remains to be determined.

According to the result of the sequence analysis in *ECRG 4* gene, we found that there were CpG islands in the promoter region, exon 1 and part of intron 1 of the gene. Many tumor suppressor genes are downregulated by promoter methylation during the development and progression of cancer, and hypermethylation of gene-promoter regions is being revealed as one of the most frequent mechanisms in loss of gene function, thus detection of CpG methylation is important to understand the gene regulation of cancer^[8,9]. It has been reported that the expression of some tumor suppressor genes, such as *p16^{INK4a}*, *p16^{INK4b}*, *FHIT* and *E-cadherin* are commonly downregulated by CpG island hypermethylation in ESCC^[10-13]. However, the reason for reducing expression of *ECRG 4* in ESCC is unknown.

In order to determine the mechanism involved in the downregulation of *ECRG 4* in ESCC, we have examined the methylation status of the 5' CpG island in promoter region of the *ECRG 4* gene in 5 human cell lines, which include 3 esophageal cancer cell lines, 2 normal esophageal epithelia and 20 cases with ESCC and adjacent tissues. The methylation status of the cell lines and tissues were compared with the expression of the *ECRG 4* gene in the same samples by RT-PCR respectively.

MATERIALS AND METHODS

Cell lines and tissue samples

Five cell lines, including 3 esophageal cancer cell line-NEC,

EC109 and EC9706; 1 gastric cancer cell line- GLC and 1 human embryo kidney cell line-Hek293 were used in this study. All cell lines were routinely cultured in 1640 medium (Gibco) supplemented with 10 % fetal bovine serum (Hyclone) at 37 °C with 5 % CO₂. 20 pairs of ESCC and corresponding tissues adjacent to the tumors were obtained from surgically removed specimens of individual patients who underwent an operation at the Cancer Hospital in Linxian County which has the highest age-adjusted mortality rate of this cancer. Two normal esophageal epithelia were collected from healthy individuals by biopsy. All the samples were frozen at -70 °C before RNA and DNA were extracted with standard method as described previously^[14].

Bisulfite treatment of DNA

Genomic DNA was treated with sodium bisulfite as described by Herman *et al*^[15]. Briefly, 1 g DNA was denatured by adding freshly prepared NaOH with the final concentration 0.3 M for 15 min in a 37 °C water bath. The denatured DNA was then diluted in 30 µl freshly prepared 10 mM hydroquinone (Sigma) and 520 µl freshly prepared 3 M sodium bisulfite (Sigma) at pH 5.0. The DNA was incubated at 50 °C for 16 h and subsequently purified by the Wizard DNA Clean-Up System Kit (A7280; Promega).

20 µg of human placenta genomic DNA was incubated for 24 h with 20 units of *SssI* (New England Biolabs) as described in the instruction manual and the methylated DNA was treated by bisulfite and purified by the Wizard DNA Clean-Up System Kit (A7280; Promega) as described above.

Design of primers and SsPCR condition

Primers were designed according to the CpG island of the sense strand of the *ECRG 4* gene. The strand-specific primers for the treated CpG island were used to amplify a 220 bp fragment containing 16 CpG sites and 4 cis-acting elements, and they were: 5' -AGTGGGGGA GTT AAG GAG ATA TT -3' (forward), and 5' -CCC CTA AAC TCC AAA ACC AA -3' (reverse). PCR was performed in a GeneAmp 2400 thermocycler (Perkin-Elmer, Norwalk, CT) with a 25 µl reaction mixture containing about 100 ng DNA, 1.6 µmol each primer, 400 µmol each dNTPs, 1.25 U LA Taq with 1× LA reaction buffer (TaKaRa). Thermal cycles were: at 94 °C for 2 min, then 40 cycles at 94 °C for 30 sec, at 52 °C for 30 sec, at 72 °C for 1 min and 30 sec followed by extension at 72 °C for 7 min. The PCR products were detected in 1.5 % agarose gels.

Analysis for methylation by DHPLC

The ssPCR products of *ECRG 4* were introduced into the mobile phase at an injection volume of 5 µl by the autosampler on a WAVE DNA Fragment Analysis System (Transgenomic) identical to that described by Deng *et al*^[16]. Non-denaturing analysis was conducted at 48 °C and partially denaturing analysis was conducted at 56 °C, which was predicted by

WAVEMaker.

The ssPCR product from the *SssI* and bisulfite treated human placenta genomic DNA was the positive control of the experiment.

DNA cloning and sequencing

The PCR products amplified with primers specific either for the methylated or for the unmethylated DNA were purified and cloned into the pMD18-T Easy Vector (Promega) and sequenced on an ABI 377 automated sequencer (Applied Biosystems) by using M13 primers.

RT-PCR detection

Total RNA was isolated from cells and tissues using Trizol reagent (Invitrogen). Reverse transcription was carried out with the SuperScript TM First-Strand Synthesis System (Invitrogen). Approximately 3 µg total RNA was used in each reverse transcription reaction and the final volume was 20 µl. The ORF of *ECRG 4* gene was amplified using the primers 5' -GGT TCT CCC TCG CAG CAC CT -3' (forward), and 5' -CAG CGT GTG GCA AGT CAT GGT TAG T -3' (reverse). PCR was performed in a GeneAmp 2400 thermocycler (Perkin-Elmer, Norwalk, CT) with a 25 µl reaction mixture containing 1 µl reverse transcription products, 200 pmol each primer, 200 µmol each dNTPs, 1.5 mM Mg²⁺, 2.0 U PLATINUM pfx DNA polymerase with 1× reaction buffer (Promega). Thermal cycles were: at 95 °C for 2 min, then 30 cycles at 95 °C for 30 sec, at 62 °C for 30 sec, at 72 °C for 1 min followed by extension at 72 °C for 7 min. The β-actin transcripts in each sample were also amplified as internal controls to normalize the amount of *ECRG 4* specific products.

RESULTS

The promoter hypermethylation in *ECRG 4* gene

Based on the flanking DNA sequences of the *ECRG 4*-core promoter region, PCR primers were designed to amplify a 220 bp fragment containing the 16 CpG sites (Figure 1). Using the ssPCR-specific primers, a 220 bp product was successfully obtained from each bisulfite-treated sample, which was detected by 1.5 % agarose gels and DHPLC size analysis, and the specific band (Figure 2) and the single chromatogram peak (Figure 3) were obtained respectively. The agarose gel detection and the size analysis on DHPLC all indicating the quality and quantity of the ssPCR products were high and the products could be used in the methylation analysis on DHPLC. Figure 4a shows the detection of methylated and unmethylated CpG islands in ssPCR products by DHPLC. Compared with the peak of positive control from the *SssI* treated human fetal DNA, the methylated and unmethylated samples could be easily discerned. The different proportion of methylated peak represented the different methylation levels in different samples. To confirm the reliability of the ssPCR products of

```

agtgggggag ccaaggagac accccagcgc tgggatccgg caagtctcc ctcttgagtg
CAAT box CAAT
ccagggggcc tcgtcccttc tccgatgcc ttctgccctt ccttggtct ccgaaccca
box
gcttgctcta accgctttcg ctgaggcag cgctggccac gcgcccccg cgcgagcgg
BARBIE box
ttctcgtgg ccaagcatcc ttggccttgg agccccggg
CAAT box

```

Figure 1 The sequence of *ECRG 4* fragment for bisulfite- DHPLC analysis. The fragment contains 4 cis-acting elements and 16 CpG sites in shadow. The 5' and 3' primers are in the frames of the two ends of the fragment respectively.

the *ECRG4* promoter region, either the methylated or the unmethylated DNA was cloned and sequenced (Figure 5). The cytosines in the CpG sites of methylated ssPCR products remained unchanged, but the cytosines of unmethylated products were converted to thymines. The promoter methylation of *ECRG4* gene in esophageal tissues is shown in Table 1. A high frequency of methylation was observed in 12 cancer tissues, 3 tumor adjacent tissues and 3 cell lines (EC 9706, EC 109 and GLC). No methylation peak was obtained in the two normal esophageal epithelia, the other tumor and adjacent tissues and the two cell lines (NEC and Hek293).

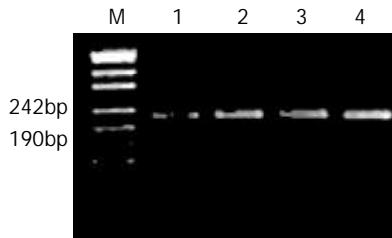


Figure 2 The 1.5% agarose gel detection of the ssPCR products of *ECRG4*. M; pUC19 DNA/*Msp I Hap II* Marker. 1, 2, 3, 4; four tissue samples.

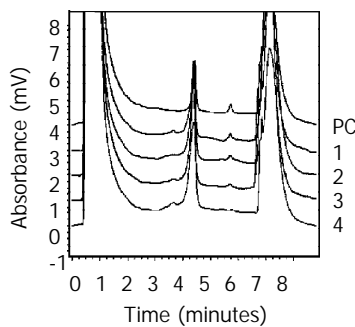


Figure 3 The sizing analysis of ssPCR products of *ECRG4* on DHPLC at 48 °C. PC was the product from the *Sss I* treated human placenta genomic DNA. 1, 2, 3, 4; the same samples as in Figure 2.

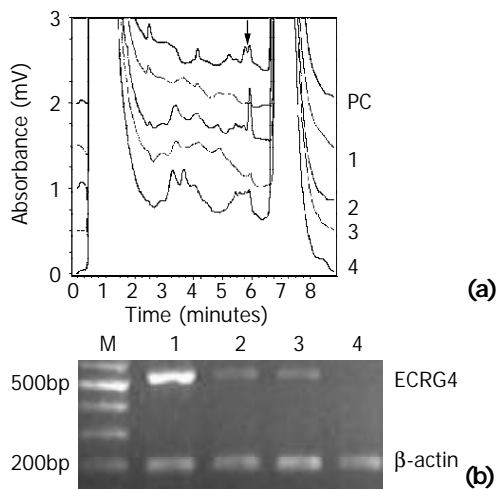


Figure 4 (a) The methylation detection of ssPCR products at 56 °C on DHPLC. The methylation peak was emphasized by the arrow. PC was the product from the *SssI* treated human placenta genomic DNA. 1, 2, 3, 4; the same samples as Figure 2. **(b)** The expression level of *ECRG4* by RT-PCR using the primer set flanking the ORF of the gene in the same samples was detected on DHPLC. The β -Actin gene was amplified as internal control. M; 1 kb DNA Ladder Marker. 1, 2, 3, 4; the same samples as Figure 2.

The expression level of *ECRG4* gene was different, and a high frequency of methylation was revealed in 12 (8 unexpressed and 4 lowly expressed) of the 15 (80%) cancer tissues and the 3 of the 4 unexpressed cell lines. No methylation peak was observed in the two highly expressed normal esophageal epithelia and the methylation frequency was low (3/20) among the 20 cases in the highly expressed adjacent tissues.

Expression of *ECRG4* gene related to methylation

The expression level of the *ECRG4* gene in the tissues and cell lines was examined by RT-PCR (Figure 4b). Out of 20 esophageal cancer tissues, nine were unexpressed, six were lowly expressed and five were highly expressed compared with the adjacent tissues and the 2 normal esophageal epithelia. In addition, 4 out of the 5 human cell lines were also unexpressed. The methylation was observed in 12 (8 unexpressed and 4 lowly expressed) of the 15 (80.0%) cancer tissues and the 3 unexpressed cell lines (Table 1 and Table 2). Among the normal tissues corresponding to the 12-methylation cancer tissues, nine were highly expressed and unmethylated; three were lowly expressed or unexpressed and methylated (Table 1). No methylation peak was obtained in the highly expressed samples, including the two normal esophageal epithelia, the cell line Hek293 and the other tumor and adjacent tissues. The results demonstrated that the expression of *ECRG4* was downregulated by CpG island hypermethylation in human esophageal squamous cell carcinoma.

Table 1 The expression and methylation of *ECRG4* in ESCC

Cases	Gender	Pathological stage	Expression		Methylation	
			Normal	Cancer	Normal	Cancer
N1	F ^a			+++ ^c		-
N2	F			++		-
1	M ^b	Moderate	++	+ ^d	- ^f	+ ^g
2	F	Moderate	+	-	-	+
3	M	Moderate	++	++	-	-
4	M	Moderate	++	++	-	-
5	F	Moderate	++	- ^e	-	+
6	F	Moderate	+	+	+	+
7	M	Moderate	++	++	-	-
8	F	Poor	++	-	-	+
9	M	Moderate	++	++	-	-
10	M	Poor	++	-	-	+
11	F	Moderate	+	+	+	+
12	F	Moderate	++	-	-	+
13	F	Moderate	++	++	-	-
14	M	Moderate	++	+	-	+
15	M	Moderate	++	-	-	+
16	F	Moderate	++	-	-	+
17	M	Moderate	-	-	+	-
18	F	Moderate	++	+	-	-
19	M	Moderate	++	+	-	-
20	M	Moderate	++	-	-	+

^a, Female; ^b, Male; ^c+, high expression; ^d+, low expression; ^e-, unexpression; ^f-, unmethylation; ^g+, methylation.

Table 2 The expression and methylation of *ECRG4* in cell lines

Cell lines	Expression	Methylation
NEC	- ^a	- ^c
EC109	-	+ ^d
EC9706	-	+
GLC	-	+
Hek293	+ ^b	-

^a-, unexpression; ^b+, expression; ^c-, unmethylation; ^d+, methylation.

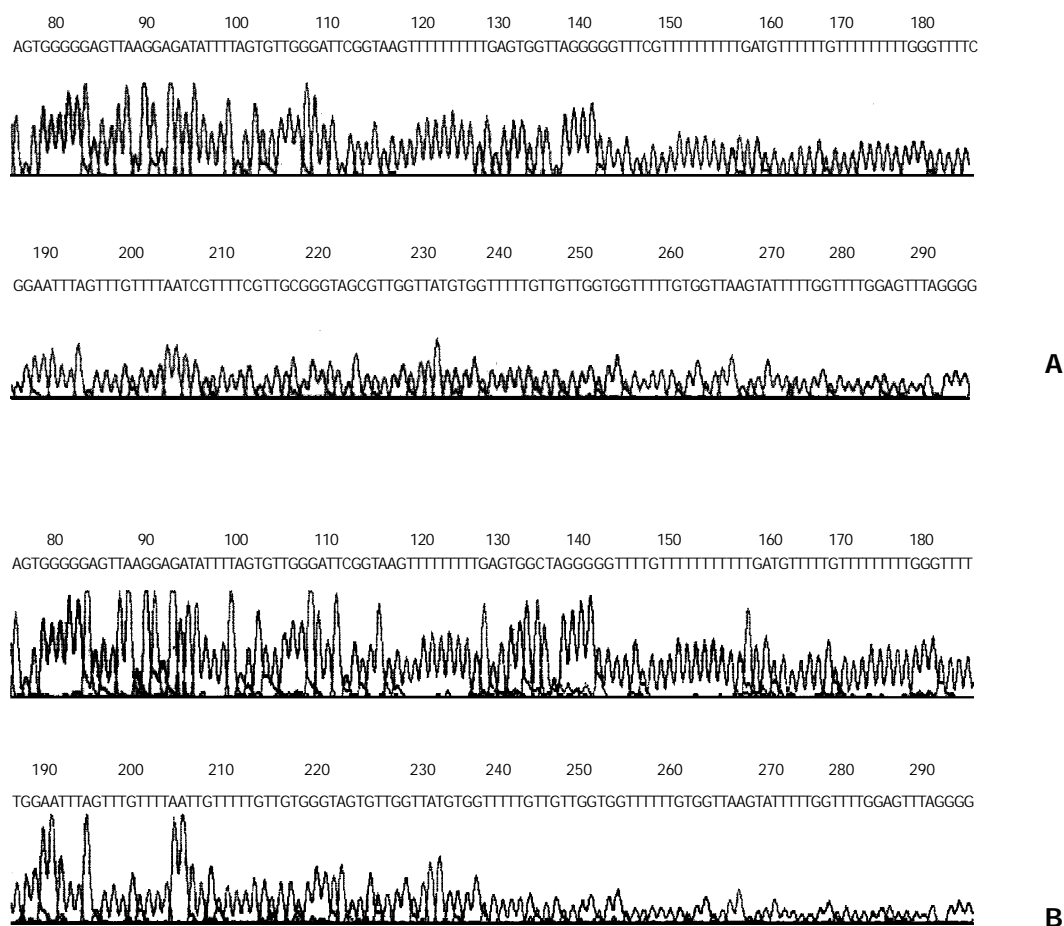


Figure 5 Sequencing of ssPCR products of the *ECRG4* gene promoter region. All cytosines in CpG dinucleotides in the methylated *ECRG4* remain as cytosines, indicating methylation (A), while all cytosines in unmethylated *ECRG4* have been converted to thymidines, indicating unmethylation (B).

DISCUSSION

We used a high-throughput methylation assay, bisulfite-DHPLC assay to examine the methylation status of the *ECRG 4* gene promoter in ESCC. The results demonstrated for the first time that downregulated expression of *ECRG 4* in ESCC was associated with CpG island methylation in the core promoter region of the gene. These findings suggest that inactivation by the promoter hypermethylation of *ECRG 4* is a common molecular event in ESCC and it may be involved in the development of this cancer, since this epigenetic change of the *ECRG 4* gene was not found in the normal epithelium and immortalizing cell line Hek293. Eads *et al* reported that DNA hypermethylation was an early epigenetic alteration in the multistep progression of the esophageal adenocarcinoma, because they found that the premalignant tissue was significantly more methylated than the normal tissue^[17]. Then, we can speculate that the inactivation by hypermethylation of *ECRG 4* might be an early event in the progression of ESCC carcinogenesis.

Because of the extent of methylation at various CpG sites of most genes, especially a novel identified gene is unknown, it is hard to design good MSP primers or MethyLight probes for methylated templates, which require full methylation at all CpG sites in their mating region^[15,18]. However, the ssPCR for bisulfite-modified templates are not influenced by the extent of methylation of CpGs, because no CpG site exists in the primer sequence and the primer for modified DNA can amplify both methylated and unmethylated templates. Deng *et al* had compared the bisulfite-DHPLC with other methylation detection method, and demonstrated the bisulfite-DHPLC assay could be used to detect methylation in homoallelic and heteroallelic CpG islands in cell lines and tissues rapidly and

reliably^[16]. In the present study, we also confirmed the reliability of bisulfite-DHPLC assay by DNA sequencing.

Abnormal hypermethylation of CpG islands associated with tumor suppressor genes can lead to repression of gene expression and contribute significantly to tumorigenesis of many kinds of tumors, such as esophageal cancer, gastric cancer, lung cancer, breast cancer and cervical cancer^[19-23]. Furthermore, each tumor type has a characteristic set of genes with an increased propensity to become methylated, and an individual tumor within a single patient has a unique epigenetic fingerprint^[24]. Determining tumor-type specific and patient-specific fingerprints may provide biomarkers that can be used in diagnosis, such as cancer detection, cancer chemoprediction and prognostics^[25,26]. The recent study has been repleted with the examples of hypermethylation of CpG islands in the promoter region of more than 40 lung cancer related genes to analyse methylation patterns of multiple genes. They want to obtain complex DNA methylation signatures, which can provide a useful and highly specific tool for lung cancer diagnosis^[27].

The promoter hypermethylation of the ESCC-related genes such as, *p16^{INK4a}*, *p15^{INK4b}*, *hMLH1*, *E-cadherin*, *Chfr* and HLA class I genes, has been shown to be a common epigenetic event in this cancer and the studies of these genes suggest that hypermethylation of key genes may be used in combination with other molecular changes, such as *p53* mutation, in the development of biomarkers for predicting the risk for ESCC^[28-30]. Our present study extended the findings of methylation signature in ESCC, and the methylation in more ESCC-related genes was studied, better understanding of the mechanisms underlying tumor progression in this cancer was

obtained, so that improved diagnosis and therapy can be facilitated.

In summary, our study demonstrated that aberrant methylation of CpG islands in the core promoter of the *ECRG 4* gene was a frequent molecular event in ESCC and proved for the first time that loss or lower expression of *ECRG 4* was associated with *ECRG 4* CpG island methylation. These results indicate that the inactivation of *ECRG 4* gene by hypermethylation in ESCC may be involved in the carcinogenesis of the cancer.

REFERENCES

- 1 **Lu SH.** Alterations of oncogenes and tumor suppressor genes in esophageal cancer in China. *Mutat Res* 2000; **462**: 343-353
- 2 **Lu SH, Hsieh LL, Luo FC, Weinstein IB.** Amplification of the EGF receptor and *c-myc* genes in human esophageal cancer. *Int J Cancer* 1988; **42**: 502-505
- 3 **Yang ZQ, Imoto I, Fukuda Y, Pimkhaokham A, Shimada Y, Imamura M, Sugano S, Nakamura Y, Inazawa J.** Identification of a novel gene, *GASCI*, within an amplicon at 9p23-24 frequently detected in esophageal cancer cell lines. *Cancer Res* 2000; **60**: 4735-4739
- 4 **Daigo Y, Nishiwaki T, Kawasoe T, Tamari M, Tsuchiya E, Nakamura Y.** Molecular cloning of a candidate tumor suppressor gene, *DLC1*, from chromosome 3p21.3. *Cancer Res* 1999; **59**: 1966-1972
- 5 **Sasaki S, Nakamura T, Arakawa H, Mori M, Watanabe T, Nagawa H, Croce CM.** Isolation and characterization of a novel gene, *hRFI*, preferentially expressed in esophageal cancer. *Oncogene* 2002; **21**: 5024-5030
- 6 **Su T, Liu HL, Lu SX, Zhao XJ, Zhou CX, Jin SQ.** Cloning and identification of cDNA fragment related to human esophageal cancer. *Chinese J Oncology* 1998; **20**: 254-257
- 7 **Bi MX, Han WD, Lu SX.** Using lab on-line to clone and identify the esophageal cancer related gene 4. *Acta Biochimica et Biophysica Sinica* 2001; **33**: 257-261
- 8 **Jones PA.** DNA methylation and cancer. *Oncogene* 2002; **21**: 5358-5360
- 9 **Esteller M.** CpG island hypermethylation and tumor suppressor genes: a booming present, a bright future. *Oncogene* 2002; **21**: 5427-5440
- 10 **Xing EP, Nie Y, Song Y, Yang GY, Cai YC, Wang LD, Yang CS.** Mechanisms of inactivation of *p14ARF*, *p15^{INK4b}* and *p16^{INK4a}* genes in human esophageal squamous cell carcinoma. *Clin Cancer Res* 1999; **5**: 2704-2713
- 11 **Wong DJ, Barrett MT, Stoger R, Emond MJ, Reid BJ.** *P16^{INK4a}* promoter is hypermethylated at a high frequency in esophageal adenocarcinomas. *Cancer Res* 1997; **57**: 2619-2622
- 12 **Si HX, Tsao SW, Lam KY, Srivastava G, Liu Y, Wong YC, Shen ZY.** E-cadherin expression is commonly downregulated by CpG island hypermethylation in esophageal carcinoma cells. *Cancer Lett* 2001; **173**: 71-78
- 13 **Tanaka H, Shimada Y, Harada H, Shinoda M, Hatooka S, Imamura M, Ishizaki K.** Methylation of the 5' CpG island of the FHIT gene is closely associated with transcriptional inactivation in esophageal squamous cell carcinomas. *Cancer Res* 1998; **58**: 3429-3434
- 14 **Blin N, Stafford DW.** A general method for isolation of high molecular weight DNA from eukaryotes. *Nucleic Acid Res* 1976; **3**: 2303-2308
- 15 **Herman JG, Graff JR, Myohanen S, Nelkin BD, Baylin SB.** Methylation-specific PCR: a novel PCR assay for methylation status of CpG islands. *Proc Natl Acad Sci USA* 1996; **93**: 9821-9826
- 16 **Deng DJ, Deng GR, Smith MF, Zhou J, Xin HJ, Powell SM, Lu YY.** Simultaneous detection of CpG methylation and single nucleotide polymorphism by denaturing high performance liquid chromatography. *Nucleic Acid Res* 2002; **30**: e13
- 17 **Eads CA, Lord RV, Wickramasinghe K, Long TI, Kurumboor SK, Bernstein L, Peters JH, DeMeester SR, DeMeeste TR, Skinner KA, Laird PW.** Epigenetic patterns in the progression of esophageal adenocarcinoma. *Cancer Res* 2001; **61**: 3410-3418
- 18 **Eads CA, Danenberg KD, Kawakami K, Saltz LB, Blake C, Shibata D, Danenberg PV, Laird PW.** MethyLight: a high-throughout assay to measure DNA methylation. *Nucleic Acid Res* 2000; **28**: e32
- 19 **Tokugawa T, Sugihara H, Tani T, Hattori T.** Modes of silencing of *p16* in development of esophageal squamous cell carcinoma. *Cancer Res* 2002; **62**: 4938-4944
- 20 **Oue N, Shigeishi H, Kuniyasu H, Yokozaki H, Yuraoka K, Ito R, Yasui W.** Promoter hypermethylation of *MGMT* is associated with protein loss in gastric carcinoma. *Int J Cancer* 2001; **93**: 805-809
- 21 **Palmisano WA, Divine KK, Saccomanno G, Gilliland FD, Baylin SB, Herman JG, Belinsky SA.** Predicting lung cancer by detecting aberrant promoter methylation in sputum. *Cancer Res* 2000; **60**: 5954-5958
- 22 **Widschwendter M, Jones PA.** DNA methylation and breast carcinogenesis. *Oncogene* 2002; **21**: 5462-5482
- 23 **Virmanani AK, Muller C, Rathi A, Zochbauer-Mueller S, Mathis M, Gazdar AF.** Aberrant methylation during cervical carcinogenesis. *Clin Cancer Res* 2001; **7**: 584-589
- 24 **Costello JF, Fruhwald MC, Smiraglia DJ, Rush LJ, Robertson GP, Gao X, Wright FA, Feramisco JD, Peltomaki P, Lang JC, Schuller DE, Yu L, Bloomfield CD, Caligiuri MA, Yates A, Nishikawa R, Su HH, Petrelli NJ, Zhang X, O' Dorisio MS, Held WA, Cavenee WK, Plass C.** Aberrant CpG-island methylation has non-random and tumor-type-specific patterns. *Nat Genet* 2000; **24**: 132-138
- 25 **Jones PA, Laird PW.** Cancer epigenetics comes of age. *Nat Genet* 1999; **21**: 163-167
- 26 **Beck S, Olek A, Walter J.** From genomics to epigenomics: a loftier view of life. *Nat Biotechnol* 1999; **17**: 1144
- 27 **Tsou JA, Hagen JA, Carpenter CL, Laird-Offringa IA.** DNA methylation analysis: a powerful new tool for lung cancer diagnosis. *Oncogene* 2002; **21**: 5450-5461
- 28 **Nie Y, Liao J, Zhao X, Song Y, Yang GY, Wang LD, Yang CS.** Detection of multiple gene hypermethylation in the development of esophageal squamous cell carcinoma. *Carcinogenesis* 2002; **23**: 1713-1720
- 29 **Shibata Y, Haruki N, Kuwabara Y, Ishiguro H, Shinoda N, Sato A, Kimura M, Koyama H, Toyama T, Nishiwaki T, Kudo J, Terashita Y, Konishi S, Sugiura H, Fujii Y.** *Chfr* expression is downregulated by CpG island hypermethylation in esophageal cancer. *Carcinogenesis* 2002; **23**: 1695-1699
- 30 **Nie Y, Yang G, Song Y, Zhao X, So C, Liao J, Wang LD, Yang CS.** DNA hypermethylation is a mechanism for loss of expression of the HLA class I genes in human esophageal squamous cell carcinomas. *Carcinogenesis* 2001; **22**: 1615-1623

Edited by Zhang JZ and Wang XL

Expression of a plant-associated human cancer antigen in normal, premalignant and malignant esophageal tissues

Jun Fu, Ping Qu, Mo Li, Hai-Mei Tian, Zhen-Hai Zheng, Xin-Wen Zheng, Wei Zhang

Jun Fu, Ping Qu, Mo Li, Hai-Mei Tian, Wei Zhang, Central Laboratory for Tumor Biology, Cancer Hospital (Institute), Peking Union Medical College and Chinese Academy of Medical Sciences, Beijing 100021, China

Zhen-Hai Zheng, Xin-Wen Zheng, Zheng's Cancer Institute, Linshou 050500, HeBei Province, China

Correspondence to: Professor Wei Zhang, Central Laboratory for Tumor Biology, Cancer Institute, Peking Union Medical College and Chinese Academy of Medical Sciences, Beijing 100021, China. zhangwe@public.bta.net.cn

Telephone: +86-10-67718679 **Fax:** +86-10-67718679

Received: 2002-12-24 **Accepted:** 2003-03-05

Abstract

AIM: To study the relationship between the expression profiles of a plant-associated human cancer antigen and carcinogenesis of esophagus and its significance.

METHODS: We analyzed expression of a plant-associated human cancer antigen in biopsy specimens of normal ($n=29$), mildly hyperplastic ($n=29$), mildly ($n=30$), moderately ($n=27$) and severely dysplastic ($n=29$) and malignant esophageal ($n=30$) tissues by immunohistochemistry.

RESULTS: The plant-associated human cancer antigen was mainly confined to the cytoplasm and showed diffuse type of staining. Positive staining was absent or weak in normal (0/30) and mildly hyperplastic tissue samples (2/29), while strong staining was observed in severe dysplasia (23/29) and carcinoma *in situ* (24/30). There was significant difference of its expression between normal mucosa and severely dysplastic tissues ($P<0.001$) or carcinoma *in situ* ($P<0.001$). Significant difference was also observed between mild dysplasia and severe dysplasia ($P<0.001$) or carcinoma *in situ* ($P<0.001$). An overall trend toward increased staining intensity with increasing grade of dysplasia was found. There was a linear correlation between grade of lesions and staining intensity ($r=0.794$, $P<0.001$). Samples from esophageal cancer showed no higher levels of expression than those in severely dysplastic lesions ($P>0.05$).

CONCLUSION: The abnormal expression of this plant-associated human cancer antigen in esophageal lesions is a frequent and early finding in the normal-dysplasia-carcinoma sequence in esophageal carcinogenesis. It might contribute to the carcinogenesis of esophageal cancer. The abnormal expression of this plant-associated human cancer antigen in esophageal lesion tissues may serve as a potential new biomarker for early identification of esophageal cancer.

Fu J, Qu P, Li M, Tian HM, Zheng ZH, Zheng XW, Zhang W. Expression of a plant-associated human cancer antigen in normal, premalignant and malignant esophageal tissues. *World J Gastroenterol* 2003; 9(6): 1179-1181

<http://www.wjgnet.com/1007-9327/9/1179.asp>

INTRODUCTION

Despite three decades of progress in cancer treatment, esophageal cancer remains a significant health problem worldwide with a very low 5-year survival rate and a rapid increase in its incidence^[1-4]. Esophageal squamous cell carcinoma is believed to develop progressively through a dysplasia-carcinoma sequence^[5,6]. The evolution of sequential histological changes from normal to dysplasia and carcinoma *in situ* suggests that specific biomarkers may be expressed at different points in the evolution of esophageal carcinoma^[7]. Therefore, research directed toward the discovery of new biomarkers that can aid in the early detection of esophageal neoplasm has been intensified in recent years.

In the 1990s, Dr. Zhen-Hai Zheng separated and identified a glycoprotein (molecular weight: 46 kilo-dalton) from a lower plant. Early experiments demonstrated its stimulatory activity on the growth of esophageal cancer cells. Recently the differential stimulatory effects of this plant antigen on isolated lymphocytes from patients with dysplasia or breast cancer have been confirmed. Their experiments also suggested that this plant antigen might have an associated counterpart cancer antigen in human.

In this research, we aimed to study the relationship between expression profiles of this human cancer antigen and carcinogenesis of esophagus and its significance.

MATERIALS AND METHODS

Tissue specimens

Biopsy specimens were obtained from the Cancer Hospital (Chinese Academy of Medical Sciences) in Beijing. These samples were taken from patients with morphologically normal ($n=29$), mildly hyperplastic ($n=29$) esophageal mucosa, mildly ($n=30$), moderately ($n=27$) or severely ($n=29$) dysplastic lesions, or squamous carcinomas *in situ* ($n=30$). All samples were routinely fixed in 10 % buffered formalin, embedded in paraffin, and cut into 4 μ m sections. Samples were selected based on the pathological diagnosis and reviewed by a pathologist to ensure the correct diagnosis.

Reagents

SP-ABC kit was purchased from Beijing Zhong Shan Biotechnology Co. Ltd. Rabbit polyclonal antibody anti-plant antigen was kindly provided by professor Zhen-Hai Zheng, diluted to $2 \times 10^{-2} \text{g} \cdot \text{L}^{-1}$ before use.

Immunohistochemistry

The immunohistochemical localization of the plant-associated human cancer antigen was performed using a modified ABC technique^[8]. Briefly, tissue sections were deparaffinized in xylene and rehydrated in a series of ethanol solutions (100-50 %). The sections were then microwaved for 15 min to restore antigens in 0.01M citric acid solutions. The endogenous peroxidase activity was blocked by incubation in a 3 % hydrogen peroxide solution for 20 min at 23 °C. This was followed by preincubation with 1.5 % normal sheep serum to minimize nonspecific binding of the second antibody. The

sections were incubated at 4 °C overnight with rabbit polyclonal antibody anti-plant protein. After being washed three times in PBS, the sections were incubated with biotinylated sheep anti-rabbit IgG for 20 min at 37 °C and were washed three times in PBS. Sections were then incubated with streptavidin-peroxidase for 20 min at 37 °C, followed by 2 min staining with DAB-H₂O₂ solution and nuclear counterstained with hematoxylin. For negative controls, the rabbit anti-plant protein polyclonal antibody was replaced by normal rabbit serum.

Review and scoring of the section

The stained sections were reviewed and scored independently by two investigators using an Olympus microscope. The intensity of staining was graded on a scale of 0 to 3 as follows: 0 meaning the amounts of positive cells were less than 10 %; 1, weak positive, the amounts of positive cells were more than 10 %, but less than 30 %; 2, positive, the amounts of positive cells were more than 30 % but less than 50 %; and 3, strong positive, the amounts of positive cells were more than 50 %^[9]. The grading for each section used for data analysis was the highest intensity seen on the section.

Statistical analysis

The mean values of the staining intensity for different grades of diseases were compared by analysis of variance. Linear regression analysis was done to evaluate the linear correlation between lesion severity and staining intensity. Statistical analysis was made using Fisher's exact test to determine the

association between normal or dysplastic tissues and tumors. *P* values were generated using SPSS 10.0 for Windows. Statistical significance was accepted at the *P*<0.05 level.

RESULTS

Our finding suggested that the plant-associated human cancer antigen was mainly confined to the cytoplasm and showed diffuse type of staining, enormous nuclear staining could also be observed in severe dysplastic and carcinoma *in situ* tissue samples. Only background staining was observed in basal layers underlying epithelium. Staining was absent to weak in normal and mildly hyperplastic tissue samples (Figure 1-6). Positive staining was absent to weak in normal (0/30) and mildly hyperplastic tissue samples (2/29), while high positive rate was observed in severe dysplasia (23/29) and carcinoma *in situ* (24/30).

There was significant difference of its expression between normal mucosa and severely dysplastic tissues (*P*<0.001) or esophageal cancer (*P*<0.001). Significant difference was also observed between mild dysplasia and severe dysplasia (*P*<0.001) or esophageal cancer (*P*<0.001) (Table 1). Samples from esophageal cancer showed no higher levels of its expression than seen in severely dysplastic lesions (*P*>0.05). An overall trend toward increased staining intensity with increasing grade of dysplasia was found. There was a linear correlation between grade of lesion and staining intensity (*r*=0.794, *P*<0.001) (Table 2).

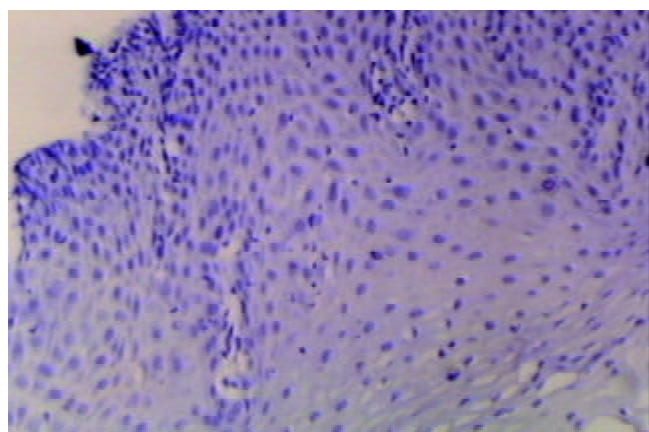


Figure 1 The expression of plant-associated human cancer antigen in normal esophageal tissues. Avidin-biotin complex staining, ABC, ×100.

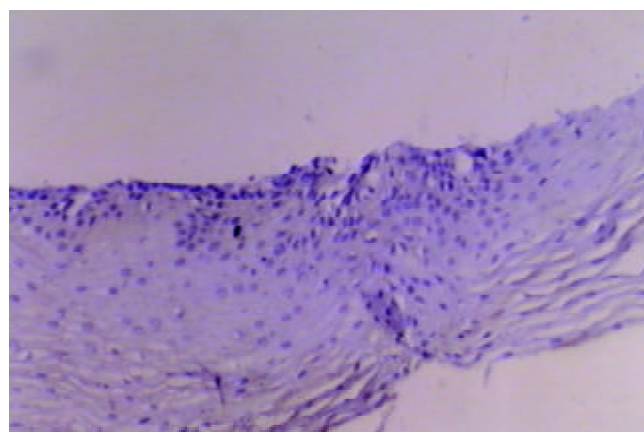


Figure 3 The expression of plant-associated human cancer antigen in mild dysplasia. Avidin-biotin complex staining, ABC, ×100.

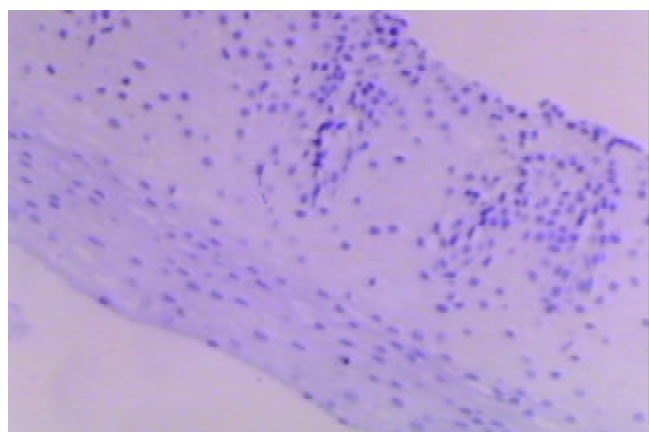


Figure 2 The expression of plant-associated human cancer antigen in mild hyperplasia. Avidin-biotin complex staining, ABC, ×100.

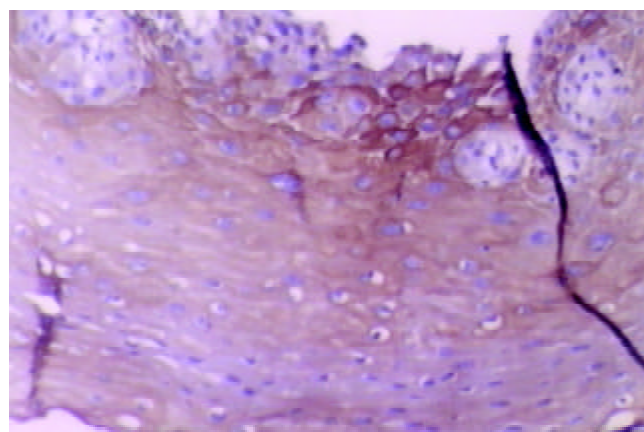


Figure 4 The expression of plant-associated human cancer antigen in moderate dysplasia. Avidin-biotin complex staining, ABC, ×100.

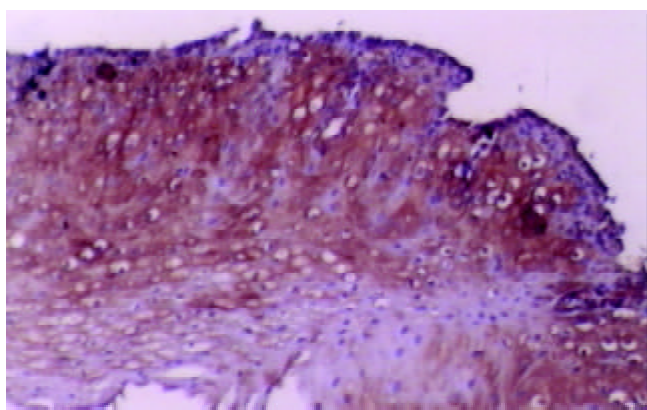


Figure 5 The expression of plant-associated human cancer antigen in severe dysplasia. Avidin-biotin complex staining, ABC, $\times 100$.

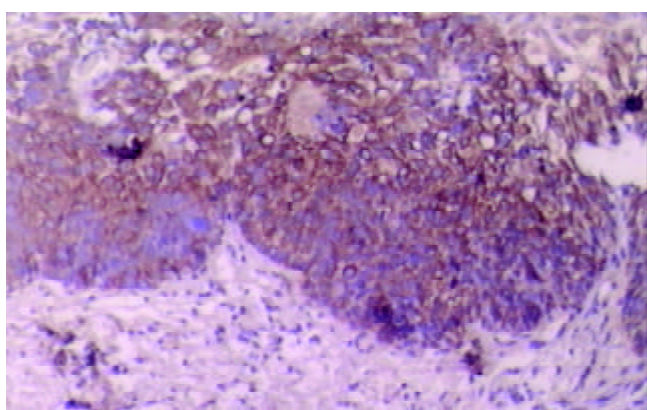


Figure 6 The expression of plant associated-human cancer antigen in carcinoma *in situ*. Avidin-biotin complex staining, ABC, $\times 100$.

Table 1 Expression of the plant-associated human cancer antigen in different esophageal tissues

Esophageal tissues	Total cases	Positive staining	Negative staining	%Positive
Normal	29	0	18	0
Hyperplasia	29	2	27	6.9
Dysplasia				
Mild	30	8	22	26.7
Moderate	27	17	10	63.0
Severe	29	23	6	79.3
^a CIN	30	24	6	80.0

^aCIN: Carcinoma *in situ*.

Table 2 Staining intensity of the plant-associated human cancer antigen expressed in different esophageal tissues

Histologic diagnosis	Total cases	Staining intensity ^a	Biopsies staining with intensity >2 (%)
Normal	29	0	0
Dysplasia			
Mild	30	0.27 \pm 0.52	3.3
Moderate	27	1.00 \pm 0.93	25.9
Severe	29	1.38 \pm 0.96	41.4
CIN	30	1.33 \pm 0.92	43.3

^aExpressed as mean staining intensity \pm standard deviation. Intensity of staining was graded on a scale of 0 to 3.

DISCUSSION

We have evaluated esophageal mucosal expression of the plant-associated human cancer antigen in a variety of normal, precancerous or malignant esophageal tissue specimens. Esophageal biopsy specimens with normal histology or low-grade dysplasia did not express significant levels of this human cancer antigen. Its intensive expression was observed in high-grade dysplastic and malignant lesions. There was an overall trend toward increased staining intensity with increasing grade of dysplasia, and the largest difference was observed between mild and severe dysplastic lesions, suggesting that its up-regulation of expression may be involved in esophageal carcinogenesis. Since esophageal carcinogenesis is a multi-stage process, early detection is very crucial^[10,11]. This human cancer antigen might be a useful diagnostic marker for advanced dysplasia and could serve as a useful target for biological treatment and for bio-prevention in high-risk patients diagnosed having dysplasia or esophageal carcinoma.

In this report, we also studied the expression distribution of this human cancer antigen in abnormal human sections. Although this antigen was mainly expressed in cytoplasm, enormous nuclear staining could also be observed in severely dysplastic and malignant tissue samples. Combined with previous conclusions, our finding suggested that this protein might be involved in signal transduction pathway or cell cycle control. Its intracellular translocation from cytoplasm to nuclei might play an important role in the transition from low-grade dysplasia to severe lesions and neoplasm. The mechanism of action of this cancer antigen in esophageal carcinogenesis still awaits further studies.

The ability to identify the plant-associated human cancer antigen in esophageal biopsy specimens from patients with dysplasia may provide a useful method for early detection, identification of high-risk patients, monitoring response to therapy. Further studies are needed to separate and identify this protein and its encoding gene in order to fully understand the regulatory mechanism underlying its aberrant expression and its role in esophageal carcinogenesis.

REFERENCES

- 1 **Mc Cann J.** Esophageal cancers: changing character, increasing incidence. *J Natl Cancer Inst* 1999; **91**: 497-498
- 2 **Flood WA, Forastiere AA.** Esophageal cancer. *Curr Opin Oncol* 1995; **7**: 381-386
- 3 **Flood WA, Forastiere AA.** Esophageal cancer. *Cancer Treat Res* 1998; **98**: 1-40
- 4 **Blot WJ.** Esophageal cancer trends and risk factors. *Semin Oncol* 1994; **21**: 403-410
- 5 **Liu FS, Wang QL, Goldman H.** Pathology of the gastrointestinal tract. Philadelphia: Saunders 1992: 439-458
- 6 **Haggitt RC.** Barrette's esophagus, dysplasia, and adenocarcinoma. *Human Pathol* 1994; **25**: 982-993
- 7 **Stemmermann G, Heffelfinger SC, Noffsinger A.** The molecular biology of esophageal and gastric cancer and their precursors: oncogenes, tumor suppressor genes, and growth factors. *Hum Pathol* 1994; **25**: 968-981
- 8 **Zhang W, Rashid A, Wu H, Xu XC.** Differential expression of retinoic acid receptors and P53 protein in normal, premalignant, and malignant esophageal tissues. *J Cancer Res Clin Oncol* 2001; **127**: 237-242
- 9 **Xu M, Jin YL, Fu J, Huang H, Chen SZ, Qu P, Tian HM, Liu ZY, Zhang W.** The abnormal expression of retinoic acid receptor- β , P53 and Ki67 protein in normal, premalignant and malignant esophageal tissues. *World J Gastroenterol* 2002; **8**: 200-202
- 10 **Kelloff GJ, Boone CW, Steele VK, Perloff M, Crowell J, Doody LA.** Development of chemopreventive agents for lung and upper aerodigestive tract cancers. *J Cell Biochem Suppl* 1993; **17F**: 2-17
- 11 **Lippman SM, Lee JJ, Sabichi AL.** Cancer chemoprevention: progress and promise. *J Natl Cancer Inst* 1998; **90**: 1514-1515

Upregulated expression of Ezrin and invasive phenotype in malignantly transformed esophageal epithelial cells

Zhong-Ying Shen, Li-Yan Xu, Ming-Hua Chen, En-Min Li, Jin-Tao Li, Xian-Ying Wu, Yi Zeng

Zhong-Ying Shen, Li-Yan Xu, Ming-Hua Chen, Jin-Tao Li, Xian-Ying Wu, Department of Pathology, Medical College of Shantou University, Shantou, 515031, Guangdong Province China

En-Min Li, Department of Biochemistry, Medical College of Shantou University, Shantou, 515031, China

Yi Zeng, Institute of Virology, Chinese Academy of Preventive Medicine, Beijing 100052, China

Supported by the National Natural Science Foundation of China (No. 39830380, 39900069), Research and Development Foundation of Shantou University (L00012) and the Chinese National Human Genome Center, Beijing

Correspondence to: Professor Zhong-Ying Shen, Department of Pathology, Medical College of Shantou University, Shantou 515031, Guangdong Province, China. zhongyingshen@yahoo.com

Telephone: +86-754-8538621 **Fax:** +86-754-8537516

Received: 2003-03-12 **Accepted:** 2003-04-19

Abstract

AIM: To investigate the correlation between ezrin expression and invasive phenotype formation in malignantly transformed esophageal epithelial cells.

METHODS: The experimental cell line employed in the present study was originated from the progressive induction of a human embryonic esophageal epithelial cell line (SHEE) by the E6E7 genes of human papillomavirus (HPV) type 18. The cells at the 35th passage after induction called SHEEIMM were in a state of immortalized phase and used as the control, while that of the 85th passage denominated as SHEEMT represented the status of cells that were malignantly transformed. The expression changes of ezrin and its mRNA in both cell passages were respectively analyzed by RT-PCR and Western blot. Invasive phenotype was assessed *in vivo* by inoculating these cells into the severe combined immunodeficient (SCID) mice via subcutaneous and intraperitoneal injection, and *in vitro* by inoculating them on the surface of the amnion membranes, which then was determined by light microscopy and scanning electron microscopy.

RESULTS: Upregulated expression of ezrin protein and its mRNA was observed in SHEEMT compared with that in SHEEIMM cells. The SHEEMT cells inoculated in SCID mice were observed forming tumor masses in both visceral organs and soft tissues in a period of 40 days with a special propensity to invading mesentery and pancreas, but did not exhibit hepatic metastases. Pathologically, these tumor cells harboring larger nucleus, nucleolus and less cytoplasm could infiltrate and destroy adjacent tissues. In the *in vitro* study, the inoculated SHEEMT cells could grow in cluster on the amniotic epithelial surface and intrude into the amniotic stroma. In contrast, unrestricted growth and invasiveness were not found in SHEEIMM cells in both *in vivo* and *in vitro* experiment.

CONCLUSION: The upregulated ezrin expression is one of the important factors that are possibly associated with the

invasive phenotype formation in malignantly transformed esophageal epithelial cells.

Shen ZY, Xu LY, Chen MH, Li EM, Li JT, Wu XY, Zeng Y. Upregulated expression of Ezrin and invasive phenotype in malignantly transformed esophageal epithelial cells. *World J Gastroenterol* 2003; 9(6): 1182-1186

<http://www.wjgnet.com/1007-9327/9/1182.asp>

INTRODUCTION

It has been well known that cancer cells can invade and destroy surrounding tissues by their disseminative potency. This acquired malignant property is believed recently to be determined by the abnormal changes of expression patterns of certain genes such as c-met, urokinase type plasminogen activator receptor or ezrin and so on^[1-9]. Therefore, the correlation between the invasive phenotype of tumor cells and the aberrant expression of these genes has become a focus of attention by the worldwide oncologists.

Induced by E₆E₇ genes of human papilloma virus (HPV) type 18, we have established both kinds of immortalized and malignantly transformed cells from a human embryonic esophageal epithelial cell line (SHEE)^[10]. At early passages after induction, the cell did not display any abnormal growth ability in soft agar and nude mice^[11-13]. At the 20th passage, the cell was noted to be immortalized with the appearance of telomerase^[14, 15]. At the 30th passage, the cell manifested as a phenotype of biphasic differentiation^[16]. While cultivated over 60 passages, the cell exhibited atypical morphological changes and chromosomal alterations that were suspected to be a kind of premalignant transformation^[17]. Over 85 passages, the cell was observed having harbored a property of malignant transformation shown by its unrestricted growth in the nude mice and invasion to the surrounding tissues^[18, 19]. Obviously, this process of malignant transformation of SHEE cells induced by E₆E₇ genes of HPV type 18 possesses a progressive and stepwise characteristic, which is no doubt a good cell model suitable for the study of correlations between abnormal gene expression and corresponding malignant phenotype formation in tumorigenesis.

Differential display analysis of RNA samples isolated from the SHEEIMM and SHEEMT cells has been performed in our previous study. There were 15 up-regulated and 6 down-regulated genes being identified by the cDNA microarray method (Data to be published), in which ezrin was one of the up-regulated genes that have been found existed in certain diseases and tumors. Being a membrane-cytoskeleton linker, ezrin protein is located in cytoplasm and is rich in microvilli and cell surface structures with the function involved in the formation of microvilli and intercellular junctions, as well as the cell motility and invasive behavior of malignant tumors^[20-28]. Up to the present, however, there have been few reports concerned about how the ezrin expressed in the malignant transformation of esophageal epithelial cells and what was its relation to the invasiveness formation of tumor cells, which are of both theoretical and practical importance in the

investigation of cancerogenesis. Thus, our present study was conducted to identify the correlation between the ezrin gene expression and invasive phenotype formation in malignantly transformed esophageal epithelial cells.

MATERIALS AND METHODS

Cell lines and cell culture

The experimental cells came from our laboratory, and were established by the progressive induction of SHEE cell line with the E6E7 genes of HPV type 18. The 35th, 85th passages of induced cells were employed in the present study. The cells at the 35th passage called SHEEIMM were in a state of immortalized phase, while that of the 85th passage denominated as SHEEMT represented the status of cells that were malignantly transformed. Both passages of cells were continuously cultivated in flasks with medium 199 (GIBCO) supplemented by 10 % fetal bovine serum (FBS), 100 U·ml⁻¹ penicillin and 100 U·ml⁻¹ streptomycin at 37 °C in a humidified atmosphere containing 5 % of CO₂.

RT-PCR

Total RNA was extracted from SHEEIMM and SHEEMT cells using the Trizol reagent (Invitrogen). The first-strand cDNA synthesis was performed with 1 µg total RNA and carried out at 42 °C for 1 h followed by at 95 °C for 5 min and at 0-5 °C for 5 min according to protocol of reverse transcription system (Promega). The synthesized cDNA was diluted to 100 µl with TE and stored at -20 °C until use. In the following experiment, 5 µl of cDNA was amplified in a 25 µl PCR reaction volume with Advantage 2 PCR Kit (CLONTECH). Both of the ezrin primer 5' CGGGCGCTCTAAGGGTTCT3' (sense), 5' TGCCTTTGCAAAGCTTTTATTTCA3' (antisense) and GAPDH primer 5' GAAGGTGAAGGTCCGAGTC 3' (sense), 5' GAAGATGGTGATGGGATTTCC 3' (antisense) were synthesized by Genecore Company (Shanghai). After prepared by routine procedures, PCR products were visualized by electrophoresis on 1 % agarose gel stained with ethidium bromide and quantitated with Gelworks 1D Intermediate software (version 3.51, Kodak).

Western blot

Western blot was used to detect ezrin protein expressed by experimental cells. Confluent cells of 3 flasks were washed three times with ice-cold PBS and then lysed in buffer containing 50 mM Tris-HCl (pH 8.0), 150 mM NaCl, 100 µg·ml⁻¹ phenyl-methyl-sulfonyl fluoride (PMSF) and 1 % Triton X-100 for 30 min on ice. After removal of cell debris by centrifugation at 12 000 g for 5 min, 50 µl of supernatant was boiled for 5 min in the sample buffer and separated by 10 % SDS-PAGE, which was then transferred onto the nitrocellulose membrane (Pall Corporation). After non-specific reactivity was blocked by 5 % fat-free milk in TBST (10 mM Tris-HCl, pH 7.5, 150 mM NaCl, 0.05 % Tween 20) for 1 h at room temperature, the membrane was incubated in turn with monoclonal antibody of mouse against human ezrin p81 (Maixin-Bio) and anti-mouse IgG-HRP antibody. Reactive protein was finally detected by ECL chemiluminescence system (Santa Cruz).

Oncogenesis and invasive potency of SHEE *in vivo*

SCID mice (C.B-17/IcrJ-scid nu/nu) were from Animal Laboratory Center, Chinese Academy of Medical Sciences. For the determination of their oncogenesis and invasive potency, SHEEIMM and SHEEMT cells were cultured in flasks with fresh medium to reconstitute their surface protein. After digested and washed twice with PBS, they were counted and

resuspended in PBS solution (10×10⁶·ml⁻¹) until use. Then SCID mice were anesthetized with 7 % chloralhydrate followed by intraperitoneal and subcutaneous inoculation with the both passages of cells. That is, 2×10⁶ SHEEMT or SHEEIMM cells in 0.2 ml PBS were injected into the peritoneal cavity in 5 mice and into the right axilla of the same number of animals. Instead, the control mice were injected only with 0.2 ml of PBS. The experimental animals were checked daily and all were killed on after day 40 inoculation by an overdose of anesthetic. Tissues from tumor mass, mesentery, pancreas and gastrointestinal tract were sampled and prepared with the routine method to produce thin paraffin sections (5 µm) stained by hematoxylin and eosin for the assessment of tumor invasion.

Invasive potency of SHEE *in vitro*

Tumor cell invasion *in vitro* was assessed by using a fresh fetal amnion, which was cultured in 199 medium supplemented with 10 % FBS. In the experiment, a piece of amnion and 50 000 SHEEIMM or SHEEMT cells were in turn added to one well of a 24-well plate and incubated together for 24 h and 72 h, and then were washed for several times with PBS. Then the samples, including the piece of amnion and cells adhering to it, were fixed with 2.5 % glutaraldehyde and post-fixed with 2 % osmium tetroxide. After full dehydration with gradient concentrations of ethanol, the samples were adhered to an aluminium stub and sprayed plating with gold for 3 minutes (EIKD, IB-3, Hitachi), which were further examined by Hitachi H300 electron microscope with the attachment of scanning apparatus.

RESULTS

Expressive alterations of ezrin and its mRNA

The ezrin mRNA detected by electrophoresis on 1 % agarose gel was shown as a band of 3 032 bp segment, whose expression was observed to be significantly up-regulated in SHEEMT by RT-PCR assay compared with that expressed in SHEEIMM cells as displayed in Figure 1. The same difference was also noted in the expression of ezrin protein between both of the cell passages (Figure 2).

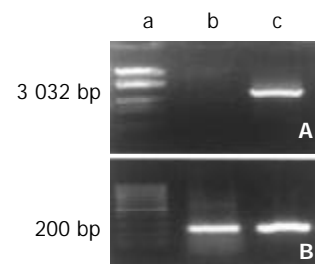


Figure 1 RT-PCR assay of ezrin mRNA. The expression of ezrin mRNA was significantly increased in SHEEMT compared with that in SHEEIMM cells. A. Ezrin; B. GAPDH: a. Marker; b. SHEEIMM; c. SHEEMT.



Figure 2 Western blot analysis of ezrin protein expression. The ezrin protein was exhibited as a band of 81-kDa segment, whose expression was up-regulated in SHEEMT compared with that in SHEEIMM cells. Lane a: SHEEIMM; lane b: SHEEMT.

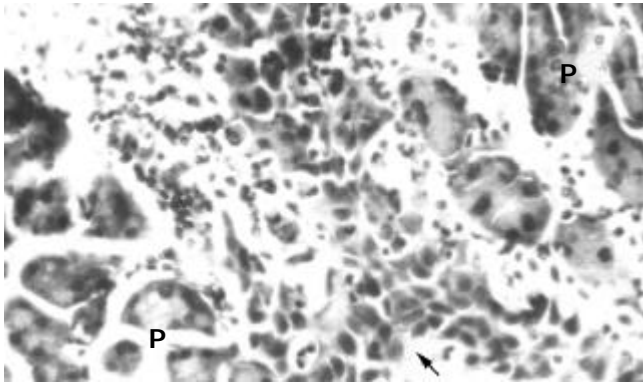


Figure 3 The inoculated SHEEMT cells (arrow) invaded into the parenchyma of pancreas (P) (HE, $\times 200$).

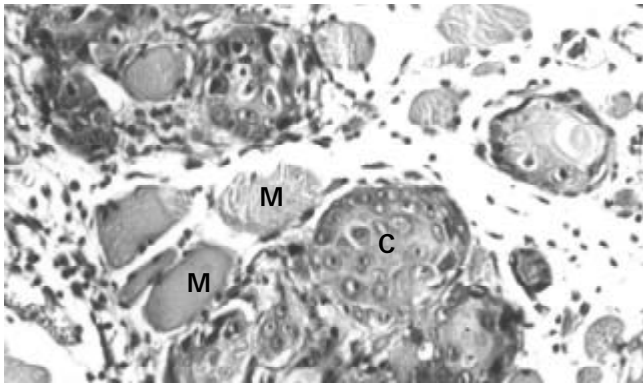


Figure 4 Tumor formation in subcutaneous tissue inoculated with SHEEMT cells (C), the latter was also shown to invade and destroy nearby muscle fibers (M). (HE, $\times 200$).

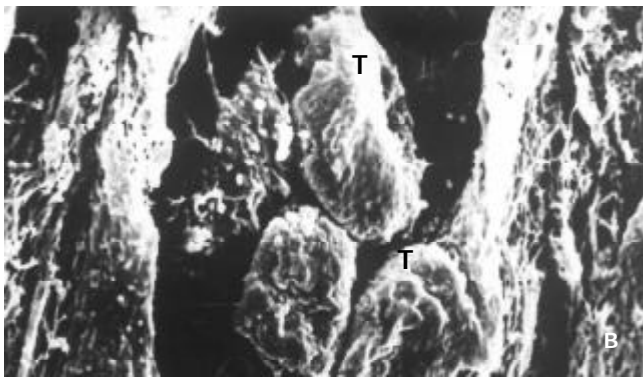
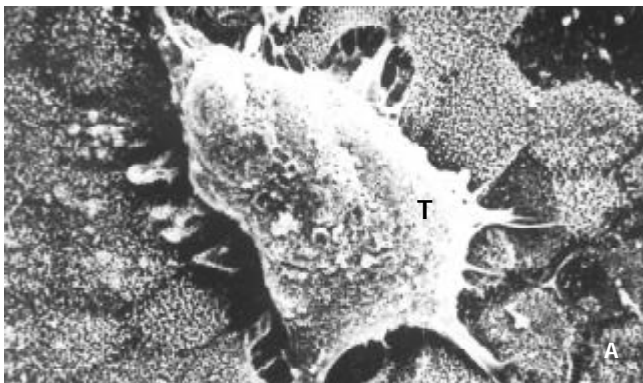


Figure 5 The invasiveness of inoculated SHEEMT cells on amniotic epithelium was demonstrated by scanning electron microscopy. A. A cluster of SHEEMT cells (T) grew on the amniotic epithelial surface (bar, 5μ); B. On the cutting surface, SHEEMT cells (T) were observed invading into the amnion stroma (bar, 50μ).

Oncogenesis and invasiveness in SCID mice

After inoculated into the SCID mice, SHEEMT cells were noted growing rapidly and forming tumor masses in 40 days. In peritoneal cavity, tumors were observed occurring on the mesentery, pancreas, urinary cyst, sub-diaphragm etc. with a special propensity for invading mesentery and pancreas, but did not exhibit any signs of hepatic metastases. Histological examination revealed that these tumor cells did not only grow on the organ surface, but also invade into adjacent tissues (Figure 3). In the subcutaneous tissue of the right axilla, tumor mass was observed macroscopically forming on the thoracic wall and penetrating into the thoracic cavity. Pathologically, these tumor cells harboring larger nucleus, nucleolus and less cytoplasm could infiltrate and destroy adjacent muscular fibers (Figure 4). Once transplanted, tumors could keep be passed to other SCID mice. In contrast, SHEEIMM cells were not found to form tumors in inoculated tissue by gross examination.

Invasive potency in vitro

After inoculated on the amnion, SHEEMT cells were shown growing in cluster on the epithelial surface with the formation of pseudopod that intruded into the gap between intercellular junctions (Figure 5A). On the cutting surface, SHEEMT cells were observed invading into the amnion stroma (Figure 5B). It was not found that the inoculated SHEEIMM cells could adhere to or colonize on the amniotic epithelium.

DISCUSSION

Invasive potency is one of the most important features of malignant tumors and is involved in a critical cascade of events such as extracellular matrix degradation, cell migration and colonization in the assaulted tissue. The invasive phenotype formation of malignant cells requires up-regulated expression of certain adhesive molecules, enzymes and related genes responsible for the interaction between cancer cells and extracellular matrix^[29]. Several co-factors have been reported to be involved in the process of invasion and metastasis^[30-32] besides ezrin that has been considered as an important molecule contributing to the malignantly transformation of cells. In addition to combining with adhesion molecules such as E-cadherin and catenin implicated in cell-cell and cell-matrix adhesion^[33], ezrin plays a critical role in the determination of invasiveness of cancer cells^[34].

In the present study, we investigated the expression of ezrin and its mRNA in a malignantly transformed esophageal epithelial cell line SHEEMT and further demonstrated its unrestricted growth and invasive potency in both *in vivo* and *in vitro* circumstances. The experimental results revealed that the expression of ezrin protein and its mRNA was significantly upregulated in SHEEMT compared with that in SHEEIMM cells. The SHEEMT cells inoculated to SCID mice could form tumor masses in both visceral organs and soft tissues in a period of 40 days. Pathologically, these tumor cells harboring larger nucleus, nucleolus and less cytoplasm could infiltrate and destroy adjacent tissues. In the *in vitro* study, the inoculated SHEEMT cells could grow in cluster on the amniotic epithelial surface and intrude into the amniotic stroma. In contrast, unrestricted growth and invasive property were not found in the SHEEIMM cells that were used as the control in both *in vivo* and *in vitro* experiments. As to our knowledge, this is one of the few reports concerned about how the ezrin gene expresses and what is its relation to the invasiveness formation in malignantly transformed esophageal epithelial cells.

New technology in molecular medicine allows global descriptions of complex expression patterns of genes responsible for the malignant properties of tumors^[35-38]. With the two representative passages of cells described above, we

have defined the profile of genes involved in the invasiveness of tumor cells using a sensitive cDNA microarray in a previous study. We found that increased expression of ezrin protein in SHEEMT cells was in accordance with their acquisition of the invasive potency^[39]. Based on these observations, we therefore speculated that ezrin might be an important candidate of genes in charge of the invasive behaviors of malignantly transformed esophageal epithelial cells, as reported in lymphoma and astrocytic tumors^[40, 41]. However, recent work in this field has also focused on the identification of ezrin-binding molecules, including CD₄₄, CD₄₃, intercellular adhesion molecule^[42-44] and syndecan-2^[45]. Moreover, modulation of the ERM protein ezrin by Merlin and NF-2 has been reported in other literatures^[46-48]. In the meanwhile, we have demonstrated that following expression of MMP₂ and MMP₉, highly invasive potency was developed in SHEEMT cells (Data to be published). All these suggest the invasiveness of tumor cells is determined by multiple genes and co-factors with complicated cellular signal pathways. Therefore, future works are necessitated to demonstrate more exactly the roles of ezrin and related molecules in the formation of invasive potency of cancer cells by the gene knockout technique and other powerful tools.

REFERENCES

- 1 **Ueda M**, Terai Y, Yamashita Y, Kumagai K, Ueki K, Yamaguchi H, Akise D, Hung YC, Ueki M. Correlation between vascular endothelial growth factor-C expression and invasion phenotype in cervical carcinomas. *Int J Cancer* 2002; **98**: 335-343
- 2 **Nestl A**, Von Stein OD, Zatloukal K, Thies WG, Herrlich P, Hofmann M, Sleeman JP. Gene expression patterns associated with the metastatic phenotype in rodent and human tumors. *Cancer Res* 2001; **61**: 1569-1577
- 3 **Comoglio PM**, Tamagnone L, Boccaccio C. Plasminogen-related growth factor and semaphorin receptors: a gene superfamily controlling invasive growth. *Exp Cell Res* 1999; **253**: 88-99
- 4 **Janneau JL**, Maldonado-Estrada J, Tachdjian G, Miran I, Motte N, Saulnier P, Sabourin JC, Cote JF, Simon B, Frydman R, Chaouat G, Bellet D. Transcriptional expression of genes involved in cell invasion and migration by normal and tumoral trophoblast cells. *J Clin Endocrinol Metab* 2002; **87**: 5336-5339
- 5 **Guo Y**, Pakneshan P, Gladu J, Slack A, Szyf M, Rabbani SA. Regulation of DNA methylation in human breast cancer. Effect on the urokinase-type plasminogen activator gene production and tumor invasion. *J Biol Chem* 2002; **277**: 41571-41579
- 6 **Jiang Y**, Xu W, Lu J, He F, Yang X. Invasiveness of hepatocellular carcinoma cell lines: contribution of hepatocyte growth factor, c-met, and transcription factor Ets-1. *Biochem Biophys Res Commun* 2001; **286**: 1123-1130
- 7 **Orian-Rousseau V**, Chen L, Sleeman JP, Herrlich P, Ponta H. CD44 is required for two consecutive steps in HGF/c-Met signaling. *Genes Dev* 2002; **16**: 3074-3086
- 8 **Loktionov A**, Watson MA, Stebbings WS, Speakman CT, Bingham SA. Plasminogen activator inhibitor-1 gene polymorphism and colorectal cancer risk and prognosis. *Cancer Lett* 2003; **189**: 189-196
- 9 **Tokunou M**, Niki T, Eguchi K, Iba S, Tsuda H, Yamada T, Matsuno Y, Kondo H, Saitoh Y, Imamura H, Hirohashi S. c-MET expression in myofibroblasts: role in autocrine activation and prognostic significance in lung adenocarcinoma. *Am J Pathol* 2001; **158**: 1451-1463
- 10 **Shen ZY**, Xu LY, Chen MH, Shen J, Cai WJ, Zeng Y. Progressive transformation of immortalized esophageal epithelial cells. *World J Gastroenterol* 2002; **8**: 976-981
- 11 **Shen ZY**, Cen S, Cai WJ, Teng ZP, Shen J, Hu Z, Zeng Y. Immortalization of human fetal esophageal epithelial cells induced by E6 and E7 genes of human papilloma virus 18. *Zhonghua Shiyan He Linchuang Bingduxue Zazhi* 1999; **13**: 121-123
- 12 **Shen ZY**, Xu LY, Chen Xh, Cai WJ, Shen J, Chen JY, Huang TH, Zeng Y. The genetic events of HPV-immortalized esophageal epithelium cells. *Int J Mol Med* 2001; **8**: 537-542
- 13 **Shen ZY**, Shen J, Cai WJ, Cen S, Zeng Y. Biological characteristics of human fetal esophageal epithelial cell line immortalized by the E6 and E7 gene of HPV type 18. *Zhonghua Shiyan He Linchuang Bingduxue Zazhi* 1999; **13**: 209-212
- 14 **Shen ZY**, Xu LY, Li C, Cai WJ, Shen J, Chen JY, Zeng Y. A comparative study of telomerase activity and malignant phenotype in multistage carcinogenesis of esophageal epithelial cells induced by human papillomavirus. *Int J Mol Med* 2001; **8**: 633-639
- 15 **Shen ZY**, Xu LY, Li EM, Cai WJ, Chen MH, Shen J, Zeng Y. Telomere and telomerase in the initial stage of immortalization of esophageal epithelial cell. *World J Gastroenterol* 2002; **8**: 357-362
- 16 **Shen ZY**, Xu LY, Chen MH, Cai WJ, Shen J, Chen JY, Hon CQ, Zeng Y. Biphasic differentiation of immortalized esophageal epitheliums induced by HPV18E6E7. *Bingdu Xuebao* 2001; **17**: 210-214
- 17 **Shen ZY**, Cen S, Shen J, Cai W, Xu J, Teng Z, Hu Z, Zeng Y. Study of immortalization and malignant transformation of human embryonic esophageal epithelial cells induced by HPV18E6E7. *J Cancer Res Clin Oncol* 2000; **126**: 589-594
- 18 **Shen ZY**, Cai WJ, Shen J, Xu JJ, Cen S, Teng ZP, Hu Z, Zeng Y. Human papilloma virus 18E6E7 in synergy with TPA induced malignant transformation of human embryonic esophageal epithelial cells. *Bingdu Xuebao* 1999; **15**: 1-6
- 19 **Shen ZY**, Shen J, Cai WJ, Chen JY, Zeng Y. Identification of malignant transformation in the immortalized esophageal epithelial cells. *Zhonghua Zhongliu Zazhi* 2002; **24**: 107-109
- 20 **Mangeat P**, Roy C, Martin M. ERM proteins in cell adhesion and membrane dynamics. *Trends Cell Biol* 1999; **9**: 187-192
- 21 **Scherer SS**, Xu T, Crino P, Arroyo EJ, Gutmann DH. Ezrin, radixin, and moesin are components of Schwann cell microvilli. *J Neurosci Res* 2001; **65**: 150-164
- 22 **Ohtani K**, Sakamoto H, Rutherford T, Chen Z, Satoh K, Naftolin F. Ezrin, a membrane-cytoskeletal linking protein, is involved in the process of invasion of endometrial cancer cells. *Cancer Lett* 1999; **147**: 31-38
- 23 **Makitie T**, Carpen O, Vaheri A, Kivela T. Ezrin as a prognostic indicator and its relationship to tumor characteristics in uveal malignant melanoma. *Invest Ophthalmol Vis Sci* 2001; **42**: 2442-2449
- 24 **Ohtani K**, Sakamoto H, Rutherford T, Chen Z, Kikuchi A, Yamamoto T, Satoh K, Naftolin F. Ezrin, a membrane-cytoskeletal linking protein, is highly expressed in atypical endometrial hyperplasia and uterine endometrioid adenocarcinoma. *Cancer Lett* 2002; **179**: 79-86
- 25 **Tokunou M**, Niki T, Saitoh Y, Imamura H, Sakamoto M, Hirohashi S. Altered expression of the ERM proteins in lung adenocarcinoma. *Lab Invest* 2000; **80**: 1643-1650
- 26 **Johnson MW**, Miyata H, Vinters HV. Ezrin and moesin expression within the developing human cerebrum and tuberous sclerosis-associated cortical tubers. *Acta Neuropathol* 2002; **104**: 188-196
- 27 **Mykkanen OM**, Gronholm M, Ronty M, Lalowski M, Salmikangas P, Suila H, Carpen O. Characterization of human palladin, a microfilament-associated protein. *Mol Biol Cell* 2001; **12**: 3060-3073
- 28 **Gautreau A**, Pouillet P, Louvard D, Arpin M. Ezrin, a plasma membrane-microfilament linker, signals cell survival through the phosphatidylinositol 3-kinase/Akt pathway. *Proc Natl Acad Sci USA* 1999; **96**: 7300-7305
- 29 **Gonzalez RR**, Devoto L, Campana A, Bischof P. Effects of leptin, interleukin-lalpha, interleukin-6, and transforming growth factor-beta on markers of trophoblast invasive phenotype: integrins and metalloproteinases. *Endocrine* 2001; **15**: 157-164
- 30 **Chen Z**, Fadiel A, Feng Y, Ohtani K, Rutherford T, Naftolin F. Ovarian epithelial carcinoma tyrosine phosphorylation, cell proliferation, and ezrin translocation are stimulated by interleukin lalpha and epidermal growth factor. *Cancer* 2001; **92**: 3068-3075
- 31 **Tran Quang C**, Gautreau A, Arpin M, Treisman R. Ezrin function is required for ROCK-mediated fibroblast transformation by the Net and Dbl oncogenes. *EMBO J* 2000; **19**: 4565-4576
- 32 **Stapleton G**, Malliri A, Ozanne BW. Downregulated AP-1 activity is associated with inhibition of Protein-Kinase-C-dependent CD44 and ezrin localization and upregulation of PKC theta in A431 cells. *J Cell Sci* 2002; **115**: 2713-2724

- 33 **Si HX**, Tsao SW, Lam KY, Srivastava G, Liu Y, Wong YC, Shen ZY, Cheung AL. E-cadherin expression is commonly downregulated by CpG island hypermethylation in esophageal carcinoma cells. *Cancer Lett* 2001; **173**: 71-78
- 34 **Hiscox S**, Jiang WG. Ezrin regulates cell-cell and cell-matrix adhesion, a possible role with E-cadherin/beta-catenin. *J Cell Sci* 1999; **112**: 3081-3090
- 35 **Schindelmann S**, Windisch J, Grundmann R, Kreienberg R, Zeillinger R, Deissler H. Expression profiling of mammary carcinoma cell lines: correlation of in vitro invasiveness with expression of CD24. *Tumour Biol* 2002; **23**: 139-145
- 36 **Zhan F**, Cao L, Hu C, Li G. Differentially expressed cDNA sequences homologous with known genes in human nasopharyngeal carcinoma. *Hunan Yike Daxue Xuebao* 1999; **24**: 103-106
- 37 **Khanna C**, Khan J, Nguyen P, Prehn J, Caylor J, Yeung C, Trepel J, Meltzer P, Helman L. Metastasis-associated differences in gene expression in a murine model of osteosarcoma. *Cancer Res* 2001; **61**: 3750-3759
- 38 **Wang KC**, Cheng AL, Chuang SE, Hsu HC, Su JJ. Retinoic acid-induced apoptotic pathway in T-cell lymphoma: Identification of four groups of genes with differential biological functions. *Exp Hematol* 2000; **28**: 1441-1450
- 39 **Shen J**, Chen MH, Zheng RM, Chen JJ, Shen ZY. Detection of tumor cell invasion in vitro by scanning electron microscopy. *Dianzi Xianwei Xuebao* 2000; **19**: 313-314
- 40 **Geiger KD**, Stoldt P, Schlote W, Derouiche A. Ezrin immunoreactivity is associated with increasing malignancy of astrocytic tumors but is absent in oligodendrogliomas. *Am J Pathol* 2000; **157**: 1785-1793
- 41 **Akisawa N**, Nishimori I, Iwamura T, Onishi S, Hollingsworth MA. High levels of ezrin expressed by human pancreatic adenocarcinoma cell lines with high metastatic potential. *Biochem Biophys Res Commun* 1999; **258**: 395-400
- 42 **Harrison GM**, Davies G, Martin TA, Jiang WG, Mason MD. Distribution and expression of CD44 isoforms and Ezrin during prostate cancer-endothelium interaction. *Int J Oncol* 2002; **21**: 935-940
- 43 **Legg JW**, Lewis CA, Parsons M, Ng T, Isacke CM. A novel PKC-regulated mechanism controls CD44 ezrin association and directional cell motility. *Nat Cell Biol* 2002; **4**: 399-407
- 44 **Guan XQ**, Wang CJ, Li YY. Effects of Ezrin on differentiation and adhesion of hepatocellular carcinoma. *Ai Zheng* 2002; **21**: 281-284
- 45 **Granes F**, Urena JM, Rocamora N, Vilaro S. Ezrin links syndecan-2 to the cytoskeleton. *J Cell Sci* 2000; **113**: 1267-1276
- 46 **Gronholm M**, Sainio M, Zhao F, Heiska L, Vaheri A, Carpen O. Homotypic and heterotypic interaction of the neurofibromatosis 2 tumor suppressor protein merlin and the ERM protein ezrin. *J Cell Sci* 1999; **112**: 895-904
- 47 **Meng JJ**, Lowrie DJ, Sun H, Dorsey E, Pelton PD, Bashour AM, Groden J, Ratner N, Ip W. Interaction between two isoforms of the NF2 tumor suppressor protein, merlin, and between merlin and ezrin, suggests modulation of ERM proteins by merlin. *J Neurosci Res* 2000; **62**: 491-502
- 48 **Gutmann DH**, Sherman L, Seftor L, Haipek C, Hoang Lu K, Hendrix M. Increased expression of the NF2 tumor suppressor gene product, merlin, impairs cell motility, adhesion and spreading. *Hum Mol Genet* 1999; **8**: 267-275

Edited by Zhu L and Wang XL

Research and control of well water pollution in high esophageal cancer areas

Xiu-Lan Zhang, Bing Zhang, Xing Zhang, Zhi-Feng Chen, Jun-Zhen Zhang, Shuo-Yuang Liang, Fan-Shu Men, Shu-Liang Zheng, Xiang-Ping Li, Xiu-Lan Bai

Xiu-Lan Zhang, Zhi-Feng Chen, Shuo-Yuang Liang, Cancer Institute, the Fourth Hospital of Hebei Medical University, Shijiazhuang 050011, Hebei Province, China

Bing Zhang, Xing Zhang, School of Public Health, Hebei Medical University, Shijiazhuang 050017, Hebei Province, China

Jun-Zhen Zhang, the Fourth Hospital of Hebei Medical University, Shijiazhuang 050011, Hebei Province, China

Fan-Shu Men, Shu-Liang Zheng, Xiang-Ping Li, Cixian Cancer Institute, Cixian County, Hebei Province, China

Xiu-Lan Bai, Chichen Health Center, Chichen County, Hebei Province, China

Supported by Ministry of Education of China, No.85-914-01-01

Correspondence to: Dr. Xiu-Lan Zhang, Cancer Institute, the Fourth Hospital of Hebei Medical University, 12 Jian Kang Lu, Shijiazhuang 050011, Hebei Province, China. czf@xinhuanet.com

Telephone: +86-311-5825709 Fax: +86-311-6077634

Received: 2002-10-08 Accepted: 2002-12-22

Abstract

AIM: In order to detect risk factors for esophageal cancer, a national research program was carried out during the Eighth Five-Year Plan (from 1991 to 1995).

METHODS: Cixian County and Chichen County in Hebei Province were selected as the index and the control for the study fields with higher or lower incidence of esophagus cancer in China, respectively. In these areas, we investigated the pollution of three nitrogenous compounds in well water for drinking and the use of nitrogen fertilizer in farming.

RESULTS: In well water, nitrate nitrogen, nitrite nitrogen and ammonia nitrogen were 8.77 mg/L, 0.014 mg/L and 0.009 mg/L in Cixian County in 1993, respectively. They were significantly higher than their levels (3.84 mg/L, 0.004 mg/L and 0.004 mg/L) in Chichen County ($P < 0.01$, $t = 6.281$, $t = 3.784$, $t = 3.775$). There was a trend that the nitrogenous compounds in well water increased from 1993 to 1996. The amount of nitrogen fertilizer used in farming was 787.6 kg per hectare land in Cixian County in 1991, significantly higher than 186 kg per hectare in Chichen County ($t = 9.603$, $P < 0.001$).

CONCLUSION: These investigations indicate that the pollution of nitrogenous compounds in well water for drinking is closely related to the use of nitrogen fertilizer in farming, and there is a significantly positive correlation between the level of three nitrogenous compounds in well water and the mortality of esophageal cancer (correlation coefficient = 0.5992). We suggest that improvement of well system for drinking water quality should be an effective measure for esophageal cancer prevention and control in rural areas.

Zhang XL, Zhang B, Zhang X, Chen ZF, Zhang JZ, Liang SY, Men FS, Zheng SL, Li XP, Bai XL. Research and control of well water pollution in high esophageal cancer areas. *World J Gastroenterol* 2003; 9(6): 1187-1190

<http://www.wjgnet.com/1007-9327/9/1187.asp>

INTRODUCTION

It is well known that the chief causes of most cancers are environmental, dietary and lifestyle factors. In China, there is a special area around the Taihang Mountain with the highest incidence of esophageal cancer. Esophageal cancer has been studied in this rural area for a long time^[1-3]. These studies indicate some relationship between local environmental factors and esophageal cancer^[4-8]. Among these, nitrogenous compounds in well water for drinking is considered as a possible risk factor for esophageal cancer because of its close relationship with local people's life^[7,8]. In this rural area, well is the main water source for drinking. It is polluted usually by nitrogenous compounds. In order to identify the effect of nitrogenous compound pollution on esophageal cancer, we designed a 2×2 cross-sectional study for factor analysis during the Eighth Five-Year Plan (from 1991 to 1995). The research program for investigating the relationship between drinking water pollution and esophageal cancer was carried out. It also included a step of improvement in well water quality and pollution control.

MATERIALS AND METHODS

Study fields

According to mortality, two counties from Hebei Province were selected for the present study fields, Cixian County as index and Chichen County as control, respectively. From 1974 to 1976, the mortality per 100 000 of esophageal cancer standardized by Chinese population in Cixian County and in Chichen County was 147.7 and 8.3 in male, and 79.33 and 2.8 in female, respectively. Cixian County is located at the southern part of Hebei Province and the eastern foot of the Taihang Mountain. There are 354 villages under 35 local town governments in Cixian County. It covers an area of 1 015 Km² and has a population of 580 000.

Well registration

Before the investigation, a team for the program was organized. The investigators and other work staff were trained based on the program guideline. From the end of 1991 to the beginning of 1992, we completed registration of the wells located in 101 villages (9 towns) in Cixian County and made well file. The registered items of well file included (1) position, (2) type, (3) depth, (4) enclosing wall, (5) wall structure, (6) pipeline, (7) pollution source within 10 meter distance, (8) served population, and (9) served time. According to the well registration, we started a consecutive monitor on the pollution of three nitrogenous compounds (nitrate nitrogen, nitrite nitrogen and ammonia nitrogen) in the selected wells. Meanwhile, we investigated the amount of nitrogen fertilizer used in farming per year in the study fields.

Nitrogenous compounds examination

The level of ammonia nitrogen in water was analyzed by Nessler's reagent method. The amount of nitrate nitrogen and of nitrite nitrogen was tested in terms of Cadmium column

reduction method. The water samples were collected according to the routine method^[9-12].

Statistical analysis

Statistical analysis was performed by *t* test, and linear correlation was used for analysis on the relationship between three nitrogenous compounds and mortality of esophageal cancer. Two-tailed *P* value of less than 0.05 was defined as statistically significant.

RESULTS

Among 9 towns in Cixian County, there were three types of well served for drinking water, manual-pump well, motor-pump well and non-pump well. Non-pump well was main type, about 554 were built in these areas. This type of well had a big opening mouth without pipe, enclosing wall and cover. Recently, some new motor-pump wells were built. They were 200 meter in depth with brick wall. These old and new wells provided drinking water for 130 952 people. In the control areas, 1/3 of wells was about 8 meters and 2/3 was less than 40 meters in depth. The depth of water varied with season. The served time of wells was different. The oldest one, for example, the Longwangmiao Well of the Xiguanglu Village of the Guanglu Town had a history of 300 years, and the new one was only 2 years.

The pollution of nitrogenous compounds in drinking water was a big health problem. We found that 41.2 % of the motor-pump wells and 88.5 % of non-pump wells existed pollution sources within 10 meter distance, for example, excrement and urine from the residents and animals, and pollution sources increased year by year. The monitoring data from the sampled wells showed that nitrate nitrogen, nitrite nitrogen and ammonia nitrogen in Cixian County were significantly higher than those in Chichen County (*P*<0.01), and the pollution increased gradually from 1993 to 1996 (Table 1). They were 20.6 %, 50.5 % and 33.3 % higher than the state permissive level, respectively. The amount of nitrogen fertilizer used in Cixian County's farming was significantly higher than in Chichen County (*P*<0.01), and there was an increasing trend (Table 2). The time trend of three nitrogen compounds in relation to the use of nitrogen fertilizer is shown in Figure 1, Figure 2 and Figure 3 for Cixian County and Chichen County, respectively.

Table 1 Three nitrogenous compounds pollution (mg/L) of the well water in Cixian County and Chichen County from 1993 to 1996

	Numbers of well	1993	1994	1995	1996
Nitrate nitrogen					
Cixian	33	8.770 ^b	13.381 ^b	14.473 ^b	19.554 ^b
Chichen	31	3.829	4.452	4.351	8.022
Ratio (Cixian/Chichen)		2.29	3.00	3.33	2.44
Nitrite nitrogen					
Cixian	33	0.0144 ^b	0.0629 ^b	0.0407 ^b	0.0101 ^b
Chichen	31	0.0039	0.0094	0.0085	0.0020
Ratio (Cixian/Chichen)		3.69	6.69	4.79	5.05
Ammonia nitrogen					
Cixian	33	0.0094 ^b	0.0256 ^b	0.0237	0.0117 ^b
Chichen	31	0.0039	0.0029	0.0230	0.0028
Ratio (Cixian/Chichen)		2.41	8.82	1.03	4.18

^b*P*<0.01, There was a significant difference between two counties.

Table 2 Farming use of nitrogen fertilizer (kg/hectare) in Cixian County and Chichen County from 1991 to 1996

	1991	1992	1993	1994	1995	1996
Cixian	787.6	825.1	1293.1	1213.6	1251.1	1053.1
Chichen	186.0 ^b	202.5 ^b	196.5 ^b	201.0 ^b	220.5 ^b	219.0 ^b
Ratio (Cixian/Chichen)	4.20	4.07	6.58	6.04	5.67	4.81

^b*P*<0.01, There was a significant difference between two counties.

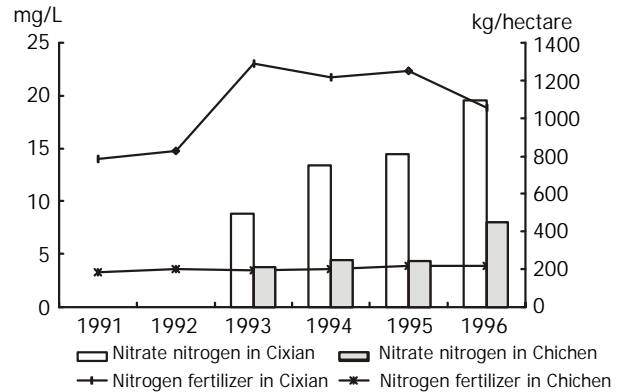


Figure 1 Time trend of nitrate nitrogen in relation to the farming use of nitrogen fertilizer in Cixian County and Chichen County.

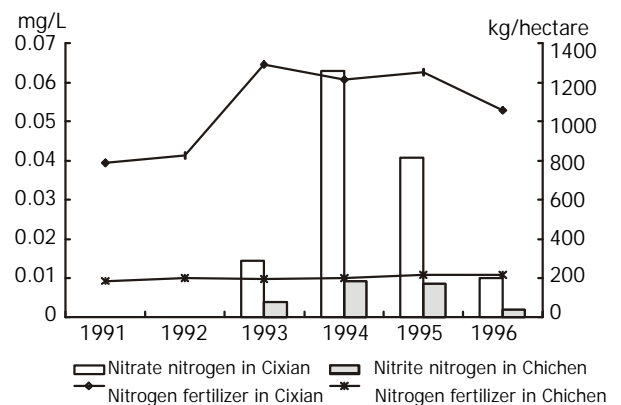


Figure 2 Time trend of nitrite nitrogen in relation to the farming use of nitrogen fertilizer in Cixian County and Chichen County.

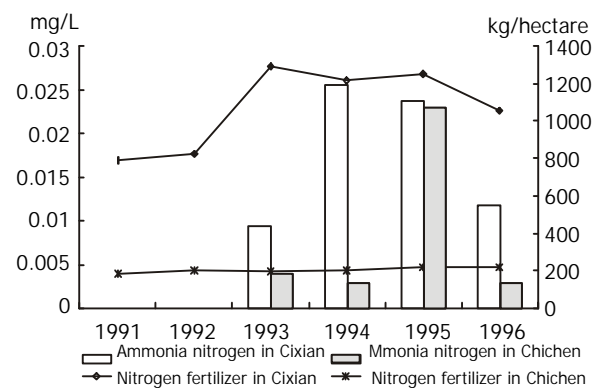


Figure 3 Time trend of ammonia nitrogen in relation to the farming use of nitrogen fertilizer in Cixian County and Chichen County.

DISCUSSION

It has been proven in animal experiments that nitrosamine compounds (NOC) are a kind of strong carcinogen and can

cause tumor in different animal tissues and organs^[13-21]. The epidemiological investigation has also demonstrated an increased risk of human gastric cancer with food intake polluted by nitrosamine compounds^[22,23]. Nitrate and nitrite are precursors of NOC^[24,25].

If well water contains a large amount of three nitrogenous compounds, and serve as main water source, there may be two harmful effects on local people's health. One is that three nitrogenous compounds would accumulate in plants and in crops^[25-29]. Usually, nitrate is easily reduced to nitrite, and then it is synthesized into NOC. The other harmful effect is that local people and livestock or poultry would have an increased intake of three nitrogenous compounds through the drinking water^[30-32]. These nitrogenous compounds with ammonia can be changed to a strong carcinogen, NOC, in stomach since its pH value is 1-3 from gastric acid^[33].

The present investigation showed that the pollution of three nitrogenous compounds in the index area with high risk of esophageal cancer was significantly higher than that in the control area ($P < 0.01$). The mortality ratio between Cixian County and Chichen County was 17.9 (147.7 per 100 000 / 8.3 per 100 000) in male, and 28.5 (79.3/2.8) in female in the period of 1974 through 1976. There was a positive correlation between the nitrate nitrogen, nitrite nitrogen in well water and mortality of esophageal cancer in the study fields. The present findings indicate that heavy pollution of nitrogenous compounds in drinking water in the index area is a possible risk factor for esophageal cancer.

There were two possible pollution sources of nitrogenous compounds for well in the investigated fields, living garbage or excrement and farming nitrogen fertilizer. In comparison of the two counties, we found that the amount of nitrogen fertilizer used in farming in Cixian County was significantly higher than that in Chichen County, and the pollution of nitrate nitrogen and nitrite nitrogen in well water had a similar trend (Figure 1 and Figure 2). It can be understood that the nitrate nitrogen and nitrite nitrogen in well water come mainly from the pollution of farming nitrogen fertilizer. The amount of ammonia nitrogen in well has not a regular change. Its pollution to the drinking water is possibly resulted from the excrement of local people and animals other than farming nitrogen fertilizer.

Based on these evidences, well water pollution control of three nitrogenous compounds will be one of the important measures for the primary prevention of esophageal cancer in the higher risk areas. The study revealed that water quality improvement had a beneficial effect on gastric cancer prevention^[34]. At the beginning of the Ninth Five-Year Plan (1996-2000), a program for improvement of water supply system in the index area was started. Initial effect was observed (Table 3). There was a significant decline of three nitrogenous compounds in well water after several years' pollution control. These findings indicate that the program for improvement in water supply system is successful for pollution control. Whether pollution control of nitrogenous compounds contributes to incidence decline of esophageal cancer in the higher risk area, needs further study and more evidence.

Table 3 Three nitrogenous compounds (mg/L) in well water before and after well reconstruction

No. of well	Nitrate nitrogen		Nitrite nitrogen		Ammonia nitrogen	
	Before	After	Before	After	Before	After
12#	14.9621	8.0097	0.0077	0.0033	0.0131	0.0048
14#	8.9890	1.9099	0.0208	0.0067	0.0127	0.0053
29#	18.4929	0.0000	0.2929	0.0100	0.0459	0.0087

12#, 14#, 29# are the number of the sampled well.

Based on the presently investigated results, measures for pollution prevention and control in the areas with high risk of esophageal cancer should include: (1) The first measure is to improve the health consciousness of local people on drinking water, and to develop the type of deep well with pipeline. (2) The second is to focus on the environmental hygiene surrounding the well. It includes garbage control near water source, and sanitary management of excrement and urine. (3) The third is to establish and to improve the system management of water source, and to supply clean water with pipeline. (4) The fourth is to build high quality lavatory and to prevent its pollution to well water. (5) The fifth is to encourage local farmers to use rational formula fertilization in order to decrease effectively organic nitrogen pollution in the environment.

REFERENCES

- Hou J**, Lin PZ, Chen ZF, Wang GQ, Liu KG, Li SS, Meng FS, Du CL. Survey on esophageal cancer in Cixian County. *Zhongliu Fangzhi Yanjiu* 1998; **25**: 73-75
- Yokokawa Y**, Ohta S, Hou J, Zhang XL, Li SS, Ping YM, Nakajima T. Ecological study on the risks of esophageal cancer in Cixian, China: the importance of nutritional status and the use of well water. *Int J Cancer* 1999; **83**: 620-624
- Qiao YL**, Hou J, Yang L, He YT, Liu YY, Li LD, Li SS, Lian SY, Dong ZW. The Trends and preventive strategies of esophageal cancer in high-risk areas of Taihang Mountains, China. *Zhongguo Yixue Kexue Yuan Xuebao* 2000; **23**: 10-14
- Zhuo XG**, Watanabe S. Factor analysis of digestive cancer mortality and food consumption in 65 Chinese counties. *J Epidemiol* 1999; **9**: 275-284
- Li WJ**, Zhu MJ, Chen PP, Lu WQ, Wang Q, Shi BQ. Study on dietary pattern and nutrients intakes of residents in areas of high and low incidence of esophageal cancer. *Weisheng Yanjiu* 1997; **26**: 351-355
- Wang H**, Wei H, Ma J, Luo X. The fumonisin B1 content in corn from North China, a high risk area of esophageal cancer. *J Environ Pathol Toxicol Oncol* 2000; **19**: 139-141
- Li WJ**, Lu WQ, Zhu MJ, Shi BQ, Wang Q. Determination of copper, zinc, iron and calcium in wheat and maize and three nitrogen compounds in high and low risk areas of esophageal cancer. *Weisheng Yanjiu* 1998; **27**: 69-71
- Zhang XL**, Li SS, Zhang WZ. Investigation and study on drinking water in Cixian County. *Zhongguo Zhongliu* 1996; **5**: 12-14
- Hao CJ**. The Practical handbook for environmental monitoring and water analysis. Harbin: Harbin Industrial University Press 1986
- Ministry of Public Health**. The people's republic of China, the standardized method for drinking water testing. Beijing: China Standard Bureau Press 1986
- Environmental Protective Bureau**. Ministry of urban and rural construction & environment protection analytical method for environmental monitoring. Beijing: Chinese Environmental Science Press 1986
- Chinese Environmental Monitoring Center**. The handbook of quality assurance for environmental monitoring on water. Beijing: Chemical Industry Press 1984
- Opitz OG**, Harada H, Suliman Y, Rhoades B, Sharpless NE, Kent R, Kopelovich L, Nakagawa H, Rustgi AK. A mouse model of human oral-esophageal cancer. *J Clin Invest* 2002; **110**: 761-769
- Fong LY**, Nguyen VT, Farber JL. Esophageal cancer prevention in zinc-deficient rats: rapid induction of apoptosis by replenishing zinc. *J Natl Cancer Inst* 2001; **93**: 1525-1533
- Straif K**, Weiland SK, Bungers M, Holtherrich D, Taeger D, Yi S, Keil U. Exposure to high concentrations of nitrosamines and cancer mortality among a cohort of rubber workers. *Occup Environ Med* 2000; **57**: 180-187
- Qi GY**, Shu SC, You CF, Chen SW, Song Y. A case-control study on the influential factors of esophageal cancer. *Zhongguo Manxingbing Yu Fangyu Kongzhi* 2001; **9**: 15-14,34
- Lin K**, Shen ZY, Cai SS, Lu SX, Guo LP. Investigation on nitrosamines in the diets of the inhabitants of high-risk area for esophageal cancer in the southern China and analysis of the correlation factors. *Weisheng Yanjiu* 1997; **26**: 266-269

- 18 **Lin K**, Shen W, Shen Z, Wu Y, Lu S. Dietary exposure ad urinary excretion of total N- nitroso compounds, nitrosamino acids and volatile nitrosamine in inhabitants of high- and low- risk areas for esophageal cancer in Southern China. *Int J Cancer* 2002; **102**: 207-211
- 19 **Zhang GS**, He YT, Hou J. A case control study on risk factor of esophageal cancer in Cixian County. *Sichuan Zhongliu FangZhi* 2000; **13**: 65-67
- 20 **Wilp J**, Zwickenpflug W, Richter E. Nitrosation of dietary myosmine as risk factor of human cancer. *Food Chem Toxicol* 2002; **40**: 1223-1228
- 21 **Siddiqi M**, Kumar R, Fazili Z, Spiegelhalter B, Preussmann R. Increased expoure to dietary amines and nitrate in a popalation at high risk of oesophageal and gastric cancer in Kashmir. *Carcinogenesis* 1992; **13**: 1331-1335
- 22 **Cai L**, Zheng ZL, Zhang ZF. Risk factors for the gastric cardia cancer: a case-control study in Fujian Province. *World J Gastroenterol* 2003; **9**: 214-218
- 23 **Ye WM**, Yi YN, Luo RX, Zhou TS, Lin RT, Chen GD. Diet and gastric cancer: a casecontrol study in Fujian Province, China. *World J Gastroenterol* 1998; **4**: 516-518
- 24 **Rogers MA**, Vaughan TL, Davis S, Thomas DB. Consumption of nitrate, nitrite, and nitrosodimethylamine and the risk of upper aerodigestive tract cancer. *Cancer Epidemiol Biomarkers Prev* 1995; **4**: 29-36
- 25 **Yang XF**, Wang KJ, Jia YS, Lian BQ, Li T, Li SD, Du C, Yan JG. Epidemiological investigation on cancer mortality of the workers exposed to nitrite compounds. *Zhonghua Laodongwei Shengzhi Yebing Zazhi* 1996; **14**: 293-295
- 26 **Li W**, Lu W, Zhu M, Shi B. Determination of copper, zinc, iron and calcium in wheat and maize and three nitrogen compounds in high and low risk areas of esophageal cancer. *Weisheng Yanjiu* 1998; **27**: 69-71
- 27 **Lu SH**, Camus AM, Ji C, Wang YL, Wang MY, Bartsch H. Mutagenicity in salmonella typhimurium of N-3-methylbutyl- N-1-methyl-acetonyl-nitrosamine and N-methyl-N-benzyl nitrosamine, N-nitrosation products isolated from corn-bread contaminated with commonly occurring moulds in Linshien County, a high incidence area for oesophageal cancer in Northern China. *Carcinogenesis* 1980; **1**: 867-870
- 28 **Guo LP**, Zhang FS, Wang XR, Mao DR, Chen XP. Effect of long-term fertilization on soil nitrate distribution. *J Environ Sci* 2001; **13**: 58-63
- 29 **Ramos C**, Agut A, Lidon AL. Nitrate leaching in important crops of the Valencian Community region. *Environ Pollut* 2002; **118**: 215-223
- 30 **Barrett JH**, Parslow RC, McKinney PA, Law GR, Forman D. Nitrate in drinking water and the incidence of gastric, esophageal, and brain cancer in Yorkshire, England. *Cancer Causes Control* 1998; **9**: 153-159
- 31 **Lu WQ**, Chen JL, Li WJ, Wang Y, Ddong WZ, Zhu MJ, Wang Q. Analysis on three nitrogen compounds of the drinking water in high and low risk areas of esophageal cancer. *Zhongguo Zhongliu* 2000; **9**: 227
- 32 **Shrestha RK**, Ladha JK. Nitrate pollution in groundwater and strategies to reduce pollution. *Water Sci Technol* 2002; **45**: 29-35
- 33 **Mayne ST**, Risch HA, Dubrow R, Chow WH, Gammon MD, Vaughan TL, Farrow DC, Schoenberg JB, Stanford JL, Ahsan H, West AB, Rotterdam H, Blot WT, Fraumeni JF Jr. Nutrient intake and risk of subtypes of esophageal and gastric cancer. *Cancer Epidemiol Biomarkers Prev* 2001; **10**: 1055-1062
- 34 **Wang ZQ**, He J, Chen W, Chen Y, Zhou TS, Lin YC. Relationship between different sources of drinking water, water quality improvement and gastric cancer mortality in Changle County-A retrospective-cohort study in high incidence area. *World J Gastroenterol* 1998; **4**: 45-47

Edited by Wen CY and Wang XL

Development of an oral DNA vaccine against MG7-Ag of gastric cancer using attenuated *salmonella typhimurium* as carrier

Chang-Cun Guo, Jie Ding, Bo-Rong Pan, Zhao-Cai Yu, Quan-Li Han, Fan-Ping Meng, Na Liu, Dai-Ming Fan

Chang-Cun Guo, Jie Ding, Zhao-Cai Yu, Quan-Li Han, Fan-Ping Meng, Na Liu, Dai-Ming Fan, Institute of Digestive Disease, Xijing Hospital, Fourth Military Medical University, Xi'an 710032, Shaanxi Province, China

Bo-Rong Pan, Oncology Center, Xijing Hospital, 127 Changle West Road, Xi'an 710032, Shaanxi Province, China

Supported by the National Natural Science Foundation of China, No. 39870742

Correspondence to: Professor Dai-Ming Fan, Institute of Digestive Disease, Xijing Hospital, Fourth Military Medical University, Xi'an 710032, Shaanxi Province, China. daimfan@fmmu.edu.cn

Telephone: +86-29-3375229

Received: 2002-08-24 **Accepted:** 2002-10-21

Abstract

AIM: To develop an oral DNA vaccine against gastric cancer and evaluate its efficacy in mice.

METHODS: The genes of the MG7-Ag mimotope and a universal Th epitope (Pan-DR epitope, PADRE) were included in the PCR primers. By PCR, the fusion gene of the two epitopes was amplified. The fusion gene was confirmed by sequencing and was then cloned into pcDNA3.1(+) plasmid. The pcDNA3.1(+)-MG7/PADRE was used to transfect an attenuated *Salmonella typhimurium*. C57BL/6 mice were orally immunized with 1×10^8 cfu *Salmonella* transfectants. *Salmonella* harboring the empty pcDNA3.1(+) plasmid and phosphate buffer saline (PBS) were used as negative controls. At the 6th week, serum titer of MG7-Ag specific antibody was detected by ELISA. At the 8th week cellular immunity was detected by an unprimed proliferation test of the spleenocytes by using a [3 H]-thymidine incorporation assay. Ehrlich ascites carcinoma cells expressing MG7-Ag were used as a model in tumor challenge assay to evaluate the protective effect of the vaccine.

RESULTS: Serum titer of antibody against MG7-Ag was significantly higher in mice immunized with the vaccine than that in control groups (0.841 vs 0.347, $P < 0.01$; 0.841 vs 0.298, $P < 0.01$), while *in vitro* unprimed proliferation assay of the spleenocytes showed no statistical difference between those three groups. Two weeks after tumor challenge, 2 in 7 immunized mice were tumor free, while all the mice in the control groups showed tumor formation.

CONCLUSION: Oral DNA vaccine against the MG7-Ag mimotope of gastric cancer is immunogenic. It can induce significant humoral immunity against tumor in mice, and the vaccine has partially protective effects.

Guo CC, Ding J, Pan BR, Yu ZC, Han QL, Meng FP, Liu N, Fan DM. Development of an oral DNA vaccine against MG7-Ag of gastric cancer using attenuated *salmonella typhimurium* as carrier. *World J Gastroenterol* 2003; 9(6): 1191-1195

<http://www.wjgnet.com/1007-9327/9/1191.asp>

INTRODUCTION

Gastric cancer is the most common malignant tumor in China and the second most common malignancy around the world. Conventional intervention measures such as operation and chemotherapy work poorly in treating gastric cancer. And with few tumor-specific antigens identified, there are few effective vaccines developed to combat gastric cancer. MG7-Ag, discovered by our institute, is a kind of gastric cancer-specific tumor-associated antigen. Detecting the serum anti-MG7-Ag antibody serves as a preliminary test in the diagnosis for gastric cancer and could be used for the surveillance of relapse and the appraisal of treatment efficacy^[1]. MG7-Ag can be used as an indicator for high risk of malignant change in stomach mucosa dysplasia^[2]. Primary study showed that MG7-Ag could elicit significant specific immune response against gastric cancer, suggesting that it could be an excellent target for cancer vaccine development. However, due to its unknown identity, it is much difficult to isolate and purify MG7-Ag from tumor tissues. Recently, we have identified the mimotopes of MG7-Ag by screening the phage display library, and the mimotopes could mimic the primary antigen efficiently, as shown by *in vitro* and *in vivo* assays^[3,4]. We reported here for the first time the development of an oral DNA vaccine by using the MG7-Ag mimotope of gastric cancer.

MATERIALS AND METHODS

Plasmids and bacteria

The plasmid pcDNA3.1(+) was purchased from Invitrogen Corporation. And the pEGFP plasmid containing the enhanced green fluorescence protein (EGFP) gene was purchased from Clontech Corporation. Attenuated *Salmonella typhimurium* SL3261 strain was used as the oral vector to develop the vaccine.

Construction of eukaryotic expression vector of MG7-Ag mimotope fused with a helper T cell epitope PADRE

Two pairs of PCR primers (P_{1.1}, P_{1.2} and P_{2.1}, P_{2.2}) were designed by using Primer Premiere 5.0 software. The sense primers (P_{1.1} and P_{2.1}) were both 5' -CGATGTACGGGCCAGATA TACGCG-3', corresponding to the 209-232 bp sequence of pcDNA3.1(+). Reverse primer P_{1.2} was 5' -ACTTCCTC CTCCTTTGTATGCACA TGAGGTTTCATGGTGCAA GCTTCCTACCGCCCATTTGCGT, corresponding to the reverse complementary sequence of 768-785 bp sequence of pcDNA3.1(+), Hind III digestion site, Kozak sequence, and the sequence of the MG7-Ag mimotope. Reverse primer P_{2.2} was 5' -TTAAGCAGCAGCTTTAAGTGTCCAAGCAGCCAC AAATTTAGCACTTCCTCCTCCTTTTGTATGCA-3', corresponding to the reverse complementary sequence of the MG7-Ag mimotope and the universal Th epitope PADRE. Two PCR reactions were performed to incorporate the mimotope and the PADRE into a fragment of pcDNA3.1(+) plasmid. In this case, the pcDNA3.1 fragment was used as a carrier to facilitate further manipulations. For the first PCR reaction, template was plasmid pcDNA3.1(+), and primers were P_{1.1} and P_{1.2}. By using the product of the first PCR as template, a second PCR was performed with primers P_{2.1} and P_{2.2} to incorporate

the PADRE epitope into the yielding fragment. The final PCR product was visualized by agarose electrophoresis and was then cloned into pUCm-T vector and sequenced on ABI PRISM™ 377 sequencer. Then, the PCR product was subcloned into pcDNA3.1(+) vector from the pUCm-T vector. By restrictive enzyme digestion with *Hind* III, the non-relevant plasmid fragment was removed from the final recombinant vector pcDNA3.1(+)-MG7/PADRE. The vector was sequenced to confirm the proper encoding sequence.

Construction of oral DNA vaccine and in vitro experiment using attenuated *Salmonella typhimurium* as the oral DNA vector

To get the oral DNA vaccine, the pcDNA3.1(+)-MG7/PADRE vector was transduced into the attenuated *Salmonella typhimurium* SL3261 by electroporation (2.5 kV, 25 μF, 200 Ω, pulse time 0.0326S). Plasmid in the *Salmonella* transfectant was extracted and used as template, and PCR was performed by using primer P_{1,1} and primer P_{2,2} to verify the successful transfection. The PCR product underwent agarose electrophoresis for visualization. An *in vitro* experiment was performed by using the SL3261 strain as the oral vector of DNA vaccine according to reference^[5]. Briefly, eukaryotic expression vector of the enhanced green fluorescence protein was transduced into the attenuated *Salmonella typhimurium* SL3261. The transfectants were coincubated with murine peritoneal macrophage at 37 °C for 30 min. SL3261 harboring the empty pcDNA3.1(+) plasmid was used as negative control. Gentamycin was added into the culture media to kill the extracellular bacteria. Four hours later, tetracycline was added to kill the intracellular bacteria. The infected macrophages were cultured for 48 hours, and were then examined by flow cytometry (FCM) for the expression of green fluorescence protein.

Immunization of the mice and immune response examination

Thirty-five female 4-week-aged C57BL/6J mice weighing 15-20g were used in the immunization assay. They were randomly divided into 3 groups, which were orally given the PBS solution (10 mice, PBS control), the attenuated *Salmonella* SL3261 harboring the empty pcDNA3.1(+) plasmid (10 mice, empty control) or the oral DNA vaccine SL3261 strain harboring the pcDNA3.1(+)-MG7/PADRE (15 mice, immunization group).

Before immunization, all the mice were starved overnight and pre-administered with 100 μl 10 g/L NaHCO₃ solution. Each time, 100 μl PBS (pH7.6) was given to the mice in PBS control group, and 1×10⁸ *Salmonella typhimurium* were given to the mice in the empty control and immunization group. PBS and *Salmonella typhimurium* were given to the mice by orogastric inoculation. Immunization was repeated every two weeks. At the 6th week after the first immunization, sera from the mice (5 mice from each group) were prepared and 1:80 diluted. By coating KATO III cells expressing the MG7-Ag on the plates, a cellular ELISA was performed to detect the antibody against MG7-Ag. At the 8th week, the splenocyte suspension was prepared, and an unprimed proliferation test of the splenocytes was performed by a [³H]-thymidine incorporation assay^[6] with a few modifications. Briefly, splenocyte suspension of the mice from three groups was prepared. 1×10⁶ cells were plated into each well of 96-well plate. Into each well, 1×10⁵ mytocin C-pretreated autologous antigen-presenting cells (APC) were added. The cells were incubated with 50 μg/ml synthetic MG7-Ag mimotope peptide for 4 hours. The cells were washed and cultured for 3 days. Then cells were incubated for 6 hours with 74MBq/L of [³H]thymidine. The plates were harvested, and the proliferative response of the splenocytes was examined by measuring the β counts of the cells. To further investigate the efficacy of the oral DNA vaccine, the tumor challenge assay was performed. Ehrlich ascites carcinoma cells (EAC) were immunostained with MG7 antibody to verify the presence of the MG7-Ag. Then 1×10⁷ EAC cells were injected into the abdominal cavity of the mice in each group. The number of tumor-bearing mice and the survival rate of each group were observed.

RESULTS

Construction of the oral DNA vaccine

By PCR, MG7-Ag mimotope and PADRE were fused together and incorporated into a fragment of the pcDNA3.1(+) (Figure 1). The proper coding of the epitopes was confirmed by sequencing (Figure 2). The PCR product was subcloned into pcDNA3.1(+). And by *Hind* III digestion, the fragment of the pcDNA3.1 in the PCR product was removed (Figure 3).

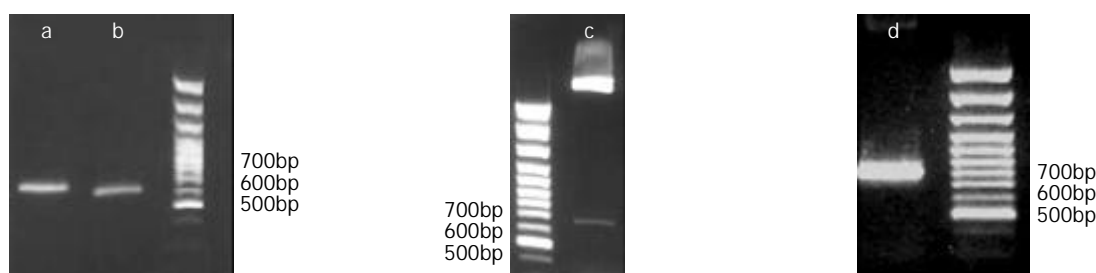


Figure 1 Incorporation of the epitope gene into the pcDNA3.1 fragment by PCR: A product of 620bp was amplified by the first PCR (a), and a fragment of 660bp was amplified by the second PCR (b).

Figure 2 *Hind* III digestion of the recombinant plasmid after subcloning the PCR product into pcDNA3.1(+) from the pUCm-T vector: A fragment of 660bp was released (c), which corresponded to the size of the carrier fragment.

Figure 4 PCR identification of the pcDNA3.1(+)-MG7/PADRE plasmid harbored by the *Salmonella typhimurium* SL3261: By PCR, a fragment of 800bp was amplified (d), suggesting the existence of epitope genes and removal of carrier fragment.

```

AAG CTT GCC ACC ATG AAA CCT CAT GTG CAT ACA AAA GGA GGA GGA AGT GCT AAA TTT
Hind III   Kozak   M   K   P   H   V   H   T   K   G   G   G   S   A   K   F
                GTG GCT GCT TGG ACA CTT AAA GCT GCT GCT TAA
                V   A   A   W   T   L   K   A   A   A   Z

```

Figure 3 Sequencing of PCR product (partial sequence): By PCR, the two epitopes were fused together and incorporated into a pcDNA3.1 fragment. The amino acid sequence of KPHVHTKGGGS corresponded to the sequence of MG7-Ag mimotope. AKFVAAWTLKAAZ corresponds to the sequence of universal Th epitope PADRE.

The pcDNA3.1(+)-MG7/PADRE was transduced into the attenuated *Salmonella typhimurium* SL3261 by electroporation. Plasmid from the transfectant was extracted and used as template. By PCR, it was verified that the plasmid harbored by the SL3261 transfectant was pcDNA3.1(+)-MG7/PADRE (Figure 4).

In vitro assay using *Salmonella typhimurium* as oral DNA vaccine vector

Forty-eight hours after infection with *Salmonella typhimurium*, fluorescence intensity of macrophages infected by the *Salmonella* harbouring the pcDNA3.1(+)-EGFP was 0.927 and the percentage of fluorescent cells was 40.6 %, which was significantly higher than that of the control (0.345 $P < 0.01$ and 3.8 % $P < 0.01$ respectively). Our result showed that pcDNA3.1(+)-EGFP plasmid was transferred into the macrophages from the bacteria and was expressed by the macrophages, suggesting that the SL3261 strain could be used as the oral DNA vaccine vector.

Immune response induced by the oral DNA vaccine

No diarrhea was seen in the mice given the *Salmonella typhimurium* harbouring either the vaccine DNA or the empty pcDNA3.1(+) vector. And no *Salmonella* infection-associated death occurred in the end of the experiments. Six weeks after the first immunization, serum titre of the antibody against MG7-Ag was significantly increased in the vaccine-immunized mice, while no significant titre of MG7 antibody was detected in the control groups. There was a significant difference between the vaccine-immunized group and the control groups ($P < 0.05$), while no difference was detected between the two control groups ($P < 0.05$, Table 1). *In vitro* unprimed proliferation assay of the splenocytes showed no statistical difference between those three groups (Table 2), suggesting no significant cellular immunity was elicited.

Table 1 Cellular ELISA detection of antibody in the immune serum (OD₄₅₀, $\bar{x} \pm s$)

Group	OD ₄₅₀
PBS control	0.298±0.017
Empty vector control	0.347±0.062
Vaccination group	0.841±0.136

Paired Student *t*-test was used to investigate the difference between two groups.

Table 2 *In vitro* unprimed assay of splenocytes (Radiation count/min cpm $\bar{x} \pm s$)

Group	Radiation count (cpm)
PBS control	2981±389.8
Empty vector control	3158±416.7
Vaccination group	2896±335.4

Paired student *t*-test was used to investigate the difference between two groups.

By immunohistochemical staining, it was found that MG7-Ag was expressed in the EAC cells, both on the membrane and in the cytoplasm (Figure 5), indicating that the EAC cells can be used to challenge the mice to investigate the protective ability of the oral DNA vaccine. Two weeks after the challenge, all the mice in the control groups developed neoplastic ascites, which was confirmed by microscopic observation of the cells in ascites. However, 2 in the 7 vaccinated mice were tumor free. All the mice in the control group died 4 weeks after the

primary challenge, while the tumor-free mice in the immunization group survived 8 weeks after the challenge with no signs of tumor formation. Our results suggested that the oral DNA vaccine was partially protective.

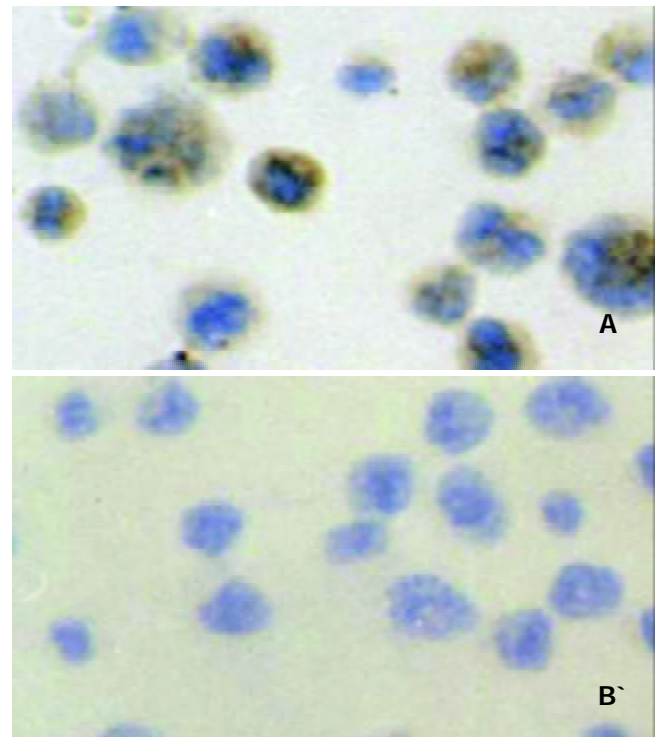


Figure 5 Immunohistochemical staining of the Ehrlich ascites carcinoma cells (EAC): Positive signal was seen in the cytoplasm and membrane of the EAC cells (A). When stained with a negative control monoclonal antibody (anti-E-tag antibody), the EAC cells showed no positive staining (B).

DISCUSSION

Attenuated strains of *Salmonella typhimurium* have been widely used as vehicles for delivery and expression of vaccine antigens. Attenuated *Salmonella typhimurium* strains expressing antigens from bacteria, viruses and parasites have been proved efficient as well as safe in combating respective pathogens^[7]. Due to mutations in their genome, attenuated *Salmonella typhimurium* lost their pathogenicity but remained to be invasive. When used as the oral vehicle, they can invade the M cells and the intestinal epithelial cells and penetrate the mucosal barrier of the intestine. Subsequently, they can be uptaken by the macrophages and dendritic cells (DC) in the lamina propria and the Peyer's patch. The intracellular bacteria would not undergo lysis in the lysosomes immediately but survive for a period of time due to unknown reasons. The intracellular bacteria could provide a reservoir of antigen, so these features of the *Salmonella typhimurium* strains make them an excellent vehicle of oral vaccines. The use of attenuated *Salmonella typhimurium* as oral DNA vaccine carrier was first reported by Darji and his colleagues^[8]. They found that when used as the carrier of DNA vaccines, the *Salmonella* could deliver the eukaryotic vector to the host cells through the unknown mechanism and the eukaryotic vector could be expressed by the host cells. Further study by Paglia *et al* suggested that attenuated *Salmonella typhimurium* could deliver the eukaryotic vector to the dendritic cells in the spleen^[9]. Other studies suggested the expression of eukaryotic vectors in dendritic cells in the mesenteric nodes and Peyer's patch was detected early after inoculation^[10-12]. Oral DNA vaccines developed by using *Salmonella typhimurium* as carrier

can provide a context similar to intracellular bacteria infection and render the body danger signals. Besides, the DC cells are excellent antigen presenting cells and have high expression of costimulatory molecules. So it is not surprising that the oral DNA vaccines can evoke significant immune response, especially CTL response^[5, 11, 13, 14]. In this study, we used an attenuated *Salmonella typhimurium* strain SL3261 (*S. typhimurium* WARY hisG46 aroA del407 Fusaricres etc, R+M+), which genotype is much the same as SL7207. We found that it could also act as the carrier of DNA vaccine, which was safe to mice.

CD4+ T cells (T helper cells, Th) play important roles in modulating immune response: They can facilitate the activation of CTL cells by cross-priming, produce various cytokines for the activation of T and B cells, upregulate the costimulatory molecules on APC cells and enhance their ability of antigen processing and presenting. In order to enhance the efficacy of the DNA vaccine, we fused the MG7-Ag mimotope with a universal T helper cell epitope PADRE, which was developed by Alexander *et al*^[15]. They introduced the anchoring motif of MHC molecules into the polyalanine backbone and found that the PADRE could bind to most of the human HLA-DR alleles and certain mouse class II alleles and elicit strong CD4+ T cell response; the epitopes were approximately 1000 times more powerful than natural T cell epitopes. PADRE has been used as the adjuvant for various epitopes including B cell epitope, CTL epitope and carbohydrate epitope and was proved to be efficient in enhancing the immunogenicity of these epitopes. Ishioka *et al*^[16] developed a minigene vaccine by including PADRE in tandem with multiple CTL epitopes with no spacer between them, and found that though the affinity of the CTL epitopes varied much, PADRE could still provide adjuvant effects on the induction of strong CTL response. Their study suggested that spacers were not necessarily needed in designing the multi-epitope minigene DNA vaccines. Therefore we fused the PADRE directly with the mimotope gene. To guarantee the efficient expression of the minigene, we included a Kozak sequence to right upstream the ATG initiation codon of the fusion gene. Kozak sequence is a specific sequence for the recognition and initiation of the transcription for the eukaryotic ribosome. The study suggested that Kozak sequence was necessary for correct and efficient expression of minigene vaccine^[17].

MG7-Ag of gastric cancer was discovered by our institute, and we found that the immunogenicity of the MG7-Ag was located in the carbohydrate chain of the glycoprotein. Due to its unknown identity, MG7-Ag is hard to be isolated from tumor tissue. Our institute has successfully identified the anti-MG-Ag antibodies using phage display method^[18,19]. Thus we identified the mimic peptides of MG7-Ag by screening the phage display peptide library with the MG7 antibody and then used it as the target for vaccine development. DNA vaccine of mimotope was first reported by Kieber-Emmons *et al*^[20], and the feasibility to develop DNA vaccine of mimotopes was further confirmed by Lesinski *et al*^[21]. In both studies, the DNA vaccine of mimotope induced strong humoral immune response. And in the former study, no significant CTL response was elicited. As shown by Monzavi-Karbassi *et al*, the mimic peptides could induce carbohydrate antigen reactive T cell response^[22]. Therefore, absence of significant specific T cell response in Kieber-Emmons' s study and our study might be due to the immunogen type of the primary antigen. However, the oral DNA vaccine developed by us was shown to be partially protective as shown by the tumor challenge assay though no significant difference was seen in the ³H-Tdr incorporation assay. The inconsistency between the results of tumor challenge assay and the ³H-Tdr incorporation assay might be due to the following reasons: (1) The inaccuracy of

the ³H-Tdr incorporation assay in determining the T cell response. More accurate methods include ⁵¹Cr-releasing assay and ELISPOT. Moreover in our study, we did not purify CD8+ T cells for ³H-Tdr incorporation assay. The existence of other types of cells might affect the results. (2) The sample included in the tumor challenge assay was too small. Much larger samples would be needed to further confirm the protective effect of the oral DNA vaccine.

Due to its various mechanisms of multi-drug resistance, gastric cancer often responds poorly to chemotherapy^[23, 24]. Cancer vaccines have been proved a powerful adjuvant intervention in gastric cancer management. Study showed that gastric cancer antigens could induce specific immune response^[25]. We reported here the first attempt to develop an oral DNA vaccine against gastric cancer antigen mimotope. The oral DNA vaccine against MG7-Ag mimotope is immunogenic. It can induce significant immune response against gastric cancer and may be partially protective in mice. Our results verified the feasibility to develop oral DNA vaccine of mimotopes and efficacy as well as safety of *Salmonella typhimurium* as oral DNA vaccine carriers.

REFERENCES

- 1 **Zhang XY**. Some recent works on diagnosis and treatment of gastric cancer. *World J Gastroenterol* 1999; **5**: 1-3
- 2 **Liu J**, Hu JL, Zhang XY, Qiao TD, Chen XT, Wu KC, Ding J, Fan DM. The value of MG7 antigen in predicting cancerous change in dysplastic gastric mucosa. *Int J Clin Pract* 2002; **56**: 169-172
- 3 **Xu L**, Qiao T, Chen B. Mimic epitope recognized by monoclonal antibody MG7 against gastric cancer through screening phage displayed random peptide library. *Zhonghua Yixue Zazhi* 2000; **80**: 304-307
- 4 **Xu L**, Xu H, Ma F. Immunogenicity of phage-displayed tumor antigen-mimic peptide. *Zhonghua Zhongliu Zazhi* 2001; **23**: 187-189
- 5 **Xiang R**, Lode HN, Chao TH, Ruehlmann JM, Dolman CS, Rodriguez F, Whitton JL, Overwijk WW, Restifo NP, Reisfeld RA. An autologous oral DNA vaccine protects against murine melanoma. *Proc Natl Acad Sci U S A* 2000; **97**: 5492-5497
- 6 **Pinilla-Ibarz J**, Cathcart K, Korontsvit T, Soignet S, Bocchia M, Caggiano J, Lai L, Jimenez J, Kolitz J, Scheinberg DA. Vaccination of patients with chronic myelogenous leukemia with bcr-abl oncogene breakpoint fusion peptides generates specific immune responses. *Blood* 2000; **95**: 1781-1787
- 7 **Sirard JC**, Niedergang F, Kraehenbuhl JP. Live attenuated *Salmonella*: a paradigm of mucosal vaccines. *Immunol Rev* 1999; **171**: 5-26
- 8 **Darji A**, Guzman CA, Gerstel B, Wachholz P, Timmis KN, Wehland J, Chakraborty T, Weiss S. Oral somatic transgene vaccination using attenuated *S. typhimurium*. *Cell* 1997; **91**: 765-775
- 9 **Paglia P**, Medina E, Arioli I, Guzman CA, Colombo MP. Gene transfer in dendritic cells, induced by oral DNA vaccination with *Salmonella typhimurium*, results in protective immunity against a murine fibrosarcoma. *Blood* 1998; **92**: 3172-3176
- 10 **Darji A**, zur Lage S, Garbe AI, Chakraborty T, Weiss S. Oral delivery of DNA vaccines using attenuated *Salmonella typhimurium* as carrier. *FEMS Immunol Med Microbiol* 2000; **27**: 341-349
- 11 **Cochlovius B**, Stassar MJ, Schreurs MW, Benner A, Adema GJ. Oral DNA vaccination: antigen uptake and presentation by dendritic cells elicits protective immunity. *Immunol Lett* 2002; **80**: 89-96
- 12 **Hopkins SA**, Niedergang F, Corthesy-Theulaz IE, Kraehenbuhl JP. A recombinant *Salmonella typhimurium* vaccine strain is taken up and survives within murine Peyer' s patch dendritic cells. *Cell Microbiol* 2000; **2**: 59-68
- 13 **Niethammer AG**, Primus FJ, Xiang R, Dolman CS, Ruehlmann JM, Ba Y, Gillies SD, Reisfeld RA. An oral DNA vaccine against human carcinoembryonic antigen (CEA) prevents growth and dissemination of Lewis lung carcinoma in CEA transgenic mice. *Vaccine* 2001; **20**: 421-429
- 14 **Zheng B**, Woo PC, Ng M, Tsoi H, Wong L, Yuen K. A crucial role of macrophages in the immune responses to oral DNA vaccina-

- tion against hepatitis B virus in a murine model. *Vaccine* 2001; **20**: 140-147
- 15 **Alexander J**, Sidney J, Southwood S, Ruppert J, Oseroff C, Maewal A, Snoke K, Serra HM, Kubo RT, Sette A. Development of high potency universal DR-restricted helper epitopes by modification of high affinity DR-blocking peptides. *Immunity* 1994; **1**: 751-761
- 16 **Ishioka GY**, Fikes J, Hermanson G, Livingston B, Crimi C, Qin M, del Guercio MF, Oseroff C, Dahlberg C, Alexander J, Chesnut RW, Sette A. Utilization of MHC class I transgenic mice for development of minigene DNA vaccines encoding multiple HLA-restricted CTL epitopes. *J Immunol* 1999; **162**: 3915-3925
- 17 **An LL**, Rodriguez F, Harkins S, Zhang J, Whitton JL. Quantitative and qualitative analyses of the immune responses induced by a multivalent minigene DNA vaccine. *Vaccine* 2000; **18**: 2132-2141
- 18 **Yu ZC**, Ding J, Nie YZ, Fan DM, Zhang XY. Preparation of single chain variable fragment of MG(7) mAb by phage display technology. *World J Gastroenterol* 2001; **7**: 510-514
- 19 **Nie YZ**, He FT, Li ZK, Wu KC, Cao YX, Chen BJ, Fan DM. Identification of tumor associated single-chain Fv by panning and screening antibody phage library using tumor cells. *World J Gastroenterol* 2002; **8**: 619-623
- 20 **Kieber-Emmons T**, Monzavi-Karbassi B, Wang B, Luo P, Weiner DB. Cutting edge: DNA immunization with minigenes of carbohydrate mimotopes induce functional anti-carbohydrate antibody response. *J Immunol* 2000; **165**: 623-627
- 21 **Lesinski GB**, Smithson SL, Srivastava N, Chen D, Widera G, Westerink MA. A DNA vaccine encoding a peptide mimic of *Streptococcus pneumoniae* serotype 4 capsular polysaccharide induces specific anti-carbohydrate antibodies in Balb/c mice. *Vaccine* 2001; **19**: 1717-1726
- 22 **Monzavi-Karbassi B**, Cunto-Amesty G, Luo P, Lees A, Kieber-Emmons T. Immunological characterization of peptide mimetics of carbohydrate antigens in vaccine design strategies. *Biologicals* 2001; **29**: 249-257
- 23 **Han Y**, Han ZY, Zhou XM, Shi R, Zheng Y, Shi YQ, Miao JY, Pan BR, Fan DM. Expression and function of classical protein kinase C isoenzymes in gastric cancer cell line and its drug-resistant sublines. *World J Gastroenterol* 2002; **8**: 441-445
- 24 **Wang X**, Lan M, Shi YQ, Lu J, Zhong YX, Wu HP, Zai HH, Ding J, Wu KC, Pan BR, Jin JP, Fan DM. Differential display of vincristine-resistance-related genes in gastric cancer SGC7901 cell. *World J Gastroenterol* 2002; **8**: 54-59
- 25 **Chen Q**, Ye YB, Chen Z. Activation of killer cells with soluble gastric cancer antigen combined with anti-CD(3) McAb. *World J Gastroenterol* 1999; **5**: 179-180

Edited by Zhang JZ

A gene encoding an apurinic/apyrimidinic endonuclease-like protein is up-regulated in human gastric cancer

Gang-Shi Wang, Meng-Wei Wang, Ben-Yan Wu, Xiao-Bing Liu, Wei-Di You, Xin-Yan Yang

Gang-Shi Wang, Meng-Wei Wang, Ben-Yan Wu, Wei-Di You, Xin-Yan Yang, Department of Gerontal Gastroenterology, General Hospital of Chinese PLA, Beijing 100853, China

Xiao-Bing Liu, Department of Pathology, General Hospital of Chinese PLA, Beijing 100853, China

Supported by Key Project Grant of Medical Sciences of the Tenth Five-Year Plan of Chinese PLA; Grant number: 01Z035

Correspondence to: Gang-Shi Wang, MD., Ph.D., Department of Gerontal Gastroenterology, General Hospital of Chinese PLA, Beijing 100853, China. wanggangshi@hotmail.com

Received: 2003-01-14 **Accepted:** 2003-03-03

Abstract

AIM: To identify the gene that may predispose to human gastric cancer and to analyze its expression in gastric cancer and non-tumorous gastric mucosa.

METHODS: Cancer, para-tumor, and non-tumor gastric tissues were studied for gene expression profile using fluorescent differential display reverse transcription polymerase chain reaction (DDRT-PCR). The differentially expressed bands of interest were analyzed by cloning, Northern blotting, and sequencing. The sequencing results were compared with the GenBank database for homology and conserved domain analysis. *In situ* hybridization with DIG-labeled cRNA probes was used to detect the expression of gene in paraffin embedded gastric adenocarcinoma and non-cancerous tissues.

RESULTS: A gene expressed higher in tumor and para-tumor tissues than in their non-tumor counterparts of all 7 tested gastric adenocarcinoma patients was identified by means of DDRT-PCR analysis. It was named *GCRG213* (gastric cancer related gene 213). Northern blot confirmed the differential expression. *GCRG213* (GenBank No. AY053451) consisted of 1094 base pairs with an open reading frame (ORF) which encoded 142 amino acids. The deduced amino acid sequence contained a putative conserved domain, apurinic/apyrimidinic endonuclease (APE). *In situ* hybridization analysis showed that *GCRG213* was expressed higher in gastric cancer tissues than in their corresponding non-tumor ones. Precancerous lesions of gastric adenocarcinoma showed a high *GCRG213* expression, too. No difference of the expression patterns was found between the early and advanced gastric cancer.

CONCLUSION: A gene named *GCRG213* was identified in human gastric adenocarcinoma. It encoded an APE-like protein which was probably a new member of the APE family. *GCRG213* was over-expressed not only in gastric cancer, but also in its precancerous lesions. The role of *GCRG213* expression in carcinogenesis needs further study.

Wang GS, Wang MW, Wu BY, Liu XB, You WD, Yang XY. A gene encoding an apurinic/apyrimidinic endonuclease-like protein is up-regulated in human gastric cancer. *World J Gastroenterol* 2003; 9(6): 1196-1201

<http://www.wjgnet.com/1007-9327/9/1196.asp>

INTRODUCTION

Gastric cancer is the second most common cause of cancer-related deaths in the world. It is widely accepted that genetic alterations play an important role in the pathogenesis of gastric cancer^[1,2]. The expression of oncogenes such as c-met, c-myc, ras, c-erbB-2^[3-5], the inactivation of tumor-suppressor genes, such as p53, p16, Rb, DCC, APC^[6-12]; and the abnormal transcription of genes related to metastasis, such as nm23, CD44, and E-cadherin^[12,13], have been reported in patients with gastric adenocarcinoma. Recent data showed that cancer related genes such as COX-2^[14,15], survivin^[16,17], metallothionein II and RUNX3, etc.^[18-22] were also expressed abnormally in gastric cancer. With the development of molecular biology techniques, such as cDNA array and differential display reverse transcription polymerase chain reaction (DDRT-PCR), some novel genes or cDNA fragments closely related to the development of human gastric cancer were identified recently^[23-32]. However, the genetic factors in human gastric cancer and their mechanisms of carcinogenesis remain uncertain and deserve further study. We, therefore, used DDRT-PCR to screen the human intestinal-type gastric adenocarcinoma and its precursor lesions for the differential expression of gastric cancer related genes (GCRGs).

In our previous reports, we described a cDNA fragment which was upregulated in human gastric cancer tissues. Two subclones, *GCRG213* and *GCRG224*, were subsequently identified. *GCRG224* was overexpressed in almost all gastric mucosal epithelia but only in a small portion of gastric cancer and precancerous lesions^[33]. In this study, we investigated the subclone, *GCRG213* and found that it was a gene encoding an apurinic/apyrimidinic endonuclease (APE)-like protein. *GCRG213* was overexpressed in gastric cancer and in its precancerous lesions.

MATERIALS AND METHODS

Patients and tissue acquisition

Fresh primary intestinal-type gastric adenocarcinoma, para-tumor tissues and non-cancerous gastric mucosal tissues were collected from 7 patients (male: 4, female: 3; mean age: 51±18 years old) during surgical operation for the differential display analyses of genes. The para-tumor tissues were collected at 1.0 cm away from the tumor mass. Three other sets of fresh gastric adenocarcinoma and non-cancerous gastric tissues were used for Northern blot analysis. Specimens of paraffin embedded gastric adenocarcinoma (male: 21, female: 11; mean age 57±8 years old) and their corresponding noncancerous tissues were collected for *in situ* hybridization analysis. Of the 32 cases of gastric adenocarcinoma, 15 cases were early gastric cancer while the other 17 cases were advanced carcinoma. The diagnosis of cancer was confirmed through histological findings.

Differential display, cloning and sequencing

Total RNA was extracted from tissues using TRIzol reagent (Life Technologies, Inc., Rockville, Maryland) according to the instructions of the manufacturer. The fluorescent differential display was performed as previously described^[34]. The primers used in the assay were T₁₂GG vs. ARP-8: 5' TGGTAAAGGG3'

(Genomx Corporation, Foster City, CA). The intensity of differentially expressed bands was quantified by Image Quant software (Molecular Dynamics, Sunnyvale, CA). The differentially expressed cDNA fragments were sub-cloned and sequenced as described previously^[33]. The sequenced cDNA was analyzed via the BLAST program for matches in the GenBank database^[35], and DNASIS software (Hitachi Software Engineering America Ltd., San Bruno, CA) was used for bioinformatic analysis.

Northern blot analysis

Dig Northern Starter Kit (Roche Diagnostic Corporation, Indianapolis, IN) was used. The procedure of hybridization was performed according to the manufacturer's protocol. Anti-sense cRNA probe labeled with digoxigenin was generated from a digested cDNA insert by means of *in vitro* transcription. Digoxigenin labeled sense cRNA probe was used as a negative control. The hybridization signals were visualized with chemiluminescence which is recorded on X-ray films. The exposure time was 10 minutes.

In situ hybridization

All specimens were fixed in 10 % neutral buffered formalin and embedded in paraffin. A series of 5 µm thick sections were cut for analysis. *In situ* hybridization (ISH) was performed as previously described^[36,37] using anti-sense cRNA probe labeled with digoxigenin. Briefly, the slides were dried at 40 °C overnight, dewaxed, rehydrated and pretreated with DEPC-treated PBS containing Triton X-100. The sections were then permeabilized with 20 µg/ml RNase-free proteinase K (Merck, Darmstadt, Germany) for 20 min, incubated at 37 °C for at least 20 min with prehybridization buffer. Each section was overlaid with 30 µl of hybridization buffer containing 10 ng of digoxigenin-labeled cRNA probe and incubated at 42 °C

overnight. The positive signal for GCRG213 mRNA was finally detected by using NBT/BCIP as substrate. Sense cRNA probes were used as negative control. The presentation of blue staining in cytoplasm was considered positive. The positive staining of cytoplasm was semi-quantified as Grade ± barely detectable light blue, Grade 1+: diffuse light blue, Grade 2+: blue staining, and Grade 3+: dark blue. More than 100 non-tumor or tumor cells were quantified in each measurement, and more than one measurement was required to confirm the diagnosis. Consequent slides with H&E staining were then reviewed to compare the histological patterns to the staining patterns in the ISH preparations.

Informed consents

The study protocol was approved by the Institutional Review Board of the hospital under the guidelines of the 1975 Declaration of Helsinki. Written informed consents were obtained from patients.

RESULTS

Identification of a human gastric cancer related gene

One differentially expressed cDNA band named W2 was found to be more abundant in the tumor and paratumor samples in all tested patients. W2 was sub-cloned into a pGEM-T easy vector, and confirmed by EcoR I digestion. Two subclones, *GCRG213* and *GCRG224*, were subsequently identified^[33]. Sequencing results showed that *GCRG213* consisted of 1094 base pairs with an open reading frame (ORF) which encoded 142 amino acids with an estimated molecular weight of 16.4 kDa (Figure 1). This nucleotide sequence data were submitted to GenBank with accession No. AY053451. BLASTN analysis revealed that *GCRG213* shared 88 % homology with human

```

3 GTA AAG GGA TCA ATG CAA CAA GAA GAG CTA ACT ATC CTA AAT ATA TAT GCA CCT AAT ACA 62
1 M Q Q E E L T I L N I Y A P N T 20

63 AGA GCA CCC AGA TTC ATA AAG CAA GTC CTT AGA GAC CTA CAA AGA GAC TTA GAT TCC CAC 122
21 R A P R F I K Q V L R D L Q R D L D S H 40

123 ACA ATA ATA ATG GGA GAC TTT AAC ACC CAA CTG TCA ATA TTA GAA AGA TCA ACA AGG CAG 182
41 T I I M G D F N T Q L S I L E R S T R Q 60

183 AAG GTT AAC AAA GAT ATC CAG GAC CTG AAC TCA GCT CTG CAA CAA ACA GAC CCA ATA GAC 242
61 K V N K D I Q D L N S A L Q Q T D P I D 80

243 ATC CAC AGA ACT CTC CAC CCC AAA TCA ACA GAG TGT ACA TTC TTC TCA GCA CCA CAT CTC 302
81 I H R T L H P K S T E C T F F S A P H L 100

303 ACT TAT TCT AAA TTT GGC CAC ATA ATT GGA AGT AAA GCA CTC CTC ACC AAA TGT AAA AGA 362
101 T Y S K F G H I I G S K A L L T K C K R 120

363 ACA GAA ATC ACA ACA GAC TGT CTC TCA GAC CAC AGT GCG ATC AAA TTC GAA CTT AGG ATT 422
121 T E I T T D C L S D H S A I K F E L R I 140

423 AAG AAG CTC ACT CAA AAC TGA ACA ACT ACA TGG AAA CTG AAT AAT TTG CTC CTG AAT GAC 482
141 K K L T Q N * 160

483 TAC TGG GTA AAT AAC AAA ATG AAG GCAGAA ATA AAG ATG TTC TTT GAA ACC AAT GAG AAC 542
543 AAA GAC ACA ATG TAC CAG AAT CTC TGG GAC ACA TTT AAA GCA GTG TGT AGG GGG AAATTG 602
603 ATA GCA CTA AAT GCC CAG AAG AGA AAG CAG GAA AGA TCT AAA ATT GAC CCC CTA ACATCA 662
663 CAA TTA AAA GTA CTA GAG AAG AAA AAG CAA ACA CAT TCA AAAGCTGGCAGA AGG AAA AAA 722
723 TAA GAT CAG AGC AGA GCT GAA GGA GAC AGA GAC ACA AAA AACCCCTCAAAA AAG CAATGA 782
783 ATC CAG GAG CTT GTT TTT TGA AAA GAT CAA CAA AAT TGA TAG ACT GCT AGC AAG ACT AAT 842
843 AAA GAG AAA AGA GAG AGG AAT CAA ATA GAT GCA ATA AAA TGA TAA AGG GGA TAT CAC CAC 902
903 TGA GCC CAG GGA AAT AAA AAC TAC CAT CAG AGA ATA CTA TAA ACG CCT ATA CAC AAA TAA 962
963 ACT TGA ACA TCT GGA AGA AAT GGA TAA ATT CTG GGA CAC ATA CAC CCT TGC AAG ACT AAA 1022
1023 CCA GGA AGA GGT TGA ATC TCT GAA TAG ACC AAT AAC AAG TTC TGA AGT TGA GGC AGT AAT 1082
1083 TAA TAG CCT ACC AAA AAA AAA AAA 1106

```

Figure 1 Sequence of the human *GCRG213* cDNA. The DNA sequence encoding the predicted start (ATG) and stop (TGA) codons is bolded and underlined. Three possible polyadenylation signals (AATAAA) are in italics. The protein encoded by the open reading frame is indicated in the single-letter code below the DNA sequence.

retrotransposable LINE-1 element LRE2. Through conserved domain database search in GenBank, a putative conserved domain, apurinic/aprimidinic endonuclease 1 (APE), was detected in the deduced amino acid sequence of *GCRG213*-

ORF, it shared 61.0 % alignment with the C-terminal region of APE conserved domain (Figure 2). Northern blot analysis showed that *GCRG213* was over-expressed in tumor tissues than in their non-tumor counterparts (Figure 3).



Figure 2 NCBI conserved domain search results. A: *GCRG213* ORF produced significant alignments with gnl | Pfam | pfam 01260 AP_endonuclease1, AP endonuclease family 1; CD-length =250 residues, only 61.0 % aligned; Score=88.2 bits (217), Expect=3e-19. B: Human APE protein produced significant alignments with gnl | Pfam | pfam01260 AP_endonuclease1, AP endonuclease family 1; CD-length=250 residues, 100.0 % aligned. Score=161 bits (407), Expect=1e-40. *GCRG213*-ORF contained residues such as Y171, D210, N212, D308 and H309 (arrowed) that are important for the endonuclease activity of APE.

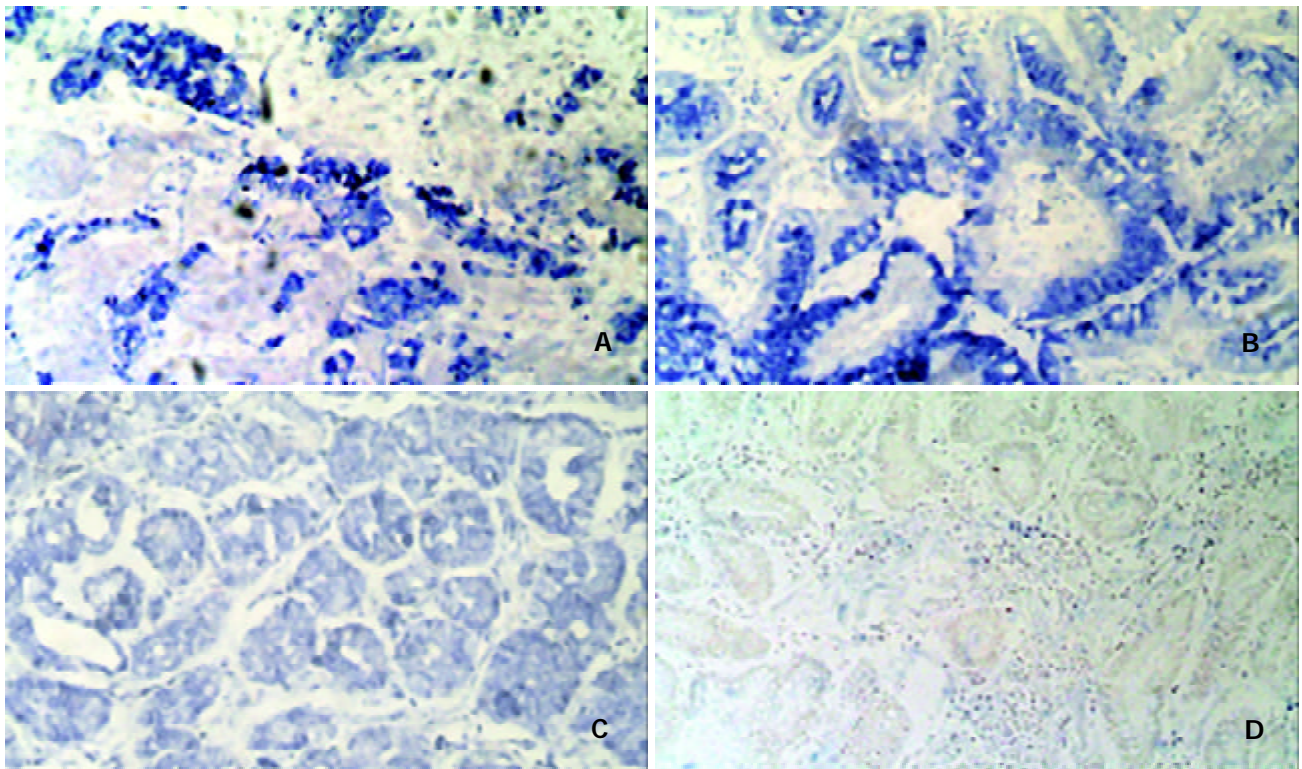


Figure 4 *In situ* hybridization analysis of *GCRG213* in formalin-fixed, paraffin-embedded tissues with a digoxigenin-labeled anti-sense probe, NBT/BCIP was used as alkaline phosphatase substrates, the expression appeared as cytoplasmic staining (blue precipitates). (A) gastric adenocarcinoma invading into the muscle layer showed grade 2+ ~ 3+ staining, (B) gastric IM epithelium showed grade 2+ ~ 3+ staining, (C) normal gastric glands showed grade ± ~ + staining, (D) negative control. Magnification was 10x10.

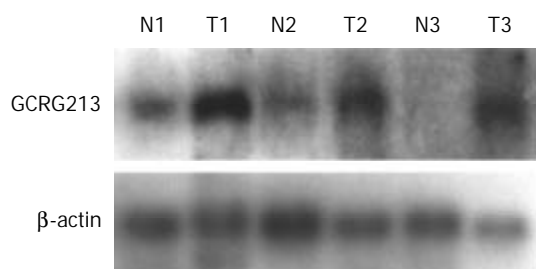


Figure 3 Northern blot analysis of *GCRG213* in human gastric tissues. *GCRG213* showed higher expression in tumor tissues than in non-tumorous ones. The expression of β -actin served as an internal control. N: non-tumorous tissue; T: tumor; 1-3: patient number.

In situ hybridization

GCRG213 expression was analyzed at the mRNA level using *in situ* hybridization. The hybridization signal appeared as a blue color in cytoplasm.

Both the early and advanced gastric cancer tissues were stained grade 2+ ~ 3+. Eight of the 17 cases of advanced adenocarcinoma showed an invasion of cancer into the muscle layer, with all eight cases showing grade 3+ staining in the invading tumor cells (Figure 4A). Dysplasia tissues at the para-tumor region were found in 22 patients. 15/22 dysplasia tissues showed grade 2+ ~ 3+ staining of *GCRG213* expression while the rest showed grade 1+ staining. Nineteen patients had intestinal metaplasia (IM) epithelia at the para-tumor tissue. 9/19 IM showed grade 2+ ~ 3+ staining, the rest showed non-staining to grade 1+ staining (Figure 4B). All normal gastric glands showed grade \pm ~ + staining (Figure 4C).

DISCUSSION

In the present study, we used differential display to study the gene expression profile of human gastric cancer. One cDNA fragment, named by us as gastric cancer related gene 213 (*GCRG213*), was up-regulated in the gastric adenocarcinoma tissues of all 7 tested patients. Northern blot analysis confirmed the differential expression of *GCRG213*. As for the consistent up-regulation in gastric cancer tissues, further studies are necessary to confirm the role of *GCRG213* and its expression pattern in tumors.

The nucleotide sequence of *GCRG213* shared 88 % homology with human retrotransposable LINE1 element LRE2. LINE-1 elements are very ancient, they constitute 20 % or more of some mammalian genomes and presumably play a role in the evolution, structure, and function of mammalian genomes. LINE-1 elements contain regulatory signals and encode two proteins: one is an RNA-binding protein and the other is an APE-like enzyme which has both endonuclease and reverse transcriptase activities^[38,39]. BLASTP analysis in this study showed that the deduced amino acid sequence of *GCRG213*-ORF shared 84 % homology with the N terminal of LINE-1 ORF2 where the repair nuclease domain of APE exists.

We proposed that *GCRG213*-ORF be a new APE-like protein based on the following facts. First, APE conserved domain could be detected in *GCRG213*-ORF and the latter shared homology with the C terminal of human APE protein which is of particular relevance to the endonuclease function of APE. Furthermore, *GCRG213*-ORF also contains residues proposed to be important to the endonuclease activity of APE (Y171, D210, N212, D308 and H309)^[40-42].

AP endonucleases have been divided into two families based on their amino acid sequence identity to either exonuclease III or Endo IV. Typically, the exonuclease III family of endonucleases accounts for approximately 95 % of

the repair activity in the organism. In mammals, the predominant AP endonuclease is APE (also called HAP1 or APEX), an enzyme that belongs to the ExoIII family^[42]. Human APE plays an important role in the base excision repair machinery of eukaryotic cells^[40]. The DNA repair activity of APE resides in the C-terminal region^[41].

Many mechanisms such as hydrolysis of purine or pyrimidine, ionizing radiation, UV irradiation, and N-glycosylases may act on endogenous apurinic/aprimidinic sites to modify DNA bases^[40-43]. Unrepaired apurinic/aprimidinic sites result in mutations during DNA replication. Apart from its DNA repair function, APE exhibits as Redox-factor-1 which is important for the activation of transcription factors, such as activator protein 1, p53 and nuclear factor kappa B. APE also regulates the transactivation and pro-apoptotic functions of p53^[41]. Therefore, a role of APE in human tumorigenesis has been suggested.

APE protein is expressed in a wide range of human cells. Through immunohistochemistry detection, APE can be mainly localized in nucleus or cytoplasm or both^[44] depending on the cell type. Elevated expression of APE has been reported in a number of tumors such as prostate, ovarian, cervical, colorectal and germ cell tumors, malignant gliomas, whereas the cellular localization (nuclear/cytoplasmic ratio) differs in some neoplasia (colorectal carcinomas, epithelial ovarian cancers, primary breast carcinomas and thyroid carcinomas)^[45-54]. In breast cancer, APE protein expression correlates with lymph node status and angiogenesis^[51] while in head-and-neck cancer, nuclear expression of APE is associated with its resistance to chemoradiotherapy and poor outcome^[55]. In this study, *GCRG213* overexpressed in gastric intestinal metaplasia and dysplasia of the stomach as well as early and advanced gastric adenocarcinoma. The patterns of *GCRG213* expression in cancerous tissue of the early gastric cancer did not differ significantly from those in the advanced gastric carcinoma. Thus, the *GCRG213* expression appears "early" in the stage of gastric adenocarcinoma. This expression pattern is consistent with that of APE in cervical, prostate, colorectal cancer and their premalignant lesions^[45-47] reported.

There are two immediate implications of these findings of elevated *GCRG213* expression in cancers. First, if the expression of *GCRG213* could be modulated downward to, or below normal levels in the cancer cells, there may be an effect on the progression of the cancer or, the cells may become more sensitive to chemotherapeutic treatment. The latter presumes that the increase in AP endonuclease activity result in increased DNA repair activity, protecting more cancer cells against base damage than normal cells.

In conclusion, a gene, *GCRG213*, overexpressed in tumors was identified in this study. Because of the similarity of the expression pattern in tumors between APE and *GCRG213*, as well as the 61 % alignment between the amino acid sequences of *GCRG213*-ORF and APE conserved domain, it is likely that *GCRG213*-ORF is a new member of the APE family. A greater understanding of alterations in the function of *GCRG213* in human cancers may explore its epidemiological and therapeutic significance.

ACKNOWLEDGEMENTS

The authors would like to thank Dr. Sien-Sing Yang, the Cathay General Hospital, Taipei, Taiwan and Timothy K Lee, Ph.D., FDA, U.S.A. for their comments.

REFERENCES

- Gonzalez CA**, Sala N, Capella G. Genetic susceptibility and gastric cancer risk. *Int J Cancer* 2002; **100**: 249-260

- 2 **El-Rifai W**, Powell SM. Molecular biology of gastric cancer. *Semin Radiat Oncol* 2002; **12**: 128-140
- 3 **Nakajima M**, Sawada H, Yamada Y, Watanabe A, Tatsumi M, Yamashita J, Matsuda M, Sakaguchi T, Hirao T, Nakano H. The prognostic significance of amplification and overexpression of c-met and c-erbB-2 in human gastric carcinomas. *Cancer* 1999; **85**: 1894-1902
- 4 **Takehana T**, Kunitomo K, Kono K, Kitahara F, Iizuka H, Matsumoto Y, Fujino MA, Ooi A. Status of c-erbB-2 in gastric adenocarcinoma: a comparative study of immunohistochemistry, fluorescence in situ hybridization and enzyme-linked immunosorbent assay. *Int J Cancer* 2002; **98**: 833-837
- 5 **Yoo J**, Park SY, Robinson RA, Kang SJ, Ahn WS, Kang CS. ras Gene mutations and expression of Ras signal transduction mediators in gastric adenocarcinomas. *Arch Pathol Lab Med* 2002; **126**: 1096-1100
- 6 **Chang MS**, Kim HS, Kim CW, Kim YI, Lan Lee B, Kim WH. Epstein-Barr virus, p53 protein, and microsatellite instability in the adenoma-carcinoma sequence of the stomach. *Hum Pathol* 2002; **33**: 415-420
- 7 **Gurel S**, Dolar E, Yerci O, Samli B, Ozturk H, Nak SG, Gulden M, Memik F. Expression of p53 protein and prognosis in gastric carcinoma. *J Int Med Res* 1999; **27**: 85-89
- 8 **Liu XP**, Tsushimi K, Tsushimi M, Kawauchi S, Oga A, Furuya T, Sasaki K. Expression of p21(WAF1/CIP1) and p53 proteins in gastric carcinoma: its relationships with cell proliferation activity and prognosis. *Cancer Lett* 2001; **170**: 183-189
- 9 **Sato K**, Tamura G, Tsuchiya T, Endoh Y, Usaba O, Kimura W, Motoyama T. Frequent loss of expression without sequence mutations of the DCC gene in primary gastric cancer. *Br J Cancer* 2001; **85**: 199-203
- 10 **Lee JH**, Abraham SC, Kim HS, Nam JH, Choi C, Lee MC, Park CS, Juhng SW, Rashid A, Hamilton SR, Wu TT. Inverse relationship between APC gene mutation in gastric adenomas and development of adenocarcinoma. *Am J Pathol* 2002; **161**:611-618
- 11 **Zhou Y**, Gao SS, Li YX, Fan ZM, Zhao X, Qi YJ, Wei JP, Zou JX, Liu G, Jiao LH, Bai YM, Wang LD. Tumor suppressor gene p16 and Rb expression in gastric cardia precancerous lesions from subjects at a high incidence area in northern China. *World J Gastroenterol* 2002; **8**: 423-425
- 12 **Waki T**, Tamura G, Tsuchiya T, Sato K, Nishizuka S, Motoyama T. Promoter methylation status of E-cadherin, hMLH1, and p16 genes in nonneoplastic gastric epithelia. *Am J Pathol* 2002; **161**: 399-403
- 13 **Hsieh HF**, Yu JC, Ho LI, Chiu SC, Harn HJ. Molecular studies into the role of CD44 variants in metastasis in gastric cancer. *Mol Pathol* 1999; **52**: 25-28
- 14 **van Rees BP**, Saukkonen K, Ristimaki A, Polkowski W, Tytgat GN, Drilenburg P, Offerhaus GJ. Cyclooxygenase-2 expression during carcinogenesis in the human stomach. *J Pathol* 2002; **196**: 171-179
- 15 **Kikuchi T**, Itoh F, Toyota M, Suzuki H, Yamamoto H, Fujita M, Hosokawa M, Imai K. Aberrant methylation and histone deacetylation of cyclooxygenase 2 in gastric cancer. *Int J Cancer* 2002; **97**: 272-277
- 16 **Krieg A**, Mahotka C, Krieg T, Grabsch H, Muller W, Takeno S, Suschek CV, Heydthausen M, Gabbert HE, Gerharz CD. Expression of different survivin variants in gastric carcinomas: first clues to a role of survivin-2B in tumour progression. *Br J Cancer* 2002; **86**: 737-743
- 17 **Yu J**, Leung WK, Ebert MP, Ng EK, Go MY, Wang HB, Chung SC, Malfertheiner P, Sung JJ. Increased expression of survivin in gastric cancer patients and in first degree relatives. *Br J Cancer* 2002; **87**: 91-97
- 18 **Ebert MP**, Gunther T, Hoffmann J, Yu J, Miehle S, Schulz HU, Roessner A, Korc M, Malfertheiner P. Expression of metallothionein II in intestinal metaplasia, dysplasia, and gastric cancer. *Cancer Res* 2000; **60**: 1995-2001
- 19 **Li QL**, Ito K, Sakakura C, Fukamachi H, Inoue K, Chi XZ, Lee KY, Nomura S, Lee CW, Han SB, Kim HM, Kim WJ, Yamamoto H, Yamashita N, Yano T, Ikeda T, Itohara S, Inazawa J, Abe T, Hagiwara A, Yamagishi H, Ooe A, Kaneda A, Sugimura T, Ushijima T, Bae SC, Ito Y. Causal relationship between the loss of RUNX3 expression and gastric cancer. *Cell* 2002; **109**: 113-124
- 20 **Bai YQ**, Yamamoto H, Akiyama Y, Tanaka H, Takizawa T, Koike M, Kenji Yagi O, Saitoh K, Takeshita K, Iwai T, Yuasa Y. Ectopic expression of homeodomain protein CDX2 in intestinal metaplasia and carcinomas of the stomach. *Cancer Lett* 2002; **176**: 47-55
- 21 **Saitoh T**, Mine T, Katoh M. Up-regulation of WNT8B mRNA in human gastric cancer. *Int J Oncol* 2002; **20**: 343-348
- 22 **Li Z**, Wang Y, Song J, Kataoka H, Yoshii S, Gao C, Wang Y, Zhou J, Ota S, Tanaka M, Sugimura H. Genomic structure of the human beta-PIX gene and its alteration in gastric cancer. *Cancer Lett* 2002; **177**: 203-208
- 23 **Yoshikawa Y**, Mukai H, Hino F, Asada K, Kato I. Isolation of two novel genes, down-regulated in gastric cancer. *Jan J Cancer Res* 2000; **91**: 459-463
- 24 **Wang G**, Wang M, You W, Li H. Cloning and primary expression analyses of down-regulated cDNA fragment in human gastric cancer. *Zhonghua Yixue Yichuanxue Zazhi* 2001; **18**: 43-47
- 25 **Wang JH**, Chen SS. Screening and identification of gastric adenocarcinoma metastasis-related genes by using cDNA microarray coupled to FDD-PCR. *Shengwu Huaxue Yu Shengwu Wuli Xuebao (Shanghai)* 2002; **34**: 475-481
- 26 **Wang X**, Lan M, Shi YQ, Lu J, Zhong YX, Wu HP, Zai HH, Ding J, Wu KC, Pan BR, Jin JP, Fan DM. Differential display of vincristine-resistance-related genes in gastric cancer SGC7901 cell. *World J Gastroenterol* 2002; **8**: 54-59
- 27 **Saitoh T**, Mine T, Katoh M. Molecular cloning and expression of proto-oncogene FRAT1 in human cancer. *Int J Oncol* 2002; **20**: 785-789
- 28 **Line A**, Stengrevics A, Slucka Z, Li G, Jankevics E, Rees RC. Serological identification and expression analysis of gastric cancer-associated genes. *Br J Cancer* 2002; **86**: 1824-1830
- 29 **Lee S**, Baek M, Yang H, Bang YJ, Kim WH, Ha JH, Kim DK, Jeoung DI. Identification of genes differentially expressed between gastric cancers and normal gastric mucosa with cDNA microarrays. *Cancer Lett* 2002; **184**: 197-206
- 30 **Liu LX**, Liu ZH, Jiang HC, Qu X, Zhang WH, Wu LF, Zhu AL, Wang XQ, Wu M. Profiling of differentially expressed genes in human gastric carcinoma by cDNA expression array. *World J Gastroenterol* 2002; **8**: 580-585
- 31 **El-Rifai W**, Smith MF Jr, Li G, Beckler A, Carl VS, Montgomery E, Knuutila S, Moskaluk CA, Frierson HF Jr, Powell SM. Gastric cancers overexpress DARPP-32 and a novel isoform, t-DARPP. *Cancer Res* 2002; **62**: 4061-4064
- 32 **Wang GS**, Wang MW, Wu BY, You WD. A lamin-like protein gene is down-regulated in human gastric cancer. *Zhonghua Yixue Yichuanxue Zazhi* 2003; **20**: in press
- 33 **Wang GS**, Wang MW, Wu BY, You WD, Yang XY. A novel gene, GCRG224, is differentially expressed in human gastric mucosa. *World J Gastroenterol* 2003; **9**: 30-34
- 34 **Wang GS**, Wang MW, You WD, Wang HF, Feng MF. Fluorescent mRNA differential display technique. *Zhongguo Yingyong Shenglixue Zazhi* 2000; **16**: 373-376
- 35 **Altschul SF**, Madden TL, Schäffer AA, Zhang J, Zhang Z, Miller W, Lipman DJ. Gapped BLAST and PSI-BLAST: a new generation of protein database search programs. *Nucleic Acids Res* 1997; **25**: 3389-3402
- 36 **Komminoth P**. Digoxigenin as an alternative probe labeling for *in situ* hybridization. *Diagn Mol Pathol* 1992; **1**: 142-150
- 37 **Komminoth P**, Merk FB, Leav I, Wolfe HJ, Roth J. Comparison of 35S- and digoxigenin-labeled RNA and oligonucleotide probes for *In situ* hybridization. Expression of mRNA of the seminal vesicle secretion protein II and androgen receptor genes in the rat prostate. *Histochemistry* 1992; **98**: 217-228
- 38 **Furano AV**. The biological properties and evolutionary dynamics of mammalian LINE-1 retrotransposons. *Prog Nucleic Acid Res Mol Biol* 2000; **64**: 255-294
- 39 **Volff JN**, Korting C, Froschauer A, Sweeney K, Scharlt M. Non-LTR retrotransposons encoding a restriction enzyme-like endonuclease in vertebrates. *J Mol Evol* 2001; **52**: 351-360
- 40 **Fritz G**. Human APE/Ref-1 protein. *Int J Biochem Cell Biol* 2000; **32**: 925-929
- 41 **Evans AR**, Limp-Foster M, Kelley MR. Going APE over ref-1. *Mutat Res* 2000; **461**: 83-108
- 42 **Wilson DM 3rd**, Barsky D. The major human abasic endonuclease:

- formation, consequences and repair of abasic lesions in DNA. *Mutat Res* 2001; **485**: 283-307
- 43 **Meira LB**, Devaraj S, Kisby GE, Burns DK, Daniel RL, Hammer RE, Grundy S, Jialal I, Friedberg EC. Heterozygosity for the mouse Apex gene results in phenotypes associated with oxidative stress. *Cancer Res* 2001; **61**: 5552-5557
- 44 **Duguid JR**, Eble JN, Wilson TM, Kelley MR. Differential cellular and subcellular expression of the human multifunctional apurinic/aprimidinic endonuclease (APE/ref-1) DNA repair enzyme. *Cancer Res* 1995; **55**: 6097-6102
- 45 **Kakolyris S**, Kaklamanis L, Engels K, Turley H, Hickson ID, Gatter KC, Harris AL. Human apurinic endonuclease 1 expression in a colorectal adenoma-carcinoma sequence. *Cancer Res* 1997; **57**: 1794-1797
- 46 **Kelley MR**, Cheng L, Foster R, Tritt R, Jiang JZ, Broshears J, Koch M. Elevated and altered expression of the multifunctional DNA base excision repair and redox enzyme Ape1/ref-1 in prostate cancer. *Clin Cancer Res* 2001; **7**: 824-830
- 47 **Xu Y**, Moore DH, Broshears J, Liu L, Wilson TM, Kelley MR. The apurinic/aprimidinic endonucleases (APE/ref-1) DNA repair enzyme is elevated in premalignant and malignant cervical cancer. *Anticancer Res* 1997; **17**: 3713-3719
- 48 **Schindl M**, Oberhuber G, Pichlbauer EG, Obermair A, Birner P, Kelley MR. DNA repair-redox enzyme apurinic endonuclease in cervical cancer: evaluation of redox control of HIF-1alpha and prognostic significance. *Int J Oncol* 2001; **19**: 799-802
- 49 **Herring CJ**, West CM, Wilks DP, Davidson SE, Hunter RD, Berry P, Forster G, MacKinnon J, Rafferty JA, Elder RH, Hendry JH, Margison GP. Levels of the DNA repair enzyme human apurinic/aprimidinic endonuclease (APE1, APEX, Ref-1) are associated with the intrinsic radiosensitivity of cervical cancers. *Br J Cancer* 1998; **78**: 1128-1133
- 50 **Moore DH**, Michael H, Tritt R, Parsons SH, Kelly MR. Alterations in the expression of the DNA repair/redox enzyme APE/ref-1 in epithelial ovarian cancers. *Clin Cancer Res* 2000; **6**: 602-609
- 51 **Kakolyris S**, Kaklamanis L, Engels K, Fox SB, Taylor M, Hickson ID, Gatter KC, Harris AL. Human AP endonuclease 1 (HAP1) protein expression in breast cancer correlates with lymph node status and angiogenesis. *Br J Cancer* 1998; **77**: 1169-1173
- 52 **Robertson KA**, Bullock HA, Tritt R, Zimmerman E, Ulbright TM, Foster RS, Einhorn LH, Kelley MR. Altered expression of Ape1/ref-1 in germ cell tumors and overexpression in NT2 cells confers resistance to bleomycin and radiation. *Cancer Res* 2001; **61**: 2220-2225
- 53 **Bobola MS**, Blank A, Berger MS, Stevens BA, Silber JR. Apurinic/aprimidinic endonuclease activity is elevated in human adult gliomas. *Clin Cancer Res* 2001; **7**: 3510-3518
- 54 **Russo D**, Arturi F, Bulotta S, Pellizzari L, Filetti S, Manzini G, Damante G, Tell G. Ape1/Ref-1 expression and cellular localization in human thyroid carcinoma cell lines. *J Endocrinol Invest* 2001; **24**: RC10-RC12
- 55 **Koukourakis MI**, Giatromanolaki A, Kakolyris S, Sivridis E, Georgoulas V, Funtzilias G, Joclspm ID, Gatter KC, Harris AL. Nuclear expression of human apurinic/aprimidinic endonuclease (HAP1/Ref-1) in head-and-neck cancer is associated with resistance to chemoradiotherapy and poor outcome. *Int J Radiat Oncol Biol Phys* 2001; **50**: 27-36

Edited by Zhao P

Is p53 gene mutation an indicator of the biological behaviors of recurrence of hepatocellular carcinoma?

I-Shyan Sheen, Kuo-Shyang Jeng, Ju-Yann Wu

I-Shyan Sheen, Liver Research Unit, Chang Gung Memorial Hospital, Taipei, Taiwan

Kuo-Shyang Jeng, Department of Surgery, Mackay Memorial Hospital, Mackay Junior School of Nursing, Taipei, Taiwan

Ju-Yann Wu, Medical Research, Mackay Memorial Hospital, Taipei, Taiwan

Supported by grants from the Department of Health National Science Council, Executive Yuan, Taiwan. No. NSC 84-2331-B-195-002

Correspondence to: Kuo-Shyang Jeng, M.D., F.A.C.S., Department of Surgery, Mackay Memorial Hospital, No. 92, Sec 2, Chung-San North Road, Taipei, Taiwan. issheen.jks@msa.hinet.net

Telephone: +86-2-25433535 **Fax:** +86-2-27065704

Received: 2003-03-04 **Accepted:** 2003-03-21

Abstract

AIM: To evaluate mutant p53 gene in primary hepatocellular carcinoma and to investigate the correlation between it and the recurrence of hepatocellular carcinoma.

METHODS: Mutations of p53 gene were examined using anti-human p53 monoclonal antibody and immunohistochemical staining in 79 resected hepatocellular carcinomas. The correlations among variables of p53 positivity and invasiveness, disease free interval and survival were studied. In addition, in those who developed recurrence, the correlation among p53 positivity, clinical features and post-recurrence survival were also studied.

RESULTS: Of these 79 cases, 64 (81 %) had p53 mutation. Those patients with mutant p53 positivity had significantly more tumor recurrence (76.6 % vs 40.0 %, $P=0.0107$). However, the COX proportional hazards model showed that p53 overexpression had only weak correlations with recurrence free interval and survival time ($P=0.088$ and 0.081), which was probably related to the short duration of follow-up. The invasiveness variables may be predictors of HCC recurrence. On univariate analysis, more patients with mutant p53 positivity had vascular permeation [78.1 vs 40.0 %, $P=0.0088$, O.R. (odds ratio) =5.3], grade II-IV differentiation (98.4 vs 80.0 %, $P=0.0203$, O.R. =15.7), no complete capsule (82.8 vs 53.3 %, $P=0.0346$, O.R. =4.2) and daughter nodules (60.9 vs. 33.3 %, $P=0.0527$, O.R. =3.1) than patients with negative p53 staining. On multivariate analysis, only vascular permeation and grade of differentiation remained significant ($P=0.042$ and 0.012). There was no statistically significant correlation between the status of p53 in the primary lesion and the clinical features of recurrent hepatocellular carcinomas examined, including extrahepatic metastasis ($P=0.1103$) and the number of recurrent tumors ($P=1.000$) except for disease over more than one segment in the extent of recurrent tumors ($P=0.0043$). The post-recurrence median survival was lower in patients in whom p53 mutation had been detected in the primary lesion with a weak significance (3.42 months vs 11.0 months, $P=0.051$).

CONCLUSION: Our findings suggest that p53 mutation

correlates significantly with invasiveness including vascular permeation, grade of cellular differentiation, incomplete capsule and multinodular lesions. Hepatocellular carcinomas with p53 mutations had more tumor recurrence and p53 mutation may also influence disease recurrence interval and survival time. Hepatocellular carcinomas with p53 mutations recur more extensively with a shorter survival. Therefore, p53 mutation in the primary lesion is useful as an indicator of the biological behavior of recurrent hepatocellular carcinomas.

Sheen IS, Jeng KS, Wu JY. Is p53 gene mutation an indicator of the biological behaviors of recurrence of hepatocellular carcinoma? *World J Gastroenterol* 2003; 9(6): 1202-1207

<http://www.wjgnet.com/1007-9327/9/1202.asp>

INTRODUCTION

Hepatocellular carcinoma (HCC) is one of the most common types of malignant tumors that carry a poor prognosis. During the last 10 years, efforts have been made worldwide toward earlier detection and safer surgical resection of HCC. However, despite these recent diagnostic and therapeutic advances, postoperative recurrence is still common^[1-4]. How to predict recurrence before resection is a challenging problem for surgeons. Certain characteristics related to HCC recurrence have been reported widely and variably in the literatures^[1-11]. Risk factors which have been mentioned include vascular permeation, absence of capsule, presence of daughter nodules, histological grade of tumor differentiation, tumor size, associated cirrhosis, hepatitis B virus (HBV) infection, hepatitis C virus (HCV) infection, daughter nodules, and adequate section margin, etc.

The cellular wild-type p53 gene on chromosome 17p is an established tumor suppressor gene^[12-14]. It regulates the cell cycle of DNA repair and synthesis, and also programmed cell death. Once it is mutated, loss of normal function leads to the evolution of neoplasm. Moreover, the speed of tumor growth and invasion may also be enhanced. When mutated, this gene may have transforming properties and can be stained immunohistochemically^[15-21]. Its prognostic significance in some types of human cancer has been reported. The relationship between hepatocellular carcinoma (HCC) and overexpression of the mutant p53 gene have been studied in different countries^[15-32]. The results are varied. In addition, mutation of the p53 gene was emphasized in advanced but not in early hepatocellular carcinoma^[33,34]. However, the correlation between the clinical significance of such p53 mutations and the clinical recurrence of HCC has rarely been clarified.

In this study, we did immunohistochemical staining to investigate the overexpression of p53 protein in HCC in a series of patients. The correlation of the clinical and pathological variables of HCC, recurrence of HCC and the biological behaviors of the mutant p53 gene were studied. The goal of this study was to elucidate the possible role of p53 mutations in the prediction of recurrent HCCs.

MATERIALS AND METHODS

Patients

One hundred patients with HCC who underwent hepatectomy at Mackay Memorial Hospital, between January 1993 and December 1997 whose tissue specimens (formalin fixed, paraffin wax embedded) were histopathologically found to have no degeneration or necrosis were selected for this study. Clinical details were available from medical records of all patients. Seventy-nine patients entered this study and twenty-one cases were excluded for the following reasons: (1) immediate operative mortality, (2) failure to obtain p53 results due to severe, extensive tumor necrosis, some of which probably resulted from preoperative transcatheter hepatic arterial chemoembolization (TACE), (3) incomplete follow-up, and (4) causes of death not related to liver disease. The mean age of patients was 52.4 ± 16.6 years (range 16-82) with a male to female ratio of 2:1 (52:27). All received curative resections. The surgical operations included major resections (15 partial lobectomies, 31 lobectomies and 9 extended lobectomies) and minor resections (19 segmentectomies, 3 subsegmentectomies and 2 wedge resections). After resection, all patients were followed up at our out-patient-clinic receiving regular clinical assessment, periodic abdominal ultrasonography (every 2 to 3 months during the first 5 years, then every 4 to 6 months thereafter) to detect tumor recurrence, serum alpha-fetoprotein (AFP) and liver biochemistry (every 2 months during the first 2 years, then every 4 months during the following 3 years, and every 6 months thereafter). Abdominal computed tomography was also done (every 6 months during the first year, then every year).

Methods

Five-micron-thick formalin-fixed and paraffin embedded sections were cut, deparaffinized and rehydrated with graded alcohol and xylene. Endogenous peroxidase was blocked using 3% H_2O_2 for 5 minutes, followed by a brief wash in Tris buffer, pH 7.2. Sections were rehydrated and heated in citrate buffer, pH 6.0, in a microwave oven at 500 watts for 10 minutes to retrieve the antigen. The tissues were stained with a monoclonal mouse anti-human p53 antibody (DAKO-p53, clone DO-7, Dako Corp, Carpinteria, Calif. U.S.A.) and a labeled streptavidin-biotin staining kit (DAKO LSAB kit, alkaline phosphatase system 40). They were incubated with the antibody at a dilution of 1:100 (in Tris-HCl buffer) for one hour at room temperature. The peroxidase reaction used 3,3'-diaminobenzidine tetrahydrochloride as chromogen and the slides were counterstained with hematoxylin. Two independent, blinded observers evaluated all tissue sections. Only nuclear staining was regarded as positive. Cases were scored as negative when no cell was stained even at a concentration as high as 1:10 in a triplicate study. A known colon adenocarcinoma with diffuse p53 nuclear accumulation was stained in parallel as the positive control. For negative controls, we used buffer instead of the specific primary antibody.

We used light microscopy to search for the highest concentration of reactive staining nuclei in each p53 staining section and counted 1 000 cells from the most aggressive area of the tumor to represent the tumor's behavior and reduce count variability. Specific staining was identified by the presence of a red reaction product in the nuclei and was graded as negative (0), slight (+), moderate (++) or strong (+++) immunostaining, with the distribution as diffuse or focal. The percentage of nuclei immunostained was estimated and was scored without knowledge of the grade of tumor differentiation.

The differences of p53 overexpression in diverse clinicopathologic parameters were evaluated. Parameters included the presence of associated liver cirrhosis (confirmed

from the operative findings and also from the pathological examination of the specimen), HBV surface antigen (HBsAg), hepatitis C virus (HCV) infection (antibody to HCV, anti-HCV), Child-Pugh classification of liver reserve, serum alpha fetoprotein (AFP) titer, tumor size (<3 cm, 3-10 cm, >10 cm), cell differentiation grade (Edmondson and Steiner grade I vs II-IV), encapsulation (complete, infiltration by HCC or absent), vascular permeation (including vascular invasion and/or tumor thrombi within the portal vein or hepatic vein), and presence of daughter nodules (Table 1). The time lapse between the postoperation till the detection of recurrence is defined as the recurrence free interval. During the follow-up (median 3 years, range 2 to 5 years), 55 patients had tumor recurrence (48 intrahepatic, and 7 both intrahepatic and extrahepatic) and 43 patients died. We also correlated the p53 overexpression with the outcomes. In these 55 patients with recurrence, the correlation between p53 mutation of the primary lesion (presence or absence) and recurrence was studied. The following prognostic factors after recurrence were also analyzed: extrahepatic metastasis (presence or absence), the number (solitary or multiple) and the extent of recurrent tumors (affecting more than or less than one segment), treatment for recurrent tumor (surgical or nonsurgical treatment), and survival time after recurrence.

Table 1 Characteristics of 79 patients with HCC

Characteristics	n (%)
Age (years, mean \pm S.D.)	52.4 \pm 16.6
Male	52 (65.8)
Liver cirrhosis	57 (72.2)
Child class A:B	55:24 (70:30)
Tumor size small (<3 cm): median (3-10 cm): large (>10 cm)	24:25:30 (30.4:31.6:38.0)
HBsAg (+)	60 (75.9)
Anti-HCV (+)	41 (51.9)
AFP: normal: >1000ng/ml	30:20(38.0:25.3)
Edmondson grade: I:II:III:IV	4:30:42:3(5.1:38.0:53.2:3.8)
Capsule: absent: incomplete: complete	54:7:18(68.4:8.9:22.8)
Vascular permeation	56 (70.9)
Daughter nodules	44 (55.7)
Resection, major: minor	55:24 (69.6:30.4)

Notes: HCC: hepatocellular carcinoma; HBsAg: hepatitis B surface antigen; Anti-HCV: antibody to hepatitis C virus; AFP: alpha-fetoprotein; Edmondson grade: Edmondson-Steiner grade of cellular differentiation.

Statistical analysis

The data were tested with statistical programs (BMDP), Student's *t*-test or Mann-Whitney test for continuous variables, chi-square test or Fisher's exact test for categorical variables, and logistic regression and COX proportional hazards model for multivariate analysis. *P* value < 0.05 was defined as statistically and significantly different.

RESULTS

Among the 79 patients, 64 (81 %) patients had a p53-positive result. Among the 64 patients with immunopositivity, 29 patients (45 %) had moderate (++) immunostaining and 3 patients (4.7 %) had strong (++++) immunostaining. The correlations between a positive oncoprotein p53 and patient characteristics are shown in Table 2. Age, gender, positivity of HBsAg or Anti-HCV, levels of AFP, liver cirrhosis, Child-Pugh class A or B, and size of the HCC showed no statistically

significant difference between p53 positive and negative groups. From univariate analysis, a significant correlation was found between p53 over-expression and vascular permeation (78.1 vs 40.0 %, $P=0.0088$, odds ratio (O.R.)=5.357), grade of differentiation (Edmondson-Steiner grade I vs. II to IV, 98.4 vs 80.0 %, $P=0.0203$, O.R.=15.750), complete capsule vs infiltration or absent capsule (82.8 vs 53.3 %, $P=0.0346$, O.R.=4.200), and presence of daughter nodules (60.9 vs 33.3 %, $P=0.0527$, O.R.=3.120) (Table 2). From multivariate analysis, only vascular permeation and grade of differentiation remained significant ($P=0.042$ and 0.012 , respectively).

Table 2 Comparison of characteristics between p53 positive and negative groups

Characteristics	P53 Positive (n=64)	P53 Negative (n=15)	P (UV)
Age (years)	52.8	48.3	n.s.
Male	65.6 %	66.7 %	n.s.
Liver cirrhosis	76.6 %	53.3 %	n.s.
Child class A	68.8 %	73.3 %	n.s.
Tumor ≤ 3 cm	34.4 %	13.3 %	n.s.
>10 cm	35.9 %	40.0 %	n.s.
HBsAg (+)	78.1 %	66.7 %	n.s.
Anti-HCV (+)	53.1 %	46.6 %	n.s.
AFP <20 ng/mL	37.5 %	40.0 %	n.s.
>1 000 ng/mL	21.9 %	40.0 %	n.s.
Edmondson grade I ^a	1.6 %	20.0 %	0.0203
Capsule complete	17.2 %	46.7 %	0.0346
Daughter nodules	60.9 %	33.3 %	0.0527
Vascular permeation ^b	78.1 %	40.0 %	0.0088

Notes: P (UV): The P value by univariate analysis; In multivariate analysis, the significant variables of ^a and ^b: P values were 0.0120 and 0.0420 respectively; HBsAg: hepatitis B surface antigen; Anti-HCV: antibody to hepatitis C virus; AFP: alpha-fetoprotein; Edmondson grade: Edmondson-Steiner grade of cellular differentiation; n.s.: no statistical significance; O.R.: odds ratio.

Table 3 shows that patients with p53 positivity had more tumor recurrence (76.6 % vs 40.0 %, $P=0.0107$) and more death (59.4 % vs 33.3 %, $P=0.0683$). After analysis with the COX proportional hazards model, p53 overexpression had only a weak correlation with recurrence free interval and survival time ($P=0.088$ and 0.081). Factors influencing HCC recurrence and time lapse to recurrence were vascular permeation ($P=0.0002$, O.R.=5.36), complete capsule ($P=0.0160$, O.R.=3.10), and p53 positivity ($P=0.088$, O.R.=2.29) (Table 4). The significant variables affecting death resulting from recurrence included vascular permeation ($P<0.0001$, O.R.=8.35) and p53 positivity ($P=0.081$, O.R.=2.38).

Table 3 Correlation of p53 with the outcome of patients with HCC

Outcome	p53 positive (n=64)	p53 negative (n=15)	P value
Morbidity of surgery (%)	6.3	6.7	n.s.
Recurrence (%) (number)	76.6 (49)	40.0 (6)	0.0107
Death ^a (%)	59.4	33.3	0.0683
Recurrence free interval (median, months)	8.3	39.1	0.0880
Duration of survival (median, months)	11.8	41.9	0.0810

Notes: n.s.: no statistical significance; Death^a: patients died of recurrence.

Table 4 Factors influencing tumor recurrence and death of patients in multivariate analysis

Variables	P	O.R.
Recurrence		
Vascular permeation	0.0002	5.36
Complete capsule	0.0160	3.10
p53 positivity	0.0880	2.29
Death		
Vascular permeation	<0.0001	8.35
p53 positivity	0.0810	2.38

Note: O.R: odds ratio.

In 55 patients with recurrent HCCs, there was no statistically significant correlation between the status of mutant p53 positivity in the primary lesion and the treatment for recurrent tumors, and the clinical features of recurrent HCCs examined, i.e. the existence of extrahepatic metastasis ($P=0.113$), and the number of recurrent tumors ($P=1.000$), except for the extent of recurrent tumors over one hepatic segment ($P=0.0043$). The median survival after recurrence was shorter (3.42 months vs 11 months) in those with p53 mutation with a weak significance ($P=0.051$) (Table 5).

Table 5 Correlation between the clinical features of recurrent hepatocellular carcinoma and the presence of a p53 mutation in the primary lesion

The clinical features	P53 Positive (n=49)	P53 Negative (n=6)	P
Extrahepatic metastasis (number) (%)	24 (49.0)	3 (50.0)	0.1130
Multiple-recurrent tumors (number) (%)	34 (69.4)	4 (66.7)	1.0000
Extent of recurrent tumors:	34 (69.4)	5 (83.3)	0.0043
More than one segment (number) (%)			
Median survival after recurrence (Months)	3.4	11.0	0.0510
Treatment for recurrent tumors			
Surgery (number) (%)	0	1 ^a (16.7)	n.s.
Non-surgical ^b (number) (%)	20 (40.8)	3 (50.0)	
No treatment (number) (%)	29 (59.2)	2 (33.3)	

Notes: n.s.: no statistical significant; ^a: A 55 year old man had a resection of segment II and III; ^b: The Non-surgical treatments included transcatheter arterial chemoembolization and percutaneous ethanol injection.

DISCUSSION

P53 gene mutation has been identified in over half of human tumors, including HCC, and is the most common genetic abnormality in human cancers^[13, 17, 20, 25, 34-42]. Its inactivation by mutation is thought to be a fundamentally important step in carcinogenesis. In addition, the correlation among p53 gene alteration and diagnosis, assessment of tumor progression, recurrence, or cancer prognosis has been investigated and reported^[24,28,33]. Recently, Nagao *et al*^[43] and Saegusa *et al*^[44] found p53 overexpression to be strongly associated with proliferation activity of HCC cells by immunohistochemical studies. Lowe *et al.* demonstrated that a few point mutations on p53 which thus inactivated the gene produced treatment-resistant tumors^[45,46]. They suggested p53 status was an important determinant of tumor response to therapy. This indicates that recurrent HCCs with p53 mutation therefore either have a high proliferation rate or are resistant to treatment. Our results supported theirs from a clinical point of view, and also suggested that the high malignant potential was caused by the

p53 mutation. The positive rate of the mutant p53 gene in our HCC patients was 81 %. A wide range in the incidence of p53 mutations from 0 to over 70 % has been reported, with a lower frequency than in other types of cancer, except for special populations in China and Africa. Factors related to the wide variation in positivity may include different thresholds of positivity adopted, different anti-p53 antibodies used, geographical variations and differences in the molecular mechanisms of hepatocarcinogenesis, such as aflatoxin exposure. Some authors have raised a question of whether p53 protein over-expression can represent p53 gene mutation in neoplasms^[47]. Hall mentioned a very close correlation between p53 expression and mutations of the p53 gene and found that most antibodies gave the same results^[48]. The high recurrence rate after resection is one of the main factors in the poor outcome for HCC patients^[1-6, 10, 11]. Tumor recurrence limits the long-term survival. However, tumor recurrence is well correlated with tumor invasiveness. Tumor invasiveness may be determined from vascular permeation, the grade of cell differentiation, infiltration or absence of capsule and presence of daughter lesion. According to our study, they are also all compatible with oncoprotein p53 positivity. In our study, p53 protein over-expression correlated well with tumor recurrence ($P=0.0107$). To analyze the factors relating to HCC recurrence and death, vascular invasion, complete capsule, and p53 positivity correlated well with recurrence and only vascular permeation and p53 positivity correlated with death. A weak association with both recurrence free interval and duration of survival with mutation of the p53 gene was found. The weak correlation may be attributed to the short duration of follow-up (2 to 5 years, median 3 years) in this study.

Vascular permeation indicating tumor invasiveness, consists of either tumor invasion of the hepatic vein, portal vein and/or hepatic artery, or tumor thrombi within the vessels. It may be detected preoperatively by ultrasonography, arteriography or portography, intraoperative ultrasonography or direct observation, or postoperative pathological examination of surgical specimens. Vascular permeation is the most consistent significant prognostic factor of postoperative tumor recurrence^[10]. In our univariate analysis, the positive p53 status was significantly related to vascular permeation and in the COX model, patients with vascular permeation had significantly shorter recurrence free intervals and survival periods.

Whether the grade of differentiation of HCC is a determinant of recurrence after resection has been debated for a long time. The association of grade of anaplasia (Edmondson-Steiner's classification) with p53 positivity also varied in reports^[28,49,50]. In our series, less overexpression of p53 and less recurrence were found in patients with well differentiated tumors (Edmondson-Steiner's grade I) than in those with grade II to IV tumors. The histological differentiation of the HCCs in this study correlated with p53 mutations, and the incidence of p53 mutations increased with increased dedifferentiation. Our findings were consistent with previous reports showing p53 mutation to be associated with the progression of HCC as a late event in hepatocarcinogenesis^[33, 34].

The exact mechanism of capsular formation is not known. A tumor capsule may act as a barricade preventing the spread of cancer cells and has a positive role in the prognosis of HCC. The invaded capsule was regarded as incomplete in our series. We found the overexpression rate of p53 was similar in patients with no capsule and incomplete capsule (87.1 % vs 85.7 %), but was significantly lower in those with a complete capsule (17.2 %, $P=0.0346$) (Table 2). Other authors had different findings^[23,24,49,50]. Multifocal HCCs are also a controversial issue. Some consider them an early metastasis via the portal vein, but some consider them multicentric. The former is a

poor prognostic factor but the latter might not be^[51]. Without the aid of molecular biology, it is difficult to differentiate daughter nodules, intrahepatic metastatic nodules and multicentric HCC. In the present study, we selected daughter nodules as intrahepatic metastasis according to the criteria of the Liver Cancer Study Group of Japan in order to assess the clinical outcome after recurrence. As for the evaluation of prognosis after recurrence, Ikeda *et al.*^[1] reported that the most significant factor affecting the survival time of patients with intrahepatic recurrence was the number of tumor nodules at the time of recurrence. Those with daughter nodules showed a higher mutant p53 positive rate than the group with solitary HCC ($P=0.0527$). This might suggest that most daughter nodules favor intrahepatic metastasis.

Tumor size has been emphasized as one of the significant prognostic factors^[2-5] because vascular invasion and daughter lesions may increasingly develop as the tumor grows. In our study, no significant correlation between p53 positivity and tumor size was found. In addition, tumor size also had no significant correlation with histological grade, vascular invasion, recurrence free interval or survival in our patients. From our experience, some large HCCs may be the result of expansive growth and may have slow intraportal or distant spread.

The implications of our results, nevertheless, are that the immunohistochemical detection of p53 is a valuable tool for prediction of recurrence in patients after resection or for identifying subgroups of patients who may be at higher risk. There is some discrepancy between our results and the findings of previous studies on the role of p53 expression in determining the prognosis of patients with HCC. These discrepancies, however, might reflect important variables of selection, such as number of patients, histological type of tumors, tumor stage, period of follow-up, and type of antibody used. All the patients entering our study had received curative resections.

Prognosis after recurrence in relation to p53 mutations in the primary lesion is rarely reported in the literatures. Our findings suggest that HCCs with p53 mutations have a higher malignant potential. Matsuda *et al.*^[52] found that the postrecurrence survival of patients with repeat surgery was better than that of patients who were treated conservatively. However, from our study, the type of treatment for recurrent HCCs did not affect the postrecurrent survival because the choice of treatment was closely related to the number and extent of recurrent tumors and the liver function of the remnant. The majority of our patients had diffused multiple recurrent nodules over the liver remnant. Repeat surgery was undertaken on only one patient. In our study, the postrecurrent survival was weakly lower ($P=0.051$) in patients with p53 mutations in their primary lesion than in those without them.

We thus consider the status of p53 mutations in the primary lesion to be useful as a predictor affecting both the recurrence after resection and the prognosis after recurrence, even before the pathologic findings of recurrent HCCs are known. Therefore, it is important in the follow-up of patients after resection of HCCs. In conclusion, patients with p53 mutations have a worse prognosis than patients without such mutations, including survival after recurrence. Therefore, p53 mutation in the primary lesion is considered useful as an indicator of the biological behavior of recurrent HCCs.

REFERENCES

- 1 **Ikeda K**, Saitoh S, Tsubota A, Arase Y, Chayama K, Kumada H, Watanabe G, Tsurumaru M. Risk factors for tumor recurrence and prognosis after curative resection of hepatocellular carcinoma. *Cancer* 1993; **71**: 19-25

- 2 **Arii S**, Tanaka J, Yamazoe Y, Minematsu S, Morino T, Fujita K, Maetani S, Tobe T. Predictive factors for intrahepatic recurrence of hepatocellular carcinoma after partial hepatectomy. *Cancer* 1992; **69**: 913-919
- 3 **Shirabe K**, Kanematsu T, Matsumata T, Adachi E, Akazawa K, Sugimachi K. Factors linked to early recurrence of small hepatocellular carcinoma after hepatectomy: univariate and multivariate analysis. *Hepatology* 1991; **14**: 802-805
- 4 **Jwo SC**, Chiu JH, Chau GY, Loong CC, Lui WY. Risk factors linked to tumor recurrence of human hepatocellular carcinoma after hepatic resection. *Hepatology* 1992; **16**: 1367-1371
- 5 **Nagao T**, Inoue S, Goto S, Mizuta T, Omori Y, Kawano N, Morioka Y. Hepatic resection for hepatocellular carcinoma. *Ann Surg* 1987; **205**: 33-40
- 6 **Sasaki Y**, Imaoka S, Masutani S, Ohashi I, Ishikawa O, Koyama H, Iwanaga T. Influence of coexisting cirrhosis on long-term prognosis after surgery in patients with hepatocellular carcinoma. *Surgery* 1992; **112**: 515-521
- 7 **Lai EC**, Ng IO, Ng MM, Lok AS, Tam PC, Fan ST, Choi TK, Wong J. Long-term results of resection for large hepatocellular carcinoma: a multivariate analysis of clinicopathological features. *Hepatology* 1990; **11**: 815-818
- 8 **Hsu HC**, Wu TT, Wu MZ, Sheu JC, Lee CS, Chen DS. Tumor invasiveness and prognosis in resected hepatocellular carcinoma. *Cancer* 1988; **61**: 2095-2099
- 9 **Hsu HC**, Sheu JC, Lin YH, Chen DS, Lee CS, Hwang LY, Beasley RP. Prognostic histologic features of resected small hepatocellular carcinoma (HCC) in Taiwan. *Cancer* 1985; **56**: 672-680
- 10 **el-Assal ON**, Yamanoi A, Soda Y, Yamaguchi M, Yu L, Nagasue N. Proposal of invasiveness score to predict recurrence and survival after curative hepatic resection for hepatocellular carcinoma. *Surgery* 1997; **122**: 571-577
- 11 **Jeng KS**, Chen BF, Lin HF. En bloc resection for extensive hepatocellular carcinoma: is it advisable? *World J Surg* 1994; **18**: 834-839
- 12 **Bartek J**, Bartkova J, Vojtesek B, Staskova Z, Lukas J, Rejthar A, Kovarik J, Midgley CA, Gannon JV, Lane DP. Aberrant expression of the p53 oncoprotein is a common feature of a wide spectrum of human malignancies. *Oncogene* 1991; **6**: 1699-1703
- 13 **Hollstein M**, Sidransky D, Vogelstein B, Harris CC. p53 mutations in human cancers. *Science* 1991; **253**: 49-53
- 14 **Baker SJ**, Fearon ER, Nigo JM, Hamilton SR, Preisinger AC, Jessup JM, vanTuinen P, Ledbetter DH, Barker DF, Nakamura Y. Chromosome 17 deletions and p53 gene mutations in colorectal carcinomas. *Science* 1989; **244**: 217-221
- 15 **Collier JD**, Carpenter M, Burt AD, Bassendine MF. Expression of mutant p53 protein in hepatocellular carcinoma. *Gut* 1994; **35**: 98-100
- 16 **Livni N**, Eid A, Ilan Y, Rivkind A, Rosenmann E, Blendis LM, Shouval D, Galun E. p53 expression in patients with cirrhosis with and without hepatocellular carcinoma. *Cancer* 1995; **75**: 2420-2426
- 17 **Saegusa M**, Takano Y, Kishimoto H, Wakabayashi G, Nohga K, Okudaira M. Comparative analysis of p53 and c-myc expression and cell proliferation in human hepatocellular carcinomas- an enhanced immunohistochemical approach. *J Cancer Res Clin Oncol* 1993; **119**: 737-744
- 18 **D'Errico A**, Grigioni WF, Fiorentino M, Baccarini P, Grazi GL, Mancini AM. Overexpression of p53 protein and Ki67 proliferative index in hepatocellular carcinoma: an immunohistochemical study on 109 Italian patients. *Pathol Int* 1994; **44**: 682-687
- 19 **Ng IOL**, Srivastava G, Chung LP, Tsang SW, Ng MM. Overexpression and point mutations of p53 tumor suppressor gene in hepatocellular carcinomas in Hong Kong Chinese people. *Cancer* 1994; **74**: 30-37
- 20 **Cohen C**, DeRose PB. Immunohistochemical p53 in hepatocellular carcinoma and liver cell dysplasia. *Mod Pathol* 1994; **7**: 536-539
- 21 **Zhao M**, Zhang NX, Laissue JA, Zimmermann A. Immunohistochemical analysis of p53 protein overexpression in liver cell dysplasia and in hepatocellular carcinoma. *Virchows Arch* 1994; **424**: 613-621
- 22 **Hollstein MC**, Wild CP, Bleicher F, Chutimataewin S, Harris CC, Srivatanakul P, Montesano R. p53 mutations and aflatoxin B1 exposure in hepatocellular carcinoma patients from Thailand. *Int J Cancer* 1993; **53**: 51-55
- 23 **Vesey DA**, Hayward NK, Cooksley WGE. p53 gene in hepatocellular carcinomas from Australia. *Cancer Detect Prev* 1994; **18**: 123-130
- 24 **Pierre LP**, Flejou JF, Fabre M, Bedossa P, Belghiti J, Gayral F, Franco D. Overexpression of p53: a rare event in a large series of white patients with hepatocellular carcinoma. *Hepatology* 1992; **16**: 1171-1175
- 25 **Sheu JC**, Huang GT, Lee PH, Chung JC, Chou HC, Lai MY, Wang JT, Lee HS, Shih LN, Yang PM. Mutation of p53 gene in hepatocellular carcinoma in Taiwan. *Cancer Res* 1992; **52**: 6098-6100
- 26 **Kress S**, Jahn UR, Buchmann A, Bannasch P, Schwarz M. p53 mutations in human hepatocellular carcinomas from Germany. *Cancer Res* 1992; **52**: 3220-3223
- 27 **Wee A**, The M, Raju C. p53 expression in hepatocellular carcinoma in a population in Singapore with endemic hepatitis B virus infection. *J Clin Pathol* 1995; **48**: 236-238
- 28 **Hsu HC**, Tseng HJ, Lai PL, Lee PH, Peng SY. Expression of p53 gene in 184 unifocal hepatocellular carcinomas: association with tumor growth and invasiveness. *Cancer Res* 1993; **53**: 4691-4694
- 29 **Debuire B**, Paterlini P, Pontisso P, Basso G, May E. Analysis of the p53 gene in European hepatocellular carcinomas and hepatoblastomas. *Oncogene* 1993; **8**: 2303-2306
- 30 **Shieh YSC**, Nguyen C, Vocal MV, Chu HW. Tumor suppressor p53 gene in hepatitis C and B virus-associated human hepatocellular carcinoma. *Int J Cancer* 1993; **54**: 558-562
- 31 **Nishida N**, Fukuda Y, Kokuryu H, Toguchida J, Yandell DW, Ikenega M. Role and mutational heterogeneity of the p53 gene in hepatocellular carcinoma. *Cancer Res* 1993; **53**: 368-372
- 32 **Bressac B**, Kew M, Wands J, Ozturk M. Selective G to T mutations of p53 gene in hepatocellular carcinoma from southern Africa. *Nature* 1991; **350**: 429-431
- 33 **Tanaka S**, Toh Y, Adachi E, Matsumata T, Mori R, Sugimachi K. Tumor progression in hepatocellular carcinoma may be mediated by p53 mutation. *Cancer Res* 1993; **53**: 2884-2887
- 34 **Oda T**, Tsuda H, Scarpa A, Sakamoto M, Hirohashi S. p53 gene mutation spectrum in hepatocellular carcinoma. *Cancer Res* 1992; **52**: 6358-6364
- 35 **Puisieux A**, Ponchel F, Ozturk M. p53 as a growth suppressor gene in HBV-related hepatocellular carcinoma cells. *Oncogene* 1993; **8**: 487-490
- 36 **Bressac B**, Galvin KM, Liang TJ, Isselbacher KJ, Wands JR, Ozturk M. Abnormal structure and expression of p53 gene in human hepatocellular carcinoma. *Proc Natl Acad Sci USA* 1990; **87**: 1973-1977
- 37 **Slagle BL**. p53 mutations and hepatitis B virus: cofactors in hepatocellular carcinoma. *Hepatology* 1995; **21**: 597-599
- 38 **Nishida N**, Fukuda Y, Kokuryu H, Toguchida J, Yandell DW, Ikenega M. Role and mutational heterogeneity of the p53 gene in hepatocellular carcinoma. *Cancer Res* 1993; **53**: 368-372
- 39 **Scorson KA**, Zhou YZ, Butel JS, Slagle BL. p53 mutations cluster at codon 249 in hepatitis B virus-positive hepatocellular carcinomas from China. *Cancer Res* 1992; **52**: 1635-1638
- 40 **Goldblum JR**, Bartos RE, Carr KA, Frank TS. Hepatitis B and alterations of the p53 tumor suppressor gene in hepatocellular carcinoma. *Am J Surg Pathol* 1993; **17**: 1244-1251
- 41 **Harris CC**, Hollstein M. Clinical implications of the p53 tumor-suppressor gene. *NEJM* 1993; **329**: 1318-1327
- 42 **Finlay CA**, Hinds PW, Levine AJ. The p53 proto-oncogene can act as a suppressor of transformation. *Cell* 1989; **57**: 1083-1093
- 43 **Nagao T**, Kondo F, Sato T, Nagato Y, Kondo Y. Immunohistochemical detection of aberrant p53 expression in hepatocellular carcinoma: correlation with cell proliferative activity indices, including mitotic index and MIB-1 immunostaining. *Hum Pathol* 1995; **26**: 326-333
- 44 **Saegusa M**, Takano Y, Kishimoto H, Wakabayashi G, Nohga K, Okudaira M. Comparative analysis of p53 and c-myc expression and cell proliferation in human hepatocellular carcinomas- an enhanced immunohistochemical approach. *J Cancer Res Clin Oncol* 1993; **119**: 737-744
- 45 **Lowe SW**, Rulley HE, Jacks T, Housman DE. p53-dependent apoptosis modulates the cytotoxicity of anticancer agents. *Cell* 1993; **74**: 957-967

- 46 **Lowe SW**, Bodis S, McClatchey A, Remington L, Ruley HE, Fisher DE, Housman DE, Jacks T. p53 status and the efficacy of cancer therapy *in vivo*. *Science* 1994; **266**: 807-810
- 47 **Wynford-Thomas D**. P53 in tumor pathology: can we trust immunocytochemistry? *J Pathol* 1992; **166**: 329-330
- 48 **Hall PA**, Lane DP. p53 in tumor pathology: can we trust immunohistochemistry? *J Pathol* 1994; **172**: 1-4
- 49 **Sugo H**, Takamori S, Kojima K, Beppu T, Futagawa S. The significance of p53 mutations as an indicator of the biological behavior of recurrent hepatocellular carcinomas. *Surg Today* 1999; **29**: 849-855
- 50 **Hayashi H**, Sugio K, Matsumata T, Adachi E, Takenaka K, Sugimachi K. The clinical significance of p53 gene mutation in hepatocellular carcinomas from Japan. *Hepatology* 1995; **22**: 1702-1707
- 51 **Nakano S**, Haratake J, Okamoto K, Takeda S. Investigation of resected multinodular hepatocellular carcinoma: assessment of unicentric or multicentric genesis from histological and prognosis viewpoint. *Am J Gastroenterol* 1994; **9**: 189-193
- 52 **Matsuda Y**, Ito T, Oguchi Y, Nakajima K, Izukura T. Rationale of surgical management for recurrent hepatocellular carcinoma. *Ann Surg* 1993; **217**: 28-34

Edited by Xu XQ

Transcatheter arterial embolization treatment in patients with hepatocellular carcinoma and risk of pulmonary metastasis

Shee-Chan Lin, Shou-Chuan Shih, Chin-Roa Kao, Sun-Yen Chou

Shee-Chan Lin, Shou-Chuan Shih, Chin-Roa Kao, Sun-Yen Chou, Division of Gastroenterology, Department of Internal Medicine, Mackay Memorial Hospital, Taipei, Taiwan, China
Correspondence to: Dr. Shee-Chan Lin, Chief of Division of Gastroenterology, Department of Internal Medicine, Mackay Memorial Hospital, 92, Sec. 2, Chung San North Road, Taipei, Taiwan, China. sheechan@ms2.mmh.org.tw
Telephone: +86-2-25433535 **Fax:** +86-2-25433642
Received: 2003-02-25 **Accepted:** 2003-03-16

Abstract

AIM: To investigate the relationship between transcatheter arterial embolization (TAE) and pulmonary metastasis in subjects with hepatocellular carcinoma (HCC).

METHODS: A total of 287 patients with HCC followed up for more than 1 week were included. 102 patients underwent transcatheter arterial embolization (TAE group) and 185 received conservative treatment (control group). The patients' chest x-rays and chest CT scans were examined for pulmonary metastasis.

RESULTS: Patients with TAE had a median survival of 19.3 months while that of the control group was only 10.0 months ($P < 0.05$). Pulmonary metastasis occurred in 14 (13.7 %) patients in the TAE group and 14 (7.6 %) patients in the control group, there was no significant difference ($P > 0.05$). The 1-year, 2-year and 5-year cumulative incidence of pulmonary metastasis was 11.8 %, 17.6 % and 24.0 % in the TAE group and 7.0 %, 13.0 % and 21.7 % in the control group, respectively ($P > 0.05$). On the univariate analysis, tumor size, abnormal serum alanine aminotransferase levels and heterogeneity on sonography were significantly associated with pulmonary metastasis. However, on the multivariate analysis, only tumor size was significantly predictive of pulmonary metastasis.

CONCLUSION: TAE is effective on prolonging survival of patients with HCC. It does not significantly increase the risk of pulmonary metastasis. Tumor size is the only significant predictive factor associated with lung metastasis.

Lin SC, Shih SC, Kao CR, Chou SY. Transcatheter arterial embolization treatment in patients with hepatocellular carcinoma and risk of pulmonary metastasis. *World J Gastroenterol* 2003; 9(6): 1208-1211
<http://www.wjgnet.com/1007-9327/9/1208.asp>

INTRODUCTION

Hepatocellular carcinoma (HCC) is the most common cancer in Taiwan and certain other parts of the world where hepatitis B virus infection is hyperendemic^[1]. HCC has a dismal overall prognosis, with 94 % of affected individuals dying of the disease^[2]. Treatment leading to long-term survival generally includes resection or ablative therapy for small or localized

hepatic tumors^[3-6]. Unfortunately, patients with HCC are usually diagnosed at a late stage when few can be treated with surgical resection. Factors indicating unresectability are (1) large or multicentric liver tumors, (2) the presence of metastatic disease, and (3) insufficient functional hepatic reserve^[3]. Therapies other than surgical resection include systemic or infusional chemotherapy, hepatic artery ligation or embolization, and radiolabeled antibodies^[7]. Transcatheter arterial embolization (TAE) has been performed for the treatment of unresectable HCC^[8,9] and has been shown to be able to prolong survival^[7, 10-11]. One study found survival of post-TAE to be comparable to that of post-hepatectomy^[12].

However, it has been suggested that TAE-induced necrosis might result in hematogenous dissemination from the primary tumor^[13]. The lung is the most common site of extrahepatic metastasis in HCC^[14]. A higher incidence of pulmonary metastasis following TAE in patients with HCC has been reported. However, the subjects who developed lung metastasis in that series were followed for a longer period than those without metastasis^[15]. We designed this case control study to evaluate the risk of pulmonary metastasis in patients with HCC following TAE, taking into account duration of follow up.

MATERIALS AND METHODS

Patients

Patients with HCC diagnosed from January 1996 to December 1999 at our hospital were included in this study. Diagnosis of HCC was based on high serum alpha-fetoprotein (AFP) values, ultrasonography, computed tomography (CT), and angiographic findings with or without needle biopsy or aspiration cytological examination. Patients who had pulmonary metastasis before or within 1 week after admission or who died within 1 week after admission were excluded, as were those eligible for surgical resection or percutaneous ethanol injection. There were 102 patients receiving TAE treatment during the study period. We selected another 185 patients with HCC who had refused either TAE or chemotherapy as a control group.

Methods

TAE was performed with lipiodol mixed with gelatin particles at an interval of 12 to 16 weeks. All patients were followed until death or December 31, 2000. Chest x-rays were taken at each admission or every 3 months in the outpatient clinic. Multiple nodules in the lung fields on chest x-ray and chest CT scans were diagnosed as pulmonary metastasis. Liver ultrasonography was performed every 3 months. Tumor size and sonographic patterns were recorded. Tumors with both hyper-echoic and hypo-echoic patterns were classified as heterogeneous. The presence of portal vein thrombosis was evaluated with a combination of ultrasonography, angiography and CT. Tumor stage was assessed according to the staging system described by Okuda *et al*^[8].

Statistical analysis

Statistical analysis was performed using the χ^2 test to compare

differences between groups. Results were given as the mean \pm standard deviation. Comparisons between group means were performed using Student's *t* test. Survival time was calculated from the time of cancer diagnosis until death or December 31, 2000. The time from the date of the diagnosis of cancer to the date of pulmonary metastasis or December 31, 2000 was calculated for analysis of cumulative incidence of pulmonary metastasis. The cumulative probability of survival and the cumulative incidence of pulmonary metastasis were calculated using the Kaplan-Meier method, and the difference between groups was compared using the log-rank test^[16]. Univariate and multivariate analyses using Cox proportional hazard models were performed to evaluate clinical parameters associated with pulmonary metastasis and calculate odds ratios (OR). The parameters included in the analysis were age, sex, serum albumin levels, bilirubin levels, AST and ALT values, AFP value, presence of cirrhosis, presence of ascites, presence of encephalopathy, Child scores, tumor size, sonographic pattern, uni- or multifocal tumor, presence of tumor halo, presence of portal vein thrombosis, stage of the disease, and TAE therapy. Significant parameters in the univariate analyses were analyzed with multivariate analysis. The level of significance was set at $P < 0.05$.

RESULTS

Demographic and clinical characteristics, liver function tests, and tumor characteristics did not differ significantly between the TAE and control groups (Table 1). Patients who had received TAE had a median survival time of 19.3 months compared with only 10.0 months for controls. The 6 month, one-year and two-year survival rate was 83 %, 59.1 % and 47.5 % respectively, in the TAE group, and 66.8 %, 43.7 % and 25.7 %, respectively, in the control group ($P < 0.001$, Figure 1). Pulmonary metastasis developed in 14 (13.7 %) patients in the TAE group and 14 (7.6 %) patients in the control group ($P > 0.05$). There was no significant difference in the cumulative incidence of pulmonary metastasis between these two groups. The 1-year, 2-year, 3-year, and 5-year cumulative incidence of pulmonary metastasis was 11.8 %, 17.6 %, 17.6 % and 24 % in the TAE group, 7 %, 13 %, 21.7 % and 21.7 % in the control group, respectively ($P > 0.05$, Figure 2).

Table 1 Clinical characteristics of patients with hepatocellular carcinoma

Parameters	TAE group (n=102)	Control group (n=185)	P
Male (%)	75 (74.3%)	148 (80%)	NS
Age (years)*	56.7 \pm 10.5	56.8 \pm 13.7	NS
Albumin (g/dl)*	3.51 \pm 0.57	3.40 \pm 0.61	NS
Bilirubin (mg/dl)*	2.02 \pm 7.17	1.30 \pm 1.25	NS
ALT (IU/ml)*	68.4 \pm 63.6	63.0 \pm 57.1	NS
Prolonged Prothrombin time*	1.38 \pm 1.25	1.48 \pm 1.11	NS
Encephalopathy (%)	6 (5.9%)	14 (7.6%)	NS
Cirrhosis (%)	76 (74.5%)	121 (65.4%)	NS
Ascites (%)	14 (13.7%)	32 (17.3%)	NS
Multicentric tumors (%)	19 (18.6%)	39 (21.1%)	NS
Heterogeneous echopattern (%)	34 (33.4%)	72 (39.1%)	NS
Encapsulated tumors (%)	49 (48.0%)	76 (41.1%)	NS
PV thrombosis (%)	23 (22.5%)	58 (31.4%)	NS
Large tumor size (%)	56 (54.9%)	103 (55.7%)	NS

Data expressed as means \pm standard deviation, comparison with unpaired Student's *t* test. NS=not significant.

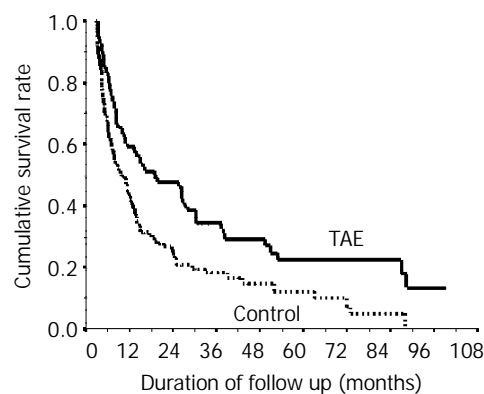


Figure 1 Survival curves of patients with HCC treated with TAE and untreated controls.

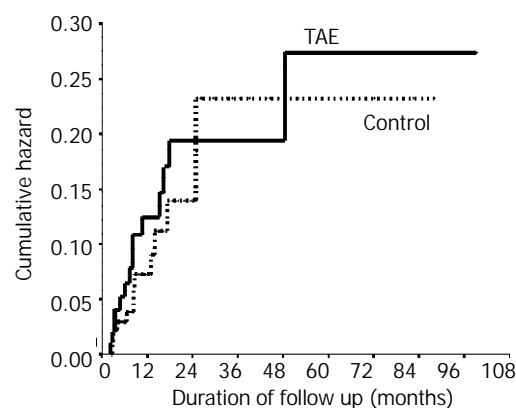


Figure 2 Cumulative incidence of pulmonary metastasis in patients with HCC treated with TAE or untreated controls.

On the univariate analysis using the Cox proportional hazard model, tumor size (OR 2.34), abnormal serum ALT levels (OR 1.94) and heterogeneous sonographic pattern (OR 2.08) were significantly associated with the risk of pulmonary metastasis. However, on multivariate analysis only tumor size was significantly predictive of pulmonary metastasis (OR 2.24, 95 % CI 1.37 to 6.45).

DISCUSSION

It is believed that manipulation of tumor with TAE will increase the risk of hematogenous metastasis due to an increase in activity of serum type IV collagen-degrading enzyme^[17], or a decrease in activity of the tumor invasion-inhibiting factor^[18]. The disruption of tissue architecture resulting from ischemic necrosis after the TAE treatment may facilitate the dissemination of neoplastic cells^[19]. The incidence of extrahepatic recurrence of HCC is increased in patients who receive preoperative TAE treatment compared to those who undergo surgery alone^[20]. However, in our study, the incidence of pulmonary metastasis after the TAE therapy was not significantly increased. TAE patients also experienced longer survival and were followed longer than untreated controls (Figure 1). The 1-year, 2-year, 3-year and 5-year cumulative incidence of lung metastasis did not differ between the two groups.

The overall incidence of pulmonary metastasis in our series was 7.2 %, lower than that from an autopsy series of HCC reported in Japan^[21]. There may be several reasons for this discrepancy. We excluded patients with obvious pulmonary metastasis within 1 month after the diagnosis of cancer, although we could not exclude the presence of micro-metastasis. Our diagnosis of metastatic disease was based on

multi-nodular lesions on the chest x-ray and confirmed by chest CT. Most of our patients with metastasis had lesions larger than 3 mm on the chest film. Peters reported that pulmonary metastasis larger than 1 cm in size was rare and that, in 55 % of cases, lung metastasis was only recognizable microscopically^[22]. We would expect the actual incidence of pulmonary metastasis in our series to be more than 10 %, but this could not be documented, in part because autopsy is not well accepted in Taiwan. However, as both TAE and control groups initially included patients without clinically detectable metastasis, we believe that our results are still valid, as the subjects were similar at baseline.

It has been reported in an autopsy study that the HCC tumor size and invasion of the portal vein were associated with pulmonary metastasis^[21]. In another study of patients with long survival, the same association was found, with the coexistence of pulmonary metastasis, a large tumor size and portal vein invasion being the final event leading to death^[23]. In our series, on univariate analysis only large tumor size, a heterogeneous echo pattern, or abnormal alanine aminotransferase levels were associated with an increased incidence of pulmonary metastasis.

When HCC is small, the sonographic pattern is homogeneous and hypo-echoic. Most small hepatomas progress from hypoechoic to heterogeneous hyperechoic patterns when they grow larger^[24]. In general, small hepatomas without necrosis are hypoechoic; medium-sized tumors have a hypoechoic periphery and a hyperechoic center. The hypoechoic periphery corresponds to viable tumor and the hyperechoic core corresponds to central coagulation necrosis. Large tumors with extensive necrosis have an irregular mixed-echo pattern^[25]. A significant correlation between the incidence of metastasis and extent of necrosis in the primary tumor has been reported^[26]. The heterogeneous sonographic pattern of the tumor therefore implies later stage disease with more potential of extrahepatic metastasis. The serum alanine aminotransferase level correlates with hepatocellular damage. Tumor necrosis releases alanine aminotransferase enzymes into the blood flow. These observations likely explain our finding of an association on the univariate analysis between these factors and pulmonary metastasis. The fact that tumor size was the only independent predictor of metastasis on the multivariate analysis is thus understandable, as large tumors are almost invariable heterogeneous on sonography and associated with abnormal alanine aminotransferase levels.

Unfortunately, about 80 % of all our patients with HCC were not treated (data not shown). The reasons for lack of specific treatment in the control group varied. Most of them did not have regular serum AFP screening or sonographic examination and some already had late-stage HCC with a poor general condition and were thus too unwell for any specific treatment. Some did not trust Western medicine and tried Chinese herbal medicine instead. Only 20 % of our patients with HCC received treatment, 21 % undergoing surgical resection or percutaneous ethanol injection and 75 % of them being treated with TAE. More frequent sonographic screening of patients at high risk for HCC is important for earlier detection of smaller tumors.

In conclusion, TAE therapy is effective on prolonging survival of some patients with HCC. In our series, TAE did not increase the incidence of pulmonary metastasis. The larger the tumor, the higher the risk for pulmonary metastasis.

REFERENCES

- 1 **Beasley RP**, Hwang LY, Lin CC, Chien CS. Hepatocellular carcinoma and hepatitis B virus. A prospective study of 22 707 men in Taiwan. *Lancet* 1981; **2**: 1129-1133
- 2 **Rustgi V**. Epidemiology of hepatocellular cancer. *Ann Intern Med* 1988; **108**: 390-397
- 3 **Curley SA**, Levin B, Rich TA. Liver and bile ducts. In: Abeloff MD, Armitage JO, Lichter AS. eds. *Clinical Oncology*. New York: Churchill Livingstone, Inc, 1995: 1305-1372
- 4 **Nagasue N**, Kohno H, Chang YC, Taniura H, Yamanoi A, Uchida M, Kimoto T, Takemoto Y, Nakamura T, Yukaya H. Liver resection for hepatocellular carcinoma: results of 229 consecutive patients during 11 years. *Ann Surg* 1993; **217**: 375-384
- 5 **Curley SA**, Izzo F, Ellis LM, Nicolas Vauthey J, Vallone P. Radiofrequency ablation of hepatocellular cancer in 110 patients with cirrhosis. *Ann Surg* 2000; **232**: 381-391
- 6 **Livraghi T**, Bolondi L, Lazzaroni S, Marin G, Morabito A, Rapaccini GL, Salmi A, Torzilli G. Percutaneous ethanol injection in the treatment of hepatocellular carcinoma in cirrhosis. *Cancer* 1992; **69**: 925-929
- 7 **Di Bisceglie AM**, Rustgi VK, Hoofnagle JH, Dusheiko GM, Lotze MT. NIH conference: hepatocellular carcinoma. *Ann Intern Med* 1988; **108**: 390-401
- 8 **Okuda K**, Ohtsuki T, Obata H, Tomimatsu M, Okazaki N, Hasegawa H, Nakajima Y, Ohnishi K. Natural history of hepatocellular carcinoma and prognosis in relation to treatment: study of 850 patients. *Cancer* 1985; **56**: 918-928
- 9 **Yamada R**, Sato M, Kawabata M, Nakatsuka H, Nakamura K, Takashima S. Hepatic artery embolization in 120 patients with unresectable hepatoma. *Radiology* 1983; **148**: 397-401
- 10 **Mondazzi L**, Bottelli R, Brambilla G, Rampoldi A, Rezakovic I, Zavaglia C, Alberti A, Ideo G. Transarterial oily chemoembolization for the treatment of hepatocellular carcinoma: a multivariate analysis of prognostic factors. *Hepatology* 1994; **19**: 1115-1123
- 11 **Hsieh MY**, Chang WY, Wang LY, Chen SC, Chuang WL, Lu SN, Wu DK. Treatment of hepatocellular carcinoma by transcatheter arterial chemoembolization and analysis of prognostic factors. *Cancer Chemotherapy & Pharmacology* 1992; **31**: S82-85
- 12 **Yoshimi F**, Nagao T, Inoue S, Kawano N, Muto T, Gunji T, Ohnishi S, Imawari M. Comparison of hepatectomy and transcatheter arterial chemoembolization for the treatment of hepatocellular carcinoma: necessity for prospective randomized trial. *Hepatology* 1992; **16**: 702-706
- 13 **Bonfil RD**, Bustuoabad OD, Ruggiero RA, Meiss RP, Pasqualini CD. Tumor necrosis can facilitate the appearance of metastasis. *Clin Exp Metastasis* 1988; **6**: 121-129
- 14 **Lee YT**, Geer DA. Primary liver cancer: pattern of metastasis. *J Surg Oncol* 1987; **36**: 26-31
- 15 **Liou TC**, Shih SC, Kao CR, Chou SY, Lin SC, Wang HY. Pulmonary metastasis of hepatocellular carcinoma associated with transarterial chemoembolization. *J Hepatol* 1995; **23**: 563-568
- 16 **Peto R**, Pike MC, Armitage P, Breslow NE, Cox DR, Howard SV, Mantel N, McPherson K, Peto J, Smith PG. Design and analysis of randomized clinical trials requiring prolonged observation of each patient: II. Analysis and examples. *Br J Cancer* 1977; **35**: 1-39
- 17 **Hashimoto N**, Kobayashi M, Tsuji T. Serum type IV collagen-degrading enzyme in hepatocellular carcinoma with metastasis. *Acta Med Okayama* 1988; **42**: 1-6
- 18 **Isoai A**, Giga-Hama Y, Shinkai K, Mukai M, Akedo H, Kumagai H. Tumor invasion-inhibiting factor 2: primary structure and inhibitory effect on invasion in vitro and pulmonary metastasis of tumor cells. *Cancer Res* 1992; **52**: 1422-1426
- 19 **Boix L**, Bruix J, Castells A. Circulating mRNA for alpha-fetoprotein in patients with hepatocellular carcinoma. Evidence of tumor dissemination after transarterial embolization. *Hepatology* 1996; **24**: 349
- 20 **Peters RL**. Pathology of hepatocellular carcinoma. Okuda K, Peters, RL, eds. *Hepatocellular carcinoma*. New York: John Wiley & Son Inc, 1976: 107-168
- 21 **Wu CC**, Ho YZ, Ho WL, Wu TC, Liu TJ, Peng FK. Preoperative transcatheter arterial chemoembolization for resectable large hepatocellular carcinoma: a reappraisal. *Br J Surg* 1995; **82**: 122-126
- 22 **Sawabe M**, Nakamura T, Kanno J, Kasuga T. Analysis of mor-

- phological factors of hepatocellular carcinoma in 98 autopsy cases with respect to pulmonary metastasis. *Acta Pathol Jpn* 1987; **37**: 1389-1404
- 23 **Falkson G**, Cnaan A, Schutt AJ, Ryan LM, Falkson HC. Prognostic factors for survival in hepatocellular carcinoma. *Cancer Res* 1988; **48**: 7314-7318
- 24 **Sheu JC**, Chen DS, Sung JL, Chuang CN, Yang PM, Lin JT, Yang PC. Hepatocellular carcinoma: US evolution in the early stage. *Radiology* 1985; **155**: 463-467
- 25 **Yang R**, Kopecky KK, Rescorla FJ, Galliani CA, Grosfeld JL. Changes of hepatoma echo patterns with tumor growth. A study of the microanatomic basis in a rat model. *Invest Radiol* 1993; **28**: 507-512
- 26 **Nishizaki T**, Matsumata T, Kanematsu T, Yasunaga C, Sugimachi K. Surgical manipulation of VX2 carcinoma in the rabbit liver evokes enhancement of metastasis. *J Surg Res* 1990; **49**: 92-97

Edited by Xu XQ

Changes in survival patterns in urban Chinese patients with liver cancer

Xi-Shan Hao, Ke-Xin Chen, Peizhong Peter Wang, Tom Rohan

Xi-Shan Hao, Ke-Xin Chen, Tianjin Cancer Institute and Hospital, Tianjin Medical University, Tianjin 300060, China

Peizhong Peter Wang, Department of Public Health Sciences, University of Toronto, Toronto, Canada

Tom Rohan, Department of Epidemiology and Social Medicine, Albert Einstein College of Medicine, Bronx, U.S.A

Correspondence to: Dr. P. Peter Wang, ACREU, Toronto Western Hospital Research Institute, University Health Network, MP 10-327, 399 Bathurst Street, Toronto, Ontario M5T 2S8, Canada. wang@uhnres.utoronto.ca

Telephone: +1-416-603-5800 Ext: 3174 **Fax:** +1-416-603-6288

Received: 2003-02-26 **Accepted:** 2003-03-16

Abstract

AIM: To examine the survival patterns and determinants of primary liver cancer in a geographically defined Chinese population.

METHODS: Primary liver cancer cases ($n=13\ 685$) diagnosed between 1981 and 2000 were identified by the Tianjin Cancer Registry. Age-adjusted and age-specific incidence rates were examined in both males and females. Proportional hazards (Cox) regression was utilized to explore the effects of time of diagnosis, sex, age, occupation, residence, and hospital of diagnosis on survival.

RESULTS: Crude and age-adjusted incidence rates in the study period were: 27.4/100 000 and 26.3/100 000 in males; and 11.5/100 000 and 10.4/100 000 in females, respectively. Cox regression analyses indicated that there was a significant improvement in survival rates over time. Industrial workers and older people had relatively poor survival rates. The hospital in which the liver cancer was diagnosed was a statistically significant predictor of survival; patients diagnosed in city hospitals were more likely to have better survival than those diagnosed in community/district hospitals.

CONCLUSION: Patients diagnosed in recent years appeared to have a better outcome than those diagnosed in early times. There were also significant survival disparities with respect to occupation and hospital of diagnosis, which suggest that socioeconomic status may play an important role in determining prognosis.

Hao XS, Chen KX, Wang PP, Rohan T. Changes in survival patterns in urban Chinese patients with liver cancer. *World J Gastroenterol* 2003; 9(6): 1212-1215
<http://www.wjgnet.com/1007-9327/9/1212.asp>

INTRODUCTION

Liver cancer is a fairly common malignancy world wide^[1-5], especially in developing countries^[6-9]. In China, primary liver cancer is the third and fourth most common cancer in men and women with the age-adjusted incidence rates of 28.2/100 000 and 9.8/100 000 respectively in Shanghai^[10]. Population-based

survival data on cancer are indispensable in providing real, unbiased, average outcome of cancer patients. While liver cancer is a major cause of cancer-related mortality in China, little is known about its survival patterns over time. The objective of this study was two-fold: (1) to examine a specific hypothesis regarding the survival patterns of liver cancer in the studied urban Chinese population; (2) to examine the factors affecting such survival patterns. The objectives were achieved by analysing the data from the Tianjin Cancer Registry. The Tianjin Cancer Registry Centre is one of the members of the International Agency for Research on Cancer (IARC) of the World Health Organization. The cancer incidence data from Tianjin have been included in IARC official publications: "Cancer Incidence in Five Continents" since 1981. As Tianjin Cancer Registry is one of the few internationally accredited cancer registries in China, the results have important implications.

MATERIALS AND METHODS

Data

Tianjin, the third largest city in China, has a population about 10 million, of which about 98 % belongs to the Han ethnic group. The Tianjin Cancer Registry was established in 1978 and became operational in 1981^[11-13]. While the registry covers the whole city, data from six urban districts, which include approximately 4-million people, have been computerized and evaluated here. A city by-law requires that all physicians are responsible for filling out a report form for each new diagnosis of cancer. Practically, the task of cancer reporting is delegated to the medical record unit at each hospital. Thus, cancer cases are normally reported when patients are discharged from or die in the hospital. Information collected on the cancer reporting card includes name, sex, current age or date of birth, address, reporting hospital or medical institute, date (month and year) of diagnosis, four digit ICD-9 codes, and occupation. The Centre for Disease Control in Tianjin performs an annual quality control examination in at least 20 randomly selected hospitals in Tianjin to ensure that each hospital meets the standard cancer case reporting protocol. The evaluation results are used as part of the overall hospital report card, which is further used for hospital excellence ranking. A monetary incentive is offered for each cancer case reported, which is normally paid to the medical record unit rather than to individual physicians. Patients from other parts of China or those without permanent residence in Tianjin are not reflected in the current registry data.

All death certificates, which are the second source of cancer registration, are registered both at the district public health unit (DPHU) and the local police station. The DPHU routinely reviews all death certificates and identifies deaths, which are directly or indirectly caused by cancers. All cancer cases identified through death certificates are checked against the existing database at the Tianjin Cancer Institute for possible double or multiple reporting. In this study, we included all primary liver cancer patients (ICD-9 codes 155.1, 155.2). Numbers in each age-sex specific population for the six urban districts were obtained from the Tianjin Police Head Office,

which enumerates the Tianjin urban population based on people's unique resident cards.

Analyses

Univariate and bivariate descriptive analyses were performed prior to multivariate analyses. Proportional hazards regression (Cox model)^[14-20] was used to examine the effects of various factors on survival time for the study population. The proportional hazards model can be expressed as:

$$h(t; X) = h_0(t) \exp(\mathbf{b}' X)$$

where $h(t; X)$ is the hazard function of T at time t given a regression vector X; h_0 is the unspecified baseline hazard function. The SAS PROC PHREG procedure was used to examine the specified survival model. The time variable (in days) was defined as the interval between the date of diagnosis and date of death. The covariates included in the survival analyses were age, sex, occupation, year of diagnosis, and residence. To best capture the impact of age on survival time, we explored different ways to categorize it in our regression models. As the incidence rates of liver cancer are very low in children, in our final model, we used ages 0-19 years as one group (baseline) and 10-year intervals thereafter to get stable estimates for the regression coefficients. Treating age categories as dummy variables in the model did not result in a better goodness of fit than simply introducing age as an ordered categorical variable with one degree of freedom.

Residence was introduced as a binary variable. As Hexi district is generally regarded as the best neighbourhood in Tianjin, it was used as a reference group and coded as "0". Other districts were coded as "1" and compared to Hexi district. Self-reported occupations were collapsed into 4-broad mutually exclusive categories: professionals and managers (such as teachers, medical doctors), service industry workers (such as

salespeople), industry workers, and others. The professional and manager group was treated as the reference category. Year of diagnosis was treated as single year in Poisson regression and grouped into four categories in Cox regression analysis: 1981-1985 (reference category), 1986-1990, 1991-1995, and 1996-2000. Hospital of diagnosis was dichotomized to community/district hospitals (reference category) and city hospitals. Community hospitals normally provide walk-in service in their districts but do not provide surgical operations. District hospitals provide in-patient service and day-surgery operations in their districts. City general hospitals and speciality hospitals, which normally have advanced technology and research programs, provide a wide range of service to all Tianjin residents referred by community or district hospitals and sometimes patients from other parts of China.

RESULTS

In total, 13 685 cancer cases were identified during the study period (1981-2000) and 70.6 % occurred in males. The mean age at diagnosis for the study population was 62.2 years (61.3 and 64.3 years for males and females, respectively) with a median survival time of 151 days. As shown in Table 1, diagnosis based on death certificate only (DCO) was less than 1 %. Most cancer cases were reported from city (75.1 %) or district hospitals (15.5 %) and most cases were diagnosed based on either medical imaging (60.6 %) or histology (28.4 %). While there are few gender differences with respect to the age at diagnosis and types of hospitals of diagnosis, males were more likely than females to be administrators or professionals.

The crude and age-adjusted incidence rates for the entire study period were 27.4/100 000 and 26.3/100 000 respectively for males. The corresponding rates were 11.5/100 000 and 10.4/100 000 for females.

Table 1 Characteristics of liver cancer cases diagnosed during 1981 to 2000, Tianjin, China

Variable	Category	Male		Female		Total	
		n	%	n	%	n	%
Sex	Male	-	-	-	-	9666	70.63
	Female	-	-	-	-	4019	29.37
Age	0-19	19	0.20	18	0.45	37	0.27
	20-29	64	0.66	24	0.60	88	0.64
	30-39	360	3.72	119	2.96	479	3.50
	40-49	1118	11.57	284	7.07	1402	10.24
	50-59	2443	25.27	728	18.11	3171	23.17
	60-69	3155	32.64	1395	34.71	4550	33.25
	70-79	2009	20.78	1129	28.09	3138	22.93
	80+	498	5.15	322	8.1	820	5.99
Type of diagnosis	Clinical only	981	10.15	473	11.77	1454	10.62
	Medical imaging only	5934	61.39	2353	58.55	8287	60.56
	Histology at local site	2710	28.04	1176	29.26	3886	28.40
	Surgical examination or autopsy	14	0.14	8	0.20	22	0.16
	Death certificate only	1	0.01	1	0.02	2	0.01
	Unknown	26	0.27	8	0.20	34	0.25
Occupation	Professionals and administrators	3193	33.03	390	9.7	3583	26.18
	Service industry workers	1220	12.62	334	8.31	1554	11.36
	Industry workers	3937	40.73	989	24.61	4926	36.00
	All others	1316	13.62	2306	57.38	3622	26.46
Type of reporting hospital	City general or specified hospitals	7306	75.58	2968	73.85	10274	75.07
	District general hospital	1495	15.47	624	15.53	2119	15.48
	Community hospital	865	8.95	427	10.62	1292	9.44

Table 2 displays the results from the proportional hazard regression analyses. Older age and female gender were associated with poor survival rates, with relative risks of 1.06 (95 % CI: 1.01, 1.11) and 1.08 (95 % CI: 1.05, 1.09) respectively. Hospital of diagnosis was a statistically significant predictor of survival time. Patients diagnosed in city hospitals tended to live longer than those diagnosed in district or community hospitals, with relative risk of death of 0.76 (95 % CI: 0.73, 0.79). The results showed that period of diagnosis was a statistically significant predictor of patients' survival time. Patients diagnosed in more recent years were likely to live longer than those diagnosed in earlier years with a relative risk of 0.85 (95 % CI: 0.83, 0.86) for every 5-year increment.

Table 2 Proportional hazards analyses of liver cancer diagnosed between 1981 and 2000 in Tianjin urban districts

Variable	Category	Relative risk	95 % CI
Sex	Male	1	
	Female	1.06	1.01, 1.11
Age	0-19	1	
	Every 10-years increase	1.08	1.05, 1.09
Period of diagnosis	1981-1985	1	
	Every 5-years increase	0.85	0.83, 0.86
Residence	Hexi District (advantaged)	1	
	Other districts	1.02	0.97, 1.08
Occupation	Administrators	1	
	Service industry workers	1.06	0.99, 1.13
	Industry workers	1.08	1.03, 1.13
	All others	0.97	0.91, .102
Hospital	District or community hospitals	1	
	City general or speciality hospitals	0.76	0.73, 0.79

DISCUSSION

In this study, we described the survival patterns for primary liver cancer in a Chinese urban population over the last 20 years. To the best of our knowledge, this was the first study of its kind ever reported from China. Given the inconsistencies in the literature regarding liver cancer incidence trends^[21-26] and survival patterns^[27-32], this study provides another piece of useful information for this disease. As Tianjin has a first-class cancer treatment centre and facilities, patients from other parts of China often seek treatment in Tianjin. It is relatively uncommon that Tianjin residents travel to other parts of China for treatment. There is no conceivable reason that this pattern had changed during the study period. Moreover, regardless of where a Tianjin patient gets treated, his/her cancer status would eventually be reflected in the death certificates, which are one source of our cancer registration data.

Based on clinical patients in Qidong, which has the highest liver cancer incidence rates in China, Chen *et al*^[31] reported that females had a more favourable prognosis than males. In this study, we found that females had slightly poor survival rate than males. As the magnitude of the reported survival difference was small, the results were unlikely to be conclusive. Nevertheless, the discrepancy between the two studies may be related to the differences in study population, such as, clinical setting versus population based or rural (Qidong) versus urban (Tianjin). The last four decades have seen a significant improvement in liver cancer treatment in China^[33]. While the current study only had a span of 20 years, the improvement in survival was apparent. The changes may be explained by improvements in liver cancer clinical management in this city. For example, unpublished data indicate the proportion of liver cancer patients who undergo surgery for their condition has

increased substantially in Tianjin.

This study has several limitations. First, we only included urban residents and were unable to compare the differences between rural and urban populations. Since China is a vast country with significant variations in economic conditions, the reported results may only be applicable to urban Chinese residents. Second, as the Tianjin Cancer Registry only records cancer related deaths (direct and indirect), it is possible that liver cancer patients who died from other causes, such as traffic accidents, were not reflected in our data bases. As a result, the observed survival time as reflected in the cancer registry data, might have been inflated. However, given that liver cancer is a fast progressive condition and a dominant majority of liver cancer patients die from it or its complications, it is unlikely that the problem related to non-liver cancer deaths would have altered the observed survival patterns greatly. Furthermore, since the possible artificially better survival caused by omission of non-liver cancer deaths would have been more in evidence for patients diagnosed in early periods, the true survival advantage for the patients diagnosed in recent years could be even greater. Third, we did not have information on cancer stage and treatment and were unable to estimate their impact on the observed survival pattern. It was possible that some of the observed survival advantage in later periods could be attributed to the cancer stage shift over time. Thus, studies on the changes in cancer stage and treatment over time are needed to address these questions.

ACKNOWLEDGEMENTS

Tianjin Cancer Registry is jointly funded by the Tianjin Health Bureau and the Tianjin Cancer Institute. All computations were prepared at Tianjin Cancer Institute and the responsibility for the use and interpretation of these data is entirely that of the authors. The authors thank the International Agency for Research on Cancer (IARC) for their technological support. We are grateful to Dr. Qi-Long Yi, University of Toronto, for his statistical advice.

REFERENCES

- 1 **Benhamiche AM**, Faivre C, Minello A, Clinard F, Mitry E, Hillon P, Faivre J. Time trends and age-period-cohort effects on the incidence of primary liver cancer in a well-defined French population: 1976-1995. *J Hepatol* 1998; **29**: 802-806
- 2 **Anderson IB**, Sorensen TI, Prener A. Increase in incidence of disease due to diagnostic drift: primary liver cancer in Denmark, 1943-85. *Bmj* 1991; **302**: 437-440
- 3 **Chiesa R**, Donato F, Portolani N, Favret M, Tomasoni V, Nardi G. Primary liver cancer in a high-incidence area in north Italy: etiological hypotheses arising from routinely collected data. *Eur J Epidemiol* 1995; **11**: 435-442
- 4 **El-Serag HB**, Mason AC. Rising incidence of hepatocellular carcinoma in the United States. *N Engl J Med* 1999; **340**: 745-750
- 5 **Kobayashi M**, Ikeda K, Saitoh S, Suzuki F, Tsubota A, Suzuki Y, Arase Y, Murashima N, Chayama K, Kumada H. Incidence of primary cholangiocellular carcinoma of the liver in Japanese patients with hepatitis C virus-related cirrhosis. *Cancer* 2000; **88**: 2471-2477
- 6 **Miyakawa Y**, Yoshizawa H. Increasing incidence of hepatocellular carcinoma associated with hepatitis C virus infection in Japan. *Indian J Gastroenterol* 2001; **20**: C95-96
- 7 **Parkin DM**, Srivatanakul P, Khlat M, Chenvidhya D, Chotiwan P, Insiripong S, L' Abbe KA, Wild CP. Liver cancer in Thailand. I. A case-control study of cholangiocarcinoma. *Int J Cancer* 1991; **48**: 323-328
- 8 **Srivatanakul P**, Parkin DM, Khlat M, Chenvidhya D, Chotiwan P, Insiripong S, L' Abbe KA, Wild CP. Liver cancer in Thailand. II. A case-control study of hepatocellular carcinoma. *Int J Cancer* 1991; **48**: 329-332
- 9 **Shea KA**, Fleming LE, Wilkinson JD, Wohler-Torres B, McKinnon

- JA. Hepatocellular carcinoma incidence in Florida. Ethnic and racial distribution. *Cancer* 2001; **91**: 1046-1051
- 10 **International Agency for Research on Cancer.** Cancer Incidence in Five Continents, Vol. VII. *Lyon, IARC* 1997
- 11 **Chen KX,** He M, Dong SF, Wang JF. Incidence, mortality and survival rates of female breast cancer in Tianjin, China. *Zhonghua Zhongliu Zazhi* 2002; **24**: 573-579
- 12 **Wang QS,** Lin XP. An approach to use cancer registration to assess cancer risks by occupation and industry. *Zhonghua Liuxing Bingxue Zazhi* 1997; **18**: 331-333
- 13 **Guo Z.** Mortality analysis of malignant neoplasms and cardiovascular diseases 1979-1983 in Tianjin. *Zhonghua Liuxing Bingxue Zazhi* 1985; **6**: 353-355
- 14 **Wang PP,** Haines CS. Childhood and adolescent leukaemia in a North American population. *Int J Epidemiol* 1995; **24**: 1100-1109
- 15 **Contal C,** Mallet A. Checking the Cox model in a real situation. *Rev Epidemiol Sante Publique* 2000; **48**: 490-501
- 16 **Fu JH,** Rong TH, Li XD, Ma GW, Hu Y, Min HQ. Cox regression analysis of the prognostic factors of unresectable esophageal carcinoma after stenting. *Ai Zheng* 2003; **22**: 91-94
- 17 **Averbook BJ,** Fu P, Rao JS, Mansour EG. A long-term analysis of 1018 patients with melanoma by classic Cox regression and tree-structured survival analysis at a major referral center: Implications on the future of cancer staging. *Surgery* 2002; **132**: 589-602; discussion 602-604
- 18 **Steinbach D,** Hermann J, Littlewood T, Zintl F. Risk group definition in children with acute myeloid leukemia by calculating individual risk factors on the basis of a multivariate stepwise Cox regression analysis. *Leuk Lymphoma* 2001; **42**: 1289-1295
- 19 **Boberg KM,** Rocca G, Egeland T, Bergquist A, Broome U, Caballeria L, Chapman R, Hultcrantz R, Mitchell S, Pares A, Rosina F, Schrupf E. Time-dependent Cox regression model is superior in prediction of prognosis in primary sclerosing cholangitis. *Hepatology* 2002; **35**: 652-657
- 20 **de Bruijne MH,** le Cessie S, Kluin-Nelemans HC, van Houwelingen HC. On the use of Cox regression in the presence of an irregularly observed time-dependent covariate. *Stat Med* 2001; **20**: 3817-3829
- 21 **Law MG,** Roberts SK, Dore GJ, Kaldor JM. Primary hepatocellular carcinoma in Australia, 1978-1997: increasing incidence and mortality. *Med J Aust* 2000; **173**: 403-405
- 22 **Saracci R,** Repetto F. Time trends of primary liver cancer: indication of increased incidence in selected cancer registry populations. *J Natl Cancer Inst* 1980; **65**: 241-247
- 23 **Yu MC,** Yuan JM, Govindarajan S, Ross RK. Epidemiology of hepatocellular carcinoma. *Can J Gastroenterol* 2000; **14**: 703-709
- 24 **Bosch FX,** Ribes J. Epidemiology of liver cancer in Europe. *Can J Gastroenterol* 2000; **14**: 621-630
- 25 **Bosch FX,** Ribes J, Borrás J. Epidemiology of primary liver cancer. *Semin Liver Dis* 1999; **19**: 271-285
- 26 **Taylor-Robinson SD,** Foster GR, Arora S, Hargreaves S, Thomas HC. Increase in primary liver cancer in the UK, 1979-94. *Lancet* 1997; **350**: 1142-1143
- 27 **Lee CL,** Ko YC. Survival and distribution pattern of childhood liver cancer in Taiwan. *Eur J Cancer* 1998; **34**: 2064-2067
- 28 **Tang ZY,** Yu YQ, Zhou XD, Chen QM. Factors influencing primary liver cancer resection survival rate. *Chin Med J (Engl)* 1981; **94**: 749-754
- 29 **Walker AR,** Walker BF, Serobe W, Paterson A, Isaacson C, Segal I. Survival of blacks with liver cancer in Soweto, Johannesburg, South Africa. *Trop Gastroenterol* 1986; **7**: 169-172
- 30 **Zhou X,** Tang Z, Yu Y. Changing prognosis of primary liver cancer: some aspects to improve long-term survival. *Zhonghua Zhongliu Zazhi* 1996; **18**: 211-213
- 31 **Chen J,** Sankaranarayanan R, Li W. Population-based survival analysis of primary liver cancer in a high-incidence area-Qidong, China during 1972-1991. *Zhonghua Yufang Yixue Zazhi* 1997; **31**: 149-152
- 32 **Faivre J,** Forman D, Esteve J, Obradovic M, Sant M. Survival of patients with primary liver cancer, pancreatic cancer and biliary tract cancer in Europe. *Eur J Cancer* 1998; **34**: 2184-2190
- 33 **Wu M.** Clinical advances in primary liver cancer in China. *Hepatogastroenterology* 2001; **48**: 29-32

Edited by Zhang JZ

Loss of fragile histidine triad protein in human hepatocellular carcinoma

Po Zhao, Xin Song, Yuan-Yuan Nin, Ya-Li Lu, Xiang-Hong Li

Po Zhao, Xin Song, Yuan-Yuan Nin, Ya-Li Lu, Xiang-Hong Li,
Department of Pathology, Chinese PLA General Hospital, Beijing 100853, China

Correspondence to: Dr. Po Zhao, Department of Pathology, Chinese PLA General Hospital, 28 Fuxing Road, Beijing 100853, Beijing China. zhaopo@plagh.com.cn

Telephone: +86-10-66937954

Received: 2002-12-22 **Accepted:** 2003-02-11

Abstract

AIM: To investigate the expression of fragile histidine triad (FHIT) gene protein, Fhit, which is recently thought to be a candidate tumor suppressor. Abnormal expression of fragile histidine triad has been found in a variety of human cancers, but little is known about its expression in human hepatocellular carcinogenesis and evolution.

METHODS: Sections of 83 primary human hepatocellular carcinoma with corresponding para-neoplastic liver tissue and 10 normal liver tissue were evaluated immunohistochemically for Fhit protein expression.

RESULTS: All normal liver tissue and para-neoplastic liver tissue showed a strong expression of Fhit, whereas 50 of 83 (65.0 %) carcinomas showed a marked loss or absence of Fhit expression. The differences of Fhit expression between carcinoma and normal or para-neoplastic liver tissue were highly significant ($P=0.000$). The proportion of carcinomas with reduced Fhit expression showed an increasing trend (a) with decreasing differentiation or higher histological grade ($P=0.219$); (b) in tumors with higher clinical stage III and IV (91.3 %, $P=0.000$), compared with tumors with lower stage I and II (27.6 %); and (c) in cancers with bigger tumor size (>50 mm) (75.0 %, $P=0.017$), compared with smaller tumor size (≤ 50 mm).

CONCLUSION: FHIT inactivation seems to be both an early and a later event, associated with carcinogenesis and progression to more aggressive hepatocellular carcinomas. Thus, evaluation of Fhit expression by immunohistochemistry in hepatocellular carcinoma may provide important diagnostic and prognostic information in clinical application.

Zhao P, Song X, Nin YY, Lu YL, Li XH. Loss of fragile histidine triad protein in human hepatocellular carcinoma. *World J Gastroenterol* 2003; 9(6): 1216-1219

<http://www.wjgnet.com/1007-9327/9/1216.asp>

INTRODUCTION

Fragile histidine triad gene (FHIT) has been cloned and mapped to chromosomal region 3p14.2^[1]. It spans the t(3:8) +(p14.2;q24) translocation breakpoint found in familial renal cell carcinoma and encompasses the most common human fragile site, FRA3B^[2,3]. Alterations of FHIT and its expression have been found in primary tumors and cell lines of the lung^[4,5],

breast^[6-8], head and neck^[9], esophageal^[10-12], stomach^[13-15], colon and rectum^[16-18], pancreas^[19], kidney^[20,21], cervix^[22-25], and hepatocellular carcinomas^[26-30]. Allelic deletion of FHIT and abnormal expression of FHIT protein (Fhit) in lung cancer are associated with smoking history and poor prognosis^[31,32]. The finding of decreased expression of Fhit in 93 % of precancerous lesions of the lung suggests that this gene may be used as a molecular marker for early diagnosis and prognosis of lung cancers^[32]. However, there are only a few reports that evaluated FHIT in hepatocellular carcinoma in a small number of cases so far^[30] and further investigation of Fhit protein expression during hepatocellular carcinogenesis is required. Liver cancer, like lung cancer, is thought to be induced by carcinogens such as major viral and environmental risk factors. Therefore, it is imperative to determine whether FHIT plays a role in the development of hepatocellular carcinoma which has been ranked the second in cancer mortality in China since 1990s and is increasing in the rate of its incidence among males in many countries. In this study, 10 normal liver tissues and 83 hepatocellular carcinomas with their corresponding para-neoplastic liver tissues were examined for Fhit expression by immunohistochemistry. It was found that the expression of Fhit was altered in a high proportion of hepatocellular carcinomas and the loss of Fhit expression was associated with more advanced stage of the tumor.

MATERIALS AND METHODS

Specimens

Paraffin embedded sections of 83 hepatocellular carcinomas with corresponding para-neoplastic tissues and 10 normal liver tissues as controls were obtained from the Department of Pathology, Chinese People's Liberation Army General Hospital. The patients included 71 men and 12 women with the mean age of 52 ± 9.67 years (range 10-76 years). Of these patients, 15 were at grade I, 39 at grade II and 29 at grade III according to histological grading; and 4 were at stage I, 33 at stage II, 46 at stage III and 4 at stage IV according to clinical staging of UICC. In terms of size, 44 tumors were bigger than and 39 were equal to or smaller than 50 mm in diameter.

Immunohistochemical determination of Fhit

All specimens were fixed in 10 % buffered formalin and embedded in paraffin. Paraffin blocks were sectioned into 4- μ m thickness and the sections were mounted onto APES-coated glass slides. The slides were deparaffinized in xylene twice for 10 minutes, rehydrated through graded ethanol to distilled water, incubated for 30 minutes with 3 % hydrogen peroxidase-methanol to inhibit endogenous peroxidase activity, and heated in 0.01M citrate buffer (pH 6.0) in a microwave oven for 5 minutes at 100 °C for antigen retrieval. After cooled down at room temperature for 30 minutes, the slides were blocked for 15 minutes in PBS containing 10 % normal goat serum, incubated at 4 °C overnight in a humidified chamber with rabbit polyclonal antibody to human Fhit (Zymed Laboratories Inc., South San Francisco, CA) at 1:200 dilution in blocking solution. The sections were then rinsed in PBS and incubated

for 30 minutes with biotinylated secondary antibody (Histostain-SP, Zymed), rinsed again in PBS and incubated for 30 minutes in streptavidin-HRP (Histostain-SP, Zymed). 3, 3'-Diaminobenzidine was used as the chromogen. Slides were counterstained for 3 minutes with hematoxylin solution. Normal liver tissue was used as the positive control for each lesion, whereas the primary antibody was replaced by normal rabbit serum IgG with a similar dilution or PBS for the negative control.

Evaluation of score

Both the extent and intensity of immunostaining were considered when scoring Fhit protein expression according to Hao *et al.*^[18]. The intensity of positive staining was scored as 0, negative; 1, weak; 2, moderate; 3, strong as in normal liver. The extent of positive staining was scored as 0, <5%; 1, >5-25%; 2, >25-50%; 3, >50-75%; 4, >75% of the hepatocytes in the respective lesions. The final score was determined by multiplying the intensity score and the extent score, yielding a range from 0 to 12. Scores 9-12 were defined as preserved or strong staining (++), 5-8 as weak staining (+) and 0-4 as markedly reduced or negative expression (-).

Statistical analysis

Fisher's exact test (two sided) and Pearson Chi square's test for trends in proportions were used to assess the associations between Fhit expression and pathological indices. A $P < 0.05$ was considered statistically significant.

RESULTS

Fhit expression in normal, para-neoplastic tissue and carcinoma

Fhit was strongly expressed in the cytoplasm of hepatocytes in all 10 normal liver and 83 para-neoplastic tissues (Figure 1A). Some stromal cells, such as lymphocytes, plasma cells and macrophages, also expressed Fhit in both nucleus and cytoplasm. The expression of Fhit was strong in 33, weak in 21 and negative in 29 hepatocellular carcinomas (Table 1). The carcinomas with markedly reduced or loss of Fhit expression were observed in 50 (65.2%) cases, whereas those with expression of Fhit equal to normal liver were observed in 33 (34.8%) cases. In cases with reduced expression of Fhit, both the extent and intensity of Fhit staining were reduced markedly (Figure 1B).

Table 1 Levels of Fhit expression in hepatocellular carcinomas, para-neoplastic tissues and normal liver tissues

	n	Fhit score		
		-	+	++
HCC	83	29	21	33
Para-neoplastic tissue ^b	83	0	0	83
Normal liver tissue ^b	10	0	0	10

^b $P=0.000$, vs hepatocellular carcinomas.

Relationship between Fhit expression and histological grade, clinical stage and tumor size

The percentage of carcinomas with reduced expression of Fhit increased from 46.7% (7 of 15) in well-differentiated cancers (grade I) to 53.8% (21 of 39) in moderately differentiated cancers (grade II) and to 75.8% (22 of 29) in poorly differentiated cancers (grade III), although this association of increased histological grade of tumors with decreased Fhit expression was not statistically significant ($P > 0.05$, Table 2). Nevertheless, the decrease in expression of Fhit was

significantly associated with more advanced clinical stage of the tumors. Whereas 21.6% (8 of 37) stage I and II cases showed reduced expression of Fhit, the percentage of stage III and IV cases with reduced expression of Fhit increased to 91.3% (42 of 46) ($P=0.000$, Table 2). In addition, the carcinomas with reduced expression of Fhit protein were found in 75% (33 of 44) of tumors greater than 50 mm in diameter, compared with 43.6% (17 of 39) of tumors 50 mm or smaller in diameter ($P=0.017$).

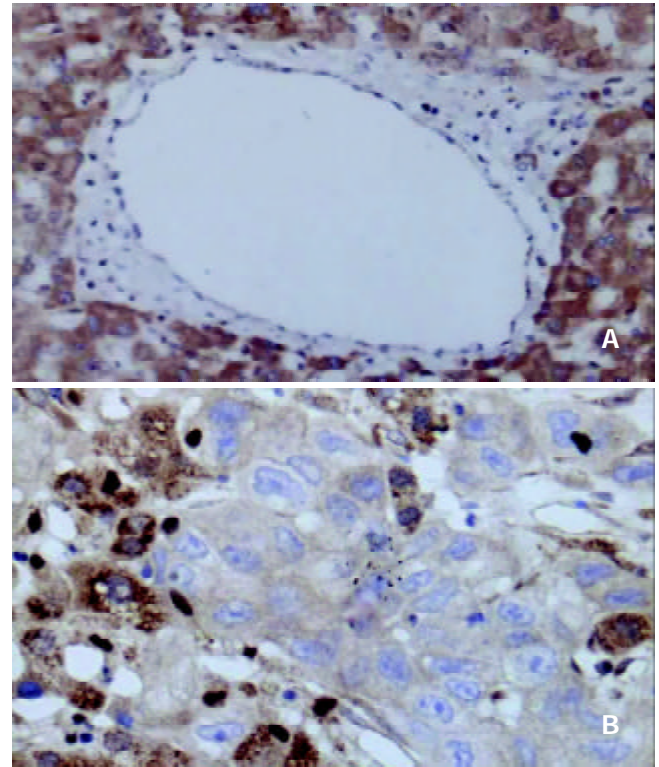


Figure 1 (A) Strong positive staining of Fhit in normal liver tissue SP $\times 100$ (B) Negative staining of Fhit in invading hepatocellular carcinoma (upper right) compared with strong positive staining of Fhit in para-neoplastic liver tissue (lower left) (SP $\times 400$).

Table 2 Relationship between Fhit expression and clinicopathological indice

	n	Fhit score		
		-	+	++
Histological grade				
Grade I	15	3	4	8
Grade II	39	12	9	18
Grade III	29	14	8	7
Clinical stage				
Stage I-II	37	4	4	29
Stage III-IV	46	25	17	4
Size (mm)				
≤ 50	39	10	7	22
> 50	44	19	14	11

DISCUSSION

Fhit protein is expressed in most types of normal human tissues but has been found to be frequently reduced or lost in a variety of human tumors due to alterations in its gene transcription or gene deletion^[1]. It has thus been suggested that FHIT gene is a candidate tumor suppressor gene for multiple carcinomas. Fhit,

the FHIT gene protein, is a member of histidine triad family and the mechanism of its suppression on tumor cells remains obscure^[1-3]. The following possible mechanisms have been considered as a tumor suppressor^[33]: First, the tumor-suppressing function of Fhit might be to catabolize ApppA (Ap₃A) or related substrates. Ap₃A is an analogue of ATP, which can provide phosphates as a substrate to raise the activity of protein kinase. Loss of Fhit protein may lead to the loss of Ap₃A hydrolase activity and the resulting elevated levels of Ap₃A or similar compounds may enhance the transductive signals of growth, thus contribute to carcinogenesis. Second, the activity of Fhit on mRNA cap analogs raises the possibility that failure of a decapping function might be tumorigenic, however, the properties of Fhit are quite different from those of enzymes known to decap mRNA, making this an unlikely mechanism. Third, the tumor-suppressing function of Fhit might be signaling by Fhit-substrate complexes or compounds as an active form of Fhit, which may be more important than its role of hydrolase. Fourth, Fhit might have a nucleotide-independent role as a tumor suppressor^[33].

Yuan *et al.*^[30] found that 4 of 9 cell lines and 5 of 10 primary hepatocellular carcinomas did not express Fhit protein or only expressed reduced levels of Fhit. Consistent with their results, we found that 50 of 83 (65.2 %) primary hepatocellular carcinomas showed markedly reduced or loss of expression of Fhit, suggesting that loss of Fhit protein might be related to the carcinogenesis of hepatocytes. Furthermore, decreasing expression of Fhit protein with higher histological grading, and more significantly with advanced clinical stages (stage III and IV) of primary tumors and bigger tumor size (>50 mm in diameter) suggests that loss of Fhit expression is strongly associated with the development and progression of hepatocellular carcinoma. Similar association between loss of FHIT function and the stage, grade and poor prognosis of tumors has been noted in lung cancer^[4-5], colorectal carcinoma^[18] and advanced breast cancer^[8].

In summary, expression of Fhit is reduced or lost in a significant proportion of hepatocellular carcinomas and especially in more advanced stages of primary tumors. Thus, detection of Fhit protein expression by immunohistochemistry in hepatocellular lesions may provide important diagnostic and prognostic information in practical clinical application.

REFERENCES

- 1 **Croce CM**, Sozzi G, Huebner K. Role of FHIT in human cancer. *J Clin Oncol* 1999; **17**: 1618-1624
- 2 **Huebner K**, Druck T, Siprashvili Z, Croce CM, Kovatich A, McCue PA. The role of deletions at the FRA3B/FHIT locus in carcinogenesis. *Recent Results Cancer Res* 1998; **154**: 200-215
- 3 **Druck T**, Berk L, Huebner K. FHITness and cancer. *Oncol Res* 1998; **10**: 341-345
- 4 **Fong KM**, Biesterveld EJ, Virmani A, Wistuba I, Sekido Y, Bader SA, Ahmadian M, Ong ST, Rassoool FV, Zimmerman PV, Giaccone G, Gazdar AF, Minna JD. FHIT and FRA3B 3p14.2 allele loss are common in lung cancer and preneoplastic bronchial lesions and are associated with cancer-related FHIT cDNA splicing aberrations. *Cancer Res* 1997; **57**: 2256-2267
- 5 **Sozzi G**, Tornielli S, Tagliabue E, Sard L, Pezzella F, Pastorino U, Minoletti F, Pilotti S, Ratcliffe C, Veronese ML, Goldstraw P, Huebner K, Croce CM, Pierotti MA. Absence of Fhit protein in primary lung tumors and cell lines with FHIT gene abnormalities. *Cancer Res* 1997; **57**: 5207-5212
- 6 **Negrini M**, Monaco C, Vorechovsky I, Ohta M, Druck T, Baffa R, Huebner K, Croce CM. The FHIT gene at 3p14.2 is abnormal in breast carcinomas. *Cancer Res* 1996; **56**: 3173-3179
- 7 **Bieche I**, Latil A, Becette V, Lidereau R. Study of FHIT transcripts in normal and malignant breast tissue. *Genes Chromosomes Cancer* 1998; **23**: 292-299
- 8 **Campiglio M**, Pekarsky Y, Menard S, Tagliabue E, Pilotti S, Croce CM. FHIT loss of function in human primary breast cancer correlates with advanced stage of the disease. *Cancer Res* 1999; **59**: 3866-3869
- 9 **Virgilio L**, Shuster M, Gollin SM, Veronese ML, Ohta M, Huebner K, Croce CM. FHIT gene alterations in head and neck squamous cell carcinomas. *Proc Natl Acad Sci U S A* 1996; **93**: 9770-9775
- 10 **Zou TT**, Lei J, Shi YQ, Yin J, Wang S, Souza RF, Kong D, Shimada Y, Smolinski KN, Greenwald BD, Abraham JM, Harpaz N, Meltzer SJ. FHIT gene alterations in esophageal cancer and ulcerative colitis (UC). *Oncogene* 1997; **15**: 101-105
- 11 **Michael D**, Beer DG, Wilke CW, Miller DE, Glover TW. Frequent deletions of FHIT and FRA3B in Barrett's metaplasia and esophageal adenocarcinomas. *Oncogene* 1997; **15**: 1653-1659
- 12 **Menin C**, Santacatterina M, Zamboni A, Montagna M, Parenti A, Ruol A, D'Andrea E. Anomalous transcripts and allelic deletions of the FHIT gene in human esophageal cancer. *Cancer Genet Cytogenet* 2000; **119**: 56-61
- 13 **Tamura G**, Sakata K, Nishizuka S, Maesawa C, Suzuki Y, Iwaya T, Terashima M, Saito K, Satodate R. Analysis of the fragile histidine triad gene in primary gastric carcinomas and gastric carcinoma cell lines. *Genes Chromosomes Cancer* 1997; **20**: 98-102
- 14 **Baffa R**, Veronese ML, Santoro R, Mandes B, Palazzo JP, Rugge M, Santoro E, Croce CM, Huebner K. Loss of FHIT expression in gastric carcinoma. *Cancer Res* 1998; **58**: 4708-4714
- 15 **Lee SH**, Kim WH, Kim HK, Woo KM, Nam HS, Kim HS, Kim JG, Cho MH. Altered expression of the fragile histidine triad gene in primary gastric adenocarcinomas. *Biochem Biophys Res Commun* 2001; **284**: 850-855
- 16 **Ohta M**, Inoue H, Cotticelli MG, Kastury K, Baffa R, Palazzo J, Siprashvili Z, Mori M, McCue P, Druck T. The FHIT gene, spanning the chromosome 3p14.2 fragile site and renal carcinoma-associated t (3;8) breakpoint, is abnormal in digestive tract cancers. *Cell* 1996; **84**: 587-597
- 17 **Thiagalasingam S**, Lisitsyn NA, Hamaguchi M, Wigler MH, Willson JK, Markowitz SD, Leach FS, Kinzler KW, Vogelstein B. Evaluation of the FHIT gene in colorectal cancers. *Cancer Res* 1996; **56**: 2936-2939
- 18 **Hao XP**, Willis JE, Pretlow TG, Rao JS, MacLennan GT, Talbot IC, Pretlow TP. Loss of fragile histidine triad expression in colorectal carcinomas and premalignant lesions. *Cancer Res* 2000; **60**: 18-21
- 19 **Sorio C**, Baron A, Orlandini S, Zamboni G, Pederzoli P, Huebner K, Scarpa A. The FHIT gene is expressed in pancreatic ductular cells and is altered in pancreatic cancers. *Cancer Res* 1999; **59**: 1308-1314
- 20 **Hadaczek P**, Siprashvili Z, Markiewski M, Domagala W, Druck T, McCue PA, Pekarsky Y, Ohta M, Huebner K, Lubinski J. Absence or reduction of Fhit expression in most clear cell renal carcinomas. *Cancer Res* 1998; **58**: 2946-2951
- 21 **Werner NS**, Siprashvili Z, Fong LY, Marquitan G, Schroder JK, Bardenheuer W, Seeber S, Huebner K, Schutte J, Opalka B. Differential susceptibility of renal carcinoma cell lines to tumor suppression by exogenous Fhit expression. *Cancer Res* 2000; **60**: 2780-2785
- 22 **Greenspan DL**, Connolly DC, Wu R, Lei RY, Vogelstein JT, Kim YT, Mok JE, Munoz N, Bosch FX, Shah K, Cho KR. Loss of FHIT expression in cervical carcinoma cell lines and primary tumors. *Cancer Res* 1997; **57**: 4692-4698
- 23 **Yoshino K**, Enomoto T, Nakamura T, Nakashima R, Wada H, Saitoh J, Noda K, Murata Y. Aberrant FHIT transcripts in squamous cell carcinoma of the uterine cervix. *Int J Cancer* 1998; **76**: 176-181
- 24 **Birrer MJ**, Hendricks D, Farley J, Sundborg MJ, Bonome T, Walts MJ, Geradts J. Abnormal Fhit expression in malignant and premalignant lesions of the cervix. *Cancer Res* 1999; **59**: 5270-5274
- 25 **Wu R**, Connolly DC, Dunn RL, Cho KR. Restored expression of fragile histidine triad protein and tumorigenicity of cervical carcinoma cells. *J Natl Cancer Inst* 2000; **92**: 338-344
- 26 **Chen YJ**, Chen PH, Chang JG. Aberrant FHIT transcripts in hepatocellular carcinomas. *Br J Cancer* 1998; **77**: 417-420
- 27 **Schlott T**, Ahrens K, Ruschenburg I, Reimer S, Hartmann H, Droese M. Different gene expression of MDM2, GAGE-1, -2 and FHIT in hepatocellular carcinoma and focal nodular hyperplasia. *Br J Cancer* 1999; **80**: 73-78
- 28 **Keck CL**, Zimonjic DB, Yuan BZ, Thorgeirsson SS, Popescu NC.

- Nonrandom breakpoints of unbalanced chromosome translocations in human hepatocellular carcinoma cell lines. *Cancer Genet Cytogenet* 1999; **111**: 37-44
- 29 **Gramantieri L**, Chieco P, Di Tomaso M, Masi L, Piscaglia F, Brillanti S, Gaiani S, Valgimigli M, Mazziotti A, Bolondi L. Aberrant fragile histidine triad gene transcripts in primary hepatocellular carcinoma and liver cirrhosis. *Clin Cancer Res* 1999; **5**: 3468-3475
- 30 **Yuan BZ**, Keck-Waggoner C, Zimonjic DB, Thorgeirsson SS, Popescu NC. Alterations of the FHIT gene in human hepatocellular carcinoma. *Cancer Res* 2000; **60**: 1049-1053
- 31 **Burke L**, Khan MA, Freedman AN, Gemma A, Rusin M, Guinee DG, Bennett WP, Caporaso NE, Fleming MV, Travis WD, Colby TV, Trastek V, Pairolero PC, Tazelaar HD, Midthun DE, Liotta LA, Harris CC. Allelic deletion analysis of the FHIT gene predicts poor survival in non-small cell lung cancer. *Cancer Res* 1998; **58**: 2533-2536
- 32 **Sozzi G**, Pastorino U, Moiraghi L, Tagliabue E, Pezzella F, Ghirelli C, Tornielli S, Sard L, Huebner K, Pierotti MA, Croce CM, Pilotti S. Loss of FHIT function in lung cancer and preinvasive bronchial lesions. *Cancer Res* 1998; **58**: 5032-5037
- 33 **Pace HC**, Garrison PN, Robinson AK, Barnes LD, Draganescu A, Rosler A, Blackburn GM, Siprashvili Z, Croce CM, Huebner K, Brenner C. Genetic, biochemical, and crystallographic characterization of Fhit-substrate complexes as the active signaling form of Fhit. *Proc Natl Acad Sci U S A* 1998; **95**: 5484-5489

Edited by Liu HX

PPAR γ pathway activation results in apoptosis and COX-2 inhibition in HepG2 cells

Ming-Yi Li, Hua Deng, Jia-Ming Zhao, Dong Dai, Xiao-Yu Tan

Ming-Yi Li, Dong Dai, Xiao-Yu Tan, Department of General Surgery, Affiliated Hospital of Guangdong Medical College, Zhanjiang 524001, Guangdong Province, China

Hua Deng, Department of Biochemistry & Molecular Biology, Beijing Institute for Cancer Research, Da Hong-Luo Chang Street, Beijing 100034, China

Jia-Ming Zhao, Central Laboratory, Affiliated Hospital of Guangdong Medical College, Zhanjiang 524001, Guangdong Province, China

Correspondence to: Ming-Yi Li, Department of General Surgery, Affiliated Hospital of Guangdong Medical College, Zhanjiang 524001, Guangdong Province, China. zjmyli@sohu.com

Telephone: +86-759-2387613

Received: 2002-11-06 **Accepted:** 2003-01-28

Abstract

AIM: To investigate whether troglitazone (TGZ), the peroxisome proliferator-activated receptor (PPAR) gamma ligand, can induce apoptosis and inhibit cell proliferation in human liver cancer cell line HepG2 and to explore the molecular mechanisms.

METHODS: [3-(4,5)-dimethylthiazol-2-yl]-2,5-diphenyl tetrazolium bromide (MTT), [³H] Thymidine incorporation, Hoechst33258 staining, DNA ladder, enzyme-linked immunosorbent assay (ELISA), RT-PCR, Northern and Western blotting analyses were employed to investigate the effect of TGZ on HepG2 cells and related molecular mechanisms.

RESULTS: TGZ was found to inhibit the growth of HepG2 cells and to induce apoptosis. During the process, the expression of COX-2 mRNA and protein and Bcl-2 protein was down-regulated, while that of Bax and Bak proteins was up-regulated, and the activity of caspase-3 was elevated. Furthermore, the level of PGE₂ was decreased transiently after 12 h of treatment with 30 μ M troglitazone.

CONCLUSION: TGZ inhibits cell proliferation and induces apoptosis in HepG2 cells, which may be associated with the activation of caspase-3-like proteases, down-regulation of the expression of COX-2 mRNA and protein, Bcl-2 protein, the elevation of PGE₂ levels, and up-regulation of the expressions of Bax and Bak proteins,

Li MY, Deng H, Zhao JM, Dai D, Tan XY. PPAR γ pathway activation results in apoptosis and COX-2 inhibition in HepG2 cells. *World J Gastroenterol* 2003; 9(6): 1220-1226

<http://www.wjgnet.com/1007-9327/9/1220.asp>

INTRODUCTION

Peroxisome proliferator-activated receptors (PPARs) are transcription factors belonging to the nuclear receptor gene family. PPARs bind to specific response elements as heterodimers with the retinoid X receptor and activate

transcription in response to a variety of endogenous and exogenous ligands, including some polyunsaturated fatty acids, arachidonic acid metabolites, and some anti-diabetic drugs and non-steroidal anti-inflammatory drugs^[1-6]. Recently, PPARs subfamily has been defined as PPAR α , PPAR β and PPAR γ . Three PPAR isoforms differ in their tissue distribution and ligand specificity. PPAR α is predominantly expressed in tissues exhibiting high catabolic rate of fatty acids, whereas PPAR β expression is ubiquitous, and its physiological role is not clear. PPAR γ is expressed predominantly in adipose tissue, the adrenal gland, spleen, large colon and the immune system. Several lines of evidence indicate that PPAR γ plays an important role in regulating adipocyte differentiation and glucose homeostasis. Both PPAR α and PPAR γ have been shown to be involved in anti-inflammatory reactions mediated by arachidonic acid metabolites. PPAR α binds to, and is activated by leukotriene B₄, and its level is regulated at the transcriptional level by anti-inflammatory glucocorticoids^[7-15]. PPAR γ is activated by prostaglandin D₂ metabolite 15-deoxy- $\Delta^{12,14}$ prostaglandin J₂ (15 d-PGJ₂) and synthetic anti-diabetic thiazolidinedione drugs, resulting in down-regulation of the expression of pro-inflammatory genes and inhibition of tumor cell growth^[16,17].

Cyclooxygenase (COX) is a rate-limiting enzyme, catalyzing the initial step in biosynthesis of prostaglandins (PGs) from arachidonic acid^[18,19]. COX is encoded by two separate genes, COX-1 and COX-2, both of which participate in formation of a variety of eicosanoids including PGD₂, PGE₂, PGI₂, PGF_{2 α} , and thromboxane A. COX-1 is expressed constitutionally in most tissues and has been proposed to be a house-keeping gene, which is involved in cytoprotection of gastric mucosa, vasodilation in kidney, and control of platelet aggregation. In contrast, COX-2 is an inducible immediate-early gene that is upregulated by various stimuli including mitogens, cytokines, growth factors, and tumor promoters. Previous studies have demonstrated that COX-2 expression is aberrantly increased in (various) human epithelial cancers in colorectum, esophagus, stomach, lung, and bladder^[20-39]. These findings suggest that up-regulation of COX-2 may be a common mechanism in epithelial carcinogenesis. Recently, PPAR γ ligands was found to suppress COX-2 expression in fetal hepatocytes^[40] and in macrophage-like differentiated U937 cells^[41]. However, other authors reported that 15d-PGJ₂ induced the expression of COX-2 in immortalized epithelial^[42] and colorectal cancer cells^[43]. The mechanisms for the different regulation of COX-2 expression by PPAR γ ligands remain to be elucidated. In the present study, we wanted to investigate the effect of PPAR γ activation on cell growth and apoptosis, and to investigate underlying mechanism in regard to the expression of COX-2 and Bcl-2 members in HepG2 cells.

MATERIALS AND METHODS

Cell culture

Human liver cancer cell line HepG2 was provided by the American Type Culture Collection. Cells were grown in RPMI-1640 medium supplemented with 15 % new born bovine serum, penicillin G (100 kU · L⁻¹) and kanamycin (0.1g/L) at 37 °C in

the 5 % CO₂ incubator. Cells were grown on 96-well plates for MTT assay, [³H] thymidine incorporation and DNA fragmentation enzyme-linked immunosorbent assay (ELISA). For the experiment, cells were grown in fresh serum-free medium, incubated for 6 hours, and treated with experimental reagents.

MTT cell viability assay

Cell growth was assessed by a modified MTT assay. About 2×10⁵ cells/well were plated in 96-well microtiter plates and incubated overnight. Cells were then treated with troglitazone for 48 h in various concentrations. Then 10 μ l stock MTT (0.5 g/L) was added to each well, and the cells were further incubated at 37 °C for 4 h. After supernatant was removed, 100 μ l of 0.04 M HCl in isopropanol was added to each well to solubilize the formazan products. The absorbance at the wavelength of 570 nm was measured by a micro-ELISA reader. The negative control well contained medium only. The ratios of the absorbance of treated cells relative to those of the control wells were calculated and expressed as percentage of growth inhibition.

[³H] thymidine incorporation

Cells were planted in 96-well plates and grown for 24 h after being starved by growing in the serum-free medium for 48 h. Then, they were treated with troglitazone for 48 h and labeled with 5 μ Ci of [³H] thymidine for 4 h. Radioactivity was detected using a Beckman L5 counter, after the reaction was washed and stopped with 5 % trichloro acetic acid and the cells solubilized in 0.5 % of 0.25 N sodium hydroxide. Each experiment was done in quadruplicates and repeated at least three times.

Hoechst 33258 staining

Cells were fixed with 4 % formaldehyde in phosphate-buffered saline (PBS) for 10 min, stained by Hoechst 33258 (10 mg/L) for 1 hour, and subjected to fluorescence microscopy. After treatment with troglitazone, morphologic changes, including reduction in cell size and nuclear chromatin condensation, were observed.

DNA ladder demonstration

After induction of apoptosis, cells (7×10⁶/sample, both attached and detached cells) were lysed with 150 μ l hypotonic lysis buffer (edetic acid 10 mM, 0.5 % Triton X-100, Tris-HCl, pH7.4) for 15 min on ice and were precipitated with 2.5 % polyethylene glycol and 1 M NaCl for 15 min at 4 °C. After centrifugation at 16 000×g for 10 min at room temperature, the supernatant was treated with proteinase K (0.3 g/L) at 37 °C for 1 h and precipitated with isopropanol at -20 °C. After centrifugation, each pellet was dissolved in 10 μ l of Tris-EDTA (pH 7.6) and electrophoresed on a 1.5 % agarose gel containing ethidium bromide. DNA ladder pattern was identified under ultraviolet light.

Detection of DNA fragmentation

HepG2 cells were grown in 96-well plates. The cells were incubated with various dose of troglitazone for 48 h. DNA fragmentation was detected using an enzyme-linked immunosorbent assay (ELISA) kit (Roche). This assay was based on a quantitative sandwich enzyme-immunoassay directed against cytoplasmic histone-associated DNA fragments. Briefly, the cells were incubated in 200 μ l of lysis buffer. After centrifugation, 20 μ l of the supernatant was reacted overnight at 4 °C in streptavidin-coated wells with 80 μ l of biotinylated anti-histone antibody and peroxidase-conjugated anti-DNA antibody. After washing, the immunocomplex-bound peroxidase

was probed with 2,2'-azino-di[3-ethylbenzthiazoline sulfonate] for spectrophotometric detection at 405 nm.

TUNEL reaction

TUNEL reaction was done using apoptosis detection system (Cayman). Cells were fixed overnight at 4 °C with 4 % paraformaldehyde in PBS. The samples were washed three times with PBS and permeabilized by 0.2 % Triton X-100 in PBS for 15 min on ice. After washed twice, cells were equilibrated at room temperature for 15 to 30 min in equilibration buffer (potassium cacodylate 200 mM, dithiothreitol 0.2 mM, bovine serum albumin 0.25 g/L, and cobalt chloride 2.5 mM in 25 mM Tris-HCl, pH 6.6), and then incubated in a solution containing 5 μ M fluorescein-12-dUTP, 10 μ M dATP, 100 μ M edetic acid, and terminal deoxynucleotidyl transferase at 37 °C for 1.5 h in a dark chamber. The tailing reaction was terminated by 2×standard saline citrate (SSC). The samples were washed three times with PBS and analyzed by fluorescence microscopy. At least 1000 cells were counted, and the percentage of TUNEL-positive cells was determined.

RNA isolation and northern blotting

After incubation with different doses of troglitazone for 6 h, cells were washed with RPMI. Total RNA was extracted from adherent cells using Rneasy Mini kits (Sigma) as described previously^[37]. 30 mg of total RNA from each sample was separated on agarose/formaldehyde gels and transferred to nylon membranes. The membrane was hybridized with probes for COX-2 and for GAPDH as a reference.

RT-PCR for COX-2

Total RNA was extracted from cells using TRIzolTM (Sigma). COX-2 and beta-actin mRNA were detected by polymerase-chain-reaction following reverse transcription- (RT-PCR) as described^[37]. Primers for beta-actin were: sense 5' -ATCTGGCACCACCTTCTACAATGAGCTGCG-3', antisense 5' -CGTCATACTCCTGCTTGCTGATCCACATCTGC-3'.

Western blotting analysis

The cells were lysed in a lysis buffer (hepes 25 mM, Triton X-100 1.5 %, sodium deoxycholate 1 %, SDS 0.1 %, NaCl 0.5 M, edetic acid 5 mM, NaF 50 mM, sodium vanadate 0.1 mM, phenylmethylsulfonyl fluoride (PMSF) 1 mM and leupeptin 0.1 g/L, pH7.8) at 4 °C with sonication. The lysates were centrifuged at 15 000 g for 15 min and the concentration of the protein in each lysate was determined with Coomassie brilliant blue G-250. Loading buffer (42 mM Tris-HCl, containing 10 % glycerol, 2.3 % SDS, 5 % 2-mercaptoethanol and 0.002 % bromophenol blue) was then added to each lysate, which was subsequently boiled for 3 min and then electrophoresed on a SDS-polyacrylamide gel. Proteins were transferred onto a nitrocellulose filter and incubated separately with the antibodies against Bcl-2, Bax, Bak, Bcl-x_L and COX-2, and then labeled with peroxidase-conjugated secondary antibodies. The reactions were visualized using the enhanced chemiluminescence reagent (Sigma). The results were approved by repeating the reactions 2 times.

Evaluation of PGE2 production

To determine the levels of PGE2, HepG2 cells were treated with different concentrations of troglitazone for 24 h. The quantity of PGE2 in supernatants was immediately determined with the PGE2 Enzyme Immunoassay kit (Caymen Chemical) according to the manufacturer's instructions. Data were recorded using a Dynatech MR50000 microplate reader and normalized to micrograms of protein.

Assessment of caspase-3 activity

Caspase-3 activity was evaluated using a caspase assay kit following instructions of the manufacturer. In brief, caspase-3 fluorogenic substrate (Ac-DEVD-AMC or Ac-IETD-AMC) was incubated with JTE522-treated cell for 1 h at 37 °C, then AMC released from Ac-DEVD-AMC or Ac-IETD-AMC was detected using a fluorometric plate reader with an excitation wavelength of 380nm and an emission wavelength of 420-460nm.

Statistical analysis

Data were presented as the mean \pm standard error, unless otherwise indicated. Multiple comparisons were examined for significant differences using analysis of variance, followed by individual comparisons with the Bonferroni post-test. Comparisons between two groups were made with the Student *t* test. $P < 0.05$ was considered significant.

RESULTS

Effects of PPAR γ activation on cell proliferation and cell viability

HepG2 cells were incubated with various doses of troglitazone for 48 h. MTT assay showed that troglitazone significantly inhibited cell viability. The inhibition was dependent on dose of troglitazone administered (Figure 1A). Application of troglitazone also resulted in a reduction of [³H] thymidine uptake in a dose-dependent manner (Figure 1B).

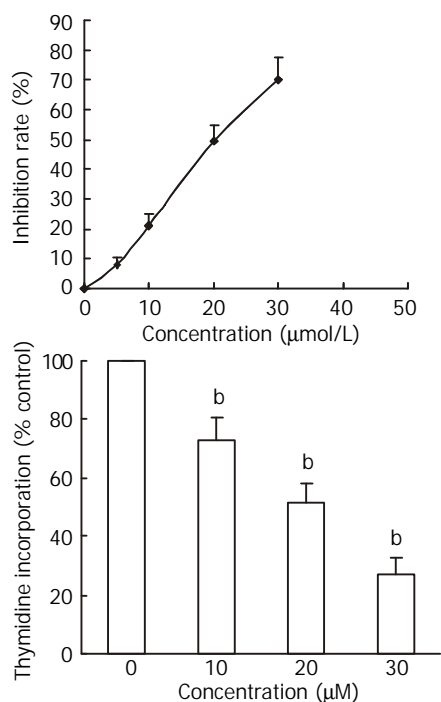


Figure 1 Effect of TGZ on growth of HepG2 cells. HepG2 cells were incubated with various concentrations of TGZ for 48 h: (A) MTT assay; (B) [³H] thymidine uptake assay. The value was represented as mean \pm SEM ($n=3$). ^b $P < 0.01$ versus corresponding control group.

Influence of PPAR γ activation on apoptosis

Effect of PPAR γ activation on apoptosis was assessed by staining with Hoechst 33258, TUNEL reaction, DNA fragmentation demonstration on an agarose gel and by ELISA. The initiating effect of PPAR γ activation on apoptosis was confirmed in HepG2 cell, the morphologic changes included reduction in cell size and nuclear chromatin condensation visualized by Hoechst 33258 staining. The apoptotic index was also increased by treatment with different concentration of troglitazone from

3.2 \pm 1.2 % to 53 \pm 2.6 %. Agarose gel electrophoresis showed DNA ladder pattern in the exposed HepG2 cells (Figure 2). The PPAR γ pathway-induced apoptosis was further demonstrated in quantitative measurement of cytoplasmic histone-associated DNA fragment by ELISA. As shown in Figure 3, troglitazone induced significant increase in DNA fragmentation in a dose-dependent manner.

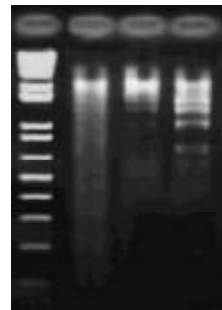


Figure 2 DNA ladder pattern formation in HepG2 cells after treatment with TGZ. Cells were treated with TGZ for 48 h and the formation of oligonucleosomal fragments was determined by 1.5 % agarose gel electrophoresis: M) DNA markers; 1) control; 2) 10 μ M TGZ; 3) 30 μ M TGZ.

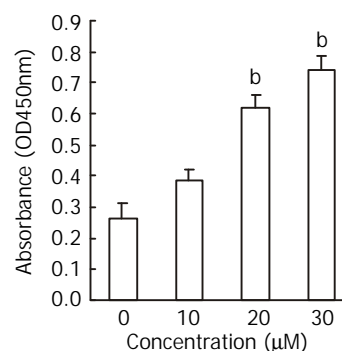


Figure 3 DNA fragmentation by ELISA assay, as measured by absorbance (OD 450 values). HepG2 cells cultured for 48 h in the presence of TGZ resulted in dose dependent DNA fragmentation. ^a $P < 0.05$, ^b $P < 0.01$ compared to respective control.

Down-regulation of COX-2 associated with the PPAR γ activation

The fact that the COX-2 promoter contains a PPRE indicates that COX-2 might be one of the downstream targets of the PPAR γ pathway. In the present study, COX-2 expression was observed in HepG2 cells treated with vehicle or 30 μ M troglitazone. After 6, 12, 24 and 48 h of the treatment, cells were harvested. COX-2 mRNA was analysed by RT-PCR (4A) and Northern blotting (4B), and its translation product was demonstrated by Western blotting (4C). As shown in Figure 4, no significant change was detected during the first 6 h of treatment when compared with the control. After treatment with 30 μ M troglitazone for 12 h, the expression of COX-2 was inhibited.

Effects of PPAR γ activation on expression levels of Bcl-2, Bcl-x_L, Bax and Bak

To further elucidate the mechanisms of troglitazone-induced apoptosis in HepG2 cells, we assessed the involvement of bcl-2 family proteins in the process by Western blotting. Expression of Bax protein was up-regulated 6 h after 20 μ M troglitazone treatment and remained elevated to 24 h. Expression level of Bak protein was also elevated 12 h after the treatment with 30 μ M troglitazone and declined at 48 h. On the contrary, Bcl-2

protein expression was down-regulated at 6 h and undetectable at 24 h. No significant change was observed in the expression of bcl-x_L protein (Figure 5).

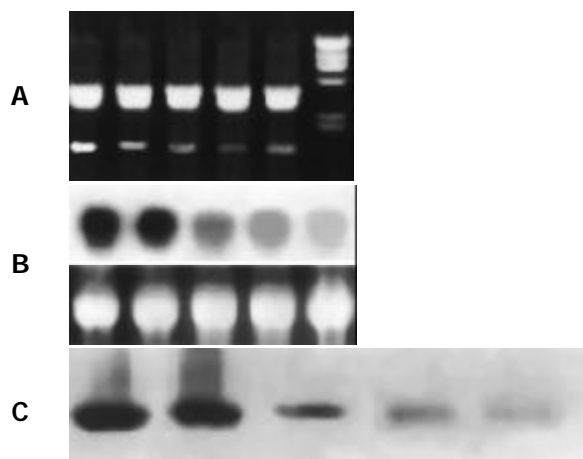


Figure 4 Effect of TGZ on the expression of COX-2 mRNA and protein in human liver cancer cell line HepG2 cells: (A) RT-PCR; (B) Northern blot; (C): Western blot.

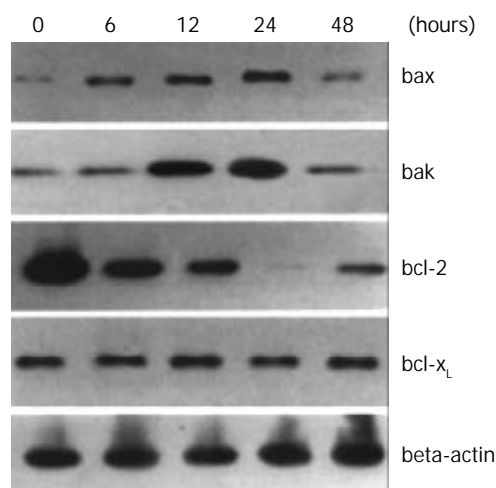


Figure 5 Effects of TGZ on the levels of bcl-2, bcl-x_L, bax and bak proteins in HepG2 cells at indicated time.

Effects of PPAR γ activation on PGE₂ production

The levels of PGE₂ in vehicle controls were always high throughout the culture. When HepG2 cells were treated with 30 μ M troglitazone, PGE₂ concentration decreased transiently at 12 h (Figure 6).

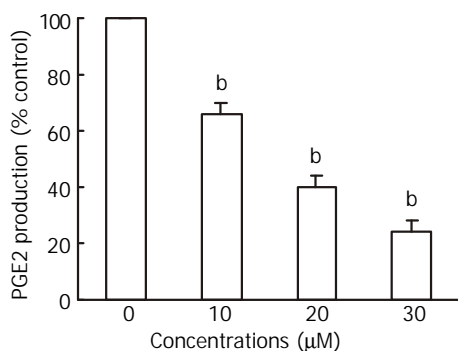


Figure 6 Effect of TGZ on the production of PGE₂. The value was represented as mean \pm SEM ($n=3$). ^b $P<0.01$ compared to respective control.

Change in caspase-3 activity associated with PPAR γ activation

In consideration of frequent involvement of caspases activation in apoptosis, caspase-3 activity was assessed in HepG2 cell, treated with 20 μ M troglitazone. As shown in Figure 7, the caspase-3 activity increased with the treatment, the reaction was time-dependent.

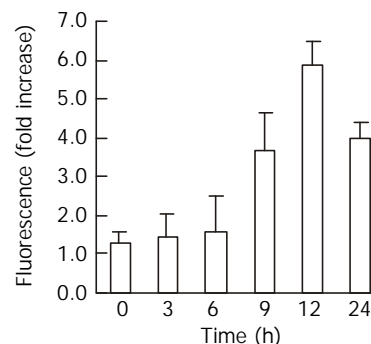


Figure 7 Effect of TGZ on the activity of caspase-3. The value was represented as mean \pm SEM ($n=3$).

DISCUSSION

Potent effects of PPAR γ on cell proliferation and cell cycling have been described. PPAR γ ligands can trigger cell cycle arrest in NIH3T3 cells and HIB-1B cells^[44]. PPAR γ ligands can also induce terminal differentiation and withdrawal of human liposarcoma cells from the cell cycle^[45]. Importantly, PPAR γ ligands have been found to slow down the progression of advanced liposarcoma in humans^[46]. Given the expression of PPAR γ in nonadipose tissues, the effect of PPAR γ on human breast cancer, gastric cancer, prostate cancer, colon cancer and transitional cell, bladder cancer have been explored. Treatment of cultured breast cancer cells with troglitazone results in cell growth arrest and promotes differentiation^[47]. Troglitazone has also been shown to inhibit tumor growth and induce apoptosis in human breast cancer cells *in vitro* and in BNX mice. Moreover, another PPAR γ ligand, GW7845, has been shown to decrease tumor incidence, tumor growth and tumor burden I, the NMU induced mammary carcinoma^[48]. These data suggest that PPAR γ ligands may be used as novel, nontoxic and selective chemotherapeutic agents for human breast cancers. In the present study, our results have shown that activation of PPAR γ by troglitazone inhibits cell growth and induces apoptosis in human liver cancer HepG2 cells. We confirmed that the induction of apoptosis was mediated through down-regulation of COX-2 and Bcl-2 expression, and up-regulation of Bax and Bak expression. The down-regulation of COX-2 was coincident with down-regulation of the production of PGE₂. The activity of Caspase-3 was increased after treatment with 30 μ M PPAR γ ligand troglitazone in a time-dependent manner.

Meade *et al.* have demonstrated that COX-2 expression is enhanced by peroxisome proliferators, including some fatty acids, PGs and NSAIDs, as well as the prototypical peroxisome proliferator WY-14, 643, in mammary and colonic epithelial cells, presumably through PPAR α ^[49]. Yang *et al.* showed that activation of PPAR pathway by ciglitazone induced apoptosis and inhibition of COX-2 expression in human colon cancer cells HT-29^[50], but the result was not approved in an observation by Lefebvre *et al.*^[51]. Our data showed that PPAR γ activation inhibited the expression of COX-2. The discrepancy may be caused by different cell types used in these groups.

Overexpression of COX-2 plays important roles in cell adhesion, apoptosis and angiogenesis. Numerous epidemiological studies suggest that use of nonsteroidal anti-inflammatory drugs

(NSAIDs) decreases the incidence of gastrointestinal cancers and COX-2 is recognized as a major target of NSAIDs^[52-64]. Inhibition of COX-2 by NSAIDs or COX-2 specific inhibitors causes cell death in cancer cells, indicating that COX-2 may be used as an important molecular target for prevention and therapy in gastrointestinal cancers^[65-70]. The mechanism of COX-2 expression remains unclear. Subbaramaiah and colleagues have shown that PPAR γ can inhibit COX-2 expression.

In the present study, the levels of PGE₂ were decreased in a time-dependent manner after the treatment with 30 μ M troglitazone, and were correlated with the change in COX-2 expression. This is in agreement with previous observations in other cell lines^[71-73]. Thus, excessively synthesized PGE₂ mediated by overexpression of COX-2 is believed to play an important role in neoplasia formation. Inhibition of COX-2 activity may at least partly explain the chemopreventative effect of activated PPAR pathway in human liver cancer.

Apoptosis is characterized by a series of distinct morphological and biochemical changes. Several apoptosis-related genes have been found. One group of apoptosis regulatory genes is the Bcl-2 family^[74-79]. Of these genes, Bcl-2, Bcl-x_L are antiapoptotic, whereas Bax, Bcl-x_s, Bak, Bad and Bik are proapoptotic. In this study, overexpression of Bax and Bak, and suppression of the expression of Bcl-2 were found during the apoptosis induced by PPAR γ activation. These data confirm the role of these proteins in troglitazone-induced apoptosis in HepG2 cells. In addition, the activity of caspase-3 was also found to be elevated during the apoptotic process induced by PPAR γ activation.

In summary, we have shown that activation of PPAR γ by troglitazone induces apoptosis in HepG2 cells through down-regulation of the expression of COX-2 and bcl-2, up-regulation of bax and bak, and activation of caspase-3. Consistent with other potential chemopreventive agents in human liver cancer model, we believe that COX-2, bak, bax, bcl-2 and caspase-3 play some roles in the process of PPAR γ activation-induced apoptosis. These serve as potential targets for future drugs or therapies for prevention and treatment of liver cancer.

REFERENCES

- 1 **Evans RM**. The steroid and thyroid hormone receptor superfamily. *Science* 1988; **240**: 889-895
- 2 **Spiegelman BM**. PPAR gamma: adipogenic regulator and thiazolidinedione receptor. *Diabetes* 1998; **47**: 507-514
- 3 **Blumberg B**, Evans RM. Orphan unclear receptors-new ligands and new possibilities. *Genes Dev* 1998; **12**: 3149-3155
- 4 **Desvergne B**, Wahli W. Peroxisome proliferator-activated receptors: nuclear control of metabolism. *Endocr Rev* 1999; **20**: 649-688
- 5 **Murao K**, Ohyama T, Imachi H, Ishida T, Cao WM, Takahara J. Ealpha stimulation of MCP-1 expression is mediated by the Akt/PKB signal transduction pathway in vascular endothelial cells. *Biochem Biophys Res Commun* 2000; **276**: 791-796
- 6 **Willson TM**, Brown PJ, Sternbach DD, Henke BR. The PPARs: from orphan receptors to drug discovery. *J Med Chem* 2000; **43**: 527-550
- 7 **Wu GD**. Nuclear receptor to prevent colon cancer. *N Engl J Med* 2000; **342**: 651-653
- 8 **Zhu Y**, Qi C, Korenberg JR. Structural organization of mouse peroxisome proliferator-activated receptor γ (mRNA γ) gene: alternative promoter use and different splicing yield two mPPAR γ isoforms. *Pro Natl Acad Sci USA* 1995; **92**: 7921-7925
- 9 **Fajas L**, Fruchart JC, Auwerx J. PPAR γ mRNA: A distinct PPAR γ mRNA subtype transcribed from an independent promoter. *FEBS Lett* 1998; **438**: 55-60
- 10 **Fajas L**, Auboeuf D, Raspe E. The organization, promoter analysis, and expression of the human PPAR γ gene. *J Biol Chem* 1997; **272**: 18779-18789
- 11 **Escher P**, Wahli W. Peroxisome proliferator-activated receptors: Insight into multiple cellular functions. *Mut Res* 2000; **448**: 121-138
- 12 **Shao D**, Rangwala SM, Bailey ST. Interdomain communication regulating ligand binding by PPAR. *Nature* 1998; **396**: 377-380
- 13 **Moras D**, Gronemeyer H. The nuclear receptor ligand-binding domain: Structure and function. *Curr Opin Cell Biol* 1998; **3**: 384-391
- 14 **Leibowitz MD**, Fievet C, Hennuyer N. Activation of PPARdelta alters lipid metabolism in db/db mice. *FEBS Lett* 2000; **473**: 333-336
- 15 **Liang YC**, Tsai SH, Tsai DC, Lin-Shiau SY, Lin JK. Suppression of inducible cyclooxygenase and nitric oxide synthase through activation of Peroxisome proliferator-activated receptor γ by flavonoids in mouse macrophages. *FEBS Lett* 2001; **496**: 12-18
- 16 **Kubota T**, Koshizuka K, Williamson EA. Ligand for Peroxisome proliferator-activated receptor α has potent antitumor effect against human prostate cancer both *in vitro* and *in vivo*. *Cancer Res* 1998; **58**: 3344-3352
- 17 **Takahashi N**, Okumaura T, Motomura W. Activation of PPARgamma inhibits cell growth and induces apoptosis in human gastric cancer cells. *FEBS Lett* 1999; **455**: 135-139
- 18 **Dubois RN**, Abramson SB, Crofford L. Cyclooxygenase in biology and disease. *FASEB J* 1993; **12**: 1063-1073
- 19 **Herschman HR**. Prostaglandin synthase 2. *Biochem Biophys Acta* 1996; **1299**: 125-140
- 20 **Eberhart CE**, Coffey RJ, Radhika A. Up-regulation of cyclooxygenase-2 during sporadic colorectal carcinogenesis. *J Pathol* 1999; **187**: 295-301
- 21 **Ristimaki A**, Honkonen N, Jankala H. Expression of cyclooxygenase-2 in human gastric carcinoma. *Cancer Res* 1998; **58**: 2929-2934
- 22 **Mahammed SI**, Knapp DW, Bostwick DG. Expression of cyclooxygenase-2 in human invasive transitional cell carcinoma of the urinary bladder. *Cancer Res* 1999; **59**: 5647-5650
- 23 **Yang ZY**, Rorison KA. Cyclooxygenase-2-selective antagonists do not inhibit growth of colorectal carcinoma cell lines. *Cancer Letters* 1998; **122**: 25-30
- 24 **Kusuhara H**, Komatsu H, Sugahara K. Reactive oxygen species are involved in the apoptosis induced by NSAIDs in cultured gastric cells. *Eur J Pharmacol* 1999; **383**: 331-337
- 25 **Tanaka K**, Pracyk JB, Takeda K, Yu ZX, Finkel T. Expression of Id1 results in apoptosis of cardiac myocytes through a redox-dependent mechanism. *J Biol Chem* 1998; **273**: 25922-25928
- 26 **Kim YB**, Kim GE, Cho NH, Pyo HR, Shim SJ, Chang SK, Park HC, Suh CO, Park TK, Kim BS. Overexpression of cyclooxygenase-2 is associated with a poor prognosis in patients with squamous cell carcinoma of the uterine cervix treated with radiation and concurrent chemotherapy. *Cancer* 2002; **95**: 531-539
- 27 **Ferrandina G**, Legge F, Ranelletti FO, Zannoni GF, Maggiano N, Evangelisti A, Mancuso S, Scambia G, Lauriola L. Cyclooxygenase-2 expression in endometrial carcinoma. *Cancer* 2002; **95**: 801-807
- 28 **Tang X**, Sun YJ, Half E, Kuo MT, Sinicrope F. Cyclooxygenase-2 overexpression inhibits death receptor 5 expression and confers resistance to tumor necrosis factor-related apoptosis-inducing ligand-induced apoptosis in human colon cancer cells. *Cancer Res* 2002; **62**: 4903-4908
- 29 **Staats P**. Pain Management and beyond. evolving concepts and treatments involving cyclooxygenase inhibition. *J Pain Symptom Manage* 2002; **24**: S4
- 30 **Lin DT**, Subbaramaiah K, Shah JP, Dannenberg AJ, Boyle JO. Cyclooxygenase-2: A novel molecular target for the prevention and treatment of head and neck cancer. *Head Neck* 2002; **24**: 792-799
- 31 **Jiang XH**, Lam SK, Lin MC, Jiang SH, Kung HF, Slosberg ED, Soh JW, Weinstein IB, Wong BC. Novel target for induction of apoptosis by cyclo-oxygenase-2 inhibitor SC-236 through a protein kinase C-beta(1)-dependent pathway. *Oncogene* 2002; **21**: 6113-6122
- 32 **He Q**, Luo X, Huang Y, Sheikh MS. Apo2L/TRAIL differentially modulates the apoptotic effects of sulindac and a COX-2 selective non-steroidal anti-inflammatory agent in Bax-deficient cells. *Oncogene* 2002; **21**: 6032-6040

- 33 **Kirkpatrick K**, Ogunkolade W, Elkak A, Bustin S, Jenkins P, Ghilchik M, Mokbel K. The mRNA expression of cyclo-oxygenase-2 (COX-2) and vascular endothelial growth factor (VEGF) in human breast cancer. *Curr Med Res Opin* 2002; **18**: 237-241
- 34 **Tapiero H**, Ba GN, Couvreur P, Tew KD. Polyunsaturated fatty acids (PUFA) and eicosanoids in human health and pathologies. *Biomed Pharmacother* 2002; **56**: 215-222
- 35 **Badawi AF**, Habib SL, Mohammed MA, Abadi AA, Michael MS. Influence of cigarette smoking on prostaglandin synthesis and cyclooxygenase-2 gene expression in human urinary bladder cancer. *Cancer Invest* 2002; **20**: 651-656
- 36 **Gallo O**, Masini E, Bianchi B, Bruschini L, Paglierani M, Franchi A. Prognostic significance of cyclooxygenase-2 pathway and angiogenesis in head and neck squamous cell carcinoma. *Hum Pathol* 2002; **33**: 708-714
- 37 **Li HL**, Zhang HW, Chen DD, Zhong L, Ren XD, Si-Tu R. JTE-522, a selective COX-2 inhibitor, inhibits cell proliferation and induces apoptosis in RL95-2 cells. *Acta Pharmacol Sin* 2002; **23**: 631-637
- 38 **Li HL**, Chen DD, Li XH, Zhang HW, Lu YQ, Ye CL, Ren XD. Changes of NF-kB, p53, Bcl-2 and caspase in apoptosis induced by JTE-522 in human gastric adenocarcinoma cell line AGS cells: role of reactive oxygen species. *World J Gastroenterol* 2002; **8**: 431-435
- 39 **Li HL**, Chen DD, Li XH, Zhang HW, Lu JH, Ren XD, Wang CC. JTE-522-induced apoptosis in human gastric adenocarcinoma cell line AGS cells by caspase activation accompanying cytochrome C release, membrane translocation of Bax and loss of mitochondrial membrane potential. *World J Gastroenterol* 2002; **8**: 217-223
- 40 **Callejas NA**, Castrillo A, Bosca L, Martin-Sanz P. *J Pharmacol Exp Ther* 1999; **288**: 1235-1241
- 41 **Inoue H**, Tanabe T, Umeson K. Feedback control of cyclooxygenase-2 expression through PPAR α . *J Biol Chem* 2000; **275**: 28028-28032
- 42 **Meadc EA**, McIntyre M, Zimmerman GA, Prescott SM. *J Biol Chem* 1999; **274**: 8328-8334
- 43 **Chinery R**, Coffey RJ, Graves-Deal R, Kirkland SC, Sanchez SC, Morrow JD. Prostaglandin J2 and 15-deoxy-delta12,14-prostaglandin J2 induce proliferation of cyclooxygenase-depleted colorectal cancer cells. *Cancer Res* 1999; **59**: 2739-2746
- 44 **Altiock S**, Xu M, Spiegelman BM. PPAR γ induces cell cycle withdrawal: inhibition of E2F/DP DNA-binding activity via down-regulation of PP2A. *Genes & Dev* 1997; **11**: 1987-1998
- 45 **Tontonoz P**, Singer S, Forman BM. Terminal differentiation of human liposarcoma cell induced by ligands for peroxisome proliferator-activated receptor and the retinoid X receptor. *Proc Natl Acad USA* 1997; **94**: 237-241
- 46 **Demetri GD**, Fletcher CD, Mueller E. Induction of solid tumor differentiation by the peroxisome proliferator-activated receptor-gamma ligand troglitazone in patients with liposarcoma. *Proc Natl Acad USA* 1999; **96**: 3951-3956
- 47 **Mueller E**, Sarraf P, Tontonoz P. Terminal differentiation of human breast cancer through PPAR γ . *Mol Cell* 1998; **1**: 465-470
- 48 **Suh N**, Wang Y, Williams CR. A new ligand for the peroxisome proliferator-activated receptor-gamma, GW7845, inhibits rat mammary carcinogenesis. *Cancer Res* 1999; **59**: 5671-5673
- 49 **He TC**, Chan TA, Vogelstein B, Kinzler KW. PPAR δ is a APC-regulated target of nonsteroidal anti-inflammatory drugs. *Cell* 1999; **99**: 335-345
- 50 **Yang LW**, Frucht H. Activation of the PPAR pathway induces apoptosis and COX-2 inhibition in HT-29 human colon cancer cells. *Carcinogenesis* 2001; **22**: 1379-1383
- 51 **Lefebvre AM**, Chen I, Desreuxaux P, Najib I, Auwerx J. Activation of peroxisome proliferator-activated receptor gamma promotes the development of colon tumors in C57BL/6J-APC^{Min/+} mice. *Nature Med* 1998; **4**: 1053-1057
- 52 **Lednicer D**. Tracing the Origins of COX-2 Inhibitors' Structures. *Curr Med Chem* 2002; **9**: 1457-1461
- 53 **Kawabe A**, Shimada Y, Uchida S, Maeda M, Yamasaki S, Kato M, Hashimoto Y, Ohshio G, Matsumoto M, Imamura M. Expression of cyclooxygenase-2 in primary and remnant gastric carcinoma: comparing it with p53 accumulation, *Helicobacter pylori* infection, and vascular endothelial growth factor expression. *J Surg Oncol* 2002; **80**: 79-88
- 54 **Kong G**, Kim EK, Kim WS, Lee KT, Lee YW, Lee JK, Paik SW, Rhee JC. Role of cyclooxygenase-2 and inducible nitric oxide synthase in pancreatic cancer. *J Gastroenterol Hepato* 2002; **17**: 914-921
- 55 **Liu CM**, Hong CY, Shun CT, Hsiao TY, Wang CC, Wang JS, Hsiao M, Lin SK. Inducible cyclooxygenase and interleukin 6 gene expressions in nasal polyp fibroblasts: possible implication in the pathogenesis of nasal polyposis. *Arch Otolaryngol Head Neck Surg* 2002; **128**: 945-951
- 56 **Maitra A**, Ashfaq R, Gunn CR, Rahman A, Yeo CJ, Sohn TA, Cameron JL, Hruban RH, Wilentz RE. Cyclooxygenase 2 expression in pancreatic adenocarcinoma and pancreatic intraepithelial neoplasia: an immunohistochemical analysis with automated cellular imaging. *Am J Clin Pathol* 2002; **118**: 194-201
- 57 **Carlton PS**, Gopalakrishnan R, Gupta A, Habib S, Morse MA, Stoner GD. Piroxicam is an ineffective inhibitor of N-nitrosomethylbenzylamine-induced tumorigenesis in the rat esophagus. *Cancer Res* 2002; **62**: 4376-4382
- 58 **Hoozemans JJ**, Bruckner MK, Rozemuller AJ, Veerhuis R, Eikelenboom P, Arendt T. Cyclin D1 and cyclin E are co-localized with cyclo-oxygenase 2 (COX-2) in pyramidal neurons in Alzheimer disease temporal cortex. *J Neuropathol Exp Neurol* 2002; **61**: 678-688
- 59 **Wei M**, Wanibuchi H, Morimura K, Iwai S, Yoshida K, Endo G, Nakae D, Fukushima S. Carcinogenicity of dimethylarsinic acid in male F344 rats and genetic alterations in induced urinary bladder tumors. *Carcinogenesis* 2002; **23**: 1387-1397
- 60 **Sunayama K**, Konno H, Nakamura T, Kashiwabara H, Shoji T, Tsuneyoshi T, Nakamura S. The role of cyclooxygenase-2 (COX-2) in two different morphological stages of intestinal polyps in APC (Delta474) knockout mice. *Carcinogenesis* 2002; **23**: 1351-1359
- 61 **Wu T**, Han C, Lunz JG, Michalopoulos G, Shelhamer JH, Demetris AJ. Involvement of 85-kd cytosolic phospholipase A (2) and cyclooxygenase-2 in the proliferation of human cholangiocarcinoma cells. *Hepatology* 2002; **36**: 363-373
- 62 **Wardlaw SA**, Zhang N, Belinsky SA. Transcriptional regulation of basal cyclooxygenase-2 expression in murine lung tumor-derived cell lines by CCAAT/enhancer-binding protein and activating transcription factor/cAMP response element-binding protein. *Mol Pharmacol* 2002; **62**: 326-333
- 63 **Shah T**, Ryu S, Lee HJ, Brown S, Kim JH. Pronounced radiosensitization of cultured human cancer cells by COX inhibitor under acidic microenvironment. *Int J Radiat Oncol Biol Phys* 2002; **53**: 1314-1318
- 64 **Lew JI**, Guo Y, Kim RK, Vargish L, Michelassi F, Arenas RB. Reduction of Intestinal Neoplasia With Adenomatous Polyposis Coli Gene Replacement and COX-2 Inhibition Is Additive. *J Gastrointest Surg* 2002; **6**: 563-568
- 65 **Qiu DK**, Ma X, Peng YS, Chen XY. Significance of cyclooxygenase-2 expression in human primary hepatocellular carcinoma. *World J Gastroenterol* 2002; **8**: 815-817
- 66 **Tian G**, Yu JP, Luo HS, Yu BP, Yue H, Li JY, Mei Q. Effect of nimesulide on proliferation and apoptosis of human hepatoma SMMC-7721 cells. *World J Gastroenterol* 2002; **8**: 483-487
- 67 **Wu YL**, Sun B, Zhang XJ, Wang SN, He HY, Qiao MM, Zhong J, Xu JY. Growth inhibition and apoptosis induction of Sulindac on Human gastric cancer cells. *World J Gastroenterol* 2001; **7**: 796-800
- 68 **Wang X**, Lan M, Wu HP, Shi YQ, Lu J, Ding J, Wu KC, Jin JP, Fan DM. Direct effect of croton oil on intestinal epithelial cells and colonic smooth muscle cells. *World J Gastroenterol* 2002; **8**: 103-107
- 69 **Niu ZS**, Li BK, Wang M. Expression of p53 and C-myc genes and its clinical relevance in the hepatocellular carcinoma and pericarcinomatous tissues. *World J Gastroenterol* 2002; **8**: 822-826
- 70 **Chen Q**, Yang GW, An LG. Apoptosis of hepatoma cells SMMC-7721 induced by Ginkgo biloba seed polysaccharide. *World J Gastroenterol* 2002; **8**: 832-836
- 71 **Taketo MM**. Cyclooxygenase-2 inhibitors in tumorigenesis. *J Natl Cancer Inst* 1998; **90**: 1529-1536

- 72 **Zimmermann KC**, Sarbia M, Weber AA, Borchard F, Gabbert HE, Schror K. Cyclooxygenase-2 expression in human esophageal carcinoma. *Cancer Res* 1999; **59**: 198-204
- 73 **Tjandrawinata RR**, Dahiya R, Hughes FM. Induction of cyclooxygenase-2 mRNA by prostaglandin E2 in human prostatic carcinoma cells. *Br J Cancer* 1997; **75**: 1111-1118
- 74 **Zhao AG**, Zhao HL, Jin XJ, Yang JK, Tang LD. Effects of Chinese Jianpi herbs on cell apoptosis and related gene expression in human gastric cancer grafted onto nude mice. *World J Gastroenterol* 2002; **8**: 792-796
- 75 **Liu S**, Wu Q, Ye XF, Cai JH, Huang ZW, Su WJ. Induction of apoptosis by TPA and VP-16 is through translocation of TR3. *World J Gastroenterol* 2002; **8**: 446-450
- 76 **Xu CT**, Huang LT, Pan BR. Current gene therapy for stomach carcinoma. *World J Gastroenterol* 2001; **7**: 752-759
- 77 **Wu YL**, Sun B, Zhang XJ, Wang SN, He HY, Qiao MM, Zhong J, Xu JY. Growth inhibition and apoptosis induction of Sulindac on Human gastric cancer cells. *World J Gastroenterol* 2001; **7**: 796-800
- 78 **Hou L**, Li Y, Jia YH, Wang B, Xin Y, Ling MY. Molecular mechanism about lymphogenous metastasis of hepatocarcinoma cells in mice. *World J Gastroenterol* 2001; **7**: 532-536
- 79 **Xu AG**, Li SG, Liu JH, Gan AH. Function of apoptosis and expression of the proteins Bcl-2, p53 and C-myc in the development of gastric cancer. *World J Gastroenterol*. 2001; **7**: 403-406

Edited by Su Q and Wang XL

Clinical significance of vascular endothelial growth factor expression and neovascularization in colorectal carcinoma

Shu Zheng, Ming-Yong Han, Zuo-Xiang Xiao, Jia-Ping Peng, Qi Dong

Shu Zheng, Ming-Yong Han, Zuo-Xiang Xiao, Jia-Ping Peng, Qi Dong, Cancer Institute, Zhejiang University, Hangzhou 310009, Zhejiang Province, China

Correspondence to: Professor Shu Zheng, Cancer Institute, Zhejiang University, Hangzhou 310009, Zhejiang Province, China

Telephone: +86-571-87214404 **Fax:** +86-571-87214404

Received: 2003-03-02 **Accepted:** 2003-04-01

Abstract

AIM: To clarify the association of vascular endothelial growth factor (VEGF) and microvascular density (MVD) expression with the angiogenesis and prognosis of colorectal cancer.

METHODS: A total of 97 cases of colorectal carcinomas were examined by immunohistochemical staining (SP method), using anti-VEGF and anti-factor CD34⁺ monoclonal antibodies.

RESULTS: VEGF positive staining was obtained in 68 out of 97 cases (70.1 %), and observed mainly in the cytoplasm of tumor cells, and also frequently in stromal cells. VEGF expression was more intense in poorly differentiated adenocarcinoma in comparison with others, but there was no significant correlation between VEGF expression and age, sex and stage. A significant correlation was found between the MVD and grades, and there was no significant relationship between the MVD and age, sex, and stage. The MVD in the VEGF positive group (68 cases) was higher than that in the negative group. Upon multivariate analysis, the significant variables were stage, tumor grade and MVD; VEGF expression was not an independent prognostic factor.

CONCLUSION: The expression of VEGF has a significant correlation with MVD; MVD expression has prognostic value but VEGF has not in colon cancer.

Zheng S, Han MY, Xiao ZX, Peng JP, Dong Q. Clinical significance of vascular endothelial growth factor expression and neovascularization in colorectal carcinoma. *World J Gastroenterol* 2003; 9(6): 1227-1230

<http://www.wjgnet.com/1007-9327/9/1227.asp>

INTRODUCTION

Angiogenesis is an essential process required for the growth and metastatic ability of solid tumors^[1]. Some studies demonstrated that an increase in microvascular density (MVD) was found to be closely associated with the expression of vascular endothelial growth factor (VEGF), and that MVD and VEGF expression had a prognostic value in predicting metastasis of various malignant solid tumors^[2,3]. Several studies have noted that the level of VEGF expression, a strong angiogenic factor, correlates with neovascularity and tumor progression in human breast and brain cancers and experimental tumor models^[4,5]. In this study, we investigated

the correlation of the VEGF and MVD in the tumor tissue of patients with colon cancer.

MATERIALS AND METHODS

Patients and tumor specimens

Tumor specimens from 97 patients resected for colorectal cancers, from the Second Affiliated Hospital of Zhejiang University (Hangzhou, China) from March 1993 to September 1995 were assessed. The age of the patients ranged from 36 to 74 years; 58 were male and 39 were female; average age, male 57.5 years old, female 61.5 years old. The patients were staged according to operation and pathological findings with UICC TNM classification: 9 (9.3 %) in stage I, 38 (39.2 %) in stage II, 32 (32.9 %) in stage III, and 18 (18.6) in stage IV.

Immunohistochemistry

Specimens were fixed in a 10 % formaldehyde solution and embedded in paraffin. Sections, 5 μ m thick, were cut and mounted on glass slides. Immunohistochemical staining was performed using the avidin-biotin method. Staining for VEGF was performed using an anti-VEGF monoclonal antibody (MAb) (Calbiochem, Cambridge, UK). Staining for vascular endothelial cells was performed using an anti-CD34 MAb (DAKO, Copenhagen, Denmark). Briefly, formalin-fixed, paraffin-embedded 5 μ m tissue sections were deparaffinised with xylene, dehydrated in ethanol and incubated with 3 % hydrogen peroxidase for 5 min. After washed with phosphate-buffered saline (PBS), tissue sections were incubated in 10 % normal bovine serum for 20 min, followed by an overnight incubation with anti-VEGF (1:50) antibody or anti-CD34 antibody (1:50). Biotinylated goat antimouse and antirabbit immunoglobulins were used as secondary antibodies. Peroxidase-conjugated avidin was used as a dilution of 1:500. Finally, 0.02 % diaminobenzidine and 1 % hydrogen peroxide in PBS were used as the substrate. Normal mouse IgG diluted to an equivalent protein concentration was used as a control in place of the primary antibody. Counterstaining was performed with haematoxylin.

Any single brown-stained cell that indicates an endothelial cell stained with CD34 was counted as a single vessel. Branching structures were counted as a single vessel, unless there was a break in the continuity of the structure. The stained sections were screened at 5 times magnification, to identify the areas of highest vascular density. After the area of highest neovascularization was identified, individual vessel counts were performed at $\times 200$ magnification.

Evaluation of VEGF expression

For the evaluation of VEGF expression, immunostaining was classified in two groups, corresponding to the percentage of immunoreactive cells; the cut-off point to distinguish low from high VEGF expression was 25 % of positive carcinoma cells.

Statistical analysis

Statistical comparisons for significance were made with the Student's *t* test and χ^2 test. Multivariate analysis was performed

using the Cox's regression multiple hazard model. $P < 0.05$ was considered statistically significant.

RESULTS

VEGF expression

Positive staining was obtained in 68 out of 97 cases (70.1 %) and a typical immunohistochemical staining is shown in Figure 1. VEGF immunoreactivity was observed mainly in the cytoplasm of tumor cells, and also frequently in stromal cells. The distribution of VEGF-staining was not continuous in the whole slide of the specimen. VEGF expression was more intense in poorly differentiated adenocarcinoma in comparison with other tumors ($P = 0.014$), but there was no significant correlation between VEGF expression and age, sex and stage (Table 1).

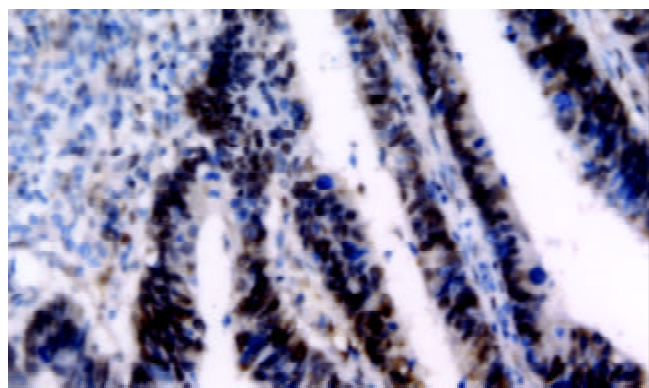


Figure 1 VEGF expression in colorectal cancer specimen. VEGF immunoreactivity was observed mainly in the cytoplasm of tumor cells, and also frequently in stromal cells.

Table 1 Relationship between clinicopathologic factors and VEGF expression ($n=97$)

Variables	n (%)	VEGF expression		P value
		+ n(%)	- n(%)	
Age				
<45 years	36	26(72.2)	10(27.8)	
>45 years	61	42(68.8)	19(31.2)	
Sex				
Male	58	41(74.1)	17(25.9)	
Female	39	27(68.9)	12(31.1)	
Different differentiation				
Well	28	15(51.1)	13(48.9)	
Moderate	36	26(72.2)	10(27.8)	
Poor	33	27(81.8)	6(18.2)	0.014
Stage				
I	9	7(77.8)	2(22.2)	
II	38	27(71.1)	11(28.9)	
III	32	23(72.2)	9(27.8)	
IV	18	11(61.5)	7(38.5)	

$P < 0.05$ vs Well differentiated group.

Microvascular density (MVD)

Any single brown-stained cell that indicates an endothelial cell stained with CD34 was counted as a single vessel (Figure 2). The median MVD was 187.6 ± 17.3 . A significant correlation was found between the MVD and different grade (0.028), and there was no significant relationship between the MVD and age, sex, and stage (Table 2).

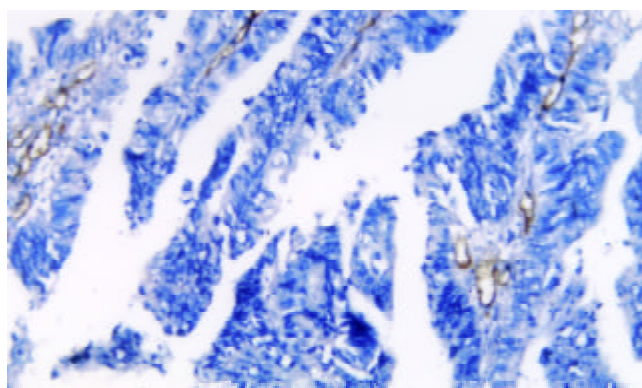


Figure 2 Microvascular density in colorectal cancer specimen. The single brown-stained cell indicates an endothelial cell that was stained for the presence of CD34.

Table 2 Relationship between clinicopathologic factors and MVD ($n=97$)

Variables	n	MVD		P value
		high MVD	low MVD	
Age				
<45 years	36	20(55.6)	16(44.4)	
>45 years	61	33(54.3)	28(45.7)	
Sex				
Male	58	32(55.2)	26(44.8)	
Female	39	21(53.8)	18(46.2)	
Different differentiation				
Well	28	12(42.9)	16(57.1)	
Moderate	36	20(55.6)	16(44.4)	
Poor	33	21(63.6)	12(36.4)	0.028
Stage				
I	9	5(55.6)	4(44.4)	
II	38	20(52.6)	18(47.4)	
III	32	18(56.3)	14(43.7)	
IV	18	10(55.6)	8(44.4)	

$P < 0.05$ vs Well differentiated group.

Table 3 Relationship between MVD and VEGF expression

Variable	MVD	P value
VEGF (+)	213.4±12.8	
Expression (-)	138.7±19.4	0.027

$P < 0.05$ vs VEGF (-) group.

Table 4 Multivariate analysis of overall survival by Cox proportional hazards model

Variable	Categories	Hazard ratio	SEM	P value
Age	>45 years versus <45 years	1.877	0.3796	
Sex	Male versus female	1.216	0.4071	
Differentiation	Poor versus others	2.361	0.2438	0.0217
Stage	I, II versus III, IV	2.973	0.1976	0.0012
VEGF	(+) versus (-)	1.164	0.3874	
MVD	>187.6 versus <187.6	2.526	0.2126	0.0314

$P < 0.05$ vs Stage I, II group.

Association between VEGF expression and MVD

The MVD in the VEGF positive group was 213.4 ± 12.8 , and that in the negative group was 138.7 ± 19.4 . MVD in the VEGF

positive group was higher than that in the negative group ($P=0.027$) (Table 3).

Multivariate analysis

Upon multivariate analysis of all patients, the significant variables were stage, tumor grade and MVD. Age, sex, VEGF expression were not independent prognostic factors (Table 4).

DISCUSSION

Microvasculature is important in cancer growth and metastasis because it is involved in the transport of various nutrients to the tumor cells^[1,2]. In this process of tumor growth and angiogenesis numerous angiogenic factors are involved. In recent years several of these factors have been identified^[3-6]. One of the most important regulators of angiogenesis is VEGF. It induces the vascular stroma not only as a direct endothelial cell mitogen, but also as a potent mediator of microvessel permeability. This ability of VEGF to induce fenestrations on microvessels has been demonstrated in experimental tumors^[7,8].

The VEGF is overexpressed in a variety of benign tissues and malignant human tumors. The expression of VEGF suggests that it plays a role in luminal secretion by increasing local vascular permeability^[9]. In neuroendocrine tumors the high levels of VEGF expression could indicate a role for VEGF in the release of gastrointestinal hormones through the regulation of baseline permeability of the normal microcirculation^[10]. The high level of VEGF expression in some malignant tumors, such as breast cancer, non-small cell lung cancer, bladder cancer and gastric cancer, is a characteristic feature of these tumors. Several studies have demonstrated that high microvessel density is a useful indicator for poor prognosis in these cancers^[11-15].

CD34 antigen is expressed on immature human haematopoietic precursor cells and is progressively lost during maturation^[16,17]. In normal resting tissues, anti-CD34 antibodies are predominantly reacted with the luminal endothelial membrane, whereas the abluminal membrane is negative or only weakly positive. In contrast, significant staining of the endothelial abluminal microprocesses (EAM) has been found in tumor stroma^[18]. It has been shown that CD34 is a marker for EAM during angiogenesis and the antigenicity of CD34 is preserved by freezing, or ethanol, and formalin fixation^[19].

Microvessel density (MVD) and expression of VEGF act as a highly specific inducer of angiogenesis. Strong VEGF expression and high MVD are considered important parameters of tumor angiogenesis and related to poor survival probability in vulvar cancer patients^[20,21]. In primary breast cancer, MVD and VEGF serve as a parameter for determining tumor biological, metastatic potential and prognosis^[22]. VEGF is highly related to angiogenesis of gastric carcinoma and promotes growth, invasion and metastasis of gastric carcinoma, VEGF expression and MVD are predictors for the biological behavior of gastric carcinoma^[21,23]. In primary liver cancer, besides tumor stage, satellite nodules and portal vein embolus, the MVD and VEGF expressions are also of prognostic significance^[24]. Intense VEGF staining was found in the majority of advanced primary SCCs, lymph node metastases, and human SCCs in severe combined immunodeficient mice, where no dysplasia, CIS, or early SCCs showed intense immunostaining. Suggesting a role for VEGF in both clinical and experimental HNSCC^[25,26]. By univariate analysis, VEGF expression and MVD in the biopsy specimens were significant predictors of bladder cancer recurrence. By multivariate analysis, only VEGF expression was an independent prognostic factor^[27]. The metastatic potency of NPC tissue and the prognosis of the patients with NPC could be estimated by measuring MVD and the expression of VEGF in NPC tissue^[28].

Previously it was demonstrated that in prostate tumors, angiogenesis measured as microvessel density (MVD) was associated with tumor stage as well as WHO grade and was an independent predictor of clinical outcome. Vascular endothelial growth factor (VEGF) is a major inducer of angiogenesis^[29]. The relationship between VEGF expression and MVD in ovarian carcinoma suggests that in conjunction with the established clinicopathologic prognostic parameters of ovarian carcinoma, VEGF expression may enhance the predictability of patients at high risk for tumor progression who are potential candidates for further aggressive therapy^[30]. But MVD in synovial sarcomas did not correlate with prognosis or VEGF expression, angiogenesis in synovial sarcoma might be controlled by angiogenesis activators other than VEGF^[31]. In patients with invasive cervical cancer VEGF expression has no prognostic value in contrast with the MVD^[32].

In this study, we found positive VEGF staining was obtained in 68 out of 97 cases (70.1 %), VEGF immunoreactivity was observed mainly in the cytoplasm of tumor cells, and also frequently in stromal cells. VEGF expression was more intense in poorly differentiated adenocarcinoma in comparison with other tumors, but there was no significant correlation between VEGF expression and age, sex and stage. A significant correlation was found between the MVD and different grade, and there was no significant relationship between the MVD and age, sex, and stage. MVD in the VEGF positive group was higher than that in the negative group. Upon multivariate analysis, the significant variables were stage, tumor grade and MVD; VEGF expression was not an independent prognostic factor. We conclude that MVD but not VEGF expression has prognostic value in colon cancer.

REFERENCES

- 1 **Folkman J.** Tumor angiogenesis. *Adv Cancer Res* 1985; **43**: 175-203
- 2 **Decaussin M, Sartelet H, Robert C, Moro D, Claraz C, Brambilla C, Brambilla E.** Expression of vascular endothelial growth factor (VEGF) and its two receptors in non-small cell lung carcinoma (NSCLCs): correlation with angiogenesis and survival. *J Pathol* 1999; **188**: 369-377
- 3 **Folkman J, Klagsbrun M.** Angiogenic factors. *Science* 1987; **235**: 442-447
- 4 **Burian M, Quint C, Neuchrist C.** Angiogenic factors in laryngeal carcinomas: do they have prognostic relevance? *Acta Otolaryngol* 1999; **119**: 289-292
- 5 **Giatromanolaki A, Koukourakis MI, Stathopoulos GP, Kapsoritakis A, Paspatis G, Kakolyris S, Sivridis E, Georgolias V, Harris AL, Gatter KC.** Angiogenic interactions of vascular endothelial growth factor, of thymidine phosphorylase, and of p53 protein expression in locally advanced gastric cancer. *Oncol Res* 2000; **12**: 33-41
- 6 **Li Z, Shimada Y, Uchida S, Maeda M, Kawabe A, Mori A, Itami A, Kano M, Watanabe G, Imaura M.** TGF- α as well as VEGF, PD-ECGF and bFGF contribute to angiogenesis of esophageal squamous cell carcinoma. *Int J Oncol* 2000; **17**: 453-460
- 7 **Roberts WG, Palade GE.** Increased microvascular permeability and endothelial fenestration induced by vascular endothelial growth factor. *J Cell Sci* 1995; **108**: 2369-2379
- 8 **Fujimoto K, Hosotani R, Wada M, Lee JU, Koshiba T, Miyamoto Y, Tsuji S, Nakajima S, Doi R, Imamura M.** Expression of two angiogenic factors, vascular endothelial growth factor and platelet-derived endothelial cell growth factor in human pancreatic cancer, and its relationship to angiogenesis. *Eu J Cancer* 1998; **34**: 1439-1447
- 9 **Zhang L, Scott PA, Turley H, Leek R, Lewis CE, Gatter KC, Harris AL, Mackenzie IZ, Rees MC, Bicknell R.** Validation of anti-vascular endothelial growth factor antibodies for immunohistochemical localization of VEGF in tissue sections: expression of VEGF in the human endometrium. *J Pathol* 1998; **185**: 402-408
- 10 **Terris B, Scozec JY, Rubbia L, Bregeaud L, Pepper MS,**

- Ruszniewski P, Belghiti J, Flejou J, Degott C. Expression of vascular endothelial growth factor in digestive neuroendocrine tumours. *Histopathology* 1998; **32**: 133-138
- 11 **Uchida S**, Shimada Y, Watanabe G, Tanaka H, Shibagaki I, Miyahara T, Ishigami S, Imamura M. In oesophageal squamous cell carcinoma vascular endothelial growth factor is associated with p53 mutation, advanced stage and poor prognosis. *Br J Cancer* 1998; **77**: 1704-1709
- 12 **de-Jong JS**, van-Diest PJ, van-der-Valk P, Baak JP. Expression of growth factors, growth-inhibiting factors, and their receptors in invasive breast cancer. *J Pathol* 1998; **184**: 53-57
- 13 **Koomagi R**, Volm M. Tissue-factor expression in human non-small-cell lung carcinoma measured by immunohistochemistry: correlation between tissue factor and angiogenesis. *Int J Cancer* 1998; **79**: 19-22
- 14 **Aikawa H**, Takahashi H, Fujimura S, Sato M, Endo C, Sakurada A, Kondo T, Tanita T, Matsumura Y, Ono S, Saito Y, Sagawa M. Immunohistochemical study on tumor angiogenic factors in non-small cell lung cancer. *Anticancer Res* 1999; **19**: 4305-4309
- 15 **Neuchrist C**, Quint C, Pammer A, Burian M. Vascular endothelial growth factor (VEGF) and microvessel density in squamous cell carcinomas of the larynx: an immunohistochemical study. *Acta Otolaryng* 1999; **119**: 732-738
- 16 **Watt SM**, Karhi K, Gatter K, Furley AJ, Katz FE, Healy LE, Altass LJ, Bradley NJ, Sutherland DR, Levinsky R. Distribution and epitope analysis of the cell membrane glycoprotein associated with human hematopoietic progenitor cells. *Leukemia* 1987; **1**: 417-426
- 17 **El-Assal ON**, Yamanoi A, Soda Y, Yamaguchi M, Igarashi M, Yamamoto A, Nabika T, Nagasue N. Clinical significance of microvessel density and vascular endothelial growth factor expression in hepatocellular carcinoma and surrounding liver: possible involvement of vascular endothelial growth factor in the angiogenesis of cirrhotic liver. *Hepatology* 1998; **27**: 1554-1562
- 18 **Schlingemann RO**, Rietveld FJ, de Waal RM, Bradley NJ, Skene AI, Davies AJ, Greaves MF, Denekamp J, Ruiter DJ. Leukocyte antigen CD34 is expressed by a subset of cultured endothelial cells and on endothelial abluminal microprocesses in the tumor stroma. *Lab Invest* 1990; **62**: 690-696
- 19 **Traweek ST**, Kandalaf PL, Mehta P, Battifora H. The human hematopoietic progenitor cell antigen (CD34) in vascular neoplasia. *Am J Clin Pathol* 1991; **96**: 25-31
- 20 **Ogura Y**, Sato K, Kato T, Saito K, Enomoto K. Immunohistochemical analysis of expression of angiogenic factors and tumor angiogenesis in superficial bladder cancer. *Nippon Hinyokika Gakkai Zasshi* 1998; **89**: 529-537
- 21 **Obermair A**, Kohlberger P, Bancher Todesca D, Tempfer C, Sliutz G, Leodolter S, Reinthaller A, Kainz C, Breitenecker G, Gitsch G. Influence of microvessel density and vascular permeability factor/vascular endothelial growth factor expression on prognosis in vulvar cancer. *Gynecol Oncol* 1996; **63**: 204-209
- 22 **Jiang X**, Huang X, Li J. The correlation between tumor angiogenesis and lymph node metastasis in primary breast carcinoma. *Zhonghua Waikexue* 1997; **35**: 583-585
- 23 **Lu M**, Jiang Y, Wang R. The relationship of vascular endothelial growth factor and angiogenesis to the progression of gastric carcinoma. *Zhonghua Binglixue Zazhi* 1998; **27**: 278-281
- 24 **Xia J**, Yang B, Ye S. Clinico-pathological significance of microvessel density and VEGF expression in primary liver cancer. *Zhonghua Zhongliu Zazhi* 1998; **20**: 440-442
- 25 **Ikeguchi M**, Oka S, Saito H, Kondo A, Tsujitani S, Maeta M, Kaibara N. The expression of vascular endothelial growth factor and proliferative activity of cancer cells in gastric cancer. *Langenbecks Arch Surg* 1999; **384**: 264-270
- 26 **Sauter ER**, Nesbit M, Watson JC, Klein-Szanto A, Litwin S, Herlyn M. Vascular endothelial growth factor is a marker of tumor invasion and metastasis in squamous cell carcinoma of the head and neck. *Clin Cancer Res* 1999; **5**: 775-782
- 27 **Inoue K**, Slaton JW, Karashima T, Yoshikawa C, Shuin T, Sweeney P, Millikan R, Dinney CP. The prognostic value of angiogenesis factor expression for predicting recurrence and metastasis of bladder cancer after neoadjuvant chemotherapy and radical cystectomy. *Clin Cancer Res* 2000; **6**: 4866-4873
- 28 **Guang WH**, Sunagawa M, Jie En L, Shimada S, Gang Z, Tskeshi Y, Kosugi T. The relationship between microvessel density, the expression of vascular endothelial growth factor, and the extension of nasopharyngeal carcinoma. *Laryngoscope* 2000; **110**: 2066-2069
- 29 **Strohmeier D**, Rossing C, Bauerfeind A, Kaufmann O, Schlechte H, Bartsch G, Loening S. Vascular endothelial growth factor and its correlation with angiogenesis and p53 expression in prostate cancer. *Prostate* 2000; **45**: 216-224
- 30 **Shen GH**, Ghazizadeh M, Kawanami O, Shimizu H, Jin E, Araki T, Sugisaki Y. Prognostic significance of vascular endothelial growth factor expression in human ovarian carcinoma. *Br J Cancer* 2000; **83**: 196-203
- 31 **Kawauchi S**, Fukuda T, Tsuneyoshi M. Angiogenesis does not correlate with prognosis or expression of vascular endothelial growth factor in synovial sarcomas. *Oncol Rep* 1999; **6**: 959-964
- 32 **Tjalma W**, Weyler J, Weyn B, Van-Marck E, Van-Daele A, Van-Dam P, Goovaerts G, Buytaert P. The association between vascular endothelial growth factor, microvessel density and clinicopathological features in invasive cervical cancer. *Eur J Obstet Gynecol Reprod Biol* 2000; **92**: 251-257

Edited by Zhang JZ

Effects of KAI1/CD82 on biological behavior of human colorectal carcinoma cell line

Li Liu, De-Hua Wu, Zu-Guo Li, Guang-Zhi Yang, Yan-Qing Ding

Li Liu, Zu-Guo Li, Guang-Zhi Yang, Yan-Qing Ding, Department of Pathology, the First Military Medical University, Guangzhou 510515, Guangdong Province, China

De-Hua Wu, Department of Radiation Oncology, Nanfang Hospital, the First Military Medical University, Guangzhou 510515, Guangdong Province, China

Supported by the National Natural Science Foundation, No. 31070423, the Natural Science Foundation of Guangdong Province, No. 990385, 970335 and the Natural Science Foundation of PLA of China, No. 01MA128

Correspondence to: Dr Yang-Qing Ding, Department of Pathology, the First Military Medical University, Guangzhou 510515 Guangdong Province, China. dyq@fimmu.com

Telephone: +86-20-61642148 **Fax:** +86-20-61642148

Received: 2002-12-22 **Accepted:** 2003-02-11

Abstract

AIM: To investigate the effects of KAI1/CD82 on biological behavior of colorectal carcinoma cells.

METHODS: KAI1 cDNA was transfected into highly malignant colorectal carcinoma cell line, LoVo, which had low level of endogenous KAI1 expression, and established stable transfectant clones with high KAI1/CD82 expression. The cell-cell adhesion, cell aggregation, cell-matrix adhesion and cell invasion assay were performed to determine whether KAI1 transfectant could have an effect on proliferation, adhesion and tumor metastasis in comparison with the control transfectant cells.

RESULTS: KAI1 expression did not alter *in vitro* cell proliferation. But the KAI1 transfectant cells exhibited significantly increased homotypic cell-cell adhesion and cell aggregation in comparison with the control transfectant cells ($P < 0.05$). Furthermore, KAI1 expression significantly suppressed the cell adhesion to extracellular matrix components and *in vitro* cell invasion in KAI1-transfected LoVo cells. The data indicated that KAI1 expression significantly suppressed the metastatic potential of KAI1-transfected LoVo cells.

CONCLUSION: Our results suggest that KAI1 might function as a negative regulator of colorectal carcinoma metastasis.

Liu L, Wu DH, Li ZG, Yang GZ, Ding YQ. Effects of KAI1/CD82 on biological behavior of human colorectal carcinoma cell line. *World J Gastroenterol* 2003; 9(6): 1231-1236
<http://www.wjgnet.com/1007-9327/9/1231.asp>

INTRODUCTION

KAI1, a newly identified metastatic suppressor gene for prostatic cancer, is located on human chromosome 11p11.2. It was originally isolated by Dong in 1995^[1,2]. KAI1 mRNA, is ubiquitously expressed with abundant expression in the surface

epithelium of the major epithelial tissues, including prostate, breast, bladder, and gastrointestinal tract^[3,4]. Its protein product, CD82, belongs to TM4SF (transmembrane four superfamily) or TST (tetra span transmembrane) superfamily, many of which, including KAI1, are CD antigens present on the surface of leukocytes^[5,6]. Four hydrophobic transmembrane domains and one large extracellular hydrophilic domain containing 3 potential N-glycosylation sites are thought to function in cell-cell and cell-matrix interactions. At least three TM4SF members are implicated in metastasis, including CD9/MRP-1, CD63/ME491, and CD82/KAI1^[7]. KAI1 and other TM4SF members have been demonstrated to bind to each other, integrins, and E-cadherin, and other surface molecules to relay extracellular signals to signal transduction pathways that are important in cellular adhesion, invasive motility, and metastasis suppression^[8-10].

The role of KAI1 in tumor progression may not be limited to prostatic cancer. It was reported to be important in preventing the development of metastases in a wide variety of human tumor types, including several cancers such as cervical^[11], breast^[12], pancreatic^[13], esophageal^[14], and ovarian cancer^[15]. Therefore, we transfected KAI1 plasmid into highly malignant colorectal carcinoma cell line, LoVo, and examined cell proliferation, adhesion and invasion. The aim of this study was to determine whether KAI1 could suppress the invasive or metastatic ability of colorectal carcinoma cells.

MATERIALS AND METHODS

Cell lines and culture conditions

LoVo cell line was derived from human colon adenocarcinoma established from the metastatic nodule resected from a 56-year-old Caucasian man with colon adenocarcinoma in 1972. ECV304 cell line was derived from human umbilical cord transformed endothelium. Both cell lines were cultured in RPMI-1640 medium supplemented with 10 % heat-inactivated fetal bovine serum (FBS) and 100 U/ml penicillin/streptomycin. All cells were grown in 5 % CO₂ humidified atmosphere at 37 °C, and harvested for analysis at 80-90 % confluency.

Transfection and selection of the expressing cells

pCMV-KAI1 plasmid was a generous gift from Carl Barrett. 1.6 kb KAI1 cDNA inserting at salI sites was inserted into the xhoI site of pCMV-neo-xhoI vector to construct pCMV-KAI1. This plasmid was transfected into LoVo cell using the cationic polymer transfection reagent (jetPEI transfection reagent was purchased from Dakewe Biotechnology Company). The transfection proposal was as follows: the cells were plated at 6-well plate 1d before the transfection. 3 µg pCMV-KAI1 plasmid was diluted to 100 µl 150 mM NaCl and 6 µl jetPEI solution was diluted to 100 µl 150 mM NaCl. 100 µl jetPEI solution was added to the 100 µl DNA solution and vortex the solution immediately. Then the mixture was added drop-wise onto the serum containing medium in each well after incubated for 30 min at room temperature. After incubated for 48 h at 37 °C, 5 % CO₂ in a humidified atmosphere, the transfectants named LoVo-KAI1 were isolated by growing them in G418-containing medium (700 µg/ml) and G418-resistant clones

were established in two weeks. The pCMV-neo (purchased from Stratagene Company) vector alone was also transfected into LoVo cells to generate neo transfected control clones, designated as LoVo-neo.

In situ hybridization (ISH) assay

To prepare digoxigenin-labeled KAI1-DNA probes for *in situ* hybridization, PCR amplification was performed with a forward primer 5' -AGTCCTCCCTGCTGCTGTGTG-3' and reverse primer 5' -TCAGTCAGGGTGGGCAAGAGG-3' and a 1 030 bp KAI1 fragment was achieved^[16]. The probes were labeled by Dig DNA Labeling and detecting Kit (purchased from Roche Company). Blot hybridization of Dig-labeled probe showed the labeling efficiency. ISH was performed according to the description of the enhanced sensitive ISH detection kit (purchased from Boster Biotechnology Company). Briefly, the cells that were incubated in cover slip for 24 hour and fixed with 95 % ethanol were washed with PBS (phosphate-buffered saline) three times. The endogenous peroxidases were blocked by incubating with 0.5 % H₂O₂ for 30 min at room temperature. The cells were subsequently treated for 10 min with triton X-100 and for 40 s with 3 % pepsin. At 37 °C the cells were prehybridized for 3 h and hybridized overnight. The final concentrations of the labeled probes were 150 pg/μl. After hybridization, excess probe was removed by washing in 2×SSC, 0.5×SSC, 0.2×SSC respectively. The cells were incubated with an antidigoxigenin antibody conjugated biotin for 120 min at room temperature and then added strept-avidin biotin complex for 30 min. For color reaction, diaminobenzidine (DAB) was used. If the ISH signals were present, the cytoplasm would be full of brown granules. The control was LoVo-neo cell group.

Immunohistochemistry (IHC) assay

The fixed cells were subjected to immunostaining by using an ultrasensitive S-P technique (Maixin Biotechnology Company). Endogenous peroxidases were blocked by incubating with 0.5 % H₂O₂ for 30 min at room temperature. The cells were subsequently treated for 10 min with triton X-100 and for 40 s with 3 % pepsin. The cells were incubated for 30 min at 37 °C with normal nonimmune serum before incubation at 4 °C with specific monoclonal KAI1-antibody (BD Pharmingen Technical Company) used at a dilution of 1:100 overnight. The cells were then treated with biotin-conjugated second antibody before adding streptavidin-peroxidase. For color reaction, diaminobenzidine was used. If the IHC signals were present, the cytoplasm and membrane were stained brown. The control was LoVo-neo cell group.

Growth curve

LoVo-KAI1 Cells were prepared by trypsinization. The cells were resuspended at a concentration of 10⁴ cells/ml in RPMI 1640 10 % FCS and then 100 μl aliquots were dispensed into 96 well microtiter plates. The cells were incubated for 1,2,3,4,5,6 day respectively and MTT assay was performed by adding 20 μl MTT (5 mg/ml) for 4 h. When the MTT incubation was completed, the supernatants were removed. 150 μl dimethyl sulfoxide (DMSO) was added to each well. The A value of each well was measured with a microplate reader at 570 nm 15 min later. All experiments were performed in triplicate. The control was LoVo-neo cell group.

Cell-cell adhesion assay

Cell-cell adhesion assays were performed using 96-well plates. The cells were cultured in 96-well plates and in confluence without vacant space. Other homotypic cells were harvested with 0.25 % trypsin and resuspended to a density of 10⁵ cells/ml in RPMI-1640 without FCS. Then the cells of 100 μl were

added into each well with already cultured homotypic cells and recovered for 60 min, 90 min at 37 °C. Non-adherent cells were collected by gentle washing with PBS and the washed cells were counted. The number of cell-cell adhesion was calculated using the following formula: The number of cell-cell adhesion = total number of added cells - the number of cells being washed. The experiments were performed in triplicate and repeated three times. The control was LoVo-neo cell group.

Cell-cell aggregation assay^[17]

12-well plate was coated with 1 % agar. And then single cell suspension (10⁵/ml) was washed by PBS three time after the cells were detached from the culture flasks with 0.25 % trypsin. The cells (1 ml) were added to 12-well plate and incubated at 37 °C with rotary shaking (70 r/min) for 5 h. The number of single cell was counted by haemocytometer. The cell-cell aggregation rate was then measured as ((total number of cells - single cells)/(total number of cells)) × 100 %.

Cell-matrix adhesion^[18]

96-well plates were incubated with 75 μl fibronectin (50 μg/ml) for 45 min and blocked with BSA (10 mg/ml). The cells were harvested as described for cell-cell adhesion assay. The cells (10⁵ cells/ml) of 100 μl were added to each well and allowed to attach 2 h at 37 °C. After washed with PBS twice to withdraw the non-adherent cells, 20 μl MTT was added for 4 h and 200 μl DMSO was added as above. The value of each well was measured with a microplate reader at 570 nm 15 min later. The experiments were performed in triplicate. The control was LoVo-neo cell group.

In vitro invasion assay

This assay was based on the principle of Boyden chamber^[19]. The top and bottom of Boyden chamber (Corning Company) were separated by polycarbonate filter with 8 μm pore size. The top chamber was prepared by coating the filter with 50 μg of diluted matrigel and incubated for 30 min. The bottom chamber was prepared with 5 % FBS as a chemoattractant. After 24 h, 48 h incubation, the noninvasive cells were removed with a cotton swab. The cells that had migrated through the membrane and stuck to the lower surface of the membrane were fixed with methanol and stained with hematoxylin. For quantification, the cells were counted under a microscope in five predetermined fields at ×200. The control was LoVo-neo cell group.

Monolayer cells invasion assay

ECV304 cells were cultured in cover slip and confluence without vacant space. LoVo-KAI1 cells were harvested with 0.25 % trypsin and resuspended to a density of 10⁵ cells/ml in RPMI-1640 with 2 % FBS and 10⁵ cells were added to the surface of ECV304 cells. After interaction for 24 h, the cells were washed with PBS and fixed immediately with 95 % ethanol. The cells that had migrated through the ECV304 cells and grown under ECV304 cells were counted. For quantification, the cells were counted under a microscope in five random fields at ×200. The experiments were performed in triplicate and the control was LoVo-neo cell group.

Statistical analysis

The comparison was made using Student *t*-test with a single contrast of LoVo-neo. The *P* value <0.05 was considered to be significant.

RESULTS

Transfection of KAI1 cDNA and selection of stable clones

To clarify whether KAI1 could suppress colorectal cancer

invasion and metastasis, we transfected KAI1 full-length cDNA into colorectal carcinoma LoVo cell lines. An expression vector was transfected as a negative control. After transfection and G418 selection for two weeks, 10 of each growing clone were picked and screened to confirm the transgene by *in situ* hybridization and immunohistochemistry. The probes for ISH were about 1 000 bp. (Figure 1). The blot hybridization was used to evaluate the efficiency of Dig-labeling probe (Figure 2). KAI1 mRNA expression in LoVo-KAI1 cell was located in the cytoplasm by *in situ* hybridization. LoVo-KAI1 cells were full of brown granules, but the LoVo-neo cells were negative (Figure 3). KAI1 protein expression was detected by immunohistochemistry and located in the cytoplasm and membrane. LoVo-KAI1 cells displayed positive immunostaining and LoVo-neo cells displayed negative staining (Figure 4). The results suggested that KAI1 was expressed in mRNA and protein level.

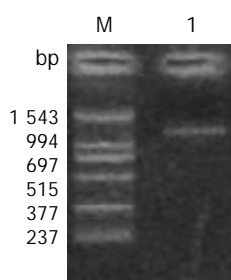


Figure 1 1 % gelose electrophoretogram of the product of PCR (1 030 bp). M: PCR marker; 1: PCR product.

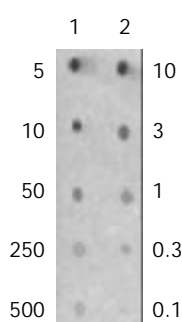


Figure 2 Blot hybridization of Dig-labeled probe to show the labeling efficiency. Column 1: Dig-labeling probe; Column 2: standard control (unit: pg/ μ l).

Growth curve

Growth curve showed LoVo-KAI1 cells and LoVo-neo cells existing no difference in proliferation ability (Figure 5). The result demonstrated that KAI1 gene had no effect on cell proliferation ability.

Cell-cell adhesion assay

After interaction of homotypic cells in 60 min and 90 min, cell-cell adhesion was analyzed (Figure 6). These data suggested KAI1 gene could increase adhesion of homotypic cells.

Cell-cell aggregation assay

Aggregation observed in the LoVo-KAI1 cells was very different from that of the LoVo-neo cells. The LoVo-KAI1 cells formed large multicellular aggregates containing many cells, whereas the aggregates formed by LoVo-neo cells were much smaller and rarely contained more than a few cells (Figure 7). The number of LoVo-KAI1 cells aggregation (64.8 ± 4.4) was much larger than that of LoVo-neo cells (58.6 ± 3.5) ($P < 0.05$).

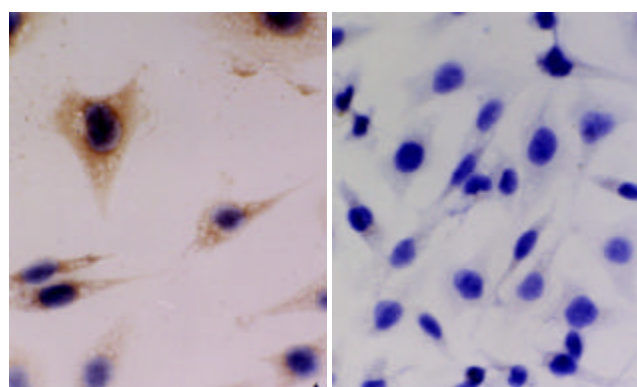


Figure 3 Expression of KAI1 in LoVo-KAI1 cell and LoVo-neo cell by *in situ* hybridization. The left picture: Expression of LoVo-KAI1 cells ($\times 400$) showed that the positive expression (brown granule) located in cytoplasm. The right picture: Expression of LoVo-neo cells ($\times 400$) was negative.

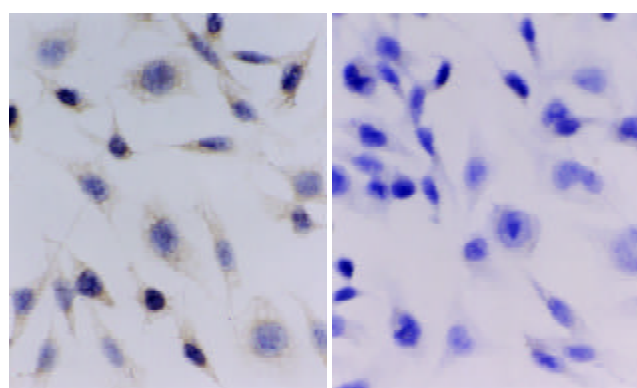


Figure 4 Expression of CD82 in LoVo-KAI1 cells and LoVo-neo cells by immunohistochemistry. The left picture: Detection of LoVo-KAI1 cells ($\times 400$) was positive, the cytoplasm and the membrane were stained brown. The right picture: Detection of LoVo-neo cells ($\times 400$) was negative.

Cell-matrix adhesion assay

All LoVo-neo cells attached to fibronectin and the surface of fibronectin appeared the phenomena of degradation while most LoVo-KAI1 cells attached to fibronectin and no degradation occurred. MTT assay showed OD_{570} in LoVo-KAI1 cells was 0.164 ± 0.011 and OD_{570} in LoVo-neo cells was 0.499 ± 0.023 . Attachment of LoVo-neo cells to fibronectin were demonstrated to be much higher compared to attachment of LoVo-KAI1 cells ($P < 0.01$).

In vitro invasion assay

An *in vitro* cell invasion assay was performed based on the principle of the Boyden chamber assay. The matrigel matrix served as a reconstituted basement membrane *in vitro*. The number of cells migrating through the Matrigel matrix was counted and the result was presented in Figure 8, 9. The LoVo-KAI1 cells showed significantly reduced invasiveness as compared with LoVo-neo cells ($P < 0.01$). These data indicated that the enhanced expression of KAI1 in LoVo-KAI1 cells was associated with reduced invasive ability.

Monolayer cells invasion assay

After cultured for 24 h, some tumor cells had invaded the ECV304 cells and migrated through the monolayer cells of ECV304. The invasive number of LoVo-KAI1 cells was 6.33 ± 1.74 and that of LoVo-neo was 17.67 ± 4.73 . The invasive ability of the LoVo-KAI1 cells was significantly reduced compared with that of the LoVo-neo cells ($P < 0.05$).

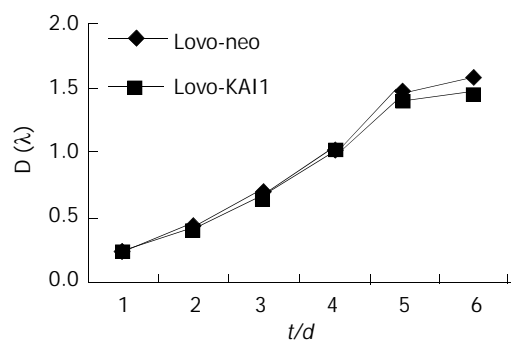


Figure 5 Growth curve of LoVo-KAI1 and LoVo-neo ($P < 0.05$).

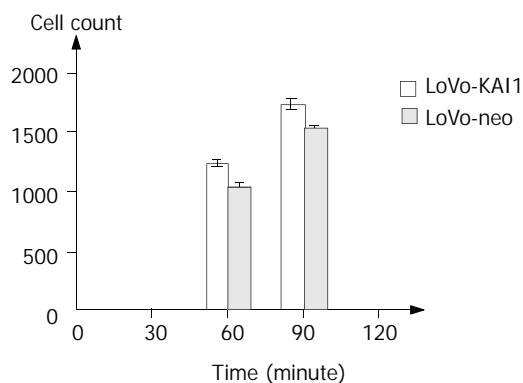


Figure 6 Adhesion of homotypic cells: The cell-cell adhesion ability in LoVo-KAI1 cells was significantly increased as compared with that of LoVo-neo cells ($P < 0.01$).

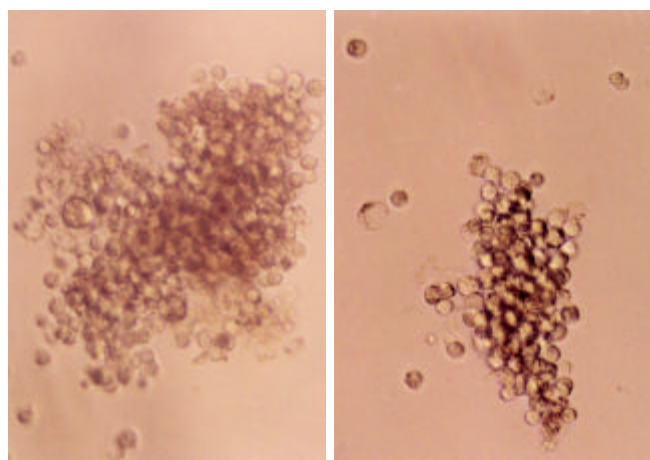


Figure 7 The cells aggregation pictures. The left picture: The LoVo-KAI1 cells formed large multicellular aggregates. The right picture: The LoVo-neo cells formed smaller aggregates.

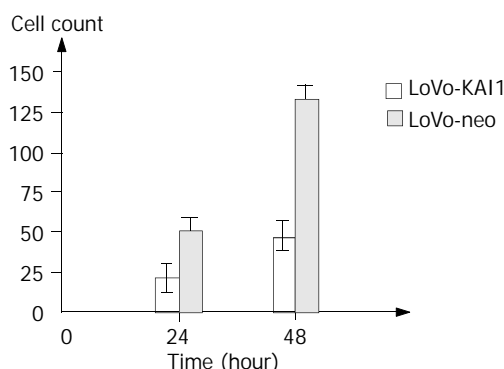


Figure 8 The invasion assay: The invasive number of LoVo-KAI1 cells was significantly reduced compared with that of LoVo-neo cells ($P < 0.01$).

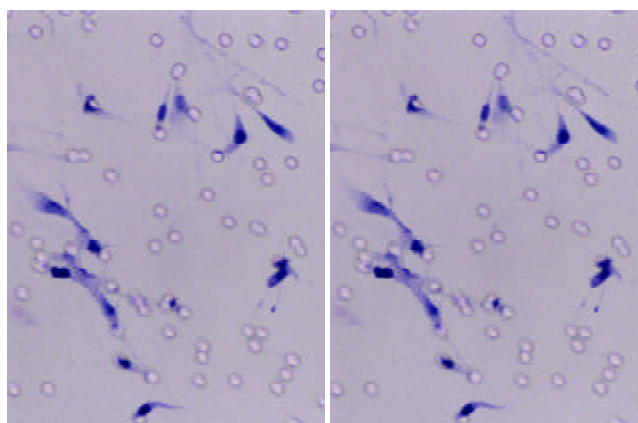


Figure 9 The invasion ability of LoVo-KAI1 cells and LoVo-neo cells by modified Boyden chamber. The left picture: LoVo-KAI1 cell invasion picture ($\times 200$). The right picture: LoVo-neo cell invasion picture ($\times 200$).

DISCUSSION

Loss of the function of metastasis suppressor genes is an important step in the progression of a tumor type. KAI1 is thought to be one of such metastasis suppressor genes because it has been shown to suppress the ability of human prostatic cancer cells to metastasize when the tumor is transplanted into nude mice^[1] and because KAI1 mRNA expression is reduced in advanced pancreatic cancer^[20], it enables the pancreatic cancer cells to spread to lymph nodes and distant organs. Furthermore, transfer of the KAI1 gene into mammary cancer cells has been shown to lead to suppression of their metastatic potential, whereas their primary tumor growth is not affected.

In our previous studies, KAI1 gene expression at protein level was inversely correlated with the metastatic potential of some established colorectal carcinoma cell lines. Maurer *et al* also demonstrated that the progression of colorectal cancer was associated with decreased expression of KAI1^[21]. To further elucidate the effect of KAI1 on colorectal carcinoma cell behavior, we transfected KAI1 cDNA into highly malignant colon adenocarcinoma cell lines, LoVo, which have low level of endogenous KAI1 expression. Consistent with the studies of prostatic cancer^[2], breast cancer^[12] cells by Dong and Yang, our data also indicated that KAI1 expression did not alter *in vitro* cell proliferation.

To determine if KAI1 expression was reflected in changes of intercellular adhesion, we used cell-cell adhesion assay and cell-cell aggregation assay. We found KAI1 could increase homotypic cells adhesion and the transfectants formed large multicellular aggregates than non-transfected cells. In terms of cell-matrix, our results showed that KAI1 could reduce the transfected cells adhesion to fibronectin as compared with the controls. Member of the TM4SF family of proteins associated with each other and specific integrins^[22], suggesting that they might be involved in cell-cell and cell-matrix interactions. Current thinking suggests that these interactions are involved in the formation of multiprotein complexes within the cell membrane that include cell surface receptors, specific integrins and TM4SF proteins. Consequently, a reduced expression of TM4SF proteins might reasonably be expected to have profound effects on cell-cell and cell-matrix interactions. An important avenue of further investigation will be to determine precisely the functions and location of TM4SF-integrin complexes. In this context, Berditchevski^[23] has recently provided evidence that TM4SF can modulate integrin signaling and point to a mechanism by which TM4SF proteins regulate cell adhesion.

Our data showed KAI1 could decrease invasive ability in

the transfected cells to a reconstituted basement membrane and endothelium compared to the controls. And there is also accumulated evidence that KAI1 is involved in the reduction of invasive tumor cells. Imai demonstrated that decreased KAI1 gene expression might be associated with increased invasive ability of oral squamous cell carcinoma^[24]. Takaoka's study also suggested that reduced KAI1 gene expression might contribute to the invasiveness and metastatic ability of colon cancer cells^[25]. How does reduced TM4SF expression cause changes of invasive ability in tumor cells? It was hypothesized that tetraspanins might be implicated in the assembly of integrin-containing signaling complexes, thus modulating the function of integrin receptors in cell migration^[26]. Sugiura's results indicated that integrin-tetraspanin protein complexes played an important role in regulating protrusive activity of the tumor cells and contributed to ECM-induced production of MMP-2, and as a consequence, the invasive ability of cells^[27].

Our *in vitro* study are consistent with *in vivo* observations that reduced KAI1 expression is associated with invasive human colorectal carcinoma. Muneyuki and Lombardi found that KAI1 expression was closely correlated with clinicopathological factors for colorectal cancers and appeared to be a useful prognostic marker^[28-30].

KAI1 has been extensively studied for its involvement in the progression of different human cancers. The mechanism of down-regulation is also analyzed although it exists much debate. Mashimo recently found a putative p53 consensus-binding site within the promoter region of KAI1 and demonstrated that the loss of p53 function, which is commonly observed in many types of cancer, leads to the down-regulation of KAI1 gene, which may result in the progression of metastasis^[31]. But Uzawa's data suggest that the down-regulation of KAI1 is not associated with either mutation, allelic loss, methylation of the promoter, or p53 regulation^[32]. Our previous study also demonstrated that mutation of KAI1 gene, methylation of CpG islands and abnormality of p53 were not related to low expression of KAI1.

Our results demonstrated a significantly increased adhesion to homotypic cells and decreased adhesion to extracellular matrix components and lower level of invasiveness. In conclusion, KAI1 has a close relationship with tumor adhesion and invasion and the effect of KAI1 appears to be directly targeted on tumor metastasis. Through our studies, we wish colorectal carcinoma cells would be more homotypical adhesion, less adhesive to matrix, less invasive^[33] that are necessary for metastasis.

REFERENCES

- Dong JT**, Lamb PW, Rinker-Schaeffer CW, Vukanovic J, Ichikawa T, Isaacs JT, Barrett JC. KAI1, a metastasis suppressor gene for prostate cancer on human chromosome 11p11.2. *Science* 1995; **268**: 884-886
- Dong JT**, Isaacs WB, Barrett JC, Isaacs JT. Genomic organization of the human KAI1 metastasis-suppressor gene. *Genomics* 1997; **41**: 25-32
- Petty HR**, Worth RG, Todd R F 3rd. Interactions of integrins with their partner proteins in leukocyte membranes. *Immunol Res* 2002; **25**: 75-95
- Maecker HT**, Todd SC, Levy S. The tetraspanin superfamily: molecular facilitators. *FASEB J* 1997; **11**: 428-442
- White A**, Lamb PW, Barrett JC. Frequent downregulation of the KAI1(CD82) metastasis suppressor protein in human cancer cell lines. *Oncogene* 1998; **16**: 3143-3149
- Okochi H**, Mine T, Nashiro K, Suzuki J, Fujita T, Furue M. Expression of tetraspanins transmembrane family in the epithelium of the gastrointestinal tract. *J Clin Gastroenterol* 1999; **29**: 63-67
- Adachi M**, Taki T, Konishi T, Huang CI, Higashiyama M, Miyake M. Novel staging protocol for non-small-cell lung cancers according to MRP-1/CD9 and KAI1/CD82 gene expression. *J Clin Oncol* 1998; **16**: 1397-1406
- Rubinstein E**, Le Naour F, Lagaudriere Gesbert C, Billard M, Conjeaud H, Boucheix C. CD9, CD63, CD81, and CD82 are components of a surface tetraspan network connected to HLA-DR and VLA integrins. *Eur J Immunol* 1996; **26**: 2657-2665
- Bienstock RJ**, Barrett JC. KAI1, a prostate metastasis suppressor: prediction of solvated structure and interactions with binding partners; integrins, cadherins, and cell-surface receptor proteins. *Mol Carcinog* 2001; **32**: 139-153
- Hashida H**, Takabayashi A, Tokuhara T, Taki T, Keiichi K, Kohno N, Yamaoka Y, Migake M. Integrin alpha3 expression as a prognostic factor in colon cancer: association with MRP-1/CD9 and KAI1/CD82. *Int J Cancer* 2002; **97**: 518-525
- Liu FS**, Chen JT, Dong JT, Hsieh YT, Lin AJ, Ho ES, Hung MJ, Lu CH. KAI1 metastasis suppressor gene is frequently down-regulated in cervical carcinoma. *Am J Pathol* 2001; **159**: 1629-1634
- Yang X**, Wei LL, Tang C, Slack R, Mueller S, Lippman ME. Overexpression of KAI1 suppresses *in vitro* invasiveness and *in vivo* metastasis in breast cancer cells. *Cancer Res* 2001; **61**: 5284-5288
- Friess H**, Guo XZ, Tempia Caliera AA, Fukuda A, Martignoni ME, Zimmermann A, Korc M, Buchler MW. Differential expression of metastasis-associated genes in papilla of Vater and pancreatic cancer correlates with disease stage. *J Clin Oncol* 2001; **19**: 2422-2432
- Miyazaki T**, Kato H, Shitara Y, Yoshikawa M, Tajima K, Masuda N, Shouji H, Tsukada K, Nakajima T, Kuwano H. Mutation and expression of the metastasis suppressor gene KAI1 in esophageal squamous cell carcinoma. *Cancer* 2000; **89**: 955-962
- Liu FS**, Dong JT, Chen JT, Hsieh YT, Ho ES, Hung MJ. Frequent down-regulation and lack of mutation of the KAI1 metastasis suppressor gene in epithelial ovarian carcinoma. *Gynecol Oncol* 2000; **78**: 10-15
- Tagawa K**, Arihiro K, Takeshima Y, Hiyama E, Yamasaki M, Inai K. Down-regulation of KAI1 messenger RNA expression is not associated with loss of heterozygosity of the KAI1 gene region in lung adenocarcinoma. *Jpn J Cancer Res* 1999; **90**: 970-976
- Whittard JD**, Akiyama SK. Activation of beta1 integrins induces cell-cell adhesion. *Exp Cell Res* 2001; **263**: 65-76
- Jackson P**, Kingsley EA, Russell PJ. Inverse correlation between KAI1 mRNA levels and invasive behaviour in bladder cancer cell lines. *Cancer Lett* 2000; **156**: 9-17
- Itoh F**, Yamamoto H, Hinoda Y, Imai K. Enhanced secretion and activation of matrilysin during malignant conversion of human colorectal epithelium and its relationship with invasive potential of colon cancer cells. *Cancer* 1996; **77**: 1717-1721
- Guo X**, Friess H, Graber HU, Kashiwagi M, Zimmermann A, Korc M, Buchler MW. KAI1 expression is up-regulated in early pancreatic cancer and decreased in the presence of metastases. *Cancer Res* 1996; **56**: 4876-4880
- Maurer CA**, Graber HU, Friess H, Beyermann B, Willi D, Netzer P, Zimmermann A, Buchler MW. Reduced expression of the metastasis suppressor gene KAI1 in advanced colon cancer and its metastases. *Surgery* 1999; **126**: 869-880
- Shibagaki N**, Hanada K, Yamashita H, Shimada S, Hamada H. Overexpression of CD82 on human T cells enhances LFA-1/ICAM-1-mediated cell-cell adhesion: functional association between CD82 and LFA-1 in T cell activation. *Eur J Immunol* 1999; **29**: 4081-4091
- Berditchevski F**, Odintsova E. Characterization of integrin-tetraspanin adhesion complexes: role of tetraspanins in integrin signaling. *J Cell Biol* 1999; **146**: 477-492
- Imai Y**, Sasaki T, Shinagawa Y, Akimoto K, Fujibayashi T. Expression of metastasis suppressor gene (KAI1/CD82) in oral squamous cell carcinoma and its clinic-pathological significance. *Oral Oncol* 2002; **38**: 557-561
- Takaoka A**, Hinoda Y, Satoh S, Adachi Y, Itoh F, Adachi M, Imai K. Suppression of invasive properties of colon cancer cells by a metastasis suppressor KAI1 gene. *Oncogene* 1998; **16**: 1443-1453
- Hemler ME**, Mannion BA, Berditchevski F. Association of TM4SF proteins with integrins: relevance to cancer. *Biochim Biophys Acta* 1996; **1287**: 67-71

- 27 **Muneyuki T**, Watanabe M, Yamanaka M, Shiraishi T, Isaji S. KAIL/CD82 expression as a prognostic factor in sporadic colorectal cancer. *Anticancer Res* 2001; **21**: 3581-3587
- 28 **Mikami T**, Ookawa K, Shimoyama T, Fukuda S, Saito H, Munakata A. KAI1, CAR, and Smad4 expression in the progression of colorectal tumor. *J Gastroenterol* 2001; **36**: 465-469
- 29 **Lombardi DP**, Geradts J, Foley JF, Chiao C, Lamb PW, Barrett JC. Loss of KAI1 expression in the progression of colorectal cancer. *Cancer Res* 1999; **59**: 5724-5731
- 30 **Sugiura T**, Berditchevski F. Function of alpha3 beta1-tetraspanin protein complexes complexes in tumor cell invasion. Evidence for the role of the complexes in production of matrix metalloproteinase 2(MMP-2). *J Cell Biol* 1999; **146**: 1375-1389
- 31 **Mashimo T**, Watabe M, Hirota S, Hosobe S, Miura K, Tegtmeyer PJ, Rinker-Shaeffer CW, Watabe K. The expression of the KAI1 gene, a tumor metastasis suppressor, is directly activated by p53. *Proc Natl Acad Sci USA* 1998; **95**: 11307-11311
- 32 **Uzawa K**, Ono K, Suzuki H, Tanaka C, Yakushiji T, Yamamoto N, Yokoe H, Tanzawa H. High prevalence of decreased expression of KAI1 metastasis suppressor in human oral carcinogenesis. *Clin Cancer Res* 2002; **8**: 828-835
- 33 **Geradts J**, Maynard R, Birrer MJ, Hendricks D, Abbondanzo SL, Fong KM, Barrett JC, Lombardi DP. Frequent loss of KAI1 expression in squamous and lymphoid neoplasms. An immunohistochemical study of archival tissues. *Am J Pathol* 1999; **154**: 1665-1671

Edited by Wu XN

Cyclooxygenase-2 expression and angiogenesis in colorectal cancer

Bin Xiong, Tao-Jiao Sun, Hong-Yin Yuan, Ming-Bo Hu, Wei-Dong Hu, Fu-Lin Cheng

Bin Xiong, Tao-Jiao Sun, Hong-Yin Yuan, Ming-Bo Hu, Wei-Dong Hu, Fu-Lin Cheng, Department of Oncology, Affiliated Zhongnan Hospital of Wuhan University, Wuhan 430071, Hubei Province, China
Supported by Hubei Province Natural Science Foundation, No.2000J054

Correspondence to: Dr. Bin Xiong, Department of Oncology, Affiliated Zhongnan Hospital of Wuhan University, Wuhan 430071, Hubei Province, China. xbxh@public.wh.hb.cn

Telephone: +86-27-87325716

Received: 2003-01-11 **Accepted:** 2003-03-10

Abstract

AIM: Cyclooxygenase-2 is involved in a variety of important cellular functions, including cell growth and differentiation, cancer cell motility and invasion, angiogenesis and immune function. However, the role of cyclooxygenase-2 as an angiogenic factor in colorectal cancer tissue is still unclear. We investigated the relationship between cyclooxygenase-2 and angiogenesis by analyzing the expression of cyclooxygenase-2 in colorectal cancer tissue, as well as its association with vascular endothelial growth factor (VEGF) and microvascular density (MVD).

METHODS: The expression of cyclooxygenase-2, VEGF, as well as MVD was detected in 128 cases of colorectal cancer by immunohistochemical staining. The relationship between the cyclooxygenase-2 and VEGF expression and MVD was evaluated. Our objective was to determine the effect of cyclooxygenase-2 on the angiogenesis of colorectal cancer tissue.

RESULTS: Among 128 cases of colorectal cancer, 87 were positive for cyclooxygenase-2 (67.9 %), and 49 for VEGF (38.3 %), respectively. The microvessel counts ranged from 23 to 142, with a mean of 51.7 (standard deviation, 19.8). The expression of cyclooxygenase-2 was correlated significantly with the depth of invasion, stage of disease, metastasis (lymph node and liver), VEGF expression and MVD. Patients in T3-T4, stage III-IV and with metastasis had much higher expression of cyclooxygenase-2 than patients in T1-T2, stage I-II and without metastasis ($P < 0.05$). The positive expression rate of VEGF (81.6 %) in the cyclooxygenase-2 positive group was higher than that in the cyclooxygenase-2 negative group (18.4 %, $P < 0.05$). Also, the microvessel count (56 ± 16) in cyclooxygenase-2 positive group was significantly higher than that in cyclooxygenase-2 negative group (43 ± 12 , $P < 0.05$). The microvessel count in tumors with positive cyclooxygenase-2 and VEGF was the highest (60 ± 18 , 41-142, $P < 0.05$), whereas that in tumors with negative cyclooxygenase-2 and VEGF was the lowest (39 ± 16 , 23-68, $P < 0.05$).

CONCLUSION: Cyclooxygenase-2 may be associated with tumor progression by modulating the angiogenesis in colorectal cancer tissue and used as a possible biomarker.

Xiong B, Sun TJ, Yuan HY, Hu MB, Hu WD, Cheng FL. Cyclooxygenase-2 expression and angiogenesis in colorectal cancer. *World J Gastroenterol* 2003; 9(6): 1237-1240
<http://www.wjgnet.com/1007-9327/9/1237.asp>

INTRODUCTION

Angiogenesis has been postulated to play an important role in the development of malignant tumors^[1-5]. Increased vascularity may allow not only an increase in tumor growth but also a greater chance of hematogenous tumor embolization^[6]. An association between poor prognosis and increase in microvascular density (MVD) of tumor has been reported in certain tumors^[7-10]. This neoangiogenesis depends on the production of angiogenic factors by tumor cells and normal cells^[11-15].

Cyclooxygenase (COX) is a key enzyme in prostaglandin biosynthesis^[16]. Two COX isoforms, COX-1 and COX-2, have been identified. COX-1 is constitutively expressed and involved in general cell functions, whereas COX-2 is an inducible enzyme that is up-regulated in response to various stimuli, including growth factors and mitogens^[17-22]. An enhanced expression of COX-2 has been found in many tumors, such as the lung, the breast, the esophagus and colon cancer^[23-26]. Recent studies have demonstrated that COX-2 could affect carcinogenesis via several different mechanisms^[27-35]. COX-2 has been also reported to induce angiogenesis^[36-39]. COX-2 may be related to development of colorectal cancer, however, its association with angiogenesis in colorectal cancer tissue still remains unclear. To determine the role of COX-2 expression in angiogenesis of colorectal cancer, we examined the VEGF and MVD in colorectal cancer tissue, and then compared the findings with the expression of COX-2 protein.

MATERIALS AND METHODS

Patients

A total of 128 cases of colorectal adenocarcinoma patients who had undergone surgical resection in the Affiliated Zhongnan Hospital of Wuhan University (Wuhan, China) from January 1999 to September 2002 were included. COX-2, VEGF immunohistochemical staining and MVD counting were performed. There were 73 men and 55 women, and their age ranged from 23 to 74 years (means, 56 ± 11 years). Among the 128 patients, 26 were well differentiated adenocarcinoma, 57 moderately differentiated adenocarcinoma and 45 poorly differentiated adenocarcinoma. According to Duke's staging criteria, 37 cases were stage I, 41 stage II, 39 stage III and 11 stage IV.

Methods

Immunohistochemistry: All the tissue specimens were fixed in 100 mL L^{-1} neutral formalin and embedded in paraffin. Five- μ m thick sections were dewaxed in xylene and dehydrated in ethanol. Tissue sections were washed three times in 0.05 mol L^{-1} PBS, and incubated in endogenous peroxidase blocking solution. Non-specific antibody binding was blocked by pretreatment with PBS containing 5 g L^{-1} bovin serum albumin. Sections were then rinsed in PBS and incubated overnight at 4 °C with diluted anti-COX-2, anti-VEGF and anti-CD34 antibodies. The steps were performed using immunostain kit according to the manufacturer's

instructions. PBS was used as substitutes of antibody for negative control. The sections were examined under light microscope. Anti-VEGF polyclonal antibody and anti-CD34 monoclonal antibody were purchased from Bosden Co. (Wuhan, China). Anti-COX-2 polyclonal antibody was purchased from Santa Cruz Co. (USA). S-P detection kit was purchased from Fuzhou Maixin Co. (Fuzhou, China). Anti-COX-2 polyclonal antibody was diluted to 1:75. Anti-VEGF polyclonal antibody and anti-CD34 monoclonal antibody were impromptu type.

Results: Positive evaluation for COX-2 was performed according to the following scoring system^[16]: staining intensity was graded as weak (1), moderate (2), or strong (3), and area of staining positivity as <10 percent (0) of all cells stained in the cytoplasm as viewed by microscope, 10 to 40 percent (1), 40 to 70 percent (2), or ≥ 70 percent (3). A total for grade and area of 3 or more was defined as positive expression and less than 3 as negative. Positive signal for VEGF was located in the cytoplasm or/and cell membrane^[2]. Immunoreactivity was graded as follows: +, ≥ 10 percent stained tumor cells; -, <10 percent stained tumor cells^[2]. The microvessel counting procedures have been described in the published studies^[2]. Briefly, the stained sections were screened at a magnification of $\times 100$ ($\times 10$ objective and $\times 10$ ocular lens) under a light microscope to identify 3 regions of the section with the highest microvessel density. Microvessels were counted in these areas at a magnification of $\times 200$, and the average numbers of microvessels were recorded. The average number is known as MVD of the tumor.

Statistical analysis

The difference between each group was analyzed by Chi-square test. $P < 0.05$ was considered significant.

RESULTS

COX-2 expression in colorectal cancer and clinicopathologic findings

COX-2 was expressed in the cytoplasm of cancer cells (Figure 1). COX-2 expression in primary tumor was noted in 67.9 % (87/128). The correlation between COX-2 expression and the clinicopathologic findings is shown in Table 1. The expression of COX-2 was significantly correlated with depth of invasion, stage of disease, metastasis (lymph node and liver). Patients in T3-T4, stage III-IV, with metastasis had much higher COX-2 expression than patients in T1-T2, stage I-II, without metastasis ($P < 0.05$). The expression of COX-2 was not correlated with age, gender and differentiation degree of the tumor ($P > 0.05$).

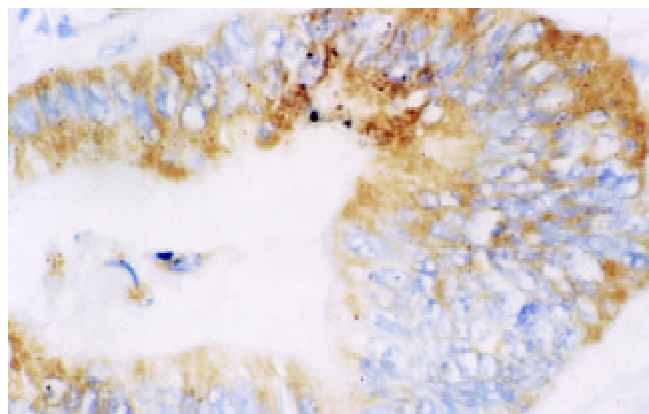


Figure 1 Expression of COX-2 mainly in cytoplasm of tumor cells, S-P, $\times 400$.

Table 1 Clinicopathologic characteristics of colorectal cancer with expression of COX-2

Variable	n	COX-2 Positive n(%)	COX-2 Negative n(%)
Sex			
Male	73	50(68.5)	23(31.5)
Female	55	37(67.3)	18(32.7)
Age(y)		54 \pm 12	56 \pm 15
Histological differentiation			
Well	26	17(65.4)	9 (34.6)
Moderate	57	40(70.2)	17(29.8)
Poor	45	30(66.7)	15(33.3)
Depth of invasion			
T1-T2	81	48(59.3)	33(40.7)
T3-T4	47	39(83.0)	8 (17.0) ^a
Metastasis			
Present	50	42(84.0)	8 (16.0)
Absent	78	45(57.7)	33(42.3) ^a
Duke's stage			
A	37	15(40.5)	22(59.5)
B	41	28(68.3)	13(31.7)
C+D	50	44(88.0)	6 (12.0) ^a
VEGF expression			
Positive	49	40(81.6)	9 (18.4)
Negative	79	47(59.5)	32(40.5) ^a
MVD ($\bar{x}\pm s$)		56 \pm 16	43 \pm 12 ^a

^a $P < 0.05$, vs positive.

Relationship between COX-2 and VEGF expression and MVD

VEGF was localized mainly in the cytoplasm and cell membrane of the tumor cells (Figure 2). VEGF expression was detected in 49 tumors (38.3 %), and COX-2 expression was correlated closely with VEGF expression (Table 1). The positive expression rate of VEGF (81.6 %) in the COX-2 positive group was higher than that in the COX-2 negative group (18.4 %) ($P < 0.05$).

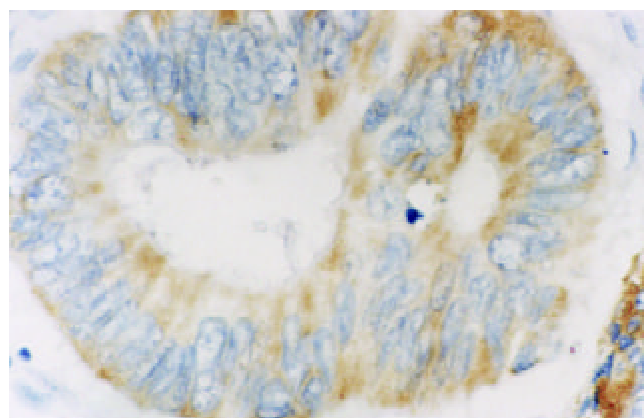


Figure 2 VEGF expression mainly in cytoplasm and membrane of tumor cell, S-P, $\times 400$.

The number of microvessel counts in all cases was 23-142 ($\bar{x}\pm s$, 50 \pm 19). Moreover, the microvessel counts were 56 \pm 16 in COX-2 positive tumors and 43 \pm 12 in COX-2 negative tumors ($P < 0.05$, Table 1). COX-2 expression, VEGF expression and MVD were significantly correlated with one another ($r=0.5635, 0.2812, 0.5253$, respectively, $P < 0.05$). The microvessel counts in tumors with both positive COX-2 and VEGF were the highest (60 \pm 18, 41-142; $P < 0.05$). The

microvessel counts in tumors with both negative COX-2 and VEGF were the lowest (39±16, 23-68; $P<0.05$). The microvessel counts in tumors with positive COX-2 and negative VEGF were 50±16 (29-130), and that in tumors with negative COX-2 and positive VEGF were 51±18 (30-132), lower than that in tumors with both positive COX-2 and VEGF ($P<0.05$). The microvessel counts in tumors with positive COX-2 and negative VEGF were not different from that in tumors with negative COX-2 and positive VEGF ($P>0.05$).

DISCUSSION

Angiogenesis is essential for tumor growth and metastasis. The process of angiogenesis is the outcome of an imbalance between positive and negative angiogenic factors produced by both tumor cells and normal cells. Numerous angiogenic factors have been described. Of these, VEGF plays a key role in the angiogenesis in colorectal cancer^[1-15]. VEGF is a multi-functional cytokine, and has direct relationship with angiogenesis. The factors that regulate VEGF expression in tumor and non-tumor cells have now been elucidated^[10-28]. COX-2 is an inducible enzyme catalyzing the conversion of arachidonic acid to biologically active prostanoids. COX-2 modulates the growth and function of many cells, including those with malignant transformation. The over-expression of COX-2 has been reported in tissue from patients with different carcinoma, and is believed to play a role in tumor transformation and progression, as well as in tumor regression^[23-33]. Recent experimental studies showed that COX-2 could inhibit cell apoptosis, regulate angiogenesis, and was associated with matrix metalloproteinases (MMP)^[16-48]. Uefuji *et al*^[45] studied the correlation of COX-2 and angiogenesis of gastric cancer, and found COX-2 might regulate angiogenesis.

COX-2 was overexpressed in approximately 80 percent of colorectal cancer cases^[16], but the role of COX-2 in angiogenesis of colorectal cancer tissue has not been identified yet. This study found that the expression of VEGF and MVD in positive COX-2 group was significantly higher than that in COX-2 negative group. The expression of COX-2 was significantly correlated with the expression of VEGF. It demonstrated that COX-2 might be correlated indirectly with angiogenesis through an up-regulation of the expression of VEGF. The expression of COX-2 was also significantly correlated with MVD in colorectal cancer. It indicates that COX-2 may modulate angiogenesis directly or indirectly through up-regulating the expression of other angiogenic factors. The microvessel counts in tumors that were both positive COX-2 and VEGF were the highest of all. It suggests that COX-2 and VEGF may co-modulate angiogenesis.

COX-2 expression was detected in 87 tumors (67.9 %). The expression of COX-2 was correlated significantly with the depth of invasion, stage of disease and metastasis (lymph node and liver). Patients in T3-T4, stage C-D and with metastasis had much higher expression of COX-2 than patients in T1-T2, stage A-B and without metastasis ($P<0.05$). It suggests that COX-2 is closely related to the invasion and metastasis of colorectal cancer, and COX-2 may be used as a possible biomarker.

REFERENCES

- 1 **Gunsilius E**, Tschmelitsch J, Eberwein M, Schwelberger H, Spizzo G, Kahier CM, Stockhammer G, Lang A, Petzer AL, Gastl G. In vivo release of vascular endothelial growth factor from colorectal carcinomas. *Oncology* 2002; **62**: 313-317
- 2 **Xiong B**, Gong LL, Zhang F, Hu MB, Yuan HY. TGFβ1 expression and angiogenesis in colorectal cancer tissue. *World J Gastroenterol* 2002; **8**: 496-498
- 3 **Tsuji T**, Sasaki Y, Tanaka M, Hanabata N, Hada R, Munakata A. Microvessel morphology and vascular endothelial growth factor expression in human colonic carcinoma with or without metastasis. *Lab Invest* 2002; **82**: 555-562
- 4 **Uthoff SM**, Duchrow M, Schmidt MH, Broll R, Bruch HP, Strik MW, Galandiuk S. VEGF isoforms and mutations in human colorectal cancer. *Int J Cancer* 2002; **101**: 32-36
- 5 **Shaheen RM**, Tseng WW, Davis DW, Liu W, Reinmuth N, Vellagas R, Wiczorek AA, Ogura Y, McConkey DJ, Drazan KE, Bucana CD, McMahon G, Ellis LM. Tyrosine kinase inhibition of multiple angiogenesis growth factor receptors improves survival in mice bearing colon cancer liver metastasis by inhibition of endothelial cell survival mechanisms. *Cancer Res* 2001; **61**: 1464-1468
- 6 **Dachs GU**, Tozer GM. Hypoxia modulated gene expression: angiogenesis, metastasis and therapeutic exploitation. *Eur J Cancer* 2000; **36**: 1649-1660
- 7 **Sumiyoshi Y**, Yamashita Y, Maekawa T, Sakai N, Shirakusa T, Kikuchi M. Expression of CD44, vascular endothelial growth factor, and proliferating cell nuclear antigen in severe venous invasional colorectal cancer and its relationship to liver metastasis. *Surg Today* 2000; **30**: 323-327
- 8 **Kondo Y**, Arai S, Mori A, Furutani M, Chiba T, Imamura M. Enhancement of angiogenesis, tumor growth, and metastasis by transfection of vascular endothelial growth factor into LoVo human colon cancer cell line. *Clin Cancer Res* 2000; **6**: 622-630
- 9 **Ellis LM**, Takahashi Y, Liu W, Shaheen RM. Vascular endothelial growth factor in human colon cancer: biology and therapeutic implications. *Oncologist* 2000; **5**(Suppl 1): 11-15
- 10 **Jia L**, Chen TX, Sun JW, Na ZM, Zhang HH. Relationship between microvessel density and proliferating cell nuclear antigen and prognosis in colorectal cancer. *Shijie Huaren Xiaohua Zazhi* 2000; **8**: 74-76
- 11 **Teraoka H**, Sawada T, Nishihara T, Yashiro M, Ohira M, Ishikawa T, Nishino H, Hirakawa K. Enhanced VEGF production and decreased immunogenicity induced by TGF-β1 promote liver metastasis of pancreatic cancer. *Br J Cancer* 2001; **85**: 612-617
- 12 **Mancuso P**, Burlini A, Pruneri G, Goldhirsch A, Martinelli G, Bertolini F. Resting and activated endothelial cells are increased in the peripheral blood of cancer patients. *Blood* 2001; **97**: 3658-3661
- 13 **Carmeliet P**, Jain RK. Angiogenesis in cancer and other diseases. *Nature* 2000; **407**: 249-257
- 14 **Liu DH**, Zhang W, Su YP, Zhang XY, Huang YX. Constructions of eukaryotic expression vector of sense and antisense VEGF165 and its expression regulation. *Shijie Huaren Xiaohua Zazhi* 2001; **9**: 886-891
- 15 **Yamauchi T**, Watanabe M, Kubota T, Hasegawa H, Ishii Y, Endo T, Kabeshima Y, Yorozuya K, Yamamoto K, Mukai M, Kitajima M. Cyclooxygenase-2 expression as a new marker for patients with colorectal cancer. *Dis Colon Rectum* 2002; **45**: 98-103
- 16 **Qiu DK**, Ma X, Peng YS, Chen XY. Significance of cyclooxygenase-2 expression in human primary hepatocellular carcinoma. *World J Gastroenterol* 2002; **8**: 815-817
- 17 **Wu QM**, Li SB, Wang Q, Wang DH, Li XB, Liu CZ. The expression of COX-2 in esophageal carcinoma and its relation to clinicopathologic characteristics. *Shijie Huaren Xiaohua Zazhi* 2001; **9**: 11-14
- 18 **Wu HP**, Wu KC, Li L, Yao LP, Lan M, Wang X, Fan DM. Cloning of human cyclooxygenase-2 (COX-2) encoding gene and study of gastric cancer cell transfected with its antisense vector. *Shijie Huaren Xiaohua Zazhi* 2000; **8**: 1211-1217
- 19 **Cao Y**, Prescott SM. Many actions of cyclooxygenase-2 in cellular dynamics and in cancer. *J Cell Physiol* 2002; **190**: 279-286
- 20 **Koki AT**, Masferrer JL. Celecoxib: A specific COX-2 inhibitor with anticancer properties. *Cancer Control* 2002; **9**(Suppl 2): 28-35
- 21 **Kakiuchi Y**, Tsuji S, Tsujii M, Murata H, Kawai N, Yasumaru M, Kimura A, Komori M, Irie T, Miyoshi E, Sasaki Y, Hayashi N, Kawano S, Hori M. Cyclooxygenase-2 activity altered the cell-surface carbohydrate antigens on colon cancer cells and enhanced liver metastasis. *Cancer Res* 2002; **62**: 1567-1572
- 22 **Hida T**, Kozaki K, Ito H, Miyaishi O, Tatematsu Y, Suzuki T, Matsuo K, Sugiura T, Ogawa M, Takahashi T, Takahashi T. Significant growth inhibition of human lung cancer cells both *in vitro* and *in vivo* by the combined use of a selective cyclooxygenase-2 inhibitor, JTE-522, and conventional anticancer agents. *Clin Cancer Res* 2002; **8**: 2443-2447

- 23 **Yamada H**, Kuroda E, Matsumoto S, Matsumoto T, Yamada T, Yamashita U. Prostaglandin E2 down-regulates viable bacilli calmette-guerin-induced macrophage cytotoxicity against murine bladder cancer cell MBT-2 *in vitro*. *Clin Exp Immunol* 2002; **128**: 52-58
- 24 **Harizi H**, Juzan M, Pitard V, Moreau JF, Gualde N. Cyclooxygenase-2-issued prostaglandin E2 enhances the production of endogenous IL-10, which down-regulates dendritic cell functions. *J Immunology* 2002; **168**: 2255-2263
- 25 **Kundu N**, Fulton AM. Selective cyclooxygenase(COX)-1 or COX-2 inhibitors control metastasis disease in a murine model of breast cancer. *Cancer Res* 2002; **62**: 2343-2346
- 26 **Leahy KM**, Ornberg RL, Wang Y, Zweifel BS, Koki AT, Masferrer JL. Cyclooxygenase-2 inhibition by celecoxib reduces proliferation and induces apoptosis in angiogenic endothelial cells *in vivo*. *Cancer Res* 2002; **62**: 625-631
- 27 **Hansen-Petrik MB**, McEntee MF, Jull B, Shi H, Zemel MB, Whelan J. Prostaglandin E2 protects intestinal tumors from non-steroidal anti-inflammatory drug-induced regression in Apc^{Min/+} Mice. *Cancer Res* 2002; **62**: 403-408
- 28 **Waskewich C**, Blumenthal RD, Li H, Stein R, Goldenberg DM, Burton J. Celecoxib exhibits the greatest potency amongst cyclooxygenase(COX) inhibitors for growth inhibition of COX-2-negative hematopoietic and epithelial cell lines. *Cancer Res* 2002; **62**: 2029-2033
- 29 **Jones MK**, Szabo IL, Kawanaka H, Husain SS, Tarnawski AS. von Hippel Lindau tumor suppressor and HIF-1 α : new targets of NSAIDs inhibition of hypoxia-induced angiogenesis. *FASEB J* 2002; **16**: 264-266
- 30 **Kvirkvelia N**, Vojnovic I, Warner TD, Athie-Morales V, Free P, Rayment N, Chain BM, Rademacher TW, Lund T, Roitt IM, Delves PJ. Placentally derived prostaglandin E2 acts via the EP4 receptor to inhibit IL-2 dependent proliferation of CTLL-2 T cell. *Clin Exp Immunol* 2002; **127**: 263-269
- 31 **Adam L**, Mazumdar A, Sharma T, Jones TR, Kumar R. A three-dimensional and temporo-spatial model to study invasiveness of cancer cells by heregulin and prostaglandin E2. *Cancer Res* 2001; **61**: 81-87
- 32 **Dannhardt G**, Ulbrich H. In-vitro test system for the evaluation of cyclooxygenase-1(COX-1) and cyclooxygenase-2(COX-2) inhibitors based on a single HPLC run with UV detection using bovine aortic coronary endothelial cells(BAECs). *Inflamm Res* 2001; **50**: 262-269
- 33 **Bae SH**, Jung ES, Park YM, Kim BS, Kim BK, Kim DG, Ryu WS. Expression of cyclooxygenase-2(COX-2) in hepatocellular carcinoma and growth inhibition of hepatoma cell lines by a COX-2 inhibitor, NS-398. *Clin Cancer Res* 2001; **7**: 1410-1418
- 34 **Yang WL**, Frucht H. Activation of the PPAR pathway induces apoptosis and COX-2 inhibition in HT-29 human colon cancer cells. *Carcinogenesis* 2001; **22**: 1379-1383
- 35 **Dohadwala M**, Luo J, Zhu L, Lin Y, Dougherty GJ, Sharma S, Huang M, Pold M, Batra RK, Dubinett SM. Non-small cell lung cancer cyclooxygenase-2 dependent invasion is mediated by CD44. *J Biol Chem* 2001; **276**: 20809-20812
- 36 **Dempke W**, Rie C, Grothey A, Schmoll HJ. Cyclooxygenase-2: a novel target for cancer chemotherapy? *J Cancer Res Clin Oncol* 2001; **127**: 411-417
- 37 **Gilroy DW**, Saunders MA, Wu KK. COX-2 expression and cell cycle progression in human fibroblasts. *Am J Physiol Cell Physiol* 2001; **281**: C188-194
- 38 **Chen WS**, Wei SJ, Liu JM, Hsiao M, Kou-Lin J, Yang WK. Tumor invasiveness and liver metastasis of colon cancer cells correlated with cyclooxygenase-2(COX-2) expression and inhibited by a COX-2 selective inhibitor, *Etodolac*. *Int J Cancer* 2001; **91**: 894-899
- 39 **Rozić JG**, Chakraborty C, Lala PK. Cyclooxygenase inhibitors retard murine mammary tumor progression by reducing tumor cell migration, invasiveness and angiogenesis. *Int J Cancer* 2001; **93**: 497-506
- 40 **Williams CS**, Tsujii M, Reese J, Dey SK, DuBois RN. Host cyclooxygenase-2 modulates carcinoma growth. *J Clin Invest* 2000; **105**: 1589-1594
- 41 **Marrogi A**, Pass HI, Khan M, Metheng-Barlow LJ, Harris CC, Gerwin BI. Human meothelioma sample overexpress both cyclooxygenase-2(COX-2) and inducible nitric oxide synthase (NOS2): *In vitro* antiproliferative effects of a COX-2 inhibitor. *Cancer Res* 2000; **60**: 3696-3700
- 42 **Uefuji K**, Ichikura T, Mochizuki H. Cyclooxygenase-2 expression is related to prostaglandin biosynthesis and angiogenesis in human gastric cancer. *Clin Cancer Res* 2000; **6**: 135-138
- 43 **Attiga FA**, Fernandez PM, Weeraratna AT, Manyak MJ, Patierno SR. Inhibitors of prostaglandin synthesis inhibit human prostate tumor cell invasiveness and reduce the release of matrix metalloproteinases. *Cancer Res* 2000; **60**: 4629-4637
- 44 **Shao J**, Sheng H, Inoue H, Morrow JD, DuBois RN. Regulation of constitutive cyclooxygenase-2 expression in colon carcinoma cells. *J Biol Chem* 2000; **275**: 33951-33956
- 45 **Masferrer JL**, Leahy KM, Koki AT, Zweifel BS, Settle SL, Woerner BM, Edwards DA, Flickinger AG, Moore RJ, Seibert K. Antiangiogenic and antitumor activities of cyclooxygenase-2 inhibitors. *Cancer Res* 2000; **60**: 1306-1311
- 46 **Reddy BS**, Hirose Y, Lubet R, Steele V, Kelloff G, Paulson S, Seibert K, Rao CV. Chemoprevention of colon cancer by specific cyclooxygenase-2 inhibitor, Celecoxib, administered during different stages of carcinogenesis. *Cancer Res* 2000; **60**: 293-297
- 47 **Hsueh CT**, Chiu CF, Kelsen DP, Schwartz GK. Selective inhibition of cyclooxygenase-2 enhances mitomycin-C induced apoptosis. *Cancer Chemother Pharmacol* 2000; **45**: 389-396
- 48 **Hida T**, Kozaki K, Muramatsu H, Masuda A, Shimizu S, Mitsudomi T, Sugiura T, Ogawa M, Takahashi T. Cyclooxygenase-2 inhibitor induces apoptosis and enhances cytotoxicity of various anticancer agents in non-small cell lung cancer cell lines. *Clin Cancer Res* 2000; **6**: 2006-2011

Synergistic antitumor effect of TRAIL and doxorubicin on colon cancer cell line SW480

Li-Hong Xu, Chang-Sheng Deng, You-Qing Zhu, Shi-Quan Liu, Dong-Zhou Liu

Li-Hong Xu, Chang-Sheng Deng, You-Qing Zhu, Department of Gastroenterology, Zhongnan Hospital of Wuhan University, Wuhan 430071, Hubei Province China

Shi-Quan Liu, Department of Oncology, Zhongnan Hospital of Wuhan University, Wuhan 430071, Hubei Province China

Dong-Zhou Liu, Department of Nephrology, Renmin Hospital of Wuhan University, Wuhan 430060, Hubei Province China

Correspondence to: Li-Hong Xu, Department of Gastroenterology, Zhongnan Hospital of Wuhan University, Donghu Road 169, Wuhan 430071, Hubei Province China. hqy222@yahoo.com.cn

Telephone: +86-27-87330254

Received: 2002-12-28 **Accepted:** 2003-02-15

Abstract

AIM: TRAIL (tumor necrosis factor-related apoptosis-inducing ligand) has been reported to specifically induce apoptosis of cancer cells although only a small percentage of cell lines were sensitive to it. Cell lines not responding to TRAIL *in vitro* were said to be more prone to apoptosis when TRAIL was combined with another anticancer agent. Generally, factors affecting drug-sensitivity involve many apoptosis-related proteins, including p53. The expression of wild-type p53 gene was proposed as an important premise for tumor cells responding to chemotherapy. The present study was to investigate the cell killing action of TRAIL on colon cancer cell line SW480, its synergistic effect with doxorubicin, and the possible mechanisms.

METHODS: SW480 cells were cultured in the regular condition and incubated with different levels of agents. Morphologic changes in these cells after treatment were observed under phase-contrast microscope and cytotoxicity by TRAIL alone and in combination with doxorubicin was quantified by a 1-day microculture tetrazolium dye (MTT) assay. In addition, flow cytometry assay (FCM) and transmission electron microscopy were used to detect apoptosis among these cells. Variation of p53 protein level among different groups according to concentrations of agents was measured by Western blot assay.

RESULTS: (1) SW480 cells were not sensitive to TRAIL, with $IC_{50} > 1 \text{ mg} \cdot \text{L}^{-1}$ and dose-independent cytotoxicity. (2) SW480 cells were sensitive to doxorubicin at a certain degree, with dose-dependent cytotoxicity and $IC_{50} = 65.25 \pm 3.48 \text{ } \mu\text{mol} \cdot \text{L}^{-1}$. (3) TRAIL could synergize with doxorubicin to kill SW480 cells effectively, which was represented by the boosted killing effect of doxorubicin on these cells. IC_{50} of doxorubicin against SW480 cells sharply reduced when it was combined with TRAIL. (4) Subtoxic TRAIL ($100 \text{ } \mu\text{g} \cdot \text{L}^{-1}$), combined with subtoxic doxorubicin ($0.86 \text{ } \mu\text{mol} \cdot \text{L}^{-1}$), could kill SW480 cells sufficiently. Cytotoxicity by MTT assay arrived at $80.12 \pm 2.67 \%$, which was significantly higher than that by TRAIL or doxorubicin alone, with $P = 0.006$ and 0.003 respectively. This killing effect was partly due to apoptosis. It was proved by large amounts of apoptotic cells under phase-contrast microscopy, cell apoptosis rate of $76.82 \pm 1.93 \%$ by FCM assay and typical apoptotic

morphology observed through transmission electron microscopy. Increase of apoptosis after combined treatment had no relation with protein level of p53 ($P > 0.05$).

CONCLUSION: SW480 cells are not sensitive to TRAIL, but TRAIL can synergize with lower concentration of doxorubicin to induce apoptosis effectively. The status of p53 protein is not involved in the mechanism of synergistic apoptosis. It suggests the potential therapeutic applicability of the combination of TRAIL with doxorubicin against colon cancers.

Xu LH, Deng CS, Zhu YQ, Liu SQ, Liu DZ. Synergistic antitumor effect of TRAIL and doxorubicin on colon cancer cell line SW480. *World J Gastroenterol* 2003; 9(6): 1241-1245

<http://www.wjgnet.com/1007-9327/9/1241.asp>

INTRODUCTION

The rapid induction of apoptosis by TRAIL (tumor necrosis factor-related apoptosis-inducing ligand) preferentially in tumor cells but not in normal cells has implied its potential use in therapy of malignancies^[1,2]. Recent studies indicated that many cancer cells *in vitro* were resistant to apoptosis-inducing effect of TRAIL^[3,4]. Enhancement of the antitumor activity of TRAIL by metabolic inhibitors has led to later studies encompassing the augmentation of antitumor effects of several kinds of chemotherapy or radiation therapy by TRAIL^[5-13].

Doxorubicin has been the regular chemotherapeutic agents for its strong cell killing ability. But severe systemic toxicity limited its use in the clinical treatment of cancer. Reduction of its dose and maintenance of its high efficacy will be necessary in the future treatment of tumors. More efforts have been made to explore the combination of chemodrugs with some other agents^[14].

MATERIALS AND METHODS

Materials

SW480 cell line was purchased from ATCC and maintained in Roswell Park Memorial Institute (RPMI)-1640 medium (Gibco) supplemented with $2 \text{ mmol} \cdot \text{L}^{-1}$ L-glutamine (Gibco), $100 \text{ kU} \cdot \text{L}^{-1}$ penicillin (Gibco), $100 \text{ g} \cdot \text{L}^{-1}$ streptomycin (Gibco) and $100 \text{ ml} \cdot \text{L}^{-1}$ heat-inactivated fetal bovine serum (Gibco), hereafter referred to as complete medium. Recombinant human soluble TRAIL (rhsTRAIL) was purchased from Pepro Tech, USA. Doxorubicin, p53 Mab and MTT were respectively from Sigma Co, Santa Cruz Company and Amresco Co.

Methods

Cytotoxicity assay Cytotoxicity was determined by MTT assay. In brief, the cells were cultured in 96-well microtiter plates under $50 \text{ ml} \cdot \text{L}^{-1} \text{ CO}_2$ in a humidified atmosphere at $37 \text{ }^\circ\text{C}$. Each well was then incubated for 4 h with MTT solution (final concentration $0.45 \text{ g} \cdot \text{L}^{-1}$, Sigma Chemical, St.Louis, MO) under the same condition. Culture medium in each well was discarded and replaced with $100 \text{ } \mu\text{L}$ of dissolving solution (DMSO). The absorbance of each well was determined by a spectrophotometer

with a 490 nm wavelength. The percentage of cell viability was calculated by multiplying the ratio absorbance of the sample versus the control by 100. Doxorubicin IC_{50} was determined as a doxorubicin concentration showing 50 % cell growth inhibition as compared with control cell growth.

Antitumor activity of doxorubicin and/or TRAIL The cells were placed at 4×10^4 cells/well in 96-well microtiter plates. After 24 h culture for cell adherence to the plate, doxorubicin and/or TRAIL were added to each well at a given concentration. Detection of cell viability by MTT assay was performed following further incubation of the cells with doxorubicin and/or TRAIL for another 24 h. One well treated by the complete medium with neither doxorubicin nor TRAIL served as a control. The experiments were repeated in triplicate, and the percentage of cell viability was expressed as mean \pm standard deviation.

Flow cytometry This analysis was conducted with a Facscan flow cytometer (Becton Dickinson, Mountain View, CA). It was to quantify cell apoptosis by the propidium iodide method. In brief, the cells were harvested by trypsinization at 24 hours after treatment and washed twice with PBS (pH 7.2). The medium and PBS were placed in tubes and centrifuged. A total of 1 ml of hypotonic buffer (propidium iodide, 50 mg \cdot L $^{-1}$, in 1 ml \cdot L $^{-1}$ sodium citrate, Rnase plus 1 ml \cdot L $^{-1}$ Triton X-100; sigma) was added directly to the tubes and gently pipetted off. The tubes were placed at 4 $^{\circ}$ C in the dark for half an hour before flow cytometry analysis. The propidium iodide fluorescence of individual nuclei was measured in the red fluorescence and the data were registered in a logarithmic scale. At least 10^4 cells of each sample were analyzed each time. Apoptotic nuclei appeared as a broad hypodiploid DNA peak before the G_1 phase of cell cycle, which was easily distinguished from the narrow hyperdiploid DNA peak at the G_1 phase or later G_2 and S phase.

Transmission electron microscopy Transmission electron microscopy was used to observe apoptosis directly through morphological changes at the subcellular level. In brief, the cells were cultured in the regular condition for 24 h. Then, TRAIL (100 μ g \cdot L $^{-1}$), doxorubicin (0.86 μ mol \cdot L $^{-1}$), their combination or the complete culture medium was added to them and maintained for another 24 h. After these, the cells were subsequently trypsinized, harvested, fixed in glutaral, immersed with Epon 821, imbedded in capsules and converged. Ultrathin sections of 60 nm were finally prepared and stained with uranyl acetate and lead citrate. Cell morphology was measured by transmission electron microscope.

Western blot analysis for p53 protein expression p53 levels following treatment with doxorubicin and/or TRAIL were investigated by Western blot analysis. The cells were incubated with the medium alone, doxorubicin alone, TRAIL alone, or the combination of doxorubicin and TRAIL at 37 $^{\circ}$ C for 24 h. The cells were lysed in a lysis buffer consisting of 1 mmol \cdot L $^{-1}$ dithiothreitol, 1 mmol \cdot L $^{-1}$ phenylmethyl sulphonyl fluoride, 5 mg \cdot L $^{-1}$ leupeptin, 1 mmol \cdot L $^{-1}$ NaF, 10 mmol \cdot L $^{-1}$ β -glycerophosphate, 2 mmol \cdot L $^{-1}$ Natrium orthovanadate, 50 mmol \cdot L $^{-1}$ HEPES, 250 mmol \cdot L $^{-1}$ NaCl, 1 mmol \cdot L $^{-1}$ EDTA, and 1 % Nonidet P-40. After centrifuged for 7 min at 14 000 g, the supernatant was collected and the total protein amount was determined by SPECTRAMax 250. Twelve μ g/lane of proteins were boiled in a sample buffer for 1 min at 100 $^{\circ}$ C, electrophoresed in a multigel 10/20, and then transferred to Immobilon-P membranes (Millipore). Nonspecific antibody bindings were blocked by preincubation of the membranes for 1 h with a 5 % skim milk suspension. Then the membranes were incubated for 1 h with the polyclonal rabbit anti-human p53 antibody (1:200) (Santa Cruz, Delaware, CA), followed by further incubation overnight with horseradish peroxidase conjugated anti-rabbit IgG (1:2 000) (Santa Cruz). After each

antibody incubation, the membranes were washed three times by Tris-buffer saline. To visualize the protein bands, ECL Western blot detection reagents (Amersham, Buckinghamshire, UK) were used and the membranes were exposed to X-ray film.

Statistical analysis

All determinations were made in triplicate, and the results were expressed as the mean \pm standard deviation (S.D.). Statistical significance was determined by Student's *t*-test. A *P* value of 0.05 or less was considered significant.

RESULTS

Effect of TRAIL or doxorubicin on SW480 cells

MTT assay demonstrated that SW480 cells were not sensitive to TRAIL. No dose-dependent cytotoxicity of TRAIL on these cells was found at the concentrations from 0 μ g \cdot L $^{-1}$, 10 μ g \cdot L $^{-1}$, 100 μ g \cdot L $^{-1}$, 500 μ g \cdot L $^{-1}$, to 1 mg \cdot L $^{-1}$, (as shown in Figure 1). IC_{50} was above 1 mg \cdot L $^{-1}$ which was significantly higher than 0.4 μ g \cdot L $^{-1}$ of TRAIL-sensitive leukaemic cell line Jurkat. 100 μ g \cdot L $^{-1}$ TRAIL could only affect 5.8 % of these cells, a subtoxic concentration. By contrast, SW480 cells responded to doxorubicin sensitively, with obvious dose-dependent cytotoxicity and IC_{50} of 65.25 ± 3.48 μ mol \cdot L $^{-1}$. 0.86 μ mol \cdot L $^{-1}$ doxorubicin could not damage any cell, also a subtoxic concentration (as shown in Figure 2). All values by MTT assay were proved by flow cytometry assay and apoptosis applauded parallel with cytotoxicity.

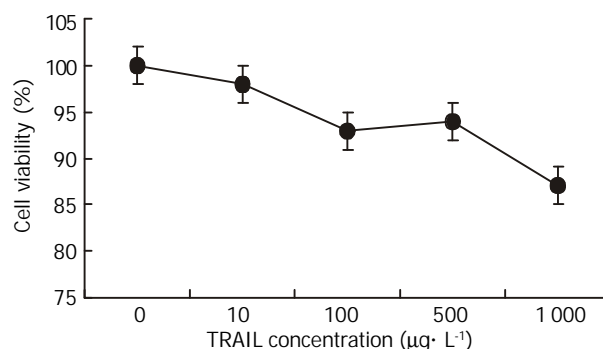
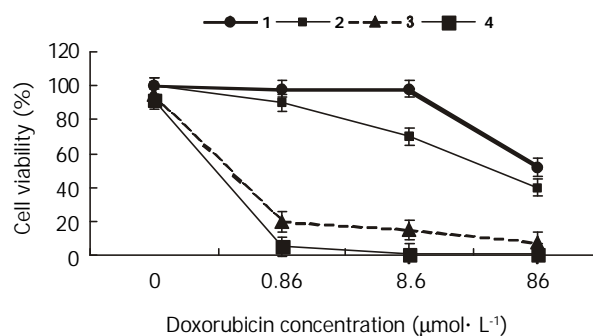


Figure 1 Effect of TRAIL on SW480 cells. SW480 cells were treated with TRAIL at the concentrations of 0, 10, 100, 500 and 1 000 μ g \cdot L $^{-1}$ for 24 h. Cell growth inhibition was assessed by MTT assay and confirmed by flow cytometry assay. Compared with TRAIL-sensitive leukaemic cell line Jurkat (IC_{50} 0.42 μ g \cdot L $^{-1}$), SW480 cells (IC_{50} >1 000 μ g \cdot L $^{-1}$) were not responsive to TRAIL at concentration more than 100 times those active on Jurkat.



1, 2, 3, 4 was respectively doxorubicin with TRAIL 0, 10, 100, 1000 μ g \cdot L $^{-1}$.

Figure 2 Effect of TRAIL and doxorubicin on SW480 cells SW480 cells were treated with doxorubicin alone or a combination of doxorubicin with TRAIL at different concentrations. The combination resulted in the reduction of doxorubicin IC_{50} in cells ($P < 0.05$). Doxo-

rubicin IC₅₀ was 65.25±3.48 when cells were treated by doxorubicin alone, while it was further reduced with the increased concentrations of TRAIL. Doxorubicin IC₅₀ was 43.17±2.54 μmol·L⁻¹ when it was combined with 10 μg·L⁻¹ of TRAIL, 0.51±0.02 μmol·L⁻¹ IC₅₀ when combined with 100 μg·L⁻¹ TRAIL, and 0.44±0.02 μmol·L⁻¹ IC₅₀ when combined with 1 000 μg·L⁻¹ TRAIL.

Effect of TRAIL and doxorubicin on SW480 cells

SW480 cells were treated by doxorubicin alone, TRAIL alone, and a combination of doxorubicin and TRAIL, and cell viability after each treatment was determined by MTT assay. The cell growth inhibitory effects of the combined treatment were synergistic and more significant in proportion to the increasing concentrations of TRAIL as compared with doxorubicin alone. Furthermore, TRAIL could cause a decrease in doxorubicin IC₅₀ (as shown in Figure 2).

Effect of subtoxic TRAIL with subtoxic doxorubicin on SW480 cells

Subtoxic concentration TRAIL of 100 μg·L⁻¹, with subtoxic concentration doxorubicin of 0.86 μmol·L⁻¹ was capable of killing 80.12±2.67 % cells by MTT assay. Much more apoptotic cells were observed under phase-contrast microscope in the group treated by this combination compared with those treated by TRAIL or doxorubicin alone. Flow cytometry assay also measured apoptosis rate of 76.82±1.93 % and obvious pre-G₁ apoptotic DNA peak among the cells (as shown in Figure 3). And electron microscopy observed a large number of apoptosis cells in them (as shown in Figure 4).

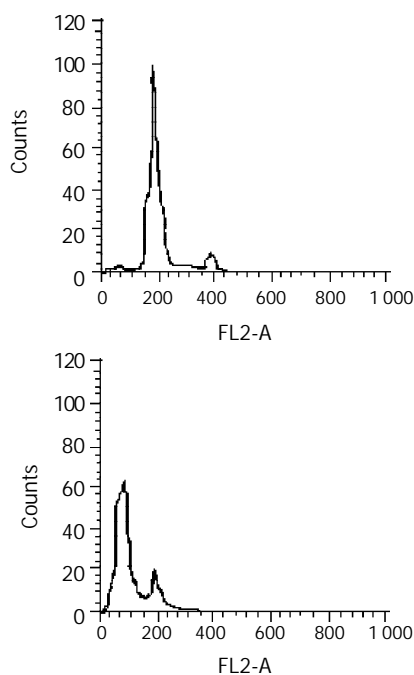


Figure 3 Apoptosis assay by flow cytometry. SW480 cells were treated with doxorubicin (0.86 μmol·L⁻¹) alone, TRAIL (100 μg·L⁻¹) alone or a combination of them for 24 h. The apoptosis-inducing effect was quantified by PI stain flow cytometry assay. A: There was no hypodiploid DNA peak before G₁ phase which was similar to normal cells when treated with TRAIL (100 μg·L⁻¹) or doxorubicin (0.86 μmol·L⁻¹) alone. B: There was an obvious hyperdiploid DNA peak before G₁ phase in combination treatment, with apoptotic rate of 76.82±1.93 %. It was in accordance with cytotoxicity by MTT assay.

Protein level of mutant p53 before and after treatment of TRAIL and/or doxorubicin

SW480 cells were treated with 100 μg·L⁻¹ TRAIL alone, 0.86 μmol·L⁻¹ doxorubicin alone, and their combination or complete

control medium for 24 h. The protein level of mutant p53 was not different among them, with P>0.05 (as shown in Figure5). Variation of agent concentration turned out similar result.

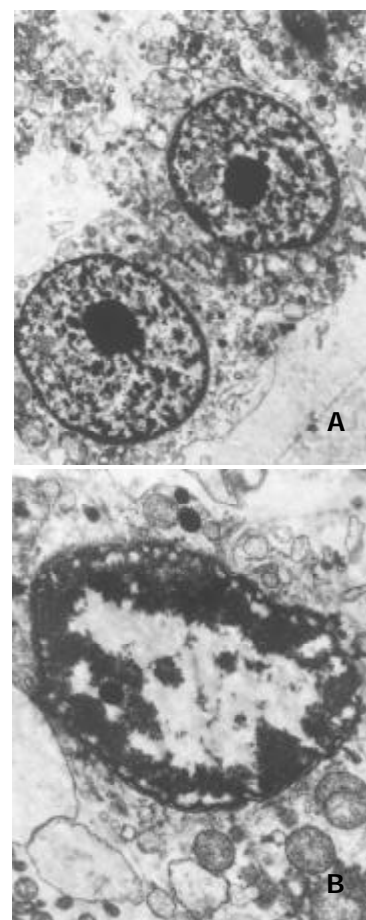


Figure 4 Subcellular morphology of SW480 cells under treatment of TRAIL (100 μg·L⁻¹), doxorubicin (0.86 μmol·L⁻¹), or the combination of them. The electron microscopic morphology was observed after 24 hours treatment at the given concentration. A: TRAIL (100 μg·L⁻¹) or doxorubicin (0.86 μmol·L⁻¹) alone didn't affect the morphology of cells, with complete construction and evenly distributed chromatin (×5 000). B: The combination of TRAIL (100 μg·L⁻¹) and doxorubicin (0.86 μmol·L⁻¹) induced apoptosis in many cells, presented as condensed chromatin, distributing along nuclear perimeter (×15 000).

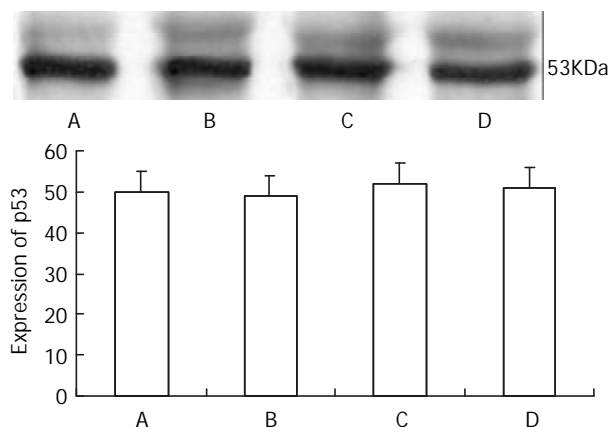


Figure 5 p53 protein level by Western blot assay. They were detected after 24 hours of treatment. A, B, C, D were respectively normal control, TRAIL (100 μg·L⁻¹), doxorubicin (0.86 μmol·L⁻¹) and TRAIL (100 μg·L⁻¹) + doxorubicin (0.86 μmol·L⁻¹) groups. There was no difference in p53 protein expression among these four groups (P>0.05).

DISCUSSION

TRAIL, also named Apo-2L, is a new member of the TNF cytokine family. It resembles Fas/Apo-2L in its amino acid sequence, as well as in its ability to induce apoptosis. It conducts or regulates the activities via a set of receptors on the surface of various cells^[15-24]. TRAIL has attracted much interest for a profound feature since its discovery in 1995. That is the selectivity of killing cells, namely, TRAIL only induces apoptosis in transformed or tumor cells, but does not damage the normal ones^[1,2]. There was a proposal for its clinical use after a series of *in vitro* experimentations. But a variety of cancer cells of breast, lung, prostate, colon and bladder were reported resistant to the effect of TRAIL^[5-7].

Results in this study demonstrated that colon cancer cell line SW480 was relatively resistant to TRAIL, compared with TRAIL-sensitive leukaemic cell line Jurkat. The mechanisms of the underlying resistance was not clear update^[7-9]. The conditions of decoy receptors, caspase-inhibition protein (FLIP), caspases and some apoptosis-related genes might attribute to the different responses^[25-34]. It's necessary to find a way to reverse the resistance if it is used in clinic in the future. Previous articles indicated some chemotherapeutic drugs could sensitize the cancer cells to TRAIL-mediated apoptosis^[10-15]. Doxorubicin is a member of antibiotics, specifically for cancer cells. It belongs to the classical chemotherapeutic agents, with high anti-cancer efficacy. However, severe cardiac toxicity limits its broad use in clinic. Reducing concentration and maintaining efficacy of doxorubicin should be necessary for continuing its work. This study also demonstrated the sensitivity of SW480 cells to doxorubicin and its synergistic effect with TRAIL when percentage of cell viabilities were significantly decreased by the combined treatment at any dose as compared with those treated by doxorubicin or TRAIL alone. The degrees of growth inhibition were greater accompanied by the increased concentrations of TRAIL. Furthermore, augmentation of the cytotoxic effect of doxorubicin with TRAIL was significant even at low Doxorubicin ($0.86 \mu\text{mol} \cdot \text{L}^{-1}$) and low TRAIL ($100 \mu\text{g} \cdot \text{L}^{-1}$) concentrations in SW480 cells. It presented the evidence that TRAIL could reduce the dose of doxorubicin against tumor cells, which ultimately resulted in minimizing risks for systemic side effects while increasing the efficacy of doxorubicin, suggesting the clinical applicability of this combination for colon cancers.

Concentrations of TRAIL that were completely inactive on their own, boosted the activity of doxorubicin in the SW480 cells. This correlated well with the increased ability of this drug when combined with TRAIL to induce apoptosis and it did not correlate with the status of p53. Mutant-type p53 was said to contribute to drug-resistance of most cancer cells^[27, 28]. The precise mechanisms enabling TRAIL to augment the cytotoxicity of chemotherapeutic agents in the p53 mutant-type cells have not been extensively investigated; however, recent evidence has suggested several possibilities: First, the augmentation of TRAIL-induced apoptosis by adriamycin or 5FU in p53 wild- and mutant-type breast cancer cell lines was mediated through a selective activation of caspases by these agents^[28]. Subsequent investigations demonstrated that caspase activation, which was not observed with TRAIL or doxorubicin alone, became more evident after the combined treatment in p53 mutant-type cell lines. These findings implied that the up-regulation of intracellular apoptotic signaling events contributed to overcome resistance to TRAIL alone even in p53 mutant-type cells. Second, the increase of KILLER/DR5 expression by certain genotoxic stresses, which resulted in the enhancement of TRAIL, is regulated in a p53-dependent and -independent manner^[29, 30]. Finally, another TRAIL receptor, DR4, which transmitted a death signal through its binding with

TRAIL, is regulated in a p53-independent manner^[31-34].

The finding that TRAIL could boost the activity of doxorubicin against colorectal carcinoma cells should have important therapeutic implications. Since TRAIL itself is thought to have no apparent toxicity to normal cells and to be safe in systemic administration, the combination of doxorubicin and TRAIL will result in minimization of the toxicity and maximization of the antitumor activity.

REFERENCES

- Ashkenazi A**, Pai RC, Fong S, Leung S, Lawrence DA, Marsters SA, Blackie C, Chang L, McMurtrey AE, Hebert A, De Forge L, Koumenis IL, Lewis D, Harris L, Bussiere J, Koeppen H, Shahrokh Z, Schwall RH. Safety and antitumor activity of recombinant soluble Apo2 ligand. *J Clin Invest* 1999; **104**: 155-162
- Lin T**, Huang X, Gu J, Zhang L, Roth JA, Xiong M, Curley SA, Yu Y, Hunt KK, Fang B. Long-term tumor-free survival from treatment with the GFP-TRAIL fusion gene expressed from the hTERT promoter in breast cancer cells. *Oncogene* 2002; **21**: 8020-8028
- Jang YJ**, Park KS, Chung HY, Kim HI. Analysis of the phenotypes of Jurkat clones with different TRAIL-sensitivity. *Cancer Lett* 2003; **194**: 107-117
- Naumann U**, Waltereit R, Schulz JB, Weller M. Adenoviral (full-length) Apo2L/TRAIL gene transfer is an ineffective treatment strategy for malignant glioma. *J Neurooncol* 2003; **61**: 7-15
- Gliniak B**, Le T. Tumor necrosis factor-related apoptosis-inducing ligand's antitumor activity *in vivo* is enhanced by the chemotherapeutic agent CPT-11. *Cancer Res* 1999; **59**: 6153-6158
- Jin Z**, Dicker DT, El-Deiry WS. Enhanced sensitivity of G1 arrested human cancer cells suggests a novel therapeutic strategy using a combination of simvastatin and TRAIL. *Cell Cycle* 2002; **1**: 82-89
- Hernandez A**, Wang QD, Schwartz SA, Evers BM. Sensitization of human colon cancer cells to TRAIL-mediated apoptosis. *J Gastrointest Surg* 2001; **5**: 56-65
- Hietakangas V**, Poukkula M, Heiskanen KM, Karvinen JT, Sistonen L, Eriksson JE. Erythroid differentiation sensitizes K562 leukemia cells to TRAIL-induced apoptosis by downregulation of c-FLIP. *Mol Cell Biol* 2003; **23**: 1278-1291
- Keane MM**, Ettenberg SA, Nau MM, Russell EK, Lipkowitz S. Chemotherapy augments TRAIL-induced apoptosis in breast cell lines. *Cancer Res* 1999; **59**: 734-741
- Vignati S**, Codegani A, Polato F, Brogginini M. Trail activity in human ovarian cancer cells: potentiation of the action of cytotoxic drugs. *Eur J Cancer* 2002; **38**: 177-183
- Mizutani Y**, Nakanishi H, Yoshida O, Fukushima M, Bonavida B, Miki T. Potentiation of the sensitivity of renal cell carcinoma cells to TRAIL-mediated apoptosis by subtoxic concentrations of 5-fluorouracil. *Eur J Cancer* 2002; **38**: 167-176
- Shimoyama S**, Mochizuki Y, Kusada O, Kaminishi M. Supra-additive antitumor activity of 5FU with tumor necrosis factor-related apoptosis-inducing ligand on gastric and colon cancers *in vitro*. *Int J Oncol* 2002; **21**: 643-648
- Wei XC**, Wang XJ, Chen K, Zhang L, Liang Y, Lin XL. Killing effect of TNF-related apoptosis inducing ligand regulated by tetracycline on gastric cancer cell line NCI-N87. *World J Gastroenterol* 2001; **7**: 559-562
- Chen XX**, Lai MD, Zhang YL, Huang Q. Less cytotoxicity to combination therapy of 5-fluorouracil and cisplatin than 5-fluorouracil alone in human colon cancer cell lines. *World J Gastroenterol* 2002; **8**: 841-846
- Sheridan JP**, Marsters SA, Pitti RM, Gurney A, Skubtch M, Baldwin D, Ramakrishnan L, Gray CL, Baker K, Wood WL, Goddard AD, Godowski P, Ashkenazi A. Control of TRAIL-induced apoptosis by a family of signaling and decoy receptors. *Science* 1997; **277**: 818-821
- Schneider P**, Thome M, Burns K, Bodmer JL, Hofmann K, Kataoka T, Holler N, Tschopp J. TRAIL receptors 1 (DR4) and 2 (DR5) signal FADD-dependent apoptosis and activate NF- κ B. *Immunity* 1997; **7**: 831-836
- Walczak H**, Degli-Esposti MA, Johnson RS, Smolak PJ, Waugh JY, Boiani N, Timour MS, Gerhart MJ, Schooley KA, Smith CA,

- Goodwin RG, Rauch CT. TRAIL-R2: a novel apoptosis-mediating receptor for TRAIL. *EMBO J* 1997; **16**: 5386-5397
- 18 **Strater J**, Hinz U, Walczak H, Mechtersheimer G, Koretz K, Herfarth C, Moller P, Lehnert T. Expression of TRAIL and TRAIL receptors in colon carcinoma: TRAIL-R1 is an independent prognostic parameter. *Clin Cancer Res* 2002; **8**: 3734-3740
- 19 **Degli-Esposti MA**, Smolak PJ, Walczak H., Waugh J, Huang CP, Dubose RF, Goodwin RG, Smith CA. Cloning and characterization of TRAIL-R3, a novel member of the emerging TRAIL receptor family. *J Exp Med* 1997; **186**: 1165-1170
- 20 **Degli-Esposti MA**, Dougall WC, Smolak PJ, Waugh JY, Smith CA, Goodwin RG. The novel receptor TRAIL-R4 induces NF- κ B and protects against TRAIL-mediated apoptosis, yet retains an incomplete death domain. *Immunity* 1997; **7**: 813-820
- 21 **Marsters SA**, Sheridan JP, Pitti RM, Huang A, Skubtch M, Baldwin D, Yuan J, Gurney A, Goddard AD, Godowski P, Ashkenazi A. A novel receptor for Apo2L/TRAIL contains a truncated death domain. *Curr Biol* 1997; **7**: 1003-1006
- 22 **Pan G**, Ni J, Yu G, Wei YF, Dixit VM. TRUNDD, a new member of the TRAIL receptor family that antagonizes TRAIL signaling. *FEBS Lett* 1998; **424**: 41-45
- 23 **Emery JG**, McDonnell P, Burke MB, Deen KC, Lyn S, Silverman C, Dul E, Appelbaum ER, Eichman C, DiPrinzio R, Dodds RA, James IE, Rosenberg M, Lee JC, Young PR. Osteoprotegerin is a receptor for the cytotoxic ligand TRAIL. *J Biol Chem* 1998; **273**: 14363-14367
- 24 **Shipman CM**, Croucher PI. Osteoprotegerin is a soluble decoy receptor for tumor necrosis factor-related apoptosis-inducing ligand/apo2 ligand and can function as a paracrine survival Factor for human myeloma cells. *Cancer Res* 2003; **63**: 912-916
- 25 **Griffith TS**, Lynch DH. TRAIL: a molecule with multiple receptors and control mechanisms. *Curr. Opin Immunol* 1998; **10**: 559-563
- 26 **Grotzer MA**, Eggert A, Zuzak TJ, Janss AJ, Marwaha S, Wiewrodt BR, Ikegakin, Brodeur GM, Phillips PC. Resistance to TRAIL-induced apoptosis in primitive neuroectodermal brain tumor cells correlates with a loss of caspase-8 expression. *Oncogene* 2000; **19**: 4604-4610
- 27 **Xu SQ**, El-Deiry WS. P21^{WAF1/CIP1} inhibits initiator caspase cleavage by TRAIL death receptor DR4. *Biochem Biophys Res Commun* 2000; **269**: 179-190
- 28 **Xu M**, Jin YL, Fu J, Huang H, Chen SZ, Qu P, Tian HM, Liu ZY, Zhang W. The abnormal expression of retinoic acid receptor- β , p53 and Ki67 protein in normal, premalignant and malignant esophageal tissues. *World J Gastroenterol* 2002; **8**: 200-202
- 29 **Siervo-Sassi RR**, Marrangoni AM, Feng X, Naoumova N, Winans M, Edwards RP, Lokshin A. Physiological and molecular effects of Apo2L/TRAIL and cisplatin in ovarian carcinoma cell lines. *Cancer Lett* 2003; **190**: 61-72
- 30 **Ng CP**, Zisman A, Bonavida B. Synergy is achieved by complementation with Apo2L/TRAIL and actinomycin D in Apo2L/TRAIL-mediated apoptosis of prostate cancer cells: role of XIAP in resistance. *Prostate* 2002; **53**: 286-299
- 31 **Lee KY**, Park JS, Jee YK, Rosen GD. Triptolide sensitizes lung cancer cells to TNF-related apoptosis-inducing ligand (TRAIL)-induced apoptosis by inhibition of NF-kappaB activation. *Exp Mol Med* 2002; **34**: 462-468
- 32 **Kelly MM**, Hoel BD, Voelkel-Johnson C. Doxorubicin pretreatment sensitizes prostate cancer cell Lines to TRAIL induced apoptosis which correlates with the loss of c-FLIP expression. *Cancer Biol Ther* 2002; **1**: 520-527
- 33 **Thomas RP**, Farrow BJ, Kim S, May MJ, Hellmich MR, Evers BM. Selective targeting of the nuclear factor-kappaB pathway enhances tumor necrosis factor-related apoptosis-inducing ligand-mediated pancreatic cancer cell death. *Surgery* 2002; **132**: 127-134
- 34 **Shetty S**, Gladden JB, Henson ES, Hu X, Villanueva J, Haney N, Gibson SB. Tumor necrosis factor-related apoptosis inducing ligand (TRAIL) up-regulates death receptor 5 (DR5) mediated by NFkappaB activation in epithelial derived cell lines. *Apoptosis* 2002; **7**: 413-420

Edited by Wu XN

Role of inducible nitric oxide synthase expression in aberrant crypt foci-adenoma-carcinoma sequence

Mei-Hua Xu, Chang-Sheng Deng, You-Qing Zhu, Jun Lin

Mei-Hua Xu, Chang-Sheng Deng, You-Qing Zhu, Jun Lin,
Department of Gastroenterology, Zhongnan Hospital, Wuhan
University, Wuhan 430071, Hubei Province China

Correspondence to: Mei-Hua Xu, Zhongnan Hospital, Wuhan
University, Wuhan 430071 Hubei Province, China. xmh-11@163.com

Telephone: +86-27-87330404

Received: 2002-07-18 **Accepted:** 2002-09-12

Abstract

AIM: To investigate the expression of inducible nitric oxide synthase (iNOS) in aberrant crypt foci (ACF) -adenoma-carcinoma sequence and its relation with tumor cell apoptosis, proliferation and angiogenesis.

METHODS: The expression of iNOS, proliferating cell nuclear antigen (PCNA) and microvessel density (MVD) in different stages of colorectal cancer were studied by immunohistochemical method from 30 normal tissues, 30 nonhyperplastic ACF, 30 hyperplastic ACF, 30 dysplastic ACF, 30 adenomas and 60 carcinomas. The apoptotic cells were detected by terminal deoxynucleotidyl transferase-mediated dUTP-biotin nick end labeling (TUNEL) method using an Apop Tag *in situ* detection kit.

RESULTS: The immunoreactivity of iNOS significantly increased in the transition from hyperplastic ACF to dysplastic ACF. This transition was associated with a significant decrease in the apoptotic index (AI) (0.73 ± 0.37 vs 0.61 ± 0.35 , $P<0.05$) and significant increases in the PCNA labeling index (LI) (27.3 ± 2.80 vs 40.3 ± 3.11 , $P<0.01$) and microvessel density (MVD) (55 ± 11.5 vs 70 ± 13.2 , $P<0.01$). The expression of iNOS was in low levels and positively correlated with PCNA-LI ($r=0.812$, $P<0.01$) and MVD ($r=0.863$, $P<0.01$) during transition from normal mucosa to nonhyperplastic ACF and hyperplastic ACF. The expression of iNOS was in high levels and positively correlated with AI ($r=0.901$, $P<0.01$) after transition from hyperplastic ACF to dysplastic ACF, adenoma and carcinoma.

CONCLUSION: The results suggest that the transition from hyperplastic ACF to dysplastic ACF may be a crucial step in the ACF-adenoma-carcinoma sequence, in which iNOS plays an important role by regulating tumor cell apoptosis, proliferation and angiogenesis.

Xu MH, Deng CS, Zhu YQ, Lin J. Role of inducible nitric oxide synthase expression in aberrant crypt foci-adenoma-carcinoma sequence. *World J Gastroenterol* 2003; 9(6): 1246-1250
<http://www.wjgnet.com/1007-9327/9/1246.asp>

INTRODUCTION

Aberrant crypt foci (ACF) are recently described colorectal lesions that might be related to the earliest steps in multistage colorectal carcinogenesis^[1]. Nitric oxide (NO) is an important

bioactive agent and signaling molecule that mediates a variety of physical actions and may contribute to the pathogenesis of a variety of disorders including cancer^[2-6]. Several studies implicate iNOS in colorectal tumorigenesis^[7-9], but none has evaluated the expression of iNOS in ACF-adenoma-carcinoma sequence. In this study, TUNEL technique and immunohistochemical staining were used to detect biologic parameters of tumor and compare the state of apoptosis, proliferation, MVD and iNOS expression in ACF-adenoma-carcinoma sequence. The purpose was to find out the relationship between aberrant expression of iNOS and colorectal carcinogenesis and the possible mechanism.

MATERIALS AND METHODS

Tissue specimens

Human colorectal tissues were obtained from Zhongnan Hospital and the People's Hospital of Wuhan University and Hubei Cancer Hospital. We collected 90 ACF and their adjacent normal mucosa from 32 colorectal carcinomas (CRC) (19 males and 13 females; mean age, 54 ± 7.5 years). 30 adenomas (18 males and 12 females; mean age, 51 ± 7.3 years) and 60 carcinomas were included in this study. The cancer patients included 32 males and 28 females that had 7 Dukes' stage A, 24 stage B, 12 stage C, and 17 stage D. There were 22 well-differentiated CRCs, 26 moderately differentiated and 12 poorly differentiated CRCs. All specimens were routinely fixed in 10 % buffered formalin, embedded in paraffin, and cut into 5 μ m sections. Each of the 5 sections was stained with hematoxylin and eosin for classification.

Sampling of ACF

Immediately after bowel resection, freshly resected colorectal segments were opened longitudinally, and the mucosa from macroscopically normal segments were dissected from the underlying layers, spread over on a piece of filter paper, and fixed in 10 % buffered formalin solution. 24 hours later, the fixed mucosal strips were immersed in 0.2 % methylene blue solution for 5 to 10 minutes and screened under 40 \times magnification for ACF. Methylene blue-stained ACF were easily distinguished from normal crypts by their deeper blue color, larger diameter, and the shape of their crypt orifices (oval, serrated, or slit-like)^[10]. Randomly selected ACF were microdissected with a rim of normal surrounding mucosa, paraffin embedded, and serially cut perpendicular to the surface.

Histochemical detection of apoptosis and determination of apoptotic index

Apoptotic cell tissue sections were detected by terminal deoxynucleotidyl transferase-mediated dUTP-biotin nick end labeling (TUNEL) method using an Apop Tag *in situ* detection kit according to the manufacturer's instructions. Morphologic characteristics of apoptosis were chromatin condensation, nuclear disintegration, and formation of crescent caps of condensed chromatin at the nuclear periphery. The apoptotic index (AI) was expressed as the ratio of positively stained cells

to total cells evaluated for each tissue section after counting 1 000 cells at 5 areas randomly selected for counting less than 400-fold magnification.

Immunohistochemical staining and evaluation of the sections
 SP kit was used. The primary antibodies were iNOS polyclonal antibody (ready to use, Boster, Wuhan), PCNA monoclonal antibody (ready to use, Maxin, Fujian) and CD34 monoclonal antibody (ready to use, Maxin, Fujian), respectively. Before staining, the sections were heated in microwave heated in 0.01 mol/L citric acid solution for antigen retrieval. PBS was substituted for primary antibodies as negative control. The stained sections were reviewed and scored independently by two investigators using an Olympus microscope. The extent and intensity of immunoreactivity for iNOS of all specimens were recorded. The following scale was used to express the extent of positivity: 0, ≤5 %; 1, >5-25 %; 2, >25-50 %; 3, >50-75 %; 4, >75 %. The intensity of iNOS expression was scored as follows: 0, negative; 1, weak; 2, moderate; 3, strong. The final score, obtained by multiplying the intensity and extent of positivity scores, ranged from 0-12. Scores of 0- 4 were defined as “markedly reduced” or “no expression”; Scores 5-8 were defined as “intermediate expression”; and scores of 9-12 were defined as “strong expression”^[11]. The PCNA labeling index (LI) was expressed as the ratio of cells positively stained for PCNA to all epithelial cells in at least 5 areas randomly selected for counting less than 200-fold magnification. For microvessel density (MVD) determination, 5 areas were randomly selected and counted less than 200-fold magnification. The average count was recorded and expressed as the absolute number of vessels per 0.74 mm² (per × 200 field) for each case.

Statistical analysis

T test was used for comparison of the means. The positivity of iNOS protein was analyzed by Fisher exact probability method. For the tendency of AI, LI and MVD in the ACF-adenoma-carcinoma sequence analysis of variance was performed based on the trend test. *P* value less than 0.05 was regarded as statistically significant.

RESULTS

Expression of iNOS in ACF-adenoma-carcinoma sequence

Although most cases of normal mucosa, nonhyperplastic ACF and hyperplastic ACF showed intermediate, weak or absent iNOS expression, the expression of iNOS increased markedly during transition from hyperplastic ACF to dysplastic ACF (*P*<0.01) (Table 1, Figure 1). Greater than 70 % of cases of dysplastic ACF, adenoma or carcinoma showed strong expression of iNOS. We found no relationship between expression of iNOS and the Ducks’ classification and the differentiation of cancer.

Table 1 iNOS expression in normal mucosa-ACF-adenoma-carcinoma sequence

	iNOS expression			Total
	Strong	Intermediate	Weak or absent	
Normal mucosa	3	6	21	30
Nonhyperplastic ACF	6	8	16	30
Hyperplastic ACF	8	10	12	30
Dysplastic ACF	26	2	2	30
Adenoma	24	4	2	30
Carcinoma	41	10	9	60

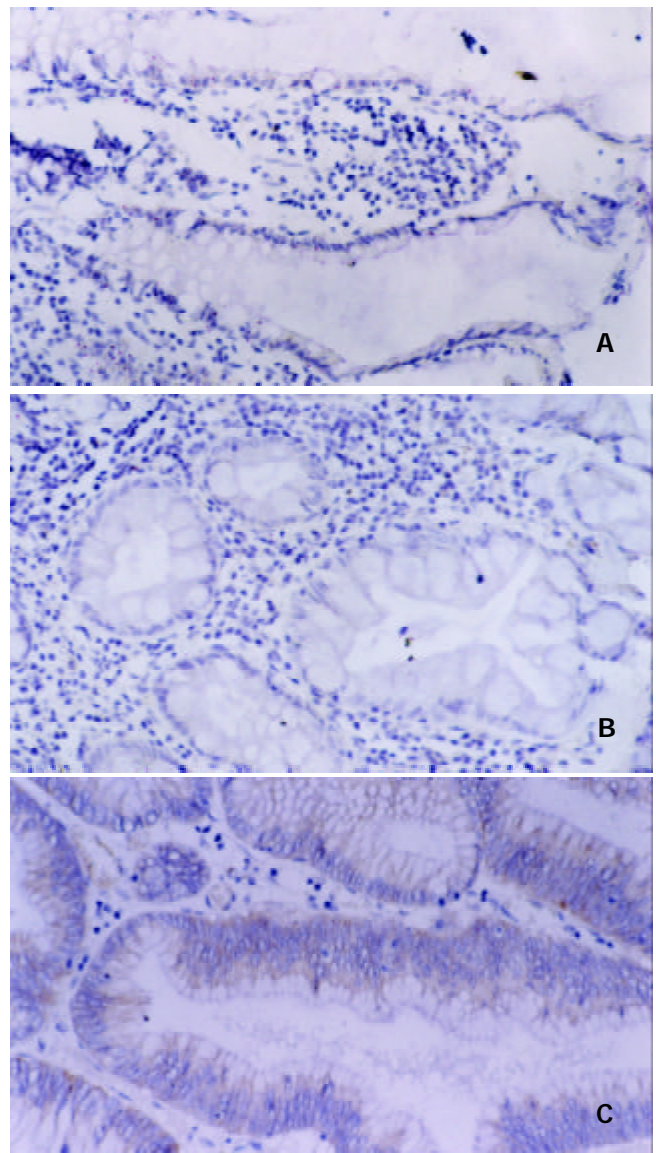


Figure 1 Immunohistochemical analysis for iNOS protein in ACF. (A) weak staining was observed in the cytoplasm of nonhyperplastic ACF. (SP method, ×200). (B) weak staining was observed in the cytoplasm of hyperplastic ACF. (SP method, ×200). (C) strong staining was observed in the cytoplasm of dysplastic ACF. (SP method, ×200).

Table 2 Changes in AI, PCNA-LI, and MVD in ACF-adenoma-carcinoma sequence ($\bar{x}\pm s$)

	<i>n</i>	AI (%)	PCNA-LI (%)	MVD (MVD /0.74mm ²)
Normal mucosa	30	0.21±0.13	12.1±2.48	50±10.3
Nonhyperplastic ACF	30	0.28±0.16	14.7±2.47	52±10.6
Hyperplastic ACF	30	0.73±0.37 ^{ab}	27.3±2.80 ^{ab}	55±11.5
Dysplastic ACF	30	0.61±0.35 ^{abc}	40.3±3.11 ^{abd}	70±13.2 ^{abd}
Adenoma	30	0.58±0.25 ^{abc}	45.4±3.24 ^{abd}	80±14.7 ^{abde}
Carcinoma	60	0.49±0.43 ^{abde}	52.2±3.17 ^{abdf}	95±13.3 ^{abdf}

^a*P*<0.01, vs normal mucosa; ^b*P*<0.01, vs nonhyperplastic ACF; ^c*P*<0.05, vs hyperplastic ACF; ^d*P*<0.01, vs Hyperplastic ACF; ^e*P*<0.05, vs dysplastic ACF; ^f*P*<0.01, vs dysplastic ACF.

Changes in AI, PCNA-LI, and MVD in ACF-adenoma-carcinoma sequence

Apoptotic index was highest in hyperplastic ACF, whereas it significantly decreased after transition to dysplastic ACF

(Figure 2), adenoma and carcinoma ($P<0.05$). Conversely, the proliferative activity as determined by PCNA-LI gradually increased during ACF (Figure 3)-adenoma-carcinoma

sequence ($P<0.01$). Microvessel density significantly increased after the transition to dysplastic ACF (Figure 4), and further elevated in adenoma and carcinoma ($P<0.01$) (Table 2).

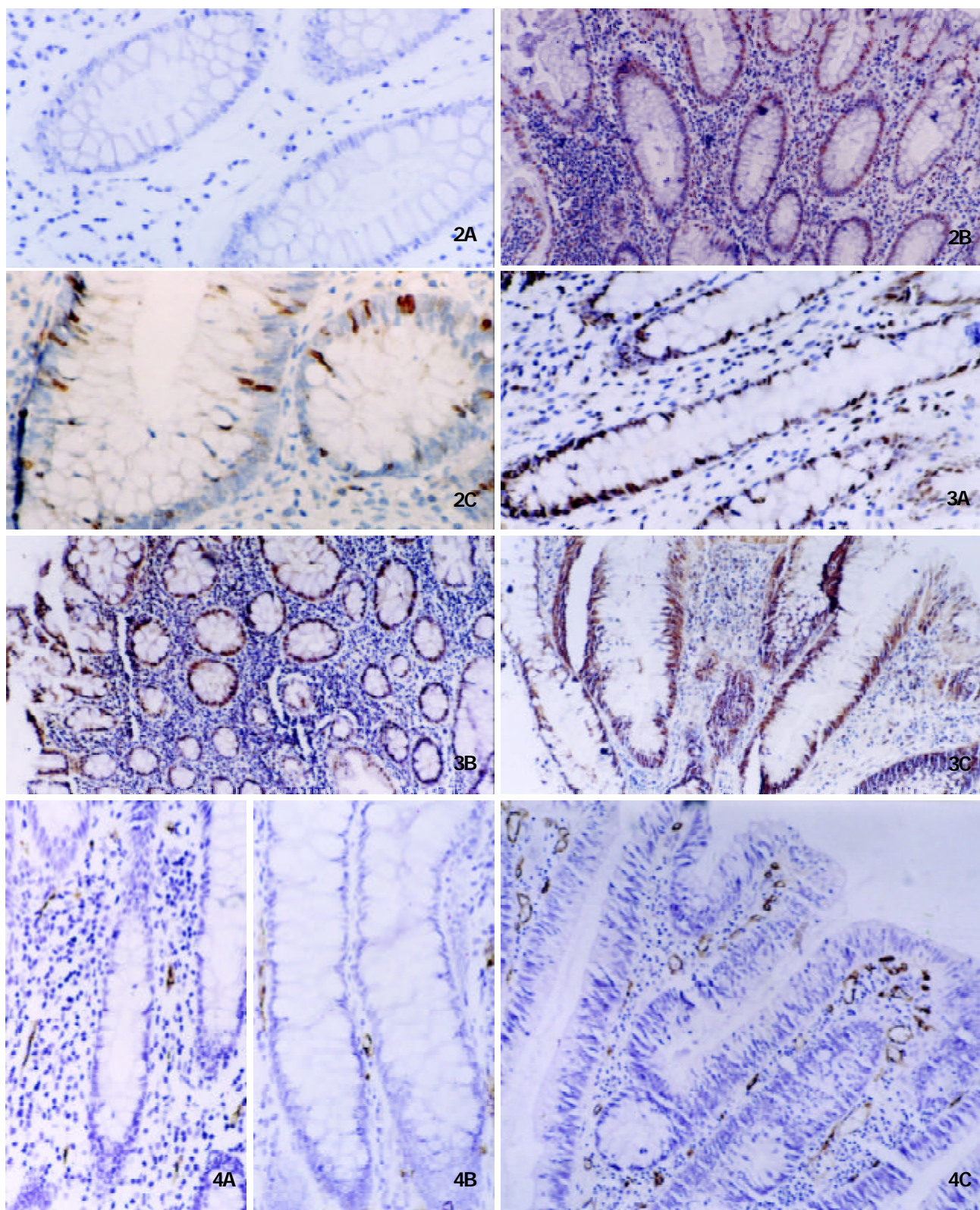


Figure 2 Histochemical detection of apoptosis by TUNEL in ACF. Few apoptotic cells were detected in nonhyperplastic ACF (Panel A, original magnification $\times 200$), and more apoptotic cells were detected in hyperplastic ACF (Panel B, original magnification $\times 100$) whereas they decreased significantly after transition to dysplastic ACF (Panel C, original magnification $\times 200$).

Figure 3 Immunohistochemistry of PCNA protein in ACF. PCNA expression was gradually increased from nonhyperplastic ACF (Panel A, original magnification $\times 200$), hyperplastic ACF (Panel B, original magnification $\times 100$) to dysplastic ACF (Panel C, original magnification $\times 100$).

Figure 4 Immunohistochemistry of CD34 protein in ACF. MVD determined by anti-CD34 antibody was low in nonhyperplastic ACF (Panel A, original magnification $\times 200$) and hyperplastic ACF (Panel B, original magnification $\times 200$) whereas significantly increased in dysplastic ACF (Panel C, original magnification $\times 200$).

Correlations between iNOS expression and biologic parameters

The expression of iNOS was in low level and positively correlated with PCNA-LI ($r=0.812$, $P<0.01$) and MVD ($r=0.863$, $P<0.01$) during transition from normal mucosa to nonhyperplastic ACF and hyperplastic ACF. The expression of iNOS was in high level and positively correlated with AI ($r=0.901$, $P<0.01$) after transition to dysplastic ACF, adenoma and carcinoma.

DISCUSSION

The development of colorectal carcinoma usually occurs via the adenoma-carcinoma sequence^[12,13]. The search for the earliest morphological precursors led to the description of ACF. Currently, there is a tendency to consider ACF as putative preneoplastic lesions that could represent one of the earliest stages of the multistep colorectal carcinogenesis^[11,14]. Alteration of enzymes, specifically hexosaminidase, and carcinoembryonic antigen expression have been identified in ACF. Genetic mutations that include APC suppressor gene and k-ras gene as well as beta-catenin gene have been found in ACF^[15,16]. Genomic instability, manifested as altered lengths of microsatellites and oligo A sequences similar to alterations that occur in neoplasm, has been identified in some ACF^[17]. Morphological alterations from nonhyperplasia to hyperplasia to varying degrees of dysplasia have been found in ACF^[18]. One study suggested that some hyperplastic ACF can develop into the adenomatous type^[19]. In a carcinogen-induced colonic tumorigenesis model, these lesions may show dysplastic morphology and precede formation of adenomas and adenocarcinomas. Phenotypic and genetic abnormalities in ACF have been postulated as evidence that ACF are preneoplastic and the smallest lesions preceding adenoma and carcinoma. Recently, there was a direct evidence of the existence of an ACF-adenoma-carcinoma sequence^[20].

A disturbance in the balance between cell proliferation and cell loss, or apoptosis may underlie neoplastic development^[21-27]. In this study, we noticed that in normal mucosa the apoptotic cells were identified in colorectal surface epithelium and formed "an apoptotic zone". Proliferative cells were seen in the basal region of the mucosa glands and formed "a proliferating zone". However in colorectal carcinoma, apoptotic cells and proliferative cells clustered all over the tumor tissue. This phenomenon elucidated that the regulation of apoptosis and proliferation had already been beyond control. Angiogenesis also played a crucial role in tumorigenesis^[28-32]. In this study, we demonstrated that MVD increased gradually in ACF-adenoma-carcinoma sequence. This change indicated that the regulation of growth of vessel was also disordered.

We investigated iNOS expression in human colorectal cancer with respect to tumor staging. Only low levels were found in the surrounding normal tissue, nonhyperplastic ACF and hyperplastic ACF. However, we found markedly increased iNOS in dysplastic ACF, adenoma and carcinoma. After transition to dysplastic ACF, adenoma and carcinoma, iNOS activity decreased with increasing staging. The markedly increased iNOS expression during hyperplastic ACF-dysplastic ACF transition suggested that the increase of iNOS expression might be an early event in the development of colorectal tumor. The different expression of iNOS in the epithelial cells in ACF-adenoma-carcinoma sequence may provide important clues that host factor regulates iNOS differently in different tumor stages.

During transition from normal mucosa to nonhyperplastic ACF and hyperplastic ACF, the expression of iNOS was at low levels. This transition was associated with a gradual increase in the AI, PCNA-LI and MVD. Several reports suggest that low concentrations of NO and iNOS induce angiogenesis

and enhance the growth rate of tumor^[33]. Increased proliferation might result in a state of lacking of nutrients, competition for growth factors or oxygen starvation and then in turn induce apoptosis^[34]. Our results demonstrated that the initial neoplastic transformation was associated with a remarkable increase in rates of both proliferation and apoptosis, which suggested the increased instability of colorectal mucosa in this process. The immunoreactivity of iNOS significantly increased during the transition from hyperplastic ACF to dysplastic ACF. The perturbation of tissue homeostasis derived from the increased proliferation and decreased apoptosis detected at this transition. Microvessel density (MVD) was found markedly increased at this transition. These results suggested that the transition from hyperplastic ACF to dysplastic ACF might be a crucial step in the ACF-adenoma-carcinoma sequence, in which iNOS might play an important role. The expression of iNOS was in high level and associated with a significant increase in the PCNA-LI, MVD and marked decrease in the AI after transition to dysplastic ACF, adenoma and carcinoma. With the decreased expression of iNOS, AI decreased gradually and was lowest in carcinoma in this process. Several reports suggest that high concentrations of NO and iNOS are cytotoxic and can induce apoptosis^[33]. Because the increased instability of colorectal mucosa in former stages led to the formation of "supper clone" and the micro-environmental changes such as expression of EGF and TGF- α in the tumor tissues^[35,36], epithelial cells maintained at hyperproliferation and increased angiogenesis was present after transition to dysplastic ACF, adenoma and carcinoma. These results elucidate that iNOS might be an important factor of colorectal carcinogenesis by regulating tumor cell apoptosis, proliferation and angiogenesis. What may cause the overexpression of iNOS after transition to dysplastic ACF, adenoma and carcinoma remains unclarified and awaits further study.

REFERENCES

- 1 **Bird RP.** Role of aberrant crypt foci in understanding the pathogenesis of colon cancer. *Cancer lett* 1995; **93**: 55-71
- 2 **Holian O,** Wahid S, Atten MJ, Attar BM. Inhibition of gastric cancer cell proliferation by resveratrol: role of nitric oxide. *Am J Physiol Gastrointest Liver Physiol* 2002; **282**: G809-816
- 3 **Zhang K,** Deng CS, Zhu YQ, Yang YP, Zhang YM. Significance of nuclear factor- κ B, cyclooxygenase 2 and inducible nitric oxide synthase expression in human ulcerative colitis tissues. *Shijie Huaren Xiaohua Zazhi* 2002; **10**: 575-578
- 4 **Diao TJ,** Yuan TY, Li YL. Immunologic role of nitric oxide in acute rejection of golden hamster to rat liver xenotransplantation. *World J Gastroenterol* 2002; **8**: 746-751
- 5 **Bing RJ,** Miyataka M, Rich KA, Hanson N, Wang X, Slosser HD, Shi SR. Nitric oxide, prostanoids, cyclooxygenase, and angiogenesis in colon and breast cancer. *Clin Cancer Res* 2001; **7**: 3385-3392
- 6 **Song ZJ,** Gong P, Wu YE. Relationship between the expression of iNOS, VEGF, tumor angiogenesis and gastric cancer. *World J Gastroenterol* 2002; **8**: 591-595
- 7 **Amb S,** Merriam WG, Bennett WP, Felley-Bosco E, Ogunfusika MO, Oser SM, Klein S, Shields PG, Billiar TR, Harris CC. Frequent nitric oxide synthase-2 expression in human colon adenomas: implication for tumor angiogenesis and colon cancer progression. *Cancer Res* 1998; **58**: 334-341
- 8 **Rao CV,** Kawamori T, Hamid R, Reddy BS. Chemoprevention of colonic aberrant crypt foci by an inducible nitric oxide synthase-selective inhibitor. *Carcinogenesis* 1999; **20**: 641-644
- 9 **Nozoe T,** Yasuda M, Honda M, Inutsuka S, Korenaga D. Immunohistochemical expression of cytokine induced nitric oxide synthase in colorectal carcinoma. *Oncol Rep* 2002; **9**: 521-524
- 10 **Nucci MR,** Robinson CR, Longo P, Campbell P, Hamilton SR. Phenotypic and genotypic characteristics of aberrant crypt foci in human colorectal mucosa. *Hum pathol* 1997; **28**: 1396-1407
- 11 **Hao XP,** Willis JE, Pretlow TG, Rao JS, MacLennan GT, Talbot IC, Pretlow TP. Loss of fragile histidine triad expression in

- colorectal carcinomas and premalignant lesions. *Cancer Res* 2000; **60**: 18-21
- 12 **Li A**, Yonezawa S, Matsukita S, Hasui K, Goto M, Tanaka S, Imai K, Sato E. Comparative study for histology, proliferative activity, glycoproteins, and p53 protein between old and recent colorectal adenomas in Japan. *Cancer Lett* 2001; **170**: 45-52
- 13 **Luo MJ**, Lai MD. Identification of differentially expressed genes in normal mucosa, adenoma and adenocarcinoma of colon by SSH. *World J Gastroenterol* 2001; **7**: 726-731
- 14 **Bird RP**, Good CK. The significance of aberrant crypt foci in understanding the pathogenesis of colon cancer. *Toxicol Lett* 2000; **112-113**: 395-402
- 15 **Yuan P**, Sun MH, Zhang JS, Zhu XZ, Shi DR. APC and K-ras gene mutation in aberrant crypt foci of human colon. *World J Gastroenterol* 2001; **7**: 352-356
- 16 **Takahashi M**, Mutoh M, Kawamori T, Sugimura T, Wakabayashi K. Altered expression of beta-catenin, inducible nitric oxide synthase and cyclooxygenase-2 in azoxymethane-induced rat colon carcinogenesis. *Carcinogenesis* 2000; **21**: 1319-1327
- 17 **Pedroni M**, Sala E, Scarselli A, Borghi F, Menigatti M, Benatti P, Percesepe A, Rossi G, Foroni M, Losi L, Di Gregorio C, De Pol A, Nascimbeni R, Di Betta E, Salerni B, de Leon MP, Roncucci L. Microsatellite instability and mismatch-repair protein expression in hereditary and sporadic colorectal carcinogenesis. *Cancer Res* 2001; **61**: 896-899
- 18 **Bouzuorene H**, Chaubert P, Seelentag W, Bosman FT, Saraga E. Aberrant crypt foci in patients with neoplastic and nonneoplastic colonic disease. *Hum pathol* 1999; **30**: 66-71
- 19 **Otori K**, Sugiyama K, Hasebe T, Fukushima S, Esumi H. Emergence of adenomatous aberrant crypt foci (ACF) from hyperplastic ACF with concomitant increase in cell proliferation. *Cancer res* 1995; **55**: 4743-4746
- 20 **Shpitz B**, Hay K, Medline A, Bruce WR, Bull SB, Gallinger S, Stern H. Natural history of aberrant crypt foci. A surgical approach. *Dis Colon Rectum* 1996; **39**: 763-767
- 21 **Wang LD**, Zhou Q, Wei JP, Yang WC, Zhao X, Wang LX, Zou JX, Gao SS, Li YX, Yang CS. Apoptosis and its relationship with cell proliferation, p53, Waf1p21, bcl-2 and c-myc in esophageal carcinogenesis studied with a high-risk population in northern China. *World J Gastroenterol* 1998; **4**: 287-293
- 22 **Liu HF**, Liu WW, Fang DC, Men RP. Expression and significance of proapoptotic gene Bax in gastric carcinoma. *World J Gastroenterol* 1999; **5**: 15-17
- 23 **Sun BH**, Zhao XP, Wang BJ, Yang DL, Hao LJ. FADD and TRADD expression and apoptosis in primary human hepatocellular carcinoma. *World J Gastroenterol* 2000; **6**: 223-227
- 24 **Jia XD**, Han C. Chemoprevention of tea on colorectal cancer induced by dimethylhydrazine in Wistar rats. *World J Gastroenterol* 2000; **6**: 699-703
- 25 **Zhang Z**, Yuan Y, Gao H, Dong M, Wang L, Gong YH. Apoptosis, proliferation and p53 gene expression of *H. pylori* associated gastric epithelial lesions. *World J Gastroenterol* 2001; **7**: 779-782
- 26 **Oda T**, Takahashi A, Miyao N, Yanase M, Masumori N, Itoh N, Sato MA, Kon SI, Tsukamoto T. Cell proliferation, apoptosis, angiogenesis and growth rate of incidentally found renal cell carcinoma. *Int J Urol* 2003; **10**: 13-18
- 27 **Hao X**, Du M, Bishop AE, Talbot IC. Imbalance between proliferation and apoptosis in the development of colorectal carcinoma. *Virchows Arch* 1998; **433**: 523-527
- 28 **Tanigawa N**, Amaya H, Matsumura M, Lu C, Kitaoka A, Matsuyama K, Muraoka R. Tumor angiogenesis and mode of metastasis in patients with colorectal cancer. *Cancer Res* 1997; **57**: 1043-1046
- 29 **Xiong B**, Gong LL, Zhang F, Hu MB, Yuan HY. TGFβ1 expression and angiogenesis in colorectal cancer tissue. *World J Gastroenterol* 2002; **8**: 496-498
- 30 **Minagawa N**, Nakayama Y, Hirata K, Onitsuka K, Inoue Y, Nagata N, Itoh H. Correlation of plasma level and immunohistochemical expression of vascular endothelial growth factor in patients with advanced colorectal cancer. *Anticancer Res* 2002; **22**: 2957-2963
- 31 **Fan YF**, Huang ZH. Angiogenesis inhibitor TNP-470 suppresses growth of peritoneal disseminating foci of human colon cancer line Lovo. *World J Gastroenterol* 2002; **8**: 853-856
- 32 **Tao HQ**, Lin YZ, Wang RN. Significance of vascular endothelial growth factor messenger RNA expression in gastric cancer. *World J Gastroenterol* 1998; **4**: 10-13
- 33 **Thomsen LL**, Miles DW. Role of nitric oxide in tumour progression: lessons from human tumours. *Cancer Metastasis Rev* 1998; **17**: 107-118
- 34 **Sinicrope FA**, Roddey G, McDonnell TJ, Shen Y, Cleary KR, Stephens LC. Increased apoptosis accompanies neoplastic development in the human colorectum. *Clin Cancer Res* 1996; **2**: 1999-2006
- 35 **Wang Q**, Wu JS, Gao DM, Lai DL, Ma QJ. Significance of EGF receptor and TGF-α messenger RNA expression in colorectal carcinoma. *Shijie Huaren Xiaohua Zazhi* 1999; **7**: 590-592
- 36 **Xia L**, Yuan YZ, Xu CD, Zhang YP, Qiao MM, Xu JX. Effects of epidermal growth factor on the growth of human gastric cancer cell and the implanted tumor of nude mice. *World J Gastroenterol* 2002; **8**: 455-458

Distribution and anti-HBV effects of antisense oligodeoxynucleotides conjugated to galactosylated poly-L-lysine

Su-Jun Zheng, Sen Zhong, Jian-Jun Zhang, Feng Chen, Hong Ren, Cun-Liang Deng

Su-Jun Zheng, Jian-Jun Zhang, Hong Ren, Institute of Viral Hepatitis, Chongqing University of Medical Sciences, Chongqing 400016, China

Sen Zhong, Feng Chen, Cun-Liang Deng, Department of Infectious Diseases, Luzhou Medical College Hospital, Luzhou 646000, Sichuan Province, China

Supported by the Natural Science Foundation of China, No. 39370648

Correspondence to: Sen Zhong, Department of Infectious Diseases, Luzhou Medical College Hospital, Luzhou 646000, China. zhongsenz@yahoo.com.cn

Telephone: +86-830-2392712-5419

Received: 2002-12-08 **Accepted:** 2003-01-08

Abstract

AIM: To describe distribution of the phosphorothioated antisense oligodeoxynucleotides (PS-asODNs) conjugated to galactosylated poly-L-lysine (Gal-PLL) in mice, and to observe their effects on expression of HBV gene in the 2.2.15 cells and transgenic mice.

METHODS: According to the result of direct sequencing of PCR amplified products, a 16 mer phosphorothioate analogue of the antisense oligodeoxynucleotides (PS-asODNs) directed against the HBV U₅-like region was conjugated to the hepatotropic Gal-PLL molecules. Its distribution was demonstrated using asODNs labeled with ³²P at the 5' terminus with a T4-polynucleotide Kinase. Its inhibition effect on HBV expression was observed in the transfected 2.2.15 cells and transgenic mice.

RESULTS: The Gal-PLL and asODNs could form stable complex at a molar ratio of 2:1. As shown in the HBV-transfected 2.2.15 cells, the inhibition effects of asODNs alone and asODNs conjugated to Gal-PLL, at 10 μmol/L for both, on HBsAg and HBeAg production were different, the former being 70 % and 58 %, respectively, and the latter being 96 % and 82 %, respectively. A more pronounced reduction was also observed in viral DNA load in the culture supernatant for the test with Gal-PLL-asODNs. Among many mouse organs, livers retained more asODNs molecules after administration. The preferential concentration in liver was found to be 52.14 % for Gal-PLL-asODNs, as high as 2.38-fold of that for asODNs (21.9 %). Both elements decreased gradually in liver, with 2.9 % of the former, 5.99 % of the latter retained 24 hours after the administration. The injection interval, therefore, was recommended to be 24 hours. In the transgenic mice, serum HBsAg decreased significantly ($P < 0.01$) at the 12th day after administering Gal-PLL-asODNs, the serum HBV DNA turned negative in 4 of the 6 mice.

CONCLUSION: Antisense oligodeoxynucleotides conjugated to Gal-PLL can be concentrated in liver and intaked by hepatocytic cells. This may result in specific inhibition of expression and replication of HBV *in vitro* and *in vivo*.

Zheng SJ, Zhong S, Zhang JJ, Chen F, Ren H, Deng CL. Distribution and anti-HBV effects of antisense oligodeoxynucleotides conjugated to galactosylated poly-L-lysine. *World J Gastroenterol* 2003; 9(6): 1251-1255

<http://www.wjgnet.com/1007-9327/9/1251.asp>

INTRODUCTION

The antisense oligodeoxynucleotides (asODNs) have been demonstrated previously to be effective for inhibition of HBV gene expression and viral replication *in vitro* and *in vivo*, being potential new agents for anti-HBV therapy^[1-4]. However, there are still some hinders for their potential application. First, their molecules must be water soluble and can penetrate the lipophilic cell membrane. Second, they must be resistant enough to enzymatic degradation to allow their concentration in liver. Third, They must be bound specifically to the target HBV sequence. In the present study, a 16-mer phosphorothioate analogue of the antisense oligonucleotides (PS-asODNs) directed against the HBV U₅-like region was synthesized and then conjugated to hepa tropic galactosylated poly-L-lysine (Gal-PLL). The anti-HBV effects of asODNs and Gal-PLL-asODNs were demonstrated in the 2.2.15 cells and transgenic mice. In addition, distribution of asODNs was studied in mice.

MATERIALS AND METHODS

PCR product sequencing

PCR was conducted using the primer pair P₁/ P₂ in a 50 μl system with the initial denaturation temperature at 94 °C for 4 min, followed by 30 cycles at 94 °C for 30 s, at 55 °C for 30 s and at 72 °C for 40 s. The reaction was for the pre-C and C genes of HBV (ayw1 subtype). The sequence of the PCR primers pair was as follows: P₁: 5' -AAGGTCTTTGTACTAGGAGGC-3' (1 761-1 781); P₂: 5' -TTCCCGATACAGAGCTGAGGC-3' (2 000-2 020). The PCR products were as long as 260 bp and were sequenced using the method given by the Pharmacia T₇kit.

Cells and cell culture

2.2.15 cell line, human hepatoblastoma Hep G2 cell line stably transfected by HBV genome^[5-7], were cultured in PRMI1640 medium at 37 °C under 5 % CO₂, pH: 7.2-7.4, which contained 15 % fetal calf serum, 2 mmol/L glutamine, 0.1 mu/L penicillin and streptomycin, and 380 mg/L G418 (Sigma).

Preparation of targeting antisense ODNs

A targeting water soluble DNA carrier was prepared by coupling galactose and poly-L-lysine using the method of Schwartz and Gray^[8], with their molar ratio being 10:1. A 16-mer phosphorothioated antisense oligodeoxynucleotide (5' -CATGCCCCAAAGCCAC-3'), corresponding to the nucleotides 1 980-1 905, and complementary to preC/C regions of HBV genome (ayw1 subtype), was synthesized. As a reference molecule, another 16-mer phosphorothioated oligodeoxynucleotide (5' -AGTCACTCAGTCAGTC-3'),

unrelated to the HBV sequence, was prepared. By agarose gel (2.5 %) electrophoresis, conjunctive ratio of Gal-PLL to PS-asODNs was identified^[9].

Anti-viral effect of PS-asODNs in vitro

The 2.2.15 cells were incubated for 60 h, and then were transferred to the medium containing asODNs, HBV-specific Gal-PLL-asODNs, HBV-unrelated Gal-PLL-ODNs, or the medium without any oligodeoxynucleotides. The concentration of ODNs in the media was 10 $\mu\text{mol/L}$. 72 h later, the 2.2.15 cells were transferred to the ordinary medium for 72 h, then 200 μl of supernatant was used for the ELISA reaction for HBsAg and HBeAg, HBV DNA was detected by dot hybridization.

Animals

Kunming mice, (weighing 20 g in average) were used to describe the distribution of asODNs. HBV transgenic mice, were provided by 458 Hospital of PLA in Guangzhou, China, whose expression of HBsAg (126-930 ng/ml) was well documented in the previous studies^[10,11].

Radiolabeling of asODNs

The ³²P-labelling of asODNs was at 5' terminus with T4-polynucleotide kinase (Amersham) in the reaction mixture containing asODNs 6.6 $\mu\text{g}/20 \mu\text{l}$, [γ -³²P] ATP 90 μl (10 mCi/ml), 10 \times buffer 18 μl , T4-polynucleotide kinase 9 μl and deionized water 43 μl for 1.5 h. The reaction was stopped by adding 9 μl 0.5M EDTA (pH 8.0). The product was extracted by chloroform and separated using Sephadex-G50. Using the same method, the reaction was carried out twice.

Distribution of as ODNs in Kunming mice

A total number of 24 Kunming mice were equally divided randomly into two groups, one for asODNs and the other for Gal-PLL-asODNs. The labeled asODNs were equally divided into 25 pieces, each piece for 200 μl , with the radioactivity of 9.42×10^6 cpm. Twelve pieces of asODNs were mixed with Gal-PLL at a molar ratio of 1:2, and were incubated at room temperature for 60 min. Twenty-four pieces of asODNs were administered intravenously via tail vein to 24 mice, respectively. At 2 min, 30 min, 1 h, 4 h, 13 h, 24 h following intravenous administration, 2 animals were sacrificed for each group at each time point, their blood and organs were collected for determination of total radioactivity using liquid scintillation counter.

Anti-HBV effects of Gal-PLL-asODNs in the transgenic mice

Twelve mice, strongly positive for HBsAg and carrying HBV DNA in serum were equally divided into Gal-PLL-asODNs and control groups. Gal-PLL was then mixed with asODNs in a molar ratio of 2:1 at room temperature. The mixture was then administered intravenously via the tail vein in a dose of 15 $\mu\text{g/g}$ weight/d of asODNs for successive 12 days. The same volume of saline was used for the control mice by the same means. Blood samples were collected at the venous plexus behind orbital cavity before, or 12 days after the treatment. Sera were separated by incubating at 37 $^{\circ}\text{C}$ for 30 min and centrifuged, and stored at -20 $^{\circ}\text{C}$ for use. Being diluted at 1:100 with normal saline, the sera were subjected to the ELISA for HBsAg and nested PCR (TakaRa Biotechnology Co.) for viral DNA, with its product being 230 bp in size.

RESULTS

PCR and sequencing of PCR products

Figure 1 shows that the band of PCR product was between the

size of 221-298bp. The sequence of the 132bp product was: 5' -CCAGCACCATGCAACTTTTTCACCTCTGCC-TAATCATCTCTTGTTCATGTCCTACTGTTCAAGCCTCCAA-GCTGTGCCTTGGGTGGCTTTGGGGCATGGACATC-GACCCTTATAAAGAATTTGGAGCTACTG-3'. This was in accordance with the corresponding sequence of HBV genome (ayw1 subtype) which contained the preC region (1 816-1 902), U₅-like sequence (1 857-1 918) and partial poly-A addition signal sequence (1 919-1 962)^[12,13].

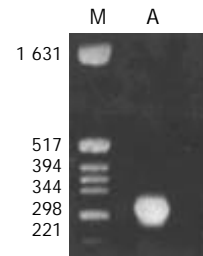


Figure 1 Amplification of HBV DNA in the 2.2.15 cells with PCR. The PCR products were resolved on 1.5 % agarose gel. M: Molecule weight marker; A: HBV DNA in 2.2.15 cells.

The complexon of Gal-PLL and asODNs

Gal-PLL at different concentrations was incubated with asODNs, and the proper molar ratio for their binding was assessed by agarose gel electrophoresis. The binding was detectable at the molar ratio of 1:1, and complete at the molar ratio of 2:1 or more (Figure 2).

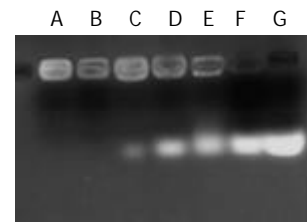


Figure 2 Analysis of Gal-PLL/asODNs complex formation at different molar ratios. A: Gal-PLL/asODNs=3:1; B: Gal-PLL/asODNs=2:1; C: Gal-PLL/asODNs=1.75:1; D: Gal-PLL/asODNs=1.5:1; E: Gal-PLL/asODNs=1:1; F: Gal-PLL/asODNs=0.5:1; G: Gal-PLL/asODNs=0:1.

Effects of antisense ODNs on HBV gene expression in vitro

As shown in Table 1, after incubation of 2.2.15 cells with asODNs for 8.5 days, the inhibition rates of HBsAg, HbeAg were 70 % and 50 %, respectively, while those with Gal-PLL-asODNs were 96 % and 82 %, respectively. Only slightly negative effects were observed for the reference agent Gal-PLL-ODNs on expression of HBsAg (19 %) and HBeAg (10 %). The Gal-PLL-asODNs treatment was shown to markedly reduce the amount of HBVDNA in the 2.2.15 cells and the culture medium, compared with free asODNs and conjugated HBV-unrelated Gal-PLL-ODNs.

Table 1 Inhibition of asODNs on HBsAg and HBeAg secretion in 2.2.15 cells (P/N values $\bar{x} \pm s$)

Groups	HBsAg	Inhibitory rate (%)	HBeAg	Inhibitory rate (%)
Cell control	9.4 \pm 0.16		15.10 \pm 0.15	
PS-asODNs	4.30 \pm 0.25	70	7.60 \pm 1.10	58
Gal-PLL:PS-asODNs	2.40 \pm 0.26	96	4.50 \pm 0.42	82
Gal-PLL:PS-ODNs	8.10 \pm 0.13	19	13.80 \pm 0.76	10

Distribution of asODNs in mice

Plasma level of asODNs declined rapidly after intravenous administration, with its half-life being approximately 1-2 min, and 7.6 % of asODNs was left in circulation one hour later. Among organs examined, liver retained more asODNs (21.9 %) 30 min after the administration, and the retained molecules decreased gradually, with 2.93 % of them detected 24 hours later. At the time point of 30 min, the retained radioactivity listed in the order of intensity was as following: liver> kidney > lung> heart > spleen> brain (Figure 3).

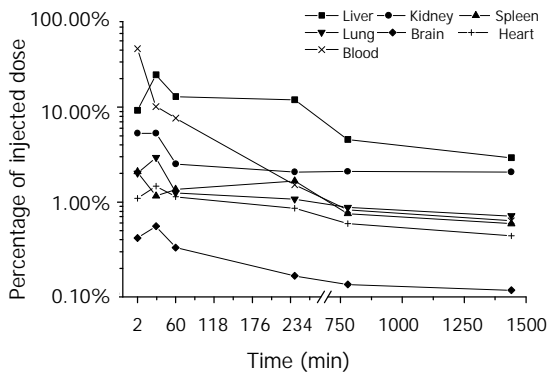


Figure 3 Distribution of asODNs in Kunming mice ($n=2$).

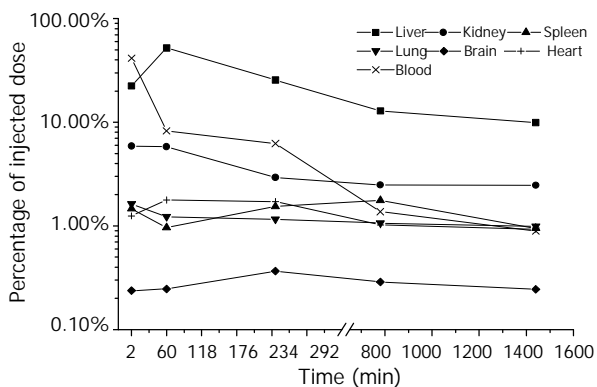


Figure 4 Distribution of Gal-PLL-asODNs in Kunming mice ($n=2$).

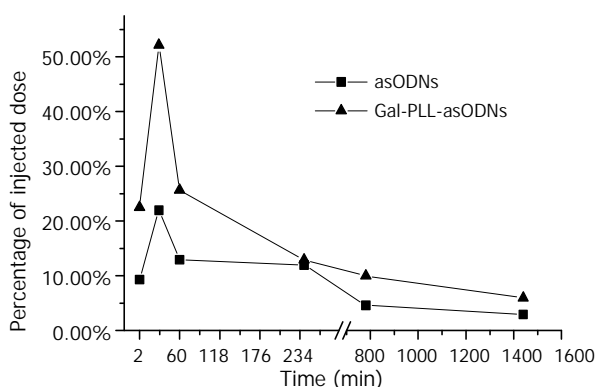


Figure 5 Comparison of the amount retained in liver between asODNs and Gal-PLL-asODNs ($n=2$).

Distribution of Gal-PLL-asODNs in mice

The elimination process of Gal-PLL-asODNs from bloodstream was similar to that of asODNs, with its half-life being 1-2 minutes. Less Gal-PLL-asODNs was shown to be retained in the circulation at the time points of 30 min (8.26 %), 60 min (6.24 %) than asODNs (10.17 % for 30 min, 7.65 % for 60 min) at the corresponding time points. Up to 52.14 % of

Gal-PLL-asODNs was shown to be in liver at the time point of 30 min, and only 5.99 % of the activity was retained in liver 24 hours after its administration. Kidney was the second radioactivity concentrating organ, retaining 5.89 % of injected Gal-PLL-asODNs at the time point of 2 min. The amount in the brain was the smallest (Figure 4). In comparison to that for asODNs, more radioactivity for Gal-PLL-asODNs was retained in liver at each time points (Figure 5). Evidently, Gal-PLL had prompted hepatic intake of asODNs. It might enhance the preferential concentration of agent in liver, with a factor of 8.98-fold to kidney, 42.66-fold to lung, 54.24-fold to spleen. However, there were only few asODNs in liver for both groups 24 hours later (5.99 % and 2.93 %, respectively).

Inhibition of viral protein expression by antisense oligonucleotides in vivo

After treatment for 12 days, serum HBsAg decreased significantly in the Gal-PLL-PSODNs treated group ($P<0.01$); in contrast, no apparent change was detected after treatment with HBV-unrelated Gal-PLL-ODNs (Table 2). In serum HBsAg level, as shown in Figure 6, serum HBV DNA turned negative in 4 of the 6 (66.7 %) Gal-PLL-asODNs treated transgenic mice, but it remained unchanged in the control mice.

Table 2 Change of serum HBsAg (the value of OD) between pretreatment and posttreatment in HBV transgenic mice

Groups	Pieces (n)	Days of therapy	
		Pretreatment	The 12th day
Normal saline	6	1.335±0.769	1.262±0.765 ^a
Gal-PLL-asODNs	6	1.608±0.658	0.733±0.547 ^b

Note: Matched t test analysis showed that, compared with pretreatment, ^a $P>0.05$; ^b $P<0.01$.

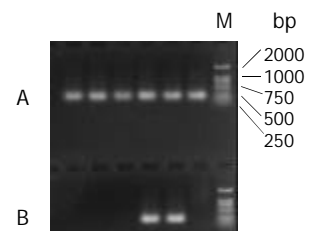


Figure 6 Products of HBV DNA nested-PCR in the mice serum after 12 days treatment. Lane A: Products of HBVDNA nested-PCR in serum after normal saline treatment; Lane B: Products of HBVDNA nested-PCR in serum after asODNs treatment. M: Molecule weight marker.

DISCUSSION

The 2.2.15 cells were shown to carry HBVDNA, being a useful model for screening of HBV-specific asODNs. Exonucleases and endonucleases were identified in serum, cells, and other body fluid, both being able to degrade ODNs. Nucleoside modifications may enhance the resistance of ODNs to nuclease digestion. Among them, phosphorothioate oligodeoxynucleotides were found to be more stable in cell culture medium, cells, the cell extraction, serum, tissue and urine. PSODNs, therefore, were used as a drug in this study.

Foreign DNA can be introduced into cells by transfection using several protocols, including electroporation, liposome and calcium phosphate-mediated procedure. In addition, some DNA delivery systems have been designed for binding foreign gene to target cells^[14,15]. The DNA-carrier system consisting

of an asialoglycoprotein (asialoorosomucoid, ASOR) covalently linked to poly-L-lysine has been used as a hepatotropic ligand to bring a foreign gene preferentially to hepatocytes via asialoglycoprotein receptors^[16-23].

For this purpose, Gal-PLL was prepared in this laboratory previously. Its selective affinity to hepatocytes was demonstrated *in vitro*, proposed to be mediated by asialoglycoprotein receptors on hepatocytes membrane^[24-30]. In this study, the optimized molar ratio 2:1 between Gal-PLL and ODNs was estimated to be 2:1, being in agreement with the reported data (17). Gal-PLL was also suggested to be useful as a liver-targeting plasmid DNA carrier *in vivo*^[27, 28, 30, 31]. This was approved in this study.

The distribution of different ODNs *in vivo* may vary with their length and sequence^[32], and this should be clarified before gene therapy. More than a half of asODNs conjugated to Gal-PLL was shown to be retained in liver, being 2.38-fold of that to free asODNs. In order to avoid the possible interference by plasma HBV DNA in HBV infected animal, normal Kunming mice were used to explore the distribution of asODNs *in vivo*.

According to the data presented, Gal-PLL appears to be a more favorable hepatotropic ligand for gene delivery *in vivo* regarding its convenient preparation and stability, as compared to other compounds such as the well characterized tetra-antennary cluster galactoside L₃G₄^[33].

Considering the dynamic of asODNs, free or conjugated to Gal-PLL, asODNs in liver were 2.97 % and 5.99 %, respectively, 24 hrs after administration, the recommended drug injection interval was 24 hours.

In the same condition of experiment, the inhibition rates of HBsAg and HBeAg by asODNs were 70 % and 58 %, respectively, while those of HBsAg and HBeAg by Gal-PLL-asODNs were 96 % and 82 %, These data indicate that asODNs conjugated to Gal-PLL can block HBV gene expression more efficiently *in vitro*.

HBV transgenic mice were proved to be the suitable animal model for screening anti-HBV drugs^[10,11,34,35,36]. In the present study, a pronounced inhibition was observed by Gal-PLL-asODNs treatment. In addition, serum HBVDNA turned negative in 4 of the 6 transgenic mice. These data show the potential application significance of Gal-PLL-asODNs as an anti-HBV agent.

REFERENCES

- Jensen KD**, Kopeckova P, Kopecek J. Antisense oligonucleotides delivered to the lysosome escape and actively inhibit the hepatitis B virus. *Bioconjug Chem* 2002; **13**: 975-984
- Liu S**, Sun W, Cao Y. Study on anti-HBV effects by antisense oligodeoxynucleotides *in vitro*. *Zhonghua Yufang Yixue Zazhi* 2001; **35**: 338-340
- Robaczewska M**, Guerret S, Remy JS, Chemin I, Offensperger WB, Chevallier M, Behr JP, Podhajska AJ, Blum HE, Trepo C, Cova L. Inhibition of hepadnaviral replication by polyethylenimine-based intravenous delivery of antisense phosphodiester oligodeoxynucleotides to the liver. *Gene Ther* 2001; **8**: 874-881
- Soni PN**, Brown D, Saffie R, Savage K, Moore D, Gregoriadis G, Dusheiko GM. Biodistribution, stability, and antiviral efficacy of liposome-entrapped phosphorothioate antisense oligodeoxynucleotides in ducks for the treatment of chronic duck hepatitis B virus infection. *Hepatology* 1998; **28**: 1402-1410
- Sells MA**, Chen ML, Acs G. Production of hepatitis B virus particles in Hep G2 cells transfected with cloned hepatitis B virus DNA. *Proc Natl Acad Sci USA* 1987; **84**: 1005-1009
- Acs G**, Sells MA, Purcell RH, Price P, Engle R, Shapiro M, Popper H. Hepatitis B virus produced by transfected Hep G2 cells causes hepatitis in chimpanzees. *Proc Natl Acad Sci USA* 1987; **84**: 4641-4644
- Sells MA**, Zelent AZ, Shvartsman M, Acs G. Replicative inter-mediate of hepatitis B virus in Hep G2 cells that produce infectious virions. *J Virol* 1988; **62**: 2836-2844
- Schwartz BA**, Gray GR. Proteins containing reductively aminated disaccharides. Synthesis and chemical characterization. *Arch Biochem Biophys* 1977; **181**: 542-549
- Zhong S**, Zhang D, Wen S. Inhibition of hepatitis B viral gene expression and replication *in vitro* by targeted antisense oligonucleotides. *Zhonghua Yixue Zazhi* 1995; **75**: 392-395, 444
- Xiong Y**, Jia Y, Wang H, Liu G, Ren H, Zhuo Z, Zhang D. Hepatitis B virus transgenic mice for the model of anti-hepatitis B virus drug study. *Zhonghua Ganzangbing Zazhi* 2001; **9**: 19-21
- Xiong YL**, Jia YZ, Wang HM, Liu GZ, Zhang YJ. High-level hepatitis B virus expression in transgenic mice. *Chuanranbing Xinx* 2000; **13**: 164-165
- Miller RH**, Kaneko S, Chung CT, Girones R, Purcell RH. Compact organization of the hepatitis B virus genome. *Hepatology* 1989; **9**: 322-327
- Galibert F**, Mandart E, Fitoussi F, Tiollais P, Charnay P. Nucleotide sequence of the hepatitis B virus genome (subtype ayw) cloned in *E. coli*. *Nature* 1979; **281**: 646-650
- Wu CH**, Wilson JM, Wu GY. Targeting genes: delivery and persistent expression of a foreign gene driven by mammalian regulatory elements *in vivo*. *J Biol Chem* 1989; **264**: 16985-16987
- Lu XM**, Fischman AJ, Jyawook SL, Hendricks K, Tompkins RG, Yarmush ML. Antisense DNA delivery *in vivo*: liver targeting by receptor mediated uptake. *J Nucl Med* 1994; **35**: 269-275
- Nakazono K**, Ito Y, Wu CH, Wu GY. Inhibition of hepatitis B virus replication by targeted pretreatment of complexed antisense DNA *in vitro*. *Hepatology* 1996; **23**: 1297-1303
- Wu GY**, Walton CM, Wu CH. Targeted polynucleotides for inhibition of hepatitis B and C viruses. *Croat Med J* 2001; **42**: 463-466
- Wu GY**, Wu CH. Specific inhibition of hepatitis B viral gene expression *in vitro* by targeted antisense oligonucleotides. *J Biol Chem* 1992; **267**: 12436-12439
- Martinez Fong D**, Mullersman JE, Purchio AF, Armendariz Borunda J, Martin ezHernandez A. Nonenzymatic glycosylation of poly-L-lysine: a new tool for targeted gene delivery. *Hepatology* 1994; **20**: 1602-1608
- Guo J**, Zhou YX, Yao ZQ, Wang SQ, Weng SM, Wang BC. Specific delivery to liver cells by asialoglycoprotein modified antisense oligodeoxynucleotides *in vitro* and *in vivo*. *Zhonghua Chuanranbing Zazhi* 1997; **15**: 16-19
- Dini L**, Falasca L, Lentini A, Mattioli P, Piacentini M, Piredda L, Autuori F. Galactose specific receptor modulation related to the onset of apoptosis in rat liver. *Eur J Cell Biol* 1993; **61**: 329-337
- Anderson WF**. Human gene therapy. *Science* 1992; **256**: 808-813
- Walton CM**, Wu CH, Wu GY. A DNA delivering system containing listeriolysin O results in enhanced hepatocyte directed gene expression. *World J Gastroenterol* 1999; **5**: 465-469
- Zhang J**, Chen F, Zhong S, Tang K, Shi X, Wang M, Peng J. Anti-HBV effect of targeted antisense RNA against HBV C gene. *Zhonghua Ganzangbing Zazhi* 2000; **8**: 169-170
- Zhong S**, Wen S, Zhang D, Wang Q, Wang S, Ren H. Inhibition of HBV gene expression by antisense oligonucleotides using galactosylated poly(L-lysine) as a hepatotropic carrier. *Zhonghua Shiyan He Linchuang Bingduxue Zazhi* 2001; **15**: 150-153
- Zhong S**, Wen SM, Zhang DF, Wang QL, Wang SQ, Ren H. Sequencing of PCR amplified HBV DNA pre-c and c regions in the 2.2.15 cells and antiviral action by targeted antisense oligonucleotide directed against sequence. *World J Gastroenterol* 1998; **4**: 434-436
- Yang CQ**, Wang JY, He BM, Liu JJ, Guo JS. Glyco-poly-L-lysine is better than liposomal delivery of exogenous genes to rat of liver. *World J Gastroenterol* 2000; **6**: 526-531
- Yang CQ**, Wang JY, Fang GT, Liu JJ, Guo JS. A comparison between intravenous and peritoneal route on liver targeted uptake and expression of plasmid delivered by Glyco-poly-L-lysine. *World J Gastroenterol* 2000; **6**: 508-512
- Chen YP**, Zhang L, Lu QS, Feng XR, Luo KX. Lactosamination of liposomes and hepatotropic targeting research. *World J Gastroenterol* 2000; **6**: 593-596

- 30 **Yang C**, Wang J, Wen S, Liu J, Guo J. Comparative studies of different carriers and introducing routes on the effects of liver targeted uptake of exogenous gene. *Zhonghua Ganzangbing Zazhi* 2000; **8**: 227-229
- 31 **Mani SA**, Harish S, Vathsala PG, Rangarajan PN, Padmanaban G. Receptor-mediated gene delivery approach demonstrates the role of 5'-proximal DNA region in conferring phenobarbitone responsiveness to CYP2B2 gene in rat liver *in vivo*. *Biochem Biophys Res Commun* 2000; **268**: 734-739
- 32 **Biessen EA**, Vietsch H, Kuiper J, Bijsterbosch MK, Berkel TJ. Liver uptake of phosphodiester oligodeoxynucleotides is mediated by scavenger receptors. *Mol Pharmacol* 1998; **53**: 262-269
- 33 **Biessen EA**, Vietsch H, Rump ET, Fluiter K, Kuiper J, Bijsterbosch MK, van Berkel TJ. Targeted delivery of oligodeoxynucleotides to parenchymal liver cells *in vivo*. *Biochem J* 1999; **340**: 783-792
- 34 **Morrey JD**, Korba BE, Sidwell RW. Transgenic mice as a chemotherapeutic model for hepatitis B virus infection. *Antivir Ther* 1998; **3**(Suppl 3):59-68
- 35 **Morrey JD**, Bailey KW, Korba BE, Sidwell RW. Utilization of transgenic mice replicating high levels of hepatitis B virus for antiviral evaluation of lamivudine. *Antiviral Res* 1999; **42**: 97-108
- 36 **Julander JG**, Sidwell RW, Morrey JD. Characterizing antiviral activity of adefovir dipivoxil in transgenic mice expressing hepatitis B virus. *Antiviral Res* 2002; **55**: 27-40

Edited by SuQ

Cross-reactivity of hypervariable region 1 chimera of hepatitis C virus

Bing-Shui Xiu, Shi-Gan Ling, Xiao-Guo Song, He-Qiu Zhang, Kun Chen, Cui-Xia Zhu

Bing-Shui Xiu, Shi-Gan Ling, Xiao-Guo Song, He-Qiu Zhang, Kun Chen, Cui-Xia Zhu, Laboratory of Molecular Virology, Institute of Basic Medical Sciences, Academy of Military Medical Sciences, Beijing 100850, China

Supported by National 10th Five-Year Plan of Science and Technology Brainstorm Project, No. 2001BA708B06 and a grant from Natural Science Foundation of Beijing, No.7002031

Correspondence to: Professor Shi-Gan Ling, Laboratory of Molecular Virology, Institute of Basic Medical Sciences, Academy of Military Medical Sciences, Beijing 100850, P.R.China. lingsg@nic.bmi.ac.cn

Telephone: 010-66932308 **Fax:** +86-10-68285718

Received: 2003-01-04 **Accepted:** 2003-02-16

Abstract

AIM: To analyze the amino acid sequences of hypervariable region 1 (HVR1) of HCV isolates in China and to construct a combinatorial chimeric HVR1 protein having a very broad high cross-reactivity.

METHODS: All of the published HVR1 sequences from China were collected and processed with a computer program. Several representative HVR1's sequences were formulated based on a consensus profile and homology within certain subdivision. A few reported HVR1 mimotope sequences were also included for a broader representation. All of them were cloned and expressed in *E.coli*. The cross-reactivity of the purified recombinant HVR1 antigens was tested by ELISA with a panel of sera from HCV infected patients in China. Some of them were further ligated together to form a combinatorial HVR1 chimera.

RESULTS: Altogether 12 HVR1s were selected and expressed in *E.coli* and purified to homogeneity. All of these purified antigens showed some cross-reactivity with sera in a 27 HCV positive panel. Recombinant HVR1s of No. 1, 2, 4, and 8# showing broad cross-reactivities and complementarity with each other, were selected for the ligation elements. The chimera containing these 4 HVR1s was highly expressed in *E.coli*. The purified chimeric antigen could react not only with all the HCV antibody positive sera in the panel but also with 90/91 sera of HCV-infected patients.

CONCLUSION: The chimeric antigen was shown to have a broad cross-reactivity. It may be helpful for solving the problem caused by high variability of HCV, and in the efforts for a novel vaccine against the virus.

Xiu BS, Ling SG, Song XG, Zhang HQ, Chen K, Zhu CX. Cross-reactivity of hypervariable region 1 chimera of hepatitis C virus. *World J Gastroenterol* 2003; 9(6): 1256-1260
<http://www.wjgnet.com/1007-9327/9/1256.asp>

INTRODUCTION

Hepatitis C virus (HCV) is a major etiological agent of non-A,

non-B hepatitis worldwide^[1-3], and HVR1, the N-terminal 27 amino acid residues of the putative HCV envelope protein E2, is known as the principal neutralization epitopes up to date^[4-7]. Antibodies to HVR1 in human sera have been shown to block viral attachment to human cell lines *in vitro* and to protect chimpanzees from HCV infection *in vivo*^[8-10]. The HVR1 sequence is highly variable, and is the greatest obstacle for the vaccine development and immune therapy^[11,12]. However, the highly variable HVR1s have been shown to have some cross-reactivities with each other, indicating that a broadly cross-reactive HVR1 peptide or their cocktails are helpful to solving the problem^[13]. Data were accumulated in this study all over the world^[14-17].

In China, HVR1 sequences of different HCV isolates have been reported by many authors, but few studies were on HVR1 cross-reactivity. Integrating the HVR1 sequences reported in China together with some published mimotopes, 12 representative HVR1 sequences were selected using bioinformatics technology. All of the representative HVR1 sequences were cloned and expressed, and their cross-reactivity was studied with a panel of 27 HCV positive sera. Finally we obtained an HVR1 fusion antigen broadly cross-reactive with the HCV-infected sera.

MATERIALS AND METHODS

Human sera

Samples of HCV-infected sera were obtained from blood donor applicants in Beijing Red Cross Blood Center and from chronic HCV-infected patients from 302 Hospital of PLA. All were positive for HCV antibodies using the 2nd-generation ELISA kit. (Ortho Diagnostics, Raritan N.J).

Selection of representative HVR1 sequences

All of the HVR1 sequences published in China were loaded into database and their consensus sequence was obtained by BASIC program according to the frequency of amino acid residues. All of these HVR1 sequences were divided into several groups according to their alignment, and one sequence was chosen as the representative from each group. All of the work above was operated on Goldkey (a molecular biology software developed by our institute). Some HVR1 sequences or mimotopes published were chosen as representative ones for their high cross-reactivity with sera of HCV infected patients from other countries.

Construction of expression plasmid HVR1-1 # to 12

The representative HVR1 sequences were modified considering the *Escherichia coli*'s favorable codon usage. The coding genes were synthesized chemically and to facilitate further ligation, two linkers with a specially designed restriction endonuclease site were incorporated into their N- and C-terminals respectively. The N terminal arm is F1 (5'-gc ctc gag ggt ggt gga tct -3'), The C terminal arm is R1 (5'-gc tct aga acc tcc acc act -3'). The fragments were digested with XhoI and XbaI enzymes and inserted into the expressing plasmid pBVIL1 digested by the same restrictive enzymes. In

the same way, 12 different pBVIL1-HVR1 constructs were prepared and the HVR1 genes were expressed as fusion protein with IL1 β in *E. coli*.

Construction of the chimeric plasmid

According to the cross-reactivity with the HCV antibodies positive sera panel, several HVR1s were chosen to ligate together one by one as illustrated in Figure 1. The plasmid pBVIL1-HVR1-1# (pHVR1#) was chosen as a vector digested by Xba I and BamH I, while the plasmid pBVIL1-HVR1-2#, was chosen as the donor of pattern, amplified using constant primer F2 (5' gc act agt ggt ggt gga tct 3') and R2 (5'cg gga tcc tta gga aga cac aaa 3') which annealed to C-terminal of IL1 β . The PCR product was digested with *Spe* I and *Bam*H I, and inserted into the digested vector, pBVIL1-HVR1-1#. Owe to the same cohesive end of the endonuclease Xba I and *Spe* I, the digested PCR fragment could accurately linked to the digested plasmid and the new ligated site could be digested by neither of them.

The pBVIL1-HVR1-1+2# had the same enzyme sites with pHVR1# and so it could be used as a new vector and connected with other HVR1 gene fragments. In this way, the pBVIL1-chimeric-HVR1 was constructed to contain four HVR1 genes, HVR1-1#, HVR1-4#, HVR1-6# and HVR1-8#.

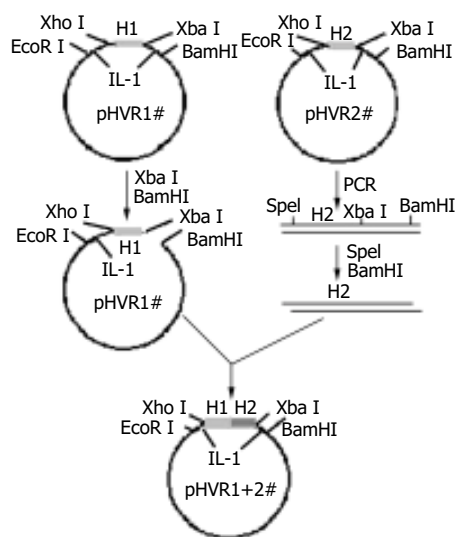


Figure 1 Four different HVR1 gene fragments were cloned on pBVIL-1. HVR1-2 gene fragment was ligated with pBVIL-1-HVR1-1 (pHVR1#). The new pHVR1+2 had the same site with pHVR1#, and the HVR1-4# gene fragments could be ligated by the same way. After 3 cycles, the chimera HVR1 plasmid was constructed.

Purification of representative HVR1-1-12# and the chimeric antigen

The plasmids carrying HVR1 fragments were transformed into HB101 as routine, and were examined for their orientation and nucleic acid sequences. The transformed HB101 was grown overnight, diluted 1:20 with fresh LB-medium and further incubated at 37 °C to an OD₆₀₀ of 0.6. After induction for 4 h at 42 °C the bacteria were harvested by centrifugation, and lysed by sonication. All of the recombinant proteins existed in inclusion bodies, and could be dissolved in a solution containing 8 M urea. The recombinant proteins were isolated and purified consecutively by Q-Sepharose-FF and Sephadex G50 chromatography.

ELISA

Microplates were coated with 0.3 μ g recombinant HVR1

peptide in 100 mM phosphate buffer (pH7.4) by incubation overnight at 4 °C. The plates were then blocked with the phosphate buffer containing 0.2 % BSA at 4 °C for 3 h, and then incubated with 100 μ l of the serum sample 1:10 diluted with a sample buffer (100 mM sodium phosphate buffer, pH7.5 containing 10 % goat serum and 0.05 % Tween) at 37 °C for 1 h. After being washed for five times with 100 mM phosphate buffer (pH7.5) containing 0.05 % Tween, the plates were then incubated for 30 min at 37 °C with 1:25 000 diluted HRP-conjugated monoclonal antibody against human IgG. After washing, the reaction was visualized in the substrate buffer (50 mM sodium phosphate-citric acid buffer, pH5.0 containing 0.4 mg/ml TMB and 0.4 μ l/ml of 30 % hydrogen peroxide). The reaction was stopped by adding 50 μ l of 2 M sulfuric acid, and the absorbance was measured in a microplates ELISA reader at 450 nm.

RESULTS

Determination of 12 representative peptides

A total number of 123 sequences on HVR1 were reported in China, and the derived consensus profile of them is shown in Figure 2A. Some amino acid residues of HVR1 were shown to be hypervariable, while those at position 385, 389, 406, 409 were conserved. The sequence on first line was defined as CCS (Chinese consensus sequence), whose amino acid residues emerged most frequently. CCS was chosen as the first representative sequence, named HVR1-1#, being different at some positions from Puntoriero's consensus sequence^[13] (Figure 2B). The homology of the 123 sequences was analyzed using the Goldkey software, and divided into 6 groups, HVR1-2 to 7# according to their alignment to CCS. In this way 6 sequences named were obtained. HVR1-8# 9# were from GenBank (L19383, S24080), both being broadly cross-reactive with mice sera induced by mimotopes. HVR1-10# and 11# were sequences for the mimotope R9 and M122 respectively (Puntoriero *et al.*, 1998), and HVR1-12# reported by Watanabe^[14].

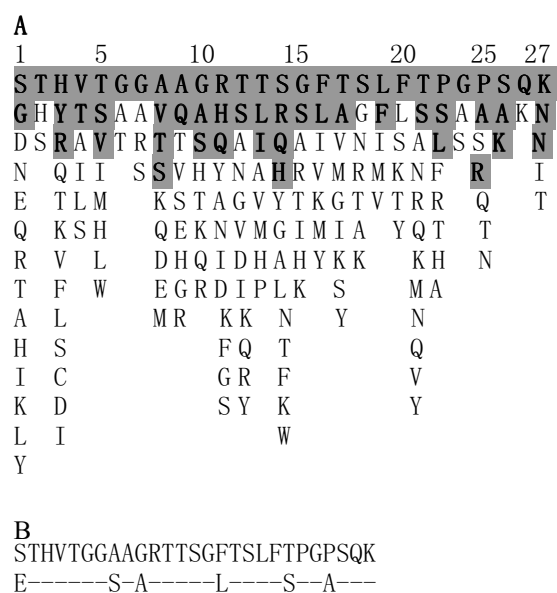


Figure 2 Derivation of the Chinese consensus sequence. (A) Consensus pattern of the 123 natural variants of the HCV HVR1 sequence used in this work. Shaded residues accounted alone for 80 % of the observed frequency. Residues were listed in decreasing order of observed frequency from top to bottom. The first line was Chinese consensus sequence (CCS). (B) The Chinese consensus sequence (upper) was different with Puntoriero's (lower). Dashes indicate residues identical to the upper line.

Reactivity of representative peptide with sera of panel I

Twelve representative HVR1 gene as shown in Figure 3, were expressed in *E.coil* fused with human IL-1 β . The HVR1/IL-1 β fusion protein migrated at the expected position of about 21 kD (Figure 4). Twenty-seven HCV patients' sera were used as panel I to show the cross-reactivities of 12 representative HVR1 by ELISA. As shown in Figure 5, all of the HVR1 peptide reacted with more than one serum. No reactivity was detected to IL-1 β in sera of panel I, and none of the anti-HCV negative sera reacted with the 12 recombinant peptides. The most broadly cross-reactive HVR1 was HVR1-11#, and the Chinese consensus sequence (CCS) which showed a higher cross-reactivity too.

We took HVR1-1,2,4,8# as components for the best cocktail, because these 4 HVR1 peptides showed complementary reactivities to the sera in panel I, as showed in Figure 5. There overall cross-reactivity was found to be 25/27.

1#	STHVTGGAAGRITTSGFTSLFTPGPSQK
2#	STHVTGGVQGHSLRGLTSLFTSGPAQK
3#	ITRVTGGVQGHSLRSLTSLFTPGPAQK
4#	STHVTGAVQGRSLQSFSTFLSPGPSQK
5#	DTHVTGGAARGASGLANLFTSGPAQK
6#	GFYVTGGATAHTASGFASLFTTIGSKQN
7#	TTHVTAGTAAHATSSFTKLFAPGAKQN
8#	NTYVTGSSAAHTTSRFTSLFSPGPQQN
9#	ETHTSGGSVARAAFGLTSLFSPGKSN
10#	TTTTTGGVQGHTRGLVRLFLSLGSKQN
11#	DTIVTGGQAAARTQSFSTSLFPPGPSQK
12#	DTIVTGGQAAARTQSFSTSLFTPGPSQK

Figure 3 The amino acid sequence of 12 representative HVR1 sequences. Amino acid residues were indicated by standard single-letter codes.

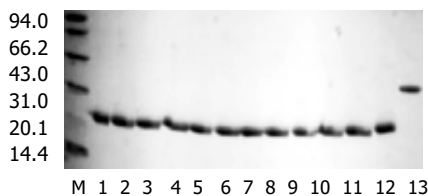


Figure 4 The Coomassie stain after SDS-PAGE of 12 purified representative and chimera HVR1 antigen. M. marker; 1-12. 12 purified representative HVR1 antigen; 13. chimera HVR1 antigen.

Reactivity of chimera HVR1 antigen with panel I and panel II

HVR1-1#, 2#, 4# and 8# were ligated one by one in tandem within plasmid pBVIL1. The chimeric protein was expressed in HB101 and further purified (Figure 4).

As expected, a broader reactive spectrum was observed for the chimeric HVR1 antigen. It was shown to be reactive with all of the sera of panel I, including sera 73# and 39# which were not reactive with any single HVR1 (Figure 5). For more data 91 sera from HCV-infected patients were also used for the assay as panel II, with 90 reactive with chimera antigen (Table 1). The data indicated that application of the chimera protein helped to acquire a higher cross-reactivity.

Table 1 Reactivity of F4HVR1 with another panel (91 sera of HCV infected patient)

OD difference between sera and co	No. of reactive sera	The adding up percent of total sera
>2.0	56	61.5
1.5-2.0	14	76.9
1.0-1.5	13	91.2
0.5-1.0	6	97.8
0.371	1	98
0.065	1	

The cutoff of the ELISA was as defined in Figure 5.

DISCUSSION

HVR1, which contains a principal neutralization epitope in HCV, is important for the development of HCV vaccine^[4-7]. Due to the high mutation rate of HVR1, there are now hundreds of HVR1 isolates reported, presenting a great obstacle for HCV vaccine development^[18-21]. It was suggested that to select a highly cross-reactive HVR1 antigen could solve the variability problem^[22-27], thus highlighted the importance to study the cross-reactivity of HVR1.

Most of the work about the cross-reactivity of HVR1 focused on single HVR1 antigen. However we think the cross-reactivity of single HVR1 is limited. Recently, multi-epitope chimeric antigen was used to improve the sensitivity of HCV immunoassay reagents^[28,29]. Here we provided evidence for enhancing the cross-reactivity by constructing a chimeric antigen that incorporates several representative HVR1 peptides.

Considering geographical variation of HVR1^[30-33], we gave

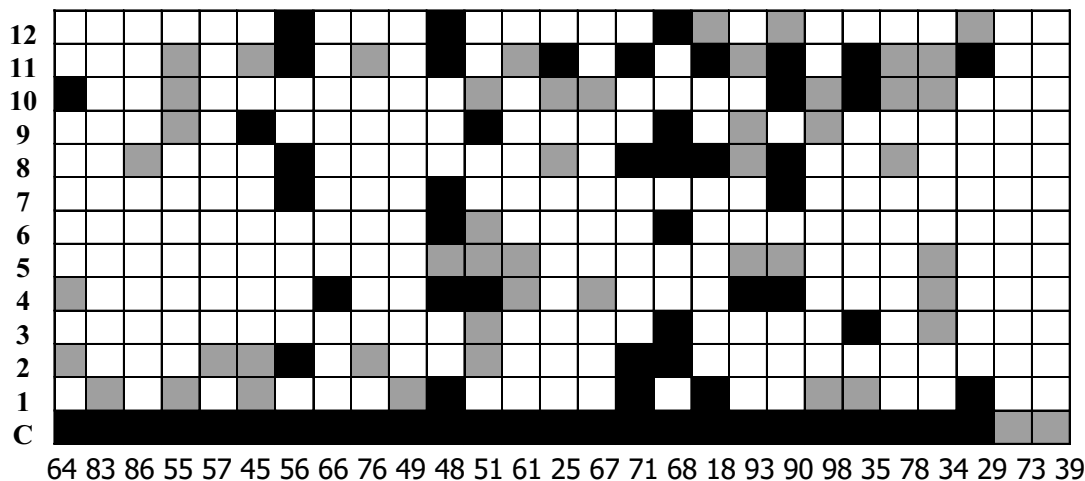


Figure 5 Reaction of the 12 representative HVR1s and chimera HVR1 antigen (C) with 27 sera from HCV-infected patients. HVR1 names are indicated at the left of each column. For each serum (indicated on the bottom of each column) average values (A450) have been determined from two independent experiments. The mean of 10 sera from non-infected individuals plus 4SD defined the cutoff (co). Results were expressed as the difference between the average value of the HCV antibody positive sera and co. Strong positive values (>0.5) are indicated in black. And weak positive values (0.15-0.5).

priority to Chinese sequence when we selected representative HVR1 sequences. The differences between CCS and Puntoriero's suggest the HVR1 variant found in China differs to a certain extent from what occurred elsewhere^[14]. The chimeric antigen contains 3 representative HVR1 sequences coming from China, and showed broad cross-reactivity with sera of the HCV-infected patients.

The reported HVR1 antigen or mimotope could cross-react with no more than 80 % of sera containing HCV antibodies^[22-27]. Chimeric HVR1 antigen could cross-react with 90/91 (98 %) of tested sera. The results also suggested that most of HCV infected patients could generate some antibodies against HVR1. The possible association between HVR1 antibody and the self-limiting course of HCV infection and a more favorable response to interferon^[34-40], remains to be evaluated in the following study.

Evidently, the reaction spectrum of the chimera HVR1 antigen include the total cross-reactivity of the representative HVR1 antigen contained. Interestingly, the chimera HVR1 antigen could react with sera 73# and 39#, which are not definitely reactive with any of the four representative HVR1. In our consideration, those samples might react with some of the representative HVR1 used for ligation, but reactions are too weak to be detected. The OD value would be elevated when 4 HVR1 is added up together.

In this study, we used a prepared chimeric antigen instead of synthetic peptides^[41-43]. The antigen may also be used in the study for the HCV vaccine. In addition, the chimeric antigen is fused with IL-1 β . The latter part contains a nano-peptide sequence. It may act as an immune adjuvant^[44-46], promoting a strong immune response when injected.

In summary, the chimeric HVR1 antigen, containing several representative HVR1 fragments, can show very high cross-reactivity, which may be helpful to overcome the variability of HCV. The chimeric HVR1 antigen is of potential application for HCV vaccination and immune therapy.

REFERENCES

- Alter HJ. To C or not to C. these are the questions. *Blood* 1995; **85**: 1681-1695
- Choo QL, Kuo G, Weiner AJ, Overby LR, Bradley DW, Houghton M. Isolation of a cDNA clone derived from a blood-borne non-A, non-B viral hepatitis genome. *Science* 1989; **244**: 359-362
- Sela B. New approaches to immune against hepatitis C virus *Harefuah* 2002; **141**: 1076-1080
- Esumi M, Rikihisa T, Nishimura S, Goto J, Mizuno K, Zhou YH, Shikata T. Experimental vaccine activities of recombinant E1 and E2 glycoproteins and hypervariable region 1 peptides of hepatitis C virus in chimpanzees. *Arch Virol* 1999; **144**: 973-980
- Farci P, Alter HJ, Wong DC, Miller RH, Govindarajan S, Engle R, Shapiro M, Purcell RH. Prevention of hepatitis C virus infection in chimpanzees after antibody-mediated in vitro neutralization. *Proc Natl Acad Sci U S A* 1994; **91**: 7792-7796
- Cerino A, Meola A, Segagni L, Furione M, Marciano S, Triyatni M, Liang TJ, Nicosia A, Mondelli MU. Monoclonal antibodies with broad specificity for hepatitis C virus hypervariable region 1 variants can recognize viral particles. *J Immunol* 2001; **167**: 3878-3886
- Farci P, Shimoda A, Wong D, Cabezon T, De Gioannis D, Strazzer A, Shimizu Y, Shapiro M, Alter HJ, Purcell RH. Prevention of hepatitis C virus infection in chimpanzees by hyperimmune serum against the hypervariable region 1 of the envelope 2 protein. *Proc Natl Acad Sci U S A* 1996; **93**: 15394-15399
- Zhou YH, Takekoshi M, Maeda F, Ihara S, Esumi M. Recombinant antibody Fab against the hypervariable region 1 of hepatitis C virus blocks the virus adsorption to susceptible cells *in vitro*. *Antiviral Res* 2002; **56**: 51-59
- Goto J, Nishimura S, Esumi M, Makizumi K, Rikihisa T, Nishihara T, Mizuno K, Zhou Y, Shikata T, Fujiyama S, Tomita K. Prevention of hepatitis C virus infection in a chimpanzee by vaccination and epitope mapping of antiserum directed against hypervariable region 1. *Hepato Res* 2001; **19**: 270-283
- Zibert A, Schreier E, Roggendorf M. Antibodies in human sera specific to hypervariable region 1 of hepatitis C virus can block viral attachment. *Virology* 1995; **208**: 653-661
- Korenaga M, Hino K, Katoh Y, Yamaguchi Y, Okuda M, Yoshioka K, Okita K. A possible role of hypervariable region 1 quasispecies in escape of hepatitis C virus particles from neutralization. *J Viral Hepat* 2001; **8**: 331-340
- Gao G, Buskell Z, Seeff L, Tabor E. Drift in the hypervariable region of the hepatitis C virus during 27 years in two patients. *J Med Virol* 2002; **68**: 60-67
- Scarselli E, Cerino A, Esposito G, Silini E, Mondelli MU, Traboni C. Occurrence of antibodies reactive with more than one variant of the putative envelope glycoprotein (gp70) hypervariable region 1 in viremic hepatitis C virus-infected patients. *J Virol* 1995; **69**: 4407-4412
- Puntoriero G, Meola A, Lahm A, Zucchelli S, Ercole BB, Tafi R, Pezzanera M, Mondelli MU, Cortese R, Tramontano A, Galfre' G, Nicosia A. Towards a solution for hepatitis C virus hypervariability: mimotopes of the hypervariable region 1 can induce antibodies cross-reacting with a large number of viral variants. *EMBO J* 1998; **17**: 3521-3533
- Watanabe K, Yoshioka K, Ito H, Ishigami M, Takagi K, Utsunomiya S, Kobayashi M, Kishimoto H, Yano M, Kakumu S. The hypervariable region 1 protein of hepatitis C virus broadly reactive with sera of patients with chronic hepatitis C has a similar amino acid sequence with the consensus sequence. *Virology* 1999; **264**: 153-158
- Mondelli MU, Cerino A, Segagni L, Meola A, Cividini A, Silini E, Nicosia A. Hypervariable region 1 of hepatitis C virus: immunological decoy or biologically relevant domain? *Antiviral Res* 2001; **52**: 153-159
- Rispeter K, Lu M, Behrens SE, Fumiko C, Yoshida T, Roggendorf M. Hepatitis C virus variability: sequence analysis of an isolate after 10 years of chronic infection. *Virus Genes* 2000; **21**: 179-188
- Fan X, Di Bisceglie AM. Genetic characterization of hypervariable region 1 in patients chronically infected with hepatitis C virus genotype 2. *J Med Virol* 2001; **64**: 325-333
- Lin HJ, Seeff LB, Barbosa L, Hollinger FB. Occurrence of identical hypervariable region 1 sequences of hepatitis C virus in transfusion recipients and their respective blood donors: divergence over time. *Hepatology* 2001; **34**: 424-429
- Lu L, Nakano T, Orito E, Mizokami M, Robertson BH. Evaluation of accumulation of hepatitis C virus mutations in a chronically infected chimpanzee: comparison of the core, E1, HVR1, and NS5b regions. *J Virol* 2001; **75**: 3004-3009
- Ray SC, Wang YM, Laeyendecker O, Ticehurst JR, Villano SA, Thomas DL. Acute hepatitis C virus structural gene sequences as predictors of persistent viremia: hypervariable region 1 as a decoy. *J Virol* 1999; **73**: 2938-2946
- Zucchelli S, Roccasecca R, Meola A, Ercole BB, Tafi R, Dubuisson J, Galfre G, Cortese R, Nicosia A. Mimotopes of the hepatitis C virus hypervariable region 1, but not the natural sequences, induce cross-reactive antibody response by genetic immunization. *Hepatology* 2001; **33**: 692-703
- Roccasecca R, Folgari A, Ercole BB, Puntoriero G, Lahm A, Zucchelli S, Tafi R, Pezzanera M, Galfre G, Tramontano A, Mondelli MU, Pessi A, Nicosia A, Cortese R, Meola A. Induction of cross-reactive humoral immune response by immunization with mimotopes of the hypervariable region 1 of the hepatitis C virus. *Int Rev Immunol* 2001; **20**: 289-300
- Roccasecca R, Folgari A, Ercole BB, Puntoriero G, Lahm A, Zucchelli S, Tafi R, Pezzanera M, Galfre G, Tramontano A, Mondelli MU, Pessi A, Nicosia A, Cortese R, Meola A. Mimotopes of the hyper variable region 1 of the hepatitis C virus induce cross-reactive antibodies directed against discontinuous epitopes. *Mol Immunol* 2001; **38**: 485-492
- Li C, Candotti D, Allain JP. Production and characterization of monoclonal antibodies specific for a conserved epitope within hepatitis C virus hypervariable region 1. *J Virol* 2001; **75**: 12412-12420
- Shang D, Zhai W, Allain JP. Broadly cross-reactive, high-affinity antibody to hypervariable region 1 of the hepatitis C virus in rabbits. *Virology* 1999; **258**: 396-405

- 27 **Zhou YH**, Moriyama M, Esumi M. Multiple sequence-reactive antibodies induced by a single peptide immunization with hypervariable region 1 of hepatitis C virus. *Virology* 1999; **256**: 360-370
- 28 **Yagi S**, Kashiwakuma T, Yamaguchi K, Chiba Y, Ohtsuka E, Hasegawa A. An epitope chimeric antigen for the hepatitis C virus serological screening test. *Biol Pharm Bull* 1996; **19**: 1254-1260
- 29 **Paolini R**, Marson P, Vicarioto M, Ongaro G, Viero M, Girolami A. Anti-hepatitis C virus serology in patients affected with congenital coagulation defects: a comparative study using three second generation ELISA tests. *Transfus Sci* 1994; **15**: 303-311
- 30 **Bosch FX**, Ribes J. Epidemiology of liver cancer in Europe. *Can J Gastroenterol* 2000; **14**: 621-630
- 31 **Simmonds P**. Viral heterogeneity of the hepatitis C virus. *J Hepatol* 1999; **31**(Suppl 31): 54-60
- 32 **Cai Q**, Zhang X, Tian L, Yuan M, Jin G, Lu Z. Variant analysis and immunogenicity prediction of envelope gene of HCV strains from China. *J Med Virol* 2002; **67**: 490-500
- 33 **Oliveira ML**, Bastos FI, Sabino RR, Paetzold U, Schreier E, Pauli G, Yoshida CF. Distribution of HCV genotypes among different exposure categories in Brazil. *Braz J Med Biol Res* 1999; **32**: 279-282
- 34 **Zibert A**, Meisel H, Kraas W, Schulz A, Jung G, Roggendorf M. Early antibody response against hypervariable region 1 is associated with acute self-limiting infections of hepatitis C virus. *Hepatology* 1997; **25**: 1245-1249
- 35 **Lechner S**, Rispeter K, Meisel H, Kraas W, Jung G, Roggendorf M, Zibert A. Antibodies directed to envelope proteins of hepatitis C virus outside of hypervariable region 1. *Virology* 1998; **243**: 313-321
- 36 **Isaguliant MG**, Widell A, Zhang SM, Sidorchuk A, Levi M, Smirnov VD, Santantonio T, Diepolder HM, Pape GR, Nordenfelt E. Antibody responses against B-cell epitopes of the hypervariable region 1 of hepatitis C virus in self-limiting and chronic human hepatitis C followed-up using consensus peptides. *J Med Virol* 2002; **66**: 204-217
- 37 **Del Porto P**, Puntoriero G, Scotta C, Nicosia A, Piccolella E. High prevalence of hypervariable region 1-specific and -cross-reactive CD4(+) T cells in HCV-infected individuals responsive to IFN-alpha treatment. *Virology* 2000; **269**: 313-324
- 38 **Hjalmarsson S**, Blomberg J, Grillner L, Pipkorn R, Allander T. Sequence evolution and cross-reactive antibody responses to hypervariable region 1 in acute hepatitis C virus infection. *J Med Virol* 2001; **64**: 117-124
- 39 **Hattori M**, Yoshioka K, Aiyama T, Iwata K, Terazawa Y, Ishigami M, Yano M, Kakumu S. Broadly reactive antibodies to hypervariable region 1 in hepatitis C virus-infected patient sera: relation to viral loads and response to interferon. *Hepatology* 1998; **27**: 1703-1710
- 40 **Pawlotsky JM**, Germanidis G, Frainais PO, Bouvier M, Soulier A, Pellerin M, Dhumeaux D. Evolution of the hepatitis C virus second envelope protein hypervariable region in chronically infected patients receiving alpha interferon therapy. *J Virol* 1999; **73**: 6490-6499
- 41 **Zhou YH**, Sugitani M, Esumi M. Sequences in the hypervariable region 1 of hepatitis C virus show only minimal variability in the presence of antibodies against hypervariable region 1 during acute infection in chimpanzees. *Arch Virol* 2002; **147**: 1955-1962
- 42 **Wang Y**, Hao F, Huang Y. Molecular design and immunoreactivity studies of multiple antigen peptide corresponding to hypervariable region 1 sequence of hepatitis C virus. *Zhonghua Ganzangbing Zazhi* 2000; **8**: 48-50
- 43 **Duenas-Carrera S**, Vina A, Garay HE, Reyes O, Alvarez-Lajonchere L, Guerra I, Gonzalez LJ, Morales J. Immunological evaluation of Escherichia coli-derived hepatitis C virus second envelope protein (E2) variants. *J Pept Res* 2001; **58**: 221-228
- 44 **Bockmann S**, Mohrdieck K, Paegelow I. Influence of interleukin-1 beta on bradykinin-induced responses in guinea pig peritoneal macrophages. *Inflamm Res* 1999; **48**: 56-62
- 45 **Akasu T**, Tsurusaki M. Effects of interleukin-1 beta on neurons in mammalian pelvic ganglia. *Kurume Med J* 1999; **46**: 143-150
- 46 **Boraschi D**, Tagliabue A. Interleukin-1 and interleukin-1 fragments as vaccine adjuvants. *Methods* 1999; **19**: 108-113

Edited by Su Q and Wang XL

TT virus infection in patients with chronic hepatitis B and response of TTV to lamivudine

Javier Moreno Garcia, Rafael Barcena Marugan, Gloria Moraleda Garcia, M Luisa Mateos Lindeman, Jesus Fortun Abete, Santos del Campo Terron

Javier Moreno Garcia, Rafael Barcena Marugan, Gloria Moraleda Garcia, Santos del Campo Terron, Department of Gastroenterology, Hospital Ramon y Cajal, Madrid, Spain

M Luisa Mateos Lindeman, Department of Microbiology, Hospital Ramon y Cajal, Madrid, Spain

Jesus Fortun Abete, Department of Infectious Diseases, Hospital Ramon y Cajal, Madrid, Spain

Supported by Fundacion Manchega de Investigacion Docencia en Gastroenterologia

Correspondence to: Dr. Rafael Barcena Marugan, Department of Gastroenterology, Hospital Ramon y Cajal, Ctra. Colmenar, Km 9.1, 28034 Madrid, Spain. rbarcena.hrc@salud.madrid.org

Telephone: +34-91-3368093 **Fax:** +34-91-7291456

Received: 2003-02-25 **Accepted:** 2003-03-16

Abstract

AIM: To investigate the responses of TT virus (TTV) and hepatitis B virus (HBV) to a long-term lamivudine therapy.

METHODS: Sixteen patients infected with both TTV and HBV were treated with lamivudine 100 mg daily for 30 months. Blood samples were drawn at the beginning of the therapy and subsequently at month 3, 6, 9, 12 and 30. Serum TTV was quantified by real time PCR and serum HBV was detected by hybridization assay and nested polymerase chain reaction.

RESULTS: TTV infection was detected in 100 % of HBV-infected patients. Loss of serum TTV DNA after one year of treatment occurred in 1/16 (6 %) patients. At the end of therapy, TTV DNA was positive in 94 % of them. The decline of HBV viremia was evident at 3 months after therapy and the response rate was 31 %, 44 %, 63 %, 50 % and 50 % at month 3, 6, 9, 12 and 30, respectively.

CONCLUSION: TTV replication is not sensitive to lamivudine and is highly prevalent in HBV-infected patients.

Garcia JM, Marugan RB, Garcia GM, Lindeman MLM, Abete JF, Terron SC. TT virus infection in patients with chronic hepatitis B and response of TTV to lamivudine. *World J Gastroenterol* 2003; 9(6): 1261-1264

<http://www.wjgnet.com/1007-9327/9/1261.asp>

INTRODUCTION

TT virus (TTV) was recently discovered in a patient with post-transfusional hepatitis of unknown etiology^[1]. Its genome is a circular, single-stranded DNA of negative polarity, which shares similarities with the members of the Circoviridae family^[2]. In contrast to DNA viruses, TTV isolates exhibit a high level of genetic heterogeneity^[3]. TTV presents an extreme diffusion of active infection throughout the world^[4]. Its presence in blood products could indicate that TTV can be transmitted through transfusion^[5]. Although it has been proposed that TT virus might be responsible for the small

proportion of acute and chronic forms of hepatitis that still remain unsolved, no other illness has yet been attributed to the virus.

Hepatitis B virus (HBV) causes transient and chronic infections of the liver, which may progress to cirrhosis and eventually to hepatocellular carcinoma (HCC)^[6]. Interferon (IFN)-alpha is the only approved drug for the treatment of chronic HBV infection, but the recent registration of lamivudine, a dideoxycytidine analogue that inhibits both the HIV and HBV reverse transcriptases, has provided new perspectives for the treatment of chronic HBV infection^[7, 8]. Coinfection of TTV and HBV is commonly seen because both viruses share the same transmission routes such as blood transfusion^[9]. In previous studies, IFN therapy has been reported effective against TTV^[10], but the possible susceptibility of the virus to lamivudine treatment has not yet been investigated. Thus, the aims of this study were: (1) to know the impact of TTV in patients with chronic hepatitis B; (2) to investigate the response of TTV to lamivudine therapy; and (3) to evaluate whether the outcome of long term lamivudine therapy in chronic hepatitis B is influenced by a TTV coinfection.

MATERIALS AND METHODS

Patients

The study group consisted of 16 patients (12 males and 4 females; mean age: 52.62 years; range: 33 and 66 years) with chronic dual HBV and TTV infection. The diagnosis of chronic hepatitis was made on the basis of clinical and histological results. Patients included 15 cases of liver cirrhosis and 1 hepatocarcinoma. In 9 patients the transmission route was unknown, 2 had a history of blood transfusion, 2 developed HBV infection after liver transplantation, 1 had primary biliary cirrhosis and 2 were addicts to alcohol. At the beginning of the therapy, all patients were positive to HBV DNA by solution hybridization assay and had elevated alanine aminotransferase (ALT) levels that were 3 times of the upper normal limit (normal range: 5-45 IU/L). Nine patients were hepatitis B e antigen (HBeAg) positive, 5 had antibodies against HBeAg (anti-HBe) and 2 patients were negative to both HBeAg and anti-HBe.

Ten patients underwent liver transplantation; 8 of them for HBV-related liver cirrhosis. The remaining 2 patients without evidence of HBV infection before allograft developed a *de novo* post-transplant HBV infection.

Lamivudine (Glaxo Wellcome, UK) was given orally to all patients at a dose of 100 mg daily for 30 months. Blood samples were taken at the baseline time and subsequently were obtained at month 3, 6, 9, 12 and 30. To evaluate the effects of lamivudine, levels of ALT, TTV DNA and HBV DNA and viral serological markers were evaluated at each time. HBV complete responders to lamivudine therapy were defined as patients showing clearance of serum HBV DNA by nested polymerase chain reaction (PCR) and normal ALT levels at 30 months of treatment. All patients gave written informed consent before the enrollment in the study, which was approved by the ethics committees of the hospital.

Detection and quantification of TTV DNA

TTV DNA quantification was carried out with a real time PCR by the SYBR Green approach using primers targeting the untranslated region (UTR) of the viral genome: forward primer T801: 5'-GCTACGTCCTAACCACG-3', position 6 to 25; reverse primer T935: 5'-CTGCGGTGTGTAACCTACC-3', position 185 to 204^[11]. Total DNA was purified from 200 μ l of serum using the High Pure Viral Nucleic Acid Kit (Roche Diagnostic, Mannheim, Germany) and eluted in a final volume of 50 μ l. Real time PCR was done using 2 μ l of the eluted DNA with 0.2 μ M of each primer in 23 μ l 2 \times SYBR Green PCR mix (Qiagen). The cycling conditions were: 95 $^{\circ}$ C for 10 min to activate the DNA polymerase followed by 45 cycles of amplification: 95 $^{\circ}$ C for 15 sec, 62 $^{\circ}$ C for 30 sec and 72 $^{\circ}$ C for 30 sec.

HBV markers

Hepatitis B surface antigen (HBsAg), hepatitis B e antigen (HBeAg) and antibodies to HBsAg, HBeAg and hepatitis B c antigen (HBcAg) were determined by immunoassay (EIA; Abbott Laboratories, N Chicago, IL). Serum HBV DNA levels at the beginning of lamivudine therapy were quantified using Abbott hybridization assay. Viral DNA during the following time points was detected by nested PCR^[12].

Statistical analysis

Statistical analysis was performed using Student's *t* test. Data were analyzed with the computer program SPSS (SPSS Inc., Chicago, IL, USA). A probability (*P*) value of less than 0.05 was considered statistically significant.

RESULTS

Detection and response of TTV to lamivudine therapy

Sixteen patients doubly infected with TTV and HBV were monitored for levels of both viruses in serum, at selected time points, during the lamivudine treatment by real time and nested PCR methodology, respectively. Of the 16 patients, serum TTV DNA could be detected in all of them by real time PCR at the beginning of lamivudine therapy, with TTV values that ranged between 8.7×10^3 to 1.9×10^8 genomes per ml of serum (mean: 5.7×10^8 genomes/ml). After 30 months of lamivudine treatment, 15/16 patients (94 %) still had TTV DNA in serum and TTV values ranged between 3×10^4 to 4.2×10^8 genomes per ml of serum (mean: 4.3×10^7 genomes/ml). The patient who became negative to TTV DNA lost this marker after 12 months of treatment and he still remained TTV DNA negative until the end of therapy. The TTV DNA value of this patient at baseline time point was 8×10^4 viral genomes per ml of serum. However, this patient did not respond to the lamivudine therapy and he was serum HBV DNA positive at each time point. With respect to the 15 positive TTV DNA patients, at the end of the treatment and relative to baseline levels, 1 patient (7 %) showed unchanged serum TTV DNA levels, 6 patients (40 %) had 6 times of reduction of serum TTV load and 8 cases (53 %) presented 8 times of increase of the levels of TTV DNA in serum.

Changes in serum TTV DNA concentration with respect to HBV non-responsive and responsive patients to lamivudine treatment were also analyzed. It was found that there was no statistically significant difference when basal and final serum samples were compared between both groups (Table 1) or when basal and final serum samples were compared in the same group (Table 2).

Finally, serum TTV DNA values in patients with or without liver transplants were evaluated as well. Once again, there were not significant differences when baseline and final serum

samples were compared between non-transplanted and transplanted patients (Table 3) or when baseline and final serum samples were compared between non-transplanted or transplanted patients (Table 4).

Table 1 Comparison of serum TTV DNA concentration changes before treatment and at the end of treatment

	Non-responders (n=7)	Responders (n=8)	<i>P</i> ^a
Before treatment	4.6×10^7	8.0×10^7	0.66
End of treatment	1.1×10^8	3.4×10^7	0.29

TTV DNA concentration was expressed as viral genomes/ml of serum. ^aStudent's *t*-test, HBV non-responsive patients vs. responsive patients to lamivudine therapy.

Table 2 Changes of TTV DNA concentration in HBV non-responsive and responsive patients to lamivudine therapy

	Before treatment	End of treatment	<i>P</i> ^a
Non-responders (n=7)	4.6×10^7	1.1×10^8	0.60
Responders (n=8)	8.0×10^7	3.4×10^7	0.55

TTV DNA concentration was expressed as viral genomes/ml of serum. ^aStudent's *t*-test, before vs at the end of treatment.

Table 3 Comparison of serum TTV DNA concentration changes before treatment and at the end of treatment

	Non-transplanted (n=5)	Transplanted (n=10)	<i>P</i> ^a
Before treatment	1.2×10^7	8.9×10^7	0.22
End of treatment	8.8×10^6	1.0×10^8	0.07

TTV DNA concentration was expressed as viral genomes/ml of serum. ^aStudent's *t*-test, non-transplanted vs. transplanted patients.

Table 4 Changes in TTV DNA concentration in non-transplanted and transplanted patients

	Before treatment	End of treatment	<i>P</i> ^a
Non-transplanted (n=5)	1.2×10^7	8.8×10^6	0.59
Transplanted (n=10)	8.9×10^7	1.0×10^8	0.87

TTV DNA concentration was expressed as viral genomes/ml of serum. ^aStudent's *t*-test, before vs at the end of treatment.

HBV response to lamivudine treatment

At the baseline time point, HBV DNA values ranged between 4.2×10^9 and 8.4×10^{11} DNA genomes per ml of serum (mean: 1.2×10^{11} genomes/ml). The decline of HBV viremia was clearly evident at month 3 after therapy and the response rate was 31 %, 44 %, 63 %, 50 % and 50 % at month 3, 6, 9, 12 and 30, respectively. When compared between responsive and non-responsive patients, the responders had almost 4 times the value of the non-responder ones but the difference was not significant (2.6×10^{11} vs 7×10^{10} genomes per ml of serum, respectively). Also, there was no significant difference in baseline of ALT levels between responsive and non-responsive patients (117 IU/L vs. 123 IU/L, respectively). However, differences were statistically significant in post-treatment ALT levels between responsive and non-responsive patients (37 IU/L vs 128 IU/L, respectively; *P*=0.03). Of the 5 HBeAg positive patients, 2 seroconverted to anti-HBe by month 12. The other 3 patients still remained HBeAg positive after 30 months of lamivudine therapy. In the 2 HBeAg and anti-HBe negative patients, they

developed anti-HBe by month 3.

With respect to the 10 liver transplant recipients, 4 patients (40 %) started to receive lamivudine treatment after recurrent allograft re-infection. In these cases, serum HBV DNA was still detectable after 30 months of therapy. However, in those 6 patients who started lamivudine administration before liver transplantation as a prophylaxis regimen, 5 (50 %) lost viral DNA at month 3 of treatment, and then they underwent liver allograft and remained HBV DNA negative throughout the therapy. By contrast, the remaining patient developed a recurrent HBV infection at month 6 of post-transplant.

DISCUSSION

Since TTV was discovered a few years ago, many studies have been done trying to assess whether it causes liver disease; however, there is still a poor understanding of its molecular properties and pathogenic potential.

This study shows, in agreement with other groups, that TTV infection is chronic and characterized by the continued presence of high virus loads in serum with wide variations ranging between 10^3 and 10^8 genomes per ml^[13, 14]. Over a period of 30 months, 96 % of the patients presented high TTV DNA levels; however, in some individuals, viremia levels fluctuated extensively while they remained essentially constant in others.

Different epidemiological studies have clearly indicated that TTV can behave as a transmissible blood-borne virus sharing common transmission routes with the hepatitis viruses. Then, coinfection of TTV is frequently observed in patients with chronic hepatitis B^[9]. One important finding in our study is that 100 % of patients infected with HBV were TTV DNA-positive by real-time PCR. These results suggest that the prevalence of TTV infection is very high in the HBV-infected population. However, our results are in disagreement with other studies that reported TTV DNA rates between 15 % and 36 %^[15-17]. One explanation for this result might be due to the different primers used for the detection of TTV DNA; we used a set of primers that already showed 92 % positivity to TTV in healthy adults in Japan^[11]. Another possible explanation why these patients were TTV positive is their histological status: 94 % of them presented cirrhosis. A TTV well-recognized feature is that TTV infection is chronic and tends to last many years, so it could be that TTV infection is more prevalent in patients with advanced HBV-associated liver disease than in those with stable disease.

However, the most novel and interesting information that emerged from this study is that lamivudine treatment in a regimen of 100 mg daily and for a period of 30 months did not inhibit TTV replication in patients coinfecting with HBV and TTV. Only one individual (6 %) of the 16 patients enrolled in the study became serum TTV DNA negative after 12 months of therapy. This observation could suggest that this patient lost TTV in a spontaneous way and not by effect of lamivudine on TTV replication.

With respect to the effect of lamivudine treatment of chronic hepatitis B, this study confirms earlier reports where HBV infection responded positively to lamivudine treatment^[18-20]. The response of HBV to lamivudine treatment was not affected with the concurrent TTV infection. This observation can be explained by two reasons. Firstly, the changes observed in ALT values during the lamivudine treatment period were correlated with the change of HBV DNA in chronic hepatitis B; it seemed that ALT dynamic was unrelated to TTV viremia. Secondly, TTV viremia was not related to different HBV DNA levels, so TTV did not seem to interfere with HBV replication. Thus, in agreement with many other published studies, TTV may lack clinical association with liver disease in these patients^[21, 22].

Finally, it has been suggested a relationship between an

increased TTV viral load and host immunological disorders^[23]. In immunosuppressed patients, such as recipients of liver transplants, TTV viremia could be higher than that in individuals without liver allografts. However, we did not find any significant difference in TTV viral load when both groups were compared, even if transplanted patients had always higher TTV titers. Based on our results it seems that immune system is not involved in elevated TTV viremia in HBV patients, although more extensive studies need to be performed to prove this hypothesis.

In conclusion, during the lamivudine therapy for chronic hepatitis B, disappearance of TTV does not occur in the majority of the HBV-infected patients which supports the interpretation that lamivudine does not inhibit TTV replication. Moreover, this study shows the highly prevalence of TTV infection in patients with chronic hepatitis B, but without any effect on the course of HBV infection.

REFERENCES

- 1 **Nishizawa T**, Okamoto H, Konishi K, Yoshizawa H, Miyakawa Y, Mayumi M. A novel DNA virus (TTV) associated with elevated transaminase levels in posttransfusion hepatitis of unknown etiology. *Biochem Biophys Res Commun* 1997; **241**: 92-97
- 2 **Miyata H**, Tsunoda H, Kazi A, Yamada A, Khan MA, Murakami J, Kamahora T, Shiraki K, Hino S. Identification of a novel GC-rich 113-nucleotide region to complete the circular, single-stranded DNA genome of TT virus, the first human circovirus. *J Virol* 1999; **73**: 3582-3586
- 3 **Hijikata M**, Takahashi K, Mishiro S. Complete circular DNA genome of a TT virus variant (isolate name SANBAN) and 44 partial ORF2 sequences implicating a great degree of diversity beyond genotypes. *Virology* 1999; **260**: 17-22
- 4 **Abe K**, Inami T, Asano K, Miyoshi C, Masaki N, Hayashi S, Ishikawa K, Takebe Y, Win KM, El Zayadi AR, Han KH, Zhang DY. TT virus infection is widespread in the general populations from different geographic regions. *J Clin Microbiol* 1999; **37**: 2703-2705
- 5 **Matsumoto A**, Yeo AE, Shih JW, Tanaka E, Kiyosawa K, Alter HJ. Transfusion-associated TT virus infection and its relationship to liver disease. *Hepatology* 1999; **30**: 283-288
- 6 **Lee WM**. Hepatitis B virus infection. *N Engl J Med* 1997; **337**: 1733-1745
- 7 **Eron JJ**, Benoit SL, Jemsek J, MacArthur RD, Santana J, Quinn JB, Kuritzkes DR, Fallon MA, Rubin M. Treatment with lamivudine, zidovudine, or both in HIV-positive patients with 200 to 500 CD4+ cells per cubic millimeter. North American HIV Working Party. *N Engl J Med* 1995; **333**: 1662-1669
- 8 **Dienstag JL**, Perrillo RP, Schiff ER, Bartholomew M, Vicary C, Rubin M. A preliminary trial of lamivudine for chronic hepatitis B infection. *N Engl J Med* 1995; **333**: 1657-1661
- 9 **Kao JH**, Chen W, Chen PJ, Lai MY, Chen DS. TT virus infection in patients with chronic hepatitis B or C: influence on clinical, histological and virological features. *J Med Virol* 2000; **60**: 387-392
- 10 **Nishizawa Y**, Tanaka E, Orii K, Rokuhara A, Ichijo T, Yoshizawa K, Kiyosawa K. Clinical impact of genotype 1 TT virus infection in patients with chronic hepatitis C and response of TT virus to alpha-interferon. *J Gastroenterol Hepatol* 2000; **15**: 1292-1297
- 11 **Takahashi K**, Hoshino H, Ohta Y, Yoshida N, Mishiro S. Very high prevalence of TT virus (TTV) infection in general population of Japan revealed by a new set of PCR primers. *Hepatol Res* 1998; **12**: 233-239
- 12 **Lindh M**, Gonzalez JE, Norkrans G, Horal P. Genotyping of hepatitis B virus by restriction pattern analysis of a pre-S amplicon. *J Virol Methods* 1998; **72**: 163-174
- 13 **Lefrere JJ**, Roudot-Thoraval F, Lefrere F, Kanfer A, Mariotti M, Lerable J, Thauvin M, Lefevre G, Rouger P, Girot R. Natural history of the TT virus infection through follow-up of TTV DNA-positive multiple-transfused patients. *Blood* 2000; **95**: 347-351
- 14 **Oguchi T**, Tanaka E, Orii K, Kobayashi M, Hora K, Kiyosawa K. Transmission of and liver injury by TT virus in patients on maintenance hemodialysis. *J Gastroenterol* 1999; **34**: 234-240

- 15 **Lai YC**, Hu RT, Yang SS, Wu CH. Coinfection of TT virus and response to interferon therapy in patients with chronic hepatitis B or C. *World J Gastroenterol* 2002; **8**: 567-570
- 16 **Naoumov NV**, Petrova EP, Thomas MG, Williams R. Presence of a newly described human DNA virus (TTV) in patients with liver disease. *Lancet* 1998; **352**: 195-197
- 17 **Tanaka H**, Okamoto H, Luengrojanakul P, Chainuvati T, Tsuda F, Tanaka T, Miyakawa Y, Mayumi M. Infection with an unenveloped DNA virus (TTV) associated with posttransfusion non-A to G hepatitis in hepatitis patients and healthy blood donors in Thailand. *J Med Virol* 1998; **56**: 234-238
- 18 **Lai CL**, Chien RN, Leung NW, Chang TT, Guan R, Tai DI, Ng KY, Wu PC, Dent JC, Barber J, Stephenson SL, Gray DF. A one-year trial of lamivudine for chronic hepatitis B. Asia Hepatitis Lamivudine Study Group. *N Engl J Med* 1998; **339**: 61-68
- 19 **Leung NW**, Lai CL, Chang TT, Guan R, Lee CM, Ng KY, Lim SG, Wu PC, Dent JC, Edmundson S, Condreay LD, Chien RN. Extended lamivudine treatment in patients with chronic hepatitis B enhances hepatitis B e antigen seroconversion rates: results after 3 years of therapy. *Hepatology* 2001; **33**: 1527-1532
- 20 **Leung N**. Liver disease-significant improvement with lamivudine. *J Med Virol* 2000; **61**: 380-385
- 21 **Gimenez-Barcons M**, Fornis X, Ampurdanes S, Guilera M, Soler M, Soguero C, Sanchez-Fueyo A, Mas A, Bruix J, Sanchez-Tapias JM, Rodes J, Saiz JC. Infection with a novel human DNA virus (TTV) has no pathogenic significance in patients with liver diseases. *J Hepatol* 1999; **30**: 1028-1034
- 22 **Forns X**, Hegerich P, Darnell A, Emerson SU, Purcell RH, Bukh J. High prevalence of TT virus (TTV) infection in patients on maintenance hemodialysis: frequent mixed infections with different genotypes and lack of evidence of associated liver disease. *J Med Virol* 1999; **59**: 313-317
- 23 **Touinssi M**, Gallian P, Biagini P, Attoui H, Vialettes B, Berland Y, Tamalet C, Dhiver C, Ravaux I, De Micco P, De Lamballerie X. TT virus infection: prevalence of elevated viremia and arguments for the immune control of viral load. *J Clin Virol* 2002; **21**: 135-141

Edited by Xu XQ and Zhu LH

Antralization at the edge of proximal gastric ulcers: Does *Helicobacter pylori* infection play a role?

Harry Hua-Xinag Xia, Shiu Kum Lam, Wai Man Wong, Wayne Hsing Cheng Hu, Kam Chuen Lai, Sau Hing Wong, Suet Yi Leung, Siu Tsan Yuen, Nicholas A. Wright, Benjamin Chun-Yu Wong

Harry Hua-Xinag Xia, Shiu Kum Lam, Wai Man Wong, Wayne Hsing Cheng Hu, Kam Chuen Lai, Sau Hing Wong, Benjamin Chun-Yu Wong, Department of Medicine, The University of Hong Kong, Hong Kong SAR, China

Suet Yi Leung, Siu Tsan Yuen, Department of Pathology, The University of Hong Kong, Hong Kong SAR, China

Nicholas A. Wright, Histopathology Unit, London Research Institute, Cancer Research, UK

Supported by the Seed Funding for Basic Research 2001 (301/01), The University of Hong Kong, and a competitive earmarked research grant from the Research Grants Council of Hong Kong Special Administrative Region, China (HKU7318/01M) to HH-X Xia

Correspondence to: Dr Benjamin CY Wong, Department of Medicine, The University of Hong Kong, Queen Mary Hospital, Hong Kong, China. bcywong@hku.hk

Telephone: +852-28554541 **Fax:** +852-28725828

Received: 2003-03-04 **Accepted:** 2003-03-08

Abstract

AIM: To determine the prevalence of antralization at the edge of proximal gastric ulcers, and the effect of *H. pylori* eradication on the mucosal appearances.

METHODS: Biopsies were taken from the antrum, body and the ulcer edge of patients with benign proximal gastric ulcers before and one year after treatment. Gastric mucosa was classified as antral, transitional or body type. *H. pylori* positive patients received either triple therapy, or omeprazole.

RESULTS: Patients with index ulcers in the incisura, body or fundus ($n=116$) were analyzed. Antral-type mucosa was more prevalent at the ulcer edge in *H. pylori*-positive patients than *H. pylori*-negative patients (93 % vs 60 %, OR=8.95, 95 %CI: 2.47-32.4, $P=0.001$). At one year, there was a significant reduction in the prevalence of antralization (from 93 % to 61 %, $P=0.004$) at the ulcer edge in patients with *H. pylori* being eradicated. However, there was no difference in the prevalence of antralization at the ulcer edge in those with persistent infection.

CONCLUSION: *H. pylori* infection is associated with antralization at the edge of proximal gastric ulcers, which may be reversible in some patients after eradication of the infection.

Xia HHX, Lam SK, Wong WM, Hu WHC, Lai KC, Wong SH, Leung SY, Yuen ST, Wright NA, Wong BCY. Antralization at the edge of proximal gastric ulcers: Does *Helicobacter pylori* infection play a role? *World J Gastroenterol* 2003; 9(6): 1265-1269
<http://www.wjgnet.com/1007-9327/9/1265.asp>

INTRODUCTION

Peptic ulcer disease is common, and is associated with considerable mortality due to complications such as bleeding

and perforation^[1]. *H. pylori* infection is now recognized to be a major cause for peptic ulcer, accounting for up to 90 % of duodenal ulcer cases and 80 % of gastric ulcer cases, with the use of non-steroidal anti-inflammatory drugs being another major cause^[2-4]. While gastric metaplasia in duodenum has been identified to be an important morphopathological change in the development of *H. pylori*-associated duodenal and prepyloric ulcer^[5-7], the mucosal morpho-pathogenesis of gastric ulcer, which occurs predominantly along the body-antrum transitional zone (particularly at the gastric incisura), remains unclear. Previous studies have observed a stem-cell-derived "ulcer-associated cell lineage" (UACL) at the sites of chronic gastrointestinal ulceration, commonly found in the borders of Crohn's ulcers in small bowel, and in gastroduodenal ulceration^[8-11]. In the literature, UACL was usually described as pseudopyloric (or pyloric) metaplasia, because it has morphological similarities to pyloric glands^[8, 9], and similar changes can occur in other tissues, such as gall bladder, bile ducts, and pancreatic ducts, often associated with malignant transformation of these tissues^[12-16]. In the stomach, pseudopyloric metaplasia is specifically defined as a replacement of specialized glands by mucous-secreting glands in the gastric body or at the body-antrum junction^[17], a concept identical to "antralization" as described in our previous studies^[18, 19].

In a previous study, we have demonstrated that in the absence of *H. pylori* infection, the gastric incisura mucosa belongs to either body-type or transitional type in most (82 %) individuals, suggesting that normal incisura mucosa is histologically distinct from the antral mucosa, but more homologous to the body and fundus mucosa^[18]. However, *H. pylori* infection is associated with the presence of antral (pyloric)-type mucosa in the proximal stomach (i.e. gastric incisura, body and fundus), indicating that *H. pylori* infection may be a causal factor for antralization of the proximal stomach^[18]. Thus, it is conceivable that *H. pylori*-induced antralization may play an important pathogenic role in proximal gastric ulceration, and eradication of *H. pylori* infection may reverse antralization to normal transitional or body type mucosa, and thus reduce the risk for ulcer relapse. Therefore, the present study was carried out to determine the prevalence of antralization at the edge of proximal gastric ulcer in relation to *H. pylori* infection, and the effect of *H. pylori* eradication on the mucosal appearances.

MATERIALS AND METHODS

Patients

One hundred and sixteen patients with newly diagnosed uncomplicated benign-looking proximal gastric ulcers (>5 mm in diameter and >1 mm in depth) at the Endoscopy Unit of Department of Medicine, Queen Mary Hospital were included in the study. The location of gastric ulcers and demographic and clinical characteristics of these patients were summarized in Table 1. Exclusion criteria at entry included patients who had been taking aspirin or non-steroidal anti-inflammatory drugs (NSAIDs) over the past year, or taking antibiotics, H₂ receptor blockers, bismuth or proton pump inhibitors in the

preceding 4 weeks, patients with previous gastric surgery, and those with a histological diagnosis of gastric carcinoma or lymphoma.

Informed written consent was obtained from all patients who participated in the trial. This project was approved by the Ethics Committee of the University of Hong Kong.

Table 1 The demographic clinical characteristics of the patients initially recruited, according to the location of gastric ulcers ($n=116$)

	Ulcer location		
	Incisura ($n=91$)	Body ($n=23$)	Fundus ($n=2$)
Age (mean \pm SD)	59.5 \pm 13.3	69.3 \pm 10.2	51.0 \pm 11.2
Gender (male/female)	60/31	17/6	2/0
Smoking (yes/no)	44/46	11/12	1/1
<i>H.pylori</i> status (positive/negative)	81/10	19/4	1/1

Diagnosis of *H. pylori* infection

During the first endoscopy, three biopsies were taken at the gastric antrum within 3 cm of the pylorus at the lesser curvature, two at the midway between the pylorus and cardioesophageal junction at the greater curvature, and four from the edge of gastric ulcer. When the ulcer was present in the body, the body biopsies were taken at least 3 cm apart from the ulcer. One antral biopsy was used for a rapid urease test (RUT) and the rest were sent for the detection of *H. pylori* infection and histological examination after haematoxylin & eosin (H&E) staining. All patients then received a ^{13}C -urea breath test following a standard protocol measured by an isotope ratio mass spectrometer^[20]. The definition of *H. pylori* infection in this study required that at least two of the three tests (the RUT, histology and ^{13}C -urea breath test) were positive. The absence of *H. pylori* infection required all three tests to be negative. This definition was used as the "gold standard" in this study.

Histological examination

Slides were read by experienced pathologists who were blinded to all clinical and endoscopic information, including the RUT results. The mucosa of gastric biopsies taken from different sites was classified as antral (mucous-secreting or pyloric) type, body (acid-secreting or oxyntic) type or transitional (junctional) type according to the definitions set out in the updated Sydney system^[21]. The characteristic feature of antral-type mucosa was the presence of coiled and branching antral glands, which were lined by mucus cells that were interspersed with endocrine cells (chiefly G and D types), and a few parietal cells. The glands in body-type mucosa were straight tubes that constituted acid-producing parietal cells along with scattered mucus cells in their upper portion and mainly chief cells in their lower portion, with scattered argyrophilic endocrine cells. Transitional type mucosa was a mixture of the architectural features and cell types found in the antral and body type mucosae^[21].

Treatment and endoscopy at one year

One hundred and one patients received triple therapy consisting of clarithromycin 250 mg, metronidazole 300 mg each given 4 times daily for 2 weeks and sucralfate 1 gm 4 times daily for 4 weeks ($n=54$), or acid suppression therapy consisting of omeprazole 20 mg daily for one year ($n=47$). Successful eradication was indicated if the rapid urease test, histological examination by H&E and Giemsa staining and ^{13}C -urea breath test were all negative at week 6 after treatment. 65 patients (male/female 44/21, age (mean \pm SD) 61.9 \pm 11.0 years) received either triple therapy ($n=28$), or omeprazole ($n=37$), with ulcers

completely healed at 12 weeks. Upper endoscopy and ^{13}C -urea breath test were repeated at month 12. Gastric biopsies were obtained from the antrum, body and ulcer site (visible scar area in 47 of 53 (90.6 %) cases with a healed ulcer) or the edge of ulcer in 12 patients with relapsed ulcers, and assessed as described above. Successful eradication was indicated if the rapid urease test, histological examination by H&E and Giemsa staining and ^{13}C -urea breath test were all negative at week 6 or month 12 after treatment. The histological characteristics of these biopsies were compared with those biopsies taken at the first endoscopy. Histological improvement of gastric mucosa over the period of one year was defined as changes from antral to transitional or body, or from transitional to body-type, whereas worsening of gastric mucosa was defined as changes from body to transitional or antral, or from transitional to antral-type. An upper endoscopy and a ^{13}C -urea breath test were repeated at month 12 for 65 patients (male/female 44/21, age (mean \pm SD) 61.9 \pm 11.0 years) who had their ulcers completely healed 12 weeks after treatment. Gastric biopsies were obtained from the antrum, body and ulcer site (visible scar area) in 47 of 53 (90.6 %) cases with a healed ulcer or the edge of ulcer in 12 patients with relapsed ulcers, and assessed as described above. The histological characteristics of these biopsies were compared with those biopsies taken at the first endoscopy. Histological improvement of gastric mucosa over the period of one year was defined as changes from antral to transitional or body, or from transitional to body-type, whereas worsening of gastric mucosa was defined as changes from body to transitional or antral, or from transitional to antral-type.

Statistical analysis

The Chi-squared test (with Yates' correction if required), the Fisher's exact test or McNemar test was used for categorical variables, and odds ratios (OR) and 95 % confidence interval (CI) were estimated where appropriate. All tests were carried out using the SPSS system (version 10.0, SPSS Inc. Chicago, Illinois, USA). All *P* values calculated were two-tailed. The alpha level of significance was set at $P<0.05$.

RESULTS

The presence of antral-type mucosa in the gastric body and at the edge of proximal gastric ulcers

Of the 116 patients, 91 had the index ulcers at the incisura, 23 in the body and 2 in the fundus. Of these, 101 were *H. pylori*-positive and 15 were *H. pylori*-negative. All biopsies taken from the antrum showed antral-type mucosa. Overall, antral-type mucosa was present in the gastric body in 6 (5.2 %) patients and at the edge of proximal gastric ulcers in 103 (88.8 %) patients. Of *H. pylori*-positive patients 6 (5.9 %) had antral-type mucosa and 4 (4 %) had transitional type mucosa whereas all (100 %) of *H. pylori*-negative patients had body-type mucosa at the gastric body. Antral-type mucosa was present at the edge of proximal gastric ulcers in 93.1 % (94/101) of *H. pylori*-positive patients and 60 % (9/15) of *H. pylori*-negative patients (OR=8.95, 95 % CI: 2.47-32.4, $\chi^2=14.35$, $P=0.001$) (Figure 1). In *H. pylori*-positive patients, 81 had ulcers at the incisura, 19 at the body and one at the fundus. In the presence of *H. pylori* infection, there was no difference in the prevalence of antral-type mucosa at the ulcer edge at different gastric sites: 92.6 % (75/81) at the incisura, 94.7 % (18/19) at the body and 100 % (1/1) at the fundus. In *H. pylori*-negative patients, antral-type mucosa was present at the edges of ulcers in 70 % (7/10), 50 % (2/4) and 0 % (0/1) of patients when the ulcer occurred at the incisura, body and fundus, respectively.

Changes of gastric mucosa in the gastric body and at the edge of proximal gastric ulcers at one year

Of the 65 patients who were followed up for one year, 28 had *H. pylori* infection eradicated and 27 had persistent infection. Of the 12 patients with ulcers relapse, one (3.6 %) was from patients in whom *H. pylori* infection was eradicated and 11 (29.7 %) were from those with persistent infection (OR=11.4, 95 % CI: 1.38-94.9, $\chi^2=5.61$, $P=0.018$).

There was a significant reduction in the prevalence of antral-type mucosa at both the gastric body (from 7.1 % to 0 %) and the gastric ulcer sites (from 92.9 % to 60.7 %, $P=0.004$, McNemar test) in patients in whom *H. pylori* infection was eradicated. However, there was no difference in the prevalence of antral-type mucosa when *H. pylori* infection was persistent (Figure 2).

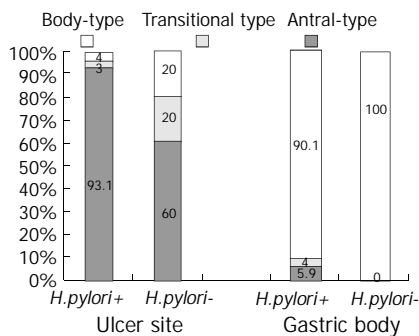


Figure 1 Prevalence of antral-type mucosa at the edge of proximal gastric ulcers and non-ulcerated gastric body in *H. pylori*-positive patients (*H. pylori*+, n=101) and those without *H. pylori* infection (*H. pylori*-, n=15).

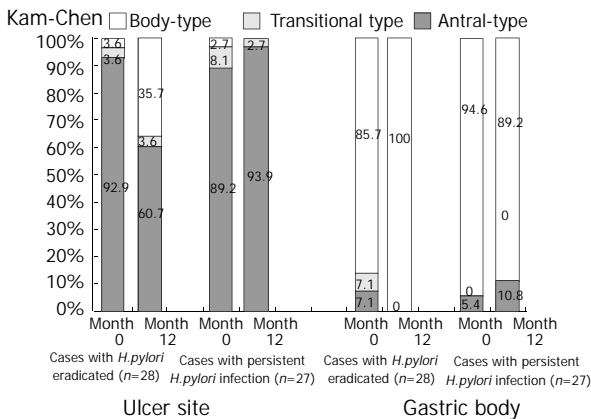


Figure 2 Presence of antral-type mucosa at the edge of proximal gastric ulcers and non-ulcerated gastric body in patients with *H. pylori* eradicated (n=28) and in those with persistent infection (n=37) before (month 0) and 12 months after treatment.

Table 2 Changes of gastric mucosa at the edge of proximal gastric ulcers and gastric body one year after treatment, in relation to post-treatment *H. pylori* status, treatment regimens, ulcer relapse and ulcer location (n=65)

	Mucosal type change (%)					
	Ulcer edge			Gastric body		
	Improvement ^a (n=11)	No change ^b (n=49)	Worsening ^c (n=5)	Improvement (n=5)	No change (n=58)	Worsening (n=2)
<i>H. pylori</i> infection						
Eradicated (n=28)	35.7 ^d	64.3	0	14.3	85.7	0
Persistent (n=37)	2.7	83.8	13.5	2.7	91.9	5.4
Ulcer location						
Incisura (n=52)	15.4	76.9	7.7	5.8	90.4	3.8
Body (n=13)	23.1	69.2	7.7	15.4	84.6	0

^a, Improvement, antral-type (A)→transitional type (T), A→body-type (B), or T→B; ^b, No change, A→A, T→T or B→B; ^c, Worsening, T→A, B→A or B→T. ^d, $P<0.001$, compared with persistent infection.

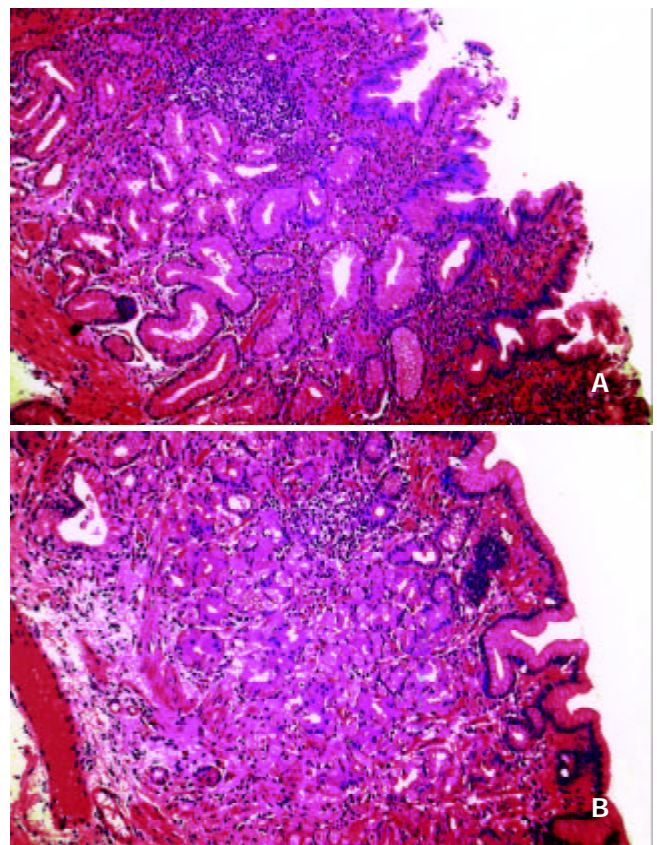


Figure 3 Gastric mucosa at the ulcer edge before and after eradication of *H. pylori* infection in the same patient. A, biopsy of the ulcer edge before *H. pylori* eradication showing antral-type gastric mucosa with severe active chronic inflammation; B, biopsy of the healed ulcer site after *H. pylori* eradication showing body-type gastric mucosa with presence of parietal and chief cells in the gastric glands and mild residual chronic inflammation. Haematoxylin & eosin (H&E) staining $\times 250$.

Histological improvement of gastric mucosa was observed in 14 (21.5 %) patients; 3 at the gastric body, 9 at the ulcer site and 2 at both sites (Figure 3). Histological improvement of gastric mucosa at the ulcer sites was more common in patients in whom *H. pylori* was eradicated than those with persistent infection (35.7 % vs 2.7 %, OR=20.0, 95 % CI: 2.37-168.6, $\chi^2=12.35$, $P<0.001$) (Table 2). When patients with relapsed ulcers were excluded, the association remained unchanged (37.0 % vs 3.8 %, OR=14.71, 95 % CI: 1.72-125.7, $\chi^2=8.87$, $P=0.003$). Similarly, triple therapy was associated with a higher rate of histological improvement at the ulcer site, compared to omeprazole treatment (31.0 % vs 5.6 %, OR=7.65, 95 % CI: 1.50-39.0, $\chi^2=5.72$, $P=0.017$). Gastric mucosa at the ulcer site was improved in more patients with cured ulcers than those

with relapsed ulcers, although the difference did not reach statistical significance (20.8 % vs 0 %, $P=0.109$). There was no difference in histological improvement between patients with ulcers at the body/fundus and those with ulcers at the incisura (23.1 % vs 15.4 %, $OR=1.65$, 95 % $CI: 0.37-7.35$, $P=0.804$) (Table 2). Age and gender were not associated with histological improvement (data not shown).

Overall, 7 (10.8 %) patients had worsened histology after treatment; 5 at the ulcer edge and the other 2 at the gastric body (Table 2). All of these patients had persistent *H. pylori* infection; 6 were treated with omeprazole and one with triple therapy. 3 (75 %) of these patients had ulcer relapsed.

DISCUSSION

In the present study, approximately 90 % of patients with proximal gastric ulcers had antral-type mucosa at the ulcer edge, and *H. pylori* infection was associated with a higher prevalence of antralization in the proximal gastric ulceration. Moreover, eradication of *H. pylori* infection resulted in histological improvement at the ulcer edge of 36 % of patients in 12 months, whereas the persistence of the infection was accompanied by worsening of histology (14 %). These findings suggest that *H. pylori* infection contributes to antralization, which may, in turn, play an important role in gastric ulceration.

H. pylori-associated antralization is believed to be a consequence of direct insults of chronic *H. pylori* infection, as a host defense and reparative response to the mucosal damage caused by organisms. As demonstrated in our previous study and in the present study, *H. pylori* infection is associated with antralization (or pseudopyloric metaplasia) at the gastric incisura and less frequently at the body and fundus^[18]. It has been established that *H. pylori* infection induces apoptosis of gastric epithelial cells, and subsequently stimulates cell proliferation in the gastric mucosa^[22]. Hanby *et al* reported that mucous neck cells formed an important cell lineage which secretes a series of peptides including the spasmolytic polypeptide, or trefoil family factor 2 (TFF-2) with luminal protective functions^[23]. It has been suggested that pseudopyloric metaplasia occurs in the body glands as a result of hyperplasia of mucous neck cells, and represents a mucosal response to damage associated with *H. pylori* infection^[18, 23]. Indeed, Schmidt *et al* reported that the spasmolytic polypeptide-expressing metaplastic (SPEM) lineage was closely associated with fundic *H. pylori* infection^[24]. Thus, we propose that the hyperplastic mucous neck cells move both upwards and particularly downwards in the oxyntic tubule, replace the specialized parietal and chief cells, and create a mucous cell lineage. This process can occur focally, occupying a single oxyntic tubule, groups of tubules, or on a fairly massive scale with many tubules involved^[25]. Eventually a mucous gland, which resembles pyloric glands, is formed, and thus antralization of proximal gastric mucosa follows. It is most likely that the weakened antralized mucosa in the proximal stomach is prone to be further damaged by *H. pylori*, resulting in ulceration even in the presence of subnormal acid production^[26]. Therefore, in the presence of persistent chronic infection with *H. pylori*, this defense and reparative mechanism probably facilitates rather than prevents the development of ulceration.

In the present study, eradication of *H. pylori* infection led to histological improvement, and persistent infection was associated with the development of antralization in the proximal stomach. These observations may have implications for the prevention of the development of gastric cancer, as we have previously reported that antralization of gastric incisura is strongly associated with precancerous lesions such as gastric atrophy and intestinal metaplasia^[18]. It has been shown that

the time-dependent progression of gastritis in grade (development of atrophy and intestinal metaplasia) and in extent (spreading of gastritis by pyloro-cardial extension) is correlated with the development of gastric cancer in the distal and angular stomach^[27], and that atrophic gastritis and intestinal metaplasia progress and exhibit a cephaloid shift (i.e. pyloro-cardial extension) in chronic *H. pylori* infection^[28]. Therefore, it is hypothesized that the initial events in gastric carcinogenesis occur at the junction of the oxyntic and antral mucosae, and it is the antral type mucosa that is prone to gastric atrophy and intestinal metaplasia, and expansion of antral mucosa towards the proximal stomach (either by pyloro-cardial extension or by differentiation) may be associated with an increased risk of developing intestinal metaplasia^[29]. However, gastric atrophy and intestinal metaplasia are unlikely to regress after eradication of *H. pylori* infection although this is controversial^[30-33]. On the other hand, the reversibility of antralization at the proximal gastric mucosa may provide a new hallmark in the chemoprevention of gastric cancer, although further studies on the role of antralization in gastric carcinogenesis are required. If the proposals of Schmidt *et al*^[24] are confirmed, the prevention or reversal of SPEM might be critical.

Sampling error might account for the difference in improvement of gastric mucosa between patients with *H. pylori* eradication and those with persistent infection. For example, biopsies may be more correctly taken at the edge of active ulcers than healed ulcers. In most cases, ulcer scars are visible, which helps to improve the accuracy of the biopsy site.

Notably, the rate of antralization reached 60 % (9/15) for patients with proximal ulcers but without *H. pylori* infection, suggesting that certain other factors that result in gastric mucosal damage also lead to antralization and gastric ulceration. In the present study, there were no documented records on the causes of *H. pylori*-negative gastric ulcers, and thus we were unable to identify the potential factors that may lead to antralization. Some NSAID users who were unaware of NSAID use at entry might have been included. Previously, Lanas *et al* demonstrated that between 13 % and 22 % of patients with gastrointestinal bleeding and perforation who claimed not to have used aspirin had objective evidence of current aspirin intake^[34, 35]. If this were the case in the present study, then NSAID use would account for proximal gastric ulcer in up to 3 of the 15 patients. Nevertheless, the significance of NSAID use and other factors in antralization of proximal stomach remains to be clarified.

In conclusion, *H. pylori* infection is associated with antralization at the edge of proximal gastric ulcers, which may be reversible in a proportion of patients after eradication of *H. pylori* infection. Antralization in the proximal stomach may play an important role in the pathogenesis of gastric ulceration.

REFERENCES

- 1 Westbrock JI, Rushworth RL. The epidemiology of peptic ulcer mortality 1953-1989: a birth cohort analysis. *Int J Epidemiol* 1993; **22**: 1085-1092
- 2 Anonymous. NIH Consensus Conference. *Helicobacter pylori* in peptic ulcer disease. NIH consensus development panel on *Helicobacter pylori* in peptic ulcer disease. *Helicobacter pylori* in peptic ulcer disease. *JAMA* 1994; **272**: 65-69
- 3 Xia HHX, Wong BCY, Wong KW, Wong SY, Wong WM, Lai KC, Hu WHC, Chan CK, Lam SK. Clinical and endoscopic characteristics of non-*Helicobacter pylori*, non-NSAID duodenal ulcers: a long-term prospective study. *Aliment Pharmacol Ther* 2001; **15**: 1875-1882
- 4 Xia HHX, Phung N, Kalantar JS, Talley NJ. Demographic and endoscopic characteristics of *Helicobacter pylori*-positive and negative peptic ulcer disease. *Med J Aust* 2000; **173**: 515-519
- 5 Carrick J, Lee A, Hazell S, Rakston M, Daskalopoulos G.

- Campylobacter pylori*, duodenal ulcer, and gastric metaplasia: possible role of functional heterotopic tissue in ulcerogenesis. *Gut* 1989; **30**: 790-797
- 6 **Taha AS**, Dahill S, Nakshabendi I, Lee FD, Sturrock RD, Russell RI. Duodenal histology, ulceration, and *Helicobacter pylori* in the presence or absence of non-steroidal anti-inflammatory drugs. *Gut* 1993; **34**: 1162-1166
 - 7 **Olbe L**, Fandriks L, Hamlet A, Svennerholm AM. Conceivable mechanisms by which *Helicobacter pylori* provokes duodenal ulcer disease. *Best Pract Res Clin Gastroenterol* 2000; **14**: 1-12
 - 8 **Longman RJ**, Douthwaite J, Sylvester PA, Poulson R, Corfield AP, Thomas MG, Wright NA. Coordinated localisation of mucins and trefoil peptides in the ulcer associated cell lineage and the gastrointestinal mucosa. *Gut* 2000; **47**: 792-800
 - 9 **Pera M**, Heppell J, Poulson R, Teixeira FV, Williams J. Ulcer associated cell lineage glands expressing trefoil peptide genes are induced by chronic ulceration in ileal pouch mucosa. *Gut* 2001; **48**: 792-796
 - 10 **Hanby AM**, Jankowski JA, Elia G, Poulson R, Wright NA. Expression of the trefoil peptides pS2 and human spasmodic polypeptide (hSP) in Barrett's metaplasia and the native oesophageal epithelium: delineation of epithelial phenotype. *J Pathol* 1994; **173**: 213-219
 - 11 **Wright NA**, Poulson R, Stamp GW, Hall PA, Jeffery RE, Longcroft JM, Rio MC, Tomasetto C, Chambon P. Epidermal growth factor (EGF/URO) induces expression of regulatory peptides in damaged human gastrointestinal tissues. *J Pathol* 1990; **162**: 279-284
 - 12 **Roberts IS**, Stoddart RW. Ulcer-associated cell lineage ('pylori metaplasia') in Crohn's disease: a lectin histochemical study. *J Pathol* 1993; **171**: 13-19
 - 13 **Callea F**, Sergi C, Fabbretti G, Brisigotti M, Cozzutto C, Medicina D. Precancerous lesions of the biliary tree. *J Surg Oncol* 1993; **3 (Suppl)**: 131-133
 - 14 **Sasaki M**, Yamato T, Nakanuma Y, Ho SB, Kim YS. Expression of MUC2, MUC5AC and MUC6 apomucins in carcinoma, dysplasia and non-dysplastic epithelia of the gallbladder. *Pathol Inter* 1999; **49**: 38-44
 - 15 **Yamagiwa H**. Mucosal dysplasia of gallbladder: isolated and adjacent lesions to carcinoma. *Jpn J Cancer Res* 1989; **80**: 238-243
 - 16 **Bakotic BW**, Robinson MJ, Sturm PD, Hruban RH, Offerhaus GJ, Albores-Saavedra J. Pylori gland adenoma of the main pancreatic duct. *Am J Surg Pathol* 1999; **23**: 227-231
 - 17 **Dixon MF**. Atrophy, metaplasia and dysplasia - a risk for gastric cancer: are they reversible? In: Hunt R, Tytgat G, editors. *Helicobacter pylori*. Basic Mechanisms to Clinical Cure. Lancaster: Kluwer 1998; pp336-353
 - 18 **Xia HHX**, Kalantar J, Talley NJ, Ma Wyatt J, Adams S, Cheung K. Antral-type mucosa in the gastric incisura (antralization) - a link between *Helicobacter pylori* infection and intestinal metaplasia? *Am J Gastroenterol* 2000; **95**: 114-121
 - 19 **Xia HHX**, Zhang G-S, Talley NJ, Wong BC, Yang Y, Henwood C, Wyatt JM, Adams S, Cheung K, **Xia B**, Zhu YQ, Lam SK. Topographic association of gastric epithelial expression of Ki-67, Bax and Bcl-2 expression with antralization in the gastric incisura, body and fundus. *Am J Gastroenterol* 2002; **97**: 3123-3131
 - 20 **Wong BCY**, Wong WM, Wang WH, Wang WH, Tang VSY, Young J, Lai KC, Yuen ST, Leung SY, Hu WHC, Chan CK, Hui WM, Lam SK. An evaluation of invasive and non-invasive tests for the diagnosis of *Helicobacter pylori* infection in Chinese. *Aliment Pharmacol Ther* 2001; **15**: 505-511
 - 21 **Dixon MF**, Genta RM, Yardley JH, Correa P. And the participants in the International Workshop on the Histopathology of Gastritis, Houston 1994. Classification and grading of gastritis. The updated Sydney System. *Am J Surg Pathol* 1996; **20**: 1161-1181
 - 22 **Xia HHX**, Talley NJ. Apoptosis in gastric epithelium induced by *Helicobacter pylori* infection: implications in gastric carcinogenesis. *Am J Gastroenterol* 2001; **96**: 16-26
 - 23 **Hanby AM**, Poulson R, Playford RJ, Wright NA. The mucous neck cell in the human gastric corpus: a distinctive, functional cell lineage. *J Pathol* 1999; **187**: 331-337
 - 24 **Schmidt PH**, Lee JR, Joshi V, Playford RJ, Poulson R, Wright NA, Goldenring JR. Identification of a metaplastic cell lineage associated with human gastric adenocarcinoma. *Lab Invest* 1999; **79**: 639-646
 - 25 **Wright NA**. Mechanisms involved in gastric atrophy. In: Hunt R, Tytgat G, editors. *Helicobacter pylori*. Basic Mechanisms to Clinical Cure 2000. Dordrecht: Kluwer 2000; pp239-247
 - 26 **Dixon MF**. Patterns of inflammation linked to ulcer disease. *Best Pract Res Clin Gastroenterol* 2000; **14**: 27-40
 - 27 **Sipponen P**, Kimura K. Intestinal metaplasia, atrophic gastritis and stomach cancer: trends over time. *Eur J Gastroenterol Hepatol* 1994; **6 (Suppl 1)**: S79-S83
 - 28 **Sakaki N**, Kozawa H, Egawa N, Tu Y, Sanaka M. Ten-year prospective follow-up study on the relationship between *Helicobacter pylori* infection and progression of atrophic gastritis, particularly assessed by endoscopic findings. *Aliment Pharmacol Ther* 2002; **16 (Suppl 2)**: 198-203
 - 29 **Seery JP**. A reinterpretation of the events in gastric carcinogenesis. *Med Hypoth* 1991; **35**: 179-181
 - 30 **Genta RM**. Atrophy, metaplasia and dysplasia: are they reversible? *Ital J Gastroenterol Hepatol* 1998; **30 (Suppl 3)**: S324-S325
 - 31 **Satoh K**. Does eradication of *Helicobacter pylori* reverse atrophic gastritis or intestinal metaplasia? Data from Japan. *Gastroenterol Clin North Am* 2000; **29**: 829-835
 - 32 **Dixon MF**. Prospects for intervention in gastric carcinogenesis: reversibility of gastric atrophy and intestinal metaplasia. *Gut* 2001; **49**: 2-4
 - 33 **Xia HHX**, Wong BCY, Lam SK. *Helicobacter pylori* infection and gastric cancer. *Asian J Surg* 2001; **24**: 217-221
 - 34 **Lanas A**, Sekar C, Hirschowitz BI. Objective evidence of aspirin use in both ulcer and nonulcer upper and lower gastrointestinal bleeding. *Gastroenterology* 1992; **103**: 862-869
 - 35 **Lanas A**, Serano P, Bajador E, Esteva F, Benito R, Sainz R. Evidence of aspirin use in both upper and lower gastrointestinal perforation. *Gastroenterology* 1997; **112**: 683-689

Edited by Zhang JZ

• *H.pylori* •

Clinicopathologic study of mucosa-associated lymphoid tissue lymphoma in gastroscopic biopsy

Hong Cheng, Jun Wang, Chuan-Shan Zhang, Pei-Song Yan, Xiao-Hui Zhang, Pei-Zhen Hu, Fu-Cheng Ma

Hong Cheng, Chuan-Shan Zhang, Pei-Song Yan, Xiao-Hui Zhang, Pei-Zhen Hu, Fu-Cheng Ma, Department of Pathology, Xijing Hospital, Fourth Military Medical University, Xi'an 710033, Shaanxi Province, China

Jun Wang, Department of Pathology, Shaanxi Traditional Chinese Medicine College, Xianyang 712083, Shaanxi Province, China

Correspondence to: Dr Hong Cheng, Department of Pathology, Xijing Hospital, Fourth Military Medical University, Xi'an 710033, Shaanxi Province, China. nelson@fmmu.edu.cn

Telephone: +86-29-3375497

Received: 2003-01-15 **Accepted:** 2003-02-22

Abstract

AIM: To explore and discuss the clinicopathologic characteristics of mucosa-associated lymphoid tissue (MALT) lymphoma in gastroscopic biopsy specimen.

METHODS: A retrospective study of 26 cases of lymphoma diagnosed by gastroscopic biopsy during 1999 to 2001 from gastroscopy files of Xijing Hospital was made. The diagnostic criteria were adopted according to the new classification of non-Hodgkin's lymphoma.

RESULTS: Twenty-six cases of primary gastric lymphoma consisting of 15 men and 11 women, aged between 23 to 76 years were recruited from 6 225 cases who received gastroscopy. All of them were diagnosed by both endoscopic findings and histological examinations. Histologically, 23 cases were MALToma (low grade) and 3 cases lymphoblastic lymphoma (high grade). Immunohistochemically, all cases were CD20 positive, while CK and EMA were negative.

CONCLUSION: The majority of the cases of primary low-grade gastric lymphoma have morphologic and clinical features that justify their inclusion in the category of low-grade lymphoma of mucosa associated lymphoid tissue.

Cheng H, Wang J, Zhang CS, Yan PS, Zhang XH, Hu PZ, Ma FC. Clinicopathologic study of mucosa-associated lymphoid tissue lymphoma in gastroscopic biopsy. *World J Gastroenterol* 2003; 9(6): 1270-1272

<http://www.wjgnet.com/1007-9327/9/1270.asp>

INTRODUCTION

Primary gastric lymphoma is the most common extra nodal lymphoma, and the vast majority of them are of B cell origin. Most of the low-grade gastric lymphomas are of the mucosa-associated lymphoid tissue (MALT) type^[1-4]. The concept of MALT lymphoma was first proposed in 1983 by Isaacson and Wright^[1]. Histologically it is characterized by centrocyte-like cells, often with plasmacytic differentiation, and accompanied by lymphoepithelial lesions. The histopathological criteria for the diagnosis of gastric MALToma have largely been based on analysis of partial gastrectomy specimens. From routine biopsy diagnosis by gastroscopy, it is very difficult to

distinguish MALToma from reactive lymphoid hyperplasia on small pieces of tissue. In this article, twenty-six cases were retrospectively analyzed with regard to criteria of diagnosis and clinicopathologic characteristics.

MATERIALS AND METHODS

Materials

During the period of 1999-2001, 6 225 cases received gastroscopy in Xijing Hospital and 26 cases of gastric lymphoma were diagnosed according to the new classification of lymphoid neoplasms. The patients (11 women and 15 men) ranged in age from 23 to 76 years. According to the new classification of lymphoid neoplasms^[2], all the histology of MALToma was established if the following criteria were met: (1) invasion of epithelial structures resulting in "lymphoepithelial lesions"; (2) small lymphocytes, marginal zone cells and/or monocytoid B cells; (3) infiltration of diffuse, perifollicular, interfollicular, or even follicular type due to colonization of reactive follicles. Tissue specimens were embedded in paraffin, sectioned and stained with haematoxylin-eosin and immunohistochemical method.

Immunohistochemical analysis

Immunohistochemical staining of CD20, CD45, CD45RO, Keratin and EMA were performed on paraffin-embedded sections by using the monoclonal antibody (Dako, Copenhagen, Denmark). For antigen retrieval, the deparaffinized slides were microwaved in 0.01 mol/L sodium citrate buffer (pH 6.0) for 10 minutes. Endogenous peroxidase activity was inhibited by hydrogen peroxidase. The sections were incubated with the monoclonal antibody (1:100) overnight at room temperature, and then the detection was performed by the avidin-biotin peroxidase complex method. The sections were counterstained with hematoxylin. PBS buffer solution was substituted for the first antibodies as the negative control, whereas the lymphoma cases were used as positive control.

RESULTS

Clinical data

There were 26 cases of MALToma, of them 15 were males and 11 females, with age ranging from 23 to 76 years. Clinical manifestations were epigastric discomfort, abdominal pain, dyspepsia, fever, melena and mucous stool. Endoscopic evaluation showed the location of 5 cases in gastric body, 4 in gastric antrum, 15 in gastric body and antrum, 1 in gastric angulus and 1 in gastric fundus. By endoscopic diagnosis, 9 cases were gastric cancer and 17 cases were gastric ulcer.

Pathological data

Based on the appearance of biopsy specimens, all 26 cases were gastric lymphomas, of them 23 were MALToma (low grade) and 3 lymphoblastic lymphoma (high grade).

Macroscopically, MALToma could be categorized into erosion and ulcerative types; the size of tumor varied from millet to rice. The lymphomatous cells infiltrated into the

mucosa, sub-mucosa and muscular layer diffusely or locally. Typical features of a low-grade mucosa-associated lymphoma with an organized architectural arrangement including lymphoid follicles, centrocyte-like cells and classical lymphoepithelial lesions were seen. Lymphoid follicles were seen and the germinal centers were partly or entirely replaced by lymphoma cells. Dendritic cells and macrophages with chromophilic bodies disappeared. This phenomenon is called follicular colonization. Lymphoepithelial lesion was shown in which there were clusters of pleomorphic, mitotically active lymphomatous cells infiltration locally and gastric glands destroyed (Figure 1). The neoplastic cells presented a serial cell lineage of small lymphocyte, centrocyte-like cell, monocyte-like B cell, lymphoplasma cell, and also centroblast like cells. In all these cells, several kinds were in a mixed distribution, but usually one kind was predominant. Immunohistochemically, all cases of MALTomas were CD20 positive (Figure 2) and CD45 positive. CK and EMA were negative in all cases.

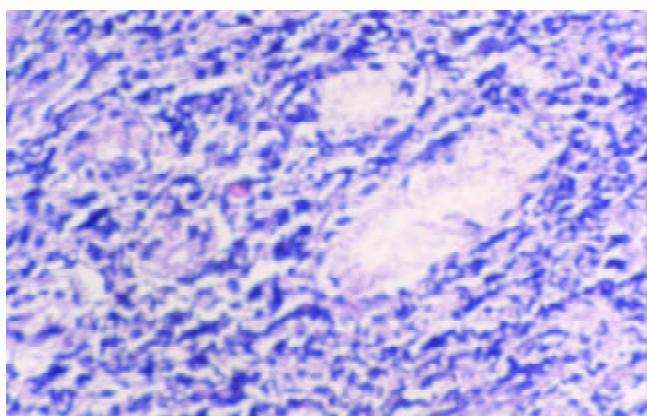


Figure 1 Neoplastic lymphocytes infiltrated into and destroyed glands forming lymphoepithelial lesion. HE $\times 200$.

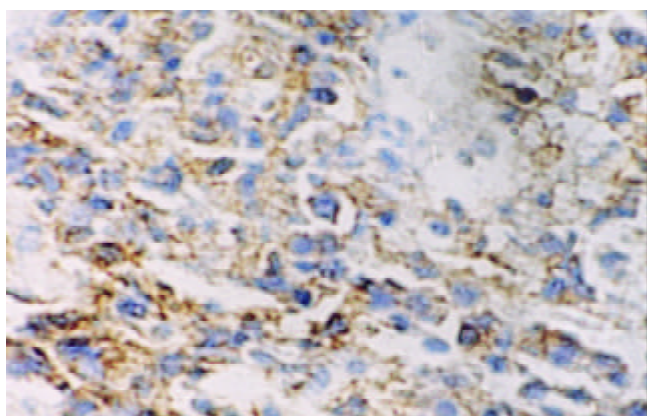


Figure 2 Neoplastic lymphocytes infiltrated into mucosa membrane, with positive CD20. Envision method. $\times 400$.

DISCUSSION

The gastrointestinal tract is the most frequently involved extranodal site of origin for non-Hodgkin's lymphoma, accounting for 12-15 % of all non-Hodgkin's lymphomas and 30-40 % of all extranodal lymphomas^[1,5]. The lymphomas in the stomach arise from MALT. Usually they are not present in the stomach but acquired following *H. pylori* infection of the gastric mucosa. *H. pylori*, a microaerophilic Gram-negative rod, has been proposed as the causative agent for low-grade primary gastric lymphoma of MALT^[6-10]. Presenting features

of primary gastric lymphomas are nonspecific, with dyspepsia, vague epigastric pain, nausea and vomiting^[11-15]. Fever with night sweats and elevated lactate dehydrogenase levels are very uncommon. By endoscopy, diffuse gastritis, thickened gastric folds, erosions and occasionally ulcers are more common findings. Although any region of the stomach may be involved, most MALTomas arise in the antrum or the distal body, the sites commonly colonized by *H. pylori*. Histologically, the prominent lymphoepithelial lesion on endoscopic biopsy specimens is one of the most important features for the diagnosis of MALToma of the stomach^[2, 16-18]. They are seen in 100 % of the biopsy specimens. It is a key point for the diagnosis of MALToma that the infiltrating lymphocytes showed homogeneity in marginal zone cells, small lymphocytes, or monocytoid B cells^[2, 16-18]. All of the three types of cells comprise low-grade lymphomas with a dense infiltrate of a superficial and peripheral plasma cell component. Cytologically, neoplastic lymphocytes are characterized by cellular heterogeneity, including centrocyte like cells (small, atypical cells, but with more abundant cytoplasm), monocytoid B cells, small lymphocytes, and plasma cells. Occasionally large cells (centroblast or immunoblast like) are present in most cases. If reactive follicles are present, neoplastic cells will occupy the marginal zone and/or the interfollicular region. When neoplastic lymphocytes take on a follicular pattern, it is called follicular colonization.

Therefore, the diagnosis of gastric MALToma is based on (1) prominent lymphoepithelial lesions; (2) dense lymphoid infiltrate with marginal zone cells, small lymphocytes, or monocytoid B cells. Lymphoepithelial lesions are considered as the characteristic features of MALToma. Nest formation could also be found in the inflammatory and reactive status, it might be difficult to distinguish them from the real lymphoepithelial lesions. In such cases, immunohistochemistry may be helpful. The former is several leukocytes of polyclone and the latter is the lymphocytes of mono-clone. Follicular colonization is easy to be misjudged as reactive follicles. The following morphological characteristics and immunophenotype may be helpful for the differentiation^[14-18]: (1) Follicular colonization has no dendritic cells or macrophages with chromophilic bodies. (2) Centrocyte like cell is the immunophenotype of B cells in the marginal area, rather than at the germinal center. Both lymphoepithelial lesion and follicular colonization are characteristic features for diagnosis, but they could only be seen in some of the cases. If one case is highly suspected for MALToma of the stomach, repeated biopsy should be performed if clinically indicated and then, immunohistochemistry and molecular biology technique should be done.

Understanding primary gastric lymphomas is undergoing rapid and significant transformation from both clinicopathological and therapeutic standpoints. The most important new developments in therapy are the use of *H. pylori* eradication as the initial treatment for localized low-grade primary gastric lymphomas, and the use of chemoradiation over a surgical approach for localized high-grade primary gastric lymphoma^[19-30]. Patients with low-grade primary gastric lymphoma should be treated with *H. pylori* eradication therapy as most patients respond with prompt amelioration of dyspeptic symptoms, although histological regression may take several months. Patients need to be followed-up with serial endoscopies. If no histologically proven lymphoma regression occurs, then biopsy should be done to rule out the presence of co-existing high-grade primary gastric lymphoma. The finding of high-grade primary gastric lymphoma usually indicates the need for more aggressive treatment with chemotherapy and radiotherapy. Surgery is an option in cases of significant

hemorrhage or perforation. With appropriate treatment, the long-term survival is 70-80 % for limited-stage disease and 50-60 % for advanced stage disease.

REFERENCES

- Stolte M**, Bayerdorffer E, Morgner A, Alpen B, Wundisch T, Thiede C, Neubauer A. *Helicobacter* and gastric MALT lymphoma. *Gut* 2002; **50**(Suppl 3): III 19-24
- Isaacson PG**, Muller-Hermelink HK, Paris MA, Berger F, Nathwani BN, Swerdlow SH, Harris NL. Extranodal marginal zone B-cell lymphoma of mucosa-associated lymphoid tissue (MALT lymphoma). In Jaffe ES, Harris NL, Stein H, Vardiman JW eds. World Health Organization Classification of Tumours. Pathology and genetics of tumours of haematopoietic and lymphoid tissues. Lyon: IARC Press 2001: 157-160
- Zhou Q**, Xu TR, Fan QH, Zhen ZX. Clinicopathologic study of primary intestinal B cell malignant lymphoma. *World J Gastroenterol* 1999; **5**: 538-540
- Salam I**, Durai D, Murphy JK, Sundaram B. Regression of primary high-grade gastric B-cell lymphoma following *Helicobacter pylori* eradication. *Eur J Gastroenterol Hepatol* 2001; **13**: 1375-1378
- Delchier JC**, Lamarque D, Levy M, Tkoub EM, Copie-Bergman C, Deforges L, Chaumette MT, Haioun C. *Helicobacter pylori* and gastric lymphoma: high seroprevalence of CagA in diffuse large B-cell lymphoma but not in low-grade lymphoma of mucosa-associated lymphoid tissue type. *Am J Gastroenterol* 2001; **96**: 2324-2328
- Go MF**, Smoot DT. *Helicobacter pylori*, gastric MALT lymphoma, and adenocarcinoma of the stomach. *Semin Gastrointest Dis* 2000; **11**: 134-141
- Wotherspoon AC**, Dogliani C, Diss TC, Pan L, Moschini A, de Boni M, Isaacson PG. Regression of primary low-grade B-cell gastric lymphoma of mucosa-associated lymphoid tissue type after eradication of *Helicobacter pylori*. *Lancet* 1993; **342**: 575-577
- Furusyo N**, Kanamoto K, Nakamura S, Yao T, Suekane H, Yano Y, Ariyama I, Hayashi J, Kashiwagi S. Rapidly growing primary gastric B-cell lymphoma after eradication of *Helicobacter pylori*. *Intern Med* 1999; **38**: 796-799
- Montalban C**, Santon A, Boixeda D, Bellas C. Regression of gastric high grade mucosa associated lymphoid tissue (MALT) lymphoma after *Helicobacter pylori* eradication. *Gut* 2001; **49**: 584-587
- Miki H**, Kobayashi S, Harada H, Yamanoi Y, Uraoka T, Sotozono M, Ohmori M. Early stage gastric MALT lymphoma with high-grade component cured by *Helicobacter pylori* eradication. *J Gastroenterol* 2001; **36**: 121-124
- Gretschel S**, Hunerbein M, Foss HD, Krause M, Schlag PM. Regression of high-grade gastric B-cell lymphoma after eradication of *Helicobacter pylori*. *Endoscopy* 2001; **33**: 805-807
- Morgner A**, Miehle S, Fischbach W, Schmitt W, Muller-Hermelink H, Greiner A, Thiede C, Schetelig J, Neubauer A, Stolte M, Ehninger G, Bayerdorffer E. Development of early gastric cancer 4 and 5 years after complete remission of *Helicobacter pylori* associated gastric low grade marginal zone B cell lymphoma of MALT type. *World J Gastroenterol* 2001; **7**: 248-253
- Morgner A**, Miehle S, Fischbach W, Schmitt W, Muller-Hermelink H, Greiner A, Thiede C, Schetelig J, Neubauer A, Stolte M, Ehninger G, Bayerdorffer E. Complete remission of primary high-grade B-cell gastric lymphoma after cure of *Helicobacter pylori* infection. *J Clin Oncol* 2001; **19**: 2041-2048
- Bouzourene H**, Haefliger T, Delacretaz F, Saraga E. The role of *Helicobacter pylori* in primary gastric MALT lymphoma. *Histopathology* 1999; **34**: 118-123
- Morgner A**, Lehn N, Andersen LP, Thiede C, Bennedsen M, Trebesius K, Neubauer B, Neubauer A, Stolte M, Bayerdorffer E. *Helicobacter heilmannii*-associated primary gastric low-grade MALT lymphoma: complete remission after curing the infection. *Gastroenterology* 2000; **118**: 821-828
- Hiyama T**, Haruma K, Kitadai Y, Masuda H, Miyamoto M, Ito M, Kamada T, Tanaka S, Uemura N, Yoshihara M, Sumii K, Shimamoto F, Chayama K. Clinicopathological features of gastric mucosa-associated lymphoid tissue lymphoma: a comparison with diffuse large B-cell lymphoma without a mucosa-associated lymphoid tissue lymphoma component. *J Gastroenterol Hepatol* 2001; **16**: 734-773
- Tang CC**, Shih LY, Chen PC, Chen TC. Simultaneous occurrence of gastric adenocarcinoma and low-grade gastric lymphoma of mucosa-associated lymphoid tissue. *Chang Gung Med J* 2002; **25**: 115-121
- Papa A**, Cammarota G, Tursi A, Gasbarrini A, Gasbarrini G. *Helicobacter pylori* eradication and remission of low-grade gastric mucosa-associated lymphoid tissue lymphoma: a long-term follow-up study. *J Clin Gastroenterol* 2000; **31**: 169-171
- Xue FB**, Xu YY, Wan Y, Pan BR, Ren J, Fan DM. Association of *H. pylori* infection with gastric carcinoma: a Meta analysis. *World J Gastroenterol* 2001; **7**: 801-804
- Wang RT**, Wang T, Chen K, Wang JY, Zhang JP, Lin SR, Zhu YM, Zhang WM, Cao YX, Zhu CW, Yu H, Cong YJ, Zheng S, Wu BQ. *Helicobacter pylori* infection and gastric cancer: evidence from a retrospective cohort study and nested case-control study in China. *World J Gastroenterol* 2002; **8**: 1103-1107
- Lu XL**, Qian KD, Tang XQ, Zhu YL, Du Q. Detection of *H. pylori* DNA in gastric epithelial cells by *in situ* hybridization. *World J Gastroenterol* 2002; **8**: 305-307
- Vandenplas Y**. *Helicobacter pylori* infection. *World J Gastroenterol* 2000; **6**: 20-31
- Hu PJ**. *Hp* and gastric cancer: challenge in the research. *Shijie Huaren Xiaohua Zazhi* 1999; **7**: 1-2
- Quan J**, Fan XG. Progress in experimental research of *Helicobacter pylori* infection and gastric carcinoma. *Shijie Huaren Xiaohua Zazhi* 1999; **7**: 1068-1069
- Guo CQ**, Wang YP, Ma SW, Ding GY, Li LC. Study on *Helicobacter pylori* infection and p53, c-erbB-2 gene expression in carcinogenesis of gastric mucosa. *Shijie Huaren Xiaohua Zazhi* 1999; **7**: 313-315
- Xiao SD**, Liu WZ. Current status in treatment of *Hp* infection. *Shijie Huaren Xiaohua Zazhi* 1999; **7**: 3-4
- Begum S**, Sano T, Endo H, Kawamata H, Urakami Y. Mucosal change of the stomach with low-grade mucosa-associated lymphoid tissue lymphoma after eradication of *Helicobacter pylori*: follow-up study of 48 cases. *J Med Invest* 2000; **47**: 36-46
- Yamashita H**, Watanabe H, Ajioka Y, Nishikura K, Maruta K, Fujino MA. When can complete regression of low-grade gastric lymphoma of mucosa-associated lymphoid tissue be predicted after *Helicobacter pylori* eradication? *Histopathology* 2000; **37**: 131-140
- Urakami Y**, Sano T, Begum S, Endo H, Kawamata H, Oki Y. Endoscopic characteristics of low-grade gastric mucosa-associated lymphoid tissue lymphoma after eradication of *Helicobacter pylori*. *J Gastroenterol Hepatol* 2000; **15**: 1113-1119
- Alpen B**, Thiede C, Wundisch T, Bayerdorffer E, Stolte M, Neubauer A. Molecular diagnostics in low-grade gastric marginal zone B-cell lymphoma of mucosa-associated lymphoid tissue type after *Helicobacter pylori* eradication therapy. *Clin Lymphoma* 2001; **2**: 103-108

Expression and cell-specific localization of cholecystokinin receptors in rat lung

Bin Cong, Shu-Jin Li, Yi-Ling Ling, Yu-Xia Yao, Zhen-Yong Gu, Jun-Xia Wang, Hong-Yu You

Bin Cong, Shu-Jin Li, Yi-Ling Ling, Yu-Xia Yao, Zhen-Yong Gu, Department of Pathophysiology, Hebei Medical University, Shijiazhuang 050017, Hebei Province, China
Jun-Xia Wang, Hong-Yu You, Molecular Biological Laboratory, Hebei Medical University, Shijiazhuang 050017, Hebei Province, China

Supported by National Natural Science Foundation of China, No. 39570304

Correspondence to: Professor Yi-Ling Ling, Department of Pathophysiology, Hebei Medical University, Shijiazhuang 050017, Hebei Province, China. lingyiling@163.net

Telephone: +86-311-6265645

Received: 2003-01-04 **Accepted:** 2003-02-11

Abstract

AIM: To elucidate whether CCK receptors exist in lung tissues and their precise cellular localization in the lung.

METHODS: CCK-AR and CCK-BR mRNA expression and cellular distribution in the rat lung were detected by highly sensitive method of *in situ* reverse transcription-polymerase chain reaction (RT-PCR) and conventional *in situ* hybridization.

RESULTS: CCK-AR and CCK-BR gene positive signals were observed in bronchial epithelial cells, alveolar epithelial cells, pulmonary macrophages and vascular endothelial cells of the rats' lung by *in situ* RT-PCR. The hybridization signals of CCK-AR were relatively faint. By *in situ* hybridization, however, only the signals of CCK-BR but not CCK-AR were detected in the lung, and the positive staining was only found in vascular endothelial cells and macrophages.

CONCLUSION: CCK-AR and CCK-BR gene were present in pulmonary vascular endothelial cells, macrophages, bronchial epithelial cells and alveolar epithelial cells, which play an important role in mediating the regulatory actions of CCK-8 on these cells.

Cong B, Li SJ, Ling YL, Yao YX, Gu ZY, Wang JX, You HY. Expression and cell-specific localization of cholecystokinin receptors in rat lung. *World J Gastroenterol* 2003; 9(6): 1273-1277
<http://www.wjgnet.com/1007-9327/9/1273.asp>

INTRODUCTION

Cholecystokinin (CCK) is a gut-brain peptide that exerts a variety of physiological actions in the gastrointestinal tract and central nervous system (CNS) through cell surface CCK receptors^[1]. CCK receptors have been pharmacologically classified into two subtypes CCK-A receptor (CCK-AR) and CCK-B receptor (CCK-BR) according to their affinity for the peptide agonists CCK and gastrin, which share the same COOH-terminal pentapeptide amide sequence but differ in sulfation at the sixth (gastrin) and seventh (CCK) tyrosyl residues^[2]. CCK-AR is highly selective to sulfated analogues

of CCK and the antagonist L-364 718, whereas CCK-BR has similarly high affinity to both sulfated and nonsulfated peptide analogues of CCK/gastrin peptides and the antagonist L-365 260^[2]. CCK-AR is found principally in the gastrointestinal tract and selective areas of the CNS, while CCK-BR is found principally in the CNS and selective areas of the gastrointestinal tract, on pancreatic acinar cells and parietal cells^[3,4]. CCK binds to CCK-AR present on a variety of gastrointestinal target tissues including pancreatic acini, islets, gastric mucosa and gallbladder to induce pancreatic enzyme secretion, insulin secretion, release of pepsinogen and gallbladder contraction^[5]. CCK-BR in the CNS regulates feeding, anxiety and memory, etc^[3]. CCK-AR and CCK-BR are also expressed in the neoplastic cells such as pancreatic cancer cells^[6,7], gastric cancer cells^[8,9], colonic cancer cells^[10] and small cell lung cancer cells^[11-13] where they may stimulate cell growth. In addition, CCK-BR is also present on T lymphocytes^[14,15] to regulate lymphocytes proliferation^[16,17]. These data suggested that CCK receptors were widely distributed around various kinds of tissues and their presence provided the structural basis for CCK to exert a broad array of physiological action.

Our previous data demonstrated that CCK-8, as an intestinal neuropeptide, not only protected gastric mucosa against alcohol-induced injury^[18-20], but also was a potent protective agent against acute lung injury by LPS^[21,22]. It obviously reduced the pulmonary artery hypertension (PAH) and lessened the inflammatory lesion in lung tissues of endotoxin shock (ES) rats^[21,22]. Moreover, CCK-8 could inhibit the reduction of endothelial-dependent relaxation of isolated pulmonary artery to acetylcholine (ACh) induced by LPS^[23]. Stretton and Barnes reported that CCK-8 produced a concentration-dependent contractile response in guinea-pig trachea and this effect was antagonized by the CCK receptor antagonists dibutyl cyclic guanosine monophosphate and L-364 718^[24]. These data indicated that there might be CCK receptors in the lung tissues to mediate the action of CCK-8. However, whether CCK receptors are present in lung tissues and their precise cellular localization remains unclear. In the present study, we detected the cellular localization of CCK receptors in the rats' lung using highly sensitive method of *in situ* RT-PCR.

MATERIALS AND METHODS

Animal model and tissue preparation

Healthy Sprague-Dawley rats (weighing 180-220 g BW) were anaesthetized with urethane (1 g/kg). Lung tissues were dissected from the rats. The inferior lobe of right lung was fixed in 4 % paraformaldehyde for 1 h and embedded in paraffin for *in situ* hybridization and *in situ* RT-PCR.

Primers and probe

The primers and probe of CCK receptor were designed according to Mostein's report^[25]. The sequences of CCK-AR primers were 5' -CTC GCT CGC CCA GAA CTC TAC CAA GGA ATC AAA TTT GAT GC-3' (sense) and 5' -CTG GTT CGG CCC ATG GAG CAG AGG TGC TCA TGT GGC TGT AG-3' (antisense). The sequences of CCK-BR primers were

5'-CTC GCT CGC CCA GAA CTC TAC CTA GGA CTC CAC TTT GA-3' (sense) and 5'-CTG GTT CGG CCC ACG CAC CAC CCG CTT CTT AGC CAG CA-3' (antisense). The sequences of CCK-AR and CCK-BR probes were respectively 5'-CGG GGG CCG GGG ACT TCT GCA AGT AAC AGC CAT CAC TAT CCT CAT A-3' and 5'-AGC TAC GCT GGT TAC AGG CCG GCA GCC CCC GTT-3'. The oligonucleotide probes were labeled with alkaline phosphatase (Boehringer Mannheim). All the primers and probes were synthesized by Sangon Corporation (Shanghai).

In situ RT-PCR

The sections (5 μ m) were baked and deparaffinized to water, and then treated with 0.2 mol/L HCl and EDTA. The slides were pretreated with 0.1 % proteinase K at 37 °C for 12 min to prevent background staining and inactivate endogenous enzyme. Then the tissues were treated overnight in a Rnase-free DNAase solution (Boehringer Mannheim) at 37 °C. The *in situ* reverse transcription step was performed in 30 μ l solution containing 2 μ mol/L CCK-AR or CCK-BR primers and 1 U/ μ l AMV-RT at 42 °C for 1.5 h. Then the slides were overlain with 50 μ l *in situ* PCR reaction mixture containing 1 \times PCR buffer, 4.5 mmol/L MgCl₂, 0.2 μ mol/L dNTPs, 1 μ mol/L each of primers, and 10 U Taq polymerase (Perkin Elmer). The PCR was performed at conditions of initial denaturation at 94 °C for 2 min, followed by 30 cycles of denaturation at 94 °C for 1.5 min, annealing at 55 °C for 1 min, and extension at 72 °C for 1 min. PCR-amplified products were detected with alkaline phosphatase (AP)-labeled CCK-AR and CCK-BR oligonucleotide probes (2 pmol/ml) at 37 °C for 24 h. The slides were then developed in NBT/BCIP solutions at room temperature for 48 h. To stop the color reaction, the slides were washed in distilled water and mounted with glycerol.

Controls

The brain sections were used as positive control. A series of negative controls were performed to guarantee the specificity of the method of *in situ* RT-PCR. Samples pretreated with RNase were used as negative control. Other five negative controls were samples treated without AMV-RT, or Taq polymerase, or primers, or probes specified or unspecified.

In situ hybridization

The procedure was carried out the same way as *in situ* RT-PCR, but without the RT-PCR steps.

RESULTS

The positive and negative controls of in situ RT-PCR

The rat brain sections expressed both CCK-AR and CCK-BR. The hybridization signal was present in the neuron. There was no positive signal in RNase-pretreated samples. Omission of AMV-RT, or Taq polymerase, or primers, or probes prevented specific staining (Figure 1, Table 1).

Table 1 Negative controls for *in situ* RT-PCR

Reagent	a	b	c	d	e	f
AMV-RT	√	√	√	√	×	√
Taq polymerase	√	√	√	×	√	√
Primers	√	√	×	√	√	√
Probes	√	×	√	√	√	√
RNase	√	×	×	×	×	×
Probes (Unspecified)	×	√	×	×	×	×
Signal	-	-	±	-	-	-

In situ expression of CCK-BR gene in rat lungs

By *in situ* RT-PCR, CCK-BR mRNA stainings (dark blue color) were found in bronchial mucosal epithelial cells, endothelial cells, alveolar epithelial cells and macrophages (Figure 2). By *in situ* hybridization, however, CCK-BR mRNA staining was only seen in endothelial cells and macrophages (Figure 3).

In situ expression of CCK-AR gene in rat lungs

By *in situ* RT-PCR, the hybridization signals of CCK-AR mRNA were also found in bronchial mucosal epithelial cells, endothelial cells, alveolar epithelial cells and macrophages, and the hybridization signals of CCK-AR were weaker than those of CCK-BR (Figure 4). By *in situ* hybridization, however, no expression of CCK-AR mRNA was detected (Figure 5).

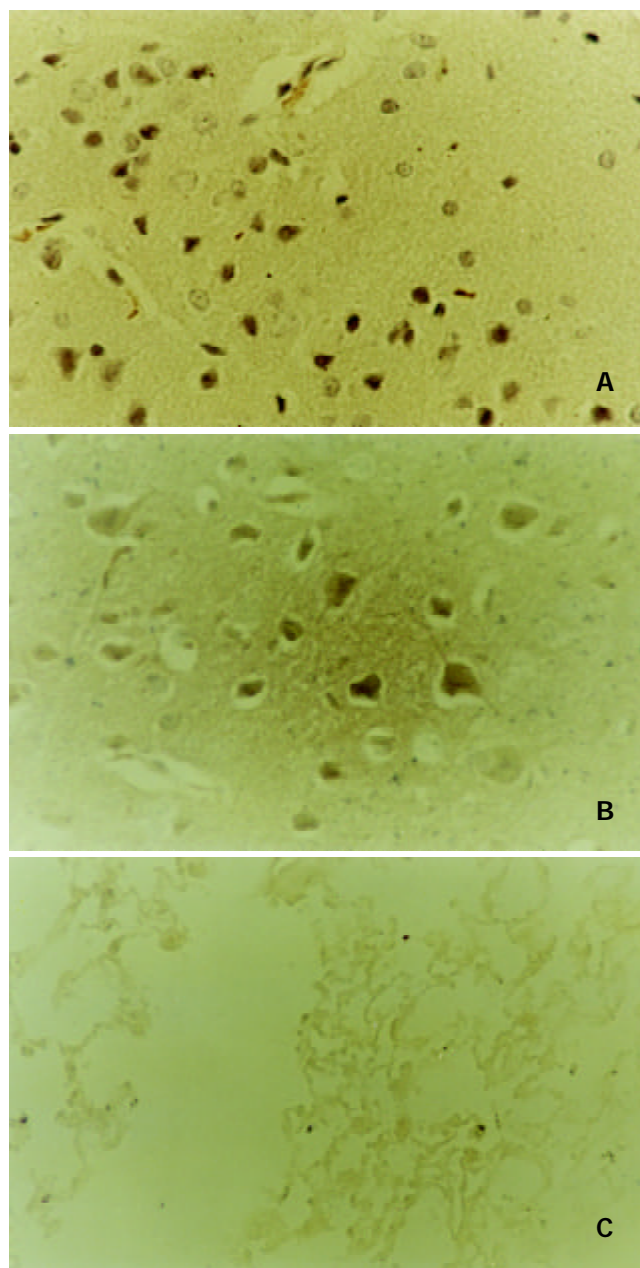


Figure 1 Appearance of positive and negative control tissue section for detecting *in situ* expression of CCK-AR and CCK-BR gene by *in situ* RT-PCR. (A) *In situ* expression of CCK-BR gene in the brain of SD rats (\times 400). (B) *In situ* expression of CCK-AR gene in the brain of SD rats (\times 400). (C) Negative control section from the lung tissue of SD rats (\times 200).

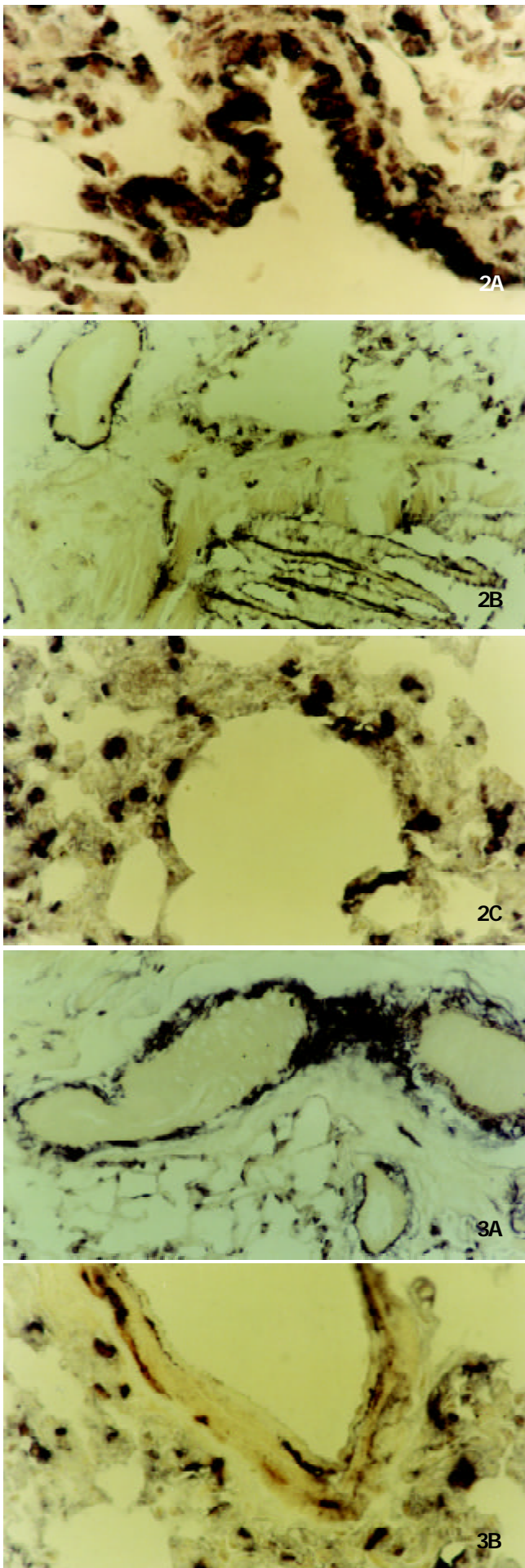


Figure 2 Localization of CCK-BR gene in the lung tissues of

SD rats by *in situ* RT-PCR ($\times 400$). (A) Expression of CCK-BR gene in bronchial mucosal cells. (B) Expression of CCK-BR gene in vascular endothelial cells. (C) Expression of CCK-BR gene in macrophages and alveolar epithelial cells.

Figure 3 Localization of CCK-BR mRNA in rat lung tissues by *in situ* hybridization. (A) Expression of CCK-BR gene in vascular endothelial cells ($\times 100$). (B) Expression of CCK-BR gene in vascular endothelial cells and macrophages ($\times 400$).

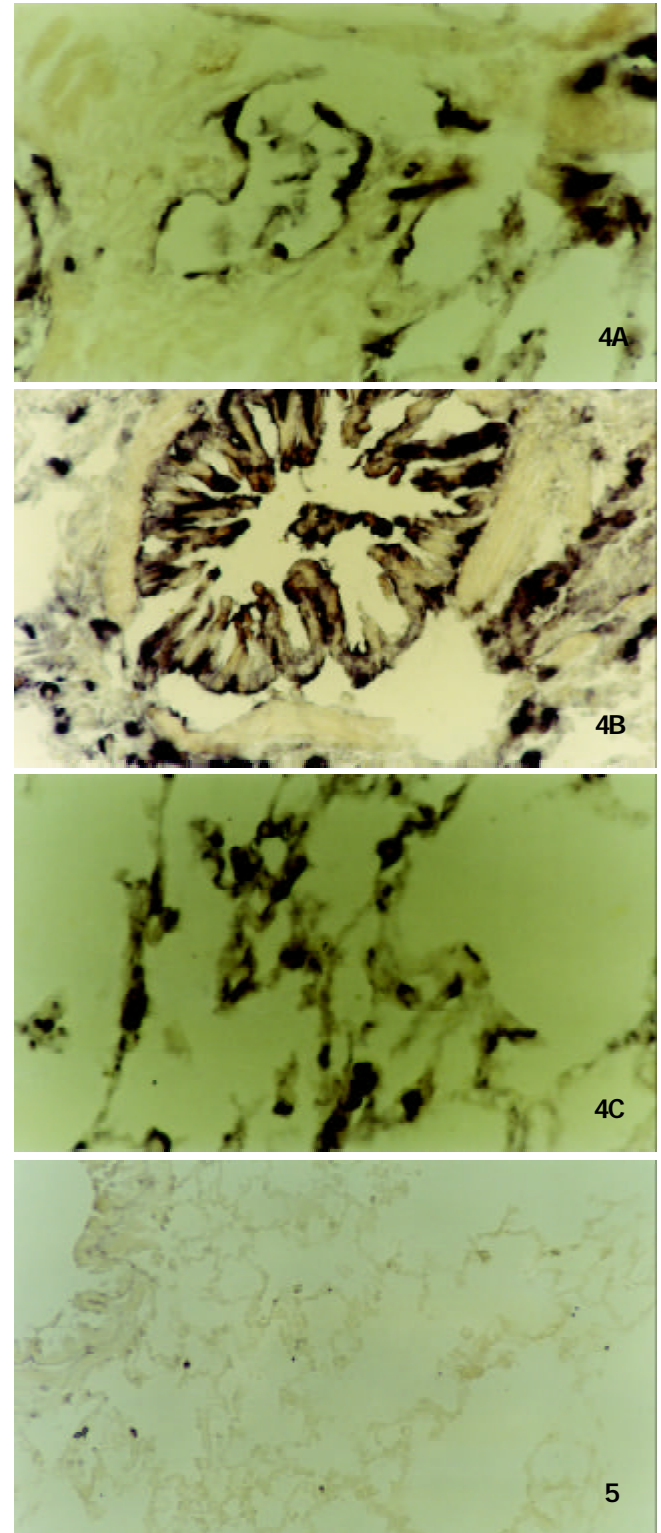


Figure 4 *In situ* expression of CCK-AR gene in the lung tissues of SD rats, detected by *in situ* RT-PCR ($\times 400$). (A) Expression of CCK-AR gene in vascular endothelial cells. (B) Expression of CCK-AR gene in bronchial mucosal cells and macrophages. (C) Expression of CCK-AR gene in alveolar epithelial cells.

Figure 5 No positive signal of CCK-AR gene was detected in lung tissues by *in situ* hybridization ($\times 200$).

DISCUSSION

In situ RT-PCR is a novel molecular biological technique that combines the high sensitivity of RT-PCR for generating a cDNA from small amounts of mRNA with cellular localization of *in situ* hybridization. The sensitivity of *in situ* hybridization is 10-20 copies per cell when detecting the single-copy and low-copy (less than 10 copies) target DNA or RNA in tissues, while using *in situ* RT-PCR could significantly enhance the sensitivity for detecting the target DNA or RNA^[26]. In the present study, we detected the *in situ* expression of CCK receptors by two methods of *in situ* hybridization and *in situ* RT-PCR. By *in situ* hybridization, only little amount of CCK-BR gene staining was found in vascular endothelial cells and macrophages, whereas by *in situ* RT-PCR, both CCK-AR and CCK-BR mRNA expressions were detected in bronchial mucosal cells and alveolar epithelial cells other than endothelial cells and macrophages. Our results also demonstrated that the sensitivity of *in situ* RT-PCR was obviously higher than that of *in situ* hybridization. Large amounts of cDNA were amplified by specially designed target-specific primers and followed by hybridization with highly specific probes^[27]. So the specific binding of nucleotide on the basis of base complementation was performed twice, which increased the specificity of *in situ* RT-PCR. High sensitivity and specificity made *in situ* RT-PCR a favorable technique to study the *in situ* expression and cellular distribution of target gene in tissues. To further ensure the specific results, we designed six negative controls: First, omission of AMV-RT prevented the positive staining, indicating that genome DNA was completely digested. Second, omission of Taq polymerase produced negative results, suggesting endogenous polymerase was inactive. Third, omission of primers produced weak positive reaction which was the results of little amounts of cDNA binding with specific probes, and it confirmed the specificity of the primers. Fourth, addition of RNase produced negative results, confirming that mRNA was detected during RT-PCR. Fifth, omission of specific probes and addition of nonspecific probes produced negative reaction, confirming the specificity of the probes. Sixth, addition of unlabeled specific probes prevented the positive staining, indicating that endogenous alkaline phosphatase was inactive.

Using *in situ* RT-PCR, we found that CCK-AR and CCK-BR were present in the rats' lungs. It is the first report about the distribution of CCK receptors in lung tissues. The results of *in situ* RT-PCR also demonstrated the cellular localization of CCK receptors in lung tissues: vascular endothelial cells, macrophages, bronchial epithelial cells and alveolar epithelial cells. Our previous study showed that exposure of rabbit pulmonary artery to LPS or TNF- α led to significant reduction of endothelial-dependent relaxation to ACh and enhancement of contractile response to phenylephrine, which could be reversed by CCK-8^[23,28]. This may be the mechanisms of CCK-8 to abolish PAH during endotoxin shock. The present study showed that pulmonary vascular endothelial cells expressed both CCK-AR and CCK-BR gene. So CCK-8 may bind to CCK receptors on pulmonary vascular endothelial cells to mediate its effects on isolated pulmonary artery. Gu *et al*^[29] reported that CCK-8 protected cultured bovine pulmonary artery endothelial cells (BPAEC) against the detrimental effect of LPS such as lipoperoxide damages and cell apoptosis as well as LPS-induced peroxynitrite formation, which might be in part reversed by proglumide, a nonspecific CCK receptor antagonist. These data suggested that there might be CCK receptors on BPAEC. Therefore, CCK receptors on pulmonary endothelial cells may mediate effects of CCK-8 on pulmonary vascular such as regulating the reactivity of pulmonary vascular to vasoactive agents and protecting the endothelial cells against damages.

Our present study also demonstrated existence of CCK-AR and CCK-BR gene expression in pulmonary macrophages. It is well known that activation of macrophages plays a critical role in inducing the inflammatory response^[30]. Macrophages stimulated by LPS or other inflammatory factors produce and release large quantities of various proinflammatory cytokines including TNF- α , IL-1 β , IL-6 etc. Overproduction of these cytokines can result in systemic inflammatory response syndrome (SIRS) and multiple organ dysfunction syndrome (MODS), which might lead to death^[31]. So controlling the overactivation of macrophages may be an effective measure in preventing the generation and development of SIRS and MODS. In another study, we found that CCK-8 could inhibit LPS-induced TNF- α release and gene expression in rat pulmonary interstitial macrophages (PIMs) *in vitro*^[32,33]. The study about its upstream signalling mechanisms demonstrated that CCK-8 inhibited LPS-induced NF- κ B activity and I κ B degradation in PIMs, which was abrogated by proglumide^[33]. Furthermore, LPS-induced expression of LPS receptor CD14 on PIMs could be downregulated by CCK-8 *in vitro*^[32]. These data suggested that CCK-8 might bind to CCK receptors on pulmonary macrophages to interfere with the activation of macrophages during inflammation. But the cellular signal transduction mechanisms through which CCK receptors mediated in macrophages were not fully clarified. Other than pulmonary macrophages, several functions of murine peritoneal macrophages were negatively modulated by CCK-8 including the production of superoxide anion, phagocytosis and mobility^[34,35]. Therefore, CCK receptors on macrophages provide the structural basis for CCK-8 to regulate the functions and activation of macrophages, which may be beneficial to the control of inflammatory responses.

In addition, CCK-AR and CCK-BR mRNA expressions were observed on bronchial epithelial cells and alveolar epithelial cells in this study. Stretton and Barnes reported that CCK-8 produced a concentration-dependent contractile response in guinea-pig trachea and this effect was antagonized by the CCK receptor antagonists dibutyryl cyclic guanosine monophosphate and L-364 718^[24]. So the CCK receptors present on bronchial epithelial cells may mediate the regulatory effect of CCK-8 on the tonus of bronchus. The functions of CCK receptors on alveolar epithelial cells remain unclear.

In summary, we successfully detected CCK-AR and CCK-BR mRNA expression in rats' lung tissues and clarified their cellular localization using *in situ* RT-PCR. To our knowledge, this is the first report about the CCK receptors gene expression in lung tissues. CCK receptors present on pulmonary endothelial cells, macrophages, bronchial epithelial cells and alveolar epithelial cells play an important role in mediating effects of CCK-8 such as protecting endothelial cells against damages, inhibiting the overactivation of macrophage and regulating the pulmonary vascular tonus and bronchial tonus.

REFERENCES

- 1 **Crawley JN**, Corwin RL. Biological actions of cholecystokinin. *Peptides* 1994; **15**: 731-755
- 2 **Wank SA**. Cholecystokinin receptors. *Am J Physiol* 1995; **269**: G628-G646
- 3 **Noble F**, Roques BP. CCK-B receptor: chemistry, molecular biology, biochemistry and pharmacology. *Progress in Neurobiol* 1999; **58**: 349-379
- 4 **Kulaksiz H**, Arnold R, Goke B, Maronde E, Meyer M, Fahrenholz F, Forssmann WG, Eissele R. Expression and cell-specific localization of the cholecystokinin B/gastrin receptor in the human stomach. *Cell Tissue Res* 2000; **299**: 289-298
- 5 **Wank SA**. G protein-coupled receptors in gastrointestinal physiology I. CCK receptors: an exemplary family. *Am J Physiol* 1998; **274**: G607-G613

- 6 **Smith JP**, Verderame MF, McLaughlin P, Martenis M, Ballard E, Zagon IS. Characterization of the CCK-C (cancer) receptor in human pancreatic cancer. *Int J Mol Med* 2002; **10**: 689-694
- 7 **Clerc P**, Leung-Theung-Long S, Wang TC, Dockray GJ, Bouisson M, Delisle MB, Vaysse N, Pradayrol L, Fourmy D, Dufresne M. Expression of CCK2 receptors in the murine pancreas: proliferation, transdifferentiation of acinar cells, and neoplasia. *Gastroenterology* 2002; **122**: 428-437
- 8 **Pagliocca A**, Wroblewski LE, Ashcroft FJ, Noble PJ, Dockray GJ, Varro A. Stimulation of the gastrin-cholecystokinin(B) receptor promotes branching morphogenesis in gastric AGS cells. *Am J Physiol Gastrointest Liver Physiol* 2002; **283**: G292-G299
- 9 **Henwood M**, Clarke PA, Smith AM, Watson SA. Expression of gastrin in developing gastric adenocarcinoma. *Br J Surg* 2001; **88**: 564-568
- 10 **Fontana MG**, Moneghini D, Villanacci V, Donato F, Rindi G. Effect of cholecystokinin-B gastrin receptor blockade on chemically induced colon carcinogenesis in mice: follow-up at 52 weeks. *Digestion* 2002; **65**: 35-40
- 11 **Reubi JC**, Schaer JC, Waser B. Cholecystokinin(CCK)-A and CCK-B/gastrin receptors in human tumors. *Cancer Res* 1997; **57**: 1377-1386
- 12 **Matsumori Y**, Katakami N, Ito M, Taniguchi T, Iwata N, Takaishi T, Chihara K, Matsui T. Cholecystokinin-B/gastrin receptor: a novel molecular probe for human small cell lung cancer. *Cancer Res* 1995; **55**: 276-279
- 13 **Behr TM**, Jenner N, Radetzky S, Behe M, Gratz S, Yucekent S, Raue F, Becker W. Targeting of cholecystokinin-B/gastrin receptors in vivo: preclinical and initial clinical evaluation of the diagnostic and therapeutic potential of radiolabelled gastrin. *Eur J Nucl Med* 1998; **25**: 424-430
- 14 **Dornand J**, Roche S, Michel F, Bali JP, Cabane S, Favero J, Magous R. Gastrin-CCK-B type receptors on human T lymphoblastoid Jurkat cells. *Am J Physiol* 1995; **268**: G522-529
- 15 **Oiry C**, Gagne D, Cottin E, Bernad N, Galleyrand JC, Berge G, Lignon MF, Eldin P, Le Cunff M, Leger J, Clerc P, Fourmy D, Martinez J. CholecystokininB receptor from human Jurkat lymphoblastic T cells is involved in activator protein-1-responsive gene activation. *Mol Pharmacol* 1997; **52**: 292-299
- 16 **Medina S**, Rio MD, Cuadra BD, Guayerbas N, Fuente MD. Age-related changes in the modulatory action of gastrin-releasing peptide, neuropeptide Y and sulfated cholecystokinin octapeptide in the proliferation of murine lymphocytes. *Neuropeptides* 1999; **33**: 173-179
- 17 **De la Fuente M**, Carrasco M, Del Rio M, Hernanz A. Modulation of murine lymphocyte functions by sulfated cholecystokinin octapeptide. *Neuropeptides* 1998; **32**: 225-33
- 18 **Mercer DW**, Cross JM, Smith GS, Miller TA. Protective action of gastrin-17 against alcohol-induced gastric injury in the rat: role in mucosal defense. *Am J Physiol* 1997; **273**: G365-G373
- 19 **Mercer DW**, Cross JM, Chang L, Lichtenberger LM. Bombesin prevents gastric injury in the rat: role of gastrin. *Dig Dis Sci* 1998; **43**: 826-833
- 20 **Mercer DW**, Smith GS, Miller TA. Cyclooxygenase inhibition attenuates cholecystokinin-induced gastroprotection. *Dig Dis Sci* 1998; **43**: 468-475
- 21 **Ling YL**, Huang SS, Wang LF, Zhang JL, Wan M, Hao RL. Cholecystokinin octapeptide reverses experimental endotoxin shock. *Shengli Xuebao* 1996; **48**: 390-394
- 22 **Ling YL**, Cong B, Gu ZY, Li SJ, Zhou XH. Inhibitory effect of cholecystokinin octapeptide on pulmonary arterial hypertension during endotoxic shock. *Zhongguo Xueshu Qikan Wenzhai* 2000; **6**: 890-892
- 23 **Gu ZY**, Ling YL, Meng AH, Cong B, Hung SS. Effects of cholecystokinin-octapeptide on the response of rabbit pulmonary artery induced by LPS *in vitro*. *Zhongguo Bingli Shengli Zazhi* 1999; **15**: 484-487
- 24 **Stretton CD**, Barnes PJ. Cholecystokinin-octapeptide constricts guinea-pig and human airways. *Br J Pharmacol* 1989; **97**: 675-682
- 25 **Monstein HJ**, Nylander AG, Salehi A, Chen D, Lundquist I, Hakanson R. Cholecystokinin-A and cholecystokinin-B/gastrin receptor mRNA expression in the gastrointestinal tract and pancreas of the rat and man. *Scand J Gastroenterol* 1996; **31**: 383-390
- 26 **Bartlett JM**. Approaches to the analysis of gene expression using mRNA: a technical overview. *Mol Biotechnol* 2002; **21**: 149-160
- 27 **Peters J**, Krams M, Wacker HH, Carstens A, Weisner D, Hamann K, Menke M, Harms D, Parwaresch R. Detection of rare RNA sequences by single-enzyme in situ reverse transcription-polymerase chain reaction. *Am J Pathol* 1997; **150**: 469-476
- 28 **Meng AH**, Ling YL, Wang DH, Gu ZY, Li SJ, Zhu TN. Role of nitric oxide in cholecystokinin-octapeptide alleviation of tumor necrosis factor- α induced changes in rabbit pulmonary arterial reactivity. *Shengli Xuebao* 2001; **53**: 478-482
- 29 **Gu ZY**. Peroxynitrite-mediated pulmonary vascular injury induced by endotoxin and the protective role of cholecystokinin. *Shengli Kexue Jinzhan* 2001; **32**: 135-137
- 30 **Tobias PS**, Tapping RI, Gegner JA. Endotoxin interactions with lipopolysaccharide-responsive cells. *Clin Infect Dis* 1999; **28**: 476-481
- 31 **Salomao R**, Rigato O, Pignatari AC, Freudenberg MA, Galanos C. Bloodstream infections: epidemiology, pathophysiology and therapeutic perspectives. *Infection* 1999; **27**: 1-11
- 32 **Li SJ**, Cong B, Yan YL, Yao YX, Ma CL, Ling YL. Cholecystokinin octapeptide inhibits the *in vitro* expression of CD14 in rat pulmonary interstitial macrophages induced by lipopolysaccharide. *Chin Med J (English Issue)* 2002; **115**: 276-279
- 33 **Cong B**, Li SJ, Yao YX, Zhu GJ, Ling YL. Effect of cholecystokinin octapeptide on tumor necrosis factor α transcription and nuclear factor- κ B activity induced by lipopolysaccharide in rat pulmonary interstitial macrophages. *World J Gastroenterol* 2002; **8**: 718-723
- 34 **De la Fuente M**, Campos M, Del Rio M, Hernanz A. Inhibition of murine peritoneal macrophage functions by sulfated cholecystokinin octapeptide. *Regul Pept* 1995; **55**: 47-56
- 35 **De la Fuente M**, Medina S, Del Rio M, Ferrandez MD, Hernanz A. Effect of aging on the modulation of macrophage functions by neuropeptides. *Life Sci* 2000; **67**: 2125-2135

Effect of caffeic acid phenethyl ester on proliferation and apoptosis of hepatic stellate cells *in vitro*

Wen-Xing Zhao, Jing Zhao, Chong-Li Liang, Bing Zhao, Rong-Qing Pang, Xing-Hua Pan

Wen-Xing Zhao, Jing Zhao, Chong-Li Liang, Bing Zhao, Rong-Qing Pang, Xing-Hua Pan, Medical Laboratory of Kunming General Hospital, Chengdu Command, Kunming 650032, Yunnan Province, China

Supported by Natural Science Foundation of Yunnan Province for Younth, No. 1999C0034Q, No. 2000C0031Q

Correspondence to: Dr. Wen-Xing Zhao, Medical Laboratory of Kunming General Hospital, Chengdu Command, 212 Dagan Road, Kunming 650032, Yunnan Province, China. zwx-zzh@sohu.com

Telephone: +86-871-4074771 **Fax:** +86-871-4074771

Received: 2002-12-07 **Accepted:** 2003-01-08

Abstract

AIM: To investigate the role of nuclear factor- κ B (NF- κ B) inhibitor caffeic acid phenethyl ester (CAPE) in the proliferation, collagen synthesis and apoptosis of hepatic stellate cells (HSCs) of rats.

METHODS: The HSCs from rats were isolated and cultured in Dulbecco's Modified Eagle's Medium (DMEM) and treated with CAPE. The proliferation and collagen synthesis of HSCs were determined by 3 H-TdR and 3 H-proline incorporation respectively, and the expression of type I, III procollagen genes was further explored by *in situ* hybridization. Apoptosis cell indices (AIs) were examined using terminal deoxynucleotidyl transferase-mediated DIG-dUTP nick end labeling (TUNEL).

RESULTS: In activated HSC in culture, CAPE significantly inhibited 3 H-TdR and 3 H-proline incorporation by HSCs at concentrations of 5 μ mol/L and 10 μ mol/L respectively. CAPE also reduced the type I procollagen gene expression ($P < 0.05$) at higher concentration. Apoptosis of HSC was induced by CAPE and the AIs were time- and dose-dependently increased from 2.82 ± 0.73 % to 7.66 ± 1.25 % at 12 h ($P < 0.01$) and from 3.15 ± 0.88 % to 10.61 ± 2.88 % at 24 h ($P < 0.01$).

CONCLUSION: CAPE inhibits proliferation and collagen synthesis of HSC at lower concentration and induces HSC apoptosis at higher concentration.

Zhao WX, Zhao J, Liang CL, Zhao B, Pang RQ, Pan XH. Effect of caffeic acid phenethyl ester on proliferation and apoptosis of hepatic stellate cells *in vitro*. *World J Gastroenterol* 2003; 9 (6): 1278-1281

<http://www.wjgnet.com/1007-9327/9/1278.asp>

INTRODUCTION

Liver fibrosis is a progressive pathological process involving multi-cellular and molecular events that ultimately lead to deposition of excess matrix proteins in the extracellular space. It is generally accepted that HSC is the most pathogenetically relevant cell type for the development of liver fibrosis^[1-5]. During liver injury and inflammation, quiescent HSCs transdifferentiate into activated-type HSCs, also termed

myofibroblasts (MFBs), which result in accumulation of a cell type that provides main collagenous and non-collagenous components of the extracellular fibrotic matrix, contribute to diminished degradation of extracellular matrix by the expression of tissue inhibitors of metalloproteinases (TIMPs) and also produce an array of proinflammatory cytokines and chemokines involving the development of liver fibrosis^[3-11].

It has recently been shown that the recovery from established experimental fibrosis can occur through the apoptosis of HSC, which is associated with reduction of collagen and expression of TIMPs in liver. Apoptosis, therefore, plays an important role in the resolution of fibrosis by eliminating the sources of both the neomatrix and TIMPs, and thereby facilitates net matrix degradation^[12-15]. Activation and apoptosis of HSCs could play a central role in turnover of liver fibrosis.

Recent research showed that cultured HSC underwent a rapid and persistent induction of a high-mobility NF- κ B DNA binding complex, and the activation of NF- κ B in cultured HSC was required for activated phenotype of HSCs and might be anti-apoptotic for HSCs^[16-19]. In this study, we investigated the effect of NF- κ B inhibitor CAPE on the proliferation, collagen synthesis and apoptosis of HSCs.

MATERIALS AND METHODS

Materials

Wistar rats, male, 450-500 g of body mass, were provided by the Center for Laboratory Animal of Kunming General Hospital. DMEM and FBS were obtained from GIBCO. CAPE and collagenase were purchased from SIGMA, 3 H-TdR and 3 H-proline were provided by Beijing Institute of Atomic Energy, RNA Mimi Kit and DIG DNA Labeling and Detecting Kit were respectively obtained from Gene and Boehringer Mannheim.

Methods

Isolation and culture of HSCs HSCs were isolated from normal liver by sequential *in situ* perfusion with collagenase, as previously described^[20,21]. Briefly, the livers were perfused first with Ca^{2+} - and Mg^{2+} - free solution for 10 min at 37 °C, and next with 0.05 % (w/v) collagenase solution for 30 min at 37 °C, the digested liver were excised, dispersed in D-Hanks, and filtered through gauze. The residual hepatocytes were removed by two low-speed centrifugation (50 g, 4 °C, 2 min). The stellate-cell enriched fraction was obtained by centrifugation with a triple-layered (9, 11, and 17 %) Nycodenz cushion (1 400 \times g, 4 °C 20 min). The cells in the upper-layer were washed and seeded onto uncoated plastic tissue culture plate in DMEM supplemented with 10 % FBS and grown for 14 days. Purity and viability of freshly isolated HSC were determined by Desmin immunohistochemistry and trypan-blue stain respectively.

3 H-TdR and 3 H-proline uptake by HSC Passaged HSCs were cultured in 24-well plates for 48 h and then treated with CAPE at concentrations of 0.0, 1.0, 2.5, 5.0, 10.0, 20.0, and 40.0 μ mol/L for 24 h. CAPE was dissolved in DMSO. The cells were then labeled with 1 μ ci/ml 3 H-TdR or 1 μ ci/ml 3 H-proline

respectively. After washed with D-Hanks, the HSCs were digested with trypsin and absorbed on glass fiber filter paper. The cells were then washed once with 10 % trichloroacetic acid and three times with saline and dried overnight at 80 °C, the radioactivity (CPM) of each sample was counted using liquid-scintillation analyzer.

Expression of procollagen gene in HSC Type I and III procollagen gene sequences were enquired from GeneBank of National Center of Biotechnology Information, and primers that amplified the procollagen genes were designed with OLIGO microsoft according to the gene sequences and synthesized by Sangon Company. The primers were 5' -CGA TGG ATT CCC GTT CGA GTA C-3' and 5' -GTC CAC AAC CCT GTA GGT G-3' for type I procollagen gene, 5' -GGA AAC AGC AAA TTC ACT TAC A-3' and 5' -TCA CTT GCA CTG GTT GAT AAG A-3' for type III procollagen gene. The RNA was extracted from the skin of newborn ICR mice by RNA mini kit, the genes were amplified by RT-PCR and procollagen gene probes were labeled with PCR and DIG-dUTP. HSCs cultured in 24-well plates were treated with 20 μmol/L CAPE for 24 h and the procollagen gene expression was detected according to the previously described procedure^[22].

Apoptosis assay Passaged HSCs were cultured for 48 h and then cultured in 5 % FBS DMEM and treated with CAPE at predetermined concentrations of 0.0, 20.0, and 40.0 μmol/L for 12 h and 24 h, the cells were fixed in formaldehyde solution and stained with TUNEL reaction solution containing DIG-dUTP and terminal deoxynucleotide transferase for 60 min at 37 °C. DIG was detected by anti-DIG-AP conjugate and colorimetric substrate NBT/BCIT. Positive cells were counted under microscope.

RESULTS

Characteristics of HSCs

Freshly isolated HSCs were round-shaped with many yellow-coloured droplets in cytoplasm, after 2-3 days in culture on uncoated plastic surface, the cells had spread and showed a typical 'star'-like configuration. More than 80 % of freshly isolated cells were desmin-positive, and the cell viability was about 90 % according to trypan-blue staining.

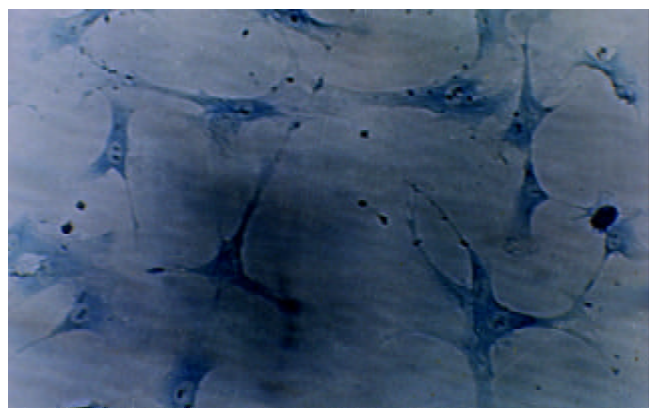


Figure 1 The hepatic stellate cells stained with toluidine after cultured for 10 days after isolation ($\times 66$).

Effect of CAPE on ^3H -TdR and ^3H -proline incorporation by HSC

We observed the effect of CAPE on ^3H -TdR and ^3H -proline incorporation by cultured HSCs. As shown in Figure 2, CAPE significantly and dose-dependently suppressed the incorporation of ^3H -TdR and ^3H -proline by HSCs. The median inhibitory concentrations were 5 and 10 μmol/L respectively for ^3H -TdR and ^3H -proline. These concentrations were lower, especially for the inhibition of HSCs proliferation, indicating

that CAPE was a potent inhibitor for proliferation, and collagen synthesis.

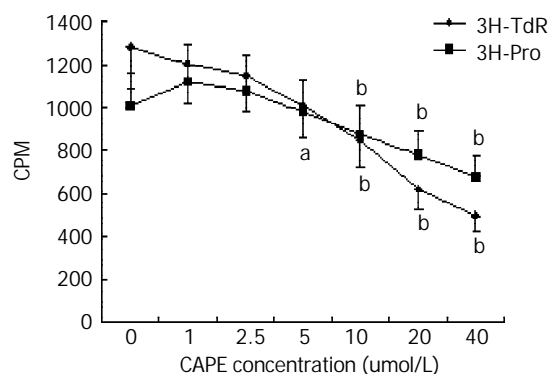


Figure 2 Effects of CAPE on ^3H -TdR and ^3H -proline uptake by HSCs. ^a $P < 0.05$; ^b $P < 0.01$ vs groups without CAPE treatment.

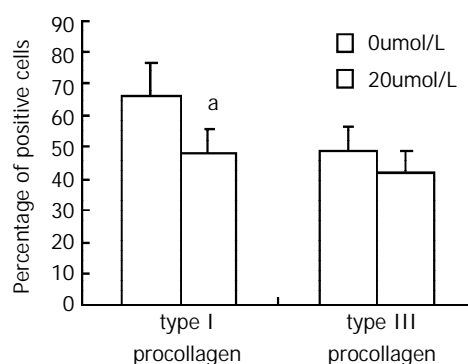


Figure 3 Effect of CAPE on type I and III procollagen gene expression. ^a $P < 0.05$ vs the group without CAPE treatment.

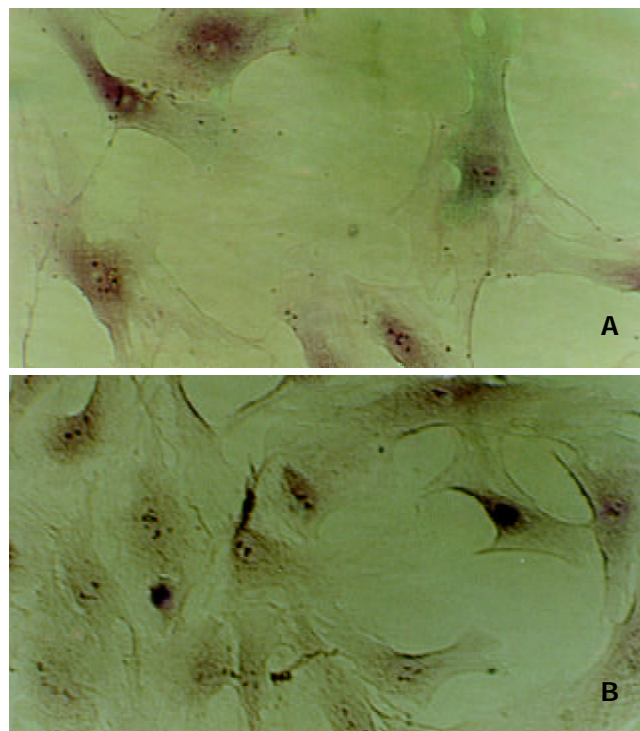


Figure 4 Apoptotic HSCs detected by TUNEL without (A) or with 40 μmol/L CAPE treatment (B).

Effects of CAPE on procollagen gene expression

Type I and III collagens are the main components of extracellular matrix in liver fibrosis. *In situ* hybridization

analysis of type I and III procollagen genes showed that positive HSCs were reduced by CAPE at the concentration of 20 $\mu\text{mol/L}$. And the reduction of type I procollagen gene expression was statistically significant, indicating that CAPE suppressed the procollagen gene expression.

Apoptosis of HSC induced by CAPE

Apoptosis of HSC was demonstrated by TUNEL, the nucleus of apoptotic HSCs were stained with violet blue (Figure 4). After treatment with CAPE, AIs were time- and dose-dependently increased from $2.82 \pm 0.73\%$ to $7.66 \pm 1.25\%$ at 12h and from $3.15 \pm 0.88\%$ to $10.61 \pm 2.88\%$ at 24 h. The data indicated that CAPE induced HSC apoptosis at higher concentrations (Figure 5).

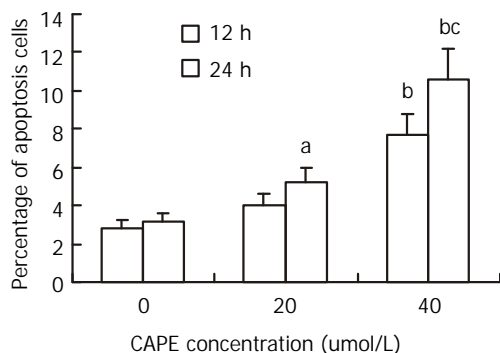


Figure 5 Effects of CAPE on HSC apoptosis. ^a $P < 0.05$; ^b $P < 0.01$ vs the groups without CAPE treatment; ^c $P < 0.01$ vs the group with 40 $\mu\text{mol/L}$ CAPE treated for 12 h.

DISCUSSION

HSCs, previously termed as fat or vitamin A-storing cells or Ito cells, localized in close proximity to sinusoidal endothelial cell and hepatocyte in the space of Disse, are the most pathogenetically relevant cell type for development of liver fibrosis^[2-5]. Activated HSCs in liver tissue provide virtually most main components of ECM, contribute to diminished degradation of ECM by expressing TIMPs, and produce an array of proinflammatory cytokines and chemokines involving the development of liver fibrosis^[3-11]. It is generally accepted that HSCs are important target cells for the treatment of liver fibrosis^[5,23].

In our study, we observed that the NF- κB inhibitor CAPE inhibited the proliferation and collagen synthesis of HSCs. CAPE dose-dependently suppressed the incorporation of ^3H -TdR and ^3H -proline by HSCs. This indicated CAPE inhibited the proliferation of HSCs. Because the reduction of either total cell number or collagen synthesis may contribute to the reduction of ^3H -proline incorporation by HSCs, the expressions of type I and type III procollagen genes were further explored in HSCs. Our data showed that the procollagen gene expressions were reduced by CAPE, and the reduction of ^3H -proline uptake partially indicated that CAPE inhibited collagen synthesis, in addition to the reduction of HSC number.

CAPE, a structural relative of flavonoids that is an active component of propolis from honeybee hives, has been shown to inhibit the growth of different types of cells including endothelial cells, keratinocyte and tumor cells, which involves in nuclear factor, protein kinase C and cytokine signal transduction^[24-29]. CAPE inhibited the proliferation and collagen synthesis of HSCs, properly by reducing the reactive oxygen intermediates, this is consistent with the antioxidant property of CAPE^[30,31]. Previous studies showed that reactive oxidant species induced HSCs activation and collagen gene expression *in vivo* and *in vitro*^[32-35]. The antioxidant phenolic

compounds reduced the proliferation and collagen synthesis by suppressing inositol phosphate metabolism, tyrosine and protein kinase activation^[33,36]. Since CAPE is a structural relative of flavonoids, CAPE probably inhibits the proliferation and collagen synthesis of HSCs similarly. Other mechanisms might include inhibition of the expression of COX2 and activation of NF- κB by CAPE, which are associated with the phenotype of activated HSCs^[37,38].

Activated HSCs undergo auto-apoptosis in serum-deprived DMEM and in experimental fibrosis induced by CCl_4 . P^{75} and Fas have already been identified as molecules associated with the apoptosis of HSCs, which were expressed in HSCs. Apoptosis of HSCs can be induced by nerve growth factor and soluble Fas-ligand^[39,40]. The recovery from established experimental fibrosis is relevant to the apoptosis of HSCs, which contributes to the reduction of neomatrix synthesis and expression of TIMPs. Recent reports showed the persistent activation of NF- κB was induced in activated but not in quiescent HSCs, which is required for activated phenotype of HSCs and may be antiapoptotic for HSCs^[16-18]. CAPE is a potent and specific inhibitor of NF- κB , CAPE inhibits the activation of NF- κB induced by TNF and other inflammatory agents including phorbol ester, ceramide, hydrogen peroxide, *etc*^[41]. Our data showed the AIs of HSCs were increased by CAPE, the inhibition of NF- κB activation by CAPE probably played a key role in HSC apoptosis. CAPE inhibited the activation of NF- κB and the expression of proinflammatory cytokines TNF- α and IL-1 β ; CAPE also induced apoptosis in macrophages^[42], similar results were observed in leucocytes as well^[43]. However, CAPE induced apoptosis of tumor cells by regulating the expression of caspas-3, bcl-2, bax and P^{53} ^[44-46]. For HSCs, the mechanism of apoptosis induced by CAPE needs further investigation.

CAPE has been shown to be a pharmacologically safe compound with known antiinflammatory, antimutagenic, anticarcinogenic, antioxidant, and immunomodulatory effects^[37,47]. Therefore, CAPE might have a therapeutic role in liver fibrosis by inhibiting the proliferation or inducing the apoptosis of HSCs.

REFERENCES

- Brenner DA, Waterboer T, Choi SK, Lindquist JN, Stefanovic B, Burchardt E, Yamauchi M, Gillan A, Rippe RA. New aspects of hepatic fibrosis. *J Hepatol* 2000; **32**(Suppl 1): 32-38
- Benyon RC, Iredale JP. Is liver fibrosis reversible. *Gut* 2000; **46**: 443-446
- Rockey DC. The cell and molecular biology of hepatic fibrogenesis. Clinical and therapeutic implications. *Clin Liver Dis* 2000; **4**: 319-355
- Arthur MJ. Fibrogenesis II. Metalloproteinases and their inhibitors in liver fibrosis. *Am J physiol Gastrointest liver Physiol* 2000; **279**: G245-249
- Bataller R, Brenner DA. Hepatic stellate cells as a target for the treatment of liver fibrosis. *Semin Liver Dis* 2001; **21**: 437-451
- Yao XX, Tang YW, Yao DM, Xiu HM. Effects of Yigan Decoction on proliferation and apoptosis of hepatic stellate cells. *World J Gastroenterol* 2002; **8**: 511-514
- Reeves HL, Friedman SL. Activation of hepatic stellate cells-a key issue in liver fibrosis. *Front Biosci* 2002; **7**: d808-826
- Gressner AM. The up and down of hepatic stellate cells in tissue injury: apoptosis restore cellular homeostasis. *Gastroenterology* 2001; **120**: 1285-1287
- Wang JY, Zhang QS, Guo JS, Hu MY. Effects of glycyrrhetic acid on collagen metabolism of hepatic stellate cells at different stages of liver fibrosis in rats. *World J Gastroenterol* 2001; **7**: 115-119
- Marra F. Chemokines in liver inflammation and fibrosis. *Front Biosci* 2002; **7**: d1899-1914
- Gressner AM. The cell biology of liver fibrosis-an imbalance of proliferation, growth arrest and apoptosis of myofibroblasts. *Cell Tissue Res* 1998; **292**: 447-454

- 12 **Benyon RC**, Arthur MJ. Extracellular matrix degradation and the role of hepatic stellate cells. *Semin Liver Dis* 2001; **21**: 373-384
- 13 **Issa R**, Williams E, Trim N, Kendall T, Arthur MJ, Reichen J, Benyon RC, Iredale JP. Apoptosis of hepatic stellate cells: involvement in resolution of biliary fibrosis and regulation by soluble growth factors. *Gut* 2001; **48**: 548-557
- 14 **Wright MC**, Issa R, Smart DE, Trim N, Murray GI, Primrose JN, Arthur MJ, Iredale JP, Mann DA. Gliotoxin stimulates the apoptosis of human and rat hepatic stellate cells and enhances the resolution of liver fibrosis in rats. *Gastroenterology* 2001; **121**: 685-698
- 15 **Liu XJ**, Yang L, Mao YQ, Wang Q, Huang MH, Wang YP, Wu HB. Effects of the tyrosine protein kinase inhibitor genistein on the proliferation, activation of cultured rat hepatic stellate cells. *World J Gastroenterol* 2002; **8**: 739-745
- 16 **Hellerbrand C**, Jobin C, Licato LL, Sartor RB, Brenner DA. Cytokines induced NF- κ B in activated but not in quiescent rat hepatic stellate cells. *Am J Physiol* 1998; **275**: G269-278
- 17 **Saile B**, Matthes N, El Armouche H, Neubauer K, Ramadori G. The bcl, NF κ B and p53/p21WAF1 systems are involved in spontaneous apoptosis and in the anti-apoptotic effect of TGF- β or TNF- α on activated hepatic stellate cells. *Eur J Cell Biol* 2001; **80**: 554-561
- 18 **Elsharkawy AM**, Wright MC, Hay RT, Arthur MJ, Hughes T, Bahr MJ, Degitz K, Mann DA. Persistent activation of nuclear factor- κ B in cultured rat hepatic stellate cells involves the induction of potentially novel Rel-like factors and prolonged changes in the expression of I κ B family proteins. *Hepatology* 1999; **30**: 761-769
- 19 **Murphy FR**, Issa R, Zhou X, Ratnarajah S, Nagase H, Arthur MJ, Benyon C, Iredale JP. Inhibition of apoptosis of activated hepatic stellate cells by tissue inhibitor of metalloproteinase-1 is mediated via effects on matrix metalloproteinase inhibition: implications for reversibility of liver fibrosis. *J Biol Chem* 2002; **277**: 11069-11076
- 20 **Kawada N**, Klein H, Decker K. Eicosanoid-mediated contractility of hepatic stellate cells. *Biochem J* 1992; **285**: 367-371
- 21 **Zhou Y**, Shimizu I, Lu G, Itonaga M, Okamura Y, Shono M, Honda H, Inoue S, Muramatsu M, Ito S. Hepatic stellate cells contain the functional estrogen receptor beta but not the estrogen receptor alpha in male and female rats. *Biochem Biophys Res Commun* 2001; **286**: 1059-1065
- 22 **Zhao W**, Liang C, Chen Z, Pang R, Zhao B, Chen Z. Luteolin inhibits proliferation and collagen synthesis of hepatic stellate cells. *Zhonghua Ganzhangbing Zazhi* 2002; **10**: 204-206
- 23 **Beljaars L**, Meijer DK, Poelstra K. Targeting hepatic stellate cells for cell-specific treatment of liver fibrosis. *Front Biosci* 2002; **7**: e214-222
- 24 **Song YS**, Park EH, Jung KJ, Jin C. Inhibition of angiogenesis by propolis. *Arch Pharm Res* 2002; **25**: 500-504
- 25 **Maffia P**, Ianaro A, Pisano B, Borrelli F, Capasso F, Pinto A, Ialenti A. Beneficial effects of caffeic acid phenethyl ester in a rat model of vascular injury. *Br J Pharmacol* 2002; **136**: 353-360
- 26 **Mahmoud NN**, Carothers AM, Grunberger D, Bilinski RT, Churchill MR, Martucci C, Newmark HL, Bertagnolli MM. Plant phenolics decrease intestinal tumors in an animal model of familial adenomatous polyposis. *Carcinogenesis* 2000; **21**: 921-927
- 27 **Zheng ZS**, Xue GZ, Grunberger D, Prystowsky JH. Caffeic acid phenethyl ester inhibits proliferation of human keratinocytes and interferes with the EGF regulation of ornithine decarboxylase. *Oncol Res* 1995; **7**: 445-452
- 28 **Usia T**, Banskota AH, Tezuka Y, Midorikawa K, Matsushige K, Kadota S. Constituents of Chinese propolis and their antiproliferative activities. *J Nat Prod* 2002; **65**: 673-676
- 29 **Huleihel M**, Ishano V. Effect of propolis extract on malignant cell transformation by moloney murine sarcoma virus. *Arch Virol* 2001; **146**: 1517-1526
- 30 **Uz E**, Sogut S, Sahin S, Var A, Ozyurt H, Gulec M, Akyol O. The protective role of caffeic acid phenethyl ester (CAPE) on testicular tissue after testicular torsion and detorsion. *World J Urol* 2002; **20**: 264-270
- 31 **Son S**, Lewis BA. Free radical scavenging and antioxidative activity of caffeic acid amide and ester analogues: structure-activity relationship. *J Agric Food Chem* 2002; **50**: 468-472
- 32 **Greenwel P**, Dominguez-Rosales JA, Mavi G, Rivas-Estilla AM, Rojkind M. Hydrogen peroxide: a link between acetaldehyde-elicited alpha1(I) collagen gene up-regulation and oxidative stress in mouse hepatic stellate cells. *Hepatology* 2000; **31**: 109-116
- 33 **Kawada N**, Seki S, Inoue M, Kuroki T. Effect of antioxidants, reveratrol, quercetin and N-acetylcysteine, on the functions of cultured rat hepatic stellate cells and kupffer cells. *Hepatology* 1998; **27**: 1265-1274
- 34 **Svegliati-Baroni G**, Saccomanno S, van Goor H, Jansen P, Benedetti A, Moshage H. Involvement of reactive oxygen species and nitric oxide radicals in activation and proliferation of rat hepatic stellate cells. *Liver* 2001; **21**: 1-12
- 35 **Poli G**. Pathogenesis of liver fibrosis: role of oxidative stress. *Mol Aspects Med* 2000; **21**: 49-98
- 36 **Nagaoka T**, Banskota AH, Tezuka Y, Saiki I, Kadota S. Selective antiproliferative activity of caffeic acid phenethyl ester analogues on highly liver-metastatic murine colon 26-L5 carcinoma cell line. *Bioorg Med Chem* 2002; **10**: 3351-3359
- 37 **Gallois C**, Habib A, Tao J, Moulin S, Maclouf J, Mallat A, Lotersztajn S. Role of NF- κ B in the antiproliferative effect of endothelin-1 and tumor necrosis factor- α in human hepatic stellate cells. *J Biol Chem* 1998; **273**: 23183-23190
- 38 **Cheng J**, Imanishi H, Liu W, Iwasaki A, Ueki N, Nakamura H, Hada T. Inhibition of the expression of alpha-smooth muscle actin in human hepatic stellate cell line, LI90, by a selective cyclooxygenase 2 inhibitor, NS-398. *Biochem Biophys Res Commun* 2002; **297**: 1128-1134
- 39 **Trim N**, Morgan S, Evans M, Issa R, Fine D, Afford S, Wilkins B, Iredale J. Hepatic stellate cells express the low affinity nerve growth factor receptor p75 and undergo apoptosis in response to nerve growth factor stimulation. *Am J Pathol* 2000; **156**: 1235-1243
- 40 **Gong W**, Pecci A, Roth S, Lahme B, Beato M, Gressner AM. Transformation-dependent susceptibility of rat hepatic stellate cells to apoptosis induced by soluble Fas ligand. *Hepatology* 1998; **28**: 492-502
- 41 **Natarajan K**, Singh S, Burke TR Jr, Grunberger D, Aggarwal BB. Caffeic acid phenethyl ester is a potent and specific inhibitor of activation of nuclear transcription factor NF- κ B. *Pro Natl Acad Sci USA* 1996; **93**: 9090-9095
- 42 **Lu B**, Wang L, Medan D, Toledo D, Huang C, Chen F, Shi X, Rojanasakul Y. Regulation of Fas (CD95)-induced apoptosis by nuclear factor-kappaB and tumor necrosis factor-alpha in macrophages. *Am J Physiol Cell Physiol* 2002; **283**: C831-838
- 43 **Orban Z**, Mitsiades N, Burke TR Jr, Tsokos M, Chrousos GP. Caffeic acid phenethyl ester induces leukocyte apoptosis, modulates nuclear factor-kappa B and suppresses acute inflammation. *Neuroimmunomodulation* 2000; **7**: 99-105
- 44 **Nomura M**, Kaji A, Ma W, Miyamoto K, Dong Z. Suppression of cell transformation and induction of apoptosis by caffeic acid phenethyl ester. *Mol Carcinog* 2001; **31**: 83-89
- 45 **Chen YJ**, Shiao MS, Hsu ML, Tsai TH, Wang SY. Effect of caffeic acid phenethyl ester, an antioxidant from propolis, on inducing apoptosis in human leukemic HL-60 cells. *J Agric Food Chem* 2001; **49**: 5615-5619
- 46 **Chen YJ**, Shiao MS, Wang SY. The antioxidant caffeic acid phenethyl ester induces apoptosis associated with selective scavenging of hydrogen peroxide in human leukemic HL-60 cells. *Anticancer Drugs* 2001; **12**: 143-149
- 47 **Isla MI**, Nieva-Moreno MI, Sampietro AR, Vattuone MA. Antioxidant activity of argentine propolis extracts. *J Ethnopharmacol* 2001; **76**: 165-170

Isolation and analysis of a novel gene over-expressed during liver regeneration

Yu-Chang Li, Cun-Shuan Xu, Wu-Lin Zhu, Wen-Qiang Li

Yu-Chang Li, Cun-Shuan Xu, Wen-Qiang Li, College of Life Science, Henan Normal University, Xinxiang 453002, Henan Province, China

Wu-Lin Zhu, Xinxiang Medical College, Xinxiang 453002, Henan Province, China

Supported by a grant from Key Scientific and Technical Problem of Henan Province No.0122031900

Correspondence to: Dr. Yu-Chang Li, College of Life Science, Henan Normal University, Xinxiang 453002, Henan Province, China. ycli_us@yahoo.com

Telephone: +86-373-3328084 **Fax:** +86-373-3326609

Received: 2002-12-05 **Accepted:** 2003-03-03

Abstract

AIM: To isolate and analyze a novel gene over-expressed during liver regeneration.

METHODS: Total RNA of regenerating liver was extracted from liver tissue after 0-4-36-36-36 hr short interval successive partial hepatectomy (SISPH). Reverse transcription-polymerase chain reaction was used to synthesize double strand cDNA, after the tissue was digested by proteinase K and Sfi A/B. The double-strand cDNA was ligated to λ TriplEx2. λ phage packaging reaction was performed and *E. coli* XL1-Blue was infected for titering and amplifying. One expressed sequence tag was probed by Dig and phage *in situ* hybridization was carried out to isolate positive clones. Positive recombinant λ TriplEx2 was converted to the corresponding pTriplEx2, and bioinformatics was used to analyze full-length cDNA.

RESULTS: We isolated a novel full-length cDNA during liver regeneration following SISPH.

CONCLUSION: We have succeeded in cloning a novel gene, based on bioinformatics. We postulate that this gene may function in complicated network in liver regeneration. On the one hand, it may exert initiation of liver regeneration via regulating nitric oxide synthesis. On the other hand, it may protect damaged residue lobus following SISPH.

Li YC, Xu CS, Zhu WL, Li WQ. Isolation and analysis of a novel gene over-expressed during liver regeneration. *World J Gastroenterol* 2003; 9(6): 1282-1286

<http://www.wjgnet.com/1007-9327/9/1282.asp>

INTRODUCTION

Liver regeneration is a system suitable for investigating normally regulated growth^[1-4]. After surgical removal of 70 % of the mass of a healthy liver (two-thirds hepatectomy), residual tissue enlarges to make up for the mass of removed substance in entirety, in small animals, this process usually lasts 5 to 7 days^[5-7].

The growth response after partial hepatectomy is governed by priming and progression through the cell cycle^[2,6,8]. The

priming phase coincides with loss of growth inhibition and represents the G₀ to G₁ transition, whereas the progression phase acts on promoting cell replication and represents the G₁ to S transition. Priming involves the activation of a group of non-specific factors, which are necessary, but not sufficient for the S phase completion; they comprise the nuclear factor for kappa chains (NF- κ) in B cells, signal transducer and activator of transcription-3 (STAT3), activator protein-1 (AP-1), CCAAT enhancer binding protein, and several immediate early genes like epithelial growth factor (EGF), tumor necrosis factor-alpha (TNF- α , IL-6), insulin, and matrix changes^[9-15]. The priming step is reversible until the cells have crossed the so-called G₁ checkpoint, the cells thereupon being irreversibly committed for replication. Moreover, the initiation of the growth response depends on complex interactions among hepatocytes and nonparenchymal cells, the extracellular matrix (ECM), endocrine, autocrine, paracrine, and neuroregulatory factors, oxygen free radicals, metabolites, and nutrients^[2,6,9,16]. Progression signals include hepatocyte growth factor (HGF), transforming growth factor-alpha (TGF- α), EGF and insulin. The regulation of hepatic regenerative process depends on a number of myriad factors that ultimately modulate immediate-early, delayed-early, and liver-specific gene expression^[2,6,9,17-20].

The termination of hepatic regeneration still remains an enigma. A variety of factors have been touted as growth inhibitors/terminators during the regenerative response once recovery of the liver mass has been achieved. TGF- β and activins are regarded as potent inhibitors involved in the termination response^[21,22]. TGF- β is a fibrogenic cytokine secreted by hepatic stellate cells, TGF- β mRNA, almost undetectable in normal liver, increases within 3-4 h after partial hepatectomy, and attains a plateau after 48-72 h. TGF- β 1 overexpression in transgenic mice inhibits the abundance of the cyclin-dependent kinase activating tyrosine phosphatase cdc25A protein, and is associated with increased binding of histone deacetylase 1 to p130 in the liver^[23]. Activin A (the homodimer of the inhibin β A chain) inhibits but follistatin (anactivin-binding protein) promotes hepatocyte proliferation. Whereas activin A is a negative regulator of hepatocyte proliferation, mice deficient in both activin β C and activin β E, are not different from wild-type mice with respect to liver development and the regenerative response after partial hepatectomy. The activin system also plays a significant role in the dynamics of the ECM, in particular fibronectin; ECM components are reconstructed during desinualization and hepatocyte cluster formation. After rat liver injury and partial hepatectomy, hepatocyte activin A receptors are down-regulated at 24 hr and normalized at 72 hr. This phenomenon may be involved in rendering hepatocytes responsive to mitogenic stimuli, whereas increased activin A levels stimulate stellate cell production of fibronectin, important for the growth and proper placement of regenerating hepatocytes^[24].

Despite the research efforts, our knowledge on the regulatory mechanisms of cell growth, differentiation and tissue organization is limited. There may be some unknown factors that may play important roles in the process of liver regeneration. To acquire a better understanding on the

mechanisms involved, some researchers have established a series of successive partial hepatectomy (SPH) models. These mainly include the long interval successive partial hepatectomy (LISPH) in which an interval of more than three weeks is applied as described by Wu *et al.*, the SPH model where a one-third hepatectomy 2 weeks after a two-thirds hepatectomy is performed as described by Takeshi *et al.*^[25], and the short interval successive partial hepatectomy (SISPH) model (0-4-40-76-112 hr) which has an interval of 4 and/or 36 h because the cells would re-enter into dedifferentiation stage after 4 hr and reach the peak of cell division after 36 hr following partial hepatectomy as described by Xu *et al.*^[26]. Studies have demonstrated that SISPH could provide more useful materials for analyzing the mechanism of liver regeneration^[27]. We have begun identifying and characterizing some genes that are strongly expressed in liver regeneration. We took 0 h and 112 hr as driver and tester respectively in 0-4-36-36-36hr SISPH model and a suppression subtracted hybridization (SSH) method was performed^[28-30]. Then we constructed a forward-subtractive cDNA library from which we have cloned 53 up-regulated expressed sequence tags (ESTs). Among these, nine ESTs were 100 % homologous to GenBank and 44 ESTs were homologous to GenBank. one of these ESTs was found to be a novel gene in GenBank. In the present study, we have used one subtracted probe from suppression subtracted library in liver regeneration and isolated its full-length cDNA from cDNA library by the phage *in situ* hybridization method. Based on bioinformatics, we suggest that it might play important roles in the regulation of initiation of liver regeneration.

MATERIALS AND METHODS

Establishment of the SISPH model

Adult Spargue-Dawley rats (weighing 200-250 g) were provided by the Experimental Animal House of Henan Normal University, and the 0-4-36-36-36 hr SISPH model was made according to the method described by Xu *et al.*^[26]. Lobus external sinister and lobus centralis sinister, lobus centralis, lobus dexter and lobus candatus were removed one by one at four different time points, i.e. at 4, 36, 36 and 36 hr (total time: 4 hr, 40 hr, 76 hr, 112 hr), respectively. The fourth resected liver lobus was washed with precooled phosphate- buffered saline (PBS) thoroughly, then the sample was frozen in liquid nitrogen and transferred to the -80 °C freezer for storage.

Primers

A1: 5'-ATTCTAGAGGCCGAGCGGCCGACATG-d (T)₃₀N-3'
 A2: 5'-AAGCAGTFFTATCAACGCAGAGT-3'
 A3: 5'-TCGAGCGGCCCGCCGGCAGGT-3'
 A4: 5'-AGCGTGGTCGCGCCGAGGT-3'
 A5: 5'-TCCGAGATCTGGACGAGC-3'
 A6: 5'-TAATACGACTCACTATAGGG-3'

Among these primers, A1 was used for synthesis of first cDNA strand, A1/A2 were used to amplify cDNA, A3/A4 were used to probe expressed sequence tag with Dig, A5/A6 were used to detect full length cDNA.

RNA Isolation

Total RNA was isolated from 112 h liver tissue samples following SISPH by the method described by Chomczynski and Sacchi^[31]. Tissues were homogenized and extracted twice with acidic guanidinium isothiocyanate-phenol-chloroform. The poly(A)⁺ RNA fraction was isolated by oligo-dT cellulose chromatography (Pharmacia Diagnostics AB, Uppsala, Sweden). The purity and integrity of total RNA were monitored by absorbance of ultraviolet spectrometer at 260/280 nm, and electrophoresis was carried out on a denaturing formaldehyde agarose gel and the gel was stained with ethidium bromide.

RT-PCR

300 ng mRNA was reversely transcribed to single-stranded cDNA by Powerscriptase at 42 °C for 1hr. First-strand cDNA was synthesized with a Sfi IB-oligo(dT) adapter-primer (A1). The resulting single strand cDNA was amplified by PCR using CDSIII/3' primer (A1) and 5' primer (A2) following parameters: 94 °C for 45 s, 68 °C for 6 min.

cDNA library construction

The double strand cDNA synthesis and library construction were carried out mainly according to the manual of SMART cDNA Library Construction Kit (Clontech, Heidelberg, Germany). After second-strand synthesis and ligation of Sfi IA adapters, cDNA was digested by Sfi IA/Sfi IB, generating cDNA flanked by Sfi IA sites at 5' ends and /Sfi IB sites at the 3' ends. Digested cDNAs were size-fractionated with Sephacryl S-500 spin columns and ligated into the λTriplEx2 express vector predigested by Sfi IA/Sfi IB. The resulting concatomers were packaged by using Gigapack Gold packaging extracts. After titration, aliquots of primary packaging mixture were stored in 7 % DMSO at -80 °C as primary library stocks. At the same time, the ratio of white (recombinant) to total (white + blue (nonrecombinant)) assay was determined^[32]. The remainder was amplified to establish stable library stocks.

Probe labeling and Phage in situ hybridization

A novel EST related to liver regeneration was probed with A3/A4 primers according to the user manual of Dig Probe Synthesis kit (Roche Diagnostics, Mannheim, Germany). Thermal cycle parameters were 94 °C for 2 min, 25 cycles including a denaturation step at 94 °C for 15sec, an annealing step at 68 °C for 30sec, extension at 72 °C for 1 min and 30sec, and a final extension step at 72 °C for 7 min. The amplified phage cDNA library was diluted in 1×λ dilution buffer to obtain a concentration of 10⁴ pfu/ml and then to infect *E. coli* XL1-Blue. Host bacterial cells were absorbed by phage at 37 °C for 15 min and the indicated volume of melted LB top agarose/MgSO₄ was added. The mixture was inverted once and poured onto a prewarmed, dry LB/MgSO₄ plate. The plate was inverted and incubated at 37 °C until plaques became distinctly visible. A nylon filter was numbered and placed onto the LB soft top agarose, then the filter was marked in three asymmetric locations. After 2 min, the filter was peeled off carefully. The filter was placed in petri dishes orderly containing DNA denaturing solution for 5 min, neutralizing solution for 5 min, or 2×SSC for 5 min. Hybridization and wash procedures were performed according to Sambrook^[33]. When positive signal appeared the process was performed as above for the secondary and tertiary screening until single clone was obtained. Then recombinant λTriplEx2 was converted to the corresponding pTriplEx2. Plasmid was extracted and sent to TaKaRa (Dalian, China) for sequencing analysis.

RESULTS

RT-PCR

The mRNA was isolated from the 112 h liver tissue following SISPH. A modified oligo (dT) primer (A1 primer) primed the first-strand synthesis reaction. The resulting single strand cDNA was amplified by PCR using CDSIII/3' primer (A1) and 5' primer (A2) derived from SMART oligonucleotide (Figure 1).

Determination of cDNA library

The unamplified library and amplified library were titered when *E. coli* XL1-Blue was infected by λphage. The plaques were counted and cDNA library was calculated respectively as

follows: pfu/ml=number of plaques × dilution × 10³ μl/ml/μl of diluted phage plated. Results showed that unamplified cDNA library and amplified library were 6 × 10⁶ pfu/ml and 6 × 10¹⁰ pfu/ml respectively. X-gal/IPTG was used to assess recombination efficiency. Among 500-1 000 plaques, the ratio of white (recombinant) to total (recombinant and blue (nonrecombinant)) was 99.52 %. These data suggest that the cDNA library was successfully established.

Screening result and bioinformatics

Figure 2 shows the tertiary positive clone screened by phage *in situ* hybridization. After conversion of a recombinant λTriplEx2 to the corresponding pTriplEx2, the tertiary positive clones were analyzed by PCR with the sequencing primers A5/A6. The length detected by electrophoresis was consistent with the sequencing result and its full length cDNA was 1 354 bp (Figure 3). We identified that its ORF region encodes 344 amino acids, its start codon AUG was in 47-49 nucleotide and its termination codon TAG was in 1 079-1 081 nucleotides, and the sequence followed by TAG was polyA (Figure 4). It was compared with other sequences in the GenBank through Internet by BLAST and found to be 98.8 % homologous to mouse arginase. The sequence has been deposited in the GenBank database (accession No. AF508019).

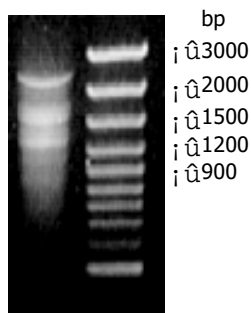


Figure 1 Gel electrophoresis of double strand cDNA. Lane 1: Double strand cDNA; lane 2: DNA mass marker.

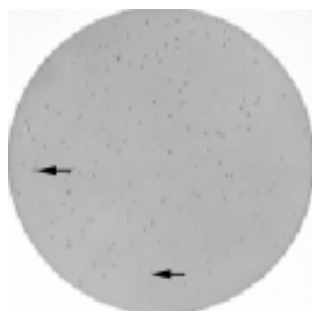


Figure 2 Tertiary screening result of positive clones. Arrows point the positive clones.

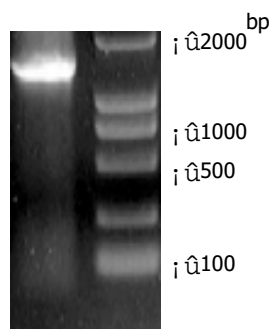


Figure 3 Detection of cDNA full length gel electrophoresis. Lane 1: 1 354bp; lane 2: DNA mass maker.

```

1 gttgcaccgagccggttctcctagggtaatccocctccctgccaatc
47 atgttcctgaggagcagcgcctccctcctccacgggcaaatt
   M F L R S S A S R L L H G Q I
92 ccttgctcctgacgagatccgtccactctgtagctatagtgga
   P C V L T R S V H S V A I V G
137 gccccctctcggggacagaagaagctaggagtggaatatggtcca
   A P S R G Q K K L G V E Y G P
182 gctgccattcgagaagctggcttgcctgaagaggctctccagggtg
   A A I R E A G L L K R L S R L
227 ggatgccacctaaaagactttggagacttgagtttactaatgtc
   G C H L K D F G D L S F T N V
272 ccacaagataatccctacaataatctggttgatcctcctgtca
   P Q D N P Y N N L V V Y P R S
317 gtgggccttgccaaccaggaactggctgaagtggtagtagagct
   V G L A N Q E L A E V V S R A
362 gtgtcagggtgctacagctgtgtcaccatgggaggagaccacagc
   V S G G Y S C V T M G G D H S
407 ctggcaataggtagcattatcggctcaccgccggcaccgccagac
   L A I G T I I G H A R H R P D
452 tgtgtcatctgggttgatgctcatgcggaattaatacacctctc
   C V I W V D A H A D I N T P L
497 gtatctggaaatatacatggacagccacttcccttctcatcaaa
   V S G N I H G Q P L S F L I K
542 gaactacaagacaaggtaccacaactgccaggattttcctggatc
   E L Q D K V P Q L P G F S W I
587 aaaccttgcctctctcccccataattgtgtacattggcctgaga
   K P C L S P P N I V Y I G L R
632 gatgtggagcctcctgaacattttatgtttatgacatccagtat
   D V E P P E H F I F Y D I Q Y
677 ttttccatgagagagattgatogacttgggatccagaagggtgatg
   F S M R E I D R L G I Q K V M
722 gaacagacatttgatcggctgattggcaaaaggcagaggccaatc
   E Q T F D R L I G K R Q R P I
767 cacctgagttttgatattgatgactttgaccctaaattggctcca
   H L S F D I D A F D P K L A P
812 gccacaggaacccctgtttaggggattaacctacagagaagga
   A T G T P V V G G L T Y R E G
857 gtgtatattactgaagaaatacataatacagggttgctgtcagct
   V Y I T E E I H N T G L L S A
902 ctggatgaagtcaatcctcatttggccacttctgaggaagaggcc
   L D E V N P H L A T S E E E A
947 aaggcaacagccagactagcagtgatgtgattgcttcaagtttt
   K A T A R L A V D V I A S S F
992 ggtcagacaagagaaggcattgtctatgaccaccttctactcct
   G Q T R E G I V Y D H L P T P
1037 agttcaccacacgaatcagaaaatgaagaatgtgtgagaatttag
   S S P H E S E N E E C V R I *
1081 GAAATACTGTACTCTGGCACCTTTCACAACAGCATTCCAGAGTTGCAAGGCAGGGACAG
1141 ATATGAAATGGCTGTCTGGATCAATATTGCCTTAATGAGAATCTGTGCACTCTCACAA
1201 CTGTAAAACCTCCTTCTCTATTTTGGTCACCAACACTGTAATGTATTTTTTGTGTTTTT
1261 TGAAGTTTACAAGCTATAATGTTATACATGTAAGTTTGAAGGAGTCATAAACAACATTT
1321 ATTACCTTAGTATATCATAAAAAAAAAAAAAAAAAA
    
```

Figure 4 The full length of cDNA and its amino acid sequence.

DISCUSSION

To understand and elucidate the mechanism of liver regeneration, we established short interval successive partial hepatectomy, and attached great importance to seeking some novel differential display genes responsible for cell differentiation and dedifferentiation by suppression subtracted hybridization (SSH) to obtain a bulk of up-regulated and down-

regulated expressed sequence tags (ESTs) in liver regeneration. In the 0-4-36-36-36h SISPH model, we took 0h and 112 hr as driver and tester respectively, and performed the SSH method. Then we constructed a forward-subtractive cDNA library from which we cloned 53 up-regulated ESTs. The 53 up-regulated ESTs may be classified as following: (1) Related to positive/negative major acute phase protein (MAPP) mRNA genes, such as serum amyloid A, transferrin, haptoglobin, alpha acid glycoprotein and fibrinogen like factor; (2) Related to mitochondrial oxidative phosphorylation genes such as ankyrin protein and mitochondrial cytochrome oxidase subunits I, II, III genes; (3) Related to protein synthesis genes such as mitochondrial ribosomal protein 63 (Mrp63); (4) Related to cell division genes, such as microtubulin associated protein (MAP); and (5) Related to signal transduction genes; for example, arginase gene may be related to NO signal pathway and regulate hepatic regeneration together with NO synthase I.

5' end cDNA is not completely reversely transcribed in constructing traditional cDNA library, which leads to some defaults in cloning full-length cDNA. In our study, we adopted a switching mechanism at 5' end of RNA transcript and successfully resolved this shortcoming. Moreover, the cDNA library we constructed may simultaneously express three open reading frames, and thus enables us to study from nucleic acid and protein aspects^[34].

Arginase is an important enzyme in ornithine cycle^[35]. In liver regeneration this enzyme is expressed highly, which may regulate the process of generating NO. Recent work has suggested that NO synthase (NOS) is necessary for liver regeneration^[36-38]. Arginase and NOS require the same substrate amino acid L-arginine, thereby they compete for the same substrate in liver regeneration^[38,39]. In our study, arginase was up-regulated, suggesting the involvement of arginase in regulating NO signal pathway.

Lepoivre *et al* proved that inducible NO could inhibit mouse DNA synthesis in hepatocellular carcinoma (HCC) *in vitro*. TA3 cell may stimulate L-arginine to produce nitrite in condition of adding IFN- γ or not adding LPS. NO affects nucleotide reductase activity by binding unferrohemoglobin, therefore, to inhibit DNA synthesis^[40]. NO may trigger phagocyte into G1 but negatively correlate with DNA synthesis of hepatocytes.

The increase of NO concentration in residue lobus following partial hepatectomy depends on gradual recovery of hepatocyte function. NO may expand vascular smooth muscle in liver to inhibit leukocyte adhesion and platelet aggregation, to improve microcirculation and reduce fat accumulation and deposition in liver accordingly. In normal state, arginine granted may enhance arginine transportation and NO synthesis by hepatocytes^[41,42]. Thereby up-regulated arginine will protect damaged liver, to some extent, following SISPH.

In conclusion, we succeeded in cloning a novel gene, based on bioinformatics. We postulate that this gene may function in complicated network in liver regeneration. On the one hand, it may exert initiation of liver regeneration via regulating NO synthesis. On the other hand, it may protect damaged residue lobus following SISPH. More detailed studies are required to clarify the biological functions of this gene in liver regeneration.

REFERENCES

- 1 **Stolz DB**, Mars WM, Petersen BE, Kim TH, Michalopoulos GK. Growth factor signal transduction immediately after two-thirds partial hepatectomy in the rat. *Cancer Res* 1999; **59**: 3954-3960
- 2 **Michalopoulos GK**, DeFrances MC. Liver regeneration. *Science* 1997; **276**: 60-66
- 3 **Fausto N**, Webber EM. Control of liver growth. *Crit Rev Eukaryot Gene Expr* 1993; **3**: 117-135
- 4 **Diehl AM**, Rai RM. Liver regeneration 3: Regulation of signal transduction during liver regeneration. *FASEB J* 1996; **10**: 215-227
- 5 **Zimmermann A**. Liver regeneration: the emergence of new pathways. *Med Sci Monit* 2002; **8**: RA53-63
- 6 **Ankoma-Sey V**. Hepatic regeneration-revisiting the myth of Prometheus. *News Physiol Sci* 1999; **14**: 149-155
- 7 **Xu CS**, Xia M, Lu AL, Li XY, Li YH, Zhao XY, Hu YH. Changes in the content and activity of HSC70/HSP68, proteinase and phosphatases during liver regeneration. *Sheng Li Xue Bao* 1999; **51**: 548-556
- 8 **Cressman DE**, Greenbaum LE, DeAngelis RA, Ciliberto G, Furth EE, Poli V, Taub R. Liver failure and defective hepatocyte regeneration in interleukin-6-deficient mice. *Science* 1996; **274**: 1379-1383
- 9 **Xia M**, Xue SB, Xu CS. Shedding of TNFR1 in regenerative liver can be induced with TNF alpha and PMA. *World J Gastroenterol* 2002; **8**: 1129-1133
- 10 **Mohn KL**, Laz TM, Melby AE, Taub R. Immediate-early gene expression differs between regenerating liver, insulin-stimulated H-35 cells, and mitogen-stimulated Balb/c 3T3 cells. Liver-specific induction patterns of gene 33, phosphoenolpyruvate carboxykinase, and the jun, fos, and egr families. *J Biol Chem* 1990; **265**: 21914-21921
- 11 **Cressman DE**, Diamond RH, Taub R. Rapid activation of the Stat3 transcription complex in liver regeneration. *Hepatology* 1995; **21**: 1443-1449
- 12 **Cressman DE**, Greenbaum LE, Haber BA, Taub R. Rapid activation of post-hepatectomy factor/nuclear factor kappa B in hepatocytes, a primary response in the regenerating liver. *J Biol Chem* 1994; **269**: 30429-30435
- 13 **Hsu JC**, Laz T, Mohn KL, Taub R. Identification of LRF-1, a leucine-zipper protein that is rapidly and highly induced in regenerating liver. *Proc Natl Acad Sci USA* 1991; **88**: 3511-3515
- 14 **Taub R**. Liver regeneration 4: transcriptional control of liver regeneration. *FASEB J* 1996; **10**: 413-427
- 15 **Block GD**, Locker J, Bowen WC, Petersen BE, Katyal S, Strom SC, Riley T, Howard TA, Michalopoulos GK. Population expansion, clonal growth, and specific differentiation patterns in primary cultures of hepatocytes induced by HGF/SF, EGF and TGF alpha in a chemically defined (HGM) medium. *J Cell Biol* 1996; **132**: 1133-1149
- 16 **Bonney RJ**, Hopkins HA, Walker PR, Potter VR. Glycolytic isoenzymes and glycogen metabolism in regenerating liver from rats on controlled feeding schedules. *Biochem J* 1973; **136**: 115-124
- 17 **Walker PR**, Potter VR. Isozyme studies on adult, regenerating, precancerous and developing liver in relation to findings in hepatomas. *Adv Enzyme Regu* 1972; **10**: 339-364
- 18 **Tsanev R**, Sendov B. A model of the regulatory mechanism of cellular multiplication. *J Theor Biol* 1966; **12**: 327-341
- 19 **Loyer P**, Glaise D, Cariou S, Baffet G, Meijer L, Guguen-Guillouzo C. Expression and activation of cdk's (1 and 2) and cyclins in the cell cycle progression during liver regeneration. *J Biol Chem* 1994; **269**: 2491-2500
- 20 **Fausto N**. Liver regeneration. *J Hepatol* 2000; **32**(Suppl 1): 19-31
- 21 **Bouzahzah B**, Fu M, Iavarone A, Factor VM, Thorgeirsson SS, Pestell RG. Transforming growth factor-beta1 recruits histone deacetylase 1 to a p130 repressor complex in transgenic mice *in vivo*. *Cancer Res* 2000; **60**: 4531-4537
- 22 **Webber EM**, FitzGerald MJ, Brown PI, Bartlett MH, Fausto N. Transforming growth factor-alpha expression during liver regeneration after partial hepatectomy and toxic injury, and potential interactions between transforming growth factor-alpha and hepatocyte growth factor. *Hepatology* 1993; **18**: 1422-1431
- 23 **Nakamura T**, Sakata R, Ueno T, Sata M, Ueno H. Inhibition of transforming growth factor beta prevents progression of liver fibrosis and enhances hepatocyte regeneration in dimethylnitrosamine-treated rats. *Hepatology* 2000; **32**: 247-255
- 24 **Lau AL**, Kumar TR, Nishimori K, Bonadio J, Matzuk MM. Activin betaC and betaE genes are not essential for mouse liver growth, differentiation, and regeneration. *Mol Cell Biol* 2000; **20**: 6127-6137
- 25 **Aoki T**, Murakami M, Niiya T, Murai N, Shimizu Y, Kato H, Kusano M. Capacity of hepatic regeneration following a second partial hepatectomy in rats. *Hepatol Res* 2001; **21**: 228-241

- 26 **Xu CS**, Li YC, Lin JT, Zhang HY, Zhang YH. Cloning and analyzing the up-regulated expression of transthyretin-related gene (LR(1)) in rat liver regeneration following short interval successive partial hepatectomy. *World J Gastroenterol* 2003; **9**: 148-151
- 27 **Lu AL**, Xu CS. Effect of heat shock on change of HSC70/HSP68, acid and alkaline phosphatases before and after rat partial hepatectomy on HSC/HSP68, acid and alkaline phosphatases. *World J Gastroenterol* 2000; **6**: 730-733
- 28 **Diatchenko L**, Lau YF, Campbell AP, Chenchik A, Moqadam F, Huang B, Lukyanov S, Lukyanov K, Gurskaya N, Sverdlov ED, Siebert PD. Suppression subtractive hybridization: a method for generating differentially regulated or tissue-specific cDNA probes and libraries. *Proc Natl Acad Sci USA* 1996; **93**: 6025-6030
- 29 **Nishizuka S**, Tsujimoto H, Stanbridge EJ. Detection of differentially expressed genes in HeLa x fibroblast hybrids using subtractive suppression hybridization. *Cancer Res* 2001; **61**: 4536-4540
- 30 **Shridhar V**, Sen A, Chien J, Staub J, Avula R, Kovats S, Lee J, Lillie J, Smith DI. Identification of underexpressed genes in early- and late-stage primary ovarian tumors by suppression subtraction hybridization. *Cancer Res* 2002; **62**: 262-270
- 31 **Chomczynski P**, Sacchi N. Single-step method of RNA isolation by acid guanidinium thiocyanate-phenol-chloroform extraction. *Anal Biochem* 1987; **162**: 156-159
- 32 **Hagen FS**, Gray CL, Kuijper JL. Assaying the quality of cDNA libraries. *Biotechniques* 1988; **6**: 340-345
- 33 **Sambrook J**, Fritsch EF, Maniatis T. Molecular Cloning: A laboratory Manual. 2nd ed. *New York: Cold Spring Harbor* 1989: 18-24
- 34 **Young RA**, Davis RW. Efficient isolation of genes by using antibody probes. *Proc Natl Acad Sci USA* 1983; **80**: 1194-1198
- 35 **Brebner LD**, Balinsky JB. Changes in activities of urea cycle enzymes in early stages of liver regeneration after partial hepatectomy in rats. *Life Sci* 1983; **32**: 1391-1400
- 36 **Rai RM**, Lee FY, Rosen A, Yang SQ, Lin HZ, Koteish A, Liew FY, Zaragoza C, Lowenstein C, Diehl AM. Impaired liver regeneration in inducible nitric oxide synthase-deficient mice. *Proc Natl Acad Sci USA* 1998; **95**: 13829-13834
- 37 **Hortelano S**, Dewez B, Genaro AM, Diaz-Guerra MJ, Bosca L. Nitric oxide is released in regenerating liver after partial hepatectomy. *Hepatology* 1995; **21**: 776-786
- 38 **Tenu JP**, Lepoivre M, Moali C, Brollo M, Mansuy D, Boucher JL. Effects of the new arginase inhibitor N (omega)-hydroxy-nor-L-arginine on NO synthase activity in murine macrophage. *Nitric Oxide* 1999; **3**: 427-438
- 39 **Liu ZW**, Zhao MJ, Li ZP. Identification of up-regulated genes in rat regenerating liver tissue by suppression subtractive hybridization. *Shengwu Huaxue Yu Shengwu Wuli Xuebao (Shanghai)* 2001; **33**: 191-197
- 40 **Lepoivre M**, Flaman JM, Bobe P, Lemaire G, Henry Y. Quenching of the tyrosyl free radical of ribonucleotide reductase by nitric oxide. Relationship to cytostasis induced in tumor cells by cytotoxic macrophages. *J Biol Chem* 1994; **269**: 21891-21897
- 41 **Obolenskaya M**, Schulze-Specking A, Plaumann B, Frenzer K, Freudenberg N, Decker K. Nitric oxide production by cells isolated from regenerating rat liver. *Biochem Biophys Res Commun* 1994; **204**: 1305-1311
- 42 **Obolenskaya M**, Vanin AF, Mordvintcev PI, Mulsch A, Decker K. Epr evidence of nitric oxide production by the regenerating rat liver. *Biochem Biophys Res Commun* 1994; **202**: 571-576

Edited by Xia HHX

Expression of insulin-like growth factor 1 and insulin-like growth factor 1 receptor and its intervention by interleukin-10 in experimental hepatic fibrosis

Xiao-Zhong Wang, Zhi-Xin Chen, Li-Juan Zhang, Yun-Xin Chen, Dan Li, Feng-Lin Chen, Yue-Hong Huang

Xiao-Zhong Wang, Zhi-Xin Chen, Li-Juan Zhang, Yun-Xin Chen, Dan Li, Feng-Lin Chen, Yue-Hong Huang, Department of Gastroenterology, Affiliated Union Hospital, Fujian Medical University, Fuzhou, 350001, Fujian Province, China

Supported by Science and Technology fund of Fujian Province, No. 2003D05

Correspondence to: Xiao-Zhong Wang, Department of Gastroenterology, Affiliated Union Hospital, Fujian Medical University, Fuzhou, 350001, Fujian Province, China. drwangxz@pub6.fz.fj.cn

Telephone: +86-591-3322384

Received: 2002-12-28 **Accepted:** 2003-02-11

Abstract

AIM: To study the expression of IGF-1 and IGF-1R and its intervention by interleukin-10 in the course of experimental hepatic fibrosis.

METHODS: Hepatic fibrosis was induced in rats by carbon tetrachloride intoxication and liver specimens were taken from the rats administered CCl₄ with or without IL-10 treatment and the animals of the control group. Immunoreactivities for insulin-like growth factor-1 (IGF-1) and IGF-1 receptor (IGF-1R) were demonstrated by immunohistochemistry, and their intensities were evaluated in different animal groups.

RESULTS: The positive levels for IGF-1 and IGF-1R were increased with the development of hepatic fibrosis, with the positive signals localized in cytoplasm and/or at the plasmic membrane of hepatocytes. The positive signals of IGF-1 and IGF-1R were observed more frequently ($P < 0.01$) in the CCl₄-treated group (92.0 % and 90.0 %) compared to those in the control group. The positive signals decreased significantly ($P < 0.05$) in IL-10-treated group. The responses in IGF-1 and IGF-1R expression correlated with the time of IL-10 treatment.

CONCLUSION: The expression of IGF-1 and IGF-1R immunoreactivities in liver tissue seems to be up-regulated during development of hepatic fibrosis induced by CCl₄, and exogenous IL-10 inhibits the responses.

Wang XZ, Chen ZX, Zhang LJ, Chen YX, Li D, Chen FL, Huang YH. Expression of insulin-like growth factor 1 and insulin-like growth factor 1 receptor and its intervention by interleukin-10 in experimental hepatic fibrosis. *World J Gastroenterol* 2003; 9 (6): 1287-1291

<http://www.wjgnet.com/1007-9327/9/1287.asp>

INTRODUCTION

Hepatic fibrosis is a common pathological change resulted from various chronic hepatic injuries, which is characterized by an increase of extracellular matrix (ECM) deposition in the Disse's

space and the imbalance between synthesis and degeneration of ECM. It is a change before cirrhosis^[1-6]. Many studies suggested that cytokines play important roles during hepatic fibrosis with different mechanisms^[1,7-16]. There is a contrary effect of insulin-like growth factor-1 (IGF-1) on rat hepatic stellate cells (HSC) *in vivo* and *in vitro*. IGF-1 and its receptor (IGF-1R) may play a significant role in hepatic fibrosis. The rat hepatic fibrosis model was established and the immunoreactivities for IGF-1 and IGF-1R in rat liver tissues were assessed to show the possible involvement of IGF-1 and IGF-1R in the process of hepatic fibrosis and the effect of interleukin-10 on this change.

MATERIALS AND METHODS

Materials

One hundred clean male Sprague-Dawley rats weighing 140-180 g (Provided by Shanghai Experimental Animal Center) were divided randomly into 3 groups. The control group (group C) included 24 rats; the model group (group M) included 40 rats and the IL-10 treated group (group T) included 36 rats. All the rats were bred under routine conditions.

Methods

Preparation of rats The rats of group C were injected intraperitoneally with saline 2 ml·kg⁻¹ twice a week. The rats of group M and group T were injected intraperitoneally with 50 % CCl₄ (dissolved in castor oil) 2 ml·kg⁻¹ twice a week. From the third week, the rats of group T were injected intraperitoneally with IL-10 4 ug·kg⁻¹ (dissolved in saline) 20 minutes before they were injected with CCl₄. All injections were given on Monday and Thursday. To the fifth week, 3 rats in group M and 2 rats in group T died; to the seventh week, 8 rats in group M and 4 rats in group T died; to the ninth week, 10 rats in group M, 6 rats in group T and 3 rats in group C died. In the 5,7,9 week, 10 rats of groups M and T and 7 rats of control group were sacrificed and their livers were taken. The specimens were fixed in 10 % formalin and embedded with paraffin. Sections were stained by hematoxylin and eosin and evaluated by pathologists.

Immunohistochemistry and data evaluation The rat liver tissues were sectioned at a thickness of 4 μm. The sections were deparaffinized with xylene, dehydrated with graded ethanol, incubated in PBS containing 3 % H₂O₂ to block endogenous peroxidase activity and then incubated in PBS containing 0.1M citrate to saturate nonspecific binding sites. After incubation with rabbit anti-rat IGF-1 or IGF-1R monoclonal antibody (American Neomarkers Company), the reactions were with the instance S-P immunohistochemistry reagents (American Zymed Company). And then, the sections were incubated in a buffer containing 3, 3-diaminobenzidine tetrahydrochloride (DAB) and H₂O₂ to produce a brown reaction product, then were dehydrated and coverslipped. The reactions were graded according to their intensities and percentage of the positive cell as follows: negative=0, stained yellowish=1, stained with deep yellows or brown=2; the percentage of stained cell: <5 %=0, 6 % to

25 % = 1, 26 % to 50 % = 2, >50 % = 3. Then the eventual result was by these two scores according to the following predefined definitions: 0 to 1 = negative (-), 2 to 3 = positive (+), 4 and above 4 = strongly positive (++) . Ridit analysis described the difference between groups.

RESULTS

Expression of IGF-1 and IGF-1R in the liver tissues of the three groups

The positive rates of IGF-1 in the control group, the CCl₄-treated group and the CCl₄-and IL-10-treated group were 38.1 %, 92.0 % and 71.4 %, respectively. Those of IGF-1R were 33.3 %, 80.0 % and 64.3 %, respectively. The granular positive products were localized in the cytoplasm and/or at the membrane, but not in the nuclei. In group C, IGF-1 and IGF-1R signals were weak, mainly located in the perivenular area (Figure 1,2). In group M, the expression increased obviously with the development of hepatic fibrosis, and the positive cells distributed

throughout the hepatic lobule (Figure 3,4). In group T, the changes were less pronounced than in group M (Figure 5,6).

Intensities of IGF-1 and IGF-1R immunoreactivities

The comparison of IGF-1 and IGF-1R system expression levels in groups C, M and T is listed in Table 1. Ridit analysis showed a significant difference among the three groups ($P < 0.01$). Expression levels of the IGF-1 and IGF-1R in group M were found to be higher than that in group C ($P < 0.01$). In group T, after the treatment with IL-10, the immunoreactivities for IGF-1 and IGF-1R decreased ($P < 0.01$ and $P < 0.05$, respectively). The data for IGF-1 and IGF-1R reactivities in different stages of hepatic fibrosis are listed in Table 2. With the development of hepatic fibrosis, intensities of IGF-1 and IGF-1R immunoreactivities increased significantly ($P < 0.05$). The data for IGF-1 and IGF-1R immunoreactivities in different stages of hepatic fibrosis in group T are listed in Table 3. A significant decrease was observed in IGF-1 and IGF-1R expression with the IL-10 treatment ($P < 0.05$).

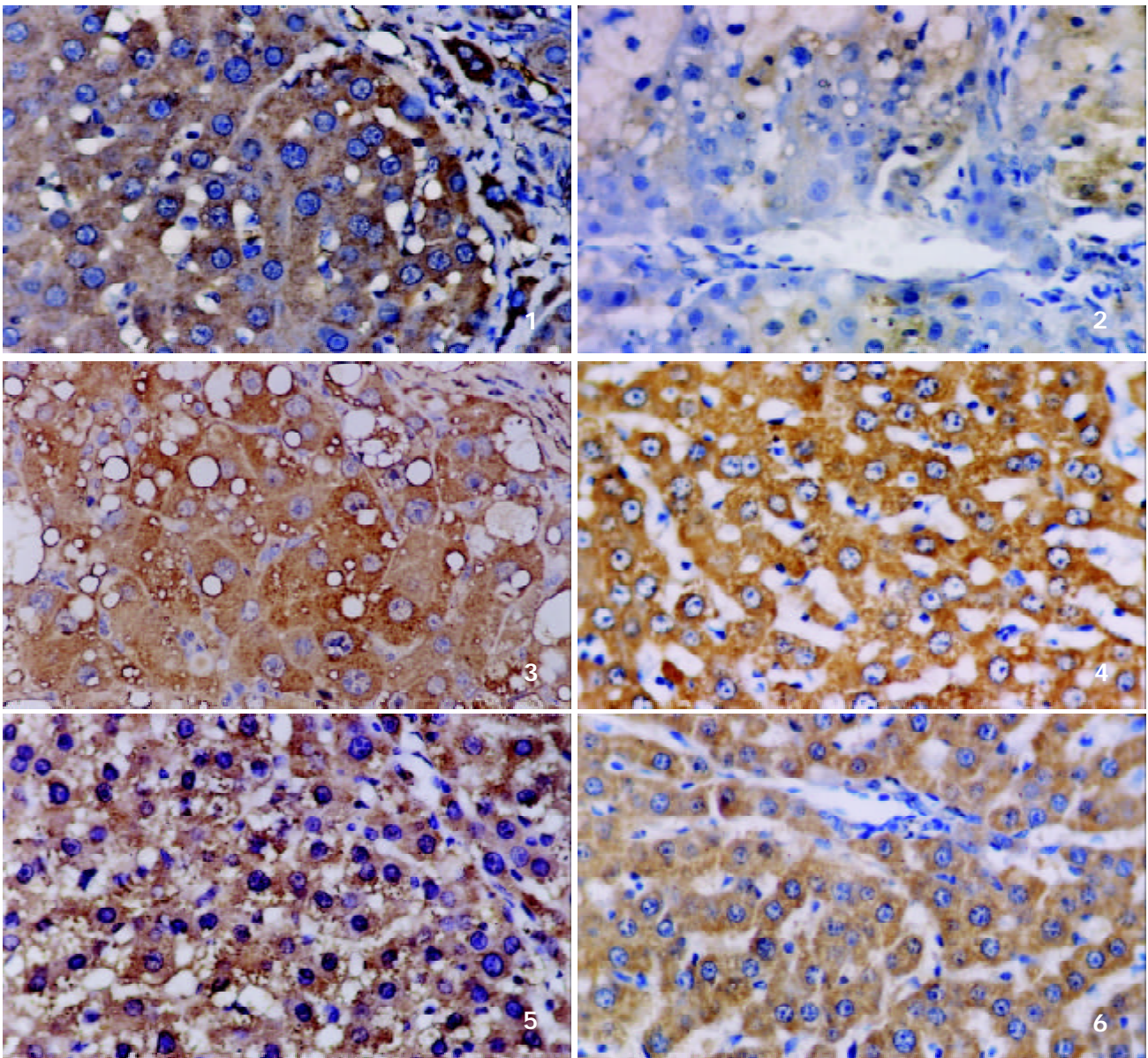


Figure 1 IGF-1 positively expressed cell in group C S-P method $\times 400$.

Figure 2 IGF-1R positively expressed cell in group C S-P method $\times 400$.

Figure 3 IGF-1 positively expressed cell in group M S-P method $\times 400$.

Figure 4 IGF-1R positively expressed cell in group M S-P method $\times 400$.

Figure 5 IGF-1 positively expressed cell in group T S-P method $\times 400$.

Figure 6 IGF-1R positively expressed cell in group T S-P method $\times 400$.

Table 1 Intensities for IGF-1/IGF-1R immunoreactivities in groups C, M and T

Group	n	IGF-1				Ridit value	IGF-1R			
		-	+	++			-	+	++	Ridit value
C	21	13	8	0	0.302 ^{acf}	14	7	0	0.331 ^{ac}	
M	25	2	10	13	0.689 ^{acd}	5	8	12	0.666 ^{ace}	
T	28	8	16	4	0.480 ^{adf}	10	16	2	0.478 ^{ae}	

^a $P < 0.01$ vs among three groups, ^c $P < 0.01$ group M vs group C
^d $P < 0.01$, ^e $P < 0.05$ group M vs group T, ^f $P < 0.05$ group C vs group T.

Table 2 Intensities for IGF-1 and IGF-1R immunoreactivities in different time points of hepatic fibrosis induced by CCl₄

Week	n	IGF-1				Ridit value	IGF-1R			
		-	+	++			-	+	++	Ridit value
5 wk	8	0	1	7	0.683 ^{ab}	0	1	7	0.710 ^{ab}	
7 wk	8	0	4	4	0.510 ^a	2	3	3	0.445 ^a	
9 wk	9	2	5	2	0.329 ^{ab}	3	4	2	0.362 ^{ab}	

^a $P < 0.05$ vs among three groups, ^b $P < 0.05$, 5 wk vs 9 wk.

Table 3 Intensities for IGF-1 and IGF-1R immunoreactivities in different periods of hepatic fibrosis in group T

Week	n	IGF-1				Ridit value	IGF-1R			
		-	+	++			-	+	++	Ridit value
5 wk	10	0	7	3	0.678 ^{ab}	1	7	2	0.661 ^{ab}	
7 wk	9	3	5	1	0.468 ^{ab}	3	6	0	0.488 ^a	
9 wk	9	5	4	0	0.333 ^{ab}	6	3	0	0.334 ^{ab}	

^a $P < 0.05$ vs among three groups, ^b $P < 0.05$, 5 wk vs 9 wk.

DISCUSSION

Hepatic fibrosis is the early stage of hepatic cirrhosis, characterized by accumulation of excessive extracellular matrix, necrosis, nodular regeneration of hepatocytes and formation of fibrous septum^[1-6]. Cytokines play important roles in the formation and regression of hepatic fibrosis^[1,7-16].

In the present study, up-regulated expression of IGF-1 and IGF-1R was observed in liver tissues injured by CCl₄-intoxication, and was positively correlated with the development of hepatic fibrosis. However, the response was less pronounced in IL-10- treated group.

Insulin-like growth factors (IGFs) include two related homologous polypeptides: IGF-1 and IGF-2, which have similar structure and activity *in vitro*, but different biological effect *in vivo*. Activation of mitosis and induction or acceleration of differentiation are their major functions, which are mediated through IGF-1R by means of autocrine, paracrine and endocrine mechanisms. IGF-1R is a transmembrane tyrosine kinase receptor. After binding with its ligand, intracellular transcription and synthesis of proteins are activated and regulated through a series of signal transduction. This gives rise to insulin-like metabolic effects and promotes proliferation and differentiation of cells. It is also involved in the maintenance of transformed cell phenotypes. Its expression is essential for the transforming function of cell cycle-related protooncogenes and viral oncogenes^[17,18]. In addition, IGF-1 and IGF-1R have an anti-apoptosis effect on different cells^[13]. Liver is the main organ of IGF-1, but the function of IGF-1 and IGF-1R in hepatic fibrosis still remains controversial. Many authors

have observed a decreased serum concentration of IGF-1 and insulin-like growth factor-binding protein 3 (IGFBP3) in patients with hepatic cirrhosis, this change is correlative with cirrhosis progression. With the treatment of recombinant somatotropin, the serum concentration increased along with the improvement of protein synthesis and liver metabolism. For these patients, the IGF-1 concentration below 10 nmol/L was considered an unfavored response to the treatment and poor prognosis^[19-31]. Castilla *et al* and Myguez *et al* reported that the histological parameters in hepatic fibrosis animals were improved after being treated with exogenous IGF-1. So IGF-1 might act as an antifibrogenic factor^[32,33]. On the contrary, other researches speculated IGF-1 had a great influence on hepatic stellate cell (HSC), which was the main producer of ECM, such as activating proliferation, inhibiting apoptosis, accelerating the secretion of collagen type I, etc^[13,34]. The function of IGF-1 also seems to be regulated by IGF-BP, IGF-1R and other cytokines^[22-30].

The present study observed and evaluated IGF-1 expression with the fibrosis progression, which might be a compensatory reaction to the continuous loss of hepatocytes in the CCl₄-treated animals. We consider that IGF-1 may stimulate the replication of hepatocytes and interfere with fibrosis. The discordance was observed between the IGF-1 level in liver tissue and that in serum, with the former higher and the latter lower, this is likely due to the decrease of IGF-1 released from hepatocytes to blood circulation. In other words, the hepatocytic secretion of IGF-1 maybe regulated by means of autocrine under such a situation. The positive correlation between the expression of IGF-1 and IGF-1R and the fibrosis progression may be helpful for fibrosis staging.

IL-10 is an antifibrogenic cytokine produced by Th2 cells, macrophages, stellate cells and hepatocytes^[35-47]. It has been reported the deficiency of IL-10 prompted fibrosis probably by its failure in inhibiting the overproduction of TGF- β ₁ and TNF- α . The latter two cytokines are secreted by macrophages and can enhance synthesis of collagen type I^[48]. The knock-out experiments (IL-10-/-mice) indicated that endogenous IL-10 actually relieved CCl₄-induced fibrosis^[49-51]. In our previous study, exogenous IL-10 was found to be able to inhibit the progress of fibrosis and might be used for treatment. Similar results were also reported by Nelson, but its mechanism remains obscure^[52,53]. The present study showed that IGF-1 and IGF-1R expression decreased with the improvement of fibrosis after treatment with IL-10. It seems that antifibrogenic effect of IL-10 is associated with down-regulation of IGF-1/IGF-1R. More works are demanded to clarify whether this action is regulated by IGF-1 and IGF-1R or the decrease of IGF-1R expression is only a phenomenon of hepatic cirrhosis remission.

REFERENCES

- 1 **Friedman SL.** Cytokines and fibrogenesis. *Semi Liver Dis* 1999; **19**: 129-140
- 2 **Liu HL,** Li XH, Wang DY, Yang SP. Matrix metalloproteinase-2 and tissue inhibitor of metalloproteinase-1 expression in fibrotic rat liver. *World J Gastroenterol* 2000; **6**: 881-884
- 3 **Du WD,** Zhang YE, Zhai WR, Zhou XM. Dynamic changes of type I, III and IV collagen synthesis and distribution of collagen-producing cells in carbon tetrachloride-induced rat liver fibrosis. *World J Gastroenterol* 1999; **5**: 397-403
- 4 **Wang JY,** Guo JS, Yang CQ. Expression of exogenous rat collagenase *in vitro* and in a rat model of liver fibrosis. *World J Gastroenterol* 2002; **8**: 901-907
- 5 **Nie QH,** Cheng YQ, Xie YM, Zhou YX, Cao YZ. Inhibiting effect of antisense oligonucleotides phosphorothioate on gene expression of TIMP-1 in rat liver fibrosis. *World J Gastroenterol* 2001; **7**: 363-369
- 6 **Vaillant B,** Chiramonte MG, Cheever AW, Soloway PD, Wynn TA. Regulation of hepatic fibrosis and extracellular matrix genes

- by the th response: new insight into the role of tissue inhibitors of matrix metalloproteinases. *J Immunol* 2001; **167**: 7017-7026
- 7 **Zhang GL**, Wang YH, Teng HL, Lin ZB. Effects of aminoguanidine on nitric oxide production induced by inflammatory cytokines and endotoxin in cultured rat hepatocytes. *World J Gastroenterol* 2001; **7**: 331-334
- 8 **Daniluk J**, Szuster-Ciesielska A, Drabko J, Kandefer-Szerszen M. Serum cytokine levels in alcohol-related liver cirrhosis. *Alcohol* 2001; **23**: 29-34
- 9 **Von Baehr V**, Docke WD, Plauth M, Liebenthal C, Kupferling S, Lochs H, Baumgarten R, Volk HD. Mechanisms of endotoxin tolerance in patients with alcoholic liver cirrhosis: role of interleukin 10, interleukin 1 receptor antagonist, and soluble tumour necrosis factor receptors as well as effector cell desensitisation. *Gut* 2000; **47**: 281-287
- 10 **Si XH**, Yang LJ. Extraction and purification of TGF β and its effect on the induction of apoptosis of hepatocytes. *World J Gastroenterol* 2001; **7**: 527-531
- 11 **Weng HL**, Cai WM, Liu RH. Animal experiment and clinical study of effect of gamma2interferon on hepatic fibrosis. *World J Gastroenterol* 2001; **7**: 42-48
- 12 **Li D**, Zhang LJ, Chen ZX, Huang YH, Wang XZ. Effects of TNF α , IL-6 and IL-10 on the development of experimental rat liver fibrosis. *Shijie Huaren Xiaohua Zazhi* 2001; **9**: 1242-1245
- 13 **Issa R**, Williams E, Trim N, Kendall T, Arthur MJP, Reichen J, Benyon RC, Iredale JP. Apoptosis of hepatic stellate cells: involvement in resolution of biliary fibrosis and regulation by soluble growth factors. *Gut* 2001; **48**: 548-557
- 14 **Gong JP**, Dai LL, Liu CA, Wu CX, Shi YJ, Li SW, Li XH. Expression of CD14 protein and its gene in liver sinusoidal endothelial cells during endotoxemia. *World J Gastroenterol* 2002; **8**: 551-554
- 15 **Wang JY**, Wang XL, Liu P. Detection of serum TNF- α , IFN- β , IL-6 and IL-8 in patients with hepatitis B. *World J Gastroenterol* 1999; **5**: 38-40
- 16 **Assy N**, Paizi M, Gaitini D, Baruch Y, Spira G. Clinical implication of VEGF serum levels in cirrhotic patients with or without portal hypertension. *World J Gastroenterol* 1999; **5**: 296-300
- 17 **Kalebic T**, Tsokos M, Helman LJ. *In vivo* treatment with antibody against IGF-1 receptor suppresses growth of human rhabdomyosarcoma and down-regulates p34^{cdc2}. *Cancer Res* 1994; **54**: 5531-5534
- 18 **Zhou P**, Zhou ZC, Chen WS, Liu WW, Fang DC, Yang JM. Effect of IGF-1R antisense gene on the morphology of hepatoma cell line SMMC-7721. *Shijie Huaren Xiaohua Zazhi* 2002; **10**: 279-282
- 19 **Gayan-Ramirez G**, van de Castele M, Rollier H, Fevery J, Vanderhoydonc F, Verhoeven G, Decramer M. Biliary cirrhosis induces type Iix/b fiber atrophy in rat diaphragm and skeletal muscle, and decreases IGF-I mRNA in the liver but not in muscle. *J Hepatol* 1998; **29**: 241-249
- 20 **Donaghy A**, Ross R, Wicks C, Hughes SC, Holly J, Gimson A, Williams R. Growth hormone therapy in patients with cirrhosis: a pilot study of efficacy and safety. *Gastroenterology* 1997; **113**: 1617-1622
- 21 **Moller S**, Juul A, Becker U, Henriksen JH. The acid-labile subunit of the ternary insulin-like growth factor complex in cirrhosis: relation to liver dysfunction. *J Hepatol* 2000; **32**: 441-446
- 22 **Ormarsdottir S**, Ljunggren O, Mallmin H, Olofsson H, Blum WF, Loof L. Circulating levels of insulin-like growth factors and their binding proteins in patients with chronic liver disease: lack of correlation with bone mineral density. *Liver* 2001; **21**: 123-128
- 23 **Assy N**, Hochberg Z, Amit T, Shen-Orr Z, Enat R, Baruch Y. Growth hormone-stimulated insulin-like growth factor (IGF) I and IGF-binding protein-3 in liver cirrhosis. *J Hepatol* 1997; **27**: 796-802
- 24 **Assy N**, Hochberg Z, Enat R, Baruch Y. Prognostic value of generation of growth hormone-stimulated insulin-like growth factor-I (IGF-I) and its binding protein-3 in patients with compensated and decompensated liver cirrhosis. *Dig Dis Sci* 1998; **43**: 1317-1321
- 25 **Shmueli E**, Miell JP, Stewart M, Alberti KG, Record CO. High insulin-like growth factor binding protein 1 levels in cirrhosis: link with insulin resistance. *Hepatology* 1996; **24**: 127-133
- 26 **Moller S**, Gronbaek M, Main K, Becker U, Skakkebaek NE. Urinary growth hormone (U-GH) excretion and serum insulin-like growth factor 1 (IGF-1) in patients with alcoholic cirrhosis. *J Hepatol* 1993; **17**: 315-320
- 27 **Donaghy A**, Ross R, Gimson A, Hughes SC, Holly J, Williams R. Growth hormone, insulinlike growth factor-1, and insulinlike growth factor binding proteins 1 and 3 in chronic liver disease. *Hepatology* 1995; **21**: 680-688
- 28 **Moller S**, Juul A, Becker U, Flyvbjerg A, Skakkebaek NE, Henriksen JH. Concentrations, release, and disposal of insulinlike growth factor (IGF)-binding proteins (IGFBP), IGF-I, and growth hormone in different vascular beds in patients with cirrhosis. *J Clin Endocrinol Metab* 1995; **80**: 1148-1157
- 29 **Kratsch J**, Blum WF, Schenker E, Keller E. Regulation of growth hormone (GH), insulin-like growth factor (IGF)I, IGF binding proteins -1, -2, -3 and GH binding protein during progression of liver cirrhosis. *Exp Clin Endocrinol Diabetes* 1995; **103**: 285-291
- 30 **Ottesen LH**, Bendtsen F, Flyvbjerg A. The insulin-like growth factor binding protein 3 ternary complex is reduced in cirrhosis. *Liver* 2001; **21**: 350-356
- 31 **Santolaria F**, Gonzalez-Gonzalez G, Gonzalez-Reimers E, Martinez-Riera A, Milena A, Rodriguez-Moreno F, Gonzalez-Garcia C. Effects of alcohol and liver cirrhosis on the GH-IGF-I axis. *Alcohol Alcohol* 1995; **30**: 703-708
- 32 **Muguerza B**, Castilla-Cortazar I, Garcia M, Quiroga J, Santidrian S, Prieto J. Antifibrogenic effect *in vivo* of low doses of insulinlike growth factor-I in cirrhotic rats. *Biochim Biophys Acta* 2001; **1536**: 185-195
- 33 **Castilla-Cortazar I**, Garcia M, Muguerza B, Quiroga J, Perez R, Santidrian S, Prieto J. Hepatoprotective effects of insulin-like growth factor 1 in rats with carbon tetrachloride-induced cirrhosis. *Gastroenterology* 1997; **113**: 1682-1691
- 34 **Svegliati-Baroni G**, Ridolfi F, Di Sario A, Casini A, Marucci L, Gaggiotti G, Orlandoni P, Macarri G, Peregon L, Benedetti A, Folli F. Insulin and insulin-like growth factor 1 stimulate proliferation and type I collagen accumulation by human hepatic stellate cells: differential effects on signal transduction pathways. *Hepatology* 1999; **29**: 1743-1751
- 35 **Di Marco R**, Xiang M, Zaccone P, Leonardi C, France S, Meroni P, Nicoletti F. Concanavalin A-induced hepatitis in mice is prevented by interleukin (IL)-10 and exacerbated by endogenous IL-10 deficiency. *Autoimmunity* 1999; **31**: 75-83
- 36 **Louis H**, Le Moine O, Peny MO, Gulbis B, Nisol F, Goldman M, Deviere J. Hepatoprotective role of interleukin 10 in galactosamine/lipopolysaccharide mouse liver injury. *Gastroenterology* 1997; **112**: 935-942
- 37 **Louis H**, Le Moine O, Peny MO, Quertinmont E, Fokan D, Goldman M, Deviere J. Production and role of interleukin-10 in concanavalin A-induced hepatitis in mice. *Hepatology* 1997; **25**: 1382-1389
- 38 **Hill DB**, D'Souza NB, Lee EY, Burikhanov R, Deaciuc IV, de Villiers WJ. A role for interleukin-10 in alcohol-induced liver sensitization to bacterial lipopolysaccharide. *Alcohol Clin Exp Res* 2002; **26**: 74-82
- 39 **Santucci L**, Fiorucci S, Chiorean M, Brunori PM, Di Matteo FM, Sidoni A, Migliorati G, Morelli A. Interleukin 10 reduces lethal and hepatic injury induced by lipopolysaccharide in galactosamine-sensitized mice. *Gastroenterology* 1996; **111**: 736-744
- 40 **Howard M**, O'Garra A. Biological properties of interleukin 10. *Immunol Today* 1992; **13**: 198-200
- 41 **De Vries JE**. Immunosuppressive and anti-inflammatory properties of interleukin 10. *Ann Med* 1995; **27**: 537-541
- 42 **Wakkach A**, Cottrez F, Groux H. Can interleukin-10 be used as a true immunoregulatory cytokine? *Eur Cytokine Netw* 2000; **11**: 153-160
- 43 **Oberholzer A**, Oberholzer C, Moldawer LL. Interleukin-10: a complex role in the pathogenesis of sepsis syndromes and its potential as an anti-inflammatory drug. *Crit Care Med* 2002; **30**: S58-63
- 44 **Weng S**, Leng X, Wei Y. Interleukin-10 inhibits the activation of cultured rat hepatic stellate cells induced by Kupffer cells. *Zhonghua Yixue Zazhi* 2002; **82**: 104-107
- 45 **Louis H**, Le Moine A, Quertinmont E, Peny MO, Geerts A, Goldman M, Le Moine O, Deviere J. Repeated concanavalin A challenge in mice induces an interleukin 10-producing phenotype and liver fibrosis. *Hepatology* 2000; **31**: 381-390
- 46 **Nagano T**, Yamamoto K, Matsumoto S, Okamoto R, Tagashira

- M, Ibuki N, Matsumura S, Yabushita K, Okano N, Tsuji T. Cytokine profile in the liver of primary biliary cirrhosis. *J Clin Immunol* 1999; **19**: 422-427
- 47 **Wang XZ**, Zhang LJ, Li D, Huang YH, Chen ZX, Li B. Effects of transmitters and interleukin-10 on rat hepatic fibrosis induced by CCl₄. *World J Gastroenterol* 2003; **9**: 539-543
- 48 **Nagaki M**, Tanaka M, Sugiyama A, Ohnishi H, Moriwaki H. Interleukin-10 inhibits hepatic injury and tumor necrosis factor- α and interferon- γ mRNA expression induced by staphylococcal enterotoxin B or lipopolysaccharide in galactosamine-sensitized mice. *J Hepatol* 1999; **31**: 815-824
- 49 **Thompson K**, Maltby J, Fallowfield J, Mcaulay M, Millward-Sadler H, Sheron N. Interleukin-10 expression and function in experimental murine liver inflammation and fibrosis. *Hepatology* 1998; **28**: 1597-1606
- 50 **Louis H**, Van Laethem JL, Wu W, Quertinmont E, Degraef C, Van den Berg K, Demols A, Goldman M, Le Moine O, Geerts A, Deviere J. Interleukin-10 controls neutrophilic infiltration, hepatocyte proliferation, and liver fibrosis induced by carbon tetrachloride in mice. *Hepatology* 1998; **28**: 1607-1615
- 51 **Demols A**, Van Laethem JL, Quertinmont E, Degraef C, Delhaye M, Geerts A, Deviere J. Endogenous interleukin-10 modulates fibrosis and regeneration in experimental chronic pancreatitis. *Am J Physiol Gastrointest Liver Physiol* 2002; **282**: G1105-1112
- 52 **Zhang LJ**, Wang XZ, Huang YH. Effect of interleukin-10 on experimental liver fibrosis. *Zhonghua Xiaohu Zazhi* 2002; **22**: 179-180
- 53 **Nelson DR**, Lauwers GY, Lau JY, Davis GL. Interleukin-10 treatment reduces fibrosis in patients with chronic hepatitis C: a pilot trial of interferon nonresponders. *Gastroenterology* 2000; **118**: 655-660

Edited by Su Q

Experimental study of effect of Ganyanping on fibrosis in rat livers

Wang-Xian Tang, Zi-Li Dan, Hong-Mei Yan, Cui-Huan Wu, Guo Zhang, Mei Liu, Qin Li, Shao-Bai Li

Wang-Xian Tang, Zi-Li Dan, Guo Zhang, Mei Liu, Qin Li, Shao-Bai Li, Institute of Liver Diseases, Tongji Hospital, Tongji Medical College, Huazhong University of Science and Technology, Wuhan 430030, Hubei Province, China

Hong-Mei Yan, The 7th Hospital of Wuhan, Wuhan 430071, Hubei Province, China

Cui-Huan Wu, Department of Pathology, Tongji Medical College, Huazhong University of Science and Technology, Wuhan 430030, Hubei Province, China

Supported by the Natural Science Foundation of Hubei Province, No. 1999 J151

Correspondence to: Professor Wang-Xian Tang, Institute of Liver Diseases, Tongji Hospital, Tongji Medical College, Huazhong University of Science and Technology, Wuhan 430030, Hubei Province, China. tangwx@tjh.tjmu.edu.cn

Telephone: +86-27-83662873 **Fax:** +86-27-83615970

Received: 2002-11-06 **Accepted:** 2003-02-11

Abstract

AIM: To observe the effects of Ganyanping on CCl₄-induced hepatic fibrosis in rats.

METHODS: The rats were separated randomly into five groups. Groups A to group D, each consisting of 15 rats, were for different tests, while 8 rats were used as normal controls (N). For group D, CCl₄ was injected subcutaneously, at a dosage of 3 ml/kg for 9 weeks. For group A, Ganyanping was administered via gastric tube at a dosage of 10 ml/kg. For group B, the treatment with Ganyanping was started 4 weeks after CCl₄ administration. In group C, Ganyanping was administered 8 weeks after the intoxication, and treatment lasted for 4 weeks. Liver tissues were fixed in 10 % formalin and embedded in paraffin. Pathologic changes, particularly fibrosis, were evaluated on the HE and V-G-stained sections. Ten middle-power fields were randomly selected for assessment of collagen deposition.

RESULTS: Loss of normal hepatic architecture, some with pseudo-lobule formation, was observed in group D, while hepatocytes steatosis and fibrosis were less pronounced in the animals treated with Ganyanping. Pseudo-lobule formation was not evident in the latter groups. The total collagen area and ratio were 840.23±81.65 and 7.0±0.9, respectively in group D, the ratio being reduced greatly in the Ganyanping-treated groups (148.73±45.89 and 1.16±0.33, respectively). The activities of MAO and ACP were elevated and that of SDH in group D decreased in the hepatic tissue as compared to the control group. The treatment with Ganyanping abrogated these enzymatic changes.

CONCLUSION: Our data approved that Ganyanping could improve the microcirculation in the liver, reduce oxygen-derived free radicals, and enhance the cellular metabolism and immune function, all resulting in an anti-fibrotic effect. Hence, Ganyanping can protect the liver from fibrosis. It

may be a safe and effective preparation for patient with fibrosis.

Tang WX, Dan ZL, Yan HM, Wu CH, Zhang G, Liu M, Li Q, Li SB. Experimental study of effect of Ganyanping on fibrosis in rat livers. *World J Gastroenterol* 2003; 9(6): 1292-1295
<http://www.wjgnet.com/1007-9327/9/1292.asp>

INTRODUCTION

Ganyanping, a preparation of Chinese herbs proposed by Li Shaobai *et al*^[1] has been used in clinical and experimental fields for many years. It has been shown to be protective for the animal liver against injury by D-GalN and cirrhosis caused by CCl₄ intoxication^[2-6]. In this study, the effects of Ganyanping on liver fibrosis used a CCl₄-intoxication model. The V-G and enzyme histochemistry techniques were employed to observe the effects of Ganyanping.

MATERIALS AND METHODS

Reagents

CCl₄ (Beijing Chemical Factory, Lot No. 20000225) was diluted to 40 % in vegetable oil (Southseas Oils & Fats Industrial (CHI Wan) Limited, Grade One, Lot No. KO'SOF Ts88). Ganyanping tablet preparation (Lot No.20001110) was provided by the Institute of Liver Disease, Tongji Hospital, Tongji Medical College, consisting of Radix Astragali seu Hedysari, Radix Salviae Miltiorrhizae, Rhizoma polygoni Cuspidati and other herbs. The tablets were prepared in the Chinese Medicine Pharmacy of Tongji Hospital. The powder of Ganyanping was dissolved into water (1.2 g/ml) before use.

Animals

68 Wistar rats (♂ & ♀, 38 for ♂ and 30 for ♀), weighing between 170 and 250 g, were provided by the Laboratory Animal Center of Tongji Medical College. The rats were separated randomly into five groups. Group N, normal control, consisted of 8 rats. For group A to group D, rats (15 for each) were treated with CCl₄ by subcutaneous injection at a dosage of 3 ml/kg for 9 weeks. For group A, Ganyanping (10 ml/kg) was also administered via gastric tube along with the CCl₄ intoxication. For group B, Ganyanping treatment was started 4 weeks later and lasted for the remaining 5 weeks. For group C, Ganyanping was given after 8 weeks of CCl₄ administration, and the treatment lasted for 4 weeks. Ganyanping was administered in the form of an aqueous suspension (2 g/ml). After 9 weeks, the overnight fasting animals were anesthetized with sodium pentobarbital (30 mg/kg, per injection). Blood was taken from inferior vena cava for the estimation of biochemical parameters including values of ALT, AST, and concentrations of protein and albumin.

Pathological observations

Hepatic tissues were fixed with formalin and embedded with paraffin. The sections were stained with hematoxylin and eosin.

Samples for electron microscopy were fixed in 25 g/L glutaraldehyde buffer for two hours, then with osmium acid, dehydrated in acetone, and embedded with epoxy resin. The sections were observed under an electron microscope (OPTON EM10C, Carl Zeiss Company, Made in Germany, No.5166, voltage is 60KV).

V-G staining and enzymatic reactions

Van Gieson's method was used to demonstrate collagen fibers^[7]. HPIAS-1000 auto medical image analyzing system was used for quantitative assessment of collagen fibers in liver. Ten middle power fields were selected randomly for the total area occupied by collagen fibers and its ratio against the total area observed. Activity of monoamine oxidase (MAO) was demonstrated using 15 μm -thick frozen sections with the chayen method, that of succinic dehydrogenase (SDH) was visualized using lojda method, that of ALP with culling method, and that of ACP with Bancroft method^[8]. NOS was shown using NADPH method^[9].

Statistics

Statistical analysis with ANOVA: Data were presented as $\bar{x}\pm s$. Significant differences were determined by using ANOVA in statistical software SPSS11.0. Results were considered significant when $P<0.05$.

RESULTS

Histologic and ultrastructural findings

Liver sample from group D showed loss of normal lobular architecture. The parenchyma showed steatosis, cellular swelling, necrosis, and was divided into rounded nodules, separated by bands of fibrous tissues, while in groups A, B and C, the steatosis was not severe and the fibrosis was not so pronounced, without any pseudo-lobule observed (Figures 1, 2). Hepatocellular degeneration was frequently seen in the intoxicated animals under electron microscope, characterized by marked swelling of mitochondria, loss of rough endoplasmic reticulum structures and distention of them. Glycogen particles were greatly reduced and more lipid droplets were found in the cytoplasmic compartment. In some hepatocytes, nuclear irregularity was noted, lipid droplets and some components resembling rough endoplasmic reticulum (nuclear or pseudo-nuclear inclusions) were also found within the nuclei. A few lipid droplets were found in the cytoplasm in the Ganyanping-treated groups (Figures 3, 4).

VG staining

Fibrosis was shown in group D by VG staining, with hepatic parenchyma separated by the rough, red-stained fibrotic septa. The change was less pronounced in the Ganyanping-treated groups. The total collagen-deposited area and ratio in group D, but not in the Ganyanping-treated groups ($P<0.05$), were increased compared to those in the control group ($P<0.001$) (Table1, Figures 5, 6).

Table 1 Area occupied by fibrotic septa and its ratio to the total area examined

Groups	n	Area covered by fibrotic septa (μm^2)	Ratio (%)
N	8	35.30 \pm 13.86 ^b	0.32 \pm 0.18 ^b
A	15	200.74 \pm 33.84 ^a	1.63 \pm 0.45 ^a
B	15	148.73 \pm 45.89 ^a	1.16 \pm 0.33 ^a
C	15	158.73 \pm 40.89 ^a	1.12 \pm 0.28 ^a
D	15	840.23 \pm 81.65	7.00 \pm 0.90

^a $P<0.05$ vs Group D, ^b $P<0.001$ vs Group D.

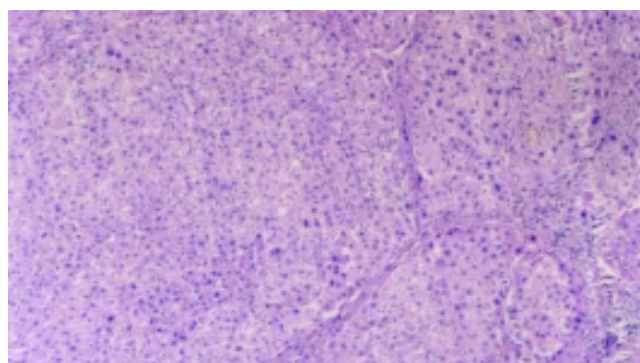


Figure 1 Loss of normal lobular architecture, some had pseudo lobule formation in the CCl_4 intoxicated groups. HE \times 100.

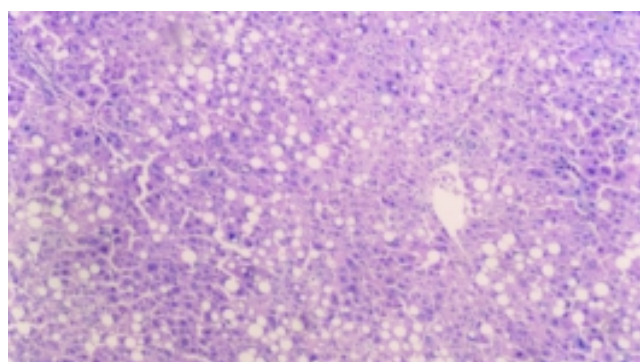


Figure 2 Steatosis was not severe and fibrosis was not so pronounced, without any pseudo-lobule formation in the Ganyanping-treated groups. HE \times 100.

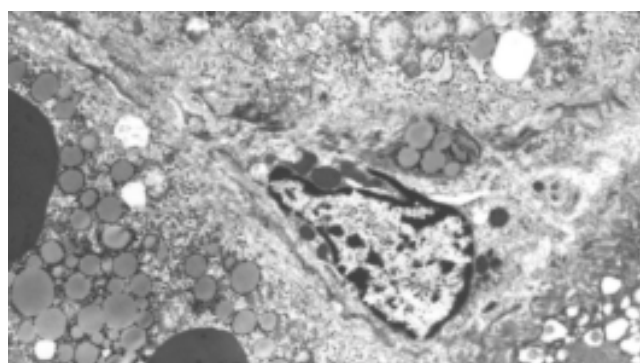


Figure 3 The numbers of hepatic stellate cells and collagen fibrils increased in Disse's space and hepatocellular degeneration were frequently seen in the CCl_4 intoxicated groups. \times 4 000.

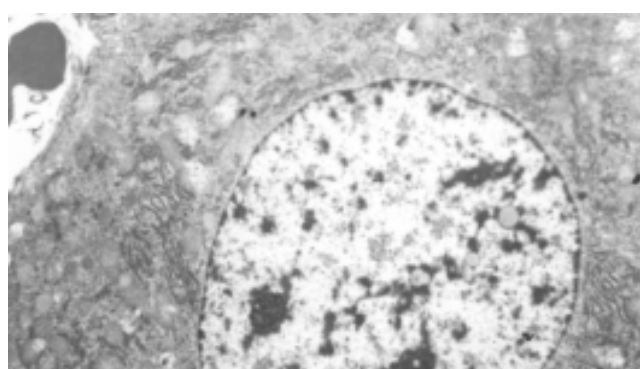


Figure 4 Most of hepatocytes showed basically normal ultrastructure and a few lipid droplets were found in the cytoplasm in the Ganyanping-treated groups. \times 4 000.

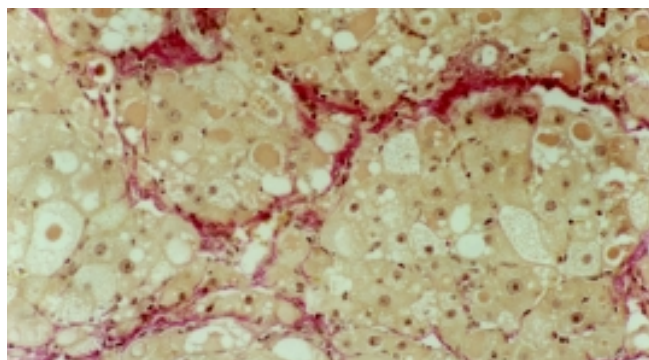


Figure 5 Hepatic parenchyma separated by the rough, red-stained fibrotic septa in the CCl₄ intoxicated groups. VG×200.

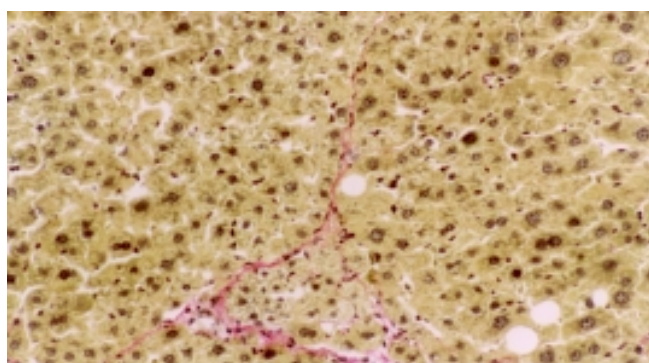


Figure 6 Collagen fibrosis was less pronounced in the Ganyanping-treated groups. VG×200.

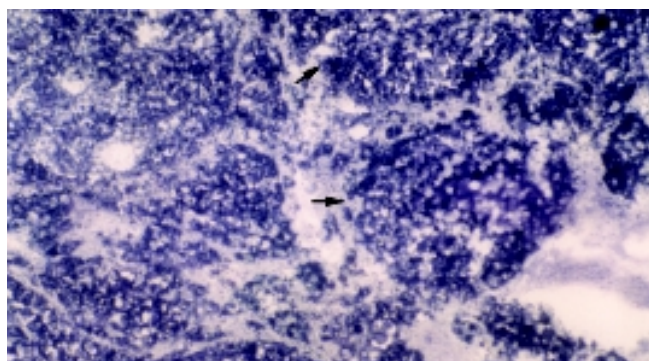


Figure 7 Increase in the activities of MAO(+++) in the CCl₄ intoxicated groups. ×75.

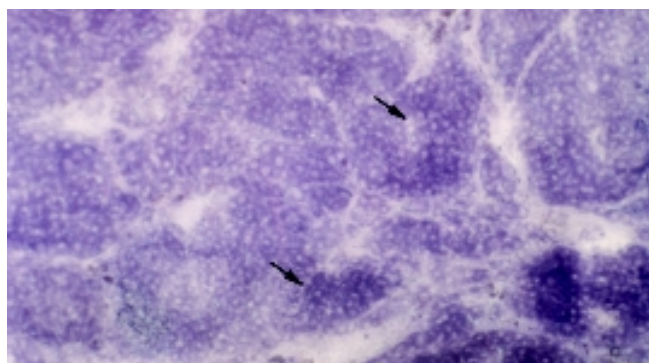


Figure 8 Decrease in the activities of MAO in the Ganyanping-treated groups (++) . ×75.

Enzymatical reactions

Activities of MAO, SDH, ALP and NOS were demonstrated in

frozen sections with the procedures described above. Those for MAO and ACP were found to be elevated and that of SDH was reduced in group D compared to those in the control group. The changes were not so marked in any of the Ganyanping-treated groups (Tables 2, 3; Figures 7, 8).

Table 2 Semiquantitative assessment of enzymatic activities in different liver samples

Groups	n	MAO	SDH	ACP	LDH	NOS	ALP
N	8	++	+++	+	++	++	++
A	15	++	+++	++	+ _i ŷ	++	++
B	15	++	+++	+	++	++	++
C	15	++	+++	+	++	++	++
D	15	+++ _i ü	+++ _i ŷ	+++ _i ü	+ _i ŷ	++	++

+: positive; ++: moderately positive; +++: strongly positive; _iü activity enhancement; _iŷ activity weakened.

Table 3 Quantitative observation of the liver enzymatic activities (mean absorbance)

Groups	n	MAO	SDH	ACP	LDH
N	8	0.2042±0.041 ^a	0.4057±0.030 ^a	0.1160±0.0338 ^a	0.1685±0.0103
A	15	0.3201±0.066 ^a	0.2917±0.045 ^a	0.1623±0.0246 ^a	0.1948±0.0319
B	15	0.3308±0.079 ^a	0.3380±0.103 ^a	0.2101±0.0342 ^a	0.1331±0.0071
C	15	0.1835±0.060 ^a	0.3939±0.0434 ^a	0.1884±0.0542 ^a	0.1757±0.0216
D	15	0.5022±0.149	0.1819±0.1049	0.4235±0.0727	0.1656±0.0145

^aP<0.05 vs group D.

DISCUSSION

It remains a problem to prevent cirrhosis or to control its progression in patients with a chronic liver disease^[10,11]. Great efforts have been made to find safe and effective drugs. Recent clinical and experimental observations have demonstrated that Chinese medicines might be of some preventive and therapeutic values against fibrosis^[12-20]. Ganyanping, prepared according to the regime of Li Shaobai *et al*^[21], has been used for many years for this purpose. However, its effect and associated mechanism need further experimental evidence. For this reason, we used CCl₄ to induce liver fibrosis and investigated herein the effects of Ganyanping on fibrosis.

Liver fibrosis is a pathologic process associated with over production and deposition of collagen fibers^[22, 23] and other extracellular matrix (ECM) components^[24-27] resulted from various hepatic diseases. It is considered a necessary intermediate step between liver parenchyma injury and cirrhosis^[28]. Activation of hepatic stellate cells (HSCs) has been shown to be one of the critical steps during hepatic fibrosis^[29-34]. It is associated to a number of pathological factors, resulting in ECM deposition and hepatic fibrosis. This was also observed in the fibrosis caused by CCl₄ intoxication, and this process could be effectively controlled by treatment with Ganyanping. The preparation was found to be inhibitory in the collagen production.

MAO is used as a marker for evaluating hepatic function in cirrhosis, its elevation indicating liver damage^[35]. An increase in MAO activity was observed in the intoxication group. Ganyanping was found to be able to abrogate this change. Thus, Ganyanping is considered to have some anti-cirrhotic effect. SDH is a rate-limiting enzyme in the tricarboxylic acid cycle^[36,37]. The elevation of its activities reflects more active metabolism. Our data indicate the treatment with Ganyanping might be helpful for liver parenchyma cells to

maintain this SDH activity through the intoxication. The treatment was also shown to be helpful for stabilizing the lysosome membrane in chronic hepatic injury, reflected by its interference to ACP values of the animals received intoxication. In the present study, activity of NOS was shown to be reduced in the CCl₄-intoxicated group, but the effect was partially abrogated by the treatment with Ganyanping, indicating that the treatment might help the liver to recover its function through the stress caused by CCl₄ administration.

In summary, Ganyanping was found to play some anti-fibrotic role. According to the theory of traditional Chinese medicine, Ganyanping may possess multiple pharmaceutical effects, such as invigorating “qi” and activating “blood”, dispersing stagnated hepatic “qi” and facilitating the discharge of “bile”, delivering “heat” and “toxins”, and eliminating “dampness” in view of its composition. Our experimental data have proved that Ganyanping could reduce oxygen-derived free radicals, and enhance the cellular metabolism and immune function, all resulting in an anti-fibrotic effect. Ganyanping may be used as a safe and effective preparation for patients with fibrosis.

REFERENCES

- 1 **Li XG**, Li SB, Wang TC, Tang WX, Du LJ, Zhang WY. Protective Effect of Gan Yanping on Con A induced liver injury. *Zhonghua Ganzhangbing Zazhi* 1996; **4**: 243-244
- 2 **Tang WX**, Yu DX, Dan ZL, Zhang WY, Du LJ, Li SB. Study on protective effect of Traditional Chinese herbs (Gan Yanping) on acute liver injury induced by D-GalN in rats. *Tongji Yike Daxue Xuebao* 1998; **27**: 56-58
- 3 **Tang WX**, Yu DX, Dan ZL, Du LJ, Zhang WY, Li SB. An experimental study on the effect of Gan Yanping on Collagen Fiber in rat Chronic Liver Induced by CCl₄. *Weichang Bingxue He Ganbingxue Zazhi* 1998; **7**: 167-169
- 4 **Du LJ**, Tang WX, Dan ZL, Zhang WY, Li SB. Protective effect of gan yanping on CCl₄ induced liver fibrosis in rats. *Shijie Huaren Xiaohua Zazhi* 1998; **6**: 22-23
- 5 **Du LJ**, Tang WX, Dan ZL, Zhang WY, Li SB. Study of protective effect of GanYanping in acute liver injury model. *Tongji Yike Daxue Xuebao* 1997; **26**: 149-151
- 6 **Tang WX**, Du LJ, Zhang WY, Xiong XK, Zhang Y. Histochemistry study on the protective effect of Gan Yanping from liver injury induced by D-GalN in rats. *Zhongguo Zuzhi Huaxue He Xibao Huaxue Zazhi* 1996; **5**: 397-340
- 7 **Wei HS**, Li DG, Lu HM, Zhan YT, Wang ZR, Huang X, Zhang J, Chang JL, Xu OF. Effects of AT1 receptor antagonist, losartan, on rat hepatic induced by CCl₄. *World J Gastroenterol* 2000; **6**: 540-545
- 8 **Pen CN**, Wang Y, Niu JZ, Weng JG, Shi SS, Shun PW, Piao YJ, Li SG, She Y, Guo SG, Peng JY, Ge ZH, Xie JY, Xiong XK. Histochemistry.1. Beijing: People's Medical Publishing Company 2001: 392-528
- 9 **Punkt K**, Zaitsev S, Vwlnr M, Schreiter T, Fitzl G, Buchwalow LB. Myopathy-dependent changes in activity of ATPase SDH and GPDH and NOS expression in the different fibre types of hamster muscles. *Acta histochem* 2002; **104**: 15-22
- 10 **Zeng MD**. Treatment of liver fibrosis. *Zhonghua Ganzhangbing Zazhi* 2001; **9**: 68-69
- 11 **Dai WJ**, Jiang HC. Advances in gene therapy of liver cirrhosis: a review. *World J Gastroenterol* 2001; **7**: 1-8
- 12 **Zheng LN**, Han T, Wang BE, Ma XM, Jia JD, Qian SC, Gao YT. Effect of Bupleurum on collagen content in hepatic stellate cell media *in vitro*. *Tianjing YiKe Daxue Xuebao* 2001; **7**: 502-504
- 13 **Cheng ML**, Wu YY, Huang KF, Luo TY, Ding YS, Lu YY, Liu RC, Wu J. Clinical study on the treatment of liver fibrosis due to hepatitis B by IFN- α 1 and traditional medicine preparation. *World J Gastroenterol* 1999; **5**: 267-269
- 14 **Liu P**, Liu C, Xu LM, Xue HM, Liu CH, Zhang ZQ. Effects of Fuzheng Huayu 319 recipe on liver fibrosis in chronic hepatitis B. *World J Gastroenterol* 1998; **4**: 348-353
- 15 **Li JM**. Recent condition of traditional chinese herb on treatment of fibrosis. *Tianjing Zhongyi Xueyuan Xuebao* 2002; **21**: 37-38
- 16 **Cai DY**, Zhao G, Chen JC, Ye GM, Bing FH, Fan BW. Therapeutic effect of Zijin capsule in liver fibrosis in rats. *World J Gastroenterol* 1998; **4**: 260-263
- 17 **Li JC**, Ding SP, Xu J. Regulating effect of Chinese herbal medicine on the peritoneal lymphatic stomata in enhancing ascites absorption of experimental hepatofibrotic mice. *World J Gastroenterol* 2002; **8**: 333-337
- 18 **Liu P**, Hu YY, Liu C, Zhu DY, Xue HM, Xu ZQ, Xu LM, Liu CH, Gu HT, Zhang ZQ. Clinical observation of salvianolic acid B in treatment of liver fibrosis in chronic hepatitis B. *World J Gastroenterol* 2002; **8**: 679-685
- 19 **Shen BS**, Wong XG, Qiao HC, Lu ZH, Han Q, Wang W, Guan HL. Preventive effect of Sanjia Yigan granule in hepatofibrosis in rats. *Shijie Huaren Xiaohua Zazhi* 1998; **6**: 386-388
- 20 **Liu CH**, Hu YY, Wang XL, Liu P, Xu LM. Effects of salvianolic acid-A on NIH/3T3 fibroblast proliferation, collagen synthesis and gene expression. *World J Gastroenterol* 2000; **6**: 361-364
- 21 **Du LJ**, Tang WX, Zhang WY, Li SB. Effect of Gan Yanping on Cytokines in acute liver injury induced by D-GalN in rats. *Zhongxiyi Jiehe Ganbingxue Zazhi* 1998; **8**: 28-30
- 22 **Wang AM**, Wang BE, Yang YW, Zhang B, Jiang LA, Du SC. Interstitial collagenase gene expression in patients with liver disease. *Linchuang Gandanbing Zazhi* 2000; **16**: 90-91
- 23 **Nie QH**, Cheng YQ, Xie YM, Zhou YX, Cao YZ. Inhibiting effect of antisense oligonucleotides phosphorothioate on gene expression of TIMP-1 in rat liver fibrosis. *World J Gastroenterol* 2001; **7**: 363-369
- 24 **Wang TL**, Wang BE, Zhang HH, Liu X, Dan ZP, Zhang J, Ma H, Li XM, Li NZ. Pathology study of the therapeutic effect on HBV-related liver fibrosis with herbal compound 861. *Zhongguo Weichang Bingxue He Ganbingxue Zazhi* 1998; **7**: 148-150
- 25 **Wang TL**, Zhang B, Jie J. Effect of anti-fibrosis compound on collagen expression of hepatic cells in experimental liver fibrosis of rats. *World J Gastroenterol* 2000; **6**: 877-880
- 26 **George J**, Rao KR, Stem R, Chandrakasan G. Dimethylnitrosamine-induced liver injury in rats: the early deposition of collagen. *Toxicology* 2001; **156**: 129-138
- 27 **Wang BE**. Hepatic stellate cell and Fibrosis. *Zhonghua Ganzhangbing Zazhi* 2000; **8**: 197-199
- 28 **Wang GY**, Cai WM, Wang JQ, Weng HR, Cheng F. An experimental study of histological quantitative method in the diagnosis of hepatic fibrosis. *Zhonghua Ganzhangbing Zazhi* 1998; **6**: 201-202
- 29 **Cheng ML**, Wu J, Wang HQ, Xue LM, Tan YZ, Ping L, Li CX, Huang NH, Yao YM, Ren LZ, Ye L, Li L, Jia ML. Effect of Maotai liquor in inducing metallothioneins and on hepatic stellate cells. *World J Gastroenterol* 2002; **8**: 520-523
- 30 **Wei HS**, Lu HM, Li DG, Zhan YT, Wang ZR, Huang X, Cheng JL, Xu QF. The regulatory role of AT 1 receptor on activated HSCs in hepatic fibrogenesis: effects of RAS inhibitors on hepatic fibrosis induced by CCl₄. *World J Gastroenterol* 2000; **6**: 824-828
- 31 **Zhan YT**, Zhan CY, Chen YW, Li DG. Hepatic stellate cell and Fibrosis. *Linchuang Gandanbing Zazhi* 2000; **16**: 71-73
- 32 **Lou Y**, Dai LL, Shen DM. Research progress of hepatic stellate cell and fibrosis. *Zhonghua Ganzhangbing Zazhi* 2000; **8**: 251-252
- 33 **Liu J**, Zhao FD, Jia SJ, Han QR. The study of VG staining for liver fibrosis of chronic liver diseases. *Jilin Yixueyuan Xuebao* 1998; **18**: 21-22
- 34 **Ma H**, Wang BE, Ma XM, Jia JD. Effect of compound 861 on rat hepatic cell collagen synthesis and degradation *in vitro*. *Zhonghua Ganzhangbing Zazhi* 1999; **7**: 30-32
- 35 **Wang W**, Liu HL. Significance and change of HA, LN and MAO of hepatitis B patients' serum. *Bao Tou Yixue Zazhi* 2001; **17**: 41-42
- 36 **Shah V**, Toruner M, Haddad F, Cadelina G, Papapetropoulos A, Choo K, Sessa WC, Groszmann RJ. Impaired endothelial nitric oxide synthase activity associated with enhanced caveolin binding in experimental cirrhosis in the rat. *Gastroenterology* 1999; **117**: 1222-1228
- 37 **Song BC**, Yin SY, Tang WX, Xiong XK. Study on enzyme histochemistry of experimental cirrhosis liver. *Zhongguo Zuzhi Huaxue he Xibao Huaxue Zazhi* 1999; **8**: 47-50

NF- κ B activation and zinc finger protein A20 expression in mature dendritic cells derived from liver allografts undergoing acute rejection

Ming-Qing Xu, Wei Wang, Lan Xue, Lv-Nan Yan

Ming-Qing Xu, Wei Wang, Lv-Nan Yan, Department of General Surgery, West China (Huaxi) Hospital, Sichuan University, Chengdu 610041, Sichuan Province, China

Lan Xue, 208 PLA Hospital, Changchun 130021, Jilin Province, China

Correspondence to: Dr Ming-Qing Xu, Department of General Surgery, West China Hospital, Sichuan University, Chengdu 610041, Sichuan Province, China. xumingqing@hotmail.com

Telephone: +86-28-85582968

Received: 2002-12-22 **Accepted:** 2003-02-16

Abstract

AIM: To investigate the role of NF- κ B activation and zinc finger protein A20 expression in the regulation of maturation of dendritic cells (DCs) derived from liver allografts undergoing acute rejection.

METHODS: Sixty donor male SD rats and sixty recipient male LEW rats weighing 220-300 g were randomly divided into whole liver transplantation group and partial liver transplantation group. Allogeneic (SD rat to LEW rat) whole and 50 % partial liver transplantation were performed. DCs from liver grafts 0 hour and 4 days after transplantation were isolated and propagated in the presence of GM-CSF *in vitro*. Morphological characteristics and phenotypical features of DCs propagated for 10 days were analyzed by electron microscopy and flow cytometry, respectively. NF- κ B binding activity, IL-12p70 protein and zinc finger protein A20 expression in these DCs were measured by EMSA and Western blotting, respectively. Histological grading of rejection was determined.

RESULTS: Allogeneic whole liver grafts showed no signs of rejection on day 4 after the transplantation. In contrast, allogeneic partial liver grafts demonstrated moderate to severe rejection on day 4 after the transplantation. After propagation for 10 days in the presence of GM-CSF *in vitro*, DCs from allogeneic whole liver grafts exhibited features of immature DC with absence of CD40 surface expression, these DCs were found to exhibit detectable but very low level of NF- κ B activity, IL-12 p70 protein and zinc finger protein A20 expression. Whereas, DCs from allogeneic partial liver graft 4 days after transplantation displayed features of mature DC, with high level of CD40 surface expression, and as a consequence, higher expression of IL-12p70 protein, higher activities of NF- κ B and higher expression of zinc finger protein A20 compared with those of DCs from whole liver grafts ($P < 0.001$).

CONCLUSION: These results suggest that A20 expression is up-regulated in response to NF- κ B activation in mature DCs derived from allogeneic liver grafts undergoing acute rejection. Given the NF- κ B inhibition function of this gene, it is suggested that their expression survives to limit NF- κ B activation and maturation of DCs,

and consequently inhibits the acute rejection and induces acceptance of liver graft.

Xu MQ, Wang W, Xue L, Yan LN. NF- κ B activation and zinc finger protein A20 expression in mature dendritic cells derived from liver allografts undergoing acute rejection. *World J Gastroenterol* 2003; 9(6): 1296-1301

<http://www.wjgnet.com/1007-9327/9/1296.asp>

INTRODUCTION

Dendritic cells (DCs) are specialized antigen-presenting cells (APCs) that play an essential role in the activation of lymphocytes^[1-10]. Among APCs, which also include macrophages and B cells, only DCs are believed to be capable of activating naive T cells. DC function is regulated by their state of maturation. Immature DCs resident in nonlymphoid tissues such as normal liver are deficient at antigen capture and progressing processing^[11,12]. "Maturation" of DC can be induced by microbial stimuli, proinflammatory cytokines, as well as through interaction with CD40L-CD40 cross-linking^[13-20]. The control of DC maturation and activation plays an important role in regulating their T cell priming functions^[21]. Significantly, engagement of CD40 expressed on DCs with CD40L expressed on T cells not only stimulates maturation and cytokine production but also enhances DC survival and activation^[19, 22, 23]. Mature DCs are highly immunogenic due to high levels of expression of MHC I and II, costimulatory and adhesion molecules, including B7-1, B7-2, CD40, and ICAM-1^[11-19]. In the case of experimental skin, heart, or kidney allografts, mature dendritic cells resident in donor tissue have been implicated as the principal instigators of rejection. Whereas, DCs derived from normal liver display an immature phenotype with absence of costimulatory molecules (CD40, CD80 and CD86) surface expression, low levels of MHC class I and II, and as a consequence, low stimulatory capacity for naive allogeneic T cells. Unlike mature DC, these liver-derived immature DCs do not induce detectable levels of intracytoplasmic IFN- γ in allogeneic CD4⁺ cells in 72-h MLR, and elicit very low levels of CTLs *in vitro*^[11, 12]. It has been observed that liver-derived^[11, 24] or bone marrow-derived immature DCs^[25], propagated *in vitro* and lacking surface costimulatory molecules, can prolong heart or pancreatic islet allograft survival. Whereas, marked augmentation of DCs numbers and maturation of DCs in liver allografts by donor treatment with the hematopoietic growth factor fms-like tyrosine kinase 3 (Flt3) ligand (FL) results in acute liver graft rejection^[26, 27].

Although the significance of DCs as regulators of transplantation immunity is beyond doubt, little is known about intracellular mechanisms specifically responsible for regulation of DC activation and maturation. Previous studies have suggested that NF- κ B may play a key role in DC maturation^[20, 28-30], and NF- κ B inhibition could impair the maturation and function of DC^[28, 29].

A20 is a zinc finger protein originally identified as a TNF-

inducible gene product in endothelial cells (EC), and has been shown to be dependent upon NF- κ B for its expression. A20 is expressed in a variety of cell types including fibroblasts, B, T, and β -cells in response to different stimuli including LPS, IL-1 and CD40 cross-linking^[31-36]. A20 is itself a NF- κ B-dependent gene and is part of a negative regulatory loop critical for modulation of cell activation^[37, 38]. A20 serves a broad cytoprotective function in EC by protecting EC from apoptosis and down-regulating inflammatory responses via NF- κ B inhibition^[39]. A20^{-/-} knock-out mice are born cachectic and die within 3 weeks from severe and uncontrolled inflammation that further confirms the potent anti-inflammatory function of A20^[40]. A20 is also part of the physiologic NF- κ B-dependent survival response of hepatocytes to injury, limited expression of A20 in hepatocytes drastically improves the fate of mice in the D-gal/LPS model of toxic FHF where A20 protects hepatocytes from apoptosis and promotes the liver regeneration^[37]. In addition, investigation has shown that A20 expression is up-regulated in human renal allografts in response to immune injury inferred by acute rejection, and the result suggests that A20 could limit graft injury^[41].

Although A20 is a very effective inhibitor of NF- κ B activation induced by LPS, IL-1 and CD40 cross-linking, little is known about the role of A20 in the regulation of maturation of DCs derived from allogeneic liver grafts accompanied by acute rejection.

The purpose of the present study was to investigate the binding activity of NF- κ B DNA and A20 expression in mature DCs derived from allogeneic partial liver grafts undergoing acute rejection in rats. Attempts were made also to correlate A20 expression in DCs derived from liver grafts with the acceptance of allogeneic liver grafts.

MATERIALS AND METHODS

Animals

Sixty donor male SD rats and sixty recipient male LEW rats weighing 220-300 g were randomly divided into whole liver transplantation group and partial liver transplantation group. Allogeneic whole and 50 % partial liver transplantation were performed using a SD to LEW combination. The animals were purchased from Chinese Academy of Sciences and Sichuan University. They were maintained with a 12-hour light/dark cycle in a conventional animal facility with water and commercial chow provided ad libitum, with no fasting before the transplantation.

Liver transplantation

All operations were performed under ether anesthesia in clean but not sterile conditions. All surgical procedures were performed from 8 a.m to 5 p.m. Donors and recipients of similar weight (± 10 g) were chosen. Liver reduction was achieved by removing the left lateral lobe and the two caudate lobes, which resulted in a 50 % reduction of the liver mass. Whole liver transplantation (WLT) and partial liver transplantation (PLT) were performed according to the method described in our previous study^[42].

Histology

Part of liver tissues was sectioned and preserved in 10 % formalin, embedded in paraffin, cut with microtome, and stained with hematoxylin and eosin. The histological grading of rejection was determined according to the criteria described by Williams.

Propagation and purification of liver graft-derived DC populations

DCs from liver graft 0 hour and 4 days after the transplantation

were propagated in GM-CSF from nonparenchymal cells (NPC) isolated from collagenase-digested liver graft tissue, as described by Lu *et al.*^[24]. Nonadherent cells, released spontaneously from proliferating cell clusters, were collected after culture for 10 days, and purified by centrifugation 500 \times g, for 10 minutes at room temperature on a 16 % w/v metrizamide gradient (DC purity 80-85 %).

Morphological and phenotypical features of DCs

Morphological characteristics of DCs derived from liver graft were observed by electron microscopy. Expression of cell surface molecules was quantitated by flow cytometry as described in our previous study^[42]. Aliquots of 2×10^5 DCs propagated for 10 days *in vitro* were incubated with the following primary mouse anti-rat mAbs against OX62, CD40 (Serotec, USA), or rat IgG as an isotype control for 60 minutes on ice (1 μ g/ml diluted in PBS/1.0 % FCS). The cells were washed with PBS/1.0 % FCS and labeled with FITC-conjugated goat anti-mouse IgG, diluted 1/50 in PBS/1.0 % FCS for 30 minutes on ice. At the end of this incubation, cells were washed, propidium iodide/PBS were added, and the cells were subsequently analyzed in an FACS-4200 flow cytometer (Becton-Dickinson, USA).

Isolation of nuclear proteins

Nuclear proteins were isolated from DCs extract by placing the sample in 0.9 ml of ice-cold hypotonic buffer [10 mM \cdot L⁻¹ HEPES (pH7.9), 10 mM \cdot L⁻¹ KCl, 0.1 mM \cdot L⁻¹ EDTA, 0.1 mM \cdot L⁻¹ ethylene glycol tetraacetic acid, 1 mM \cdot L⁻¹ DTT; Protease inhibitors (aprotinin, pepstatin, and leupeptin, 10 mg \cdot L⁻¹ each)]. The homogenates were incubated on ice for 20 minutes, vortexed for 20 seconds after adding 50 μ l of 10 % Nonide-P40, and then centrifuged for 1 minutes at 4 $^{\circ}$ C in an Eppendorf centrifuge. Supernatants were decanted, the nuclear pellets after a single wash with hypotonic buffer without Nonide-P40 were suspended in an ice-cold hypertonic buffer [20 mM \cdot L⁻¹ HEPES (pH7.9), 0.4 M \cdot L⁻¹ NaCl, 1 mM \cdot L⁻¹ EDTA, 1 mM \cdot L⁻¹ DTT; Protease inhibitors], incubated on ice for 30 minutes at 4 $^{\circ}$ C, mixed frequently, and centrifuged for 15 minutes at 4 $^{\circ}$ C. The supernatants were collected as nuclear extracts and stored at -70 $^{\circ}$ C. Concentrations of total proteins in the samples were determined according to the method of Bradford.

Electrophoretic mobility shift assay (EMSA) for NF- κ B activation of DCs

NF- κ B binding activity was performed in a 10- μ l binding reaction mixture containing 1 \times binding buffer [50 mg \cdot L⁻¹ of double-stranded poly (dI-dC), 10 mM \cdot L⁻¹ Tris-HCl (pH7.5), 50 mM \cdot L⁻¹ NaCl, 0.5 mM \cdot L⁻¹ EDTA, 0.5 mM \cdot L⁻¹ DTT, 1 mM \cdot L⁻¹ MgCl₂, and 100 ml \cdot L⁻¹ glycerol], 5 μ g of nuclear protein, and 35 fmol of double-stranded NF- κ B consensus oligonucleotide (5' -AGT TGA GGG GAC TTT CCC AGG-3') that was endly labeled with γ -³²P (111TBq mM⁻¹ at 370 GBq⁻¹) using T4 polynucleotide kinase. The binding reaction mixture was incubated at room temperature for 20 minutes and analyzed by electrophoresis on 7 % nondenaturing polyacrylamide gels. After electrophoresis, the gels were dried by Gel-Drier (Biol-Rad Laboratories, Hercules, CA) and exposed to Kodak X-ray films at -70 $^{\circ}$ C.

Western blotting for IL-12 p70 and zinc finger protein A20 expression in DCs

DCs cultured for 10 days *in vitro* were starved in serum-free medium for 4 hours at 37 $^{\circ}$ C. These cells were washed twice in cold PBS, resuspended in 100 μ l lysis buffer (1 % Nonidet-P40, 20 mM Tris-HCl, pH8.0, 137 mM NaCl, 10 % glycerol,

2 mM EDTA, 10 $\mu\text{g} \cdot \text{mL}^{-1}$ leupeptin, 10 $\mu\text{g} \cdot \text{mL}^{-1}$ aprotinin, 1 mM PMSF, and 1 mM sodium orthovanadate), and total cell lysates were obtained. The homogenates were centrifuged at 10 000 \times g for 10 minutes at 4 $^{\circ}\text{C}$. Cell lysates (20 μg) were electrophoresed on SDS-PAGE gels, and transferred to PVDC membranes for Western blot analysis. Briefly, PVDC membranes were incubated in a blocking buffer for 1 hour at room temperature, then incubated for 2 hours with Abs raised against IL-12 p70 and A20 (Santa Cruz, CA). The membranes were washed and incubated for 1 hour with HRP-labeled IgG. Immunoreactive bands were visualized by ECL detection reagent. The binding bands were quantified by scanning densitometer of a Bio-Image Analysis System. The results were expressed as relative optical density.

Statistics analysis

Statistic analysis of data was performed using the Student's *t*-test; $P < 0.05$ was considered statistically significant.

RESULTS

Histological rejection

Histological rejection features of allografted livers were compared between the whole and partial groups on day 4 after the transplantation, allogeneic whole liver grafts demonstrated no rejection. In contrast, partial liver grafts demonstrated moderate to severe rejection, including inflammatory cellular infiltration in the portal tract, endotheliitis, bile duct damage and hepatocytes necrosis.

Phenotypic characteristics of liver graft-derived DCs propagated in vitro

As shown in our previous study^[42], after cultured for 10 days in the presence of GM-CSF, DCs both from whole and partial liver grafts displayed typical morphological features of DC, including anomalous shape, bigger body, and numerous longer dendrites. Flow cytometry showed 80-85 % of these DCs strongly expressed rat DC - specific OX62 antigen molecule, which suggested that high purity DCs were obtained. Flow cytometric analysis showed that DCs from whole liver grafts and from partial liver grafts 0 hour after the transplantation were negative for the costimulatory molecule CD40 expression, which was an immature phenotype (CD40⁻), whereas DCs from partial liver graft 4 days after the transplantation showed high level of CD40 expression, which was a mature phenotype (CD40⁺). These results suggested maturation of DCs resident in allogeneic partial liver graft undergoing acute rejection.

IL-12 p70 protein expression in DCs derived from allogeneic partial liver grafts

Our previous study showed that IL-12 p35 and IL-12 p40 subunit expressions were significantly up-regulated in mature DCs derived from allogeneic partial liver grafts undergoing acute rejection^[42]. In the present study, we evaluated IL-12 p70 expression in DCs from allogeneic liver grafts. As shown in Figure 1, DCs derived from both whole and partial liver grafts 0 hour after the transplantation expressed detectable but very low level of IL-12 p70, and expression level of IL-12 p70 in DCs from whole liver graft 4 days after transplantation was not elevated compared with those of DCs from whole liver graft 0 hour after the transplantation ($P > 0.05$). However, expression of IL-12 p70 in DCs from partial liver graft 4 days after transplantation was markedly increased, and their expression levels were significantly higher than those of DCs both from partial liver graft 0 hour and whole liver graft 4 days after transplantation ($P < 0.001$).

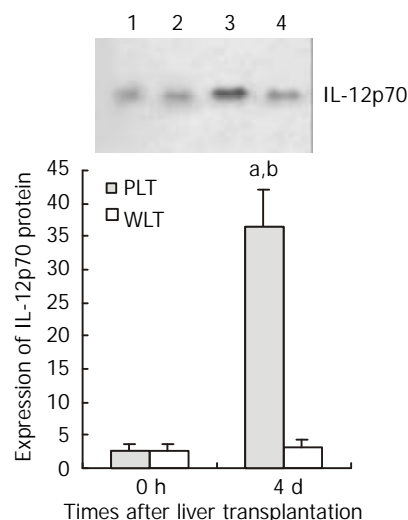


Figure 1 Expression of IL-12 p70 in liver graft - derived DCs by Western blotting. Lanes 1, 2: Expression of IL-12 p70 in DCs from partial liver graft and whole liver graft 0 hour after transplantation. Lanes 3, 4: Expression of IL-12 p70 in DCs from partial liver graft and whole liver graft 4 days after transplantation. ^a $P < 0.001$ vs 4d WLT group; ^b $P < 0.001$ vs 0 hour PLT group.

Electrophoretic mobility shift assay (EMSA) for NF- κ B activation of DCs

As shown in Figure 2, EMSA analysis showed detectable but very low level of NF- κ B activity of DCs derived from both whole and partial liver grafts 0 hour after transplantation, and NF- κ B activity of DCs from whole liver graft 4 days after transplantation was not increased compared with those of DCs from liver graft 0 hour after transplantation ($P > 0.05$). However, NF- κ B activity of DCs from partial liver graft 4 days after transplantation was significantly elevated compared with those of DCs from partial liver graft 0 hour and whole liver graft 4 days after transplantation ($P < 0.001$).

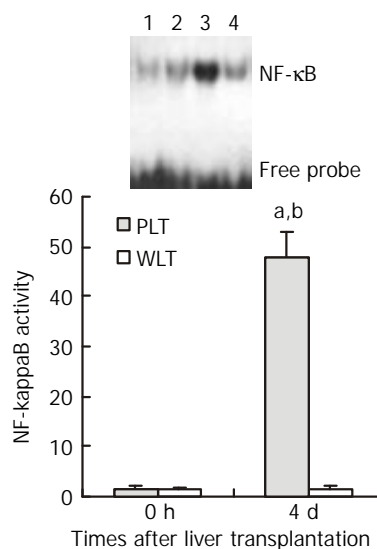


Figure 2 NF- κ B activation of DCs derived from allogeneic liver grafts. Lanes 1, 2: NF- κ B activation of DCs from partial liver graft and whole liver graft 0 hour after transplantation. Lanes 3, 4: NF- κ B activation of DCs from partial liver graft and whole liver graft 4 days after transplantation. ^a $P < 0.001$ vs 4 d WLT group; ^b $P < 0.001$ vs 0 hour PLT group.

A20 protein expression in DCs derived from partial liver allografts

In order to investigate the intracellular mechanisms specifically

responsible for regulation of DC activation and maturation, we evaluated NF- κ B inhibitor zinc finger protein A20 expression in DCs derived from allogeneic liver grafts. As shown in Figure 3, DCs from both whole and partial liver grafts 0 hour after the transplantation expressed detectable but very low level of A20, and expression level of A20 in DCs derived from whole liver graft 4 days after transplantation was not increased compared with those of DCs from whole liver graft 0 hour after transplantation ($P>0.05$). However, expression of A20 in DCs from partial liver graft 4 days after transplantation was markedly up-regulated, and its expression level was significantly higher than those of DCs both from partial liver graft 0 hour and whole liver graft 4 days after transplantation ($P<0.001$).

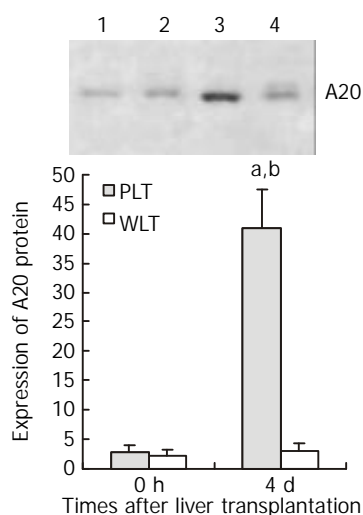


Figure 3 Expression of A20 protein in DCs derived from allogeneic liver grafts. Lanes 1, 2: Expression of A20 protein in DCs from partial liver graft and whole liver graft 0 hour after transplantation. Lanes 3, 4: Expression of A20 protein in DCs from partial liver graft and whole liver graft 4 days after transplantation. ^a $P<0.001$ vs 4 d WLT group; ^b $P<0.001$ vs 0 hour PLT group.

DISCUSSION

Despite the emergence of DCs as key cellular players in the immune system, the signal transduction events that regulate DC maturation and function have been poorly understood. This study was conducted to explore whether NF- κ B activation and its inducible expression gene of A20 could be detected in mature DCs derived from liver allograft undergoing acute rejection. Our aim was to determine whether A20 gene is involved in NF- κ B inhibition of these mature DCs. In the present study, it has been shown that engagement of CD40 on DCs derived from allogeneic partial liver grafts undergoing acute rejection leads to a powerful NF- κ B activation of these mature DCs, and as a consequence, leads to high level expression of the protective gene A20 in these DCs. Expression of this gene in mature DCs derived from liver graft undergoing acute rejection is consistent with their known potential to be induced in response to NF- κ B activation.

It has been shown that DCs derived from allogeneic partial liver grafts undergoing acute rejection displayed mature phenotypic high level CD40 expression and NF- κ B activation. Although resting DCs residing in normal liver tissues display only low levels of CD40, B7, and MHC class II molecule expression^[11, 12, 24]. The ischemia/reperfusion injury which is consecutive to the transplantation procedure will rapidly activate them. In addition, partial hepatectomy has been reported to induce the expression of MHC II on Kupffer cell.

Interstitial dendritic cells and sinusoidal endothelium in rats, together with the up-regulated TNF- α production after partial hepatectomy would induce the expression of B7 and CD40 molecules on DCs^[16]. These factors could stimulate maturation of DCs derived from partial liver grafts. These mature DCs may contribute to the allogeneic liver graft rejection induction. Previously other studies showed that mature DC could provide signals able to trigger T cell proliferation after TCR engagement^[43, 44]. These accessory, or "costimulatory" signals, are consecutive to interactions between costimulatory molecules present on activated DC such as B7, CD40, and OX40-ligand and their respective counter-receptors, CD28, CD40-ligand, and OX40, on T cell membranes. Several intracellular signals follow the engagement of costimulatory molecules. Interactions of CD40L, CD28, and OX40 with their ligands on DCs activate the transcription factor NF- κ B in both T cells and DCs^[29, 30]. In turn, NF- κ B initiates the transcription of numerous genes involved in immune activation, such as chemokines and cytokines^[20, 30], and also of costimulatory molecules themselves. For instance, CD40 ligation on the APC will up-regulate its expression of B7 molecules. This initiates positive feedback loops ultimately contributing to T cell expansion^[45]. Among the costimulatory molecules, CD40 and B7 seem to play a crucial role in alloreactive responses. Indeed, blockade of both CD40 and B7 molecules at the time of transplantation prevents allograft rejection and induces alloreactive T cell anergy^[46, 47]. In the present study, DCs derived from allogeneic partial liver grafts undergoing acute rejection demonstrated high level expression of CD40, which could interact with the CD40-ligand on T cells, leading to a powerful NF- κ B activation and high level of IL-12p70 expression in these mature DCs. Given an essential role for NF- κ B transcription in LPS- and CD40L - induced expression of IL-12 (IL-12 p35, p40 and p70) in DCs^[20], IL-12 is a key inducer of liver graft rejection^[26], together with high level of IL-12 p35 and IL-12 p40 protein expression in the mature DCs derived from allogeneic liver grafts undergoing acute rejection^[42]. Our results suggest that NF- κ B may play a key role in the maturation of DCs derived from allogeneic liver grafts undergoing acute rejection.

To provide further insights into potential intracellular mechanisms responsible for maturation regulation of DCs derived from allogeneic liver grafts undergoing acute rejection, we measured the protective A20 gene expression in these DCs. Zinc finger protein A20 is a potent inhibitor of NF- κ B^[31], and although other studies have shown A20 is mainly expressed in endothelial and infiltrating mononuclear cells of human renal allografts undergoing acute rejection^[41], little is known about whether it is also involved in the regulation of DC maturation and activation. Our results first demonstrate that high level A20 expression is detected in the mature DCs (which present significant NF- κ B activation) derived from acute rejecting liver allografts, but few A20 is detected in the immature DCs (which present few NF- κ B activation) derived from nonrejecting liver allografts. Given A20 is itself a NF- κ B - dependent gene and is part of a negative regulatory loop critical for modulation of cell activation^[37, 38], together with NF- κ B which may play a key role in the maturation of DCs derived from liver allografts undergoing acute rejection, it is suggested that A20 expression in these mature DCs derived from liver allografts undergoing acute rejection survives to inhibit NF- κ B activation and to limit maturation of these DCs, and as a consequence to limit the graft rejection.

In summary, we demonstrate for the first time an association between NF- κ B activation and expression of the protective gene A20 and maturation of DCs derived from liver allografts undergoing acute rejection. NF- κ B binding activity and A20 expression in these mature DCs are strongly up-regulated in

response to acute rejection. NF- κ B may play a key role in the maturation of DCs derived from allogeneic liver grafts undergoing acute rejection, and A20 expression in these mature DCs derived from liver allografts undergoing acute rejection survives to inhibit NF- κ B activation and to limit maturation of these DCs.

REFERENCES

- Zhang JK**, Chen HB, Sun JL, Zhou YQ. Effect of dendritic cells on LPAK cells induced at different times in killing hepatoma cells. *Shijie Huaren Xiaohua Zazhi* 1999; **7**: 673-675
- Li MS**, Yuan AL, Zhang WD, Chen XQ, Tian XH, Piao YT. Immune response induced by dendritic cells induce apoptosis and inhibit proliferation of tumor cells. *Shijie Huaren Xiaohua Zazhi* 2000; **8**: 56-58
- Luo ZB**, Luo YH, Lu R, Jin HY, Zhang BP, Xu CP. Immunohistochemical study on dendritic cells in gastric mucosa of patients with gastric cancer and precancerous lesions. *Shijie Huaren Xiaohua Zazhi* 2000; **8**: 400-402
- Li MS**, Yuan AL, Zhang WD, Liu SD, Lu AM, Zhou DY. Dendritic cells *in vitro* induce efficient and special anti-tumor immune response. *Shijie Huaren Xiaohua Zazhi* 1999; **7**: 161-163
- Wang FS**, Xing LH, Liu MX, Zhu CL, Liu HG, Wang HF, Lei ZY. Dysfunction of peripheral blood dendritic cells from patients with chronic hepatitis B virus infection. *World J Gastroenterol* 2001; **7**: 537-541
- Zhang JK**, Li J, Chen HB, Sun JL, Qu YJ, Lu JJ. Antitumor activities of human dendritic cells derived from peripheral and cord blood. *World J Gastroenterol* 2002; **8**: 87-90
- Tang ZH**, Qiu WH, Wu GS, Yang XP, Zou SQ, Qiu FZ. The immunotherapeutic effect of dendritic cells vaccine modified with interleukin-18 gene and tumor cell lysate on mice with pancreatic carcinoma. *World J Gastroenterol* 2002; **8**: 908-912
- Zhang J**, Zhang JK, Zhuo SH, Chen HB. Effect of a cancer vaccine prepared by fusions of hepatocarcinoma cells with dendritic cells. *World J Gastroenterol* 2001; **7**: 690-694
- Banchereau J**, Briere F, Caux C, Davoust J, Lebecque S, Liu YJ, Pulendran B, Palucka K. Immunobiology of dendritic cells. *Annu Rev Immunol* 2000; **18**: 767-811
- Banchereau J**, Steinman RM. Dendritic cells and the control of immunity. *Nature* 1998; **392**: 245-252
- Khanna A**, Morelli AE, Zhong CP, Takayama T, Lu LN, Thomson AW. Effects of liver-derived dendritic cell progenitors on Th1- and Th2-like cytokine responses *in vitro* and *in vivo*. *J Immunol* 2000; **164**: 1346-1354
- Morelli AE**, O'Connell PJ, Khanna A, Logar AJ, Lu LN, Thomson AW. Preferential induction of Th1 responses by functionally mature hepatic (CD8 α^+ and CD8 α^+) dendritic cells: association with conversion from liver transplant tolerance to acute rejection. *Transplantation* 2000; **69**: 2647-2657
- Hertz CJ**, Kiertscher SM, Godowski PJ, Bouis DA, Norgard MV, Roth MD, Modlin RL. Microbial lipopeptides stimulate dendritic cell maturation via Toll-like receptor 2. *J Immunol* 2001; **166**: 2444-2450
- Thoma-Uszynski S**, Kiertscher SM, Ochoa MT, Bouis DA, Norgard MV, Miyake K, Godowski PJ, Roth MD, Modlin RL. Activation of toll-like receptor 2 on human dendritic cells triggers induction of IL-12, but not IL-10. *J Immunol* 2000; **165**: 3804-3810
- Kaisho T**, Takeuchi O, Kawai T, Hoshino K, Akira S. Endotoxin-induced maturation of MyD-88 deficient dendritic cells. *J Immunol* 2001; **166**: 5688-5694
- Kitamura H**, Iwakabe K, Yahata T, Nishimura S, Ohta A, Ohmi Y, Sato M, Takeda K, Okumura K, Van Kaer L, Kawano T, Taniguchi M, Nishimura T. The natural killer T (NKT) cell ligand α -galactosylceramide demonstrates its immunopotentiating effect by inducing interleukin (IL)-12 production by dendritic cells and IL-12 receptor expression on NKT cells. *J Exp Med* 1999; **189**: 1121-1128
- Nagayama H**, Sato K, Kawasaki H, Enomoto M, Morimoto C, Tadokoro K, Juji T, Asano S, Takahashi TA. IL-12 responsiveness and expression of IL-12 receptor in human peripheral blood monocyte-derived dendritic cells. *J Immunol* 2000; **165**: 59-66
- Visintin A**, Mazzoni A, Spitzer JH, Wyllie DH, Dower SK, Segal DM. Regulation of Toll-like receptor in human monocytes and dendritic cells. *J Immunol* 2001; **166**: 249-255
- Corinti S**, Albanesi C, la Sala A, Pastore S, Girolomoni G. Regulatory activity of autocrine IL-10 on dendritic cell functions. *J Immunol* 2001; **166**: 4312-4318
- Ouaaz F**, Arron J, Zheng Y, Choi Y, Beg AA. Dendritic cell development and survival require distinct NF- κ B subunits. *Immunity* 2002; **16**: 257-270
- Josien R**, Li HL, Ingulli E, Sarma S, Wong BR, Vologodskaya M, Steinman RM, Choi Y. TRANCE, a tumor necrosis factor family member, enhances the longevity and adjuvant properties of dendritic cells *in vivo*. *J Exp Med* 2000; **191**: 495-502
- Miga AJ**, Masters SR, Durell BG, Gonzalez M, Jenkins MK, Maliszewski C, Kikutani H, Wade WF, Noelle RJ. Dendritic cell longevity and T cell persistence is controlled by CD154-CD40 interactions. *Eur J Immunol* 2001; **31**: 959-965
- Cella M**, Scheidegger D, Palmer-Lehmann K, Lane P, Lanzavecchia A, Alber G. Ligation of CD40 on dendritic cells triggers production of high levels of interleukin-12 and enhances T cell stimulatory capacity: T-T help via APC activation. *J Exp Med* 1996; **184**: 747-752
- Lu L**, Woo J, Rao AS, Li Y, Watkins SC, Qian S, Starzl TE, Demetris AJ, Thomson AW. Propagation of dendritic cell progenitors from normal mouse liver using granulocyte/macrophage colony-stimulating factor and their maturational development in the presence of type-1 collagen. *J Exp Med* 1994; **179**: 1823-1834
- Khanna A**, Steptoe RJ, Antonysamy MA, Li W, Thomson AW. Donor bone marrow potentiates the effect of tacrolimus on nonvascularized heart allograft survival: association with microchimerism and growth of donor dendritic cell progenitors from recipient bone marrow. *Transplantation* 1998; **65**: 479-485
- Li W**, Lu L, Wang Z, Wang L, Fung JJ, Thomson AW, Qian S. IL-12 antagonism enhances apoptotic death of T cells within hepatic allografts from Flt3 ligand-treated donors and promotes graft acceptance. *J Immunol* 2001; **166**: 5619-5628
- Steptoe RJ**, Fu F, Li W, Drakes ML, Lu L, Demetris AJ, Qian S, McKenna HJ, Thomson AW. Augmentation of dendritic cells in murine organ donors by Flt3 ligand alters the balance between transplant tolerance and immunity. *J Immunol* 1997; **159**: 5483-5491
- Rescigno M**, Martino M, Sutherland CL, Gold MR, Ricciardi-Castagnoli P. Dendritic cell survival and maturation are regulated by different signaling pathways. *J Exp Med* 1998; **188**: 2175-2180
- Verhasselt V**, Vanden Berghe W, Vanderheyde N, Willems F, Haegeman G, Goldman M. N-acetyl-L-cysteine inhibits primary human T cell responses at the dendritic cell level: association with NF- κ B inhibition. *J Immunol* 1999; **162**: 2569-2574
- Mann J**, Oakley F, Johnson PW, Mann DA. CD40 induces interleukin-6 gene transcription in dendritic cells. *J Biol Chem* 2002; **277**: 17125-17138
- Zetoun F**, Murthy AR, Shao Z, Hlaing T, Zeidler MG, Li Y, Vincenz C. A20 inhibits NF- κ B activation downstream of multiple Map3 kinases and interacts with the I kappa B signalosome. *Cytokine* 2001; **15**: 282-298
- Klinkenberg M**, Van-Huffel S, Heynink K, Beyaert R. Functional redundancy of the zinc fingers of A20 for inhibition of NF- κ B activation and protein-protein interactions. *FEBS Lett* 2001; **498**: 93-97
- Hofer-Warbinek R**, Schmid JA, Stehlik C, Binder BR, Lipp J, deMartin R. Activation of NF- κ B by XIAP, the X chromosome-linked inhibitor of apoptosis, in endothelial cells involves TAK1. *J Biol Chem* 2000; **275**: 22064-22068
- Beyaert R**, Heynink K, Van-Huffel S. A20 and A20-binding proteins as cellular inhibitors of nuclear factor- κ B-dependent gene expression and apoptosis. *Biochem Pharmacol* 2000; **60**: 1143-1151
- Sarma V**, Lin Z, Clark L, Rust BM, Tewari M, Noelle RJ, Dixit VM. Activation of the B-cell surface receptor CD40 induces A20, a novel zinc finger protein that inhibits apoptosis. *J Biol Chem* 1995; **270**: 12343-12346
- Kupfner JG**, Arcaroli JJ, Yum HK, Nadler SG, Yang KY, Abraham E. Role of NF- κ B in endotoxemia-induced alterations of lung

- neutrophil apoptosis. *J Immunol* 2001; **167**: 7044-7051
- 37 **Heyninck K**, De Valck D, Vanden Berghe W, Van Crielinge W, Contreras R, Fiers W, Haegeman G, Beyaert R. The zinc finger protein A20 inhibits TNF-induced NF- κ B-dependent gene expression by interfering with an RIP- or TRAF2-mediated transactivation signal and directly binds to a novel NF- κ B-inhibiting protein ABIN. *J Cell Biol* 1999; **145**: 1471-1482
- 38 **Arvelo MB**, Cooper JT, Longo C, Daniel S, Grey ST, Mahiou J, Czismadia E, Abu-Jawdeh G, Ferran C. A20 protects mice from D-galactosamine/LPS acute toxic lethal hepatitis. *Hepatology* 2002; **35**: 535-543
- 39 **Ferran C**, Stroka DM, Badrichani AZ, Cooper JT, Wrighton CJ, Soares M, Grey ST, Bach FH. A20 inhibits NF- κ B activation in endothelial cells without sensitizing to tumor necrosis factor-mediated apoptosis. *Blood* 1998; **91**: 2249-2258
- 40 **Lee EG**, Boone DL, Chai S, Libby SL, Chien M, Lodolce JP, Ma A. Failure to regulate TNF-induced NF-kappaB and cell death responses in A20-deficient mice. *Science* 2000; **289**: 2350-2354
- 41 **Avihingsanon Y**, Ma N, Czismadia E, Wang C, Pavlakis M, Giraldo M, Strom TB, Soares MP, Ferran C. Expression of protective genes in human renal allografts: a regulatory response to injury associated with graft rejection. *Transplantation* 2002; **73**:1079-1085
- 42 **Xu MQ**, Yao ZX. Functional changes of dendritic cells derived from allogeneic partial liver graft undergoing acute rejection in rats. *World J Gastroenterol* 2003; **9**: 141-147
- 43 **Lechler R**, Ng WF, Steinman RM. Dendritic cells in transplantation: friend or foe? *Immunity* 2001; **14**: 357-368
- 44 **Matzinger P**. Graft tolerance: a duel of two signals. *Nat Med* 1999; **5**: 616-617
- 45 **Stout RD**, Suttles J. The many roles of CD40 in cell-mediated inflammatory responses. *Immunol Today* 1996; **17**: 487- 492
- 46 **Larsen CP**, Elwood ET, Alexander DZ, Ritchie SC, Hendrix R, Tucker-Burden C, Cho HR, Aruffo A, Hollenbaugh O, Linsley PS, Winn KJ, Pearson TC. Long-term acceptance of skin and cardiac allografts after blocking CD40 and CD28 pathways. *Nature* 1996; **381**: 434-438
- 47 **Kirk AD**, Harlan DM, Armstrong NN, Davis TA, Dong Y, Grag GS, Hong X, Thomas D, Fechner JH Jr, Knechtle SJ. CTLA4-Ig and anti-CD40 ligand prevent renal allograft rejection in primates. *Proc Natl Acad Sci USA* 1997; **94**: 8789-8794

Edited by Xu XQ

Celecoxib inhibits proliferation and induces apoptosis via prostaglandin E₂ pathway in human cholangiocarcinoma cell lines

Gao-Song Wu, Sheng-Quan Zou, Zheng-Ren Liu, Zhao-Hui Tang, Ju-Hua Wang

Gao-Song Wu, Sheng-Quan Zou, Zheng-Ren Liu, Zhao-Hui Tang, Ju-Hua Wang, Department of General Surgery, Tongji Hospital, Tongji Medical College, Huazhong University of Science and Technology, Wuhan, 430030, Hubei Province, China

Correspondence to: Gao-Song Wu, Department of General Surgery, Tongji Hospital, 1095 Jiefang Road, Wuhan, 430030, Hubei Province, China. wugaosong9172@sina.com

Telephone: +86-27-83662851 **Fax:** +86-27-83662851

Received: 2002-04-26 **Accepted:** 2002-06-11

Abstract

AIM: To evaluate the roles and mechanisms of celecoxib in inducing proliferation inhibition and apoptosis of human cholangiocarcinoma cell lines.

METHODS: Cyclooxygenase-2-overexpressing human cholangiocarcinoma cell line QBC939 and cyclooxygenase-2-deficient human cholangiocarcinoma cell line SK-CHA-1 were used in the present study. The anti-proliferative effect was measured by methabenzthiazuron (MTT) assay; apoptosis was determined by transferase-mediated dUTP nick end labeling (TUNEL) detection and transmission electron microscopy (TEM). Cell cycle was analyzed by flow cytometry (FCM). The PGE₂ levels in the supernatant of cultured cholangiocarcinoma cells were quantitated by enzyme-linked immunosorbent assay (ELISA).

RESULTS: Celecoxib suppressed the production of PGE₂ and inhibited the growth of QBC939 cells. Celecoxib at 10, 20, and 40 μmol/L inhibited PGE₂ production by 26 %, 58 %, and 74 % in QBC939 cells. The PGE₂ level was much lower constitutively in SK-CHA-1 cells (18.6±3.2) compared with that in QBC939 (121.9±5.6) cells ($P<0.01$) and celecoxib had no significant influence on PGE₂ level in the SK-CHA-1 cells. The PGE₂ concentration in SK-CHA-1 cells also reduced but not significantly after treatment with celecoxib. The PGE₂ concentration in SK-CHA-1 cells was (16.5±2.9) ng/well, (14.8±3.4) ng/well, (13.2±2.0) ng/well and (12.6±3.1) ng/well respectively, when pre-treated with 1 μmol/L, 10 μmol/L, 20 μmol/L and 40 μmol/L of celecoxib for 48 h ($P>0.05$, vs control). The anti-proliferation effect of celecoxib (20 μmol/L) on QBC939 cells was time-dependent, it was noticeable on day 2 (OD490=0.23±0.04) and became obvious on day 3 (OD490=0.31±0.07) to day 4 (OD490=0.25±0.06), and the OD490 in the control group (day 1) was 0.12±0.03 ($P<0.01$, vs control). The anti-proliferation effect of celecoxib could be abolished by the addition of 200 pg/mL PGE₂. The proliferation of SK-CHA-1 cells was inhibited slightly by celecoxib, the cell density OD490 in the presence of celecoxib and in control group was 0.31±0.04 and 0.42±0.03 respectively on day 2 ($P>0.05$), 0.58±0.07 and 0.67±0.09 respectively on day 3 ($P>0.05$), and 0.71±0.08 and 0.78±0.06 respectively on day 4 ($P>0.05$). Celecoxib induced proliferation inhibition and apoptosis by G₁-S cell cycle arrest: the percentage of QBC939 cells in G₀-G₁ phase after treatment with 40 μmol/L (74.66±6.21) and 20 μmol/L (68.63±4.36) celecoxib increased significantly compared

with control cells (54.41±5.12, $P<0.01$). The percentage of SK-CHA-1 cells in G₀-G₁ phase after treatment with various concentrations of celecoxib didn't change significantly compared with control cells. The TUNEL index was much higher in QBC939 cells treated with 20 μmol/L celecoxib for 2 d (0.063±0.018) and for 4 d (0.102±0.037) compared with control cells (0.017±0.004, $P<0.01$).

CONCLUSION: The current *in vitro* study indicates that inhibition of proliferation and induction of apoptosis in human cholangiocarcinoma cells by cyclooxygenase-2 specific inhibitor celecoxib may involve in COX-dependent mechanisms and PGE₂ pathway. Celecoxib as a chemopreventive and chemotherapeutic agent might be effective primarily on COX-2-expressing cholangiocarcinoma.

Wu GS, Zou SQ, Liu ZR, Tang ZH, Wang JH. Celecoxib inhibits proliferation and induces apoptosis via prostaglandin E₂ pathway in human cholangiocarcinoma cell lines. *World J Gastroenterol* 2003; 9(6): 1302-1306

<http://www.wjgnet.com/1007-9327/9/1302.asp>

INTRODUCTION

Prostaglandins (PGs) are important in the proliferation of various types of cancer cells^[1-13]. PGs are synthesized by two isoforms of cyclooxygenase (COX) enzymes, COX-1 and COX-2, each of which displays distinct physiological profile. Inducible isozyme COX-2 has been shown to be important in carcinogenesis^[14-26]. PGE₂ is the major metabolite of arachidonic acid in many human cells^[27,28]. The selective COX-2 inhibitors are currently being evaluated for their effectiveness as chemopreventive and chemotherapeutic agents^[29-32]. However, the effects of specific inhibitor of COX-2 on the proliferation of human carcinoma cells remain to be investigated. There are many controversies on whether or not these effects are mediated predominantly through the inhibition of COX-2 activity and prostaglandin synthesis^[33]. Our previous studies have demonstrated that overexpression of COX-2 may play a crucial role in the carcinogenesis and development of extra-hepatic cholangiocarcinoma. In this study we aimed to explore the effects and mechanism of celecoxib and the role of PGE₂ in inducing proliferation inhibition and apoptosis of COX-2 overexpressing human cholangiocarcinoma cell line QBC939 and COX-2-deficient human cholangiocarcinoma cell line SK-CHA-1.

MATERIALS AND METHODS

Materials

Human extra-hepatic cholangiocarcinoma cells SK-CHA-1 were a gift from Professor A. Knuth (Frankfurt, Germany)^[35], and human cholangiocarcinoma cell line QBC939 was established by Professor Wang SG in the Third Military Medical University, China, and was offered to us as a gift^[34]. Both cells were maintained as mono-layers in Dulbecco's modified Eagle's medium (DMEM) supplemented with 10 %

fetal bovine serum (FBS, Gibco, USA.), 100 units/ml penicillin and 100 mg/ml streptomycin in a humidified atmosphere of 95 % air and 5 % CO₂ at 37 °C. They were subcultivated every 3–5 d and given fresh medium every other day. Cholangiocarcinoma cells at 70–80 % subconfluent were employed in all experiments. PGE₂ ELISA detection kit was purchased from Jingmei Biotech Co., Wuhan, China. TUNEL kit was purchased from Boster Co., Wuhan, China. PGE₂ was purchased from Sigma, USA. Celecoxib was synthesized by Dr. Mei ZN (Wuhan University, China) and given to us as a gift^[36]. Stock solution was prepared in dimethylsulfoxide (DMSO) and stored at -20 °C. In all experiments DMSO final concentration in the medium was ≤0.1 %.

Methods

MTT assay The human cholangiocarcinoma cells QBC939 and SK-CHA-1 proliferation status were determined by MTT assay. Cholangiocarcinoma cells were seeded at a density of 1×10⁴ cells per well in flat-bottomed 96-well microplates. 12 h after incubation, cells were treated with celecoxib (40, 20, 10, or 0 μmol/L respectively). In some experiments 200 pg/mL PGE₂ was added to cells prior to addition of celecoxib. After 1, 2, 3, or 4 days' incubation, 20 μl MTT (5 g/L) was added to each well and incubated for 4 h. Supernatant was then removed and 150 μl DMSO was added. It was shaken for 5 min until the crystal was dissolved. OD_{490nm} value was measured by an enzyme-linked immunoabsorbent assay reader. The negative control well had no cells and was used as zero point of absorbance. Each well was read three times in triplicate.

TUNEL Preparation of specimens: cholangiocarcinoma cells QBC939 were subcultured on coverslips in 6-well culture plates. After 12 h, cells were treated with 20 μmol/L celecoxib. Every day medium and celecoxib were changed. After 2 and 4 d the coverslips were taken out and fixed with 4 % fresh polyformaldehyde in PBS (pH 7.4–7.6) for 30 min at room temperature. Cell apoptosis was measured by TUNEL method according to the instruction of the kit. Cells were washed with PBS for 2 min, 3 times, followed by washing with distilled water for 2 min, 3 times. Cells were soaked in fresh 3 % H₂O₂ for 10 min, and then rinsed with distilled water for 2 min, 3 times. Cells were digested with proteinase K (diluted 1:100 by TBS) for 5 min at 37 °C, and were rinsed with distilled water for 2 min, 3 times. Labelling buffer (20 μl/sample) was added to keep the slides wet. TDT and DIG-d-UTP (1 μl each) were mixed in 18 μl labelling buffer. The redundant liquid was removed and labelling reagent (20 μl/sample) was added. The slides were put in a humidified box and incubated for 2 h at 37 °C. The slides were washed with TBS for 2 min, 3 times. Blocking solution (50 μl/sample) was added to the slides for 30 min at room temperature. The blocking solution was removed from the slides. The biotin-DIG antibody was diluted with a blocking solution at a ratio of 1:100, and 50 μl/sample of it was added to the slides. The slides were kept in a humidified box, incubated at 37 °C for 30 min, and followed by washing with TBS for 5 min, 3 times. SABC was diluted to 1:100 with TBS and added to the slides. They were incubated at 37 °C for 30 min and washed with TBS for 5 min, 3 times. BCIP/NBT was diluted to 1:20 with TBS, and added to the slides. They were incubated at 37 °C for 10–30 min. The reaction was monitored under microscope: when purplish red was developed, the slides were washed with distilled water. After being stained with nuclear fast red, the slides were sealed with glycerite. Substitution of PBS for TUNEL staining solution was used as negative control. Three hundred cells were counted, and the TUNEL index was expressed as the number of positive cells/the total number of cells.

ELISA The PGE₂ levels in the supernatant of cultured human

cholangiocarcinoma cells QBC939 and SK-CHA-1 were quantitated by ELISA. Cells were seeded into 4.0×10⁵/well microplates and allowed to adhere overnight. The cells were then incubated in the presence or absence of celecoxib for 24 h. The supernatants were aspirated and centrifuged to prepare for the detection of PGE₂. Supernatant (0.5 ml) was added into 1 N HCl (0.1 ml) and centrifuged for 10 min at room temperature, then 1.2 N NaOH (0.1 ml) was used to neutralize the acidified samples. Standard solution (200 μl per well) or activated samples were added into the microplates. Then the steps for ELISA were performed as instructed. The value of OD of each well was measured at 450nm. The supernatants were harvested in triplicates and the experiment was performed twice.

FCM Human cholangiocarcinoma cells QBC939 and SK-CHA-1 were trypsinized and plated in 6-well culture dishes in the presence of celecoxib (40, 20, 10, 0 μmol/L respectively). After 48 h, cells were harvested, centrifuged at low speed and fixed in 70 % ethanol. After overnight incubation at 4 °C, cells were stained with 50 μg/ml propidium iodide in the presence of RNase A (10 μg/ml) and 0.1 % Triton X-100 and measured with a flow cytometer. The experiments were repeated three times.

TEM After treatment with celecoxib for 3 d cholangiocarcinoma cells QBC939 were digested by 0.25 % trypsin and collected. Cells were rinsed with PBS and fixed with 3 % glutaraldehyde for 30 min. After routine embedding and sectioning, cells were examined under electron microscope.

Statistical analysis

Data were expressed as mean ± standard deviation. Student's *t*-test was used for statistical analysis. *P*<0.05 indicates significant difference.

RESULTS

PGE₂ production

The concentration of PGE₂ in culture medium of each cell line treated with or without celecoxib is shown in Figure 1. Celecoxib at 10 μmol/L inhibited PGE₂ production in QBC939 cells by 26 %. With 20 μmol/L and 40 μmol/L of celecoxib, PGE₂ production was further inhibited by 58 % and 74 %, which were statistically significant (*P*<0.01, *vs* control). The PGE₂ level was much lower constitutively in SK-CHA-1 cells (18.6±3.2) compared with that in QBC939 (121.9±5.6) cells (*t* test, *P*<0.01). The PGE₂ concentration in SK-CHA-1 cells was also reduced, but not significantly after treatment with celecoxib. The PGE₂ concentration in SK-CHA-1 cells was (16.5±2.9) ng/well, (14.8±3.4) ng/well, (13.2±2.0) ng/well and (12.6±3.1) ng/well respectively, when pre-treated with 1 μmol/L, 10 μmol/L, 20 μmol/L and 40 μmol/L of celecoxib for 48 h (*P*>0.05, *vs* control).

Celecoxib inhibition on cholangiocarcinoma cells growth

QBC939 and SK-CHA-1 cells were incubated in the presence or absence of celecoxib (20 μmol/L) and the cell density OD₄₉₀ was measured. As shown in Figure 2, proliferation inhibition of QBC939 by celecoxib was time-dependent: it was noticeable on day 2 (OD₄₉₀=0.23±0.04) and became obvious on day 3 (OD₄₉₀=0.31±0.07) to day 4 (OD₄₉₀=0.25±0.06), and the OD₄₉₀ in the control group (day 1) was 0.12±0.03 (*P*<0.01, *vs* control). The proliferation of SK-CHA-1 cells was inhibited slightly by celecoxib, but the effect was not statistically significant (Figure 3). The cell density OD₄₉₀ in the presence of celecoxib and in control group was 0.31±0.04 and 0.42±0.03 respectively on day 2 (*P*>0.05), 0.58±0.07 and 0.67±0.09 respectively on day 3 (*P*>0.05), and 0.71±0.08 and 0.78±0.06 respectively on day 4 (*P*>0.05).

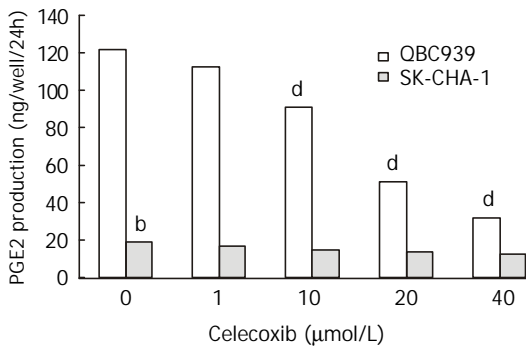


Figure 1 ELISA for PGE₂ detection using supernatants from QBC939 and SK-CHA-1 cells pre-treated with celecoxib at various concentrations for 48 h. Celecoxib at 10 μmol/L inhibited PGE₂ production in QBC939 cells by 26 %. With 20 μmol/L and 40 μmol/L of celecoxib, PGE₂ production was further inhibited by 58 % and 74 %, which were statistically significant (^a $P < 0.01$, vs control). The PGE₂ level was much lower constitutively in SK-CHA-1 cells (18.6 ± 3.2) compared with that in QBC939 (121.9 ± 5.6) cells (t test, ^b $P < 0.01$). The PGE₂ concentration in SK-CHA-1 cells was also reduced, but not significantly after treatment with celecoxib. The PGE₂ concentration in SK-CHA-1 cells was (16.5 ± 2.9) ng/well, (14.8 ± 3.4) ng/well, (13.2 ± 2.0) ng/well and (12.6 ± 3.1) ng/well respectively, when pre-treated with 1 μmol/L, 10 μmol/L, 20 μmol/L and 40 μmol/L of celecoxib for 48 h ($P > 0.05$, vs control).

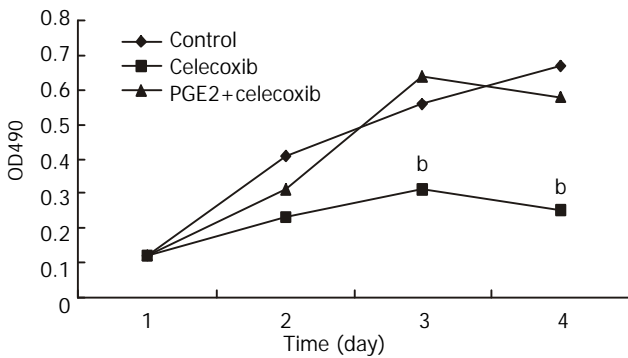


Figure 2 Growth curves of QBC939 cells in the presence of celecoxib, celecoxib + PGE₂ and control group. Proliferation inhibition of QBC939 by celecoxib (20 μmol/L) was time-dependent: it was noticeable on day 2 and became significant on day 3 to 4 (^b $P < 0.01$, vs control). The anti-proliferation effect of celecoxib on QBC939 cells was abolished by pre-added PGE₂ (200 pg/mL).

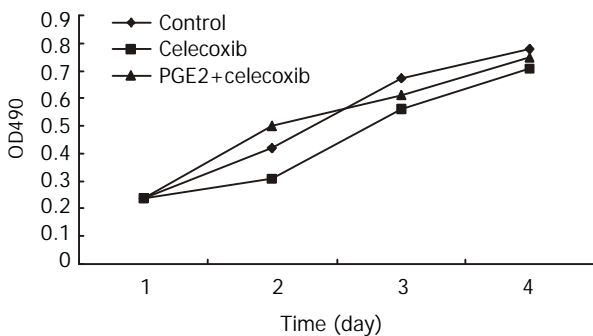


Figure 3 Growth curves of SK-CHA-1 cells in the presence of celecoxib, celecoxib + PGE₂ and control group. The proliferation of SK-CHA-1 cells was inhibited slightly by celecoxib, the cell density OD490 in the presence of celecoxib and in control group was 0.31 ± 0.04 and 0.42 ± 0.03 respectively on day 2 ($P > 0.05$), 0.58 ± 0.07 and 0.67 ± 0.09 respectively on day 3 ($P > 0.05$), and 0.71 ± 0.08 and 0.78 ± 0.06 respectively on day 4 ($P > 0.05$).

PGE₂ abolished the anti-proliferation effect of celecoxib on QBC939 cells

To investigate whether the anti-proliferation effect of celecoxib on QBC939 cells was due to suppression of PGE₂ production by QBC939 cells, 200 pg/mL PGE₂ was added to QBC939 cells prior to the addition of celecoxib, and MTT assay was performed (Figure 2). The anti-proliferation effect of celecoxib on QBC939 cells was abolished by PGE₂. However, addition of 200 pg/mL PGE₂ had no significant influence on the proliferation of SK-CHA-1 cells when pre-treated with 20 μmol/L celecoxib (Figure 3).

Apoptosis induction and detection

The TUNEL index of QBC939 cells treated with 20 μmol/L celecoxib for 2 d (0.063 ± 0.018) and 4 d (0.102 ± 0.037) was much higher compared with control cells (0.017 ± 0.004, $P < 0.01$).

Celecoxib induces G₁-S cell cycle arrest

Cell cycle analysis by flow cytometry showed that the percentage of QBC939 cells in G₀-G₁ phase after treatment with 40 μmol/L (74.66 ± 6.21) and 20 μmol/L (68.63 ± 4.36) increased significantly compared with control cells (54.41 ± 5.12, $P < 0.01$, Figure 4). The percentage of SK-CHA-1 cells in G₀-G₁ phase after treatment with various concentrations of celecoxib did not change significantly compared with control cells.

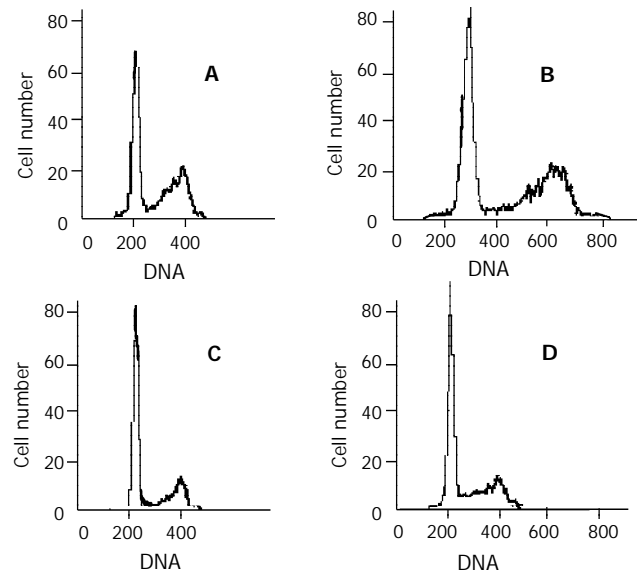


Figure 4 Cell cycle analysis. Representative flow cytometry data from QBC939 cells after 48 h in the presence of various concentration of celecoxib: 0 μmol/L (A), 10 μmol/L (B), 20 μmol/L (C) and 40 μmol/L (D). The percentage of QBC939 cells in G₀-G₁ phase after treatment with 40 μmol/L (74.66 ± 6.21) and 20 μmol/L (68.63 ± 4.36) of celecoxib increased significantly compared with control cells (t test, $P < 0.01$).

Electron micrography of apoptosis of cholangiocarcinoma cells

QBC939 cells were treated for 3 d with 20 μmol/L of celecoxib. The chromatin became condensed and attached to the inner surface of nuclear membrane.

DISCUSSION

A substantial body of evidence indicates that COX and PGs are important in carcinogenesis. COX catalyzes the synthesis of PGs from arachidonic acid. Several PGs, most notably PGE₂, can promote tumorigenesis by stimulating angiogenesis, inhibiting immune surveillance^[37-40], modulating several signal

transduction pathways^[41-44]. Several studies have demonstrated that COX-2 selective inhibitor celecoxib has significant efficacy in animal cancer models: celecoxib inhibited intestinal tumor multiplicity by up to 71 % compared with controls in the Min mouse model and inhibited colorectal tumor burden in the rat azoxymethane (AOM) model^[45-48]. Recently celecoxib has been approved by FDA to reduce the number of adenomatous colorectal polyps in patients with familial adenomatous polyposis (FAP). However, the exact mechanisms that account for the anti-proliferative effects of celecoxib are still not fully understood. It is still controversial that whether or not these effects are mediated predominantly through the inhibition of COX-2 activity and prostaglandin synthesis. Several studies have shown both COX-dependent and COX-independent mechanisms are involved in non-steroidal anti-inflammatory drug (NSAIDs) induced growth in human colorectal tumor cells^[49].

Our previous studies have demonstrated that overexpression of COX-2 may play a crucial role in the carcinogenesis and development of extra-hepatic cholangiocarcinoma. In the present study we found the PGE₂ level was much lower constitutively in COX-2-deficient human cholangiocarcinoma cell line SK-CHA-1 cells than that in COX-2 overexpressing human cholangiocarcinoma cell line QBC939. In this study we have shown that the proliferation of QBC939 cells was inhibited by celecoxib in a time- and dose-dependent manner. Our study also showed celecoxib had no significant influence on the SK-CHA-1 cells. These findings indicate that COX-2 inhibitor might be an effective anti-proliferative agent, especially against cancer cells that express COX-2 and produce high-level PGE₂. Our data demonstrated that celecoxib suppressed the production of PGE₂ in QBC939 cells, and the anti-proliferative effect of celecoxib could be abolished by addition of PGE₂. These results suggest that COX-2 might play a central role in production of PGE₂ and the specific inhibition of COX-2 inhibits proliferation and induces apoptosis of QBC939 cells via suppression of PGE₂ production. Our data also indicate that celecoxib inhibits proliferation and induces apoptosis of human cholangiocarcinoma QBC939 cells by an accumulation of cells in the G₀/G₁ phase and the inhibition of G₀/G₁ phase transition to S phase.

In summary, our results in the present study demonstrate that inhibition of proliferation and induction of apoptosis by celecoxib in human cholangiocarcinoma cells may involve in COX-dependent mechanisms and PGE₂ pathway and these findings also suggest that celecoxib, as a chemopreventive and chemotherapeutic agent may be effective primarily on COX-2-expressing cholangiocarcinoma.

REFERENCES

- Bostrom PJ**, Aaltonen V, Soderstrom KO, Uotila P, Laato M. Expression of cyclooxygenase-1 and -2 in urinary bladder carcinomas in vivo and in vitro and prostaglandin E2 synthesis in cultured bladder cancer cells. *Pathology* 2001; **33**: 469-474
- Fan XM**, Wong BC, Lin MC, Cho CH, Wang WP, Kung HF, Lam SK. Interleukin-1beta induces cyclo-oxygenase-2 expression in gastric cancer cells by the p38 and p44/42 mitogen-activated protein kinase signaling pathways. *J Gastroenterol Hepatol* 2001; **16**: 1098-1104
- Wu GS**, Zou SQ, Luo XW, Wu JH, Liu ZR. Proliferative activity of bile from congenital choledochal cyst patients. *World J Gastroenterol* 2003; **9**: 184-187
- Chasseing NA**, Hofer E, Bordenave RH, Shanley C, Rumi LS. Bone marrow fibroblasts in patients with advanced lung cancer. *Braz J Med Biol Res* 2001; **34**: 1457-1463
- Berger S**, Siegert A, Denkert C, Kobel M, Hauptmann S. Interleukin-10 in serous ovarian carcinoma cell lines. *Cancer Immunol Immunother* 2001; **50**: 328-333
- Venza I**, Giordano L, Piraino G, Medici N, Ceci G, Teti D. Prostaglandin E2 signalling pathway in human T lymphocytes from healthy and conjunctiva basal cell carcinoma-bearing subjects. *Immunol Cell Biol* 2001; **79**: 482-489
- Chen X**, Yang CS. Esophageal adenocarcinoma: a review and perspectives on the mechanism of carcinogenesis and chemoprevention. *Carcinogenesis* 2001; **22**: 1119-1129
- McHowat J**, Creer MH, Rickard A. Stimulation of protease activated receptors on RT4 cells mediates arachidonic acid release via Ca²⁺ independent phospholipase A2. *J Urol* 2001; **165**: 2063-2067
- Krishnan K**, Ruffin MT, Normolle D, Shureiqi I, Burney K, Bailey J, Peters-Golden M, Rock CL, Boland CR, Brenner DE. Colonic mucosal prostaglandin E2 and cyclooxygenase expression before and after low aspirin doses in subjects at high risk or at normal risk for colorectal cancer. *Cancer Epidemiol Biomarkers Prev* 2001; **10**: 447-453
- Lim JW**, Kim H, Kim KH. Nuclear factor-kappaB regulates cyclooxygenase-2 expression and cell proliferation in human gastric cancer cells. *Lab Invest* 2001; **81**: 349-360
- Akhtar M**, Cheng Y, Magno RM, Ashktorab H, Smoot DT, Meltzer SJ, Wilson KT. Promoter methylation regulates *Helicobacter pylori*-stimulated cyclooxygenase-2 expression in gastric epithelial cells. *Cancer Res* 2001; **61**: 2399-2403
- Sheng H**, Shao J, Washington MK, DuBois RN. Prostaglandin E2 increases growth and motility of colorectal carcinoma cells. *J Biol Chem* 2001; **276**: 18075-18081
- Faas FH**, Dang AQ, White J, Schaefer R, Johnson D. Increased prostatic lysophosphatidylcholine acyltransferase activity in human prostate cancer: a marker for malignancy. *J Urol* 2001; **165**: 463-468
- Tian G**, Yu JP, Luo HS, Yu BP, Yue H, Li JY, Mei Q. Effect of Nimesulide on proliferation and apoptosis of human hepatoma SMMC-7721 cells. *World J Gastroenterol* 2002; **8**: 483-487
- Wu YL**, Sun B, Zhang XJ, Wang SN, He HY, Qiao MM, Zhong J, Xu JY. Growth inhibition and apoptosis induction of Sulindac on Human gastric cancer cells. *World J Gastroenterol* 2001; **7**: 796-800
- Cheng J**, Imanishi H, Iijima H, Shimomura S, Yamamoto T, Amuro Y, Kubota A, Hada T. Expression of cyclooxygenase 2 and cytosolic phospholipase A(2) in the liver tissue of patients with chronic hepatitis and liver cirrhosis. *Hepatol Res* 2002; **23**: 185-195
- Davies G**, Martin LA, Sacks N, Dowsett M. Cyclooxygenase-2 (COX-2), aromatase and breast cancer: a possible role for COX-2 inhibitors in breast cancer chemoprevention. *Ann Oncol* 2002; **13**: 669-678
- Seno H**, Oshima M, Ishikawa TO, Oshima H, Takaku K, Chiba T, Narumiya S, Taketo MM. Cyclooxygenase 2- and prostaglandin E(2) receptor EP(2)-dependent angiogenesis in Apc (Delta716) mouse intestinal polyps. *Cancer Res* 2002; **62**: 506-511
- Zimmermann KC**, Sarbia M, Weber AA, Borchard F, Gabbert HE, Schror K. Cyclooxygenase-2 expression in human esophageal carcinoma. *Cancer Res* 1999; **59**: 198-204
- Gupta S**, Srivastava M, Ahmad N, Sakamoto K, Bostwick DG, Mukhtar H. Lipoxygenase-5 is overexpressed in prostate adenocarcinoma. *Cancer* 2001; **91**: 737-743
- Weddle DL**, Tithoff P, Williams M, Schuller HM. Beta-adrenergic growth regulation of human cancer cell lines derived from pancreatic ductal carcinomas. *Carcinogenesis* 2001; **22**: 473-479
- Ristimaki A**, Nieminen O, Saukkonen K, Hotakainen K, Nordling S, Haglund C. Expression of cyclooxygenase-2 in human transitional cell carcinoma of the urinary bladder. *Am J Pathol* 2001; **158**: 849-853
- Kulkarni S**, Rader JS, Zhang F, Liapis H, Koki AT, Masferrer JL, Subbaramaiah K, Dannenberg AJ. Cyclooxygenase-2 is overexpressed in human cervical cancer. *Clin Cancer Res* 2001; **7**: 429-434
- Tong BJ**, Tan J, Tajeda L, Das SK, Chapman JA, DuBois RN, Dey SK. Heightened expression of cyclooxygenase-2 and peroxisome proliferator-activated receptor-delta in human endometrial adenocarcinoma. *Neoplasia* 2000; **2**: 483-490
- Uefuji K**, Ichikura T, Mochizuki H. Expression of cyclooxygenase-2 in human gastric adenomas and adenocarcinomas. *J Surg Oncol* 2001; **76**: 26-30

- 26 **Kokawa A**, Kondo H, Gotoda T, Ono H, Saito D, Nakadaira S, Kosuge T, Yoshida S. Increased expression of cyclooxygenase-2 in human pancreatic neoplasms and potential for chemoprevention by cyclooxygenase inhibitors. *Cancer* 2001; **91**: 333-338
- 27 **Kakiuchi Y**, Tsuji S, Tsujii M, Murata H, Kawai N, Yasumaru M, Kimura A, Komori M, Irie T, Miyoshi E, Sasaki Y, Hayashi N, Kawano S, Hori M. Cyclooxygenase-2 activity altered the cell-surface carbohydrate antigens on colon cancer cells and enhanced liver metastasis. *Cancer Res* 2002; **62**: 1567-1572
- 28 **Sumitani K**, Kamijo R, Toyoshima T, Nakanishi Y, Takizawa K, Hatori M, Nagumo M. Specific inhibition of cyclooxygenase-2 results in inhibition of proliferation of oral cancer cell lines via suppression of prostaglandin E2 production. *J Oral Pathol Med* 2001; **30**: 41-47
- 29 **Hosomi Y**, Yokose T, Hirose Y, Nakajima R, Nagai K, Nishiwaki Y, Ochiai A. Increased cyclooxygenase 2 (COX-2) expression occurs frequently in precursor lesions of human adenocarcinoma of the lung. *Lung Cancer* 2000; **30**: 73-81
- 30 **Tsubouchi Y**, Mukai S, Kawahito Y, Yamada R, Kohno M, Inoue K, Sano H. Meloxicam inhibits the growth of non-small cell lung cancer. *Anticancer Res* 2000; **20**: 2867-2872
- 31 **Souza RF**, Shewmake K, Beer DG, Cryer B, Spechler SJ. Selective inhibition of cyclooxygenase-2 suppresses growth and induces apoptosis in human esophageal adenocarcinoma cells. *Cancer Res* 2000; **60**: 5767-5772
- 32 **Grubbs CJ**, Lubet RA, Koki AT, Leahy KM, Masferrer JL, Steele VE, Kelloff GJ, Hill DL, Seibert K. Celecoxib inhibits N-butyl-N-(4-hydroxybutyl)-nitrosamine-induced urinary bladder cancers in male B6D2F1 mice and female Fischer-344 rats. *Cancer Res* 2000; **60**: 5599-5602
- 33 **Sabine G**, Irmgard T, Elien N, Lutz B, Gerd G. COX-2 independent induction of cell cycle arrest and apoptosis in colon cancer cells by the selective COX-2 inhibitor of celecoxib. *FASEB* 2001; **15**: 2742-2744
- 34 **Knuth A**, Gabbert H, Dippold W, Klein O, Sachsse W, Bitter-Suermann D, Prellwitz W. Biliary adenocarcinoma. Characterisation of three new human tumor cell lines. *J Hepatol* 1985; **1**: 579-596
- 35 **Wang SG**, Han BL, Duan HC, Chen YS, Peng ZM. Establishment of the extrahepatic cholangiocarcinoma cell line. *Zhonghua Shiyian Waike Zazhi* 1997; **14**: 67-68
- 36 **Mei ZY**, Shi Z, Wang XH, Luo XD. Synthesis of COX-2 Inhibitor Celecoxib. *Zhongguo Yiyao Gongye Zazhi* 2000; **31**: 433-434
- 37 **Soslow RA**, Dannenberg AJ, Rush D, Woerner BM, Khan KN, Masferrer J, Koki AT. COX-2 is expressed in human pulmonary, colonic, and mammary tumors. *Cancer* 2000; **89**: 2637-2645
- 38 **Vanaja DK**, Grossmann ME, Celis E, Young CY. Tumor prevention and antitumor immunity with heat shock protein 70 induced by 15-deoxy-delta12,14-prostaglandin J2 in transgenic adenocarcinoma of mouse prostate cells. *Cancer Res* 2000; **60**: 4714-4718
- 39 **O'Byrne KJ**, Dalglish AG, Browning MJ, Steward WP, Harris AL. The relationship between angiogenesis and the immune response in carcinogenesis and the progression of malignant disease. *Eur J Cancer* 2000; **36**: 151-169
- 40 **Morecki S**, Yacovlev E, Gelfand Y, Trembovler V, Shohami E, Slavin S. Induction of antitumor immunity by indomethacin. *Cancer Immunol Immunother* 2000; **48**: 613-620
- 41 **Jang BC**, Sanchez T, Schaefer HJ, Trifan OC, Liu CH, Creminon C, Huang CK, Hla T. Serum withdrawal-induced post-transcriptional stabilization of cyclooxygenase-2 mRNA in MDA-MB-231 mammary carcinoma cells requires the activity of the p38 stress-activated protein kinase. *Biol Chem* 2000; **275**: 39507-39515
- 42 **Paik JH**, Ju JH, Lee JY, Boudreau MD, Hwang DH. Two opposing effects of non-steroidal anti-inflammatory drugs on the expression of the inducible cyclooxygenase. Mediation through different signaling pathways. *J Biol Chem* 2000; **275**: 28173-28179
- 43 **Subbaramaiah K**, Michaluart P, Sporn MB, Dannenberg AJ. Ursolic acid inhibits cyclooxygenase-2 transcription in human mammary epithelial cells. *Cancer Res* 2000; **60**: 2399-2404
- 44 **Higashi Y**, Kanekura T, Kanzaki T. Enhanced expression of cyclooxygenase (COX)-2 in human skin epidermal cancer cells: evidence for growth suppression by inhibiting COX-2 expression. *Int J Cancer* 2000; **86**: 667-671
- 45 **Takahashi M**, Mutoh M, Kawamori T, Sugimura T, Wakabayashi K. Altered expression of beta-catenin, inducible nitric oxide synthase and cyclooxygenase-2 in azoxymethane-induced rat colon carcinogenesis. *Carcinogenesis* 2000; **21**: 1319-1327
- 46 **Jacoby RF**, Cole CE, Tutsch K, Newton MA, Kelloff G, Hawk ET, Lubet RA. Chemopreventive efficacy of combined piroxicam and difluoromethylornithine treatment of Apc mutant Min mouse adenomas, and selective toxicity against Apc mutant embryos. *Cancer Research* 2000; **60**: 1864-1870
- 47 **Reddy BS**, Rao CV, Seibert K. Evaluation of cyclooxygenase-2 inhibitor for potential chemopreventive properties in colon carcinogenesis. *Cancer Research* 1996; **56**: 4566-4569
- 48 **Kawamori T**, Rao CV, Seibert K, Reddy BS. Chemopreventive activity of celecoxib, a selective cyclooxygenase -2 inhibitor, against colon carcinogenesis. *Cancer Research* 1998; **58**: 409-412
- 49 **Richter M**, Weiss M, Weinberger I, Furstenberger G, Marian B. Growth inhibition and induction of apoptosis in colorectal tumor cells by cyclooxygenase inhibitors. *Carcinogenesis* 2001; **22**: 17-25

Effects of melatonin on the expression of iNOS and COX-2 in rat models of colitis

Wei-Guo Dong, Qiao Mei, Jie-Ping Yu, Jian-Ming Xu, Li Xiang, Yu Xu

Wei-Guo Dong, Jie-Ping Yu, Yu Xu, Department of Gastroenterology, Renmin Hospital, Wuhan University, Wuhan 430060, Hubei Province, China

Qiao Mei, Jian-Ming Xu, Li Xiang, Department of Gastroenterology, the First Affiliated Hospital, Anhui Medical University, Hefei 230032, Anhui Province, China

Correspondence to: Wei-Guo Dong, Department of Gastroenterology, Renmin Hospital, Wuhan University, Wuhan 430060, China. dongwg@public.wh.hb.cn

Telephone: +86-27-88041911 Ext 7737

Received: 2002-11-26 **Accepted:** 2003-01-13

Abstract

AIM: To investigate the effects of melatonin (MT) on the expression of inducible nitric oxide synthase (iNOS) and cyclooxygenase-2 (COX-2) in rat models of colitis.

METHODS: Healthy adult Sprague-Dawley (SD) rats of both sexes, weighing 280 ± 30 g, were employed in the present study. The rat models of colitis were induced by either acetic acid or 2,4,6-trinitrobenzene sulfonic acid (TNBS) enemas. The experimental animals were randomly divided into melatonin treatment and model control group that were intracolically treated daily with melatonin at doses of 2.5, 5.0, 10.0 mg·kg⁻¹ and equal amount of saline respectively from 24 h following induction of colitis in rats inflicted with acetic acid enema and the seventh day in rats with TNBS to the end of study. A normal control group of rats treated with neither acetic acid nor TNBS but saline enema was also included in the study. On the 28th day of the experiment, the rat colon mucosal damage index (CDMI) was calculated, and the colonic prostaglandin E₂ (PGE₂), nitric oxide (NO), as well as the iNOS and COX-2 expression were also determined biochemically or immunohistochemically.

RESULTS: CDMI increased to 2.87 ± 0.64 and 3.12 ± 1.12 respectively in rats treated with acetic acid and TNBS enema, which was in accordance with the significantly elevated colonic NO and PGE₂ contents, as well as the up-regulated colonic iNOS and COX-2 expression in both of the two rat models of colitis. With treatment by melatonin at the doses of 5.0 and 10.0 mg·kg⁻¹, CDMI in both models of rat colitis was significantly decreased ($P < 0.05-0.01$), which accorded synchronously and unanimously with the reduced colonic NO and PGE₂ content, as well as the down-regulated expression of colonic iNOS and COX-2.

CONCLUSION: Melatonin has a protective effect on colonic injury induced by both acetic acid and TNBS enemas, which is probably via a mechanism of local inhibition of iNOS and COX-2 expression in colonic mucosa.

Dong WG, Mei Q, Yu JP, Xu JM, Xiang L, Xu Y. Effects of melatonin on the expression of iNOS and COX-2 in rat models of colitis. *World J Gastroenterol* 2003; 9(6): 1307-1311
<http://www.wjgnet.com/1007-9327/9/1307.asp>

INTRODUCTION

Inflammatory bowel disease (IBD) consists of a group of illnesses with chronic inflammation of the gastrointestinal tract, which causes life-impairing symptoms, necessitates long-term dependence on powerful drugs, and often results in debilitating surgery and even death. Although the etiology remains unclear, IBD appears to result from a dysregulated immune response. In recent years, plenty of studies have shown that nitric oxide (NO) and prostaglandin (PG) as the main inflammatory mediators take part in the pathogenesis of inflammatory bowel disease, with enhanced expression of inducible nitric oxide synthase (iNOS) and cyclooxygenase-2 (COX-2) in the morbid colonic mucosa^[1,2]. Meanwhile, it has been noted melatonin (MT) normally produced mainly in the gastrointestinal tract besides the pineal gland bears a number of beneficial properties including anti-oxidation, anti-inflammation and immunoregulation^[3-15], and could alleviate colonic injury caused by both dextran sulfate sodium^[16] and dinitrobenzene sulfonic acid^[17] in rats. It is reasonable to extrapolate that the protective roles of melatonin might be related to its effect on the expression of iNOS and COX-2 in local tissue. We therefore performed the present study in an attempt to confirm this hypothesis.

MATERIALS AND METHODS

Animals

Healthy adult Sprague-Dawley (SD) rats of both sexes, weighing 280 ± 30 g, were employed in the study. They were purchased from the Experimental Animal Center, Anhui Medical University, housed in a temperature conditioned room (22-24 °C) with a 12 h light-dark cycle, allowed access to standard rat chow and water ad libitum, and acclimatized to the surroundings for one week prior to the experiments. The study protocol was in accordance with the guideline for animal research and was approved by the Ethical and Research Committee of the hospital.

Reagents

Melatonin, TNBS, and N-1-naphthylenediamine hydrochloride came from Sigma Corp. Acetic acid was purchased from Bangbu Chemical Corp. PGE₂ assay kit was from Radio-immunity Institute of PLA General Hospital. Immunohistochemical assay kits for iNOS and COX-2 were provided by Beijing Zhongshan Reagent Corp. Other reagents used in the present study were all with a quality of analytical grade.

Experimental protocol

Rat model of colitis induced with either acetic acid or TNBS enema was described in the literature^[18, 19]. According to different treatment regimens, the experimental animals were randomly divided into melatonin treatment and model control group that were intracolically treated under anesthesia with melatonin at doses of 2.5, 5.0, 10.0 mg·kg⁻¹ and equal amount of saline respectively and daily (8:00 am) from 24

h following induction of colitis in rats inflicted with acetic acid enema and the seventh day in rats after TNBS treatment to the end of the experiment. A normal control group of rats treated with neither acetic acid nor TNBS but saline enema was also included in the study. On the 28th day of the experiment, the animals were killed and the colon mucosal damage index (CMDI) was evaluated with the methods reported elsewhere^[19, 20]. At the same time, colon tissue prostaglandin E₂ (PGE₂) and nitric oxide (NO), as well as the expression of iNOS and COX-2 were determined biochemically or immunohistochemically.

Determination of NO and PGE₂

Colonic specimen was prepared to a concentration of 20 g · L⁻¹ by adding dehydrated alcohol-saline (1:4), and then centrifuged at 4 000 g for 30 min, 4 °C. Two milliliters of the supernatant were added into 0.1 ml of HCL (0.1 mol · L⁻¹) and further adjusted pH to 3.5 by 0.05 mol · L⁻¹ of NaOH. After mixed with ethyl acetate 5 ml for 2 min, they were centrifuged at 1 500 g for 15 min. Repeat the procedures above and the sample solution was evaporated to dryness by N₂ and stored at -20 °C until analysis. The samples were dissolved to 1 ml of phosphate buffered saline, from which 0.1 ml of specimen was taken to perform the PGE₂ measurement following the manufacturer's instruction of the assay kit^[21]. The colonic tissue NO was detected as described in the literature^[22].

Immunohistochemistry detection

The expression of iNOS and COX-2 in colon tissue was exhibited immunohistochemically as reported before^[23], in which the employed first polyclonal antibody was 1:80 rabbit-anti-rat-iNOS and 1:50 goat-anti-rat-COX-2, and the second antibody was biotinylation goat-anti-rabbit IgG and biotinylation rabbit-anti-goat IgG respectively. The iNOS or COX-2 negatively expressed cells were manifested as blue-stained nuclei and the positive cell was with brown-yellow cytoplasm or nuclear membrane. The expression of target protein was further semiquantitated according to the percentage of positively-stained cells, in which positive cells appeared less than 5 %, from 6 % to 30 %, from 31 % to 70 % and more than 71 % were scored as 0, 1, 2 and 3 respectively.

Statistical analysis

Experimental results were analyzed by ANOVA and *t*-tests for multiple comparisons between groups. Data were finally expressed as mean ± standard error of the mean. *P* value less than 0.05 was considered statistically significant.

RESULTS

Protective effects of melatonin on rat colonic lesion

Pronounced pathological changes of colonic mucosa similar to that in human IBD were observed in rats with colitis induced by both acetic acid and TNBS enema, which were in accordance with the colon mucosal damage index that was significantly increased in these experimental animals compared with normal controls (*P*<0.01). Local treatment with different doses of melatonin by enema could effectively reduce the severity of gut injury and the CMDI was significantly decreased in a dose dependent manner in rats treated by melatonin compared with that in model control animals (*P*<0.05-0.01, Table 1).

Effects of MT on NO content and iNOS expression

In normal controls, colonic iNOS expression was mainly observed on histocytes, neutrophils and smooth muscle

cells with a sparse distribution in epithelial cells. The NO content and the expression of iNOS in colonic tissue were synchronously and significantly increased in rats inflicted with both acetic acid and TNBS enema compared with that of the normal controls (*P*<0.01), which were significantly inhibited by different doses of melatonin employed in the present study (*P*< 0.05-0.01 vs. Model control, Table 2, 3, Figure 1).

Table 1 Effects of MT on CMDI in rats with experimental colitis ($\bar{x}\pm s$, *n*=8)

Group	Doses (mg · kg ⁻¹)	CMDI	
		Acetic acid	TNBS
Normal control		0.0±0.0	0.0±0.0
Model control		2.87±0.64 ^a	3.12±1.12 ^a
Melatonin	2.5	2.12±0.83 ^b	2.33±0.51
Melatonin	5.0	1.75±0.88 ^c	1.66±0.81 ^b
Melatonin	10.0	1.12±0.35 ^c	1.75±0.88 ^b

^a*P*<0.01 vs. Normal control; ^b*P*<0.05, ^c*P*<0.01 vs. Model control.

Table 2 Effects of MT on the colonic NO and PGE₂ levels in rats with experimental colitis ($\bar{x}\pm s$, *n*=8)

Group	Doses (mg · kg ⁻¹)	NO (μmol · g ⁻¹ tissue)		PGE ₂ (ng · g ⁻¹ tissue)	
		Acetic acid	TNBS	Acetic acid	TNBS
Normal control		0.174±0.044	0.287±0.069	43.1±32.1	43.1±32.1
Model control		0.327±0.090 ^b	0.533±0.068 ^b	184.5±96.3 ^b	181.3±51.7 ^b
Melatonin	2.5	0.230±0.017 ^d	0.403±0.042 ^d	89.1±59.1 ^c	109.0±33.3 ^d
Melatonin	5.0	0.218±0.018 ^d	0.380±0.029 ^d	76.4±23.6 ^c	89.8±37.7 ^d
Melatonin	10.0	0.189±0.029 ^d	0.340±0.019 ^d	57.1±23.2 ^d	85.9±39.2 ^d

^a*P*<0.05, ^b*P*<0.01, vs. normal control; ^c*P*<0.05, ^d*P*<0.01 vs. model control.

Effects of melatonin on PGE₂ content and COX-2 expression

Compared with normal group, the content of PGE₂ and the expression of COX-2 in rat colitis, the number of positive granules and the degree of staining were enhanced significantly. The content of PGE₂ was decreased after different doses of melatonin were given by enema. The expression of COX-2 was inhibited by melatonin, which proved that melatonin decreased the synthesis of PGE₂ and it might be related with inhibition of the expression of COX-2 (Figure 2, Table 2, 3).

Table 3 Effects of MT on the colonic expression of iNOS and COX-2 semi-quantitated in rats with experimental colitis ($\bar{x}\pm s$, *n*=6)

Group	Doses (mg · kg ⁻¹)	iNOS		COX-2	
		Acetic acid	TNBS	Acetic acid	TNBS
Normal control		0.3±0.5	0.3±0.5	0.2±0.4	0.2±0.4
Model control		2.2±0.9 ^b	2.3±0.8 ^b	1.8±0.9 ^b	2.2±0.9 ^b
Melatonin	2.5	1.3±0.5 ^c	1.5±0.5 ^c	1.2±0.4	1.7±0.8
Melatonin	5.0	0.5±0.5 ^d	1.2±0.8 ^c	1.0±0.6	1.3±0.8
Melatonin	10.0	0.3±0.5 ^d	0.7±0.8 ^d	0.5±0.5 ^c	0.8±0.8 ^c

^a*P*<0.05, ^b*P*<0.01 vs. Normal control; ^c*P*<0.05, ^d*P*<0.01 vs. Model control.

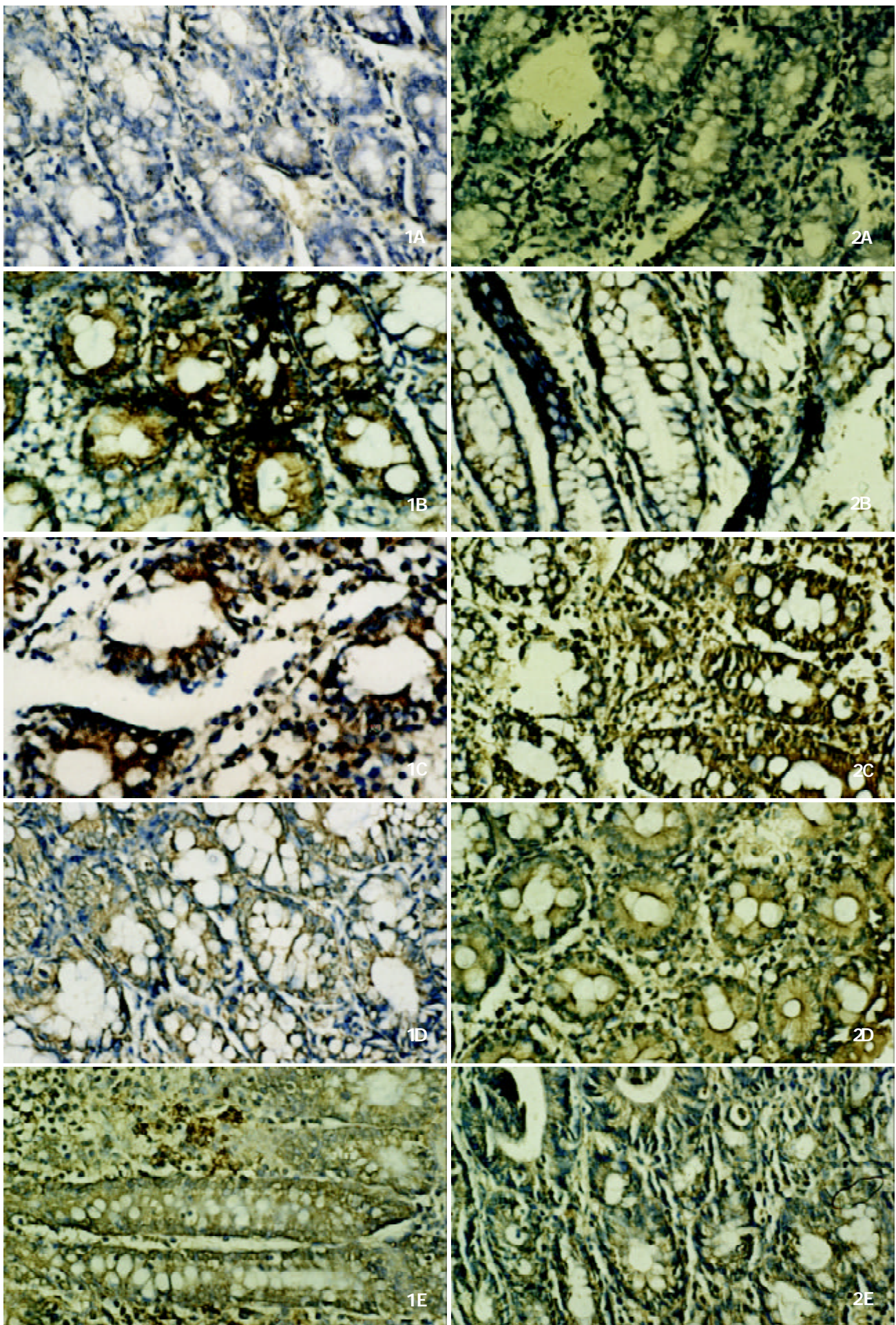


Figure 1 Abnormal expression of iNOS in colonic tissue of rats with colitis induced by both acetic acid and TNBS enemas and its

improvement by melatonin. A. Immunohistochemical localization of iNOS in normal control, which was manifested as fine brown granules distributed mainly in the cytoplasm of histocytes, neutrophils and smooth muscle cells. B. Positively stained granules for iNOS were significantly increased in both number and intensity in colonic tissue of model control rats. (a) Acetic acid treated rats; (b) TNBS treated rats. C. The colonic iNOS expression was significantly reduced in both acetic acid (a) and TNBS (b) treated rats after intervened with 10.0 mg·kg⁻¹ of melatonin.

Figure 2 Abnormal expression of COX-2 in colonic tissue of rats with colitis induced by acetic acid or TNBS enema and its improvement by melatonin, which was in accordance with the observation in clonic iNOS expression. A. Positively stained COX-2 granules in colonic tissue of normal control rats. B. iNOS expression was significantly increased as manifested by the augmented and intensified positively stained granules in colonic tissue of model control rats. (a) Acetic acid treated rats; (b) TNBS treated rats. C. The colonic COX-2 expression was significantly reduced in both acetic acid (a) and TNBS (b) treated rats after intervened with 10.0 mg·kg⁻¹ of melatonin.

DISCUSSION

Although the etiology of IBD remains unclear, dysregulated immune response has been widely accepted as a possible mechanism in the pathogenesis of inflammatory bowel disease. Numerous reports have revealed that certain local bioactive agents including NO and PGE₂ are involved in colonic injury by various inducers^[1,2]. Meddleton and other authors^[24,25] found NO concentration was rather higher in ulcerative colitis patients with obviously strengthened iNOS activity. As an important inflammatory mediator, NO could react with superoxide anion to form more poisonous nitrite anion, which then disturbs the function of inflammatory cells and further impairs the colonic mucosa^[26,27]. PGE₂, another major local inflammatory mediator that might come from activated eosinophils and monocytes^[28], is also considered as a marker of colitis. In the two rat models of colitis respectively induced by acetic acid and TNBS in the present study, the mucosal NO and PGE₂ contents in the morbid colon were significantly increased with enhanced expression of iNOS and COX-2, which was in accordance with the previous reports.

Melatonin, a major hormone produced in pineal gland, was also found in recent years to be secreted for a certain amount from gastrointestinal tract and played an important role in the adjustment of gastrointestinal function^[7-14]. As a potent antioxidant agent that could clear oxygen-derived free radicals, inhibit the activation of NF-κB and reduce inflammatory response, melatonin has been widely used to treat inflammatory bowel diseases^[29,30]. Pentney and his coworker^[16] have shown melatonin could reduce the severity of dextran-induced colitis in mice. Protective effects of melatonin on dinitrobenzene sulfonic acid induced colitis have been proved by Cuzzocrea and his colleagues^[17]. In the present investigation, melatonin was demonstrated to reduce colonic lesions induced by acetic acid and TNBS enemas, which combined with the reports above, suggested that the protective effect of melatonin on the induced colitis might be universal. The present study also revealed the improvement of colonic lesions by melatonin accorded synchronously and unanimately with the decrease of colonic NO and PGE₂ content, as well as the down-regulated expression of colonic iNOS and COX-2, which indicates the improvement is probably via a mechanism of local inhibition of iNOS and COX-2 expression in the colonic mucosa. Further studies are needed to explore other mechanisms involved in the protection of colonic mucosa by melatonin.

REFERENCES

- 1 **Sakamoto C.** Roles of COX-1 and COX-2 in gastrointestinal pathophysiology. *J Gastroenterol* 1998; **33**: 618-624
- 2 **Kankuri E,** Asmawi MZ, Korpela R, Vapaatalo H, Moilanen E. Induction of iNOS in a rat model of acute colitis. *Inflammation* 1999; **23**: 141-152
- 3 **Vural H,** Sabuncu T, Arslan SO, Aksoy N. Melatonin inhibits lipid peroxidation and stimulates the antioxidant status of diabetic rats. *J Pineal Res* 2001; **31**: 193-198
- 4 **Cuzzocrea S,** Reiter RJ. Pharmacological action of melatonin in shock, inflammation and ischemial-reperfusion injury. *Eur J*

- 5 **Bubenik GA.** Gastrointestinal melatonin: localization, function, and clinical relevance. *Dig Dis Sci* 2002; **47**: 2336-2348
- 6 **Maestroni GJ.** The immunotherapeutic potential of melatonin. *Expert Opin Investig Drug* 2001; **10**: 467-476
- 7 **Sjoblom M,** Jedstedt G, Flemstrom G. Peripheral melatonin mediates neural stimulation of duodenal mucosal bicarbonate secretion. *J Clin Invest* 2001; **108**: 625-633
- 8 **Sener-Muratoglu G,** Paskaloglu K, Arbak S, Hurdag C, Ayanoglu-Dulger G. Protective effect of famotidine, omeprazole, and melatonin against acetylsalicylic acid-induced gastric damage in rats. *Dig Dis Sci* 2001; **46**: 318-330
- 9 **Otsuka M,** Kato K, Murai I, Asai S, Iwasaki A, Arakawa Y. Roles of nocturnal melatonin and the pineal gland in modulation of water-immersion restraint stress-induced gastric mucosal lesions in rats. *J Pineal Res* 2001; **30**: 82-86
- 10 **Bubenik GA.** Localization, physiological significance and possible clinical implication of gastrointestinal melatonin. *Biol Signals Recept* 2001; **10**: 350-366
- 11 **Cabeza J,** Motilva V, Martin MJ, de la Lastra CA. Mechanisms involved in gastric protection of melatonin against oxidant stress by ischemia-reperfusion in rats. *Life Sci* 2001; **68**: 1405-1415
- 12 **Bandyo Padhyay D,** Biswas K, Bandyopadhyay U, Reiter RJ, Banerjee RK. Melatonin protects against stress-induced gastric lesion by scavenging the hydroxyl radical. *J Pineal Res* 2000; **29**: 143-151
- 13 **Messner M,** Huether G, Lorf T, Ramadori G, Schworer H. Presence of melatonin in the human hepatobiliary-gastrointestinal tract. *Life Sci* 2001; **69**: 543-551
- 14 **Ustundag B,** Kazez A, Demirbag M, Canatan H, Halifeoglu I, Ozercan IH. Protective effect of melatonin on antioxidative system in experimental ischemia-reperfusion of rat small intestine. *Cell Physiol Biochem* 2000; **10**: 229-236
- 15 **Poon AM,** Mak AS, Luk HT. Melatonin and 2^[125I]iodomelatonin binding sites in the human colon. *Endocr Res* 1996; **22**: 77-94
- 16 **Pentney PT,** Bubenik GA. Melatonin reduces the severity of dextran-induced colitis in mice. *J Pineal Res* 1995; **19**: 31-39
- 17 **Cuzzocrea S,** Mazzon E, Serraino I, Lepore V, Terranova ML, Ciccolo A. Melatonin reduces dinitrobenzene sulfonic acid-induced colitis. *J Pineal Res* 2001; **30**: 1-12
- 18 **Morris GP,** Beck PL, Herridge MS. Hapten-induced model of chronic inflammation and ulceration in the rat colon. *Gastroenterol* 1989; **96**: 795-803
- 19 **Mei Q,** Yu JP, Xu JM, Wei W, Xiang L, Yue L. Melatonin reduces colon immunological injury in rats by regulating activity of macrophages. *Acta Pharmacol Sin* 2002; **23**: 882-886
- 20 **Millar AD,** Rampton DS, Chander CL, Claxson AW, Blades S, Coumbe A. Evaluating the antioxidant potential of new treatments for inflammatory bowel disease using a rat model of colitis. *Gut* 1996; **39**: 407-415
- 21 **Raab Y,** Sundberg C. Mucosal synthesis and release of prostaglandin E2 from activated eosinophils and macrophages in ulcerative colitis. *Am J Gastroenterol* 1995; **90**: 614-620
- 22 **Shechter H,** Gruener N, Shuval HI. A micromethod for the determination of nitrite in blood. *Anal Chim Acta* 1972; **60**: 93-99
- 23 **Luo YQ,** Wu KC, Sun AH, Pan BR, Zhang XY, Fan DM. Significance of COX-1, COX-2 and iNOS expression in superficial gastritis, gastric mucosa atypical hyperplasia and gastric carcinoma. *Zhonghua Xiaohua Zazhi* 2000; **20**: 223-226
- 24 **Southey A,** Tanaka S, Murakami T. Pathophysiological role of nitric oxide in rat experimental colitis. *Int J Immunopharmacol* 1997; **19**: 669-676

- 25 **Middleton SJ**, Shorthouse M, Hunter JO. Increased nitric oxide synthesis in ulcerative colitis. *Lancet* 1993; **341**: 465-469
- 26 **Dijkstra G**, Moshage H, van Dullemen HM, de Jager-Krikken A, Tiebosch AT, Kleibeuker JH, Jansen PL, van Goor H. Expression of nitric oxide synthases and formation of nitrotyrosine and reactive oxygen species in inflammatory bowel disease. *J Pathol* 1998; **186**: 416-421
- 27 **El-Shenawy SM**, Abdel-Salam OM, Baiuomy AR, El-Batran S, Arbid MS. Studies on the anti-inflammatory and anti-nociceptive effects of melatonin in the rat. *Pharmacol Res* 2002; **46**: 235-243
- 28 **Schmidt C**, Baumeister B, Kipnowski J. Alteration of prostaglandin E₂ and leukotriene B₄ synthesis in chronic inflammatory bowel disease. *Hepatogastroenterology* 1996; **43**: 1508-1512
- 29 **Reiter RJ**, Melchiorri D, Sewerynek E, Poeggeler B, Barlow-Walden L, Chuang J. A review of the evidence supporting Melatonin's role as an antioxidant. *J Pineal Res* 1995; **18**: 1-11
- 30 **Bubenik GA**, Blask DE, Brown GM, Maestroni GJ. Prospects of the clinical utilization of melatonin. *Biol Signals Recept* 1998; **7**: 195-219

Edited by Zhu L

Rapid mitogen-activated protein kinase by basic fibroblast growth factor in rat intestine after ischemia/reperfusion injury

Xiao-Bing Fu, Yin-Hui Yang, Tong-Zhu Sun, Wei Chen, Jun-You Li, Zhi-Yong Sheng

Xiao-Bing Fu, Yin-Hui Yang, Tong-Zhu Sun, Wei Chen, Jun-You Li, Zhi-Yong Sheng, Wound Healing and Cell Biology Laboratory, Burns Institute, 304 Hospital, Trauma Center of Postgraduate Medical College, Beijing 100037, China

Supported in part by the National Basic Science and Development Programme (973 Programme, No.G1999054204), Grant for National Distinguished Young Scientists No. 39525024, Grant for National Natural Science Foundation of China, No. 39900054, 30170966

Correspondence to: Professor Xiao-Bing Fu, Wound Healing and Cell Biology Laboratory, 304 Hospital, Burns Institute, Trauma Center of Postgraduate Medical College, 51 Fu Cheng Road, Beijing 100037, China. fuxb@cgw.net.cn

Telephone: +86-10-66867396 **Fax:** +86-10-88416390

Received: 2003-03-04 **Accepted:** 2003-04-01

Abstract

AIM: Previous studies showed that exogenous basic fibroblast growth factor (bFGF or FGF-2) could improve physiological dysfunction after intestinal ischemia/reperfusion (I/R) injury. However, the mechanisms of this protective effect of bFGF are still unclear. The present study was to detect the effect of bFGF on the activities of mitogen-activated protein kinase (MAPK) signaling pathway in rat intestine after I/R injury, and to investigate the protective mechanisms of bFGF on intestinal ischemia injury.

METHODS: Rat intestinal I/R injury was produced by clamping the superior mesenteric artery (SMA) for 45 minutes and followed by reperfusion for 48 hours. Seventy-eight Wistar rats were used and divided randomly into sham-operated group (A), normal saline control group (B), bFGF antibody pre-treated group (C), and bFGF treated group (D). In group A, SMA was separated without occlusion. In groups B, C and D, SMA was separated and occluded for 45 minutes, then, released for reperfusion for 48 hours. After the animals were sacrificed, blood and tissue samples were taken from the intestine 45 minutes after ischemia in group A and 2, 6, 24, and 48 hours after reperfusion in the other groups. Phosphorylated forms of p42/p44 MAPK, p38 MAPK and stress activated protein kinase/C-Jun N-terminal kinase (SAPK/JNK) were measured by immunohistochemistry. Plasma levels of D-lactate were examined and histological changes were observed under the light microscope.

RESULTS: Intestinal I/R injury induced the expression of p42/p44 MAPK, p38 MAPK, and SAPK/JNK pathways and exogenous bFGF stimulated the early activation of p42/p44 MAPK and p38 MAPK pathways. The expression of phosphorylated forms of p42/p44 MAPK was primarily localized in the nuclei of crypt cells and in the cytoplasm and nuclei of villus cells. The positive expression of p38 MAPK was localized mainly in the nuclei of crypt cells, very few in villus cells. The activities of p42/p44 MAPK and p38

MAPK peaked 6 hours after reperfusion in groups B and C, while SAPK/JNK peaked 24 hours after reperfusion. The activities of p42/p44 MAPK and p38 MAPK peaked 2 hours after reperfusion in group D and those of SAPK/JNK were not changed in group B. D-lactate levels and HE staining showed that the intestinal barrier was damaged severely 6 hours after reperfusion; however, histological structures were much improved 48 hours after reperfusion in group D than in the other groups.

CONCLUSION: The results indicate that intestinal I/R injury stimulates the activities of MAPK pathways, and that p42/p44 MAPK and p38MAPK activities are necessary for the protective effect of exogenous bFGF on intestinal I/R injury. The protective effect of bFGF on intestinal dysfunction may be mediated by the early activation of p42/p44 MAPK and p38 MAPK signaling pathways.

Fu XB, Yang YH, Sun TZ, Chen W, Li JY, Sheng ZY. Rapid mitogen-activated protein kinase by basic fibroblast growth factor in rat intestine after ischemia/reperfusion injury. *World J Gastroenterol* 2003; 9(6): 1312-1317

<http://www.wjgnet.com/1007-9327/9/1312.asp>

INTRODUCTION

Previous studies have shown that intestinal ischemia/reperfusion (I/R) injury reduce the expression of endogenous basic fibroblast growth factor (bFGF) in rats, and the intravenous administration of exogenous bFGF could induce the expression of endogenous bFGF and improve the physiological functions of the intestine, lung, kidney, and other internal organs after I/R injury^[1-6]. However, the protective mechanisms of bFGF on intestinal I/R injury remain unknown.

Mitogen-activated protein kinase (MAPK) cascade, a cytoplasmic protein kinase that requires dual phosphorylation on specific threonine and tyrosine residues for their activation, can transmit mitogen or differentiation signals from the cell surface into the nucleus, thus regulating the gene expression^[7-10]. P42/p44 MAPK, p38MAPK and stress activated protein kinase/C-Jun N-terminal kinase (SAPK/JNK) are three important members of the MAPK family. The purpose of the present study was to detect the activities of mitogen-activated protein kinase (MAPK) signaling pathway in rat intestine after administration of bFGF, and to investigate the protective mechanisms of bFGF on intestinal (I/R) injury.

Rat intestinal I/R injury was produced by clamping the superior mesenteric artery (SMA) for 45 minutes and by different durations of reperfusion^[11]. The activities of p42/p44 MAPK, p38 MAPK, and SAPK/JNK were measured after administration of bFGF or bFGF monoclonal antibody. The results indicate that the early activation of p42/p44 MAPK and p38 MAPK is necessary for the protective effect of bFGF on intestinal I/R injury.

MATERIALS AND METHODS

Animal model

Seventy-eight healthy Wistar rats weighing 220 ± 20 g (Animal Center, Academy of Military Medical Sciences, Beijing) were used. All animals were housed in the laboratory and given free access to food and water for 1 week before being used. The animal was under anesthesia by 3 % sodium pentobarbital (40 mg/kg), a middle incision was made. The superior mesenteric artery (SMA) was identified and freed by blunt dissection. A microvascular clamp was placed at the root of SMA to cause complete cessation of blood flow for 45 minutes, and thereafter the clamp was loosened to form reperfusion injury^[1,11]. After 2, 6, 24 and 48 hours reperfusion, the animals were sacrificed and blood samples and intestinal tissue biopsies were taken. Blood samples were centrifuged and serum was frozen to measure plasma D-lactate. Tissue biopsies were fixed with 4 % paraformaldehyde.

In this study, all operations were performed under aseptic conditions. The animal experiments were approved by the local animal management committee.

Experimental design

The animals were randomly divided into four groups: sham-operated (A), normal saline control (B), bFGF monoclonal antibody (Sigma, St. Louis, MO, USA) pre-treated (C) and bFGF (Sigma, St. Louis, MO, USA) treated groups (D). In group A, SMA was freed but without occlusion and blood samples and tissue biopsies were taken 45 minutes after exposure of the SMA. In groups B and D, 0.15 ml saline or 0.15 ml saline plus bFGF (2 μ g/rat) was injected immediately 45 minutes after SMA occlusion from the tail vein. In group C, 0.15 ml saline plus bFGF monoclonal antibody (25 μ g/rat) was injected right before SMA occlusion from tail vein for pre-treatment.

Measurement of phosphorylated forms of p42/p44 MAPK, p38 MAPK and SAPK/JNK

Formalin-fixed, paraffin-embedded small intestinal tissues were used to measure the expression of phosphorylated forms of p42/p44 MAPK, p38 MAPK, and SAPK/JNK by immunohistochemistry. Immunohistochemical staining was performed according to the instructions of the PowerVision™ kit (Santa Cruze, USA). Briefly, sections (5 μ m) were dewaxed and rehydrated in graded alcohols. Endogenous peroxidase activity was quenched, and antigen retrieval was performed by heating for 20 minutes at 100 °C in 0.01 mol/L sodium citrate. The primary monoclonal antibodies for p42/p44 MAPK, p38 MAPK and SAPK/JNK (Cell Signaling Technology, Inc., USA) were diluted to 1:100 in buffer and incubated for 40 minutes at 37 °C. The sections were then incubated with HRP-conjugated secondary antibodies (Santa Cruz, USA) for 20 minutes at 37 °C. Positive expression was detected with diaminobenzidine (DAB) (Sigma, St. Louis, MO, USA). The sections were lightly counterstained with hematoxylin, dehydrated in graded alcohol, and mounted. For negative control, the sections were processed similarly but PBS was used as primary antibodies instead of the MAPKs monoclonal antibodies.

The result of positive staining was semi-quantitatively defined as -, +, ++ and +++. This was observed under microscope with 10 times eyepiece and 40 times objective. “-” represents no visible positive staining, “+” less than 10 stained cells and “++” 10-30 stained cells, while “+++” represents more than 30 positively stained cells within one high power field.

Measurement of plasma D-lactate

The levels of plasma D-lactate were measured with modified Brandt's method^[12]. Briefly, heparinized blood was centrifuged at 3 200 rpm for 10 min and 2 ml of the plasma was deproteinized with 0.2 ml perchloric acid (PCA) (1/10 vol),

mixed and kept in an ice bath for 10 min. The denatured protein solution was centrifuged at 3 200 rpm for 10 min and the supernatant solution was removed. To 1.4 ml of supernatant solution, 0.12 ml KON was added and they were mixed for 20 s. Precipitant KClO₄ was removed by centrifugation at 3 200 rpm for 10 min. The supernatant solution and neutralized-protein-free plasma were used to measure the absorbency at 340 nm. Plasma D-lactate concentration was expressed as mmol/L.

Histological observation

Paraformaldehyde fixed, paraffin embedded small intestine samples were also cut 5 μ m in thickness, deparaffinized in xylene, rehydrated in graded ethanol, and then stained with haematoxylin-eosin (HE) for histological observation under light microscope (Olympus, Japan).

Statistical analysis

Data were expressed as mean \pm standard error. Comparisons between groups of data were analyzed by Student's *t*-test. *P* values <0.05 were considered statistically significant.

RESULTS

Activities of p42/p44 MAPK and p38 MAPK

Quantitative immunohistochemical results for phosphorylated forms of p42/p44 MAPK and p38 MAPK were evaluated (Tables 1 and 2). The expression of activated p42/p44 MAPK was localized in the cytoplasm and nuclei of villus cells and in the nuclei of crypt cells, mainly in the epithelium and villus cells (Figure 1). Activated p38 MAPK was localized primarily in the nuclei of crypt cells, very few in villus cells (Figure 2). There was a consistent correlation between positive expression levels and the intensity of p42/p44 MAPK and p38 MAPK. The positive expression of p42/p44 MAPK and p38 MAPK was weak in the sham-operated intestinal tissues and ischemic tissues. However, the number of positive staining cells increased with high staining intensity after reperfusion injury. In the normal saline and bFGF antibody pre-treated groups, the number of positive staining cells of p42/p44 MAPK (Figures 1B and C) and p38 MAPK (Figures 2B and C) increased 2 hours after reperfusion, peaked at 6th hours, and decreased from 24 to 48 hours. In the bFGF treated group, however, the number of positive staining cells and the intensity of p42/p44 MAPK and p38 MAPK peaked 2 hours after reperfusion (Figures 1D and 2D) and decreased afterwards, but they were still higher than those in the sham-operated control at 48 hours. Compared with the normal saline and bFGF treated groups, the intensity of p42/p44 MAPK and p38 MAPK positive staining in the bFGF antibody pretreated group was weaker from 2 hours to 48 hours after reperfusion.

Activities of SAPK/JNK

Weak staining of SAPK/JNK was observed in small intestine after I/R injury. Positive staining was localized in the nuclei and cytoplasm of villus and crypt cells. The staining, however, was weak without much difference among the groups (Table 3). The positive staining of SAPK/JNK in bFGF treated group was slightly higher only at 24 hours after reperfusion. Among all the groups, the positive staining of SAPK/JNK was weaker than that of p42/p44 MAPK and p38 MAPK.

Changes of plasma D-lactate levels

Plasma D-lactate levels were measured 2, 6, 24, and 48 hours after reperfusion in all groups. They were elevated 2 hours after reperfusion in all groups, peaked at 6th hour, and decreased to nearly normal 48 hours later (Table 4). The levels at 45 min after ischemia in the sham-operated group were served as controls.

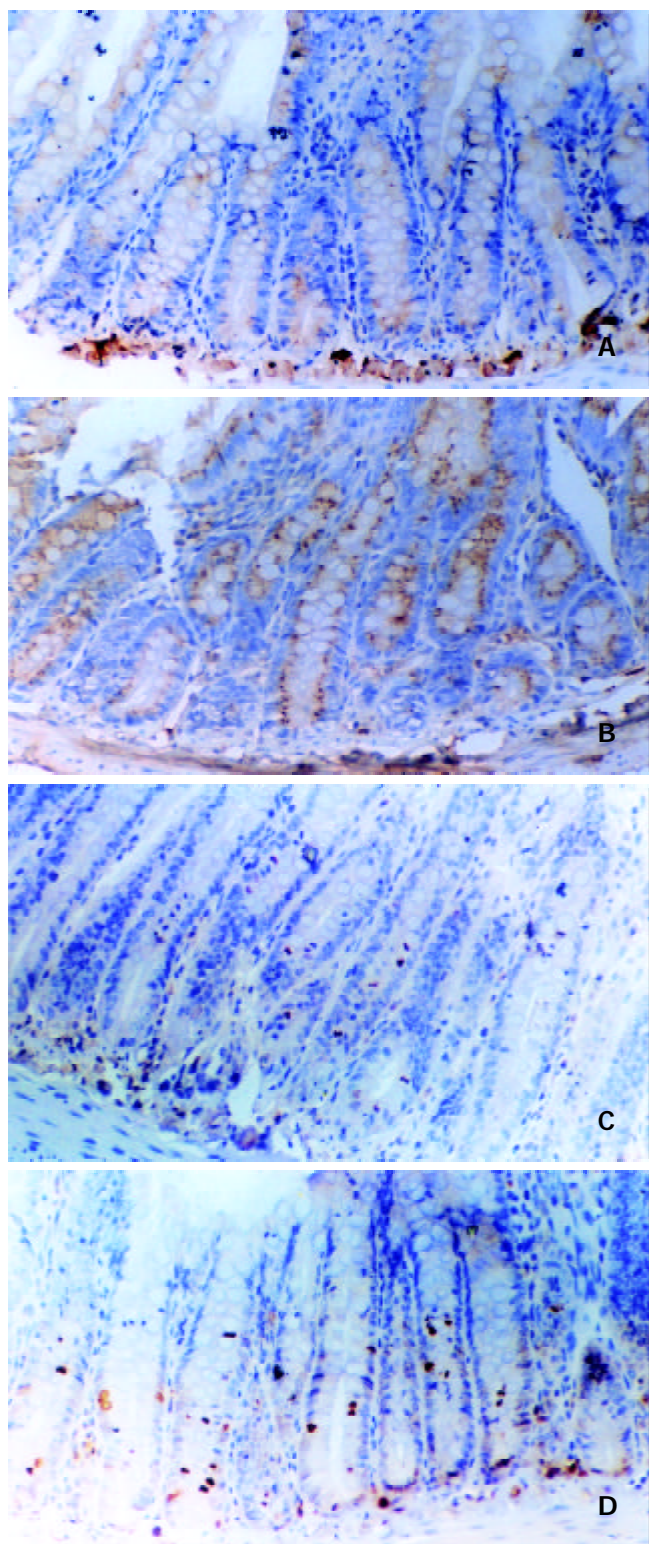


Figure 1 Immunohistochemical staining of phosphorylated p42/p44 MAPK in intestinal biopsies in rats after ischemia/reperfusion injury (SP×200). A: Negative control of p42/p44 MAPK staining. There was no positive expression signal in this group. B: The expression of phosphorylated p42/p44 in intestinal biopsies in the saline control group 2 hours after reperfusion. The activated p42/p44 MAPK expression was localized in the cytoplasm and nuclei of villus cells and in the nuclei of crypt cells, mainly in the epithelium and villus cells. C: Phosphorylated p42/p44 staining in the bFGF antibody pre-treated group. The number of positive cells and intensity in this group were weaker compared with those in the saline control and bFGF treated groups. D: The expression of phosphorylated p42/p44 in the bFGF treated group 2 hours

after reperfusion. The activated p42/p44 MAPK expression was localized in the cytoplasm and nuclei of villus cells and in the nuclei of crypt cells, mainly in the epithelium and villus cells. The number of positive cells in this group was more than that in the bFGF antibody pre-treated group. ISH×400.

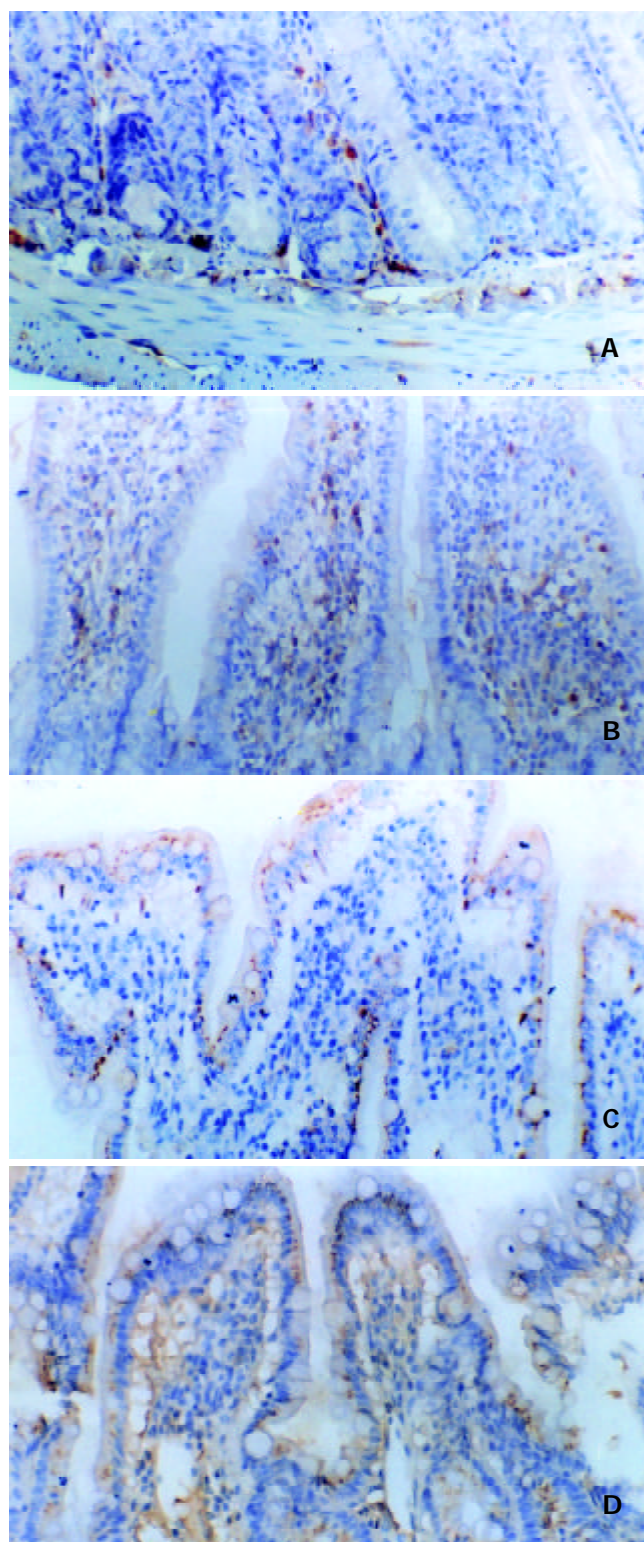


Figure 2 Immunohistochemical staining of phosphorylated p38 MAPK in intestinal biopsies in rats after ischemia/reperfusion injury (SP×200). A: Negative control of p38 MAPK staining. There was no positive expression signal in this group. B: Phosphorylated p38 MAPK staining in the saline control group 2 hours after reperfusion. Few p38 MAPK positive expression were localized in the cytoplasm and nuclei of villus cells and in the nuclei of crypt cells, mainly in the

Table 1 Semi-quantitative results of immunohistochemical staining for phosphorylated forms of p42/p44 MAPK in different groups

Groups	Pre-injury	2 hrs post-injury	6 hrs post-injury	24 hrs post-injury	48 hrs post-injury
Group B	-	++	++	+	++
Group C	-	+	++	+	+
Group D	-	+++	+++	+	+

“-” represents no visible positive staining, “+” less than 10 stained cells and “++” 10-30 stained cells, while “+++” represents more than 30 positively stained cells within one high power field.

Table 2 Semi-quantitative results of immunohistochemical staining for phosphorylated forms of p38 MAPK in different groups

Groups	Pre-injury	2 hrs post-injury	6 hrs post-injury	24 hrs post-injury	48 hrs post-injury
Group B	-	++	++	+	++
Group C	-	+	++	+	+
Group D	-	+++	++	+	+

“-” represents no visible positive staining, “+” less than 10 stained cells and “++” 10-30 stained cells, while “+++” represents more than 30 positively stained cells within one high power field.

Table 3 Semi-quantitative results of immunohistochemical staining for phosphorylated forms of SAPK/JNK in different groups

Groups	Pre-injury	2 hrs post-injury	6 hrs post-injury	24 hrs post-injury	48 hrs post-injury
Group B	-	+	+	++	+
Group C	-	+	+	+	+
Group D	-	+	+	++	+

“-” represents no visible positive staining, “+” less than 10 stained cells and “++” 10-30 stained cells, while “+++” represents more than 30 positively stained cells within one high power field.

Table 4 The changes of plasma D-lactate levels at different time points in three groups (mmol/L) ($\bar{x}\pm s$)

Groups	Animal numbers	Control	2 hours	6 hours	24 hours	48 hours
Group B	24	0.332±0.132	0.372±0.090	0.397±0.096	0.463±0.147	0.511±0.179
Group C	24	0.332±0.132	0.309±0.079	0.327±0.098	0.415±0.177 ^a	0.425±0.208 ^a
Group D	24	0.332±0.132	0.369±0.124	0.407±0.089	0.475±0.128	0.537±0.098

^a $P < 0.05$ vs compared with control.

epithelium and villus cells. C: P38 MAPK staining in the bFGF antibody pre-treated group. The number of positive cells and localization of p38 MAPK positive cells were similar with those in the saline group. D: Phosphorylated p38 staining in the bFGF treated group 2 hours after reperfusion. Activated p38 MAPK was localized primarily in the nuclei of crypt cells, few in villus cells. The number of positive cells was more than that in the saline control and bFGF antibody pre-treated groups. In the bFGF treated group, the number of positive expression cells of p38 MAPK as well as its intensity peaked 2 hours after reperfusion.

Histological evaluation

Intestinal I/R injury resulted in the damage of intestinal barrier and the increase of mucosal permeability. HE staining showed partial loss of the mucosa 2 hours after reperfusion. 6 hours after reperfusion, however, the damage of intestinal epithelial cells, hemorrhage and necrosis were observed and accompanied by inflammatory cell infiltration into the intestinal wall. Histological structure of the intestinal mucosa was markedly improved after administration of bFGF.

DISCUSSION

Intestinal I/R injury causes release of bacteria and toxin from the gut into the host blood circulation and changes of inflammatory factors, cytokines and growth factors, resulting in damage to the intestinal barrier and other internal organs^[1-3,13-17]. We found that administration of exogenous basic fibroblast growth factor (bFGF) could reduce the intestinal injury caused by I/R insult. However, the mechanisms of this protective effect of bFGF are not elucidated. bFGF is expressed in many normal adult tissues and has mitogenic activity in a wide variety of cells of mesenchymal, neuronal, and epithelial origins, and regulates events in normal embryonic development, angiogenesis, wound repair, and neoplasia^[18-20]. Also, it can regulate migration and replication of intestinal epithelial cells in culture^[21]. Recent studies have shown that L-glutamine, tumor necrosis factor- α and epidermal growth factor (EGF) stimulate proliferation of intestinal crypt cells by activating the MAPK pathway, and that p42/p44 MAPK activities are necessary for both cell cycle progression and differentiation of the intestinal cells^[22-25]. In many other cell types, growth factor controls proliferation and differentiation

via the MAPK pathway. MAPK is a common signal pathway to transmit the mitogen or the differentiating signals from the cell surface to the nucleus, and thus ultimately regulates different gene expression^[26-28]. Hence, we hypothesized that MAPK activation might be involved in the regulation of bFGF signals in the process of intestinal barrier repair.

To investigate this hypothesis, we evaluated changes of the activated MAPK signal pathway after administration of bFGF and bFGF antibodies. We found that intestinal I/R injury stimulated the activities of phosphorylated forms of the p42/p44 MAPK and p38MAPK pathways, and increased the SAPK/JNK activity slightly. p42/p44 MAPK and p38MAPK activities were increased 2 hours after reperfusion, and peaked at 6 hours. At the same time, the levels of SAPK/JNK increased slightly 24 hours after reperfusion compared with those of the normal control. Phosphorylated forms of p42/p44 MAPK were mainly localized in the nuclei of crypt cells and in the cytoplasm and nuclei of villus cells, whereas those of p38MAPK were primarily localized in the nuclei of crypt cells, few in villus cells. After administration of bFGF, the expression of both p42/p44 MAPK and p38MAPK was quickly stimulated, and the activation of both p42/p44 MAPK and p38MAPK peaked 2 hours after reperfusion, declined gradually to normal at 48 hours. A coherence was noted between the changes of p42/p44 MAPK and p38MAPK and histological findings. These results indicate that intestinal I/R injury induces the activities of the MAPK pathways, and p42/p44 MAPK and p38MAPK activities are necessary for the protective effects of exogenous bFGF on intestinal I/R injury. The early stimulation of the p42/p44 MAPK and p38MAPK signal pathways may mediate the protective effects of bFGF on intestinal dysfunction.

MAPK family is composed of "extracellular signal regulated" p42/p44 MAPK, "stress-regulated" MAPK (SR-MAPKs), stress-activated protein kinases (SAPKs)/c-Jun N-terminal kinases (JNKs) and p38-MAPKs. On stimulation, MAPKs are translated into the nucleus where they may phosphorylate nuclear transcription factors and thus regulate gene expression. The four principal differentiated cell lineages of intestinal epithelium are derived from common multipotent stem cells located near the base of each crypt. These crypt stem cells divide to produce daughter stem cells as well as more rapidly replicating transit cells, which in turn undergo 4-6 rapid cell divisions in the proliferative zone located in the lower half of each crypt^[29,30]. Factors determining whether cells continue to proliferate, cease dividing, and begin to differentiate, appear to operate during the first gap phase (G1) of the cell cycle. P42/p44 is activated during G0 to G1 transition, and the activity remains elevated up to S phase entry, implicating this family of protein kinases in the control of G1 progression^[31,32]. Activation of p42/p44 MAPK is also necessary for growth factor-dependent proliferation of some cell lines.

We propose the possible mechanisms of the protective effects of bFGF on intestinal I/R injury be involved in the activation of MAPK pathway. First, to protect the survival of intestinal stem cells within crypt and mediate the proliferation and differentiation of these cells. Intestinal epithelium is maintained by continuous and rapid replacement of differentiated epithelial cells by replication of undifferentiated epithelial cells. Exogenous bFGF markedly enhances the survival of crypt stem cells before and after irradiation injury^[33]. Microvascular endothelial apoptosis is the primary lesion leading to stem cell dysfunction, while endothelial apoptosis could be inhibited by intravenous bFGF^[34]. Second, to regulate the inflammation reactions after I/R injury. The TNF translation by IL-10 is inhibited mainly by inhibiting the activation of the p38 MAPK pathway^[35]. This is necessary for maintenance of immune homeostasis in the gut.

In the perfused heart, ischemia/reperfusion activates stress-

regulated MAPKs, direct pharmacological activation of p38 triggers delayed preconditioning of the heart, and there is minimal activation of the p42/p44 MAPK subfamily by heart I/R injury^[35-37]. Yet phosphorylation of p42/p44 MAPK occurs consistently in the grey matter penumbra of brain tissue after ischemic stroke, and may be associated with neuronal survival and/or angiogenic activity in the recovering brain tissue^[38]. The results indicate that the MAPK pathways respond differently to ischemic injury in different sites.

The changes of serum D (-)-lactate were used as a predictor of intestinal I/R injury in this study. D (-)-lactate is the stereoisomer of mammalian L (+)-lactate. Mammalian tissue does not produce D (-)-lactate and only slowly metabolizes it. It is a strict product of bacterial fermentation. Since mammals do not possess the enzyme systems to rapidly metabolize D (-)-lactate^[11, 39,40], the released D (-)-lactate will pass through the gut barrier and liver in an unchanged form and appear in the peripheral blood. As intestinal ischemia injury causes mucosal injury and subsequent bacterial proliferation, D (-)-lactate is released from gut into the circulation. In this study, the serum D (-)-lactate level was increased after injury, but in the bFGF treated group, it was not significantly increased as in the control group, indicating that bFGF exerts a positive protective effect on the mucosal barrier and decreases the intestinal permeability.

In summary, intestinal I/R injury induces the activities of the MAPK pathways, and p42/p44 MAPK and p38MAPK activities are necessary for the protective effect of exogenous bFGF on intestinal I/R injury. The protective effect of bFGF on intestinal dysfunction may be mediated by the early stimulation of the p42/p44 MAPK and p38 MAPK signaling pathways.

REFERENCES

- 1 **Fu XB**, Sheng ZY, Wang YP, Ye YX, Xu MH, Sun TZ, Zhou BT. Basic fibroblast growth factor reduces the gut and liver morphologic and functional injuries after ischemia and reperfusion. *J Trauma* 1997; **42**: 1080-1085
- 2 **Yang YH**, Fu XB, Sun TZ, Jiang LX, Gu XM. bFGF and TGF β expression in rat kidneys after ischemic/reperfusion gut injury and its relationship with tissue repair. *World J Gastroenterol* 2000; **6**: 147-149
- 3 **Fu XB**, Yang YH, Sun XQ, Sun TZ, Gu XM, Sheng ZY. Protective effects of endogenous basic fibroblast growth factor activated by 2, 3 butanedion monocime on functional changes of ischemic intestine, liver and kidney in rats. *Zhongguo Weizhongbing Jijiu Yixue* 2000; **12**: 69-72
- 4 **Yang YH**, Fu XB, Sun TZ, Jiang LX, Gu XM. The effect of exogenous basic fibroblast growth factor on hepatic endogenous basic fibroblast growth factor and fibroblast growth factor receptor expression after intestinal ischemia-reperfusion injury. *Zhongguo Weizhongbing Jijiu Yixue* 1999; **11**: 734-736
- 5 **Fu XB**, Yang YH, Sun TZ, Sun XQ, Gu XM, Chang GY, Sheng ZY. Effect of inhibition or anti-endogenous basic fibroblast growth factor on functional changes in intestine, liver and kidneys in rats after gut ischemia-reperfusion injury. *Zhongguo Weizhongbing Jijiu Yixue* 2000; **12**: 465-468
- 6 **Yang YH**, Fu XB, Sun TZ, Jiang LX, Gu XM. Renal endogenous expression of basic fibroblast growth factor and transforming growth factor β after intestinal ischemia-reperfusion injury. *Zhongguo Weizhongbing Jijiu Yixue* 1999; **11**: 203-205
- 7 **Marshall CJ**. Specificity of receptor tyrosine kinase signaling: transient versus sustained extracellular signal-regulated kinase activation. *Cell* 1995; **80**: 179-185
- 8 **Seeger R**, Krebs EG. The MAPK signaling cascade. *FASEB J* 1995; **9**: 726-735
- 9 **Marais R**, Wynne J, Treisman R. The SRF accessory protein Elk-1 contains a growth factor-regulated transcriptional activation domain. *Cell* 1993; **73**: 381-393
- 10 **Nishida E**, Gotoh Y. The MAP kinase cascade is essential for diverse signal transduction pathways. *Trends Biochem Sci* 1993; **18**: 128-131

- 11 **Sun XQ**, Fu XB, Zhang R, Lu Y, Deng Q, Jiang XG, Sheng ZY. Relationship between plasma D(-)-lactate and intestinal damage after severe injuries in rats. *World J Gastroenterol* 2001; **7**: 555-558
- 12 **Qin RY**, Zou SQ, Wu ZD, Qiu FZ. Influence of splanchnic vascular infusion on the content of endotoxins in plasma and the translocation of intestinal bacteria in rats with acute hemorrhage necrosis pancreatitis. *World J Gastroenterol* 2000; **6**: 577-580
- 13 **Wang XJ**, Luo XD, Luo Q, Yang ZC. Effects of sera from burn patients on human hepatocytic viscoelasticity. *World J Gastroenterol* 1998; **4**: 60
- 14 **Zhang P**, Yang WM, Shui WX, Du YG, Jin GY. Effect of Chinese herb mixture, shock decoction on bacterial translocation from the gut. *World J Gastroenterol* 2000; **6**(Suppl 3): 74
- 15 **Zhu L**, Yang ZC, Li A, Cheng DC. Protective effect of early enteral feeding on postburn impairment of liver function and its mechanism in rats. *World J Gastroenterol* 2000; **6**: 79-83
- 16 **Li YS**, Li JS, Li N, Jiang ZW, Zhao YZ, Li NY, Liu FN. Evaluation of various solutions for small bowel graft preservation. *World J Gastroenterol* 1998; **4**: 140-143
- 17 **Zhang GL**, Wang YH, Ni W, Teng HJ, Lin ZB. Hepatoprotective role of ganoderma lucidum polysaccharide against BCG in duced immune liver injury in mice. *World J Gastroenterol* 2002; **8**: 728-733
- 18 **Liu XJ**, Yang L, Mao YQ, Wang Q, Huang MH, Wang YP, Wu HB. Effects of the tyrosine protein kinase inhibitor genistein on the proliferation, activation of cultured rat hepatic stellate cells. *World J Gastroenterol* 2002; **8**: 739-745
- 19 **Brandt RB**, Siegel SA, Waters MG, Bloch MH. Spectrophotometric assay for D(-)-Lactate in plasma. *Anal Biochem* 1980; **102**: 39-46
- 20 **Basilico C**, Moscatelli D. The FGF family of growth factors and oncogenes. *Adv Cancer Res* 1992; **59**: 115-165
- 21 **Dignass AU**, Tsunekawa S, Podolsky DK. Fibroblast growth factors modulate intestinal epithelial cell growth and migration. *Gastroenterology* 1994; **106**: 1254-1262
- 22 **Estival A**, Monzat V, Miquel K, Gaubert F, Hollande E, Korc M, Vaysse N, Clemente F. Differential regulation of fibroblast growth factor receptor-1 mRNA and protein by two molecular forms of basic FGF. *J Biol Chem* 1996; **271**: 5663-5670
- 23 **Nice EC**, Fabri L, Whitehead RH, James R, Simpson RJ, Burgess AW. The major colonic cell mitogen extractable from colonic mucosa is an N-terminally extended form of basic fibroblast growth factor. *J Biol Chem* 1991; **266**: 14425-14430
- 24 **Rhoads JM**, Argenzio RA, Chen W, Rippe RA, Westwick JK, Cox AD, Berschneider HM, Brenner DA. L-glutamine stimulates intestinal cell proliferation and activates mitogen-activated protein kinases. *Am J Physiol* 1997; **272**: G943-G953
- 25 **Oliver BL**, Sha'afi RI, Hajjar JJ. Transforming growth factor-alpha and epidermal growth factor activate mitogen-activated protein kinase and its substrates in intestinal epithelial cells. *Proc Soc Exp Biol Med* 1995; **210**: 162-170
- 26 **Goke M**, Kanai M, Lgnch-Devaney K, Podolsky DK. Rapid mitogen-activated protein kinase activation by transforming growth factor alpha in wounded rat intestinal epithelial cells. *Gastroenterology* 1998; **114**: 697-705
- 27 **Aliaga JC**, Deschenes C, Beaulieu JF, Calvo EL, Rivard N. Requirement of the MAP kinase cascade for cell cycle progression and differentiation of human intestinal cells. *Am J Physiol* 1999; **277**:G631-G641
- 28 **Gordon JI**, Hermiston ML. Differentiation and self-renewal in the mouse gastrointestinal epithelium. *Curr Opin Cell Biol* 1994; **6**: 795-803
- 29 **Potten CS**, Booth C, Pritchard DM. The intestinal epithelial stem cell: the mucosal governor. *Int J Exp Pathol* 1997; **78**: 219-243
- 30 **Brondello JM**, McKenzie FR, Sun H, Tonks NK, Pouyssegur J. Constitutive MAP kinase phosphatase (MKP-1) expression blocks G1 specific gene transcription and S-phase entry in fibroblasts. *Oncogene* 1995; **10**: 1895-1904
- 31 **Meloche S**, Seuwen K, Pages G, Pouyssegur J. Biphasic and synergistic activation of p44MAPK (ERK1) by growth factors: correlation between late phase activation and mitogenicity. *Mol Endocrinol* 1992; **6**: 845-854
- 32 **Houchen CW**, George RJ, Sturmoski MA, Cohn SM. FGF-2 enhances intestinal stem cell survival and its expression is induced after radiation injury. *Am J Physiol* 1999; **276**: G249-G258
- 33 **Paris F**, Fuks Z, Kang A, Capodiceci P, Juan G, Ehleiter D, Haimovitz-Friedman A, Cordon-Cardo C, Kolesnick R. Endothelial apoptosis as the primary lesion initiating intestinal radiation damage in mice. *Science* 2001; **293**: 293-297
- 34 **Kontoyiannis D**, Kotlyarov A, Carballo E, Alexopoulou L, Blackshear PJ, Gaestel M, Davis R, Flavell R, Kollias G. Interleukin-10 targets p38 MAPK to modulate ARE-dependant TNF mRNA translation and limit intestinal pathology. *EMBO J* 2001; **20**: 3760-3770
- 35 **Clerk A**, Fuller SJ, Michael A, Sugden PH. Stimulation of "stress-regulated" mitogen-activated protein kinases (stress-activated protein kinases/c-Jun N-terminal kinases and p38-mitogen-activated protein kinases) in perfused rat hearts by oxidative and other stresses. *J Biol Chem* 1998; **273**: 7228-7234
- 36 **Zhao TC**, Taher MM, Valerie KC, Kukreja RC. p38 triggers late preconditioning elicited by anisomycin in heart: involvement of NF-KB and iNOS. *Circ Res* 2001; **89**: 915-922
- 37 **Tong H**, Chen W, London RE, Murphy E, Steenbergen C. Preconditioning enhances glucose uptake is mediated by p38 MAP kinase not by phosphatidylinositol 3-kinase. *J Biol Chem* 2000; **275**: 11981-11986
- 38 **Slevin M**, Krupinski J, Slowik A, Rubio F, Szczudlik A, Gaffney J. Activation of MAP kinase (ERK-1/ERK-2), tyrosine kinase and VEGF in the human brain following acute ischaemic stroke. *Neuroreport* 2000; **11**: 2759-2764
- 39 **Murray MJ**, Barbose JJ, Cobb CF. Serum D (-)-lactate levels as a predictor of acute intestinal ischemia in a rat model. *J Surg Res* 1993; **54**: 507-509
- 40 **Murray MJ**, Gonze MD, Nowak LR, Cobb CF. Serum D (-)-lactate levels as an aid to diagnosing acute intestinal ischemia. *Am J Surg* 1994; **167**: 575-578

Edited by Zhang JZ and Zhu LH

Role of nitric oxide and peroxynitrite anion in lung injury induced by intestinal ischemia-reperfusion in rats

Jun-Lin Zhou, Guo-Hua Jin, Yi-Ling Yi, Jun-Lan Zhang, Xin-Li Huang

Jun-Lin Zhou, Department of Hand Surgery, Third Affiliated Hospital, Hebei Medical University, Shijiazhuang 050051, Hebei Province, China

Guo-Hua Jin, Department of Liver Medicine, Third Affiliated Hospital, Hebei Medical University, Shijiazhuang 050051, Hebei Province, China

Yi-Ling Yi, Jun-Lan Zhang, Xin-Li Huang, Department of Pathophysiology, Hebei Medical University, Shijiazhuang 050017, Hebei Province, China

Correspondence to: Dr. Jun-Lin Zhou, Department of Hand Surgery, Third Affiliated Hospital, Hebei Medical University, Shijiazhuang 050051, Hebei Province, China. zhjunlin@yahoo.com

Telephone: +86+311-7027951 Ext 3117

Received: 2003-01-18 **Accepted:** 2003-03-10

Abstract

AIM: To evaluate effects of nitric oxide (NO) and peroxynitrite anion (ONOO⁻) on lung injury following intestinal ischemia-reperfusion (IR) in rats.

METHODS: A rat model of intestinal ischemia was made by clamping superior mesenteric artery and lung injury was resulted from reperfusion. The animals were randomly divided into 3 groups: sham operation (Sham), 2 h ischemia followed by 2 h reperfusion (IR) and IR pretreated with aminoguanidine (AG) - an inhibitor of inducible NO synthase (iNOS) 15 minutes before reperfusion (IR+AG). The lung malondialdehyde (MDA) and nitrate/nitrite (NO₂⁻/NO₃⁻) contents and morphological changes were examined. Western blot was used to detect the iNOS protein expression. Immunohistochemical staining was used to determine the change of nitrotyrosine (NT) - a specific "footprint" of ONOO⁻.

RESULTS: The morphology revealed evidence for lung edema, hemorrhage and polymorphonuclear sequestration after intestinal IR. Compared with sham group, lung contents of MDA and NO₂⁻/NO₃⁻ in IR group were significantly increased (12.00±2.18 vs 23.44±1.25 and 76.39±6.08 vs 140.40±4.34, *P*<0.01) and the positive signals of iNOS and NT were also increased in the lung. Compared with IR group, the contents of MDA and NO₂⁻/NO₃⁻ in IR+AG group were significantly decreased (23.44±1.25 vs 14.66±1.66 and 140.40±4.34 vs 80.00±8.56, *P*<0.01) and NT staining was also decreased.

CONCLUSION: Intestinal IR increases NO and ONOO⁻ production in the lung, which may be involved in intestinal IR-mediated lung injury.

Zhou JL, Jin GH, Yi YL, Zhang JL, Huang XL. Role of nitric oxide and peroxynitrite anion in lung injury induced by intestinal ischemia-reperfusion in rats. *World J Gastroenterol* 2003; 9 (6): 1318-1322

<http://www.wjgnet.com/1007-9327/9/1318.asp>

INTRODUCTION

A devastating consequence of tissue reperfusion is the damage

in organs uninvolved in the initial ischemic insult^[1]. Multiple organ dysfunction syndrome (MODS), as it is known, is the leading cause of death in critically ill patients and is a documented consequence of gut reperfusion^[2-5]. Although systemic inflammatory characteristic of MODS can result in damage to any organ, onset of the syndrome is usually heralded by the development of respiratory insufficiency^[2-9]. The pathophysiology of lung injury associated with intestinal ischemia-reperfusion (IIR) probably involves a variety of inflammatory and vasoactive mediators. Recently, the production of large amounts of nitric oxide (NO), a free radical produced by the inducible isoform of NO synthase (iNOS) has been implicated as a cytotoxic factor in a variety of pathophysiological processes, including various forms of inflammation and circulatory shock^[10-14]. The cytotoxic effects of NO are in part, mediated by peroxynitrite anion (ONOO⁻), a reactive oxidant species formed from NO and superoxide at an almost diffusion-controlled rate^[15-18]. The production of ONOO⁻ has been demonstrated in various lung injury^[19-21]. However, no evidence exists about its change and role in the lung injury following IIR. The major aim of the present study, therefore, was to determine the change and role of iNOS and peroxynitrite in lung injury induced by IIR.

MATERIALS AND METHODS

Animal model^[22]

Male healthy Sprague-Dawley rats (250-300 g) were anesthetized with intraperitoneal administration of sodium pentobarbital (40 mg·kg⁻¹) and secured in a supine position on a heated restraining board at 37 °C after being shaved. Following midline laparotomy, a microvascular clip was placed across the superior mesenteric artery (SMA) for 120 minutes. Removal of the clip allowed reperfusion for 120 minutes. This degree of IIR is consistently associated with intestinal, hepatic and pulmonary injury with a 12-hour mortality rate of 100 %.

Experimental protocols

To determine the effect of iNOS induction on the peroxynitrite formation and the lung injury, aminoguanidine (AG), an inhibitor of iNOS^[23], was used. The rats were randomly divided into 3 groups (*n*=8 in each): Sham, IR and IR+AG. The surgical sham group underwent full surgical preparation including isolation of the SMA without occlusion. After that they were followed for the same aggregate period of time. The IR group received 2 h of ischemia and 2 h of reperfusion. The IR + AG group was given AG (10 mg·kg⁻¹ intravenously, Sigma, USA) 15 min before reperfusion. The animals in IR group and sham group were treated with equal volume of the vehicle (normal saline solution, NS; 1 ml·kg⁻¹). All animals were killed by exsanguination at designated time. Both lungs were harvested immediately for the following detection.

Lung histology

The right middle lung lobe was harvested and fixed in 10 % formalin. After embedded in paraffin, sections of 8 μm were stained with hematoxylin and eosin for light microscopy.

Assessments of lung malondialdehyde (MDA) content

The right base of lung was harvested and immediately homogenized on ice in 9 volumes saline. The homogenates were centrifuged at 4 000 r·min⁻¹ at 4 °C for 10 min. The MDA content in the supernatants was measured using MDA assay kit (Nanjing Jiancheng Corp. China).

Lung nitrite/nitrate (NO₂⁻/NO₃⁻) detection

NO₂⁻/NO₃⁻ production, an indicator of NO synthesis, was measured in the lung homogenate with a NO assay kit (Nanjing Jiancheng Corp. China) following the manufacturer's instruction.

Western blotting analysis for iNOS

The left lung was homogenized with PBS (pH 7.2) and centrifuged at 4 °C, 18 000 r·min⁻¹ for 10 min. After precipitated unsolubilized fraction was discarded, the protein concentration in the supernatant was determined by Coomassie blue dye-binding assay (Nanjing Jiancheng Corp. China). Aliquots (30 µg) of protein from each sample were electrophoresed on a 120 g·L⁻¹ SDS-polyacrylamide gel for 4 hour at 100V. The protein samples were transferred onto a nitrocellulose membrane (Amersham, USA). The membrane was then probed with polyclonal rabbit anti-rat iNOS antibody (1:50 dilution, Santa Cruz Co., USA) for 2 hours at 37 °C. After 3 washes with TPBS, blots were visualized with the use of an amplified HRP kit (Wuhan Boshide, China). The presence of iNOS was indicated by the development of brown color.

Immunohistochemical analysis of NT

Tyrosine nitration, a specific "footprint" of peroxynitrite formation^[16], was detected in the left lung by immunohistochemical technique. The left lung was harvested and fixed in 10 % formalin. Sections of 8 µm thickness of lung tissue were treated with 0.3 % H₂O₂ in methanol to block endogenous peroxidase activity. Immunohistochemical staining was performed using rabbit polyclonal antibody against NT (1:50 dilution, Cayman Chemical, USA) by indirect streptavidin/peroxidase technique (SP kit, Zymed Co., USA). Experiments were performed following the manufacturer's instruction. Paraffin-embedded sections were incubated with polyclonal anti-rat NT antibody for 12 hours at 4 °C after antigen retrieval. Biotinylated IgG was added as second antibody. Horseradish peroxidase labeled streptomycin-avidin complex was used to detect second antibody. Slides were stained with diaminobenzidine, and examined under light microscope. The brown or dark brown stained cytoplasm was considered as positive.

Statistical analysis

Values were expressed as mean ±SD (\bar{x} ±s). Statistical analyses were performed using paired Student's *t* test. *P*<0.05 was considered significant.

RESULTS

Pathological alternations of lung tissue

The histological structure of alveolar and mesenchymal cells was normal in the lungs of sham group, while the lung tissues from the IR group were significantly damaged, with pulmonary edema, hemorrhage and inflammatory cell infiltration. Administering AG before reperfusion could attenuate significantly the lung injury as showed by light microscope (Figure 1).

Change of MDA content

The lung MDA content was increased significantly in IR group

when compared with the sham control (*P*<0.05). Compared with the IR group, the MDA content was decreased markedly in IR +AG group (*P*<0.05) (Table 1).

Table 1 Changes of MDA and NO₂⁻/NO₃⁻ contents in lung tissue after IIR with pretreatment of AG in rats (\bar{x} ±s, n=8)

Groups	MDA (nmol.ml ⁻¹)	NO ₂ ⁻ /NO ₃ ⁻ (umol.L ⁻¹)
Sham	12.00±2.18	76.39±6.08
IR	23.44±1.25 ^a	140.40±4.34 ^a
IR+AG	14.66±1.66 ^c	80.00±8.56 ^c

^a*P*<0.05 vs Sham group. ^c*P*<0.05 vs IR group.

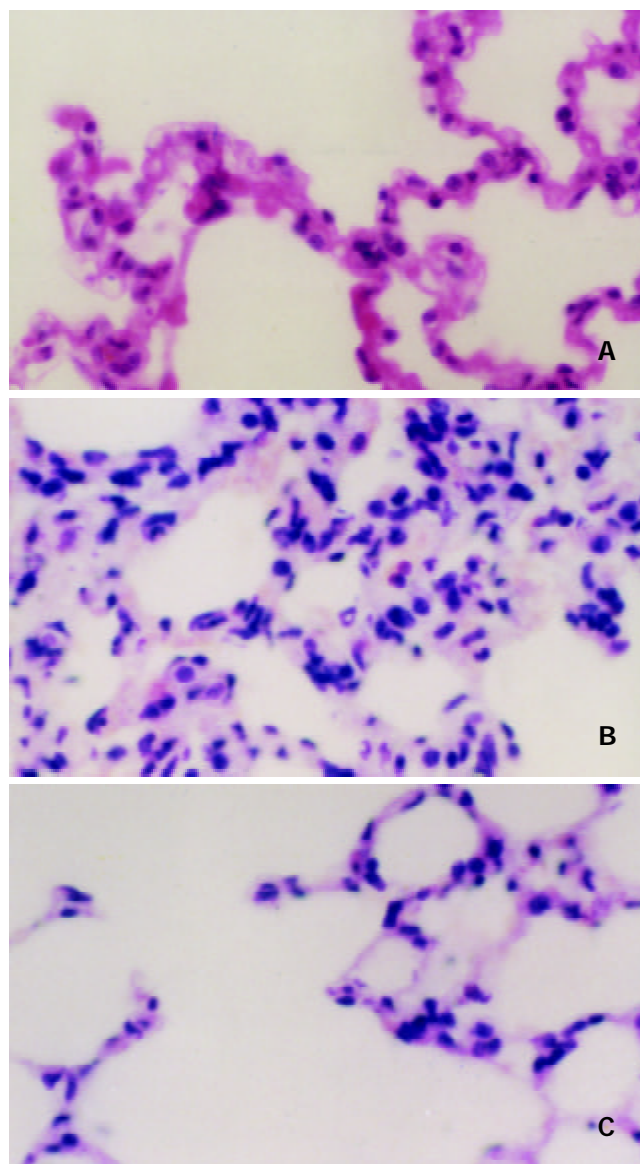


Figure 1 Light microscopic observation on the lung after IIR with pretreatment of AG in rats (HE×400). A. The normal lung tissue structure was found in sham group. B. Lung edema, hemorrhage and inflammatory cells sequestration were found in the IR group. C. Decreased morphological changes induced by the intestinal IR were found in the IR+AG group.

Change of nitrite/nitrate

Compared with the sham group, the lung content of nitrite/nitrate in IR group was increased significantly (*P*<0.05). Compared with the IR group, the content of nitrite/nitrate in IR+AG group was decreased significantly (*P*<0.05) (Table 1).

Change of iNOS expression

Western blotting showed that weak positive signal was found in the lung in sham group. In contrast, marked increase of iNOS protein expression was found in the IR group. There was still notable positive signal in the IR+AG group (Figure 2).

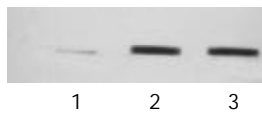


Figure 2 Western blotting analysis of iNOS in rat lung after IIR with pretreatment of AG in rats. 1. Sham; 2. IR; 3. IR+AG.

Change of NT formation

The formation of peroxynitrite in the lung sections was demonstrated by immunohistochemical staining with monoclonal anti-NT antibodies. In the sham group, no brown deposits were present in lung sections. In contrast, very strong staining was observed in lung tissue sections from the IR group. Compared with the IR group, the immunostaining for NT in the IR+AG group decreased significantly, indicating that inhibition of iNOS activity and decrease of NO production could reduce the peroxynitrite formation (Figure 3).

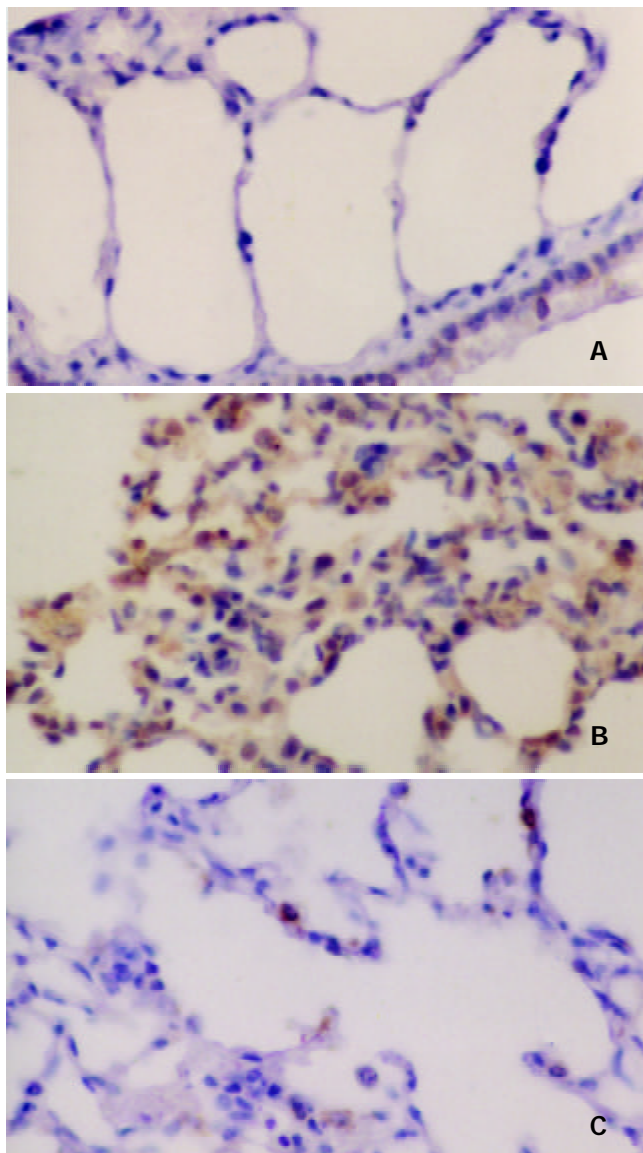


Figure 3 Immunohistochemical analysis of NT in the lung after IIR with pretreatment of AG in rats. SP stain $\times 400$. A. No

positive signal was found in the lung in sham group. B. Intense positive NT staining was found in the IR group. C. Positive NT staining decreased in the IR+AG group.

DISCUSSION

The lung is one of the very important target organs in multiple organ dysfunction syndrome (MODS) or multiple system organ failure (MOSF) caused by severe injury^[1-9]. It has been found that in addition to the direct trauma, the lung could also be damaged by indirect injury such as gut, liver and skeletal muscle reperfusion, as well as aortic occlusion-reperfusion and circulatory shock^[1-9]. The present results showed that 2 h of intestinal ischemia followed by 2 h of reperfusion induced lung injury, manifested as the histological evidence of lung edema, hemorrhage and PMN infiltration. Moreover, the IIR mediated lung injury was oxygen-dependent, as indicated by the increase in the levels of MDA, an established marker of oxidative stress.

The mechanism of respiratory failure after intestinal I/R is complex and poorly understood. Under the condition of an inadequate mucosal blood flow, the gut barrier function can be progressively impaired and invaded by bacteria or endogenous endotoxin^[24-26]. This process is associated with activation of systemic inflammatory mediators including bacteriotoxin, inflammatory mediators, such as tumor necrosis factor (TNF) and interleukin (IL) and immunocytokines^[26-31]. In addition, several recent observations implicate that NO may be an important participant in the pulmonary response to IIR^[32]. It has been suggested that nitric oxide (NO), produced from endothelial constitutive nitric oxide synthase (eNOS), may be an important protective molecule at the onset of the IR of the small bowel. In this regard, inhibitors of endogenous NO production greatly exacerbate the increase in epithelial permeability and cardiovascular dysfunction in the reperfused post-ischemia intestine^[32-34], while administration of NO donors prevents the early rise in epithelial permeability and tissue dysfunction^[35,36]. Excess NO production has been attributed to a second NOS (induced NOS, iNOS) that is not present under normal condition but can be induced in response to systemic inflammatory states, including IR. The induction of iNOS has been implicated in the pathogenesis of IIR and it was reported that inhibition of iNOS activity and nitric oxide production could attenuate the intestinal ischemia/reperfusion injury^[37-40]. In the present experiment, we studied the contribution of iNOS to the IIR-induced lung injury. The results demonstrated that 2 h of intestinal ischemia followed by 2 h of reperfusion up-regulated significantly the lung iNOS expression, accompanied by the elevation of pulmonary nitrate/nitrite (stable metabolites of NO) level. This is consistent with the findings of Virlos IT, *et al*^[34] who demonstrated that pulmonary iNOS activity in rats subjected to IIR was significantly increased. The effect of increased iNOS expression on IIR-induced lung injury was indirectly assessed by administration of AG, a selective inhibitor of iNOS. The results that *in vivo* treatment with AG reduced markedly the nitrate/nitrite levels and the lung injury demonstrated that the induction of iNOS and the excessive NO production in the lung following intestinal IR involved in the IIR-induced lung injury.

Though the cytotoxic actions of the excessive NO production may be involved in several potential mechanisms, recent studies suggested that peroxynitrite, may be a key mediator for cytotoxicity of excess NO generation and is involved in many pathological processes^[15-18]. The cytotoxic processes triggered by peroxynitrite include initiation of lipid peroxidation, inhibition of mitochondrial respiration, inhibition of membrane pumps, depletion of glutathione, and damage to DNA with subsequent activation of poly (ADP-ribose) synthetase and

concomitant cellular energy depletion^[19-21, 41, 42]. Peroxynitrite is now generally considered an oxidant more toxic than either NO or superoxide anion alone. Furthermore, it has been shown that a major product of the reaction of peroxynitrite with protein is the addition of a nitro group in the ortho position of tyrosine to form NT which could be detected by antibodies specific to protein NT^[16]. The present results of immunohistochemical staining with monoclonal anti-NT antibodies demonstrated that peroxynitrite formation occurred in the reperfusion phase of ischemic intestine. The results also suggested that the formation of peroxynitrite was correlated with iNOS expression and involved in the IIR-induced lung injury, because inhibiting iNOS activity with AG reduced significantly the NT immunoreactivity and attenuated the IIR-induced lung injury. The cytotoxic actions of iNOS-NO and peroxynitrite may be associated with their damages to the endothelial barrier, their oxidant to the membrane lipid and the triggering of the PMN sequestration in the lung, manifested as the detection of lung MDA content and the observation of the lung pathological changes.

In summary, the present results demonstrate that the systemic inflammatory response and lung injury occur following IIR with an increase of NO, iNOS expression and the formation of peroxynitrite in the lung. Inhibition of iNOS prevented the lung injury and the formation of NT, suggesting that excessive NO production and peroxynitrite formation are cytotoxic to the cell and tissue and are involved in the secondary lung injury induced by the IIR. These results may partially explain the mechanism of MOF and suggest that inhibiting peroxynitrite may be a novel pharmacological approach to prevent cell injury and MOF.

REFERENCES

- 1 **Carden DL**, Granger DN. Pathophysiology of ischemia-reperfusion injury. *J Pathol* 2000; **190**: 255-266
- 2 **Rotstein OD**. Pathogenesis of multiple organ dysfunction syndrome: gut origin, protection, and decontamination. *Surg Infect (Larchmt)* 2000; **1**: 217-225
- 3 **Fu XB**, Yang YH, Sun TZ, Gu XM, Jiang LX, Sun X Q, Sheng ZY. Effect of intestinal ischemia-reperfusion on expression of endogenous basic fibroblast growth factor and transforming growth factor betain lung and its relation with lung repair. *World J Gastroenterol* 2000; **6**: 353-355
- 4 **Wu XT**, Li JS, Zhao XF, Zhuang W, Feng XL. Modified techniques of heterotopic total small intestinal transplantation in rats. *World J Gastroenterol* 2002; **8**: 758-762
- 5 **Mitsuoka H**, Schmid-Schonbein GW. Mechanisms for blockade of in vivo activator production in the ischemic intestine and multi-organ failure. *Shock* 2000; **14**: 522-527
- 6 **Yassin MM**, Harkin DW, Barros D' Sa AA, Halliday MI, Rowlands BJ. Lower limb ischemia-reperfusion injury triggers a systemic inflammatory response and multiple organ dysfunction. *World J Surg* 2002; **26**: 115-121
- 7 **Zhou JL**, Zhu XG, Ling T, Zhang JQ, Chang JY. Effect of endogenous carbon monoxide on oxidant-mediated multiple organ injury following limb ischemia-reperfusion in rats. *Zhongguo Xiufu Chongjian Waie Zazhi* 2002; **16**: 273-276
- 8 **Rezende-Neto JB**, Moore EE, Melo de Andrade MV, Teixeira MM, Lisboa FA, Arantes RM, de Souza DG, da Cunha-Melo JR. Systemic inflammatory response secondary to abdominal compartment syndrome: stage for multiple organ failure. *J Trauma* 2002; **53**: 1121-1128
- 9 **Weinbroum AA**, Shapira I, Abraham RB, Szold A. Mannitol dose-dependently attenuates lung reperfusion injury following liver ischemia reperfusion: a dose-response study in an isolated perfused double-organ model. *Lung* 2002; **180**: 327-338
- 10 **Tavaf-Motamen H**, Miner TJ, Starnes BW, Shea-Donohue T. Nitric oxide mediates acute lung injury by modulation of inflammation. *J Surg Res* 1998; **78**: 137-142
- 11 **Wangle F**, Patel M, Razavi HM, Weicker S, Joseph MG, McCormack DG, Mehta S. Role of inducible nitric oxide synthase in pulmonary microvascular protein leak in murine sepsis. *Am J Respir Crit Care Med* 2002; **165**: 1634-1639
- 12 **Li H**, Forstermann U. Nitric oxide in the pathogenesis of vascular disease. *J Pathol* 2000; **190**: 244-254
- 13 **Hofseth LJ**, Saito S, Hussain SP, Espey MG, Miranda KM, Araki Y, Jhappan C, Higashimoto Y, He P, Linke SP, Quezado MM, Zurer I, Rotter V, Wink DA, Appella E, Harris CC. Nitric oxide-induced cellular stress and p53 activation in chronic inflammation. *Proc Natl Acad Sci U S A* 2003; **100**: 143-148
- 14 **Qin JM**, Zhang YD. Intestinal expressions of eNOSmRNA and iNOSmRNA in rats with acute liver failure. *World J Gastroenterol* 2001; **7**: 652-656
- 15 **Cuzzocrea S**, Zingarelli B, Caputi AP. Role of constitutive nitric oxide synthase and peroxynitrite production in a rat model of splanchnic artery occlusion shock. *Life Sci* 1998; **63**: 789-799
- 16 **Pryor WA**, Squadrito GL. The chemistry of peroxynitrite: a product from the reaction of nitric oxide with superoxide. *Am J Physiol* 1995; **268**: L699-L722
- 17 **Szabo C**. The pathophysiological role of peroxynitrite in shock, inflammation, and ischemia-reperfusion injury. *Shock* 1996; **6**: 79-88
- 18 **Zhao KS**, Liu J, Yang GY, Jin C, Huang Q, Huang X. Peroxynitrite leads to arteriolar smooth muscle cell membrane hyperpolarization and low vasoreactivity in severe shock. *Clin Hemorheol Microcirc* 2000; **23**: 259-267
- 19 **Gu ZY**, Ling Y, Cong B. Peroxynitrite mediated acute lung injury induced by lipopolysaccharides in rats. *Zhonghua Yixue Zazhi* 2000; **80**: 58-61
- 20 **Laskin DL**, Fakhrzadeh L, Laskin JD. Nitric oxide and peroxynitrite in ozone-induced lung injury. *Adv Exp Med Biol* 2001; **500**: 183-190
- 21 **Gu ZY**. Peroxynitrite-mediated pulmonary vascular injury induced by endotoxin and the protective role of cholecystokinin. *Shengli Kexue Jinzhan* 2001; **32**: 135-137
- 22 **Turnage RH**, Kadesky KM, Bartula L, Myers SI. Intestinal reperfusion up regulates inducible nitric oxide synthase activity within the lung. *Surgery* 1995; **118**: 288-293
- 23 **Zhang GL**, Wang YH, Teng HL, Lin ZB. Effects of aminoguanidine on nitric oxide production induced by inflammatory cytokines and endotoxin in cultured rat hepatocytes. *World J Gastroenterol* 2001; **7**: 331-334
- 24 **Turnage RH**, Guice KS, Oldham KT. Endotoxemia and remote organ injury following intestinal reperfusion. *J Surg Res* 1994; **56**: 571-578
- 25 **Olanders K**, Sun Z, Borjesson A, Dib M, Andersson E, Lasson A, Ohlsson T, Andersson R. The effect of intestinal ischemia and reperfusion injury on ICAM-1 expression, endothelial barrier function, neutrophil tissue influx, and protease inhibitor levels in rats. *Shock* 2002; **18**: 86-92
- 26 **Yao Y**, Yu Y, Chen J. The effect of intestinal ischemia/reperfusion on increased sensitivity to endotoxin and its potential mechanism. *Zhonghua Zhengxing Shaoshang Waie Zazhi* 1999; **15**: 301-304
- 27 **Ishii H**, Ishibashi M, Takayama M, Nishida T, Yoshida M. The role of cytokine-induced neutrophil chemoattractant-1 in neutrophil-mediated remote lung injury after intestinal ischaemia/reperfusion in rats. *Respirology* 2000; **5**: 325-331
- 28 **Yan GT**, Hao XH, Xue H, Wang LH, Li YL, Shi LP. Interleukin-1beta expression and phospholipase A(2) activation after intestinal ischemia/reperfusion injury. *Shengli Xuebao* 2002; **54**: 28-32
- 29 **Souza DG**, Cassali GD, Poole S, Teixeira MM. Effects of inhibition of PDE4 and TNF-alpha on local and remote injuries following ischaemia and reperfusion injury. *Br J Pharmacol* 2001; **134**: 985-994
- 30 **Wada K**, Montalto MC, Stahl GL. Inhibition of complement C5 reduces local and remote organ injury after intestinal ischemia/reperfusion in the rat. *Gastroenterology* 2001; **120**: 126-133
- 31 **Zhao H**, Montalto MC, Pfeiffer KJ, Hao L, Stahl GL. Murine model of gastrointestinal ischemia associated with complement-dependent injury. *J Appl Physiol* 2002; **93**: 338-345
- 32 **Khanna A**, Rossman JE, Fung HL, Caty MG. Attenuated nitric oxide synthase activity and protein expression accompany intestinal ischemia/reperfusion injury in rats. *Biochem Biophys Res Commun* 2000; **269**: 160-164

- 33 **Tavaf-Motamen H**, Miner TJ, Starnes BW, Shea-Donohue T. Nitric oxide mediates acute lung injury by modulation of inflammation. *J Surg Res* 1998; **78**: 137-142
- 34 **Virlos IT**, Inglott FS, Williamson RC, Mathie RT. Differential expression of pulmonary nitric oxide synthase isoforms after intestinal ischemia-reperfusion. *Hepatogastroenterol* 2003; **50**: 31-36
- 35 **Kalia N**, Brown NJ, Hopkinson K, Stephenson TJ, Wood RF, Pockley AG. FK409 inhibits both local and remote organ damage after intestinal ischaemia. *J Pathol* 2002; **197**: 595-602
- 36 **Ward DT**, Lawson SA, Gallagher CM, Conner WC, Shea-Donohue T. Sustained nitric oxide production via l-arginine administration ameliorates effects of intestinal ischemia-reperfusion. *J Surg Res* 2000; **89**: 13-19
- 37 **Turnage RH**, Wright JK, Iglesias J, LaNoue JL, Nguyen H, Kim L, Myers S. Intestinal reperfusion-induced pulmonary edema is related to increased pulmonary inducible nitric oxide synthase activity. *Surgery* 1998; **124**: 457-462
- 38 **Xia G**, Lara-Marquez M, Luquette MH, Glenn S, Haque A, Besner GE. Heparin-binding EGF-like growth factor decreases inducible nitric oxide synthase and nitric oxide production after intestinal ischemia/reperfusion injury. *Antioxid Redox Signal* 2001; **3**: 919-930
- 39 **Takada K**, Yamashita K, Sakurai-Yamashita Y, Shigematsu K, Hamada Y, Hioki K, Taniyama K. Participation of nitric oxide in the mucosal injury of rat intestine induced by ischemia-reperfusion. *J Pharmacol Exp Ther* 1998; **287**: 403-407
- 40 **Suzuki Y**, Deitch EA, Mishima S, Lu Q, Xu D. Inducible nitric oxide synthase gene knockout mice have increased resistance to gut injury and bacterial translocation after an intestinal ischemia-reperfusion injury. *Crit Care Med* 2000; **28**: 3692-3696
- 41 **Jagtap P**, Soriano FG, Virag L, Liaudet L, Mabley J, Szabo E, Hasko G, Marton A, Lorigados CB, Gallyas F Jr, Sumegi B, Hoyt DG, Baloglu E, VanDuzer J, Salzman AL, Southan GJ, Szabo C. Novel phenanthridinone inhibitors of poly (adenosine 5'-diphosphate-ribose) synthetase: potent cytoprotective and antishock agents. *Crit Care Med* 2002; **30**: 1071-1082
- 42 **Cuzzocrea S**, McDonald MC, Mazzon E, Dugo L, Serraino I, Threadgill M, Caputi AP, Thiemeermann C. Effects of 5-aminoisoquinolinone, a water-soluble, potent inhibitor of the activity of poly (ADP-ribose) polymerase, in a rodent model of lung injury. *Biochem Pharmacol* 2002; **63**: 293-304

Edited by Zhang JZ

Effects of n-3 fatty acid, fructose-1,6-diphosphate and glutamine on mucosal cell proliferation and apoptosis of small bowel graft after transplantation in rats

Xiao-Ting Wu, Jie-Shou Li, Xiao-Fei Zhao, Ning Li, Yu-Kui Ma, Wen Zhuang, Yong Zhou, Gang Yang

Xiao-Ting Wu, Yu-Kui Ma, Wen Zhuang, Yong Zhou, Gang Yang, Department of General Surgery, West China Hospital, Sichuan University, Chengdu 610041, Sichuan Province, China

Jie-Shou Li, Ning Li, Research Institute of General Surgery, Nanjing General Hospital of PLA, Clinical School of Medical College, Nanjing University, Nanjing 210002, Jiangsu Province, China

Xiao-Fei Zhao, Sichuan Reproductive Health Institute, Chengdu 610041, Sichuan Province, China

Supported by the State Education Commission Research Foundation for Returned Overseas Chinese Scholars Abroad (1997) 436

Correspondence to: Professor Xiao-Ting Wu, Department of General Surgery, West China Hospital, Sichuan University, 37 Guo Xue Rd., Chengdu 610041, Sichuan Province, China. wxt1@medmail.com.cn
Telephone: +86-28-85422480 **Fax:** +86-28-85422411

Received: 2002-09-13 **Accepted:** 2002-11-21

Abstract

AIM: To evaluate the effects of n-3 fatty acids (n-3FA), fructose-1,6-diphosphate (FDP) and glutamine (GLN) on mucosal cell proliferation and apoptosis of small bowel graft.

METHODS: One hundred and ninety-six inbred strain Wistar rats were grouped as donors and recipients, and underwent heterotopic small bowel transplantation (SBT). n-3FA, FDP and GLN were administered via gastric tube as well as venous infusion for 10 days before and after surgery, respectively. The proliferation and apoptosis of mucosal cells were analyzed with flow cytometry and *in situ* cell death detection kits.

RESULTS: Apparent apoptosis and minor proliferation of mucosal cells of small bowel graft after transplantation were observed. A higher mucosal cell proliferative index and lower apoptotic index were found in all small bowel grafts after supplying with n-3FA, FDP and GLN.

CONCLUSION: Nutritional support with n-3FA, FDP and GLN promotes mucosal cell proliferation significantly, and prevents mucosal cell from undergoing apoptosis with different degrees. These regulatory effects on the apoptosis alter the structure and absorption function of transplanted small bowel favorably.

Wu XT, Li JS, Zhao XF, Li N, Ma YK, Zhuang W, Zhou Y, Yang G. Effects of n-3 fatty acid, fructose-1,6-diphosphate and glutamine on mucosal cell proliferation and apoptosis of small bowel graft after transplantation in rats. *World J Gastroenterol* 2003; 9(6): 1323-1326

<http://www.wjgnet.com/1007-9327/9/1323.asp>

INTRODUCTION

The atrophy and malabsorption of transplanted small intestine are the main obstacles to small bowel transplantation (SBT). The effects of n-3 fatty acids (n-3FA), fructose-1, 6-diphosphate (FDP) and glutamine (GLN) on mucosal cell

proliferation and apoptosis of small bowel graft were evaluated. The mechanisms of mucosal atrophy and malabsorption of small bowel graft were studied at cellular and molecular levels.

MATERIALS AND METHODS

Animals

One hundred and ninety-six inbred male Wistar rats (180-310 g) purchased from Shanghai Animal Center of Chinese Academy of Medical Sciences were housed in laminar-flow cabinets under specific pathogen-free (SPF) condition. All studies on rats were conducted in accordance with the "Guideline for the Care and Use of Laboratory Animals" by National Institute of Health. The protocol approved by Shanghai Medical Experimental Animal Care Committee was followed during study. The rats were divided into 5 groups with 10 rats in each group. Group (1) was treated with non-essential amino acids. Group (2) was treated with FDP, group (3) with n-3FA, group (4) with GLN and group (5) with n-3FA+FDP+GLN. A modified heterotopic SBT was utilized^[1]. End to side anastomosis between graft abdominal aorta and recipient abdominal aorta was performed. The left kidney of recipient was resected. The portal vein of graft was anastomosed to the left renal vein of the recipient. Fistulizations of the distal and proximal ends of graft were performed through left abdominal wall.

Administration of special nutrition

In group (3) and (5), n-3FA (Sigma Company, USA), 1 mL·d⁻¹, was given via gastric tube to both donor and recipient 10 days before and after operation, respectively. All animals received TPN. The dosage of FDP was 1 g·kg⁻¹·d⁻¹ (Foscama Company, Italy). The nutritional solution in group (4) contained 2 % GLN (Ajinomoto company, Japan). L-alanine, glycine, L-proline and L-serine were applied to the nutritional solution of group (1), (2) and (3). The nitrogen and calorie in the nutritional solution were equal in each group.

Specimen collection

Prior to transplantation, 5 cm of jejunum distal to the treitz ligament of graft was resected as baseline samples. Ten days postoperative TPN support, 5 cm of proximal jejunum of the graft in the recipient was resected for examination.

Preparation of specimen

Flow cytometry The mucosae of the specimen were scissored into tiny pieces in saline and filtered to get cell suspension. The nucleus was stained by hypotonic propidium iodide at 4 °C over night.

TdT-mediated X-dUTP nick end labeling (TUNEL method) The specimen was sectioned in 3 μm-thick and dehydrated through 70-90 % ethanol in series. After digestion with proteinase K (20 μg·mL⁻¹), the work solution of TUNEL was added. The reaction was terminated with ddH₂O. The positive nucleus was stained with brownish yellow. Ten fields were selected randomly from each section under light microscope.

Two thousand mucosal cells were examined from each section. The apoptotic index (AI) was calculated with the formula: AI = (number of positive cells/total number of cells examined)×100 %.

Flow cytometry analysis

Epics XL flow cytometer (Coulter Company, USA) was used in the analysis. The proportions of cells in stage G₁, S and G₂ were calculated in 10 000 cells examined. The proliferative index (PI) indicating the proliferation of mucosal cells was calculated using the formula: PI = [(S+G₂)/(G₁+S+G₂)]×100 %.

Statistical analysis

Newman-Keuls' *s q* test and Student' *s t* test were used. The statistical analysis software package stata 5.0 was used for the tests, and *P*<0.05 was considered statistically significant.

RESULTS

Flow cytometry

All the data from flow cytometry study are showed in Table 1.

Table 1 Changes of proliferation of graft mucosal cells in each group ten days before and after SBT and TPN ($\bar{x}\pm s$)

Group	Stage of cell cycle	Before SBT and TPN (%)	After SBT and TPN (%)	<i>P</i>
(1)	G ₁	94.73±2.33	94.08±2.15	0.7440
	G ₂	0.38±0.31	1.38±1.44	0.3296
	S	4.88±2.42	4.55±0.92	0.8480
	PI	5.25±2.29	5.85±2.26	0.7682
(2)	G ₁	96.22±2.96 ^b	86.14±4.08 ^b	0.0011 ^b
	G ₂	0.88±1.20 ^a	3.06±1.12	0.0140 ^a
	S	2.90±1.78 ^b	10.78±3.06 ^b	0.0007 ^b
	PI	3.78±2.96 ^b	13.84±4.05 ^b	0.0011 ^b
(3)	G ₁	90.94±4.37 ^b	83.12±2.59 ^b	0.0069 ^b
	G ₂	1.96±1.12 ^a	3.86±0.96 ^a	0.0497 ^a
	S	7.10±3.98 ^a	13.02±3.39 ^a	0.0211 ^a
	PI	9.06±4.39 ^b	16.88±2.59 ^b	0.0071 ^b
(4)	G ₁	95.52±1.57 ^b	81.03±4.98 ^b	0.0002 ^b
	G ₂	0.63±0.60 ^b	5.93±1.62 ^b	0.0016 ^b
	S	4.02±1.57 ^b	13.52±4.70 ^b	0.0011 ^b
	PI	4.65±1.48 ^b	18.97±5.01 ^b	0.0002 ^b
(5)	G ₁	90.48±3.21 ^b	80.52±0.95 ^b	0.0053 ^b
	G ₂	2.52±2.06	5.02±1.43	0.0674
	S	6.96±2.96 ^a	14.22±1.77	0.0148 ^a
	PI	9.48±3.24 ^b	19.24±0.94 ^b	0.0057 ^b

^a*P*<0.05, ^b*P*<0.01 vs before SBT.

G₁ stage No change of the proportion of graft mucosal cells in G₁ stage in group (1) was observed after transplantation. Most cells remained at G₁ stage. However, the proportions of graft mucosal cells in G₁ stage in the rest groups after transplantation decreased significantly.

G₂ stage Changes of proportion of graft mucosal cells in G₂ stage of group (1) and (5) after transplantation were not obvious. The proportions of graft mucosal cells in G₂ stage in the rest groups increased with great statistical significance.

S stage Following transplantation the change of proportion of graft mucosal cells in S stage was increased significantly in all groups except group (1).

PI Compared with the baseline before transplantation, the PI of graft mucosal cells changed significantly in all groups except group (1).

Apoptosis in situ

Group (1) After SBT, the number of graft mucosal cells with apoptosis was increased. The AI was increased significantly after transplantation (Table 2). The AI in group (1) was significantly higher than those in other groups.

Group (2) The AI of graft mucosal cells increased after SBT and TPN with significant difference (Table 2). The AI in group (2) was higher than those in other groups with significance.

Group (3) The AI of graft mucosal cells after transplantation increased slightly without significance compared with baseline (Table 2). The AI was similar among groups (3), (4) and (5) without any significant difference.

Group (4) The AI of graft mucosal cells in group (4) was similar to that in group (5), decreased slightly after SBT without significant difference (Table 2).

Group (5) No change of the AI of graft mucosal cells was observed after SBT (Table 2).

Table 2 Change of AI of graft mucosal cells in each group ten days before and after SBT and TPN ($\bar{x}\pm s$)

Group	Before SBT and TPN (%)	After SBT and TPN (%)	<i>P</i>
(1)	25.50±5.43 ^b	40.50±3.24 ^b	0.0041 ^b
(2)	24.63±1.70 ^a	30.88±2.50 ^a	0.0447 ^a
(3)	24.25±1.32	25.63±1.38	0.2141
(4)	25.00±2.68	23.63±0.85	0.4863
(5)	23.75±0.87	24.00±1.68	0.8130

^a*P*<0.05, ^b*P*<0.01 vs before SBT.

DISCUSSION

Rejection of graft will not occur in organ transplantation between two individuals from same strain of inbred animals. Thus, the effect of special nutrition on the transplanted small intestine could be observed in our research without the influence of transplant immunological factors.

Our results indicated that the proliferation of graft mucosal cells after SBT in group (1) was obviously less active than that before SBT. Most cells were rested in stage G₁. The ratios of cells in stage S over stage G₂ decreased, which suggested that DNA synthesis in graft mucosal cells after SBT reduced, and that mucosal cells were at rest stage instead of active proliferation. These changes in cytodynamics might be the underlying cause of cytopathy of graft with the characteristics of atrophy and malabsorption.

Compared with the results of group (1), after SBT the proliferation of graft mucosal cells in rest groups was more active. The ratios of cells in stage S over stage G₂ increased, which suggested that n-3FA, FDP and GLN contributed to the proliferation and repair of graft mucosal cells, and were helpful in preventing atrophy and maintaining the normal structure and function of intestinal mucus.

The number of apoptotic cells and AI of graft mucosal cells in groups (1) and (2) after SBT and TPN increased significantly compared with those before SBT and TPN. On the contrary, those of groups (3), (4) and (5) did not change obviously. The AI in groups (2), (3), (4) and (5) after SBT and TPN decreased significantly in comparison with that in group (1). The result suggested that n-3FA, FDP and GLN could inhibit the apoptosis of graft mucus after SBT to a certain degree.

GLN might influence the graft in several ways, in which it promotes the proliferation of graft mucosal cells and inhibits the cell apoptosis. (1) GLN offers the energy and metabolic substrate which are necessary to the proliferation of intestine mucosal cells^[2-15], including carbon chains for energy releasing

(30 mol ATP/mol) and nitrogen for synthesis of amino acid, protein and nuclear acid. (2) GLN also participates in the synthesis of glutathione (GSH). Administration of exogenous GLN will result in high level of GSH. It is indicated in some experiments that GSH could antagonize the oxidation injury to the biomembrane caused by oxygen-derived free radicals, and improve the survival of cells^[16-19]. (3) GLN may indirectly stimulate the secretion of hormones which are beneficial to the nutrition of intestine, and improve the hormone environment of intestinal mucosal cells. This may help establish normal physiological metabolism and the balanced proliferation and apoptosis of intestinal mucosal cells^[20]. (4) The apoptosis of host cells could be induced by bacterial and viral infections^[21]. GLN may improve the structure and function of the transplanted intestine and reduce bacterial translocation, which could prevent infection and reduce apoptosis^[22-32].

It is not clear why FDP could promote proliferation of mucosal cells of intestinal graft and inhibit apoptosis. The possible reasons might include: (1) As a kind of potent energy substrate, FDP can offer plenty of ATP quickly whether it is on normal or stress occasion, such as ischemia or anoxia^[33,34]. So, FDP can meet the energy need of proliferation of intestinal mucosal cells with quick metabolism. (2) As a promoter of energy synthesis, FDP may activate pyruvate kinase and phosphofructokinase on stress occasion, such as ischemia or anoxia. These enzymes may promote the metabolism of carbohydrate to offer adequate energy^[33], which is helpful to cell proliferation. The products of zymolysis could be decomposed in the energy-producing process^[35]. Thus tissue damage caused by these products could be avoided and the inducing factors of apoptosis were reduced. (3) FDP could reduce the retention of intracellular calcium at stress, and inhibit endogenous calcium dependent endonuclease which is important to nuclear changes in apoptosis^[36]. (4) The cell injuries during ischemia/reperfusion and cold storage of graft are associated with apoptosis^[37-39]. FDP could inhibit the production of toxic oxygen group by activated polymorphonuclear leukocyte and scavenge the hypoxanthine accumulated in the tissues during ischemia and reperfusion^[40]. Thus, the apoptosis caused by these factors could be reduced^[41].

The mechanism of n-3FA in improving the proliferation of mucosal cell of intestinal graft and inhibiting apoptosis is not clear. It may involve the following factors: (1) As a kind of energy substrate, n-3FA could offer energy for the proliferation of mucosal cells. (2) n-3FA could be esterified into phospholipid and neutral lipid which are essential to neogenetic mucosal cells as important component of structure membrane^[42-45]. (3) n-3FA could inhibit the production of IL-1 α , IL-1 β and TNF secreted by monocytes. It is indicated that IL-1 β and TNF can promote apoptosis^[46]. (4) Apoptosis might be one of the ways of cell death in rejection after allogeneic transplantation^[47,48]. As a kind of immunosuppressant^[49-51], n-3FA could inhibit the apoptosis of graft cells through immunosuppression.

In conclusion, special nutrition with n-3FA, FDP and GLN after SBT can promote the proliferation of graft mucosal cells and inhibit apoptosis. Our results may provide new ways to treat intestinal atrophy and malabsorption after SBT.

REFERENCES

- 1 **Wu XT**, Li JS, Zhao XF, Zhuang W, Feng XL. Modified techniques of heterotopic total small intestinal transplantation in rats. *World J Gastroenterol* 2002; **8**: 758-762
- 2 **Windmueller HG**, Spaeth AE. Uptake and metabolism of plasma glutamine by the small intestine. *J Biol Chem* 1974; **249**: 5070-5079
- 3 **Zhang W**, Bain A, Rombeau JL. Insulin-like growth factor-I (IGF-I) and glutamine improve structure and function in the small bowel allograft. *J Surg Res* 1995; **59**: 6-12
- 4 **Klimberg VS**, Souba WW, Salloum RM, Holley DT, Hautamaki RD, Dolson DJ, Copeland EM 3rd. Intestinal glutamine metabolism after massive small bowel resection. *Am J Surg* 1990; **159**: 27-32
- 5 **Marks SL**, Cook AK, Reader R, Kass PH, Theon AP, Greve C, Rogers QR. Effects of glutamine supplementation of an amino acid-based purified diet on intestinal mucosal integrity in cats with methotrexate-induced enteritis. *Am J Vet Res* 1999; **60**: 755-763
- 6 **Fox AD**, Kripke SA, De Paula J, Berman JM, Settle RG, Rombeau JL. Effect of aglutamine supplemented enteral diet on methotrexate induced enteritis. *JPEN* 1988; **12**: 325-331
- 7 **Gu Y**, Wu ZH. The anabolic effects of recombinant human growth hormone and glutamine on parenterally fed, short bowel rats. *World J Gastroenterol* 2002; **8**: 752-757
- 8 **Colomb V**, Darcy-Vrillon B, Jobert A, Guihot G, Morel MT, Corriol O, Ricour C, Duee PH. Parenteral nutrition modifies glucose and glutamine metabolism in rat isolated enterocytes. *Gastroenterology* 1997; **112**: 429-436
- 9 **Cherbuy C**, Darcy-Vrillon B, Morel MT, Pegorier JP, Duee PH. Effect of germfree state on the capacities of isolated rat colonocytes to metabolize n-butyrate, glucose, and glutamine. *Gastroenterology* 1995; **109**: 1890-1899
- 10 **Wilmore DW**. Glutamine and the gut. *Gastroenterology* 1994; **107**: 1885-1901
- 11 **Minami H**, Morse EL, Adibi SA. Characteristics and mechanism of glutamine-dipeptide absorption in human intestine. *Gastroenterology* 1992; **103**: 3-11
- 12 **Dejong CH**, Kampman MT, Deutz NE, Soeters PB. Altered glutamine metabolism in rat portal drained viscera and hindquarter during hyperammonemia. *Gastroenterology* 1992; **102**: 936-948
- 13 **Rhoads JM**, Keku EO, Quinn J, Woosely J, Lecce JG. L-glutamine stimulates jejunal sodium and chloride absorption in pig rotavirus enteritis. *Gastroenterology* 1991; **100**: 683-691
- 14 **Klein S**. Glutamine: an essential nonessential amino acid for the gut. *Gastroenterology* 1990; **99**: 279-281
- 15 **Firmansyah A**, Penn D, Leenthal E. Isolated colonocyte metabolism of glucose, glutamine, n-butyrate, and beta-hydroxybutyrate in malnutrition. *Gastroenterology* 1989; **97**: 622-629
- 16 **Yu JC**, Jiang ZM, Li DM. Glutamine: a precursor of glutathione and its effect on liver. *World J Gastroenterol* 1999; **5**: 143-146
- 17 **Yagi M**, Sakamoto K, Inoue T, Fukushima W, Muraoka K, Ii T, Iyobe T, Iwasa K, Hashimoto T, Shimizu K, Izumi R, Miyazaki I. Effect of a glutamine-enriched elemental diet on regeneration of the small bowel mucosa following isotransplantation of small intestine. *Transplant Proc* 1994; **26**: 2297-2298
- 18 **Scheppach W**, Dusel G, Kuhn T, Loges C, Karch H, Bartram HP, Richter F, Christl SU, Kasper H. Effect of L-glutamine and n-butyrate on the restitution of rat colonic mucosa after acid induced injury. *Gut* 1996; **38**: 878-885
- 19 **Xu Y**, Nguyen Q, Lo DC, Czaja MJ. c-myc-Dependent hepatoma cell apoptosis results from oxidative stress and not a deficiency of growth factors. *J Cell Physiol* 1997; **170**: 192-199
- 20 **Petronini PG**, Urbani S, Alfieri R, Borghetti AF, Guidotti GG. Cell susceptibility to apoptosis by glutamine deprivation and rescue: survival and apoptotic death in cultured lymphoma-leukemia cell lines. *J Cell Physiol* 1996; **169**: 175-185
- 21 **Thompson CB**. Apoptosis in the pathogenesis and treatment of disease. *Science* 1995; **267**: 1456-1462
- 22 **Schroeder P**, Schweizer E, Blomer A, Deltz E. Glutamine prevents mucosal injury after small bowel transplantation. *Transplant Proc* 1992; **24**: 1104
- 23 **Klimberg VS**, Souba WW, Dolson DJ, Salloum RM, Hautamaki RD, Plumley DA, Mendenhall WM, Bova FJ, Khan SR, Hackett RL, Bland KI, Copeland III EM. Prophylactic glutamine protects the intestinal mucosa from radiation injury. *Cancer* 1990; **66**: 62-68
- 24 **Zhang W**, Frankel WL, Singh A, Laitin E, Klurfeld D, Rombeau JL. Improvement of structure and function in orthotopic small bowel transplantation in the rat by glutamine. *Transplantation* 1993; **56**: 512-517
- 25 **Li JY**, Lu Y, Hu S, Sun D, Yao YM. Preventive effect of glutamine on intestinal barrier dysfunction induced by severe trauma. *World J Gastroenterol* 2002; **8**: 168-171
- 26 **Yoshida S**, Matsui M, Shirouzu Y, Fujita H, Yamana H, Shirouzu K. Effects of glutamine supplements and radiochemotherapy on

- systemic immune and gut barrier function in patients with advanced esophageal cancer. *Ann Surg* 1998; **227**: 485-491
- 27 **Yoshida S**, Leskiw MJ, Schluter MD, Bush KT, Nagele RG, Lanza-Jacoby S, Stein TP. Effect of total parenteral nutrition, systemic sepsis, and glutamine on gut mucosa in rats. *Am J Physiol* 1992; **263**: E368-373
- 28 **Burke DJ**, Alverdy JC, Aoys E, Moss GS. Glutamine-supplemented total parenteral nutrition improves gut immune function. *Arch Surg* 1989; **124**: 1396-1399
- 29 **Rhoads JM**, Argenzio RA, Chen W, Graves LM, Licato LL, Blikslager AT, Smith J, Gatzky J, Brenner DA. Glutamine metabolism stimulates intestinal cell MAPKs by a cAMP-inhibitable, Raf-independent mechanism. *Gastroenterology* 2000; **118**: 90-100
- 30 **De Blaauw I**, Deutz NE, van der Hulst RR, von Meyenfeldt MF. Glutamine depletion and increased gut permeability in nonanorectic, non-weight-losing tumor-bearing rats. *Gastroenterology* 1997; **112**: 118-126
- 31 **Tremel H**, Kienle B, Weilemann LS, Stehle P, Furst P. Glutamine dipeptide-supplemented parenteral nutrition maintains intestinal function in the critically ill. *Gastroenterology* 1994; **107**: 1595-1601
- 32 **Scheppach W**, Loges C, Bartram P, Christl SU, Richter F, Dusel G, Stehle P, Fuerst P, Kasper H. Effect of free glutamine and alanyl-glutamine dipeptide on mucosal proliferation of the human ileum and colon. *Gastroenterology* 1994; **107**: 429-434
- 33 **Jurgens TM**, Hardin CD. Fructose-1,6-bisphosphate as a metabolic substrate in hog ileum smooth muscle during hypoxia. *Mol Cell Biochem* 1996; **154**: 83-93
- 34 **Trimarchi GR**, Arcadi FA, Imperatore C, Ruggeri P, Costa G. Effects of fructose-1,6-bisphosphate on microsphere-induced cerebral ischemia in the rat. *Life Sci* 1997; **61**: 611-622
- 35 **Hassinen IE**, Nuutinen EM, Ito K, Nioka S, Lazzarino G, Giardina B, Chance B. Mechanism of the effect of exogenous fructose 1,6-bisphosphate on myocardial energy metabolism. *Circulation* 1991; **83**: 584-593
- 36 **Pozzilli C**, Lenzi GL, Argentino C, Carolei A, Rasura M, Signore A, Bozzao L, Pozzilli P. Imaging of leukocytic infiltration in human cerebral infarcts. *Stroke* 1985; **16**: 251-255
- 37 **Takeuchi K**, Cao-Danh H, Friehs I, Glynn P, D'Agostino D, Simplaceanu E, McGowan FX, del Nido PJ. Administration of fructose 1,6-diphosphate during early reperfusion significantly improves recovery of contractile function in the postischemic heart. *J Thorac Cardiovasc Surg* 1998; **116**: 335-343
- 38 **Sun JX**, Farias LA, Markov AK. Fructose 1-6 diphosphate prevents intestinal ischemic reperfusion injury and death in rats. *Gastroenterology* 1990; **98**: 117-126
- 39 **Farias LA**, Smith EE, Markov AK. Prevention of ischemic-hypoxic brain injury and death in rabbits with fructose-1,6-diphosphate. *Stroke* 1990; **21**: 606-613
- 40 **Chu SJ**, Chang DM, Wang D, Chen YH, Hsu CW, Hsu K. Fructose-1,6-diphosphate attenuates acute lung injury induced by ischemia-reperfusion in rats. *Crit Care Med* 2002; **30**: 1605-1609
- 41 **Raff MC**. Social controls on cell survival and cell death. *Nature* 1992; **356**: 397-400
- 42 **Teo TC**, DeMichele SJ, Selleck KM, Babayan VK, Blackburn GL, Bistrian BR. Administration of structured lipid composed of MCT and fish oil reduces net protein catabolism in enterally fed burned rats. *Ann Surg* 1989; **210**: 100-107
- 43 **Endres S**, Ghorbani R, Kelley VE, Georgilis K, Lonnemann G, van der Meer JW, Cannon JG, Rogers TS, Klempner MS, Weber PC, Schaefer EJ, Wolff SM, Dinarello CA. The effect of dietary supplementation with n-3 polyunsaturated fatty acids on the synthesis of interleukin-1 and tumor necrosis factor by mononuclear cells. *N Engl J Med* 1989; **320**: 265-271
- 44 **Dinarello CA**, Cannon JG, Wolff SM, Bernheim HA, Beutler B, Cerami A, Figari IS, Palladino MA Jr, O'Connor JV. Tumor necrosis factor (cachectin) is an endogenous pyrogen and induces production of interleukin 1. *J Exp Med* 1986; **163**: 1433-1450
- 45 **Thiele J**, Zirbes TK, Lorenzen J, Kvasnicka HM, Dresbach S, Manich B, Leder LD, Niederle N, Diehl V, Fischer R. Apoptosis and proliferation (PCNA labelling) in CML-a comparative immunohistological study on bone marrow biopsies following interferon and busulfan therapy. *J Pathol* 1997; **181**: 316-322
- 46 **Steller H**. Mechanisms and genes of cellular suicide. *Science* 1995; **267**: 1445-1449
- 47 **Krams SM**, Egawa H, Quinn MB, Villanueva JC, Garcia-Kennedy R, Martinez OM. Apoptosis as a mechanism of cell death in liver allograft rejection. *Transplantation* 1995; **59**: 621-625
- 48 **Ito H**, Kasagi N, Shomori K, Osaki M, Adachi H. Apoptosis in the human allografted kidney. Analysis by terminal deoxynucleotidyl transferase-mediated DUTP-biotin nick end labeling. *Transplantation* 1995; **60**: 794-798
- 49 **Prickett JD**, Robinson DR, Steinberg AD. Dietary enrichment with the polyunsaturated fatty acid eicosapentaenoic acid prevents proteinuria and prolongs survival in NZB x NZW F1 mice. *J Clin Invest* 1981; **68**: 556-559
- 50 **Kelley VE**, Ferretti A, Izui S, Strom TB. A fish oil diet rich in eicosapentaenoic acid reduces cyclooxygenase metabolites, and suppresses lupus in MRL-lpr mice. *J Immunol* 1985; **134**: 1914-1919
- 51 **Kelley VE**, Kirkman RL, Bastos M, Barrett LV, Strom TB. Enhancement of immunosuppression by substitution of fish oil for olive oil as a vehicle for cyclosporine. *Transplantation* 1989; **48**: 98-102

Effects of glutamine on intestinal permeability and bacterial translocation in TPN-rats with endotoxemia

Lian-An Ding, Jie-Show Li

Lian-An Ding, Jie-Show Li, Clinical College of Nanjing University Medical School, 305 East Zhongshan Road, Nanjing 210002 Jiangsu Province, China

Correspondence to: Lian-An Ding, Associate Professor of Nanjing University Medical School, 210002 Jiangsu Province, China. dlahaolq@hotmail.com

Telephone: +86-25-4827110-58088 **Fax:** +86-25-4803956

Received: 2002-10-17 **Accepted:** 2002-12-20

Abstract

AIM: To evaluate the protective effect and mechanism of glutamine on the intestinal barrier function in total parenteral nutrition (TPN) rats with trauma or endotoxemia.

METHODS: To perform prospective, randomized and controlled animal experimentation of rats with surgical trauma, TPN and endotoxemia, thirty-four male, adult Sprague Dawley rats were divided into four groups: control group ($n=8$), TPN group ($n=9$), trauma and endotoxemia group (LPS, $n=8$) and trauma plus endotoxemia supplemented with glutamine in TPN solution group (Gln group, $n=9$). All groups except the control group were given TPN solutions in 7-day experimental period. For Gln group, 1 000 mg/kg/d of glutamine was added to TPN solution during day 1-6. On the 7th day all the animals were gavaged with lactulose (66 mg) and mannitol (50 mg) in 2 ml of normal saline. Then 24 h urine with preservative was collected and kept at -20 °C. On day 8, under intra-peritoneal anesthesia using 100 mg/kg ketamin, the intestine, liver, mesenteric lymph nodes and blood were taken for examination.

RESULTS: The body weight of LPS group decreased most among the four groups. The structure of small intestinal mucosa in TPN group, LPS group and Gln group showed impairments of different degrees, and the damage of small intestinal mucosa in Gln group was remarkably alleviated. The concentrations of interleukins in small intestine mucosa were lower (for IL-4 and IL-6) or the lowest (IL-10) in Gln group. The IgA level in the blood plasma and the mucosa of Gln group was the highest among all of the groups. The urine lactulose/mannitol test showed that the intestinal permeability in LPS group was lower than that in TPN group ($P<0.001$), but there was no difference between LPS group and Gln group. The rate of bacterial translocation in Gln group was lower than that in LPS group ($P<0.02$).

CONCLUSION: Prophylactic treatment with glutamine could minimize the increments of intestinal permeability and bacterial translocation caused by trauma and endotoxemia in rats treated with TPN.

Ding LA, Li JS. Effects of glutamine on intestinal permeability and bacterial translocation in TPN-rats with endotoxemia. *World J Gastroenterol* 2003; 9(6): 1327-1332

<http://www.wjgnet.com/1007-9327/9/1327.asp>

INTRODUCTION

Trauma, burn, infection, surgical operations and the use of intravenous alimentionation over a long period can damage the barrier function of the intestine, leading to atrophy of the intestinal mucosa, increase of mucosal permeability, decrease of immunity, and occurrence of bacterial/endotoxin translocation^[1-5]. If the causes could not be removed or the stress is too severe when the intestinal barrier is protected, the damage of the intestinal mucosa would become more severe and multiple organ dysfunction syndrome (MODS) would ensue. These adverse outcomes are commonly seen clinically and methods of their prevention need to be investigated. Therefore we studied the mechanism of protective effect of glutamine on the intestinal barrier function in TPN rats with trauma and endotoxemia.

MATERIALS AND METHODS

Experimental animals and grouping

Adult, healthy male Sprague-Dawley rats, with body weight of 150-180 g (supplied by Shanghai Experimental Animal Center, the Chinese Academy of Sciences) were used. The rats were fed for over a week in our lab for their adaptation and then were put into metabolic cages for 5-7 days. The temperature in the animal rooms was 17-21 °C with 60 % humidity and illumination of 12 h/day (6:00-18:00). During the adaptation period all rats were fed with regular rat chow and tap water ad libitum. When the rat's weight reached 200-300 g, thirty-four rats were chosen randomly and divided into four groups: 1. control group ($n=8$), fed rat chow and tap water freely; 2. TPN group ($n=9$), infused with a whole nutrients solution through a central venous catheter, and with drinking water ad libitum; 3. LPS group (trauma + TPN + endotoxemia, $n=8$), in which an exploratory laparotomy and central venous catheterization served as the trauma. After this, TPN was their sole nutrition source plus drinking water ad libitum. On the 7th day 5 mg/kg of lipopolysaccharide (LPS) was injected intraperitoneally; 4. Gln group, (trauma + TPN + endotoxemia + glutamine, $n=9$) in which all the treatments were the same as LPS group but on days 2-6, 1 000 mg/kg/d glutamine (Dipeptiven) was added to TPN solution. All groups except the control one received isonitrogenous, isocaloric and isovolumic TPN solution during the 7-day period. All the protocols and procedures were approved by our University Committee of Animal Experiment Administration.

Intravenous nutrients and other relevant chemicals

TPN ingredients 11.4 % compound amino acids injection (Novamin), 20 % mid-long chain fat emulsion (Lipovenoes MCT), Dipeptiven (alanyl-glutamine dipeptide solution), multivitamin mixture (Soluvit, Vitalipid) and a trace element mixture (Addamel), all from Sino-Sweden and Fresenius Pharmaceutical Corp. LTD.

Chemicals and reagents Lipopolysaccharide (LPS, from *E. Coli*, 055: B5) was purchased from Sigma Co.; IL-4 from Diaclone Co. of France; IL-6 and IL-10, from Biosource Co., USA; and IgA, from Bethyl Co. USA.

Experimental model

Operation procedures Under anaesthesia of 100 mg/kg of ketamin injected into the animals intraperitoneally, the TPN model was constructed and a rotary transfusion apparatus was used for TPN infusion^[6,7]. For surgical trauma, the animal's abdomen after shaving and incision (4 cm in length) was exposed and examined from the epigastrium to the pelvic cavity. The incision was sutured in double layers with silk suture No. 1 and operation was performed aseptically.

TPN solution The rats were put in the metabolic cages after surgical recovery. Each rat received 230 cal/kg body wt of calories and 1.42 g nitrogen/kg each day in 50 ml of TPN solution. The ratio of glucose to lipid in this solution was 2:1, and nonprotein calorie to nitrogen (kcal/g), 137:1. Multivitamins, electrolytes, trace elements and 500 units of heparin were also included in the TPN solution. All the nutrient solutions were prepared under aseptic conditions daily and the infusion was done with an injecting micropump continuously and uniformly during 24 h each day. The TPN infusion was started immediately after recovery from the laparotomy. On the first and last days of the experiment, each rat was given half of the total calories without any changes of other TPN ingredients.

Inducing endotoxemia On the 7th day of the experiment, 5 mg/kg of LPS in 5 ml of sterile distilled water was injected into the animals' peritoneal cavity to cause a septic state.

Lactulose and mannitol solution gavage On the 7th day of the experiment, 66 mg of lactulose and 50 mg of mannitol dissolved in 2 ml of normal saline were gavaged. Twenty-four hour urine was collected, with the volume recorded and 0.2 ml of mercury salicylosulfide added. Then 5 ml of the urine specimen was stored at -20 °C until measured.

Samples preparation and measurements

Twenty-four hours after gavaging with lactulose and mannitol and injecting endotoxin, 100 mg/kg of ketamine was injected intraperitoneally as an anesthetic. After the laparotomy was done, tissue and blood samples were collected and examinations were performed.

Bacteriological test 0.5 ml of blood from the portal vein was drawn for culture. One gram of anterior lobe liver tissue and about 0.5 g mesenteric lymph nodes were excised. Each sample was put in a tissue homogenizer and an equivalent amount of normal saline was added before they were homogenized. The specimens were sent to microbiological laboratory for aerobic culture and bacterial identification by morphological and biochemical examinations.

Bacterial culture (1) 10 µl homogenates of the lymph nodes and liver homogenates were separately taken and put on blood agar plates. Another 10 µl lymph nodes and liver homogenates were mixed with 10 ml saline for a dilution and the diluted samples were inoculated also on blood agar plates. (2) 0.5 ml of portal vein blood was inoculated into 4.5 ml of common broth for bacterial enrichment of 16 hours, then 20 µl of the enrichment solution was inoculated on blood agar plates. (3) The cultured media were put in a CO₂ incubator at 35 °C for 24-48 hours. If there was no bacterial growth, they would be regarded as negative, but if there was growth, it would be further identified.

Identification of bacteria First, Gram stained smears were made to determine whether they were coccus or bacillus and G+ or G-. Second, biochemical and serological identifications were made using standard and routine methods.

Preparation and examination of small intestine specimens The whole small intestine below the Treitz ligament was excised and immediately placed in icy 0.9 % saline. The intestine was opened longitudinally and the contents of the intestine were washed out with icy saline. Two cm of proximal jejunum and distal ileum was cut and put into 10 % neutral formalin solution

promptly and sent to be examined histologically.

Histological examination of intestinal mucosa Specimens were embedded in paraffin, 4 µm sections made and stained with H.E., analyzed with an HPIAS-1000 Multimedia Color Analysis System. Three low power (10×10) fields in each slide were read. The length of 5 villi, the depth of 5 crypts and the thickness of the mucosa at 5 sites were read and analyzed. The average value was calculated and documented. All the manipulations were done blindly by two experienced pathologists.

Bloodletting and animal execution Three ml of blood from the right ventricle was drawn and 1 250 u of heparin was added. The blood was centrifuged and the serum was stored at -70 °C. Then the animals were sacrificed by exsanguination.

Lactulose/mannitol test The lactulose and mannitol concentrations in the preserved urine sample were measured by a high-performance liquid chromatograph (Waters Co., USA). The ion-exchange column used was bought from Transgenomic Co., USA. The ratio between the two sugars was then calculated.

Identification of the interleukins About 5 cm intestine segments from the upper, middle and lower paste were resected and then the surfaces of the mucosa were dried with cotton swabs. The mucous membrane of the icy specimens was scraped, weighed and divided into two equal parts. They were immediately put into liquid nitrogen and then stored at -70 °C. For the tests, the specimens were melted to room temperature, and 1 ml normal saline was added before homogenates were made. The homogenates were then centrifuged for 15 minutes at 4 °C and then IL-4, IL-6 and IL-10 in the supernatants were measured with ELISA method described by Kudsk^[8]. The results were described as pg/g of mucosal tissue of the small intestine.

Determination of IgA The frozen samples of blood plasma and the mucosa of the small intestine were melted to room temperature and the concentration of IgA in them was measured by ELISA method. The results were shown as IgA µg/ml of blood plasma and IgA µg/g of small intestinal mucosa.

Statistical analysis

All the values were expressed as the mean ±SD. One-way ANOVA was used to check the differences between them. ChiSquare test was used to check the differences of bacterial translocation rates between the groups. When *P* was less than 0.05, the difference was considered statistically significant. The degree of correlation was described using Pearson Correlation coefficient. Software SPSS10.0 was used in all statistical analyses.

RESULTS

Body weight

The body weight changes of the animals in each group are illustrated in Figure 1. At the beginning of the experiment there was no difference in the body weight of the animals among the groups. At the end of the experiment, the body weight decrease was greatest in the animals of LPS group.

Morphology and morphometry of small intestinal mucous membrane

The degree of damage of villi and crypts and the thinning of mucous membrane in jejunum and ileum were most significant in LPS group among all groups (Figure 2 and 3).

Interleukins of small intestinal mucosal tissue

The concentrations of IL-4 and IL-6 in Gln group were the lowest among these groups except control group. IL-10 level in Gln

group was also the lowest among the four groups, and it was significantly lower than that in TPN group ($P<0.01$, Figure 4).

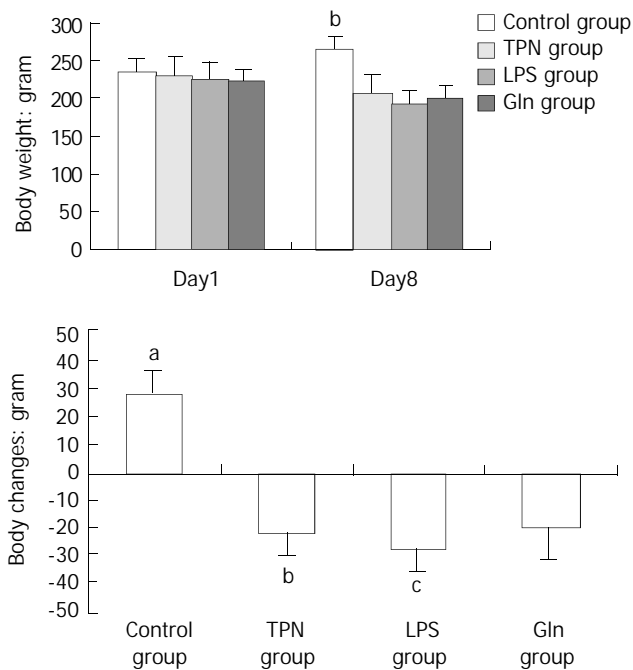


Figure 1 Graphs of body weight changes. (a) Graphs of body weights of animals at the start and end of the experiment; Day 1 means the date when experiments started; Day 8 means the date when experiments ended; $^bP<0.001$, vs control group, TPN group, and Gln group; (b) The illustration of body weight increase or decrease at the endpoint of the experiment; $^aP<0.001$, vs TPN group, LPS group and Gln group; $^bP<0.02$, vs LPS group; $^cP<0.03$, vs Gln group.

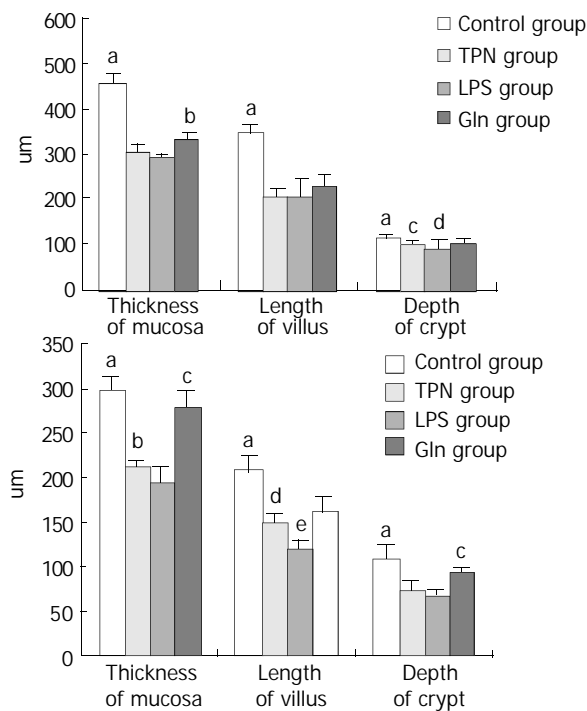


Figure 3 Graphs of morphometry of small intestinal mucosa. (a) Morphometry of jejunal mucous membrane; $^aP<0.01$, vs TPN group, LPS group and Gln group; $^bP<0.01$, vs TPN group and LPS group; $^cP<0.02$, vs LPS group; $^dP<0.04$, vs Gln group; (b) Morphometry of ileal mucous membrane; $^aP<0.004$, vs TPN group, LPS group and Gln group; $^bP<0.005$, vs LPS group; $^cP<0.02$, vs Gln group; $^dP<0.02$, vs Gln group; $^eP<0.001$, vs TPN group and Gln group.

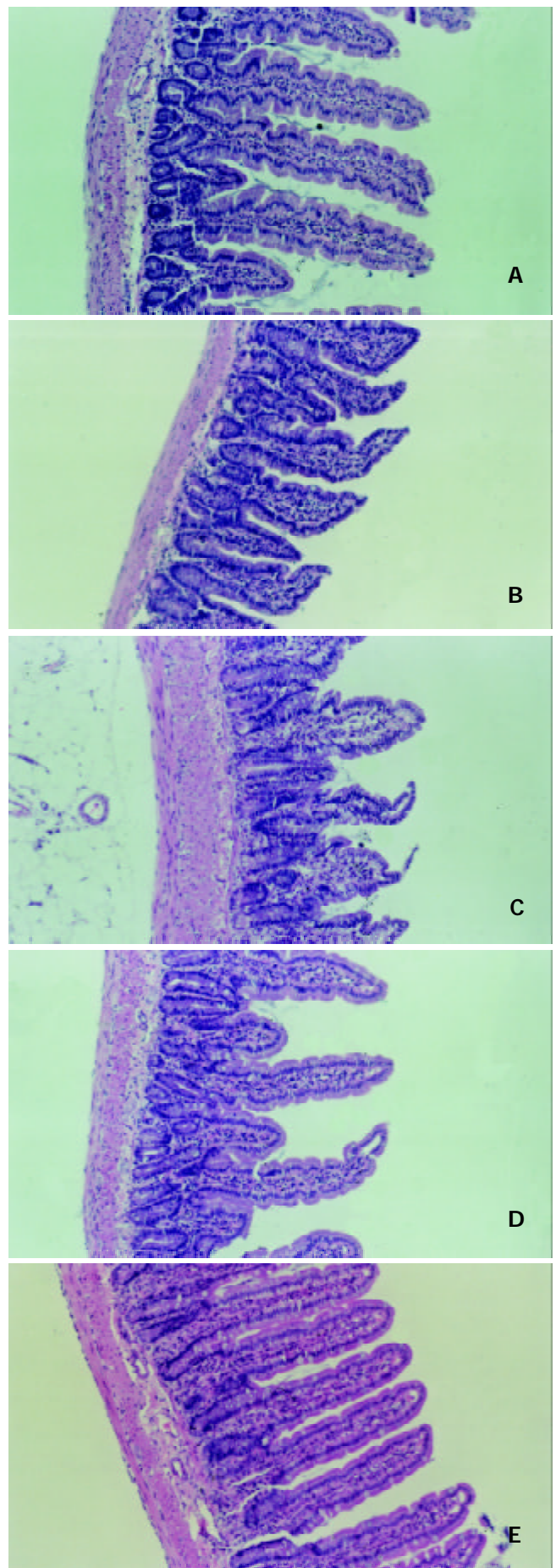


Figure 2 Alterations of structure in mucous membrane of small intestine under microscope. A. The normal structure of jejunum mucosa in normal group rats; B. The normal structure of ileal mucosa in normal group rats; C. Slice of the structure of ileal

mucosa in TPN group. The section shows an evident damage in mucosal architecture. The villi become shorter, blunted and swollen. Infiltration of leukocytes occurs within the lamina propria. The lymphatic ducts in lamina propria reveal dilatation and edematous; D. Slice of the jejunal mucosa of LPS group. The villi are more sparse and shorter than control group. It also shows infiltration of leukocytes within lamina propria, and dilatation of lymphatic ducts in lamina propria; E. The section of ileum mucosa of Gln group. The morphology of ileal mucosa is similar to that of control group (B).

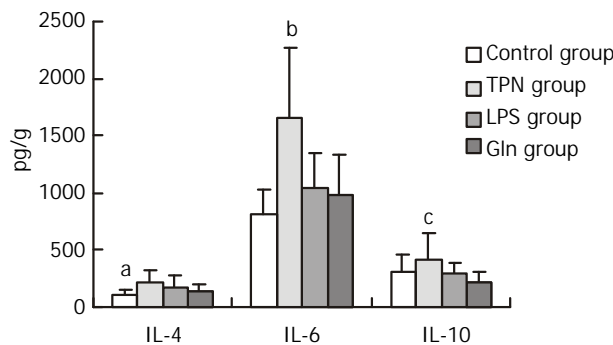


Figure 4 Graph of interleukins in mucous membrane of small intestine. ^a $P < 0.02$, vs TPN group; ^b $P < 0.001$, vs Control group, LPS group, Gln group; ^c $P < 0.01$, vs Gln group.

IgA levels in plasma and small intestinal mucous membrane

IgA levels in blood plasma in Gln group were the highest among the four groups, and so was that in small intestinal mucosa. There was a positive correlation for IgAs level between those in plasma and small intestinal mucosa ($r = 0.961$, $P < 0.04$, Table 1).

Table 1 IgA Levels in blood plasma and small intestinal mucous membrane

	Blood plasma IgA (ug/ml)	Mucosal tissue IgA (ug/g)
Control Group	146.73±50.98 ^a	507.48±167.39 ^c
Group TPN	133.94±64.41 ^b	544.62±100.78 ^d
Group LPS	194.52±111.18	611.89±171.60
Group Gln	255.13±160.59	827.89±279.96

Note: Values were expressed as mean ± SD; ^a $P < 0.02$, vs Gln group; ^b $P < 0.04$, vs Gln group; ^c $P < 0.01$, vs Gln group; ^d $P < 0.02$, vs Gln group; There 's a positive correlation for IgA levels in blood plasma and mucosal tissues ($r = 0.961$, $P < 0.04$).

Correlation of IgA with interleukines

There was no significant correlation between IgA level in plasma and mucosa with the level of interleukins in mucosal tissue of small intestine (Table 2).

Table 2 Correlation of IgAs with interleukins

	IgA of blood plasma			IgA of mucous membrane		
	IL-4	IL-6	IL-10	IL-4	IL-6	IL-10
r value	-0.562	-0.584	-0.744	-0.614	-0.373	-0.396
P value	0.438	0.416	0.256	0.386	0.627	0.604
Correlation ^a	no	no	no	no	no	no

Note: Values were expressed as mean ± SD; ^aThere was no correlations between each IgA level in plasma and mucosal tissue with that of three interleukins respectively in intestinal mucosa.

Lactulose and mannitol (L/M) test

The recovery rates of lactulose and mannitol in the urine of TPN group, LPS group and Gln group were increased. The ratio of L/M was the biggest in LPS group, and the value of the ratio in LPS group was not different statistically from that in Gln group (Figure 5).

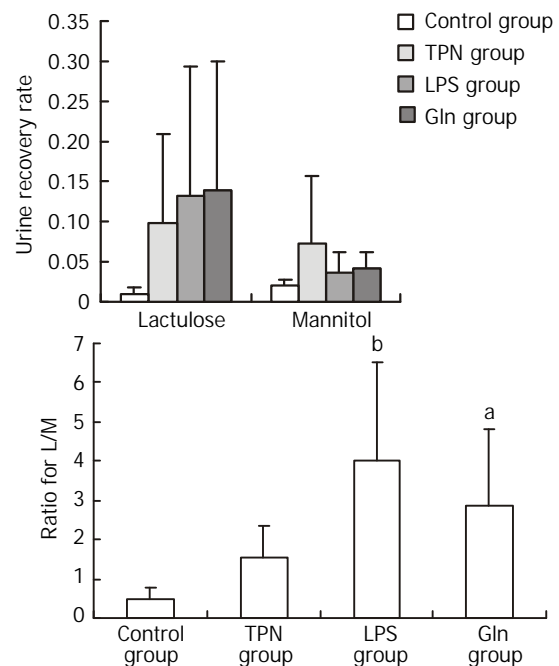


Figure 5 Illustration of dual sugar test. (a) Recovery rate of urine for lactulose and mannitol; (b) Graphic of intestinal permeability expressed by L/M ratio. ^a $P < 0.003$, vs control group; ^b $P < 0.001$, vs control groups and TPN groups.

Bacterial identification and translocation

The results of bacterial culture were labeled as positive when the CFU found per gram of tissue (or ml of blood) was more than or equivalent to $10^{3[9]}$. In LPS group the rate of bacterial translocation was the highest. The second highest rate was seen in TPN group. The logarithm of the number of translocated bacteria correlated positively with the bacterial translocation rate (Table 3). The bacteria translocated, in order of frequency, were proteus, *E. coli*, enterococcus and other Gram negative bacteria. One or two, even three bacteria were usually recovered from the same organ when translocation was present^[6,9].

Table 3 Bacteriologic tests

	MLN	Liver	PVB	Rate of BT	Logarithm of TB
Control group	3/8	0/8	0/8	12.5% (3/24) ^a	0.5414±1.4799 ^d
TPN group	4/9	4/9	4/9	44.4% (12/27)	2.3279±2.3609
LPS group	5/8	6/8	7/8	75.0% (18/24) ^b	3.0782±2.2824 ^c
Gln group	2/8	5/8	3/8	41.7% (10/24) ^c	1.5845±2.3209

Note: Values were expressed as mean ± SD; MLN, mesenteric lymph node; PVB, portal vein blood; BT, bacterial translocation; TB, translocated bacteria; BTR, rate of BT; ^a $P < 0.01$, vs TPN group and LPS group; ^b $P < 0.02$, vs Gln group; ^c $P < 0.03$, vs group control; ^d $P < 0.01$, vs TPN group and LPS group; ^e $P < 0.01$, vs Gln group; The rate of bacterial translocation is positively correlated to the logarithm of the number of translocated bacteria ($r = 0.978$, $P < 0.022$, $P < 0.03$).

DISCUSSION

Damage of intestinal barrier function and the resulting bacterial

translocation and endotoxemia caused by stress was well documented in the literature^[1-4, 10-14]. How to protect this barrier function and prevent bacterial translocation and toxemia during stress are important research topics^[15-17].

Animal experiments showed some good results in protecting intestinal barrier function and decreasing bacterial translocation, toxemia and enterogenous infection by various measures^[6, 8, 9, 15, 17-22, 30]. Glutamine has many biological functions^[23, 24]. It comprises more than 50 percent of the body's free amino acid pool and is a precursor for synthesis of nucleic acids and glutathione. It is the main fuel for rapid proliferating and dividing cells such as enterocytes, lymphocytes, and other immunocytes etc. It can promote hyperplasia of the epithelial cells of ileum and colon^[25]. The structure and function of small intestinal mucosa are maintained and the increment of intestinal permeability is reduced when glutamine is supplemented to animals fed parenterally^[26-28]. Besides, glutamine could enhance body's immunity through immune modulation^[8, 24, 29]. Results from a series of experiments and clinical investigations indicate that supplementation with glutamine parenterally and/or enterally has improved the gut barrier function and body's immunity when used in human and animals^[13, 17, 23, 29-35]. It has been generally accepted that glutamine could maintain intestinal barrier function through the improvement of architecture of small intestinal mucosa. Formerly, researches along this line usually paid attention to only one aspect of the functions of the intestinal barrier. For this reason, no interrelationship among the permeability and immunity of intestinal mucosa and bacterial translocation was discussed or fully explained^[6, 11, 30].

It is known that the cause of the damage of intestinal permeability in animals fed with TPN is mainly the atrophy of intestinal mucous membrane^[11, 34]. The mechanism of the increase of intestinal permeability caused by endotoxin is very complicated. It may relate to many inflammation mediators such as cytokines, vasoactive amines and oxygen free radicals^[16, 36]. The problem needs further investigation. Our experiment showed that injection of LPS intraperitoneally to rats indeed led to impairment of gut barrier function and an increase in bacterial translocation. Although there were no differences in body weight change when comparing that in glutamine-supplemented group with those in TPN group and LPS group, the damage of architecture of small intestinal mucosa in the former, especially in mucous membrane of ileum, was greatly alleviated than those in the latter two groups.

Glutamine has a visible effect on the secretion of interleukins in mucous membrane of small intestine. The three interleukins in small intestinal mucosa in glutamine group were lower (for IL-4 and IL-6) or lowest (IL-10) than those in other groups of our experiment. There are different opinions about the effects of interleukins on intestinal barrier function. Some authors mentioned that intestinal IL-4 and IL-10 were important in maintaining IgA concentration in the respiratory and alimentary tracts and in the blood^[8]. In the present experiment, we have not found a correlation between IgA level and IL-4 and IL-10 levels in intestinal mucosa. It has been considered that type II cytokines such as IL-4 and IL-10 have an anti-inflammatory function and then it could alleviate tissue and cell damage caused inflammatory mediators and type I cytokines such as IL-6^[37-39]. But there was a report that held a completely different opinion^[40]. We could see from our experiment that glutamine could reduce secretion of interleukins, and it seems that the lower interleukin concentrations are beneficial in reducing the damage of intestinal permeability^[40].

It is known that the digestive tract is the largest immune organ in human body and intestinal mucosal IgA is the first defense line of intestine immunity barrier. This has an important function in preventing bacterial adherence and translocation

within intestinal lumen. In our experiment, the IgA levels in blood and intestinal mucosa in glutamine group were the highest among all groups. There was statistically significant difference between the mucosal IgA levels in glutamine group and those in the control and TPN groups. This result meant that the alleviation of bacterial translocation rate in animals supplemented with glutamine correlated with the increase of IgA secretion in mucous membrane of the small intestine. There was a positive correlation between IgA levels in mucous membrane and blood plasma. It confirmed that the intestine is a vital organ for IgA secretion^[32].

Many changes of the immunological indicators in our experiment did not reach a statistically significant level. The reason for this might be that our experiment and observation period ended at the time when the peak of stress reaction had just passed and the animals had no sufficient recovery time^[12]. In this experiment we have made a model in which the animal is injured by laparotomy and parenteral nutrition, and endotoxemia is caused by an injection with a higher dosage of LPS intraperitoneally 6 days after the injury. The protective mechanism of glutamine on gut barrier was investigated. We found that the model simulated well the conditions of the clinical infectious complications.

In summary, using 1 000 mg/kg/d glutamine parenterally can alleviate the atrophy and impairment of the mucous membrane of small intestine in rats. It can also increase the concentration of IgA and decrease concentrations of IL-4, IL-6 and IL-10 that are secreted by the mucous membrane of small intestine. Thus, the immune function of the small intestinal mucosa was modulated and the damage of gut barrier caused by trauma and endotoxemia was alleviated. The rate of bacterial translocation was also decreased. Changes of intestinal permeability measured with the dual sugar test did not completely correlated with alterations of gut barrier function^[41].

ACKNOWLEDGEMENTS

We would like to thank Prof. Shao Haifeng and Prof. Xu Genbao for their technical guidance and help; we are grateful to the staff of Animal Lab. and Institute of General Surgery for their selfless work and support in this investigation.

REFERENCES

- 1 **Swank GM**, Deitch EA. Role of the gut in multiple organ failure: bacterial translocation and permeability changes. *World J Surg* 1996; **20**:411-417
- 2 **Berg RD**. Bacterial translocation from the gastrointestinal tract. *Trends Microbiol* 1995; **3**: 149-154
- 3 **Wilmore DW**, Smith RJ, O' Dwyer ST, Jacobs DO, Ziegler TR, Wang XD. The gut: A central organ after surgical stress. *Surgery* 1988; **104**: 917-923
- 4 **van Der Hulst RR**, von Meyenfeldt MF, van Kreel BK, Thunnissen FB, Brummer R, Arends JW, Soeters PB. Gut permeability, intestinal morphology, and nutritional depletion. *Nutrition* 1998; **14**: 1-6
- 5 **Carrico JC**, Meakins JL, Marshall JC, Fry D, Maier RV. Multiple-Organ-Failure Syndrome. *Arch Surg* 1986; **121**: 196-208
- 6 **Eizaguirre I**, Aldazabal P, Barrena MJ, Garcia-Arenzana JM, Ariz C, Candelas S, Tovar JA. Effect of growth hormone on bacterial translocation in experimental short-bowel syndrome. *Pediatr Surg Int* 1999; **15**: 160-163
- 7 **Zhou X**, Li YX, Li N, Li JS. Effect of bowel rehabilitative therapy on structural adaptation of remnant small intestine: animal experiment. *World J Gastroenterol* 2001; **7**: 66-73
- 8 **Kudsk KA**, Wu Y, Fukatsu K, Zarzaur BL, Johnson CD, Wang R, Hanna MK. Glutamine-enriched total parenteral nutrition maintains intestinal interleukin-4 and mucosal immunoglobulin A levels. *JPEN* 2000; **24**: 270-274
- 9 **Huang KF**, Chung DH, Herndon DN. Insulinlike growth factor

- 1 (IGF-1) reduces gut atrophy and bacterial translocation after severe burn injury. *Arch Surg* 1993; **128**: 47-54
- 10 **Naaber P**, Smidt I, Tamme K, Liigant A, Tapfer H, Mikelsaar M, Talvik R. Translocation of indigenous microflora in an experimental model of sepsis. *J Med Microbiol* 2000; **49**: 431-439
- 11 **MacFie J**. Enteral versus parenteral nutrition: the significance of bacterial translocation and gut-barrier function. *Nutrition* 2000; **16**: 606-611
- 12 **Deich EA**, Ma WJ, Ma L, Berg RD, Specian RD. Protein malnutrition predisposes to inflammatory-induced gut-origin septic states. *Ann. Surg* 1990; **211**: 560-567
- 13 **MacFie J**, O' Boyle C, Mitchell CJ, Buckley PM, Johnstone D, Sudworth P. Gut origin of sepsis: a prospective study investigating associations between bacterial translocation, gastric microflora, and septic morbidity. *Gut* 1999; **45**: 223-228
- 14 **Reynolds JV**, Murchan P, Leonard N, Clarke P, Keane FB, Tanner WA. Gut barrier failure in experimental obstructive jaundice. *J Surg Res* 1996; **62**: 11-16
- 15 **Chen K**, Okuma T, Okamura K, Tabira Y, Kaneko H, Miyauchi Y. Insulin-like growth factor-I prevents gut atrophy and maintains intestinal integrity in septic rats. *JPEN* 1995; **19**: 119-124
- 16 **Mishima S**, Xu D, Deitch EA. Increase in endotoxin-induced mucosal permeability is related to increased nitric oxide synthase activity using the Ussing chamber. *Crit Care Med* 1999; **27**: 880-886
- 17 **Fukushima R**, Saito H, Inoue T, Fukatsu K, Inaba T, Han I, Furukawa S, Lin MT, Muto T. Prophylactic treatment with growth hormone and insulin-like growth factor 1 improve systemic bacterial clearance and survival in a murine model of burn-induced gut-derived sepsis. *Burns* 1999; **25**: 425-430
- 18 **Vazquez I**, Gomez-de-Segura IA, Grande AG, Escribano A, Gonzalez-Gancedo P, Gomez A, Diez R, De Miguel E. Protective effect of enriched diet plus growth hormone administration on radiation-induced intestinal injury and on its evolutionary pattern in the rat. *Deg Dis Sci* 1999; **44**: 2350-2358
- 19 **Ziegler TR**, Leader LM, Jonas CR, Griffith DP. Adjunctive therapies in nutritional support. *Nutrition* 1997; **13** (Suppl 9): 64S-72S
- 20 **Chen DL**, Wang WZ, Wang JY. Epidermal growth factor prevents gut atrophy and maintains intestinal integrity in rats with acute pancreatitis. *World J Gastroenterol* 2000; **6**: 762-765
- 21 **Gu Y**, Wu ZH. The anabolic effects of recombinant human growth hormone and glutamine on parenterally fed, short bowel rats. *World J Gastroenterol* 2002; **8**: 752-757
- 22 **Zhou X**, Li N, Li JS. Growth hormone stimulates remnant small bowel epithelial cell proliferation. *World J Gastroenterol* 2000; **6**: 909-913
- 23 **Heys SD**, Ashkanani F. Glutamine. *Br J Surg* 1999; **86**: 289-290
- 24 **Pichard C**, Kudsk KA. From nutrition support to pharmacologic nutrition in the ICU. *Germany, Springer* 2000: 30-31
- 25 **Scheppach W**, Loges C, Bartram P, Christl SU, Richter F, Dusel G, Stehle P, Fuerst P, Kasper H. Effect of free glutamine and alanyl-glutamine dipeptide on mucosal proliferation of the human ileum and colon. *Gastroenterology* 1994; **107**: 429-434
- 26 **Van Der Hulst RR**, Van Kreel BK, Von Meyenfeldt MF, Brummer RJ, Arends JW, Deutz NE, Soeters PB. Glutamine and the preservation of gut integrity. *Lancet* 1993; **341**: 1363-1365
- 27 **Khan J**, Iiboshi Y, Cui L, Wasa M, Sando K, Takagi Y, Okada A. Alanyl-glutamine-supplemented parenteral nutrition increases luminal mucus gel and decreases permeability in the rat small intestine. *JPEN* 1999; **23**: 24-31
- 28 **Li JY**, Lu Y, Hu S, Sun D, Yao YM. Preventive effect of glutamine on intestinal barrier dysfunction induced by severe trauma. *World J Gastroenterol* 2002; **8**: 168-171
- 29 **Burke DJ**, Alverdy JC, Aoys E, Moss GS. Glutamine-supplemented total parenteral nutrition improves gut immune function. *Arch Surg* 1989; **124**: 1396-1399
- 30 **Scopa CD**, Koureleas S, Tsamandas AC, Spiliopoulou I, Alexandrides T, Filos KS, Vagianos CE. Beneficial effects of growth hormone and insulin-like growth factor 1 on intestinal bacterial translocation, endotoxemia, and apoptosis in experimentally jaundiced rats. *J Am Coll Surg* 2000; **190**: 423-431
- 31 **Juby LD**, Rothwell J, Axon AT. Lactulose/mannitol test: an ideal screen for celiac disease. *Gastroenterol* 1989; **96**: 79-85
- 32 **Hulsewé KW**, van Acker BA, von Meyenfeldt MF, Soeters PB. Nutritional depletion and dietary manipulation: effects on the immune response. *World J Surg* 1999; **23**: 536-544
- 33 **Byrne TA**, Morrissey TB, Nattakom TV, Ziegler TR, Wilmore DW. Growth hormone, glutamine, and a modified diet enhance nutrient absorption in patients with severe short bowel syndrome. *JPEN* 1995; **19**: 296-302
- 34 **Sugiura T**, Tashiro T, Yamamori H, Takagi K, Hayashi N, Itabashi T, Toyoda Y, Sano W, Nitta H, Hirano J, Nakajima N, Ito I. Effects of total parenteral nutrition on endotoxin translocation and extent of the stress response in burned rats. *Nutrition* 1999; **15**: 570-575
- 35 **Foitzik T**, Kruschewski M, Kroesen AJ, Hotz HG, Eibl G, Buhr HJ. Does glutamine reduce bacterial translocation? A study in two animal models with impaired gut barrier. *Int J Colorectal Dis* 1999; **14**: 143-149
- 36 **O' Dwyer ST**, Michie HR, Ziegler TR, Revhaug A, Smith RJ, Wilmore DW. A single dose of endotoxin increases intestinal permeability in healthy humans. *Arch Surg* 1988; **123**: 1459-1464
- 37 **Welsh FK**, Farmery SM, MacLennan K, Sheridan MB, Barclay GR, Guillou PJ, Reynolds JV. Gut barrier function in malnourished patients. *Gut* 1998; **42**: 396-401
- 38 **Lyons A**, Kelly JL, Rodrick ML, Mannick JA, Lederer JA. Major injury induces increased production of interleukin-10 by cells of the immune system with a negative impact on resistance to infection. *Ann Surg* 1997; **226**: 450-460
- 39 **Rongione AJ**, Kusske AM, Ashley SW, Reber HA, McFadden DW. Interleukin-10 prevents early cytokine release in severe intraabdominal infection and sepsis. *J Surg Res* 1997; **70**: 107-112
- 40 **McKay DM**, Baird AW. Cytokine regulation of epithelial permeability and ion transport. *Gut* 1999; **44**: 283-289
- 41 **O' Boyle CJ**, Mac Fie J, Dave K, Sagar PS, Poon P, Mitchell CJ. Alterations in intestinal barrier function do not predispose to translocation of enteric bacteria in gastroenterologic patients. *Nutrition* 1998; **14**: 358-362

Edited by Wu XN

Establishment of transgenic mice carrying the gene of human nuclear receptor NR5A2 (hB1F)

Shui-Liang Wang, Hua Yang, You-Hua Xie, Yuan Wang, Jian-Zhong Li, Long Wang, Zhu-Gang Wang, Ji-Liang Fu

Shui-Liang Wang, Hua Yang, Jian-Zhong Li, Ji-Liang Fu, Department of Medical Genetics, Second Military Medical University, Shanghai 200433, China

You-Hua Xie, Yuan Wang, Institute of Biochemistry and Cell Biology, Shanghai Institute for Biological Sciences, Chinese Academy of Sciences, Shanghai 200031, China

Long Wang, Zhu-Gang Wang, Ji-Liang Fu, Shanghai Nanfang Research Center for Model Organisms, Shanghai 201203, China

Supported by the National Natural Science Foundation of China, No.39830360, and the National "863" High Technology Research and Development Program of China, No. 2001AA221261

Correspondence to: Professor. Ji-Liang Fu, Department of Medical Genetics, Second Military Medical University, 800 Xiangyin Road, Shanghai 200433, China. jlfu@guomai.sh.cn

Telephone: +86-21-25070027 **Fax:** +86-21-25070027

Received: 2002-12-05 **Accepted:** 2003-01-02

Abstract

AIM: Human hepatitis B virus enhancer II B1 binding factor (hB1F) was cloned and characterized as a novel member of the Ftz-F1 (NR5A) nuclear receptor subfamily. Although progresses have recently been made, its biological function remains largely unidentified. The aim of this study was to establish an hB1F transgenic mouse model to promote the functional study of hB1F.

METHODS: Transgene fragments were microinjected into fertilized eggs of mice. The manipulated embryos were transferred into the oviducts of pseudopregnant female mice. The offsprings were identified by PCR and Southern blot analysis. Transgene expression was analyzed with RT-PCR and Western blot analysis. Transgenic founder mice were used to establish transgenic mouse lineages. The F1 and F2 mice were identified by PCR analysis.

RESULTS: Seven mice were identified as carrying copies of transgene. RT-PCR and Western blotting results showed that the transgene was expressed in heart, liver, lung, kidney and stomach in one of the transgenic mouse lineages. Genetic analysis of the transgenic mice demonstrated that the transgene was integrated into the chromosome at a single site, and was transmitted stably.

CONCLUSION: In this study we established an hB1F transgenic mouse model, which will facilitate the investigation of the biological function of hB1F *in vivo*.

Wang SL, Yang H, Xie YH, Wang Y, Li JZ, Wang L, Wang ZG, Fu JL. Establishment of transgenic mice carrying the gene of human nuclear receptor NR5A2 (hB1F). *World J Gastroenterol* 2003; 9(6): 1333-1336

<http://www.wjgnet.com/1007-9327/9/1333.asp>

INTRODUCTION

Nuclear receptor (NR) is a superfamily of eukaryotic transcription factors that are crucial for gene regulation and

development. Members of this superfamily include receptors for steroid and non-steroid hormones as well as a large number of orphan receptors whose regulatory ligands have not been identified^[1,2]. *Fushi tarazu* factor 1 (Ftz-F1) is one of the six subfamilies of the NR superfamily^[3], which has been nominated as NR5^[4]. Members of the Ftz-F1 subfamily all possess a particular Ftz-F1 box located at the C-terminal of the DNA-binding domain (DBD) and bind to their response elements as monomer.

Human hepatitis B virus (HBV) enhancer II B1 binding factor (hB1F) has been cloned and characterized as a novel member of the Ftz-F1 subfamily^[5]. hB1F (also known as NR5A2, CPF, and hFTF) binds specifically to the B1 element in the enhancer II of HBV and activates its function, thus regulating the viral gene expression and replication. RT-PCR and 3' -RACE have previously revealed that utilization of two polyadenylation signals results in the 3.8 and 5.2 kb transcripts^[6,7]. hB1F is the human homologue of the mouse transcription factor mLRH-1. It has been reported that NR5A2 may play an important role in regulating the liver-specific expression of several genes^[8]. Recent findings demonstrate that NR5A2 is a critical transcription factor in the bile acid biosynthesis pathway^[9,10] and may also regulate the expression of bile acid and cholesterol transporters in the liver and intestine^[11,12].

To facilitate the functional studies of hB1F, we reported here the establishment of transgenic mice carrying hB1F gene. 7 transgenic mice were identified by PCR and Southern blotting and used as founders to establish transgenic mouse lineages. The results of the F1 identification with PCR showed that the transgenes could be transmitted stably. RT-PCR and Western blotting analysis demonstrated that the transgenes expressed in multiple tissues of transgenic mice.

MATERIALS AND METHODS

Plasmid

pcDNA3-hB1F contains the full length hB1F cDNA under the control of CMV promoter. A Flag tag was placed upstream to the hB1F coding sequence to facilitate the characterization of the expressed protein.

Animals

C57 and CBA mice were maintained by Shanghai Nanfang Research Center for Model Organisms. Transgenic mice were raised, and bred in the Laboratory Animal Centre of Second Military Medical University.

Generation of transgenic mice

The 6.9 kb linearized pcDNA3-hB1F was purified from agarose gel with QIAGEN gel extraction kit (Qiagen, CA, USA), adjusted to a final concentration of 1 µg/ml in TE buffer and used as the DNA solution in microinjection. The F1 female hybrids of C57 and CBA mice were hormonally superovulated and mated with F1 male hybrids. Next morning the fertilized one-cell eggs were collected from the oviduct. The eggs were microinjected with the DNA solution under a microscope. The injected fertilized eggs were transplanted into the oviduct of pseudo-pregnant F1 hybrids of C57 and CBA mice.

Identification of transgenic mice

Founder (G0) mice were identified by PCR and Southern blotting analysis. For PCR, DNA was extracted from tails with Genomic DNA MINIPREPES kit (Sangon Inc. China). PCR amplification was performed with hB1F primers (P1: 5'-CCGACAAGTGGTACATGGAA-3' P2: 5'-CTGCTGCGGGTAGTTACACA-3') and pcDNA3 primers (P3: 5'-ATGCGGTGGGCTCTATG-3' P4: 5'-CGGCTCCATCCGAGTA-3') which would produce 300 bp and 1 353 bp fragments from mice carrying the transgene, respectively. For Southern blotting, genomic DNA was digested overnight with HindIII and subjected to electrophoresis on a 1.0 % agarose gel. DNA was transferred onto nylon membrane (MILLIPORE Co., Ltd, London, UK). Hybridization was performed under a stringent condition with a randomly-primed (α - 32 P)-labeled hB1F probe.

Expression of the transgene

One of the transgenic mouse lineages was used to study the expression of transgene. Total RNA was isolated from tissues with the TRIzol reagent (Invitrogen, CA, USA), according to manufacturer's instructions. First strand cDNA was synthesized by reverse transcription (Promega, USA). Semiquantitative RT-PCR reactions were performed using primer pairs 5'-CCGACAAGTGGTACATGGAA-3' and 5'-CTGCTGCGGGTAGTTACACA-3' for hB1F cDNA, and 5'-AACTTTGGCATTGTGGAAGG-3' and 5'-TGTGAGGGAGATGCTCAGT G-3' for mouse glyceraldehyde-3-phosphate dehydrogenase (GAPDH) cDNA, which resulted in the generation of 300 bp and 600 bp products, respectively. PCR was performed for 30 cycles at 94 °C for 1 min, at 57 °C for 1 min, and at 72 °C for 1 min. PCR products were electrophoresed on 1.5 % agarose gels. Signals were quantified by density analysis of the digital images using BioStar image software, version 2.

For Western blotting, protein samples from tissues were prepared according to the protocols by the manufacturer (Santa Cruz Biotechnology, Inc. WA, USA). 50 μ g protein of each sample was electrophoresed on 10 % SDS-polyacrylamide gel and transferred to PVDF membrane. Membranes were blocked with 5 % (w/v) non-fat milk in Tween-TBS (TBST) overnight at 4 °C and incubated with anti-Flag antibody (Sigma, USA) at a dilution of 1:500 in TBST for 2 h at room temperature. Membranes were washed three times with TBST and incubated with a secondary antibody (horseradish peroxidase-conjugated anti-mouse IgG) at a dilution of 1:2 000 at room temperature for 1 h. Immunodetection was carried out with an enhanced chemiluminescence kit (Amersham Pharmacia Biotech, USA).

Transmission of transgene

To study the transmission of transgene in mice, transgenic founder mice were mated to normal C57 mice to produce the first generation (F1) transgenic mice which were identified by PCR analysis using hB1F primers P1 and P2, and primers P5 (5'-GTTGGAGGTCGCTGAGTA-3') and P6 (5'-AGTAGGAAAGTCCCATAGGTC-3'), yielding 300 bp and 500 bp products, respectively, from mice carrying the transgene. The F1 mice of the same founder carrying the transgene were mated between brother and sister mice to produce the second generation (F2). The F2 transgenic mice were identified by the same methods for the F1 transgenic mice.

RESULTS

Establishment of hB1F transgenic mice

The transgene fragment containing the full length hB1F cDNA was microinjected into the male pronucleus of 653 fertilized

oocytes of F1 hybrids between C57 and CBA mice. The injected eggs were implanted into the oviducts of 24 pseudo-pregnant foster mothers, of which 13 mice became pregnant and gave birth to 97 offsprings. Eleven offspring mice were identified to carry the hB1F cDNA as demonstrated by PCR analysis (Figure 1), seven out of which were further confirmed by Southern blotting analysis (Figure 2). The ratio of transgene integration was 11.3 % and 7.2 %, respectively, by PCR and Southern blotting analysis.

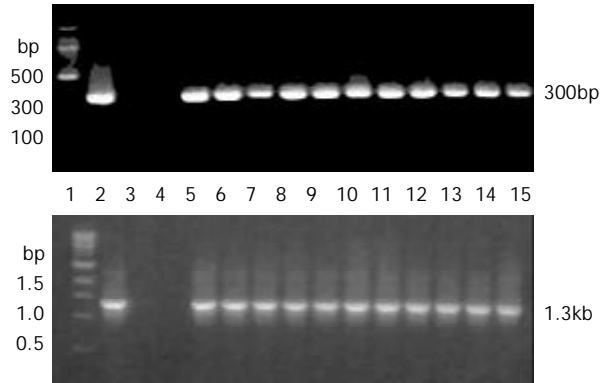


Figure 1 PCR results of transgenic mice. 1: DNA molecular weight marker, up 100bp ladder, down 1kb ladder; 2: Positive control (pcDNA3-hB1F); 3: Negative control (normal mouse); 4: Water as template; 5-15: Transgenic founder mice; Up: P1-P2 primers amplified; Down: P3-P4 primers amplified.



Figure 2 Genomic DNA Southern blotting results of transgenic mice. 1: Positive control (pcDNA3-hB1F); 2: Negative control (normal mouse); 3-13: Transgenic founder mice.

hB1F transgene expressed in multiple tissues of transgenic mice

As the transgene was driven by the CMV promoter, to study if it can express in multiple tissues of transgenic mice, we analysed the tissue expression profile of the hB1F transgene by RT-PCR and Western blot. The results (Figure 3, Figure 4) showed that the hB1F transgene was expressed in the heart, liver, lung, stomach and kidney, but not in intestine and encephalon.

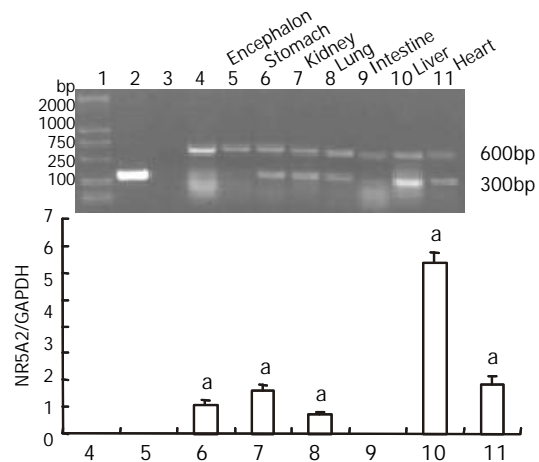


Figure 3 RT-PCR results of transgene expression. 1: DNA molecular weight marker DL 2000; 2: Positive control (pcDNA3-hB1F); 3: Negative control (non-reversely transcribed RNA); 4: C57 mouse liver; 5-11: Transgenic mice tissues. $^aP < 0.05$.

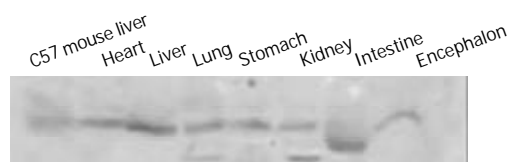


Figure 4 Western blotting analysis of transgene expression.

Genetics of transgenic mice

To establish the transgenic mouse lineages, founder mice were mated to C57 mice to produce F1 mice. Among 128 mice of the first generation, 60 were identified as carrying hB1F cDNA transgene by PCR analysis (Figure 5). The ratio of transgene transmission was 46.9%. The F1 mice from the same founder were mated each other to produce the F2 mice. 45 out of 64 F2 mice were hB1F transgenic mice, with a ratio of transgene transmission of 70.3%. These results showed that the inheritance of hB1F transgene was in accordance with Mendel's laws, and the transgene was integrated into the chromosome in a single site and could be transmitted stably.

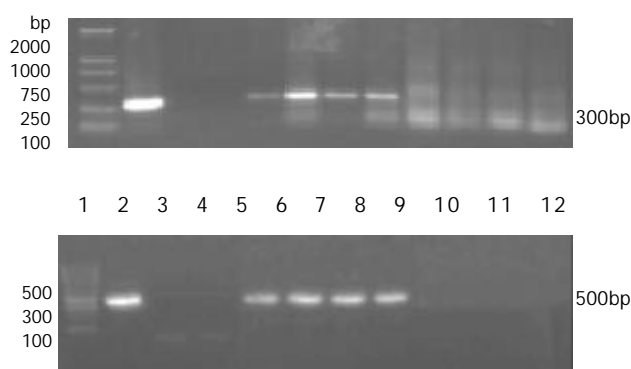


Figure 5 Partial PCR results of F1 transgenic mice. 1: DNA molecular weight marker, up DL 2000, down 100bp ladder; 2: Positive control (pcDNA3-hB1F); 3: Negative control (normal mouse); 4: Water as control; 5-12: F1 mice; Up: P1-P2 primers amplified; Down: P5-P6 primers amplified.

DISCUSSION

hB1F (NR5A2) is a novel member of the FTZ-F1 nuclear receptor subfamily. It was originally cloned based on its interaction with hepatitis B virus (HBV) enhancer II B1 element^[5]. It has been shown to be a critical regulator of HBV gene expression and replication. Recent studies have revealed that hB1F is mainly involved in the regulation of cholesterol related gene expression in the hepatic-intestinal system. hB1F and its mouse homolog mLRH-1 are essential for the transcription of the gene encoding cholesterol 7 α hydroxylase (CYP7A1), the first and rate limiting enzyme in bile acid biosynthesis^[6,9,10]. Together with two other nuclear receptors, FXR and SHP, and hB1F/mLRH-1 can mediate the feedback effect of bile acids on the transcription of CYP7A1. Moreover, hB1F/mLRH-1 can also regulate the expression of sterol 12 α -hydroxylase (CYP8B1)^[13], multidrug resistance protein-3 (MRP-3)^[11], cholesterol ester transport protein (CETP)^[12] and aromatases^[14]. There is evidence that mLRH-1 may also regulate the expression of several critical transcriptional factors, such as HNF1, HNF3 β and HNF4^[15]. It is possible that hB1F/mLRH-1 may exert broad influences on many genes by regulating these important factors. Since the regulation of cholesterol and bile acid homeostats is complicated, prone to be influenced by various genetic and environmental factors, it is vital to establish a transgenic or knock-out animal model for the studies of the biological role

that hB1F plays in a living organism. The strategy to knock out mLRH-1 in mice has not been successful, due to early embryo lethality (personal communication), which suggests that hB1F/mLRH-1 has yet unidentified crucial functions during embryogenesis. The attempt to generate hB1F transgenic mice has not been reported either. To our knowledge, we have generated the first transgenic mice carrying and expressing the hB1F transgene.

In vivo hB1F/mLRH-1 is mainly expressed in the liver and pancreas. However, weak expression of hB1F has also been detected in other tissues such as heart, lung, skeletal muscle and intestine^[5,6]. Recent studies have also demonstrated that hB1F is expressed abundantly in human ovary, testis^[16] and preadipocytes^[14], as well as in human adrenal and placenta in small amount^[16], thus hB1F has a broader expression tissue profile than previously thought. In this study, the hB1F transgene was expressed in multiple tissues, most of which are capable of expressing endogenous hB1F *in vivo*. Therefore, the hB1F transgenic mice we generated in this study is an invaluable animal model, for investigating hB1F function not only in hepatic tissues, but also in other tissues, which may ultimately reveal the yet unidentified biological functions of hB1F.

In conclusion, we reported here the successful generation of a transgenic mouse model expressing the orphan nuclear receptor hB1F (NR5A2). Future studies will focus on the physiological and pathological changes in this mouse model using powerful analytic methods e.g. microarray comparisons of gene expression profiles between normal and transgenic mice.

REFERENCES

- 1 **Beato M**, Herrlich P, Schutz G. Steroid hormone receptors: many actors in search of a plot. *Cell* 1995; **83**: 851-857
- 2 **Kastner P**, Mark M, Chambon P. Non-steroid nuclear receptors: what are genetic studies telling us about their role in real life? *Cell* 1995; **83**: 859-869
- 3 **Laudet V**. Evolution of the nuclear receptor superfamily: early diversification from an ancestral orphan receptor. *J Mol Endocrinol* 1997; **19**: 207-226
- 4 **Nuclear Receptors Nomenclature Committee**. A unified nomenclature system for the nuclear receptor superfamily. *Cell* 1999; **97**: 161-163
- 5 **Li M**, Xie YH, Kong YY, Wu X, Zhu L, Wang Y. Cloning and characterization of a novel human hepatocyte transcription factor, hB1F, which binds and activates enhancer II of hepatitis B virus. *J Biol Chem* 1998; **273**: 29022-29031
- 6 **Nitta M**, Ku S, Brown C, Okamoto AY, Shan B. CPF: an orphan nuclear receptor that regulates liver-specific expression of the human cholesterol 7 α -hydroxylase gene. *Proc Natl Acad Sci USA* 1999; **96**: 6660-6665
- 7 **Zhang CK**, Lin W, Cai YN, Xu PL, Dong H, Li M, Kong YY, Fu G, Xie YH, Huang GM, Wang Y. Characterization of the genomic structure and tissue-specific promoter of the human nuclear receptor NR5A2 (hB1F) gene. *Gene* 2001; **273**: 239-249
- 8 **Galameau L**, Pare JF, Allard D, Hamel D, Levesque L, Tugwood JD, Green S, Belanger L. The alpha1-fetoprotein locus is activated by a nuclear receptor of the Drosophila FTZ-F1 family. *Mol Cell Biol* 1996; **16**: 3853-3865
- 9 **Goodwin B**, Jones SA, Price RR, Watson MA, McKee DD, Moore LB, Galardi C, Wilson JG, Lewis MC, Roth ME, Maloney PR, Willson TM, Kliewer SA. A regulatory cascade of the nuclear receptors FXR, SHP-1, and LRH-1 represses bile acid biosynthesis. *Mol Cell* 2000; **6**: 517-526
- 10 **Lu TT**, Makishima M, Repa JJ, Schoonjans K, Kerr TA, Auwerx J, Mangelsdorf DJ. Molecular basis for feedback regulation of bile acid synthesis by nuclear receptors. *Mol Cell* 2000; **6**: 507-515
- 11 **Inokuchi A**, Hinoshita E, Iwamoto Y, Kohno K, Kuwano M, Uchiumi T. Enhanced expression of the human multidrug resis-

- tance protein 3 by bile salt in human enterocytes: A transcriptional control of a plausible bile acid transporter. *J Biol Chem* 2001; **276**: 46822-46829
- 12 **Luo Y**, Liang CP, Tall AR. The orphan nuclear receptor LRH-1 potentiates the sterol-mediated induction of the human CETP Gene by Liver X Receptor. *J Biol Chem* 2001; **276**: 24767-24773
- 13 **del Castillo-Olivares A**, Gil G. A1pha-fetoprotein transcription factor is required for the expression of sterol 12 alpha-hydroxylase, the specific enzyme for cholic acid synthesis. Potential role in the bile acid-mediated regulation of gene transcription. *J Biol Chem* 2000; **275**: 17793-17799
- 14 **Clyne CD**, Speed CJ, Zhou J, Simpson ER. Liver receptor homologue-1 (LRH-1) regulates expression of aromatase in preadipocytes. *J Biol Chem* 2002; **277**: 20591-20597
- 15 **Pare JF**, Roy S, Galarneau L, Belanger L. The mouse fetoprotein transcription factor (FTF) gene promoter is regulated by three GATA elements with tandem E-box and Nkx motifs, and FTF in turn activates the HNF3beta, HNF4a1pha and HNF1a1pha gene promoters. *J Biol Chem* 2001; **276**: 13136-13144
- 16 **Sirianni R**, Seely JB, Attia G, Stocco DM, Carr BR, Pezzi V, Rainey WE. Liver receptor homologue-1 is expressed in human steroidogenic tissues and activates transcription of genes encoding steroidogenic enzymes. *J Endocrinol* 2002; **174**: R13-17

Edited by Xia HHX

Gene-expression analysis of single cells-nested polymerase chain reaction after laser microdissection

Xin Shi, Jörg Kleeff, Zhao-Wen Zhu, Bruno Schmied, Wen-Hao Tang, Arthur Zimmermann, Markus W. Büchler, Helmut Friess

Xin Shi, Jörg Kleeff, Zhao-Wen Zhu, Bruno Schmied, Markus W. Büchler, Helmut Friess, Department of General Surgery, University of Heidelberg, Im Neuenheimer Feld 110, D-69120 Heidelberg, Germany

Xin Shi, Wen-Hao Tang, Department of General Surgery, Zhongda Hospital, Southeast University, Nanjing 210009, Jiangsu Province, P. R. China

Arthur Zimmermann, Institute of Pathology, University of Bern, Inselspital, CH-3010 Bern, Switzerland

Correspondence to: Helmut Friess, M.D. Department of General Surgery, University of Heidelberg, Im Neuenheimer Feld 110, D-69120 Heidelberg, Germany. helmut_friess@med.uni-heidelberg.de

Telephone: +49-6221-566900 **Fax:** +49-6221-566903

Received: 2002-12-30 **Accepted:** 2003-03-12

Abstract

AIM: The structural and functional characteristics of cells are dependent on the specific gene expression profile. The ability to study and compare gene expression at the cellular level will therefore provide valuable insights into cell physiology and pathophysiology.

METHODS: Individual cells were isolated from frozen colon tissue sections using laser microdissection. DNA as well as RNA were extracted, and total RNA was reversely transcribed to complementary DNA (cDNA). Both DNA and cDNA were analyzed by nested polymerase chain reaction (PCR). The quality of isolated DNA and RNA was satisfactory.

RESULTS: Single cells were successfully microdissected using an ultraviolet laser micromanipulator. Nested PCR amplification products of DNA and cDNA of single cells could clearly be visualized by agarose gel electrophoresis.

CONCLUSION: The combined use of laser microdissection and nested-PCR provides an opportunity to analyze gene expression in single cells. This method allows the analysis and identification of specific genes which are involved in physiological and pathophysiological processes in a complex of variable cell phenotypes.

Shi X, Kleeff J, Zhu ZW, Schmied B, Tang WH, Zimmermann A, Büchler MW, Friess H. Gene-expression analysis of single cells-nested polymerase chain reaction after laser microdissection. *World J Gastroenterol* 2003; 9(6): 1337-1341
<http://www.wjgnet.com/1007-9327/9/1337.asp>

INTRODUCTION

Techniques for isolating a specific cell population from a tissue complex for subsequent analysis of its molecular and biochemical contents have long been critical in cellular and molecular biology. To this end, various microdissection techniques have been developed to reduce contamination of surrounding cells^[1-3]. Microdissection originally involved manual or micromanipulator guidance of a needle to scrape

off an area of interest of a thin tissue section^[4]. Selective ultraviolet radiation fractionation, which relies on negative selection and ablation of the unwanted areas of the tissue on the slide, provides a technical advancement in this field^[1]. Micromanipulators and microdissection have improved the accuracy and reliability of microdissection; however, it remains an intrinsically slow, technique-dependent process of procuring pure cell populations from tissues. Modern techniques, such as flow cytometry with cell sorting and affinity-labeled magnetic beads, allow separation of cell subpopulations from heterogeneous pools of single cells in suspension. To apply these techniques to tissues, there is a requirement for the dissolution of intercellular adhesion and the formation of a suspension of individual cells, which is not generally practical in solid tissues and may change the characteristics of the isolated cells. Perhaps the biggest breakthrough in this approach and one that is rapidly gaining popularity is laser microdissection (LM)^[5,6]. LM can be used to collect individual cells or specific cell populations from complex tissues without any contamination, and an individual operator can collect many samples in a single session.

The use of LM to obtain pure cell populations has so far been applied to DNA analysis^[5], protein analysis^[7] and mRNA analysis^[8]. A variety of approaches are routinely used to assess the expression of specific genes in cells and tissues, such as Northern blot and RNase protection assay. The quantity of mRNA that can be harvested from a single cell is on the order of 1 pg at best. Thus, the techniques used to analyze gene expression are limited when applied to single cells. Nested PCR has proved to be a sensitive and specific procedure^[9], and the use of nested PCR increases both the sensitivity and specificity of the standard PCR assay^[10,11].

We now present an approach that allows analysis of DNA and mRNA down to the cellular level within intact tissue sections using a combination of LM and nested PCR.

MATERIALS AND METHODS

Preparation of tissue sections

Normal colon tissues were obtained from operation specimens in which a partial colon resection was performed for colon cancer. The Human Subject Committee of the University of Bern approved the studies. Immediately following surgical removal, tissues were snap-frozen in liquid nitrogen and maintained at -80 °C until use. Tissues were embedded in Tissue Tek OCT medium (VWR Scientific Products Corporation, San Diego, CA, USA) and sectioned at 8 µm in a cryostat, mounted on uncoated glass slides, and immediately stored at -80 °C once air dried. Slides containing frozen sections were fixed in 70 % ethanol for 2 min, stained with hematoxylin and eosin, then dehydrated in 70 %, 94 % and 100 % alcohol (each for 2 minutes) and finally dehydrated for 2 minutes in xylene.

Laser microdissection

The ultraviolet-laser Robot-Microbeam (P.A.L.M., Wolfratshausen, Germany) used for microdissection consists

of a nitrogen laser of high-beam precision (wavelength 337nm) coupled to an inverted microscope (Axiovert 135; Zeiss, Jena, Germany) via the epifluorescence illumination path. The microscope stage and micromanipulator are digitally controlled and moved by a computer mouse. The high photon density within the laser focus catapults the material to the cap without any heating effect—a so-called cold ablation—so that DNA and RNA would not degrade during microdissection. With the combination of laser-manipulated microdissection (LMM) and the laser pressure catapulting (LPC) technique, single cells could be processed in seconds^[12].

DNA extraction from microdissected samples

DNA was extracted using DNA extraction solution with 100 mM Tris-HCl, pH 8.0, 400 µg/ml proteinase K (Sigma, Deisenhofen, Germany). After incubation at 37 °C for 3 h, the samples were boiled to inactivate proteinase K. After centrifugation, the supernatants of the DNA extraction buffer, now containing DNA from the microdissected cells, were used for nested PCR.

RNA isolation from microdissected samples and reverse transcription

Total RNA was independently isolated by means of a modification of the RNA microisolation protocol, as described previously^[13]. Briefly, caps were placed in Eppendorf tubes containing guanidinium isothiocyanate buffer, inverted several times, extracted with phenol/chloroform/isoamyl alcohol, and precipitated with sodium acetate and glycogen carrier (10 µg/µl) in isopropanol. After initial recovery and resuspension of the RNA pellet, a DNase treatment was performed for 2 h at 37 °C using 10 units of DNase (Roche Diagnostics, Mannheim, Germany) in the presence of 10 units of RNase inhibitor (Roche Diagnostics, Mannheim, Germany), followed by re-extraction and precipitation. The pellet was resuspended in 24 µl of RNase-free water. 12 µl of total RNA was reversely transcribed into complementary DNA (cDNA) using random hexamers according to the manufacturer's instructions (Roche Diagnostics, Rotkreuz, Switzerland)^[14]. For each cDNA reaction tube, an identical tube containing the same amount of RNA was prepared as a negative control (mock RT). In these tubes, the same amount of water was substituted for reverse transcriptase. After incubation, the reaction was terminated by heating to 95 °C for 10 min. The cDNA preparations were used immediately or stored at -20 °C until use.

Gene analysis by nested PCR

The human beta-actin gene, a ubiquitously and constitutively expressed gene, was used as the target gene^[15] for nested PCR. This approach involves the use of two pairs of PCR primers. The primers were synthesized by Amplimmun (Amplimmun AG, Madulain, Switzerland); the sequence is shown in Table 1. PCR amplification was carried out using beta-actin-outer primers in a final volume of 25 µl with a Perkin-Elmer GeneAmp System 9700 using 0.625U of Taq DNA polymerase (Roche Diagnostics GmbH, Mannheim, Germany). Cycling conditions were as follows: 35 cycles of denaturation at 94 °C for 1 min, annealing at 62 °C for 1 min, and elongation at 72 °C for 2.5 min. The first PCR cycle was preceded by denaturation at 94 °C for 3 min, and the last PCR cycle was followed by incubation at 72 °C for 8 min. Nested PCR was performed using 0.5 µl of the first PCR product as a template. The PCR cycling conditions for the beta-actin-inner primers were the same as above except for an annealing temperature of 60 °C. The amplification products were analyzed by electrophoresis on 1 % agarose gels and stained with ethidium bromide.

Table 1 β-actin primers used for nested PCR analysis

Primer	Sequence	Primer size (bp)	Size of PCR products (bp)
β-actin-outer			
Forward primer	GGC ATC CTC ACC CTG AAG TA	20	494
Reverse primer	CCA TCT CTT GCT CGA AGT CC	20	
β-actin-inner			
Forward primer	AAA TCT GGC ACC ACA CCT TC	20	240
Reverse primer	AGG GCA TAC CCC TCG TAG AT	20	

RESULTS

Laser microdissection of cells from cryostat sections

Eight-micrometer cryostat sections were prepared from normal colon tissues. Single colon mucosa cells were selected and cut with LM and catapulted by LPC under visual control (Figure 1). For LPC, the setting of laser energy was sufficiently high to catapult the microdissected cells into the microcentrifuge cap. Cell clusters of interest were also selected and laser-microdissected under visual control (Figure 2). The laser precisely circumscribed a selected area or a single cell, which yielded a clear-cut gap between selected and non-selected areas.

DNA analysis in microdissected cells by nested PCR

100 cells, 10 cells and 1 cell were microdissected from normal colon sections. Samples were digested by proteinase K and boiled for 10 min to denature proteinase K. After centrifugation, the supernatants were used for PCR with the beta-actin-outer primers. The amplification products were analyzed by electrophoresis on 1 % agarose gels; the results are shown in Figure 3A. The bands from a complete section, 100 cells, and 10 cells could be clearly visualized. Nested PCR was performed using 0.5 µl of the first PCR product as a template; the amplification results are shown in Figure 3B. Amplification products from single cells could be clearly visualized by agarose gel electrophoresis after nested PCR. Control amplifications without DNA templates did not yield any signal.

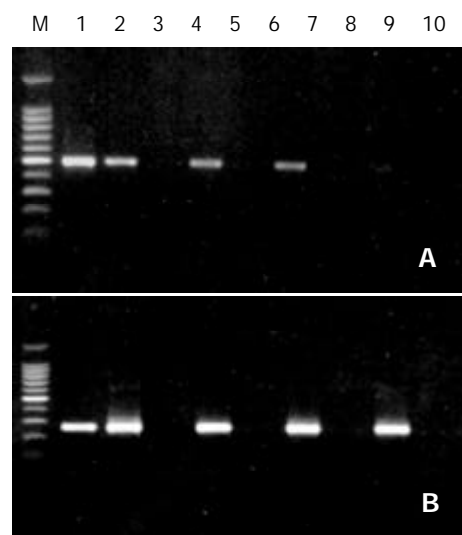


Figure 2 Amplification results from nested PCR of colon cells after laser microdissection. Nested PCR amplification products of DNA of single cells could clearly be visualized by agarose gel electrophoresis. A: Amplification results of β-actin-outer primers. B: Amplification results of β-actin-inner primers. M: DNA markers (upper to lower: 2000, 1000, 900, 800, 700, 600, 500, 400, 300, 200, and 100 bp). 1: PCR positive control; 2: one complete section; 3, 4, 6 and 8 are 100, 10 and 1 cell(s), respectively; 3, 5, 7 and 9 are negative controls of 2, 4, 6 and 8; 10: PCR negative control.

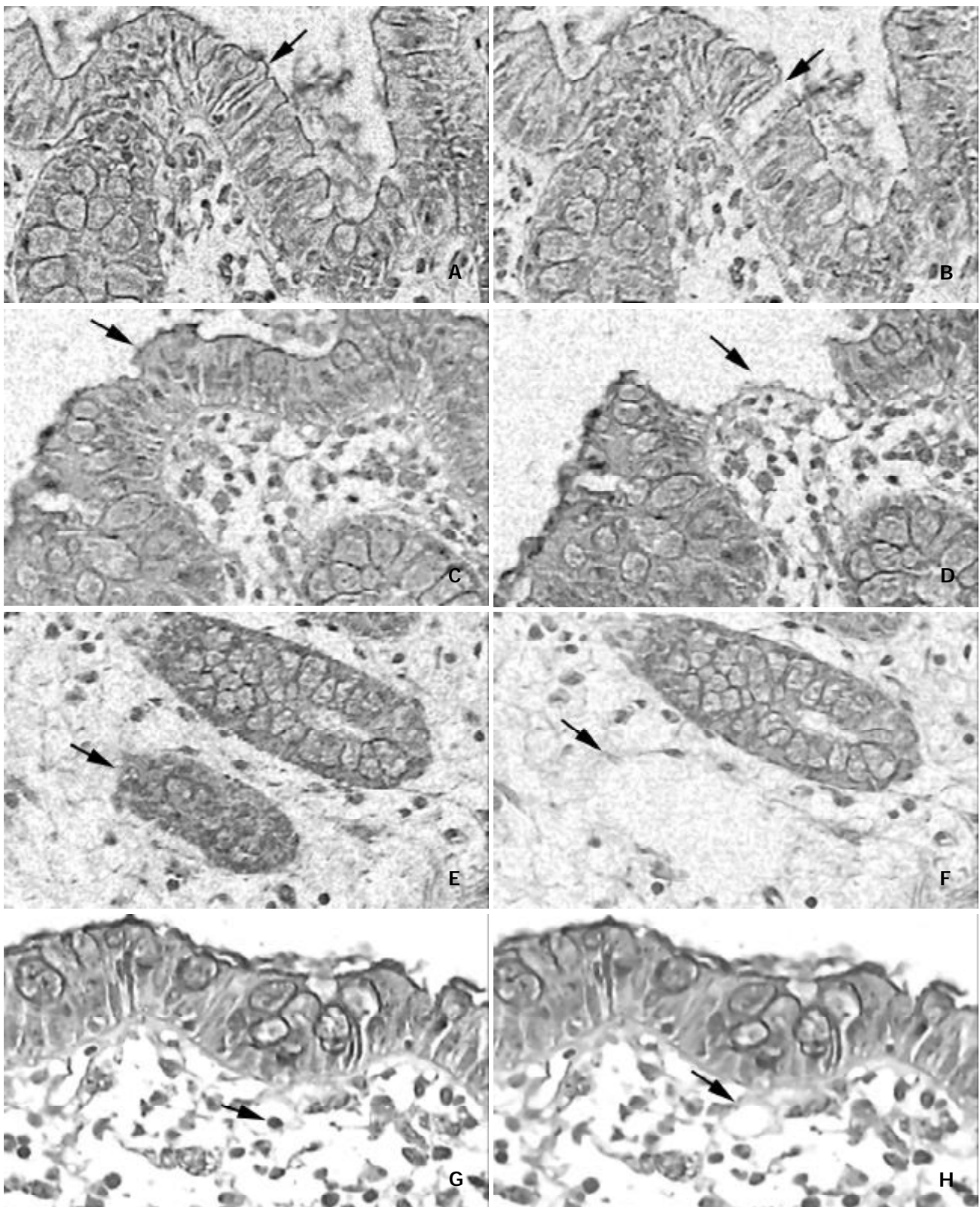


Figure 1 Examples of laser microdissection in colon tissues (hematoxylin and eosin, magnification $\times 200$). Single cells were picked by combination laser-manipulated microdissection (LMM) and laser pressure catapulting (LPC). A, C, E, G: Before Laser microdissection. B, D, F, H: Using LMM, the laser precisely circumcised selected cells, yielding a cut gap between selected and non-selected areas. Then the selected cells were catapulted using the LPC technique. A-F: Typical images before and after LMM and LPC. G, H: Laser microdissection could also be used to cut out the nucleus of a selected cell.

mRNA expression in microdissected cells by nested PCR

Normal colon RNA was obtained from complete sections, 200 cells, 100 cells, 10 cells and single cells. cDNA was transcribed from total RNA. The amplification products were analyzed by electrophoresis on 1 % agarose gels; the results are shown in Figure 3C. Signals from complete sections could

be clearly visualized. However, the signals from 200 cells and 100 cells could only be seen on the original gels, and the signals from 10 cells and single cells were below the level of detection. Nested PCR was performed using 0.5 μ l of the first PCR product as a template; the amplification results are shown in Figure 3D. Amplification products of even single

cells could be clearly visualized by agarose gel electrophoresis. Control amplifications without cDNA templates did not yield any signal.

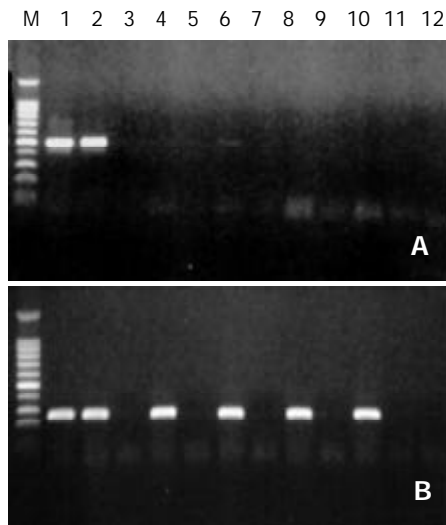


Figure 3 Amplification results from nested RT-PCR for cDNA of single cells after laser microdissection. A: Amplification results of β -actin-outer primers. B: Amplification results of β -actin-inner primers. M: DNA markers (upper to lower: 2000, 1000, 900, 800, 700, 600, 500, 400, 300, 200, and 100 bp). 1: PCR positive control; 2: one complete section; 4, 6, 8 and 10 are 200, 100, 10 and 1 cell(s), respectively; 3, 5, 7, 9 and 11 are negative controls of 2, 4, 6, 8 and 10; 12: PCR negative control.

DISCUSSION

In this study, single colon mucosa cells could be selectively microdissected and collected from frozen tissue sections under direct microscopic visualization using LM. Microdissected mucosa cells were used for further gene analysis using nested PCR.

Most tissues are composed of a number of different cell types, and cellular heterogeneity in most tissues is very complex. In normal or developing organs, specific cells express different genes and undergo complex molecular changes both in response to internal control signals, signals from adjacent cells, and humoral stimuli. In disease pathologies, the diseased cells of interest, such as precancerous cells or invading groups of cancer cells, are surrounded by these heterogeneous tissue elements. The percentage of non-neoplastic cells present in such specimens can be as high as 95 %^[16]. This tissue heterogeneity has proved one of the major obstacles to molecular research using current methods, since varying numbers of normal cells could mask the presence of single abnormal cells when analysis of its gene expression and total DNA or RNA from heterogeneous tissue is used^[17-24].

LM is a new method for performing microdissection of selected regions down to a single cell^[5,6,25]. There have been other reports describing methods to collect specific regions of tissue, such as graded sieving of glomeruli or pancreatic islet cells^[26,27] and isolation of suspension of proximal tubular cells^[28]. These methods make it possible to obtain relatively pure and large amounts of samples; however, it is difficult to avoid possible contamination of other tissue compartments, which can cause problems with sensitive RT-PCR methods. Using LM, our study has shown that it is feasible to examine mRNA expression of single cells without the risk of contamination by neighboring cells. If more than one cell is needed, single unwanted cells can selectively be destroyed from the tissue section using LM, resulting in an area composed of a

homogenous cell population. Utilizing a computer-controlled microscope stage, the cells of interest are visually selected and marked and their positions are stored electronically. The stage then automatically goes to and moves around the selected cells, while the laser fires with a preselected pulse energy and repetition rate. With a further slightly defocused laser shot, the target cells can selectively be catapulted into a microcentrifuge cap using LPC for further study. As reported in this article, this method allows gene analysis in the particular tissue region isolated from the frozen cryostat specimen, avoiding the contamination of other cells.

The quantity of mRNA that can be harvested from a single cell is approximately 1 pg at best. Therefore, to obtain meaningful gene-expression data, well-optimized or specialized amplification protocols must be applied. Using conventional PCR, the theoretical limit of detection is one copy of a single-stranded DNA molecule, and so with efficient harvesting of cytoplasm and a well-optimized PCR protocol, single-cell PCR is feasible^[29]. However, this is not a trivial undertaking, and identifying the expression of rare or particularly labile transcripts would prove to be technically demanding^[30].

In this study, amplification signals from DNA of single cells were only faintly present in the agarose gels, and amplification signals from cDNA could not be visualized by gel electrophoresis. Therefore, certain modifications to this approach have to be applied to provide more comprehensive single-cell expression analysis. In this study, a straightforward method of expanding the results obtained from single-cell PCR involves the use of nested PCR. Essentially, a primary conventional PCR increases the target concentration so that a second PCR reaction can be carried out to assay for the presence or absence of gene expression. The present study has shown that nested PCR is feasible for the analysis of gene expression after LM, even at the cellular level, and that this approach has the advantage of being relatively simple to apply. Further studies on the gene expression profiles of single microdissected cells will provide novel insight into different physiological and pathophysiological processes.

REFERENCES

- 1 **Shibata D**, Hawes D, Li ZH, Hernandez AM, Spruck CH, Nichols PW. Specific genetic analysis of microscopic tissue after selective ultraviolet radiation fractionation and the polymerase chain reaction. *Am J Pathol* 1992; **141**: 539-543
- 2 **Becker I**, Becker KF, Rohrl MH, Minkus G, Schutze K, Hofler H. Single-cell mutation analysis of tumors from stained histologic slides. *Lab Invest* 1996; **75**: 801-807
- 3 **Whetsell L**, Maw G, Nadon N, Ringer DP, Schaefer FV. Polymerase chain reaction microanalysis of tumors from stained histological slides. *Oncogene* 1992; **7**: 2355-2361
- 4 **Going JJ**, Lamb RF. Practical histological microdissection for PCR analysis. *J Pathol* 1996; **179**: 121-124
- 5 **Emmert-Buck MR**, Bonner RF, Smith PD, Chuaqui RF, Zhuang Z, Goldstein SR, Weiss RA, Liotta LA. Laser capture microdissection. *Science* 1996; **274**: 998-1001
- 6 **Bonner RF**, Emmert-Buck M, Cole K, Pohida T, Chuaqui R, Goldstein S, Liotta LA. Laser capture microdissection: Molecular analysis of tissue. *Science* 1997; **278**: 1481-1483
- 7 **Hao J**, Jackson L, Calaluce R, McDaniel K, Dalkin BL, Nagle RB. Investigation into the mechanism of the loss of laminin 5 (alpha3beta3gamma2) expression in prostate cancer. *Am J Pathol* 2001; **158**: 1129-1135
- 8 **Fink L**, Seeger W, Ermert L, Hanze J, Stahl U, Grimminger F, Kummer W, Bohle RM. Real-time quantitative RT-PCR after laser-assisted cell picking. *Nat Med* 1998; **4**: 1329-1333
- 9 **Yan Z**, Surmeier DJ. D5 dopamine receptors enhance Zn2+-sensitive GABA(A) currents in striatal cholinergic interneurons through a PKA/PP1 cascade. *Neuron* 1997; **19**: 1115-1126
- 10 **Bochet P**, Audinat E, Lambolez B, Crepel F, Rossier J, Iino M,

- Tsuzuki K, Ozawa S. Subunit composition at the single-cell level explains functional properties of a glutamate-gated channel. *Neuron* 1994; **12**: 383-388
- 11 **Massengill JL**, Smith MA, Son DI, O' Dowd DK. Differential expression of K4-AP currents and Kv3.1 potassium channel transcripts in cortical neurons that develop distinct firing phenotypes. *J Neurosci* 1997; **17**: 3136-3147
- 12 **Nagasawa Y**, Takenaka M, Matsuoka Y, Imai E, Hori M. Quantitation of mRNA expression in glomeruli using laser-manipulated microdissection and laser pressure catapulting. *Kidney Int* 2000; **57**: 717-723
- 13 **Sgroi DC**, Teng S, Robinson G, LeVangie R, Hudson JR Jr, Elkahoun AG. *In vivo* gene expression profile analysis of human breast cancer progression. *Cancer Res* 1999; **59**: 5656-5661
- 14 **Conejo JR**, Kleeff J, Koliopoulos A, Matsuda K, Zhu ZW, Goecke H, Bicheng N, Zimmermann A, Korc M, Friess H, Buchler MW. Syndecan-1 expression is up-regulated in pancreatic but not in other gastrointestinal cancers. *Int J Cancer* 2000; **88**: 12-20
- 15 **Efferth T**, Fabry U, Osieka R. Leptin contributes to the protection of human leukemic cells from cisplatin cytotoxicity. *Anti-cancer Res* 2000; **20**: 2541-2546
- 16 **Becker I**, Becker KF, Rohrl MH, Hofler H. Laser-assisted preparation of single cells from stained histological slides for gene analysis. *Histochem Cell Biol* 1997; **108**: 447-451
- 17 **Shi X**, Gao NR, Guo QM, Yang YJ, Huo MD, Hu HL, Friess H. Relationship between overexpression of NK-1R, NK-2R and intestinal mucosal damage in acute necrotizing pancreatitis. *World J Gastroenterol* 2003; **9**: 160-164
- 18 **Lin JS**, Song YH, Kong XJ, Li B, Liu NZ, Wu XL, Jin YX. Preparation and identification of anti-transforming growth factor beta1 U1 small nuclear RNA chimeric ribozyme *in vitro*. *World J Gastroenterol* 2003; **9**: 572-577
- 19 **Yue H**, Na YL, Feng XL, Ma SR, Song FL, Yang B. Expression of p57(kip2), Rb protein and PCNA and their relationships with clinicopathology in human pancreatic cancer. *World J Gastroenterol* 2003; **9**: 377-380
- 20 **Wang GS**, Wang MW, Wu BY, You WD, Yang XY. A novel gene, GCRG224, is differentially expressed in human gastric mucosa. *World J Gastroenterol* 2003; **9**: 30-34
- 21 **Liu JW**, Tang Y, Shen Y, Zhong XY. Synergistic effect of cell differential agent-II and arsenic trioxide on induction of cell cycle arrest and apoptosis in hepatoma cells. *World J Gastroenterol* 2003; **9**: 65-68
- 22 **Shi M**, Wang FS, Wu ZZ. Synergetic anticancer effect of combined quercetin and recombinant adenoviral vector expressing human wild-type p53, GM-CSF and B7-1 genes on hepatocellular carcinoma cells *in vitro*. *World J Gastroenterol* 2003; **9**: 73-78
- 23 **Tang NH**, Chen YL, Wang XQ, Li XJ, Yin FZ, Wang XZ. Construction of IL-2 gene-modified human hepatocyte and its cultivation with microcarrier. *World J Gastroenterol* 2003; **9**: 79-83
- 24 **Xiong LJ**, Zhu JF, Luo DD, Zen LL, Cai SQ. Effects of pentoxifylline on the hepatic content of TGF-beta1 and collagen in Schistosomiasis japonica mice with liver fibrosis. *World J Gastroenterol* 2003; **9**: 152-154
- 25 **Schutze K**, Lahr G. Identification of expressed genes by laser-mediated manipulation of single cells. *Nat Biotechnol* 1998; **16**: 737-742
- 26 **Troyer DA**, Kreisberg JJ. Isolation and study of glomerular cells. *Methods Enzymol* 1990; **191**: 141-152
- 27 **Figliuzzi M**, Zappella S, Morigi M, Rossi P, Marchetti P, Remuzzi A. Influence of donor age on bovine pancreatic islet isolation. *Transplantation* 2000; **70**: 1032-1037
- 28 **Vinay P**, Gougoux A, Lemieux G. Isolation of a pure suspension of rat proximal tubules. *Am J Physiol* 1981; **241**: F403-F411
- 29 **Jin L**, Thompson CA, Qian X, Kuecker SJ, Kulig E, Lloyd RV. Analysis of anterior pituitary hormone mRNA expression in immunophenotypically characterized single cells after laser capture microdissection. *Lab Invest* 1999; **79**: 511-512
- 30 **Dixon AK**, Richardson PJ, Pinnock RD, Lee K. Gene-expression analysis at the single-cell level. *Trends Pharmacol Sci* 2000; **21**: 65-70

Edited by Zhu LH

Rapid detection of the known SNPs of CYP2C9 using oligonucleotide microarray

Si-Yuan Wen, Hui Wang, Ou-Jun Sun, Sheng-Qi Wang

Si-Yuan Wen, Hui Wang, Ou-Jun Sun, Sheng-Qi Wang, Beijing Institute of Radiation Medicine, Beijing 100850, China

Supported by a grant from the State 863 High Technology Project of China, No. 2002AA2Z3411

Correspondence to: Professor Sheng-Qi Wang, Beijing Institute of Radiation Medicine, No. 27 Taiping Road, Beijing 100850, China. sqwang@nic.bmi.ac.cn

Telephone: +86-10-66932211 Fax: +86-10-66932211

Received: 2002-11-12 Accepted: 2002-12-18

Abstract

AIM: Cytochrome P450 2C9 (CYP2C9) is a polymorphic enzyme responsible for the metabolism of a large number of clinically important drugs. Individuals with mutant enzymes may risk serious side effects under routine therapy with certain drugs metabolized by CYP2C9. In order to facilitate the detection of the known SNPs of CYP2C9, an allele-specific oligonucleotide (ASO) based microarray was made.

METHODS: An oligonucleotide microarray was made to facilitate the SNP (single nucleotide polymorphism) screening and was applied for the detection of CYP2C9 polymorphism in 62 high blood pressure (HBP) patients who received Irbesartan for treatment. Part of the genotyping results was confirmed by direct sequencing. And the relation between CYP2C9 polymorphism and therapeutic outcome of Irbesartan was statistically analyzed.

RESULTS: Heterozygous alleles of CYP2C9*1/*3 were found in 7 out of 62 subjects. No mutant alleles of CYP2C9*2, *4 and *5 and no homozygous mutant alleles were detected. The 7 heterozygous CYP2C9*1/*3 and 13 random wild type DNA samples were subjected to direct sequencing with purified PCR products and same genotyping results were obtained with the 20 DNA samples. There was no significant difference in the odds of effectiveness of Irbesartan between the wild type (normal) group and CYP2C9*1/*3 (mutant) group ($P>0.05$).

CONCLUSION: The oligonucleotide microarray made in this study is a reliable assay for detecting the CYP2C9 known alleles and the heterozygous CYP2C9*1/*3 has no significant effects on the therapeutic outcome of Irbesartan.

Wen SY, Wang H, Sun OJ, Wang SQ. Rapid detection of the known SNPs of CYP2C9 using oligonucleotide microarray. *World J Gastroenterol* 2003; 9(6): 1342-1346
<http://www.wjgnet.com/1007-9327/9/1342.asp>

INTRODUCTION

Pharmacogenetics was established on the fact that certain genetic polymorphisms may cause significantly different responses among individuals on exposure to a particular drug^[1-3]. Recent advances in the understanding of the molecular genetics of drug-metabolizing enzymes (DME), particularly

cytochrome P450, have enabled the molecular basis of many polymorphisms to be elucidated and the genotyping assays to be developed^[4-6].

Cytochrome P450 is one of the key enzymatic mechanisms for the metabolism of drugs, pesticides, environmental pollutants, and carcinogens^[7-9]. In this superfamily, CYP2C9^[10-12] is a polymorphic enzyme responsible for the metabolism of a large number of clinically important drugs such as S-warfarin, phenytoin, tolbutamide, losartan and nonsteroidal anti-inflammatory drugs. To date, 5 alleles of CYP2C9 including the wild type CYP2C9*1 and the mutants CYP2C9*2 (430C-T), CYP2C9*3 (1075A-C), CYP2C9*4 (1076T-C) and CYP2C9*5 (1080C-G) have been found (www.imm.ki.se/cypalleles). In the four mutant alleles, single nucleotide variations in the exon 3 and exon 7 cause amino acid substitutions Arg144Cys, Ile359Leu, Ile359Thr and D360E, respectively, and therefore lead to a slow metabolizing capacity of the enzymes. The altered pharmacogenetics may result in prolonged or shortened effect time. The individuals with mutant enzymes risk serious side effects under routine therapy with certain drugs metabolized by CYP2C9. So frequent variants of CYP2C9 should be analyzed in participants of clinical trials where the enzymes may play a key role.

In order to facilitate the detection of the known SNPs of CYP2C9, an ASO (allele-specific oligonucleotide) hybridization based microarray was made, which could simultaneously screen the 4 mutant alleles of CYP2C9 of 10 individuals, and was applied for the detection of CYP2C9 polymorphism in 62 hypertension patients who received Irbesartan for treatment. Irbesartan is a selective antagonist of the AT1 receptor of angiotensin II receptor (AT1R) used in the treatment of hypertension and congestive heart failure^[13,14]. Previous studies indicate that Irbesartan is mainly metabolized by CYP2C9 to the inactive form^[15].

MATERIALS AND METHODS

DNA samples

A total of 62 peripheral blood samples were collected from unrelated HBP patients who received Irbesartan for treatment and the therapeutic outcome was classified as outstanding (11 persons), effective (38 persons) and failed (13 persons). Genomic DNA was extracted with the Genomic DNA purification kit (Promega) and quantified by UV spectrophotometer (DU® 640, Beckman coulter).

Oligonucleotides synthesis

Oligonucleotides (primers or probes) were synthesized using automatic DNA synthesizer (ABi 391A). For signal detection, the reverse primers were fluorescein (Cy3) labeled at 5' end. A probe was synthesized with the 3' end amino-modified to have a primary NH₂ group for immobilization onto aldehyde-coated slides, and the NH₂ group was linked by a polyethyleneglycol spacer to a specific allele-discriminating sequence, which was 16-17 nucleotides in length with a nucleotide complimentary to either the normal or mutant allele in the middle of the sequence. A list of oligonucleotides used in this study is presented in Table 1.

Table 1 Oligonucleotides used in this study

##	Sequence (5' --3')	Application
C1	CAC ATG GCT GCC CAG TGT CAG CTT C	Primers used to amplify exon3 and exon7 fragments of CYP2C9 containing SNP sites. C2* and C4* were fluorescein (Cy3) labeled at 5' end.
C2*	GGC CAC CCC TGA AAT GTT TCC AAG	
C3	ACG TGT GAT TGG CAG AAA CCG GAG C	
C4*	GGG ACT TCG AAA ACA TGG AGT TGC AG	
C1Tf	ATT GAG GAC <u>T</u> GT GTT CAA GAG GAA GC	Primers used to construct mutant templates. The variant bases (indicated by underlines) were introduced when synthesized.
C1Tr	CTT CCT CTT GAA CAC <u>A</u> GT CCT C	
C2Tf	CCT ACA CAG ATG CTG TGG TGC AC	
C2T1	CTG GTG GGG AGA AGG TCA <u>A</u> GG TAT CTC	
C2T2	CTG GTG GGG AGA AGG TCA <u>G</u> TG TAT CTC	
C2T3	CTG GTG GGG AGA <u>A</u> GC TCA ATG TAT CTC	
P1	TTG AGG ACC <u>G</u> TG TTC AA - spacer- NH ₂	Pairs of probes with one base difference (indicated with underline) for SNP discrimination, immobilized on aldehyde-coated slides surface with 3' end primary NH ₂ group.
P2	TTG AGG ACT <u>T</u> GTG TTC AA - spacer- NH ₂	
P3	GAG ATA C <u>A</u> T TGA CCT TC - spacer- NH ₂	
P4	GAG ATA C <u>C</u> T TGA CCT TC - spacer- NH ₂	
P5	GAG ATA C <u>A</u> T TGA CCT TC - spacer- NH ₂	
P6	GAG ATA C <u>A</u> C TGA CCT TC - spacer- NH ₂	
P7	TAC ATT G <u>A</u> C CTT CTC C - spacer- NH ₂	
P8	TAC ATT G <u>A</u> G CTT CTC C - spacer- NH ₂	

PCR amplification

The 2 target segments containing the SNP sites to be typed were amplified by PCR in one tube. Asymmetric PCR method was used to generate single-stranded target segments. The ratio of forward primer to reverse primer (fluorescein labeled) was optimized at 1:40 in a PCR reaction (data not shown). Reaction mixtures of 20 μ L contained 100 μ M dNTP, 0.5 μ M forward primer, 20 μ M reverse primer, 100 ng of a genomic DNA or 40 ng of a plasmid DNA, 1* PCR buffer and 1 U Taq enzyme. Amplification was conducted in a thermal cycler (PTC-100™ programmable thermal controller, MJ. Research Inc) under the following conditions: initial denaturation (5 min at 94 °C) followed by 40 cycles of denaturation (30 sec at 94 °C), annealing (30 sec at 62 °C) and extension (30 sec at 72 °C). A final extension step was carried out for 5 min at 72 °C. The PCR products were analyzed by 2 % agarose gel electrophoresis.

Construction of standard templates

DNA segments of wild type or mutant CYP2C9 were subcloned to PGEM®T4-vector (Promega) according to the protocol. The plasmids were used as standard wild type or mutant templates for the optimization of hybridization conditions and establishment of signal intensity ratio of match to mismatch after verification by sequencing. The artificial heterozygous templates were constructed by mixing equal amounts of wild type and mutant plasmid DNA. To introduce a mutant nucleotide at specific position in a DNA segment, site-directed mutagenesis method^[16] with mutant primers was used.

Preparation of DNA microarrays

The 3' end amino-modified probes were diluted to a final concentration of 20 μ mol/L in spotting solutions (3*SSC and 0.01 % SDS). The spotting solutions were transferred into 96-well plates in volumes of 10 μ L and spotted to aldehyde-coated glass slides with a microarray printer (Cartisan), which deposited 0.5 nL at each spotting site, resulting in spots of 200 μ m in diameter. Each probe was spotted in duplicate. The humidity during spotting was 70 % and the temperature was kept at 23 °C. After spotting, slides were incubated for another 1 h under the same conditions and stored at room temperature for at least 1 day before use. The pattern of slide and array format are shown in Figure 3.

Hybridization and signal detection

Two μ L of the single-stranded Cy3-labeled target PCR products was mixed with 10 μ L hybridization solution (5*SSC, 0.1 % SDS, 1 % salmon DNA), and the 12 μ L final volume was transferred to the hybridization area on the glass slide. The slide was incubated in 40 °C water bath for 30 min in a hybridization chamber. After incubation, the slide was washed sequentially in washing solution A (1*SSC, 0.2 % SDS), washing solution B (0.2*SSC) and washing solution C (0.1 *SSC) for 1 min each.

The glass slides were scanned using the confocal Scanarray 3 000 (GSI Lumonics), with excitation at 540 nm and emission at 570 nm (Cy3). Sixteen-bit TIFF images of 10 μ m resolution were analyzed. After subtraction of local background, the average signal intensity of the duplicate spots of each probe was used to calculate the signal ratios defining the genotypes.

Direct sequencing with PCR products

Part of the DNA samples was subjected to direct sequencing using DNA sequencer (CEQ™ 2000XL DNA analysis system, Beckman) to confirm the results. PCR reaction was carried out in 50 μ L solution and the PCR products were purified to be the sequencing templates with PCR products purification kit (Promega).

Statistical analysis

Statistics was made by χ^2 test.

RESULTS

Determination of the signal intensity ratio of match to mismatch

According to the hybridization result of standard wild type or mutant plasmid templates, under the optimized hybridization and stringent washing conditions, there was a great difference in signal intensities between the perfect match and the single base mismatch probes. The ratio of match to mismatch of signal pairs was above 4 at least. Detection of heterozygous alleles was a hard point for microarray. In the present study, the hybridization results of the heterozygous templates showed that the signal intensity ratio of the probe pair corresponding to heterozygous alleles was below 2.5 (the ratio was always

the stronger to the weaker). Typical results are shown in Figure 1. Repeated experiments with genomic DNA gave a statistically similar result (data not shown). So the ratio value above 4 or below 2.5 was considered sensible for genotype judgement while sample with the ratio value within 2.5-4 should be re-genotyped.

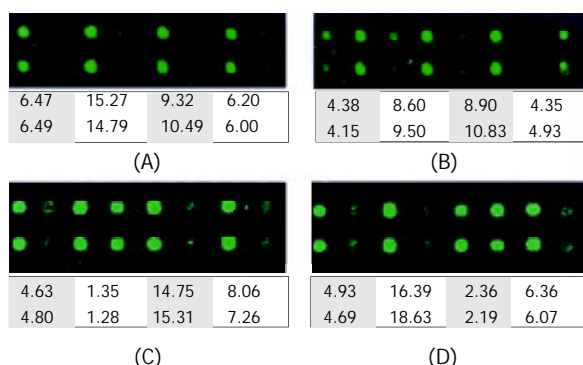


Figure 1 The TIF image of hybridization results of (A) wildtype template, (B) mutant template, (C) heterozygous template of CYP2C9*1/CYP2C9*3, and (D) heterozygous template of CYP2C9*1/CYP2C9*4. The discriminating power of a pair of probes was represented by the ratio of match to mismatch listed below.

Genotype results of 62 DNA samples by DNA microarray

In the genotype result of the 62 samples determined by the microarray, heterozygous alleles of CYP2C9*1/*3 were found in 7 out of 62 subjects. No heterozygous or homozygous mutant alleles of CYP2C9*2, *4 and *5 were detected. Repeated experiments gave the same result. A brief procedure is illustrated in Figure 2 and Figure 3.



Figure 2 2 % agarose gel electrophoresis of the PCR products of 10 samples. 1-10: PCR products of 10 DNA samples, M: DGL2000 marker.

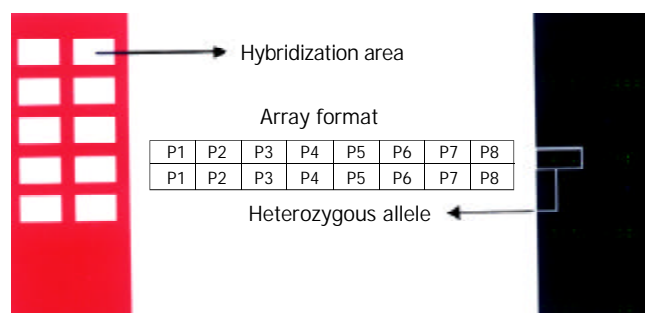


Figure 3 Array format and microarray hybridization result of 10 samples.

DNA samples genotyped by direct sequencing

To confirm the genotype result determined by microarray, the 7 heterozygous CYP2C9*1/*3 and 13 random wild type DNA samples were subjected to direct sequencing with purified PCR products. The same genotype results were obtained with the

20 DNA samples typed with two methods. The typical sequencing results of the heterozygous CYP2C9*1/*3 and wild type are compared in Figure 4.

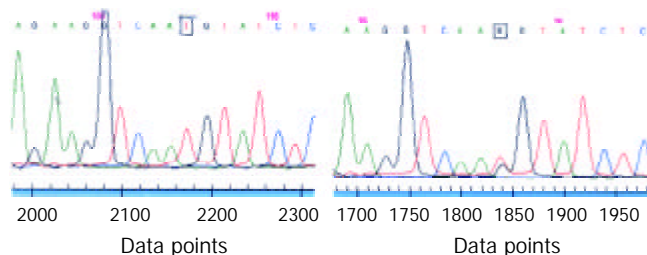


Figure 4 Part of the sequencing results. The letters in square indicate wildtype and heterozygous of CYP2C9*1/CYP2C9*3 (1075A-C) in two samples.

Allele frequency and effects of CYP2C9 polymorphism on therapeutic outcome of Irbesartan

The microarray described here is a reliable assay for detecting the CYP2C9 known alleles. The analysis of 62 HBP patients DNA samples yielded frequencies for CYP known alleles (Table 2) that were in agreement with previous study^[7,17,18]. There was no significant difference in the odd of effectiveness of Irbesartan between the wild type (normal) group and the CYP2C9*1/*3 (mutant) group (Table 3, P>0.05).

Table 2 CYP2C9 allele frequency in the study population

Allele	Number of alleles	Frequency %
*2	0/124	0
*3	7/124	5.6
*4	0/124	0
*5	0/124	0

Table 3 Therapeutic outcome of Irbesartan in wild type group and CYP2C9*1/*3 group

	Effective	Failed
Wild type	43	12
CYP2C9*1/*3	6	1

P>1 (χ² test), no significant difference in the odd of effectiveness of Irbesartan between wild type group and CYP2C9*1/*3 group.

DISCUSSION

Single nucleotide polymorphism (SNP) is the most common variation form in human genome^[19-21]. The early methods to type SNPs include SSCP, RFLP, AS-PCR, etc^[22-24], making genotyping judgement coupled with gel electrophoresis analysis. The methods above are unfit for a large scale screening due to the limitation of detection methods. With the advance of organic fluorescence labeling and detection technology, significant change has taken place in genotyping technology. Molecular beacon^[25], TaqMan^[26] probe methods, which detect fluorescence signal in homologous reaction, and DNA microarray^[27-29], which is based on hybridization coupled with solid phase reaction, make genotyping easier and more accurate. In the newly developed technologies, DNA microarray is more preferable in the genetic linkage and association study between large number of genetic markers and phenotypic traits in pharmacogenomics, disease genomics etc, due to its parallel detection of a large quantity of genetic markers.

Fluorescence-labeled sample preparation is a critical step in microarray genotyping. The quality and amount of genomic DNA used as template in PCR reaction are essential to the hybridization results. In the present study, the two target segments containing the SNP sites to be typed were PCR amplified in one tube. Asymmetric PCR method was used to generate single-stranded target segments complimentary to the probes.

The fluorescence signal intensity and discriminating power (ratio of match to mismatch) of the probe pairs are the key results from microarray for genotyping judgement, which can be affected by many factors. When other conditions (the quality and amount of single stranded PCR products, the quality of aldehyde-coated slides, hybridization/washing conditions, etc) are strictly controlled, the specific sequence context of the probes is the determining factor. Because there was no simultaneous mutation reported in the CYP2C9 known alleles, the probes were designed without consideration of crosslink of SNP sites of 1075A-C, 1076T-C, 1080C-G, any two of which were assumed normal when the other one was set as SNP site to be typed. The assumption reduced the number of probe to be designed and was confirmed by the genotyping result in the present study. Four pairs of probes were designed to discriminate the normal and the four mutant alleles. However, as an improvement to probe redundancy, all possible probe patterns should be fabricated. In probe design, the probes were chosen to have a common algorithmically calculated T_m value of 50±2 °C with length of 16-17 nt. Under the optimized hybridization/washing conditions, the P1/P2 and P7/P8 probe pairs had a less intense signal and discriminating power than the P3/P4 and P5/P6 pairs. The signal intensity ratio value above 4 or below 2.5 is considered a critical limit for genotype judgement. When the value fell into 2.5-4, the sample should be re-genotyped.

The allele frequency of CYP2C9 determined in this study was in accordance with the published data. Yoon YR *et al.*^[17] showed that there were no CYP2C9*2 (430C-T) allele in Asian population. Dickmann *et al.*^[18] found CYP2C9*5 (1080C-G) only in Black people. In the present study, heterozygous CYP2C9*1/*3 (1075A-C) were detected in 7 out of 62 unrelated Chinese. There were marked ethnic/geographic differences in the distribution of allelic variants of many DMEs^[30]. It is of obvious importance that such ethnic/geographic differences be taken into account in routine pharmacogenetic diagnosis or screening. Considering that it is challenging to optimize oligonucleotide probes to achieve global maximum discrimination of many genetic variants simultaneously, it is of importance to reduce the probe number to ensure the reproducibility and reliability of ASO hybridization based-microarray genotyping performance. For example, microarray for genotyping frequent SNP sites (>1 %) in DME-coding gene specific to Chinese should be made and applied in Chinese population.

There were no homozygous mutants detected in the studied population, and there may be other factors that affect the effectiveness of Irbesartan, such as the polymorphism in drug targets (ATIR), other potential mutation sites in CYP2C9, etc. The results of genotyping in this study suggest that there is no significant difference in the odd of effectiveness of Irbesartan between the wild type group and CYP2C9*1/*3 group. Provided that the heterozygous individuals have prolonged effective time, a better therapeutic outcome may be obtained as long as no additional side-effects occur.

REFERENCES

- Nebert DW**, Mckinnon RA, Puga A. Human drug-metabolizing enzyme polymorphism: effects on risk of toxicity and cancer. *DNA Cell Biol* 1996; **15**: 273-280
- Shi MM**, Bleavins MR, De La Iglesia FA. Pharmacogenetic application in drug development and clinical trials. *Drug Metabolism Disposition* 2001; **29**: 591-595
- Krynetski EY**, Evans WE. Genetic polymorphism of thiopurine S-methyltransferase: molecular mechanism and clinical importance. *Pharmacology* 2000; **61**: 136-146
- Cronin MT**, Pho M, Dutta D, Frueh F, Schwarcz L, Brennan T. Utilization of new technologies in drug trials and discovery. *Drug Metabolism Disposition* 2001; **29**: 586-590
- Shi MM**. Enabling large-scale pharmacogenetics studies by high-throughput mutation detection and genotyping technologies. *Clin Chem* 2001; **47**: 164-172
- Broude NE**, Woodward K, Cavallo R, Cantor CR, Englert D. DNA microarrays with stem-loop DNA probe: preparations and applications. *Nucleic Acids Research* 2001; **29**: E92
- Zhu GJ**, Yu YN, Li X, Qian YL. Cloning of cytochrome P-450 2C9 cDNA from human liver and its expression in CHL cells. *World J Gastroenterol* 2002; **8**: 318-322
- Cai L**, Yu SZ, Zhan ZF. Cytochrome P450 2E1 genetic polymorphism and gastric cancer in Changde, Fujian Province. *World J Gastroenterol* 2001; **7**: 792-795
- Cheng JW**. Cytochrome p450-mediated cardiovascular drug interactions. *Heart Dis* 2000; **2**: 254-258
- Aithal GP**, Day CP, Kesteven PJ, Daly AK. Association of polymorphisms in the cytochrome P450 CYP2C9 with warfarin dose requirement and risk of bleeding complications. *Lancet* 1999; **353**: 717-719
- Kidd RS**, Curry TB, Gallagher S, Edeki T, Blaisdell J, Goldstein JA. Identification of a null allele of CYP2C9 in an African-American exhibiting toxicity to phenytoin. *Pharmacogenetics* 2001; **11**: 803-808
- Goldstein JA**. Clinical relevance of genetic polymorphisms in the human CYP2C subfamily. *Br J Clin Pharmacol*. 2001; **52**: 349-355
- Timmermans PB**. Pharmacological properties of angiotensin II receptor antagonists. *Can J Cardio* 1999; **15**(Suppl. F): 26F-28F
- Graham MR**, Allcock NM. Irbesartan substitution for valsartan or losartan in treating hypertension. *Ann Pharmacother* 2002; **36**: 1840-1844
- Yasar U**, Tybring G, Hidestrand M, Oscarson M, Ingelman-Sundberg M, Dahl ML, Eliasson E. Role of CYP2C9 polymorphism in losartan oxidation. *Drug Metab Dispos* 2001; **29**: 1051-1056
- Li T**, Liang H, Yan F, Lu S. Site-directed mutagenesis of atrial natriuretic peptide gene and effect of the mutations on its diuretic activity in nephrotic rats. *Zhonghua Yixue Zazhi* 2002; **82**: 1324-1327
- Yoon YR**, Shon JH, Kim MK, Lim YC, Lee HR, Park JY, Cha JJ, Shin JG. Frequency of cytochrome P450 2C9 mutant alleles in a Korean population. *Br J Clin Pharmacol* 2001; **51**: 277-280
- Dickmann LJ**, Rettie AE, Kneller MB, Kim RB, Wood AJ, Stein CM. Identification and functional characterization of a new CYP2C9 variant (CYP2C9*5) expressed among African American. *Mol Pharmacol* 2001; **60**: 382-387
- Gu HF**. Single nucleotide polymorphisms (SNPs) and SNP databases. *Zhonghua Yixue Yichuanxue Zazhi* 2001; **18**: 479-481
- Kwok PY**. Methods for genotyping single nucleotide polymorphisms. *Annu Rev Genomics Hum Genet* 2001; **2**: 235-258
- Roses AD**. Pharmacogenetics. *Hum Mol Genet* 2001; **10**: 2261-2267
- Hsieh KP**, Lin YY, Cheng CL, Lai ML, Lin MS, Siest JP, Huang JD. Novel mutations of CYP3A4 in Chinese. *Drug Metab Dispos* 2001; **29**: 268-273
- Oda Y**, Kobayashi M, Ooi A, Muroishi Y, Nakanishi I. Genotypes of glutathione S-transferase M1 and N-acetyltransferase 2 in Japanese patients with gastric cancer. *Gastric Cancer* 1999; **2**: 158-164
- Hersberger M**, Marti-Jaun J, Rentsch K, Hanseler E. Rapid detection of the CYP2D6*3, CYP2D6*4, and CYP2D6*6 alleles by tetra-primer PCR and of the CYP2D6*5 allele by multiplex long PCR. *Clin Chem* 2000; **46**: 1072-1077
- Li JJ**, Geyer R, Tan W. Using molecular beacons as a sensitive fluorescence assay for enzymatic cleavage of single-stranded DNA. *Nucleic Acids Res* 2000; **28**: E52

- 26 **Kleiber J**, Walter T, Haberhausen G, Tsang S, Babel R, Rosenstraus M. Performance characteristics of a quantitative, homogeneous TaqMan RT-PCR test for HCV RNA. *J Mol Diagn* 2000; **2**: 158-166
- 27 **O'Meara D**, Ahmadian A, Odeberg J, Lundeberg J. SNP typing by apyrase-mediated allele-specific primer extension on DNA microarrays. *Nucleic Acids Res* 2002; **30**: e75
- 28 **Iwasaki H**, Ezura Y, Ishida R, Kajita M, Kodaira M, Knight J, Daniel S, Shi M, Emi M. Accuracy of genotyping for single nucleotide polymorphisms by a microarray-based single nucleotide polymorphism typing method involving hybridization of short allele-specific oligonucleotides. *DNA Res* 2002; **9**: 59-62
- 29 **Huber M**, Mundlein A, Dornstauder E, Schneeberger C, Tempfer CB, Mueller MW, Schmidt WM. Accessing single nucleotide polymorphisms in genomic DNA by direct multiplex polymerase chain reaction amplification on oligonucleotide microarrays. *Anal Biochem* 2002; **303**: 25-33
- 30 **Bertilsson L**. Geographical/interracial difference in polymorphic drug oxidation. *Clin. Pharmacokinet* 1995; **29**: 192-209

Edited by Pang LH

Identification of RanBMP interacting with *Shigella flexneri* IpaC invasin by two-hybrid system of yeast

Xiao Yao, Heng-Liang Wang, Zhao-Xing Shi, Xiao-Yu Yan, Er-Ling Feng, Bo-Lun Yang, Liu-Yu Huang

Xiao Yao, Bo-Lun Yang, College of Environmental and Chemical Engineering, Xi'an Jiaotong University, Xi'an 710049, Shaanxi Province, China

Heng-Liang Wang, Zhao-Xing Shi, Xiao-Yu Yan, Er-Ling Feng, Liu-Yu Huang, Beijing Institute of Biotechnology, Beijing 100071, China

Supported by Capital "248" Key Innovation Project (H010210360119) and State key Research and Development Project (G1999054103)

Correspondence to: Liu-Yu Huang, Beijing Institute of Biotechnology, 20 Dongdajie, Fengtai, Beijing 100071, China. huangly@nic.bmi.ac.cn

Telephone: +86-10-66948836 **Fax:** +86-10-63833521

Received: 2002-12-22 **Accepted:** 2003-01-14

Abstract

AIM: Bacillary dysentery caused by *Shigella flexneri* is still a threat to human health. Of four invasion plasmid antigen proteins (IpaA, B, C and D), IpaC plays an important role in the pathogenicity of this pathogen. The purpose of this study was to investigate the proteins interacting with IpaC in the host cell during the pathogenic process of this disease.

METHODS: By applying two-hybrid system, the bait plasmid containing *ipaC* gene was constructed and designated pGBKT-*ipaC*. The bait plasmid was transformed AH109, and proved to express IpaC and then HeLa cDNA library plasmids were introduced into the above transformed AH109. The transformation mixture was plated on medium lacking Trp, Leu, and His in the initial screen, then restreaked on medium lacking Trp, Leu, His and Ade. Colonies growing on the selection medium were further assayed for β -galactosidase activity. BLAST was carried out in the database after sequencing the inserted cDNA of the positive library plasmid.

RESULTS: Among the 2×10^6 transformants, 64 positive clones were obtained as determined by activation of His, Ade and LacZ reporter genes. Sequence analysis revealed that cDNA inserts of two colonies were highly homologous to a known human protein, RanBPM.

CONCLUSION: These results provide evidence that IpaC may be involved in the invasion process of *S. flexneri* by interacting with RanBPM, and RanBPM is most likely to be the downstream target of IpaC in the cascade events of *S. flexneri* infection.

Yao X, Wang HL, Shi ZX, Yan XY, Feng EL, Yang BL, Huang LY. Identification of RanBMP interacting with *Shigella flexneri* IpaC invasin by two-hybrid system of yeast. *World J Gastroenterol* 2003; 9(6): 1347-1351

<http://www.wjgnet.com/1007-9327/9/1347.asp>

INTRODUCTION

Shigella is a Gram-negative bacterium responsible for intestinal diseases ranging from mild watery diarrhea to bacillary

dysentery in humans. The severe forms of shigellosis are due to colonization and destruction of the colonic mucosa by this invasive pathogen. The infectious potential of *Shigella* is very high, since as few as 100 microorganisms administered orally are sufficient to cause dysentery in volunteers. Each year, at least a billion cases of diarrheal diseases account for about three million deaths. In the developing world, children under 5 years of age are the most susceptible victims, with over half a million deaths occurred annually worldwide^[1].

The phenotype which is essential to the pathogenicity of *S. flexneri* is encoded by a 31kb sequence^[2,3] located on the 200kb large virulence plasmid^[4,5]. One locus in this fragment, composed of the *ipa* operon (invasion plasmid antigen), is necessary to encode and secrete the effectors, the Ipa proteins or invasins. The *ipa* operon encodes four secreted proteins: IpaB(62kDa), IpaC(42kDa), IpaD(37kDa) and IpaA(70kDa), which elicit the formation of the entry focus via localized actin polymerization^[6]. The Ipa proteins are rapidly secreted from *S. flexneri* when the bacterium comes into contact with epithelial cells^[7-10]. Following their secretion, IpaB and IpaC are found as part of a protein complex and this complex is absolutely required for entry into epithelial cells^[7,11,12]. Latex beads coated with anti-IpaC antibodies have been used to recover the extracellular Ipa complex containing IpaB and IpaC, and were shown to be internalized in HeLa cells through the formation of membrane ruffles similar to those induced upon bacterial entry^[13]. These results have led to the proposal that IpaB and IpaC play major roles in the entry of *shigella* into epithelial cells.

Although IpaB is undoubtedly important for *S. flexneri* invasion^[14-17], a great deal of foci were shifted to IpaC as a potential effector of *S. flexneri* invasion when purified IpaB was shown not to possess *in vitro* membranolytic activity^[11], and purified IpaC was demonstrated to have such activities consistent with its contribution to invasion^[18]. Effector-related functions that have been demonstrated for purified IpaC include: enhanced invasion of cultured cells by *S. flexneri* at nanomolar IpaC concentrations^[16,19]; induced uptake of virulence plasmid-cured at micromolar IpaC concentrations^[24]; association with model phospholipid membranes^[16,21]; and triggering of cytoskeletal changes in cultured cells^[22,27]. Additional activities associated with IpaC also include *in vitro* reconstitution into complexes with IpaB, which may promote the uptake of non-invasive strains of *Escherichia coli*^[12, 19].

Shigellosis provides a model to study how a pathogenic microorganism can subvert an integrated defense barrier and interact with the host cells, which in turn facilitates invasion at the early stage of the process. A major challenge is to understand the role of Ipa proteins in entry into epithelial cells. In order to investigate the mechanism of IpaC in the entry process, two-hybrid system was exploited to identify the proteins in host cells that interacted with IpaC invasin.

MATERIALS AND METHODS

Materials

The strains and plasmids used in this study are listed in Table 1.

Table 1 Strains and plasmids

	Relevant characteristics	Source
Strains		
<i>S. flexneri</i> 2a, 2 457T	Wild type, Nal ^r	Maurelli AT
<i>E. coli</i> DH5 α	SupE44, Δ lacU169 (ϕ 80 lacZ Δ M15), hsdR17, recA1, endA1, gyrA96, thi-1, relA1, Nal ^r	Our lab
<i>S. cerevisiae</i> AH109	MATa, trp1-901, leu2-3, ura3-52, his3-200, gal4 Δ , gal80 Δ , LYS2::GAL1 _{UAS} -GAL1 _{TATA} -HIS3, GAL2 _{UAS} -GAL2 _{TATA} -ADE2, URA3::MEL1 _{UAS} -MEL1 _{TATA} -LacZ	Clontech
Plasmids		
pGBKT7	GAL4 DNA-BD, TRP1, c-Myc epitope tag, Km ^r	Clontech
pGBKT- <i>ipaC</i>	GAL4 DNA-BD fusion of <i>IpaC</i> , TRP1, c-Myc epitope tag, Km ^r	This study
pACT2	GAL4 DNA-AD, HA epitope, LEU2, Ap ^r	Clontech
pLAM5 ⁻ -1	GAL4 DNA-BD fusion of the human lamin C, TRP1, a false-positive detection plasmid, Ap ^r	Clontech
p1	A positive library plasmid	This study

Human HeLa MATCHMAKER cDNA library (HL4048AH), c-Myc monoclonal antibody, YPD medium, minimal SD base and DO supplement medium were purchased from Clontech. Peroxidase-conjugated goat anti-mouse IgG was from Santa Cruz. Mini- and Megapreps plasmid kits were obtained from Promega. Restriction endonucleases and T4 DNA ligase were purchased from New England Biolabs. Taq DNA polymerase, deoxyribonucleotides, and PCR fragment recovery kit were from TaKaRa. Primers for the 5' and 3' ends of *ipaC* gene, P1 and P2, were synthesized in our lab.

Methods

Growth and maintenance of strains *Shigella flexneri* 2a was grown at 37 °C with constant stirring in trypticase soy broth (TSB). Prior to use, the bacteria were streaked onto trypticase soy agar (TSA) containing 0.025 % Congo red so that colonies binding the dye could be selected. Bacteria that had lost the invasion plasmid were not able to bind this dye and thus appeared white in the presence of Congo red. Yeast strain AH109 was grown at 30 °C with vigorous shaking in YPAD. Antibiotics were used at the following concentrations: ampicillin (Ap), 100 mg · L⁻¹; kanamycin (Km), 50 mg · L⁻¹; nalidixic acid (Nal), 40 mg · L⁻¹.

Construction of bait plasmid Isolation of plasmid and all other molecular biology procedures were carried out according to the standard published procedures^[22]. *ipaC* gene was amplified by PCR in a standard 100- μ l reaction containing 2.5 mM MgCl₂, 0.25 mM of each dNTP, 100 pmol of P1 and P2 primers, 10 μ l boiled *S. flexneri*, and 5U Taq DNA polymerase. Reactions were allowed to proceed in a Perkin-Elmer 2400 thermal cycler programmed for 30 cycles (94 °C, 30 s; 56 °C, 30 s; and 72 °C, 90 s) with one additional cycle for 7 min at 72 °C. PCR product was purified by agarose gel electrophoresis, digested by NcoI and SalI, then ligated into the pGBKT7 plasmid digested by NcoI and SalI. The ligation products were then transformed into *E. coli* DH5 α . The insert of *ipaC* gene was then confirmed by PCR using the conditions described above. To confirm if the *ipaC* gene was fused in frame to the coding sequence of the GAL4 DNA-binding domain, the plasmids were subjected to double-stranded DNA sequencing with T7 sequencing primer according to the manufacturer's specifications.

Yeast transformation The lithium acetate (LiAc)-mediated method was performed to transform DNA into yeast as described in the reference^[23]. In brief, the yeast competent cells were prepared and suspended in a LiAc solution with the plasmids DNA to be transformed, along with excess carrier DNA. Polyethylene glycol (PEG) with an appropriate amount of LiAc was then added and the mixture of DNA and yeast was incubated at 30 °C. After incubation, DMSO was added and the cells were heat shocked at 42 °C. The cells were then

plated on the appropriate medium to select transformants. The amount of plasmids used for transformation was 0.1 μ g except that 50 μ g library plasmid was used.

SDS-PAGE and western blot analysis Extraction of yeast protein sample was carried out by using urea/SDS method as described in reference^[24]. SDS-PAGE was performed using the standard procedure of Laemmli^[22]. The samples were resolved on a 12 % polyacrylamide gel. The samples could be stained with Coomassie brilliant blue R250, or the proteins electroblotted to NC membranes for western blot analysis using a Bio-Rad Transblot Semi-dry Blotter according to the manufacturer's instructions. Western blot analysis was performed as previously described^[22,25]. Briefly, the membranes were blocked following protein transfer by incubation in TBS (50 mM Tris-HCl pH7.4, 5 % BSA, 500 mM NaCl) and then incubated with c-Myc monoclonal antibody diluted in TBS containing 0.1 % Tween 20 (v/v). After several rinses in the same buffer, the membrane was incubated with HRP-conjugated secondary antibody in the same buffer. The membrane was then rinsed in TBS containing 10 mM EDTA, 0.5 M NaCl, and 0.1 % Tween 20 (w/v). Blots were developed using TBS (50 mM Tris-HCl pH7.4, 5 % BSA, 500 mM NaCl) containing 0.7 mg/ml 3,3'-diaminobenzidine (DAB) and 0.003 % H₂O₂, finally terminated with 2M H₂SO₄.

Two-hybrid strategy Before the screening process, intrinsic activation function of the bait was tested as demonstrated by a bait-testing assay. To perform the two-hybrid screening, the bait plasmid pGBKT-*ipaC* was transformed into the yeast strain AH109. The HeLa cDNA libraries were extracted from *E. coli* and introduced into the AH109 transformed with the bait. Cells were first spread on plates lacking Leu, Trp and His, and containing 1mM 3-aminotriazole to select colonies by prototrophy for histidine. The His⁺ colonies were streaked on selective plates lacking Leu, Trp, His and Ade. The His⁺, Ade⁺ colonies were assayed for expression of β -galactosidase by an X-Gal overlay assay, and blue colonies were streaked twice on selective plates. After that, individual His⁺, Ade⁺, LacZ⁺ colonies were cultured in liquid SD synthetic medium. Yeast DNA was recovered and transformed into *E. coli* DH5 α by electroporation. The insert carried by the prey plasmid in each of the selected clones was amplified by PCR and grouped. Representative plasmids from each group were retransformed back into yeast to test their interaction with *IpaC*. The cDNA inserts were subjected to sequencing.

RESULTS

Construction of bait plasmid

PCR primers for the 5' and 3' ends of *ipaC* gene were designed as follows based on its published sequences^[26]: P1, 5' -

CGGCCATGGTAATAGAAGCTGATGTTGC-3' containing an *NcoI* restriction site and 18 bases of the 5' end of *ipaC* gene; and P2, 5' -GCGTCCGACTTAAGCTCGAATGTTAC-3' containing a *Sall* restriction site and 18 bases of the 3' end of *ipaC* gene. After amplification of *ipaC* gene by PCR, there was a band of about 1.1kb by agarose gel electrophoresis (data not shown). The fragment was purified, digested by *NcoI* and *Sall*, and cloned into the *NcoI* and *Sall* sites of pGBKT7. The resulting plasmid was designated as pGBKT-*ipaC* (Figure 1). Sequencing revealed that the *ipaC* gene was fused in the correct reading frame with the coding sequence of GAL4 DNA-binding domain (data not shown).

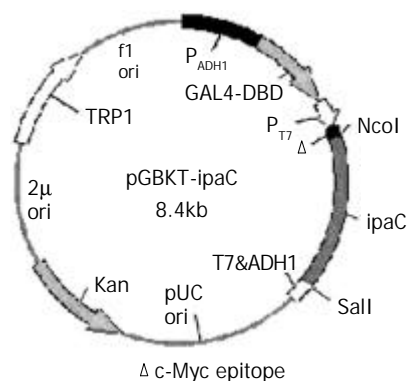


Figure 1 Construction of recombinant plasmid expressing IpaC.

Expression of *IpaC* in yeast

SDS-PAGE and western blotting were carried out with the protein extracted from yeast AH109, AH109 transformed with pGBKT7 and pGBKT-*ipaC* (Figure 2). An approximate 20kDa GAL4 DNA binding domain containing c-Myc epitope tag was expressed in AH109 transformed with pGBKT7, while a 62kDa peptide was expressed in AH109 transformed with pGBKT-*ipaC*. This showed that IpaC could be expressed in frame with the GAL4 DNA binding domain and the bait plasmid could be used in two-hybrid screening.

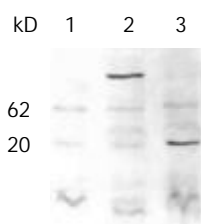


Figure 2 Western blot analysis of the fused expression of IpaC with c-Myc monoclonal antibody as a primary antibody. Lane 1, AH109; lane 2, AH109 transformed with pGBKT-*ipaC*; lane 3, AH109 transformed with pGBKT7.

Two-hybrid screening

In order to identify whether the fused bait protein could activate the expression of reporter genes, yeast containing the bait plasmid (pGBKT-*ipaC*) and yeast containing the empty vector of library (pACT2) were tested as demonstrated by a bait-testing assay (Table 2). The results indicated that IpaC was devoid of transcriptional activity and could be used as bait in a yeast two-hybrid assay.

The bait plasmid and cDNA library were sequentially transformed into yeast strain AH109. Initial screening of 2×10^6 colonies of a human HeLa MATCHMAKER cDNA library identified 92 clones that showed specific activation of His reporter gene. Further testing of the specificity of interaction

screening on selective media lack of Trp, Leu, His, Ade and by β -galactosidase assay showed that only 64 colonies interacted specifically with the bait BD-IpaC protein, but not with fusion proteins between BD and human lamin C (Table 3).

Table 2 Detection of transcriptional activity of bait fusion protein in AH109

Transformed plasmids	Growth on SD His ⁻	X-Gal
pGBKT- <i>ipaC</i>	-	white
pGBKT- <i>ipaC</i> + pACT2	-	white

Table 3 Verification of the interaction in positive clones

Transformed plasmids	β -Gal activity
1 p1	white
2 p1 + pGBKT7	white
3 p1 + pLAM5' -1	white
4 p1 + pGBKT- <i>ipaC</i>	blue

Sequence analysis of the clones revealed that two independent colonies (p1 and p25) contained the same gene. A database search using the BLAST program showed that this gene encoded the protein which had as much as 99 % homology with RanBPM (GenBank accession number AB055311). The two library colonies isolated from the yeast-two hybrid assay contained amino acid sequences that were upstream of the BPM55 start codon, but were within the coding region of BPM90. The resulting product of p1 contained 584 C-terminal amino acids of RanBPM, which fused in the frame with the GAL4 activation domain.

DISCUSSION

An important step in *S. flexneri* infection is bacterial invasion of colonic epithelial cells, as characterized by host cytoskeletal rearrangements at the site of bacterial contact^[27]. These localized changes in the host cytoskeleton lead to the formation of filopodia that combine and trap the pathogen within a membrane-bound vacuole that is rapidly lysed, thereby providing the bacterium with access to the host cell cytoplasm^[6]. Evidence indicates that IpaC is necessary and sufficient to promote the formation of filopodial extensions localized at the edge of fibroblastic cells^[21]. These extensions appear within seconds after exposure of permeabilized cells to IpaC. The data presented above and those from other laboratories indicate that IpaC proteins play an important role in this process.

Current understanding of the role of *S. flexneri* Ipa proteins in epithelial cell invasion is primarily based on deletion mutagenesis, genetic complementation, and immunological analyses^[12-14,28,29]. To better understand the roles of the Ipa proteins in the pathogenesis of shigellosis, it is necessary to isolate proteins that interact with Ipa proteins in host cells. The two-hybrid system is an effective genetic method to identify protein-protein interaction and has been increasingly used^[30,31]. Therefore, we exploited a two-hybrid screen to identify the IpaC-interacting protein in host cells. The foci of infection of this pathogen are human colonic epithelial cells, so a library prepared from them should be used in our screening. Unfortunately, it is not commercially available. The mechanism of entry of *Shigella* into cells has been studied extensively in cultured cell lines. Of these cell lines, HeLa was derived from human epithelial cells and has been frequently used in the invasion of *S. flexneri*^[32-35]. Therefore a HeLa cDNA library was used instead in our screening. Two library colonies that were isolated in the yeast-two hybrid assay contained amino

acid sequences with high homology to RanBPM.

RanBPM was originally identified by its interaction with Ran, a small Ras-like GTPase. Ran shuttles between the nucleus and the cytoplasm to complete its GTPase cycle, carrying out nucleocytoplasmic transport of macromolecules and inducing microtubule self-assembly by interacting with distinct Ran binding protein^[36,37]. RanBPM was initially identified as a 55kD protein (BPM55) which contains 500 amino acids^[37]. A subsequent report has shown that BPM55 is a truncated protein and the full-sized RanBPM is a 90kD protein (BPM90) which contains 729 amino acids^[38]. Here we demonstrated that the function domain within BPM90 was able to interact with IpaC *in vivo*. RanBPM was predominantly localized both in the nucleus and in the cytoplasmic region surrounding the centrosome^[38]. When truncated RanBPM was overexpressed in green monkey kidney COS7 cells, the multiple spots which were colocalized with γ -tubulin were formed and acted as ectopic microtubule nucleation sites, resulting in a reorganization of microtubule network^[37]. The function of BPM90 is still unclear, but it has recently been linked to the Ras/Erk signaling pathway^[39].

Actin filaments and microtubule (MT) arrays have been regarded as constituting separate cytoskeletal systems with distinct functions. However, it has become clear that the cell's system of cytoskeletal filaments and its network of signaling pathways are intimately linked and function cooperatively to generate a cell phenotype tailored to the immediate conditions of the cell^[40]. When a signal occurs, the structural responses driven by the cytoskeleton are usually complex, such as establishing new axes of polarity, making and breaking contacts, moving or dividing, especially generating protrusions as observed in the entry process of *S. flexneri*.

Taken the data presented above together, we therefore become greatly interested in possible involvement of IpaC in the signaling cascade resulting in massive cytoskeletal rearrangements (Figure 3).

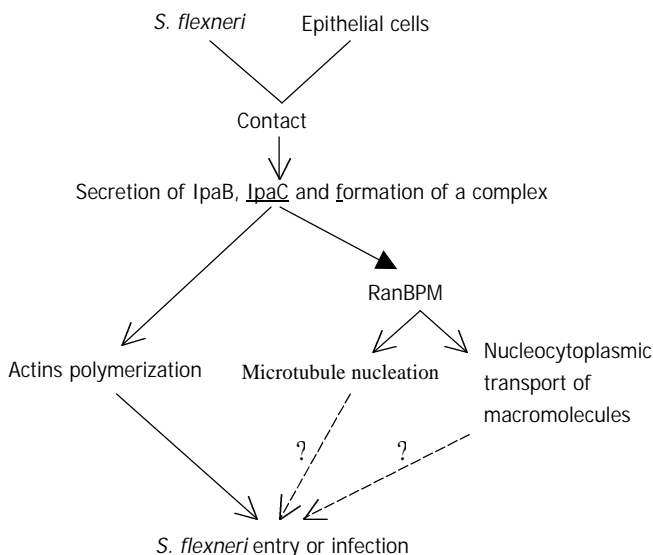


Figure 3 A schematic diagram of possible IpaC signaling cascade in *S. flexneri* entry.

The early step of infection is the invasion of epithelial cells of the colon. As bacteria contact the cell surface, Ipa invasins are secreted through the specialized secretory apparatus, two of which (IpaB and IpaC) form a complex. IpaC has hydrophobic regions that form transmembrane helices and insert into cell membrane^[41]. This complex constitutes the primary effector of *Shigella* entry and is able to activate entry via its interaction with the host cell membrane. Then IpaC stimulates localized accumulation of filamentous actin at the site of bacterial contact. Meanwhile IpaC also leads to

microtubule nucleation and/or nucleocytoplasmic transport of macromolecules possibly by interacting with RanBPM. So it is likely that IpaC elicits major rearrangements of host cell cytoskeleton, and these cytoskeletal filaments function cooperatively and form bundles supporting the membrane projections which achieve bacterial entry. Both the pathogen and the host cell actively contribute to this process.

This is the first report that IpaC interacts with RanBPM identified by two-hybrid screening. This information provides an important step in studying the protein-protein interaction that occurs in the host cells during initiation of *Shigella* pathogenesis. Although our understanding of the mechanisms that govern *Shigella* entry and actin-based intracellular motility has improved at a considerable pace, many questions remain open. In particular, it will be interesting to establish various connections between signaling pathways involved in *Shigella* entry and responses linked to the ipa proteins. Understanding how these responses integrate together and act in a concerted manner to induce bacterial entry will represent another exciting field of investigations.

ACKNOWLEDGMENTS

We would like to thank Prof. Qi-Nong Ye for his technical assistance and helpful discussions. We also thank Prof. Jian-Guang Zhou, Dr. Hao Zhang for their support in this project. We acknowledge the technical assistance of De-Hui He, Kun Hu and Zhi-Yong Gao.

REFERENCES

- Lindberg AA, Pal T. Strategies for development of potential candidate *Shigella* vaccine. *Vaccine* 1993; **11**: 168-179
- Maurelli AT, Baudry B, d' Hauteville H, Hale TL, Sansonetti PJ. Cloning of plasmid DNA sequences involved in invasion of HeLa cells by *Shigella flexneri* *Infect Immun* 1985; **49**: 164-171
- Sasakawa C, Kamata K, Sakai T, Makino S, Yamada M, Okada N, Yoshikawa M. Virulence-associated genetic regions comprising 31 kilobases of the 230-kilobase plasmid in *Shigella flexneri* 2a. *J Bacteriol* 1988; **170**: 2480-2484
- Sansonetti PJ, Kopecko DJ, Formal SB. Involvement of a large plasmid in the invasive ability of *Shigella flexneri*. *Infect Immun* 1987; **55**: 2681-2688
- Sansonetti PJ, Hale TL, Dammin GJ, Kapfer C, Collins HH Jr, Formal SB. Alterations in the pathogenicity of *Escherichia coli* K-12 after transfer of plasmid and chromosomal genes from *Shigella flexneri*. *Infect Immun* 1983; **39**: 1392-1402
- Clerc P, Sansonetti PJ. Entry of *Shigella flexneri* into HeLa cells: evidence for directed phagocytosis involving actin polymerization and myosin accumulation. *Infect Immun* 1987; **55**: 2681-2688
- Parsot C, Menard R, Gounon P, Sansonetti PJ. Enhanced secretion through the *Shigella flexneri* Mxi-Spa translocon leads to assembly of extracellular proteins into macromolecular structures. *Mol Microbiol* 1995; **16**: 291-300
- Watarai M, Tobe T, Yoshikawa M, Sasakawa C. Contact of *Shigella* with host cells triggers release of Ipa invasins and is an essential function of invasiveness. *EMBO J* 1995; **14**: 2461-2470
- Menard R, Sansonetti P, Parsot C. The secretion of the *Shigella flexneri* Ipa invasins is activated by epithelial cells and controlled by IpaB and IpaD. *EMBO J* 1994; **13**: 5293-5302
- Watarai M, Tobe T, Yoshikawa M, Sasakawa C. Disulfide oxidoreductase activity of *Shigella flexneri* is required for release of Ipa proteins and invasion of epithelial cells. *Proc Natl Acad Sci USA* 1995; **92**: 4927-4931
- Menard R, Sansonetti P, Parsot C, Vasselon T. Extracellular association and cytoplasmic partitioning of the IpaB and IpaC invasins of *S. flexneri*. *Cell* 1994; **79**: 515-525
- Menard R, Prevost MC, Gounon P, Sansonetti P, Dehio C. The secreted Ipa complex of shigella flexneri promotes entry into mammalian cells. *Proc Natl Acad Sci USA* 1996; **93**: 1254-1258
- Menard R, Sansonetti PJ, Parsot C. Nonpolar mutagenesis of the ipa genes defines IpaB, IpaC and IpaD as effectors of *Shigella*

- flexneri* entry into epithelial cells. *J Bacteriol* 1993; **175**: 5899-5906
- 14 **High N**, Mounier J, Prevost MC, Sansonetti PJ. IpaB of *Shigella flexneri* causes entry into epithelial cells and escape from the phagocytic vacuole. *EMBO J* 1992; **11**: 1991-1999
- 15 **Skoudy A**, Mounier J, Aruffo A, Ohayon H, Gounon P, Sansonetti P, Tran Van Nhieu G. CD44 binds to the *Shigella* IpaB protein and participates in bacterial invasion of epithelial cells. *Cell Microbiol* 2000; **2**: 19-33
- 16 **Tran N**, Serfis AB, Davis R, Osiecki JC, Coye L, Picking WL, Picking WD. Interaction of *Shigella flexneri* IpaC with model membranes correlate with effects on cultured cells. *Infect Immun* 2000; **68**: 3710-3715
- 17 **Tran Van Nhieu G**, Bourdet-Sicard R, Dumenil G, Blocker A, Sansonetti PJ. Bacterial signals and cell responses during *Shigella* entry into epithelial cells. *Cell Microbiol* 2000; **2**: 187-193
- 18 **Marquart ME**, Picking WL, Picking WD. Soluble invasion plasmid antigen C (IpaC) from *Shigella flexneri* elicits epithelial cell responses related to pathogen invasion. *Infect Immun* 1996; **64**: 4182-4187
- 19 **Davis R**, Marquart ME, Lucius D, Picking WD. Protein-protein interactions in the assembly of *Shigella flexneri* invasion plasmid antigens IpaB and IpaC into protein complexes. *Biochim Biophys Acta* 1998; **1429**: 45-56
- 20 **De Geyter C**, Vogt B, Benjelloun-Touimi Z, Sansonetti PJ, Ruyschaert JM, Parsot C, Cabiaux V. Purification of IpaC, a protein involved in entry of *Shigella flexneri* into epithelial cells and characterization of its interaction with lipid membranes. *FEBS Lett* 1997; **400**: 149-154
- 21 **Tran Van Nhieu G**, Caron E, Hall A, Sansonetti PJ. IpaC induces actin polymerization and filopodia formation during *Shigella* entry into epithelial cell. *EMBO J* 1999; **18**: 3249-3262
- 22 **Sambrook J**, Fritsch EF, Maniatis T. Molecular cloning: a laboratory manual. 2nd ed. New York: Cold Spring Harbour Press 1989
- 23 **Gietz D**, St Jean A, Woods RA, Schiestl RH. Improved method for high efficiency transformation of intact yeast cells. *Nucleic Acids Res* 1992; **20**: 1425
- 24 **Printen JA**, Sprague GF. Jr. Protein-protein interactions in the yeast pheromone response pathway: Ste5p interacts with all members of the MAP kinase cascade. *Genetics* 1994; **138**: 609-619
- 25 **Burnette WN**. "West blotting": electrophoretic transfer of proteins from SDS-PAGE to unmodified nitrocellulose and radiographic detection with antibody and radiiodinated protein A. *Anal Biochem* 1981; **112**: 195-203
- 26 **Venkatesan MM**, Buysse JM, Kopecko DJ. Characterization of invasion plasmid antigen genes (ipaBCD) from *Shigella flexneri*. *Proc Natl Acad Sci USA* 1988; **85**: 9317-9321
- 27 **LaBrec EH**, Schneider H, Magnani TJ, Formal SB. Epithelial cell penetration as an essential step in the pathogenesis of bacillary dysentery. *J Bacteriol* 1988; **88**: 1503-1518
- 28 **Sasakakawa C**, Komatsu K, Tobe T, Suzuki T, Yoshikawa M. Eight genes in region 5 that form an operon are essential for invasion of epithelial cells by *Shigella flexneri* 2a. *J Bacteriol* 1993; **175**: 2334-2346
- 29 **Mills JA**, Buysse JM, Oaks EV. *Shigella flexneri* invasion plasmid antigens B and C: Epitope location and characterization with monoclonal antibodies. *Infect Immun* 1988; **56**: 2933-2941
- 30 **Fields S**, Sternglanz R. The two-hybrid system: an assay for protein-protein interactions. *Trends Genet* 1994; **10**: 286-292
- 31 **Li K**, Wang L, Cheng J, Zhang LX, Duan HJ, Lu YY, Yang JZ, Liu Y, Hong Y, Xia XB, Wang G, Dong J, Li L, Zhong YW, Chen JM. Screening and cloning of gene of hepatocyte protein 1 interacting with HCV core protein. *Shijie huaren xiaohua zazhi* 2001; **9**: 1379-1383
- 32 **Skoudy A**, Nhieu GT, Mantis N, Arpin M, Mounier J, Gounon P, Sansonetti P. A functional role for ezrin during *Shigella flexneri* entry into epithelial cells. *J Cell Sci* 1999; **112** (Pt 13): 2059-2068
- 33 **Tran Van Nhieu G**, Ben-Ze'ev A, Sansonetti PJ. Modulation of bacterial entry into epithelial cells by association between vinculin and the *Shigella* IpaA invasin. *EMBO J* 1997; **16**: 2717-2729
- 34 **Pal T**, Hale TL. Plasmid-associated adherence of *Shigella flexneri* in a HeLa cell model. *Infect Immun* 1989; **57**: 2580-2582
- 35 **Zhong QP**. Pathogenic effects of O-polysaccharide from *Shigella flexneri* strain. *World J Gastroenterol* 1999; **5**: 245-248
- 36 **Bischoff FR**, Ponstingl H. Mitotic regulator protein RCC1 is complexed with a nuclear ras-related polypeptide. *Proc Natl Acad Sci USA* 1991; **88**: 10830-10834
- 37 **Nakamura M**, Masuda H, Horii J, Kuma K, Yokoyama N, Ohba T, Nishitani H, Miyata T, Tanaka M, Nishimoto T. When overexpressed, a novel centrosomal protein, RanBPM, causes ectopic microtubule nucleation similar to gamma-tubulin. *J Cell Biol* 1998; **143**: 1041-1052
- 38 **Nishitani H**, Hirose E, Uchimura Y, Nakamura M, Umeda M, Nishii K, Mori N, Nishimoto T. Full-sized RanBPM cDNA encodes a protein possessing a long stretch of proline and glutamine within the N-terminal region, comprising a large protein complex. *Gene* 2001; **272**: 25-33
- 39 **Wang D**, Li Z, Messing EM, Wu G. Activation of Ras/Erk pathway by a novel MET-interaction protein RanBPM. *J Biol Chem* 2002; **277**: 36216-36222
- 40 **Hollenbeck P**. Cytoskeleton: microtubules get the signal. *Curr Biol* 2001; **11**: R820-823
- 41 **Blocker A**, Gounon P, Larquet E, Niebuhr K, Cabiaux V, Parsot C, Sansonetti P. The tripartite type III secretion of *Shigella flexneri* inserts IpaB and IpaC into host membranes. *J Cell Biol* 1999; **147**: 683-693

Construction and expression of a humanized M₂ autoantigen trimer and its application in the diagnosis of primary biliary cirrhosis

Xiao-Hua Jiang, Ren-Qian Zhong, Sheng-Qian Yu, Yin Hu, Weng-Weng Li, Xian-Tao Kong

Xiao-Hua Jiang, Department of Laboratory Medicine, 85 Hospital the Chinese PLA, Shanghai 200052, China

Ren-Qian Zhong, Weng-Weng Li, Xian-Tao Kong, Clinical Immunology Center of the Chinese PLA, Changzheng Hospital, Second Military Medical University, Shanghai 200003, China

Sheng-Qian Yu, Department of Nephrology, Changzheng Hospital, Second Military Medical University, Shanghai 200003, China

Yin Hu, Department of Basic Science, Shanghai University of Engineering Science, Shanghai 200335, China

Correspondence to: Dr Xiao-Hua Jiang, Department of Laboratory Medicine, 85 Hospital of the Chinese PLA, Huashan Road, Shanghai 200052, China. jhlulu@citiz.net

Telephone: +86-21-62528805 **Fax:** +86-21-33110236

Received: 2002-07-18 **Accepted:** 2002-08-07

Abstract

AIM: To construct and express a humanized M₂ autoantigen trimer designated as BPO and to apply it in the diagnosis of primary biliary cirrhosis (PBC).

METHODS: cDNA fragments encoding M₂-reactive epitopes of pyruvate dehydrogenase complex E₂ (PDC-E₂), branched chain 2-oxo-acid dehydrogenase complex E₂ (BCOADC-E₂) and 2-oxo-glutarate dehydrogenase complex E₂ (OGDC-E₂) were amplified with PCR using total RNA extracted from human peripheral mononuclear blood cells. The fragments were cloned into the plasmid vector pQE-30 and then transferred into *E. coli* M15 (pREP4) for expression, which was induced by isopropylthio-β-D-galactoside. The expressed recombinant BPO protein was demonstrated by SDS-PAGE, Western-blotting and Immunoabsorption test, its antigenic reactivity and specificity were identified with seven M₂-positive sera confirmed at Euroimmun Research Center (Germany). Using the purified BPO, M₂ antibodies in sera from patients with PBC and other liver related diseases were detected with ELISA.

RESULTS: The expressed BPO was observed with both antigenic reactivity and specificity of M₂ autoantigens. The determination of M₂ antibodies by BPO with ELISA was more sensitive than using the Euroimmun's kit with the coefficients of variation less than 10 % in both interassay and intraassay. With the newly established method, M₂ antibodies were found in 100 % (20/20) of patients with PBC. Six cases of liver disease with unknown etiology and 1 patient with drug induced liver injury had detectable levels of serum M₂ antibodies. There were also 2 patients with autoimmune cholangitis and 1 with autoimmune hepatitis showing M₂-antibody positive.

CONCLUSION: Compared with the routine immunofluorescence assay and commercially available assay kit using porcine heart mitochondrial protein as the antigen, the detection system established in the present study shows higher sensitivity and specificity and may be used as a powerful tool for the diagnosis of PBC.

Jiang XH, Zhong RQ, Yu SQ, Hu Y, Li WW, Kong XT. Construction and expression of a humanized M₂ autoantigen trimer and its application in the diagnosis of primary biliary cirrhosis. *World J Gastroenterol* 2003; 9(6): 1352-1355

<http://www.wjgnet.com/1007-9327/9/1352.asp>

INTRODUCTION

Primary biliary cirrhosis (PBC) is a chronically progressive cholestatic liver disease with autoimmune basis. According to some reports, the incidence of this disease has been consistently increased in recent years^[1-4]. One of the remarkable features of PBC is the appearance of high titre antimitochondrial antibodies (AMA) in the patient's sera. Generally, these antibodies are categorized into nine subgroups termed M₁-M₉ according to the antigens they recognize, in which only M₂ antibodies are considered specific for PBC patients that are detectable years or decades before the clinical and histological diagnosis^[5-11].

The major autoantigens recognized by M₂ antibodies are the members of 2-oxo-acid dehydrogenase complex including pyruvate dehydrogenase complex E₂ (PDC-E₂), branched chain 2-oxo-acid dehydrogenase complex E₂ (BCOADC-E₂) and 2-oxo-glutarate dehydrogenase complex E₂ (OGDC-E₂), whose immunodominant epitopes have been mapped within lipoyl domains. Antibodies to these corresponding autoantigens have been reported in PBC patients with a positive rate of 95 %, 53-55 % and 39-88 % respectively^[6,12]. However, when all of these antibodies are determined simultaneously, the patients with PBC can be diagnosed as high as 92-100 %^[13-16]. These facts suggest such a possibility that if there is a constructed antigen containing the specific immunodominant epitopes and the antibodies above can be detected synchronously, the diagnosis of PBC patients would be more specific, sensitive and convenient.

Therefore, we designed and constructed a M₂ autoantigen trimer (BPO) expression vector, which could coexpress the immunodominant lipoyl domains of PDC-E₂, BCOADC-E₂ and OGDC-E₂ from human origin, in an attempt to establish a more accurate and sensitive method with BPO to detect M₂ antibodies in patients with PBC. Besides, because it has never been reported that M₂ antibodies were found in other liver related diseases other than PBC^[17-20], a survey to detect M₂ antibodies under these circumstances with our constructed M₂ autoantigen trimer was also included in the present study.

MATERIALS AND METHODS

Patients

Eight groups of adult patients with both sexes who were treated in Shanghai Changzheng Hospital were enrolled in the present study. Group 1 consisted of 20 patients with PBC diagnosed on the criteria: the presence of AMA and at least one of the followings: (1) Elevation of serum alkaline phosphatase (ALP) and/or gamma glutamyl transpeptidase (γ-GT). (2) Liver biopsy with PBC characteristics^[21]. Group 2 consisted of 5 patients with autoimmune hepatitis (AIH)^[22]. Two patients diagnosed

as autoimmune cholangitis (AIC) were included in group 3, and group 4 was composed of 18 patients diagnosed as liver disease with unknown etiology (LDUE) that was defined as lack of obvious causes including drug use, alcohol abuse, exposure to hepatotoxic medication or chemicals and virus infection. Group 5 consisted of 8 patients with drug induced liver injury (DILI). Group 6 enrolled 201 patients with other liver diseases (Post-viral hepatitis and liver cirrhosis, $n=153$; Obstructive jaundice, $n=25$; Acute hepatitis A, $n=15$; Hepatic abscess, $n=3$; Wilson's disease, $n=1$; Cardiac cirrhosis, $n=4$). Thirty-three patients with various autoimmune diseases (AID) (Rheumatoid arthritis, $n=12$; Systemic lupus erythmatosus, $n=12$; Polymyositis, $n=4$; Vasculitis, $n=3$; Hashimoto's thyroiditis, $n=2$) were included in group 7 and 1 225 healthy volunteers taking a health checkup aged less than 28 served as the control. In the experiment, fasting serum from each patient was prepared with routine procedures and stored at -20°C until further analysis.

Materials

Reverse transcriptase and PCR amplification system were purchased from Roche Company (U.S.A). Restriction endonucleases and T₄DNA ligase were from New England Biolabs (U.S.A). Plasmid vector pQE-30 and *E.coli* M15 (prep 4) were from Qiagen Company (Germany). Indirect immunofluorescence (IIF) test kit for AMA and Western-blotting kit for M₂ antibodies were all from Euroimmun Company (Germany).

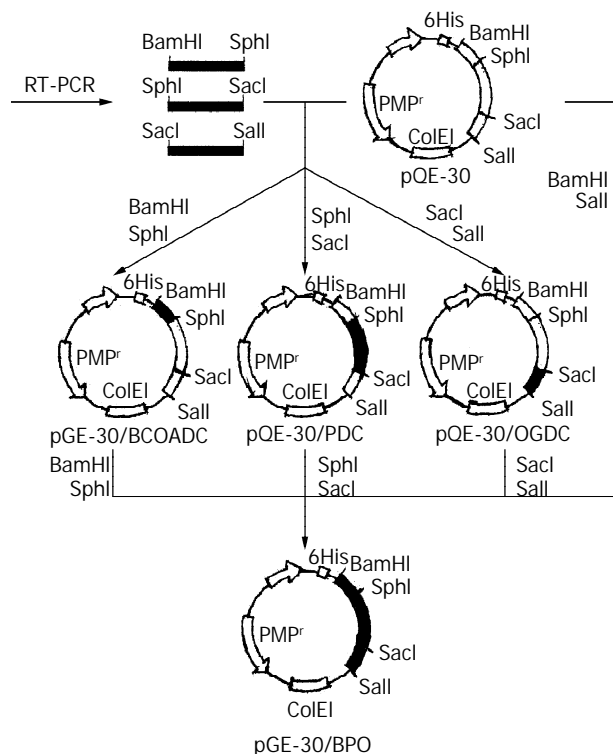


Figure 1 Construction protocol of recombinant plasmids.

Expression and identification of M₂ autoantigen trimer

Recombinant plasmids were constructed as illustrated in Figure 1. Briefly, total RNA was extracted from human peripheral mononuclear blood cells. The objective cDNAs were synthesized by reverse transcriptase and used as the template to amplify the immunodominant epitopes of BCOADC-E₂, PDC-E₂ and OGDC-E₂ with polymerase chain reaction. The PCR products were digested with relevant restriction endonuclease and purified cDNA fragments were inserted into the expression vector pQE-30 to form recombinant plasmids

pQE-30/BCOADC-E₂, pQE-30/PDC-E₂, pQE-30/OGDC-E₂ and pQE-30/BPO respectively. The pQE-30/BPO was then transferred into *E. Coli* M15 (pREP4) and induced by isopropylthio- β -D-galactoside to express BPO protein, which was finally confirmed with SDS-PAGE, Western-blotting and Immunoabsorption test.

The antigenic reactivity and specificity of the recombinant BPO trimer were identified with seven M₂-positive sera confirmed at Euroimmun Research Center (Germany) by immunoblotting using beef heart mitochondrial preparations.

Detection of M₂ antibodies with BPO

The obtained recombinant BPO protein fused with the 6 \times His affinity tag in the N-terminus was purified by Ni-NTA affinity chromatography under denaturing conditions. After renatured by removing denaturants slowly with dialysis, the BPO protein was used as the specific antigen to detect M₂ antibodies with the routine procedures of ELISA. The coefficients of variation for this assay method, the mean OD \pm SD for the control sera, as well as the critical OD value for the positive determination were respectively calculated or defined based on the experimental results. The measurements of M₂ antibodies and AMA with Euroimmun's kits as a comparison of the present assay method were also simultaneously performed in the study.

RESULTS

Identification of expressed M₂ autoantigen trimer

The segment analysis by restriction endonuclease digestion confirmed that inserted cDNA sequences in the constructed plasmids were completely consistent with that of the published data (Figure 2). The molecular mass of BPO protein was examined by SDS-PAGE in 15 % polyacrylamide gel, in which a specific 42 KD protein band was clearly visualized (Figure 3).

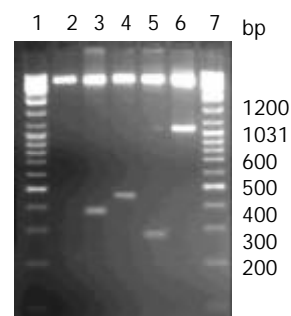


Figure 2 Segment analysis of recombinant plasmids by restriction endonuclease digestion. 1, 7. Markers; 2. pQE-30 (Bamh1); 3. pQE-30/BCOADC-E₂ (Bamh1+Sph1); 4. pQE-30/PDC-E₂ (Sph1+Sac1); 5. p30/OGDC-E₂ (Sac1+Sall); 6. pQE-30/BPO (Bamh1+Sall).

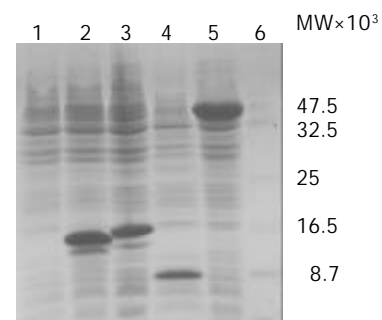


Figure 3 Expression products of recombinant plasmids detected by SDS-PAGE stained with Coomassie Brilliant Blue R-

250. Lane 1: pQE-30 (control); Lane 2: pQE-30/BCOADC-E₂; Lane 3: pQE-30/PDC-E₂; Lane 4: pQE-30/OGDC-E₂; Lane 5: pQE-30/BPO; Lane 6: protein marker.

The expressed BPO protein could react with all of the seven M₂-positive sera confirmed at Euroimmun Research Center (Germany) by immunoblotting using beef heart mitochondrial preparations, which identified the antigenic reactivity of the recombinant BPO trimer (Figure 4). When mixed beforehand with the lysates of *E. coli* expressing BPO overnight, the sera became M₂-negative by Western-blotting, which confirmed the BPO specificity determined by the immunodominant epitopes of PDC-E₂, BCOADC-E₂ and OGDC-E₂.

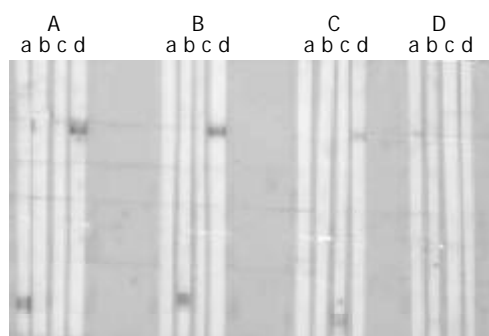


Figure 4 Immunoreactivity of sera against recombinant proteins. Three M₂ antibody positive sera (A, B, C) and a M₂ antibody negative serum (D) were probed with SDS-PAGE-separated recombinant proteins of BCOADC-E₂ (lane a), PDC-E₂ (lane b), OGDC-E₂ (lane c), BPO (lane d).

Effectiveness of BPO in the detection of M₂ antibodies

The coefficients of variation for the detection of M₂ antibodies by BPO with ELISA were less than 10 % in both interassay and intraassay. The mean OD \pm SD for the control sera was 0.073 \pm 0.046. The critical OD value for positive was defined as \geq 0.303 based on the mean control value + 5 SD.

M₂ antibodies in patients with PBC

In the patients with PBC who were AMA positive determined by IIF test kit, the positive rate of M₂ antibodies detected by BPO with ELISA and Euroimmun's kit was 100 % (20/20) and 80 % (16/20) respectively (Table 1).

Table 1 AMA and M₂ antibodies in patients with different diseases

Group	n	AMA positive	M ₂ - positive		AASLD's guideline (+)
			Euroimmun's kit	ELISA	
PBC	20	20	16	20	20
AIH	5	0	0	1	0
AIC	2	0	1	2	0
LDUE	18	7	6	6	6
DILI	8	1	1	1	1
Other liver diseases	201	ND	ND	0	ND
AID	33	3	0	0	0
Control	1225	ND	ND	0	ND

PBC: primary biliary cirrhosis; AIH: autoimmune hepatitis; AIC: autoimmune cholangitis; LDUE: liver disease with unknown etiology; DILI: drug induced liver injury; AID: autoimmune disease; AMA: antimitochondrial antibodies; ND: not done.

M₂ antibodies in patients with other diseases

Seven patients with liver disease of unknown etiology were all AMA positive; However, only one was M₂ antibody negative and didn't agree with the guideline by the American Association for the Study of Liver Diseases (AASLD), and his plasma ALP and γ -GT were in normal range but alanine aminotransferase was elevated (120 U/L). The other 6 patients with M₂ antibody positive had no specific symptoms except the unexplained elevation of serum ALP (187-1 525 U/L) and γ -GT (88-2 685 U/L).

One patient with drug induced liver injury was demonstrated as M₂ antibody positive by both ELISA and Euroimmun's kit, whose additional laboratory data were as follows: AMA positive, antinuclear antibodies positive, ALP 153 U/L, γ -GT 321 U/L; alanine aminotransferase 281 U/L, aspartate transaminase 225 U/L, total bilirubin 25 μ mol/L (normal < 18 μ mol/L). This patient suffered from lymphatic tuberculosis and had taken rifampisin for one year before the onset of liver disease. He was in agreement with the AASLD's guideline.

It was noteworthy that the sera from 1 AIH and 2 AIC patients with AMA negative had detectable M₂ antibody by BPO with ELISA, while they were M₂ antibody negative with the Euroimmun's kit. The prominent elevation of plasma ALP and γ -GT was observed in all of the three patients.

No M₂ antibody positive sera were found in control, other liver disease and the AID group by BPO with ELISA.

DISCUSSION

In the guideline by AASLD in 2000 and the standards by other researchers, AMA has long been used as an important marker for the primary biliary cirrhosis^[21, 23]; however, only M₂ antibodies are considered as specific for the PBC diagnosis. Other AMA sub-types have been found in drug-induced disorders, cardiomyopathies, systemic lupus erythematosus, rheumatoid arthritis, tuberculosis, syphilis and hepatitis C, indicating the nonspecific nature of AMA in the diagnosis of PBC^[24]. Besides, there were about 5-17 % of the patients with biochemical and histological features compatible with PBC not having detectable AMA with the IIF method^[25-34]. To get better diagnostic results, approaches to detect M₂ antibodies by ELISA or Western-blotting using recombinant antigen of PDC-E₂, BCOADC-E₂ and OGDC-E₂ have been reported in several literatures^[15-17].

In 2001, Miyakawa and his coworkers^[35] developed a new ELISA for the detection of M₂ antibody using porcine heart mitochondrial protein as the antigen. The sensitivity of this method was only 78 %, despite the specificity was 100 %. In the present study, we employed BPO as the antigen to determine M₂ antibodies with ELISA, which was more sensitive than the Euroimmun's kit. The reason for this was partially because the antigen used in our approach was derived from human sources instead of that from porcine used in Euroimmun's kit. The antigen heterogeneity might affect the assay results^[36]. Furthermore, the three major autoantigens, BCOADC-E₂, PDC-E₂ and OGDC-E₂, with no cross-reactivity between, were constructed together as a trimer by molecular biological techniques, which could provide more positive chance for the detection of M₂ antibodies. Therefore, the use of this recombinant molecule offered a rapid, simple and sensitive ELISA for the immunodiagnosis of PBC.

According to the investigation by James and his associates^[3], the incidence of PBC has been increased in recent years. In northern England, the prevalence of PBC from 201.9 per 10⁶ adults and 541.4 per 10⁶ women over 40 in 1987 rose to 334.6 and 939.8 respectively in 1994. Owing to the lack of sensitive diagnostic methods, there have no reliable data related to the epidemiology of PBC in China so far and more seriously,

clinical doctors have not yet paid appropriate attention to this disease. We checked 10 patients with liver cirrhosis hospitalized in January, February and April in 2000 whose serum immunological variables showed no signs of viral infection, and the reason for liver cirrhosis seemed unclear. However, 7 of the 10 patients were found M₂ antibody positive by the detailed studies at the Euroimmun Research Center (Germany). In the past six months since we detected M₂ antibody by BPO with ELISA for the PBC diagnosis, over 120 patients' sera have been examined, in which 69 demonstrated M₂ antibody positive and 30 cases with comparatively complete clinical data listed in this paper. Our recent research and the related domestic reports in 2001 indicate that PBC is probably not so rare in China as it has been thought^(4, 37).

REFERENCES

- 1 **James OF**, Bhopal R, Howel D, Gray J, Burt AD, Metcalf JV. Primary biliary cirrhosis once rare, now common in the United Kingdom? *Hepatology* 1999; **30**: 390-394
- 2 **Metcalf J**, James O. The geoepidemiology of primary biliary cirrhosis. *Semin Liver Dis* 1997; **17**: 13-22
- 3 **Metcalf JV**, Bhopal RS, Gray J, Howel D, James OF. Incidence and prevalence of primary biliary cirrhosis in the city of Newcastle upon Tyne, England. *Int J Epidemiol* 1997; **26**: 830-836
- 4 **Medina J**, Jones EA, Garcia Monzon C, Moreno Otero R. Immunopathogenesis of cholestatic autoimmune liver diseases. *Eur J Clin Invest* 2001; **31**: 64-71
- 5 **Heathcote EJ**. Evidence-based therapy of primary biliary cirrhosis. *Eur J Gastroenterol Hepatol* 1999; **11**: 607-615
- 6 **Joplin RE**, Neuberger JM. Immunopathology of primary biliary cirrhosis. *Eur J Gastroenterol Hepatol* 1999; **11**: 587-593
- 7 **Metcalf JV**, Mitchison HC, Palmer JM, Jones DE, Bassendine MF, James OF. Natural history of early primary biliary cirrhosis. *Lancet* 1996; **348**: 1399-1402
- 8 **Kisand KE**, Metskula K, Kisand KV, Kivik T, Gershwin ME, Uibo R. The follow-up of asymptomatic persons with antibodies to pyruvate dehydrogenase in adult population samples. *J Gastroenterol* 2001; **36**: 248-254
- 9 **Koizumi H**, Onozuka Y, Shibata M, Sano K, Ooshima Y, Morizane T, Ueno Y. Positive rate of anti-mitochondrial antibody in Japanese corporate workers. *Rinsho Byori* 2000; **48**: 966-970
- 10 **Turchany JM**, Uibo R, Kivik T, Van de Water J, Prindiville T, Coppel RL, Gershwin ME. A study of antimitochondrial antibodies in a random population in Estonia. *Am J Gastroenterol* 1997; **92**: 124-126
- 11 **Nakano T**, Inoue K, Hirohara J, Arita S, Higuchi K, Omata M, Toda G. Long-term prognosis of primary biliary cirrhosis (PBC) in Japan and analysis of the factors of stage progression in asymptomatic PBC (a-PBC). *Hepatol Res* 2002; **22**: 250-260
- 12 **Migliaccio C**, Van de Water J, Ansari AA, Kaplan MM, Coppel RL, Lam KS, Thompson RK, Stevenson F, Gershwin ME. Heterogeneous response of antimitochondrial autoantibodies and bile duct apical staining monoclonal antibodies to pyruvate dehydrogenase complex E₂: the molecule versus the mimic. *Hepatology* 2001; **33**: 792-801
- 13 **Kitami N**, Komada T, Ishiji H, Shimizu H, Adachi H, Yamaguchi Y, Kitamura T, Oide H, Miyazaki A, Ishikawa M. Immunological study of anti-M₂ in antimitochondrial antibody-negative primary biliary cirrhosis. *Intern Med* 1995; **34**: 496-501
- 14 **Jones DE**. Autoantigens in primary biliary cirrhosis. *J Clin Pathol* 2000; **53**: 813-821
- 15 **Miyakawa H**, Tanaka A, Kikuchi K, Matsushita M, Kitazawa E, Kawaguchi N, Fujikawa H, Gershwin ME. Detection of antimitochondrial autoantibodies in immunofluorescent AMA-negative patients with primary biliary cirrhosis using recombinant autoantigens. *Hepatology* 2001; **34**: 243-248
- 16 **Kitami N**, Ishii H, Shimizu H, Adachi H, Komada T, Mikami H, Yokoi Y, Sato N. Immunoreactivity to M₂ proteins in antimitochondrial antibody-negative patients with primary biliary cirrhosis. *J Gastroenterol Hepatol* 1994; **9**: 7-12
- 17 **Jensen WA**, Jois JA, Murphy P, De Giorgio J, Brown B, Rowley MJ, Mackay IR. Automated enzymatic mitochondrial antibody assay for the diagnosis of primary biliary cirrhosis. *Clin Chem Lab Med* 2000; **38**: 753-758
- 18 **Leung PS**, van de Water J, Coppel RL, Nakanuma Y, Munoz S, Gershwin ME. Molecular aspects and the pathological basis of primary biliary cirrhosis. *J Autoimmun* 1996; **9**: 119-128
- 19 **Strassburg CP**, Manns MP. Autoimmune tests in primary biliary cirrhosis. *Baillieres Best Pract Res Clin Gastroenterol* 2000; **14**: 585-599
- 20 **Quaranta S**, Shulman H, Ahmed A, Shoenfeld Y, Peter J, McDonald GB, Van de Water J, Coppel R, Ostlund C, Worman HJ, Rizzetto M, Tsuneyama K, Nakanuma Y, Ansari A, Locatelli F, Paganin S, Rosina F, Manns M, Gershwin ME. Autoantibodies in human chronic graft-versus-host disease after hematopoietic cell transplantation. *Clin Immunol* 1999; **91**: 106-116
- 21 **Parikh Patel A**, Gold EB, Worman H, Krivy KE, Gershwin ME. Risk factors for primary biliary cirrhosis in a cohort of patients from the United States. *Hepatology* 2001; **33**: 16-21
- 22 **Ma X**, Qiu DK. Relationship between autoimmune hepatitis and HLA-DR4 and DR β allelic sequences in the third hypervariable region in Chinese. *World J Gastroenterol* 2001; **7**: 718-721
- 23 **Heathcote EJ**. Management of primary biliary cirrhosis. The American association for the study of liver diseases practice guidelines. *Hepatology* 2000; **31**: 1005-1013
- 24 **Strassburg CP**, Jaeckel E, Manns MP. Anti-mitochondrial antibodies and other immunological tests in primary biliary cirrhosis. *Eur J Gastroenterol Hepatol* 1999; **11**: 595-601
- 25 **Michieletti P**, Wanless IR, Katz A, Scheuer PJ, Yeaman SJ, Bassendine MF, Palmer JM, Heathcote EJ. Antimitochondrial antibody negative primary biliary cirrhosis: a distinct syndrome of autoimmune cholangitis. *Gut* 1994; **35**: 260-265
- 26 **Lacerda MA**, Ludwig J, Dickson ER, Jorgensen RA, Lindor KD. Antimitochondrial antibody-negative primary biliary cirrhosis. *Am J Gastroenterol* 1995; **90**: 247-249
- 27 **Heathcote J**. Autoimmune cholangitis. *Gut* 1997; **40**: 440-442
- 28 **Ikuno N**, Scealy M, Davies JM, Whittingham SF, Omagari K, Mackay IR, Rowley MJ. A comparative study of antibody expressions in primary biliary cirrhosis and autoimmune cholangitis using phage display. *Hepatology* 2001; **34**: 478-486
- 29 **Kinoshita H**, Omagari K, Whittingham S, Kato Y, Ishibashi H, Sugi K, Yano M, Kohno S, Nakanuma Y, Penner E, Wieserska Gadek J, Reynoso Paz S, Gershwin ME, Anderson J, Jois JA, Mackay IR. Autoimmune cholangitis and primary biliary cirrhosis-an autoimmune enigma. *Liver* 1999; **19**: 122-128
- 30 **Invernizzi P**, Crosignani A, Battezzati PM, Covini G, De Valle G, Larghi A, Zuin M, Podda M. Comparison of the clinical features and clinical course of antimitochondrial antibody-positive and -negative primary biliary cirrhosis. *Hepatology* 1997; **25**: 1090-1095
- 31 **Kaserer K**, Exner M, Mosberger I, Penner E, Wrba F. Characterization of the inflammatory infiltrate in autoimmune cholangitis. A morphological and immunohistochemical study. *Virchows Arch* 1998; **432**: 217-222
- 32 **Mayo MJ**, Lipsky PE, Miller SN, Stastny P, Combes B. Similar T-cell oligoclonality in antimitochondrial antibody-positive and -negative primary biliary cirrhosis. *Dig Dis Sci* 2001; **46**: 345-351
- 33 **Fujioka S**, Yamamoto K, Okamoto R, Miyake M, Ujike K, Shimada N, Terada R, Miyake Y, Nakajima H, Piao CY, Iwasaki Y, Tanimizu M, Tsuji T. Laparoscopic features of primary biliary cirrhosis in AMA-positive and AMA-negative patients. *Endoscopy* 2002; **34**: 318-321
- 34 **Nakajima M**, Shimizu H, Miyazaki A, Watanabe S, Kitami N, Sato N. Detection of IgA, IgM, and IgG subclasses of anti-M₂ antibody by immunoblotting in autoimmune cholangitis: is autoimmune cholangitis an early stage of primary biliary cirrhosis? *J Gastroenterol* 1999; **34**: 607-612
- 35 **Miyakawa H**, Kikuchi K, Jong Hon K, Kawaguchi N, Yajima R, Ito Y, Maekubo H. High sensitivity of a novel ELISA for anti-M₂ in primary biliary cirrhosis. *J Gastroenterol* 2001; **36**: 33-38
- 36 **Miyakawa H**, Kawaguchi N, Kikuchi K, Fujikawa H, Kitazawa E, Matsushita M. Definition of antigen specificity for antimitochondrial proteins detected by Western blotting using native mitochondrial proteins in primary biliary cirrhosis. *Hepatol Res* 2001; **21**: 101-107
- 37 **Zhang F**, Jia J, Wang B, Qian L, Yin S, Wang Y, Cui Y, You H, Ma H, Wang H, Zhang C. Clinical characteristics of primary biliary cirrhosis: a report of 45 cases. *Zhonghua Nei Ke Za Zhi* 2002; **41**: 163-167

Functional brain imaging in irritable bowel syndrome with rectal balloon-distention by using fMRI

Yao-Zong Yuan, Ran-Jun Tao, Bin Xu, Jing Sun, Ke-Min Chen, Fei Miao, Zhong-Wei Zhang, Jia-Yu Xu

Yao-Zong Yuan, Ran-Jun Tao, Bin Xu, Jing Sun, Jia-Yu Xu, Department of Gastroenterology, Ruijin Hospital, Shanghai Second Medical University, Shanghai 200025, China

Ke-Min Chen, Fei Miao, Zhong-Wei Zhang, Department of Radiology, Ruijin Hospital, Shanghai Second Medical University, Shanghai 200025, China

Correspondence to: Dr. Yao-Zong Yuan, Department of Gastroenterology, Ruijin Hospital, Shanghai Second Medical University, Shanghai 200025, China. yyz28@hotmail.com

Telephone: +86-21-64370045-665242 **Fax:** +86-21-64150773

Received: 2002-11-19 **Accepted:** 2003-01-02

Abstract

AIM: Irritable bowel syndrome (IBS) is characterized by abdominal pain and changes in stool habits. Visceral hypersensitivity is a key factor in the pathophysiology of IBS. The aim of this study was to examine the effect of rectal balloon-distention stimulus by blood oxygenation level-dependent functional magnetic resonance imaging (BOLD-fMRI) in visceral pain center and to compare the distribution, extent, and intensity of activated areas between IBS patients and normal controls.

METHODS: Twenty-six patients with IBS and eleven normal controls were tested for rectal sensation, and the subjective pain intensity at 90 ml and 120 ml rectal balloon-distention was reported by using Visual Analogue Scale. Then, BOLD-fMRI was performed at 30 ml, 60 ml, 90 ml, and 120 ml rectal balloon-distention in all subjects.

RESULTS: Rectal distention stimulation increased the activity of anterior cingulate cortex (35/37), insular cortex (37/37), prefrontal cortex (37/37), and thalamus (35/37) in most cases. At 120 ml of rectal balloon-distention, the activation area and percentage change in MR signal intensity of the regions of interest (ROI) at IC, PFC, and THAL were significantly greater in patients with IBS than that in controls. Score of pain sensation at 90 ml and 120 ml rectal balloon-distention was significantly higher in patients with IBS than that in controls.

CONCLUSION: Using fMRI, some patients with IBS can be detected having visceral hypersensitivity in response to painful rectal balloon-distention. fMRI is an objective brain imaging technique to measure the change in regional cerebral activation more precisely. In this study, IC and PFC of the IBS patients were the major loci of the CNS processing of visceral perception.

Yuan YZ, Tao RJ, Xu B, Sun J, Chen KM, Miao F, Zhang ZW, Xu JY. Functional brain imaging in irritable bowel syndrome with rectal balloon-distention by using fMRI. *World J Gastroenterol* 2003; 9(6): 1356-1360

<http://www.wjgnet.com/1007-9327/9/1356.asp>

INTRODUCTION

Irritable bowel syndrome (IBS) is the most common disorder

seen in gastroenterological practice^[1,2]. The disorder affects approximately 15 % to 20 % of the world's population and is predominately found in women^[2]. It comprises a group of functional bowel disorders in which abdominal discomfort or pain is associated with defecation or a change in bowel habit, and with features of disordered defecation^[3,4]. The pathophysiology of the symptom remains unclear, and visceral hypersensitivity or decreased pain thresholds to distension of the gut is considered to be a biologic marker for IBS and is present in most patients with this gastrointestinal disorder^[5]. Possibly, there are dysfunctions in the processing of sensory stimuli in the "brain-gut" axis that may cause visceral hypersensitivity and secondary motility changes^[6]. The central nervous system is believed to play a strong modulatory or etiological role in the pathophysiology of the disease^[7].

In animals, the perception of somatovisceral pain is derived from the expression of the immediate early gene c-fos^[8-11]. Numerous positron emission tomography (PET)^[12-15] or functional magnetic resonance imaging (fMRI)^[16-18] studies have dealt with the central processing of somatic pain in humans. In contrast, the neural networks involved in the perception of visceral pain in humans, especially rectal pain, have been the subjects of a limited number of functional brain imaging studies^[19-23].

Previous studies of somatic pain using PET scanning to measure the regional cerebral blood flow have suggested that the anterior cingulate cortex (ACC), prefrontal cortex (PFC), insular cortex (IC), and thalamus (THAL) are important loci in pain perception^[12,24]. Studies of visceral pain have generally suggested that these brain centers are important in sensation. fMRI is an alternative technique to measure changes in regional cerebral activity during stimulation. Using fMRI, the cerebral loci activated by rectal distention were also characterized in healthy volunteers^[22].

In this study, we examined the effect of rectal balloon-distention stimulus by blood oxygenation level-dependent functional magnetic resonance imaging (BOLD-fMRI) in the visceral pain center and to compare the distribution, extent, and intensity of activated areas between irritable bowel Syndrome (IBS) patients and normal controls.

MATERIALS AND METHODS

Subjects

Eleven normal right-handed control subjects (6 men and 5 women; age, 24-49 years; average age, 39 years) and twenty-six right-handed patients with IBS (12 men and 14 women; age, 18-61 years; average age, 47 years) participated in the study. All volunteers were free of any gastrointestinal complaint. The IBS patients were all diagnosed in Ruijin Hospital, and met the Rome II criteria for IBS^[4], which include at least 12 weeks, not necessarily to be consecutive in the preceding 12 months of abdominal discomfort or pain that has two of the following three features: (1) Relieved with defecation; (2) Onset associated with a change in frequency of stool; (3) Onset associated with a change in form (appearance) of stool. Each patient underwent a basic evaluation to exclude organic disease including a history, physical examination, and colonoscopy.

Distention protocol

Subjects reclined on the magnetic resonance imaging (MRI) table with head resting on a beanbag saddle that reduced head motion. A plastic balloon (Medtronic Synectics, USA) was placed in rectum at 10-15 cm from the anal margin. First, the subjects were tested for the rectal sensation, including the thresholds for sensation of gas, defecation and pain. Second, subjects reported the subjective pain intensity at 90 ml and 120 ml rectal balloon-distention by using visual analogue scale (0=no pain, 10=unbearable pain). Then, fMRI scanning was begun. Subjects were instructed to expect 4 series of rectal stimuli. Each set of distention included 3 stimuli of the same volume lasting 30 seconds each, with a 30-second rest period in between. The balloon inflation and deflation for each stimulus required an average of 6 seconds. The baseline volume during the rest periods was 0 ml. The first series of stimulus volume was 30 ml, the second 60 ml, the third 90 ml, and the last 120 ml.

MRI scanning

BOLD imaging was performed on a 1.5-T GE Signa MRI system. Each scanning consisted of a T1-weighted (the parameters included TR/TE=400 ms/14 ms, matrix=256×256, NEX=1). Next, four 10-mm-thick slices aligned at an approximately 20° angle above the anterior commissure-posterior commissure line to include the ACC, IC, PFC, and THAL. A functional scan was performed using echo planar imaging, and a matrix of 64×64, NEX=1. The pulse sequence parameters included a 90° flip-angle with a TR (image repetition rate)/TE (effective echo time) of 3 000 ms/60 ms. Each run consisted of 3 repetitions of 30 seconds of rest, followed by 30 seconds of stimulus. In each 30-second period, 10 parameters were collected, 60 data during each series.

Data processing and analysis

Data analysis was performed using correlation-coefficient tool in Functional software (AW3.2, SUN workstation). The confidence level was 0.05. Brain areas thought to mediate painful sensation included the ACC, the IC, the PFC, and THAL. These regions of interest (ROI) were identified and circled on the high-resolution anatomic images by a radiologist, who was blind to the identity of the patient and to the active pixels. The regional cerebral activation was evaluated by the percentage area of ROI and the percentage change in MR signal intensity of ROI. The percentage area of ROI was calculated by the formula: the percentage area of ROI = the pixels of ROI/the total pixels of selected pain center ×100%. The percentage change in MR signal intensity of ROI = (the MR signal intensity during stimulation - the Mean baseline signal)/the mean baseline signal ×100%. The average percentage change in MR signal intensity was calculated for each subject at each stimulus volume in each ROI. To exclude the influence of balloon inflation and deflation, the first and the tenth MR signal intensity of the rest and stimulus phase were eliminated.

Statistical analysis

The data were expressed as means ±SEM. For comparison of means, an unpaired Student's *t* test was used. The primary comparisons were the thresholds for sensation and VAS score between IBS patients and controls. Secondary analysis included the percentage of ROI and the average percentage change in MR signal intensity of ROI comparing IBS patients with controls. Statistically significant differences by 2-tailed *t* tests were defined by $P < 0.05$.

RESULTS

Rectal sensation test

In the control group, the average thresholds for sensation of

gas, defecation and pain were 28 ml, 127 ml, and 208 ml. They were 24 ml, 90 ml, and 150 ml respectively in IBS group. The thresholds for sensation of defecation and pain were significantly lower in IBS group than in control group ($P < 0.05$, Figure 1).

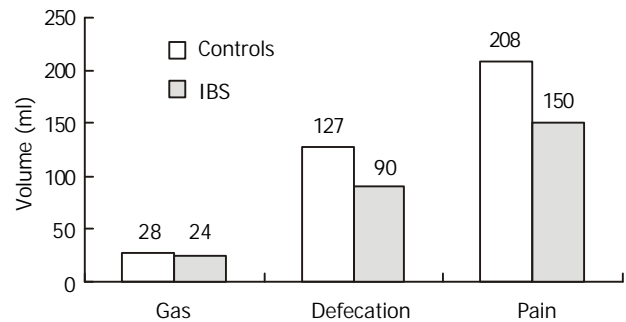


Figure 1 Rectal sensation test (the thresholds for sensation).

VAS score

At 30 ml rectal distention, subjects generally sensed a very-low-intensity stimulation, using the terms "gas", "mildly felt". At 60 ml rectal distention, some IBS patients expressed sensation of defecation. At 90 ml rectal distention, a large number of IBS patients and some normal controls expressed sensation of stool, associated with mild-moderate pain, and VAS score was 4.42 ± 2.00 vs 2.71 ± 1.78 . At 120 ml rectal distention, most IBS patients reported moderate-severe painful sensation, and VAS score was 5.90 ± 1.84 vs 3.95 ± 2.04 . In this study, three IBS patients could not tolerate 120 ml rectal distention. The VAS score of 90 ml and 120 ml rectal distention (painful rectal distention) was significantly higher in IBS patients than in control ($P < 0.05$, Figure 2).

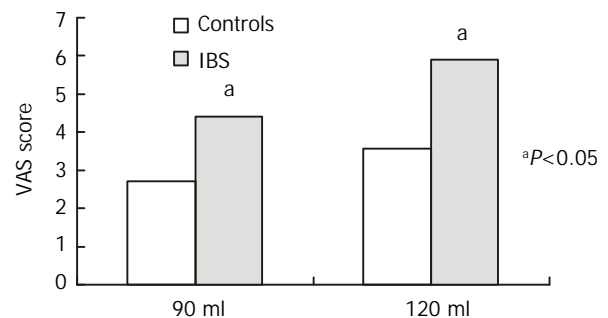


Figure 2 Subjective pain intensity.

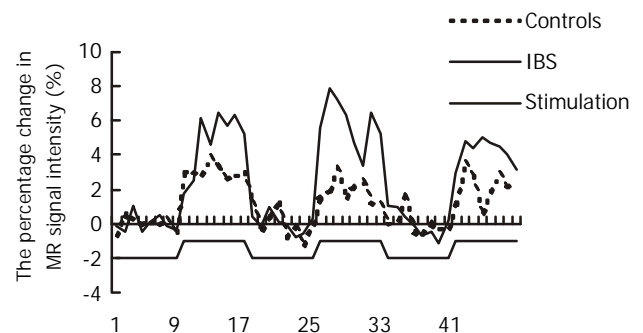


Figure 3 The percentage change in MR signal intensity time course of PFC in response to 3 rectal distentions at 90 ml.

Functional brain imaging

The time course of rectal stimulation sensation center response indicated immediate increase and rapid decline in BOLD signal

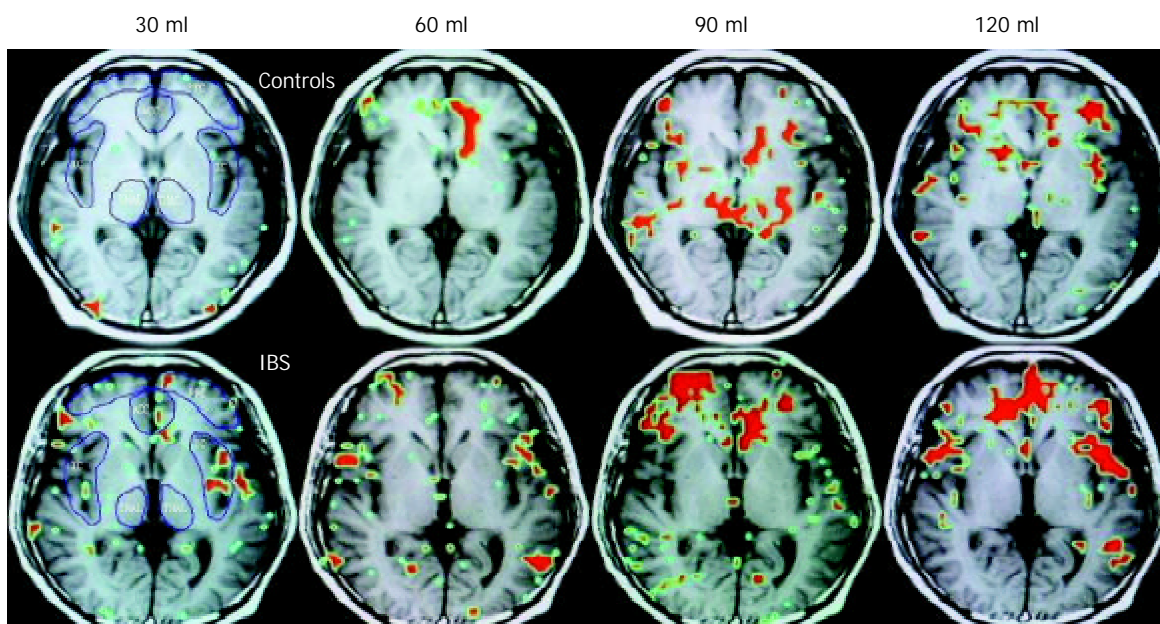


Figure 4 Functional brain map. The red area is the ROI.

in parallel with the mechanical distending stimulus (Figure 3). For both IBS patients and control subjects, rectal distention stimulation increased the activity of anterior cingulate cortex (35/37), insular cortex (37/37), prefrontal cortex (37/37), and thalamus (35/37) in most cases.

In patients with IBS, the average percentage area of ROI increased in parallel with rectal distention volumes in the IC, PFC, and THAL, only that in PFC had statistical significance ($P < 0.05$). In controls, this increasing tendency only occurred in the ACC (Figure 4). At 120 ml rectal distention, the average percentage area of ROI and the average percentage change in MR signal intensity of ROI in the IC, PFC, and THAL were significantly greater in patients with IBS than in control subjects ($P < 0.05$, Figure 5 and 6).

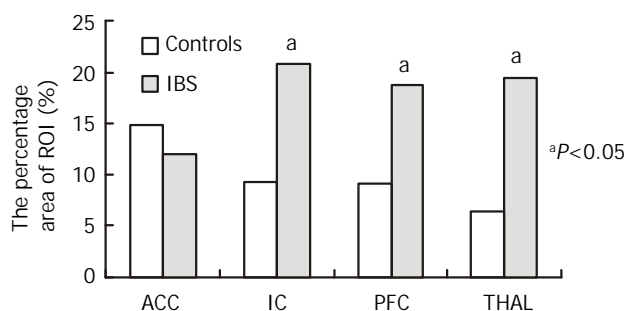


Figure 5 The average area of ROI at 120ml rectal distention.

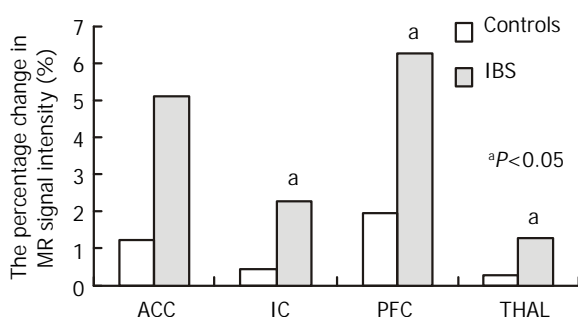


Figure 6 The percentage change in MR signal intensity of ROI at 120 ml rectal distention.

DISCUSSION

FMRI is a useful technology to measure changes in regional CNS blood oxygenation, which is in parallel with regional metabolic activity^[25-27]. The BOLD technology detects changes in the ratio of deoxyhemoglobin to oxyhemoglobin. When brain-center neurons are metabolically active, there is an increase in local blood flow and a relative increase in the amount of oxyhemoglobin, and an increase in magnetic resonance signal^[25-29]. Accordingly, the magnetic resonance signal in a given pixel will increase above baseline if the region is activated in response to stimulation. FMRI offers advantages over PET such as direct anatomic correlation, avoidance of radioisotopes, and acceptable signal-to-noise ratio that do not require large numbers of stimuli. fMRI images give similar results as PET^[30,31].

It showed that fMRI has adequate sensitivity to measure regional cerebral blood flow changes in response to visceral - in this case rectal - stimulation. Activity in the 4 selected CNS pain centers, ACC, IC, PFC, and THAL, promptly increase with rectal distention stimulation. The 4 selected pain centers are components of the brain’s pain-processing system^[12,24,32,33]. Current studies pointed to the THAL as a relay center, connecting afferent signals from the spinothalamic tract and spinoreticular tracts to higher centers such as the cingulate, prefrontal, and insular cortices^[34,35]. The IC is believed to mediate primarily visceral sensations (taste, smell, gastric, colonic, and other visceral inputs) including rectal stimuli, whereas the ACC is thought to mediate the affective or “emotional” content of sensory information. The insular cortex neurons distributed between the taste area and the visceral area receive convergent inputs from baroreceptor, chemoreceptor, gustatory and nociceptive organs and may have roles in taste aversion or in regulation of visceral responses^[36]. Using positron emission tomography (PET), Craig’s^[37] group found contralateral activity correlated with graded cooling stimuli only in the dorsal margin of the middle/posterior insula in humans. Furthermore, Krushel^[38] referred to the region of convergence in the agranular insular cortex as the visceral cortex, and suggested its involvement in the efficient integration of specific visceral sensory stimuli with correlated limbic or motivational consequences. The visceral cortex may help regulate the organism’s visceral response to stress.

The PFC is thought to exert higher executive functions in pain perception^[39]. There are several different functional

divisions of the PFC, including the dorsolateral, ventromedial, and orbital sectors. Each of these regions plays some role in affective processing that shares the feature of representing affect in the absence of immediate rewards and punishments as well as in different aspects of emotional regulation^[40].

In this study, the thresholds for sensation of defecation and pain were significantly lower in IBS group than in control group, and VAS score was significantly higher in IBS patients than in controls. The results were similar to the previous studies^[41]. Normal volunteers and IBS patients had significant cerebral activation in the 4 selected brain centers (ACC, IC, PFC, and THAL) during distention stimulation at 30 ml, 60 ml, 90 ml, and 120 ml. Significant differences in cerebral activation (both the percentage area and the percentage change in MR signal intensity of ROI) were found between IBS patients and controls. In IBS patients, there was significantly greater area of ROI of the PFC with 120 ml distention than with other volume distention. Conversely, in control subjects there was no significant increase in activation of these areas with 120 ml distention compared with others. Furthermore, at 120 ml rectal distention, there was significantly greater activation of the IC, PFC, and THAL in patients with IBS than in control subjects. In summary, by a variety of measures, it is possible that IC and PFC responses to visceral pain in IBS are greater than that in controls.

There were several studies about the CNS activity in response to visceral stimulation by using PET and fMRI, but the results differed. Silverman^[20] found a lack of activation within the ACC or PFC with nonpainful stimuli, and reported activation of PFC in response to rectal pain only in IBS and the ACC only in normal subjects. In contrast, more recently Mertz^[23], using fMRI, observed that pain led to a greater activation of the ACC than nonpainful stimuli. In Bernstein's^[42] study, they also found that normal controls and subjects with IBD and IBS shared similar loci of activations to visceral sensations of stool and pain. A significantly higher percentage of pixels activated in the anterior cingulate gyrus over both pain and stool conditions for the control group than for the IBS group and for the IBS group than for the IBD group ($P < 0.035$). In another study, Bonaz *et al* revealed significant deactivations within the right insula, the right amygdala, and the right striatum^[7]. There were gender differences in cortical representation of rectal distension in healthy humans. Male subjects showed localized clusters of fMRI activity primarily in the sensory and parietooccipital regions, whereas female subjects also showed activity in the anterior cingulate and insular regions^[43]. Thus, somatic and visceral sensation including pain perception can be studied noninvasively in humans with functional brain imaging techniques. Positron emission tomography and functional magnetic resonance imaging have identified a series of cerebral regions involved in the processing of somatic pain, including the anterior cingulate, insular, prefrontal, inferior parietal, primary and secondary somatosensory, and primary motor and premotor cortices, the thalamus, hypothalamus, brain stem, and cerebellum^[44]. Experimental evidence supports possible specific roles for individual structures in processing the various dimensions of pain^[44].

In conclusion, our data conform that fMRI is an objective brain imaging technique to measure the change in regional cerebral activation exactly. Using fMRI, some patients with IBS could be detected having visceral hypersensitivity in response to painful rectal balloon-distention. In this study, IC and PFC of IBS patients are the major loci in CNS processing of visceral perception.

REFERENCES

- 1 **Olden KW**. Diagnosis of irritable bowel syndrome. *Gastroenterology* 2002; **122**: 1701-1714
- 2 **Foxx-Orenstein AE**, Clarida JC. Irritable bowel syndrome in women: the physician-patient relationship evolving. *J Am Osteopath Assoc* 2001; **101**: S12-16
- 3 **Camilleri M**, Prather CM. The irritable bowel syndrome: Mechanisms and a practical approach to management. *Ann Intern Med* 1992; **116**: 1001-1008
- 4 **Thompson WG**, Longstreth GF, Drossman DA, Heaton KW, Irvine EJ, Muller-Lissner SA. Functional bowel disorders and functional abdominal pain. *Gut* 1999; **45** (Suppl 2): II43-47
- 5 **Verne GN**, Price DD. Irritable bowel syndrome as a common precipitant of central sensitization. *Curr Rheumatol Rep* 2002; **4**: 322-328
- 6 **Blomhoff S**, Diseth TH, Jacobsen MB, Vatn M. Irritable bowel syndrome-a multifactorial disease in children and adults. *Tidsskr Nor Laegeforen* 2002; **122**: 1213-1217
- 7 **Bonaz B**, Baciu M, Papillon E, Bost R, Gueddah N, Le Bas JF, Fournet J, Segebarth C. Central processing of rectal pain in patients with irritable bowel syndrome: an fMRI study. *Am J Gastroenterol* 2002; **97**: 654-661
- 8 **Menetrey D**, Gannon A, Levine JD, Basbaum AI. Expression of c-fos protein in interneurons and projection neurons of the rat spinal cord in response to noxious somatic, articular, and visceral stimulation. *J Comp Neurol* 1989; **285**: 177-195
- 9 **Bonaz B**, Plourde V, Tache Y. Abdominal surgery induces fos immunoreactivity in the rat brain. *J Comp Neurol* 1994; **349**: 212-222
- 10 **Traub RJ**, Silva E, Gebhart GF, Solodkin A. Noxious colorectal distention induced c-Fos protein in limbic brain structures in the rat. *Neurosci Lett* 1996; **215**: 165-168
- 11 **Bonaz B**, Riviere PJ, Sinniger V, Pascaud X, Junien JL, Fournet J, Feuerstein C. Fedotozine, a kappa-opioid agonist, prevents spinal and supra-spinal Fos expression induced by a noxious visceral stimulus in the rat. *Neurogastroenterol Motil* 2000; **12**: 135-148
- 12 **Casey KL**, Minoshima S, Berger KL, Koeppe RA, Morrow TJ, Frey KA. Positron emission tomographic analysis of cerebral structures activated specifically by repetitive noxious heat stimuli. *J Neurosurg* 1994; **71**: 802-807
- 13 **Craig AD**, Reiman EM, Evans A, Bushnell MC. Functional imaging of an illusion of pain. *Nature* 1996; **384**: 258-260
- 14 **Rainville P**, Duncan GH, Price DD, Carrier B, Bushnell MC. Pain effect encoded in human anterior cingulate but not somatosensory cortex. *Science* 1997; **277**: 968-971
- 15 **Coghill RC**, Sang CN, Maisog JM, Iadarola MJ. Pain intensity processing within the human brain: A bilateral, distributed mechanism. *J Neurophysiol* 1999; **82**: 1934-1943
- 16 **Talbot JD**, Marrett S, Evans AC, Meyer E, Bushnell MC, Duncan GH. Multiple representations of pain in human cerebral cortex. *Science* 1991; **251**: 1355-1358
- 17 **Derbyshire SW**, Jones AK, Gyulai F, Clark S, Townsend D, Firestone LL. Pain processing during three levels of noxious stimulation produces differential patterns of central activity. *Pain* 1997; **73**: 431-445
- 18 **Apkarian AV**, Gelnar PA, Krauss BR, Szevenenyi NM. Cortical responses to thermal pain depend on stimulus size: A functional MRI study. *J Neurophysiol* 2000; **83**: 3113-3122
- 19 **Rothstein RD**, Stecker M, Reivich M, Alavi A, Ding XS, Jaggi J, Greenberg J, Ouyang A. Use of positron emission tomography and evoked potentials in the detection of cortical afferents from the gastrointestinal tract. *Am J Gastroenterol* 1996; **91**: 2372-2376
- 20 **Silverman DH**, Munakata JA, Ennes H, Mandelkern MA, Hoh CK, Mayer EA. Regional cerebral activity in normal and pathological perception of visceral pain. *Gastroenterology* 1997; **112**: 64-72
- 21 **Bouras EP**, O'Brien TJ, Camilleri M, O'Connor MK, Mullan BP. Cerebral topography of rectal stimulation using single photon emission computerized tomography. *Am J Physiol* 1999; **277**: G687-694
- 22 **Baciu MV**, Bonaz BL, Papillon E, Bost RA, Le Bas JF, Fournet J, Segebarth CM. Central processing of rectal pain: A functional MR imaging study. *Am J Neuroradiol* 1999; **20**: 1920-1924
- 23 **Mertz H**, Morgan V, Tanner G, Pickens D, Price R, Shyr Y, Kessler R. Regional cerebral activation in irritable bowel syndrome and control subjects with painful and nonpainful rectal distention. *Gastroenterology* 2000; **118**: 842-848
- 24 **Derbyshire SW**, Jones AK, Devani P, Friston KJ, Feinmann C,

- Harris M, Pearce S, Watson JD, Frackowiak RS. Cerebral responses to pain in patients with atypical facial pain measured by positron emission tomography. *J Neurol Neurosurg Psychiatry* 1994; **57**: 1166-1172
- 25 **Fox PT**, Raichle ME. Focal physiological uncoupling of cerebral blood flow and oxidative metabolism during somatosensory stimulation in human subjects. *Proc Natl Acad Sci USA* 1986; **83**: 1140-1144
- 26 **Le Bihan D**, Jezzard P, Haxby J, Sadato N, Rueckert L, Mattay V. Functional magnetic resonance imaging of the brain. *Ann Intern Med* 1995; **122**: 296-303
- 27 **Kwong KK**, Belliveau JW, Chesler DA, Goldberg IE, Weisskoff RM, Poncelet BP, Kennedy DN, Hoppel BE, Cohen MS, Turner R. Dynamic magnetic resonance imaging of human brain activity during primary sensory stimulation. *Proc Natl Acad Sci USA* 1992; **89**: 5675-5679
- 28 **Bandettini PA**, Wong EC, Hinks RS, Tikofsky RS, Hyde JS. Time course EPI of human brain function during task activation. *Magn Reson Med* 1992; **25**: 390-397
- 29 **Bandettini PA**, Jesmanowicz A, Wong EC, Hyde JS. Processing strategies for time course data sets in functional MRI of the human brain. *Magn Reson Med* 1993; **30**: 161-173
- 30 **Belliveau JW**, Kennedy DN Jr, McKinstry RC, Buchbinder BR, Weisskoff RM, Cohen MS, Vevea JM, Brady TJ, Rosen BR. Functional mapping of the human visual cortex by magnetic resonance imaging. *Science* 1991; **254**: 716-719
- 31 **Yousry TA**, Schmid UD, Jassoy AG, Schmidt D, Eisner WE, Reulen HJ, Reiser MF, Lissner J. Topography of the cortical motor hand area: prospective study with functional MR imaging and direct motor mapping at surgery. *Radiology* 1995; **195**: 23-29
- 32 **Rosen SD**, Paulesu E, Nihoyannopoulos P, Tousoulis D, Frackowiak RS, Frith CD, Jones T, Camici PG. Silent ischemia as a central problem: regional brain activation compared in silent and painful myocardial ischemia. *Ann Intern Med* 1996; **124**: 939-949
- 33 **Aziz Q**, Andersson JL, Valind S, Sundin A, Hamdy S, Jones AK, Foster ER, Langstrom B, Thompson DG. Identification of human brain local processing esophageal sensation using positron emission tomography. *Gastroenterology* 1997; **113**: 50-59
- 34 **Devinsky O**, Morrell MJ, Vogt BA. Contributions of anterior cingulate cortex to behaviour. *Brain* 1995; **118**: 279-306
- 35 **Cechetto DF**, Saper CB. Role of the cerebral cortex in autonomic function. In: Loewy AD, Spyer KM, eds. Central regulation of autonomic function. *New York: Oxford University* 1990: 208-223
- 36 **Hanamori T**, Kunitake T, Kato K, Kannan H. Responses of neurons in the insular cortex to gustatory, visceral, and nociceptive stimuli in rats. *J Neurophysiol* 1998; **79**: 2535-2545
- 37 **Craig AD**, Chen K, Bandy D, Reiman EM. Thermosensory activation of insular cortex. *Nat Neurosci* 2000; **3**: 184-190
- 38 **Krushel LA**, van der Kooy D. Visceral cortex: integration of the mucosal senses with limbic information in the rat agranular insular cortex. *J Comp Neurol* 1988; **270**: 39-54, 62-63
- 39 **Kupfermann I**. Localization of higher cognitive and affective functions: the association cortices. In Kandell E, Schwartz J, Jessell T, eds. Principles of neuroscience. 3rd ed. *East Norwalk, CT: Appleton & Lange* 1991: 823-838
- 40 **Davidson RJ**. Anxiety and affective style: role of prefrontal cortex and amygdala. *Biol Psychiatry* 2002; **51**: 68-80
- 41 **Rogers J**. Testing for and the role of anal and rectal sensation. *Bailliers Clin Gastroenterol* 1992; **6**: 179-191
- 42 **Bernstein CN**, Frankenstein UN, Rawsthorne P, Pitz M, Summers R, McIntyre MC. Cortical mapping of visceral pain in patients with GI disorders using functional magnetic resonance imaging. *Am J Gastroenterol* 2002; **97**: 319-327
- 43 **Kern MK**, Jaradeh S, Arndorfer RC, Jesmanowicz A, Hyde J, Shaker R. Gender differences in cortical representation of rectal distension in healthy humans. *Am J Physiol Gastrointest Liver Physiol* 2001; **281**: G1512-1523
- 44 **Ladabaum U**, Minoshima S, Owyang C. Pathobiology of visceral pain: molecular mechanisms and therapeutic implications V. Central nervous system processing of somatic and visceral sensory signals. *Am J Physiol Gastrointest Liver Physiol* 2000; **279**: G1-6

Edited by Wu XN

Tuberculosis of pancreas and peripancreatic lymph nodes in immunocompetent patients: experience from China

Feng Xia, Ronnie Tung-Ping Poon, Shu-Guang Wang, Ping Bie, Xue-Quan Huang, Jia-Hong Dong

Feng Xia, Shu-Guang Wang, Ping Bie, Xue-Quan Huang, Jia-Hong Dong, Institute of Hepatobiliary Surgery, Southwest Hospital, Third Military Medical University, Chongqing 400038, China

Ronnie Tung-Ping Poon, Center for the Study of Liver Disease and Department of Surgery, University of Hong Kong Medical Centre, Queen Mary Hospital, Hong Kong, China

Correspondence to: Dr. Jia-Hong Dong, Institute of Hepatobiliary Surgery, Southwest Hospital, Third Military Medical University, Chongqing 400038, China. drfxia@hotmail.com

Telephone: +86-23-65387419 **Fax:** +86-23-65430233

Received: 2002-10-04 **Accepted:** 2002-11-16

Abstract

AIM: To determine the clinical, radiographic and laboratory characteristics, diagnostic methods, and therapeutic variables in immunocompetent patients with tuberculosis (TB) of the pancreas and peripancreatic lymph nodes.

METHODS: The records of 16 patients (6 male, 10 female; mean age 37 years, range 18-56 years) with tuberculosis of the pancreas and peripancreatic lymph nodes from 1983 to 2001 in the Southwest Hospital were analyzed retrospectively. In addition, 58 similar cases published in Chinese literature were reviewed and summarized. We reviewed the clinical, radiographic and laboratory findings, diagnostic methods, therapeutic approaches, and outcome in the patients. Criteria for the diagnosis of pancreatic tuberculosis were the presence of granuloma in histological sections or the presence of *Mycobacterium tuberculosis* DNA by polymerase chain reaction (PCR).

RESULTS: Predominant symptoms consisted of abdominal nodule and pain (75 %), anorexia/weight loss (69 %), malaise/weakness (64 %), fever and night sweats (50 %), back pain (38 %) and jaundice (31 %). Swelling of the head of the pancreas with heterogeneous attenuation echo was detected with ultrasound in 75 % (12/16). CT scan showed pancreatic mass with heterogeneous hypodensity focus in all patients, with calcification in 56 % (9/16) patients, and peripancreatic nodules in 38 % (6/16) patients. Anemia and lymphocytopenia were seen in 50 % (8/16) patients, and pancytopenia occurred in 13 % (2/16) patients. Hypertransaminasemia, elevated alkaline phosphatase (AP) and GGT were seen in 56 % (9/16) patients. The erythrocyte sedimentation rate (ESR) was elevated in 69 % (11/16) cases. Granulomas were found in 75 % (12/16) cases, and in 38 % (6/16) cases caseous necrosis tissue was found. Laparotomy was performed in 75 % (12/16) cases, and ultrasound-guided fine needle aspiration (FNA) was done in 63 % (10 of 16). The most commonly used combinations of medications were isoniazid/rifampin/streptomycin (63 %, $n=10$) and isoniazid/rifampin pyrazinamide/streptomycin or ethambutol (38 %, $n=6$). The duration of treatment lasted for half or one year and treatment was successful in all cases. The characteristics of 58 cases from Chinese literature were also summarized.

CONCLUSION: Tuberculosis of the pancreas and peripancreatic lymph nodes should be considered as a diagnostic possibility in patients presenting with a pancreatic mass, and diagnosis without laparotomy is possible if only doctors are aware of its clinical features and investigate it with appropriate modalities. Pancreatic tuberculosis can be effectively cured by antituberculous drugs.

Xia F, Poon RTP, Wang SG, Bie P, Huang XQ, Dong JH. Tuberculosis of pancreas and peripancreatic lymph nodes in immunocompetent patients: experience from China. *World J Gastroenterol* 2003; 9(6): 1361-1364

<http://www.wjgnet.com/1007-9327/9/1361.asp>

INTRODUCTION

Tuberculosis (TB) is a potentially systemic disease that can infect any organ and system. It was a prevalent disease in the developing countries about 50 years ago, but its incidence has been controlled with the availability of effective anti-tuberculous drugs. However, the last decade has witnessed a rise in the incidence of tuberculosis even in developed countries. In the United States, the Centers for Disease Control reported that the incidence of TB was significantly greater in 1994 than in 1985^[1]. Nowadays, TB is often an acquired immune deficiency syndrome (AIDS)-defining illness in individuals found to be human immunodeficiency virus (HIV) antibody-positive; however, it can still cause a devastating disease in immunocompetent hosts^[1,2]. In China, there is a revival trend in the incidence of TB although AIDS remains uncommon nationally.

Abdominal infection with tuberculosis commonly affects the spleen, liver, and ileocecal region^[2,3]. Pancreatic tuberculosis is an extremely rare disease, especially when it is isolated in the pancreas. There were a few case reports published before in literature, but its clinical characteristics remain unclear^[4-6]. In this retrospective study, we reported 16 patients with TB of the pancreas and peripancreatic lymph nodes, and summarized the clinical features of 58 similar cases in the Chinese language literature where the HIV antibody status of the patients was either negative or not stated. The clinical, radiographical and laboratory findings, diagnostic methods, therapeutic approaches, and outcome in patients in an endemic area were reviewed in this study.

MATERIALS AND METHODS

The records of 16 patients who were admitted to Hepatobiliary Surgery Center, Southwest Hospital, Third Military Medical University, Chongqing, China with TB of the pancreas and peripancreatic lymph nodes between 1983 and 2001 were reviewed. The clinical, radiographic and laboratory findings, diagnostic methods, therapeutic approaches, and outcome in these patients were summarized. Ten patients were screened for anti-HIV antibodies. Criteria for the diagnosis of pancreatic TB were (1) paraffin-embedded tissues with granuloma or (2) the presence of *Mycobacterium tuberculosis* DNA by

polymerase chain reaction (PCR). IS 6110-specific primers, which could amplify all *M. tuberculosis* complex strains, were used for amplification. In addition, all available bacteriological and histological studies were performed to confirm the diagnosis. The clinical and laboratory features of patients were collected from the casebooks. Details of follow-up were obtained from medical records. In addition, 58 similar cases published in the Chinese literature were also reviewed and summarized.

RESULTS

A total of 16 patients with TB of the pancreas and peripancreatic lymph nodes had been documented. Six patients were male and 10 were female, with a mean age of 37 years (range 18-56 years). Eight patients had predisposing factors. Six patients had a history of pulmonary TB or TB of lymph nodes, one had diabetes mellitus, and one had connective tissue disease.

Presenting symptoms and physical findings

Predominant symptoms consisted of fever, abdominal pain, abdominal nodule, back pain, jaundice, malaise/weakness, anorexia/weight loss and night sweats. In twelve patients with abdominal nodule and pain, eleven had anorexia/weight loss, ten had malaise/weakness, eight had fever and night sweats, six had back pain, and five had jaundice.

Fever, usually the intermittent type, was present in eight patients. The mean duration of fever prior to the diagnosis was 23 days (range 11-35 days).

Radiographic findings

Chest X-rays revealed relic of TB focus in 8 patients, 6 with pneumonitis. All of the patients had been examined with ultrasound and computed tomography (CT) scan. Twelve patients showed swollen head of the pancreas with ultrasound image of heterogeneous attenuation echo. Four patients were demonstrated to have inner heterogeneous attenuation echo in head or body of the pancreas. CT scan showed pancreatic mass with heterogeneous hypodensity focus in all of the patients, with calcification in 9 of 16 patients, and peripancreatic nodules in 6 of 16 patients (Figures 1, 2 and 3). Endoscopic retrograde cholangiopancreatography had been performed for 12 cases, and 2 cases had pancreatic duct dilatation. Magnetic resonance imaging and digital subtraction angiogram had been done for 6 patients, and the results showed pancreatic nodules and/or peripancreatic mass.

Tuberculin skin test

Tuberculin skin test was performed on 9 patients before initiation of therapy. Four in 9 were positive (≥ 10 mm of induration) to 5TU of intradermally purified protein derivative (PPD).

Haematology and biochemistry

In 8 patients, anemia and lymphocytopenia were seen. Pancytopenia occurred in 2 patients. Hypertransaminasemia, elevated alkaline phosphatase (AP) and GGT were seen in 9 patients, respectively. The erythrocyte sedimentation rate (ESR) was elevated in 11 cases.

Results of smears and mycobacterial cultures

Secretions and body fluids were examined microscopically and cultured in 9 patients. Acid-fast bacilli were demonstrated in 1 case, and cultures for *M. tuberculosis* were positive in 4 out of 9 specimens tested. Anti-TB drug susceptibility was studied in 4 patients, and two *M. tuberculosis* strains were sensitive to the major anti-TB drugs including isoniazid (INH), rifampin

(RMP), pyrazinamide (PZA), streptomycin (SM), and ethambutol (EMB). The other 2 cases were not sensitive to rifampin, isoniazid and streptomycin, respectively.



Figure 1 Mass with heterogeneous hypodensity located in the head of pancreas. The body and tail of the pancreas appeared atrophy, and with enlarged main pancreatic duct.



Figure 2 Pancreas appeared swollen diffusely with heterogeneous enhancement and vague margin. A circle lymph nodes showed enhancement under pancreas.



Figure 3 Calcification of pancreatic TB occurred under the body of the pancreas and retroperitoneal lymph nodes.

Biopsy data

Granuloma was found in 12 cases among specimens harvested from the pancreas and peripancreatic nodule by laparotomy (12 of 16) and ultrasound-guided fine needle aspiration (FNA) (10 of 16). Caseous necrosis tissue was found in 6 of 16 cases, and results of smears showed that there were Langhans' giant cells, epithelioid cells and lymphocytes. Seven of the 16 patients had combined TB in the liver, bile duct or spleen.

Initial diagnosis

Eleven of 16 patients were initially given a diagnosis of pancreatic tumor. The diagnosis of pancreatic TB had been firstly confirmed for only three of 16 cases. Another three cases were diagnosed with retroperitoneal tumor.

Treatment regimen and outcome

Biopsy and/or FNA were done for all of the patients. Twelve in 16 cases received laparotomy. In one case, cholangiojejunostomy was performed for CBD obstruction, and in another two cases splenectomy was performed for splenic tuberculosis. All 16 patients received treatment with antitubercotics for TB. The most commonly used combinations were INH/RMP/SM ($n=10$) and INH/RMP/PZA/SM or EMB ($n=6$). The therapeutic duration lasted for a half or one year.

Twelve patients received follow-up from a half to 14 years. No recurrence of TB was found in the pancreas or other organs. In 11 patients, follow-up CT scans in abdomen were available. Resolution was complete in all patients. The mean time to resolution was 132 days (range 78-186 days).

Literature review

A total of 58 cases of pancreatic TB have been described in the Chinese language literature^[7-17]. Fifteen of the 58 patients were stated to be HIV antibody-negative, and the HIV status of the other patients was not confirmed. All of the 58 patients were diagnosed by histological appearance being consistent with characteristics of tuberculosis, or positive organisms by acid-fast staining, culture of *Mycobacterium tuberculosis* or PCR analysis. Twenty patients were male and 36 were female, with a mean age 43.5 years (from 14 to 73). The main symptoms were epigastric pain and discomfort (37 cases), fever (31 cases), weight loss (23 cases) and anorexia (21 cases). The other unusual symptoms included malaise/weakness (11 cases), back pain (9 cases), nausea/vomiting (8 cases), jaundice (6 cases), night sweats (6 cases), upper gastrointestinal bleeding (3 cases), cough (3 cases) and diarrhea (1 case). The duration of symptoms prior to presentation ranged from 5 days to 5 months (mean 2.6 months). Thirteen cases gave a past history of TB pneumonia (10 cases) and TB lymph nodes (3 cases). The appearance of the chest X-ray was reported in 49 cases. There was relic of TB focus in 14 patients, 9 with pneumonitis. 34 patients received tuberculin skin testing, of which 21 were positive. Single or multiple modalities of investigation were performed for the patients. Ultrasound revealed pancreatic mass in 38 cases and failed to do so in another 9 cases. Abdominal CT scan was used in 41 cases and reported pancreatic mass and/or peripancreatic nodules in all cases. MRI was performed in 19 cases and also showed a mass in all instances. ERCP found abnormalities with CBD and pancreatic duct in 7 cases. Abdominal X-ray showed focal calcification in 6 cases and DSA located a mass in 4 cases. Ultrasound-guided fine needle aspiration was performed in 21 cases and was successful in diagnosis in 14 cases. Laparoscopic biopsy was performed in 7 cases and confirmed diagnosis in all cases. Fifteen patients had combined TB in other organs.

The initial diagnoses included pancreatic tumor (35), chronic pancreatitis (7), retroperitoneal tumor (5), acute pancreatitis (4) and pancreatic TB (3). Thirty-nine patients underwent laparotomy, 24 for biopsy, 12 for FNA, 5 for pus cavity draining, 4 for choledochojejunostomy, 2 for pancreatoduodenectomy, and 1 for celiac ganglia resection. Pathological report showed granuloma in 27 patients. Acid-fast bacilli were demonstrated in 14 of 27 cases, and cultures for *M. tuberculosis* were positive in 8 out of 19 specimens tested.

The treatment details were given in 41 of 58 cases. The common agents were isoniazid, rifampicin, streptomycin, pyrazinamide and ethambutol. Combinations of 3 or 4 drugs were used for 36 patients. The duration of treatment was recorded in 28 cases, ranging from 3 to 12 months. 24 patients were reported to have resolution after treatment for 3 to 12 months. One death was reported among the 58 cases.

DISCUSSION

We have presented a description of a series of 16 cases with tuberculosis of the pancreas and peripancreatic lymph nodes in immunocompetent patients. Having reviewed Chinese literature we found 58 similar cases and summarized their clinical findings. Pancreatic TB is extremely rare. Diagnosis remains difficult for most of the patients, and it is especially difficult to differentiate pancreatic TB from pancreatic tumor. Our series and review of Chinese literature revealed several clinical characteristics as follows: (1) pancreatic TB is mostly suffered by young people, with a predominance of female over male. In contrast, pancreatic tumor is common in old people; (2) some patients have a history of TB in past, and most of them come from areas with high prevalence of active tuberculosis; (3) the patients often present with epigastric pain, fever and weight loss; (4) ultrasound and CT scan show pancreatic mass and peripancreatic nodules, sometimes with focal calcification; (5) FNA and laparoscopic biopsy are the diagnostic procedures of choice for patients with a high suspicion of pancreatic TB. It can lead to confirmed diagnosis and hence avoids laparotomy. Treatment using combination of 3 or 4 antituberculous drugs is effective for most patients. However, attention should be paid to the possibility of drug resistance to some agents that have been used for a long time.

Recently, the incidence of tuberculosis is increasing^[1-6]. Cases of pancreatic TB are being reported with increasing frequency, too^[18-22]. The reasons may be related to evolutionary changes in the biology of the mycobacterium, drug resistance, and new populations with immunological deficits. Cases related to acquired immunodeficiencies, AIDS or immunosuppression for transplantation have been reported more frequently. Jenney *et al.* had reviewed English language literature before 1998. A total of 37 cases of pancreatic TB in patients not stated to be HIV antibody-positive was found^[23]. The authors concluded that it was important to consider the diagnosis of TB when a patient presented with epigastric pain, fever and weight loss and a mass lesion in the pancreas by diagnostic imaging. Three forms of mycobacterial infection of the pancreas have been described as follows: (1) generalized (military) tuberculosis, in which *Mycobacterium tuberculosis* is the agent; (2) spread to the pancreas from celiac and other retroperitoneal lymph nodes, in which *Mycobacterium bovis* is the main agent to be considered; (3) primary localized pancreatic tuberculosis due to *Mycobacterium tuberculosis*, which may reflect a point of origin from the intestinal tract^[24-32].

In conclusion, tuberculosis of the pancreas and peripancreatic lymph nodes in immunocompetent patients is rare and could present a diagnostic challenge. However, if doctors are aware of its clinical features and conduct appropriate investigations with multiple modalities including CT scan and ultrasound-guided FNA or laparoscopic biopsy, diagnosis of pancreatic tuberculosis without laparotomy is possible and the disease can be effectively treated with antituberculous drugs.

REFERENCES

- 1 **Babu RD**, John V. Pancreatic tuberculosis: case report and review of the literature. *Trop Gastroenterol* 2001; **22**: 213-214
- 2 **Evans JD**, Hamanaka Y, Olliff SP, Neoptolemos JP. Tuberculosis of the pancreas presenting as metastatic pancreatic carcinoma. A case report and review of the literature. *Dig Surg* 2000; **17**: 183-187
- 3 **Turan M**, Sen M, Koyuncu A, Aydin C, Elaldi N, Arici S. Pancreatic Pseudotumor due to Peripancreatic Tuberculous Lymphadenitis. *Pancreatol* 2002; **2**: 561-564
- 4 **Suri S**, Gupta S, Suri R. Computed tomography in abdominal tuberculosis. *Br J Radiol* 1999; **72**: 92-98
- 5 **Tanabe N**, Ikematsu Y, Nishiwaki Y, Kida H, Murohisa G, Ozawa T, Hasegawa S, Okawada T, Toritsuka T, Waki S. Pancreatic tuberculosis. *J Hepatobiliary Pancreat Surg* 2002; **9**: 515-518

- 6 **Shan YS**, Sy ED, Lin PW. Surgical resection of isolated pancreatic tuberculosis presenting as obstructive jaundice. *Pancreas* 2000; **21**: 100-101
- 7 **Li XH**, Wang YL, Yao YM. A case of local portal hypertension caused by pancreatic TB. *Zhonghua Gandan Waike Zazhi* 1999; **4**: 28-28
- 8 **Zhao MF**, Yang JF. Analysis of 11 cases pancreatic tuberculosis. *Zhonghua Putong Waike Zazhi* 2000; **15**: 292-293
- 9 **Tang TJ**. A case of misdiagnosis of pancreatic tuberculosis. *Chuanbei Yixueyuan Xuebao* 2000; **3**: 15-15
- 10 **Li GC**, Yao L. Analysis of 18 cases of pancreatic tuberculosis. *Zhongguo Shiyong Waike Zazhi* 1998; **18**: 755-756
- 11 **Zhao LB**, Hao F. Analysis of misdiagnosis of 4 cases pancreatic tuberculosis and a literature review. *Shiyong Yiyao Zazhi* 1998; **11**: 23-24
- 12 **Hou JX**, Fan YH. Diagnosis and treatment of pancreatic tuberculosis. *Zhonghua Jiehe He Huxi Zazhi* 1998; **21**: 689-689
- 13 **Li Z**, Wu LH, Pei SJ. A report of 3 cases of misdiagnosis of pancreatic tuberculosis. *Linchuang Wuzhen Wuzhi* 2000; **8**: 17-17
- 14 **Zhao JP**, Chen ZX. The diagnosis and treatment of Tuberculosis of pancreas and peripancreatic lymph nodes. *Zhongguo Jijiu Yixue* 1999; **19**: 737-737
- 15 **Zhong SX**, Zhao P. A report of 8 cases of pancreatic tuberculosis. *Zhonghua Waike Zazhi* 1996; **34**: 476-478
- 16 **Sun PL**, Chen TX. Three cases of pancreatic tuberculosis. *Xin Xiaohua Binxue Zazhi* 1997; **5**: 11-11
- 17 **Zhou XX**, Yin J. A report of 4 cases of pancreatic tuberculosis. *Zhonghua Chaosheng Yingxiangxue Zazhi* 1998; **7**: 373-373
- 18 **Ladas SD**, Vaidakis E, Lariou C, Anastasiou K, Chalevelakis G, Kintzonidis D, Raptis SA. Pancreatic tuberculosis in non-immunocompromised patients: reports of two cases, and a literature review. *Eur J Gastroenterol Hepatol* 1998; **10**: 973-976
- 19 **Demir K**, Kaymakoglu S, Besisik F, Durakoglu Z, Ozdil S, Kaplan Y, Boztas G, Cakaloglu Y, Okten A. Solitary pancreatic tuberculosis in immunocompetent patients mimicking pancreatic carcinoma. *J Gastroenterol Hepatol* 2001; **16**: 1071-1074
- 20 **Kouraklis G**, Glinavou A, Karayiannakis A, Karatzas G. Primary tuberculosis of the pancreas mimicking a pancreatic tumor. *Int J Pancreatol* 2001; **29**: 151-153
- 21 **Chaudhary A**, Negi SS, Sachdev AK, Gondal R. Pancreatic tuberculosis: still a histopathological diagnosis. *Dig Surg* 2002; **19**: 389-392
- 22 **Yokoyama T**, Miyagawa S, Noike T, Shimada R, Kawasaki S. Isolated pancreatic tuberculosis. *Hepatogastroenterology* 1999; **46**: 2011-2014
- 23 **Jenney AW**, Pickles RW, Hellard ME, Spelman DW, Fuller AJ, Spicer WJ. Tuberculosis pancreatic abscess in an HIV antibody-negative patient: case report and review. *Scand J Infect Dis* 1998; **30**: 99-104
- 24 **Franco-Paredes C**, Leonard M, Jurado R, Blumberg HM, Smith RM. Tuberculosis of the pancreas: report of two cases and review of the literature. *Am J Med Sci* 2002; **323**: 54-58
- 25 **Riaz AA**, Singh A, Robshaw P, Isla AM. Tuberculosis of the pancreas diagnosed with needle aspiration. *Scand J Infect Dis* 2002; **34**: 303-304
- 26 **Echenique Elizondo M**, Amondarain Arratibel J, Compton CC, Warshaw AL. Tuberculosis of the pancreas. *Surgery* 2001; **129**: 114-116
- 27 **Akhan O**, Pringot J. Imaging of abdominal tuberculosis. *Eur Radiol* 2002; **12**: 312-323
- 28 **Ozden I**, Emre A, Demir K, Balci C, Poyanli A, Ilhan R. Solitary pancreatic tuberculosis mimicking advanced pancreatic carcinoma. *J Hepatobiliary Pancreat Surg* 2001; **8**: 279-283
- 29 **Kwon AH**, Inui H, Kamiyama Y. Preoperative laparoscopic examination using surgical manipulation and ultrasonography for pancreatic lesions. *Endoscopy* 2002; **34**: 464-468
- 30 **Small G**, Wilks D. Pancreatic mass caused by Mycobacterium tuberculosis with reduced drug sensitivity. *J Infect* 2001; **42**: 201-202
- 31 **Chen CH**, Yang CC, Yeh YH, Yang JC, Chou DA. Pancreatic tuberculosis with obstructive jaundice-a case report. *Am J Gastroenterol* 1999; **94**: 2534-2536
- 32 **Karia K**, Mathur SK. Tuberculous cold abscess simulating pancreatic pseudocyst. *J Postgrad Med* 2000; **46**: 33-34

Edited by Zhang JZ

Prevalence of anti-ulcer drug use in a Chinese cohort

Tzeng-Ji Chen, Li-Fang Chou, Shinn-Jang Hwang

Tzeng-Ji Chen, Shinn-Jang Hwang, Department of Family Medicine, Taipei Veterans General Hospital and National Yang-Ming University School of Medicine, Taipei, Taiwan, China

Li-Fang Chou, Department of Public Finance, National Chengchi University, Taipei, Taiwan, China

Correspondence to: Professor Shinn-Jang Hwang, Department of Family Medicine, Taipei Veterans General Hospital, 201, Sec. 2, Shih-Pai Road, Taipei 11217, Taiwan, China. sjhwang@vghtpe.gov.tw

Telephone: +86-2-28757458 **Fax:** +86-2-28737901

Received: 2003-02-25 **Accepted:** 2003-03-16

Abstract

AIM: To estimate the age-specific prevalence of anti-ulcer drug use and to calculate the usage of different anti-ulcer drugs over 5 years within the universal health insurance program in Taiwan area.

METHODS: The National Health Insurance Research Database in Taipei supplied the cohort data sets of 200 000 people. The ambulatory and inpatient claims of the cohort from 1997 to 2001 were analyzed. The anti-ulcer drugs included all drug items of the group A02B (drugs for treatment of peptic ulcer) in the Anatomical Therapeutic Chemical classification system (version 2000). The amount of drug usage was measured in unit of defined daily dose.

RESULTS: Among the totally 13 034 393 visits with 56 672 631 ambulatory prescription items, there were 398 150 (0.7 %) prescribed items of anti-ulcer drugs in 378 855 (2.9 %) visits. Among the 107 649 admissions with 5 762 312 inpatient prescription items, there were 24 598 (0.4 %) prescribed items of anti-ulcer drugs in 11 548 (10.7 %) admissions. The annual prevalence of anti-ulcer drug use was 9.6 % in 1997, 11.6 % in 1998, 15.4 % in 1999, 14.5 % in 2000, and 15.9 % in 2001 respectively. The 5-year prevalence was 36.1 %. The age-specific prevalence among the people younger than 20 years was 9.2 % in 2001 and 23.7 % during the 5-year period. Cimetidine not only was the most popular ingredient among anti-ulcer drugs (57 634 cimetidine users in 70 729 all anti-ulcer drug users during the 5-year period) but also had the largest prescribed amount (42.3 % of DDDs for all anti-ulcer drug users during the 5-year period). The annually prescribed amount of anti-ulcer drugs had grown from 4.9 DDDs/1000 inhabitants/day in 1997 to 7.5 in 2001. This increase was largely attributed to H₂-receptor antagonists and the expanding number of users.

CONCLUSION: Prescribing of anti-ulcer drugs is indeed popular among the Chinese population in Taiwan area. The disproportionate use of anti-ulcer drugs by children demands further investigation.

Chen TJ, Chou LF, Hwang SJ. Prevalence of anti-ulcer drug use in a Chinese cohort. *World J Gastroenterol* 2003; 9(6):1365-1369 <http://www.wjgnet.com/1007-9327/9/1365.asp>

INTRODUCTION

In the past three decades, the invention of several revolutionary

anti-ulcer drugs, *e.g.* H₂-receptor antagonists, synthetic prostaglandins, proton pump inhibitors, and cytoprotective agents, has changed the physicians' treatment patterns in gastroenterology and greatly improved the ulcer-healing rate of patients with peptic ulcer disease^[1-6]. In spite of effectiveness and popularity, the cost of these drugs has also aroused concern in the health care systems of developed countries^[7-11]. The concern has been aggravating in recent years because of expanding use of proton pump inhibitors in treating gastroesophageal reflux disease. Although prescribing of these potent acid-suppressing drugs is popular, their patterns of utilization have been infrequently documented in national surveys^[12-21].

In Taiwan area, a single and universal health insurance program started in 1995 and covered nearly all inhabitants (21 653 555 beneficiaries at the end of 2001)^[22]. The prescription drug benefits are included in the insurance. Because all claims data for the reimbursement purpose are in electronic form and available to researchers, we can perform a survey of anti-ulcer drug use among the Chinese population in Taiwan area.

The aims of this study were twofold: to estimate the age-specific prevalence of anti-ulcer drug use and to calculate the usage of different anti-ulcer drugs over 5 years within the universal health insurance program in Taiwan area. The strengths of our study were to use the longitudinal data sets of a representative cohort of 200 000 people and to adopt the unit of international standards in measuring the anti-ulcer drug usage.

MATERIALS AND METHODS

Data sources

We obtained 4 cohort data sets (R01-4) from the National Health Insurance Research Database (NHIRD; <http://www.nhri.org.tw/nhird/>) in Taipei in November 2002. The total 200 000 people in these 4 cohort data sets had been randomly sampled from 23 753 407 people who were ever insured under the universal health insurance program in Taiwan area from March 1, 1995 to December 31, 2000. Not every person of the cohort was insured through the study period because of new birth, death, immigration, and emigration. The cohort data sets contained all insurance claims of 200 000 people from 1996 to 2001. The structure of the insurance claim files had been described in details in our previous study^[23].

In the current study, we analyzed the ambulatory and inpatient files of the cohort data sets from 1997 to 2001. Totally, there were 13 034 393 visits, 56 672 631 ambulatory prescription items, 107 649 admissions, and 5 762 312 inpatient prescription items.

Besides, we obtained a complete file of 21 146 approved drug items of Western medicine in Taiwan area from the web site of the Bureau of National Health Insurance (BNHI; <http://www.nhi.gov.tw/>; accessed January 12, 2002). Each drug of different brand, strength and form was officially assigned a unique code for use in the claims file. The BNHI also offered a list of ATC codes (the Anatomical Therapeutic Chemical classification system, version 2000)^[24] for each drug item.

Study design

The anti-ulcer drugs in our study included all drug items of the group A02B (drugs for treatment of peptic ulcer, renamed to 'drugs for peptic ulcer and gastroesophageal reflux disease')

in 2002) in the ATC classification system. This group of drugs has 5 subgroups of the fourth level: A02BA (H₂-receptor antagonists, H₂RA), A02BB (prostaglandins), A02BC (proton pump inhibitors, PPI), A02BD (combinations for eradication of *Helicobacter pylori*), and A02BX (other drugs for treatment of peptic ulcer, renamed to 'other drugs for peptic ulcer and gastroesophageal reflux disease' in 2002). A total of 428 anti-ulcer drug items, including the original brands and generics, have been registered in Taiwan area since 1995. Some drugs might be no more available on the market or not reimbursable by the insurance during the study period.

In estimating the age-specific prevalence of anti-ulcer drug use, we first identified the people receiving anti-ulcer drug items in each year. Because the number of people in the cohort fluctuated during the study period, we calculated the number of the denominator in each year by excluding those people who were not insured at any time of that year. A person's age in a year was defined as the difference between her/his birthday and the end of that year. In estimating the 5-year age-specific prevalence from 1997 to 2001, we took December 31, 2001 as the index date to calculate a person's age.

In describing the distribution of anti-ulcer drug prescriptions among the cohort, we calculated the number of recipients and the total prescribed amount for each ingredient (ATC 5th level) in each year. Supposed that the cohort did not take anti-ulcer drugs before the base year of 1997, the number of new anti-ulcer drug users was additionally computed for each year after 1997. The prescribed amounts of anti-ulcer drugs were measured in unit of defined daily dose (DDD) by ATC classification system^[24]. The original dose of each prescription was converted to a number of DDDs according to the DDD of the ingredient. Some anti-ulcer drugs (e.g. cetraxate, urogastone, and gefarnate) lacked either ATC codes or DDDs; we used the most commonly prescribed daily doses as their DDDs. For international comparison, the numbers of DDDs per 1,000 inhabitants per day were also computed.

Statistical analysis

The database software of Microsoft SQL Server 2000 was used

for data linkage and processing. The regular statistics were displayed.

RESULTS

General information of the cohort

Among the 200 000-people cohort, only 195 971 people were eligible during the 5-year study period. The other 4 029 people who had dropped out of the insurance before 1997 would not be included in the following analyses. The number of eligible people varied from year to year (Table 1). There were more men than women (100 257 vs. 95 654), and the status of sex was unknown in 60 persons.

General information of anti-ulcer drug prescriptions

During the 5-year study period, 356 distinct anti-ulcer drugs had existed in the cohort data sets. The drugs belonged to 18 ingredients of ATC 5th level. At the ambulatory sector, there were 398 150 (0.7 %) prescribed items of anti-ulcer drugs in 378 855 (2.9 %) visits; at the inpatient sector, there were 24 598 (0.4 %) prescribed items in 11 548 (10.7 %) admissions.

Age specific prevalence of anti-ulcer drug use

In 1997, as high as 9.6 % (17 414/180 781) of eligible cohort received anti-ulcer drugs. The percentage increased by two-thirds to 15.9 % (29 181/183 976) in 2001. More than a third (36.1 %) of the cohort had ever received anti-ulcer drugs during the 5-year study period. Generally, the prevalence of anti-ulcer drug use increased with age. Another noteworthy finding was that anti-ulcer drugs had been prescribed to an appreciable percentage of children and adolescents (Table 1).

Recipients of anti-ulcer drugs by ingredient

Cimetidine was the most popular ingredient of anti-ulcer drugs among the cohort, followed by sucralfate, ranitidine, famotidine, omeprazole, pirenzepine, and lansoprazole (Table 2). The majority of new anti-ulcer drug users in each year were also attributed to cimetidine.

Table 1 Age distribution of patients receiving anti-ulcer drugs and age-specific prevalence of anti-ulcer drug use from 1997 to 2001

	1997	1998	1999	2000	2001	1997-2001
Sampling cohort						
0 - 19 years	57388	56427	55448	54684	51029	52103
20 - 39 years	62613	63765	64848	65219	63800	69425
40 - 59 years	39809	41420	42922	44241	45432	47663
60 years and older	20971	21836	22489	23093	23715	26780
Total	180781	183448	185707	187237	183976	195971
Patients with anti-ulcer drugs						
0 - 19 years	2965	3611	5171	4634	4712	12339
20 - 39 years	5345	6741	9249	8788	9673	23741
40 - 59 years	4933	6213	8277	8113	8664	20166
60 years and older	4172	4787	5905	5643	6132	14483
Total	17415	21352	28602	27178	29181	70729
Prevalence of anti-ulcer drug use						
0 - 19 years	5.2 %	6.4 %	9.3 %	8.5 %	9.2 %	23.7 %
20 - 39 years	8.5 %	10.6 %	14.3 %	13.5 %	15.2 %	34.2 %
40 - 59 years	12.4 %	15.0 %	19.3 %	18.3 %	19.1 %	42.3 %
60 years and older	19.9 %	21.9 %	26.3 %	24.4 %	25.9 %	54.1 %
Total	9.6 %	11.6 %	15.4 %	14.5 %	15.9 %	36.1 %

Table 2 Recipients of anti-ulcer drugs by main ingredient from 1997 to 2001 (number of new users in parentheses)

ATC ^a coding	Group/ingredient name	1997	1998	1999	2000	2001	1997-2001
A02BA	H ₂ RA						
	01 Cimetidine	11538	15793 (11340)	22905 (14525)	22356 (10564)	24305 (9667)	57634
	02 Ranitidine	1588	1852 (1482)	2262 (1757)	2283 (1611)	2579 (1802)	8240
	03 Famotidine	974	1143 (953)	1401 (1113)	1526 (1216)	1669 (1232)	5488
	04 Nizatidine	187	255 (221)	295 (236)	199 (157)	137 (108)	909
	06 Roxatidine	89	98 (82)	87 (76)	83 (67)	97 (80)	394
A02BB	Prostaglandins						
	01 Misoprostol	128	145 (129)	156 (135)	150 (112)	88 (68)	572
A02BC	PPIS						
	01 Omeprazole	709	913 (807)	1168 (990)	1150 (917)	1445 (1156)	4579
	02 Pantoprazole	-	1(1)	84 (84)	147 (133)	273 (255)	473
	03 Lansoprazole	151	391 (365)	531 (459)	647 (537)	785 (643)	2155
	04 Rabeprazole	-	-	-	-	31 (31)	31
A02BX	Other drugs						
	01 Carbenoxolone	287	260 (219)	337 (271)	155 (105)	199 (164)	1046
	02 Sucralfate	3463	3192 (2510)	3107 (2301)	2390 (1506)	2173 (1390)	11170
	03 Pirenzepine	1177	1197 (937)	1181 (857)	731 (454)	625 (351)	3776
	05 Bismuth subcitrate	329	299 (266)	271 (223)	173 (141)	142 (111)	1070
	06 Proglumide	113	61 (53)	36 (34)	3 (3)	8 (5)	208
	07 Gefarnate	248	295 (270)	416 (363)	326 (265)	203 (161)	1307
	- Cetraxate	356	101 (81)	72 (59)	48 (40)	41 (37)	573
	- Urogastrone	192	46 (34)	42 (32)	14 (12)	6 (5)	275
Total		17415	21352 (14423)	28602 (16611)	27178 (11660)	29181 (10622)	70729

^aATC=Anatomical therapeutic chemical classification system.

Table 3 Total prescribed amount of anti-ulcer drugs by main ingredient from 1997 to 2001 (unit of measurement: numbers of defined daily doses [DDDs])

ATC ^a coding	Group/ingredient name	1997	1998	1999	2000	2001
A02BA	H ₂ RA					
	01 Cimetidine	114145	151403	221528	198255	221836
	02 Ranitidine	57329	62357	69780	69954	88034
	03 Famotidine	33366	40063	51198	52852	53108
	04 Nizatidine	8943	12304	12282	8269	5305
	06 Roxatidine	3493	3057	3215	2847	4460
A02BB	Prostaglandins					
	01 Misoprostol	2244	3649	5594	4534	1941
A02BC	PPIS					
	01 Omeprazole	26635	33587	46429	43589	57193
	02 Pantoprazole	-	14	2593	4845	9276
	03 Lansoprazole	5840	14276	19624	24860	31023
	04 Rabeprazole	-	-	-	-	864
A02BX	Other drugs					
	01 Carbenoxolone	5708	4164	4768	1945	1918
	02 Sucralfate	26172	20170	15942	10960	9898
	03 Pirenzepine	7575	7378	5925	3868	3942
	05 Bismuth subcitrate	7999	6104	5213	2686	2754
	06 Proglumide	1010	459	198	12	31
	07 Gefarnate	14379	17859	26568	16682	8972
	- Cetraxate	4072	1254	849	615	657
	- Urogastrone	5067	1272	1151	232	32
Total		323976	379370	492856	447005	501243
	Ambulatory sector	297213	355837	465326	420144	470924
	Inpatient sector	26764	23532	27530	26861	30319
DDDs / 1000 inhabitants / day		4.9	5.7	7.3	6.5	7.5

^aATC=Anatomical therapeutic chemical classification system.

Total prescribed amounts of anti-ulcer drugs

Measured in unit of DDDs, cimetidine again had the largest prescribed amount (42.3 %) of all anti-ulcer drugs among the cohort during the 5-year study period (Table 3). It was then followed by ranitidine (16.2 %), famotidine (10.8 %), omeprazole (9.7 %), and lansoprazole (4.5 %). The majority of anti-ulcer drugs were used at the ambulatory sector (93.7 % of total DDDs).

The total prescribed amount of anti-ulcer drugs grew from 4.9 DDDs/1 000 inhabitants/day in 1997 to 7.5 in 2001 (Table 3). This increase was attributed to the expanded number of users because the average prescribed amount of anti-ulcer drugs per user in a year remained relatively stable (18.7 ± 54.8 DDDs in 1997, 17.9 ± 41.0 in 1998, 17.3 ± 51.0 in 1999, 16.5 ± 40.5 in 2000, and 17.3 ± 40.8 in 2001).

On the other hand, H₂-receptor antagonists and proton pump inhibitors had contributed to the growth of the total prescribed amount of anti-ulcer drugs during the study period (Figure 1). While H₂-receptor antagonists had the largest share of growth, proton pump inhibitors had the highest growth rate. In the meantime, the usage of prostaglandins had remained stable, but other drugs for treatment of peptic ulcer had fewer users and smaller prescribed amount totally.

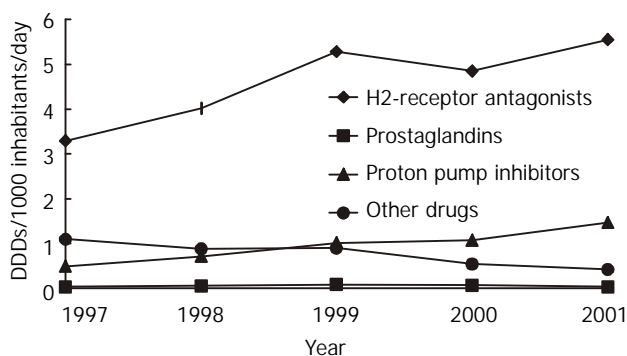


Figure 1 Trend of total prescribed amount of anti-ulcer drugs by pharmacological subgroups from 1997 to 2001.

DISCUSSION

To the best of our knowledge, our study might be one of the few reports that surveyed the anti-ulcer drug use in the Chinese population. Only with the computerization of insurance reimbursement, pharmacoepidemiological studies of such a large scale could be feasible. Besides, the person-based sampling in our study could estimate both the total amount and prevalence of drug use among the population.

Our study revealed that prescribing of anti-ulcer drugs was indeed popular in Taiwan. Nearly a sixth of the population received anti-ulcer drugs covered by the health insurance in 2001 and more than a third of the population had been exposed to such drugs during the 5 years. But the total usage of anti-ulcer drugs in Taiwan was not high in international comparison. According to the statistics of the OECD (Organization for Economic Co-operation and Development), 8 countries supplied their national consumption of anti-ulcer drugs in 1998: Australia (38.8 DDDs/1 000 inhabitants/day), Sweden (29.0), Iceland (28.1), Denmark (16.5), Norway (16.0), Czech Republic (13.1), Finland (12.4), and Slovakia (8.7)^[25]. In contrast, Taiwan had only 5.7 DDDs/1 000 inhabitants/day of anti-ulcer drugs in the same year. However, the statistics has not been adjusted by age.

In the 1990s, the developed countries experienced a drastic increase of anti-ulcer drug consumption since the introduction of proton pump inhibitors. For example, the national consumption of anti-ulcer drugs in Sweden increased from 9.2 DDDs/1 000 inhabitants/day in 1990 to 34.4 in 2000^[25]. During

the 5 years of our study, a growing trend of anti-ulcer drugs was also observed in Taiwan. But the increase was largely attributed to H₂-receptor antagonists and expanding user group. The explanation might be that the reimbursement policy of the health insurance in Taiwan limited the use of expensive proton pump inhibitors on the one hand and loosened the regulation over the much cheaper generics of H₂-receptor antagonists on the other hand.

While overuse of proton pump inhibitors has become a research topic^[26,27], our study found that at least the children in Taiwan might be disproportionately exposed to anti-ulcer drugs. Because children were generally not able to receive upper gastrointestinal endoscopy, their use of anti-ulcer drugs could be seldom justified. It demanded further studies to explore such a situation in Taiwan.

Our study with insurance claims in Taiwan had some limitations. At first, the drug use outside the insurance was not included in the analysis. However, the majority of anti-ulcer drugs, including the low-dose cimetidine, were prescription-only drugs in Taiwan. Besides, the compulsory health insurance covered nearly all inhabitants in Taiwan and reimbursed most prescription-only drugs. The use of anti-ulcer drugs at the private market should be of a less significant scale.

Secondly, the actual duration of drug treatment was not computed in our study because of missing dosage frequency in the inpatient files of the NHIRD data sets. Instead, we calculated the cumulated numbers of DDDs for each person as a proxy of treatment duration. But the DDD is arbitrarily set for trend and international comparisons. It does not consider the dosing at the specific conditions of children, elderly, and other risk groups. However, our data showed that the yearly amount of anti-ulcer drugs per user was low on average. It might be inferred that most people took anti-ulcer drugs only for a short term.

Thirdly, the purpose of cohort data sets in the NHIRD was to trace a cohort retrospectively and prospectively. The people of the cohort were chosen in 2000 and it was planned to follow them up continuously in the next years. Thus, the data sets of 2001 did not include anyone born after December 31, 2000. The denominator in 2001 should be smaller than the actual number of people and the prevalence correspondingly became a little overestimated.

Finally, we did not analyze the distribution of diagnoses in our study because a claims diagnosis served for the purpose of reimbursement and was seldom verified. The NHIRD data sets did provide the information whether the patients had received the endoscopic or radiological examinations of upper gastrointestinal tract. But no laboratory findings were routinely transmitted to the insurer in electronic form. Conventional epidemiological surveys are still needed to understand the prevalence of peptic ulcer and gastroesophageal reflux disease in Taiwan.

ACKNOWLEDGMENTS

This study was based in part on data from the National Health Insurance Research Database provided by the Bureau of National Health Insurance, Department of Health and managed by National Health Research Institutes in Taiwan. The interpretation and conclusions contained herein do not represent those of Bureau of National Health Insurance, Department of Health or National Health Research Institutes.

REFERENCES

- 1 **Molinder H**, Wallander MA, Svärdsudd K, Bodemar G. The introduction of H₂-receptor antagonists to Scandinavia: effects of expert's opinions. *Scand J Gastroenterol* 1998; **33**: 224-230

- 2 **Soll AH.** Medical treatment of peptic ulcer disease: practice guidelines. *JAMA* 1996; **275**: 622-629
- 3 **Howden CW,** Hunt RH. Guidelines for the management of *Helicobacter pylori* infection. *Am J Gastroenterol* 1998; **93**: 2330-2338
- 4 **DeVault KR,** Castell DO. Updated guidelines for the diagnosis and treatment of gastroesophageal reflux disease. *Am J Gastroenterol* 1999; **94**: 1434-1442
- 5 **Andersen IB,** Bonnevie O, Jørgensen T, Sørensen TIA. Time trends for peptic ulcer disease in Denmark, 1981-1993: analysis of hospitalization register and mortality data. *Scand J Gastroenterol* 1998; **33**: 260-266
- 6 **Thors H,** Svanes C, Thjodleifsson B. Trends in peptic ulcer morbidity and mortality in Iceland. *J Clin Epidemiol* 2002; **55**: 681-686
- 7 **McGavock H,** Webb CH, Johnston GD, Milligan E. Market penetration of new drugs in one United Kingdom region: implications for general practitioners and administrators. *BMJ* 1993; **307**: 1118-1120
- 8 **McManus P,** Marley J, Birkett DJ, Lindner J. Compliance with restrictions on the subsidized use of proton pump inhibitors in Australia. *Br J Clin Pharmacol* 1998; **46**: 409-411
- 9 **Cromwell DM,** Bass EB, Steinberg EP, Yasui Y, Ravich WJ, Hendrix TR, McLeod SF, Moore RD. Can restrictions on reimbursement for anti-ulcer drugs decrease Medicaid pharmacy costs without increasing hospitalizations? *Health Serv Res* 1999; **33**: 1593-1610
- 10 **O' Connor JB,** Provenzale D, Brazer S. Economic considerations in the treatment of gastroesophageal reflux disease: a review. *Am J Gastroenterol* 2000; **95**: 3356-3364
- 11 **Lucas LM,** Gerrity MS, Anderson T. A practice-based approach for converting from proton pump inhibitors to less costly therapy. *Eff Clin Pract* 2001; **4**: 263-270
- 12 **Thors H,** Sigurdsson H, Oddsson E, Thjodleifsson B. Survey of prescriptions for peptic ulcer drugs (ACT class A02B) in Iceland. *Scand J Gastroenterol* 1994; **29**: 988-994
- 13 **Roberts SJ,** Bateman DN. Prescribing of antacids and ulcer-healing drugs in primary care in the north of England. *Aliment Pharmacol Ther* 1995; **9**: 137-143
- 14 **Goudie BM,** McKenzie PE, Cipriano J, Griffin EM, Murray FE. Repeat prescribing of ulcer healing drugs in general practice-prevalence and underlying diagnosis. *Aliment Pharmacol Ther* 1996; **10**: 147-150
- 15 **Moride Y,** Melnychuk D, Monette J, Abenhaim L. Determinants of initiation and suboptimal use of anti-ulcer medication: a study of the Quebec older population. *J Am Geriatr Soc* 1997; **45**: 853-856
- 16 **Morales Suárez-Varela MM,** Pérez-Benajas MA, Girbes Pelechano VJ, Llopis-González A. Antacid (A02A) and antiulcer (A02B) drug prescription patterns: Predicting factors, dosage and treatment duration. *Eur J Epidemiol* 1998; **14**: 363-372
- 17 **Bashford JNR,** Norwood J, Chapman SR. Why are patients prescribed proton pump inhibitors? Retrospective analysis of link morbidity and prescribing in the General Practice Research Database. *BMJ* 1998; **317**: 452-456
- 18 **Martin RM,** Lim AG, Kerry SM, Hilton SR. Trends in prescribing H₂-receptor antagonists and proton pump inhibitors in primary care. *Aliment Pharmacol Ther* 1998; **12**: 797-805
- 19 **Prach AT,** McGilchrist MM, Murray FE, Johnston DA, MacDonald TM. Prescription of acid-suppressing drugs in relation to endoscopic diagnosis: a record-linkage study. *Aliment Pharmacol Ther* 1999; **13**: 397-405
- 20 **Boutet R,** Wilcock M, MacKenzie I. Survey on repeat prescribing for acid suppression drugs in primary care in Cornwall and the Isles of Scilly. *Aliment Pharmacol Ther* 1999; **13**: 813-817
- 21 **Jones MI,** Greenfield SH, Jowett S, Bradley CP, Seal R. Proton pump inhibitors: a study of GPs' prescribing. *Fam Pract* 2001; **18**: 333-338
- 22 **Bureau of National Health Insurance.** 2001 National Health Insurance Annual Statistical Report. Taipei: *Bureau of National Health Insurance* 2002
- 23 **Liu JY,** Chen TJ, Hwang SJ. Concomitant prescription of non-steroidal anti-inflammatory drugs and antacids in the outpatient setting of a medical center in Taiwan: A prescription database study. *Eur J Clin Pharmacol* 2001; **57**: 505-508
- 24 Guidelines for ATC Classification and DDD Assignment, 3rd ed. Oslo: *WHO Collaborating Centre for Drug Statistics Methodology* 2000
- 25 OECD Health Data 2001. Paris: *OECD (Organisation for Economic Co-operation and Development)* 2001
- 26 **Naunton M,** Peterson GM, Bleasel MD. Overuse of proton pump inhibitors. *J Clin Pharm Ther* 2000; **25**: 333-340
- 27 **Nardino RJ,** Vender RJ, Herbert PN. Overuse of acid-suppressive therapy in hospitalized patients. *Am J Gastroenterol* 2000; **95**: 3118-3122

Edited by Xu XQ

***In situ* expression and significance of B7 costimulatory molecules within tissues of human gastric carcinoma**

Xiao-Li Chen, Xu-Dong Cao, An-Jing Kang, Kang-Min Wang, Bao-Shan Su, Yi-Li Wang

Xiao-Li Chen, An-Jing Kang, Kang-Min Wang, Bao-Shan Su, Department of Pathology, Second Hospital of Xi'an Jiaotong University, Xi'an 710004, Shaanxi Province, China

Xu-Dong Cao, Medical School of Shihezi University, Shihezi 832002, Xinjiang Uygur Autonomous Region, China

Yi-Li Wang, Institute of Immunopathology, Medical School of Xi'an Jiaotong University, Xi'an 710061, Shaanxi Province, China

Correspondence to: Dr. Xiao-Li Chen, Department of Pathology, Second Hospital of Xi'an Jiaotong University, Xi'an 710004, Shaanxi Province, China. chenxiaoli64.student@sina.com

Telephone: +86-29-8546322

Received: 2002-10-25 **Accepted:** 2002-11-16

Abstract

AIM: To explore the role and significance of costimulatory molecules B7H1, B7H2 and ICOS within tissues of human gastric carcinoma and the possible mechanisms in tumor escape.

METHODS: mRNA expressions of costimulatory molecules including B7H1, B7H2, ICOS and B7-1 in tissues of human gastric carcinoma were investigated by *in situ* hybridization using digoxigenin-labeled oligonucleotide-probes. The tissue of chronic gastric ulcer was used as a control. All data were analyzed by SPSS statistic software.

RESULTS: At the site of gastric carcinoma, mRNA expression levels of B7H1, B7H2 and ICOS were much higher than that of B7-1. Their mRNA positive expression indexes were 0.512 ± 0.333 , 0.812 ± 0.454 , 0.702 ± 0.359 and 0.293 ± 0.253 , respectively. The positively stained cells were mainly tumor infiltrating lymphocytes (TILs), and some tumor cells. The difference between them was greatly significant $P < 0.005$. The mRNA expression levels of four molecules were not correlated to the pathological grade and metastasis of gastric carcinoma.

CONCLUSION: ICOS-B7H costimulatory pathway may be predominant at the site of gastric carcinoma. B7-1 mRNA might be the basis of ICOS-B7H interaction. ICOS-B7H interaction induces the production of IL-10 which inhibits the antitumor immune responses. Therefore, it is supposed that ICOS-B7H costimulatory pathway may be involved in the negative regulation of cell-mediated immune responses.

Chen XL, Cao XD, Kang AJ, Wang KM, Su BS, Wang YL. *In situ* expression and significance of B7 costimulatory molecules within tissues of human gastric carcinoma. *World J Gastroenterol* 2003; 9(6): 1370-1373

<http://www.wjgnet.com/1007-9327/9/1370.asp>

INTRODUCTION

Tumor immunity is primarily cell-mediated. The tumor antigen leads to anti-tumor immune response of the host. A body of evidences have shown that the specific activation of

lymphocytes requires two signals; one is provided by T-cell receptor complex coupled to CD3/MHC peptide antigen, and the other is costimulatory signal delivered by interaction of costimulatory molecules with their ligands expressed on antigen presenting cells (APCs). In the absence of costimulatory signals, antigen-MHC complex interaction may lead to T-cell clonal anergy or deletion, and thus, the effective cellular immune response can not be induced. Furthermore, there are evidences that activation of lymphocyte subpopulation with different function needs unique costimulation factors. Therefore, investigation of costimulators on infiltrating lymphocytes and tumor cells at the tumor site and of their significance will be of great help in developing new methods of anti-tumor immunotherapy. Cell-mediated immunity is the main mechanism of anti-tumor immunity of the host. With presentation of antigen recognition and deepening of the understanding of activated T-cells, it is believed that in the presence of costimulatory signals, effective anti-tumor immune response presents tumor antigen multi-peptide to T cells and stimulates T-cell immune response. B7 is an important costimulatory molecule. Most tumors lack or have a low expression of B7-1, so they do not induce effective anti-tumor immune response. The tumor cells escape from immune system of the host and continue to grow^[1-15]. Although many *in vitro* experiments support this idea, *in situ* studies on human tumors have shown that most tumor tissues express the B7-1 or B7-2 molecules. So the idea meets challenges. An *in vitro* study on new members of B7 family - B7H1, B7H2 and ICOS suggested that the role of ICOS-B7H costimulatory pathway stimulated IL-10 production and induced secretion of Th2 type cytokines. The present study was to explore the role and biological significance of ICOS-B7H costimulatory signals and the possible mechanisms in tumor escape, and to provide the theoretical foundation for designing effective schemes of immunotherapy of carcinoma.

MATERIALS AND METHODS

Patients

17 patients with gastric carcinoma (10 metastatic, and 7 non-metastatic) and 6 patients with gastric ulcer were identified by pathological diagnosis at the Department of Pathology, Second Hospital of Xi'an Jiaotong University. The fresh tissue samples were instantly fixed in 10% formalin, and embedded in paraffin according to routine procedures. Tonsil tissue served as a positive control.

Main reagents

Digoxigenin (DIG)-labeling and detection kits were purchased from Boehringer Mannheim Company in Germany. Solution for *in situ* hybridization was mixed with diethyl pyrocarbonate (DEPC) water. All apparatuses were baked at 180 °C for four hours and DEPC water was digested with RNase.

Specimens

Sections (4-5 μm) cut from the tissue block were de-paraffined in 65 °C oven for 24 hours and then stored at -70 °C until being used.

Labeling of oligonucleotide probes and detection of their sensitivities

Labeling On the ice, 4 μ l reaction buffer (vial 1), 4 μ l CoCl_2 solution (vial 2), 1 μ l probe (100 pmol), 1 μ l DIG-dUTP solution (vial 2), 1 μ l dATP solution (vial 4), 1 μ l terminal transferase (vial 5) and 8 μ l DEPC water, were consecutively added into an eppendorf tube, and carefully mixed and incubated at 37 °C for 15 minutes. 2 μ l stopping solution (prepared by mixing 1 μ l glycogen solution (vial 9) with 200 μ l 0.2 mol/L EDTA solution) was added into the tube to stop the labeling reaction. Then, 2.5 μ l 4mol/L CrCl_2 and 75 μ l pro-cold pure alcohol were added to deposit the labeled. After the supernatants were drained out, the probe was washed with 50 μ l 70 % pre-cold alcohol and dried with a frozen dry machine, and stored at -20 °C until being used.

Detection of sensitivity Sensitivity of each probe was measured by the detection kit following the manufacturer's instructions. The lowest concentration for positive staining was 1.25 pmol/ml. The oligonucleotide probe sequences were as follow. B7-1 5' -CAT GAA GCT GTG GTT GGT TG-3' ; B7H1 5' -TGC TTG TCC AGG TGA CTT CG-3' ; B7H2 5' -CCA TCG CTC TGA CTT CCT TC-3' ; and ICOS 5' -TTC AGC TGG CAA CAA AGT TG-3' .

Hybridization

Sections stored at -70 °C were recovered at room temperature, deparaffined in dimethylbenzene, and hydrated in gradient alcohol. They were digested in 0.5 μ g/ml fresh proteinase K solution at room temperature for 20 minutes, and fixed in 4 % poly-formaldehyde for 20 minutes after digestion was stopped in 0.2 % glycine, and then repeatedly rinsed with 1 \times PBS for 10 minutes. The sections were treated in 0.2N HCl solution at room temperature for 10 minutes, rinsed with DEPC water for 3 minutes; and dehydrated in gradient alcohol. At 42 °C in a bio-hybridization oven, all sections were pre-hybridized for 2 hours, and then hybridized for 20 hours. After hybridization, they were rinsed with 2 \times SSC for two times, 15 minutes each, rinsed with 1 \times SSC for 30 minutes and finally with buffer I solution (pH 7.5) for 6 minutes.

Detection

50 μ l blocking reagent (containing 8 % normal goat serum, 0.3 % Triton X-100 buffer I) was instilled onto each section. The sections were incubated at 37 °C for one hour and a half, and then 30 μ l anti-DIG-AP conjugate (1:500) was added onto each section, and all sections were incubated at 37 °C for two hours and rinsed with buffer I two times, 15 minutes each, then rinsed with buffer III (100 mmol/L Tris-HCl, 100 mmol/L NaCl and 50 mmol/L MgCl_2 , pH 9.5) for 5 minutes, and stained with NBT-BCIP at 20 °C for 12 hours. Finally, the reaction was stopped with buffer IV solution (10 mmol/L Tris-HCl, and 1 mmol/L EDTA, pH 8.0), and the sections were washed in running water, counterstained with methyl green, dehydrated, cleaned in xylene and coverslipped.

Evaluation of results

Under a light microscope, positively hybridized signals were mainly located in the infiltrating lymphocytes and colored purple blue. Reactivity was scored using a semi-quantitative method. First, each section was randomly scored one thousand cells. The positive cell ratio in each section was calculated. Then, according to the staining intensity of positive cells, results were graded as following: intense 3+, moderate 2+, weak 1+ and negative, a score of 3, 2, 1, 0 was assigned respectively. Finally, the positive cell ratio multiplied with staining intensity score of the positive cells was regarded as positive index of mRNA expression of costimulatory molecules.

Control experiment

Expression of ICOS mRNA of the chronic tonsillitis lymphocytes was regarded as a positive control. The results were negative control when no probe was used.

Statistical analysis

All data were expressed as $\bar{x}\pm s$ and analyzed by SPSS statistic software. Differences in values were considered significant if $P<0.05$.

RESULTS

mRNA expression of costimulatory molecules within tissues of human gastric carcinoma

At the site of gastric carcinoma, positive cells for B7H1, B7H2, ICOS were mainly tumor infiltrating lymphocytes (Figure 1). Some positive cells were tumor cells. Their mRNA positive expression indexes were 0.512 ± 0.333 , 0.812 ± 0.454 and 0.702 ± 0.359 , respectively. B7-1 mRNA was expressed on tumor cells and TILs (Figure 2), with a positive expression index being 0.293 ± 0.253 . The mRNA expression levels of B7H1, B7H2 and ICOS were significantly higher than that of B7-1 (all $P<0.05$).

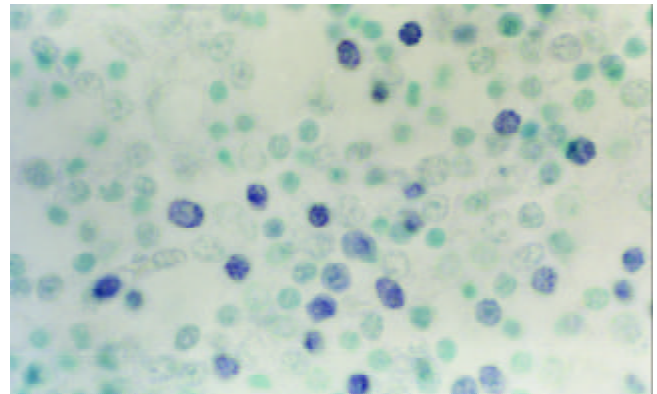


Figure 1 B7H1 mRNA expression of tumor infiltrating lymphocytes (TILs) within tissues of human gastric carcinoma (*In situ* hybridization, NBT-BCIP Staining, counterstained with methyl green, $\times 1000$).

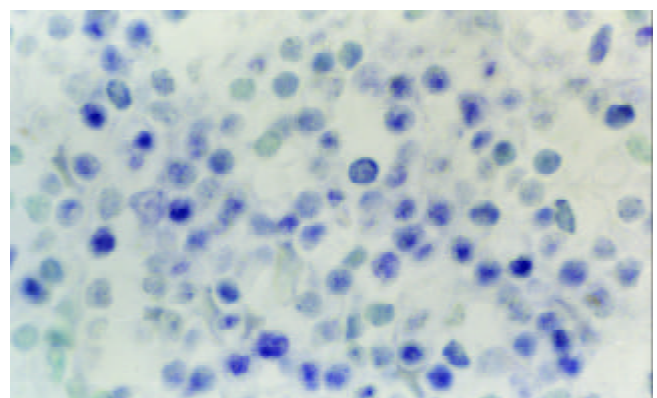


Figure 2 B7-1 mRNA expression of tumor infiltrating lymphocytes (TILs) within tissues of human gastric carcinoma (*In situ* hybridization, NBT-BCIP Staining, counterstained with methyl green, $\times 1000$).

Expression of costimulatory molecules in relation to metastasis of gastric carcinoma

The expression levels of B7-1, B7H1, B7H2 and ICOS had no statistical significance between metastasis and non-metastasis

of gastric carcinoma ($P>0.05$), which suggested that expressions of costimulatory molecules at tumor site were not correlated to the metastasis of tumor.

Expression of costimulatory molecules in relation to differentiation of gastric carcinoma

mRNA expression levels of B7-1, B7H1 and ICOS on infiltrating lymphocytes at the tumor site was not significantly different between well-differentiated and poorly-differentiated. However, the expression level of B7H2 mRNA was significantly higher in well-differentiated than in poorly-differentiated (1.040 ± 0.400 vs 0.651 ± 0.436 , $P=0.047$). mRNA expression of B7-1 was greatly lower than that of B7H1, B7H2 and ICOS in both well-differentiated and poorly-differentiated gastric carcinoma which might indicate that function of B7-1 was different from other costimulatory molecules in gastric carcinoma.

Expression of costimulatory molecules in comparison between gastric carcinoma and gastric ulcer

In the tissue of gastric ulcer, the expression levels of B7-1, B7H1, B7H2 and ICOS on infiltrating lymphocytes were higher than those in gastric carcinoma. But there was no difference in the expression of B7H1, B7H2 and ICOS between the tissues of gastric carcinoma and gastric ulcer except B7-1. The effect of costimulators in the gastric ulcer was not clear.

DISCUSSION

Cell-mediated immunity is the main mechanism of antitumor immunity of the host. With presentation of antigen identification and deepening of the understanding of T-cells activated, it is believed that in the presence of costimulatory signals, effective antitumor immune response presents tumor antigen multi-peptide to T cells and stimulates T-cell immune response^[16-18]. B7 is an important costimulatory molecule. Most tumors lack or have a low expression of B7-1, so they do not induce effective antitumor immune response. The tumor cells escape from immune system of the host and continue to grow. Though many *in vitro* experiments support this idea, *in situ* studies on human tumors have shown that most tumor tissues express the B7-1 or B7-2 molecules^[19]. So the idea meets challenges.

The effective anti-tumor immune response requires three factors, including immunogenicity, costimulatory signals and Th1 type cytokines. In the past, it was emphasized that cytokines or/antigen essence determined the classification of immune responses. Generally, weak immunogenicity of tumor cells primarily induced Th2 response^[20]. In recent years, studies on costimulatory signals *in vitro* have shown that different costimulatory signals play a determinant role in immune response type. There might be Th2 predominant costimulatory signals in human tumor site. The present study has detected mRNA expression of B7H1, B7H2 and ICOS within the tissue of human gastric carcinoma, using *in situ* hybridization with DIG-labeled oligonucleotide probes. The results suggest that tumor infiltrating lymphocytes in tissue of gastric carcinoma express high levels of recently discovered members of B7 costimulatory family, B7H1, B7H2 and ICOS^[21-26]. Compared with mRNA expression level of B7-1, difference was dramatically significant. But mRNA expression levels of B7H1, B7H2 and ICOS were not correlated to the pathological grade and metastasis of gastric carcinoma. The experiments^[27-35] *in vitro* have verified that the interaction between B7h and ICOS stimulates the proliferation of T-cells and production of Th2 cytokines, preferentially secretion of IL-10. This is probably the main reason that Th2 cytokines may predominate at the tumor immune- microenvironment of gastric carcinoma, and thus the type of immune response shifts from Th1 to Th2. There was an

increase of Th2 cytokine-IL-10 in tumor immune- microenvironment of gastric carcinoma^[36].

In this study, we have also observed the expression of B7-1 in the tissue of gastric carcinoma, and found that tumor infiltrating lymphocytes (TIL) and tumor cells expressed low gastric carcinoma levels of B7-1 mRNA. Now that there were costimulatory molecules in the tissues of gastric carcinoma, why did not the host produce the effective antitumor immune response? With the further study of immunology and tumor immunology, a new concept related to interaction between TIL and tumor cells was introduced. That is the tumor microenvironment. This theory supposes that immune system of the host cannot eliminate tumors because there are many inhibitors of tumor immunity at the site of tumor microenvironment. For example, tumor cells produce TGF- β , PGE₂ and so on, which are accumulated at tumor site and interfere with the activity of recruited immunocytes. Activated immunosuppressive cells further augment the immunodepression mechanism in tumor microenvironment. In addition, a recent study^[27] has shown that B7-1 costimulation also enhances the up-regulation effects of ICOS costimulation which results in the increase of Th2 cytokines, preferentially inducing the secretion of IL-10.

The present experimental results suggest that the tumor infiltrating lymphocytes in the tissues of gastric carcinoma express high levels of B7H1, B7H2 and ICOS mRNA. Some tumor cells also express them but the expression levels are low. This indicates that there are costimulatory signal pathways in the site of gastric carcinoma. Since the interaction between B7H1, B7H2 and ICOS stimulates proliferation of T cells by various ways and induces secretion of IL-10. IL-10 is known to be an immune inhibitor, which down-regulates function of Th1 type cells, and inhibits antitumor immune response of the body, and thus the body is in the state of immune inhibition. Therefore, it is supposed that although interaction between B7H1, B7H2 and ICOS delivers costimulatory signals to T-cells, promotes their activation, the effective antitumor immunity can not be induced. Tumor cells can escape from the immunosurveillance of the host and continue to grow. This is due to the fact that many inhibitors at tumor site have blocked the role of specifically activated T cells. As far as most tumors are concerned, the host's immunoreaction can not eliminate the tumor because Th2 type response is stimulated, or it can be recognized by immune system of the body. Maybe there are other regulation mechanisms. The present study indicates that costimulatory pathways might exist at the tumor site with different functions. ICOS-B7h pathway is predominant and plays an important role in negative regulation of cell-mediated immune response. This finding might provide a new approach for designing effective immune-therapy of carcinoma.

REFERENCES

- 1 Ellis JH, Burden MN, Vinogradov DV, Linge C, Crowe JS. Interactions of CD80 and CD86 with CD28 and CTLA4. *J Immunol* 1996; **156**: 2700-2709
- 2 Guinan EC, Gribben JG, Boussiotis VA, Freeman GJ, Nadler LM. Pivotal role of the B7:CD28 pathway in trans-plantation tolerant and tumor immunity. *Blood* 1994; **84**: 3261-3282
- 3 Ikemizu S, Gilbert RJ, Fennelly JA, Collins AV, Harlos K, Jones EY, Stuart DI, Davis SJ. Structure and dimerization of a soluble form of B7-1. *Immunity* 2000; **12**: 51-60
- 4 Hung K, Hayashi R, Lafond-Walker A, Lowenstein C, Pardoll D, Levitsky H. The central role of CD4⁺ T cells in the antitumor immune response. *J Exp Med* 1998; **188**: 2357-2368
- 5 Ganss R, Hanahan D. Tumor microenvironment can restrict the effectiveness of activated antitumor lymphocytes. *Cancer Res* 1998; **58**: 4673-4681
- 6 Denfeld RW, Dietrich A, Wuttig C, Tanczos E, Weiss JM,

- Vanscheidt W, Schopf E, Simon JC. In situ expression of B7 and CD28 receptor families in human malignant melanoma: relevance for T cell-mediated anti-tumor immunity. *Int J Cancer* 1995; **62**: 259-265
- 7 **Salvadori S**, Martinelli G, Zier K. Resection of solid tumors reverses T cell defects and restores protective immunity. *J Immunol* 2000; **164**: 2214-2220
 - 8 **Yu X**, Fournier S, Allison JP, Sharpe AH, Hodes RJ. The role of B7 costimulation in CD4/CD8 T cell homeostasis. *J Immunol* 2000; **164**: 3543-3553
 - 9 **Martin-Fontecha A**, Moro M, Crosti MC, Veglia F, Casorati G, Dellabona P. Vaccination with mouse mammary adenocarcinoma cells coexpressing B7-1 (CD80) and B7-2 (CD86) discloses the dominant effect of B7-1 in the induction of antitumor immunity. *J Immunol* 2000; **164**: 698-704
 - 10 **Kinoshita K**, Tesch G, Schwarting A, Maron R, Sharpe AH, Kelley VR. Costimulation by B7-1 and B7-2 is repaired for autoimmune disease in MRL-Fas mice. *J Immunol* 2000; **164**: 6046-6056
 - 11 **Geldhof AB**, Raes G, Bakkus M, Devos S, Thielemans K, De Baetselier P. Expression of B7-1 by highly metastatic mouse T lymphomas induces optimal natural killer cell-mediated cytotoxicity. *Cancer Res* 1995; **55**: 2730-2733
 - 12 **Huang M**, Wang J, Lee P, Sharma S, Mao JT, Meissner H, Uyemura K, Modlin R, Wollman J, Dubinett SM. Human non-small cell lung cancer cells express a type 2 cytokine pattern. *Cancer Res* 1995; **55**: 3847-3853
 - 13 **Romagnani S**. The Th1/Th2 paradigm. *Immunol Today* 1997; **18**: 263-266
 - 14 **Fujii H**, Inobe M, Kimura F, Murata J, Murakami M, Onishi Y, Azuma I, Uede T, Saiki I. Vaccination of tumor cells transfected with the B7-1 (CD80) gene induces the antimetastatic effect and tumor immunity in mice. *Int J Cancer* 1996; **66**: 219-224
 - 15 **Wu TC**, Huang AY, Jaffee EM, Levitsky HI, Pardoll DM. A reassessment of the role of B7-1 expression in tumor rejection. *J Exp Med* 1995; **182**: 1415-1421
 - 16 **Judge TA**, Tang A, Turka LA. Immunosuppression through blockade of CD28:B7-mediated costimulatory signals. *Immunol Res* 1996; **15**: 38-49
 - 17 **Hu JY**, Wang S, Zhu JG, Zhou GH, Sun QB. Expression of B7 costimulation molecules by colorectal cancer cells reduce tumorigenicity and induces anti-tumor immunity. *World J Gastroenterol* 1999; **5**: 147-151
 - 18 **Ren XF**, Luo KX. Expression of B7 and liver diseases. *Shijie Huaren Xiaohua Zazhi* 1999; **7**: 415-416
 - 19 **Guo J**, Si L, Wang Y. An in situ study on immunostimulatory molecules in cancer cells within the cervical carcinoma tissues. *Zhonghua Yixue Zazhi* 2000; **80**: 342-345
 - 20 **Song YJ**, Yang ZY, Dong JH. Th1/Th2 cells and immune tolerance of transplantation. *Shijie Huaren Xiaohua Zazhi* 2001; **9**: 794-796
 - 21 **Dong H**, Zhu G, Tamada K, Chen L. B7H1, a third member of the B7 family, co-stimulates T cell proliferation and interleukin-10 secretion. *Nat Med* 1999; **5**: 1365-1369
 - 22 **Wang S**, Zhu G, Chapoval AI, Dong H, Tamada K, Ni J, Chen L. Costimulation of T cells by B7-H2, a B7-like molecule that binds ICOS. *Blood* 2000; **96**: 2808-2813
 - 23 **McAdam AJ**, Chang TT, Lumelsky AE, Greenfield EA, Boussiotis VA, Duke-Cohan JS, Chernova T, Malenkovich N, Jabs C, Kuchroo VK, Ling V, Collins M, Sharpe AH, Freeman GJ. Mouse inducible costimulatory molecule (ICOS) expression is enhanced by CD28 costimulation and regulate differentiation of CD4⁺ T cells. *J Immunol* 2000; **165**: 5035-5040
 - 24 **Dong C**, Juedes AE, Temann UA, Shresta S, Allison JP, Ruddle NH, Flavell RA. ICOS costimulatory receptor is essential for T-cell activation and function. *Nature* 2001; **409**: 97-101
 - 25 **McAdam AJ**, Greenwald RJ, Levin MA, Chernova T, Malenkovich N, Ling V, Freeman GJ, Sharpe AH. ICOS is critical for CD40-mediated antibody class switching. *Nature* 2001; **409**: 102-105
 - 26 **Tafuri A**, Shahinian A, Bladt F, Yoshinaga SK, Jordana M, Wakeham A, Boucher LM, Bouchard D, Chan VS, Duncan G, Odermatt B, Ho A, Itie A, Horan T, Whoriskey JS, Pawson T, Penninger JM, Ohashi PS, Mak TW. ICOS is essential for effective T-helper-cell responses. *Nature* 2001; **409**: 105-109
 - 27 **Hutloff A**, Dittrich AM, Beier KC, Eljaschewitsch B, Kraft R, Anagnostopoulos I, Kroczeck RA. ICOS is an inducible T-cell costimulatory structurally and functionally related to CD28. *Nature* 1999; **397**: 263-266
 - 28 **Liu X**, Bai XF, Wen J, Gao JX, Liu J, Lu P, Wang Y, Zheng P, Liu Y. B7H costimulates clonal expansion of, and cognate destruction of tumor cells by, CD8(+) T lymphocytes *in vivo*. *J Exp Med* 2001; **194**: 1339-1348
 - 29 **Guo J**, Stolina M, Bready JV, Yin S, Horan T, Yoshinaga SK, Senaldi G. Stimulatory effects of B7-related protein-1 on cellular and humoral immune responses in mice. *J Immunol* 2001; **166**: 5578-5584
 - 30 **Riley JL**, Blair PJ, Musser JT, Abe R, Tezuka K, Tsuji T, June CH. ICOS costimulation requires IL-2 and can be prevented by CTLA-4 engagement. *J Immunol* 2001; **166**: 4943-4948
 - 31 **Yoshinaga SK**, Whoriskey JS, Khare SD, Sarmiento U, Guo J, Horan T, Shih G, Zhang M, Coccia MA, Kohno T, Tafuri-Bladt A, Brankow D, Campbell P, Chang D, Chiu L, Dai T, Duncan G, Elliott GS, Hui A, McCabe SM, Scully S, Shahinian A, Shaklee CL, Van G, Mak TW. T-cell co-stimulation through B7RP-1 and ICOS. *Nature* 1999; **402**: 827-832
 - 32 **Tamatani T**, Tezuka K, Hanzawa-Higuchi N. AILIM/ICOS: a novel lymphocyte adhesion molecule. *Int Immunol* 2000; **12**: 51-55
 - 33 **Mages HW**, Hutloff A, Heuck C, Buchner K, Himmelbauer H, Oliveri F, Kroczeck RA. Molecular cloning and characterization of murine ICOS and identification of B7h as ICOS ligand. *Eur J Immunol* 2000; **30**: 1040-1047
 - 34 **Tamura H**, Dong H, Zhu G, Sica GL, Flies DB, Tamada K, Chen L. B7-H1 costimulation preferentially enhances CD28-independent T-helper cell function. *Blood* 2001; **97**: 1809-1816
 - 35 **Beier KC**, Hutloff A, Dittrich AM, Heuck C, Rauch A, Buchner K, Ludewig B, Ochs HD, Mages HW, Kroczeck RA. Induction, binding specificity and function of human ICOS. *Eur J Immunol* 2000; **30**: 3707-3717
 - 36 **Liu P**, Si LS, Li R, Lai BC, Wang YL. Dynamic change of the local immune environment of human gastric carcinoma during the progress of this disease. *Xi'an Yike Daxue Xuebao* 2001; **22**: 408-410

Edited by Xia HHX and Wang XL

Late course accelerated hyperfractionated radiotherapy for clinical T₁₋₂ esophageal carcinoma

Kuai-Le Zhao, Yang Wang, Xue-Hui Shi

Kuai-Le Zhao, Yang Wang, Xue-Hui Shi, Department of Radiation Oncology, Cancer Hospital, Fudan University, Shanghai 200032, China
Correspondence to: Kuai-Le Zhao, Department of Radiation Oncology, Cancer Hospital, Fudan University, Shanghai 200032, China. kuaile_z@sina.com
Telephone: +86-21-64175590-3900
Received: 2002-11-06 **Accepted:** 2003-01-08

Abstract

AIM: This retrospective study was designed to analyze the results and the failure patterns of late course accelerated hyperfractionated radiotherapy for clinical T₁₋₂N₀M₀ esophageal carcinoma.

METHODS: From Aug. 1994 to Feb. 2001, 56 patients with clinical T₁₋₂ esophageal carcinoma received late course accelerated hyperfractionated radiotherapy in Cancer Hospital, Fudan University. All patients had been histologically proven to have squamous cell carcinoma (SCC) and were diagnosed to be T₁₋₂N₀M₀ by CT scan. All patients were treated with conventional fractionation (CF) irradiation during the first two-thirds course of the treatment to a dose of about 41.4Gy/23fx/4 to 5 weeks, which was then followed by accelerated hyperfractionation irradiation using reduced fields, twice daily at 1.5Gy per fraction, to a dose about 27Gy/18 fx. Thus the total dose was 67-70Gy/40-43fx/40-49 d.

RESULTS: The 1-, 3- and 5-year overall survival was 90.9 %, 54.6 %, 47.8 % respectively. The 1-, 3- and 5-year local control rate was 90.9 %, 84.5 % and 84.5 %, respectively. Twenty-five percent (14/56) patients had distant metastasis and/or lymph nodes metastasis alone. Eight point nine percent (5/56) patients had local disease alone. Another 3.6 % (2/56) patients had regional relapse and distant metastasis.

CONCLUSION: Late course accelerated hyperfractionated radiotherapy is effective on clinical T₁₋₂ esophageal carcinoma. The main failure pattern is distant metastasis.

Zhao KL, Wang Y, Shi XH. Late course accelerated hyperfractionated radiotherapy for clinical T₁₋₂ esophageal carcinoma. *World J Gastroenterol* 2003; 9(6): 1374-1376
<http://www.wjgnet.com/1007-9327/9/1374.asp>

INTRODUCTION

Surgery has been the main treatment method for clinical T₁₋₂ esophageal carcinoma. But the treatment of upper thoracic esophageal carcinoma is challenging. The intimate relationship of the esophagus to the airway, arch of the aorta, and recurrent laryngeal nerve poses special technical problems. Radiotherapy is as effective as surgery, and preserves esophagus.

In 1988, Shi designed the schedule of late course accelerated hyperfractionated radiotherapy (LCAF) on SCC of the esophagus. The results were very encouraging. The 5-year survival and local control rate were markedly improved in the

LCAF group. Compared with CF radiotherapy, the 5-year overall survival of 34 % versus 15 % was statistically significant, the local control rate was 55 % versus 21 %^[1]. However, the outcome of clinical T₁₋₂ esophageal carcinoma treated with LCAF has not been investigated extensively. Therefore, we conducted a retrospective evaluation of clinical T₁₋₂ patients treated with LCAF.

MATERIALS AND METHODS

Materials

From August 1994 to February 2001, 56 patients with clinical T₁₋₂N₀M₀ SCC of esophagus were treated by LCAF radiotherapy in the Department of Radiation Oncology, Cancer Hospital, Fudan University. All patients had detailed medical records. Pretreatment evaluation generally included history and physical examination, complete blood cell count, chest radiograph, chest computed tomographic (CT) scan, esophageal barium examination, ultrasonic examination for abdomen, including liver, kidney, spleen, and retroperitoneal lymph nodes. All patients were restaged according to the TNM classification of the International Union Against Cancer (devised in 1997). The patients' eligibility for this study was as follows: (1) Primary lesion was single, and a flat plane separating the esophageal mass from the periesophageal structures was visible on all CT sections. (2) Mediastinal and upper abdominal lymph nodes were smaller than 5 mm on short-axis diameter. And (3) No supraclavicular lymph nodes and distant metastasis. The patients' clinical characteristics are listed in Table 1.

Table 1 Pretreatment characteristics

Characteristic	n	%
Age(years)		
<65	30	53.6
≥65	26	46.4
Median		59.5
Range		40-74
Gender		
Male	41	73.2
Female	15	26.8
T stage		
T1	2	3.7
T2	54	96.3
Site		
Cervical	2	3.6
Upper-thoracic	19	33.9
Middle-thoracic	34	60.7
Lower-thoracic	1	1.8
Length (cm)		
≤5	25	44.6
>5	31	55.4
Median		5.8
Range		2.0-9.0
Thickness of wall (cm)		
≤1.5	42	75.0
>1.5	14	25
Median		1.2
Range		0.5-2.7

Methods

Radiation source was 6MV or 18 MV linear accelerator. The design of the radiation fields was based on the diagnosis by CT and barium examinations. For patients with lesions in cervical region, two anterior oblique fields with wedge filters were used. For patients with lesions in the thoracic a three-field approach was used: one anterior and two posterior oblique portals. The width of the fields was adjusted to cover gross tumor with 2 cm to 3 cm margins to include the subclinical lesions and the length of the field should cover clinical tumors with 3 cm to 5 cm extended margin at both ends of the lesion. All patients received 1.8Gy per fraction, five fractions a week during the first two thirds of the course of radiotherapy to a dose of about 41.4Gy/23fx/4 to 5 weeks. This was then followed by accelerated hyperfractionation using reducing fields, twice daily at 1.5Gy per fraction with a minimum interval of 6 hours between fractions. The dose contributed by the accelerated technique was about 27Gy. The total dose given to the clinical tumor was 67-70Gy/40-43fx/40-49d. No prophylactic irradiation was given to the supraclavicular region. Details of the schedule had been reported previously^[1].

End-points in this analysis were overall survival and local control. Death from any cause was calculated from the date of radiotherapy until death or last follow-up evaluation. Patterns of failure were first failure (local, regional, or distant), time to any local failure, and time to any distant metastasis. If recurrences occurred within 60 days of each other, they were counted simultaneously. The time to these end points was calculated from the date of treatment until disease relapse or last follow-up.

Four patients were lost to follow-up. Median follow-up for the survival patients was 38.0 months (range 5-67 months), follow-up rate was 92.9 %.

The statistics was done by SPSS (Version 10.0). Survival rate and local control rate were estimated by the Kaplan-Meier method.

RESULTS

Acute toxicities (RTOG)

The incidence of grade 1, 2, 3 and 4 of acute radiation-induced bronchitis was 19.6 % (11/56), 17.9 % (10/56), 3.6 % (2/56), and 1.8 % (1/56), respectively. The incidence of grade 1, 2, 3 and 4 of acute radiation-induced esophagitis was 25.0 % (14/56), 46.4 % (26/56), 10.7 % (6/56), and 0 % (0 cases), respectively.

Late complications (SOMA)

Three patients (53.6 %) developed grade 2 radiation-induced late esophageal stenosis, and one patient (1.8 %) developed grade 3 esophageal stenosis (the patient had required dilatation). One patient (1.8 %) developed grade 2 late pulmonary fibrosis. Two patients (3.6 %) died of late complications (1 case died of pulmonary fibrosis, 1 case died of myelitis).

Survival rates and local control rates

The overall survival curve and the local control rates for all patients are shown in Figure 1, 2. The overall survival rate at 1-, 3- and 5-year was 90.9 %, 54.6 % and 47.8 %, respectively. The local control rate at 1-, 3- and 5-years was 90.9 %, 84.5 % and 84.5 %, respectively.

Failure patterns

The patterns of first failure are listed in Table 2. The main first failures were local regional failure and distant metastasis (including lymph metastasis). Twenty-five percent (14/56) patients had distant metastasis and/or lymph nodes metastasis alone. Eight point nine percent (5/56) had local disease alone.

Another 3.6 % (2/56) had local regional relapse and distant metastasis. The median local regional failure time was 9 months (rang: 0-18 months). The median distant metastasis time was 17.5 months (rang: 7-65 months).

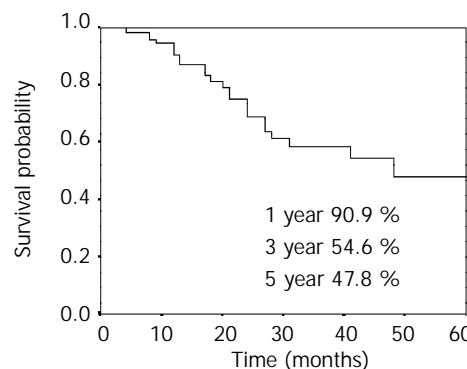


Figure 1 The overall survival rates for clinical T₁₋₂ esophageal carcinoma treated with LCAF radiotherapy.

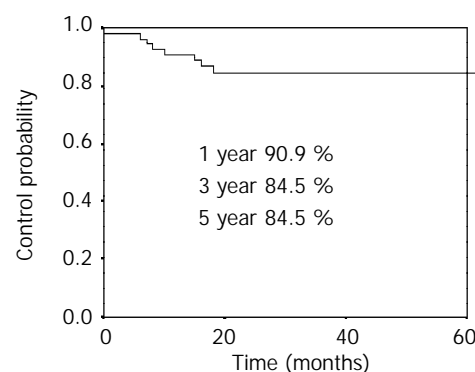


Figure 2 The local control rates for clinical T₁₋₂ esophageal carcinoma treated by LCAF radiotherapy.

Table 2 First treatment failures

First failure	n	%
None	31	55.4
Local/regional only	5	8.9
Distant only	14	25.0
Local/regional/distant	2	3.6
Hemorrhage	1	1.8
Complications	2	3.6
Unknown	1	1.8
Total	56	100

DISCUSSION

Surgery is the main treatment for clinical T₁₋₂ esophageal carcinoma. In a nationwide surgical series from 1983 to 1987 in Japan^[2], the survival rate of 127 patients with mucosal tumors was 92.26 % at 1 year, 81.09 % at 3 years, and 89.85 % at 5 years. A total of 533 patients with submucosal tumor had survival rate of 83.51 % at 1 year, 66.76 % at 3 years, and 59.66 % at 5 years. T₁ classification by UICC (1987) combines mucosal and submucosal tumors. Seven hundred forty patients with invasion to the muscularis propria, equal to T₂ by UICC classification, had survival rate of 69.86 % at 1 year, 41.88 % at 3 years, and 34.47 % at 5 years. Because a nearly total esophagectomy is often required, higher mortality and morbidity occur often. Orringer^[3] reported 800 patients with cancer of the intrathoracic esophagus and cardia treated with transhiatal esophagectomy. Major complications included

anastomotic leaks (13 %), recurrent laryngeal nerve injury (7 %), wound infection (3 %), pulmonary complications (2 %), bleeding (1 %), and chylothorax (1 %). More than 90 % of patients were discharged within 21 days of hospitalization. Complications were more severe in the patients with carcinoma of upper thoracic esophagus. The operation of upper thoracic esophageal cancer is challenging. The intimate relationship of the esophagus to the airway, arch of the aorta, and recurrent laryngeal nerve poses special technical problems. The survival rate is often lower, and the mortality and morbidity are often higher. Vigneswaran^[4] reported 49 patients treated with extended esophagectomy. There was one postoperative death (2.0 %). Fifteen patients (30.6 %) had a cervical anastomotic leak, and all occurred in patients with a gastric conduit. Leaks occurred in 5 of 10 (50 %) substernally placed stomachs and in 10 of 36 (27.7 %) transposed through the esophageal bed. Wound infection occurred in five patients. Postoperative vocal cord paralysis developed in 11 patients (22.4 %) and was unilateral in 10 and bilateral in one. Six patients developed pulmonary complications. Ten patients (20.8 %) developed mild to severe late dysphagia, which was a result of benign stenosis in eight patients and recurrent carcinoma in two. Four patients required dilatations.

Chemoradiotherapy has been widely used in Western countries. Reports on definitive chemoradiotherapy for clinical T₁₋₂ esophageal carcinoma are few. Zenone *et al.* concluded that the combined multimodality therapy, might be an alternative to radical surgery, based on 5-year survival of 56.3 % for T₁ patients and 29.8 % for T₂ patients^[5]. Roca *et al.* also suggested the feasibility of organ preservation in a report using intensive chemoradiotherapy^[7]. Murakami *et al.* reported in a randomized study comparing chemoradiation with surgery that overall 1- and 3-year survival rates were 100 % and 83 % in the T₁/protocol group versus 82 % and 72 % in the T₁/surgery group ($P=0.36$), and 100 % and 51 % in the T₂/protocol group, versus 95 % and 68 % in the T₂/surgery group ($P=0.61$), respectively. There was no treatment-related mortality in either group. The rate of esophageal conservation was 92 % in the T₁/protocol group and 58 % in the T₂/protocol group^[2]. These results indicate that chemoradiation for clinical T₁₋₂ patients is a feasible radical treatment. However, there has been no report that compares surgery and chemoradiotherapy. Although there was a significant improvement in local control and overall survival with combined multimodality therapy compared with radiation therapy alone, the combined treatment had more severe and life-threatening hematologic side effects. Grade 3-5 acute toxicity was seen in 64 % of patients treated by concurrent chemoradiotherapy, much higher than 28 % in patients treated by radiotherapy alone. Approximately 80 % of patients completed chemotherapy according to the protocol guidelines.

In China, Shi^[1] modified the concomitant boost schedule designed by Anderson Cancer Center to LCAF radiotherapy on SCC of the esophagus. The results were very encouraging. The 5-year survival and local control rate were markedly improved in the LCAF group. Compared with CF radiotherapy, the 5-year overall survival was 34 % versus 15 % which was statistically significant, the local control rate was 55 % versus 21 %. Henceforth, more randomized and retrospective trials confirmed the results^[7-9]. LCAF radiotherapy is the most

frequently used radiotherapeutic management for localized SCC of esophageal carcinoma in some cancer hospitals in China including our department.

The survival rate and local control rate are comparable with operation and chemoradiotherapy in the patients treated with LCAF radiotherapy alone. Esophagus can be preserved, and the severe complications can be decreased. In the retrospective study, most patients were clinical stage T₂N₀M₀, at upper thoracic and middle thoracic. The 5-year survival rate was 47.8 %, and the 5-year local control rate was 84.5 %. Grade 3-5 acute radiation-induced toxicities were 16.1 %. The incidence of grade 3-5 late complications was 7.0 %.

In analyzing failure patterns, there was significant difference between the patients in early-stage and advanced-stage. Local/regional recurrence was the main reason of failure in the advanced patients treated with conventional radiotherapy. Forty-two percent patients died of local recurrence, and nineteen percent patients died of metastasis in the advanced patients treated with LCAF radiotherapy^[1]. Forty-five percent patients had local regional disease as the first failure, distant metastasis as the first failure occurred in 13 % of concurrent chemoradiotherapy^[2]. In our retrospective study, distant metastasis rate (28.6 %) increased significantly, and local regional recurrent rate (12.5 %) decreased markedly.

REFERENCES

- 1 **Shi XH**, Yao WQ, Lui TF. Late course accelerated fractionation in radiotherapy of esophageal carcinoma. *Radiother Oncol* 1999; **51**: 21-26
- 2 **Murakami M**, Kuroda Y, Nakajima T, Okamoto Y, Mizowaki T, Kusumi F, Hajiro K, Nishimura S, Matsusue S, Takeda H. Comparison between chemoradiation protocol intended for organ preservation and conventional surgery for clinical T1-T2 esophageal carcinoma. *Int J Radiat Oncol Biol Phys* 1999; **45**: 277-284
- 3 **Orringer MB**, Marshall B, Iannettoni MD. Transhiatal esophagectomy: clinical experience and refinements. *Ann Surg* 1999; **230**: 392-400
- 4 **Vigneswaran WT**, Trastek VF, Pairolero PC, Deschamps C, Daly RC, Allen MS. Extended esophagectomy in the management of carcinoma of the upper thoracic esophagus. *J Thorac Cardiovascular Surg* 1994; **107**: 901-907
- 5 **Zenone T**, Romestaing P, Lambert R, Gerard JP. Curative non-surgical combined treatment of squamous cell carcinoma of the Oesophagus. *Eur J Cancer* 1992; **28A**: 1380-1386
- 6 **Roca E**, Pennella E, Sardi M, Carraro S, Barugel M, Milano C, Fiorini A, Giglio R, Gonzalez G, Kneitschel R, Aman E, Jarentchuk A, Blajman C, Nadal J, Santarelli MT, Navigante A. Combined intensive chemoradiotherapy for organ preservation in patients with resectable and non-resectable oesophageal cancer. *Eur J Cancer* 1996; **32A**: 429-432
- 7 **Wang WD**. Conventional radiotherapy boosted with late course hyperfractionation in patient with esophageal cancer (abstr.). *Zhonghua Fangshe Zhongliuxue Zazhi* 2001; **10**: 30
- 8 **Wang Y**, Shi XH, He SQ, Yao WQ, Wang Y, Guo XM, Wu GD, Zhu LX, Liu TF. Comparison between continuous accelerated hyperfractionated and late-course accelerated hyperfractionated radiotherapy for esophageal carcinoma. *Int J Radiat Oncol Biol Phys* 2002; **54**: 131-136
- 9 **Zhao KL**, Wang Y, Shi XH. Analysis of outcome and failure reasons of late accelerated hyperfractionation radiotherapy for esophageal carcinoma. *Zhonghua Fangshe Zhongliuxue Zazhi* 2000; **10**: 14-16

Multiple immune disorders in unrecognized celiac disease: a case report

Giorgio La Villa, Pietro Pantaleo, Roberto Tarquini, Lino Cirami, Federico Perfetto, Francesco Mancuso, Giacomo Laffi

Giorgio La Villa, Pietro Pantaleo, Roberto Tarquini, Federico Perfetto, Francesco Mancuso, Giacomo Laffi, Dipartimento di Medicina Interna, Università degli Studi di Firenze, Firenze, Italia
Lino Cirami, Unità Operativa di Nefrologia, Dialisi e Trapianto, Azienda Ospedaliera Careggi, Firenze, Italia

Supported by grants from the Ministero dell'Istruzione, dell'Università e della Ricerca and the University of Florence

Correspondence to: Giacomo Laffi, MD, Department of Internal Medicine, University of Florence School of Medicine, viale Morgagni, 85 - 50134 Firenze, Italy. g.laffi@dmi.unifi.it

Telephone: +39-55-4296538 **Fax:** +39-55-417123

Received: 2002-11-26 **Accepted:** 2002-12-22

Abstract

We reported a female patient with unrecognized celiac disease and multiple extra intestinal manifestations, mainly related to a deranged immune function, including macroamilasemia, macrolipasemia, IgA nephropathy, thyroiditis, and anti-b2-glicoprotein-1 antibodies, that disappeared or improved after the implementation of a gluten-free diet.

La Villa G, Pantaleo P, Tarquini R, Cirami L, Perfetto F, Mancuso F, Laffi G. Multiple immune disorders in unrecognized celiac disease: a case report. *World J Gastroenterol* 2003; 9(6): 1377-1380
<http://www.wjgnet.com/1007-9327/9/1377.asp>

INTRODUCTION

Celiac disease (CD), the most common life-long food sensitive enteropathy in humans, is characterized by malabsorption, chronic inflammation of small intestine mucosa, villous atrophy and crypt hyperplasia, which occur as a consequence of the ingestion of wheat gluten or related rye and barley proteins^[1,2]. CD is strongly associated with HLA-DQ2, coded by the DQA1*0501 and DQB1*02 alleles, and/or the DQ8 (DQA1*03, DQB1*0302 alleles), but a role of non-HLA genes has also been postulated^[2,3]. The current prevalence of celiac disease has increased from 1:1 000 to 1:300 inhabitants, or even more^[4]. Typical symptoms include chronic diarrhea, abdominal distension, and failure to thrive^[2,5]. However, only few patients with CD show clinical malabsorption, while most patients have subtle symptoms, if any^[6]. Therefore, the disease is clearly under diagnosed^[2,7]. The recent introduction of tests for IgA anti-endomysial antibodies and the anti-tissue transglutaminase test has proved promising with a sensitivity and specificity of over 95 %^[2, 8, 9].

Celiac disease may be associated with a wide range of diseases^[2, 8], including thyroid, dermatological and lymphoproliferative disorders, mainly intestinal lymphomas^[2]. Furthermore, there is a greater than expected prevalence of immune disorders in CD patients^[2, 10-12] as well as of CD in patients with autoimmune diseases^[13-15].

The current report dealt with a female patient with unrecognized CD and recurrent miscarriage, macroamilasemia, macrolipasemia, IgA nephropathy, and thyroiditis that

disappeared or improved when a correct diagnosis was made and the patient was given a gluten-free diet.

CASE REPORT

A 34 years old, non drinker, non smoking woman, was admitted to the third Medical Clinic, Careggi University Hospital, Florence because of hyper-amilasemia and hyper-lipasemia of unknown origin. The patient had acute meningitis at the age of three. At age of 23, she was admitted to hospital because of syncope, referred to acute gastroenteritis complicated by metabolic acidosis; laboratory evaluation performed on that occasion showed iron deficient anemia, polyclonal hypergammaglobulinemia, elevated erythrocyte sedimentation rate (ESR), reduced C3 levels and circulating antinuclear antibodies (1:80), that led to suspicion of a not otherwise specified collagen disease. Iron deficiency was unresponsive to supplement of oral iron, while it improved following intravenous therapy. The patient had two spontaneous abortions when aged 30 and 31 years, respectively, both at the 16th week of gestation. During admission because of the second abortion, a thorough investigation was performed that was negative for potential causes of fetal demise, including fasting glucose, basal FSH, LH and estradiol levels on day 3 of a natural cycle, TSH and prolactin levels, antinuclear antibodies, antibodies against infectious agents, hysterosalpingography and genetic karyotyping of the couple. On that occasion, she was found to have hyperamilasemia and hyperlipasemia, together with the previously reported laboratory alterations; so further investigations were performed including CT, which turned out to be negative for any pancreatic disease.

At the time of admission to our hospital unit, physical examination was completely negative. Routine blood analysis showed anemia (Ht: 32.8 %, Hb: 11.2 g/dL), thrombocytosis (452 000 platelets/mL), high ESR (124 mm/h), low plasma albumin (3.05 g/dL), and high levels of IgA (1 100 mg/dL) and IgM (369 mg/dL) with no monoclonal component. The patient also had low ferritin (<9 mg/mL) and tetrahydrofolate levels (1.9 ng/ml; normal range 3-17 ng/mL). A coagulation study showed the presence of lupus anticoagulant (Table 1). Enzyme studies confirmed a remarkable increase of serum amylase (1 196 IU/L), pancreatic isoamylase fraction (798 IU/L), and serum lipase (1 650 IU/L). On the other hand, urinary amylase excretion was normal (120, normal value <1 500 IU/day), and ultrasound examination of the pancreas was normal. A chromatographic assay was therefore performed at another Institution (Ospedali Riuniti, Padova, Italy), which demonstrated the presence of macroamilasemia and macrolipasemia.

Our patient had iron-deficient anemia, which was refractory to oral iron supplementation, a well known presenting sign of CD^[2,6,16], together with low albumin and tetrahydrofolate levels. In addition, she had macroamilasemia and macrolipasemia which could be associated with CD^[17]. Therefore, a search was performed for circulating anti-gliadin, anti-endomysial and anti-transglutaminase (TTG) antibodies. Detection of these antibodies (Table 1) led us to perform upper gastrointestinal tract endoscopy and duodenal biopsy, which confirmed the diagnosis of CD. A gluten free diet was therefore introduced.

Due to the patient's clinical history of repeated abortions and the results of coagulation studies, other autoantibodies such as anti-thyreoglobulin (1:40) and anti- β 2-glycoprotein-1 antibodies (24 UI/mL) were detected. Further characterization of the latter antibodies showed that IgG was 6.3 (normal range < 9) and IgM 48.7 (normal range < 5) IU/mL. All parameters of thyroid function were within the normal range.

Urinalysis showed glomerular proteinuria (0.7 g/day), microscopic hematuria, hyaline and granular casts; creatinine clearance (74 mL/min) was reduced with respect to the patient's age. These results raised the suspicion of IgA nephropathy, but the patient did not consent to undergo kidney biopsy. HLA analysis revealed the presence of HLA DQB1*02. The main laboratory data during the first admission at our unit and the follow up are shown in Table 1.

Table 1 Main results of laboratory studies in baseline conditions and after implementation of gluten free diet

Parameter (normal values)	Baseline determinations	Gluten free diet	
		6 th month	24 th month
Serum amylase (IU/L) (< 220)	1196	146	132
Serum lipase (UI/L) (< 200)	1650	39	ND
Ig A (mg/dL) (60-318)	1100	119	155
Immunocomplexes (meq/mL) (< 5)	6.5	ND	ND
Antigliadin antibodies IgA (%) (< 7)	96.9	5.8	ND
Antigliadin antibodies IgG (%) (< 12)	61	18.5	ND
Antiendomysial antibodies	Positive	Positive	ND
Anti-transglutaminase antibodies (UI/L) (<8)	20.5	ND	ND
Anti-thyreoglobulin antibodies (ND)	1:40	ND	ND
Total b2 GP 1 antibodies (IU/mL) (< 4 IU/mL)	24	ND	ND
Lupus anticoagulant	Positive	ND	ND
Creatinine clearance (mL/min) (70-120 mL/min)	74.07	88.05	107
Protein excretion rate (mg/24h)	322	2268	320

IU=international units; ND=not detectable.

After six months of controlled gluten free diet, the patient's body weight increased 12 kg; laboratory investigations demonstrated normalization of serum amylase, serum lipase and immunoglobulin levels; antigliadin, anti- β 2-glycoprotein-1 and anti-thyreoglobulin antibodies were no longer detectable, but antiendomysial antibodies were still present. Endoscopy showed a normal appearance of duodenal mucosa, and duodenal biopsy revealed a partial recovery of duodenal morphology. Due to the persistence of proteinuria (2.3 g/day), microscopic hematuria and hyaline and granular casts, a kidney biopsy showed that it was IgA nephropathy.

After 18 months of gluten-free diet, antiendomysial antibodies disappeared; creatinine clearance increased (Table 1), but proteinuria further worsened (2.9 g/day, Table 1), and albumin levels were still low.

After 24 months of gluten-free diet, a new duodenal biopsy showed complete recovery of villous architecture. Renal function further improved and proteinuria markedly decreased (Table

1). Amylase, lipase, and immunoglobulin levels were within the normal range. Anti- β 2-glycoprotein-1, anti-thyreoglobulin, antigliadin, antiendomysial and anti-TTG antibodies were undetectable. A coagulation study was normal (Table 1).

DISCUSSION

The increased prevalence of immune disorders in patients with CD is well recognized^[2, 10-12]. The association between CD and other immune disorders may be due to the sharing of a common genetic background, such as HLA antigens. However, in a very large study, involving 909 patients with celiac disease, Ventura and his associates^[12] found that the development of immune disorders in CD was clearly related to the duration of exposure to gluten. It is also interesting to note that multiple immune diseases in CD patients are uncommon. In the study of Ventura *et al.*^[12], only 15/909 patients had two kinds of immune manifestations and only one patient had three kinds of immune manifestations.

In this report, we described a female patient with unrecognized CD, who developed several clinical and/or sub clinical immune diseases.

Macroamylasemia with or without macrolipasemia occurs in approximately 0.4 % of general population and about 2.5-5.9 % of patients have hyperamylasemia^[18, 19]. It may be either an isolated, benign condition without pathological significance or may be associated with underlying diseases such as lymphoma, AIDS, carcinoma, liver disease and autoimmune disorders. The macroamylase complex is formed by amylase bound with serum proteins, commonly IgG and/or IgA. This molecule is too large to be filtered by the kidney and excreted in the urine, so it accumulates in plasma, whereas urinary amylase is normal or even low, a finding that should point to the correct diagnosis. Similarly, the macrolipase complex is a macroenzyme formed by association of polyclonal IgA with lipase. The incidental finding of macroamylasemia, if unrecognized, directs the diagnostic work-up to the pancreas and patients undergo unnecessary examinations and even surgery. Some case reports dealt with the occurrence of macroamylasemia with or without macrolipasemia in adult and pediatric patients with CD^[20-23]; in the large study by Rabsztyń *et al.*^[17], 21 out of 124 newly diagnosed CD patients (16.9 %) had macroamylasemia. Interestingly, serum macroamylase usually remained elevated despite strict gluten free diet^[17], and only in few cases, macroamylasemia and macrolipasemia disappeared after gluten free diet^[22, 23], as it occurred in our patient.

IgA nephropathy is the most common glomerulonephritis and is considered a relatively benign disease. However, longitudinal follow-up studies demonstrated that about 20 % of patients would progress to end stage of renal disease within 20 years from its onset. Patients with IgA nephropathy often have circulating IgA-antigliadin antibodies. However, lack of IgA-antireticulin, IgA-antiendomysium antibodies or jejunal mucosal atrophy suggests that most of these patients do not have latent CD^[24-26]. On the other hand, oral immunization with gliadin can induce IgA nephropathy in mice^[27]. Data on the association between CD and IgA nephropathy in humans are controversial, and only few cases of IgA nephropathy had definite CD and showed remission or improvement of renal disease after gluten withdrawal^[28, 29]. In our patient, the effect of gluten free diet on proteinuria was delayed, since this parameter showed increments at the 6th and the 18th month, despite the disappearance of antigliadin antibodies and normalization of IgA levels.

Patients with insulin-dependent diabetes mellitus, autoimmune thyroid disease, Addison's disease, and alopecia aerata are at increased risk of CD. A recent study addressed whether patients

with more than one autoimmune endocrine disorder were even more susceptible to CD or had celiac-type mucosal inflammation. Seven out of the 62 patients studied (11 %) were found to have CD; in addition, 2 had minor villous deterioration and 5 had an increased density of mucosal intraepithelial gamma-delta+ T-cells. HLA-DQ2 or DQ8 alleles were found in all subjects with mucosal changes^[30]. The association of CD with autoimmune thyroiditis has been proved. A study in 172 patients with autoimmune thyroiditis found a 10-fold higher prevalence of CD in this population than expected^[31]. The Authors concluded that the association of CD with autoimmune thyroid disease was not surprising as they shared common immunopathogenesis and suggested that it was advisable to screen patients with autoimmune thyroid disease for CD as there might be an increased risk for gluten intolerance^[31]. In our patient, anti-thyroglobulin antibodies disappeared after six months of gluten free diet. This finding confirmed that autoimmune thyroid disease and CD may share a common pathogenetic mechanism and that the disappearance of the immunological activation due to intestinal inflammation may lead to normalization of concomitant immune disorders.

Antiphospholipid antibodies, the most commonly detected of which are lupus anticoagulant, anticardiolipin and anti- β 2-glycoprotein-1 antibodies, are associated with the so-called antiphospholipid syndrome, a syndrome of arterial and venous thrombotic disease, thrombocytopenia, and fetal wastage^[32, 33]. Antiphospholipid antibodies are found in young, apparently healthy subjects with a prevalence of 1-5 %. Their prevalence increases with age, especially among elderly patients with coexistent chronic diseases, and is even higher in patients with autoimmune diseases. Untreated patients with CD also have an increased prevalence (about 14 %) of anticardiolipin antibodies^[34, 35], a phenomenon that Di Sabatino *et al.*^[35] found that an increased susceptibility of peripheral blood lymphocytes would undergo Fas-mediated apoptosis which resulted in immunogenic exposure of phospholipids with subsequent production of autoantibodies. As we know, lupus anticoagulant was observed in one patient^[36], while the female patient reported here had both lupus anticoagulant and anti- β 2-glycoprotein I antibodies which disappeared within 6 months after the introduction of gluten free diet.

Untreated CD in women resulted in a 8.9-fold increase in the relative risk of pregnancy miscarriage and in an about 30 % reduction of the baby's birth weight. Both miscarriage frequency and babies' low birth weight would normalize in response to gluten free diet^[37, 38]. Antiphospholipid antibodies were also associated with an unusually high proportion of pregnancy losses after the 10th week of gestation^[32, 33]. Our patient therefore had two different risk factors for abortion, both related to untreated CD. Unfortunately, it was not possible to establish whether the gluten-free diet corrected her miscarriage tendency, since until now the patient did not wish to plan a new pregnancy.

In conclusion, we found a high prevalence of immune diseases and a large number of organ-specific autoantibodies in a patient with CD. Although both CD and the other manifestations of a deranged immunity might be explained on the basis of a common genetic predisposition to this kind of disorders, some findings suggest that CD itself is responsible for the initiation of the immunological response. Indeed, persistent stimulation by some proinflammatory cytokines, such as interferon γ and tumor necrosis factor α , could induce further processing of autoantigens and their presentation to T lymphocytes by macrophage-type immunocompetent cells. As a matter of fact, the prevalence of immune diseases among patients with CD seems proportional to the time of exposure to gluten^[12], and many immune alterations disappear following

the recognition of CD and appropriate treatment, just as it occurred in our patient.

ACKNOWLEDGEMENT

The authors gratefully acknowledged Rosanna Abbate, MD (Dipartimento dell' area critica medico-chirurgica) and Antonio Calabrò, MD (Dipartimento di Fisiopatologia clinica, University of Florence), for their kind help in revising the manuscript.

REFERENCES

- 1 **Cook HB**, Burt MJ, Collett JA, Whitehead MR, Frampton CM, Chapman BA. Adult coeliac disease: prevalence and clinical significance. *J Gastroenterol Hepatol* 2000; **15**: 1032-1036
- 2 **Farrell RJ**, Kelly CP. Celiac sprue. *New Eng J Med* 2002; **346**: 180-188
- 3 **Badenhoop K**, Dieterich W, Segni M, Hofmann S, Hufner M, Usadel KH, Hahn EG, Schuppan D. HLA DQ2 and/or DQ8 is associated with celiac disease-specific autoantibodies to tissue transglutaminase in families with thyroid autoimmunity. *Am J Gastroenterol* 2001; **96**: 1648-1649
- 4 **Hernell O**, Ivarsson A, Persson LA. Coeliac disease: effect of early feeding on the incidence of the disease. *Early Hum Dev* 2001; **65** (Suppl): S153-160
- 5 **Kennedy NP**, Feighery C. Clinical features of coeliac disease today. *Biomed Pharmacother* 2000; **54**: 373-380
- 6 **Fasano A**, Catassi C. Current approaches to diagnosis and treatment of celiac disease: an evolving spectrum. *Gastroenterology* 2001; **120**: 635-651
- 7 **Tronccone R**, Greco L, Auricchio S. The controversial epidemiology of coeliac disease. *Acta Paediatr* 2000; **89**: 140-141
- 8 **Koop I**, Ilchmann R, Izzi L, Adragna A, Koop H, Barthelmes H. Detection of autoantibodies against tissue transglutaminase in patients with celiac disease and dermatitis herpetiformis. *Am J Gastroenterol* 2000; **95**: 2009-2014
- 9 **Gillett HR**, Freeman HJ. Serological testing in screening for adult celiac disease. *Can J Gastroenterol* 1999; **13**: 265-269
- 10 **Cooper BT**, Holmes GKT, Cooke WT. Coeliac disease and immunological disorders. *Br Med J* 1978; **1**: 537-539
- 11 **Collin P**, Reunala T, Pukkala E, Lappala P, Keyrilainen O, Pasternack A. Coeliac disease-associated disorders and survival. *Gut* 1994; **35**: 1215-1218
- 12 **Ventura A**, Magazzù G, Greco L. Duration of exposure to gluten and risk for autoimmune disorders in patients with celiac disease. *Gastroenterology* 1999; **117**: 297-303
- 13 **Collin P**, Salmi J, Hallstrom O, Oksa H, Oksala H, Maki M, Reunala T. High frequency of coeliac disease in adult patients with type-I diabetes. *Scand J Gastroenterol* 1989; **24**: 81-84
- 14 **Pococco M**, Ventura A. Coeliac disease and insulin-dependent diabetes mellitus: a causal association. An Italian multicentre study. *Acta Paediatr* 1995; **84**: 1432-1433
- 15 **Lepore L**, Martellosi S, Pennesi M, Falcini F, Ermini ML, Ferrari R, Peticarari S, Presani G, Lucchesi A, Lapini M, Ventura A. Prevalence of coeliac disease in patients with juvenile chronic arthritis. *J Pediatr* 1996; **129**: 311-313
- 16 **Carroccio A**, Iannitto E, Montalto G, Tumminiello M, Campagna P, Lipari MG, Notarbartolo A, Iacono G. Sideropenic anemia and celiac disease: one study, two points of view. *Dig Dis Sci* 1998; **43**: 673-678
- 17 **Rabsztyan A**, Green PH, Berti I, Fasano A, Perman JA, Horvath K. Macroamylasemia in patients with celiac disease. *Am J Gastroenterol* 2001; **96**: 1096-1100
- 18 **Quilez C**, Martinez J, Gomez A, Trigo C, Palazon JM, Belda G, Perez-Mateo M. Chronic elevation of enzymes of pancreatic origin in asymptomatic patients. *Gastroenterol Hepatol* 1998; **21**: 209-211
- 19 **Yoshida E**, Tsuruoka T, Suzuki M, Asahara M, Okazaki T, Kadohno N, Kanno T. Sex and age distribution of patients with macroamylasemia found in the daily isoenzyme analysis. *Rinsho Byori* 1998; **46**: 473-478
- 20 **Rajvanshi P**, Chowdhury JR, Gupta S. Celiac sprue and macroamylasemia: potential clinical and pathophysiological implications. Case study. *J Clin Gastroenterol* 1995; **20**: 304-306

- 21 **Garcia-Gonzalez M**, Defarges-Pons V, Monescillo A, Hernandez F, Cano-Ruiz A. Macrolipaseemia and celiac disease. *Am J Gastroenterol* 1995; **90**: 2233-2234
- 22 **Bonetti G**, Serricchio G, Giudici A, Bettonagli M, Vadacca GB, Bruno R, Coslovich E, Moratti R. Hyperamylasemia due to macroamylasemia in adult gluten enteropathy. *Scand J Clin Lab Invest* 1997; **57**: 271-273
- 23 **Barera G**, Bazzigaluppi E, Viscardi M, Renzetti F, Bianchi C, Chiumello G, Bosi E. Macroamylasemia attributable to gluten-related amylase autoantibodies: a case report. *Pediatrics* 2001; **107**: E93
- 24 **Rostoker G**, Laurent J, Andre C, Cholin S, Lagrue G. High levels of IgA antigliadin antibodies in patients who have IgA mesangial glomerulonephritis but not coeliac disease (letter). *Lancet* 1988; **1**: 356-357
- 25 **Sategna-Guidetti C**, Ferfaglia G, Bruno M, Pulitano R, Roccatello D, Amore A, Coppo R. Do IgA antigliadin and IgA antiendomysium antibodies show there is latent coeliac disease in primary IgA nephropathy? *Gut* 1992; **33**: 476-478
- 26 **Ots M**, Uibo O, Metskula K, Uibo R, Salupere V. IgA-antigliadin antibodies in patients with IgA nephropathy: the secondary phenomenon? *Am J Nephrol* 1999; **19**: 453-458
- 27 **Amore A**, Emancipator SN, Roccatello D, Gianoglio B, Peruzzi L, Porcellini MG, Piccoli G, Coppo R. Functional consequences of the binding of gliadin to cultured rat mesangial cells: bridging immunoglobulin A to cells and modulation of eicosanoid synthesis and altered cytokine production. *Am J Kidney Dis* 1994; **23**: 290-301
- 28 **Fomasieri A**, Sinico RA, Maldifassi P, Bernasconi P, Vegni M, D' Amico G. IgA-antigliadin antibodies in IgA mesangial nephropathy (Berger's disease). *Br Med J* 1987; **295**: 78-80
- 29 **Woodrow G**, Innes A, Boyd SM, Burden RP. A case of IgA nephropathy with coeliac disease responding to a gluten-free diet. *Nephrol Dial Transplant* 1993; **8**: 1382-1383
- 30 **Kaukinen K**, Collin P, Mykkanen AH, Partanen J, Maki M, Salmi J. Celiac disease and autoimmune endocrinologic disorders. *Dig Dis Sci* 1999; **44**: 1428-1433
- 31 **Berti I**, Trevisiol C, Tommasini A, Citta A, Neri E, Geatti O, Giammarini A, Ventura A, Not T. Usefulness of screening program for celiac disease in autoimmune thyroiditis. *Dig Dis Sci* 2000; **45**: 403-406
- 32 **Levine JS**, Branch DW, Rauch J. The antiphospholipid syndrome. *New Eng J Med* 2002; **346**: 752-763
- 33 **Stone S**, Khamashta MA, Poston L. Placentation, antiphospholipid syndrome and pregnancy outcome. *Lupus* 2001; **10**: 67-74
- 34 **Lerner A**, Blank M, Lahat N, Shoenfeld Y. Increased prevalence of autoantibodies in coeliac disease. *Dig Dis Sci* 1998; **43**: 723-726
- 35 **Di Sabatino A**, D' Alò S, Millimaggi D, Ciccocioppo R, Parroni R, Sciarpa G, Cifone MG. Apoptosis and peripheral blood lymphocyte depletion in coeliac disease. *Immunology* 2001; **103**: 435-440
- 36 **Chiurazzi F**, Poggi V, Greco L, Rotoli B. Lupus anticoagulant and coeliac disease: a case report. *Haematologica* 1987; **72**: 357-359
- 37 **Hozyasz KK**. Pregnancy outcomes in celiac women. *Am J Gastroenterol* 2000; **95**: 1373-1374
- 38 **Norgard B**, Fonager K, Sorensen HT, Olsen J. Birth outcomes of women with celiac disease: a nationwide historical cohort study. *Am J Gastroenterol* 1999; **94**: 2435-2440

Edited by Xu XQ

Hepato-splenic lymphoma: a rare entity mimicking acute hepatitis: A case report

Federico Perfetto, Roberto Tarquini, Francesco Mancuso, Simonetta di Lollo, Silvia Tozzini, Giampiero Bellesi, Giacomo Laffi

Federico Perfetto, Roberto Tarquini, Francesco Mancuso, Giacomo Laffi, Department of Internal Medicine, University of Florence, Italy

Simonetta di Lollo, Silvia Tozzini, Department of Human Pathology and Oncology, University of Florence, Italy

Giampiero Bellesi, Department of Hematology, University of Florence, Italy

Correspondence to: Professor Giacomo Laffi, Department of Internal Medicine, University of Florence, Viale Pieraccini, 18, Zip Code 50139 Firenze, Italy. g.laffi@mednuc2.dfc.unifi.it

Telephone: +39-55-4223549 **Fax:** +39-55-4223549

Received: 2002-10-10 **Accepted:** 2002-11-04

Abstract

We reported a case of non-Hodgkin's lymphoma where liver involvement was the predominant clinical manifestation. A 27-year old man presented with markedly elevated serum aspartate aminotransferase, alanine aminotransferase and lactate dehydrogenase, reduced prothrombin activity, thrombocytopenic purpura and hepato-splenomegaly without adenopathy. Viral, toxic, autoimmune and metabolic liver diseases were excluded. Bone marrow biopsy showed an intracapillary infiltration of T-lymphocytes with no evidence of lipid storage disease. Because of a progressive spleen enlargement, splenectomy was performed. Histological examination showed lymphomatous intrasinusoid invasion of the spleen. Immunohistochemical investigation revealed the T phenotype of the neoplastic cells: CD45+, CD45RO+, CD3+, CD4-, CD8-, TIA1-. About 50 % of the lymphoid cells expressed CD56 antigen. The diagnosis of hepatosplenic T cell lymphoma was done. The patient was treated with chemotherapy, which induced a complete remission. Eighteen months later, he had a first relapse with increased aspartate aminotransferase, alanine aminotransferase, lactate dehydrogenase, thrombocytopenic purpura and blast in the peripheral blood. In spite of autologous bone marrow transplantation, he died twenty months after the diagnosis. Even in the absence of a mass lesion or lymphadenopathy, hepatosplenic T-cell lymphoma should be considered in the differential diagnosis of a patient whose clinical course is atypical for acute hepatic dysfunction.

Perfetto F, Tarquini R, Mancuso F, di Lollo S, Tozzini S, Bellesi G, Laffi G. Hepato-splenic lymphoma: a rare entity mimicking acute hepatitis: A case report. *World J Gastroenterol* 2003; 9 (6): 1381-1384

<http://www.wjgnet.com/1007-9327/9/1381.asp>

INTRODUCTION

Liver and splenic involvement is commonly seen during a malignant lymphoma, but rarely occurs as a prominent clinical feature at diagnosis. Hepatosplenic lymphoma is a rare and poorly recognized entity^[1] characterized by neoplastic

proliferation of T-cell bearing a gd or, more rarely, ab clonal rearrangement of the receptor (TCR). This lymphoma shows a specific morphological pattern characterized by a preferential hepatic sinusoids and splenic red pulp involvement without lymphadenopathy and discrete or absent bone marrow involvement. Moreover the diagnosis is complicated in several cases by the presence of misleading symptoms. We reported the case of a young man without palpable lymphadenopathy and clinical and laboratory presentations resembling an acute liver disease.

CASE REPORT

A 27-year old caucasian man was admitted in an Internal Medicine unit in February 1999 because of fever (38 °C), malaise, anorexia, and erythematous macules and papules on the face, trunk and arms. The patient referred similar but transient cutaneous lesions in the previous two-months. Laboratory investigations yielded the following results: aspartate aminotransferase (AST) 240 IU/L (normal range: 0-37 IU/L), alanine aminotransferase (ALT) 520 IU/L (normal range: 0-40 IU/L), γ -glutamyl-transpeptidase (γ -GT) 46 IU/L (normal range: 11-43 IU/L), alkaline phosphatase (ALP) 298 IU/L (normal range: 60-270 IU/L) and platelets 120×10^9 /L (normal range: $130-400 \times 10^9$ /L). Serological tests for Epstein Barr virus (EBV) showed a positivity for nuclear antigen (IgG 248 ACU/ml) (normal value: <56 ACU/ml) whereas serology for hepatitis A (HAV), hepatitis B (HBV) and hepatitis C (HCV) viruses was negative. Physical examination showed a mild hepato-splenomegaly. There was no palpable lymphadenopathy.

Two weeks later he was transferred to our Internal Medicine unit with the clinical diagnosis of "acute hepatitis with hepato-splenomegaly and recidivant purpuric exanthema". Physical examinations showed an enlarged tender liver (2 cm below the rib border) and splenomegaly (2 cm below the rib border) without peripheral lymphadenopathy. The cutaneous lesions of the trunk and the face were already present as purpuric palpable papules. Fever was absent. Abdominal ultrasonography revealed a mild hepatomegaly and splenomegaly (major axis of 18 cm), without ascite and abdominal lymphadenomegaly. Doppler sonography revealed an increased blood flow in the spleen and the portal vein without obstruction of the main hepatic veins. An upper gastrointestinal endoscopy did not reveal esophageal varices. Chest x-rays at the time of admission yielded normal findings. Liver function test showed AST 498 IU/L, ALT 958 IU/L, γ -GT 49 IU/L, ALP 426 IU/L, total bilirubin 1.15 mg/dl (normal range: 0.2-1.0 mg/dl) and lactate dehydrogenase (LDH) 1 234 U/L (normal range 190-450 IU/L). Peripheral blood counts showed hemoglobin 16.1 g/dl, hematocrit 45 %, leukocytes 4.9×10^9 /L with normal differential count and platelets 80×10^9 /L. Coagulation indices showed prothrombin activity 53 % (normal range: 90-100 %), international normal ratio 1.4, activated partial thromboplastin time 53 sec (normal range: 25-40 sec) and fibrinogen 267 mg/dl (normal range: 200-400 mg/dl). Albumin levels were 4.25 g/dl (normal range: 3.3-5.1 g/dl) and γ -globulin were 1.44 g/dl (normal range:

0.84-1.44 g/dl). Serological tests were negative for HAV, HBV, HCV, cytomegalovirus and human herpes simplex N° 1, 2, and 6. EBV serologic findings were heterophile test (heterophile antibody) negative, viral capsid antigen (VCA) immunoglobulin IgM negative and IgG positive. Serological tests exploring infective agents able to induce an acute hepatitis such as Chlamydia pneumoniae, Bartonella spp, Borrelia burgdorferi, Toxoplasma gondii, Coxsackie virus groups A and B (N° 1-6) and Echovirus, were negative as well as the serological test for Rickettsia and Parvovirus B19. Results of serology for human immunodeficient virus (HIV) 1 and 2 including cDNA Polymerase Chain Reaction and the screening of the antigen p24 of HIV1 were negative. Serum α -fetoprotein and carcinoembryonic antigens were within the normal range. To exclude autoimmune disease, serological tests for anti-nuclear, anti-mitochondrial, anti-liver/kidney microsomal (LKM), and anti-smooth muscle (ASM) were performed but the results were negative; cryoglobulins and circulating immune complexes were absent. Serum ceruloplasmine levels, circulating serum copper levels, 24-h urine excretion of copper and α 1-antitrypsin levels were in the normal range and Kayser Fleischer rings were absent on slit-lamp examination. To exclude a thrombocytopenia induced by EDTA (pseudothrombocytopenia) blood was drawn on test tube with sodium citrate as anticoagulant but the result confirmed the presence of a true thrombocytopenia. Anti-platelet antibodies were negative in two consecutive different samples and reticulate platelets were in the normal range. Toxic (including also ingestion of hepatotoxic mushrooms such as Amanita Phalloides) and drugs inducing hepatitis were excluded by a careful and detailed personal and family history. During the following weeks, patient complained increasing fatigue and tenderness in the upper left quadrant and physical examination revealed an enlarged spleen that extended his lower pole 4-cm below the rib border. Liver function tests continued to rise with AST 658 IU/L, ALT 1 074 IU/L, γ -GT 72 IU/L, ALP 473 IU/L, and LDH 1 365 U/L. Serum β -2 microglobulin levels were 2.4 mg/dl; (normal range: 1.2-2.5 mg/dl). Coagulation indices showed prothrombin activity 51 %, international normal ratio 1.4, fibrinogen 146 mg/dl and activated partial thromboplastin time 42.4 sec without serological evidence of circulating anticoagulants such as lupus anticoagulant or anticardiolipin antibodies. A decreased activity of coagulation factor II (57 %; normal range: 70-120 %), VII (58 %; normal range: 70-120 %) and X (41 %; normal range: 70-120 %) were also demonstrated, despite i.v. Vitamin K treatment; factor VIII activity was also reduced (63.9 %; normal range: 70-150). The bleeding time was slightly prolonged (8 minutes and 20 seconds; normal range: 3-7 min.) Because of coagulopathy and thrombocytopenia percutaneous liver biopsy was not performed. Biopsy of the skin showed neither vasculitis findings nor lymphoproliferative disease. An abdominal CT scan revealed a massive enlargement of the spleen (20 cm of sagittal diameter and 14 cm of antero-posterior diameter) and mild hepatomegaly without either focal lesions or abdominal lymphadenomegaly. Thorax and neck CT scan yielded normal findings. Although in type 1 Gaucher disease the liver function tests were not so seriously altered, the presence of hepatomegaly with a progressive and massive splenomegaly together with thrombocytopenia prompted us to undergo the patient to bone marrow examination and to a measurement of acid β -glucosidase activity in circulating leukocyte cells. Although β -glucosidase activity was slightly decreased (5.5 nmol/mg/h; normal range: 8-15.1 nmol/mg/h), the bone marrow examination did not reveal the presence of the characteristics of Gaucher cells with the typical "wrinkled paper" cytoplasm. However, an intracapillary T-lymphocytes

infiltration was observed. The circulating leukocytes were $14.6 \times 10^9/L$ (normal range: 4.8-8.5) with absolute lymphocytosis ($8.8 \times 10^9/L$, normal range: 1.6-2.4). Immunophenotype of circulating lymphocytes showed that CD3 positive lymphocytes were about $5.4 \times 10^9/L$ (normal range: 1.1-1.7), CD4 positive lymphocytes were $2.5 \times 10^9/L$ (normal range: 0.65-1.4), CD8 positive lymphocytes were $3.01 \times 10^9/L$ (normal range: 0.32-0.90) with CD4 to CD8 ratio of 0.8 % (normal range: 1-1.5 %) and CD19 positive lymphocytes were $1.23 \times 10^9/L$ (normal range: 0.2-0.4). Circulating T lymphocytes (65 % of overall; $5.65 \times 10^9/L$) bearing the ab type of TCR were 92.5 % (normal range: 90-95 %) while circulating T lymphocytes bearing gd TCR were about 7.5 % (normal range: 5-10 %). Over half (60 %) of circulating leukocytes were small to medium sized lymphoid cell with moderate amount of pale, agranular cytoplasm without villous projections. Some lymphocytes showed round or folding nucleus, with moderate clumped chromatin surrounding a small nucleolus. In spite of the opportunity to perform a transjugular liver biopsy, the presence of massive splenomegaly with pain in the left upper abdominal quadrant and early satiety, urged us to do splenectomy which was performed in April 1999. The histologic examination of the spleen revealed a hepatosplenic lymphoma. After the splenectomy, skin lesions disappeared, liver enzyme values progressively decreased and coagulation indices showed normalization in one week. As expected, platelets count increased until $738 \times 10^9/L$ one week after the splenectomy and decreased to $417 \times 10^9/L$ one month later. In the post surgical period, patient was treated with 4 cycles of chemotherapy (Fi2/89; epirubicine, vincristine, bleomycine and cyclophosphamide). This resulted in a complete clinical remission with negative bone marrow biopsy. In view of autologous bone marrow transplantation (ABMT) he was treated with 2 cycles of chemotherapy (BAVEC-MiMA; BiCNU, adriablastine, vepeside, vincristine, mitoxantrone, methotrexate and cytosine arabinoside). In January 2000, he was submitted to three consecutive leukapheresis but, unfortunately, the number of peripheral circulating levels of CD34 positive cells was not sufficient for the ABMT and the patient refused new leukapheresis. Two other cycles of BAVEC-MiMA chemotherapy were performed as intensive consolidation therapy after the remission. One month later (May 2000), the patient was admitted to a hematological unit because of fatigue, malaise and erythematous papules of the face and trunk similar to those that characterized the beginning of the disease. Significant laboratory values included AST 225 IU/L, ALT 255 IU/L, LDH 1773 U/L, platelets $46 \times 10^9/L$ and leukocytes $27.9 \times 10^9/L$, the latter characterized by medium and large size lymphocytes with cleaved and folding nucleus. The immunophenotype of circulating lymphocytes was NK (CD16+, CD56+, CD2+, CD7+; CD8 were expressed on about 63 % of NK population while CD3 was negative). He was treated with four weekly infusions of chemotherapy (MACOP-B; vincristine, adriamycine, bleomycine, cyclophosphamide, methotrexate and prednisone) with normalization of liver enzyme values, peripheral blood counts and skin lesions. The second relapse occurred 10 weeks later. Patient was readmitted in the same hematological unit for salvage ABMT. One-month later, he developed an acute leukemia. The patient died in December 2000, twenty months after the diagnosis. Post-mortem examination was not performed.

MATERIALS AND METHODS

Informed consent for all procedures was obtained from the patient. Bone marrow specimen was fixed in 10 % buffered formalin and processed according to standard technique. Paraffin sections were stained with hematoxylin-eosin, Giemsa,

PAS and Gomori method. Biopsy of the skin and specimens of the spleen were fixed in 10 % buffered formalin, and in B5; paraffin sections were stained with hematoxylin-eosin, Giemsa and PAS. An immunohistochemical investigation was performed on bone marrow and spleen sections according to streptavidin-biotin method. Monoclonal antibodies were used for detection of CD45, CD20, CD79a, CD10, CD45RO, CD30, CD15, CD56, CD8, CD4, TIA-1, AE1/AE3, EMA, HMB45, MIB1 antigens, and polyclonal antibodies for CD3 and S-100 protein detection. The positive reaction was revealed using diaminobenzidin as chromogen.

Histologic findings

Biopsy of the skin showed a moderate aspecific lymphoid infiltration of perivascular space associated with erythrocytes. Bone marrow biopsy showed intense eritroid and megakaryocytic hyperplasia and a mild hypoplasia of myeloid compartment. Moreover an important intracapillary infiltration of medium-sized T-lymphocytes (CD45+, CD3+, scattered CD56+, CD 20-) was observed (Figure 1). The spleen weight was 3 000 g. Microscopic examination showed the presence of a diffuse intrasinuses infiltrate in the red pulp of medium-sized T-lymphoid cells with round to irregular nuclei and moderately abundant pale cytoplasm (Figure 2). All neoplastic cells expressed CD45, CD45RO and CD3 membrane antigens (Figure 3), whereas they were CD4-, CD8- and TIA-1-. CD56 antigen was positive on about 50 % of the T-lymphoid cells (Figure 4). The diagnosis of hepatosplenic T cell lymphoma was done. Because of the unavailability of frozen sections, the analysis of gd TCR expression was not done.

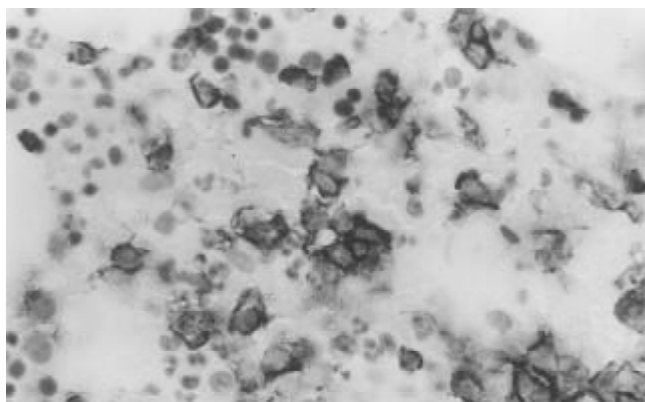


Figure 1 Immunohistochemical analysis of the bone marrow: the neoplastic cells within sinuses were CD3 positive and scattered CD56 positive (insert).

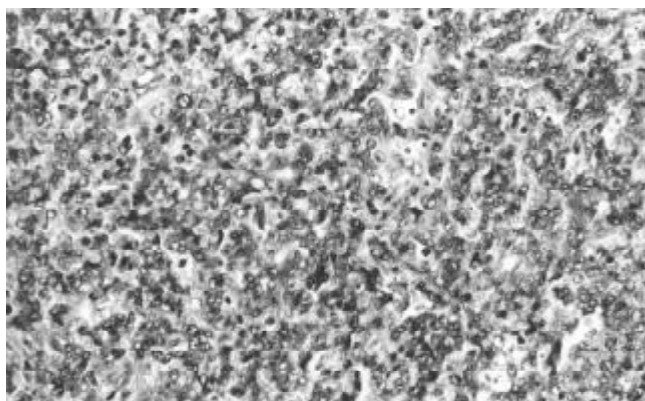


Figure 2 Clusters of medium-sized cells seeped through the red pulp of spleen.

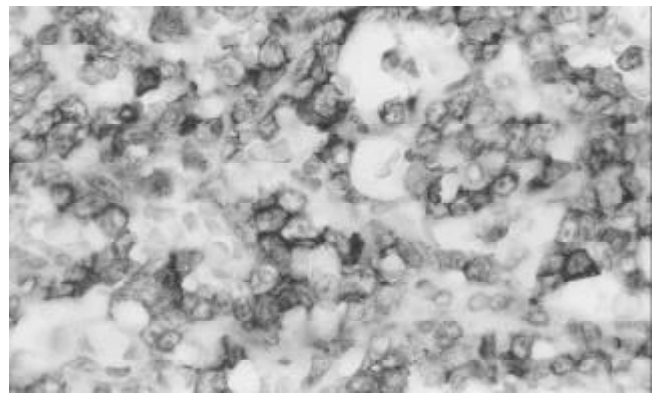


Figure 3 The neoplastic cells were CD3 positive in the spleen.

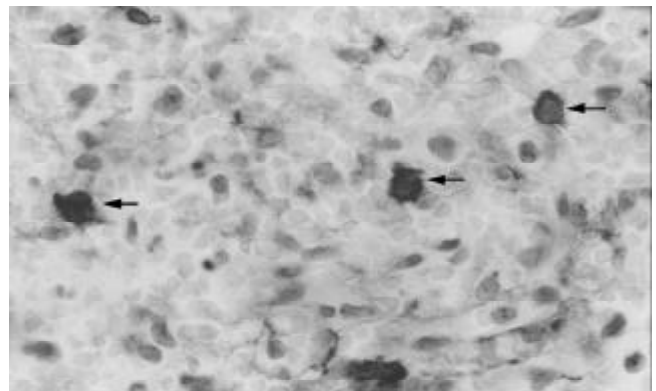


Figure 4 The neoplastic cells were scattered CD56 positive (arrows) in the spleen.

DISCUSSION

Lymphomatous involvement of the liver has been described in three clinical situations: disseminated disease, primary liver lymphoma and hepatosplenic T-cell lymphoma. Secondary hepatic involvement by lymphoma is relatively common and indicates advanced disease. Non-Hodgkin's primary lymphoma of the liver is an uncommon entity, often clinically indistinguishable from more commonly occurring primary carcinoma and metastatic neoplasms; the correct diagnosis is based on liver biopsy or even on post-mortem examination because of lacking of suggestive clinical or imaging features. The hepatosplenic T-cell lymphoma has been recognized by Farcet *et al.* in 1990^[1] as a distinct entity characterized by a $\gamma\delta$ T lymphocytes sinusal infiltration of the red pulp of the spleen and by sinusoidal infiltration of the liver without lymph node involvement^[2]. Because of its striking uniformity with respect to clinical, morphological and immunophenotypical features, this lymphoma was listed as a provisional entity in the Revised European-American Lymphoma (REAL) classification^[3]. Later on, it has been incorporated as a distinct entity in the WHO classification of lymphoid neoplasms^[4] and termed hepatosplenic $\gamma\delta$ T-cell lymphoma. Since then, to our knowledge, 45 cases have been described^[5]. According to Weidmann revision, clinical symptoms at presentation are hepato-splenomegaly, constitutional symptoms and less frequently jaundice due to hepatic involvement. The predominant laboratory findings are reduced peripheral blood cells ranging from hemolytic anemia (Coombs negative) to thrombocytopenia or pancytopenia, high levels of LDH and mild increase of liver enzymes. Moreover, recently, 14 cases of hepatosplenic lymphoma expressing $\alpha\beta$ TCRs have been described^[6].

These $\alpha\beta$ lymphomas fulfill all the clinical, morphological and immunophenotypical criteria required for the diagnosis

of hepatosplenic lymphoma, with the exception of the female preponderance (11/14 patients) and age of distribution (more wide than the $\gamma\delta$ counterpart). Early diagnosis of this lymphoma, even if mandatory, is complicated in several cases because of the absence of lymphadenomegaly, not specific bone marrow involvement and normal peripheral blood cell counts. The diagnosis of hepatosplenic T-cell lymphoma in the case we reported had considerable difficulties because its clinical and laboratory features were similar to acute hepatitis. As a matter of fact, the liver chemistry evaluation was typical of hepatic inflammatory disease with hepatocellular necrosis (about tenfold increase of AST and ALD and threefold increase of LDH) and impaired synthesis of liver coagulation factors whereas, the mild increase of ALP level together with normal levels of serum β -2 microglobulin and γ -GT were unusual for a lymphoproliferative disease of the liver. Probably these unusual laboratory findings were related to the quite exclusive sinusoidal infiltration by lymphoid cells without or with minimal portal involvement. However, this clinical presentation prompted us to exclude all causes of acute liver diseases such as viral hepatitis drugs, toxins, chemical ingestion and/or exposition, vascular abnormalities, autoimmune hepatitis and metabolic diseases. As the present case illustrated, an early diagnosis of hepatosplenic lymphoma was unlikely to be possible on bone marrow specimen alone. According to Galaurd^[7] even when the hepatosplenic involvement is clear, the presence of few T-cells within bone marrow sinus is neither specific nor conclusive without a molecular analysis on frozen tissue. Liver biopsy, which is another way to confirm the diagnosis of hepatosplenic T-cell lymphoma, was not performed in this case because of the presence of coagulopathy and thrombocytopenia. Nevertheless, the presence of an intracapillary infiltrate by T lymphocytes on the bone marrow specimen as well as the progressive and symptomatic enlargement of the spleen prompted us to suspect the presence of a lymphoproliferative disease and consequently to perform splenectomy. As reported in literature, splenectomy was the cornerstone for the diagnosis of hepatosplenic T-cell lymphoma. Immunophenotype studies on the spleen specimens showed the typical pattern of hepatosplenic T-cell lymphoma characterized by expression of CD45 and CD3 antigens and by double negativity for CD4 and CD8 antigens. The NK cell associated antigen CD56 expression has been reported in approximately 70-100 % of hepatosplenic T-cell lymphoma^[8, 9]. The presence in the bone marrow of T-lymphocytes bearing the CD56 antigen could explain the late involvement of peripheral blood by lymphoid cell with NK immunophenotype. Furthermore, in contrast with other previous investigations, in all specimens of the spleen examined, neoplastic cells were negative for TIA-1 (restricted intracellular antigen, also called granular membrane protein of 17 Kd, GMP 17), a very sensitive marker of cytosol granules independent of their activation status. Concerning the recurrence of cutaneous skin lesions, a skin biopsy, performed early in the course of disease, showed only a moderate and aspecific lymphoid infiltration of perivascular spaces, without the morphological and immunophenotypical findings that characterized the peripheral lymphoma involving the skin. Although thrombocytopenia was not severe, a complete remission of skin lesions was achieved

after its correction. It seems likely to ascribe these purpuric lesions to the reduced number of circulating platelets, but a cytotoxic activity of cutaneous T lymphocytes could have a role in the pathogenesis of these skin lesions. As the present case illustrated that the prognosis for this type of lymphoma is poor. Complete remission was reported only in few patients after chemotherapy (second and third generation regime for high-grade lymphomas), followed by autologous and allogenic bone marrow or peripheral stem cell transplantation. The median survival time was 8 months (range 0-42 month)^[5].

In conclusion, the current report described the unusual clinical presentations of hepatosplenic lymphoma. This patient, in fact, shared several distinctive features including: 1) the initial clinical presentations mimicking an acute hepatitis, 2) the presence of cutaneous lesions, contemporary with the hepatosplenic involvement and 3) a negativity of TIA-1 expression of lymphoid T cells. Even in the absence of a mass lesion or lymphadenopathy, hepatosplenic T-cell lymphoma should be included in the differential diagnosis of an acute hepatic dysfunction in young patient who shows no evidence of viral, toxic, autoimmune or metabolic liver disease.

REFERENCES

- 1 **Farcet JP**, Gaulard P, Marolleau JP, Le Couedic JP, Henni T, Gourdin MF, Divine M, Haioun C, Zafrani S, Goossens M. Hepatosplenic T-cell lymphoma: sinusal/sinusoidal localization of malignant cells expressing the T-cell receptor gamma delta. *Blood* 1990; **75**: 2213-2219
- 2 **Gaulard P**, Zafrani S, Mavier P, Rocha FD, Farcet JP, Divine M, Haioun C, Piau deau Y. Peripheral T cell lymphoma presenting as predominant liver disease: a report of three cases. *Hepatology* 1986; **6**: 864-868
- 3 **Harris NL**, Jaffe ES, Stein H, Banks PM, Chan JK, Cleary ML, Delsol G, De Wolf-Peters C, Falini B, Gatter KC. A revised European-American Lymphoma of lymphoid neoplasms: a proposal from the International Lymphoma Study Group. *Blood* 1994; **84**: 1361-1392
- 4 **Harris NL**, Jaffe ES, Diebold J, Flandrin G, Muller-Hermelink HK, Vardiman J. Lymphoma classification-from controversy to consensus: the R.E.A.L. and WHO Classification of lymphoid neoplasms. *Ann Oncol* 2000; **11**: 3-10
- 5 **Weidmann E**. Hepatosplenic T cell lymphoma. A review on 45 cases since the first report describing the disease as a distinct lymphoma entity in 1990. *Leukemia* 2000; **14**: 991-997
- 6 **Macon WR**, Levy NB, Kurtin PJ, Salhany KE, Elkhalfia MY, Casey TT, Craig FE, Vnencak-Jones CL, Gulley ML, Park JP, Cousar JB. Hepatosplenic alpha beta lymphomas: a report of 14 cases and comparison with hepatosplenic gammadelta lymphomas. *Am J Surg Pathol* 2001; **25**: 285-296
- 7 **Gaulard P**, Kanavaros P, Farcet JP, Rocha FD, Haioun C, Divine M, Reyes F, Zafrani ES. Bone marrow histologic and immunohistochemical findings in peripheral T cell lymphoma: a study of 38 cases. *Hum Pathol* 1991; **22**: 331-338
- 8 **Cooke CB**, Krenacs L, Steller-Stevenson M, Greiner TC, Raffeld M, Kingma DW, Abruzzo L, Frantz C, Kaviani M, Jaffe ES. Hepatosplenic T cell lymphoma: a distinct clinicopathologic entity of cytotoxic gd T cell origin. *Blood* 1996; **88**: 4265-4274
- 9 **Salhany KE**, Feldman M, Kahn MJ, Perrit D, Schretzenmair RD, Wilson DM, DiPaola RS, Glick AD, Kant JA, Nowell PC, Khan MJ. Hepatosplenic gammadelta lymphoma: ultrastructural, immunophenotypic, and functional evidence for cytotoxic T lymphocyte differentiation. *Hum Pathol* 1997; **28**: 674-685